

PERFORMANCE ASSESSMENT for the SALTSTONE DISPOSAL FACILITY at the SAVANNAH RIVER SITE



October 2009

Prepared by: SRR Closure & Waste Disposal Authority
Aiken, SC 29808



Prepared for U.S. Department of Energy Under Contract No. DE-AC09-09SR22505

REVISION SUMMARY

| REV. # | DESCRIPTION | DATE OF ISSUE |
|---------------|--|----------------------|
| A | Initial Issue to DOE-SR (Draft issued under No. LWO-RIP-2009-00011). | 03/31/2009 |
| B | Issued for DOE Low-Level Waste Federal Review Group (LFRG) Review (Draft issued under No. LWO-RIP-2009-00011). | 06/25/2009 |
| 0 | Initial Issue | 10/29/2009 |

TABLE OF CONTENTS

| | |
|---|--------------|
| TABLE OF CONTENTS | iii |
| LIST OF FIGURES | x |
| LIST OF TABLES | xxi |
| ACRONYMS / ABBREVIATIONS | xxvii |
| ACRONYMS / ABBREVIATIONS | xxvii |
| 1.0 EXECUTIVE SUMMARY | 31 |
| 2.0 INTRODUCTION | 33 |
| 2.1 <i>General Approach</i> | 33 |
| 2.1.1 Previous Performance Assessments and Composite Analyses..... | 33 |
| 2.1.1.1 1992 Radiological Performance Assessment..... | 33 |
| 2.1.1.2 2002 Special Analysis: Reevaluation of the Inadvertent Intruder, Groundwater, Air, and Radon Analyses for the SDF..... | 34 |
| 2.1.1.3 2005 Special Analysis: Revision of Saltstone Vault 4 Disposal Limits | 34 |
| 2.1.1.4 2005 Performance Objective Demonstration Document | 35 |
| 2.1.1.5 Impact on Composite Analysis | 35 |
| 2.1.2 Modeling Process..... | 35 |
| 2.2 <i>General Facility Description</i> | 37 |
| 2.2.1 Savannah River Site..... | 37 |
| 2.2.2 Saltstone Facility..... | 37 |
| 2.3 <i>Facility Life Cycle</i> | 38 |
| 2.4 <i>Related Documents</i> | 38 |
| 2.4.1 Groundwater Protection Management Program | 38 |
| 2.4.2 End State Vision | 38 |
| 2.4.3 SRS Long Range Comprehensive Plan | 39 |
| 2.5 <i>Performance Criteria</i> | 40 |
| 2.5.1 DOE O 435.1-1 Performance Objectives and Requirements | 40 |
| 2.5.2 10 CFR 61 Performance Objectives | 41 |
| 2.6 <i>Summary of Key Assessment Assumptions</i> | 42 |
| 2.6.1 General SDF Facility Modeling Assumptions..... | 42 |
| 2.6.2 Site Characteristics Assumptions..... | 42 |
| 2.6.3 Facility Design Assumptions | 42 |
| 2.6.4 Stabilized Contaminants Characteristic Assumptions | 42 |
| 2.6.4.1 Inventory | 42 |
| 2.6.4.2 Waste Form..... | 43 |
| 2.6.5 Integrated Site Conceptual Model Assumptions | 43 |
| 2.6.5.1 Degradation and Contaminant Movement | 43 |
| 2.6.5.2 Infiltration and Erosion Control..... | 44 |
| 3.0 DISPOSAL FACILITY CHARACTERISTICS | 45 |
| 3.1 <i>Site Characteristics</i> | 45 |

| | | |
|---------|--|-----|
| 3.1.1 | Geography and Demography | 45 |
| 3.1.1.1 | SRS Site Description..... | 45 |
| 3.1.1.2 | Closure Site Description | 50 |
| 3.1.1.3 | Population Distribution | 52 |
| 3.1.1.4 | Land Use – Present and Planned..... | 53 |
| 3.1.2 | Meteorology and Climatology | 53 |
| 3.1.2.1 | General SRS Climate | 53 |
| 3.1.2.2 | Meteorological Data Collection..... | 54 |
| 3.1.2.3 | Data Pertinent to PA Modeling..... | 56 |
| 3.1.3 | Ecology | 56 |
| 3.1.4 | Geology, Seismology, and Volcanology | 58 |
| 3.1.4.1 | Regional and Site-Specific Topography | 59 |
| 3.1.4.2 | Local Geology and Soils..... | 63 |
| 3.1.4.3 | Seismology..... | 65 |
| 3.1.5 | Hydrogeology | 69 |
| 3.1.5.1 | Regional Hydrogeology | 69 |
| 3.1.5.2 | Characterization of Local Hydrogeology..... | 75 |
| 3.1.5.3 | Groundwater Flow in the GSA | 83 |
| 3.1.5.4 | Surface-Water Flow in the GSA..... | 85 |
| 3.1.6 | Geochemistry | 88 |
| 3.1.7 | Natural Resources | 89 |
| 3.1.7.1 | Water Resources | 89 |
| 3.1.8 | Natural and Background Radiation..... | 92 |
| 3.2 | <i>Principal Facility Design Features</i> | 93 |
| 3.2.1 | SDF Vaults and Future Disposal Cells | 94 |
| 3.2.1.1 | Vault 1..... | 97 |
| 3.2.1.2 | Vault 4..... | 104 |
| 3.2.1.3 | Disposal Unit 2 and FDCs | 112 |
| 3.2.1.4 | Grout Transfer Lines..... | 125 |
| 3.2.2 | Conceptual Closure Cap | 125 |
| 3.2.2.1 | Closure Cap Background | 125 |
| 3.2.2.2 | Scoping Level Evaluation | 126 |
| 3.2.2.3 | Closure Cap Layout Scenario | 126 |
| 3.2.2.4 | Physical Stability Requirements | 126 |
| 3.2.2.5 | Conceptual Closure Cap General Design Features..... | 127 |
| 3.2.2.6 | Site Preparation | 133 |
| 3.2.2.7 | Closure Cap Performance without Degradation | 134 |
| 3.2.2.8 | Closure Cap Degradation Mechanisms..... | 136 |
| 3.2.2.9 | Open Issues for Further Design | 138 |
| 3.3 | <i>Saltstone Disposal Facility Radionuclide and Chemical Inventory</i> | 139 |
| 4.0 | ANALYSIS OF PERFORMANCE | 147 |
| 4.1 | <i>Overview of Analysis</i> | 148 |
| 4.2 | <i>Integrated Site Conceptual Model of Facility Performance</i> | 150 |
| 4.2.1 | Radionuclide Screening | 151 |

| | | |
|---------|--|-----|
| 4.2.1.1 | Evaluation of Radionuclides in Principal Decay Chains | 154 |
| 4.2.1.2 | Evaluation of Radionuclides Identified in WCS..... | 156 |
| 4.2.1.3 | Evaluation of Remaining Radionuclides | 157 |
| 4.2.1.4 | Groundwater Modeling Initial Inventory..... | 161 |
| 4.2.1.5 | Air Pathways Modeling Initial Inventory | 161 |
| 4.2.2 | Source Term Release | 162 |
| 4.2.3 | Radionuclide Transport..... | 165 |
| 4.2.3.1 | Transport Model Approach..... | 165 |
| 4.2.3.2 | Model Material Properties | 182 |
| 4.2.4 | Exposure Pathways and Scenarios..... | 218 |
| 4.2.4.1 | Member of the Public Exposure Pathways | 218 |
| 4.2.4.2 | Intruder Exposure Pathways | 224 |
| 4.3 | <i>Modeling Codes</i> | 234 |
| 4.3.1 | Modeling Codes Utilized | 234 |
| 4.3.1.1 | Hydrologic Evaluation of Landfill Performance (HELP) Model | 234 |
| 4.3.1.2 | PORFLOW | 235 |
| 4.3.1.3 | GoldSim | 238 |
| 4.3.1.4 | CAP-88 | 239 |
| 4.3.1.5 | STADIUM® | 240 |
| 4.3.2 | Software QA and Validation..... | 240 |
| 4.3.3 | Modeling Codes Summary | 242 |
| 4.4 | <i>Closure System Modeling</i> | 242 |
| 4.4.1 | Individual Vault and FDC Modeling | 243 |
| 4.4.1.1 | Vault 1 Modeling | 243 |
| 4.4.1.2 | Vault 4 Modeling | 245 |
| 4.4.1.3 | Disposal Cells 2A and 2B (and FDC) Modeling | 247 |
| 4.4.2 | Systems and Potential Degradation | 249 |
| 4.4.2.1 | Vault 1 Degradation Cases..... | 250 |
| 4.4.2.2 | Vault 4 Degradation Cases..... | 257 |
| 4.4.2.3 | FDC Degradation Cases (Typical)..... | 262 |
| 4.4.3 | Evaluation of Integrated System Behavior | 264 |
| 4.4.3.1 | Closure Cap..... | 264 |
| 4.4.3.2 | Disposal Unit Roof | 264 |
| 4.4.3.3 | Saltstone..... | 265 |
| 4.4.3.4 | Disposal Unit Walls and Floor..... | 265 |
| 4.4.3.5 | Vadose Zone Surrounding the SDF Disposal Units | 266 |
| 4.4.4 | Modeling Process..... | 266 |
| 4.4.4.1 | PORFLOW Modeling Process..... | 268 |
| 4.4.4.2 | GoldSim Modeling Process | 304 |
| 4.5 | <i>Airborne and Radon Analysis</i> | 322 |
| 4.5.1 | Air and Radon Pathway Conceptual Model | 322 |
| 4.5.1.1 | Air and Radon Pathway Diffusive Transport Model | 327 |
| 4.5.1.2 | Summary of Key Air and Radon Pathways Assumptions | 333 |
| 4.5.2 | Saltstone Disposal Facility Air Pathways Model | 333 |
| 4.5.2.1 | Source Term Development | 334 |

| | | |
|------------|--|------------|
| 4.5.2.2 | Implementation of Partitioning Coefficients in PORFLOW | 337 |
| 4.5.2.3 | Effective Air Diffusion Coefficients..... | 342 |
| 4.5.2.4 | Air Pathways Model Results..... | 342 |
| 4.5.2.5 | Saltstone Disposal Facility Radon Analysis | 350 |
| 4.5.2.6 | Radon Pathway Model Results | 354 |
| 4.6 | <i>Biotic Pathways</i> | 358 |
| 4.6.1 | Bioaccumulation Factors | 358 |
| 4.6.1.1 | Bioaccumulation Factor Methodology | 358 |
| 4.6.2 | Human Health Exposure Parameters (Consumption Rates) | 371 |
| 4.6.2.1 | Human Health Exposure Parameters Methodology..... | 371 |
| 4.7 | <i>Dose Analysis</i> | 375 |
| 4.7.1 | Dose Conversion Factors | 375 |
| 4.7.1.1 | Internal DCFs..... | 375 |
| 4.7.1.2 | External DCFs..... | 376 |
| 4.7.2 | Member of the Public Dose Analysis | 380 |
| 4.7.3 | Intruder Dose Analysis | 380 |
| 4.7.4 | Analysis Approach..... | 380 |
| 5.0 | RESULTS OF ANALYSES | 381 |
| 5.1 | <i>Source Term (Analysis Results) Assumptions</i> | 381 |
| 5.2 | <i>Environmental Transport of Radionuclides</i> | 381 |
| 5.2.1 | Groundwater Concentrations at 100m | 382 |
| 5.2.2 | Key Radionuclide Determination | 425 |
| 5.2.3 | Groundwater Concentrations at the Seeplines | 426 |
| 5.3 | <i>Air Pathways and Radon Analysis</i> | 426 |
| 5.3.1 | Air Pathways Dose..... | 427 |
| 5.3.2 | Instantaneous Radon Flux..... | 428 |
| 5.4 | <i>Biotic Pathways</i> | 430 |
| 5.4.1 | Member of the Public at the 100m Well Dose Pathways | 430 |
| 5.4.1.1 | Member of the Public at the 100m Well Ingestion Dose Pathways | 430 |
| 5.4.1.2 | Member of the Public at the 100m Well Direct Exposure Dose Pathways | 433 |
| 5.4.1.3 | Member of the Public at the 100m Well Inhalation Dose Pathways | 434 |
| 5.5 | <i>Dose Analysis</i> | 436 |
| 5.5.1 | Member of the Public at 100m Groundwater Pathways Dose Results | 437 |
| 5.5.1.1 | Member of the Public 100m Peak Annual Groundwater Pathways Dose | 437 |
| 5.5.1.2 | Individual Radionuclide Contributions to the MOP 100m Peak Annual Groundwater Pathways Dose | 440 |
| 5.5.1.3 | Individual Disposal Unit Contributions to a MOP 100m Peak Annual Groundwater Pathways Dose | 443 |
| 5.5.1.4 | Individual Pathways Contributions to a MOP 100m Peak Annual Groundwater Pathways Dose | 443 |
| 5.5.1.5 | Member of the Public 100m Peak Annual Groundwater Pathways Dose Results for 40,000 years..... | 447 |
| 5.5.2 | Member of the Public All-Pathways Dose Results..... | 448 |
| 5.6 | <i>Uncertainty and Sensitivity Analyses</i> | 449 |

| | | |
|------------|--|------------|
| 5.6.1 | Uncertainty and Sensitivity Analyses using Probabilistic Modeling..... | 449 |
| 5.6.1.1 | GoldSim SDF Model | 450 |
| 5.6.2 | GoldSim Benchmarking | 450 |
| 5.6.2.1 | Benchmarking Between the GoldSim and PORFLOW Models..... | 450 |
| 5.6.2.2 | Saltstone Disposal Facility PA Benchmarking Activities and Results | 451 |
| 5.6.2.3 | Benchmarking Adjustments and Results | 451 |
| 5.6.3 | Parameters Evaluated in the SDF Probabilistic Model..... | 477 |
| 5.6.3.1 | Saltstone Disposal Facility Case Scenarios | 477 |
| 5.6.3.2 | Radionuclide Inventory..... | 484 |
| 5.6.3.3 | Distribution Coefficient Values | 486 |
| 5.6.3.4 | Transition Times between Chemical States..... | 487 |
| 5.6.3.5 | SDF Lower Vadose Zone Thickness | 488 |
| 5.6.3.6 | Well Depth..... | 488 |
| 5.6.3.7 | Bioaccumulation Factors and Human Health Exposure Parameters | 489 |
| 5.6.3.8 | Saturated Zone Flow Modeling Parameters..... | 494 |
| 5.6.4 | Uncertainty/Sensitivity Analysis using the SDF Probabilistic Model..... | 495 |
| 5.6.5 | Sensitivity Analysis using the SDF Probabilistic Model..... | 505 |
| 5.6.5.1 | Introduction to SDF Probabilistic Model Sensitivity Analysis..... | 505 |
| 5.6.5.2 | Model Fitting and Validation..... | 506 |
| 5.6.5.3 | Summary Statistics for Endpoints..... | 509 |
| 5.6.5.4 | Case A Partial Dependence Plots..... | 512 |
| 5.6.5.5 | Case C Partial Dependence Plots..... | 524 |
| 5.6.5.6 | Summary of the SDF Probabilistic Model Sensitivity Analysis..... | 535 |
| 5.6.6 | Single Parameter Sensitivity Analyses | 535 |
| 5.6.6.1 | Alternate Disposal Unit Case Sensitivity Analysis using the PORFLOW Deterministic Model | 535 |
| 5.6.6.2 | No Closure Cap Sensitivity Analysis using the PORFLOW Deterministic Model | 541 |
| 5.6.6.3 | Materials Degradation Sensitivity Analysis using the PORFLOW Deterministic Model | 542 |
| 5.6.6.4 | Inventory Sensitivity Analysis using the PORFLOW Deterministic Model | 548 |
| 5.6.6.5 | Synergistic Sensitivity Analysis Using the PORFLOW Deterministic Model | 548 |
| 5.6.6.6 | Oxidized Concrete Sensitivity Analysis Using the PORFLOW Deterministic Model | 550 |
| 5.6.6.7 | Increased Saltstone Hydraulic Conductivity Sensitivity Analysis Using the PORFLOW Deterministic Model | 551 |
| 5.7 | <i>ALARA Analysis</i> | 552 |
| 6.0 | INADVERTENT INTRUDER ANALYSIS | 554 |
| 6.1 | <i>Groundwater Concentrations at 1m</i> | 554 |
| 6.2 | <i>Acute Exposure Scenarios</i> | 587 |
| 6.2.1 | Acute Intruder Ingestion Dose Pathways – Ingestion of Resuspended Drill Cuttings..... | 587 |

| | | |
|-------------|--|------------|
| 6.2.2 | Acute Intruder Inhalation Dose Pathways – Inhalation of Drill Cuttings..... | 588 |
| 6.2.3 | Acute Intruder Direct Exposure Dose Pathways – Direct Exposure to Drill Cuttings..... | 589 |
| 6.3 | <i>Chronic Exposure Scenarios</i> | 589 |
| 6.3.1 | Chronic Intruder Ingestion Dose Pathways | 589 |
| 6.3.2 | Chronic Intruder Direct Exposure Dose Pathways | 593 |
| 6.3.3 | Chronic Intruder Inhalation Dose Pathways | 594 |
| 6.4 | <i>Intruder Analysis Results</i> | 597 |
| 6.5 | <i>Intruder Uncertainty/Sensitivity Analysis</i> | 598 |
| 6.5.1 | Intruder Probabilistic Uncertainty Analysis | 599 |
| 6.5.2 | Intruder Probabilistic Sensitivity Analysis | 604 |
| 6.5.3 | Intruder Single Parameter Sensitivity Analysis | 604 |
| 6.5.3.1 | Impact of Drilling into a SDF Disposal Unit on Acute Intruder..... | 604 |
| 6.5.3.2 | Impact of Drilling into a SDF Disposal Unit on Chronic Intruder | 605 |
| 7.0 | INTERPRETATION OF RESULTS | 607 |
| 7.1 | <i>Performance Assessment Results</i> | 607 |
| 7.1.1 | Integrated System Behavior | 607 |
| 7.1.1.1 | Closure Cap..... | 608 |
| 7.1.1.2 | Saltstone Disposal Unit Roof..... | 609 |
| 7.1.1.3 | Saltstone..... | 609 |
| 7.1.1.4 | Disposal Unit Walls and Floor..... | 610 |
| 7.1.1.5 | Vadose Zone Surrounding SDF Disposal Units | 611 |
| 7.1.2 | 100m Groundwater Pathways Doses | 611 |
| 7.1.3 | All-Pathways Dose | 612 |
| 7.1.4 | Intruder Dose | 612 |
| 7.1.5 | Airborne Dose..... | 613 |
| 7.1.6 | Radon Flux..... | 613 |
| 7.1.7 | Groundwater Protection | 613 |
| 7.2 | <i>Conservatisms Included in the SDF Performance Assessment</i> | 613 |
| 7.2.1 | Closure Cap..... | 613 |
| 7.2.2 | Integrated Site Conceptual Model | 614 |
| 7.2.3 | Volatile Radionuclide and Radon Analysis | 614 |
| 7.2.4 | Other Factors Affecting Results | 615 |
| 8.0 | PERFORMANCE EVALUATION..... | 616 |
| 8.1 | <i>Use of Performance Assessment Results</i> | 616 |
| 8.2 | <i>Further Work</i> | 617 |
| 9.0 | PREPARERS | 622 |
| 10.0 | REFERENCES..... | 635 |
| 11.0 | GLOSSARY | 647 |

APPENDICES

| | |
|--|--------------|
| APPENDIX A: 100-METER RADIOLOGICAL AND CHEMICAL CONCENTRATIONS..... | A-1 |
| <i>A.1: 100-Meter Radiological and Chemical Concentrations at the Upper Three Runs Aquifer – Upper Zone.....</i> | <i>A.1-1</i> |
| <i>A.2: 100-Meter Radiological and Chemical Concentrations at the Upper Three Runs Aquifer – Lower Zone.....</i> | <i>A.2-1</i> |
| <i>A.3: 100-Meter Radiological and Chemical Concentrations at the Gordon Aquifer.....</i> | <i>A.3-1</i> |
| <i>A.4: 100-Meter Radiological and Chemical Concentrations – Case B.....</i> | <i>A.4-1</i> |
| <i>A.5: 100-Meter Radiological and Chemical Concentrations – Case C.....</i> | <i>A.5-1</i> |
| <i>A.6: 100-Meter Radiological and Chemical Concentrations – Case D.....</i> | <i>A.6-1</i> |
| <i>A.7: 100-Meter Radiological and Chemical Concentrations – Case E.....</i> | <i>A.7-1</i> |
| APPENDIX B: SEEPLINE KEY RADIONUCLIDE AND CHEMICAL CONCENTRATIONS..... | B-1 |
| APPENDIX C: 100-METER KEY RADIONUCLIDE CONCENTRATIONS FOR 40,000 YEARS..... | C-1 |
| APPENDIX D: 100-METER KEY RADIONUCLIDE AND CHEMICAL CONCENTRATIONS FOR SELECTED SOURCES..... | D-1 |
| APPENDIX E: CONCENTRATIONS OF KEY RADIONUCLIDE AT 100-METERS AND THE SEEPLINE..... | E-1 |
| <i>E.1: Concentrations of Key Radionuclides at 100-Meters and the Seepline.....</i> | <i>E.1-1</i> |
| <i>E.2: Comparison of 100-Meter Concentrations Per Aquifer.. ..</i> | <i>E.2-1</i> |
| APPENDIX F: 1-METER RADIOLOGICAL AND CHEMICAL CONCENTRATIONS..... | F-1 |
| <i>F.1: 1-Meter Radiological and Chemical Concentrations at the Upper Three Runs Aquifer – Upper Zone.....</i> | <i>F.1-1</i> |
| <i>F.2: 1-Meter Radiological and Chemical Concentrations at the Upper Three Runs Aquifer – Lower Zone.....</i> | <i>F.2-1</i> |
| <i>F.3: 1-Meter Radiological and Chemical Concentrations at the Gordon Aquifer.....</i> | <i>F.3-1</i> |
| APPENDIX G: CONCRETE MATERIAL DEGRADATION SENSITIVITY..... | G-1 |
| <i>G.1: Concrete Material Degradation Sensitivity – Accelerated Degradation.....</i> | <i>G.1-1</i> |
| <i>G.2: Concrete Material Degradation Sensitivity – Decreased Degradation.....</i> | <i>G.2-1</i> |
| APPENDIX H: FLOW SENSITIVITY (NO CLOSURE CAP)..... | H-1 |
| APPENDIX I: DATA VERIFICATION..... | I-1 |
| APPENDIX J: SALTSTONE HYDRAULIC CONDUCTIVITY SENSITIVITY..... | J-1 |
| APPENDIX K: VAULT 1 AND 4 OXIDIZED CONCRETE SENSITIVITY..... | K-1 |
| APPENDIX L: ALTERNATIVE SENSITIVITY DETERMINISTIC CASES..... | L-1 |

LIST OF FIGURES

| | |
|---|----|
| Figure 2.1-1: Saltstone Disposal Facility PA Modeling Relationships | 36 |
| Figure 3.1-1: Physical Location of Savannah River Site | 46 |
| Figure 3.1-2: Location of SRS and Adjacent Areas | 47 |
| Figure 3.1-3: SRS Operational Area Location Map | 49 |
| Figure 3.1-4: Layout of the GSA | 50 |
| Figure 3.1-5: Anticipated Layout of SDF | 51 |
| Figure 3.1-6: SRS Meteorological Monitoring Network | 55 |
| Figure 3.1-7: Regional Geological Provinces of Eastern U.S. | 60 |
| Figure 3.1-8: Regional Geologic Provinces of South Carolina | 61 |
| Figure 3.1-9: GSA Topography | 62 |
| Figure 3.1-10: General Soil Associations for SRS | 64 |
| Figure 3.1-11: Historical Seismic Events in the Southeast..... | 66 |
| Figure 3.1-12: Seismic Events within a 50 Mile Radius of SRS | 67 |
| Figure 3.1-13: Regional Scale Faults for SRS and Vicinity | 68 |
| Figure 3.1-14: Regional NW to SE Cross Section..... | 70 |
| Figure 3.1-15: Comparison of Chronostratigraphic, Lithostratigraphic, and Hydrostratigraphic Units in the SRS Region | 71 |
| Figure 3.1-16: Potentiometric Surface of the UTR Aquifer | 73 |
| Figure 3.1-17: Potentiometric Surface of the Gordon Aquifer | 74 |
| Figure 3.1-18: Hydrostratigraphic Picks in GSAD..... | 76 |
| Figure 3.1-19: Laboratory Determined Permeability Data in GSAD | 77 |
| Figure 3.1-20: Multiple Well Pump Test Data in GSAD | 78 |
| Figure 3.1-21: Single Well Pump Test Data in GSAD | 79 |
| Figure 3.1-22: Slug Test Data in GSAD..... | 80 |
| Figure 3.1-23: Locations of CPT and Well Boreholes at Z-Area | 82 |
| Figure 3.1-24: Conceptual Diagram of Groundwater Flow beneath the GSA | 84 |
| Figure 3.1-25: Savannah River Basin Dams..... | 86 |
| Figure 3.1-26: SRS Watershed Boundaries and Major Tributaries | 87 |
| Figure 3.1-27: Major Sources of Radiation Exposure in the Vicinity of SRS..... | 93 |
| Figure 3.2-1: Saltstone Disposal Facility Aerial View | 95 |
| Figure 3.2-2: SDF Anticipated FDC Layout..... | 96 |

| | |
|--|-----|
| Figure 3.2-3: Vault 1 and Vault 4 Arrangement after Initial Construction | 98 |
| Figure 3.2-4: Vault 1 Photograph | 99 |
| Figure 3.2-5: Vault 1 Plan View | 100 |
| Figure 3.2-6: Vault 1 Interior Elevation Marks | 101 |
| Figure 3.2-7: Vault 1 Cross Section..... | 102 |
| Figure 3.2-8: Vault 4 Photograph | 105 |
| Figure 3.2-9: Vault 4 Roof Plan View | 106 |
| Figure 3.2-10: Vault 4 Cross Section..... | 107 |
| Figure 3.2-11: Vault 4 Permanent Roof Plan Details (Cells B through L)..... | 111 |
| Figure 3.2-12: Interior View of Vault 4 Roof..... | 112 |
| Figure 3.2-13: Vendor Example of Cylindrical, FDC Type Tank..... | 113 |
| Figure 3.2-14: Future Disposal Cell Cross-Section | 115 |
| Figure 3.2-15: Future Disposal Cell Roof-Column Detail..... | 119 |
| Figure 3.2-16: Roof Plan for Future Disposal Cell (Typical)..... | 120 |
| Figure 3.2-17: Future Disposal Cell Wall Detail | 121 |
| Figure 3.2-18: Future Disposal Cell Base Details | 123 |
| Figure 3.2-19: Placement of Lower Mud Mat for Disposal Unit 2 During Construction (Typical for FDCs)..... | 124 |
| Figure 3.2-20: Saltstone Disposal Facility Conceptual Closure Cap Layers..... | 131 |
| Figure 3.2-21: Closure Cap Side Slope and Toe Detail..... | 132 |
| Figure 3.2-22: Saltstone Closure Cap Year 0 (intact) Average Water Balance..... | 135 |
| Figure 4.1-1: SDF Modeling Input Relationships..... | 149 |
| Figure 4.2-1: Location of Z-Area and GSA Layout | 166 |
| Figure 4.2-2: SDF Overall Performance Assessment Model..... | 167 |
| Figure 4.2-3: Average Water Balance Through SDF Closure Cap Over Time | 168 |
| Figure 4.2-4: Contaminant Release and Transportation from Saltstone (Condition 1) | 170 |
| Figure 4.2-5: Contaminant Release and Transport from Saltstone (Condition 2) | 171 |
| Figure 4.2-6: General Flow of Groundwater Away from the SDF..... | 173 |
| Figure 4.2-7: GSA Boundary Conditions | 174 |
| Figure 4.2-8: North-South Cross Section of GSA/PORFLOW Computational Mesh for GSA..... | 175 |
| Figure 4.2-9: Perspective View of GSA/PORFLOW Computational Mesh | 175 |

| | |
|--|-----|
| Figure 4.2-10: North-South Cross Section of GSA/PORFLOW Model - Horizontal Hydraulic Conductivity Variations | 176 |
| Figure 4.2-11: North-South Cross Section of GSA/PORFLOW Model - Vertical Hydraulic Conductivity Variations | 177 |
| Figure 4.2-12: General Separations Area Database Relationship..... | 178 |
| Figure 4.2-13: Water Table Contour Maps for GSA | 179 |
| Figure 4.2-14: Comparison of (a) GSA/PORFLOW Model Predicted and (b) Hand-Contoured 2003 Water Table Maps..... | 180 |
| Figure 4.2-15: Vertical Hydraulic Conductivity of Lower Lateral Drainage Layer..... | 184 |
| Figure 4.2-16: Porosity of Lower Lateral Drainage Layer | 184 |
| Figure 4.2-17: Backfill Characteristic Curves | 185 |
| Figure 4.2-18: Drainage Layer Characteristic Curves | 186 |
| Figure 4.2-19: Hydraulic Parameters of HDPE-GCL Layer | 187 |
| Figure 4.2-20: Locations and Base Elevations of Disposal Units within SDF..... | 189 |
| Figure 4.2-21: Long Term Average Water Table Near SDF | 190 |
| Figure 4.2-22: Characteristic Curve for Lower Vadose Zone | 193 |
| Figure 4.2-23: Characteristic Curves for Low Quality Concrete..... | 198 |
| Figure 4.2-24: Characteristic Curves for Medium Quality Concrete | 198 |
| Figure 4.2-25: Characteristic Curves for High Quality Concrete | 199 |
| Figure 4.2-26: Characteristic Curve for Fractured Concrete | 199 |
| Figure 4.2-27: Characteristic Curves for Saltstone..... | 200 |
| Figure 4.2-28: Simulated Progression of Ettringite Front | 201 |
| Figure 4.2-29: Conceptual Model of a Generic Moving Ettringite Front..... | 202 |
| Figure 4.2-30: STADIUM® Simulation Results for Vaults 1 and 4 | 203 |
| Figure 4.2-31: STADIUM® Simulation Results for FDCs | 203 |
| Figure 4.2-32: Power Law Fit to Data on Figure 4.2-26 | 204 |
| Figure 4.2-33: Power Law Fit to Data on Figure 4.2-27 | 204 |
| Figure 4.2-34: Comparison of Correlation to Original STADIUM® Results Vaults 1 and 4..... | 206 |
| Figure 4.2-35: Comparison of Correlation to Original STADIUM® Results for FDC..... | 206 |
| Figure 4.2-36: Hydraulic Conductivity for Vault 1 and 4 Concrete | 210 |
| Figure 4.2-37: Diffusion Coefficient for Vaults 1 and 4 Concrete | 210 |

| | |
|---|-----|
| Figure 4.2-38: Hydraulic Conductivity and Diffusion Coefficient for Vault 4 Concrete Roof..... | 211 |
| Figure 4.2-39: Hydraulic Conductivity and Diffusion Coefficient for FDC Concrete Roof/Floor..... | 211 |
| Figure 4.2-40: Hydraulic Conductivity and Diffusion Coefficient for FDC Concrete Wall | 212 |
| Figure 4.2-41: Pseudo-sorption Coefficient as a Function of Reduction Capacity for Tc-99 Simulations..... | 214 |
| Figure 4.2-42: Hydraulic Conductivity and Diffusion Coefficient for HDPE Lining of FDCs After Closure | 217 |
| Figure 4.2-43: Member of the Public Exposure Pathways | 222 |
| Figure 4.2-44: Chronic Intruder Agricultural (Post-Drilling) Scenario..... | 226 |
| Figure 4.3-1: SDF PA Modeling Code Integration..... | 236 |
| Figure 4.3-2: SDF PA Modeling Code Integration – Details of Water Flow and Transport..... | 237 |
| Figure 4.4-1: Conceptual Model for SDF Vault 1 | 244 |
| Figure 4.4-2: Conceptual Model for the SDF Vault 4 | 246 |
| Figure 4.4-3: Conceptual Model for FDC (Typical)..... | 248 |
| Figure 4.4-4: Model Scenario Case A (Base Case) | 251 |
| Figure 4.4-5: Characteristic Curves for Gravel..... | 253 |
| Figure 4.4-6: Model Scenario Case C..... | 254 |
| Figure 4.4-7: Model Scenario Case E..... | 255 |
| Figure 4.4-8: Characteristic Curves for Degraded Saltstone | 256 |
| Figure 4.4-9: Model Scenario Case B..... | 259 |
| Figure 4.4-10: Model Scenario Case D..... | 260 |
| Figure 4.4-11: Saltstone Disposal Facility PA Modeling Relationships | 267 |
| Figure 4.4-12: Simulated Groundwater Flow paths in GSA/PORFLOW Modeling..... | 268 |
| Figure 4.4-13: Source and Seepage Nodes in GSA/PORFLOW Modeling..... | 269 |
| Figure 4.4-14: SDF Modeling from GSA Scale Model..... | 270 |
| Figure 4.4-15: SDF Modeling Showing Source Nodes and Perimeters | 272 |
| Figure 4.4-16: SDF Modeling Showing Divisional Sectors | 273 |
| Figure 4.4-17: SDF Vault 1 Modeling Showing Stream Tracers | 274 |
| Figure 4.4-18: SDF Vault 4 Modeling Showing Stream Tracers | 275 |
| Figure 4.4-19: SDF FDC Modeling Showing Stream Tracers | 276 |
| Figure 4.4-20: Vault 1 Material Zones for PORFLOW Vadose Zone Modeling..... | 277 |

| | |
|--|-----|
| Figure 4.4-21: Vault 1 Gridding for PORFLOW Vadose Zone Modeling..... | 278 |
| Figure 4.4-22: Vault 1 Upper Corner Detail for PORFLOW Vadose Zone Modeling | 278 |
| Figure 4.4-23: Vault 1 Lower Corner Detail for PORFLOW Vadose Zone Modeling | 279 |
| Figure 4.4-24: FDC Material Zones for PORFLOW Vadose Zone Modeling | 279 |
| Figure 4.4-25: FDC Gridding for PORFLOW Vadose Zone Modeling..... | 280 |
| Figure 4.4-26: FDC Upper Corner Detail for PORFLOW Vadose Zone Modeling | 280 |
| Figure 4.4-27: FDC Lower Corner Detail for PORFLOW Vadose Zone Modeling | 281 |
| Figure 4.4-28: Vault 4 Material Zones for PORFLOW Vadose Zone Modeling..... | 281 |
| Figure 4.4-29: Vault 4 Gridding for PORFLOW Vadose Zone Modeling..... | 282 |
| Figure 4.4-30: Vault 4 Upper Corner Detail for PORFLOW Vadose Zone Modeling | 282 |
| Figure 4.4-31: Vault 4 Lower Corner Detail for PORFLOW Vadose Zone Modeling | 283 |
| Figure 4.4-32: Vault 1 Saturation and Darcy Velocity Fields Base Case at 100 Years | 284 |
| Figure 4.4-33: Vault 1 Saturation and Darcy Velocity Fields Base Case at 1,000 Years | 284 |
| Figure 4.4-34: Vault 1 Saturation and Darcy Velocity Fields Base Case at 5,000 Years | 285 |
| Figure 4.4-35: Vault 1 Saturation and Darcy Velocity Fields Base Case at 10,000 Years | 285 |
| Figure 4.4-36: FDC Saturation and Darcy Velocity Fields Base Case at 100 Years..... | 286 |
| Figure 4.4-37: FDC Saturation and Darcy Velocity Fields Base Case at 1,000 Years..... | 286 |
| Figure 4.4-38: FDC Saturation and Darcy Velocity Fields Base Case at 5,000 Years..... | 287 |
| Figure 4.4-39: FDC Saturation and Darcy Velocity Fields Base Case at 10,000 Years..... | 287 |
| Figure 4.4-40: Vault 4 Saturation and Darcy Velocity Fields Base Case at 100 Years | 288 |
| Figure 4.4-41: Vault 4 Saturation and Darcy Velocity Fields Base Case at 1,000 Years | 288 |
| Figure 4.4-42: Vault 4 Saturation and Darcy Velocity Fields Base Case at 5,000 Years | 289 |
| Figure 4.4-43: Vault 4 Saturation and Darcy Velocity Fields Base Case at 10,000 Years | 289 |
| Figure 4.4-44: Vault 1 Saturation and Darcy Velocity Fields Fast Flow Path Case C at 100 Years | 292 |
| Figure 4.4-45: Vault 1 Saturation and Darcy Velocity Fields Fast Flow Path Case C at 1,000 Years | 293 |
| Figure 4.4-46: Vault 1 Saturation and Darcy Velocity Fields Fast Flow Path Case C at 5,000 Years | 293 |
| Figure 4.4-47: Vault 1 Saturation and Darcy Velocity Fields Fast Flow Path Case C at 10,000 Years | 294 |
| Figure 4.4-48: FDC Saturation and Darcy Velocity Fields Fast Flow Path Case C at 100 Years | 294 |

| | |
|---|-----|
| Figure 4.4-49: FDC Saturation and Darcy Velocity Fields Fast Flow Path Case C at 1,000 Years | 295 |
| Figure 4.4-50: FDC Saturation and Darcy Velocity Fields Fast Flow Path Case C at 5,000 Years | 295 |
| Figure 4.4-51: FDC Saturation and Darcy Velocity Fields Fast Flow Path Case C at 10,000 Years | 296 |
| Figure 4.4-52: Vault 4 Saturation and Darcy Velocity Fields Fast Flow Path Case C at 100 Years | 296 |
| Figure 4.4-53: Vault 4 Saturation and Darcy Velocity Fields Fast Flow Path Case C at 1,000 Years | 297 |
| Figure 4.4-54: Vault 4 Saturation and Darcy Velocity Fields Fast Flow Path Case C at 5,000 Years | 297 |
| Figure 4.4-55: Vault 4 Saturation and Darcy Velocity Fields Fast Flow Path Case C at 10,000 Years | 298 |
| Figure 4.4-56: VZMS Layout and Instrumentation at Slit Trenches | 300 |
| Figure 4.4-57: Basis for PORFLOW Model and VZMS Data Comparison..... | 301 |
| Figure 4.4-58: PORFLOW Model and VZMS Tritium Data Comparison..... | 301 |
| Figure 4.4-59: Surveyed Seepelines Compared to GSA/PORFLOW Model Simulation | 302 |
| Figure 4.4-60: Comparison of GSA/PORFLOW Groundwater Pathlines to a Tritium Plume | 303 |
| Figure 4.4-61: Comparison of GSA/PORFLOW Groundwater Pathlines to Contaminant Plumes Emanating from F-Area | 304 |
| Figure 4.4-62: Top Level of the GoldSim SDF Model..... | 306 |
| Figure 4.4-63: Container “ <i>TheVaults</i> ” | 308 |
| Figure 4.4-64: Container “ <i>Vault_2</i> ” | 309 |
| Figure 4.4-65: Element “ <i>Waste</i> ” | 311 |
| Figure 4.4-66: Container “ <i>VaultCells</i> ” | 312 |
| Figure 4.4-67: Container “ <i>UnsatZone</i> ” | 315 |
| Figure 4.4-68: Sample Velocity Table - Grout | 317 |
| Figure 4.4-69: Sample Velocity Table - Dirt..... | 318 |
| Figure 4.4-70: Saltstone Disposal Facility Streamlines..... | 320 |
| Figure 4.4-71: Saltstone Disposal Facility Sectors | 321 |
| Figure 4.5-1: Schematic of PORFLOW Model Grid for Vault 1 Air and Radon..... | 324 |
| Figure 4.5-2: Schematic of PORFLOW Model Grid for FDC Air and Radon..... | 325 |

| | |
|---|-----|
| Figure 4.5-3: Schematic of PORFLOW Model Grid for Vault 4 Air and Radon..... | 326 |
| Figure 4.5-4: Ci Flux at Land Surface for Modeled Radionuclides in Vault 1 for DDA Saltstone..... | 343 |
| Figure 4.5-5: Ci Flux at Land Surface for Modeled Radionuclides in Vault 1 for ARP/ MCU Saltstone..... | 343 |
| Figure 4.5-6: Ci Flux at Land Surface for Modeled Radionuclides in FDCs for SWPF Saltstone..... | 344 |
| Figure 4.5-7: Ci Flux at Land Surface for Modeled Radionuclides in Vault 4 for DDA Saltstone..... | 344 |
| Figure 4.5-8: Ci Flux at Land Surface for Modeled Radionuclides in Vault 4 for ARP/ MCU Saltstone..... | 345 |
| Figure 4.5-9: Radioactive Decay Chains Leading to Rn-222 | 352 |
| Figure 4.5-10: Rn-222 Flux at Land Surface Resulting from Unit Source Term for Vault 1 DDA Saltstone | 354 |
| Figure 4.5-11: Rn-222 Flux at Land Surface from Unit Source Term for Vault 1 ARP/ MCU Saltstone..... | 355 |
| Figure 4.5-12: Rn-222 Flux at Land Surface from Unit Source Term for FDC Saltstone | 355 |
| Figure 4.5-13: Rn-222 Flux at Land Surface from Unit Source Term for Vault 4 DDA Saltstone..... | 356 |
| Figure 4.5-14: Rn-222 Flux at Land Surface from Unit Source Term for Vault 4 ARP/ MCU Saltstone..... | 356 |
| Figure 5.2-1: SDF 1m and 100m Modeled Cells and Sectors | 383 |
| Figure 5.2-2: SDF Vault 1 Modeling Showing Stream Tracers | 385 |
| Figure 5.2-3: SDF Vault 4 Modeling Showing Stream Tracers | 386 |
| Figure 5.2-4: SDF Future Disposal Cell Modeling Showing Stream Tracers | 387 |
| Figure 5.2-5: Contaminant Plume Leaving SDF – Plan View..... | 389 |
| Figure 5.2-6: Contaminant Plume Leaving SDF – South/North Cross Section View..... | 390 |
| Figure 5.2-7: Contaminant Plume Leaving SDF – East/West Cross Section View | 390 |
| Figure 5.2-8: PORFLOW SDF Seepage Evaluation Sectors | 426 |
| Figure 5.5-1: 100m MOP Peak Groundwater Pathways Dose within 10,000 Years, Sectors A-L | 439 |
| Figure 5.5-2: 100m MOP Peak Groundwater Pathways Dose within 20,000 Years, Sectors A-L | 439 |
| Figure 5.5-3: Contributors to the Sector B 100m Peak Groundwater Pathways Dose, 10,000 Years | 440 |

| | |
|---|-----|
| Figure 5.5-4: Contributors to the Sector B 100m Peak Groundwater Pathways Dose, 20,000 Years | 441 |
| Figure 5.5-5: Contributors to the Sector I 100m Peak Groundwater Pathways Dose, 20,000 Years | 441 |
| Figure 5.5-6: 100m MOP Peak Water Ingestion Dose within 10,000 Years, Sectors B and I..... | 445 |
| Figure 5.5-7: 100m MOP Peak Fish Ingestion Dose within 10,000 Years, Sectors B and I..... | 446 |
| Figure 5.5-8: 100m MOP Peak Vegetable Ingestion Dose within 10,000 Years, Sectors B and I..... | 447 |
| Figure 5.5-9: 100m MOP Peak Groundwater Pathways Dose within 40,000 Years, Sectors B and I..... | 448 |
| Figure 5.6-1: Vault 1 Ra-226 Flux Comparison | 453 |
| Figure 5.6-2: Vault 1 I-129-Flux Comparison | 454 |
| Figure 5.6-3: Vault 1 Tc-99 Flux Comparison | 454 |
| Figure 5.6-4: Vault 4 Ra-226 Flux Comparison | 456 |
| Figure 5.6-5: Vault 4 I-129 Flux Comparison | 456 |
| Figure 5.6-6: Vault 4 Tc-99 Flux Comparison | 457 |
| Figure 5.6-7: FDC Ra-226 Flux Comparison | 458 |
| Figure 5.6-8: FDC I-129 Flux Comparison | 458 |
| Figure 5.6-9: FDC Tc-99 Flux Comparison | 459 |
| Figure 5.6-10: South Sectors Concentration Comparisons – Case A | 461 |
| Figure 5.6-11: North Sectors Concentration Comparisons – Case A | 462 |
| Figure 5.6-12: Fish Ingestion Dose Pathway Comparisons – Case A | 463 |
| Figure 5.6-13: MOP Dose Comparisons – Case A | 464 |
| Figure 5.6-14: Concentration Comparisons in Sector B – Case B | 465 |
| Figure 5.6-15: Concentration Comparisons in Sector I – Case B..... | 466 |
| Figure 5.6-16: MOP Comparisons – Case B | 467 |
| Figure 5.6-17: Concentration Comparisons in Sector B – Case C | 468 |
| Figure 5.6-18: Concentration Comparisons in Sector I – Case C..... | 469 |
| Figure 5.6-19: MOP Comparisons – Case C | 470 |
| Figure 5.6-20: Concentration Comparisons in Sector B – Case D | 472 |
| Figure 5.6-21: Concentration Comparisons in Sector I – Case D..... | 472 |
| Figure 5.6-22: MOP Dose Comparisons – Case D | 473 |

| | |
|---|-----|
| Figure 5.6-23: Concentration Comparisons in Sector B – Case E..... | 474 |
| Figure 5.6-24: Concentration Comparisons in Sector I – Case E..... | 475 |
| Figure 5.6-25: MOP Dose Comparisons – Case E | 476 |
| Figure 5.6-26: Flow Profile through Saltstone in Vault 1 for Cases A, C, and E..... | 480 |
| Figure 5.6-27: Flow Profile through Vault 1 Wall for Cases A, C, and E..... | 480 |
| Figure 5.6-28: Flow Profile through Saltstone in Vault 4 for Cases A through E..... | 482 |
| Figure 5.6-29: Flow Profile through Vault 4 Wall for Cases A through E..... | 482 |
| Figure 5.6-30: Flow Profile through Saltstone in the FDCs for Cases A through E | 483 |
| Figure 5.6-31: Flow Profile through the Wall of the FDCs for Cases A through E | 484 |
| Figure 5.6-32: Saltcake Sample to Prediction Ratio..... | 486 |
| Figure 5.6-33: Mean Dose to a MOP, Any Sector within 20,000 Years – All Cases..... | 496 |
| Figure 5.6-34: Mean Dose to a MOP, Any Sector within 20,000 Years – Case A | 497 |
| Figure 5.6-35: Mean Dose to a MOP, Any Sector within 20,000 Years – Case B..... | 497 |
| Figure 5.6-36: Mean Dose to a MOP, Any Sector within 20,000 Years – Case C..... | 498 |
| Figure 5.6-37: Mean Dose to a MOP, Any Sector within 20,000 Years – Case D | 498 |
| Figure 5.6-38: Mean Dose to a MOP, Any Sector within 20,000 Years – Case E..... | 499 |
| Figure 5.6-39: Peak Mean Dose to a MOP, Any Sector – All Cases | 500 |
| Figure 5.6-40: Peak Mean Dose to a MOP, Any Sector - Case A..... | 500 |
| Figure 5.6-41: Peak Mean Dose to a MOP, Any Sector – Case C | 501 |
| Figure 5.6-42: Statistical Time History of a MOP Dose, Sector B within 20,000 Years – Case A | 504 |
| Figure 5.6-43: Statistical Time History of a MOP Dose, Sector B within 20,000 Years – Case C | 504 |
| Figure 5.6-44: Example of a Result Probability Density and Partial Dependence Plot | 508 |
| Figure 5.6-45: Max MOP Dose, Any Sector within 10,000 Years – Case A | 512 |
| Figure 5.6-46: Max MOP Dose, Any Sector within 20,000 Years – Case A | 513 |
| Figure 5.6-47: Max MOP Dose, Sector B within 10,000 Years – Case A | 514 |
| Figure 5.6-48: Max MOP Dose, Sector B within 20,000 Years – Case A | 515 |
| Figure 5.6-49: Max MOP Dose, Sector J within 10,000 Years – Case A | 516 |
| Figure 5.6-50: Max MOP Dose, Sector J within 20,000 Years – Case A | 517 |
| Figure 5.6-51: Max Concentration of Tc-99 at Sector B within 20,000 Years – Case A..... | 518 |
| Figure 5.6-52: Max Concentration of Tc-99 at Sector J within 20,000 Years – Case A..... | 519 |

| | |
|---|-----|
| Figure 5.6-53: Max Concentration of I-129 at Sector B within 20,000 Years – Case A..... | 520 |
| Figure 5.6-54: Max Concentration of I-129 at Sector J within 20,000 Years – Case A..... | 521 |
| Figure 5.6-55: Max Concentration of Ra-226 at Sector B within 20,000 Years – Case A..... | 522 |
| Figure 5.6-56: Max Concentration of Ra-226 at Sector J within 20,000 Years – Case A..... | 523 |
| Figure 5.6-57: Max MOP Dose, Any Sector within 10,000 Years – Case C | 524 |
| Figure 5.6-58: Max MOP Dose, Any Sector within 20,000 Years – Case C | 525 |
| Figure 5.6-59: Max MOP Dose, Sector B within 10,000 Years – Case C..... | 526 |
| Figure 5.6-60: Max MOP Dose, Sector B within 20,000 Years – Case C..... | 527 |
| Figure 5.6-61: Max MOP Dose, Sector J within 10,000 Years – Case C..... | 528 |
| Figure 5.6-62: Max MOP Dose, Sector J within 20,000 Years – Case C..... | 528 |
| Figure 5.6-63: Max Concentration of Tc-99, Sector B within 20,000 Years – Case C | 529 |
| Figure 5.6-64: Max Concentration of Tc-99, Sector J within 20,000 Years – Case C..... | 530 |
| Figure 5.6-65: Mass Concentration of I-129, Sector B within 20,000 Years – Case C..... | 531 |
| Figure 5.6-66: Mass Concentration of I-129, Sector J within 20,000 Years – Case C..... | 532 |
| Figure 5.6-67: Mass Concentration of Ra-226, Sector B within 20,000 Years – Case C..... | 533 |
| Figure 5.6-68: Mass Concentration of Ra-226, Sector J within 20,000 Years – Case C..... | 534 |
| Figure 5.6-69: 100m Peak Groundwater Pathways Dose Sectors B and I, Case B | 538 |
| Figure 5.6-70: 100m Peak Groundwater Pathways Dose Sectors B and I, Case C | 538 |
| Figure 5.6-71: 100m Peak Groundwater Pathways Dose Sectors B and I, Case D..... | 539 |
| Figure 5.6-72: 100m Peak Groundwater Pathways Dose Sectors B and I, Case E | 539 |
| Figure 5.6-73: 100m Peak Groundwater Pathways Dose Sector B, Case A through E..... | 540 |
| Figure 5.6-74: 100m Peak Groundwater Pathways Dose Sector I, Case A through E..... | 540 |
| Figure 5.6-75: Peak Groundwater Pathways Dose Sectors B and I, No Closure Cap Case | 542 |
| Figure 5.6-76: Diffusion Coefficient Compared To Hydraulic Conductivity for Saltstone Materials Palette..... | 544 |
| Figure 5.6-77: Unsaturated Hydraulic Conductivity Estimate for Cracked/Un-cracked Disposal Unit Concrete | 544 |
| Figure 5.6-78: Ettringite Front Position for Accelerated Sulfate Attack Vault 1 | 545 |
| Figure 5.6-79: Ettringite Front Position for Accelerated Sulfate Attack FDCs..... | 545 |
| Figure 5.6-80: Ettringite Front Position for Accelerated Sulfate Attack Vault 4 | 546 |
| Figure 5.6-81: Peak Groundwater Pathways Dose Sector B, Materials Degradation Sensitivity Analysis | 547 |

| | |
|---|-----|
| Figure 5.6-82: Peak Groundwater Pathways Dose Sector I, Materials Degradation Sensitivity Analysis | 547 |
| Figure 5.6-83: Peak Groundwater Pathways Dose, Sectors B and I - Synergistic Case and Base Case | 549 |
| Figure 5.6-84: Peak Groundwater Pathways Dose Sectors B and I, Vault 1 and 4 - Oxidized Concrete Case and Base Case | 551 |
| Figure 5.6-85: Peak Groundwater Pathways Dose, Sectors B and I, Increased Saltstone Hydraulic Conductivity Case and Base Case..... | 552 |
| Figure 6.4-1: Chronic Intruder Dose Results | 598 |
| Figure 6.5-1: Mean Dose to the Chronic Intruder, Any Sector – All Cases | 599 |
| Figure 6.5-2: Mean Dose to the Chronic Intruder, Any Sector – Case A..... | 600 |
| Figure 6.5-3: Mean Dose to the Chronic Intruder, Any Sector – Case C | 600 |
| Figure 6.5-4: Total Chronic IHI Dose in Sector B – Case A..... | 602 |
| Figure 6.5-5: Total Chronic IHI Dose in Sector J – Case A | 602 |
| Figure 6.5-6: Total Chronic IHI Dose in Sector B – Case C | 603 |
| Figure 6.5-7: Total Chronic IHI Dose in Sector J – Case C | 603 |
| Figure 6.5-8: Peak Acute Intruder Dose Assuming Drilling into a SDF Disposal Unit..... | 605 |
| Figure 6.5-9: Peak Chronic Intruder Dose for 20,000 Years Assuming Drilling into a SDF Disposal Unit | 606 |
| Figure 7.1-1: Peak Groundwater Pathways Dose and Key Radionuclide Doses for Sector B - Base Case..... | 607 |
| Figure 7.1-2: Model Input Timeline for Various SDF Modeling Segments..... | 608 |

LIST OF TABLES

| | |
|--|-----|
| Table 1.0-1: Comparison of SDF Results with Performance Measures | 32 |
| Table 2.5-1: Maximum Contaminant Levels | 41 |
| Table 3.1-1: Population Distribution and Percent of Region for Counties and Selected Communities | 52 |
| Table 3.1-2: Characterization and Monitoring Data in the GSAD | 81 |
| Table 3.1-3: Water Quality in the Savannah River Upstream and Downstream from SRS (Calendar Year 2007)..... | 90 |
| Table 3.1-4: Water Quality in UTR | 91 |
| Table 3.1-5: Groundwater Monitoring Results for Outcrops to UTR | 92 |
| Table 3.2-1: Vault 1 Concrete Formulations | 103 |
| Table 3.2-2: Vault 4 Concrete Formulations | 108 |
| Table 3.2-3: Future Disposal Cell Tested Concrete Mix | 117 |
| Table 3.2-4: Generic SDF Conceptual Closure Cap Layers | 128 |
| Table 3.2-5: Function of the SDF Conceptual Closure Cap Layers | 129 |
| Table 3.2-6: Closure Cap Potential Degradation Mechanisms | 137 |
| Table 3.2-7: Closure Cap Estimated Infiltration Rates | 138 |
| Table 3.3-1: Vault 1 Projected Radionuclide Inventory at Closure | 139 |
| Table 3.3-2: Vault 1 Projected Chemical Inventory at Closure | 140 |
| Table 3.3-3: Vault 4 Projected Radionuclide Inventory at Closure | 141 |
| Table 3.3-4: Vault 4 Projected Chemical Inventory at Closure | 142 |
| Table 3.3-5: FDC Projected Radionuclide Inventory at Closure | 143 |
| Table 3.3-6: FDC Projected Chemical Inventory at Closure | 144 |
| Table 3.3-7: Total Projected SDF Disposal Units' Radionuclide Inventory at Closure | 145 |
| Table 3.3-8: Total Projected SDF Disposal Units' Chemical Inventory at Closure | 146 |
| Table 4.2-1: Summary of Age - Redox States in Cementitious Material | 151 |
| Table 4.2-2: Radionuclides Requiring Further Evaluation | 154 |
| Table 4.2-3: Decay Series for Neptunium, Thorium, Uranium, and Actinium | 155 |
| Table 4.2-4: Initial Inventory Isotopes from Principal Decay Chains | 156 |
| Table 4.2-5: SDF Inventory Radionuclides | 156 |
| Table 4.2-6: Continued Evaluation of Radionuclides | 157 |
| Table 4.2-7: Ingredients of Saltstone and Clean Grout..... | 163 |

| | |
|--|-----|
| Table 4.2-8: Key Constituents in the Infiltrating Solutions Analyzed..... | 164 |
| Table 4.2-9: Transitions for Saltstone and FDC Concrete..... | 164 |
| Table 4.2-10: Hydraulic Head Residuals Between GSA/PORFLOW Model and Field Data through 2006..... | 181 |
| Table 4.2-11: SDF Closure Cap Material Properties | 182 |
| Table 4.2-12: Hydraulic Parameters for Lower Lateral Drainage Layer | 185 |
| Table 4.2-13: Estimated Depth of Vadose Zone for SDF Disposal Units | 191 |
| Table 4.2-14: Hydraulic Properties of Vadose Zone Material..... | 192 |
| Table 4.2-15: Recommended K_d Values for Backfill and the Vadose Zone | 194 |
| Table 4.2-16: Cementitious Material Properties | 197 |
| Table 4.2-17: Chemical Transition Times for Cementitious Materials | 213 |
| Table 4.2-18: Recommended K_d Values for Cementitious Materials..... | 215 |
| Table 4.2-19: Lower Vadose Zone and Effective Saturated Zone Soil Properties..... | 218 |
| Table 4.2-20: Crosswalk of Potential Exposure Pathways for MOP Receptors..... | 219 |
| Table 4.2-21: Crosswalk of Potential Exposure Pathways for Intruder Receptors..... | 229 |
| Table 4.4-1: Material Parameters for Vault 1 Conceptual Model | 244 |
| Table 4.4-2: Material Parameters for Vault 4 Conceptual Model | 246 |
| Table 4.4-3: Material Parameters for FDC Conceptual Model..... | 248 |
| Table 4.4-4: Cases Postulated for SDF Vaults and FDCs | 250 |
| Table 4.4-5: Hydraulic Properties of Gravel..... | 252 |
| Table 4.4-6: Occurrences of Model Changes by Case for Vault 1 | 257 |
| Table 4.4-7: Occurrences of Model Changes by Case for Vault 4 | 261 |
| Table 4.4-8: Hydraulic Properties of Sand | 262 |
| Table 4.4-9: Occurrences of Model Changes by Case for FDCs..... | 263 |
| Table 4.4-10: PORFLOW Materials Palette for SDF | 291 |
| Table 4.5-1: Vertical Layer Sequence/Thickness for Vault 1 and Cover Material | 329 |
| Table 4.5-2: Vertical Layer Sequence/Thickness for FDC and Cover Material..... | 329 |
| Table 4.5-3: Vertical Layer Sequence/Thickness for Vault 4 and Cover Material | 330 |
| Table 4.5-4: Particle Density, Total Porosity, Average Saturation, and Air-filled Porosity Vault 1..... | 331 |
| Table 4.5-5: Particle Density, Total Porosity, Average Saturation, and Air-filled Porosity FDCs | 331 |

| | |
|--|-----|
| Table 4.5-6: Particle Density, Total Porosity, Average Saturation, and Air-Filled Porosity Vault 4..... | 332 |
| Table 4.5-7: Radionuclides and Compounds of Interest for Air and Radon Pathway Analysis..... | 334 |
| Table 4.5-8: Gases for Each Radionuclide, their Reaction with Aqueous Component, and Equilibrium Constants | 335 |
| Table 4.5-9: Parameters Used in Estimating Apparent Henry's Law Constants | 336 |
| Table 4.5-10: Radionuclides of Interest, Dominant Gas Under Saltstone Conditions, and Apparent Henry's Law Constant | 336 |
| Table 4.5-11: Apparent Henry's Law Constant and Partitioning Coefficient | 338 |
| Table 4.5-12: Effective Air Diffusion Coefficients for Vault 1 and Closure Cap | 339 |
| Table 4.5-13: Effective Air Diffusion Coefficients for FDCs and Closure Cap | 340 |
| Table 4.5-14: Effective Air Diffusion Coefficients for Vault 4 and Closure Cap | 341 |
| Table 4.5-15: SRS Boundary for DDA Saltstone in Vault 1 | 345 |
| Table 4.5-16: 100m Dose for DDA Saltstone in Vault 1 | 346 |
| Table 4.5-17: SRS Boundary Dose for ARP/MCU Saltstone in Vault 1 | 346 |
| Table 4.5-18: 100m Dose for ARP/MCU Saltstone in Vault 1 | 347 |
| Table 4.5-19: SRS Boundary Dose for SWPF Saltstone in FDCs..... | 347 |
| Table 4.5-20: 100m Dose for SWPF Saltstone in FDCs | 348 |
| Table 4.5-21: SRS Boundary Dose for DDA Saltstone in Vault 4..... | 348 |
| Table 4.5-22: 100m Dose for DDA Saltstone in Vault 4..... | 349 |
| Table 4.5-23: SRS Boundary Dose for ARP/MCU Saltstone in Vault 4..... | 349 |
| Table 4.5-24: 100m Dose for ARP/MCU Saltstone in Vault 4 | 350 |
| Table 4.5-25: Peak Rn-222 Flux over 10,000 Years for Vault 1 DDA Saltstone..... | 357 |
| Table 4.5-26: Peak Rn-222 Flux over 10,000 Years for Vault 1 ARP/MCU Saltstone | 357 |
| Table 4.5-27: Peak Rn-222 Flux over 10,000 Years for FDCs SWPF Saltstone | 357 |
| Table 4.5-28: Peak Rn-222 Flux over 10,000 Years for Vault 4 DDA Saltstone..... | 357 |
| Table 4.5-29: Peak Rn-222 Flux over 10,000 Years for Vault 4 ARP/MCU Saltstone | 358 |
| Table 4.6-1: Soil-to-Vegetable Transfer Factors (Unitless) | 360 |
| Table 4.6-2: Feed-to-Milk Transfer Factors (d/L) | 363 |
| Table 4.6-3: Feed-to-Meat Transfer Factors (d/kg) | 366 |
| Table 4.6-4: Water-to-Fish Bioaccumulation Factors (L/kg) | 369 |
| Table 4.6-5: Crop Exposure Times and Productivity | 373 |

| | |
|---|-----|
| Table 4.6-6: Physical Parameters..... | 373 |
| Table 4.6-7: Individual Exposure Times and Consumption Rates | 374 |
| Table 4.7-1: Internal and External DCFs..... | 377 |
| Table 5.2-1: Key Model Parameters | 382 |
| Table 5.2-2: Aquifer Travel Distance to SDF 100m Boundary | 388 |
| Table 5.2-3: Radiological 100m Concentrations for UTR-UZ Sectors A through E | 392 |
| Table 5.2-4: Radiological 100m Concentrations for UTR-UZ Sectors F through J..... | 395 |
| Table 5.2-5: Radiological 100m Concentrations for UTR-UZ Sectors K and L | 398 |
| Table 5.2-6: Radiological 100m Concentrations for UTR-LZ Sectors A through E..... | 400 |
| Table 5.2-7: Radiological 100m Concentrations for UTR-LZ Sectors F through J | 403 |
| Table 5.2-8: Radiological 100m Concentrations for UTR-LZ Sectors K and L | 406 |
| Table 5.2-9: Radiological 100m Concentrations for GAU Sectors A through E | 408 |
| Table 5.2-10: Radiological 100m Concentrations for GAU Sectors F through J..... | 411 |
| Table 5.2-11: Radiological 100m Concentrations for GAU Sectors K and L | 414 |
| Table 5.2-12: Chemical 100m Concentrations for UTR-UZ Sectors A through E | 416 |
| Table 5.2-13: Chemical 100m Concentrations for UTR-UZ Sectors F through J..... | 417 |
| Table 5.2-14: Chemical 100m Concentrations for UTR-UZ Sectors K and L | 418 |
| Table 5.2-15: Chemical 100m Concentrations for UTR-LZ Sectors A through E..... | 419 |
| Table 5.2-16: Chemical 100m Concentrations for UTR-LZ Sectors F through J | 420 |
| Table 5.2-17: Chemical 100m Concentrations for UTR-LZ Sectors K and L..... | 421 |
| Table 5.2-18: Chemical 100m Concentrations for Gordon Aquifer Sectors A through E | 422 |
| Table 5.2-19: Chemical 100m Concentrations for GAU Sectors F through J..... | 423 |
| Table 5.2-20: Chemical 100m Concentrations for GAU Sectors K and L | 424 |
| Table 5.2-21: Determination of Key Radionuclides | 425 |
| Table 5.3-1: Total Projected SDF Inventory of Gaseous Radionuclides..... | 427 |
| Table 5.3-2: Vault 1 10,000 Year Dose at 100m | 427 |
| Table 5.3-3: Vault 4 10,000 Year Peak Dose at 100m | 428 |
| Table 5.3-4: FDCs 10,000 Year Peak Dose at 100m..... | 428 |
| Table 5.3-5: SDF Inventory of Radionuclides Producing Rn-222 | 429 |
| Table 5.3-6: Peak Rn-222 Flux above Vault 1 | 429 |
| Table 5.3-7: Peak Rn-222 Flux above Vault 4 | 429 |
| Table 5.3-8: Peak Rn-222 Flux above FDCs..... | 429 |

| | |
|--|-----|
| Table 5.5-1: 100m MOP Peak Groundwater Pathways Dose by Sector..... | 437 |
| Table 5.5-2: Sector B 100m MOP Peak Groundwater Pathways Dose in 10,000 Years | 440 |
| Table 5.5-3: Sector I 100m MOP Peak Groundwater Pathways Dose in 20,000 Years..... | 442 |
| Table 5.5-4: 100m MOP Peak Groundwater Pathways Dose at Peak Years, Sectors B and I..... | 443 |
| Table 5.5-5: 100m MOP Peak Dose Groundwater Pathways Contributions, Sector B..... | 444 |
| Table 5.5-6: 100m MOP Peak Water Ingestion Doses, Sectors B and I | 444 |
| Table 5.5-7: 100m MOP Peak Fish Ingestion Doses, Sectors B and I | 444 |
| Table 5.5-8: 100m MOP Peak Vegetable Ingestion Doses, Sectors B and I..... | 445 |
| Table 5.5-9: 100m MOP Peak Annual All-Pathways Dose Contributors | 449 |
| Table 5.6-1: Adjustment Multiplicative Factors on Flow Values..... | 455 |
| Table 5.6-2: Disposal Unit Cases..... | 478 |
| Table 5.6-3: Case Probability by Disposal Unit Type | 479 |
| Table 5.6-4: Radionuclide Inventory Uncertainty in GoldSim Model | 486 |
| Table 5.6-5: Distribution Coefficient Variability in the GoldSim Model | 487 |
| Table 5.6-6: Pore Volume Transition Uncertainty in the GoldSim Model..... | 487 |
| Table 5.6-7: Probability of Well Driller Exposure from Each Aquifer | 488 |
| Table 5.6-8: Contaminant Transfer Ratios Between Aquifers..... | 489 |
| Table 5.6-9: Crop Exposure Time and Productivity Stochastics..... | 490 |
| Table 5.6-10: Pathway Physical Parameter Stochastics | 490 |
| Table 5.6-11: Consumption Rate, Pathway Exposure Time and Transport Stochastics | 491 |
| Table 5.6-12: Summary for Selected SDF Endpoints – Case A Only | 502 |
| Table 5.6-13: Summary for Selected SDF Endpoints – Case C Only | 503 |
| Table 5.6-14: Most Sensitive Parameters for Endpoints of Interest – Case A | 510 |
| Table 5.6-15: Most Sensitive Parameters for Endpoints of Interest – Case C..... | 511 |
| Table 5.6-16: 100m Peak Dose for Key Radionuclides within 20,000 Years by Sector for Cases A through E | 537 |
| Table 5.6-17: 100m Peak Groundwater Pathways Dose within 20,000 Years for Sectors B and I for No Closure Cap Sensitivity Comparison..... | 541 |
| Table 5.6-18: Disposal Unit Component Failure Times, Base Case and 10 Times Sulfate Case..... | 543 |
| Table 5.6-19: 100m Peak Groundwater Pathways Dose within 20,000 Years for Sectors B and I for Materials Degradation Sensitivity Comparison..... | 546 |

| | |
|---|-----|
| Table 5.6-20: 100m Peak Groundwater Pathways Dose within 20,000 Years for Sectors B and I for Synergistic Sensitivity Comparison | 549 |
| Table 5.6-21: 100m Peak Groundwater Pathways Dose within 20,000 Years for Sectors B and I for Vault 1 and 4 Oxidized Concrete Sensitivity Comparison..... | 550 |
| Table 5.6-22: 100m Peak Groundwater Pathways Dose within 20,000 Years for Sectors B and I for Increased Saltstone Hydraulic Conductivity Sensitivity Comparison | 552 |
| Table 6.1-1: Radiological 1m Concentrations for UTR-UZ Sectors A through E | 555 |
| Table 6.1-2: Radiological 1m Concentrations for UTR-UZ Sectors F through J | 558 |
| Table 6.1-3: Radiological 1m Concentrations for UTR-UZ Sectors K and L | 561 |
| Table 6.1-4: Radiological 1m Concentrations for UTR-LZ Sectors A through E..... | 563 |
| Table 6.1-5: Radiological 1m Concentrations for UTR-LZ Sectors F through J | 566 |
| Table 6.1-6: Radiological 1m Concentrations for UTR-LZ Sectors K and L | 569 |
| Table 6.1-7: Radiological 1m Concentrations for Gordon Aquifer Sectors A through E | 571 |
| Table 6.1-8: Radiological 1m Concentrations for Gordon Aquifer Sectors F through J | 574 |
| Table 6.1-9: Radiological 1m Concentrations for Gordon Aquifer Sectors K and L | 577 |
| Table 6.1-10: Chemical 1m Concentrations for UTR-UZ Sectors A through E | 579 |
| Table 6.1-11: Chemical 1m Concentrations for UTR-UZ Sectors F through J | 580 |
| Table 6.1-12: Chemical 1m Concentrations for UTR-UZ Sectors K and L | 581 |
| Table 6.1-13: Chemical 1m Concentrations for UTR-LZ – Sectors A through E..... | 582 |
| Table 6.1-14: Chemical 1m Concentrations for UTR-LZ Sectors F through J | 583 |
| Table 6.1-15: Chemical 1m Concentrations for UTR-LZ Sectors K and L..... | 584 |
| Table 6.1-16: Chemical 1m Concentrations for Gordon Aquifer Sectors A through E | 585 |
| Table 6.1-17: Chemical 1m Concentrations for Gordon Aquifer Sectors F through J | 586 |
| Table 6.1-18: Chemical 1m Concentrations for Gordon Aquifer Sectors K and L | 587 |
| Table 6.4-1: Chronic Intruder Peak Dose Contributors in 10,000 Years..... | 597 |
| Table 6.4-2: Chronic Intruder 10,000 Year Peak Dose Contributors by Radionuclide..... | 597 |
| Table 6.5-1: Determination of 100m Multiplier for Intruder Uncertainty Analyses | 599 |
| Table 6.5-2: Summary Statistics for Chronic Intruder (IHI) Endpoints – Cases A and C | 601 |
| Table 8.1-1: Comparison of SDF Results with Performance Measures | 616 |
| Table 8.2-1: PA Maintenance Activities to Address NRC TER Factors | 619 |

ACRONYMS / ABBREVIATIONS

| | |
|----------------|---|
| ALARA | As Low As Reasonably Achievable |
| ARP | Actinide Removal Process |
| ASTM | American Society of Testing and Materials |
| BMF | Benchmarking Factors |
| C&IS | Computer and Information Security |
| CA | Composite Analysis |
| CAB | Citizens Advisory Board |
| CAP-88 | Clean Air Act Assessment Package – 1988 |
| CERCLA | Comprehensive Environmental Response, Compensation, and Liability Act |
| CFD | Computational Fluid Dynamics |
| CFR | Code of Federal Regulations |
| cfs | cubic feet per second |
| CLM | Central Climatology Site |
| CPT | Cone Penetration Test |
| CSFII | Continuing Survey of Food Intakes by Individuals |
| CSH | Calcium Silicate Hydrate |
| CSRA | Central Savannah River Area |
| d | Day(s) |
| D&D | Deactivation and Decommissioning |
| DCF | Dose Conversion Factors |
| DCG | Derived Concentration Guide |
| DCS | Distributed Control System |
| DDA | Deliquification, Dissolution, and Adjustment |
| DOE | United States Department of Energy |
| DOE-HQ | Department of Energy – Headquarters |
| DOE-SR | Department of Energy – Savannah River Operations Office |
| DRF | Dose Release Factors |
| DSA | Documented Safety Analysis |
| DWPF | Defense Waste Processing Facility |
| EFH | Exposure Factors Handbook |
| E _h | Measure of reduction (or oxidation) potential |
| EPA | United States Environmental Protection Agency |
| EPDM | Ethylene-propylene Monomer |

| | |
|--------|---|
| ERDMS | Environmental Restoration Data Management System |
| ETF | Effluent Treatment Facility |
| FDC | Future Disposal Cells |
| FMF | Fuel Material Facility |
| FTF | F-Tank Farm |
| FTF PA | F-Tank Farm Performance Assessment |
| GAU | Gordon Aquifer Unit |
| GBM | Gradient Boosting Models |
| GCL | Geosynthetic Clay Liner |
| GM | Geometric Mean |
| GS | General Service |
| GSA | General Separations Area |
| GSAD | General Separations Area Database |
| GSD | Geometric Standard Deviation |
| GTG | GoldSim Technology Group LLC |
| GW | Groundwater |
| HDPE | High Density Polyethylene |
| HELP | Hydrologic Evaluation of Landfill Performance |
| HTF | H-Tank Farm |
| ICRP | International Commission on Radiological Protection |
| IHI | Inadvertent Human Intruder |
| INEEL | Idaho National Engineering and Environmental Laboratory |
| ISCM | Integrated Site Conceptual Model |
| ISMS | Integrated Safety Management System |
| ITP | In-Tank Precipitation Facility |
| LAZ | Lower Aquifer Zone |
| LFRG | DOE Low-Level Waste Federal Review Group |
| LLW | Low-Level Waste |
| MCL | Maximum Contaminant Levels |
| MCU | Modular Caustic Side Solvent Extraction Unit |
| MEI | Maximally Exposed Individual |
| MOP | Member of the Public |
| MP | Management Policy |
| MQB | McQueen Branch |
| MSL | Mean Sea Level |

| | |
|--------|---|
| NC | Not Calculated |
| NCRP | National Council on Radiation Protection and Measurements |
| ND | Non-Detectable |
| NDAA | National Defense Authorization Act |
| NERP | National Environmental Research Park |
| NESHAP | National Emissions Standards for Hazardous Air Pollutants |
| NPDES | National Pollutant Discharge Elimination System |
| NR | Not Reported |
| NRC | United States Nuclear Regulatory Commission |
| NRMP | Natural Resources Management Plan |
| ORNL | Oak Ridge National Laboratories |
| OUO | Official Use Only |
| PA | Performance Assessment |
| PMP | Probable Maximum Precipitation |
| PODD | Performance Objective Demonstration Document |
| PS | Production Support |
| PVC | Polyvinyl Chloride |
| QA | Quality Assurance |
| QAMP | Quality Assurance Management Program |
| QC | Quality Control |
| RCRA | Resource Conservation and Recovery Act |
| RESRAD | RESidual RADioactivity Computer Software |
| ROI | Region of Influence |
| SA | Special Analysis |
| SC | Safety Class |
| SCDHEC | South Carolina Department of Health and Environmental Control |
| SCS | Soil Conservation Service |
| SD | Standard Deviation |
| SDF | Saltstone Disposal Facility |
| SDF PA | Saltstone Disposal Facility Performance Assessment |
| SDWA | Federal Safe Drinking Water Act |
| SGCP | Soil and Groundwater Closure Project |
| SI | Sensitivity Indices |
| SMA | Strong Motion Accelerometer |
| SPF | Saltstone Production Facility |

| | |
|--------|--|
| SQAP | Software Quality Assurance Plan |
| SREL | Savannah River Ecology Laboratory |
| SRNL | Savannah River National Laboratory |
| SRR | Savannah River Remediation |
| SRS | Savannah River Site |
| SS | Safety Significant |
| SS&ES | Safeguards, Security & Emergency Services |
| SWPF | Salt Waste Processing Facility |
| TCCZ | Tan Clay Confining Zone |
| TCLP | Toxicity Characteristic Leaching Procedure |
| TEDE | Total Effective Dose Equivalent |
| TER | Technical Evaluation Report |
| U.S.C. | United States Code |
| UAZ | Upper Aquifer Zone |
| USACE | United States Army Corps of Engineers |
| USDA | United States Department of Agriculture |
| USGS | United States Geological Survey |
| UTR | Upper Three Runs |
| UTR-LZ | Upper Three Runs – Lower Zone |
| UTR-UZ | Upper Three Runs – Upper Zone |
| UV | Ultraviolet |
| VZMS | Vadose Zone Monitoring System |
| WAC | Waste Acceptance Criteria |
| WCS | Waste Characterization System |
| WES | Waterways Experiment Station |
| WQS | Water Quality Standard |
| WSRC | Washington Savannah River Company |
| WWTF | Waste Water Treatment Facility |

1.0 EXECUTIVE SUMMARY

This Performance Assessment (PA) for the Savannah River Site (SRS) was prepared to support the operation and eventual closure of the Saltstone Disposal Facility (SDF). This PA was prepared to demonstrate compliance with the pertinent requirements of the United States Department of Energy (DOE) Order 435.1, Change 1, *Radioactive Waste Management*, Chapter IV, and Title 10, of the Code of Federal Regulations (CFR) Part 61, *Licensing Requirements for Land Disposal of Radioactive Waste*, Subpart C as required by the *Ronald W. Reagan National Defense Authorization Act (NDAA) for Fiscal Year 2005*, Section 3116. [DOE O 435.1-1, 10 CFR 61, NDAA_3116]

Requirements in both DOE O 435.1-1 and 10 CFR 61 stipulate that a PA should provide reasonable assurance that Low-Level Waste (LLW) disposal will comply with specified performance objectives. DOE O 435.1-1 and 10 CFR 61 both require assessments of impacts to hypothetical inadvertent intruders. DOE O 435.1-1 also requires assessments for impacts to water resources. These assessments were performed to address a 10,000 year performance period after facility closure (which encompasses the DOE O 435.1-1 1,000 year compliance period). [DOE O 435.1-1, 10 CFR 61]

The point of compliance for the performance measures, relevant to the all-pathways and air pathways performance objectives, as well as the impact on water resources assessment requirements, must correspond to the point of highest projected dose or concentration beyond a 100m buffer zone surrounding the disposed waste following the assumed end of active institutional controls. For the performance measure relevant to radon, the point of compliance is the disposal facility surface. For the performance measure relevant to an inadvertent intruder, the point of compliance is the disposal facility after the assumed end of active institutional controls, 100 years after facility closure.

SRS is located in south-central South Carolina, approximately 100 miles from the Atlantic coast. The SDF is located in Z-Area, which is in the central region of SRS. Z-Area consists of approximately 161 acres. The Saltstone Facility consists of two facility segments, one is the Saltstone Production Facility (SPF), which receives and treats salt solution to produce saltstone. Saltstone is a cementitious waste form made by mixing salt solution, from the liquid waste tanks in the F- and H-Tank Farms (FTF and HTF) of SRS, with a dry mix containing blast furnace slag, fly ash, and cement. The second facility segment is the SDF which consists of two existing disposal units (Vaults 1 and 4) and will include future disposal cells (FDCs). FDCs will be constructed as needed to coordinate with salt processing rates with 64 FDCs assumed for this PA. The SDF is permitted as a Class 3 Landfill per South Carolina Department of Health and Environmental Control (SCDHEC) regulations. [DHEC_09-09-2008]

Radiological dose to human receptors is analyzed in this PA in the all-pathways analysis, the inadvertent intruder analysis, and the air pathways analysis, for comparison to the relevant performance measures. Seventy isotopes were modeled for the groundwater transport and intruder analyses, and eight were modeled in the air pathways analysis. Radon fluxes were also evaluated. The pathways identified that result in potential dose contributions were; (1) leaching

from the saltstone waste form resulting in contamination of the local groundwater, and (2) gaseous diffusion into the atmosphere above the disposal units. For the inadvertent intruder analysis, only the chronic intruder agriculture scenario was considered to result in credible potential exposure.

The SDF PA employed a hybrid modeling approach. In this approach, the PORFLOW computer code was used to model groundwater flow and transport to provide radionuclide concentrations used for the calculation of dose for comparison to the relevant performance measures. Uncertainty and sensitivity analyses were performed via probabilistic analyses using the GoldSim computer code. The probabilistic sensitivity analysis was supplemented with multiple deterministic sensitivity analyses using the PORFLOW code.

As shown in Table 1.0-1, all of the regulatory limits are met within the 10,000 year period of compliance.

Table 1.0-1: Comparison of SDF Results with Performance Measures

| Performance Measure | | Limit | Result |
|---------------------|------------------------|--|---|
| DOE O 435.1-1 | All-Pathways Dose | 25 mrem/yr | 1.4 mrem/yr |
| DOE O 435.1-1 | Intruder Dose | 500 mrem acute 100 mrem/yr chronic | N/A - acute 1.9 mrem/yr - chronic |
| DOE O 435.1-1 | Air Pathways Dose | 10 mrem/yr | <4E-09 mrem/yr |
| DOE O 435.1-1 | Radon Flux | 20 pCi/m ² /s at ground surface | 2.0E-13 pCi/m ² /s |
| DOE O 435.1-1 | Groundwater Protection | Total β/γ 4 mrem/yr Total α 15 pCi/L Total U 30 µg/L Total Ra 5 pCi/L | 1.16 mrem/yr 1.9 pCi/L 8.0E-9 µg/L 1.9 pCi/L |
| 10 CFR 61.41 | All-Pathways Dose | 25 mrem/yr | 1.4 mrem/yr |
| 10 CFR 61.42 | Intruder Dose | 500 mrem/yr | 1.9 mrem/yr |

N/A = Not applicable

MCL = Maximum Contaminant Level

The results of the Composite Analysis (CA) for SRS showed that the predominant source of radionuclides contributing to the calculated dose at the identified points of assessment were facilities other than the SDF. [WSRC-RP-97-311_OUO] The points of assessment for the CA were the mouths of Upper Three Runs (UTR) and Fourmile Branch, where stream water is undiluted by the Savannah River, but still accessible by a hypothetical Member of the Public (MOP). Other points of assessment include the Savannah River at Highway 301 and the water treatment plants at Beaufort-Jasper, South Carolina, and Port Wentworth, Georgia. [WSRC-RP-97-311_OUO] Based on these points of assessment, it is concluded that the impact of this SDF PA results on the CA are negligible.

2.0 INTRODUCTION

The potential radiological dose to receptors is typically evaluated with a PA model that simulates the release of radionuclides from the disposal site, transport of radionuclides through the environment, and exposure of potential receptors from residual material. The PA provides the technical basis for demonstrating compliance with the performance objectives of DOE O 435.1-1 and 10 CFR 61. [DOE O 435.1-1, 10 CFR 61]

2.1 General Approach

The SDF PA is used to fulfill the DOE O 435.1-1 requirement that an assessment be prepared and maintained for DOE LLW disposed after September 26, 1988. The PA must provide reasonable assurance that the facility design and method of disposal will comply with the performance objectives of the order, which ensure protection of public health and safety in limiting doses to a MOP and limiting releases of radon. The PA must also, for purposes of establishing limits on radionuclides that may be buried near-surface, assess impacts to a hypothetical intruder and impacts to water resources.

2.1.1 Previous Performance Assessments and Composite Analyses

2.1.1.1 1992 Radiological Performance Assessment

A radiological PA was issued in 1992 following the design and construction of the Saltstone Facility (1992 PA). [WSRC-RP-92-1360] The 1992 PA was written in accordance with the requirements contained in DOE O 5820.2A (note, DOE O 5820.2A was canceled by the issuance of DOE O 435.1-1, Chg. 1). The inventory assumption for this initial evaluation was the decontaminated salt solution stream from the In-Tank Precipitation Facility (ITP) and the concentrate stream from the Effluent Treatment Facility (ETF). The 1992 PA evaluated waste material in SDF Vaults 1 and 4 and projected the results for FDCs, assuming rectangular disposal units. The groundwater evaluation point for this and future performance objective compliance reviews was a hypothetical well at a point 100m from the disposal units. The groundwater pathways performance objective assumed in the 1992 PA was a dose of 4 mrem/yr from direct ingestion, for all radionuclides combined. The groundwater pathways analysis was quantitative in nature, while the air pathways was a qualitative evaluation, which concluded that the air pathways was insignificant compared to the groundwater pathways. The intruder scenarios were evaluated in a qualitative fashion. The dose calculations in the 1992 PA were based on the anticipated inventory and determined to be within performance limits. In 1998, an addendum was developed for the 1992 PA in order to address comments from the DOE PA Peer Review Panel and DOE Headquarters (DOE-HQ). [WSRC-RP-98-00156] There was no change in the conclusions of the 1992 PA based upon the 1998 Addendum. [WSRC-RP-92-1360, WSRC-RP-98-00156]

2.1.1.2 2002 Special Analysis: Reevaluation of the Inadvertent Intruder, Groundwater, Air, and Radon Analyses for the SDF

In 2002, a Special Analysis (SA) (2002 SA) was performed. [WSRC-TR-2002-00456] The 2002 SA was prepared in response to updated facility inventory information as a result of suspended ITP operations and replacing that waste stream with expected low curie salt solution feed. DOE O 435.1-1 had also been promulgated and the 2002 SA used this order for a compliance determination. Rather than using a specific radionuclide list for evaluation, as was used in the 1992 PA, a radionuclide screening evaluation was performed using National Council on Radiation Protection and Measurements (NCRP) methodology. [NCRP-123 Vol. 1] The screening yielded one new radionuclide of interest, Np-237. Rather than calculating specific doses from a fixed radionuclide inventory, the 2002 SA calculated radionuclide inventory limits against specific objectives of 25 mrem/yr from all-pathways, 10 mrem/yr from the air pathways, and the United States Environmental Protection Agency (EPA) MCLs for the groundwater pathways. [WSRC-TR-2002-00456, SCDHEC R.61-58] The 1992 PA doses for a specific radionuclide inventory were utilized to determine the individual radionuclide limits. For beta-gamma radionuclides the MCL limit is 4 mrem/yr from the direct ingestion groundwater pathways and 15 pCi/L for alpha radionuclides. Since Np-237 was not included in the 1992 PA, the limit for this radionuclide was calculated in the 2002 SA. The air pathways was a quantitative analysis in the 2002 SA. The anticipated low curie salt solution feed inventory was then compared to the limits. The results of the intruder and groundwater and air pathways analyses demonstrated compliance with DOE O 435.1-1. [WSRC-TR-2002-00456, WSRC-RP-92-1360]

2.1.1.3 2005 Special Analysis: Revision of Saltstone Vault 4 Disposal Limits

Updated information on the SDF feed solutions, modeling methods, closure cap design, and evaluations were captured in a 2005 Special Analysis (2005 SA). [WSRC-TR-2005-00074] The 2005 SA supplements the analyses in the 1992 PA and supersedes the analyses in the 2002 SA. The 2005 SA evaluates the SDF against the specific performance objectives of DOE O 435.1-1 and 10 CFR 61. [WSRC-TR-2005-00074, WSRC-RP-92-1360, WSRC-TR-2002-00456]

The salt waste inventory was updated to reflect current estimates of the total inventory expected to be disposed of in Vault 4, including Deliquification, Dissolution, and Adjustment (DDA), as well as the anticipated decontaminated solution from the Salt Waste Processing Facility (SWPF). The 2005 SA recalculated groundwater transport and air transport. An all-pathways analysis included residential and agricultural pathways. The radionuclide limits were calculated for specific exposure pathways and a limit determined for each pathway at the most restrictive exposure time period between 100 and 10,000 years after closure. The most restrictive limit for any pathway for each radionuclide was chosen as the limit, and thus a sum-of-fractions for any waste inventory would be conservative. The 2005 SA includes many sensitivity evaluations, but it only included limits for the SDF Vault 4. [WSRC-TR-2005-00074] The intruder scenarios were also recalculated and determined to be in compliance with the DOE O 435.1-1 requirements.

2.1.1.4 2005 Performance Objective Demonstration Document

Removal and disposal of low-activity salt waste is critical in order to establish empty tank space for future tank waste processing operations, including the Actinide Removal Process (ARP), Modular Caustic Side Solvent Extraction Unit (MCU), and the SWPF. It will also ensure that vitrification of the high-activity fraction will be able to continue uninterrupted.

The ability to dispose of the low-activity salt stream in the SDF required determination of compliance with NDAA Section 3116. One requirement of NDAA Section 3116 is to demonstrate compliance with the performance objectives set out in Subpart C of Part 61 of Title 10 Code of Federal Regulation. [NDAA_3116, 10 CFR 61] The Performance Objective Demonstration Document (PODD) was developed to demonstrate compliance with 10 CFR 61 Subpart C and was presented in a format that would meet the requirements of NDAA Section 3116. [CBU-PIT-2005-00146]

The PODD addressed the disposal of solidified low-activity salt waste streams into the SDF as saltstone and its compliance with performance objectives for near-surface disposal of radioactive waste. Specifically, this PODD demonstrated and documented that the solidified low-activity salt streams from SRS salt processing activities will meet the performance objectives set out in 10 CFR 61 Subpart C by assuming all future salt solution inventory was placed in Vault 4. [10 CFR 61, CBU-PIT-2005-00146]

2.1.1.5 Impact on Composite Analysis

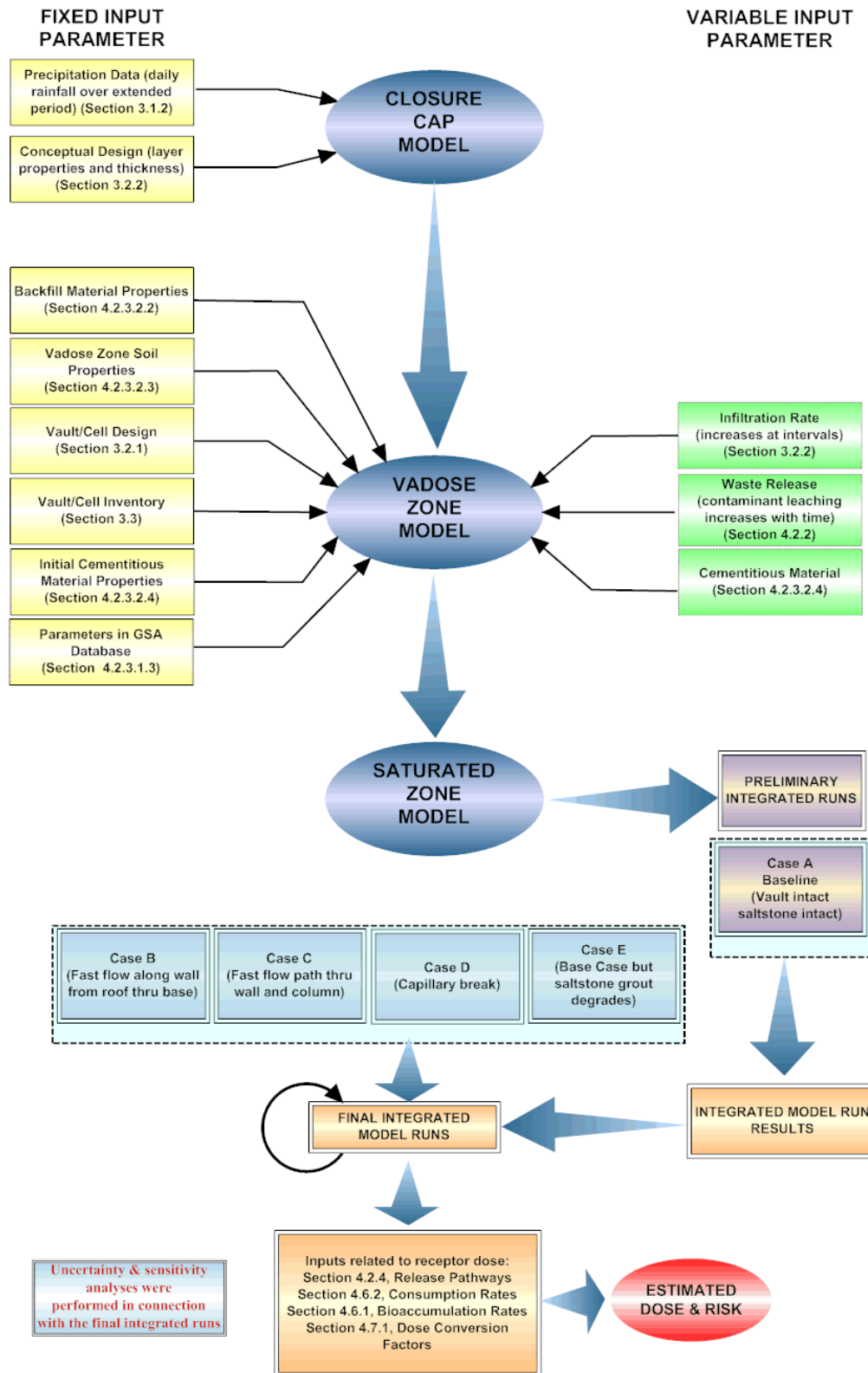
The results of the CA for SRS concluded that the predominant sources of radionuclides contributing to the calculated dose at the identified points of assessment were facilities other than the SDF. [WSRC-RP-97-311_OUO] The SDF was found to be a relatively insignificant source of the major radionuclides. The points of assessment for the CA were the mouths of UTR and Fourmile Branch, where stream water is undiluted by the Savannah River, but still accessible to a future MOP. Other points of assessment included the Savannah River at the Highway 301 bridge and the water treatment plants at Beaufort-Jasper, South Carolina and Port Wentworth, Georgia. These were all selected based on considerations that the points of maximum concentration accessible by the public, will be consistent with site plans for future land use and control. [WSRC-RP-97-311_OUO]

The primary dose limit of 100 mrem/yr, and dose constraint of 30 mrem/yr, are applicable to the CA. This SDF PA considers performance measures for groundwater and air (media by which a MOP may be exposed to radionuclides at the points of assessment) that are considerably less than these limits and constraints. Also, the points of assessment for the CA are far enough removed from the vicinity of Z-Area that considerable dispersion and decay in transit would occur. [WSRC-RP-97-311_OUO] Therefore, it is concluded that the impact of this SDF PA results on the CA are negligible.

2.1.2 Modeling Process

Figure 2.1-1 illustrates the general process followed in implementing the Integrated Site Conceptual Model (ISCM) for the PA. This figure shows the key inputs of the three model components (closure cap, vadose zone, and saturated zone).

Figure 2.1-1: Saltstone Disposal Facility PA Modeling Relationships



Some inputs involve fixed parameters that do not change over time. These are generally shown on the left side of the figure. The inputs on the right side of the figure do change over time. The manner in which an input changes is described in the section of this document as identified in the input blocks of Figure 2.1-1.

As shown in Figure 2.1-1, a base case scenario was identified for model runs, which were accomplished using the applicable computer codes identified in Section 4.3. This scenario was analyzed by running the model using different combinations.

The results of the preliminary model runs were analyzed. Based on these analyses, the model was refined. After these refinements were made, the final model runs were performed. Uncertainty and sensitivity analyses, as shown in Figure 2.1-1, were performed in connection with and incorporated into the final model runs.

The final result of this process produced predicted contaminant concentrations in groundwater. The data for radiological contaminants were used in combination with the inputs related to receptors shown on Figure 2.1-1 to estimate the potential dose to a hypothetical MOP or an intruder.

2.2 General Facility Description

2.2.1 Savannah River Site

SRS is located in south-central South Carolina, approximately 100 miles from the Atlantic Coast. The major physical feature at SRS is the Savannah River, approximately 20 miles which serves as the southwestern boundary of the site and the South Carolina-Georgia border. SRS encompasses portions of Aiken, Barnwell, and Allendale Counties in South Carolina. SRS occupies an almost circular area of approximately 310 square miles, or 198,344 acres, and contains production, service, and research and development areas. The developed areas occupy less than 10% of the SRS area while the remainder of the site is undeveloped forest or wetlands.

2.2.2 Saltstone Facility

The Saltstone Facility consists of two facility segments, the SPF, which receives and treats salt solution to produce solidified saltstone, and the SDF, which consists of existing vaults and projected FDCs used for the final disposal of the solidified saltstone. The SPF is permitted as a wastewater treatment facility per SCDHEC *Standards for Waste Water Facility Construction*. [SCDHEC R.61-67, DHEC_10-03-2006] The SDF is permitted as a Class 3 Landfill per SCDHEC R.61-107.19, *SWM: Solid Waste Landfills and Structural Fill*. [DHEC_09-09-2008] The SPF and SDF are also covered by the overall SRS Air Quality Permit. [TV-0080-0041] The only radiological requirements unique to the SDF are contained in the landfill permit for radionuclide concentrations in the saltstone waste form. The permit concentrations are consistent with DDA material reflected in the estimated inventory presented in Section 3.3 of this PA. The Saltstone Waste Acceptance Criteria (WAC) reflects the most restrictive limit from the permit, DSA, or the PA. SRS also maintains a Linking Document Database that identifies all permit requirements and their implementing documents to ensure the requirements are addressed. [X-SD-Z-00001, X-ESR-Z-00007]

2.3 Facility Life Cycle

Construction of Vaults 1 and 4 of SDF were completed between February 1986 and July 1988. The SPF started radioactive operations June 1990. Disposal into Vault 1 occurred intermittently from June 1990 to September 1996. Disposal into Vault 4 began in January 1997 and continues now. FDCs will be constructed as needed in coordination with salt processing production rates. Operation of the SDF is expected to continue until 2030.

2.4 Related Documents

This PA provides the technical basis and results to be used to demonstrate compliance with the pertinent requirements for LLW management per DOE O 435.1-1 and its associated manual (DOE M 435.1-1). Additional context has been added to address NDAA Section 3116. The *Radioactive Waste Management Manual* and *Format and Content Guide for U.S. Department of Energy Low-Level Waste Disposal Facility Performance Assessments and Composite Analyses-DRAFT* were also relied on for guidance. [DOE M 435.1-1, DOE Format Guide_OUO] The PA was influenced by, and has an influence on, other documents that are discussed in this section.

2.4.1 Groundwater Protection Management Program

The SDF Closure Plan will document requirements for protection of water resources. The appropriate measures for protection of water resources have been determined to be the EPA Safe Drinking Water Act (SDWA) MCLs (<http://www.epa.gov/safewater/contaminants/index.html#mcls>). The MCLs for the radionuclides are based on 4 mrem/yr for beta-gamma emitting nuclides, 15 pCi/L for alpha emitting nuclides and 5 pCi/L for radium. The MCLs are listed with the 100m results for the SDF in Section 5.2.

The plan for protection of groundwater at SRS is documented in the *SRS Groundwater Protection Management Program*. [WSRC-TR-2004-00152] The hydrogeology information utilized in this SDF PA is consistent with that in the groundwater protection program. The *SRS Groundwater Protection Program* is focused on those activities regulated by external agencies (i.e., the State of South Carolina and the EPA). [WSRC-TR-2004-00152] Consistent with guidance for preparing the PA, the requirement of DOE O 435.1-1 to identify impacts to water resources has been addressed by assessing the projected concentrations of radioactive or chemical contaminants at closure against standards for public drinking water supplies established by the EPA.

2.4.2 End State Vision

The *SRS End State Vision* focuses on site facilities and areas that are the responsibility of the DOE Office of Environmental Management, which includes SDF and SPF. [PIT-MISC-0089_OUO] This document describes planned end states for these facilities and areas. Like the *Long Range Comprehensive Plan*, which is addressed below, the *SRS End State Vision* is founded on the following basic assumptions about land ownership and use. [PIT-MISC-0041_OUO, PIT-MISC-0089_OUO]

- The entire site will be owned and controlled by the federal government in perpetuity
- The property will be used only for industrial purposes
- Site boundaries will remain unchanged
- Residential use will not be allowed onsite

DOE solicited public input into the *SRS End State Vision*. The document contains an appendix that addresses public comments received, including recommendations/endorsement from the SRS Citizens Advisory Board (CAB). [PIT-MISC-0089_OUO]

2.4.3 SRS Long Range Comprehensive Plan

The *Long Range Comprehensive Plan* provides the framework for integrating the SRS mission and vision with ecological, economic, cultural, and social factors in a regional context and to support decision-making for near-term and long-term use of the site. This plan reflects a cooperative working relationship between DOE and the state of South Carolina. [PIT-MISC-0041_OUO]

The *Long Range Comprehensive Plan* describes the current site conditions, defines a vision for the evolution of the site over the next 50 years, outlines actions to achieve the vision, and guides the allocation of resources toward attainment of that vision. This plan provides guidance and direction for the future physical development of the site and provides a framework within which detailed analyses will be conducted to determine the courses of action required to reach optimum site configuration. The plan is based on specific assumptions. If these assumptions were to change, the plan would be updated to reflect the changed conditions. Chapter 3 of the *Long Range Comprehensive Plan* contains the Future Land Use Plan. [PIT-MISC-0041_OUO] Guidelines on which SRS land use is based include:

- Giving priority to protection of workers and the public
- Maintaining site security
- Maintaining other appropriate institutional controls
- Considering worker, public, and environmental risks, benefits, and costs
- Restricted use programs for units regulated under the Comprehensive Environmental Response, Compensation and Liability act (CERCLA) of 1980, Title 42, United States Code (U.S.C) §§ 9601 et seq., as amended by the Superfund Amendments and Reauthorization Act of 1986. Pub. L. 99-499, or under the Resource Conservation and Recovery Act (RCRA) Federal law of the United States contained in Title 42, U.S.C. §§6901-6992k [www.epa.gov/superfund/policy/cercla.htm, <http://www.epa.gov/epawaste/laws-regs/rcrahistory.htm>]
- Maintaining existing SRS boundaries
- Continuing federal ownership of the land
- Prohibiting residential use of any SRS land

DOE considered stakeholder input on future use of the site property, as was solicited in development of the *SRS End State Vision*. Chapter 3 of the *Long Range Comprehensive Plan* describes future use of the site that was developed with input from public meetings,

workshops, and consultation with state and federal agencies. [PIT-MISC-0041_OUO, PIT-MISC-0089_OUO]

2.5 Performance Criteria

2.5.1 DOE O 435.1-1 Performance Objectives and Requirements

The DOE LLW disposal performance objectives are defined in DOE M 435.1-1 IV.P (1). DOE-HQ issued a letter from Mr. Rispoli to Mr. Allison, *Compliance with DOE M 435.1-1 Waste Incidental to Reprocessing Requirements and Implementation of Section 3116(a) of the National Defense Authorization Act for Fiscal Year 2005 (NDAA)*, which offers guidance and clarification to avoid duplication of efforts concerning the requirements in DOE O 435.1-1 when the requirements of NDAA Section 3116 are also applicable. [DOE_02-09-2006]

The DOE LLW disposal performance objectives (DOE M 435.1-1 IV.P (1)) are:

Low-level waste disposal facilities shall be sited, designed, operated, maintained, and closed so that a reasonable expectation exists that the following performance objectives will be met for waste disposed of after September 26, 1988:

- (a) Dose to representative members of the public shall not exceed 25 mrem (0.25 mSv) in a year Total Effective Dose Equivalent (TEDE) from all exposure pathways, excluding the dose from radon and its progeny in air.*
- (b) Dose to representative members of the public via the air pathway shall not exceed 10 mrem (0.10 mSv) in a year TEDE, excluding the dose from radon and its progeny.*
- (c) Release of radon shall be less than an average flux of 20 pCi/m²/s (0.74 Bq/m²/s) at the surface of the disposal facility. Alternatively, a limit of 0.5 pCi/l (0.0185 Bq/l) of air may be applied at the boundary of the facility.*

The DOE O 435.1-1 requirement for assessment of the protection of water resources is found in DOE M 435.1-1.IV.P (2) (g), which states:

- (g) For purposes of establishing limits on radionuclides that may be disposed of near-surface, the performance assessment shall include an assessment of impacts to water resources.*

The guide for DOE O 435.1 states “DOE M 435.1-1 does not specify the level of protection for water resources that should be used in a performance assessment for a specific LLW disposal facility. Rather a site-specific approach, in accordance with a hierarchical set of criteria should be followed.” [DOE G 435.1-1]

At SRS, the appropriate measure for protection of water resources has been determined to be the Safe Drinking Water Act MCLs. The MCLs are shown in Table 2.5-1.

Table 2.5-1: Maximum Contaminant Levels

| Component | MCL |
|-----------------|-----------|
| Beta-Gamma Dose | 4 mrem/yr |
| Gross Alpha | 15 pCi/L |
| Radium | 5 pCi/L |

The DOE O 435.1-1 requirement for assessment of inadvertent intruder analysis is found in DOE M 435.1-1.IV.P (2) (h), which states:

(h) For purposes of establishing limits on the concentration of radionuclides that may be disposed of near-surface, the performance assessment shall include an assessment of impacts calculated for a hypothetical person assumed to inadvertently intrude for a temporary period into the low-level waste disposal facility. For intruder analyses, institutional controls shall be assumed to be effective in deterring intrusion for at least 100 years following closure. The intruder analyses shall use performance measures for chronic and acute exposure scenarios, respectively, of 100 mrem (1mSv) in a year and 500 mrem (5mSv) total effective dose equivalent excluding radon in air.

The order specifies that the PA shall include calculations for a 1,000 year period after closure of potential doses to representative future MOPs and potential releases from the facility to provide a reasonable expectation that the performance objectives identified are not exceeded. The point of compliance must correspond to the point of highest projected dose or concentration beyond a 100m buffer zone surrounding the disposed waste.

2.5.2 10 CFR 61 Performance Objectives

NDAA Section 3116 identifies 10 CFR 61 performance objectives as also applicable to the SDF. It also specifies the criteria for DOE to classify waste as non-high level waste for purposes of onsite disposition. NDAA Section 3116 is applicable only to South Carolina and Idaho. [NDAA_3116] The applicable performance objectives for this SDF PA are reproduced below. Section 61.43 for radiation protection during operations and Section 61.44 for site stability are not subjects that will use the PA as a technical basis in future closure documents and are therefore not discussed.

“Section 61.40 General requirement.”

Land disposal facilities must be sited, designed, operated, closed, and controlled after closure so that reasonable assurance exists that exposures to humans are within the limits established in the performance objectives in Sections 61.41 through 61.44.”

“Section 61.41 Protection of the general population from releases of radioactivity.”

Concentrations of radioactive material, which may be released to the general environment in ground water, surface water, air, soil, plants, or animals must not result in an annual dose exceeding an equivalent of 25 millirems to the whole body, 75 millirems to the

thyroid, and 25 millirems to any other organ of any member of the public. Reasonable effort should be made to maintain releases of radioactivity in effluents to the general environment as low as is reasonably achievable.”

“Section 61.42 Protection of individuals from inadvertent intrusion.

Design, operation, and closure of the land disposal facility must ensure protection of any individual inadvertently intruding into the disposal site and occupying the site or contacting the waste at any time after active institutional controls over the disposal site are removed.”

2.6 Summary of Key Assessment Assumptions

Numerous assumptions and predictions were made in assessing the performance of the SDF over the 10,000 year period of performance. A summary of the key assumptions supporting the SDF PA analyses are discussed in this section.

2.6.1 General SDF Facility Modeling Assumptions

The *Long Range Comprehensive Plan* assumes that the entire site will be owned and controlled by the federal government in perpetuity. [PIT-MISC-0041_OUO] However, for the purpose of this PA only, no federal protection of the SDF is assumed beyond the 100 year period of institutional control. The period of compliance will span 10,000 years following closure. A 100 year period of institutional control is assumed to begin in year 2030. A list of specific key model assumptions can be found in Table 5.2-1.

2.6.2 Site Characteristics Assumptions

The SDF flow model used available data to simulate a future precipitation rate and the resulting infiltration rate is expected to change over time as the closure cap degrades. The characterization and monitoring data for the SRS General Separations Area (GSA) is extensive and provided a clear understanding of hydrogeology of the SDF and is a reasonable data set to represent long term conditions.

2.6.3 Facility Design Assumptions

A low-infiltration closure cap will be placed above the SDF disposal units and is expected to perform as described in Section 3.2.2. Tables 3.2-4 and 3.2-7 and Figure 3.2-20 provide specific design and performance values.

2.6.4 Stabilized Contaminants Characteristic Assumptions

2.6.4.1 Inventory

The estimate of residual saltstone in the SDF disposal units is expected to sufficiently bound the actual inventory and is described in Section 3.3. The groundwater concentrations at 100m are the highest concentration at 100m or further from the SDF based on the contaminant plume evidence in Figures 5.2-5 through 5.2-7 and the discussion in Section

5.2.1. An initial radionuclide screening process was developed and performed to support characterization efforts and is applicable to SDF PA modeling as described in Section 4.2.1.

2.6.4.2 Waste Form

Saltstone is a cementitious waste form created through the mixing of a salt solution (that originates in the SRS F-and H-Area liquid waste storage tanks) with a dry mix containing blast furnace slag, fly ash, and cement per Table 4.2-7. Table 4.2-7 contains the nominal formulation that was analyzed to support this PA revision. Additional work is being conducted to evaluate the sensitivity of modeling parameters to changes in the formula. These activities are presented in Section 8.2 as ongoing future work. The SPF currently utilizes operating procedures to control the formulation of the saltstone. A review of a number of premix feed batches indicated that the variability of the dry materials is within plus or minus 3% of the nominal formulation at the 95% confidence interval. The results of the ongoing work will be used in conjunction with the operational information to evaluate any impacts as part of PA maintenance.

Over the course of time, the mobile contaminants in the closed SDF disposal units are expected to be released and gradually migrate downward through unsaturated soil to the hydrogeologic units comprised of the shallow aquifers underlying the SDF.

2.6.5 Integrated Site Conceptual Model Assumptions

2.6.5.1 Degradation and Contaminant Movement

The mechanism generally controlling the release of contaminants from SDF is the adsorption characteristic of the saltstone expressed by the K_d (distribution coefficient) which is element dependent and differs as the saltstone E_h (oxidation potential or measure of reduction potential) and pH (measure of acidity or basicity) conditions change over time. Contaminant concentrations in saltstone are not generally expected to be limited by solubility. The degradation of the disposal unit concrete (walls, roof, and floor) is dominated by internal sulfate attack from the saltstone as described in Section 4.2.3.2.4. Wherever possible, a best estimate value was chosen for input variables. The rates of contaminant release and movement from saltstone are principally controlled by these factors:

- Chemical and physical properties (e.g., K_d) of the saltstone, disposal units, and soil (Tables 4.2-15, 4.2-16 and 4.2-18)
- Physical properties (e.g., void structure and hydraulic conductivity, etc.) and state (e.g., integrity) of the waste form and disposal unit and soil (Tables 4.2-14, 4.2-16, 4.2-19 and Figures 4.2-36 through 4.2-40)
- Chemical properties (e.g., reduction capacity) and state (e.g., E_h and pH) of the waste form and disposal unit (Table 4.2-17)
- Moisture flux to the saltstone through the disposal unit from the overlying soil (Table 3.2-7)

The FDCs are designed for a dual role that limits releases of contaminants out of the disposal unit and limits the migration of oxygen into the disposal unit via dissolved oxygen in moisture, thus delaying oxidation of the saltstone. The SDF is designed to retain Tc-99 through the use of slag-bearing saltstone and disposal unit concrete mixes, which create a

low E_h environment. The groundwater concentrations are assumed to be the highest concentration in the area at 100m or farther from the SDF.

Five disposal unit scenarios were employed in the groundwater model to simulate potential conditions in the SDF closure system over the 10,000 year performance period. While only one scenario (Case A) was simulated in the baseline analysis, the other four were considered in the deterministic sensitivity and probabilistic analyses.

2.6.5.2 Infiltration and Erosion Control

Erosion control is maintained via the closure cap as detailed in Section 3.2.2.4. The erosion barrier maintains a minimum 10 feet of clean material above the disposal unit to act as an intruder deterrent. Infiltration control of the SDF is expected to operate as estimated in Section 3.2.2.

3.0 DISPOSAL FACILITY CHARACTERISTICS

Section 3.1 provides information regarding site characteristics with more detailed information furnished for those characteristics that influence the contaminant transport modeling assumptions provided in Section 4.

- Section 3.1.1 provides a general description and layout of SRS and the SDF to orient the reader.
- Section 3.1.2 describes meteorological and climatological data collection at SRS.
- Section 3.1.3 provides a general description of SRS ecology of the site for information purposes.
- Section 3.1.4 provides information regarding the geology, seismology, and volcanology of SRS that is used to determine appropriate modeling parameters.
- Section 3.1.5 provides information regarding the hydrogeology of SRS that determine the modeling assumptions related to the flow of surface water and groundwater.
- Section 3.1.6 identifies the sources of information available regarding the geochemistry of the soils and cementitious material that determine the modeling assumptions related to the migration of radionuclides to the environment.
- Sections 3.1.7 and 3.1.8 address natural resource management of the site and sources of natural and background radiation exposure, respectively, for information purposes.

Section 3.2 describes the design of existing SDF disposal units and the SDF closure cap concept.

- Section 3.2.1 provides the design and construction of the SDF vaults and FDCs.
- Section 3.2.2 provides the design performance requirements and constructability requirements for the conceptual SDF closure cap, and the results of the infiltration analysis of the closure cap presented in WSRC-STI-2008-00244.

Section 3.3 presents the estimated inventory of the radionuclides and chemicals in the disposal units at the time of SDF closure.

3.1 Site Characteristics

Evaluation of radionuclide transport from the SDF, and of human exposure resulting from release of radionuclides to the environment, requires careful consideration of factors affecting transport processes and exposure potential. Topographic features and hydrogeologic characteristics strongly affect the direction and flow of radionuclides potentially released from the closure site. Projected land use and population distributions affect the estimation of human exposure. In this section, the relevant natural and demographic characteristics of Z-Area and the surrounding area are discussed.

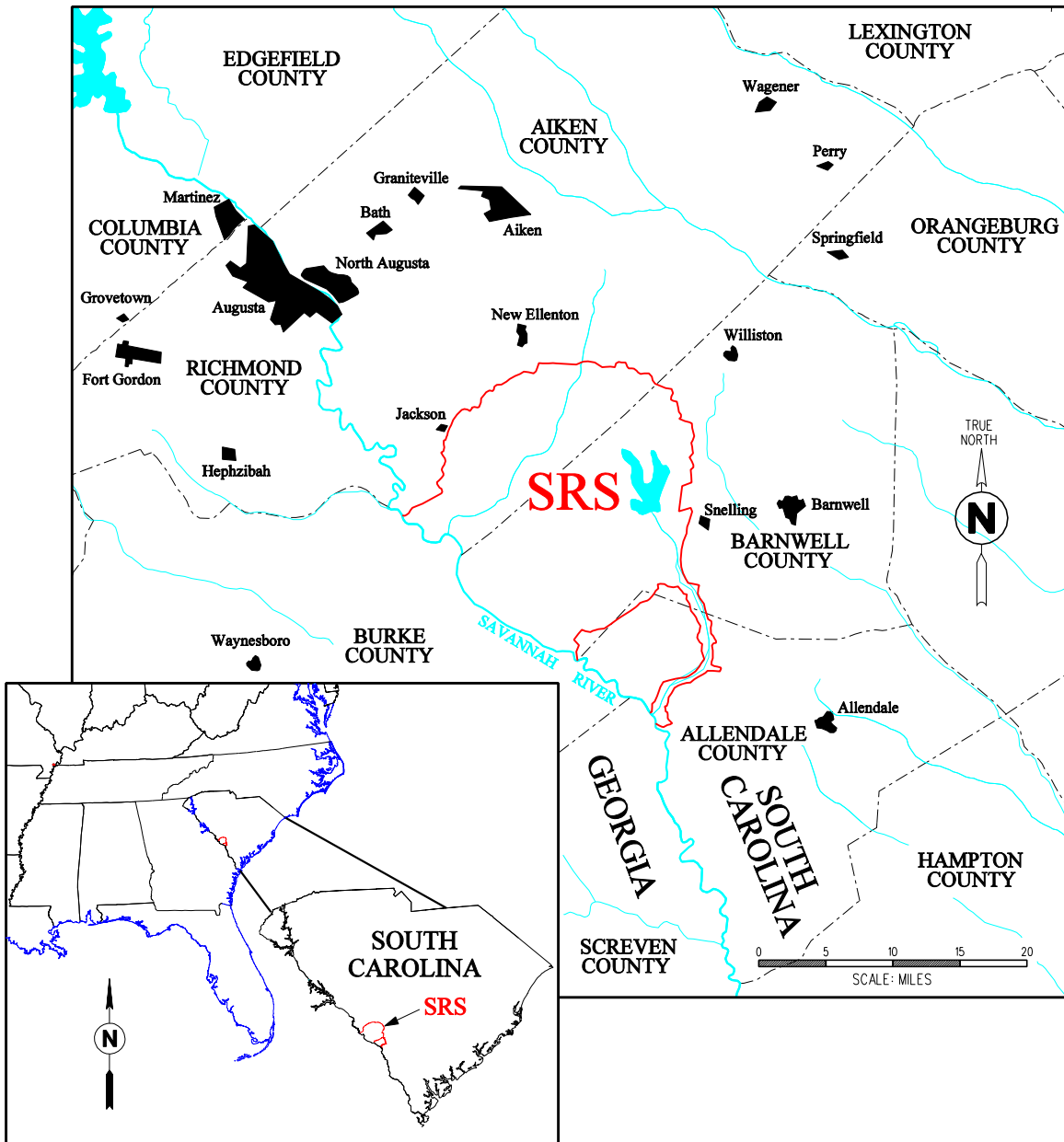
3.1.1 Geography and Demography

3.1.1.1 SRS Site Description

SRS, one of the facilities in the DOE complex, was constructed starting in the early 1950s to produce nuclear materials (such as Pu-239 and tritium). The site covers approximately 310 square miles in South Carolina and borders the Savannah River. SRS encompasses 198,344 acres in Aiken, Allendale, and Barnwell counties of South Carolina. The site is

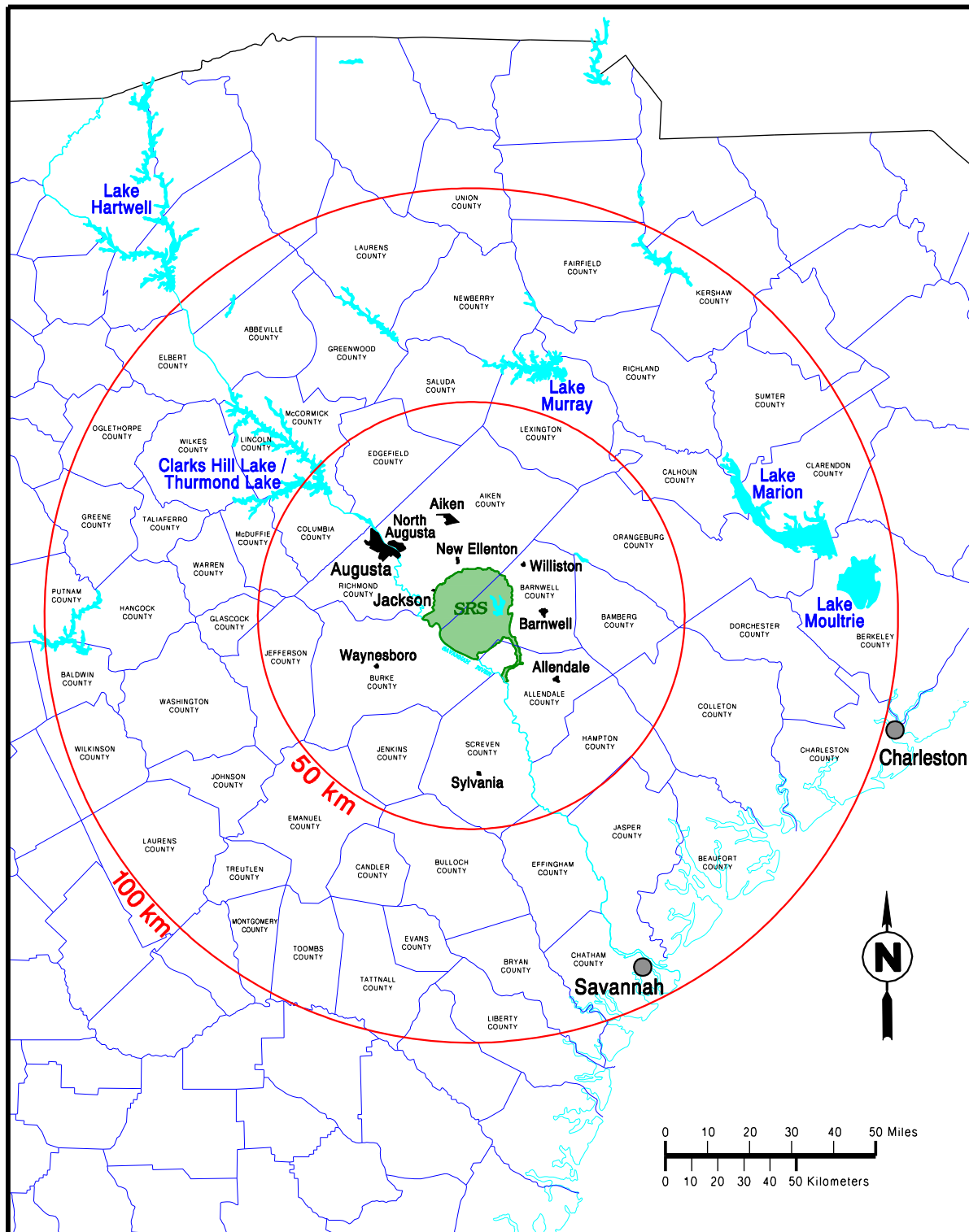
approximately 12 miles south of Aiken, South Carolina, and 15 miles southeast of Augusta, Georgia, as shown in Figure 3.1-1. [WSRC-STI-2008-00057]

Figure 3.1-1: Physical Location of Savannah River Site



Prominent geographic features within 30 miles of SRS include the Savannah River and Clarks Hill Lake (also known as Thurmond Lake), shown in Figure 3.1-2. The Savannah River forms the southwest boundary of SRS. Clarks Hill Lake is the largest nearby public recreational area. This reservoir lies on the Savannah River approximately 40 miles upstream of the center of SRS.

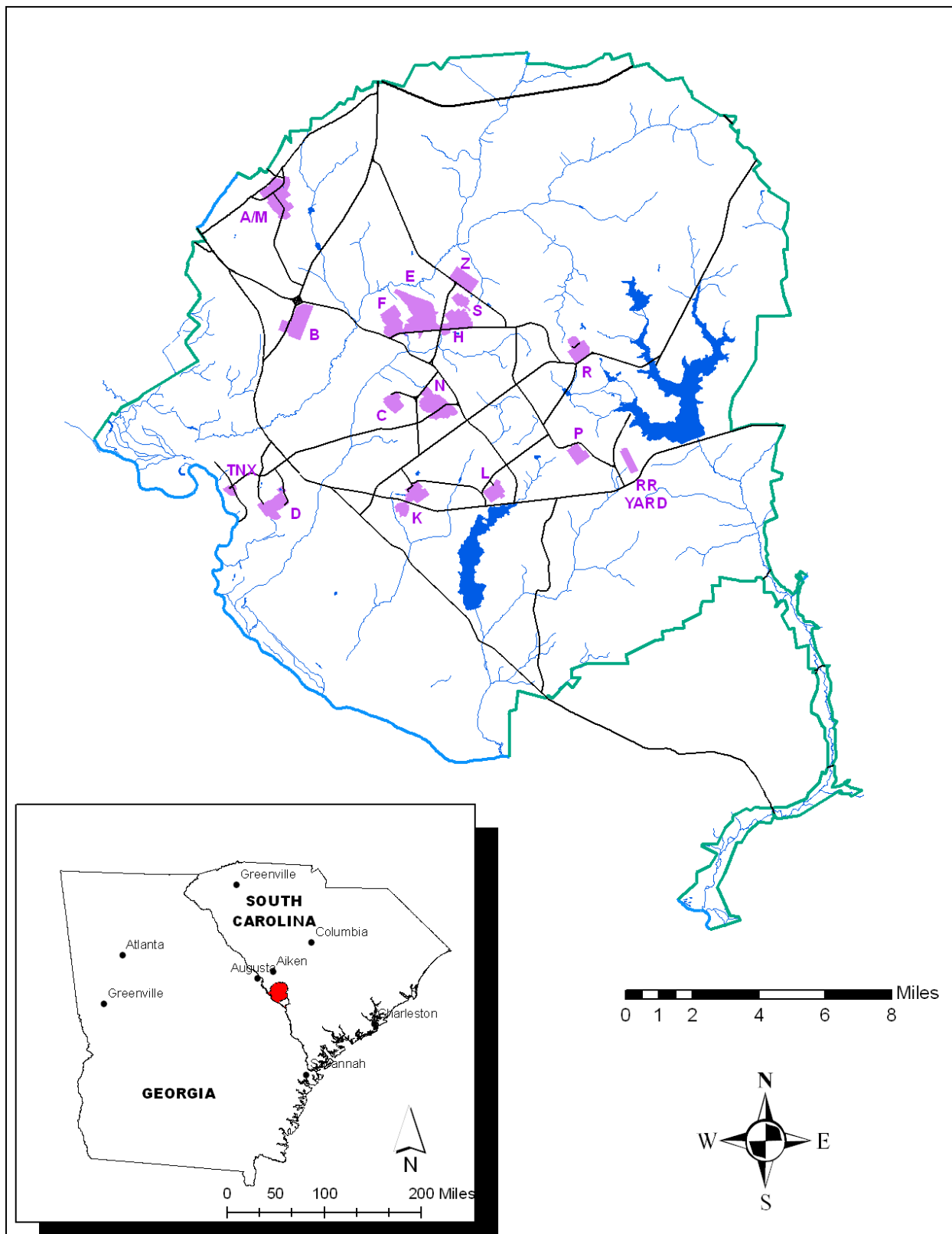
Figure 3.1-2: Location of SRS and Adjacent Areas



Within the SRS boundary, prominent water features include Par Pond and L Lake, shown in Figure 3.1-3. Par Pond, a former reactor cooling water impoundment, covers approximately 2,700 acres and lies in the eastern sector of SRS. L Lake, another former reactor cooling water impoundment, covers approximately 1,000 acres and lies in the southern sector of SRS. [WSRC-IM-2004-00008, pg 1.4-11]

Figure 3.1-3 also shows the major operational areas at SRS. Prominent operational areas, both past and present, include, Separations (F- and H-Areas), Waste Management Operations (E-, F-, and H-Areas), Reactor Areas (C, K, L, P, R), and Defense Waste Processing (S- and Z-Areas). The Savannah River National Laboratory (SRNL) and Savannah River Ecology Laboratory (SREL) are located in A-Area. Administrative and support services are located in B-Area and construction administration activities are located in N-Area. D-Area is the coal-fired powerhouse that provides steam to SRS. M-Area and TNX have undergone Deactivation and Decommissioning (D&D).

Figure 3.1-3: SRS Operational Area Location Map



3.1.1.2 Closure Site Description

The Saltstone Facility is located in Z-Area, which is in the central region of SRS. Figure 3.1-4 presents the area known as the GSA. The GSA is located atop a ridge running southwest-northeast that forms the drainage divide between UTR to the north and Fourmile Branch to the south. The GSA contains the F- and H-Area Separations Facilities, the S-Area Defense Waste Processing Facility (DWPF), the Z-Area Saltstone Facility, and the E-Area LLW Facility. Z-Area consists of approximately 161 acres, and is situated northeast of DWPF. Figure 3.1-5 illustrates the anticipated layout of SDF. While the figure presents the anticipated FDC locations, numbering of the units are placeholders and may not match the final disposal unit numbers.

Surface drainage in Z-Area, which includes the Saltstone Facility, is toward UTR, northwest to north, and toward McQueen Branch, northeast and southeast.

Z-Area was chosen for the SDF site based on considerations of depth to the water table, available surface area, surface topography, proximity to the wastewater generated on site, and distance to surface water and the public. [WSRC-RP-92-1360]

Figure 3.1-4: Layout of the GSA

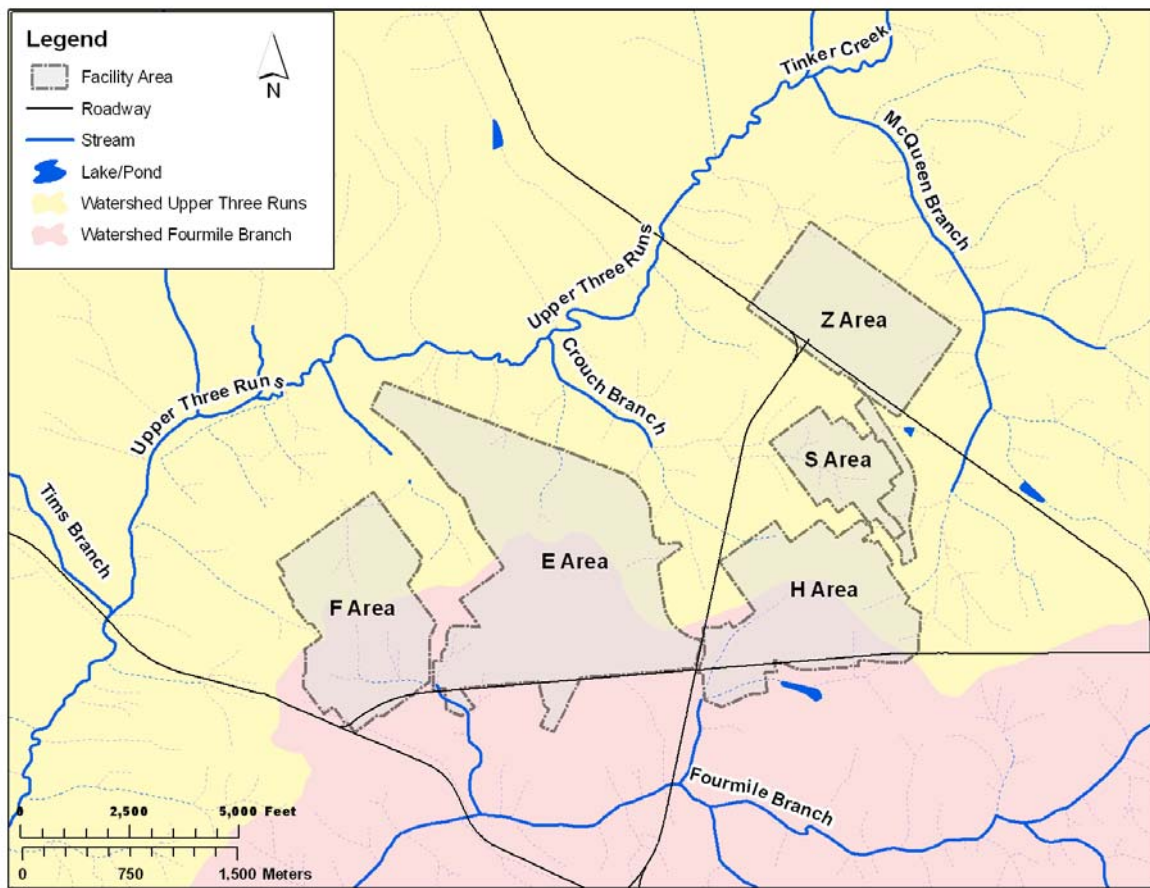
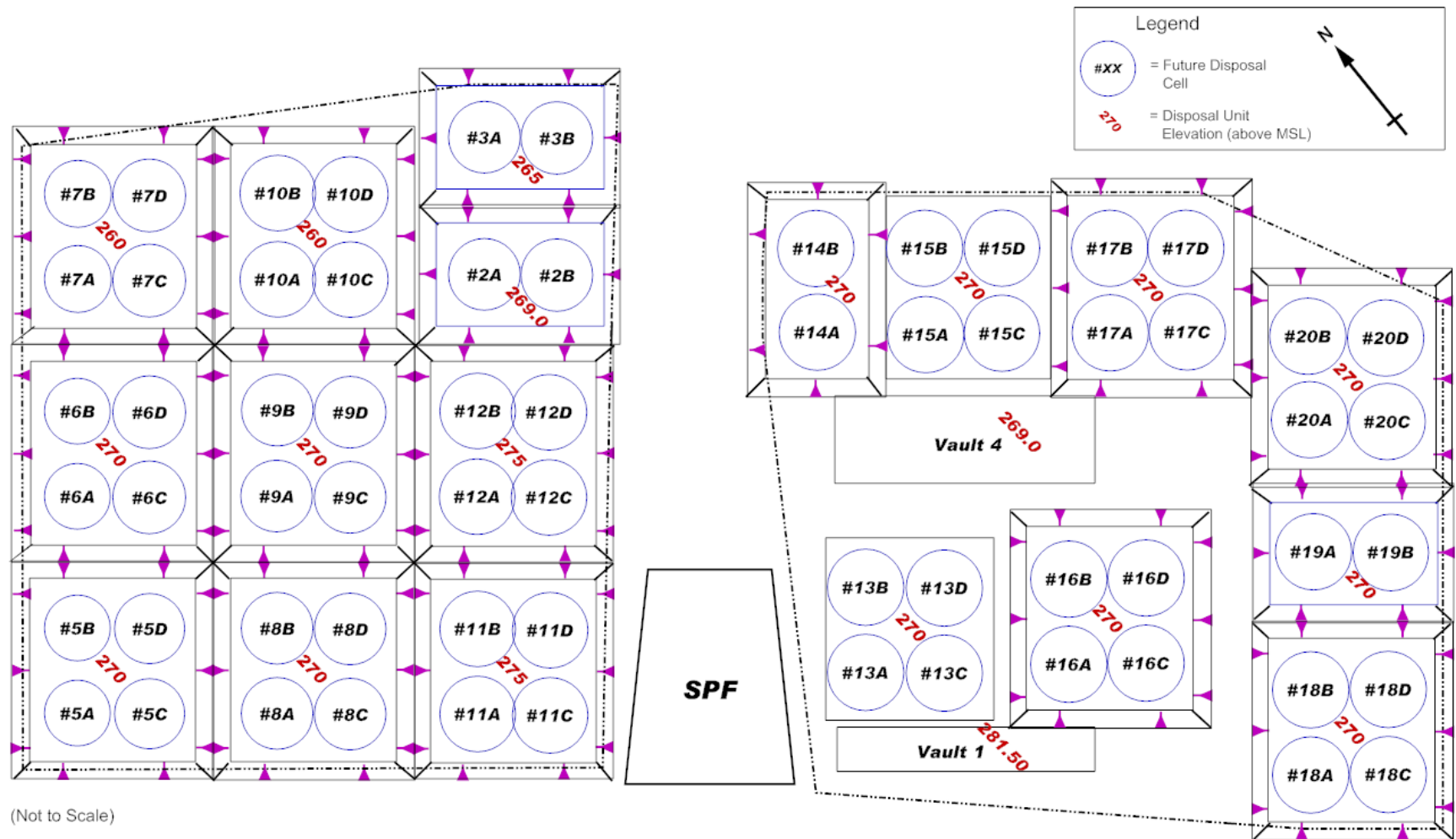


Figure 3.1-5: Anticipated Layout of SDF



Note: Figure presents the anticipated FDC locations, numbering of the units are placeholders and may not match the final disposal unit numbering.

3.1.1.3 Population Distribution

According to U.S. Census Bureau data, the estimated 2008 population in the eight-county region of influence (ROI) was 550,675. Four of the counties lie in South Carolina and include Aiken, Allendale, Bamberg, and Barnwell. The other four counties lie in Georgia and include Burke, Columbia, Richmond, and Screven (see Figure 3.1-2). The ROI includes the counties immediately adjacent to SRS and the counties where the majority of SRS workers reside. Approximately 84% of the ROI live in the following three counties, Aiken (28%), Richmond (36.2%) and Columbia (20.1%). Only approximately 16% of this region population lives in the remaining counties as shown in Table 3.1-1. [www.factfinder.census.gov]

Table 3.1-1: Population Distribution and Percent of Region for Counties and Selected Communities

| Jurisdiction | 2008 Population Estimate ^a | 2008 % Region |
|---------------------------|---------------------------------------|---------------|
| SOUTH CAROLINA | | |
| Aiken County | 154,071 | 28 |
| Aiken, City | 29,434 | 5.4 |
| Jackson, Town | 1,647 | 0.3 |
| New Ellenton, Town | 2,227 | 0.4 |
| North Augusta, City | 20,712 | 3.8 |
| Allendale County | 10,447 | 1.9 |
| Allendale, Town | 3,659 | 0.7 |
| Bamberg County | 15,307 | 2.8 |
| Bamberg, Town | 3,432 | 0.6 |
| Barnwell County | 22,872 | 4.2 |
| Barnwell, City | 4,783 | 0.9 |
| GEORGIA | | |
| Burke County | 22,732 | 4.1 |
| Columbia County | 110,627 | 20.1 |
| Richmond County | 199,486 | 36.2 |
| Screven County | 15,133 | 2.7 |
| Eight-County Total | 550,675 | |

(a) 2008 Population estimates based on 2000 population census and are provided by the U.S. Census Bureau, Population Estimates Program, www.factfinder.census.gov; data for births, deaths, and domestic and international migration were used by the U.S. Census Bureau to update the 2000 base counts.

From 2000 to 2008 the population in the eight-county region grew an estimated 5.8%. Columbia County had the highest estimated growth at approximately 23.9% followed by Aiken County with an estimated growth of approximately 8.1% and Burke County with an estimated growth of 2.2%. Allendale, Bamberg, Barnwell, Richmond, and Screven Counties experienced a net population loss. Calculations are based on information obtained from the U.S. Census Bureau website, www.factfinder.census.gov.

Population projections and further information regarding the eight-county region around SRS (see Table 3.1-1) can be found in the *High-Level Waste Tank Closure Final Environmental Impact Statement*. [DOE-EIS-0303]

3.1.1.4 Land Use – Present and Planned

Land within a 5 mile radius of SDF is entirely within SRS boundaries and is currently used either for industrial purposes or as forested land. Current land use within the entire GSA is classified as heavy nuclear industrial. Plans for the future of SRS are addressed in two key planning documents identified below and described in Sections 2.4.2 and 2.4.3.

- The *SRS End State Vision* (PIT-MISC-0089_OUO)
- The *Savannah River Site (SRS) Long Range Comprehensive Plan* (PIT-MISC-0041_OUO)

3.1.2 Meteorology and Climatology

3.1.2.1 General SRS Climate

The SRS region has a humid subtropical climate characterized by relatively short, mild winters and long, warm, and humid summers. Summer-like conditions typically last from May through September, when the area is frequently under the influence of a western extension in the semi-permanent Atlantic subtropical anticyclone (i.e., the ‘Bermuda’ high). Winds in summer are light and cold fronts generally remain well north of the area. Daily high temperatures during the summer months exceed 90°F on more than half of all days on average. Scattered afternoon and evening thunderstorms are common. The influence of the Bermuda high begins to diminish during the fall as continental air masses become more prevalent, resulting in lower humidity and more moderate temperatures.

Average rainfall during the fall is usually the least of the four seasons. In the winter months, mid-latitude low pressure systems and associated fronts often migrate through the region. As a result, conditions frequently alternate between warm, moist, subtropical air from the Gulf of Mexico region and cool, dry, polar air. The Appalachian Mountains to the north and northwest of SRS help to moderate the extremely cold temperatures that are associated with occasional outbreaks of Arctic air. Consequently, less than one-third of winter days have minimum temperatures below freezing on average, and days with temperatures below 20°F are infrequent. Measurable snowfall occurs on an average of once every two years. Tornadoes occur more frequently in spring than the other seasons of the year. Although spring weather is somewhat windy, temperatures are usually mild and humidity is relatively low. [WSRC-TR-2007-00118]

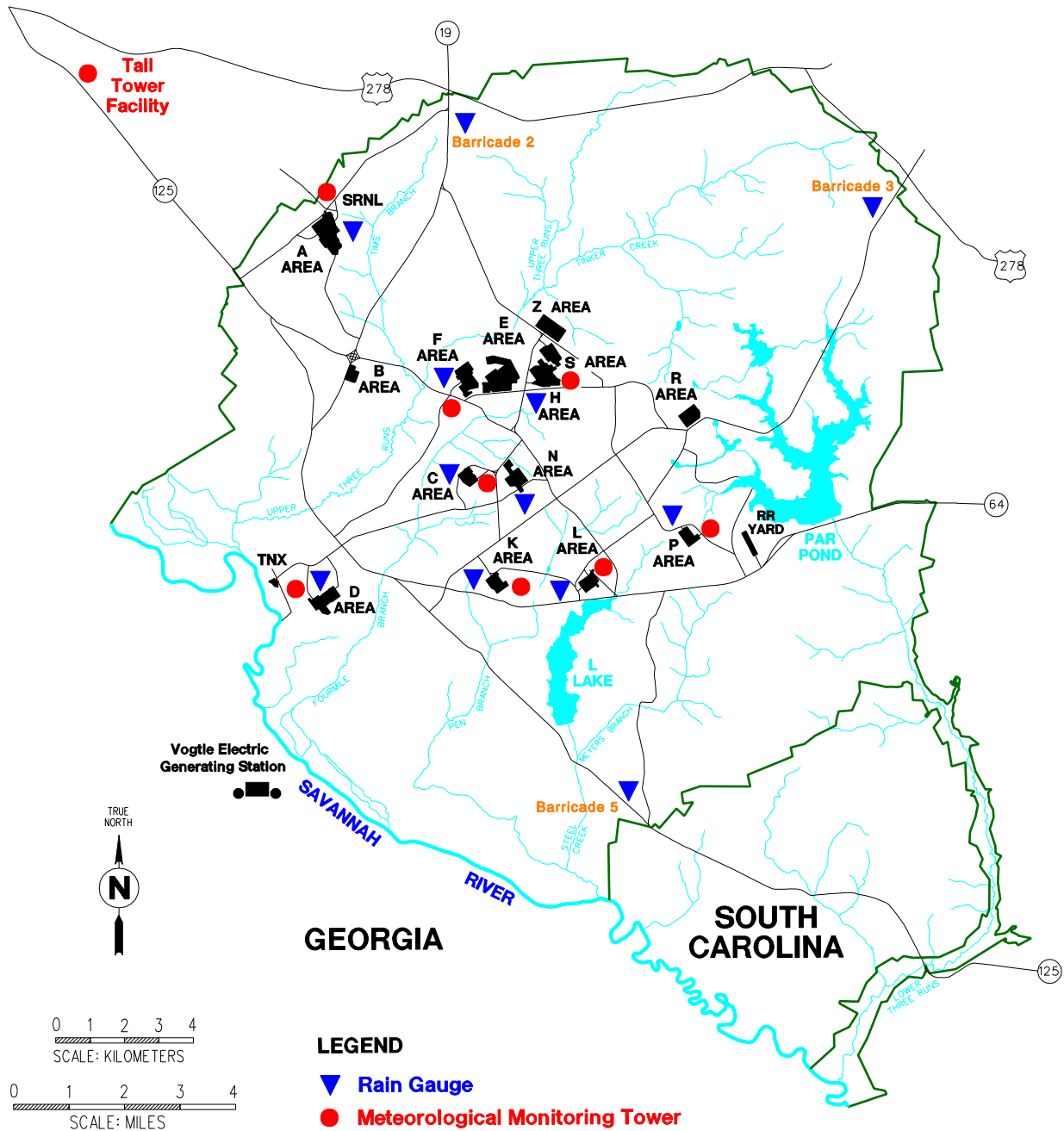
3.1.2.2 *Meteorological Data Collection*

Meteorological data is collected at SRS from a network of nine primary monitoring stations (Figure 3.1-6). Towers located adjacent to each of eight areas (A-, C-, D-, F-, H-, K-, L-, and P-Areas) are equipped to measure wind direction and wind speed at 201.3 feet above ground and to measure temperature and dew point at both 6.6 feet (2m) and 201.3 feet above ground. Temperature and dew point are also measured at 2m. A ninth tower near N-Area, known as the Central Climatology Site (CLM) is instrumented with wind, temperature, and dew point sensors at four levels; (1) 6.6 feet (13.2 feet for wind), (2) 59.4 feet, (3) 118.8 feet, and (4) 201.3 feet. The CLM site is also equipped with an automated tipping bucket rain gauge, a barometric pressure sensor, and a solar radiometer near the tower at ground level. Data acquisition units at each station record a measurement from each instrument at one-second intervals. Every 15 minutes, 900 data points are processed to generate statistical summaries for each variable, including averages and instantaneous maxima. The results are uploaded to a relational database for permanent archival.

In addition, the Tall Tower facility, near Beech Island, South Carolina, provides a set of high-quality meteorological measurements that is unique to the southeast United States. This facility utilizes fast-response sonic anemometers, water vapor sensors, barometric pressure sensors, slow-response temperature sensors and relative humidity sensors. Data is collected at 100 feet, 200 feet, and 1,000 feet above ground level. Spread-spectrum modems at each measurement level transmit raw data to a redundant set of personal computers at the SRNL. Data processing software on the personal computers determine mean values and other statistical quantities every 15 minutes and uploads the results to the relational database.

Precipitation measurements are collected from a network of 13 rain gauges across SRS (Figure 3.1-6). Twelve of these gauges are read manually by security or operations personnel once per day, usually around 6 am. The daily data is reported to the SRNL Atmospheric Technologies Center, where it is technically reviewed and manually entered into a permanent electronic database. The other is an automated rain gauge at the CLM previously addressed above.

Figure 3.1-6: SRS Meteorological Monitoring Network



[WSRC-TR-2007-00118]

3.1.2.3 Data Pertinent to PA Modeling

Weather data pertinent to the PA modeling are atmospheric dispersion, precipitation, and air temperature. Each is discussed below.

3.1.2.3.1 Atmospheric Dispersion

Since the mid-1970s, a 5 year database of meteorological conditions at SRS is updated in order to support dose calculations for accident or routine release scenarios for onsite and offsite populations. The meteorological database includes wind speed, wind direction, temperature, dew point, and horizontal and vertical turbulence intensities. The most recent database is for the time period January 1, 2002 through December 31, 2006, and consists of one-hour time averages of temperature and dew-point; wind speed, direction, and turbulence. [WSRC-STI-2007-00613] This data is used to determine Dose Release Factor (DRFs) in the evaluation for air pathways dose modeling described in Section 4.5.

3.1.2.3.2 Precipitation

Compilations of rainfall data obtained from meteorological data collection described above for years 1952 through 2006 for the site and for years 1961 through 2006 are provided in WSRC-STI-2008-00244. An average precipitation of 48.5 inches per year results from the 55 year monitoring period for the site, and 49 inches per year from the 46 year monitoring period. This data is used to determine appropriate rainfall assumptions for the performance evaluation of infiltration through the closure cap described in Section 3.2.2 and evaluated in WSRC-STI-2008-00244.

3.1.2.3.3 Air Temperature

A compilation of air temperature data obtained from meteorological data collection described above for years 1968 through 2005 is provided in WSRC-STI-2008-00244. For this 37 year period, the annual average air temperature is approximately 64°F with an average monthly air temperature from a low of approximately 46°F, to a high of approximately 81°F. This data is used to determine appropriate assumptions for the performance evaluation of infiltration through the closure cap described in Section 3.2.2 and evaluated in WSRC-STI-2008-00244.

3.1.3 Ecology

Comprehensive descriptions of SRS ecological resources and wildlife can be found in *SRS Ecology: Environmental Information Document* and are briefly discussed in this section. [WSRC-TR-2005-00201]

SRS supports abundant terrestrial and semi-aquatic wildlife, as well as a number of species considered threatened or endangered. Since the early 1950s, the Site has changed from 67% forest and 33% agriculture to 94% forest, with the remainder in aquatic habitats and developed areas. Wildlife populations correspondingly shifted from forest-farm edge-utilizing species to a predominance of forest-dwelling species. SRS now supports 44 species of amphibians, 60 species of reptiles, 255 species of birds, and 55 species of mammals. These populations include urban wildlife, several commercially and recreationally important species, and a few threatened or endangered species. Protection and restoration of all flora and fauna to a point where their existence is not jeopardized are principal goals of federal and

state environmental programs. Those species of plants and animals afforded governmental protection are collectively referred to as “species of concern.” [WSRC-TR-2005-00201]

SRS has extensive, widely distributed wetlands, most of which are associated with floodplains, creeks, or impoundments. In addition, approximately 200 Carolina bays occur on SRS. Carolina bays are unique wetland features of the southeastern United States. They are isolated wetland habitats dispersed throughout the uplands of SRS. The approximately 200 Carolina bays on SRS exhibit extremely variable hydrogeology and a range of plant communities from herbaceous marsh to forested wetland. [DOE-EIS-0303]

The Savannah River bounds SRS to the southwest for approximately 20 miles. The river floodplain supports an extensive swamp, covering approximately 15 square miles of SRS; with a natural levee separating the swamp from the river. Timber was cut in the swamp from the turn of the century until 1951, when the Atomic Energy Commission assumed control of the area. At present, the swamp forest is comprised of two kinds of forested wetland communities. Areas that are slightly elevated and well-drained are characterized by a mixture of oak species, as well as red maple, sweet gum, and other hardwood species. Low-lying areas that are continuously flooded are dominated by second-growth bald cypress and water tupelo. [DOE-EIS-0303]

SRS supports abundant herpetofauna because of its temperate climate and diverse habitats. The species of herpetofauna include 17 salamanders, 27 frogs and toads, one crocodilian, 13 turtles, nine lizards, and 36 snakes. The class Amphibia is represented on site by two orders, 11 families, 16 genera, and 44 species. The Reptilia are represented by three orders, 12 families, 41 genera, and 59 species. [WSRC-TR-2005-00201]

Waterfowl and wading birds, as well as many upland species, use SRS aquatic habitats year round. Sixty-seven percent use Carolina bays and emergent marshes. This type of habitat is used by 68% of the upland species. Edge or shoreline areas accounted for high numbers of upland birds at Carolina bays and emergent marshes, stream, and small drainage corridors, and river swamp habitats. The aquatic birds are most common in large and small open water habitat. [WSRC-TR-2005-00201]

More than 255 species of birds can be found at SRS. Large mammals inhabiting the site include white-tailed deer and feral hogs. Raccoon, beaver, and otter are relatively common throughout the wetlands of SRS. In addition, the gray fox, opossum, bobcat, gray squirrel, fox squirrel, eastern cottontail, mourning dove, northern bobwhite, and eastern wild turkey are common at SRS. Threatened or endangered plant and animal species known to occur or that might occur on the overall SRS include the smooth purple coneflower, wood stork, red-cockaded woodpecker, and short nose sturgeon.

The SDF is located within a densely developed, industrialized area of SRS. The immediate area provides habitat for only those animal species typically classified as urban wildlife. Species commonly encountered in this type of urban landscape include the Southern toad, green anole, rat snake, rock dove, European starling, house mouse, opossum, and feral cats and dogs. Grasses and landscaped areas within SDF also provide some marginal terrestrial wildlife habitat. A number of ground-foraging bird species (e.g., American robin, killdeer, and mourning dove) and small mammals (e.g., cotton mouse, cotton rat, and Eastern

cottontail) that use lawns and landscaped areas around buildings may be present at certain times of the year, depending on the level of human activity (e.g., frequency of mowing). Pine plantations managed for timber production by the U.S. Forest Service (under an interagency agreement with DOE) occupy surrounding areas.

The UTR seepline area is located in a bottomland hardwood forest community. The canopy layer of this bottomland forest is dominated by sweet gum, red maple, and red bay. Sweet bay is also common. The understory consists largely of saplings of these same species, as well as a herbaceous layer of smilax, dog hobble, giant cane, poison ivy, chain fern, and hepatica. At the seepline's upland edge, scattered American holly and white oak occur. Dominant along Fourmile Branch in this area are tag alder, willow, sweet gum, and wax myrtle. [DOE-EIS-0303]

No endangered or threatened fish or wildlife species have been recorded near the UTR seepline. The seepline and associated bottomland community do not provide habitat favored by endangered or threatened fish and wildlife species known to occur at SRS. The American alligator is the only federally protected species that could potentially occur in the area of the seepline. [DOE-EIS-0303]

According to summaries of studies on UTR documented in the *SRS Ecology Environmental Information Document*, the macro invertebrate communities of UTR drainage are unusual. [WSRC-TR-2005-00201] They include many rare species and contain species not often found living together in the same freshwater system. Since UTR is a spring-fed stream and is colder and generally clearer than most surface water at its low elevation, species typical of unpolluted streams in northern North America or the southern Appalachian Mountains are found here along with lowland (Atlantic Coastal Plain) species.

The fish community of UTR is typical of third- and higher-order streams on SRS that have not been greatly affected by industrial operations, with shiners and sunfish dominating collections. The smaller tributaries of UTR are dominated by shiners and other small-bodied species (i.e., pirate perch, madtoms, and darters) indicative of un-impacted streams in the Atlantic Coastal Plain. In the 1970s, the United States Geological Survey (USGS) designated UTR as a National Hydrological Benchmark Stream due to its high water quality and rich fauna. However, this designation was rescinded in 1992 due to increased development of the UTR watershed north of SRS site boundaries. [DOE-EIS-0303]

3.1.4 Geology, Seismology, and Volcanology

Regional and local information on the geologic and seismic characteristics of the SDF are presented in this section. Because SRS is not located within a region of active plate tectonics characterized by volcanism, volcanology is not an issue of concern in this PA, and thus further discussion of this topic is omitted from the following discussion. [WSRC-IM-2004-00008]

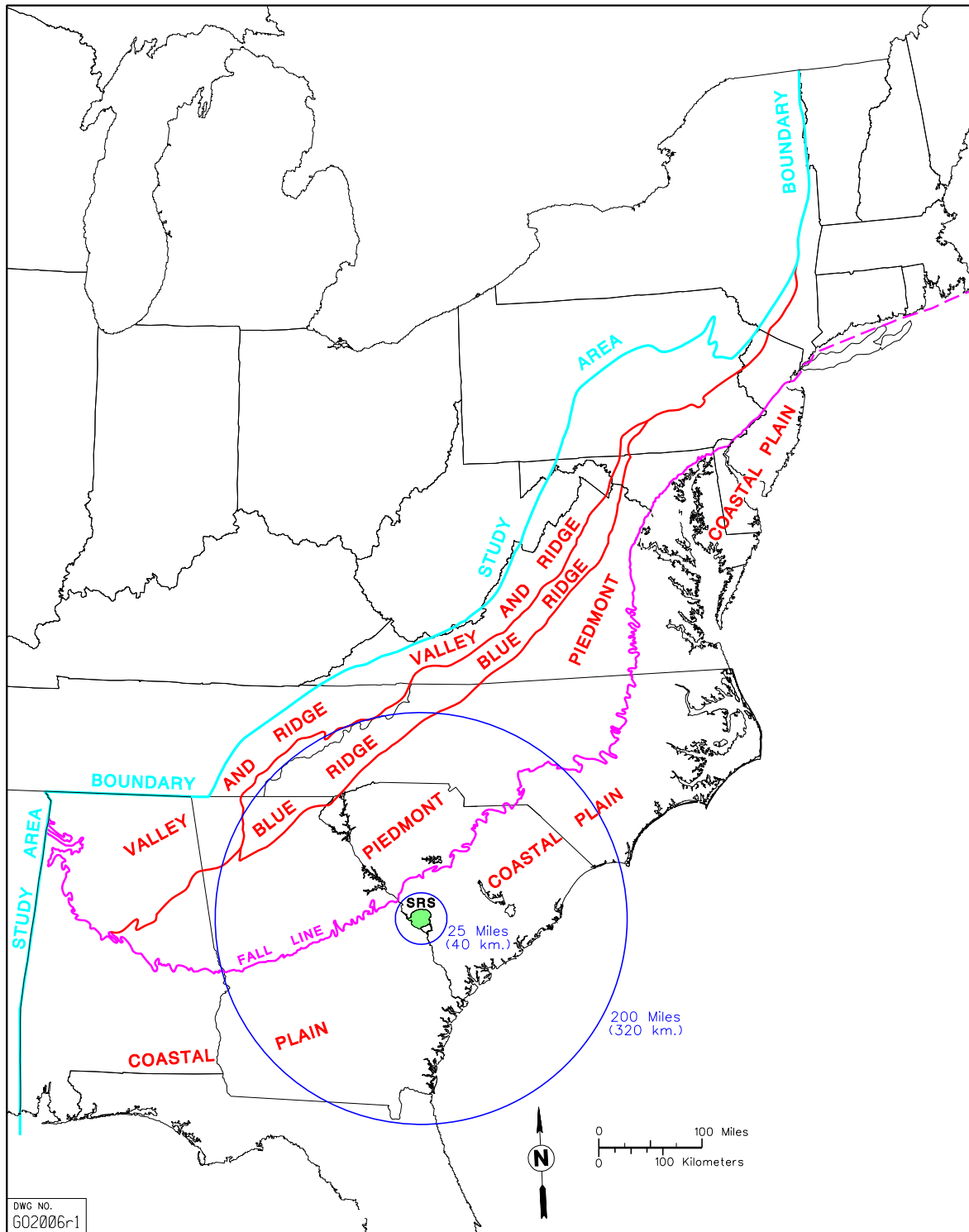
3.1.4.1 *Regional and Site-Specific Topography*

SRS is on the Atlantic Coastal Plain, Physiographic Province approximately 25 miles southeast of the fall line that separates the relatively unconsolidated Coastal Plain sediments. Beneath the Coastal Plain sedimentary sequence are two geologic terranes: (1) the Dunbarton basin, a Triassic-Jurassic Rift basin, filled with lithified terrigenous and lacustrine sediments, and (2) a crystalline terrane of metamorphosed sedimentary and igneous rock that may range in age from Precambrian to late Paleozoic from the crystalline igneous and metamorphic rocks of possibly late Precambrian to late Paleozoic age in the Piedmont Province. Early to middle Mesozoic (Triassic to Jurassic) rocks occur in isolated fault-bounded valleys either exposed within the crystalline belts or buried beneath the Coastal Plain sediments. The Coastal Plain sediments were derived from erosion of the crystalline rocks during late Mesozoic (Cretaceous) in stream and river valleys and are represented locally by gravel deposits adjacent to present-day streams and by sediments filling upland depressions (sinks and Carolina Bays). The Cretaceous and younger sediments are not significantly indurated. The total thickness of the sediment package at SRS varies between approximately 700 feet at the northwest boundary and 1,200 feet at the southeast boundary. [WSRC-TR-95-0046]

Figure 3.1-7 shows the relationship of SRS to overall regional geological provinces, and Figure 3.1-8 details the regional physiographic provinces in South Carolina. As can be seen on Figure 3.1-8, much of SRS lies within the Aiken Plateau, and this Plateau slopes to the southeast approximately 5 feet per mile. The Plateau is bounded by the Savannah and Congaree Rivers and extends from the fall line to the Orangeburg Escarpment. The highly dissected surface of the Aiken Plateau is characterized by broad interfluvial areas with narrow, steep-sided valleys. Local relief can be as much as 300 feet. Figure 3.1-9 shows the topography and 10 foot contour lines of the GSA. [WSRC-TR-95-0046]

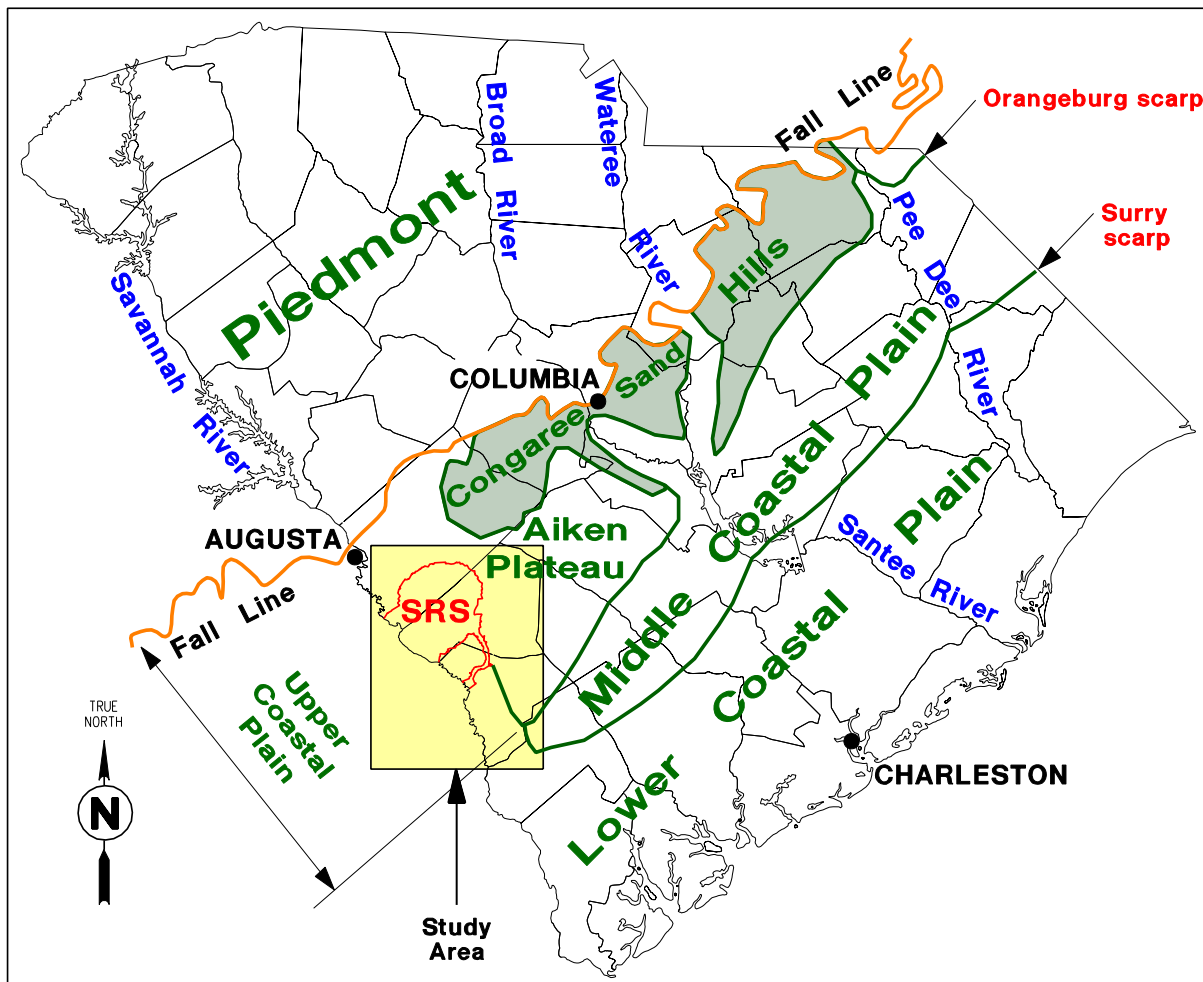
Currently, SDF storm water drainage is diverted indirectly to McQueen Branch, which drains into Tinker Creek near its junction with UTR and will be unaffected by SDF operations and closure activities. The installation of the SDF closure cap (Section 3.2.2) may necessitate changes to the SDF drainage system which will be designed later as part of the overall closure of SDF.

Figure 3.1-7: Regional Geological Provinces of Eastern U.S.



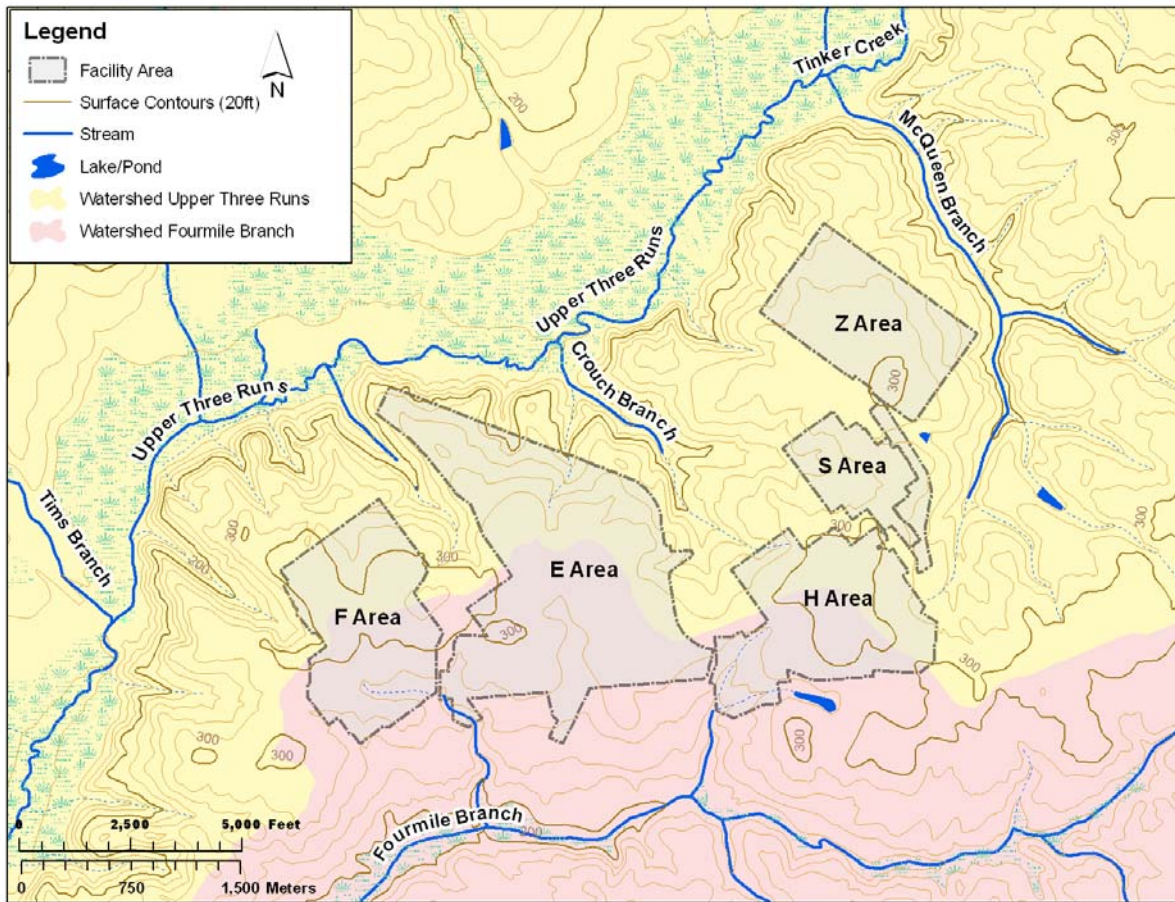
[WSRC-TR-2000-00310, Figure 1]

Figure 3.1-8: Regional Geologic Provinces of South Carolina



[WSRC-TR-95-0046, Figure 2-3]

Figure 3.1-9: GSA Topography



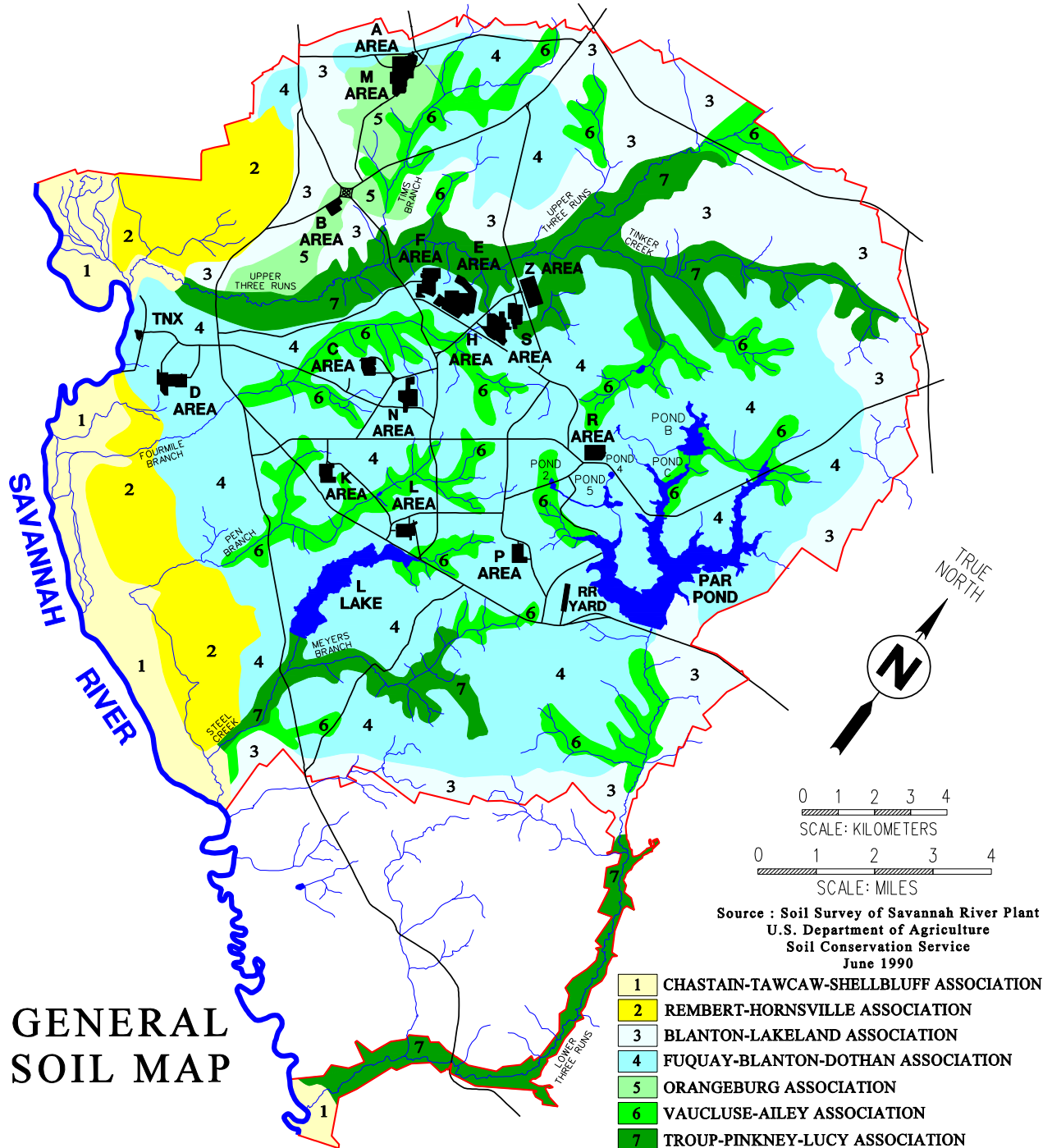
3.1.4.2 Local Geology and Soils

The vadose zone is comprised of the middle to late Miocene-age “Upland Unit,” that extends over much of SRS, including Z-Area. The term “Upland Unit” is an informal name used to describe sediments at higher elevations located in the Upper Coastal Plain in southwestern South Carolina. This area has also been referred to as the Aiken Plateau. The occurrence of cross-bedded, poorly sorted sands with clay lenses in the Aiken Plateau indicates fluvial deposition (high-energy channel deposits to channel-fill deposits) with occasional transitional marine influence. This depositional environment results in wide differences in lithology and presents a very complex system of transmissive and confining beds or zones. The lower surface of the “Upland Unit” is very irregular due to erosion of the underlying formations.

A notable feature of the “Upland Unit” is its compositional variability. This formation predominantly consists of red-brown to yellow-orange, gray, and tan colored, coarse to fine grained sand, pebbly sand with lenses and beds of sandy clay and clay. Vertically upward through the unit, sorting of grains becomes poorer, clay beds become more abundant and thicker, and sands become more argillaceous and indurated. In some areas, small-scale joints and fractures, both of which are commonly filled with sand or silt, traverse the unit. The mineralogy of the sands and pebbles primarily consists of quartz, with some feldspar. In areas to the east-southeast, sediments may become more phosphatic and dolomitic. The soils in the “Upland Unit” may contain as much as 20% to 40% clay. [DOE-EIS-0303]

SRS is comprised of seven major soil associations. They are, Chastin-Tawcaw-Shellbluff; Rembert-Hornsville; Blanton-Lakeland; Fuquay-Blanton-Dothan; Orangeburg; Vacluse-Ailey; and Troup-Pinkney-Lucy. Figure 3.1-10 delineates the general soil associations for SRS. Details regarding these associations may be found in the *Soil Survey of the Savannah River Plant Area, Parts of Aiken, Barnwell and Allendale Counties, South Carolina*. [<http://soildatamart.nrcs.usda.gov/Manuscripts/SC696/0/savannah.pdf>]

Figure 3.1-10: General Soil Associations for SRS



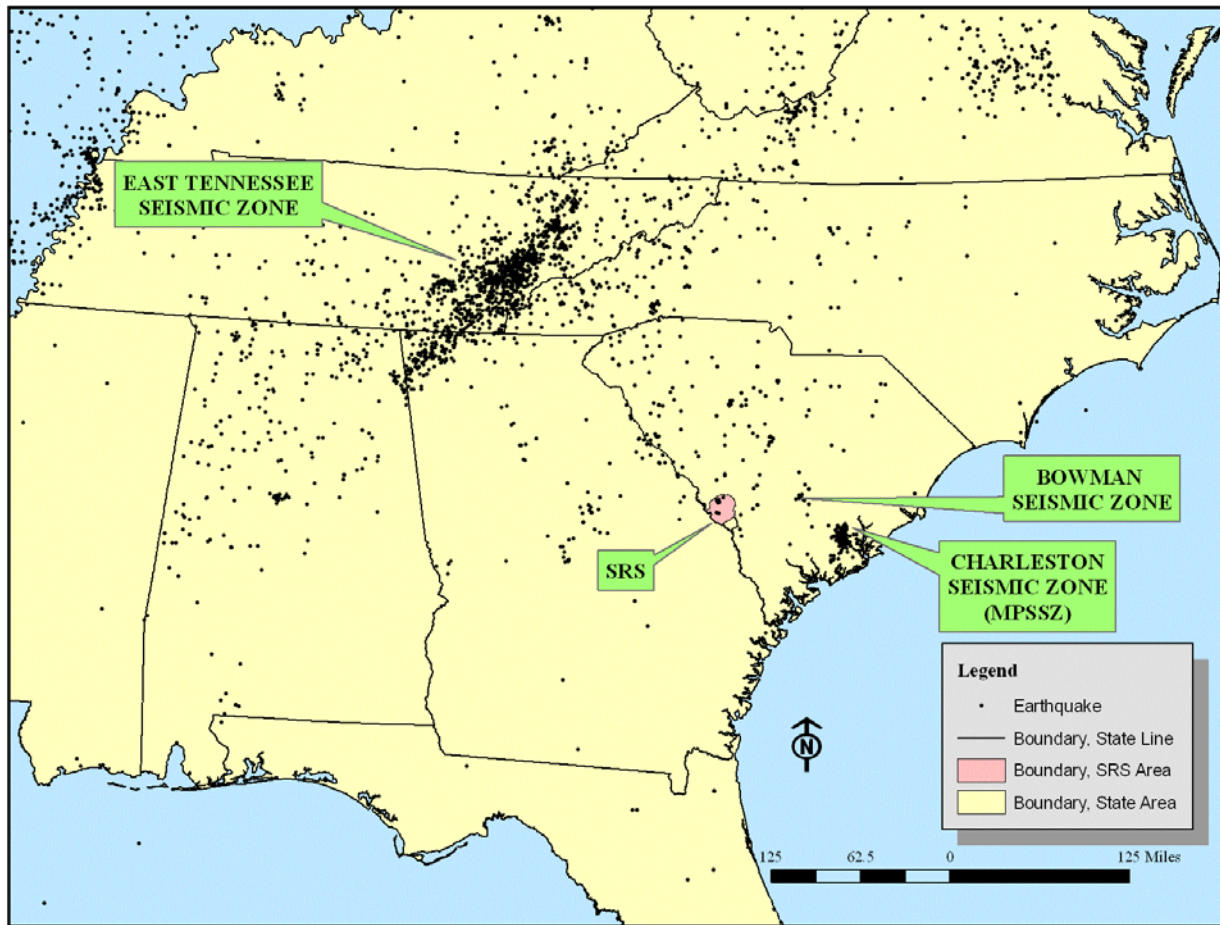
The overall general soil association for Z-Area is the Fuquay-Blanton-Dothan. The most predominant soil types within Z-Area are classified as Udorthents. Udorthents consist of well drained soils that formed in heterogeneous materials, which are the spoil or refuse from excavations and major construction operations. Udorthents range from sandy to clayey, depending upon the source of material or geologic parent material. Udorthents are most commonly associated with well drained to excessively drained upland soils. A few small, poorly drained areas that have spoil are also included. Typical profiles for Udorthents are not shown due to the lack of consolidation within short distances. Clayey soil has demonstrated good retention for most radionuclides. There are also areas that consist of cross-bedded, poorly sorted sand with lenses and layers of silt and clay.

A more detailed description of the geology and soils of the Z-Area can be found in a report titled *Hydrogeologic Framework of West-Central South Carolina* (PIT-MISC-0112) and supplemented with later investigations as reported in WSRC-TR-96-0399, Volumes 1 and 2, and SED-GTE-2008-002.

3.1.4.3 Seismology

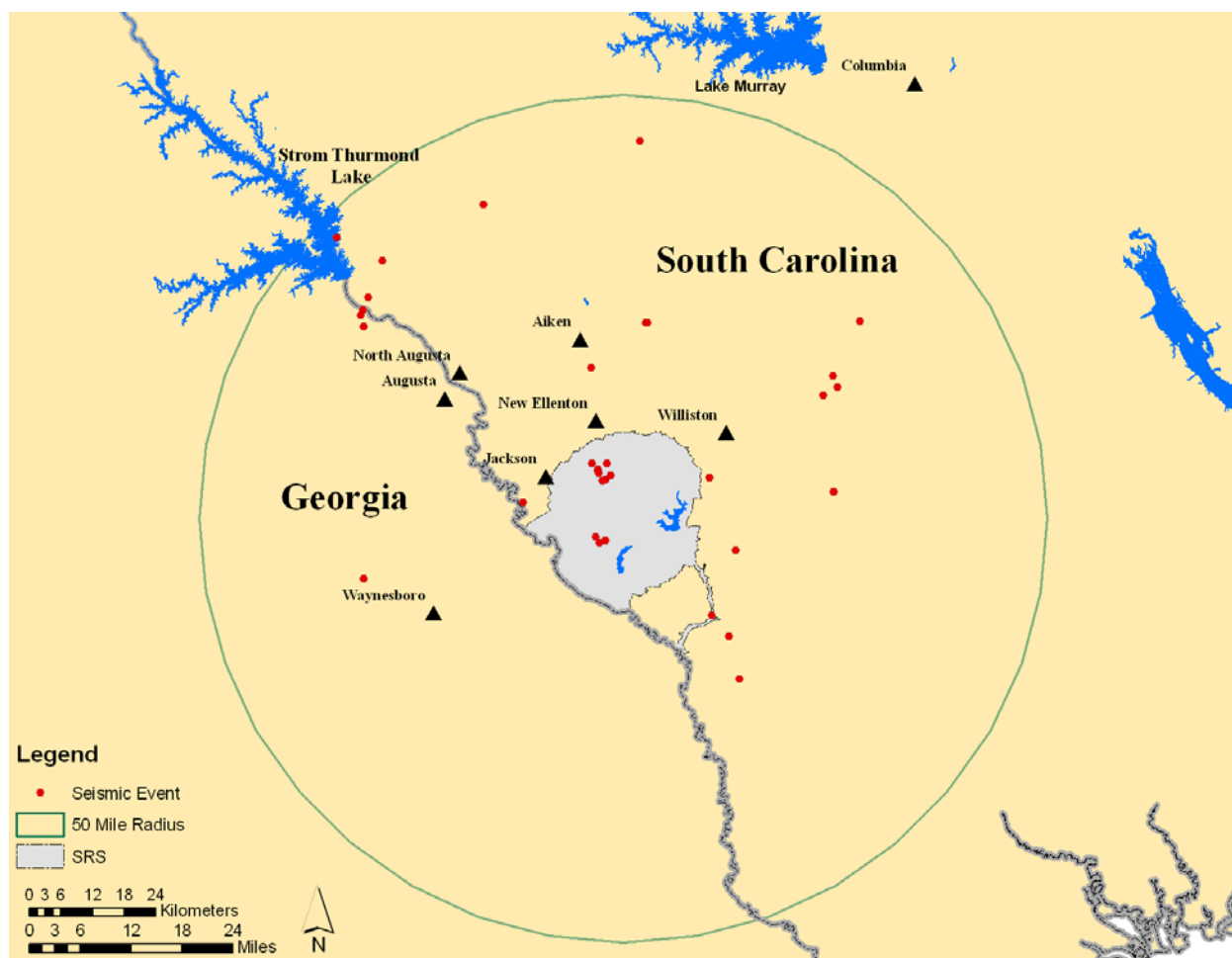
The seismic history of the Southeastern United States (of which SRS is a part) spans a period of nearly three centuries and is dominated by the Charleston earthquake of August 31, 1886 (estimated magnitude of 7.0). The historical database for the region is essentially composed of two data sets extending back to as early as 1698. The first set is comprised of pre-network, mostly qualitative data (1698-1974), and the second set covers the relatively recent period of instrumentally recorded or post-network seismicity, 1974 through April, 2009. Figure 3.1-11 shows the locations of historical seismic events in the Southeast. Figure 3.1-12 denotes the epicenter locations of seismic events within a 50 mile radius of SRS. [WSRC-MS-2003-00617, http://neic.cr.usgs.gov/neis/last_event_states/]

Figure 3.1-11: Historical Seismic Events in the Southeast



[Note: Map information can be found at http://neic.cr.usgs.gov/neis/last_event_states/]

Figure 3.1-12: Seismic Events within a 50 Mile Radius of SRS

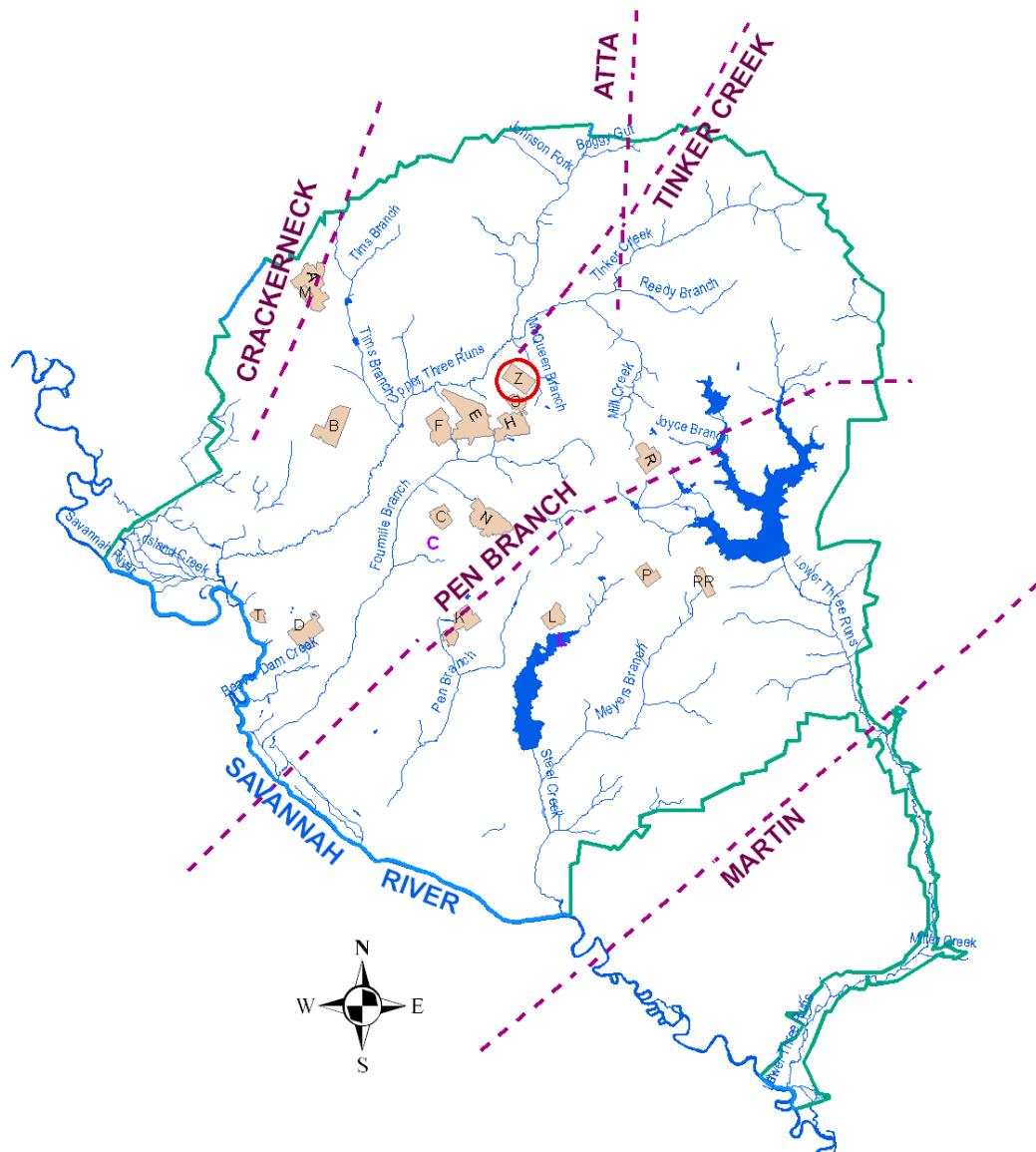


[WSRC-MS-2003-00617, http://neic.cr.usgs.gov/neis/last_event_states/]

The most recent event occurring within a 50 mile radius of SRS was on March 27, 2009, with a magnitude of 2.6. No damage to SRS was recorded. However, there have been four earthquakes with epicenter locations within SRS. They occurred on June 9, 1985 (magnitude of 2.6); August 5, 1988 (magnitude of 2.0); May 17, 1997 (magnitude of 2.3), and October 8, 2001 (magnitude of 2.6). No Strong Motion Accelerometers (SMAs) were triggered as a result of these earthquakes. Note that additional seismic events with epicenter locations within SRS occurred shortly after the October 2001 earthquake however, these seismic events were attributed to aftershocks and not actual earthquakes. [WSRC-MS-2003-00617]

In particular, Z-Area, because of its proximity to the Tinker Creek fault, could be subject to potential activity of the Tinker Creek fault, which is associated with activity of the Coastal Plain sediments. A seismic evaluation of Z-Area shows that soils beneath Z-Area are not susceptible to significant liquefaction for earthquakes leaving a peak ground acceleration less than or equal to 0.17g. [K-CLC-Z-00001] Figure 3.1-13 shows the locations of regional scale faults.

Figure 3.1-13: Regional Scale Faults for SRS and Vicinity



[WSRC-TR-2000-00310, Figure 10]

In 1976, a short-period seismic network was established. This network continues to be upgraded and in 1999 a 10-station SMA network was installed throughout the complex. Detailed information regarding seismic characteristics at SRS can be found in the Documented Safety Analysis (DSA) document, WSRC-IM-2004-00008.

Seismic considerations are included in the design of the SDF closure cap to ensure seismic induced degradation mechanisms are addressed. Section 3.2.2 discusses the design of the SDF closure cap which will appropriately consider and handle static loading induced settlement, seismic induced liquefaction and subsequent settlement, and seismic induced slope instability.

3.1.5 Hydrogeology

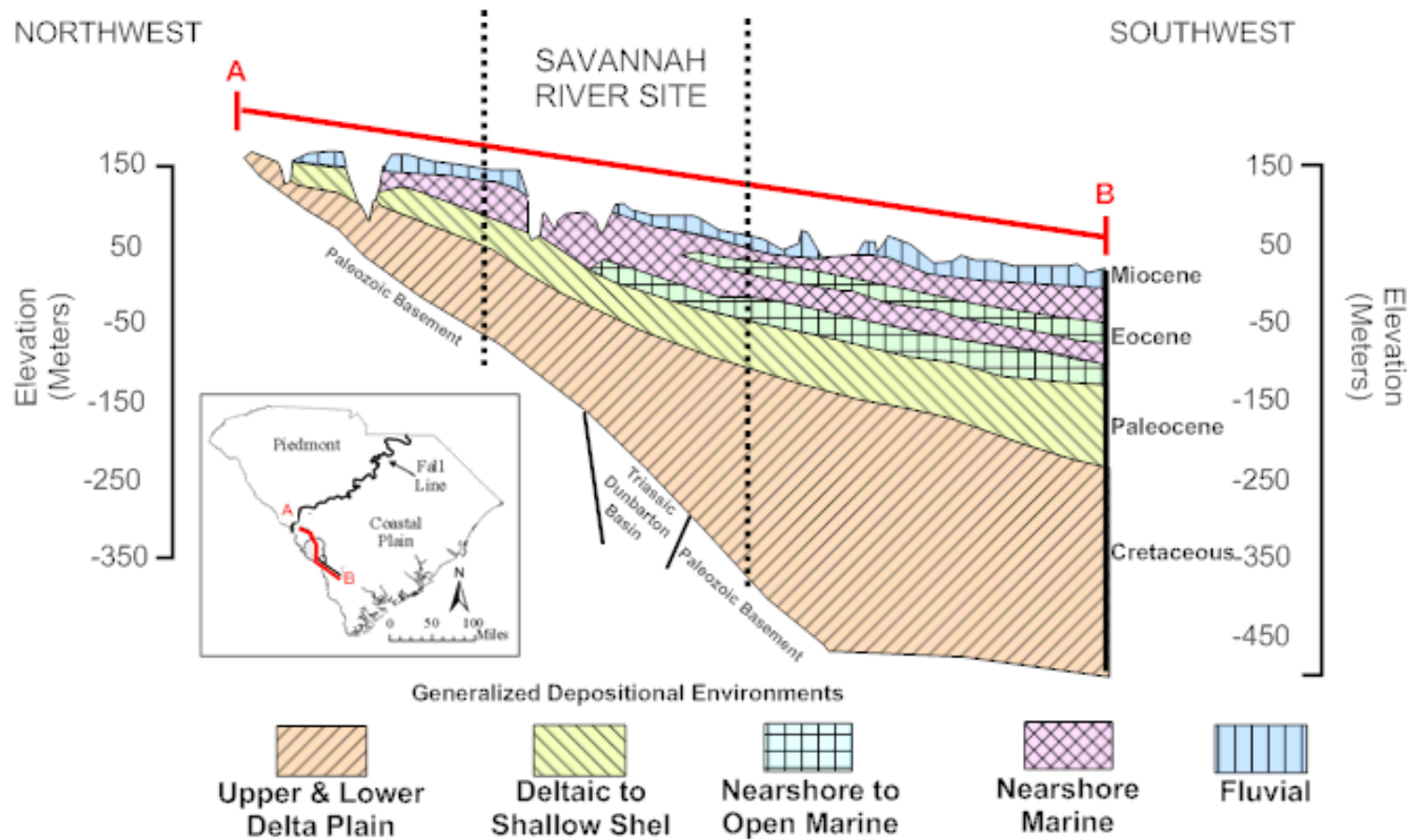
An understanding of the hydrogeology of SDF is required in order for an estimate of the fate and transport of the residual SDF contaminants to be modeled. Characterization and monitoring data in the SRS GSA is extensive and provides a clear understanding of hydrogeology containing the SDF, and permitted generation of the General Separations Area Database (GSAD). Additional background information supporting this conclusion is presented in Section 3.1.5.2.

3.1.5.1 Regional Hydrogeology

SRS lies in the Atlantic Coastal Plain, a southeast-dipping wedge of unconsolidated and semi-consolidated sediment, which extends from its contact with the Piedmont Province at the Fall Line to the continental shelf edge. Sediments range in geologic age from Late Cretaceous to Recent and include sands, clays, lime stones, and gravels. This sedimentary sequence ranges in thickness from essentially zero at the Fall Line to more than 4,000 feet at the Atlantic Coast. At SRS, coastal plain sediments thicken from approximately 700 feet at the northwestern boundary to approximately 1,200 feet at the southeastern boundary of the site and form a series of aquifers and confining or semi-confining units. Aquifer systems include the Floridian, Dublin and Midville systems. [WSRC-TR-96-0399-Vol. 1]




Figure 3.1-14 shows a generalized cross section of the sedimentary strata and their corresponding depositional environments for the Upper Coastal Plain down-dip through SRS into the Lower Coastal Plain. Figure 3.1-15 shows the regional lithologic units and their corresponding hydrostratigraphic units at SRS. This classification system is consistent with the established system, and is now widely used as SRS standard. [WSRC-TR-96-0399-Vol. 1, WSRC-TR-95-0046, WSRC-STI-2008-00057, Page 7-1]

Figure 3.1-14: Regional NW to SE Cross Section



[WSRC-STI-2006-00198]

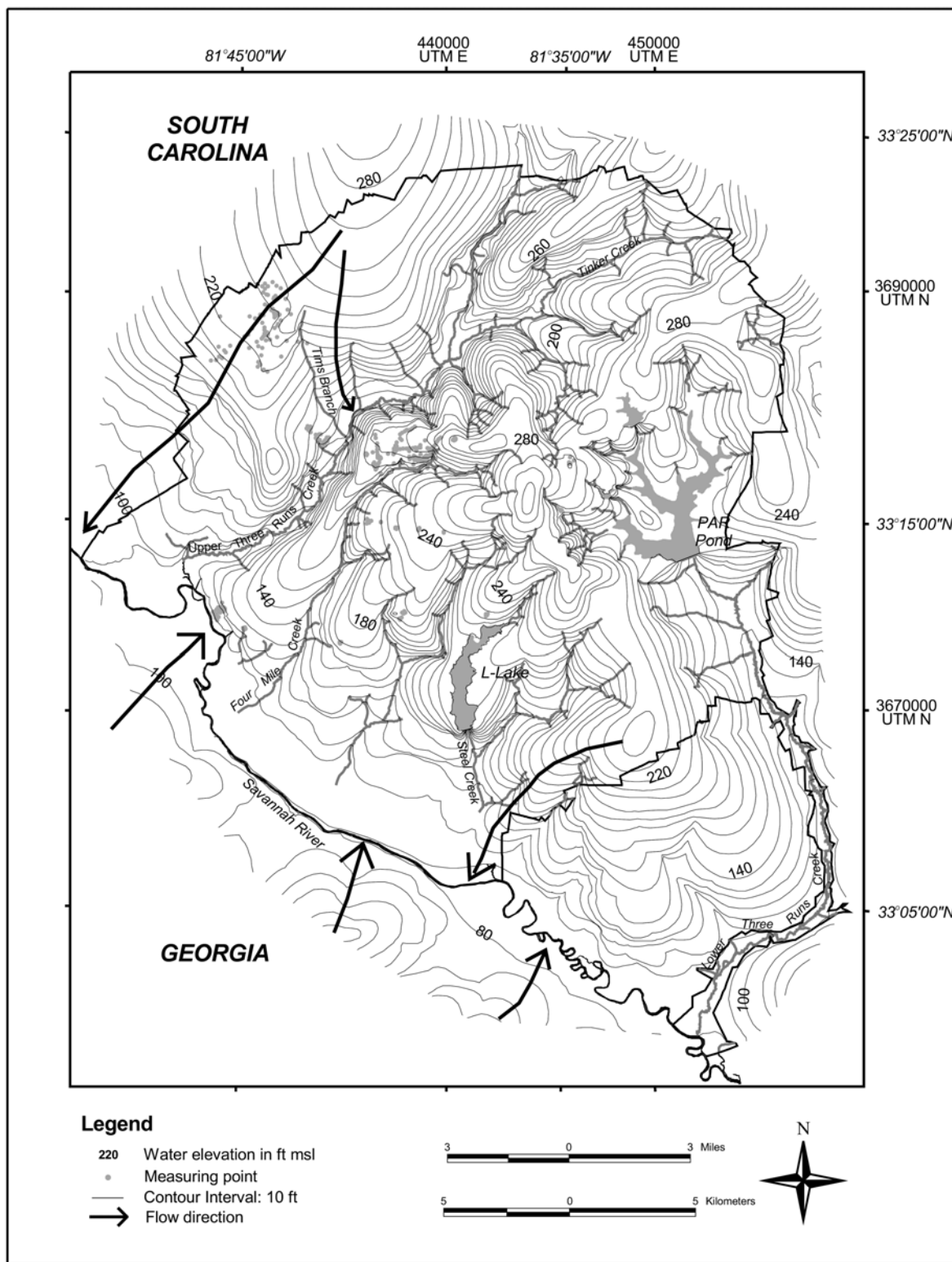
Figure 3.1-15: Comparison of Chronostratigraphic, Lithostratigraphic, and Hydrostratigraphic Units in the SRS Region

| CHRONOSTRATIGRAPHIC UNITS | | | LITHOSTRATIGRAPHIC UNITS (Modified from Fallaw and Price, 1995) | | | HYDROSTRATIGRAPHIC UNITS (Modified from Aadland et al., 1995) | | | | |
|---------------------------|------------|------------------|--|------------------------------------|--------------------------|--|-----------------------|--------------------------------|--------------------------------|--|
| ERA | System | Series | Group | Formation | | | | | | |
| CENOZOIC | Tertiary | Miocene(?) | | "Upland" unit | | Upper Aquifer Zone (UAZ) | | Upper Three Runs Aquifer | Floridan Aquifer System | |
| | | Eocene | Barnwell Group | Tobacco Road Sand | |  | | | | |
| | | | | Dry Branch Formation | Twiggs Clay Mbr. | | | | | |
| | | | | | Griffins Landing Mbr. | | | | | |
| | | | | | Irwinton Sand Mbr. | | | | | |
| | | | Clindfield Formation | | Lower Aquifer Zone (LAZ) | | | | | |
| | | Orangeburg Group | Santee Formation | | | | | | | |
| | | | Warley Hill Formation | | | | Gordon Confining Unit | | | |
| | | | Congaree Formation | | | | Gordon Aquifer Unit | | | |
| | | Paleocene | Black Mingo Group | Fourmile Branch Formation | | | | | | |
| | | | | Snapp Formation | | | | | | |
| | | | | Lang Syne Formation | | | | | | |
| | | | | Sawdust Landing Formation | | | | Crouch Branch Confining Unit | | |
| MESOZOIC | Cretaceous | Upper Cretaceous | Lumbee Group | Steel Creek Formation | | Crouch Branch Aquifer | | Meyers Branch Confining System | Dublin-Midville Aquifer System | |
| | | | | Black Creek Group | |  | | | | |
| | | | | Middendorf Formation | | McQueen Branch Aquifer | | | | |
| | | | | Cape Fear Formation | |  | | | | |
| LATE(?) PROTEROZOIC | Triassic | | Newark Supergroup | Sedimentary Rock (Dunbarton Basin) | | | | | | |
| | | | | Crystalline Basement Rock | | Piedmont Hydrogeologic Province | | | | |

[WSRC-STI-2008-00057, WSRC-TR-96-0399-Vol. 1]

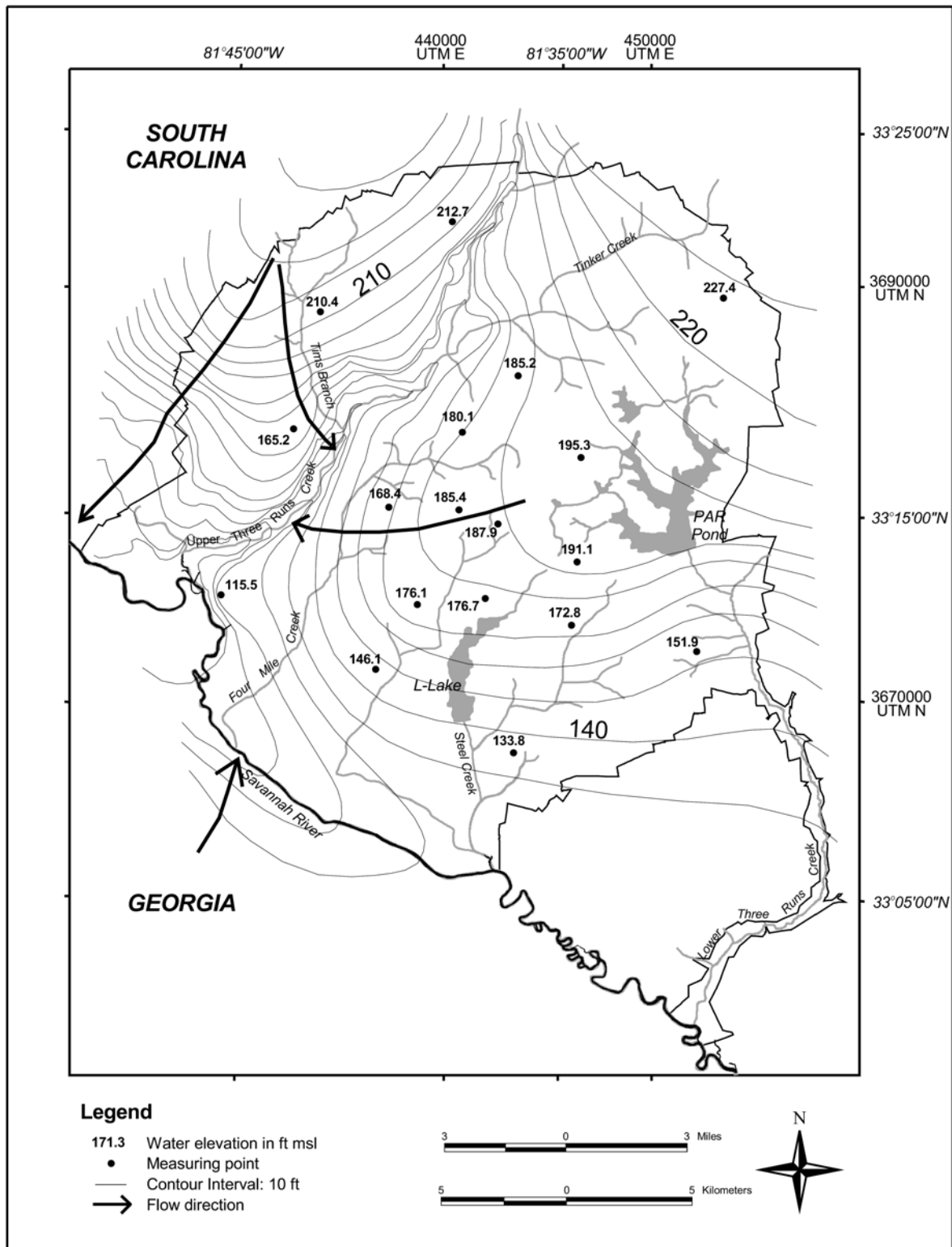
Figures 3.1-16 and 3.1-17 illustrate potentiometric maps of the UTR and Gordon Aquifers. Groundwater within the Floridan Aquifer system flows toward streams and swamps and into the Savannah River at rates ranging from inches to several hundred feet per year. The depth to which nearby streams cut into sediments, the lithology of the sediments, and the orientation of the sediment formations control the horizontal and vertical movement of the groundwater. The valleys of smaller perennial streams, such as Fourmile Branch, McQueen Branch, and Crouch Branch in the GSA, allow discharge from the shallow saturated geologic formations. The valleys of major tributaries of the Savannah River (e.g., UTR) drain formations of greater depth. With the release of water to the streams, the hydraulic head of the aquifer unit releasing the water can become less than that of the underlying unit. If this occurs, groundwater has the potential to migrate upward from the lower unit to the overlying unit. [DOE-EIS-0303]

Figure 3.1-16: Potentiometric Surface of the UTR Aquifer



[WSRC-STI-2008-00057-SRS Maps, Page 18]

Figure 3.1-17: Potentiometric Surface of the Gordon Aquifer



[WSRC-STI-2008-00057-SRS Maps, Page 19]

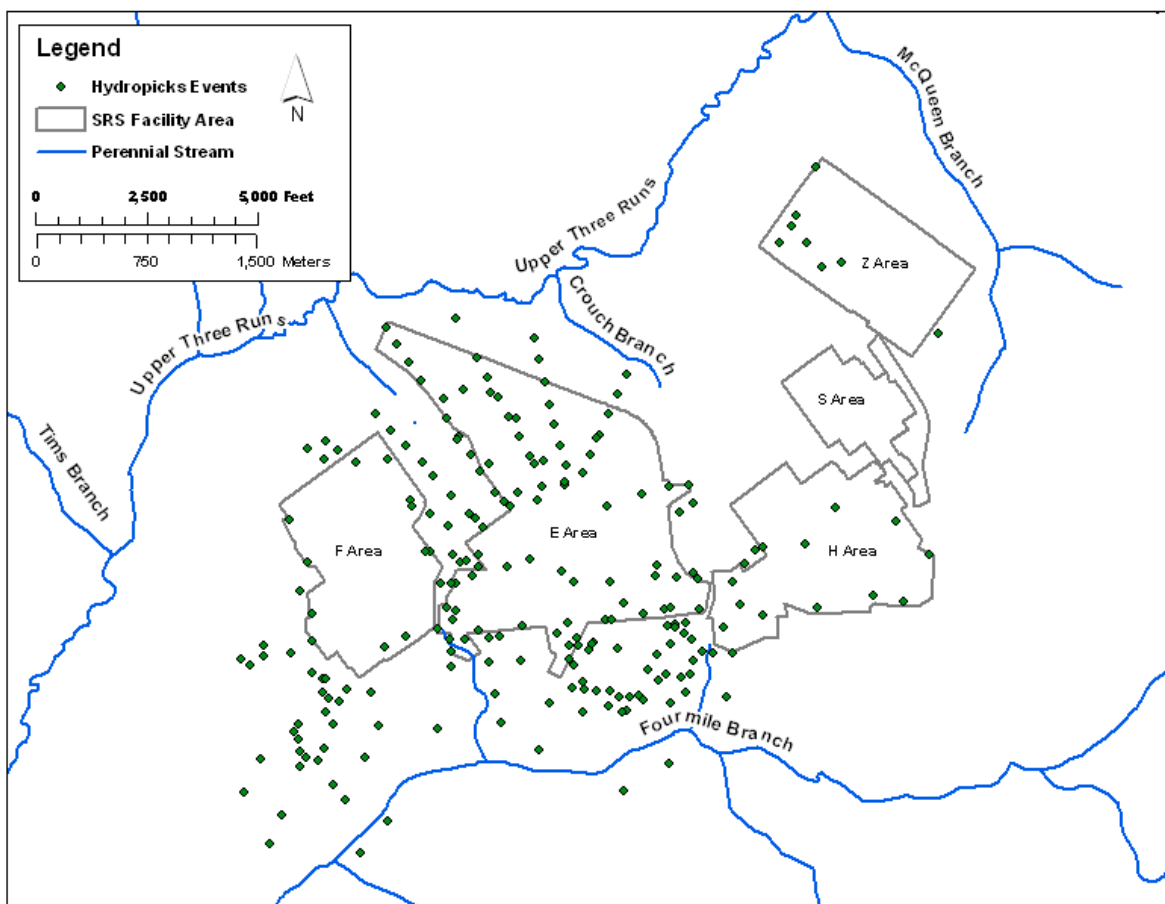
3.1.5.2 *Characterization of Local Hydrogeology*

The GSA has been the focus of numerous geological and hydrogeologic investigations. Early work included installation of monitoring wells in the 1950's and 1960's. Further characterization and monitoring were conducted in the area during the 1970's through present time, largely to support groundwater monitoring and decommissioning activities. The GSAD was developed using field data and interpretations for the GSA and vicinity through 1996. Although characterization and monitoring have been ongoing, the additional data has not altered fundamental understanding of groundwater flow patterns and gradients in the GSA. The GSAD is a subset of site-wide data sets of soil lithology and groundwater information. Figure 3.1-18 shows the location of all hydrostratigraphic picks used in the GSAD. Picks were made based on a combination of geophysical logs, Cone Penetration Test (CPT) logs, and core descriptions. Figures 3.1-19 through 3.1-22 shows locations of laboratory permeability data, multiple well pump tests, single well pump tests, and slug test data used in the GSAD. Table 3.1-2 presents a summary of the characterization and monitoring data in the GSAD. This data provides detailed understanding of local hydrogeology beneath the SDF. See WSRC-TR-96-0399, Volumes 1 and 2 for a more comprehensive discussion of the data set. The GSAD, comprising SRS characterization and monitoring data and interpretations is used as the basis of hydrogeologic input values into the computational model for groundwater flow and contaminant transport.

The transport and flow groundwater modeling requires an understanding of the subsurface geologic and hydrodynamic conditions at the SDF site. Contained within the Dry Branch Formation, the hydrostratigraphic unit, known (at SRS) as the Tan Clay Confinement Zone (TCCZ), is of particular interest because it acts locally as an aquitard, supporting a water table and retarding the downward flow of groundwater. The presence or absence, thickness, and extent of this unit are important inputs into groundwater flow and transport models that are in turn used to demonstrate expected compliance with applicable groundwater regulatory requirements.

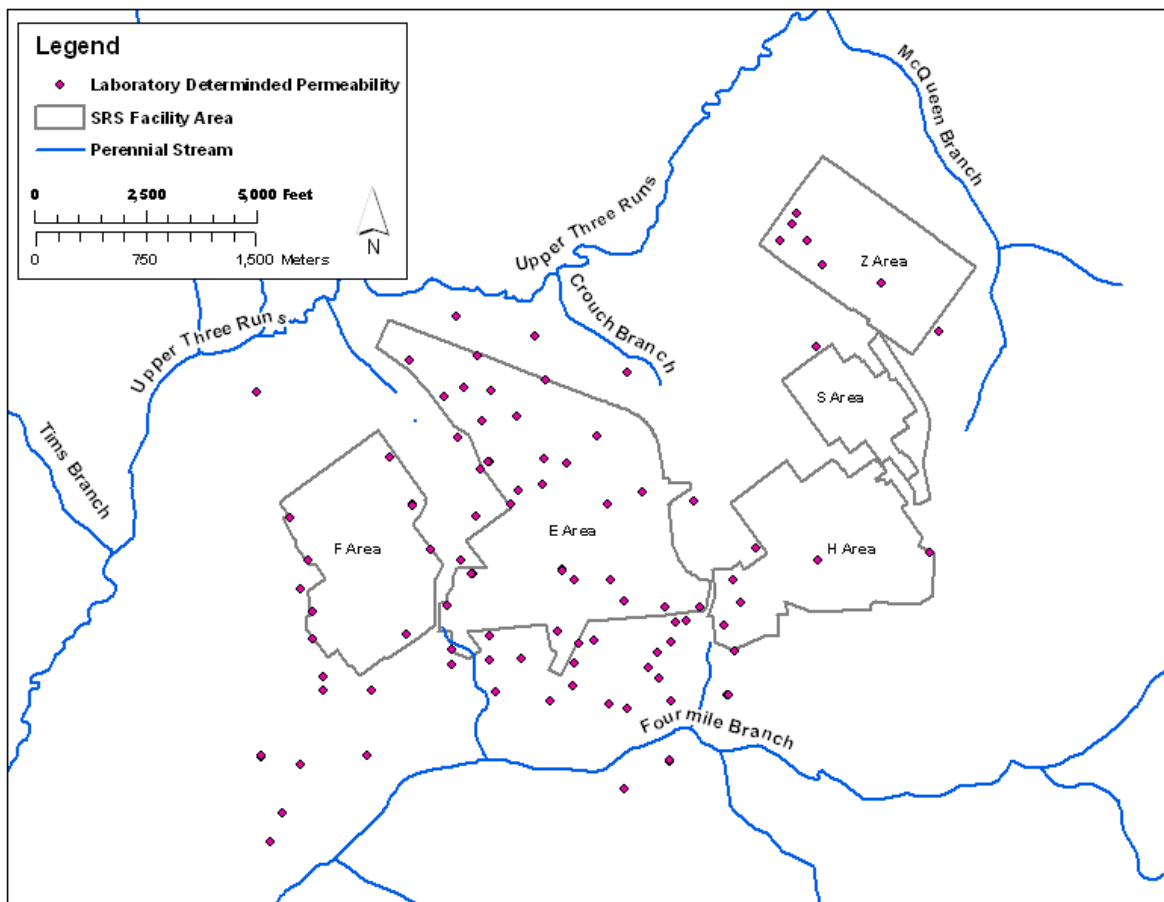
Since the issuance of WSRC-TR-96-0399, additional CPTs and well boreholes have been completed in Z-Area. A review of this information was recently conducted to examine the TCCZ in the modeling region of interest for this PA. Figure 3.1-23 shows the locations of the CPTs and boreholes interpreted for this effort and the locations of active groundwater monitoring wells. Results from this examination revealed that the TCCZ is present in every borehole and CPT evaluated at the Saltstone Facility site. [SED-GTE-2008-002, SRNS-TR-2008-00310]

Figure 3.1-18: Hydrostratigraphic Picks in GSAD



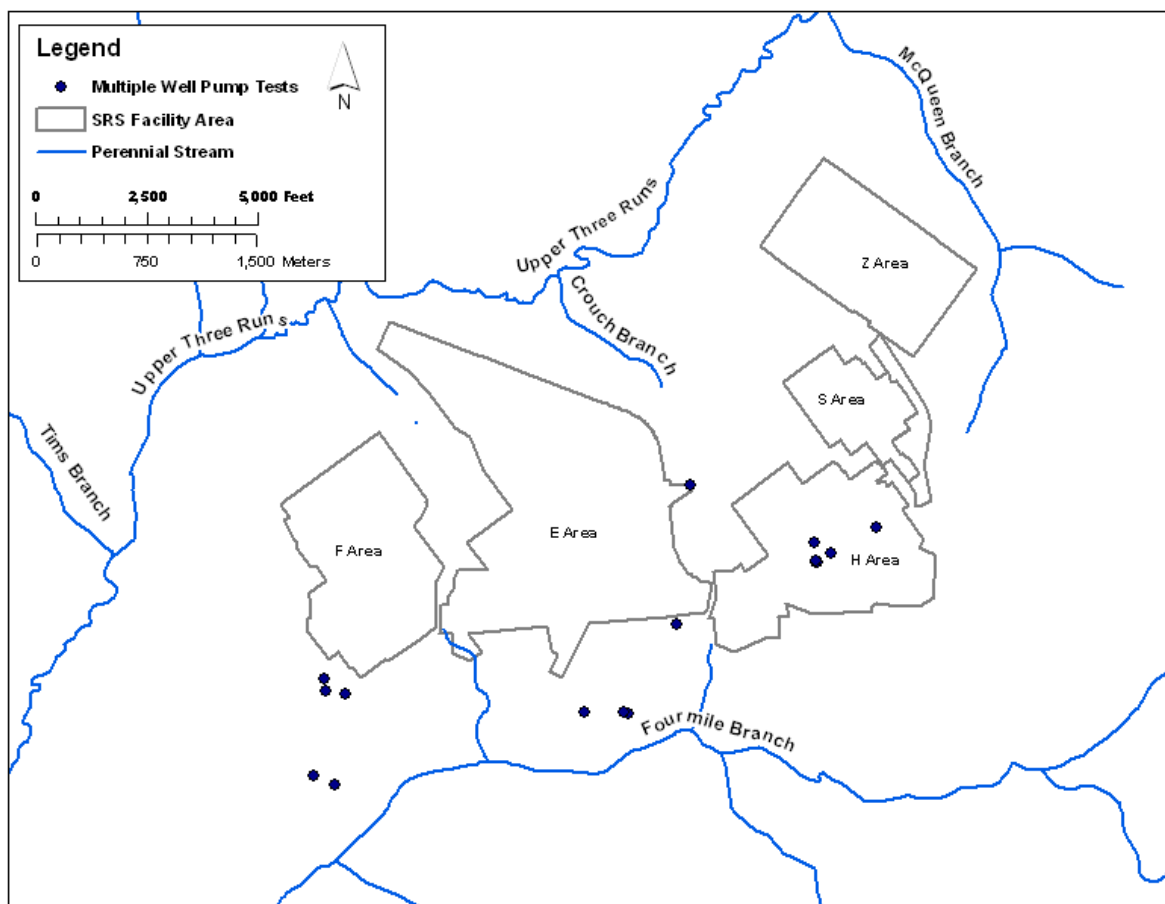
[WSRC-TR-96-0399-Vol. 2]

Figure 3.1-19: Laboratory Determined Permeability Data in GSAD



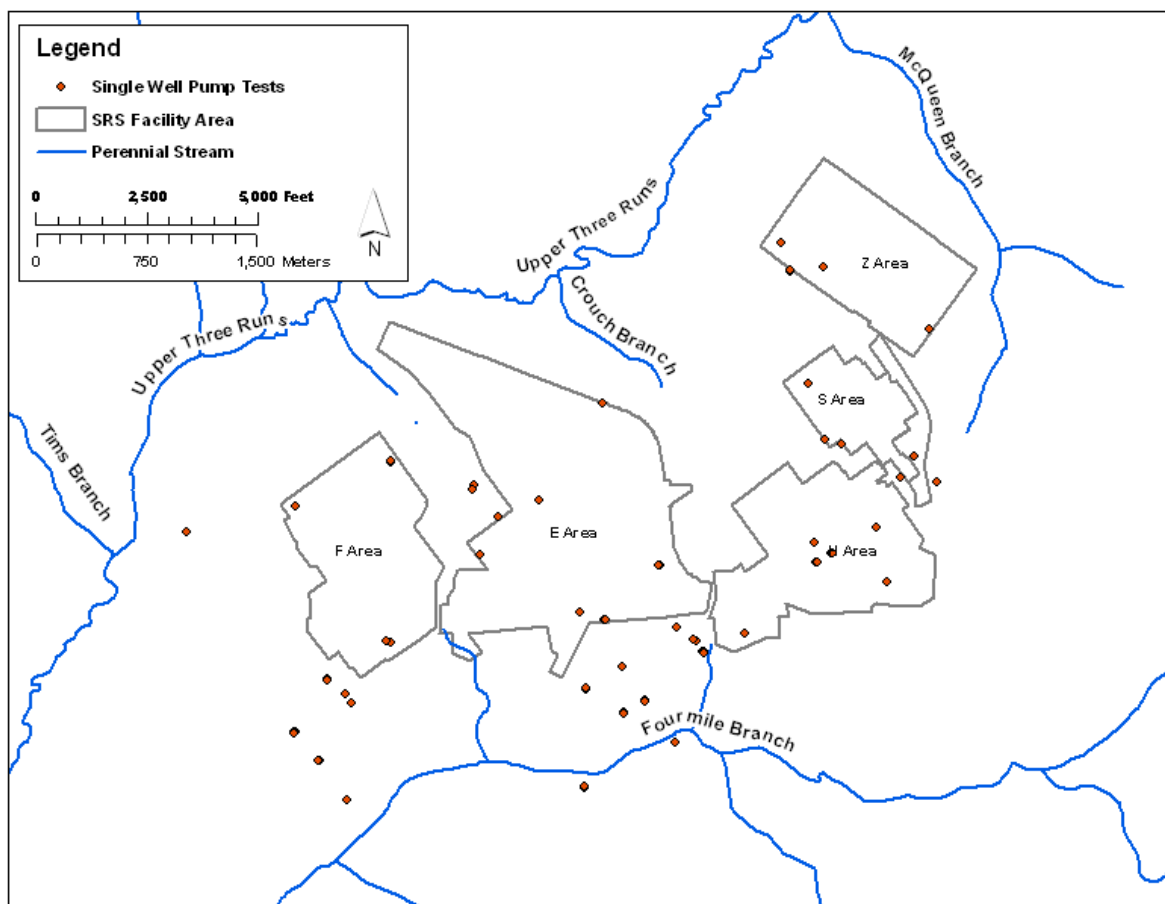
[SRNL-ESB-2007-00035]

Figure 3.1-20: Multiple Well Pump Test Data in GSAD



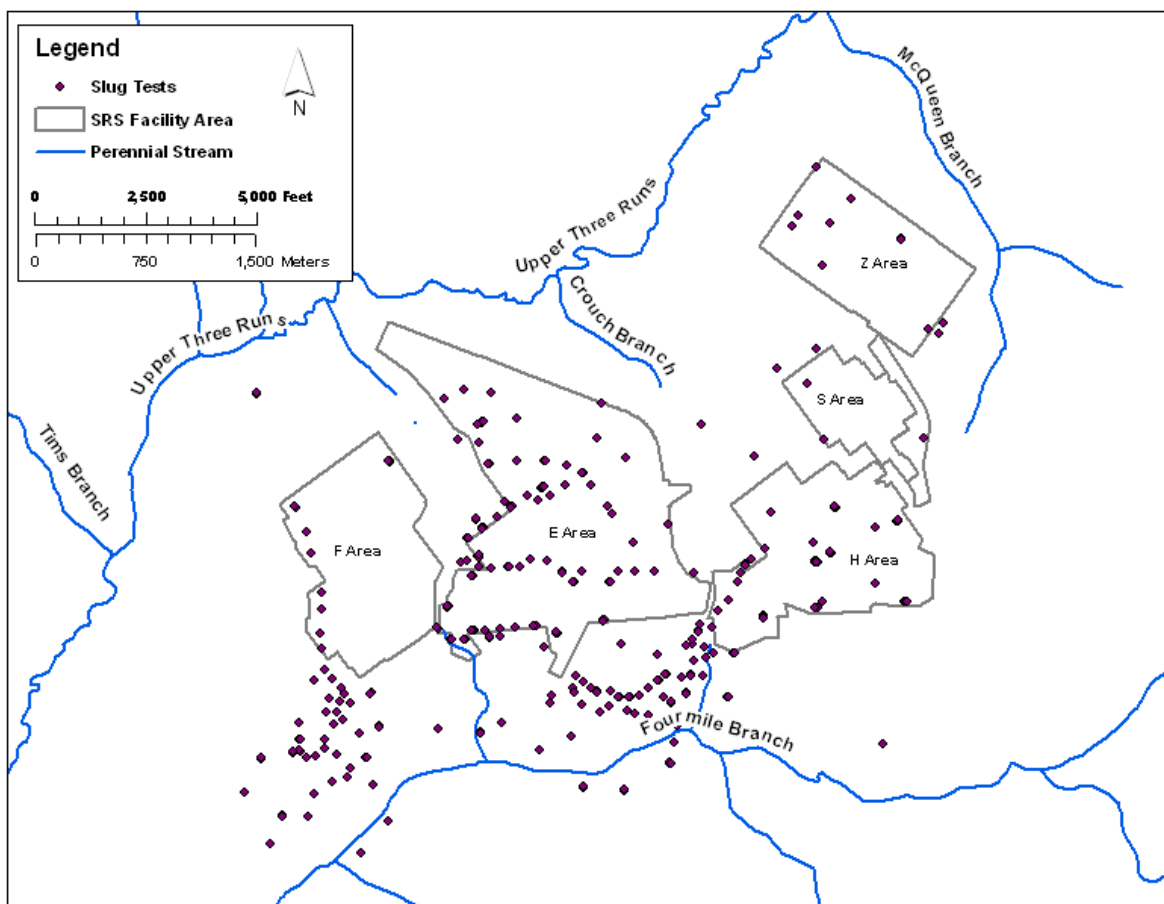
[WSRC-TR-96-0399-Vol. 2]

Figure 3.1-21: Single Well Pump Test Data in GSAD



[WSRC-TR-96-0399-Vol. 2]

Figure 3.1-22: Slug Test Data in GSAD

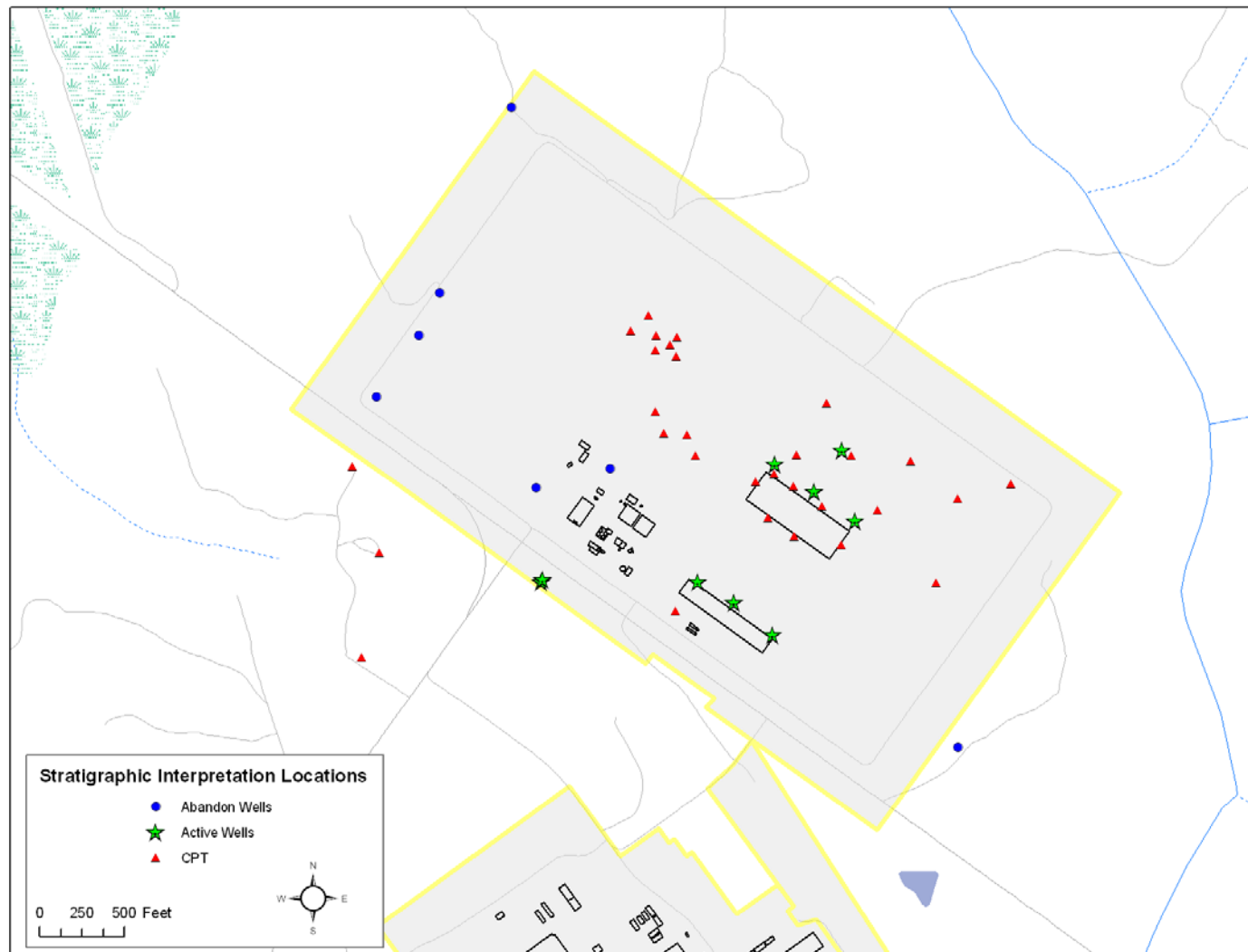


[WSRC-TR-96-0399-Vol. 2]

Table 3.1-2: Characterization and Monitoring Data in the GSAD

| Data Type | Quantity | Reference |
|--|-----------------------------------|------------------------------------|
| Sediment Core Descriptions | 204 Locations; ~37,500 feet | WSRC-TR-96-0399- Vol. 1, App. B |
| Tops of Hydrostratigraphic Units/Zones | | |
| Gordon Aquitard | 52 Locations | WSRC-TR-96-0399- Vol. 1, App. A |
| Gordon Aquifer | 146 Locations | |
| Green Clay Aquitard | 161 Locations | |
| Upper Three Runs - Lower Zone (UTR-LZ) | 222 Locations | |
| Tan Clay Aquitard | 225 Locations | |
| Permeability Measurements | | |
| Pumping Tests | 85 Values | WSRC-TR-96-0399- Vol. 2, App. B |
| Slug Tests | 481 Values | |
| Laboratory Permeability | 258 Values | |
| Water Levels | | |
| Gordon Aquifer | 79 Locations | WSRC-TR-96-0399- Vol. 2, App. C |
| UTR-LZ | 173 Locations | |
| Upper Three Runs - Upper Zone (UTR-UZ) | 387 Locations | |

Figure 3.1-23: Locations of CPT and Well Boreholes at Z-Area



Note: Reproduced from Figure 1 of SED-GTE-2008-002 and Figure 1 of SRNS-TR-2008-00310.

3.1.5.3 *Groundwater Flow in the GSA*

The Aiken Plateau is dissected by numerous streams near Z-Area that greatly influence the local groundwater system. Z-Area lies on a local topographic high, at approximately 300 feet above sea level. Z-Area is bound by McQueen Branch in the northeast and UTR in the northwest. The local relief is approximately 160 feet. McQueen Branch is a tributary of UTR and UTR drains into the Savannah River, approximately 10 miles southwest of Z-Area. Upper Three Runs lies approximately 4,000 feet from the northwest corner of Z-Area. The east corner of Z-Area is located approximately 500 feet from McQueen Branch. McQueen Branch and Crouch Branch are incised into the topographic high, southeast and southwest of Z-Area, such that their headwaters come within approximately 3,300 feet of each other at approximately 4,600 feet south of Z-Area. The elevations of both tributaries range from approximately 150 feet to 250 feet. [WSRC-RP-92-1360]

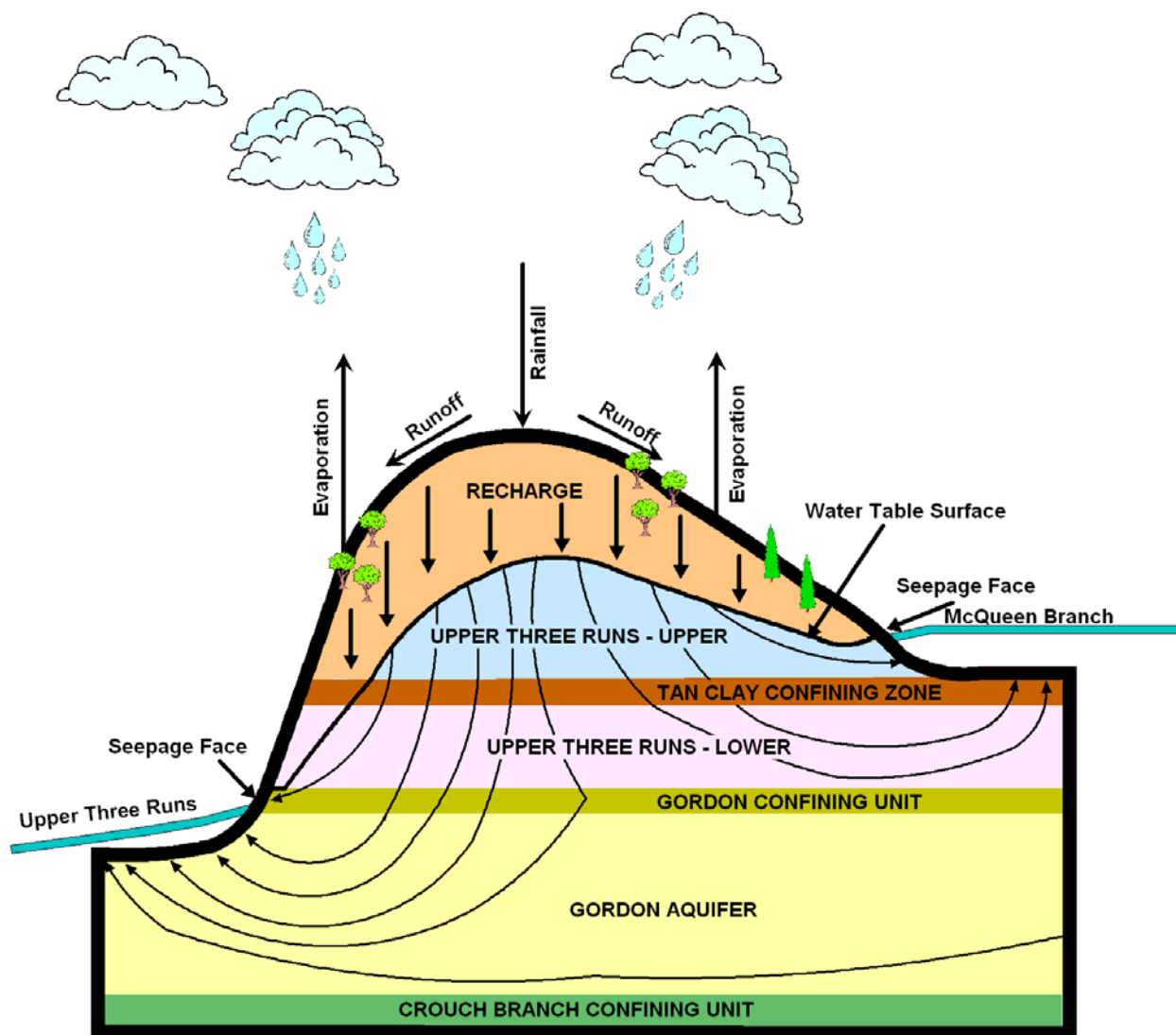
Except in the vicinity of the creeks, the water table in Z-Area occurs in the “Upland Unit” of the southwestern South Carolina Coastal Plain. The average water table beneath the SDF is approximately 210 feet to 230 feet mean sea level (MSL) with the probable maximum water table calculated to be approximately 234 feet to 248 feet MSL. For perspective, the disposal unit base elevations above MSL of existing Vaults 1 and 4, and FDCs 2A and 2B are 281.5 feet, 269 feet, and 269 feet, respectively. The horizontal gradient ranges from 0.002 in the southern part of Z-Area to 0.05 at the northeastern hill slope. [DPST-83-607, WSRC-TR-2005-00131, WSRC-RP-92-1360]

The watershed of UTR drains approximately 190 square miles of the Upper Coastal Plain northeast of the Savannah River. Significant tributaries to this creek are Tinker Creek, which is a headwaters branch that comes in north of Z-Area, and Tims Branch, which connects up south of Z-Area. There are no lakes or flow control structures on UTR or its tributaries. The stream channel has a low gradient and is meandering. Its floodplain ranges in width from 0.25 to 0.99 miles and is heavily forested with hardwoods. [WSRC-RP-92-1360]

Two smaller tributaries of UTR, McQueen Branch and Crouch Branch, are located northeast to southeast and west of Z-Area respectively. Both tributaries receive runoff from Z-Area. McQueen Branch has a drainage area of approximately 4.25 square miles and Crouch Branch has a drainage area of approximately 1.08 square miles. [WSRC-RP-92-1360]

Figure 3.1-24 is a cross-sectional schematic representation of groundwater flow patterns in the UTR and Gordon Aquifers along a north-south cross-section running through the GSA, shown with significant vertical exaggeration. [WSRC-TR-96-0399-Vol. 1 & 2]

Figure 3.1-24: Conceptual Diagram of Groundwater Flow beneath the GSA



[NOT TO SCALE]

3.1.5.4 *Surface-Water Flow in the GSA*

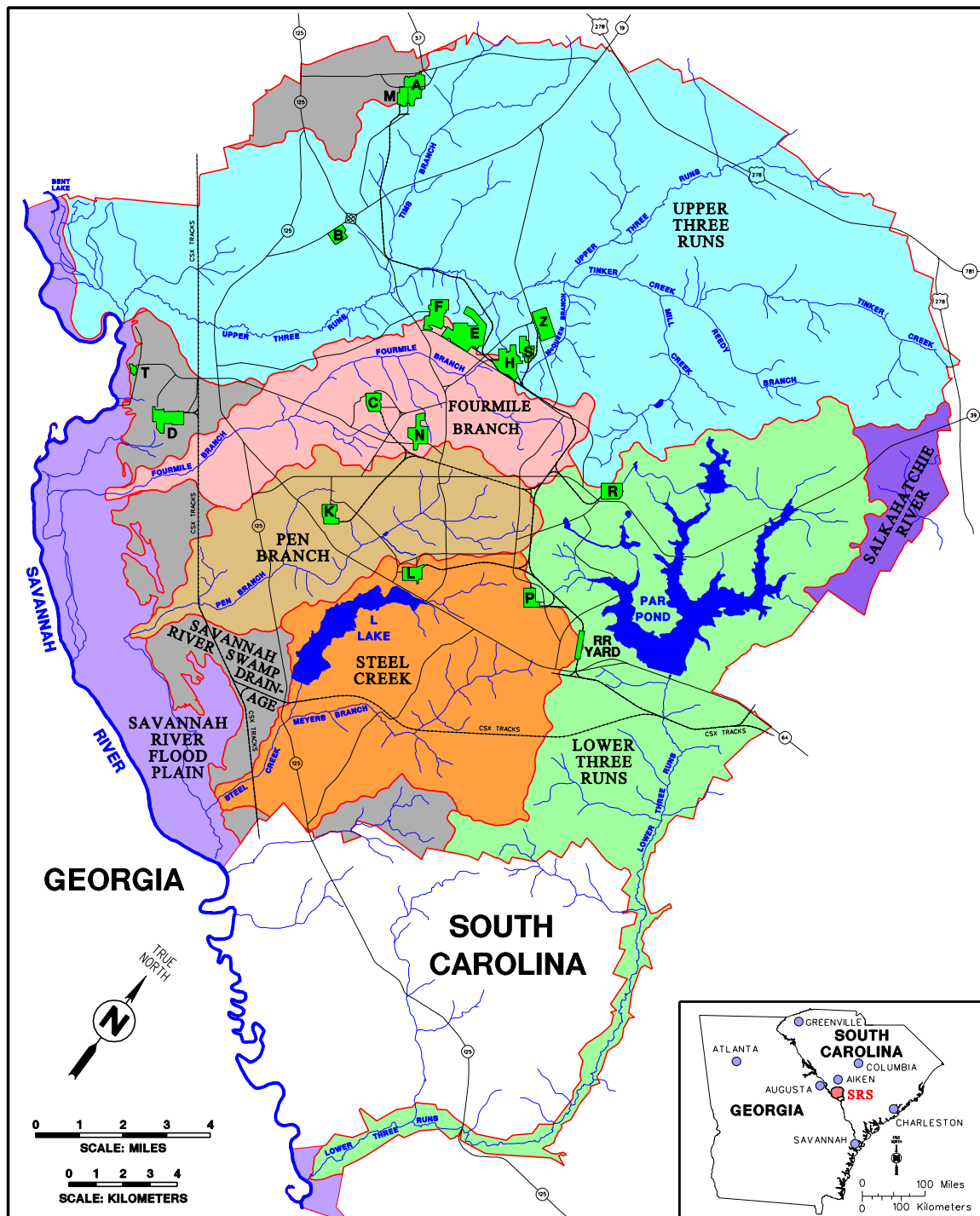
The Savannah River, which forms the boundary between Georgia and South Carolina, is the principal surface-water system near SRS. The river adjoins the site along its southwestern boundary for a distance of approximately 20 miles, and the site is 160 river-miles from the Atlantic Ocean. Five upstream reservoirs, Jocassee, Keowee, Hartwell, Richard B. Russell, and Strom Thurmond (Clarks Hill Lake), minimize the effects from droughts and the impacts of low flow on downstream water quality, and fish and wildlife resources in the river. Figure 3.1-25 shows the Savannah River Basin dams. The long-term yearly Savannah River flow averages approximately 10,400 cubic feet per second (cfs) at SRS. For 2007, the annual average measured flow rate was 6,090 cfs. [WSRC-TR-2005-00201, WSRC-STI-2008-00057]

The major tributaries on SRS are UTR, Fourmile Branch, Pen Branch, Steel Creek, and Lower Three Runs. These tributaries drain all of SRS with the exception of a small area on the northeast side, which drains to a tributary of the Salkehatchie River. Figure 3.1-26 graphically depicts the relative sizes of the watersheds within SRS. Each of these streams originates on the Aiken Plateau in the Coastal Plain and descends 50 to 200 feet before discharging into the Savannah River. The source of most of the surface water on SRS is either natural rainfall, water pumped from the Savannah River and used for cooling site facilities, or groundwater discharging to surface streams. The streams, which historically have received varying amounts of effluent from SRS operations, are not commercial sources of water. Downstream of SRS, Savannah River supplies domestic water and is used for commercial and sport fishing, boating, and other recreational activities. [DOE-EIS-0303, page 3-7]

NORTH CAROLINA



Figure 3.1-26: SRS Watershed Boundaries and Major Tributaries



South Carolina Department of Health and Environmental Control regulate the physical properties and concentrations of chemicals and metals in SRS effluents under the National Pollutant Discharge Elimination System (NPDES) program. In addition to regulating biological Water Quality Standards (WQS) for SRS waters, SCDHEC has classified the Savannah River and SRS streams as “Freshwaters.” “Freshwaters” are defined as surface water suitable for; (1) primary and secondary contact recreation and as a drinking water source after treatment in accordance with SCDHEC requirements, (2) fishing for the survival and propagation of a balanced indigenous aquatic community of fauna and flora, and (3) industrial and agricultural uses. [WSRC-STI-2008-00057, DOE-EIS-0303]

The longest of the SRS streams, UTR is a large stream in the northern part of SRS that discharges to the Savannah River. It drains an area of over 195 square miles and is approximately 25 miles long, with its lower 17 miles within SRS boundaries. This stream receives more water from underground sources than other SRS streams and is the only stream with headwaters arising outside the site. It is the only major tributary on SRS that has not received thermal discharges. The UTR valley has meandering channels, especially in the lower reaches, and its floodplain ranges in width from 0.25 to 1 mile. It has a steep southeastern side and gently sloping northwestern sides. [DOE-EIS-0303]

Flood hazard recurrence frequencies have been calculated for the various SRS site areas. The 100 year, 1,000 year, and 10,000 year flood water levels for UTR Basin near Z-Area is approximately 152, 154, and 157 feet above MSL, respectively. [WSRC-TR-99-00369] As shown in Section 4.2.3, the lowest elevation of a disposal unit within the SDF is 260 feet above MSL; thus the highest period flood water level of approximately 157 feet above MSL is approximately 103 feet below the lowest elevation of saltstone material. In addition, the lowest elevation of the lower foundation layer, at the bottom of the side slope, of the conceptual closure cap is approximately 257 feet above MSL, which is approximately 100 feet above the highest flood water level of 157 feet. [WSRC-STI-2008-00244] Therefore, flooding is not a concern for this PA.

3.1.6 Geochemistry

The migration of radionuclides in the subsurface environment is dependent on physical and chemical parameters or properties of cementitious materials, soils, and groundwater. Studies and analyses have been conducted to determine appropriate K_d values. The data used in the radionuclide transport model is presented in Sections 4.2.2 and 4.2.3.2 specific to the GSA and is not reproduced in this section.

3.1.7 Natural Resources

Natural resources at SRS are managed under the *Natural Resources Management Plan* (NRMP) prepared for the DOE by the United States Department of Agriculture (USDA) and fosters the following principles, which govern SRS natural resource management:

- All work will be done in accordance with Integrated Safety Management Procedures found in DOE Policy 450.4, *Safety Management System Policy*
- Environmental stewardship activities will be compatible with future SRS missions.
- SRS will continue to protect and manage SRS natural resources
- Sustainable resource management will be applied to SRS natural resources
- Close cooperation will be maintained among organizations when managing and protecting SRS natural resources
- The results of research, monitoring, and operational findings will be used in the management of SRS natural resources
- Restoration of native communities and species will continue
- Employees, customers, stakeholders, state natural resource officials, and regulators will be invited to participate in the natural resource planning process
- SRS will maintain the area as a National Environmental Research Park (NERP) [NRMP-2005]

3.1.7.1 Water Resources

SRS monitors non-radioactive liquid discharges to surface waters through the NPDES, as mandated by the EPA Clean Water Act. [www.epw.senate.gov/water.pdf] As required by EPA and SCDHEC, SRS has NPDES permits in place for discharges to the waters of the United States and South Carolina. These permits establish the specific sites to be monitored, parameters to be tested, and monitoring frequency, as well as analytical, reporting, and collection methods. [WSRC-STI-2008-00057, page 4-7] Continuous surveillance monitoring of site streams occurs downstream of several process areas to detect and quantify levels of radioactivity in effluents transported to the Savannah River. [WSRC-STI-2008-00057, page 5-3]

Table 3.1-3 characterizes Savannah River water quality both upstream and downstream of SRS. Table 3.1-4 characterizes water quality in the UTR upstream and downstream of the GSA.

Table 3.1-3: Water Quality in the Savannah River Upstream and Downstream from SRS (Calendar Year 2007)

| Parameter | Unit of Measure | Upstream | | Downstream | |
|---------------------------|-----------------|----------|----------------------|------------|----------------------|
| | | Minimum | Maximum ^a | Minimum | Maximum ^a |
| Aluminum | mg/L | 0.062 | 0.97 | 0.0777 | 0.622 |
| Cadmium | mg/L | ND | ND | ND | ND |
| Chromium | mg/L | ND | ND | ND | ND |
| Copper | mg/L | ND | 0.0388 | ND | 0.0083 |
| Dissolved Oxygen | mg/L | 6.1 | 11.1 | 6.2 | 10.1 |
| Gross Alpha Radioactivity | pCi/L | ND | 1.26 | ND | 1.55 |
| Lead | mg/L | ND | ND | ND | 0.0023 |
| Mercury | mg/L | ND | 0.000023 | ND | 0.000024 |
| Nickel | mg/L | ND | 0.003 | ND | 0.0066 |
| Nitrate (as N) | mg/L | 0.18 | 0.57 | 0.19 | 0.41 |
| pH | pH units | 5.9 | 7.1 | 6.6 | 16.1 ^b |
| Phosphate | mg/L | 0.032 | 0.18 | 0.084 | 0.17 |
| Suspended solids | mg/L | 1 | 47 | 4 | 15 |
| Temperature | °F | 52.5 | 78.6 | 53.2 | 82.4 |
| Tritium | pCi/L | ND | 229 | 140 | 1,060 |
| Zinc | mg/L | ND | 0.0087 | ND | 0.0173 |

Notes: Information extracted from WSRC-STI-2008-00057 accompanying data files. Parameters are those DOE routinely measures as a regulatory requirement or as part of ongoing monitoring programs. (ND) indicates non detectable.

(a) The maximum listed concentration is the highest single result found during one sampling event.

(b) Highest one month sample, next highest value reported was 7.2 pH unit.

Table 3.1-4: Water Quality in UTR

| | Temperature (°F) | pH | Dissolved Oxygen (mg/L) | Total Suspended Solids (mg/L) |
|---|---------------------|-----------|----------------------------|----------------------------------|
| Sampling Location: UTR (Upstream of GSA) | | | | |
| Mean | 61 | 5.9 | 9.1 | 4.6 |
| Range | 51 - 70 | 5.4 - 6.7 | 4.4 - 14 | 3 - 9 |
| Sampling Location: UTR (Downstream of GSA) | | | | |
| Mean | 65 | 6.5 | 9.6 | 6.2 |
| Range | 52 - 74 | 5.2 - 7.6 | 6.4 - 16 | 4 - 11 |

[WSRC-STI-2008-00057]

➤ **Groundwater**

The SDWA was enacted in 1974 to protect public drinking water supplies. [<http://www.epa.gov/safewater/contaminants/index.html#mcls>] SRS domestic water is supplied by 17 separate systems, all of which utilize groundwater sources. The A-Area, D-Area, and K-Area systems are actively regulated by SCDHEC, while the remaining smaller water systems receive a reduced level of regulatory oversight. [WSRC-STI-2008-00057]

Table 3.1-5 provides the summary of maximum groundwater monitoring results for those areas that most likely outcrop to UTR. [WSRC-STI-2008-00057, SRNS-TR-2008-00310] It should be noted that these are maximum values generally associated with wells very close to the contaminant source areas and not stream concentrations. By the time the groundwater reaches a stream it has lower contaminant concentrations because of natural attenuation processes.

Continued environmental monitoring, a condition for the SRS Z-Area Saltstone Industrial Solid Waste Permit, #025500-1603 (DHEC_9-09-2008), ensures the timely response to any potential impacts to the groundwater. Environmental monitoring includes the following:

- Maintaining a groundwater monitoring system
 - Collecting and analyzing groundwater samples
 - Assessing and providing corrective actions for any groundwater impact
 - Providing semi-annual, annual, and biennial reports on the results of the groundwater monitoring analyses
- [DHEC_9-09-2008]

Table 3.1-5: Groundwater Monitoring Results for Outcrops to UTR

| Location | Major Contaminants | Units | 2006 Maximum | MCL | 2007 Maximum | Likely Outcrop Point |
|----------|--------------------|-------|-------------------|------------------------|------------------|-----------------------------|
| E-Area | Tritium | pCi/L | 33,600,000 | 20,000 | 30,800,000 | UTR/Crouch Branch in North |
| | TCE | ppb | 750 | 5 | 370 | |
| F-Area | TCE | ppb | 78.9 | 5 | 52.2 | UTR/Crouch Branch in North |
| | Tritium | pCi/L | 91,500 | 20,000 | 73,000 | |
| | Gross alpha | pCi/L | 2,030 | 15 | 2,120 | |
| | Beta | pCi/L | 1,620 | 4 mrem/yr ^a | 380 | |
| H-Area | Tritium | pCi/L | 80,400 | 20,000 | 67,200 | UTR/Crouch Branch in North |
| | Gross alpha | pCi/L | 98 | 15 | 25.5 | |
| | Beta | pCi/L | 116 | 4 mrem/yr ^a | 55.6 | |
| Location | Major Contaminants | Units | 2007 Maximum | MCL | 2008 Maximum | Likely Outcrop Point |
| Z-Area | Tritium | pCi/L | 5,360 | 20,000 | 4,980 | UTR/McQueen Branch in North |
| | Gross alpha | pCi/L | 10.4 ^b | 15 | 6.8 ^b | |
| | Beta | pCi/L | 6.2 ^b | 4 mrem/yr ^a | ND | |

(a) The activity (pCi/L) equivalent to 4 mrem/yr varies according to which specific beta emitters are present in the sample. [WSRC-STI-2008-00057, Page 7-9]

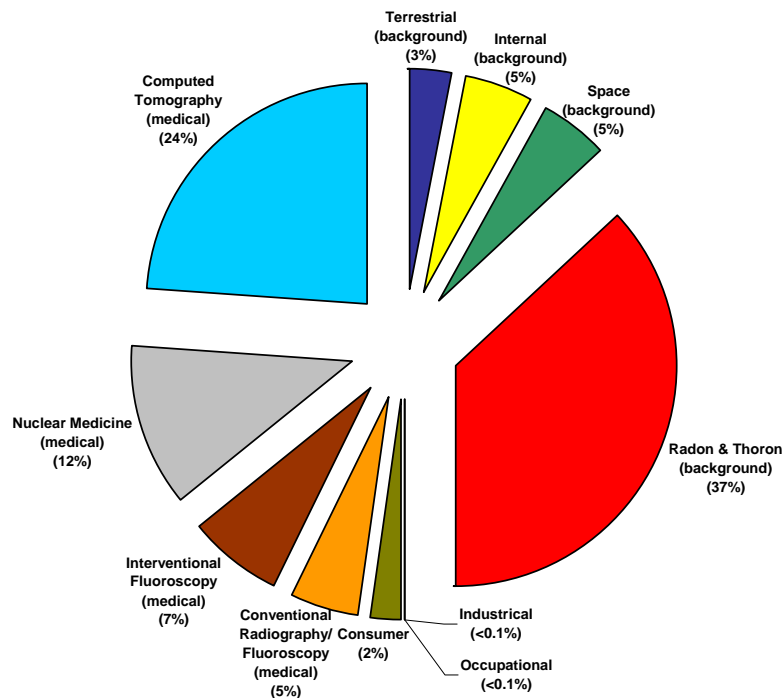
(b) Analytical results indicate that the analyte was identified but the result is approximate due to its low concentration in relation to the detection limit [SRNS-TR-2008-00310, page 18]

ND = Not detected.

3.1.8 Natural and Background Radiation

All human beings are exposed to sources of ionizing radiation that include naturally occurring and man-made sources. Individual's average dose contribution estimates from various sources were obtained from the review information presented in NCRP Report 160 and are shown in Figure 3.1-27. [NCRP-160] On average, a person living in either the United States or the Central Savannah River Area (CSRA) receives an annual radiation dose of approximately 620 mrem. The dose from SRS operations to the maximally exposed offsite individual during calendar year 2007 was estimated to be 0.1 mrem. [WSRC-STI-2008-00057, page 6-7]

Figure 3.1-27: Major Sources of Radiation Exposure in the Vicinity of SRS



The major source of radiation exposure to an average MOP in the CSRA is attributed to naturally occurring radiation (311 mrem/yr) and medical exposure (300 mrem/yr). This naturally occurring radiation is often referred to as natural background radiation and includes dose from background radon and its decay products (228 mrem/yr), cosmic radiation (33 mrem/yr), internal radionuclides occurring naturally in the body (29 mrem/yr), and natural radioactive material in the ground (21 mrem/yr). The dominant medical sources include dose from computed tomography (147 mrem/yr), nuclear medicine (77 mrem/yr), and radiography/fluoroscopy (77 mrem/yr). The remainder of the dose is from consumer products (13 mrem/yr), industrial/educational/research activities (<1 mrem/yr), and occupational exposure (<1 mrem/yr). [NCRP-160]

3.2 Principal Facility Design Features

The Saltstone Facility consists of two facility segments; (1) the SPF, which receives and treats the salt solution to produce saltstone, and (2) the SDF, which consists of disposal units used for the final disposal of the saltstone. Both the SPF and the SDF are located in Z-Area.

Construction of SPF and the first two SDF disposal units were completed between February 1986 and July 1988 and radioactive operations began in June 1990. The first disposal unit constructed is designated Vault 1 and is described in Section 3.2.1.1. The next disposal units constructed were originally designated Vaults 6 and 7 and are now identified as Vault 4, and are described in Section 3.2.1.2. Future disposal units are called FDCs and will be constructed on a “just-in-time” basis in coordination with salt processing production rates and will be constructed in pairs with the first set of FDCs numbered 2A and 2B. The next set to be constructed will be

numbered 3A and 3B and subsequent FDCs will be numbered consecutively starting with 5A and 5B. Disposal cells 2A and 2B are currently in the construction phase and are described in Section 3.2.1.3. [WSRC-STI-2006-00198, SRNS-STI-2008-00045]

Above grade structures, utilities, and equipment, will be removed from the SDF and SPF area prior to installation of the closure cap. Thus no ancillary equipment that will impact the modeling will remain prior to final closure.

A maximum elevation difference of 25 feet from the finished grade level of Vault 1 to the finished grade level of some FDC groupings is anticipated. In addition, a maximum elevation difference of 45 feet from the top of Vault 1 to the top of some FDC groupings is anticipated. The SPF (i.e., buildings, dry feed silos, etc) will not be covered by a closure cap, but will undergo D&D.

3.2.1 SDF Vaults and Future Disposal Cells

The SDF currently includes two completed disposal units, two FDCs under construction, and is anticipated to eventually include a total of sixty-four FDCs. Figure 3.2-1 provides an aerial view of the SDF, showing the locations of Vault 1 and 4, and the site for FDCs 2A and 2B. Figure 3.2-2 provides a layout of the anticipated SDF FDC groups.

Figure 3.2-1: Saltstone Disposal Facility Aerial View

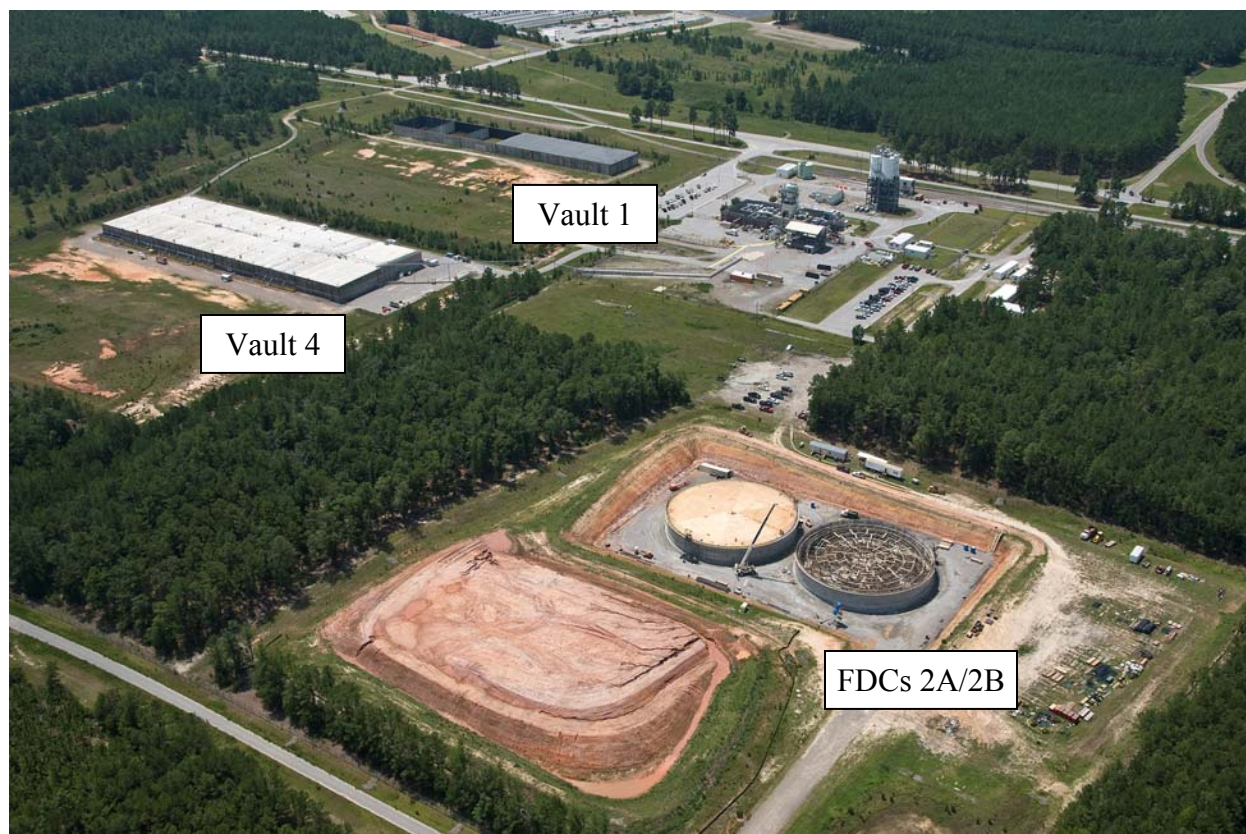
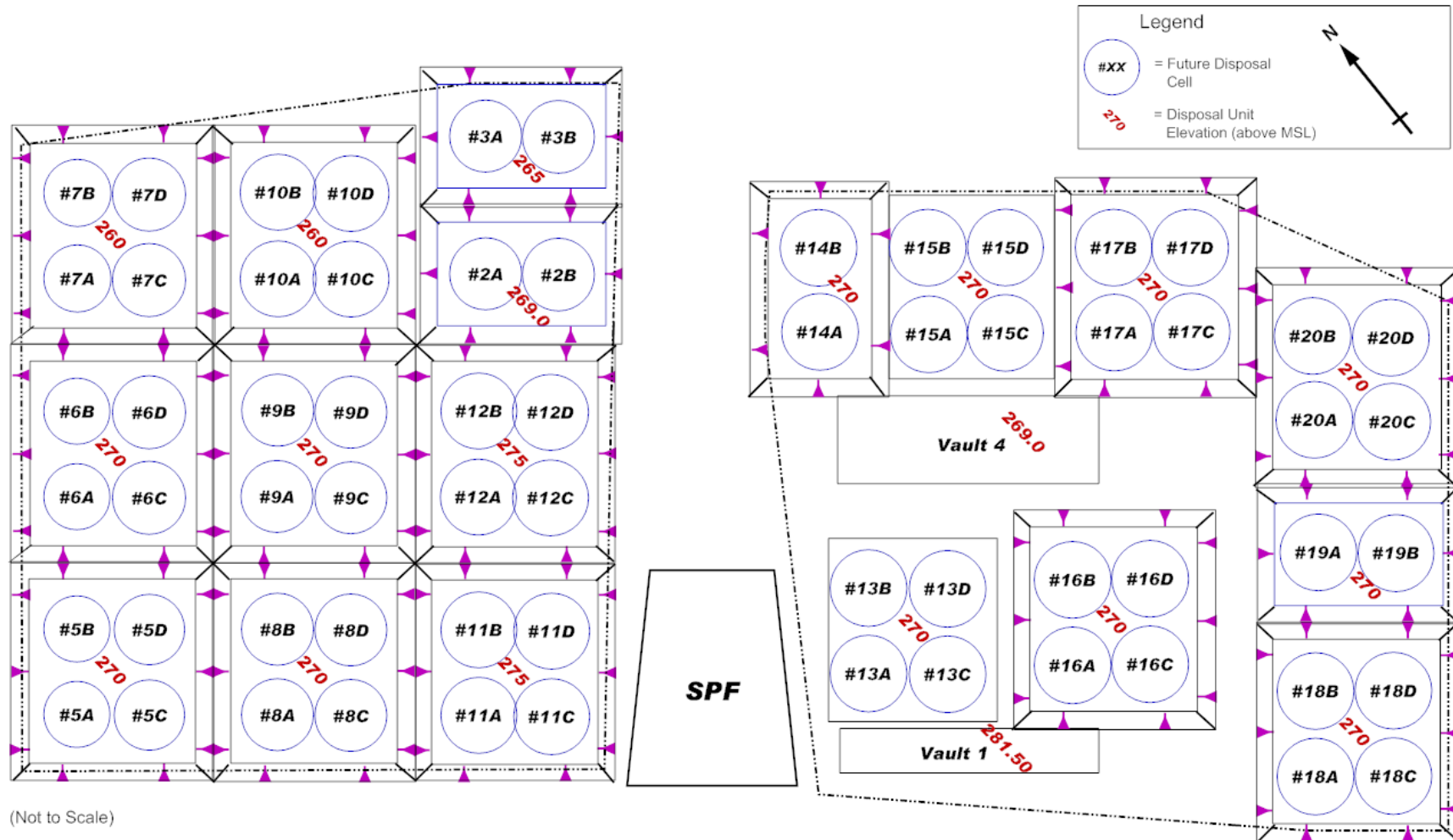


Figure 3.2-2: SDF Anticipated FDC Layout



Note: Figure presents the anticipated FDC locations, numbering of the units are placeholders and may not match the final disposal unit numbering.

3.2.1.1 Vault 1

Vault 1 is rectangular in shape and is divided into six equal individual cells. The walls and floor of the vault are reinforced concrete and designed for gravity loads. A rolling roof was originally installed on Vault 1, but has since been removed (see Figures 3.2-3 and 3.2-4). Cells A, B, and C have been filled with grout, clean capped, and the permanent roof sealed. Figure 3.2-3 shows Vault 1 prior to the construction of the permanent roof. Figure 3.2-4 shows Vault 1 conditions as of this document.

3.2.1.1.1 Vault 1 History

Construction on Vault 1 was completed in two phases; (1) the working slab, foundation, interior walls, and exterior walls, and (2) the permanent roof (only on cells that contain waste, Cells A, B and C). Vault 1 experienced cracks from construction and operational events dating back to 1988. Document ESH-WPG-2006-00132, *Z-Area Industrial Solid Waste Landfill Vault Cracking*, provides a history of the cracking experienced with Vault 1 and the repairs and remediation actions conducted to limit future weeping from the vault. The general mechanism for water weeping from the cracks in the Vault 1 walls stems from construction cracks and/or that of hydrostatic head exerting a force on the wall from the accumulation of water in the gap that forms between the saltstone monolith and the vault wall. The source of water within the gap was from rainwater intrusion and water resulting from the grout curing process and flush water from cleaning the transfer lines after a grout transfer into the vault. To limit further accumulation of rainwater in the gap between the saltstone monolith and the vault walls the following actions were taken, a foam sealant was installed in the gap between the vault roof and the wall; flashing was installed over the edge of the vault roof and wall; and an Ethylene-Propylene Diene Monomer (EPDM) membrane was applied over the entire roof surface. In addition, a polymer sealant was applied to the inside surface of the outside walls of the remaining cells to seal any shrinkage cracks developed during the saltstone curing process.

Environmental monitoring, discussed in Section 3.1.7.1, ensures the timely response to any potential impacts to the groundwater resulting from Vault 1 seepage.

3.2.1.1.2 Vault 1 Dimensions

Vault 1 is an above-grade, rectangular, reinforced concrete disposal unit. Vault 1 is approximately 600 feet long, 100 feet wide and 27 feet high. It is divided into two units each 100 feet x 300 feet, with a 3 inch separation gap between the units. Each unit is further divided into three cells of approximately 100 feet x 100 feet. The 100 foot dimension is taken from the centerline of 18 inch thick concrete walls; thus the interior dimensions of the cells are 98 feet - 6 inches. Thus, Vault 1 is comprised of six 100 feet x 100 feet cells. Figure 3.2-4 provides an exterior photograph of Vault 1, Figure 3.2-5 and Figure 3.2-6 provide plan and elevation view information for the disposal unit and Figure 3.2-7 provides a cross-section of the disposal unit (including the saltstone and clean grout cap).

The Vault 1 system filled with saltstone consists of the following from lowest elevation to highest elevation:

- Controlled compacted backfill soil base
- 4 inch thick, concrete working slab
- 2 foot thick, reinforced concrete, floor slab
- 18 inch thick, reinforced concrete walls
- 24 feet of saltstone poured into the cell from above
- Minimum 6 inch thick clean grout cap
- Poured-in-place concrete roof with approximately 2% slope
[W780625, C-CC-Z-0010, WSRC-STI-2006-00198]

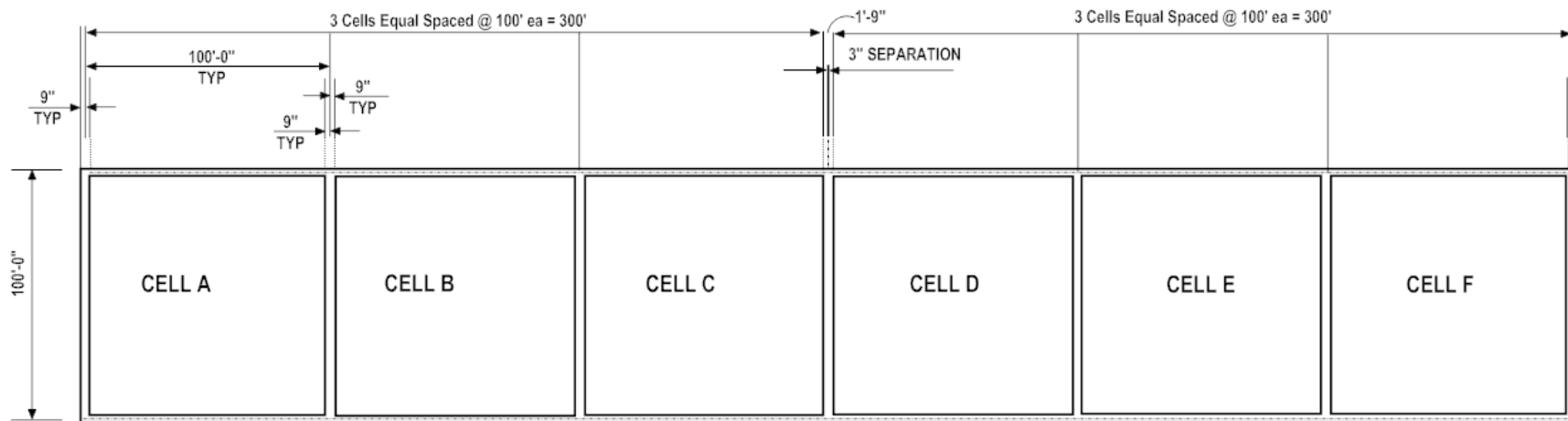
Figure 3.2-3: Vault 1 and Vault 4 Arrangement after Initial Construction



Figure 3.2-4: Vault 1 Photograph



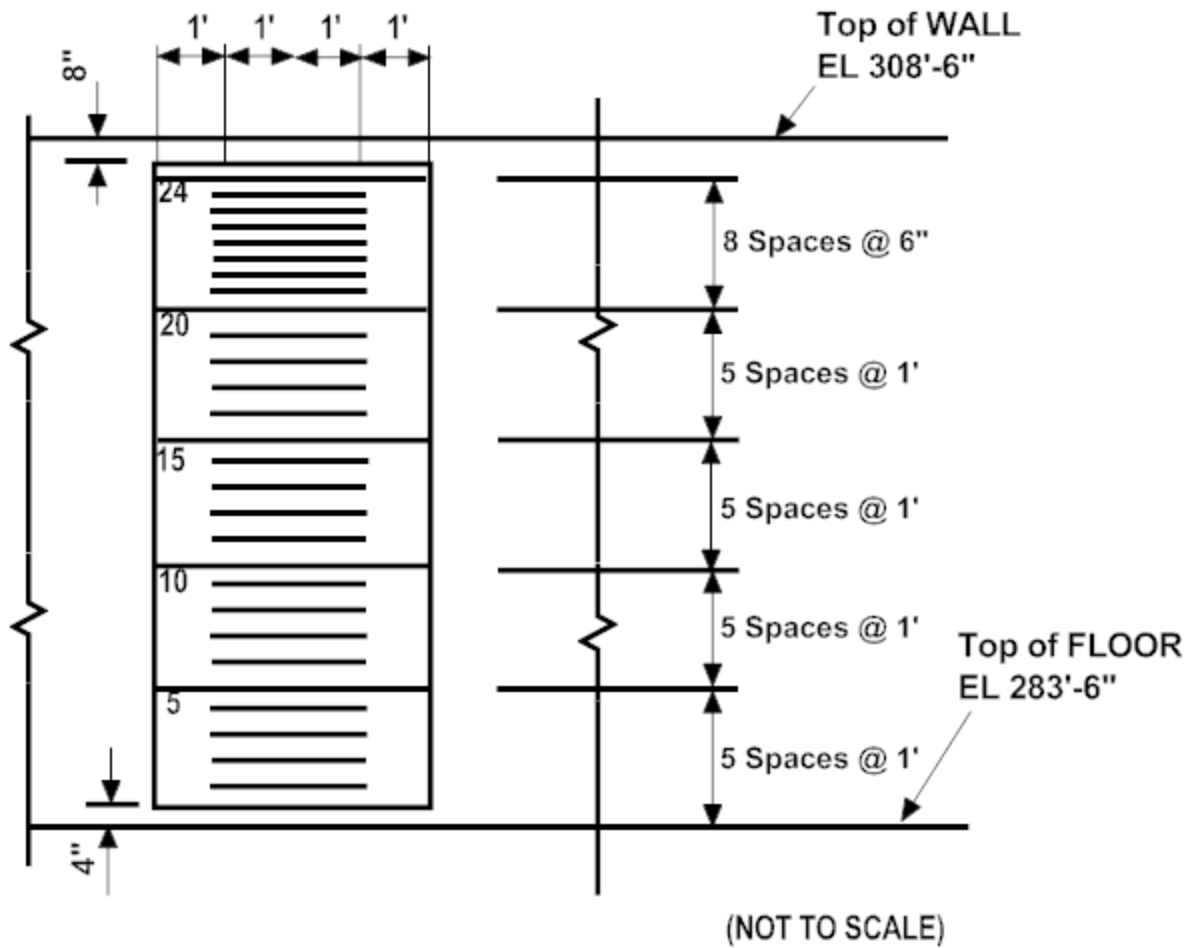
Figure 3.2-5: Vault 1 Plan View



(NOT TO SCALE)

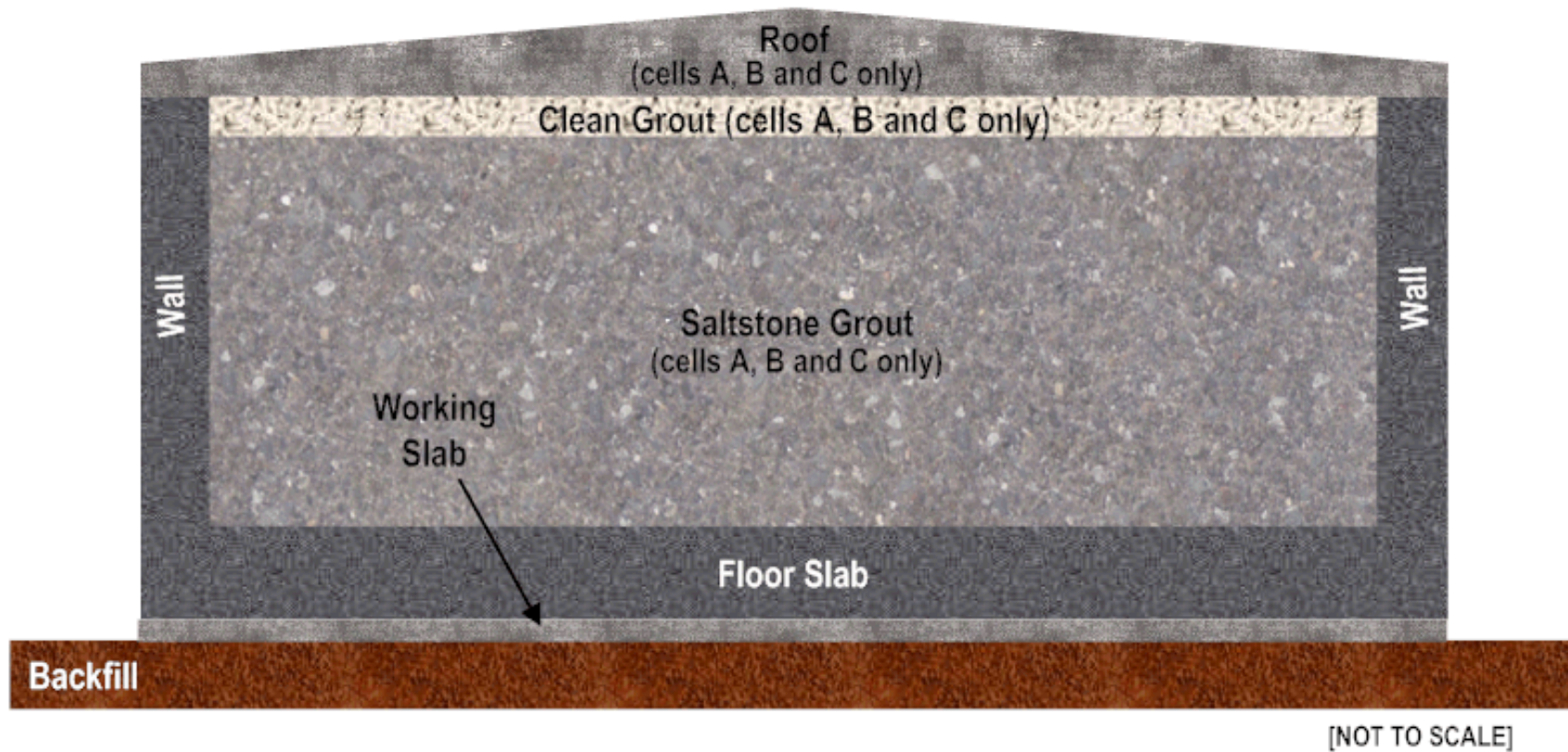
[W780625]

Figure 3.2-6: Vault 1 Interior Elevation Marks



[W780625]

Figure 3.2-7: Vault 1 Cross Section



3.2.1.1.3 Vault 1 Concrete Specification

The concrete mixes used in the foundation and walls of Vault 1 are listed in Table 3.2-1.

Table 3.2-1: Vault 1 Concrete Formulations

| Ingredient | Working Slab Quantity (lbs/yd³) | Floor Slab and Walls Quantity (lbs/yd³) | Roof Quantity (lbs/yd³) |
|--|---|---|---|
| Type II ASTM C 150 cement | 413 | 419 | 400 |
| Grade 120 ASTM C 989 Blast Furnace Slag | 0 | 278 | 0 |
| Type F ASTM C 618 Fly Ash | 73 | 0 | 70 |
| Sand (ASTM C 33) | 1,356 | 1,133 | 1,149 |
| No. 67 ASTM C 33 Aggregate (maximum 0.75 inches) | 1,698 | 1,798 | 1,900 |
| Water (maximum) | 272 | 268 | 292 |
| Water to Cementitious Material Ratio | 0.56 | 0.385 | 0.62 |
| Minimum Compressive Strength at 28 days | 2,000 psi | 4,000 psi | 3,000 psi |

[WSRC-STI-2006-00198]

3.2.1.1.4 Vault 1 Roof, Wall and Base

The Vault 1 roof has a minimum thickness of 6 inches and is poured-in-place concrete with approximately 2% slope. Cells A, B and C have been filled and the permanent roof installed. Cells D, E, and F contain no saltstone and have no roof (see Figure 3.2-4). The 18 inch thick walls, and 24 inch thick floor slab are reinforced concrete with a compressive strength of 4,000 psi. The working slab with a thickness of 4 inches has a compressive strength of 2,000 psi. [W780625]

3.2.1.2 Vault 4

3.2.1.2.1 Vault 4 History

The original construction on Vault 4 included the working slab, floor slab, exterior walls, and interior walls. This work was performed in 1988 and at that time the Vault 4 was referred to as Vaults 6 and 7. The walls and floor slab of the vault are of reinforced concrete construction. In 1996, Vault 4 was modified with a permanent roof prior to introduction of grout to provide operational flexibility; this allows for more than two partially filled cells at any one time and reduces potential rainwater intrusion. The permanent concrete roof was painted with a dura-cool coating for heat dissipation, not as a waterproof coating. The roof joints, however, allowed small amounts of rainwater to enter the vault cells and condensation associated with operation continues to occur. This resulted in wall cracking similar to that experienced in Vault 1. Therefore, joint sealing and cell draining was instituted to remediate the liquid accumulation. Figure 3.2-3 shows Vault 4 prior to the construction of permanent roof.

Cell A contains 10,000 drums of Fuel Material Facility (FMF) non-hazardous saltcrete generated from the operation of the Waste Water Treatment Facility (WWTF) at FMF. Cell A also contains the wooden pallets used in the movement of the FMF drums (one pallet to four drums). [ESH-FSS-9000373] The inventory associated with the waste and wooden pallets has been included in the Vault 4 inventory accounting in Section 3.3. The metal 55 gallon drums were completely filled with contaminated waste by combining the liquid FMF WWTF waste with dry concrete mix in a batch mixer and pouring into the drums. The void space in Cell A surrounding the drums is filled with clean grout.

Eight cells in Vault 4 have been modified with a drainage system designed to relieve the hydrostatic head on the vault walls. This sheet drain system (details in Section 3.2.1.2.5) will collect any liquid that may appear between the solidified grout and the vault wall, returning the liquid through pipes to the SPF to be used in the production of grout.

Environmental monitoring, discussed in Section 3.1.7.1, ensures the timely response to any potential impacts to the groundwater resulting from vault weepage.

3.2.1.2.2 Vault 4 Dimensions

Vault 4 is an above-grade, rectangular, reinforced concrete vault. It is approximately 600 feet long, 200 feet wide and 30 feet high. Vault 4 is divided into two units each, 200 feet x 300 feet, with a 3 inch separation gap between the units. Each unit is further divided into six cells of approximately 100 feet x 100 feet. Thus, Vault 4 is comprised of twelve 100 feet x 100 feet cells. The 100 foot dimension is taken from the centerline of 18 inch thick concrete walls; thus the interior dimensions of the cells are 98 feet - 6 inches. Figure 3.2-8 provides an exterior view of Vault 4, Figure 3.2-9 provides a roof plan view, and Figure 3.2-10 provides a cross section view (the saltstone and clean grout cap are not shown for clarity). [W828992, C-CC-Z-0013, WSRC-STI-2006-00198]

The Vault 4 system, when filled with saltstone consists of the following from lowest elevation to highest:

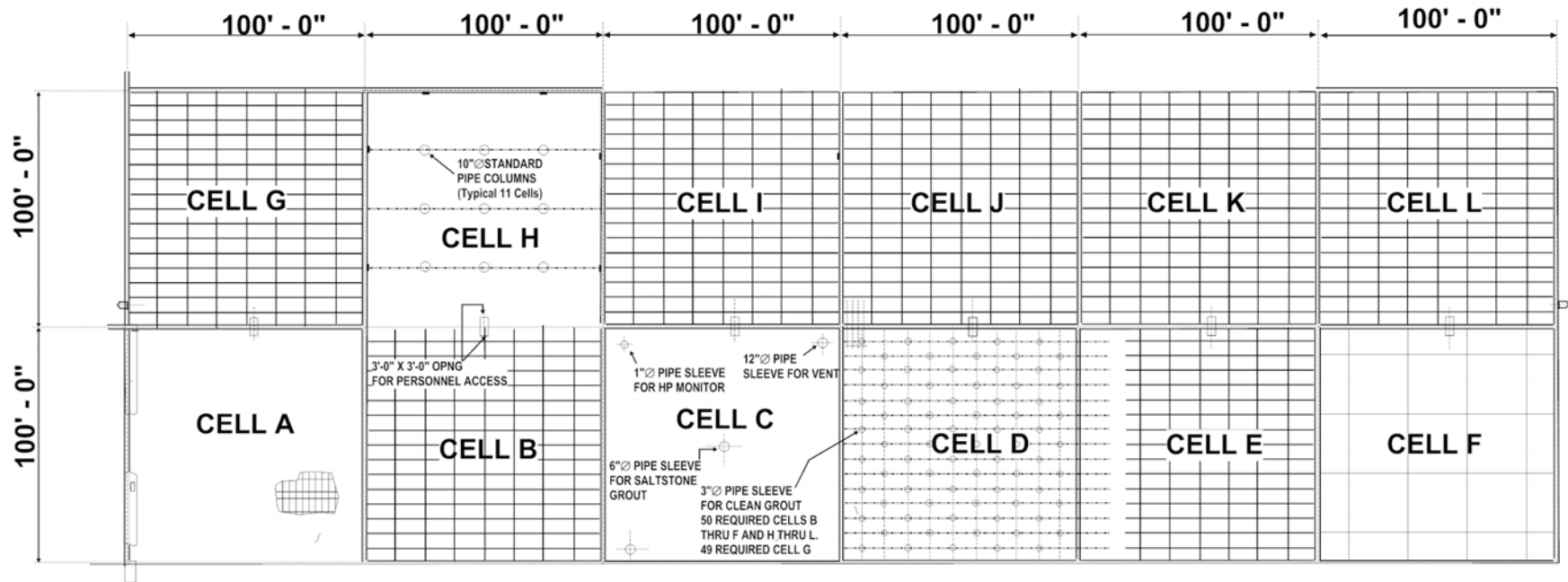
- Controlled compacted backfill soil base
- 4 inch thick, concrete working slab
- 2 foot thick reinforced concrete floor slab
- 18 inches thick, reinforced concrete walls
- 10 inch diameter roof support columns filled with lean concrete (except in Cell A)
- Sheet drain system (all cells except A, C, G and I)
- 24 feet - 9 inches (maximum) of saltstone, poured in from above (except Cell A)
- Drums of low-activity waste, encapsulated by clean grout (Cell A only)
- 15 inches thick clean grout cap (all cells)
- Poured-in-place concrete over steel decking roof with approximately 2% slope (except Cell A)
- Concrete encased wire mesh roof with approximately 2% slope (Cell A only)

[C-CC-Z-0013, C-CS-Z-0002, WSRC-STI-2006-00198, W828992, W828993]

Figure 3.2-8: Vault 4 Photograph



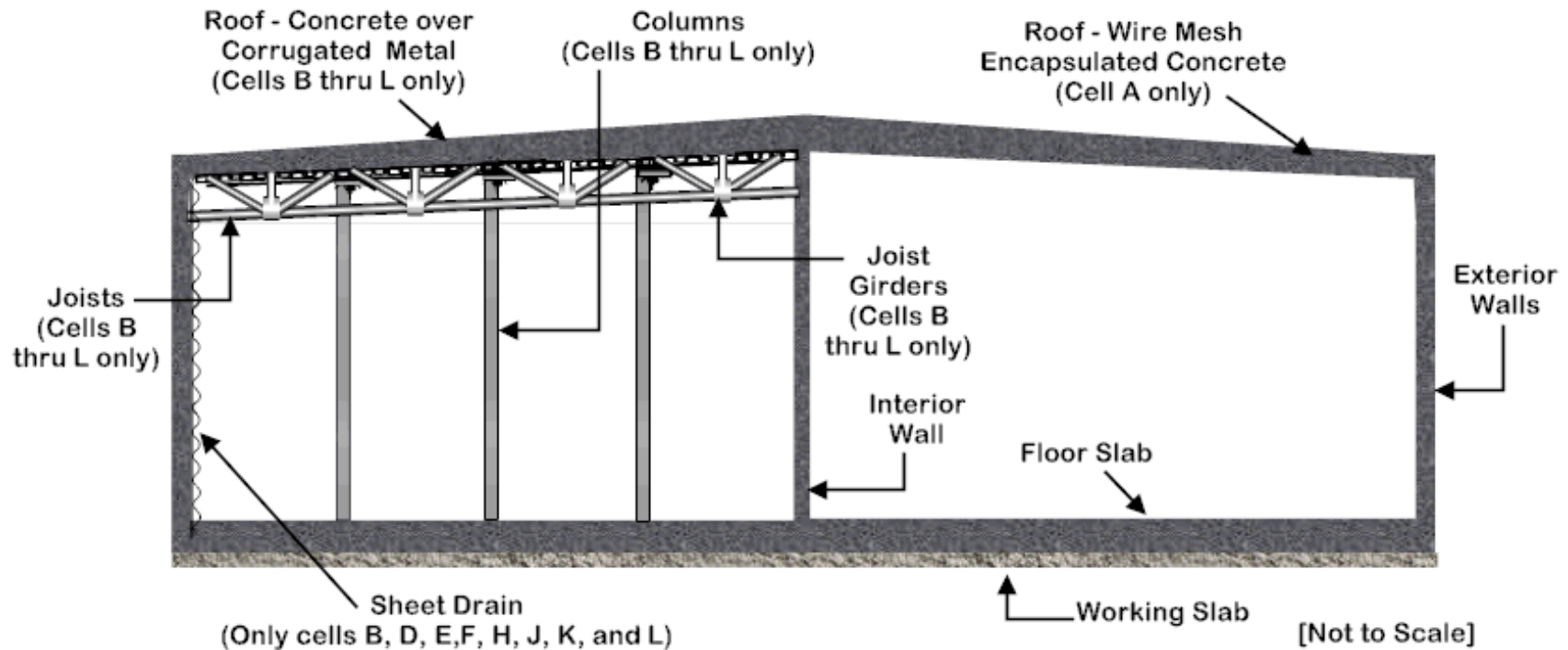
Figure 3.2-9: Vault 4 Roof Plan View



(NOT TO SCALE)

[C-CC-Z-0012]

Figure 3.2-10: Vault 4 Cross Section



Note: For clarity, roof and wall penetrations, drain lines and piping are not shown

[W828993, C-CC-Z-0012, C-CS-Z-0002]

3.2.1.2.3 Vault 4 Concrete Specification

The concrete mixes used in the working slab, floor slab, walls, and roof of Vault 4 are described in Table 3.2-2.

Table 3.2-2: Vault 4 Concrete Formulations

| Ingredient | Working Slab Quantity (lbs/yd³) | Floor Slab and Walls to 25 feet Quantity (lbs/yd³) | Walls above 25 feet and Roof (lbs/yd³) |
|--|---|--|--|
| Type II, ASTM C150 Cement | 413 | 419 | 466 |
| Grade 120, ASTM C 989 Blast Furnace Slag | 0 | 278 | 0 |
| Type F, ASTM C 618 Fly Ash | 73 | 0 | 62 |
| ASTM C 33 Sand | 1,356 | 1,133 | 1,190 |
| No. 67, ASTM C 33 Aggregate (maximum 0.75 inches) | 1,698 | 1,798 | 1,800 |
| Water (maximum) | 273 (32.7 gal) | 254 (30.4 gal) | 296 (35.5 gal) |
| Water to Cementitious Material Ratio | 0.56 | 0.36 | 0.56 |
| Minimum Compressive Strength at 28 days | 2,000 psi | 4,000 psi | 4,000 psi |

[SRNL-EST-2005-00105]

3.2.1.2.4 Vault 4 Walls, Columns, and Floor

The initial walls and floor slab of the vault are of reinforced concrete construction with the walls designed for gravity loads plus the hydrostatic head associated with the saltstone. The original wall height for Vault 4 was 25 feet. In 1996, the walls of the vault (exterior and interior) were extended 1 foot – 6 inches in height, to allow for the installation of a concrete roof. The exterior and interior vault walls are 1 foot – 6 inches thick.

Each Vault 4 cell contains two or three 1 inch diameter through-wall drain lines in the bottom of an exterior wall. Each cell also contains a 2 inch diameter, through-wall, schedule 40, stainless steel pipe through the exterior wall of Cells B, D, E, F, H, J, K, and L, in order to transfer the collected liquids from inside the cell to the SPF. Finally, partial penetrations exist in Vault 4 exterior walls from anchor bolts used for ladders, and pipe supports. [WSRC-STI-2006-00198]

Cells B through L each contain nine equally spaced roof support columns comprised of concrete-filled 10 inch diameter, schedule 40 carbon steel pipes (Figure 3.2-9 and Figure 3.2-11). [C-CS-Z-0002, C-CC-Z-0012] The floor is a 2 foot reinforced concrete slab which was placed on top of a separate 4 inch concrete working slab (see Table 3.2-2 for concrete formulations).

3.2.1.2.5 Vault 4 Sheet Drains

Cells B, D, E, F, H, J, K, and L have sheet drains (polystyrene sheet with 0.437 inch dimples covered on one side with a non-woven, needle-punched polypropylene filter fabric) installed on the walls to limit the build up of hydrostatic head by removing drainwater and condensate from the cells. Figure 3.2-10 depicts the sheet drains in Vault 4. [WSRC-STI-2006-00198]

The sheet drains were installed to mitigate potential cracking of the vault walls due to hydrostatic head created by drainwater. The sheet drain collects free water that accumulates in the narrow gap between the vault wall and the saltstone waste form. The sheet drain also acts as a barrier to keep water away from the wall. [WSRC-STI-2006-00198]

This drainwater collection system consists of the sheet drains placed against the vault walls and a polyvinyl chloride (PVC) piping system that collects the water for transfer back to SPF to be re-fed into the dry feeds mix to form grout. The drainwater collection system will be emptied, will be filled with grout, and will permanently remain in place within the vault after the operational period. [CBU-ENG-2003-00103]

3.2.1.2.6 Vault 4 Roof

Cell A of Vault 4 contains drums of low-activity waste that have been filled with concrete grout and covered with a roof comprised of wire mesh and a 3 inch concrete topping. At least 15 inches of clean concrete grout exists between the waste drums and the concrete topping below the top of the cell. [C-CC-Z-0012]

The remaining cells in Vault 4 are covered with a sloped (approximately 2%), permanent roof consisting of 6 inch thick poured-in-place concrete over 20 gauge corrugated metal, supported by steel joists and 10 inch diameter standard pipe columns filled with lean

concrete. The roof is painted with a dura-cool coating to help heat dissipation. [C-CS-Z-0002]

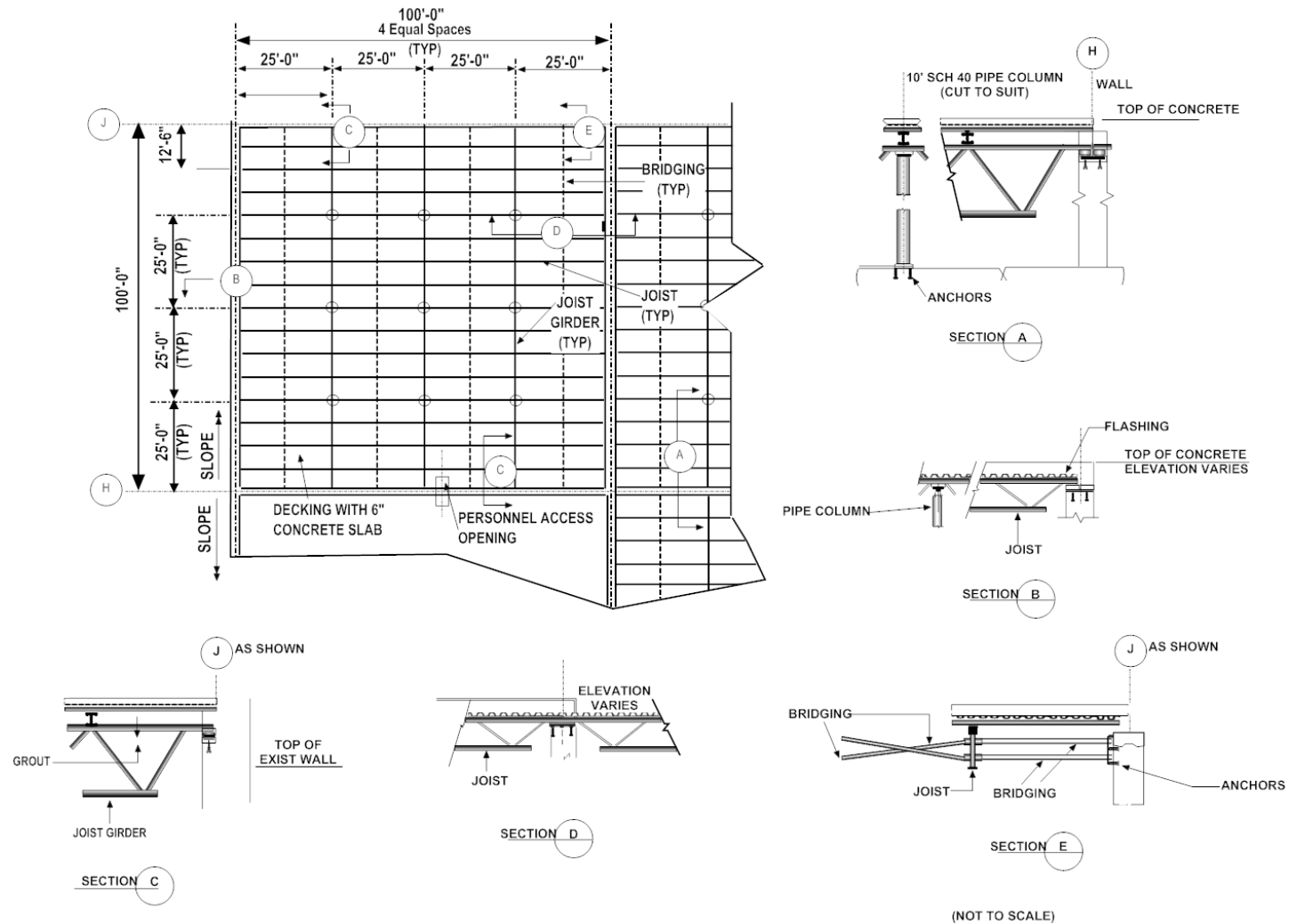
The design includes fifty, 3 inch pipes that penetrate the roof of each cell, except Cell A. These pipes provide capped ports for pouring clean grout into the cell. The pipes are evenly spaced across the roof, allowing complete coverage of the cell. Each pipe will be filled with grout and capped when the cell is closed. The grouting and capping process will be designed and installed to prevent these 50 penetrations from becoming a potential flow path in the future. Figures 3.2-9 and Figure 3.2-11 show details related to the Vault 4 roof. Figure 3.2-12 is a photograph of the interior of the Vault 4 roof. [C-CS-Z-0002]

Vault 4 contains the following penetrations in the roof of each cell, except for Cell A whose roof contains no penetrations:

- Fifty, 3 inch diameter pipe sleeves per cell for the clean cap pour (49 in cell G)
- Two, 12 inch diameter pipe sleeves per cell for venting
- One, 6 inch diameter pipe sleeve per cell for pouring saltstone
- One, 3 foot x 3 foot personnel/camera access opening per cell
- One, 1 inch diameter pipe sleeve per cell for radiological monitoring

[C-CS-Z-0002]

Figure 3.2-11: Vault 4 Permanent Roof Plan Details (Cells B through L)



[C-CS-Z-0002]

Figure 3.2-12: Interior View of Vault 4 Roof



3.2.1.3 *Disposal Unit 2 and FDCs*

3.2.1.3.1 Future Disposal Cell Design Information

FDCs will be constructed in Z-Area, and the projected locations are presented in Figure 3.1-5. The design details for FDCs are projected to be the same as Disposal Unit 2, which is currently under construction. Cone penetration tests, geotechnical boreholes, test pits, and laboratory testing were performed at the footprint of Disposal Unit 2 to a depth of over 100 feet below the surface. Subsurface conditions were characterized and soil properties were determined using site-specific data as well as existing data from surrounding areas. [WSP-SSF-2005-00023] Seismic stability analyses have been conducted for the Disposal Unit 2 site and are documented in K-ESR-Z-00001. Figure 3.2-13 is a photograph of a concrete tank similar in design to Disposal Unit 2.

Figure 3.2-13: Vendor Example of Cylindrical, FDC Type Tank



[www.dutchlandinc.com/product_pages/circulair_5_lewistown.html]

Disposal Unit 2 basic construction design is to be Class III sulfate resistant concrete floor slab, upper mud mat, and pre-stressed Class III sulfate resistant concrete walls. The main components of the pre-stressed walls are to consist of pre-cast panels of Class III sulfate resistant concrete mix, a steel shell diaphragm, reinforcing bars, pre-stressing wires, and Type II shotcrete fill. The disposal unit is to include a carbon steel diaphragm of 26 gauge (0.179 inch) thickness in association with the prefabricated concrete panels (core walls), which will be sealed mechanically between panels, with no welding involved. The diaphragm has been designed to help prevent water seepage out of the concrete disposal unit over the life of typical concrete water storage tanks. The water tight attribute is seen as a superior design feature over the Vault 1 and Vault 4 designs. The steel diaphragm is to have no horizontal joints. Vertical reinforcing bars will be installed to resist bending moments, shrinkage, and temperature stresses. High strength pre-stressing wires are to be installed around the disposal unit and then tightened to design specifications. The disposal unit wall pre-stressing is designed to carry the hydraulic load and to help facilitate the walls being in compression. Shotcrete is to be used during various stages of the disposal unit construction to protect the reinforcing bars and pre-stressing wires. The reinforcing steel, pre-stressing wire, and steel shell diaphragm are all to be of carbon steel construction. [WB00001K-004]

3.2.1.3.2 Future Disposal Cell Expected Dimensions

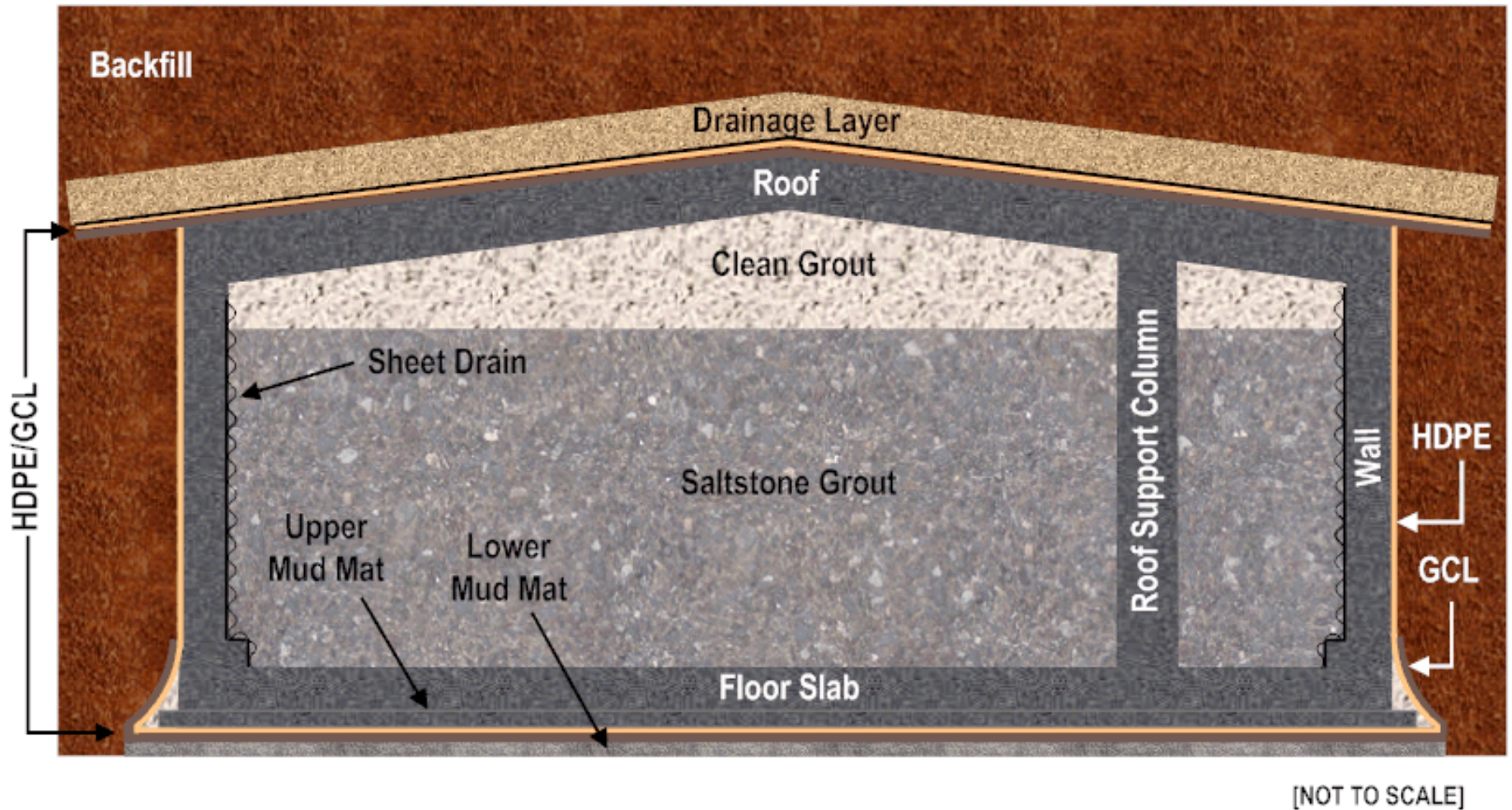
The design details for FDCs are projected to be the same as Disposal Unit 2 currently under construction. Disposal Unit 2 design consists of two identical cells, Cell 2A and 2B. The diameter of both cells is to be 150 feet, with an interior height of 22 feet (this height will increase to 23.5 feet at the center of the cell). The cylindrical, reinforced concrete cell will be constructed below grade to the roof (additional information can be found in Section 3.2.1.3.1). The location of the cell had been prepared at the time of the SDF PA issuance by excavating, and then stockpiling the native soil to be used as backfill around the completed cell. [C-CG-Z-00030]

Each FDC is to consist of the following:

- Controlled compacted backfill soil base.
- 4 inch thick lower concrete mud-mat. [WB00001K-004]
- Geosynthetic Clay Liner (GCL) consisting of a minimum 0.75 lbs/ft² sodium bentonite covered by a 100 mil High Density Polyethylene (HDPE) liner above the lower mud-mat. [WB00001K-004, C-SPP-Z-00006, Sections 02378 and 02379, WSP-SSF-2005-00023]
- 4 inch thick upper mud-mat of Class III sulfate resistant concrete. [WB00001K-004, WSP-SSF-2005-00023]
- Minimum 8 inch thick cast-in-place floor slab of Class III sulfate resistant concrete. [WB00001K-004, WSP-SSF-2005-00023]
- Minimum 8 inch thick pre-cast walls of Class III sulfate resistant concrete. [WB00001K-004, WSP-SSF-2005-00023]
- Shotcrete placed on the exterior of the walls to cover the reinforcing bar and the layers of prestressing wire. The shotcrete thickness ranges from more than 5 inches to approximately 1.5 inches with an average thickness of approximately 2.3 inches. [WB00001K-004]
- The exterior side of the walls covered with a 100 mil HDPE geomembrane. [WB00001K-004]
- 48 roof support columns of Class III sulfate resistant concrete, 14 inch diameter, with a typical spacing of approximately 20 foot centers. [WB00001K-004]
- Maximum 20 feet of saltstone or other cementitious waste form poured into the disposal unit through a roof penetration. [WSRC-STI-2006-00198]
- Minimum of 2 feet, clean non-radioactive grout cap layer poured into the disposal unit through roof penetrations to fill between the saltstone and roof. [WSRC-STI-2006-00198]
- Minimum 8 inch thick roof of Class III sulfate resistant concrete with a minimum 2% slope (in place prior to the saltstone pour). [WB00001K-004]
- Roof penetrations will exist for personnel access, ventilation, sheet drain, thermocouple trees, monitoring (temperature and cameras), and saltstone (or other cementitious waste form) pouring. [WB00001K-004, C-CH-Z-00014]

Figure 3.2-14 provides the expected, typical cross-section of a FDC. [WB00001K-004]

Figure 3.2-14: Future Disposal Cell Cross-Section



Note: For clarity, roof penetrations are not shown, please refer to Figure 3.2-16 for the roof plan.

3.2.1.3.3 Future Disposal Cell Concrete Specification

The waste stream to be disposed of in the FDCs will be high in sulfates, which can attack hardened concrete. Due to this high sulfate nature the FDCs upper mud mat, floor slab, walls, and roof are to be constructed with a Class III sulfate resistant concrete mix. This concrete mix is designed to retard the ingress and movement of water. Pozzolans and slag are to be added to the cement to reduce the water to cementitious materials ratio. This will also help reduce the saturated hydraulic conductivity of the concrete. In addition, the walls are to be constructed with wire pre-stressing and the exterior is to be backfilled allowing for the walls to be under compression, further minimizing water penetration into the walls. Table 3.2-3 presents a suitable FDC concrete mix formula. [SRNL-STI-2008-00421]

The concrete attributes important to the SDF FDC are:

- Low hydraulic conductivity
- High pH
- Low E_h
- High degradation resistance
- High sulfate attack resistance

Recent concrete studies examined two potential FDC concrete mixes. [SRNL-STI-2008-00421] Both mixes produced acceptable results for use as FDC concrete. It is expected that further concrete mix testing will be conducted during the operational phase of the SDF. It is expected that continued studies and testing, may develop alternative FDC concrete mixes with the important attributes listed above (see Section 8.2).

Table 3.2-3: Future Disposal Cell Tested Concrete Mix

| Ingredient | Material Quantity (lbs/yd³) |
|--|---|
| Type V cement (Lehigh T-V #2 ; ASTM C 150) | 213 |
| Grade 100 Blast furnace slag (Holcim Grade 100 Slag; ASTM C 989) | 284 |
| Silica Fume (W. R. Grace Silica Fume; ASTM C 1240) | 47.3 |
| Type F Fly ash (SEFA Group, Class "F" Fly Ash; ASTM C 618) | 165.7 |
| Sand (Natural Washed Sand; ASTM C 33) | 911 |
| Aggregate (#67 Granite; ASTM C 33) | 1850 |
| Water (maximum; gal/yd ³) | 32.3 |
| Maximum water to cementitious material ratio | 0.38 |
| Grace WRDA 35 (oz/cwt c+p) | 5 |
| Grace Darex II (oz/cwt c+p) | 0.4 to 0.5 |
| Grace Adva 380 (oz/cwt c+p) | 3 to 4 |

[SRNL-STI-2008-00421]

3.2.1.3.4 Future Disposal Cell Roof

The roof will be designed to be formed and poured in place using Class III sulfate resistant concrete with a minimum thickness of 8 inches. The roof will be poured over 20 gauge corrugated metal supported by steel joists. The roof will be constructed with a minimum slope of 2% to allow adequate storm water runoff. Figures 3.2-15 and Figure 3.2-16 depict additional details regarding the roof.

Roof penetrations will be available for ventilation, sheet drain, thermocouple trees, closed circuit television, and grout poring. The penetrations will be steel pipes, except for the sheet drain, which will be chlorinated PVC. Figure 3.2-16 depicts a typical roof plan for the FDCs showing many of the penetrations, for details see WB00001K-004. The roof penetrations will be sealed in a manner to prevent rain infiltration using neoprene gasket material. After the FDC is filled, the roof mounted items will be removed and the penetrations will be filled in a manner that makes them equivalent to the rest of the roof specifications. The GCL-HDPE liner system will be extended over the roof prior to installation of the closure cap.

3.2.1.3.5 Future Disposal Cell Walls and Columns

The walls are designed to be constructed of pre-cast Class III sulfate resistant concrete panels with a minimum thickness of 8 inches. Wall joints are to be sealed using Class III sulfate resistant concrete mix. There are to be no wall or floor penetrations. Figure 3.2-17 depicts the wall design details.

A continuous, steel shell diaphragm is designed to be installed surrounding the pre-cast concrete panels. The steel shell wall joints are to be sealed watertight by injecting with a polysulfide material from the bottom to the top. Pre-stressing wires are to be installed around the circumference of the disposal unit wall. The pre-stressing wires are to be covered with shotcrete for protection as described in Section 3.2.1.3.2.

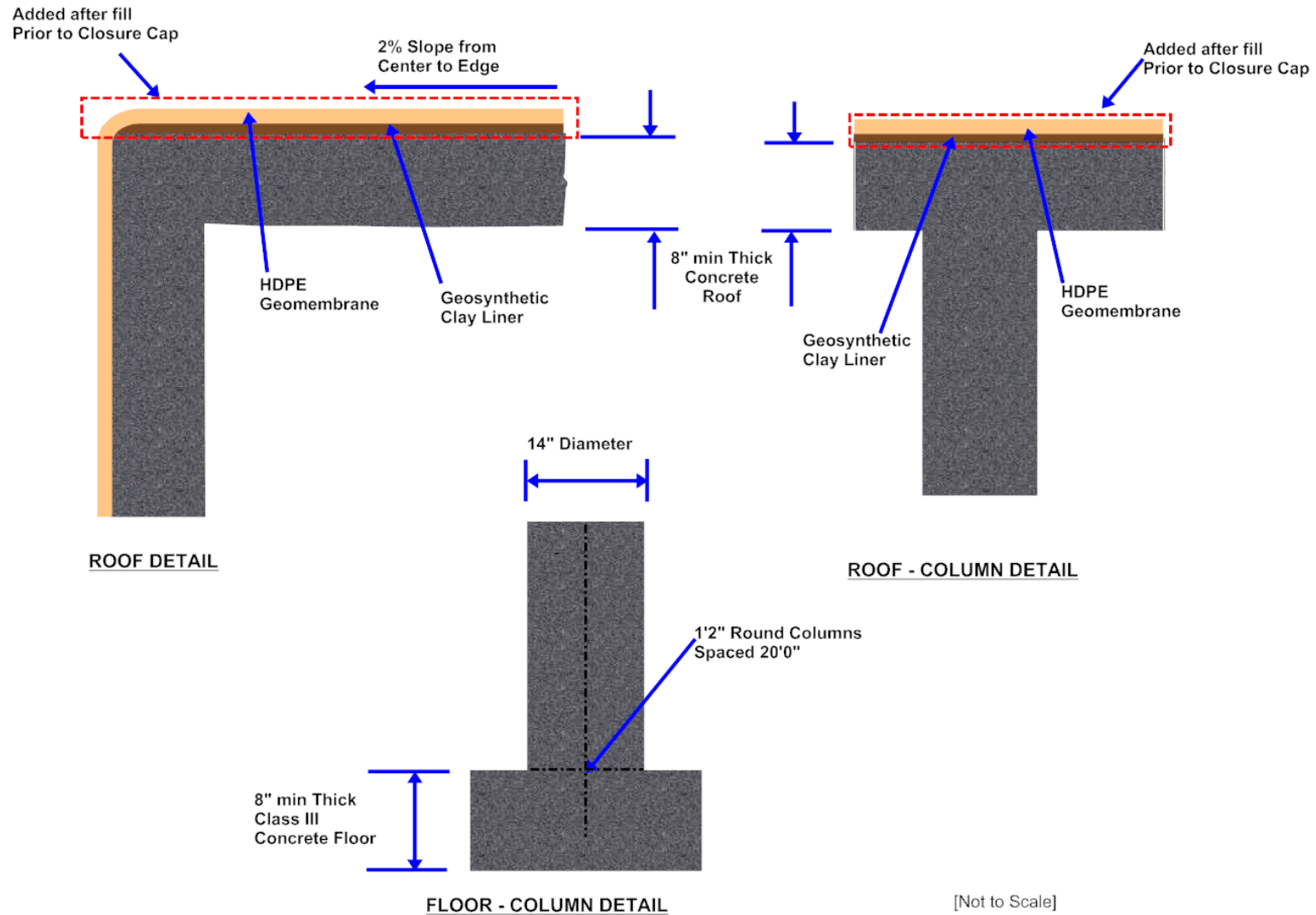
The HDPE-GCL liner system designed to be beneath the disposal unit's upper mud mat is to be hermetically sealed to an identical liner system surrounding the walls (see Section 3.2.1.3.6 for addition details on floor design). This HDPE liner design will extend the entire height of the disposal unit, while the GCL will extend to a height of approximately 2 feet above the upper mud mat. The design for the HDPE-GCL has the installation resuming on the roof. Figures 3.2-15 and Figure 3.2-17 depict the liner system on the walls and the roof. [C-SPP-Z-00006]

Each FDC is designed with 48 columns to support the roof. Typical column spacing is expected to be approximately at 20 foot centers. The anticipated typical construction is shown on Figure 3.2-15.

All FDCs are designed to have sheet drains (polystyrene sheet with 0.437 inch dimples covered on one side with a non-woven, needle-punched polypropylene filter fabric) installed on the walls. These are to be installed to mitigate potential cracking of the FDC by limiting the build up of hydrostatic head created by drainwater on the walls. The sheet drain collects free water that accumulates in the narrow gap between the FDC wall and the saltstone waste form. Additionally, it acts as barrier to keep water away from the wall. [WSRC-STI-2006-00198]

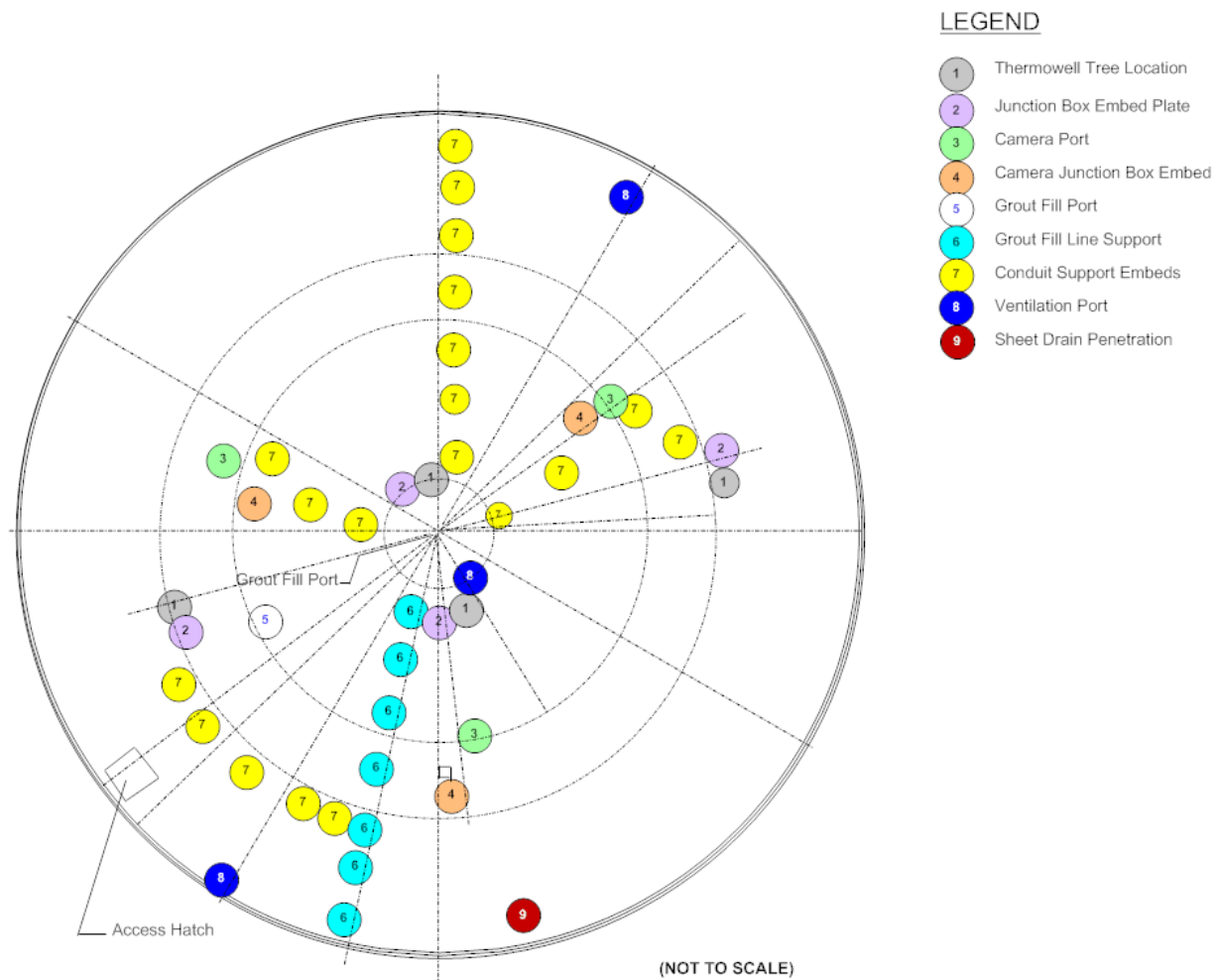
The drainwater collection system design consists of the sheet drains and a PVC piping system that collects the water for transfer back to the process via a roof penetration (shown in Figure 3.2-16) to be re-fed into the dry feeds mix to form grout. The drainwater collection system will be emptied, will be filled with grout, and will permanently remain in place within the vault after the operational period. [CBU-ENG-2003-00103]

Figure 3.2-15: Future Disposal Cell Roof-Column Detail



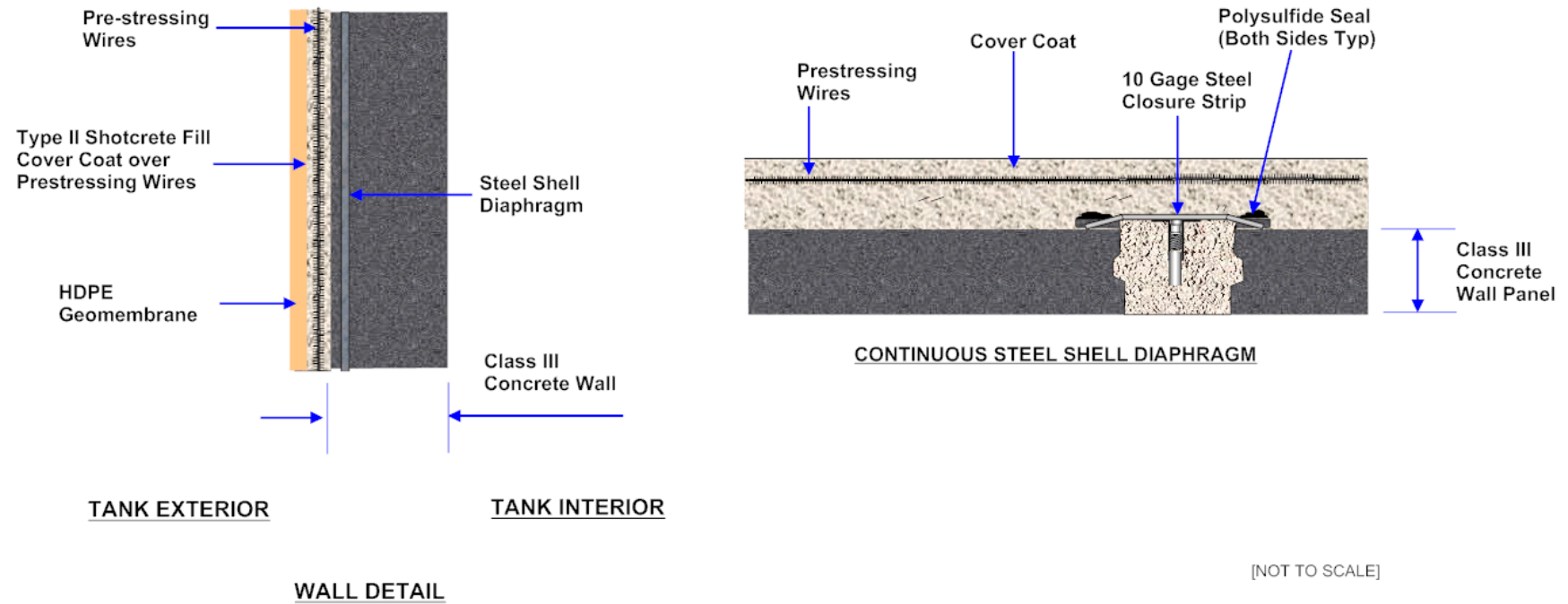
[WB00001K-004, WSRC-STI-2008-00244, C-SPP-Z-00006]

Figure 3.2-16: Roof Plan for Future Disposal Cell (Typical)



Note: Not all penetrations are shown.
[WB00001K-004, C-CH-Z-00014]

Figure 3.2-17: Future Disposal Cell Wall Detail



[WB00001K-004

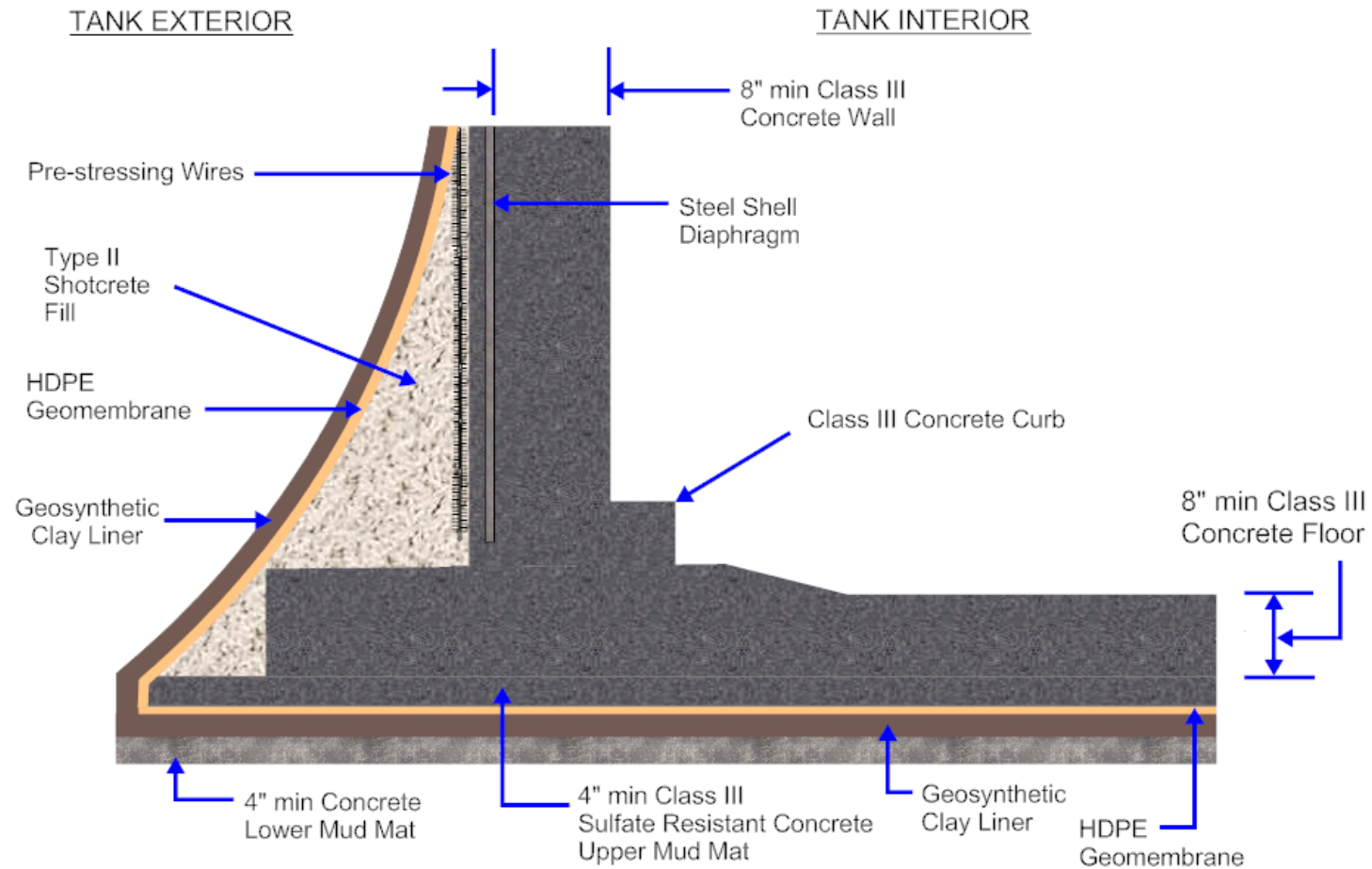
3.2.1.3.6 Future Disposal Cell Floor

The existing grade will be excavated for the base layers. The base layers will consist of the components as shown in Figure 3.2-18.

There will be two circular concrete mud mats, upper and lower, each with a thickness of 4 inches. The lower mud mat will be constructed on the (excavated) compacted grade. A GCL will be installed over the lower mud mat. The GCL will consist of “bentonite sandwiched between two geotextiles.” Bentonite, the hydraulically functional portion of a GCL, is the general term given to swelling type montmorillonite clay which formed as the stable alteration product of volcanic ash. Bentonite is expected to remain mineralogically and chemically stable. A 100 mil HDPE liner with hermetically sealed joints will be installed above of the GCL. The upper mud mat with a minimum thickness of 4 inches consisting of Class III sulfate resistant concrete will be poured on top of the GCL-HDPE in order to protect the GCL-HDPE during construction. A circular Class III sulfate resistant concrete mix concrete floor slab will be poured in place with a minimum thickness of 8 inches. The disposal units concrete, in conjunction with the encasing HDPE geomembrane form a composite advective and diffusive barrier to contaminant migration. [WB00001K-004, WSP-SSF-2005-00023, C-SPP-Z-00006]

Figure 3.2-19 is a photograph of the placement of the lower mud mat prior to the installation of the GCL for Disposal Unit 2A/2B, currently under construction. It is expected to be typical for FDCs.

Figure 3.2-18: Future Disposal Cell Base Details



[WB00001K-004, C-SPP-Z-000006]

**Figure 3.2-19: Placement of Lower Mud Mat for Disposal Unit 2 During Construction
(Typical for FDCs)**



3.2.1.3.7 Future Disposal Cell Interior Coating

An evaluation has been conducted on potential interior coating and lining options and is provided in WSRC-TR-2008-00090, *Saltstone Vault #2 Interior Lining Review*. The use of a coating will be to mitigate sulfate attack from short-term saltstone bleed water penetration (through surface cracks and by capillary suction) and diffusion of sulfate from the pore fluid of the cured saltstone. The sulfates are inherent in the salt solution waste stream that is mixed with dry materials to form grout by the SPF. For the service conditions anticipated, the evaluation recommends a mat-reinforced epoxy-novolac thermosetting lining. Flexible or elastomeric coatings such as flexible epoxies, polyureas and polyurethanes cannot be recommended at this time, primarily due to concern over chemical degradation at peak temperatures as well as lower radiation resistance. However, these may be options for FDCs with lower radioactivity levels or thermal conditions, or if more flexible systems are required. The evaluation has concluded that under the anticipated conditions, mat-reinforced thermosetting polymer linings are expected to maintain high integrity during initial disposal unit operations and for the first 50 to 100 years of service, after which protection is not assumed. This is based on several assumptions including, limited oxidation, gradual temperature decline, tolerable radiation dose with minimal dose rate effects, minimal differential settlement, and proper installation. [WSRC-TR-2008-00090] Because a two foot

clean group cap is to be placed over the saltstone, the concentration of sulfate that would diffuse to the roof is reduced. Therefore, a coating/barrier is not anticipated for the roof. [WSRC-TR-2008-00090]

Modeling will consider the effects of the coating on material degradation but a coating layer is not depicted in the physical model. [WSRC-TR-2008-00090]

3.2.1.4 Grout Transfer Lines

A grout line will be installed from the SPF to the disposal units. Appropriate pipe supports and shielding will be installed along the grout line run. The grout line will be equipped with a three-way valve that will allow the grout to be pumped to Cell A or B. In order to avoid the interference with the shielding, the three-way valve handle will be positioned in the field. The grout line shielding requirements may be revised for future designs based on waste concentrations. Since the grout lines will be cleaned and/or removed prior to area closure, they are not included in the model. [WSP-SSF-2005-00023]

3.2.2 Conceptual Closure Cap

An engineered closure cap will be installed over the SDF following the closure of the final disposal unit. The closure cap description is based on an SRNL report (WSRC-STI-2008-00244) concerning the SDF closure cap concept and estimated initial infiltration. The closure cap design and infiltration information is preliminary and conceptual in nature, being consistent with a scoping level concept. However, it does provide sufficient information for planning purposes, to evaluate the closure cap configuration relative to its constructability and functionality, and to estimate infiltration over time through modeling. It is not intended to constitute final design. Final design and a re-evaluation of infiltration will be performed near the end of the operational period. Technological advances, increased knowledge, and improved modeling capabilities are all likely prior to closure and will result in improvements in both the final closure cap design and infiltration estimates. [WSRC-STI-2008-00244]

3.2.2.1 Closure Cap Background

The SDF closure cap is primarily intended to provide physical stabilization of the site, minimize infiltration, and provide an intruder deterrent. Two closure caps are anticipated to be constructed over the SDF disposal units at the end of the operational period. The operational period is that period of time during which waste will be mixed with grout and placed in the disposal units and the disposal units will be topped off with clean grout. During the operational period, active SDF facility maintenance sufficient to prevent both infiltration of rainwater into the disposal units and subsurface discharge out of the disposal units is assumed. After installation of the closure cap, a 100 year institutional control period is assumed to begin, during which active SDF maintenance will be conducted sufficient to prevent pine forest succession and to repair any significant erosion. After the institutional control period, a 10,000 year post-closure performance period is assumed to begin, during which no active SDF maintenance will be conducted. Degradation of the closure cap will accelerate once active SDF maintenance has ceased. [WSRC-STI-2008-00244]

3.2.2.2 *Scoping Level Evaluation*

An evaluation of the SDF closure cap layout was conducted in order to determine the maximum slope length that should be considered for the conceptual closure cap physical stability and for determination of the infiltration through the closure cap. Current case scenarios reflect the results of the evaluation. [WSRC-STI-2008-00244]

3.2.2.3 *Closure Cap Layout Scenario*

The initial closure cap layout evaluated was a “C”-shaped closure cap covering the northern and southern disposal unit areas, with the hollow of the “C” in the process buildings area. The larger, northern area was used to determine that the most likely construction scenario, including a cap with longest slopes running to the northeast and southwest from a central northwest-southeast oriented peak. The longest cap surface-slopes were estimated at 825 feet, with the length of the peak, or cap apex, of 1,380 feet. The cap for the southern disposal unit area was not anticipated to be any larger than that of the northern area, so infiltration for a second cap would be expected to be no greater than the scenario modeled herein. [WSRC-STI-2008-00244]

Upon completion of a detailed cap configuration drawing based on the earlier C-shaped configuration, it was determined that relocating some of the anticipated disposal unit locations would allow both the previously assumed maximum 825 foot surface slope length and a more functional drainage system. The current conceptual design includes two distinct closure caps over the north and south groupings of disposal units as depicted in Figure 3.2-2.

3.2.2.4 *Physical Stability Requirements*

Calculations have been made in order to determine closure cap requirements for physical stability. Stability calculations for the following key components of the closure cap are provided in detail in WSRC-STI-2008-00244:

- Vegetative soil cover
- Erosion barrier
- Side slope
- Toe of the side slope

The calculations resulted in the following conclusions:

- A 1.5% slope over an 825 feet slope length for the vegetative soil cover is considered physically stable (i.e., prevents the initiation of gully during a probable maximum precipitation (PMP) event). Maximum acceptable slopes for portions of the closure cap with slope lengths less than 825 feet may be greater than 1.5%, if determined they are physically stable during the actual closure cap design process.
- An erosion barrier consisting of 12 inches thick riprap with a D_{50} (median size) of 2.5 inches on a 825 feet long, 1.5% slope is considered physically stable (i.e., prevents any riprap movement during a PMP event). Based upon the D_{50} of 2.5 inches, rock consistent with type B riprap from Table F-3 of NUREG-1623 or size R-20 riprap from Table 1 of ASTM D 6092-97 is suitable for use in the erosion barrier.
- Side slope riprap that is 24 inches thick with a D_{50} (median size) of 10.1 inches on a 300 feet long, 33.3% slope receiving drainage from a 825 feet long, 1.5% slope is

considered physically stable (i.e., prevents any riprap movement during a PMP event). Based upon the D_{50} of 10.1 inches, rock consistent with type D riprap from Table F-3 of NUREG-1623 or size R-150 riprap from Table 1 of ASTM D 6092-97 is suitable for use on the side slopes.

- Toe of the side slope riprap that is 42 inches thick, extends out 20 feet from the side slope, and has a D_{50} (median size) of 12.82 inches is considered physically stable (i.e., prevents any riprap movement due to receiving runoff from the 1.5%, 825 feet top slope and 33.3%, 300 feet side slope during a PMP event). Based upon the D_{50} of 12.82 inches, rock consistent with type D riprap from Table F-3 of NUREG-1623 or size R-300 riprap from Table 1 of ASTM D 6092-97 is suitable for use on the toe.

Erosion barrier, side slope, and toe riprap size may be smaller for portions of the closure cap with shorter slope lengths than those used to determine the requirements outlined above, if it is determined that the smaller sized riprap is stable under a PMP event during the actual closure cap design process. [WSRC-STI-2008-00244]

3.2.2.5 Conceptual Closure Cap General Design Features

It is anticipated that the SDF closure cap will consist of the layers outlined in Table 3.2-4 and depicted from top to bottom on Figure 3.2-20. Table 3.2-5 provides an overview of the function of each of these layers. Figure 3.2-21 illustrates the significant features associated with the conceptual design of the side slope and toe of the conceptual SDF closure cap evaluated in WSRC-STI-2008-00244. Cross sectional views of the conceptual SDF closure cap are provided in WSRC-STI-2008-00244.

Table 3.2-4: Generic SDF Conceptual Closure Cap Layers

| Layer ¹ | Layer Thickness (in) |
|---|---|
| Vegetative Cover | N/A |
| Topsoil | 6 |
| Upper Backfill | 30 |
| Erosion Barrier | 12 |
| Geotextile Fabric | NC |
| Middle Backfill | 12 (minimum, will increase from cap apex to toe due to difference between surface slope and upper drainage layer slope) |
| Geotextile Filter Fabric | 0.1 (minimum) |
| Upper Lateral Drainage Layer | 12 |
| Geotextile Fabric | NC |
| HDPE Geomembrane | 0.06 (60 mil) |
| Geosynthetic Clay Liner | 0.2 |
| Foundation Layer (backfill with bentonite admix) | 12 |
| Lower Backfill Layer | 12 (minimum, will increase from cap toe to apex due to upper drainage layer slope) |
| Geotextile Filter Fabric ² | NC |
| Lower Drainage Layer, extends approximately 25-ft from disposal unit ² | 24 |
| Geotextile Fabric ² | NC |
| HDPE Geomembrane | 0.1 |
| Geosynthetic Clay Liner | 0.2 |

[WSRC-STI-2008-00244, Table 4]

(1) The layers are arranged in the table to reflect their order from top to bottom in the SDF closure cap.

(2) Layer is above each disposal unit and does not cover the entire SDF area.

Note: Detailed explanations and functions of the layers are provided in Table 3.2-5.

NC = Not Calculated

Table 3.2-5: Function of the SDF Conceptual Closure Cap Layers

| Layer | Function |
|------------------------------|--|
| Vegetative Cover | The vegetative cover will be established to promote runoff, minimize erosion, and promote evapotranspiration. The initial vegetative cover will be a persistent grass such as Bahia. If it is determined that bamboo is a climax species that prevents or greatly slows the intrusion of pine trees, bamboo will be planted as the final vegetative cover at the end of the 100 year institutional control period. |
| Topsoil | The topsoil will be designed to support a vegetative cover, promote runoff, prevent the initiation of gulying, and provide water storage for the promotion of evapotranspiration. |
| Upper Backfill | The upper backfill will be designed to increase the elevation of the closure cap to that necessary for placement of the topsoil and to provide water storage for the promotion of evapotranspiration. |
| Erosion Barrier | The erosion barrier will be designed to prevent riprap movement during a PMP event and therefore form a barrier to further erosion and gully formation (i.e., provide closure cap physical stability). It will be used to maintain a minimum 10 feet of clean material above the disposal unit to act as an intruder deterrent. It will also act to preclude burrowing animals from access to underlying closure cap layers. It also provides minimal water storage for the promotion of evapotranspiration. |
| Geotextile Fabric | This geotextile fabric will be designed to prevent the penetration of erosion barrier stone into the underlying middle backfill and to prevent piping of the middle backfill through the erosion barrier voids. |
| Middle Backfill | The middle backfill will provide water storage for the promotion of evapotranspiration in the event that the topsoil and upper backfill are eroded away since the overlying erosion barrier provides only minimal such water storage. |
| Geotextile Filter Fabric | This geotextile fabric will be designed to provide filtration between the overlying middle backfill layer and the underlying lateral drainage layer. This filtration will allow water to freely flow from the middle backfill to the lateral drainage layer while preventing the migration of soil from the middle backfill to the lateral drainage layer. |
| Upper Lateral Drainage Layer | The upper lateral drainage layer will be a 1 foot thick coarse sand layer designed to: <ul style="list-style-type: none"> Divert infiltrating water away from the underlying disposal unit and transport the water to the perimeter drainage system, in conjunction with the underlying composite hydraulic barrier (i.e., HDPE geomembrane and GCL), and Provide the necessary confining pressures to allow the underlying GCL to hydrate properly. |
| Geotextile Fabric | This geotextile fabric will be a non-woven geotextile fabric designed to protect the underlying HDPE geomembrane from puncture or tear during placement of the overlying lateral drainage layer. |

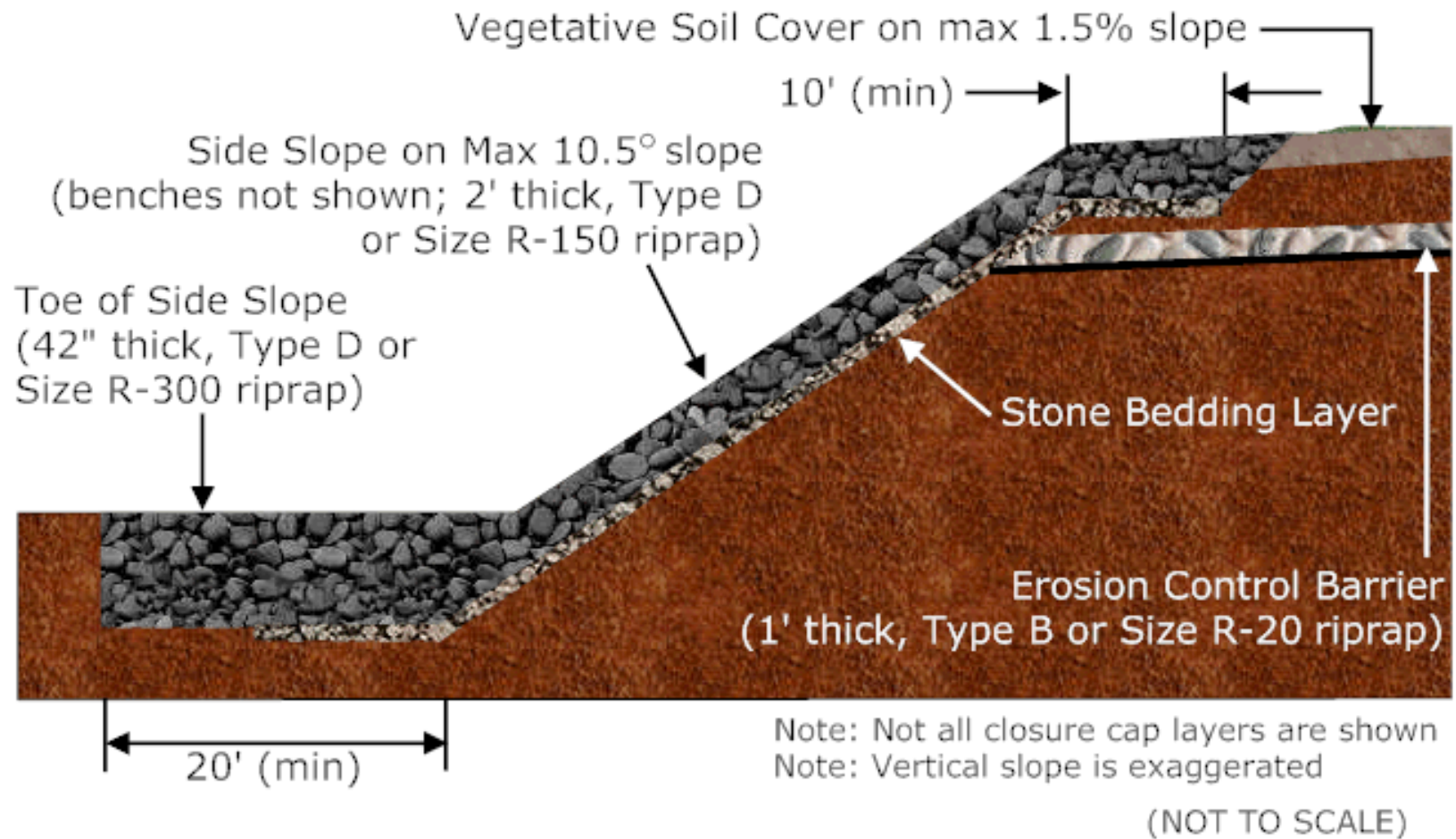
Table 3.2-5: Function of the SDF Conceptual Closure Cap (Continued)

| Layer | Function |
|--|---|
| HDPE Geomembrane | The HDPE geomembrane will form a composite hydraulic barrier in conjunction with the GCL. The composite hydraulic barrier will be designed to promote lateral drainage through the overlying lateral drainage layer and minimize infiltration to the disposal unit. |
| Geosynthetic Clay Liner | The GCL will form a composite hydraulic barrier described above in conjunction with the HDPE geomembrane. As part of the composite hydraulic barrier the GCL is designed to hydraulically plug any holes that may develop in the HDPE geomembrane. |
| Foundation Layer | Provide structural support and required contours for slope of 4% for overlying layers. Provide relatively low-permeability layer directly above lower backfill. |
| Lower Backfill | The lower backfill layer will be designed to: <ul style="list-style-type: none"> • Provide structural support for the rest of the overlying closure cap • Produce the required contours and produce a slope of 4% for the overlying layers • Produce the maximum 3:1 side slopes of the closure cap • Provide a suitable surface for installation of the GCL (i.e., a soil with a moderately low permeability and a smooth surface free from deleterious materials) • Promote drainage of infiltrating water away from and around the disposal units |
| Layers Above Each Disposal unit | |
| Geotextile Filter Fabric | Designed to provide filtration between the overlying lower backfill layer and the underlying lower drainage layer while preventing the migration of soil from the lower backfill to the lower drainage layer. |
| Lower Drainage Layer | Extends approximately 25 feet from each disposal unit, designed primarily to prevent buildup of hydraulic head on top of the disposal unit. The portion of this drainage layer extending beyond each disposal unit roof edge will be constructed atop backfill material. |
| Geotextile Fabric | Designed to protect the underlying HDPE geomembrane from puncture or tear during placement of the overlying lower drainage layer. |
| HDPE Geomembrane | Designed to form a composite hydraulic barrier in conjunction with the GCL. The composite hydraulic barrier will be designed to promote lateral drainage through the overlying lower drainage layer and minimize infiltration to the disposal units. |
| GCL | Forms a composite hydraulic barrier described above and designed to hydraulically plug any holes that may develop in the HDPE geomembrane. |

Figure 3.2-20: Saltstone Disposal Facility Conceptual Closure Cap Layers



Figure 3.2-21: Closure Cap Side Slope and Toe Detail



3.2.2.6 Site Preparation

Site preparation will be required to ready the SDF area for installation of the closure cap. The exact nature of such site preparation has not yet been determined; however it will need to address the following:

- Above grade structures, utilities, and other interferences that could interfere with closure cap construction
- Existing surfaces (soils, asphalt, riprap, disposal unit, etc.) over which the closure cap will be constructed
- Placement of GCL, HDPE, and geotextile fabric layers on each FDC prior to placement of lower drainage layer above each FDC (the HDPE above each FDC will be welded to the HDPE on the FDC's sides)

The SPF, along with above grade structures, utilities, etc. that could interfere with closure cap construction will be removed from the SDF area prior to closure cap installation. The existing surfaces (i.e., soils and riprap) over which the closure cap is to be constructed will have been prepared prior to closure cap construction. Preparation includes removing 3 to 6 inches of existing soil surface to eliminate any topsoil and vegetation present, rough grading to establish a base elevation, and then compacting with a vibratory roller. Additionally existing riprap will be removed or the voids within the existing riprap surfaces will be filled to eliminate subsidence potential. [WSRC-STI-2008-00244]

Detailed information regarding the purpose, design, and constructability of each of the SDF closure cap layers listed in Tables 3.2-4 and 3.2-5 are provided in WSRC-STI-2008-00244.

3.2.2.6.1 Closure Cap Preparation Above Each Disposal Unit

As described in WSRC-STI-2008-00244, a lower drainage layer will be placed over each FDC. Prior to placing the lower drainage layer on top of the disposal unit, a GCL layer will overlay the disposal unit. This GCL layer will be covered with a HDPE layer which is then covered with a geotextile fabric. Finally, the lower drainage layer will be placed on top of the geotextile fabric. Because the lower drainage layer, the geotextile fabric, GCL, and HDPE layers are placed directly above each disposal unit and are not contiguous across the closure cap, they are not considered part of the SDF closure cap. Further details regarding the lower drainage layer, the geotextile fabric, GCL, and HDPE layers are provided in WSRC-STI-2008-00244.

3.2.2.6.2 Vegetative Cover

A vegetative cover will be established to promote runoff, minimize erosion, and promote evapotranspiration. The topsoil will be fertilized, seeded, and mulched to provide a vegetative cover. The initial vegetative cover is expected to be a persistent grass such as Bahia. During seeding and establishment of the initial grass, appropriate mulch, erosion control fabric, or similar substances will be used to protect the surface. [WSRC-STI-2008-00244]

The area will be repaired through transplanting or replanting to ensure that a self maintaining cover is developed. If it is determined that bamboo is a climax species that prevents or greatly slows the intrusion of pine trees, it will be planted as the final vegetative cover at the end of the 100 year institutional control period. Pine trees are typically assumed to be the most deeply rooted naturally occurring climax plant species which will degrade the GCL through root penetration. In contrast, bamboo is a shallow-rooted species, which will not degrade the GCL. Additionally bamboo, in the SRS climate, evapotranspires year round, minimizes erosion, and can sustain growth with minimal maintenance. A study conducted by the USDA Soil Conservation Service (SCS) has shown that two species of bamboo (*Phyllostachys bissetii* and *Phyllostachys rubromarginata*) will quickly establish a dense ground cover. [WSRC-MS-92-513] All work in association with the vegetative cover shall be performed in accordance with the approved drawings, plans, and specifications of the final design, which will be produced near the end of the operational period. [WSRC-STI-2008-00244]

3.2.2.6.3 Closure Cap Side Slopes and Toe

The toe of closure cap side slopes will consist of a riprap layer. The intention of this riprap is to; (1) stabilize the underlying gravel bedding layer, (2) provide erosion protection to the toe, (3) transition flow from the side slope to adjacent areas, and (4) provide gully intrusion protection to the embankment. This riprap layer will extend at least 20 feet from the toe of the side slope as shown in Figure 3.2-21.

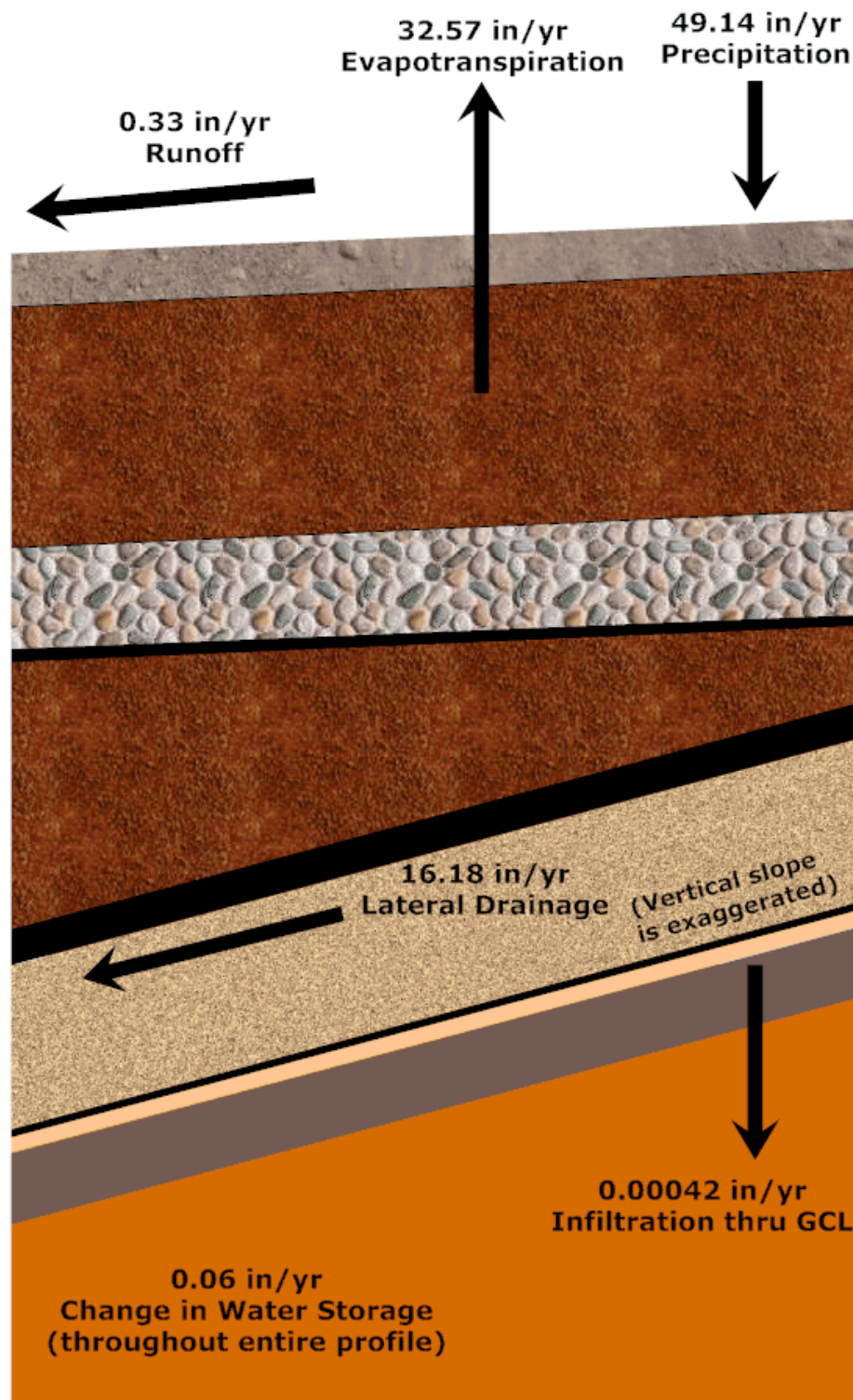
The closure cap side slopes will be placed at a maximum 10.5° slope and have a riprap surface with an underlying gravel bedding layer to prevent gully formation on the side slopes and to provide long-term slope stability. The side slope riprap and underlying gravel bedding layer will extend from the toe of the side slope, up the side slope, and onto the top slope for at least 10 feet, as shown in Figure 3.2-21.

An integrated drainage system will be designed and built to handle the runoff from the closure cap and drainage from the closure cap lateral drainage layers. The runoff and lateral drainage will be directed to a system of riprap lined ditches, which will be designed in accordance with NUREG-1623. The riprap lined ditches will direct the water away from the SDF closure cap as a whole and will be constructed around the perimeter of the SDF closure cap. The ditches will discharge into sedimentation basins as necessary for sediment control. [WSRC-STI-2008-00244]

3.2.2.7 Closure Cap Performance without Degradation

Figure 3.2-22 depicts the Hydrologic Evaluation of Landfill Performance (HELP) model configuration and results for the recommended closure cap configuration in the undegraded condition. The material properties utilized in this assessment of the closure cap configuration are provided in WSRC-STI-2008-00244.

Figure 3.2-22: Saltstone Closure Cap Year 0 (intact) Average Water Balance



[WSRC-STI-2008-00244]

3.2.2.8 *Closure Cap Degradation Mechanisms*

Potential SDF closure cap degradation mechanisms presented in this section are discussed in context of the base case land use scenario (i.e., institutional control to pine forest, land use scenario). This scenario assumes a 100 year institutional control period following SDF closure cap construction during which the closure cap is maintained. At the end of institutional control, it is assumed that a pine forest succeeds the cap's original vegetative cover. [WSRC-STI-2008-00244]

Table 3.2-6 provides a list of potential SDF closure cap degradation mechanisms that were taken into consideration for the estimation of infiltration through the closure cap over time. The table lists the potential degradation mechanisms associated with each of the major SDF closure cap layers (other than backfill layers located below the erosion barrier). Waste layer subsidence is not considered an applicable degradation mechanism to the SDF closure cap, since the disposal units will be filled with saltstone. Additionally, chemical degradation from contact with waste leachate is generally not applicable to the closure cap layers, since they are located above the waste layer. For the SDF closure cap, waste is contained within the disposal unit, located a minimum of 7 feet below any closure cap layer that could be significantly affected by leachate (i.e., erosion barrier, HDPE geomembrane, and the GCL). Therefore chemical degradation of the SDF closure cap by leachate is not considered applicable. [WSRC-STI-2008-00244]

Finally, degradation of sand layers due to mineral precipitation and microbial growth are primarily degradation mechanisms associated with leachate collection layers rather than closure cap lateral drainage layers. Leachate collection layers receive leachate containing both organic and inorganic degradation products from the waste; whereas closure cap lateral drainage layers only receive non-contaminated water from infiltration (in the case of SRS, infiltrating water is very low in both mineral and organic content). Therefore mineral precipitation and microbial growth within the lateral drainage layer is not considered an applicable degradation mechanism. Since waste layer subsidence, chemical (waste leachate) degradation, and mineral precipitation and microbial growth within the lateral drainage layer are not applicable to the SDF closure cap, they will not receive further consideration. WSRC-STI-2008-00244 discusses the other potential SDF closure cap degradation mechanisms outlined in Table 3.2-6. [WSRC-STI-2008-00244]

Based on the identified degradation mechanisms, Table 3.2-7 presents the estimated infiltration rate change over the performance period and beyond.

Table 3.2-6: Closure Cap Potential Degradation Mechanisms

| Affected Layer | Potential Degradation Mechanism |
|--------------------------------|---|
| All | Static loading induced settlement Seismic induced liquefaction and subsequent settlement Seismic induced slope instability Seismic induced lateral spread Seismic induced direct rupture due to faulting Waste layer subsidence ^a |
| Vegetative cover | Succession Stressors (droughts, disease, fire, and biological) |
| Soil above the erosion barrier | Erosion Desiccation (wet-dry cycles) |
| Erosion barrier | Weathering (Dissolution) Biological (root penetration, burrowing animals) Chemical (waste leachate) ^b |
| Lateral drainage layers | Silting-in Biological (root penetration; upper drainage layer only) Mineral precipitation and microbial growth ^c |
| HDPE geomembrane | Ultraviolet (UV) radiation Antioxidant depletion Thermal oxidation High energy irradiation Tensile stress cracking Biological (microbial, root penetration, burrowing animals) Chemical (waste leachate) ^b |
| Geosynthetic clay liner | Slope stability Freeze-thaw cycles Dissolution Divalent cations (Ca^{+2} , Mg^{+2} , etc.) Desiccation (wet-dry cycles) Biological (root penetration, burrowing animals) Chemical (waste leachate) ^b |

- (a) Waste layer subsidence is not considered applicable to the SDF closure cap since the disposal units are filled with grout.
- (b) Chemical degradation of the erosion barrier, HDPE geomembrane, and GCL from leachate associated within the disposal units is not considered applicable to the SDF closure cap, since the erosion barrier, HDPE geomembrane, and GCL will be located above the disposal units.
- (c) Mineral precipitation and microbial growth within the lateral drainage layers is not considered applicable to the SDF closure cap, since infiltrating SRS water is very low in both mineral and organic content and the layers will not contact waste leachate.

Table 3.2-7: Closure Cap Estimated Infiltration Rates

| Year | Average Annual Infiltration thru GCL (in/yr) |
|-------------|---|
| 0 | 0.00042 |
| 100 | 0.00333 |
| 180 | 0.04520 |
| 220 | 0.05676 |
| 300 | 0.17110 |
| 380 | 0.47236 |
| 460 | 0.72342 |
| 560 | 1.0211 |
| 1,000 | 2.2638 |
| 1,800 | 4.340 |
| 3,200 | 6.795 |
| 5,412 | 10.6 |
| 5,600 | 10.6 |
| 10,000 | 10.6 |
| >10,000 | 10.6 |

[WSRC-STI-2008-00244]

3.2.2.9 Open Issues for Further Design

Listed below are open issues related to the SDF closure cap concept, particularly in regard to degradation issues, which will be addressed as the design concept matures.

- Is bamboo a climax species that prevents or greatly slows the intrusion of pine trees?
- What are the requirements for the lower backfill layer particularly in terms of its ability to drainwater away from and around the disposal units?
- What is the estimated weathering rate of the erosion barrier, toe of side slopes, and side slopes stone (assumed granite) based upon natural or archaeological analogs and available literature?
- What material should be used to fill the stone voids of the erosion barrier to prevent loss of overlying material into the erosion barrier?
- Should a sodium bentonite or calcium bentonite GCL be utilized?
- Is the 50 foot extension of the closure cap beyond the sides of the disposal units sufficient to prevent infiltration at the side slopes, the perimeter drainage system, or the natural surrounding land surface from impacting contaminant transport out of the disposal units?

The final design must allow the free transport of water out of the lateral drainage layer into the side slope riprap, while at the same time preventing sand movement from the lateral drainage layer into the side slope riprap.

The current design concept makes conservative assumptions about these open issues, and is acceptable for use for PA modeling. [WSRC-STI-2008-00244]

3.3 Saltstone Disposal Facility Radionuclide and Chemical Inventory

The development of the waste inventory in the SDF disposal units at time of closure is provided in SRNS-J2100-2008-00004, *Estimated Inventory for the Saltstone Disposal Facility*. Tables 3.3-1 through 3.3-6 provide the estimated radionuclide and chemical inventory in the disposal units. The uncertainty and variability associated with these values are presented in Section 5.6.3.2. All radionuclides have been decayed to October 1, 2030 (expected date of SDF closure).

Table 3.3-1: Vault 1 Projected Radionuclide Inventory at Closure

| Radionuclide | Projected Inventory at Closure (Ci) | Radionuclide | Projected Inventory at Closure (Ci) |
|--------------|-------------------------------------|--------------|-------------------------------------|
| Am-241 | 4.7E-04 | Pu-242 | 9.0E-04 |
| Ba-137m | 4.1E+00 | Ra-226 | 6.4E-07 |
| C-14 | 1.3E+00 | Rh-106 | 1.5E-10 |
| Cl-36 | 7.6E-04 | Ru-106 | 1.5E-10 |
| Co-60 | 8.2E-05 | Sb-125 | 1.6E-01 |
| Cs-137 | 4.3E+00 | Sb-126 | 1.4E-01 |
| Eu-152 | 1.8E-03 | Sb-126m | 1.0E+00 |
| Eu-154 | 2.3E-04 | Se-79 | 3.0E-01 |
| H-3 | 6.1E+00 | Sn-126 | 1.0E+00 |
| I-129 | 1.1E-01 | Sr-90 | 6.9E-03 |
| K-40 | 7.6E-04 | Tc-99 | 1.1E+02 |
| Nb-93m | 2.5E-01 | Te-125m | 3.8E-02 |
| Nb-94 | 2.5E-03 | Th-229 | 3.0E-01 |
| Ni-59 | 3.5E-02 | Th-230 | 4.1E-01 |
| Ni-63 | 7.8E-01 | U-233 | 2.8E-01 |
| Np-237 | 4.5E-03 | U-234 | 2.8E-01 |
| Pd-107 | 1.9E-03 | U-235 | 3.2E-03 |
| Pt-193 | 3.7E-01 | U-236 | 3.2E-03 |
| Pu-238 | 7.8E-03 | U-238 | 7.4E-03 |
| Pu-239 | 1.2E-02 | Y-90 | 6.9E-03 |
| Pu-240 | 1.2E-02 | Zr-93 | 2.5E-01 |
| Pu-241 | 9.8E-03 | Total | 1.3E+02 |

Note: Due to the smaller number of radionuclides analyzed during disposal operations, the Vault 1 inventory contains fewer radionuclides than the other disposal units.

Table 3.3-2: Vault 1 Projected Chemical Inventory at Closure

| Chemical | Projected Inventory at Closure (kg) |
|-----------------|--|
| Ag | 2.0E+01 |
| As | 4.4E+01 |
| Ba | 2.0E+01 |
| Cd | 3.9E+02 |
| Cr | 1.8E+02 |
| Hg | 1.5E+00 |
| NO ₂ | 7.4E-01 |
| NO ₃ | 3.4E+01 |
| Pb | 2.3E+01 |
| Se | 6.1E+01 |

Note: In the model the inventories provided in Tables 3.3-1 and 3.3-2 are doubled to account for the potential filling of the three empty cells in Vault 1 with similar waste currently in Vault 1 with low level contaminated materials (e.g., failed contaminated equipment).

Table 3.3-3: Vault 4 Projected Radionuclide Inventory at Closure

| Radionuclide | Projected Inventory at Closure (Ci) | Radionuclide | Projected Inventory at Closure (Ci) |
|---------------------|--|---------------------|--|
| Ac-227 | 1.6E-05 | Pa-231 | 9.3E-05 |
| Al-26 | 3.4E-01 | Pd-107 | 5.0E-02 |
| Am-241 | 1.3E+02 | Pm-147 | 4.1E-01 |
| Am-242m | 6.7E-02 | Pr-144 | 1.8E-09 |
| Am-243 | 1.8E+00 | Pt-193 | 1.0E+01 |
| Ba-137m | 2.8E+05 | Pu-238 | 9.1E+03 |
| Bk-249 | 1.8E-28 | Pu-239 | 3.8E+02 |
| C-14 | 2.7E+01 | Pu-240 | 1.2E+02 |
| Ce-144 | 1.8E-09 | Pu-241 | 2.4E+03 |
| Cf-249 | 6.5E-13 | Pu-242 | 8.1E-01 |
| Cf-251 | 1.2E+00 | Pu-244 | 1.6E-02 |
| Cf-252 | 1.8E-18 | Ra-226 | 4.1E+00 |
| Cl-36 | 3.0E-03 | Ra-228 | 1.6E-06 |
| Cm-242 | 6.7E-02 | Rh-106 | 9.1E-07 |
| Cm-243 | 2.1E-01 | Ru-106 | 9.1E-07 |
| Cm-244 | 1.3E+02 | Sb-125 | 5.7E+00 |
| Cm-245 | 9.2E-01 | Sb-126 | 9.0E-01 |
| Cm-247 | 3.9E-06 | Sb-126m | 6.4E+00 |
| Cm-248 | 1.2E-13 | Se-79 | 4.6E+01 |
| Co-60 | 4.6E-01 | Sm-151 | 4.2E+01 |
| Cs-134 | 5.2E-01 | Sn-126 | 6.4E+00 |
| Cs-135 | 5.4E+00 | Sr-90 | 2.4E+05 |
| Cs-137 | 3.0E+05 | Tc-99 | 5.8E+02 |
| Eu-152 | 9.7E-02 | Te-125m | 1.4E+00 |
| Eu-154 | 1.2E+01 | Th-229 | 2.5E+01 |
| Eu-155 | 6.8E-01 | Th-230 | 7.5E+00 |
| H-3 | 2.6E+02 | Th-232 | 3.2E-04 |
| I-129 | 2.8E-01 | U-232 | 4.4E-02 |
| K-40 | 3.0E-03 | U-233 | 2.4E+01 |
| Na-22 | 1.5E-01 | U-234 | 2.6E+01 |
| Nb-93m | 8.4E+00 | U-235 | 4.7E-01 |
| Nb-94 | 8.7E-02 | U-236 | 7.7E-01 |
| Ni-59 | 4.0E-01 | U-238 | 5.9E-01 |
| Ni-63 | 2.2E+01 | Y-90 | 2.4E+05 |
| Np-237 | 6.1E-01 | Zr-93 | 8.4E+00 |
| | | Total | 1.1E+06 |

Table 3.3-4: Vault 4 Projected Chemical Inventory at Closure

| Chemical | Projected Inventory at Closure (kg) |
|-----------------|---|
| Ag | 2.7E+01 |
| As | 1.0E+03 |
| Ba | 2.6E+01 |
| Cd | 3.8E+01 |
| Cr | 3.5E+03 |
| Cu | 8.8E+02 |
| F | 3.5E+03 |
| Fe | 6.9E+02 |
| Hg | 9.8E+02 |
| Mn | 4.1E+02 |
| Ni | 8.9E+01 |
| NO ₂ | 4.0E+05 |
| NO ₃ | 4.3E+06 |
| Pb | 4.5E+02 |
| Se | 5.2E+03 |
| U | 2.8E+02 |
| Zn | 1.3E+03 |

Table 3.3-5: FDC Projected Radionuclide Inventory at Closure

| Radionuclide | Projected Inventory per Disposal Unit at Closure (Ci) | Radionuclide | Projected Inventory per Disposal Unit at Closure (Ci) |
|---------------------|--|---------------------|--|
| Ac-227 | 1.7E-07 | Pa-231 | 9.8E-07 |
| Al-26 | 1.9E-01 | Pd-107 | 5.6E-03 |
| Am-241 | 1.4E+00 | Pm-147 | 7.7E-02 |
| Am-242m | 5.9E-04 | Pr-144 | 3.6E-10 |
| Am-243 | 3.7E-02 | Pt-193 | 1.1E+00 |
| Ba-137m | 2.2E+01 | Pu-238 | 1.7E+02 |
| Bk-249 | 1.8E-28 | Pu-239 | 1.5E+01 |
| C-14 | 2.0E+00 | Pu-240 | 4.1E+00 |
| Ce-144 | 3.6E-10 | Pu-241 | 4.2E+01 |
| Cf-249 | 6.7E-13 | Pu-242 | 3.9E-03 |
| Cf-251 | 2.3E-14 | Pu-244 | 1.6E-05 |
| Cf-252 | 1.8E-18 | Ra-226 | 7.8E-07 |
| Cl-36 | 4.2E-04 | Ra-228 | 8.7E-05 |
| Cm-242 | 6.3E-19 | Rh-106 | 1.2E-06 |
| Cm-243 | 2.1E-04 | Ru-106 | 1.2E-06 |
| Cm-244 | 9.5E-01 | Sb-125 | 2.4E-01 |
| Cm-245 | 2.4E-04 | Sb-126 | 1.2E+00 |
| Cm-247 | 7.1E-14 | Sb-126m | 8.2E+00 |
| Cm-248 | 7.4E-14 | Se-79 | 1.4E+00 |
| Co-60 | 5.4E-02 | Sm-151 | 5.9E+01 |
| Cs-134 | 1.5E-05 | Sn-126 | 8.2E+00 |
| Cs-135 | 1.3E-04 | Sr-90 | 3.7E+01 |
| Cs-137 | 2.3E+01 | Tc-99 | 5.4E+02 |
| Eu-152 | 9.8E-02 | Te-125m | 5.8E-02 |
| Eu-154 | 1.8E+00 | Th-229 | 3.9E-02 |
| Eu-155 | 1.3E-01 | Th-230 | 1.9E-01 |
| H-3 | 3.0E+01 | Th-232 | 1.4E-03 |
| I-129 | 3.8E-01 | U-232 | 3.1E-04 |
| K-40 | 4.2E-04 | U-233 | 3.7E-02 |
| Na-22 | 6.9E-02 | U-234 | 1.3E-01 |
| Nb-93m | 3.7E-01 | U-235 | 3.0E-03 |
| Nb-94 | 3.8E-03 | U-236 | 1.6E-02 |
| Ni-59 | 8.4E-02 | U-238 | 1.0E-01 |
| Ni-63 | 2.4E+00 | Y-90 | 3.7E+01 |
| Np-237 | 5.0E-02 | Zr-93 | 3.7E-01 |
| | | Total | 1.0E+03 |

Table 3.3-6: FDC Projected Chemical Inventory at Closure

| Chemical | Projected Inventory per Disposal Unit at Closure (kg) |
|-----------------|--|
| Ag | 3.4E-01 |
| As | 1.6E+02 |
| Ba | 1.7E+00 |
| Cd | 8.0E+00 |
| Cr | 4.0E+02 |
| Cu | 2.9E+02 |
| F | 2.0E+02 |
| Fe | 3.5E+01 |
| Hg | 1.5E+02 |
| Mn | 1.1E+02 |
| Ni | 2.2E+01 |
| NO ₂ | 7.7E+04 |
| NO ₃ | 2.2E+05 |
| Pb | 9.7E+01 |
| Se | 5.5E+02 |
| U | 9.6E+00 |
| Zn | 4.0E+02 |

The projected total inventory of radionuclides and chemicals to be disposed in all SDF disposal units are listed in Tables 3.3-7 and 3.3-8, respectively.

Table 3.3-7: Total Projected SDF Disposal Units' Radionuclide Inventory at Closure

| Radionuclide | Projected Inventory at Closure (Ci) | Radionuclide | Projected Inventory at Closure (Ci) |
|--------------|-------------------------------------|--------------|-------------------------------------|
| Ac-227 | 2.7E-05 | Pa-231 | 1.6E-04 |
| Al-26 | 1.3E+01 | Pd-107 | 4.1E-01 |
| Am-241 | 2.2E+02 | Pm-147 | 5.3E+00 |
| Am-242m | 1.0E-01 | Pr-144 | 2.5E-08 |
| Am-243 | 4.2E+00 | Pt-193 | 8.1E+01 |
| Ba-137m | 2.8E+05 | Pu-238 | 2.0E+04 |
| Bk-249 | 1.2E-26 | Pu-239 | 1.3E+03 |
| C-14 | 1.6E+02 | Pu-240 | 3.8E+02 |
| Ce-144 | 2.5E-08 | Pu-241 | 5.1E+03 |
| Cf-249 | 4.4E-11 | Pu-242 | 1.1E+00 |
| Cf-251 | 1.2E+00 | Pu-244 | 1.7E-02 |
| Cf-252 | 1.2E-16 | Ra-226 | 4.1E+00 |
| Cl-36 | 3.1E-02 | Ra-228 | 5.6E-03 |
| Cm-242 | 6.7E-02 | Rh-106 | 7.8E-05 |
| Cm-243 | 2.2E-01 | Ru-106 | 7.8E-05 |
| Cm-244 | 1.9E+02 | Sb-125 | 2.1E+01 |
| Cm-245 | 9.4E-01 | Sb-126 | 7.8E+01 |
| Cm-247 | 3.9E-06 | Sb-126m | 5.3E+02 |
| Cm-248 | 4.9E-12 | Se-79 | 1.4E+02 |
| Co-60 | 3.9E+00 | Sm-151 | 3.8E+03 |
| Cs-134 | 5.2E-01 | Sn-126 | 5.3E+02 |
| Cs-135 | 5.4E+00 | Sr-90 | 2.4E+05 |
| Cs-137 | 3.0E+05 | Tc-99 | 3.5E+04 |
| Eu-152 | 6.4E+00 | Te-125m | 5.2E+00 |
| Eu-154 | 1.3E+02 | Th-229 | 2.8E+01 |
| Eu-155 | 9.0E+00 | Th-230 | 2.0E+01 |
| H-3 | 2.2E+03 | Th-232 | 9.0E-02 |
| I-129 | 2.5E+01 | U-232 | 6.4E-02 |
| K-40 | 3.1E-02 | U-233 | 2.7E+01 |
| Na-22 | 4.6E+00 | U-234 | 3.5E+01 |
| Nb-93m | 3.2E+01 | U-235 | 6.7E-01 |
| Nb-94 | 3.3E-01 | U-236 | 1.8E+00 |
| Ni-59 | 5.8E+00 | U-238 | 7.0E+00 |
| Ni-63 | 1.8E+02 | Y-90 | 2.4E+05 |
| Np-237 | 3.8E+00 | Zr-93 | 3.2E+01 |
| | | Total | 1.1E+06 |

Table 3.3-8: Total Projected SDF Disposal Units' Chemical Inventory at Closure

| Chemical | Projected Inventory at Closure (kg) |
|-----------------|--|
| Ag | 6.9E+01 |
| As | 1.1E+04 |
| Ba | 1.5E+02 |
| Cd | 9.4E+02 |
| Cr | 2.9E+04 |
| Cu | 1.9E+04 |
| F | 1.6E+04 |
| Fe | 2.9E+03 |
| Hg | 1.1E+04 |
| Mn | 7.5E+03 |
| Ni | 1.5E+03 |
| NO ₂ | 5.3E+06 |
| NO ₃ | 1.8E+07 |
| Pb | 6.7E+03 |
| Se | 4.0E+04 |
| U | 8.9E+02 |
| Zn | 2.7E+04 |

Note: In the model the inventories provided in Tables 3.3-1 and 3.3-2 are added to the inventories provided in Tables 3.3-7 and 3.3-8, respectively, to account for the potential filling of the three empty cells in Vault 1 with similar waste currently in Vault 1.

4.0 ANALYSIS OF PERFORMANCE

The purpose of this section is to provide the technical basis for the analysis of performance for the closed SDF.

Section 4.1 provides an overview of the ISCM comprised of three components; (1) closure cap, (2) vadose zone, and (3) saturated zone.

Section 4.2 describes the ISCM approach for waste release.

- 4.2.1 presents the analysis conducted to perform the screening of radionuclides for the groundwater pathways and airborne pathways.
- 4.2.2 presents details of the source term release and the analyses performed to estimate the release of contaminants from SDF.
- 4.2.3 describes the assumed radionuclide transport mechanisms and parameters used for groundwater pathways modeling to estimate exposures to a MOP and the inadvertent intruder for various scenarios.
- 4.2.4 defines the MOP and intruder exposure pathways used for dose calculation.

Section 4.3 describes various computer codes utilized in this PA, their purpose and integration. The computer codes discussed in the section are, HELP, PORFLOW, GoldSim, and The Clean Air Act Assessment Package – 1988 (CAP-88).

Section 4.4 describes the integrated closure system, including the SDF existing vault and FDC modeling dimensions and case scenarios for potential conditions. The modeling processes used in PORFLOW and GoldSim are detailed in this section.

Section 4.5 describes the ISCM and modeling assumptions to estimate the potential flux of gaseous radionuclides at the ground surface for the air pathways analysis. Results are provided based on the assumed inventory of radionuclides susceptible to volatilization. A radon analysis is also completed by presenting the ISCM, modeling assumptions, and the results of the Rn-222 surface flux analysis based on source inventories of the parent radionuclides that generate Rn-222.

Section 4.6 presents the factors for each element necessary in the biotic dose pathway model.

- 4.6.1 presents the bioaccumulation factors used in the analysis.
- 4.6.2 presents consumption rates for human health exposure.

Section 4.7 presents the internal and external Dose Conversion Factors (DCFs) utilized in the various dose pathway models.

4.1 Overview of Analysis

The purpose of this section is to describe the ISCM used for evaluating the performance of the SDF closure system following Saltstone Facility closure.

This ISCM is used to evaluate the migration of contaminants from the SDF and is illustrated in Figure 4.1-1. It comprises three related conceptual models that represent the SDF closure system and the environmental media through which contaminants may migrate.

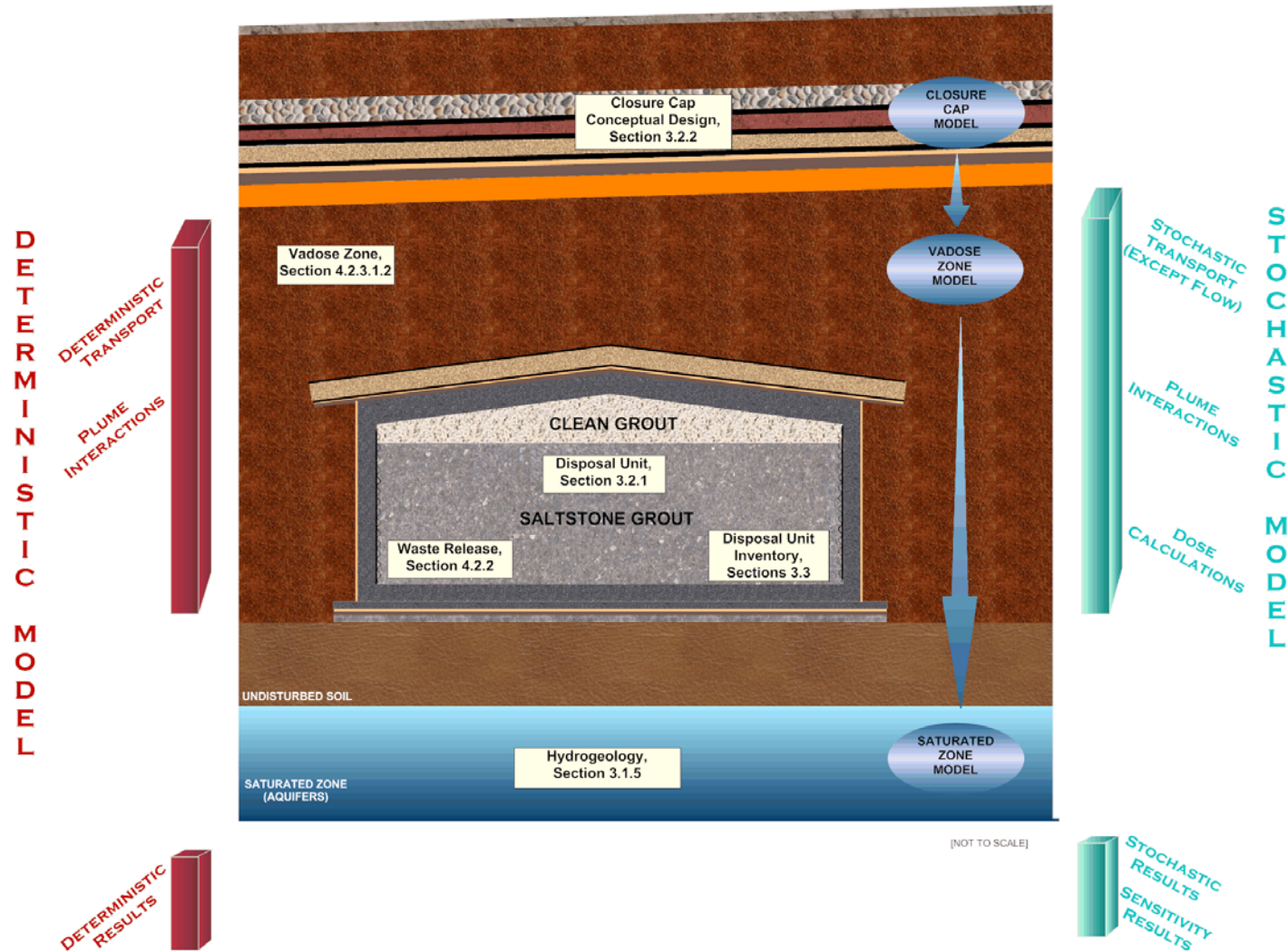
- Closure cap model
- Vadose zone model
- Saturated zone model

Computer codes utilized in the modeling of the ISCM are described in Section 4.3.

Figure 4.1-1 also depicts the relationship between the deterministic and stochastic modeling efforts associated with this PA. Details of the deterministic and stochastic models are discussed further in Section 4.3.

The ISCM described in this section is used to simulate the release of radiological and chemical contaminants from the existing Vaults 1 and 4 and the 64 FDCs in the SDF, and the migration of the contaminants thorough soil and groundwater. Vaults 1 and 4 and the FDCs are described in detail in Section 3.2.1. The ISCM output is used with other information described throughout Section 4 to predict impacts of contaminants on human receptors through various pathways and exposure routes (described in detail in Section 4.2.4). Although the ISCM focuses mainly on the groundwater exposure pathways, the air pathways are also taken into account. For example, inhalation of volatile radioactive contaminants in water from a contaminated well or stream is accounted for in the inputs related to human receptor impacts.

Figure 4.1-1: SDF Modeling Input Relationships



4.2 Integrated Site Conceptual Model of Facility Performance

The ISCM simulates the release of radiological and chemical contaminants from the SDF disposal units. The mechanism generally controlling the release of contaminants from the saltstone is the adsorption characteristic of the saltstone, expressed by the K_d , which is element dependent and differs as the saltstone E_h and pH conditions change over time (e.g., from a reducing cementitious medium to an oxidized cementitious medium). Change in pH or from reducing to oxidized states is treated as a function of the pore water volume that travels through the saltstone. The volume of pore water traveling through the saltstone is dependent on the infiltration rate into the saltstone and the hydraulic conductivity and molecular diffusion of the saltstone. The release of some species, most notably Tc-99, is highly influenced by E_h conditions. Tc-99 is relatively insoluble in cementitious materials under reducing conditions and mobile under oxidized conditions. Blast furnace slag is included in the saltstone dry mix to create reducing conditions that immobilize Tc-99.

This ISCM approach considers the integrity of the proposed SDF closure cap, the cementitious barriers of each disposal unit (roof, walls, and floor), and the saltstone. These key elements control overall contaminant release and transport to groundwater exposure points. Flow into and out of the disposal unit is impacted by the material properties of the closure cap, the cementitious materials comprising the disposal unit, and the saltstone material. Time varying degradation of the closure cap and cementitious materials is included in the model and is described in Sections 3.2.2.8 and 4.2.3.2, respectively.

Chemical degradation of reducing cementitious materials (saltstone and disposal unit concrete) control the chemical composition of the pore fluids passing through the saltstone, and ultimately influences the release of contaminants from the waste form as described in Section 4.2.2. This chemical degradation of the cementitious material is modeled by transitions from one defined age-redox state to another. The “age” of the cementitious material is determined based on the pH level of the pore liquid traversing through the cementitious material. A pH level of 11 or greater indicates Region II (middle age) and a lower pH level indicates Region III (old age), as defined in ISSN 1019-0643 (hereafter referred to as Region II, or III). Oxidation potential plays a key role in the adsorption and solubility of contaminants in the cementitious material where an E_h less than zero is a reducing environment and an E_h greater than zero is an oxidizing environment. The cementitious materials in the model are assigned an age-redox state based on the pH and E_h of the system, which transitions as the pH decreases (from Region II to Region III) and the E_h increases (from reducing conditions to oxidizing conditions). Table 4.2-1 summarizes the results of an analysis conducted on the saltstone and FDC cementitious materials to determine the number of pore liquid volumes required to transition from one age-redox state to another. [SRNL-TR-2008-00283] This analysis is discussed further in Section 4.2.2. The results of this analysis are representative of the saltstone and concrete material in Vaults 1 and 4 and the FDCs.

Table 4.2-1: Summary of Age - Redox States in Cementitious Material

| Age-Redox State Transition | Number of Pore Liquid Volumes | |
|--|-------------------------------|------------------------|
| | Saltstone | Disposal Unit Concrete |
| Region II Reducing → Region III Reducing | 2,274 ^a | N/A |
| Region III Reducing → Region III Oxidizing | 2,734 ^a | N/A |
| Region II Reducing → Region II Oxidizing | 2,806 ^b | N/A |
| Region II Oxidizing → Region III Oxidizing | 10,422 ^b | N/A |
| Region II Reducing → Region II Oxidizing | N/A | 3,230 |
| Region II Oxidizing → Region III Oxidizing | N/A | 4,206 |

[SRNL-TR-2008-00283]

(a) Pore fluid is groundwater with no contact to disposal unit concrete

(b) Pore fluid is groundwater equilibrated with middle age disposal unit concrete

4.2.1 Radionuclide Screening

An initial radionuclide screening process was developed and performed to support characterization efforts and is applicable to SDF PA modeling. Document number CBU-PIT-2005-00228 identifies how SRS performed a screening of radionuclides by initially evaluating 849 isotopes. Of the original 849 isotopes, 159 remained on the list and 690 were excluded from further consideration.

This screening process, to exclude isotopes, used the following information:

- Physical properties of each radioisotope such as half-life and decay mechanism
- Source and handling of the waste based on isotope production mechanisms and time since the isotope was produced
- Screening factors for ground disposal of radionuclides developed in NCRP-123, which convert a quantity of each radionuclide to a dose

The screening process performed in the initial screening was presented in CBU-PIT-2005-00228 as follows. A radionuclide may be screened by multiple steps. Table A8 of CBU-PIT-2005-00228 identifies the results of screening for each radionuclide.

Step 1: Identify isotopes that have part of any of the four decay series, (Actinium, Neptunium, Thorium, or Uranium) and retain them for further analysis because the SDF waste is known to contain the first member of each of the series.

Step 2: Identify isotopes that have high-level waste sludge characterization versus supernate character for saltstone information and retain these for further analysis since they have been determined likely to be present in the waste, and of importance to some aspect of the program. Note that this step may identify isotopes for inclusion that could have been screened out at some later step if they had not been designated.

Next, the remaining list of radionuclides was examined to eliminate those isotopes that can be excluded based on the criteria presented in the following evaluation steps; those that have very long half-lives (and correspondingly low specific activity), and those that have been screened out using the most up-to-date method presented in NCRP-123. There are conservative assumptions made in NCRP-123 to develop the screening criteria compared to the actual closure conditions in the SDF. Several of the model conservatisms include: the waste remained buried for as little as two years, the waste is exhumed and spread over a small area, and the quantity of drinking water consumed is higher than that assumed in Section 4. Although the assumptions are different than in the closure conditions for SDF, they are conservative compared to the SDF and the screening criteria are therefore appropriate for screening radionuclides for inclusion in the PA modeling.

Step 3: Identify isotopes for which there is no dose conversion information (typically very long lived and essentially stable isotopes). The two most comprehensive sources of this information are the NCRP-123 and the U.S. EPA Risk Assessment. Both of these sources were consulted. [www.epa.gov/radiation/heast]

Step 4: Identify isotopes that have been screened out in NCRP-123 using the screening methodology for ground disposal.

The next part of the screening process to eliminate isotopes employs some general information about an assumed residual inventory of radionuclides in high-level waste sludge that is an order of magnitude or more than expected at closure.

Step 5: Identify those isotopes that would result in hypothetical exposure to a MOP of 1 mrem/yr or less assuming there is a large activity level (1m Ci) of any isotope remaining in the waste and use the screening factors from NCRP-123. Note that this analysis includes the exposure due to all daughter radionuclides.

Step 6: Identify those isotopes that would result in hypothetical exposure to a MOP of 1 mrem/yr or less assuming there is a large mass (1,000 lbs) of any isotope remaining in the waste, and using the screening factors from NCRP-123. Note that this analysis includes the exposure due to all daughter radionuclides.

Step 7: Identify isotopes that would not be in the waste due to their physical properties (e.g., present as a gas and released in the reactor or during fuel processing).

More specific information about the waste at SRS is used to identify those radionuclides which can be excluded based on the history of the site waste.

Step 8: Employ information about the age of the SDF waste (minimum of 15 years) to identify those radionuclides that would not be expected to be in the waste at the time of closure due to their short half-lives. Restrict this analysis to those isotopes that have no on-going source and decay directly to stable products so that no isotopes with significant daughters are prematurely eliminated.

Step 9: Employ information about the age of the SDF waste (minimum of 15 years) to identify those radionuclides that would not be expected to be in the waste at the time of closure due to their short half-lives. Apply this analysis to those isotopes that have no

on-going source and decay to short-lived daughters (less than 1 year) and then to stable products so that no isotopes with significant daughters are prematurely eliminated.

Next, some basic information about the duration of institutional control combined with specific isotope characteristics can be used to eliminate radionuclides that are not going to be of future concern to a MOP or worker exposure.

Step 10: Employ detailed decay scheme information to identify short-lived isotopes with no ongoing sources that will decay to stable isotopes in multiple short steps. This step requires the careful review of each individual decay scheme. Although there is not a general rule of thumb, it is obvious from inspection of the decay chain that both the parent and the daughters are effectively extinct.

Step 11: Employ detailed decay scheme information to identify those short-lived isotopes with no ongoing sources that will decay to a longer lived isotope that is separately tracked. Once this decay has happened, the short-lived parent isotope is no longer of interest.

Step 12: Employ detailed decay scheme information and an assumed period of institutional control (100 years) to identify those isotopes with no ongoing sources that will decay to a stable isotope during the period of institutional control.

Step 13: Employ detailed decay scheme information and an assumed period of institutional control (100 years) to identify those isotopes with no ongoing sources that will decay to a longer lived isotope that is separately tracked during the period of institutional control. Once this decay has happened, the parent isotope is no longer of interest.

The isotopes remaining on the list that have not been identified for either inclusion or exclusion can now be examined. Many of the isotopes on the list were not created in SRS reactors. This is because the initial list of isotopes for evaluation was pulled from a variety of sources and includes isotopes of interest for many different reasons due to SRS activities other than just reactor operations.

Step 14: The remaining isotopes are now identified as those isotopes that require further analysis (i.e., pathway and/or inventory specific screening).

The results of the screening process yielded 159 remaining radionuclides for evaluation. These remaining radionuclides are presented in Table 4.2-2.

Table 4.2-2: Radionuclides Requiring Further Evaluation

| | | | | | | |
|---------|--------|---------|--------|---------|---------|--------|
| Ac-225 | Bk-250 | Eu-152 | Nb-94 | Po-213 | Rh-106 | Th-227 |
| Ac-227 | C-14 | Eu-154 | Ni-59 | Po-214 | Rn-219 | Th-228 |
| Ac-228 | Ca-41 | Eu-155 | Ni-63 | Po-215 | Rn-220 | Th-229 |
| Ag-108m | Ce-144 | Fe-60 | Np-236 | Po-216 | Rn-222 | Th-230 |
| Al-26 | Cf-249 | Fr-221 | Np-237 | Po-218 | Ru-106 | Th-231 |
| Am-241 | Cf-250 | Fr-223 | Np-239 | Pr-144 | Sb-125 | Th-232 |
| Am-242 | Cf-251 | Gd-148 | Np-240 | Pt-193 | Sb-126 | Th-234 |
| Am-242m | Cf-252 | H-3 | Pa-231 | Pu-236 | Sb-126m | Ti-44 |
| Am-243 | Cl-36 | Hf-178m | Pa-233 | Pu-238 | Se-79 | Tl-207 |
| Am-246 | Cm-242 | Hf-182 | Pa-234 | Pu-239 | Si-32 | Tl-208 |
| At-217 | Cm-243 | Hg-194 | Pb-202 | Pu-240 | Sm-146 | Tl-209 |
| At-218 | Cm-244 | Ho-166m | Pb-205 | Pu-241 | Sm-147 | Tl-210 |
| Ba-137m | Cm-245 | I-129 | Pb-209 | Pu-242 | Sm-151 | U-232 |
| Be-10 | Cm-246 | Ir-192 | Pb-210 | Pu-243 | Sn-121m | U-233 |
| Bi-207 | Cm-247 | Ir-192m | Pb-211 | Pu-244 | Sn-126 | U-234 |
| Bi-210 | Cm-248 | K-40 | Pb-212 | Pu-246 | Sr-90 | U-235 |
| Bi-210m | Cm-250 | La-137 | Pb-214 | Ra-223 | Ta-182 | U-236 |
| Bi-211 | Co-60 | La-138 | Pd-107 | Ra-224 | Tb-157 | U-238 |
| Bi-212 | Co-60m | Lu-176 | Pm-145 | Ra-225 | Tb-158 | U-240 |
| Bi-213 | Cs-134 | Mn-53 | Pm-147 | Ra-226 | Tc-97 | Y-90 |
| Bi-214 | Cs-135 | Mo-93 | Po-210 | Ra-228 | Tc-98 | Zr-93 |
| Bk-247 | Cs-137 | Na-22 | Po-211 | Rb-87 | Tc-99 | |
| Bk-249 | Eu-150 | Nb-93m | Po-212 | Re-186m | Te-125m | |

4.2.1.1 Evaluation of Radionuclides in Principal Decay Chains

Each of the 159 remaining radionuclides from the screening presented in CBU-PIT-2005-00228 was evaluated to determine if it would be included in the SDF PA modeling. Fifty-four of the 159 isotopes were part of the decay series for actinium, neptunium, thorium or uranium (these four decay series are presented in Table 4.2-3). Because tank farm waste storage tanks, which feed the stabilized salt waste, contain waste that is known to include the first member of these four series, isotopes in these decay chains were addressed in the PA modeling. The GoldSim and PORFLOW modeling software accounted for decay and progeny in-growth as time progresses, which ensures the daughter products were addressed even if they were not assigned an initial inventory. Therefore, the other daughter product radionuclides were removed from modeling consideration and were not assigned an initial SDF inventory. The 14 isotopes from these four decay chains, for which an initial inventory was used in the modeling, are listed in Table 4.2-4.

Table 4.2-3: Decay Series for Neptunium, Thorium, Uranium, and Actinium

| Neptunium Series | Thorium Series | Uranium Series | Actinium Series |
|------------------|------------------|----------------|-----------------|
| Cf-249 | Pu-244 | Pu-242 | Cm-243 |
| ↓ | ↓ | ↓ | ↓ |
| Cm-245 | U-240 | U-238 | Pu-239 |
| ↓ | ↓ | ↓ | ↓ |
| Pu-241 | Np-240m | Th-234 | U-235 |
| ↓ | ↓ | ↓ | ↓ |
| Am-241 | Pu-240 | Pa-234m | Th-231 |
| ↓ | ↓ | ↓ | ↓ |
| Np-237 | U-236 | U-234 | Pa-231 |
| ↓ | ↓ | ↓ | ↓ |
| Pa-233 | Th-232 | Th-230 | Ac-227 |
| ↓ | ↓ | ↓ | ↓ |
| U-233 | Ra-228 | Ra-226 | Th-227 |
| ↓ | ↓ | ↓ | ↓ |
| Th-229 | Ac-228 | Rn-222 | Ra-223 |
| ↓ | ↓ | ↓ | ↓ |
| Ra-225 | Th-228 | Po-218 | Rn-219 |
| ↓ | ↓ | ↓ | ↓ |
| Ac-225 | Ra-224 | Pb-214 | Po-215 |
| ↓ | ↓ | ↓ | ↓ |
| Fr-221 | Rn-220 | Bi-214 | Pb-211 |
| ↓ | ↓ | ↓ | ↓ |
| At-217 | Po-216 | Po-214 | Bi-211 |
| ↓ | ↓ | ↓ | ↓ |
| Bi-213 | Pb-212 | Pb-210 | Tl-207 |
| ↓ ↓ | ↓ | ↓ | ↓ |
| Po-213 Tl-209 | Bi-212 | Bi-210 | Pb-207 |
| ↓ ↓ | ↓ ↓ | ↓ | |
| Pb-209 | Po-212 Tl-208 | Po-210 | |
| ↓ | ↓ ↓ | ↓ | |
| Bi-209 | Pb-208 | Pb-206 | |

Note: Only decay modes of greater than 1% included.
[CBU-PIT-2005-00228]

Table 4.2-4: Initial Inventory Isotopes from Principal Decay Chains

| | | | | | | |
|--------|--------|--------|--------|--------|-------|-------|
| Ac-227 | Np-237 | Pu-241 | Ra-228 | Th-230 | U-233 | U-235 |
| Am-241 | Pa-231 | Ra-226 | Th-229 | Th-232 | U-234 | U-238 |

4.2.1.2 Evaluation of Radionuclides Identified in WCS

In addition to the 14 isotopes from the four decay chains (the decay series in Table 4.2-3), for which an initial inventory was used in modeling, there were 56 additional isotopes that were determined by the Waste Characterization System (WCS) to possibly be present in tank farm waste tanks, which are the source of inventory for the SDF. WCS is an electronic information system that tracks projected radionuclide inventories based on process histories, sample analysis, composition studies, and theoretical relationships. WCS is routinely (i.e., monthly) updated to reflect changes in waste inventory resulting from waste generation facilities, other waste tanks, evaporator operation, and waste processing. Special analyses were performed to determine radionuclide inventories that had not been historically tracked in WCS. Examples of special analyses include fission yield ratios to other radionuclides and equations for progeny radionuclides in terms of the appropriate parent radionuclide. The inventory of each isotope that was used in the modeling is provided in Section 3.3, which presents the expected inventory in the disposal units at the time of closure. An inventory was developed for the 70 isotopes presented in Table 4.2-5. Note, not all radionuclides included in the inventory were modeled in GoldSim. Refer to Appendix I Table I6-1 for a listing of those radionuclides not included in the GoldSim modeling.

Table 4.2-5: SDF Inventory Radionuclides

| | | | | | | |
|---------|--------|--------|--------|--------|---------|--------|
| Ac-227 | Cf-251 | Cs-134 | Nb-93m | Pu-238 | Sb-125 | Th-230 |
| Al-26 | Cf-252 | Cs-135 | Nb-94 | Pu-239 | Sb-126 | Th-232 |
| Am-241 | Cl-36 | Cs-137 | Ni-59 | Pu-240 | Sb-126m | U-232 |
| Am-242m | Cm-242 | Eu-152 | Ni-63 | Pu-241 | Se-79 | U-233 |
| Am-243 | Cm-243 | Eu-154 | Np-237 | Pu-242 | Sm-151 | U-234 |
| Ba-137m | Cm-244 | Eu-155 | Pa-231 | Pu-244 | Sn-126 | U-235 |
| Bk-249 | Cm-245 | H-3 | Pd-107 | Ra-226 | Sr-90 | U-236 |
| C-14 | Cm-247 | I-129 | Pm-147 | Ra-228 | Tc-99 | U-238 |
| Ce-144 | Cm-248 | K-40 | Pr-144 | Rh-106 | Te-125m | Y-90 |
| Cf-249 | Co-60 | Na-22 | Pt-193 | Ru-106 | Th-229 | Zr-93 |

4.2.1.3 Evaluation of Remaining Radionuclides

The remaining 89 isotopes from Table 4.2-2 are screened out of the initial inventory for the reasons described in Table 4.2-6.

Table 4.2-6: Continued Evaluation of Radionuclides

| Isotope | Half-life* | Reason for Elimination from Initial Inventory | Decay Chain |
|---------|-----------------|--|--|
| Ac-225 | 10 days | Generated by Np-237 decay in modeling; short half-life | See Table 4.2-3. |
| Ac-228 | 6.15 hours | Generated by Th-232 decay in modeling; short half-life | See Table 4.2-3. |
| Ag-108m | 438 years | No decay source | Ag-108m → Ag-108 → Cd-108 (stable) and Pd-108 (stable) |
| Am-242 | 16 hours | Decay from Am-242m in modeling | Am-242m → Am-242 → Cm-242 → Pu-238 → U-234 (in Uranium Series) |
| Am-246 | 39 minutes | Ancestors not present, decays to U-238 series | Cm-250 → Pu-246 → Am-246 → Cm-246 → Pu-242 → U-238 (in Uranium Series) |
| At-217 | <1 second | Generated by Np-237 decay in modeling; short half-life | See Table 4.2-3. |
| At-218 | 1.5 seconds | Generated by U-238 decay in modeling; short half-life | Decay mode less than 1% of Po-218 decay. |
| Be-10 | 1,510,000 years | No decay source | Be-10 → Ba-10 (stable) Long-lived naturally occurring isotope |
| Bi-207 | 32.9 years | Ancestors not present | At-207 → Po-207 → Bi-207 → Pb-207 (stable) |
| Bi-210 | 5 days | Generated by U-238 decay in modeling; short half-life | See Table 4.2-3. |
| Bi-210m | 3,040,000 years | No decay source | Bi-210m → Tl-206 → Pb-206 (stable) |
| Bi-211 | 2.14 seconds | Generated by U-235 decay in modeling; short half-life | See Table 4.2-3. |
| Bi-212 | 60.55 minutes | Generated by Th-232 decay in modeling; short half-life | See Table 4.2-3. |
| Bi-213 | 45.6 minutes | Generated by Np-237 decay in modeling; short half-life | See Table 4.2-3. |
| Bi-214 | 20 minutes | Generated by U-238 decay in modeling; short half-life | See Table 4.2-3. |
| Bk-247 | 1,380 years | Ancestors not present, decays to U-235 series | Cf-247 → Bk-247 → Am-243 → Np-239 → Pu-239 → U-235 (in Actinium Series) |
| Bk-250 | 3.2 hours | Ancestors not present, decays to U-238 series | Md-258 → Es-254 → Bk-250 → Cf-250 → Cm-246 → Pu-242 → U-238 (in Uranium Series); Cm-250 → Bk-250 → Cf-250 → Cm-246 → Pu-242 → U-238 (in Uranium Series) |

Table 4.2-6: Continued Evaluation of Radionuclides (Continued)

| Isotope | Half-life* | Reason for Elimination from Initial Inventory | Decay Chain |
|----------------|-------------------|--|--|
| Ca-41 | 102,000 years | No decay source | Ca-41 → K-41 (stable) |
| Cf-250 | 13.1 years | Ancestors not present, decays to U-238 series | Md-258 → Es-254 → Bk-250 → Cf-250 → Cm-246 → Pu-242 → U-238 (in Uranium Series) Cm-250 → Bk-250 → Cf-250 → Cm-246 → Pu-242 → U-238 |
| Cm-246 | 4760 years | Ancestors not present, decays to U-238 series | Cf-250 → Cm-246 → Pu-242 → U-238 (in Uranium Series); Es-250m → Cf-250 and Bk-246 → Cm-246 → Pu-242 → U-238 (in Uranium Series) Cm-250 → Pu-246 → Am-246 → Cm-246 → Pu-242 → U-238 (in Uranium Series) |
| Cm-250 | 8,300 years | No decay source | Cm-250 → Pu-246 → Am-246 → Cm-246 → Pu-242 → U-238 (in Uranium Series) |
| Co-60m | 10.5 seconds | Ancestors not present | Fe-60 → Co-60m → Co-60 → Ni-60 (stable) |
| Eu-150 | 36.9 years | No decay source | Eu-150 → Sm-150 (stable) |
| Fe-60 | 1,500,000 years | No decay source | Fe-60 → Co-60m → Co-60 → Ni-60 (stable) |
| Fr-221 | 5 minutes | Generated by Np-237 decay in modeling; short half-life | See Table 4.2-3. |
| Fr-223 | 22 minutes | Generated by U-235 decay in modeling; short half-life | See Table 4.2-3. |
| Gd-148 | 70.9 years | No decay source | Gd-148 → Sm-144 (stable) |
| Hf-178m | 31 years | No decay source | Hf-178m → Hf-178 (stable) |
| Hf-182 | 8,900,000 years | Ancestors not present | Hf-182m → Hf-182 → Ta-182 → W-182 (stable) |
| Hg-194 | 444 years | Ancestors not present | [Ti-194 and Ti-194m] → Hg-194 → Au-194 → Pt-194 (stable) |
| Ho-166m | 1200 years | No decay source | Ho-166m → Er-166 (stable) |
| Ir-192 | 74 days | Ancestors not present | Ir-192m → Ir-192 → Pt-192 (stable) or Os-192 (stable) |
| Ir-192m | 241 years | No decay source | Ir-192m → Ir-192 → Pt-192 (stable) or Os-192 (stable) |
| La-137 | 60,000 years | Ancestors not present | Ce-137m → Ce-137 → La-137 → Ba-137 (stable); Pr-137 → Ce-137 → La-137 → Ba-137 (stable) |
| La-138 | 1.02E+11 years | No decay source | La-138 → Ce-138 (stable) Long-lived naturally occurring isotope |
| Lu-176 | 3.76E+10 years | No decay source | Lu-176 → Hf-176 (stable) Long-lived naturally occurring isotope |

Table 4.2-6: Continued Evaluation of Radionuclides (Continued)

| Isotope | Half-life* | Reason for Elimination from Initial Inventory | Decay Chain |
|----------------|-------------------|--|--|
| Mn-53 | 374,000 years | No decay source | Mn-53 → Cr-53 (stable) |
| Mo-93 | 4,000 years | Ancestors not present | [Mo-93m and Tc-93 and Tc-93m] → Mo-93 → Nb-93m → Nb-93 (stable) |
| Np-236 | 1,540 years | No decay source | Np-236 → U-236 → Th-232 (in Thorium Series); Np-236 → Pu-236 Np-236a → U-232 to Th-228 (in Thorium Series) |
| Np-239 | 2.4 days | Decay from Am-243 in modeling; short half-life | Cf-247 → Bk-247 → Am-243 → Np-239 → Pu-239 → U-235 (in Actinium Series); Es-255 → Bk-251 or Fm-255 → Cf-251 → Cm-247 → Pu-243 → Am-243 → Np-239 → Pu-239 → U-235 (in Actinium Series) |
| Np-240 | 62 minutes | Decay from Pu-244 in modeling; short half-life | Cf-252 → Cm-248 → Pu-244 → U-240 → Np-240 → Pu-240 → U-236 → Th-232 in Thorium Series |
| Pa-233 | 27 days | Generated by Np-237 decay in modeling; short half-life | See Table 4.2-2. |
| Pa-234 | 6.7 hours | Generated by U-238 decay in modeling; short half-life | See Table 4.2-2. |
| Pb-202 | 52,500 years | Ancestors not present | Po-202 → Bi-202 → Pb-202 → [Tl-202 and Hg-198 (stable)]; Tl-202 → Hg-202 (stable) |
| Pb-205 | 1.73E+07 years | Ancestors not present | Po-205 → Bi-205 → Pb-205 → Tl-205 (stable) |
| Pb-209 | 3.3 hours | Generated by Np-237 decay in modeling; short half-life | See Table 4.2-3. |
| Pb-210 | 22 years | Generated by U-238 decay in modeling | See Table 4.2-3. |
| Pb-211 | 36 minutes | Generated by U-235 decay in modeling; short half-life | See Table 4.2-3. |
| Pb-212 | 10.6 hours | Generated by Th-232 decay in modeling; short half-life | See Table 4.2-3. |
| Pb-214 | 27 minutes | Generated by U-238 decay in modeling; short half-life | See Table 4.2-3. |
| Pm-145 | 18 years | Ancestors not present | Gd-145 → Eu-145 → Sm-145 → Pm-145 → Nd-145 (stable) |
| Po-210 | 138 days | Generated by U-238 decay in modeling | See Table 4.2-3. |
| Po-211 | <1 second | Generated by U-235 decay in modeling; short half-life | Decay mode less than 1% of Bi-211 decay. |
| Po-212 | <1 second | Generated by Th-232 decay in modeling; short half-life | See Table 4.2-3. |

Table 4.2-6: Continued Evaluation of Radionuclides (Continued)

| Isotope | Half-life* | Reason for Elimination from Initial Inventory | Decay Chain |
|----------------|-------------------|--|---|
| Po-213 | <1 second | Generated by Np-237 decay in modeling; short half-life | See Table 4.2-3. |
| Po-214 | <1 second | Generated by U-238 decay in modeling; short half-life | See Table 4.2-3. |
| Po-215 | <1 second | Generated by U-235 decay in modeling; short half-life | See Table 4.2-3. |
| Po-216 | <1 second | Generated by Th-232 decay in modeling; short half-life | See Table 4.2-3. |
| Po-218 | 3 minutes | Generated by U-238 decay in modeling; short half-life | See Table 4.2-3. |
| Pu-236 | 3 years | Ancestors not present, decays to Th-228 series | Cf-244 → Cm-240 → Pu-236 → U-232 → Th-228 (in Thorium Series) |
| Pu-243 | 5 hours | Decay from Cf-251 in modeling | Cf-251 → Cm-247 → Pu-243 → Am-243 → Np-239 → Pu-239 → U-235 (in Actinium Series) |
| Pu-246 | 11 days | Ancestors not present | Cm-250 → Pu-246 → Am-246 → Cm-245 Pu-241 (in Neptunium Series); |
| Ra-223 | 11 days | Generated by U-235 decay in modeling; short half-life | See Table 4.2-3. |
| Ra-224 | 3.6 days | Generated by Th-232 decay in modeling; short half-life | See Table 4.2-3. |
| Ra-225 | 15 days | Generated by Np-237 decay in modeling; short half-life | See Table 4.2-3. |
| Rb-87 | 4.97E+10 years | Ancestors not present | [Kr-87 and Sr-87m] → Rb-87 → Sr-87 (stable) |
| Re-186m | 200,000 years | No decay source | Re-186m → Re-186 → Os-186 → W-182 (stable) |
| Rn-219 | 4 seconds | Generated by U-235 decay in modeling; short half-life | See Table 4.2-3. |
| Rn-220 | 56 seconds | Generated by Th-232 decay in modeling; short half-life | See Table 4.2-3. |
| Rn-222 | 4 days | Generated by U-238 decay in modeling; short half-life | See Table 4.2-3. |
| Si-32 | 132 years | No decay source | Si-32 → P-32 → S-32 (stable) |
| Sm-146 | 1.03E+08 years | Ancestors not present | [Gd-146 and Tb-150] → Eu-146 → Sm-146 → Nd-142 (stable); Eu-150m → Gd-150 → Sm-146 → Nd-142 (stable) |
| Sm-147 | 1.06E+11 years | Decay from Pm-147 in modeling | Pr-147 → Nd-147 → Pm-147 → Sm-147 → Nd-143 (stable); Tb-147 → Gd-147 → Eu-147 → Sm-147 → Nd-143 (stable) |
| Sn-121m | 44 years | No decay source | Sn-121m → Sn-121 → Sb-121 (stable) |

Table 4.2-6: Continued Evaluation of Radionuclides (Continued)

| Isotope | Half-life* | Reason for Elimination from Initial Inventory | Decay Chain |
|---------|-----------------|--|---|
| Ta-182 | 114 days | Ancestors not present; short half-life | Hf-182m → Hf-182 → Ta-182 → W-182 (stable) |
| Tb-157 | 71 years | Ancestors not present | Ho-157 → Dy-157 → Tb-157 → Gd-157 (stable) |
| Tb-158 | 180 years | No decay source | Tb-158 → Gd-158 (stable) |
| Tc-97 | 4,210,000 years | Ancestors not present | [Ru-97 and Tc-97m] → Tc-97 → Mo-97 (stable) |
| Tc-98 | 4,200,000 years | No decay source | Tc-98 → Ru-98 (stable) |
| Th-227 | 19 days | Generated by U-235 decay in modeling; short half-life | See Table 4.2-3 |
| Th-228 | 1.9 years | Generated by Th-232 decay in modeling; short half-life | See Table 4.2-3 |
| Th-231 | 25.5 hours | Generated by U-235 decay in modeling; short half-life | See Table 4.2-3 |
| Th-234 | 24 days | Generated by U-238 decay in modeling; short half-life | See Table 4.2-3 |
| Ti-44 | 60 years | No decay source | Ti-44 → Sc-44 → Ca-44 (stable) |
| Tl-207 | 5 minutes | Generated by U-235 decay in modeling; short half-life | See Table 4.2-3 |
| Tl-208 | 3 minutes | Generated by Th-232 decay in modeling; short half-life | See Table 4.2-3 |
| Tl-209 | 2.2 minutes | Generated by Np-237 decay in modeling; short half-life | See Table 4.2-3 |
| Tl-210 | 1.3 minutes | Generated by U-238 decay in modeling; short half-life | Decay mode less than 1% of Bi-214 decay. |
| U-240 | 14 hours | Decay from Cf-252 in modeling; short half-life | Cf-252 → Cm-248 → Pu-244 → U-240 → Np-240 → Pu-240 → U-236 → Th-232 (in Thorium Series) |

*Half-life years obtained from the April 2005 Nuclear Wallet Cards. [PIT-MISC-0072]

4.2.1.4 Groundwater Modeling Initial Inventory

No further screening was performed on the initial inventories listed in Section 3.3 for the purpose of groundwater modeling

4.2.1.5 Air Pathways Modeling Initial Inventory

The methodology used for airborne pathways screening was based on the NCRP-123 atmospheric screening methodology, and accounted for the fact that the radionuclides of concern are constrained by the actual disposal unit inventory and the limited number of radionuclides susceptible to volatilization.

The steps in the airborne pathways screening are as follows:

Step 1: The initial list of radionuclides of concern for the airborne pathways is taken from the actual disposal unit inventories. From the 70 candidate radionuclides in Table 4.2-4, only those radionuclides assumed to have a measurable inventory at closure are subject to further evaluation.

Step 2: As discussed in the *Atmospheric Pathway Screening Analysis for the E-Area Low-Level Waste Facility*, some fundamental principles of physics and chemistry are applied to further reduce the number of radionuclides required to be analyzed for the airborne pathways. [WSRC-STI-2006-00159] The PA only considers times after final facility closure. Once the SDF is closed and capped, there are only two possible ways for radionuclides to be released to the atmosphere. One is by particulates produced by intrusion, which is considered in a different pathway analysis in the PA, and the other is to be released as a gas. The list of elements in the initial disposal unit inventory were reviewed and only those that were judged to have the potential to form a vapor phase in the waste form were considered for further analysis in the PA. The following elements are judged to have the potential to form a vapor phase in the waste form, Ar, As, At, Br, C, Cl, F, Ge, H, Hg, I, Kr, N, O, P, S, Sb, Se, Sn, and Xe. These elements have a total of 137 associated individual radionuclides. Of these 137 radionuclides, only C-14, Cl-36, H-3, I-129, Sb-125, Se-79, and Sn-126 are present in the actual SDF inventory.

4.2.2 Source Term Release

Saltstone is a cementitious waste form made by mixing salt solution originating from SRS liquid waste storage tanks in FTF and HTF with a dry mix containing blast furnace slag, fly ash, and cement or lime. The primary soluble salts present in the salt solution in descending order are sodium nitrate, sodium hydroxide, sodium nitrite, sodium aluminum hydroxide ($\text{NaAl}(\text{OH})_4$), sodium carbonate, and sodium sulfate. The primary solid components of saltstone in descending order are silicon dioxide, aluminum oxide, calcium oxide, magnesium oxide, and iron (III) oxide. Solidified saltstone is a dense, alkaline, reducing, micro-porous, monolithic, cementitious matrix, consisting of solids such as calcium aluminosilicate and containing a solution of salts within its pore structure. The pore fluid consists predominately of sodium, nitrate, and nitrite. The clean grout, made from process water, has a bulk composition similar to saltstone. Table 4.2-7 presents the approximate weight percentages of the ingredients for saltstone and clean grout for the nominal formulation. [WSRC-STI-2006-00198] Additional work is being conducted to evaluate the sensitivity of modeling parameters to changes in the formula as presented in Section 8.2. The SPF currently utilizes operating procedures to control the formulation of the saltstone via the Distributed Control System (DCS). These procedures include a Use Every Time procedure for verifying the DCS settings for premix blending (Manual SW24.5, Section 2.11) and Use Every Time procedures for either automatic (Manual SW24.5, Section 2.4) or manual (Manual SW24.5, Section 2.5) operations of the premix blending system. A review of 31 premix feed batches in January of 2009 indicated that the variability of the dry materials is within plus or minus 3% of the nominal formulation at the 95% confidence interval for flyash and slag and within plus or minus two percent for cement. [LWO-WSE-

2009-00038] The results of the ongoing work will be used in conjunction with the available, and any new, operational information to evaluate any impacts as part of PA maintenance.

Table 4.2-7: Ingredients of Saltstone and Clean Grout

| Ingredient | Quantity (wt%) | |
|---|----------------|-------------|
| | Saltstone | Clean Grout |
| Blast furnace slag (grade 100 or 120) | 25 | 28 |
| Cement (ASTM C 150 Type II) or lime | 3 | 6 |
| Fly ash (Class F) | 25 | 28 |
| Salt solution (average 28% by weight salts) | 47 | N/A |
| Water (maximum) | N/A | 38 |

Contaminant concentrations in saltstone are not generally expected to be limited by solubility. Transport is assumed to be primarily controlled by sorption that can be adequately represented by a linear isotherm (i.e., a constant soil-solute K_d). The release of some species, most notably Tc-99, is strongly controlled by E_h conditions. Saltstone and most SDF disposal unit concretes contain blast furnace slag to produce reducing conditions that greatly inhibit Tc-99 release.

An analysis was conducted and documented in SRNL-TR-2008-00283 to estimate the E_h and pH transitions in the saltstone and disposal unit concrete. Chemical degradation of reducing saltstone and disposal unit concrete controls the chemical composition of the pore fluids passing through the saltstone, and ultimately influences the release of contaminants from the waste form. Simulations were done using *The Geochemist's Workbench*® Release 6.0 (a geochemical modeling software computer code developed by the University of Illinois) to estimate the chemical degradation of the reducing cementitious materials. The simulations estimated chemical changes as a function of the number of pore volumes of infiltrate water that react with grout minerals. This information provides step changes in E_h and pH of pore fluids in saltstone and disposal unit concrete with the number of pore volumes of reacting fluid passing through these forms. The simulations do not consider physical degradation, such as fracturing, even though physical degradation may ultimately affect the rate of chemical degradation by influencing the rate that infiltration passes through the grout. The effect of physical degradation is addressed in Section 4.2.3.2.4.

Simulations were run in a “flush” mode. This mode mimics column experiments where for each pore volume of infiltrate that enters the column, an equal volume of reacted infiltrate exits and is analyzed. Each pore volume of fluid equilibrates with cementitious minerals. All transports of dissolved ions were assumed to be the result of advective flow of the infiltrating fluid. In this conceptual model, the initial saltstone and disposal unit concrete pore fluids were flushed out with the first pore volume of infiltrate. Thus, issues with high ionic strengths and calculation of activity coefficients by the extended Debye-Hückel method were ignored.

Three cases were run for saltstone and one case for FDC concrete. Saltstone is encased in disposal unit concrete so it was assumed that the origin of the infiltrate into saltstone was groundwater with or without interaction with the disposal unit concrete. The first case represents a situation where a “fast flow” path is created through the disposal unit concrete and un-reacted groundwater directly contacts saltstone. For the second case, infiltrate groundwater was equilibrated with an oxidized disposal unit concrete in Region III (old age) and defined as “groundwater equilibrated with calcite.” For the third case, infiltrate groundwater was equilibrated with an oxidized FDC concrete in Region II (middle age) and defined as “groundwater equilibrated with Calcium Silicate Hydrate (CSH) ($\text{CaSiO}_3 \cdot \text{H}_2\text{O}$).” For the FDC concrete, the infiltrate was un-reacted groundwater. Table 4.2-8 presents the key constituents for the three infiltrating solutions analyzed.

Table 4.2-8: Key Constituents in the Infiltrating Solutions Analyzed

| Constituent | Groundwater (GW) | GW + CSH | GW + Calcite |
|---------------------------------|-------------------------|-----------------|---------------------|
| Ca (mol/L) | 6.2E-5 | 2.9E-3 | 4.5E-4 |
| Cl (mol/L)* | 9.4E-5 | 1.3E-4 | 1.32E-4 |
| Dissolved CO_2 (mol/L) | 9.8E-5 | 7.0E-6 | 7.6E-5 |
| Dissolved O_2 (mol/L) | 2.5E-4 | 2.5E-4 | 2.5E-4 |
| Na (mol/L) | 4.2E-5 | 4.2E-5 | 4.2E-5 |
| pH | 5.4 | 11.1 | 8.3 |

*chloride concentrations are adjusted to achieve charge balance

Further details on the mineralogical composition of the saltstone and FDC concrete, as well as thermodynamic data used in these simulations using *The Geochemist's Workbench®* Release 6.0, are provided in SRNL-TR-2008-00283. Table 4.2-9 provides the results of these simulations for the saltstone and FDC concrete.

Table 4.2-9: Transitions for Saltstone and FDC Concrete

| Case | E_h Transition | | pH Transition | |
|-----------------------------|------------------------------------|--------------------|-----------------------|-----------------------|
| | Pore Volume | Value Range | Pore Volume | Value Range |
| Saltstone with GW | 2,734 | -0.45 to +0.66 | 2,274 | 11.0 to 9.5 |
| Saltstone with GW + calcite | 2,775 | -0.45 to +0.61 | 2,558 | 11.0 to 10.3 |
| Saltstone with GW + CSH | 2,806 | -0.45 to +0.56 | 10,422 (extrapolated) | 11.0 to (not defined) |
| FDC concrete with GW | 3,230 | -0.46 to +0.57 | 4,206 (extrapolated) | 11.0 to (not defined) |

As indicated in Table 4.2-9, saltstone transitions from a reducing environment to an oxidizing environment (E_h turns positive) prior to transitioning from middle age (initial condition of saltstone) to old age (pH is less than 11) when groundwater is equilibrated with CSH. Based on the infiltration rate through the closure cap and entering the disposal units, saltstone remains in its initial condition of a reducing middle age cementitious material throughout the performance period. Thus, the sorption coefficients used to simulate the release of contaminants from the saltstone are the K_d values shown in Table 4.2-18 for reducing middle age cementitious material.

4.2.3 Radionuclide Transport

Over the course of time, the mobile contaminants in the closed SDF disposal units are expected to be released and gradually migrate downward through unsaturated soil to the hydrogeologic units comprising the shallow aquifers underlying the SDF. Some contaminants will be transported via groundwater through near surface aquifers and out crop at either McQueen Branch or UTR. Exposure to contaminants could occur through various pathways associated with groundwater, surface water uses, and air exposure. Figure 4.2-1 shows the location of the Z-Area within the GSA, which is bounded by UTR to the north, Fourmile Branch to the south, and McQueen Branch to the east.

4.2.3.1 Transport Model Approach

Figure 4.1-1 illustrates the transport model, which is broken up into three component conceptual models; (1) the closure cap, (2) the vadose zone, and (3) the saturated zone (i.e., the aquifers). Simplifying model assumptions have been made for each of these distinct layers or zones. Figure 4.2-2 illustrates the overall SDF PA model and provides an overview for the discussion that follows.

4.2.3.1.1 Transport Model – Closure Cap

In the closure cap conceptual model, the SDF is covered by two large closure caps. The closure cap conceptual design and the expected performance of the closure cap are described in Section 3.2.2 based on WSRC-STI-2008-00244. The closure cap design provides a basis for modeling the net infiltration of water to the vadose zone (including waste locations). The infiltration rate through the closure cap is dependent on the assumed precipitation rates as discussed in Section 3.2.3 and evaluated in WSRC-STI-2008-00244. The average water balance through the closure cap over time is shown in Figure 4.2-3 based on data obtained from WSRC-STI-2008-00244.

Figure 4.2-1: Location of Z-Area and GSA Layout

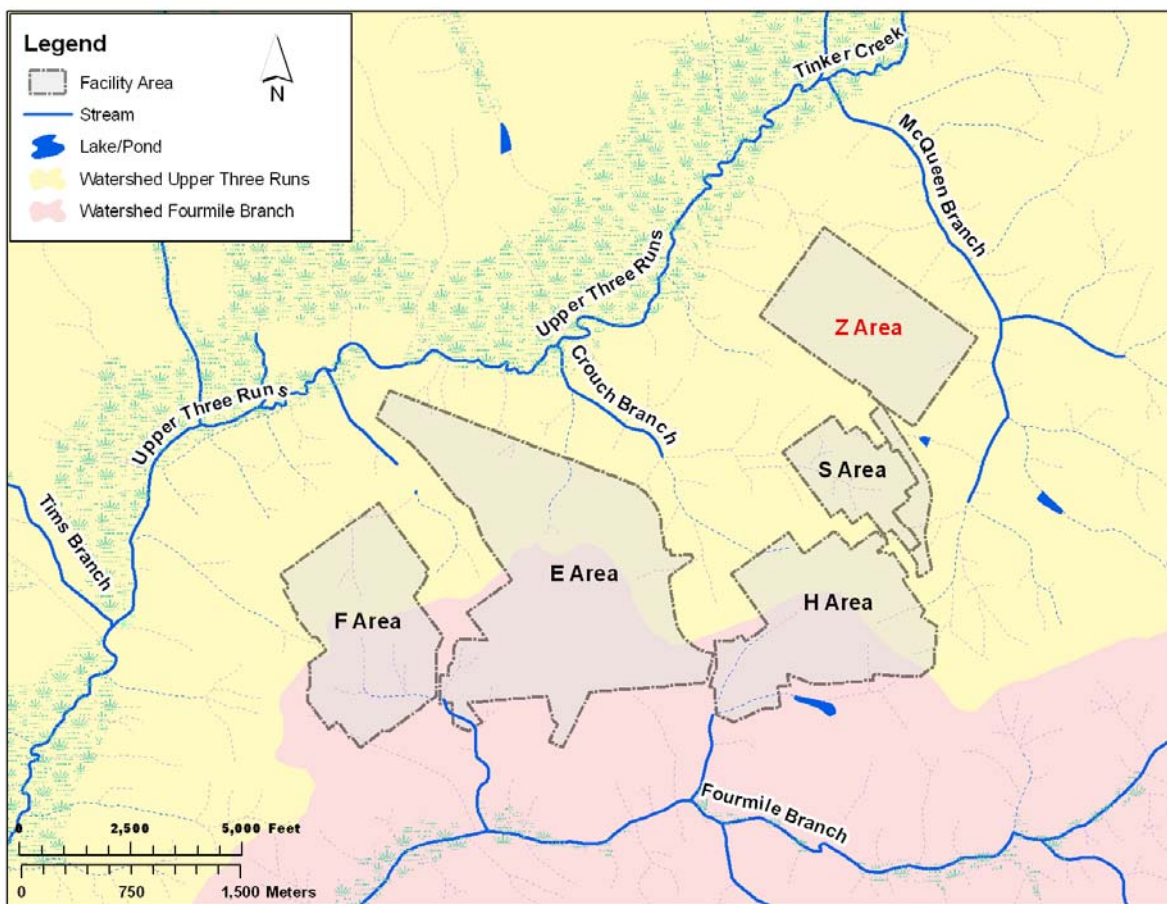
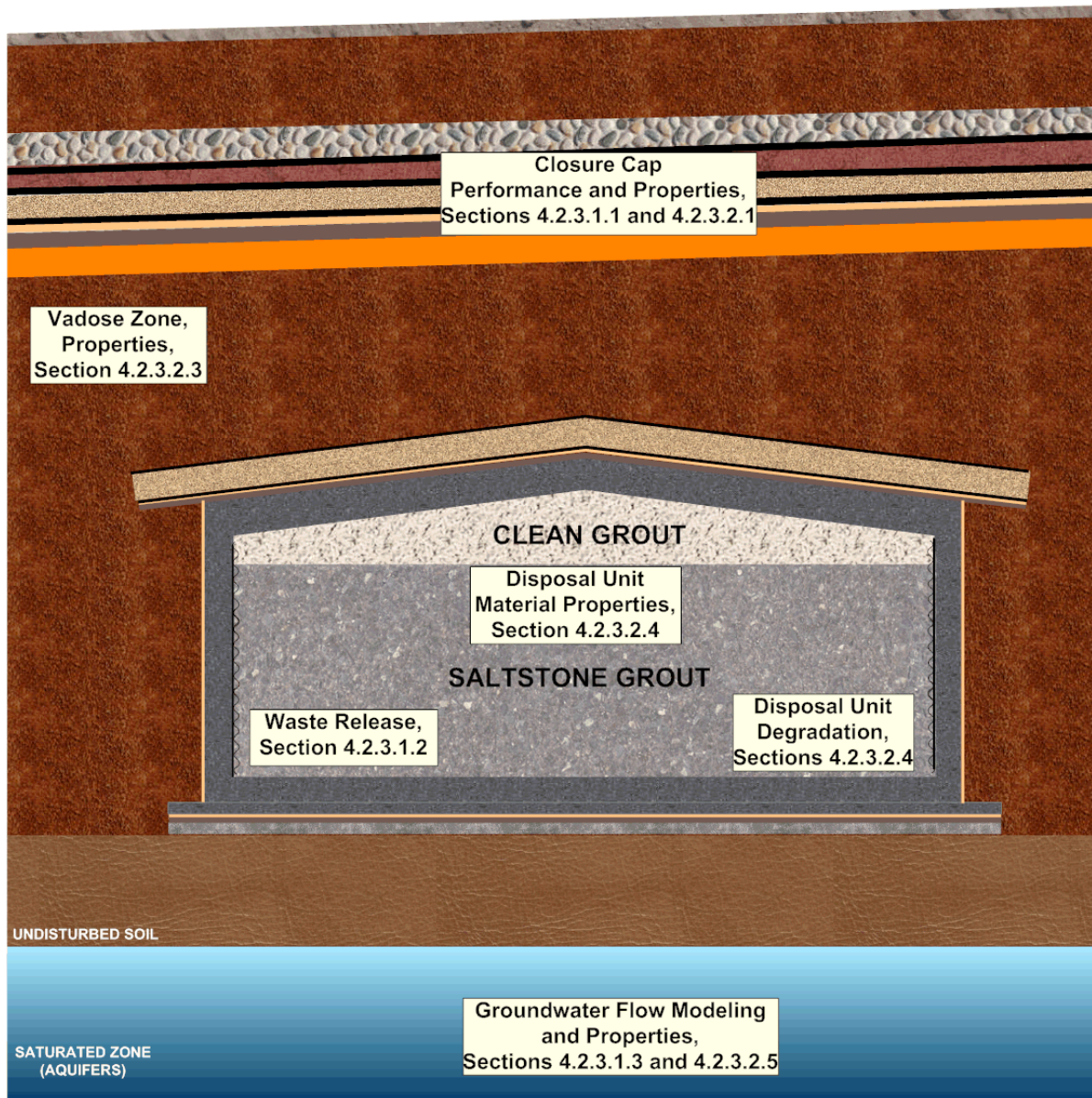
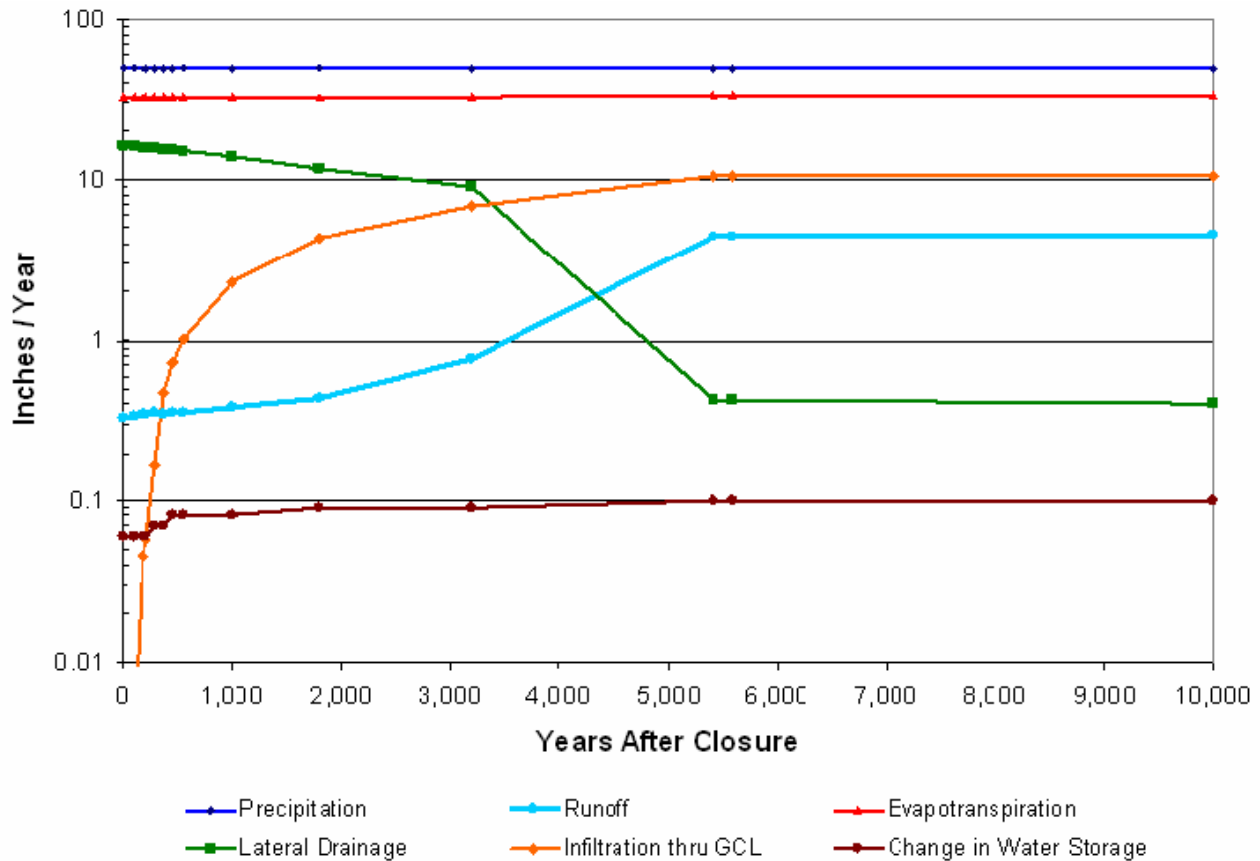


Figure 4.2-2: SDF Overall Performance Assessment Model



[NOT TO SCALE]

Figure 4.2-3: Average Water Balance Through SDF Closure Cap Over Time



[WSRC-STI-2008-00244]

4.2.3.1.2 Transport Model – Vadose Zone (Vaults, FDC and Unsaturated Soils)

The area directly below the SDF closure cap in the conceptual model is considered the vadose zone for modeling purposes. The vadose zone contains the potential contamination sources in SDF (i.e., Vaults 1, 4, and the FDCs) and the surrounding unsaturated soil, both undisturbed and backfilled. The individual SDF disposal unit closure systems are included in the vadose zone. Infiltration predicted to pass through the HDPE-GCL liners of the SDF closure cap is considered a boundary flow condition for the vadose zone analysis. A full description of the soil properties of the SDF vadose zone is provided in Section 4.2.3.2. Over the course of time, the mobile contaminants in the closed SDF are likely to be released from the disposal unit and gradually migrate downward through unsaturated soil via advection-dominated transport. Transport of some contaminant species will be significantly retarded by sorption to native and backfilled soils.

At a conceptual level, the mechanisms that can control release of contaminants from the saltstone are dissolution (i.e., dissolving solid fraction of saltstone contaminants into a solvent and yielding a contaminant solution), sorption, diffusion, dispersion, and advection. After saltstone curing, contaminants will generally be partitioned as a dissolved fraction, an

adsorbed fraction, and a remaining fraction incorporated into the solid matrix. Contaminants bound in the solid matrix of the monoliths are primarily released into the pore fluid through the process of dissolution. Contaminants are also released to pore fluid through desorption. Contaminants dissolved in the pore fluid move through the saltstone by molecular diffusion (contaminants moving from higher to lower concentration via molecular motion), mechanical dispersion (movement of contaminants from areas of higher to lower concentrations via non-ideal flows), and advection (transport by bulk motion of the fluid). The rates of contaminant release and movement from saltstone by these mechanisms are principally controlled by these factors:

- Chemical and physical properties of the contaminants (e.g., sorption coefficient or K_d)
- Physical properties (e.g., void structure and hydraulic conductivity, etc.) and state (e.g., integrity) of the waste form and disposal unit
- Chemical properties (e.g., reduction capacity) and state (e.g., E_h and pH) of the waste form and disposal unit
- Moisture flux to the saltstone through the disposal unit from the overlying soil

The basic design concept of the SDF is controlled release of contaminants over very long time periods. While functioning as designed, the SDF closure cap prevents perched water above the disposal unit and reduces water infiltration through the saltstone monolith. When the facility is relatively hydraulically intact, the predominant potential contaminant release mechanism is diffusion (Figure 4.2-4). As time passes the closure cap, the drainage layer, and the saltstone flow properties will degrade and may allow water movement through the closure cap, disposal unit, and saltstone monolith (Figure 4.2-5). Advective transport becomes increasingly important, as indicated by the increasing water velocity through the saltstone. Both diffusion and advective movement of dissolved contaminants from the saltstone monolith are enhanced under saturated conditions.

Figure 4.2-4: Contaminant Release and Transportation from Saltstone (Condition 1)

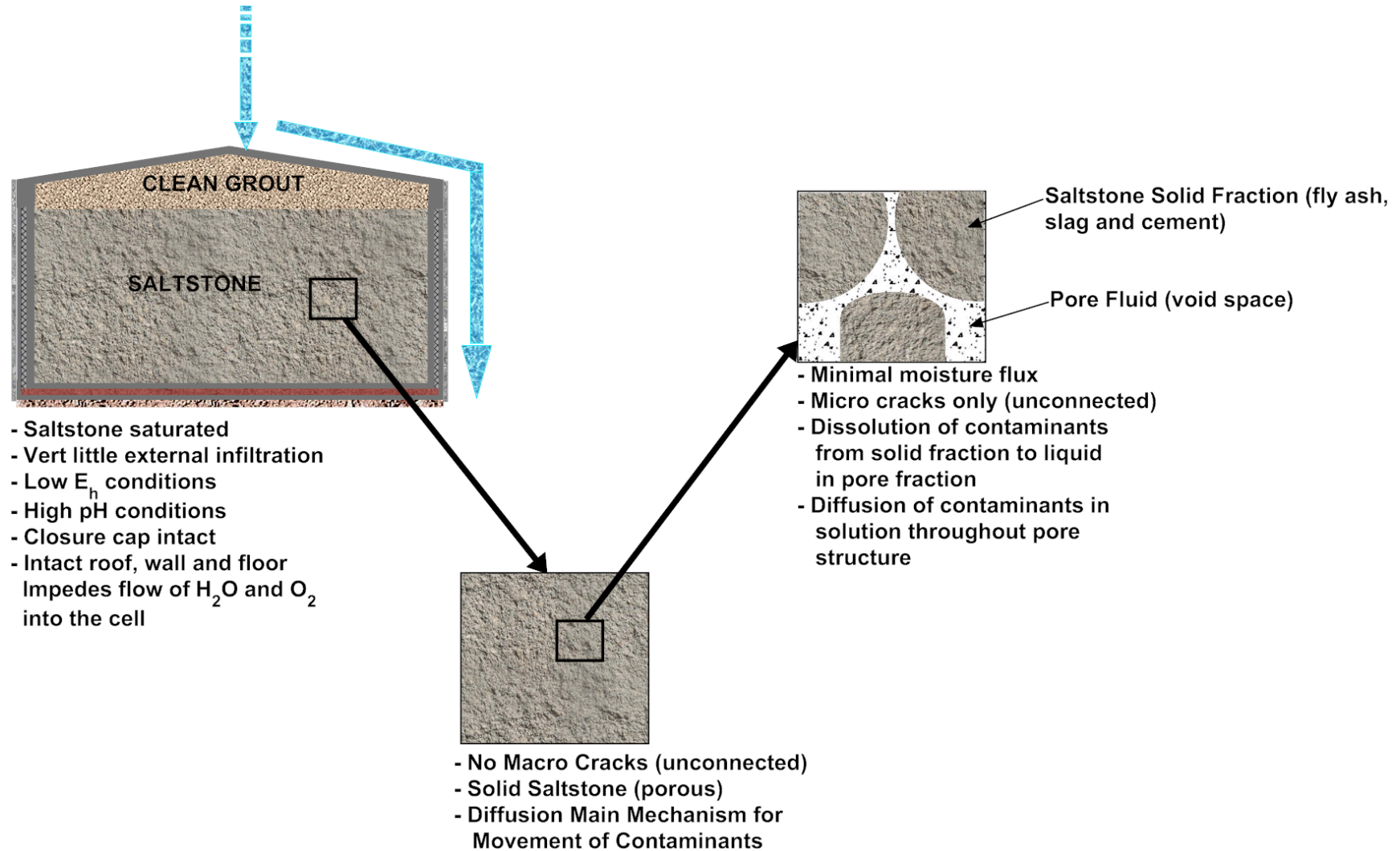
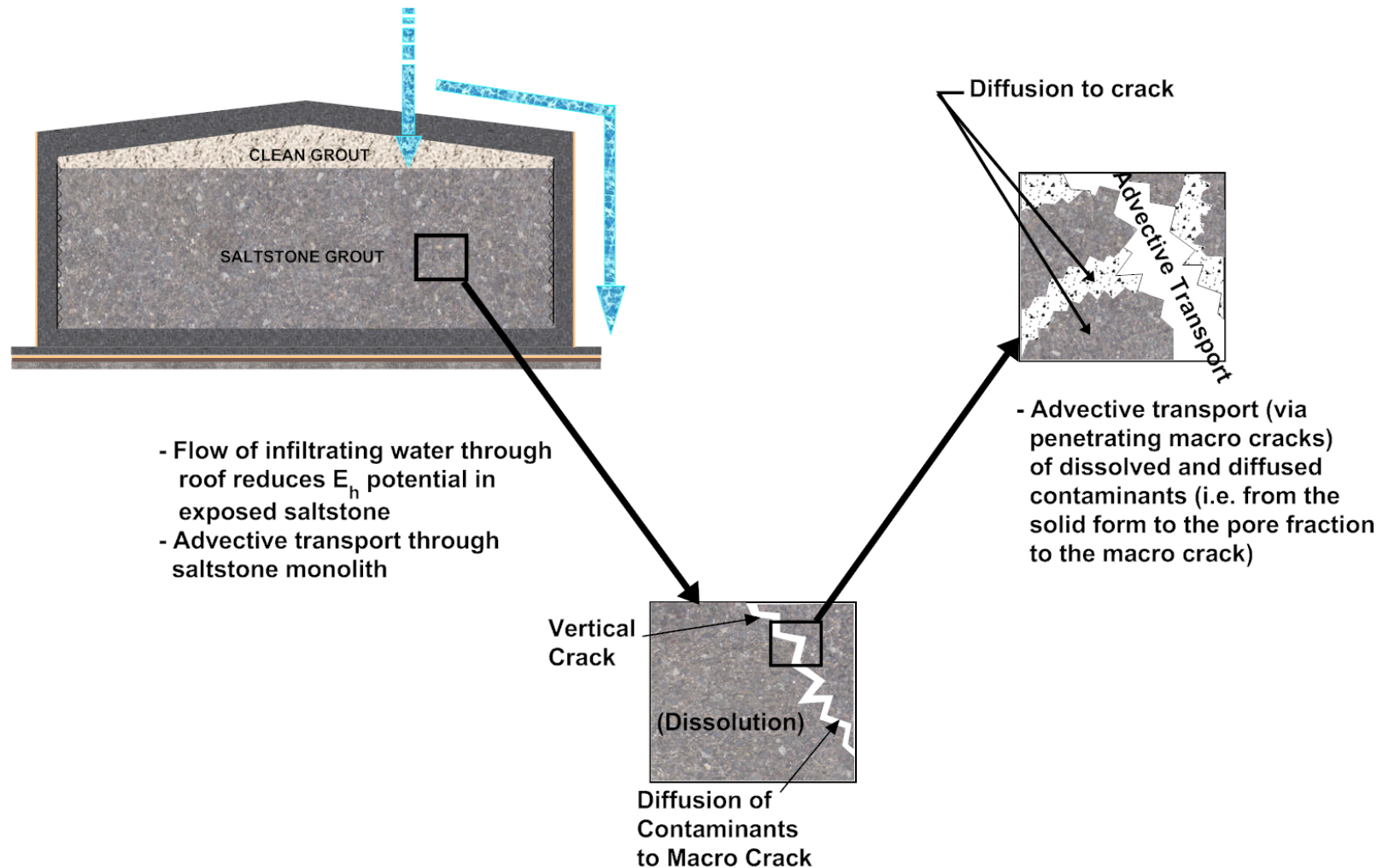


Figure 4.2-5: Contaminant Release and Transport from Saltstone (Condition 2)



Transport of certain species will be retarded by sorption to a varying degree, depending on K_d values of the retarding material. Redox and pH may affect solubility and sorption. For example, some contaminant species are highly sensitive to redox conditions, most notably technetium. Tc-99 is relatively mobile under oxidized conditions, but essentially immobile under reducing conditions. The SDF is designed to retain Tc-99 through the use of slag-bearing saltstone and disposal unit concrete mixes, which create a low E_h environment. It is assumed that oxygen from the environment outside the disposal unit will migrate via moisture into the SDF over time, slowly oxidizing the slag and releasing Tc-99.

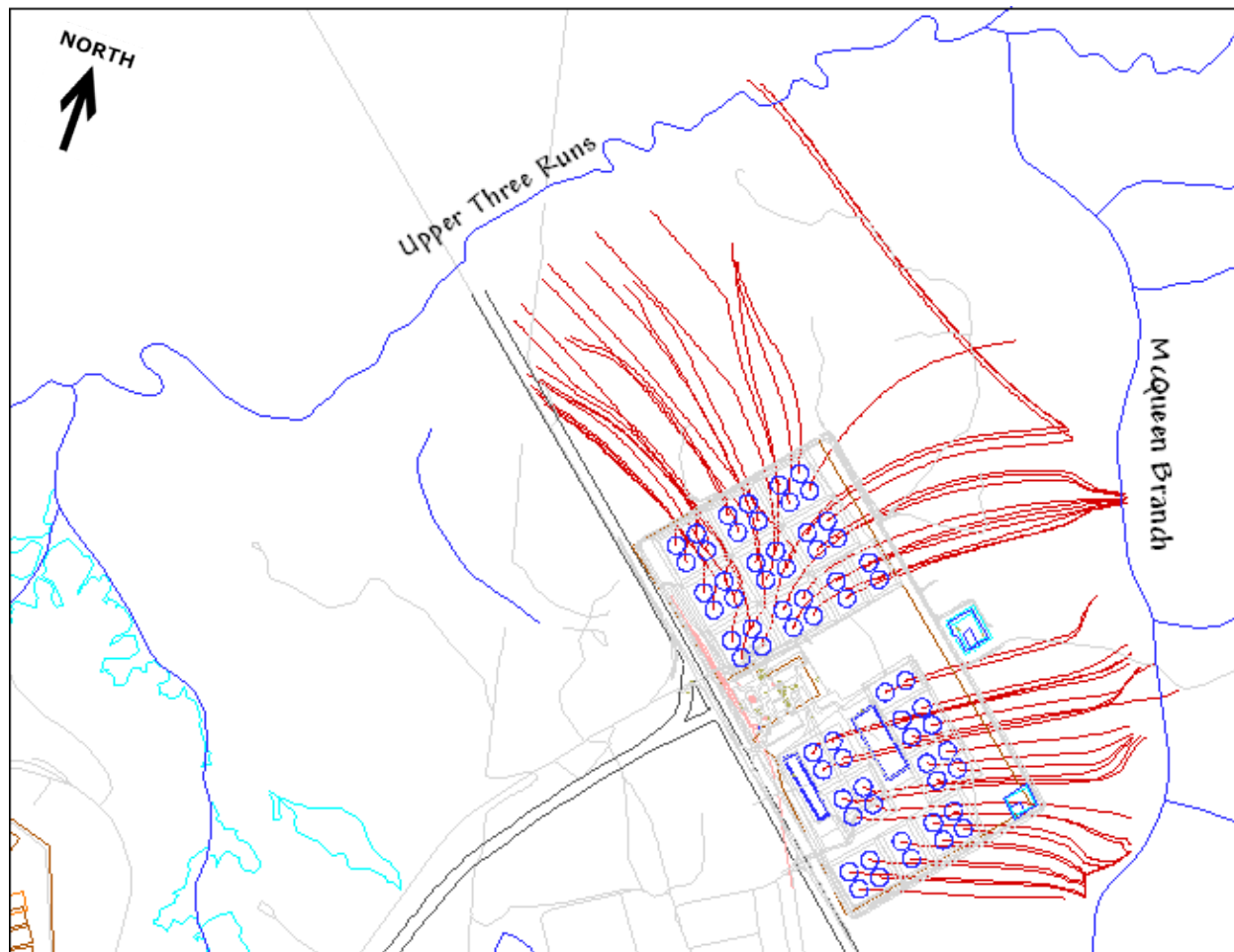
The SDF disposal units are designed, in part, for a dual role that limits releases of contaminants out of the disposal units, and limits the migration of oxygen into the disposal unit via dissolved oxygen in moisture, thus delaying oxidation of the saltstone. For example, the walls and floor of the FDCs are designed with a series of concrete layers and incorporate a HDPE barrier. Two separate HDPE systems are also incorporated into the closure cap system above the disposal units. A GCL (bentonite) layer is designed into the closure cap, the base layers, and the lower part of the wall system of the FDCs. Carbon steel is incorporated into the wall system. These materials are in place as a form of defense in-depth protection, and tend to limit the migration of dissolved oxygen into the disposal units and saltstone.

4.2.3.1.3 Transport Model – Saturation Zone

Contaminant flux crossing the water table will enter hydrogeologic units comprising the shallow aquifers underlying the SDF disposal units. The SDF straddles a groundwater divide between UTR and McQueen Branch. Some contaminants will be transported via groundwater through near surface aquifers and outcrop at either McQueen Branch or UTR. Exposure to contaminants could occur through various pathways associated with groundwater, surface water uses, and air exposure. Figure 4.2-1 shows the location of the SDF within the GSA, bound by UTR to the north, Fourmile Branch to the south, and McQueen Branch to the east.

Figure 4.2-6 illustrates the general flow of groundwater away from the FDCs of the SDF. The stream trace lines in Figure 4.2-6 were generated by the PORFLOW computer code, using the GSAD. The GSAD is a regional groundwater model used for saturated zone transport evaluations for all facilities within the GSA.

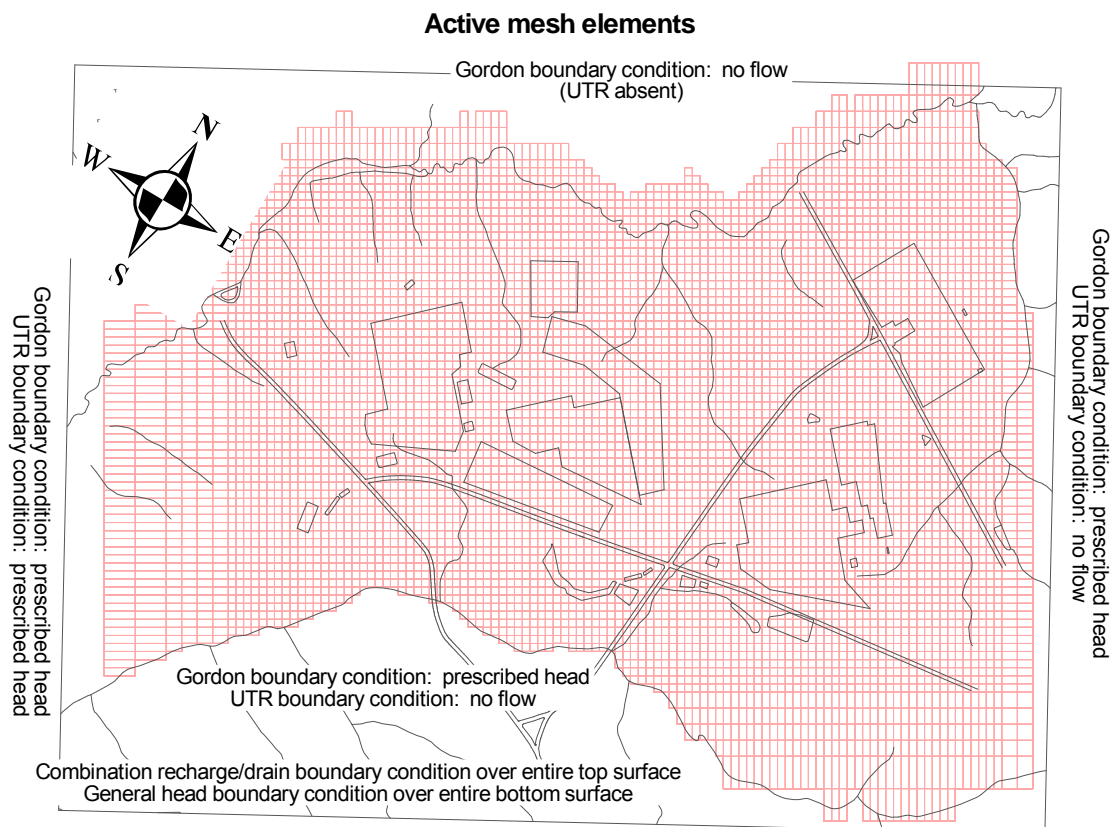
Figure 4.2-6: General Flow of Groundwater Away from the SDF



➤ **Groundwater Flow Simulation**

Groundwater flow in the much larger scale saturated zone or aquifer model is controlled by net infiltration or recharge over a broad area surrounding the SDF. While vadose flow simulations reflect lower infiltration due to the SDF cover system, no credit is taken for reduced infiltration in the aquifer model. That is, flow exiting the vadose zone model at the water table is not used to define local recharge beneath the SDF in the aquifer model. Rather, an average infiltration based on field studies is used to define the recharge portion of the combined recharge/drain boundary condition applied uniformly over the upper boundary of the GSA model. [WSRC-TR-96-0399-Vol. 2] For saturated zone contaminant transport, the contaminant flux leaving the bottom of the vadose zone model becomes the source of contamination entering the aquifer.

Figure 4.2-7: GSA Boundary Conditions



[WSRC-TR-96-0399-Vol. 2]

The aerial resolution of the aquifer model is 200 feet square except in peripheral areas. There are 108 grid blocks along the east-west axis, and 77 blocks along the north-south axis. The vertical resolution varies depending on hydrogeologic unit and terrain/hydrostratigraphic surface variations as depicted in Figure 4.2-8. Each hydrostratigraphic surface is defined by numerous “picks” ranging in number from approximately 52 to 225 depending on the surface. The Upper Zone of UTR (UTR-UZ) Aquifer Unit is represented with up to 10 finite elements in the vertical direction. The vadose zone is included in the model. The UTR Lower Zone (UTR-LZ) contains five finite elements while the TCCZ separating the aquifer zones is modeled with two vertical elements. The Gordon Confining Unit and Gordon Aquifer each contain two elements, for a total of 21 vertical elements from ground surface to the bottom of the Gordon Aquifer. The grid comprises 102,294 active cells as depicted in Figure 4.2-9 representing the three-dimensional (3-D) combination of the plan view information in Figure 4.2-7 and example section view information as presented in Figure 4.2-8.

Figure 4.2-8: North-South Cross Section of GSA/PORFLOW Computational Mesh for GSA

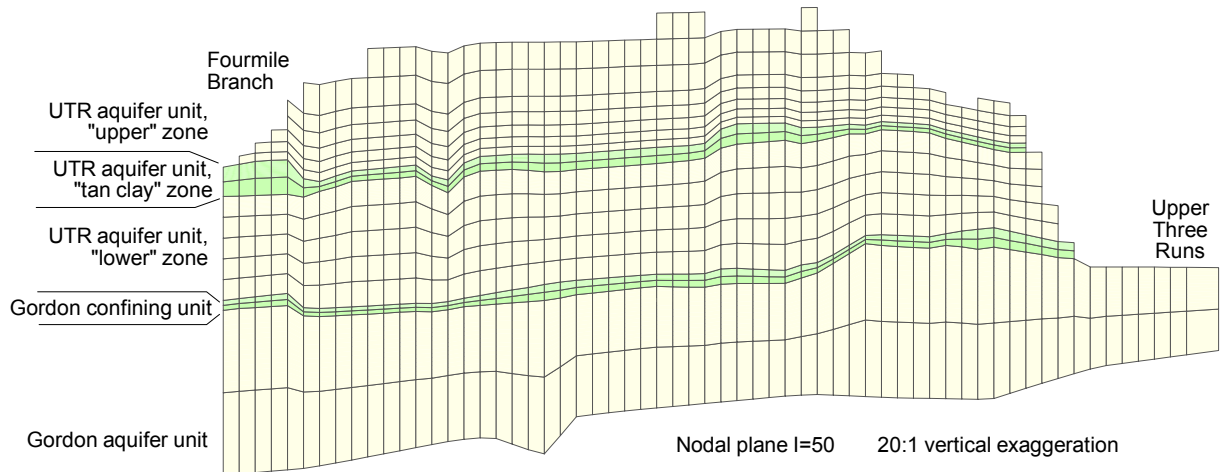
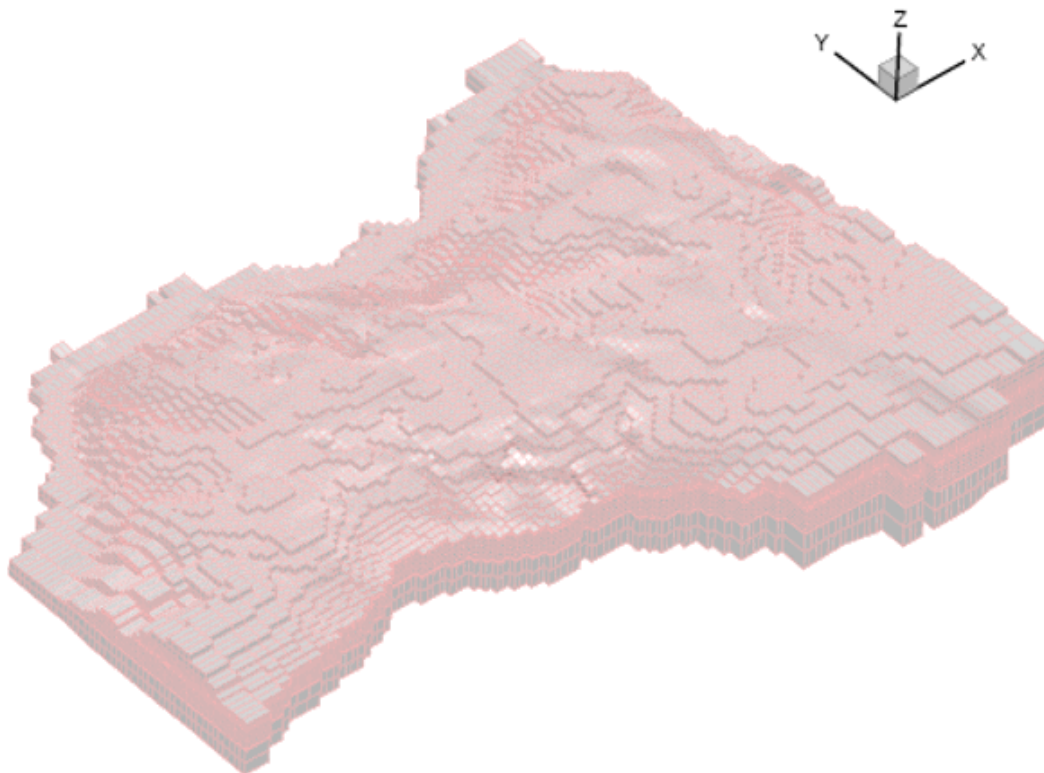


Figure 4.2-9: Perspective View of GSA/PORFLOW Computational Mesh



Hydraulic conductivity values in the model are based on characterization from the GSAD discussed in Section 3.1.5. The conductivity field is heterogeneous within hydrogeologic units and reflects variations present in the characterization data. The average horizontal conductivities in the saturated UTR-UZ, UTR-LZ, and Gordon Aquifer are approximately 10, 13, and 38 ft/d, respectively. The average vertical conductivities for the TCCZ and the Gordon Confining Unit are $6.0\text{E-}3$ and $1.0\text{E-}5$ ft/d, respectively. Figures 4.2-10 and 4.2-11 illustrate the horizontal and vertical hydraulic conductivity field models, respectively, along a representative cross section. The GSA/PORFLOW model was calibrated and validated using measured well water levels.

Figure 4.2-10: North-South Cross Section of GSA/PORFLOW Model - Horizontal Hydraulic Conductivity Variations

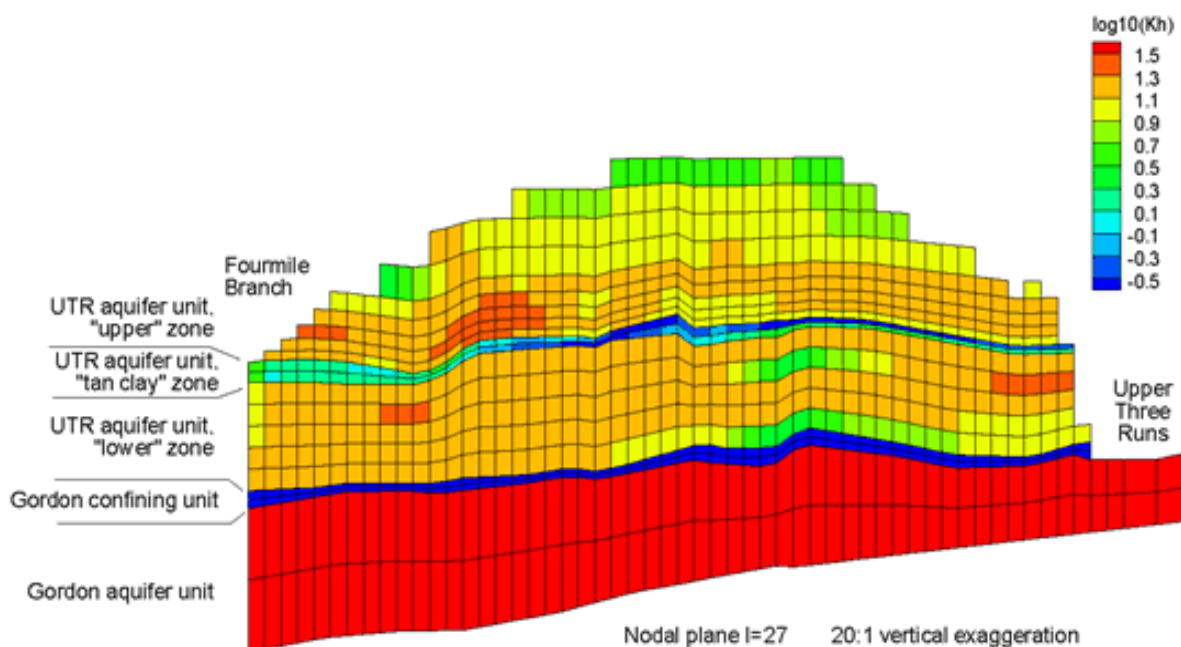
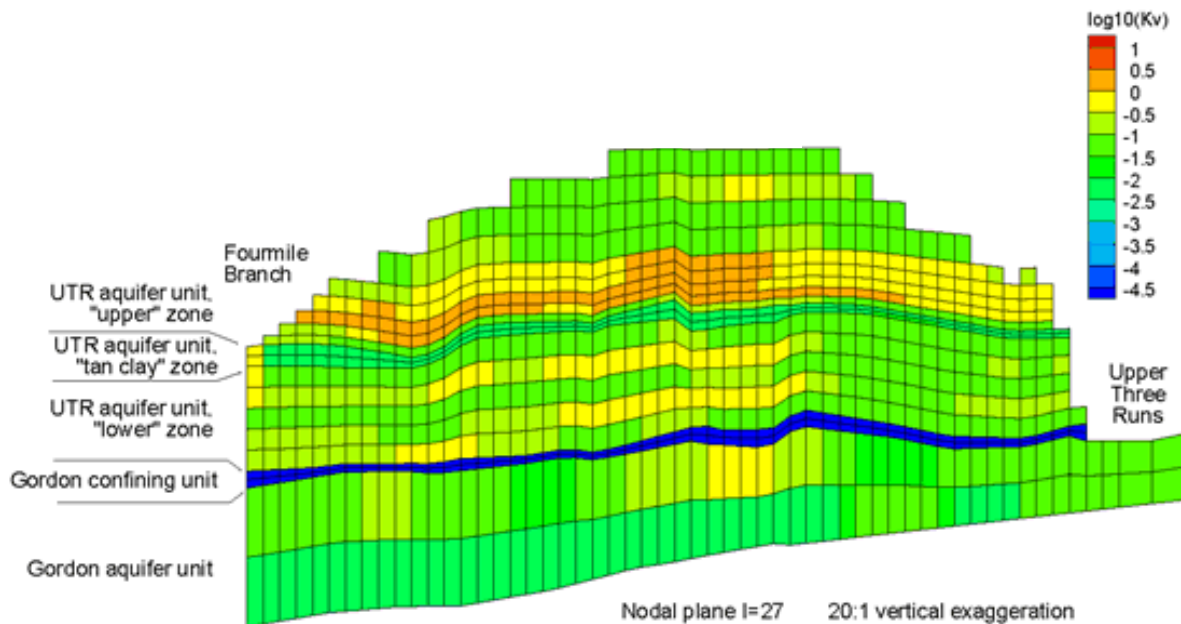


Figure 4.2-11: North-South Cross Section of GSA/PORFLOW Model - Vertical Hydraulic Conductivity Variations



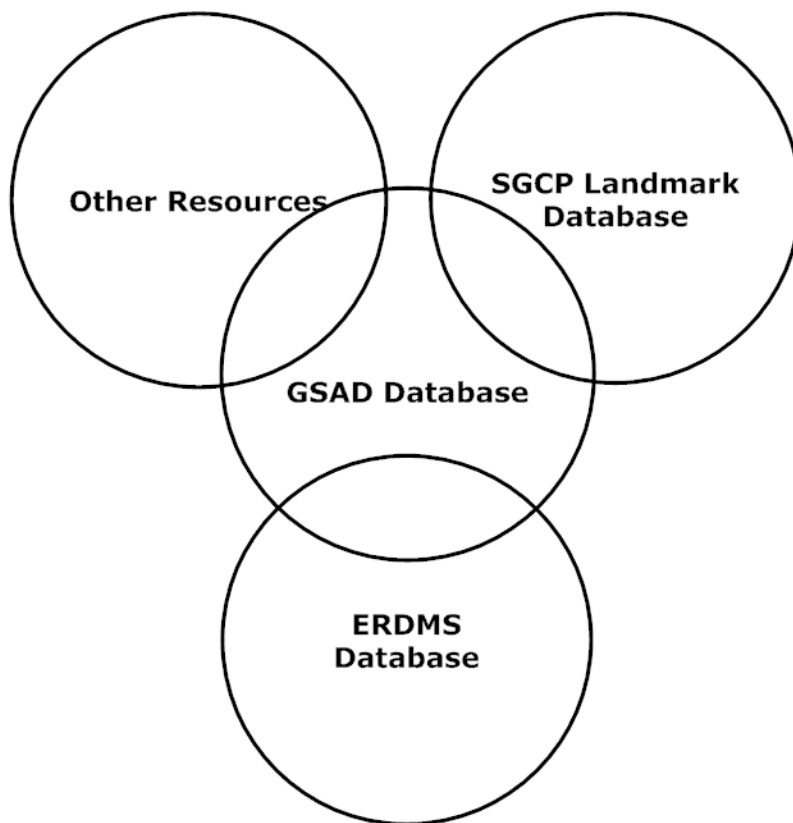
The average natural recharge over the entire model domain is 14.7 in/yr. [WSRC-TR-2004-00106] Various man-made features (e.g., basins) provide additional recharge in localized areas. The estimated discharge rates to UTR and Fourmile Branch within the model domain are 18.2 and 2.6 ft³/sec, respectively. [WSRC-TR-2004-00106] The simulated discharge rates are 11.4 and 3.8 ft³/sec, respectively. Predicted seepage faces are consistent with field observations. Simulated hydraulic heads, vertically-averaged over the entire thickness of the UTR-LZ, UTR-UZ, and Gordon Aquifer, agree with potentiometric maps based on measured heads. Simulated flow directions, vertically-averaged over the entire thickness of the aquifer zones, agree with conceptual models of groundwater flow.

➤ **Adequacy of GSAD Data Set for Groundwater Flow Simulation**

additional data has not altered fundamental understanding of groundwater flow patterns and gradients in the GSA. The GSAD is a subset of site-wide data sets of soil lithology and groundwater information. These larger sets of data are captured in the Environmental Restoration Data Management System (ERDMS) database, SGCP landmark database, and other resources. The relationship between GSAD and the full set of data is pictured in Figure 4.2-12.

The GSAD includes field data and interpretations collected in the GSA through 1996. Although characterization and monitoring have been ongoing, the

Figure 4.2-12: General Separations Area Database Relationship



During the 1980s and early 1990s, significant work was conducted within the GSA to better define the hydrogeology including installation of well clusters, continuous core descriptions, and geophysical logs associated with the deepest well in the cluster. At that point, the Hydrostratigraphy of the GSA was considered sufficiently defined, and no additional characterization was planned. Since the mid 1990s, wells have been installed to better define plumes, and CPT logs have been generated for structural/seismic and vadose zone monitoring purposes.

The hydrostratigraphic unit known as the TCCZ is of particular interest to a SDF PA analysis because the TCCZ can act locally as an aquitard, supporting a water table and retarding the downward flow of groundwater. The presence or absence, thickness, and extent of this unit are important inputs into contaminant transport simulations used in this PA. The TCCZ was recently reviewed and interpreted with new and pertinent subsurface geologic data for Z-Area. [SED-GTE-2008-002] The results of this review supplement and confirm previous interpretations regarding the TCCZ beneath the SDF. Results from this examination revealed that the TCCZ is present in every borehole and CPT evaluated at the SDF site. Section 3.1.5.2 discusses more details of this review.

In order to evaluate the need to update the original GSAD to incorporate new hydrogeologic information, two evaluations were conducted.

Figure 4.2-13 shows recent hand-drawn water table contour map for the GSA based on water level data collected in 1995, 1998 and 2003. Contours were developed using mean water levels from SRS wells, field verification of perennial stream reaches, and the USGS 1:24000 scale topography data. [WSRC-MS-95-0524, WSRC-TR-98-00045, and WSRC-TR-2003-00250] These contour maps are consistent with each other indicating that there has not been a significant change in our understanding of long-term average water table conditions in the GSA since the mid 1990s.

Figure 4.2-13: Water Table Contour Maps for GSA

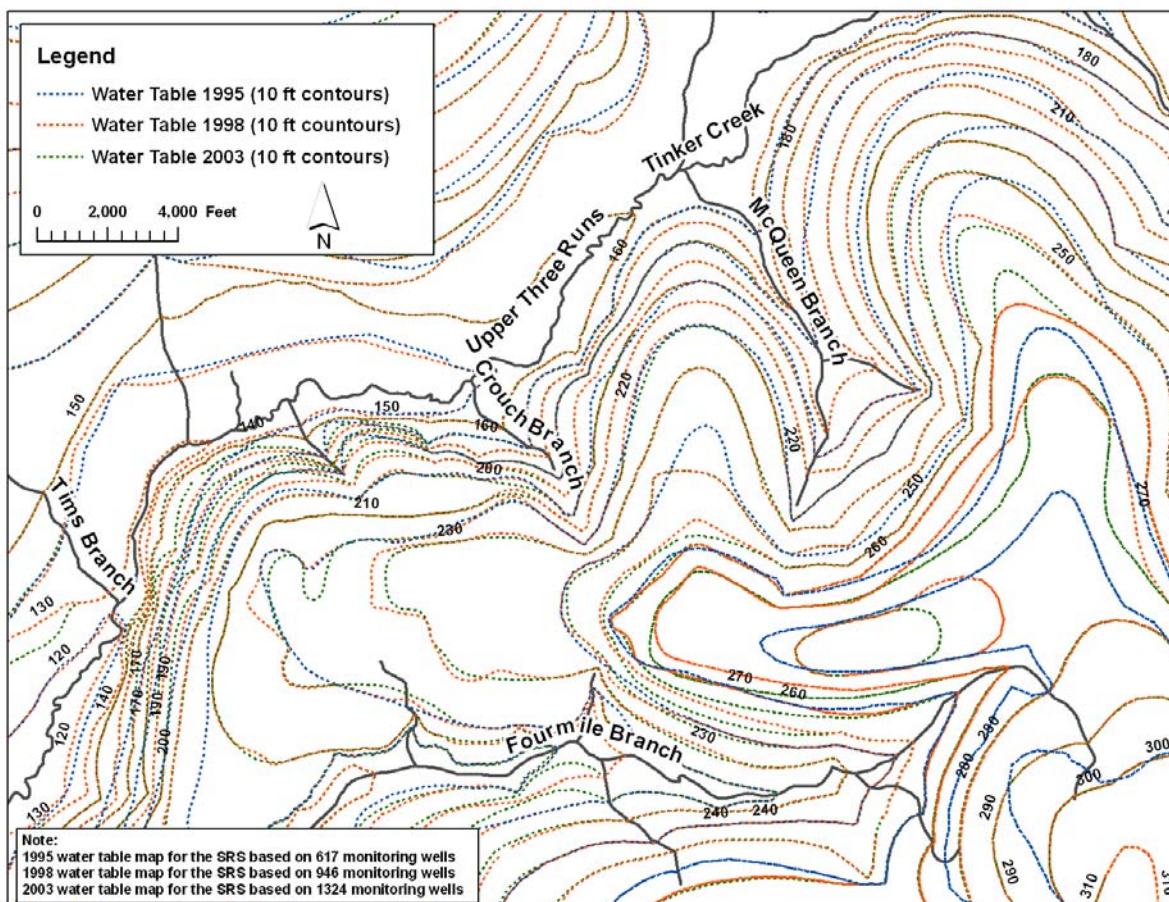


Figure 4.2-14 provides a comparison of the 2003 hand-drawn, contoured water table map and the water table predicted by the GSA/PORFLOW model.

Figure 4.2-14: Comparison of (a) GSA/PORFLOW Model Predicted and (b) Hand-Contoured 2003 Water Table Maps

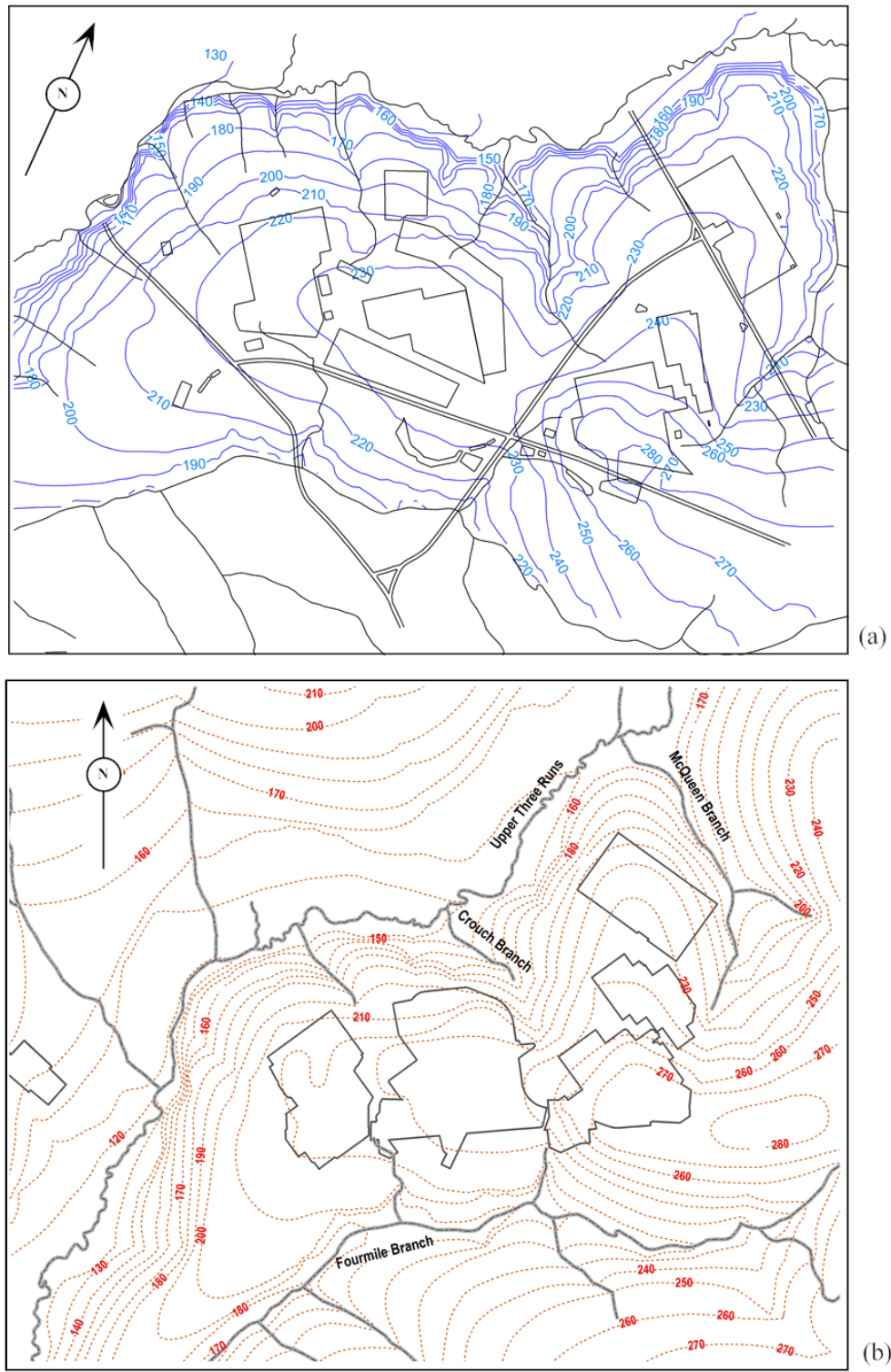


Table 4.2-10 summarizes hydraulic head residuals between the model and the field data. [WSRC-TR-2004-00106, Section 3.1] Table 4.2-10 also summarizes more recent well water level data through 2006, available as a result of new well installations and continued monitoring. The agreement between the model and the data set through 2006 is similar to that of the original data set.

Table 4.2-10: Hydraulic Head Residuals Between GSA/PORFLOW Model and Field Data through 2006

| Aquifer Zone | Number of Wells | Median Residual (feet) | Average Residual (feet) | Root-Mean-Square Residual (feet) | Minimum Residual (feet) | Maximum Residual (feet) |
|------------------------|-----------------|------------------------|-------------------------|----------------------------------|-------------------------|-------------------------|
| Up to 1995 Data | 638 | N/A | N/A | N/A | N/A | N/A |
| Gordon | 79 | -0.0 | -0.5 | 1.7 | -4.7 | 2.5 |
| UTR-LZ | 173 | +0.8 | +0.6 | 4.6 | -9.4 | 27.0 |
| UTR-UZ | 386 | -0.1 | -0.5 | 3.4 | -15.2 | 10.0 |
| Up to 2006 Data | 917 | N/A | N/A | N/A | N/A | N/A |
| Gordon | 94 | +0.3 | -0.0 | 1.5 | -3.8 | 2.6 |
| UTR-LZ | 272 | +1.1 | +1.0 | 4.7 | -11.9 | 27.0 |
| UTR-UZ | 551 | +0.8 | +0.1 | 3.5 | -16.8 | 14.5 |

The data collection and quality review process employed in constructing the GSAD is described in *Summary of the Quality Review Process for General Separations Area Aquifer Model Database*. [SRNL-ESB-2007-00001]

As noted earlier, the ISCM of subsurface water flow and contaminant transport comprises three principal elements; (1) the closure cap, (2) the vadose zone, and (3) the saturated zone, as illustrated in Figure 4.1-1.

➤ **Transport Model Interfaces**

A prescribed rainfall condition in the form of daily rainfall values over an extended period of time is the primary input or external boundary condition to the closure cap flow analysis. The closure cap model produces a net infiltration rate at the bottom of the closure cap that becomes a flow boundary condition to the adjoining vadose zone. Water infiltrating the closure cap is assumed to be free of contaminants, so the concentration is set to zero at the top boundary of the vadose zone.

Groundwater flow in the much larger scale saturated zone or aquifer model is controlled by net infiltration or recharge over a broad area surrounding the SDF. While vadose flow simulations reflect lower infiltration due to the SDF cover system, no credit is taken for reduced infiltration in the aquifer model. That is, flow exiting the vadose zone model at the water table is not used to define local recharge beneath the SDF in the aquifer model. Rather, an average infiltration based on field studies is used to define the recharge portion of the combined recharge/drain boundary condition applied uniformly over the upper boundary of the GSA model. [WSRC-TR-96-0399-Vol. 2] For saturated zone contaminant transport, the contaminant flux leaving the bottom of the vadose zone model becomes the source of contamination entering the aquifer.

Each water table flux contribution from an individual SDF disposal unit is assigned to the aquifer transport grid by uniformly distributing the flux to those water table cells with centroids lying within the footprint of the disposal unit.

4.2.3.2 Model Material Properties

Relevant material properties for the three conceptual models in the ISCM form a key part of the performance assessment and are provided in this section.

4.2.3.2.1 Closure Cap Material Properties

The conceptual design and detailed description of the closure cap are provided in Section 3.2.2. Table 4.2-11 provides the material properties of the closure cap obtained from WSRC-STI-2008-00244 that are pertinent to the transport model. Table 3.2-6 provides the time-variant infiltration rates based on the analysis presented in Section 3.2.2.

Table 4.2-11: SDF Closure Cap Material Properties

| Layer | Thickness (inches) | Saturated Hydraulic Conductivity (cm/sec) |
|--|--------------------|---|
| Topsoil | 6 | 3.1E-03 |
| Upper Backfill | 30 | 4.1E-05 |
| Erosion Barrier | 12 | 1.3E-04 |
| Middle Backfill Layer | 12 | 4.1E-05 |
| Upper Lateral Drainage Layer | 12 | 5.0E-02 |
| HDPE Geomembrane | 0.06 | 2.0E-13 |
| GCL | 0.2 | 5.0E-09 |
| Foundation Layer (backfill with bentonite admix) | 12 | 1.0E-06 |
| Lower Backfill | 72 ^a | 1.0E-03 |

(a) Thickness of this layer is based on expected nominal thickness rather than the minimum thickness specified in Section 3.2.2. The performance of the closure cap is not appreciably impacted by the thickness of this layer.

4.2.3.2.2 Material Properties Above the Disposal Unit

This portion of the overall SDF closure ISCM focuses on the region between the bottom of the closure cap and the top of the disposal units. This area includes the lower drainage layer and the HDPE-GCL layer above the disposal unit roof.

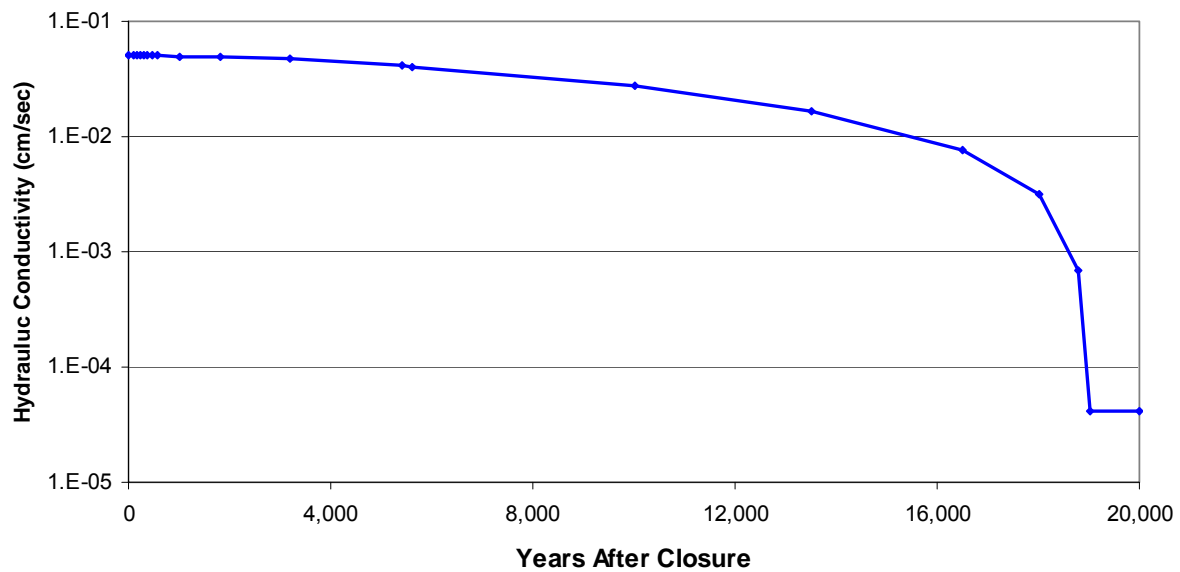
Prior to the placement of the closure cap, each disposal unit will be prepared by sealing all penetrations. Each FDC will be provided a smooth surface free of material that may be deleterious to the membrane material layers that will overlay each disposal unit. Directly above each FDC there will be placed a GCL layer, followed by a HDPE layer, and then it will be topped with a geotextile fabric. The geotextile fabric will also be placed above Vaults 1 and 4. A 2 foot thick lower lateral drainage layer will be placed above the geotextile fabric overlying the disposal units. This lower lateral drainage layer will extend approximately 25 feet from each disposal unit, draining to the backfill material that will be placed adjacent to the disposal units. The lateral drainage layer will be designed to do the following:

- Divert infiltrating water away from the underlying disposal unit and transport the water beyond each disposal unit perimeter in conjunction with the underlying composite hydraulic barrier (i.e., HDPE geomembrane and GCL for the FDCs) and prevent perched water on top of the FDCs
- Provide the necessary confining pressures to allow the GCL underlying the FDCs to hydrate properly

The lower lateral drainage layer will be sloped at the same degree as the roof of the disposal units (i.e., 2%). The lower lateral drainage layer will be hydraulically connected to the foundation layer (lower backfill) of the closure cap in order to divert and transport as much infiltrating water as possible away from the underlying disposal unit. A geotextile filter fabric will be placed between the lower lateral drainage layer and the foundation layer of the closure cap.

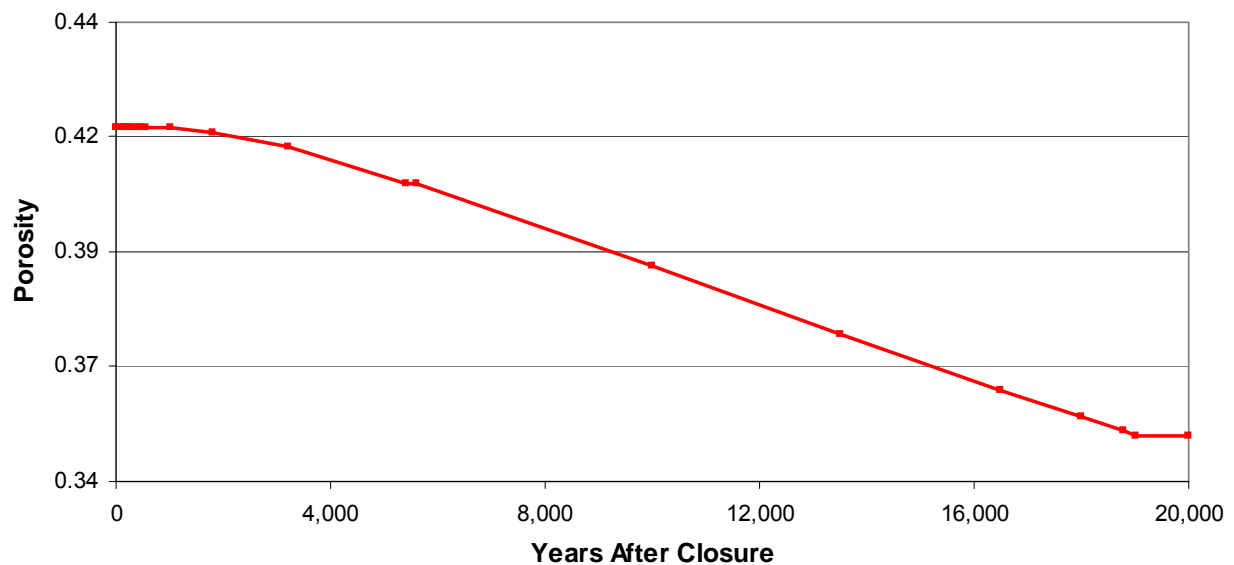
The hydraulic properties of the backfill layer above the drainage layer are not expected to change; however, over time colloidal clay will migrate with the water-flux from the lower backfill layer to the underlying 2 foot thick lower lateral drainage layer. This water-flux driven clay will accumulate in the lower drainage layer from the bottom up. The thickness of the clay filled portion increases with time, while the thickness of the unfilled portion decreases with time, which will result in an overall decrease in hydraulic conductivity and the porosity of the drainage layer. Figures 4.2-15 and 4.2-16 illustrate the decrease in the vertical hydraulic conductivity and porosity based on analyses described in WSRC-STI-2008-00244 and presented in SRNL-STI-2009-00115. The decrease in the horizontal hydraulic conductivity follows the curve illustrated in Figure 4.2-15 for the reduction in the vertical hydraulic conductivity. After approximately 19,000 years, the hydraulic conductivity and porosity of the lower lateral drainage layer are estimated to be similar to those for the overlying backfill layer as shown in Table 4.2-12. Figures 4.2-17 and 4.2-18 illustrate the characteristic curves for the backfill layer and the drainage layer, respectively.

Figure 4.2-15: Vertical Hydraulic Conductivity of Lower Lateral Drainage Layer



[SRNL-STI-2009-00115]

Figure 4.2-16: Porosity of Lower Lateral Drainage Layer

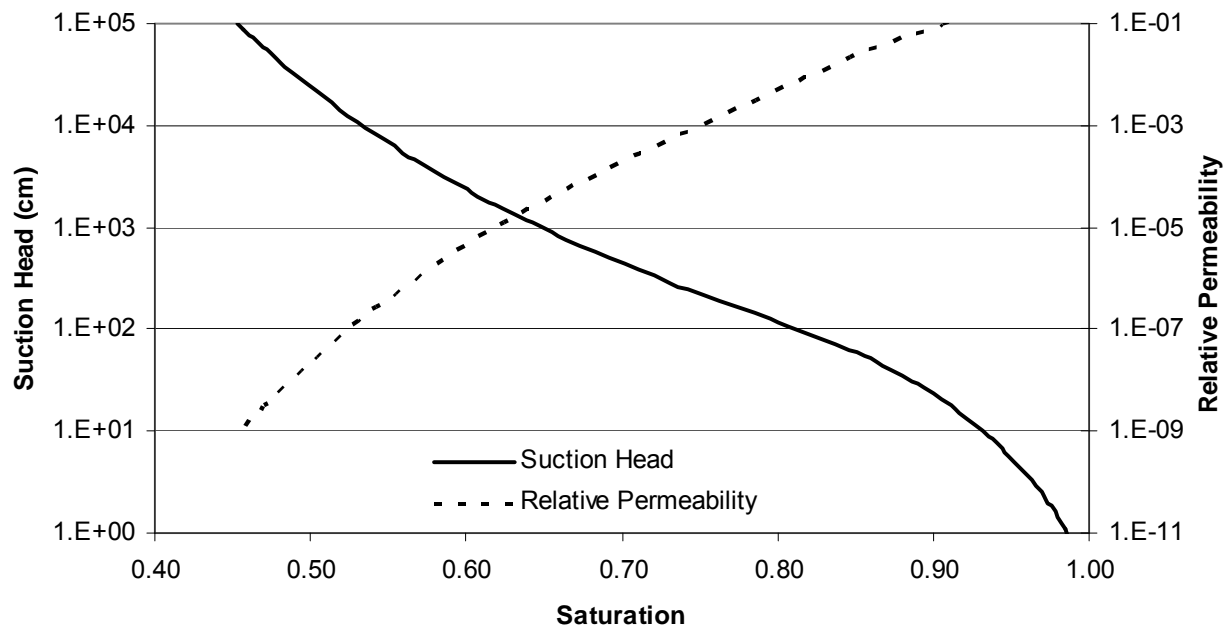


[SRNL-STI-2009-00115]

Table 4.2-12: Hydraulic Parameters for Lower Lateral Drainage Layer

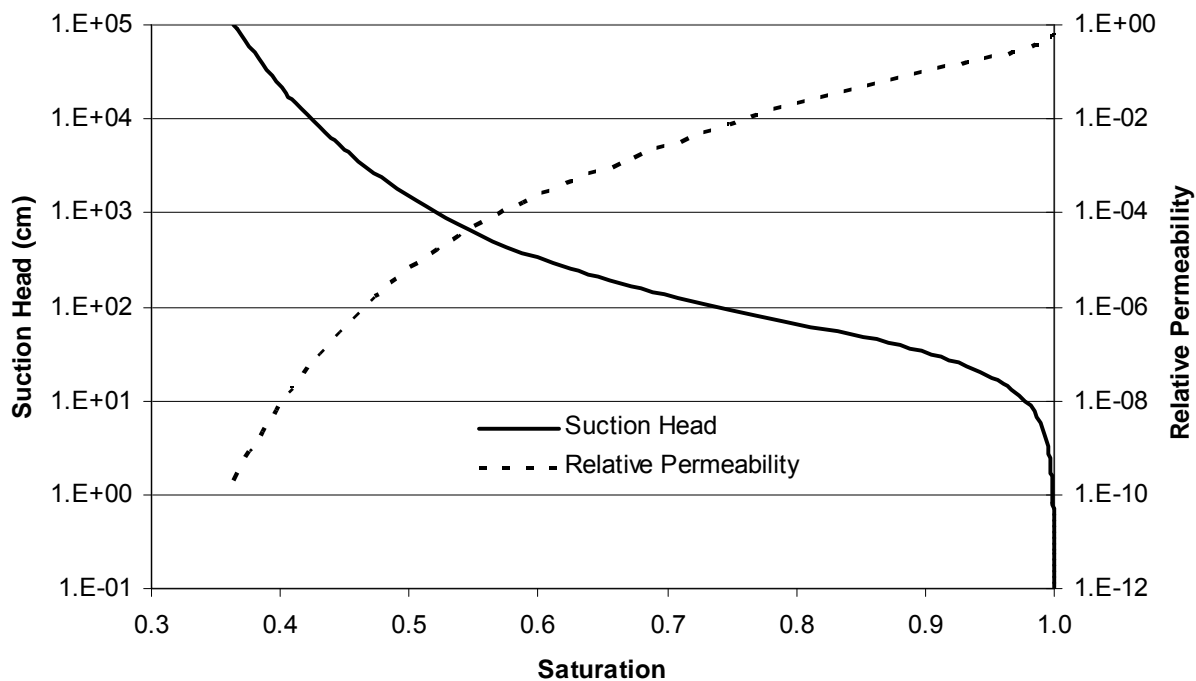
| Time Period | Conductivity (cm/sec) | Porosity | Reference |
|------------------------------------|--|----------|---------------------|
| Initially (Sand drainage layer) | 5.0E-02 (vertical) 5.0E-02 (horizontal) | 0.417 | WSRC-STI-2008-00244 |
| After 19,013 years (Backfill) | 4.1E-05 (vertical) 7.6E-05 (horizontal) | 0.35 | SRNL-STI-2009-00115 |

Figure 4.2-17: Backfill Characteristic Curves



[WSRC-STI-2006-00198, Table 5-21]

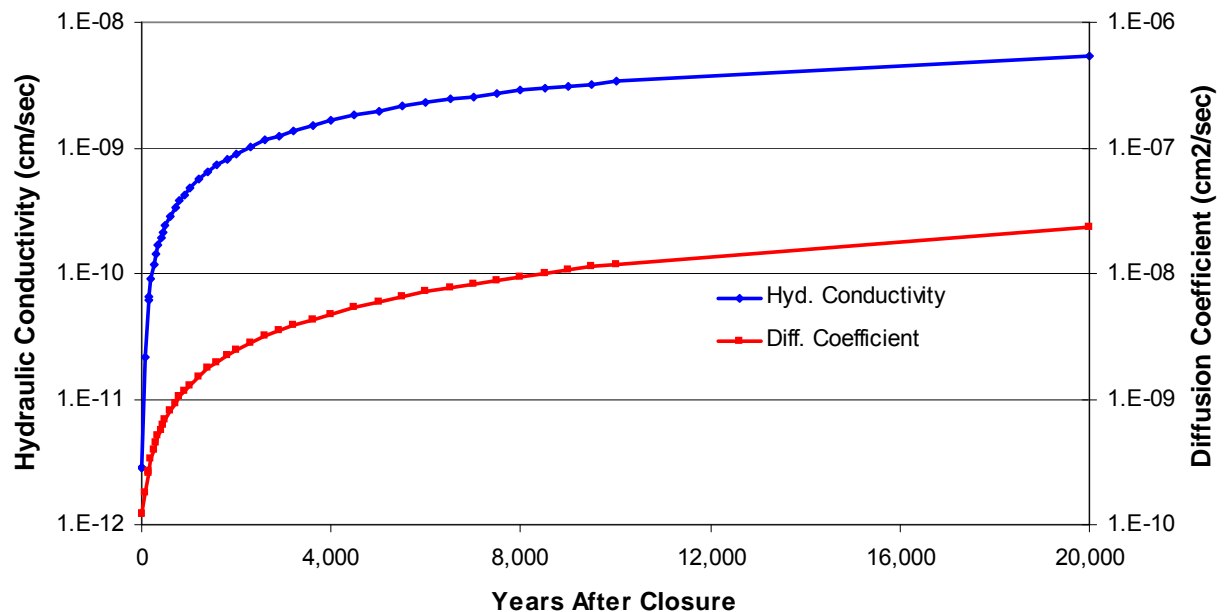
Figure 4.2-18: Drainage Layer Characteristic Curves



[WSRC-STI-2006-00198, Table 5-20]

The geomembrane composite layer below the drainage layer and overlying each FDC will also undergo degradation, which will result in the increase in the hydraulic conductivity and diffusion associated with this composite layer. Initially, the HDPE-GCL composite layer has a hydraulic conductivity of $2.8\text{E-}12$ cm/sec and a D_e (effective diffusion coefficient) of $1.2\text{E-}10$ cm²/sec. Over time, holes will generate within the HDPE as the membrane becomes increasingly susceptible to brittle stress cracking, which is analyzed as part of the performance assessment of the proposed closure cap design. In addition, the GCL will experience divalent cation degradation from the conversion of the initial sodium bentonite to calcium-magnesium-bentonite. These degradation mechanisms for the HDPE and GCL are described in WSRC-STI-2008-00244 and have been similarly evaluated for the HDPE-GCL composite layer in SRNL-STI-2009-00115. The results of this evaluation are illustrated in Figure 4.2-19, which shows the increase in the hydraulic parameters of the HDPE-GCL for 20,000 years after SDF closure. For modeling purposes, the characteristic curves for backfill, shown on Figure 4.2-17, are assumed applicable to the HDPE-GCL layer.

Figure 4.2-19: Hydraulic Parameters of HDPE-GCL Layer



[SRNL-STI-2009-00115]

4.2.3.2.3 Vadose Zone Material Properties

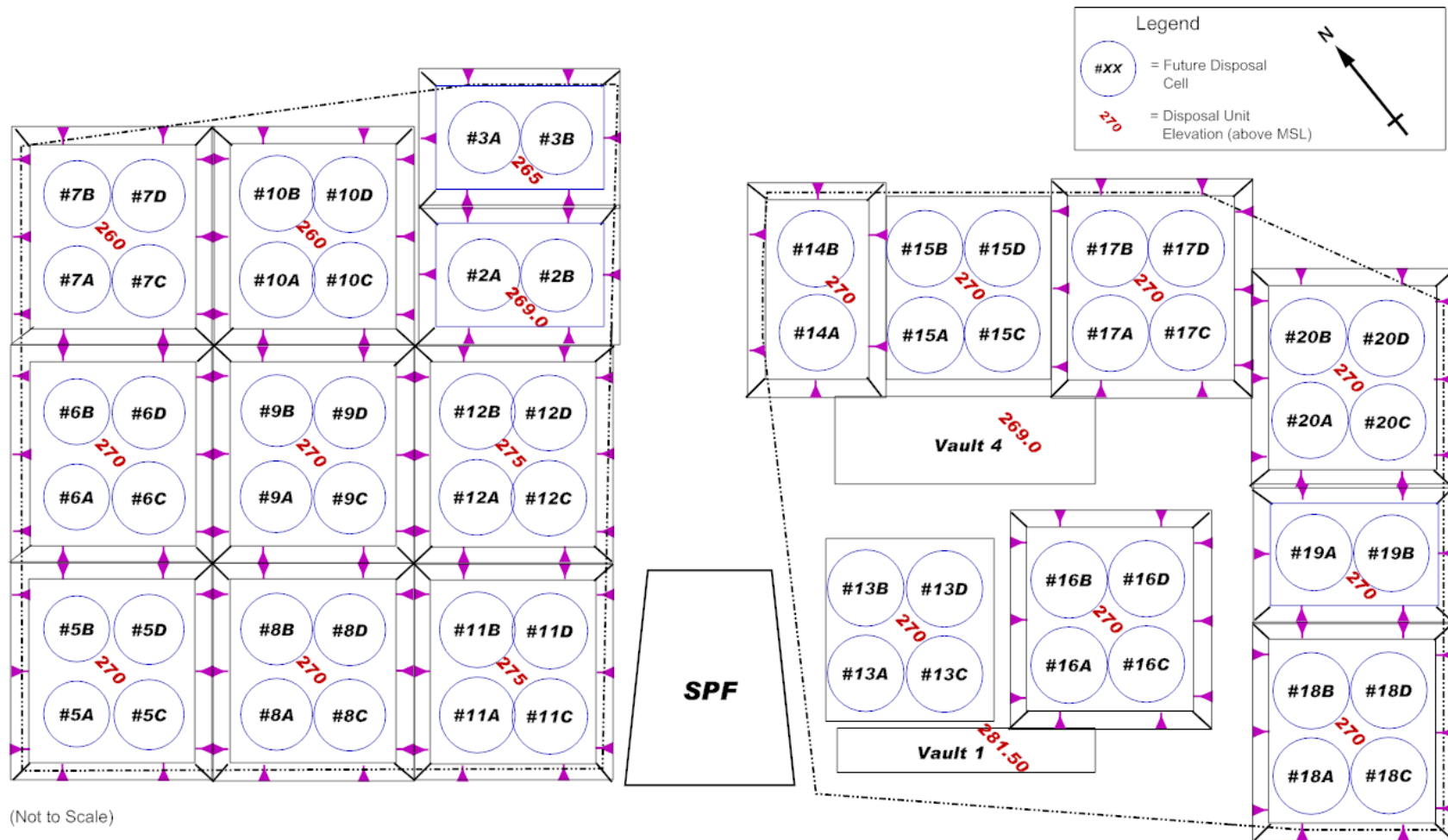
This portion of the overall SDF closure ISCM focuses on the region between the existing grade and the top of the water table (excluding the disposal units themselves). This area includes the undisturbed, unsaturated soil under the disposal units and the backfilled soil around the FDCs. The parameters of concern include:

- Vadose zone thickness under the SDF disposal units
- Saturated D_e
- Average total porosity
- Average dry bulk density
- Average particle density
- Saturated horizontal hydraulic conductivity
- Saturated vertical hydraulic conductivity
- K_d values
- Characteristic curves (suction head, saturation, and relative permeability)

➤ **Vadose Zone Background** This section briefly describes the basis for the vadose zone input parameters. The source of information for the parameters is WSRC-STI-2006-00198, which can be consulted for additional details.

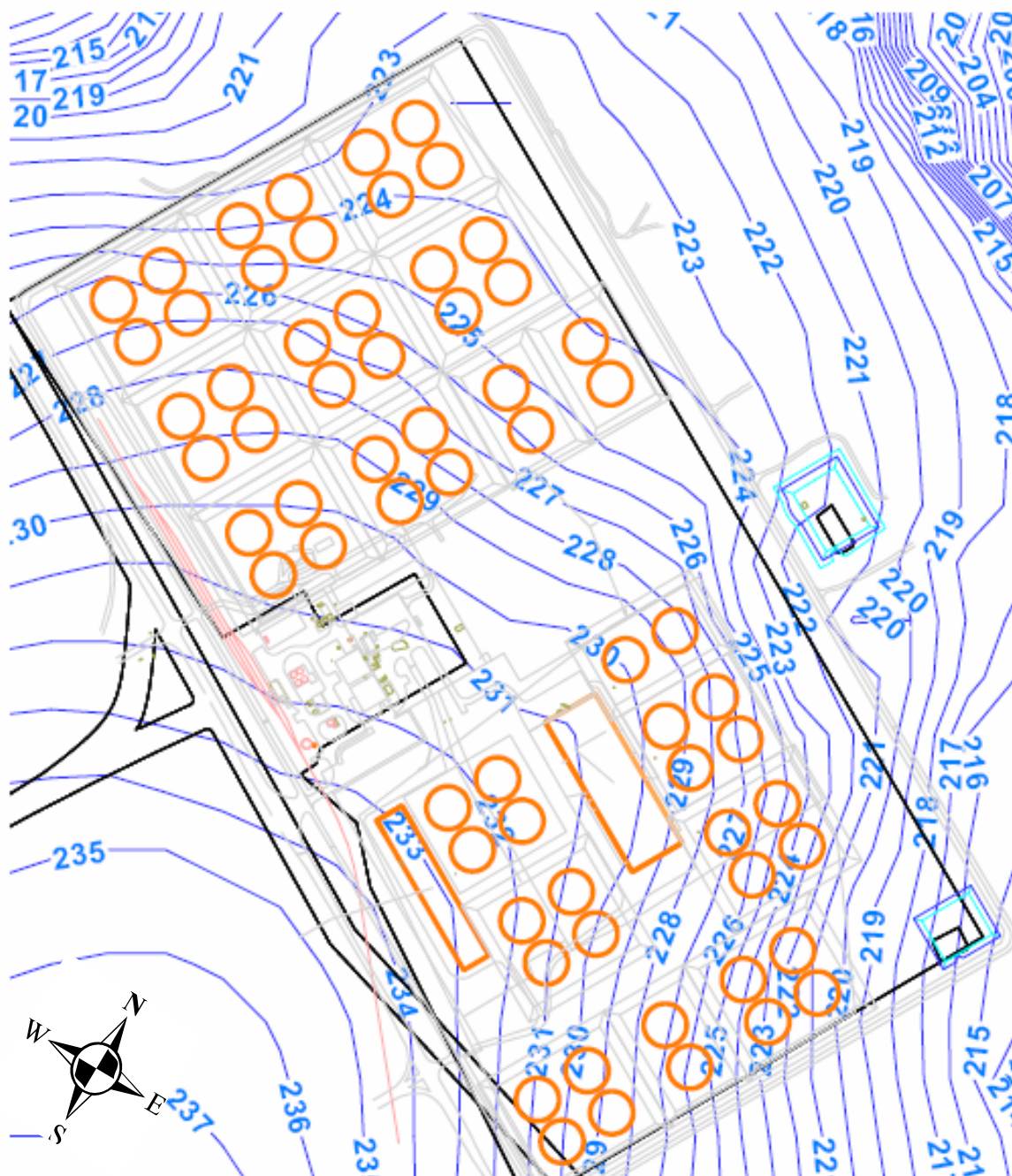
The vadose zone at the SDF can be divided into two regions, an Upper Vadose Zone and a Lower Vadose Zone. The Upper Vadose Zone (above 264 feet above MSL) consists of finer-grained sediments and typically displays a higher gamma ray, CPT friction ratio, and pore pressure response. The Lower Vadose Zone (below 264 feet above MSL) has a higher sand content and generally exhibits a lower gamma ray, CPT friction ratio, and pore pressure response. Figure 4.2-20 illustrates the anticipated locations and base elevations of the SDF disposal units. The base elevations for Vaults 1 and 4 are described as the bottom of the floor slab, which rests on top of the disposal unit's four inch thick working slab. The base elevation for the FDCs is described as the bottom of the lower mud mat, which is described in Section 3.2.1.3. As indicated in Figure 4.2-20, the base of the disposal units are each located within the Upper Vadose Zone with the FDCs being backfilled with the excavated material from the Upper Vadose Zone. Figure 4.2-21 shows water table contours obtained from the GSA/PORFLOW model (Figure 62 of SRNL-STI-2009-00115). The depth of the vadose zone (distance from the base of the disposal unit to the water table) is presented in Table 4.2-13. To facilitate the modeling for the FDCs, the thickness of the vadose zone below the FDCs was modeled as 42 feet, which is the arithmetic average of the thickness of the vadose zone for the 64 FDCs.

Figure 4.2-20: Locations and Base Elevations of Disposal Units within SDF



Note: Figure presents the anticipated FDC locations, numbering of the units are placeholders and may not match the final disposal unit numbering.

Figure 4.2-21: Long Term Average Water Table Near SDF



[SRNL-STI-2009-00115, Figure 62]

Table 4.2-13: Estimated Depth of Vadose Zone for SDF Disposal Units

| SDF Disposal Unit | Disposal Unit Base Elevation (Feet above MSL)¹ | Estimated Elevation of Water Table (Feet above MSL) | Estimated Depth of Vadose Zone (Feet) |
|-----------------------------------|--|--|--|
| Vault 1 (existing) | 281.5 | 233.5 | 48 |
| Vault 4 (existing) | 269 | 230.6 | 38.4 |
| Disposal Cells 2A / 2B (future) | 269 | 225.5 | 43.5 |
| Disposal Cells 3A / 3B (future) | 265 | 224.3 | 40.7 |
| Disposal Cells 5A – 5D (future) | 270 | 226.5 | 43.5 |
| Disposal Cells 6A – 6D (future) | 270 | 224.2 | 45.8 |
| Disposal Cells 7A – 7D (future) | 260 | 223.7 | 36.3 |
| Disposal Cells 8A – 8D (future) | 270 | 228.8 | 41.2 |
| Disposal Cells 9A – 9D (future) | 270 | 226.8 | 43.2 |
| Disposal Cells 10A – 10D (future) | 260 | 224.4 | 35.6 |
| Disposal Cells 11A – 11D (future) | 275 | 230.4 | 44.6 |
| Disposal Cells 12A – 12D (future) | 275 | 228.4 | 46.6 |
| Disposal Cells 13A – 13D (future) | 270 | 232.1 | 37.9 |
| Disposal Cells 14A / 14B (future) | 270 | 229.2 | 40.8 |
| Disposal Cells 15A – 15D (future) | 270 | 228.3 | 41.7 |
| Disposal Cells 16A – 16D (future) | 270 | 230.9 | 39.1 |
| Disposal Cells 17A – 17D (future) | 270 | 225.5 | 44.5 |
| Disposal Cells 18A – 18D (future) | 270 | 229.8 | 40.2 |
| Disposal Cells 19A / 19B (future) | 270 | 226.5 | 43.5 |
| Disposal Cells 20A – 20D (future) | 270 | 222.3 | 47.7 |

(1) Base elevation for Vaults 1 and 4 is at the bottom of the disposal unit floor slab and for the FDCs at the bottom of the lower mud mat.

➤ **Vadose Zone Material Properties Upper and Lower Vadose Zone**

The physical and chemical properties of the vadose zone soils surrounding and below the SDF disposal units are

required for the ISCM. Vadose zone material properties required for the modeling are:

- Saturated D_e
- Average total porosity, average dry bulk density
- Average particle density, saturated horizontal hydraulic conductivity
- Saturated vertical hydraulic conductivity, and K_d values

The properties are modeled as not changing over time because of the relative stability of the soil grains and structure. Table 4.2-14 provides the material properties for the backfill and the Upper and Lower Vadose Zones from WSRC-STI-2006-00198. Backfill surrounding the FDCs will be composed mostly of excavated soil from the Upper Vadose Zone that has been disturbed and compacted upon placement around constructed FDC. For modeling purposes, the hydraulic properties of the backfill material will be used rather than the hydraulic properties of the Upper Vadose Zone. As indicated in Table 4.2-14, the properties of the Upper Vadose Zone (characteristic of more clayey stratified soils) would retard the movement of water through the zone to a greater extent than that of the backfill (characteristic of clayey and sandy isotropic soils) and the Lower Vadose Zone (characteristic of more sandy stratified soils). Thus, the transport model conservatively assumed backfill material properties for the backfilled material and that the undisturbed soil beneath the disposal units has the characteristics of the Lower Vadose Zone. Figure 4.2-22 presents the characteristic curves for the Lower Vadose Zone. The characteristic curves for the backfill material is presented in Figure 4.2-17.

Table 4.2-14: Hydraulic Properties of Vadose Zone Material

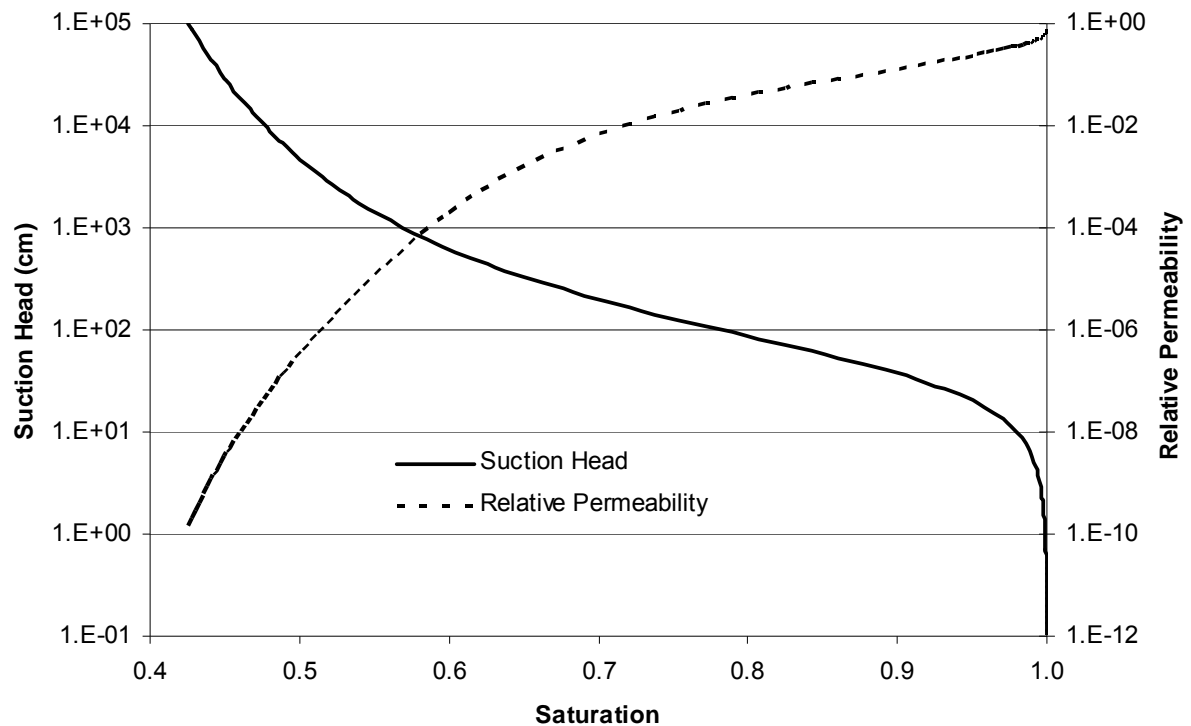
| Material Zone | Saturated Effective Diffusion Coefficient D_e (cm ² /sec) | Average Total Porosity (%) | Average Dry Bulk Density (g/cm ³) | Average Particle Density (g/cm ³) | Saturated Horizontal Hydraulic Conductivity (cm/sec) | Saturated Vertical Hydraulic Conductivity (cm/sec) |
|---------------|--|----------------------------|---|---|--|--|
| Upper Vadose | 5.3E-06 | 39 | 1.65 | 2.7 | 6.2E-05 | 8.7E-06 |
| Backfill | 5.3E-06 | 35 | 1.71 | 2.63 | 7.6E-05 | 4.1E-05 |
| Lower Vadose | 5.3E-06 | 39 | 1.62 | 2.66 | 3.3E-04 | 9.1E-05 |

[WSRC-STI-2006-00198, Table 5-18]

Recommended K_d values for all soil zones were taken from recent compilations of geotechnical data prepared in support of site PA modeling. Estimates of the K_d values for each element and soil type were provided. These values were based primarily on SRS site-specific experimental data, some central value of literature, or on expert judgment, with SRS site-specific experimental data being the preferred information source. Table

4.2-15 provides these values for the PORFLOW modeled vadose zone for the SDF disposal units.

Figure 4.2-22: Characteristic Curve for Lower Vadose Zone



[WSRC-STI-2006-00198, Table 5-19]

Table 4.2-15: Recommended K_d Values for Backfill and the Vadose Zone

| Element | Soils Media | | | |
|---------|--------------------------|------|------------------------------|------|
| | Backfill Soil (mL/g)* | Ref. | Vadose Zone Soil (mL/g)** | Ref. |
| Ac | 8,500 | a | 1,100 | a |
| Ag | 150 | b | 60 | b |
| Al | 1,300 | b | 1,300 | b |
| Am | 8,500 | a | 1,100 | a |
| Ar | 0 | a | 0 | a |
| As | 200 | b | 100 | b |
| At | 0.6 | a | 0 | a |
| Ba | 17 | a | 5 | a |
| Bk | 8,500 | a | 1,100 | a |
| C | 0 | a | 0 | a |
| Cd | 10 | b | 4 | b |
| Ce | 1,500 | b | 1,000 | b |
| Cf | 8,500 | a | 1,100 | a |
| Cl | 0 | a | 0 | a |
| Cm | 8,500 | a | 1,100 | a |
| Co | 30 | a | 7 | a |
| Cr | 10 | b | 4 | b |
| Cs | 250 | a | 50 | a |
| Cu | 70 | b | 50 | b |
| Eu | 8,500 | a | 1,100 | a |
| F | 0 | b | 0 | b |
| Fe | 400 | b | 200 | b |
| Fr | 250 | a | 50 | a |
| Gd | 8,500 | a | 1,100 | a |
| H | 0 | a | 0 | a |
| Hg | 1,000 | b | 800 | b |
| I | 0.6 | a | 0 | a |
| K | 60 | b | 10 | b |
| Mn | 200 | b | 15 | b |
| N | 0 | b | 0 | b |
| Na | 25 | b | 5 | b |
| Nb | 0 | a | 0 | a |
| Ni | 30 | a | 7 | a |
| Np | 35 | a | 0.6 | a |

Table 4.2-15: Recommended K_d Values for Backfill and the Vadose Zone (Continued)

| Element | Soils Media | | | |
|---------|--------------------------|------|------------------------------|------|
| | Backfill Soil (mL/g)* | Ref. | Vadose Zone Soil (mL/g)** | Ref. |
| Pa | 35 | a | 0.6 | a |
| Pb | 5,000 | a | 2,000 | a |
| Pd | 30 | b | 7 | b |
| Pm | 0 | c | 0 | c |
| Po | 5,000 | a | 2,000 | a |
| Pr | 0 | c | 0 | c |
| Pt | 0 | c | 0 | c |
| Pu | 5,900 | a | 270 | a |
| Ra | 17 | a | 5 | a |
| Rb | 250 | a | 50 | a |
| Re | 0.2 | a | 0.1 | a |
| Rh | 0 | c | 0 | c |
| Rn | 0 | a | 0 | a |
| Ru | 0 | c | 0 | c |
| Sb | 2,500 | b | 2,500 | b |
| Se | 1,000 | a | 1,000 | a |
| Sm | 8,500 | a | 1,100 | a |
| Sn | 5,000 | a | 2,000 | a |
| Sr | 17 | a | 5 | a |
| Tc | 1.8 | d | 0.6 | d |
| Te | 1,000 | a | 1,000 | a |
| Th | 2,000 | a | 900 | a |
| U | 300 | a | 200 | a |
| V | 0 | c | 0 | c |
| Y | 0 | c | 0 | c |
| Zn | 200 | e | 100 | e |
| Zr | 2,000 | a | 900 | a |

* Backfill soil represented by clayey sediment.

** Vadose zone soil represented by sandy sediment.

- (a) WSRC-TR-2006-00004
- (b) SRNL-RPA-2007-00006
- (c) Assigned a value of zero
- (d) SRNL-TR-2009-00019
- (e) SRS-REG-2007-00036

4.2.3.2.4 Cementitious Material Properties

The hydraulic and physical properties of the cementitious materials associated with the SDF disposal units after closure (i.e., roof and walls, base, clean grout fill and saltstone) are integral to the ISCM. Property estimates for cementitious materials associated with the SDF are utilized as input to the PA modeling. Some properties are expected to remain the same over time and are modeled as such. These include, dry bulk density (pb), particle density (pp), and the water retention characteristic curves. The cementitious materials in the SDF can be grouped into five categories.

1. Low quality concrete associated with the lower mud mat for the FDCs
2. Medium quality or ordinary concrete associated with the roof of Vaults 1 and 4 and the clean grout used to cap the interior of the disposal units after filling with saltstone
3. High quality concrete associated with the wall and base of Vaults 1 and 4 and the concrete for the FDCs, including the upper mud mats
4. “Fractured concrete” associated with the existing walls of Vaults 1 and 4, which have experienced macroscopic cracks and have been modeled with an increased hydraulic conductivity based on analysis presented in SRNL-STI-2009-00115
5. Saltstone

The physical properties used in the modeling (dimensions) associated with each of these categories are presented in Section 4.4 for Vaults 1 and 4 and the FDCs and represent the nominal formulations for each. For saltstone, additional work is being conducted to evaluate the sensitivity of modeling parameters to changes in the formula as presented in Section 8.2. The results of the ongoing work will be used in conjunction with the available, and any new, operational information to evaluate any impacts as part of PA maintenance. The hydraulic properties associated with each of these cementitious material categories are presented in Table 4.2-16.

Characteristic curves for the cementitious materials are presented in Figures 4.2-23 through 4.2-27. These characteristic curves are based on WSRC-STI-2006-00198, except for “fractured concrete,” which is based on SRNL-STI-2009-00115. A detailed discussion on the assumptions associated with the characteristic curves for fractured concrete is presented on pages 95 through 99 of SRNL-STI-2009-00115. In the fractured cases, the fractures become unsaturated under certain conditions.

Table 4.2-16: Cementitious Material Properties

| Material | Porosity (%) | Dry Bulk Density (g/cm³) | Particle Density ρ_p (g/cm³) | Hydraulic Conductivity $k_{h,v}$ (cm/sec) | Effective Diffusion Coefficient D_e (cm²/sec) |
|--|---------------------|--|--|---|--|
| Low quality concrete ^b | 21.1 | 2.06 | 2.61 | 1.0E-08 | 8.0E-07 |
| Medium (ordinary) quality concrete – Vault 1 roof | 14.5 | 2.20 | 2.57 | 5.0E-09 | 1.0E-07 |
| Medium (ordinary) quality concrete – Vault 4 roof | 13.6 | 2.21 | 2.56 | 5.0E-09 | 1.0E-07 |
| High quality concrete – Vaults 1 & 4 walls and base ^c | 12.0 | 2.24 | 2.55 | 3.1E-10 | 5.0E-08 |
| Fractured walls in Vault 1 and 4 ^d | 12.0 | 2.24 | 2.55 | 1.7E-01 | 5.0E-08 |
| High quality concrete – FDCs ^c | 11.0 | 2.22 | 2.49 | 9.3E-11 | 5.0E-08 |
| Saltstone and clean grout cap ^c | 58.0 | 1.01 | 2.40 | 2.0E-09 | 1.0E-07 |

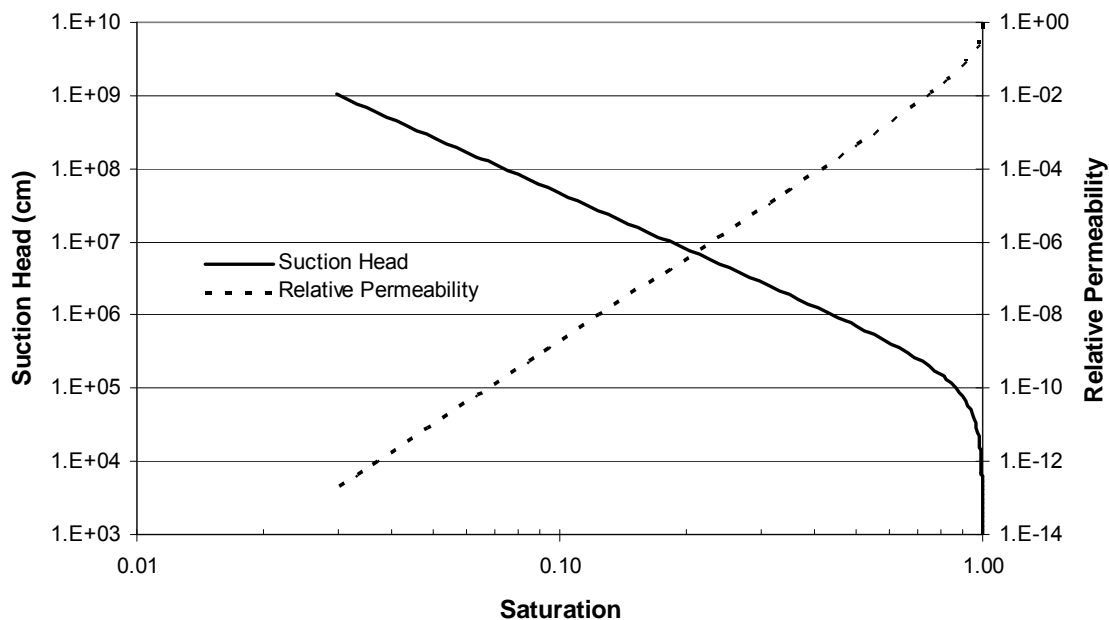
(a) Unless otherwise noted, values obtained from Table 6-47 of WSRC-STI-2006-00198

(b) Material assumed for the lower mud mats of the FDCs

(c) Values obtained from SRNL-STI-2008-00421 with D_e obtained from WSRC-STI-2006-00198 for high quality concrete

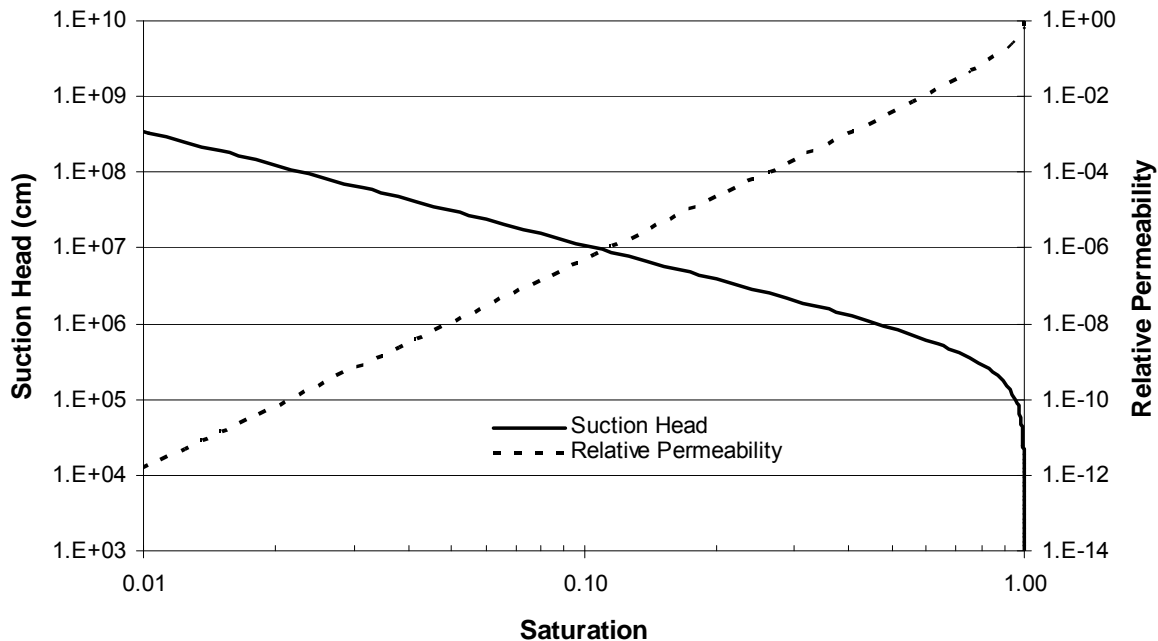
(d) The presence of macroscopic cracks in the exterior walls of Vaults 1 and 4 has been evaluated in SRNL-STI-2009-00115 and modeled by an increase in the hydraulic conductivity and the use of a developed characteristic curve for “fractured concrete”.

Figure 4.2-23: Characteristic Curves for Low Quality Concrete



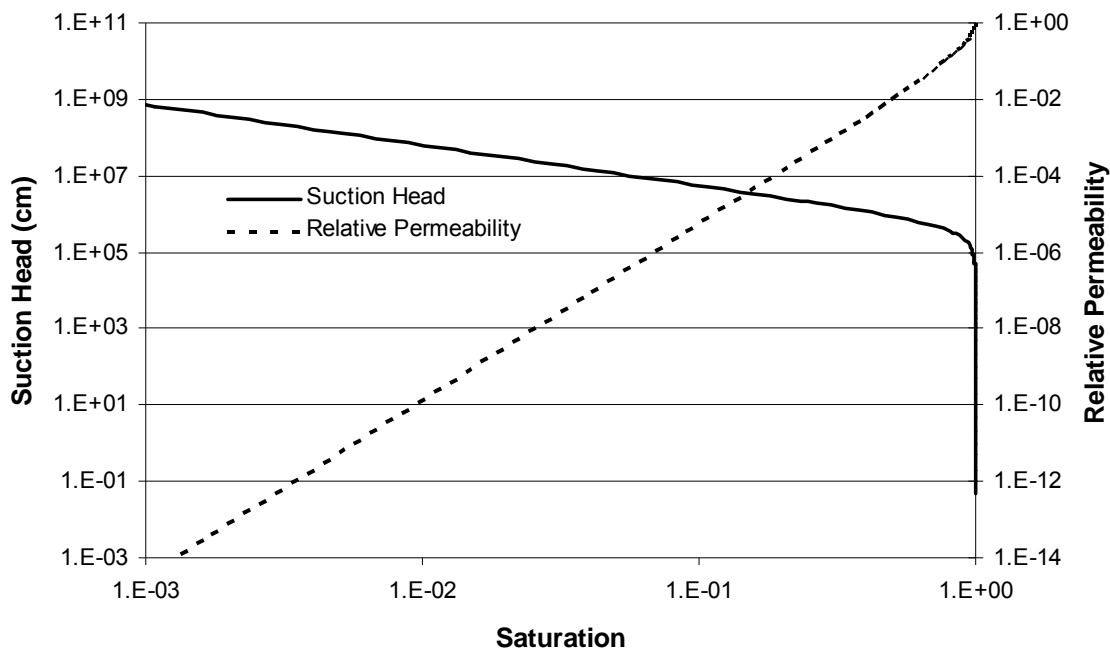
[WSRC-STI-2006-00198, Table 6-48]

Figure 4.2-24: Characteristic Curves for Medium Quality Concrete



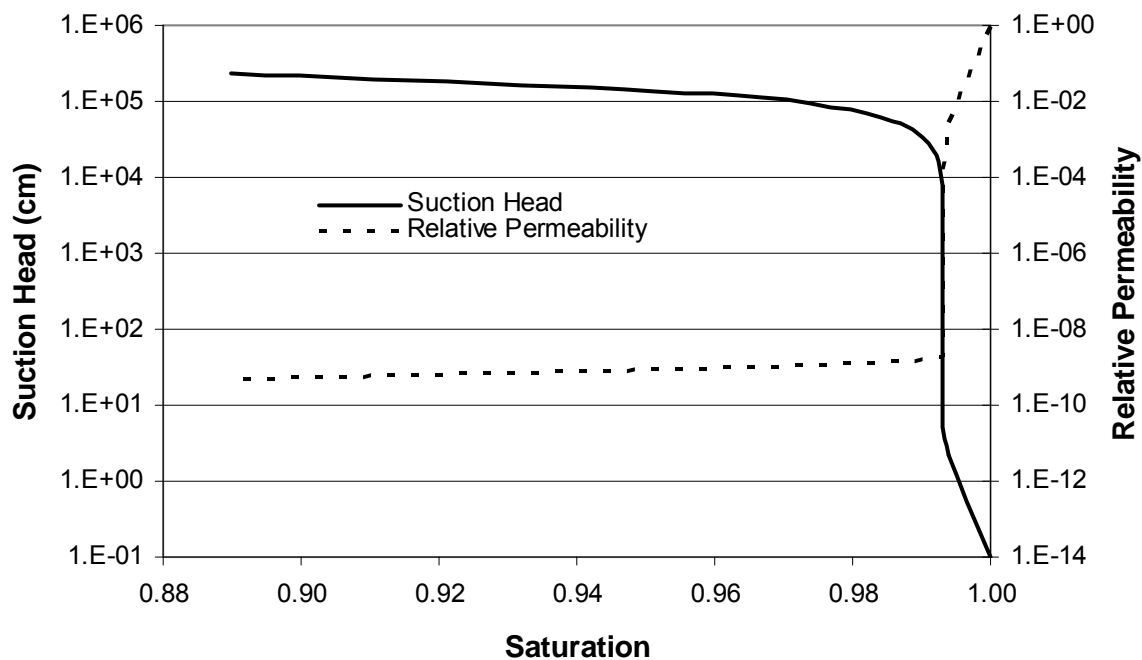
[WSRC-STI-2006-00198, Table 6-48]

Figure 4.2-25: Characteristic Curves for High Quality Concrete



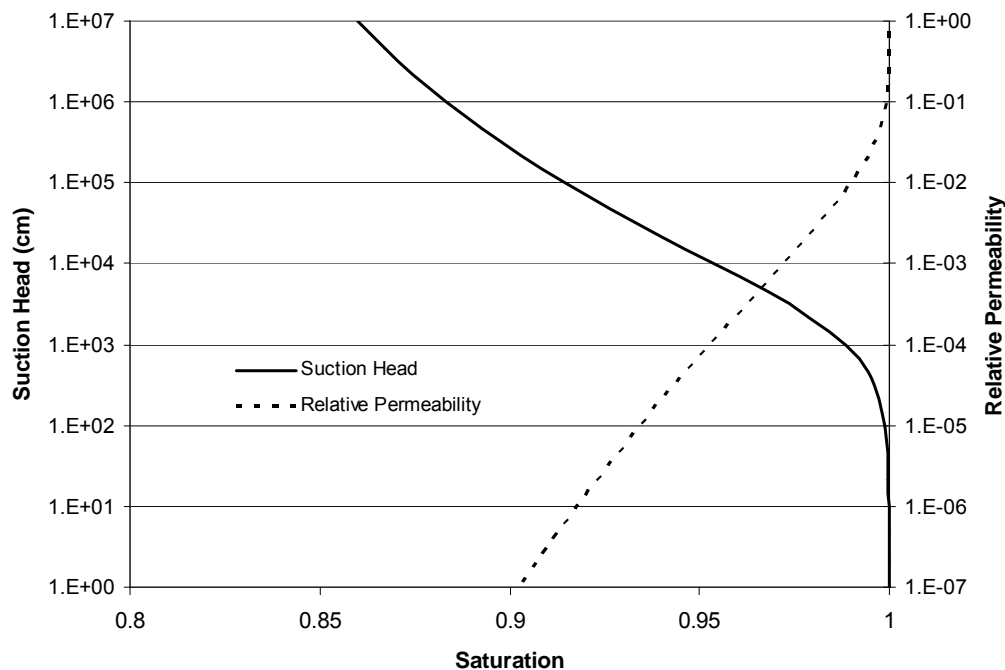
[WSRC-STI-2006-00198, Table 6-48]

Figure 4.2-26: Characteristic Curve for Fractured Concrete



[SRNL-STI-2009-00115]

Figure 4.2-27: Characteristic Curves for Saltstone



[WSRC-STI-2007-00649]

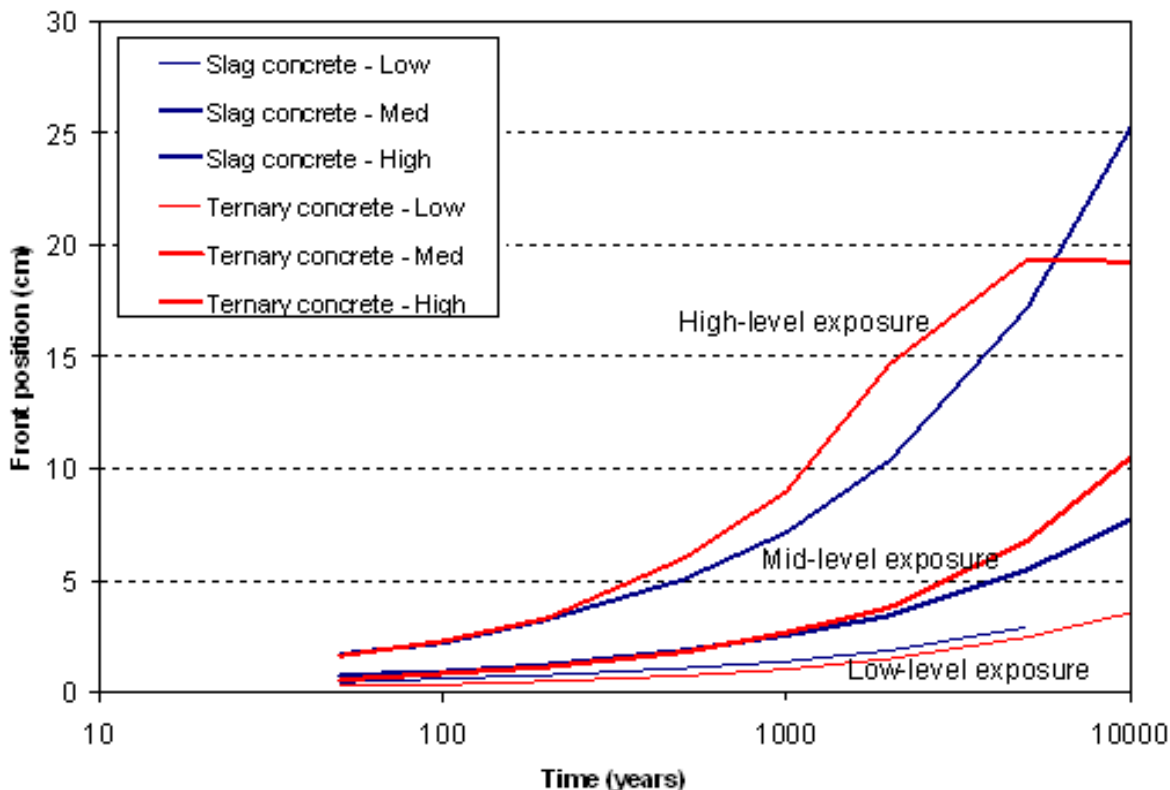
➤ Concrete Degradation

Degradation of the disposal unit concrete (walls, roof, and base) is believed to be dominated by external sulfate attack. Sulfate is present in saltstone feedwater and, after grout curing, remains at significant concentrations in pore water. Sulfate reacts with cement paste and creates ettringite, an expansive mineral phase often associated with spalling or cracking. External sulfate attack involves coupled porous medium transport, chemical reaction, and fracture mechanics. These effects have not yet been fully simulated in a satisfactory coupled manner, and sulfate attack modeling remains an open research topic. Nonetheless, reactive transport models have been developed that adequately simulate ettringite formation as a result of dissolved sulfate reacting with cement minerals. Among these, a leading code is STADIUM®, a proprietary code developed by SIMCO Technologies Inc. in collaboration with Laval University. STADIUM® simulations, combined with an assumption that physical damage results from ettringite formation, were used to predict disposal unit concrete degradation.

SIMCO Technologies Inc. used their STADIUM® code to simulate ettringite formation in Vaults 1 and 4 and FDC concretes under specific conditions. Degradation of hydraulic properties is estimated by assuming concrete ahead of the ettringite front retains its initial properties while concrete behind the front is cracked or otherwise degraded. SIMCO used the STADIUM® code to simulate the advance of an ettringite front through surrogate disposal unit concretes representing FDC wall thickness of 20 cm (8 inches) and a wall thickness of 46 cm (18 inches) for Vaults 1 and 4. In the model simulations extending over 10,000 years, one side of the concrete was exposed to a saltstone leachate

simulant while the other boundary contacted vadose zone soil at 100% relative humidity. Three compositions were considered, corresponding to high, medium, and low sulfate concentration, 0.2, 0.02, and 0.002 mol/L SO_4^{2-} . Figure 4.2-28, reproduced from SRNS-STI-2008-00050, summarizes the STADIUM® results. Note that in Figure 4.2-28 “Slag Concrete” refers to Vault 1 and 4 concrete and “Ternary Concrete” refers to FDC concrete. Further information on the SIMCO work is provided SRNS-STI-2008-00050.

Figure 4.2-28: Simulated Progression of Ettringite Front



➤ **Concrete Physical Degradation**

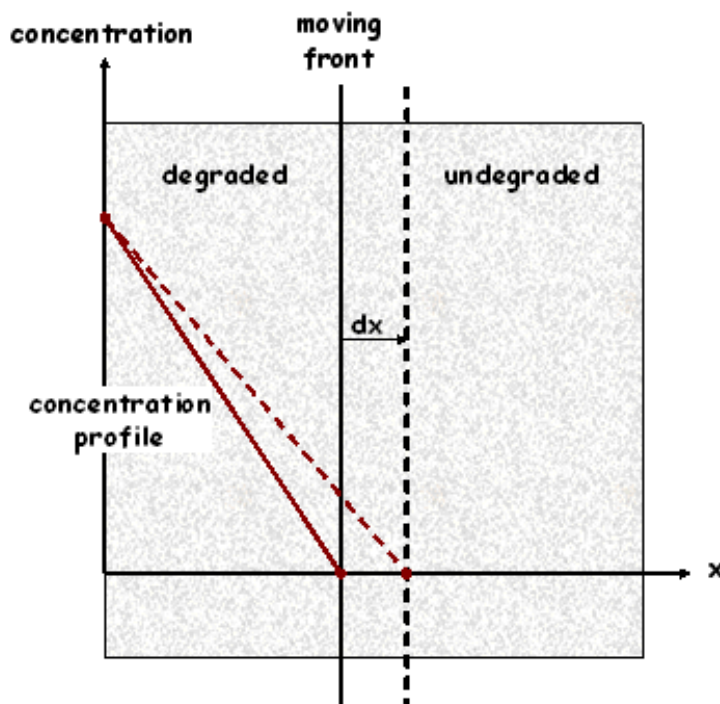
Figure 4.2-29 illustrates a generic moving front that consumes reactants that are delivered to the front through quasi-steady diffusion. The latter implies that the timescale of diffusion is much shorter than the timescale of the moving front, which is expected for sulfate attack. As the front advances, the diffusion length increases, slowing both the reactant delivery and the further advance of the front. A differential equation describing the movement of the front is

$$R \frac{dx}{dt} = \frac{nD_e c}{x} \quad (1)$$

where x is front position (e.g., cm), t is time (s), R is a reaction capacity (mol/cm), n is porosity, D_e is effective diffusion coefficient (cm^2/s), and c is a fixed aqueous concentration of reactant at $x = 0$ (mol/ cm^3). The analytic solution to Equation (1) is

$$x = \left[\frac{2nD_e c t}{R} \right]^{1/2} \quad (2)$$

Figure 4.2-29: Conceptual Model of a Generic Moving Ettringite Front



Thus, a square root dependence on porosity, diffusion coefficient, exposure concentration and time can be anticipated in STADIUM® result (conceptual model depicted in Figure 4.2-28). For a given SDF disposal unit and leachate exposure scenario, the position of the ettringite front, as predicted by STADIUM®, is indeed proportional to the square root of time, as shown by the linear correlations in Figures 4.2-30 and 4.2-31 which plot x against \sqrt{t} . The leading coefficient or proportionality factor indicated in the plots varies with sulfate concentration in a non-linear manner. A power-law function of sulfate concentration fits the proportionality factor data with adequate agreement, as shown in Figures 4.2-32 and 4.2-33. The power-law relationship appears as a straight-line when plotted in log-log coordinates.

Figure 4.2-30: STADIUM® Simulation Results for Vaults 1 and 4

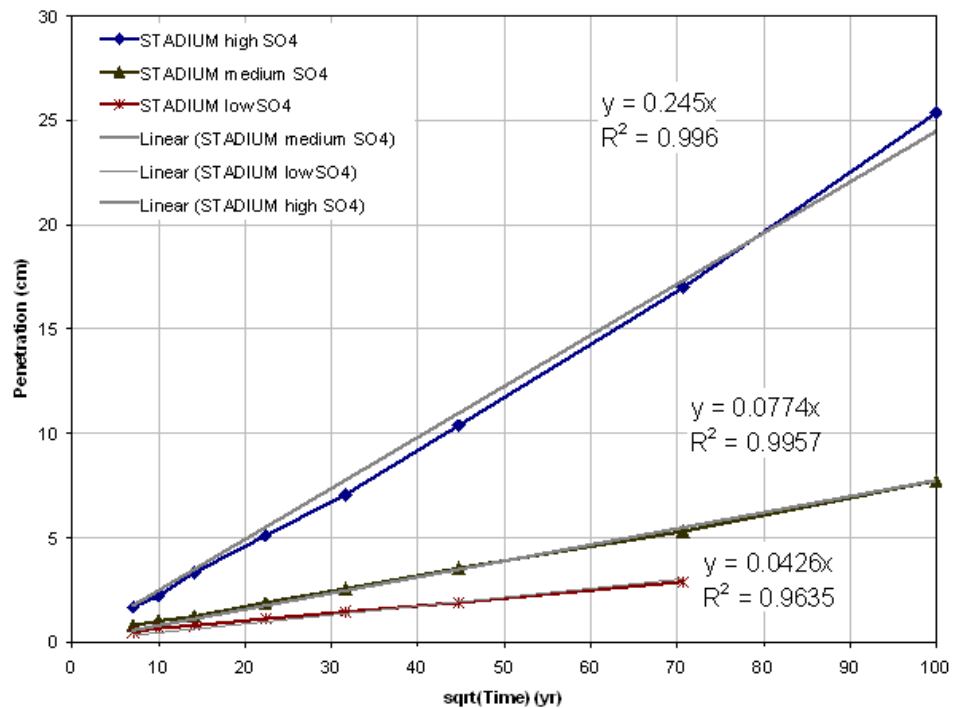


Figure 4.2-31: STADIUM® Simulation Results for FDCs

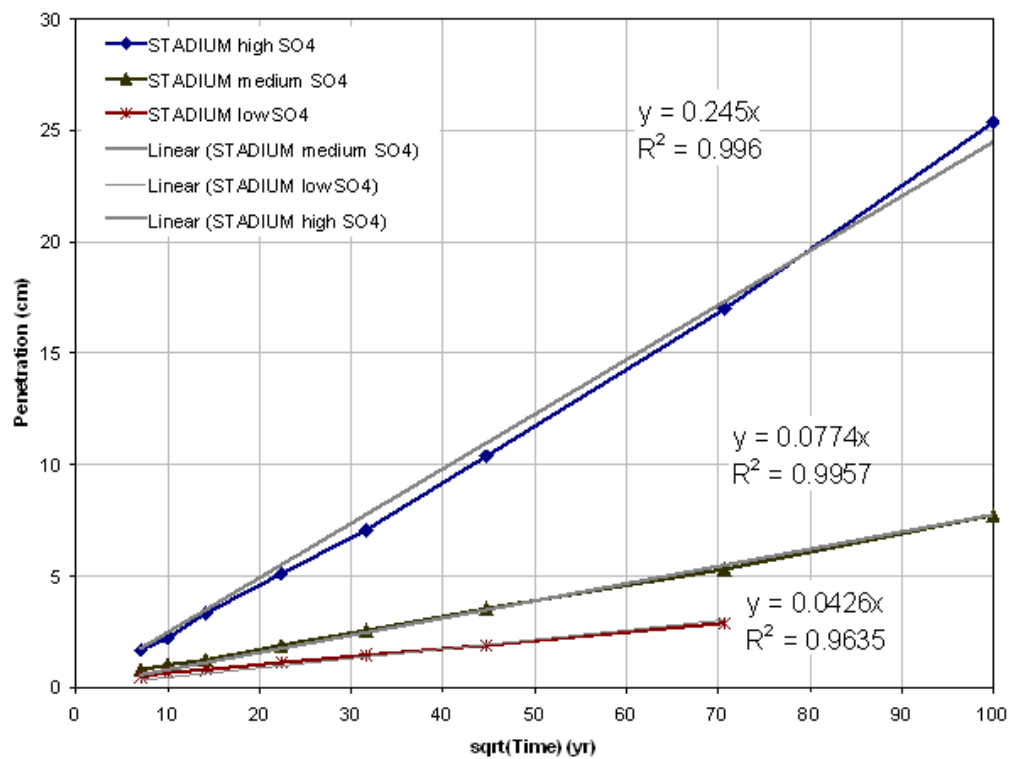


Figure 4.2-32: Power Law Fit to Data on Figure 4.2-26

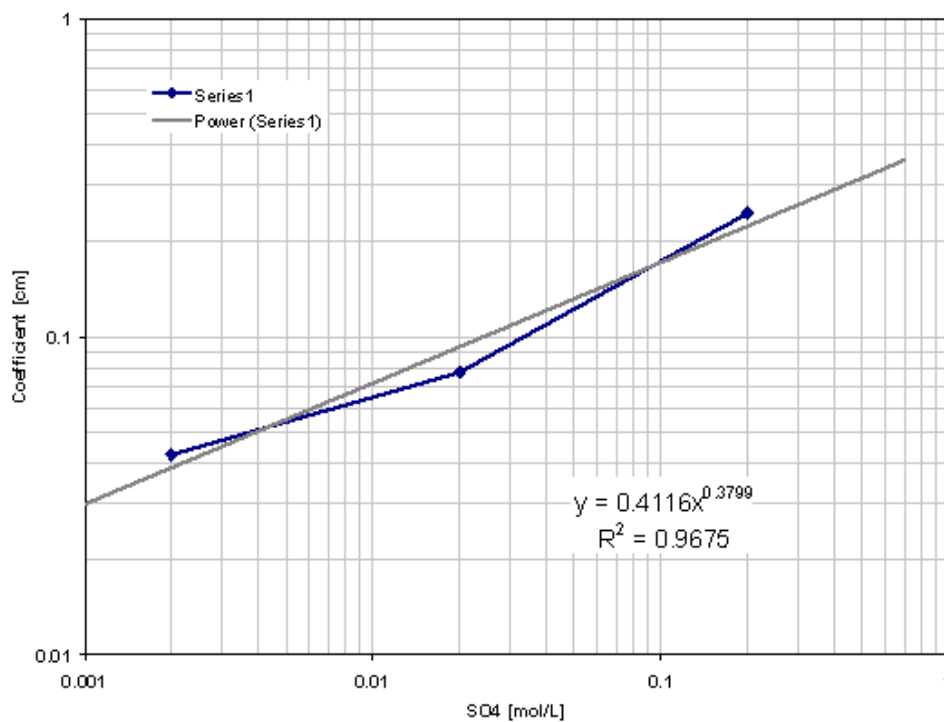
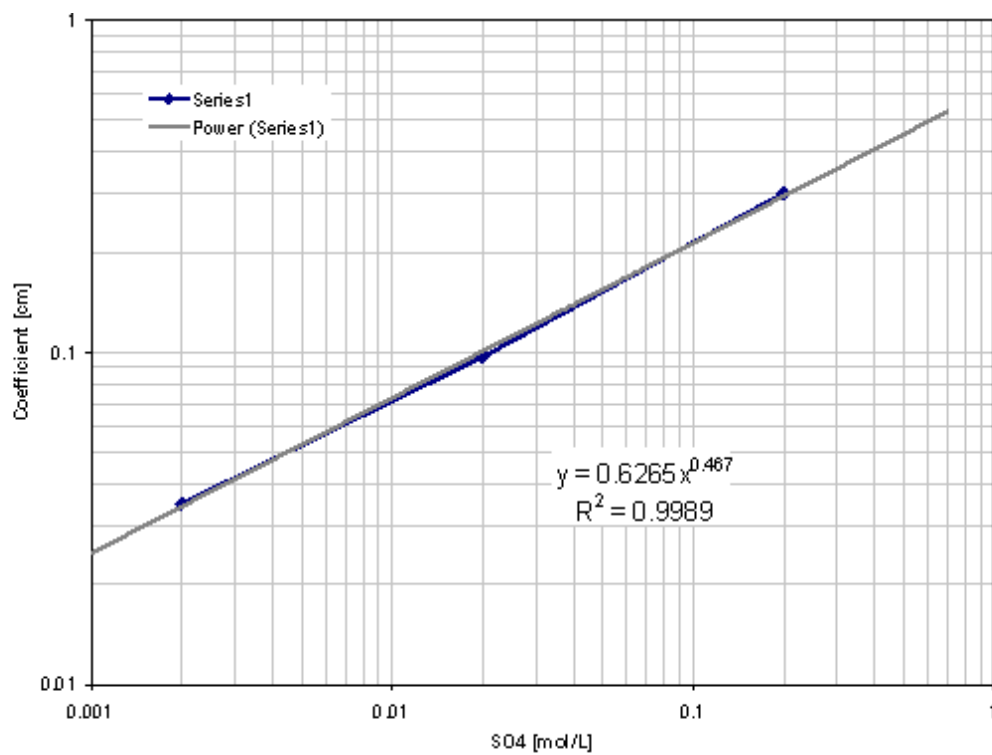


Figure 4.2-33: Power Law Fit to Data on Figure 4.2-27



Combining the correlations in Figures 4.2-30 through 4.2-33 produces an equation for the front position (x) as a function of time (t) and sulfate concentration (c) of the form

$$x = Ac^B \sqrt{t} \quad (3)$$

where A and B are constants specific to Vaults 1 and 4 and the FDCs.

For Vaults 1 and 4 in particular,

$$A = 0.412 \frac{\text{cm}}{(\text{mol/L})^B \sqrt{\text{yr}}} \quad (4)$$

$$B = 0.380 \quad (5)$$

For the FDCs,

$$A = 0.626 \frac{\text{cm}}{(\text{mol/L})^B \sqrt{\text{yr}}} \quad (6)$$

$$B = 0.467 \quad (7)$$

Figures 4.2-34 and 4.2-35 compare the semi-empirical correlations to the original STADIUM® predictions for Vaults 1 and 4 and the FDCs, respectively. In Figure 4.2-35, the semi-empirical correlation is artificially extended beyond the medium thickness (20 cm), whereas the STADIUM® results reflect the finite dimension of the material.

Figure 4.2-34: Comparison of Correlation to Original STADIUM® Results Vaults 1 and 4

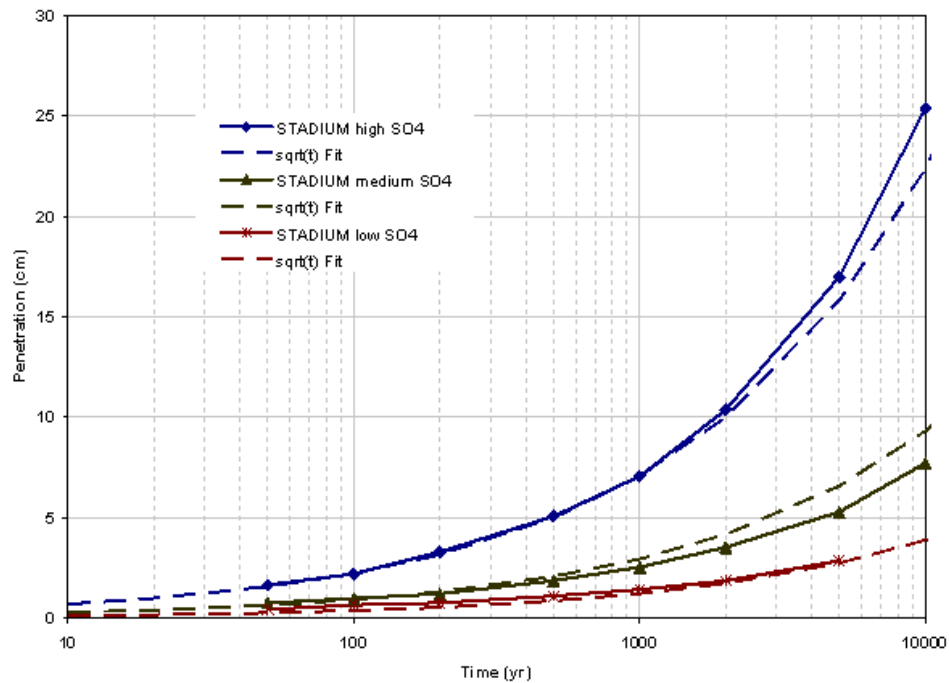
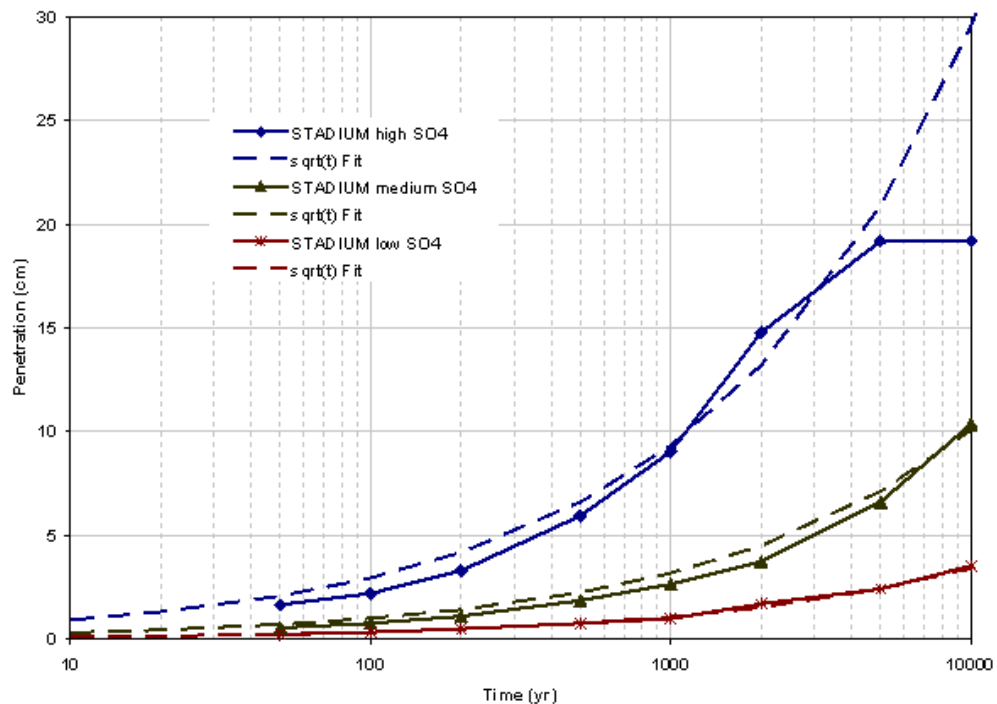


Figure 4.2-35: Comparison of Correlation to Original STADIUM® Results for FDC



Further inspection of Equation (2) indicates that the constant B should be approximately 0.5, which can be seen by rewriting Equation (2) as

$$x = \left[\frac{2nD_e c}{R} \right]^{0.5} \sqrt{t} = Ac^{0.5} \sqrt{t} \quad (8)$$

where the factor, A, is defined as

$$A = \left[\frac{2nD_e}{R} \right]^{0.5} \quad (9)$$

The empirical values of 0.380 and 0.467 are consistent with the predicted value, and further support the conceptual model of Figure 4.2-29.

The STADIUM® simulations assumed a nominal diffusion coefficient of $\sim 10^{-7} \text{ cm}^2/\text{s}$ for ionic transport. Based on Equation (2), Equation (3) can be further generalized as

$$x = Ac^B \sqrt{\frac{D_e}{D_{\text{ref}}}} \sqrt{t} \quad (10)$$

where $D_{\text{ref}} = 10^{-7} \text{ cm}^2/\text{s}$ is implicitly embedded in the empirical constant A. The rate of change in the front position is

$$\frac{dx}{dt} = Ac^B \sqrt{\frac{D_e}{D_{\text{ref}}}} \frac{1}{2\sqrt{t}} \quad (11)$$

Equation (10) is based on constant values of sulfate concentration and diffusion coefficient. If the front speed under changing conditions is assumed to follow Equation (11) at any instant in time

$$\frac{dx}{dt} = Ac(t)^B \sqrt{\frac{D_e(t)}{D_{\text{ref}}}} \frac{1}{2\sqrt{t}} \quad (12)$$

then the front position for varying sulfate concentration and diffusion coefficient can be computed by integrating Equation (12) as

$$x = \int_0^T Ac(t)^B \sqrt{\frac{D_e(t)}{D_{\text{ref}}}} \frac{1}{2\sqrt{t}} dt \quad (13)$$

where T is cumulative time. Equation (13) can be numerically evaluated for arbitrary variations in concentration and diffusion coefficient.

The STADIUM® code simulates coupled transport and chemical reaction, but does not consider damage mechanics. Thus, the model does not predict whether physical damage will occur, nor does it consider the impact on transport properties if damage does occur. To define concrete degradation from STADIUM® results, two key assumptions are made:

- (1) Transport properties, with respect to predicting ettringite front position, are unchanged by passage of the front.
- (2) The presence of ettringite coincides with physical damage to concrete, for the purpose of estimating effective transport properties for saltstone contaminant release.

Assumption (1) would be accurate if ettringite formation does not damage the concrete, or if changes in morphology do not significantly increase transport properties for the given exposure conditions. An example of the latter, spalling or cracking under unsaturated conditions may not accelerate sulfate attack, because the fractures would be dewatered with sufficient suction, and relatively inactive. On the other hand, Assumption (1) would not be accurate under saturated conditions, for which cracks/fractures typically control transport. Assumption (1) may be neutral, or non-conservative, if cracking accelerates attack. Assumption (2) may be neutral, or conservative, if damage does not in fact occur.

With these key assumptions and the front position defined by Equation (13), effective transport properties can be estimated by averaging the intact and degraded regions. Using saturated hydraulic conductivity (K) as an example,

$$\Delta x K_{\text{eff}}^p = \Delta x_i K_i^p + \Delta x_d K_d^p \quad (14)$$

or equivalently

$$K_{\text{eff}} = \left[\frac{\Delta x_i K_i^p + \Delta x_d K_d^p}{\Delta x} \right]^{1/p} \quad (15)$$

where $-1 \leq p \leq +1$ and Δx denotes thickness. The subscripts "i" and "d" refer to the intact and degraded regions ahead and behind the front respectively, and "eff" is the effective (composite) value. Arithmetic averaging corresponds to $p = 1$ and harmonic averaging is obtained with $p = -1$. The former would be used for transport parallel to the ettringite front, and the latter for transport transverse to the front.

The sulfate concentration indicated in Equation (13) is a pore water value at the interface between saltstone and the disposal unit concrete. When sulfate laden saltstone is conceptually brought into contact with clean disposal unit concrete (physically when a waterproof interior coating degrades), the interface concentration will equilibrate to an

intermediate value depending on the properties of the two porous media. The interface concentration can be estimated using analytic solutions for diffusion in semi-infinite regions as described in SRNL-STI-2009-00115. Over time, the assumption of diffusion in semi-infinite domains will break down. This is due to the finite thickness of the disposal unit and/or advection becoming dominant, causing the concentration to decline. Nonetheless, the interface concentration is assumed to be constant for the purpose of estimating concrete degradation, which is expected to be conservative. For either vault or FDC roof concrete, an interface concentration can be computed for the saltstone and clean grout and the concentration at the underside of the roof on the opposite side of the clean grout can be estimated from another analytic solution for diffusion in a semi-infinite region.

Using the equations derived above and computed interface sulfate concentrations, estimates of degradation to disposal unit concrete hydraulic conductivities and diffusion coefficient from sulfate attack have been developed in SRNL-STI-2009-00115 and are illustrated in Figures 4.2-36 through 4.2-40. Figures 4.2-36 and 4.2-37 illustrate the increase in the hydraulic conductivity and diffusion coefficient, respectively, for the walls and base of Vaults 1 and 4 and the roof for Vault 1. The thickness of the Vault 4 roof (4 inches) is such that the ettringite front travels the full thickness of the roof within 10,000 years after closure and the increase in the hydraulic conductivity and diffusion coefficient is illustrated in Figure 4.2-38. Figure 4.2-39 illustrates the increase of hydraulic conductivity and diffusion coefficient from sulfate attack to the roof and base of the FDCs and Figure 4.2-40 illustrates the increase of hydraulic conductivity and diffusion coefficient from sulfate attack to the FDC walls. [SRNL-STI-2009-00115]

Figure 4.2-36: Hydraulic Conductivity for Vault 1 and 4 Concrete

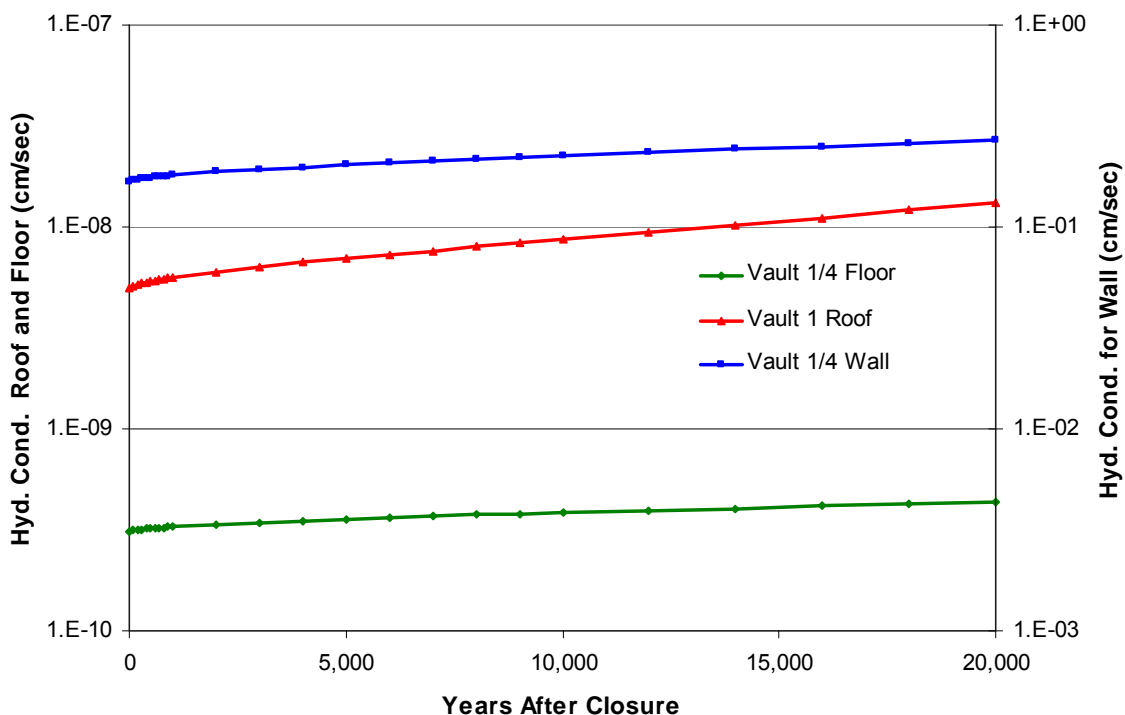


Figure 4.2-37: Diffusion Coefficient for Vaults 1 and 4 Concrete

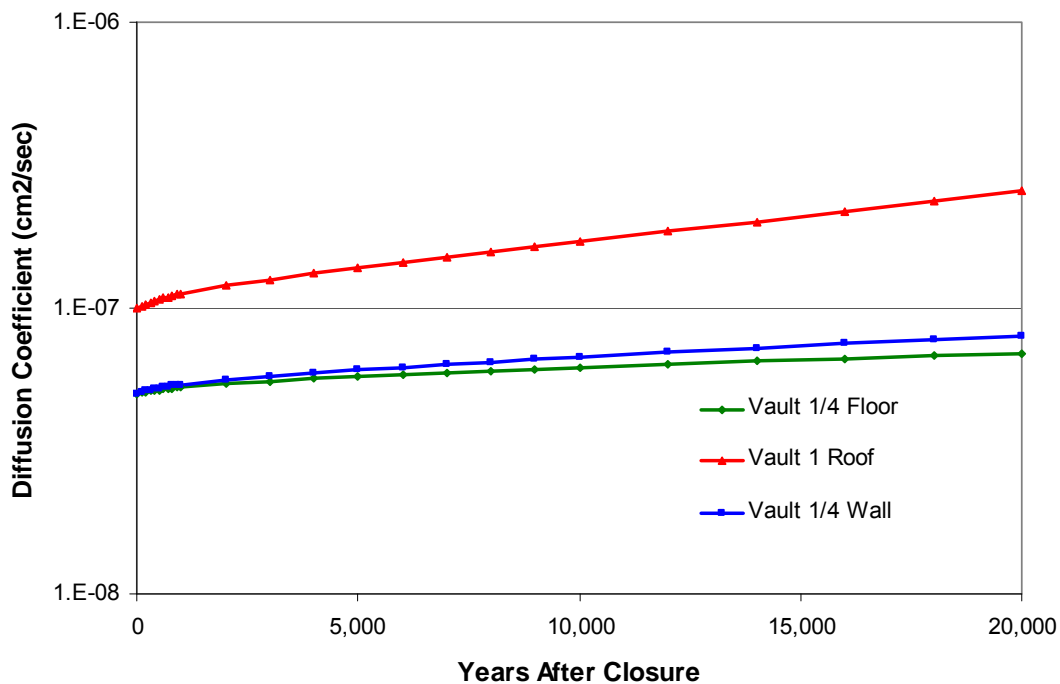


Figure 4.2-38: Hydraulic Conductivity and Diffusion Coefficient for Vault 4 Concrete Roof

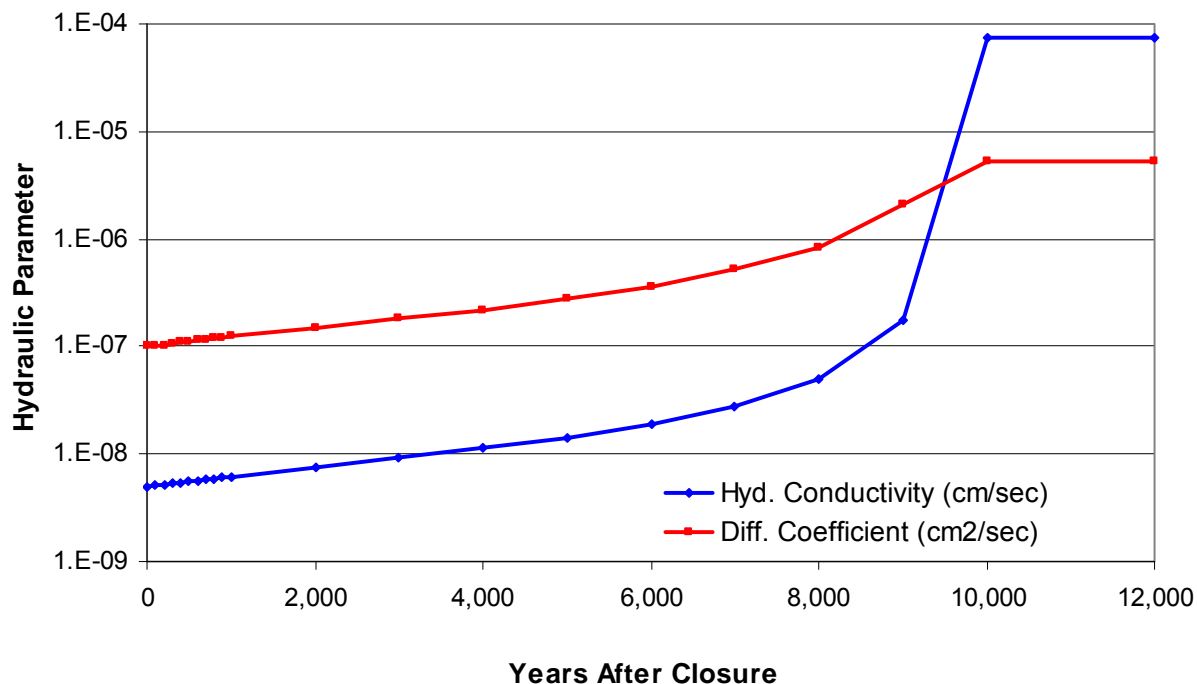


Figure 4.2-39: Hydraulic Conductivity and Diffusion Coefficient for FDC Concrete Roof/Floor

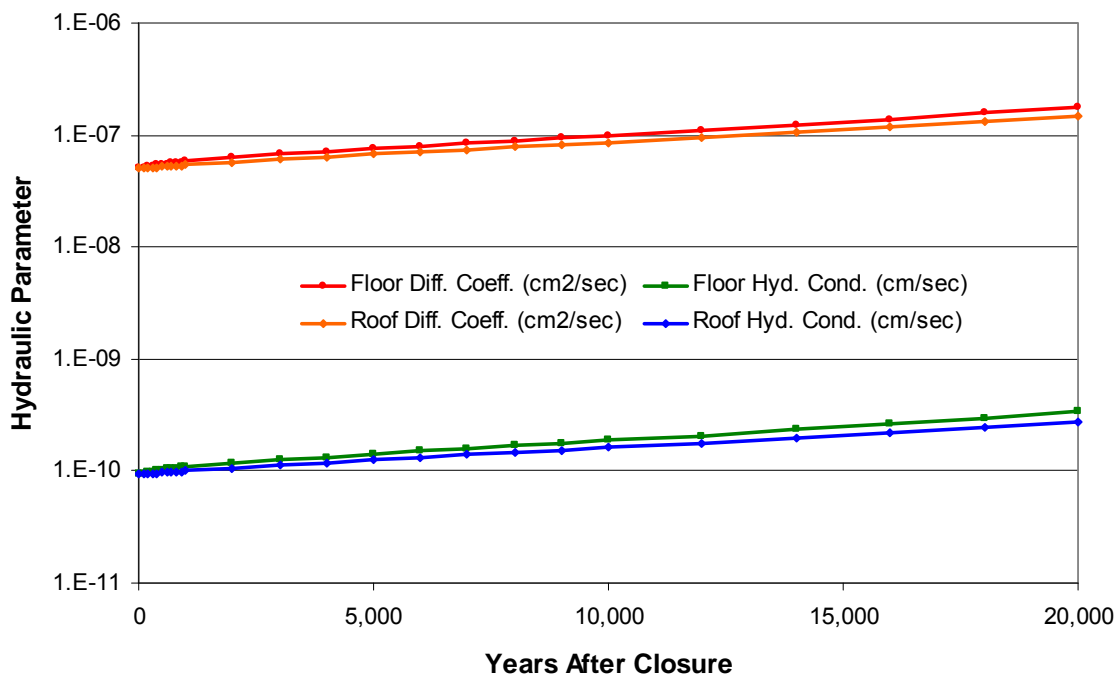
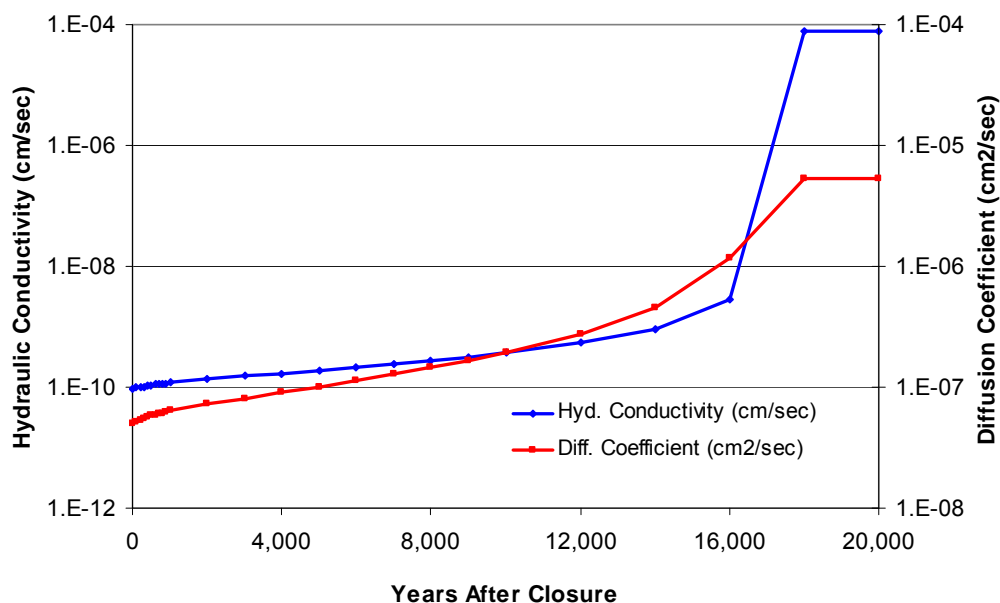


Figure 4.2-40: Hydraulic Conductivity and Diffusion Coefficient for FDC Concrete Wall



➤ **Saltstone Physical Degradation**

In the ISCM base case, degradation of the saltstone material is not assumed to occur during the performance period. Saltstone is designed to indefinitely immobilize contaminants in a low permeability medium. The potential for physical degradation is uncertain. The formation of expansive mineral phases in saltstone from exposure to rainwater or rainwater equilibrated with cement, using a reactive transport model, was investigated. The volumetric change was observed to be small in comparison to the pore space. The investigation concluded that "fracturing that initiates in pores by expansive phase precipitation is unlikely to occur in saltstone because the maximum amount of porosity filled is 34%". [WSRC-STI-2008-00236] However, a case scenario (Section 4.4.2) was developed to address the consequences of a hypothetical degraded saltstone condition. Degraded saltstone is assumed to take the form of cracked grout and has been modeled by increasing its hydraulic conductivity to a value of $1.7\text{E-}3$ cm/sec and modifying the characteristic curves based on the analysis presented in SRNL-STI-2009-00115.

➤ **Cementitious Materials Chemical Degradation**

Beyond the concrete and saltstone degradation processes discussed above, the mineral compositions of cementitious materials are expected to slowly change as water flows through pores and reacts with the solid matrices. Reduced materials will oxidize with exposure to dissolved oxygen in groundwater (increasing E_h), and pH will decrease as acidic groundwater dissolves the cement paste. These E_h and pH changes will affect sorption coefficient values and generally increase the rate of contaminant transport. Technetium is particularly sensitive to redox conditions, being practically insoluble at low E_h and relatively mobile under oxidized conditions. Section 4.2.2 describes the analysis conducted to evaluate the transitions from reducing to oxidizing conditions and

from middle age to old age cementitious materials. The number of pore water volumes passing through the disposal unit and the corresponding transitions to different chemical conditions is included in the SDF modeling. Table 4.2-17 presents the transition times for the various cementitious materials as computed within the PORFLOW model.

Table 4.2-17: Chemical Transition Times for Cementitious Materials

| Cementitious Material | Vault 1 | | Vault 4 | | FDCs | |
|-----------------------|-----------------------------------|-----------------------|-----------------------------------|-----------------------|-----------------------------------|-----------------------|
| | E _h Transition (years) | pH Transition (years) | E _h Transition (years) | pH Transition (years) | E _h Transition (years) | pH Transition (years) |
| Roof | N/A ¹ | 25,400 | N/A ¹ | 16,547 | 25,640 | 27,387 |
| Clean Grout | NR | NR | NR | NR | NR | NR |
| Saltstone | NR | NR | NR | NR | NR | NR |
| Wall | 20,781 | 21,043 | 15,519 | 16,018 | 16,334 | 16,753 |
| Floor ² | NR | NR | NR | NR | 22,498 | 23,274 |

(1) Material is oxidized at the start of the model.

(2) Includes the Upper Mud Mat for the FDCs.

NR = Not reported, computed transition time greater than 30,000 years

[SRNL-STI-2009-00115]

➤ **Cementitious Material
K_d Values**

The K_d values are necessary for cementitious materials through which contaminants have the potential to travel (e.g., saltstone and the walls and floor of the disposal units, including the upper and lower mud mats of the FDCs). Table 4.2-18 provides K_d values for cementitious materials as a function of aging and whether the material is reducing or oxidizing. The K_d values in this table are based on SRS site-specific data, values from literature, or engineering judgment, with SRS site-specific data being the preferred basis. The K_d for an element in concrete is also dependent on the pH of the concrete pore water, which in turn is dependent upon the amount of water (number of pore water volumes) that has passed through the concrete over time.

As indicated in Table 4.2-17, saltstone remains as reducing middle age throughout the performance period, as does the Vault 1 concrete and the Vault 4 floor concrete. The Vault 4 and FDC walls will transition from reducing middle age, to oxidizing middle age, and then to oxidizing old age during the performance period. When an E_h or pH transition is reached, according to Table 4.2-17, the K_d material changes to "oxidizing" (if in a "reducing" condition), or "old", respectively. This approach to K_d assignments applies to all species except Tc-99.

A more sophisticated shrinking-core treatment of oxidation is used for Tc-99 transport simulations, as presented in SRNL-STI-2009-00115. The shrinking core model is predicated on the reduction capacity of the cementitious materials, which is supported by site-specific test data presented in SRNS-STI-2008-00045 Table 8. The saltstone grout will start with a high reduction capacity, which will inhibit Tc-99 release as supported by data in WSRC-STI-2007-00640 and ISSN 1019-0643, and with site specific testing information in WSRC-RP-2005-01674, DPST-87-523, and LBNL-54094, with the reduction capacity of the grout decreasing over time. Reduction capacity and oxygen

concentration are explicitly tracked in each grid cell of the numerical model. Oxygen entering the disposal unit by liquid phase transport oxidizes the slag, thereby depleting the reduction capacity. Gas phase transport is ignored because the slag bearing materials are practically 100% saturated with water. Also, oxygen in the soil effectively stays at its saturation value, 1.06 meq e-/L, in the model due to higher liquid transport rates relative to the reducing materials. When the reduction capacity in a disposal unit has been consumed, previously immobile Tc-99 is made mobile. Tc-99 is made immobile in the model by setting K_d to 1,000 mL/g. The 1,000 mL/g used as the pseudo K_d in the shrinking core model is pessimistic compared to the value of 5,000 mL/g recommended in Table 11, and experimental results in Table 2, of WSRC-STI-2007-00640 and was chosen to maximize the magnitude of Tc-99 release peaks (Note: SRNS-STI-2008-00045 contained Tc-99 test results inconsistent with previous reducing cementitious material work but these results have been attributed to questionable experimental performance, have been discarded, and further experimental work recommended). Figure 4.2-41 illustrates how the sorption coefficient is artificially varied to achieve Tc-99 immobilization and release as a function of local reduction capacity. A cubic Hermitian polynomial defines a smooth variation in the transition zone between 0 and 0.005 meq e-/mL. The underlying physical process is not one of sorption, rather K_d variation is simply used as a convenient means to control Tc-99 release in the model. Accordingly, Figure 4.2-41 identifies K_d as a "pseudo-sorption coefficient" to call attention to its non-physical nature. Because of the introduction of a chemical reaction equation for slag oxidation, the time stepping was reduced from 1 year increments to 0.05 year increments for Tc-99 simulations to eliminate numerical instabilities. [SRNL-STI-2009-00115]

Figure 4.2-41: Pseudo-sorption Coefficient as a Function of Reduction Capacity for Tc-99 Simulations.

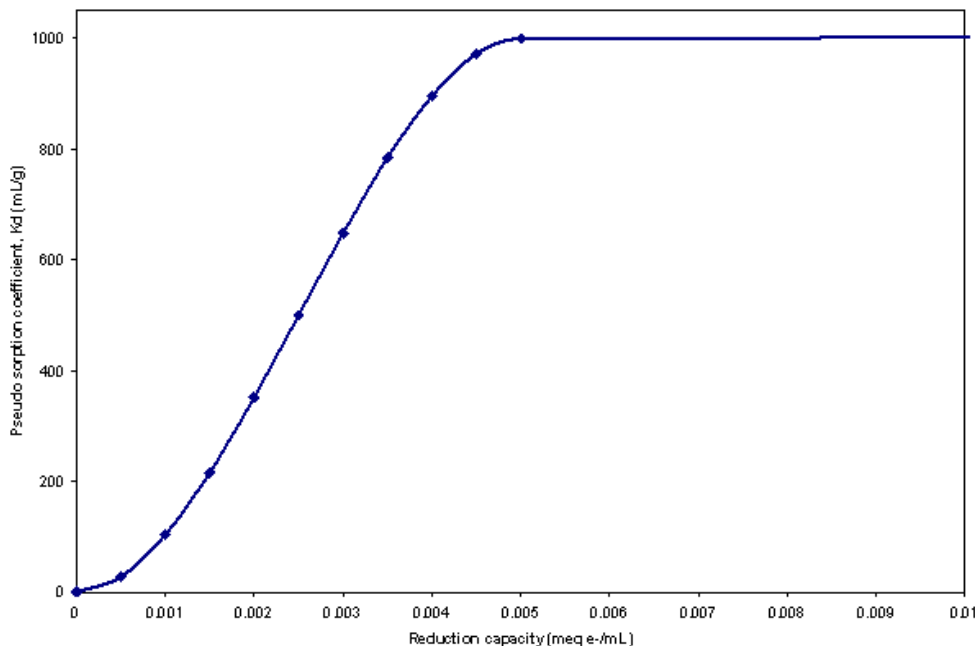


Table 4.2-18: Recommended Kd Values for Cementitious Materials

| Element | Reducing Cementitious Material | | | | Oxidized Cementitious Material | | | |
|---------|--------------------------------|-------------------|----------------|------|--------------------------------|-------------------|----------------|------|
| | Young Age (mL/g) | Middle Age (mL/g) | Old Age (mL/g) | Ref. | Young Age (mL/g) | Middle Age (mL/g) | Old Age (mL/g) | Ref. |
| Ac | 5,000 | 5,000 | 1,000 | a | 6,000 | 6,000 | 600 | a |
| Ag | 1 | 1 | 0.1 | a | 1 | 1 | 0.1 | a |
| Al | 5,000 | 5,000 | 1,000 | a | 6,000 | 6,000 | 600 | a |
| Am | 5,000 | 5,000 | 1,000 | b | 6,000 | 6,000 | 600 | a |
| Ar | 0 | 0 | 0 | a | 0 | 0 | 0 | a |
| As | 1,000 | 1,000 | 100 | a | 1,000 | 1,000 | 100 | a |
| At | 2 | 10 | 4 | a | 8 | 15 | 4 | a |
| Ba | 0.5 | 3 | 20 | a | 100 | 100 | 70 | a |
| Bk | 5,000 | 5,000 | 1,000 | a | 6,000 | 6,000 | 600 | a |
| C | 20 | 10 | 0 | a | 20 | 10 | 0 | a |
| Cd | 5,000 | 5,000 | 1,000 | b | 4,000 | 4,000 | 1,000 | a |
| Ce | 5,000 | 5,000 | 1,000 | b | 6,000 | 6,000 | 600 | a |
| Cf | 5,000 | 5,000 | 1,000 | a | 6,000 | 6,000 | 600 | a |
| Cl | 20 | 20 | 2 | a | 20 | 20 | 2 | a |
| Cm | 5,000 | 5,000 | 1,000 | a | 6,000 | 6,000 | 600 | a |
| Co | 5,000 | 5,000 | 1,000 | b | 4,000 | 4,000 | 1,000 | a |
| Cr | 5,000 | 5,000 | 1,000 | a | 20 | 20 | 2 | a |
| Cs | 0 | 2 | 10 | b | 2 | 20 | 10 | a |
| Cu | 1 | 1 | 0.1 | a | 1 | 1 | 0.1 | a |
| Eu | 5,000 | 5,000 | 1,000 | a | 6,000 | 6,000 | 600 | a |
| F | 20 | 20 | 2 | a | 20 | 20 | 2 | a |
| Fe | 5,000 | 5,000 | 1,000 | a | 6,000 | 6,000 | 600 | a |
| Fr | 0 | 2 | 10 | a | 2 | 20 | 10 | a |
| Gd | 5,000 | 5,000 | 1,000 | a | 6,000 | 6,000 | 600 | a |
| H | 0 | 0 | 0 | a | 0 | 0 | 0 | a |
| Hg | 1,000 | 1,000 | 300 | b | 300 | 300 | 300 | a |
| I | 5 | 9 | 0 | b | 8 | 15 | 4 | a |
| K | 0 | 2 | 10 | a | 2 | 20 | 10 | a |
| Mn | 100 | 100 | 10 | a | 100 | 100 | 10 | a |
| N | 0 | 0 | 0 | a | 0 | 0 | 0 | a |
| Na | 0.5 | 1 | 0.5 | a | 0.5 | 1 | 0.5 | a |
| Nb | 1,000 | 1,000 | 500 | a | 1,000 | 1,000 | 500 | a |
| Ni | 5,000 | 5,000 | 1,000 | a | 4,000 | 4,000 | 1,000 | a |
| Np | 4,000 | 4,000 | 3,000 | b | 1,600 | 1,600 | 250 | a |
| Pa | 5,000 | 5,000 | 500 | b | 1,600 | 1,600 | 250 | a |

Table 4.2-18: Recommended K_d Values for Cementitious Materials (Continued)

| Element | Reducing Cementitious Material | | | | Oxidized Cementitious Material | | | |
|-----------------|--------------------------------|-------------------|----------------|------|--------------------------------|-------------------|----------------|------|
| | Young Age (mL/g) | Middle Age (mL/g) | Old Age (mL/g) | Ref. | Young Age (mL/g) | Middle Age (mL/g) | Old Age (mL/g) | Ref. |
| Pb | 500 | 500 | 250 | a | 500 | 500 | 250 | a |
| Pd | 5,000 | 5,000 | 1,000 | a | 4,000 | 4,000 | 1,000 | a |
| Pm | 0 | 0 | 0 | c | 0 | 0 | 0 | c |
| Po | 500 | 500 | 250 | a | 500 | 500 | 250 | a |
| Pr | 0 | 0 | 0 | c | 0 | 0 | 0 | c |
| Pt | 0 | 0 | 0 | c | 0 | 0 | 0 | c |
| Pu | 10,000 | 10,000 | 10,000 | f | 10,000 | 10,000 | 1,000 | f |
| Ra | 0.5 | 3 | 20 | a | 100 | 100 | 70 | a |
| Rb | 0 | 2 | 10 | a | 2 | 20 | 10 | a |
| Re | 5,000 | 5,000 | 5,000 | a | 0.8 | 0.8 | 0.5 | a |
| Rh | 0 | 0 | 0 | c | 0 | 0 | 0 | c |
| Rn | 0 | 0 | 0 | a | 0 | 0 | 0 | a |
| Ru | 0 | 0 | 0 | c | 0 | 0 | 0 | c |
| Sb | 5,000 | 5,000 | 1,000 | a | 100 | 100 | 2 | a |
| Se | 300 | 300 | 300 | b,e | 300 | 300 | 150 | a |
| Sm | 5,000 | 5,000 | 1,000 | a | 6,000 | 6,000 | 600 | a |
| Sn | 5,000 | 5,000 | 2,000 | b | 4,000 | 4,000 | 2,000 | a |
| Sr | 0.5 | 3 | 20 | b | 3 | 30 | 15 | a |
| Tc ^d | 5,000 | 5,000 | 5,000 | a | 0.8 | 0.8 | 0.5 | a |
| Te | 300 | 300 | 150 | a | 300 | 300 | 150 | a |
| Th | 5,000 | 5,000 | 500 | a | 5,000 | 5,000 | 500 | a |
| U | 2,500 | 2,500 | 2,500 | b | 250 | 250 | 70 | a |
| V | 0 | 0 | 0 | c | 0 | 0 | 0 | c |
| Y | 5,000 | 5,000 | 1,000 | b | 5,000 | 5,000 | 500 | a |
| Zn | 5,000 | 5,000 | 1,000 | a | 4,000 | 4,000 | 1,000 | a |
| Zr | 5,000 | 5,000 | 500 | a | 5,000 | 5,000 | 500 | a |

(a) WSRC-STI-2007-00640

(b) SRNS-STI-2008-00045

(c) Assigned a value of zero

(d) An explicit redox simulation coupled with a reduction capacity dependent pseudo- K_d value is used (Figure 4.2-41) in the PORFLOW analysis for reducing cementitious material on SRNL-STI-2009-00115.

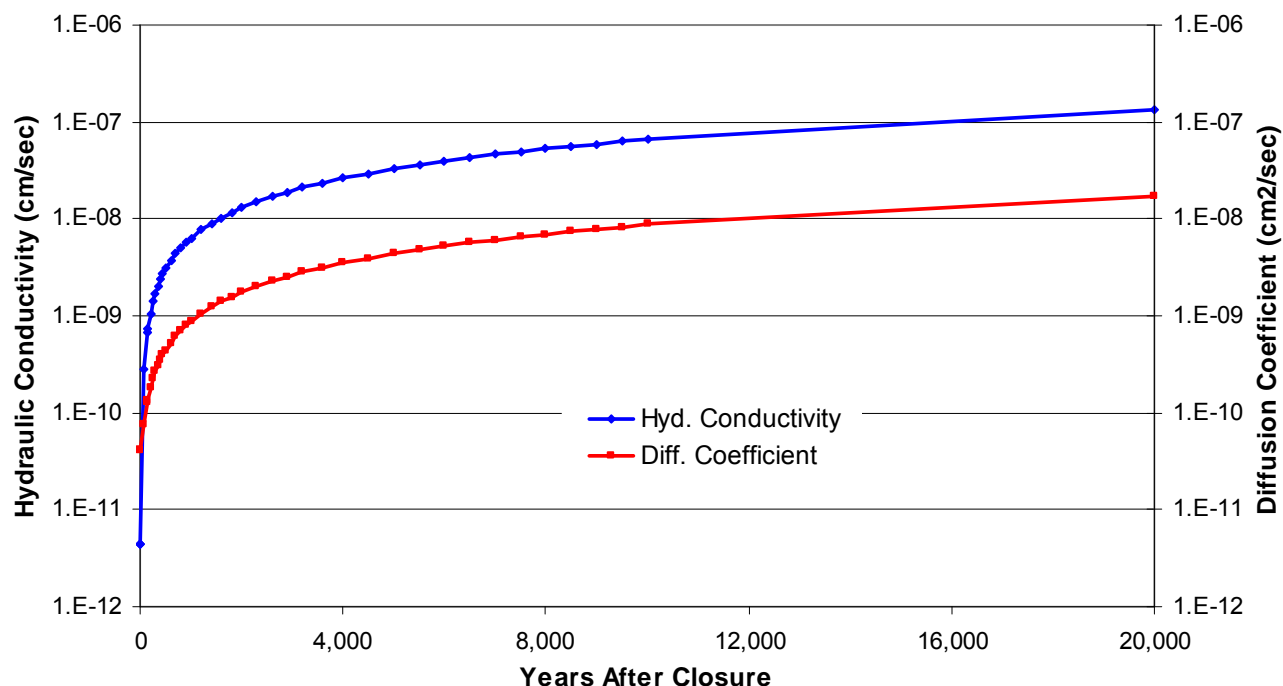
(e) It was discovered after the runs were complete that the reducing, old age value should have been 150 mL/g in SRNS-STI-2008-00045, but this state is not achieved in the modeling runs so does not impact any results.

(f) WSRC-TR-2009-00019

➤ **HDPE Properties and Degradation**

An HDPE liner, though not cementitious material, is attached to the exterior of the wall of the FDCs, and its properties and degradation are included to complete the discussion of FDC material degradation. A 100 mil (0.1 inch) thick HDPE liner is attached to the wall and will undergo degradation via the generation of holes and cracks. Initially the HDPE is assumed to have a hydraulic conductivity of $2.0\text{E-}13$ cm/sec and an D_e of $4.0\text{E-}11$ cm²/sec. [WSRC-STI-2008-00244, SRNL-STI-2009-00115] Utilizing the degradation analysis described in the evaluation of the proposed closure cap, WSRC-STI-2008-00244, and assuming the holes or tears of the HDPE are filled with soil having properties of backfill (Table 4.2-14) the degradation of the HDPE as a function of time after SDF closure has been estimated in SRNL-STI-2009-00115 and is illustrated in Figure 4.2-42.

Figure 4.2-42: Hydraulic Conductivity and Diffusion Coefficient for HDPE Lining of FDCs After Closure



4.2.3.2.5 Saturated Zone Hydraulic Properties

Within the GSAD, soils with a saturated hydraulic conductivity greater than $1.0\text{E-}07$ cm/sec are defined as sandy and those with a saturated hydraulic conductivity less than $1.0\text{E-}07$ cm/sec are classified as clay, for the purpose of defining transport properties (i.e., K_d and D_e). [WSRC-STI-2006-00198] For consistency with the vadose zone soils, the saturated zone soils within the GSA model that are defined as sandy are assigned the D_e of the Lower Vadose Zone (i.e., $5.3\text{E-}06$ cm²/sec) and those defined as clay are assigned that of the vadose zone clay (i.e., $4.0\text{E-}06$ cm²/sec).

Table 4.2-19 provides a summary of the saturated zone soils hydraulic properties (as represented by the vadose zone soil properties) and the model input used to represent these values.

Table 4.2-19: Lower Vadose Zone and Effective Saturated Zone Soil Properties

| Actual/Model | Porosity (%) | Dry Bulk Density (g/cm ³) | Particle Density (g/cm ³) | Saturated Effective Diffusion Coefficient D _e (cm ² /sec) |
|--|----------------|---------------------------------------|---------------------------------------|---|
| Lower Vadose Zone | 39 (total) | 1.62 | 2.66 | 5.3E-06 |
| Saturated Zone Soil (Effective Properties for Modeling Purposes) | 25 (effective) | 1.04 (effective) | 1.39 (effective) | Sandy: 5.3E-06 Clay: 4.0E-06 |

[WSRC-STI-2006-00198, Section 5.6.1]

4.2.4 Exposure Pathways and Scenarios

In order to calculate receptor doses, MOP and intruder exposure pathways were defined. The primary mechanism for transport of radionuclides from the SDF is expected to be leaching to the groundwater and subsequent human consumption.

4.2.4.1 Member of the Public Exposure Pathways

The pathways for a MOP release to be used in the PA analyses are presented in Table 4.2-20 and discussed below. Table 4.2-20 also indicates whether detailed dose calculations are included as part of the PA. The scenarios are not assumed to occur until after the 100 year institutional control period ends, during which no active SDF facility maintenance will be conducted. The consumption rates and bioaccumulation factors that are used in conjunction with the pathways are discussed in detail in Section 4.6.

Table 4.2-20: Crosswalk of Potential Exposure Pathways for MOP Receptors

| Release Mechanism from Soil | Primary Pathway | Secondary Pathway | Tertiary Pathway | Exposure Route | MOP at well |
|------------------------------------|------------------------|--------------------------|-------------------------|------------------------|--------------------|
| Groundwater release at Stream | Stream water | Drinking Water | N/A | Ingestion | N/A |
| Groundwater release at Stream | Stream water | Showering | N/A | Dermal | N/A |
| Groundwater release at Stream | Stream water | Showering | N/A | Inhalation | N/A |
| Groundwater release at Stream | Stream water | Showering | N/A | Ingestion (accidental) | N/A |
| Groundwater release at Stream | Stream water | Swimming | N/A | Inhalation | X |
| Groundwater release at Stream | Stream water | Swimming | N/A | Dermal | O |
| Groundwater release at Stream | Stream water | Swimming | N/A | Ingestion (accidental) | X |
| Groundwater release at Stream | Stream water | Swimming, Fishing | Direct Rad Emissions | External Exposure | X |
| Groundwater release at Stream | Stream water | Fish | N/A | Ingestion | X |
| Groundwater release at Stream | Stream water | Shellfish | N/A | Ingestion | O |
| Volatilization | Ambient Air (vapors) | Plume Rad Exposure | N/A | External Exposure | X |
| Volatilization | Ambient Air (vapors) | Livestock | Meat | Ingestion | X |
| Volatilization | Ambient Air (vapors) | Livestock | Milk | Ingestion | X |
| Volatilization | Ambient Air (vapors) | Garden Vegetables | N/A | Ingestion | X |
| Volatilization | Ambient Air (vapors) | Garden Fodder | Livestock - Meat | Ingestion | X |
| Volatilization | Ambient Air (vapors) | Garden Fodder | Livestock - Milk | Ingestion | X |

Table 4.2-20: Crosswalk of Potential Exposure Pathways for MOP Receptors (Continued)

| Release Mechanism from Soil | Primary Pathway | Secondary Pathway | Tertiary Pathway | Exposure Route | MOP at well |
|-----------------------------|-----------------------|-------------------|------------------|------------------------|-------------|
| Groundwater at Well | Well Water | Drinking Water | N/A | Ingestion | X |
| Groundwater at Well | Well Water | Showering | N/A | Dermal | O |
| Groundwater at Well | Well Water | Showering | N/A | Inhalation | X |
| Groundwater at Well | Well Water | Showering | N/A | Ingestion (accidental) | X |
| Groundwater at Well | Well Water | Livestock | N/A | Ingestion | X |
| Groundwater at Well | Well Water | Milk | N/A | Ingestion | X |
| Groundwater at Well | Well Water Irrigation | Garden Vegetables | N/A | Ingestion | X |
| Groundwater at Well | Well Water Irrigation | Garden Fodder | Livestock - Meat | Ingestion | X |
| Groundwater at Well | Well Water Irrigation | Garden Fodder | Livestock - Milk | Ingestion | X |

X = addressed quantitatively

O = addressed qualitatively

4.2.4.1.1 Scenario with Well Water as Primary Water Source

The primary water source for the MOP release pathway is assumed to be a well drilled into the groundwater aquifers.

In the groundwater well dose analysis, doses are calculated using water from a well for domestic purposes. Exposure pathways involving the use of contaminated well water are assumed to occur as presented in Table 4.2-20 and Figure 4.2-43.

- Direct ingestion of well water
- Ingestion of milk and meat from livestock (e.g., dairy and beef cattle) that drink well water
- Ingestion of vegetables grown in garden soil irrigated with well water
- Ingestion of milk and meat from livestock (e.g., dairy and beef cattle) that eat fodder from pasture irrigated with well water.
- Ingestion and inhalation of well water while showering

The following exposure pathways involving the use of contaminated surface water (from the applicable stream) for recreational use are assumed to occur:

- Direct irradiation during recreational activities (e.g., swimming, fishing) from stream water
- Dermal contact with stream water during recreational activities (e.g., swimming, fishing)
- Incidental ingestion and inhalation of stream water during recreational activities
- Ingestion of fish from the stream water

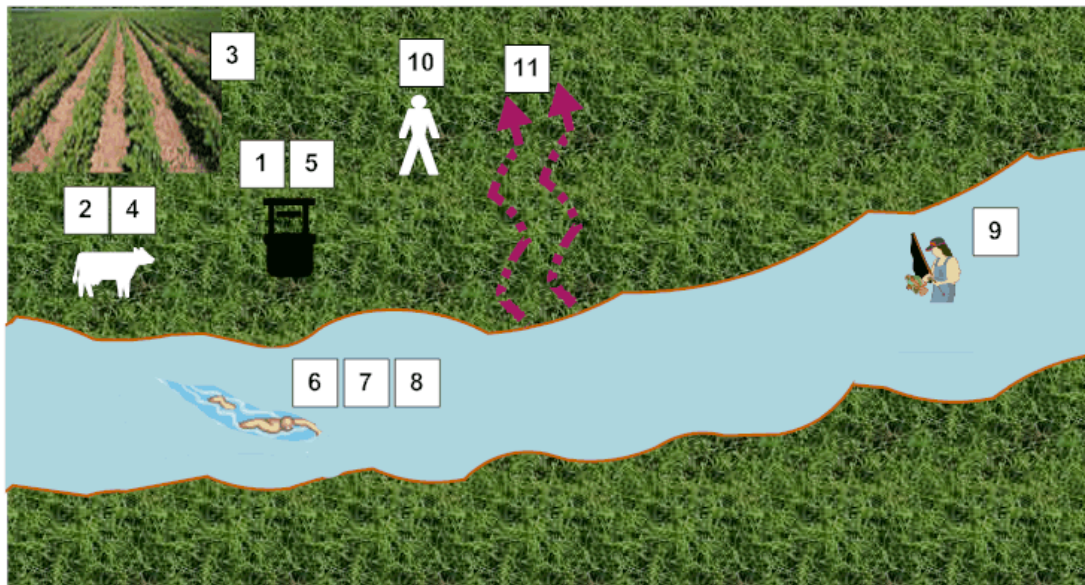
Additional exposure pathways could involve releases of radionuclides into the air from the water taken from the well (i.e., volatile radionuclides such as H-3, C-14, I-129). Exposures from the air pathways may include:

- Direct plume shine
- Inhalation

There are other secondary and indirect pathways that contribute relatively minor doses to a receptor when compared to direct pathways such as ingestion of milk and meat. These pathways include:

- Inhalation of well water used for irrigation
- Inhalation of dust from the soil that was irrigated with well water
- Ingestion of soil that was irrigated with well water
- Direct radiation exposure from radionuclides deposited on the soil that was irrigated with well water

Figure 4.2-43: Member of the Public Exposure Pathways



SCENARIO WITH WELL WATER AS PRIMARY WATER SOURCE

1. Direct ingestion of well water
2. Ingestion of milk and meat from livestock (e.g., dairy and beef cattle) that drink well water
3. Ingestion of vegetables grown in garden soil irrigated with well water
4. Ingestion of milk and meat from livestock (e.g., dairy and beef cattle) that eat fodder from pasture irrigated with well water
5. Ingestion and inhalation of well water while showering
6. Direct irradiation during recreational activities (e.g., swimming, fishing) from stream water
7. Dermal contact with stream water during recreational activities (e.g., swimming, fishing)
8. Incidental ingestion and inhalation of stream water during recreational activities
9. Ingestion of fish from the stream water
10. Direct plume shine
11. Inhalation

4.2.4.1.2 Basis for Release Pathways

Table 4.2-20 was prepared to provide a list of the SDF exposure pathways identified as candidates for detailed analysis. The list of candidates was developed based on a review of SRS PA analyses and U.S. Nuclear Regulatory Commission (NRC) documents. [CBU-PIT-2005-00146, NUREG-0782, NUREG-0945 (VOL. 1), NUREG-1573] Those activities at SRS that could bring humans in contact with stabilized contaminants (e.g., water use, hunting, fishing, recreational activities such as swimming and boating, habitation in dwellings, and other unique activities that involve water use or ground disturbance) were

considered (with emphasis on local practices), to ensure that any pathways unique to SRS were taken into account. The *SRS Ecology Environmental Information Document* was used as a source of relevant environmental information and conditions at SRS. [WSRC-TR-2005-00201] For example, the *SRS Ecology Environmental Information Document* was used to identify potential wild game available on site, potential bio-intrusion candidates (flora and fauna), and the potential for the presence of fish and/or shellfish in the creeks bordering the SDF.

Those potential pathways planned for quantified analysis are denoted with an “X” for the various receptors. Quantified analysis will not be performed for potential pathways denoted with an “O” (Table 4.2-20). NUREG-1854 states that transport pathways may be excluded from a PA if it can be demonstrated that either there is limited potential for radionuclides to be released into a particular pathway, or the pathway is not viable (e.g., water is not potable). Other pathways were marked as N/A due to the nature of the scenario making them impossible (e.g., a garden that receives 100% of its irrigation water from a well cannot also receive water from a stream).

4.2.4.1.3 Inputs and Assumptions Related to Public Release Pathways

The following assumptions were made regarding the pathways related to the MOP resident scenario using water from a well or stream:

- The stabilized contaminants release mechanisms to include leaching to the groundwater and volatilization to the surface. Well drilling is not a release mechanism, since any well drilling associated with the MOP scenarios will be outside the SDF buffer zone, and therefore will not disturb the stabilized contaminants.
- Bio-intrusion and/or erosion are not considered credible mechanisms for significant stabilized contaminant disturbance based on the depth and form of the stabilized contaminant. The stabilized contaminants will be at least 12 feet below the erosion control barrier of the closure cap. No mechanism was identified that would result in stabilized contaminant disturbance and dispersal such that the dose to a MOP (outside the SDF buffer zone) would be impacted.
- In the well water as primary water source scenario, well water will be used as a primary potable water source for a residence near the well (e.g., drinking water, showering) and will be used by the resident as a primary water source for agriculture (e.g., irrigation, livestock water).
- The resident can use a stream for recreational activities (e.g., swimming, fishing).
- Any wild game ingested (deer, wild pigs) would merely offset ingested livestock, and would result in a lower total dose since the livestock raised near SDF would be more affected by SDF stabilized contaminants than transient wild game.
- There are two creeks, UTR and McQueen Branch, from which ingestion of finfish with contamination is possible. These creeks were conservatively assumed to be a source of dietary fish, but shellfish were excluded because UTR and McQueen Branch are not significant sources of edible shellfish and shellfish play an insignificant role in local diets in relation to other ingested contributors to dose such as livestock, milk, and vegetables (local invertebrate consumption is a total of 2 kg/yr). [WSRC-TR-2005-00201, WSRC-STI-2007-00004]

- Since there is no substantive water source readily available at the well site, pathways related to water-related commercial activities were not postulated. Based on the relative proximity of a large natural water source (i.e., the Savannah River), it is not assumed that a man-made body of water would be created at a MOP resident site.
- The dose associated with dermal absorption of radionuclides is considered insignificant because, unlike some chemicals, radionuclides are generally absorbed into the body very poorly.
- The quantities of water ingested during the relatively short activities of showering (10 min/d) and swimming (8.9 hr/yr) are negligibly small and are not addressed independently. The impact of these activities is addressed by the “direct ingestion of well water” pathways (i.e., they are included in the 337 liters of water that is assumed to be ingested every year). [WSRC-STI-2007-00004]

4.2.4.2 Intruder Exposure Pathways

The stabilized contaminant materials after SDF closure will be located in areas protected by significant materials, which are clearly distinguishable from the surrounding soil and make drilling not an impractical scenario based on regional drilling practices. Regional drilling conditions are such that a barrier like the grout fill would cause drillers to stop operations and move the drilling location.

The dose pathways for an inadvertent intruder are presented in Table 4.2-21 and discussed below. Table 4.2-21 indicates whether detailed dose calculations are required.

The consumption rates and bioaccumulation factors that are used in conjunction with the Table 4.2-21 proposed pathways are discussed in detail in Section 4.6.

In order to calculate the dose to an inadvertent intruder, the following intruder scenarios were considered:

- Acute Intruder-Drilling Scenario
- Acute Intruder-Construction Scenario
- Acute Intruder-Discovery Scenario
- Chronic Intruder Agricultural (Post-Drilling) Scenario
- Chronic Intruder-Resident Scenario
- Chronic Intruder-Recreational Hunting and Fishing Scenario
- Bio-intrusion Scenario

4.2.4.2.1 Acute Intruder-Drilling Scenario

In a drilling scenario, an acute intruder is assumed to be the person or persons who install a water well and are exposed to drill cuttings during well installation. Regional drilling conditions are such that a barrier such as the grout fill would cause well drillers to stop operations and move to another drilling location.

Since no natural resources other than water have been identified in the SDF, no additional drilling scenarios were postulated.

4.2.4.2.2 Acute Intruder- Construction Scenario

This scenario involves stabilized contaminants below the depth of typical construction excavations. The intruder is assumed to dig a basement excavation to a depth of approximately 10 feet. It is assumed that the intruder does not recognize the hazardous nature of the material excavated. During the excavation of the basement, the intruder is exposed to the exhumed stabilized contaminants by inhalation of re-suspended contaminated soil and external irradiation from contaminated soil.

Since the disposal depth of the stabilized contaminants in the SDF disposal units will be at least 12 feet below the erosion control barrier of the SDF closure cap, the acute intruder-construction scenario is not considered applicable.

4.2.4.2.3 Acute Intruder- Discovery Scenario

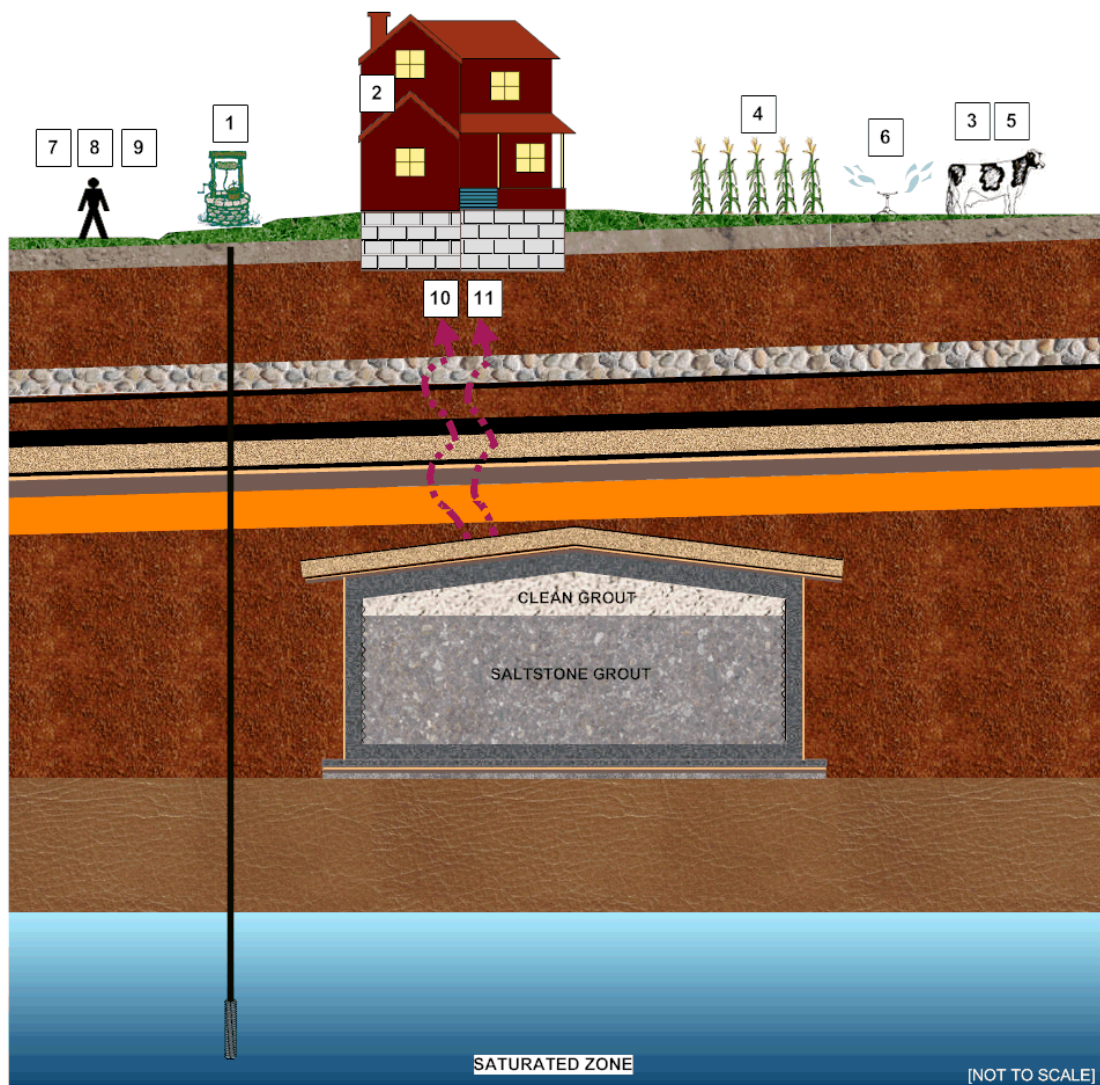
The intruder-discovery scenario is conceptualized as a modification of the intruder-construction scenario. The basis for the intruder-discovery scenario is the same as the intruder-construction scenario, except the exposure time is reduced. The scenario involves the intruder excavating a basement to a depth of approximately 10 feet. The intruder is assumed to recognize that he or she is digging into very unusual soil immediately upon encountering the stabilized waste and leaves the site. Consequently, the exposure time is reduced. Similar to the intruder-construction scenario, the intruder-discovery scenario was not considered for further analysis due to the disposal depth of the stabilized contaminants in the disposal units below the SDF closure cap.

4.2.4.2.4 Chronic Intruder Agricultural (Post-Drilling) Scenario

In this scenario, it is assumed that after the end of active institutional controls, a farmer lives on, and consumes food crops grown and animals raised on the disposal area. This scenario is credible for the Saltstone Facility. The chronic intruder agriculture (i.e., post-drilling) scenario is an extension of the acute intruder drilling scenario. It is assumed in this scenario that an intruder lives in a building with a basement near the well drilled as part of the intruder-drilling scenario and engages in agricultural activities on the contaminated site. The soil used for agricultural purposes is assumed to be contaminated by irrigation well water. There are no contaminated cuttings from drilling the well.

The exposure pathways for the intruder (Figure 4.2-44) are the same as those for a MOP exposed to well water, including the secondary and indirect pathways. Exposure pathways involving the use of contaminated surface water are not assumed to occur.

Figure 4.2-44: Chronic Intruder Agricultural (Post-Drilling) Scenario



1. Direct ingestion of well water
2. Ingestion and inhalation of well water while showering
3. Ingestion of milk and meat from livestock (e.g., dairy and beef cattle) that drink well water
4. Ingestion of vegetables grown in garden soil irrigated with well water
5. Ingestion of milk and meat from livestock (e.g., dairy and beef cattle) that eat fodder from pasture irrigate with well water
6. Inhalation of well water used for irrigation
7. Inhalation of dust from the soil that was irrigated with well water
8. Ingestion of soil that was irrigated with well water
9. Direct radiation exposure from radionuclides deposited on the soil that was irrigated with well water
10. Direct plume shine through basement of residence
11. Inhalation through basement of residence

4.2.4.2.5 Chronic Intruder- Resident Scenario

In this scenario, it is assumed that after the end of active institutional controls, an intruder (i.e., the resident intruder) inadvertently constructs a house at, and lives on the waste disposal area, including the use of well water. The intruder-resident scenario involves the same pathways as the chronic intruder agriculture (i.e., post-drilling) scenario, with the potential for additional pathways associated with a house constructed over stabilized contaminants. This scenario is applicable to the Saltstone Facility. The pathways uniquely associated with construction of a residence over stabilized contaminants are considered because of the depth of the stabilized contaminants under the closure cap.

4.2.4.2.6 Chronic Intruder- Recreational Hunting and Fishing Scenario

In this scenario, a hunter/fisher is assumed to inadvertently visit the site, perhaps on a periodic basis, and consumes game and fish taken from the site. Given the significant exposure pathways, the inadvertent intruder is postulated to experience as part of the intruder agriculture scenario (e.g., use of well water as potable water and ingestion of livestock and vegetables raised using well water); the intruder-hunter/fisher scenario is bounded by the chronic intruder agriculture scenario and does not require unique analysis.

4.2.4.2.7 Bio-Intrusion Scenario

The bio-intrusion scenario assumes that an intruder moves onto the site and does not excavate into the stabilized contaminants. Rather, radioactivity is brought to the surface by plants through root uptake and burrowing animals. Bio-intrusion is not considered a credible mechanism for significant stabilized contaminant disturbance, based on the stabilized contaminant depth and form. The stabilized contaminants will be significantly below ground. The stabilized contaminants are contained within grouted disposal units. Of the likely burrowing animal residents at SRS, only one burrower, the Florida Harvester Ant, is expected to burrow below 2m, and then, only 5% of its burrows are expected to be that deep. [WSRC-RP-92-1360] Assuming the SDF cover reverts to pine forest in the future, the pine trees could also pose a bio-intrusion risk, with a mature pine having roots from 6 to 12 feet deep. [WSRC-TR-2003-00436] These bio-intrusion depths will not be deep enough to reach the principal SDF stabilized contaminant inventory at closure, which is below at least 12 feet of material under the erosion control barrier of the closure cap and at least 2 feet of clean grout covering the contaminated grout. Even if a pine tree root were to reach the stabilized waste, no significant stabilized contaminant dispersal would be anticipated. The amount of contamination excavated from animal burrows or vegetative intrusion is far less than that involved in the agricultural (intruder-drilling) scenarios for drilling a domestic well into the underlying aquifers. Therefore the bio-intrusion scenario is bounded by the chronic agricultural (post drilling) scenario.

Table 4.2-21 was prepared to provide a list of all the SDF exposure pathways identified as candidates for detailed analysis. The list of candidates was developed based on a review of SRS PA analyses and NRC documents. [CBU-PIT-2005-00146, NUREG-0782, NUREG-0945 (VOL. 1), NUREG-1573] Those human activities at SRS that could bring humans in contact with stabilized contaminants (e.g., water use, hunting, fishing, recreational activities such as swimming and boating, habitation in dwellings and other unique activities that involve

water use or ground disturbance) were considered (with emphasis on local practices), to ensure that any pathways unique to SRS were taken into account. Those potential pathways that had quantitative analysis are denoted with an “X” for the various receptors. Quantitative analysis was not performed for potential pathways denoted with an “O”, based on the applicable justifications provided. NUREG-1854 states that transport pathways may be excluded from performance analysis if it can be demonstrated that there is limited potential for radionuclides to be released into a particular pathway, or the pathway is not viable (e.g., water is not potable). Other pathways were excluded due to the nature of the scenario making them impossible (e.g., a garden that receives 100% of its irrigation water from a well can’t also receive water from a stream).

Table 4.2-21: Crosswalk of Potential Exposure Pathways for Intruder Receptors

| Release Mechanism from Soil | Primary Pathway | Secondary Pathway | Tertiary Pathway | Exposure Route | Acute Intruder | Chronic Intruder |
|------------------------------------|--|----------------------------|-------------------------|------------------------|-----------------------|-------------------------|
| Drill Cuttings | Fugitive Dust Generation during drilling | Ambient Air (particulates) | N/A | Inhalation | N/A | N/A |
| Drill Cuttings | Biotic Uptake | Garden Vegetables | N/A | Ingestion | N/A | N/A |
| Drill Cuttings | Biotic Uptake | Garden Fodder | Livestock - Meat | Ingestion | N/A | N/A |
| Drill Cuttings | Biotic Uptake | Garden Fodder | Livestock - Milk | Ingestion | N/A | N/A |
| Drill Cuttings | Drill Cuttings dropped on surface | Direct Soil Contact | N/A | Ingestion | N/A | N/A |
| Drill Cuttings | Drill Cuttings dropped on surface | Direct Soil Contact | N/A | Dermal | N/A | N/A |
| Drill Cuttings | Drill Cuttings dropped on surface | Direct Rad Emissions | N/A | External Exposure | N/A | N/A |
| Groundwater release at Stream | Stream water | Drinking Water | N/A | Ingestion | N/A | N/A |
| Groundwater release at Stream | Stream water | Showering | N/A | Dermal | N/A | N/A |
| Groundwater release at Stream | Stream water | Showering | N/A | Inhalation | N/A | N/A |
| Groundwater release at Stream | Stream water | Showering | N/A | Ingestion (accidental) | N/A | N/A |
| Groundwater release at Stream | Stream water | Swimming | N/A | Inhalation | N/A | X |
| Groundwater release at Stream | Stream water | Swimming | N/A | Dermal | N/A | O |
| Groundwater release at Stream | Stream water | Swimming | N/A | Ingestion (accidental) | N/A | X |

Table 4.2-21: Crosswalk of Potential Exposure Pathways for Intruder Receptors (Continued)

| Release Mechanism from Soil | Primary Pathway | Secondary Pathway | Tertiary Pathway | Exposure Route | Acute Intruder | Chronic Intruder |
|------------------------------------|---------------------------|--|----------------------------|-----------------------|-----------------------|-------------------------|
| Groundwater release at Stream | Stream water | Swimming, Fishing | Direct Rad Emissions | External Exposure | N/A | X |
| Groundwater release at Stream | Stream water | Fish | N/A | Ingestion | N/A | X |
| Groundwater release at Stream | Stream water | Shellfish | N/A | Ingestion | N/A | O |
| Groundwater release at Stream | Stream water to Livestock | Livestock | Meat | Ingestion | N/A | N/A |
| Groundwater release at Stream | Stream Water Irrigation | Garden Vegetables | N/A | Ingestion | N/A | N/A |
| Groundwater release at Stream | Stream Water Irrigation | Garden Fodder | Livestock - Meat | Ingestion | N/A | N/A |
| Groundwater release at Stream | Stream Water Irrigation | Garden Fodder | Livestock - Milk | Ingestion | N/A | N/A |
| Groundwater release at Stream | Stream Water Irrigation | Fugitive Dust Generation during Irrigation | Ambient Air (particulates) | Inhalation | N/A | N/A |
| Groundwater release at Stream | Stream Water Irrigation | Ambient Air (vapors) from Irrigation | N/A | Inhalation | N/A | N/A |
| Groundwater release at Stream | Stream Water Irrigation | Direct Soil Contact | N/A | Ingestion | N/A | N/A |
| Groundwater release at Stream | Stream Water Irrigation | Direct Rad Emissions | N/A | External Exposure | N/A | X |
| Volatilization | Ambient Air (vapors) | N/A | N/A | Inhalation | N/A | X |
| Volatilization | Ambient Air (vapors) | Plume Rad Exposure | N/A | External Exposure | N/A | X |

Table 4.2-21: Crosswalk of Potential SDF Exposure Pathways for Intruder Receptors by Stabilized Salt Waste (Continued)

| Release Mechanism from Soil | Primary Pathway | Secondary Pathway | Tertiary Pathway | Exposure Route | Acute Intruder | Chronic Intruder |
|-----------------------------|-----------------------|--|----------------------------|------------------------|----------------|------------------|
| Volatilization | Ambient Air (vapors) | Livestock | Meat | Ingestion | N/A | O |
| Volatilization | Ambient Air (vapors) | Livestock | Milk | Ingestion | N/A | O |
| Volatilization | Ambient Air (vapors) | Garden Vegetables | N/A | Ingestion | N/A | O |
| Volatilization | Ambient Air (vapors) | Garden Fodder | Livestock – Meat | Ingestion | N/A | O |
| Volatilization | Ambient Air (vapors) | Garden Fodder | Livestock – Milk | Ingestion | N/A | O |
| Well | Well Water | Drinking Water | N/A | Ingestion | N/A | X |
| Well | Well Water | Showering | N/A | Dermal | N/A | O |
| Well | Well Water | Showering | N/A | Inhalation | N/A | X |
| Well | Well Water | Showering | N/A | Ingestion (accidental) | N/A | X |
| Well | Well Water | Livestock | N/A | Ingestion | N/A | X |
| Well | Well Water | Milk | N/A | Ingestion | N/A | X |
| Well | Well Water Irrigation | Garden Vegetables | N/A | Ingestion | N/A | X |
| Well | Well Water Irrigation | Garden Fodder | Livestock – Meat | Ingestion | N/A | X |
| Well | Well Water Irrigation | Garden Fodder | Livestock – Milk | Ingestion | N/A | X |
| Well | Well Water Irrigation | Fugitive Dust Generation during Irrigation | Ambient Air (particulates) | Inhalation | N/A | X |

Table 4.2-21: Crosswalk of Potential SDF Exposure Pathways for Intruder Receptors by Stabilized Salt Waste (Continued)

| Release Mechanism from Soil | Primary Pathway | Secondary Pathway | Tertiary Pathway | Exposure Route | Acute Intruder | Chronic Intruder |
|-----------------------------|-----------------------------------|--------------------------------------|------------------|-------------------|----------------|------------------|
| Well | Well Water Irrigation | Ambient Air (vapors) from Irrigation | N/A | Inhalation | N/A | X |
| Well | Well Water Irrigation | Direct Soil Contact | N/A | Ingestion | N/A | X |
| Well | Well Water Irrigation | Direct Soil Contact | Surface Soil | Dermal | N/A | O |
| Well | Well Water Irrigation | Direct Rad Emissions | N/A | External Exposure | N/A | X |
| Direct radiation | Residence over waste vault or FDC | Direct Rad Emissions | N/A | External Exposure | N/A | X |

X = addressed quantitatively

O = addressed qualitatively

4.2.4.2.8 Inputs and Assumptions Related to Intruder Release Pathways

The following assumptions were made regarding the pathways related to the intruder scenario using water from a well or stream.

The stabilized contaminant release mechanisms to the intruder are leaching of stabilized contaminants to the groundwater and volatilization of the stabilized contaminants to the surface. Well drilling into a waste disposal unit is not considered a credible release mechanism, since local practices would cause a well driller to choose a new location before the stabilized contaminants were disturbed. The local well drillers expect to reach good drinking water aquifers at no more than 150 to 200 feet while drilling through sandy soil (no drilling through high-strength geologic materials). A driller would not expend the effort and equipment damage required to drill through the concrete/grout covering the stabilized contaminant waste inventory. Even if the driller did not realize that he had struck a waste disposal unit, and simply thought he had a layer of high-strength geologic materials, local experience would tell him that moving the drill site a short distance would avoid the impediment. Nevertheless, an intruder drilling into the stabilized waste while attempting to drill a well is investigated in the sensitivity analysis.

- Well water will be used by the inadvertent intruder as a primary potable water source (e.g., drinking water, showering) and is used as a primary water source for agriculture (e.g., irrigation, livestock water).
- The inadvertent intruder can use a nearby stream for recreational activities (e.g., swimming, fishing).
- Any wild game ingested (deer, wild pigs) would merely offset ingested livestock, and would result in a lower total dose since the livestock raised near SDF would be more affected by SDF stabilized contaminants than transient wild game.
- There are two creeks (UTR and McQueen Branch) from which ingestion of finfish with contamination is possible. These creeks were conservatively assumed to be a source of dietary fish, but shellfish were excluded because UTR and McQueen Branch are not significant sources of edible shellfish and shellfish play an insignificant role in local diets in relation to other ingested contributors to dose such as livestock, milk, and vegetables. [WSRC-TR-2005-00201, WSRC-STI-2007-00004]
- Since there is no significant water source readily available at the well site, pathways related to water-related commercial activities were not postulated. Based on the relative proximity of a large natural water source (i.e., the Savannah River), it is not assumed that a man-made body of water would be created at a MOP resident site.
- The quantities of water ingested during the relatively short activities of showering (10 min/d) and swimming (8.9 hr/yr) are negligibly small and are not addressed independently. The impact of these activities is addressed by the “direct ingestion of well water” pathways (i.e., they are included in the 337 liters of water that is assumed to be ingested every year). [WSRC-STI-2007-00004]

The dose associated with dermal absorption of radionuclides is insignificant because unlike some chemicals, radionuclides are generally absorbed into the body very poorly. Tritium is

an exception to this rule, but tritium is found in such relatively small concentrations in the groundwater that it would not be a significant contributor to dose.

4.3 Modeling Codes

In the process of completing the PA for the SDF, a variety of modeling codes were utilized to perform various media transport, radiological dose and risk assessment calculations for compliance with performance objectives and risk evaluations. The purpose of this section is to present the modeling codes used and describe the modeling code integration. A brief description is provided for each modeling code, which includes the function of the code, available code manuals or technical documents for the applicable code revision, reasons for selection of the particular code, and available quality assurance (QA) documentation for the code.

4.3.1 Modeling Codes Utilized

The HELP model is a quasi-two-dimensional water balance model designed to conduct landfill water balance analyses. The HELP model was used to generate water infiltration estimates through the final closure cap for use in PA calculations. HELP model infiltration estimates form the input to subsequent flow and contaminant transport models.

4.3.1.1 *Hydrologic Evaluation of Landfill Performance (HELP) Model*

The HELP model requires the input of weather, soil and design data. It provides estimates of runoff, evapotranspiration, lateral drainage, vertical percolation (i.e., infiltration), hydraulic head and water storage for the evaluation of various landfill designs. United States Army Corps of Engineers (USACE) personnel at the Waterways Experiment Station (WES) in Vicksburg, Mississippi developed the HELP model, under an interagency agreement with the EPA. [EPA-600-R-94-168b] As such, the HELP model is an EPA sanctioned model for conducting landfill water balance analyses. HELP model version 3.07, issued on November 1, 1997, is the latest version of the model and was the version used for the SDF PA calculations. The HELP model was used at SRS during the development of calculations supporting the PA and is the code used by the Soil and Groundwater Closure Project (SGCP) during CERCLA closure evaluations. [www.epa.gov/superfund/policy/cercla.htm, CBU-PIT-2005-00146] While other codes for closure cap infiltration calculations exist, the HELP model is a proven code that is appropriate for use at SRS. It is public domain software available from the WES website <http://www.wes.army.mil/el/elmodels/helpinfo.html>. EPA and the USACE have provided a user's guide associated with the HELP model that includes instructions for HELP model use. [EPA-600-R-94-168a]

Engineering documentation provides information on the source language used to write the code, the hardware necessary to operate the code, data generation methodologies available for use, and the methods of solution. [EPA-600-R-94-168b]

HELP verification test reports exist, which compare the model's drainage layer estimates to the results of large-scale physical models and compare the model's water balance estimates to "field data from a total of 20 landfill cells at seven sites in the United States". [PB87-227104, PB87-227518]

The *Saltstone Disposal Facility Closure Cap Concept and Infiltration Estimates* report, WSRC-STI-2008-00244, identifies and reports eight water balance and infiltration studies that have been conducted in and around SRS by various organizations, including SRNL, USGS, State University of New York at Brockport, Pennsylvania State University, University of Arizona, and the Desert Research Institute. Findings from these studies are summarized in Section 3.2 of WSRC-STI-2008-00244. The summary shows that evapotranspiration dominates the water balance distribution of precipitation at SRS, which is also the case for the analyses conducted for SDF.

In summary, additional comparison studies to support HELP appropriateness in humid environments are not needed since the limitations of the software result in conservative infiltration estimates. However, continuing efforts will be made to update the HELP code with more sophisticated software to further enhance PA evaluations.

The Software Quality Assurance Plan (SQAP) for the HELP model version used for the SDF PA calculations is documented within Q-SQA-A-00005.

4.3.1.2 PORFLOW

PORFLOW is a commercial Computational Fluid Dynamics (CFD) tool developed by Analytic & Computational Research, Inc. (www.acricfd.com/software/porflow/). PORFLOW numerically solves problems involving transient or steady state fluid flow, heat, salinity, and mass transport in multi-phase, variably saturated, porous or fractured media with dynamic phase change. PORFLOW was used in SDF PA modeling to calculate fluid flow and contaminant transport in the vadose and saturated zones. PORFLOW transport results were utilized by subsequent modeling codes to calculate radiological doses and perform human health and ecological risk evaluations. PORFLOW flow results were also utilized by GoldSim to conduct contaminant transport via another computational tool. Another use of PORFLOW was to calculate vapor phase radionuclide diffusion to the ground surface from stabilized contaminants material for use in air transport calculations. Figures 4.3-1 and 4.3-2 illustrate the integration of PORFLOW in the modeling efforts and provide additional detail of the integration and steps of PORFLOW calculations for fluid flow and contaminant transport.

Figure 4.3-1: SDF PA Modeling Code Integration

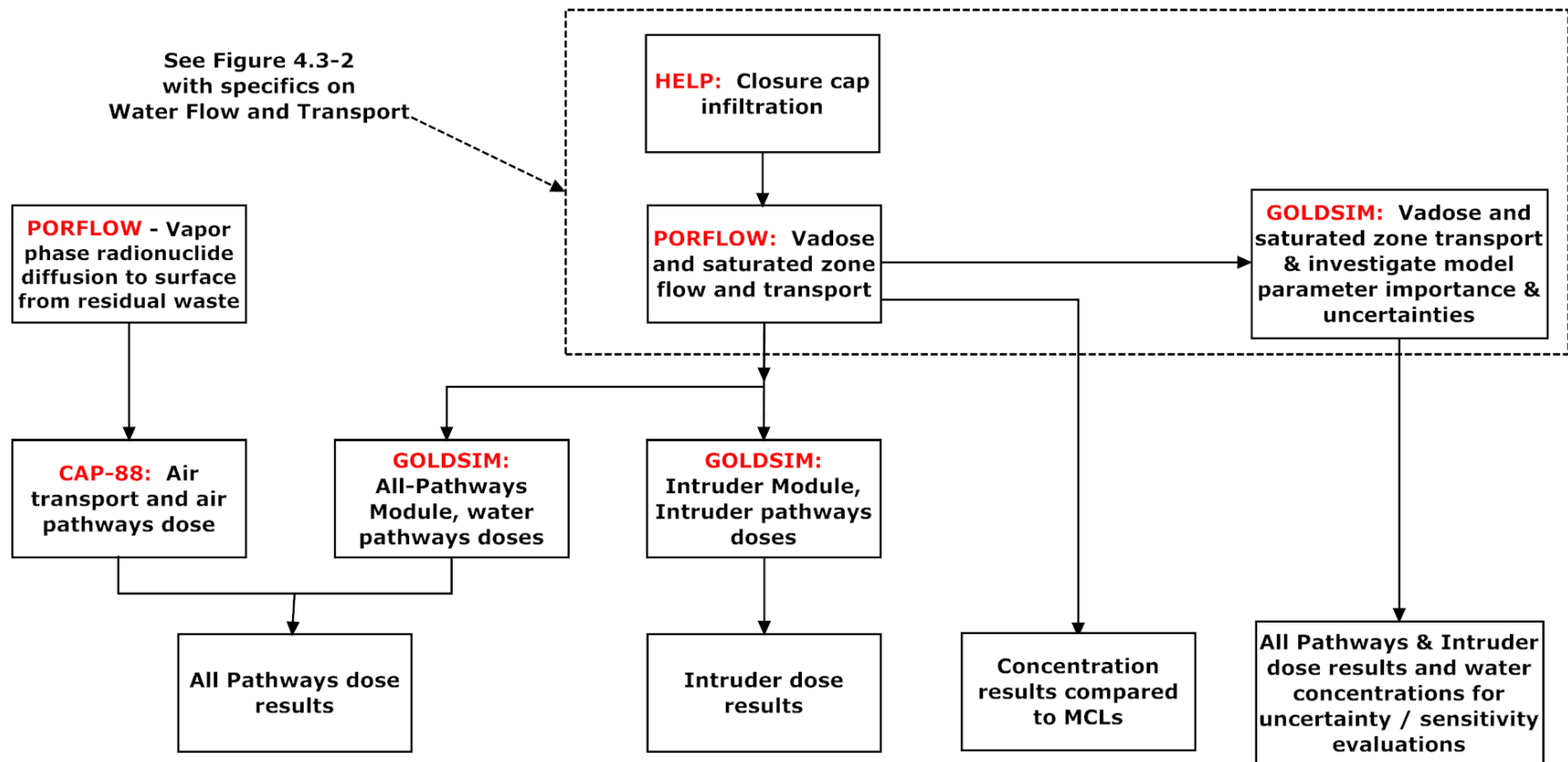
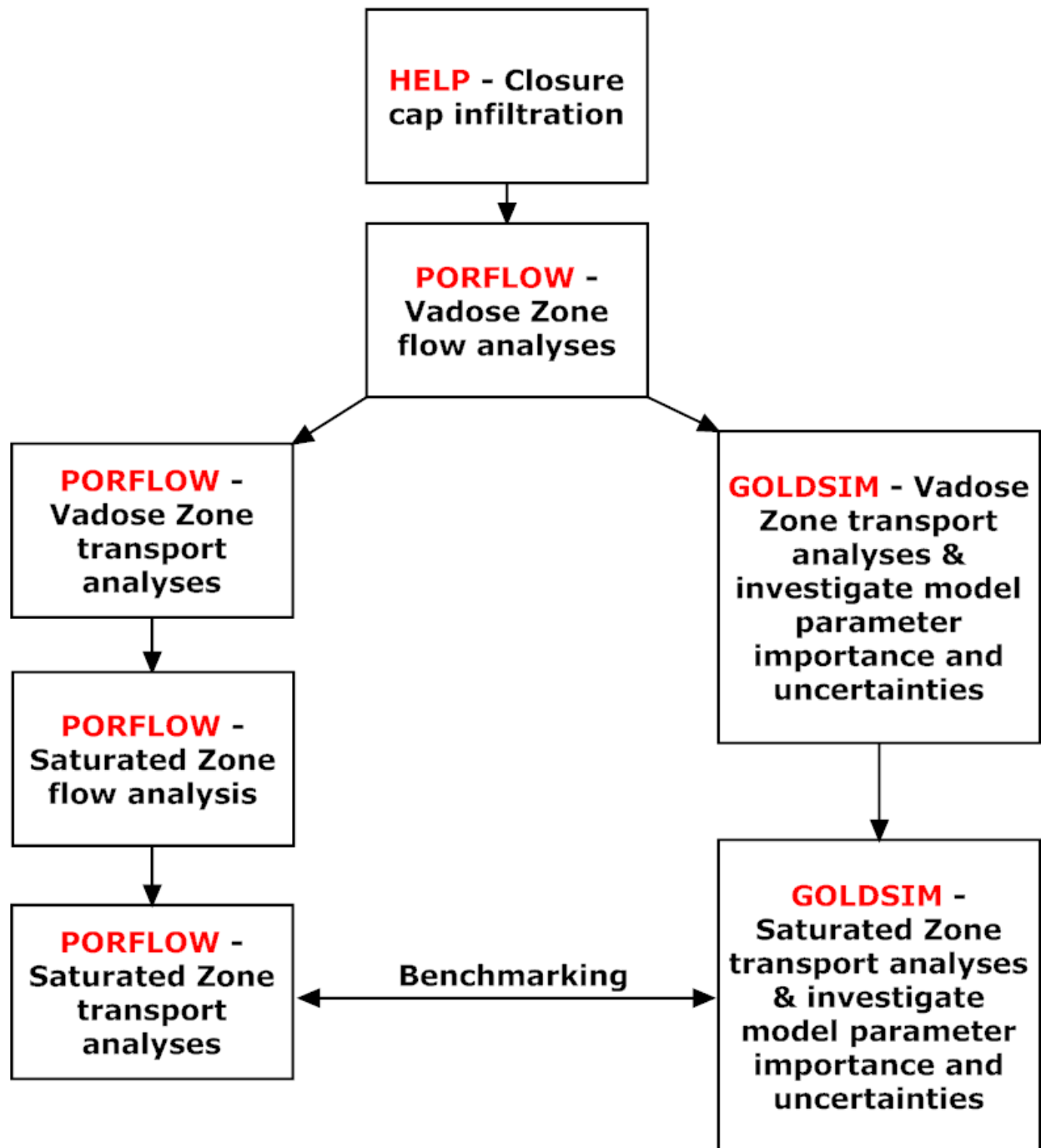


Figure 4.3-2: SDF PA Modeling Code Integration – Details of Water Flow and Transport



PORFLOW options include porous/fractured media which may be anisotropic and heterogeneous, arbitrary sources (injection or pumping wells) which may be present and, chemical reactions or radioactive decay which may take place. PORFLOW accommodates alternate fluid and media property relations and complex and arbitrary boundary conditions. The geometry may be 2-D or 3-D, Cartesian or Cylindrical and the mesh may be structured or unstructured, giving maximum flexibility to the user. PORFLOW version 6.10.3 was used for PA porous medium flow and transport analyses because its capabilities met program needs, core software functions have been verified through vendor and QA testing, and SRS personnel were experienced in applying PORFLOW in PA analyses. PORFLOW was used at SRS for calculations supporting the FTF PA and used by Idaho National Engineering and Environmental Laboratory (INEEL) for analyses supporting closure of the Tank Farm Facility. [SRS-REG-2007-00002_OUO, DOE-ID-10966] For the SDF PA, PORFLOW is an appropriate code because it can accommodate calculations in both the saturated and unsaturated zones and more importantly has the ability to simulate first-order decay and progeny in-growth associated with radionuclide chains, which is necessary for calculations involving radioactive stabilized contaminant disposal.

Analytic & Computational Research, Inc. has provided the following documentation associated with PORFLOW:

- A user's guide (ACRi-2002), which provides instructions for PORFLOW use
- Validation data for PORFLOW (ACRi-1994)

SQAP for the PORFLOW version used for the SDF PA calculations is covered by WSRC-SQP-A-00028 and G-TR-G-00002.

Data and modeling used for the performance of the PORFLOW model are documented in SRNL-STI-2009-00115 and have been peer reviewed and management approved. The scope of SRNL-STI-2009-00115 includes:

- SDF disposal unit performance
- Numerical model development of vadose zone flow and transport
- Numerical model development of aquifer flow and transport
- Simulations of vadose zone flow and transport
- Simulations of aquifer flow and transport

4.3.1.3 GoldSim

GoldSim is a commercial program developed by GoldSim Technology Group LLC (GTG) that is a user-friendly, highly graphical, Windows-based program for carrying out dynamic probabilistic simulations of complex systems, to support management and decision-making in engineering, science and business.

GoldSim was used to assist in developing uncertainty analyses for the SDF PA and identifying, from the parameters modeled in GoldSim, the important input parameters in the groundwater transport model. GoldSim utilized the flow field outputs from PORFLOW to perform transport calculations and subsequent dose calculations for evaluation of input parameter importance and calculation uncertainties. GoldSim was used to evaluate parameter importance, while developing the initial model for PORFLOW and provides

feedback to the PORFLOW modelers on areas requiring additional attention. GoldSim was also used to perform all-pathways and intruder analyses by utilizing the contaminant transport results from PORFLOW to calculate groundwater pathways and inadvertent intruder doses. Figures 4.3-1 and 4.3-2 illustrate the integration of GoldSim in the modeling effort and provide additional detail of the integration and steps of GoldSim calculations for fluid flow and contaminant transport.

GoldSim was designed to facilitate the construction of large, complex models. The user can build a model of a system in a hierarchical, modular manner, such that the model can evolve and add detail as more knowledge regarding the system is obtained. Other features, such as the ability to manipulate arrays, the ability to “localize” parts of a model, and the ability to assign version numbers to a model, which is constantly being modified and improved, further facilitate the construction and management of large models. GoldSim has an extensive internal database of units and conversion factors allowing the user to enter data and display results in any units and/or define customized units. GoldSim ensures dimensional consistency in models and carries out all of the unit conversions internally eliminating the need to carry out (error-prone) unit conversions. The user can dynamically link external programs or spreadsheets directly into a GoldSim model. GoldSim was also specifically designed to support the addition of customized modules (program extensions) to address specialized applications.

GoldSim version 9.60 is used for PA porous medium transport and dose analyses because its capabilities meet program needs, allows for ease of input changes and output visualization and is used by other DOE sites (e.g., Nevada Test Site, Yucca Mountain) and the NRC.

GoldSim Technology Group LLC provides a two volume user’s guide and a separate guide for data validation. [GTG-2007 Vol. 1 and Vol. 2, GTG-2006b] The SQAP for GoldSim is covered by G-SQA-A-00011.

4.3.1.4 CAP-88

CAP-88 computer model is a set of computer programs, databases and associated utility programs developed by the EPA for use in the estimation of dose and risk from radionuclide emissions to air. [<http://www.epa.gov/rpdweb00/assessment/CAP88/aboutcap88.html>] CAP-88 was used in the SDF PA to estimate the annual dose to Maximally Exposed Individuals (MEI) considering plume and ground gamma-shine, and inhalation and foodstuff ingestion pathways using the vapor phase radionuclide diffusion to the surface results from PORFLOW.

CAP-88 was developed by the EPA and is used to demonstrate compliance with 40 CFR 61 National Emissions Standards for Hazardous Air Pollutants (NESHAPs), Subpart H, and National Emission Standards for Emissions of Radionuclides other than Radon from DOE facilities. CAP-88 uses a modified Gaussian plume equation to estimate the average dispersion of radionuclides released from up to six sources at the same release location with different release heights. [<http://www.epa.gov/rpdweb00/assessment/CAP88/aboutcap88.html>] Assessments are done for a circular grid with a radius up to 50 miles. CAP-PC Version 1.0 is still in use today at SRS because prior personal computer versions of CAP-88 do not allow for adjustment of site-specific parameters of significance to SRS and it is

already being used at SRS for NESHAP compliance. CAP88-PC is the code used at SRS by the SGCP during CERCLA closure evaluations. In addition, CAP88-PC was used by INEEL during the development of calculations supporting their Tank Farm Facility, and was used at SRS for development of calculations supporting the FTF. [DOE-ID-10966, SRS-REG-2007-00002_OUO]

A user's manual, which provides instruction for use of the CAP88-PC Version 1.0 is available. [EPA-402-B-92-001] The SQAP for the CAP-88 version used for the SDF PA calculations is covered by Q-SQP-A-00002.

4.3.1.5 STADIUM®

The STADIUM® code (Software for Transport and Degradation in Unsaturated Materials) is a proprietary code developed by SIMCO Technologies Inc. to predict short and long-term behavior and service life of concrete. [STADIUM® User Guide] STADIUM® was used by SIMCO Technologies Inc. as a subcontractor to SRS for the SDF PA to support the calculations of the ettringite front movement from sulfate reactions, and thus degradation front, through the disposal unit concrete as described in Section 4.2.3.2.4. The results of the calculations in Section 4.2.3.2.4 were used in the PORFLOW model.

STADIUM® was developed by SIMCO Technologies Inc. for the assessment of concrete degradation for concrete civil infrastructures such as bridges, roads, and parking structures. The code is a finite element analysis software product that predicts time to initiate corrosion, identifies causes and progress of degradation, and develops optimal rehabilitation strategies to extend service life. STADIUM® allows the user to input specific parameters about the cementitious material being evaluated and environmental conditions of exposure.

A user guide (STADIUM® User Guide), which provides information on calculation methodologies and instructions for use, is available at http://www.mslexperts.com/slm/stadium_help/index.html. STADIUM® has been validated via comparison to both laboratory tests and to field conditions of existing structures. The comparisons are provided in the user guide and show that STADIUM® reproduced the results for both the laboratory and field materials tests. [STADIUM® User Guide] The work by SIMCO Technologies Inc. as reported in SRNS-STI-2008-00050 used testing of laboratory prepared samples of the SDF concrete formulations to input the material parameters into STADIUM®.

4.3.2 Software QA and Validation

General requirements for QA are described in *Quality Assurance Manual*, Manual 1Q, Procedure 2-1 *Quality Assurance Program*. The SQAP requirements are described in Manual 1Q, Procedure 20-1, *Software Quality Assurance Manual* (Manual 1Q 20-1). The software QA implementation reports that are referenced for the specific software codes are located in Section 4.3.1. The hierarchy of SRS documents is described as follows:

Management Policies (MP), WSRC 1-01, Policy 4.2 Quality Assurance contains SRS' policy statement regarding the Company's commitment to provide products and services which meet or exceed the requirements and expectations of our customers. The MP is to be implemented in a manner to support implementation of SRS imperatives of safety, disciplined operations, cost effectiveness, continuous improvement, and teamwork. SRS

has established and implemented an Integrated Safety Management System (ISMS). The QA program is consistent with, and an integral part, of the SRS ISMS. The policy requires that the program include appropriate procedures to comply with legal, regulatory, contractual, and corporate requirements related to quality. The policy also requires that the SRS QA program comply with DOE O 414.1C, 10 CFR 830, Subpart A, and the *Quality Assurance Management Plan* (QAMP). [WSRC-RP-92-225] The QA Program applies in a manner which contributes to the safe, reliable, and environmentally sound operation of SRS. It incorporates a graded approach commensurate with risk in the definition and application of QA/Quality Control (QC) requirements. The QAMP provides for the prevention of errors as well as the detection and correction of deficient conditions and incorporates an assessment process for identifying opportunities for continuous improvement. The focus of quality improvement is to reduce the variability of every process that influences the quality and value of SRS products or services. [WSRC 1-01 MP 4.2, WSRC-RP-92-225]

Management Policies Manual WSRC 1-01, Procedure 4.2, Quality Assurance describes the requirements and responsibilities for execution of the SRS QA Program for implementing DOE O 414.1C, and 10 CFR 830, Subpart A. [WSRC 1-01 MP 4.2] *Quality Assurance Requirements for Nuclear Facility Applications* and other consensus standards are used in the development of the QAMP. [ASME NQA-1-2004, ASME NQA-1a-2005, ASME NQA-1b-2007] The plan has been jointly approved by SRS and Department of Energy – Savannah River Operations Office (DOE-SR) and serves as the basis for the establishment of the procedures. [WSRC-RP-92-225]

Quality Assurance Manual 1-0, Procedure 2-1, Quality Assurance Program provides the structure and procedures for achieving and verifying the SRS requirements for quality. The manual consists of a series of QA Procedures which describe applicable QA requirements. Furthermore, Procedure 2-1, Section B states that the QA Program has been developed to be responsive to the requirements of DOE O 414.1C, and DOE *Nuclear Safety Management*, Title 10 CFR 830, Subpart A. Because of the size and complexity of SRS and its varied products, services, and missions, the program has been defined in a standard framework of company policy, procedures, and instructions to be used by the implementing organizations to perform quality-related activities. [Manual 1Q 2-1]

Conduct of Engineering and Technical Support Procedure Manual E-7, Procedure 2.60, Technical Reviews (E7 Manual 2.60) is the QA implementing procedure for performing technical reviews. The end use of data drives the level of review required. Design Verification, the highest level review, must be performed for work affecting Safety Significant (SS)/Safety Class (SC) systems. Design Check is the next lower level of review and is required for all Production Support (PS) and General Service (GS) design output documents. Because the work associated with the PA and associated documents are not associated with SS or SC systems, the Design Check represents the appropriate level of rigor.

A design checker assures the technical accuracy of the design document by performing the following Design Check activities:

- A mathematical check, if appropriate
- A review for correct use of technical input, including quality requirements
- A review of the approach used and reasonableness of the output
- An administrative check (page numbers, etc.)

A design checker must meet the following criteria to perform a Design Check:

- Did not participate in the development of the portion of the document being checked
- Is knowledgeable in the area of the design or analysis for which they review
- Is capable of performing similar design or analysis activities
- Has security clearance for access to sufficient information to perform the Design Check

Between 2002 and 2004 SRNL developed, piloted and then implemented technical review guidelines incorporating the E7 Manual 2.60 requirements for performing Design Checks and Design Verification by document review. These guidelines also meet the requirements for review of Type 2 Calculations contained in the E7 Manual, Procedure 2.31 *Engineering Calculations* (E7 Manual 2.31). The guidelines provide a flowchart to map the SRNL technical review process, lines of inquiry for performing reviews, a checklist for communicating instructions, and best management practices to set a benchmark for management expectations.

Software QA is conducted in accordance with the requirements of Manual 1Q 20-1 through the development and execution of the SQAP. This procedure fulfills the requirements of DOE O 414.1.C and 10 CFR 830, Subpart A. The QA plans and processes used by SRS to verify the inputs and outputs for the different modeling codes used are provided in the code specific descriptions in Section 4.3.1.

4.3.3 Modeling Codes Summary

In conclusion, Figures 4.3-1 and 4.3-2 present the approach to modeling code integration used for the SDF PA. Of importance in the implementation of the modeling integration shown in Figures 4.3-1 and 4.3-2 is the assurance that the input data to the various codes is verified to be accurate. Documentation of the verification of the model input traced from source documents to modeling input and to appropriate sections within this PA, has been performed and is described in Appendix I of this document.

4.4 Closure System Modeling

This section describes how the SDF design elements and their associated properties were represented in the computer modeling codes. The closure system conceptual design was an aphysical simplification of the actual SDF system design, which is required for analytical modeling. Certain disposal unit features and design elements are by necessity omitted in the conceptual model, and are discussed in Section 4.4.1.

This section also describes how the SDF closure system is expected to behave in the future, and what modeling scenarios are used to depict system behavior over time. Because it is difficult to predict with a high level of certainty just what changes may occur to the closed SDF disposal units over the 10,000 year performance period, this section describes a range of potential conditions to which the closed disposal units may be subjected. While the baseline analysis (represented through the PORFLOW SDF model) reflected the best estimate of future closure system behavior, the probabilistic analysis (represented through the GoldSim SDF model) considered a variety of possible scenarios. In addition to analyzing differing scenarios in the 10,000 year performance period, the transport models were all run to at least 20,000 years for the purposes of determining peak concentrations that occur after the 10,000 year performance period.

4.4.1 Individual Vault and FDC Modeling

The initial conceptual design, which is required for analytical modeling, is a physical simplification of the actual disposal unit design, described in Section 3.2.1. Certain disposal unit features and design elements have been, by necessity, omitted in the initial conceptual model. The disposal unit design features not included in the initial conceptual design may be addressed in subsequent conceptual models. A number of general modeling decision guidelines were followed for the initial conceptual design for all disposal units.

1. The intent of the initial conceptual model is to capture disposal unit dimensions and relative material differences for each discrete disposal unit segment.
2. Each discrete disposal unit segment/area is represented as homogeneous, ignoring interior elements (e.g., rebar) and/or penetrations through the area.
3. The salient features of the concrete which have direct bearing on the performance of the material in the transport model (e.g., thickness and chemical properties) are included in the model.

4.4.1.1 Vault 1 Modeling

The Vault 1 conceptual model used in the SDF PA modeling is illustrated in Figure 4.4-1. Table 4.4-1 provides additional information on the dimensions used in the model. Only half of the vault in the short dimension is modeled, taking advantage of symmetry about the centerline. The 4 inch thick concrete working slab located below Vault 1, described in Section 3.2.1.1, is replaced in the model with lower vadose zone soil material. In addition, weeping cracks in the wall associated with Vault 1 saltstone filling are included in the model through initial property definitions and degradation. To conservatively assess the potential for contaminants within the walls, the model assumes the available void space in the walls to be filled with pore fluid containing the same concentration of contaminants as in the vault cells. Based on 12% porosity for the concrete walls as shown in Table 4.2-16, an estimated 0.65% of the vault inventory resides in the walls of the vault.

Figure 4.4-1: Conceptual Model for SDF Vault 1



[NOT TO SCALE]

Table 4.4-1: Material Parameters for Vault 1 Conceptual Model

| Material Zone | Thickness | Material Type |
|-------------------|----------------|------------------------------------|
| Backfill Layer | 4 feet (min) | Backfill ^a |
| Drainage Layer | 2 feet | Sand ^d |
| Roof (2 % slope) | 6 inches (min) | Ordinary Concrete ^b |
| Clean Grout Cap | 6 inches | Ordinary Concrete ^b |
| Saltstone | 24 feet | Saltstone ^b |
| Floor Slab | 2 feet | High Quality Concrete ^b |
| Wall ^c | 18 inches | High Quality Concrete ^c |

(a) Hydraulic properties for material type provided in Section 4.2.3.2.3

(b) Hydraulic properties for material type provided in Section 4.2.3.2.4

(c) Hydraulic properties for “cracked concrete” in Section 4.2.3.2.4

(d) Hydraulic properties for sand in Section 4.2.3.2.2

4.4.1.2 Vault 4 Modeling

The Vault 4 conceptual model used in the SDF PA modeling is illustrated in Figure 4.4-2 with additional information on the dimensions in Table 4.4-2. The PA model is a simplification of the actual physical infrastructure of Vault 4. Only half of the Vault 4, in the short dimension is modeled, taking advantage of symmetry.

Specific areas where these modeling simplifications are implemented for Vault 4 are highlighted below:

- Cells B through L each contain nine equally spaced roof support columns comprised of concrete filled 10 inch diameter, schedule 40 carbon steel pipes. These columns are accounted for in the model as potential fast flow paths as described in Section 4.4.2.
- The girders, joists, and steel decking that form and support the concrete roof in Cells B through L will be completely encased in saltstone or clean grout upon vault closure and are not explicitly included in the model.
- Embedded piping penetrating the roof of Cells B through L for saltstone fill, clean grout cap fill, monitoring, and venting are not included in the present model. Final closure will result in a configuration such that the roof model assumptions are met.
- Drain lines and piping, discussed in Section 3.2.1.2.4, will be addressed when the cell is closed to ensure wall assumptions are met and will not be included in the modeling.
- The sheet drain system, discussed in Section 3.2.1.2.5, is included in the model as potential fast flow paths as described in Section 4.4.2.
- Weeping cracks, associated with Vault 4 saltstone filling, are included in the model through initial property definitions and degradation.
- A tubing bundle, with flammable gas sampling tubes, is installed in two of the 12 Vault 4 cells. The tubing bundles are suspended in Vault 4 during operations, but will be grouted and capped prior to filling the cells with the clean grout cap. The tube bundles are not explicitly included in the initial Vault 4 modeling.
- In addition, to conservatively assess the potential for contaminants within the walls, the model assumes the available void space in the walls to be filled with pore fluid containing the same concentration of contaminants as in the vault cells. Based on 12% porosity for the concrete walls as shown in Table 4.2-16, an estimated 0.50% of the vault inventory resides in the walls of the vault.
- Cell A contains 10,000 drums of FMF non-hazardous saltcrete generated from the operations of the WWTF at FMF. Cell A also contains the wooden pallets used in the movement of the FMF drums (one pallet to four drums). [ESH-FSS-9000373] The inventory associated with the waste and wooden pallets has been included in the Vault 4 inventory accounting in Section 3.3. The void space in Cell A surrounding the drums is filled with clean grout. While not specifically modeled as a transport barrier, the FMF drums are accounted for in the model as potential fast flow paths as described in Section 4.4.2.

Figure 4.4-2: Conceptual Model for the SDF Vault 4

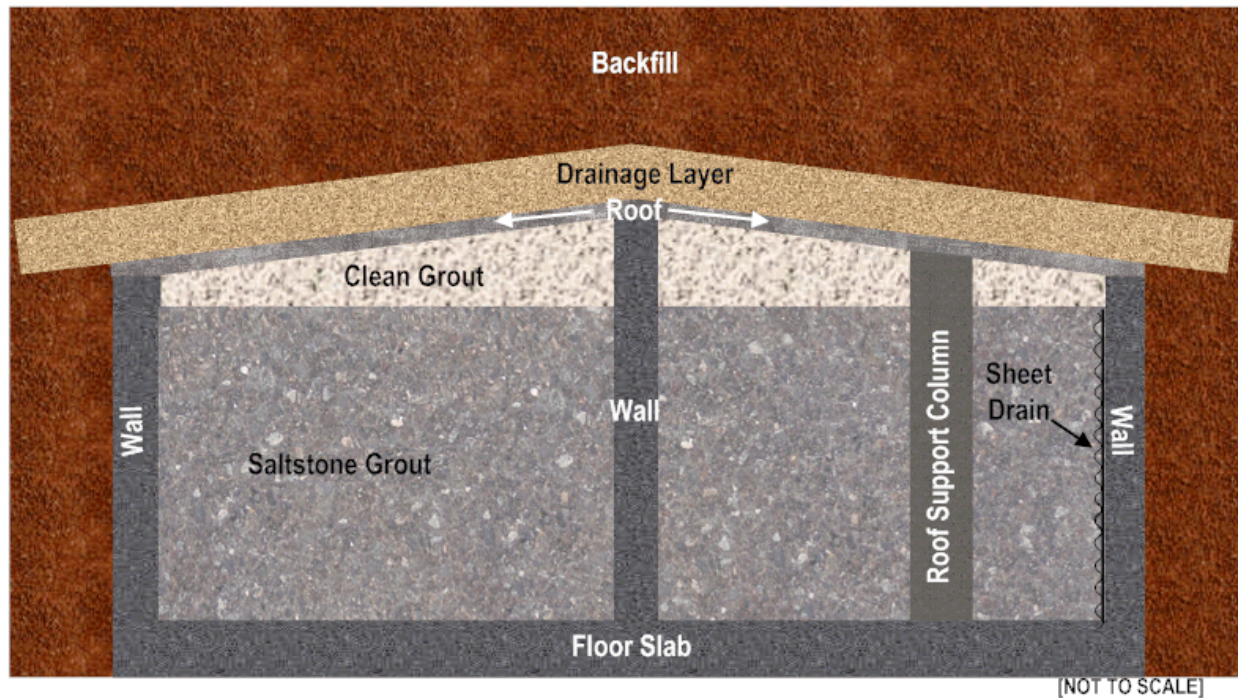


Table 4.4-2: Material Parameters for Vault 4 Conceptual Model

| Material Zone | Thickness | Material Type |
|-------------------|-------------------|------------------------------------|
| Backfill Layer | 24 feet (min) | Backfill ^a |
| Drainage Layer | 2 feet | Sand ^d |
| Roof (2 % slope) | 4 inches | Ordinary Concrete ^b |
| Clean Grout Cap | 17.4 inches (min) | Ordinary Concrete ^b |
| Saltstone | 24.75 feet | Saltstone ^b |
| Floor Slab | 2 feet | High Quality Concrete ^b |
| Wall ^c | 18 inches | High Quality Concrete ^c |

- (a) Hydraulic properties for material type provided in Section 4.2.3.2.3
(b) Hydraulic properties for material type provided in Section 4.2.3.2.4
(c) Hydraulic properties for “cracked concrete” in Section 4.2.3.2.4
(d) Hydraulic properties for sand in Section 4.2.3.2.2

4.4.1.3 Disposal Cells 2A and 2B (and FDC) Modeling

The FDCs conceptual model used in the SDF PA modeling is illustrated in Figure 4.4-3 and Table 4.4-3. Areas where significant modeling simplifications are implemented for the FDCs are highlighted below:

- The walls, roof and floor slab of the FDCs are composed of steel bar reinforced concrete. The salient features of the concrete which have direct bearing on the performance of the material in the transport model (e.g., thickness and chemical properties) are included.
- The pre-cast concrete panels that comprise the walls include additional elements (e.g., pre-stressing wires, seismic restraint cables and at least 1 inch of shotcrete cover with Type II concrete) that are not included in the model.
- The interior of the walls and floor slab will be coated to retard the degradation of concrete from sulfate attack. The coating as a layer is not specifically modeled; however, the coating on the walls and floor slab is utilized to justify no degradation of the walls and floor slab during the 100 year period of institutional control after SDF closure.
- The interior of the disposal units include 48, 14 inch diameter, steel bar reinforced Type II concrete support columns that are included in the model as potential fast flow paths as described in Section 4.4.2.
- The disposal units rest on two 4 inch thick mud mats separated by a 0.1m thick HDPE liner and a GCL. The upper mud mat is Class III, sulfate resistant concrete. The mud mats extend beyond the footprint of the disposal unit floor slab and will be modeled as such.
- A sheet drain system exists along the interior of the wall and is included in the model to address potential fast flow paths as described in Section 4.4.2.
- The HDPE-GCL placed on the top and bottom of each FDC is 0.3 inch thick; however, the model assumes a 1 inch thickness to mitigate numerical convergence difficulties and increases the hydraulic conductivity, as stated in Section 4.2.3.2.2, by a factor of 3.33 to compensate. These layers are not present in the Vaults 1 and 4 design.
- The HDPE placed on the exterior of the wall of each FDC is 0.1 inch thick; however the model assumes a 1 inch thickness to mitigate numerical convergence difficulties and increases the hydraulic conductivity, as stated in Section 4.2.3.2.2, by a factor of 10 to compensate.

Figure 4.4-3: Conceptual Model for FDC (Typical)

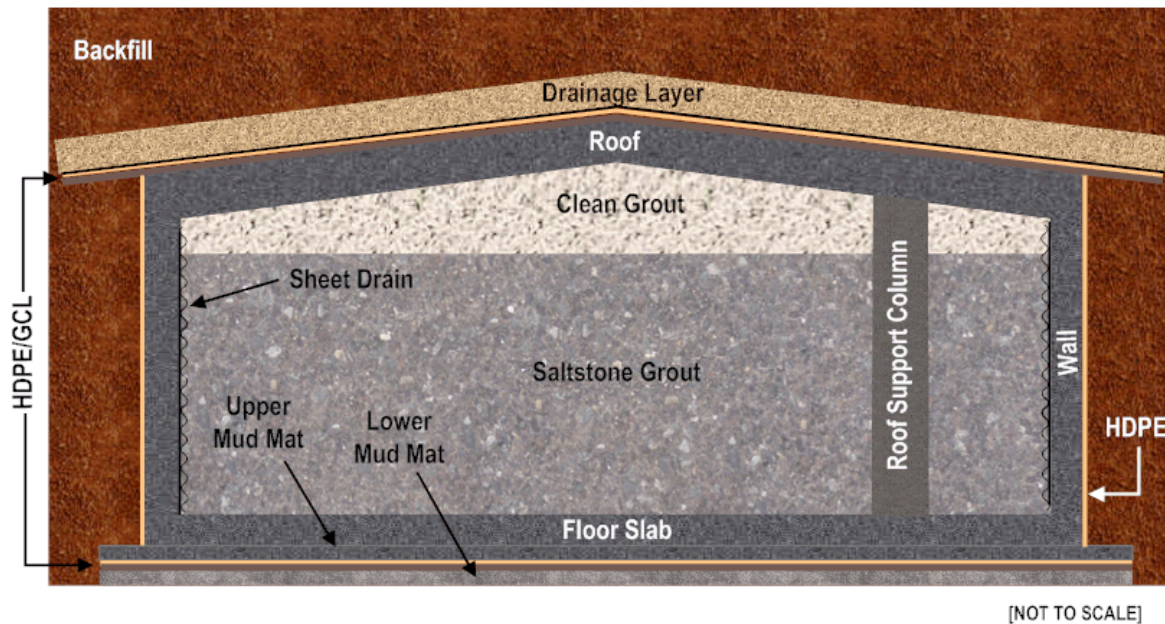


Table 4.4-3: Material Parameters for FDC Conceptual Model

| Material Zone | Thickness | Material Type |
|---------------------------|--------------|------------------------------------|
| Backfill Layer | 7 feet (min) | Backfill ^a |
| Drainage Layer | 2 feet | Sand |
| HDPE-GCL | 1 inch | HDPE-GCL ^b |
| Roof (2 % slope) | 8 inches | High Quality Concrete ^c |
| Clean Grout Cap | 2 feet (min) | Saltstone ^c |
| Saltstone | 20 feet | Saltstone ^c |
| Floor Slab | 8 inches | High Quality Concrete ^c |
| Upper Mud Mat | 4 inches | High Quality Concrete ^c |
| HDPE-GCL | 1 inch | HDPE-GCL ^b |
| Lower Mud Mat | 4 inches | Low Quality Concrete ^c |
| Radial Orientation | | |
| Wall | 8 inches | High Quality Concrete ^c |
| Shotcrete (not shown) | 6 inches | Backfill ^a |
| HDPE | 1 inch | HDPE ^b |

(a) Hydraulic properties for material type provided in Section 4.2.3.2.3

(b) Hydraulic properties for material type provided in Section 4.2.3.2.2

(c) Hydraulic properties for material type provided in Section 4.2.3.2.4

4.4.2 Systems and Potential Degradation

The SDF is designed to contain salt waste through; (1) immobilization of initially liquid salt feedwater in the form of a monolithic, low permeability, low E_h , saltstone, and (2) encapsulation of the saltstone within the SDF disposal unit, which comprises a barrier to advection and release to the environment, as well as slowing the ingress of oxygen from outside the disposal unit to the saltstone monolith. The design intent is to limit contaminant release to a controlled and low rate. Over time, disposal unit materials are expected to degrade through a variety of mechanisms, leading to higher contaminant releases.

The dominant form of SDF disposal unit physical degradation is expected to be sulfate attack resulting from exposure to sulfate remaining in saltstone pore water after curing. The dominant form of chemical degradation will likely be loss of reducing (low E_h) conditions that keep technetium, neptunium, and plutonium in relatively insoluble form. Oxidization is expected to occur via dissolved oxygen transport through saturated pore space and micro cracks in the disposal unit wall. Section 4.2.3.2.4 discusses the chemical and physical degradation of the disposal unit concrete. The HDPE-GCL liner systems supplement the primary concrete barrier for the roof and floor (including the upper mud mat of the FDCs) and a HDPE liner supplements the primary concrete barrier for the wall of the FDCs. The HDPE-GCL and HDPE liner systems also degrade over time and their degradation is discussed in Section 4.2.3.2.2. Contaminant release is dominated by diffusion early, but is eventually advection controlled after sufficient closure cap, disposal unit roof, and saltstone degradation.

Another possible physical degradation mode is formation of preferential or fast flow paths that allow infiltration to enter the disposal units and contact waste-bearing saltstone directly, prior to general disposal unit failure. Credible fast flow path mechanisms include large scale cracks due to seismic events or differential settlement, shrinkage cracks, vertical sheet drains, degraded steel columns and roof supports, roof penetrations and bleed water drain piping. Fast flow path scenarios also accelerate slag oxidation in the vicinity of the conduits, further accelerating release of E_h sensitive species (e.g., Tc-99).

To assess the intended, as designed, performance of SDF disposal units and conceivable alternative scenarios, several case scenarios have been conceptually identified for subsequent numerical modeling. The conceptual modeling that derived the alternative scenarios is intended to capture the variability in the three disposal unit design features (Vault 1, Vault 4 and FDC). Each case or scenario discussed below is meant to represent a potential outcome. In developing these scenarios, the intent was to capture each outcome rather than to predict the cause of the outcome. For example, in the scenario where the FDC has fast flow paths based on cracks and sheet drains (Cases B and C), the intent was for these fast flow paths to represent any fast flow path that might develop in an FDC over the 10,000 year period of performance, rather than an attempt to predict the cause of the fast flow path. The results of the sensitivity cases are discussed in Section 5.6.6.1. Case A, considered the Base Case, reflects the expected condition where intact disposal unit concrete and saltstone lead to a diffusion-dominated release, prior to the cover system and the disposal units becoming significantly degraded. Other cases were postulated for diagnostic purposes, to better understand the range of possible disposal unit behavior. Case B assumes that a fast flow path

forms between saltstone and the Vault 4 wall and the walls of the FDCs at time zero, due to the presence of a sheet drain at the wall and connecting breaches through the roof and floor (including the upper and lower mud mat for the FDCs). This case is not applicable to Vault 1 because Vault 1 does not have sheet drain systems. Case C is similar to Case B with additional fast flow paths passing through the saltstone interior, possibly due to corrosion of support columns (in Vault 4 and the FDCs), or fissures in response to differential settlement. Case D is similar to Case A, except that an intact sheet drain creates a capillary break, precluding transport across the gap under unsaturated conditions. Because Vault 1 does not have sheet drain systems, this case is not applicable to Vault 1. Case E is similar to Case A in that no fast flow paths exist and the sheet drain system does not create a capillary break; however, the saltstone is postulated to be severely degraded at time zero. These cases are more fully described in the following sections and are summarized in Table 4.4-4. For each case a figure is provided to conceptually illustrate the model described. Note that the figures illustrating the different cases will consistently use a conceptual pictorial of an FDC even though the cases may also be appropriate for Vaults 1 and 4.

Table 4.4-4: Cases Postulated for SDF Vaults and FDCs

| Case | Vault 1 | Vault 4 | FDCs |
|-------------|--|---|--|
| A | <u>Base Case</u> vault wall degraded, saltstone intact | <u>Base Case</u> vault wall degraded, saltstone intact | <u>Base Case</u> disposal unit wall intact, saltstone intact |
| B | N/A (no sheet drains) | <u>Fast flow walls</u> fast flow along walls from roof thru floor, vault wall degraded | <u>Fast flow walls</u> fast flow along walls from roof thru floor (including upper and lower mud mats) |
| C | <u>Fast flow walls & crack</u> fast flow along cracks from roof thru floor, vault wall degraded | <u>Fast flow walls & crack</u> fast flow along walls and cracks from roof thru floor vault wall degraded | <u>Fast flow walls & columns</u> fast flow along walls and columns from roof thru floor (including upper and lower mud mats) |
| D | N/A (no sheet drains) | <u>Capillary break</u> Base Case with capillary break at sheet drains | <u>Capillary break</u> Base Case with capillary break at sheet drains |
| E | <u>Saltstone severely degraded</u> vault wall degraded | <u>Saltstone severely degraded</u> vault wall degraded | <u>Saltstone severely degraded</u> disposal unit wall intact |

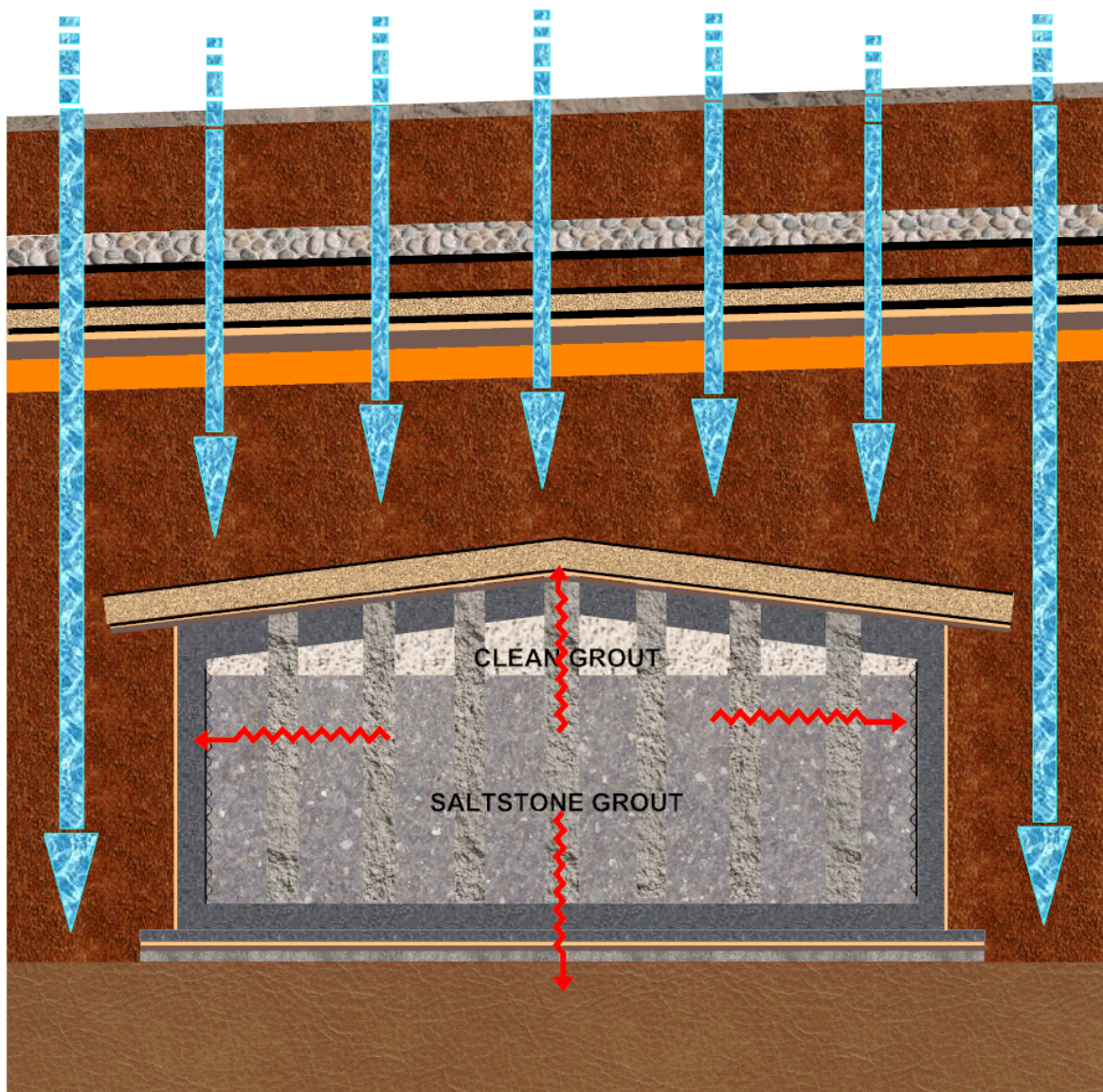
4.4.2.1 Vault 1 Degradation Cases

To assess the potential impact of Vault 1 degradation, a conceptual model was developed that included three degradation cases for the deterministic groundwater modeling (it should be noted that Case B and D are not applicable to Vault 1).

Case A is the Base Case where the disposal unit is modeled in the scenario that is most expected for the duration of the performance period. Figure 4.4-4 conceptually illustrates this Base Case. The major aspects for this expected degradation case are:

- Closure cap performs as described in Sections 4.2.3.2.1 and 4.2.3.2.2
- Infiltration from the closure cap enters the disposal unit through pores within the cementitious material
- The saltstone is not degraded
- Model parameters are as shown in Table 4.4-1
- The disposal unit concrete degrades as described in Section 4.2.3.2.4

Figure 4.4-4: Model Scenario Case A (Base Case)



Case C acknowledges the potential of cracks forming outside and within the disposal unit causing a “fast flow” path to develop from the top of the upper backfill layer, through the lateral drainage layer, the concrete roof, the clean grout cap, the saltstone, the base layers, and finally the native soil to the aquifer. This fast flow path is modeled as a 2 inch wide slot, located in the center of the disposal unit, traversing the length, and having material and hydraulic properties associated with gravel as indicated in Table 4.4-5 and Figure 4.4-5. Figure 4.4-6 conceptually illustrates Case C. The major aspects for this case are:

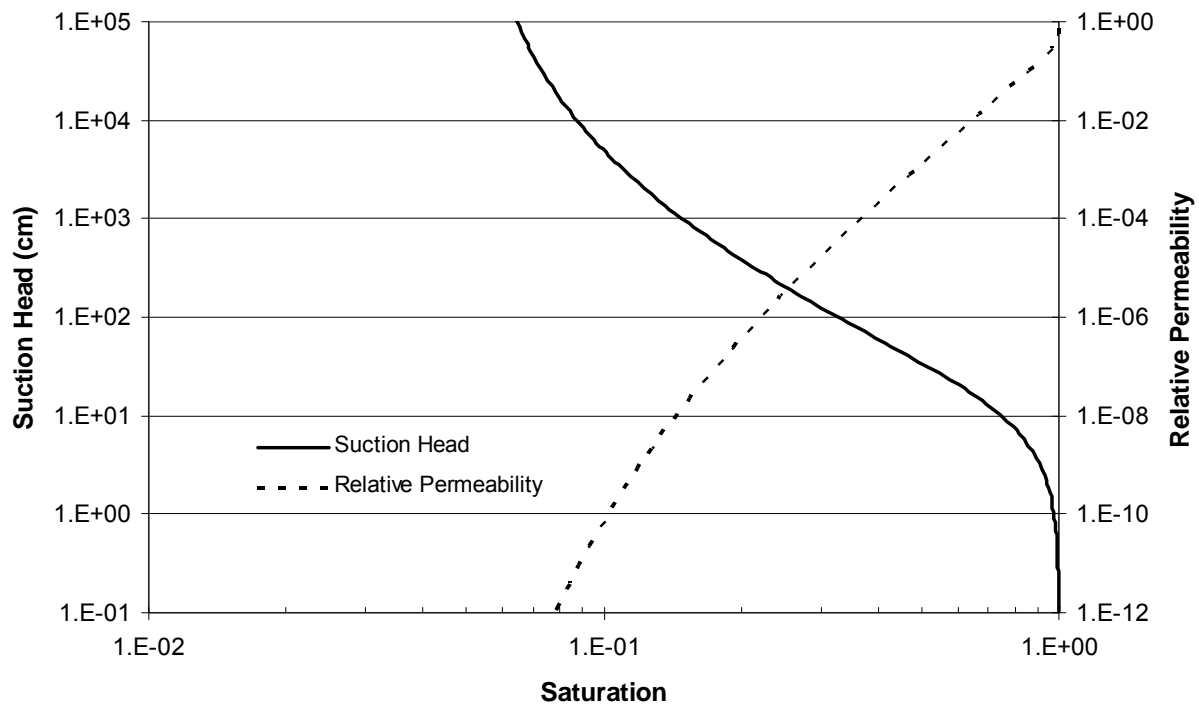
- Closure cap performs as described in Sections 4.2.3.2.1 and 4.2.3.2.2
- Infiltration from the closure cap enters the disposal unit through pores within the cementitious material as well as through the fast flow path described above
- Fast flow path is modeled as a 2 inch wide slot with material and hydraulic properties associated with gravel located in the center of the saltstone monolith
- The K_d values are assumed zero within the fast flow path
- The saltstone is not degraded
- Model parameters are as shown in Table 4.4-1
- The disposal unit concrete physically degrades as described in Section 4.2.3.2.4

Table 4.4-5: Hydraulic Properties of Gravel

| Saturated Effective Diffusion Coefficient D_e (cm²/sec) | Average Total Porosity (%) | Average Dry Bulk Density (g/cm³) | Average Particle Density (g/cm³) | Saturated Horizontal Hydraulic Conductivity (cm/sec) | Saturated Vertical Hydraulic Conductivity (cm/sec) |
|--|---|--|--|---|---|
| 9.4E-06 | 30 | 1.82 | 2.60 | 1.5E-01 | 1.5E-01 |

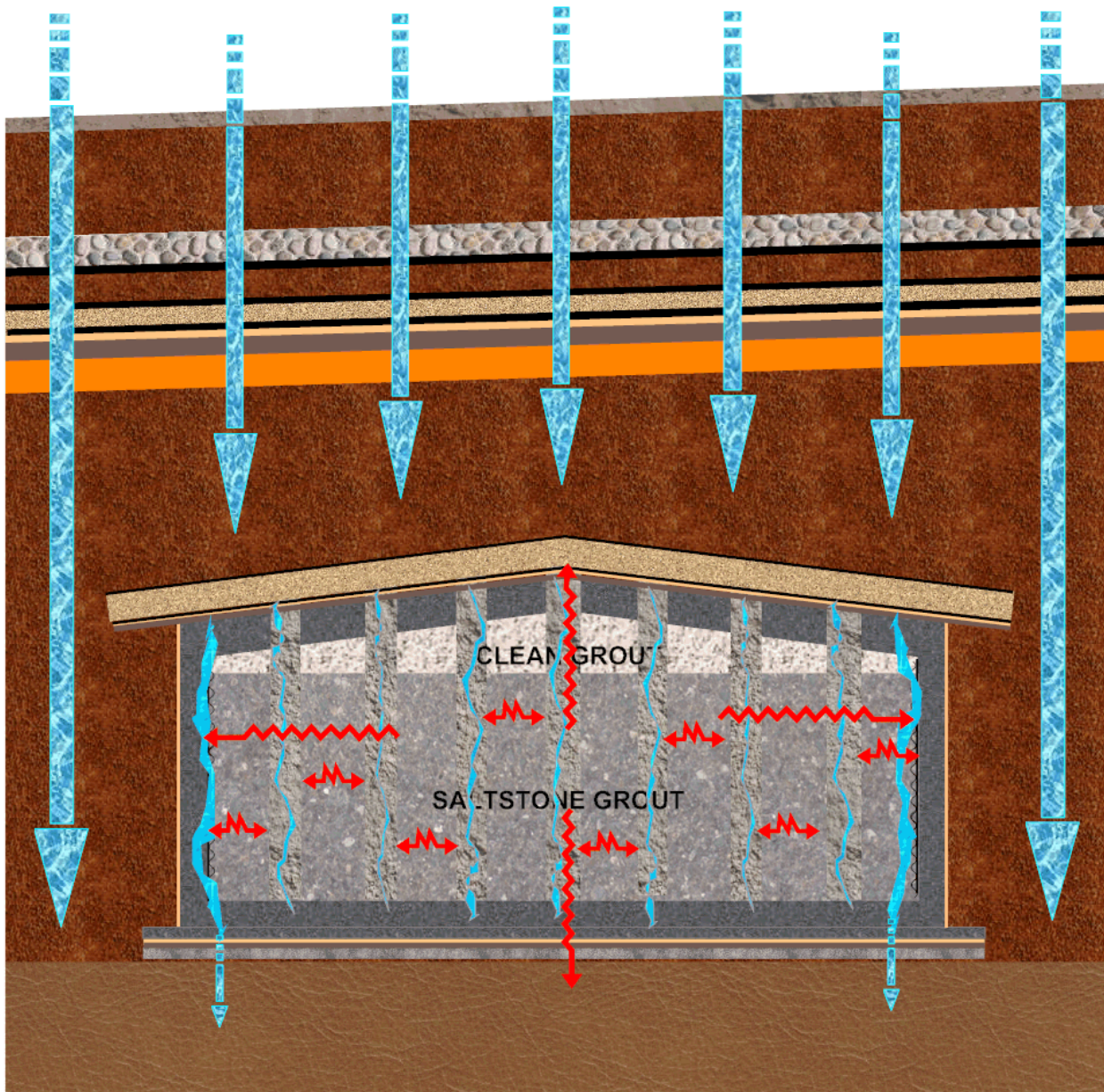
[WSRC-STI-2006-00198, Table 5-18]

Figure 4.4-5: Characteristic Curves for Gravel



[WSRC-STI-2006-00198, Table 5-22]

Figure 4.4-6: Model Scenario Case C



Note: For Vault 1 the fast flow paths are only associated with cracks in the saltstone monolith. For Vault 4 and the FDCs additional fast flow paths are depicted along the walls to model the sheet drain system (see Section 4.4.2.2) and through the support columns.

Case E postulates that the saltstone degrades, as described in Section 4.2.3.2.4, but retains the other model parameters of Case A. Figure 4.4-7 conceptually illustrates Case E. The major aspects for this case are:

- Closure cap performs as described in Sections 4.2.3.2.1 and 4.2.3.2.2
- Infiltration from the closure cap enters the disposal unit through pores within the cementitious material
- The saltstone is degraded, as described in Section 4.2.3.2.4 and in the analysis presented in SRNL-STI-2009-00115, resulting in a greater than 800,000 fold increase in the hydraulic conductivity within the saltstone, from the Base Case at time zero. The characteristic curves for the degraded saltstone condition are based on SRNL-STI-2009-00115 and are presented in Figure 4.4-8
- Model parameters are as shown in Table 4.4-1
- The disposal unit concrete degrades as described in Section 4.2.3.2.4

Figure 4.4-7: Model Scenario Case E

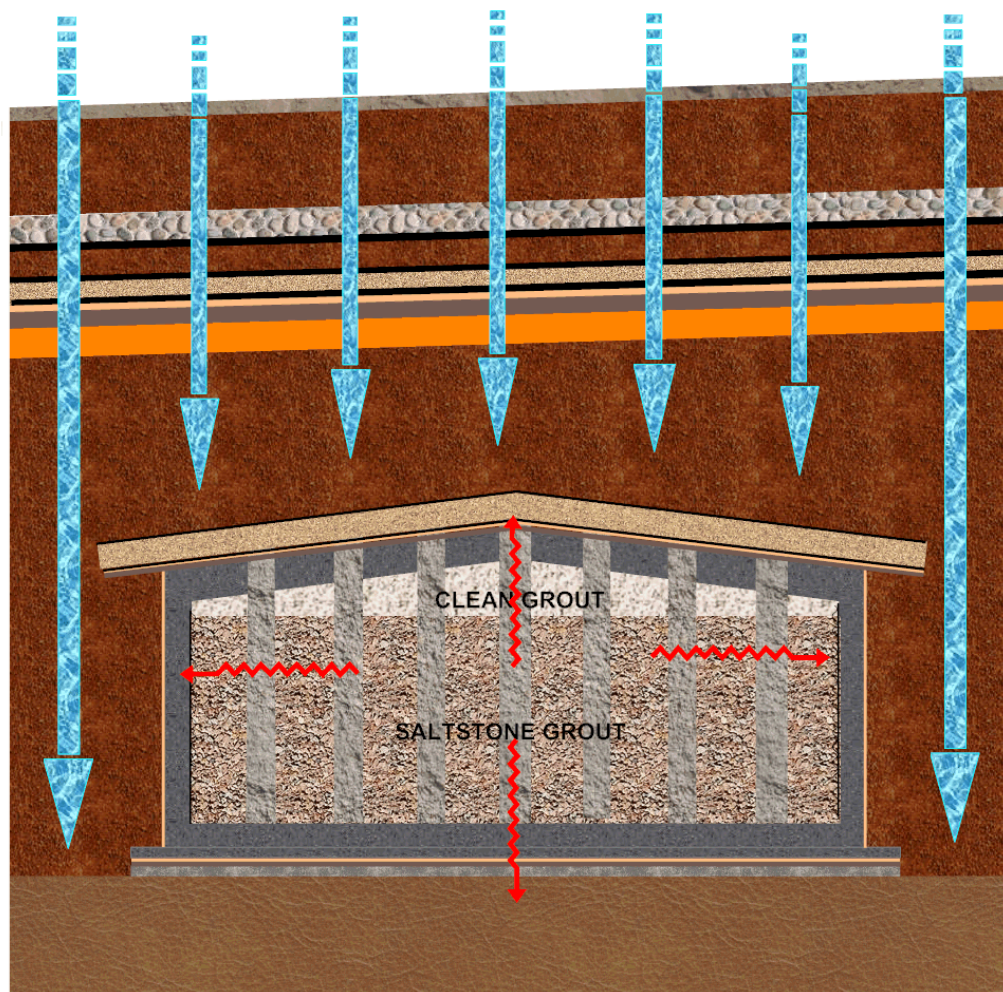
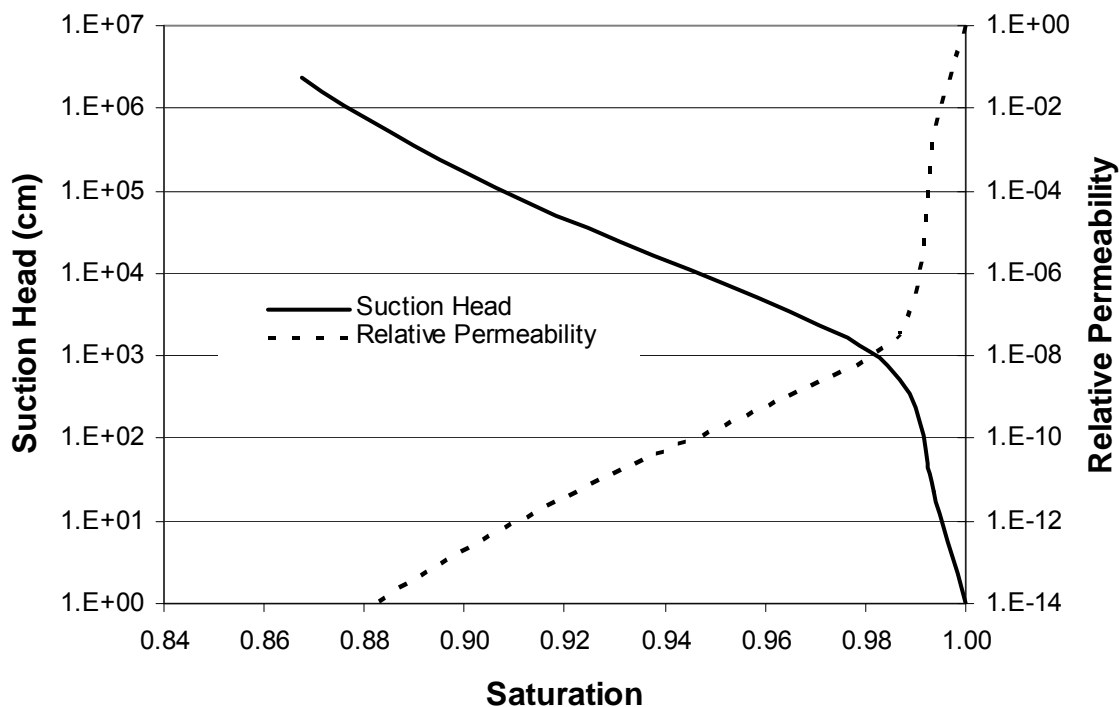


Figure 4.4-8: Characteristic Curves for Degraded Saltstone



Both Cases C and E accelerate the chemical degradation of disposal unit concrete. The increase in water infiltration due to the fast flow path and the change in the hydraulic properties of the saltstone, due to saltstone degradation, may potentially reduce the time that the pore volumes are reached that correspond to the chemical transition states described in Sections 4.2.2 and 4.2.3.2.4. Table 4.4-6 summarizes the performance of the degradation model for Vault 1 for these three applicable cases.

Table 4.4-6: Occurrences of Model Changes by Case for Vault 1

| Change in Model Parameters | Time of Occurrence for Given Case (years after closure) | | | |
|--|--|---------------------|---------------------|---------------------|
| | Analytical Value | Value in Model | | |
| | Case A | Case A | Case C | Case E |
| Degradation of closure cap ^a | 5,412 ^a | 5,500 ^b | 5,500 ^b | 5,500 ^b |
| Lateral drainage layer degrades to backfill properties | 19,013 ^c | 20,000 ^d | 20,000 ^d | 20,000 ^d |
| Wall concrete transitions from reducing to oxidizing | 20,781 ^b | 20,781 ^b | 20,968 ^b | 11,626 ^e |
| Wall concrete transitions from middle age to old age | 21,043 ^b | 21,043 ^b | 22,193 ^b | 13,669 ^e |

- (a) Most significant degradation occurs within 1,000 years, more than a 5,000 fold increase in infiltration rate, and an additional degradation factor of less than five, until complete degradation in 5,412 years (WSRC-STI-2008-00244)
- (b) Obtained from review of PORFLOW related files
- (c) Table 22 of SRNL-STI-2009-00115
- (d) Appendix E of SRNL-STI-2009-00115
- (e) Appendix F of SRNL-STI-2009-00115

4.4.2.2 Vault 4 Degradation Cases

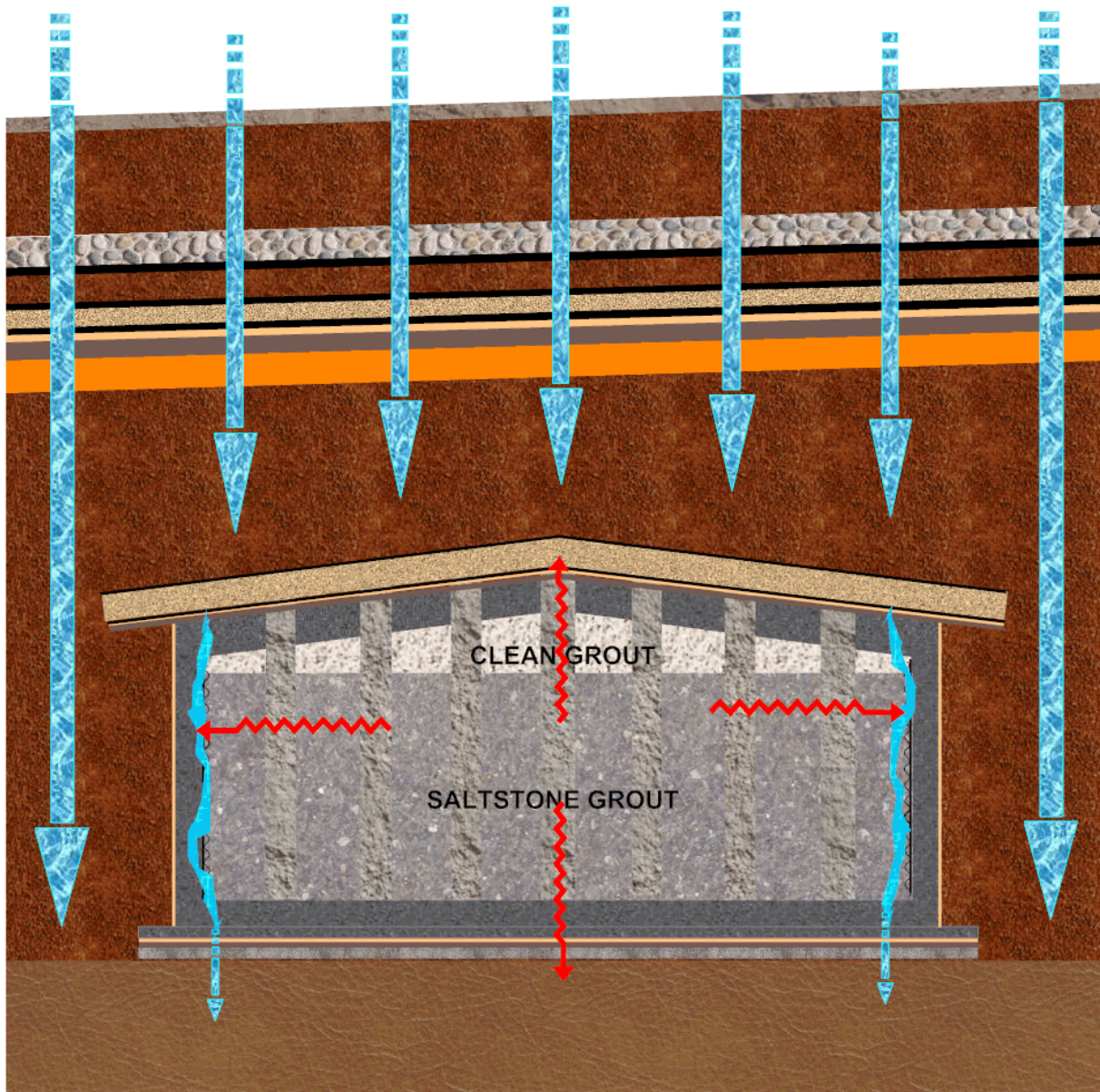
To assess the likely impact of Vault 4 degradation, the modeling of Cases A, C, and E that are addressed in Section 4.4.2.1 for Vault 1 are also utilized for Vault 4. Because eight of the 12 cells within Vault 4 contain a sheet drain system (Section 3.2.1.2), two additional cases were modeled, and Case C was modified to access the sheet drain systems. The existence of the support columns in all the cells of Vault 4 (except Cell A) was included in the modeling for the fast flow path in Case C.

Case A is the Base Case where the disposal unit was modeled in the scenario that is most expected for the duration of the performance period. The major aspects for this expected case are as described for Vault 1 and illustrated in Figure 4.4-4, with the exception that the model parameters are shown in Table 4.4-2 for Vault 4.

Case B, conceptually illustrated in Figure 4.4-9, acknowledges the potential that the in-place sheet drain system degrades to the extent that a fast flow path will exist between the saltstone and the walls. This allows advective flow of water from the top of the upper backfill layer, through the lateral drainage layer, the concrete roof, the clean grout cap, the saltstone, the disposal unit base layers, and finally, through the native soil to the aquifer. This fast flow path is modeled as a 2 inch wide slot, located along the dividing wall between cells and also along the interior of the outside wall, traversing the length of the disposal unit, and having material and hydraulic properties associated with gravel as indicated in Table 4.4-5. The major aspects for this case are:

- Closure cap performs as described in Sections 4.2.3.2.1 and 4.2.3.2.2
- Infiltration from the closure cap enters the disposal unit through pores within the cementitious material as well as through the fast flow paths described above
- Fast flow paths are modeled as 2 inch wide slots with material and hydraulic properties associated with gravel located along the dividing wall between cells and the interior of the outside wall
- The K_d values are assumed zero within the fast flow paths
- The saltstone is not degraded
- Model parameters are as shown in Table 4.4-2
- The disposal unit concrete physically degrades as described in Section 4.2.3.2.4

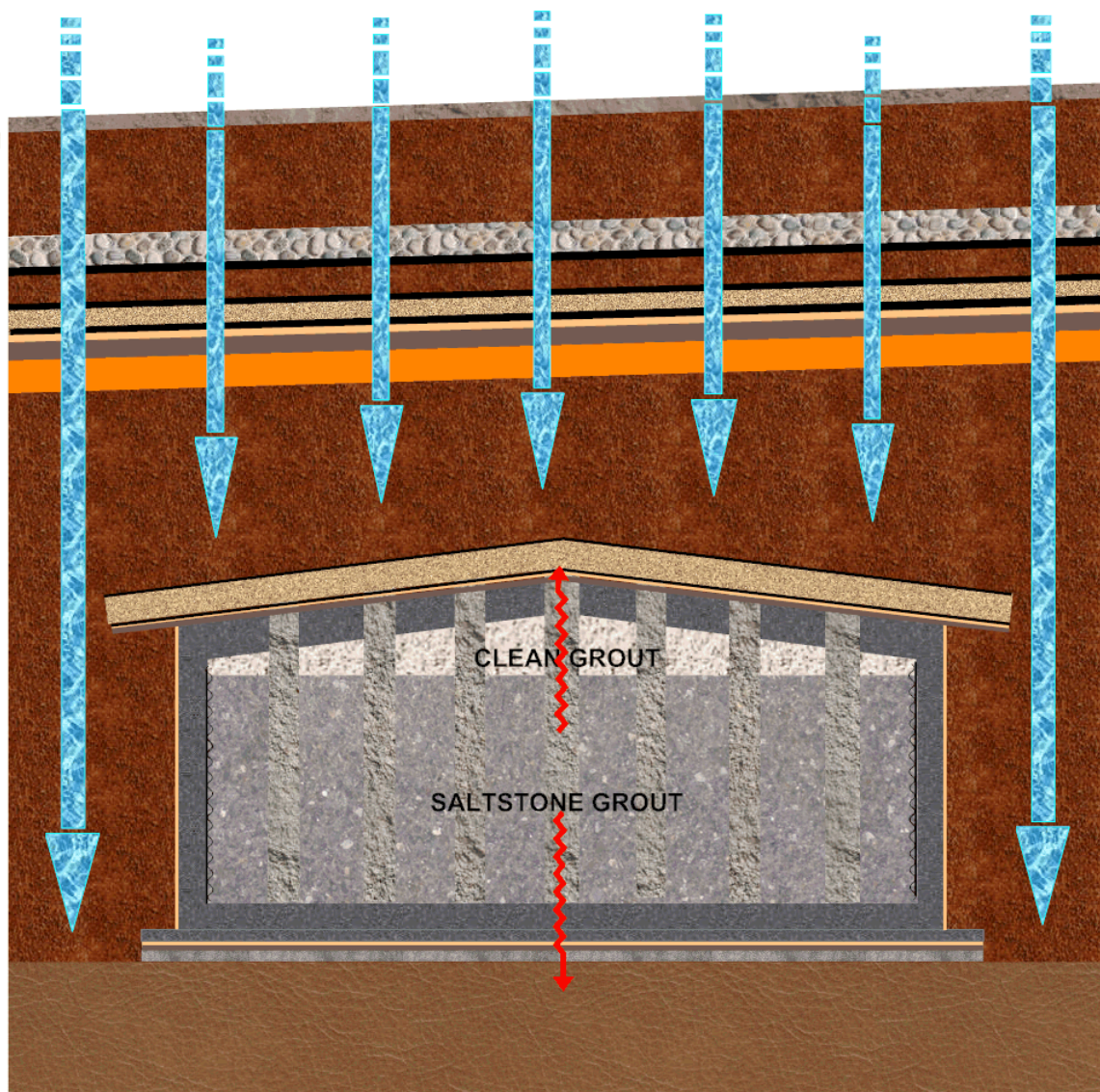
Figure 4.4-9: Model Scenario Case B



Case C, conceptually illustrated in Figure 4.4-6, is the same as Case B, but with the addition of the fast flow path addressed in Case C for Vault 1. Thus, Case C for Vault 4 is modeled with three 2 inch wide slots, two slots for the sheet drain systems and an additional slot in the center of the saltstone monolith to model postulated cracks or degradation of the support columns in Vault 4.

Case D postulates that the in-place sheet drain system provides a capillary break between the saltstone and the walls of the cell, thus precluding transport across the gap under unsaturated conditions. The major aspects of this case are as indicated for Case B, except that the 2 inch slots are modeled with a very small hydraulic conductivity, $5.0\text{E-}15$ cm/sec, to simulate an impervious layer. Figure 4.4-10 conceptually illustrates Case D.

Figure 4.4-10: Model Scenario Case D



Case E is the same as described above for Vault 1, except that the model parameters are as indicated in Table 4.4-2.

Case B, C, and E accelerate the chemical degradation of disposal unit concrete. The increase in water infiltration (due to the fast flow paths) and the change in the hydraulic properties of the saltstone (due to saltstone degradation) may potentially reduce the time it takes to reach the chemical transition states described in Sections 4.2.2 and 4.2.3.2.4, since more pore water may travel through the cementitious materials. Case D reduces the flow of water through the saltstone monolith; therefore, chemical degradation of the disposal unit concrete occurs later than the other cases. Table 4.4-7 summarizes the performance of the conceptual model for Vault 4 for these five cases.

Table 4.4-7: Occurrences of Model Changes by Case for Vault 4

| Change in Model Parameters | Time of Occurrence for Given Case (years after closure) | | | | | |
|--|---|---------------------|---------------------|---------------------|---------------------|---------------------|
| | Analytical Value | Value in Model | | | | |
| | Case A | Case A | Case B | Case C | Case D | Case E |
| Degradation of closure cap | 5,412 ^a | 5,500 ^b | 5,500 ^b | 5,500 ^b | 5,500 ^b | 5,500 ^b |
| Vault roof degrades to backfill properties | 10,000 ^c | 10,000 ^d | 10,000 ^d | 10,000 ^d | 10,000 ^d | 10,000 ^d |
| Wall concrete transitions from reducing to oxidizing | 15,519 ^e | 15,519 ^e | 3,987 ^e | 3,069 ^e | 15,555 ^e | 5,134 ^e |
| Wall concrete transitions from middle age to old age | 16,018 ^e | 16,018 ^e | 5,016 ^e | 3,363 ^e | 16,052 ^e | 5,836 ^e |
| Lateral drainage layer degrades to backfill properties | 19,013 ^f | 20,000 ^g | 20,000 ^g | 20,000 ^g | 20,000 ^g | 20,000 ^g |

- (a) Most significant degradation occurs within 1,000 years, more than a 5,000 fold increase in infiltration rate, an additional degradation factor of less than five until complete degradation in 5,412 years WSRC-STI-2008-00244)
- (b) Obtained from review of PORFLOW related files
- (c) Table 36 of SRNL-STI-2009-00115
- (d) Roof degrades by more than a factor of 500 within the first 9,000 years and an additional factor of less than 30 until complete degradation in 10,000 years (Appendix E of SRNL-STI-2009-00115)
- (e) Appendix F of SRNL-STI-2009-00115
- (f) Table 22 of SRNL-STI-2009-00115
- (g) Appendix E of SRNL-STI-2009-00115

4.4.2.3 FDC Degradation Cases (Typical)

To assess the likely impact of degradation for the FDCs, the conceptual modeling of Cases A through E that are addressed in Section 4.4.2.2 for Vault 4 are also utilized for the FDCs. The figures illustrating these cases are as identified in Section 4.4.2.2. The FDCs will contain a sheet drain system and will have roof support columns as described in Section 3.2.1.3. The major aspects for the five cases for the FDCs are the same as described above for Vault 4, with the following modifications:

- Model parameters are as shown in Table 4.4-3.
- Fast flow paths in Cases B and C used to simulate degraded conditions of the sheet drain system is a 2 inch wide annular space around the interior of the outer wall of the disposal unit and extends through the layers from the lower backfill layer to the aquifer, including the upper and lower mud mats.
- Case C contains two fast flow paths each a 2 inch wide annular space, with one adjacent to the wall and the other located within the saltstone monolith approximately 14 feet from the centerline of the disposal unit with hydraulic properties associated with sand vs. gravel for Vault 1 and 4 is shown in Table 4.4-8. The characteristic curve for sand is provided in Figure 4.2-17.

Table 4.4-8: Hydraulic Properties of Sand

| Saturated Effective Diffusion Coefficient D_e (cm²/sec) | Average Total Porosity (%) | Average Dry Bulk Density (g/cm³) | Average Particle Density (g/cm³) | Saturated Horizontal Hydraulic Conductivity (cm/sec) | Saturated Vertical Hydraulic Conductivity (cm/sec) |
|--|-----------------------------------|--|--|---|---|
| 8.0E-06 | 38 | 1.65 | 2.66 | 5.0E-04 | 2.8E-04 |

[WSRC-STI-2006-00198, Table 5-18]

Cases B, C, and E accelerate the chemical degradation of FDC concrete. The increase in water infiltration (due to the fast flow paths) and the change in the hydraulic properties of the saltstone (due to saltstone degradation) reduce the time it takes to reach the chemical transition states described in Sections 4.2.2 and 4.2.3.2.4, since more pore water may travel through the cementitious materials. Case D reduces the flow of water through the saltstone monolith; therefore, chemical degradation of the FDC concrete occurs later than the other cases. Table 4.4-9 summarizes the performance of the conceptual model for the FDCs for these five cases.

Table 4.4-9: Occurrences of Model Changes by Case for FDCs

| Change in Model Parameters | Time of Occurrence for Given Case (years after closure) | | | | | |
|--|---|---------------------|---------------------|---------------------|---------------------|---------------------|
| | Analytical Value | Value in Model | | | | |
| | Case A | Case A | Case B | Case C | Case D | Case E |
| Degradation of HDPE layer outside FDC wall | 6,000 ^c | 6,000 ^c | 6,000 ^c | 6,000 ^c | 6,000 ^c | 6,000 ^c |
| Degradation of HDPE-GCL above and below FDCs | 7,500 ^d | 7,500 ^d | 7,500 ^d | 7,500 ^d | 7,500 ^d | 7,500 ^d |
| Complete degradation of closure cap | 5,412 ^a | 5,500 ^b | 5,500 ^b | 5,500 ^b | 5,500 ^b | 5,500 ^b |
| Wall concrete transitions from reducing to oxidizing | 16,344 ^g | 16,344 ^g | 15,784 ^g | 15,803 ^g | 16,349 ^g | 15,631 ^g |
| Wall concrete transitions from middle age to old age | 16,753 ^g | 16,753 ^g | 16,027 ^g | 16,052 ^g | 16,757 ^g | 15,841 ^g |
| Wall degrades to backfill properties | 18,000 ^c | 20,000 ^f | 20,000 ^f | 20,000 ^f | 20,000 ^f | 20,000 ^f |
| Lateral drainage layer degrades to backfill properties | 19,013 ^h | 20,000 ⁱ | 20,000 ⁱ | 20,000 ⁱ | 20,000 ⁱ | 20,000 ⁱ |
| Upper mud mat transitions from reducing to oxidizing | 22,177 ^g | 22,177 ^g | 20,079 ^g | 20,896 ^g | 22,207 ^g | 20,262 ^g |
| Floor concrete transitions from reducing to oxidizing | 22,498 ^g | 22,498 ^g | 21,820 ^g | 21,559 ^g | 22,514 ^g | 22,198 ^g |
| Upper mud mat transitions from middle age to old age | 22,871 ⁶ | 22,871 ^g | 21,421 ^g | 21,118 ^g | 22,906 ^g | 22,304 ^g |
| Floor concrete transitions from middle age to old age | 23,274 ^g | 23,274 ^g | 22,385 ^g | 22,043 ^g | 23,293 ^g | 22,938 ^g |
| Floor and upper mud mat degrade to native soil properties ⁽ⁱ⁾ | 40,000 ^k | 50,000 ^l | 50,000 ^l | 50,000 ^l | 50,000 ^l | 50,000 ^l |
| Roof degrades to backfill properties | 40,000 ^j | 20,000 ⁱ | 20,000 ⁱ | 20,000 ⁱ | 20,000 ⁱ | 20,000 ⁱ |

- (a) Most significant degradation occurs within 1,000 years, more than a 5,000 fold increase in infiltration rate, an additional degradation factor of less than 5 until complete degradation in 5,412 years [SRNL-STI-2009-00115]
- (b) Obtained from PORFLOW related files
- (c) HDPE continually degrades with a degradation factor of more than 600 within the first 6,000 years and an additional degradation factor of 3 at 20,000 years (Appendix E of SRNL-STI-2009-00115)
- (d) HDPE-GCL continually degrades with a degradation factor of more than 400 within the first 7,500 years and an additional degradation factor of 2 at 20,000 years [Appendix E of SRNL-STI-2009-00115]
- (e) Table 31 of SRNL-STI-2009-00115
- (f) Most significant degradation occurs within the first 15,000 years with a degradation factor of over 60,000 and an additional degradation factor of less than 15 at 20,000 years [Appendix E of SRNL-STI-2009-00115]
- (g) Appendix F of SRNL-STI-2009-00115
- (h) Table 22 of SRNL-STI-2009-00115
- (i) Appendix E of SRNL-STI-2009-00115
- (j) Table 33 of SRNL-STI-2009-00115
- (k) Table 32 of SRNL-STI-2009-00115
- (l) Most significant degradation occurs within the first 20,000 years with a degradation factor of over 40,000 and an additional degradation factor of less than 80 at 50,000 years [Appendix E of SRNL-STI-2009-00115]

4.4.3 Evaluation of Integrated System Behavior

Upon the closure of SDF, there is an opportunity for the stabilized contaminants to leach from distinct disposal units. The various individual system behaviors that were evaluated have been presented for the various types of disposal units in Section 4.4.2. The analysis of the Base Case (Case A) through the PORFLOW SDF model provided results reflecting the best estimate of closure system behavior. These independent modeling scenarios for the disposal units are melded together in the probabilistic analysis to produce integrated results.

The grid for the saturated zone was such that the disposal units can be individually resolved. Explicit representation of individual sources enables investigation of potential plume overlap from separate sources. Integrated system behavior, as measured by concentration at exposure points, was simulated by applying contaminant flux transients for chosen disposal units and cases to appropriately located grid cells.

Provided below is a short description of the integrated conceptual model process flow from the closure cap to the saturated zone. The integrated conceptual model consists of different segments, some of which were represented by independent sub-models. For example, the geochemistry model developed different sorption coefficients for different chemical states. The chemical state used in the model was determined in PORFLOW based on the PORFLOW calculated pore volumes. It should be noted that since the sub-models were developed independently and may have different levels of conservatism, some shared input parameters may have different values from sub-model to sub-model. For example, the vadose sub-model considered the impact of the SDF cover system on infiltration, but the aquifer transport sub-model took no credit for reduced infiltration. Emphasis was placed on ensuring that individual sub-models were defensible. The fact that two model segments may assume different values for the same parameter was not considered significant if the sub-models were valid and defensible.

The model process flow description below describes how each individual model segment was integrated into the entire model and how its behavior was depicted. The degradation case timelines associated with the various model segments for Vaults 1 and 4, and Disposal Unit 2A (a typical FDC), are provided in Tables 4.4-6, 4.4-7, and 4.4-9, respectively.

The simplified model flow process for a FDC is provided below.

4.4.3.1 Closure Cap

A flow rate leaving the closure cap over time was determined in the closure cap sub-model. The infiltration rate into the closure cap top was based on the rainfall rates and the closure cap material properties (which are discussed in detail in Section 4.2.3.2.1). The flow rate out of the cap was calculated using the HELP code, with the closure cap modeled as degrading over time. The flow rate through the closure cap reaches a steady state value at approximately year 5,412. Table 3.2-7 provides the time-variant infiltration rates based on the closure cap analysis presented in Section 3.2.2.

4.4.3.2 Disposal Unit Roof

The flow leaving the closure cap travels to the disposal unit, with the flow rate being affected by the backfill layer and lateral drainage layer above the concrete roof. Based on the relative

hydraulic properties of the two materials (soil vs. concrete), some flow was directed around the disposal unit into the surrounding soil, while some flow travels downward toward the roof. For the FDCs, an HPDE-GCL layer overlays the roof and is an additional barrier to the flow to the roof. Degradation of the HDPE-GCL layer was modeled as changing over time and is discussed in Section 4.2.3.2.2. The concrete material properties (which are discussed in detail in Section 4.2.3.2.4) were modeled as changing over time. The only disposal unit roof material properties of concern are the hydraulic properties, since the disposal unit roof impacts flow, but does not retard contaminant transport (contaminant transport was not modeled as occurring in the roof). The disposal unit roof hydraulic properties were degraded as depicted in the figures in Section 4.2.3.2.4.

4.4.3.3 *Saltstone*

Water enters the top of the disposal unit and travels downward into the saltstone. The saltstone material properties (e.g., hydraulic conductivity, diffusion coefficient, which are discussed in detail in Section 4.2.2 and 4.2.3.2.4) were modeled as changing over time. In some degradation cases used in the sensitivity analyses (Section 4.4.2), fast flow paths through the grout were modeled resulting in a higher flow rate through the grout. A cementitious materials analysis was performed to determine the time it would take to transition from reducing to oxidizing state and from middle age to old age. Analysis indicated that during the performance period the saltstone remained in its initial state of reducing middle age.

The saltstone inventory (contaminants) was assumed to be distributed homogeneously throughout the saltstone. Contaminant release was assumed to be controlled by sorption coefficient (K_d values) as described in Section 4.2.2, and the K_d values associated with reducing, middle age concrete provided in Table 4.2-18. Because of the importance of Tc-99 in the model, a more sophisticated analysis was developed to determine a time varying K_d value for Tc-99 as described in Section 4.2.3.2.4.

The saltstone material properties of principal concern are the hydraulic properties. The saltstone hydraulic properties influence the water flow rate through the disposal unit. The earlier the saltstone degrades, the earlier the flow rate through the disposal unit reaches a steady state maximum flow. Case E, described in Section 4.4.2, assumes the saltstone monolith to be in a degraded state, described in Section 4.2.3.2.4, throughout the performance period.

4.4.3.4 *Disposal Unit Walls and Floor*

Contaminants leaving the saltstone monolith enter the concrete walls and floor of the SDF disposal units. For Vaults 1 and 4, contaminants are assumed to be present in the vault walls initially. Disposal unit concrete material properties (which are discussed in detail in Section 4.2.3.2.4) are modeled as changing over time. These changes are depicted in Figures 4.2-37 through 4.2-41 of Section 4.2.3.2.4. The material properties of the concrete impact both the flow rate through the disposal unit base and the K_d value.

Contaminant transport is retarded by the wall and floor concrete (including the upper and lower mud mat for the FDCs), with some radionuclides being slowed greatly depending on their K_d values. Table 4.2-18 provides K_d values for cementitious materials as a function of

aging, with the grout “age” dependent on the pH of the concrete pore water, which in turn is dependent upon the amount of water (number of pore water volumes) that has passed through the concrete over time. A description of pore water chemistry modeling is provided in Section 4.2.3.2.4 and discussed in the context of the various degradation cases in Section 4.4.2. As the disposal unit chemistry changes, the concrete transitions from reducing to oxidizing and from middle age to old age and the associated K_d values are modeled as changing.

4.4.3.5 *Vadose Zone Surrounding the SDF Disposal Units*

After contaminants exit the floor (the lower mud mat of the FDCs) or the walls, they enter the vadose zone (e.g., soil) surrounding the disposal units, which is discussed in detail in Section 4.2.3.2.2. The vadose zone material properties impact the flow rate through the soil and the associated K_d values, with both being important to the model. The vadose zone depth below each disposal unit can vary depending on the disposal unit involved, as shown in Table 4.2-13. The vadose zone material properties are not modeled as changing over time. In the probabilistic model however, the vadose zone thickness was allowed to vary, which impacts transport time through the soil.

4.4.4 *Modeling Process*

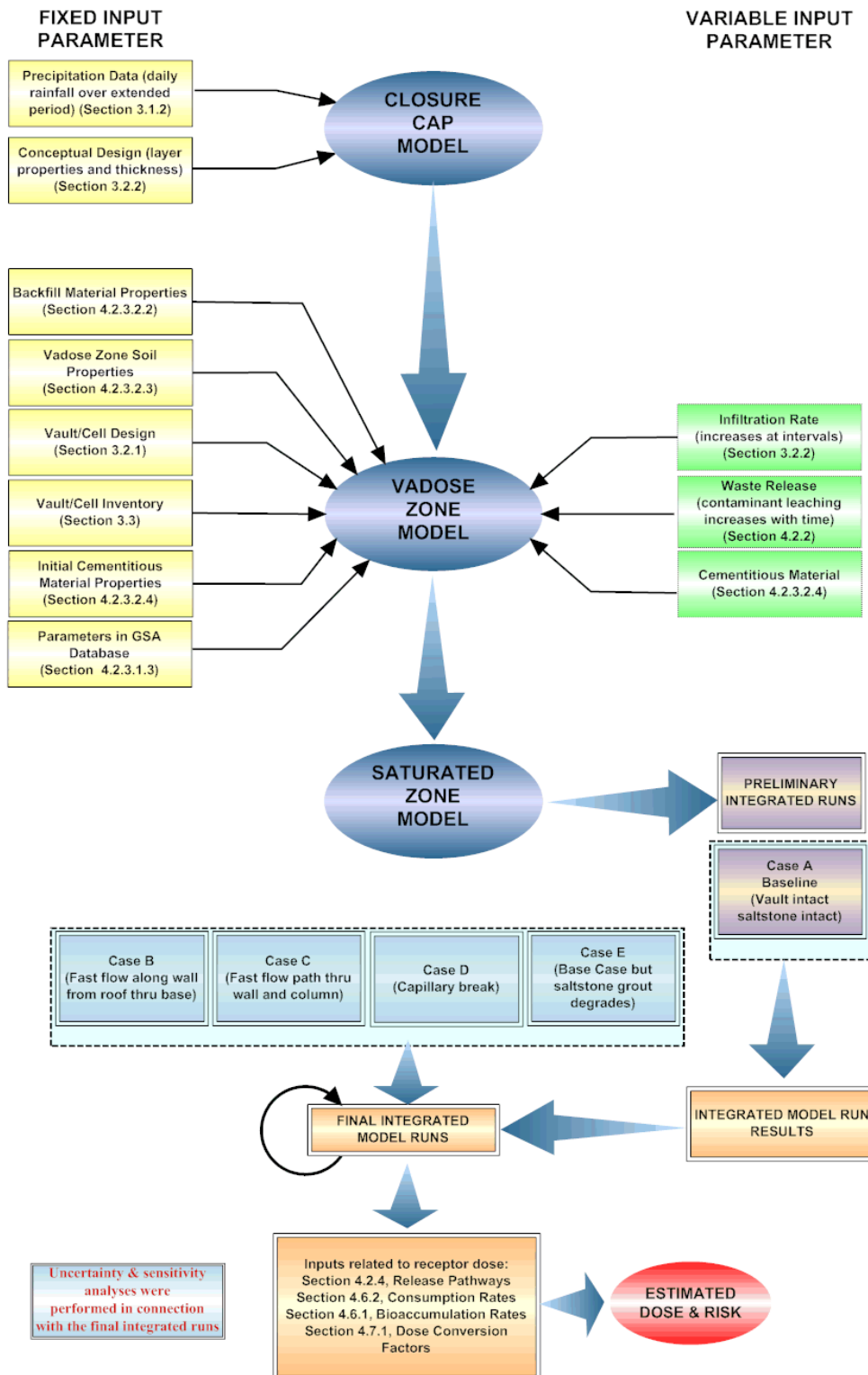
Figure 4.4-11 illustrates the general process followed in implementing the ISCM and presents the three component models and their key inputs.

Some inputs, as indicated on Figure 4.4-11, involved fixed parameters that do not change over time. These are generally shown on the left side of the figure. The inputs on the right side of the figure do change over time.

As shown in Figure 4.4-11, and as explained previously, five Vault 4 and FDC degradation case scenarios and three Vault 1 case scenarios were used for the probabilistic model runs, which were accomplished using the applicable computer codes identified in Section 4.3. These cases were analyzed by running the model using different combinations as discussed above. The PORFLOW SDF model was used to simulate the flow behavior for the various cases. The Base Case results are reflected through Case A, PORFLOW SDF contaminant transport modeling. Uncertainty and sensitivity analyses were also performed using the multiple cases and variations of the individual parameters modeled as part of a case. The GoldSim model used the PORFLOW SDF model flow results and other parameter distributions to provide a range of possible outcomes, and to identify those parameters of most interest.

The Base Case analysis provided baseline contaminant concentrations in groundwater. The data for radiological contaminants was used in combination with the inputs related to receptor dose shown on Figure 4.4-11 to calculate impacts on various receptors.

Figure 4.4-11: Saltstone Disposal Facility PA Modeling Relationships



4.4.4.1 PORFLOW Modeling Process

4.4.4.1.1 Regional (GSA) and Local (SDF) Modeling in PORFLOW

The PORFLOW computer code was used to model SDF flow (for all degradation cases) and transport. Regional GSA modeling in PORFLOW was developed using the original GSA/PORFLOW 200 foot x 200 foot grid depicted in Figure 4.2-7, with the primary focus on seepage concentrations. Figure 4.4-12 shows simulated groundwater pathlines emanating from the SDF based on the GSA/PORFLOW model. The groundwater flow paths discharge to either UTR or McQueen Branch. A groundwater divide is observed to pass through the northwest half of the SDF. Figure 4.4-13 shows the "Source" and "Seepage" nodes used in GSA scale seepage modeling. The source nodes for Vaults 1 and 4 are identified as grid cells with centroids lying within the footprint of each existing vault. For FDCs, the closest single grid cell is chosen to represent the source. Seepage nodes occur where groundwater discharges to ground surface, and are segregated by aquifer; (Gordon Aquifer Unit (GAU), Lower Aquifer Zone (LAZ), Upper Aquifer Zone (UAZ)), and the tributaries UTR and McQueen Branch.

Figure 4.4-12: Simulated Groundwater Flow paths in GSA/PORFLOW Modeling

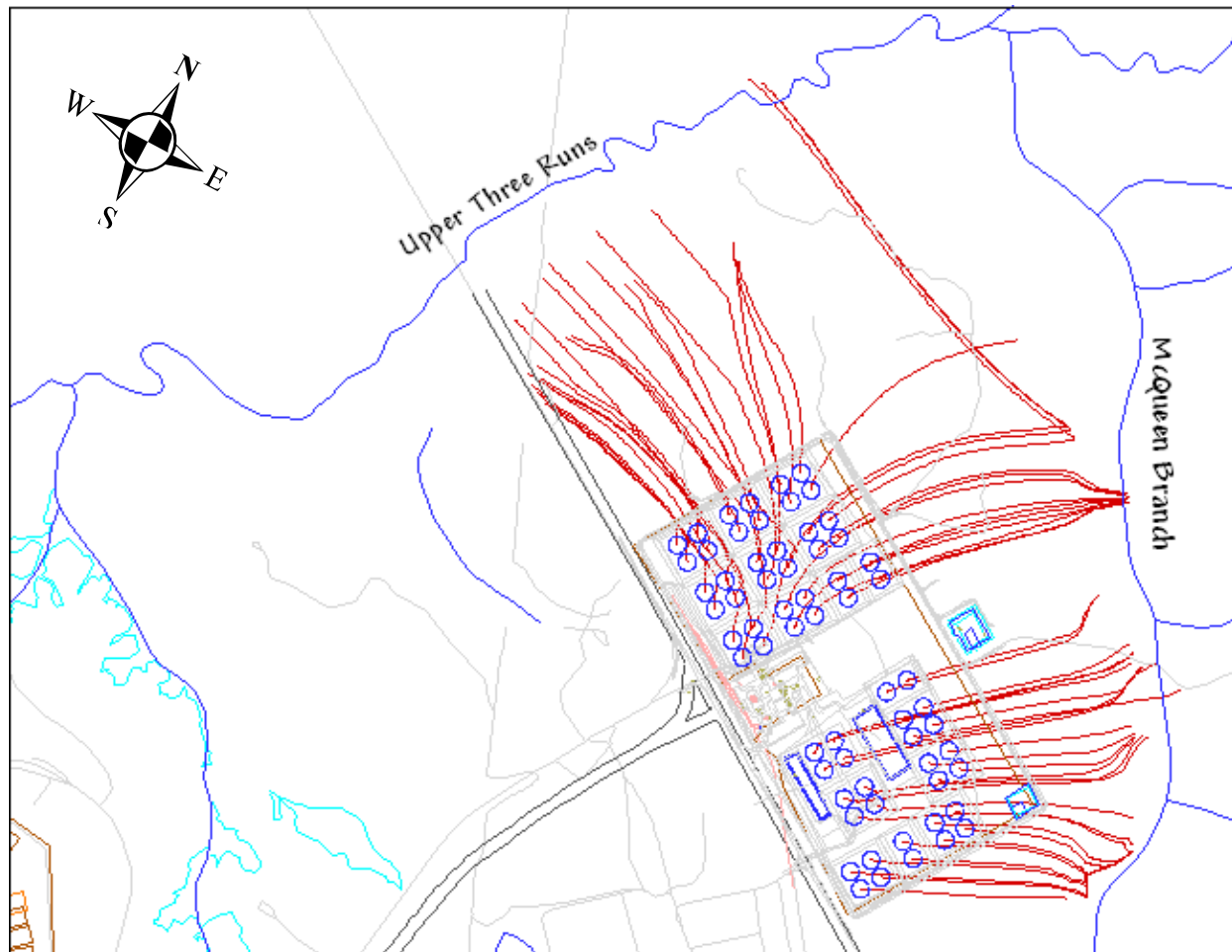
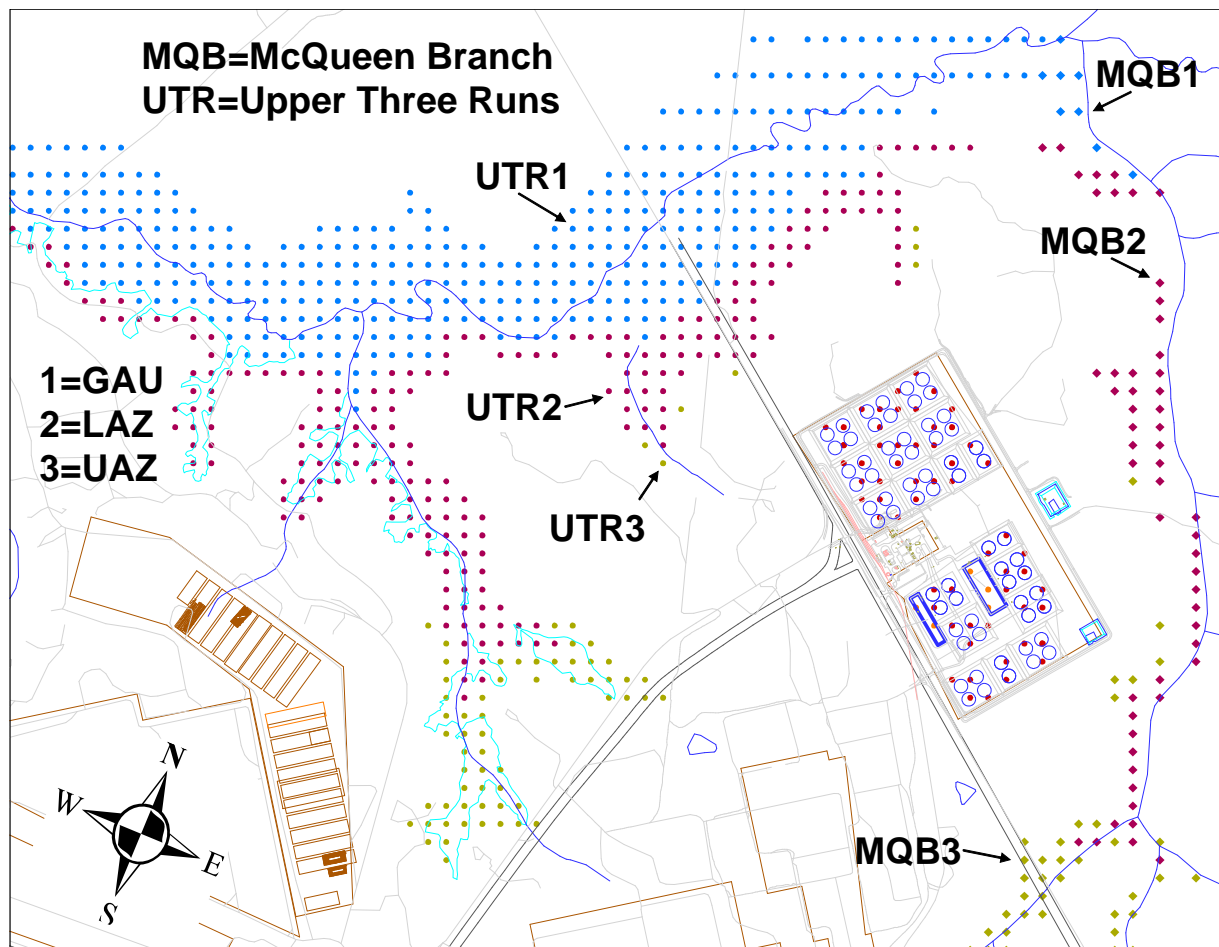
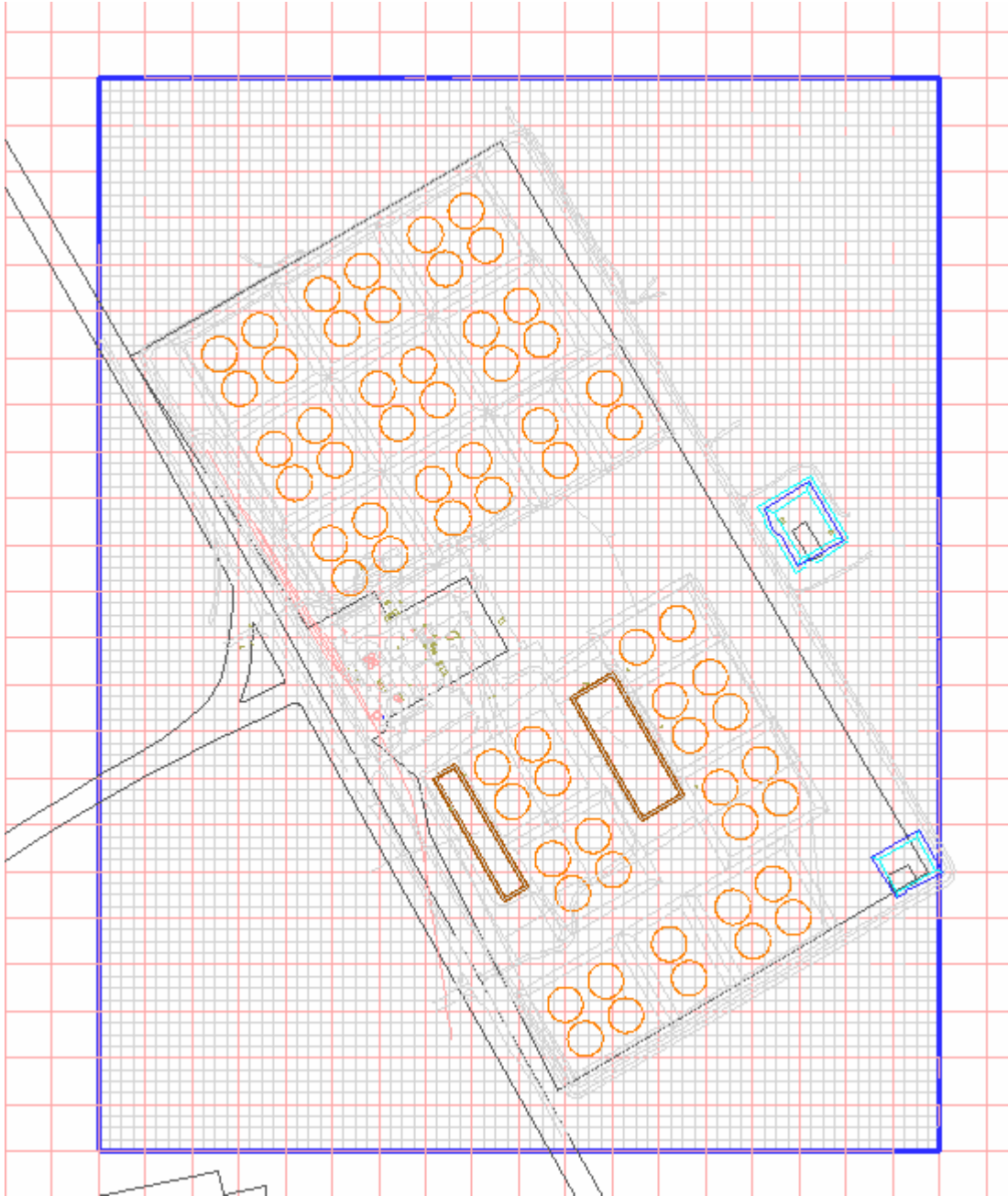


Figure 4.4-13: Source and Seepage Nodes in GSA/PORFLOW Modeling



Local SDF modeling was developed from the GSA scale model using a 50 foot x 50 foot grid refinement, with the primary focus on the 1m and 100m concentrations (Figure 4.4-14). A grid resolution finer than 200 feet x 200 feet was required to avoid excessive numerical dispersion at the local scale. The SDF velocity field was generated directly from the coarser scale GSA velocity model by subdividing the 200 foot x 200 foot grid cells and using a mass-conserving linear interpolation scheme to assign velocities to the refined 50 foot x 50 foot mesh, rather than a separate flow model requiring its own boundary conditions and properties. [SRNL-STI-2009-00115] This approach ensured strict consistency between the two aquifer flow fields, apart from resolution. The SDF velocity field included the entire vertical extent of the GSA model within the horizontal confines of the SDF domain.

Figure 4.4-14: SDF Modeling from GSA Scale Model



"Source" nodes were identified as grid cells with centroids lying within the footprint of each disposal unit (Figure 4.4-15). Also shown are 1m and 100m nodes comprising the groundwater assessment perimeter surrounding SDF disposal units. Using mathematical parlance, the 1m nodes were created by first defining the convex hull of all disposal units. The convex hull can be thought of as a taut rubber band enveloping the collection of disposal units. The 1m perimeter cells were defined as those grid nodes that adjoin on any side or corner with nodes inside the convex hull of source regions. The 100m nodes were constructed by defining 100m buffer zones for each disposal unit, and joining these with the convex hull of the source zones. By definition, the 100m perimeter nodes adjoin at least one buffer node on a face or corner. For diagnostic purposes, the 1m and 100m assessment perimeters were divided into sectors labeled A-L (Figure 4.4-16). For the 1m distance, the collection of sector nodes coincide exactly with the 1m nodes depicted in Figure 4.4-15, except the upgradient nodes were omitted. For the 100m sector nodes, the original 100m perimeter was slightly modified to lie exactly 100m beyond the 1m perimeter for consistency.

Figure 4.4-15: SDF Modeling Showing Source Nodes and Perimeters

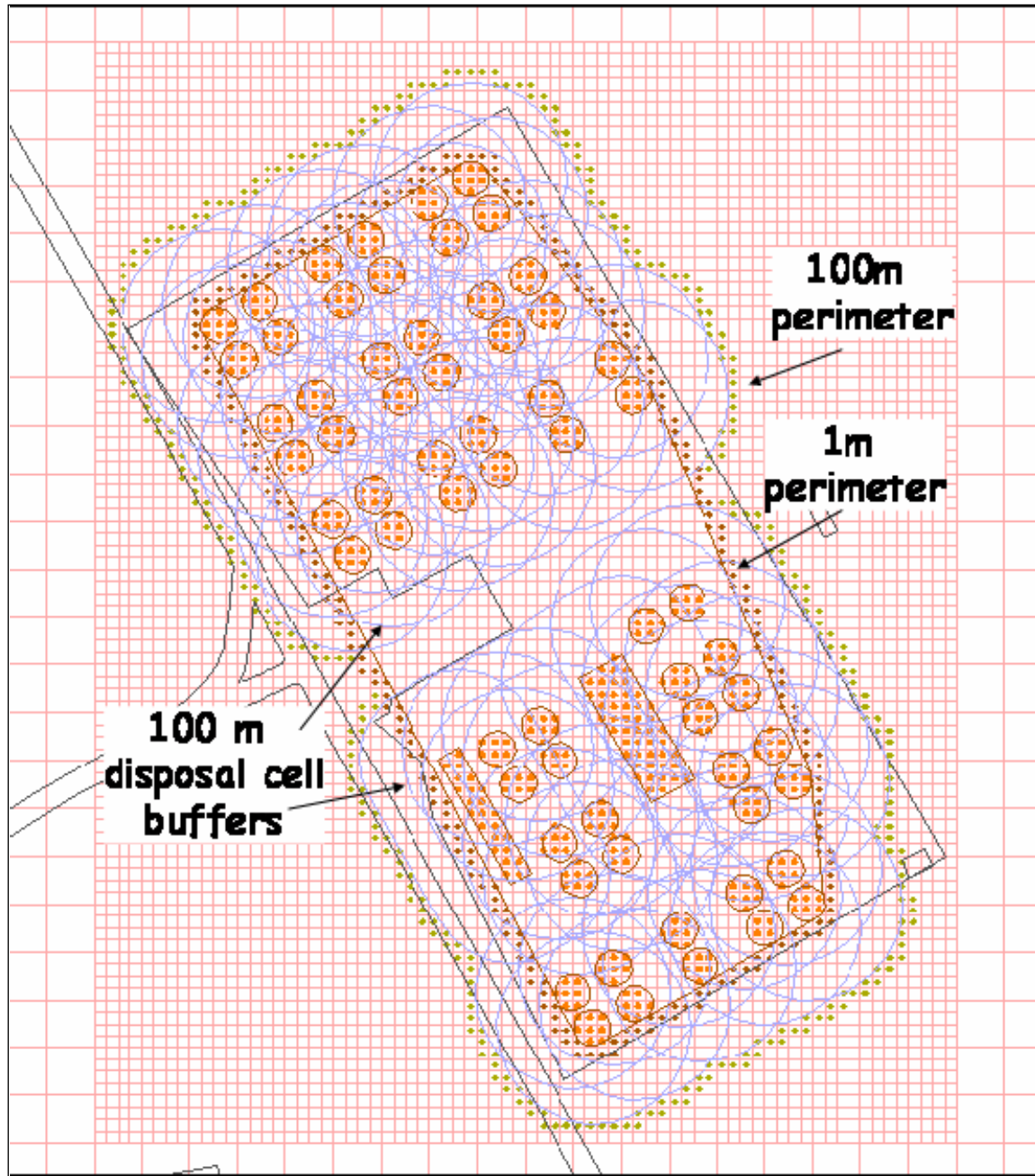
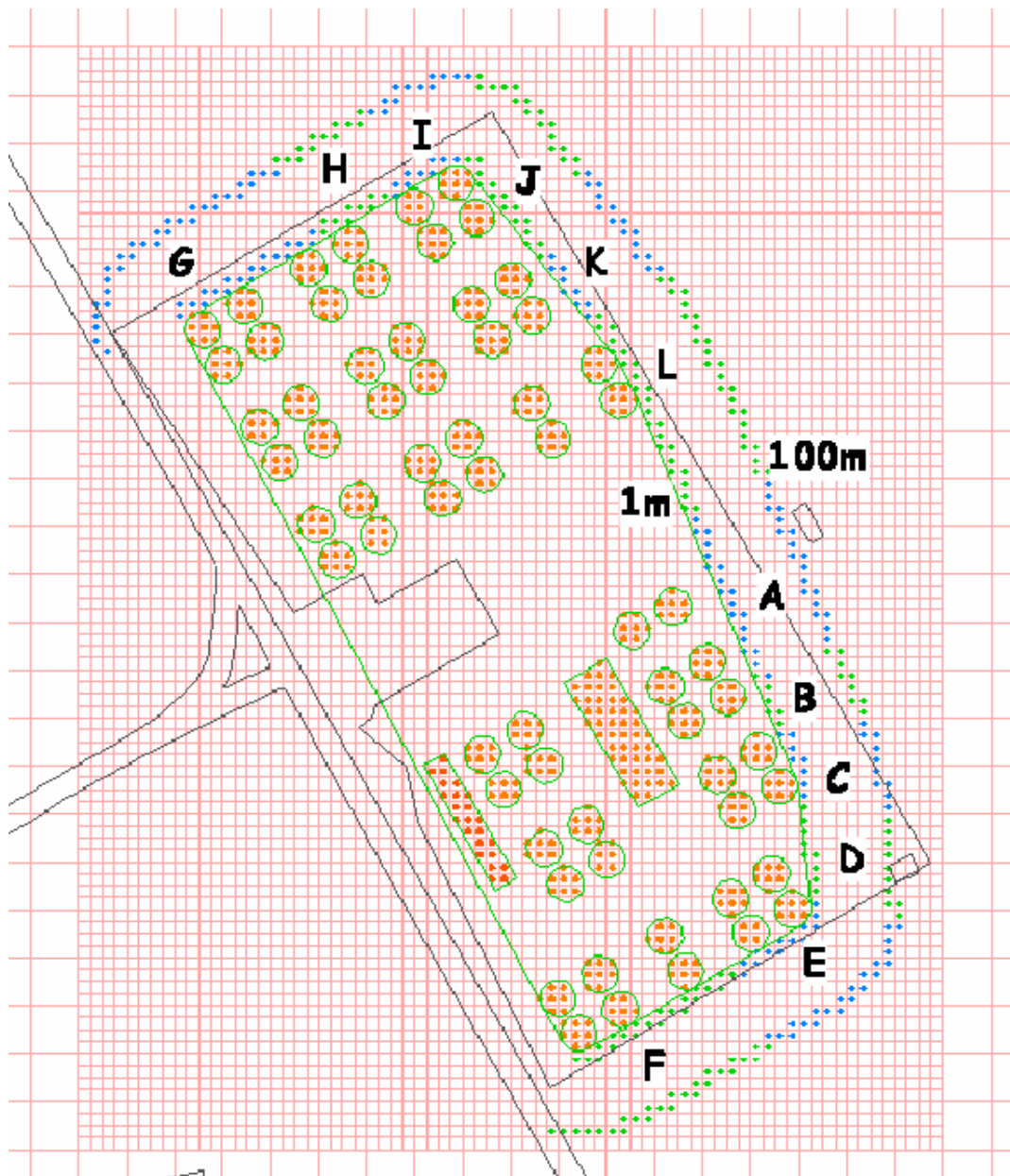


Figure 4.4-16: SDF Modeling Showing Divisional Sectors



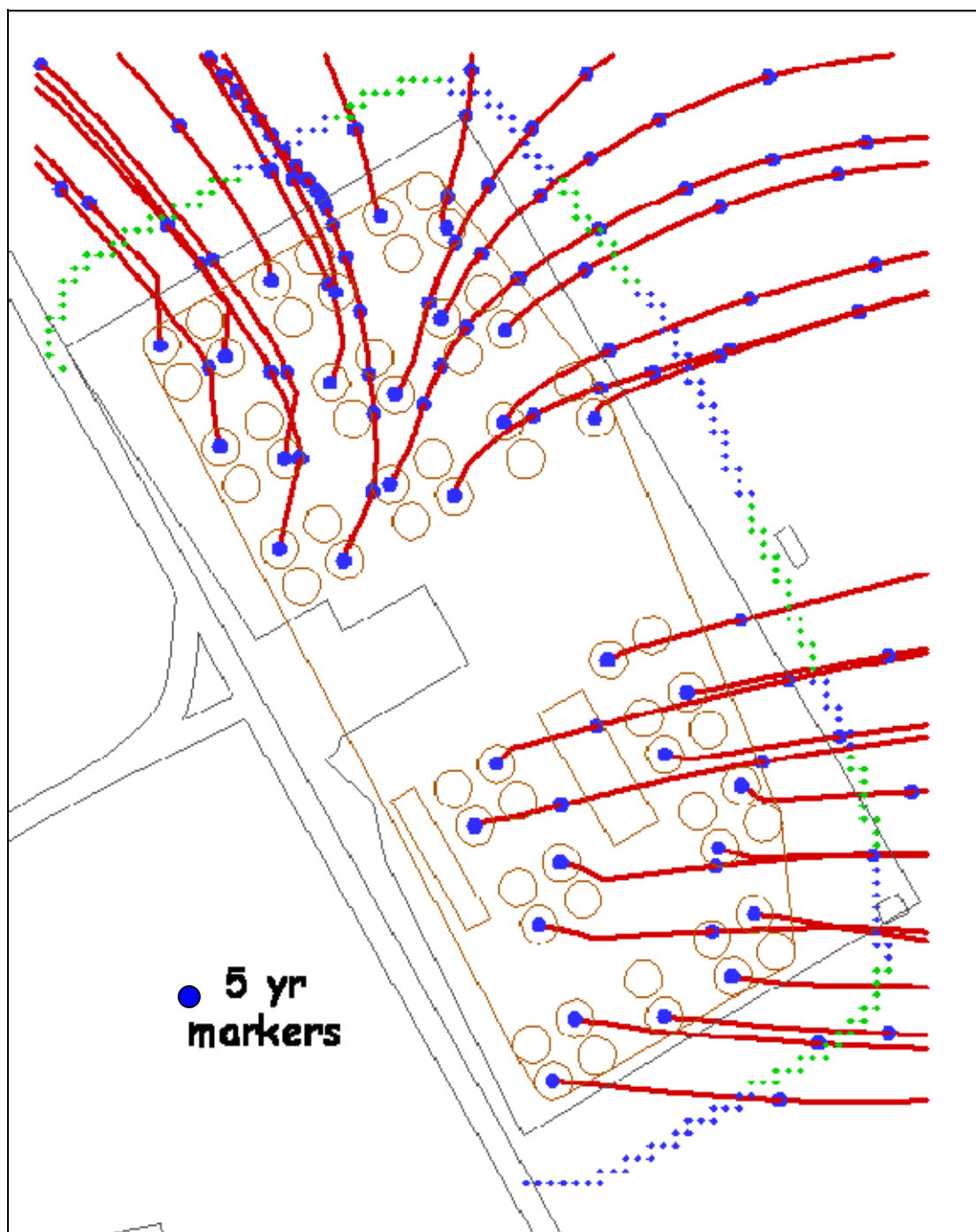
The stream traces from the SDF disposal units are shown in Figures 4.4-17 through 4.4-19. Five year time markers (blue dots) indicate travel times in the saturated zone between sources and the 100m perimeter ranging from under 10 years to several decades depending on location within the SDF. In aquifer transport modeling, hydrodynamic dispersion is represented by longitudinal and transverse dispersivities of 10m and 1m, respectively, which are 10% and 1% of a nominal 100m plume travel distance. Both the GSA and SDF scale models have been shown to preserve mass to adequate tolerances. [WSRC-TR-2004-00106, Q-SQP-G-00003]

[illegible]

Figure 4.4-18: SDF Vault 4 Modeling Showing Stream Tracers



Figure 4.4-19: SDF FDC Modeling Showing Stream Tracers



4.4.4.1.2 Disposal Unit Modeling in PORFLOW

For computational efficiency, the existing disposal units were modeled in two-dimensions (2-D) in PORFLOW. The long, rectangular Vaults 1 and 4 were represented in 2-D Cartesian coordinates as a transverse slice through Vaults 1, 4, and surrounding vadose zone soils, that implicitly neglect end effects. The FDCs were modeled in 2-D cylindrical coordinates by a radial cut (unit radian pie wedge), that implicitly assumed symmetry about the centerline axis. Up to 18 distinct material zones were defined in PORFLOW to represent different materials and to reflect different flow scenarios (e.g., fast flow paths). Approximately 7,000 grid blocks were used to represent each of the three different disposal unit types (grid varies with disposal unit type). Graphic depictions of the PORFLOW material zones and grids for the various disposal unit types, including corner details, are provided in Figures 4.4-20 through 4.4-31.

Figure 4.4-20: Vault 1 Material Zones for PORFLOW Vadose Zone Modeling

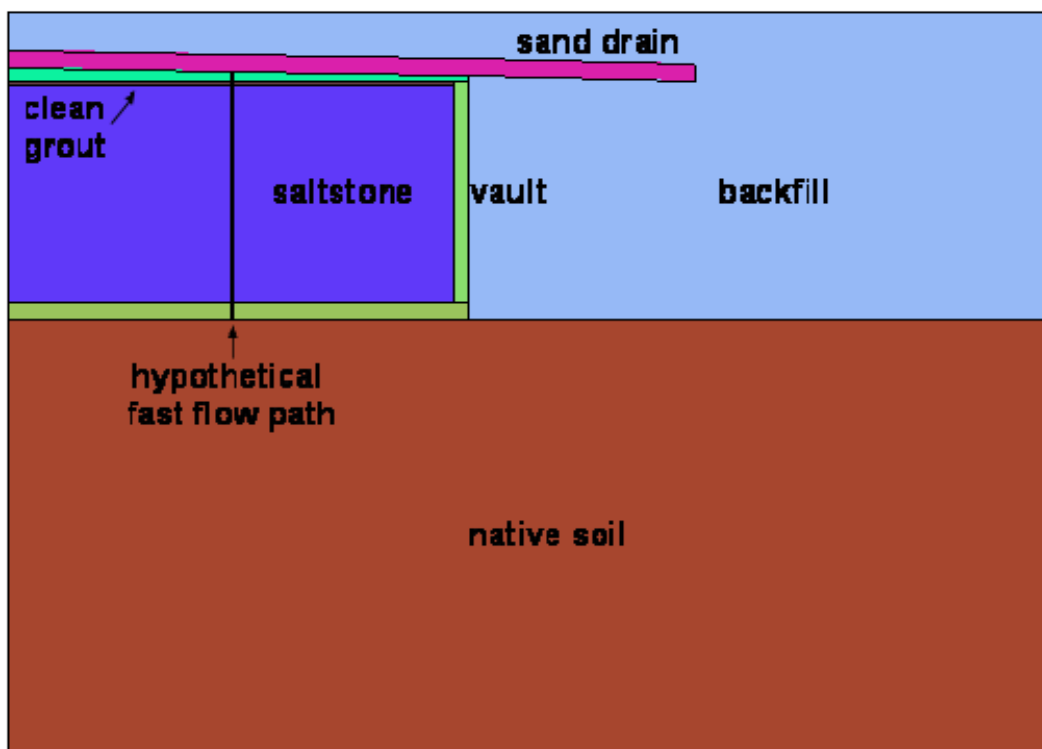


Figure 4.4-21: Vault 1 Gridding for PORFLOW Vadose Zone Modeling

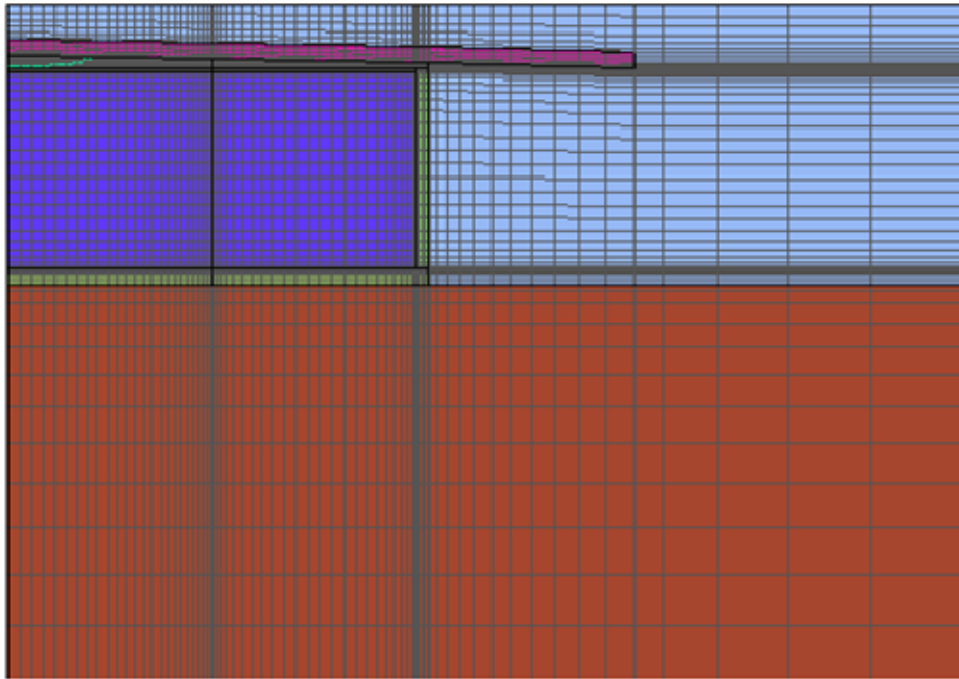


Figure 4.4-22: Vault 1 Upper Corner Detail for PORFLOW Vadose Zone Modeling



Figure 4.4-23: Vault 1 Lower Corner Detail for PORFLOW Vadose Zone Modeling

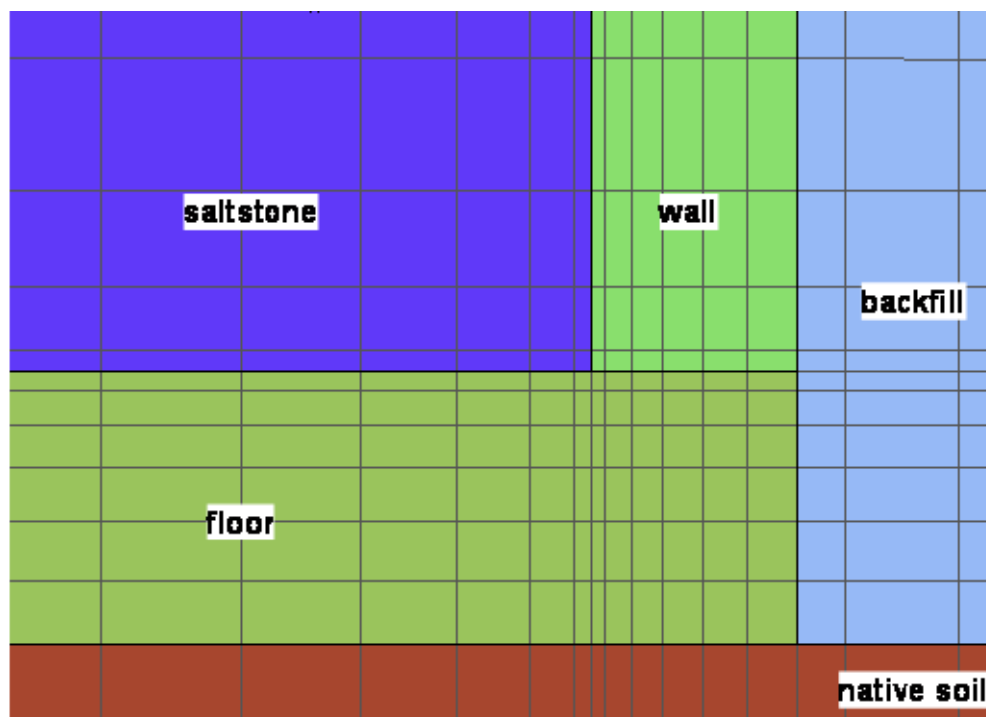


Figure 4.4-24: FDC Material Zones for PORFLOW Vadose Zone Modeling

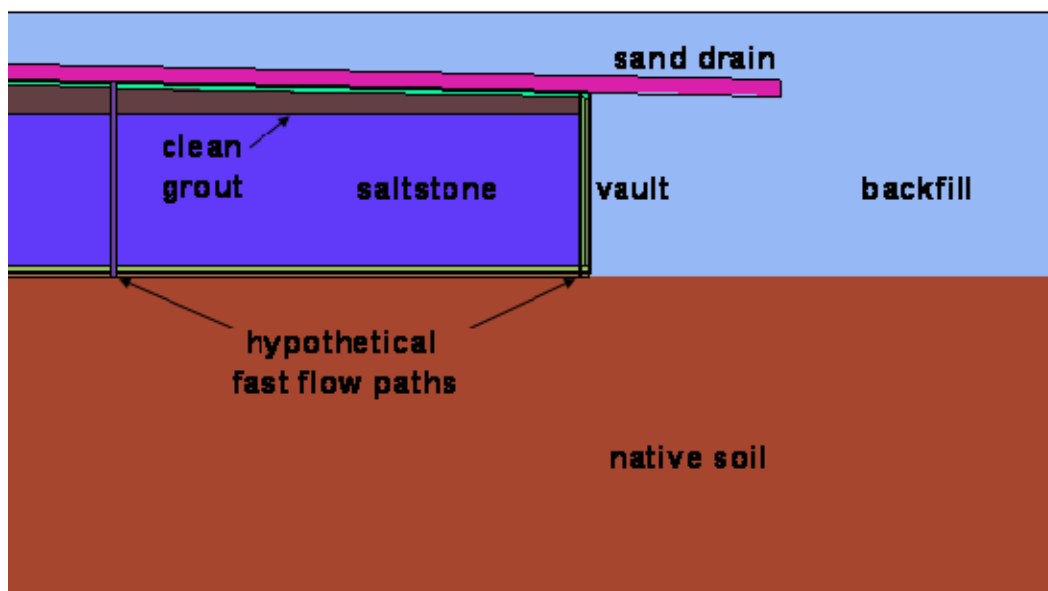


Figure 4.4-25: FDC Gridding for PORFLOW Vadose Zone Modeling

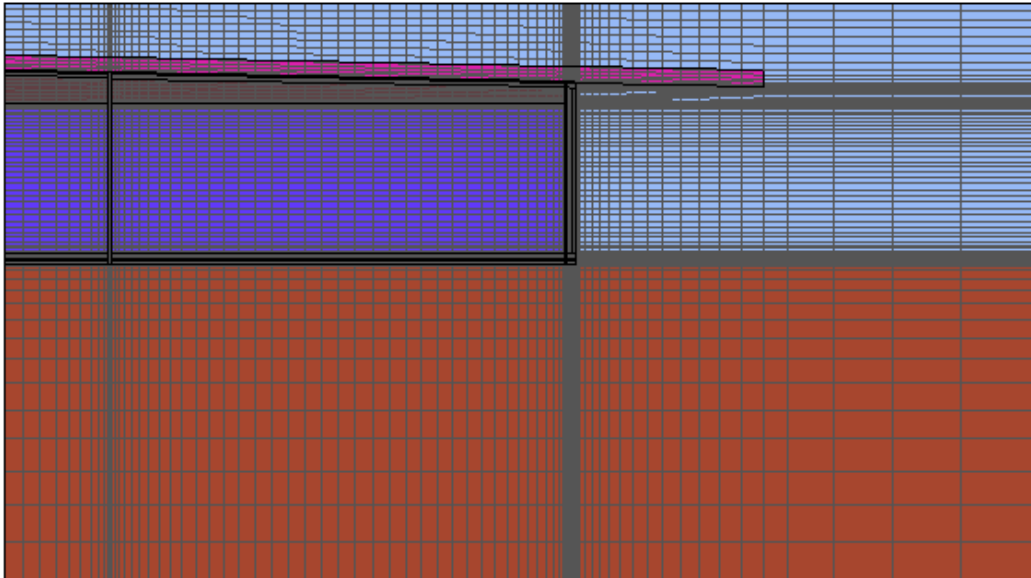


Figure 4.4-26: FDC Upper Corner Detail for PORFLOW Vadose Zone Modeling

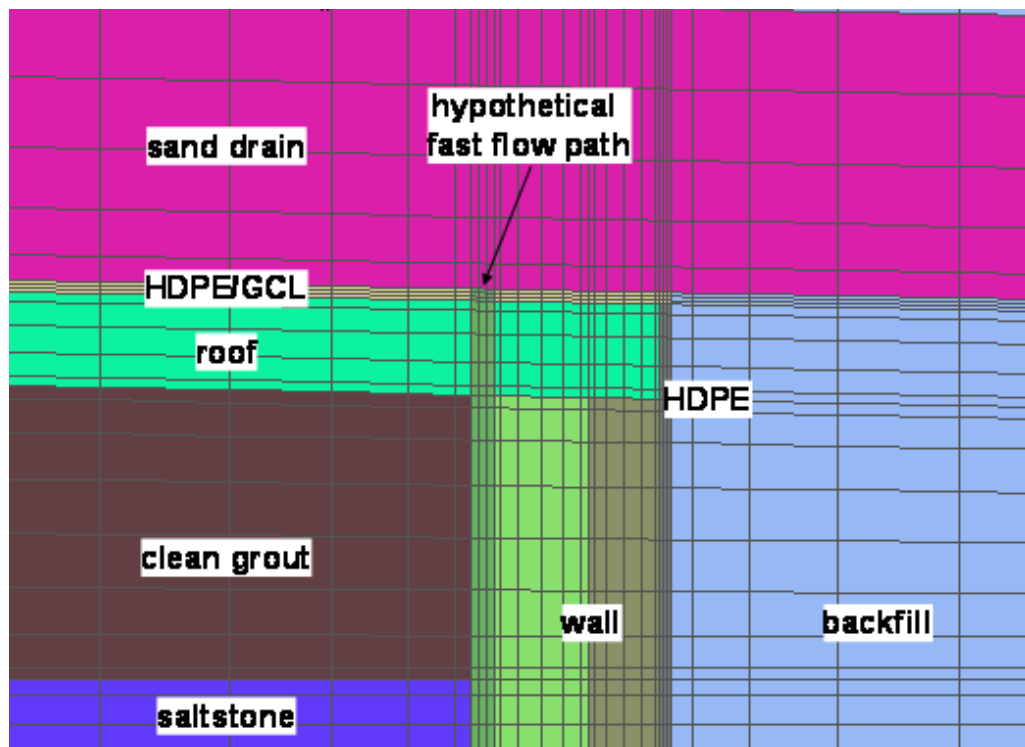


Figure 4.4-27: FDC Lower Corner Detail for PORFLOW Vadose Zone Modeling

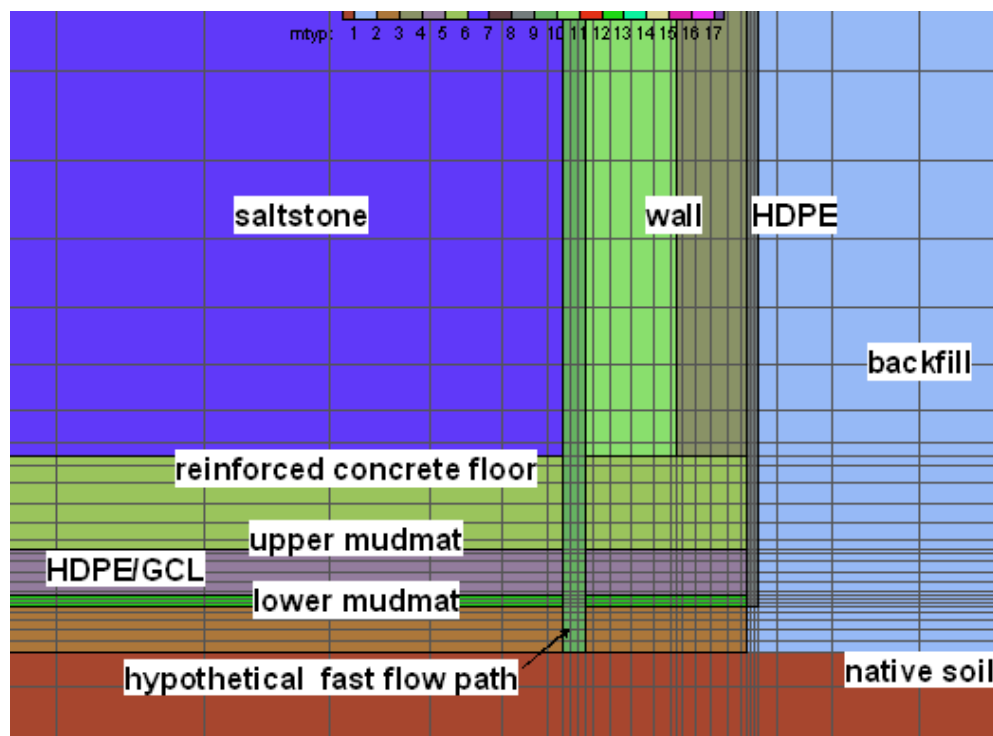


Figure 4.4-28: Vault 4 Material Zones for PORFLOW Vadose Zone Modeling

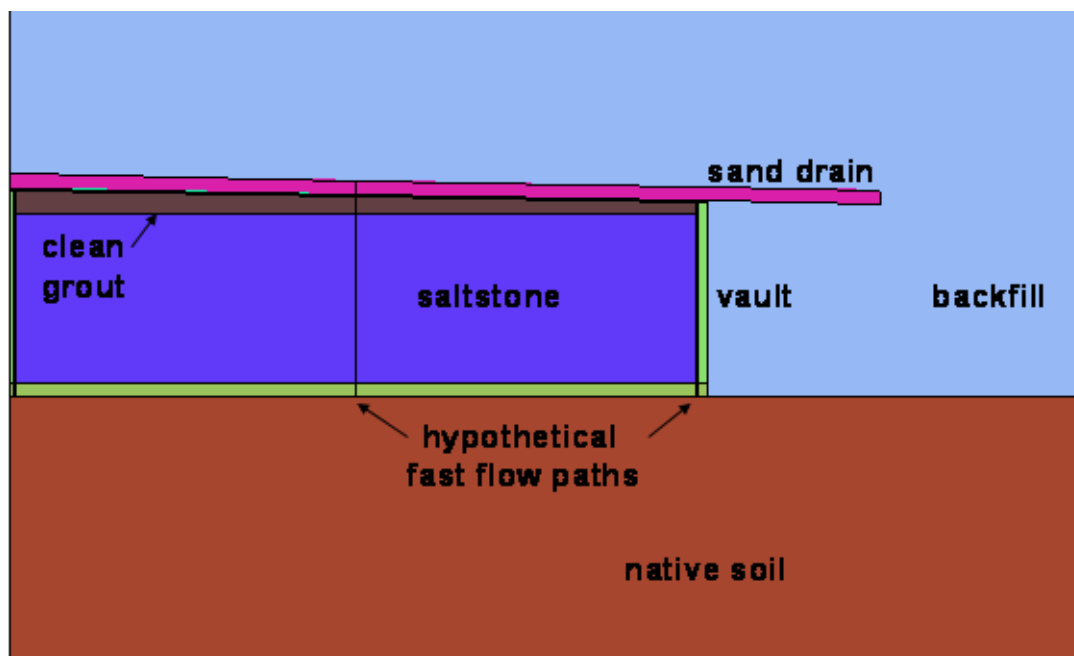


Figure 4.4-29: Vault 4 Gridding for PORFLOW Vadose Zone Modeling

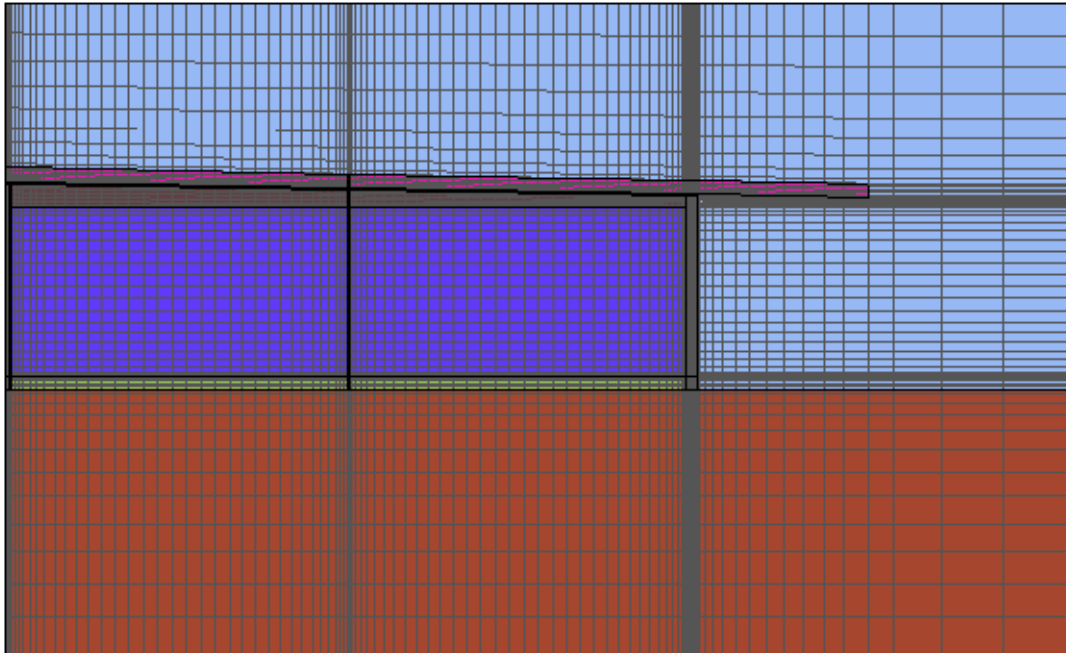


Figure 4.4-30: Vault 4 Upper Corner Detail for PORFLOW Vadose Zone Modeling

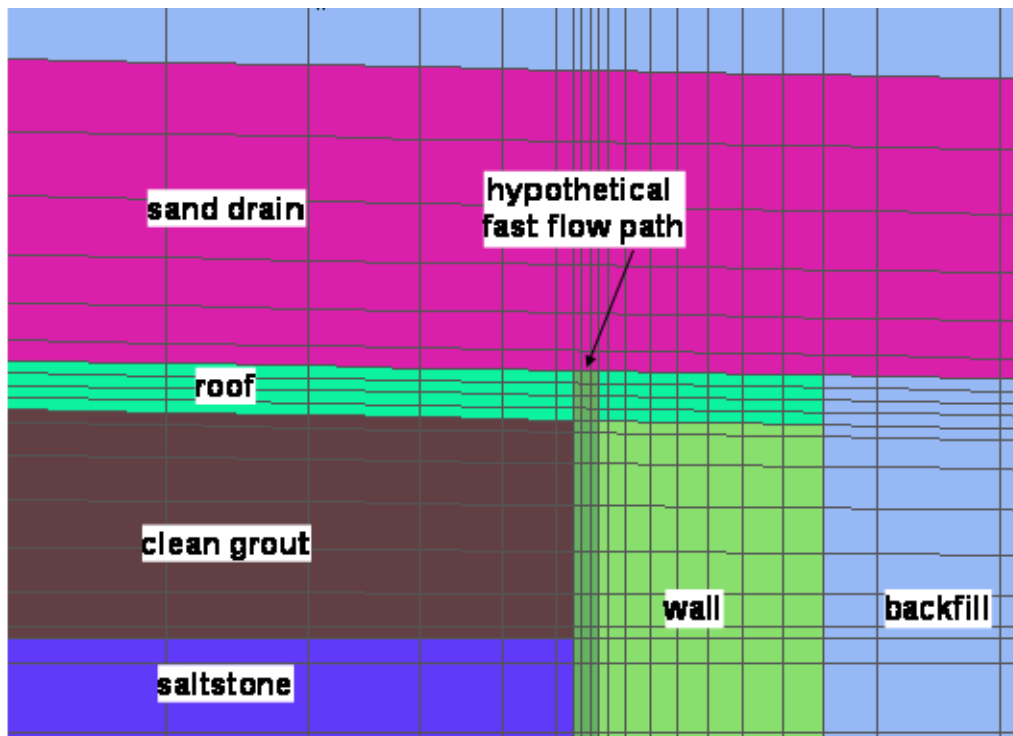
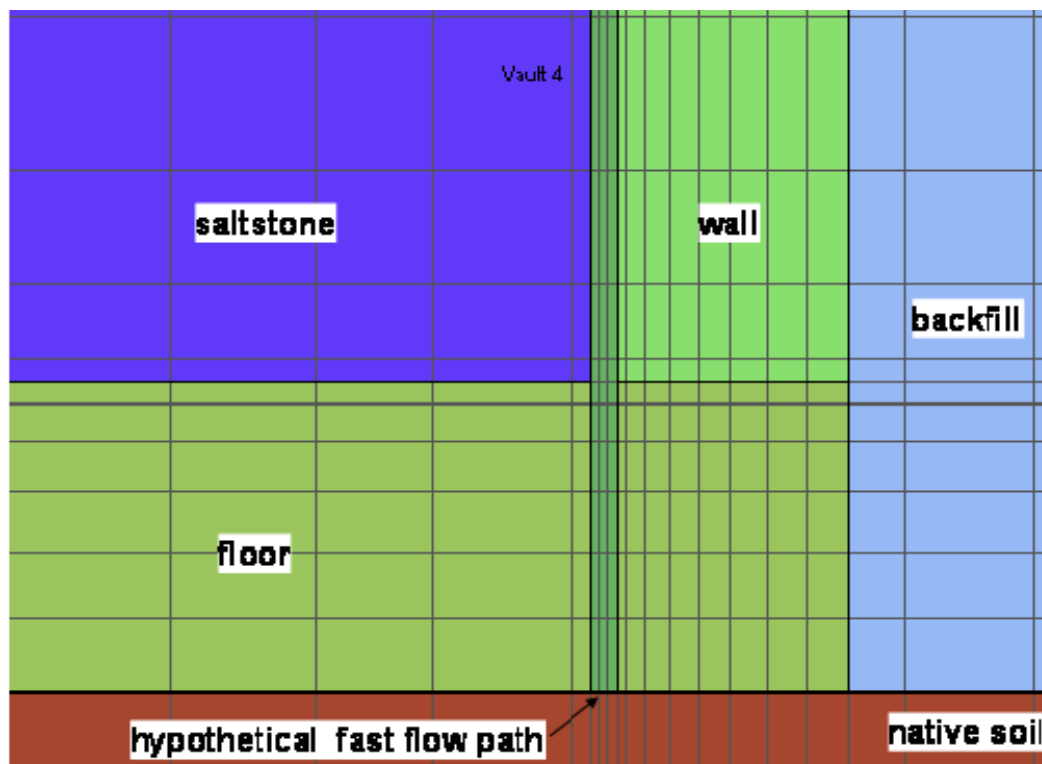
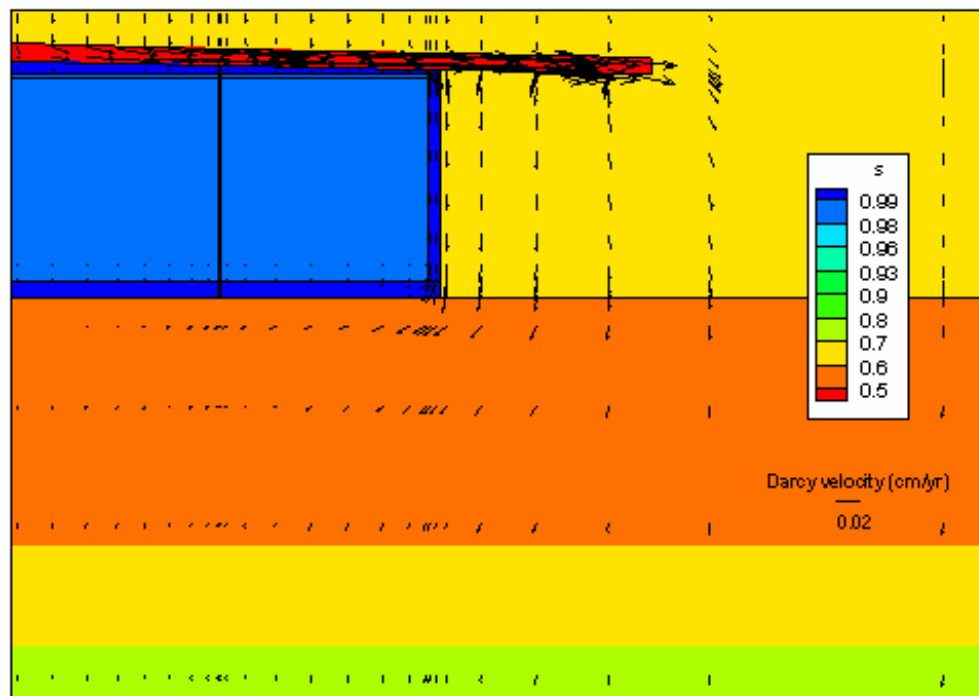


Figure 4.4-31: Vault 4 Lower Corner Detail for PORFLOW Vadose Zone Modeling



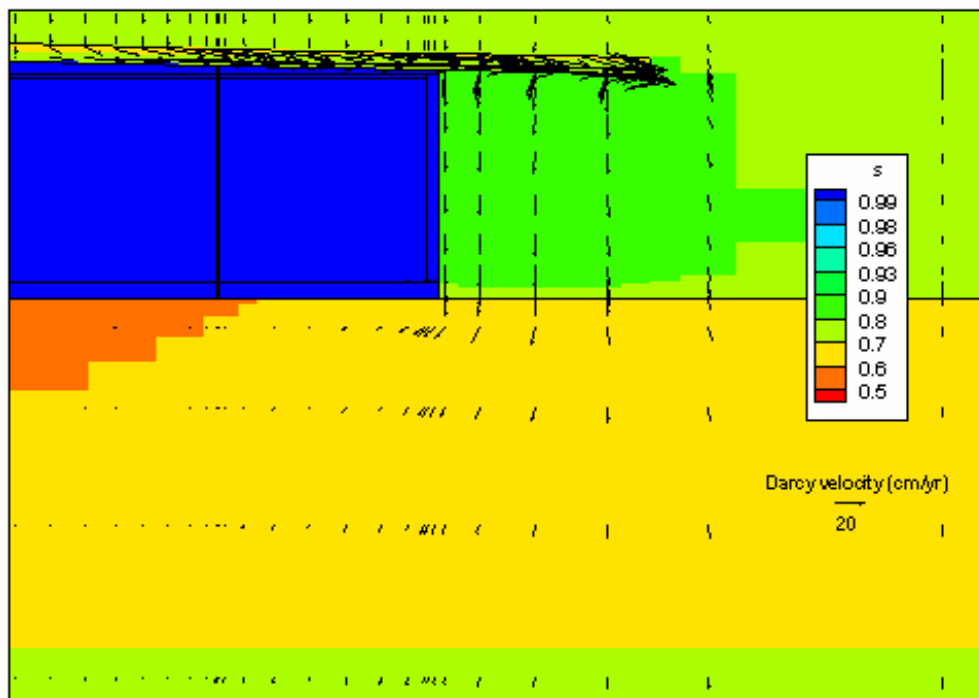
Depth to the water table was modeled as a uniform distance for each particular disposal unit type (i.e., one depth for all FDCs) using an average of the values in Table 4.2-13 for the associated disposal unit type. The chosen grid resolution was a compromise between two competing objectives; (1) resolution of thin geometric features (e.g., sheet drains, HDPE-GCL liners) and sharp flow field transitions (e.g., pond water flowing over roof edge), and (2) achieving reasonable computer storage and runtimes. Each grid extends at least 30 feet beyond the outside edge of a disposal unit to represent average conditions away from the disposal unit. At certain angles, obstructions such as adjacent FDCs are present at shorter distances. However, these features generally have an insignificant impact on water table flux. PORFLOW material properties for native, undisturbed soil utilize Section 4.2.3.2.2 parameters for vadose zone soil and Section 4.2.3.2.2 parameters for backfill soil. Figures 4.4-32 through 4.4-43 display the simulated flow fields for the various disposal unit types over time for the Base Case A simulations. The figures are color coded to show the areas of highest saturation (dark blue) and have arrows, which denote the Darcy Velocity. The figures show how PORFLOW models flow and how flow changes over time, affected by disposal unit changes (e.g., cap degradation, concrete degradation).

Figure 4.4-32: Vault 1 Saturation and Darcy Velocity Fields Base Case at 100 Years



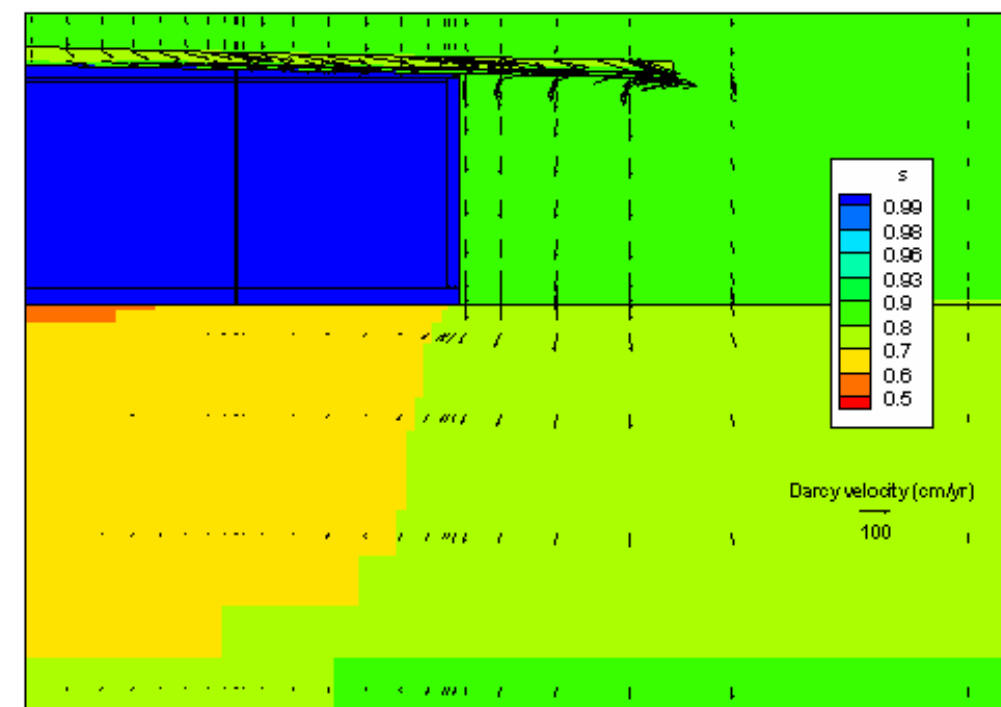
s = saturation

Figure 4.4-33: Vault 1 Saturation and Darcy Velocity Fields Base Case at 1,000 Years



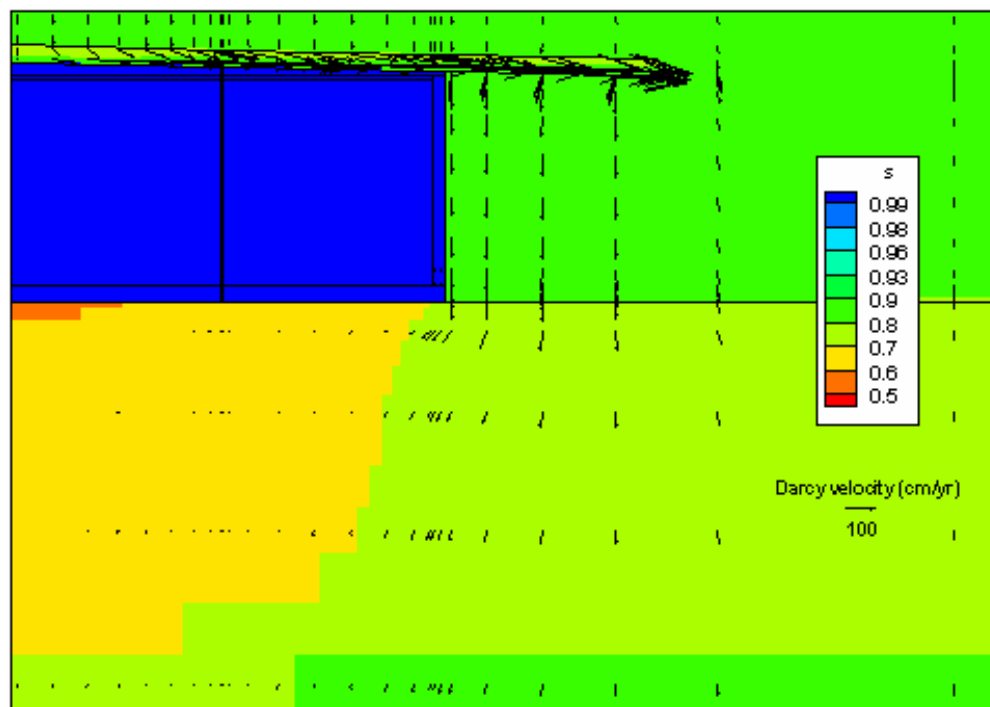
s = saturation

Figure 4.4-34: Vault 1 Saturation and Darcy Velocity Fields Base Case at 5,000 Years



s = saturation

Figure 4.4-35: Vault 1 Saturation and Darcy Velocity Fields Base Case at 10,000 Years



s = saturation

Figure 4.4-36: FDC Saturation and Darcy Velocity Fields Base Case at 100 Years

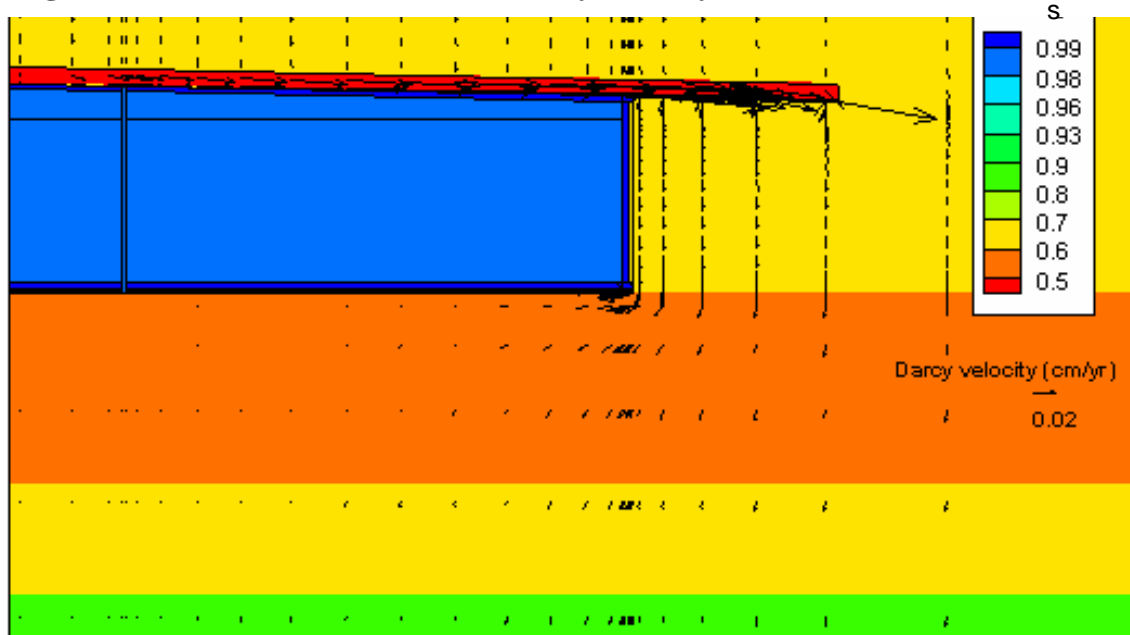


Figure 4.4-37: FDC Saturation and Darcy Velocity Fields Base Case at 1,000 Years

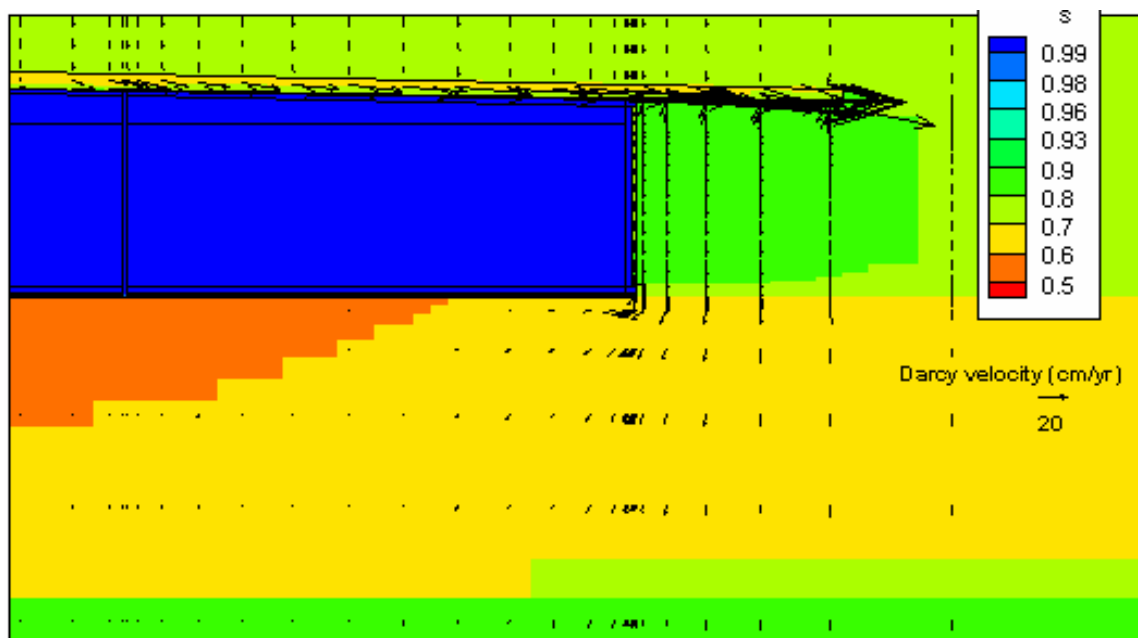


Figure 4.4-38: FDC Saturation and Darcy Velocity Fields Base Case at 5,000 Years

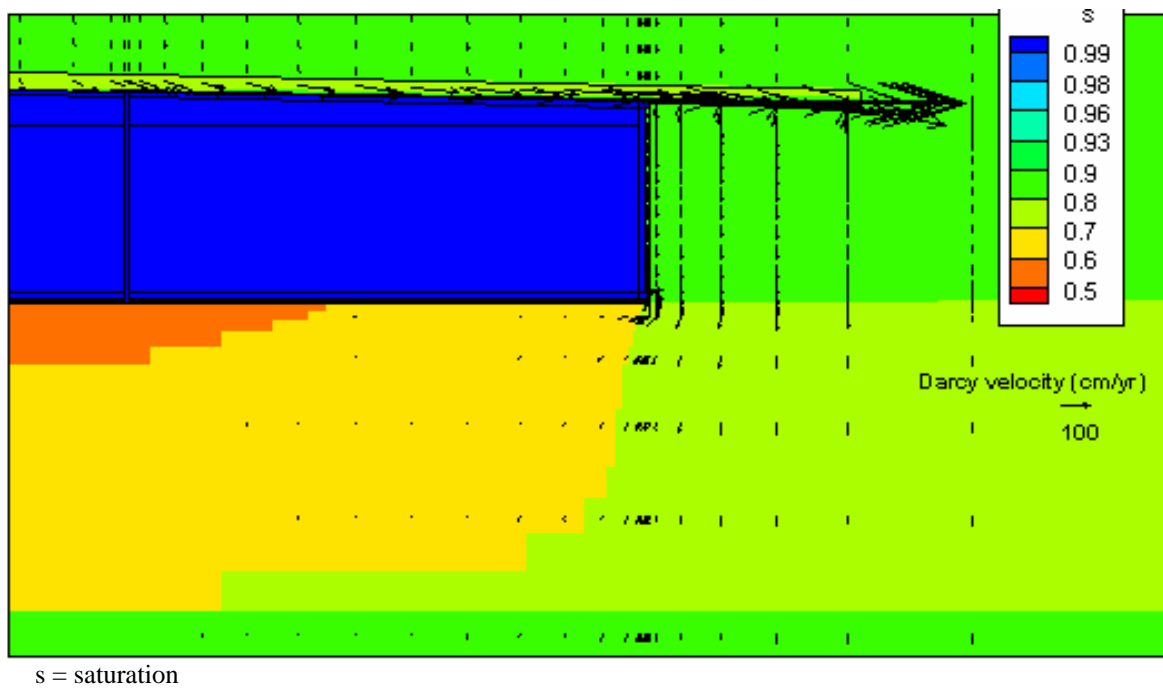


Figure 4.4-39: FDC Saturation and Darcy Velocity Fields Base Case at 10,000 Years

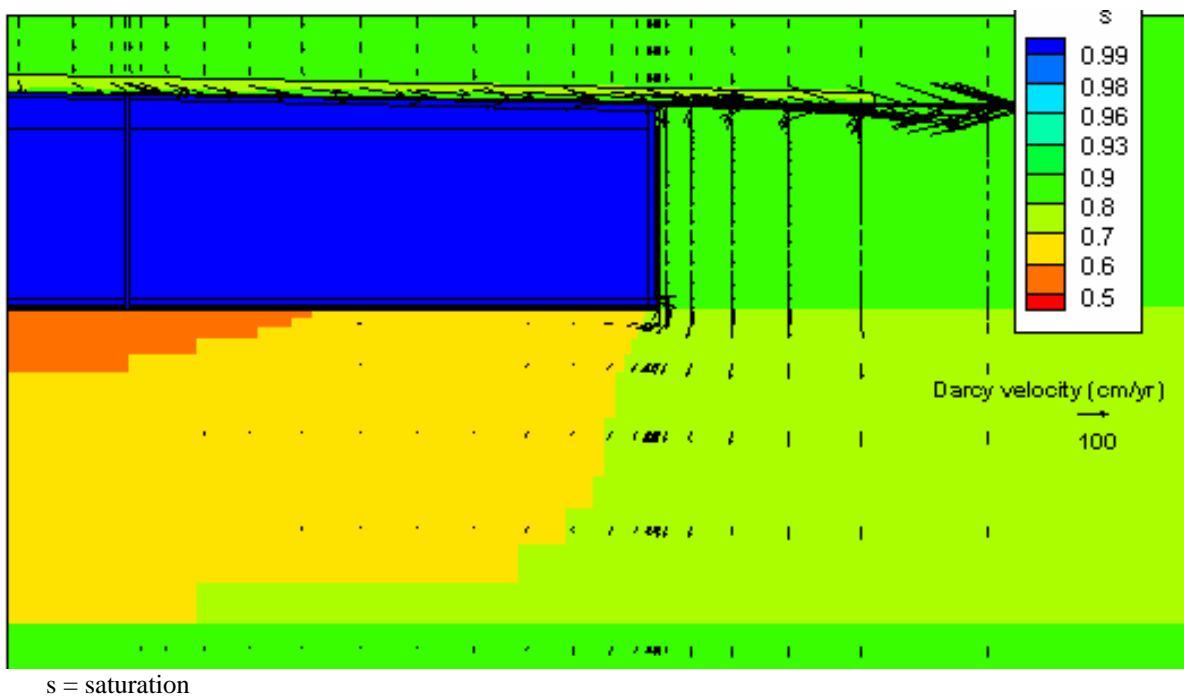


Figure 4.4-40: Vault 4 Saturation and Darcy Velocity Fields Base Case at 100 Years

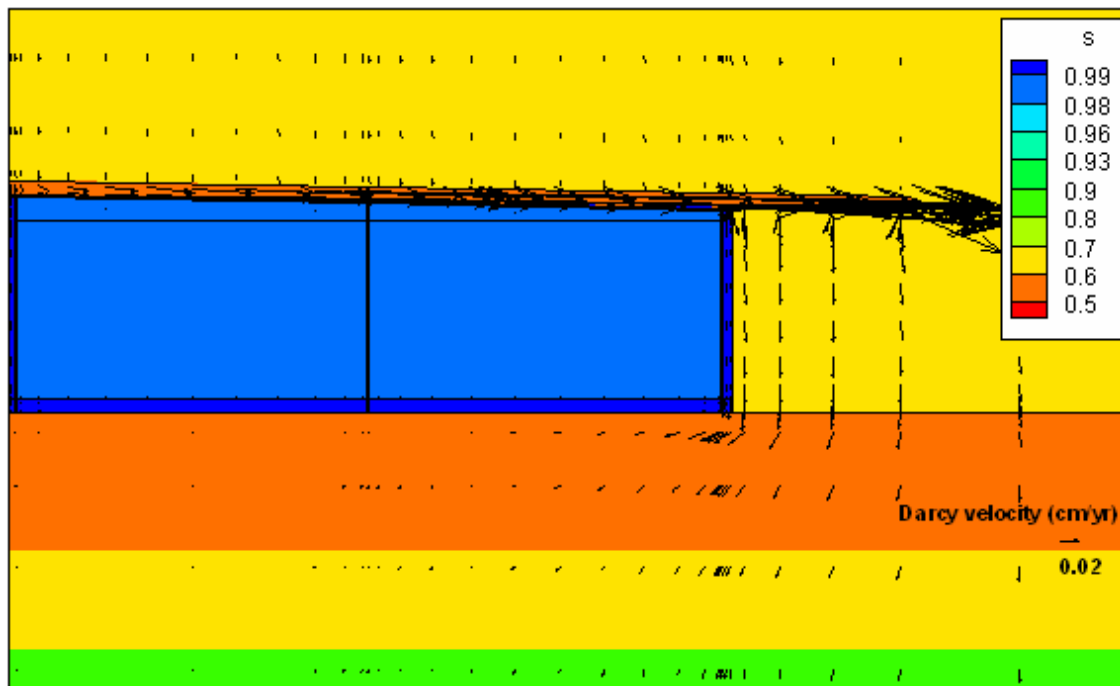


Figure 4.4-41: Vault 4 Saturation and Darcy Velocity Fields Base Case at 1,000 Years

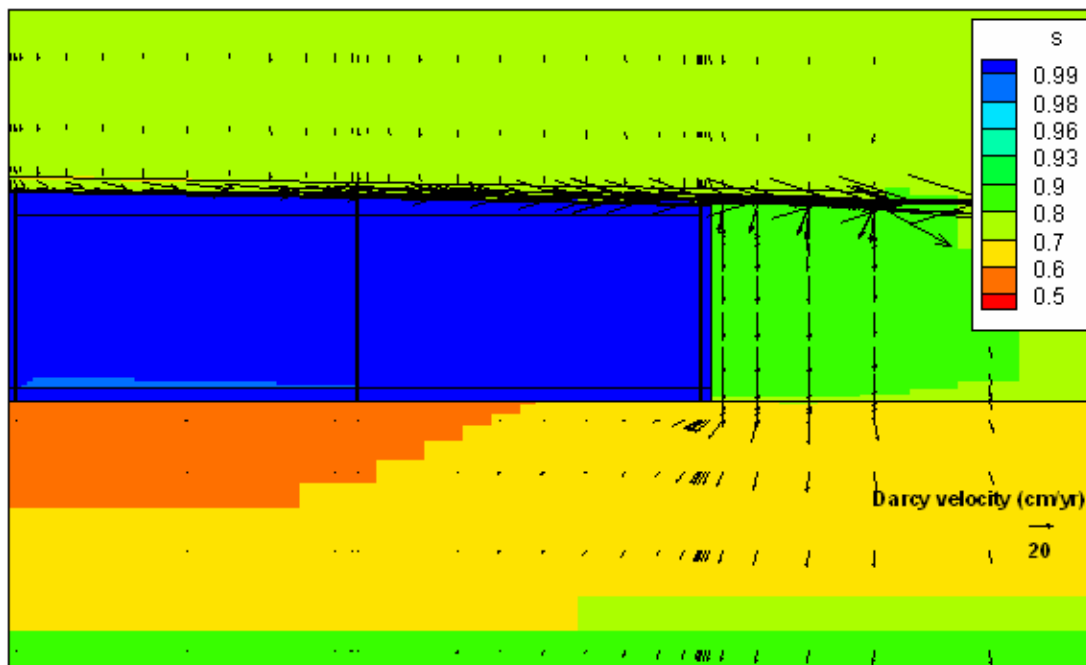
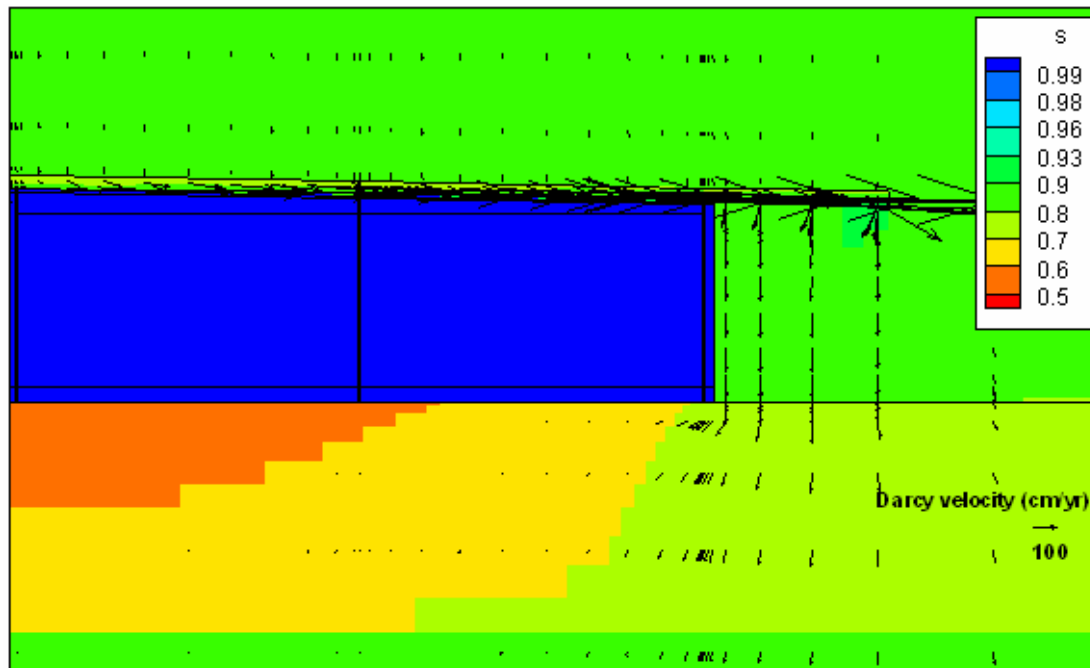
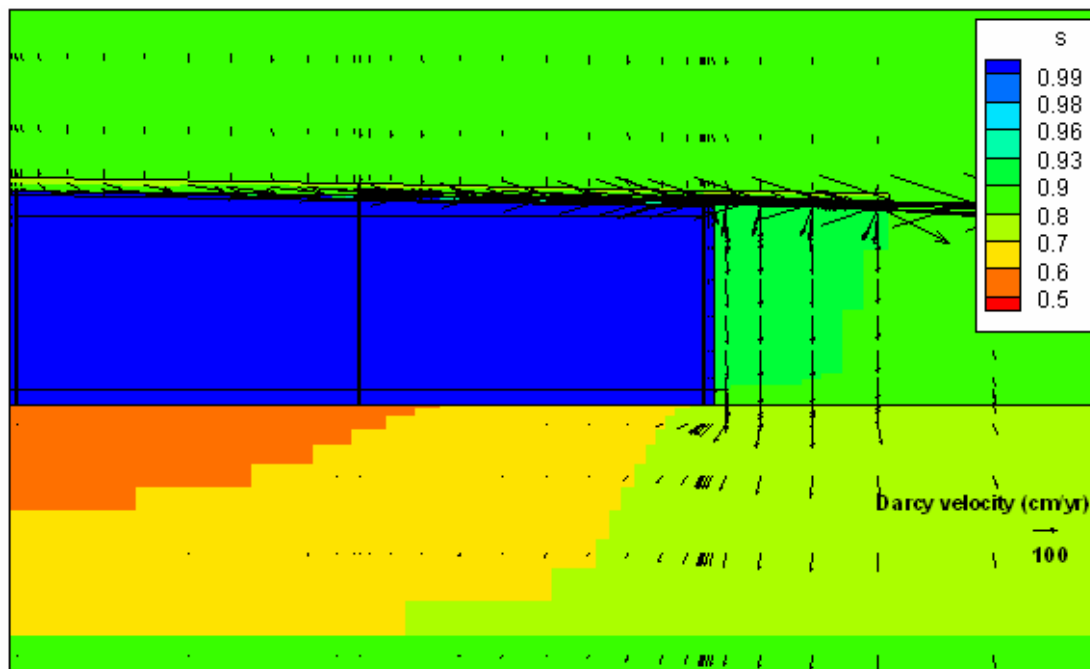


Figure 4.4-42: Vault 4 Saturation and Darcy Velocity Fields Base Case at 5,000 Years



s = saturation

Figure 4.4-43: Vault 4 Saturation and Darcy Velocity Fields Base Case at 10,000 Years



s = saturation

Hydrodynamic dispersion is a result of molecular diffusion and differential small-scale advective transport due to porous-medium heterogeneity. These plume spreading processes were controlled in PORFLOW modeling through specification of a D_e and longitudinal and transverse dispersivities, respectively. A non-zero diffusion coefficient was assigned in vadose transport modeling (e.g., Table 4.2-19). However, dispersivities were set to zero because most materials are homogeneous (e.g., concrete) or relatively so (e.g., backfilled soil). This modeling assumption somewhat underestimated plume spreading in the vadose zone, which generally produced higher peak fluxes at the water table. Preferential flow pathways through cracks, fractures, or other discrete features were modeled using one of two methods, depending on scale. Small-scale features were implicitly represented as a general increase in saturated hydraulic conductivity within a porous medium formulation. Large-scale features were explicitly represented in a porous medium formulation as discrete zones of high permeability (e.g., sand seam). A porous, rather than fractured, medium approach was considered desirable because; (1) smaller scale crack/fracture geometry and other properties have not been quantitatively defined for the degraded material of interest; and (2) the scenarios of interest for the SDF PA can be adequately represented in the simpler porous medium approach.

Material properties were independently defined for each grid zone, but are not necessarily different, depending on scenario. Properties were defined as the product of three factors:

- Base value from a materials palette, a time-invariant constant
- Time-dependent factor (1), typically intended to represent baseline physical changes
- Time-dependent factor (2), typically intended for uncertainty/sensitivity analysis perturbations

The materials palette used in PORFLOW SDF modeling is provided in Table 4.4-10, as taken from SRNL-STI-2009-000115 Table 13. The latter two factors defining properties can be arbitrary piecewise-linear functions. They are functionally identical, and differ only in intended usage.

Water flux results were recorded at a 1 year frequency and aquifer concentrations were monitored on 20 year intervals. Tc-99 vadose zone simulations were run at a 0.05 year time-step to avoid numerical inaccuracies. The selected step sizes were a compromise between two competing objectives; (1) resolution of concentration peaks from relatively mobile species that migrate as a pulse, and (2) achieving reasonable computer runtimes. A 20 year recording frequency for aquifer concentrations avoided significantly slower runtimes caused by frequent accessing of many output files. Aquifer simulations for selected cases and species were re-run at a 1 year time-step and data recording frequency to validate the choice of a 2.5 year time-step and 20 year monitoring frequency. The results from these base model and sensitivity runs included peak groundwater concentrations at 100m regardless of aquifer and sector. Comparing these groundwater peak concentrations between the 1 year time-step model and the base model time-steps indicated that the greatest difference was less than 2% on peak concentration and a variance of no more than 12 years for the incidence of peak concentration. For transport modeling, a fixed time-step of 1 year was chosen for vadose zone simulations and 2.5 years for the saturated zone.

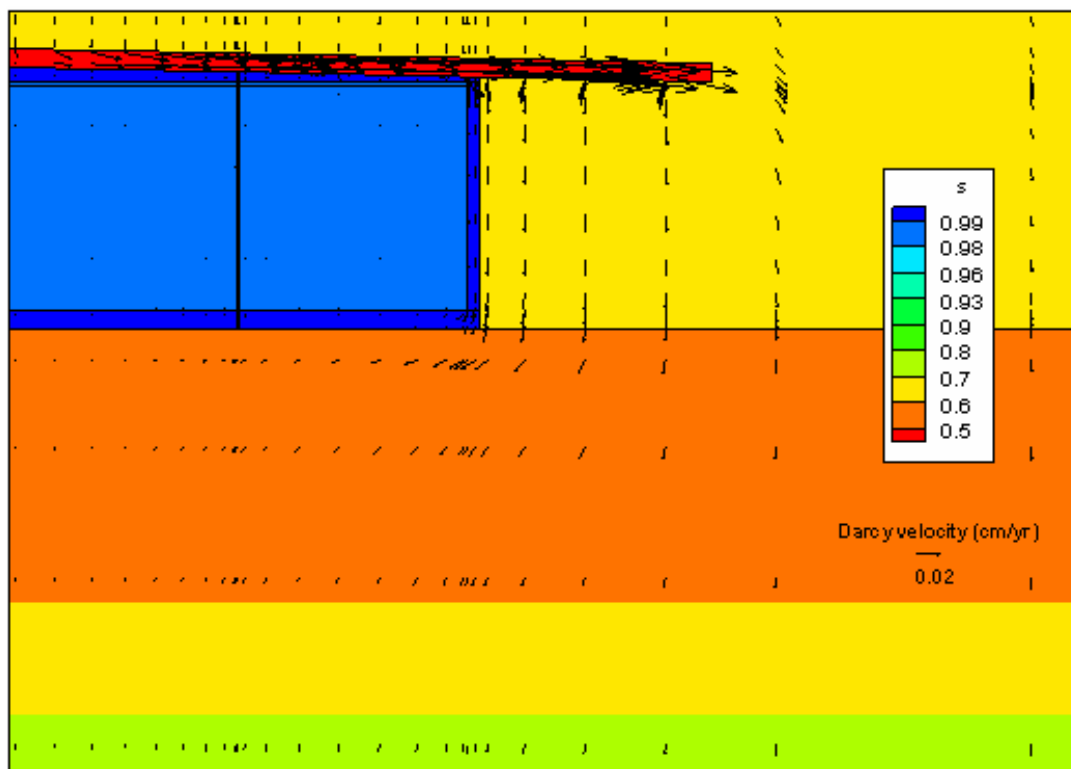
Table 4.4-10: PORFLOW Materials Palette for SDF

| Material | Horizontal conductivity | Vertical conductivity | Effective Diffusion Coefficient | Porosity | Bulk density | Particle density | Soil curves |
|-----------------------|-------------------------|-----------------------|---------------------------------|-----------------|----------------------------|----------------------------|--------------------|
| numerical model id | K_h cm/s | K_v cm/s | D_e cm ² /s | η unitless | ρ_b g/cm ³ | ρ_s g/cm ³ | numerical model id |
| native_soil | 3.3E-04 | 9.1E-05 | 5.3E-06 | 0.39 | 1.62 | 2.66 | LowerVz |
| backfill | 7.6E-05 | 4.1E-05 | 5.3E-06 | 0.35 | 1.71 | 2.63 | CcBackfill |
| Sand | 5.0E-04 | 2.8E-04 | 8.0E-06 | 0.38 | 1.65 | 2.66 | Sand |
| Gravel | 1.5E-01 | 1.5E-01 | 9.4E-06 | 0.30 | 1.82 | 2.60 | Gravel |
| vault1_wall_uncracked | 3.1E-10 | 3.1E-10 | 5.0E-08 | 0.120 | 2.24 | 2.55 | Concrete_Qhigh |
| vault1_wall | 1.67E-01 | 1.7E-01 | 5.0E-08 | 0.120 | 2.24 | 2.55 | FracturedConcrete |
| vault1_floor | 3.1E-10 | 3.1E-10 | 5.0E-08 | 0.120 | 2.24 | 2.55 | Concrete_Qhigh |
| vault1_roof | 5.0E-09 | 5.0E-09 | 1.0E-07 | 0.145 | 2.20 | 2.57 | Concrete_Qmedium |
| vault4_wall_uncracked | 3.1E-10 | 3.1E-10 | 5.0E-08 | 0.120 | 2.24 | 2.55 | Concrete_Qhigh |
| vault4_wall | 1.67E-01 | 1.7E-01 | 5.0E-08 | 0.120 | 2.24 | 2.55 | FracturedConcrete |
| vault4_floor | 3.1E-10 | 3.1E-10 | 5.0E-08 | 0.120 | 2.24 | 2.55 | Concrete_Qhigh |
| vault4_roof | 5.0E-09 | 5.0E-09 | 1.0E-07 | 0.136 | 2.21 | 2.56 | Concrete_Qmedium |
| vault2_wall | 9.3E-11 | 9.3E-11 | 5.0E-08 | 0.110 | 2.22 | 2.49 | Concrete_Qhigh |
| vault2_floor | 9.3E-11 | 9.3E-11 | 5.0E-08 | 0.110 | 2.22 | 2.49 | Concrete_Qhigh |
| vault2_roof | 9.3E-11 | 9.3E-11 | 5.0E-08 | 0.110 | 2.22 | 2.49 | Concrete_Qhigh |
| saltstone | 2.0E-09 | 2.0E-09 | 1.0E-07 | 0.580 | 1.01 | 2.40 | Saltstone |
| saltstone_cracked | 1.67E-03 | 1.7E-03 | 1.0E-07 | 0.580 | 1.01 | 2.40 | FracturedSaltstone |
| z_clean_cap | 2.0E-09 | 2.0E-09 | 1.0E-07 | 0.580 | 1.01 | 2.40 | Saltstone |
| HDPE | 2.0E-13 | 2.0E-13 | 4.0E-11 | 0.30 | 1.50 | 2.14 | CcBackfill |
| HDPE_GCL | 2.8E-12 | 2.8E-12 | 1.2E-10 | 0.30 | 1.50 | 2.14 | CcBackfill |
| concrete_mat | 1.0E-08 | 1.0E-08 | 8.0E-07 | 0.211 | 2.06 | 2.61 | Concrete_Qlow |
| sheet_drain | 1.5E-01 | 1.5E-01 | 9.4E-06 | 0.30 | 1.82 | 2.60 | Gravel |
| sand_drain | 5.0E-02 | 5.0E-02 | 8.0E-06 | 0.417 | 1.65 | 2.66 | Sand |
| impervious | 5.0E-15 | 5.0E-15 | 1.0E-13 | 0.30 | 1.50 | 2.14 | Concrete_Qmedium |
| column_crack | 5.0E-04 | 2.8E-04 | 8.0E-06 | 0.38 | 1.65 | 2.66 | Sand |

➤ **Fast Flow Path Modeling
in PORFLOW**

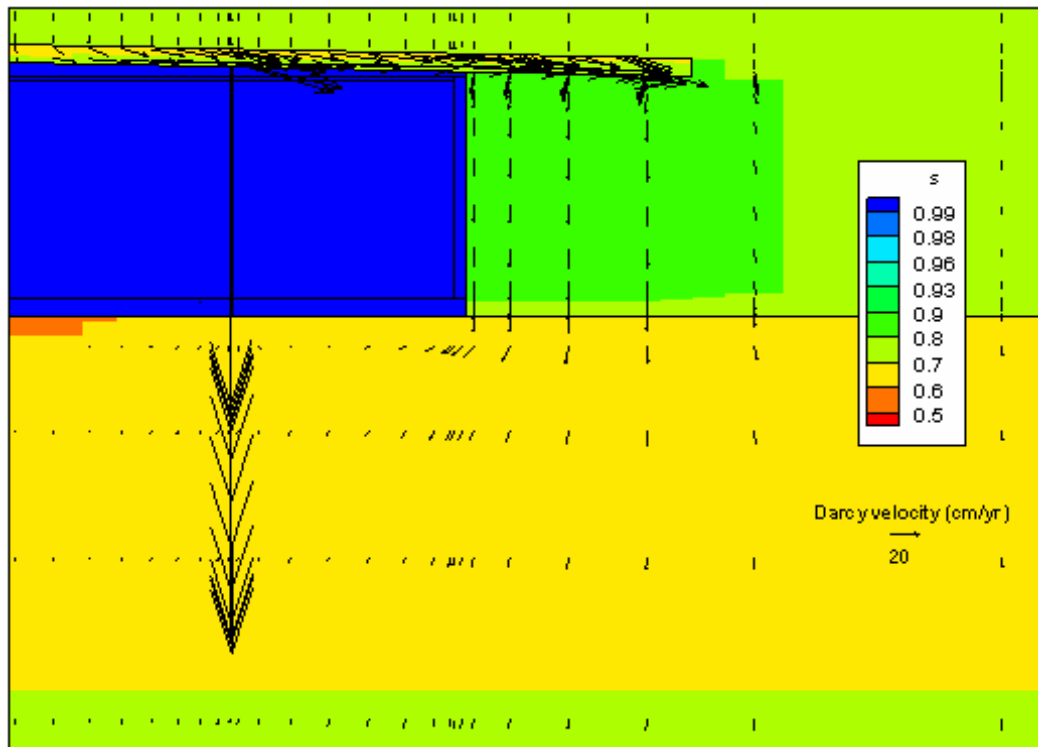
PORFLOW was used early in the analysis process to do scoping runs for the various degradation cases described in Section 4.4.2. To represent the effect of a hypothetical fast flow path through a disposal unit, the PORFLOW model incorporated a high conductivity vertical leg extending through the roof and floor to form a conduit between the sand drain and undisturbed soil beneath the disposal unit. For the FDCs, this fast flow path was modeled as a radial slice (i.e., fast flow ring) through the entire axisymmetric model. The materials occupying the fast flow zones were assumed to have high conductivity and diffusion coefficient relative to backfilled and native soils, and no adsorption was assumed (i.e., $K_d = 0$ for all radiological and chemical transport). The hypothetical fast flow paths collect water that would otherwise be shed off the disposal unit roof, and direct it to the interior of the disposal unit where it can contact saltstone waste. Figures 4.4-44 through 4.4-55 display simulated flow fields for the various disposal unit types over time for fast flow path Case C. Arrows on the plots are proportional to Darcy Velocity, and indicate high values in the hypothetical fast flow paths, especially at later times when cap infiltration is higher. As discussed in Section 4.4.2, each disposal unit had unique fast flow path assumptions based on their specific design (e.g., Vault 1 did not assume a sheet drain fast flow path because there are no sheet drains in Vault 1).

Figure 4.4-44: Vault 1 Saturation and Darcy Velocity Fields Fast Flow Path Case C at 100 Years



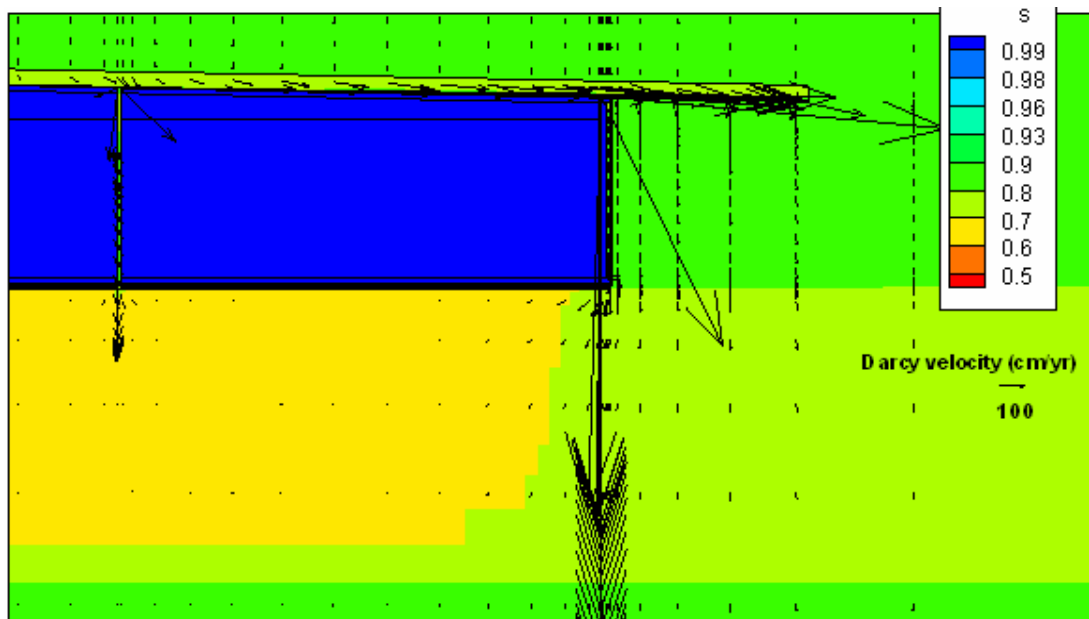
s = saturation

Figure 4.4-45: Vault 1 Saturation and Darcy Velocity Fields Fast Flow Path Case C at
1,000 Years



s = saturation

Figure 4.4-46: Vault 1 Saturation and Darcy Velocity Fields Fast Flow Path Case C at
5,000 Years



s = saturation

Figure 4.4-47: Vault 1 Saturation and Darcy Velocity Fields Fast Flow Path Case C at 10,000 Years

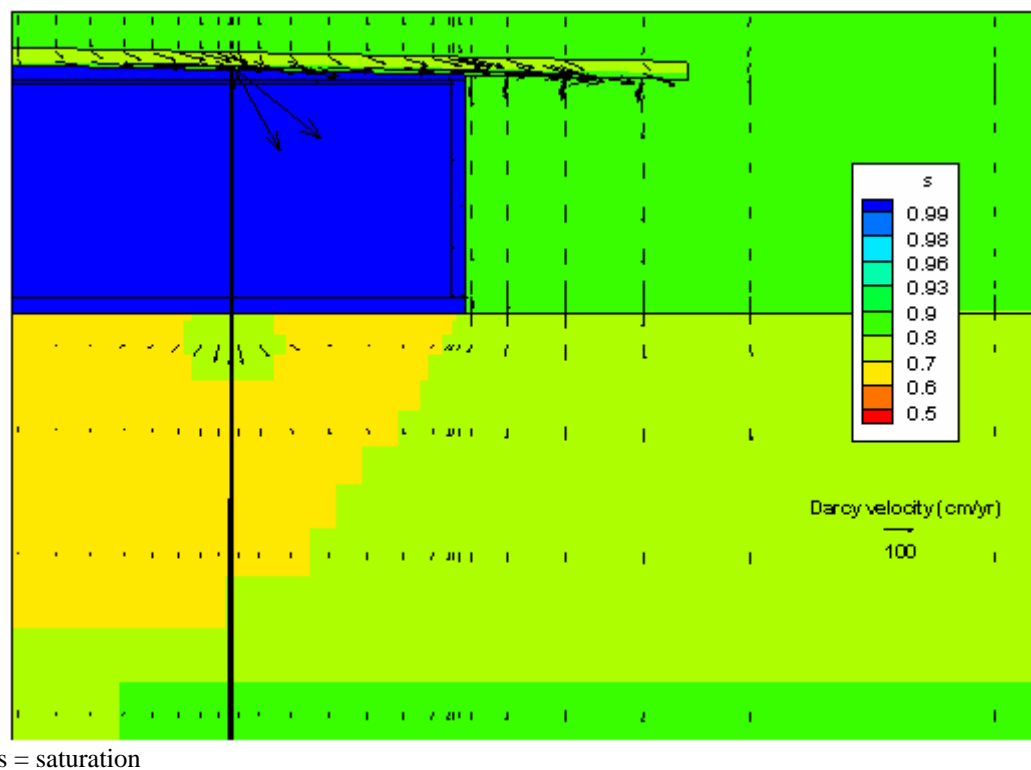


Figure 4.4-48: FDC Saturation and Darcy Velocity Fields Fast Flow Path Case C at 100 Years

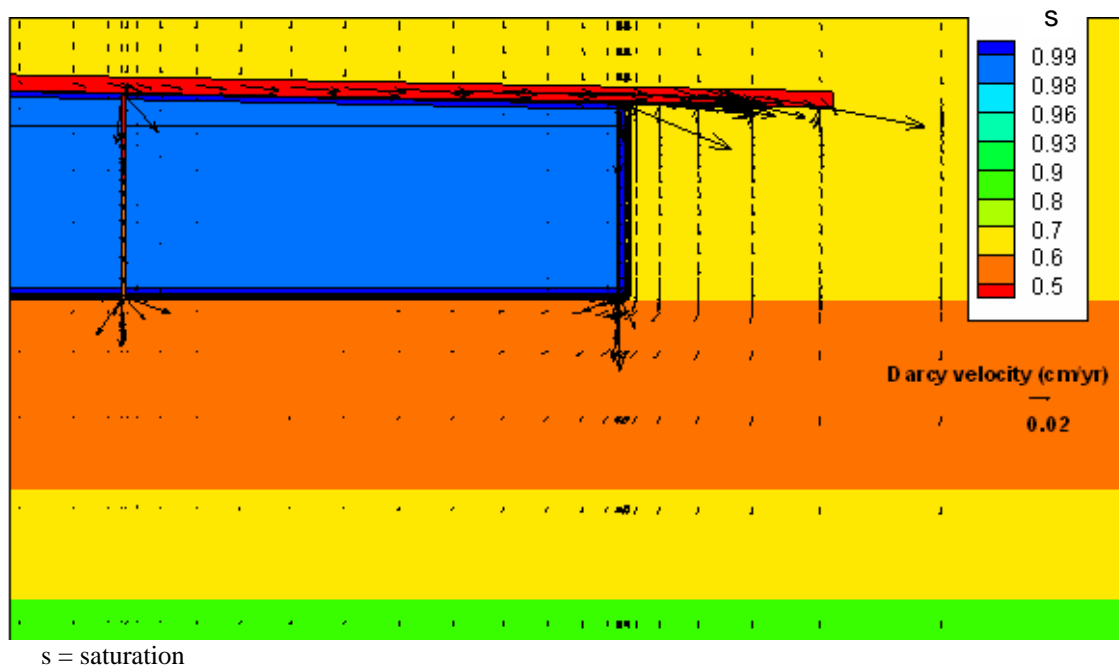
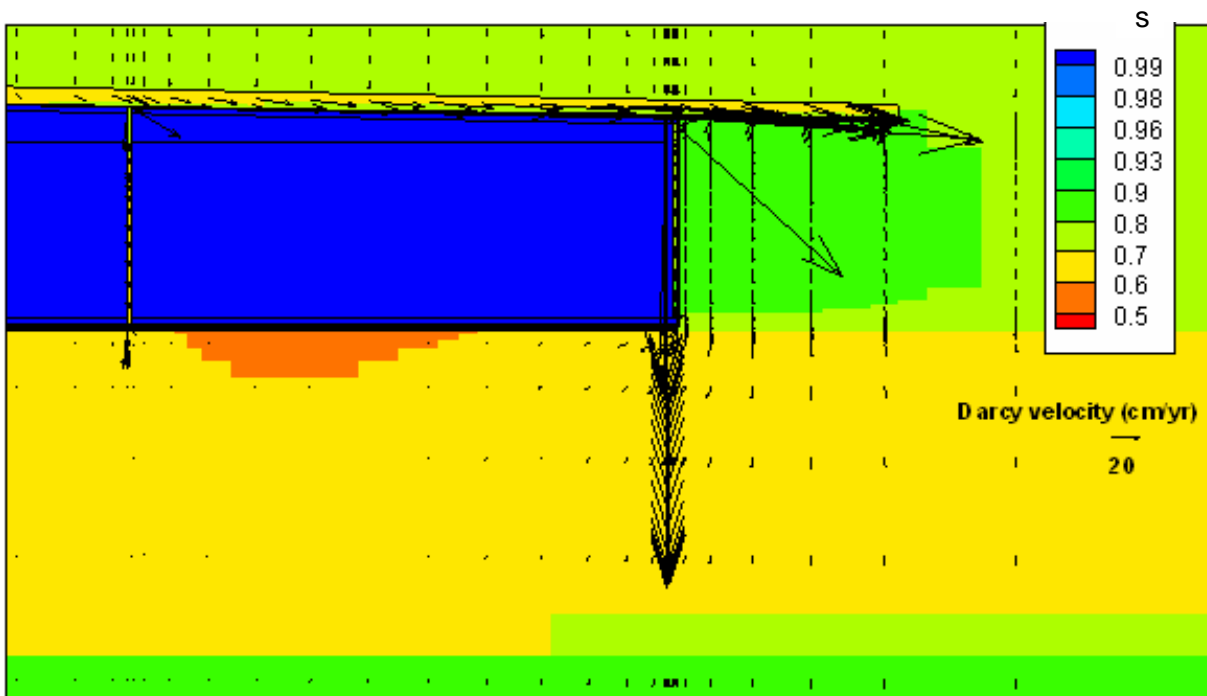
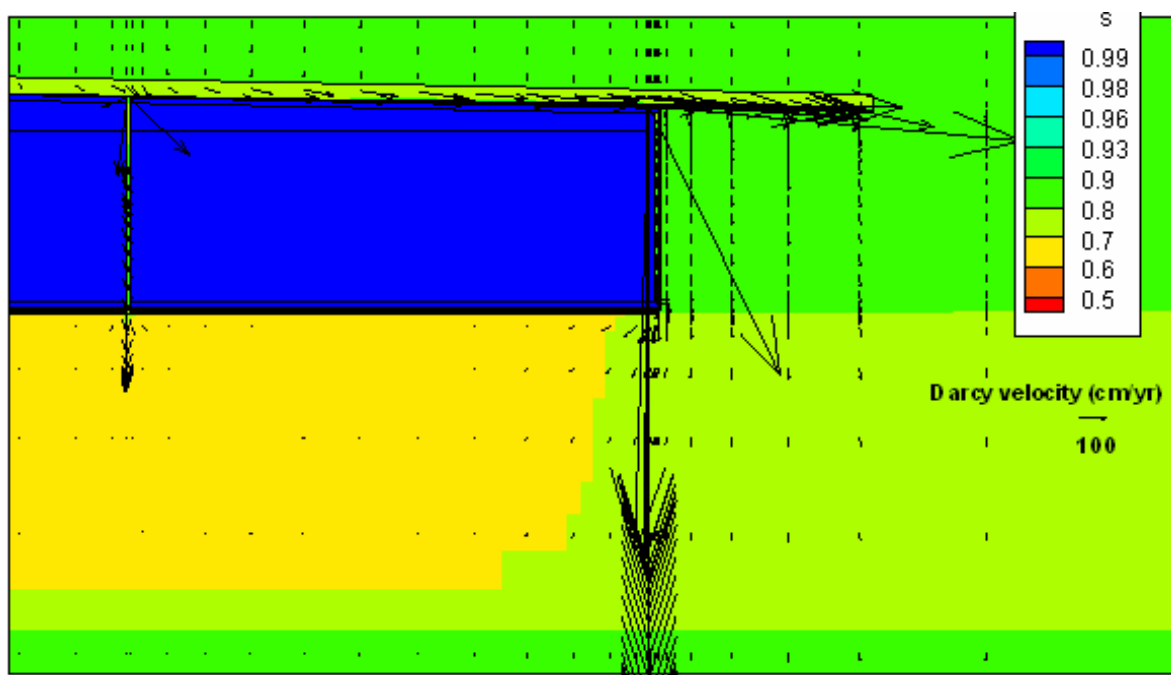


Figure 4.4-49: FDC Saturation and Darcy Velocity Fields Fast Flow Path Case C at 1,000 Years



s = saturation

Figure 4.4-50: FDC Saturation and Darcy Velocity Fields Fast Flow Path Case C at 5,000 Years



s = saturation

Figure 4.4-51: FDC Saturation and Darcy Velocity Fields Fast Flow Path Case C at 10,000 Years

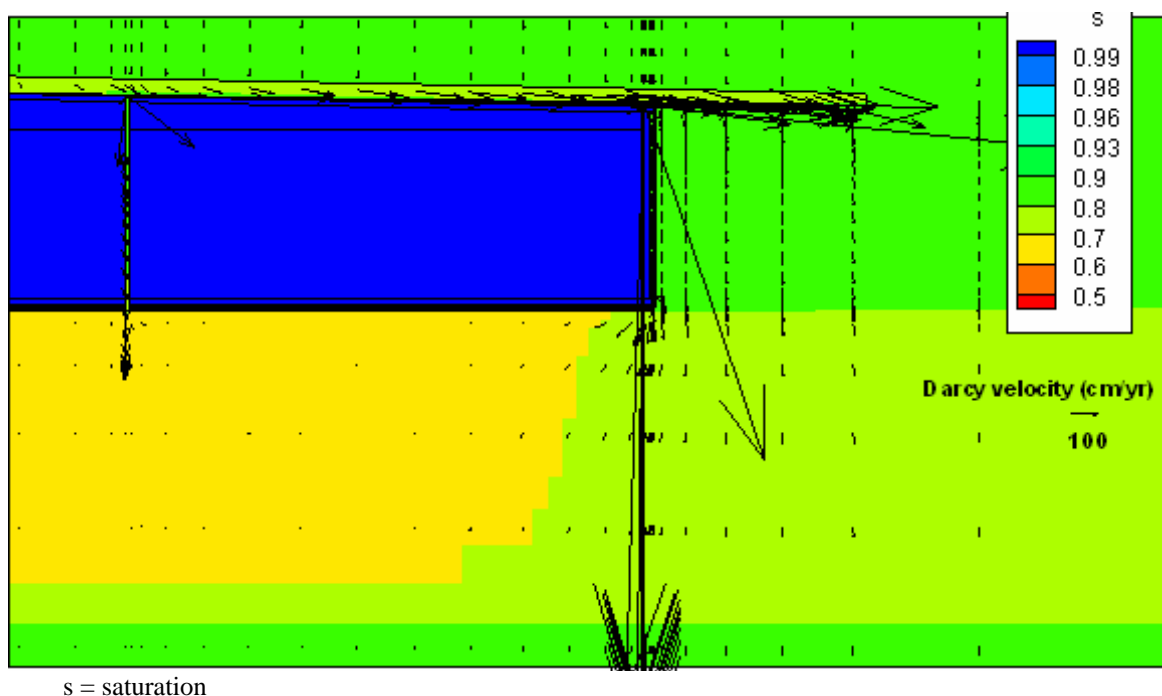


Figure 4.4-52: Vault 4 Saturation and Darcy Velocity Fields Fast Flow Path Case C at 100 Years

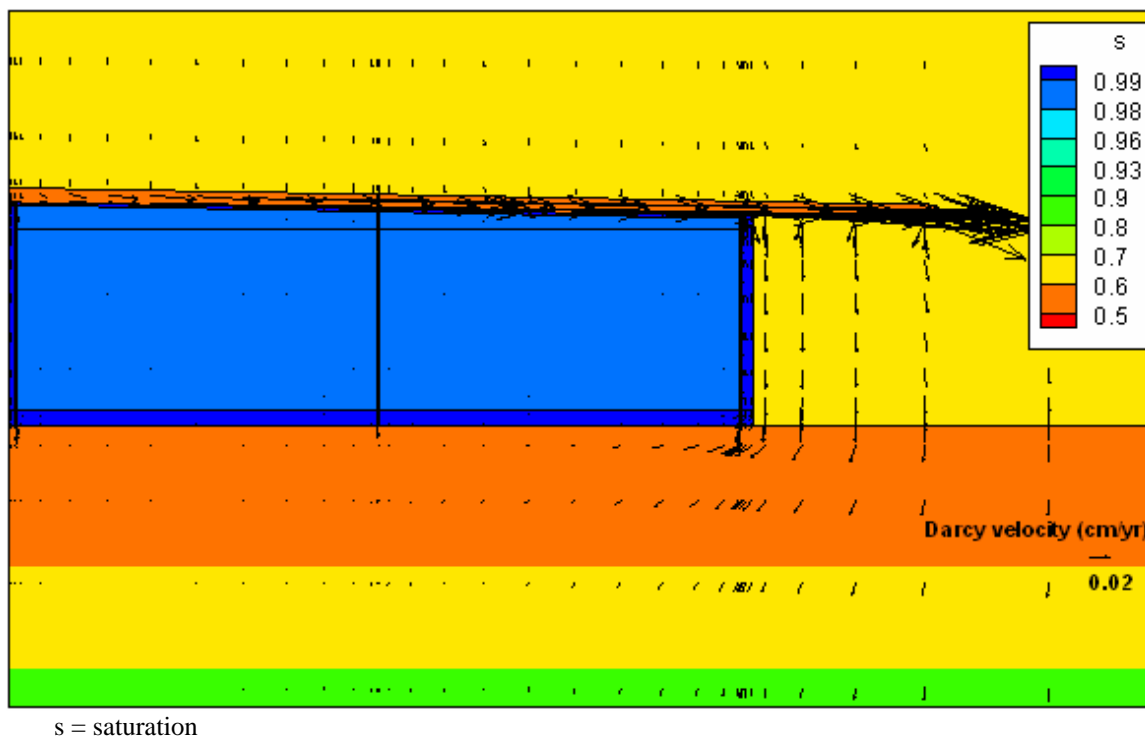


Figure 4.4-53: Vault 4 Saturation and Darcy Velocity Fields Fast Flow Path Case C at
1,000 Years

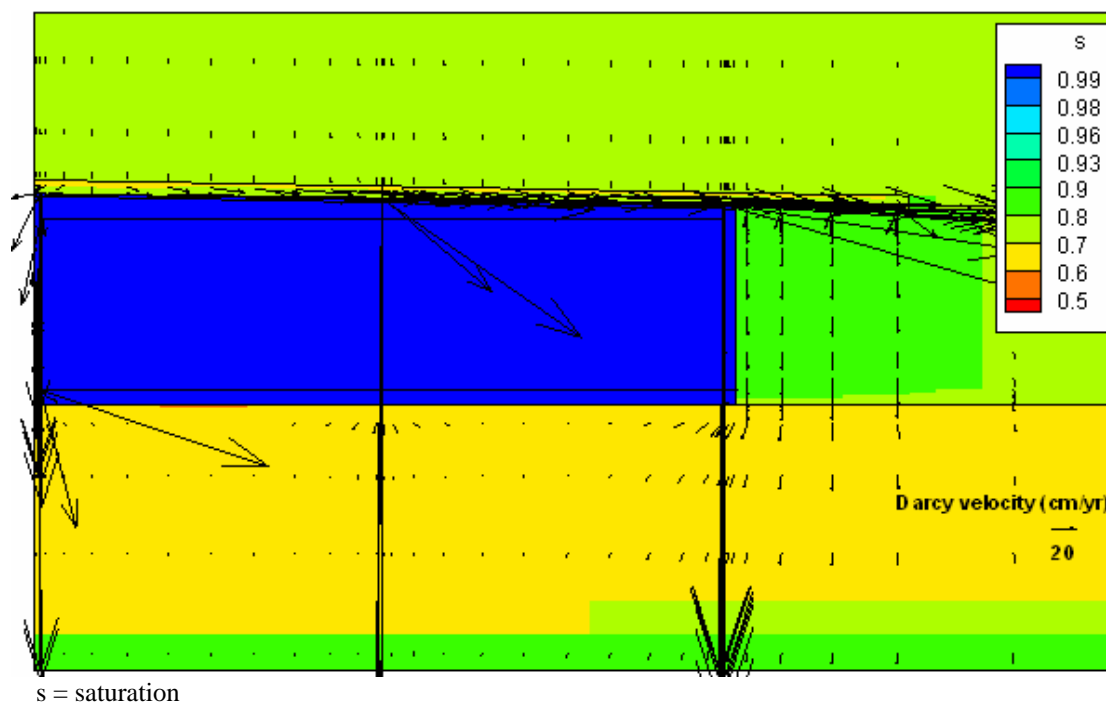


Figure 4.4-54: Vault 4 Saturation and Darcy Velocity Fields Fast Flow Path Case C at
5,000 Years

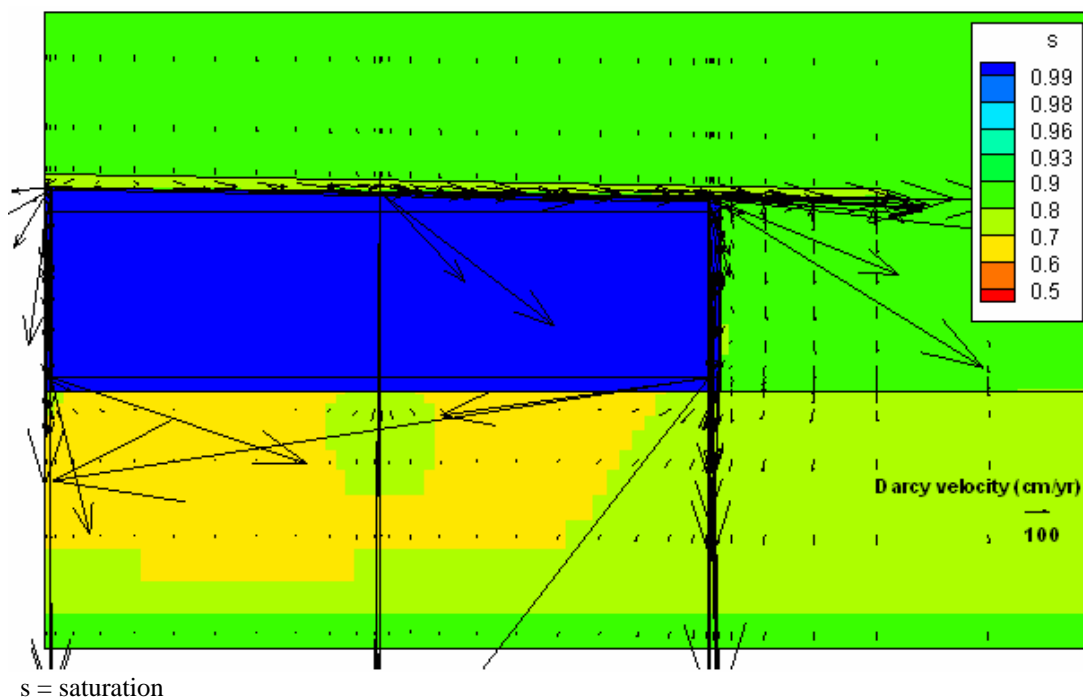
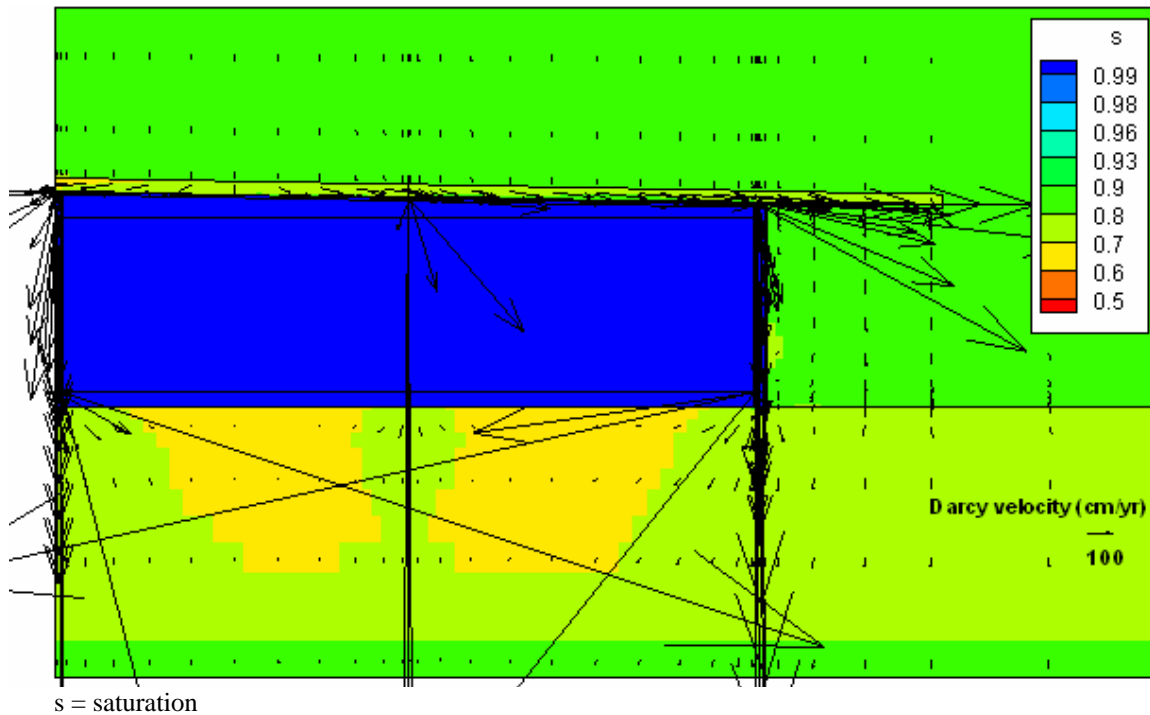


Figure 4.4-55: Vault 4 Saturation and Darcy Velocity Fields Fast Flow Path Case C at 10,000 Years



➤ **Vadose and Aquifer Model Validation in PORFLOW**

Additional PORFLOW validation was performed beyond code verification exercises and GSA/SDF model development. Using characterization and monitoring data, aspects of the PORFLOW vadose zone and aquifer models were validated against independent field data, as identified below. Additional detail can be obtained in the associated references.

Vadose zone

- Soil suction and water content from Vadose Zone Monitoring System (VZMS) in E-Area [WSRC-STI-2006-00198, Section 5.8]
- Tracer test pore velocity [WSRC-TR-2007-00283, Section 4.0]
- Tritium migration beneath the E-Area Slit Trenches

Aquifer

- Surveyed seepines [WSRC-TR-2004-00106]
- Pathline comparisons to existing plumes (herein)

The VZMS monitors soil conditions beneath and alongside solid waste disposal trenches in E-Area under uncapped infiltration conditions (Figure 4.4-56). E-Area is located in the GSA. Field measurements using tensiometers and neutron probes indicate that soil suction ranges from approximately 50 to 200 cm, while water content varies between approximately 0.15

and 0.30. The latter values suggest water saturation between 35% and 75%. Infiltration over the affected area was estimated to be 30 cm/yr (12 in/yr). Using the “Upper Vadose Zone” and “Lower Vadose Zone” soil properties recommended in WSRC-STI-2006-00198 and adopted for SDF PA modeling, a PORFLOW representation of E-Area conditions produced suction head and saturation values of 83 cm and 91% in the upper vadose zone, and 170 cm and 72% in the lower vadose zone.

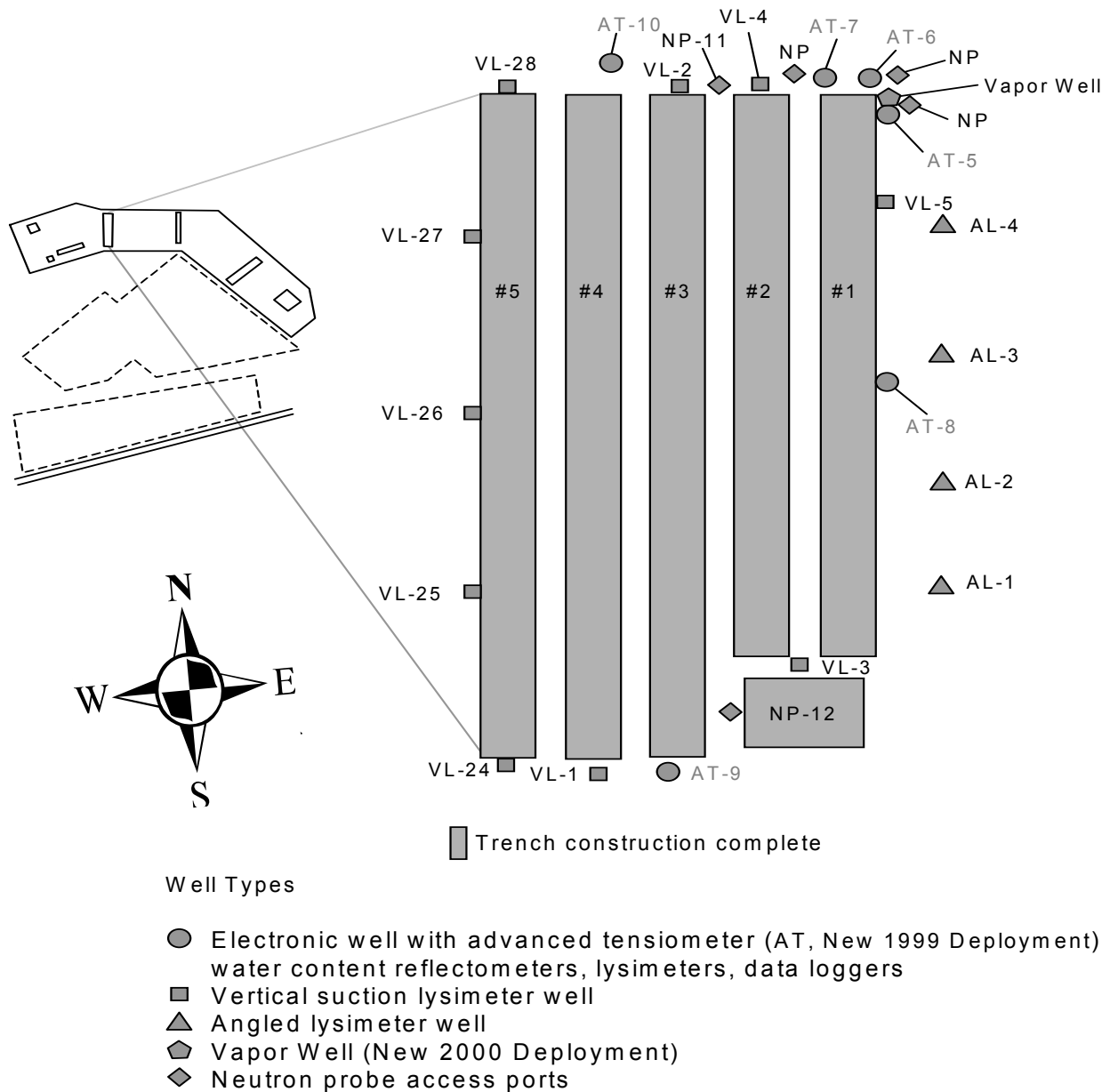
A series of field and laboratory tracer experiments have been conducted at SRS under uncapped (normal infiltration) conditions. The PORFLOW model described above produced pore velocities of approximately 34 in/yr and 43 in/yr for the upper and lower vadose zones. Together, the tracer test data indicated a pore velocity of approximately 45 in/yr for the same infiltration, which was similar to the model simulations.

A PORFLOW vadose zone model, similar to that used for SDF PA simulations, was compared to tritium concentration data from the VZMS (Figure 4.4-57). Concentration data was grouped according to elevation (high/low) and location (center/edge), relative to a disposal trench (Figure 4.4-57). The concentration data exhibited large variability, as is commonly observed with point measurements (Figure 4.4-58). Being equivalent to a spatial average representation, the PORFLOW predictions did not reflect the data scatter, but did appear to be roughly consistent with the measurement trends.

GSA/PORFLOW model predictions of seepelines bordering the GSA were compared to field surveys (Figure 4.4-59). The seepage data was not used in model development or calibration. The simulated seepage faces were generally consistent with the field observations.

The GSA contains a number of tritium plumes not associated with the SDF. Being un-retarded, tritium is an ideal tracer of groundwater flow and thus can be informative in the adequacy of the GSA/PORFLOW model to reflect actual conditions. Groundwater pathlines from the GSA/PORFLOW model were compared to an existing tritium plume map. The model pathlines on the right of Figure 4.4-60 were observed to be consistent with plume trajectory, deduced from actual monitoring well data shown in the inset on the lower left of the figure. Simulated pathlines were also compared to F-Area plumes, with good agreement (Figure 4.4-61).

Figure 4.4-56: VZMS Layout and Instrumentation at Slit Trenches



[WSRC-STI-2006-00198, Section 5.8]

Figure 4.4-57: Basis for PORFLOW Model and VZMS Data Comparison

**Two-dimensional
vadose flow and
transport models**

Predictions:

**Flux in
Ci/yr per Ci**

**Concentrations in
pCi/L per Ci/cm**

ground
surface

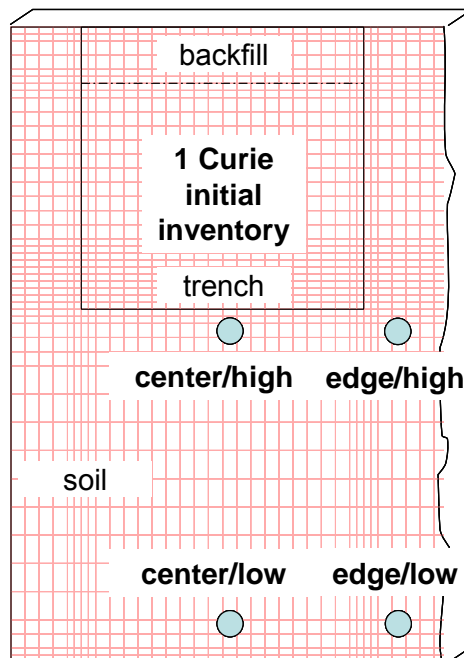


Figure 4.4-58: PORFLOW Model and VZMS Tritium Data Comparison

**All data
referenced
to average
inventory**

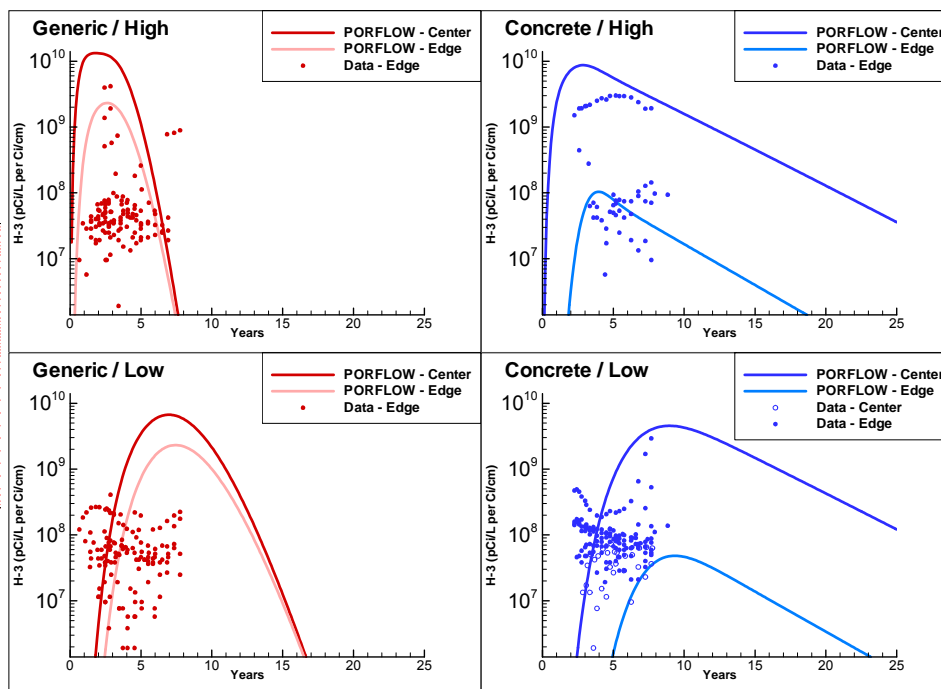
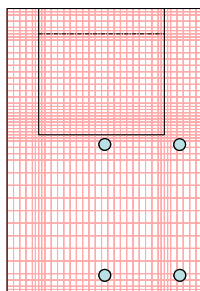
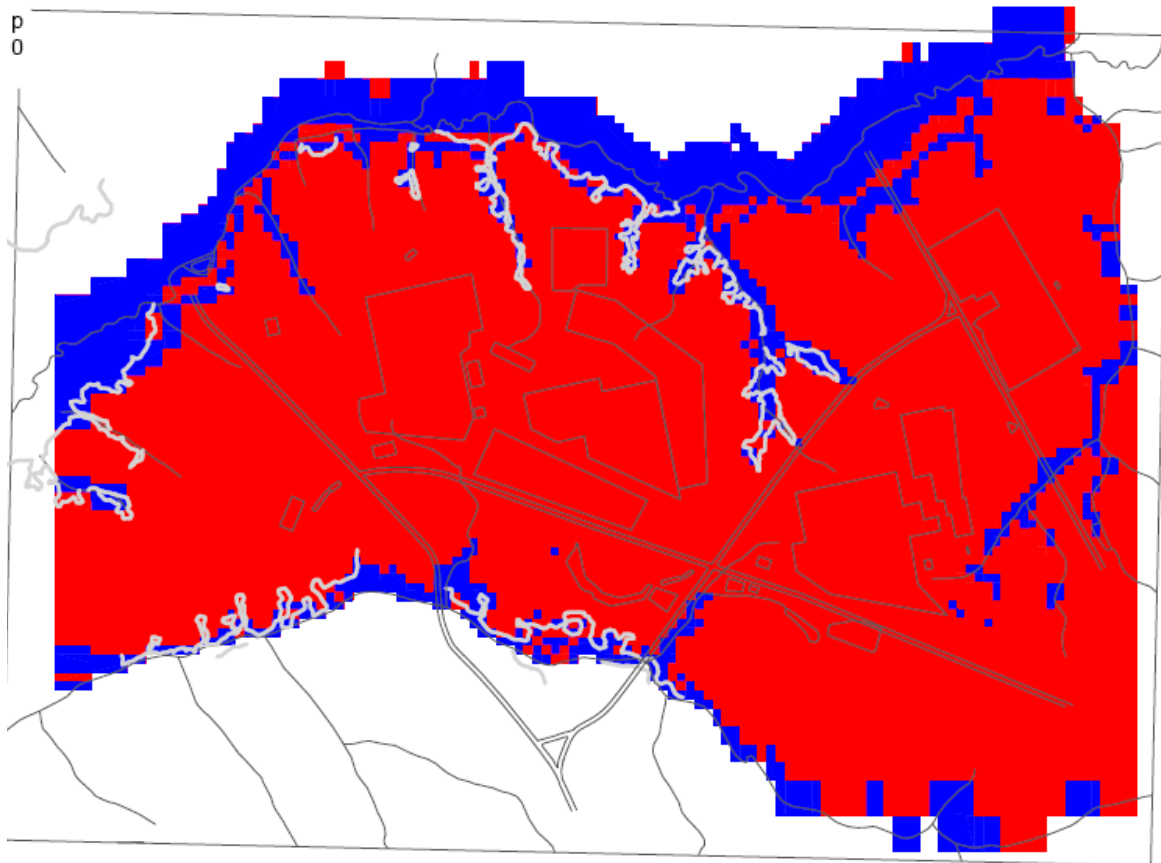
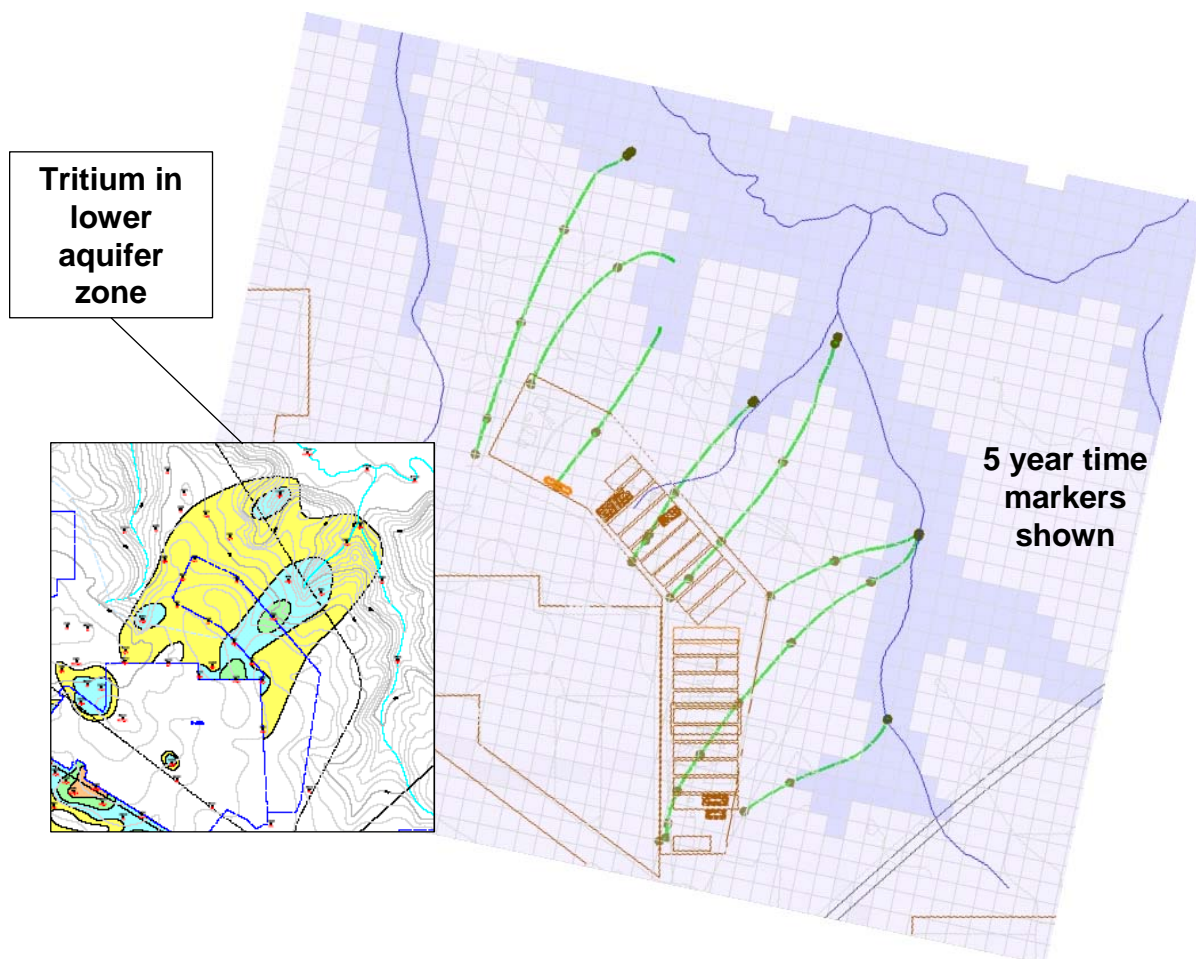


Figure 4.4-59: Surveyed Seepelines Compared to GSA/PORFLOW Model Simulation



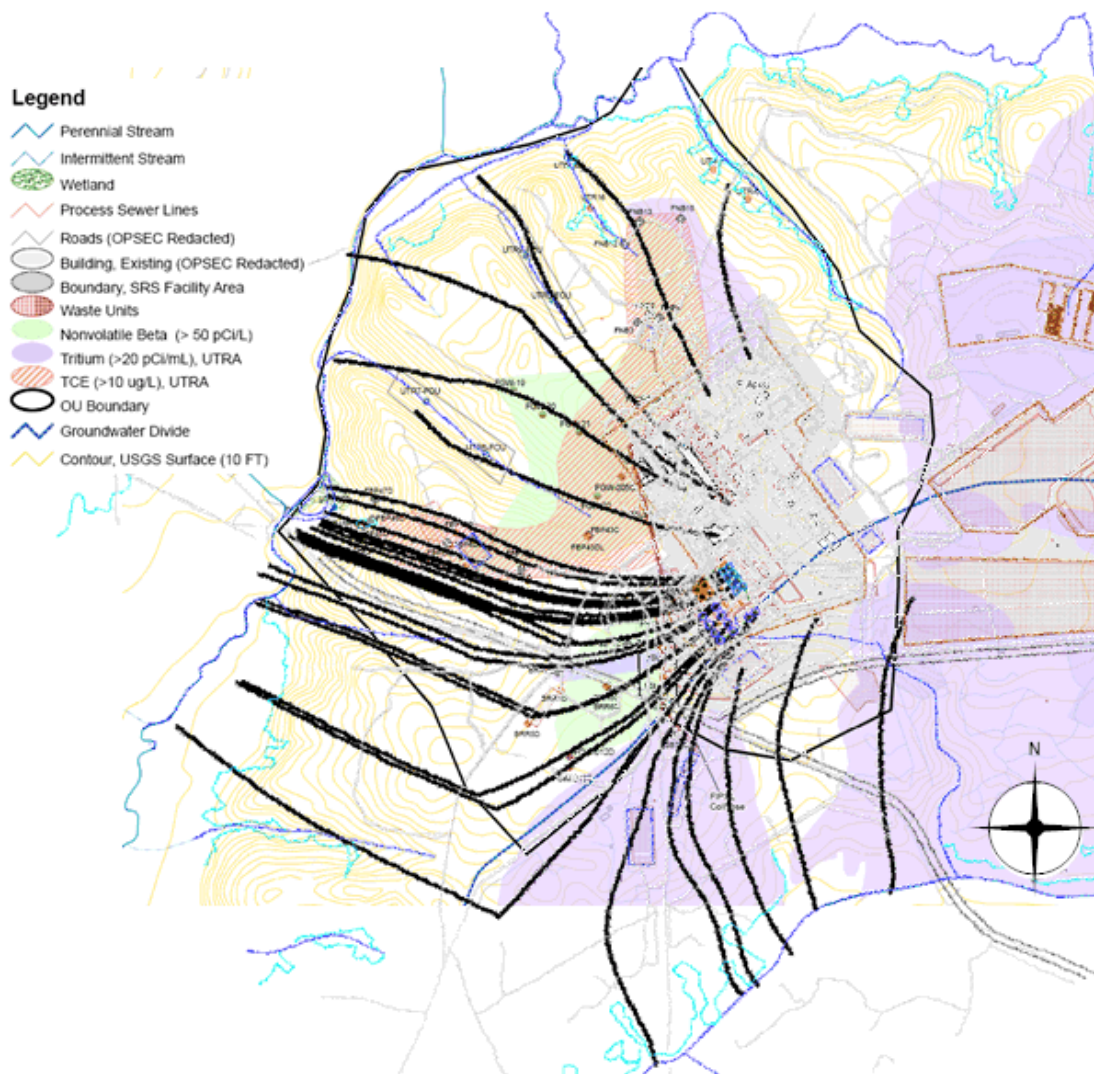
Note: Seepage predicted at interface of recharge (red) areas and discharge (blue) areas with surveyed seepage location shown in white trace lines. [WSRC-TR-2004-00106]

Figure 4.4-60: Comparison of GSA/PORFLOW Groundwater Pathlines to a Tritium Plume



Note: Comparison of GSA/PORFLOW Goundwater Pathlines to a Tritium Plume Emanating from the E-Area Mixed Waste Management Facility.

Figure 4.4-61: Comparison of GSA/PORFLOW Groundwater Pathlines to Contaminant Plumes Emanating from F-Area



4.4.4.2 GoldSim Modeling Process

In order to address uncertainty and sensitivity of the modeling of the SDF, a probabilistic model was constructed. This model was necessarily simpler than the PORFLOW groundwater model in its environmental transport calculations, but included additional calculations that can not be performed in PORFLOW. The GoldSim systems analysis software, developed by GTG, is uniquely suited to probabilistic PA (more information on GoldSim fundamentals is available at the website: www.goldsim.com). This program was developed for the task, and incorporated many features that made it particularly useful, such as integrated solutions of physically-based differential equations from radioactive decay and in-growth, to chemical partitioning and diffusion. With its whiteboard-style graphical user

interface, rich toolset of built-in function and the ability to define expressions governing relationships between model entities, GoldSim allows modelers to quickly build transparent radiological PA models. The GoldSim model is a one-dimensional (1-D) model versus a 3-D model (like PORFLOW), so some additional tasks, such as creation of a ring of wells surrounding the SDF (described below), were required during modeling. Validation of the 1-D GoldSim model versus the 3-D PORFLOW model is explicitly addressed in the GoldSim benchmarking discussion (Section 5.6.2).

In addition to aiding in uncertainty and sensitivity modeling, a separate model was used to calculate dose results using concentration inputs from PORFLOW (rather than concentrations calculated by the GoldSim SDF model using the SDF rad and non-rad inventories). This “dose calculator” GoldSim model is described in 4.4.4.2.2.

4.4.4.2.1 Model Layout and Structure

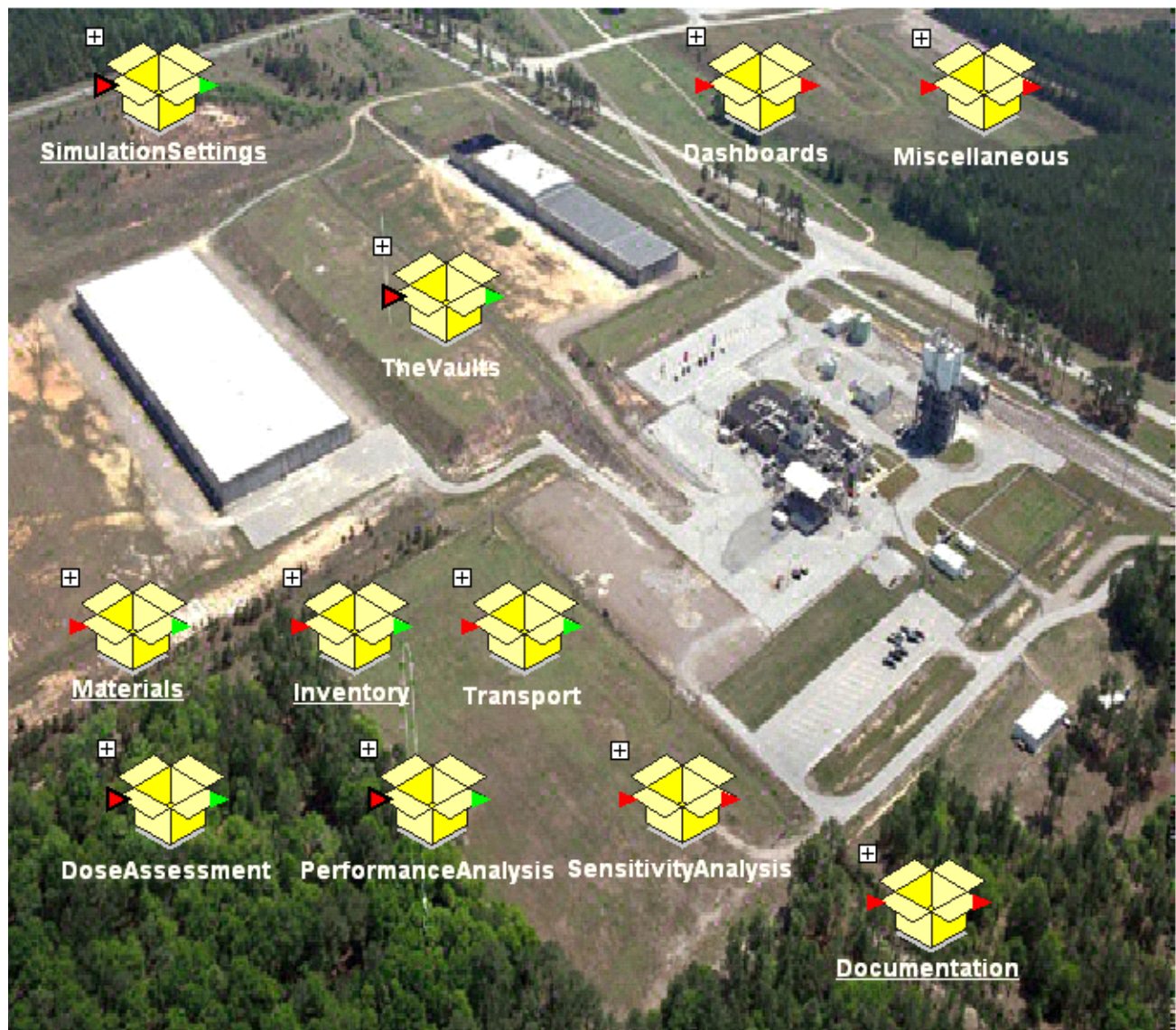
This section discusses the GoldSim implementation of the SDF model, and is organized to present the model structure and functionality roughly in the order that the calculations operate. This order starts with the definition of model domain and then continues with materials and transport phenomena to the calculation of dose results and their interpretation. This discussion applies to model version “SDF v1.013.gsm”.

This section discusses the stochastic SDF model, which is described in the *Saltstone Disposition Facility Stochastic Transport and Fate Model Description* report (SRNL-TR-2009-00051). The SDF model incorporates lessons learned from the FTF modeling effort (SRS-REG-2007-00002_OUO). Figure 4.4-62 shows the top level of the transport and fate model. The model was implemented in the GoldSim modeling environment. The various GoldSim containers will be discussed in the following sections. The discussion will focus on FDCs, but is applicable to all disposal unit types. Differences existing in the modeling of the different disposal unit types will be described as necessary. The GoldSim element names will be referred to in italics.

A brief overview of the major model elements are:

- *TheVaults* – contains the elements necessary for contaminant transport
- *Materials* – contains the material definitions and properties used in *TheVaults*
- *Inventory* – contains the source term information
- *Transport* – contains the flows used in the *TheVaults* for contaminant transport
- *DoseAssessment* – contains all dose related data and calculations

Figure 4.4-62: Top Level of the GoldSim SDF Model



4.4.4.2.2 Modeling Philosophy

This section contains a brief description of why the model was designed as it is. The primary driver in the design of this model was that it is a stochastic model. Its statistics were generated using a Monte Carlo simulation, which involved running the model many times. As such, the model must be designed such that it gives reasonable results in as short a run time as possible. Some of the short run-time requirements were met because the modeling environment was 1-D and performed only a transport simulation, (i.e., it did not perform a flow field calculation).

It was determined that the analysis to support the SDF PA would not use solubility limits. This provided an additional avenue through which run-times could be reduced. Solubility confers a non-linearity, whereas a K_d provides one with a linear formulation. This linear formulation allows for the modeling of only one FDC. Results for all the other disposal units can then be scaled from the results of one calculation, thereby saving considerable computational time. The implications of these underlying paradigms will be discussed in detail in this section.

➤ **Container**
The Vaults

The Vaults, as shown in Figure 4.4-63, is where the transport of contaminants was calculated. The containers, *Vault_1*, *Vault_2*, and *Vault_4* contain the transport calculations for each of the disposal units, with *Vault_1* representing Vault 1, *Vault_4* representing Vault 4, and *Vault_2* representing the FDCs. *VaultData* contains the geometric data for all three disposal unit types. *PlumeCalc_Sectors* contains the information necessary to calculate the plume function for each disposal unit relative to the sectors they affect. This will be described in detail in the plume discussion that follows.

Figure 4.4-63: Container “*TheVaults*”

Vault Types of the Salt Disposal Facility

The three vault types are modeled here. One model for each vault type. The details of the treatment of the multiple Vault 2s is in the Vault_2 container. For all models a large number (130 cells) is used to minimize numerical dispersion.

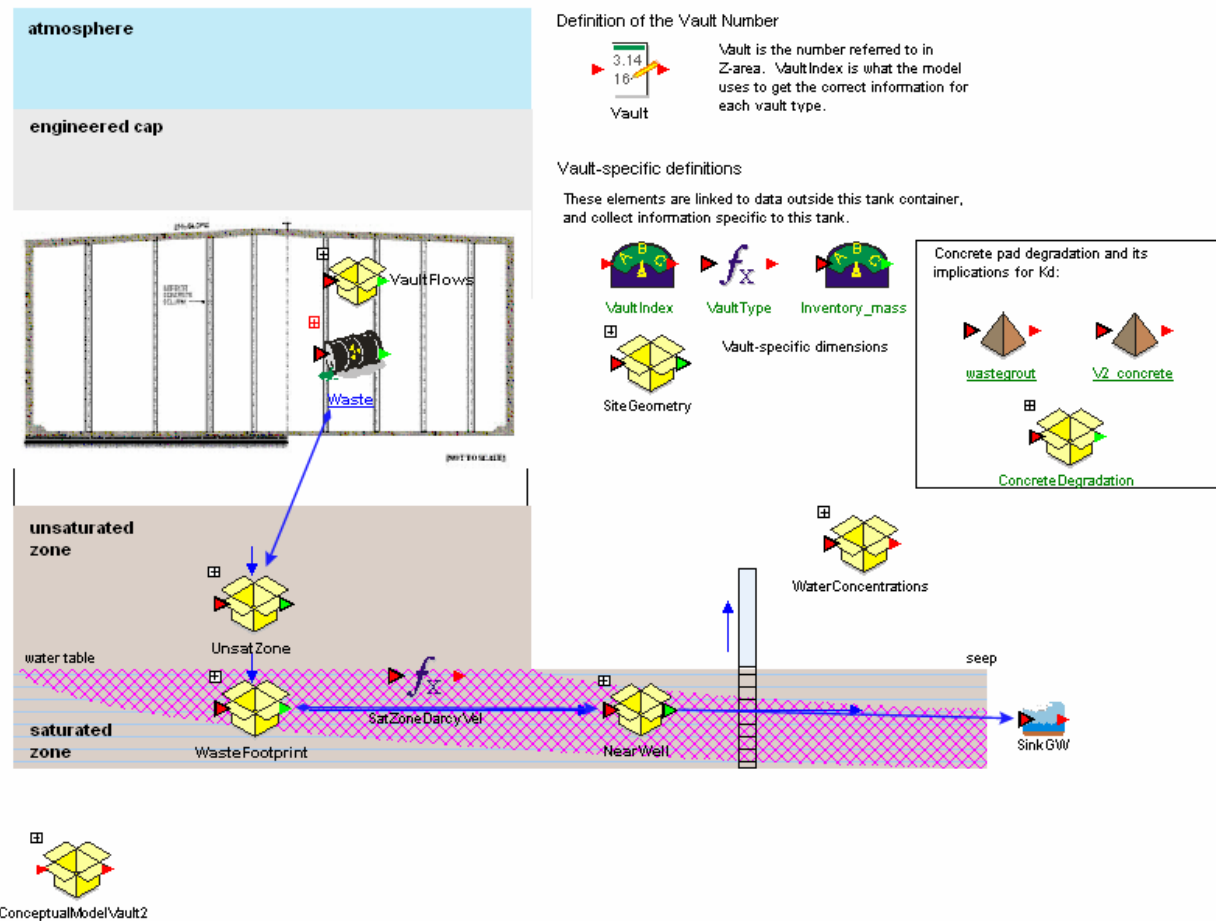


➤ Container *Vault2*

This section will be the main discussion on the transport section of the model. Any differences between the disposal units will be noted, but in most cases, those differences are minor. The discussion will focus on FDCs (shown in Figure 4.4-64), but as noted earlier, is applicable to all disposal unit types. Detailed descriptions of this container's sub-elements follow.

Figure 4.4-64: Container “Vault_2”

Vault 2 Model



⇒ **Concrete Degradation Modeling**

The concrete degradation model, as implemented in the GoldSim model, was one which affected only the chemistry of the concrete. The degradation affect on flow was implicitly applied through the PORFLOW flow rates. The degradation affected the K_d and was based on the number of pore water flushes. A local definition of the solids waste grout and *V2_concrete* is in each disposal unit. By doing this, each disposal unit could have its chemical properties change independently, but as always, all the FDCs changed at the same time. PORFLOW analyses showed that the floors of the three disposal unit types did not experience the change from reducing to oxidizing in 20,000 years, so it was not included in this model.

- The *ConcreteDegradation* container holds the calculations of pore volume flushes which affect the K_d of the cementitious materials. *PreviousValues* elements had to be used because the code reported a recursive loop. The *Selector* elements determine which set of K_d are used based on *NumberOfFlushes[Grout,Wall]*. There are two data elements that are benchmarking factors (BMF) applied to Tc-99's K_d . Tc-99 was treated differently in PORFLOW from all the other radionuclides. These BMF's are to account for those formulations and are discussed in detail in Section 5.6.2.
- The *PoreFlushes* container evaluates the selector elements to determine which set of K_d are to be used by the grout and the wall. This was thought to be a potentially important phenomenon in controlling the waste release so the number of pore flushes was described by a stochastic element. Two transitions are considered; (1) is the transition from middle reducing to middle oxidizing, and (2) is from middle oxidizing to old oxidizing. The disposal unit concrete has different K_d than the grout, hence the two separate pathways.

⇒ **Flow Modeling**

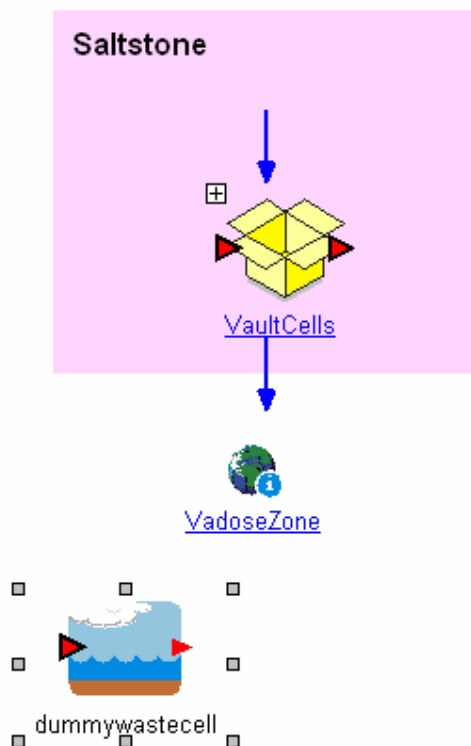
The Container *VaultFlows* determined the flow through the waste zone. This container used various GoldSim elements in modeling flow. The Element *Configuration* contains the probability of occurrence of different degradation cases. The Element *TimePeriodSelector* determined which of the PORFLOW time periods the calculation is in. The Element *PF_Flow[grout,Dirt,UZ,Wall]* picks the infiltration from the tables in Transport by choosing the appropriate time period and degradation case. The [Grout, Dirt, and UZ] elements refer to vectors such that a vertical gradient of the flow was supplied to the model. The [Wall] was a single value, as an examination of the PORFLOW results showed this to be a reasonable assumption. A detailed discussion of the abstraction of the flow data is provided below. The Element *UnsatDarcyFlux_[Grout, Dirt, UZ, Wall]* determined whether to use a natural infiltration rate or a PORFLOW generated flow rate.

- **Element *Waste*** The Element *Waste* (Figure 4.4-65) contained the transport cells at the waste form elevations in *VaultCells*. *BypassFraction* is a stochastic on how much flow bypasses the waste form.

Figure 4.4-65: Element “Waste”



The Waste Cell



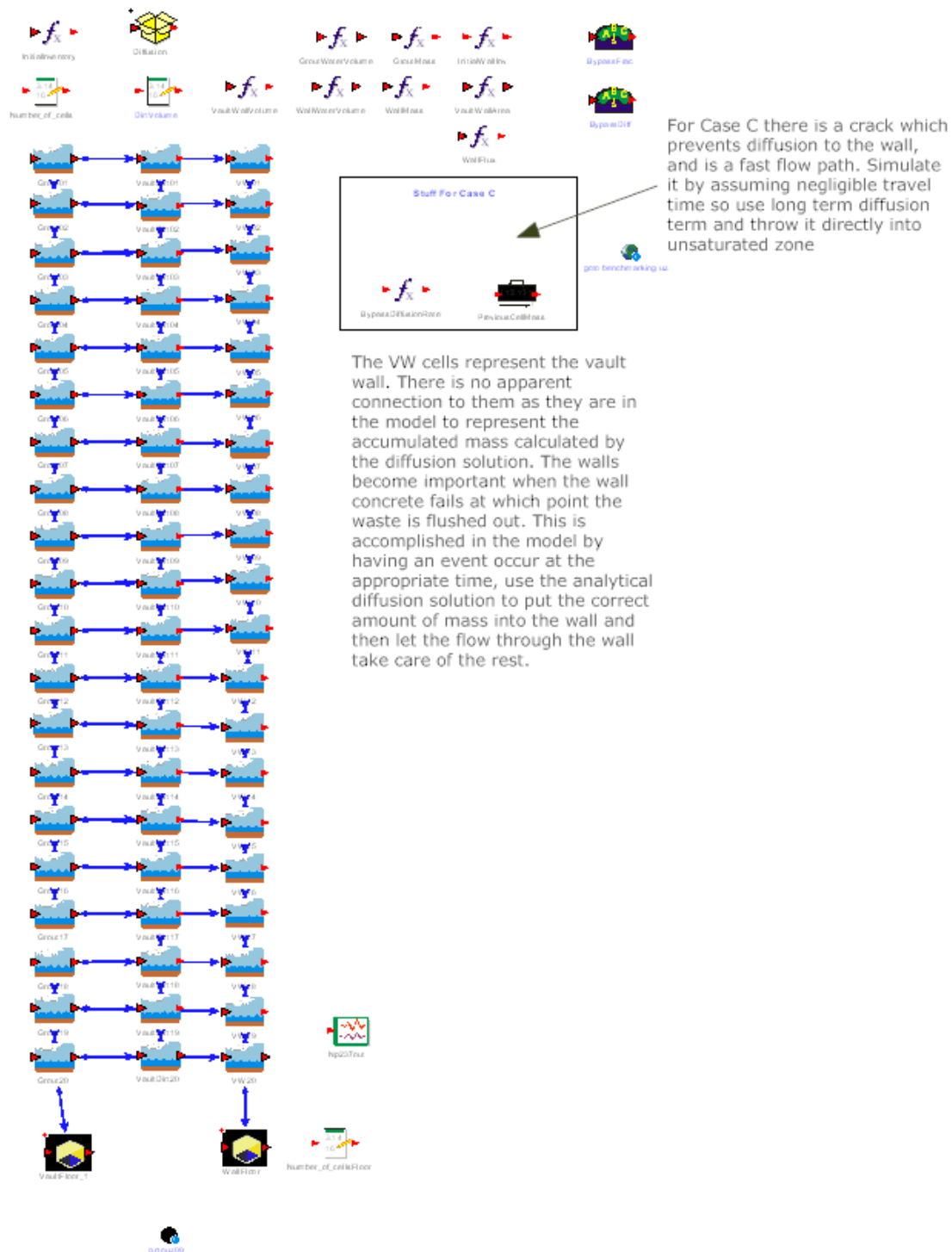
The inflow of Water from above is controlled by the overlying engineered cap and tank backfill grouts. The infiltration through these materials is calculated externally to this model by PorFlow, and is provided in the container \\ContaminantTransport\\WaterTransport\\PorFlow_Inflows

The flow through waste is implied by setting the appropriate rate of flow out of the Cell, and GoldSim assumes that the water necessary to make up the deficit is uncontaminated.

Water flows out of the waste into the concrete pad below.

- **Container *VaultCells*** The container *VaultCells* (Figure 4.4-66) was where the transport of contaminants from the waste was performed and is the “top” of the transport model. The top boundary of the model is the top of the waste (saltstone). Therefore, the flow boundary conditions were applied at this level. It should be noted that there are three parallel flow paths in this model, *GroutNN*, *VWnn*, and *DirtNN* (where “NN” corresponds to a computational cell (in this case, a GoldSim mixing cell element)). These three paths were necessary for several reasons. First, diffusion was an important element of waste transport and must be considered. Second, because diffusion was considered, the flow rates in the grout, wall, and dirt were quite different, which resulted in vastly different transport rates of the contaminants. As a result of this conceptual model formulation, the model will be referred to as a pseudo 2-D model.

Figure 4.4-66: Container “VaultCells”



Grout Cells - The grout cells are the cells which contain saltstone. The cells transport contaminants by advection and diffusion. The advective transport was done in the classic 1-D methodology and accounted for transport in the z-direction. The diffusive transport was done in the r-direction (for a FDC design) or the x-direction (for Vaults 1 and 4) and this was what gave the model its pseudo-2-D behavior.

The grout cells' advection was accomplished by applying a flow boundary condition abstracted from PORFLOW (a discussion of the flow abstraction is provided later). The grout diffusion was accomplished by the use of an analytical model of a shrinking core. The solution specified the amount of mass which must be transferred each time-step from the grout to the disposal cell wall and dirt.

This diffusion method was chosen over implementation of the GoldSim diffusion paradigm for several reasons. First, there was an issue with the implementation of the GoldSim diffusion model. The model requires a tortuosity. This was an issue with all diffusion models, not just the GoldSim implementation. Second, was the issue of discretization. A nodalization study was undertaken and it showed that approximately 400 cells would be necessary to reasonably calculate the diffusive term. This number of coupled cells would make for long run times, on the order of minutes rather than seconds, for one realization. Since this model was designed to be the uncertainty and sensitivity model, it must be able to run many realizations. In order to run a stochastic analysis of 10,000 realizations, one would be looking at perhaps weeks rather than overnight. Third, the important stochastic parameters in the diffusion equation appeared in both the analytic solution and the GoldSim implementation. Therefore, one can assess those parameters equally well in either formulation.

Dirt Cells - The dirt cells represent those cells contiguous to the waste zone to which diffusion may occur. Unlike the grout cells, the flow in the dirt cells can vary considerably. This was because of the cap drain, which channels the runoff into this region. The flow varied greatly in the z-direction and not nearly as much in the r-direction. Each dirt cell had its own flow rate. Note that in GoldSim, flow is important only as a mechanism by which the contaminant mass may be transported. No mass balance was performed on the water as its use to essentially provide the timing of the transport (if one was not concerned about the concentration, which in this instance was not a concern). The dirt cells' volume was given as a unit volume. At this point, concentration was not a concern, only the transport. The concentration was accounted for at the transition from the dirt cells to the unsaturated zone cells beneath the disposal unit. The output of the bottom cell of the dirt column, *VaultDirt20*, connected directly with the inlet cell of the *UnsatZone*, bypassing the disposal unit floor.

Initial Inventories - There were two initial inventories, one for the saltstone and one for the disposal unit walls. The initial FDC wall inventory was zero, as radionuclides are not expected to diffuse through the cells' liners. Vaults 1 and 4 walls were modeled as having an initial inventory due to vault wall weeping (see Sections 4.4 1.1 and 4.4.1.2 for further details). The initial wall inventories were determined during

benchmarking, as discussed in Section 5.6.2 and the benchmarking report (SRNL-TR-2009-00052). The fractions of inventory in the wall and saltstone add up to 1. The total initial inventory for each radionuclide in each disposal unit is 1 Ci.

Container VaultFloor - *Vaultfloor* was in the model for two reasons; it provided for a different material type than the grout, and it can have a different flow than the grout. It is the area directly under the saltstone monolith. The disposal unit floor consists of clean concrete, because at the beginning of the simulation no contamination is contained in the floor. During a simulation, the floor can have the affect of being a contaminant “sponge,” thereby adding to the retardation of the contaminant transport.

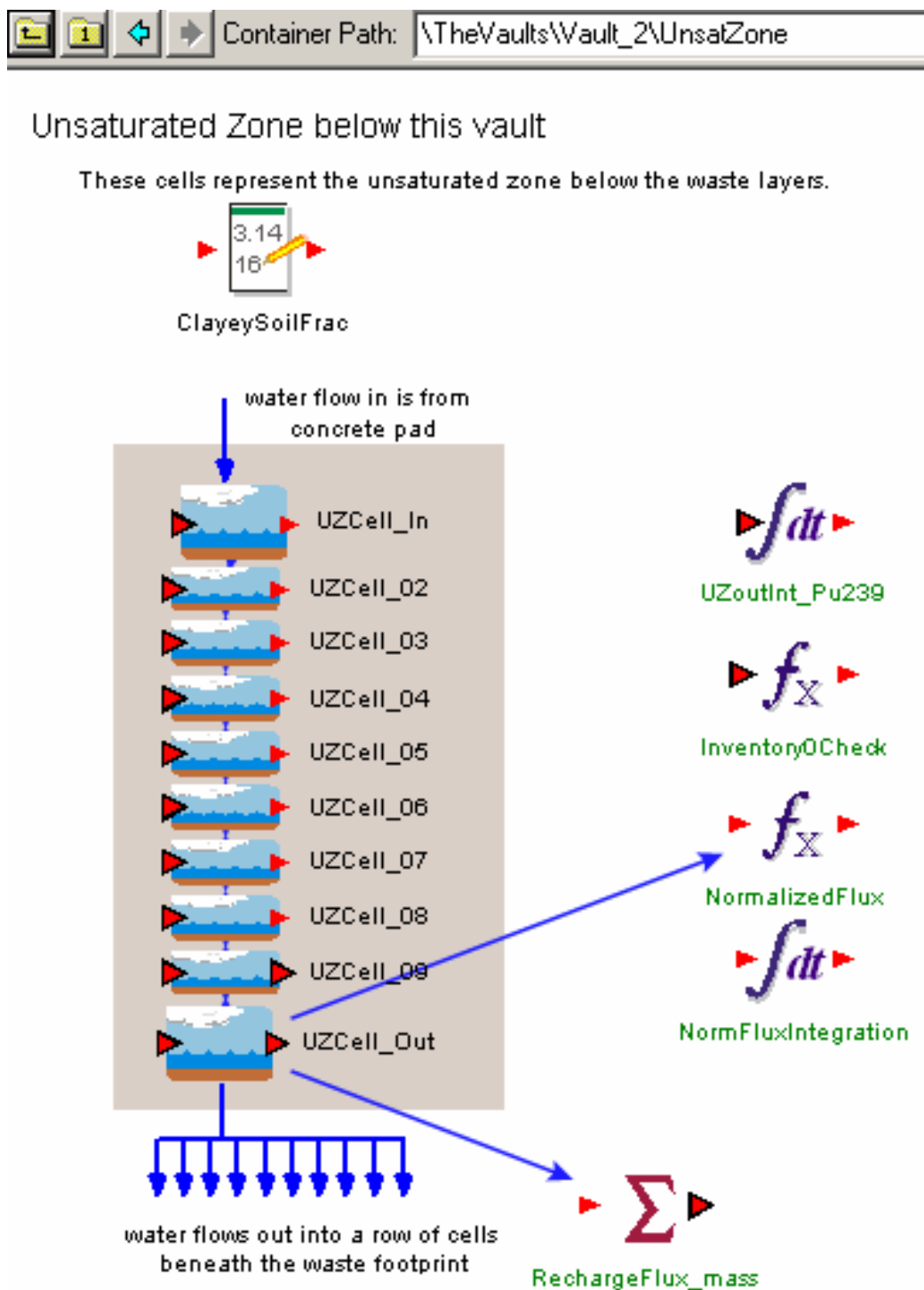
Container WallFloor - The *WallFloor* container was in the model to account for the manner in which it was modeled in PORFLOW. This will be discussed in detail in Section 5.6.2. As modeled in PORFLOW, the wall sat on the floor which allowed for a separate flow path and perhaps a different material depending on disposal unit type. This caused the wall flow to be diverted around the floor into the dirt contiguous to the floor, flow around the floor, and then move under the disposal unit beneath the floor due to the lower suction in the drier dirt. The *WallFloor* container’s elements provided for a means by which these phenomena could be simulated by having both concrete and dirt flow paths.

Bypass Elements - There are several element names containing “Bypass.” These were used for Case C, where there is assumed to be a circumferential crack isolating the grout from the disposal unit wall. When this is the case, there can be no diffusion between the saltstone and the other two flow paths, but there can be between the grout and the flowing medium in the crack. This was simulated by assuming the travel time in the crack was insignificant, so that the diffusive flux term was applied directly to the unsaturated zone. The modeling assumption in PORFLOW was that the crack extended through the disposal unit floor, therefore, the preceding assumption was correct.

Container Diffusion - This container was the local implementation of the analytical diffusion model. Each disposal unit type has its own implementation, but, because of the linear modeling paradigm implemented for disposal unit cells, all FDCs behave in an identical manner.

➤ **Container UnsatZone** The Container *UnsatZone* (Figure 4.4-67) represents the flow field between the bottom of the disposal unit floor and the top of the saturated zone. Consistent with the PORFLOW modeling, a representative height was used for this flow zone. The height is a stochastic element so that the affect of varying distance to the water table may be assessed. Note that the height will vary for all FDCs in an identical manner. Nodalization studies performed for the SDF PA showed that the number of mixing cells used for this model should adequately model the unsaturated zone for any reasonable heights. The porous medium is a mixture of clayey and sandy soil. Benchmarking showed the *ClayeySoilFrac*[tion] to be zero. The inlet flow paths to *UZCell_In* are *VF5* (vault floor), *WFD05* (wall floor dirt), and *VW20* (vault wall). The outlet flow was evenly divided among the *WasteFootprint* cells.

Figure 4.4-67: Container “UnsatZone”



➤ **Saturated Zone Modeling** The saturated zone consists of two elements, *WasteFootprint* and *NearWell*. *WasteFootprint* is the section of the saturated zone directly under the waste zone. *NearWell* is the 100m boundary.

Container *WasteFootPrint* - This container contains 10 mixing cells. Its purpose is to account for the time delay of the upstream waste leaving the shadow of the waste form. This proved to be important in the FTF PA, and as the SDF model was being developed, it was not known if this would be an important phenomenon here or not. It turns out that it was not important because the flow streamlines tend to be perpendicular to the long dimensions of Vaults 1 and 4, but the model structure was not changed once this became known. The porous medium is saturated sandy soil.

Container *NearWell* - *NearWell* represents the distance from the downstream edge of the waste form's shadow to the point of interest, the 100m boundary. It consists of a number of mixing cells. Previous modeling efforts showed a fairly fine discretization was necessary in order to avoid undue numerical dispersion.

A plume function was used to account for plume overlap. Its implementation in this model is discussed later. The use of the plume function in conjunction with the factors mentioned above, leads one to model in the following manner. When using a plume function, one could run an arbitrarily small flow area model, thereby causing the calculated concentrations to be higher than expected. The plume function was used as a correction to that arbitrary concentration, by analytically solving a dispersion equation. The reason a transport mechanism was needed, was to have the correct timing of events. One could think of it as determining the arrival of a breakthrough curve. In this case, the timing is important because of radioactive decay. PORFLOW was taken as the benchmark, so one could obtain timing information from it. All that was necessary to determine was where along the GoldSim cell network, the timing agreed with the PORFLOW data. The GoldSim concentration at that point then could be used as the input to the plume function, which would then supply a concentration to be used in the dose calculation. In essence, what was important to the model was that there was a sufficient number of mixing cells to represent different places in time. The spatial aspect was removed so that one set of cells could be used to represent all the FDCs.

➤ **Inventory** Two inventory classes were used in this model. They are described in the following sections.

Disposal Unit Inventory - The *Inventory* container was where the disposal unit inventory was defined. *Vault_Inventories* contains a unit curie for each of the disposal unit types. *[South,North]VaultSourceMultipliers* is where the fractional curie was applied to each disposal unit cell for each radionuclide. The uncertainties applied to the inventories were based on a plus/minus fraction of the nominal inventory. Therefore, within each of the Multiplier containers was an element *Nominal[North, South]SourceInventory*. These values were used in container *InventoryUncertainty*. This container contains three containers, one for each of the disposal unit's inventory uncertainty. The uncertainty values were passed back to the

Multipliers elements and it was that value that was passed to the dose calculation. Inventory uncertainty is discussed further in Section 5.6.3.2.

Post-drilling Inventory - This inventory, *AgInventory*, was available for use in the Inadvertent Human Intruder (IHI) analysis. It represented the drill cuttings inventory if one were to drill into a disposal unit cell.

➤ **Flow Abstraction** This section is a discussion of the algorithm used to extract the 2-D flow field from the PORFLOW unsaturated zone analysis into the GoldSim 1-D advective model. GoldSim does not calculate flow fields, it uses them as boundary conditions.

PORFLOW generates its time dependent flow files by running 44 independent, steady-state flow runs, with each of the 44 representing a period in time. Each of those flow runs generates an output file, which contains the Darcy velocities for each computational cell. The coordinates are either x-y for the rectangular, (Vaults 1 and 4), or r-z for the FDCs. Regardless, the output format is the same (except that the r-z is flipped from the x-y).

A natural basic script was written to interrogate the output files and to summarize the results in an Excel workbook. For the waste and dirt zones, the files were interrogated at 20 different elevations, corresponding to the 20 mixing cells used to represent each, 10 radial locations for the grout and four for the dirt. An average was then taken for each elevation and a table was constructed of time period versus elevation. Figure 4.4-68 shows a small section of one of these tables. "Time Period" corresponds to the PORFLOW time periods and "i=37", etc., corresponds to a PORFLOW elevation index. "TI44" is the last time period. If one were to read across a row, one would note that the velocities are essentially the same, as one would expect for the grout for Case A.

Figure 4.4-68: Sample Velocity Table - Grout

| | A | B | C | D | E | F | G | H | I | J | K | L |
|----|-------------|----------|----------|----------|----------|----------|----------|----------|----------|----------|----------|----------|
| 1 | Time Period | i=37 | i=40 | i=43 | i=44 | i=45 | i=47 | i=48 | i=49 | i=51 | i=52 | i=53 |
| 2 | TI44 | -0.26922 | -0.25867 | -0.24622 | -0.24389 | -0.242 | -0.23967 | -0.23889 | -0.23833 | -0.23789 | -0.23778 | -0.23744 |
| 3 | TI43 | -0.25778 | -0.24933 | -0.23944 | -0.23767 | -0.23667 | -0.23489 | -0.23444 | -0.23378 | -0.23344 | -0.23356 | -0.23356 |
| 4 | TI42 | -0.10443 | -0.10753 | -0.11247 | -0.11392 | -0.11551 | -0.11794 | -0.11877 | -0.11956 | -0.12078 | -0.12122 | -0.12189 |
| 5 | TI41 | -0.09174 | -0.09391 | -0.09693 | -0.09793 | -0.09888 | -0.10078 | -0.10158 | -0.1022 | -0.10322 | -0.10361 | -0.10401 |
| 6 | TI40 | -0.08559 | -0.08754 | -0.09022 | -0.09111 | -0.092 | -0.09363 | -0.09441 | -0.09499 | -0.09584 | -0.09622 | -0.09656 |
| 7 | TI39 | -0.08266 | -0.08454 | -0.08707 | -0.08791 | -0.08874 | -0.09036 | -0.09103 | -0.0916 | -0.09253 | -0.09279 | -0.0931 |
| 8 | TI38 | -0.0688 | -0.07046 | -0.07254 | -0.07319 | -0.07384 | -0.07498 | -0.07539 | -0.07577 | -0.07621 | -0.07632 | -0.07639 |
| 9 | TI37 | -0.0674 | -0.06901 | -0.07103 | -0.07164 | -0.07229 | -0.07341 | -0.07382 | -0.07418 | -0.0746 | -0.0747 | -0.07478 |
| 10 | TI36 | -0.06601 | -0.06757 | -0.06953 | -0.07016 | -0.07074 | -0.07184 | -0.07226 | -0.07257 | -0.07299 | -0.07311 | -0.07317 |
| 11 | TI35 | -0.0646 | -0.06613 | -0.06803 | -0.06867 | -0.06921 | -0.07029 | -0.0707 | -0.07101 | -0.07141 | -0.07156 | -0.07158 |
| 12 | TI34 | -0.0632 | -0.06471 | -0.06653 | -0.06712 | -0.06768 | -0.06871 | -0.06912 | -0.06944 | -0.06982 | -0.06993 | -0.06997 |
| 13 | TI33 | -0.06178 | -0.06324 | -0.06507 | -0.06562 | -0.06619 | -0.06719 | -0.06756 | -0.06789 | -0.06826 | -0.06837 | -0.06839 |
| 14 | TI32 | -0.06038 | -0.06181 | -0.06358 | -0.06413 | -0.06469 | -0.06562 | -0.06601 | -0.06631 | -0.0667 | -0.06679 | -0.0668 |
| 15 | TI31 | -0.05897 | -0.06034 | -0.06207 | -0.06263 | -0.06312 | -0.06408 | -0.06443 | -0.06472 | -0.0651 | -0.06518 | -0.06523 |

Figure 4.4-69 shows a similar table for the dirt zone, with several columns left out. "i=37" in the innermost node and "i=73" the outermost. The total horizontal distance is approximately 20 feet, so one can see the steep flow gradient in this zone.

Figure 4.4-69: Sample Velocity Table - Dirt

| Time Period | i=37 | i=40 | i=43 | i=44 | i=45 | i=62 | i=64 | i=66 | i=69 | i=73 |
|-------------|----------|----------|----------|----------|----------|----------|----------|----------|----------|----------|
| TI44 | -103.467 | -105.633 | -107.133 | -107.933 | -108.367 | -127.067 | -130.3 | -134.2 | -140.433 | -147.133 |
| TI43 | -112.2 | -106 | -106.867 | -106.967 | -107.733 | -126.933 | -131.133 | -136 | -144.533 | -153.867 |
| TI42 | -114.2 | -114.667 | -116.9 | -117.7 | -118.767 | -155.133 | -162.667 | -171 | -186.267 | -204.433 |
| TI41 | -114.2 | -114.667 | -116.9 | -117.7 | -118.8 | -155.133 | -162.667 | -171.333 | -186.633 | -204.767 |
| TI40 | -114.2 | -114.667 | -116.9 | -117.7 | -118.8 | -155.133 | -162.667 | -171.333 | -186.633 | -204.767 |
| TI39 | -114.2 | -114.667 | -116.9 | -117.7 | -118.8 | -155.133 | -162.667 | -171.333 | -186.633 | -204.767 |
| TI38 | -72.7333 | -72.6333 | -72.6667 | -72.7 | -72.7333 | -73.2667 | -73.2667 | -73.2667 | -73.2 | -73.1 |

Examination of the flow profiles in the disposal unit walls showed them to be essentially uniform. Therefore, one value was used to represent each of the time periods for disposal unit wall flow.

➤ **Diffusion Model** PORFLOW analyses showed diffusion to be an important mechanism for the transport of contaminant from the waste form to the external environment. Because of the relative durability of the saltstone, the major contributor to contaminants at the compliance points was the disposal unit wall. The mechanism by which contaminants get to the disposal unit wall outside environment is diffusion. This section will discuss the implementation of an analytical solution to diffusive mass transfer.

The GoldSim diffusion methodology was first used in order to assess its efficacy. Nodalization studies showed that for a reasonably well converged solution, a 2-D cell structure of over 400 coupled mixing cells would be required. This would have had a very adverse effect on the run-time of the model, so an alternative approach was required.

The alternative approach used was developed by the PORFLOW modelers to determine penetration into the concrete and its effect on Tc-99 release. The model is a shrinking core model, which accounts for the concentration gradient as a function of time. The shrinking core model required by the GoldSim fate and transport model is somewhat more complicated than the shrinking core model required by the PORFLOW analysis, in that the GoldSim has three components which must be considered; (1) the saltstone, (2) the wall, and (3) the dirt.

Diffusion Model Implementation - The diffusion model was implemented for each of the three disposal unit types. It should be noted that the solution was valid only for those radionuclides which exist at $t=0$, that is, the model does not explicitly recognize in-growth. However, in-growth was implicit to the model via the species concentrations used as arguments in the model. This was not seen to be a major shortcoming. The benchmarking process allowed for the model to be fine-tuned such that its behavior was quite similar to the fully coupled diffusion model implemented by PORFLOW.

The GoldSim implementation of the model had two purposes, to simulate the mass transfer into the dirt outside of the disposal unit, and the build-up or decrease of the contaminant mass in the disposal unit wall. The dirt was seen as an infinite sink, that is, there was no increasing concentration in the mixing cells making up the dirt column. This was a valid assumption, because the flow rate in the dirt was great

enough that all contaminants, which diffuse during one time-step, are advected out of that cell during the time-step.

Several idiosyncrasies of GoldSim make implementation of the diffusion model used in PORFLOW challenging. The idea behind the implementation is that the analytical solution will dictate the amount of mass transported by diffusion. Mass transfer is accomplished in the model by the use of a direct transfer pathway. However, this requires a fractional rate of transfer. This requires checks to ensure that a negative transfer can not occur, that no more mass than is in the mixing cell can be transferred, and that there must be a non-zero mass (so that there is not a divide by zero) when computing the fraction to be transferred. These requirements led to much of the model revision required during benchmarking.

GoldSim sees a recursive loop if the mass transfer rate is based on the current time-step's mass. The use of a *PreviousValue* element was required. Due to the rate of change and the size of the time-steps, the use of a previous time-step value did not significantly affect the results.

Diffusion Model Implementation for FDC Case C - FDC Case C is a special case for the implementation of the diffusion solution. Case C assumes that a complete, circumferential crack occurs between the saltstone and the disposal unit wall and that the crack continues through the floor of the disposal unit, including the upper and lower mud mats of the FDCs. This crack constitutes a fast flow path. The crack in the SDF disposal unit diverts flow from the saltstone, which in this case is the waste form. Therefore, although the infiltration rate is greater, it is likely that less waste will be affected by the flow.

The circumferential crack isolates the saltstone grout from the rest of system in the radial direction. Therefore, the only diffusive path is that from the saltstone to the crack. The high flow rate in the crack makes it appear as an infinite sink to the saltstone's diffusive flux. This is analogous to the appearance of the dirt in the typical case. Because of the assumption that the circumferential crack extends through the floor of the disposal unit, including the upper and lower mud mats of the FDCs, and the travel time in the crack is insignificant compared to the time-steps, the direct mass transfer pathway is from the saltstone to the unsaturated zone inlet mixing cell.

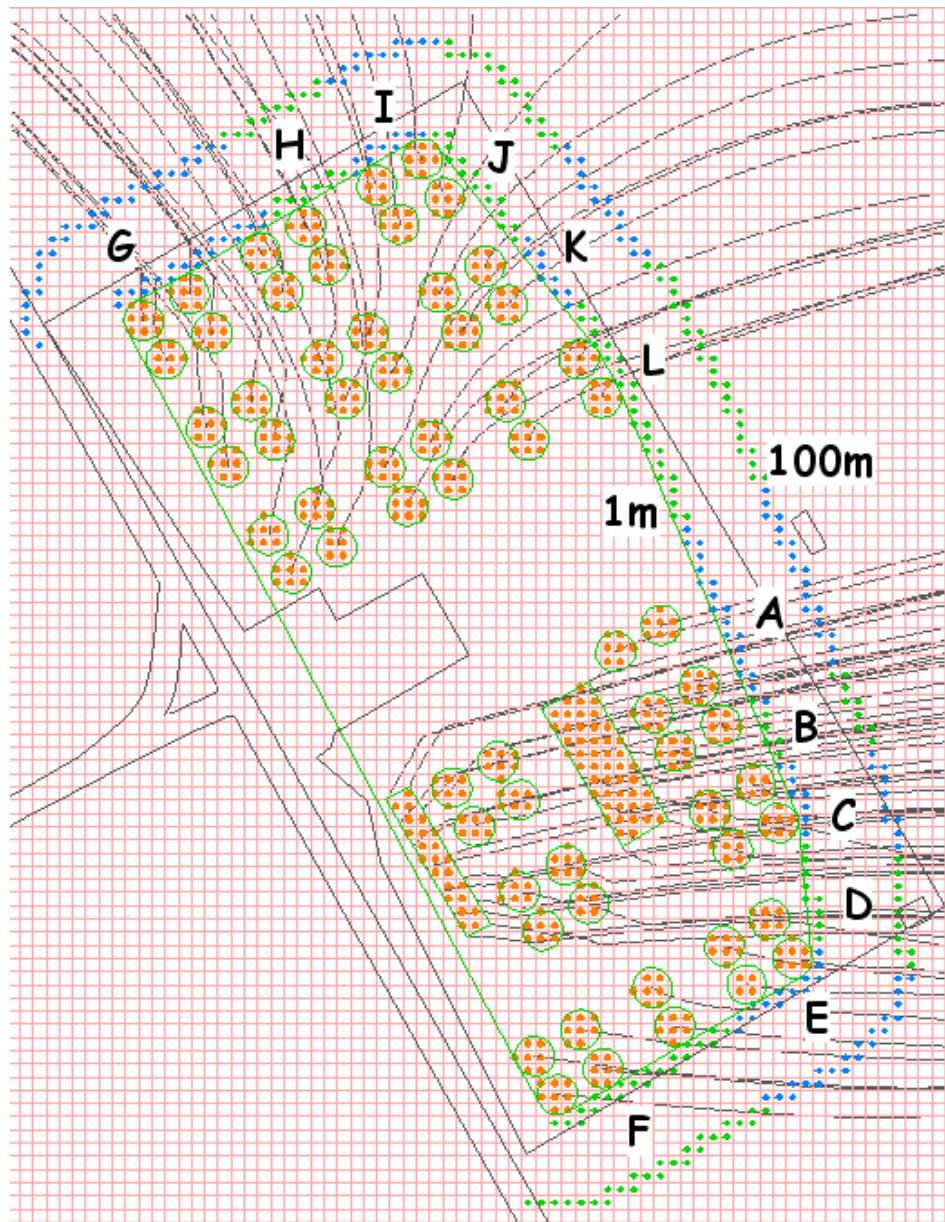
➤ **Plume Model**

The plume model was implemented for all SDF disposal units to account for plume overlap. Using the 12 flow sectors defined by PORFLOW (see Figure 4.4-70) and 66 disposal units, a matrix of 66 x 12, or 792 elements, was created. Many of those elements will have no affect on the superposition of the plumes, and although those elements cannot be eliminated from the matrix, their affect can be neglected. The logic used for setting up the plume overlap calculation is presented below.

The plume function was designed to calculate a factor to account for transverse dispersion of the contaminant. In order for this to happen, a reference point must be chosen. The point chosen for this analysis was the center of the PORFLOW calculated plume, as evidenced by the streamlines shown in Figure 4.4-70. The data to be supplied

was the maximum value in any computational cell in any aquifer in a sector. The data can move during a calculation, which made the calibration even more problematic. The decision was made to use the center node of each sector as the sectors' reference point. Therefore, the plume function is calculating the spread of a plume from where a disposal cell's streamline crosses the 100m boundary to the center of a sector at the 100m boundary.

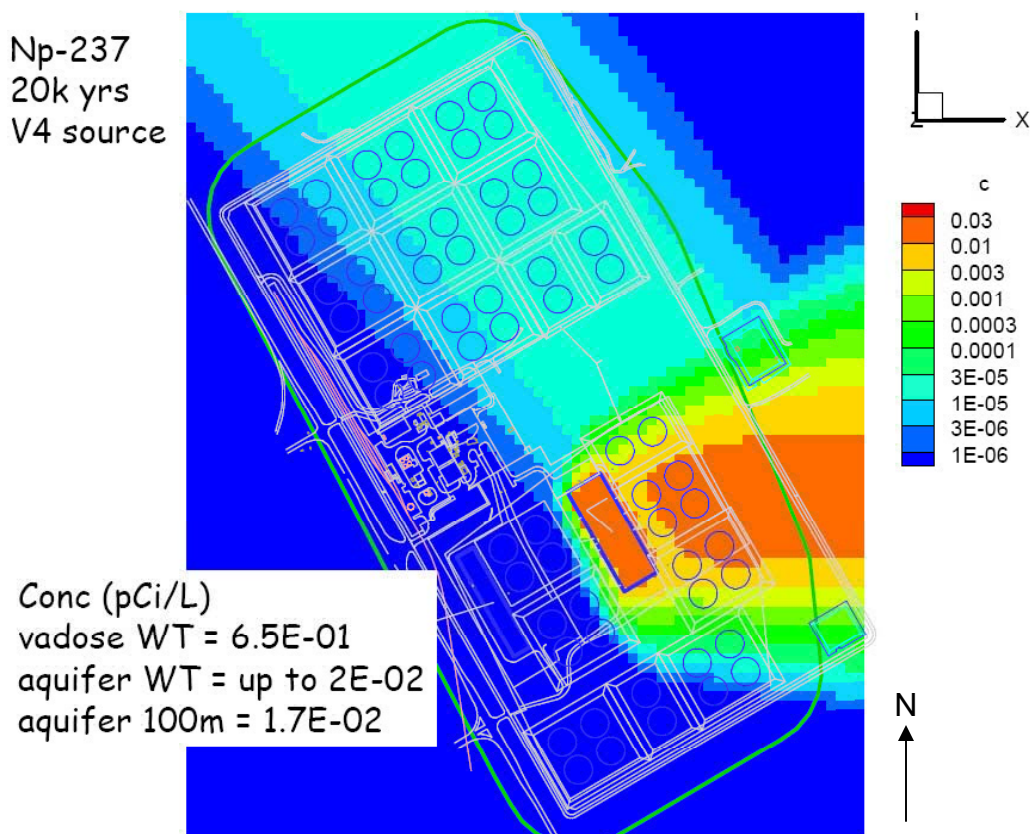
Figure 4.4-70: Saltstone Disposal Facility Streamlines



Values for plume overlap are calculated only for plumes which may reasonably be thought to interact. The model did not simulate any plume interaction between the north and south section of the SDF, nor were there any interactions between plumes on opposite sides of the flow divide. The term “plume interaction” is used here to represent the case where contaminants from multiple sources feed the same point in space. The PORFLOW model has three aquifers, the lowest of which is essentially isolated from the top two.

Figure 4.4-71 is a plan view of the highest PORFLOW concentration simulated at any depth, i.e., the plume centerline projected onto a map view. The figure shows that the majority of the contamination from Vault 4 flows in an eastwardly direction, traveling through shallow aquifer zones. However, there is a small contribution in sectors to the north, resulting from deeper migration into the Gordon aquifer (which flow to the north-northwest). While the Vault 4 contribution of some contaminants may be small in absolute terms, relative to the contributions from the FDCs, the contribution may be significant. The northern flow occurs in the lowest, isolated aquifer. To be consistent with how PORFLOW passes its data to the dose calculator, the contribution to the mixing cell concentrations was accommodated during the benchmarking process.

Figure 4.4-71: Saltstone Disposal Facility Sectors



4.4.4.2.3 GoldSim Dose Calculator Model Description

The contaminant concentrations used by the stand alone GoldSim dose calculator were obtained from the PORFLOW SDF model. The dose model obtained 1m, 100m, and seepage contaminant concentrations from the SDF PORFLOW model. The concentration data was provided for the Base Case and the various sensitivities. The 100m concentrations were provided for all 12 sectors. For the 1m and seepage concentrations, only single maximum concentrations were provided for each case/sensitivity. The concentrations were then subjected to the applicable exposure pathways (discussed in Sections 5.4, 6.2, and 6.3) to calculate doses for different scenarios, sectors, pathways, etc.

4.5 Airborne and Radon Analysis

This section describes the details associated with computing the dose to the MEI due to radioactive disposals in the SDF. The simulation period for the air and radon pathway was 10,000 years and covered only the time period following closure cap installation. The following cases were simulated.

- Vault 1 with DDA saltstone as the representative waste
- Vault 1 with ARP/MCU saltstone as the representative waste
- FDCs with SWPF saltstone as the representative waste
- Vault 4 with DDA saltstone as the representative waste
- Vault 4 with ARP/MCU saltstone as the representative waste

[Material properties taken from SRNL-STI-2008-00421]

The method employed and the key aspects of the analysis performed are discussed in the sections that follow. For the radon pathway, the peak flux at the ground surface of Rn-222 was calculated for five parent radionuclides for each disposal unit and waste degradation case. The dose to the MEI was also calculated for eight radionuclides based on the gaseous flux of each at the land surface for each disposal unit and waste degradation case.

The method chosen was a hybrid approach where most parameters were set to their best estimate values (i.e., based on available site-specific measurements or engineering judgment), while other parameters were set to conservative/bounding values. The conceptual PORFLOW transport model used for the air and radon pathway analysis has imbedded within it biases that were intended to be conservative where possible. The conceptual model for both the air and radon pathway analysis was the same and the PORFLOW transport model used for both pathways utilized the same input files. Section 4.5.1 and its associated subsections discuss the conceptual model for the air and radon pathway analysis. Sections 4.5.2 and 4.5.3 discuss the details specific to each analysis.

4.5.1 Air and Radon Pathway Conceptual Model

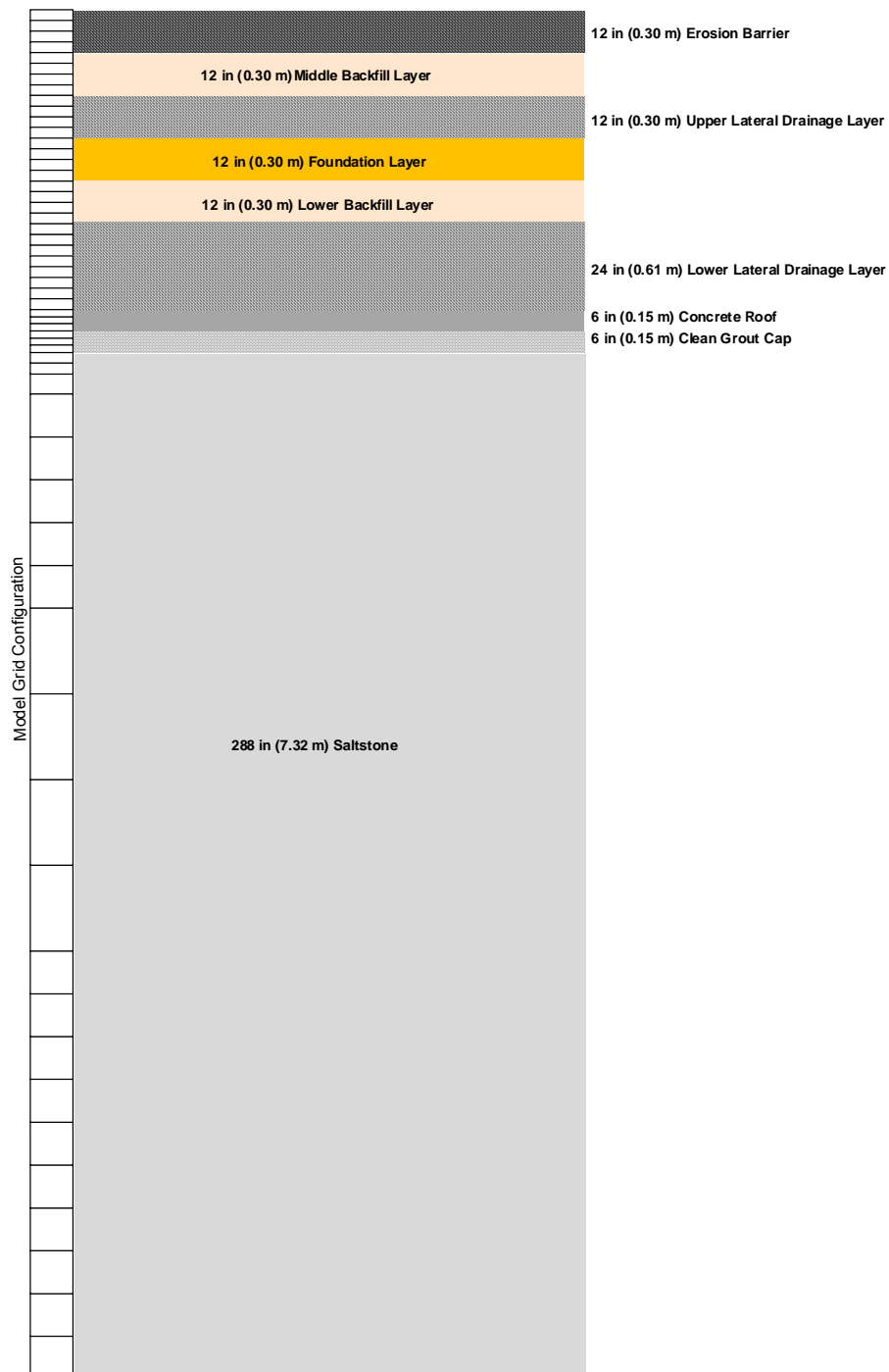
The approach taken focuses primarily on a baseline scenario where nominal settings for many of the input parameters have been conservatively chosen. The main analysis tool employed was the PORFLOW code, which simulated the transport of radionuclide chains (i.e., parents and daughters) in porous media. The flux of radioactive gasses at the land surface above the disposal units was evaluated for the closure degradation case given in WSRC-STI-2008-00244. Gaseous radionuclides within the waste zone diffused outward into

the air-filled pore space of the overlying materials. Ultimately, some of the radionuclides emanated at the land surface. As such, air was the medium through which they diffused. It was assumed that fluctuations in atmospheric pressure at the land surface, that could induce small pulses of air movement into and out of the shallow soil profile over relatively short periods of time, would have a zero net effect when averaged over longer time periods. Thus, advective transport of radionuclides in air-filled soil pores was not considered to be a significant process when compared to the rate of air diffusion.

The closure cap as described in WSRC-STI-2008-00244 consists of a top soil layer, an upper backfill layer, an erosion barrier layer, a geotextile fabric, a middle backfill layer, a geotextile fabric, an upper lateral drainage layer, a geotextile fabric, a HDPE geomembrane, a GCL, a foundation layer (backfill with bentonite admix), a lower backfill layer, a geotextile filter fabric, and a lower drainage layer. The geotextile fabrics, the HDPE geomembrane, and the GCL were excluded from this analysis. By excluding these materials, the analysis was more conservative as these materials would be expected to significantly reduce gaseous flux at the land surface (not including the geotextile fabrics). The HDPE geomembrane would have very low gaseous diffusion coefficient and the GCL would have very little air-filled porosity, since it would be at or near saturation. The top soil layer and the upper backfill layer were also excluded from the baseline analysis, since they are located above the erosion barrier and are therefore subject to erosion. For the purposes of this analysis, it was assumed that those components situated below the top of the erosion barrier remain intact for the duration of the simulation (10,000 years).

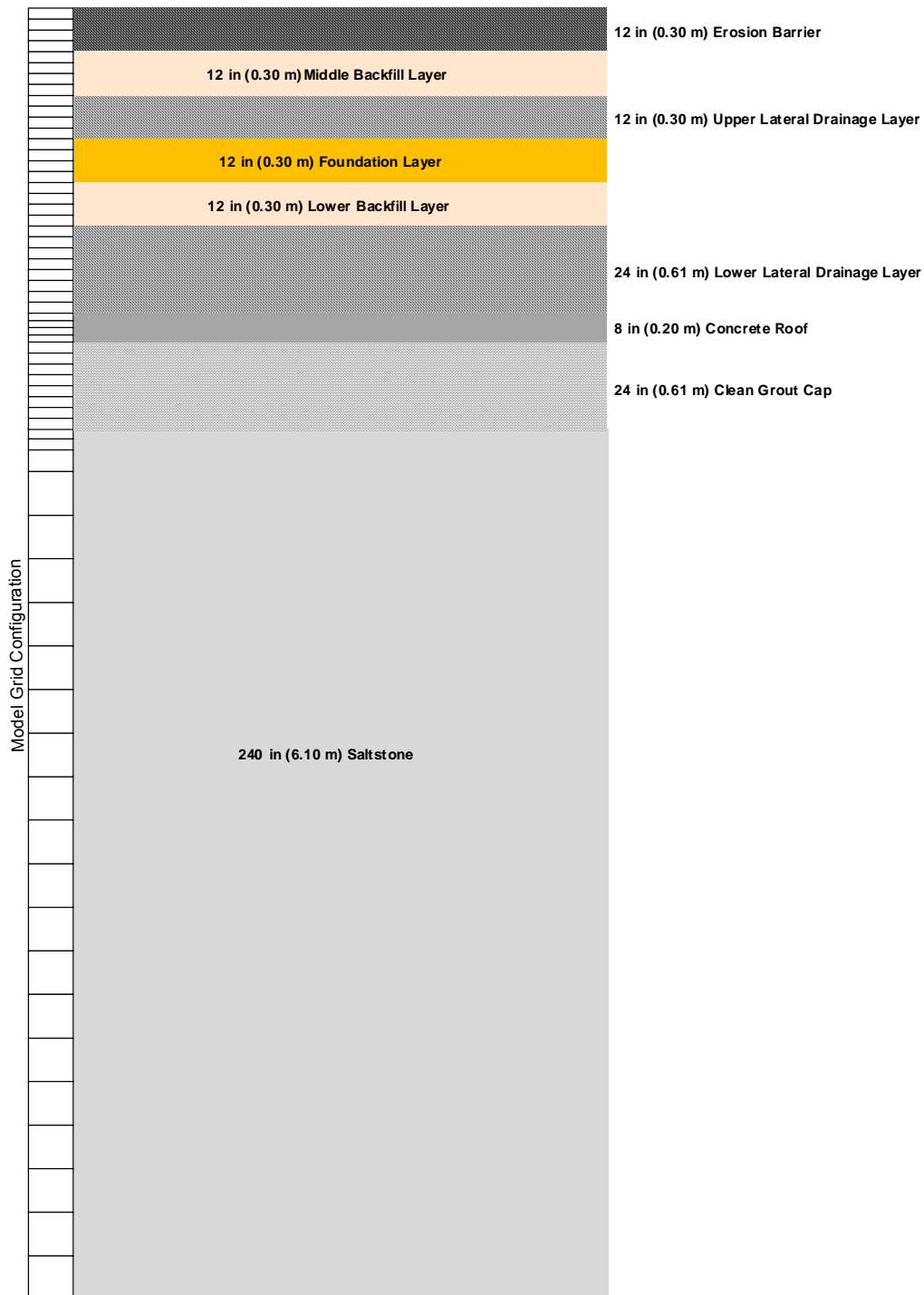
Three disposal unit designs were considered in this analysis; Vault 1, Vault 4, and the FDCs. Schematics of the models for the three designs, including the closure cap materials, are given in Figure 4.5-1, Figure 4.5-2 and Figure 4.5-3. [SRNL-STI-2008-00447] As mentioned previously, Vaults 1 and 4 are assumed to contain either DDA or ARP/MCU saltstone. It was assumed that FDCs will be filled primarily with SWPF saltstone.

Figure 4.5-1: Schematic of PORFLOW Model Grid for Vault 1 Air and Radon



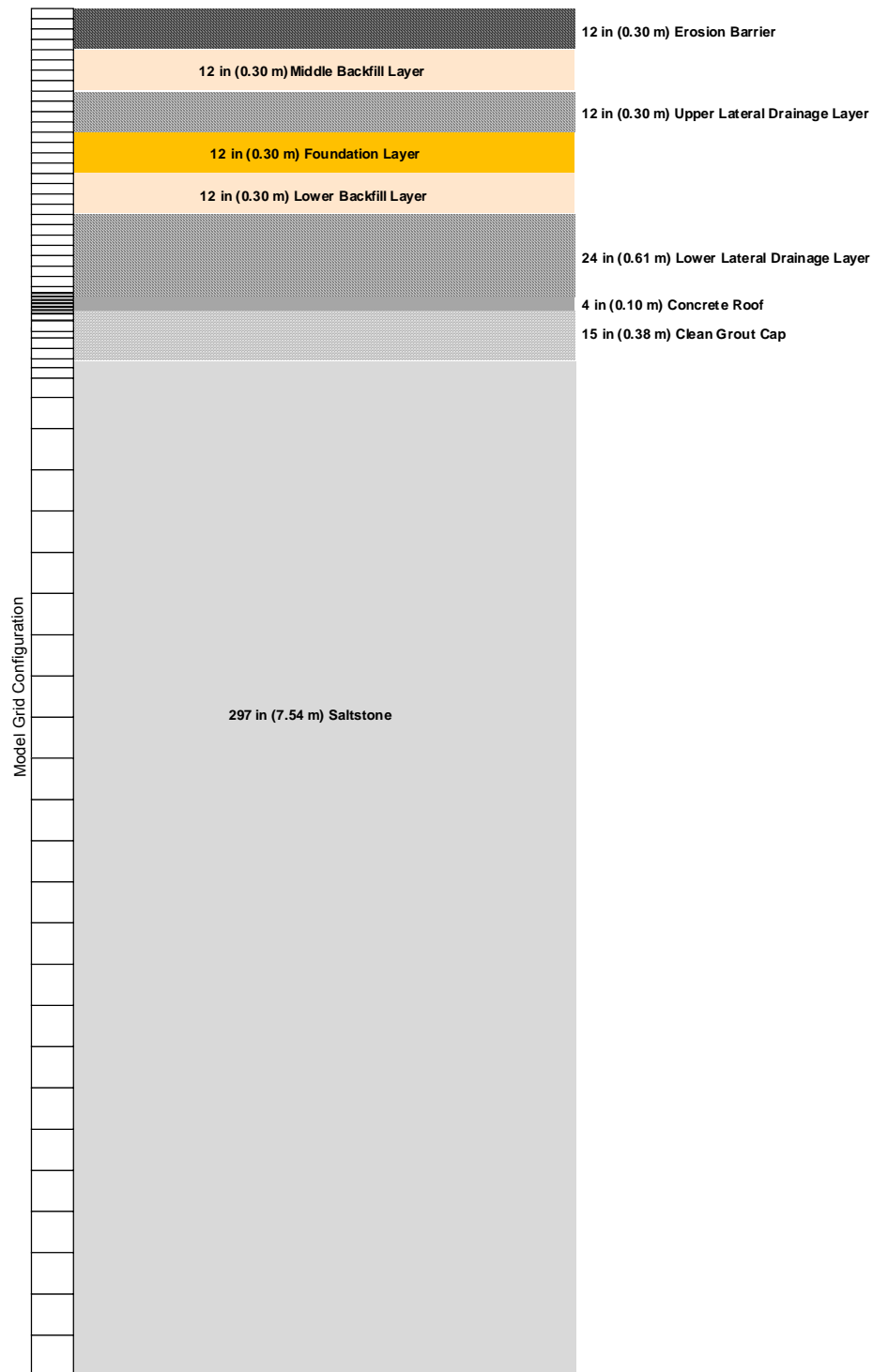
Note: For conservatism the model grid does not include the following layers, topsoil; upper backfill, geotextile fabric, HPDE geomembrane, and GCL.

Figure 4.5-2: Schematic of PORFLOW Model Grid for FDC Air and Radon



Note: For conservatism the model grid does not include the following layers; topsoil, upper backfill, geotextile fabric, HPDE geomembrane, and GCL.

Figure 4.5-3: Schematic of PORFLOW Model Grid for Vault 4 Air and Radon



Note: For conservatism the model grid does not include the following layers; topsoil, upper backfill, geotextile fabric, HPDE geomembrane, and GCL.

4.5.1.1 Air and Radon Pathway Diffusive Transport Model

A 1-D PORFLOW based diffusive transport model was created for each disposal unit. PC-based PORFLOW Version 6.10.3 was used to conduct the simulations. [ACRi PORFLOW-QA-2008-1] PORFLOW has been widely used at SRS and in the U.S. DOE complex to address major issues related to groundwater and nuclear waste management.

The governing equation for mass transport of species k in the fluid phase is given by

$$\frac{\partial C_k}{\partial t} + \frac{\partial}{\partial x_i} \left(\frac{V_i}{R_f} C_k \right) = \frac{\partial}{\partial x_i} \left(\frac{D_{ij}}{R_f} \frac{\partial C_k}{\partial x_j} \right) + \gamma_k$$

Where:

| | | |
|------------|---|---|
| C_k | = | concentration of species k , Ci/m ³ |
| V_i | = | fluid velocity in the i^{th} direction, m/yr |
| D_{ij} | = | molecular diffusion coefficient for the species, m ² /yr |
| R_f | = | retardation factor |
| γ_k | = | net decay of species k , Ci/m ³ yr |
| i, j | = | direction index |
| t | = | time, yr |
| x | = | distance coordinate, m |

This equation was solved within PORFLOW to evaluate transient radionuclide transport above the disposal units and to estimate gaseous radionuclide flux at the land surface over time. For this analysis, the advection term was disabled within PORFLOW and only the diffusive and net decay terms were evaluated.

The boundary conditions imposed on the entire model domain included:

- No-flux specified for all radionuclides along sides and bottom
($\partial C / \partial X = 0$ at $x=0$, $x=1$ and $\partial C / \partial Y = 0$ at $y=0$)
- Species concentration set to 0 at land surface (top of erosion barrier)
($C = 0$ at $y=y_{\text{max}}$)

These boundary conditions force all of the gaseous radionuclides to move upward from the waste disposal zone to the land surface. In reality, some lateral and downward diffusion occurs in the air-filled pores surrounding the waste zone; hence, ignoring this lateral and downward movement has the effect of increasing the flux at the land surface. This should introduce some conservatism in the calculated results. Simulations were conducted in transient mode for diffusive transport in air, with results being obtained over 10,000 years.

The initial condition imposed on the domain, except for the waste zone, included:

- Species concentration set to 0 at time = 0
($C=0$ for $0 \leq x \leq 1$ at $t=0$ and $C=0$ for $0 \leq y \leq y_{\max}$ at $t=0$)

For the air pathways analysis, the initial conditions for the model assumed a 1 Ci inventory of each radionuclide uniformly spread over the waste zone. For the radon pathway analysis, an emanation factor of 0.25 was applied, resulting in an initial inventory of 0.25 Ci for each parent radionuclide uniformly spread over the waste zone.

4.5.1.1.1 Grid Construction

The model grid for Vault 1 and overlying cover materials was constructed as a node mesh 3 nodes wide by 58 nodes high. This mesh creates a vertical stack of 56 model elements.

Figure 4.5-1 shows a schematic of the PORFLOW model grid. The model grid for Disposal Unit 2A/2B FDCs and overlying cover materials was constructed as a node mesh, 3 nodes wide by 64 nodes high. This mesh creates a vertical stack of 62 model elements. Figure 4.5-2 shows a schematic of the PORFLOW model grid. The model grid for Vault 4 and overlying cover materials was constructed as a node mesh, 3 nodes wide by 68 nodes high. This mesh creates a vertical stack of 66 model elements. Figure 4.5-3 shows a schematic of the PORFLOW model grid. In each case, the model grid extends upward to the top of the erosion barrier since this is the minimum possible cover thickness that could exist during the simulation period. A set of consistent units was employed in the simulations for length, mass and time, these being meters, grams and years, respectively.

4.5.1.1.2 Material Zone Properties and Other Input Parameters

Material properties utilized within the 1-D numerical model for each disposal unit were specified for 9 material zones defined within the model domain. The vertical layer sequence and associated thickness for each disposal unit is given in Table 4.5-1, Table 4.5-2, and Table 4.5-3. Each material zone was assigned values of particle density, total porosity, average saturation, air-filled porosity, and air density. An effective air diffusion coefficient was used for each radionuclide and material layer. Therefore, tortuosity was assigned a unit value in each material zone. An air fluid density of $1.24\text{E}+3 \text{ g/m}^3$ at standard atmospheric conditions was used in the transport simulations. [SRNL-STI-2008-00447]

Table 4.5-1: Vertical Layer Sequence/Thickness for Vault 1 and Cover Material

| Layer | Thickness (in) | Thickness (ft) | Thickness (m) |
|------------------------------|-------------------|-------------------|------------------|
| Erosion barrier | 12 | 1 | 0.30 |
| Middle backfill layer | 12 | 1 | 0.30 |
| Upper lateral drainage layer | 12 | 1 | 0.30 |
| Foundation layer | 12 | 1 | 0.30 |
| Lower backfill layer | 12 | 1 | 0.30 |
| Lower drainage layer | 24 | 2 | 0.61 |
| Concrete Roof | 6 | 0.5 | 0.15 |
| Clean Grout | 6 | 0.5 | 0.15 |
| DDA or ARP/MCU Saltstone | 288 | 24 | 7.32 |

[SRNL-STI-2008-00447]

Table 4.5-2: Vertical Layer Sequence/Thickness for FDC and Cover Material

| Layer | Thickness (in) | Thickness (ft) | Thickness (m) |
|------------------------------|-------------------|-------------------|------------------|
| Erosion barrier | 12 | 1 | 0.30 |
| Middle backfill layer | 12 | 1 | 0.30 |
| Upper lateral drainage layer | 12 | 1 | 0.30 |
| Foundation layer | 12 | 1 | 0.30 |
| Lower backfill layer | 12 | 1 | 0.30 |
| Lower drainage layer | 24 | 2 | 0.61 |
| Concrete Roof | 8 | 0.67 | 0.20 |
| Clean Grout | 24 | 2 | 0.61 |
| SWPF Saltstone | 240 | 20 | 6.10 |

[SRNL-STI-2008-00447]

Table 4.5-3: Vertical Layer Sequence/Thickness for Vault 4 and Cover Material

| Layer | Thickness (in) | Thickness (ft) | Thickness (m) |
|------------------------------|---------------------------|---------------------------|--------------------------|
| Erosion barrier | 12 | 1 | 0.30 |
| Middle backfill layer | 12 | 1 | 0.30 |
| Upper lateral drainage layer | 12 | 1 | 0.30 |
| Foundation layer | 12 | 1 | 0.30 |
| Lower backfill layer | 12 | 1 | 0.30 |
| Lower drainage layer | 24 | 2 | 0.61 |
| Concrete Roof | 4 | 0.33 | 0.10 |
| Clean Grout | 15 | 1.25 | 0.38 |
| DDA or ARP/MCU Saltstone | 297 | 24.75 | 7.55 |

[SRNL-STI-2008-00447]

Material properties for the saltstone and disposal unit concretes were taken from SRNL-STI-2008-00421 and are listed in Table 4.5-4, Table 4.5-5, and Table 4.5-6. Material properties for the closure cap components are also presented and were taken from WSRC-STI-2008-00244. Average saturation values for the saltstone cap and concrete roof were taken from the SDF PA vadose zone model. Additionally, the grout cap was assumed to have the same material properties as saltstone. The air-filled porosity of the saltstone cap and concrete roof were calculated from the total porosity and average saturation.

**Table 4.5-4: Particle Density, Total Porosity, Average Saturation, and Air-filled Porosity
Vault 1**

| Layer | Particle Density (g/cm ³) | Total Porosity (fraction) | Average Saturation (fraction) | Air-filled Porosity (fraction) |
|------------------------------|---------------------------------------|---------------------------|-------------------------------|--------------------------------|
| Erosion barrier | 2.65 | 0.150 | 0.88 | 0.017 |
| Middle backfill layer | 2.63 | 0.350 | 0.96 | 0.012 |
| Upper lateral drainage layer | 2.65 | 0.417 | 0.61 | 0.162 |
| Foundation layer | 2.63 | 0.350 | 0.86 | 0.048 |
| Lower backfill layer | 2.63 | 0.350 | 0.76 | 0.082 |
| Lower drainage layer | 2.65 | 0.417 | 0.00 | 0.417 |
| Concrete Roof | 2.53 | 0.120 | 0.98 | 0.032 |
| Clean Grout DDA | 2.37 | 0.550 | 0.98 | 0.011 |
| Clean Grout ARP/MCU | 2.38 | 0.590 | 0.98 | 0.012 |
| DDA Saltstone | 2.37 | 0.550 | 0.98 | 0.011 |
| ARP/MCU Saltstone | 2.38 | 0.590 | 0.98 | 0.012 |

[SRNL-STI-2008-00447]

**Table 4.5-5: Particle Density, Total Porosity, Average Saturation, and Air-filled Porosity
FDCs**

| Layer | Particle Density (g/cm ³) | Total Porosity (fraction) | Average Saturation (fraction) | Air-filled Porosity (fraction) |
|------------------------------|---------------------------------------|---------------------------|-------------------------------|--------------------------------|
| Erosion barrier | 2.65 | 0.150 | 0.88 | 0.017 |
| Middle backfill layer | 2.63 | 0.350 | 0.96 | 0.012 |
| Upper lateral drainage layer | 2.65 | 0.417 | 0.61 | 0.162 |
| Foundation layer | 2.63 | 0.350 | 0.86 | 0.048 |
| Lower backfill layer | 2.63 | 0.350 | 0.76 | 0.082 |
| Lower drainage layer | 2.65 | 0.417 | 0.00 | 0.417 |
| Concrete Roof | 2.50 | 0.110 | 0.98 | 0.002 |
| Clean Grout | 2.42 | 0.580 | 0.99 | 0.009 |
| SWPF Saltstone | 2.42 | 0.580 | 0.99 | 0.009 |

[SRNL-STI-2008-00447]

**Table 4.5-6: Particle Density, Total Porosity, Average Saturation, and Air-Filled Porosity
Vault 4**

| Layer | Particle Density (g/cm ³) | Total Porosity (fraction) | Average Saturation (fraction) | Air-filled Porosity (fraction) |
|------------------------------|---------------------------------------|---------------------------|-------------------------------|--------------------------------|
| Erosion barrier | 2.65 | 0.150 | 0.88 | 0.017 |
| Middle backfill layer | 2.63 | 0.350 | 0.96 | 0.012 |
| Upper lateral drainage layer | 2.65 | 0.417 | 0.61 | 0.162 |
| Foundation layer | 2.63 | 0.350 | 0.86 | 0.048 |
| Lower backfill layer | 2.63 | 0.350 | 0.76 | 0.082 |
| Lower drainage layer | 2.65 | 0.417 | 0.00 | 0.417 |
| Concrete Roof | 2.53 | 0.120 | 0.98 | 0.002 |
| Clean Grout DDA | 2.37 | 0.550 | 0.99 | 0.008 |
| Clean Grout ARP/MCU | 2.38 | 0.590 | 0.99 | 0.009 |
| DDA Saltstone | 2.37 | 0.550 | 0.99 | 0.008 |
| ARP/MCU Saltstone | 2.38 | 0.590 | 0.99 | 0.009 |

[SRNL-STI-2008-00447]

Infiltration evaluations were performed through the closure cap materials over time as the closure cap degraded using the HELP model. [WSRC-STI-2008-00244] Values for total porosity and volumetric moisture content for the closure cap materials and foundation layers were taken from this analysis. These values were used to calculate the average saturation and air-filled porosity for the closure cap materials. The maximum air-filled porosity for each material layer over the 10,000 year simulation was utilized since this represented the greatest air-filled porosity in which a gas could diffuse. Tables 4.5-4, 4.5-5, and 4.5-6 provide the values of particle density, total porosity, average saturation, and air-filled porosity, utilized for all the layers in each case simulated.

4.5.1.2 Summary of Key Air and Radon Pathways Assumptions

The following are the key air and radon pathways analysis assumptions associated with each disposal unit simulation:

- The waste in Vault 1 can be represented by either DDA or ARP/MCU saltstone
- The waste to be placed in future disposal units can be represented by SWPF saltstone
- The waste in Vault 4 can be represented by either DDA or ARP/MCU saltstone
- The clean grout cap for each disposal unit has the same material properties as saltstone
- Exclusion of the top soil, upper backfill, HDPE geomembrane, and GCL make the model more conservative
- Exclusion of all geotextile fabrics has no impact on the model
- The final closure cap is assumed to remain physically stable below the top of the erosion barrier for the duration of the simulation (10,000 years)

4.5.1.2.1 Measures Implemented to Ensure Conservative Results

In this analysis, several conditions introduce conservatism into the calculations. These include:

- The use of boundary conditions that force all of the gaseous radionuclides to move upward from the waste disposal zone to the land surface. In reality, some of the gaseous radionuclides diffuse sideways and downward in the air-filled pores surrounding the waste zone; hence ignoring this has the effect of increasing the flux at the land surface.
- Not taking credit for the removal of radionuclides by pore water moving vertically downward through the model domain. This mechanism would likely remove some dissolved radionuclides, and therefore its omission has the effect of increasing the estimate of instantaneous radionuclide flux at the land surface in simulations conducted as a part of this investigation.
- Exclusion of the HDPE geomembrane and the GCL. Inclusion of these materials in the model would significantly reduce the gaseous flux at the land surface due to their material properties (i.e., low air-filled porosity and/or low effective gaseous diffusion coefficient).
- Exclusion of the cover materials above the erosion barrier (i.e., top soil and upper backfill layers). Excluding these materials shortens the diffusion pathways and could increase the flux at the land surface.
- Use of the minimum closure cap thickness in the model.

4.5.2 Saltstone Disposal Facility Air Pathways Model

A screening analysis was conducted to determine the radionuclides of interest for the air pathways analysis. [WSRC-STI-2006-00159] These radionuclides included C-14, Cl-36, I-129, Se-79, Sb-125, Sn-126, and H-3. Subsequent to the screening analysis, Tc-99 was added to the list of radionuclides of interest. A summary of the radionuclides and compounds of interest is presented in Table 4.5-7.

Table 4.5-7: Radionuclides and Compounds of Interest for Air and Radon Pathway Analysis

| Radionuclide | Half-life ¹ (yrs) | Approximate Atomic Wt. | Molecular form in gaseous state | Molecular Wt. |
|--------------|------------------------------|------------------------|---------------------------------|---------------|
| Cl-36 | 3.01E+05 | 36 | Cl ₂ | 72 |
| C-14 | 5.70E+03 | 14 | CO ₂ | 46 |
| H-3 | 12.3E+00 | 3 | H ₂ | 6 |
| I-129 | 1.57E+07 | 129 | I ₂ | 258 |
| Rn-222 | 1.05E-02 | 222 | Rn | 222 |
| Sb-125 | 2.76E+00 | 125 | Sb | 125 |
| Se-79 | 2.95E+05 | 79 | Se | 79 |
| Sn-126 | 2.30E+05 | 126 | Sn | 126 |
| Tc-99 | 2.11E+05 | 99 | Tc | 99 |

(1) PIT-MISC-0072

4.5.2.1 Source Term Development

The source term for the simulations was assumed to be 1 Ci of each radionuclide, which was distributed uniformly throughout the liquid filled pores of the saltstone material layer. The radionuclides were then allowed to partition between the pore fluid and the air-filled pores. Partitioning coefficients equivalent to apparent Henry's Law constants were estimated using *The Geochemist's Workbench*® Release 6.0, Henry's Law for solutions is:

$$m_i = f_i H$$

where m_i is the molality (mol/kg) of constituent i in the aqueous phase, f_i is the fugacity of constituent in the gas phase, and H is Henry's Law constant. Both the solution and the gas phase were assumed to behave ideally. This makes the fugacity of a constituent equal to the partial pressure of that constituent in the gas phase. Thus, the units of the Henry's Law constant are:

$$\frac{\text{moles}}{\text{atm} \times \text{kg}}$$

Here, these are considered apparent Henry's Law constants because most of these gases dissociate in solution to species other than the aqueous species of the gas. For example, CO₂ gas dissolved in water at a pH of 11 exists primarily as the carbonate ion CO₃.

The gases considered for each radionuclide, their reactions with their aqueous component, and the equilibrium constants for these reactions are shown in Table 4.5-8. In all cases the fugacity of one gas for each element was higher by several orders of magnitude than the fugacity of the other gases. The highest fugacity was chosen for the estimate of the apparent Henry's Law constant for a radionuclide.

Table 4.5-8: Gases for Each Radionuclide, their Reaction with Aqueous Component, and Equilibrium Constants

| Contaminant | Gas Species | Reaction | Log K (25°C) |
|--------------|-------------------|--|--------------|
| C-14 | CO ₂ | CO _{2(g)} + H ₂ O = HCO ₃ ⁻ + H ⁺ | -7.82 |
| Cl-36 | Cl ₂ | Cl _{2(g)} + H ₂ O = 2Cl ⁻ + 2H ⁺ + ½O ₂ | 3.03 |
| Cl-36 | HClO ₄ | HClO _{4(g)} = Cl ⁻ + 2O ₂ + H ⁺ | 33.38 |
| Cl-36 | HCl | HCl _(g) = Cl ⁻ + H ⁺ | 6.31 |
| H-3 | H ₂ O | H ₂ O _(g) = H ₂ O _(l) | 1.50 |
| I-129 | I ₂ | I _{2(g)} + H ₂ O = 2I ⁻ + ½O ₂ + 2H ⁺ | -21.53 |
| I-129 | HI | HI _(g) = I ⁻ + H ⁺ | 9.31 |
| Sb-125, 126 | SbCl ₃ | SbCl _{3(g)} + 3H ₂ O = Sb(OH) ₃ ⁰ + 3Cl ⁻ + 3H ⁺ | 4.83 |
| Sb-125, 126 | SbCl ₅ | SbCl _{5(g)} + 4H ₂ O = Sb(OH) ₃ ⁰ + 5Cl ⁻ + ½O ₂ + 5H ⁺ | 2.74 |
| Sb-125, 126 | SbH ₃ | SbH _{3(g)} + 3/2O ₂ = Sb(OH) ₃ ⁰ | 143.11 |
| Se-79 | H ₂ Se | H ₂ Se _(g) + 3/2O ₂ = SeO ₃ ⁻² + 2H ⁺ | 71.83 |
| Se-79 | SeCl ₄ | SeCl _{4(g)} + 3H ₂ O = SeO ₃ ⁻² + 4Cl ⁻ + 6H ⁺ | 13.78 |
| Sn-121m, 126 | SnCl ₄ | SnCl _{4(g)} = Sn ⁺⁴ + 4Cl ⁻ | 15.85 |
| Sn-121m, 126 | SnH ₄ | SnH _{4(g)} + 4H ⁺ = 4H ₂ + Sn ⁺⁴ | 20.10 |

The assumptions used in the calculations are documented in Table 4.5-9. The E_h and pH values are from estimations made in SRNL-TR-2008-00283 for middle aged saltstone pore water conditions. The Henry's Law constants for most of the gases vary considerably with these parameters, though differently for each gas. The ionic strength of the solution was fixed at 0.015 molal primarily by Na⁺ and Cl⁻, to be in the range of the extended Debye-Hückel method of calculating activity coefficients used by *The Geochemist's Workbench*® Release 6. Nitrate is the dominant anion in the saltstone feed solution, but at equilibrium under the reducing conditions of saltstone, nitrogen exists primarily as dissolved nitrogen gas that does not contribute to ionic strength. Therefore, chloride was used to balance the sodium. The initial concentrations of the radionuclides do not matter because the apparent Henry's Law constant is the ratio of the gas fugacity to the aqueous radionuclide concentration. Thus, the ratio remains constant regardless of the total concentration of the radionuclide.

Table 4.5-9: Parameters Used in Estimating Apparent Henry's Law Constants

| Parameter | Value Used |
|-----------------|-------------|
| Cl ⁻ | 0.01 mol/kg |
| E _h | -0.45 V |
| Na ⁺ | 0.01 mol/kg |
| pH | 11.0 |
| T | 25°C |

Table 4.5-10 shows the results of the apparent Henry's Law constant estimations for partitioning the radionuclides of interest between pore water and the gas phase. Most of the apparent Henry's Law constants are so high as to be essentially meaningless, therefore, all of the radionuclide can be assumed to be in the aqueous phase. The exceptions are tritium, C-14, and possibly Se-79. The reason that elements that are often considered to be relatively volatile have such low apparent Henry's Law constants is that saltstone conditions are antithetical to the formation of gases from these elements. For example, at a pH of 5, the apparent Henry's Law constants of the radionuclides other than Tc-99 would be much lower. Likewise, the apparent Henry's Law constant for Tc-99 would be much lower if saltstone were at oxidizing conditions.

Table 4.5-10: Radionuclides of Interest, Dominant Gas Under Saltstone Conditions, and Apparent Henry's Law Constant

| Radionuclide | Gas | H (mol/atm·kg) |
|--------------|--------------------------------|-------------------|
| C-14 | CO ₂ | 1.4E+4 |
| Cl-36 | HCl | 2.3E+17 |
| I-129 | HI | 2.8E+20 |
| Sb-125, 126 | SbH ₃ | 3.3E+34 |
| Se-79 | H ₂ Se | 1.1E+6 |
| Sn-121m, 126 | SnH ₄ | 2.2E+60 |
| Tc-99 | Tc ₂ O ₇ | 1.5E+67 |
| Tritium | Water Vapor | 2.1E+3 |

The primary uncertainty in these calculations is the use of lower ionic strengths in the calculations than those estimated for saltstone pore fluids. The ionic strength of the pore fluids in fresh saltstone would be on the order of 6 molal, far higher than the 0.015 molal used here. This would lead to underestimation of the amount of a radionuclide in the gas phase for all constituents except tritium. For tritium, higher ionic strength lowers the vapor pressure of water at a given temperature, thus lowering the amount of tritium in the vapor phase. For other constituents, the high ionic strengths resulted in higher activity coefficients than those at lower ionic strengths. This caused a higher degree of partitioning of the radionuclide into the gaseous phase, sometimes referred to as the “salting out” effect. However, it is unlikely that the activity coefficients would increase by more than a factor of 10. [SRNL-STI-2008-00447] Such an increase would not significantly affect conclusions based on this analysis, particularly for Cl-36, I-129, Tc-99, Sn-126, Sb-125, or Sb-126. To account for the high ionic strength, saltstone pore fluids would require more sophisticated solution models and it is uncertain that reliable parameters required to run these models even exist for several of the radionuclides of interest.

4.5.2.2 Implementation of Partitioning Coefficients in PORFLOW

PORFLOW has the capability of partitioning radionuclides between the solid and liquid phases through a K_d . However, PORFLOW does not directly have the capability of partitioning radionuclides between the liquid and gas phases through Henry’s law. Therefore, in order to use PORFLOW to represent the transport of radionuclides through the gas phase while considering liquid-gas partitioning, Henry’s Law constants must be converted to equivalent K_d . This section outlines the method used to make the conversion.

The apparent Henry’s Law constants developed in Section 4.5.2.1 for each radionuclide were converted into pseudo-partitioning coefficients for use in PORFLOW. The conventional application of partitioning in PORFLOW involved the transfer of contaminant from solid to liquid phase via a linear and completely reversible reaction. This reaction was represented in the form of a K_d , which was used in the calculation of the retardation factor (Section 4.5.1.1, retardation factor). Distribution coefficient is defined as the concentration of contaminant in the solid phase relative to the concentration of contaminant in solution with typical units of mL/g. [SRNL-STI-2008-00447] For the air pathways analysis, the partitioning of contaminants was from the liquid to the gas phase, rather than from the solid to the liquid phase. Therefore, it was necessary to develop a relationship between the apparent Henry’s Law constants and the K_d concept used in PORFLOW. The resulting partitioning coefficients used in the PORFLOW air pathways analysis are given in Table 4.5-11.

Table 4.5-11: Apparent Henry's Law Constant and Partitioning Coefficient

| Radionuclide | H (mol/atm·kg) | Partitioning Coefficient (mL/g) |
|---------------------|---------------------------|--|
| C-14 | 1.4E+4 | 3.37E+5 |
| Cl-36 | 2.3E+17 | 5.53E+18 |
| I-129 | 2.8E+20 | 6.73E+21 |
| Sb-125, 126 | 3.3E+34 | 7.93E+35 |
| Se-79 | 1.1E+6 | 3.61E+7 |
| Sn-121m, 126 | 2.2E+60 | 5.29E+61 |
| Tc-99 | 1.5E+67 | 3.61E+68 |
| Tritium | 2.1E+3 | 5.05E+4 |

To correctly implement the partitioning coefficients in PORFLOW, it was necessary to redefine the material properties of the saltstone. The typical simulation in PORFLOW involved a solid, liquid, and a gas, with partitioning of contaminants between the solid and liquid phase (via K_d) and advective and diffusive transport occurring through the liquid phase. Inputs included the bulk density of the solid phase and the porosity of the gas-liquid phase. For gaseous diffusion problems, the particle density was that of the solid material, the porosity was the void space occupied by the gas (air-filled porosity), and the fluid density was the density of air. If the gaseous contaminants were assumed to be totally in the gas phase and the waste was assumed to be dry, then the air-filled porosity equaled the total porosity and there was no partitioning. For this analysis, the waste was assumed to be mostly saturated with the radionuclides of interest partitioned between the gas and liquid phase. In order to implement the K_d approach to partitioning, the liquid took on the role usually played by the solid in a typical groundwater transport problem. Likewise, the gas takes on the role usually played by the liquid. The solid phase could be thought of as having the role typically played by gas where it was not involved in the transport process. In this implementation, the total porosity was the content of the solid and gas phases. The air-filled porosity, which was the porosity used in the transport analysis, was determined by multiplying the total porosity by the gas saturation.

Air is the fluid through which the radioactive gasses diffuse to the ground surface. As such, the fluid density input to PORFLOW was the density of air. For each simulation, a 1 Ci inventory of each radionuclide was placed in the saltstone and partitioned between the liquid and gas phases according to the partitioning coefficients presented in Table 4.5-11. Once in the gas phase, the radionuclides diffused to the land surface based on the diffusion coefficients presented in Table 4.5-12, Table 4.5-13, Table 4.5-14, and the transport equation provided by equation 1 in section 4.5.1.1.

Table 4.5-12: Effective Air Diffusion Coefficients for Vault 1 and Closure Cap

| Radionuclide ^{a,b} | Saltstone and Clean Grout Layer (m ² /yr) | Concrete Roof (m ² /yr) | Lower Drainage Layer (m ² /yr) | Lower Backfill Layer (m ² /yr) | Foundation Layer (m ² /yr) | Upper Lateral Drainage Layer (m ² /yr) | Middle Backfill Layer (m ² /yr) | Erosion Barrier Layer (m ² /yr) |
|-----------------------------|--|--|--|--|---|---|---|---|
| C-14 | 1.93E-01 | 1.93E-01 | 7.62E+02 | 4.51E+00 | 2.40E+00 | 2.40E+00 | 9.23E+00 | 3.88E-01 |
| Cl-36 | 1.54E-01 | 1.54E-01 | 6.09E+02 | 3.61E+00 | 1.92E+00 | 7.38E+00 | 3.10E-01 | 1.61E+00 |
| H-3 | 5.35E-01 | 5.35E-01 | 2.11E+03 | 1.25E+01 | 6.64E+00 | 2.56E+01 | 1.07E+00 | 5.58E+00 |
| I-129 | 8.16E-02 | 8.16E-02 | 3.22E+02 | 1.91E+00 | 1.01E+00 | 3.90E+00 | 1.64E-01 | 8.50E-01 |
| Rn-222 | 8.79E-02 | 8.79E-02 | 3.47E+02 | 2.05E+00 | 1.09E+00 | 4.20E+00 | 1.77E-01 | 9.17E-01 |
| Sb-125 | 1.17E-01 | 1.17E-01 | 4.62E+02 | 2.74E+00 | 1.45E+00 | 5.60E+00 | 2.36E-01 | 1.22E+00 |
| Sb-126 | 1.17E-01 | 1.17E-01 | 4.61E+02 | 2.73E+00 | 1.45E+00 | 5.58E+00 | 2.35E-01 | 1.22E+00 |
| Se-79 | 1.47E-01 | 1.47E-01 | 5.82E+02 | 3.44E+00 | 1.83E+00 | 7.05E+00 | 2.96E-01 | 1.54E+00 |
| Sn-126 | 1.17E-01 | 1.17E-01 | 4.61E+02 | 2.73E+00 | 1.45E+00 | 5.58E+00 | 2.35E-01 | 1.22E+00 |
| Tc-99 | 1.32E-01 | 1.32E-01 | 5.20E+02 | 3.08E+00 | 1.63E+00 | 6.29E+00 | 2.65E-01 | 1.37E+00 |

- (a) The D_e for Rn-222 was used to determine the effective air diffusion coefficient of each radionuclide/compound based on Graham's law. [SRNL-STI-2008-00447]
- (b) The D_e for all three disposal units are the same because the average saturation assumed for each layer is the same for all three designs. [SRNL-STI-2008-00447]

Table 4.5-13: Effective Air Diffusion Coefficients for FDCs and Closure Cap

| Radionuclide ^{a,b} | Saltstone and Clean Grout Layer (m ² /yr) | Concrete Roof (m ² /yr) | Lower Drainage Layer (m ² /yr) | Lower Backfill Layer (m ² /yr) | Foundation Layer (m ² /yr) | Upper Lateral Drainage Layer (m ² /yr) | Middle Backfill Layer (m ² /yr) | Erosion Barrier Layer (m ² /yr) |
|-----------------------------|--|------------------------------------|---|---|---------------------------------------|---|--|--|
| C-14 | 1.43E-01 | 1.43E-01 | 7.62E+02 | 4.51E+00 | 2.40E+00 | 2.40E+00 | 9.23E+00 | 3.88E-01 |
| Cl-36 | 1.14E-01 | 1.14E-01 | 6.09E+02 | 3.61E+00 | 1.92E+00 | 7.38E+00 | 3.10E-01 | 1.61E+00 |
| H-3 | 3.96E-01 | 3.96E-01 | 2.11E+03 | 1.25E+01 | 6.64E+00 | 2.56E+01 | 1.07E+00 | 5.58E+00 |
| I-129 | 6.03E-02 | 6.03E-02 | 3.22E+02 | 1.91E+00 | 1.01E+00 | 3.90E+00 | 1.64E-01 | 8.50E-01 |
| Rn-222 | 6.50E-02 | 6.50E-02 | 3.47E+02 | 2.05E+00 | 1.09E+00 | 4.20E+00 | 1.77E-01 | 9.17E-01 |
| Sb-125 | 8.67E-02 | 8.67E-02 | 4.62E+02 | 2.74E+00 | 1.45E+00 | 5.60E+00 | 2.36E-01 | 1.22E+00 |
| Sb-126 | 8.63E-02 | 8.63E-02 | 4.61E+02 | 2.73E+00 | 1.45E+00 | 5.58E+00 | 2.35E-01 | 1.22E+00 |
| Se-79 | 1.09E-01 | 1.09E-01 | 5.82E+02 | 3.44E+00 | 1.83E+00 | 7.05E+00 | 2.96E-01 | 1.54E+00 |
| Sn-126 | 8.63E-02 | 8.63E-02 | 4.61E+02 | 2.73E+00 | 1.45E+00 | 5.58E+00 | 2.35E-01 | 1.22E+00 |
| Tc-99 | 9.74E-02 | 9.74E-02 | 5.20E+02 | 3.08E+00 | 1.63E+00 | 6.29E+00 | 2.65E-01 | 1.37E+00 |

- (a) The D_e for Rn-222 was used to determine the effective air diffusion coefficient of each radionuclide/compound based on Graham's law. [SRNL-STI-2008-00447]
- (b) The D_e for all three disposal units are the same because the average saturation assumed for each layer is the same for all three designs. [SRNL-STI-2008-00447]

Table 4.5-14: Effective Air Diffusion Coefficients for Vault 4 and Closure Cap

| Radionuclide ^{a,b} | Saltstone and Clean Grout Layer (m ² /yr) | Concrete Roof (m ² /yr) | Lower Drainage Layer (m ² /yr) | Lower Backfill Layer (m ² /yr) | Foundation Layer (m ² /yr) | Upper Lateral Drainage Layer (m ² /yr) | Middle Backfill Layer (m ² /yr) | Erosion Barrier Layer (m ² /yr) |
|-----------------------------|--|------------------------------------|---|---|---------------------------------------|---|--|--|
| C-14 | 1.43E-01 | 1.43E-01 | 7.62E+02 | 4.51E+00 | 2.40E+00 | 9.23E+00 | 3.88E-01 | 2.01E+00 |
| Cl-36 | 1.14E-01 | 1.14E-01 | 6.09E+02 | 3.61E+00 | 1.92E+00 | 7.38E+00 | 3.10E-01 | 1.61E+00 |
| H-3 | 3.96E-01 | 3.96E-01 | 2.11E+03 | 1.25E+01 | 6.64E+00 | 2.56E+01 | 1.07E+00 | 5.58E+00 |
| I-129 | 6.03E-02 | 6.03E-02 | 3.22E+02 | 1.91E+00 | 1.01E+00 | 3.90E+00 | 1.64E-01 | 8.50E-01 |
| Rn-222 | 6.50E-02 | 6.50E-02 | 3.47E+02 | 2.05E+00 | 1.09E+00 | 4.20E+00 | 1.77E-01 | 9.17E-01 |
| Sb-125 | 8.67E-02 | 8.67E-02 | 4.62E+02 | 2.74E+00 | 1.45E+00 | 5.60E+00 | 2.36E-01 | 1.22E+00 |
| Sb-126 | 8.63E-02 | 8.63E-02 | 4.61E+02 | 2.73E+00 | 1.45E+00 | 5.58E+00 | 2.35E-01 | 1.22E+00 |
| Se-79 | 1.09E-01 | 1.09E-01 | 5.82E+02 | 3.44E+00 | 1.83E+00 | 7.05E+00 | 2.96E-01 | 1.54E+00 |
| Sn-126 | 8.63E-02 | 8.63E-02 | 4.61E+02 | 2.73E+00 | 1.45E+00 | 5.58E+00 | 2.35E-01 | 1.22E+00 |
| Tc-99 | 9.74E-02 | 9.74E-02 | 5.20E+02 | 3.08E+00 | 1.63E+00 | 6.29E+00 | 2.65E-01 | 1.37E+00 |

- (a) The D_e for Rn-222 was used to determine the effective air diffusion coefficient of each radionuclide/compound based on Graham's law. [SRNL-STI-2008-00447]
- (b) The D_e for all three disposal units are the same because the average saturation assumed for each layer is the same for all three designs. [SRNL-STI-2008-00447]

4.5.2.3 *Effective Air Diffusion Coefficients*

A radon effective air diffusion coefficient was determined for each material type based upon the average moisture saturation for the material. [SRNL-STI-2008-00447] Subsequently, using Graham's Law, the effective air diffusion coefficient of each radionuclide or compound evaluated was determined for each material type based on the radon effective air diffusion coefficient using the following relationship:

$$D = D' \sqrt{\frac{MWT'}{MWT}}$$

where:

D = the effective diffusion coefficient of the radionuclide of interest (m²/yr)
within the material zone of interest

D' = the effective diffusion coefficient of Rn-222 (m²/yr) within the material zone
of interest

MWT' = the molecular weight of the reference radionuclide (Rn-222)

MWT = the molecular weight of the element or compound of interest

A summary of the radon effective air diffusion coefficients and the calculated effective air diffusion coefficients for each radionuclide/compound by material zone are presented in Table 4.5-12, Table 4.5-13, Table 4.5-14, and SRNL-STI-2008-00447.

4.5.2.4 *Air Pathways Model Results*

4.5.2.4.1 Air Pathways Flux to Ground Surface

Model simulations were conducted to evaluate the peak flux of each radionuclide emanating from the top of the model domain. A unit inventory of 1 Ci was assigned to the waste zone for each case simulated for each radionuclide considered in the analysis. Results were output in Ci/m²/yr per Ci/m², consistent with the set of units employed in the model, and are presented for each radionuclide in Figures 4.5-4 through 4.5-8. The material properties remained constant for each case for the simulation period. Hence, the transient gaseous flux at the land surface for each radionuclide is a function of radioactive decay. This is illustrated in Figures 4.5-4 through 4.5-8 where each radionuclide reaches the peak emission rate and subsequently declines as a function of decay. [SRNL-STI-2008-00447]

Figure 4.5-4: Ci Flux at Land Surface for Modeled Radionuclides in Vault 1 for DDA Saltstone

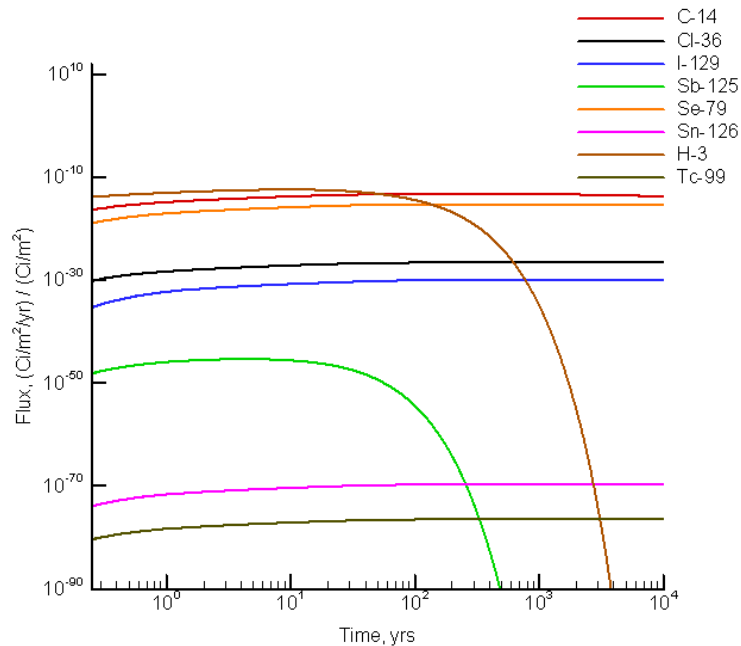


Figure 4.5-5: Ci Flux at Land Surface for Modeled Radionuclides in Vault 1 for ARP/MCU Saltstone

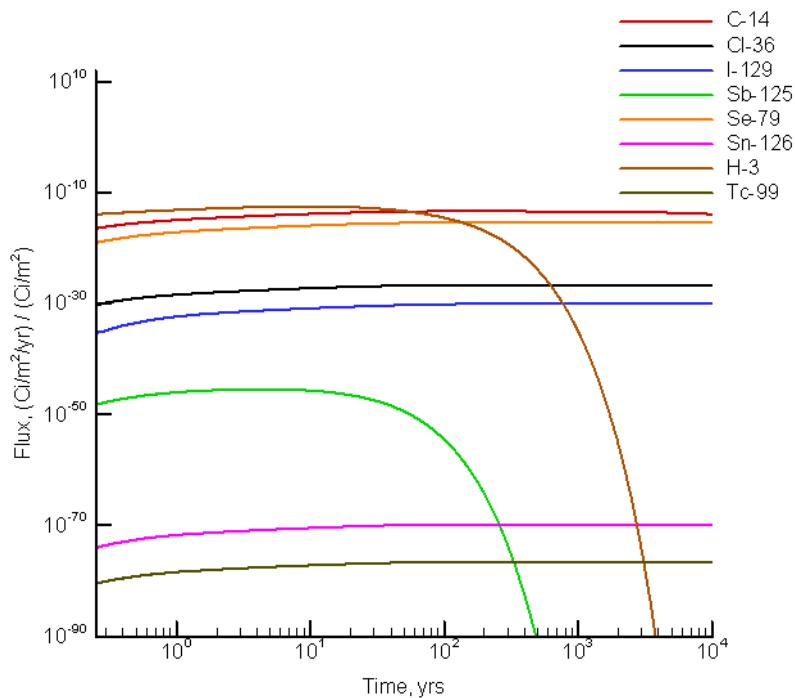


Figure 4.5-6: Ci Flux at Land Surface for Modeled Radionuclides in FDCs for SWPF Saltstone

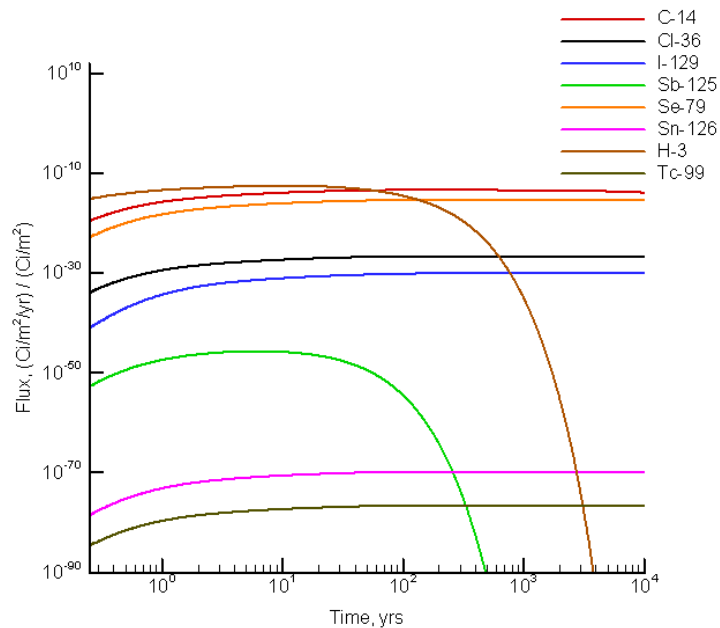
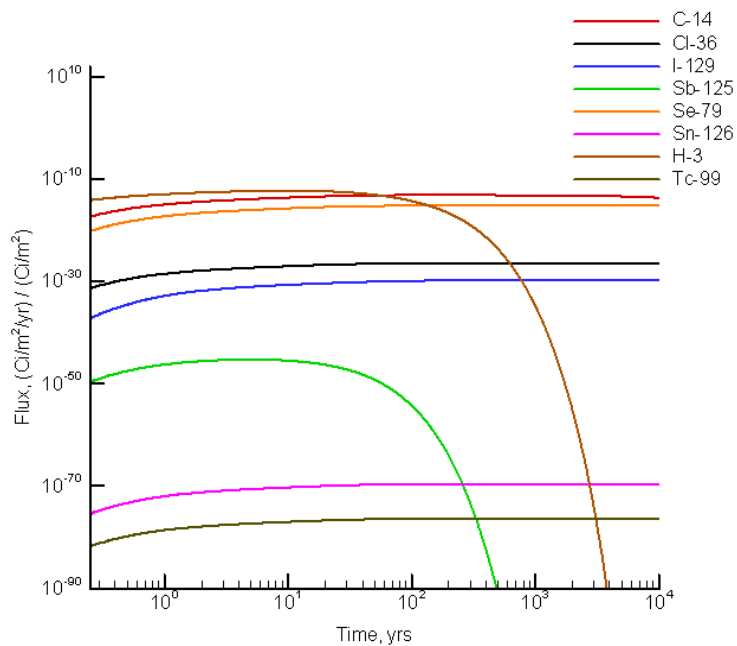
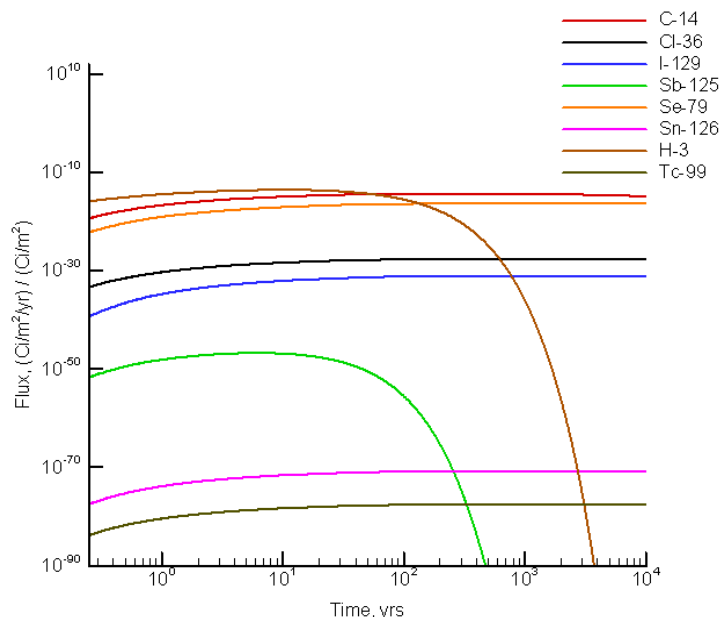


Figure 4.5-7: Ci Flux at Land Surface for Modeled Radionuclides in Vault 4 for DDA Saltstone



**Figure 4.5-8: Ci Flux at Land Surface for Modeled Radionuclides in Vault 4 for
ARP/MCU Saltstone**



The peak fluxes emanating at the land surface and the time to peak flux are presented for each case simulated in Table 4.5-15 through Table 4.5-24. The results are reported in this way to facilitate calculation of human exposure at the SRS boundary and the 100m boundary for each case simulated.

Table 4.5-15: SRS Boundary for DDA Saltstone in Vault 1

| Radionuclide | Peak Flux (Ci/m ² /yr) /Ci/m ² | Time to Peak Flux (years) | SRS Boundary DRF ^a (mrem/Ci) | Dose to MEI at SRS Boundary ^b (mrem/yr/Ci) |
|--------------|--|---------------------------|---|---|
| C-14 | 5.17E-14 | 136.7 | 1.1E-04 | 5.6E-18 |
| Cl-36 | 2.56E-27 | 281.7 | 3.6E-04 | 9.3E-31 |
| H-3 | 3.85E-13 | 9.7 | 2.3E-06 | 8.7E-19 |
| I-129 | 1.12E-30 | 763.8 | 4.8E-02 | 5.3E-32 |
| Sb-125 | 4.33E-46 | 4.4 | 6.6E-03 | 2.9E-48 |
| Se-79 | 5.12E-16 | 291.7 | 6.0E-04 | 3.1E-19 |
| Sn-126 | 2.03E-70 | 350.8 | 3.0E-01 | 6.2E-71 |
| Tc-99 | 3.36E-77 | 311.2 | 1.8E-03 | 6.0E-80 |

[SRNL-STI-2008-00415]

(a) Dose to MEI at SRS boundary = Peak Flux × SRS boundary DRF

(b) Disposal Limit = 10 mrem/yr / Dose to MEI at SRS boundary per year per curie

Table 4.5-16: 100m Dose for DDA Saltstone in Vault 1

| Radionuclide | Peak Flux (Ci/m ² /yr) /Ci/m ²) | Time to Peak Flux (years) | 100m Boundary DRF ^a (mrem/Ci) | Dose to MEI at 100m Boundary ² (mrem/yr/Ci) |
|--------------|--|---------------------------|--|--|
| C-14 | 5.17E-14 | 136.7 | 3.7E-03 | 1.9E-16 |
| Cl-36 | 2.56E-27 | 281.7 | 7.9E-03 | 2.0E-29 |
| H-3 | 3.85E-13 | 9.7 | 7.7E-05 | 3.0E-17 |
| I-129 | 1.12E-30 | 763.8 | 5.5E+00 | 6.1E-30 |
| Sb-125 | 4.33E-46 | 4.4 | 1.1E-01 | 4.8E-47 |
| Se-79 | 5.12E-16 | 291.7 | 1.1E-02 | 5.6E-18 |
| Sn-126 | 2.03E-70 | 350.8 | 4.9E+00 | 1.0E-69 |
| Tc-99 | 3.36E-77 | 311.2 | 2.9E-02 | 9.7E-79 |

[SRNL-STI-2008-00415]

(a) Dose to MEI at 100m boundary = Peak Flux × 100m boundary DRF

(b) Disposal Limit = 10 mrem/yr / Dose to MEI at 100m boundary per year per curie

Table 4.5-17: SRS Boundary Dose for ARP/MCU Saltstone in Vault 1

| Radionuclide | Peak Flux (Ci/m ² /yr) /Ci/m ²) | Time to Peak Flux (years) | SRS Boundary DRF ^a (mrem/Ci) | Dose to MEI at SRS Boundary ^b (mrem/yr/Ci) |
|--------------|--|---------------------------|---|---|
| C-14 | 4.18E-14 | 136.0 | 1.1E-04 | 4.6E-18 |
| Cl-36 | 2.07E-27 | 283.1 | 3.6E-04 | 7.5E-31 |
| H-3 | 3.12E-13 | 9.7 | 2.3E-06 | 7.1E-19 |
| I-129 | 9.02E-31 | 715.8 | 4.8E-02 | 4.3E-32 |
| Sb-125 | 3.51E-46 | 4.4 | 6.6E-03 | 2.3E-48 |
| Se-79 | 4.14E-16 | 291.7 | 6.0E-04 | 2.5E-19 |
| Sn-126 | 1.64E-70 | 350.8 | 3.0E-01 | 5.0E-71 |
| Tc-99 | 2.72E-77 | 311.2 | 1.8E-03 | 4.9E-80 |

[SRNL-STI-2008-00415]

(a) Dose to MEI at SRS boundary = Peak Flux × SRS boundary DRF

(b) Disposal Limit = 10 mrem/yr / Dose to MEI at SRS boundary per year per curie

Table 4.5-18: 100m Dose for ARP/MCU Saltstone in Vault 1

| Radionuclide | Peak Flux (Ci/m ² /yr) /Ci/m ²) | Time to Peak Flux (years) | 100m Boundary DRF ^a (mrem/Ci) | Dose to MEI at 100m Boundary ^b (mrem/yr/Ci) |
|--------------|--|---------------------------|--|--|
| C-14 | 4.18E-14 | 136.0 | 3.7E-03 | 1.5E-16 |
| Cl-36 | 2.07E-27 | 283.1 | 7.9E-03 | 1.6E-29 |
| H-3 | 3.12E-13 | 9.7 | 7.7E-05 | 2.4E-17 |
| I-129 | 9.02E-31 | 715.8 | 5.5E+00 | 5.0E-30 |
| Sb-125 | 3.51E-46 | 4.4 | 1.1E-01 | 3.9E-47 |
| Se-79 | 4.14E-16 | 291.7 | 1.1E-02 | 4.6E-18 |
| Sn-126 | 1.64E-70 | 350.8 | 4.9E+00 | 8.1E-70 |
| Tc-99 | 2.72E-77 | 311.2 | 2.9E-02 | 7.9E-79 |

[SRNL-STI-2008-00415]

(a) Dose to MEI at 100m boundary = Peak Flux × 100m boundary DRF

(b) Disposal Limit = 10 mrem/yr / Dose to MEI at 100m boundary per year per curie

Table 4.5-19: SRS Boundary Dose for SWPF Saltstone in FDCs

| Radionuclide | Peak Flux (Ci/m ² /yr) /Ci/m ²) | Time to Peak Flux (years) | SRS Boundary DRF ^a (mrem/Ci) | Dose to MEI at SRS Boundary ^b (mrem/yr/Ci) |
|--------------|--|---------------------------|---|---|
| C-14 | 4.27E-14 | 147.3 | 1.1E-04 | 4.7E-18 |
| Cl-36 | 2.12E-27 | 305.1 | 3.6E-04 | 7.7E-31 |
| H-3 | 2.97E-13 | 10.4 | 2.3E-06 | 6.7E-19 |
| I-129 | 9.22E-31 | 787.0 | 4.8E-02 | 4.4E-32 |
| Sb-125 | 2.10E-46 | 6.1 | 6.6E-03 | 1.4E-48 |
| Se-79 | 4.24E-16 | 317.5 | 6.0E-04 | 2.6E-19 |
| Sn-126 | 1.68E-70 | 379.9 | 3.0E-01 | 5.1E-71 |
| Tc-99 | 2.77E-77 | 337.1 | 1.8E-03 | 5.0E-80 |

[SRNL-STI-2008-00415]

(a) Dose to MEI at SRS boundary = Peak Flux × SRS boundary DRF

(b) Disposal Limit = 10 mrem/yr / Dose to MEI at SRS boundary per year per curie

Table 4.5-20: 100m Dose for SWPF Saltstone in FDCs

| Radionuclide | Peak Flux (Ci/m ² /yr) /Ci/m ²) | Time to Peak Flux (years) | 100m Boundary DRF ^a (mrem/Ci) | Dose to MEI at 100m Boundary ^b (mrem/yr/Ci) |
|--------------|--|---------------------------|--|--|
| C-14 | 4.27E-14 | 147.3 | 3.7E-03 | 1.6E-16 |
| Cl-36 | 2.12E-27 | 305.1 | 7.9E-03 | 1.7E-29 |
| H-3 | 2.97E-13 | 10.4 | 7.7E-05 | 2.3E-17 |
| I-129 | 9.22E-31 | 787.0 | 5.5E+00 | 5.1E-30 |
| Sb-125 | 2.10E-46 | 6.1 | 1.1E-01 | 2.3E-47 |
| Se-79 | 4.24E-16 | 317.5 | 1.1E-02 | 4.7E-18 |
| Sn-126 | 1.68E-70 | 379.9 | 4.9E+00 | 8.2E-70 |
| Tc-99 | 2.77E-77 | 337.1 | 2.9E-02 | 8.0E-79 |

[SRNL-STI-2008-00415]

(a) Dose to MEI at 100m boundary = Peak Flux × 100m boundary DRF

(b) Disposal Limit = 10 mrem/yr / Dose to MEI at 100m boundary per year per curie

Table 4.5-21: SRS Boundary Dose for DDA Saltstone in Vault 4

| Radionuclide | Peak Flux (Ci/m ² /yr) /Ci/m ²) | Time to Peak Flux (years) | SRS Boundary DRF ^a (mrem/Ci) | Dose to MEI at SRS Boundary ^b (mrem/yr/Ci) |
|--------------|--|---------------------------|---|---|
| C-14 | 7.24E-14 | 141.5 | 1.1E-04 | 7.9E-18 |
| Cl-36 | 3.59E-27 | 291.7 | 3.6E-04 | 1.3E-30 |
| H-3 | 5.23E-13 | 10.0 | 2.3E-06 | 1.2E-18 |
| I-129 | 1.56E-30 | 787.0 | 4.8E-02 | 7.4E-32 |
| Sb-125 | 5.07E-46 | 5.0 | 6.6E-03 | 3.3E-48 |
| Se-79 | 7.18E-16 | 303.6 | 6.0E-04 | 4.3E-19 |
| Sn-126 | 2.84E-70 | 363.3 | 3.0E-01 | 8.6E-71 |
| Tc-99 | 4.69E-77 | 323.9 | 1.8E-03 | 8.4E-80 |

[SRNL-STI-2008-00415]

(a) Dose to MEI at SRS boundary = Peak Flux × SRS boundary DRF

(b) Disposal Limit = 10 mrem/yr / Dose to MEI at SRS boundary per year per curie

Table 4.5-22: 100m Dose for DDA Saltstone in Vault 4

| Radionuclide | Peak Flux (Ci/m ² /yr) /Ci/m ²) | Time to Peak Flux (years) | 100m Boundary DRF ^a (mrem/Ci) | Dose to MEI at 100m Boundary ^b (mrem/yr/Ci) |
|--------------|--|---------------------------|--|--|
| C-14 | 7.24E-14 | 141.5 | 3.7E-03 | 2.7E-16 |
| Cl-36 | 3.59E-27 | 291.7 | 7.9E-03 | 2.8E-29 |
| H-3 | 5.23E-13 | 10.0 | 7.7E-05 | 4.0E-17 |
| I-129 | 1.56E-30 | 787.0 | 5.5E+00 | 8.6E-30 |
| Sb-125 | 5.07E-46 | 5.0 | 1.1E-01 | 5.6E-47 |
| Se-79 | 7.18E-16 | 303.6 | 1.1E-02 | 7.9E-18 |
| Sn-126 | 2.84E-70 | 363.3 | 4.9E+00 | 1.4E-69 |
| Tc-99 | 4.69E-77 | 323.9 | 2.9E-02 | 1.4E-78 |

[SRNL-STI-2008-00415]

(a) Dose to MEI at 100m boundary = Peak Flux × 100m boundary DRF

(b) Disposal Limit = 10 mrem/yr / Dose to MEI at 100m boundary per year per curie

Table 4.5-23: SRS Boundary Dose for ARP/MCU Saltstone in Vault 4

| Radionuclide | Peak Flux (Ci/m ² /yr) /Ci/m ²) | Time to Peak Flux (years) | SRS Boundary DRF ^a (mrem/Ci) | Dose to MEI at SRS Boundary ^b (mrem/yr/Ci) |
|--------------|--|---------------------------|---|---|
| C-14 | 4.10E-15 | 152.5 | 1.1E-04 | 4.5E-19 |
| Cl-36 | 2.04E-28 | 315.9 | 3.6E-04 | 7.4E-32 |
| H-3 | 2.79E-14 | 10.6 | 2.3E-06 | 6.3E-20 |
| I-129 | 8.86E-32 | 819.0 | 4.8E-02 | 4.2E-33 |
| Sb-125 | 1.84E-47 | 6.2 | 6.6E-03 | 1.2E-49 |
| Se-79 | 4.08E-17 | 328.8 | 6.0E-04 | 2.5E-20 |
| Sn-126 | 1.61E-71 | 391.5 | 3.0E-01 | 4.9E-72 |
| Tc-99 | 2.66E-78 | 350.8 | 1.8E-03 | 4.8E-81 |

[SRNL-STI-2008-00415]

(a) Dose to MEI at SRS boundary = Peak Flux × SRS boundary DRF

(b) Disposal Limit = 10 mrem/yr / Dose to MEI at SRS boundary per year per curie

Table 4.5-24: 100m Dose for ARP/MCU Saltstone in Vault 4

| Radionuclide | Peak Flux (Ci/m ² /yr) /Ci/m ²) | Time to Peak Flux (years) | 100m Boundary DRF ^a (mrem/Ci) | Dose to MEI at 100m Boundary ^b (mrem/yr/Ci) |
|--------------|--|---------------------------|--|--|
| C-14 | 4.10E-15 | 152.5 | 3.7E-03 | 1.5E-17 |
| Cl-36 | 2.04E-28 | 315.9 | 7.9E-03 | 1.6E-30 |
| H-3 | 2.79E-14 | 10.6 | 7.7E-05 | 2.1E-18 |
| I-129 | 8.86E-32 | 819.0 | 5.5E+00 | 4.9E-31 |
| Sb-125 | 1.84E-47 | 6.2 | 1.1E-01 | 2.0E-48 |
| Se-79 | 4.08E-17 | 328.8 | 1.1E-02 | 4.5E-19 |
| Sn-126 | 1.61E-71 | 391.5 | 4.9E+00 | 7.9E-71 |
| Tc-99 | 2.66E-78 | 350.8 | 2.9E-02 | 7.7E-80 |

[SRNL-STI-2008-00415]

(a) Dose to MEI at 100m boundary = Peak Flux × 100m boundary DRF

(b) Disposal Limit = 10 mrem/yr / Dose to MEI at 100m boundary per year per curie

4.5.2.4.2 Air Pathways Dose Calculations

An evaluation was conducted to assess the potential dose to a MEI located at the SRS boundary and the 100m location. [SRNL-STI-2008-00415] Dose to the MEI was calculated for both the SRS boundary and the 100m boundary for each case simulated using the peak flux for the 10,000 year simulation period. Dose release factors were calculated for each radionuclide potentially released from the SDF using CAP88-PC, the EPA model for NESHAP. DRFs represent the dose to the receptor exposed to 1 Ci of the specified radionuclide potentially released to the atmosphere. For the receptor located at the SRS boundary, the distance from the SDF was sufficient for an assumption of a point source. However, the DRFs for the 100m receptor required evaluation of an area source because of the close proximity of the SDF to the 100m receptor. For radionuclides not contained within the CAP88 library (Se-79, Cl-36), atmospheric transport was estimated by assigning surrogates with similar radiological properties. [SRNL-STI-2008-00415] Doses for these radionuclides were estimated by applying their dosimetric properties to the surrogate's relative air concentrations estimated by the model.

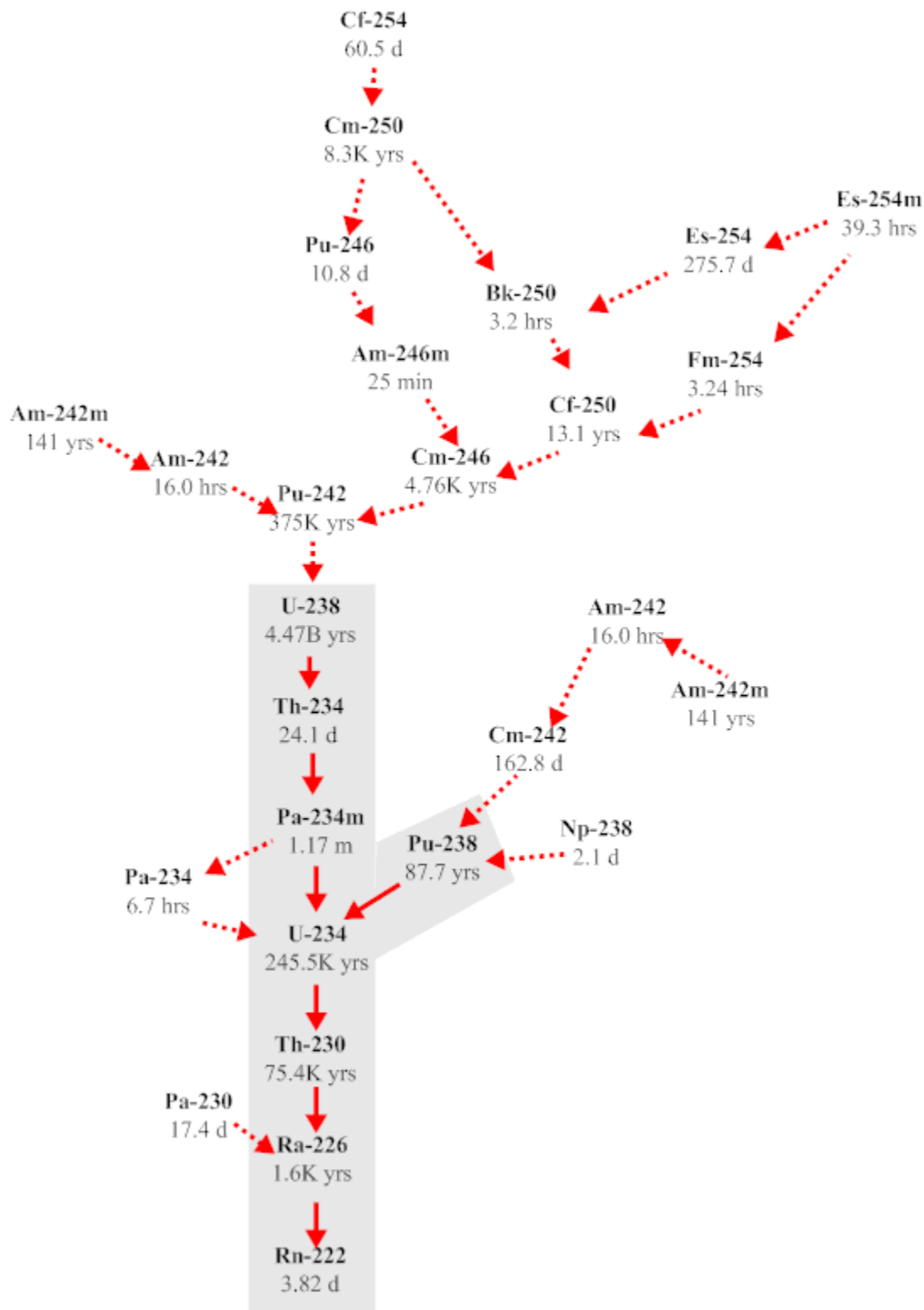
Specific SRS boundary DRFs, 100m boundary DRFs, and the calculated exposure levels for the simulation period at the SRS boundary and 100m boundary are presented in Table 4.5-15 through Table 4.5-24. [SRNL-STI-2008-00415]

4.5.2.5 Saltstone Disposal Facility Radon Analysis

This section describes the investigation conducted to evaluate the potential magnitude of radon release from Vault 1, Vault 4, and FDCs during the 10,000 year performance period. This investigation addresses only Rn-222. It was assumed that the short half-life of Rn-220 (55.6 seconds) renders it unable to escape the disposal units and migrate to the land surface via air diffusion before it is transformed by radioactive decay.

The potential parent radionuclides that can contribute to the creation of Rn-222 are illustrated in Figure 4.5-9. The diagram indicates the specific decay chains that lead to the formation of Rn-222, as well as the half-lives for each radionuclide. The extremely long half-life of U-238 ($4.47\text{E}+9$ years), causes the other radionuclides higher up on the chain of parents, to be of little concern with regard to their potential to contribute significantly to the Rn-222 flux at the land surface over the period of interest. In Figure 4.5-9, the parent radionuclides that were individually evaluated are indicated with the gray shaded area (i.e., beginning with Pu-238 and U-238). Rn-222 generated within the waste zone is in the gaseous phase and diffuses outward from this zone into the air-filled soil pores surrounding the disposal units, eventually resulting in some of the radon emanating at the land surface. As such, air is the fluid through which Rn-222 diffuses, although some Rn-222 may dissolve in residual pore water.

Figure 4.5-9: Radioactive Decay Chains Leading to Rn-222



The parent radionuclides are assumed to exist in the solid phase and therefore do not migrate upward through the air-filled pore space, although they could be leached and transported downward from the waste zone by pore water movement. This potential downward migration of the parent radionuclides was not considered in the radon analysis.

Decay chains evaluated were $\text{U-238} \rightarrow \text{Th-234} \rightarrow \text{Pa-234m} \rightarrow \text{U-234} \rightarrow \text{Th-230} \rightarrow \text{Ra-226} \rightarrow \text{Rn-222}$ and $\text{Pu-238} \rightarrow \text{U-234} \rightarrow \text{Th-230} \rightarrow \text{Ra-226} \rightarrow \text{Rn-222}$. Each parent in these chains, except Th-234 and Pa-234m, were simulated separately as the starting point of the decay chain. Th-234 and Pa-234m have extremely short half-lives compared to the other parent radionuclides in these chains. Only a fraction of the Rn-222 generated by the decay of each parent is available for migration away from its source and into open pore space. Since the Rn-222 parent radionuclides exist as oxides or in other crystalline forms, only a fraction of Rn-222 generated by decay of Ra-226 has sufficient energy to migrate away from its original location into adjacent pore space before further decay occurs (3.82 day half-life for Rn-222).

The emanation coefficient is generally defined as the fraction of the total amount of Rn-222 produced by radium decay that escapes from soil particles and enters the pore space of the medium. This is the fraction of the Rn-222 that is available for transport. In the case of the SDF, the parent radionuclides are not embedded in soil, but are contained within waste mixed with grout. Literature values for the Rn-222 emanation factor for these conditions are not available. Studies have shown the emanation factor to vary between 0.02 and 0.7 for various soil types depending primarily on moisture content. Generally, higher emanation factors are associated with higher moisture contents.

Residual Radioactivity Computer Software (RESRAD) is a model used to estimate radiation dose and risk from residual radioactive materials. This DOE and NRC approved code assumes an emanation factor of 0.25 for Rn-222, which is representative of a silty loam soil with low moisture content. For the SDF radon pathway analysis, the RESRAD default emanation factor of 0.25 was chosen, recognizing that literature values for wastes similar to the SDF are not available. To account for the emanation factor in the model, an effective source term of 0.25 Ci of parent radionuclide was utilized for each curie disposed within the facility.

Some radon dissolves in pore water, but since diffusion proceeds more slowly in that fluid, air diffusion was the only transport process by which Rn-222 was allowed to reach the land surface. This assertion was substantiated in ANL-EAD-4, *Users Manual for RESRAD Version 6*. In that report, the D_e for soil was reported to range from the radon open air diffusion coefficient of $1.0\text{E-}5 \text{ m}^2/\text{sec}$ to that of fully saturated soil, $1.0\text{E-}10 \text{ m}^2/\text{sec}$. This five order of magnitude difference was consistent with the comparison of water diffusion coefficients to air diffusion coefficients of other common molecular compounds and reported in many references. Thus, the larger volume of water-filled pore space compared to air-filled pore space (maximum of one order of magnitude difference) was inconsequential, in terms of the ability of water-dissolved radon to diffuse through water-filled pores as compared to the ability of the same compounds to diffuse as gas in the vapor-filled pore spaces.

The molecular diffusion coefficient of Rn-222 in open air is $347 \text{ m}^2/\text{yr}$. [SRNL-STI-2008-00447] A relationship between moisture saturation and the radon effective air diffusion coefficients for various pore sizes of earthen materials was established. This method was used to calculate a radon effective air diffusion coefficient for each material type based upon the average moisture saturation for the material. Tortuosity was assigned a unit value for each material type.

4.5.2.6 Radon Pathway Model Results

Model simulations were conducted to evaluate the peak instantaneous Rn-222 flux at the land surface for the simulation period of 10,000 years for each case simulated (i.e., 1 Ci of each parent). Model results were output in $\text{Ci}/\text{m}^2/\text{yr}$ per Ci/m^2 of inventory, consistent with the set of units employed in the model. Graphs of these results are shown in Figures 4.5-10 through 4.5-14, although the units were converted to $\text{pCi}/\text{m}^2/\text{sec}$ per Ci/m^2 , which were the units used to define the regulatory flux limit in DOE M 435.1-1. [DOE M 435.1-1]

The material properties remained constant for each case for the simulation period. Hence, the transient gaseous flux of Rn-222 at the land surface is a function of radioactive decay. This is illustrated in Figures 4.5-10 through Figure 4.5-14, where the flux of Rn-222 reached the peak emission rate and subsequently declined as a function of decay. The peak fluxes represent the peak Rn-222 flux per square meter at the land surface per curie of parent. The peak fluxes are presented in Table 4.5-25 through Table 4.5-29.

Figure 4.5-10: Rn-222 Flux at Land Surface Resulting from Unit Source Term for Vault 1 DDA Saltstone

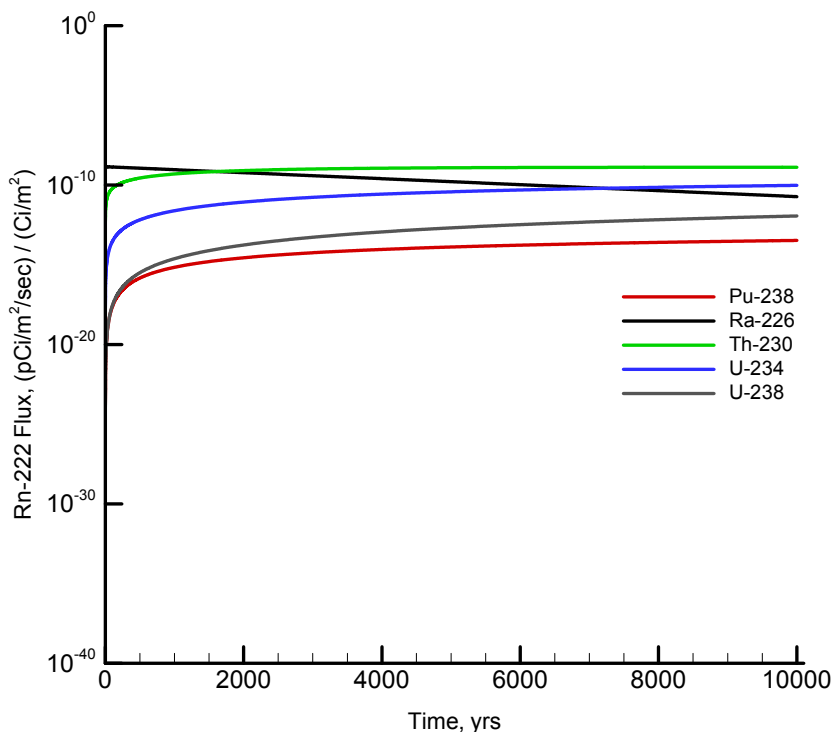


Figure 4.5-11: Rn-222 Flux at Land Surface from Unit Source Term for Vault 1
ARP/MCU Saltstone

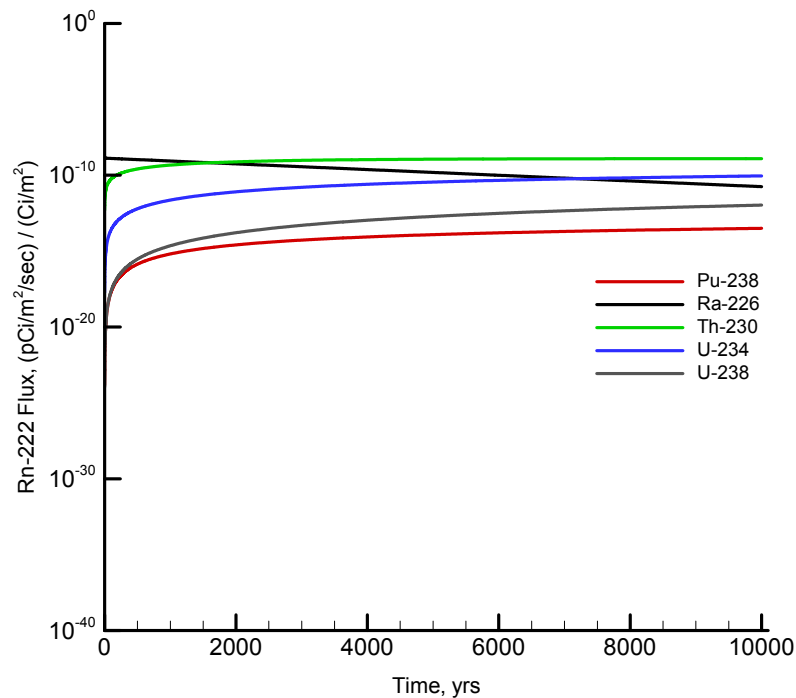


Figure 4.5-12: Rn-222 Flux at Land Surface from Unit Source Term for FDC Saltstone

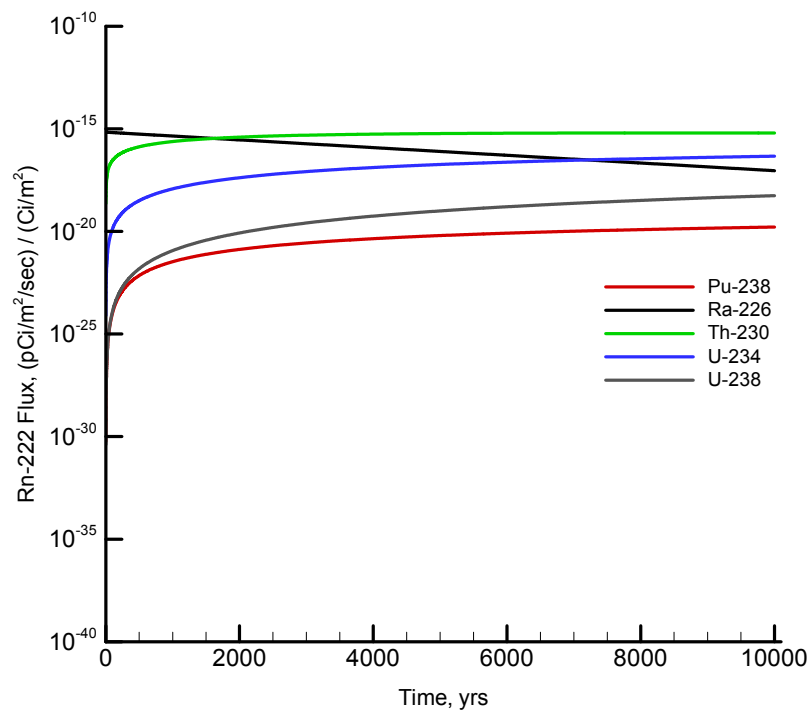


Figure 4.5-13: Rn-222 Flux at Land Surface from Unit Source Term for Vault 4 DDA
Saltstone

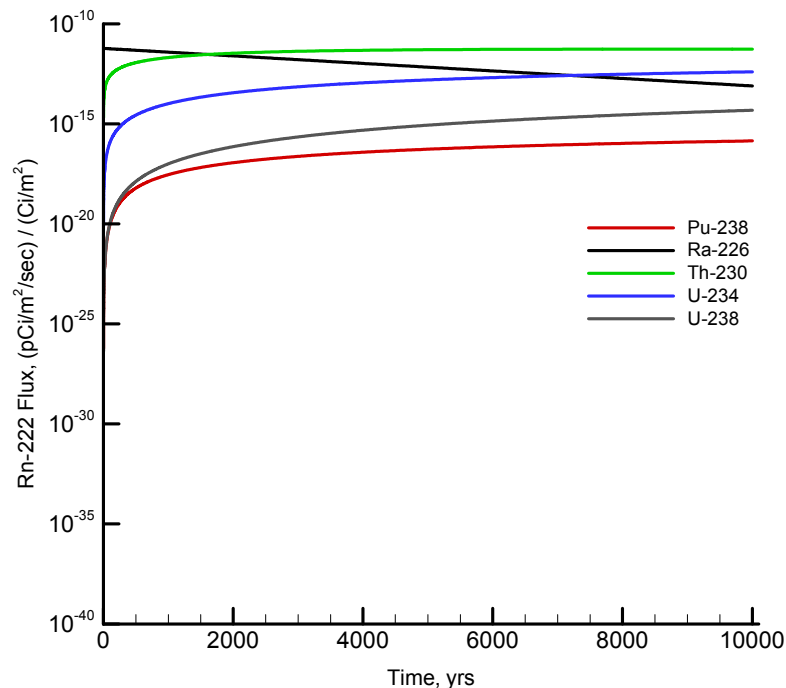


Figure 4.5-14: Rn-222 Flux at Land Surface from Unit Source Term for Vault 4
ARP/MCU Saltstone

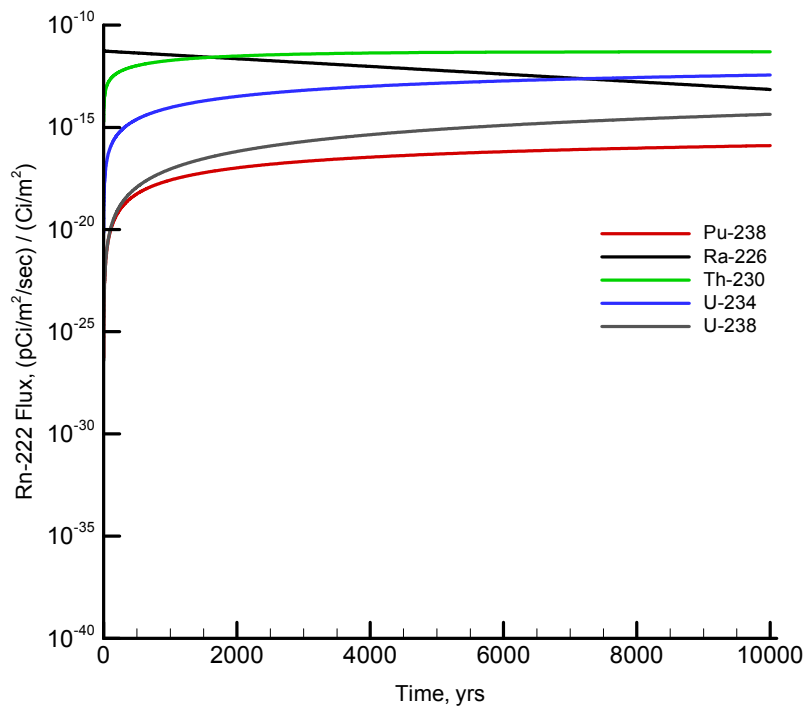


Table 4.5-25: Peak Rn-222 Flux over 10,000 Years for Vault 1 DDA Saltstone

| Parent Source (1 Ci/m ²) | Peak Instantaneous Rn-222 flux at Land Surface (pCi/m ² /sec) / (Ci/m ²) |
|--------------------------------------|---|
| Pu-238 | 3.39E-14 |
| Ra-226 | 1.43E-09 |
| Th-230 | 1.31E-09 |
| U-234 | 9.65E-11 |
| U-238 | 1.15E-12 |

Table 4.5-26: Peak Rn-222 Flux over 10,000 Years for Vault 1 ARP/MCU Saltstone

| Parent Source (1 Ci/m ²) | Peak Instantaneous Rn-222 flux at Land Surface (pCi/m ² /sec) / (Ci/m ²) |
|--------------------------------------|---|
| Pu-238 | 3.15E-14 |
| Ra-226 | 1.33E-09 |
| Th-230 | 1.22E-09 |
| U-234 | 8.96E-11 |
| U-238 | 1.07E-12 |

Table 4.5-27: Peak Rn-222 Flux over 10,000 Years for FDCs SWPF Saltstone

| Parent Source (1 Ci/m ²) | Peak Instantaneous Rn-222 flux at Land Surface (pCi/m ² /sec) / (Ci/m ²) |
|--------------------------------------|---|
| Pu-238 | 1.63E-20 |
| Ra-226 | 6.86E-16 |
| Th-230 | 6.31E-16 |
| U-234 | 4.64E-17 |
| U-238 | 5.55E-19 |

Table 4.5-28: Peak Rn-222 Flux over 10,000 Years for Vault 4 DDA Saltstone

| Parent Source (1 Ci/m ²) | Peak Instantaneous Rn-222 flux at Land Surface (pCi/m ² /sec) / (Ci/m ²) |
|--------------------------------------|---|
| Pu-238 | 1.41E-16 |
| Ra-226 | 5.92E-12 |
| Th-230 | 5.45E-12 |
| U-234 | 4.00E-13 |
| U-238 | 4.79E-15 |

Table 4.5-29: Peak Rn-222 Flux over 10,000 Years for Vault 4 ARP/MCU Saltstone

| Parent Source (1 Ci/m ²) | Peak Instantaneous Rn-222 flux at Land Surface (pCi/m ² /sec) / (Ci/m ²) |
|--------------------------------------|---|
| Pu-238 | 1.28E-16 |
| Ra-226 | 5.39E-12 |
| Th-230 | 4.96E-12 |
| U-234 | 3.64E-13 |
| U-238 | 4.35E-15 |

4.6 Biotic Pathways

The purpose of this section is to document the Bioaccumulation Factors and Human Health Exposure parameters used in the SDF PA modeling effort. Exposure pathways for the SDF PA are discussed in Section 4.2.4. Bioaccumulation Factors and Human Health Exposure parameters are used to calculate doses for each of the pathways.

4.6.1 Bioaccumulation Factors

For PA analyses at SRS, soil-to-vegetable (also known as soil-to-plant ratios or plant-to-soil ratios), feed-to-milk, feed-to-beef and water-to-fish transfer factors are the bioaccumulation factors considered. Soil-to-vegetable transfer factors determine the fraction of an element that is drawn from the soil into the edible plant. Feed-to-milk transfer factors represent the element fraction transferred from fodder to milk. Feed-to-meat transfer factors represent the element specific fraction transferred from fodder to beef. Water-to-fish transfer factors are the equilibrium ratios between concentration in aquatic foods and concentration in water.

The factors utilized were developed based on comparison to a number of other DOE facilities and generic national/global references, to establish relevance of the parameters selected and/or verify the regional differences for the Southeastern U.S. [WSRC-STI-2007-00004] The values for the parameters were based on expected values, along with a range for these values versus the specification of parameters for estimating an annual dose to the MEI.

4.6.1.1 Bioaccumulation Factor Methodology

A report entitled *Baseline Parameter Update for Human Health Input and Transfer Factors for Radiological Performance Assessments at the Savannah River Site* documents SRS evaluation and review of transfer factors. [WSRC-STI-2007-00004] This report presents additional details on factors utilized in the past and a discussion on conversion factors developed for SRS use. This report also established a single bioaccumulation factor parameter source that is up to date with existing data and maintained current via periodic reviews.

In developing the report, a comprehensive literature review was completed and references were updated to include the latest available information. In general, the values from more recent compilations were recommended, rather than those in older publications. The report includes information to establish a range of values for each element, which was used to perform uncertainty analysis.

WSRC-STI-2007-00004 recommends updating the factors using site-specific values when available, but considers *A Compendium of Transfer Factors for Agricultural and Animal Products* to be the most recent comprehensive evaluation of bioaccumulation factors and recommends this as the secondary source of values if site-specific values are not available. [PNNL-13421]

The hierarchy of document use at SRS for bioaccumulation factors is listed below:

- Site-Specific (WSRC-TR-96-0231 and SRT-EST-2003-00134)
- Other site- or regional-specific publications (i.e., CDC-2006)
- PNNL-13421
- ORNL-5786
- NCRP-123

In PNNL-13421, the hierarchy of documents used to establish transfer factors was IAEA-364, NUREG-CR-5512, and then NCRP-123. The International Atomic Energy Agency's Technical Report Series #364, *Handbook of Parameter Values for the Prediction of Radionuclide Transfer in Temperate Environments*, encompasses a wide variety of plant types and is the result of extensive background investigations. [IAEA-364] It is based on data compiled by the International Union of Radioecologists. *Residual Radioactive Contamination from Decommissioning: Technical Basis for Translating Contamination Levels to Annual Total Effective Dose Equivalent*, NUREG-CR-5512, is frequently referenced because of its large set of data and traceable references.

In general, site-specific values were used without modification where appropriate. When recent generic compilations were used, and the differences between the updated value and the currently used value were larger than two orders of magnitude, a geometric mean (GM) of the generic updated value and the currently used value was selected for averaging the ratios. This GM methodology was discussed during scoping meetings with stakeholders, accepted, and utilized in the development of the FTF PA (SRS-REG-2007-00002_OUO). This methodology was conservative for the risk significant radionuclides.

4.6.1.1.1 Bioaccumulation Parameters

The transfer factors that SRS utilized for the SDF PA appear in Table 4.6-1 through Table 4.6-4. The data in these tables were taken primarily from WSRC-STI-2007-00004.

Table 4.6-1: Soil-to-Vegetable Transfer Factors (Unitless)

| Atomic No. | Element | Soil-to-Vegetable Transfer Factors | | |
|------------|---------|------------------------------------|----------|----------|
| | | Value | Min. | Max. |
| 89 | Ac | 6.83E-05 | 6.69E-05 | 3.50E-03 |
| 47 | Ag | 1.18E-02 | 2.54E-04 | 1.50E-01 |
| 13 | Al | 1.27E-04 | 1.24E-04 | 4.00E-03 |
| 95 | Am | 6.83E-05 | 1.10E-05 | 1.70E-01 |
| 18 | Ar | 0 | 0 | 0 |
| 33 | As | 1.17E-03 | 1.17E-03 | 8.00E-02 |
| 85 | At | 2.93E-02 | 2.87E-02 | 2.00E-01 |
| 79 | Au | 3.51E-03 | 2.50E-04 | 1.00E-01 |
| 5 | B | 3.90E-01 | 1.00E-02 | 4.00E+00 |
| 56 | Ba | 2.93E-03 | 2.87E-03 | 4.00E-02 |
| 4 | Be | 2.93E-04 | 2.87E-04 | 4.00E-03 |
| 83 | Bi | 9.75E-02 | 9.56E-04 | 1.00E-01 |
| 97 | Bk | 1.00E-03 | 5.90E-05 | 1.00E-03 |
| 35 | Br | 2.93E-01 | 2.93E-01 | 7.60E-01 |
| 6 | C | 1.37E-01 | 1.37E-01 | 5.50E+00 |
| 20 | Ca | 6.83E-02 | 6.69E-02 | 5.00E-01 |
| 48 | Cd | 2.93E-02 | 2.87E-02 | 5.00E-01 |
| 58 | Ce | 3.90E-03 | 7.65E-04 | 3.00E-02 |
| 98 | Cf | 6.83E-05 | 6.50E-06 | 1.00E-02 |
| 17 | Cl | 1.37E+01 | 3.00E-01 | 7.00E+01 |
| 96 | Cm | 8.39E-05 | 2.87E-06 | 2.50E-03 |
| 27 | Co | 1.31E-02 | 1.34E-03 | 1.20E+00 |
| 24 | Cr | 8.78E-04 | 2.50E-04 | 1.00E-02 |
| 55 | Cs | 9.00E-01 | 1.10E-03 | 9.00E-01 |
| 29 | Cu | 4.88E-02 | 4.88E-02 | 1.30E-01 |
| 66 | Dy | 3.90E-03 | 7.80E-04 | 3.90E-03 |
| 68 | Er | 3.90E-03 | 7.80E-04 | 3.90E-03 |
| 99 | Es | 1.00E-03 | 5.90E-05 | 1.00E-03 |
| 63 | Eu | 3.90E-03 | 7.65E-04 | 4.00E-03 |
| 9 | F | 1.17E-03 | 1.17E-03 | 2.00E-02 |
| 26 | Fe | 9.75E-03 | 1.91E-04 | 9.75E-03 |
| 100 | Fm | 2.00E-03 | 2.00E-03 | 2.00E-03 |
| 87 | Fr | 5.85E-03 | 5.73E-03 | 3.00E-02 |
| 31 | Ga | 7.80E-05 | 7.65E-05 | 3.00E-03 |
| 64 | Gd | 3.90E-03 | 7.65E-04 | 4.00E-03 |
| 32 | Ge | 1.56E-02 | 1.53E-02 | 4.00E-01 |
| 1 | H | 4.80E+00 | 0 | 6.92E+00 |
| 2 | He | 0 | 0 | 0 |
| 72 | Hf | 1.95E-04 | 1.00E-04 | 3.00E-03 |
| 80 | Hg | 3.90E-02 | 3.82E-02 | 3.80E-01 |

Table 4.6-1: Soil-to-Vegetable Transfer Factors (Unitless) (Continued)

| Atomic No. | Element | Soil-to-Vegetable Transfer Factors | | |
|------------|---------|------------------------------------|----------|----------|
| | | Value | Min. | Max. |
| 67 | Ho | 3.90E-03 | 7.65E-04 | 4.00E-03 |
| 108 | Hs | 2.00E-03 | 2.00E-03 | 2.00E-03 |
| 53 | I | 7.80E-03 | 3.40E-04 | 5.00E-02 |
| 49 | In | 7.80E-05 | 7.65E-05 | 3.00E-03 |
| 77 | Ir | 2.93E-03 | 2.87E-03 | 3.00E-02 |
| 19 | K | 1.07E-01 | 1.05E-01 | 5.50E-01 |
| 36 | Kr | 0 | 0 | 0 |
| 57 | La | 6.83E-05 | 6.83E-05 | 2.50E-03 |
| 3 | Li | 7.80E-04 | 7.80E-04 | 1.71E-03 |
| 103 | Lr | 2.00E-03 | 2.00E-03 | 2.00E-03 |
| 71 | Lu | 7.80E-04 | 7.65E-04 | 2.50E-03 |
| 101 | Md | 2.00E-03 | 2.00E-03 | 2.00E-03 |
| 12 | Mg | 1.07E-01 | 3.00E-02 | 2.35E-01 |
| 25 | Mn | 3.90E-02 | 9.56E-03 | 3.00E-01 |
| 42 | Mo | 1.56E-01 | 1.15E-02 | 8.00E-01 |
| 7 | N | 3.50E-01 | 9.56E-03 | 1.28E+01 |
| 11 | Na | 5.85E-02 | 1.05E-02 | 3.00E-01 |
| 41 | Nb | 4.88E-03 | 9.56E-04 | 1.70E-02 |
| 60 | Nd | 3.90E-03 | 7.80E-04 | 3.90E-03 |
| 10 | Ne | 0 | 0 | 0 |
| 28 | Ni | 1.17E-02 | 1.15E-02 | 1.80E+00 |
| 102 | No | 2.00E-03 | 2.00E-03 | 2.00E-03 |
| 93 | Np | 2.54E-03 | 7.10E-04 | 1.40E-01 |
| 8 | O | 6.00E-01 | 6.00E-01 | 6.00E-01 |
| 76 | Os | 6.83E-04 | 6.83E-04 | 3.00E-02 |
| 15 | P | 6.83E-01 | 6.69E-01 | 3.50E+00 |
| 91 | Pa | 4.18E-04 | 4.78E-05 | 1.00E-02 |
| 82 | Pb | 1.17E-03 | 1.30E-04 | 1.30E-02 |
| 46 | Pd | 7.80E-03 | 7.65E-03 | 1.00E-01 |
| 61 | Pm | 3.90E-03 | 7.65E-04 | 4.00E-03 |
| 84 | Po | 1.37E-03 | 7.65E-05 | 7.00E-03 |
| 59 | Pr | 3.90E-03 | 7.65E-04 | 3.90E-03 |
| 78 | Pt | 4.88E-03 | 4.78E-03 | 1.00E-01 |
| 94 | Pu | 2.15E-04 | 3.80E-06 | 5.60E-02 |
| 88 | Ra | 4.64E-03 | 3.90E-04 | 5.50E-02 |
| 37 | Rb | 1.76E-01 | 1.34E-02 | 9.00E-01 |
| 75 | Re | 1.29E+00 | 6.83E-02 | 2.10E+02 |
| 104 | Rf | 3.00E-03 | 3.00E-03 | 3.00E-03 |
| 45 | Rh | 7.80E-03 | 7.65E-03 | 1.30E+01 |
| 86 | Rn | 0 | 0 | 0 |
| 44 | Ru | 7.80E-03 | 3.82E-03 | 5.00E-02 |

Table 4.6-1: Soil-to-Vegetable Transfer Factors (Unitless) (Continued)

| Atomic No. | Element | Soil-to-Vegetable Transfer Factors | | |
|------------|---------|------------------------------------|----------|----------|
| | | Value | Min. | Max. |
| 16 | S | 2.93E-01 | 2.87E-01 | 6.42E-01 |
| 51 | Sb | 2.49E-03 | 1.09E-04 | 1.30E-02 |
| 21 | Sc | 1.95E-04 | 1.91E-04 | 2.00E-03 |
| 34 | Se | 5.14E-02 | 4.78E-03 | 1.30E+00 |
| 14 | Si | 1.37E-02 | 1.34E-02 | 8.80E-02 |
| 62 | Sm | 3.90E-03 | 7.65E-04 | 4.00E-03 |
| 50 | Sn | 1.17E-03 | 1.15E-03 | 3.00E-01 |
| 38 | Sr | 9.75E-02 | 1.70E-02 | 1.40E+01 |
| 73 | Ta | 4.88E-03 | 4.78E-04 | 2.00E-02 |
| 65 | Tb | 3.90E-03 | 7.80E-04 | 3.90E-03 |
| 43 | Tc | 4.68E-02 | 4.68E-02 | 5.46E+00 |
| 52 | Te | 1.20E-02 | 7.65E-04 | 1.30E+00 |
| 90 | Th | 6.44E-05 | 1.62E-05 | 7.50E-03 |
| 22 | Ti | 5.85E-04 | 1.00E-04 | 3.00E-03 |
| 81 | Tl | 7.80E-05 | 7.65E-05 | 2.00E-01 |
| 69 | Tm | 7.80E-04 | 7.80E-04 | 2.00E-03 |
| 92 | U | 2.34E-03 | 7.65E-04 | 1.40E-01 |
| 23 | V | 5.85E-04 | 5.73E-04 | 3.00E-03 |
| 74 | W | 5.00E-02 | 1.91E-03 | 8.00E-01 |
| 54 | Xe | 0 | 0 | 0 |
| 39 | Y | 1.95E-03 | 1.15E-03 | 3.00E-01 |
| 70 | Yb | 7.80E-04 | 7.80E-04 | 2.00E-03 |
| 30 | Zn | 6.83E-02 | 6.83E-02 | 2.34E+00 |
| 40 | Zr | 1.95E-04 | 9.56E-05 | 1.00E-03 |

[WSRC-STI-2007-00004]

Table 4.6-2: Feed-to-Milk Transfer Factors (d/L)

| Atomic No. | Element | Feed-To-Milk Transfer Factors | | |
|------------|---------|-------------------------------|----------|----------|
| | | Value | Min. | Max. |
| 89 | Ac | 2.00E-05 | 2.00E-06 | 2.06E-05 |
| 47 | Ag | 1.58E-03 | 5.00E-05 | 5.00E-02 |
| 13 | Al | 2.06E-04 | 2.00E-04 | 2.06E-04 |
| 95 | Am | 1.50E-06 | 4.00E-07 | 5.00E-06 |
| 33 | As | 6.00E-05 | 6.00E-05 | 1.00E-04 |
| 85 | At | 1.03E-02 | 1.00E-02 | 1.03E-02 |
| 79 | Au | 5.50E-06 | 5.00E-06 | 1.00E-05 |
| 5 | B | 1.55E-03 | 1.50E-03 | 3.00E-03 |
| 56 | Ba | 4.80E-04 | 3.50E-04 | 8.00E-03 |
| 4 | Be | 9.00E-07 | 9.00E-07 | 2.00E-06 |
| 83 | Bi | 5.00E-04 | 5.00E-04 | 1.00E-03 |
| 97 | Bk | 2.00E-06 | 4.00E-07 | 2.00E-06 |
| 35 | Br | 2.00E-02 | 2.00E-02 | 2.06E-02 |
| 6 | C | 1.20E-02 | 1.05E-02 | 1.20E-02 |
| 20 | Ca | 3.00E-03 | 3.00E-03 | 1.03E-02 |
| 48 | Cd | 1.00E-03 | 1.20E-04 | 2.00E-03 |
| 58 | Ce | 3.00E-05 | 2.00E-05 | 1.00E-04 |
| 98 | Cf | 1.50E-06 | 7.50E-07 | 2.00E-06 |
| 17 | Cl | 1.70E-02 | 1.50E-02 | 2.00E-02 |
| 96 | Cm | 2.00E-05 | 2.00E-06 | 2.06E-05 |
| 27 | Co | 3.00E-04 | 3.00E-04 | 2.06E-03 |
| 24 | Cr | 1.00E-05 | 1.00E-05 | 2.20E-03 |
| 55 | Cs | 7.90E-03 | 7.00E-03 | 1.20E-02 |
| 29 | Cu | 2.00E-03 | 1.50E-03 | 1.40E-02 |
| 66 | Dy | 3.00E-05 | 2.00E-05 | 6.00E-05 |
| 68 | Er | 3.00E-05 | 2.00E-05 | 6.00E-05 |
| 99 | Es | 2.00E-06 | 4.00E-07 | 2.00E-06 |
| 63 | Eu | 3.00E-05 | 2.00E-05 | 6.00E-05 |
| 9 | F | 1.00E-03 | 1.00E-03 | 7.00E-03 |
| 26 | Fe | 3.00E-05 | 3.00E-05 | 1.20E-03 |
| 87 | Fr | 2.06E-02 | 8.00E-03 | 2.06E-02 |
| 31 | Ga | 5.00E-05 | 1.00E-05 | 5.15E-05 |
| 64 | Gd | 3.00E-05 | 2.00E-05 | 6.00E-05 |
| 32 | Ge | 7.21E-02 | 1.00E-02 | 7.21E-02 |
| 1 | H | 1.50E-02 | 0 | 1.50E-02 |
| 2 | He | 0 | 0 | 0 |
| 72 | Hf | 5.50E-07 | 5.50E-07 | 2.50E-05 |
| 80 | Hg | 4.70E-04 | 4.50E-04 | 5.00E-04 |
| 67 | Ho | 3.00E-05 | 2.00E-05 | 6.00E-05 |
| 108 | Hs | 5.00E-06 | 5.00E-06 | 5.00E-06 |

Table 4.6-2: Feed-to-Milk Transfer Factors (d/L) (Continued)

| Atomic No. | Element | Feed-to-Milk Transfer Factors | | |
|------------|---------|-------------------------------|----------|----------|
| | | Value | Min. | Max. |
| 53 | I | 9.00E-03 | 6.00E-03 | 1.20E-02 |
| 49 | In | 2.00E-04 | 1.00E-04 | 2.00E-04 |
| 77 | Ir | 2.00E-06 | 2.00E-06 | 2.06E-06 |
| 19 | K | 7.20E-03 | 7.00E-03 | 7.21E-03 |
| 57 | La | 2.00E-05 | 5.00E-06 | 6.00E-05 |
| 3 | Li | 2.06E-02 | 2.06E-02 | 5.00E-02 |
| 103 | Lr | 5.00E-06 | 5.00E-06 | 5.00E-06 |
| 71 | Lu | 2.06E-05 | 2.00E-05 | 6.00E-05 |
| 101 | Md | 5.00E-06 | 5.00E-06 | 5.00E-06 |
| 12 | Mg | 3.90E-03 | 3.90E-03 | 8.00E-03 |
| 25 | Mn | 3.00E-05 | 3.00E-05 | 3.61E-04 |
| 42 | Mo | 1.70E-03 | 1.50E-03 | 7.50E-03 |
| 7 | N | 2.50E-02 | 1.00E-02 | 2.58E-02 |
| 11 | Na | 1.60E-02 | 1.60E-02 | 4.00E-02 |
| 41 | Nb | 3.20E-05 | 4.10E-07 | 2.06E-02 |
| 60 | Nd | 3.00E-05 | 5.00E-06 | 6.00E-05 |
| 28 | Ni | 1.60E-02 | 1.00E-03 | 2.00E-02 |
| 102 | No | 5.00E-06 | 5.00E-06 | 5.00E-06 |
| 93 | Np | 5.00E-06 | 5.00E-06 | 1.00E-05 |
| 76 | Os | 5.00E-03 | 1.00E-04 | 3.50E+00 |
| 15 | P | 1.60E-02 | 1.50E-02 | 2.50E-02 |
| 91 | Pa | 5.00E-06 | 5.00E-06 | 5.15E-06 |
| 82 | Pb | 2.60E-04 | 2.50E-04 | 3.00E-04 |
| 46 | Pd | 1.00E-02 | 1.00E-04 | 1.03E-02 |
| 61 | Pm | 3.00E-05 | 2.00E-05 | 6.00E-05 |
| 84 | Po | 3.40E-04 | 3.40E-04 | 4.00E-04 |
| 59 | Pr | 3.00E-05 | 5.00E-06 | 6.00E-05 |
| 78 | Pt | 5.15E-03 | 1.00E-04 | 5.15E-03 |
| 94 | Pu | 1.10E-06 | 1.00E-07 | 2.00E-06 |
| 88 | Ra | 1.30E-03 | 4.50E-04 | 1.30E-03 |
| 37 | Rb | 1.20E-02 | 1.00E-02 | 3.00E-02 |
| 75 | Re | 1.50E-03 | 1.40E-04 | 2.00E-03 |
| 104 | Rf | 2.00E-05 | 2.00E-05 | 2.00E-05 |
| 45 | Rh | 1.00E-02 | 5.00E-04 | 1.03E-02 |
| 86 | Rn | 0 | 0 | 0 |
| 44 | Ru | 3.30E-06 | 6.00E-07 | 2.00E-05 |
| 16 | S | 1.60E-02 | 1.50E-02 | 2.00E-02 |
| 51 | Sb | 2.50E-05 | 2.50E-05 | 1.50E-03 |
| 21 | Sc | 5.00E-06 | 5.00E-06 | 6.00E-05 |
| 34 | Se | 4.00E-03 | 4.00E-03 | 4.50E-02 |
| 14 | Si | 2.00E-05 | 2.00E-05 | 2.06E-05 |

Table 4.6-2: Feed-to-Milk Transfer Factors (d/L) (Continued)

| Atomic No. | Element | Feed-to-Milk Transfer Factors | | |
|------------|---------|-------------------------------|----------|----------|
| | | Value | Min. | Max. |
| 62 | Sm | 3.00E-05 | 5.00E-06 | 6.00E-05 |
| 50 | Sn | 1.00E-03 | 1.00E-03 | 2.50E-03 |
| 38 | Sr | 2.80E-03 | 8.00E-04 | 2.80E-03 |
| 73 | Ta | 4.10E-07 | 4.10E-07 | 5.00E-06 |
| 65 | Tb | 3.00E-05 | 2.00E-05 | 6.00E-05 |
| 43 | Tc | 1.87E-03 | 2.30E-05 | 2.50E-02 |
| 52 | Te | 4.50E-04 | 2.00E-04 | 1.00E-03 |
| 90 | Th | 5.00E-06 | 5.00E-06 | 5.15E-06 |
| 22 | Ti | 7.53E-05 | 5.50E-07 | 1.03E-02 |
| 81 | Tl | 2.00E-03 | 1.00E-03 | 1.00E-02 |
| 69 | Tm | 2.06E-05 | 2.06E-05 | 6.00E-05 |
| 92 | U | 4.00E-04 | 4.00E-04 | 6.18E-04 |
| 23 | V | 2.06E-05 | 2.00E-05 | 5.00E-04 |
| 74 | W | 3.00E-04 | 3.00E-04 | 5.00E-04 |
| 39 | Y | 2.00E-05 | 1.00E-05 | 2.00E-03 |
| 70 | Yb | 2.06E-05 | 2.06E-05 | 6.00E-05 |
| 30 | Zn | 1.00E-02 | 1.00E-02 | 3.90E-02 |
| 40 | Zr | 5.50E-07 | 5.50E-07 | 3.09E-05 |

[WSRC-STI-2007-00004, Table B-2]

Table 4.6-3: Feed-to-Meat Transfer Factors (d/kg)

| Atomic No. | Element | Feed-To-Meat Transfer Factors | | |
|------------|---------|-------------------------------|----------|----------|
| | | Value | Min. | Max. |
| 89 | Ac | 4.00E-04 | 2.00E-05 | 4.00E-04 |
| 47 | Ag | 3.00E-03 | 3.00E-03 | 1.70E-02 |
| 13 | Al | 1.50E-03 | 5.00E-04 | 1.50E-03 |
| 95 | Am | 4.00E-05 | 3.50E-06 | 2.00E-04 |
| 33 | As | 2.00E-03 | 1.50E-03 | 2.00E-02 |
| 85 | At | 1.00E-02 | 1.00E-02 | 1.00E-02 |
| 79 | Au | 5.00E-03 | 2.00E-04 | 8.00E-03 |
| 5 | B | 8.00E-04 | 8.00E-04 | 8.00E-04 |
| 56 | Ba | 2.00E-04 | 1.50E-04 | 3.00E-02 |
| 4 | Be | 1.00E-03 | 1.00E-03 | 5.00E-03 |
| 83 | Bi | 4.00E-04 | 4.00E-04 | 2.00E-03 |
| 97 | Bk | 2.50E-05 | 2.00E-05 | 4.00E-05 |
| 35 | Br | 2.50E-02 | 2.00E-02 | 5.00E-02 |
| 6 | C | 3.10E-02 | 3.10E-02 | 4.89E-02 |
| 20 | Ca | 2.00E-03 | 7.00E-04 | 2.00E-03 |
| 48 | Cd | 4.00E-04 | 4.00E-04 | 1.00E-03 |
| 58 | Ce | 2.00E-05 | 2.00E-05 | 1.20E-03 |
| 98 | Cf | 4.00E-05 | 4.00E-05 | 5.00E-03 |
| 17 | Cl | 2.00E-02 | 2.00E-02 | 8.00E-02 |
| 96 | Cm | 4.00E-05 | 3.50E-06 | 2.00E-04 |
| 27 | Co | 1.00E-02 | 1.00E-02 | 3.00E-02 |
| 24 | Cr | 9.00E-03 | 2.40E-03 | 3.00E-02 |
| 55 | Cs | 5.00E-02 | 4.00E-03 | 5.00E-02 |
| 29 | Cu | 9.00E-03 | 8.00E-03 | 1.00E-02 |
| 66 | Dy | 2.00E-05 | 2.00E-05 | 5.50E-03 |
| 68 | Er | 2.00E-05 | 2.00E-05 | 4.00E-03 |
| 99 | Es | 2.50E-05 | 2.00E-05 | 2.50E-05 |
| 63 | Eu | 2.00E-05 | 2.00E-05 | 5.00E-03 |
| 9 | F | 1.50E-01 | 2.00E-02 | 1.50E-01 |
| 26 | Fe | 2.00E-02 | 2.00E-02 | 4.00E-02 |
| 100 | Fm | 2.00E-04 | 2.00E-04 | 2.00E-04 |
| 87 | Fr | 2.50E-03 | 2.50E-03 | 3.00E-02 |
| 31 | Ga | 5.00E-04 | 3.00E-04 | 5.00E-04 |
| 64 | Gd | 2.00E-05 | 2.00E-05 | 3.50E-03 |
| 32 | Ge | 7.00E-01 | 2.00E-01 | 7.00E-01 |
| 1 | H | 1.20E-02 | 0 | 1.20E-02 |
| 72 | Hf | 3.16E-05 | 1.00E-06 | 1.00E-03 |
| 80 | Hg | 2.50E-01 | 1.00E-02 | 2.50E-01 |
| 67 | Ho | 3.00E-04 | 2.00E-05 | 4.50E-03 |
| 108 | Hs | 5.00E-06 | 5.00E-06 | 5.00E-06 |

Table 4.6-3: Feed-to-Meat Transfer Factors (d/kg) (Continued)

| Atomic No. | Element | Feed-to-Meat Transfer Factors | | |
|------------|---------|-------------------------------|----------|----------|
| | | Value | Min. | Max. |
| 53 | I | 4.00E-02 | 2.90E-03 | 4.00E-02 |
| 49 | In | 8.00E-03 | 4.00E-03 | 8.00E-03 |
| 77 | Ir | 1.50E-03 | 1.50E-03 | 2.00E-03 |
| 19 | K | 2.00E-02 | 2.00E-02 | 2.00E-02 |
| 57 | La | 2.00E-03 | 2.00E-04 | 2.00E-03 |
| 3 | Li | 1.00E-02 | 1.00E-02 | 2.00E-02 |
| 103 | Lr | 2.00E-04 | 2.00E-04 | 2.00E-04 |
| 71 | Lu | 4.50E-03 | 2.00E-03 | 4.50E-03 |
| 12 | Mg | 2.00E-02 | 3.00E-03 | 2.00E-02 |
| 25 | Mn | 5.00E-04 | 4.00E-04 | 1.00E-03 |
| 42 | Mo | 1.00E-03 | 1.00E-03 | 8.00E-03 |
| 7 | N | 7.50E-02 | 1.00E-02 | 7.50E-02 |
| 11 | Na | 8.00E-02 | 3.00E-02 | 8.00E-02 |
| 41 | Nb | 2.90E-04 | 3.00E-07 | 2.80E-01 |
| 60 | Nd | 2.00E-05 | 2.00E-05 | 3.30E-03 |
| 28 | Ni | 5.00E-03 | 5.00E-03 | 5.30E-02 |
| 102 | No | 2.00E-04 | 2.00E-04 | 2.00E-04 |
| 93 | Np | 1.00E-03 | 5.50E-05 | 1.00E-03 |
| 76 | Os | 4.00E-01 | 2.00E-03 | 4.00E-01 |
| 15 | P | 5.00E-02 | 4.60E-02 | 2.00E-01 |
| 91 | Pa | 4.47E-04 | 5.00E-06 | 5.00E-03 |
| 82 | Pb | 4.00E-04 | 3.00E-04 | 8.00E-04 |
| 46 | Pd | 4.00E-03 | 2.00E-04 | 4.00E-03 |
| 61 | Pm | 2.00E-05 | 2.00E-05 | 5.00E-03 |
| 84 | Po | 5.00E-03 | 9.50E-05 | 5.00E-03 |
| 59 | Pr | 2.00E-05 | 2.00E-05 | 4.70E-03 |
| 78 | Pt | 4.00E-03 | 2.00E-04 | 4.00E-03 |
| 94 | Pu | 1.00E-05 | 5.00E-07 | 1.00E-04 |
| 88 | Ra | 9.00E-04 | 2.50E-04 | 1.00E-03 |
| 37 | Rb | 1.00E-02 | 1.00E-02 | 3.10E-02 |
| 75 | Re | 8.00E-03 | 1.00E-04 | 1.00E-02 |
| 45 | Rh | 2.00E-03 | 1.00E-03 | 2.00E-03 |
| 86 | Rn | 0 | 0 | 0 |
| 44 | Ru | 5.00E-02 | 2.00E-03 | 4.00E-01 |
| 16 | S | 2.00E-01 | 1.00E-01 | 2.00E-01 |
| 51 | Sb | 1.00E-03 | 4.00E-05 | 4.00E-03 |
| 21 | Sc | 1.50E-02 | 2.00E-03 | 1.50E-02 |
| 34 | Se | 1.50E-02 | 1.50E-02 | 1.00E-01 |
| 14 | Si | 4.00E-05 | 4.00E-05 | 3.00E-04 |
| 62 | Sm | 3.16E-04 | 2.00E-05 | 5.00E-03 |
| 50 | Sn | 8.00E-02 | 1.00E-02 | 8.00E-02 |

Table 4.6-3: Feed-to-Meat Transfer Factors (d/kg) (Continued)

| Atomic No. | Element | Feed-to-Meat Transfer Factors | | |
|------------|---------|-------------------------------|----------|----------|
| | | Value | Min. | Max. |
| 38 | Sr | 8.00E-03 | 3.00E-04 | 1.00E-02 |
| 73 | Ta | 1.34E-05 | 3.00E-07 | 6.00E-04 |
| 65 | Tb | 2.00E-05 | 2.00E-05 | 4.50E-03 |
| 43 | Tc | 6.32E-03 | 1.00E-04 | 4.00E-01 |
| 52 | Te | 7.00E-03 | 7.00E-03 | 7.70E-02 |
| 90 | Th | 4.00E-05 | 6.00E-06 | 2.00E-04 |
| 22 | Ti | 1.73E-04 | 1.00E-06 | 3.00E-02 |
| 81 | Tl | 4.00E-02 | 2.00E-03 | 4.00E-02 |
| 69 | Tm | 4.50E-03 | 2.00E-03 | 4.50E-03 |
| 92 | U | 3.00E-04 | 2.00E-04 | 8.00E-04 |
| 23 | V | 2.50E-03 | 2.50E-03 | 1.00E-02 |
| 74 | W | 4.00E-02 | 1.30E-03 | 4.50E-02 |
| 39 | Y | 1.00E-03 | 3.00E-04 | 8.00E-03 |
| 70 | Yb | 4.00E-03 | 2.00E-03 | 4.00E-03 |
| 30 | Zn | 1.00E-01 | 3.00E-02 | 1.00E-01 |
| 40 | Zr | 1.84E-04 | 1.00E-06 | 3.40E-02 |

[WSRC-STI-2007-00004, Table B-3]

Table 4.6-4: Water-to-Fish Bioaccumulation Factors (L/kg)

| Atomic No. | Element | Water-To-Fish Transfer Factors | | |
|------------|----------------|--------------------------------|----------|----------|
| | | Value | Min. | Max. |
| 89 | Ac | 2.50E+01 | 1.50E+01 | 2.50E+01 |
| 47 | Ag | 5.00E+00 | 2.30E+00 | 5.00E+00 |
| 13 | Al | 5.00E+02 | 1.00E+01 | 5.00E+02 |
| 95 | Am | 3.00E+01 | 2.10E+01 | 2.40E+03 |
| 33 | As | 1.70E+03 | 1.00E+02 | 1.70E+03 |
| 85 | At | 1.50E+01 | 1.50E+01 | 1.50E+01 |
| 79 | Au | 3.30E+01 | 3.30E+01 | 3.50E+01 |
| 56 | Ba | 4.00E+00 | 4.00E+00 | 2.00E+02 |
| 4 | Be | 1.00E+02 | 2.00E+00 | 1.00E+02 |
| 83 | Bi | 1.50E+01 | 1.00E+01 | 1.50E+01 |
| 97 | Bk | 2.50E+01 | 2.50E+01 | 2.50E+01 |
| 35 | Br | 4.00E+02 | 4.00E+02 | 4.20E+02 |
| 6 | C ¹ | 3.00E+00 | N/A | N/A |
| 20 | Ca | 4.00E+01 | 4.00E+01 | 1.00E+03 |
| 48 | Cd | 2.00E+02 | 2.00E+02 | 2.00E+02 |
| 58 | Ce | 3.00E+01 | 1.00E+00 | 5.00E+02 |
| 98 | Cf | 2.50E+01 | 2.50E+01 | 2.50E+01 |
| 17 | Cl | 5.00E+01 | 5.00E+01 | 1.00E+03 |
| 96 | Cm | 3.00E+01 | 2.10E+01 | 2.50E+02 |
| 27 | Co | 3.00E+02 | 5.00E+01 | 3.30E+02 |
| 24 | Cr | 4.00E+00 | 4.00E+00 | 2.00E+02 |
| 55 | Cs | 3.00E+03 | 2.00E+03 | 4.70E+03 |
| 29 | Cu | 2.00E+02 | 5.00E+01 | 2.00E+02 |
| 66 | Dy | 3.00E+01 | 3.00E+01 | 3.00E+01 |
| 68 | Er | 3.00E+01 | 3.00E+01 | 3.00E+01 |
| 99 | Es | 2.50E+01 | 1.00E+01 | 2.50E+01 |
| 63 | Eu | 3.00E+01 | 2.50E+01 | 5.00E+01 |
| 9 | F | 1.00E+01 | 1.00E+01 | 1.00E+01 |
| 26 | Fe | 2.00E+02 | 1.00E+02 | 2.00E+03 |
| 87 | Fr | 3.00E+01 | 3.00E+01 | 3.00E+01 |
| 31 | Ga | 4.00E+02 | 3.33E+02 | 4.00E+02 |
| 64 | Gd | 3.00E+01 | 2.50E+01 | 3.00E+01 |
| 32 | Ge | 4.00E+03 | 3.33E+03 | 4.00E+03 |
| 2 | He | 1.00E+00 | 1.00E+00 | 1.00E+00 |
| 1 | H | 1.00E+00 | 9.00E-01 | 1.00E+00 |
| 72 | Hf | 3.00E+02 | 3.33E+00 | 3.00E+02 |
| 80 | Hg | 1.00E+03 | 1.00E+03 | 1.00E+03 |
| 67 | Ho | 3.00E+01 | 2.50E+01 | 3.00E+01 |
| 53 | I | 4.00E+01 | 1.50E+01 | 5.00E+02 |
| 49 | In | 1.00E+04 | 1.00E+04 | 1.00E+05 |
| 77 | Ir | 1.00E+01 | 1.00E+01 | 1.00E+01 |

Table 4.6-4: Water-to-Fish Bioaccumulation Factors (L/kg) (Continued)

| Atomic No. | Element | Water-to-Fish Bioaccumulation Factors | | |
|------------|---------|---------------------------------------|----------|----------|
| | | Value | Min. | Max. |
| 19 | K | 1.00E+03 | 1.00E+03 | 1.00E+04 |
| 57 | La | 3.00E+01 | 2.50E+01 | 3.00E+01 |
| 71 | Lu | 2.50E+01 | 2.50E+01 | 2.50E+01 |
| 12 | Mg | 5.00E+01 | 5.00E+01 | 5.00E+01 |
| 25 | Mn | 4.00E+02 | 1.00E+02 | 4.00E+02 |
| 42 | Mo | 1.00E+01 | 1.00E+01 | 1.00E+01 |
| 7 | N | 2.00E+05 | 1.50E+05 | 2.00E+05 |
| 11 | Na | 2.00E+01 | 8.00E+00 | 1.00E+02 |
| 41 | Nb | 3.00E+02 | 2.00E+02 | 3.00E+04 |
| 60 | Nd | 3.00E+01 | 2.50E+01 | 1.00E+02 |
| 28 | Ni | 1.00E+02 | 1.00E+02 | 1.00E+02 |
| 93 | Np | 2.10E+01 | 1.00E+01 | 2.50E+02 |
| 8 | O | 1.00E+00 | 1.00E+00 | 1.00E+00 |
| 76 | Os | 1.00E+03 | 1.00E+01 | 1.00E+05 |
| 15 | P | 5.00E+04 | 1.50E+03 | 1.00E+05 |
| 91 | Pa | 1.00E+01 | 1.00E+01 | 1.13E+01 |
| 82 | Pb | 3.00E+02 | 1.00E+02 | 3.00E+02 |
| 46 | Pd | 1.00E+01 | 1.00E+01 | 1.00E+01 |
| 61 | Pm | 3.00E+01 | 2.50E+01 | 3.00E+01 |
| 84 | Po | 5.00E+01 | 5.00E+01 | 5.00E+02 |
| 59 | Pr | 3.00E+01 | 2.50E+01 | 1.00E+02 |
| 78 | Pt | 3.50E+01 | 3.50E+01 | 1.00E+02 |
| 94 | Pu | 3.00E+01 | 3.50E+00 | 4.70E+03 |
| 88 | Ra | 5.00E+01 | 5.00E+01 | 7.00E+01 |
| 37 | Rb | 2.00E+03 | 2.00E+03 | 2.00E+03 |
| 75 | Re | 1.20E+02 | 1.19E+02 | 1.20E+04 |
| 45 | Rh | 1.00E+01 | 1.00E+01 | 1.00E+01 |
| 86 | Rn | 0 | 0 | 5.70E+01 |
| 44 | Ru | 1.00E+02 | 1.00E+01 | 1.00E+02 |
| 16 | S | 8.00E+02 | 7.50E+02 | 1.00E+03 |
| 51 | Sb | 1.00E+02 | 1.00E+00 | 2.00E+02 |
| 21 | Sc | 1.00E+02 | 1.00E+02 | 1.00E+02 |
| 34 | Se | 1.70E+02 | 1.70E+02 | 2.00E+02 |
| 14 | Si | 2.00E+01 | 2.50E+00 | 2.00E+01 |
| 62 | Sm | 3.00E+01 | 2.50E+01 | 3.00E+01 |
| 50 | Sn | 3.00E+03 | 3.00E+03 | 3.00E+03 |
| 38 | Sr | 6.00E+01 | 3.00E+01 | 5.01E+02 |
| 73 | Ta | 3.00E+02 | 1.00E+02 | 3.00E+04 |
| 65 | Tb | 3.00E+01 | 2.50E+01 | 3.00E+01 |
| 43 | Tc | 2.00E+01 | 1.50E+01 | 2.00E+01 |
| 52 | Te | 4.00E+02 | 4.00E+02 | 4.00E+02 |

Table 4.6-4: Water-to-Fish Bioaccumulation Factors (L/kg) (Continued)

| Atomic No. | Element | Water-to-Fish Bioaccumulation Factors | | |
|------------|---------|---------------------------------------|----------|----------|
| | | Value | Min. | Max. |
| 90 | Th | 1.00E+02 | 3.00E+01 | 1.00E+02 |
| 22 | Ti | 1.00E+03 | 1.00E+03 | 1.00E+03 |
| 81 | Tl | 1.00E+04 | 1.00E+04 | 1.00E+04 |
| 92 | U | 1.00E+01 | 2.00E+00 | 5.00E+01 |
| 23 | V | 2.00E+02 | 1.00E+01 | 2.00E+02 |
| 74 | W | 1.00E+01 | 1.00E+01 | 1.20E+03 |
| 39 | Y | 3.00E+01 | 2.50E+01 | 3.00E+01 |
| 30 | Zn | 3.50E+02 | 3.50E+02 | 2.50E+03 |
| 40 | Zr | 3.00E+02 | 3.30E+00 | 3.00E+02 |

[WSRC-STI-2007-00004 Table B-4]

(1) SRNL-STI-2009-00178

4.6.2 Human Health Exposure Parameters (Consumption Rates)

This section documents the Human Health Exposure parameters (i.e., consumption rates) used in the SDF PA modeling effort. The parameters utilized were compared to a number of other DOE facilities and generic national references to establish relevance of the parameters selected and/or verify the regional differences for the southeastern United States. The values for the parameters recommended were based on expected values, along with a range for these values versus the specification of parameters for estimating an annual dose to the MEI.

4.6.2.1 Human Health Exposure Parameters Methodology

A report entitled *Baseline Parameter Update for Human Health Input and Transfer Factors for Radiological Performance Assessments at the Savannah River Site* documents the results of SRS evaluation and reviews of consumption rates. [WSRC-STI-2007-00004] Refer to this report for additional discussion on parameters such as water ingestion rates, crop yields, garden fractions and sizes, and exposure times. This report established a single Human Health Exposure parameters source with existing data and is maintained current via periodic reviews.

In developing the report, a comprehensive literature review was completed and references were updated to include the latest available information. In general, the values from more recent compilations were recommended, rather than those in older publications. This report includes information used to establish a range of values for each parameter that was used to perform uncertainty analysis.

A hierarchy of data sources was established to select values for human health exposure parameters. The utilization of site-specific values from the most recent and comprehensive references were given priority. Values promulgated by national or international organizations were used as representative of SRS area practices in the absence of site-specific values. The *Risk Based Screening of Radionuclide Releases from the Savannah River Site* was used as a source to validate the receptor practices in the areas surrounding SRS. [CDC-2006] The values given for the parameters are given as expected values, together with an observed range.

Site-specific information is available for most of the human health exposure parameters required to estimate doses. *Land and Water Use Characteristics in the Vicinity of the Savannah River Site* surveyed county agents in South Carolina and Georgia and compiled county-specific statistics on land and water use within a 50 mile radius of SRS. When these reports did not provide site-specific information for physical parameters and consumption rates, global data were used. [WSRC-RP-91-17, ISSN 0017-9078 Vol. 62 No. 2, Page 136] Documents ANL-EAD-4 and ANL-EAIS-8 provided data for use in RESRAD, an NRC and DOE supported dose model, based on literature review of standard values and publications. The EPA report *Exposure Factors Handbook*, summarized and recommended human health exposure parameter data for human exposure to environmental contaminants based on studies published through August 30, 1997. [EPA-600-P-95-002] NUREG-CR-5512 provided generic and site-specific human health data for estimating dose from exposure to residual radioactive contamination.

The general hierarchy of the global data use is listed below:

- Site-specific (WSRC-RP-91-17, ISSN 0017-9078 Vol. 62 No. 2, Page 136)
- Other site- or regional-specific publications (i.e., CDC-2006)
- EPA Exposure Factors Handbook (EPA-600-P-95-002)
- RESRAD Version 6 (ANL-EAD-4 and ANL-EAIS-8)
- NUREG-CR-5512

The consumption rates that SRS utilized for the SDF PA appear in Table 4.6-5 through Table 4.6-7.

Table 4.6-5: Crop Exposure Times and Productivity

| Parameter | Recommendation | | |
|---|---------------------|-----------------|------|
| | Value | Min | Max |
| Pasture exposure time to irrigation (d) | 30 | 30 | 90 |
| Vegetable crop exposure time to irrigation (d) | 70 | 60 | 90 |
| Soil exposure time period to irrigation (d) (Buildup time in soil) | 183 | 60 | 365 |
| Productivity | | | |
| Pasture grass (kg/m ²) | 1.8 | 0.7 | 2 |
| Agricultural (veg/produce) (kg/m ²) | 0.7 | 0.5 | 4 |
| Vegetable crop yield (kg/m ²) | 0.7 | 0.2 | 4 |
| Fraction of Foodstuff Produced Locally | All-pathways | Intruder | |
| Vegetables | 0.173 | 0.308 | 0 |
| Meat | 0.306 | 0.319 | 0 |
| Milk | 0.207 | 0.254 | 0 |
| Dilution Factor for Mixing of Waste in Vegetable Garden | | | |
| Agricultural scenario | 0.2 | 0.2 | 0.2 |
| Post-Drilling Scenario | 0.02 | 0.002 | 0.02 |

(a) Model conservatively assumes 1 rather than 0.5 as reported in WSRC-STI-2007-00004.
[WSRC-STI-2007-00004, Table 3-1]

Table 4.6-6: Physical Parameters

| Parameter | Recommendation | | |
|--|----------------|----------|----------|
| | Value | Min | Max |
| Area density of soil (kg/m ²) | 240 | 180 | 270 |
| Atmospheric mass loading of soil (kg/m ³) (while in garden or while in home) ^a | 1.0 E-07 | 1.0 E-09 | 3.0 E-07 |
| Depth of garden (cm) | 15 | 15 | 61 |
| Garden irrigation rate (L/d/m ²) | 3.6 | 2.08 | 5.5 |
| Fraction of the year that crops are irrigated | 0.2 | 0.2 | 0.25 |
| Crop weathering constant (L/d) | 0.0495 | 0.03 | 0.0495 |
| Fractional retention of deposition on leaves | 0.25 | 0.2 | 0.25 |
| Area of garden for family of four (m ²) | 100 | 100 | 1,000 |

(a) WSRC-STI-2007-00004, Table 3-2, provides different values for "in the garden" and "in the home." The value of 1.0E-07 (the most conservative of the values provided) is used regardless of the location of the receptor.

Table 4.6-7: Individual Exposure Times and Consumption Rates

| Parameter | Recommendation | | |
|---|---------------------|--------|--------|
| | Value | Min | Max |
| Breathing rate (m ³ /yr) | 5,548 | 1,267 | 11,600 |
| Soil consumption (kg/yr) | 0.0365 ^a | 0.0008 | 0.05 |
| Leafy vegetable consumption (kg/yr) | 21 | 18 | 43 |
| Other vegetable consumption (kg/yr) | 163 | 90 | 276 |
| Meat consumption (kg/yr) | 43 | 26 | 81 |
| Finfish consumption (kg/yr) | 9 | 2.2 | 19 |
| Seafood consumption (kg/yr) | 0 ^b | 0 | 5 |
| Milk consumption (L/yr) | 120 | 73.7 | 230 |
| Water consumption (L/yr) | 337 | 184 | 730 |
| Fodder – Beef cattle (kg/d) | 36 | 27 | 50 |
| Fodder – Milk cattle (kg/d) | 52 | 36 | 55 |
| Fraction of milk-cow intake from pasture | 0.56 | 0.5 | 1 |
| Fraction of beef-cow intake from pasture | 0.75 | 0.5 | 1 |
| Water (beef cow) (L/d) | 28 | 28 | 50 |
| Water (milk cow) (L/d) | 50 | 50 | 60 |
| Shoreline exposure (hr/yr) | 23 | 11 | 35 |
| Swimming exposure (hr/yr) | 8.9 | 8.9 | 13 |
| Boating exposure (hr/yr) | 21 | 9.1 | 31.5 |
| Showering exposure (min/d) | 10 | 10 | 30 |
| Fraction of year working in garden (/yr) | 0.01 | 0.01 | 0.08 |
| Fraction of year residing in home (/yr) | 0.7 | 0.3 | 0.7 |
| Fraction of time cattle on pasture (/yr) | 1 | 0.75 | 1 |
| Vegetable transport time (d) | 6 | 6 | 14 |
| Feed-milk-man transport time (d) | 3 | 1 | 4 |
| Time from slaughter to consumption (d) | 6 | 6 | 20 |

(a) Converts to 100 mg/d child ingestion rate in Exposure Factors Handbook (EFH) recommended for use for the agricultural scenario.

(b) Value of 2 should be used if the dose to a person downriver (i.e. Savannah area). Consumption pathway not used for intruder and resident scenario analyses.

[WSRC-STI-2007-00004, Table 4-1]

4.7 Dose Analysis

Over time, the mobile contaminants in the SDF disposal units will gradually migrate downward through unsaturated soil to the hydrogeologic units comprising the shallow aquifer underlying the SDF. Some contaminants will be transported by groundwater through the aquifers to the outcrops at UTR. Upon reaching the surface water, the contaminants could be present at the seepage line, in sediments at the bottom of streams, and at the shoreline. Human receptors could be exposed to contaminants through various pathways associated with the aquifers and surface water as described in Section 4.2.4.

The potential dose to a MOP via the air pathways was also evaluated as described in Section 4.5.

4.7.1 Dose Conversion Factors

The purpose of this section is to present the set of DCFs used in dose calculations for the SDF PA modeling effort. A comprehensive list of DCFs was prepared and included in Table 4.7-1, even though only a subset of the values listed was actually utilized in the PA modeling.

Radiation doses to humans may result from internal intake of radionuclides by inhalation, ingestion, or from external exposure to radionuclides present in the environment. Dose assessment at SRS is carried out by considering radionuclide concentrations in environmental media, factoring in human exposure conditions, and performing the conversion of exposure to dose. For internal exposure, radionuclide activity intake is calculated by combining the radioactivity concentration in environmental media (e.g., food, soil, air, and water) with the amount of environmental medium taken into the body. Then, using internal DCFs, radionuclide intake is converted into dose. To assess exposure from external sources, SRS uses external DCFs that convert radionuclide concentrations in environmental media to doses for the duration of exposure. Only internal DCFs for adults were utilized in the SDF PA.

4.7.1.1 Internal DCFs

Previous SRS PA analyses utilized the DCFs from EPA *Federal Guidance Report No. 11, Limiting Values of Radionuclide Intake and Air Concentration and Dose Conversion Factors for Inhalation, Submersion and Ingestion*, published in 1988 (EPA-520-1-88-020). The International Commission on Radiological Protection (ICRP) published new DCFs based upon updated dosimetric models in ICRP Publication 72 in 1996. [ICRP-72] The DOE has begun using the ICRP models for occupational exposure internal dose assessments at different sites, including SRS, and they are also used for SRS safety basis calculations. Safety Basis Documents, as defined in 10 CFR 830 Subpart B, are the DSA and hazard controls that provide reasonable assurance that a DOE nuclear facility can be operated safely in a manner that adequately protects workers, the public, and the environment. [10 CFR 830]

The DCFs are converted to standard units for input into the calculations by multiplying the ICRP 72 DCFs by $3.7\text{E}+06$ ($\text{Sv/Bq} \times 3.7\text{E}+6 = \text{rem}/\mu\text{Ci}$). [ICRP-72] The internal DCFs in $\text{rem}/\mu\text{Ci}$ are presented in Table 4.7-1 for the various radionuclides. For inhalation DCFs, the most likely lung absorption type from Table 2 of ICRP-72 was used if available, and if not available, the most conservative type was assumed.

Because the ICRP data is the most recent data available and is based on the most recent dosimetric models, the ICRP 72 DCFs are used for this SDF PA analysis. [ICRP-72]

4.7.1.2 External DCFs

External DCFs for uniformly distributed contamination at an infinite depth with no shielding and at 15 cm are taken from EPA *Federal Guidance Report No. 12, External Exposure to Radionuclides in Air, Water, and Soil* (EPA-402-R-93-081). The external DCFs in EPA-402-R-93-081 represent the dose rate per unit of activity of soil contaminated at various depths, reported in sensitivity indices (SI) units (Sv/s per Bq/m³). The DCFs are converted to standard units for input into PA calculations by multiplying the Federal Guidance Report No. 12 DCF by 1.168E+14 ((rem/yr per $\mu\text{Ci}/\text{m}^3$) / (Sv/s per Bq/m³)). [EPA-402-R-93-081] External DCFs in rem/yr per $\mu\text{Ci}/\text{m}^3$ are presented in Table 4.7-1 for various radionuclides.

Table 4.7-1: Internal and External DCFs

| Nuclide | Internal DCFs (rem/ μ Ci) | | External DCFs (rem/yr per μ Ci/m ³) | | |
|---------|-------------------------------|------------|---|-------------|-----------------|
| | | | Contaminated Soil | | Water Immersion |
| | Ingestion | Inhalation | Infinite Depth | 15 cm Depth | |
| Ac-225 | 8.88E-02 | 3.15E+01 | 3.98E-05 | 3.90E-05 | 1.88E-04 |
| Ac-227 | 4.07E+00 | 2.04E+03 | 3.10E-07 | 3.06E-07 | 1.52E-06 |
| Ac-228 | 1.59E-03 | 9.25E-02 | 3.74E-03 | 3.22E-03 | 1.21E-04 |
| Al-26 | 1.30E-02 | 7.40E-02 | 1.09E-02 | 9.03E-03 | 3.43E-02 |
| Am-241 | 7.40E-01 | 1.55E+02 | 2.73E-05 | 2.73E-05 | 2.20E-04 |
| Am-242 | 1.11E-03 | 6.29E-02 | 3.12E-05 | 3.12E-05 | 1.61E-04 |
| Am-242m | 7.03E-01 | 1.37E+02 | 1.06E-06 | 1.05E-06 | 8.50E-06 |
| Am-243 | 7.40E-01 | 1.52E+02 | 8.88E-05 | 8.88E-05 | 5.77E-04 |
| Ar-39 | N/A | N/A | 5.40E-07 | 5.31E-07 | 2.06E-06 |
| At-217 | N/A | N/A | 1.11E-06 | 1.01E-06 | 3.76E-06 |
| At-218 | N/A | N/A | 3.66E-06 | 3.66E-06 | 3.21E-05 |
| Ba-133 | 5.55E-03 | 1.15E-02 | 1.24E-03 | 1.15E-03 | 4.57E-03 |
| Ba-137m | N/A | N/A | 2.25E-03 | 2.00E-03 | 7.31E-03 |
| Bi-210 | 4.81E-03 | 3.44E-01 | 2.25E-06 | 2.17E-06 | 7.39E-06 |
| Bi-211 | N/A | N/A | 1.60E-04 | 1.50E-04 | 5.66E-04 |
| Bi-212 | 9.62E-04 | 1.15E-01 | 7.32E-04 | 6.26E-04 | 2.34E-03 |
| Bi-213 | 7.40E-04 | 1.11E-01 | 4.79E-04 | 4.38E-04 | 1.62E-03 |
| Bi-214 | 4.07E-04 | 5.18E-02 | 6.13E-03 | 5.09E-03 | 1.94E-04 |
| Bk-249 | 3.59E-03 | 5.92E-01 | 2.91E-09 | 2.90E-09 | 1.89E-08 |
| C-14 | 2.15E-03 | 7.40E-03 | 8.41E-09 | 8.41E-09 | 5.13E-08 |
| Ca-41 | 7.03E-04 | 3.52E-04 | N/A | N/A | N/A |
| Cd-113m | 8.51E-02 | 4.07E-01 | 4.05E-07 | 3.99E-07 | 1.57E-06 |
| Ce-144 | 1.92E-02 | 1.33E-01 | 4.49E-05 | 4.44E-5 | 2.23E-04 |
| Cf-249 | 1.30E+00 | 2.59E+02 | 1.16E-03 | 1.07E-03 | 4.03E-03 |
| Cf-250 | 5.92E-01 | 1.26E+02 | 7.40E-08 | 7.40E-08 | 1.24E-06 |
| Cf-251 | 1.33E+00 | 2.63E+02 | 3.29E-04 | 3.22E-04 | 1.45E-03 |
| Cf-252 | 3.33E-01 | 7.40E+01 | 1.10E-07 | 1.10E-07 | 1.38E-06 |
| Cl-36 | 3.44E-03 | 2.70E-02 | 1.50E-06 | 1.42E-06 | 5.23E-06 |
| Cm-242 | 4.44E-02 | 1.92E+01 | 1.07E-07 | 1.06E-07 | 1.55E-06 |
| Cm-243 | 5.55E-01 | 1.15E+02 | 3.64E-04 | 3.53E-04 | 1.52E-03 |
| Cm-244 | 4.44E-01 | 9.99E+01 | 7.87E-08 | 7.87E-08 | 1.34E-06 |
| Cm-245 | 7.77E-01 | 1.55E+02 | 2.13E-04 | 2.10E-04 | 1.03E-03 |
| Cm-246 | 7.77E-01 | 1.55E+02 | 7.26E-08 | 7.26E-08 | 1.23E-06 |
| Cm-247 | 7.03E-01 | 1.44E+02 | 1.11E-03 | 1.03E-03 | 3.82E-03 |
| Cm-248 | 2.85E+00 | 5.55E+02 | 5.49E-08 | 5.49E-08 | 9.30E-07 |
| Co-60 | 1.26E-02 | 3.70E-02 | 1.01E-02 | 8.47E-03 | 3.20E-02 |
| Cs-134 | 7.03E-02 | 2.44E-02 | 5.92E-03 | 5.22E-03 | 1.92E-02 |
| Cs-135 | 7.40E-03 | 2.55E-03 | 2.39E-08 | 2.39E-08 | 1.28E-07 |
| Cs-137 | 4.81E-02 | 1.70E-02 | 4.70E-07 | 4.60E-07 | 1.74E-06 |
| Eu-152 | 5.18E-03 | 1.55E-01 | 4.38E-03 | 3.76E-03 | 1.44E-02 |
| Eu-154 | 7.40E-03 | 1.96E-01 | 4.80E-03 | 4.11E-03 | 1.55E-02 |

Table 4.7-1: Internal and External DCF (Continued)

| Nuclide | Internal DCFs (rem/ μ Ci) | | External DCFs (rem/yr per μ Ci/ m^3) | | |
|---------|-------------------------------|------------|---|-------------|-----------------|
| | | | Contaminated Soil | | Water Immersion |
| | Ingestion | Inhalation | Infinite Depth | 15 cm Depth | |
| Eu-155 | 1.18E-03 | 2.55E-02 | 1.14E-04 | 1.14E-04 | 6.55E-04 |
| Fr-221 | N/A | N/A | 9.60E-05 | 9.23E-05 | 3.76E-04 |
| Fr-223 | 8.88E-03 | 3.29E-03 | 1.24E-04 | 1.18E-04 | 5.97E-04 |
| Gd-152 | 1.52E-01 | 7.03E+01 | N/A | N/A | N/A |
| H-3 | 6.66E-05 | 1.67E-04 | N/A | N/A | N/A |
| I-129 | 4.07E-01 | 1.33E-01 | 8.09E-06 | 8.09E-06 | 1.04E-04 |
| K-40 | 2.29E-02 | 7.77E-03 | 6.51E-04 | 5.34E-04 | 2.03E-03 |
| Kr-85 | N/A | N/A | 8.94E-06 | 8.14E-06 | 2.98E-05 |
| Mo-93 | 1.15E-02 | 2.18E-03 | 3.69E-07 | 3.69E-07 | 6.91E-06 |
| Na-22 | 1.18E-02 | 4.81E-03 | 8.55E-03 | 7.37E-03 | 2.74E-04 |
| Nb-93m | 4.44E-04 | 1.89E-03 | 6.51E-08 | 6.51E-08 | 1.21E-06 |
| Nb-94 | 6.29E-03 | 4.07E-02 | 6.05E-03 | 5.29E-03 | 1.95E-02 |
| Ni-59 | 2.33E-04 | 4.81E-04 | N/A | N/A | N/A |
| Ni-63 | 5.55E-04 | 1.78E-03 | N/A | N/A | N/A |
| Np-237 | 4.07E-01 | 8.51E+01 | 4.87E-05 | 4.86E-05 | 2.71E-04 |
| Np-238 | 3.37E-03 | 7.77E-03 | 2.15E-03 | 1.85E-03 | 6.88E-03 |
| Np-239 | 2.96E-03 | 3.44E-03 | 4.71E-04 | 4.56E-04 | 1.99E-03 |
| Np-240 | 3.03E-04 | 3.15E-04 | 4.84E-03 | 4.26E-03 | 1.60E-02 |
| Np-240m | N/A | N/A | 1.26E-03 | 1.11E-03 | 4.10E-03 |
| Pa-231 | 2.63E+00 | 5.18E+02 | 1.19E-04 | 1.12E-04 | 4.42E-04 |
| Pa-233 | 3.22E-03 | 1.44E-02 | 6.38E-04 | 6.03E-04 | 2.39E-03 |
| Pa-234 | 1.89E-03 | 1.48E-03 | 7.22E-03 | 6.28E-03 | 2.37E-02 |
| Pa-234m | N/A | N/A | 5.61E-05 | 4.91E-05 | 1.78E-04 |
| Pb-209 | 2.11E-04 | 2.07E-04 | 4.84E-07 | 4.77E-07 | 1.83E-06 |
| Pb-210 | 2.55E+00 | 4.07E+00 | 1.53E-06 | 1.53E-06 | 1.53E-05 |
| Pb-211 | 6.66E-04 | 4.07E-02 | 1.92E-04 | 1.71E-04 | 6.32E-04 |
| Pb-212 | 2.22E-02 | 6.29E-01 | 4.40E-04 | 4.23E-04 | 1.78E-03 |
| Pb-214 | 5.18E-04 | 5.18E-02 | 8.39E-04 | 7.83E-04 | 3.03E-03 |
| Pd-107 | 1.37E-04 | 2.18E-03 | N/A | N/A | N/A |
| Pm-147 | 9.62E-04 | 1.85E-02 | 3.13E-08 | 3.12E-08 | 1.64E-07 |
| Po-210 | 4.44E+00 | 1.22E+01 | 3.27E-08 | 2.86E-08 | 1.05E-07 |
| Po-211 | N/A | N/A | 2.97E-05 | 2.62E-05 | 9.66E-05 |
| Po-212 | N/A | N/A | N/A | N/A | N/A |
| Po-213 | N/A | N/A | N/A | N/A | N/A |
| Po-214 | N/A | N/A | 3.21E-07 | 2.80E-07 | 1.03E-06 |
| Po-215 | N/A | N/A | 6.35E-07 | 5.82E-07 | 2.15E-06 |
| Po-216 | N/A | N/A | 6.52E-08 | 5.69E-08 | 2.10E-07 |
| Po-218 | N/A | N/A | 3.53E-08 | 3.07E-08 | 1.13E-07 |
| Pr-144 | 1.85E-04 | 6.66E-05 | 1.58E-04 | 1.32E-04 | 4.85E-04 |
| Pu-238 | 8.51E-01 | 1.70E+02 | 9.46E-08 | 9.43E-08 | 1.33E-06 |
| Pu-239 | 9.25E-01 | 1.85E+02 | 1.85E-07 | 1.78E-07 | 1.12E-06 |

Table 4.7-1: Internal and External DCF (Continued)

| Nuclide | Internal DCFs (rem/ μ Ci) | | External DCFs (rem/yr per μ Ci/ m^3) | | |
|---------|-------------------------------|------------|---|-------------|-----------------|
| | | | Contaminated Soil | | Water Immersion |
| | Ingestion | Inhalation | Infinite Depth | 15 cm Depth | |
| Pu-240 | 9.25E-01 | 1.85E+02 | 9.17E-08 | 9.16E-08 | 1.30E-06 |
| Pu-241 | 1.78E-02 | 3.33E+00 | 3.69E-09 | 3.68E-09 | 1.89E-08 |
| Pu-242 | 8.88E-01 | 1.78E+02 | 8.00E-08 | 8.00E-08 | 1.09E-06 |
| Pu-243 | 3.15E-04 | 3.07E-04 | 4.98E-05 | 4.91E-05 | 2.70E-04 |
| Pu-244 | 8.88E-01 | 1.74E+02 | 4.72E-08 | 4.72E-08 | 8.13E-07 |
| Ra-223 | 3.70E-01 | 2.74E+01 | 3.77E-04 | 3.62E-04 | 1.58E-03 |
| Ra-224 | 2.41E-01 | 1.11E+01 | 3.20E-05 | 3.06E-05 | 1.20E-04 |
| Ra-225 | 3.66E-01 | 2.33E+01 | 6.89E-06 | 6.89E-06 | 7.58E-05 |
| Ra-226 | 1.04E+00 | 1.30E+01 | 1.99E-05 | 1.93E-05 | 8.12E-05 |
| Ra-228 | 2.55E+00 | 9.62E+00 | N/A | N/A | N/A |
| Rb-87 | 5.55E-03 | 1.85E-03 | 8.81E-08 | 8.78E-08 | 4.13E-07 |
| Re-188 | 5.18E-03 | 2.00E-03 | 2.01E-04 | 1.83E-04 | 7.31E-04 |
| Rh-106 | N/A | N/A | 8.07E-04 | 7.18E-04 | 2.62E-03 |
| Rn-219 | N/A | N/A | 1.93E-04 | 1.80E-04 | 6.83E-04 |
| Rn-220 | N/A | N/A | 1.44E-06 | 1.28E-06 | 4.71E-06 |
| Rn-222 | N/A | N/A | 1.47E-06 | 1.33E-06 | 4.86E-06 |
| Ru-106 | 2.59E-02 | 1.04E-01 | N/A | N/A | N/A |
| S-35 | 4.81E-04 | 5.18E-03 | 9.31E-09 | 9.31E-09 | 5.54E-08 |
| Sb-125 | 4.07E-03 | 1.78E-02 | 1.53E-03 | 1.38E-03 | 5.13E-03 |
| Sb-126 | 8.88E-03 | 1.04E-02 | 1.07E-02 | 9.50E-03 | 3.49E-02 |
| Sb-126m | 1.33E-04 | 7.03E-05 | 5.82E-03 | 5.19E-03 | 1.90E-02 |
| Sc-46 | 5.55E-03 | 2.52E-02 | 7.93E-03 | 6.77E-03 | 2.52E-02 |
| Se-79 | 1.07E-02 | 4.07E-03 | 1.16E-08 | 1.16E-08 | 6.93E-08 |
| Sm-151 | 3.63E-04 | 1.48E-02 | 6.16E-10 | 6.16E-10 | 9.93E-09 |
| Sn-121 | 8.51E-04 | 8.51E-04 | 1.23E-07 | 1.21E-07 | 5.37E-07 |
| Sn-121m | 1.41E-03 | 1.67E-02 | 1.23E-06 | 1.23E-06 | 1.65E-05 |
| Sn-126 | 1.74E-02 | 1.04E-01 | 9.22E-05 | 9.23E-05 | 5.56E-04 |
| Sr-90 | 1.04E-01 | 1.33E-01 | 4.40E-07 | 4.34E-07 | 1.71E-06 |
| Tc-99 | 2.37E-03 | 1.48E-02 | 7.85E-08 | 7.83E-08 | 3.67E-07 |
| Te-125m | 3.22E-03 | 1.26E-02 | 9.47E-06 | 9.46E-06 | 1.24E-04 |
| Th-227 | 3.26E-02 | 3.70E+01 | 3.26E-04 | 3.10E-04 | 1.25E-03 |
| Th-228 | 2.66E-01 | 1.48E+02 | 4.96E-06 | 4.87E-06 | 2.39E-05 |
| Th-229 | 1.81E+00 | 2.63E+02 | 2.01E-04 | 1.99E-04 | 1.00E-03 |
| Th-230 | 7.77E-01 | 5.18E+01 | 7.56E-07 | 7.46E-07 | 4.60E-06 |
| Th-231 | 1.26E-03 | 1.22E-03 | 2.28E-05 | 2.27E-05 | 1.38E-04 |
| Th-232 | 8.51E-01 | 9.25E+01 | 3.26E-07 | 3.25E-07 | 2.32E-06 |
| Th-234 | 1.26E-02 | 2.85E-02 | 1.51E-05 | 1.51E-05 | 8.92E-05 |
| Tl-207 | N/A | N/A | 1.24E-05 | 1.11E-05 | 3.95E-05 |
| Tl-208 | N/A | N/A | 1.44E-02 | 1.13E-02 | 4.49E-02 |
| Tl-209 | N/A | N/A | 8.08E-03 | 6.76E-03 | 2.59E-02 |
| U-232 | 1.22E+00 | 2.89E+01 | 5.64E-07 | 5.57E-07 | 3.76E-06 |

Table 4.7-1: Internal and External DCF (Continued)

| Nuclide | Internal DCFs (rem/ μ Ci) | | External DCFs (rem/yr per μ Ci/ m^3) | | |
|---------|-------------------------------|------------|---|-------------|-----------------|
| | | | Contaminated Soil | | Water Immersion |
| | Ingestion | Inhalation | Infinite Depth | 15 cm Depth | |
| U-233 | 1.89E-01 | 1.33E+01 | 8.74E-07 | 8.46E-07 | 4.25E-06 |
| U-234 | 1.81E-01 | 1.30E+01 | 2.51E-07 | 2.50E-07 | 2.04E-06 |
| U-235 | 1.74E-01 | 1.15E+01 | 4.51E-04 | 4.38E-04 | 1.86E-03 |
| U-236 | 1.74E-01 | 1.18E+01 | 1.34E-07 | 1.33E-07 | 1.35E-06 |
| U-238 | 1.67E-01 | 1.07E+01 | 6.45E-08 | 6.45E-08 | 9.29E-07 |
| U-240 | 4.07E-03 | 1.96E-03 | 8.90E-07 | 8.90E-07 | 1.06E-05 |
| W-181 | 2.81E-04 | 9.99E-05 | 4.78E-05 | 4.78E-05 | 3.76E-04 |
| W-185 | 1.63E-03 | 4.44E-04 | 2.71E-07 | 2.69E-07 | 1.30E-06 |
| W-188 | 7.77E-03 | 2.11E-03 | 6.05E-06 | 5.75E-06 | 2.31E-05 |
| Y-90 | 9.99E-03 | 5.55E-03 | 1.50E-05 | 1.40E-05 | 4.24E-05 |
| Zr-93 | 4.07E-03 | 3.70E-02 | N/A | N/A | N/A |

4.7.2 Member of the Public Dose Analysis

The release scenario that was analyzed to assess potential MOP doses associated with the SDF was a well drilled into the groundwater aquifers. The MOP dose pathways used in the PA analyses are discussed in detail in Section 4.2.4.1.

The consumption rates and bioaccumulation factors that are used in conjunction with the proposed pathways are discussed in detail in Section 4.6.

4.7.3 Intruder Dose Analysis

Two distinct release scenarios were analyzed to assess the potential intruder doses associated with the SDF. The intruder scenarios of concern are the Acute Intruder-Drilling Scenario and the Chronic Intruder Agricultural (Post-Drilling) Scenario. The intruder dose pathways used in the PA analyses are discussed in detail in Section 4.2.4.2.

The consumption rates and bioaccumulation factors that are used in conjunction with the proposed pathways are discussed in detail in Section 4.6.

4.7.4 Analysis Approach

The MOP and intruder exposure scenarios were analyzed for SDF to provide results to demonstrate compliance with the performance criteria. The analysis provides not only the maximum projected dose and time of occurrence, but also the dominant pathway contributing to the dose and the radionuclides responsible for the maximum dose.

The groundwater and surface water concentrations and resulting human health impacts are calculated for the Base Case using the PORFLOW computer code. The analysis approaches used for SDF are based upon the radionuclide inventories (Section 3.3), stabilized contaminant release mechanisms (Section 4.2.2), and radionuclide transport models (Section 4.2.3) as described previously in this document.

5.0 RESULTS OF ANALYSES

The purpose of this section is to present the results for the analyses described in Section 4.

Section 5.1 discusses source term assumptions associated with release of radionuclides to the groundwater beneath the SDF.

Section 5.2 presents peak groundwater concentrations for the radionuclides and chemicals discussed in Section 4.2.1. Maximum groundwater concentrations are provided for 100m from the SDF.

Section 5.3 presents the air pathways and radon release results.

Section 5.4 presents individual biotic pathways formulas used to calculate the MOP doses.

Section 5.5 presents the MOP dose analysis.

Section 5.6 presents the uncertainty and sensitivity analyses.

Section 5.7 presents the As Low As Reasonably Achievable (ALARA) analysis.

5.1 Source Term (Analysis Results) Assumptions

In the analysis, the release of radionuclides from the SDF disposal units was controlled in most cases by advective movement, which may vary with pH, and can vary with redox potential as well. The stabilized contaminant release rate is impacted by the water flow through the disposal unit and changes over time as the hydraulic properties of the saltstone and containment materials change. After a contaminant had left its applicable containment, concrete retardation and soil retardation impacted the contaminant's transport rate into the aquifers.

5.2 Environmental Transport of Radionuclides

The purpose of this section is to present the groundwater concentrations for all of the radionuclides and chemicals discussed in the source term screening section of the PA (Section 4.2.1). Maximum groundwater concentrations are presented for 100m from the SDF.

Results are presented for the three distinct aquifers modeled (UTR-UZ, UTR-LZ, and the Gordon Aquifer).

The groundwater concentrations at 100m were calculated using the PORFLOW SDF model for the Base Case discussed in Section 4.4.2. A summary of several key parameters used in the PORFLOW SDF modeling cases are provided in Table 5.2-1.

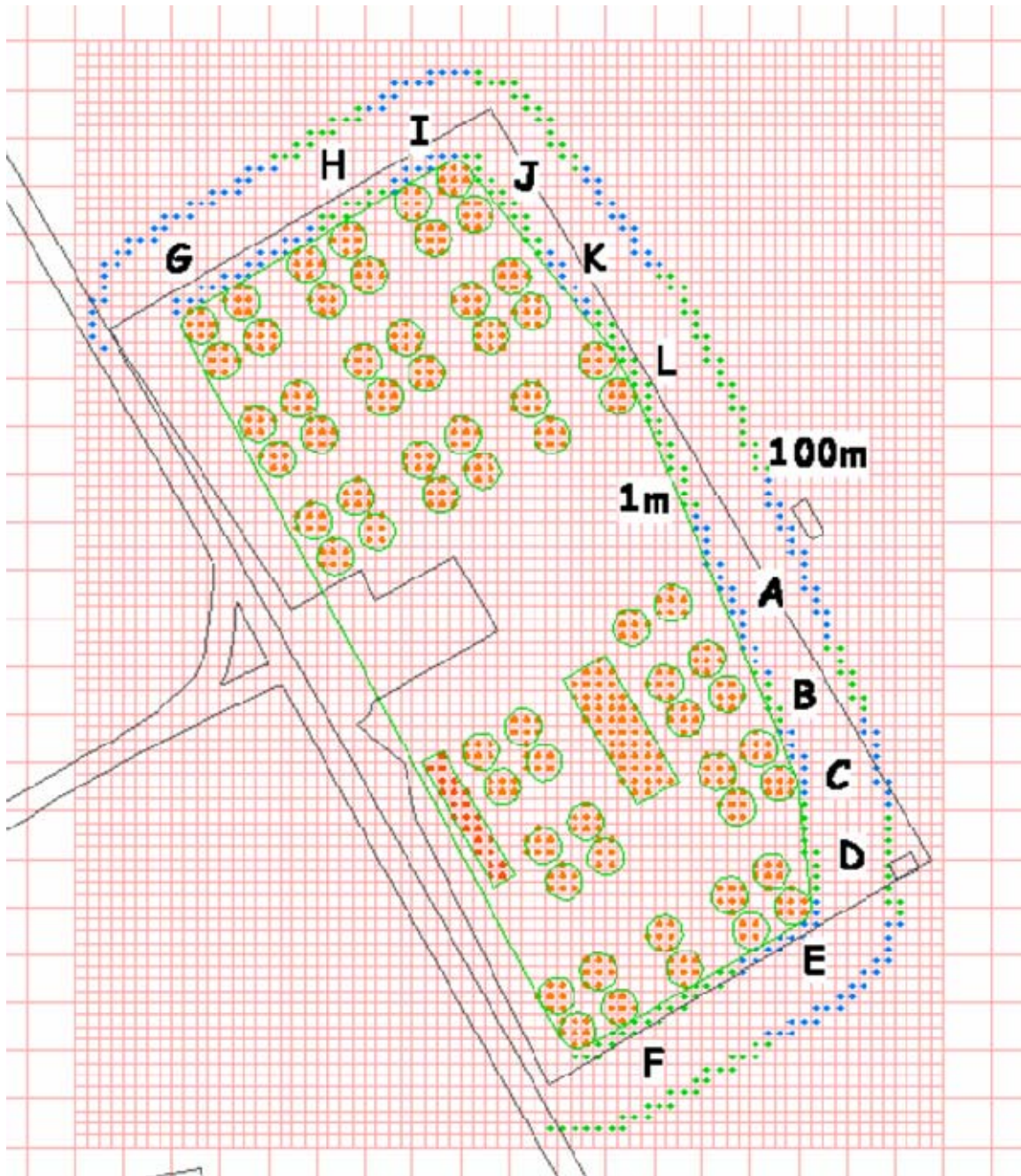
Table 5.2-1: Key Model Parameters

| SDF Parameter | Inputs |
|--|----------------------------|
| Radiological Inventory | Tables 3.3-1, 3.3-3, 3.3-5 |
| Chemical Inventory | Tables 3.3-2, 3.3-4, 3.3-6 |
| Closure Cap Estimated Infiltration Rates | Table 3.2-7 |
| Vadose K_d Values | Table 4.2-15 |
| Cementitious K_d Values | Table 4.2-18 |
| Cementitious Material Properties | Table 4.2-16 |
| FDC Walls (inches) | 8 |
| FDC Floor Slab (inches) | 8 |
| FDC Upper Mud Mat (inches) | 4 |
| FDC Lower Mud Mat (inches) | 4 |
| Vault 1 Walls (inches) | 18 |
| Vault 1 Floor Slab (inches) | 24 |
| Vault 1 Working Slab (inches) | 4 |
| Vault 4 Walls (inches) | 18 |
| Vault 4 Floor Slab (inches) | 24 |
| Vault 4 Working Slab (inches) | 4 |
| Chemical Transition of saltstone and disposal unit concrete (pore volumes) | Table 4.2-1 |
| Chemical Transition of saltstone and disposal unit concrete (years) | Table 4.2-17 |
| Significant model transitions (years) for Vault 1 | Table 4.4-6 |
| Significant model transitions (years) for Vault 4 | Table 4.4-7 |
| Significant model transitions (years) for FDCs | Table 4.4-9 |
| Disposal Unit Base Case | Case A (Section 4.4.2) |
| Vadose Zone Thickness | Table 4.2-13 |

5.2.1 Groundwater Concentrations at 100m

The 100m groundwater concentrations were calculated using the PORFLOW SDF model, which divides the area around SDF into computational cells. The blue and green dots in Figure 5.2-1 show the 1m and 100m distances from SDF. The blue and green dots also indicate the “sector” used for compilation of results. Each sector has a companion 1m and 100m field.

Figure 5.2-1: SDF 1m and 100m Modeled Cells and Sectors



Figures 5.2-2, 5.2-3, and 5.2-4 illustrate the contaminant flow via stream traces from SDF disposal units. Since the disposal units are distributed over the SDF footprint, the actual travel distance to reach the 100m boundary is often greater than 100m. Table 5.2-2 shows the approximate distances from each disposal unit to reach the 100m boundary in the direction of the flow. The stream traces (Figures 5.2-2, 5.2-3, and 5.2-4) from the SDF disposal units have 5 year time markers (blue dots) indicating travel times in the saturated zone between the source and the 100m boundary. These figures indicate that non-retarded travel times to the 100m boundary range from under 10 years to several decades depending on the source's location within the SDF and thus the aquifer or aquitard the tracer is traveling through. An example is a stream trace in Sector H which is on the groundwater divide so it travels slowly in the horizontal plane and therefore reaches the aquitard in the vertical plane causing it to move slowly near 100m.

Figure 5.2-2: SDF Vault 1 Modeling Showing Stream Tracers

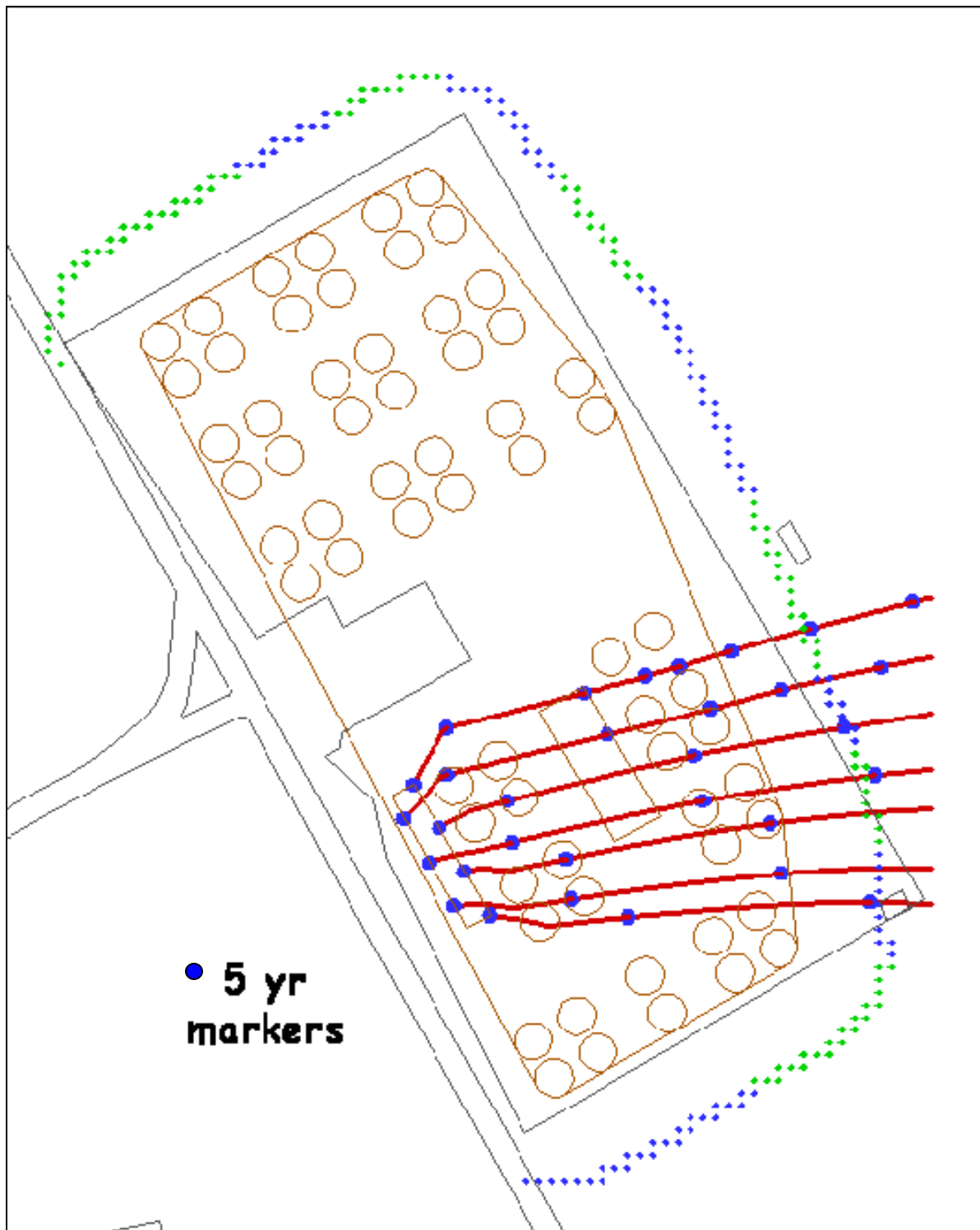


Figure 5.2-3: SDF Vault 4 Modeling Showing Stream Tracers

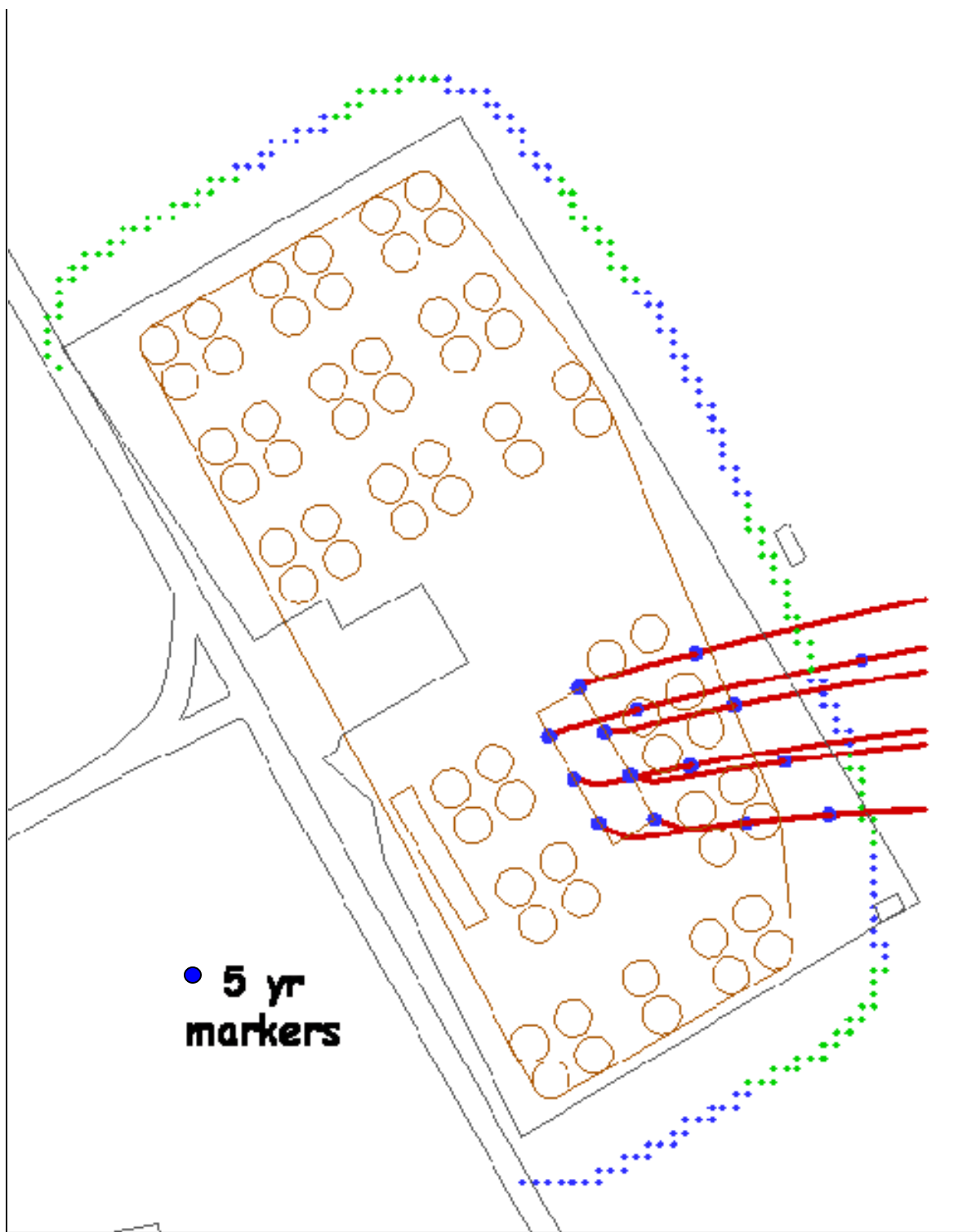


Figure 5.2-4: SDF Future Disposal Cell Modeling Showing Stream Tracers

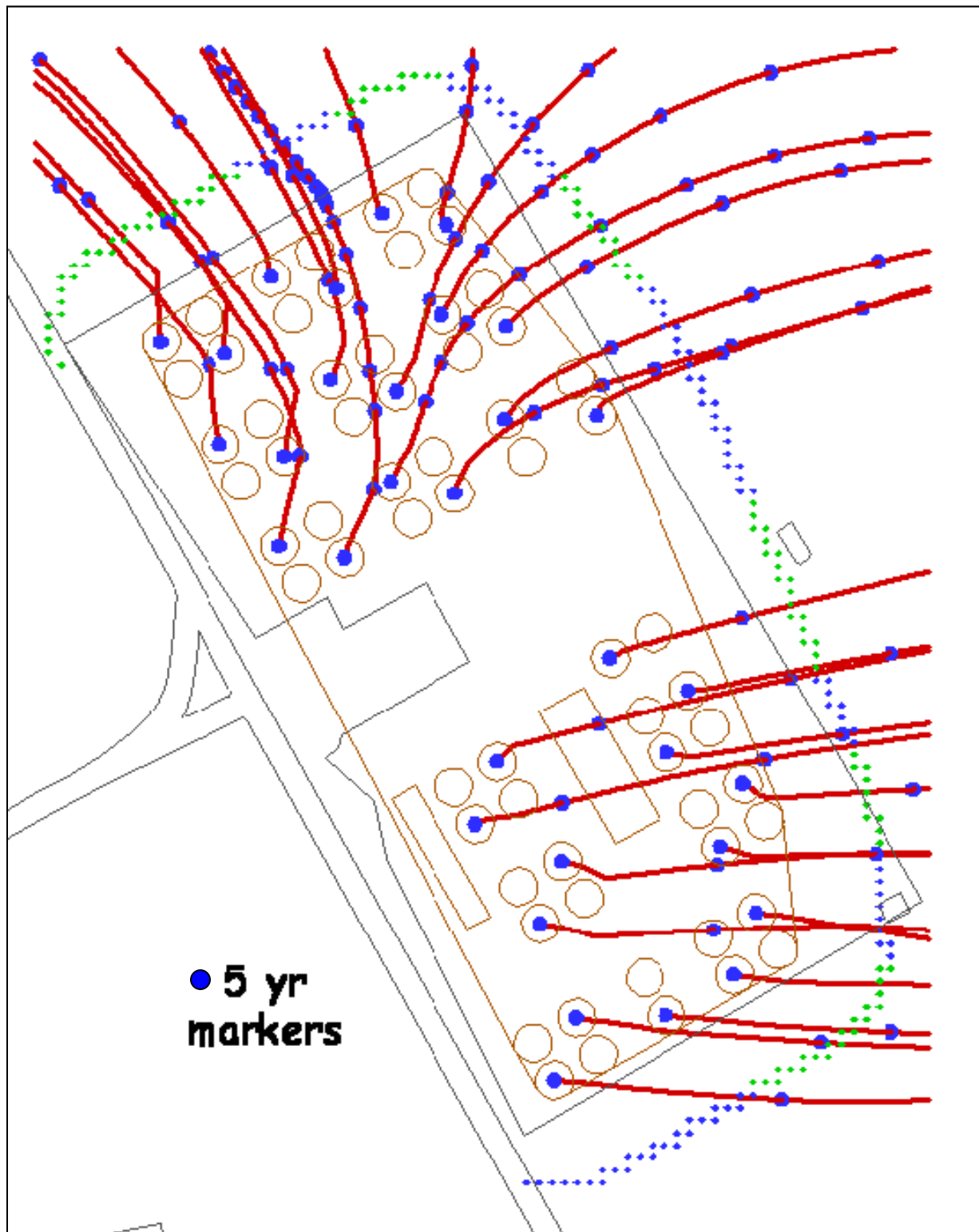


Table 5.2-2: Aquifer Travel Distance to SDF 100m Boundary

| Disposal Unit | Approximate Distance to 100m Boundary | Disposal Unit | Approximate Distance to 100m Boundary | Disposal Unit | Approximate Distance to 100m Boundary |
|---------------|---------------------------------------|---------------|---------------------------------------|---------------|---------------------------------------|
| V2A | 800 ft | V10A | 720 ft | V15C | 720 ft |
| V2B | 800 ft | V10B | 480 ft | V15D | 536 ft |
| V5A | 480 ft | V10C | 720 ft | V16A | 1,680 ft |
| V5B | 400 ft | V10D | 480 ft | V16B | 1,520 ft |
| V5C | 640 ft | V11A | 1,280 ft | V16C | 1,600 ft |
| V5D | 680 ft | V11B | 1,360 ft | V16D | 1,280 ft |
| V6A | 360 ft | V11C | 1,840 ft | V17A | 720 ft |
| V6B | 360 ft | V11D | 1,680 ft | V17B | 520 ft |
| V6C | 520 ft | V12A | 1,280 ft | V17C | 680 ft |
| V6D | 520 ft | V12B | 1,120 ft | V17D | 520 ft |
| V7A | 360 ft | V12C | 1,360 ft | V18A | 1,120 ft |
| V7B | 400 ft | V12D | 1,040 ft | V18B | 1,120 ft |
| V7C | 640 ft | V3A | 360 ft | V18C | 800 ft |
| V7D | 520 ft | V3B | 360 ft | V18D | 800 ft |
| V8A | 960 ft | V13A | 920 ft | V19A | 1,040 ft |
| V8B | 880 ft | V13B | 1,520 ft | V19B | 720 ft |
| V8C | 1,120 ft | V13C | 1,800 ft | V20A | 800 ft |
| V8D | 1,120 ft | V13D | 1,440 ft | V20B | 480 ft |
| V9A | 1,040 ft | V14A | 760 ft | V20C | 560 ft |
| V9B | 880 ft | V14B | 560 ft | V20D | 400 ft |
| V9C | 1,200 ft | V15A | 760 ft | V1 | 1,680 ft |
| V9D | 1,280 ft | V15B | 480 ft | V4 | 960 ft |

(Figure 4.2-20 identifies each disposal unit location shown in this table.)

The groundwater concentrations at 100m are the highest concentration at 100m or further from the SDF. This is supported by Figures 5.2-5, 5.2-6 and 5.2-7, which present the plume resulting from a continuous (non-depleting) source of tracer (no decay, no sorption) within the SDF disposal units. These figures show that the contaminant plumes leaving the SDF become less intense as you move away and downward. The groundwater arrangement around the SDF is such that concentrations decrease at greater distances from the inventory sources.

Figure 5.2-5: Contaminant Plume Leaving SDF – Plan View

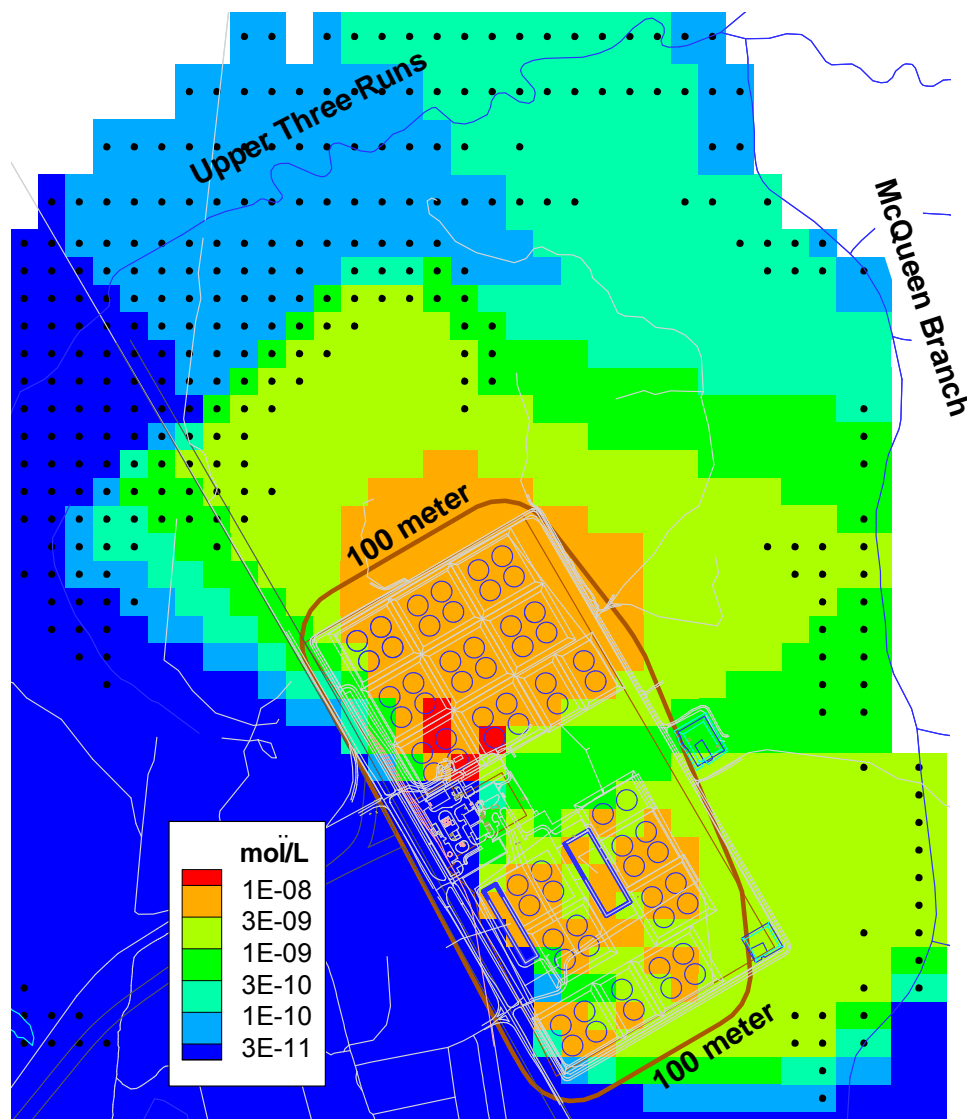
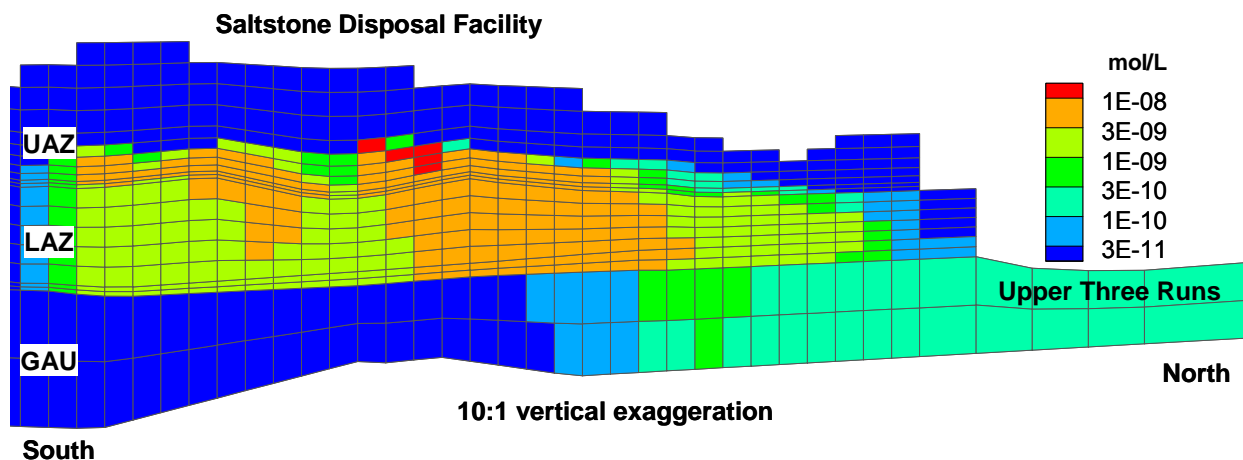
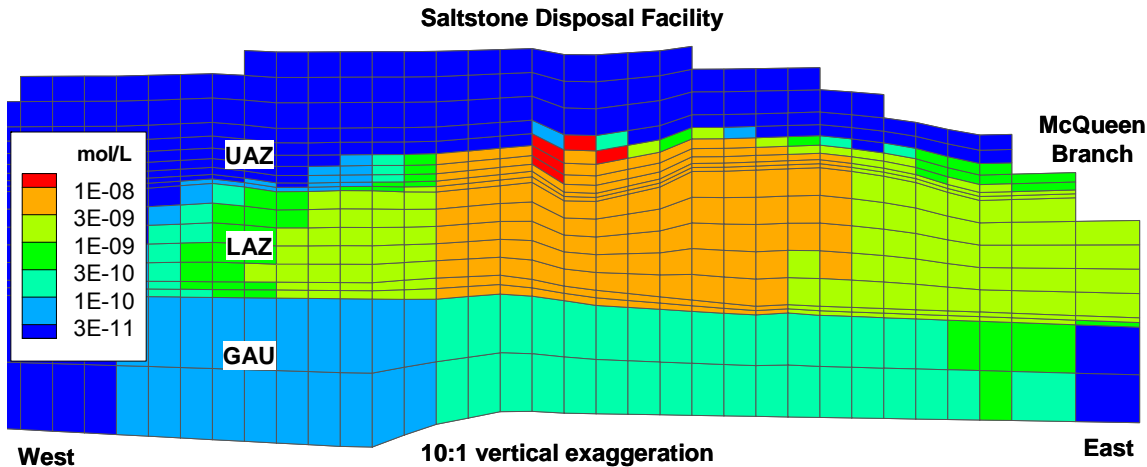


Figure 5.2-6: Contaminant Plume Leaving SDF – South/North Cross Section View



UAZ = Upper Aquifer Zone
LAZ = Lower Aquifer Zone
GAU = Gordon Aquifer Zone

Figure 5.2-7: Contaminant Plume Leaving SDF – East/West Cross Section View



UAZ = Upper Aquifer Zone
LAZ = Lower Aquifer Zone
GAU = Gordon Aquifer Zone

The PORFLOW 100m concentrations are calculated for 12 sectors (Sectors A – L), and the 1m and 100m assessment perimeters both utilize these same 12 sectors (see Figure 5.2-1). The peak concentration values for the 100m results are recorded for the three aquifer depths of concern (i.e., UTR-UZ, UTR-LZ, and Gordon Aquifer). The concentration for each aquifer represents the peak concentration in any vertical computational mesh within the aquifer. Computational

mesh layers have a vertical thickness averaging 6.6 feet in the UTR-UZ, and 12.7 feet in the UTR-LZ. No well screen averaging was used in determining the concentrations for dose calculations because the typical well screen length of 20 feet is approximate to the computational mesh height and is conservative in that the average mesh vertical thickness is less than 20 feet. Dividing the results into sectors was necessary to allow for the large amount of concentration data that is stored from PORFLOW and used by the GoldSim dose calculator model. The 12 sectors are analyzed for each radionuclide and chemical to find the maximum groundwater concentrations at 100m from the SDF. Using the sectors to determine the highest groundwater concentrations causes the calculated peak doses to be higher than they actually are, since the peak concentrations are determined for each radionuclide independent of the specific location within the sector.

Tables 5.2-3 through 5.2-11 present the peak 100m radionuclide concentrations within the 10,000 year performance period, in each sector for the three aquifers. Tables 5.2-12 through 5.2-20 show the peak 100m chemical concentrations within the 10,000 year performance period, in each sector for the three aquifers. Nitrate and nitrite are modeled as nitrogen, therefore, the MCL for nitrate plus nitrite (10,000 µg/L) is compared to the total nitrogen concentration. Tables 5.2-3 through 5.2-11 also list the MCL for each constituent with the derived values for beta and photon emitters from Table II-3 of FR-00-9654. The MCLs provided in the reference are derived for a beta-gamma dose of 4 mrem/yr. The peak concentration of each beta-gamma emitter is compared to a specific MCL to determine their fraction. To determine if the 4 mrem/yr beta-gamma limit is met, the sum of the fractions must be less than 1.0. The total alpha MCL includes Ra-226, but does not include radon or uranium. The radium MCL includes both Ra-226 and Ra-228. [SCDHEC R.61-58]

Table 5.2-3: Radiological 100m Concentrations for UTR-UZ Sectors A through E

| Radionuclide | MCL** (pCi/L) | Sector A Concentration | | Sector B Concentration | | Sector C Concentration | | Sector D Concentration | | Sector E Concentration | |
|--------------|------------------|---------------------------|---------------------|---------------------------|---------------------|---------------------------|---------------------|---------------------------|---------------------|---------------------------|---------------------|
| | | (pCi/L) | Year Peak Occurs | (pCi/L) | Year Peak Occurs | (pCi/L) | Year Peak Occurs | (pCi/L) | Year Peak Occurs | (pCi/L) | Year Peak Occurs |
| Ac-227 | NC | 9.0E-10 | 10,000 | 5.8E-08 | 10,000 | 6.4E-08 | 10,000 | 1.3E-08 | 10,000 | 7.0E-11 | 10,000 |
| Al-26 | NC | <1.0E-30 | 10,000 | 4.0E-30 | 10,000 | 3.2E-25 | 10,000 | 9.8E-28 | 10,000 | <1.0E-30 | 10,000 |
| Am-241 | Total α | <1.0E-30 | 10,000 | <1.0E-30 | 10,000 | 4.8E-27 | 10,000 | 1.8E-29 | 10,000 | <1.0E-30 | 10,000 |
| Am-242m | Total α | <1.0E-30 | 10,000 | <1.0E-30 | 10,000 | <1.0E-30 | 8,640 | <1.0E-30 | 9,160 | <1.0E-30 | 10,000 |
| Am-243 | Total α | <1.0E-30 | 10,000 | <1.0E-30 | 10,000 | 5.9E-27 | 10,000 | 2.1E-29 | 10,000 | <1.0E-30 | 10,000 |
| Ba-137m | NC | <1.0E-30 | 1,980 | <1.0E-30 | 1,840 | 2.9E-30 | 1,720 | <1.0E-30 | 1,780 | <1.0E-30 | 1,560 |
| C-14 | 2,000 | 1.2E-02 | 7,100 | 5.6E-01 | 6,100 | 6.2E-01 | 6,100 | 1.8E-01 | 7,100 | 1.1E-01 | 9,800 |
| Cf-249 | Total α | <1.0E-30 | 10,000 | <1.0E-30 | 10,000 | <1.0E-30 | 10,000 | <1.0E-30 | 10,000 | <1.0E-30 | 10,000 |
| Cf-251 | Total α | <1.0E-30 | 10,000 | <1.0E-30 | 10,000 | 4.5E-30 | 10,000 | <1.0E-30 | 10,000 | <1.0E-30 | 10,000 |
| Cl-36 | 700 | 3.9E-06 | 9,700 | 1.7E-04 | 9,600 | 1.9E-04 | 9,600 | 6.3E-05 | 9,660 | 2.1E-05 | 10,000 |
| Cm-243 | Total α | <1.0E-30 | 2,720 | <1.0E-30 | 2,660 | <1.0E-30 | 2,320 | <1.0E-30 | 2,460 | <1.0E-30 | 2,760 |
| Cm-244 | Total α | <1.0E-30 | 1,700 | <1.0E-30 | 1,740 | <1.0E-30 | 1,520 | <1.0E-30 | 1,620 | <1.0E-30 | 1,820 |
| Cm-245 | Total α | <1.0E-30 | 10,000 | <1.0E-30 | 10,000 | 3.5E-27 | 10,000 | 1.3E-29 | 10,000 | <1.0E-30 | 10,000 |
| Cm-247 | Total α | <1.0E-30 | 10,000 | <1.0E-30 | 10,000 | <1.0E-30 | 10,000 | <1.0E-30 | 10,000 | <1.0E-30 | 10,000 |
| Cm-248 | Total α | <1.0E-30 | 10,000 | <1.0E-30 | 10,000 | <1.0E-30 | 10,000 | <1.0E-30 | 10,000 | <1.0E-30 | 10,000 |
| Co-60 | 100 | <1.0E-30 | 300 | <1.0E-30 | 260 | <1.0E-30 | 260 | <1.0E-30 | 260 | <1.0E-30 | 300 |
| Cs-135 | 900 | 1.5E-03 | 10,000 | 1.2E-01 | 10,000 | 1.3E-01 | 10,000 | 2.9E-02 | 10,000 | 1.1E-04 | 10,000 |
| Cs-137 | 200 | <1.0E-30 | 1,980 | <1.0E-30 | 1,840 | 3.1E-30 | 1,720 | <1.0E-30 | 1,780 | <1.0E-30 | 1,560 |
| Eu-152 | 200 | <1.0E-30 | 1,300 | <1.0E-30 | 1,360 | <1.0E-30 | 1,200 | <1.0E-30 | 1,260 | <1.0E-30 | 1,420 |
| Eu-154 | 60 | <1.0E-30 | 860 | <1.0E-30 | 900 | <1.0E-30 | 800 | <1.0E-30 | 840 | <1.0E-30 | 940 |
| Gd-152 | NC | <1.0E-30 | 10,000 | <1.0E-30 | 10,000 | <1.0E-30 | 10,000 | <1.0E-30 | 10,000 | <1.0E-30 | 10,000 |
| H-3 | 20,000 | 2.1E-11 | 380 | 1.6E-09 | 380 | 1.8E-09 | 380 | 4.0E-10 | 380 | 2.3E-11 | 420 |
| I-129 | 1 | 4.1E-03 | 10,000 | 4.9E-02 | 10,000 | 7.2E-02 | 10,000 | 6.6E-02 | 10,000 | 7.8E-02 | 10,000 |
| K-40 | NC | 1.5E-05 | 10,000 | 3.1E-04 | 10,000 | 3.7E-04 | 10,000 | 2.3E-04 | 10,000 | 2.3E-04 | 10,000 |
| Nb-93m | 1,000 | 1.6E-03 | 10,000 | 1.1E-01 | 10,000 | 1.3E-01 | 10,000 | 2.8E-02 | 10,000 | 2.3E-04 | 10,000 |
| Nb-94 | NC | 3.4E-06 | 9,700 | 2.2E-04 | 9,700 | 2.5E-04 | 9,700 | 5.2E-05 | 9,700 | 3.4E-07 | 9,700 |

Table 5.2-3: Radiological 100m Concentrations for UTR-UZ Sectors A through E (Continued)

| Radionuclide | MCL (pCi/L)** | Sector A Concentration | | Sector B Concentration | | Sector C Concentration | | Sector D Concentration | | Sector E Concentration | |
|--------------|--------------------|---------------------------|---------------------|---------------------------|---------------------|---------------------------|---------------------|---------------------------|---------------------|---------------------------|---------------------|
| | | (pCi/L) | Year Peak Occurs | (pCi/L) | Year Peak Occurs | (pCi/L) | Year Peak Occurs | (pCi/L) | Year Peak Occurs | (pCi/L) | Year Peak Occurs |
| Ni-59 | 300 | 1.2E-06 | 10,000 | 8.8E-05 | 10,000 | 1.0E-04 | 10,000 | 2.4E-05 | 10,000 | 4.9E-07 | 10,000 |
| Ni-63 | 50 | 1.9E-13 | 1,920 | 2.1E-11 | 1,860 | 2.7E-11 | 1,840 | 5.7E-12 | 1,860 | 1.7E-14 | 1,940 |
| Np-237 | Total α | 8.5E-06 | 10,000 | 5.5E-04 | 10,000 | 6.1E-04 | 10,000 | 1.3E-04 | 10,000 | 5.9E-07 | 10,000 |
| Pa-231 | Total α | 1.2E-06 | 10,000 | 7.8E-05 | 10,000 | 8.6E-05 | 10,000 | 1.8E-05 | 10,000 | 9.4E-08 | 10,000 |
| Pb-210 | NC | 2.8E-05 | 10,000 | 1.7E-03 | 9,900 | 1.9E-03 | 9,920 | 4.6E-04 | 9,920 | 4.0E-05 | 10,000 |
| Pd-107 | NC | 1.6E-07 | 10,000 | 1.2E-05 | 10,000 | 1.3E-05 | 10,000 | 3.0E-06 | 10,000 | 3.5E-08 | 10,000 |
| Pt-193 | 3,000 | 3.7E-05 | 480 | 2.0E-03 | 460 | 2.3E-03 | 460 | 5.9E-04 | 480 | 3.7E-04 | 540 |
| Pu-238 | Total α | <1.0E-30 | 6,620 | <1.0E-30 | 6,100 | <1.0E-30 | 5,520 | <1.0E-30 | 5,700 | <1.0E-30 | 6,520 |
| Pu-239 | Total α | 8.3E-17 | 10,000 | 6.0E-13 | 10,000 | 8.6E-12 | 10,000 | 4.2E-13 | 10,000 | 9.6E-18 | 10,000 |
| Pu-240 | Total α | 1.2E-17 | 10,000 | 8.7E-14 | 10,000 | 1.2E-12 | 10,000 | 6.1E-14 | 10,000 | 1.4E-18 | 10,000 |
| Pu-241 | 300 | <1.0E-30 | 10,000 | <1.0E-30 | 10,000 | 1.9E-26 | 10,000 | 7.0E-29 | 10,000 | <1.0E-30 | 10,000 |
| Pu-242 | Total α | 2.3E-19 | 10,000 | 1.7E-15 | 10,000 | 2.4E-14 | 10,000 | 1.2E-15 | 10,000 | 2.7E-20 | 10,000 |
| Pu-244 | Total α | 4.8E-21 | 10,000 | 3.4E-17 | 10,000 | 4.9E-16 | 10,000 | 2.4E-17 | 10,000 | 5.5E-22 | 10,000 |
| Ra-226 | Total α /Ra | 1.1E-02 | 10,000 | 6.5E-01 | 9,880 | 7.2E-01 | 9,860 | 1.7E-01 | 9,840 | 1.5E-02 | 10,000 |
| Ra-228 | Total Ra | 1.1E-17 | 10,000 | 9.5E-15 | 10,000 | 3.6E-14 | 10,000 | 3.8E-15 | 10,000 | 1.2E-18 | 10,000 |
| Rn-222 | NC | 1.1E-02 | 10,000 | 6.5E-01 | 9,880 | 7.2E-01 | 9,860 | 1.7E-01 | 9,840 | 1.5E-02 | 10,000 |
| Se-79 | NC | 1.5E-29 | 10,000 | 5.7E-23 | 10,000 | 4.5E-19 | 10,000 | 2.9E-21 | 10,000 | 9.0E-29 | 10,000 |
| Sm-151 | 1,000 | <1.0E-30 | 7,980 | <1.0E-30 | 7,280 | <1.0E-30 | 6,260 | <1.0E-30 | 6,640 | <1.0E-30 | 7,540 |
| Sb-126 | NC | <1.0E-30 | 10,000 | <1.0E-30 | 10,000 | <1.0E-30 | 10,000 | <1.0E-30 | 10,000 | <1.0E-30 | 10,000 |
| Sb-126m | NC | <1.0E-30 | 10,000 | <1.0E-30 | 10,000 | 1.0E-30 | 10,000 | <1.0E-30 | 10,000 | <1.0E-30 | 10,000 |
| Sn-126 | NC | <1.0E-30 | 10,000 | <1.0E-30 | 10,000 | 1.0E-30 | 10,000 | <1.0E-30 | 10,000 | <1.0E-30 | 10,000 |
| Sr-90 | 8 | 4.9E-15 | 1,140 | 9.1E-13 | 1,100 | 1.6E-12 | 1,080 | 2.8E-13 | 1,100 | 4.8E-16 | 1,120 |
| Tc-99 | 900 | 8.0E-02 | 9,820 | 5.5E+00 | 9,800 | 6.1E+00 | 9,800 | 1.3E+00 | 9,800 | 1.3E-02 | 9,800 |
| Th-228 | Total α | 1.1E-17 | 10,000 | 9.5E-15 | 10,000 | 3.6E-14 | 10,000 | 3.8E-15 | 10,000 | 1.2E-18 | 10,000 |
| Th-229 | Total α | 8.9E-12 | 10,000 | 1.7E-09 | 10,000 | 5.8E-09 | 10,000 | 6.4E-10 | 10,000 | 1.2E-12 | 10,000 |
| Th-230 | Total α | 1.3E-13 | 10,000 | 1.6E-10 | 10,000 | 6.7E-10 | 10,000 | 6.6E-11 | 10,000 | 1.5E-14 | 10,000 |

Table 5.2-3: Radiological 100m Concentrations for UTR-UZ Sectors A through E (Continued)

| Radionuclide | MCL (pCi/L)** | Sector A Concentration | | Sector B Concentration | | Sector C Concentration | | Sector D Concentration | | Sector E Concentration | |
|--|------------------|---------------------------|---------------------|---------------------------|---------------------|---------------------------|---------------------|---------------------------|---------------------|---------------------------|---------------------|
| | | (pCi/L) | Year Peak Occurs | (pCi/L) | Year Peak Occurs | (pCi/L) | Year Peak Occurs | (pCi/L) | Year Peak Occurs | (pCi/L) | Year Peak Occurs |
| Th-232 | Total α | 1.9E-20 | 10,000 | 2.3E-17 | 10,000 | 9.8E-17 | 10,000 | 9.7E-18 | 10,000 | 2.2E-21 | 10,000 |
| U-232 | Total U* | <1.0E-30 | 4,600 | <1.0E-30 | 4,200 | <1.0E-30 | 3,780 | <1.0E-30 | 3,900 | <1.0E-30 | 4,520 |
| U-233 | Total U* | 3.2E-10 | 10,000 | 1.2E-07 | 10,000 | 4.0E-07 | 10,000 | 4.5E-08 | 10,000 | 3.5E-11 | 10,000 |
| U-234 | Total U* | 1.3E-10 | 10,000 | 1.3E-07 | 10,000 | 4.8E-07 | 10,000 | 5.2E-08 | 10,000 | 1.5E-11 | 10,000 |
| U-235 | Total U* | 2.2E-12 | 10,000 | 2.2E-09 | 10,000 | 8.1E-09 | 10,000 | 8.8E-10 | 10,000 | 2.5E-13 | 10,000 |
| U-236 | Total U* | 3.6E-12 | 10,000 | 3.5E-09 | 10,000 | 1.3E-08 | 10,000 | 1.4E-09 | 10,000 | 4.1E-13 | 10,000 |
| U-238 | Total U* | 2.7E-12 | 10,000 | 2.7E-09 | 10,000 | 1.0E-08 | 10,000 | 1.1E-09 | 10,000 | 3.1E-13 | 10,000 |
| Y-90 | 60 | 4.9E-15 | 1,140 | 9.1E-13 | 1,100 | 1.6E-12 | 1,080 | 2.8E-13 | 1,100 | 4.8E-16 | 1,120 |
| Zr-93 | 2,000 | <1.0E-30 | 10,000 | 1.1E-24 | 10,000 | 5.5E-21 | 10,000 | 4.1E-23 | 10,000 | <1.0E-30 | 10,000 |
| Total alpha | 15 | 1.1E-02 | N/A | 6.5E-01 | N/A | 7.2E-01 | N/A | 1.7E-01 | N/A | 1.5E-02 | N/A |
| Total Ra | 5 | 1.1E-02 | N/A | 6.5E-01 | N/A | 7.2E-01 | N/A | 1.7E-01 | N/A | 1.5E-02 | N/A |
| Sum of beta-gamma MCL fractions | | 4.2E-03 | N/A | 5.6E-02 | N/A | 7.9E-02 | N/A | 6.7E-02 | N/A | 7.8E-02 | N/A |

* Total uranium is evaluated in Table 5.2-12.

** MCL values for beta and photon emitters are calculated in Table II-3 of FR-00-9654 based on a beta-gamma dose of 4 mrem/yr

NC = Not Calculated

Table 5.2-4: Radiological 100m Concentrations for UTR-UZ Sectors F through J

| Radionuclide | MCL (pCi/L)** | Sector F Concentration | | Sector G Concentration | | Sector H Concentration | | Sector I Concentration | | Sector J Concentration | |
|--------------|------------------|---------------------------|---------------------|---------------------------|---------------------|---------------------------|---------------------|---------------------------|---------------------|---------------------------|---------------------|
| | | (pCi/L) | Year Peak Occurs | (pCi/L) | Year Peak Occurs | (pCi/L) | Year Peak Occurs | (pCi/L) | Year Peak Occurs | (pCi/L) | Year Peak Occurs |
| Ac-227 | NC | 4.6E-16 | 10,000 | 1.3E-19 | 10,000 | 3.2E-21 | 10,000 | 1.2E-19 | 10,000 | 1.7E-18 | 10,000 |
| Al-26 | NC | <1.0E-30 | 10,000 | <1.0E-30 | 10,000 | <1.0E-30 | 10,000 | <1.0E-30 | 10,000 | <1.0E-30 | 10,000 |
| Am-241 | Total α | <1.0E-30 | 10,000 | <1.0E-30 | 10,000 | <1.0E-30 | 10,000 | <1.0E-30 | 10,000 | <1.0E-30 | 10,000 |
| Am-242m | Total α | <1.0E-30 | 10,000 | <1.0E-30 | 8,880 | <1.0E-30 | 8,860 | <1.0E-30 | 9,060 | <1.0E-30 | 9,180 |
| Am-243 | Total α | <1.0E-30 | 10,000 | <1.0E-30 | 10,000 | <1.0E-30 | 10,000 | <1.0E-30 | 10,000 | <1.0E-30 | 10,000 |
| Ba-137m | NC | <1.0E-30 | 1,680 | <1.0E-30 | 1,580 | <1.0E-30 | 1,580 | <1.0E-30 | 1,640 | <1.0E-30 | 1,660 |
| C-14 | 2,000 | 6.8E-02 | 9,820 | 1.5E-01 | 9,780 | 9.8E-03 | 9,820 | 3.1E-02 | 9,820 | 1.4E-02 | 9,800 |
| Cf-249 | Total α | <1.0E-30 | 10,000 | <1.0E-30 | 10,000 | <1.0E-30 | 10,000 | <1.0E-30 | 10,000 | <1.0E-30 | 10,000 |
| Cf-251 | Total α | <1.0E-30 | 10,000 | <1.0E-30 | 10,000 | <1.0E-30 | 10,000 | <1.0E-30 | 10,000 | <1.0E-30 | 10,000 |
| Cl-36 | 700 | 1.3E-05 | 10,000 | 3.0E-05 | 10,000 | 1.9E-06 | 10,000 | 6.1E-06 | 10,000 | 2.8E-06 | 10,000 |
| Cm-243 | Total α | <1.0E-30 | 2,740 | <1.0E-30 | 2,400 | <1.0E-30 | 2,400 | <1.0E-30 | 2,420 | <1.0E-30 | 2,460 |
| Cm-244 | Total α | <1.0E-30 | 1,800 | <1.0E-30 | 1,560 | <1.0E-30 | 1,560 | <1.0E-30 | 1,560 | <1.0E-30 | 1,580 |
| Cm-245 | Total α | <1.0E-30 | 10,000 | <1.0E-30 | 10,000 | <1.0E-30 | 10,000 | <1.0E-30 | 10,000 | <1.0E-30 | 10,000 |
| Cm-247 | Total α | <1.0E-30 | 10,000 | <1.0E-30 | 10,000 | <1.0E-30 | 10,000 | <1.0E-30 | 10,000 | <1.0E-30 | 10,000 |
| Cm-248 | Total α | <1.0E-30 | 10,000 | <1.0E-30 | 10,000 | <1.0E-30 | 10,000 | <1.0E-30 | 10,000 | <1.0E-30 | 10,000 |
| Co-60 | 100 | <1.0E-30 | 300 | <1.0E-30 | 480 | <1.0E-30 | 460 | <1.0E-30 | 460 | <1.0E-30 | 380 |
| Cs-135 | 900 | 6.1E-06 | 10,000 | 1.3E-05 | 10,000 | 9.2E-07 | 10,000 | 2.0E-06 | 10,000 | 8.9E-07 | 10,000 |
| Cs-137 | 200 | <1.0E-30 | 1,680 | <1.0E-30 | 1,580 | <1.0E-30 | 1,580 | <1.0E-30 | 1,640 | <1.0E-30 | 1,660 |
| Eu-152 | 200 | <1.0E-30 | 1,400 | <1.0E-30 | 1,220 | <1.0E-30 | 1,220 | <1.0E-30 | 1,220 | <1.0E-30 | 1,240 |
| Eu-154 | 60 | <1.0E-30 | 800 | <1.0E-30 | 820 | <1.0E-30 | 820 | <1.0E-30 | 820 | <1.0E-30 | 820 |
| Gd-152 | NC | <1.0E-30 | 10,000 | <1.0E-30 | 10,000 | <1.0E-30 | 10,000 | <1.0E-30 | 10,000 | <1.0E-30 | 10,000 |
| H-3 | 20,000 | 1.5E-11 | 420 | 3.3E-11 | 420 | 2.2E-12 | 420 | 5.7E-12 | 420 | 2.5E-12 | 420 |
| I-129 | 1 | 5.0E-02 | 10,000 | 1.1E-01 | 10,000 | 7.2E-03 | 10,000 | 2.3E-02 | 10,000 | 1.0E-02 | 10,000 |
| K-40 | NC | 1.4E-04 | 10,000 | 3.2E-04 | 10,000 | 2.1E-05 | 10,000 | 6.5E-05 | 10,000 | 3.0E-05 | 10,000 |
| Nb-93m | 1,000 | 3.5E-09 | 10,000 | 6.7E-13 | 10,000 | 8.4E-15 | 10,000 | 3.4E-13 | 10,000 | 5.4E-12 | 10,000 |
| Nb-94 | NC | 3.6E-12 | 9,640 | 6.5E-13 | 10,000 | 3.0E-15 | 10,000 | 6.3E-15 | 10,000 | 1.4E-14 | 9,660 |

Table 5.2-4: Radiological 100m Concentrations for UTR-UZ Sectors F through J (Continued)

| Radionuclide | MCL (pCi/L)** | Sector F Concentration | | Sector G Concentration | | Sector H Concentration | | Sector I Concentration | | Sector J Concentration | |
|--------------|------------------|---------------------------|---------------------|---------------------------|---------------------|---------------------------|---------------------|---------------------------|---------------------|---------------------------|---------------------|
| | | (pCi/L) | Year Peak Occurs | (pCi/L) | Year Peak Occurs | (pCi/L) | Year Peak Occurs | (pCi/L) | Year Peak Occurs | (pCi/L) | Year Peak Occurs |
| Ni-59 | 300 | 1.1E-11 | 10,000 | 1.8E-15 | 10,000 | 7.2E-17 | 10,000 | 2.9E-15 | 10,000 | 4.0E-14 | 10,000 |
| Ni-63 | 50 | 1.0E-19 | 2,280 | 1.2E-25 | 2,840 | 8.1E-27 | 2,800 | 2.3E-25 | 2,880 | 5.9E-24 | 2,820 |
| Np-237 | Total α | 2.4E-12 | 10,000 | 1.5E-15 | 10,000 | 1.6E-17 | 10,000 | 6.3E-16 | 10,000 | 8.6E-15 | 10,000 |
| Pa-231 | Total α | 6.1E-13 | 10,000 | 1.8E-16 | 10,000 | 4.1E-18 | 10,000 | 1.6E-16 | 10,000 | 2.2E-15 | 10,000 |
| Pb-210 | NC | 2.6E-05 | 10,000 | 5.7E-05 | 10,000 | 3.7E-06 | 10,000 | 1.1E-05 | 10,000 | 5.1E-06 | 10,000 |
| Pd-107 | NC | 6.3E-13 | 10,000 | 1.3E-16 | 10,000 | 4.3E-18 | 10,000 | 1.7E-16 | 10,000 | 2.4E-15 | 10,000 |
| Pt-193 | 3,000 | 2.4E-04 | 540 | 5.3E-04 | 540 | 3.5E-05 | 540 | 1.0E-04 | 540 | 4.8E-05 | 540 |
| Pu-238 | Total α | <1.0E-30 | 6,640 | <1.0E-30 | 7,240 | <1.0E-30 | 7,220 | <1.0E-30 | 7,420 | <1.0E-30 | 7,460 |
| Pu-239 | Total α | 1.7E-24 | 10,000 | <1.0E-30 | 10,000 | <1.0E-30 | 10,000 | <1.0E-30 | 10,000 | <1.0E-30 | 10,000 |
| Pu-240 | Total α | 2.5E-25 | 10,000 | <1.0E-30 | 10,000 | <1.0E-30 | 10,000 | <1.0E-30 | 10,000 | <1.0E-30 | 10,000 |
| Pu-241 | 300 | <1.0E-30 | 10,000 | <1.0E-30 | 10,000 | <1.0E-30 | 10,000 | <1.0E-30 | 10,000 | <1.0E-30 | 10,000 |
| Pu-242 | Total α | 4.8E-27 | 10,000 | <1.0E-30 | 10,000 | <1.0E-30 | 10,000 | <1.0E-30 | 10,000 | <1.0E-30 | 10,000 |
| Pu-244 | Total α | 1.0E-28 | 10,000 | <1.0E-30 | 10,000 | <1.0E-30 | 10,000 | <1.0E-30 | 10,000 | <1.0E-30 | 10,000 |
| Ra-226 | Total α/Ra | 9.8E-03 | 10,000 | 2.2E-02 | 10,000 | 1.4E-03 | 10,000 | 4.3E-03 | 10,000 | 2.0E-03 | 10,000 |
| Ra-228 | Total Ra | 3.3E-25 | 10,000 | 8.0E-27 | 10,000 | 8.1E-28 | 10,000 | 5.6E-29 | 10,000 | 1.1E-29 | 10,000 |
| Rn-222 | NC | 9.8E-03 | 10,000 | 2.2E-02 | 10,000 | 1.4E-03 | 10,000 | 4.3E-03 | 10,000 | 2.0E-03 | 10,000 |
| Se-79 | NC | <1.0E-30 | 10,000 | 3.2E-29 | 10,000 | 3.3E-30 | 10,000 | <1.0E-30 | 10,000 | <1.0E-30 | 10,000 |
| Sm-151 | 1,000 | <1.0E-30 | 7,940 | <1.0E-30 | 6,640 | <1.0E-30 | 6,620 | <1.0E-30 | 6,740 | <1.0E-30 | 6,840 |
| Sb-126 | NC | <1.0E-30 | 10,000 | <1.0E-30 | 10,000 | <1.0E-30 | 10,000 | <1.0E-30 | 10,000 | <1.0E-30 | 10,000 |
| Sb-126m | NC | <1.0E-30 | 10,000 | <1.0E-30 | 10,000 | <1.0E-30 | 10,000 | <1.0E-30 | 10,000 | <1.0E-30 | 10,000 |
| Sn-126 | NC | <1.0E-30 | 10,000 | <1.0E-30 | 10,000 | <1.0E-30 | 10,000 | <1.0E-30 | 10,000 | <1.0E-30 | 10,000 |
| Sr-90 | 8 | 1.1E-20 | 1,120 | 2.8E-20 | 1,120 | 2.4E-21 | 1,100 | 1.5E-21 | 1,160 | 5.7E-22 | 1,160 |
| Tc-99 | 900 | 4.5E-07 | 10,000 | 5.6E-07 | 10,000 | 3.6E-08 | 10,000 | 1.1E-07 | 10,000 | 5.2E-08 | 10,000 |
| Th-228 | Total α | 3.3E-25 | 10,000 | 8.0E-27 | 10,000 | 8.1E-28 | 10,000 | 5.6E-29 | 10,000 | 1.1E-29 | 10,000 |
| Th-229 | Total α | 1.6E-17 | 10,000 | 9.6E-21 | 10,000 | 1.1E-22 | 10,000 | 4.5E-21 | 10,000 | 6.2E-20 | 10,000 |
| Th-230 | Total α | 3.8E-21 | 10,000 | 3.3E-28 | 10,000 | 3.4E-29 | 10,000 | 2.2E-30 | 10,000 | <1.0E-30 | 10,000 |
| Th-232 | Total α | 5.5E-28 | 10,000 | <1.0E-30 | 10,000 | <1.0E-30 | 10,000 | <1.0E-30 | 10,000 | <1.0E-30 | 10,000 |

Table 5.2-4: Radiological 100m Concentrations for UTR-UZ Sectors F through J (Continued)

| Radionuclide | MCL (pCi/L)** | Sector F Concentration | | Sector G Concentration | | Sector H Concentration | | Sector I Concentration | | Sector J Concentration | |
|--|------------------|---------------------------|---------------------|---------------------------|---------------------|---------------------------|---------------------|---------------------------|---------------------|---------------------------|---------------------|
| | | (pCi/L) | Year Peak Occurs | (pCi/L) | Year Peak Occurs | (pCi/L) | Year Peak Occurs | (pCi/L) | Year Peak Occurs | (pCi/L) | Year Peak Occurs |
| U-232 | Total U* | <1.0E-30 | 4,600 | <1.0E-30 | 4,920 | <1.0E-30 | 4,920 | <1.0E-30 | 5,060 | <1.0E-30 | 5,100 |
| U-233 | Total U* | 2.7E-16 | 10,000 | 3.1E-19 | 10,000 | 1.9E-21 | 10,000 | 7.4E-20 | 10,000 | 1.0E-18 | 10,000 |
| U-234 | Total U* | 3.9E-18 | 10,000 | 3.9E-25 | 10,000 | 3.9E-26 | 10,000 | 2.8E-27 | 10,000 | 5.6E-28 | 10,000 |
| U-235 | Total U* | 6.6E-20 | 10,000 | 6.4E-27 | 10,000 | 6.5E-28 | 10,000 | 4.6E-29 | 10,000 | 9.3E-30 | 10,000 |
| U-236 | Total U* | 1.1E-19 | 10,000 | 3.4E-26 | 10,000 | 3.4E-27 | 10,000 | 2.4E-28 | 10,000 | 4.9E-29 | 10,000 |
| U-238 | Total U* | 8.1E-20 | 10,000 | 2.2E-25 | 10,000 | 2.2E-26 | 10,000 | 1.6E-27 | 10,000 | 3.2E-28 | 10,000 |
| Y-90 | 60 | 1.1E-20 | 1,120 | 2.8E-20 | 1,120 | 2.4E-21 | 1,100 | 1.5E-21 | 1,160 | 5.7E-22 | 1,160 |
| Zr-93 | 2,000 | <1.0E-30 | 10,000 | <1.0E-30 | 10,000 | <1.0E-30 | 10,000 | <1.0E-30 | 10,000 | <1.0E-30 | 10,000 |
| Total alpha | 15 | 9.8E-03 | N/A | 2.2E-02 | N/A | 1.4E-03 | N/A | 4.3E-03 | N/A | 2.0E-03 | N/A |
| Total Ra | 5 | 9.8E-03 | N/A | 2.2E-02 | N/A | 1.4E-03 | N/A | 4.3E-03 | N/A | 2.0E-03 | N/A |
| Sum of beta-gamma MCL fractions | | 5.0E-02 | N/A | 1.1E-01 | N/A | 7.2E-03 | N/A | 2.3E-02 | N/A | 1.0E-02 | N/A |

* Total uranium is evaluated in Table 5.2-13.

** MCL values for beta and photon emitters are calculated in Table II-3 of FR-00-9654 based on a beta-gamma dose of 4 mrem/yr

NC = Not Calculated

Table 5.2-5: Radiological 100m Concentrations for UTR-UZ Sectors K and L

| Radionuclide | MCL (pCi/L)** | Sector K Concentration | | Sector L Concentration | |
|--------------|---------------|---------------------------|------------------|---------------------------|------------------|
| | | (pCi/L) | Year Peak Occurs | (pCi/L) | Year Peak Occurs |
| Ac-227 | NC | 2.6E-15 | 10,000 | 1.5E-11 | 10,000 |
| Al-26 | NC | <1.0E-30 | 10,000 | <1.0E-30 | 10,000 |
| Am-241 | Total α | <1.0E-30 | 10,000 | <1.0E-30 | 10,000 |
| Am-242m | Total α | <1.0E-30 | 10,000 | <1.0E-30 | 10,000 |
| Am-243 | Total α | <1.0E-30 | 10,000 | <1.0E-30 | 10,000 |
| Ba-137m | NC | <1.0E-30 | 1,760 | <1.0E-30 | 1,620 |
| C-14 | 2,000 | 3.8E-03 | 9,800 | 1.4E-02 | 9,780 |
| Cf-249 | Total α | <1.0E-30 | 10,000 | <1.0E-30 | 10,000 |
| Cf-251 | Total α | <1.0E-30 | 10,000 | <1.0E-30 | 10,000 |
| Cl-36 | 700 | 7.5E-07 | 10,000 | 2.8E-06 | 10,000 |
| Cm-243 | Total α | <1.0E-30 | 2,500 | <1.0E-30 | 2,820 |
| Cm-244 | Total α | <1.0E-30 | 1,640 | <1.0E-30 | 1,840 |
| Cm-245 | Total α | <1.0E-30 | 10,000 | <1.0E-30 | 10,000 |
| Cm-247 | Total α | <1.0E-30 | 10,000 | <1.0E-30 | 10,000 |
| Cm-248 | Total α | <1.0E-30 | 10,000 | <1.0E-30 | 10,000 |
| Co-60 | 100 | <1.0E-30 | 340 | <1.0E-30 | 300 |
| Cs-135 | 900 | 1.5E-07 | 10,000 | 1.9E-05 | 10,000 |
| Cs-137 | 200 | <1.0E-30 | 1,760 | <1.0E-30 | 1,620 |
| Eu-152 | 200 | <1.0E-30 | 1,280 | <1.0E-30 | 1,420 |
| Eu-154 | 60 | <1.0E-30 | 840 | <1.0E-30 | 820 |
| Gd-152 | NC | <1.0E-30 | 10,000 | <1.0E-30 | 10,000 |
| H-3 | 20,000 | 5.3E-13 | 420 | 2.3E-12 | 420 |
| I-129 | 1 | 2.8E-03 | 10,000 | 1.0E-02 | 10,000 |
| K-40 | NC | 7.8E-06 | 10,000 | 2.9E-05 | 10,000 |
| Nb-93m | 1,000 | 9.6E-09 | 10,000 | 2.8E-05 | 10,000 |
| Nb-94 | NC | 2.1E-11 | 9,640 | 6.4E-08 | 9,700 |
| Ni-59 | 300 | 6.0E-11 | 10,000 | 5.0E-08 | 10,000 |
| Ni-63 | 50 | 2.1E-20 | 2,700 | 2.0E-15 | 1,980 |
| Np-237 | Total α | 1.3E-11 | 10,000 | 1.4E-07 | 10,000 |
| Pa-231 | Total α | 3.4E-12 | 10,000 | 2.0E-08 | 10,000 |
| Pb-210 | NC | 1.3E-06 | 10,000 | 5.0E-06 | 10,000 |
| Pd-107 | NC | 3.6E-12 | 10,000 | 4.2E-09 | 10,000 |
| Pt-193 | 3,000 | 1.2E-05 | 560 | 4.6E-05 | 540 |
| Pu-238 | Total α | <1.0E-30 | 7,400 | <1.0E-30 | 6,920 |
| Pu-239 | Total α | <1.0E-30 | 10,000 | 2.2E-20 | 10,000 |
| Pu-240 | Total α | <1.0E-30 | 10,000 | 3.2E-21 | 10,000 |
| Pu-241 | 300 | <1.0E-30 | 10,000 | <1.0E-30 | 10,000 |
| Pu-242 | Total α | <1.0E-30 | 10,000 | 6.2E-23 | 10,000 |
| Pu-244 | Total α | <1.0E-30 | 10,000 | 1.3E-24 | 10,000 |
| Ra-226 | Total α/Ra | 4.9E-04 | 10,000 | 1.9E-03 | 10,000 |

Table 5.2-5: Radiological 100m Concentrations for UTR-UZ Sectors K and L (Continued)

| Radionuclide | MCL (pCi/L)** | Sector K | | Sector L | |
|--|---------------|-----------------------|--------------------------------|-----------------------|--------------------------------|
| | | Concentration (pCi/L) | Year Peak Concentration Occurs | Concentration (pCi/L) | Year Peak Concentration Occurs |
| Ra-228 | Total Ra | 1.6E-29 | 10,000 | 1.4E-20 | 10,000 |
| Rn-222 | NC | 4.9E-04 | 10,000 | 1.9E-03 | 10,000 |
| Se-79 | NC | <1.0E-30 | 10,000 | <1.0E-30 | 10,000 |
| Sm-151 | 1,000 | <1.0E-30 | 8,320 | <1.0E-30 | 8,060 |
| Sb-126 | NC | <1.0E-30 | 10,000 | <1.0E-30 | 10,000 |
| Sb-126m | NC | <1.0E-30 | 10,000 | <1.0E-30 | 10,000 |
| Sn-126 | NC | <1.0E-30 | 10,000 | <1.0E-30 | 10,000 |
| Sr-90 | 8 | 6.6E-23 | 1,180 | 3.1E-17 | 1,160 |
| Tc-99 | 900 | 1.2E-06 | 9,980 | 1.9E-03 | 9,820 |
| Th-228 | Total α | 1.6E-29 | 10,000 | 1.4E-20 | 10,000 |
| Th-229 | Total α | 9.4E-17 | 10,000 | 1.7E-13 | 10,000 |
| Th-230 | Total α | 5.5E-26 | 10,000 | 1.2E-16 | 10,000 |
| Th-232 | Total α | <1.0E-30 | 10,000 | 1.8E-23 | 10,000 |
| U-232 | Total U* | <1.0E-30 | 5,200 | <1.0E-30 | 4,820 |
| U-233 | Total U* | 1.5E-15 | 10,000 | 4.1E-12 | 10,000 |
| U-234 | Total U* | 8.0E-23 | 10,000 | 1.4E-13 | 10,000 |
| U-235 | Total U* | 1.3E-24 | 10,000 | 2.4E-15 | 10,000 |
| U-236 | Total U* | 2.2E-24 | 10,000 | 3.9E-15 | 10,000 |
| U-238 | Total U* | 1.7E-24 | 10,000 | 2.9E-15 | 10,000 |
| Y-90 | 60 | 6.6E-23 | 1,180 | 3.1E-17 | 1,160 |
| Zr-93 | 2,000 | <1.0E-30 | 10,000 | <1.0E-30 | 10,000 |
| Total alpha | 15 | 4.9E-04 | N/A | 1.9E-03 | N/A |
| Total Ra | 5 | 4.9E-04 | N/A | 1.9E-03 | N/A |
| Sum of beta-gamma MCL fractions | | 2.8E-03 | N/A | 1.0E-02 | N/A |

* Total uranium is evaluated in Table 5.2-14.

** MCL values for beta and photon emitters are calculated in Table II-3 of FR-00-9654 based on a beta-gamma dose of 4 mrem/yr

NC = Not Calculated

Table 5.2-6: Radiological 100m Concentrations for UTR-LZ Sectors A through E

| Radionuclide | MCL (pCi/L)** | Sector A Concentration | | Sector B Concentration | | Sector C Concentration | | Sector D Concentration | | Sector E Concentration | |
|--------------|------------------|---------------------------|---------------------|---------------------------|---------------------|---------------------------|---------------------|---------------------------|---------------------|---------------------------|---------------------|
| | | (pCi/L) | Year Peak Occurs | (pCi/L) | Year Peak Occurs | (pCi/L) | Year Peak Occurs | (pCi/L) | Year Peak Occurs | (pCi/L) | Year Peak Occurs |
| Ac-227 | NC | 1.5E-07 | 10,000 | 1.7E-07 | 10,000 | 1.6E-07 | 10,000 | 1.6E-08 | 10,000 | 9.0E-11 | 10,000 |
| Al-26 | NC | 2.2E-29 | 10,000 | 1.2E-27 | 10,000 | 2.2E-25 | 10,000 | 2.2E-28 | 10,000 | <1.0E-30 | 10,000 |
| Am-241 | Total α | <1.0E-30 | 10,000 | 2.8E-29 | 10,000 | 4.1E-27 | 10,000 | 5.0E-30 | 10,000 | <1.0E-30 | 10,000 |
| Am-242m | Total α | <1.0E-30 | 10,000 | <1.0E-30 | 9,700 | <1.0E-30 | 9,160 | <1.0E-30 | 9,600 | <1.0E-30 | 10,000 |
| Am-243 | Total α | <1.0E-30 | 10,000 | 3.2E-29 | 10,000 | 4.8E-27 | 10,000 | 5.7E-30 | 10,000 | <1.0E-30 | 10,000 |
| Ba-137m | NC | <1.0E-30 | 1,820 | 1.5E-30 | 1,780 | 8.1E-30 | 1,720 | <1.0E-30 | 1,780 | <1.0E-30 | 1,540 |
| C-14 | 2,000 | 1.4E+00 | 6,100 | 1.7E+00 | 6,100 | 1.6E+00 | 6,100 | 2.4E-01 | 7,120 | 1.5E-01 | 9,800 |
| Cf-249 | Total α | <1.0E-30 | 10,000 | <1.0E-30 | 10,000 | <1.0E-30 | 10,000 | <1.0E-30 | 10,000 | <1.0E-30 | 10,000 |
| Cf-251 | Total α | <1.0E-30 | 10,000 | <1.0E-30 | 10,000 | <1.0E-30 | 10,000 | <1.0E-30 | 10,000 | <1.0E-30 | 10,000 |
| Cl-36 | 700 | 4.3E-04 | 9,600 | 5.0E-04 | 9,600 | 4.7E-04 | 9,600 | 8.8E-05 | 9,760 | 2.9E-05 | 10,000 |
| Cm-243 | Total α | <1.0E-30 | 2,640 | <1.0E-30 | 2,540 | <1.0E-30 | 2,440 | <1.0E-30 | 2,580 | <1.0E-30 | 2,880 |
| Cm-244 | Total α | <1.0E-30 | 1,720 | <1.0E-30 | 1,660 | <1.0E-30 | 1,600 | <1.0E-30 | 1,700 | <1.0E-30 | 1,900 |
| Cm-245 | Total α | <1.0E-30 | 10,000 | <1.0E-30 | 10,000 | 2.8E-27 | 10,000 | 3.4E-30 | 10,000 | <1.0E-30 | 10,000 |
| Cm-247 | Total α | <1.0E-30 | 10,000 | <1.0E-30 | 10,000 | <1.0E-30 | 10,000 | <1.0E-30 | 10,000 | <1.0E-30 | 10,000 |
| Cm-248 | Total α | <1.0E-30 | 10,000 | <1.0E-30 | 10,000 | <1.0E-30 | 10,000 | <1.0E-30 | 10,000 | <1.0E-30 | 10,000 |
| Co-60 | 100 | <1.0E-30 | 260 | <1.0E-30 | 260 | <1.0E-30 | 240 | <1.0E-30 | 260 | <1.0E-30 | 280 |
| Cs-135 | 900 | 2.4E-01 | 10,000 | 3.1E-01 | 10,000 | 3.1E-01 | 10,000 | 3.4E-02 | 10,000 | 1.4E-04 | 10,000 |
| Cs-137 | 200 | <1.0E-30 | 1,820 | 1.6E-30 | 1,780 | 8.6E-30 | 1,720 | <1.0E-30 | 1,780 | <1.0E-30 | 1,540 |
| Eu-152 | 200 | <1.0E-30 | 1,340 | <1.0E-30 | 1,300 | <1.0E-30 | 1,260 | <1.0E-30 | 1,320 | <1.0E-30 | 1,480 |
| Eu-154 | 60 | <1.0E-30 | 900 | <1.0E-30 | 860 | <1.0E-30 | 840 | <1.0E-30 | 880 | <1.0E-30 | 980 |
| Gd-152 | NC | <1.0E-30 | 10,000 | <1.0E-30 | 10,000 | <1.0E-30 | 10,000 | <1.0E-30 | 10,000 | <1.0E-30 | 10,000 |
| H-3 | 20,000 | 3.3E-09 | 380 | 4.2E-09 | 380 | 4.2E-09 | 380 | 4.8E-10 | 380 | 3.0E-11 | 420 |
| I-129 | 1 | 1.3E-01 | 9,980 | 1.5E-01 | 10,000 | 1.2E-01 | 10,000 | 9.4E-02 | 10,000 | 1.1E-01 | 10,000 |
| K-40 | NC | 7.8E-04 | 10,000 | 9.2E-04 | 10,000 | 8.2E-04 | 10,000 | 3.7E-04 | 10,000 | 3.1E-04 | 10,000 |
| Nb-93m | 1,000 | 2.5E-01 | 10,000 | 3.0E-01 | 10,000 | 3.0E-01 | 10,000 | 3.4E-02 | 10,000 | 3.0E-04 | 10,000 |
| Nb-94 | NC | 5.7E-04 | 9,700 | 6.5E-04 | 9,700 | 6.2E-04 | 9,700 | 6.1E-05 | 9,700 | 4.4E-07 | 9,680 |

Table 5.2-6: Radiological 100m Concentrations for UTR-LZ Sectors A through E (Continued)

| Radionuclide | MCL (pCi/L)** | Sector A Concentration | | Sector B Concentration | | Sector C Concentration | | Sector D Concentration | | Sector E Concentration | |
|--------------|--------------------|---------------------------|---------------------|---------------------------|---------------------|---------------------------|---------------------|---------------------------|---------------------|---------------------------|---------------------|
| | | (pCi/L) | Year Peak Occurs | (pCi/L) | Year Peak Occurs | (pCi/L) | Year Peak Occurs | (pCi/L) | Year Peak Occurs | (pCi/L) | Year Peak Occurs |
| Ni-59 | 300 | 1.9E-04 | 10,000 | 2.3E-04 | 10,000 | 2.3E-04 | 10,000 | 2.9E-05 | 10,000 | 6.5E-07 | 10,000 |
| Ni-63 | 50 | 4.1E-11 | 1,860 | 5.9E-11 | 1,860 | 6.1E-11 | 1,840 | 6.9E-12 | 1,840 | 2.3E-14 | 1,920 |
| Np-237 | Total α | 1.4E-03 | 10,000 | 1.6E-03 | 10,000 | 1.5E-03 | 10,000 | 1.5E-04 | 10,000 | 7.5E-07 | 10,000 |
| Pa-231 | Total α | 2.0E-04 | 10,000 | 2.3E-04 | 10,000 | 2.3E-04 | 10,000 | 2.1E-05 | 10,000 | 1.2E-07 | 10,000 |
| Pb-210 | NC | 4.2E-03 | 10,000 | 4.9E-03 | 10,000 | 4.7E-03 | 10,000 | 5.7E-04 | 10,000 | 5.4E-05 | 10,000 |
| Pd-107 | NC | 2.5E-05 | 10,000 | 3.1E-05 | 10,000 | 3.1E-05 | 10,000 | 3.7E-06 | 10,000 | 4.6E-08 | 10,000 |
| Pt-193 | 3,000 | 4.9E-03 | 480 | 5.7E-03 | 480 | 5.4E-03 | 460 | 8.1E-04 | 520 | 5.0E-04 | 540 |
| Pu-238 | Total α | <1.0E-30 | 6,060 | <1.0E-30 | 5,880 | <1.0E-30 | 5,600 | <1.0E-30 | 5,840 | <1.0E-30 | 6,460 |
| Pu-239 | Total α | 1.5E-12 | 10,000 | 6.8E-12 | 10,000 | 2.2E-11 | 10,000 | 6.4E-13 | 10,000 | 2.2E-17 | 10,000 |
| Pu-240 | Total α | 2.2E-13 | 10,000 | 9.8E-13 | 10,000 | 3.2E-12 | 10,000 | 9.3E-14 | 10,000 | 3.2E-18 | 10,000 |
| Pu-241 | 300 | 2.5E-30 | 10,000 | 1.1E-28 | 10,000 | 1.6E-26 | 10,000 | 1.9E-29 | 10,000 | <1.0E-30 | 10,000 |
| Pu-242 | Total α | 4.3E-15 | 10,000 | 1.9E-14 | 10,000 | 6.0E-14 | 10,000 | 1.8E-15 | 10,000 | 6.1E-20 | 10,000 |
| Pu-244 | Total α | 8.8E-17 | 10,000 | 3.9E-16 | 10,000 | 1.2E-15 | 10,000 | 3.7E-17 | 10,000 | 1.3E-21 | 10,000 |
| Ra-226 | Total α /Ra | 1.6E+00 | 10,000 | 1.9E+00 | 9,980 | 1.8E+00 | 9,940 | 2.2E-01 | 9,880 | 2.1E-02 | 10,000 |
| Ra-228 | Total Ra | 2.0E-14 | 10,000 | 5.1E-14 | 10,000 | 7.6E-14 | 10,000 | 5.3E-15 | 10,000 | 2.1E-18 | 10,000 |
| Rn-222 | NC | 1.6E+00 | 10,000 | 1.9E+00 | 9,980 | 1.8E+00 | 9,940 | 2.2E-01 | 9,880 | 2.1E-02 | 10,000 |
| Se-79 | NC | 2.7E-22 | 10,000 | 8.1E-21 | 10,000 | 6.4E-19 | 10,000 | 1.2E-21 | 10,000 | 1.7E-28 | 10,000 |
| Sm-151 | 1,000 | <1.0E-30 | 7,240 | <1.0E-30 | 6,980 | <1.0E-30 | 6,640 | <1.0E-30 | 6,920 | <1.0E-30 | 7,720 |
| Sb-126 | NC | <1.0E-30 | 10,000 | <1.0E-30 | 10,000 | <1.0E-30 | 10,000 | <1.0E-30 | 10,000 | <1.0E-30 | 10,000 |
| Sb-126m | NC | <1.0E-30 | 10,000 | <1.0E-30 | 10,000 | <1.0E-30 | 10,000 | <1.0E-30 | 10,000 | <1.0E-30 | 10,000 |
| Sn-126 | NC | <1.0E-30 | 10,000 | <1.0E-30 | 10,000 | <1.0E-30 | 10,000 | <1.0E-30 | 10,000 | <1.0E-30 | 10,000 |
| Sr-90 | 8 | 1.8E-12 | 1,100 | 2.9E-12 | 1,080 | 3.3E-12 | 1,080 | 3.5E-13 | 1,080 | 6.5E-16 | 1,120 |
| Tc-99 | 900 | 1.3E+01 | 9,820 | 1.6E+01 | 9,820 | 1.5E+01 | 9,800 | 1.6E+00 | 9,800 | 1.7E-02 | 9,800 |
| Th-228 | Total α | 2.0E-14 | 10,000 | 5.1E-14 | 10,000 | 7.6E-14 | 10,000 | 5.3E-15 | 10,000 | 2.1E-18 | 10,000 |
| Th-229 | Total α | 4.0E-09 | 10,000 | 8.6E-09 | 10,000 | 1.3E-08 | 10,000 | 8.8E-10 | 10,000 | 1.6E-12 | 10,000 |
| Th-230 | Total α | 3.4E-10 | 10,000 | 9.1E-10 | 10,000 | 1.5E-09 | 10,000 | 9.4E-11 | 10,000 | 2.6E-14 | 10,000 |

Table 5.2-6: Radiological 100m Concentrations for UTR-LZ Sectors A through E (Continued)

| Radionuclide | MCL (pCi/L)** | Sector A Concentration | | Sector B Concentration | | Sector C Concentration | | Sector D Concentration | | Sector E Concentration | |
|--|------------------|---------------------------|---------------------|---------------------------|---------------------|---------------------------|---------------------|---------------------------|---------------------|---------------------------|---------------------|
| | | (pCi/L) | Year Peak Occurs | (pCi/L) | Year Peak Occurs | (pCi/L) | Year Peak Occurs | (pCi/L) | Year Peak Occurs | (pCi/L) | Year Peak Occurs |
| Th-232 | Total α | 5.0E-17 | 10,000 | 1.3E-16 | 10,000 | 2.2E-16 | 10,000 | 1.4E-17 | 10,000 | 3.9E-21 | 10,000 |
| U-232 | Total U* | <1.0E-30 | 4,160 | <1.0E-30 | 4,040 | <1.0E-30 | 3,820 | <1.0E-30 | 4,000 | <1.0E-30 | 4,480 |
| U-233 | Total U* | 2.6E-07 | 10,000 | 6.0E-07 | 10,000 | 8.6E-07 | 10,000 | 6.2E-08 | 10,000 | 5.0E-11 | 10,000 |
| U-234 | Total U* | 2.8E-07 | 10,000 | 6.9E-07 | 10,000 | 1.0E-06 | 10,000 | 7.3E-08 | 10,000 | 2.6E-11 | 10,000 |
| U-235 | Total U* | 4.7E-09 | 10,000 | 1.2E-08 | 10,000 | 1.7E-08 | 10,000 | 1.2E-09 | 10,000 | 4.3E-13 | 10,000 |
| U-236 | Total U* | 7.6E-09 | 10,000 | 1.9E-08 | 10,000 | 2.8E-08 | 10,000 | 2.0E-09 | 10,000 | 7.0E-13 | 10,000 |
| U-238 | Total U* | 5.7E-09 | 10,000 | 1.4E-08 | 10,000 | 2.1E-08 | 10,000 | 1.5E-09 | 10,000 | 5.3E-13 | 10,000 |
| Y-90 | 60 | 1.8E-12 | 1,100 | 2.9E-12 | 1,080 | 3.3E-12 | 1,080 | 3.5E-13 | 1,080 | 6.5E-16 | 1,120 |
| Zr-93 | 2,000 | 5.1E-24 | 10,000 | 1.4E-22 | 10,000 | 9.0E-21 | 10,000 | 2.0E-23 | 10,000 | <1.0E-30 | 10,000 |
| Total alpha | 15 | 1.6E+00 | N/A | 1.9E+00 | N/A | 1.8E+00 | N/A | 2.2E-01 | N/A | 2.1E-02 | N/A |
| Total Ra | 5 | 1.6E+00 | N/A | 1.9E+00 | N/A | 1.8E+00 | N/A | 2.2E-01 | N/A | 2.1E-02 | N/A |
| Sum of beta-gamma MCL fractions | | 1.5E-01 | N/A | 1.7E-01 | N/A | 1.4E-01 | N/A | 9.6E-02 | N/A | 1.1E-01 | N/A |

* Total uranium is evaluated in Table 5.2-15.

** MCL values for beta and photon emitters are calculated in Table II-3 of FR-00-9654 based on a beta-gamma dose of 4 mrem/yr

NC = Not Calculated

Table 5.2-7: Radiological 100m Concentrations for UTR-LZ Sectors F through J

| Radionuclide | MCL (pCi/L)** | Sector F Concentrations | | Sector G Concentrations | | Sector H Concentrations | | Sector I Concentrations | | Sector J Concentrations | |
|--------------|------------------|----------------------------|---------------------|----------------------------|---------------------|----------------------------|---------------------|----------------------------|---------------------|----------------------------|---------------------|
| | | (pCi/L) | Year Peak Occurs | (pCi/L) | Year Peak Occurs | (pCi/L) | Year Peak Occurs | (pCi/L) | Year Peak Occurs | (pCi/L) | Year Peak Occurs |
| Ac-227 | NC | 8.0E-16 | 10,000 | 1.6E-17 | 10,000 | 8.3E-17 | 10,000 | 1.1E-15 | 10,000 | 1.3E-14 | 10,000 |
| Al-26 | NC | <1.0E-30 | 10,000 | <1.0E-30 | 10,000 | <1.0E-30 | 10,000 | <1.0E-30 | 10,000 | <1.0E-30 | 10,000 |
| Am-241 | Total α | <1.0E-30 | 10,000 | <1.0E-30 | 10,000 | <1.0E-30 | 10,000 | <1.0E-30 | 10,000 | <1.0E-30 | 10,000 |
| Am-242m | Total α | <1.0E-30 | 10,000 | <1.0E-30 | 9,300 | <1.0E-30 | 9,220 | <1.0E-30 | 9,480 | <1.0E-30 | 9,780 |
| Am-243 | Total α | <1.0E-30 | 10,000 | <1.0E-30 | 10,000 | <1.0E-30 | 10,000 | <1.0E-30 | 10,000 | <1.0E-30 | 10,000 |
| Ba-137m | NC | <1.0E-30 | 1,660 | <1.0E-30 | 1,620 | <1.0E-30 | 1,620 | <1.0E-30 | 1,660 | <1.0E-30 | 1,740 |
| C-14 | 2,000 | 9.5E-02 | 9,840 | 3.4E-01 | 9,820 | 3.4E-01 | 9,820 | 3.9E-01 | 9,820 | 3.3E-01 | 9,800 |
| Cf-249 | Total α | <1.0E-30 | 10,000 | <1.0E-30 | 10,000 | <1.0E-30 | 10,000 | <1.0E-30 | 10,000 | <1.0E-30 | 10,000 |
| Cf-251 | Total α | <1.0E-30 | 10,000 | <1.0E-30 | 10,000 | <1.0E-30 | 10,000 | <1.0E-30 | 10,000 | <1.0E-30 | 10,000 |
| Cl-36 | 700 | 1.9E-05 | 10,000 | 6.7E-05 | 10,000 | 6.8E-05 | 10,000 | 7.7E-05 | 10,000 | 6.4E-05 | 10,000 |
| Cm-243 | Total α | <1.0E-30 | 2,840 | <1.0E-30 | 2,520 | <1.0E-30 | 2,500 | <1.0E-30 | 2,540 | <1.0E-30 | 2,600 |
| Cm-244 | Total α | <1.0E-30 | 1,860 | <1.0E-30 | 1,640 | <1.0E-30 | 1,620 | <1.0E-30 | 1,660 | <1.0E-30 | 1,680 |
| Cm-245 | Total α | <1.0E-30 | 10,000 | <1.0E-30 | 10,000 | <1.0E-30 | 10,000 | <1.0E-30 | 10,000 | <1.0E-30 | 10,000 |
| Cm-247 | Total α | <1.0E-30 | 10,000 | <1.0E-30 | 10,000 | <1.0E-30 | 10,000 | <1.0E-30 | 10,000 | <1.0E-30 | 10,000 |
| Cm-248 | Total α | <1.0E-30 | 10,000 | <1.0E-30 | 10,000 | <1.0E-30 | 10,000 | <1.0E-30 | 10,000 | <1.0E-30 | 10,000 |
| Co-60 | 100 | <1.0E-30 | 300 | <1.0E-30 | 460 | <1.0E-30 | 460 | <1.0E-30 | 440 | <1.0E-30 | 360 |
| Cs-135 | 900 | 8.2E-06 | 10,000 | 2.0E-05 | 10,000 | 1.7E-05 | 10,000 | 1.7E-05 | 10,000 | 1.0E-05 | 10,000 |
| Cs-137 | 200 | <1.0E-30 | 1,660 | <1.0E-30 | 1,620 | <1.0E-30 | 1,620 | <1.0E-30 | 1,660 | <1.0E-30 | 1,740 |
| Eu-152 | 200 | <1.0E-30 | 1,460 | <1.0E-30 | 1,280 | <1.0E-30 | 1,260 | <1.0E-30 | 1,300 | <1.0E-30 | 1,320 |
| Eu-154 | 60 | <1.0E-30 | 980 | <1.0E-30 | 860 | <1.0E-30 | 840 | <1.0E-30 | 860 | <1.0E-30 | 880 |
| Gd-152 | NC | <1.0E-30 | 10,000 | <1.0E-30 | 10,000 | <1.0E-30 | 10,000 | <1.0E-30 | 10,000 | <1.0E-30 | 10,000 |
| H-3 | 20,000 | 2.0E-11 | 420 | 5.7E-11 | 420 | 5.3E-11 | 420 | 5.6E-11 | 420 | 4.1E-11 | 420 |
| I-129 | 1 | 6.9E-02 | 10,000 | 2.5E-01 | 10,000 | 2.5E-01 | 10,000 | 2.9E-01 | 10,000 | 2.4E-01 | 10,000 |
| K-40 | NC | 2.0E-04 | 10,000 | 7.0E-04 | 10,000 | 7.0E-04 | 10,000 | 8.0E-04 | 10,000 | 6.5E-04 | 10,000 |
| Nb-93m | 1,000 | 6.0E-09 | 10,000 | 6.4E-11 | 10,000 | 2.2E-10 | 10,000 | 2.9E-09 | 10,000 | 4.3E-08 | 10,000 |
| Nb-94 | NC | 6.3E-12 | 9,660 | 5.6E-11 | 10,000 | 4.9E-11 | 10,000 | 2.8E-11 | 10,000 | 1.2E-10 | 10,000 |

Table 5.2-7: Radiological 100m Concentrations for UTR-LZ Sectors F through J (Continued)

| Radionuclide | MCL (pCi/L)** | Sector F Concentrations | | Sector G Concentrations | | Sector H Concentrations | | Sector I Concentrations | | Sector J Concentrations | |
|--------------|------------------|----------------------------|---------------------|----------------------------|---------------------|----------------------------|---------------------|----------------------------|---------------------|----------------------------|---------------------|
| | | (pCi/L) | Year Peak Occurs | (pCi/L) | Year Peak Occurs | (pCi/L) | Year Peak Occurs | (pCi/L) | Year Peak Occurs | (pCi/L) | Year Peak Occurs |
| Ni-59 | 300 | 1.8E-11 | 10,000 | 2.9E-13 | 10,000 | 1.9E-12 | 10,000 | 2.5E-11 | 10,000 | 3.0E-10 | 10,000 |
| Ni-63 | 50 | 1.7E-19 | 2,280 | 2.8E-23 | 2,840 | 1.6E-22 | 2,840 | 2.1E-21 | 2,860 | 6.5E-20 | 2,760 |
| Np-237 | Total α | 4.2E-12 | 10,000 | 1.3E-13 | 10,000 | 4.5E-13 | 10,000 | 5.5E-12 | 10,000 | 6.5E-11 | 10,000 |
| Pa-231 | Total α | 1.10E-12 | 10,000 | 2.1E-14 | 10,000 | 1.1E-13 | 10,000 | 1.4E-12 | 10,000 | 1.7E-11 | 10,000 |
| Pb-210 | NC | 3.5E-05 | 10,000 | 1.2E-04 | 10,000 | 1.2E-04 | 10,000 | 1.3E-04 | 10,000 | 1.1E-04 | 10,000 |
| Pd-107 | NC | 1.1E-12 | 10,000 | 1.9E-14 | 10,000 | 1.1E-13 | 10,000 | 1.5E-12 | 10,000 | 1.8E-11 | 10,000 |
| Pt-193 | 3,000 | 3.3E-04 | 540 | 1.1E-03 | 540 | 1.1E-03 | 540 | 1.2E-03 | 560 | 9.9E-04 | 560 |
| Pu-238 | Total α | <1.0E-30 | 6,560 | <1.0E-30 | 7,440 | <1.0E-30 | 7,400 | <1.0E-30 | 7,540 | <1.0E-30 | 7,880 |
| Pu-239 | Total α | 5.3E-24 | 10,000 | <1.0E-30 | 10,000 | <1.0E-30 | 10,000 | <1.0E-30 | 10,000 | <1.0E-30 | 10,000 |
| Pu-240 | Total α | 7.7E-25 | 10,000 | <1.0E-30 | 10,000 | <1.0E-30 | 10,000 | <1.0E-30 | 10,000 | <1.0E-30 | 10,000 |
| Pu-241 | 300 | <1.0E-30 | 10,000 | <1.0E-30 | 10,000 | <1.0E-30 | 10,000 | <1.0E-30 | 10,000 | <1.0E-30 | 10,000 |
| Pu-242 | Total α | 1.5E-26 | 10,000 | <1.0E-30 | 10,000 | <1.0E-30 | 10,000 | <1.0E-30 | 10,000 | <1.0E-30 | 10,000 |
| Pu-244 | Total α | 3.0E-28 | 10,000 | <1.0E-30 | 10,000 | <1.0E-30 | 10,000 | <1.0E-30 | 10,000 | <1.0E-30 | 10,000 |
| Ra-226 | Total α/Ra | 1.4E-02 | 10,000 | 4.5E-02 | 10,000 | 4.54E-02 | 10,000 | 5.1E-02 | 10,000 | 4.1E-02 | 10,000 |
| Ra-228 | Total Ra | 7.5E-25 | 10,000 | 3.1E-27 | 10,000 | 1.7E-27 | 10,000 | 4.2E-28 | 10,000 | 1.2E-29 | 10,000 |
| Rn-222 | NC | 1.4E-02 | 10,000 | 4.5E-02 | 10,000 | 4.5E-02 | 10,000 | 5.1E-02 | 10,000 | 4.1E-02 | 10,000 |
| Se-79 | NC | <1.0E-30 | 10,000 | <1.0E-30 | 10,000 | <1.0E-30 | 10,000 | <1.0E-30 | 10,000 | <1.0E-30 | 10,000 |
| Sm-151 | 1,000 | <1.0E-30 | 7,880 | <1.0E-30 | 6,940 | <1.0E-30 | 6,860 | <1.0E-30 | 7,040 | <1.0E-30 | 7,220 |
| Sb-126 | NC | <1.0E-30 | 10,000 | <1.0E-30 | 10,000 | <1.0E-30 | 10,000 | <1.0E-30 | 10,000 | <1.0E-30 | 10,000 |
| Sb-126m | NC | <1.0E-30 | 10,000 | <1.0E-30 | 10,000 | <1.0E-30 | 10,000 | <1.0E-30 | 10,000 | <1.0E-30 | 10,000 |
| Sn-126 | NC | <1.0E-30 | 10,000 | <1.0E-30 | 10,000 | <1.0E-30 | 10,000 | <1.0E-30 | 10,000 | <1.0E-30 | 10,000 |
| Sr-90 | 8 | 1.5E-20 | 1,120 | 2.6E-20 | 1,120 | 1.8E-20 | 1,140 | 1.0E-20 | 1,140 | 3.1E-21 | 1,180 |
| Tc-99 | 900 | 7.1E-07 | 10,000 | 1.4E-06 | 10,000 | 1.4E-06 | 10,000 | 1.8E-06 | 10,000 | 7.3E-06 | 10,000 |
| Th-228 | Total α | 7.5E-25 | 10,000 | 3.1E-27 | 10,000 | 1.7E-27 | 10,000 | 4.2E-28 | 10,000 | 1.2E-29 | 10,000 |
| Th-229 | Total α | 2.8E-17 | 10,000 | 1.7E-18 | 10,000 | 3.3E-18 | 10,000 | 4.0E-17 | 10,000 | 4.7E-16 | 10,000 |
| Th-230 | Total α | 8.9E-21 | 10,000 | 1.3E-28 | 10,000 | 7.2E-29 | 10,000 | 1.7E-29 | 10,000 | 1.3E-30 | 10,000 |

Table 5.2-7: Radiological 100m Concentrations for UTR-LZ Sectors F through J (Continued)

| Radionuclide | MCL (pCi/L)** | Sector F Concentrations | | Sector G Concentrations | | Sector H Concentrations | | Sector I Concentrations | | Sector J Concentrations | |
|--|------------------|----------------------------|---------------------|----------------------------|---------------------|----------------------------|---------------------|----------------------------|---------------------|----------------------------|---------------------|
| | | (pCi/L) | Year Peak Occurs | (pCi/L) | Year Peak Occurs | (pCi/L) | Year Peak Occurs | (pCi/L) | Year Peak Occurs | (pCi/L) | Year Peak Occurs |
| Th-232 | Total α | 1.3E-27 | 10,000 | <1.0E-30 | 10,000 | <1.0E-30 | 10,000 | <1.0E-30 | 10,000 | <1.0E-30 | 10,000 |
| U-232 | Total U* | <1.0E-30 | 4,540 | <1.0E-30 | 5,080 | <1.0E-30 | 5,060 | <1.0E-30 | 5,160 | <1.0E-30 | 5,320 |
| U-233 | Total U* | 4.7E-16 | 10,000 | 6.1E-17 | 10,000 | 6.3E-17 | 10,000 | 6.6E-16 | 10,000 | 7.7E-15 | 10,000 |
| U-234 | Total U* | 9.1E-18 | 10,000 | 1.5E-25 | 10,000 | 8.8E-26 | 10,000 | 2.1E-26 | 10,000 | 1.9E-27 | 10,000 |
| U-235 | Total U* | 1.5E-19 | 10,000 | 2.6E-27 | 10,000 | 1.5E-27 | 10,000 | 3.6E-28 | 10,000 | 3.3E-29 | 10,000 |
| U-236 | Total U* | 2.5E-19 | 10,000 | 1.4E-26 | 10,000 | 7.8E-27 | 10,000 | 1.9E-27 | 10,000 | 8.0E-29 | 10,000 |
| U-238 | Total U* | 1.9E-19 | 10,000 | 8.7E-26 | 10,000 | 5.0E-26 | 10,000 | 1.2E-26 | 10,000 | 3.0E-28 | 10,000 |
| Y-90 | 60 | 1.5E-20 | 1,120 | 2.6E-20 | 1,120 | 1.8E-20 | 1,140 | 1.0E-20 | 1,140 | 3.1E-21 | 1,180 |
| Zr-93 | 2,000 | <1.0E-30 | 10,000 | <1.0E-30 | 10,000 | <1.0E-30 | 10,000 | <1.0E-30 | 10,000 | <1.0E-30 | 10,000 |
| Total alpha | 15 | 1.4E-02 | N/A | 4.5E-02 | N/A | 4.5E-02 | N/A | 5.1E-02 | N/A | 4.1E-02 | N/A |
| Total Ra | 5 | 1.4E-02 | N/A | 4.5E-02 | N/A | 4.5E-02 | N/A | 5.1E-02 | N/A | 4.1E-02 | N/A |
| Sum of beta-gamma MCL fractions | | 6.9E-02 | N/A | 2.5E-01 | N/A | 2.5E-01 | N/A | 2.9E-01 | N/A | 2.4E-01 | N/A |

* Total uranium is evaluated in Table 5.2-16.

** MCL values for beta and photon emitters are calculated in Table II-3 of FR-00-9654 based on a beta-gamma dose of 4 mrem/yr

NC = Not Calculated

Table 5.2-8: Radiological 100m Concentrations for UTR-LZ Sectors K and L

| Radionuclide | MCL (pCi/L)** | Sector K Concentration | | Sector L Concentration | |
|--------------|---------------|---------------------------|---------------------|---------------------------|---------------------|
| | | (pCi/L) | Year Peak Occurs | (pCi/L) | Year Peak Occurs |
| Ac-227 | NC | 1.8E-13 | 10,000 | 1.0E-10 | 10,000 |
| Al-26 | NC | <1.0E-30 | 10,000 | <1.0E-30 | 10,000 |
| Am-241 | Total α | <1.0E-30 | 10,000 | <1.0E-30 | 10,000 |
| Am-242m | Total α | <1.0E-30 | 10,000 | <1.0E-30 | 10,000 |
| Am-243 | Total α | <1.0E-30 | 10,000 | <1.0E-30 | 10,000 |
| Ba-137m | NC | <1.0E-30 | 1,700 | <1.0E-30 | 1,600 |
| C-14 | 2,000 | 3.5E-01 | 9,800 | 2.6E-01 | 9,840 |
| Cf-249 | Total α | <1.0E-30 | 10,000 | <1.0E-30 | 10,000 |
| Cf-251 | Total α | <1.0E-30 | 10,000 | <1.0E-30 | 10,000 |
| Cl-36 | 700 | 6.8E-05 | 10,000 | 5.1E-05 | 10,000 |
| Cm-243 | Total α | <1.0E-30 | 2,620 | <1.0E-30 | 2,940 |
| Cm-244 | Total α | <1.0E-30 | 1,700 | <1.0E-30 | 1,920 |
| Cm-245 | Total α | <1.0E-30 | 10,000 | <1.0E-30 | 10,000 |
| Cm-247 | Total α | <1.0E-30 | 10,000 | <1.0E-30 | 10,000 |
| Cm-248 | Total α | <1.0E-30 | 10,000 | <1.0E-30 | 10,000 |
| Co-60 | 100 | <1.0E-30 | 340 | <1.0E-30 | 300 |
| Cs-135 | 900 | 1.4E-05 | 10,000 | 1.3E-04 | 10,000 |
| Cs-137 | 200 | <1.0E-30 | 1,700 | <1.0E-30 | 1,600 |
| Eu-152 | 200 | <1.0E-30 | 1,320 | <1.0E-30 | 1,480 |
| Eu-154 | 60 | <1.0E-30 | 880 | <1.0E-30 | 980 |
| Gd-152 | NC | <1.0E-30 | 10,000 | <1.0E-30 | 10,000 |
| H-3 | 20,000 | 4.9E-11 | 420 | 3.4E-11 | 420 |
| I-129 | 1 | 2.5E-01 | 10,000 | 1.9E-01 | 10,000 |
| K-40 | NC | 7.1E-04 | 10,000 | 5.2E-04 | 10,000 |
| Nb-93m | 1,000 | 6.6E-07 | 10,000 | 1.9E-04 | 10,000 |
| Nb-94 | NC | 1.5E-09 | 9,640 | 4.3E-07 | 9,700 |
| Ni-59 | 300 | 4.2E-09 | 10,000 | 3.5E-07 | 10,000 |
| Ni-63 | 50 | 1.6E-18 | 2,660 | 1.5E-14 | 1,960 |
| Np-237 | Total α | 9.2E-10 | 10,000 | 9.1E-07 | 10,000 |
| Pa-231 | Total α | 2.4E-10 | 10,000 | 1.3E-07 | 10,000 |
| Pb-210 | NC | 1.2E-04 | 10,000 | 8.6E-05 | 10,000 |
| Pd-107 | NC | 2.5E-10 | 10,000 | 2.8E-08 | 10,000 |
| Pt-193 | 3,000 | 1.1E-03 | 560 | 7.9E-04 | 560 |
| Pu-238 | Total α | <1.0E-30 | 7,300 | <1.0E-30 | 6,720 |
| Pu-239 | Total α | 6.9E-28 | 10,000 | 1.1E-18 | 10,000 |
| Pu-240 | Total α | 1.0E-28 | 10,000 | 1.6E-19 | 10,000 |
| Pu-241 | 300 | <1.0E-30 | 10,000 | <1.0E-30 | 10,000 |
| Pu-242 | Total α | 1.9E-30 | 10,000 | 3.1E-21 | 10,000 |
| Pu-244 | Total α | <1.0E-30 | 10,000 | 6.4E-23 | 10,000 |
| Ra-226 | Total α/Ra | 4.5E-02 | 10,000 | 3.3E-02 | 10,000 |
| Ra-228 | Total Ra | 5.7E-27 | 10,000 | 2.7E-19 | 10,000 |

Table 5.2-8: Radiological 100m Concentrations for UTR-LZ Sectors K and L (Continued)

| Radionuclide | MCL (pCi/L)** | Sector K | | Sector L | |
|--|---------------|-----------------------|--------------------------------|-----------------------|--------------------------------|
| | | Concentration (pCi/L) | Year Peak Concentration Occurs | Concentration (pCi/L) | Year Peak Concentration Occurs |
| Rn-222 | NC | 4.5E-02 | 10,000 | 3.3E-02 | 10,000 |
| Se-79 | NC | <1.0E-30 | 10,000 | 2.6E-30 | 10,000 |
| Sm-151 | 1,000 | <1.0E-30 | 8,660 | <1.0E-30 | 8,080 |
| Sb-126 | NC | <1.0E-30 | 10,000 | <1.0E-30 | 10,000 |
| Sb-126m | NC | <1.0E-30 | 10,000 | <1.0E-30 | 10,000 |
| Sn-126 | NC | <1.0E-30 | 10,000 | <1.0E-30 | 10,000 |
| Sr-90 | 8 | 8.4E-21 | 1,160 | 2.8E-16 | 1,160 |
| Tc-99 | 900 | 8.7E-05 | 10,000 | 1.3E-02 | 9,820 |
| Th-228 | Total α | 5.7E-27 | 10,000 | 2.7E-19 | 10,000 |
| Th-229 | Total α | 6.6E-15 | 10,000 | 1.2E-12 | 10,000 |
| Th-230 | Total α | 2.7E-23 | 10,000 | 2.9E-15 | 10,000 |
| Th-232 | Total α | 4.0E-30 | 10,000 | 4.3E-22 | 10,000 |
| U-232 | Total U* | <1.0E-30 | 5,120 | <1.0E-30 | 4,660 |
| U-233 | Total U* | 1.1E-13 | 10,000 | 2.9E-11 | 10,000 |
| U-234 | Total U* | 3.7E-20 | 10,000 | 3.1E-12 | 10,000 |
| U-235 | Total U* | 6.2E-22 | 10,000 | 5.2E-14 | 10,000 |
| U-236 | Total U* | 1.0E-21 | 10,000 | 8.4E-14 | 10,000 |
| U-238 | Total U* | 7.6E-22 | 10,000 | 6.4E-14 | 10,000 |
| Y-90 | 60 | 8.4E-21 | 1,160 | 2.8E-16 | 1,160 |
| Zr-93 | 2,000 | <1.0E-30 | 10,000 | <1.0E-30 | 10,000 |
| Total alpha | 15 | 4.5E-02 | N/A | 3.3E-02 | N/A |
| Total Ra | 5 | 4.5E-02 | N/A | 3.3E-02 | N/A |
| Sum of beta-gamma MCL fractions | | 2.5E-01 | N/A | 1.9E-01 | N/A |

* Total uranium is evaluated in Table 5.2-17.

** MCL values for beta and photon emitters are calculated in Table II-3 of FR-00-9654 based on a beta-gamma dose of 4 mrem/yr

NC = Not Calculated

Table 5.2-9: Radiological 100m Concentrations for GAU Sectors A through E

| Radionuclide | MCL (pCi/L)** | Sector A Concentrations | | Sector B Concentrations | | Sector C Concentrations | | Sector D Concentrations | | Sector E Concentrations | |
|--------------|------------------|----------------------------|---------------------|----------------------------|---------------------|----------------------------|---------------------|----------------------------|---------------------|----------------------------|---------------------|
| | | (pCi/L) | Year Peak Occurs | (pCi/L) | Year Peak Occurs | (pCi/L) | Year Peak Occurs | (pCi/L) | Year Peak Occurs | (pCi/L) | Year Peak Occurs |
| Ac-227 | NC | 7.8E-12 | 10,000 | 6.7E-12 | 10,000 | 3.0E-12 | 10,000 | 1.3E-13 | 10,000 | 1.0E-15 | 10,000 |
| Al-26 | NC | <1.0E-30 | 10,000 | <1.0E-30 | 10,000 | <1.0E-30 | 10,000 | <1.0E-30 | 10,000 | <1.0E-30 | 10,000 |
| Am-241 | Total α | <1.0E-30 | 10,000 | <1.0E-30 | 10,000 | <1.0E-30 | 10,000 | <1.0E-30 | 10,000 | <1.0E-30 | 10,000 |
| Am-242m | Total α | <1.0E-30 | 10,000 | <1.0E-30 | 10,000 | <1.0E-30 | 10,000 | <1.0E-30 | 10,000 | <1.0E-30 | 10,000 |
| Am-243 | Total α | <1.0E-30 | 10,000 | <1.0E-30 | 10,000 | <1.0E-30 | 10,000 | <1.0E-30 | 10,000 | <1.0E-30 | 10,000 |
| Ba-137m | NC | <1.0E-30 | 2,040 | <1.0E-30 | 2,000 | <1.0E-30 | 1,940 | <1.0E-30 | 1,980 | <1.0E-30 | 1,740 |
| C-14 | 2,000 | 2.9E-03 | 6,740 | 2.7E-03 | 6,740 | 1.3E-03 | 6,740 | 1.4E-04 | 8,260 | 1.2E-04 | 10,000 |
| Cf-249 | Total α | <1.0E-30 | 10,000 | <1.0E-30 | 10,000 | <1.0E-30 | 10,000 | <1.0E-30 | 10,000 | <1.0E-30 | 10,000 |
| Cf-251 | Total α | <1.0E-30 | 10,000 | <1.0E-30 | 10,000 | <1.0E-30 | 10,000 | <1.0E-30 | 10,000 | <1.0E-30 | 10,000 |
| Cl-36 | 700 | 8.9E-07 | 9,840 | 8.1E-07 | 9,840 | 4.2E-07 | 9,860 | 5.2E-08 | 10,000 | 2.3E-08 | 10,000 |
| Cm-243 | Total α | <1.0E-30 | 2,920 | <1.0E-30 | 2,840 | <1.0E-30 | 2,720 | <1.0E-30 | 2,860 | <1.0E-30 | 3,160 |
| Cm-244 | Total α | <1.0E-30 | 1,900 | <1.0E-30 | 1,860 | <1.0E-30 | 1,780 | <1.0E-30 | 1,880 | <1.0E-30 | 2,080 |
| Cm-245 | Total α | <1.0E-30 | 10,000 | <1.0E-30 | 10,000 | <1.0E-30 | 10,000 | <1.0E-30 | 10,000 | <1.0E-30 | 10,000 |
| Cm-247 | Total α | <1.0E-30 | 10,000 | <1.0E-30 | 10,000 | <1.0E-30 | 10,000 | <1.0E-30 | 10,000 | <1.0E-30 | 10,000 |
| Cm-248 | Total α | <1.0E-30 | 10,000 | <1.0E-30 | 10,000 | <1.0E-30 | 10,000 | <1.0E-30 | 10,000 | <1.0E-30 | 10,000 |
| Co-60 | 100 | <1.0E-30 | 300 | <1.0E-30 | 300 | <1.0E-30 | 280 | <1.0E-30 | 300 | <1.0E-30 | 320 |
| Cs-135 | 900 | 2.3E-07 | 10,000 | 2.3E-07 | 10,000 | 1.2E-07 | 10,000 | 4.8E-09 | 10,000 | 1.4E-11 | 10,000 |
| Cs-137 | 200 | <1.0E-30 | 2,040 | <1.0E-30 | 2,000 | <1.0E-30 | 1,940 | <1.0E-30 | 1,980 | <1.0E-30 | 1,740 |
| Eu-152 | 200 | <1.0E-30 | 1,480 | <1.0E-30 | 1,440 | <1.0E-30 | 1,380 | <1.0E-30 | 1,460 | <1.0E-30 | 1,600 |
| Eu-154 | 60 | <1.0E-30 | 980 | <1.0E-30 | 960 | <1.0E-30 | 920 | <1.0E-30 | 960 | <1.0E-30 | 1,080 |
| Gd-152 | NC | <1.0E-30 | 10,000 | <1.0E-30 | 10,000 | <1.0E-30 | 10,000 | <1.0E-30 | 10,000 | <1.0E-30 | 10,000 |
| H-3 | 20,000 | 2.7E-13 | 420 | 2.4E-13 | 420 | 1.2E-13 | 420 | 5.0E-15 | 420 | 5.2E-16 | 440 |
| I-129 | 1 | 2.7E-04 | 10,000 | 2.4E-04 | 10,000 | 1.4E-04 | 10,000 | 6.4E-05 | 10,000 | 7.9E-05 | 10,000 |
| K-40 | NC | 8.9E-08 | 10,000 | 7.6E-08 | 10,000 | 3.6E-08 | 10,000 | 7.7E-09 | 10,000 | 5.1E-09 | 10,000 |
| Nb-93m | 1,000 | 3.4E-05 | 10,000 | 3.1E-05 | 10,000 | 1.5E-05 | 10,000 | 6.3E-07 | 10,000 | 5.0E-09 | 10,000 |
| Nb-94 | NC | 1.2E-06 | 10,000 | 1.0E-06 | 10,000 | 5.2E-07 | 10,000 | 2.3E-08 | 10,000 | 1.6E-10 | 10,000 |
| Ni-59 | 300 | 2.5E-08 | 10,000 | 2.2E-08 | 10,000 | 1.0E-08 | 10,000 | 8.1E-10 | 10,000 | 2.6E-11 | 10,000 |
| Ni-63 | 50 | 2.1E-17 | 2,240 | 2.1E-17 | 2,220 | 1.1E-17 | 2,200 | 4.5E-19 | 2,200 | 1.4E-21 | 2,280 |

Table 5.2-9: Radiological 100m Concentrations for GAU Sectors A through E (Continued)

| Radionuclide | MCL (pCi/L)** | Sector A Concentrations | | Sector B Concentrations | | Sector C Concentrations | | Sector D Concentrations | | Sector E Concentrations | |
|--------------|------------------|----------------------------|---------------------|----------------------------|---------------------|----------------------------|---------------------|----------------------------|---------------------|----------------------------|---------------------|
| | | (pCi/L) | Year Peak Occurs | (pCi/L) | Year Peak Occurs | (pCi/L) | Year Peak Occurs | (pCi/L) | Year Peak Occurs | (pCi/L) | Year Peak Occurs |
| Np-237 | Total α | 8.3E-08 | 10000 | 7.0E-08 | 10000 | 3.1E-08 | 10000 | 1.3E-09 | 10000 | 1.1E-11 | 10,000 |
| Pa-231 | Total α | 1.0E-08 | 10000 | 8.7E-09 | 10000 | 3.9E-09 | 10000 | 1.6E-10 | 10000 | 1.3E-12 | 10,000 |
| Pb-210 | NC | 6.4E-07 | 10000 | 5.5E-07 | 10000 | 2.6E-07 | 10000 | 1.6E-08 | 10000 | 1.9E-09 | 10,000 |
| Pd-107 | NC | 3.3E-09 | 10,000 | 2.9E-09 | 10,000 | 1.3E-09 | 10,000 | 7.6E-11 | 10,000 | 1.6E-12 | 10,000 |
| Pt-193 | 3,000 | 1.9E-06 | 520 | 1.7E-06 | 520 | 8.1E-07 | 520 | 8.3E-08 | 600 | 5.9E-08 | 640 |
| Pu-238 | Total α | <1.0E-30 | 6,760 | <1.0E-30 | 6,600 | <1.0E-30 | 6,280 | <1.0E-30 | 6,520 | <1.0E-30 | 7,120 |
| Pu-239 | Total α | 3.9E-25 | 10,000 | 1.3E-24 | 10,000 | 3.6E-24 | 10,000 | 6.3E-26 | 10,000 | 1.6E-30 | 10,000 |
| Pu-240 | Total α | 5.7E-26 | 10,000 | 1.9E-25 | 10,000 | 5.3E-25 | 10,000 | 9.2E-27 | 10,000 | <1.0E-30 | 10,000 |
| Pu-241 | 300 | <1.0E-30 | 10,000 | <1.0E-30 | 10,000 | <1.0E-30 | 10,000 | <1.0E-30 | 10,000 | <1.0E-30 | 10,000 |
| Pu-242 | Total α | 1.1E-27 | 10,000 | 3.7E-27 | 10,000 | 1.0E-26 | 10,000 | 1.8E-28 | 10,000 | <1.0E-30 | 10,000 |
| Pu-244 | Total α | 2.2E-29 | 10,000 | 7.7E-29 | 10,000 | 2.1E-28 | 10,000 | 3.6E-30 | 10,000 | <1.0E-30 | 10,000 |
| Ra-226 | Total α/Ra | 2.4E-04 | 10,000 | 2.1E-04 | 10000 | 9.9E-05 | 10000 | 6.1E-06 | 10000 | 7.3E-07 | 10,000 |
| Ra-228 | Total Ra | 1.9E-23 | 10,000 | 3.4E-23 | 10000 | 4.2E-23 | 10000 | 1.2E-24 | 10000 | 3.0E-28 | 10,000 |
| Rn-222 | NC | 2.4E-04 | 10,000 | 2.1E-04 | 10000 | 9.9E-05 | 10000 | 6.1E-06 | 10000 | 7.3E-07 | 10,000 |
| Se-79 | NC | <1.0E-30 | 10,000 | <1.0E-30 | 10,000 | <1.0E-30 | 10,000 | <1.0E-30 | 10,000 | <1.0E-30 | 10,000 |
| Sm-151 | 1,000 | <1.0E-30 | 8,060 | <1.0E-30 | 7,820 | <1.0E-30 | 7,480 | <1.0E-30 | 7,780 | <1.0E-30 | 8,520 |
| Sb-126 | NC | <1.0E-30 | 10,000 | <1.0E-30 | 10,000 | <1.0E-30 | 10,000 | <1.0E-30 | 10,000 | <1.0E-30 | 10,000 |
| Sb-126m | NC | <1.0E-30 | 10,000 | <1.0E-30 | 10,000 | <1.0E-30 | 10,000 | <1.0E-30 | 10,000 | <1.0E-30 | 10,000 |
| Sn-126 | NC | <1.0E-30 | 10,000 | <1.0E-30 | 10,000 | <1.0E-30 | 10,000 | <1.0E-30 | 10,000 | <1.0E-30 | 10,000 |
| Sr-90 | 8 | 1.1E-19 | 1220 | 1.2E-19 | 1220 | 8.2E-20 | 1220 | 3.4E-21 | 1220 | 6.4E-24 | 1,240 |
| Tc-99 | 900 | 6.6E-03 | 10,000 | 5.8E-03 | 10,000 | 2.8E-03 | 10,000 | 1.8E-04 | 10,000 | 4.6E-06 | 10,000 |
| Th-228 | Total α | 1.9E-23 | 10,000 | 3.4E-23 | 10,000 | 4.2E-23 | 10,000 | 1.2E-24 | 10,000 | 3.0E-28 | 10,000 |
| Th-229 | Total α | 2.6E-12 | 10000 | 2.3E-12 | 10000 | 1.1E-12 | 10000 | 4.8E-14 | 10000 | 4.7E-16 | 10,000 |
| Th-230 | Total α | 3.8E-19 | 10000 | 7.7E-19 | 10000 | 1.1E-18 | 10000 | 2.9E-20 | 10000 | 5.5E-24 | 10,000 |
| Th-232 | Total α | 5.6E-26 | 10,000 | 1.1E-25 | 10,000 | 1.5E-25 | 10,000 | 4.3E-27 | 10,000 | <1.0E-30 | 10,000 |
| U-232 | Total U* | <1.0E-30 | 4,700 | <1.0E-30 | 4,580 | <1.0E-30 | 4,340 | <1.0E-30 | 4,520 | <1.0E-30 | 4,980 |
| U-233 | Total U* | 7.3E-11 | 10000 | 6.7E-11 | 10000 | 3.3E-11 | 10000 | 1.5E-12 | 10000 | 1.4E-14 | 10,000 |
| U-234 | Total U* | 4.9E-16 | 10000 | 9.4E-16 | 10000 | 1.3E-15 | 10000 | 3.8E-17 | 10000 | 8.2E-21 | 10,000 |

Table 5.2-9: Radiological 100m Concentrations for GAU Sectors A through E (Continued)

| Radionuclide | MCL (pCi/L)** | Sector A Concentrations | | Sector B Concentrations | | Sector C Concentrations | | Sector D Concentrations | | Sector E Concentrations | |
|--|------------------|----------------------------|---------------------|----------------------------|---------------------|----------------------------|---------------------|----------------------------|---------------------|----------------------------|---------------------|
| | | (pCi/L) | Year Peak Occurs | (pCi/L) | Year Peak Occurs | (pCi/L) | Year Peak Occurs | (pCi/L) | Year Peak Occurs | (pCi/L) | Year Peak Occurs |
| U-235 | Total U* | 8.2E-18 | 10000 | 1.6E-17 | 10000 | 2.1E-17 | 10000 | 6.4E-19 | 10000 | 1.4E-22 | 10,000 |
| U-236 | Total U* | 1.3E-17 | 10000 | 2.6E-17 | 10000 | 3.4E-17 | 10000 | 1.0E-18 | 10000 | 2.2E-22 | 10,000 |
| U-238 | Total U* | 1.0E-17 | 10,000 | 1.9E-17 | 10,000 | 2.6E-17 | 10,000 | 7.8E-19 | 10,000 | 1.7E-22 | 10,000 |
| Y-90 | 60 | 1.1E-19 | 1220 | 1.2E-19 | 1220 | 8.2E-20 | 1220 | 3.4E-21 | 1220 | 6.4E-24 | 1,240 |
| Zr-93 | 2,000 | <1.0E-30 | 10,000 | <1.0E-30 | 10,000 | <1.0E-30 | 10,000 | <1.0E-30 | 10,000 | <1.0E-30 | 10,000 |
| Total alpha | 15 | 2.4E-04 | N/A | 2.1E-04 | N/A | 9.9E-05 | N/A | 6.1E-06 | N/A | 7.3E-07 | N/A |
| Total Ra | 5 | 2.4E-04 | N/A | 2.1E-04 | N/A | 9.9E-05 | N/A | 6.1E-06 | N/A | 7.3E-07 | N/A |
| Sum of beta-gamma MCL fractions | | 2.8E-04 | N/A | 2.5E-04 | N/A | 1.4E-04 | N/A | 6.4E-05 | N/A | 7.9E-05 | N/A |

* Total uranium is evaluated in Table 5.2-18.

** MCL values for beta and photon emitters are calculated in Table II-3 of FR-00-9654 based on a beta-gamma dose of 4 mrem/yr

NC = Not Calculated

Table 5.2-10: Radiological 100m Concentrations for GAU Sectors F through J

| Radionuclide | MCL (pCi/L)** | Sector F Concentrations | | Sector G Concentrations | | Sector H Concentrations | | Sector I Concentrations | | Sector J Concentrations | |
|--------------|------------------|----------------------------|---------------------|----------------------------|---------------------|----------------------------|---------------------|----------------------------|---------------------|----------------------------|---------------------|
| | | (pCi/L) | Year Peak Occurs | (pCi/L) | Year Peak Occurs | (pCi/L) | Year Peak Occurs | (pCi/L) | Year Peak Occurs | (pCi/L) | Year Peak Occurs |
| Ac-227 | NC | 2.1E-20 | 10,000 | 5.4E-12 | 10,000 | 6.7E-12 | 10,000 | 6.4E-12 | 10,000 | 3.1E-12 | 10,000 |
| Al-26 | NC | <1.0E-30 | 10,000 | <1.0E-30 | 10,000 | <1.0E-30 | 10,000 | <1.0E-30 | 10,000 | <1.0E-30 | 10,000 |
| Am-241 | Total α | <1.0E-30 | 10,000 | <1.0E-30 | 10,000 | <1.0E-30 | 10,000 | <1.0E-30 | 10,000 | <1.0E-30 | 10,000 |
| Am-242m | Total α | <1.0E-30 | 10,000 | <1.0E-30 | 10,000 | <1.0E-30 | 10,000 | <1.0E-30 | 10,000 | <1.0E-30 | 10,000 |
| Am-243 | Total α | <1.0E-30 | 10,000 | <1.0E-30 | 10,000 | <1.0E-30 | 10,000 | <1.0E-30 | 10,000 | <1.0E-30 | 10,000 |
| Ba-137m | NC | <1.0E-30 | 1,840 | <1.0E-30 | 1,780 | <1.0E-30 | 1,800 | <1.0E-30 | 1,820 | <1.0E-30 | 1,920 |
| C-14 | 2,000 | 4.9E-05 | 10,000 | 3.9E-03 | 8,260 | 4.4E-03 | 8,240 | 4.4E-03 | 8,260 | 2.9E-03 | 9,300 |
| Cf-249 | Total α | <1.0E-30 | 10,000 | <1.0E-30 | 10,000 | <1.0E-30 | 10,000 | <1.0E-30 | 10,000 | <1.0E-30 | 10,000 |
| Cf-251 | Total α | <1.0E-30 | 10,000 | <1.0E-30 | 10,000 | <1.0E-30 | 10,000 | <1.0E-30 | 10,000 | <1.0E-30 | 10,000 |
| Cl-36 | 700 | 9.4E-09 | 10,000 | 1.2E-06 | 10,000 | 1.3E-06 | 10,000 | 1.3E-06 | 10,000 | 7.7E-07 | 10,000 |
| Cm-243 | Total α | <1.0E-30 | 3,140 | <1.0E-30 | 2,800 | <1.0E-30 | 2,780 | <1.0E-30 | 2,820 | <1.0E-30 | 2,880 |
| Cm-244 | Total α | <1.0E-30 | 2,060 | <1.0E-30 | 1,820 | <1.0E-30 | 1,800 | <1.0E-30 | 1,840 | <1.0E-30 | 1,880 |
| Cm-245 | Total α | <1.0E-30 | 10,000 | <1.0E-30 | 10,000 | <1.0E-30 | 10,000 | <1.0E-30 | 10,000 | <1.0E-30 | 10,000 |
| Cm-247 | Total α | <1.0E-30 | 10,000 | <1.0E-30 | 10,000 | <1.0E-30 | 10,000 | <1.0E-30 | 10,000 | <1.0E-30 | 10,000 |
| Cm-248 | Total α | <1.0E-30 | 10,000 | <1.0E-30 | 10,000 | <1.0E-30 | 10,000 | <1.0E-30 | 10,000 | <1.0E-30 | 10,000 |
| Co-60 | 100 | <1.0E-30 | 340 | <1.0E-30 | 440 | <1.0E-30 | 440 | <1.0E-30 | 440 | <1.0E-30 | 400 |
| Cs-135 | 900 | 3.0E-13 | 10,000 | 2.6E-08 | 10,000 | 2.7E-08 | 10,000 | 1.8E-08 | 10,000 | 9.2E-09 | 10,000 |
| Cs-137 | 200 | <1.0E-30 | 1,840 | <1.0E-30 | 1,780 | <1.0E-30 | 1,800 | <1.0E-30 | 1,820 | <1.0E-30 | 1,920 |
| Eu-152 | 200 | <1.0E-30 | 1,580 | <1.0E-30 | 1,420 | <1.0E-30 | 1,400 | <1.0E-30 | 1,420 | <1.0E-30 | 1,440 |
| Eu-154 | 60 | <1.0E-30 | 1,040 | <1.0E-30 | 940 | <1.0E-30 | 940 | <1.0E-30 | 940 | <1.0E-30 | 960 |
| Gd-152 | NC | <1.0E-30 | 10,000 | <1.0E-30 | 10,000 | <1.0E-30 | 10,000 | <1.0E-30 | 10,000 | <1.0E-30 | 10,000 |
| H-3 | 20,000 | 1.6E-16 | 440 | 1.3E-13 | 420 | 1.6E-13 | 420 | 1.4E-13 | 420 | 6.9E-14 | 420 |
| I-129 | 1 | 3.2E-05 | 10000 | 1.7E-03 | 10000 | 1.9E-03 | 10000 | 2.0E-03 | 10000 | 1.5E-03 | 10,000 |
| K-40 | NC | 1.7E-09 | 10000 | 1.3E-07 | 10000 | 1.4E-07 | 10000 | 1.3E-07 | 10000 | 8.3E-08 | 10,000 |
| Nb-93m | 1,000 | 9.0E-14 | 10000 | 1.8E-05 | 10000 | 2.2E-05 | 10000 | 2.0E-05 | 10000 | 9.3E-06 | 10,000 |
| Nb-94 | NC | 3.4E-15 | 9900 | 8.5E-07 | 10000 | 1.1E-06 | 10000 | 9.9E-07 | 10000 | 4.6E-07 | 10,000 |
| Ni-59 | 300 | 7.9E-16 | 10000 | 1.8E-08 | 10000 | 2.2E-08 | 10000 | 2.0E-08 | 10000 | 9.6E-09 | 10,000 |

Table 5.2-10: Radiological 100m Concentrations for GAU Sectors F through J (Continued)

| Radionuclide | MCL (pCi/L)** | Sector F Concentrations | | Sector G Concentrations | | Sector H Concentrations | | Sector I Concentrations | | Sector J Concentrations | |
|--------------|--------------------|----------------------------|---------------------|----------------------------|---------------------|----------------------------|---------------------|----------------------------|---------------------|----------------------------|---------------------|
| | | (pCi/L) | Year Peak Occurs | (pCi/L) | Year Peak Occurs | (pCi/L) | Year Peak Occurs | (pCi/L) | Year Peak Occurs | (pCi/L) | Year Peak Occurs |
| Ni-63 | 50 | 5.9E-27 | 2,640 | 3.3E-18 | 2,460 | 3.6E-18 | 2,460 | 2.8E-18 | 2,500 | 1.3E-18 | 2,480 |
| Np-237 | Total α | 2.2E-16 | 10,000 | 5.8E-08 | 10,000 | 7.3E-08 | 10,000 | 6.9E-08 | 10,000 | 3.4E-08 | 10,000 |
| Pa-231 | Total α | 2.7E-17 | 10,000 | 7.1E-09 | 10,000 | 9.0E-09 | 10,000 | 8.5E-09 | 10,000 | 4.2E-09 | 10,000 |
| Pb-210 | NC | 6.3E-10 | 10,000 | 4.5E-07 | 10,000 | 5.4E-07 | 10,000 | 5.1E-07 | 10,000 | 2.5E-07 | 10,000 |
| Pd-107 | NC | 4.7E-17 | 10,000 | 2.3E-09 | 10,000 | 2.8E-09 | 10,000 | 2.6E-09 | 10,000 | 1.3E-09 | 10,000 |
| Pt-193 | 3,000 | 2.1E-08 | 640 | 1.8E-06 | 580 | 2.1E-06 | 580 | 2.0E-06 | 580 | 1.2E-06 | 600 |
| Pu-238 | Total α | <1.0E-30 | 7,260 | <1.0E-30 | 10,000 | <1.0E-30 | 9,880 | <1.0E-30 | 9,820 | <1.0E-30 | 8,680 |
| Pu-239 | Total α | <1.0E-30 | 10,000 | <1.0E-30 | 10,000 | <1.0E-30 | 10,000 | <1.0E-30 | 10,000 | <1.0E-30 | 10,000 |
| Pu-240 | Total α | <1.0E-30 | 10,000 | <1.0E-30 | 10,000 | <1.0E-30 | 10,000 | <1.0E-30 | 10,000 | <1.0E-30 | 10,000 |
| Pu-241 | 300 | <1.0E-30 | 10,000 | <1.0E-30 | 10,000 | <1.0E-30 | 10,000 | <1.0E-30 | 10,000 | <1.0E-30 | 10,000 |
| Pu-242 | Total α | <1.0E-30 | 10,000 | <1.0E-30 | 10,000 | <1.0E-30 | 10,000 | <1.0E-30 | 10,000 | <1.0E-30 | 10,000 |
| Pu-244 | Total α | <1.0E-30 | 10,000 | <1.0E-30 | 10,000 | <1.0E-30 | 10,000 | <1.0E-30 | 10,000 | <1.0E-30 | 10,000 |
| Ra-226 | Total α /Ra | 2.4E-07 | 10,000 | 1.7E-04 | 10,000 | 2.1E-04 | 10,000 | 1.9E-04 | 10,000 | 9.7E-05 | 10,000 |
| Ra-228 | Total Ra | <1.0E-30 | 10,000 | 7.7E-30 | 10,000 | 8.3E-30 | 10,000 | 2.9E-30 | 10,000 | 5.8E-30 | 10,000 |
| Rn-222 | NC | 2.4E-07 | 10,000 | 1.7E-04 | 10,000 | 2.1E-04 | 10,000 | 1.9E-04 | 10,000 | 9.7E-05 | 10,000 |
| Se-79 | NC | <1.0E-30 | 10,000 | <1.0E-30 | 10,000 | <1.0E-30 | 10,000 | <1.0E-30 | 10,000 | <1.0E-30 | 10,000 |
| Sm-151 | 1,000 | <1.0E-30 | 8,720 | <1.0E-30 | 7,740 | <1.0E-30 | 7,660 | <1.0E-30 | 7,840 | <1.0E-30 | 10,000 |
| Sb-126 | NC | <1.0E-30 | 10,000 | <1.0E-30 | 10,000 | <1.0E-30 | 10,000 | <1.0E-30 | 10,000 | <1.0E-30 | 10,000 |
| Sb-126m | NC | <1.0E-30 | 10,000 | <1.0E-30 | 10,000 | <1.0E-30 | 10,000 | <1.0E-30 | 10,000 | <1.0E-30 | 10,000 |
| Sn-126 | NC | <1.0E-30 | 10,000 | <1.0E-30 | 10,000 | <1.0E-30 | 10,000 | <1.0E-30 | 10,000 | <1.0E-30 | 10,000 |
| Sr-90 | 8 | 4.5E-29 | 1,260 | 1.9E-21 | 1,380 | 2.0E-21 | 1,380 | 1.1E-21 | 1,400 | 6.1E-22 | 1,380 |
| Tc-99 | 900 | 2.3E-10 | 10,000 | 4.9E-03 | 10,000 | 5.9E-03 | 10,000 | 5.4E-03 | 10,000 | 2.6E-03 | 10,000 |
| Th-228 | Total α | < 1.0E-30 | 10,000 | 7.7E-30 | 10,000 | 8.3E-30 | 10,000 | 2.9E-30 | 10,000 | 5.8E-30 | 10,000 |
| Th-229 | Total α | 1.0E-20 | 10,000 | 8.8E-14 | 10,000 | 1.1E-13 | 10,000 | 1.0E-13 | 10,000 | 5.2E-14 | 10,000 |
| Th-230 | Total α | <1.0E-30 | 10,000 | 2.8E-28 | 10,000 | 3.6E-28 | 10,000 | 1.7E-28 | 10,000 | 2.5E-27 | 10,000 |
| Th-232 | Total α | <1.0E-30 | 10,000 | <1.0E-30 | 10,000 | <1.0E-30 | 10,000 | <1.0E-30 | 10,000 | <1.0E-30 | 10,000 |
| U-232 | Total U* | <1.0E-30 | 5,080 | <1.0E-30 | 7,200 | <1.0E-30 | 7,060 | <1.0E-30 | 7,000 | <1.0E-30 | 6,180 |

Table 5.2-10: Radiological 100m Concentrations for GAU Sectors F through J (Continued)

| Radionuclide | MCL (pCi/L)** | Sector F Concentrations | | Sector G Concentrations | | Sector H Concentrations | | Sector I Concentrations | | Sector J Concentrations | |
|--|------------------|----------------------------|---------------------|----------------------------|---------------------|----------------------------|---------------------|----------------------------|---------------------|----------------------------|---------------------|
| | | (pCi/L) | Year Peak Occurs | (pCi/L) | Year Peak Occurs | (pCi/L) | Year Peak Occurs | (pCi/L) | Year Peak Occurs | (pCi/L) | Year Peak Occurs |
| U-233 | Total U* | 3.0E-19 | 10,000 | 2.5E-12 | 10,000 | 3.1E-12 | 10,000 | 3.0E-12 | 10,000 | 1.6E-12 | 10,000 |
| U-234 | Total U* | 4.6E-28 | 10,000 | 6.4E-25 | 10,000 | 8.1E-25 | 10,000 | 3.8E-25 | 10,000 | 4.7E-24 | 10,000 |
| U-235 | Total U* | 7.6E-30 | 10,000 | 1.1E-26 | 10,000 | 1.4E-26 | 10,000 | 6.4E-27 | 10,000 | 7.8E-26 | 10,000 |
| U-236 | Total U* | 1.2E-29 | 10,000 | 1.7E-26 | 10,000 | 2.2E-26 | 10,000 | 1.0E-26 | 10,000 | 1.3E-25 | 10,000 |
| U-238 | Total U* | 9.4E-30 | 10,000 | 1.3E-26 | 10,000 | 1.7E-26 | 10,000 | 7.8E-27 | 10,000 | 9.6E-26 | 10,000 |
| Y-90 | 60 | 4.5E-29 | 1,260 | 1.9E-21 | 1,380 | 2.0E-21 | 1,380 | 1.1E-21 | 1,400 | 6.1E-22 | 1,380 |
| Zr-93 | 2,000 | <1.0E-30 | 10,000 | <1.0E-30 | 10,000 | <1.0E-30 | 10,000 | <1.0E-30 | 10,000 | <1.0E-30 | 10,000 |
| Total alpha | 15 | 2.4E-07 | N/A | 1.7E-04 | N/A | 2.1E-04 | N/A | 1.9E-04 | N/A | 9.7E-05 | N/A |
| Total Ra | 5 | 2.4E-07 | N/A | 1.7E-04 | N/A | 2.1E-04 | N/A | 1.9E-04 | N/A | 9.7E-05 | N/A |
| Sum of beta-gamma MCL fractions | | 3.2E-05 | N/A | 1.8E-03 | N/A | 1.9E-03 | N/A | 2.0E-03 | N/A | 1.5E-03 | N/A |

* Total uranium is evaluated in Table 5.2-19.

** MCL values for beta and photon emitters are calculated in Table II-3 of FR-00-9654 based on a beta-gamma dose of 4 mrem/yr

NC = Not Calculated

Table 5.2-11: Radiological 100m Concentrations for GAU Sectors K and L

| Radionuclide | MCL (pCi/L)** | Sector K Concentrations | | Sector L Concentrations | |
|--------------|--------------------|----------------------------|---------------------|----------------------------|---------------------|
| | | (pCi/L) | Year Peak Occurs | (pCi/L) | Year Peak Occurs |
| Ac-227 | NC | 2.6E-12 | 10,000 | 5.4E-12 | 10,000 |
| Al-26 | NC | <1.0E-30 | 10,000 | <1.0E-30 | 10,000 |
| Am-241 | Total α | <1.0E-30 | 10,000 | <1.0E-30 | 10,000 |
| Am-242m | Total α | <1.0E-30 | 10,000 | <1.0E-30 | 10,000 |
| Am-243 | Total α | <1.0E-30 | 10,000 | <1.0E-30 | 10,000 |
| Ba-137 m | NC | <1.0E-30 | 1,880 | <1.0E-30 | 2,240 |
| C-14 | 2,000 | 1.8E-03 | 9,280 | 2.0E-03 | 6,740 |
| Cf-249 | Total α | <1.0E-30 | 10,000 | <1.0E-30 | 10,000 |
| Cf-251 | Total α | <1.0E-30 | 10,000 | <1.0E-30 | 10,000 |
| Cl-36 | 700 | 5.1E-07 | 10,000 | 6.1E-07 | 9,840 |
| Cm-243 | Total α | <1.0E-30 | 3,540 | <1.0E-30 | 3,240 |
| Cm-244 | Total α | <1.0E-30 | 1,900 | <1.0E-30 | 2,100 |
| Cm-245 | Total α | <1.0E-30 | 10,000 | <1.0E-30 | 10,000 |
| Cm-247 | Total α | <1.0E-30 | 10,000 | <1.0E-30 | 10,000 |
| Cm-248 | Total α | <1.0E-30 | 10,000 | <1.0E-30 | 10,000 |
| Co-60 | 100 | <1.0E-30 | 380 | <1.0E-30 | 340 |
| Cs-135 | 900 | 1.7E-08 | 10,000 | 8.8E-08 | 10,000 |
| Cs-137 | 200 | <1.0E-30 | 1,880 | <1.0E-30 | 2,240 |
| Eu-152 | 200 | <1.0E-30 | 1,460 | <1.0E-30 | 1,620 |
| Eu-154 | 60 | <1.0E-30 | 960 | <1.0E-30 | 1,080 |
| Gd-152 | NC | <1.0E-30 | 10,000 | <1.0E-30 | 10,000 |
| H-3 | 20,000 | 6.8E-14 | 420 | 1.6E-13 | 420 |
| I-129 | 1 | 9.6E-04 | 10,000 | 5.2E-04 | 10,000 |
| K-40 | NC | 6.2E-08 | 10,000 | 6.4E-08 | 10,000 |
| Nb-93m | 1,000 | 8.9E-06 | 10,000 | 2.1E-05 | 10,000 |
| Nb-94 | NC | 3.8E-07 | 10,000 | 7.8E-07 | 10,000 |
| Ni-59 | 300 | 8.3E-09 | 10,000 | 1.7E-08 | 10,000 |
| Ni-63 | 50 | 1.9E-18 | 2,420 | 8.5E-18 | 2,320 |
| Np-237 | Total α | 2.8E-08 | 10,000 | 5.7E-08 | 10,000 |
| Pa-231 | Total α | 3.5E-09 | 10,000 | 7.1E-09 | 10,000 |
| Pb-210 | NC | 2.1E-07 | 10,000 | 4.3E-07 | 10,000 |
| Pd-107 | NC | 1.1E-09 | 10,000 | 2.3E-09 | 10,000 |
| Pt-193 | 3,000 | 8.8E-07 | 580 | 1.3E-06 | 520 |
| Pu-238 | Total α | <1.0E-30 | 8,200 | <1.0E-30 | 7,440 |
| Pu-239 | Total α | <1.0E-30 | 10,000 | 6.5E-29 | 10,000 |
| Pu-240 | Total α | <1.0E-30 | 10,000 | 9.4E-30 | 10,000 |
| Pu-241 | 300 | <1.0E-30 | 10,000 | <1.0E-30 | 10,000 |
| Pu-242 | Total α | <1.0E-30 | 10,000 | <1.0E-30 | 10,000 |
| Pu-244 | Total α | <1.0E-30 | 10,000 | <1.0E-30 | 10,000 |
| Ra-226 | Total α /Ra | 8.1E-05 | 10,000 | 1.7E-04 | 10,000 |
| Ra-228 | Total Ra | 1.2E-28 | 10,000 | 1.5E-25 | 10,000 |
| Rn-222 | NC | 8.1E-05 | 10,000 | 1.7E-04 | 10,000 |
| Se-79 | NC | <1.0E-30 | 10,000 | <1.0E-30 | 10,000 |

Table 5.2-11: Radiological 100m Concentrations for GAU Sectors K and L (Continued)

| Radionuclide | MCL (pCi/L)** | Sector K Concentrations | | Sector L Concentrations | |
|--|---------------|----------------------------|---------------------|----------------------------|---------------------|
| | | (pCi/L) | Year Peak Occurs | (pCi/L) | Year Peak Occurs |
| Sm-151 | 1,000 | <1.0E-30 | 9,800 | <1.0E-30 | 8,920 |
| Sb-126 | NC | <1.0E-30 | 10,000 | <1.0E-30 | 10,000 |
| Sb-126m | NC | <1.0E-30 | 10,000 | <1.0E-30 | 10,000 |
| Sn-126 | NC | <1.0E-30 | 10,000 | <1.0E-30 | 10,000 |
| Sr-90 | 8 | 1.5E-21 | 1,360 | 1.9E-20 | 1,280 |
| Tc-99 | 900 | 2.2E-03 | 10,000 | 4.5E-03 | 10,000 |
| Th-228 | Total α | 1.2E-28 | 10,000 | 1.5E-25 | 10,000 |
| Th-229 | Total α | 9.2E-14 | 10,000 | 8.9E-13 | 10,000 |
| Th-230 | Total α | 1.3E-25 | 10,000 | 9.3E-22 | 10,000 |
| Th-232 | Total α | <1.0E-30 | 10,000 | 1.4E-28 | 10,000 |
| U-232 | Total U* | <1.0E-30 | 5,800 | <1.0E-30 | 5,220 |
| U-233 | Total U* | 3.2E-12 | 10,000 | 2.5E-11 | 10,000 |
| U-234 | Total U* | 2.3E-22 | 10,000 | 1.3E-18 | 10,000 |
| U-235 | Total U* | 3.9E-24 | 10,000 | 2.2E-20 | 10,000 |
| U-236 | Total U* | 6.3E-24 | 10,000 | 3.6E-20 | 10,000 |
| U-238 | Total U* | 4.8E-24 | 10,000 | 2.7E-20 | 10,000 |
| Y-90 | 60 | 1.5E-21 | 1,360 | 1.9E-20 | 1,280 |
| Zr-93 | 2,000 | <1.0E-30 | 10,000 | <1.0E-30 | 10,000 |
| Total alpha | 15 | 8.1E-05 | N/A | 1.7E-04 | N/A |
| Total Ra | 5 | 8.1E-05 | N/A | 1.7E-04 | N/A |
| Sum of beta-gamma MCL fractions | | 9.6E-04 | N/A | 5.2E-04 | N/A |

* Total uranium is evaluated in Table 5.2-20.

** MCL values for beta and photon emitters are calculated in Table II-3 of FR-00-9654 based on a beta-gamma dose of 4 mrem/yr

NC = Not Calculated

Table 5.2-12: Chemical 100m Concentrations for UTR-UZ Sectors A through E

| Chemical | MCL (µg/L) | Sector A Concentrations | | Sector B Concentrations | | Sector C Concentrations | | Sector D Concentrations | | Sector E Concentrations | |
|----------|---------------|----------------------------|---------------------|----------------------------|---------------------|----------------------------|---------------------|----------------------------|---------------------|----------------------------|---------------------|
| | | (µg/L) | Year Peak Occurs | (µg/L) | Year Peak Occurs | (µg/L) | Year Peak Occurs | (µg/L) | Year Peak Occurs | (µg/L) | Year Peak Occurs |
| Ag | N/A | 1.1E-05 | 10,000 | 7.9E-04 | 10,000 | 8.9E-04 | 10,000 | 2.6E-04 | 10,000 | 4.2E-05 | 10,000 |
| As | 1.00E+01 | 4.8E-08 | 10,000 | 7.3E-06 | 10,000 | 1.1E-05 | 10,000 | 2.2E-06 | 10,000 | 4.9E-09 | 10,000 |
| Ba | 2.00E+03 | 9.8E-05 | 10,000 | 2.6E-03 | 10,000 | 3.1E-03 | 10,000 | 1.9E-03 | 9,760 | 6.0E-04 | 10,000 |
| Cd | 5.00E+00 | 2.0E-06 | 10,000 | 5.1E-05 | 10,000 | 6.3E-05 | 10,000 | 4.6E-05 | 10,000 | 5.7E-06 | 10,000 |
| Cr | 1.00E+02 | 2.2E-05 | 10,000 | 1.5E-03 | 10,000 | 1.7E-03 | 10,000 | 3.7E-04 | 10,000 | 4.0E-06 | 10,000 |
| Cu | N/A | 2.7E-03 | 10,000 | 5.2E-02 | 10,000 | 7.1E-02 | 10,000 | 5.4E-02 | 10,000 | 6.4E-02 | 10,000 |
| F | N/A | 2.2E-03 | 9,620 | 1.2E-01 | 9,580 | 1.3E-01 | 9,600 | 3.3E-02 | 9,620 | 1.0E-02 | 10,000 |
| Fe | N/A | 2.5E-13 | 10,000 | 2.6E-10 | 10,000 | 1.0E-09 | 10,000 | 1.1E-10 | 10,000 | 2.9E-14 | 10,000 |
| Hg | 2.00E+00 | 2.0E-28 | 10,000 | 2.1E-22 | 10,000 | 3.1E-19 | 10,000 | 3.2E-21 | 10,000 | 6.4E-29 | 10,000 |
| Mn | N/A | 1.5E-06 | 10,000 | 1.0E-04 | 10,000 | 1.1E-04 | 10,000 | 2.4E-05 | 10,000 | 1.2E-06 | 10,000 |
| N | 1.00E+04 | 2.0E+01 | 4,040 | 3.9E+02 | 4,040 | 4.6E+02 | 4,020 | 2.8E+02 | 4,020 | 3.3E+02 | 4,020 |
| Ni | N/A | 1.1E-07 | 10,000 | 8.2E-06 | 10,000 | 9.2E-06 | 10,000 | 2.0E-06 | 10,000 | 7.3E-09 | 10,000 |
| Pb | 1.50E+01 | <1.0E-30 | 10,000 | <1.0E-30 | 10,000 | <1.0E-30 | 10,000 | <1.0E-30 | 10,000 | <1.0E-30 | 10,000 |
| Se | 5.00E+00 | 1.8E-30 | 10,000 | 6.5E-24 | 10,000 | 5.1E-20 | 10,000 | 3.3E-22 | 10,000 | 3.4E-29 | 10,000 |
| U | 3.00E+01 | 1.0E-12 | 10,000 | 1.0E-09 | 10,000 | 3.7E-09 | 10,000 | 4.1E-10 | 10,000 | 1.2E-13 | 10,000 |
| Zn | N/A | 1.6E-08 | 10,000 | 2.4E-06 | 10,000 | 3.6E-06 | 10,000 | 7.1E-07 | 10,000 | 1.5E-09 | 10,000 |

Table 5.2-13: Chemical 100m Concentrations for UTR-UZ Sectors F through J

| Chemical | MCL (µg/L) | Sector F Concentrations | | Sector G Concentrations | | Sector H Concentrations | | Sector I Concentrations | | Sector J Concentrations | |
|----------|---------------|----------------------------|---------------------|----------------------------|---------------------|----------------------------|---------------------|----------------------------|---------------------|----------------------------|---------------------|
| | | (µg/L) | Year Peak Occurs | (µg/L) | Year Peak Occurs | (µg/L) | Year Peak Occurs | (µg/L) | Year Peak Occurs | (µg/L) | Year Peak Occurs |
| Ag | N/A | 2.2E-05 | 10,000 | 4.9E-05 | 10,000 | 3.4E-06 | 10,000 | 6.7E-06 | 10,000 | 2.9E-06 | 10,000 |
| As | 1.00E+01 | 1.2E-14 | 10,000 | 5.9E-19 | 10,000 | 5.7E-20 | 10,000 | 1.5E-20 | 10,000 | 4.6E-21 | 10,000 |
| Ba | 2.00E+03 | 3.9E-04 | 10,000 | 8.5E-04 | 10,000 | 5.6E-05 | 10,000 | 1.8E-04 | 10,000 | 8.0E-05 | 10,000 |
| Cd | 5.00E+00 | 1.4E-10 | 10,000 | 1.1E-13 | 10,000 | 1.0E-15 | 10,000 | 4.0E-14 | 10,000 | 5.6E-13 | 10,000 |
| Cr | 1.00E+02 | 6.8E-11 | 10,000 | 1.3E-13 | 10,000 | 6.3E-16 | 10,000 | 1.9E-14 | 10,000 | 2.6E-13 | 10,000 |
| Cu | N/A | 4.2E-02 | 10,000 | 9.3E-02 | 10,000 | 6.3E-03 | 10,000 | 1.5E-02 | 10,000 | 6.6E-03 | 10,000 |
| F | N/A | 6.6E-03 | 10,000 | 1.5E-02 | 10,000 | 9.5E-04 | 10,000 | 3.0E-03 | 10,000 | 1.4E-03 | 10,000 |
| Fe | N/A | 7.4E-21 | 10,000 | <1.0E-30 | 10,000 | <1.0E-30 | 10,000 | <1.0E-30 | 10,000 | <1.0E-30 | 10,000 |
| Hg | 2.00E+00 | <1.0E-30 | 10,000 | <1.0E-30 | 10,000 | <1.0E-30 | 10,000 | <1.0E-30 | 10,000 | <1.0E-30 | 10,000 |
| Mn | N/A | 8.2E-07 | 10,000 | 1.8E-06 | 10,000 | 1.2E-07 | 10,000 | 3.1E-07 | 10,000 | 1.4E-07 | 10,000 |
| N | 1.00E+04 | 2.1E+02 | 4,020 | 4.7E+02 | 4,020 | 3.1E+01 | 4,020 | 9.7E+01 | 4,020 | 4.5E+01 | 4,020 |
| Ni | N/A | 2.8E-15 | 10,000 | 3.1E-17 | 10,000 | 5.5E-20 | 10,000 | 1.9E-20 | 10,000 | 2.7E-21 | 10,000 |
| Pb | 1.50E+01 | <1.0E-30 | 10,000 | <1.0E-30 | 10,000 | <1.0E-30 | 10,000 | <1.0E-30 | 10,000 | <1.0E-30 | 10,000 |
| Se | 5.00E+00 | <1.0E-30 | 10,000 | 1.3E-29 | 10,000 | 1.3E-30 | 10,000 | <1.0E-30 | 10,000 | <1.0E-30 | 10,000 |
| U | 3.00E+01 | 3.0E-20 | 10,000 | 2.3E-26 | 10,000 | 2.3E-27 | 10,000 | 1.6E-28 | 10,000 | 3.3E-29 | 10,000 |
| Zn | N/A | 5.6E-16 | 10,000 | 1.5E-26 | 10,000 | 1.5E-27 | 10,000 | 3.3E-28 | 10,000 | 1.0E-26 | 10,000 |

Table 5.2-14: Chemical 100m Concentrations for UTR-UZ Sectors K and L

| Chemical | MCL (µg/L) | Sector K Concentrations | | Sector L Concentrations | |
|----------|------------|----------------------------|------------------|----------------------------|------------------|
| | | (µg/L) | Year Peak Occurs | (µg/L) | Year Peak Occurs |
| Ag | N/A | 4.6E-07 | 10,000 | 2.7E-06 | 10,000 |
| As | 1.00E+01 | 1.7E-17 | 10,000 | 3.0E-10 | 10,000 |
| Ba | 2.00E+03 | 2.1E-05 | 10,000 | 7.9E-05 | 10,000 |
| Cd | 5.00E+00 | 8.4E-10 | 10,000 | 4.8E-07 | 10,000 |
| Cr | 1.00E+02 | 4.0E-10 | 10,000 | 5.4E-07 | 10,000 |
| Cu | N/A | 1.2E-03 | 10,000 | 5.9E-03 | 10,000 |
| F | N/A | 3.7E-04 | 10,000 | 1.4E-03 | 10,000 |
| Fe | N/A | 1.3E-25 | 10,000 | 2.6E-16 | 10,000 |
| Hg | 2.00E+00 | <1.0E-30 | 10,000 | <1.0E-30 | 10,000 |
| Mn | N/A | 2.8E-08 | 10,000 | 1.3E-07 | 10,000 |
| N | 1.00E+04 | 1.2E+01 | 4,040 | 4.4E+01 | 4,040 |
| Ni | N/A | 1.6E-15 | 10,000 | 1.5E-09 | 10,000 |
| Pb | 1.50E+01 | <1.0E-30 | 10,000 | <1.0E-30 | 10,000 |
| Se | 5.00E+00 | <1.0E-30 | 10,000 | <1.0E-30 | 10,000 |
| U | 3.00E+01 | 6.2E-25 | 10,000 | 1.1E-15 | 10,000 |
| Zn | N/A | 5.7E-18 | 10,000 | 9.8E-11 | 10,000 |

Table 5.2-15: Chemical 100m Concentrations for UTR-LZ Sectors A through E

| Chemical | MCL (µg/L) | Sector A Concentrations | | Sector B Concentrations | | Sector C Concentrations | | Sector D Concentrations | | Sector E Concentrations | |
|----------|---------------|----------------------------|---------------------|----------------------------|---------------------|----------------------------|---------------------|----------------------------|---------------------|----------------------------|---------------------|
| | | (µg/L) | Year Peak Occurs | (µg/L) | Year Peak Occurs | (µg/L) | Year Peak Occurs | (µg/L) | Year Peak Occurs | (µg/L) | Year Peak Occurs |
| Ag | N/A | 2.3E-03 | 10,000 | 3.0E-03 | 10,000 | 3.0E-03 | 10,000 | 4.5E-04 | 10,000 | 5.5E-05 | 10,000 |
| As | 1.00E+01 | 1.4E-05 | 10,000 | 2.2E-05 | 10,000 | 2.4E-05 | 10,000 | 2.6E-06 | 10,000 | 6.5E-09 | 10,000 |
| Ba | 2.00E+03 | 6.7E-03 | 10,000 | 8.3E-03 | 10,000 | 7.9E-03 | 10,000 | 3.2E-03 | 9,800 | 9.4E-04 | 10,000 |
| Cd | 5.00E+00 | 1.1E-04 | 10,000 | 1.6E-04 | 10,000 | 1.5E-04 | 10,000 | 8.4E-05 | 10,000 | 7.7E-06 | 10,000 |
| Cr | 1.00E+02 | 3.6E-03 | 10,000 | 4.2E-03 | 10,000 | 4.0E-03 | 10,000 | 4.4E-04 | 10,000 | 5.3E-06 | 10,000 |
| Cu | N/A | 1.2E-01 | 10,000 | 1.4E-01 | 10,000 | 1.3E-01 | 10,000 | 6.9E-02 | 10,000 | 8.4E-02 | 10,000 |
| F | N/A | 4.6E-01 | 9,600 | 5.3E-01 | 9,600 | 5.0E-01 | 9,600 | 5.6E-02 | 9,620 | 1.4E-02 | 10,000 |
| Fe | N/A | 2.4E-09 | 10,000 | 6.0E-09 | 10,000 | 9.1E-09 | 10,000 | 6.3E-10 | 10,000 | 2.1E-13 | 10,000 |
| Hg | 2.00E+00 | 9.0E-22 | 10,000 | 1.8E-20 | 10,000 | 7.1E-19 | 10,000 | 2.3E-21 | 10,000 | 2.4E-28 | 10,000 |
| Mn | N/A | 4.2E-03 | 10,000 | 4.9E-03 | 10,000 | 4.7E-03 | 10,000 | 4.8E-04 | 10,000 | 3.1E-06 | 10,000 |
| N | 1.00E+04 | 1.0E+03 | 4,040 | 1.2E+03 | 4,040 | 1.0E+03 | 10,000 | 4.1E+02 | 4,040 | 4.6E+02 | 4,040 |
| Ni | N/A | 4.5E-05 | 10,000 | 5.6E-05 | 10,000 | 5.5E-05 | 10,000 | 6.0E-06 | 10,000 | 2.4E-08 | 10,000 |
| Pb | 1.50E+01 | <1.0E-30 | 10,000 | <1.0E-30 | 10,000 | <1.0E-30 | 10,000 | <1.0E-30 | 10,000 | <1.0E-30 | 10,000 |
| Se | 5.00E+00 | 3.1E-23 | 10,000 | 9.2E-22 | 10,000 | 7.4E-20 | 10,000 | 1.4E-22 | 10,000 | 6.2E-29 | 10,000 |
| U | 3.00E+01 | 2.2E-09 | 10,000 | 5.4E-09 | 10,000 | 8.0E-09 | 10,000 | 5.6E-10 | 10,000 | 2.0E-13 | 10,000 |
| Zn | N/A | 4.7E-06 | 10,000 | 7.2E-06 | 10,000 | 7.8E-06 | 10,000 | 8.7E-07 | 10,000 | 2.0E-09 | 10,000 |

Table 5.2-16: Chemical 100m Concentrations for UTR-LZ Sectors F through J

| Chemical | MCL (µg/L) | Sector F Concentrations | | Sector G Concentrations | | Sector H Concentrations | | Sector I Concentrations | | Sector J Concentrations | |
|----------|---------------|----------------------------|---------------------|----------------------------|---------------------|----------------------------|---------------------|----------------------------|---------------------|----------------------------|---------------------|
| | | (µg/L) | Year Peak Occurs | (µg/L) | Year Peak Occurs | (µg/L) | Year Peak Occurs | (µg/L) | Year Peak Occurs | (µg/L) | Year Peak Occurs |
| Ag | N/A | 3.0E-05 | 10,000 | 6.8E-05 | 10,000 | 5.6E-05 | 10,000 | 5.0E-05 | 10,000 | 2.9E-05 | 10,000 |
| As | 1.00E+01 | 2.1E-14 | 10,000 | 4.2E-19 | 10,000 | 2.7E-19 | 10,000 | 1.1E-19 | 10,000 | 6.4E-20 | 10,000 |
| Ba | 2.00E+03 | 6.1E-04 | 10,000 | 2.2E-03 | 10,000 | 2.2E-03 | 10,000 | 2.5E-03 | 10,000 | 2.0E-03 | 10,000 |
| Cd | 5.00E+00 | 2.5E-10 | 10,000 | 8.5E-12 | 10,000 | 2.7E-11 | 10,000 | 3.5E-10 | 10,000 | 4.2E-09 | 10,000 |
| Cr | 1.00E+02 | 1.2E-10 | 10,000 | 9.4E-12 | 10,000 | 1.5E-11 | 10,000 | 1.7E-10 | 10,000 | 2.0E-09 | 10,000 |
| Cu | N/A | 5.7E-02 | 10,000 | 1.5E-01 | 10,000 | 1.3E-01 | 10,000 | 1.3E-01 | 10,000 | 8.3E-02 | 10,000 |
| F | N/A | 9.2E-03 | 10,000 | 3.3E-02 | 10,000 | 3.3E-02 | 10,000 | 3.8E-02 | 10,000 | 3.2E-02 | 10,000 |
| Fe | N/A | 7.3E-20 | 10,000 | <1.0E-30 | 10,000 | <1.0E-30 | 10,000 | <1.0E-30 | 10,000 | 1.0E-29 | 10,000 |
| Hg | 2.00E+00 | 3.4E-35 | 10,000 | <1.0E-30 | 10,000 | <1.0E-30 | 10,000 | <1.0E-30 | 10,000 | <1.0E-30 | 10,000 |
| Mn | N/A | 1.1E-06 | 10,000 | 3.1E-06 | 10,000 | 2.9E-06 | 10,000 | 3.0E-06 | 10,000 | 2.1E-06 | 10,000 |
| N | 1.00E+04 | 3.0E+02 | 4,020 | 1.1E+03 | 4,040 | 1.1E+03 | 4,040 | 1.2E+03 | 4,040 | 1.0E+03 | 4,040 |
| Ni | N/A | 1.3E-14 | 10,000 | 6.6E-15 | 10,000 | 5.0E-15 | 10,000 | 2.0E-15 | 10,000 | 1.6E-15 | 10,000 |
| Pb | 1.50E+01 | 8.6E-44 | 10,000 | <1.0E-30 | 10,000 | <1.0E-30 | 10,000 | <1.0E-30 | 10,000 | <1.0E-30 | 10,000 |
| Se | 5.00E+00 | 2.7E-32 | 10,000 | <1.0E-30 | 10,000 | <1.0E-30 | 10,000 | <1.0E-30 | 10,000 | <1.0E-30 | 10,000 |
| U | 3.00E+01 | 7.0E-20 | 10,000 | 9.1E-27 | 10,000 | 5.2E-27 | 10,000 | 1.3E-27 | 10,000 | 3.7E-29 | 10,000 |
| Zn | N/A | 1.1E-15 | 10,000 | 4.2E-25 | 10,000 | 1.5E-25 | 10,000 | 1.3E-26 | 10,000 | 8.0E-22 | 10,000 |

Table 5.2-17: Chemical 100m Concentrations for UTR-LZ Sectors K and L

| Chemical | MCL (µg/L) | Sector K Concentrations | | Sector L Concentrations | |
|----------|------------|-------------------------|------------------|-------------------------|------------------|
| | | (µg/L) | Year Peak Occurs | (µg/L) | Year Peak Occurs |
| Ag | N/A | 4.3E-05 | 10,000 | 4.1E-05 | 10,000 |
| As | 1.00E+01 | 1.7E-15 | 10,000 | 2.8E-09 | 10,000 |
| Ba | 2.00E+03 | 2.2E-03 | 10,000 | 1.6E-03 | 10,000 |
| Cd | 5.00E+00 | 5.9E-08 | 10,000 | 3.6E-06 | 10,000 |
| Cr | 1.00E+02 | 2.8E-08 | 10,000 | 3.6E-06 | 10,000 |
| Cu | N/A | 1.1E-01 | 10,000 | 8.8E-02 | 10,000 |
| F | N/A | 3.4E-02 | 10,000 | 2.5E-02 | 10,000 |
| Fe | N/A | 2.7E-22 | 10,000 | 2.5E-14 | 10,000 |
| Hg | 2.00E+00 | <1.0E-30 | 10,000 | 1.1E-30 | 10,000 |
| Mn | N/A | 2.6E-06 | 10,000 | 2.5E-06 | 10,000 |
| N | 1.00E+04 | 1.1E+03 | 4,040 | 8.1E+02 | 4,040 |
| Ni | N/A | 1.3E-13 | 10,000 | 2.6E-08 | 10,000 |
| Pb | 1.50E+01 | <1.0E-30 | 10,000 | <1.0E-30 | 10,000 |
| Se | 5.00E+00 | <1.0E-30 | 10,000 | 1.0E-30 | 10,000 |
| U | 3.00E+01 | 2.9E-22 | 10,000 | 2.4E-14 | 10,000 |
| Zn | N/A | 5.4E-16 | 10,000 | 9.2E-10 | 10,000 |

Table 5.2-18: Chemical 100m Concentrations for Gordon Aquifer Sectors A through E

| Chemical | MCL (µg/L) | Sector A Concentrations | | Sector B Concentrations | | Sector C Concentrations | | Sector D Concentrations | | Sector E Concentrations | |
|----------|---------------|----------------------------|---------------------|----------------------------|---------------------|----------------------------|---------------------|----------------------------|---------------------|----------------------------|---------------------|
| | | (µg/L) | Year Peak Occurs | (µg/L) | Year Peak Occurs | (µg/L) | Year Peak Occurs | (µg/L) | Year Peak Occurs | (µg/L) | Year Peak Occurs |
| Ag | N/A | 4.9E-09 | 10,000 | 5.0E-09 | 10,000 | 2.9E-09 | 10,000 | 1.3E-10 | 10,000 | 1.2E-11 | 10,000 |
| As | 1.00E+01 | 1.9E-12 | 10,000 | 2.1E-12 | 10,000 | 1.6E-12 | 10,000 | 6.7E-14 | 10,000 | 1.1E-16 | 10,000 |
| Ba | 2.00E+03 | 4.5E-06 | 10,000 | 4.0E-06 | 10,000 | 2.2E-06 | 10,000 | 6.1E-07 | 10,000 | 1.1E-07 | 10,000 |
| Cd | 5.00E+00 | 1.0E-07 | 10,000 | 1.0E-07 | 10,000 | 6.3E-08 | 10,000 | 2.5E-08 | 10,000 | 1.4E-09 | 10,000 |
| Cr | 1.00E+02 | 9.3E-07 | 10,000 | 8.2E-07 | 10,000 | 4.0E-07 | 10,000 | 2.7E-08 | 10,000 | 7.2E-10 | 10,000 |
| Cu | N/A | 2.6E-06 | 10,000 | 2.5E-06 | 10,000 | 1.3E-06 | 10,000 | 1.7E-07 | 10,000 | 1.5E-07 | 10,000 |
| F | N/A | 9.3E-04 | 9,820 | 8.5E-04 | 9,820 | 4.3E-04 | 9,840 | 2.6E-05 | 9,960 | 1.1E-05 | 10,000 |
| Fe | N/A | 2.1E-18 | 10,000 | 4.2E-18 | 10,000 | 5.7E-18 | 10,000 | 1.7E-19 | 10,000 | 3.5E-23 | 10,000 |
| Hg | 2.00E+00 | <1.0E-30 | 10,000 | <1.0E-30 | 10,000 | <1.0E-30 | 10,000 | <1.0E-30 | 10,000 | <1.0E-30 | 10,000 |
| Mn | N/A | 2.5E-08 | 10,000 | 2.2E-08 | 10,000 | 9.6E-09 | 10,000 | 3.5E-10 | 10,000 | 1.3E-12 | 10,000 |
| N | 1.00E+04 | 2.1E+00 | 4,680 | 1.9E+00 | 4,660 | 1.0E+00 | 4,700 | 2.9E-01 | 4,680 | 3.7E-01 | 5,200 |
| Ni | N/A | 5.8E-09 | 10,000 | 5.0E-09 | 10,000 | 2.3E-09 | 10,000 | 8.7E-11 | 10,000 | 2.9E-13 | 10,000 |
| Pb | 1.50E+01 | <1.0E-30 | 10,000 | <1.0E-30 | 10,000 | <1.0E-30 | 10,000 | <1.0E-30 | 10,000 | <1.0E-30 | 10,000 |
| Se | 5.00E+00 | <1.0E-30 | 10,000 | <1.0E-30 | 10,000 | <1.0E-30 | 10,000 | <1.0E-30 | 10,000 | <1.0E-30 | 10,000 |
| U | 3.00E+01 | 3.8E-18 | 10,000 | 7.3E-18 | 10,000 | 9.8E-18 | 10,000 | 3.0E-19 | 10,000 | 6.4E-23 | 10,000 |
| Zn | N/A | 6.3E-13 | 10,000 | 7.0E-13 | 10,000 | 5.4E-13 | 10,000 | 2.2E-14 | 10,000 | 3.4E-17 | 10,000 |

Table 5.2-19: Chemical 100m Concentrations for GAU Sectors F through J

| Chemical | MCL (µg/L) | Sector F Concentrations | | Sector G Concentrations | | Sector H Concentrations | | Sector I Concentrations | | Sector J Concentrations | |
|----------|------------|-------------------------|------------------|-------------------------|------------------|-------------------------|------------------|-------------------------|------------------|-------------------------|------------------|
| | | (µg/L) | Year Peak Occurs | (µg/L) | Year Peak Occurs | (µg/L) | Year Peak Occurs | (µg/L) | Year Peak Occurs | (µg/L) | Year Peak Occurs |
| Ag | N/A | 2.4E-12 | 10,000 | 2.9E-10 | 10,000 | 2.9E-10 | 10,000 | 2.9E-10 | 10,000 | 9.7E-11 | 10,000 |
| As | 1.00E+01 | 3.7E-23 | 10,000 | 1.4E-15 | 10,000 | 1.4E-15 | 10,000 | 1.4E-15 | 10,000 | 3.8E-16 | 10,000 |
| Ba | 2.00E+03 | 4.0E-08 | 10,000 | 6.9E-06 | 10,000 | 6.9E-06 | 10,000 | 6.9E-06 | 10,000 | 3.3E-06 | 10,000 |
| Cd | 5.00E+00 | 5.2E-14 | 10,000 | 1.9E-07 | 10,000 | 1.8E-07 | 10,000 | 1.8E-07 | 10,000 | 4.7E-08 | 10,000 |
| Cr | 1.00E+02 | 2.5E-14 | 10,000 | 6.7E-07 | 10,000 | 8.0E-07 | 10,000 | 8.0E-07 | 10,000 | 3.5E-07 | 10,000 |
| Cu | N/A | 3.6E-08 | 10,000 | 1.4E-06 | 10,000 | 1.4E-06 | 10,000 | 1.4E-06 | 10,000 | 6.3E-07 | 10,000 |
| F | N/A | 4.6E-06 | 10,000 | 9.0E-04 | 9,940 | 1.1E-03 | 9,900 | 1.1E-03 | 9,900 | 5.8E-04 | 10,000 |
| Fe | N/A | 1.9E-30 | 10,000 | 2.0E-27 | 10,000 | 2.6E-27 | 10,000 | 2.6E-27 | 10,000 | 1.6E-26 | 10,000 |
| Hg | 2.00E+00 | <1.0E-30 | 10,000 | <1.0E-30 | 10,000 | <1.0E-30 | 10,000 | <1.0E-30 | 10,000 | <1.0E-30 | 10,000 |
| Mn | N/A | 5.8E-14 | 10,000 | 1.4E-08 | 10,000 | 1.7E-08 | 10,000 | 1.7E-08 | 10,000 | 7.5E-09 | 10,000 |
| N | 1.00E+04 | 1.5E-01 | 5,220 | 8.8E+00 | 4,740 | 9.9E+00 | 4,740 | 9.9E+00 | 4,740 | 7.6E+00 | 5,240 |
| Ni | N/A | 2.7E-19 | 10,000 | 3.8E-09 | 10,000 | 4.7E-09 | 10,000 | 4.7E-09 | 10,000 | 2.2E-09 | 10,000 |
| Pb | 1.50E+01 | <1.0E-30 | 10,000 | <1.0E-30 | 10,000 | <1.0E-30 | 10,000 | <1.0E-30 | 10,000 | <1.0E-30 | 10,000 |
| Se | 5.00E+00 | <1.0E-30 | 10,000 | <1.0E-30 | 10,000 | <1.0E-30 | 10,000 | <1.0E-30 | 10,000 | <1.0E-30 | 10,000 |
| U | 3.00E+01 | 3.5E-30 | 10,000 | 5.0E-27 | 10,000 | 6.3E-27 | 10,000 | 6.3E-27 | 10,000 | 3.6E-26 | 10,000 |
| Zn | N/A | 6.0E-24 | 10,000 | 4.5E-16 | 10,000 | 4.5E-16 | 10,000 | 4.5E-16 | 10,000 | 1.3E-16 | 10,000 |

Table 5.2-20: Chemical 100m Concentrations for GAU Sectors K and L

| Chemical | MCL (µg/L) | Sector K Concentrations | | Sector L Concentrations | |
|----------|---------------|----------------------------|---------------------|----------------------------|---------------------|
| | | (µg/L) | Year Peak Occurs | (µg/L) | Year Peak Occurs |
| Ag | N/A | 1.9E-10 | 10,000 | 1.5E-09 | 10,000 |
| As | 1.00E+01 | 2.5E-15 | 10,000 | 1.5E-13 | 10,000 |
| Ba | 2.00E+03 | 2.4E-06 | 10,000 | 3.2E-06 | 10,000 |
| Cd | 5.00E+00 | 3.8E-08 | 10,000 | 7.7E-08 | 10,000 |
| Cr | 1.00E+02 | 3.0E-07 | 10,000 | 6.3E-07 | 10,000 |
| Cu | N/A | 7.0E-07 | 10,000 | 1.2E-06 | 10,000 |
| F | N/A | 4.1E-04 | 9,940 | 6.4E-04 | 9,820 |
| Fe | N/A | 8.5E-25 | 10,000 | 5.4E-21 | 10,000 |
| Hg | 2.00E+00 | <1.0E-30 | 10,000 | <1.0E-30 | 10,000 |
| Mn | N/A | 7.1E-09 | 10,000 | 1.6E-08 | 10,000 |
| N | 1.00E+04 | 4.8E+00 | 4,720 | 2.7E+00 | 4,700 |
| Ni | N/A | 1.9E-09 | 10,000 | 3.9E-09 | 10,000 |
| Pb | 1.50E+01 | <1.0E-30 | 10,000 | <1.0E-30 | 10,000 |
| Se | 5.00E+00 | <1.0E-30 | 10,000 | <1.0E-30 | 10,000 |
| U | 3.00E+01 | 1.8E-24 | 10,000 | 1.0E-20 | 10,000 |
| Zn | N/A | 8.2E-16 | 10,000 | 5.0E-14 | 10,000 |

The 100m radionuclide and chemical concentration curves (for 20,000 years) associated with the 12 sectors and three aquifers for the Base Case, are captured in Appendix A.

- Appendix A.1 – 100m Radiological and Chemical Concentrations for the UTR-UZ (Sectors A through L)
- Appendix A.2 – 100m Radiological and Chemical Concentrations for the UTR-LZ (Sectors A through L)
- Appendix A.3 - 100m Radiological and Chemical Concentrations for the Gordon Aquifer (Sectors A through L)

To support further and varied investigation of key radionuclides (e.g., individual disposal unit contributions, peak concentrations beyond the 20,000 year evaluation period), additional 100m groundwater concentrations were calculated using the PORFLOW SDF model. Appendices A.4, A.5, A.6, and A.7 are curves representing 100m key radiological and chemical concentrations for Cases B, C, D, and E, respectively. Appendix C contains 40,000 year curves for the 100m radionuclide concentrations for all of SDF for Case A. Appendix D contains 20,000 year data curves for the 100m radionuclide concentrations for key radionuclides only for selected SDF sources (Vault 1, Vault 4, a single FDC in Sector I, and all FDCs collectively) for Case A.

5.2.2 Key Radionuclide Determination

The purpose of this section is to present the methodology used in determining which radionuclides were most significant and to document which radionuclides would be considered “key.” While all radionuclides identified in the SDF disposal unit inventory (Section 3.3) were included in 100m groundwater modeling efforts, narrowing the catalog of radionuclides to a “key” radionuclide list allowed the analysis to concentrate on the few radionuclides which posed the highest risk, and concentrated modeling efforts on the areas of greatest concern. Only the key radionuclides were included in the PORFLOW seepline modeling runs, with the doses associated with seepline concentrations for the other “non-key” rads calculated by using 35% of the applicable 100m concentrations. The 35% factor is based on the ratio seen between the bounding concentrations for the “key” radionuclides at 100m and the seepline (see Appendix E.1).

The key radionuclides were determined based on the peak all-pathways doses calculated using the 100m groundwater concentrations listed in Section 5.2.1. The peak doses for each individual radionuclide are not necessarily in the same year. Any radionuclide with a peak individual all-pathways dose (assuming Base Case pathways and assumptions) greater than 0.05 mrem/yr was considered a key radionuclide. The key radionuclide determination was conducted based on the peak all-pathways doses within 20,000 years. The screening conclusions are provided in Table 5.2-21. The resulting key radionuclides are Tc-99, I-129, Ra-226, Np-237 and Pa-231. The 0.05 mrem/yr screening threshold was considered sufficiently low enough that no radionuclides that were screened out would contribute appreciably to the peak dose results. The screening evaluation indicated that there were also no radionuclides screened with a peak dose greater than 0.02 mrem/yr but less than 0.05 mrem/yr. In order to evaluate the contribution of the key radionuclides, not only was transport of the key radionuclides modeled, but also transport of the parents of the key radionuclides; U-235 (for Pa-231), Th-230 (for Ra-226), U-234 (for Ra-226), and Pu-238 (for Ra-226) that contributed significantly to the peak dose.

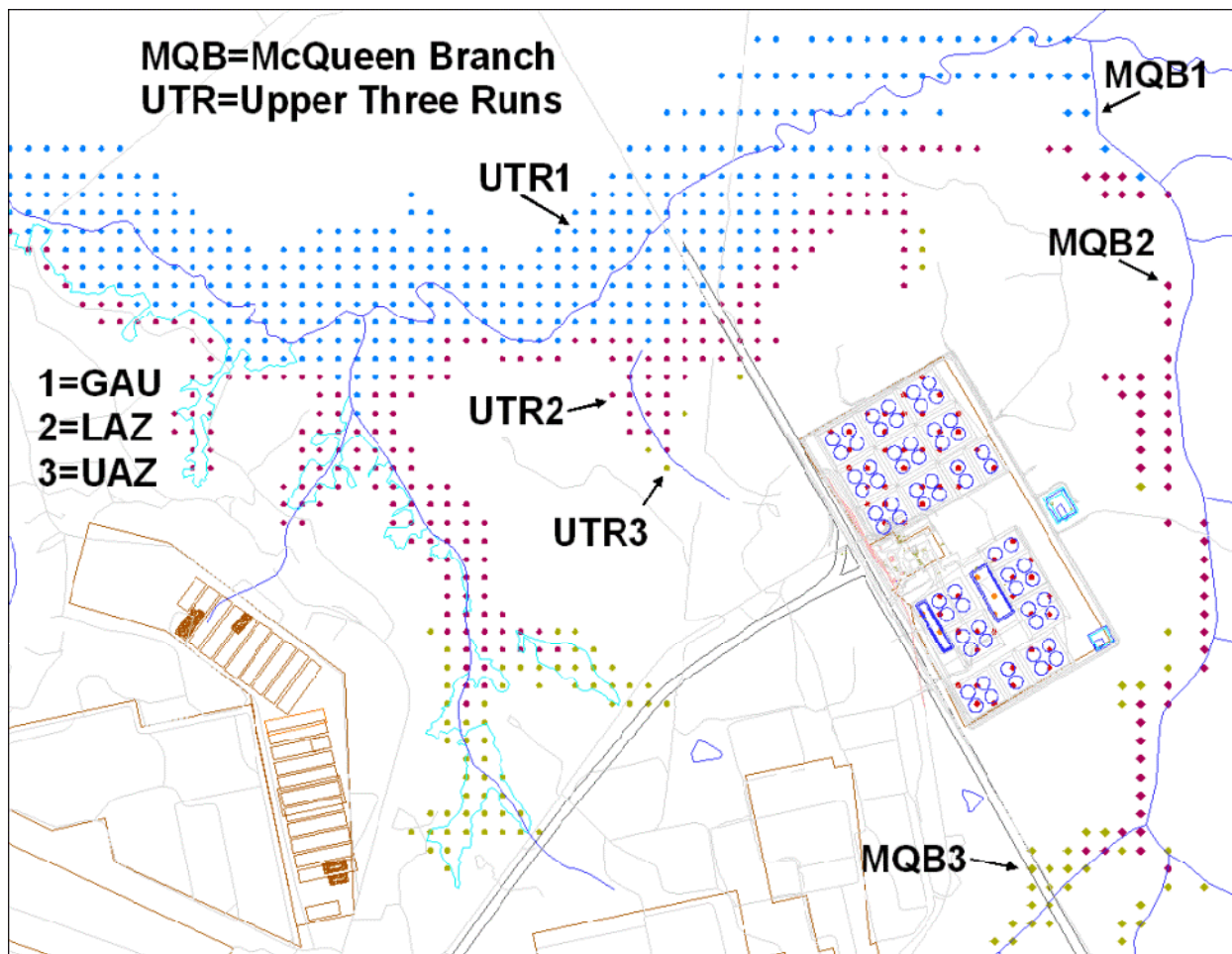
Table 5.2-21: Determination of Key Radionuclides

| Sector | Peak all-Pathways Dose Contribution in 20,000 Years (mrem/yr) | | | | |
|--------|---|-------|--------|--------|--------|
| | Tc-99 | I-129 | Ra-226 | Np-237 | Pa-231 |
| A | 0.8 | 1.3 | 1.9 | 0.1 | < 0.1 |
| B | 0.9 | 1.4 | 2.2 | 0.1 | 0.1 |
| C | 0.3 | 1.3 | 1.2 | 0.1 | < 0.1 |
| D | 0.2 | 1.1 | 0.8 | < 0.05 | < 0.05 |
| E | 0.6 | 1.3 | 1.6 | < 0.05 | < 0.05 |
| F | 0.1 | 1.0 | 0.6 | < 0.05 | < 0.05 |
| G | 0.2 | 2.4 | 0.8 | < 0.05 | < 0.05 |
| H | 0.2 | 2.4 | 0.8 | < 0.05 | < 0.05 |
| I | 0.3 | 2.7 | 0.8 | < 0.05 | < 0.05 |
| J | 0.2 | 2.3 | 0.8 | < 0.05 | < 0.05 |
| K | 0.2 | 2.4 | 0.8 | < 0.05 | < 0.05 |
| L | 0.2 | 1.9 | 0.7 | < 0.05 | < 0.05 |

5.2.3 Groundwater Concentrations at the Seepines

The seepine groundwater concentrations were calculated using the PORFLOW SDF model, which grids the GSA surrounding the SDF. Figure 5.2-8 shows the SDF seepines segregated by aquifer zones (GAU, LAZ, and UAZ) and tributaries (UTR and McQueen Branch) in relation to the SDF. The PORFLOW seepine concentrations were modeled in order to derive doses for applicable dose pathways (e.g., swimming, boating and fishing).

Figure 5.2-8: PORFLOW SDF Seepine Evaluation Sectors



5.3 Air Pathways and Radon Analysis

Section 4.5 describes the method used to determine the potential dose from airborne radionuclides at the 100m boundary. The results in that section provided a dose to a MEI per curie of inventory. The total projected SDF inventory of selected potentially airborne isotopes, as described in Section 3.3, is summarized in Table 5.3-1 for Vault 1, Vault 4 and each of the FDCs. See SRNL-STI-2008-00415 for details on the estimation of all DRFs.

Table 5.3-1: Total Projected SDF Inventory of Gaseous Radionuclides

| Radionuclide | Vault 1 Projected Inventory (Ci) | Vault 4 Projected Inventory (Ci) | FDC Projected Inventory (Ci/each cell) | Total Projected Inventory (Ci)* |
|--------------|----------------------------------|----------------------------------|--|---------------------------------|
| C-14 | 2.6E+00 | 2.7E+01 | 2.0E+00 | 1.6E+02 |
| Cl-36 | 1.5E-03 | 3.0E-03 | 4.2E-04 | 3.1E-02 |
| I-129 | 2.2E-01 | 2.8E-01 | 3.8E-01 | 2.5E+01 |
| Sb-125 | 3.2E-01 | 5.7E+00 | 2.4E-01 | 2.1E+01 |
| Se-79 | 6.0E-01 | 4.6E+01 | 1.4E+00 | 1.4E+02 |
| Sn-126 | 2.0E+00 | 6.4E+00 | 8.2E+00 | 5.3E+02 |
| H-3 | 1.2E+01 | 2.6E+02 | 3.0E+01 | 2.2E+03 |
| Tc-99 | 2.2E+02 | 5.8E+02 | 5.4E+02 | 3.5E+04 |

* Total inventory is equal to Vault 1 + Vault 4 + 64 FDCs

5.3.1 Air Pathways Dose

The dose to the MEI at 100m is estimated to be less than 4.0E-09 mrem/yr. For the air pathways, the flux of eight radionuclides was modeled. Each of these radionuclides reached peak flux within the first 1,000 years of simulation, as shown in Figures 4.5-4 through 4.5-8.

The DRFs determined in Section 4.5 were the result of analysis based on both DDA saltstone and ARP/MCU saltstone for Vaults 1 and 4. Because the DDA saltstone provided the more conservative DRFs, the dose calculations in Tables 5.3-2 and 5.3-3 use the DDA saltstone DRFs. [SRNL-STI-2008-00415] The dose for any FDCs, assumed to contain SWPF saltstone, is shown in Table 5.3-4. [SRNL-STI-2008-00415]

Table 5.3-2: Vault 1 10,000 Year Dose at 100m

| Radionuclide | Ci | Peak Flux (Ci/m ² /yr)/ (Ci/m ²) | Time to Peak Flux (yrs) | 100m DRF (mrem/Ci) | Dose to MEI at 100m (mrem/yr/Ci) | Dose to MEI ^a (mrem/yr) |
|-------------------|---------|---|-------------------------|--------------------|----------------------------------|------------------------------------|
| C-14 | 2.6E+00 | 5.2E-14 | 137 | 3.7E-03 | 1.9E-16 | 5.0E-16 |
| Cl-36 | 1.5E-03 | 2.6E-27 | 282 | 7.9E-03 | 2.0E-29 | 3.1E-32 |
| I-129 | 2.2E-01 | 1.1E-30 | 764 | 5.5E+00 | 6.2E-30 | 1.4E-30 |
| Sb-125 | 3.2E-01 | 4.3E-46 | 4 | 1.1E-01 | 4.8E-47 | 1.5E-47 |
| Se-79 | 6.0E-01 | 5.1E-16 | 292 | 1.1E-02 | 5.6E-18 | 3.4E-18 |
| Sn-126 | 2.0E+00 | 2.0E-70 | 351 | 4.9E+00 | 9.9E-70 | 2.0E-69 |
| H-3 | 1.2E+01 | 3.9E-13 | 10 | 7.7E-05 | 3.0E-17 | 3.6E-16 |
| Tc-99 | 2.2E+02 | 3.4E-77 | 311 | 2.9E-02 | 9.7E-79 | 2.1E-76 |
| Total Dose | | | | | | 8.6E-16 |

(a) Dose to MEI = Peak Flux × DRF

Table 5.3-3: Vault 4 10,000 Year Peak Dose at 100m

| Radionuclide | Ci | Peak Flux (Ci/m ² /yr)/(Ci/m ²) | Time to Peak Flux (yrs) | 100m DRF (mrem/Ci) | Dose to MEI at 100m (mrem/yr/Ci) | Dose to MEI ^a (mrem/yr) |
|-------------------|---------|---|----------------------------------|-----------------------|--|--|
| C-14 | 2.7E+01 | 7.2E-14 | 142 | 3.7E-03 | 2.7E-16 | 7.2E-15 |
| Cl-36 | 3.0E-03 | 3.6E-27 | 292 | 7.9E-03 | 2.8E-29 | 8.5E-32 |
| I-129 | 2.8E-01 | 1.6E-30 | 787 | 1.1E-01 | 1.7E-31 | 4.8E-32 |
| Sb-125 | 5.7E+00 | 5.1E-46 | 5 | 1.1E-02 | 5.6E-48 | 3.2E-47 |
| Se-79 | 4.6E+01 | 7.2E-16 | 304 | 4.9E+00 | 3.5E-15 | 1.6E-13 |
| Sn-126 | 6.4E+00 | 2.8E-70 | 363 | 7.7E-05 | 2.2E-74 | 1.4E-73 |
| H-3 | 2.6E+02 | 5.2E-13 | 10 | 5.5E+00 | 2.9E-12 | 7.5E-10 |
| Tc-99 | 5.8E+02 | 4.7E-77 | 324 | 2.9E-02 | 1.4E-78 | 7.9E-76 |
| Total Dose | | | | | | 7.5E-10 |

(a) Dose to MEI = Peak Flux × DRF

Table 5.3-4: FDCs 10,000 Year Peak Dose at 100m

| Radionuclide | Ci | Peak Flux (Ci/m ² /yr)/(Ci/m ²) | Time to Peak Flux (yrs) | 100m DRF (mrem/Ci) | Dose to MEI at 100m (mrem/yr/Ci) | Dose to MEI ^a (mrem/yr) |
|-------------------|---------|---|----------------------------------|-----------------------|--|--|
| C-14 | 2.0E+00 | 4.3E-14 | 147 | 3.7E-03 | 1.6E-16 | 3.2E-16 |
| Cl-36 | 4.2E-04 | 2.1E-27 | 305 | 7.9E-03 | 1.7E-29 | 7.0E-33 |
| I-129 | 3.8E-01 | 9.2E-31 | 787 | 1.1E-01 | 1.0E-31 | 3.9E-32 |
| Sb-125 | 2.4E-01 | 2.1E-46 | 6 | 1.1E-02 | 2.3E-48 | 5.5E-49 |
| Se-79 | 1.4E+00 | 4.2E-16 | 318 | 4.9E+00 | 2.1E-15 | 2.9E-15 |
| Sn-126 | 8.2E+00 | 1.7E-70 | 380 | 7.7E-05 | 1.3E-74 | 1.1E-73 |
| H-3 | 3.0E+01 | 3.0E-13 | 10 | 5.5E+00 | 1.6E-12 | 4.9E-11 |
| Tc-99 | 5.4E+02 | 2.8E-77 | 337 | 2.9E-02 | 8.0E-79 | 4.3E-76 |
| Total Dose | | | | | | 4.9E-11 |

(a) Dose to MEI = Peak Flux × DRF

The total peak dose for the SDF is then the sum of the dose from Vault 1 (8.6E-16 mrem/yr), the dose from Vault 4 (7.5E-10 mrem/yr) and the dose from each of the FDCs (64 x 4.9E-11 mrem/yr). The potential peak dose by the air pathway is 3.9E-09 mrem/yr.

5.3.2 Instantaneous Radon Flux

Rn-222 flux results from the decay of five radionuclides: Pu-238, Ra-226, Th-230, U-234, and U-238. As shown in Figures 4.5-10 through 4.5-14, with the exception of Ra-226, the peak flux of Rn-222 occurs at the end of the simulation period (10,000 years). [SRNL-STI-2008-00415] This is due to the long half-life for each of the parent radionuclides. For Ra-226, the peak flux of Rn-222 occurs within the first year of the simulation. The peak dose of radon for the performance period is assumed to be at 10,000 years. The total inventory of radionuclides contributing to the radon flux is summarized in Table 5.3-5.

Table 5.3-5: SDF Inventory of Radionuclides Producing Rn-222

| Radionuclide | Vault 1 Inventory (Ci) | Vault 4 Inventory (Ci) | FDC Inventory (Ci/each cell) |
|--------------|------------------------|------------------------|------------------------------|
| Pu-238 | 1.6E-02 | 9.1E+03 | 1.7E+02 |
| Ra-226 | 1.3E-06 | 4.1E+00 | 7.8E-07 |
| Th-230 | 8.2E-01 | 7.5E+00 | 1.9E-01 |
| U-234 | 5.6E-01 | 2.6E+01 | 1.3E-01 |
| U-238 | 1.5E-02 | 5.9E-01 | 1.0E-01 |

The instantaneous radon flux is found for each disposal unit by multiplying the peak flux by the total inventory of the disposal unit divided by the surface area of the unit. As shown in Tables 5.3-6, 5.3-7 and 5.3-8 the peak instantaneous radon flux, which occurs above Vault 1, is 2.0E-13 pCi/m²/sec.

Table 5.3-6: Peak Rn-222 Flux above Vault 1

| Parent Source | Vault 1 Inventory (Ci) | Vault 1 Inventory (Ci/m ²) ^a | Peak Instantaneous Rn-222 flux at Land Surface | |
|---------------|------------------------|---|--|---------------------------|
| | | | (pCi/m ² /sec) / (Ci/m ²) | (pCi/m ² /sec) |
| Pu-238 | 1.6E-02 | 2.8E-06 | 3.4E-14 | 9.5E-20 |
| Ra-226 | 1.3E-06 | 2.3E-10 | 1.4E-09 | 3.3E-19 |
| Th-230 | 8.2E-01 | 1.5E-04 | 1.3E-09 | 1.9E-13 |
| U-234 | 5.6E-01 | 1.0E-04 | 9.7E-11 | 9.7E-15 |
| U-238 | 1.5E-02 | 2.7E-06 | 1.2E-12 | 3.1E-18 |
| Total | | | | 2.0E-13 |

(a) Total area above Vault 1 is 5,574m²

Table 5.3-7: Peak Rn-222 Flux above Vault 4

| Parent Source | Vault 4 Inventory (Ci) | Vault 4 Inventory (Ci/m ²) ^a | Peak Instantaneous Rn-222 flux at Land Surface | |
|---------------|------------------------|---|--|---------------------------|
| | | | (pCi/m ² /sec) / (Ci/m ²) | (pCi/m ² /sec) |
| Pu-238 | 9.1E+03 | 8.2E-01 | 1.4E-16 | 1.2E-16 |
| Ra-226 | 3.6E-06 | 3.2E-10 | 5.9E-12 | 1.9E-21 |
| Th-230 | 7.4E+00 | 6.6E-04 | 5.5E-12 | 3.6E-15 |
| U-234 | 5.1E+00 | 4.6E-04 | 4.0E-13 | 1.8E-16 |
| U-238 | 5.9E-01 | 5.3E-05 | 4.8E-15 | 2.5E-19 |
| Total | | | | 3.9E-15 |

(a) Total area above Vault 4 is 11,148m²

Table 5.3-8: Peak Rn-222 Flux above FDCs

| Parent Source | Vault 4 Inventory (Ci) | Vault 4 Inventory (Ci/m ²) ^a | Peak Instantaneous Rn-222 flux at Land Surface | |
|---------------|------------------------|---|--|---------------------------|
| | | | (pCi/m ² /sec) / (Ci/m ²) | (pCi/m ² /sec) |
| Pu-238 | 9.1E+03 | 8.2E-01 | 1.4E-16 | 1.2E-16 |
| Ra-226 | 4.1E+00 | 3.7E-04 | 5.9E-12 | 2.2E-15 |
| Th-230 | 7.5E+00 | 6.7E-04 | 5.5E-12 | 3.7E-15 |
| U-234 | 2.6E+01 | 2.3E-03 | 4.0E-13 | 9.3E-16 |
| U-238 | 5.9E-01 | 5.3E-05 | 4.8E-15 | 2.5E-19 |
| Total | | | | 6.9E-15 |

(a) Total area above each FDC is 1642m²

5.4 Biotic Pathways

The MOP exposure pathways are discussed in detail in Section 4.2.4.1. The SDF MOP scenario with 100m well water as a primary water source is graphically represented in Figure 4.2-43. Provided below are the individual elements of the MOP biotic pathways that were identified for analysis and inclusion in the MOP scenario. The GoldSim computer code was used to calculate doses following the dose formulas provided below and utilizing the PORFLOW calculated 100m and seepage concentrations as inputs. Unless otherwise noted, formulas were based on those used in LADTAP model or in the PA for INEEL Tank Farm. [WSRC-STI-2006-00123, DOE-ID-10966] While these documents were used as guides for the formulas, ultimately the basis for all the formulas can be traced to Regulatory Guide 1.109.

5.4.1 Member of the Public at the 100m Well Dose Pathways

The MOP exposure pathways detailed below are used in calculating the dose to a MOP receptor with 100m well water as a primary water source. All transfer times are assumed negligible due to the half lives of the radionuclides and the long term analysis of the PA. Unit conversions are not explicitly stated in the equations, but are coded into GoldSim.

5.4.1.1 Member of the Public at the 100m Well Ingestion Dose Pathways

Ingestion of Water

The drinking water exposure route assumes the receptor uses a well as a drinking water source located 100m from the SDF. The incidental ingestion of water from showering and during recreational activities is assumed to be negligible when compared to ingestion of drinking water. The dose from consumption of drinking water is calculated using the following formula.

$$D = C_{GW} \times U_W \times DCF$$

were:

| | | |
|----------|---|--|
| D | = | dose from 1 year's consumption of contaminated media; in this equation, groundwater (rem/yr) |
| C_{GW} | = | radionuclide concentration in groundwater from a well (pCi/L) |
| U_W | = | human consumption rate of water (L/yr), Table 4.6-7 |
| DCF | = | ingestion dose conversion factor (rem/μCi), Table 4.7-1 |

Ingestion of Beef and Milk

The beef and dairy exposure route assumes cattle drink contaminated well water and eat contaminated fodder and the receptor in turn consumes the contaminated beef and milk from the cattle. Beef and milk are treated separately. The dose is calculated using the following formula.

Beef:

$$D = T_B \times (FF_B \times C_f \times Q_{FB} + C_{GW} \times Q_{WB}) \times DCF \times U_B \times F_B$$

Milk:

$$D = T_M \times (FF_M \times C_f \times Q_{FM} + C_{GW} \times Q_{WM}) \times DCF \times U_M \times F_M$$

where:

| | | |
|----------|---|---|
| T_B | = | beef transfer coefficient (d/kg), Table 4.6-3 |
| T_M | = | milk transfer coefficient (d/L), Table 4.6-2 |
| FF_i | = | beef or milk cattle intake fraction from irrigated field/pasture, Table 4.6-7 |
| C_f | = | radionuclide concentration in fodder (pCi/kg) |
| Q_{Fi} | = | consumption rate of fodder by beef or milk cattle (Kg/d), Table 4.6-7 |
| C_{GW} | = | radionuclide concentration in groundwater from a well (pCi/L) |
| Q_{Wi} | = | consumption rate of water by beef or milk cattle (L/d), Table 4.6-7 |
| DCF | = | ingestion dose conversion factor (rem/μCi), Table 4.7-1 |
| U_B | = | human consumption rate of beef (kg/yr), Table 4.6-7 |
| U_M | = | human consumption rate of milk (L/yr), Table 4.6-7 |
| F_B | = | fraction of meat produced locally (unitless), Table 4.6-5 |
| F_M | = | fraction of milk produced locally (unitless), Table 4.6-5 |

Ingestion of Vegetables

The dose to humans from ingestion of contaminated leafy vegetables and produce is calculated assuming two contamination routes: (1) direct deposition of contaminated irrigation water on plants and (2) deposition of contaminated irrigation water on soil followed by root uptake by plants. Leafy vegetables and produce are treated separately. The dose is calculated using:

$$D = C_{GW} \times I \times (LEAF + ROOT) \times DCF \times (U_{LV} \times k + U_{OV}) \times FV \times e^{-\lambda_e t_i}$$

$$LEAF = \frac{r \times (1 - e^{-\lambda_e t_v})}{Y_v \times \lambda}$$

$$ROOT = \frac{T_{SV} \times (1 - e^{-\lambda_i t_b})}{\rho_s \times \lambda_i}$$

$$\lambda_e = \lambda_i + \lambda_w$$

where:

| | | |
|-------------|---|--|
| C_{GW} | = | radionuclide concentration in groundwater from a well (pCi/L) |
| I | = | irrigation rate (L/d/m ²), Table 4.6-6 |
| $LEAF$ | = | radionuclide concentration in the vegetable's leaves (m ² d/kg) |
| $ROOT$ | = | radionuclide concentration in the vegetable's roots (m ² d/kg) |
| DCF | = | ingestion dose conversion factor (rem/μCi), Table 4.7-1 |
| U_{LV} | = | human consumption rate of leafy vegetables (kg/yr), Table 4.6-7 |
| U_{OV} | = | human consumption rate of other vegetables (produce) (kg/yr), Table 4.6-7 |
| k | = | fraction retention of deposition on leaves (unitless) [1] |
| FV | = | fraction of leafy vegetables and produce produced locally (unitless), Table 4.6-5 |
| r | = | fraction of material deposited on leaves that is retained (unitless), Table 4.6-6 |
| λ_e | = | weathering and radiological decay constant (L/d) |
| λ_w | = | weathering decay constant (0.0495/d) |
| t_V | = | time vegetables are exposed to irrigation (d), Table 4.6-5 |
| Y_V | = | vegetation production yield (kg/m ²), Table 4.6-5 |
| T_{StV} | = | soil to vegetable ratio (unitless), Table 4.6-1 |
| ρ_S | = | surface soil density (kg/m ²), Table 4.6-6 |
| t_b | = | buildup time of radionuclides in soil, Table 4.6-5 |
| λ_i | = | radiological decay constant |
| t_t | = | transport time (d), assumed to be zero |

Ingestion of Fish

The fish exposure route assumes fish are caught from a stream contaminated from the aquifer with the highest concentration, and the receptor in turn consumes the contaminated fish. The dose is calculated using the following formula.

$$D = C_S \times U_F \times T_F \times DCF$$

where:

| | | |
|-------|---|---|
| C_S | = | radionuclide concentration in groundwater at the seepline (pCi/L) |
| U_F | = | human consumption rate of finfish (kg/yr), Table 4.6-7 |
| T_F | = | fish bioaccumulation factor (L/kg), Table 4.6-4 |
| DCF | = | ingestion dose conversion factor (rem/μCi), Table 4.7-1 |

Ingestion of Soil

The soil ingestion exposure route assumes soil is irrigated with groundwater from a 100m well and the receptor in turn consumes the contaminated soil. For simplicity and conservatism, the soil ingested is assumed to be groundwater. This formula was derived following the approach of the previous pathway calculations. The dose is calculated using the following formula.

$$D = \frac{C_{GW} \times DCF \times U_D}{\rho_W}$$

where:

- C_{GW} = radionuclide concentration in groundwater from a well (pCi/L)
- DCF = ingestion dose conversion factor (rem/μCi), Table 4.7-1
- U_D = human consumption rate of dirt (kg/yr), Table 4.6-7
- ρ_W = density of water (g/ml)

5.4.1.2 Member of the Public at the 100m Well Direct Exposure Dose Pathways

Direct Exposure from Irrigated Soil

The irrigated soil direct exposure route assumes soil is irrigated with groundwater from a 100m well and the receptor in turn is exposed during time spent caring for a garden. The dose is calculated using the following formula.

$$D = C_D \times F_G \times DCF$$

where:

- C_D = radionuclide concentration in irrigated soil (pCi/m³)
- DCF = external dose conversion factor, 15cm (rem/yr per μCi/m³), Table 4.7-1
- F_G = fraction of time spent in garden (unitless), Table 4.6-7

Direct Exposure from Swimming

The swimming direct exposure route assumes the receptor receives dose from swimming in a stream contaminated from the aquifer with the highest concentration. The dose is calculated using the following formula.

$$D = GF_S \times t_S \times C_S \times DCF$$

where:

- DCF = external dose conversion factor, water immersion (rem/yr per $\mu\text{Ci}/\text{m}^3$), Table 4.7-1
- GF_S = swimming geometry factor, 1.0 (unitless)
- t_S = time per year spent swimming (hr/yr), Table 4.6-7
- C_S = radionuclide concentration in groundwater at the seepline (pCi/L)

Direct Exposure from Fishing/Boating

The fishing/boating direct exposure route assumes the receptor receives dose from fishing or boating in a stream contaminated from the aquifer with the highest concentration. The dose is calculated using the following formula.

$$D = GF_B \times t_B \times C_S \times DCF$$

where:

- DCF = external dose conversion factor, water immersion (rem/yr per $\mu\text{Ci}/\text{m}^3$), Table 4.7-1
- GF_B = boating geometry factor, 0.5 (unitless)
- t_B = time per year spent boating (hr/yr), Table 4.6-7
- C_S = radionuclide concentration in groundwater at the seepline (pCi/L)

5.4.1.3 Member of the Public at the 100m Well Inhalation Dose Pathways

Inhalation during Irrigation

The irrigation inhalation exposure route assumes soil is irrigated with groundwater from a 100m well and the receptor in turn is exposed by breathing while the garden is irrigated, but only during time spent caring for the garden. For simplicity and conservatism, the source material is the moisture contained within the air with equal concentrations as the groundwater. No resistance to vaporization (i.e., vapor pressure) was used. This formula was derived following the approach of the previous pathway calculations. The dose is calculated using the following formula.

$$D = \frac{C_{GW} \times DCF \times U_A \times F_G \times C_{WA}}{\rho_W}$$

where:

| | | |
|----------|---|---|
| C_{GW} | = | radionuclide concentration in groundwater from a well (pCi/L) |
| DCF | = | inhalation dose conversion factor (rem/ μ Ci), Table 4.7-1 |
| U_A | = | air intake (m^3/yr), Table 4.6-7 |
| F_G | = | fraction of time spent in garden exposed to soil irrigated with contaminated ground water (unitless), Table 4.6-7 |
| C_{WA} | = | water contained in air at ambient conditions, (g/m^3) [$10 \text{ g}/\text{m}^3$] |
| ρ_W | = | water density (g/ml) |

Inhalation during Showering

The showering inhalation exposure route assumes the receptor is exposed by breathing humid air within the shower. The source of water for the shower is a well 100m from the SDF. For simplicity and conservatism, the source material is the moisture contained within the air with equal concentrations as the groundwater. No resistance to vaporization (i.e., vapor pressure) was used, adding to the conservatism. For example, heavy elements would be greatly influenced by this assumption because they would be less likely to volatilize. This formula was derived following the approach of the previous pathway calculations. The dose is calculated using the following formula.

$$D = \frac{C_{GW} \times DCF \times U_A \times t_S \times C_{WS}}{\rho_W}$$

where:

| | | |
|----------|---|---|
| C_{GW} | = | radionuclide concentration in groundwater from a well (pCi/L) |
| DCF | = | inhalation dose conversion factor (rem/ μ Ci), Table 4.7-1 |
| U_A | = | air intake (m^3/yr), Table 4.6-7 |
| t_S | = | time spent in shower (min/d), Table 4.6-7 GoldSim uses fraction of time [$0.0069 = 10 \text{ min}/\text{d}$] |
| C_{WS} | = | water contained in air at shower conditions, (g/m^3) [$41 \text{ g}/\text{m}^3$] |
| ρ_W | = | water density (g/ml) |

Inhalation of Dust from Irrigated Soil

The irrigation soil inhalation exposure route assumes soil is irrigated with groundwater from a 100m well and the receptor is exposed by breathing dust during time spent caring for a garden. This formula was derived following the approach of the previous pathway calculations. The dose is calculated using the following formula.

$$D = \frac{U_A \times L_{SLA} \times C_D \times DCF \times F_G}{\rho_{SS}}$$

where:

| | | |
|-------------|---|---|
| U_A | = | air intake (m^3/yr), Table 4.6-7 |
| L_{SiA} | = | soil loading in air while working in a garden (kg/m^3), Table 4.6-6 |
| C_D | = | radionuclide concentration in soil irrigated with water from a well (pCi/m^3) |
| DCF | = | inhalation dose conversion factor ($\text{rem}/\mu\text{Ci}$), Table 4.7-1 |
| F_G | = | fraction of time spent in garden exposed to soil irrigated with contaminated ground water (unitless), Table 4.6-7 |
| ρ_{SS} | = | density of sandy soil (g/cm^3) |

Inhalation During Swimming

The swimming inhalation exposure route assumes a stream contaminated from the aquifer and the receptor inhales saturated air. For simplicity and conservatism, the amount of moisture contained in the inhaled air is assumed to be groundwater. The dose is calculated using the following formula.

$$D = \frac{U_A \times GF_S \times t_S \times C_{SW} \times DCF \times C_{WiA}}{\rho_W}$$

where:

| | | |
|-----------|---|---|
| U_A | = | air intake (m^3/yr), Table 4.6-7 |
| GF_S | = | swimming geometry factor, 1.0 (unitless) |
| t_S | = | time per year spent swimming (hr/yr), Table 4.6-7 |
| C_{SW} | = | radionuclide concentration in water from the stream (undiluted aquifer) (pCi/L) |
| DCF | = | inhalation dose conversion factor ($\text{rem}/\mu\text{Ci}$), Table 4.7-1 |
| C_{WiA} | = | water contained in air at ambient conditions, (g/m^3) [$10 \text{ g}/\text{m}^3$] |
| ρ_W | = | water density (g/ml) |

5.5 Dose Analysis

The peak total doses are calculated utilizing the pathways identified in Section 5.4 for a MOP at the 100m well for the Base Case (Case A). A peak dose is identified for the 10,000 year performance period. In order to provide additional insight into the modeling, a peak dose is also identified for a 20,000 year period after SDF closure. Finally, a peak dose associated with the key radionuclides is calculated through 40,000 years.

5.5.1 Member of the Public at 100m Groundwater Pathways Dose Results

The groundwater pathways peak doses for the twelve 100m sectors (A-L) are calculated using the peak concentration for each radionuclide in the Sector (a discussion of how peak concentrations are determined by sector is provided in Section 5.2). These groundwater pathways peak doses are the total dose associated with all the individual 100m well pathways identified in Section 5.4.

5.5.1.1 Member of the Public 100m Peak Annual Groundwater Pathways Dose

Table 5.5-1 shows a comparison of the 100m peak groundwater pathways doses for the twelve different 100m sectors within both 10,000 and 20,000 years. In calculating the peak groundwater pathways dose, the highest radionuclide concentration within the vertical computational meshes is used from each of the three distinct aquifers modeled (UTR-UZ, UTR-LZ, and the Gordon Aquifer).

Table 5.5-1: 100m MOP Peak Groundwater Pathways Dose by Sector

| Sector | Peak Dose in 10,000 Years | Peak Dose in 20,000 Years |
|--------|---------------------------|---------------------------|
| A | 1.2 mrem/yr | 2.6 mrem/yr (year 15,080) |
| B | 1.4 mrem/yr | 2.9 mrem/yr (year 15,080) |
| C | 0.7 mrem/yr | 2.0 mrem/yr (year 15,080) |
| D | 0.5 mrem/yr | 1.6 mrem/yr (year 15,080) |
| E | 1.0 mrem/yr | 2.3 mrem/yr (year 15,080) |
| F | 0.3 mrem/yr | 1.3 mrem/yr (year 15,080) |
| G | 0.4 mrem/yr | 2.8 mrem/yr (year 15,080) |
| H | 0.4 mrem/yr | 2.8 mrem/yr (year 15,080) |
| I | 0.4 mrem/yr | 3.1 mrem/yr (year 15,080) |
| J | 0.4 mrem/yr | 2.7 mrem/yr (year 15,080) |
| K | 0.4 mrem/yr | 2.8 mrem/yr (year 15,080) |
| L | 0.4 mrem/yr | 2.3 mrem/yr (year 15,080) |

Note: Sectors illustrated in Figure 5.2-1

The highest overall peak groundwater pathways dose in the 10,000 year performance period is associated with Sector B. The Sector B 10,000 year dose is dominated by contaminants from Vault 4. Figure 5.5-1 shows the peak doses to a 100m MOP receptor over time during the performance period (10,000 years) for the 12 100m sectors.

The highest overall peak groundwater pathways dose within 20,000 years is associated with Sector I. The 20,000 year peak dose in Sector I is dominated by contaminants from the FDCs. Figure 5.5-2 shows the 100m MOP receptor doses within 20,000 years for the 12 100m sectors.

All 12 sectors show a gradual upsweep in doses over the 10,000 year timeframe. The difference in peak dose between the sectors is attributable to variability among the individual disposal units and the difference in flow paths (see Table 5.2-2 and Figures 5.2-2, 5.2-3 and 5.2-4). A steady increase can be seen in the doses beginning in year 2,000 and reaching a plateau near year 6,500. This increase coincides with an increase in the infiltration through the closure cap system. The increase in infiltration affects all the disposal units equally, and increases infiltration from approximately 0 inches at the time of SDF closure to 10 inches from year 500 through 5,400 (see Figure 4.2-3). After year 5,400 the model uses a steady infiltration rate of 10.3 inches through the closure cap.

As indicated in Figure 5.5-1, the dose for each of the 12 sectors remains in the same relative order of magnitude during the 10,000 year period for a MOP at the 100m boundary. The results reflect the inventory of the various disposal units. Those sectors not directly impacted within 10,000 years by release from Vault 4 (i.e., Sectors E through L) have doses resulting from fish ingestion, which is tied to the seepage and is sector independent. The impact of individual radionuclides to the doses is discussed in detail in Section 5.5.1.2. Overall, Figures 5.5-1 and 5.5-2 indicate a relatively steady release of contaminants from the SDF to the environment over time. This is accomplished using the various man-made barriers available during the SDF construction and closure. There are several factors that help ensure that the key radionuclides all remain relatively immobile throughout the SDF 10,000 year performance period, (1) an effective and long lasting closure cap system, (2) a disposal unit concrete structure with sulfate resistant barriers and materials, (3) the effective binding matrix of the salt contaminants in the saltstone monolith, and (4) the reducing properties of the saltstone.

Figure 5.5-1: 100m MOP Peak Groundwater Pathways Dose within 10,000 Years, Sectors A-L

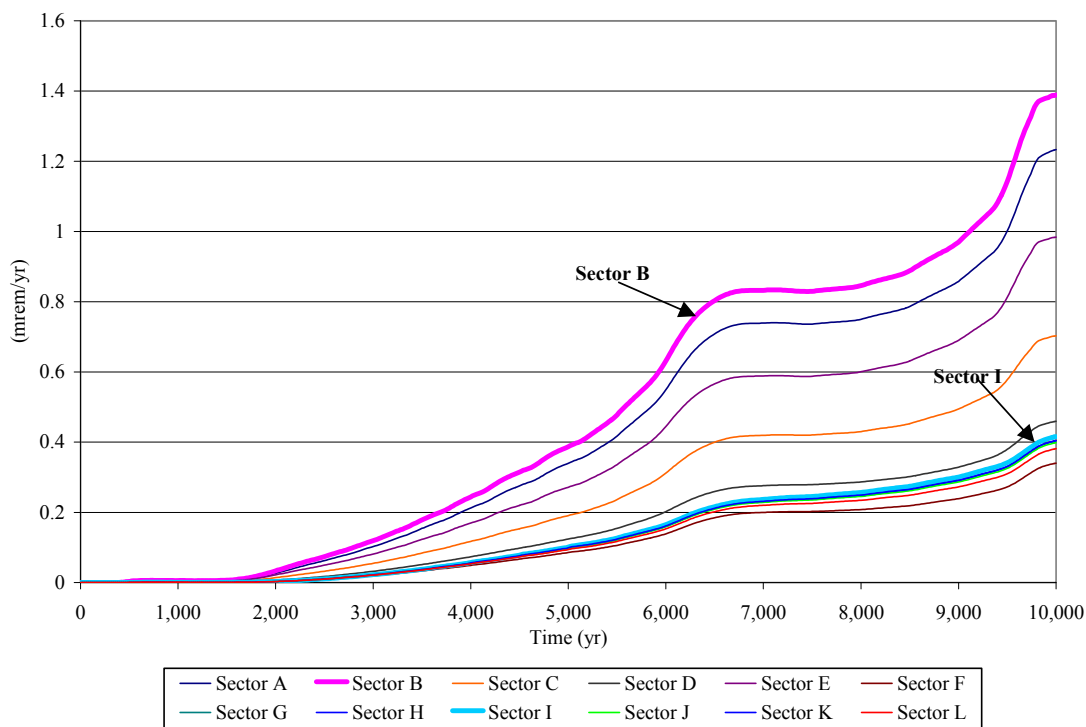
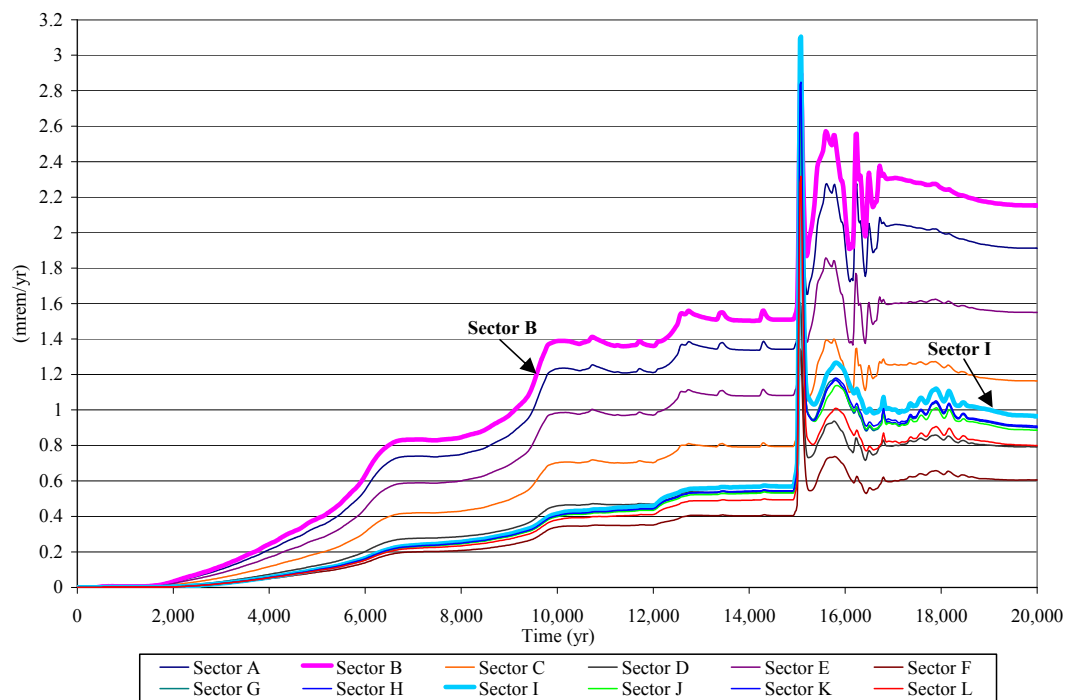


Figure 5.5-2: 100m MOP Peak Groundwater Pathways Dose within 20,000 Years, Sectors A-L



5.5.1.2 Individual Radionuclide Contributions to the MOP 100m Peak Annual Groundwater Pathways Dose

Table 5.5-2 shows the relative contribution from the key radionuclides to the Sector B 100m groundwater pathways dose over 10,000 years. Figure 5.5-3 shows the relative contribution from the key radionuclides to the 1.4 mrem/yr Sector B peak groundwater pathways dose. The peak groundwater pathways dose to a MOP at 100m during the 10,000 year performance period is primarily associated with Ra-226 (94%) and I-129 (4%). Figure 5.5-4 shows the relative contribution from the key radionuclides to the 2.9 mrem/yr Sector B peak groundwater pathways dose in 20,000 years. Figure 5.5-5 and Table 5.5-3 display the relative contributions from the key radionuclides to the Sector I 100m groundwater pathways dose over 20,000 years.

Table 5.5-2: Sector B 100m MOP Peak Groundwater Pathways Dose in 10,000 Years

| Radionuclide | Contribution to Sector B Peak dose at year 10,000 (mrem/yr) | Percentage of Total Peak Dose |
|--------------|---|-------------------------------|
| Ra-226 | 1.3 | 94% |
| I-129 | 0.05 | 4% |
| Others | <0.05 (each) | 2% (<1% each) |
| Total | 1.4 | 100% |

Figure 5.5-3: Contributors to the Sector B 100m Peak Groundwater Pathways Dose, 10,000 Years

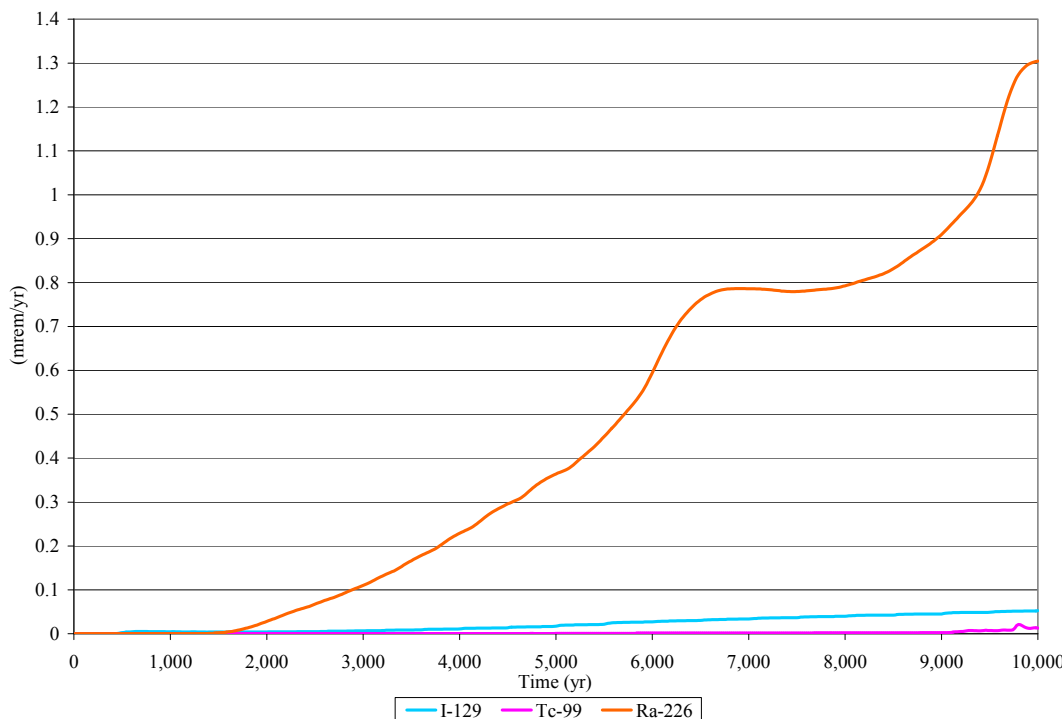


Figure 5.5-4: Contributors to the Sector B 100m Peak Groundwater Pathways Dose, 20,000 Years

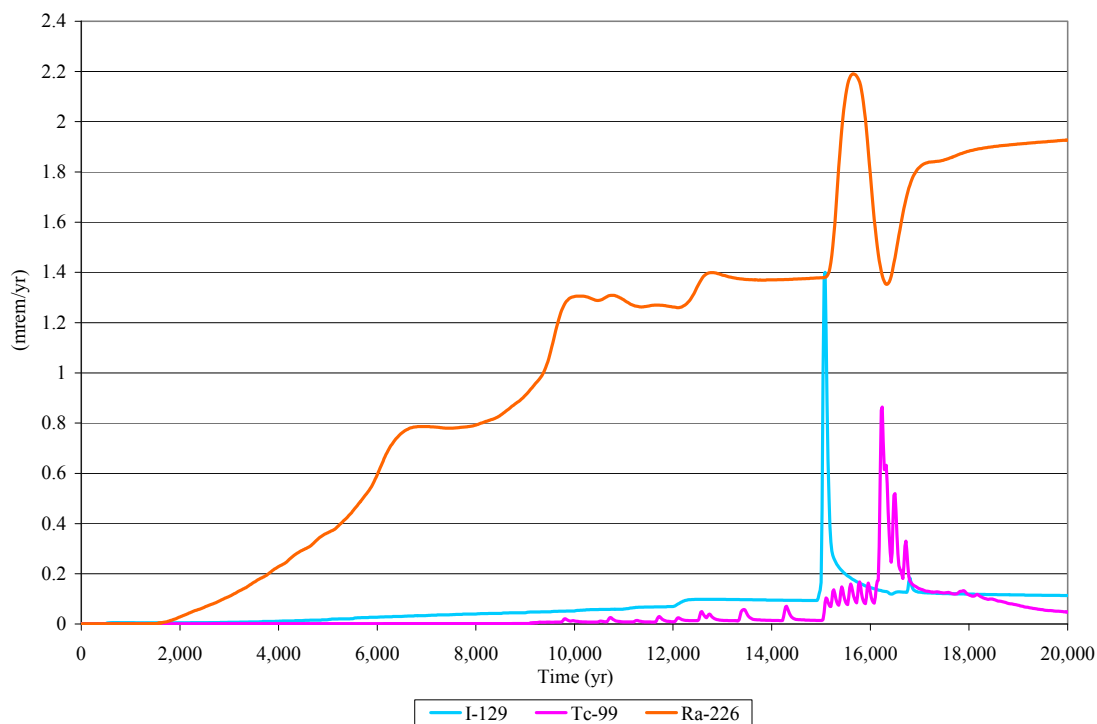


Figure 5.5-5: Contributors to the Sector I 100m Peak Groundwater Pathways Dose, 20,000 Years

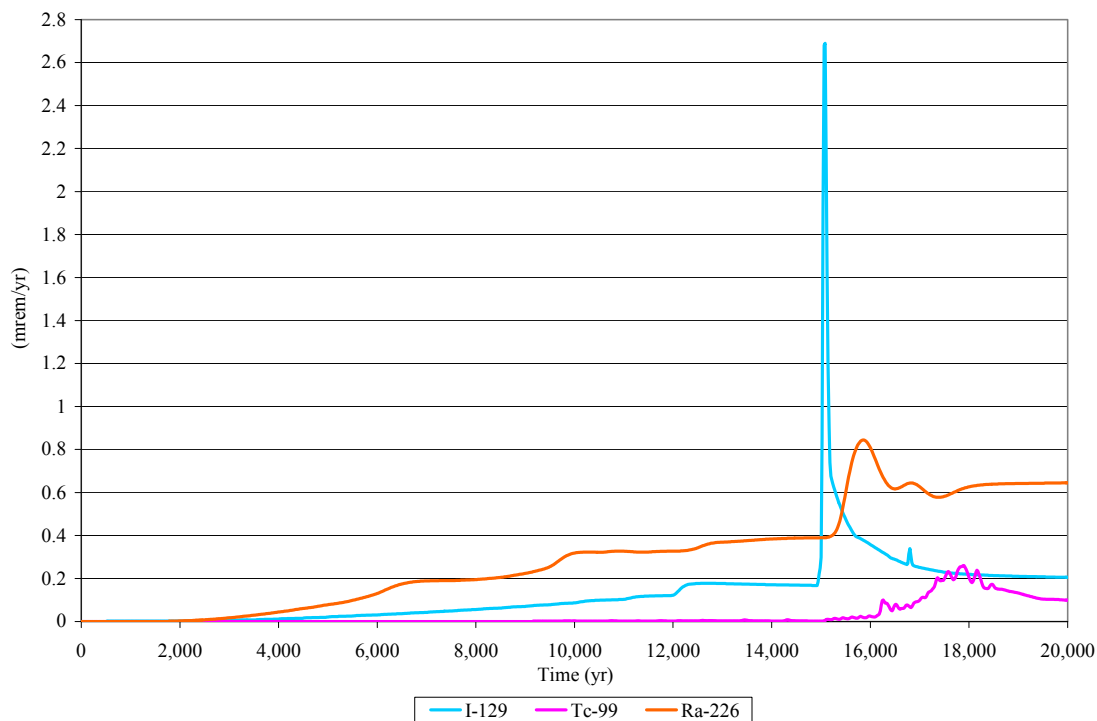


Table 5.5-3: Sector I 100m MOP Peak Groundwater Pathways Dose in 20,000 Years

| Radionuclide | Contribution to Sector I Peak Dose at Year 15,080 (mrem/yr) | Percentage of Total Peak Dose |
|---------------------|--|--|
| I-129 | 2.7 | 87% |
| Ra-226 | 0.3 | 13% |
| Others | <0.01 (each) | <1% |
| Total | 3.1 | 100% |

Sector B has the highest dose within 10,000 years because of the contribution of Ra-226. Figure 5.5-3 shows two uplifts during the 10,000 year timeframe associated with Ra-226. The first uplift of dose occurs during the 5,500 to 6,500 year timeframe, and the second Ra-226 uplift occurs during the 9,000 to 10,000 year timeframe. Ra-226 is at the 100m boundary due to it being a daughter product of Th-230, rather than as a part of the initial inventory. The 5,500 to 6,500 year uplift in Sector B Ra-226 dose is associated with the release of Ra-226, and the Ra-226 parents. Sector B receives the largest contribution of Th-230 via Vault 4. The early uplift seen in Figure 5.5-3 is associated with the steady increase of the Ra-226 parent radionuclides dispersion from the wall inventory of Vault 4, coinciding with an increase of closure cap infiltration. The later uplift is associated with the Ra-226 parent radionuclides release from Vault 4 due to the degeneration of Vault 4's roof hydraulic conductivity. The 20,000 year dose results for Sector B at 100m continue to be heavily influenced by Ra-226 with a total peak dose at 15,080 years due to the steady contribution of Ra-226, and the peak at this year associated with I-129 (i.e., the year 15,080 I-129 dose contribution is 1.4 mrem/yr), as seen in Figure 5.5-4.

As discussed earlier, Sector I produces the highest overall dose results for the 20,000 year timeframe (3.1 mrem/yr). The Sector I peak is dominated by the contribution of I-129 (87%) at year 15,080. Figures 5.5-4 and 5.5-5 show the Sector B and Sector I I-129 peaks both occur at approximately year 15,000. The reason for the uplift and the timing of the uplift is explained in the, (1) timing of the disposal unit release, (2) the material properties of I-129 (e.g., K_d), and (3) the inventory location of I-129.

- (1) The significant spike of I-129 in Sector I at 15,080 years is due to the FDC wall hydraulic conductivity increasing by four orders of magnitude at year 15,080. This factor results in the vertical spike of I-129 at 15,080 years in Figure 5.5-5.
- (2) I-129 has relatively low retardation factors in cementitious materials and soil materials that allow I-129 to move quickly through the environment to the 100m boundary once it has exited the FDC. The K_d range of I-129 in cementitious materials is 4 mL/g to 15 mL/g and in soils is 0.0 mL/g to 0.6 mL/g depending on the chemical state of the cementitious materials or solid type.

- (3) Sector I is responsible for the highest I-129 peak location at the 100m SDF boundary because of the I-129 inventory in the FDCs. As can be seen in Table 3.3-1 and Table 3.3-3, the I-129 inventory of each of Vaults 1 and 4 ($1.1\text{E-}1$ Ci and $2.8\text{E-}1$ Ci) are roughly equal to that of an individual FDCs inventory ($3.8\text{E-}1$ Ci) in Table 3.3-5. Thus, as the I-129 release becomes dominant, Sector I, which is influenced heavily by the simultaneous release of the FDC I-129 inventory, becomes the peak sector.

Since Tc-99 moves relatively quickly in an oxidized cementitious environment ($K_d = 0.8$ mL/g middle age and 0.5 mL/g old age, Table 4.2-18), once the reducing capacity in the disposal unit has been depleted, the Tc-99 moves rapidly to the 100m well. The Sector B Tc-99 peak occurs at approximately year 16,100. This peak coincides with the transition of the Vault 4 wall concrete from reducing to oxidizing conditions (Table 4.4-7).

5.5.1.3 Individual Disposal Unit Contributions to a MOP 100m Peak Annual Groundwater Pathways Dose

Table 5.5-4 shows the relative contributions from the various distinct waste sources (Vault 1, Vault 4, and the FDCs) which might contribute to the Sector B 100m MOP groundwater pathways dose at 10,000 years and to the Sector I 100m MOP groundwater pathways dose at 15,080 years (the years of the peak doses within 10,000 and 20,000 years respectively). Vault 4, which as discussed previously has an appreciable release of Ra-226 prior to year 10,000, is the primary contributor (approximately 92%) to the 100m Peak Groundwater Pathways Dose in Sector B at year 10,000. Appendix D contains the 100m radionuclide concentration curves (20,000 years) for the various distinct waste sources.

Table 5.5-4: 100m MOP Peak Groundwater Pathways Dose at Peak Years, Sectors B and I

| Waste Source | Contribution to the Sector B Peak Dose at year 10,000 (mrem/yr) | Percentage of Total Peak Dose (%) | Contribution to Sector I Peak Dose at year 15,080 (mrem/yr) | Percentage of Total Peak Dose |
|--------------|---|-----------------------------------|---|-------------------------------|
| Vault 1 | <0.1 | 3% | <0.1 | <1% |
| Vault 4 | 1.3 | 92% | 0.3 | 10% |
| FDCs | 0.1 | 5% | 2.8 | 90% |
| TOTAL | 1.4 | 100% | 3.1 | 100% |

5.5.1.4 Individual Pathways Contributions to a MOP 100m Peak Annual Groundwater Pathways Dose

As stated previously, the total peak groundwater pathways dose results are the summation of the doses associated with all the individual 100m well pathways identified in Section 5.4. Table 5.5-5 shows the relative contributions from the individual groundwater pathways to the Sector B 100m MOP receptor dose at 10,000 years (the year of the peak dose). The primary contributors are water ingestion (49% of peak dose), fish ingestion (22% of peak dose) and vegetable ingestion (22% of peak dose).

Table 5.5-5: 100m MOP Peak Dose Groundwater Pathways Contributions, Sector B

| Pathway | Associated Contribution to Sector B peak at year 10,000 (mrem/yr) | Percentage of Sector B Total Peak Dose | Sector B Principal Radionuclide Pathway Dose |
|-----------------------------|---|--|--|
| Water Ingestion | 0.7 | 49.4% | Ra-226 (95%) |
| Fish Ingestion | 0.3 | 22.3% | Ra-226 (94%) |
| Vegetable Ingestion | 0.3 | 22.2% | Ra-226 (95%) |
| Other Pathways ^a | <0.1 | 6.1% | Ra-226 (% varies by pathways) |
| TOTAL | 1.4 | 100% | |

(a) The individual pathways included in “other pathways” each contributed < 0.05 mrem/yr to the Sector B peak at year 10,000

Tables 5.5-6, 5.5-7 and 5.5-8 show the 100m peak water, fish, and vegetable ingestion doses for the 100m sectors with the highest peaks within 10,000 and 20,000 years (Sectors B and I respectively). The peak water ingestion doses for Sectors B and I are, 0.7 mrem/yr for Sector B (with Ra-226 as the principal radionuclide), and 0.1 mrem/yr for Sector I (with I-129 as the principal radionuclide). Figure 5.5-6 shows the water ingestion doses to a 100m MOP receptor over time during the performance period (10,000 years) for Sectors B and I.

The water ingestion dose is directly scalable to the assumed water consumption rate (i.e., an increase in water consumption to 730 L/yr would result in an increase of 2.17 to the water ingestion dose).

Table 5.5-6: 100m MOP Peak Water Ingestion Doses, Sectors B and I

| Sector | Peak Water Ingestion Dose in 10,000 years (mrem/yr) | Principal Radionuclide | Peak Water Ingestion Dose in 20,000 years (mrem/yr) | Principal Radionuclide |
|--------|---|------------------------|---|------------------------|
| B | 0.7 (year 10,000) | Ra-226 | 1.3 (year 16,220) | Ra-226 |
| I | 0.1 (year 10,000) | I-129 | 1.3 (year 15,080) | I-129 |

Table 5.5-7: 100m MOP Peak Fish Ingestion Doses, Sectors B and I

| Sector | Peak Fish Ingestion Dose in 10,000 years (mrem/yr) | Principal Radionuclide | Peak Fish Ingestion Dose in 20,000 years (mrem/yr) | Principal Radionuclide |
|--------|--|------------------------|--|------------------------|
| B | 0.3 (year 10,000) | Ra-226 | 0.8 (year 15,080) | I-129 |
| I | 0.3 (year 10,000) | Ra-226 | 0.8 (year 15,080) | I-129 |

Table 5.5-8: 100m MOP Peak Vegetable Ingestion Doses, Sectors B and I

| Sector | Peak Vegetable Ingestion Dose in 10,000 years (mrem/yr) | Principal Radionuclide | Peak Vegetable Ingestion Dose in 20,000 years (mrem/yr) | Principal Radionuclide |
|--------|---|------------------------|---|------------------------|
| B | 0.3 (year 10,000) | Ra-226 | 0.6 (year 16,220) | Ra-226 |
| I | < 0.05 | NA | 0.6 (year 15,080) | I-129 |

Figure 5.5-6: 100m MOP Peak Water Ingestion Dose within 10,000 Years, Sectors B and I

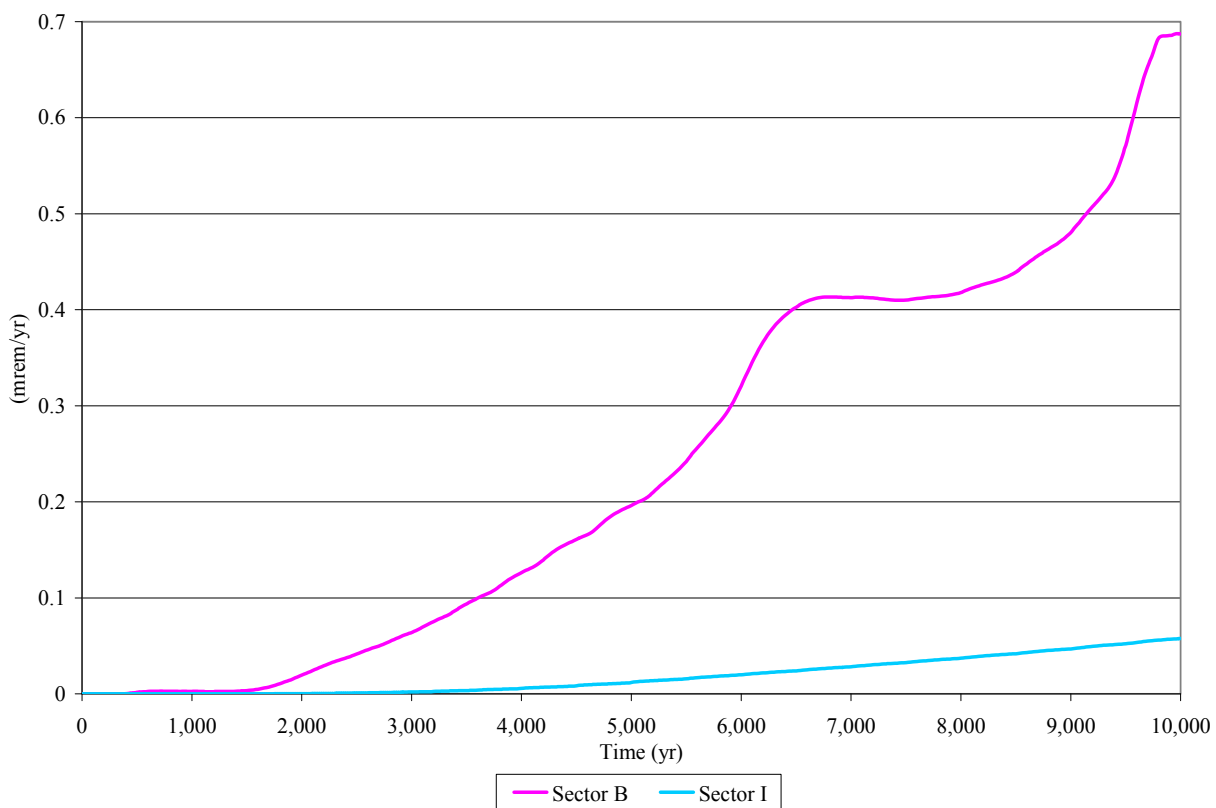


Figure 5.5-7 shows the 100m MOP receptor fish ingestion doses within 10,000 years for Sectors B and I. The peak fish ingestion doses for Sectors B and I are 0.3 mrem/yr, with Ra-226 as the principal radionuclide contributor. Note that these values are the same for Sectors B and I because the fish ingestion contribution is from the seepline location with the maximum concentration for each radionuclide, regardless of which of the sectors is being evaluated. For example, the receptor who drills a well in Sector I is allowed to fish at any seepline streams, including McQueen Branch, even though other streams (i.e., UTR) may be closer.

Figure 5.5-7: 100m MOP Peak Fish Ingestion Dose within 10,000 Years, Sectors B and I

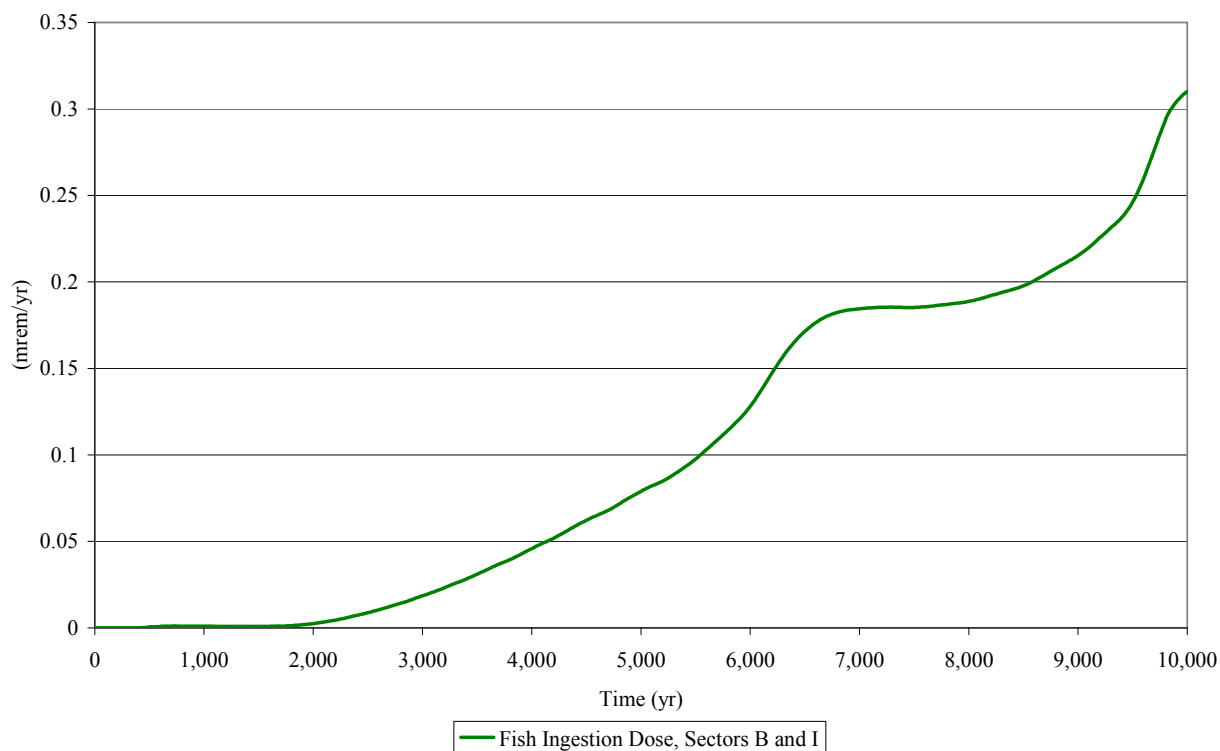
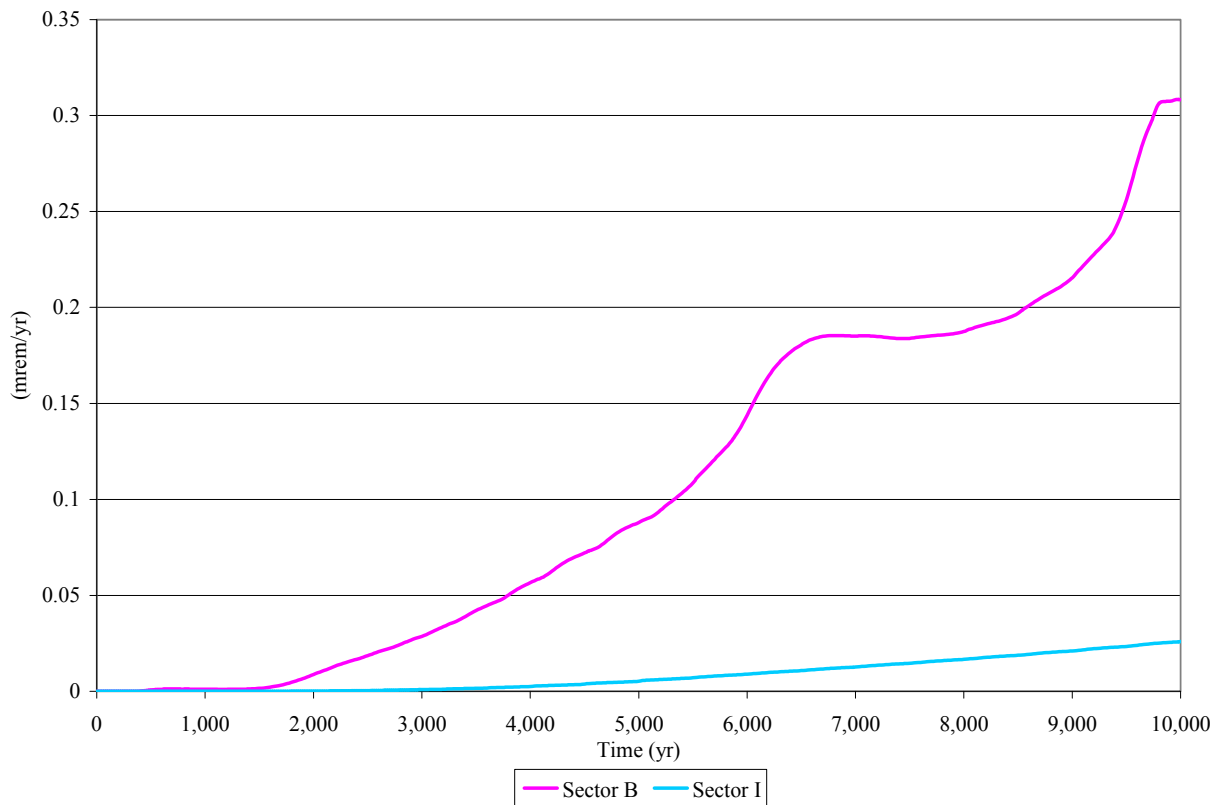


Figure 5.5-8 shows the vegetable ingestion doses to the 100m MOP receptor within 10,000 years for Sectors B and I. The peak vegetable ingestion dose for Sector B is 0.3 mrem/yr, with Ra-226 as the principal radionuclide. Sector I peak vegetable ingestion dose is <0.05 mrem/yr.

Figure 5.5-8: 100m MOP Peak Vegetable Ingestion Dose within 10,000 Years, Sectors B and I

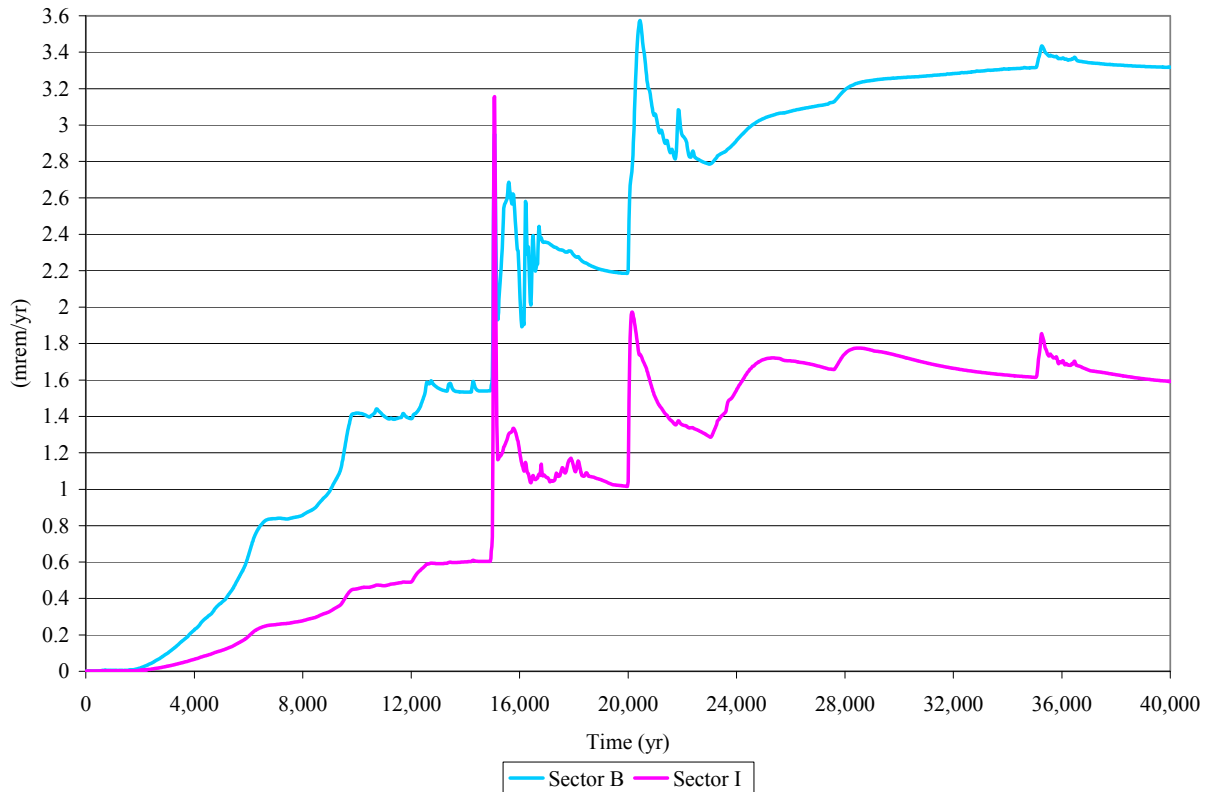


5.5.1.5 Member of the Public 100m Peak Annual Groundwater Pathways Dose Results for 40,000 years

The peak groundwater pathways doses associated with key radionuclides are calculated for 40,000 years in order that the dose behavior well past the performance period can be evaluated (Appendix C contains 40,000 year curves for the 100m key radionuclide concentrations). These peak groundwater pathways doses are the total doses associated with the individual MOP 100m pathways identified in Section 5.4. Figure 5.5-9 shows the peak 100m groundwater pathways doses over time for 40,000 years for Sectors B and I. The Sector B peak dose is approximately 3.6 mrem/yr, after year 20,000. The Sector I peak dose is approximately 3.1 mrem/yr at year 15,080.

The Sector I MOP dose peak ranges from approximately 2.0 mrem/yr to approximately 1.9 mrem/yr during the 20,000 year to 40,000 year timeframe. After 21,000 years the dose peaks for both Sector B and Sector I are not trending upward over the remainder of the 40,000 year period.

Figure 5.5-9: 100m MOP Peak Groundwater Pathways Dose within 40,000 Years, Sectors B and I



5.5.2 Member of the Public All-Pathways Dose Results

The purpose of this section is to present the total all-pathways peak doses for a MOP at 100m. The total all-pathways doses include both the groundwater and air pathways contributors.

The peak all-pathways annual dose for a MOP at 100m is calculated using the highest 100m groundwater pathways dose results during the 10,000 year performance period (from Section 5.5.1) in combination with the air pathway results (from Section 5.3). The peak all-pathways annual dose for a MOP is 1.4 mrem/yr and is associated with Sector B. The breakdown of the individual dose contributors is provided in Table 5.5-9.

Table 5.5-9: 100m MOP Peak Annual All-Pathways Dose Contributors

| Pathway | Associated Contribution to Peak at year 10,000 (mrem/yr) | Percentage of Total Peak Dose |
|-----------------------------|--|-------------------------------|
| Water Ingestion | 0.7 | 49.4% |
| Fish Ingestion | 0.3 | 22.3% |
| Vegetable Ingestion | 0.3 | 22.2% |
| Other Pathways ^a | <0.1 | 6.1% |
| Air Pathways | <0.005 | 0% |
| Total | 1.4 | 100% |

(a) The individual pathways included in "other pathways" each contributed < 0.05 mrem/yr to the Sector B peak at year 10,000.

5.6 Uncertainty and Sensitivity Analyses

The purpose of the uncertainty and sensitivity section is to consider the uncertainties in the conceptual models utilized and sensitivities of the results to the parameters used in the mathematical models. This evaluation was conducted for analyses related to a MOP, as well as those related to inadvertent intruders. These evaluations focused on key uncertainties and key sensitivities identified during modeling. The uncertainty and sensitivity analyses were primarily performed using a probabilistic model, which will be discussed in Sections 5.6.1 through 5.6.6. Section 5.6.7 will describe some additional single parameter sensitivity analyses that were performed through deterministic modeling using the PORFLOW model.

The probabilistic model, using the GoldSim systems analysis software, allows for variability of multiple parameters simultaneously, so concurrent effect of changes in the model can be analyzed, and the potential impact of changes can be assessed. This assessment allows for identification of parameters that are only of significance when varied simultaneously with another parameter. The GoldSim probabilistic model requires, as input, the abstraction of flow output from PORFLOW as described in Section 4.4.4.2.1. The deterministic model single parameter analysis, using PORFLOW, provides a method to evaluate parametric effects in isolation, so the importance of the uncertainty around a single parameter of concern can be evaluated. Although the single parameter analyses provide limited insight relative to the probabilistic uncertainty and sensitivity analyses, single parameter analyses have the advantage of using the more direct PORFLOW flow modeling, versus the abstracted flows in the SDF GoldSim model. Using both probabilistic and deterministic models for sensitivity analysis versus a single approach provides additional information concerning which parameters are of most importance to understanding dose estimates.

5.6.1 Uncertainty and Sensitivity Analyses using Probabilistic Modeling

The objective of these analyses was to investigate uncertainties that are inherent in conceptual models, mathematical models, and related data and assumptions to provide reasonable assurance that performance objectives will be met and ensure any future work focuses on issues of importance.

5.6.1.1 GoldSim SDF Model

In order to address uncertainty and sensitivity for the modeling of the SDF, a probabilistic model was constructed. This model is simpler in design than the PORFLOW groundwater model in its environmental transport calculations, but includes additional calculations that cannot be performed in PORFLOW. The GoldSim SDF model is described in detail in Section 4.4.4.2.

The probabilistic model, written using the GoldSim systems analysis software, accepts uncertainty and variability in the input parameters, the values of which can be defined using probability distributions. If a given model input (e.g., the K_d of saltstone) is given a distribution, or range of values, then this distribution is sampled in the collection of Monte Carlo runs that constitutes a probabilistic analysis. The collective uncertainty of all stochastic (probabilistic) inputs is reflected in the range and distribution of modeled results, such as water concentrations or dose to hypothetical future human receptors. If a given input parameter is given no range of input values, that is, if it is defined deterministically, then it contributes nothing to the overall uncertainty in the results. In reality, there are few parameters that have zero uncertainty. An example of a parameter without a defined range is the half-life of radionuclides.

The probabilistic model allows evaluation of the uncertainty in the PA. The results of the uncertainty analysis of this model are discussed in Section 5.6.4. Adopting a probabilistic approach also allows analysts to determine which model input parameters are the most significant to the results. This is done through sensitivity analysis, which identifies covariance between model inputs and results. Section 5.6.5 discusses the sensitivity analysis performed for the SDF model.

A benchmarking of the environmental transport calculations within a deterministic version of the GoldSim SDF model and those performed by the PORFLOW model is discussed in Section 5.6.2.

5.6.2 GoldSim Benchmarking

5.6.2.1 Benchmarking Between the GoldSim and PORFLOW Models

The probabilistic model of SDF using the GoldSim systems analysis software is described in Section 4.4.4. In order for the probabilistic results of this model to be compared to the results of the PORFLOW SDF model, obtaining a reasonable degree of agreement between the two models is needed. Ideally, the results of a deterministic Base Case (Case A) assessment using the PORFLOW model could be mimicked by a similar run in the GoldSim model. Deterministic results from both models should be comparable for the various cases and scenarios developed in the conceptual case model as well. An initial benchmarking effort for Case A and Case C is described in SRNL-TR-2009-00052. Subsequent benchmarking has been conducted to address Cases A through E and is described in this section. The term “benchmarking” has been chosen, rather than “calibration”, since this process establishes a point from which comparisons can be made rather than attempting to ensure that all results for the two models are identical for all modeling scenarios.

It is not expected that the results of the two models will be identical because there are fundamental differences in modeling platforms and differences in model approach (i.e., 2-D and 3-D process model in PORFLOW versus a 1-D system model in GoldSim).

The following sections describe the procedure used to benchmark the GoldSim SDF model to the PORFLOW SDF model and the results of that benchmarking.

5.6.2.2 *Saltstone Disposal Facility PA Benchmarking Activities and Results*

Baseline groundwater modeling was performed using the PORFLOW modeling software, a 3-D finite difference porous media flow and transport program. However, for performing a comprehensive evaluation of uncertainty and sensitivity, the PORFLOW SDF model is not optimum, since such an analysis requires the execution, integration, and analysis of more information than can be handled practically using a large process model such as PORFLOW. The PORFLOW model is used in the SDF PA for analyses of single parameter changes, but is not designed to model a large number of varying cases. For this reason, uncertainty and sensitivity analyses for the SDF PA are performed using the GoldSim systems analysis software. The GoldSim software is designed to perform probabilistic analyses of abstracted systems. To integrate the two software programs, benchmarking is required to demonstrate that the PORFLOW SDF model and the GoldSim SDF model are producing comparable results.

The purpose of the benchmarking is to ensure reasonable transport modeling agreement between the SDF PORFLOW and GoldSim models, not to calibrate the radionuclide concentration results between them. Although every attempt was made to ensure transport modeling was as similar as possible for the two models, the different solution formulations of the two codes ensured that there would be a number of differences between the two models. Before benchmarking began, the PORFLOW results were used to determine which radionuclides were most important to dose. It was found that the radionuclides of most importance to dose were Ra-226 and I-129 for Case A (see Section 5.2.2). However, the Tc-99 was also analyzed in the benchmarking as it is highly mobile during transport when released from the waste form. Benchmarking was performed using the GoldSim model in deterministic mode at two model locations, the interface between the unsaturated and saturated zones, and the 100m boundary sectors. Details on the benchmarking methodology of the SDF GoldSim model to the SDF PORFLOW model are found in SRNL-TR-2009-00052 for Cases A and C. Subsequent benchmarking, addressed below, supplements the results presented in SRNL-TR-2009-00052 and includes the other modeling scenarios in addition to Cases A and C.

5.6.2.3 *Benchmarking Adjustments and Results*

The methodology of the initial benchmarking effort described in SRNL-TR-2009-00052 is utilized in the subsequent benchmarking addressed below. Because the “shrinking core” release model for Tc-99 utilized in PORFLOW, as described in Section 4.2.3.2.4, is not explicitly modeled in GoldSim, the benchmarking conducted in SRNL-TR-2009-00052 required adjusting the K_d value for Tc-99. The Tc-99 K_d value was reduced in the reducing region by a factor of 0.3 and increased in the oxidizing region by a factor of 500. For this subsequent benchmarking effort these adjustments were retained. However, no other

elemental or radionuclide-specific adjustments made in the initial benchmarking effort have been retained.

Section 4.4.4.2 describes the GoldSim model and refers to SRNL-TR-2009-00051 for additional details. The GoldSim model utilizes the radionuclide inventories provided in Section 3.3 for all cases. PORFLOW utilizes the radionuclide inventories provided in Section 3.3 for Case A concentrations at 100m locations. PORFLOW utilizes the inventories of, and the parents of, the “Key” radionuclides described in Section 5.2.2 at the 100m locations for Cases B through E and at the stream locations for Case A. For this benchmarking effort a constraint was placed on what would be adjusted so as not to preferentially affect other radionuclides not being analyzed.

A significant departure from the initial benchmarking effort was the handling of radionuclide inventory in the walls of Vault 1 and Vault 4. The initial benchmarking effort adjusted the inventory in the vault walls to fit the modeling data obtained from PORFLOW and thus was varied for the cases analyzed (Case A and Case C). For this benchmarking effort the wall inventory in the vault walls is a fixed percentage of the vault radionuclide by vault type: 0.65% for Vault 1 and 0.5% for Vault 4 which is the same as the PORFLOW model as indicated in Sections 4.4.1.1 and 4.4.1.2.

5.6.2.3.1 Flux Benchmarking and Results for the Baseline Case – Case A

The benchmarking effort compared the flux at the interface between the unsaturated zone and the saturated zone, the concentrations at 100m distance for the various sectors shown in Section 5.2.1, and the doses to the MOP at these 100m locations.

Adjustments to the GoldSim model to benchmark the flux at the interface between the unsaturated zone and the saturated zone was restricted to applying factors to the flow values abstracted from the PORFLOW results. Section 4.4.4.2 describes the flow abstraction methodology utilized to input the flow values calculated by PORFLOW since the GoldSim model does not calculate flow; but relies on PORFLOW results. This benchmarking process merely adjusts these abstracted flow values by applying multiplicative factors to the abstracted flow values. As described in Section 4.4.4.2, the flows abstracted from PORFLOW and utilized in the GoldSim model are:

1. PF_Flowgrout – the flow of liquid through saltstone
2. PF_FlowWall – the flow of liquid through the wall of the disposal unit
3. PF_Flowdirt – the flow of liquid in the soil region adjacent to wall
4. PF_FlowUZ – the flow of liquid in the unsaturated zone below the disposal unit

For each type of disposal unit, the values of the flows described above were adjusted by a multiplicative factor. With each adjustment, the flux to the water table computed by GoldSim was compared to the flux computed by PORFLOW. Once a reasonable comparison of the flux values were observed, the adjustments were considered final.

Figures 5.6-1 through 5.6-3 illustrate the final flux benchmarking results for Vault 1 for Ra-226, I-129, and Tc-99, respectively. The final adjustments made for Case A are provided in Table 5.6-1. The rapid rise of the flux is due to the flushing of the assumed inventory in the walls for Vault 1. The behavior of the Ra-226 flux profile (Figure 5.6-1) shows good

agreement between PORFLOW (red line) and GoldSim (blue line) even though the magnitude of the flux is greater in the GoldSim model. The behavior of the I-129 flux profile (Figure 5.6-2) could have been improved with further adjustments but at the expense of the Ra-226 and Tc-99 flux curves which showed good agreement between PORFLOW and GoldSim. Because Ra-226 is the most significant contributor to dose, further adjustment was not performed.

Figure 5.6-1: Vault 1 Ra-226 Flux Comparison

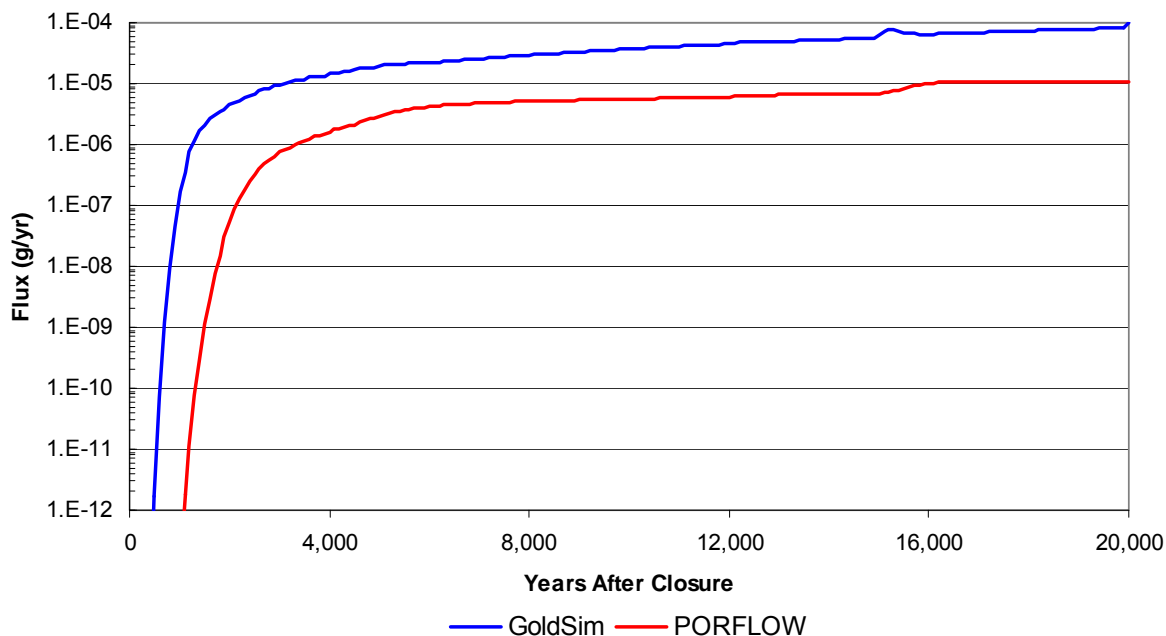


Figure 5.6-2: Vault 1 I-129-Flux Comparison

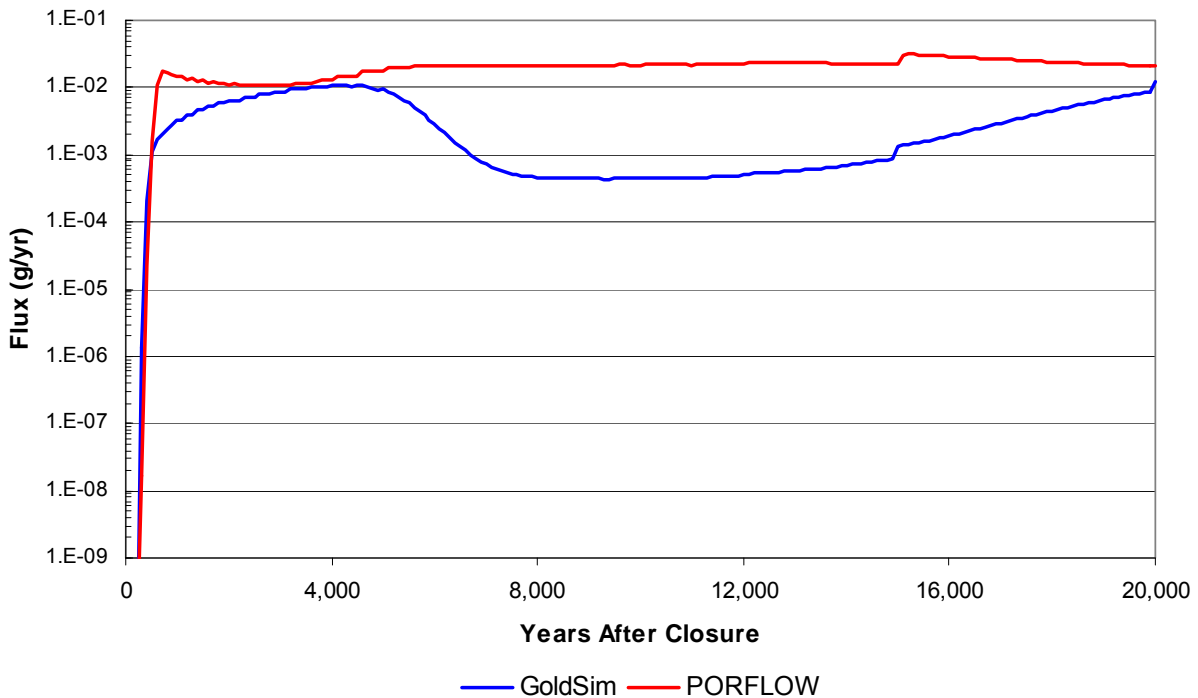


Figure 5.6-3: Vault 1 Tc-99 Flux Comparison

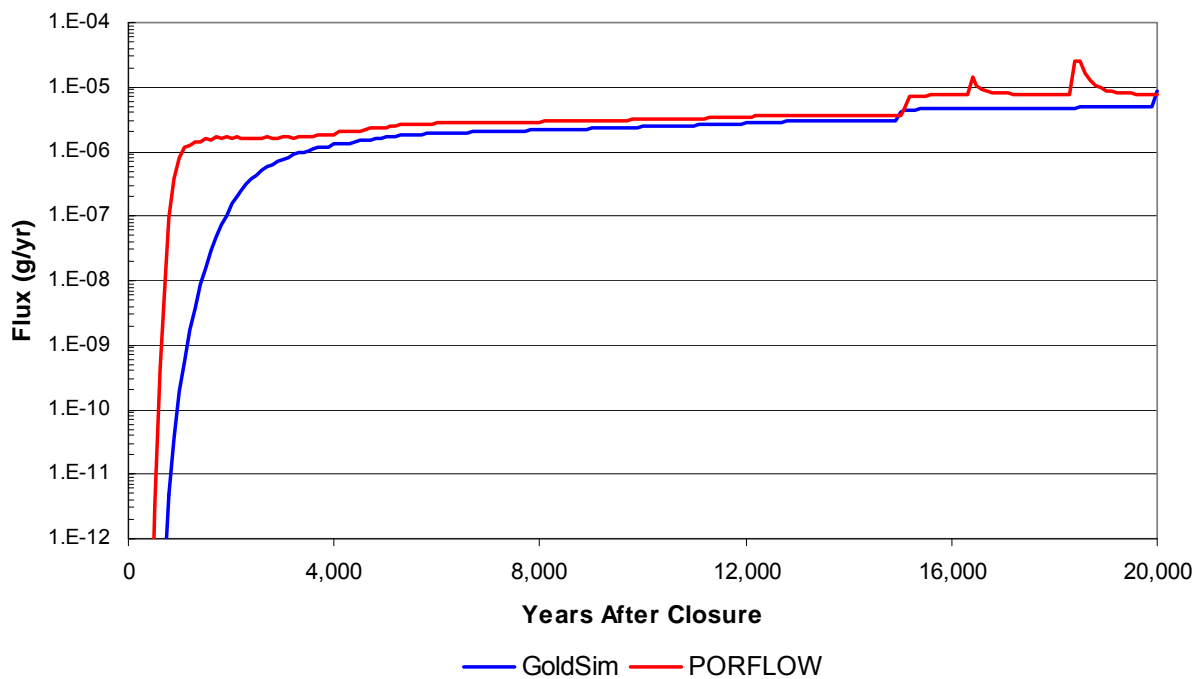


Table 5.6-1: Adjustment Multiplicative Factors on Flow Values

| GoldSim Parameter | Modeling Scenario Cases | | | | |
|-------------------|-------------------------|--------|--------|--------|--------|
| | Case A | Case B | Case C | Case D | Case E |
| Vault 1 | | | | | |
| PF_Flowgrout | 1 | 1 | 1 | 1 | 1 |
| PF_FlowWall | 0.1 | 1 | 1 | 1 | 1 |
| PF_Flowdirt | 1 | 1 | 1 | 1 | 1 |
| PF_FlowUZ | 3 | 1 | 1 | 1 | 1 |
| | | | | | |
| Vault 4 | | | | | |
| PF_Flowgrout | 0.8 | 0.3 | 1 | 1 | 0.9 |
| PF_FlowWall | 0.3 | 0.8 | 1 | 0.5 | 0.2 |
| PF_Flowdirt | 1 | 1 | 1 | 1 | 1 |
| PF_FlowUZ | 0.9 | 0.45 | 1.5 | 0.5 | 0.15 |
| | | | | | |
| FDC | | | | | |
| PF_Flowgrout | 10 | 0.15 | 1 | 1 | 1 |
| PF_FlowWall | 1 | 0.25 | 1 | 0.2 | 1 |
| PF_Flowdirt | 1 | 1 | 1 | 1 | 1 |
| PF_FlowUZ | 0.8 | 0.1 | 1 | 0.1 | 0.8 |

Figures 5.6-4 through 5.6-6 illustrate the final flux benchmarking results for Vault 4 for Ra-226, I-129, and Tc-99, respectively. The final adjustments made for Case A are presented in Table 5.6-1. The rapid rise of the flux, as in the case for Vault 1, is also due to the flushing of the assumed inventory in the walls for Vault 4. The flux profiles do not show as good agreement as shown for Vault 1 but the range of the magnitude of the fluxes is reasonable.

Figure 5.6-4: Vault 4 Ra-226 Flux Comparison

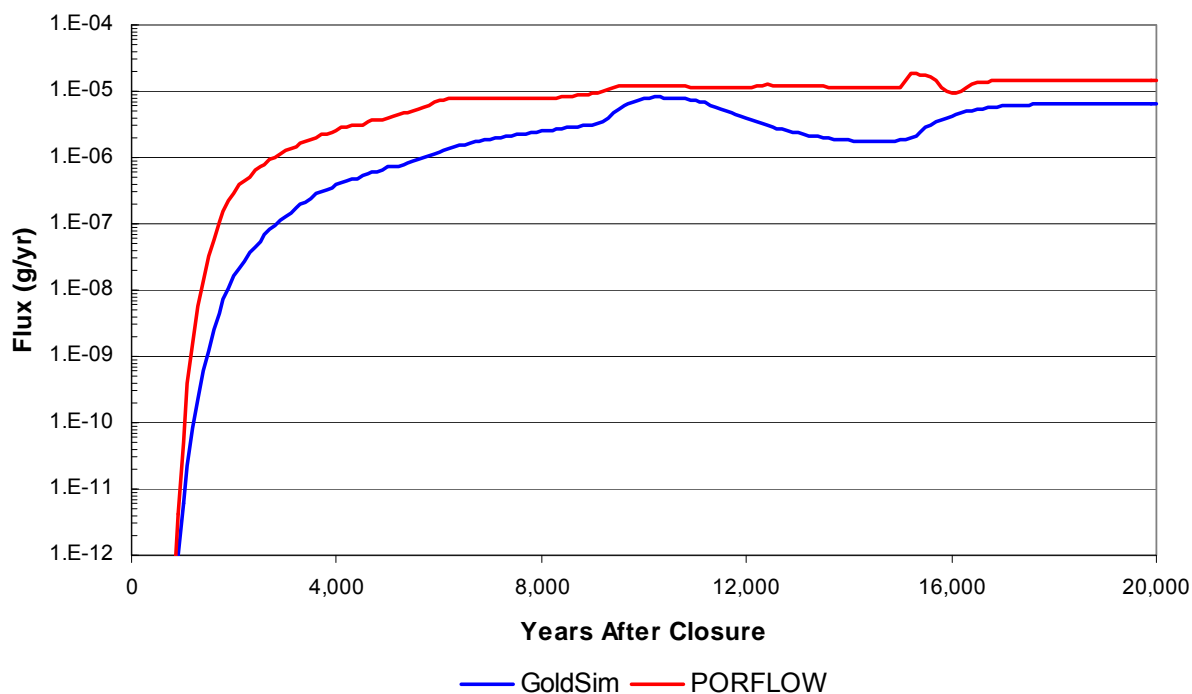


Figure 5.6-5: Vault 4 I-129 Flux Comparison

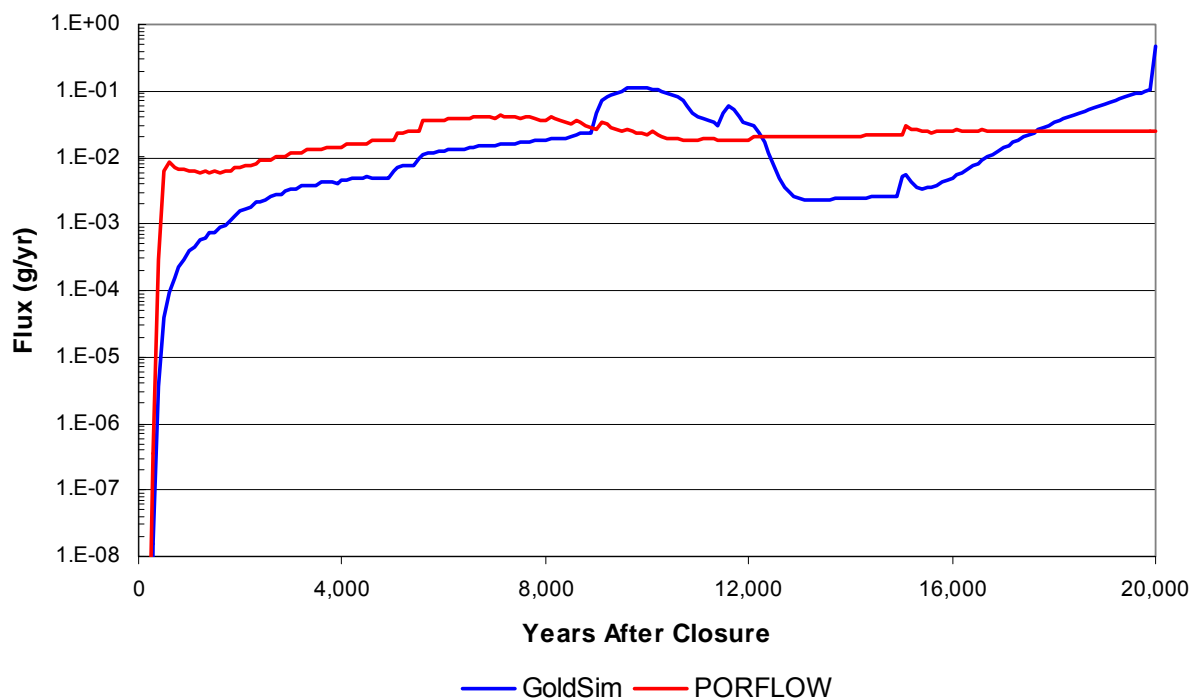
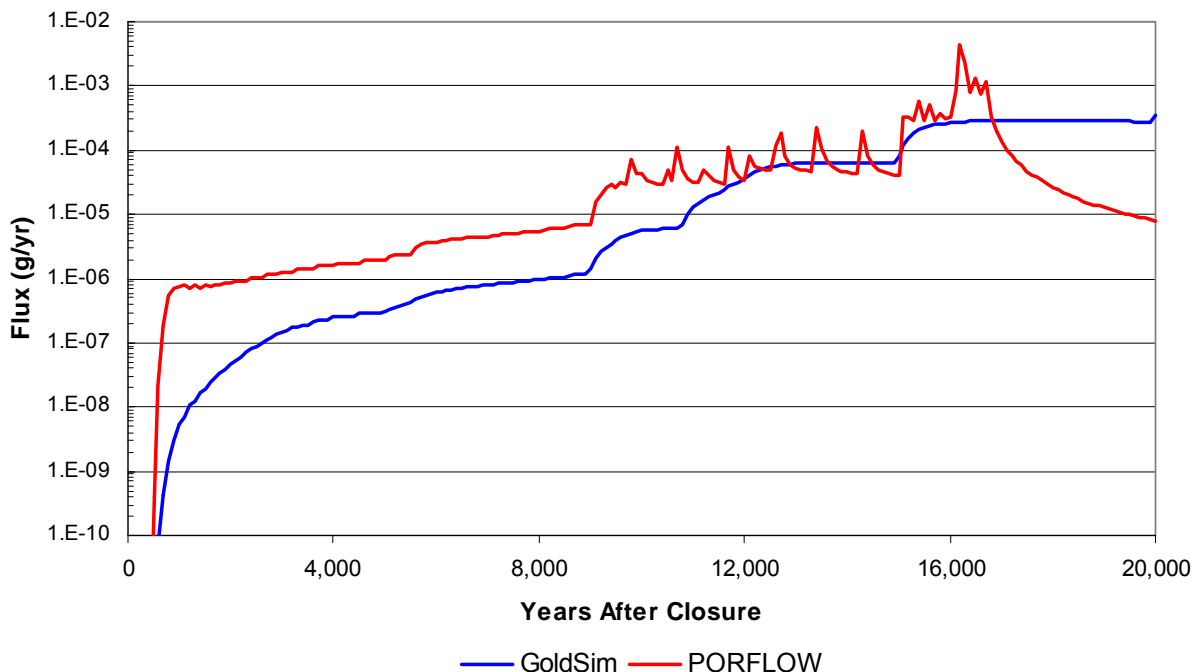


Figure 5.6-6: Vault 4 Tc-99 Flux Comparison



Figures 5.6-7 through 5.6-9 illustrate the final adjusted flux benchmarking results for an FDC for Ra-226, I-129, and Tc-99, respectively. The final adjustments made for Case A are presented in Table 5.6-1. Because there is no inventory assumed in the walls of the FDC, there is only a gradual, rather than rapid, rise in flux. The flux profiles show acceptable agreement in the later time periods when the more significant release occurs.

Figure 5.6-7: FDC Ra-226 Flux Comparison

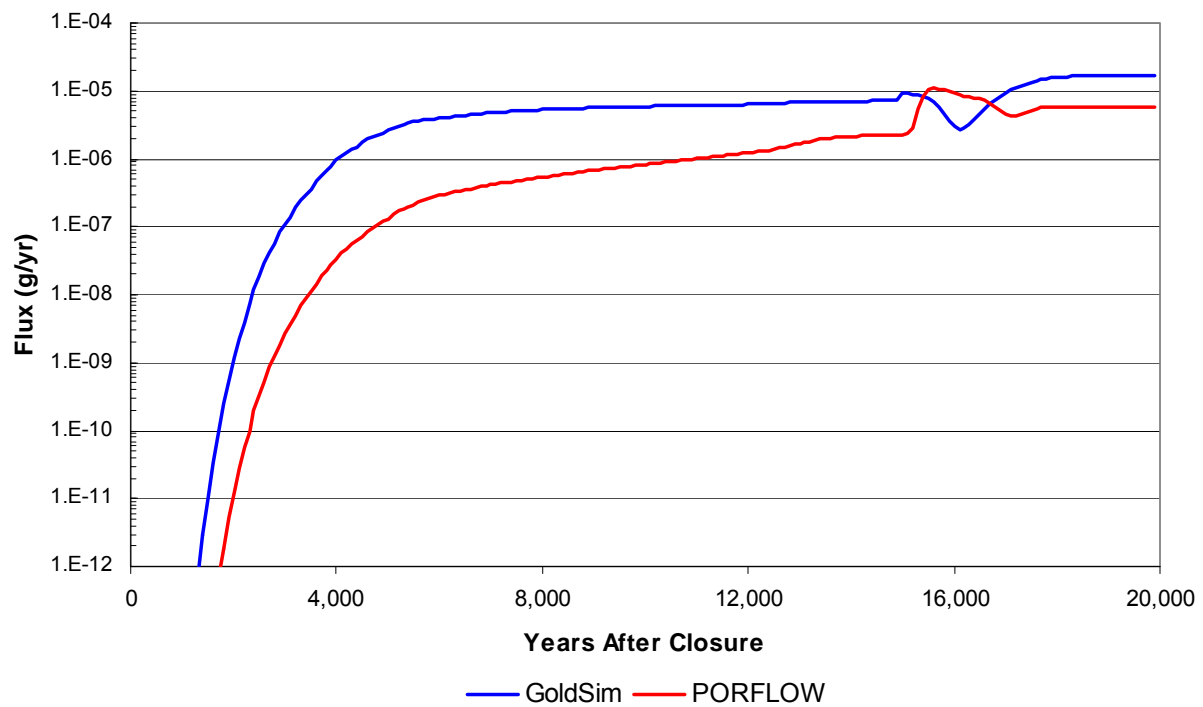


Figure 5.6-8: FDC I-129 Flux Comparison

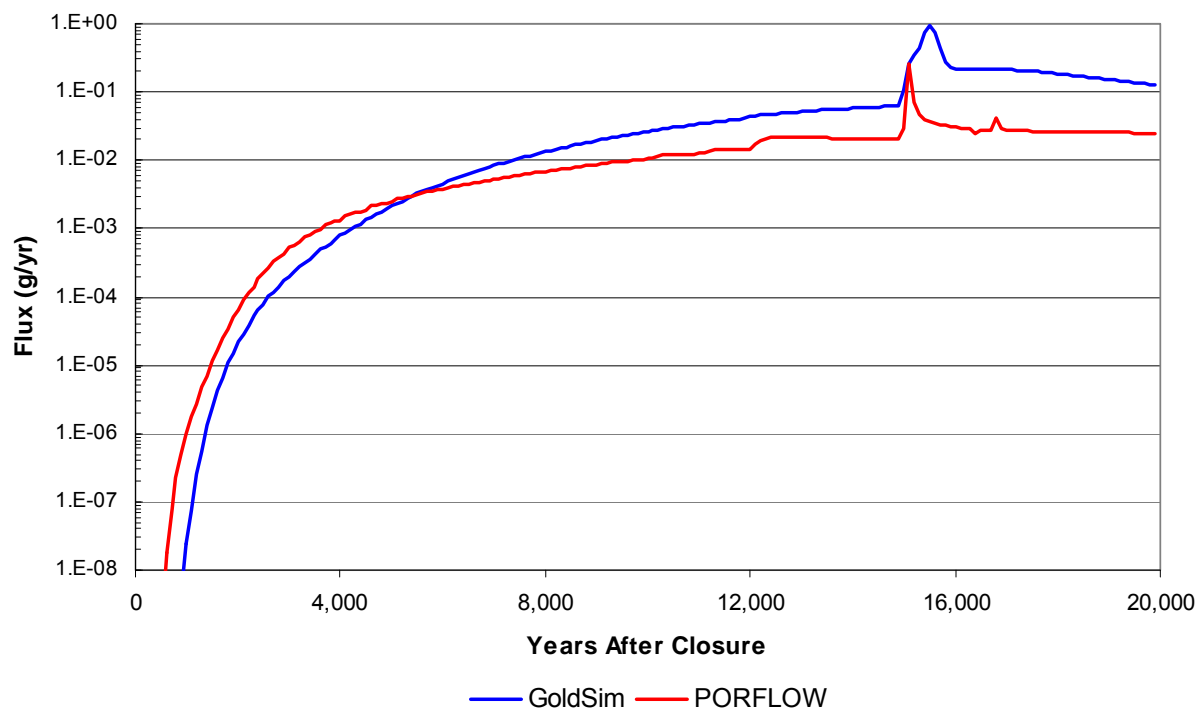


Figure 5.6-9: FDC Tc-99 Flux Comparison



5.6.2.3.2 Saturated Zone (Concentration) Benchmarking and Results – Case A

The saturated zone benchmarking described in SRNL-TR-2009-00052 was unchanged during this subsequent benchmarking effort and is reflected in the following paragraphs. Recognizing that this saturated zone benchmarking was conditional on the initial flux benchmarking which has been redone as described above; adjustments were made on the contribution of Vaults 1 and 4 to the various sectors.

The saturated zone benchmarking was challenging because of the multiple sources that can contribute to the concentrations at the various points of consideration. The arrivals of the peaks can generally be ascribed to a source, or multiple sources, due to the time-step length and the travel distance. This allowed for a relatively simple benchmarking of the saturated zone flow rate.

Because the saturated zone cell size represents an “average” saturated zone, a factor (thickness multiplied by area) was applied to all regions to account for the “dilution” shown by PORFLOW.

Two parameters adjusted after the flow rate was set were, (1) a plume factor, and (2) the contribution of Vaults 1 and 4 to unexpected regions. The plume factor was adjusted for Sector J only. In Sector J, a flow divide occurs and it was more affected than Sector I. A factor was added to donor fractions of Vaults 1 and 4 mass to the cells, normal to their main flow path.

Although there are differences between the two models' results in certain sectors, the concentration trends are similar (Figures 5.6-10 and 5.6-11) especially for Ra-226 and I-129 which are the major contributors to dose. The significant difference in concentration results for Tc-99 early in the assessment period has no adverse impact because of the Ra-226 and I-129 dominance in the dose. Note that the GoldSim model uses a 100 year time step interval for concentration calculations; but PORFLOW uses a 20 year time step interval for concentrations. The concentration comparison figures are based on 100 year time intervals.

In Figures 5.6-10 and 5.6-11, the dotted lines are GoldSim results, the solid lines are PORFLOW results. Note also that "South Sectors" and "North Sectors" refer to Sectors A through F and G through L respectively.

Figure 5.6-10: South Sectors Concentration Comparisons – Case A

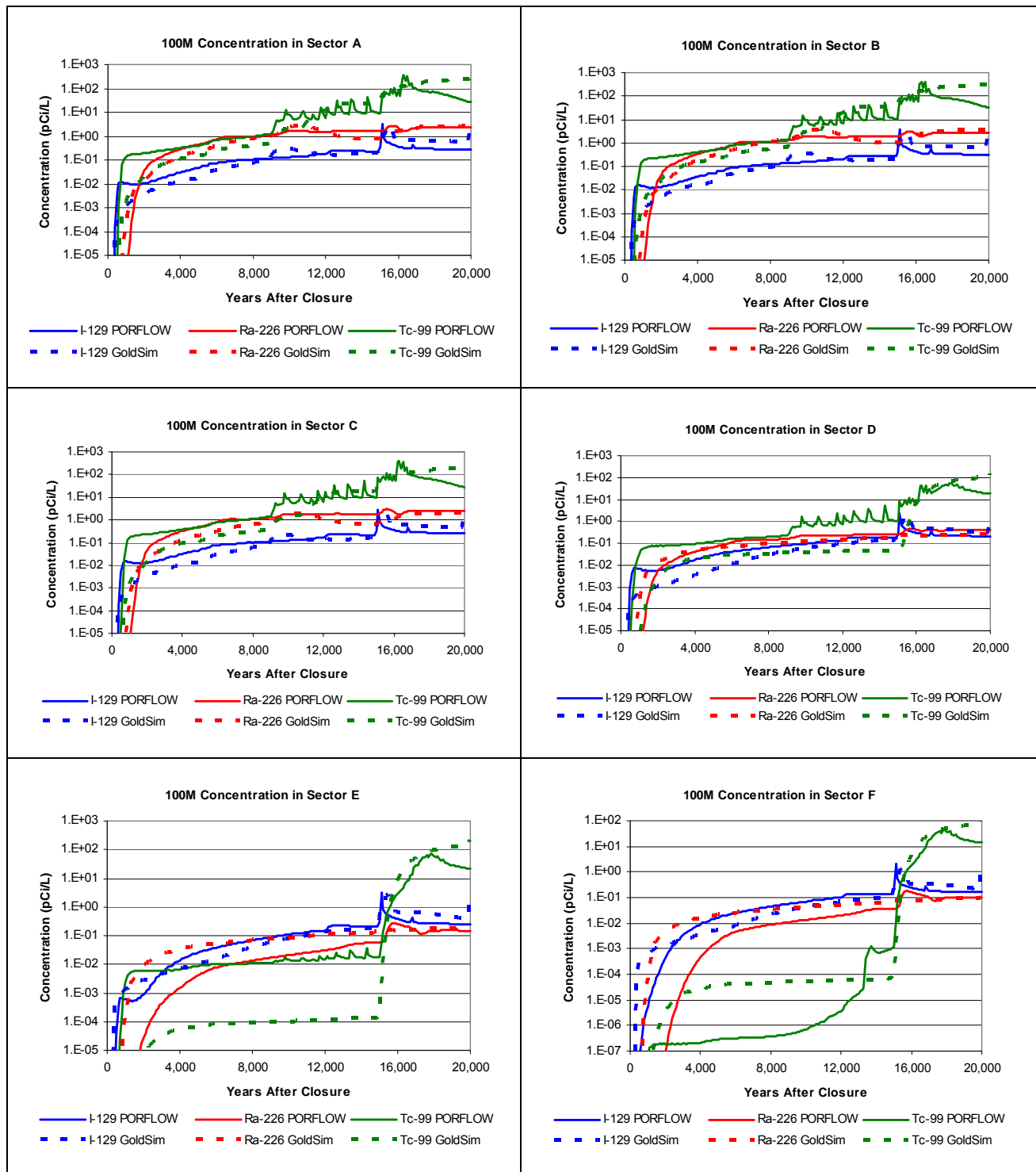
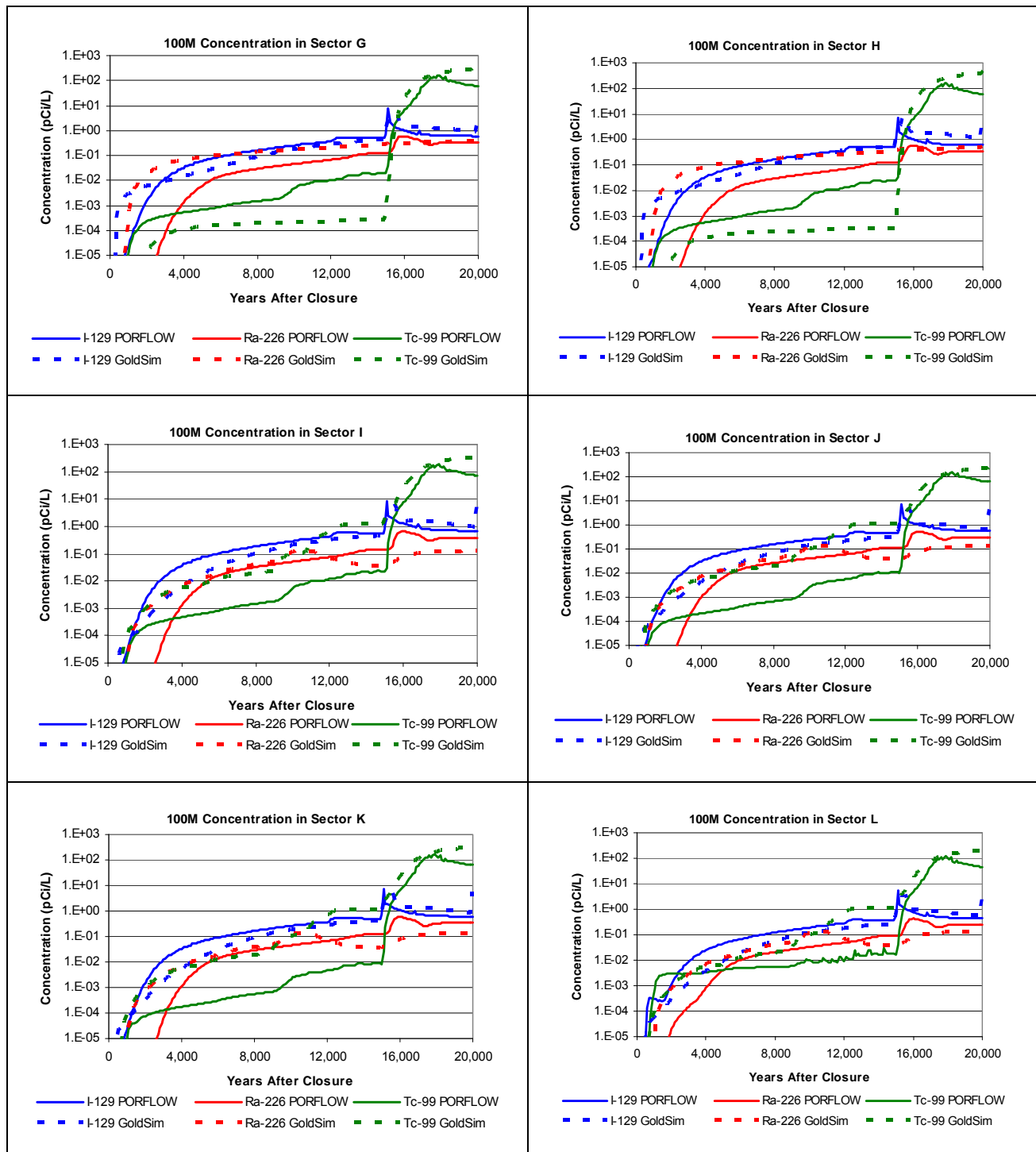


Figure 5.6-11: North Sectors Concentration Comparisons – Case A



5.6.2.3.3 Dose Comparisons – Case A

The PORFLOW model assumes that the MOP consumes fish from the stream location of highest radionuclide concentration to conservatively assess the impact of the fish ingestion pathway. In the GoldSim model the fish ingestion pathway dose was computed in each of the 12 sectors and found that Sector B provides the highest fish ingestion dose. Thus the dose to the MOP in any sector assumes that the dose contribution of fish ingestion is based on Sector B. Figure 5.6-12 illustrates the comparison of the fish ingestion dose in Sector B from the GoldSim model to the fish ingestion dose computed in PORFLOW.

Figure 5.6-12: Fish Ingestion Dose Pathway Comparisons – Case A

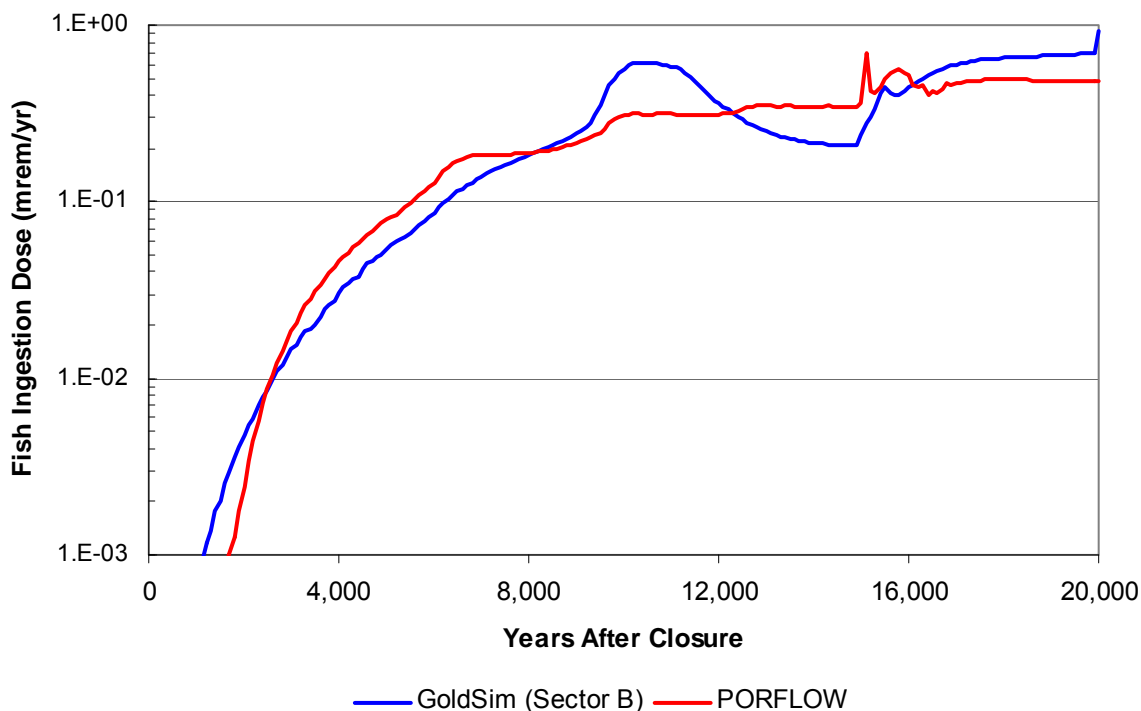
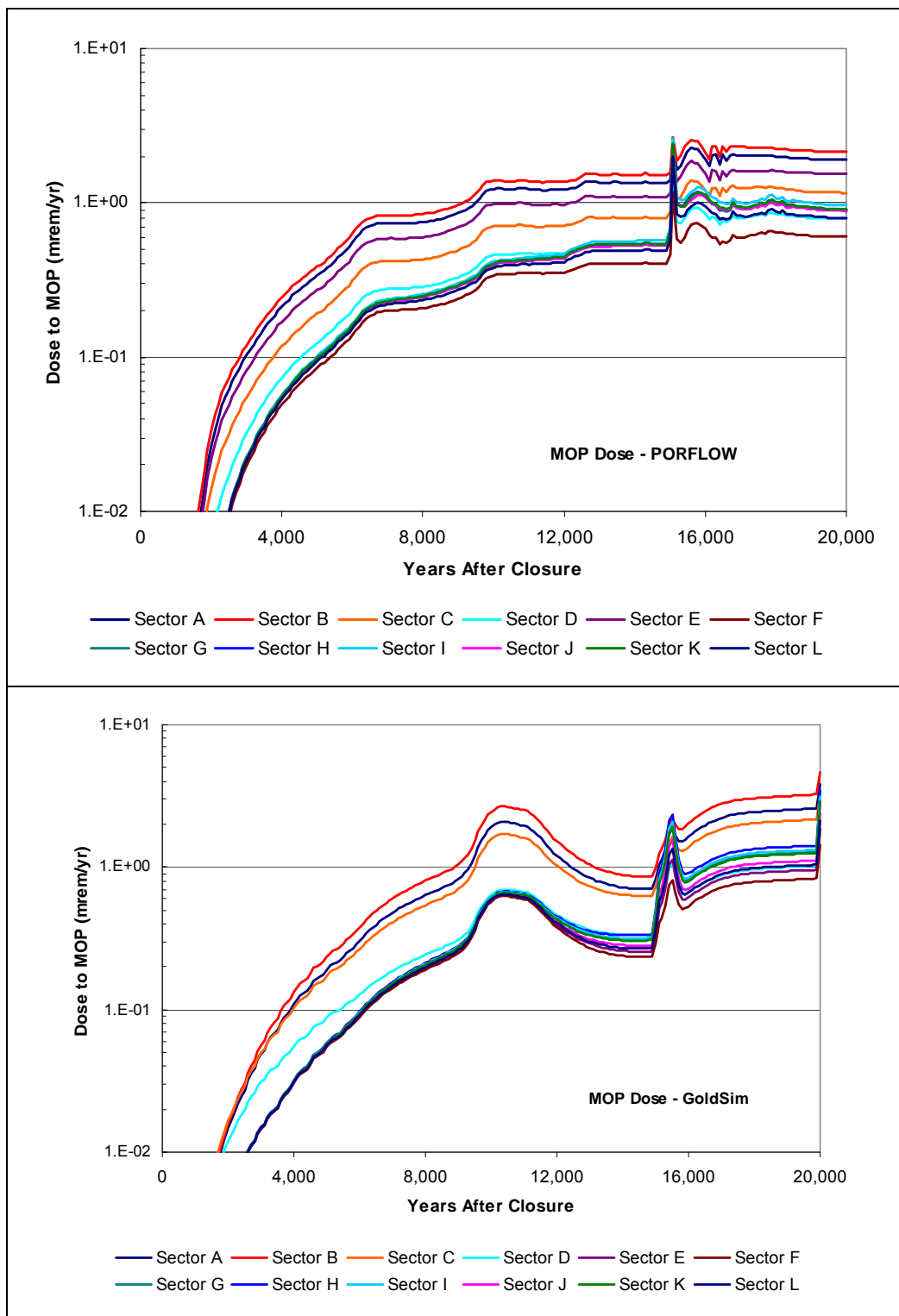


Figure 5.6-13 illustrates reasonable agreement of the magnitude of the MOP dose profiles between the GoldSim and PORFLOW models for all modeled radionuclides.

Figure 5.6-13: MOP Dose Comparisons – Case A



5.6.2.3.4 Benchmarking for Cases B Through E

Review of the benchmarking results for Case A indicate that, while comparable flux values between the GoldSim model and the PORFLOW model are desired; comparable concentration values and the resulting MOP dose between the GoldSim model and the PORFLOW model is the measure of benchmarking success.

For the remaining cases, only the multiplicative factors applied to the abstracted PORFLOW flow values are adjusted for each disposal cell type. The adjustments are summarized in Table 5.6-1. The individual case benchmarking efforts focus only on the radionuclide(s) that contribute to the majority of the dose based on the PORFLOW results. The following sections present the results of the benchmarking for Cases B through E.

5.6.2.3.5 Benchmarking Results for Case B

Figures 5.6-14 and 5.6-15 illustrate the 100m concentrations in Sector B and Sector I, respectively, for I-129 and Ra-226. Figure 5.6-14 shows excellent agreement between the GoldSim and PORFLOW models for Ra-226, which contributes more than 90% of the peak MOP dose in Sector B. Figure 5.6-15 shows reasonable agreement for Ra-226, which contributes nearly 70% of the peak MOP dose in Sector I.

Figure 5.6-16 illustrates reasonable agreement of the magnitude of the MOP dose profiles between the GoldSim and PORFLOW models for all modeled radionuclides.

Figure 5.6-14: Concentration Comparisons in Sector B – Case B

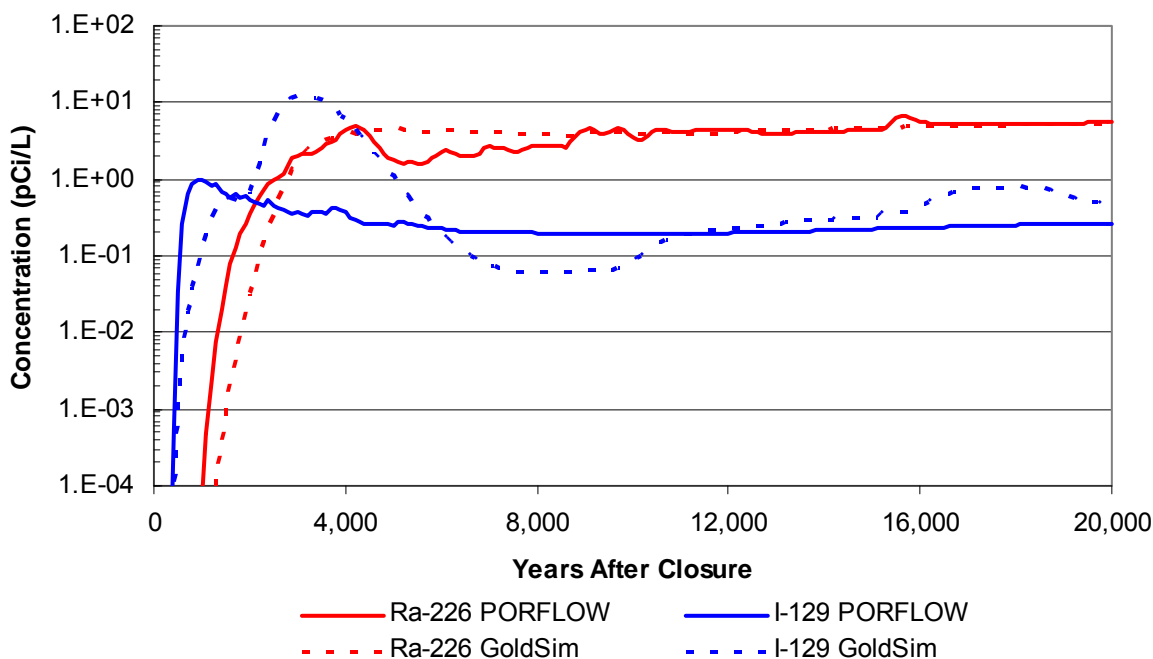


Figure 5.6-15: Concentration Comparisons in Sector I – Case B

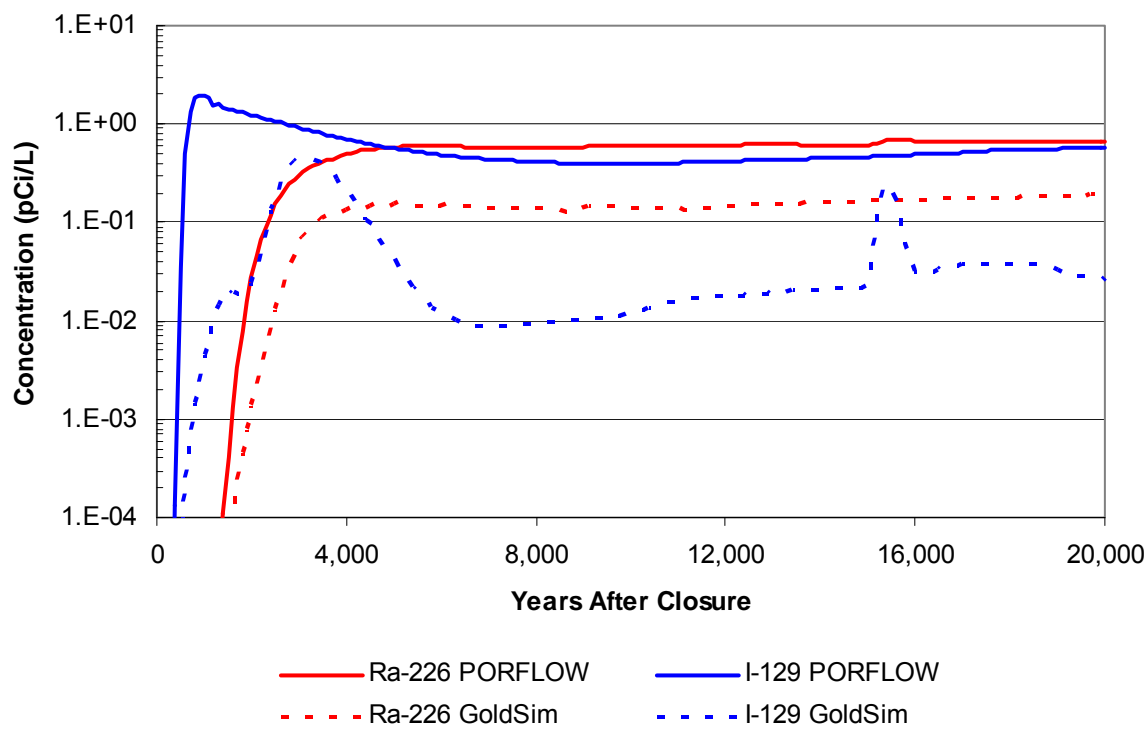
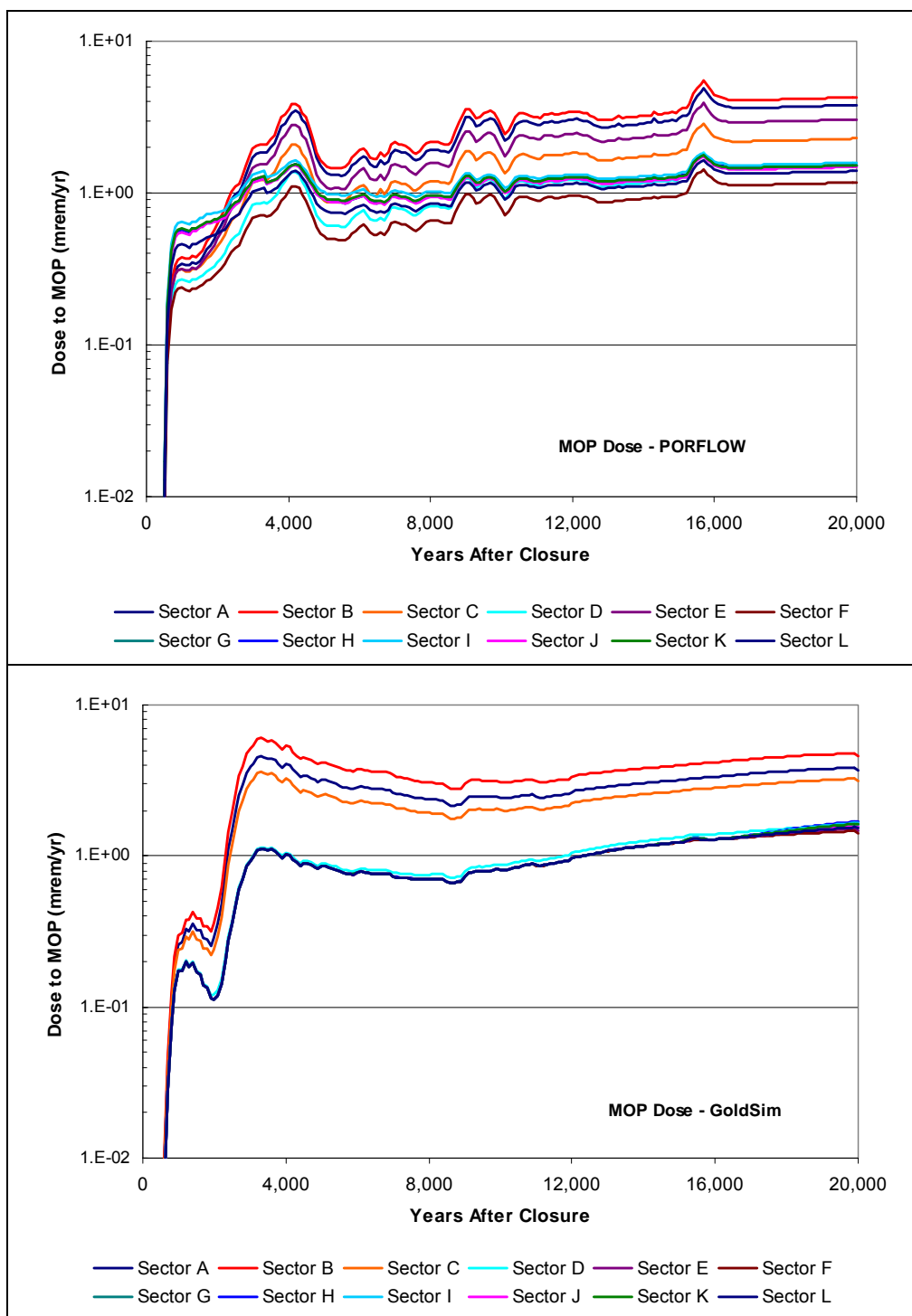


Figure 5.6-16: MOP Comparisons – Case B



5.6.2.3.6 Benchmarking and Results for Case C

Figures 5.6-17 and 5.6-18 illustrate the 100m concentrations in Sector B and Sector I, respectively, for Ra-226. Figure 5.6-14 shows excellent agreement between the GoldSim and PORFLOW models for Ra-226, which contributes nearly 93% of the peak MOP dose in Sector B. Figure 5.6-15 shows reasonable agreement for Ra-226, which contributes nearly 80% of the peak MOP dose in Sector I.

Figure 5.6-19 illustrates excellent agreement of the MOP dose profiles between the GoldSim and PORFLOW models for all modeled radionuclides during the compliance period of 10,000 years. The “upswing” of the dose curve shown in the GoldSim model is attributed to Pu-239 and Pu-240. The retardation of plutonium in the PORFLOW model caused by the disposal unit floor K_d value of 10,000 mL/g is significantly impacted by the GoldSim Case C model that assumes a direct mass transfer pathway from saltstone to the unsaturated zone.

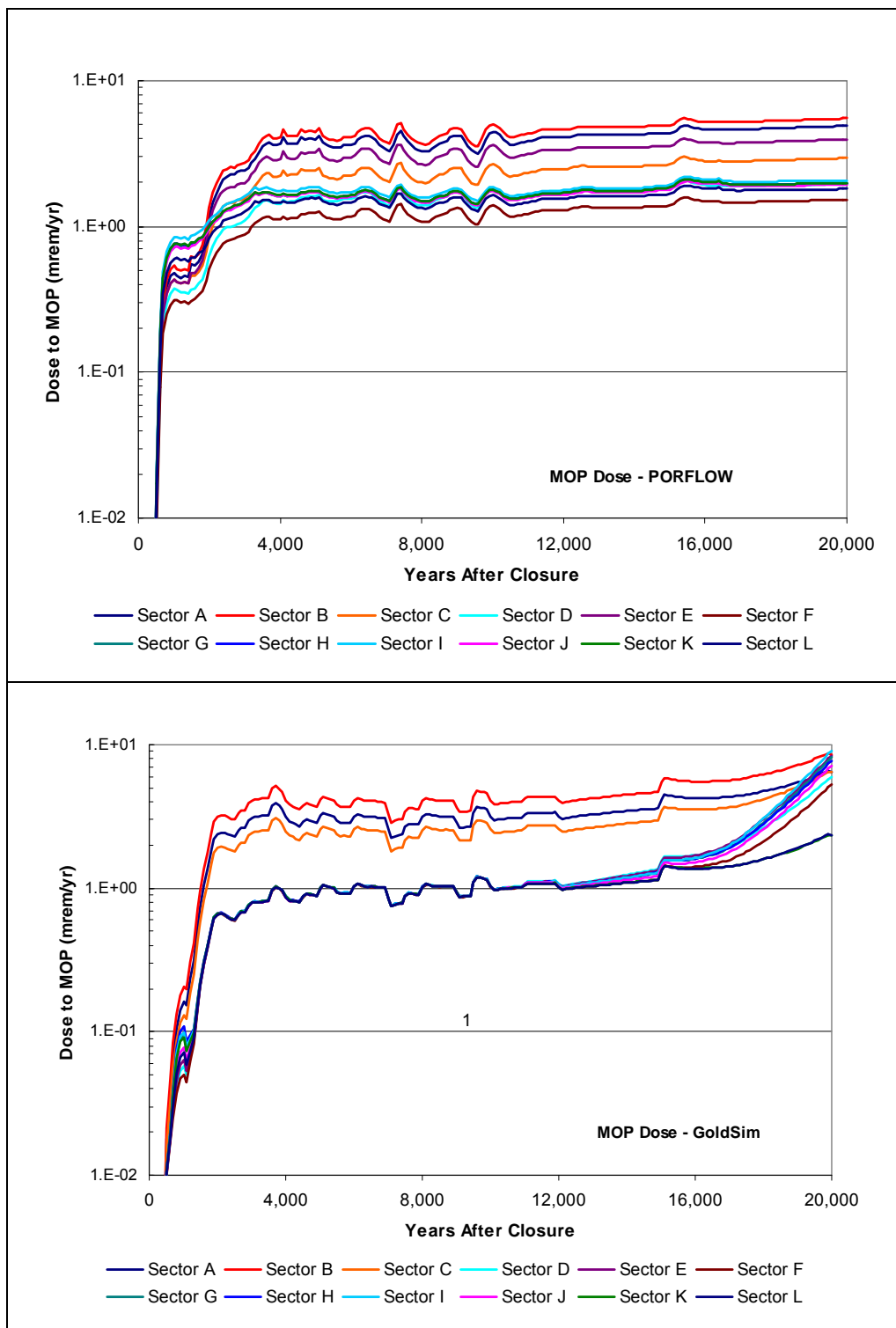
Figure 5.6-17: Concentration Comparisons in Sector B – Case C



Figure 5.6-18: Concentration Comparisons in Sector I – Case C



Figure 5.6-19: MOP Comparisons – Case C



5.6.2.3.7 Benchmarking and Results for Case D

For Case D the major contributors to the peak MOP dose in Sector B are Ra-226 (51%) and Tc-99 (40%). Figure 5.6-20 illustrates the 100m concentrations in Sector B for Ra-226 and Tc-99, and shows good agreement between PORFLOW and GoldSim models. The concentration spikes of Tc-99 shown in Figure 5.6-20 are attributed to the shrinking core model used in PORFLOW for the release of Tc-99; as the reduction capacity of the cementitious material is consumed, as discussed in Section 4.2.3.2.4. In Sector I, the peak MOP dose is predominately from Ra-226, and Figure 5.6-21 shows good agreement between the GoldSim and PORFLOW models for Ra-226, which contributes nearly 80% of the peak MOP dose.

Figure 5.6-22 illustrates the MOP dose profiles between the GoldSim and PORFLOW models for all modeled radionuclides and show excellent agreement with the magnitude of the dose profiles between the two models.

Figure 5.6-20: Concentration Comparisons in Sector B – Case D

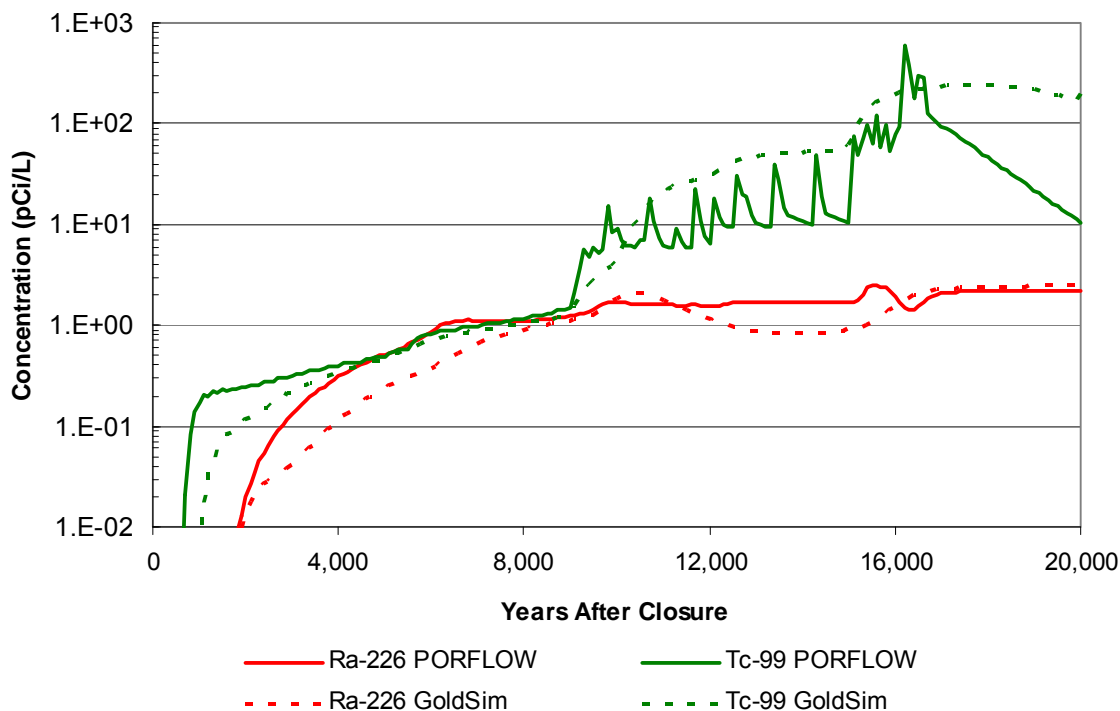


Figure 5.6-21: Concentration Comparisons in Sector I – Case D

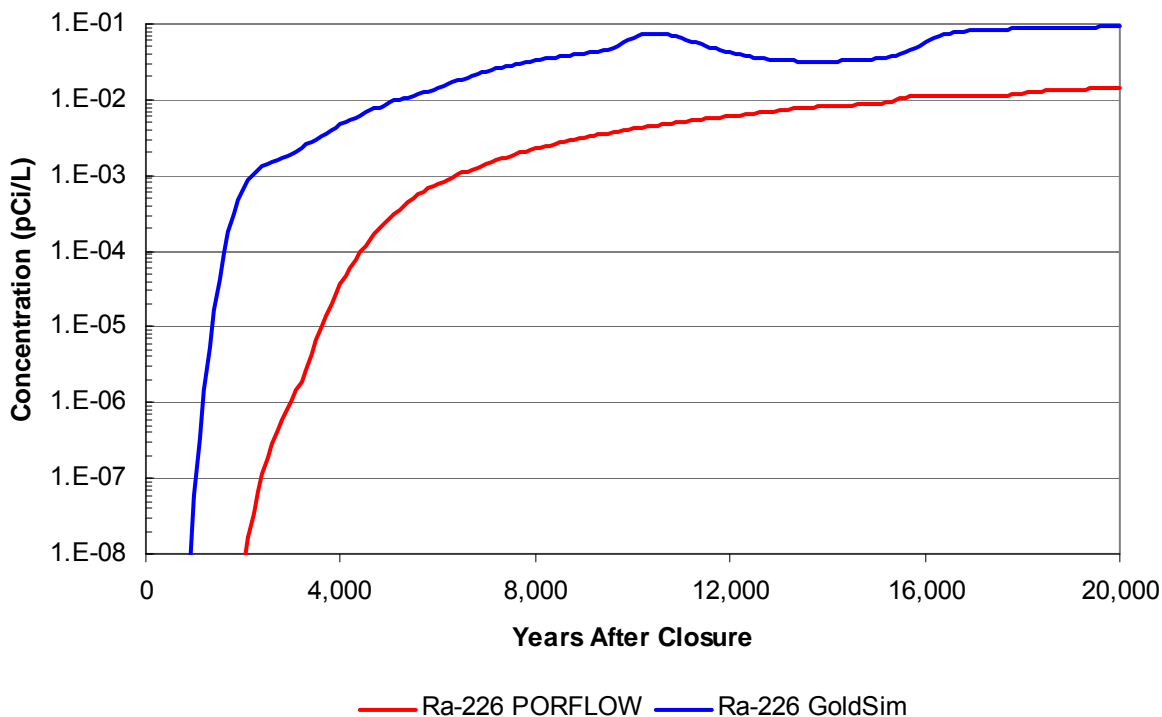
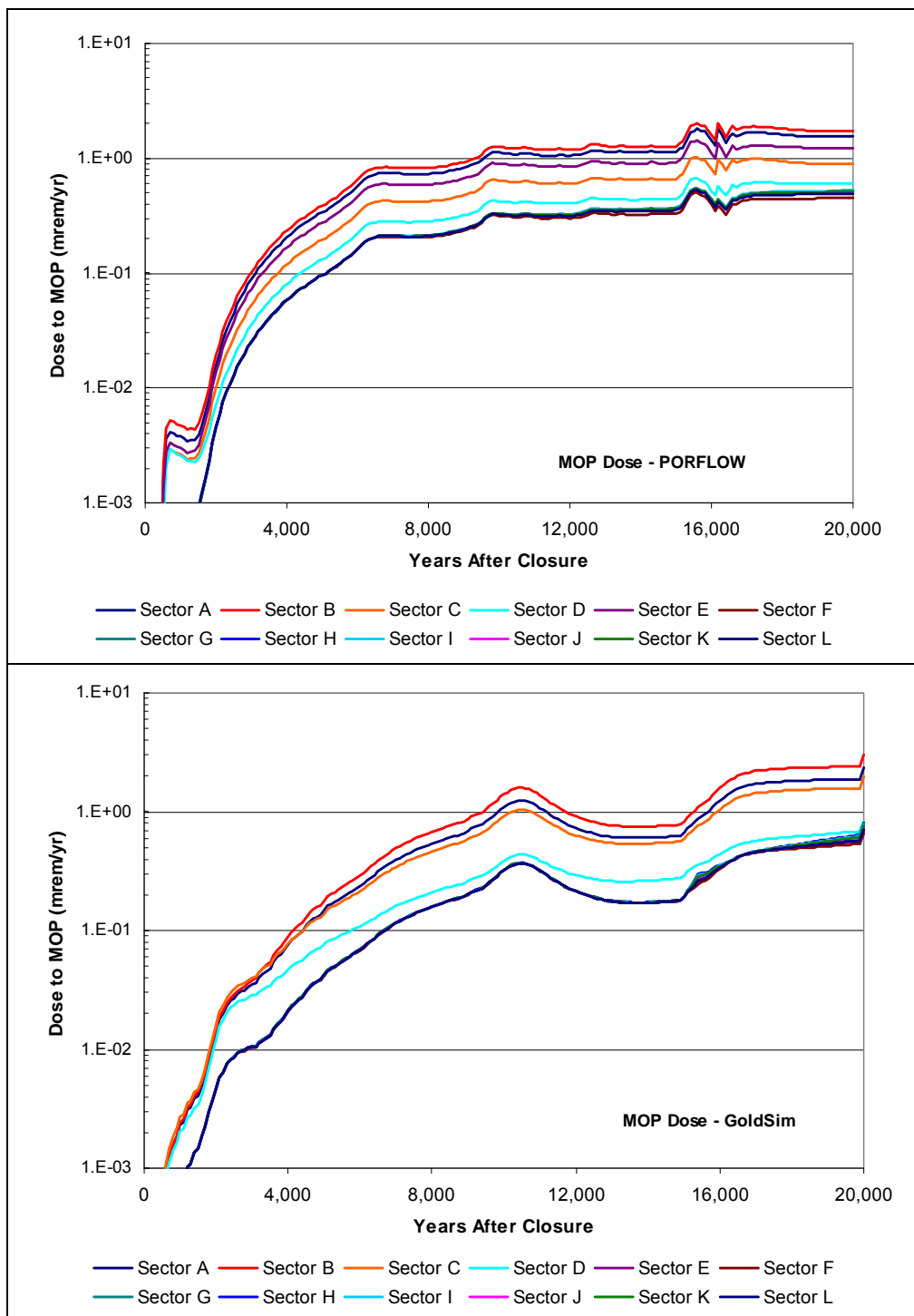


Figure 5.6-22: MOP Dose Comparisons – Case D



5.6.2.3.8 Benchmarking and Results for Case E

For Case E the peak MOP dose in Sector B is predominantly from Ra-226 (97%). Figure 5.6-23 illustrates the 100m concentrations in Sector B for Ra-226, and shows good agreement between the PORFLOW and GoldSim models. In Sector I, Ra-226 contributes 54% of the MOP peak dose and I-129 contributes 42% of the peak MOP dose. Figure 5.6-24 illustrates the 100m concentrations in Sector I for Ra-226 and I-129. Figure 5.6-24 shows good agreement for the arrival of the peak of the I-129 concentration; however, the overall behavior of the concentration profile in the GoldSim model does not have as good agreement to PORFLOW as in the other cases. This lack of general agreement to the behavior of the concentration profile is attributed to the flow abstraction used in the GoldSim model, which is influenced by the greater flow through saltstone.

Figure 5.6-25 illustrates excellent agreement of the MOP dose profiles between the GoldSim and PORFLOW models for all modeled radionuclides. The upward swing shown in the GoldSim model is attributed to the rapid increase in the liquid flow through the wall at the later time steps abstracted from the PORFLOW data.

Figure 5.6-23: Concentration Comparisons in Sector B – Case E



Figure 5.6-24: Concentration Comparisons in Sector I – Case E

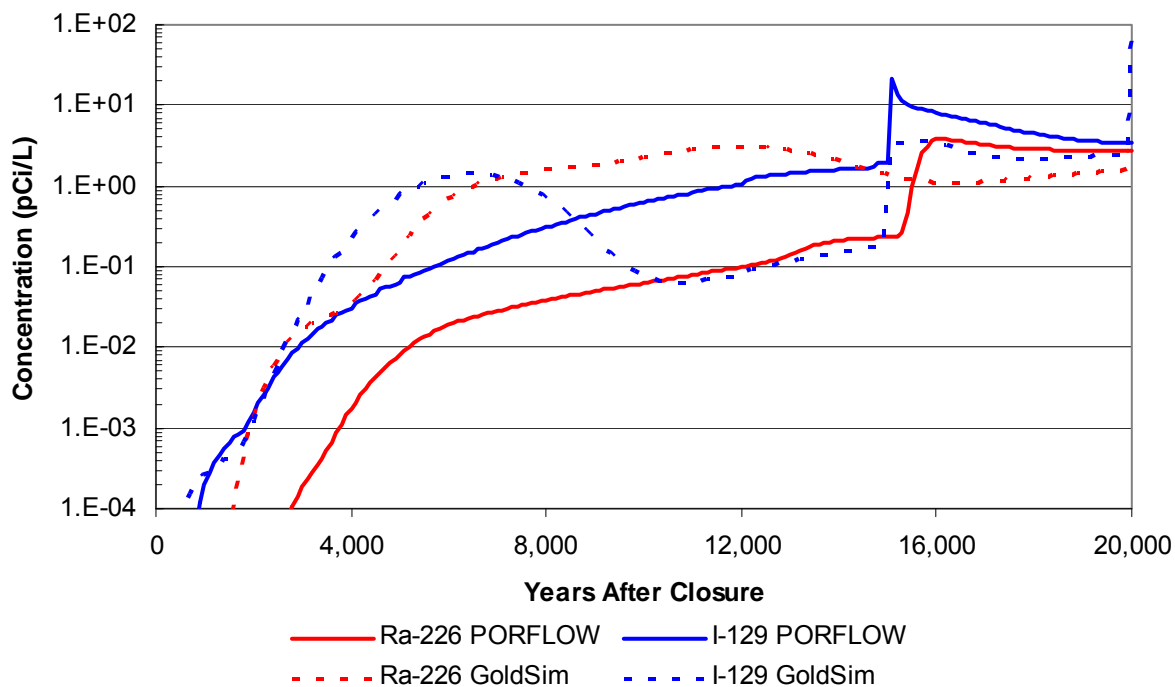
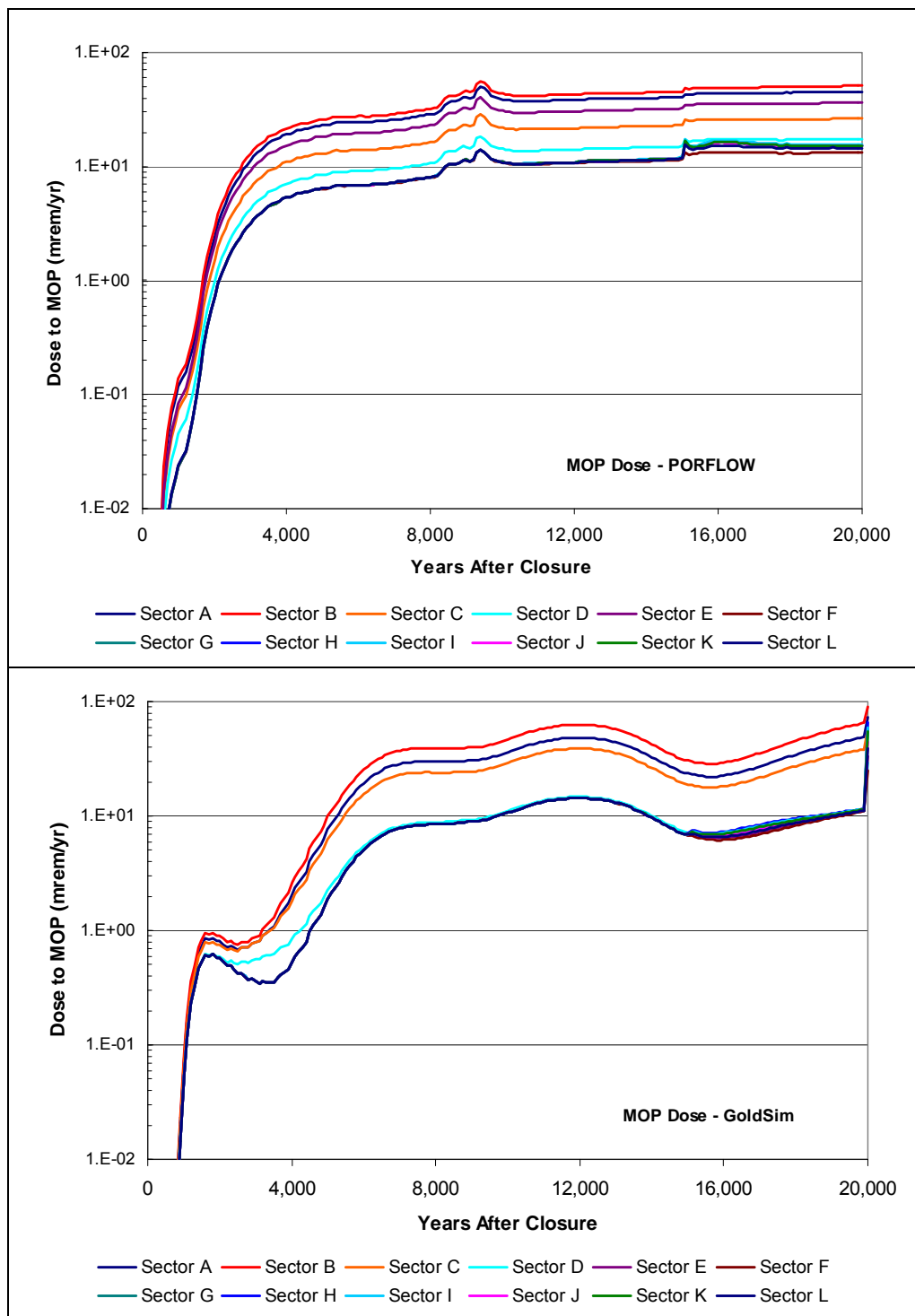


Figure 5.6-25: MOP Dose Comparisons – Case E



5.6.2.3.9 Benchmarking Summary

The objective of the benchmarking process is to demonstrate that the dose profiles between the GoldSim and PORFLOW models are similar. With similar dose profiles it can be claimed that the sensitivity and uncertainty analyses conducted using the GoldSim model is representative of the SDF conceptual model. The good to excellent agreement between the GoldSim and PORFLOW models shown in the above sections for the dose profiles, or the magnitude of the dose profiles, demonstrate that the benchmarking objective has been met.

Table 5.6-1 provides the model adjustments made to the flow values extracted from PORFLOW and used in the GoldSim model.

5.6.3 Parameters Evaluated in the SDF Probabilistic Model

In order to evaluate the most sensitive parameters, the parameters selected for evaluation in the stochastic analyses were based on modeling experience informed by the basis for the selected values and available generic and site-specific data. A thorough discussion of the parameters evaluated and the ranges considered is provided in the following discussion.

5.6.3.1 Saltstone Disposal Facility Case Scenarios

As discussed in Section 4.4.2, five different disposal unit cases are considered. The scenarios differ as to whether fast flow paths are present, what assumptions are made regarding diffusion to the disposal unit walls, and how saltstone degradation is modeled. The differences between the five analytical cases are summarized in Table 5.6-2. Depending on the disposal unit type, different probabilities of occurrence are assumed for each of the potential cases as shown in Table 5.6-3. Discrete distributions are chosen using engineering judgment informed by disposal unit design specifics, SRS PA experience, and lessons learned with a maximum entropy approach taken as a starting point for determination of the impact of various cases. Furthermore, an informal elicitation process was employed to augment the engineering judgment of the various cases and the probabilities assigned to each. The disposal unit design differences that informed the probability choices are provided below:

- Case B assumes that the sheet drainage system present in Vault 4 and the FDCs deteriorate to the extent that a channel is formed between the saltstone monolith and the walls of the disposal unit causing a fast flow path. The probability of Case B is much lower than the Base Case (Case A) because of the low likelihood that deterioration of the sheet drainage system would develop the fast flow path analyzed. Because Vault 1 does not contain a sheet drainage system, the probability of this case occurring in Vault 1 is zero. As described in Section 4.4.4.1, to represent the affect of hypothetical fast flow path in Cases B and C, the PORFLOW model incorporated a higher conductivity vertical leg extending through the roof and floor, including the upper and lower mud mats of the FDCs, to form a conduit between the sand drain and undisturbed soil beneath the disposal unit.
- Case C includes the fast flow paths caused by the deterioration of the sheet drainage system (Case B) plus the fast flow paths caused by the cracking of cementitious material in the saltstone and roof support columns. The potential for saltstone

- cracking is present in all disposal units; however, Vault 1 does not have any roof support columns and thus the potential of additional fast flow paths caused by the deterioration of the roof support columns is not present in Vault 1. The probabilities assigned to this case are much lower than the Base Case in general because “straight line” cracks are not anticipated to occur in the cementitious materials. Any degradation of the cementitious materials that does occur is expected to result in small cracks (which cause increased flow through hydraulic conductivity changes) rather than void spaces that would channel flow directly from the top of the disposal unit, through the saltstone monolith and disposal unit floor, including the upper and lower mud mats of the FDCs, and into the unsaturated zone below the disposal unit. If void spaces do develop, it is probable they would fill with material migrating downward from the materials above the void space (e.g., as the cementitious materials degrade). Cracks causing increased flow through hydraulic conductivity changes are modeled independent of the fast flow paths as addressed in Section 4.2.3.
- Case D addresses the potential that the sheet drainage system present in Vault 4 and the FDCs remains intact to form a capillary break between the saltstone monolith and the disposal unit walls, thus preventing diffusion through the walls. Similar to Case B, the probability of this case for Vault 1 is zero because Vault 1 does not have a sheet drainage system installed.
 - Case E addresses the potential for saltstone degradation. Saltstone is designed to indefinitely immobilize contaminants in a low permeability medium and the potential for its physical degradation is uncertain. As reported in Section 4.2.3, an investigation, documented in WSRC-STI-2008-00236, concludes that the fracturing initiated by expansive phase precipitation is unlikely to occur in saltstone. However, a degraded saltstone condition is postulated to occur as described in Section 4.2.3.

Table 5.6-2: Disposal Unit Cases

| Case | Fast flow paths | Saltstone Degradation |
|--------------------------|---|-----------------------|
| A (Base Case) | None | None |
| B | Fast flow path exists between the disposal unit wall and the saltstone monolith caused by deterioration of existing sheet drainage system | None |
| C | Fast flow path exists as described in Case B plus additional fast flow paths caused by cracks in the saltstone or cementitious material in the roof support columns | None |
| D | No fast flow paths and the existing sheet drainage system remains intact to form a capillary breach between saltstone and the disposal unit wall. | None |
| E | None | Yes |

Table 5.6-3: Case Probability by Disposal Unit Type

| Case | Probability by Disposal Unit Type | | |
|------|-----------------------------------|-------------|----------|
| | Vault 1 (%) | Vault 4 (%) | FDCs (%) |
| A | 95 | 85 | 85 |
| B | 0 | 5 | 5 |
| C | 4.9 | 4.9 | 4.9 |
| D | 0 | 5 | 5 |
| E | 0.1 | 0.1 | 0.1 |

Since the GoldSim SDF model is used only to model contaminant transport, flow profiles over time are abstracted from PORFLOW flow results for each of the five cases using the PORFLOW SDF model. The PORFLOW SDF model flow results are simplified into a 1-D steady state flow through the various material zones to allow use in the GoldSim SDF model. These material zones are the saltstone monolith, the walls of the disposal units, soil adjacent to the walls of the disposal units, and the unsaturated vadose zone below the disposal units. Using different flow profiles for the different cases is the method by which uncertainties in parameters affecting flow (e.g., condition of the sheet drain system for Vault 4 and the FDCs condition of support columns and saltstone) are incorporated into the uncertainty/sensitivity analysis.

Figures 5.6-26 and 5.6-27 provide flow profiles through the saltstone and the wall of Vault 1 to help illustrate the movement of water flow for the different cases associated with Vault 1. The flow profile in Figures 5.6-26 and 5.6-27 may be somewhat counterintuitive as the Case A flow produces a higher flow through the saltstone for most of the 20,000 year period. However, consideration needs to be given for the flow that is moving through the fast flow path conduits in Cases B and C, and therefore, not available to flow through the saltstone of Cases B and C. As stated earlier in this section, Vault 1 does not contain a sheet drainage system; therefore, Cases B and D are not applicable to Vault 1.

Figure 5.6-26: Flow Profile through Saltstone in Vault 1 for Cases A, C, and E

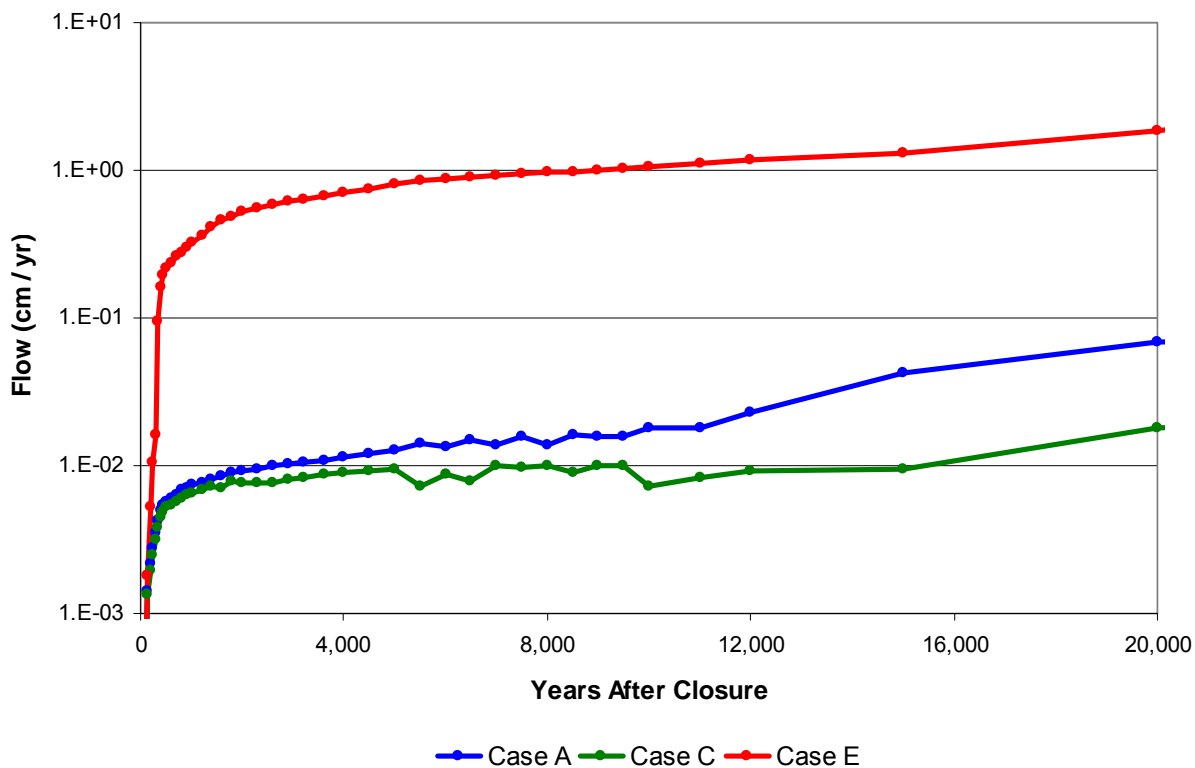


Figure 5.6-27: Flow Profile through Vault 1 Wall for Cases A, C, and E

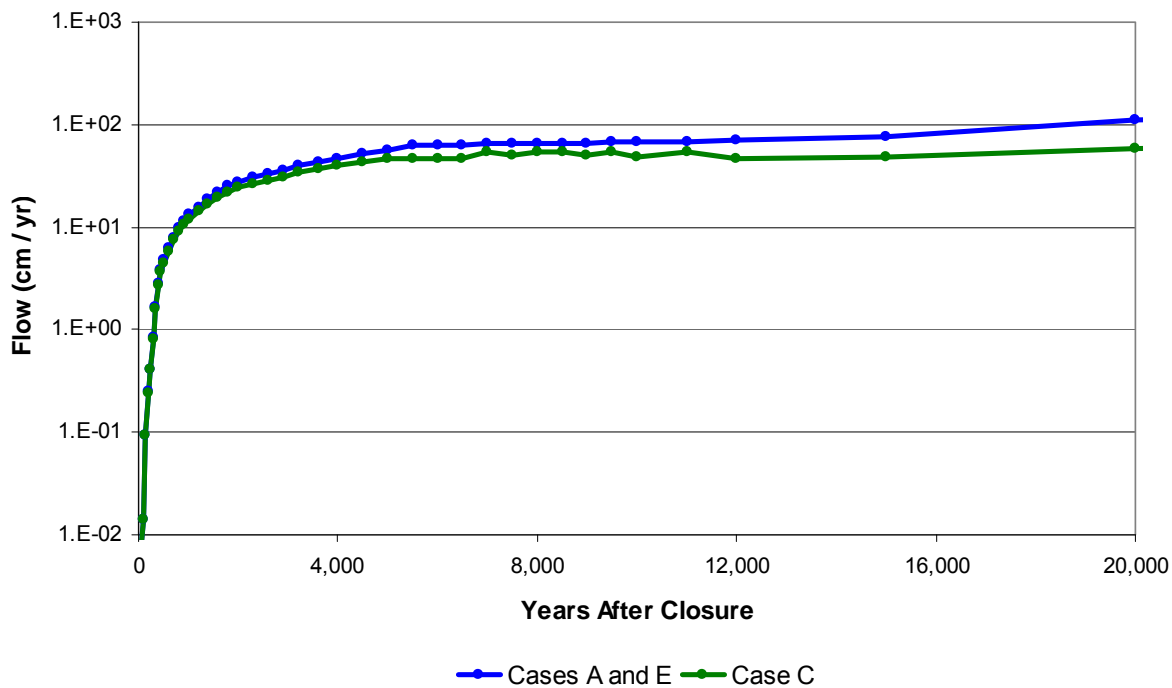


Figure 5.6-26 illustrates that because of the fast flow path postulated in Case C, flow through the saltstone is reduced from the Base Case (Case A). Similarly, Figure 5.6-27 illustrates that because of the fast flow path postulated in Case C, flow through the wall is reduced from Case A. Figure 5.6-26 illustrates that the postulated degraded condition (Case E) of the saltstone allows more flow through the saltstone than in Case A due to the lower hydraulic properties associated with the degraded condition of the saltstone. Figure 5.6-27 illustrates that the flow through the wall is not significantly impacted by the degraded condition of the saltstone.

The flow profiles through the saltstone and the wall of Vault 4 are provided in Figures 5.6-28 and 5.6-29 to help illustrate the movement of water flow for the different cases associated with Vault 4. As stated earlier in this section, Vault 4 contains a sheet drainage system; therefore, Cases B and D are applicable to Vault 4.

Similar to Vault 1, Figure 5.6-28 illustrates that the flow through the saltstone is reduced from the Base Case (Case A), for the fast flow conditions postulated in Cases B and C. See the description in Vault 1 above for the explanation for the seemingly counterintuitive results between Case A and Cases B and C. The flow profiles for Cases B and C through the saltstone illustrate the dependence on the flow through the wall as it is diverted from the saltstone to the wall as shown in Figure 5.6-29. Also, as in the case for Vault 1, the flow through the saltstone is greater for Case E, the postulated degraded saltstone condition, than in the Base Case. For Case D, where it is postulated that a capillary break exists between the saltstone and the disposal unit wall due to the presence of the sheet drain, there is no appreciable impact on the flow through the saltstone.

Figure 5.6-28: Flow Profile through Saltstone in Vault 4 for Cases A through E

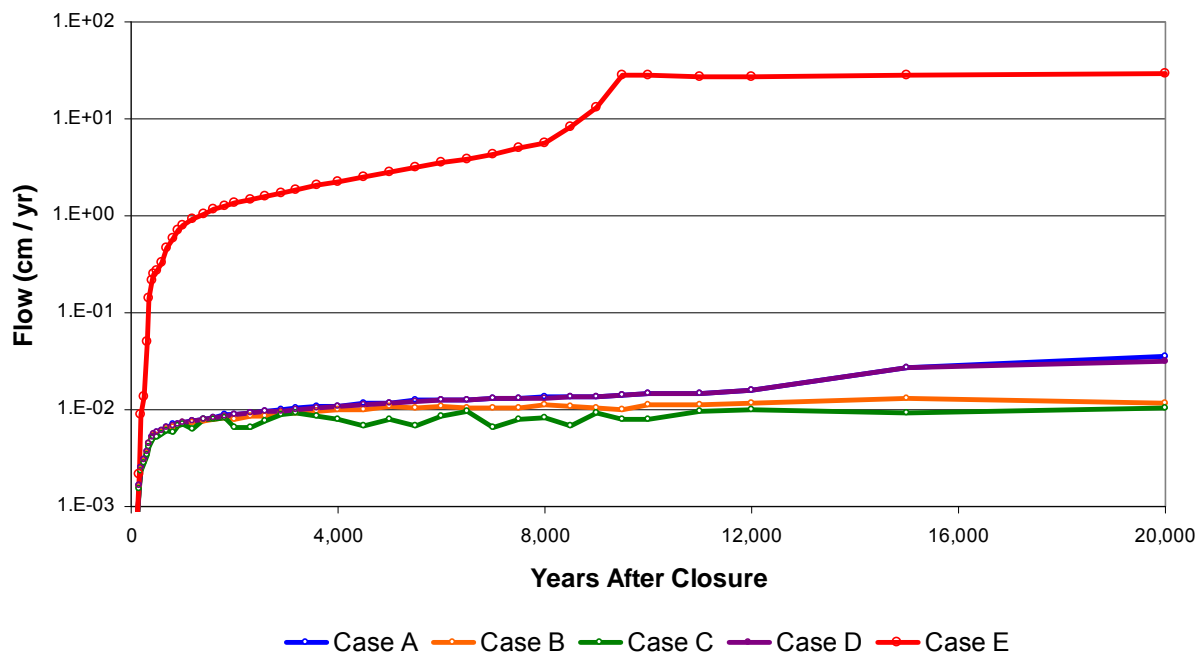
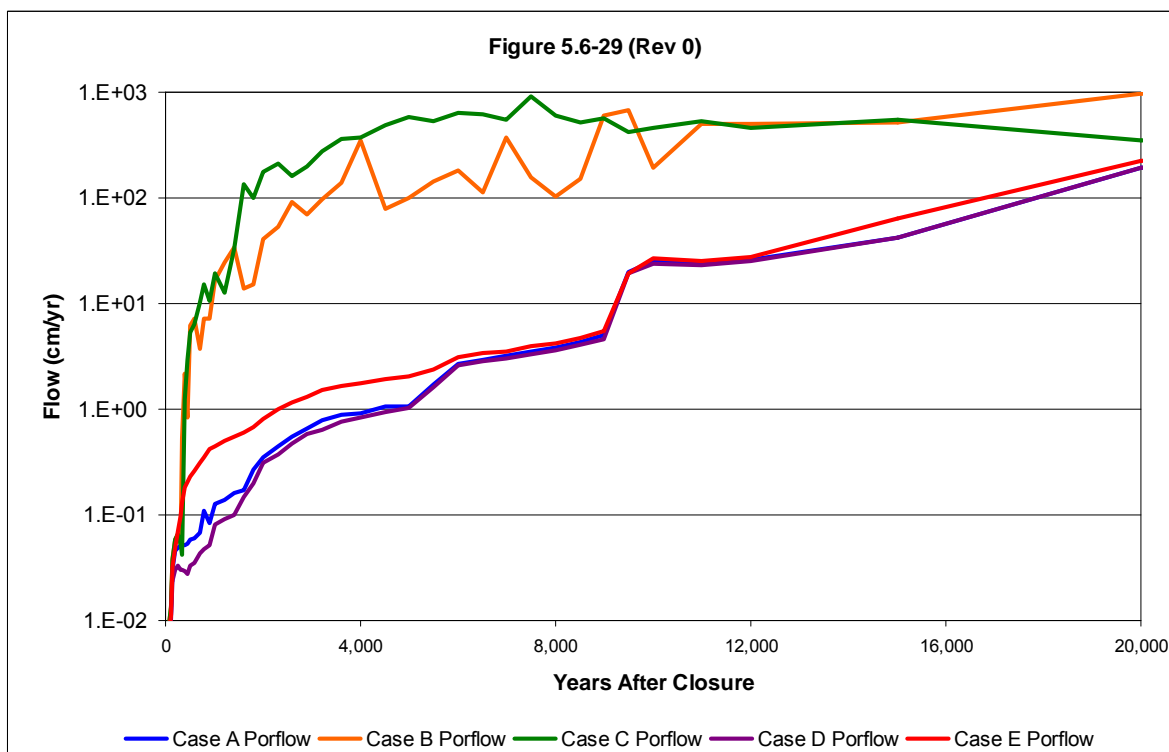


Figure 5.6-29: Flow Profile through Vault 4 Wall for Cases A through E



Similar to Vault 1, Figure 5.6-29 illustrates that the flow through the Vault 4 wall is reduced from the Base Case (Case A), for the fast flow conditions postulated in Cases B and C. Also, as in the case for Vault 1, the flow through the Vault 4 wall is not significantly impacted by Case E, the postulated degraded saltstone condition. For Case D, where it is postulated that a capillary break exists between the saltstone and the disposal unit wall, there is no appreciable impact on the flow through the Vault 4 wall. The significant changes between time-steps shown in Figure 5.6-29 for Cases B and C can be attributed to the averaging technique used to convert the 2-D flow from PORFLOW to a 1-D flow used in GoldSim.

Flow profiles through the saltstone and the wall of the FDCs are provided in Figures 5.6-30 and 5.6-31 to help illustrate the movement of water flow for the different cases associated with the FDCs. As is the case for Vault 4, the FDCs contain a sheet drainage system; therefore, Cases B and D are applicable to the FDCs.

Figure 5.6-30: Flow Profile through Saltstone in the FDCs for Cases A through E

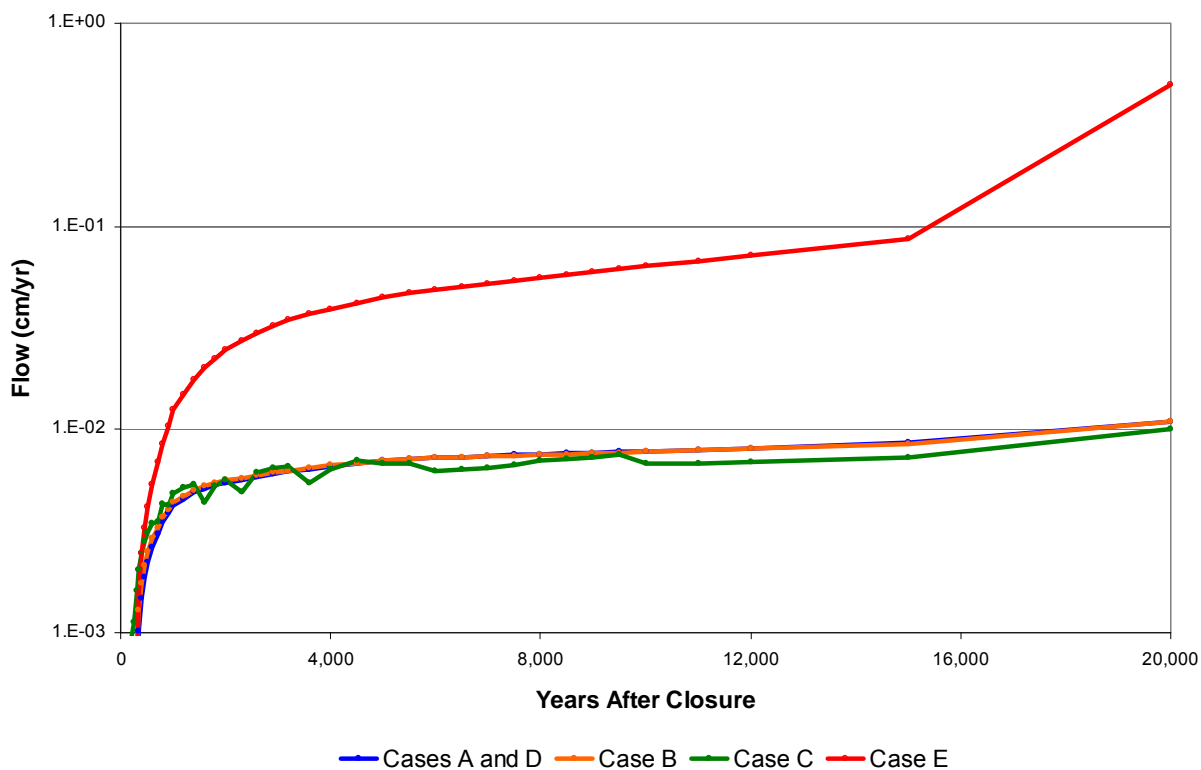
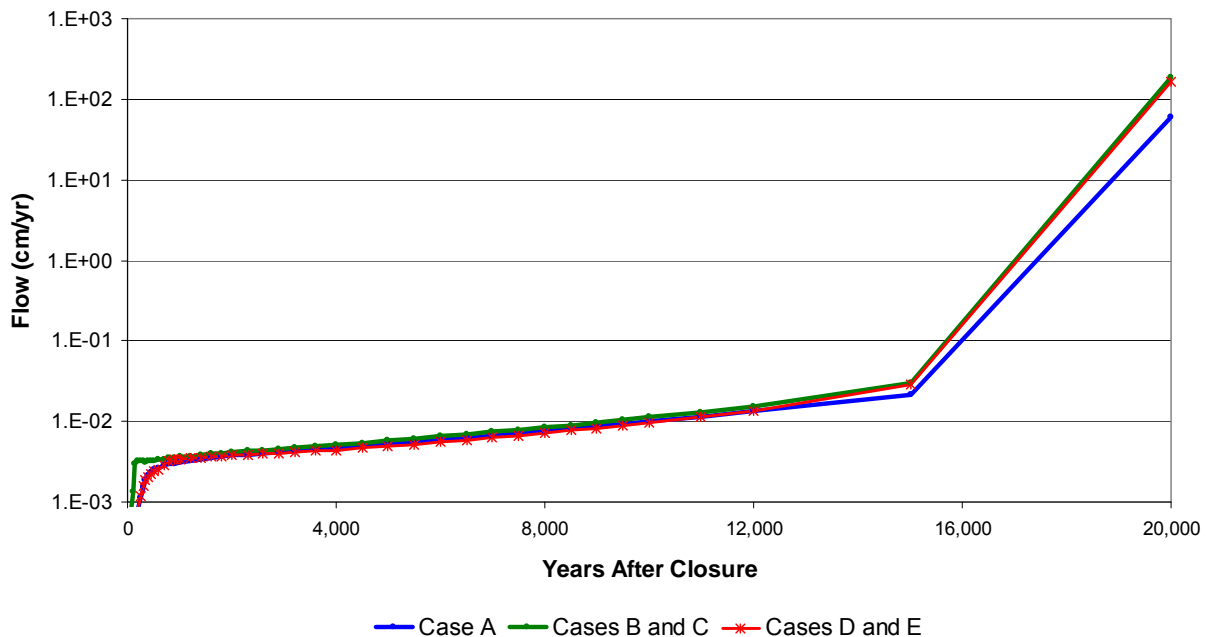


Figure 5.6-31: Flow Profile through the Wall of the FDCs for Cases A through E



Unlike Vault 4, Figure 5.6-30 illustrates that the flow through the saltstone is not significantly impacted by either of the fast flow cases (Cases B and C). As illustrated for Vault 4, Case D also does not significantly impact the flow through the saltstone for the FDCs. Also, as in the case for Vaults 1 and 4, the flow through the saltstone is greater for Case E, the postulated degraded saltstone condition, than in the Base Case (Case A).

Unlike Vault 4, Figure 5.6-31 illustrates that the flow through the wall of the FDCs is not significantly impacted by either of the fast flow cases (Cases B and C). As illustrated for Vault 4, Case D also does not significantly impact the flow through the wall for the FDCs. Also, as in the case for Vaults 1 and 4, the flow through the wall is not impacted by Case E, the postulated degraded saltstone condition.

5.6.3.2 Radionuclide Inventory

The radionuclide inventories in the SDF disposal units control the total amount of radioactive contaminants available for release. Sections 3.3 and 4.2.1 describe the basis for estimates of the radionuclide inventory in the disposal units. The baseline inventory used for each radionuclide is listed in Table 3.3-1, 3.3-3, 3.3-5, and 3.3-7. In the probabilistic analyses of this parameter, the inventory of each radionuclide is varied based on uncertainties identified in the development of the baseline inventory. The assumed waste treatments' (i.e., ARP/MCU and SWPF) effectiveness used as the basis for the Section 3.3 inventories are minimum values acceptable for the processes. Any uncertainty applied to the effectiveness would only reduce the disposal inventory and was therefore conservatively ignored in the probabilistic analyses.

Two isotope inventory variations were considered, source and location. The source variation deals with variability associated with the ability to predict inventories. This source variation not only includes material variability within the waste tanks, but also includes process treatment uncertainty and analytical uncertainty. The process treatment factors used in developing the SDF inventory were bounding. Therefore, any associated uncertainty was not included to provide conservatism in the inventory estimates. The analytical uncertainty is included in the process used to develop the inventory uncertainties below. The location variation deals with the uncertain waste disposal sequence to the disposal units. The disposal unit inventories, simply, are a total material received, after Vaults 1 and 4, averaged over all the disposal units. The actual inventory will differ based on the actual disposal order of waste removal from the various waste storage tanks. Vaults 1 and 4 are not included in the location variation.

The inventory variation was based on differences between measured and predicted inventory of salt concentrations, and not supernate concentrations. The saltstone inventory was principally based on supernate and saltcake quantities from WCS. The WCS supernate concentrations are frequently corrected based on sample analyses required for tank farm transfers. Therefore the supernate inventory is believed to be reasonably accurate, but does not allow for a study of the predicting ability of WCS. WCS also provided the overall basis for the saltcake inventories. Unlike supernate inventories, the saltcake inventories are not frequently sampled and therefore the inventories are not adjusted. This allows for a comparison of WCS predictions to sample analyses. Saltcake samples from Tanks 2, 3, 10, 25, 29, 37, 38, and 41 were used to develop a ratio of sample analysis to predicted values. Only the following isotopes were considered, C-14, Sr-90, Tc-99, I-129, Cs-137, U-238, Np-237, and Pu-239. Figure 5.6-32 illustrates these ratios for the different waste storage tanks, for several isotopes. Table 5.6-4 presents the uncertainties associated with the radionuclide inventory, developed using Figure 5.6-32 as the basis and is identified as “inventory uncertainty u” in the GoldSim model using a logarithmic-normal distribution. Note, the uncertainty assigned to Cs-137 was based more on the fact that a majority (>99%) of the Cs-137 activity originated from the supernate instead of the saltcake. Since the supernate inventories are constantly updated, generating confidence, the Cs-137 uncertainty was lower than that depicted in Figure 5.6-32. The distributions were selected based in the available data for Pu-239 presented in Figure 5.6-32 which indicates that the median of the distribution is expected to be 1.0. The values presented in Table 5.6-4 are used as multipliers to the baseline inventories presented in Section 3.3 for the uncertainty and sensitivity analysis.

Figure 5.6-32: Saltcake Sample to Prediction Ratio

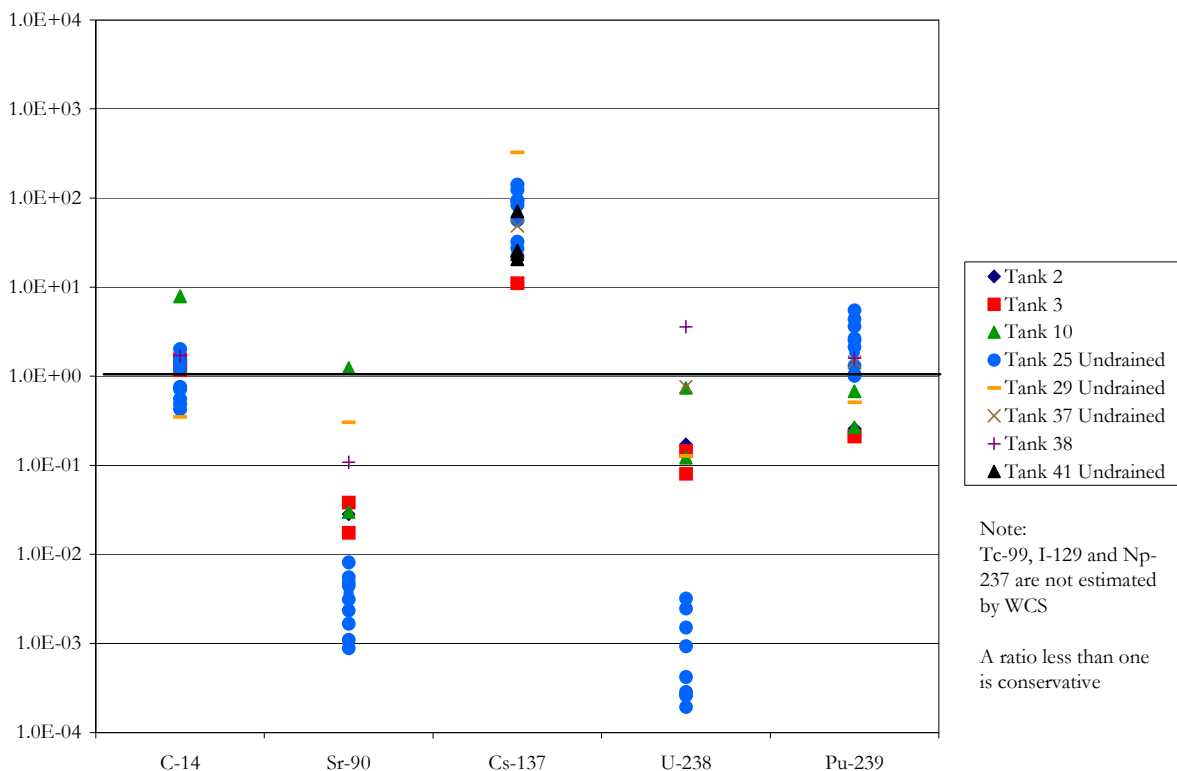


Table 5.6-4: Radionuclide Inventory Uncertainty in GoldSim Model

| Radionuclide | Minimum | Maximum | Median | Statistical Mean |
|--------------|---------|---------|--------|------------------|
| C-14 | 0.1 | 10 | 1.0 | 1.005 |
| Cs-137 | 1.0 | 10 | 1.07 | 1.081 |
| Pu-239 | 0.1 | 10 | 1.0 | 1.005 |
| Sr-90 | 0.001 | 1 | 0.94 | 0.928 |
| U-238 | 0.0001 | 10 | 1.0 | 1.005 |
| All others | 0.1 | 10 | 1.0 | 1.005 |

For the location variation on inventory, the GoldSim model randomly selected the order for which the waste tanks would be emptied and the FDCs to be filled with the constraint that the total SDF inventory presented in Table 3.3-7 would be conserved.

5.6.3.3 Distribution Coefficient Values

In the SDF model the saltstone, disposal unit concrete, and soil retard contaminant transport with their effectiveness tied to the assigned K_d values (which will vary for different elements). Tables 4.2-15 and 4.2-18 present baseline K_d values for all of the elements of interest for soils and cementitious materials, respectively. The baseline values reported in the

aforementioned tables are the GM for the truncated log-normal distributions utilized in the GoldSim model. Based on SRNL-STI-2009-00150, the distributions will be bounded as provided in Table 5.6-5.

Table 5.6-5: Distribution Coefficient Variability in the GoldSim Model

| Material Zone | Minimum | Maximum | Log-Normal Geometric Standard Deviation | |
|----------------------------------|-----------------------|-----------|---|--------------------------|
| Clayey Soils (Backfill Layer) | 0.5 x GM ^a | 1.5 x GM | GM < 4.0 mL/g | GM = 4.0 mL/g or greater |
| | | | 1.001 mL/g | 0.25 x GM |
| Sandy Soils (Vadose Zone) | 0.25 x GM | 1.75 x GM | GM < 2.7 mL/g | GM = 2.7 mL/g or greater |
| | | | 1.001 mL/g | 0.375 x GM |
| Cementitious Materials | 0.25 x GM | 1.75 x GM | GM < 2.7 mL/g | GM = 2.7 mL/g or greater |
| | | | 1.001 mL/g | 0.375 x GM |

(a) GM = Geometric Mean of the log-normal distribution defined as the baseline value presented in Table 4.2-15 for soils and Table 4.2-18 for cementitious materials.

5.6.3.4 Transition Times between Chemical States

The “Transition Times between Chemical States” in the GoldSim SDF model determined how many pore water volumes were required to pass through the saltstone or the wall concrete in the disposal units before the cementitious material transitions to a different chemistry (i.e., from reducing to oxidizing condition, or from Regions II to III). As part of the waste release modeling (discussed in detail in Section 4.2.2), the estimated transition times between various chemical phases were calculated for the saltstone and the disposal unit concrete and shown in Table 4.2-1. The analysis conducted to calculate these transition times is provided in SRNL-TR-2008-00283 and this analysis recommends a $\pm 50\%$ modeling uncertainty on the pore volumes. Thus, the GoldSim SDF model includes a stochastic analysis on transition times as shown in Table 5.6-6 using a uniform distribution with the mean value being the calculated values taken from Table 4.2-1.

Table 5.6-6: Pore Volume Transition Uncertainty in the GoldSim Model

| Transition State | Material | Mean | Minimum | Maximum |
|---|---------------------------|--------|---------|---------|
| Region II Reducing → Region II Oxidizing | Saltstone | 2,806 | 1,403 | 4,209 |
| Region II Oxidizing → Region III Oxidizing | Saltstone | 10,422 | 5,211 | 15,633 |
| Region II Reducing → Region II Oxidizing | Disposal Unit Concrete | 3,230 | 1,615 | 4,845 |
| Region II Oxidizing → Region III Oxidizing | Disposal Unit Concrete | 4,206 | 2,103 | 6,309 |

Note: Regions as found in ISSN 1019-0643

5.6.3.5 SDF Lower Vadose Zone Thickness

The lower vadose zone in the GoldSim SDF model retards contaminant transport, with its effectiveness related to the soil K_d values and the vadose zone thickness. Table 4.2-13 shows the estimated thickness of the lower vadose zone beneath each of the disposal units. The baseline model in the GoldSim SDF model uses the following vadose zone thicknesses, 50 feet for Vault 1, 40 feet for Vault 4, and 42 feet for the FDCs. Based on the data provided in WSRC-TR-2005-00131, a range of ± 16.4 feet is a reasonable variance of the unsaturated vadose zone thickness below the disposal units. A triangular distribution is used in the GoldSim SDF model for this parameter with the baseline values being the most likely values with the maximum value being the baseline plus 16.4 feet and the minimum value being the baseline minus 16.4 feet.

5.6.3.6 Well Depth

As discussed in Section 4.2.4 on exposure pathways, well water may be used as a primary potable water source for a future residence near the well (e.g., drinking water, showering) and may be used by the resident as a primary water source for agriculture (e.g., irrigation, livestock water). The hypothetical impacts to the receptor can be highly dependent on which aquifer the water is drawn. Available on-site and off-site well drilling data, as well as information from regional commercial well drillers is examined in SRS-REG-2007-00029 to determine probabilities associated with a future resident using a particular aquifer.

Based on the information obtained, SRS-REG-2007-00029 concludes that a well drilled by a professional driller would have a high probability of being located in the Gordon Aquifer or deeper. There is a possibility that a MOP receptor would choose to drill his own well and would only drill down as far as necessary to meet some short term minimum flow need (e.g., 10 gpm from the UTR-UZ), however this probability is considered reasonably small. Combining the percentages of the wells drilled in each depth range both onsite and offsite, it is reasonable to apply the probabilities in Table 5.6-7 when estimating well depths for well drilling scenarios within the GSA.

Table 5.6-7: Probability of Well Driller Exposure from Each Aquifer

| Aquifer (Depth) | % of Total in GSA |
|-------------------------------------|-------------------|
| UTR-UZ (less than 109 feet) | 13 |
| UTR-LZ (109-170 feet) | 44 |
| Gordon Aquifer (170 feet and lower) | 43 |

The GoldSim SDF model corresponds to a single representative aquifer and was benchmarked with the maximum PORFLOW calculated concentration in any aquifer within the sector. To simulate the probability that a potential well driller (MOP or intruder) might drill only as deep as the UTR-UZ, or drill deeper into the Gordon Aquifer; the well depth probabilities in Table 5.6-7 were used as a stochastic in the GoldSim SDF model. To reflect that a well at a different drill depth might have contaminant concentrations different than the

single aquifer (UTR-LZ) represented by the GoldSim SDF model, the key radionuclide concentration in each of the aquifers of interest, shown in Section 5.2.1, were compared to each other in Sector B. The concentrations in Sector B were chosen for comparison because the maximum dose within the first 10,000 years after closure occurs in Sector B, as shown in Section 5.2. The comparisons show that UTR-LZ has approximately three times the key radionuclide concentration than UTR-UZ and approximately 600 times the key radionuclide concentration than in the Gordon Aquifer. Thus, the concentration ratios between the three aquifers are approximately 35%/100%/0.2% for UTR-UZ/UTR-LZ/Gordon. The UTR-UZ and UTR-LZ concentrations are relatively similar because the aquitard that separates them (the “tan clay” layer) is a relatively ineffective flow barrier. In contrast, the aquitard that separates the Gordon Aquifer (the “green clay” layer) is very effective and there is very little downward flow into the Gordon Aquifer relatively to lateral flow along the UTR-LZ Aquifer. To conservatively assess the potential consequence of drilling into the different aquifers, the GoldSim model uses concentration ratios of 100%/100%/5%. The maximum I-129 concentration in the three aquifers shown in Section 5.2.1 result in a similar comparison provided above for nitrogen, which validates the conservatism used in the GoldSim model. Table 5.6-8 provides the relationships used in the stochastic modeling between the contaminant concentrations in the three aquifers of interest.

Table 5.6-8: Contaminant Transfer Ratios Between Aquifers

| Aquifer | Contaminant Concentration in Relation to UTR-LZ | Calculation used for Basis |
|----------------|--|--|
| UTR-UZ | 100% | Peak Concentration UTR-UZ/Peak Concentration UTR-LZ ~33% |
| UTR-LZ | 100% | N/A |
| Gordon Aquifer | 5% | Peak Concentration Gordon Aquifer/Peak Concentration UTR-LZ ~ 0.2% |

The data used in determining the ratios is provided in Appendix E.2.

5.6.3.7 Bioaccumulation Factors and Human Health Exposure Parameters

The Bioaccumulation Factors (Section 4.6.1) and Human Health Exposure (Section 4.6.2) parameters have various functions in the GoldSim SDF model, but they all assist in calculating doses for the exposure pathways. The baseline values and stochastic distributions used for various Bioaccumulation Factors and Human Health Exposure parameters are provided in Tables 5.6-9 through 5.6-11. For the transfer factors in Tables 4.6-1 through 4.6-4, only the most likely value was used in the stochastic analysis (no distributions were created for these values).

Table 5.6-9: Crop Exposure Time and Productivity Stochastics

| Parameter | Baseline⁽²⁾ | Minimum | Maximum | Mean or SD or GSD⁽³⁾ | Distribution Used |
|--|-------------------------------|----------------|----------------|--|------------------------------|
| Vegetable crop exposure times to irrigation, days ⁽¹⁾ | 70 | 60 | 90 | 7 | Normal |
| Soil exposure time period to irrigation, days (Buildup time in soil) | 183 | 60 | 365 | 212.5 | Uniform |
| Vegetable Crop Yield Productivity, kg/m ² | 0.7 | 0.2 | 4 | 1.4 | Lognormal |
| MOP Fraction of Vegetables Produced Locally | 0.173 | 0 | 0.5 | 0.224 | Triangular |
| MOP Fraction of Meat Produced Locally | 0.306 | 0 | 0.5 | 0.269 | Triangular |
| MOP Fraction of Milk Produced Locally | 0.207 | 0 | 0.5 | 0.236 | Triangular |
| Intruder Fraction of Vegetables Produced Locally | 0.308 | 0 | 0.5 | 0.269 | Triangular |
| Intruder Fraction of Meat Produced Locally | 0.319 | 0 | 0.5 | 0.273 | Triangular |
| Intruder Fraction of Milk Produced Locally | 0.254 | 0 | 0.5 | 0.251 | Triangular |

(1) Average growing time for above ground vegetables.

(2) Baseline value is the value used in the deterministic case and the Most Likely value for Triangular distributions.

(3) Mean is provided for Uniform or Triangular distribution and the SD is provided for the Normal distribution or the Geometric Standard Deviation (GSD) for the Lognormal distribution.

Table 5.6-10: Pathway Physical Parameter Stochastics

| Parameter | Baseline⁽¹⁾ | Minimum | Maximum | Mean | Distribution Used |
|--|-------------------------------|----------------|----------------|-------------|------------------------------|
| Depth of Garden, cm | 15 | 15 | 61 | 30.3 | Triangular |
| Garden Irrigation Rate, L/d/m ² | 3.6 | 2.08 | 5.5 | 0.373 | Triangular |
| Fraction of Year Garden Irrigated | 0.2 | 0.2 | 0.25 | 0.217 | Triangular |
| Garden Size, m ² | 100 | 100 | 1,000 | 400 | Triangular |

(1) Baseline value is the value used in the deterministic case and is the Most Likely value for Triangular distributions.

Table 5.6-11: Consumption Rate, Pathway Exposure Time and Transport Stochastics

| Consumption Rate Parameters | Baseline | Minimum | Maximum | Mean or SD or GSD⁽²⁾ | Distribution Used |
|--|-----------------|----------------|----------------|--|--------------------------|
| Annual Breathing Rate, m ³ /yr | 5,548 | 1,267 | 11,600 | 1,700 | Normal |
| Annual Leafy Veggie Consumption, kg/yr | 21 | 18 | 43 | 2 | Lognormal |
| Annual Other Veggie Consumption, kg/yr | 163 | 90 | 276 | 2 | Lognormal |
| Annual Beef Consumption, kg/yr | 43 | 26 | 81 | 1.8 | Lognormal |
| Annual Finfish Food Consumption, kg/yr | 9 | 2.2 | 19 | 10.1 | Triangular |
| Annual Milk Consumption, L/yr | 120 | 73.7 | 230 | 2.2 | Lognormal |
| Water Consumption Rate, L/yr | 337 | 184 | 730 | 417 | Triangular |
| Fodder Beef Cow Consumption, kg/d | 36 | 27 | 50 | 8 | Normal |
| Fodder Milk Cow Consumption, kg/d | 52 | 36 | 55 | 11 | Normal |
| Fraction of Beef Cow intake from pasture | 0.75 | 0.5 | 1 | 0.75 | Triangular |
| Fraction of Milk Cow intake from pasture | 0.56 | 0.5 | 1 | 0.69 | Triangular |
| ⁽³⁾ Water Beef Cow Consumption, L/d | 28 | 28 | 50 | 37.8 | Triangular |
| ⁽³⁾ Water Milk Cow Consumption, L/d | 50 | 50 | 60 | 54.4 | Triangular |
| Exposure Time Parameters | | | | | |
| Showering Exposure Time, min/d | 10 | 10 | 30 | 16.7 | Triangular |
| ⁽³⁾ Fraction of Year In Garden – Intruder | 0.01 | 0.01 | 0.08 | 0.04 | Triangular |

- (1) Baseline value is the value used in the deterministic case and is the Most Likely value for Triangular distributions (except as noted in Note 3).
- (2) Mean is provided for Uniform or Triangular distribution, the SD is provided for the Normal distributions or the GSD for the Lognormal distributions.
- (3) Most Likely value for Water Beef Cow Consumption is 35.3 L/d, for Water Milk Cow Consumption is 53.3 L/d, and for Fraction of Year in Garden – Intruder is 0.03.

Where available, site-specific distribution information, obtained from WSRC-STI-2007-00004 was used in determining the stochastic range to be evaluated. Where no site-specific information was available, a triangular distribution using maximum, minimum and most-likely values from WSRC-STI-2007-00004 is utilized as the distribution peak in the stochastic analysis. Although these values were not site-specific or weighted for the purpose of the stochastic analysis, they provide a wide range of possible outcomes, and better able to identify parameters of potential concern. Additional background information regarding a few parameters of interest are provided below.

5.6.3.7.1 Drinking Water Ingestion

Ingestion of water is a key usage factor for the all-pathways and inadvertent intruder analyses. The rate of contaminated water consumption varies based on assumed access to water supply.

The RESRAD 511 L/yr (1.4 L/d) average water ingestion rate updated for use in the all-pathways analysis is based on EPA surveys published in the early 1990s. [ANL-EAD-4] The 730 L/yr (2 L/d) water ingestion rates for the inadvertent intruder are taken from *Site-Specific Parameter Values for the Nuclear Regulatory Commission's Food Pathway Dose Model* (ISSN 0017-9078 Vol. 62 No. 2), and are based on rates for the MEI from Appendix I of Regulatory Guide 1.109. The average rate for ingestion of drinking water from these sources is 370 L/yr (1 L/d). These publications consider indirect ingestion of water but do not consider whether or not the water is bottled or comes from a community or commercial source.

EPA drinking water survey estimates per capita ingestion of water using data from the combined 1994, 1995, 1996, and 1998 *Continuing Survey of Food Intakes by Individuals (CSFII)*, conducted by the USDA. This publication considers indirect ingestion of water from food with water added at the final phase of food preparation and reports water consumption from community water, bottled water, water from other sources, missing source, and total water. Summary data found in the Executive Summary of EPA-822-R-00-001 (pages vii-viii) provide a 337 L/yr water ingestion rate.

According to EPA, direct water is plain water ingested directly as a beverage and indirect water is water added to foods and beverages during final preparation at home, or by food service establishments such as school cafeterias and restaurants. An example of indirect water is water added to dry cake mix. Community water is tap water from the community water supply. Bottled water is purchased, plain water. Other water is water obtained from a well or rain cistern (household's), spring (household's or public), or other source. Preparation water is water used to prepare foods and includes the water used to prepare foods at home and by local food service establishments (indirect water), as well as, water added by commercial food manufacturers. Missing water source indicates that a survey participant responded "don't know" or "not ascertained" to the survey question regarding the source of water. Total water is the sum of direct and indirect water from all sources which includes community water, bottled water, other water and missing sources. [EPA-822-R-00-001]

The EPA drinking water survey reports the mean per capita total water ingestion is 1,233 mL/person/d (450 L/yr) when viewed across genders and all age categories with 75% from community water, 13% from bottled water, 10% from other sources and 2% from non identified sources. This yields a mean of 924 mL/person/d (337 L/yr) from community water and 12.3 mL/person/d (4.5 L/yr) from other sources (well water). [EPA-822-R-00-001]

A value of 337 L/yr is used as the nominal water ingestion rate for all MOP and inadvertent intruder pathway analyses. In the stochastic analyses of this parameter, the water ingestion rate range is assumed to be as high as 730 L/yr (2 L/d), which, as discussed above, is a maximum evaluation point provided by the NRC. [Regulatory Guide 1.109] The lower range of the water ingestion rate range was set at 184 L/yr, the minimum recommended water

ingestion rate is cut in half (e.g., water or other liquids from a clean source are used instead of drinking water from a contaminated source). A triangular distribution is used in the stochastic analysis which causes the mean value for this parameter to rise well above the most likely value (417 L/yr vs. 337 L/yr).

5.6.3.7.2 Crop Yields

A survey of local practices surveyed 21 county extension agents in Georgia and South Carolina to estimate the average mass, in kilograms, of vegetation harvested in a typical square meter of garden or farmland within a 50 mile radius of SRS. [WSRC-RP-91-17] Crop yields in kg/m² were estimated for leafy vegetation (cabbage, lettuce and spinach) and other above ground vegetables (broccoli, cauliflower, green peas, lima beans, and sweet corn). Average agricultural, garden, and pasture grass productivity for farms in the 50 mile region is estimated to be 0.7 kg/m², 0.2 kg/m² and 1.8 kg/m², respectively. Because the garden productivity was estimated to be an order of magnitude lower than 10 Regulatory Guide 1.109 default, WSRC-RP-91-17 assumed the garden productivity is to be equal to agricultural productivity. This report recommends use of the site-specific value of 0.7 kg/m² as the expected value for garden productivity, and the 0.2 kg/m² should be considered in the uncertainty range.

The current assumption of the fractions of vegetables, milk, and meat intake from a local garden were based on various references with 0.5 fraction of vegetable production considered to be a maximum value. Table 13-71 of EPA-600-P-95-002 provides regional values for vegetables, milk, and meat production fractions and scenario specific values for households with gardens who raise animals for an all-pathways analysis and those for households who farm for an intruder analysis.

5.6.3.7.3 Garden Size

The garden size of 100m² for a family of four is assumed in SRS PAs, and is based on site-specific evaluation of consumption needs and annual productivity. It is assumed that a well would not be drilled for a single individual but rather for a household that includes at least two adults. As discussed in Section 4.6.2, SRS report, WSRC-RP-91-17 estimated that a person within a 50 mile radius of SRS consumes 184 kg of vegetables annually. The crop yields discussion above discusses the average garden vegetable yield of 0.2 kg/m², but recommends the use of the agricultural 0.7 kg/m², as reported in WSRC-RP-91-17. A garden size of 260m² would be required to support the annual consumption of 184 kg of vegetables for a household with two adults assuming all vegetables consumed by the adults are from their garden. Assuming that only 17% of a person's vegetables are from their home garden (EPA-600-P-95-002), roughly 100m² would be required to feed a family of four. This report recommends use of the 100m² garden size for vegetables only. However, this area is not large enough to graze livestock. ANL-EAIS-8 states that an area of 1 hectare (10,000m²) is required to graze a single milk cow. A triangular distribution using the 1,000m² as a maximum, 100m² as a minimum, and the most likely value (100m²) as the peak was utilized for garden size in the stochastic analysis.

5.6.3.7.4 Soil Exposure Time Period

For soil exposure time period to irrigation (buildup), SRS report WSRC-STI-2006-00123 recommends 40 years to indicate the life time of a facility releasing radionuclide and 0.5 of a MEI lifetime assuming the MEI is exposed at that location for their lifetime. For the intruder and MOP scenario, it is assumed that the irrigation and harvesting of vegetables occur during the first year of residence, yielding the 183 day value.

5.6.3.7.5 Foodstuff Consumption

For the inadvertent intruder, vegetable, milk and beef consumption rates are taken from ISSN 0017-9078 Vol. 62 No. 2. These values are based on county specific statistics provided by the counties within the states of South Carolina and Georgia that fall within a 50 mile radius of SRS and are based on a site-specific evaluation. Triangular distributions using values from applicable literature as maximum and minimum values, and the most likely value as the peak was utilized for consumption rates in the stochastic analysis.

5.6.3.8 *Saturated Zone Flow Modeling Parameters*

As discussed in Section 4.4.2.1, the GoldSim SDF modeling domain begins at the top of the saltstone layer and extends to a hypothetical groundwater well located 100m from the SDF boundary. The flow profiles used in the GoldSim model to represent flow through the saltstone, the walls of the disposal units, the soil contiguous to the wall, and the unsaturated soil below the disposal units are extracted from the PORFLOW model, which allows for changes in the closure cap, the lateral drainage layer, and the roof of the disposal units. The model is 1-D with downward flow represented in the unsaturated zone and predominantly horizontal flow in the saturated zone. The unsaturated zone is represented as a column underlying each disposal unit.

The water flow boundary condition for the saturated zone bulk flow is also provided by the PORFLOW model. Saturated zone modeling Base Case values were refined in the GoldSim model during the benchmarking effort to align the GoldSim model results with the PORFLOW model results, as explained in the GoldSim benchmarking discussion (Section 5.6.2). Three modeling parameters of particular importance are the Saturated Zone Width, the Saturated Zone Thickness, and the Saturated Zone Darcy Velocity, additional information for each of these parameters is provided below.

5.6.3.8.1 Saturated Zone Width and Thickness

In the GoldSim SDF model, water leaving the unsaturated zone enters the saturated zone (i.e., the aquifer) as recharge and this infiltrating water is mixed into the volume of aquifer water. The volume is determined by the flow rate and mixing volume (flow face area times flow velocity) in the aquifer. The flow face area is dependent on the width and thickness of the saturated zone. The width of the saturated zone is defined in the GoldSim model as SatWidth and is the length of the individual vaults (600 feet) and the diameter of the FDCs (150 feet). Each parameter is assigned a uniform distribution ranging from 80% to 120% of the defined value. The thickness of the aquifer is defined in the GoldSim model as SatThickness, and is assigned a Base Case value of 12m. For the stochastic modeling, the Base Case value of 12m is the mean of a normal distribution and a SD of 1.6m with

minimum and maximum values of 5m and 19m, respectively. The thickness of the saturated zone and the development of its distribution are based on review of data obtained from WSRC-TR-2005-00131, *Saltstone Disposal Facility: Determination of the Probable Maximum Water Table Elevation*, the results of the benchmarking process with the PORFLOW model, and engineering judgment.

5.6.3.8.2 Saturated Zone Darcy Velocity

In the GoldSim SDF model, the saturated zone Darcy Velocity is the primary reference for the velocity of water flowing in the aquifer. The Darcy Velocity is important to the model because it directly affects the concentration. The Base Case value used in the model is 45.7 m/yr. For the stochastic modeling, a normal distribution was utilized to determine the distribution range, with the Base Case value set as the distribution mean and 0.5 m/yr as the SD.

5.6.4 Uncertainty/Sensitivity Analysis using the SDF Probabilistic Model

A model was developed for performing the uncertainty and sensitivity analyses using the GoldSim systems analysis software. The model is not intended to predict future potential doses for comparison to performance objectives, the SDF PORFLOW model has been used for assessment of peak doses versus performance objectives. Rather, the goal of this SDF modeling is to characterize the context of uncertainty and sensitivity surrounding the PA calculations involving doses to MOP exposed via groundwater. The air and radon pathways results in Section 5.3 are such a small fraction of the performance measure that no uncertainty and sensitivity analyses were performed.

The uncertainty analysis is concerned with how the uncertainty in stochastically-defined model input parameters is propagated through the model to the selected model results, or endpoints. These model endpoints are potential radiological doses to hypothetical human receptors and aqueous concentrations of specific contaminants and groundwater concentrations of selected radionuclides.

In contrast, the sensitivity analysis (discussed in Section 5.6.5) is focused on determining which of the many input parameters (called explanatory variables) are most responsible for determining the endpoints. It is important to note that only those model parameters that are defined using a probability distribution can be assessed for uncertainty or sensitivity. The numerous parameters that are defined using a single value implicitly contain no uncertainty, and therefore, are not subject to this analysis.

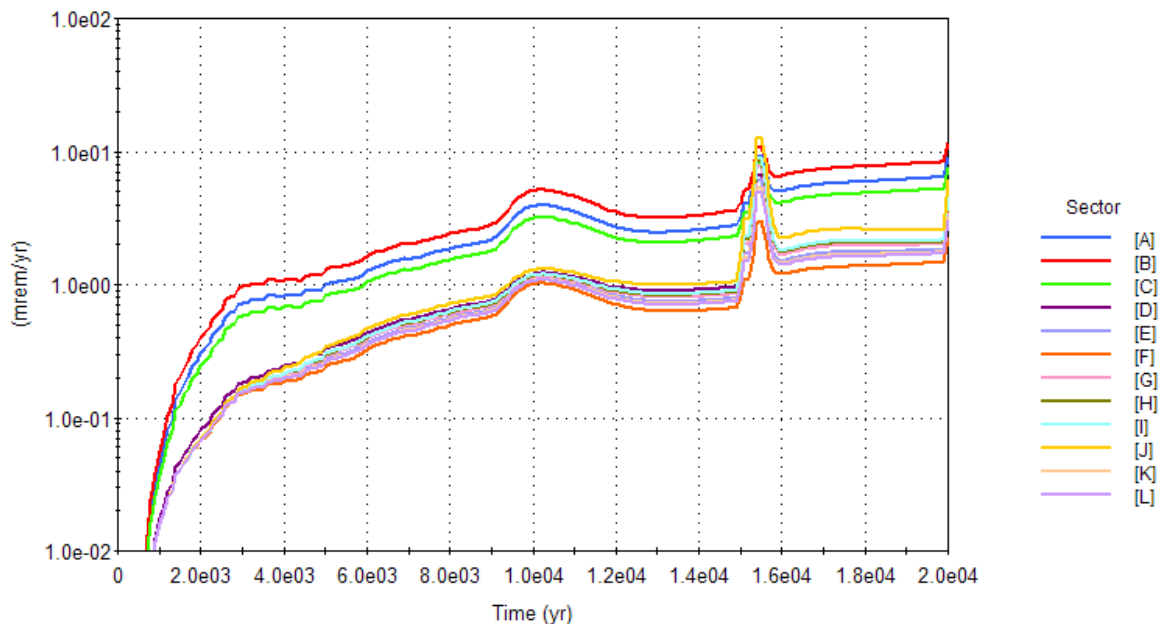
The probabilistic results of the GoldSim model are used to characterize the uncertainty manifested in the model input distributions. Some of these distributions are parameter values, (e.g., material properties or water flow rates). Others are more oriented toward scenario uncertainty, such as the stochastic parameter (variable) that selects which SDF disposal unit failure case to choose for a given realization. Together, the distributions (defined as stochastic elements in GoldSim) are intended to capture the overall uncertainty in the model. The probabilistic model uncertainty analysis does not address conceptual model uncertainty. Identification of conceptual model areas of importance is primarily accomplished through the combined sensitivity analyses (both stochastic and single parameter sensitivities). The sensitivity analyses highlight the portions of the conceptual

model that have the greatest influence on the model results (e.g., inventory, soil thickness, soil/water partition coefficients).

The SDF uncertainty/sensitivity analysis is based on 5,000 realizations of the SDF GoldSim model. The Monte Carlo analysis sampled the input distributions with Latin Hypercube Sampling. Runs were performed for Cases A through E, and for all cases combined. These runs are used to illustrate the model uncertainty. In addition, these same runs were limited to Cases A and C for the sensitivity analysis.

Before discussing these particular modeling scenarios however, their context can be illustrated by presenting a time series graph of mean doses, predicted by the model, where all cases (A through E) are chosen at random, though with non-uniform weighting. Figure 5.6-33 shows the mean dose to a MOP located in each of the defined PORFLOW sectors (Sectors A through L), at any point in time, for 20,000 years.

Figure 5.6-33: Mean Dose to a MOP, Any Sector within 20,000 Years – All Cases



Examining the behavior of the SDF by looking at some different cases in isolation, one can see which cases drive the overall behavior. The following figures present the mean value in the dose to a MOP for the various sectors for 20,000 years, examining each failure case in turn. Figure 5.6-34 presents the mean MOP dose given Case A alone followed by Figure 5.6-35 through 5.6-38 showing the results for Case B, C, D, and E, respectively. Note that the ordinate (dose) scales differ from graph to graph. The probability of each failure case occurring is provided in Section 5.6.3.1.

Figure 5.6-34: Mean Dose to a MOP, Any Sector within 20,000 Years – Case A

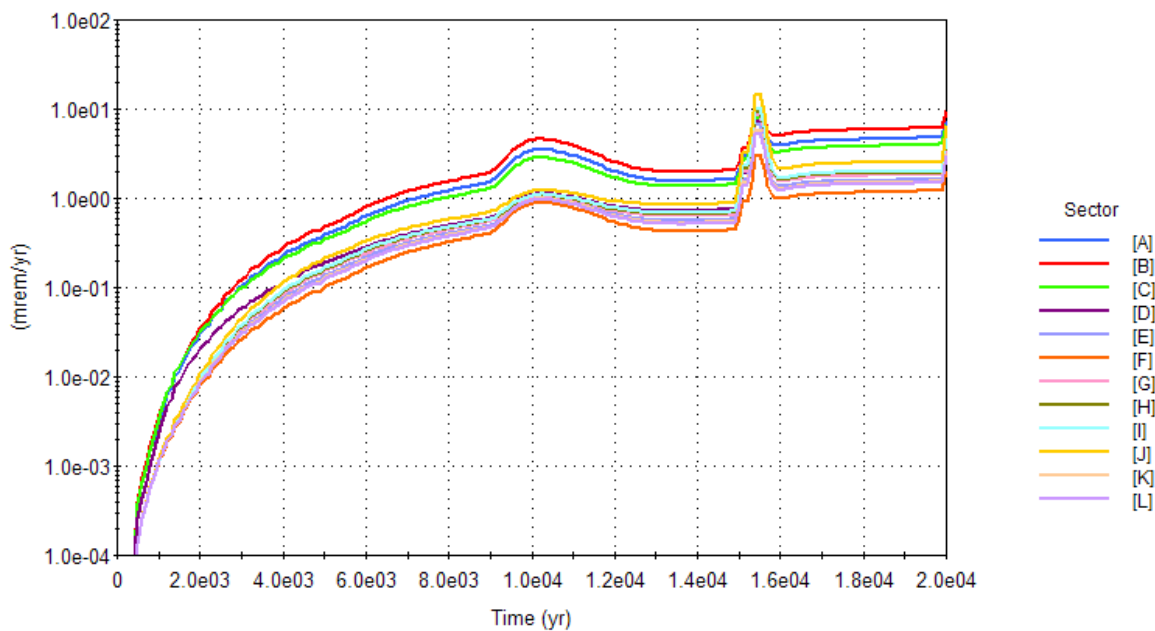


Figure 5.6-35: Mean Dose to a MOP, Any Sector within 20,000 Years – Case B

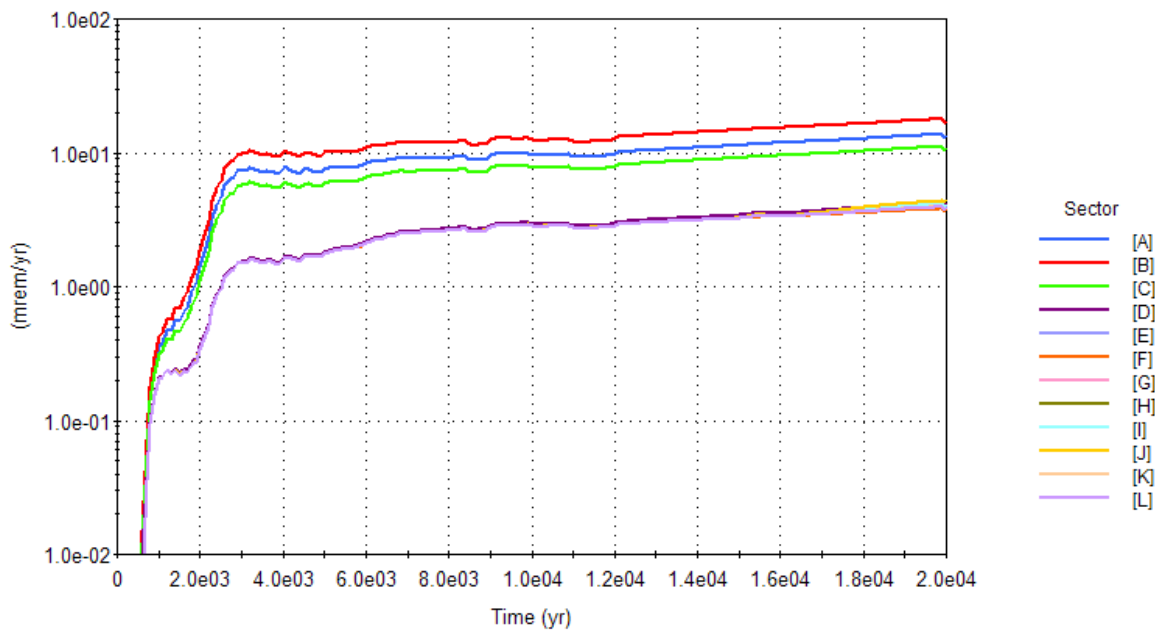


Figure 5.6-36: Mean Dose to a MOP, Any Sector within 20,000 Years – Case C

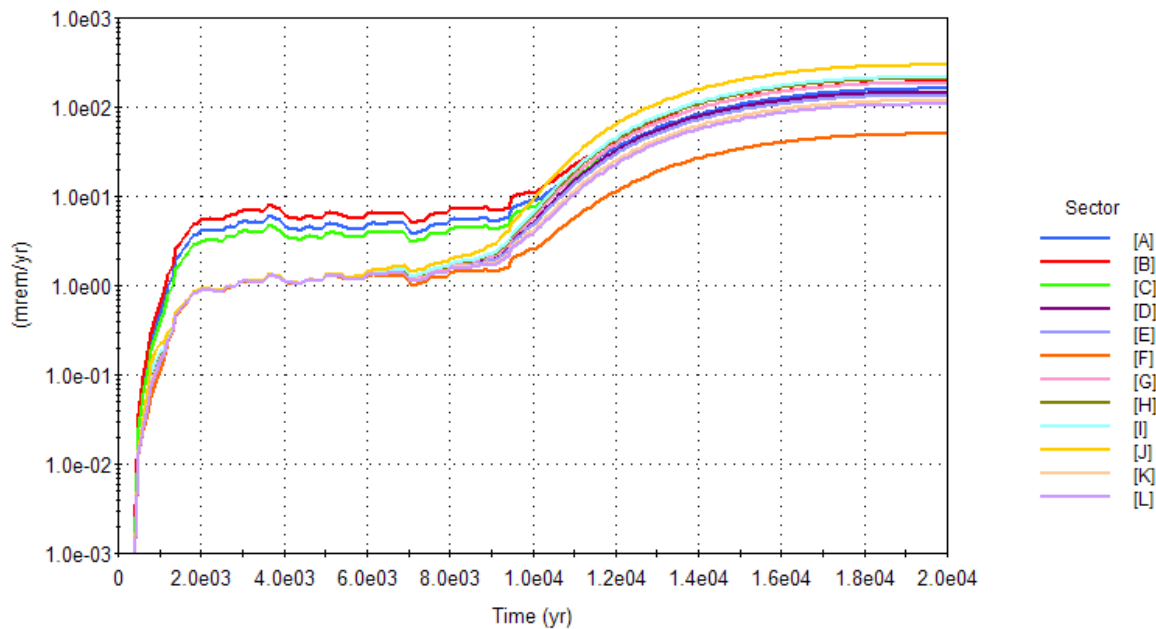


Figure 5.6-37: Mean Dose to a MOP, Any Sector within 20,000 Years – Case D

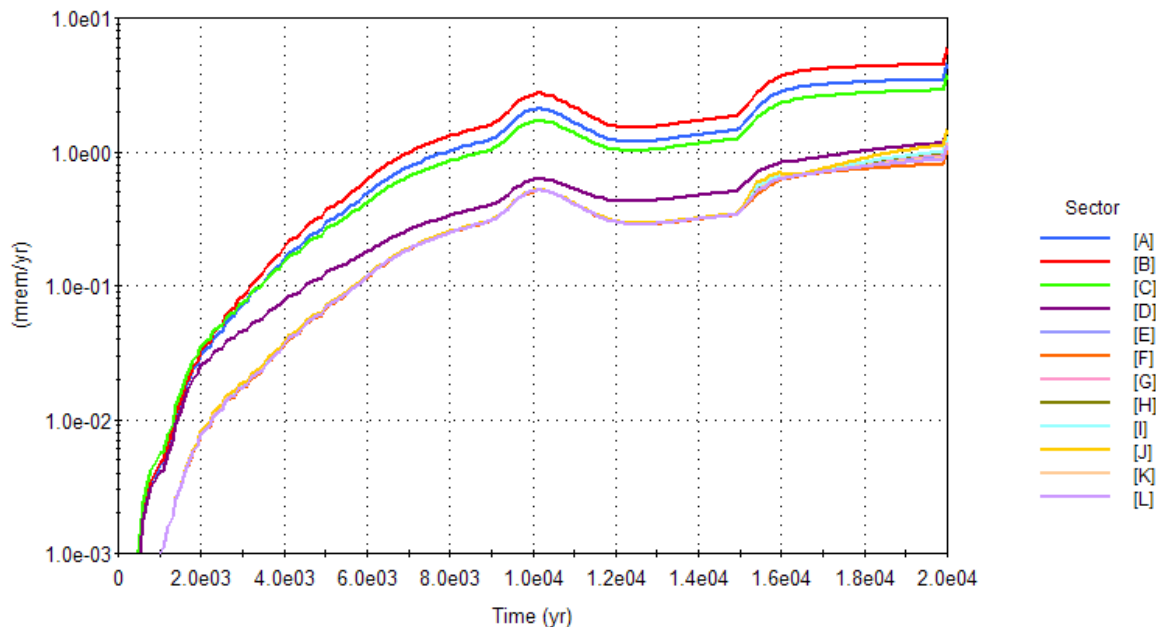
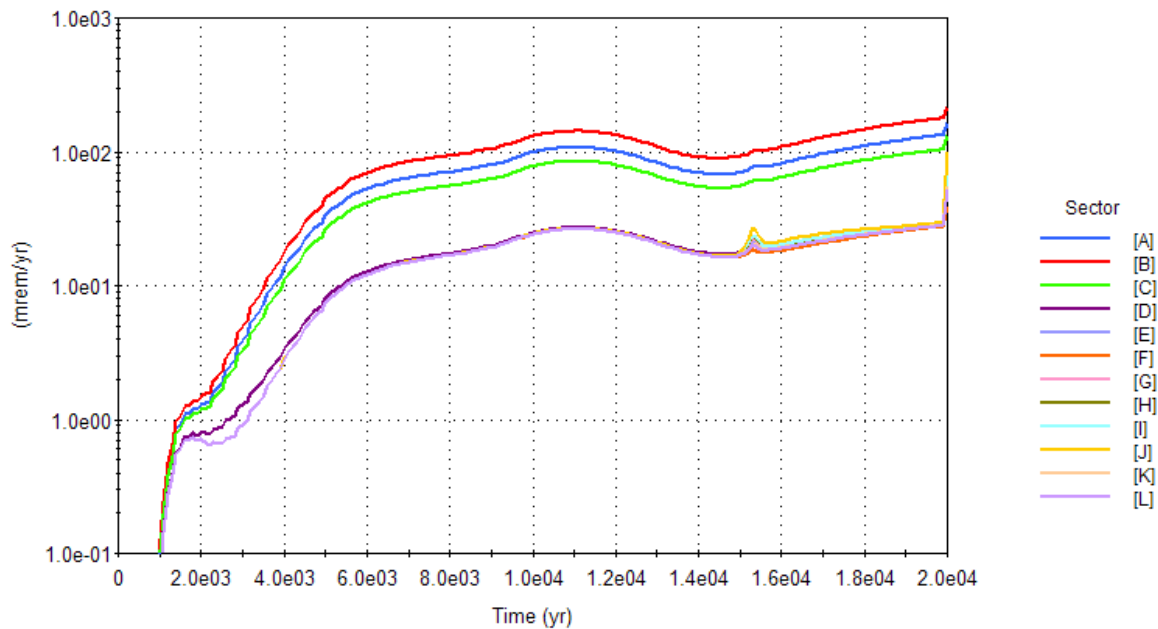


Figure 5.6-38: Mean Dose to a MOP, Any Sector within 20,000 Years – Case E



In comparing Figures 5.6-33 through 5.6-38, we can assess the relative influence of the various cases on the composite “AllCases” result. Case A has the strongest weight, since it is selected 85% of the time for the FDCs and Vault 4, and 95% of the time for Vault 1. Nevertheless, the “AllCases” result shows a maximum mean dose for Sectors B and J of just over 10 mrem/yr, slightly higher than Case A maximum for the same sector. Cases C and E are the main driver in causing higher “AllCases” mean doses, since Case C has a peak Sector J mean dose of over 300 mrem/yr and Case E has a peak Sector B dose of approximately 200 mrem/yr. Peak mean MOP dose at any time, considering all cases, is shown in Figure 5.6-39; the peak is broad, centered around 450,000 year, with a mean value of approximately 500 mrem/yr for Sector B. Of particular interest are those modeling scenarios considered most credible (Case A), and are a pessimistic fast flow case (Case C). Specific simulations were executed in order to determine the peak doses (at any time) for these two cases (shown in Figures 5.6-40 and 5.6-41). The peak dose for Case A occurs around 450,000 years, and for Case C, around 22,000 years, with peak mean values of approximately 500 mrem/yr in Sector B and 300 mrem/yr in Sector J, respectively.

Figure 5.6-39: Peak Mean Dose to a MOP, Any Sector – All Cases

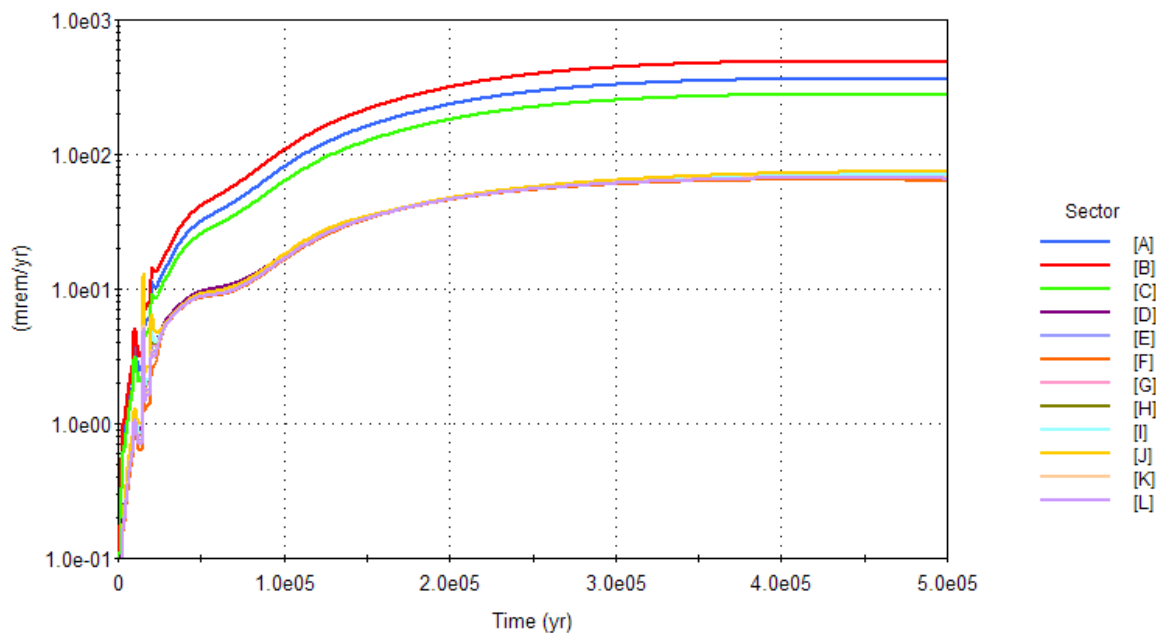


Figure 5.6-40: Peak Mean Dose to a MOP, Any Sector - Case A

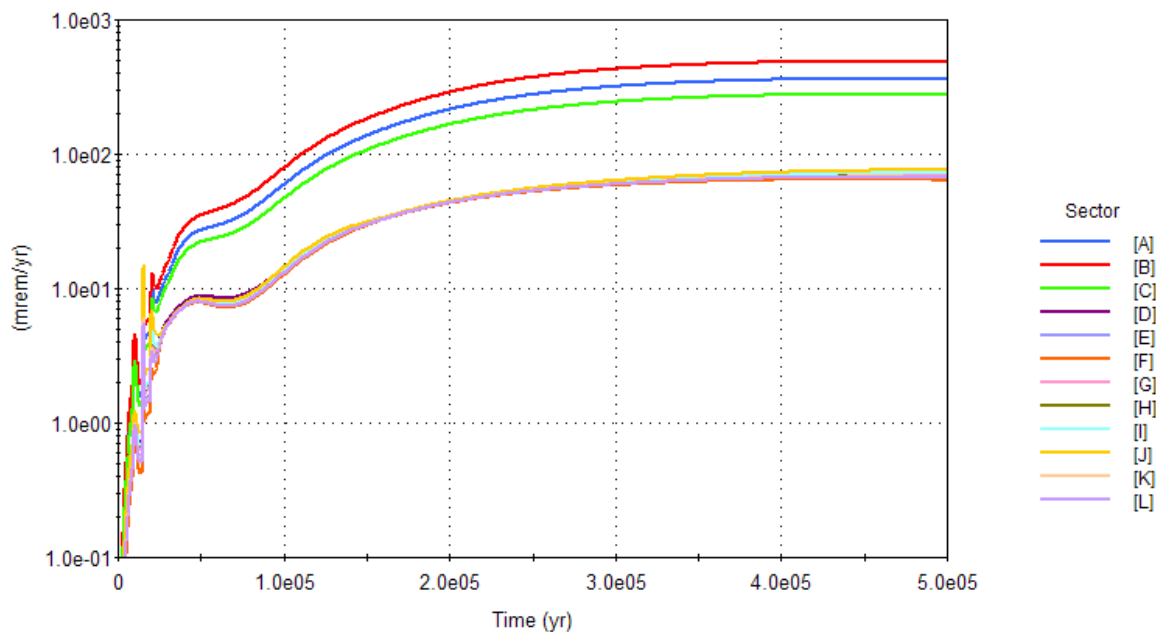
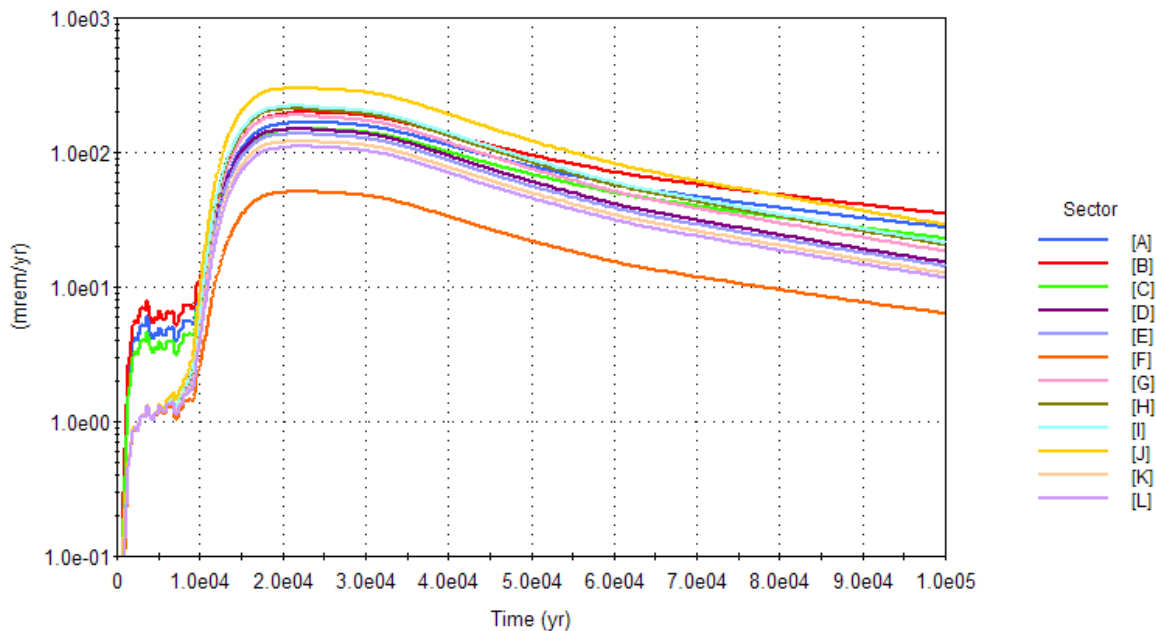


Figure 5.6-41: Peak Mean Dose to a MOP, Any Sector – Case C



Since these graphs are of mean values only, the uncertainty surrounding these values is not represented. In order to effectively communicate that uncertainty, specific cases are examined individually. These scenarios are model endpoints for doses to MOP receptors, and for groundwater concentrations of selected radionuclides. The results for the IHI receptors are provided in Section 6.5.1.

Statistics for maximum values for TEDE and groundwater concentrations are summarized in Tables 5.6-12 and 5.6-13 for failure scenarios Cases A and C respectively. The values in the tables show the statistics (mean, median, and 95th percentile) on the maximum. This is not the same thing as the statistical time histories shown in the graphs that follow, which summarize the statistical variation of endpoint values at each time-step. Since the primary goal is the reasonable assurance that the maximum dose is within the performance objective, it is necessary to examine the statistics surrounding the 5,000 realizations of maximum doses that are calculated.

Table 5.6-12: Summary for Selected SDF Endpoints – Case A Only

| Endpoint | Mean | Median (50th Percentile) | 95th Percentile |
|---|-------------|--|---------------------------------------|
| Maximum MOP dose at any Sector within 10,000 years (mrem in a year) | 4.5 | 4.0 | 9.1 |
| Maximum MOP dose at any Sector within 20,000 years (mrem in a year) | 22.0 | 12.1 | 69.5 |
| Maximum MOP dose at Sector B within 10,000 years (mrem in a year) | 4.5 | 4.0 | 9.1 |
| Maximum MOP dose at Sector B within 20,000 years (mrem in a year) | 14.9 | 11.2 | 36.3 |
| Maximum MOP dose at Sector J within 10,000 years (mrem in a year) | 1.2 | 1.1 | 2.5 |
| Maximum MOP dose at Sector J within 20,000 years (mrem in a year) | 19.5 | 9.2 | 68.7 |
| Maximum aqueous concentration of Tc-99 at Sector B within 20,000 years (pCi/L) | 537 | 512 | 825 |
| Maximum aqueous concentration of Tc-99 at Sector J within 20,000 years (pCi/L) | 739 | 673 | 1440 |
| Maximum aqueous concentration of I-129 at Sector B within 20,000 years (pCi/L) | 22.1 | 10.2 | 69.3 |
| Maximum aqueous concentration of I-129 at Sector J within 20,000 years (pCi/L) | 44.0 | 16.1 | 163 |
| Maximum aqueous concentration of Ra-226 at Sector B within 20,000 years (pCi/L) | 4.8 | 4.5 | 8.2 |
| Maximum aqueous concentration of Ra-226 at Sector J within 20,000 years (pCi/L) | 0.17 | 0.16 | 0.29 |

(based on analysis of 5,000 realizations for Case A)

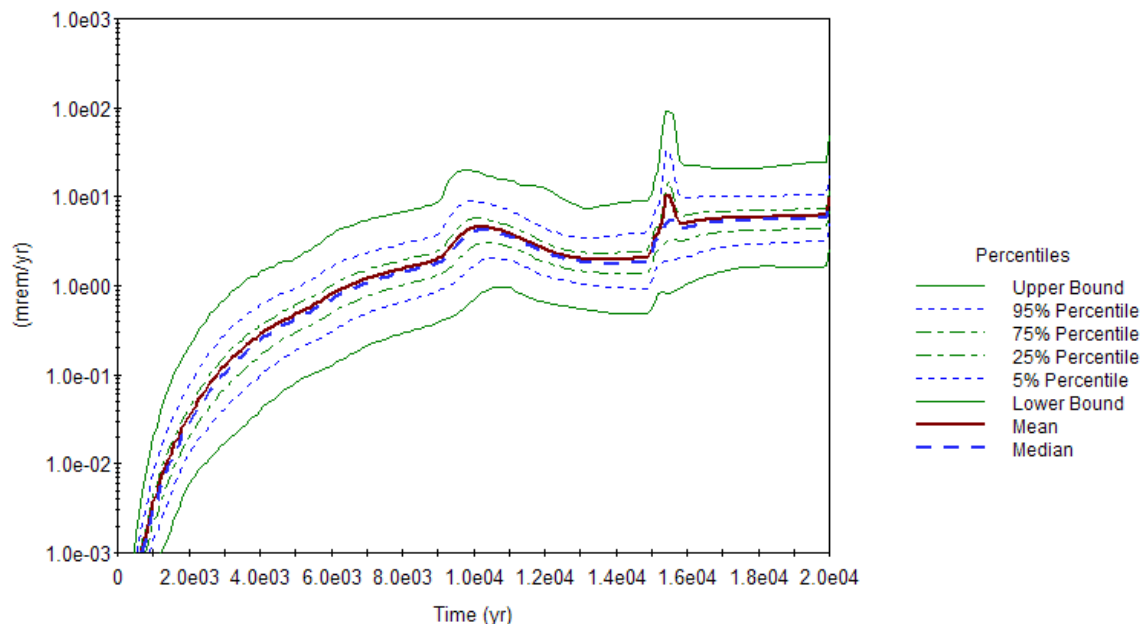
Table 5.6-13: Summary for Selected SDF Endpoints – Case C Only

| Endpoint | Mean | Median (50th Percentile) | 95th Percentile |
|---|-------------|--|---------------------------------------|
| Maximum MOP dose at any Sector within 10,000 years (mrem/yr) | 16.0 | 8.6 | 25.5 |
| Maximum MOP dose at any Sector within 20,000 years (mrem/yr) | 492 | 293 | 1590 |
| Maximum MOP dose at Sector B within 10,000 years (mrem/yr) | 12.4 | 8.6 | 20.2 |
| Maximum MOP dose at Sector B within 20,000 years (mrem/yr) | 262 | 160 | 803 |
| Maximum MOP dose at Sector J within 10,000 years (mrem/yr) | 9.4 | 2.3 | 20.1 |
| Maximum MOP dose at Sector J within 20,000 years (mrem/yr) | 431 | 212 | 1550 |
| Maximum aqueous concentration of Tc-99 at Sector B within 20,000 years (pCi/L) | 824 | 812 | 1060 |
| Maximum aqueous concentration of Tc-99 at Sector J within 20,000 years (pCi/L) | 72.5 | 65.7 | 138 |
| Maximum aqueous concentration of I-129 at Sector B within 20,000 years (pCi/L) | 1.12 | 1.08 | 1.58 |
| Maximum aqueous concentration of I-129 at Sector J within 20,000 years (pCi/L) | 0.072 | 0.045 | 0.21 |
| Maximum aqueous concentration of Ra-226 at Sector B within 20,000 years (pCi/L) | 7.8 | 7.6 | 10.8 |
| Maximum aqueous concentration of Ra-226 at Sector J within 20,000 years (pCi/L) | 0.27 | 0.27 | 0.38 |

(based on analysis of 5,000 realizations for Case C)

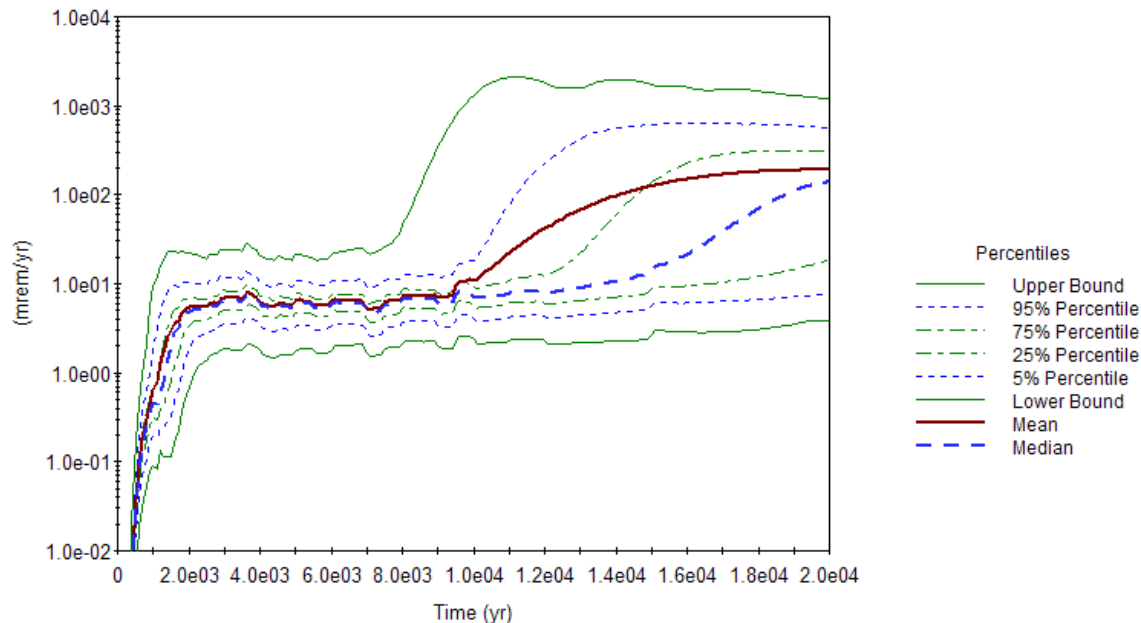
An evaluation of model uncertainty requires examination of the statistics around the results of interest as a function of time. Figure 5.6-42 shows the statistics surrounding a MOP dose for only Sector B, Case A, within 20,000 years. The maximum value of this dose is an endpoint recorded in the tables above. The statistical summary shows the percentiles of the results at any given time. That is, a single time-step would be read by placing a vertical line across the graph. Along that line, the lines showing percentiles identify the percentile of the result (MOP dose for Sector B, Case A) at that time.

Figure 5.6-42: Statistical Time History of a MOP Dose, Sector B within 20,000 Years –
Case A



The analogous situation for Case C is shown in Figure 5.6-43. That is, the statistics surrounding the MOP dose for only Sector B, Case C, within 20,000 years.

Figure 5.6-43: Statistical Time History of a MOP Dose, Sector B within 20,000 Years –
Case C



For the Case A results, the mean does not stray far from the median, but this is not true for the Case C results. The mean for Case C is sometimes up to one order of magnitude higher than the median, reaching around as high as the 85th percentile at approximately year 12,000. This indicates that there are some features of the Case C simulation that are extreme, which is also evidenced by the large upper bound values. This behavior is believed to be based on the GoldSim model that assumes, for Case C, a direct mass transfer from the saltstone to the saturated zone to simulate fast flow paths. This fast flow path GoldSim model would preferentially increase the contribution to the MOP dose from radionuclides that could have been significantly retarded by the cementitious material in the disposal unit floor (e.g., plutonium).

5.6.5 Sensitivity Analysis using the SDF Probabilistic Model

Given the uncertainties presented in Section 5.6.4, the next step was to identify those input parameters and other stochastic entities in the model that led to those uncertainties. Even in complex models, the results are often strongly dependent on only a handful of parameters. What is important for one result (e.g., the I-129 concentration) may be insignificant for another, such as the maximum dose achieved within 20,000 years. In fact, the dose to a MOP will have different sensitivities at different times, since it is driven by the presence of different radionuclides. For example, a MOP dose may be dominated by Tc-99 at one time and by I-129 at another time, and these doses will be determined by different aspects of the model (different K_{ds} , DCFs, decay chains, etc.). Extracting the important model inputs for results of interest is the subject of the sensitivity analysis.

5.6.5.1 Introduction to SDF Probabilistic Model Sensitivity Analysis

Complex modeling, such as the probabilistic modeling of the SDF, is needed to explore dynamics of systems where multiple variables interact in a nonlinear manner. The probabilistic simulation approach used in the GoldSim model propagates uncertainty regarding the explanatory variables (e.g., inputs such as physical soil properties or inventory) through the model to the predicted response (e.g., dose or concentration). Quantitative assessment of the importance of inputs is necessary when the level of uncertainty in the system response exceeds the acceptable threshold specified in the decision making framework. One of the goals of sensitivity analysis is to identify which variables have distributions that exert the greatest influence on the response.

Sensitivity analysis deals with estimating influence measures for input variables. Influence measures can be estimated in either a qualitative or quantitative context. A qualitative sensitivity analysis provides a relative ranking of the importance of input factors without incurring the computational cost of quantitatively estimating the percentage of the output variation accounted for by each input factor. For both approaches the estimates can be obtained either locally or globally within the parameter space. A local sensitivity analysis involves varying one explanatory variable while holding all other explanatory variables constant, and assessing the impact on the model response. This is local in the sense that only a minimal portion of the full explanatory variable space is explored (i.e., the point at which the explanatory variables are held constant). Although local sensitivity analysis is useful in some applications, the region of possible realizations for the model of interest is left largely unexplored. Global sensitivity analysis attempts to explore the possible realizations of the

model more completely. The space of possible realizations for the model can be explored through the use of search curves or evaluation of multi-dimensional integrals using Monte Carlo methods. However, these approaches to global sensitivity analysis become more computationally intensive as the dimensionality of the model (i.e., the number of model parameters) increases. In this case, the GoldSim SDF model includes approximately 700 stochastic parameters.

Because of the computational cost, sensitivity analysis of high-dimensional probabilistic models requires efficient algorithms for practical application. In this work, a dataset of 10,000 probabilistic model realizations (e.g., a dataset with 700 columns for the stochastic model parameters and one column for a MOP dose as the model response) were analyzed using Gradient Boosting Models (GBM). The GBM analysis provides a global sensitivity analysis that quantifies the importance of explanatory variables using SIs, which are metrics based on the explained variance in the response. [ISSN 0885-6125-Vol 40 No 2, ISSN 0885-6125 Vol 24 No 2] The implementation of GBM used here comes from the *R* statistical package named “gbm”.

5.6.5.2 *Model Fitting and Validation*

This section presents detailed discussion of the statistical methods used in the sensitivity analysis. Global sensitivity is estimated here as the proportion of the variance of the response accounted for by each explanatory variable. This estimation is conducted by fitting GBM model predictions to realizations from the GoldSim model. Variance decomposition of the fitted GBM model is then used to estimate SIs. Under this decomposition approach, the goal is to identify the most influential explanatory variables that are identified within a model. The necessary degree of model complexity is assessed using validation metrics, based on comparison of model predictions, with randomly selected subsets of the data. This approach uses the “deviance” of the model as a measure of goodness of fit. The concept of deviance is fundamental to classical statistical hypothesis tests (e.g., the common *t*-test can be derived using a deviance-based framework) and guides the model selection process applied here.

The GBM model fitting approach is based on finding the values of each explanatory variable that result in the greatest difference in mean for the corresponding subsets of the response. For example, if there were only a single explanatory variable, the GBM would identify the value of the explanatory variable that corresponds to a split of the response into two parts. This will ensure that no other split would result in corresponding groups of the response variable with a greater difference in means. When multiple explanatory variables are present, these multiple splits are referred to as “trees.” Each tree results in an estimate (e.g., prediction) of the response. As multiple potential trees are evaluated, they are compared to the observed data using a loss function. The selection of the loss function is an influential aspect of the GBM process, and depends on the distribution of the response variable. For data that are sufficiently skewed (e.g., non-normal), the absolute error loss function typically produces more reliable results.

There is a trade-off that exists when considering which loss function to use. The squared-error loss function results in better fitting models, but can do so at the expense of introducing spurious variables into the model selection process when the response distribution is

sufficiently skewed. The absolute error loss function produces model predictions with more variability, but is less likely to result in the selection of spurious variables in the model. For this application, the focus has been on using a deviance-based method to obtain models that identify the most important explanatory variables with respect to the observed variability in the response. Therefore, the squared-error function was used in these applications.

Once a GBM model is constructed, each of the explanatory variables that exist in the model can be assigned an SI. The SI is obtained through variance decomposition and can be interpreted as the percentage of variability explained in the model by a given explanatory variable. The sum of the SIs across the entire set of explanatory variables in the model will approximately equal the R^2 of the linear regression of the GoldSim output versus the GBM predictions. The R^2 values for this version of the SDF model indicate the high degree of predictive power of the GBM in fitting the GoldSim model.

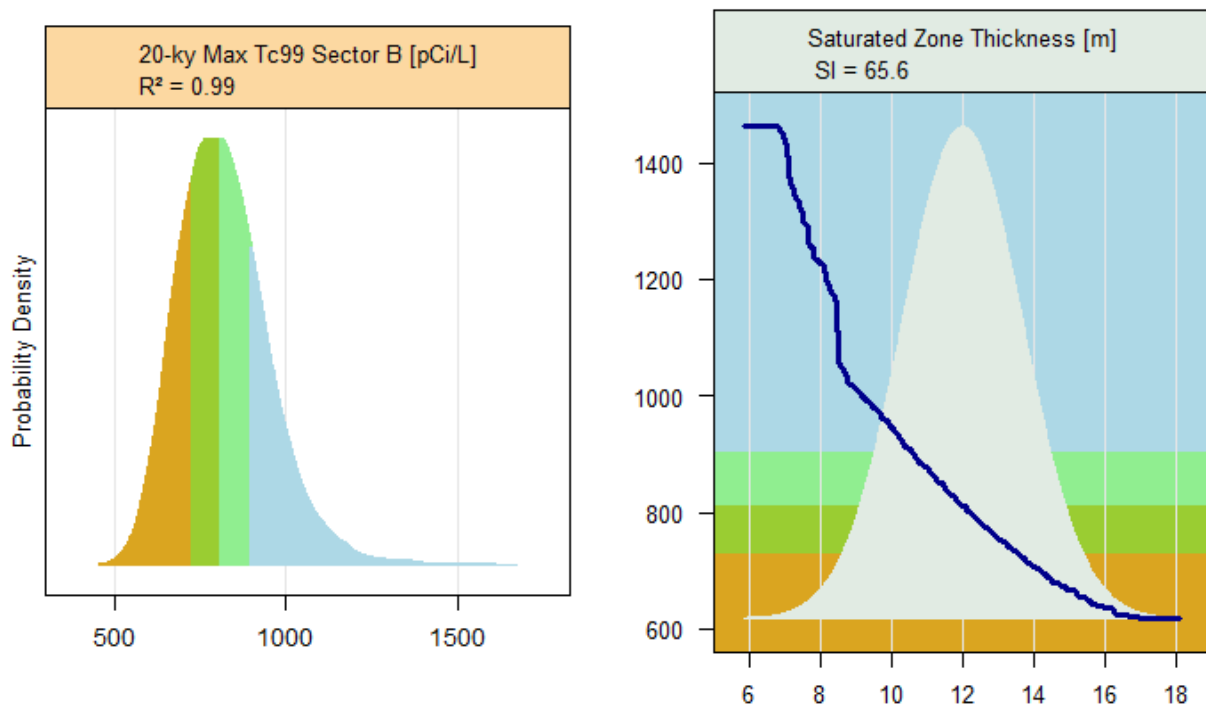
In order to assess the relationship between an individual explanatory variable and the response of interest, partial dependence plots are used (these are presented below for each identified endpoint), as shown in Figure 5.6-44. The first panel depicts a density estimate of the simulated response from the GoldSim model. The percentiles of the response distribution in this panel are shaded to provide a context for the partial dependence plots presented in the remaining panels. The colors indicate the percentile range of the response as follows:

- 1) The 0th-25th percentile region is shaded orange-brown
- 2) The 25th-50th percentile region is shaded dark yellow-green
- 3) The 50th-75th percentile region is shaded light green
- 4) The 75th-100th percentile region is shaded light blue

The y-axis scale of the partial dependence plots is in units of the response distribution (the x-axis of the first panel). Given that each parameter has a different range and strength of influence on the response, the y-axes of the partial dependence panels depict only the range of the response over which a particular parameter is influential. If the original scale of the response were maintained on each partial dependence panel, then the influence of the least influential parameter would not be visible in many cases. To counteract this scale issue, the background of the partial dependence panels is shaded to depict the percentile of the response over which the parameter is influential. For example, if the background of the partial dependence plot under the partial dependence line is light blue, then that indicates the parameter's influence on the upper end of the response distribution (i.e., the 75th to 100th percentile of the response).

The partial dependence panels in each figure show the distributions of the explanatory variables (shaded gray), and the partial dependence curve (blue line) shows changes in the response as a function of each explanatory variable. In the example provided (Figure 5.6-44), the variable has a normal input distribution, and the dependence of the result on this parameter spans nearly the entire range of the variable, with a flat (unresponsive) part at the extreme upper end.

Figure 5.6-44: Example of a Result Probability Density and Partial Dependence Plot



The partial dependence is determined through the integration across the joint density to obtain a marginal distribution. The integration is performed using a “weighted tree traversal” measure that is analogous to more common integration procedures performed with Riemann or Lebesgue measures. The vertical axis of the partial dependence plot shows the change in the response variable as a function of the changes in the explanatory variable.

With standard linear regression techniques, it is assumed that the relationship between the response and the explanatory variable is a constant (e.g., the parameter estimates in the linear model). With the GBM approach, this relationship is not constrained by assumptions of linearity, and the partial dependence plots show the data-based estimate of the relationship between the response and the explanatory variable. This is useful for understanding the influence of changes in a single explanatory variable, when integrating across all other explanatory variables.

5.6.5.3 *Summary Statistics for Endpoints*

The exporting of results from the model follows the simple procedure outlined in the SDF GoldSim model, in the *SensitivityAnalysis* container, wherein the tabulated raw data contents of the element *Endpoints_SA* are exported to a tab-delimited text file. Since each model run consisted of only 5,000 realizations.

For each endpoint, as shown in Tables 5.6-14 and 5.6-15, the most significant parameters identified by the sensitivity analysis are presented, along with the R^2 and SI for each. Relatively simple models characteristically have only a few dominant parameters, so each parameter contributes to a larger fraction of the variation in the model. For simple models, single parameters can typically impact 40% or more of the model, and occasionally 80% or even higher for some endpoints. The SDF model structure is relatively complex, and does not lend itself to easily determining which specific radionuclides are the most significant for a given dose endpoint.

Following Tables 5.6-14 and 5.6-15 in Sections 5.6.5.4 (Case A) and 5.6.5.5 (Case C) are a series of figures showing the partial dependence of each of the highest SIs for each endpoint. SIs of less than 5.0 are not reported.

Table 5.6-14: Most Sensitive Parameters for Endpoints of Interest – Case A

| Endpoint | R ² | SI Rank | Input Parameter | Sensitivity Index |
|--|----------------|---------|--|-------------------|
| Max. MOP dose at any Sector within 10,000 years | 0.94 | 1 | K _d for Ra in sandy soil | 53 |
| | | 2 | vegetable consumption – local fraction | 9.7 |
| | | 3 | saturated zone thickness | 8.1 |
| Max. MOP dose at any Sector within 20,000 years | 0.84 | 1 | K _d for I in reducing middle aged concrete | 47 |
| | | 2 | vegetable production yield | 5.5 |
| | | 3 | pore volumes to 2 nd stage - concrete | 5.3 |
| Max. MOP dose at Sector B within 10,000 years | 0.94 | 1 | K _d for Ra in sandy soil | 52 |
| | | 2 | vegetable consumption – local fraction | 9.7 |
| | | 3 | saturated zone thickness | 8.2 |
| Max. MOP dose at Sector B within 20,000 years | 0.84 | 1 | K _d for I in reducing middle aged concrete | 46 |
| | | 2 | vegetable production yield | 6.9 |
| | | 3 | saturated zone thickness | 6.0 |
| Max. MOP dose at Sector J within 10,000 years | 0.89 | 1 | K _d for I in reducing middle aged concrete | 29 |
| | | 2 | K _d for Ra in sandy soil | 24 |
| | | 3 | aquatic food consumption rate | 23 |
| Max. MOP dose at Sector J within 20,000 years | 0.82 | 1 | K _d for I in reducing middle aged concrete | 45 |
| | | 2 | pore volumes to 2 nd stage - concrete | 5.4 |
| Max. conc. of Tc-99 at Sector B within 20,000 years | 0.80 | 1 | K _d for Tc in reducing middle aged concrete | 39 |
| | | 2 | saturated zone thickness | 34 |
| | | 3 | Tc-99 tank inventory uncertainty – FDC | 6.7 |
| Max. conc. of Tc-99 at Sector J within 20,000 years | 0.58 | 1 | K _d for Tc in reducing middle aged concrete | 34 |
| | | 2 | saturated zone thickness | 14 |
| | | 3 | K _d for Tc in FDC wall/floor concrete | 6.6 |
| Max. conc. of I-129 at Sector B within 20,000 years | 0.89 | 1 | K _d for I in reducing middle aged concrete | 67 |
| | | 2 | pore volumes to 2 nd stage - concrete | 6.9 |
| Max. conc. of I-129 at Sector J within 20,000 years | 0.83 | 1 | K _d for I in reducing middle aged concrete | 56 |
| | | 2 | pore volumes to 2 nd stage - concrete | 6.7 |
| | | 3 | pore volumes to 1 st stage - concrete | 5.4 |
| Max. conc. of Ra-226 at Sector B within 20,000 years | 0.98 | 1 | K _d for Ra in sandy soil | 69 |
| | | 2 | saturated zone thickness | 16 |
| | | 3 | unsaturated zone thickness - FDCs | 9.4 |
| Max. conc. of Ra-226 at Sector J within 20,000 years | 0.98 | 1 | K _d for Ra in sandy soil | 68 |
| | | 2 | saturated zone thickness | 16 |
| | | 3 | unsaturated zone thickness - FDCs | 9.2 |

Table 5.6-15: Most Sensitive Parameters for Endpoints of Interest – Case C

| Endpoint | R ² | SI Rank | Input Parameter | Sensitivity Index |
|---|----------------|---------|--|-------------------|
| Max. MOP dose at any Sector within 10,000 years | 0.80 | 1 | K _d for Pu in clayey soil | 19 |
| | | 2 | unsaturated zone thickness – FDCs | 11 |
| | | 3 | K _d for Pu in sandy soil | 8.8 |
| Max. MOP dose at any Sector within 20,000 years | 0.88 | 1 | K _d for Pu in sandy soil | 63 |
| | | 2 | unsaturated zone thickness – FDCs | 5.5 |
| Max. MOP dose at Sector B within 10,000 years | 0.82 | 1 | K _d for Pu in clayey soil | 21 |
| | | 2 | unsaturated zone thickness – FDCs | 12 |
| | | 3 | C-14 tank inventory uncertainty – Vault 4 | 10 |
| Max. MOP dose at Sector B within 20,000 years | 0.89 | 1 | K _d for Pu in sandy soil | 70 |
| | | 2 | unsaturated zone thickness – FDCs | 5.7 |
| Max. MOP dose at Sector J within 10,000 years | 0.76 | 1 | K _d for Pu in clayey soil | 15 |
| Max. MOP dose at Sector J within 20,000 years | 0.87 | 1 | K _d for Pu in sandy soil | 48 |
| Max. conc. of Tc-99 at Sector B within 20,000 years | 0.99 | 1 | saturated zone thickness | 66 |
| | | 2 | Tc-99 tank inventory uncertainty – Vault 4 | 33 |
| Max. conc. of Tc-99 at Sector J within 20,000 years | 0.71 | 1 | K _d for Tc in reducing middle aged concrete | 30 |
| | | 2 | saturated zone thickness | 11 |
| Max. conc. of I-129 at Sector B within 20,000 years | 0.97 | 1 | K _d for I in reducing middle aged concrete | 39 |
| | | 2 | saturated zone thickness | 37 |
| | | 3 | I-129 tank inventory uncertainty – Vault 4 | 18 |
| Max. conc. of I-129 at Sector J within 20,000 years | 0.92 | 1 | K _d for I in oxidizing old concrete | 40 |
| | | 2 | K _d for I in reducing middle aged concrete | 32 |
| Max conc of Ra-226 at Sector B within 20,000 years | 0.98 | 1 | K _d for Ra in sandy soil | 43 |
| | | 2 | saturated zone thickness | 39 |
| | | 3 | Th-230 tank inventory uncertainty – Vault 4 | 9.7 |
| Max conc of Ra-226at Sector J within 20,000 years | 0.98 | 1 | K _d for Ra in sandy soil | 43 |
| | | 2 | saturated zone thickness | 39 |
| | | 3 | Th-230 tank inventory uncertainty – Vault 4 | 9.7 |

5.6.5.4 Case A Partial Dependence Plots

The partial dependence plots for Case A are shown in the figures within this section. The partial dependence plots identify the model input parameters that are most significant in determining the model endpoints identified in Table 5.6-14.

In the case of the maximum dose to a MOP at any of the sectors within 10,000 years, and assuming a Case A failure scenario only (Figure 5.6-45), the most influential parameter is the radium K_d in the material sandy soil. This is followed by relatively smaller influences by the local fraction of consumed vegetables and the saturated zone thickness.

Figure 5.6-45: Max MOP Dose, Any Sector within 10,000 Years – Case A

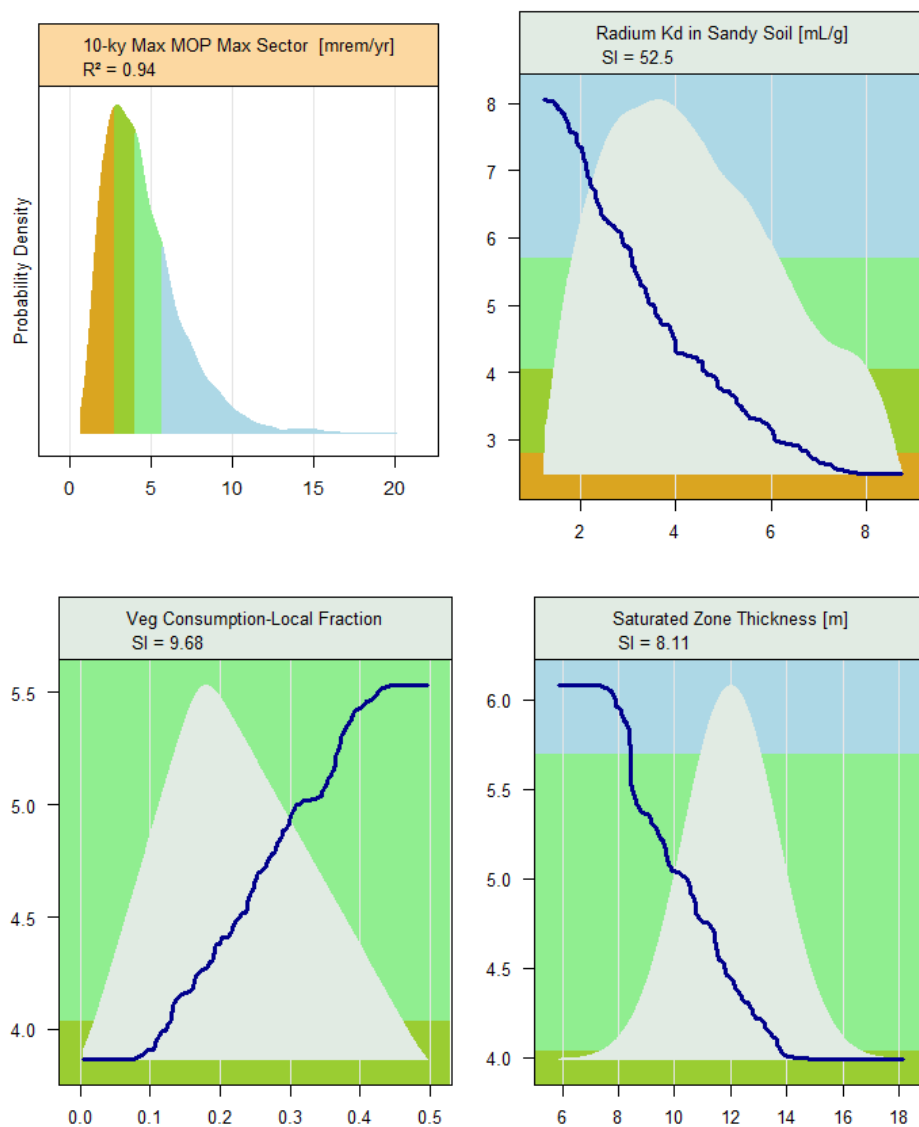
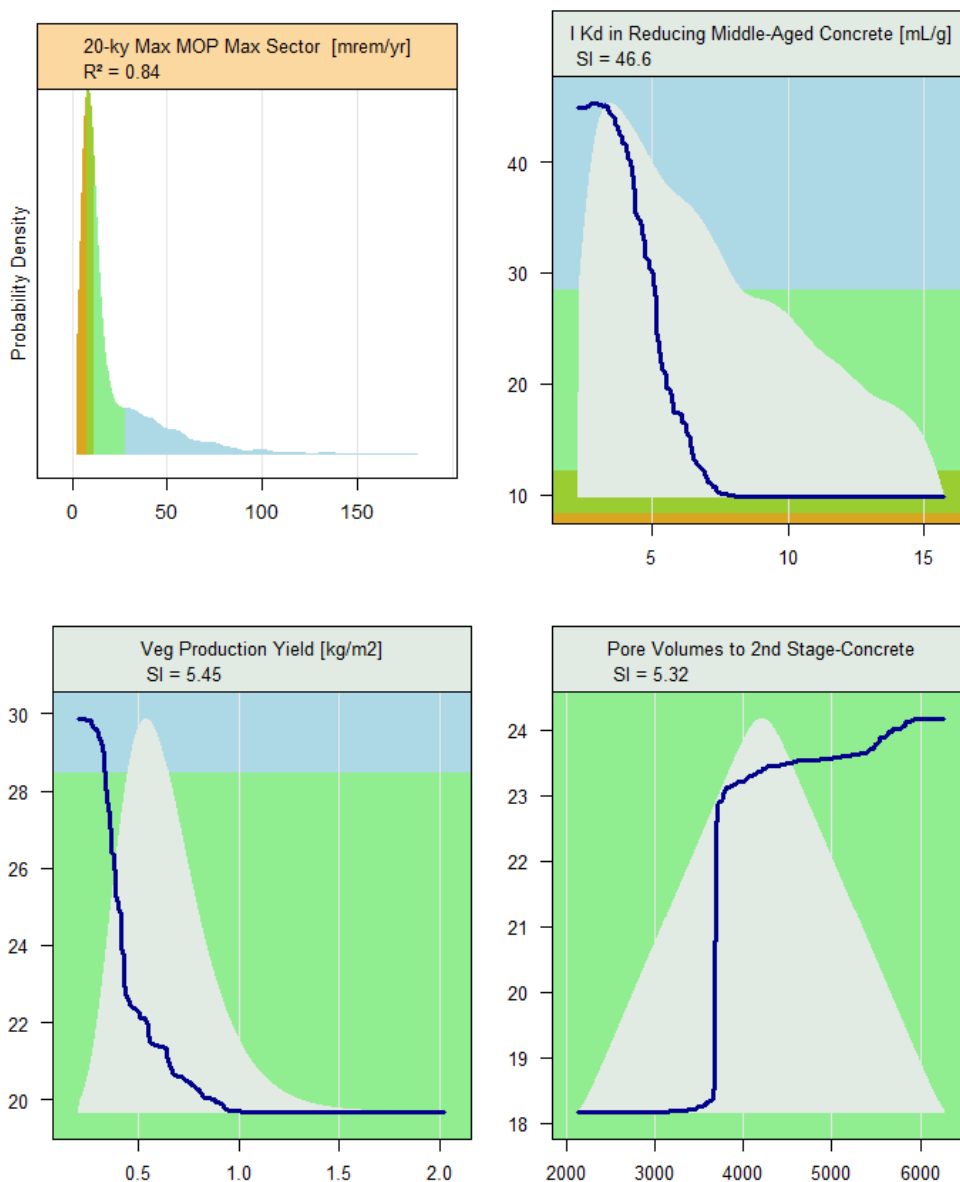


Figure 5.6-46 shows the SI plots for the same dose to a MOP at any sector, for Case A as Figure 5.6-45, but for the maximum dose within 20,000 years. Here the result is dominated by the K_d of iodine in reducing middle aged concrete. Following that, we see the vegetable production yield and the number of pore volumes required to reach the second stage of deterioration in concrete (i.e., concrete transitions from middle age oxidized to old age oxidized).

Figure 5.6-46: Max MOP Dose, Any Sector within 20,000 Years – Case A



The sensitivity analysis results for the 10,000 year maximum MOP dose within Sector B (Figure 5.6-47) shows that Sector B is apparently the most significant sector driving the dose within 10,000 years for Case A, since it essentially duplicates the sensitivity of maximum dose for all sectors within 10,000 years.

Figure 5.6-47: Max MOP Dose, Sector B within 10,000 Years – Case A

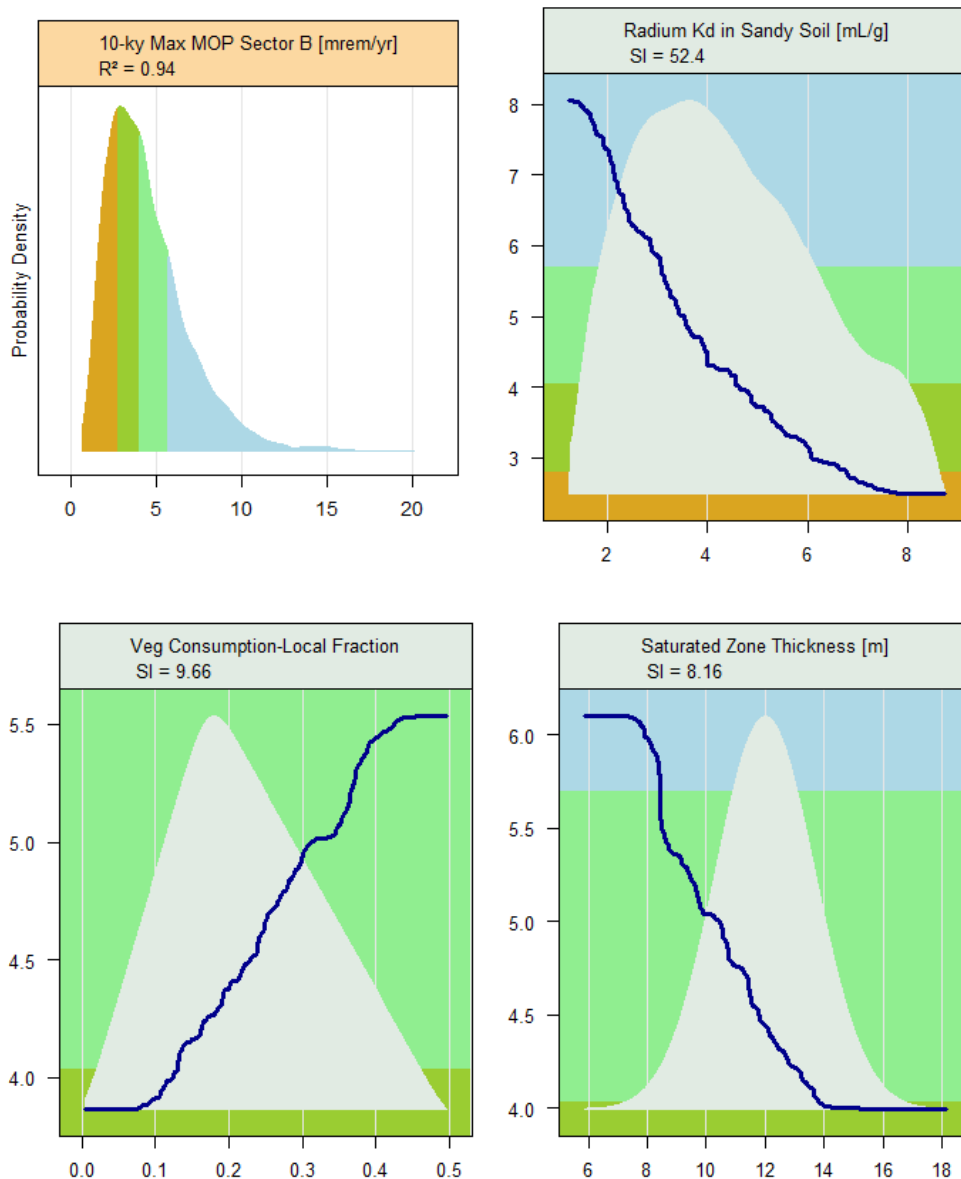
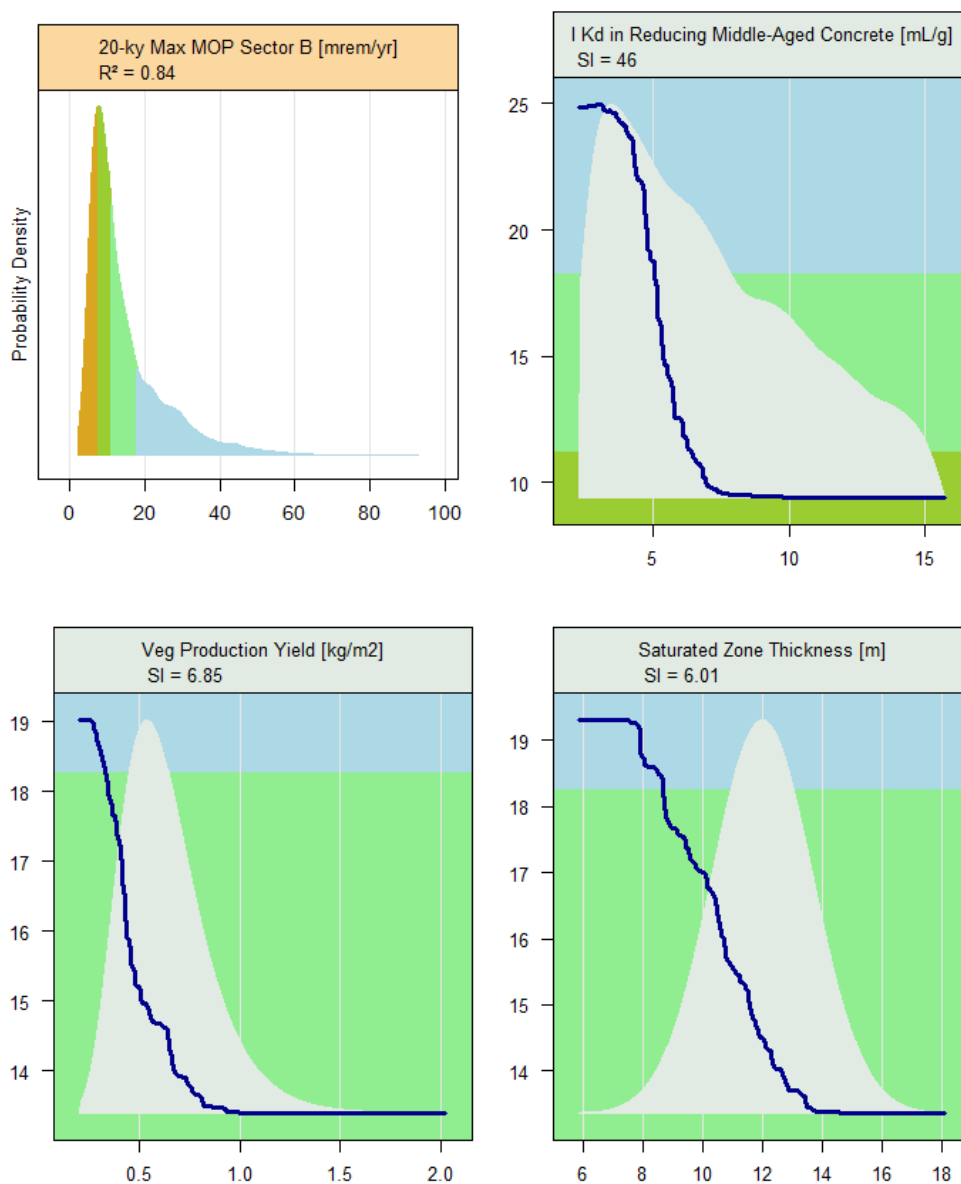


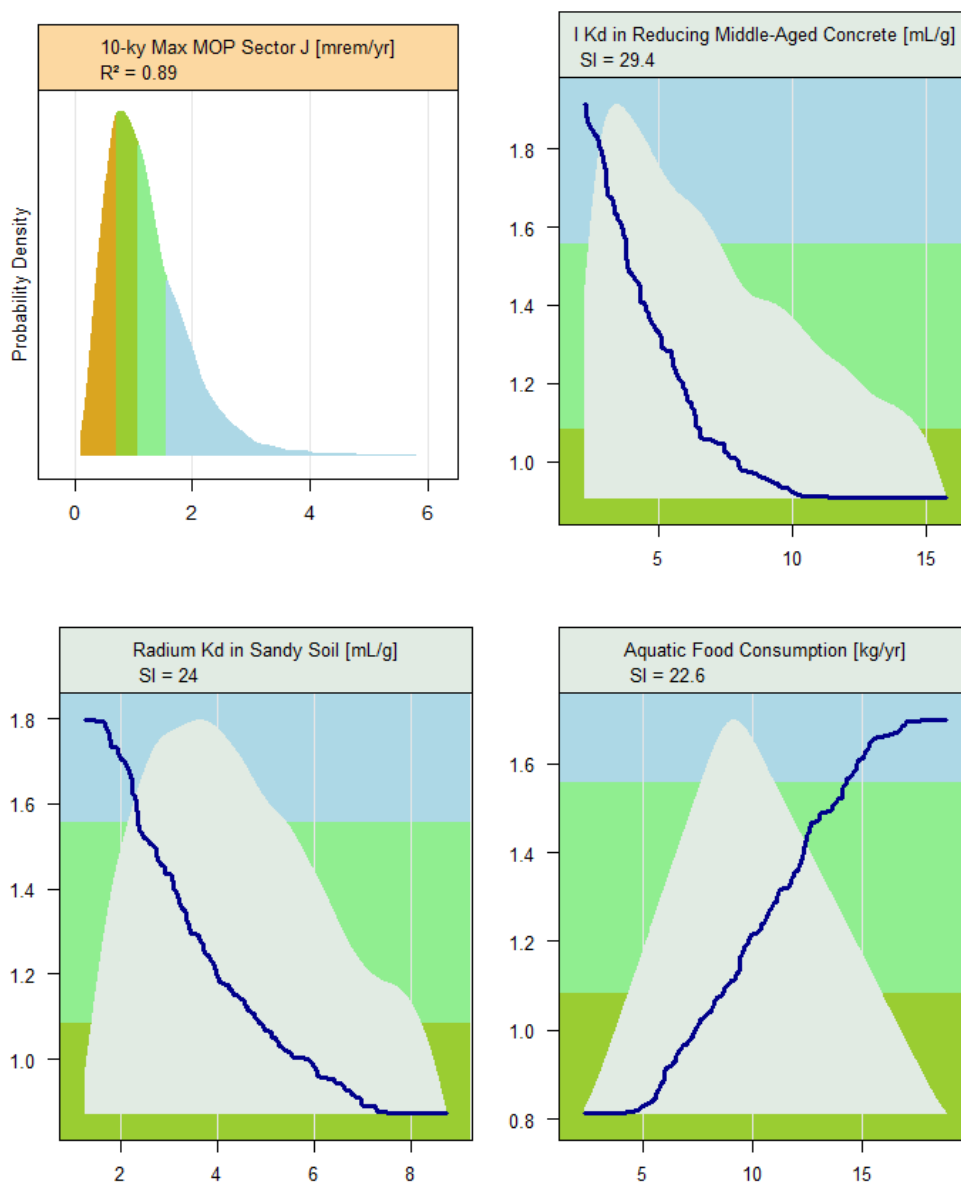
Figure 5.6-48 shows that the sensitivities for maximum MOP dose within 20,000 years in Sector B are the influential K_d for iodine in reducing middle aged concrete, the vegetable production yield, and the aquifer thickness.

Figure 5.6-48: Max MOP Dose, Sector B within 20,000 Years – Case A



The 10,000 year MOP dose within Sector J shown in Figure 5.6-49, is driven more or less equally by the K_d for iodine in reducing middle aged concrete, the radium K_d in sandy soil, and the rate of ingestion of finfish. The dependence shown for the ingestion of finfish is attributed to the GoldSim model that assumes the finfish ingestion is based on Sector B stream concentrations for all sectors.

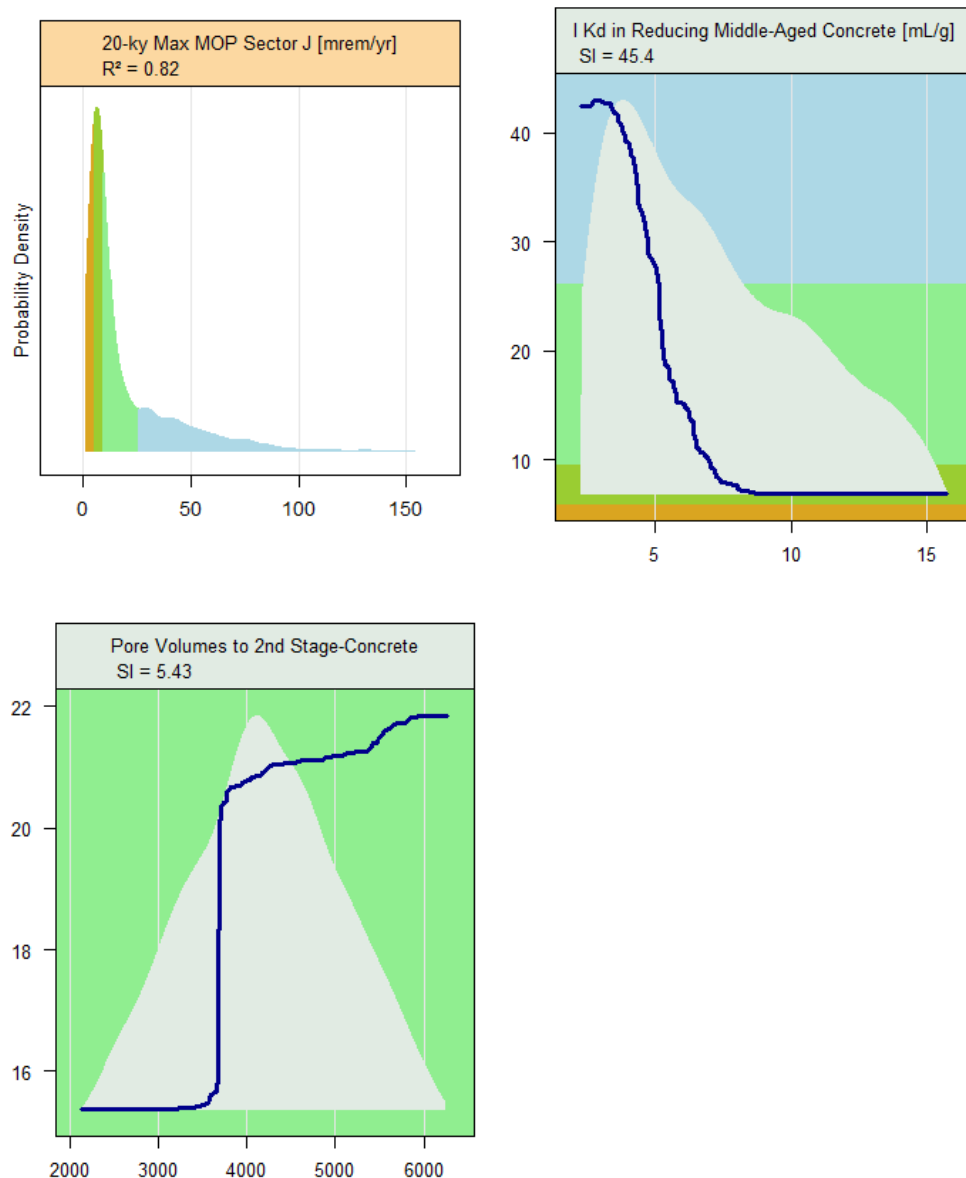
Figure 5.6-49: Max MOP Dose, Sector J within 10,000 Years – Case A



Note: Aquatic Food = finfish

Similar to results in Sector J at 10,000 years, the maximum MOP dose within 20,000 years is dominated by the K_d for iodine in reducing middle aged concrete (see Figure 5.6-50). The magnitude of the 20,000 year maximum dose for Sector J matches that of the any sector maximum dose, indicating that Sector J is determining the highest 20,000 year maximum dose.

Figure 5.6-50: Max MOP Dose, Sector J within 20,000 Years – Case A



The sensitivity analysis can also be used to examine radionuclide concentrations in groundwater at the location where a receptor might use the water. Continuing with the failure Case A scenario, Figure 5.6-51 shows the 20,000 year maximum concentration of Tc-99 at Sector B is influenced by the K_d for technetium in reducing middle aged concrete and the aquifer thickness. The inventory uncertainty factor for Tc-99 in the FDCs is of lesser influence.

Figure 5.6-51: Max Concentration of Tc-99 at Sector B within 20,000 Years – Case A

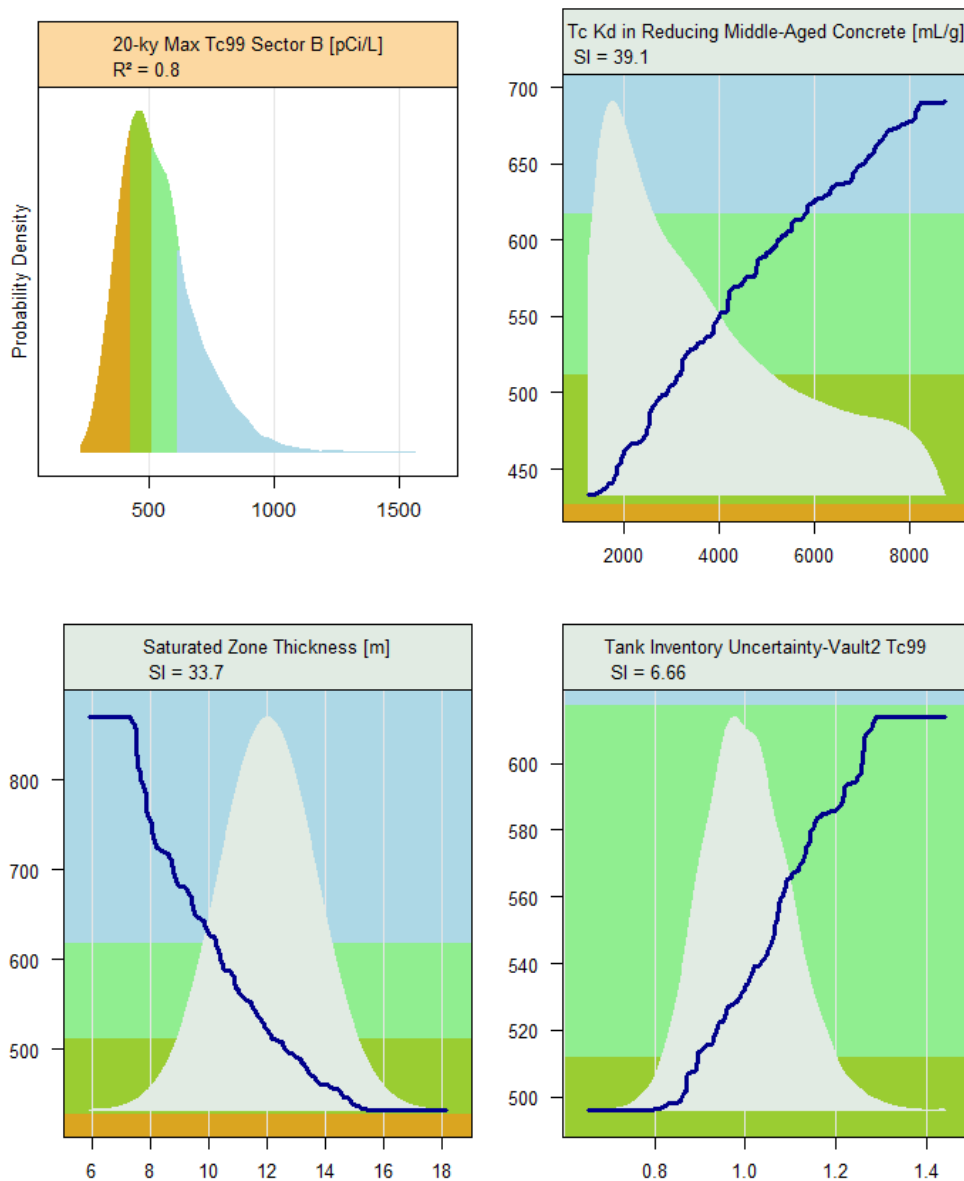


Figure 5.6-52 shows the 20,000 year maximum Tc-99 concentrations at Sector J, which are again driven principally by the technetium K_d in reducing middle aged concrete and the aquifer thickness. Finally, we also see the influence of the technetium K_d in the concrete making up the walls and floor of the FDCs.

Figure 5.6-52: Max Concentration of Tc-99 at Sector J within 20,000 Years – Case A

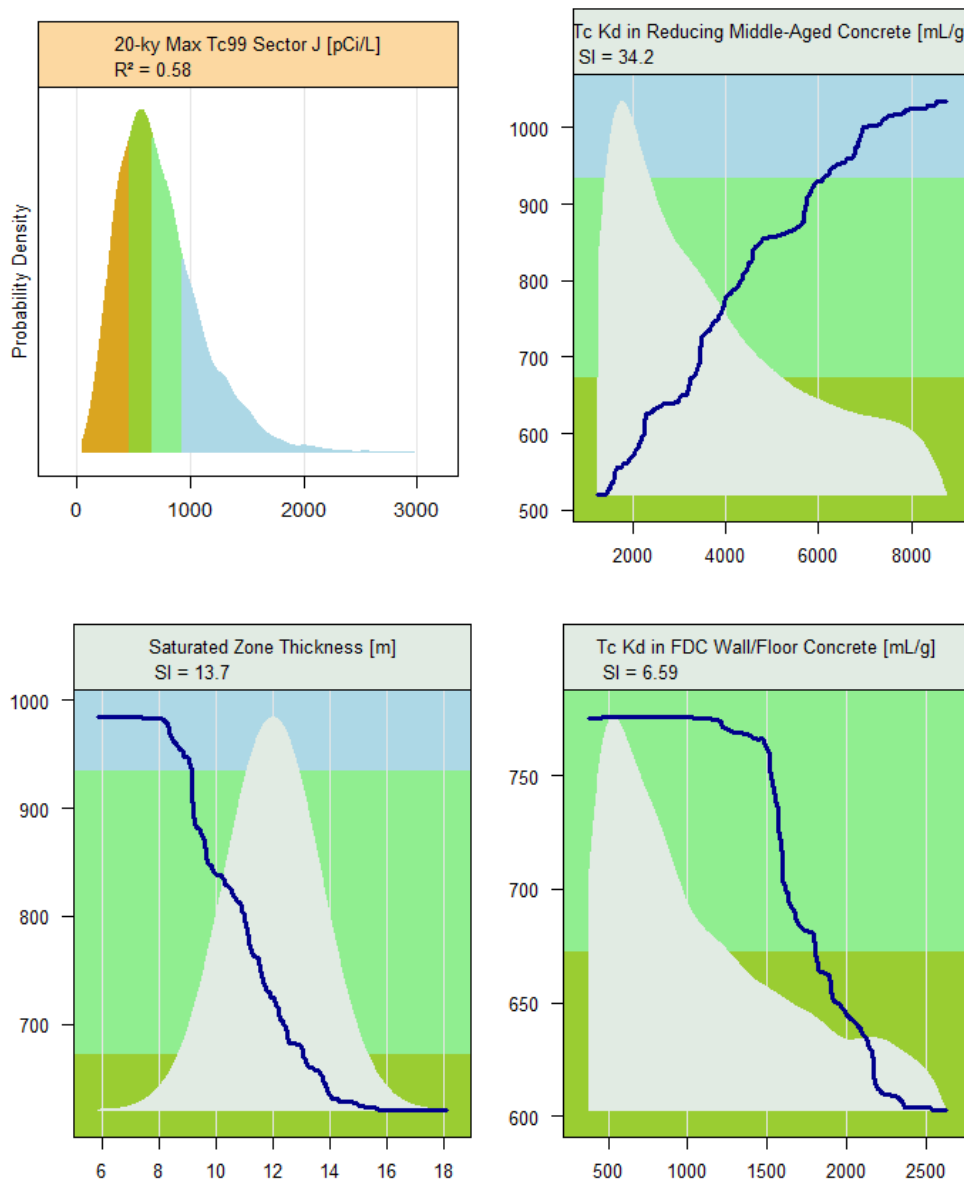


Figure 5.6-53 shows that the 20,000 year maximum groundwater concentrations for I-129 in Sector B are dominated by the iodine K_d in reducing middle aged concrete and also influenced by the number of pore volumes necessary to have the disposal unit concrete transition from middle aged oxidizing to old aged oxidizing.

Figure 5.6-53: Max Concentration of I-129 at Sector B within 20,000 Years – Case A

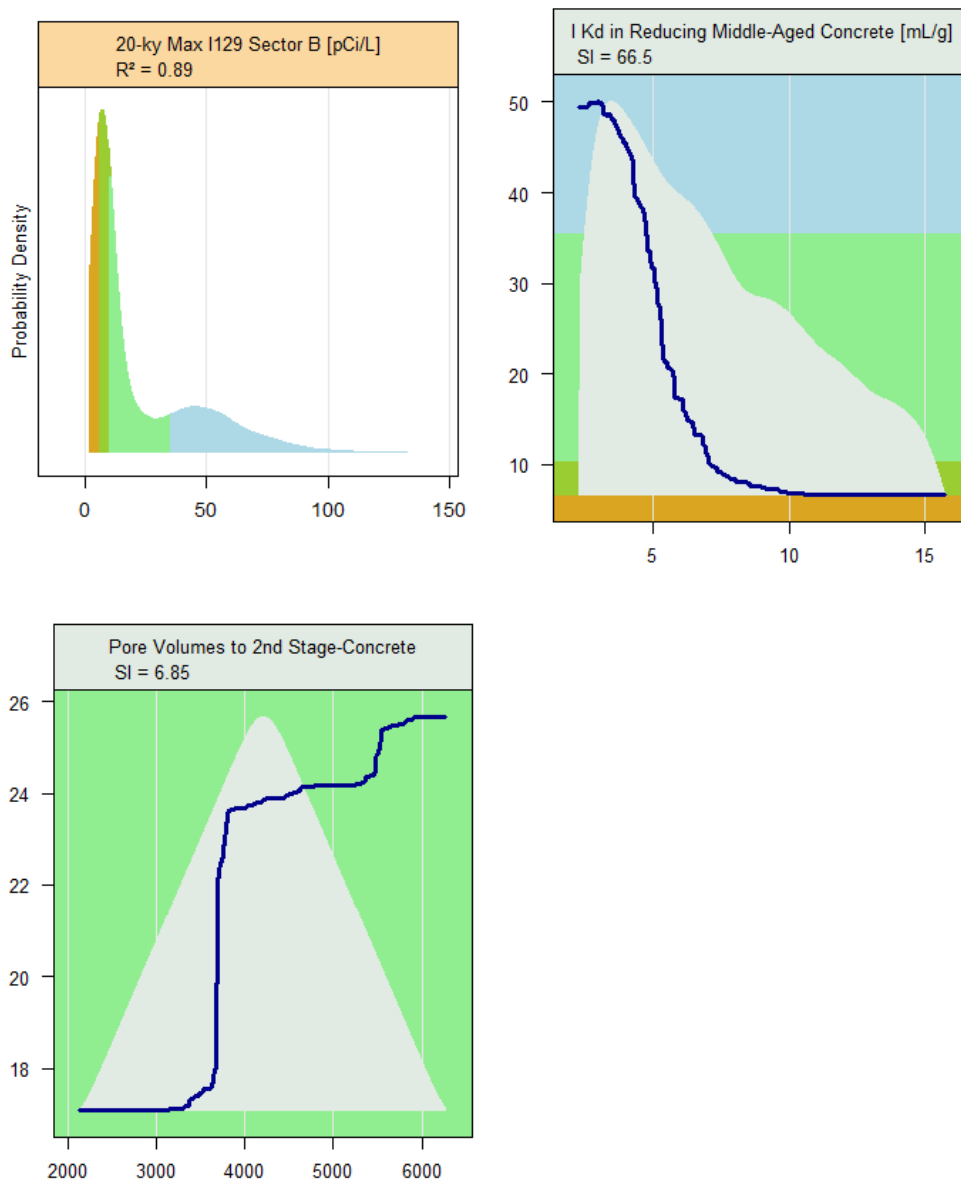


Figure 5.6-54 shows that the 20,000 year maximum concentration of I-129 at Sector J is again dominated by the reducing middle aged concrete K_d for iodine and by the pore volumes required to achieve first-stage concrete degradation (i.e., transition from middle aged reducing to middle aged oxidizing and second-stage concrete degradation from middle aged oxidizing to old aged oxidizing).

Figure 5.6-54: Max Concentration of I-129 at Sector J within 20,000 Years – Case A

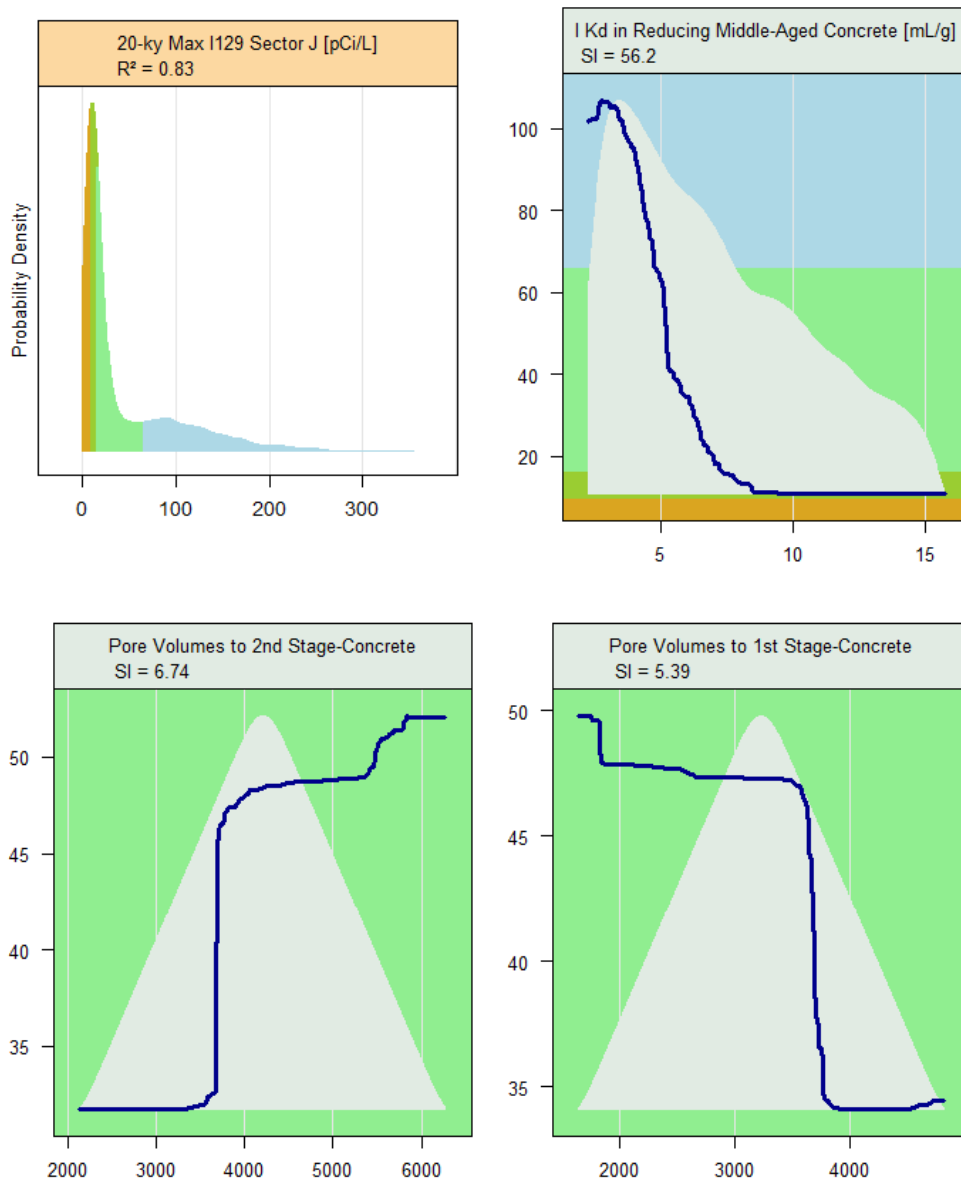


Figure 5.6-55 shows that the 20,000 year maximum concentration of Ra-226 at Sector B is driven largely by parameters related to contaminant transport, the K_d for radium in sandy soils, the aquifer thickness, and the unsaturated zone thickness below the FDCs.

Figure 5.6-55: Max Concentration of Ra-226 at Sector B within 20,000 Years – Case A

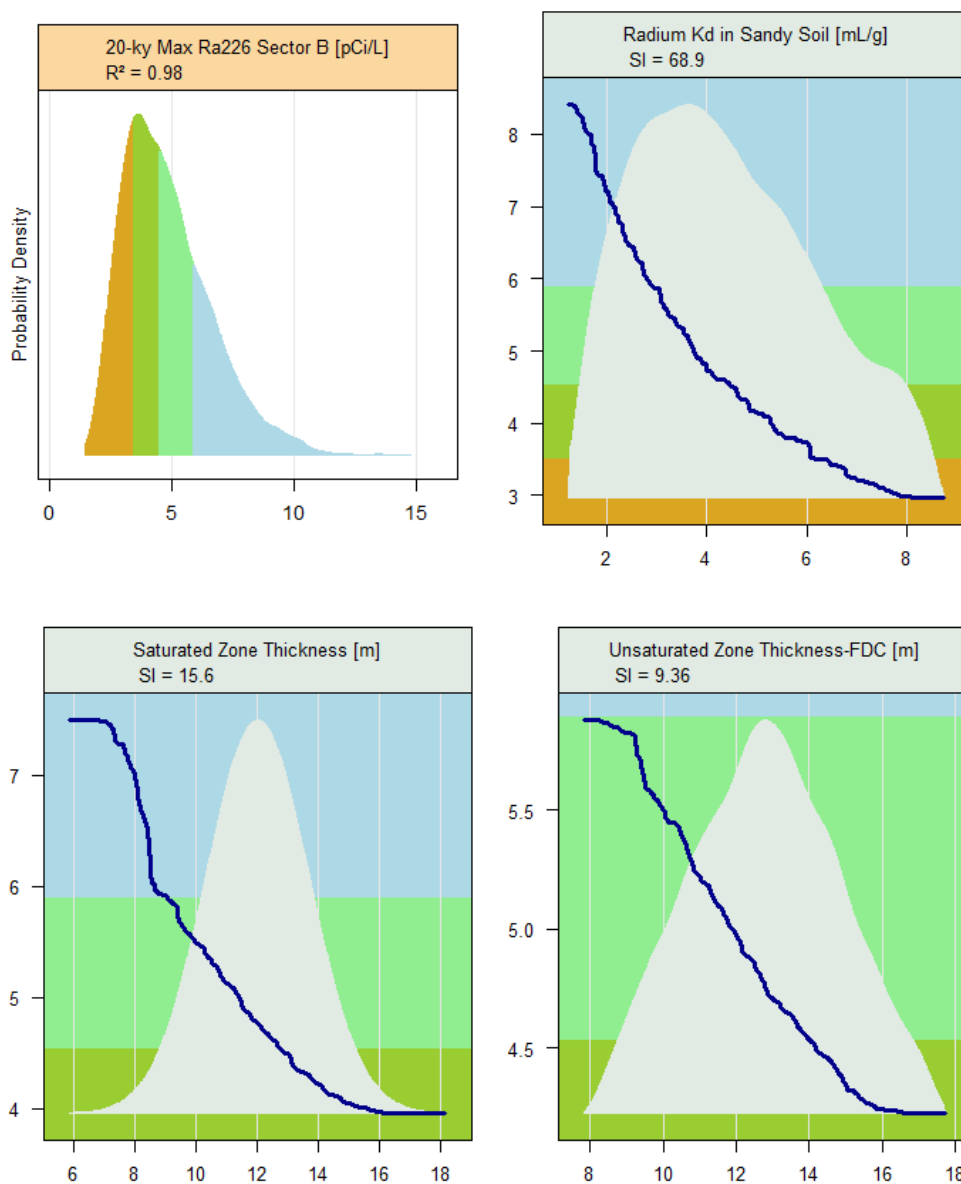
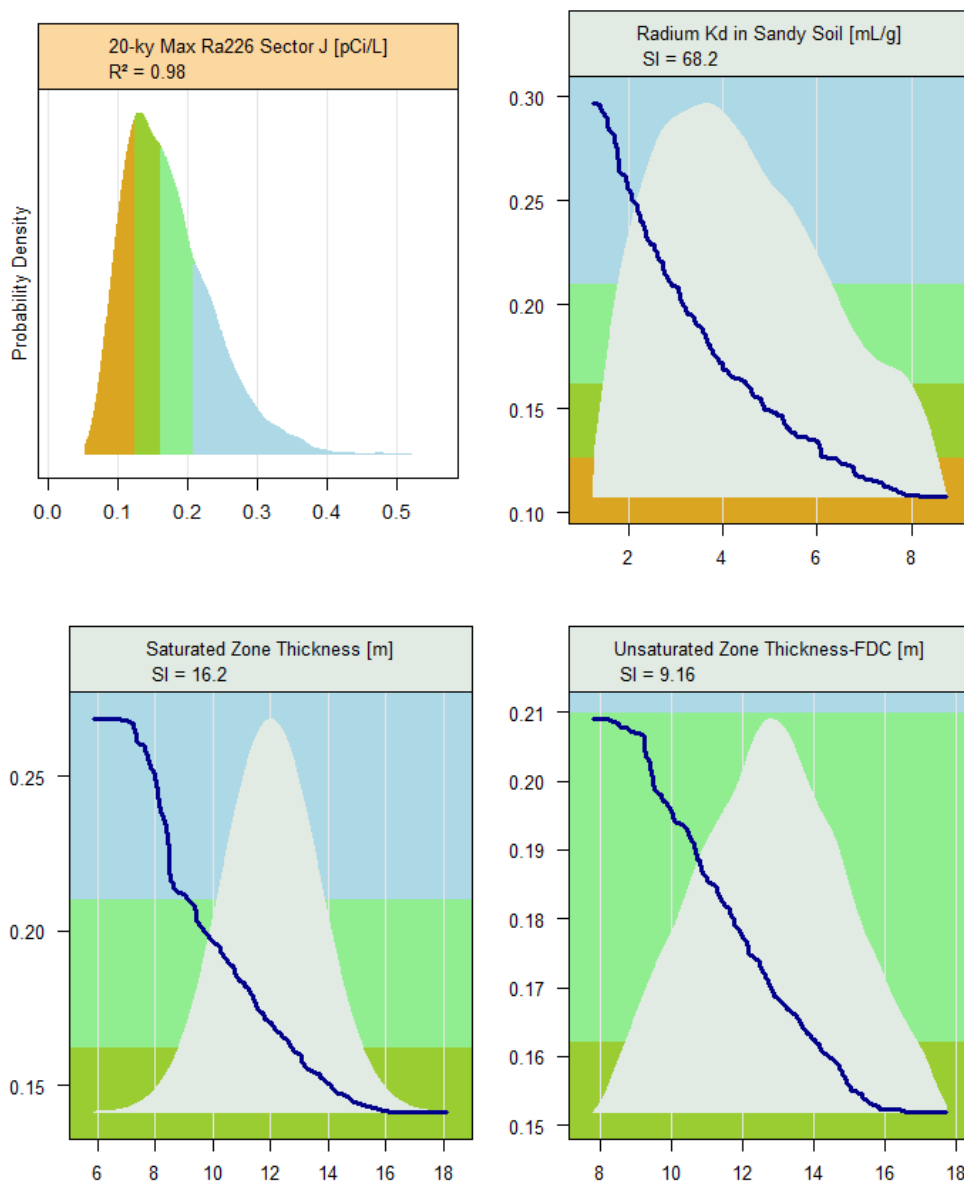


Figure 5.6-56 shows that the 20,000 year maximum concentration of Ra-226 at Sector J has essentially the same influences as that in Sector B.

Figure 5.6-56: Max Concentration of Ra-226 at Sector J within 20,000 Years – Case A



5.6.5.5 Case C Partial Dependence Plots

The partial dependence plots for Case C are shown in the figures within this section. The partial dependence plots identify the model input parameters that are most significant in determining the model endpoints identified in Table 5.6-13.

As shown in Figure 5.6-57, for Case C, the variation in the 10,000 year maximum dose to a MOP in any sector is due to the K_d for plutonium in clayey and sandy soils, and the unsaturated zone thickness for the FDCs, with none especially dominant. The dependence on Pu-239 is attributed to the modeling for Case C which assumes a direct mass transfer from saltstone to the unsaturated zone to simulate a fast flow path as discussed in at the end of Section 5.6.4.

Figure 5.6-57: Max MOP Dose, Any Sector within 10,000 Years – Case C

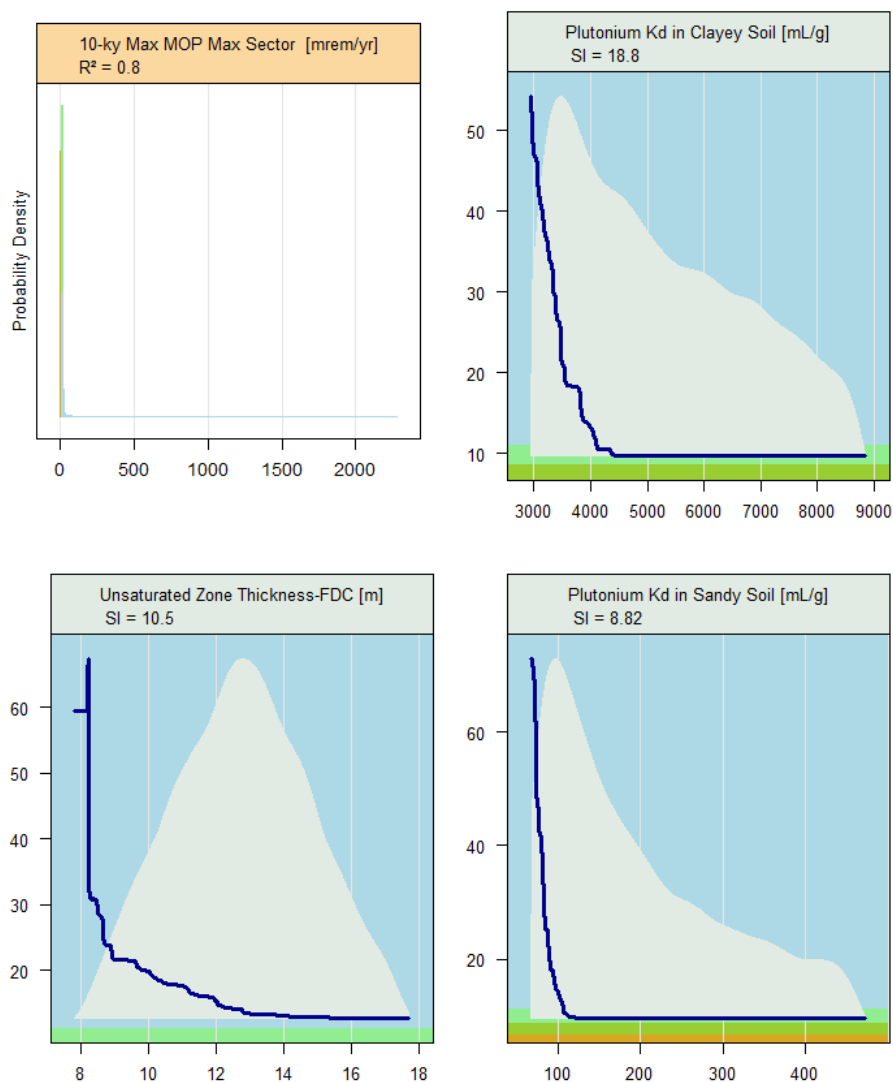


Figure 5.6-58 shows that for the maximum dose, at any sector within 20,000 years for Case C, the K_d for plutonium in sandy soils is the primary driver, followed by the vadose zone thickness below the FDCs.

Figure 5.6-58: Max MOP Dose, Any Sector within 20,000 Years – Case C

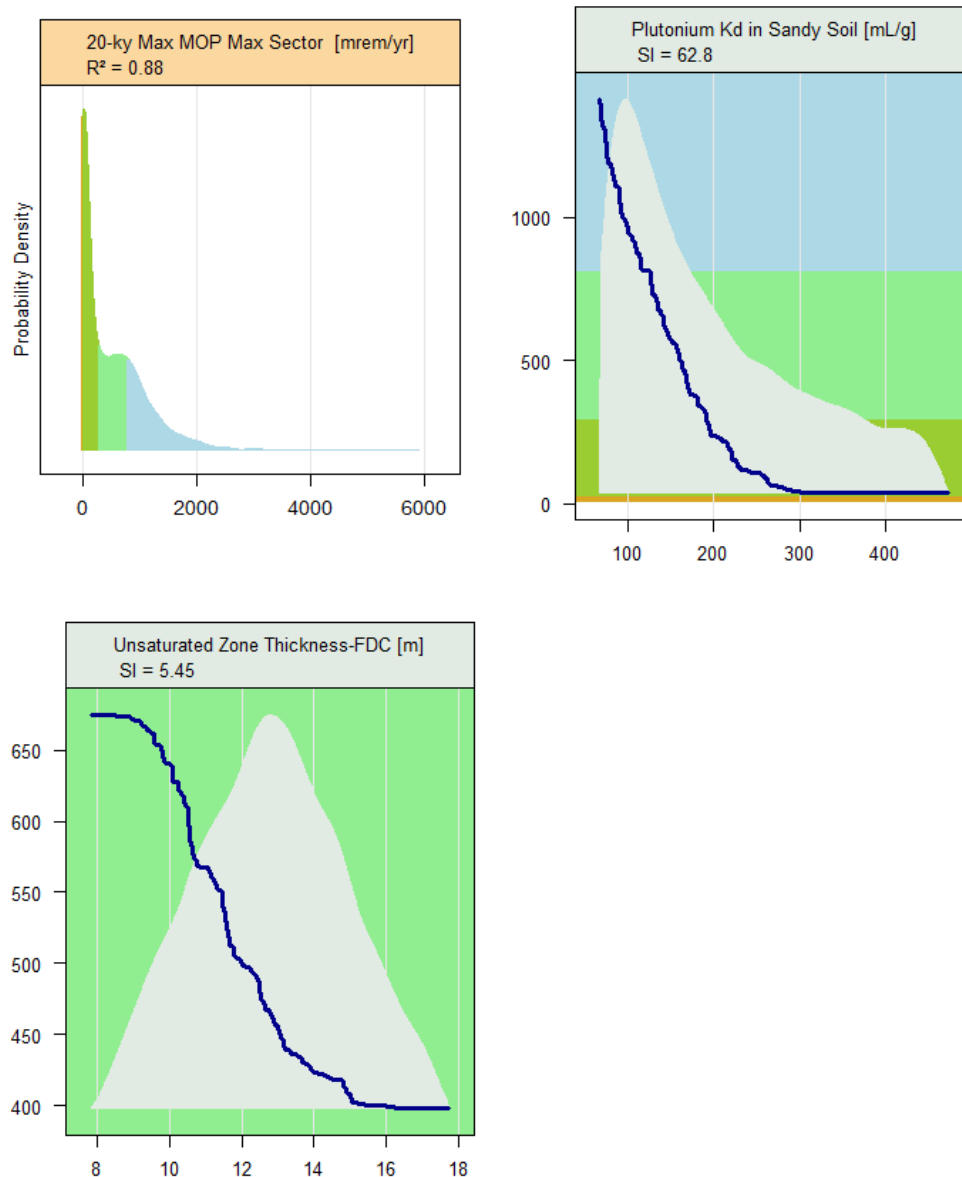


Figure 5.6-59 shows that the maximum 10,000 year MOP dose, within Sector B for Case C, has no overwhelmingly dominant parameters. The K_d of plutonium in clayey soil is greatest, followed by the vadose zone thickness for the FDCs. The third parameter identified by the sensitivity analysis is typical of a spurious influence, showing C-14, which has no influence on this dose. Overall, this is similar to the any-sector plots shown in Figure 5.6-57.

Figure 5.6-59: Max MOP Dose, Sector B within 10,000 Years – Case C

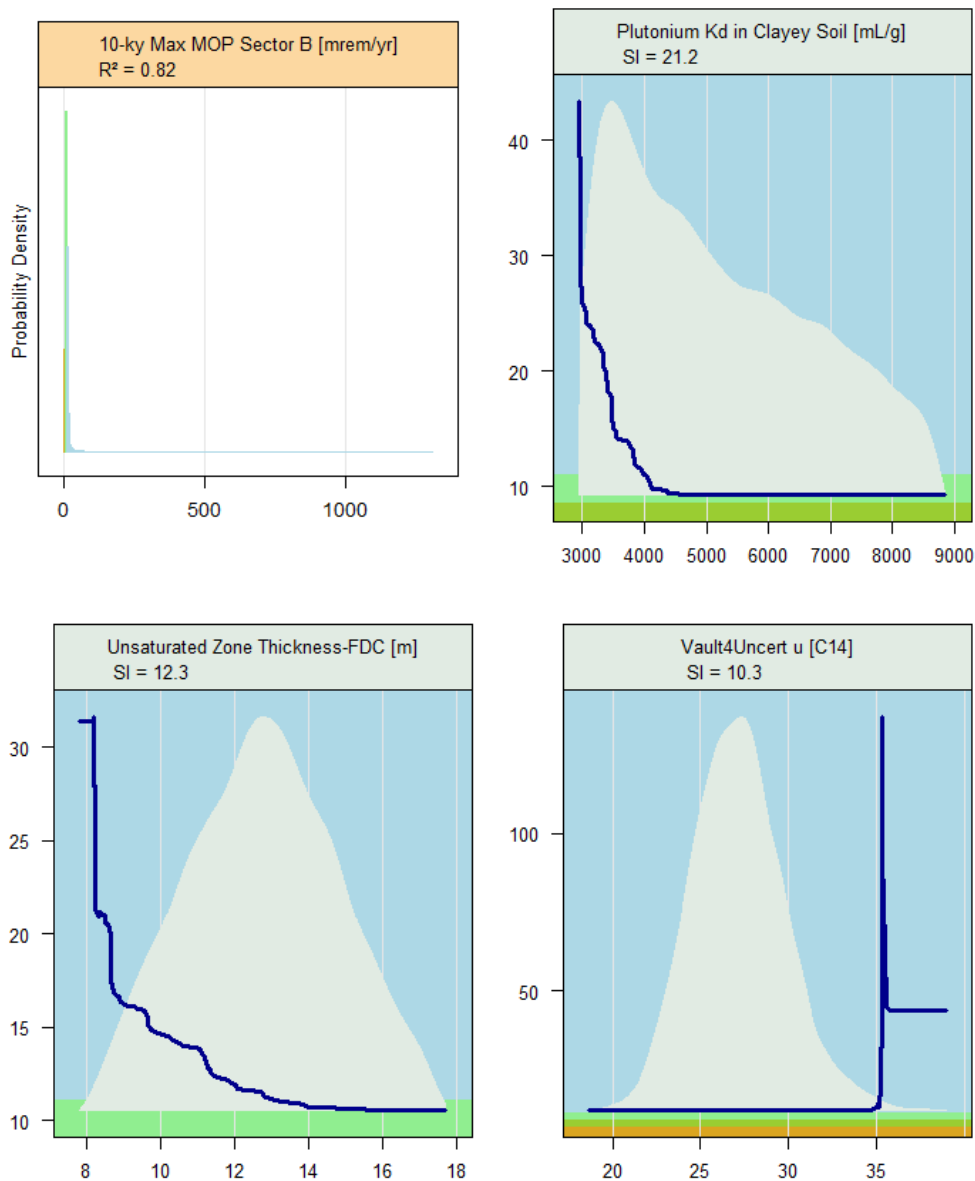


Figure 5.6-60 shows that the dominant parameters for the 20,000 year maximum dose in Sector B is similar to that of the maximum dose for any-sector, shown in Figure 5.6-58, dominated by the K_d of plutonium in sandy soil.

Figure 5.6-60: Max MOP Dose, Sector B within 20,000 Years – Case C

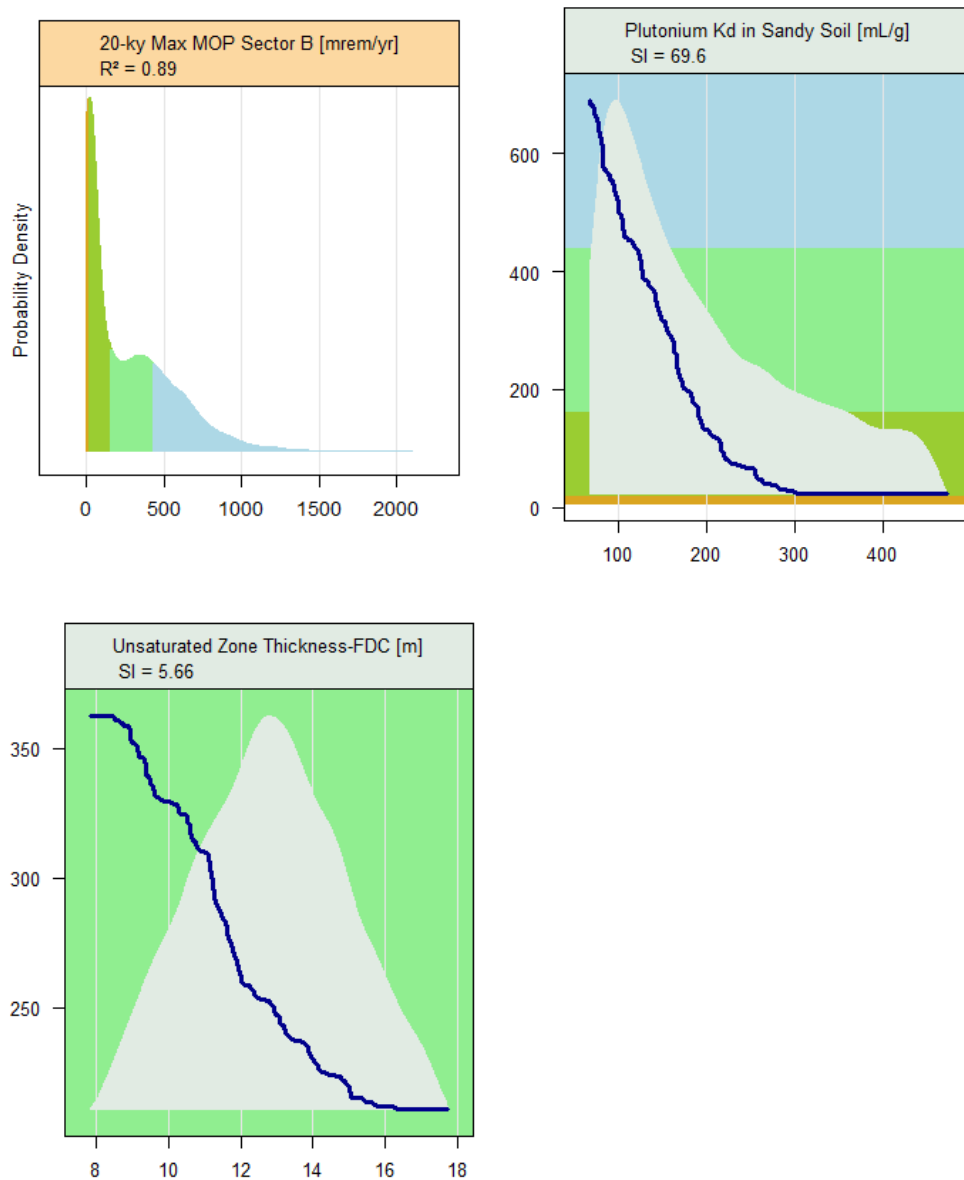
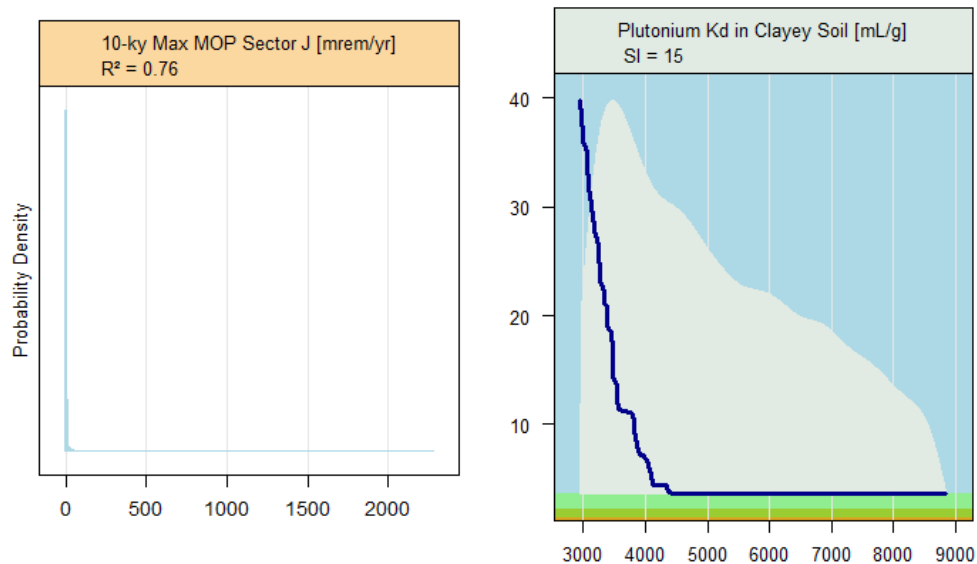


Figure 5.6-61 shows that the result for the 10,000 year maximum MOP dose for Case C in Sector J has only one minor parameter that has any credible influence, the plutonium K_d in clayey soil.

Figure 5.6-61: Max MOP Dose, Sector J within 10,000 Years – Case C



Similarly to Figure 5.6-61, Figure 5.6-62 shows that the result for the 20,000 year maximum MOP dose for Case C, in Sector J, has only one minor parameter of credible influence, plutonium K_d in sandy soil.

Figure 5.6-62: Max MOP Dose, Sector J within 20,000 Years – Case C

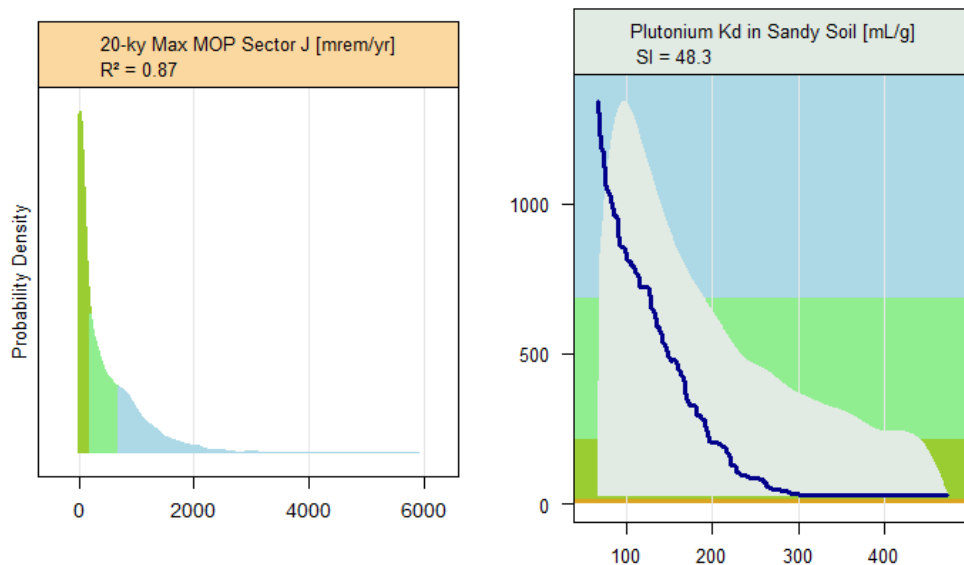


Figure 5.6-63 shows that the most sensitive parameters for Case C 20,000 year maximum concentration of Tc-99 in Sector B are the aquifer thickness and the Tc-99 uncertainty factor for the tank inventory feeding Vault 4.

Figure 5.6-63: Max Concentration of Tc-99, Sector B within 20,000 Years – Case C

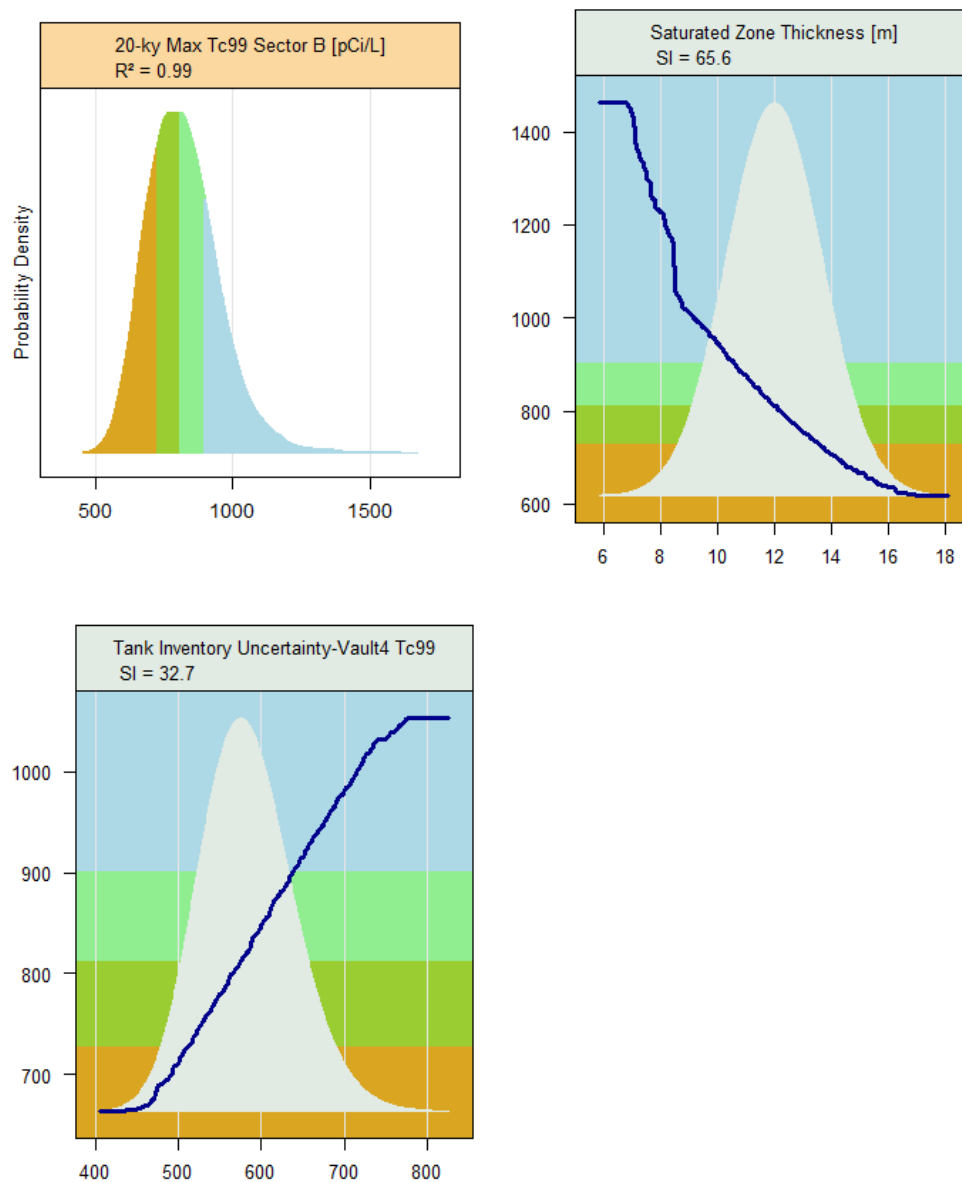


Figure 5.6-64, shows that the most sensitive parameters for the Case C 20,000 year maximum concentration of Tc-99 in Sector J are the K_d for technetium in reducing middle aged concrete and the aquifer thickness.

Figure 5.6-64: Max Concentration of Tc-99, Sector J within 20,000 Years – Case C

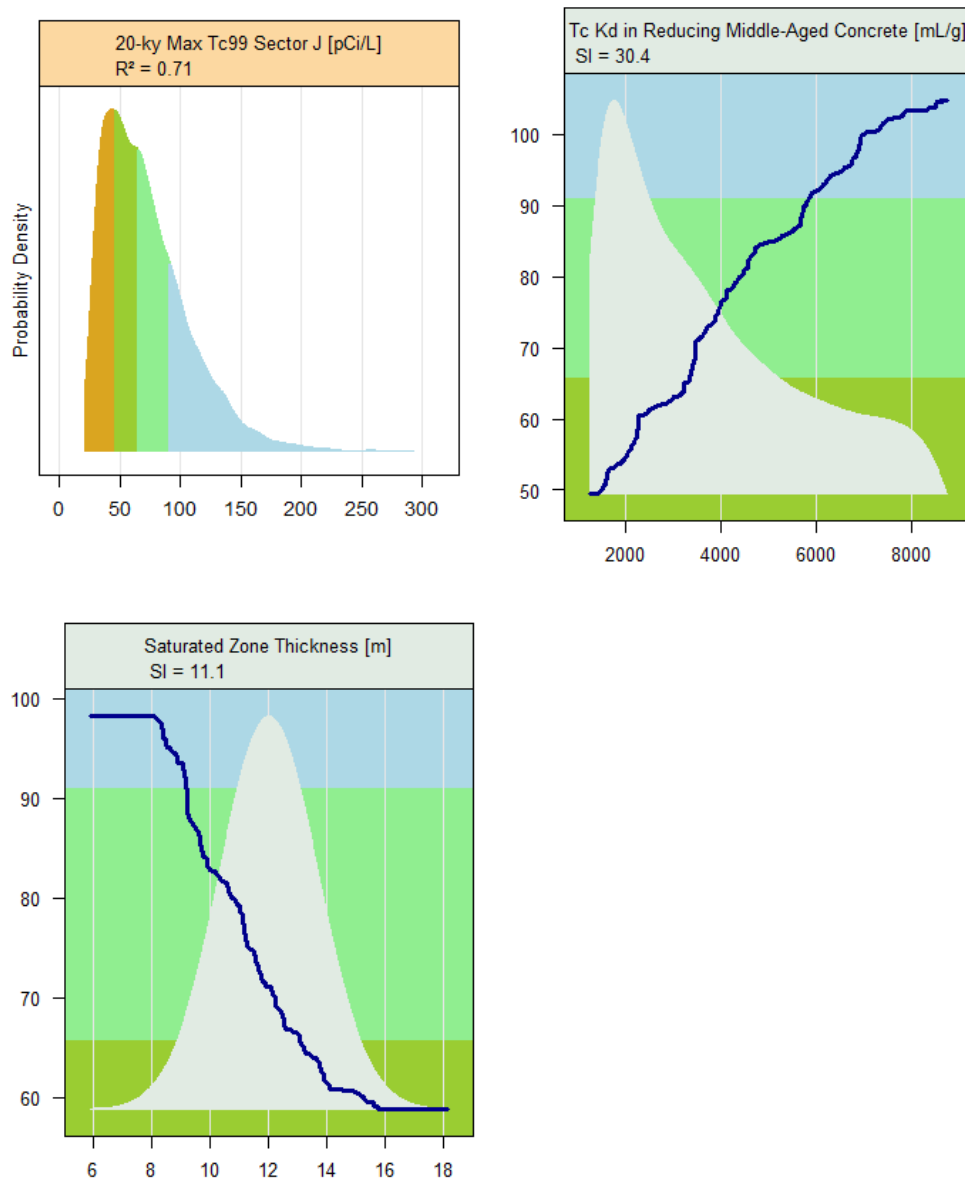
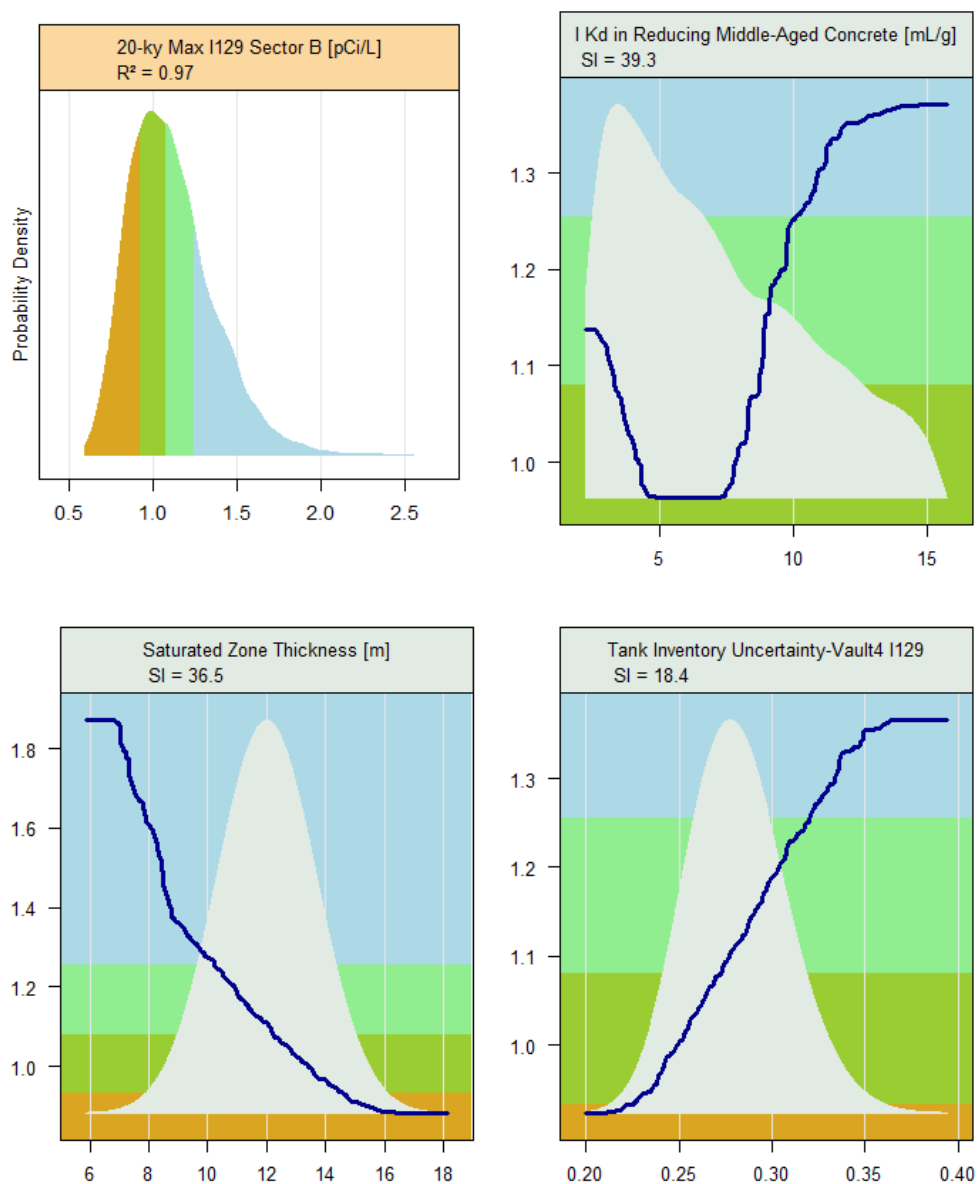


Figure 5.6-65 shows that the most sensitive parameters for the Case C 20,000 year maximum concentration of I-129 in Sector B are the K_d for iodine in reducing middle aged concrete, the aquifer thickness, and the Vault 4 inventory uncertainty factor for I-129.

Figure 5.6-65: Mass Concentration of I-129, Sector B within 20,000 Years – Case C



For the Case C 20,000 year maximum concentration of I-129 in Sector J, Figure 5.6-66 shows that the iodine K_d in oxidizing old aged and reducing middle aged concrete are the significant parameters.

Figure 5.6-66: Mass Concentration of I-129, Sector J within 20,000 Years – Case C

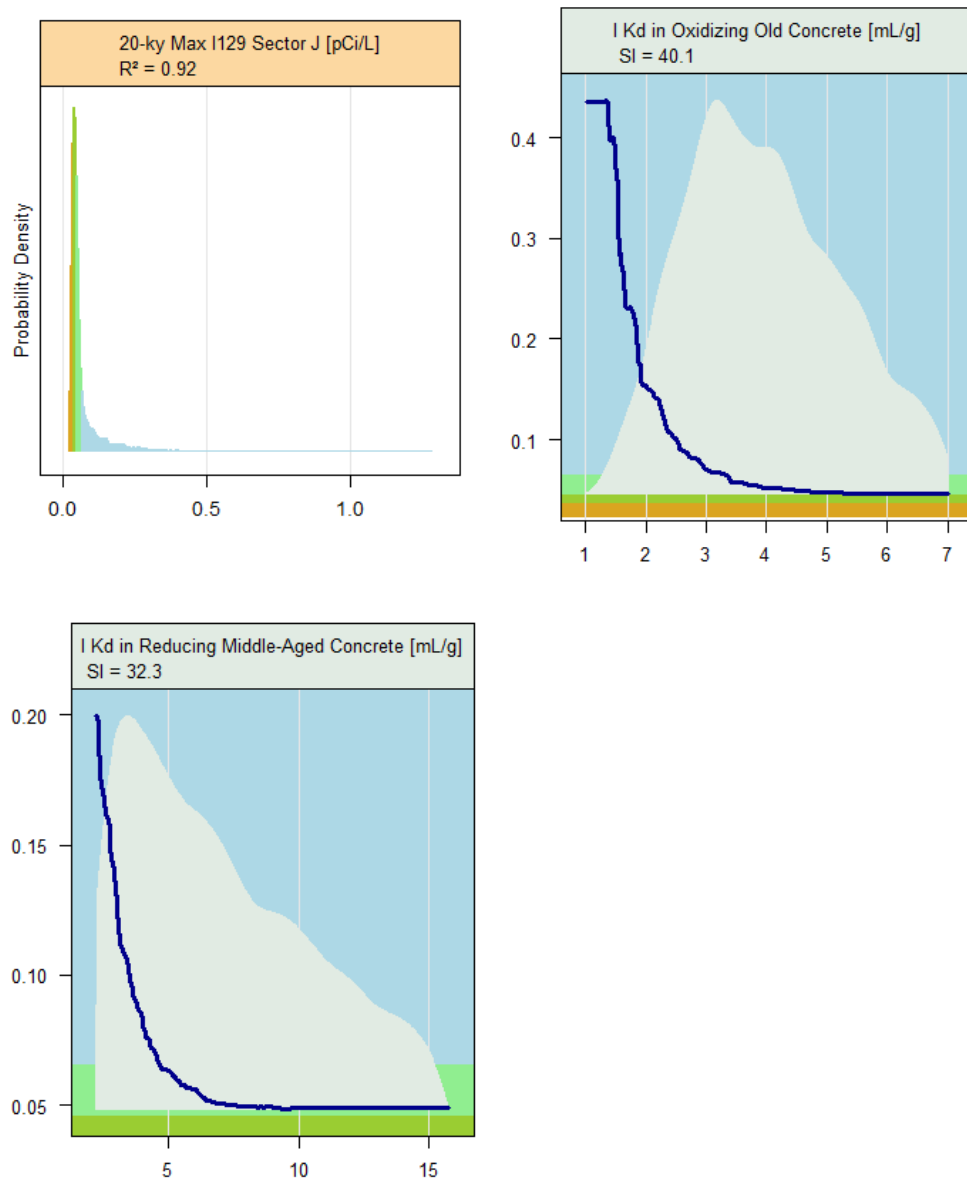


Figure 5.6-67 shows that the most sensitive parameters for the Case C 20,000 year maximum concentration of Ra-226 in Sector B are the K_d for radium in sandy soil, the aquifer thickness, and the inventory uncertainty for Ra-226 parent, Th-230, in Vault 4.

Figure 5.6-67: Mass Concentration of Ra-226, Sector B within 20,000 Years – Case C

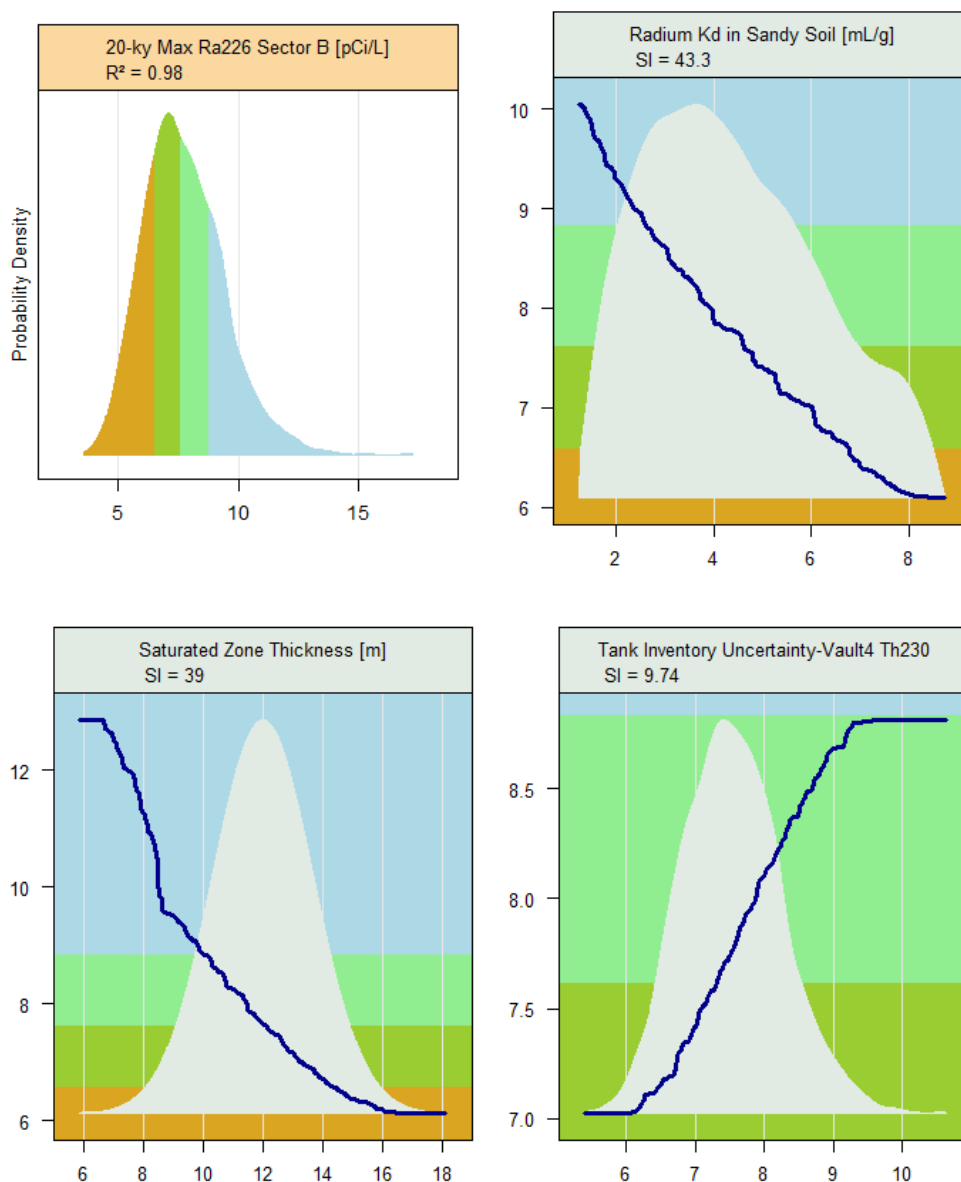
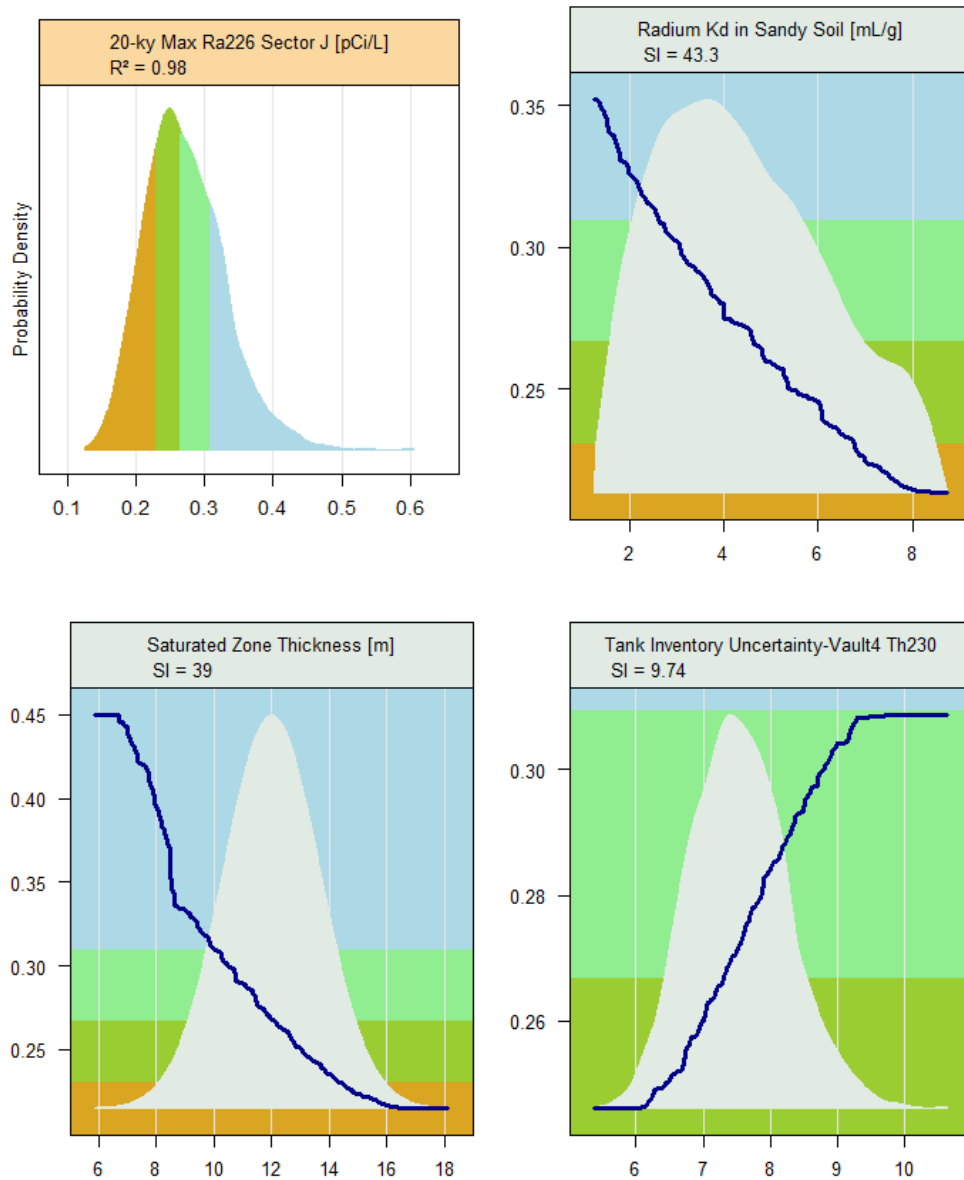


Figure 5.6-68 shows the 20,000 year maximum Ra-226 concentration in Sector J has the same drivers as for Sector B shown in Figure 5.6-67.

Figure 5.6-68: Mass Concentration of Ra-226, Sector J within 20,000 Years – Case C



5.6.5.6 Summary of the SDF Probabilistic Model Sensitivity Analysis

While the previous section contains numerous figures, the following recurring themes appeared in the sensitivity analysis:

For Case A, the following phenomena are noteworthy:

- The MOP dose in 10,000 years is influenced primarily by Ra-226 and I-129, whereas at 20,000 years it is nearly all I-129.
- The appearance of radium is most sensitive to its K_d in sandy soil, the aquifer thickness, and the thickness of the unsaturated zone beneath the FDCs.
- Iodine is most strongly influenced by its K_d in reducing middle aged concrete and the number of pore volumes of infiltrating water that flow through the disposal unit concrete, gradually degrading it.

For Case C, these are the useful results of the sensitivity analysis:

- MOP doses are strongly driven by plutonium.
- The appearance of plutonium is most sensitive to its K_d in sandy and clayey soils, and the thickness of the unsaturated zone beneath the FDCs.

Further insight into how the probabilistic sensitivity analyses results relate to the performance objectives is provided in Section 7.1.

5.6.6 Single Parameter Sensitivity Analyses

The purpose of this section is to consider the impact varying a single parameter might have on the SDF deterministic model, so that the sensitivity of the models to changes in select parameters expected to be of concern might be discovered. For the single parameter sensitivity analyses performed using the SDF PORFLOW model, 100m concentrations were calculated for the key radionuclides using the SDF PORFLOW model and the seepline doses were determined using the process described in Section 5.2.2.

5.6.6.1 Alternate Disposal Unit Case Sensitivity Analysis using the PORFLOW Deterministic Model

The sensitivity analysis results for the alternative disposal unit cases are provided in this section. Peak groundwater pathways doses were calculated using, (1) five alternative disposal unit cases discussed in Section 5.6.3.1, and (2) other parameters as modeled in the PORFLOW SDF Base Case (presented in Section 4.4). The results of these sensitivity analyses, showing the peak groundwater pathways doses for key radionuclides for Cases B through E are presented in Table 5.6-16 and Figures 5.6-69 through 5.6-74. the model parameter changes that occur for each disposal unit and each case are presented in Tables 4.4-6, 4.4-7, and 4.4-9 for Vault 1, Vault 4, and the FDCs respectively. These model changes over time are useful in the interpretation of the figures. The results indicate that peak groundwater pathways doses for Sector B, Case E produce the highest dose (57.0 mrem/yr at year 9,000) in the 10,000 year performance period compared to all other cases. As described in 5.6.3.1, Case E addresses the potential for a highly permeable saltstone and clean cap from year zero onwards through the period of performance. Case E includes no fast flow pathways.

Case E and C produce earlier increases in the dose results at 100m as compared to Case A (see Figure 5.6-73 for a compilation of Cases A-E for Sector B). The increases are due to the increase of flow through the saltstone which increases the availability of contaminants to the environment quicker. As described above and in 5.6.3.1, Case C includes fast flow paths between the saltstone monolith and the interior wall as well as fast flow paths in the saltstone. Case B includes a fast flow path between the saltstone monolith and the interior wall.

Case E increases are due to the high permeability (relatively high hydraulic conductivities of the saltstone monolith and clean cap) from year zero onward through the period of performance. When Case E is coupled with the relatively high hydraulic conductivities assumptions for the Vault 1 and 4 walls, it explains why the highest overall sector is Sector B (Sector B is dominated by the flow from Vault 1 and 4). The results also illustrate that Sector B produces the highest doses regardless of the case.

Sector I, although not as pronounced as Sector B, is similarly influenced by the relatively high hydraulic conductivities of the saltstone monolith and clean cap. The Sector I peaks at 9,000 years reflect the impact Vault 4 has on Sector I in the Gordon aquifer. The highest peak in Sector I for Case E comes near year 15,000 and is the result of the failure of the FDC walls and the subsequent effect of flushing 64 FDCs at the same time-step with higher flows. Appendix A.4 through A.7 contain data curves showing the groundwater concentrations for the disposal unit sensitivity cases.

Table 5.6-16: 100m Peak Dose for Key Radionuclides within 20,000 Years by Sector for Cases A through E

| Case | | Sectors | | | | | | | | | | | |
|------|--------------------|---------|--------|--------|--------|--------|--------|--------|--------|--------|--------|--------|--------|
| | | A | B | C | D | E | F | G | H | I | J | K | L |
| A | 10k peak (mrem/yr) | 1.2 | 1.4 | 0.7 | 0.5 | 1.0 | 0.3 | 0.4 | 0.4 | 0.4 | 0.4 | 0.4 | 0.4 |
| A | Year | 10,000 | 10,000 | 10,000 | 10,000 | 10,000 | 10,000 | 10,000 | 10,000 | 10,000 | 10,000 | 10,000 | 10,000 |
| A | 20k peak (mrem/yr) | 2.6 | 2.9 | 2.0 | 1.6 | 2.3 | 1.3 | 2.8 | 2.8 | 3.1 | 2.7 | 2.8 | 2.3 |
| A | Year | 15,080 | 15,080 | 15,060 | 15,060 | 15,060 | 15,060 | 15,080 | 15,080 | 15,080 | 15,080 | 15,080 | 15,080 |
| B | 10k peak (mrem/yr) | 3.5 | 3.896 | 2.1 | 1.4 | 2.8 | 1.1 | 1.5 | 1.5 | 1.629 | 1.5 | 1.5 | 1.4 |
| B | Year | 4,200 | 4,180 | 4,160 | 4,160 | 4,160 | 4,180 | 4,180 | 4,180 | 4,180 | 4,160 | 4,180 | 4,180 |
| B | 20k peak (mrem/yr) | 5.3 | 6.0 | 3.1 | 1.9 | 4.2 | 1.5 | 1.8 | 1.8 | 1.868 | 1.8 | 1.8 | 1.7 |
| B | Year | 15,740 | 15,740 | 15,740 | 15,720 | 15,740 | 15,740 | 15,740 | 15,740 | 15,740 | 15,740 | 15,740 | 15,740 |
| C | 10k peak (mrem/yr) | 4.52 | 5.13 | 2.75 | 1.85 | 3.72 | 1.44 | 1.85 | 1.86 | 1.95 | 1.83 | 1.86 | 1.71 |
| C | Year | 7,380 | 7,360 | 7,360 | 7,340 | 7,360 | 7,360 | 7,360 | 7,360 | 7,360 | 7,360 | 7,360 | 7,360 |
| C | 20k peak (mrem/yr) | 4.91 | 5.54 | 3.00 | 2.07 | 4.02 | 1.58 | 2.10 | 2.10 | 2.20 | 2.04 | 2.10 | 1.90 |
| C | Year | 15,420 | 15,420 | 15,400 | 15,420 | 15,400 | 15,420 | 15,420 | 15,500 | 15,500 | 15,500 | 15,500 | 15,440 |
| D | 10k peak (mrem/yr) | 1.1 | 1.275 | 0.6 | 0.4 | 0.9 | 0.3 | 0.3 | 0.3 | 0.333 | 0.3 | 0.3 | 0.3 |
| D | Year | 9,820 | 9,800 | 9,800 | 9,800 | 9,800 | 9,820 | 9,840 | 9,840 | 9,840 | 9,840 | 9,840 | 9,840 |
| D | 20k peak (mrem/yr) | 1.8 | 2.1 | 1.0 | 0.7 | 1.5 | 0.5 | 0.5 | 0.5 | 0.552 | 0.5 | 0.5 | 0.5 |
| D | Year | 16,180 | 16,180 | 15,580 | 15,580 | 15,580 | 15,580 | 15,580 | 15,580 | 15,580 | 15,580 | 15,580 | 15,580 |
| E | 10k peak (mrem/yr) | 49.87 | 56.48 | 28.61 | 18.45 | 40.30 | 14.05 | 14.15 | 14.16 | 14.17 | 14.15 | 14.16 | 14.14 |
| E | Year | 9,420 | 9,400 | 9,400 | 9,380 | 9,400 | 9,400 | 9,400 | 9,400 | 9,400 | 9,400 | 9,400 | 9,400 |
| E | 20k peak (mrem/yr) | 49.87 | 56.48 | 28.61 | 18.45 | 40.30 | 14.14 | 18.44 | 18.49 | 19.29 | 18.21 | 18.56 | 17.01 |
| E | Year | 9,420 | 9,400 | 9,400 | 9,380 | 9,400 | 15,040 | 15,060 | 15,060 | 15,060 | 15,060 | 15,060 | 15,060 |

Figure 5.6-69: 100m Peak Groundwater Pathways Dose Sectors B and I, Case B

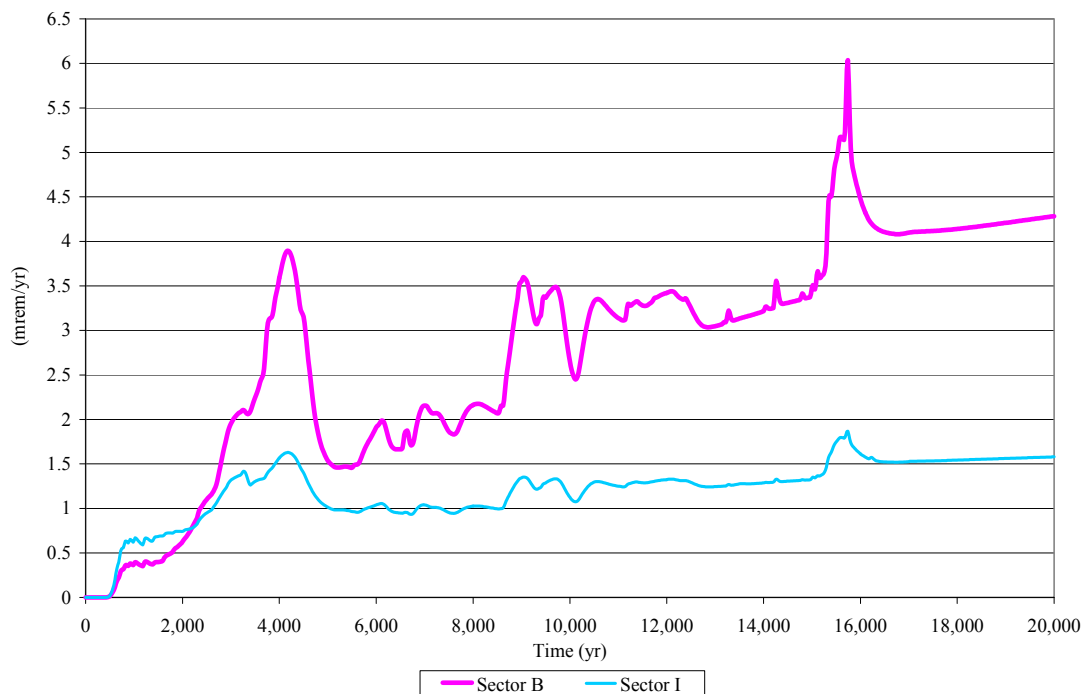


Figure 5.6-70: 100m Peak Groundwater Pathways Dose Sectors B and I, Case C

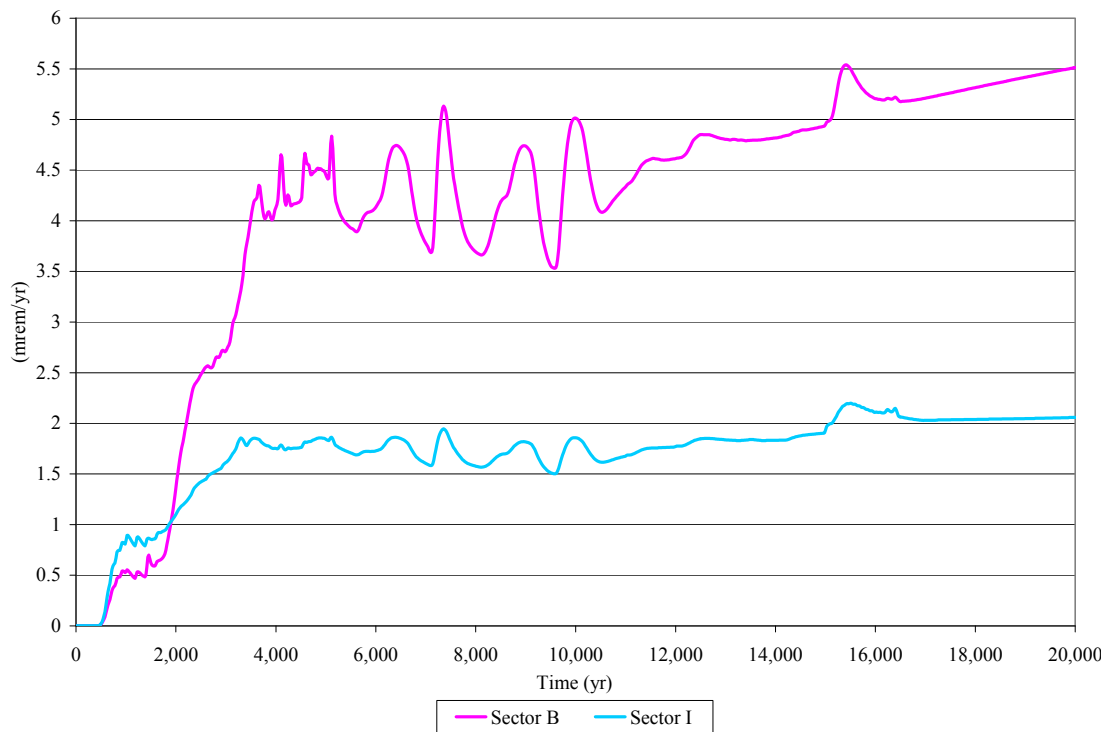


Figure 5.6-71: 100m Peak Groundwater Pathways Dose Sectors B and I, Case D

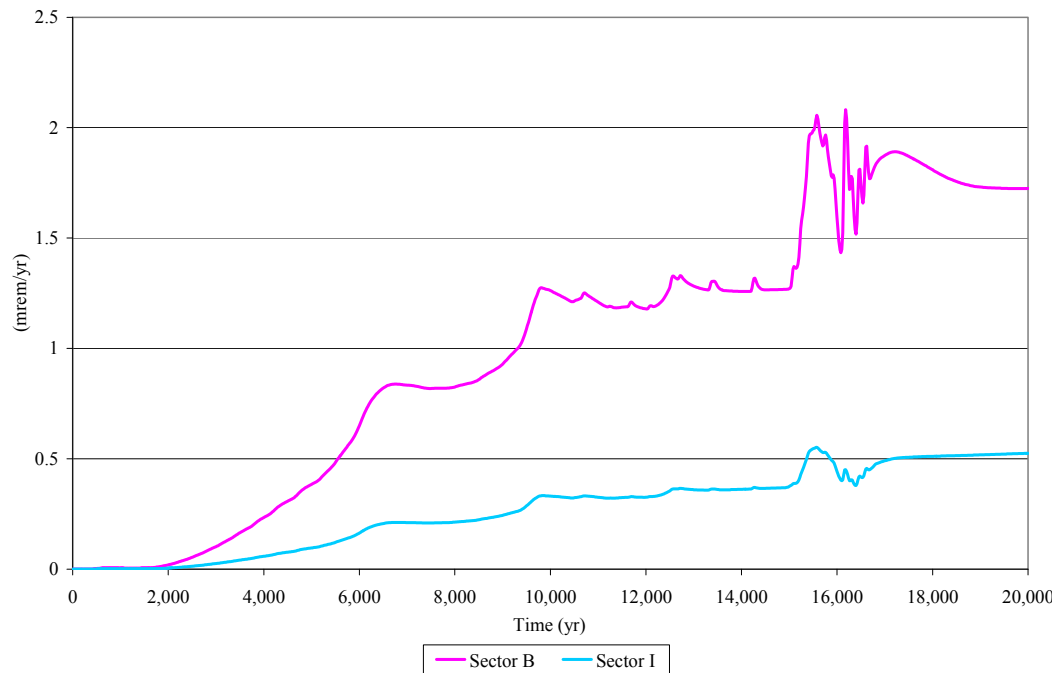


Figure 5.6-72: 100m Peak Groundwater Pathways Dose Sectors B and I, Case E

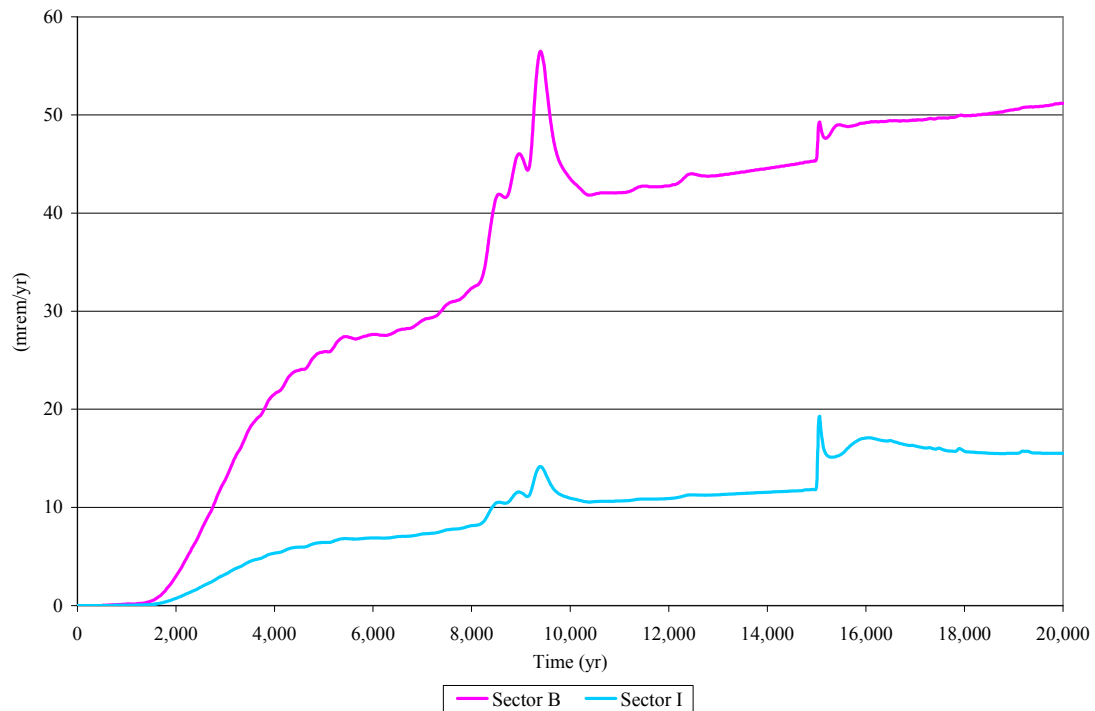


Figure 5.6-73: 100m Peak Groundwater Pathways Dose Sector B, Case A through E

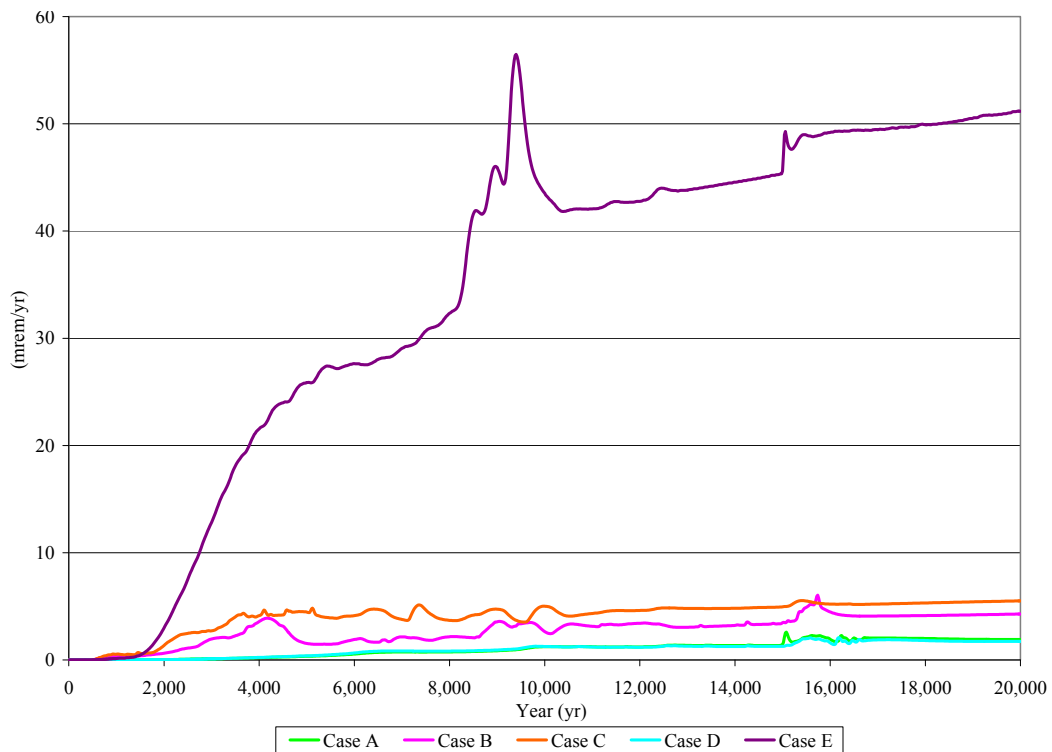
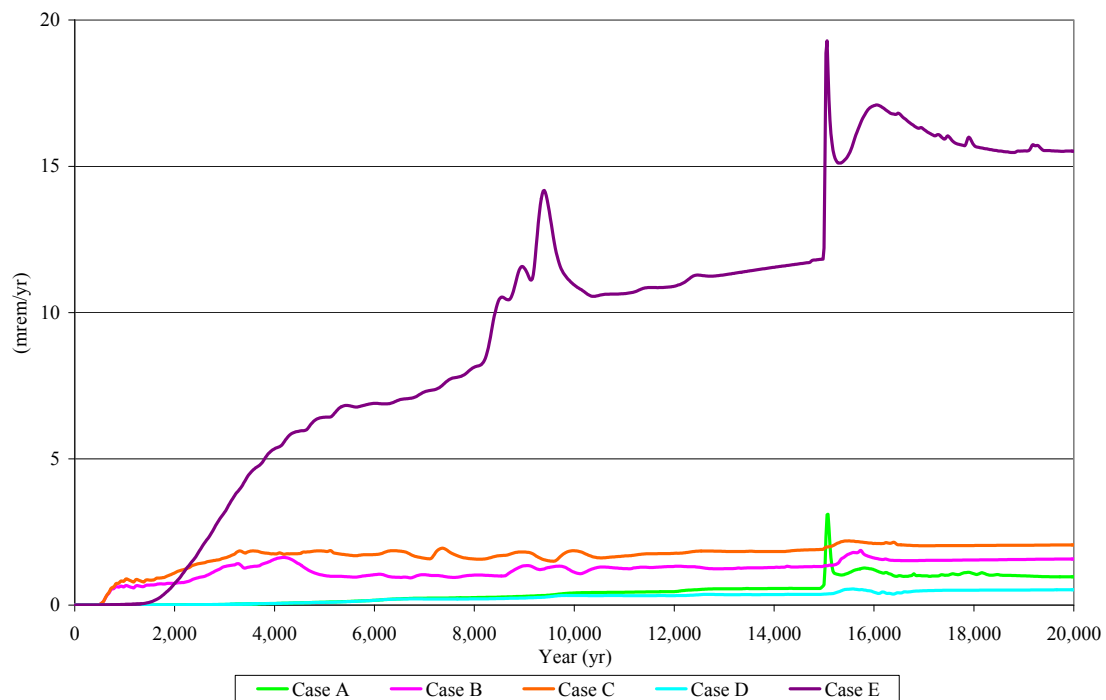


Figure 5.6-74: 100m Peak Groundwater Pathways Dose Sector I, Case A through E



5.6.6.2 No Closure Cap Sensitivity Analysis using the PORFLOW Deterministic Model

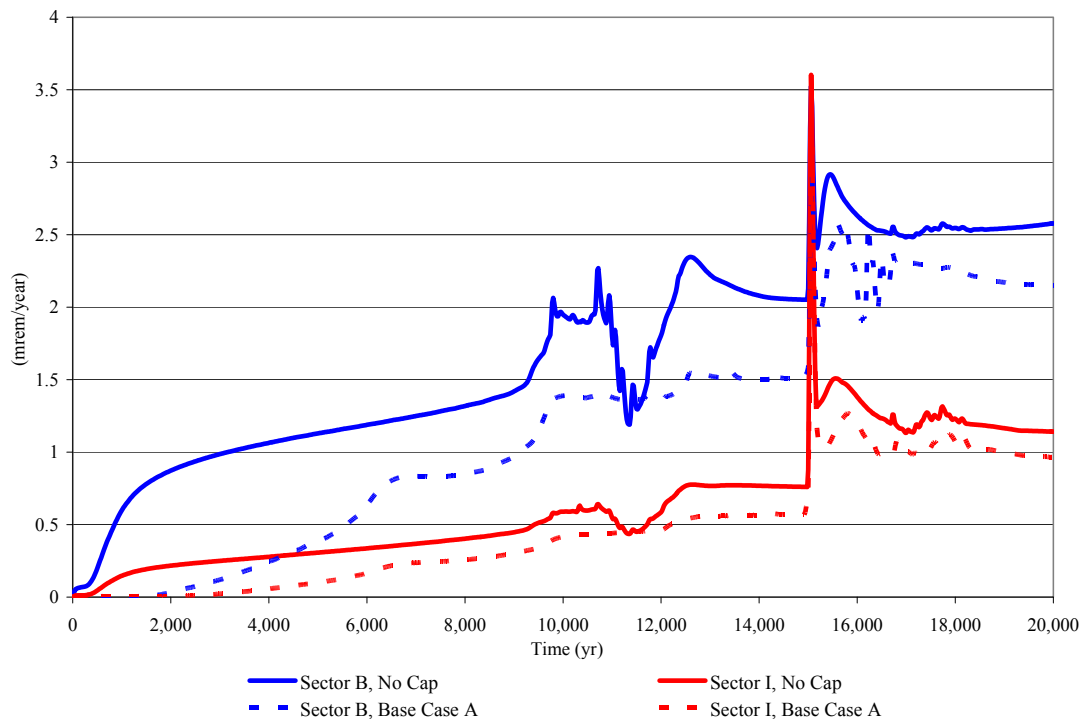
The sensitivity analysis results for the “no closure cap” case are provided in this section. The no closure cap scenario assumes that the following cap layers do not exist at time zero: the composite hydraulic barrier, the lateral drainage layers, and the erosion control layer. This scenario translates to a fixed infiltration rate of 16.45 in/yr average annual infiltration. [WSRC-STI-2008-00244] Peak groundwater pathways doses were calculated using the PORFLOW SDF Base Case parameters with the “soils only” closure cap (presented in Section 4.4).

The results of these sensitivity analyses, showing the peak groundwater pathways doses, are presented in Table 5.6-17 and Figure 5.6-75. The results show that peak groundwater pathways doses would increase without the installation of a closure cap over the SDF. Peak doses would increase by 50% for Sectors B and I in the first 10,000 years. Peak doses would increase between 12% and 50% for 10,000 and 20,000 years results.

Table 5.6-17: 100m Peak Groundwater Pathways Dose within 20,000 Years for Sectors B and I for No Closure Cap Sensitivity Comparison

| Peak Groundwater Dose | Sector B | | Sector I | |
|-------------------------------------|-----------|--------|-----------|--------|
| | Base Case | No Cap | Base Case | No Cap |
| Peak Dose in 10,000 Years (mrem/yr) | 1.4 | 2.1 | 0.4 | 0.6 |
| Year of Peak Dose | 10,000 | 9,800 | 10,000 | 10,000 |
| Peak Dose in 20,000 Years (mrem/yr) | 2.9 | 3.5 | 3.1 | 3.6 |
| Year of Peak Dose | 15,080 | 15,060 | 15,080 | 15,060 |

Figure 5.6-75: Peak Groundwater Pathways Dose Sectors B and I, No Closure Cap Case



Note: Appendix H contains data curves showing the groundwater concentrations for the no closure cap case.

5.6.6.3 Materials Degradation Sensitivity Analysis using the PORFLOW Deterministic Model

The basis and results for the disposal unit concrete degradation sensitivity analyses are provided in this section. Disposal unit concrete degradation is assumed to be driven by sulfate attack. The Base Case analysis assumes that (1) transport properties, with respect to predicting ettringite front position, are unchanged by passage of the front, and (2) the presence of ettringite, coincides with physical damage to concrete, for the purpose of estimating effective transport properties for saltstone contaminant release. [SRNL-L6200-2009-00011] A detailed discussion on materials degradation can be found in Section 4.2.3.2.

To explore the sensitivity of PORFLOW simulations to these key assumptions, two alternatives to the Base Case (Case A) assumptions are considered in this sensitivity analysis (1) diffusion coefficient, with respect to predicting ettringite front position, is assumed to locally increase after passage of the front, and (2) ettringite formation is assumed to not lead to damage. Sensitivity analysis assumption (1) (e.g., 10 times sulfate attack) is contrary to the Base Case (Case A) assumption (1) and produces faster disposal unit degradation. Sensitivity analysis assumption (2) (e.g., no sulfate attack) differs from Base Case (Case A) assumption (2) and implies no change to disposal unit properties over time.

To assign an appropriate diffusion coefficient for sensitivity analysis assumption (1), the properties of cracked concrete are considered along with the presumed state of degraded concrete behind the advancing ettringite front. Figure 5.6-76 shows a cross plot of the diffusion coefficients hydraulic conductivity for materials in SDF. An empirical curve fit indicates that diffusion coefficient varies as roughly the cube root of conductivity (power law exponent = $0.3187 \approx 1/3$):

$$\frac{D_e}{D_{ref}} \approx \left(\frac{K}{K_{ref}} \right)^{1/3} \quad (1)$$

A power law exponent of 1/3 means that a 1,000 times increase in conductivity corresponds to only a 10 times increase in diffusion coefficient.

Using Vault 1 and 4 wall concrete as a basis, Figure 5.6-77 compares the unsaturated hydraulic conductivity of cracked and uncracked concrete for the chosen crack parameters. Soil suction levels under nominal saltstone closure cap degradation conditions vary through space and time across a typical range of approximately 0.10 to approximately 0.01 centimeters. In this suction range, the conductivity of cracked concrete ranges up to three orders of magnitude higher than conductivity for uncracked concrete. Equation (1) suggests a corresponding increase in diffusion coefficient up to 10 times. Accordingly, a 10 times higher diffusion coefficient is used to predict sulfate attack for sensitivity analysis assumption (1).

The impact of a 10 times increase in diffusion coefficient is summarized in Table 5.6-18. Figures 5.6-78 through 5.6-80 show the position of the ettringite front for this accelerated sulfate attack sensitivity case. Note that the time to complete failure is less than 10,000 years for FDC components and the Vault 4 roof.

Table 5.6-18: Disposal Unit Component Failure Times, Base Case and 10 Times Sulfate Case

| Degradation Location | Time to Complete Failure | |
|-------------------------------------|--------------------------|----------------------------|
| | Base Case (yr) | 10 times Sulfate Case (yr) |
| FDC floor (including upper mud mat) | 40,000 | 5,000 |
| FDC roof | 40,000 | 7,000 |
| FDC wall | 18,000 | 3,000 |
| Vault 1 floor | >100k | 25,000 |
| Vault 1 roof | 50,000 | 12,000 |
| Vault 1 wall | >100k | 16,000 |
| Vault 4 floor | >100k | 25,000 |
| Vault 4 roof | 10,000 | 3,000 |
| Vault 4 wall | >100k | 16,000 |

Figure 5.6-76: Diffusion Coefficient Compared To Hydraulic Conductivity for Saltstone Materials Palette

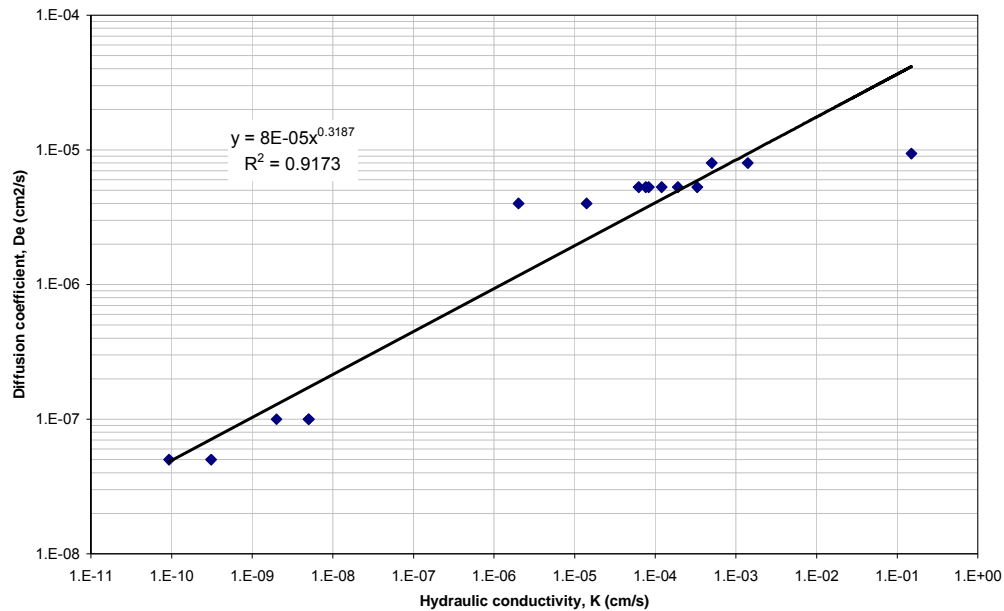
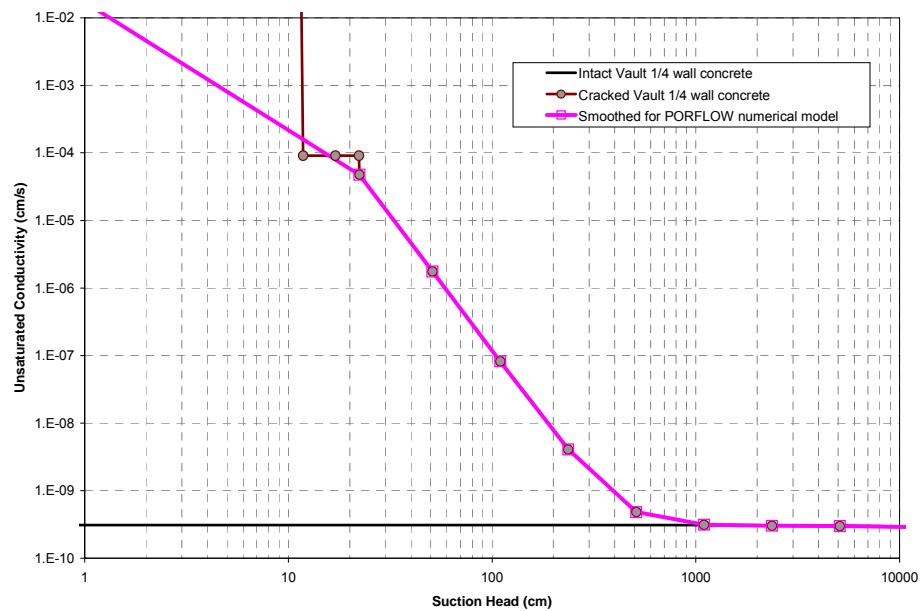


Figure 5.6-77: Unsaturated Hydraulic Conductivity Estimate for Cracked/Un-cracked Disposal Unit Concrete



(127 μ m Aperture, 1 cm Crack Spacing)

Figure 5.6-78: Ettringite Front Position for Accelerated Sulfate Attack Vault 1

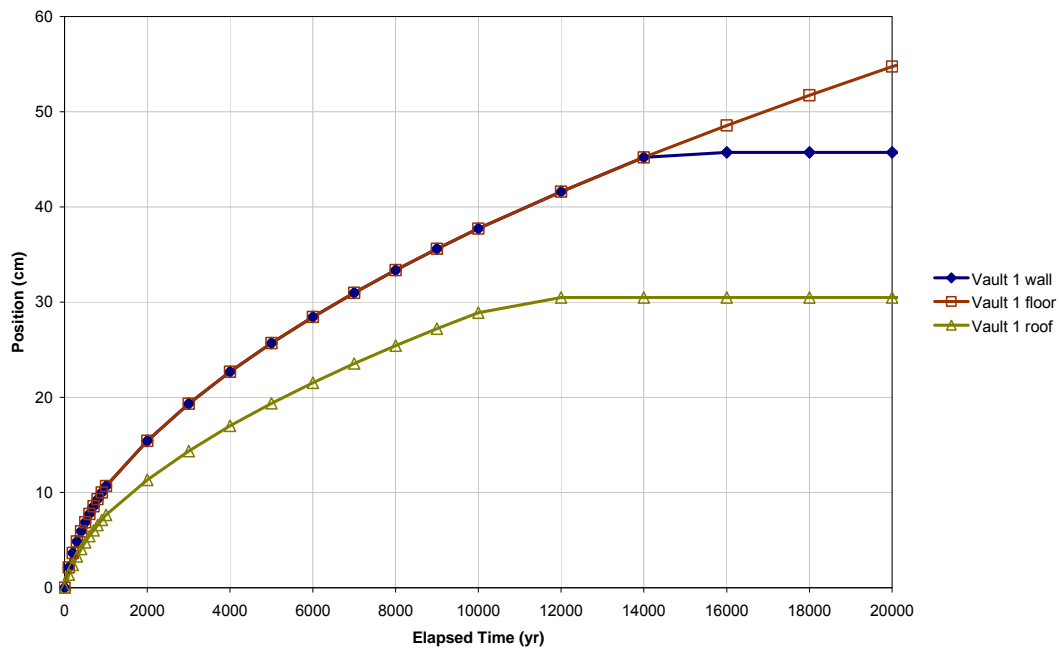


Figure 5.6-79: Ettringite Front Position for Accelerated Sulfate Attack FDCs

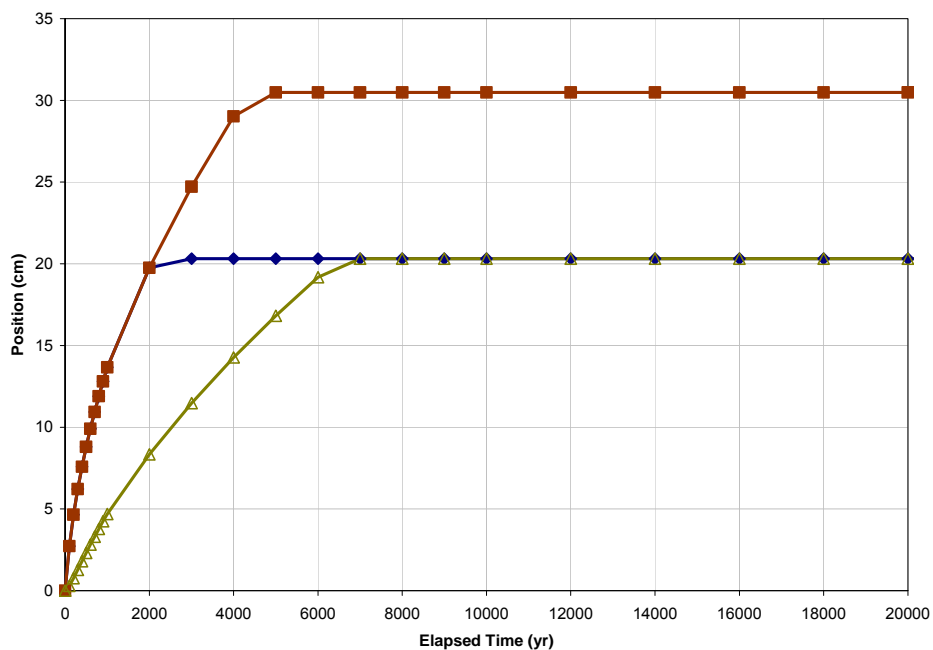
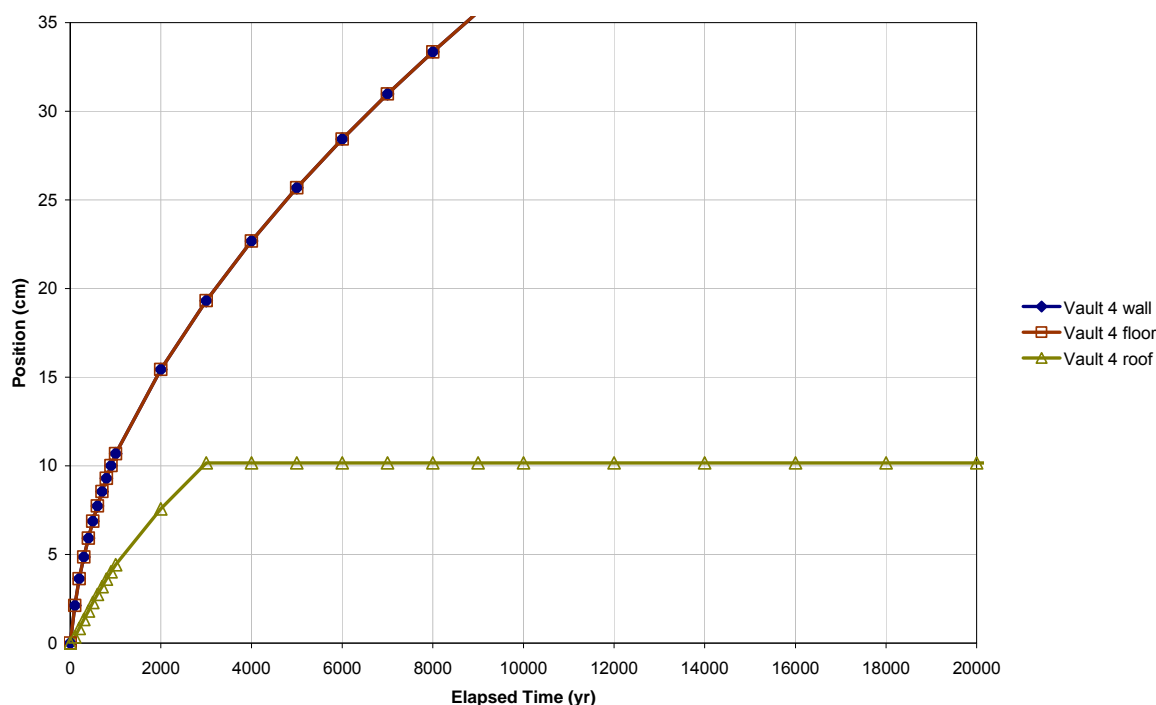


Figure 5.6-80: Ettringite Front Position for Accelerated Sulfate Attack Vault 4



Peak groundwater pathways doses were calculated using the PORFLOW SDF Base Case (presented in Section 4.4) parameters with the disposal unit concrete degradation varied by having either no sulfate or 10 times sulfate present, as described previously. The results of these sensitivity analyses, showing the peak groundwater pathways doses for the Base Case and the materials sensitivity analysis assumptions are presented in Table 5.6-19 and Figures 5.6-81 and 5.6-82. Key radionuclide and chemical concentrations at 100m for 10 times sulfate and no sulfate are presented in Appendix G.1 and G.2, respectively.

Table 5.6-19: 100m Peak Groundwater Pathways Dose within 20,000 Years for Sectors B and I for Materials Degradation Sensitivity Comparison

| Peak Groundwater Dose | Sector B | | | Sector I | | |
|-------------------------------------|-----------|--------------|------------|-----------|--------------|------------|
| | Base Case | 10 x Sulfate | No Sulfate | Base Case | 10 x Sulfate | No Sulfate |
| Peak Dose in 10,000 Years (mrem/yr) | 1.4 | 1.7 | 0.8 | 0.4 | 0.9 | 0.2 |
| Year of Peak Dose | 10,000 | 10,000 | 10,000 | 10,000 | 2,420 | 10,000 |
| Peak Dose in 20,000 Years (mrem/yr) | 2.9 | 4.8 | 2.3 | 3.1 | 1.4 | 0.6 |
| Year of Peak Dose | 15,080 | 12,140 | 15,600 | 15,080 | 12,600 | 15,600 |

Figure 5.6-81: Peak Groundwater Pathways Dose Sector B, Materials Degradation Sensitivity Analysis

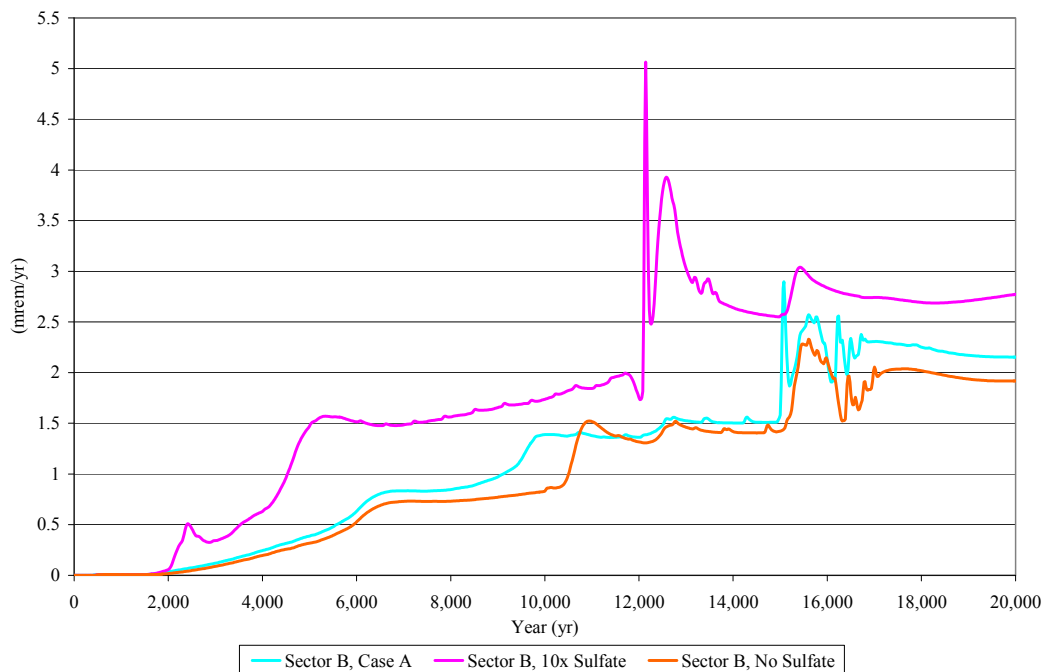
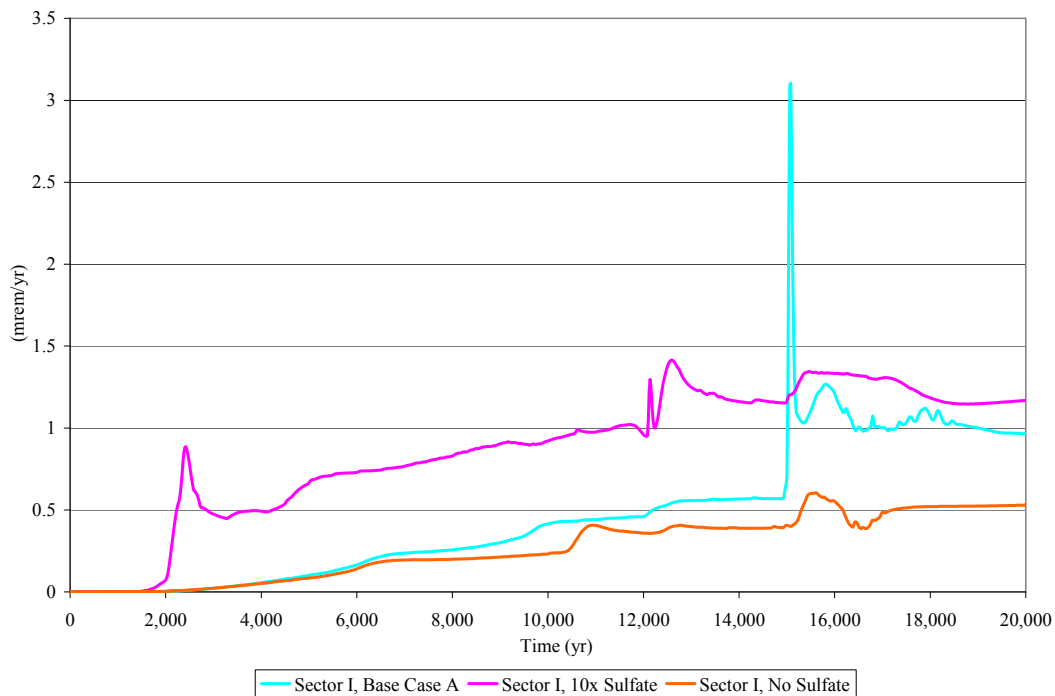


Figure 5.6-82: Peak Groundwater Pathways Dose Sector I, Materials Degradation Sensitivity Analysis



The results show that peak groundwater pathways doses are predicted to increase for both Sectors B and I in the first 10,000 years with a 10 times increase in the sulfate concentration in the saltstone (see Figures 5.6-81 and 5.6-82). The peak dose increase for Sector B during the 10,000 year timeframe is approximately 2.1%. This dose increase is due to the increase of sulfate attack on the roof, wall, and floor (including the upper mud mat for the FDCs) of the disposal units which produces faster disposal unit degradation, thus higher and quicker predicted doses. A peak dose decrease, with the 10 times increase of sulfate in Sector I during most of the 20,000 year timeframe, is expected, as the quicker release of contaminants over the 2,000 to 15,000 year time frame allows the dose under the peak dose in Case A (Base Case) at 15,000 years to be spread out. The peak occurring in Sector I, Case A at 15,000 years occurs as the simultaneous rate of 64 FDCs overcomes the otherwise higher 10 times sulfate over the 20,000 year timeframe.

5.6.6.4 *Inventory Sensitivity Analysis using the PORFLOW Deterministic Model*

During the scoping process for the PORFLOW SDF modeling runs it was confirmed that concentration scales linearly with inventory, so no explicit PORFLOW sensitivity runs were performed related to inventory. Concentration scales linearly with inventory because, as inventory is increased (or decreased), there is a direct correlation to an increase (or decrease) in results derived from concentration. Alternatives to this linear relationship are possible if the waste in the saltstone were to be controlled by solubility or a non-linear sorption isotherm. Neither of these conditions exists in the model.

5.6.6.5 *Synergistic Sensitivity Analysis Using the PORFLOW Deterministic Model*

The PORFLOW deterministic model was used to determine the impact of changing multiple material parameters to account for several potential increased degradation mechanisms from the Base Case (Case A). The simultaneous occurrence of these degraded mechanisms is a pessimistic assessment of the SDF model. The following occurrences are assumed for this synergistic sensitivity.

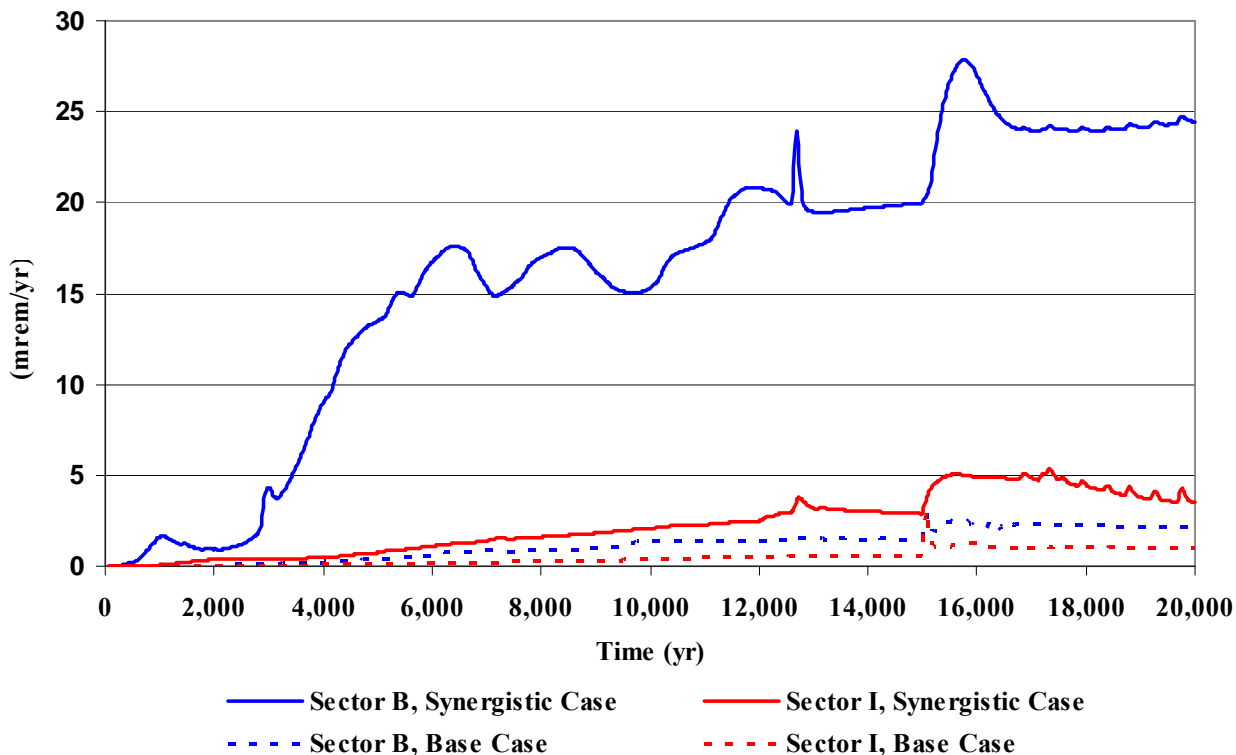
- The closure cap degrades more quickly than for Case A so that the infiltration rate of 1 in/yr (corresponding to the infiltration rate at year 560 for Case A) is assumed to occur at closure until year 560 and then continues degrading from that time forward at the rate determined for Case A.
- The concrete (walls and floor) for Vaults 1 and 4 are assumed to be middle aged oxidized concrete at closure and transition to old aged at year 500 after closure. The roof and floor of Vaults 1 and 4 also degrade hydraulically to soil properties at year 500 to account for mechanisms such as reinforcing bar corrosion. Note that Case A assumes the hydraulic properties of the walls of Vaults 1 and 4 are significantly higher than that of soil at closure.
- The FDC concrete (roof, walls, and floor) degrade chemically to oxidizing, old aged concrete and hydraulically to soil properties at year 500.
- The saltstone is assumed cracked at closure to allow for oxygen diffusion via the cracks throughout the monolith with the concentration of oxygen in the cracks fixed at 100% saturation (i. e. , non-depleting source of oxygen).

The dose comparisons of the Synergistic Case to the Base Case are shown in Table 5.6-20 and Figure 5.6-83. The results reflect an increase in the magnitude of the dose as well as earlier release times due to the parameter changes described above. The results indicate that even for this pessimistic case, the estimated dose to the MOP during the 10,000 year compliance period is less than 25 mrem/yr.

Table 5.6-20: 100m Peak Groundwater Pathways Dose within 20,000 Years for Sectors B and I for Synergistic Sensitivity Comparison

| Peak Groundwater Dose | Sector B | | Sector I | |
|-------------------------------------|-----------|------------------|-----------|------------------|
| | Base Case | Synergistic Case | Base Case | Synergistic Case |
| Peak Dose in 10,000 Years (mrem/yr) | 1.4 | 17.6 | 0.4 | 2.1 |
| Year of Peak Dose | 10,000 | 6,380 | 10,000 | 10,000 |
| Peak Dose in 20,000 Years (mrem/yr) | 2.9 | 27.8 | 3.1 | 5.4 |
| Year of Peak Dose | 15,080 | 15,760 | 15,080 | 17,320 |

Figure 5.6-83: Peak Groundwater Pathways Dose, Sectors B and I - Synergistic Case and Base Case



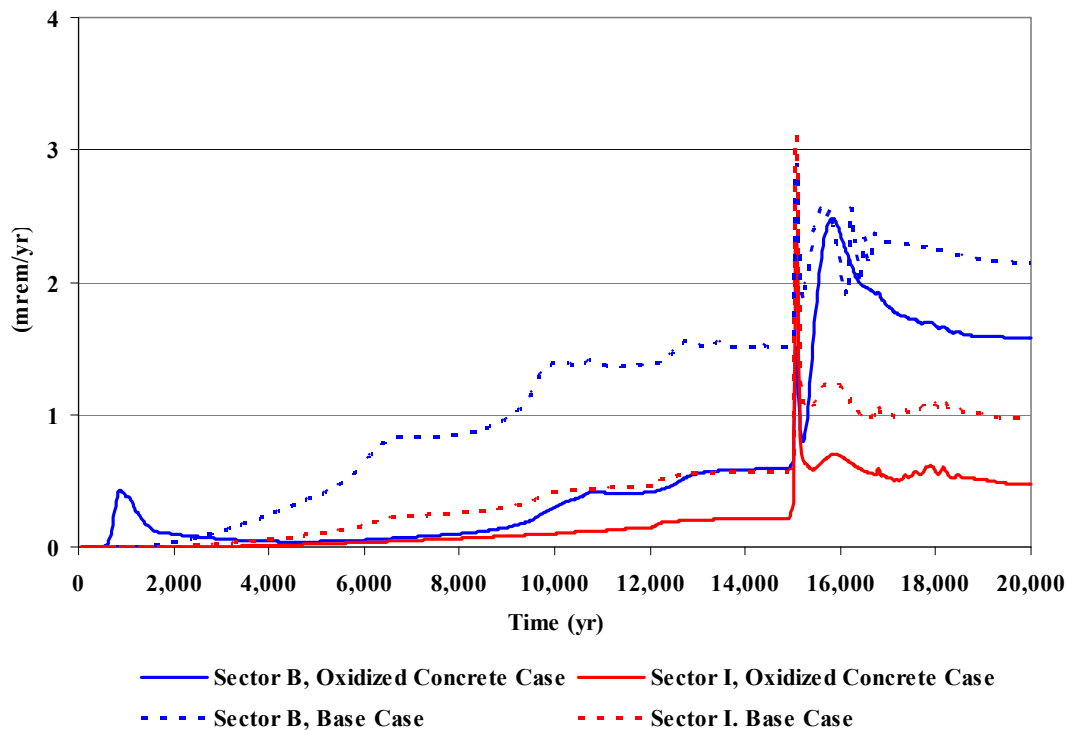
5.6.6.6 Oxidized Concrete Sensitivity Analysis Using the PORFLOW Deterministic Model

The PORFLOW deterministic model was used to determine the impact if the concrete (walls and floor) of Vaults 1 and 4 are in an oxidized condition at closure and the FDC concrete retains its Base Case degradation. In the Base Case, the roof of Vaults 1 and 4 is oxidized at closure; and within the first 20,000 years after closure, only the Vault 4 walls transition to the oxidized state as shown in Section 4.4.2. The results of this Oxidized Concrete sensitivity case are shown in Table 5.6-21 and Figure 5.6-84. The results reflect the impact of the oxidized state on two key radionuclides, Ra-226 and Tc-99. The Ra-226 concentration and dose is reduced because of an increase in K_d from 3 mL/g in a reduced state to 100 mL/g in the oxidized state. The early peak dose shown in Figure 5.6-84 for Sector B relates to the rapid release of Tc-99 from the walls of Vaults 1 and 4 because of a decrease in K_d to 0.8 mL/g in an oxidized state.

Table 5.6-21: 100m Peak Groundwater Pathways Dose within 20,000 Years for Sectors B and I for Vault 1 and 4 Oxidized Concrete Sensitivity Comparison

| Peak Groundwater Dose | Sector B | | Sector I | |
|-------------------------------------|-----------|------------------------|-----------|------------------------|
| | Base Case | Oxidized Concrete Case | Base Case | Oxidized Concrete Case |
| Peak Dose in 10,000 Years (mrem/yr) | 1.4 | 0.4 | 0.4 | 0.1 |
| Year of Peak Dose | 10,000 | 860 | 10,000 | 10,000 |
| Peak Dose in 20,000 Years (mrem/yr) | 2.9 | 2.5 | 3.1 | 2.3 |
| Year of Peak Dose | 15,080 | 15,820 | 15,080 | 15,080 |

Figure 5.6-84: Peak Groundwater Pathways Dose Sectors B and I, Vault 1 and 4 -
Oxidized Concrete Case and Base Case



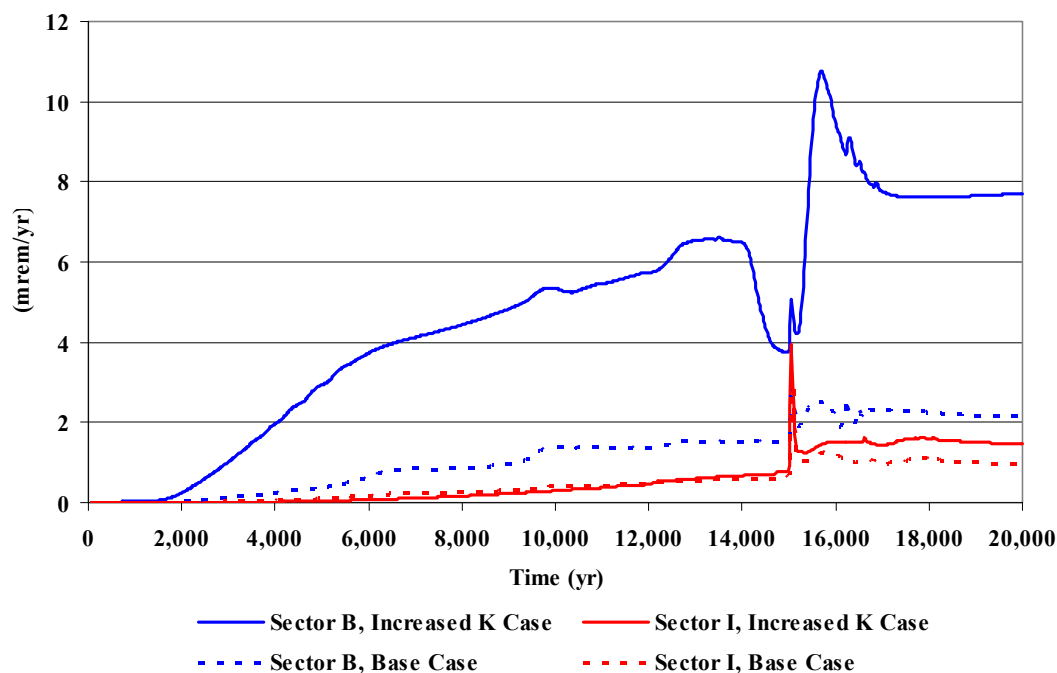
5.6.6.7 Increased Saltstone Hydraulic Conductivity Sensitivity Analysis Using the PORFLOW Deterministic Model

The PORFLOW deterministic model was used to determine the impact of a higher hydraulic conductivity for saltstone. The Base Case utilizes a hydraulic conductivity value of $2\text{E-}9$ cm/sec based on SRNL-STI-2008-00421 as shown in Table 4.2-16 and Case E assumes a degraded, fully cracked saltstone condition that results in a hydraulic conductivity of $1.7\text{E-}3$ cm/sec. Case E provides a worst case condition. This case utilizes a saltstone hydraulic conductivity of $1\text{E-}7$ cm/sec which is more pessimistic than the Base Case and represents a value higher than the experimental values determined in SRNL-STI-2008-00421. The results are shown in Table 5.6-22 and Figure 5.6-85. For this less pessimistic case for increased saltstone hydraulic conductivity, the estimated dose to the MOP is much less than 25 mrem/year.

Table 5.6-22: 100m Peak Groundwater Pathways Dose within 20,000 Years for Sectors B and I for Increased Saltstone Hydraulic Conductivity Sensitivity Comparison

| Peak Groundwater Dose | Sector B | | Sector I | |
|-------------------------------------|-----------|-----------------------------|-----------|-----------------------------|
| | Base Case | Increased Conductivity Case | Base Case | Increased Conductivity Case |
| Peak Dose in 10,000 Years (mrem/yr) | 1.4 | 5.4 | 0.4 | 0.3 |
| Year of Peak Dose | 10,000 | 9,860 | 10,000 | 10,000 |
| Peak Dose in 20,000 Years (mrem/yr) | 2.9 | 10.8 | 3.1 | 3.9 |
| Year of Peak Dose | 15,080 | 15,680 | 15,080 | 15,040 |

Figure 5.6-85: Peak Groundwater Pathways Dose, Sectors B and I, Increased Saltstone Hydraulic Conductivity Case and Base Case



5.7 ALARA Analysis

DOE's approach to radiation protection for LLW disposal units is based on the performance objectives listed in DOE O 435.1-1, which specify maximum doses for various pathways, and on the ALARA principle, which requires doses to be maintained "As Low As Reasonably Achievable." The ALARA requirement in DOE O 435.1-1 states, "Performance assessments shall include a determination that projected releases of radionuclide to the environment shall be maintained as low as reasonably achievable (ALARA)."

The goal of the ALARA process is attainment of the lowest practical dose level after taking into account social, technical, economic, and public policy considerations. SRS has a well

documented ALARA program and processes established in company level policies and procedures.

The FDCs were designed to improve the ALARA position of the SDF. The FDC are built with the following ALARA-type design elements:

- Carbon steel walls to ensure watertight containment and designed to help prevent water seepage out of the concrete disposal units over the life of typical concrete water storage tanks
- Minimum 8 inch thick pre-cast walls of Class III sulfate resistant concrete
- Interior coating to mitigate sulfate attack from short-term saltstone bleed water penetration (through surface cracks and by capillary suction), and diffusion of sulfate from the pore fluid of the cured saltstone (such a coating should be chemical, radiation, pH, and hydroxide resistant)
- A GCL consisting of bentonite sandwiched between two geotextiles will be in place above and below the FDC (the bentonite is expected to remain mineralogically and chemically stable)
- A 100 mil HDPE liner with hermetically sealed joints will completely surround the FDC
- 4 inches of Class III sulfate resistant concrete will be poured on top of the GCL-HDPE in order to protect the GCL-HDPE during construction

More details of the FDC design can be found in Section 3.2.1.3. These construction details are included in the design of the new FDCs and will enhance the ALARA position of the SDF.

For the SDF PA modeling, a 100m buffer zone surrounding SDF was evaluated after an institutional control period of 100 years. Conservatism in the PA modeling are summarized in Section 7.2. In addition, SRS land use plans indicate that the current SRS boundaries will remain unchanged. Under this plan, the land will remain under the ownership of the federal government, consistent with the site's designation as a NERP. Thus, no MOP would have unrestricted access to the SDF. Because the SDF is a much greater distance (approximately five miles) from the site boundary than 100m, and groundwater potentially affected by releases from the SDF is completely intercepted by UTR and McQueen Branch, the PA modeling results demonstrate that protection of the public is provided to a much greater degree than the performance measures require. Considerably more dispersion of any radionuclides released to groundwater or air would occur if the closest access point to the disposal facility is SRS site boundary.

The design of future FDCs will be assessed for ALARA improvements based on new operational and design information.

6.0 INADVERTENT INTRUDER ANALYSIS

This section of the PA presents the analyses of the doses to a hypothetical individual who inadvertently intrudes into the SDF closed systems after the period of institutional control has ended.

The purpose of this section is to present the inadvertent intruder results for the analyses described in Section 4 of this PA.

Section 6.1 presents peak 1m groundwater concentrations for the radionuclides and chemicals discussed in the Source Term Screening Section of the PA (Section 4.2.1).

Section 6.2 and 6.3 presents the individual biotic pathways formulas used to calculate the dose to the acute and chronic intruder.

Section 6.4 presents acute and chronic dose analyses.

Section 6.5 presents Inadvertent Intruder Uncertainty and Sensitivity Analyses.

6.1 Groundwater Concentrations at 1m

The purpose of this section is to present the 1m groundwater concentrations for all of the radionuclides and chemicals discussed in the source term screening section of the PA (Section 4.2.1). The 1m results are needed in order to determine inadvertent intruder results. Maximum groundwater concentrations are provided for the modeling cells that adjoin a perimeter boundary enveloping all source terms (Figure 5.2-1). Results are presented for the three distinct aquifers modeled.

The groundwater concentrations at 1m are calculated using the PORFLOW SDF model for the Base Case modeling case (i.e., Case A) discussed in Section 4.4. A summary of the key parameters used in the baseline PORFLOW SDF modeling case are provided in Table 5.2-1. The PORFLOW 1m concentrations are provided for 12 sectors as shown on Figure 5.2-1, with results provided for the three aquifer depths of concern (i.e., UTR-UZ, UTR-LZ and Gordon Aquifer). Dividing the results into sectors allows variability in peak concentration for different areas of the SDF to be more easily seen. The 12 sectors are evaluated for each radionuclide and chemical to find the maximum groundwater concentrations at 1m from the SDF at each computational cell for each aquifer zone and at each time-step.

Tables 6.1-1 through 6.1-9 show the peak 1m radionuclides concentrations for the three aquifers in the 10,000 year performance period. Tables 6.1-10 through 6.1-18 show the peak 1m chemical concentrations for the three aquifers in the 10,000 year performance period, the peak concentrations for each chemical in each sector, and the MCL derived values for beta and photon emitters as indicated in Table II-3 of FR-00-9654.

The 1m radionuclide and chemical concentration curves (for 20,000 years) associated with the 12 sectors and three aquifers for the Base Case, as described in Section 4.4.2, are captured in Appendix F.1, Appendix F.2, and Appendix F.3.

Table 6.1-1: Radiological 1m Concentrations for UTR-UZ Sectors A through E

| Radionuclide | MCL (pCi/L)** | Sector A Concentrations | | Sector B Concentrations | | Sector C Concentrations | | Sector D Concentrations | | Sector E Concentrations | |
|--------------|---------------|-------------------------|------------------|-------------------------|------------------|-------------------------|------------------|-------------------------|------------------|-------------------------|------------------|
| | | (pCi/L) | Year Peak Occurs | (pCi/L) | Year Peak Occurs | (pCi/L) | Year Peak Occurs | (pCi/L) | Year Peak Occurs | (pCi/L) | Year Peak Occurs |
| Ac-227 | NC | 7.0E-08 | 10,000 | 8.3E-08 | 10,000 | 8.4E-08 | 10,000 | 3.2E-08 | 10,000 | 2.9E-10 | 10,000 |
| Al-26 | NC | 4.6E-25 | 10,000 | 3.1E-23 | 10,000 | 1.0E-20 | 10,000 | 8.7E-22 | 10,000 | 4.2E-30 | 10,000 |
| Am-241 | Total α | 7.6E-27 | 10,000 | 4.1E-25 | 10,000 | 1.2E-22 | 10,000 | 1.1E-23 | 10,000 | <1.0E-30 | 10,000 |
| Am-242m | Total α | <1.0E-30 | 8,660 | <1.0E-30 | 8,240 | <1.0E-30 | 7,840 | <1.0E-30 | 8,100 | <1.0E-30 | 9,380 |
| Am-243 | Total α | 9.1E-27 | 10,000 | 5.1E-25 | 10,000 | 1.5E-22 | 10,000 | 1.4E-23 | 10,000 | <1.0E-30 | 10,000 |
| Ba-137m | NC | 1.0E-29 | 1,700 | 5.6E-29 | 1,680 | 6.0E-28 | 1,580 | 1.5E-28 | 1,600 | <1.0E-30 | 1,340 |
| C-14 | 2,000 | 6.9E-01 | 6,580 | 8.0E-01 | 6,100 | 8.2E-01 | 6,100 | 4.0E-01 | 7,100 | 2.2E-01 | 9,780 |
| Cf-249 | Total α | <1.0E-30 | 10,000 | <1.0E-30 | 10,000 | <1.0E-30 | 10,000 | <1.0E-30 | 10,000 | <1.0E-30 | 10,000 |
| Cf-251 | Total α | 6.9E-30 | 10,000 | 3.9E-28 | 10,000 | 1.2E-25 | 10,000 | 1.1E-26 | 10,000 | <1.0E-30 | 10,000 |
| Cl-36 | 700 | 2.0E-04 | 9,600 | 2.4E-04 | 9,600 | 2.4E-04 | 9,600 | 1.2E-04 | 9,620 | 4.6E-05 | 10,000 |
| Cm-243 | Total α | <1.0E-30 | 2,200 | <1.0E-30 | 2,180 | <1.0E-30 | 2,100 | <1.0E-30 | 2,180 | <1.0E-30 | 2,500 |
| Cm-244 | Total α | <1.0E-30 | 1,440 | <1.0E-30 | 1,440 | <1.0E-30 | 1,380 | <1.0E-30 | 1,440 | <1.0E-30 | 1,640 |
| Cm-245 | Total α | 5.4E-27 | 10,000 | 3.0E-25 | 10,000 | 8.8E-23 | 10,000 | 8.1E-24 | 10,000 | <1.0E-30 | 10,000 |
| Cm-247 | Total α | <1.0E-30 | 10,000 | 5.5E-29 | 10,000 | 1.6E-26 | 10,000 | 1.5E-27 | 10,000 | <1.0E-30 | 10,000 |
| Cm-248 | Total α | <1.0E-30 | 10,000 | <1.0E-30 | 10,000 | <1.0E-30 | 10,000 | <1.0E-30 | 10,000 | <1.0E-30 | 10,000 |
| Co-60 | 100 | <1.0E-30 | 240 | <1.0E-30 | 240 | <1.0E-30 | 220 | <1.0E-30 | 240 | <1.0E-30 | 260 |
| Cs-135 | 900 | 1.6E-01 | 10,000 | 2.0E-01 | 10,000 | 2.0E-01 | 10,000 | 7.9E-02 | 10,000 | 5.7E-04 | 10,000 |
| Cs-137 | 200 | 1.1E-29 | 1,700 | 5.9E-29 | 1,680 | 6.4E-28 | 1,580 | 1.5E-28 | 1,600 | <1.0E-30 | 1,340 |
| Eu-152 | 200 | <1.0E-30 | 1,120 | <1.0E-30 | 1,100 | <1.0E-30 | 1,080 | <1.0E-30 | 1,120 | <1.0E-30 | 1,280 |
| Eu-154 | 60 | <1.0E-30 | 760 | <1.0E-30 | 740 | <1.0E-30 | 740 | <1.0E-30 | 760 | <1.0E-30 | 860 |
| Gd-152 | NC | <1.0E-30 | 10,000 | <1.0E-30 | 10,000 | <1.0E-30 | 10,000 | <1.0E-30 | 10,000 | <1.0E-30 | 10,000 |
| H-3 | 20,000 | 2.2E-09 | 380 | 2.7E-09 | 380 | 2.8E-09 | 380 | 1.1E-09 | 380 | 5.8E-11 | 420 |
| I-129 | 1 | 9.2E-02 | 10,000 | 7.8E-02 | 10,000 | 1.6E-01 | 10,000 | 1.1E-01 | 10,000 | 1.6E-01 | 10,000 |
| K-40 | NC | 4.4E-04 | 10,000 | 4.4E-04 | 10,000 | 6.5E-04 | 10,000 | 4.5E-04 | 10,000 | 4.7E-04 | 10,000 |
| Nb-93m | 1,000 | 1.5E-01 | 10,000 | 1.8E-01 | 10,000 | 1.9E-01 | 10,000 | 7.4E-02 | 10,000 | 8.9E-04 | 10,000 |

Table 6.1-1: Radiological 1m Concentrations for UTR-UZ Sectors A through E (Continued)

| Radionuclide | MCL (pCi/L)** | Sector A Concentrations | | Sector B Concentrations | | Sector C Concentrations | | Sector D Concentrations | | Sector E Concentrations | |
|--------------|---------------|-------------------------|------------------|-------------------------|------------------|-------------------------|------------------|-------------------------|------------------|-------------------------|------------------|
| | | (pCi/L) | Year Peak Occurs | (pCi/L) | Year Peak Occurs | (pCi/L) | Year Peak Occurs | (pCi/L) | Year Peak Occurs | (pCi/L) | Year Peak Occurs |
| Nb-94 | NC | 2.7E-04 | 9,700 | 3.1E-04 | 9,700 | 3.2E-04 | 9,700 | 1.2E-04 | 9,680 | 1.3E-06 | 9,680 |
| Ni-59 | 300 | 1.2E-04 | 10,000 | 1.4E-04 | 10,000 | 1.5E-04 | 10,000 | 6.0E-05 | 10,000 | 1.5E-06 | 10,000 |
| Ni-63 | 50 | 3.8E-11 | 1,820 | 5.3E-11 | 1,800 | 5.7E-11 | 1,780 | 2.3E-11 | 1,780 | 1.2E-13 | 1,860 |
| Np-237 | Total α | 6.7E-04 | 10,000 | 7.9E-04 | 10,000 | 8.0E-04 | 10,000 | 3.1E-04 | 10,000 | 2.5E-06 | 10,000 |
| Pa-231 | Total α | 9.4E-05 | 10,000 | 1.1E-04 | 10,000 | 1.1E-04 | 10,000 | 4.3E-05 | 10,000 | 3.8E-07 | 10,000 |
| Pb-210 | NC | 2.1E-03 | 9,860 | 2.5E-03 | 9,820 | 2.5E-03 | 9,820 | 1.0E-03 | 9,820 | 1.0E-04 | 10,000 |
| Pd-107 | NC | 1.6E-05 | 10,000 | 2.0E-05 | 10,000 | 2.0E-05 | 10,000 | 7.9E-06 | 10,000 | 1.2E-07 | 10,000 |
| Pt-193 | 3,000 | 2.6E-03 | 460 | 3.1E-03 | 460 | 3.2E-03 | 460 | 1.4E-03 | 460 | 8.1E-04 | 540 |
| Pu-238 | Total α | <1.0E-30 | 5,580 | <1.0E-30 | 5,380 | <1.0E-30 | 5,000 | <1.0E-30 | 5,080 | <1.0E-30 | 5,820 |
| Pu-239 | Total α | 2.7E-11 | 10,000 | 1.1E-10 | 10,000 | 4.5E-10 | 10,000 | 1.4E-10 | 10,000 | 8.5E-15 | 10,000 |
| Pu-240 | Total α | 3.9E-12 | 10,000 | 1.6E-11 | 10,000 | 6.6E-11 | 10,000 | 2.0E-11 | 10,000 | 1.2E-15 | 10,000 |
| Pu-241 | 300 | 2.9E-26 | 10,000 | 1.6E-24 | 10,000 | 4.5E-22 | 10,000 | 4.2E-23 | 10,000 | <1.0E-30 | 10,000 |
| Pu-242 | Total α | 7.5E-14 | 10,000 | 3.0E-13 | 10,000 | 1.3E-12 | 10,000 | 3.8E-13 | 10,000 | 2.4E-17 | 10,000 |
| Pu-244 | Total α | 1.5E-15 | 10,000 | 6.1E-15 | 10,000 | 2.6E-14 | 10,000 | 7.8E-15 | 10,000 | 4.9E-19 | 10,000 |
| Ra-226 | Total α/Ra | 7.9E-01 | 9,820 | 9.5E-01 | 9,780 | 9.6E-01 | 9,780 | 4.0E-01 | 9,780 | 3.9E-02 | 10,000 |
| Ra-228 | Total Ra | 7.6E-14 | 10,000 | 1.9E-13 | 10,000 | 3.4E-13 | 10,000 | 1.3E-13 | 10,000 | 9.1E-17 | 10,000 |
| Rn-222 | NC | 7.9E-01 | 9,820 | 9.5E-01 | 9,780 | 9.6E-01 | 9,780 | 4.0E-01 | 9,780 | 3.9E-02 | 10,000 |
| Sb-126 | NC | 9.4E-19 | 10,000 | 2.6E-17 | 10,000 | 3.9E-15 | 10,000 | 5.0E-16 | 10,000 | 3.0E-23 | 10,000 |
| Sb-126m | NC | <1.0E-30 | 6,080 | <1.0E-30 | 5,960 | <1.0E-30 | 5,720 | <1.0E-30 | 5,900 | <1.0E-30 | 6,760 |
| Se-79 | NC | <1.0E-30 | 10,000 | 4.5E-29 | 10,000 | 5.0E-26 | 10,000 | 1.9E-27 | 10,000 | <1.0E-30 | 10,000 |
| Sm-151 | 1,000 | 1.8E-30 | 10,000 | 3.2E-28 | 10,000 | 3.6E-25 | 10,000 | 1.3E-26 | 10,000 | <1.0E-30 | 10,000 |
| Sn-126 | NC | 1.8E-30 | 10,000 | 3.2E-28 | 10,000 | 3.6E-25 | 10,000 | 1.3E-26 | 10,000 | <1.0E-30 | 10,000 |
| Sr-90 | 8 | 2.5E-12 | 1,060 | 4.3E-12 | 1,040 | 5.3E-12 | 1,040 | 2.2E-12 | 1,040 | 6.4E-15 | 1,080 |
| Tc-99 | 900 | 6.6E+00 | 9,800 | 7.9E+00 | 9,780 | 8.1E+00 | 9,780 | 3.2E+00 | 9,780 | 4.5E-02 | 9,800 |
| Th-228 | Total α | 7.6E-14 | 10,000 | 1.9E-13 | 10,000 | 3.4E-13 | 10,000 | 1.3E-13 | 10,000 | 9.1E-17 | 10,000 |

Table 6.1-1: Radiological 1m Concentrations for UTR-UZ Sectors A through E (Continued)

| Radionuclide | MCL (pCi/L)** | Sector A Concentrations | | Sector B Concentrations | | Sector C Concentrations | | Sector D Concentrations | | Sector E Concentrations | |
|--|---------------|-------------------------|------------------|-------------------------|------------------|-------------------------|------------------|-------------------------|------------------|-------------------------|------------------|
| | | (pCi/L) | Year Peak Occurs | (pCi/L) | Year Peak Occurs | (pCi/L) | Year Peak Occurs | (pCi/L) | Year Peak Occurs | (pCi/L) | Year Peak Occurs |
| Th-229 | Total α | 1.2E-08 | 10,000 | 3.1E-08 | 10,000 | 5.7E-08 | 10,000 | 2.1E-08 | 10,000 | 1.6E-11 | 10,000 |
| Th-230 | Total α | 1.5E-09 | 10,000 | 3.9E-09 | 10,000 | 7.3E-09 | 10,000 | 2.7E-09 | 10,000 | 1.6E-12 | 10,000 |
| Th-232 | Total α | 2.2E-16 | 10,000 | 5.7E-16 | 10,000 | 1.1E-15 | 10,000 | 4.0E-16 | 10,000 | 2.3E-19 | 10,000 |
| U-232 | Total U* | <1.0E-30 | 3,820 | <1.0E-30 | 3,660 | <1.0E-30 | 3,360 | <1.0E-30 | 3,440 | <1.0E-30 | 4000 |
| U-233 | Total U* | 8.4E-07 | 10,000 | 2.0E-06 | 10,000 | 3.4E-06 | 10,000 | 1.3E-06 | 10,000 | 1.1E-09 | 10,000 |
| U-234 | Total U* | 1.0E-06 | 10,000 | 2.5E-06 | 10,000 | 4.2E-06 | 10,000 | 1.6E-06 | 10,000 | 1.2E-09 | 10,000 |
| U-235 | Total U* | 1.7E-08 | 10,000 | 4.2E-08 | 10,000 | 7.1E-08 | 10,000 | 2.7E-08 | 10,000 | 2.1E-11 | 10,000 |
| U-236 | Total U* | 2.8E-08 | 10,000 | 6.8E-08 | 10,000 | 1.2E-07 | 10,000 | 4.4E-08 | 10,000 | 3.4E-11 | 10,000 |
| U-238 | Total U* | 2.1E-08 | 10,000 | 5.2E-08 | 10,000 | 8.7E-08 | 10,000 | 3.3E-08 | 10,000 | 2.6E-11 | 10,000 |
| Y-90 | 60 | 2.5E-12 | 1,060 | 4.3E-12 | 1,040 | 5.3E-12 | 1,040 | 2.2E-12 | 1,040 | 6.4E-15 | 1080 |
| Zr-93 | 2000 | 1.3E-20 | 10,000 | 3.0E-19 | 10,000 | 3.8E-17 | 10,000 | 5.2E-18 | 10,000 | 2.7E-25 | 10,000 |
| Total alpha | 15 | 8.0E-01 | N/A | 9.5E-01 | N/A | 9.7E-01 | N/A | 4.0E-01 | N/A | 3.9E-02 | N/A |
| Total Ra | 5 | 7.9E-01 | N/A | 9.5E-01 | N/A | 9.6E-01 | N/A | 4.0E-01 | N/A | 3.9E-02 | N/A |
| Sum of beta-gamma MCL fractions | | 1.0E-01 | N/A | 8.7E-02 | N/A | 1.7E-01 | N/A | 1.2E-01 | N/A | 1.6E-01 | N/A |

* Total uranium is evaluated in Table 6.1-10

** MCL values for beta and photon emitters are calculated in Table II-3 of FR-00-9654 based on a beta-gamma dose of 4 mrem/yr

NC = Not Calculated

Table 6.1-2: Radiological 1m Concentrations for UTR-UZ Sectors F through J

| Radionuclide | MCL (pCi/L)** | Sector F Concentrations | | Sector G Concentrations | | Sector H Concentrations | | Sector I Concentrations | | Sector J Concentrations | |
|--------------|------------------|----------------------------|------------------|----------------------------|------------------|----------------------------|------------------|----------------------------|------------------|----------------------------|------------------|
| | | (pCi/L) | Year Peak Occurs | (pCi/L) | Year Peak Occurs | (pCi/L) | Year Peak Occurs | (pCi/L) | Year Peak Occurs | (pCi/L) | Year Peak Occurs |
| Ac-227 | NC | 1.0E-12 | 10,000 | 1.0E-19 | 10,000 | 2.3E-19 | 10,000 | 1.6E-18 | 10,000 | 6.9E-16 | 10,000 |
| Al-26 | NC | <1.0E-30 | 10,000 | <1.0E-30 | 10,000 | <1.0E-30 | 10,000 | <1.0E-30 | 10,000 | <1.0E-30 | 10,000 |
| Am-241 | Total α | <1.0E-30 | 10,000 | <1.0E-30 | 10,000 | <1.0E-30 | 10,000 | <1.0E-30 | 10,000 | <1.0E-30 | 10,000 |
| Am-242m | Total α | <1.0E-30 | 9,540 | <1.0E-30 | 7,680 | <1.0E-30 | 7,680 | <1.0E-30 | 7,700 | <1.0E-30 | 7,720 |
| Am-243 | Total α | <1.0E-30 | 10,000 | <1.0E-30 | 10,000 | <1.0E-30 | 10,000 | <1.0E-30 | 10,000 | <1.0E-30 | 10,000 |
| Ba-137m | NC | 1.2E-30 | 1,360 | 1.2E-30 | 1,360 | 1.1E-30 | 1,360 | <1.0E-30 | 1,360 | <1.0E-30 | 1,380 |
| C-14 | 2,000 | 3.5E-01 | 9,800 | 6.3E-01 | 9,820 | 4.2E-01 | 9,800 | 5.9E-01 | 9,820 | 6.0E-01 | 9,820 |
| Cf-249 | Total α | <1.0E-30 | 10,000 | <1.0E-30 | 10,000 | <1.0E-30 | 10,000 | <1.0E-30 | 10,000 | <1.0E-30 | 10,000 |
| Cf-251 | Total α | <1.0E-30 | 10,000 | <1.0E-30 | 10,000 | <1.0E-30 | 10,000 | <1.0E-30 | 10,000 | <1.0E-30 | 10,000 |
| Cl-36 | 700 | 7.0E-05 | 10,000 | 1.2E-04 | 10,000 | 8.3E-05 | 10,000 | 1.2E-04 | 10,000 | 1.2E-04 | 10,000 |
| Cm-243 | Total α | <1.0E-30 | 2,420 | <1.0E-30 | 2,120 | <1.0E-30 | 2,140 | <1.0E-30 | 2,140 | <1.0E-30 | 2,140 |
| Cm-244 | Total α | <1.0E-30 | 1,580 | <1.0E-30 | 1,360 | <1.0E-30 | 1,360 | <1.0E-30 | 1,360 | <1.0E-30 | 1,360 |
| Cm-245 | Total α | <1.0E-30 | 10,000 | <1.0E-30 | 10,000 | <1.0E-30 | 10,000 | <1.0E-30 | 10,000 | <1.0E-30 | 10,000 |
| Cm-247 | Total α | <1.0E-30 | 10,000 | <1.0E-30 | 10,000 | <1.0E-30 | 10,000 | <1.0E-30 | 10,000 | <1.0E-30 | 10,000 |
| Cm-248 | Total α | <1.0E-30 | 10,000 | <1.0E-30 | 10,000 | <1.0E-30 | 10,000 | <1.0E-30 | 10,000 | <1.0E-30 | 10,000 |
| Co-60 | 100 | <1.0E-30 | 260 | <1.0E-30 | 440 | <1.0E-30 | 420 | <1.0E-30 | 420 | <1.0E-30 | 360 |
| Cs-135 | 900 | 4.1E-05 | 10,000 | 6.9E-05 | 10,000 | 4.8E-05 | 10,000 | 6.3E-05 | 10,000 | 6.3E-05 | 10,000 |
| Cs-137 | 200 | 1.2E-30 | 1,360 | 1.3E-30 | 1,360 | 1.2E-30 | 1,360 | <1.0E-30 | 1,360 | <1.0E-30 | 1,380 |
| Eu-152 | 200 | <1.0E-30 | 1,240 | <1.0E-30 | 1,100 | <1.0E-30 | 1,100 | <1.0E-30 | 1,100 | <1.0E-30 | 1,100 |
| Eu-154 | 60 | <1.0E-30 | 840 | <1.0E-30 | 740 | <1.0E-30 | 740 | <1.0E-30 | 740 | <1.0E-30 | 740 |
| Gd-152 | NC | <1.0E-30 | 10,000 | <1.0E-30 | 10,000 | <1.0E-30 | 10,000 | <1.0E-30 | 10,000 | <1.0E-30 | 10,000 |
| H-3 | 20,000 | 9.3E-11 | 420 | 1.6E-10 | 420 | 1.1E-10 | 420 | 1.5E-10 | 420 | 1.5E-10 | 420 |
| I-129 | 1 | 2.6E-01 | 10,000 | 4.6E-01 | 10,000 | 3.1E-01 | 10,000 | 4.3E-01 | 10,000 | 4.4E-01 | 10,000 |
| K-40 | NC | 7.6E-04 | 10,000 | 1.4E-03 | 10,000 | 9.1E-04 | 10,000 | 1.3E-03 | 10,000 | 1.3E-03 | 10,000 |
| Nb-93m | 1,000 | 7.4E-06 | 10,000 | 4.1E-13 | 10,000 | 8.0E-13 | 10,000 | 6.0E-12 | 10,000 | 3.0E-09 | 10,000 |
| Nb-94 | NC | 7.2E-09 | 9,660 | 3.2E-13 | 10,000 | 1.0E-13 | 10,000 | 1.1E-13 | 10,000 | 5.6E-12 | 9,640 |
| Ni-59 | 300 | 1.9E-08 | 10,000 | 1.9E-15 | 10,000 | 5.2E-15 | 10,000 | 3.8E-14 | 10,000 | 1.6E-11 | 10,000 |
| Ni-63 | 50 | 3.7E-16 | 2,120 | 3.4E-25 | 2,740 | 1.8E-24 | 2,680 | 1.4E-23 | 2,680 | 1.1E-20 | 2,620 |

Table 6.1-2: Radiological 1m Concentrations for UTR-UZ Sectors F through J (Continued)

| Radionuclide | MCL (pCi/L)** | Sector F Concentrations | | Sector G Concentrations | | Sector H Concentrations | | Sector I Concentrations | | Sector J Concentrations | |
|--------------|------------------|----------------------------|------------------|----------------------------|------------------|----------------------------|------------------|----------------------------|------------------|----------------------------|------------------|
| | | (pCi/L) | Year Peak Occurs | (pCi/L) | Year Peak Occurs | (pCi/L) | Year Peak Occurs | (pCi/L) | Year Peak Occurs | (pCi/L) | Year Peak Occurs |
| Np-237 | Total α | 6.1E-09 | 10,000 | 8.3E-16 | 10,000 | 1.1E-15 | 10,000 | 8.1E-15 | 10,000 | 3.5E-12 | 10,000 |
| Pa-231 | Total α | 1.3E-09 | 10,000 | 1.4E-16 | 10,000 | 3.0E-16 | 10,000 | 2.1E-15 | 10,000 | 9.0E-13 | 10,000 |
| Pb-210 | NC | 1.4E-04 | 10,000 | 2.5E-04 | 10,000 | 1.7E-04 | 10,000 | 2.3E-04 | 10,000 | 2.3E-04 | 10,000 |
| Pd-107 | NC | 1.2E-09 | 10,000 | 1.2E-16 | 10,000 | 3.1E-16 | 10,000 | 2.2E-15 | 10,000 | 9.6E-13 | 10,000 |
| Pt-193 | 3,000 | 1.3E-03 | 540 | 2.3E-03 | 540 | 1.6E-03 | 540 | 2.2E-03 | 540 | 2.2E-03 | 540 |
| Pu-238 | Total α | <1.0E-30 | 5,860 | <1.0E-30 | 6,600 | <1.0E-30 | 6,620 | <1.0E-30 | 6,640 | 2.0E-63 | 6,660 |
| Pu-239 | Total α | 2.1E-17 | 10,000 | <1.0E-30 | 10,000 | <1.0E-30 | 10,000 | <1.0E-30 | 10,000 | <1.0E-30 | 10,000 |
| Pu-240 | Total α | 3.1E-18 | 10,000 | <1.0E-30 | 10,000 | <1.0E-30 | 10,000 | <1.0E-30 | 10,000 | <1.0E-30 | 10,000 |
| Pu-241 | 300 | <1.0E-30 | 10,000 | <1.0E-30 | 10,000 | <1.0E-30 | 10,000 | <1.0E-30 | 10,000 | <1.0E-30 | 10,000 |
| Pu-242 | Total α | 5.8E-20 | 10,000 | <1.0E-30 | 10,000 | <1.0E-30 | 10,000 | <1.0E-30 | 10,000 | <1.0E-30 | 10,000 |
| Pu-244 | Total α | 1.2E-21 | 10,000 | <1.0E-30 | 10,000 | <1.0E-30 | 10,000 | <1.0E-30 | 10,000 | <1.0E-30 | 10,000 |
| Ra-226 | Total α/Ra | 5.4E-02 | 10,000 | 9.4E-02 | 10,000 | 6.4E-02 | 10,000 | 8.8E-02 | 10,000 | 9.0E-02 | 10,000 |
| Ra-228 | Total Ra | 1.5E-19 | 10,000 | 2.7E-24 | 10,000 | 2.4E-24 | 10,000 | 1.5E-24 | 10,000 | 8.0E-25 | 10,000 |
| Rn-222 | NC | 5.4E-02 | 10,000 | 9.4E-02 | 10,000 | 6.4E-02 | 10,000 | 8.8E-02 | 10,000 | 9.0E-02 | 10,000 |
| Se-79 | NC | 1.5E-23 | 10,000 | 1.3E-23 | 10,000 | 1.2E-23 | 10,000 | 6.3E-24 | 10,000 | 2.3E-24 | 10,000 |
| Sm-151 | 1,000 | <1.0E-30 | 6,800 | <1.0E-30 | 5,840 | <1.0E-30 | 5,860 | <1.0E-30 | 5,840 | <1.0E-30 | 5,860 |
| Sb-126 | NC | <1.0E-30 | 10,000 | <1.0E-30 | 10,000 | <1.0E-30 | 10,000 | <1.0E-30 | 10,000 | <1.0E-30 | 10,000 |
| Sb-126m | NC | <1.0E-30 | 10,000 | <1.0E-30 | 10,000 | <1.0E-30 | 10,000 | <1.0E-30 | 10,000 | <1.0E-30 | 10,000 |
| Sn-126 | NC | <1.0E-30 | 10,000 | <1.0E-30 | 10,000 | <1.0E-30 | 10,000 | <1.0E-30 | 10,000 | <1.0E-30 | 10,000 |
| Sr-90 | 8 | 7.7E-18 | 1,080 | 4.1E-19 | 1,060 | 3.3E-19 | 1,060 | 3.2E-19 | 1,080 | 2.7E-19 | 1,080 |
| Tc-99 | 900 | 3.9E-04 | 9,800 | 2.4E-06 | 10,000 | 1.6E-06 | 10,000 | 2.2E-06 | 10,000 | 2.2E-06 | 10,000 |
| Th-228 | Total α | 1.5E-19 | 10,000 | 2.7E-24 | 10,000 | 2.4E-24 | 10,000 | 1.5E-24 | 10,000 | 8.0E-25 | 10,000 |
| Th-229 | Total α | 5.3E-14 | 10,000 | 5.0E-21 | 10,000 | 8.1E-21 | 10,000 | 5.8E-20 | 10,000 | 2.5E-17 | 10,000 |

Table 6.1-2: Radiological 1m Concentrations for UTR-UZ Sectors F through J (Continued)

| Radionuclide | MCL (pCi/L)** | Sector F Concentrations | | Sector G Concentrations | | Sector H Concentrations | | Sector I Concentrations | | Sector J Concentrations | |
|--|------------------|----------------------------|---------------------|----------------------------|---------------------|----------------------------|---------------------|----------------------------|---------------------|----------------------------|---------------------|
| | | (pCi/L) | Year Peak Occurs | (pCi/L) | Year Peak Occurs | (pCi/L) | Year Peak Occurs | (pCi/L) | Year Peak Occurs | (pCi/L) | Year Peak Occurs |
| Th-230 | Total α | 2.8E-15 | 10,000 | 8.5E-26 | 10,000 | 7.4E-26 | 10,000 | 4.9E-26 | 10,000 | 2.6E-26 | 10,000 |
| Th-232 | Total α | 4.1E-22 | 10,000 | <1.0E-30 | 10,000 | <1.0E-30 | 10,000 | <1.0E-30 | 10,000 | <1.0E-30 | 10,000 |
| U-232 | Total U* | <1.0E-30 | 4,020 | <1.0E-30 | 4,400 | <1.0E-30 | 4,380 | <1.0E-30 | 4,400 | <1.0E-30 | 4,420 |
| U-233 | Total U* | 2.2E-12 | 10,000 | 1.3E-19 | 10,000 | 1.3E-19 | 10,000 | 9.5E-19 | 10,000 | 4.1E-16 | 10,000 |
| U-234 | Total U* | 2.1E-12 | 10,000 | 8.5E-23 | 10,000 | 7.3E-23 | 10,000 | 4.9E-23 | 10,000 | 2.7E-23 | 10,000 |
| U-235 | Total U* | 3.5E-14 | 10,000 | 1.4E-24 | 10,000 | 1.2E-24 | 10,000 | 8.1E-25 | 10,000 | 4.5E-25 | 10,000 |
| U-236 | Total U* | 5.7E-14 | 10,000 | 7.5E-24 | 10,000 | 6.4E-24 | 10,000 | 4.3E-24 | 10,000 | 2.4E-24 | 10,000 |
| U-238 | Total U* | 4.3E-14 | 10,000 | 4.8E-23 | 10,000 | 4.1E-23 | 10,000 | 2.8E-23 | 10,000 | 1.5E-23 | 10,000 |
| Y-90 | 60 | 7.7E-18 | 1,080 | 4.1E-19 | 1,060 | 3.3E-19 | 1,060 | 3.2E-19 | 1,080 | 2.7E-19 | 1,080 |
| Zr-93 | 2,000 | 5.7E-28 | 10,000 | <1.0E-30 | 10,000 | <1.0E-30 | 10,000 | <1.0E-30 | 10,000 | <1.0E-30 | 10,000 |
| Total alpha | 15 | 5.4E-02 | N/A | 9.4E-02 | N/A | 6.4E-02 | N/A | 8.8E-02 | N/A | 9.0E-02 | N/A |
| Total Ra | 5 | 5.4E-02 | N/A | 9.4E-02 | N/A | 6.4E-02 | N/A | 8.8E-02 | N/A | 9.0E-02 | N/A |
| Sum of beta-gamma MCL fractions | | 2.6E-01 | N/A | 4.6E-01 | N/A | 3.1E-01 | N/A | 4.3E-01 | N/A | 4.4E-01 | N/A |

* Total uranium is evaluated in Table 6.1-11

** MCL values for beta and photon emitters are calculated in Table II-3 of FR-00-9654 based on a beta-gamma dose of 4 mrem/yr

NC = Not Calculated

Table 6.1-3: Radiological 1m Concentrations for UTR-UZ Sectors K and L

| Radionuclide | MCL (pCi/L)** | Sector K Concentrations | | Sector L Concentrations | |
|--------------|----------------|----------------------------|------------------|----------------------------|------------------|
| | | (pCi/L) | Year Peak Occurs | (pCi/L) | Year Peak Occurs |
| Ac-227 | NC | 2.3E-14 | 10,000 | 2.78E-11 | 10,000 |
| Al-26 | NC | <1.0E-30 | 10,000 | <1.0E-30 | 10,000 |
| Am-241 | Total α | <1.0E-30 | 10,000 | <1.0E-30 | 10,000 |
| Am-242m | Total α | <1.0E-30 | 10,000 | <1.0E-30 | 9,720 |
| Am-243 | Total α | <1.0E-30 | 10,000 | <1.0E-30 | 10,000 |
| Ba-137m | NC | <1.0E-30 | 1,500 | <1.0E-30 | 1,360 |
| C-14 | 2,000 | 1.6E-01 | 9,820 | 3.51E-01 | 9,820 |
| Cf-249 | Total α | <1.0E-30 | 10,000 | <1.0E-30 | 10,000 |
| Cf-251 | Total α | <1.0E-30 | 10,000 | <1.0E-30 | 10,000 |
| Cl-36 | 700 | 3.1E-05 | 10,000 | 6.90E-05 | 10,000 |
| Cm-243 | Total α | <1.0E-30 | 2,200 | <1.0E-30 | 2,540 |
| Cm-244 | Total α | <1.0E-30 | 1,400 | <1.0E-30 | 1,660 |
| Cm-245 | Total α | <1.0E-30 | 10,000 | <1.0E-30 | 10,000 |
| Cm-247 | Total α | <1.0E-30 | 10,000 | <1.0E-30 | 10,000 |
| Cm-248 | Total α | <1.0E-30 | 10,000 | <1.0E-30 | 10,000 |
| Co-60 | 100 | <1.0E-30 | 300 | <1.0E-30 | 280 |
| Cs-135 | 900 | 1.5E-05 | 10,000 | 4.64E-05 | 10,000 |
| Cs-137 | 200 | <1.0E-30 | 1,500 | 1.05E-30 | 1,360 |
| Eu-152 | 200 | <1.0E-30 | 1,120 | <1.0E-30 | 1,100 |
| Eu-154 | 60 | <1.0E-30 | 760 | <1.0E-30 | 740 |
| Gd-152 | NC | <1.0E-30 | 10,000 | <1.0E-30 | 10,000 |
| H-3 | 20,000 | 3.6E-11 | 420 | 8.98E-11 | 420 |
| I-129 | 1 | 1.1E-01 | 10,000 | 2.57E-01 | 10,000 |
| K-40 | NC | 3.3E-04 | 10,000 | 7.57E-04 | 10,000 |
| Nb-93m | 1,000 | 1.0E-07 | 10,000 | 6.01E-05 | 10,000 |
| Nb-94 | NC | 1.9E-10 | 9,620 | 1.17E-07 | 9,680 |
| Ni-59 | 300 | 5.4E-10 | 10,000 | 9.44E-08 | 10,000 |
| Ni-63 | 50 | 4.5E-19 | 2,600 | 6.59E-15 | 1,920 |
| Np-237 | Total α | 1.2E-10 | 10,000 | 2.53E-07 | 10,000 |
| Pa-231 | Total α | 3.0E-11 | 10,000 | 3.71E-08 | 10,000 |
| Pb-210 | NC | 5.9E-05 | 10,000 | 1.38E-04 | 10,000 |
| Pd-107 | NC | 3.2E-11 | 10,000 | 8.28E-09 | 10,000 |
| Pt-193 | 3,000 | 5.5E-04 | 540 | 1.29E-03 | 540 |
| Pu-238 | Total α | <1.0E-30 | 6,700 | <1.0E-30 | 6,240 |

**Table 6.1-3: Radiological 1m Concentrations for UTR-UZ Sectors K and L
(Continued)**

| Radionuclide | MCL (pCi/L)** | Sector K Concentrations | | Sector L Concentrations | |
|--|---------------|-------------------------|------------------|-------------------------|------------------|
| | | (pCi/L) | Year Peak Occurs | (pCi/L) | Year Peak Occurs |
| Pu-239 | Total α | 6.8E-27 | 10,000 | 1.43E-17 | 10,000 |
| Pu-240 | Total α | 9.8E-28 | 10,000 | 2.08E-18 | 10,000 |
| Pu-241 | 300 | <1.0E-30 | 10,000 | <1.0E-30 | 10,000 |
| Pu-242 | Total α | 1.9E-29 | 10,000 | 3.97E-20 | 10,000 |
| Pu-244 | Total α | <1.0E-30 | 10,000 | 8.20E-22 | 10,000 |
| Ra-226 | Total α/Ra | 2.3E-02 | 10,000 | 5.29E-02 | 10,000 |
| Ra-228 | Total Ra | 6.6E-26 | 10,000 | 6.27E-19 | 10,000 |
| Rn-222 | NC | 2.3E-02 | 10,000 | 5.29E-02 | 10,000 |
| Se-79 | NC | 1.4E-26 | 10,000 | 1.13E-23 | 10,000 |
| Sm-151 | 1,000 | <1.0E-30 | 6,100 | <1.0E-30 | 6,980 |
| Sb-126 | NC | <1.0E-30 | 10,000 | <1.0E-30 | 10,000 |
| Sb-126m | NC | <1.0E-30 | 10,000 | <1.0E-30 | 10,000 |
| Sn-126 | NC | <1.0E-30 | 10,000 | <1.0E-30 | 10,000 |
| Sr-90 | 8 | 5.2E-20 | 1,100 | 1.83E-16 | 1,120 |
| Tc-99 | 900 | 1.1E-05 | 9,980 | 3.52E-03 | 9,800 |
| Th-228 | Total α | 6.6E-26 | 10,000 | 6.3E-19 | 10,000 |
| Th-229 | Total α | 8.3E-16 | 10,000 | 3.78E-13 | 10,000 |
| Th-230 | Total α | 3.9E-23 | 10,000 | 8.73E-15 | 10,000 |
| Th-232 | Total α | 5.7E-30 | 10,000 | 1.28E-21 | 10,000 |
| U-232 | Total U* | <1.0E-30 | 4,660 | <1.0E-30 | 4,300 |
| U-233 | Total U* | 1.4E-14 | 10,000 | 1.39E-11 | 10,000 |
| U-234 | Total U* | 4.6E-20 | 10,000 | 8.09E-12 | 10,000 |
| U-235 | Total U* | 7.7E-22 | 10,000 | 1.35E-13 | 10,000 |
| U-236 | Total U* | 1.3E-21 | 10,000 | 2.20E-13 | 10,000 |
| U-238 | Total U* | 9.5E-22 | 10,000 | 1.67E-13 | 10,000 |
| Y-90 | 60 | 5.2E-20 | 1,100 | 1.8E-16 | 1,120 |
| Zr-93 | 2,000 | <1.0E-30 | 10,000 | 1.47E-29 | 10,000 |
| Total alpha | 15 | 2.3E-02 | N/A | 5.3E-02 | N/A |
| Total Ra | 5 | 2.3E-02 | N/A | 5.3E-02 | N/A |
| Sum of beta-gamma MCL fractions | | 1.1E-01 | N/A | 2.6E-01 | N/A |

* Total uranium is evaluated in Table 6.1-12

** MCL values for beta and photon emitters are calculated in Table II-3 of FR-00-9654 based on a beta-gamma dose of 4 mrem/yr

NC = Not Calculated

Table 6.1-4: Radiological 1m Concentrations for UTR-LZ Sectors A through E

| Radionuclide | MCL (pCi/L)** | Sector A Concentrations | | Sector B Concentrations | | Sector C Concentrations | | Sector D Concentrations | | Sector E Concentrations | |
|--------------|------------------|----------------------------|------------------|----------------------------|------------------|----------------------------|------------------|----------------------------|------------------|----------------------------|------------------|
| | | (pCi/L) | Year Peak Occurs | (pCi/L) | Year Peak Occurs | (pCi/L) | Year Peak Occurs | (pCi/L) | Year Peak Occurs | (pCi/L) | Year Peak Occurs |
| Ac-227 | NC | 1.9E-07 | 10,000 | 1.9E-07 | 10,000 | 1.9E-07 | 10,000 | 3.7E-08 | 10,000 | 3.0E-10 | 10,000 |
| Al-26 | NC | 1.8E-23 | 10,000 | 5.1E-22 | 10,000 | 3.6E-21 | 10,000 | 8.5E-23 | 10,000 | <1.0E-30 | 10,000 |
| Am-241 | Total α | 2.8E-25 | 10,000 | 7.2E-24 | 10,000 | 4.8E-23 | 10,000 | 1.2E-24 | 10,000 | <1.0E-30 | 10,000 |
| Am-242m | Total α | <1.0E-30 | 8,820 | <1.0E-30 | 8,480 | <1.0E-30 | 8,300 | <1.0E-30 | 8,520 | <1.0E-30 | 9,720 |
| Am-243 | Total α | 3.4E-25 | 10,000 | 8.9E-24 | 10,000 | 5.9E-23 | 10,000 | 1.5E-24 | 10,000 | <1.0E-30 | 10,000 |
| Ba-137m | NC | 1.0E-28 | 1,680 | 5.5E-28 | 1,640 | 1.1E-27 | 1,600 | 9.1E-29 | 1,640 | <1.0E-30 | 1,380 |
| C-14 | 2,000 | 1.8E+00 | 6,100 | 1.9E+00 | 6,100 | 1.8E+00 | 6,100 | 4.5E-01 | 6,600 | 1.7E-01 | 9,800 |
| Cf-249 | Total α | <1.0E-30 | 10,000 | <1.0E-30 | 10,000 | <1.0E-30 | 10,000 | 3.5E-45 | 10,000 | <1.0E-30 | 10,000 |
| Cf-251 | Total α | 2.6E-28 | 10,000 | 6.8E-27 | 10,000 | 4.6E-26 | 10,000 | 1.1E-27 | 10,000 | <1.0E-30 | 10,000 |
| Cl-36 | 700 | 5.4E-04 | 9,600 | 5.6E-04 | 9,600 | 5.4E-04 | 9,600 | 1.5E-04 | 9,620 | 3.7E-05 | 10,000 |
| Cm-243 | Total α | <1.0E-30 | 2,320 | <1.0E-30 | 2,240 | <1.0E-30 | 2,220 | <1.0E-30 | 2,280 | <1.0E-30 | 2,600 |
| Cm-244 | Total α | <1.0E-30 | 1,520 | <1.0E-30 | 1,460 | <1.0E-30 | 1,460 | <1.0E-30 | 1,500 | <1.0E-30 | 1,720 |
| Cm-245 | Total α | 2.0E-25 | 10,000 | 5.2E-24 | 10,000 | 3.5E-23 | 10,000 | 8.8E-25 | 10,000 | <1.0E-30 | 10,000 |
| Cm-247 | Total α | 3.7E-29 | 10,000 | 9.5E-28 | 10,000 | 6.4E-27 | 10,000 | 1.6E-28 | 10,000 | <1.0E-30 | 10,000 |
| Cm-248 | Total α | <1.0E-30 | 10,000 | <1.0E-30 | 10,000 | <1.0E-30 | 10,000 | <1.0E-30 | 10,000 | <1.0E-30 | 10,000 |
| Co-60 | 100 | <1.0E-30 | 240 | <1.0E-30 | 240 | <1.0E-30 | 220 | <1.0E-30 | 240 | <1.0E-30 | 260 |
| Cs-135 | 900 | 4.1E-01 | 10,000 | 4.6E-01 | 10,000 | 4.5E-01 | 10,000 | 8.9E-02 | 10,000 | 5.7E-04 | 10,000 |
| Cs-137 | 200 | 1.1E-28 | 1,680 | 5.8E-28 | 1,640 | 1.2E-27 | 1,600 | 9.7E-29 | 1,640 | <1.0E-30 | 1,380 |
| Eu-152 | 200 | <1.0E-30 | 1,180 | <1.0E-30 | 1,140 | <1.0E-30 | 1,140 | <1.0E-30 | 1,180 | <1.0E-30 | 1,340 |
| Eu-154 | 60 | <1.0E-30 | 800 | <1.0E-30 | 760 | <1.0E-30 | 760 | <1.0E-30 | 780 | <1.0E-30 | 900 |
| Gd-152 | NC | <1.0E-30 | 10,000 | <1.0E-30 | 10,000 | <1.0E-30 | 10,000 | <1.0E-30 | 10,000 | <1.0E-30 | 10,000 |
| H-3 | 20,000 | 5.6E-09 | 380 | 6.3E-09 | 380 | 6.2E-09 | 380 | 1.2E-09 | 380 | 4.3E-11 | 420 |
| I-129 | 1 | 1.6E-01 | 10,000 | 1.7E-01 | 10,000 | 1.5E-01 | 10,000 | 1.2E-01 | 10,000 | 1.2E-01 | 10,000 |
| K-40 | NC | 1.0E-03 | 10,000 | 1.0E-03 | 9,980 | 9.2E-04 | 9,980 | 5.1E-04 | 10,000 | 3.7E-04 | 10,000 |
| Nb-93m | 1,000 | 3.9E-01 | 10,000 | 4.3E-01 | 10,000 | 4.2E-01 | 10,000 | 8.4E-02 | 10,000 | 9.8E-04 | 10,000 |

Table 6.1-4: Radiological 1m Concentrations for UTR-LZ Sectors A through E (Continued)

| Radionuclide | MCL (pCi/L)** | Sector A Concentrations | | Sector B Concentrations | | Sector C Concentrations | | Sector D Concentrations | | Sector E Concentrations | |
|--------------|--------------------|----------------------------|------------------|----------------------------|------------------|----------------------------|------------------|----------------------------|------------------|----------------------------|------------------|
| | | (pCi/L) | Year Peak Occurs | (pCi/L) | Year Peak Occurs | (pCi/L) | Year Peak Occurs | (pCi/L) | Year Peak Occurs | (pCi/L) | Year Peak Occurs |
| Nb-94 | NC | 7.0E-04 | 9,700 | 7.3E-04 | 9,700 | 7.0E-04 | 9,700 | 1.4E-04 | 9,700 | 1.4E-06 | 9,680 |
| Ni-59 | 300 | 3.0E-04 | 10,000 | 3.4E-04 | 10,000 | 3.3E-04 | 10,000 | 6.9E-05 | 10,000 | 1.8E-06 | 10,000 |
| Ni-63 | 50 | 1.0E-10 | 1,800 | 1.3E-10 | 1,780 | 1.3E-10 | 1,780 | 2.6E-11 | 1,780 | 1.3E-13 | 1,860 |
| Np-237 | Total α | 1.8E-03 | 10,000 | 1.8E-03 | 10,000 | 1.8E-03 | 10,000 | 3.5E-04 | 10,000 | 2.6E-06 | 10,000 |
| Pa-231 | Total α | 2.5E-04 | 10,000 | 2.6E-04 | 10,000 | 2.5E-04 | 10,000 | 4.9E-05 | 10,000 | 4.0E-07 | 10,000 |
| Pb-210 | NC | 5.4E-03 | 9,920 | 5.8E-03 | 9,820 | 5.6E-03 | 9,820 | 1.2E-03 | 9,820 | 8.8E-05 | 10,000 |
| Pd-107 | NC | 4.1E-05 | 10,000 | 4.6E-05 | 10,000 | 4.5E-05 | 10,000 | 9.0E-06 | 10,000 | 1.4E-07 | 10,000 |
| Pt-193 | 3,000 | 6.7E-03 | 460 | 7.3E-03 | 460 | 7.1E-03 | 460 | 1.6E-03 | 460 | 6.2E-04 | 540 |
| Pu-238 | Total α | <1.0E-30 | 5,440 | <1.0E-30 | 5,280 | <1.0E-30 | 5,140 | <1.0E-30 | 5,280 | <1.0E-30 | 5,940 |
| Pu-239 | Total α | 1.9E-10 | 10,000 | 6.8E-10 | 10,000 | 1.0E-09 | 10,000 | 1.2E-10 | 10,000 | 7.7E-15 | 10,000 |
| Pu-240 | Total α | 2.7E-11 | 10,000 | 9.9E-11 | 10,000 | 1.5E-10 | 10,000 | 1.7E-11 | 10,000 | 1.1E-15 | 10,000 |
| Pu-241 | 300 | 1.1E-24 | 10,000 | 2.8E-23 | 10,000 | 1.8E-22 | 10,000 | 4.7E-24 | 10,000 | <1.0E-30 | 10,000 |
| Pu-242 | Total α | 5.2E-13 | 10,000 | 1.9E-12 | 10,000 | 2.9E-12 | 10,000 | 3.2E-13 | 10,000 | 2.1E-17 | 10,000 |
| Pu-244 | Total α | 1.1E-14 | 10,000 | 3.9E-14 | 10,000 | 6.0E-14 | 10,000 | 6.6E-15 | 10,000 | 4.4E-19 | 10,000 |
| Ra-226 | Total α /Ra | 2.1E+00 | 9,840 | 2.2E+00 | 9,780 | 2.1E+00 | 9,780 | 4.6E-01 | 9,760 | 3.4E-02 | 10,000 |
| Ra-228 | Total Ra | 3.2E-13 | 10,000 | 6.9E-13 | 10,000 | 8.0E-13 | 10,000 | 1.3E-13 | 10,000 | 9.2E-17 | 10,000 |
| Rn-222 | NC | 2.1E+00 | 9,840 | 2.2E+00 | 9,780 | 2.1E+00 | 9,780 | 4.6E-01 | 9,760 | 3.4E-02 | 10,000 |
| Se-79 | NC | 3.1E-17 | 10,000 | 5.4E-16 | 10,000 | 2.7E-15 | 10,000 | 9.1E-17 | 10,000 | 5.7E-24 | 10,000 |
| Sm-151 | 1,000 | <1.0E-30 | 6,360 | <1.0E-30 | 6,120 | <1.0E-30 | 6,040 | <1.0E-30 | 6,180 | <1.0E-30 | 7,000 |
| Sb-126 | NC | 4.7E-30 | 10,000 | 3.8E-28 | 10,000 | 4.4E-27 | 10,000 | 5.3E-29 | 10,000 | <1.0E-30 | 10,000 |
| Sb-126m | NC | 3.3E-29 | 10,000 | 2.7E-27 | 10,000 | 3.2E-26 | 10,000 | 3.8E-28 | 10,000 | <1.0E-30 | 10,000 |
| Sn-126 | NC | 3.3E-29 | 10,000 | 2.7E-27 | 10,000 | 3.2E-26 | 10,000 | 3.8E-28 | 10,000 | <1.0E-30 | 10,000 |
| Sr-90 | 8 | 7.7E-12 | 1,060 | 1.2E-11 | 1,040 | 1.2E-11 | 1,040 | 2.4E-12 | 1,040 | 6.5E-15 | 1,080 |
| Tc-99 | 900 | 1.7E+01 | 9,800 | 1.8E+01 | 9,780 | 1.8E+01 | 9,780 | 3.6E+00 | 9,780 | 5.1E-02 | 9,800 |

Table 6.1-4: Radiological 1m Concentrations for UTR-LZ Sectors A through E (Continued)

| Radionuclide | MCL (pCi/L)** | Sector A Concentrations | | Sector B Concentrations | | Sector C Concentrations | | Sector D Concentrations | | Sector E Concentrations | |
|--|------------------|----------------------------|------------------|----------------------------|------------------|----------------------------|------------------|----------------------------|------------------|----------------------------|------------------|
| | | (pCi/L) | Year Peak Occurs | (pCi/L) | Year Peak Occurs | (pCi/L) | Year Peak Occurs | (pCi/L) | Year Peak Occurs | (pCi/L) | Year Peak Occurs |
| Th-228 | Total α | 3.2E-13 | 10,000 | 6.9E-13 | 10,000 | 8.0E-13 | 10,000 | 1.3E-13 | 10,000 | 9.2E-17 | 10,000 |
| Th-229 | Total α | 5.3E-08 | 10,000 | 1.2E-07 | 10,000 | 1.3E-07 | 10,000 | 2.2E-08 | 10,000 | 1.7E-11 | 10,000 |
| Th-230 | Total α | 6.6E-09 | 10,000 | 1.5E-08 | 10,000 | 1.7E-08 | 10,000 | 2.7E-09 | 10,000 | 1.6E-12 | 10,000 |
| Th-232 | Total α | 9.7E-16 | 10,000 | 2.2E-15 | 10,000 | 2.5E-15 | 10,000 | 4.0E-16 | 10,000 | 2.3E-19 | 10,000 |
| U-232 | Total U* | <1.0E-30 | 3,700 | <1.0E-30 | 3,580 | <1.0E-30 | 3,480 | <1.0E-30 | 3,580 | <1.0E-30 | 4,080 |
| U-233 | Total U* | 3.4E-06 | 10,000 | 7.1E-06 | 10,000 | 8.0E-06 | 10,000 | 1.3E-06 | 10,000 | 1.1E-09 | 10,000 |
| U-234 | Total U* | 4.2E-06 | 10,000 | 8.8E-06 | 10,000 | 9.9E-06 | 10,000 | 1.7E-06 | 10,000 | 1.3E-09 | 10,000 |
| U-235 | Total U* | 7.1E-08 | 10,000 | 1.5E-07 | 10,000 | 1.7E-07 | 10,000 | 2.8E-08 | 10,000 | 2.1E-11 | 10,000 |
| U-236 | Total U* | 1.2E-07 | 10,000 | 2.4E-07 | 10,000 | 2.7E-07 | 10,000 | 4.6E-08 | 10,000 | 3.4E-11 | 10,000 |
| U-238 | Total U* | 8.7E-08 | 10,000 | 1.8E-07 | 10,000 | 2.0E-07 | 10,000 | 3.4E-08 | 10,000 | 2.6E-11 | 10,000 |
| Y-90 | 60 | 7.7E-12 | 1,060 | 1.2E-11 | 1,040 | 1.2E-11 | 1,040 | 2.4E-12 | 1,040 | 6.5E-15 | 1,080 |
| Zr-93 | 2,000 | 3.9E-19 | 10,000 | 6.2E-18 | 10,000 | 2.9E-17 | 10,000 | 1.0E-18 | 10,000 | 8.1E-26 | 10,000 |
| Total alpha | 15 | 2.1E+00 | N/A | 2.2E+00 | N/A | 2.1E+00 | N/A | 4.6E-01 | N/A | 3.4E-02 | N/A |
| Total Ra | 5 | 2.1E+00 | N/A | 2.2E+00 | N/A | 2.1E+00 | N/A | 4.6E-01 | N/A | 3.4E-02 | N/A |
| Sum of beta-gamma MCL fractions | | 1.9E-01 | N/A | 2.0E-01 | N/A | 1.7E-01 | N/A | 1.3E-01 | N/A | 1.2E-01 | N/A |

* Total uranium is evaluated in Table 6.1-13

** MCL values for beta and photon emitters are calculated in Table II-3 of FR-00-9654 based on a beta-gamma dose of 4 mrem/yr

NC = Not Calculated

Table 6.1-5: Radiological 1m Concentrations for UTR-LZ Sectors F through J

| Radionuclide | MCL (pCi/L)** | Sector F Concentrations | | Sector G Concentrations | | Sector H Concentrations | | Sector I Concentrations | | Sector J Concentrations | |
|--------------|------------------|----------------------------|------------------|----------------------------|------------------|----------------------------|------------------|----------------------------|------------------|----------------------------|------------------|
| | | (pCi/L) | Year Peak Occurs | (pCi/L) | Year Peak Occurs | (pCi/L) | Year Peak Occurs | (pCi/L) | Year Peak Occurs | (pCi/L) | Year Peak Occurs |
| Ac-227 | NC | 1.0E-12 | 10,000 | 1.8E-17 | 10,000 | 1.0E-16 | 10,000 | 1.3E-15 | 10,000 | 4.2E-14 | 10,000 |
| Al-26 | NC | <1.0E-30 | 10,000 | <1.0E-30 | 10,000 | <1.0E-30 | 10,000 | <1.0E-30 | 10,000 | <1.0E-30 | 10,000 |
| Am-241 | Total α | <1.0E-30 | 10,000 | <1.0E-30 | 10,000 | <1.0E-30 | 10,000 | <1.0E-30 | 10,000 | <1.0E-30 | 10,000 |
| Am-242m | Total α | <1.0E-30 | 9,780 | <1.0E-30 | 8,100 | <1.0E-30 | 8,140 | <1.0E-30 | 8,200 | <1.0E-30 | 8,560 |
| Am-243 | Total α | <1.0E-30 | 10,000 | <1.0E-30 | 10,000 | <1.0E-30 | 10,000 | <1.0E-30 | 10,000 | <1.0E-30 | 10,000 |
| Ba-137m | NC | <1.0E-30 | 1,380 | <1.0E-30 | 1,480 | <1.0E-30 | 1,480 | <1.0E-30 | 1,480 | <1.0E-30 | 1,540 |
| C-14 | 2,000 | 2.0E-01 | 9,800 | 4.2E-01 | 9,820 | 4.5E-01 | 9,800 | 5.4E-01 | 9,820 | 5.2E-01 | 9,820 |
| Cf-249 | Total α | <1.0E-30 | 10,000 | <1.0E-30 | 10,000 | <1.0E-30 | 10,000 | <1.0E-30 | 10,000 | <1.0E-30 | 10,000 |
| Cf-251 | Total α | <1.0E-30 | 10,000 | <1.0E-30 | 10,000 | <1.0E-30 | 10,000 | <1.0E-30 | 10,000 | <1.0E-30 | 10,000 |
| Cl-36 | 700 | 4.0E-05 | 10,000 | 8.3E-05 | 10,000 | 8.8E-05 | 10,000 | 1.1E-04 | 10,000 | 1.0E-04 | 10,000 |
| Cm-243 | Total α | <1.0E-30 | 2,520 | <1.0E-30 | 2,240 | <1.0E-30 | 2,240 | <1.0E-30 | 2,240 | <1.0E-30 | 2,320 |
| Cm-244 | Total α | <1.0E-30 | 1,660 | <1.0E-30 | 1,440 | <1.0E-30 | 1,440 | <1.0E-30 | 1,440 | <1.0E-30 | 1,500 |
| Cm-245 | Total α | <1.0E-30 | 10,000 | <1.0E-30 | 10,000 | <1.0E-30 | 10,000 | <1.0E-30 | 10,000 | <1.0E-30 | 10,000 |
| Cm-247 | Total α | <1.0E-30 | 10,000 | <1.0E-30 | 10,000 | <1.0E-30 | 10,000 | <1.0E-30 | 10,000 | <1.0E-30 | 10,000 |
| Cm-248 | Total α | <1.0E-30 | 10,000 | <1.0E-30 | 10,000 | <1.0E-30 | 10,000 | <1.0E-30 | 10,000 | <1.0E-30 | 10,000 |
| Co-60 | 100 | <1.0E-30 | 260 | <1.0E-30 | 440 | <1.0E-30 | 420 | <1.0E-30 | 420 | <1.0E-30 | 340 |
| Cs-135 | 900 | 2.2E-05 | 10,000 | 3.1E-05 | 10,000 | 3.4E-05 | 10,000 | 4.2E-05 | 10,000 | 3.6E-05 | 10,000 |
| Cs-137 | 200 | <1.0E-30 | 1,380 | <1.0E-30 | 1,480 | <1.0E-30 | 1,480 | <1.0E-30 | 1,480 | <1.0E-30 | 1,540 |
| Eu-152 | 200 | <1.0E-30 | 1,300 | <1.0E-30 | 1,140 | <1.0E-30 | 1,140 | <1.0E-30 | 1,140 | <1.0E-30 | 1,180 |
| Eu-154 | 60 | <1.0E-30 | 860 | <1.0E-30 | 780 | <1.0E-30 | 780 | <1.0E-30 | 780 | <1.0E-30 | 800 |
| Gd-152 | NC | <1.0E-30 | 10,000 | <1.0E-30 | 10,000 | <1.0E-30 | 10,000 | <1.0E-30 | 10,000 | <1.0E-30 | 10,000 |
| H-3 | 20,000 | 5.0E-11 | 420 | 8.2E-11 | 420 | 8.8E-11 | 420 | 1.1E-10 | 420 | 9.7E-11 | 420 |
| I-129 | 1 | 1.5E-01 | 10,000 | 3.1E-01 | 10,000 | 3.3E-01 | 10,000 | 4.0E-01 | 10,000 | 3.8E-01 | 10,000 |
| K-40 | NC | 4.4E-04 | 10,000 | 8.8E-04 | 10,000 | 9.4E-04 | 10,000 | 1.1E-03 | 10,000 | 1.1E-03 | 10,000 |
| Nb-93m | 1,000 | 7.5E-06 | 10,000 | 6.5E-11 | 10,000 | 3.2E-10 | 10,000 | 4.4E-09 | 10,000 | 1.7E-07 | 10,000 |
| Nb-94 | NC | 7.3E-09 | 9,660 | 3.2E-11 | 10,000 | 2.9E-11 | 10,000 | 3.4E-11 | 10,000 | 3.5E-10 | 9,720 |
| Ni-59 | 300 | 2.0E-08 | 10,000 | 3.7E-13 | 10,000 | 2.4E-12 | 10,000 | 3.0E-11 | 10,000 | 9.8E-10 | 10,000 |
| Ni-63 | 50 | 3.6E-16 | 2,120 | 5.6E-23 | 2,780 | 4.2E-22 | 2,760 | 8.0E-21 | 2,720 | 5.5E-19 | 2,600 |

Table 6.1-5: Radiological 1m Concentrations for UTR-LZ Sectors F through J (Continued)

| Radionuclide | MCL (pCi/L)** | Sector F Concentrations | | Sector G Concentrations | | Sector H Concentrations | | Sector I Concentrations | | Sector J Concentrations | |
|--------------|------------------|----------------------------|------------------|----------------------------|------------------|----------------------------|------------------|----------------------------|------------------|----------------------------|------------------|
| | | (pCi/L) | Year Peak Occurs | (pCi/L) | Year Peak Occurs | (pCi/L) | Year Peak Occurs | (pCi/L) | Year Peak Occurs | (pCi/L) | Year Peak Occurs |
| Np-237 | Total α | 6.1E-09 | 10,000 | 1.2E-13 | 10,000 | 5.5E-13 | 10,000 | 6.6E-12 | 10,000 | 2.1E-10 | 10,000 |
| Pa-231 | Total α | 1.3E-09 | 10,000 | 2.4E-14 | 10,000 | 1.4E-13 | 10,000 | 1.7E-12 | 10,000 | 5.5E-11 | 10,000 |
| Pb-210 | NC | 7.9E-05 | 10,000 | 1.5E-04 | 10,000 | 1.6E-04 | 10,000 | 2.0E-04 | 10,000 | 1.9E-04 | 10,000 |
| Pd-107 | NC | 1.2E-09 | 10,000 | 2.3E-14 | 10,000 | 1.4E-13 | 10,000 | 1.8E-12 | 10,000 | 5.8E-11 | 10,000 |
| Pt-193 | 3,000 | 7.4E-04 | 540 | 1.4E-03 | 540 | 1.5E-03 | 540 | 1.9E-03 | 540 | 1.7E-03 | 540 |
| Pu-238 | Total α | <1.0E-30 | 5,940 | <1.0E-30 | 6,820 | <1.0E-30 | 6,840 | <1.0E-30 | 6,880 | <1.0E-30 | 7,580 |
| Pu-239 | Total α | 1.3E-17 | 10,000 | <1.0E-30 | 10,000 | <1.0E-30 | 10,000 | <1.0E-30 | 10,000 | <1.0E-30 | 10,000 |
| Pu-240 | Total α | 1.8E-18 | 10,000 | <1.0E-30 | 10,000 | <1.0E-30 | 10,000 | <1.0E-30 | 10,000 | <1.0E-30 | 10,000 |
| Pu-241 | 300 | <1.0E-30 | 10,000 | <1.0E-30 | 10,000 | <1.0E-30 | 10,000 | <1.0E-30 | 10,000 | <1.0E-30 | 10,000 |
| Pu-242 | Total α | 3.5E-20 | 10,000 | <1.0E-30 | 10,000 | <1.0E-30 | 10,000 | <1.0E-30 | 10,000 | <1.0E-30 | 10,000 |
| Pu-244 | Total α | 7.3E-22 | 10,000 | <1.0E-30 | 10,000 | <1.0E-30 | 10,000 | <1.0E-30 | 10,000 | <1.0E-30 | 10,000 |
| Ra-226 | Total α/Ra | 3.0E-02 | 10,000 | 5.9E-02 | 10,000 | 6.3E-02 | 10,000 | 7.7E-02 | 10,000 | 7.2E-02 | 10,000 |
| Ra-228 | Total Ra | 1.1E-19 | 10,000 | 2.6E-25 | 10,000 | 2.5E-25 | 10,000 | 2.1E-25 | 10,000 | 2.7E-26 | 10,000 |
| Rn-222 | NC | 3.0E-02 | 10,000 | 5.9E-02 | 10,000 | 6.3E-02 | 10,000 | 7.7E-02 | 10,000 | 7.2E-02 | 10,000 |
| Se-79 | NC | 8.4E-25 | 10,000 | 1.3E-25 | 10,000 | 1.2E-25 | 10,000 | 5.5E-26 | 10,000 | 4.6E-28 | 10,000 |
| Sm-151 | 1,000 | <1.0E-30 | 7,000 | <1.0E-30 | 6,140 | <1.0E-30 | 6,160 | <1.0E-30 | 6,200 | <1.0E-30 | 6,420 |
| Sb-126 | NC | <1.0E-30 | 10,000 | <1.0E-30 | 10,000 | <1.0E-30 | 10,000 | <1.0E-30 | 10,000 | <1.0E-30 | 10,000 |
| Sb-126m | NC | <1.0E-30 | 10,000 | <1.0E-30 | 10,000 | <1.0E-30 | 10,000 | <1.0E-30 | 10,000 | <1.0E-30 | 10,000 |
| Sn-126 | NC | <1.0E-30 | 10,000 | <1.0E-30 | 10,000 | <1.0E-30 | 10,000 | <1.0E-30 | 10,000 | <1.0E-30 | 10,000 |
| Sr-90 | 8 | 6.7E-18 | 1,080 | 1.1E-19 | 1,080 | 1.2E-19 | 1,080 | 1.3E-19 | 1,080 | 7.0E-20 | 1,100 |
| Tc-99 | 900 | 4.0E-04 | 9,800 | 1.6E-06 | 10,000 | 1.7E-06 | 10,000 | 2.3E-06 | 10,000 | 2.2E-05 | 10,000 |
| Th-228 | Total α | 1.1E-19 | 10,000 | 2.6E-25 | 10,000 | 2.5E-25 | 10,000 | 2.1E-25 | 10,000 | 2.7E-26 | 10,000 |
| Th-229 | Total α | 4.7E-14 | 10,000 | 1.1E-18 | 10,000 | 4.0E-18 | 10,000 | 4.7E-17 | 10,000 | 1.5E-15 | 10,000 |
| Th-230 | Total α | 1.9E-15 | 10,000 | 9.2E-27 | 10,000 | 9.1E-27 | 10,000 | 7.8E-27 | 10,000 | 1.2E-27 | 10,000 |
| Th-232 | Total U* | 2.8E-22 | 10,000 | <1.0E-30 | 10,000 | <1.0E-30 | 10,000 | <1.0E-30 | 10,000 | <1.0E-30 | 10,000 |
| U-232 | Total U* | <1.0E-30 | 4,080 | <1.0E-30 | 4,560 | <1.0E-30 | 4,540 | <1.0E-30 | 4,620 | <1.0E-30 | 4,820 |
| U-233 | Total U* | 1.7E-12 | 10,000 | 3.6E-17 | 10,000 | 7.1E-17 | 10,000 | 7.9E-16 | 10,000 | 2.5E-14 | 10,000 |
| U-234 | Total U* | 1.5E-12 | 10,000 | 9.6E-24 | 10,000 | 9.6E-24 | 10,000 | 8.3E-24 | 10,000 | 1.4E-24 | 10,000 |

Table 6.1-5: Radiological 1m Concentrations for UTR-LZ Sectors F through J (Continued)

| Radionuclide | MCL (pCi/L)** | Sector F Concentrations | | Sector G Concentrations | | Sector H Concentrations | | Sector I Concentrations | | Sector J Concentrations | |
|--|------------------|----------------------------|------------------|----------------------------|------------------|----------------------------|------------------|----------------------------|------------------|----------------------------|------------------|
| | | (pCi/L) | Year Peak Occurs | (pCi/L) | Year Peak Occurs | (pCi/L) | Year Peak Occurs | (pCi/L) | Year Peak Occurs | (pCi/L) | Year Peak Occurs |
| U-235 | Total U* | 2.5E-14 | 10,000 | 1.6E-25 | 10,000 | 1.6E-25 | 10,000 | 1.4E-25 | 10,000 | 2.3E-26 | 10,000 |
| U-236 | Total U* | 4.1E-14 | 10,000 | 8.5E-25 | 10,000 | 8.4E-25 | 10,000 | 7.3E-25 | 10,000 | 1.2E-25 | 10,000 |
| U-238 | 60 | 3.1E-14 | 10,000 | 5.4E-24 | 10,000 | 5.4E-24 | 10,000 | 4.7E-24 | 10,000 | 7.3E-25 | 10,000 |
| Y-90 | 2,000 | 6.7E-18 | 1,080 | 1.1E-19 | 1,080 | 1.2E-19 | 1,080 | 1.3E-19 | 1,080 | 7.0E-20 | 1,100 |
| Zr-93 | Total α | 1.6E-28 | 10,000 | <1.0E-30 | 10,000 | <1.0E-30 | 10,000 | <1.0E-30 | 10,000 | <1.0E-30 | 10,000 |
| Total alpha | 15 | 3.0E-02 | N/A | 5.9E-02 | N/A | 6.3E-02 | N/A | 7.7E-02 | N/A | 7.2E-02 | N/A |
| Total Ra | 5 | 3.0E-02 | N/A | 5.9E-02 | N/A | 6.3E-02 | N/A | 7.7E-02 | N/A | 7.2E-02 | N/A |
| Sum of beta-gamma MCL fractions | | 1.5E-01 | N/A | 3.1E-01 | N/A | 3.3E-01 | N/A | 4.0E-01 | N/A | 3.8E-01 | N/A |

* Total uranium is evaluated in Table 6.1-14

** MCL values for beta and photon emitters are calculated in Table II-3 of FR-00-9654 based on a beta-gamma dose of 4 mrem/yr

NC = Not Calculated

Table 6.1-6: Radiological 1m Concentrations for UTR-LZ Sectors K and L

| Radionuclide | MCL (pCi/L)** | Sector K Concentrations | | Sector L Concentrations | |
|--------------|---------------|----------------------------|------------------|----------------------------|------------------|
| | | (pCi/L) | Year Peak Occurs | (pCi/L) | Year Peak Occurs |
| Ac-227 | NC | 3.0E-13 | 10,000 | 1.3E-10 | 10,000 |
| Al-26 | NC | <1.0E-30 | 10,000 | <1.0E-30 | 10,000 |
| Am-241 | Total α | <1.0E-30 | 10,000 | <1.0E-30 | 10,000 |
| Am-242m | Total α | <1.0E-30 | 10,000 | <1.0E-30 | 9,880 |
| Am-243 | Total α | <1.0E-30 | 10,000 | <1.0E-30 | 10,000 |
| Ba-137m | NC | <1.0E-30 | 1,540 | <1.0E-30 | 1,420 |
| C-14 | 2,000 | 4.4E-01 | 9,800 | 3.2E-01 | 9,800 |
| Cf-249 | Total α | <1.0E-30 | 10,000 | <1.0E-30 | 10,000 |
| Cf-251 | Total α | <1.0E-30 | 10,000 | <1.0E-30 | 10,000 |
| Cl-36 | 700 | 8.6E-05 | 10,000 | 6.4E-05 | 10,000 |
| Cm-243 | Total α | <1.0E-30 | 2,320 | <1.0E-30 | 2,580 |
| Cm-244 | Total α | <1.0E-30 | 1,500 | <1.0E-30 | 1,700 |
| Cm-245 | Total α | <1.0E-30 | 10,000 | <1.0E-30 | 10,000 |
| Cm-247 | Total α | <1.0E-30 | 10,000 | <1.0E-30 | 10,000 |
| Cm-248 | Total α | <1.0E-30 | 10,000 | <1.0E-30 | 10,000 |
| Co-60 | 100 | <1.0E-30 | 300 | <1.0E-30 | 260 |
| Cs-135 | 900 | 3.1E-05 | 10,000 | 2.2E-04 | 10,000 |
| Cs-137 | 200 | <1.0E-30 | 1,540 | <1.0E-30 | 1,420 |
| Eu-152 | 200 | <1.0E-30 | 1,180 | <1.0E-30 | 1,320 |
| Eu-154 | 60 | <1.0E-30 | 800 | <1.0E-30 | 880 |
| Gd-152 | NC | <1.0E-30 | 10,000 | <1.0E-30 | 10,000 |
| H-3 | 20,000 | 8.2E-11 | 420 | 6.9E-11 | 420 |
| I-129 | 1 | 3.2E-01 | 10,000 | 2.4E-01 | 10,000 |
| K-40 | NC | 9.1E-04 | 10,000 | 6.9E-04 | 10,000 |
| Nb-93m | 1,000 | 1.2E-06 | 10,000 | 2.9E-04 | 10,000 |
| Nb-94 | NC | 2.4E-09 | 9,620 | 5.5E-07 | 9,700 |
| Ni-59 | 300 | 7.0E-09 | 10,000 | 5.0E-07 | 10,000 |
| Ni-63 | 50 | 5.4E-18 | 2,580 | 3.5E-14 | 1,880 |
| Np-237 | Total α | 1.5E-09 | 10,000 | 1.2E-06 | 10,000 |
| Pa-231 | Total α | 3.9E-10 | 10,000 | 1.7E-07 | 10,000 |
| Pb-210 | NC | 1.6E-04 | 10,000 | 1.2E-04 | 10,000 |
| Pd-107 | NC | 4.2E-10 | 10,000 | 4.1E-08 | 10,000 |
| Pt-193 | 3,000 | 1.5E-03 | 540 | 1.1E-03 | 540 |
| Pu-238 | Total α | <1.0E-30 | 6,780 | <1.0E-30 | 6,000 |
| Pu-239 | Total α | 4.5E-26 | 10,000 | 4.3E-16 | 10,000 |
| Pu-240 | Total α | 6.6E-27 | 10,000 | 6.2E-17 | 10,000 |
| Pu-241 | 300 | <1.0E-30 | 10,000 | <1.0E-30 | 10,000 |
| Pu-242 | Total α | 1.3E-28 | 10,000 | 1.2E-18 | 10,000 |
| Pu-244 | Total α | 2.6E-30 | 10,000 | 2.5E-20 | 10,000 |
| Ra-226 | Total α/Ra | 6.1E-02 | 10,000 | 4.6E-02 | 10,000 |
| Ra-228 | Total Ra | 8.0E-26 | 10,000 | 7.9E-18 | 10,000 |
| Rn-222 | NC | 6.1E-02 | 10,000 | 4.6E-02 | 10,000 |

Table 6.1-6: Radiological 1m Concentrations for UTR-LZ Sectors K and L (Continued)

| Radionuclide | MCL (pCi/L)** | Sector K Concentrations | | Sector L Concentrations | |
|--|---------------|----------------------------|------------------|----------------------------|------------------|
| | | (pCi/L) | Year Peak Occurs | (pCi/L) | Year Peak Occurs |
| Se-79 | NC | 1.1E-27 | 10,000 | 1.9E-25 | 10,000 |
| Sm-151 | 1,000 | <1.0E-30 | 6,380 | <1.0E-30 | 7,100 |
| Sb-126 | NC | <1.0E-30 | 10,000 | <1.0E-30 | 10,000 |
| Sb-126m | NC | <1.0E-30 | 10,000 | <1.0E-30 | 10,000 |
| Sn-126 | NC | <1.0E-30 | 10,000 | <1.0E-30 | 10,000 |
| Sr-90 | 8 | 7.2E-20 | 1,100 | 1.2E-15 | 1,120 |
| Tc-99 | 900 | 1.4E-04 | 10,000 | 1.7E-02 | 9,800 |
| Th-228 | Total α | 8.0E-26 | 10,000 | 7.9E-18 | 10,000 |
| Th-229 | Total α | 1.1E-14 | 10,000 | 2.5E-12 | 10,000 |
| Th-230 | Total α | 2.7E-22 | 10,000 | 1.2E-13 | 10,000 |
| Th-232 | Total α | 3.9E-29 | 10,000 | 1.8E-20 | 10,000 |
| U-232 | Total U* | <1.0E-30 | 4,720 | <1.0E-30 | 4,140 |
| U-233 | Total U* | 1.8E-13 | 10,000 | 1.2E-10 | 10,000 |
| U-234 | Total U* | 3.2E-19 | 10,000 | 1.1E-10 | 10,000 |
| U-235 | Total U* | 5.3E-21 | 10,000 | 1.8E-12 | 10,000 |
| U-236 | Total U* | 8.6E-21 | 10,000 | 2.9E-12 | 10,000 |
| U-238 | Total U* | 6.5E-21 | 10,000 | 2.2E-12 | 10,000 |
| Y-90 | 60 | 7.2E-20 | 1,100 | 1.2E-15 | 1,120 |
| Zr-93 | 2,000 | <1.0E-30 | 10,000 | 2.2E-27 | 10,000 |
| Total alpha | 15 | 6.1E-02 | N/A | 4.6E-02 | N/A |
| Total Ra | 5 | 6.1E-02 | N/A | 4.6E-02 | N/A |
| Sum of beta-gamma MCL fractions | | 3.2E-01 | N/A | 2.4E-01 | N/A |

* Total uranium is evaluated in Table 6.1-15

** MCL values for beta and photon emitters are calculated in Table II-3 of FR-00-9654 based on a beta-gamma dose of 4 mrem/yr

NC = Not Calculated

Table 6.1-7: Radiological 1m Concentrations for Gordon Aquifer Sectors A through E

| Radionuclide | MCL (pCi/L)** | Sector A Concentrations | | Sector B Concentrations | | Sector C Concentrations | | Sector D Concentrations | | Sector E Concentrations | |
|--------------|------------------|----------------------------|---------------------|----------------------------|---------------------|----------------------------|---------------------|----------------------------|---------------------|----------------------------|---------------------|
| | | (pCi/L) | Year Peak Occurs | (pCi/L) | Year Peak Occurs | (pCi/L) | Year Peak Occurs | (pCi/L) | Year Peak Occurs | (pCi/L) | Year Peak Occurs |
| Ac-227 | NC | 9.6E-12 | 10,000 | 7.1E-12 | 10,000 | 3.3E-12 | 10,000 | 2.5E-13 | 10,000 | 3.1E-15 | 10,000 |
| Al-26 | NC | <1.0E-30 | 10,000 | <1.0E-30 | 10,000 | <1.0E-30 | 10,000 | <1.0E-30 | 10,000 | <1.0E-30 | 10,000 |
| Am-241 | Total α | <1.0E-30 | 10,000 | <1.0E-30 | 10,000 | <1.0E-30 | 10,000 | <1.0E-30 | 10,000 | <1.0E-30 | 10,000 |
| Am-242m | Total α | <1.0E-30 | 10,000 | <1.0E-30 | 9,800 | <1.0E-30 | 9,580 | <1.0E-30 | 9,840 | <1.0E-30 | 10,000 |
| Am-243 | Total α | <1.0E-30 | 10,000 | <1.0E-30 | 10,000 | <1.0E-30 | 10,000 | <1.0E-30 | 10,000 | <1.0E-30 | 10,000 |
| Ba-137m | NC | <1.0E-30 | 1,900 | <1.0E-30 | 1,860 | <1.0E-30 | 1,820 | <1.0E-30 | 1,860 | <1.0E-30 | 1,660 |
| C-14 | 2,000 | 3.7E-03 | 6,740 | 3.0E-03 | 6,740 | 1.7E-03 | 6,740 | 3.0E-04 | 8,260 | 2.1E-04 | 10,000 |
| Cf-249 | Total α | <1.0E-30 | 10,000 | <1.0E-30 | 10,000 | <1.0E-30 | 10,000 | <1.0E-30 | 10,000 | <1.0E-30 | 10,000 |
| Cf-251 | Total α | <1.0E-30 | 10,000 | <1.0E-30 | 10,000 | <1.0E-30 | 10,000 | <1.0E-30 | 10,000 | <1.0E-30 | 10,000 |
| Cl-36 | 700 | 1.2E-06 | 9,840 | 9.5E-07 | 9,840 | 5.3E-07 | 9,880 | 1.1E-07 | 10,000 | 4.0E-08 | 10,000 |
| Cm-243 | Total α | <1.0E-30 | 2,620 | <1.0E-30 | 2,520 | <1.0E-30 | 2,520 | <1.0E-30 | 2,580 | <1.0E-30 | 2,880 |
| Cm-244 | Total α | <1.0E-30 | 1,700 | <1.0E-30 | 1,660 | <1.0E-30 | 1,640 | <1.0E-30 | 1,700 | <1.0E-30 | 1,900 |
| Cm-245 | Total α | <1.0E-30 | 10,000 | <1.0E-30 | 10,000 | <1.0E-30 | 10,000 | <1.0E-30 | 10,000 | <1.0E-30 | 10,000 |
| Cm-247 | Total α | <1.0E-30 | 10,000 | <1.0E-30 | 10,000 | <1.0E-30 | 10,000 | <1.0E-30 | 10,000 | <1.0E-30 | 10,000 |
| Cm-248 | Total α | <1.0E-30 | 10,000 | <1.0E-30 | 10,000 | <1.0E-30 | 10,000 | <1.0E-30 | 10,000 | <1.0E-30 | 10,000 |
| Co-60 | 100 | <1.0E-30 | 280 | <1.0E-30 | 280 | <1.0E-30 | 260 | <1.0E-30 | 280 | <1.0E-30 | 300 |
| Cs-135 | 900 | 3.8E-07 | 10,000 | 3.3E-07 | 10,000 | 1.8E-07 | 10,000 | 1.2E-08 | 10,000 | 4.9E-11 | 10,000 |
| Cs-137 | 200 | <1.0E-30 | 1,900 | <1.0E-30 | 1,860 | <1.0E-30 | 1,820 | <1.0E-30 | 1,860 | <1.0E-30 | 1,660 |
| Eu-152 | 200 | <1.0E-30 | 1,320 | <1.0E-30 | 1,280 | <1.0E-30 | 1,280 | <1.0E-30 | 1,320 | <1.0E-30 | 1,460 |
| Eu-154 | 60 | <1.0E-30 | 880 | <1.0E-30 | 860 | <1.0E-30 | 860 | <1.0E-30 | 880 | <1.0E-30 | 980 |
| Gd-152 | NC | <1.0E-30 | 10,000 | <1.0E-30 | 10,000 | <1.0E-30 | 10,000 | <1.0E-30 | 10,000 | <1.0E-30 | 10,000 |
| H-3 | 20,000 | 3.6E-13 | 420 | 2.9E-13 | 400 | 1.4E-13 | 400 | 1.1E-14 | 420 | 7.8E-16 | 440 |
| I-129 | 1 | 3.7E-04 | 10,000 | 3.1E-04 | 10,000 | 2.1E-04 | 10,000 | 1.4E-04 | 10,000 | 1.4E-04 | 10,000 |
| K-40 | NC | 1.1E-07 | 10,000 | 8.6E-08 | 10,000 | 4.7E-08 | 10,000 | 1.6E-08 | 10,000 | 7.9E-09 | 10,000 |
| Nb-93m | 1,000 | 4.5E-05 | 10,000 | 3.6E-05 | 10,000 | 1.8E-05 | 10,000 | 1.3E-06 | 10,000 | 1.5E-08 | 10,000 |
| Nb-94 | NC | 1.5E-06 | 10,000 | 1.2E-06 | 10,000 | 6.2E-07 | 10,000 | 5.0E-08 | 10,000 | 5.3E-10 | 10,000 |
| Ni-59 | 300 | 3.2E-08 | 10,000 | 2.5E-08 | 10,000 | 1.2E-08 | 10,000 | 1.6E-09 | 10,000 | 7.5E-11 | 10,000 |
| Ni-63 | 50 | 3.5E-17 | 2,180 | 3.1E-17 | 2,180 | 1.8E-17 | 2,140 | 1.1E-18 | 2,160 | 4.9E-21 | 2,240 |

Table 6.1-7: Radiological 1m Concentrations for Gordon Aquifer Sectors A through E (Continued)

| Radionuclide | MCL (pCi/L)** | Sector A Concentrations | | Sector B Concentrations | | Sector C Concentrations | | Sector D Concentrations | | Sector E Concentrations | |
|--------------|------------------|----------------------------|------------------|----------------------------|------------------|----------------------------|------------------|----------------------------|------------------|----------------------------|------------------|
| | | (pCi/L) | Year Peak Occurs | (pCi/L) | Year Peak Occurs | (pCi/L) | Year Peak Occurs | (pCi/L) | Year Peak Occurs | (pCi/L) | Year Peak Occurs |
| Np-237 | Total α | 1.0E-07 | 10,000 | 7.5E-08 | 10,000 | 3.5E-08 | 10,000 | 2.6E-09 | 10,000 | 3.2E-11 | 10,000 |
| Pa-231 | Total α | 1.3E-08 | 10,000 | 9.2E-09 | 10,000 | 4.3E-09 | 10,000 | 3.2E-10 | 10,000 | 3.9E-12 | 10,000 |
| Pb-210 | NC | 8.1E-07 | 10,000 | 6.1E-07 | 10,000 | 3.0E-07 | 10,000 | 3.2E-08 | 10,000 | 3.4E-09 | 10,000 |
| Pd-107 | NC | 4.2E-09 | 10,000 | 3.2E-09 | 10,000 | 1.5E-09 | 10,000 | 1.5E-10 | 10,000 | 4.8E-12 | 10,000 |
| Pt-193 | 3,000 | 2.5E-06 | 520 | 1.9E-06 | 520 | 9.6E-07 | 540 | 1.7E-07 | 600 | 9.3E-08 | 640 |
| Pu-238 | Total α | <1.0E-30 | 6,180 | <1.0E-30 | 6,040 | <1.0E-30 | 5,940 | <1.0E-30 | 6,020 | <1.0E-30 | 6,660 |
| Pu-239 | Total α | 4.4E-23 | 10,000 | 1.4E-22 | 10,000 | 1.8E-22 | 10,000 | 6.9E-24 | 10,000 | 1.8E-28 | 10,000 |
| Pu-240 | Total α | 6.4E-24 | 10,000 | 2.1E-23 | 10,000 | 2.6E-23 | 10,000 | 1.0E-24 | 10,000 | 2.7E-29 | 10,000 |
| Pu-241 | 300 | <1.0E-30 | 10,000 | <1.0E-30 | 10,000 | <1.0E-30 | 10,000 | <1.0E-30 | 10,000 | <1.0E-30 | 10,000 |
| Pu-242 | Total α | 1.2E-25 | 10,000 | 3.9E-25 | 10,000 | 5.0E-25 | 10,000 | 1.9E-26 | 10,000 | <1.0E-30 | 10,000 |
| Pu-244 | Total α | 2.5E-27 | 10,000 | 8.1E-27 | 10,000 | 1.0E-26 | 10,000 | 4.0E-28 | 10,000 | <1.0E-30 | 10,000 |
| Ra-226 | Total α/Ra | 3.1E-04 | 10,000 | 2.4E-04 | 10,000 | 1.2E-04 | 10,000 | 1.2E-05 | 10,000 | 1.3E-06 | 10,000 |
| Ra-228 | Total Ra | 3.2E-22 | 10,000 | 5.3E-22 | 10,000 | 5.0E-22 | 10,000 | 2.1E-23 | 10,000 | 6.2E-27 | 10,000 |
| Rn-222 | NC | 3.1E-04 | 10,000 | 2.4E-04 | 10,000 | 1.2E-04 | 10,000 | 1.2E-05 | 10,000 | 1.3E-06 | 10,000 |
| Se-79 | NC | <1.0E-30 | 10,000 | 1.2E-29 | 10,000 | 4.9E-29 | 10,000 | <1.0E-30 | 10,000 | <1.0E-30 | 10,000 |
| Sm-151 | 1,000 | <1.0E-30 | 7,220 | <1.0E-30 | 7,020 | <1.0E-30 | 6,880 | <1.0E-30 | 7,080 | <1.0E-30 | 7,840 |
| Sb-126 | NC | <1.0E-30 | 10,000 | <1.0E-30 | 10,000 | <1.0E-30 | 10,000 | <1.0E-30 | 10,000 | <1.0E-30 | 10,000 |
| Sb-126m | NC | <1.0E-30 | 10,000 | <1.0E-30 | 10,000 | <1.0E-30 | 10,000 | <1.0E-30 | 10,000 | <1.0E-30 | 10,000 |
| Sn-126 | NC | <1.0E-30 | 10,000 | <1.0E-30 | 10,000 | <1.0E-30 | 10,000 | <1.0E-30 | 10,000 | <1.0E-30 | 10,000 |
| Sr-90 | 8 | 2.9E-19 | 1,200 | 2.8E-19 | 1,200 | 2.0E-19 | 1,180 | 1.2E-20 | 1,180 | 3.0E-23 | 1,220 |
| Tc-99 | 900 | 8.4E-03 | 10,000 | 6.5E-03 | 10,000 | 3.3E-03 | 10,000 | 3.7E-04 | 10,000 | 1.4E-05 | 10,000 |
| Th-228 | Total α | 3.2E-22 | 10,000 | 5.3E-22 | 10,000 | 5.0E-22 | 10,000 | 2.1E-23 | 10,000 | 6.2E-27 | 10,000 |
| Th-229 | Total α | 3.0E-12 | 10,000 | 2.4E-12 | 10,000 | 1.2E-12 | 10,000 | 9.2E-14 | 10,000 | 1.3E-15 | 10,000 |
| Th-230 | Total α | 7.7E-18 | 10,000 | 1.5E-17 | 10,000 | 1.5E-17 | 10,000 | 6.6E-19 | 10,000 | 1.5E-22 | 10,000 |
| Th-232 | Total α | 1.1E-24 | 10,000 | 2.1E-24 | 10,000 | 2.1E-24 | 10,000 | 9.6E-26 | 10,000 | 2.1E-29 | 10,000 |
| U-232 | Total U* | <1.0E-30 | 4,260 | <1.0E-30 | 4,160 | <1.0E-30 | 4,080 | <1.0E-30 | 4,140 | <1.0E-30 | 4,640 |
| U-233 | Total U* | 8.5E-11 | 10,000 | 7.0E-11 | 10,000 | 3.6E-11 | 10,000 | 2.8E-12 | 10,000 | 3.9E-14 | 10,000 |

Table 6.1-7: Radiological 1m Concentrations for Gordon Aquifer Sectors A through E (Continued)

| Radionuclide | MCL (pCi/L)** | Sector A Concentrations | | Sector B Concentrations | | Sector C Concentrations | | Sector D Concentrations | | Sector E Concentrations | |
|--|------------------|----------------------------|---------------------|----------------------------|---------------------|----------------------------|---------------------|----------------------------|---------------------|----------------------------|---------------------|
| | | (pCi/L) | Year Peak Occurs | (pCi/L) | Year Peak Occurs | (pCi/L) | Year Peak Occurs | (pCi/L) | Year Peak Occurs | (pCi/L) | Year Peak Occurs |
| U-234 | Total U* | 8.4E-15 | 10,000 | 1.5E-14 | 10,000 | 1.5E-14 | 10,000 | 7.4E-16 | 10,000 | 2.0E-19 | 10,000 |
| U-235 | Total U* | 1.4E-16 | 10,000 | 2.6E-16 | 10,000 | 2.5E-16 | 10,000 | 1.2E-17 | 10,000 | 3.3E-21 | 10,000 |
| U-236 | Total U* | 2.3E-16 | 10,000 | 4.2E-16 | 10,000 | 4.2E-16 | 10,000 | 2.0E-17 | 10,000 | 5.3E-21 | 10,000 |
| U-238 | Total U* | 1.7E-16 | 10,000 | 3.2E-16 | 10,000 | 3.1E-16 | 10,000 | 1.5E-17 | 10,000 | 4.0E-21 | 10,000 |
| Y-90 | 60 | 2.9E-19 | 1,200 | 2.8E-19 | 1,200 | 2.0E-19 | 1,180 | 1.2E-20 | 1,180 | 3.0E-23 | 1,220 |
| Zr-93 | 2,000 | <1.0E-30 | 10,000 | <1.0E-30 | 10,000 | <1.0E-30 | 10,000 | <1.0E-30 | 10,000 | <1.0E-30 | 10,000 |
| Total alpha | 15 | 3.1E-04 | N/A | 2.4E-04 | N/A | 1.2E-04 | N/A | 1.2E-05 | N/A | 1.3E-06 | N/A |
| Total Ra | 5 | 3.1E-04 | N/A | 2.4E-04 | N/A | 1.2E-04 | N/A | 1.2E-05 | N/A | 1.3E-06 | N/A |
| Sum of beta-gamma MCL fractions | | 3.8E-04 | N/A | 3.2E-04 | N/A | 2.1E-04 | N/A | 1.4E-04 | N/A | 1.4E-04 | N/A |

* Total uranium is evaluated in Table 6.1-16

** MCL values for beta and photon emitters are calculated in Table II-3 of FR-00-9654 based on a beta-gamma dose of 4 mrem/yr
NC = Not Calculated

Table 6.1-8: Radiological 1m Concentrations for Gordon Aquifer Sectors F through J

| Radionuclide | MCL (pCi/L)** | Sector F Concentrations | | Sector G Concentrations | | Sector H Concentrations | | Sector I Concentrations | | Sector J Concentrations | |
|--------------|------------------|----------------------------|------------------|----------------------------|------------------|----------------------------|------------------|----------------------------|------------------|----------------------------|------------------|
| | | (pCi/L) | Year Peak Occurs | (pCi/L) | Year Peak Occurs | (pCi/L) | Year Peak Occurs | (pCi/L) | Year Peak Occurs | (pCi/L) | Year Peak Occurs |
| Ac-227 | NC | 1.7E-17 | 10,000 | 5.1E-12 | 10,000 | 7.0E-12 | 10,000 | 7.0E-12 | 10,000 | 5.8E-12 | 10,000 |
| Al-26 | NC | 1.7E-49 | 10,000 | <1.0E-30 | 10,000 | <1.0E-30 | 10,000 | <1.0E-30 | 10,000 | <1.0E-30 | 10,000 |
| Am-241 | Total α | <1.0E-30 | 10,000 | <1.0E-30 | 10,000 | <1.0E-30 | 10,000 | <1.0E-30 | 10,000 | <1.0E-30 | 10,000 |
| Am-242m | Total α | <1.0E-30 | 10,000 | <1.0E-30 | 9,320 | <1.0E-30 | 9,380 | <1.0E-30 | 9,420 | <1.0E-30 | 10,000 |
| Am-243 | Total α | <1.0E-30 | 10,000 | <1.0E-30 | 10,000 | <1.0E-30 | 10,000 | <1.0E-30 | 10,000 | <1.0E-30 | 10,000 |
| Ba-137m | NC | <1.0E-30 | 1,660 | <1.0E-30 | 1,660 | <1.0E-30 | 1,660 | <1.0E-30 | 1,680 | <1.0E-30 | 1,760 |
| C-14 | 2,000 | 2.1E-04 | 10,000 | 3.5E-03 | 7,780 | 4.2E-03 | 7,760 | 4.2E-03 | 7,760 | 3.5E-03 | 8,260 |
| Cf-249 | Total α | <1.0E-30 | 10,000 | <1.0E-30 | 10,000 | <1.0E-30 | 10,000 | <1.0E-30 | 10,000 | <1.0E-30 | 10,000 |
| Cf-251 | Total α | <1.0E-30 | 10,000 | <1.0E-30 | 10,000 | <1.0E-30 | 10,000 | <1.0E-30 | 10,000 | <1.0E-30 | 10,000 |
| Cl-36 | 700 | 3.9E-08 | 10,000 | 1.1E-06 | 10,000 | 1.3E-06 | 9,980 | 1.3E-06 | 9,980 | 1.0E-06 | 10,000 |
| Cm-243 | Total α | <1.0E-30 | 2,820 | <1.0E-30 | 2,500 | <1.0E-30 | 2,520 | <1.0E-30 | 2,520 | <1.0E-30 | 2,600 |
| Cm-244 | Total α | <1.0E-30 | 1,840 | <1.0E-30 | 1,640 | <1.0E-30 | 1,640 | <1.0E-30 | 1,640 | <1.0E-30 | 1,700 |
| Cm-245 | Total α | <1.0E-30 | 10,000 | <1.0E-30 | 10,000 | <1.0E-30 | 10,000 | <1.0E-30 | 10,000 | <1.0E-30 | 10,000 |
| Cm-247 | Total α | <1.0E-30 | 10,000 | <1.0E-30 | 10,000 | <1.0E-30 | 10,000 | <1.0E-30 | 10,000 | <1.0E-30 | 10,000 |
| Cm-248 | Total α | <1.0E-30 | 10,000 | <1.0E-30 | 10,000 | <1.0E-30 | 10,000 | <1.0E-30 | 10,000 | <1.0E-30 | 10,000 |
| Co-60 | 100 | <1.0E-30 | 300 | <1.0E-30 | 420 | <1.0E-30 | 400 | <1.0E-30 | 400 | <1.0E-30 | 380 |
| Cs-135 | 900 | 2.2E-12 | 10,000 | 3.9E-08 | 10,000 | 4.3E-08 | 10,000 | 3.8E-08 | 10,000 | 3.9E-08 | 10,000 |
| Cs-137 | 200 | <1.0E-30 | 1,660 | <1.0E-30 | 1,660 | <1.0E-30 | 1,660 | <1.0E-30 | 1,680 | <1.0E-30 | 1,760 |
| Eu-152 | 200 | <1.0E-30 | 1,420 | <1.0E-30 | 1,280 | <1.0E-30 | 1,280 | <1.0E-30 | 1,280 | <1.0E-30 | 1,320 |
| Eu-154 | 60 | <1.0E-30 | 960 | <1.0E-30 | 840 | <1.0E-30 | 840 | <1.0E-30 | 840 | <1.0E-30 | 880 |
| Gd-152 | NC | <1.0E-30 | 10,000 | <1.0E-30 | 10,000 | <1.0E-30 | 10,000 | <1.0E-30 | 10,000 | <1.0E-30 | 10,000 |
| H-3 | 20,000 | 8.7E-16 | 440 | 1.4E-13 | 420 | 1.8E-13 | 420 | 1.8E-13 | 420 | 1.5E-13 | 420 |
| I-129 | 1 | 1.4E-04 | 10,000 | 1.5E-03 | 10,000 | 1.6E-03 | 10,000 | 1.7E-03 | 10,000 | 1.6E-03 | 10,000 |
| K-40 | NC | 1.0E-08 | 10,000 | 1.2E-07 | 10,000 | 1.3E-07 | 10,000 | 1.3E-07 | 10,000 | 1.1E-07 | 10,000 |
| Nb-93m | 1,000 | 7.7E-11 | 10,000 | 1.8E-05 | 10,000 | 2.4E-05 | 10,000 | 2.4E-05 | 10,000 | 2.0E-05 | 10,000 |
| Nb-94 | NC | 2.4E-12 | 9,940 | 8.2E-07 | 10,000 | 1.1E-06 | 10,000 | 1.1E-06 | 10,000 | 8.8E-07 | 10,000 |
| Ni-59 | 300 | 6.2E-13 | 10,000 | 1.8E-08 | 10,000 | 2.3E-08 | 10,000 | 2.3E-08 | 10,000 | 1.8E-08 | 10,000 |
| Ni-63 | 50 | 8.0E-24 | 2,540 | 4.3E-18 | 2,400 | 5.0E-18 | 2,420 | 4.7E-18 | 2,440 | 4.5E-18 | 2,420 |

Table 6.1-8: Radiological 1m Concentrations for Gordon Aquifer Sectors F through J (Continued)

| Radionuclide | MCL (pCi/L)** | Sector F Concentrations | | Sector G Concentrations | | Sector H Concentrations | | Sector I Concentrations | | Sector J Concentrations | |
|--------------|------------------|----------------------------|------------------|----------------------------|------------------|----------------------------|------------------|----------------------------|------------------|----------------------------|------------------|
| | | (pCi/L) | Year Peak Occurs | (pCi/L) | Year Peak Occurs | (pCi/L) | Year Peak Occurs | (pCi/L) | Year Peak Occurs | (pCi/L) | Year Peak Occurs |
| Np-237 | Total α | 1.8E-13 | 10,000 | 5.5E-08 | 10,000 | 7.5E-08 | 10,000 | 7.5E-08 | 10,000 | 6.2E-08 | 10,000 |
| Pa-231 | Total α | 2.2E-14 | 10,000 | 6.8E-09 | 10,000 | 9.3E-09 | 10,000 | 9.3E-09 | 10,000 | 7.7E-09 | 10,000 |
| Pb-210 | NC | 3.5E-09 | 10,000 | 4.4E-07 | 10,000 | 5.6E-07 | 10,000 | 5.7E-07 | 10,000 | 4.6E-07 | 10,000 |
| Pd-107 | NC | 3.7E-14 | 10,000 | 2.2E-09 | 10,000 | 2.9E-09 | 10,000 | 2.9E-09 | 10,000 | 2.4E-09 | 10,000 |
| Pt-193 | 3,000 | 9.9E-08 | 640 | 1.7E-06 | 580 | 2.1E-06 | 560 | 2.1E-06 | 560 | 1.7E-06 | 560 |
| Pu-238 | Total α | <1.0E-30 | 6,620 | <1.0E-30 | 9,400 | <1.0E-30 | 9,260 | 1.4E-68 | 9,240 | <1.0E-30 | 8,160 |
| Pu-239 | Total α | <1.0E-30 | 10,000 | <1.0E-30 | 10,000 | <1.0E-30 | 10,000 | <1.0E-30 | 10,000 | <1.0E-30 | 10,000 |
| Pu-240 | Total α | <1.0E-30 | 10,000 | <1.0E-30 | 10,000 | <1.0E-30 | 10,000 | <1.0E-30 | 10,000 | <1.0E-30 | 10,000 |
| Pu-241 | 300 | <1.0E-30 | 10,000 | <1.0E-30 | 10,000 | <1.0E-30 | 10,000 | <1.0E-30 | 10,000 | <1.0E-30 | 10,000 |
| Pu-242 | Total α | <1.0E-30 | 10,000 | <1.0E-30 | 10,000 | <1.0E-30 | 10,000 | <1.0E-30 | 10,000 | <1.0E-30 | 10,000 |
| Pu-244 | Total α | <1.0E-30 | 10,000 | <1.0E-30 | 10,000 | <1.0E-30 | 10,000 | <1.0E-30 | 10,000 | <1.0E-30 | 10,000 |
| Ra-226 | Total α/Ra | 1.3E-06 | 10,000 | 1.7E-04 | 10,000 | 2.2E-04 | 10,000 | 2.2E-04 | 10,000 | 1.8E-04 | 10,000 |
| Ra-228 | Total Ra | 2.8E-30 | 10,000 | 2.1E-28 | 10,000 | 1.9E-28 | 10,000 | 1.3E-28 | 10,000 | 1.1E-27 | 10,000 |
| Rn-222 | NC | <1.0E-30 | 10,000 | 1.7E-04 | 10,000 | 2.2E-04 | 10,000 | 2.2E-04 | 10,000 | 1.8E-04 | 10,000 |
| Se-79 | NC | <1.0E-30 | 10,000 | <1.0E-30 | 10,000 | <1.0E-30 | 10,000 | <1.0E-30 | 10,000 | <1.0E-30 | 10,000 |
| Sm-151 | 1,000 | <1.0E-30 | 7,840 | <1.0E-30 | 6,940 | <1.0E-30 | 6,960 | <1.0E-30 | 7,000 | <1.0E-30 | 9,980 |
| Sb-126 | NC | <1.0E-30 | 10,000 | <1.0E-30 | 10,000 | <1.0E-30 | 10,000 | <1.0E-30 | 10,000 | <1.0E-30 | 10,000 |
| Sb-126m | NC | <1.0E-30 | 10,000 | <1.0E-30 | 10,000 | <1.0E-30 | 10,000 | <1.0E-30 | 10,000 | <1.0E-30 | 10,000 |
| Sn-126 | NC | <1.0E-30 | 10,000 | <1.0E-30 | 10,000 | <1.0E-30 | 10,000 | <1.0E-30 | 10,000 | <1.0E-30 | 10,000 |
| Sr-90 | 8 | 1.2E-26 | 1,220 | 4.1E-21 | 1,340 | 4.1E-21 | 1,360 | 3.3E-21 | 1,360 | 3.9E-21 | 1,340 |
| Tc-99 | 900 | 1.2E-07 | 10,000 | 4.7E-03 | 10,000 | 6.1E-03 | 10,000 | 6.1E-03 | 10,000 | 4.9E-03 | 10,000 |
| Th-228 | Total α | 2.8E-30 | 10,000 | 2.1E-28 | 10,000 | 1.9E-28 | 10,000 | 1.3E-28 | 10,000 | 1.1E-27 | 10,000 |
| Th-229 | Total α | 8.3E-18 | 10,000 | 8.6E-14 | 10,000 | 1.2E-13 | 10,000 | 1.2E-13 | 10,000 | 1.4E-13 | 10,000 |
| Th-230 | Total α | 6.8E-26 | 10,000 | 4.5E-26 | 10,000 | 4.5E-26 | 10,000 | 3.7E-26 | 10,000 | 1.6E-24 | 10,000 |
| Th-232 | Total α | <1.0E-30 | 10,000 | <1.0E-30 | 10,000 | <1.0E-30 | 10,000 | <1.0E-30 | 10,000 | <1.0E-30 | 10,000 |
| U-232 | Total U* | <1.0E-30 | 4,600 | <1.0E-30 | 6,700 | <1.0E-30 | 6,600 | <1.0E-30 | 6,560 | <1.0E-30 | 5,760 |
| U-233 | Total U* | 2.4E-16 | 10,000 | 2.5E-12 | 10,000 | 3.5E-12 | 10,000 | 3.5E-12 | 10,000 | 4.8E-12 | 10,000 |
| U-234 | Total U* | 8.9E-23 | 10,000 | 9.1E-23 | 10,000 | 9.0E-23 | 10,000 | 7.3E-23 | 10,000 | 2.6E-21 | 10,000 |

Table 6.1-8: Radiological 1m Concentrations for Gordon Aquifer Sectors F through J (Continued)

| Radionuclide | MCL (pCi/L) | Sector F Concentrations | | Sector G Concentrations | | Sector H Concentrations | | Sector I Concentrations | | Sector J Concentrations | |
|--|----------------|----------------------------|------------------|----------------------------|------------------|----------------------------|------------------|----------------------------|------------------|----------------------------|------------------|
| | | (pCi/L) | Year Peak Occurs | (pCi/L) | Year Peak Occurs | (pCi/L) | Year Peak Occurs | (pCi/L) | Year Peak Occurs | (pCi/L) | Year Peak Occurs |
| U-235 | Total U* | 1.5E-24 | 10,000 | 1.5E-24 | 10,000 | 1.5E-24 | 10,000 | 1.2E-24 | 10,000 | 4.4E-23 | 10,000 |
| U-236 | Total U* | 2.4E-24 | 10,000 | 2.5E-24 | 10,000 | 2.5E-24 | 10,000 | 2.0E-24 | 10,000 | 7.2E-23 | 10,000 |
| U-238 | Total U* | 1.8E-24 | 10,000 | 1.9E-24 | 10,000 | 1.9E-24 | 10,000 | 1.5E-24 | 10,000 | 5.5E-23 | 10,000 |
| Y-90 | 60 | 1.2E-26 | 1,220 | 4.1E-21 | 1,340 | 4.1E-21 | 1,360 | 3.3E-21 | 1,360 | 3.9E-21 | 1,340 |
| Zr-93 | 2,000 | <1.0E-30 | 10,000 | <1.0E-30 | 10,000 | <1.0E-30 | 10,000 | <1.0E-30 | 10,000 | <1.0E-30 | 10,000 |
| Total alpha | 15 | 1.3E-06 | N/A | 1.7E-04 | N/A | 2.2E-04 | N/A | 2.2E-04 | N/A | 1.8E-04 | N/A |
| Total Ra | 5 | 1.3E-06 | N/A | 1.7E-04 | N/A | 2.2E-04 | N/A | 2.2E-04 | N/A | 1.8E-04 | N/A |
| Sum of beta-gamma MCL fractions | | 1.4E-04 | N/A | 1.5E-03 | N/A | 1.6E-03 | N/A | 1.7E-03 | N/A | 1.6E-03 | N/A |

* Total uranium is evaluated in Table 6.1-17

** MCL values for beta and photon emitters are calculated in Table II-3 of FR-00-9654 based on a beta-gamma dose of 4 mrem/yr

NC = Not Calculated

Table 6.1-9: Radiological 1m Concentrations for Gordon Aquifer Sectors K and L

| Radionuclide | MCL (pCi/L)** | Sector K Concentrations | | Sector L Concentrations | |
|--------------|--------------------|----------------------------|------------------|----------------------------|------------------|
| | | (pCi/L) | Year Peak Occurs | (pCi/L) | Year Peak Occurs |
| Ac-227 | NC | 6.0E-12 | 10,000 | 8.3E-12 | 10,000 |
| Al-26 | NC | <1.0E-30 | 10,000 | <1.0E-30 | 10,000 |
| Am-241 | Total α | <1.0E-30 | 10,000 | <1.0E-30 | 10,000 |
| Am-242m | Total α | <1.0E-30 | 10,000 | <1.0E-30 | 10,000 |
| Am-243 | Total α | <1.0E-30 | 10,000 | <1.0E-30 | 10,000 |
| Ba-137m | NC | <1.0E-30 | 1,740 | <1.0E-30 | 2,060 |
| C-14 | 2,000 | 3.0E-03 | 7,280 | 3.3E-03 | 6,740 |
| Cf-249 | Total α | <1.0E-30 | 10,000 | <1.0E-30 | 10,000 |
| Cf-251 | Total α | <1.0E-30 | 10,000 | <1.0E-30 | 10,000 |
| Cl-36 | 700 | 8.9E-07 | 9,960 | 1.0E-06 | 9,820 |
| Cm-243 | Total α | <1.0E-30 | 3,260 | <1.0E-30 | 2,880 |
| Cm-244 | Total α | <1.0E-30 | 1,680 | <1.0E-30 | 1,880 |
| Cm-245 | Total α | <1.0E-30 | 10,000 | <1.0E-30 | 10,000 |
| Cm-247 | Total α | <1.0E-30 | 10,000 | <1.0E-30 | 10,000 |
| Cm-248 | Total α | <1.0E-30 | 10,000 | <1.0E-30 | 10,000 |
| Co-60 | 100 | <1.0E-30 | 360 | <1.0E-30 | 320 |
| Cs-135 | 900 | 5.4E-08 | 10,000 | 1.9E-07 | 10,000 |
| Cs-137 | 200 | <1.0E-30 | 1,740 | <1.0E-30 | 2,060 |
| Eu-152 | 200 | <1.0E-30 | 1,320 | <1.0E-30 | 1,460 |
| Eu-154 | 60 | <1.0E-30 | 880 | <1.0E-30 | 960 |
| Gd-152 | NC | <1.0E-30 | 10,000 | <1.0E-30 | 10,000 |
| H-3 | 20,000 | 1.6E-13 | 420 | 2.8E-13 | 420 |
| I-129 | 1 | 1.0E-03 | 10,000 | 6.6E-04 | 10,000 |
| K-40 | NC | 9.9E-08 | 10,000 | 9.9E-08 | 10,000 |
| Nb-93m | 1,000 | 2.2E-05 | 10,000 | 3.6E-05 | 10,000 |
| Nb-94 | NC | 9.1E-07 | 10,000 | 1.3E-06 | 10,000 |
| Ni-59 | 300 | 1.9E-08 | 10,000 | 2.8E-08 | 10,000 |
| Ni-63 | 50 | 5.8E-18 | 2,380 | 1.8E-17 | 2,280 |
| Np-237 | Total α | 6.5E-08 | 10,000 | 8.9E-08 | 10,000 |
| Pa-231 | Total α | 8.0E-09 | 10,000 | 1.1E-08 | 10,000 |
| Pb-210 | NC | 4.8E-07 | 10,000 | 6.9E-07 | 10,000 |
| Pd-107 | NC | 2.5E-09 | 10,000 | 3.6E-09 | 10,000 |
| Pt-193 | 3,000 | 1.6E-06 | 540 | 2.1E-06 | 520 |
| Pu-238 | Total α | <1.0E-30 | 7,740 | 3.9E-56 | 6,760 |
| Pu-239 | Total α | <1.0E-30 | 10,000 | 3.9E-26 | 10,000 |
| Pu-240 | Total α | <1.0E-30 | 10,000 | 5.6E-27 | 10,000 |
| Pu-241 | 300 | <1.0E-30 | 10,000 | <1.0E-30 | 10,000 |
| Pu-242 | Total α | <1.0E-30 | 10,000 | 1.1E-28 | 10,000 |
| Pu-244 | Total α | <1.0E-30 | 10,000 | 2.2E-30 | 10,000 |
| Ra-226 | Total α /Ra | 1.9E-04 | 10,000 | 2.6E-04 | 10,000 |
| Ra-228 | Total Ra | 7.8E-27 | 10,000 | 6.5E-24 | 10,000 |
| Rn-222 | NC | 1.9E-04 | 10,000 | 2.6E-04 | 10,000 |

**Table 6.1-9: Radiological 1m Concentrations for Gordon Aquifer Sectors K and L
(Continued)**

| Radionuclide | MCL (pCi/L)** | Sector K Concentrations | | Sector L Concentrations | |
|--|----------------|----------------------------|------------------|----------------------------|------------------|
| | | (pCi/L) | Year Peak Occurs | (pCi/L) | Year Peak Occurs |
| Se-79 | NC | <1.0E-30 | 10,000 | <1.0E-30 | 10,000 |
| Sm-151 | 1,000 | <1.0E-30 | 9,100 | <1.0E-30 | 7,940 |
| Sb-126 | NC | <1.0E-30 | 10,000 | <1.0E-30 | 10,000 |
| Sb-126m | NC | <1.0E-30 | 10,000 | <1.0E-30 | 10,000 |
| Sn-126 | NC | <1.0E-30 | 10,000 | <1.0E-30 | 10,000 |
| Sr-90 | 8 | 6.7E-21 | 1,320 | 6.3E-20 | 1,260 |
| Tc-99 | 900 | 5.1E-03 | 10,000 | 7.2E-03 | 10,000 |
| Th-228 | Total α | 7.8E-27 | 10,000 | 6.5E-24 | 10,000 |
| Th-229 | Total α | 2.2E-13 | 10,000 | 1.4E-12 | 10,000 |
| Th-230 | Total α | 1.9E-23 | 10,000 | 6.3E-20 | 10,000 |
| Th-232 | Total α | 2.8E-30 | 10,000 | 9.2E-27 | 10,000 |
| U-232 | Total U* | <1.0E-30 | 5,440 | <1.0E-30 | 4,700 |
| U-233 | Total U* | 7.6E-12 | 10,000 | 3.8E-11 | 10,000 |
| U-234 | Total U* | 3.0E-20 | 10,000 | 7.7E-17 | 10,000 |
| U-235 | Total U* | 5.1E-22 | 10,000 | 1.3E-18 | 10,000 |
| U-236 | Total U* | 8.2E-22 | 10,000 | 2.1E-18 | 10,000 |
| U-238 | Total U* | 6.2E-22 | 10,000 | 1.6E-18 | 10,000 |
| Y-90 | 60 | 6.7E-21 | 1,320 | 6.3E-20 | 1,260 |
| Zr-93 | 2,000 | <1.0E-30 | 10,000 | <1.0E-30 | 10,000 |
| Total alpha | 15 | 1.9E-04 | N/A | 2.6E-04 | N/A |
| Total Ra | 5 | 1.9E-04 | N/A | 2.6E-04 | N/A |
| Sum of beta-gamma MCL fractions | | 1.0E-03 | N/A | 6.7E-04 | N/A |

* Total uranium is evaluated in Table 6.1-18

** MCL values for beta and photon emitters are calculated in Table II-3 of FR-00-9654 based on a beta-gamma dose of 4 mrem/yr

NC = Not Calculated

Table 6.1-10: Chemical 1m Concentrations for UTR-UZ Sectors A through E

| Chemical | MCL (µg/L) | Sector A Concentrations | | Sector B Concentrations | | Sector C Concentrations | | Sector D Concentrations | | Sector E Concentrations | |
|----------|---------------|----------------------------|---------------------|----------------------------|---------------------|----------------------------|---------------------|----------------------------|---------------------|----------------------------|---------------------|
| | | (µg/L) | Year Peak Occurs | (µg/L) | Year Peak Occurs | (µg/L) | Year Peak Occurs | (µg/L) | Year Peak Occurs | (µg/L) | Year Peak Occurs |
| Ag | NC | 1.5E-03 | 10,000 | 1.8E-03 | 10,000 | 1.8E-03 | 10,000 | 8.5E-04 | 10,000 | 1.6E-04 | 10,000 |
| As | 1.00E+01 | 1.6E-05 | 10,000 | 2.4E-05 | 10,000 | 2.6E-05 | 10,000 | 1.1E-05 | 10,000 | 5.1E-08 | 10,000 |
| Ba | 2.00E+03 | 3.1E-03 | 10,000 | 3.9E-03 | 10,000 | 4.5E-03 | 10,000 | 3.1E-03 | 10,000 | 1.7E-03 | 10,000 |
| Cd | 5.00E+00 | 4.8E-05 | 10,000 | 7.0E-05 | 10,000 | 7.6E-05 | 10,000 | 5.9E-05 | 10,000 | 1.5E-05 | 10,000 |
| Cr | 1.00E+02 | 1.9E-03 | 10,000 | 2.2E-03 | 10,000 | 2.3E-03 | 10,000 | 8.8E-04 | 10,000 | 1.3E-05 | 10,000 |
| Cu | NC | 1.0E-01 | 10,000 | 8.8E-02 | 10,000 | 1.7E-01 | 10,000 | 1.1E-01 | 10,000 | 1.6E-01 | 10,000 |
| F | NC | 2.2E-01 | 9,580 | 2.6E-01 | 9,580 | 2.6E-01 | 9,580 | 1.1E-01 | 9,600 | 2.1E-02 | 10,000 |
| Fe | NC | 9.2E-09 | 10,000 | 2.3E-08 | 10,000 | 3.9E-08 | 10,000 | 1.5E-08 | 10,000 | 1.1E-11 | 10,000 |
| Hg | 2.00E+00 | 9.2E-19 | 10,000 | 1.4E-17 | 10,000 | 9.9E-16 | 10,000 | 1.6E-16 | 10,000 | 2.8E-23 | 10,000 |
| Mn | NC | 2.2E-03 | 10,000 | 2.6E-03 | 10,000 | 2.7E-03 | 10,000 | 1.0E-03 | 10,000 | 1.0E-05 | 10,000 |
| N | 1.00E+04 | 5.9E+02 | 4,020 | 5.6E+02 | 4,020 | 8.5E+02 | 4,020 | 5.6E+02 | 4,020 | 6.6E+02 | 4,020 |
| Ni | NC | 2.8E-05 | 10,000 | 3.5E-05 | 10,000 | 3.5E-05 | 10,000 | 1.4E-05 | 10,000 | 9.6E-08 | 10,000 |
| Pb | 1.50E+01 | 1.3E-30 | 10,000 | 2.3E-28 | 10,000 | 2.5E-25 | 10,000 | 9.5E-27 | 10,000 | <1.0E-30 | 10,000 |
| Se | 5.00E+00 | 1.1E-19 | 10,000 | 3.0E-18 | 10,000 | 4.5E-16 | 10,000 | 5.7E-17 | 10,000 | 6.9E-24 | 10,000 |
| U | 3.00E+01 | 8.0E-09 | 10,000 | 1.9E-08 | 10,000 | 3.3E-08 | 10,000 | 1.3E-08 | 10,000 | 9.6E-12 | 10,000 |
| Zn | NC | 5.3E-06 | 10,000 | 7.9E-06 | 10,000 | 8.6E-06 | 10,000 | 3.6E-06 | 10,000 | 1.6E-08 | 10,000 |

NC = Not Calculated

Table 6.1-11: Chemical 1m Concentrations for UTR-UZ Sectors F through J

| Chemical | MCL (µg/L) | Sector F Concentrations | | Sector G Concentrations | | Sector H Concentrations | | Sector I Concentrations | | Sector J Concentrations | |
|----------|---------------|----------------------------|---------------------|----------------------------|---------------------|----------------------------|---------------------|----------------------------|---------------------|----------------------------|---------------------|
| | | (µg/L) | Year Peak Occurs | (µg/L) | Year Peak Occurs | (µg/L) | Year Peak Occurs | (µg/L) | Year Peak Occurs | (µg/L) | Year Peak Occurs |
| Ag | NC | 1.7E-04 | 10,000 | 2.8E-04 | 10,000 | 2.0E-04 | 10,000 | 2.5E-04 | 10,000 | 2.4E-04 | 10,000 |
| As | 1.00E+01 | 1.6E-10 | 10,000 | 2.0E-17 | 10,000 | 1.7E-17 | 10,000 | 1.4E-17 | 10,000 | 9.9E-18 | 10,000 |
| Ba | 2.00E+03 | 2.3E-03 | 10,000 | 4.1E-03 | 10,000 | 2.7E-03 | 10,000 | 3.8E-03 | 10,000 | 3.9E-03 | 10,000 |
| Cd | 5.00E+00 | 2.6E-07 | 10,000 | 6.5E-14 | 10,000 | 7.4E-14 | 10,000 | 5.2E-13 | 10,000 | 2.2E-10 | 10,000 |
| Cr | 1.00E+02 | 1.3E-07 | 10,000 | 6.1E-14 | 10,000 | 3.5E-14 | 10,000 | 2.5E-13 | 10,000 | 1.1E-10 | 10,000 |
| Cu | NC | 2.7E-01 | 10,000 | 4.6E-01 | 10,000 | 3.2E-01 | 10,000 | 4.2E-01 | 10,000 | 4.2E-01 | 10,000 |
| F | NC | 3.4E-02 | 10,000 | 6.1E-02 | 10,000 | 4.1E-02 | 10,000 | 5.8E-02 | 10,000 | 5.9E-02 | 10,000 |
| Fe | NC | 1.8E-14 | 10,000 | 1.2E-29 | 10,000 | 1.0E-29 | 10,000 | 6.8E-30 | 10,000 | 3.6E-30 | 10,000 |
| Hg | 2.00E+00 | 6.7E-26 | 10,000 | 1.1E-27 | 10,000 | 9.9E-28 | 10,000 | 5.1E-28 | 10,000 | 2.0E-28 | 10,000 |
| Mn | NC | 5.3E-06 | 10,000 | 9.0E-06 | 10,000 | 6.3E-06 | 10,000 | 8.3E-06 | 10,000 | 8.2E-06 | 10,000 |
| N | 1.00E+04 | 1.1E+03 | 4,020 | 2.0E+03 | 4,020 | 1.3E+03 | 4,020 | 1.8E+03 | 4,020 | 1.9E+03 | 4,020 |
| Ni | NC | 9.5E-11 | 10,000 | 2.8E-17 | 10,000 | 3.7E-18 | 10,000 | 6.3E-19 | 10,000 | 1.8E-18 | 10,000 |
| Pb | 1.50E+01 | <1.0E-30 | 10,000 | <1.0E-30 | 10,000 | <1.0E-30 | 10,000 | <1.0E-30 | 10,000 | <1.0E-30 | 10,000 |
| Se | 5.00E+00 | 5.9E-24 | 10,000 | 5.5E-24 | 10,000 | 5.0E-24 | 10,000 | 2.6E-24 | 10,000 | 9.5E-25 | 10,000 |
| U | 3.00E+01 | 1.6E-14 | 10,000 | 5.0E-24 | 10,000 | 4.3E-24 | 10,000 | 2.9E-24 | 10,000 | 1.6E-24 | 10,000 |
| Zn | NC | 1.8E-11 | 10,000 | 6.3E-25 | 10,000 | 5.3E-25 | 10,000 | 4.1E-25 | 10,000 | 1.4E-22 | 10,000 |

NC = Not Calculated

Table 6.1-12: Chemical 1m Concentrations for UTR-UZ Sectors K and L

| Chemical | MCL (µg/L) | Sector K Concentrations | | Sector L Concentrations | |
|----------|------------|-------------------------|------------------|-------------------------|------------------|
| | | (µg/L) | Year Peak Occurs | (µg/L) | Year Peak Occurs |
| Ag | NC | 5.7E-05 | 10,000 | 1.6E-04 | 10,000 |
| As | 1.00E+01 | 3.1E-16 | 10,000 | 1.7E-09 | 10,000 |
| Ba | 2.00E+03 | 1.0E-03 | 10,000 | 2.3E-03 | 10,000 |
| Cd | 5.00E+00 | 7.5E-09 | 10,000 | 8.6E-07 | 10,000 |
| Cr | 1.00E+02 | 3.5E-09 | 10,000 | 1.0E-06 | 10,000 |
| Cu | NC | 1.0E-01 | 10,000 | 2.6E-01 | 10,000 |
| F | NC | 1.5E-02 | 10,000 | 3.4E-02 | 10,000 |
| Fe | NC | 3.5E-22 | 10,000 | 6.7E-14 | 10,000 |
| Hg | 2.00E+00 | 1.5E-30 | 10,000 | 2.0E-27 | 10,000 |
| Mn | NC | 2.0E-06 | 10,000 | 5.2E-06 | 10,000 |
| N | 1.00E+04 | 4.8E+02 | 4,020 | 1.1E+03 | 4,020 |
| Ni | NC | 9.3E-15 | 10,000 | 8.4E-09 | 10,000 |
| Pb | 1.50E+01 | <1.0E-30 | 10,000 | <1.0E-30 | 10,000 |
| Se | 5.00E+00 | 5.7E-27 | 10,000 | 4.6E-24 | 10,000 |
| U | 3.00E+01 | 3.6E-22 | 10,000 | 6.3E-14 | 10,000 |
| Zn | NC | 9.5E-17 | 10,000 | 5.7E-10 | 10,000 |

NC = Not Calculated

Table 6.1-13: Chemical 1m Concentrations for UTR-LZ – Sectors A through E

| Chemical | MCL (µg/L) | Sector A Concentrations | | Sector B Concentrations | | Sector C Concentrations | | Sector D Concentrations | | Sector E Concentrations | |
|----------|---------------|----------------------------|---------------------|----------------------------|---------------------|----------------------------|------------------|----------------------------|---------------------|----------------------------|---------------------|
| | | (µg/L) | Year Peak Occurs | (µg/L) | Year Peak Occurs | (µg/L) | Year Peak Occurs | (µg/L) | Year Peak Occurs | (µg/L) | Year Peak Occurs |
| Ag | NC | 3.8E-03 | 10,000 | 4.2E-03 | 10,000 | 4.0E-03 | 10,000 | 1.0E-03 | 10,000 | 1.6E-04 | 10,000 |
| As | 1.00E+01 | 4.4E-05 | 10,000 | 5.9E-05 | 10,000 | 6.0E-05 | 10,000 | 1.2E-05 | 10,000 | 5.2E-08 | 10,000 |
| Ba | 2.00E+03 | 8.7E-03 | 10,000 | 9.3E-03 | 10,000 | 8.9E-03 | 10,000 | 4.4E-03 | 9,780 | 1.5E-03 | 10,000 |
| Cd | 5.00E+00 | 1.6E-04 | 10,000 | 1.9E-04 | 10,000 | 1.9E-04 | 10,000 | 1.1E-04 | 10,000 | 1.9E-05 | 10,000 |
| Cr | 1.00E+02 | 4.8E-03 | 10,000 | 5.2E-03 | 10,000 | 5.0E-03 | 10,000 | 1.0E-03 | 10,000 | 1.5E-05 | 10,000 |
| Cu | NC | 1.9E-01 | 10,000 | 2.0E-01 | 10,000 | 1.8E-01 | 10,000 | 1.1E-01 | 10,000 | 1.2E-01 | 10,000 |
| F | NC | 5.8E-01 | 9,600 | 5.9E-01 | 9,600 | 5.7E-01 | 9,600 | 1.2E-01 | 9,600 | 1.7E-02 | 10,000 |
| Fe | NC | 3.8E-08 | 10,000 | 8.1E-08 | 10,000 | 9.1E-08 | 10,000 | 1.5E-08 | 10,000 | 1.1E-11 | 10,000 |
| Hg | 2.00E+00 | 2.3E-17 | 10,000 | 2.8E-16 | 10,000 | 1.0E-15 | 10,000 | 4.7E-17 | 10,000 | 1.1E-23 | 10,000 |
| Mn | NC | 5.6E-03 | 10,000 | 6.1E-03 | 10,000 | 5.9E-03 | 10,000 | 1.2E-03 | 10,000 | 9.5E-06 | 10,000 |
| N | 1.00E+04 | 1.3E+03 | 4,040 | 1.3E+03 | 4,020 | 1.1E+03 | 10,000 | 6.0E+02 | 4,020 | 5.3E+02 | 4,020 |
| Ni | NC | 7.3E-05 | 10,000 | 8.1E-05 | 10,000 | 7.9E-05 | 10,000 | 1.5E-05 | 10,000 | 9.7E-08 | 10,000 |
| Pb | 1.50E+01 | 2.4E-29 | 10,000 | 1.9E-27 | 10,000 | 2.3E-26 | 10,000 | 2.7E-28 | 10,000 | <1.0E-30 | 10,000 |
| Se | 5.00E+00 | 3.5E-18 | 10,000 | 6.1E-17 | 10,000 | 3.1E-16 | 10,000 | 1.0E-17 | 10,000 | 9.2E-25 | 10,000 |
| U | 3.00E+01 | 3.3E-08 | 10,000 | 6.8E-08 | 10,000 | 7.7E-08 | 10,000 | 1.3E-08 | 10,000 | 9.7E-12 | 10,000 |
| Zn | NC | 1.5E-05 | 10,000 | 2.0E-05 | 10,000 | 2.0E-05 | 10,000 | 3.9E-06 | 10,000 | 1.6E-08 | 10,000 |

NC = Not Calculated

Table 6.1-14: Chemical 1m Concentrations for UTR-LZ Sectors F through J

| Chemical | MCL (µg/L) | Sector F Concentrations | | Sector G Concentrations | | Sector H Concentrations | | Sector I Concentrations | | Sector J Concentrations | |
|----------|---------------|----------------------------|---------------------|----------------------------|---------------------|----------------------------|---------------------|----------------------------|---------------------|----------------------------|---------------------|
| | | (µg/L) | Year Peak Occurs | (µg/L) | Year Peak Occurs | (µg/L) | Year Peak Occurs | (µg/L) | Year Peak Occurs | (µg/L) | Year Peak Occurs |
| Ag | NC | 8.7E-05 | 10,000 | 1.2E-04 | 10,000 | 1.3E-04 | 10,000 | 1.5E-04 | 10,000 | 1.3E-04 | 10,000 |
| As | 1.00E+01 | 1.4E-10 | 10,000 | 4.1E-18 | 10,000 | 4.2E-18 | 10,000 | 4.4E-18 | 10,000 | 3.6E-17 | 10,000 |
| Ba | 2.00E+03 | 1.3E-03 | 10,000 | 2.7E-03 | 10,000 | 2.9E-03 | 10,000 | 3.5E-03 | 10,000 | 3.3E-03 | 10,000 |
| Cd | 5.00E+00 | 2.7E-07 | 10,000 | 6.8E-12 | 10,000 | 3.4E-11 | 10,000 | 4.2E-10 | 10,000 | 1.4E-08 | 10,000 |
| Cr | 1.00E+02 | 1.3E-07 | 10,000 | 6.3E-12 | 10,000 | 1.8E-11 | 10,000 | 2.0E-10 | 10,000 | 6.4E-09 | 10,000 |
| Cu | NC | 1.5E-01 | 10,000 | 2.2E-01 | 10,000 | 2.4E-01 | 10,000 | 2.9E-01 | 10,000 | 2.6E-01 | 10,000 |
| F | NC | 2.0E-02 | 10,000 | 4.1E-02 | 10,000 | 4.4E-02 | 10,000 | 5.3E-02 | 10,000 | 5.0E-02 | 10,000 |
| Fe | NC | 1.3E-14 | 10,000 | 1.2E-30 | 10,000 | 1.2E-30 | 10,000 | 9.8E-31 | 10,000 | 7.7E-28 | 10,000 |
| Hg | 2.00E+00 | 2.2E-26 | 10,000 | 1.3E-29 | 10,000 | 1.3E-29 | 10,000 | 6.1E-30 | 10,000 | <1.0E-30 | 10,000 |
| Mn | NC | 2.9E-06 | 10,000 | 4.5E-06 | 10,000 | 4.9E-06 | 10,000 | 6.0E-06 | 10,000 | 5.3E-06 | 10,000 |
| N | 1.00E+04 | 6.3E+02 | 4,020 | 1.3E+03 | 4,040 | 1.4E+03 | 4,040 | 1.7E+03 | 4,040 | 1.6E+03 | 4,040 |
| Ni | NC | 8.6E-11 | 10,000 | 3.7E-15 | 10,000 | 2.5E-15 | 10,000 | 1.8E-15 | 10,000 | 2.0E-15 | 10,000 |
| Pb | 1.50E+01 | <1.0E-30 | 10,000 | <1.0E-30 | 10,000 | <1.0E-30 | 10,000 | <1.0E-30 | 10,000 | <1.0E-30 | 10,000 |
| Se | 5.00E+00 | 3.4E-25 | 10,000 | 5.2E-26 | 10,000 | 4.9E-26 | 10,000 | 2.2E-26 | 10,000 | 1.9E-28 | 10,000 |
| U | 3.00E+01 | 1.2E-14 | 10,000 | 5.6E-25 | 10,000 | 5.6E-25 | 10,000 | 4.9E-25 | 10,000 | 7.7E-26 | 10,000 |
| Zn | NC | 1.6E-11 | 10,000 | 1.3E-24 | 10,000 | 4.1E-25 | 10,000 | 1.3E-25 | 10,000 | 1.1E-20 | 10,000 |

NC = Not Calculated

Table 6.1-15: Chemical 1m Concentrations for UTR-LZ Sectors K and L

| Chemical | MCL (µg/L) | Sector K Concentration | | Sector L Concentration | |
|----------|------------|---------------------------|------------------|---------------------------|------------------|
| | | (µg/L) | Year Peak Occurs | (µg/L) | Year Peak Occurs |
| Ag | NC | 1.1E-04 | 10,000 | 1.0E-04 | 10,000 |
| As | 1.00E+01 | 2.4E-15 | 10,000 | 1.1E-08 | 10,000 |
| Ba | 2.00E+03 | 2.8E-03 | 10,000 | 2.1E-03 | 10,000 |
| Cd | 5.00E+00 | 9.8E-08 | 10,000 | 5.8E-06 | 10,000 |
| Cr | 1.00E+02 | 4.6E-08 | 10,000 | 5.0E-06 | 10,000 |
| Cu | NC | 2.2E-01 | 10,000 | 1.9E-01 | 10,000 |
| F | NC | 4.3E-02 | 10,000 | 3.2E-02 | 10,000 |
| Fe | NC | 2.4E-21 | 10,000 | 9.0E-13 | 10,000 |
| Hg | 2.00E+00 | <1.0E-30 | 10,000 | 3.3E-25 | 10,000 |
| Mn | NC | 4.5E-06 | 10,000 | 3.8E-06 | 10,000 |
| N | 1.00E+04 | 1.4E+03 | 4,040 | 1.0E+03 | 4,020 |
| Ni | NC | 4.4E-14 | 10,000 | 4.0E-08 | 10,000 |
| Pb | 1.50E+01 | <1.0E-30 | 10,000 | <1.0E-30 | 10,000 |
| Se | 5.00E+00 | 4.5E-28 | 10,000 | 7.9E-26 | 10,000 |
| U | 3.00E+01 | 2.4E-21 | 10,000 | 8.2E-13 | 10,000 |
| Zn | NC | 5.3E-16 | 10,000 | 3.6E-09 | 10,000 |

NC = Not Calculated

Table 6.1-16: Chemical 1m Concentrations for Gordon Aquifer Sectors A through E

| Chemical | MCL (µg/L) | Sector A Concentrations | | Sector B Concentrations | | Sector C Concentrations | | Sector D Concentrations | | Sector E Concentrations | |
|----------|---------------|----------------------------|---------------------|----------------------------|---------------------|----------------------------|---------------------|----------------------------|---------------------|----------------------------|---------------------|
| | | (µg/L) | Year Peak Occurs | (µg/L) | Year Peak Occurs | (µg/L) | Year Peak Occurs | (µg/L) | Year Peak Occurs | (µg/L) | Year Peak Occurs |
| Ag | NC | 9.1E-09 | 10,000 | 8.1E-09 | 10,000 | 4.7E-09 | 10,000 | 3.3E-10 | 10,000 | 2.1E-11 | 10,000 |
| As | 1.00E+01 | 6.0E-12 | 10,000 | 6.0E-12 | 10,000 | 4.6E-12 | 10,000 | 2.8E-13 | 10,000 | 5.7E-16 | 10,000 |
| Ba | 2.00E+03 | 6.2E-06 | 10,000 | 5.1E-06 | 10,000 | 3.1E-06 | 10,000 | 1.2E-06 | 10,000 | 2.3E-07 | 10,000 |
| Cd | 5.00E+00 | 1.6E-07 | 10,000 | 1.5E-07 | 10,000 | 1.0E-07 | 10,000 | 4.9E-08 | 10,000 | 4.2E-09 | 10,000 |
| Cr | 1.00E+02 | 1.2E-06 | 10,000 | 9.3E-07 | 10,000 | 4.7E-07 | 10,000 | 5.3E-08 | 10,000 | 2.1E-09 | 10,000 |
| Cu | NC | 3.8E-06 | 10,000 | 3.2E-06 | 10,000 | 1.8E-06 | 10,000 | 3.1E-07 | 10,000 | 2.2E-07 | 10,000 |
| F | NC | 1.2E-03 | 9,800 | 9.6E-04 | 9,840 | 5.1E-04 | 9,860 | 5.6E-05 | 10,000 | 2.0E-05 | 10,000 |
| Fe | NC | 3.9E-17 | 10,000 | 7.2E-17 | 10,000 | 7.1E-17 | 10,000 | 3.5E-18 | 10,000 | 8.6E-22 | 10,000 |
| Hg | 2.00E+00 | 1.9E-30 | 10,000 | 2.0E-29 | 10,000 | 7.0E-29 | 10,000 | 1.1E-30 | 10,000 | 8.8E-38 | 10,000 |
| Mn | NC | 3.2E-08 | 10,000 | 2.4E-08 | 10,000 | 1.1E-08 | 10,000 | 7.3E-10 | 10,000 | 4.0E-12 | 10,000 |
| N | 1.00E+04 | 2.8E+00 | 4,680 | 2.3E+00 | 4,680 | 1.4E+00 | 4,680 | 6.5E-01 | 4,700 | 6.5E-01 | 5,200 |
| Ni | NC | 7.2E-09 | 10,000 | 5.4E-09 | 10,000 | 2.6E-09 | 10,000 | 1.8E-10 | 10,000 | 9.7E-13 | 10,000 |
| Pb | 1.50E+01 | <1.0E-30 | 10,000 | <1.0E-30 | 10,000 | <1.0E-30 | 10,000 | <1.0E-30 | 10,000 | <1.0E-30 | 10,000 |
| Se | 5.00E+00 | <1.0E-30 | 10,000 | 1.3E-30 | 10,000 | 5.6E-30 | 10,000 | <1.0E-30 | 10,000 | <1.0E-30 | 10,000 |
| U | 3.00E+01 | 6.5E-17 | 10,000 | 1.2E-16 | 10,000 | 1.2E-16 | 10,000 | 5.8E-18 | 10,000 | 1.5E-21 | 10,000 |
| Zn | NC | 2.0E-12 | 10,000 | 2.0E-12 | 10,000 | 1.5E-12 | 10,000 | 9.2E-14 | 10,000 | 1.9E-16 | 10,000 |

NC = Not Calculated

Table 6.1-17: Chemical 1m Concentrations for Gordon Aquifer Sectors F through J

| Chemical | MCL (µg/L) | Sector F Concentrations | | Sector G Concentrations | | Sector H Concentrations | | Sector I Concentrations | | Sector J Concentrations | |
|----------|---------------|----------------------------|---------------------|----------------------------|---------------------|----------------------------|---------------------|----------------------------|---------------------|----------------------------|---------------------|
| | | (µg/L) | Year Peak Occurs | (µg/L) | Year Peak Occurs | (µg/L) | Year Peak Occurs | (µg/L) | Year Peak Occurs | (µg/L) | Year Peak Occurs |
| Ag | NC | 1.8E-11 | 10,000 | 4.9E-10 | 10,000 | 5.1E-10 | 10,000 | 4.2E-10 | 10,000 | 4.7E-10 | 10,000 |
| As | 1.00E+01 | 3.3E-19 | 10,000 | 8.0E-15 | 10,000 | 7.4E-15 | 10,000 | 4.8E-15 | 10,000 | 9.2E-15 | 10,000 |
| Ba | 2.00E+03 | 2.1E-07 | 10,000 | 6.6E-06 | 10,000 | 6.8E-06 | 10,000 | 6.4E-06 | 10,000 | 4.8E-06 | 10,000 |
| Cd | 5.00E+00 | 3.7E-11 | 10,000 | 1.9E-07 | 10,000 | 1.8E-07 | 10,000 | 1.5E-07 | 10,000 | 9.3E-08 | 10,000 |
| Cr | 1.00E+02 | 1.8E-11 | 10,000 | 6.6E-07 | 10,000 | 8.4E-07 | 10,000 | 8.4E-07 | 10,000 | 6.8E-07 | 10,000 |
| Cu | NC | 2.4E-07 | 10,000 | 1.4E-06 | 10,000 | 1.5E-06 | 10,000 | 1.4E-06 | 10,000 | 1.4E-06 | 10,000 |
| F | NC | 1.9E-05 | 10,000 | 8.4E-04 | 9,940 | 1.1E-03 | 9,880 | 1.1E-03 | 9,900 | 8.6E-04 | 9,920 |
| Fe | NC | 3.9E-25 | 10,000 | 3.1E-25 | 10,000 | 3.0E-25 | 10,000 | 2.5E-25 | 10,000 | 9.8E-24 | 10,000 |
| Hg | 2.00E+00 | <1.0E-30 | 10,000 | <1.0E-30 | 10,000 | <1.0E-30 | 10,000 | <1.0E-30 | 10,000 | <1.0E-30 | 10,000 |
| Mn | NC | 3.9E-13 | 10,000 | 1.4E-08 | 10,000 | 1.8E-08 | 10,000 | 1.8E-08 | 10,000 | 1.5E-08 | 10,000 |
| N | 1.00E+04 | 6.5E-01 | 5,200 | 7.6E+00 | 4,720 | 8.5E+00 | 4,720 | 8.9E+00 | 4,720 | 8.0E+00 | 4,740 |
| Ni | NC | 6.9E-16 | 10,000 | 3.7E-09 | 10,000 | 4.9E-09 | 10,000 | 5.0E-09 | 10,000 | 4.1E-09 | 10,000 |
| Pb | 1.50E+01 | <1.0E-30 | 10,000 | <1.0E-30 | 10,000 | <1.0E-30 | 10,000 | <1.0E-30 | 10,000 | <1.0E-30 | 10,000 |
| Se | 5.00E+00 | <1.0E-30 | 10,000 | <1.0E-30 | 10,000 | <1.0E-30 | 10,000 | <1.0E-30 | 10,000 | <1.0E-30 | 10,000 |
| U | 3.00E+01 | 6.9E-25 | 10,000 | 7.1E-25 | 10,000 | 7.0E-25 | 10,000 | 5.7E-25 | 10,000 | 2.1E-23 | 10,000 |
| Zn | NC | 6.8E-20 | 10,000 | 2.6E-15 | 10,000 | 2.4E-15 | 10,000 | 1.6E-15 | 10,000 | 3.0E-15 | 10,000 |

NC = Not Calculated

Table 6.1-18: Chemical 1m Concentrations for Gordon Aquifer Sectors K and L

| Chemical | MCL (µg/L) | Sector K Concentration | | Sector L Concentration | |
|----------|------------|---------------------------|------------------|---------------------------|------------------|
| | | (µg/L) | Year Peak Occurs | (µg/L) | Year Peak Occurs |
| Ag | NC | 7.0E-10 | 10,000 | 3.7E-09 | 10,000 |
| As | 1.00E+01 | 2.5E-14 | 10,000 | 8.2E-13 | 10,000 |
| Ba | 2.00E+03 | 4.5E-06 | 10,000 | 5.5E-06 | 10,000 |
| Cd | 5.00E+00 | 9.6E-08 | 10,000 | 1.4E-07 | 10,000 |
| Cr | 1.00E+02 | 7.1E-07 | 10,000 | 1.0E-06 | 10,000 |
| Cu | NC | 1.3E-06 | 10,000 | 2.4E-06 | 10,000 |
| F | NC | 8.3E-04 | 9,860 | 1.0E-03 | 9,820 |
| Fe | NC | 1.2E-22 | 10,000 | 3.3E-19 | 10,000 |
| Hg | 2.00E+00 | <1.0E-30 | 10,000 | <1.0E-30 | 10,000 |
| Mn | NC | 1.7E-08 | 10,000 | 2.6E-08 | 10,000 |
| N | 1.00E+04 | 5.4E+00 | 4,720 | 3.7E+00 | 4,700 |
| Ni | NC | 4.3E-09 | 10,000 | 6.2E-09 | 10,000 |
| Pb | 1.50E+01 | <1.0E-30 | 10,000 | <1.0E-30 | 10,000 |
| Se | 5.00E+00 | <1.0E-30 | 10,000 | <1.0E-30 | 10,000 |
| U | 3.00E+01 | 2.3E-22 | 10,000 | 5.9E-19 | 10,000 |
| Zn | NC | 8.2E-15 | 10,000 | 2.7E-13 | 10,000 |

NC = Not Calculated

6.2 Acute Exposure Scenarios

The Acute Intruder Scenario description and results are not presented as a Base Case. Rather, the Acute Intruder Scenario results are presented in Section 6.5 as a sensitivity case. As discussed in Section 4.2.4.2, the stabilized contaminant materials after SDF closure will be protected by significant, long lasting materials which are clearly distinguishable from the surrounding soil and make drilling an impractical scenario based on regional drilling practices. Regional drilling conditions are such that a well driller would stop operations and move their drilling location upon encountering barriers, such as the closure cap erosion barrier, disposal unit concrete roof, or clean grout on top of the saltstone monolith.

6.2.1 Acute Intruder Ingestion Dose Pathways – Ingestion of Resuspended Drill Cuttings

The drill cuttings ingestion exposure route assumes the drill cuttings from the well installation are distributed across the garden. The receptor, in turn, is exposed by ingesting dirt. The source of material is saltstone that is assumed to be penetrated during well installation. Only the exposure from the drill cuttings is included in this calculation (this does not include any other ingestion sources). Unless otherwise noted, formulas were based on those used in LADTAP model or in the PA for the Tank Farm Facility at INEEL. [WSRC-STI-2006-00123, DOE-ID-10966]

While these documents were used as guides for the other formulas, ultimately the basis for all the formulas can be traced to Regulatory Guide 1.109. The dose is calculated using the following formula. Unit conversions are not explicitly stated in the equations, but are coded into the GoldSim dose calculator.

$$D = \frac{M_{DC} \times F_{DC} \times U_S \times DCF}{\frac{d_w^2}{4} \times \pi \times l_w \times \rho_{SS}}$$

where:

| | | |
|-------------|---|--|
| M_{DC} | = | maximum drill core activity or mass (Ci or kg) |
| F_{DC} | = | fraction of time exposed to drill cuttings (unitless) [0.0023 equates to 20 hours] |
| DCF | = | ingestion dose conversion factor (rem/μCi), Table 4.7-1 |
| U_S | = | human consumption rate of dirt (kg/yr), Table 4.6-7 |
| d_w | = | well diameter (ft) [0.667 feet] |
| l_w | = | well depth (ft) [100 feet] |
| ρ_{SS} | = | density of sandy soil (g/cm ³) |

6.2.2 Acute Intruder Inhalation Dose Pathways – Inhalation of Drill Cuttings

The drill cuttings inhalation route assumes the drill cuttings from the well installation are distributed across the garden. The receptor in turn is directly exposed during time spent in the garden. The source of material is saltstone that is assumed to be penetrated during well installation. Only the exposure from the drill cuttings is included in this calculation (this does not include any other direct exposure sources). This formula was derived following the approach of the previous pathway calculations, whose bases are found in other PA methods. The dose is calculated using the following formula.

$$D = \frac{M_{DC} \times F_{DC} \times DCF \times U_A \times L_{SiA}}{\frac{d_w^2}{4} \times \pi \times l_w \times \rho_{SS}}$$

where:

| | | |
|-------------|---|--|
| M_{DC} | = | maximum drill core activity or mass (Ci or kg) |
| F_{DC} | = | fraction of time exposed to drill cuttings (unitless) [0.0023 equates to 20 hours] |
| DCF | = | inhalation dose conversion factor (rem/μCi), Table 4.7-1 |
| l_w | = | well depth (ft) [100 feet] |
| d_w | = | well diameter (ft) [0.667 feet] |
| U_A | = | air intake (m ³ /yr), Table 4.6-7 |
| L_{SiA} | = | soil loading in air while working in a garden (kg/m ³), Table 4.6-6 |
| ρ_{SS} | = | density of sandy soil (g/cm ³) |

6.2.3 Acute Intruder Direct Exposure Dose Pathways – Direct Exposure to Drill Cuttings

The drill cuttings direct exposure route assumes the receptor is directly exposed to the drill cuttings during well drilling operations. The source of material is saltstone that is assumed to be penetrated during well installation. Only the exposure from the drill cuttings is included in this calculation (this does not include any other direct exposure sources). This formula was derived following the approach of the previous pathway calculations, whose bases are found in other PA methods. The dose is calculated using the following formula.

$$D = \frac{M_{DC} \times F_{DC} \times DCF}{\frac{d_w^2}{4} \times \pi \times l_w}$$

where:

| | | |
|----------|---|---|
| M_{DC} | = | maximum drill core activity or mass (Ci or kg) |
| F_{DC} | = | fraction of time exposed to drill cuttings (unitless) [0.0023 equates to 20 hours] |
| DCF | = | external dose conversion factor, 15 cm (rem/yr per $\mu\text{Ci}/\text{m}^3$), Table 4.7-1 |
| d_w | = | well diameter (ft) [0.667 feet] |
| l_w | = | well depth (ft) [100 feet] |

6.3 Chronic Exposure Scenarios

The exposure pathways for the SDF intruder are discussed in detail in Section 4.2.4.2. The Chronic Intruder Agricultural (Post-Drilling) Scenario analyzed in this PA is graphically represented in Figure 4.2-29. Provided below are the individual elements of the Chronic Intruder biotic pathways that were identified for analysis and inclusion in the Chronic Intruder Agricultural (Post-Drilling) Scenario dose. The GoldSim computer code was used to calculate doses following the dose formulas provided below and utilizing the PORFLOW calculated 1m concentrations as inputs. Unless otherwise noted, formulas were based on those used in LADTAP model report WSRC-STI-2006-00123 or in the PA for Idaho Tank Farm Facility, document DOE-ID-10966. While these documents were used as guides for the other formulas, ultimately the bases for all the formulas can be traced to Regulatory Guide 1.109. Unit conversions are not explicitly stated in the equations, but are coded into GoldSim.

6.3.1 Chronic Intruder Ingestion Dose Pathways

Ingestion of Water

The drinking water exposure route assumes the receptor uses a well located 1m from the SDF as a drinking water source. The incidental ingestion of water from showering and during recreational activities is assumed to be negligible when compared to ingestion of drinking water.

$$D = C_{GW} \times U_w \times DCF$$

where:

- D = dose from 1 year's consumption of contaminated media; in this equation, groundwater (rem/yr)
- C_{GW} = radionuclide concentration in groundwater from a well located at 1m (pCi/L)
- U_W = human consumption rate of water (L/yr), Table 4.6-7
- DCF = ingestion dose conversion factor (rem/ μ Ci), Table 4.7-1

Ingestion of Beef and Milk

The beef and dairy exposure route assumes cattle drink contaminated water and eat contaminated fodder and the intruder in turn consumes the contaminated beef and milk from the cattle. Beef and milk are treated separately. The dose is calculated using

Beef:

$$D = T_B \times (FF_B \times C_f \times Q_{FB} + C_{GW} \times Q_{WB}) \times DCF \times U_B \times F_B$$

Milk:

$$D = T_M \times (FF_M \times C_f \times Q_{FM} + C_{GW} \times Q_{WM}) \times DCF \times U_M \times F_M$$

where:

- T_B = beef transfer coefficient (d/kg), Table 4.6-3
- T_M = milk transfer coefficient (d/L), Table 4.6-2
- FF_i = beef or milk cattle intake fraction from irrigated field/pasture, Table 4.6-7
- C_f = radionuclide concentration in fodder (pCi/kg)
- Q_{Fi} = consumption rate of fodder by beef or milk cattle (kg/d), Table 4.6-7
- C_{GW} = radionuclide concentration in groundwater from a 1m well (pCi/L)
- Q_{Wi} = consumption rate of water by beef or milk cattle (L/d), Table 4.6-7
- DCF = ingestion dose conversion factor (rem/ μ Ci), Table 4.7-1
- U_B = human consumption rate of beef (kg/yr), Table 4.6-7
- U_M = human consumption rate of milk (L/yr), Table 4.6-7
- F_B = fraction of beef produced locally (unitless), Table 4.6-5
- F_M = fraction of milk produced locally (unitless), Table 4.6-5

Ingestion of Vegetables

The dose to humans from ingestion of contaminated leafy vegetables and produce is calculated assuming three contamination routes, (1) direct deposition of contaminated irrigation water on plants, (2) deposition of contaminated irrigation water on soil followed by root uptake by plants, and (3) deposition of contaminated drill cuttings in soil followed by root uptake by plants. Leafy vegetables and produce are treated separately. The dose is calculated using:

$$D_{IV} = D_{GW} + D_{DC}$$

where:

D_{IV} = the intruder dose from vegetable intake (rem)

D_{GW} = the vegetable dose to intruder associated with using contaminated well water (rem)

D_{DC} = the vegetable dose to intruder associated with drill cutting in the garden soil (rem)

$$D_{GW} = C_{GW} \times I \times (LEAF + ROOT) \times DCF \times (U_{LV} \times k + U_{OV}) \times FV \times e^{-\lambda_e t_i}$$

$$D_{DC} = C_{SD} \times \frac{T_{SV}}{\rho_S} \times DCF \times (U_{LV} \times k + U_{OV}) \times FV$$

$$LEAF = \frac{r \times (1 - e^{-\lambda_e t_v})}{Y_v \times \lambda}$$

$$ROOT = \frac{T_{SV} \times (1 - e^{-\lambda_i t_b})}{\rho_S \times \lambda_i}$$

$$\lambda_e = \lambda_i + \lambda_w$$

where:

C_{GW} = radionuclide concentration in groundwater from a 1m well (pCi/L)

I = irrigation rate (L/m²-d), Table 4.6-6

$LEAF$ = radionuclide concentration in the vegetable's leaves (m²d/kg)

$ROOT$ = radionuclide concentration in the vegetable's roots (m²d/kg)

DCF = ingestion dose conversion factor (rem/μCi), Table 4.7-1

U_{LV} = human consumption rate of leafy vegetables (kg/yr), Table 4.6-7

U_{OV} = human consumption rate of other vegetables (produce) (kg/yr), Table 4.6-7

k = fraction retention of deposition on leaves (unitless) [1]

| | | |
|-------------|---|---|
| FV | = | fraction of leafy vegetables and produce produced locally (unitless), Table 4.6-5 |
| r | = | fraction of material deposited on leaves that is retained (unitless), Table 4.6-6 |
| λ_e | = | weathering and radiological decay constant (L/d) |
| λ_w | = | weathering decay constant (0.0495/d) |
| t_V | = | time vegetables are exposed to irrigation (d), Table 4.6-5 |
| Y_V | = | vegetation production yield (kg/m ²), Table 4.6-5 |
| T_{SV} | = | soil to vegetable ratio (unitless), Table 4.6-1 |
| ρ_s | = | surface soil density (kg/m ²), Table 4.6-6 |
| t_b | = | buildup time of radionuclides in soil, Table 4.6-1 |
| λ_i | = | radiological decay constant |
| C_{SD} | = | concentration in soil due to drill cuttings (pCi/m ³) |
| t_t | = | transport time (d), assumed to be zero |

Ingestion of Fish

The fish exposure route assumes fish are caught from a stream contaminated from the aquifer with the highest concentration, and the receptor in turn consumes the contaminated fish. The dose is calculated using the following formula.

$$D = C_S \times U_F \times T_F \times DCF$$

where:

| | | |
|-------|---|--|
| C_S | = | radionuclide concentration in groundwater at the seep line (pCi/L) |
| U_F | = | human consumption rate of finfish (kg/yr), Table 4.6-7 |
| T_F | = | fish bioaccumulation factor (L/kg), Table 4.6-4 |
| DCF | = | ingestion dose conversion factor (rem/μCi) Table 4.7-1 |

Ingestion of Soil

The soil ingestion exposure route assumes soil is irrigated with groundwater from a well 1m from SDF and the receptor in turn consumes the contaminated soil. This formula was derived following the approach of the previous pathway calculations, whose bases are found in other PA methods. The dose is calculated using the following formula.

$$D = \frac{(C_D + C_W) \times DCF \times U_S}{\rho_{SS}}$$

where:

| | | |
|-------------|---|--|
| C_D | = | radionuclide concentration in soil contaminated with drill cuttings (pCi/m ³) |
| C_W | = | radionuclide concentration in soil irrigated with water from a 1m well (pCi/m ³) |
| DCF | = | ingestion dose conversion factor (rem/μCi), Table 4.7-1 |
| U_S | = | human consumption rate of dirt (kg/yr), Table 4.6-7 |
| ρ_{SS} | = | density of sandy soil (g/cm ³) |

6.3.2 Chronic Intruder Direct Exposure Dose Pathways

Direct Exposure from Irrigated Soil

The irrigated soil direct exposure route assumes soil is (1) irrigated with groundwater from a well 1m from the SDF, and (2) contaminated with drill cuttings. The receptor, in turn, is exposed during time spent caring for a garden. The dose is calculated using the following formula.

$$D = (C_D + C_W) \times F_G \times DCF$$

where:

| | | |
|-------|---|--|
| C_D | = | radionuclide concentration in soil contaminated with drill cuttings (pCi/m ³) |
| C_W | = | radionuclide concentration in soil irrigated with water from a 1m well (pCi/m ³) |
| DCF | = | external dose conversion factor, 15cm (rem/yr per μCi/m ³), Table 4.7-1 |
| F_G | = | fraction of time spent in garden (unitless), Table 4.6-7 |

Direct Exposure from Disposed Waste Form

The disposed waste form exposure route assumes that the resident builds a home on the disposal site with a 3m deep basement and is exposed during time spent in the basement of the home. The dose rate is calculated using the following formula and results in a value that does not account for any shielding materials between the waste form and basement of the home. The direct exposure pathway is not calculated within the GoldSim dose calculator but will be evaluated separately.

$$D = C_{SS} \times DCF \times SF$$

where:

- C_{SS} = radionuclide concentration in saltstone waste form (Ci/m³)
- DCF = external dose conversion factor, infinite soil depth (rem/yr per μ Ci/m³), Table 4.7-1
- SF = shielding factor for home (unitless) [0.7] [EPA-402-R-93-081, page 190]

Direct Exposure from Swimming

The swimming direct exposure route assumes the receptor receives dose from swimming in a stream contaminated from the aquifer with the highest concentration. The dose is calculated using the following formula.

$$D = GF_S \times t_S \times C_S \times DCF$$

where:

- DCF = external dose conversion factor, water immersion (rem/yr per μ Ci/m³), Table 4.7-1
- GF_S = swimming geometry factor (unitless) [1]
- t_S = time per year spent swimming (hr/yr), Table 4.6-7
- C_S = radionuclide concentration in groundwater at the seepline (pCi/L)

Direct Exposure from Fishing/Boating

The fishing/boating direct exposure route assumes the receptor receives dose from fishing or boating in a stream contaminated from the aquifer with the highest concentration. The dose is calculated using the following formula.

$$D = GF_B \times t_B \times C_S \times DCF$$

where:

- DCF = external dose conversion factor, water immersion (rem/yr per μ Ci/m³), Table 4.7-1
- GF_B = boating geometry factor (unitless) [0.5]
- t_B = time per year spent boating (hr/yr), Table 4.6-7
- C_S = radionuclide concentration in groundwater at the seepline (pCi/L)

6.3.3 Chronic Intruder Inhalation Dose Pathways

Inhalation during Irrigation

The irrigation inhalation exposure route assumes soil is irrigated with groundwater from a well 1m from the SDF and the intruder in turn is exposed by breathing while the garden is irrigated but only during the time spent caring for a garden. For simplicity and conservatism, the source material is the moisture contained within the air with equal concentrations as the groundwater. No resistance to vaporization (i.e., vapor pressure) was used. This formula

was derived following the approach of the previous pathway calculations, whose bases are found in other PA methods. The dose is calculated using the following formula.

$$D = \frac{C_{GW} \times DCF \times U_A \times F_G \times C_{WA}}{\rho_W}$$

where:

| | | |
|----------|---|---|
| C_{GW} | = | radionuclide concentration in groundwater from a 1m well (pCi/L) |
| DCF | = | inhalation dose conversion factor (rem/ μ Ci), Table 4.7-1 |
| U_A | = | air intake (m^3/yr), Table 4.6-7 |
| F_G | = | fraction of time spent in garden exposed to soil irrigated with contaminated ground water (unitless), Table 4.6-7 |
| C_{WA} | = | water contained in air at ambient conditions, (g/m^3) [$10 \text{ g}/\text{m}^3$] |
| ρ_W | = | water density (g/ml) |

Inhalation during Showering

The showering inhalation exposure route assumes the receptor is exposed by breathing humid air within the shower. The source of water for the shower is a well 1m from the SDF. For simplicity and conservatism, the source material is the moisture contained within the air with equal concentrations as the groundwater. No resistance to vaporization (i.e., vapor pressure) was used, adding to the conservatism. For example, heavy elements would be greatly influenced by this assumption because they would be less likely to volatilize. This formula was derived following the approach of the previous pathway calculations, whose bases are found in other PA methods. The dose is calculated using the following formula.

$$D = \frac{C_{GW} \times DCF \times U_A \times t_S \times C_{WS}}{\rho_W}$$

where:

| | | |
|----------|---|--|
| C_{GW} | = | radionuclide concentration in groundwater from a well (pCi/L) |
| DCF | = | inhalation dose conversion factor (rem/ μ Ci), Table 4.7-1 |
| U_A | = | air intake (m^3/yr), Table 4.6-7 |
| t_S | = | time spent in shower (min), Table 4.6-7 |
| | | Note: GoldSim uses fraction of time [$0.0069 = 10 \text{ min}/\text{d}$] |
| C_{WS} | = | water contained in air at shower conditions, (g/m^3) [$41 \text{ g}/\text{m}^3$] |
| ρ_W | = | water density (g/ml) |

Inhalation of Dust from Irrigated Soil

The irrigation soil inhalation exposure route assumes soil is irrigated with groundwater from a well 1m from the SDF and the receptor in turn is exposed by breathing dust during time spent caring for a garden. This formula was derived following the approach of the previous pathway calculations, whose bases are found in other PA methods. The dose is calculated using the following formula.

$$D = \frac{U_A \times L_{SiA} \times C_D \times DCF \times F_G}{\rho_{SS}}$$

where:

- U_A = air intake (m³/yr), Table 4.6-7
- L_{SiA} = soil loading in air while working in a garden (kg/m³), Table 4.6-6
- C_D = radionuclide concentration in soil irrigated with water from a well and contaminated with drill cuttings (pCi/m³)
- DCF = inhalation dose conversion factor (rem/μCi), Table 4.7-1
- F_G = fraction of time spent in garden exposed to soil irrigated with contaminated ground water (unitless), Table 4.6-7
- ρ_{SS} = density of sandy soil (g/cm³)

Inhalation During Swimming

The swimming inhalation exposure route assumes a stream contaminated from the aquifer and the receptor inhales saturated air. For simplicity and conservatism, the amount of the moisture contained in the inhaled air is assumed to be stream water. This formula was derived following the approach of the previous pathway calculations, whose bases are found in other PA methods. The dose is calculated using the following formula.

$$D = \frac{U_A \times GF_S \times t_S \times C_{SW} \times DCF \times C_{WiA}}{\rho_W}$$

where:

- U_A = air intake (m³/yr), Table 4.6-7
- GF_S = swimming geometry factor (unitless) [1]
- t_S = time per year spent swimming (hr/yr), Table 4.6-7
- C_{SW} = radionuclide concentration in water from the stream, (undiluted aquifer) (pCi/L)
- DCF = inhalation dose conversion factor (rem/μCi), Table 4.7-1
- C_{WiA} = water contained in air at ambient conditions, (g/m³) [10 g/m³]
- ρ_W = water density (g/ml)

6.4 Intruder Analysis Results

The peak total intruder doses utilize the pathways identified in Section 6.3 for the Chronic Intruder Agricultural (Post-Drilling) Scenario. The peak total doses for the Chronic Intruder Agricultural (Post-Drilling) Scenario were calculated using the maximum 1m concentrations identified in Section 6.1. A peak dose was identified for the 10,000 year performance period.

The peak Chronic Intruder Scenario doses for the SDF were calculated using the highest concentration for each radionuclide in any Sector (a discussion of how peak concentrations were determined by sector was provided in Section 6.1). These peak doses were the total dose associated with the applicable individual 1m well pathways identified in Section 6.3. The doses associated with direct exposure from the disposed waste form are not tied to groundwater concentration and were calculated separately. The direct exposure dose was shown to be negligible and therefore does not contribute to the peak dose. [SRNS-J2100-2009-00006]

The peak dose for the Chronic Intruder scenario in the 10,000 year performance period was 1.9 mrem/yr at year 10,000. The peak dose in 20,000 years was 7.2 mrem/yr at year 15,060. The peak dose in 10,000 years was primarily due to 1m well water ingestion, with 0.9 mrem/yr of the 1.9 mrem/yr from water ingestion (Table 6.4-1). The principal radionuclide contributor to the peak dose was Ra-226 (Table 6.4-2). Figure 6.4-1 presents a 20,000 year dose curve showing the peak dose during and beyond the 10,000 year compliance period.

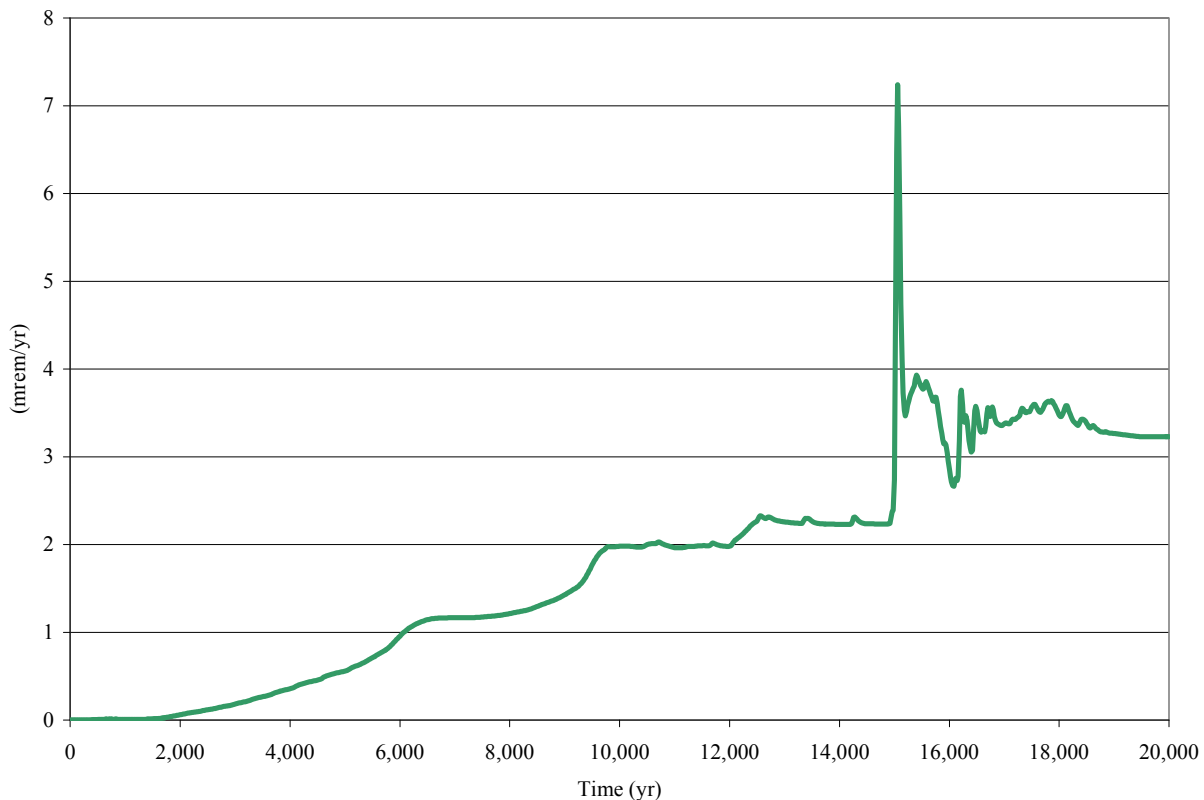
Table 6.4-1: Chronic Intruder Peak Dose Contributors in 10,000 Years

| Chronic Intruder Pathway Contributors | Contribution to Peak (mrem/yr) | Principal Radionuclide Pathway Dose (%) |
|--|---------------------------------------|--|
| Water Ingestion | 0.9 | 91% (Ra-226) |
| Fish Ingestion | 0.3 | 94% (Ra-226) |
| Vegetable Ingestion | 0.7 | 91% (Ra-226) |
| Other Pathways | <0.1 | N/A |
| Total | 1.9 | N/A |

Table 6.4-2: Chronic Intruder 10,000 Year Peak Dose Contributors by Radionuclide

| Radionuclide | Contribution to Peak at year 10,000 (mrem/yr) | % Contribution to Peak |
|---------------------|--|-------------------------------|
| Ra-226 | 1.8 | 91% |
| I-129 | 0.1 | 8% |
| Other Radionuclides | <0.01 | <1% |
| Total | 1.9 | 100% |

Figure 6.4-1: Chronic Intruder Dose Results



6.5 Intruder Uncertainty/Sensitivity Analysis

The purpose of this section is to consider the effects on the Intruder Analyses of uncertainties in the conceptual models used and sensitivities to the parameters used in the mathematical models. Further discussion on the use of the GoldSim analysis software and the methodology are provided in Sections 5.6.4 and 5.6.5. As stated in Section 6.4 the chronic intruder dose is based on the maximum 1m concentrations per sector identified in Section 6.1. For the intruder uncertainty analyses the 1m concentrations are simulated using the GoldSim calculated 100m concentrations and a multiplier factor derived from the SDF PORFLOW model concentration results. This multiplier factor is the highest ratio of the maximum 1m concentration for Case A (Appendices F.1, F.2 and F.3) to the maximum 100m concentration for Case A (Appendices A.1, A.2 and A.3), regardless of sector, for the key radionuclides identified in Section 5.2.2 as calculated by the SDF PORFLOW model. Table 6.5-1 presents the 1m to 100m concentration ratios for the key radionuclides based on SDF PORFLOW model results. This table shows that the highest ratio of 1m to 100m concentration for any key radionuclide is 1.6. The 100m concentrations computed within the GoldSim model are multiplied by the factor of 1.6 to estimate the concentrations at 1m for use in the chronic intruder uncertainty analyses.

Table 6.5-1: Determination of 100m Multiplier for Intruder Uncertainty Analyses

| Key Radionuclide | Maximum 1m Concentration (pCi/L) | Maximum 100m Concentration (pCi/L) | Ratio of 1m to 100m Concentration |
|------------------|----------------------------------|------------------------------------|-----------------------------------|
| Tc-99 | 8.3E+02 | 6.9E+02 | 1.2 |
| I-129 | 1.5E+01 | 9.5E+00 | 1.6 |
| Ra-226 | 3.8E+00 | 3.2E+00 | 1.2 |
| Np-237 | 2.4E-01 | 2.1E-01 | 1.1 |
| Pa-231 | 5.6E-02 | 5.1E-02 | 1.1 |

6.5.1 Intruder Probabilistic Uncertainty Analysis

Intruder uncertainty analyses were performed for the maximum chronic intruder dose within 20,000 years for Cases A through E. Figure 6.5-1 illustrates the time series graph of mean doses to the chronic intruder predicted by the model, by sector, where all the SDF configurations (Cases A through E) are chosen at random, though with non-uniform weighting as described in Section 5.6.3.1. This “All Cases” simulation is based on 5,000 realization runs. Additional individual simulations were run for Case A and Case C. Each of these individual simulations is also based on 5,000 realization runs. Figures 6.5-2 and 6.5-3 illustrate the time series graph of mean doses to the chronic intruder predicted by the model, by sector, for Case A and Case C, respectively.

Figure 6.5-1: Mean Dose to the Chronic Intruder, Any Sector – All Cases

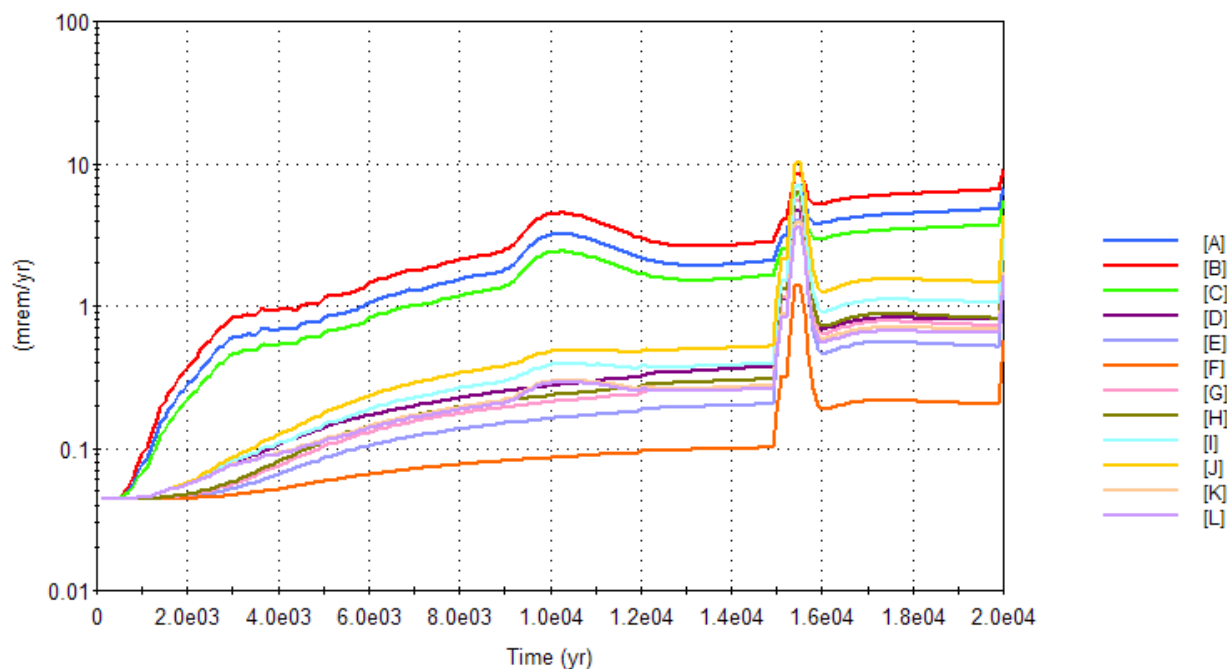


Figure 6.5-2: Mean Dose to the Chronic Intruder, Any Sector – Case A

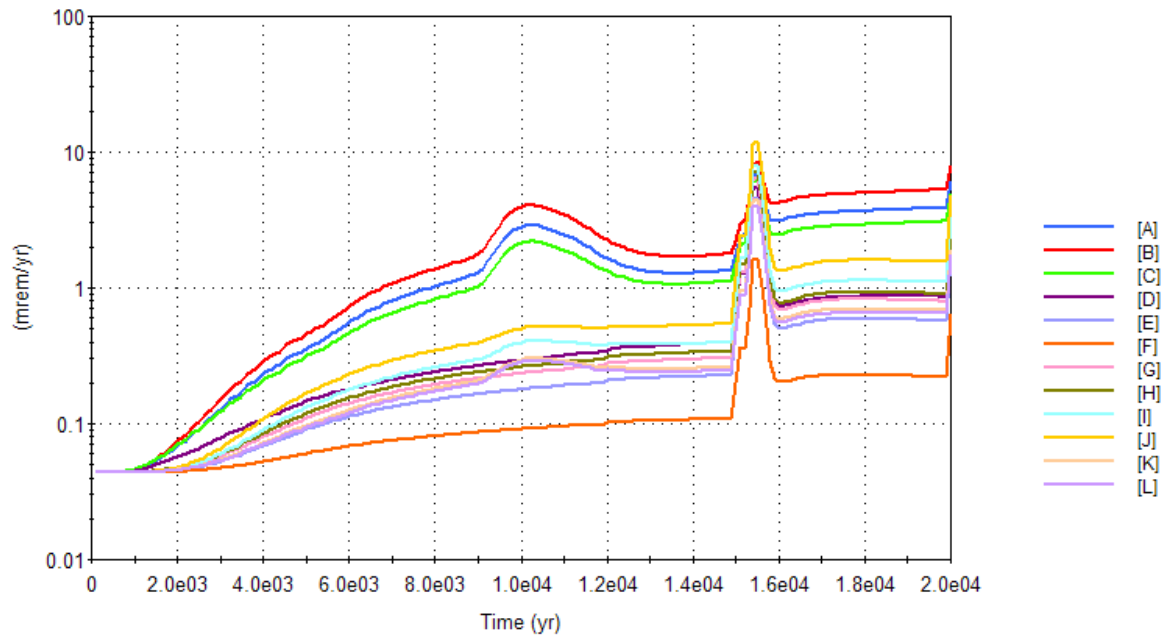
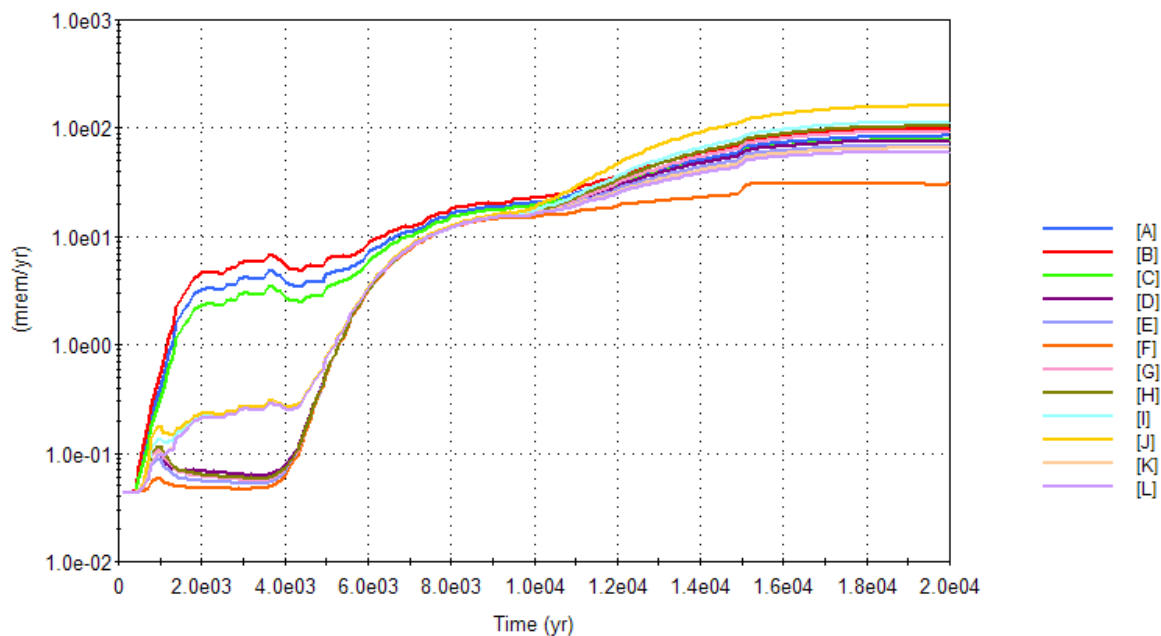


Figure 6.5-3: Mean Dose to the Chronic Intruder, Any Sector – Case C



Since these graphs are of mean values only, the uncertainty surrounding those values is not represented. In order to effectively communicate that uncertainty, Cases A and C are examined individually for the model endpoints of dose to the IHI receptor.

Statistics for maximum values for dose to the chronic intruder (IHI), at any sector, are summarized in Table 6.5-2 for Cases A and C at 10,000 years and 20,000 years. The values in Table 6.5-2 show the statistics (mean, median, and 95th percentile) on the maximum based on 1,000 realization runs for each case.

**Table 6.5-2: Summary Statistics for Chronic Intruder (IHI) Endpoints –
Cases A and C**

| Endpoint | Mean | Median (50th Percentile) | 95th Percentile |
|---|-------------|--|---------------------------------------|
| Maximum chronic IHI dose at any sector within 10,000 years (mrem/yr) for Case A | 4.0 | 3.5 | 7.8 |
| Maximum chronic IHI dose at any sector within 10,000 years (mrem/yr) for Case A | 18.2 | 10.0 | 56.5 |
| Maximum chronic IHI dose at any sector within 10,000 years (mrem/yr) for Case C | 26.9 | 9.8 | 121 |
| Maximum chronic IHI dose at any sector within 10,000 years (mrem/yr) for Case C | 254 | 160 | 807 |

An evaluation of model uncertainty requires examination of the statistics around the results of interest as a function of time. Figures 6.5-4 and 6.5-5 show the statistics surrounding the IHI dose for Case A, within 20,000 years, in Sector B and Sector J, respectively. The statistical summary shows the percentiles of the results at any given time. That is, a single time-step would be read by placing a vertical line across the graph. Along that line, the lines showing percentiles identify the percentile of the result (IHI dose for Sector B, Case A – for Figure 6.5-4) at that time. Similarly, Figures 6.5-6 and 6.5-7 show the statistics surrounding the IHI dose for Case C, within 20,000 years, in Sector B and Sector J, respectively.

Figure 6.5-4: Total Chronic IHI Dose in Sector B – Case A

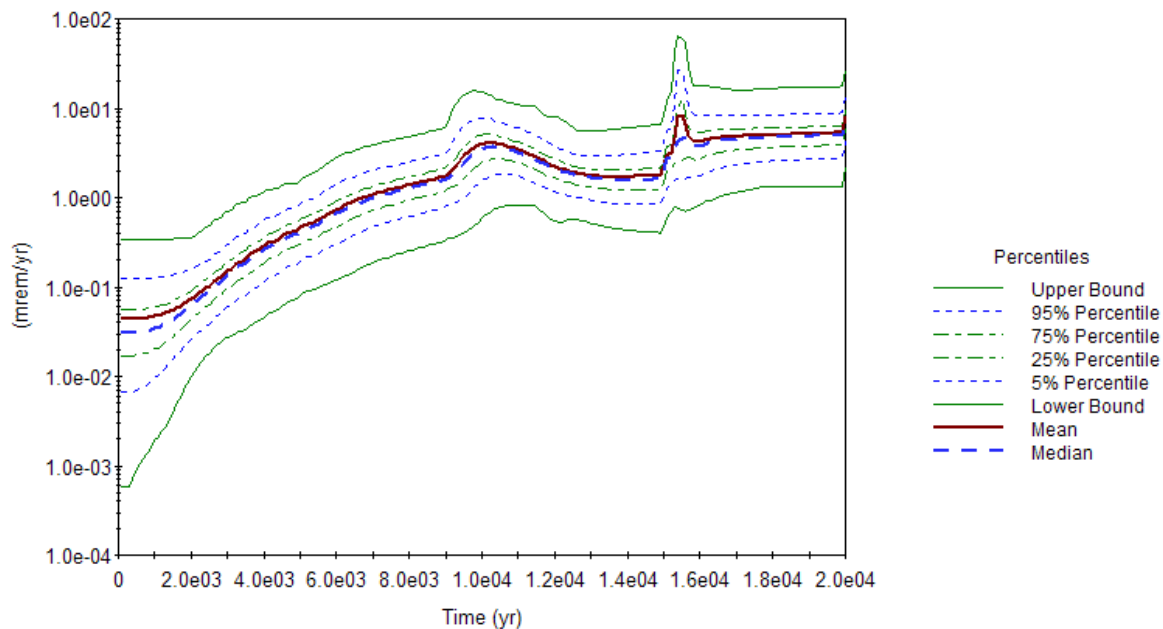


Figure 6.5-5: Total Chronic IHI Dose in Sector J – Case A

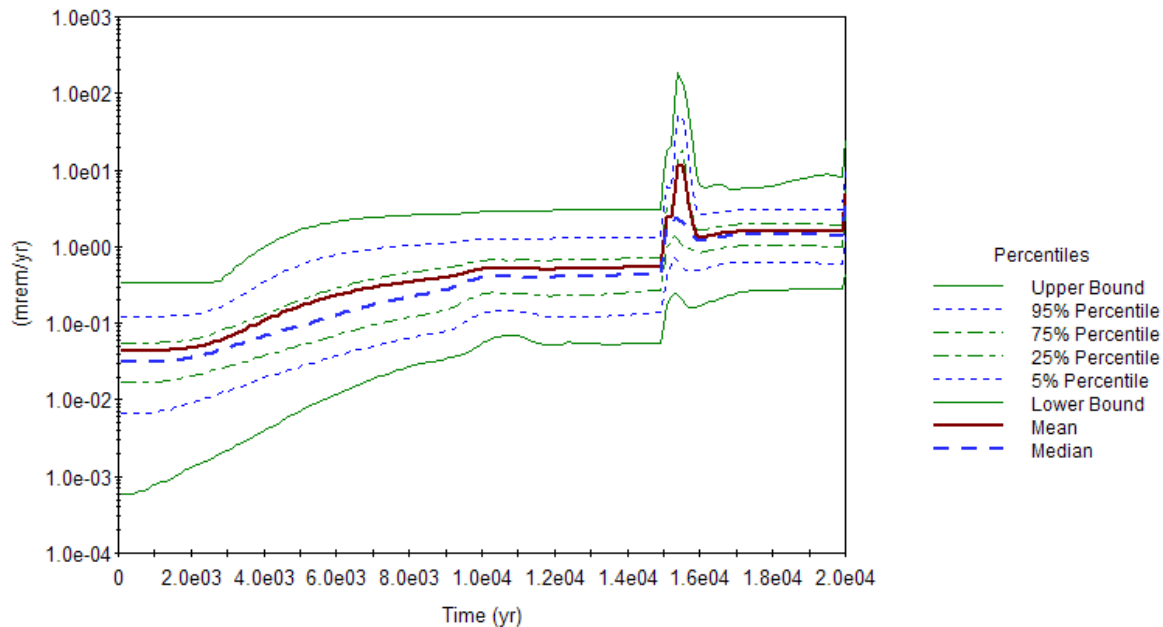


Figure 6.5-6: Total Chronic IHI Dose in Sector B – Case C

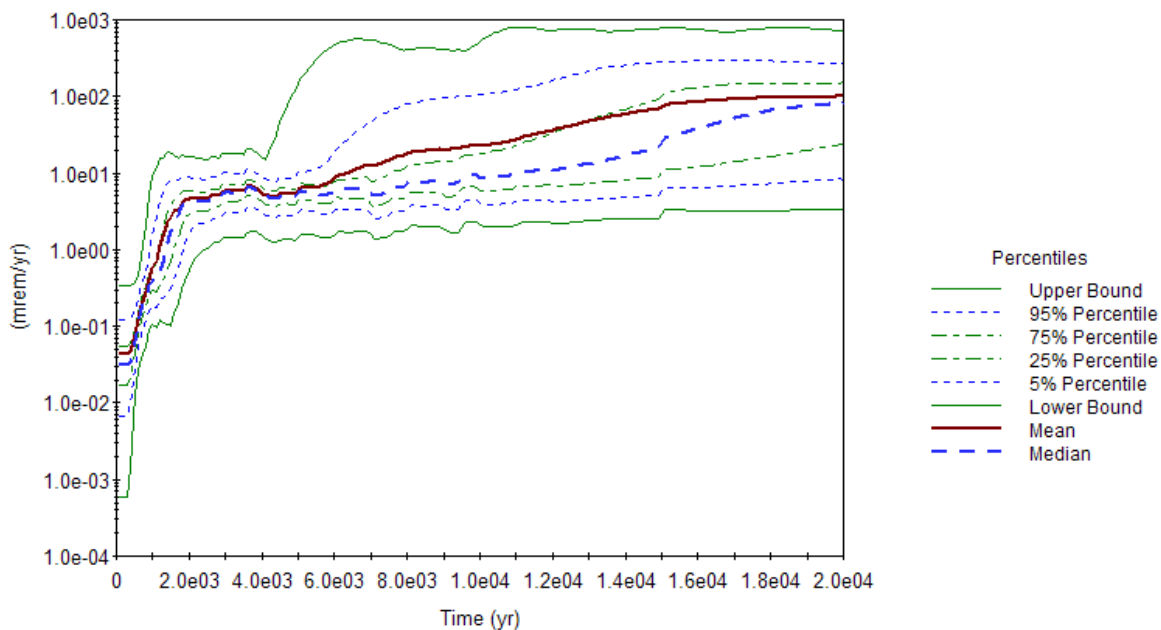
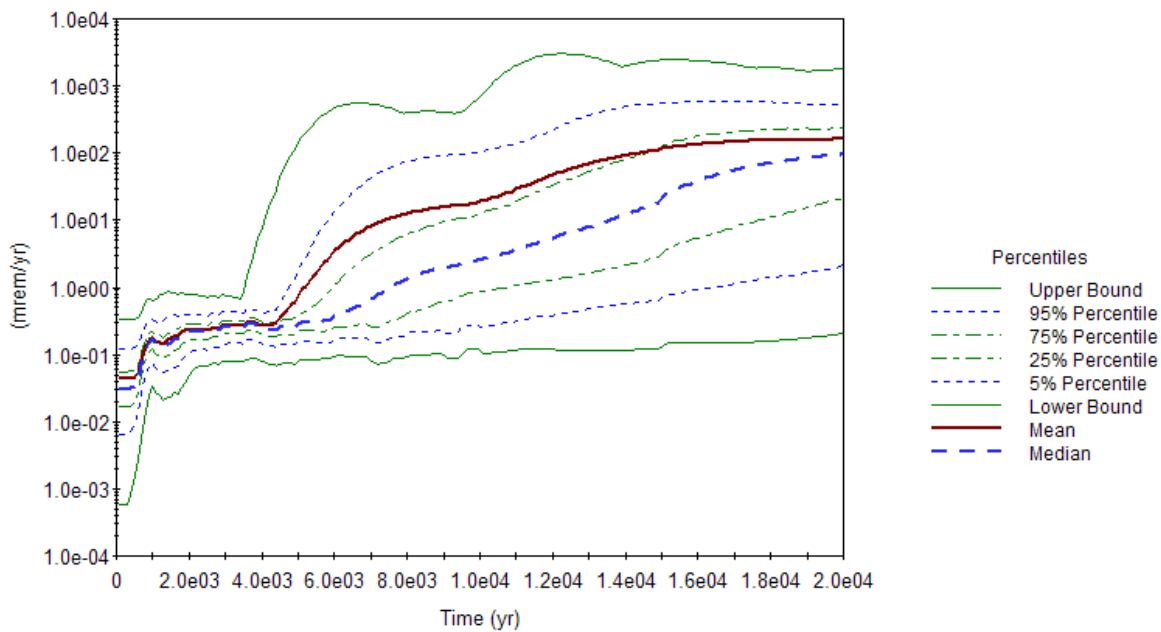


Figure 6.5-7: Total Chronic IHI Dose in Sector J – Case C



6.5.2 Intruder Probabilistic Sensitivity Analysis

The dose pathway analyses for the chronic intruder are presented in Section 6.3. The chronic intruder dose pathways are identical to the dose pathways for the MOP presented in Section 5.4 except that the groundwater concentrations are based on different well locations (e.g., the dose pathway analyses for the chronic intruder do not utilize a drill cuttings contribution). For the chronic intruder, the groundwater concentrations are taken at a 1m well; while for the MOP, the groundwater concentrations are taken at a 100m well. Therefore, the sensitivity results presented in Section 5.6.5 for the endpoints associated with the dose to the MOP are applicable to the chronic intruder, and chronic intruder dose is sensitive to the same parameters as the MOP dose, which are discussed in detail in Section 5.6.5.

6.5.3 Intruder Single Parameter Sensitivity Analysis

A single sensitivity and uncertainty analysis on the drill scenario inventory was performed using concentrations generated by SDF PORFLOW model. The concentration results were converted into chronic intruder dose results using the GoldSim dose calculator model. As discussed in Section 4.2.4.2, the stabilized contaminant materials after SDF closure will be protected by significant, long lasting materials which are clearly distinguishable from the surrounding soil and make drilling an impractical scenario based on regional drilling practices. For the intruder single parameter sensitivity analyses however, the drilling scenarios were modified to see the impact that drilling into a waste source might have on the acute and chronic intruder scenarios.

6.5.3.1 Impact of Drilling into a SDF Disposal Unit on Acute Intruder

To investigate the effect of an intruder drilling into a disposal unit (which is not considered a credible scenario per Section 4.2.4.2), a conservative SDF disposal unit drilling inventory was developed. The inventory for the intruder drilling into a disposal unit was developed by determining the hypothetical contaminant inventory of an 8 inch diameter core drilled completely through Vault 1, Vault 4 or an FDC. These three core values were compared, per radionuclide, with the highest value found in each of the three cores used for the hypothetical core inventory. [SRNS-J2100-2008-00004]

Since the disposal unit engineered barriers (e.g., closure cap erosion barrier, disposal unit, concrete roof and clean cap), will prevent drilling into the disposal unit inventory, this scenario was not considered to occur until 500 years after SDF closure. The pathways utilized for the acute intruder drilling scenario are discussed in Section 6.2. Figure 6.5-8 shows the peak acute intruder dose for 20,000 years assuming that an intruder drills into a disposal unit. The peak dose to an acute intruder is 3.76 mrem/yr at year 500 and is associated mostly with Sn-126 (65% of the year 500 peak dose). The principal exposure pathway is direct exposure to drill cuttings (86% of the year 500 peak dose).

6.5.3.2 Impact of Drilling into a SDF Disposal Unit on Chronic Intruder

The same SDF disposal unit drilling scenario utilized for the acute intruder sensitivity in Section 6.5.3.1 was utilized for the chronic intruder scenario. All other parameters from the chronic intruder scenario described in Section 6.3 were held constant. Figure 6.5-9 shows the peak chronic intruder dose for 20,000 years assuming that an intruder drills into a disposal unit. The peak dose to a chronic intruder is 15 mrem/yr at year 500.

Figure 6.5-8: Peak Acute Intruder Dose Assuming Drilling into a SDF Disposal Unit

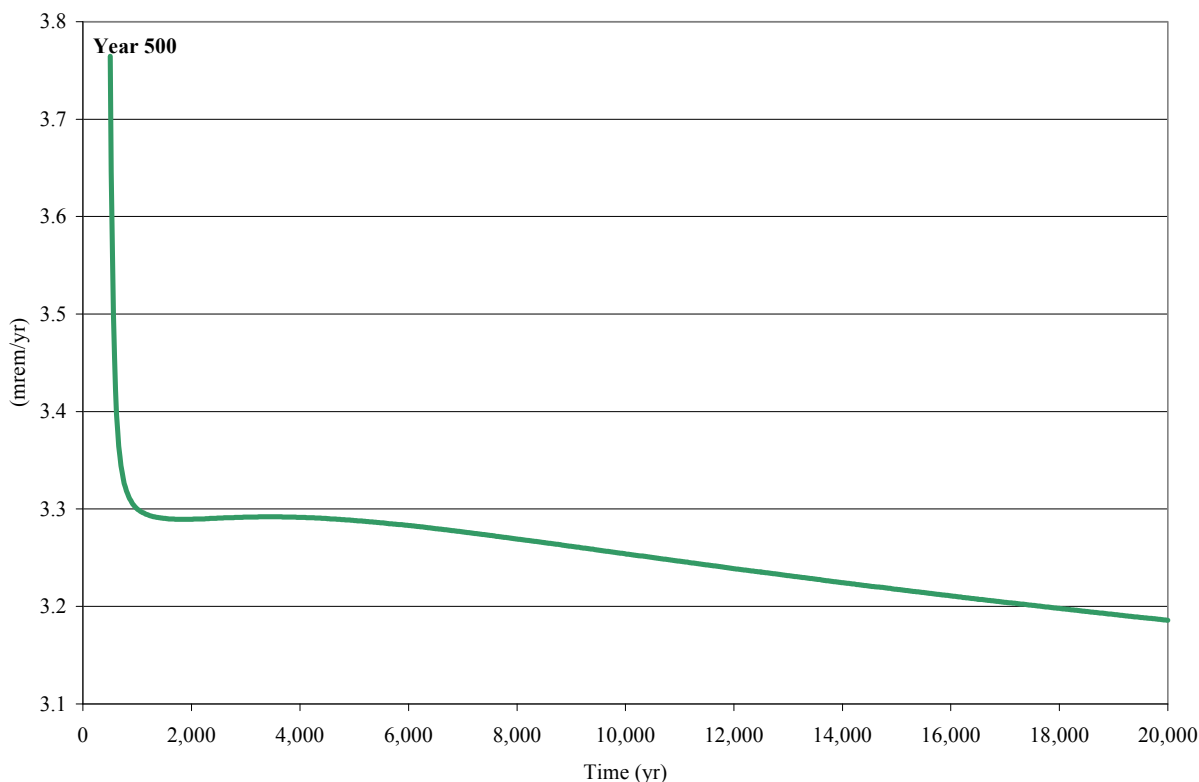
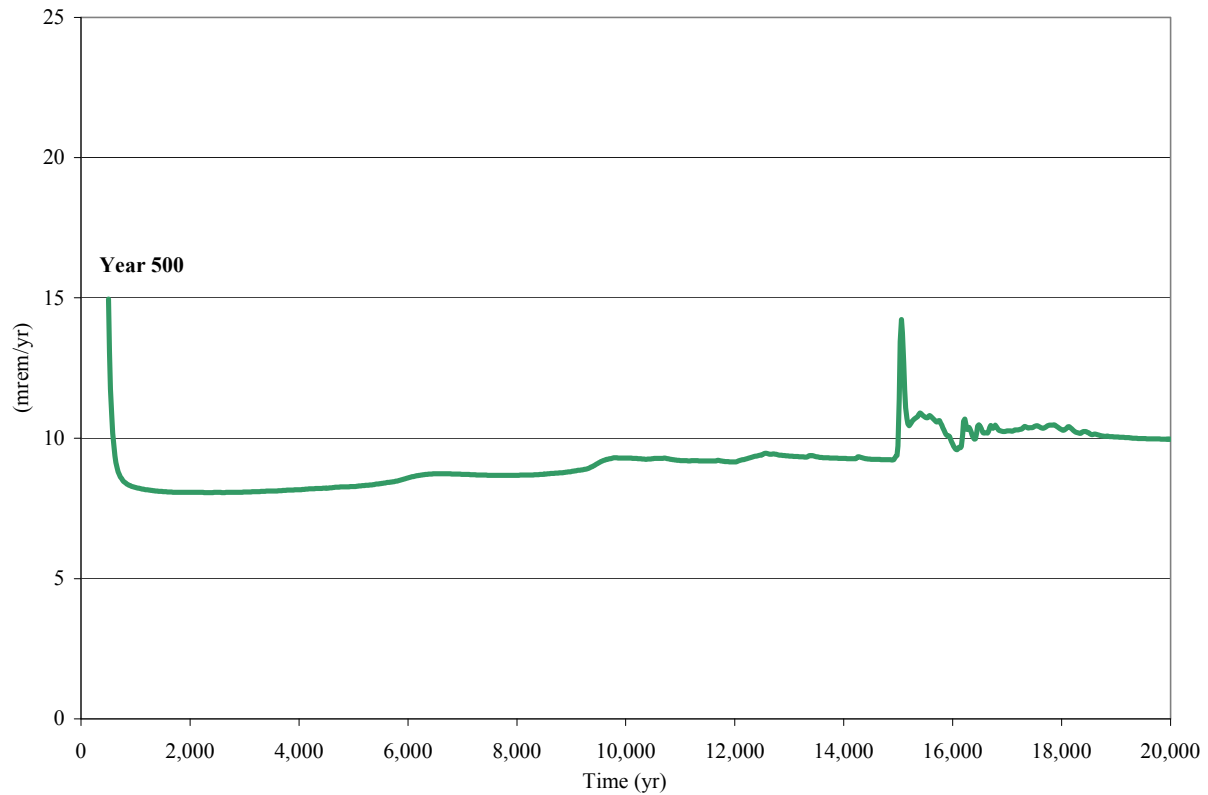


Figure 6.5-9: Peak Chronic Intruder Dose for 20,000 Years Assuming Drilling into a SDF Disposal Unit



7.0 INTERPRETATION OF RESULTS

This section provides an interpretation of results presented in Sections 5 and 6.

Section 7.1 summarizes the results presented in Sections 5 and 6.

Section 7.2 summarizes the conservatisms used in modeling.

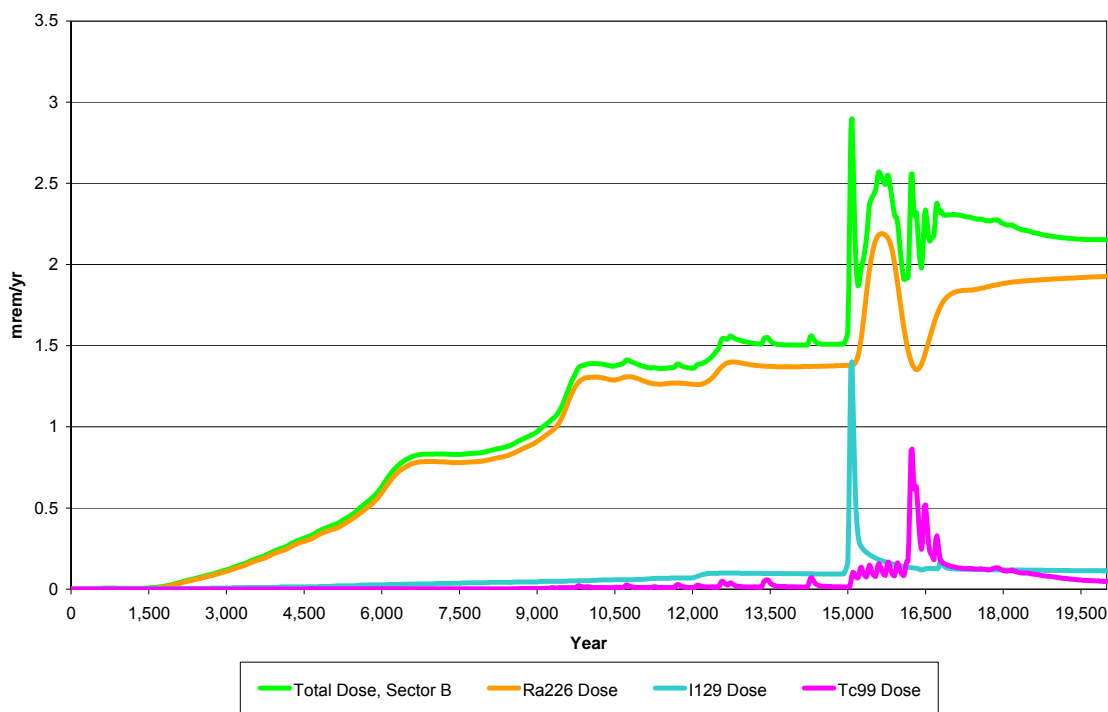
7.1 Performance Assessment Results

This section provides a summary and interpretation of the results of the Base Case (Case A) presented in Sections 5 and 6.

7.1.1 Integrated System Behavior

Provided below is a short description of the impact that various segments of the ISCM have on dose results (the segments are discussed in detail in Section 4.4.3). The timing of occurrences for model changes in this section are drawn from Tables 4.4-6, 4.4-7, and 4.4-9. For the purpose of the following discussion, the Base Case (Case A) peak groundwater total dose and individual radionuclide doses associated with Sector B will be used to illuminate segment behaviors, as illustrated in Figure 7.1-1.

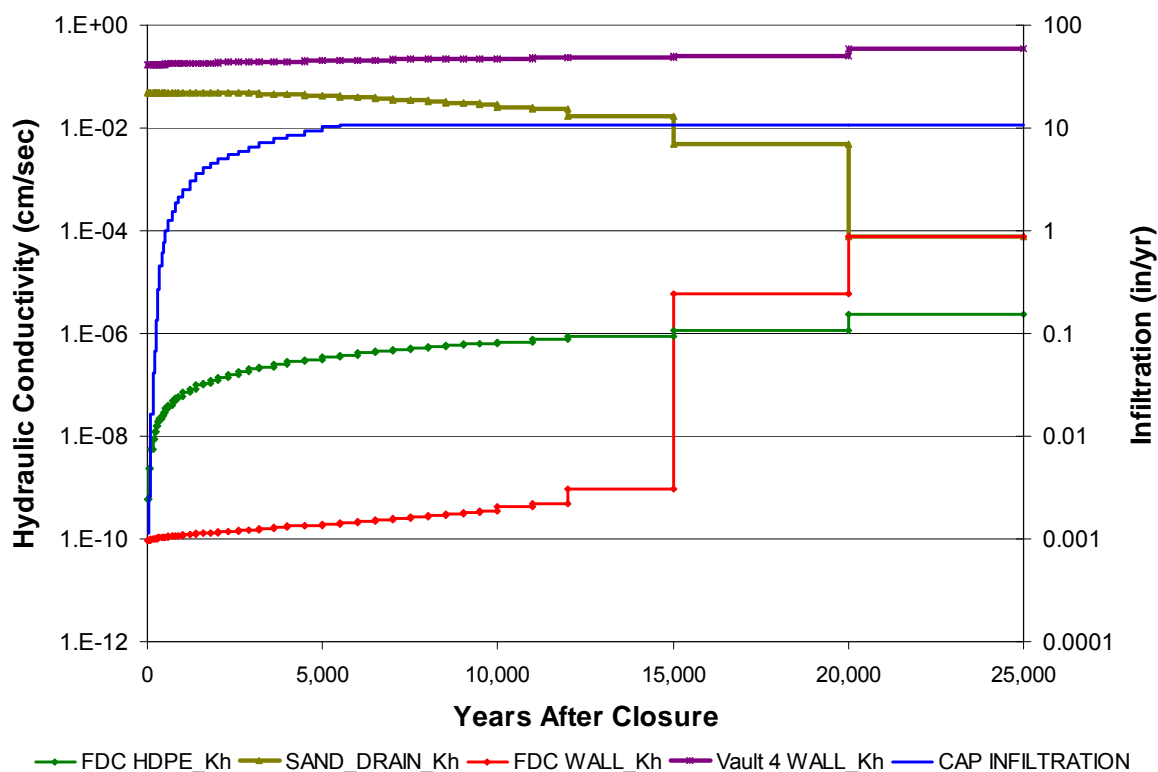
**Figure 7.1-1: Peak Groundwater Pathways Dose and Key Radionuclide Doses for Sector B
- Base Case**



7.1.1.1 Closure Cap

A flow rate leaving the closure cap over time is determined in the closure cap sub-model. The infiltration rate into the closure cap surface is based on the rainfall rates and the closure cap material properties (which are discussed in detail in Section 4.2.3.2.1). The flow rate out of the cap is calculated using the HELP code, with the closure cap modeled as degrading over time. The flow rate through the closure cap reaches a steady state value at approximately year 5,000 (see Figure 7.1-2).

Figure 7.1-2: Model Input Timeline for Various SDF Modeling Segments



A steady increase can be seen in the Sector B doses as Ra-226 is released from Vault 4 beginning in year 2,000 and comes to a plateau near year 6,500 (see Figure 7.1-1). This increase coincides with an increase in the infiltration through the closure cap system. The increase in infiltration affects all disposal units equally, and increases infiltration from approximately 0.01 inches at the time of SDF closure, to 10.6 inches from years 500 through 5,400. After year 5,400 the model uses a steady infiltration rate of 10.6 inches through the closure cap.

A sensitivity run was performed to examine the effect of losing the closure cap as an infiltration barrier. This barrier analysis showed that not having a closure cap did allow the peak dose in 10,000 years to increase as the presence of more flow early tended to accelerate transport (Figure 5.6-75). The lack of a closure cap did slightly increase the Case A 20,000 year peak dose.

7.1.1.2 *Saltstone Disposal Unit Roof*

The flow leaving the closure cap travels to the disposal unit with the flow rate being affected by the backfill layer and lateral drainage layer above the concrete roof. Based on the relative hydraulic properties of the two materials (soil vs. concrete), some flow is directed around the disposal unit into the surrounding soil, while some flow travels downward toward the roof. For the FDCs, an HDPE-GCL layer overlays the roof and is an additional barrier to the flow to the roof. Degradation of the HDPE-GCL layer is modeled as changing over time and is discussed in Section 4.2.3.2.2 (see Figure 7.1-2). The concrete roof material properties (which are discussed in detail in Section 4.2.3.2.4) are also modeled as changing over time. The only roof material property of concern are the hydraulic properties, since the roof impacts flow, but does not retard contaminant transport because the inventory is below the clean cap. The roof hydraulic properties are degraded as depicted in the figures in Section 4.2.3.2.4.

The timing of Vault 4 roof degradation affects the flow rate into the saltstone. The Sector B peak dose starts increasing slowly near year 7,500 and increases rapidly as the disposal unit roof degrades, allowing more flow, until the disposal unit roof completely degrades (to the properties of backfill) at year 10,000; at which time the dose levels off as a steady state flow is reached.

7.1.1.3 *Saltstone*

Water enters the top of the disposal unit and travels downward into the saltstone. Since the contaminants are distributed within the saltstone, contaminant release can be directly impacted by changes to the saltstone material and chemical properties. The saltstone material properties (e.g., hydraulic conductivity and contaminant retardation which are discussed in detail in Sections 4.2.2 and 4.2.3.2.4) are modeled as changing over time. In some configurations (Section 4.4.2), fast flow paths are modeled resulting in a higher flow rate through the disposal units, but not necessarily through the saltstone. A cementitious materials degradation analysis was performed to determine the time it would take to transition from a reducing to oxidizing state and from a middle age to old age state in the saltstone. Analyses results indicated that during the performance period, the saltstone remained in its initial state of reducing, middle aged.

Contaminant release is controlled by individual sorption coefficients (K_d values), as described in Section 4.2.2, and the K_d values associated with reducing (middle aged) concrete (see Table 4.2-18). Because of the importance of Tc-99 in the model, a more sophisticated analysis was developed to determine a time varying K_d value for Tc-99, as described in Section 4.2.3.2.4.

The saltstone material properties of concern are the hydraulic and chemical properties. Since the saltstone chemical properties do not change appreciably in the 20,000 year period, changes in the saltstone sorption coefficients are not a primary concern.

Sensitivity modeling in Cases B and C showed that the presence of fast flow paths causes the peak dose in 10,000 years to increase, with a decrease in the 20,000 year peaks (see Figures 5.6-73 and 5.6-74). The fast flow paths made the saltstone inventory more available for transport early, but tended to somewhat minimize the inventory available for release in later years.

Sensitivity modeling was also performed to assess the impact of severely degraded saltstone and the role of saltstone hydraulic flow changes as a transport barrier. This barrier analysis showed that the configuration reflecting severe saltstone degradation (i.e., Case E) caused the peak dose to increase significantly (see Figures 5.6-73 and 5.6-74). Since the disposal units' inventory is integral to the saltstone, changing the hydraulic properties of this barrier (i.e., the saltstone) maximizes the access of the contaminants to flow and greatly impacts the dose.

A sensitivity case was run with the hydraulic conductivity of saltstone increased by a factor of 50 from the Base Case to assess the impact on the MOP dose, without the severe saltstone degradation that was assumed for Case E. As shown in Section 5.6.6.7, the increased hydraulic conductivity of saltstone increased the peak MOP dose by a factor of three.

7.1.1.4 Disposal Unit Walls and Floor

Contaminants leaving the saltstone monolith enter the concrete walls and floor of the disposal units. Since the walls of Vaults 1 and 4 are assumed to contain contaminants, release of contaminants is impacted by the wall concrete hydraulic and chemical properties. The Vault 1 and 4 walls are assumed to be hydraulically degraded initially, so their hydraulic properties do not change significantly over time, but their chemical properties are modeled as changing over time. The FDC concrete properties (which are discussed in detail in Section 4.2.3.2.4) are modeled as changing over time and these changes are depicted in Figures 4.2-39 and 4.2-40 of Section 4.2.3.2.4. The properties of the concrete impact both the flow rate through the disposal unit and the K_d value.

Contaminant transport is retarded by the disposal unit's concrete walls and floor, with some radionuclides being slowed, greatly depending on their K_d values. Table 4.2-18 provides K_d values for cementitious materials as a function of aging, with the cementitious material "age" dependent on the pH of the concrete pore water, which in turn is dependent upon the amount of water (number of pore volumes) that has passed through the concrete over time. A description of pore water chemistry modeling is provided in Section 4.2.3.2.4 and discussed in the context of the various degradation cases in Section 4.4.2. As the disposal unit chemistry changes, the concrete transitions from reducing to oxidizing and from middle age to old age and the associated K_d values are modeled as changing.

The properties of concern for the walls and floor are both the hydraulic and chemical properties. The timing of concrete degradation affects the flow rate through the concrete. Sector B has the highest doses within 10,000 years because of the contribution of Ra-226, which is primarily associated with the Th-230 (a Ra-226 parent radionuclide) inventory modeled in the Vault 4 walls, and the fact that the Vault 4 walls are degraded from time zero.

The significant spike of I-129 at 15,080 years in all sectors is due to the FDC wall hydraulic conductivity increasing by over four orders of magnitude at year 15,000 (see Figure 7.1-2). I-129 has relatively low retardation factors in the cementitious materials and soil that allow I-129 to move quickly through the environment.

The peaks associated with Tc-99 coincide with the transition of the disposal unit wall concrete from reducing to oxidizing conditions. For the FDCs, Tc-99 release occurs as a result of wall failure due to concrete degradation which in turn accelerates wall concrete oxidation. The spike of Tc-99 near year 16,000 coincides with the oxidation of the disposal unit walls. This spike of Tc-99 is exacerbated by all 64 FDCs releasing Tc-99 at the same time. Tc-99 has low retardation factors in oxidizing cementitious materials and soil that allow Tc-99 to move quickly through the environment.

Sensitivity modeling showed the effect on the physical degradation of the floor and walls by increasing and decreasing the concentration of sulfate in the saltstone. The basis and results of this barrier analysis can be seen in Section 5.6.6.3. The primary impact of this sensitivity was to the FDCs' degradation times as indicated in Table 5.6-18.

An additional sensitivity analysis was done to show the impact on the MOP dose if the walls and floor of Vaults 1 and 4 are assumed to be oxidized, middle aged concrete at the start of closure. The oxidized condition of the vault concrete increased the release of technetium and reduced the release of radium due to the change in the K_d values from reducing to oxidized concrete. The K_d value for technetium is significantly lower in oxidized concrete than in reducing concrete; while the K_d value of Radium is higher in oxidized concrete than in reducing concrete. Thus, as shown in Section 5.6.6.6, assuming oxidized vault (Vaults 1 and 4) concrete at the start of closure results in a slightly lower MOP dose than in the Base Case.

7.1.1.5 Vadose Zone Surrounding SDF Disposal Units

After contaminants exit the floor or walls, they enter the vadose zone (i.e., soil) surrounding the SDF. The vadose zone material properties impact both the flow rate and the transport rate through the soil, with both being important to the model. The impact of the vadose zone can be very radionuclide specific depending on the K_d value for the soil for the applicable element. Radionuclides with very low K_d in soil, such as I-129 (K_d range of 0.0 to 0.6 mL/g) and Tc-99 (K_d range of 1.8 to 0.6 mL/g) are likely to contribute significantly to the peak doses, since they will move quickly in the soil. Radionuclides with higher K_d in soil, such as Ra-226 (K_d range of 17 to 5 mL/g) will have their contribution to the peak dose more distributed over time.

The effect of the soil on transport can be seen in Figure 7.1-1, when the FDC walls are modeled as significantly degraded at year 15,000. Since I-129 has a very low K_d it is transported to the 100m receptor rapidly and contributes almost immediately. Because Ra-226 and its parents have a higher K_d in soil they take longer to peak (i.e., closer to year 16,000).

7.1.2 100m Groundwater Pathways Doses

The peak 100m groundwater pathways dose in the 10,000 year performance period is 1.4 mrem/yr in Sector B. The fact that Sector B contains the peak dose is expected, since this

sector is most directly impacted by Vault 4, which has an appreciable release of Ra-226 prior to year 10,000. Vault 4 is the primary contributor (>90%) to the 100m peak groundwater pathways dose in Sector B at year 10,000. The primary pathway contributors to the peak 100m groundwater doses are water ingestion, fish ingestion, and vegetable ingestion. The 100m groundwater pathways dose during the 10,000 year performance period is primarily associated with Ra-226. While there is very little Ra-226 initially in the disposal units, the Ra-226 is a daughter product of Th-230, of which there is an appreciable quantity in Vault 4. The Ra-226 moves quickly enough in soil (e.g., $K_d < 20$ mL/g in soil) so that it is capable of reaching the 100m location within 10,000 years.

The peak 100m groundwater pathways dose within 20,000 years is associated with Sector I. Sector I is the sector most directly impacted by the FDCs. The FDCs are the primary contributors (approximately 90%) to the 100m peak groundwater pathways dose in Sector I at year 15,080. The Sector I peak is dominated by the contribution of I-129 (>85%) at year 15,080.

Uncertainties of the groundwater pathways dose results are discussed in detail in Section 5.6.4. The effect of overall uncertainty is best illustrated by Figure 5.6-33 from the probabilistic analyses, which portrays the mean doses predicted by the model, where all the SDF modeling scenarios (A through E) are chosen at random, though with non-uniform weighting. Figure 5.6-33 shows the mean dose to a MOP located in each of the defined PORFLOW Sectors (A through L), at any point in time, for 20,000 years. Overall, the peak dose occurs primarily in Sectors A, B, and C (due to the influence of Vault 4). The mean doses considering all the SDF modeling cases are below 25 mrem/yr in 10,000 years. Table 5.6-12 shows that when considering only the Base Case (i.e., Case A), the mean (4.5 mrem/yr) and 95th percentile (9.1 mrem/yr) are both below 25 mrem/yr in 10,000 years.

The probabilistic sensitivity analyses demonstrated that the groundwater doses are most sensitive to the specific radionuclide K_d values, as shown in the Section 5.6.5 tables and figures. For example, Table 5.6-14 shows that the maximum MOP dose is most sensitive to the K_d value for iodine in reducing cementitious materials and to the K_d value for radium in soil.

7.1.3 All-Pathways Dose

The peak all-pathways annual dose for a MOP at 100m is calculated using the highest 100m groundwater pathways dose results during the 10,000 year performance period in combination with the air pathways results. The peak all-pathways annual dose for a MOP is 1.4 mrem/yr and is associated with Sector B at 100m as described in Section 5.5. The all-pathways dose was dominated by the groundwater pathways, with the airborne dose contribution being negligible.

7.1.4 Intruder Dose

The peak chronic intruder scenario doses for the SDF were calculated using the highest concentration for each radionuclide in any sector (a discussion of how peak concentrations were determined by sector was provided in Section 6.1). The peak dose for the chronic intruder scenario, in the 10,000 year performance period was 1.9 mrem/yr at year 10,000. The peak dose in 20,000 years was 7.2 mrem/yr at year 15,060. The peak dose in 10,000

years was primarily due to water ingestion, with 0.9 of the 1.9 mrem/yr being due to water ingestion. The principal radionuclide contributor to the peak dose was Ra-226.

7.1.5 Airborne Dose

The annual dose from airborne releases resulted in a total dose of less than 4.0E-09 mrem/yr, principally from H-3 in the first 10 years after closure, at 100m from the SDF. These results were conservative because the flux rates were based on simplified models as described in Section 4.5.

7.1.6 Radon Flux

Using simplified models as described in Section 4.5, the peak instantaneous flux of 2.0E-13 pCi/m²/sec occurs above Vault 1 at approximately 10,000 years after closure.

7.1.7 Groundwater Protection

The radionuclide concentrations at 100m provided in Section 5.2.1 indicate that the maximum "Sum of beta-gamma MCL fractions" within the 10,000 year compliance period is 0.29, which equates to a total β/γ dose of 1.16 mrem/yr. Section 5.2.1 also indicates that the maximum total α concentration is 1.9 pCi/L and the maximum total radium concentration is 1.9 pCi/L during the compliance period. The chemical concentrations at 100m provided in Section 5.2.1 indicate that the maximum total uranium concentration is 8.0E-9 $\mu\text{g/L}$ during the compliance period.

7.2 Conservatisms Included in the SDF Performance Assessment

Numerous parameter or input value conservatisms were included in the SDF PA modeling, as discussed in previous sections. The term conservative is used in this context to indicate that the individual parameter or input assumption is thought to overstate the impact the actual value has on peak dose. The cumulative effect of these conservatisms is addressed through probabilistic modeling. A summary of key conservatisms is provided below.

7.2.1 Closure Cap

The following are some of the measures which were taken to ensure conservative HELP model infiltration results.

- The maximum slope length of the closure cap (i.e., 825 feet) was used to determine both runoff and lateral drainage for the entire cap. A significant portion of the cap will have slope lengths less than 825 feet.
- The initial saturated hydraulic conductivity of the sand used for the lateral drainage layer was taken as 5.0E-02 cm/s, which is well below the maximum (1 cm/s) in the range of values presented in the literature for various grain-size sands.
- Silting-in of the upper lateral drainage layer is assumed to begin immediately upon construction; it is assumed to result from the migration of elevated levels of colloidal clay within infiltrating water; the use of the overlying filter fabric is assumed not to reduce colloidal clay movement; and all colloidal clay that enters the layer is assumed to remain in the layer (i.e., not be flushed from the drainage layer) thus reducing its hydraulic conductivity. Silting-in may not occur, or may occur on a much-reduced scale compared to the scenario modeled.

- A saturated hydraulic conductivity was assigned to the intact portions of the HDPE geomembrane even though water transport through HDPE is a vapor diffusion process.
- The initial saturated hydraulic conductivity of the GCL was taken as 5.0E-09 cm/s even though test results indicate that the value could be significantly lower.

7.2.2 Integrated Site Conceptual Model

Several modeling assumptions were made that introduced conservatism into the timing of release of radionuclides from the SDF.

- Parametric changes associated with all the FDCs were assumed to occur simultaneously. This simplifying assumption resulted in over emphasizing the effect of releases from the FDCs.
- No HDPE-GCL layer is considered over the roof of Vault 1 and 4.
- Modeling events that affect flow are modeled as changing (sometimes drastically) at the modeling time-steps, even though the supporting analyses might reflect the change (e.g., barrier degradation) being gradual. Because fewer modeling time-steps were used after year 10,000 during flow modeling, occurrences of significance that occur after year 10,000 are grouped together at a single time in the model rather than distributed more evenly over time as would be expected. This leads to peak doses appearing more acute, as flow changes are not introduced gradually, but instead tend to be exaggerated.
- No stream dilution was assumed when calculating dose effects associated with finfish ingestion.

7.2.3 Volatile Radionuclide and Radon Analysis

The following conservatisms were used in the airborne radionuclide and radon analysis that conservatively bound the flux of radionuclides from the contaminant zone to the surface.

- The use of boundary conditions that force all of the gaseous radionuclides to move upward from the waste disposal zone to the land surface. In reality, some of the gaseous radionuclides diffuse sideways and downward in the air-filled pores surrounding the waste zone; hence, ignoring this has the effect of increasing the flux at the land surface.
- Not taking credit for the removal of radionuclides by pore water moving vertically downward through the model domain. This mechanism would likely remove some dissolved radionuclides, and therefore its omission has the effect of increasing the estimate of instantaneous radionuclide flux at the land surface.
- Exclusion of the HDPE geomembrane and the GCL. Inclusion of these materials in the model would significantly reduce the gaseous flux at the land surface due to their material properties (i.e., low air-filled porosity and/or low effective gaseous diffusion coefficient).
- Exclusion of the cover materials above the erosion barrier (i.e., top soil and upper backfill layers). Excluding these materials shortens the diffusion pathway and could increase the flux at the land surface.
- Use of the minimum closure cap thickness in the model.

7.2.4 Other Factors Affecting Results

As discussed in Section 5.2.1, the use of sectors in determining groundwater concentrations added conservatism to the peak dose results since the peak concentrations are determined for each radionuclide independent of the location and aquifer within the sector.

As discussed in Section 5.2.1, the methodology for determining seepline concentrations added conservatism to the peak dose results since the seepline concentrations are determined at each time-step for individual radionuclides independent of the specific seepline location (i.e., I-129 from UTR and Ra-226 from McQueen Branch could both be used when determining the dose at year 15,080).

8.0 PERFORMANCE EVALUATION

Summary for Section 8.0

Section 8 describes the application of the PA.

Section 8.1 describes how the PA will be used.

Section 8.2 describes future work to be done to support maintenance of the PA.

8.1 Use of Performance Assessment Results

The SDF PA is used to fulfill the DOE O 435.1-1 requirement that an assessment be prepared and maintained for DOE LLW disposed of after September 26, 1988. The results of this PA provide reasonable assurance that the facility design and method of disposal will comply with the performance objectives of DOE O 435.1-1, which ensure protection of public health and safety in limiting doses to a MOP and limiting releases of radon. The SDF PA also provides reasonable assurance that the applicable performance objectives of 10 CFR 61 will be met. This PA will also be used to establish limits on radionuclides that may be buried near-surface and assesses impacts to a hypothetical intruder and impacts to water resources. Disposal limits for each radionuclide will be calculated and incorporated into the SDF WAC based on the results of this PA.

As shown in Table 8.1-1, all of the regulatory limits for the SDF are met within the 10,000 year period of compliance.

Table 8.1-1: Comparison of SDF Results with Performance Measures

| Performance Measure | | Limit | Result |
|---------------------|------------------------|--|---|
| DOE O 435.1-1 | All-Pathways Dose | 25 mrem/yr | 1.4 mrem/yr |
| DOE O 435.1-1 | Intruder Dose | 500 mrem acute 100 mrem/yr chronic | N/A – acute 1.9 mrem/yr - chronic |
| DOE O 435.1-1 | Air Pathways Dose | 10 mrem/yr | <4E-09 mrem/yr |
| DOE O 435.1-1 | Radon Flux | 20 pCi/m ² /s At ground surface | 2.0E-13 pCi/m ² /s |
| DOE O 435.1-1 | Groundwater Protection | Total β/γ 4 mrem/yr Total α 15 pCi/L Total U 30 µg/L Total Ra 5 pCi/L | 1.16 mrem/yr 1.9 pCi/L 8.0E-9 µg/L 1.9 pCi/L |
| 10 CFR 61.41 | All-Pathways Dose | 25 mrem/yr | 1.4 mrem/yr |
| 10 CFR 61.42 | Intruder Dose | 500 mrem/yr | 1.9 mrem/yr |

8.2 Further Work

Because this PA is considered a living document for the closure of the SDF, it will be reviewed as additional information and studies are conducted to verify that it continues to bind the SDF model inputs. As additional data become available, the information will be assessed versus the PA. The following areas of future work are presented to facilitate discussion of potential PA enhancements.

Saltstone Variability

Studies may be performed to further enhance the ability of the SPF to understand and predict the variability associated with the production of saltstone. Areas of this variability include homogeneity of the saltstone mix and impacts on saltstone hydraulic properties.

Closure Cap

Research and development programs could assist in the refinement of the assumptions associated with the closure cap. These activities could include addressing data and information gaps relevant to the long-term performance of the closure cap. Also, evaluation of a replacement for the existing software code utilized in predicting the infiltration rate through the closure cap over time should be completed.

Modeling Parameters and Inputs

Future work could be planned in the area of input refinement and confirmation, especially in areas where modeling results indicate inputs are sensitive to results. For example, efforts should continue in developing an enhanced understanding of the effect sulfate has on the chemical and physical breakdown of the saltstone and concrete barriers. External sulfate attack involves coupled porous medium transport, chemical reaction, and fracture mechanics. These effects have not yet been fully simulated in a coupled manner and sulfate attack modeling remains an ongoing research topic. Further study may be warranted for an enhanced estimate of the effective transport properties for saltstone contaminant release over time including:

- Understanding of saltstone oxidation and Tc-99 release rate to strengthen overall support for this model. This work should include evaluation of gas phase transport of oxygen through the saltstone and fractures
- Studies to further improve the understanding of the extent and frequency of fractures in saltstone
- Ra-226 release modeling, including the possibility of radium co-precipitation

Modeling Uncertainty/Sensitivity Analyses

Based on the results in Sections 5.6.5 and 5.6.6 (uncertainty and sensitivity analyses), further work could be warranted in refinement of stochastic distribution parameters, especially those parameters that are sensitive to, or important to, potential dose results. The probabilistic sensitivity analyses demonstrated that the groundwater doses are most sensitive to the specific radionuclide inventories and increased emphasis will be placed on understanding and improving this area of the model uncertainty. Other areas of improvement could include enhancement of the Vaults 1 and 4 wall release model, refinement of the assumed inventory

uncertainty distributions, and applying an inventory and pore volume transition stochastic to each individual FDC. Also, the application of correlations between linked stochastics (e.g., vegetable consumption and garden size) should be considered. In addition, PORFLOW runs reflecting alternative flow barrier configurations could be used to add more flow variability to the GoldSim probability analysis.

As a result of the NRC Technical Evaluation Report (TER) on the DOE waste determination for salt waste disposal at SRS (ML053010225), a number of PA maintenance activities are already in progress or planned to address the eight factors identified in the TER. Previous work to address the eight factors completed as of the issuance of this PA revision has already been incorporated. Table 8.2-1 identifies the on-going or planned activities for each of the eight factors. As information from these maintenance activities is available, the PA will be reviewed to determine what, if any, actions are required based on the new information.

Table 8.2-1: PA Maintenance Activities to Address NRC TER Factors

| Factor | Factor Description | Related PA Maintenance Activities |
|---------------|--|---|
| 1 | The rate of waste oxidation and release of technetium from an oxidized layer of saltstone will be a key determinant of the future performance of the saltstone disposal facility and therefore whether 10 CFR 61.41 can be met. More realistic modeling will be important to achieving the performance objectives, and adequate model support is essential to providing the technical basis for the model results. It will be important to ensure that gas phase transport of oxygen through fractures will not significantly increase oxidation of technetium in the saltstone. | <ul style="list-style-type: none"> ○ PA maintenance activities to provide additional model support are described under Factor 3. |
| 2 | The extent of degradation that may influence the hydraulic isolation capabilities of the saltstone and disposal units will be a key factor in assessing whether the SDF can meet 10 CFR 61.41. Degradation mechanisms that may result in the hydraulic conductivity of degraded saltstone and disposal unit concrete being larger than 1×10^{-7} cm/s (1×10^{-1} ft/yr) need to be evaluated with multiple sources of information (e.g., modeling, analogs, experiments [especially field scale and long-term], expert elicitation) to ensure that they are unlikely to occur. It will be important to ensure that field-scale physical properties (e.g., hydraulic conductivity, effective diffusivity) of as-emplaced saltstone are not significantly different from the results of laboratory tests of smaller-scale samples performed to date. It will be important to perform additional laboratory measurements of hydraulic conductivity because the data being relied upon represent limited samples that had a small range of curing times. In addition, because there was a fairly significant amount of variability in the Toxicity Characteristic Leaching Procedure (TCLP) test results, if DOE deviates significantly from the nominal saltstone composition, DOE should perform additional tests for hydraulic conductivity and effective diffusivity that justify the parameter values used over the range of compositions. | <ul style="list-style-type: none"> ○ A long-range program plan for on-going testing of degradation mechanisms associated with cementitious hydraulic properties is being developed to identify additional field/lab testing and identify test methods and equipment. |

Table 8.2-1: PA Maintenance Activities to Address NRC TER Factors (Continued)

| Factor | Factor Description | Related PA Maintenance Activities |
|--------|---|---|
| 3 | <p>Adequate model support is essential to assessing whether the saltstone disposal facility can meet 10 CFR 61.41. The model support for (1) moisture flow through fractures in the concrete and saltstone located in the vadose zone, (2) realistic modeling of waste oxidation and release of technetium, (3) the extent and frequency of fractures in saltstone and disposal unit that will form over time, (4) the plugging rate of the lower drainage layer of the closure cap, and (5) the long-term performance of the engineering cap as an infiltration barrier is key to confirming performance assessment results.</p> | <p>(1) <u>Moisture Flow through Fractures</u></p> <ul style="list-style-type: none"> ○ A long-range program plan for on-going testing of degradation mechanisms associated with cementitious hydraulic properties is being developed to identify additional field/lab testing and identify test methods and equipment. ○ A future study will be performed to evaluate the rate of equilibration of saltstone water content. <p>(2) <u>Waste Oxidation and Technetium Release</u></p> <ul style="list-style-type: none"> ○ A long-range program plan for on-going testing of waste oxidation and release of technetium is being developed to identify additional field/lab testing and identify test methods and equipment. <p>(3) <u>Extent and Frequency of Fractures</u></p> <ul style="list-style-type: none"> ○ A long-range program plan for on-going testing of the extent and frequency of fractures is being developed to identify additional field/lab testing and identify test methods and equipment. <p>(4) <u>Plugging Rate of lower Drainage Layer</u></p> <ul style="list-style-type: none"> ○ A long-range program plan for evaluating the plugging rate of the lower drainage layer is being developed to identify additional field/lab testing and identify test methods and equipment. ○ Evaluation of a replacement for the HELP code is currently planned. <p>(5) <u>Long-Term Performance of Closure Cap</u></p> <ul style="list-style-type: none"> ○ A long-range program plan for evaluating the long-term performance of the closure cap is being developed to identify additional field/lab testing and identify test methods and equipment. |

Table 8.2-1: PA Maintenance Activities to Address NRC TER Factors (Continued)

| Factor | Factor Description | Related PA Maintenance Activities |
|---------------|--|--|
| 4 | The erosion control design is important to ensuring that 10 CFR 61.42 can be met because it eliminates pathways and scenarios for intruder dose assessments. Implementation of an adequate design that does not deviate significantly from information submitted to the NRC is important, or if it does deviate significantly that it is reviewed by NRC staff to ensure the revisions are consistent with long-term erosion control design principles. | <ul style="list-style-type: none"> Future changes to the erosion control design will need to be evaluated by the UDAQ process and will be reviewed as part of the annual PA validation and closure plan review. |
| 5 | The infiltration control design is important to ensuring that 10 CFR 61.41 can be met because the release of contaminants to the groundwater is predicted to be sensitive to the large reduction in infiltration provided by the infiltration control. It is important to ensure that the design can be implemented and will perform as designed. | <ul style="list-style-type: none"> Additional model support will be developed to substantiate assumptions about lower drainage layer plugging and long-term performance of the closure cap. A long-range program plan for evaluating the plugging rate of the lower drainage layer is being developed as well as a long-range program plan for evaluating the long-term performance of the closure cap. |
| 6 | Implementation of an adequate sampling plan is important to ensuring that 10 CFR 61.41 and 10 CFR 61.42 can be met. It is important to assess results of future sampling and confirm that current projections of the concentrations of highly radioactive radionuclides in treated salt waste (or grout) are greater than or equal to actual concentrations of highly radioactive radionuclides in treated salt waste (or grout). | <ul style="list-style-type: none"> A review of the inventory of waste disposed of in the SDF is evaluated as part of the annual PA validation. In addition, feed tank sampling is reviewed with the NRC as part of the on-going support of the NRC monitoring role. |
| 7 | To ensure that Tank 48 waste can be safely managed, future tests of the physical properties of samples that contain organic materials similar to Tank 48 waste will need to confirm that the properties of the wasteform made from this waste will provide for suitable wasteform performance such that the disposal system will be able to meet the performance objectives. The technical basis should, at a minimum, include tests for hydraulic conductivity and effective diffusivity. | <ul style="list-style-type: none"> Current plans are to treat the existing Tank 48 waste by organic destruction. The resulting material will then be treated by the Salt Waste Processing Facility prior to disposal of any material in SDF. Any additional testing or research activities required will be reviewed once the treatment method is finalized. |
| 8 | Predicted removal efficiencies of highly radioactive radionuclides by each of the planned salt waste treatment processes are a key factor in determining the radiological inventory disposed of in saltstone. The inventory, in turn, is an important factor in the determination that 10 CFR 61.41 and 10 CFR 61.42 can be met. | <ul style="list-style-type: none"> A review of the inventory of waste disposed of in the SDF is evaluated as part of the annual PA validation. In addition, inventory is one of the areas reviewed with the NRC as part of the on-going support of the NRC monitoring role. |

9.0 PREPARERS

BAGWELL, LAURA, Savannah River National Laboratory

M.S. Geology – Texas A&M University

B.S. Geology – University of South Carolina

Experience: Laura Bagwell is a Principal Engineer with SRNL. Her 17 year SRS career includes regulatory compliance for waste management facilities; soil and groundwater characterization for closure projects; and geoscience support for new missions. As a member of SRNL's Environmental Analysis Section, she supports various SRS environmental and geotechnical projects and, through the Center for Sustainable Groundwater and Soil Solutions, provides expertise for environmental characterization and remediation across the DOE complex.

Contributions: Reviewed subsurface geologic data and interpreted shallow stratigraphy and water table conditions near the Saltstone Disposal Facility.

BIRK, MARCIA, SRR/Closure & Waste Disposal Authority

B.S. Chemical Engineering – University of Minnesota, Institute of Technology

Experience: Ms. Birk has over 18 years of experience at SRS in waste management engineering and environmental compliance. In her assignment in waste management engineering, she was responsible for radioactive and chemical characterization of mixed waste to meet offsite treatment facility WAC and Department of Transportation requirements for radioactive waste shipments. She has also held responsibility for regulatory compliance and for the maintenance of RCRA permits for the Consolidated Incineration Facility and the Hazardous and Mixed Waste Storage Facilities.

Contributions: Primary development of sections related to air pathways/radon analysis. Ms. Birk also assisted in the preparation and review of various PA sections.

BURNS, HEATHER, Savannah River National Laboratory

B.S. Chemical Engineering – Vanderbilt University

Experience: Heather is a Principal Engineer/ Project Manager at SRNL with over 25 years of experience related to various waste treatments of radioactive, hazardous, and mixed solid and liquid wastes at the SRS. She has been involved with both the stabilization/solidification and the thermal destruction of these wastes. She also developed the maintenance program for performance assessments in an effort to improve waste management practices at SRS. As part of this program, she took the lead as principal investigator on improving the monitoring program at the burial grounds by leading the effort to design, install, and operate the first vadose zone monitoring program in the DOE Complex. Her current efforts have been focused on providing project management for SRNL tank farm and Saltstone Disposal Facility PAs.

Contributions: Heather provided the project management and oversight for the SRNL support of the science/research and modeling efforts for the Saltstone Disposal Facility Performance Assessment.

CRAIG, ERIKA, SRR/Closure & Waste Disposal Authority

B.S. Chemical Engineering – University of South Carolina

Experience: Ms. Craig has a background in regulatory compliance. Her experience includes environmental, health, and safety compliance with an emphasis in air quality and waste management. Prior to joining SRS, she has worked in both public and private sectors for the chemical, pulp and paper, and textile industries.

Contributions: Ms. Craig performed technical and editing reviews for various sections of the PA.

DEAN, BEN, SRR/Closure & Waste Disposal Authority

B.S. Chemical Engineering – Clemson University

Experience: With over 11 years experience, four at SRS, Mr. Dean has primarily worked with characterization of waste within the tank farms. Prior to joining WSRC, Mr. Dean spent six years in the chemical industry (chlor-alkali and fiberglass) with experience in operations, process engineering and statistics.

Contributions: Assisted in development of the waste tank characterization and exposure pathway calculations.

DIXON, KENNETH, Savannah River National Laboratory

M.E. Civil Engineering – University of South Carolina

M.S. Agricultural Engineering – University of Georgia

B.S. Agricultural Engineering – University of Georgia

Experience: Mr. Dixon is a Principal Engineer at SRNL with over 17 years of experience related to groundwater hydrology, soil and groundwater characterization and remediation, and computational simulation. He has been the principal investigator on a number of vadose zone modeling studies at SRS aimed at assessing the impacts of contaminant migration from waste sites and decommissioned building slabs. Recently his efforts have been focused on PA support including measuring the physical and hydraulic properties of various cementitious waste forms and contaminant transport modeling in support of the air and radon pathway analyses.

Contributions: Mr. Dixon is one of the principal investigators on the air and radon pathway PORFLOW analysis. Additionally, he is one of the principal investigators focusing on the measurement of the hydraulic and physical properties of cementitious waste forms.

DYER, CONNIE, SRR/Closure & Waste Disposal Authority

Experience: Ms. Dyer has over 28 years experience in both the government and commercial nuclear sectors. She has over 19 years SRS-specific multi-disciplined engineering support experience. In her assignment in the 3116 Documentation Group, she is responsible for providing technical engineering support and configuration control for site closure and technology innovation activities. Ms. Dyer is responsible for developing internal procedures and processes required for production of regulatory documents being prepared, reviewed and issued under the direction of various government/independent agencies codes, statutes and requirements (including the NRC, SCDHEC, the U.S. EPA, and various oversight committees).

Contributions: Primary development of PA document format/layout. Develop and prepare drawings, process cartoons, diagrams, sketches and flowsheet. Provide document research, editorial and consistency reviews for project engineers in addition to being responsible for providing comment tracking and incorporation.

FARFAN, EDUARDO, Savannah River National Laboratory

Ph.D. Nuclear and Radiological Engineering – University of Florida

M.S. Nuclear and Radiological Engineering – University of Florida

B.S. Nuclear Engineering – University of Florida

Experience: Eduardo B. Farfan is a Principal Engineer at SRNL. His experience includes five years teaching in Nuclear Engineering and Health Physics Departments. His research involves internal dosimetry, risk assessment, probabilistic risk assessment, radon assessment, and computational modeling. A number of his research projects have involved collaborative efforts with the Centers for Disease Control and Prevention. Additionally, Dr. Farfan holds adjunct professor appointments at Clemson University and Idaho State University and is an online professor at Excelsior College. As a member of SRNL Environmental Analysis Section's Environmental Dosimetry Group, he provides expertise for various SRS dose and risk assessment projects involving airborne and liquid radionuclide releases.

Contributions: Dr. Farfan performs dose/risk assessments using the computer models: AXAIRQ, AXAOTHER, CAP88, IMBA, LADTAP, LUDEP, LUDUC, MAXDOSE, POPDOSE, and VENTSAR.

FLACH, GREGORY, Savannah River National Laboratory

Ph D. Mechanical Engineering – North Carolina State University

M.S. Mechanical Engineering – North Carolina State University

B.S. Mechanical Engineering – University of Kentucky

Experience: Dr. Flach is a Fellow Engineer at SRNL with over 19 years of experience related to groundwater hydrology, computational simulation, and numerical code development. He has been the principal investigator on a number of groundwater modeling studies at SRS involving regional and local scale hydrology, contaminant migration from waste sites, and evaluation of environmental cleanup alternatives. Over the last decade his efforts have focused on PA and CA related projects and research involving dual-domain formulations of contaminant transport.

Contributions: Dr. Flach is one of the principal modeling investigators focusing on the PORFLOW modeling of groundwater pathways.

FLETCHER, DORI, SRR/Closure & Waste Disposal Authority

B.S. Business Administration – Southern Wesleyan University

Experience: Ms. Fletcher has over 20 years experience at SRS. Her assignments include program administration within Engineering, Construction, Project Management, and special projects. She has served as a consultant, on special project initiatives, to Bechtel Corporation (Bechtel Group) at other DOE projects. In her assignment with the 3116 Documentation Group, she is responsible for providing technical administrative support and configuration control for site closure and technology innovation activities. She supports the production process of preparing regulatory documents for, review and issue under the direction of various government/independent agency codes, statutes and requirements (including the NRC, SCDHEC, the EPA, and various oversight committees).

Contributions: Primary application of the SDF PA document format/layout. Develop and prepare drawings, process cartoons, diagrams, sketches and flowsheets. Provide document research, editorial and consistency reviews, and comment tracking and incorporation.

GEORGE, BEN, ORISE Intern

B.S. Geology – Vanderbilt University

Experience: Mr. George received his geology degree in 2005 and is currently earning a Ph.D. from Vanderbilt University in Environmental Science and Engineering with a focus on Nuclear Waste Management and Disposal. He is working as an intern in the 3116 Documentation group and also has past experience in Environmental Consulting.

Contributions: Mr. George performed quality assurance, technical, and editing reviews for various sections of the PA. He also assisted with the inadvertent intruder external exposure calculations.

JONES, WILLIAM E., Savannah River National Laboratory

M.S. Geology – East Carolina University

B.A. Anthropology – East Carolina University

Experience: Mr. Jones is a Principal Scientist at SRNL, with over 20 years of experience related to geology, groundwater hydrology, geochemistry, and geotechnical engineering. He has been involved in closure cap installation, design, and performance evaluation and principal investigator for a variety of groundwater geochemistry and environmental clean-up projects.

Contributions: Mr. Jones' focus for Saltstone has been design and long-term performance evaluation of the closure cap.

JORDAN, JEFFREY, Savannah River National Laboratory

M.S. Mechanical Engineering – Georgia Institute of Technology

B.S. Physics – Furman University

B.A. History – Furman University

Experience: Jeff is a Senior Engineer at SRNL. He has an M.S. in Mechanical Engineering with a concentration in computational simulation. He has several years of experience with computational modeling of engineered systems. He has been working with groundwater modeling and contaminant transport for the past 2 years.

Contributions: Focused on developing and evaluating the PORFLOW modeling of groundwater pathways.

KNEPP, ANTHONY

M.S. Environmental Engineering – Clemson University

Experience: Mr. Knepp is an environmental engineer and manager who has worked on various nuclear waste planning, design and cleanup projects for the Department of Energy. He directed the Single Shell Performance Assessment for the Richland Office of DOE, evaluated the environmental cleanup program at Los Alamos for the National Academy of Sciences, and provides technical direction to soil and groundwater cleanup of radioactive waste for the Department of Energy. Mr. Knepp managed the investigation of the impact of leaking radioactive waste from single shell tanks at Hanford Site, Washington.

Contributions: Mr. Knepp provided an independent technical review of the PA.

LAYTON, MARK, SRR/Closure & Waste Disposal Authority

B.S. Nuclear Engineering – University of Cincinnati

Experience: Mr. Layton has over 18 years experience at SRS in various regulatory compliance organizations. The majority of this time was spent working on HLW regulatory compliance assignments and supporting various Safety Basis activities. Mr. Layton also provided safety basis support for numerous other facilities at SRS and across the DOE complex, including Sandia, Pantex, and Oak Ridge.

Contributions: Mr. Layton assisted in the preparation and review of various PA sections. Mr. Layton also provided support to the PA modeling.

LEE, PATRICIA L. Savannah River National Laboratory

Ph D. Nuclear Engineering/Health Physics – Georgia Institute of Technology

M.S. Health Physics – Georgia Institute of Technology; Physics – Clark Atlanta University

B.S. Physics – Lincoln University (PA)

Experience: Dr. Lee is an Environmental Health Physicist with a diverse scientific background including over 18 years of experience in Health Physics. For the past 9 years, she has worked in the Savannah River National Laboratory working on and performing research associated with dose and risk assessments for a variety of SRS projects. Her support of performance assessment activities at SRS are primarily focused on inadvertent intruder analysis, air pathway modeling and site-specific input parameters.

Contributions: For this study, Dr. Lee developed the air pathway dose-release factors.

MILES, WILSON, SRR/ SALT PROJECTS

B.A. Zoology – University of Mississippi

B.S. Chemical Engineering – University of Mississippi

Experience: Mr. Miles has over 19 years of engineering experience at SRS in waste management engineering, site closure and remediation, and radioactive liquid waste processing. In his current assignment as design authority, he is responsible for Saltstone vault organic modification, design and construction of new cylindrical disposal units, and Saltstone modification to support the Tank 50 return to service effort. Mr. Miles formerly held positions as an environmental engineer for over 6 years in the CERCLA Section of the Bureau of Solid and Hazardous Waste Management at the SCDHEC.

Contributions: Identification of cylindrical disposal unit design inputs and assumptions to be used in development of PA modeling.

MILLINGS, MARGARET, Savannah River National Laboratory

M.S. Geology – University of Georgia

B.S. Geology – The University of the South

Experience: Ms. Millings is a Senior Scientist with the Savannah River National Laboratory with 9 years of experience related to groundwater and surface water hydrology, coastal plain geology and geochemistry. At SRNL she has been involved in various subsurface characterization and monitoring programs and assisted in several environmental remediation projects at the SRS.

Contributions: One of the principal investigators providing material property interpretations for the vadose zone to be used in the PORFLOW modeling; in addition, provided assistance in the review of the Tan Clay Confining Zone and water table conditions near the Saltstone Disposal Facility.

NEWMAN, JEFF, SRNS/Regulatory Integration & Environmental Services

M.S. Public Health – University of South Carolina

B.S. Public Administration – Kutztown University

Experience: Mr. Newman has experience with regulatory compliance of high-level radioactive tank system closures. He was a primary author and the regulatory lead in obtaining approval for closure of the first high level radioactive waste tanks (SRS Tanks 17 and 20) in the United States DOE complex. Mr. Newman has over 30 years of environmental experience with a broad background in regulatory interpretation and compliance. Mr. Newman formerly held a position in the Bureau of Wastewater at the SCDHEC.

Contributions: Primary technical author and modeling coordinator of the PA.

PHIFER, MARK, Savannah River National Laboratory

M.S. Civil Engineering (Environmental and Geotechnical) – University of Tennessee

B.S. Civil Engineering – Tennessee Tech

South Carolina Registered Professional Engineer (No. 12310)

Experience: Mr. Phifer is a Senior Fellow Engineer with the Savannah River National Laboratory. He has 25 years of environmental and geotechnical experience at SRS. The first 10 years included environmental regulatory compliance, civil/environmental design, project engineering (closure of a mixed waste landfill and basins (80 acres)), and management (environmental remediation technology). The subsequent 15 years have been at the Savannah River National Laboratory developing, deploying, and evaluating waste site closure, groundwater remediation, and radioactive waste disposal technologies. These technologies include horizontal and vertical barrier systems, diffusion barriers, closure caps (including their degradation), waste subsidence, low-level radioactive waste disposal facilities, cementitious barriers and waste forms, permeable reactive barriers, GeoSiphon/GeoFlow groundwater treatment systems, sulfate reduction remediation, reductive dechlorination, and vadose zone and aquifer characterization and testing. For the last 7 years Mr. Phifer has in addition worked on Performance Assessment and CA related activities.

Contributions: Mr. Phifer is one of the principal investigators focusing on closure cap configuration and degradation; infiltration estimates; soil and cementitious material hydraulic properties; and air and radon modeling.

ROSENBERGER, KENT, SRR/Closure & Waste Disposal Authority

B.S. Nuclear Engineering – Pennsylvania State University

Experience: Mr. Rosenberger has over 18 years of experience at SRS primarily in the area of radiological controls. He has spent the last several supporting tank closure and Saltstone regulatory documents including 3116 Waste Determination and Performance Assessment development. He previously has held positions in radiological engineering project and operations support and facility operational radiological control management. Mr. Rosenberger has considerable experience with the SRS HLW processes and facilities, in addition to experience with reactor, chemical separations, plutonium processing and storage, and laboratory facilities.

Contributions: Provided overall technical review and management assistance.

SHEPPARD, RICHARD, SRR/Closure & Waste Disposal Authority

M.S. Nuclear Science – University of Michigan

B.S. Mathematics – Michigan Technological University

Experience: Mr. Sheppard has over 31 years experience within the Nuclear Industry During his period of commercial nuclear industry experience his emphasis was on accident analyses and dose assessments for various commercial nuclear power plants and regulatory and licensing activities associated with construction and operation. During his period at SRS, Mr. Sheppard coordinated hazard and safety analyses for design projects at various SRS nuclear facilities. He has spent the past two years supporting the WD efforts associated with the Saltstone and the closure of waste Tanks 18 and 19.

Contributions: Mr. Sheppard assisted in the preparation of various PA sections. He also conducted data verification for the development of the PA and input to PORFLOW and GoldSim computer simulations.

STAUB, AARON, SRR/ Waste Solidification Engineering

B.S. Chemical Engineering – University of Alabama

Experience: Mr. Staub has ten years experience at SRS. During his period at SRS, his emphasis has been on chemical process development and operations for various facilities used to stabilize low-level and high-level wastes. He has experience in micro-filtration and vitrification in addition to Saltstone processing. He has spent the past two years coordinating quality improvement initiatives to define the variability and performance of the Saltstone product.

Contributions: Mr. Staub assisted in the input verification for the PA.

TAUXE, JOHN, Neptune and Company, Inc.

Ph.D. Civil Engineering – University of Texas at Austin

M.S. Civil Engineering – University of Texas at Austin

B.A. Earth Science – Wesleyan University

Experience: Dr. Tauxe has been working in the earth and environmental sciences and engineering since 1981, and has developed expertise in quantitative hydrology and hydrogeology, and in computer programming, concentrating in the modeling of contaminant fate and transport in the environment. His relevant professional experience centers on modeling in support of radiological performance assessment in a probabilistic context at several sites in the DOE complex since 1994.

Contributions: Supervised uncertainty and sensitivity analysis work within Neptune and Company and provided interpretation of these analyses.

TAYLOR, GLENN, Savannah River National Laboratory

M.S. Mechanical Engineering – University of Texas at Austin

B.S. Engineering Physics – University of Louisville

Experience: Mr. Taylor has over 29 years of experience in code development, modeling, and research. His primary emphasis has been non-equilibrium thermal-hydraulics and chemical process methods development and modeling. He has been involved with Probabilistic Risk Assessment-type analyses since the mid-1980s. He has been doing groundwater modeling and contaminant transport modeling for the past 3 years.

Contributions: One of the principal investigators that performed the GoldSim groundwater pathway transport. Glenn also provided technical oversight of the sensitivity and uncertainty analyses provided by Neptune and Company and the dose calculator provided by SRNL staff.

WALTZ, COURTNEY, SCUREF INTERN

Experience: Ms. Waltz is currently earning her B. S. in chemical engineering at the University of South Carolina. She is working as an intern in the 3116 Documentation group.

Contributions: Ms. Waltz performed quality assurance, technical, and editing reviews for various sections of the PA.

WILHITE, ELMER, Savannah River National Laboratory

M.S. Inorganic Chemistry – Washington University

B.S. Chemistry – University of Missouri, Columbia

Experience: Mr. Wilhite has 39 years experience at SRS. His assignments include environmental research, high-level and LLW research, and supervision of environmental monitoring and analytical chemistry groups. Mr. Wilhite has served as a consultant to DOE Headquarters on LLW management for 23 years. He was the chairman of the former DOE Peer Review Panel and the technical lead for DOE for the radiological assessment section of the response to the DNFSB recommendation 94-2.

Contributions: Mr. Wilhite consulted on development of the conceptual model.

10.0 REFERENCES

Note 1: Reference numbers with an – OOU designator have been classified as: “*Official Use Only, Exemption 2 -- Not Releasable to the Public or Foreign Nationals without prior approval from DOE-SR*” by SRS Computer and Information Security (C&IS), Safeguards, Security & Emergency Services (SS&ES) Department.

Note 2: References identified as (Copyright) were used in the development of this SDF PA, but are protected by copyright laws. No part of the publication may be reproduced in any form or by any means, including photocopying or electronic transmittal in any form by any means, without permission in writing from the copyright owner.

10 CFR 61, *Licensing Requirements for Land Disposal of Radioactive Waste*, U.S. Code of Federal Regulations, U.S. Nuclear Regulatory Commission, Washington DC, December 23, 2008.

10 CFR 830, *Nuclear Safety Management, U.S.*, U.S. Department of Energy, Washington DC, February 4, 2002.

40 CFR 61, Subpart H, *National Emission Standards for Hazardous Air Pollutants, Subpart H, National Emission Standards for Emissions of Radionuclides Other than Radon from Department of Energy Facilities*, U.S. Environmental Protection Agency, Washington DC, July 20, 2009.

ACRi PORFLOW-QA-2008-1, (Copyright), *Software Testing and Verification for PORFLOW, Comparison of Versions 6.10.3 and 6.20.0*, ACRi Consultants in Engineering and Environmental Services, Bel Air, CA, Rev. 1, December 1, 2008.

ACRi-1994, (Copyright), *Analytic & Computational Research, Inc, PORFLOW Validation*, Version. 2.5, Analytic and Computational Research, Inc., Bel Air, CA, March 31, 1994.

ACRi-2002, (Copyright), *Analytic & Computational Research, Inc. PORFLOW User's Manual*, Version 5.0, Analytic and Computational Research, Inc., Bel Air, CA, Rev. 5, March 25, 2002.

ANL-EAD-4, Yu, C., et al., *User's Manual for RESRAD Version 6*, Argonne National Laboratory, Argonne, IL, July 2001.

ANL-EAIS-8, Yu, C., et al., *Data Collection Handbook to Support Modeling the Impacts of Radioactive Material in Soil*, Argonne National Laboratory, Argonne, IL, April 1993.

ASME NQA-1-2008, (Copyright), *Quality Assurance Program Requirements for Nuclear Facility Applications*, The American Society of Mechanical Engineers, New York, NY, 2008.

ASME NQA-1a-2009, (Copyright), *Addenda to ASME NQA-1-2008, Quality Assurance Requirements for Nuclear Facility Applications*, The American Society of Mechanical Engineers, New York, NY August 14, 2009.

ASTM D 6092 – 97, (Reapproved 2007), (Copyright), *Guide Standard Practice for Specifying Standard Sizes of Stone for Erosion Control*, ASTM International, West Conshohocken, PA, June 1, 2008.

CBU-ENG-2003-00103, Liner, K. R., *Saltstone Vault Sheet Drain Installation*, Savannah River Site, Aiken, SC, April 30, 2003.

CBU-PIT-2005-00146, Rosenberger, K. H., et al., *Saltstone Performance Objective Demonstration Document*, Savannah River Site, Aiken, SC, Rev. 0, June 2005.

CBU-PIT-2005-00228, Hamm, B. A., *Savannah River Site High-Level-Waste Tank Farm Closure Radionuclide Screening Process (First-Level) Development and Application*, Savannah River Site, Aiken, SC, Rev. 0, November 7, 2006.

C-CC-Z-0010, *Saltstone Vault No. 1 Personal Protection Layers Plan, Sections and Detail*, Savannah River Site, Aiken, SC, Rev. 1, March 14, 1995.

C-CC-Z-0012, *Saltstone Vault No. 4 Permanent Roof Plan*, Savannah River Site, Aiken, SC, Rev. 5, July 8, 2009.

C-CC-Z-0013, *Saltstone Vault No. 4 Permanent Roof Concrete Sections and Details Sheet No. 1*, Savannah River Site, Aiken, SC, Rev. 3, July 7, 1998.

C-CG-Z-00030, *Z-Area Saltstone Site Vault #2 Finish Grading Plan*, Savannah River Site, Aiken, SC, Rev. 3, June 24, 2009.

C-CH-Z-00014, *Saltstone Storage Vault No. 2, Drain Water Collection System Piping Arrangement and Pipe Support*, Savannah River Site, Aiken, SC, Rev. 4, August 31, 2009.

C-CS-Z-0002, *Saltstone Vault 4, Permanent Roof Steel Sections & Details (Sh.2)*, Savannah River Site, Aiken, SC, Rev. 2, July 7, 1998.

CDC-2006, *Risk Based Screening of Radionuclide Releases from the Savannah River Site*, U.S. Center for Disease Control, Atlanta, GA, August 2006.

C-SPP-Z-00006, Kelley, J. P., *Saltstone Vault #2 Including Excavation, Liner and Backfill*, Savannah River Site, Aiken, SC, Rev. 1, June 30, 2008.

DHEC_09-09-2008, *Modified Permit for the Savannah River Site (SRS) Z-Area Saltstone Disposal Facility (SDF), Facility ID No. 025500-1603, Aiken County, (Class 3 Landfill Permit)*, S.C. Department of Health and Environmental Control, Columbia, SC, September 9, 2008.

DHEC_10-03-2006, *Draft Modified Permit for the Savannah River Site (SRS) Z-Area Saltstone Disposal Facility, Facility ID No. 025500-1603*, S.C. Department of Health and Environmental Control, Columbia, SC, October 3, 2006.

DOE Format Guide_OUO, DRAFT *Format and Content Guide for U.S. Department of Energy Low-Level Waste Disposal Facility Performance Assessments and Composite Analyses*, U.S. Department of Energy, Washington DC, Rev. 1, May 11, 2007. (Draft Document - Not Approved for Public Release)

DOE G 435.1-1, *Implementation Guide for use with DOE M 435.1-1*, U.S. Department of Energy, Washington DC, July 9, 1999.

DOE M 435.1-1, Chg. 1, *Radioactive Waste Management Manual*, U.S. Department of Energy, Washington DC, January 9, 2007.

DOE O 414.1C, *Quality Assurance*, U.S. Department of Energy, Washington DC, July 7, 2005.

DOE O 435.1-1, Chg. 1, *Radioactive Waste Management*, U.S. Department of Energy, Washington DC, January 9, 2007.

DOE P 450.4, *Safety Management System Policy*, U.S. Department of Energy, Washington DC, October 15, 1996.

DOE_02-09-2006, *Compliance with DOE M 435.1-1 Waste Incidental to Reprocessing (WIR) Requirements and Implementation of Section 3116(a) of the National Defense Authorization Act for Fiscal Year 2005 (NDAA)*, U.S. Department of Energy, Washington DC, February 9, 2006.

DOE-EIS-0303, *High-Level Waste Tank Closure Final Environmental Impact Statement*, U.S. Department of Energy – Savannah River, Savannah River Site, Aiken, SC, May 2002.

DOE-ID-10966, *Performance Assessment for the Tank Farm Facility at the Idaho National Engineering Environmental Laboratory, Final*, Idaho National Laboratory, Idaho Falls, ID, Rev. 1 Predecisional, April 2003.

DPST-83-607, Cook, J. R., *Estimation of High Water Table Levels at the Saltstone Disposal Site*, Savannah River Site, Aiken, SC, Rev. 0, June 27, 1983.

DPST-87-523, McIntyre, P. F., and White, E. L., *Slag Saltstone Lysimeter: Monitoring During the First Two Years*, Savannah River Site, Aiken, SC, July 14, 1987.

E7 Manual 2.31, *Conduct of Engineering and Technical Support Procedure Manual, Engineering Calculations*, Savannah River Site, Aiken, SC, Rev. 10, September 24, 2007.

E7 Manual 2.60, *Conduct of Engineering and Technical Support Procedure Manual, Technical Reviews*, Savannah River Site, Aiken, SC, Rev. 12, August 14, 2009.

EPA-402-B-92-001, Parks, B. S., *User's Guide for CAP88-PC, Version 1.0*, Office of Radiation Programs, U.S. Environmental Protection Agency, Las Vegas, NV, March 1992.

EPA-402-R-93-081, *Federal Guidance Report No. 12, External Exposure to Radionuclides in Air, Water, and Soil*, U.S. Environmental Protection Agency, Washington DC, September 1993.

EPA-520-1-88-020, *Federal Guidance Report No. 11, Limiting Values of Radionuclide Intake and Air Concentration and Dose Conversion Factors for Inhalation, Submersion and Ingestion*, U.S. Environmental Protection Agency, Washington DC, September 1988.

EPA-600-P-95-002, *Exposure Factors Handbook*, U.S. National Center for Environmental Assessment, U.S. Environmental Protection Agency, Washington DC, August 1997.

EPA-600-R-94-168a, Schroeder, P. R., Aziz, N. M., Lloyd, C. M., and Zippi, P. A., *The Hydrologic Evaluation of Landfill Performance (HELP) Model: User's Guide for Version 3*, U.S. Environmental Protection Agency Office of Research and Development, Washington DC, September 1994.

EPA-600-R-94-168b, Schroeder, P. R., Dozier, T. S., Zippi, P. A., McEnroe, B. M. Sjostrom, J. W., and Peyton, R. L., *The Hydrologic Evaluation of Landfill Performance (HELP) Model: Engineering Documentation for Version 3*, U.S. Environmental Protection Agency Office of Research and Development, Washington DC, September 1994.

EPA-822-R-00-001, *Estimated Per Capita Water Ingestion and Body Weight in the United States – An Update, Based on Data Collected by the United States Department of Agriculture’s 1994 – 1996 and 1998 Continuing Survey of Food Intakes by Individuals*, U.S. Department of Agriculture, Washington DC, October 2004.

ESH-FSS-9000373, Odum, J. V., *Naval Fuel Material Facility (FMF) Settlement Agreement 89-06-SW, Item No. 3 Final Disposal of Saltcrete Drums*, Savannah River Site, Aiken, SC, June 20, 1990.

ESH-WPG-2006-00132, Liner, K. R., *Z-Area Industrial Solid Waste Landfill Vault Cracking*, Savannah River Site, Aiken, SC, October 19, 2006.

FR-00-9654, Federal Register/Vol. 65, No. 78, *National Primary Drinking Water Regulations; Radionuclides; Notice of Data Availability; Proposed Rule*, U.S. Environmental Protection Agency, Washington DC, April 21, 2000.

G-SQA-A-00011, Swingle, R. F., *Software Quality Assurance Plan for GoldSim*, Savannah River Site, Aiken, SC, Rev. 0, August 30, 2006.

GTG-2006b (Copyright), *Verification Plan: GoldSim Version 9.21*, GoldSim Technology Group LLC, Issaquah, WA, Rev. 0, April 2006.

GTG-2007, Volumes 1 and 2, *GoldSim User’s Guide, Version 9.60*, GoldSim Technology Group LLC., Issaquah, WA, March 2007.

G-TR-G-00002, Whiteside, T., *Software Testing and Verification for PORFLOW Version 6.10.3*, Savannah River Site, Aiken, SC, Rev. 0, October 30, 2007.

http://neic.cr.usgs.gov/neis/last_event_states/, *Earthquake Hazards Program: Last Earthquake in the United States, by State*, U.S. Geological Survey, Reston VA.

<http://soildatamart.nrcs.usda.gov/Manuscripts/SC696/0/savannah.pdf>, *Soil Survey of Savannah River Plant Area, Parts of Aiken, Barnwell, and Allendale Counties, South Carolina*, U.S. Department of Agriculture, Washington DC.

<http://www.epa.gov/epawaste/laws-regs/rcrahistory.htm>, *Resource Conservation and Recovery Act (RCRA)*, Federal Law of the United States contained in Title 42 U.S.C., U.S. Environmental Protection Agency, Washington DC.

<http://www.epa.gov/rpdweb00/assessment/CAP88/aboutcap88.html>, *About CAP-88, Regulatory Context, Application Niche, Strengths and Limitations, and Validation*, U.S. Environmental Protection Agency, Washington DC.

<http://www.epa.gov/safewater/contaminants/index.html#mcls>, *Drinking Water Contaminants*, U.S. Environmental Protection Agency, Washington DC.

<http://www.wes.army.mil/el/elmodels/helpinfo.html>, *Hydrologic Evaluation of Landfill Performance (HELP): Computer Program for Landfill Confined Disposal Facility (CDF) Design*, Version 3, U.S. Army Corps of Engineers, Washington DC.

IAEA-364, (Copyright), *Handbook of Parameter Values for the Prediction of Radionuclide Transfer in Template Environments, Produced in Collaboration with the International Union of Radioecologists*, International Atomic Energy Agency, Technical Reports Series 364, International Atomic Energy Agency, Vienna, July 29, 1957.

ICRP-72, (Copyright), *Radiation Protection: ICRP Publication 72 – Age-Dependent Doses to Members of the Public from Intake of Radionuclides: Part 5 Compilation of Ingestion and Inhalation Dose Coefficients*, International Commission on Radiological Protection, Didcot, Oxfordshire, September 1996.

ISSN 0017-9078 Vol. 62 No. 2, (Copyright), Hamby, D. M., *Site-Specific Parameter Values for the Nuclear Regulatory Commission's Food Pathway Dose Model*, Health Physics Radiation Protection Journal, Charleston, SC, Rev. 0, February 1992.

ISSN 0885-6125 Vol. 24 No. 2, (Copyright), Breiman, L., *Bagging Predictors*, University of California, Berkeley, November 21, 1995.

ISSN 0885-6125 Vol. 40 No. 2, (Copyright), Dietterich, T. G., *An Experimental Comparison of Three Methods for Constructing Ensembles of Decision Trees*, Oregon State University, Corvallis, OR, January 1, 2000.

ISSN 1019-0643, (Copyright), Bradbury, M. H., and Sarott, F. A., *Sorption Databases for the Cementitious Near-Field of a L/ILW Repository for Performance Assessment*, Paul Scherrer Institute, Labor für Entsorgung, Villigen PSI, Switzerland, Rev. 0, March 1995.

K-CLC-Z-00001, McHood, M., *Liquefaction Potential for Saltstone Disposal Facility Vault No. 4*, Savannah River Site, Aiken, SC, Rev. 0, August 27, 2002.

K-ESR-Z-00001, Li, W., *Saltstone Vault No. 2 Geotechnical Investigation Report*, Savannah River Site, Aiken, SC, Rev. 0, April 30, 2008.

LBNL-54094, (Copyright), Bucher, J. J., Edelstein, N. M., Lukens, W. W., and Shuh, D. K., *Evolution of Technetium Speciation in Reducing Grout*, Lawrence Berkeley National Laboratory, Berkeley, CA, 2003.

LWO-WSE-2009-00038, Staub, A. V., *Estimation of Variability in Premix Preparation At Saltstone*, Savannah River Site, Aiken, SC, February 4, 2009.

Manual 1Q 20-1, *Quality Assurance Manual, Software Quality Assurance*, Savannah River Site, Aiken, SC, Rev. 11, December 17, 2008.

Manual 1Q 2-1, *Quality Assurance Manual, Quality Assurance Program*, Savannah River Site, Aiken, SC, Rev. 10, December 17, 2008.

Manual SW24.5, Section 2.11, *Premix Blending & Conveying System Operating Manual*, Savannah River Site, Aiken, SC, Rev. 3, February 23, 2009.

Manual SW24.5 Section 2.4, *Premix Blending System Automatic Operation*, Savannah River Site, Aiken, SC, Rev. 7, April 29, 2009.

Manual SW 24.5, Section 2.5, *Premix Blending System Manual Operation*, Savannah River Site, Aiken, SC, Rev. 9, April 29, 2009.

ML053010225, *U.S. Nuclear Regulatory Commission Technical Evaluation Report for the U.S. Department of Energy Savannah River Site Draft Section 3116 Waste Determination for Salt Waste Disposal*, U.S. Nuclear Regulatory Commission, Washington DC, December 2005.

NCRP-123, (Copyright), *Screening Models for Releases of Radionuclides to Atmosphere, Surface Water, And Ground, Volume 1 and Volume 2*, National Council on Radiation Protection and Measurements, Bethesda, MD, January 22, 1996.

NCRP-160, (Copyright), *Ionizing Radiation Exposure of the Population of the United States (2009)*, National Council on Radiation Protection and Measurements, Bethesda, MD, March, 2009.

NDAA_3116, Public Law 108-375, *Ronald W. Reagan National Defense Authorization Act for Fiscal Year 2005*, Section 3116, *Defense Site Acceleration Completion*, U.S. Department of Energy, Washington DC, October 28, 2004.

NRMP-2005, *Natural Resources Management Plan (NRMP) for the Savannah River Site*, U.S. Department of Agriculture & Forestry Service, Savannah River Site, Aiken, SC, May 2005.

NUREG-0782, *Draft Environmental Impact Statement on 10 CFR Part 61 Licensing Requirements for Land Disposal of Radioactive Waste*, U.S. Nuclear Regulatory Commission, Washington DC, September 1981.

NUREG-0945, *Final Environmental Impact Statement on 10 CFR 61 Licensing Requirements for Land Disposal of Radioactive Waste, Summary and Main Report, Vol. 1*, U.S. Nuclear Regulatory Commission, Washington DC, November 1982.

NUREG-1573, *A Performance Assessment Methodology for Low-Level Radioactive Waste Disposal Facilities*, U.S. Nuclear Regulatory Commission, Washington DC, October 2000.

NUREG-1623, Johnson, T. L., *Design of Erosion Protection for Long-Term Stabilization*, U.S. Nuclear Regulatory Commission, Washington DC, September 2002.

NUREG-1854, *NRC Staff Guidance for Activities Related to U.S. Department of Energy Waste Determinations, Draft Final Report for Interim Use*, U.S. Nuclear Regulatory Commission, Washington DC, August 2007.

NUREG-CR-5512, (PNL-7994), Kennedy, W. E., Jr., et al., *Residual Radioactive Contamination From Decommissioning, Technical Basis for Translating Contamination Levels to Annual Total Effective Dose Equivalent, Final Report, Vol. 1*, Pacific Northwest Laboratory, Richland, WA, October 1992.

ORNL-5786, Baes, C. F., III, et al., *A Review and Analysis of Parameters for Assessing Transport of Environmentally Released Radionuclides through Agriculture*, Oak Ridge National Laboratory, Oak Ridge, TN, September 1984.

PB87-227104, Schroeder, P. R., and Payton, R. L., *Verification of the Lateral Drainage Component of the HELP Model Using Physical Models*, EPA/600/2-87/049, U.S. Environmental Protection Agency, Office of Research and Development, Cincinnati, OH, July 1987.

PB87-227518, Schroeder, P. R., and Peyton, R. L., *Verification of the Hydrologic Evaluation of Landfill Performance (HELP) Model Using Field Data*, EPA/600/2-87/050, U.S. Environmental Protection Agency, Office of Research and Development, Cincinnati, OH, July 1987.

PIT-MISC-0041_OUO, *Discussion Draft, SRS Long Range Comprehensive Plan*, Savannah River Site, Aiken, SC, Rev. 0, December 2000.

PIT-MISC-0072, Tuli, J. K., *Nuclear Wallet Cards, Seventh Edition*, National Nuclear Data Center, Brookhaven National Laboratory, Upton, NY, April 2005.

PIT-MISC-0089_OUO, *Savannah River Site End State Vision*, Savannah River Site, Aiken, SC, July 26, 2005.

PIT-MISC-0112, Aadland, R., et al., *Hydrogeologic Framework of West-Central South Carolina, Report 5*, S.C. Department of Natural Resources, Columbia, SC, 1995.

PNNL-13421, Staven, L. H., et al., *A Compendium of Transfer Factors for Agricultural and Animal Products*, Pacific Northwest Laboratory, Richland, WA, June 2003.

Q-SQA-A-00005, Phifer, M. A., *Software Quality Assurance Plan for the Hydrologic Evaluation of Landfill Performance (HELP) Model*, Aiken, SC, Rev. 0, October 2006.

Q-SQP-A-00002, Farfan, E. B., *Software Quality Assurance Plan for Environmental Dosimetry*, Savannah River Site, Aiken, SC, Rev. 2, May 2007.

Q-SQP-G-00003, Flach, G. P., *Software Quality Assurance Plan for Aquifer Model Refinement Tool (MESH3D)*, Savannah River Site, Aiken, SC, Rev. 0, February 2007.

Regulatory Guide 1.109, *Regulatory Guide 1.109 Calculation of Annual Doses to Man From Routine Releases of Reactor Effluents for the Purpose of Evaluating Compliance with 10 CFR 50, Appendix I*, U.S. Nuclear Regulatory Commission, Washington DC, Rev. 1, October 1977.

SCDHEC R.61-107.19, *SWM: Solid Waste Landfills and Structural Fill*, S.C. Department of Health and Environmental Control, Columbia, SC, May 23, 2008.

SCDHEC R.61-58, *State Primary Drinking Water Regulation*, S.C. Department Of Health and Environmental Control, Columbia, SC, June 2008.

SCDHEC R.61-67, *Standards for Wastewater Facility Construction*, S.C. Department Of Health and Environmental Control, Columbia, SC, May 24, 2002.

SED-GTE-2008-002, Bagwell, L. A., and Millings, M. R., *Review of the Tan Clay Confining Zone Beneath Z Area*, Savannah River Site, Aiken, SC, February 29, 2008.

SRNL-ESB-2007-00001, Millings, M. R., et al., *Summary of the Quality Review Process for General Separations Area Aquifer Model Database*, Savannah River Site, Aiken, SC, January 2, 2007.

SRNL-ESB-2007-00035, Millings, M. R., et al., *Addendum to Integrated Hydrogeological Modeling Report of the General Separations Area (GSA) (WSRC-TR-96-0399-Vol. 2, Rev.1)*, Savannah River Site, Aiken, SC, October 24, 2007.

SRNL-EST-2005-00105, Dixon, K. L., *Concrete Mixes for Saltstone Vault 4*, Savannah River Site, Aiken, SC, June 21, 2005.

SRNL-L6200-2009-00011, Flach, G. P., *PORFLOW Sensitivity Cases for Saltstone PA*, Savannah River Site, Aiken, SC, March 18, 2009.

SRNL-RPA-2007-00006, Kaplan, D. I., *Distribution Coefficients for Various Elements of Concern to the Tank Waste Performance Assessment*, Savannah River Site, Aiken, SC, July 10, 2007.

SRNL-STI-2008-00415, Lee, P. L., and Foley, T. Q., *Air Pathway Dose Modeling for the Saltstone Disposal Facility*, Savannah River Site, Aiken, SC, Rev. 0, December 15, 2008.

SRNL-STI-2008-00421, Dixon, K. L., et al., *Hydraulic and Physical Properties of Saltstone Grouts and Vault Concretes*, Savannah River Site, Aiken, SC, Rev. 0, November 2008.

SRNL-STI-2008-00447, Dixon, K. L., et al., *Air and Radon Pathway Modeling for the Saltstone Disposal Facility*, Savannah River Site, Aiken, SC, Rev. 0, December 2008.

SRNL-STI-2009-00115, Flach, G. P., et al., *Numerical Flow and Transport Simulations Supporting the Saltstone Disposal Facility Performance Assessment*, Savannah River Site, Aiken, SC, Rev. 1, June 17 2009.

SRNL-STI-2009-00150, Kaplan, D. I., and McDowell-Boyer, L., *Distribution Coefficients (K_d s), K_d Distributions, and Cellulose Degradation Production Correction Factors for the Composite Analysis*, Savannah River Site, Aiken, SC, Rev. 1, April 7, 2009.

SRNL-STI-2009-00178, Hinton, T., et al., *Systems Model of Carbon Dynamics in Four Mile Branch on the Savannah River Site*, Savannah River Site, Aiken, SC, Rev. 1, March 25, 2009.

SRNL-TR-2008-00283, Denham, M. E., *Estimation of Eh and pH Transitions in Pore Fluids During Aging of Saltstone and Disposal Unit Concrete*, Savannah River Site, Aiken, SC, December 2008.

SRNL-TR-2009-00019, Kaplan, D. I., *Tc and Pu Distribution Coefficients, K_d Values, for the Saltstone Facility Performance Assessment*, Savannah River Site, Aiken, SC, January 16, 2009.

SRNL-TR-2009-00051, Taylor, G. A., *Saltstone Disposition Facility Stochastic Transport and Fate Model Description*, Savannah River Site, Aiken, SC, Rev. 0, March 20, 2009.

SRNL-TR-2009-00052, Taylor, G. A., *Saltstone Disposition Facility Stochastic Transport and Fate Model Benchmarking*, Savannah River Site, Aiken, SC, Rev. 1, May, 2009.

SRNS-J2100-2008-00004, Dean, W. B., *Estimated Closure Inventory for the Saltstone Disposal Facility*, Savannah River Site, Aiken, SC, Rev. 2, June 22, 2009.

SRNS-J2100-2009-00006, Rosenberger, K. H., *Evaluation of Inadvertent Intruder External Exposure from Saltstone Disposal Cell Wasteform*, Savannah River Site, Aiken, SC, Rev. 1, June 16, 2009.

SRNS-STI-2008-00045, Kaplan, D. I., et al., *Saltstone and Concrete Interactions with Radionuclides: Sorption (K_d), Desorption, and Reduction Capacity Measurements*, Savannah River Site, Aiken, SC, October 30, 2008.

SRNS-STI-2008-00050, Langton, C. A., *Evaluation of Sulfate Attack on Saltstone Vault Concrete and Saltstone*, Simco Technologies, Inc., Part 1: Final Report, Savannah River Site, Aiken, SC, Rev. 1, August 28, 2009.

SRNS-TR-2008-00310, Wells, D., *Z-Area Groundwater Monitoring Report For 2008*, Savannah River Site, Aiken SC, January 9, 2009.

SRS-REG-2007-00002_OUO, Layton, M. H., et al., *Performance Assessment for F-Tank Farm at the Savannah River Site – Final*, Savannah River Site, Aiken, SC, Rev. 0, June 27, 2008.

SRS-REG-2007-00029, Birk, M. B., *General Separations Area Well Drilling Probabilities*, Savannah River Site, Aiken, SC, Rev. 0, November 7, 2007.

SRS-REG-2007-00036, *Documentation of Personal Communication Between Kaplan, D. I., to Newman, J. L., September 9, 2007*, Savannah River Site, Aiken, SC, Rev. 0, November 13, 2007.

SRT-EST-2003-00134, Jannik, G. T., *Cesium-137 Bioconcentration Factor for Freshwater Fish in the SRS Environment*, Savannah River Site, Aiken, SC, July 15, 2003.

STADIUM® User Guide, (Copyright), *STADIUM® Software for Transport and Degradation in Unsaturated Materials, Users Guide VV2.8*, http://www.mslexperts.com/slm/stadium_help/index.html, SIMCO Technologies Inc., Quebec City, Quebec, Canada, September 2008.

TV-0080-0041, *Part 70 Air Quality Permit*, S.C. Department of Health and Environmental Control, Columbia, SC, Rev. 13, December 11, 2007.

W780625, *Saltstone Surface Disposal Vault Foundation and Floor Plan, Elevation and Sections*, Savannah River Site, Aiken, SC, Rev. 7, Feb. 24, 2004.

W828992, *Saltstone Vault 6 & 7 Plan*, Savannah River Site, Aiken, SC, Rev. 2, March 10, 2008.

W828993, *Saltstone Vault 4 Sections & Details, Concrete and Steel*, Savannah River Site, Aiken, SC, Rev. 7, July 8, 2009.

WB00001K-004, *2.9 – MG Saltstone Tanks 2A & 2B*, Savannah River Site, Aiken, SC, Rev. F, June 1, 2009.

WSP-SSF-2005-00023, Liner, K. R., *Application for Modification, Z-Area Industrial Solid Waste Landfill Permit #025500-1603, Engineering Report for Vault 2 Construction*, Savannah River Site, Aiken, SC, Rev. 1, August 20, 2007.

WSRC 1-01 MP 4.2, *Management Policies, Section 4.2, Quality Assurance*, Savannah River Site, Aiken, SC, Rev. 4, January 13, 2005.

WSRC-IM-2004-00008, *DSA Support Document - Site Characteristics and Program Descriptions*, Savannah River Site, Aiken, SC, Rev. 1, June 2007.

WSRC-MS-2003-00617, Stevenson, D. A., et al., *2001-2002 Upper Three Runs Sequence of Earthquakes at the SRS, South Carolina*, Savannah River Site, Aiken, SC, September 19, 2003.

WSRC-MS-92-513, Salvo, S. K., and Cook, J. R., *Selection and Cultivation of Final Vegetative Cover for Closed Waste Sites at the Savannah River Site, SC*, Savannah River Site, Aiken, SC, February 1993.

WSRC-MS-95-0524, Hiergesell, R. A., *Regional Water Table Map of the Savannah River Site, IQ-95*, Savannah River Site, Aiken, SC, Rev. 0, December 1995.

WSRC-RP-2005-01674, Kaplan, D. I., Hang, T., and Aleman, S. E., *Estimated Duration of the Reduction Capacity within High-Level Waste Tank*, Savannah River Site, Aiken, SC, Rev. 0, August 3, 2005.

WSRC-RP-91-17, Hamby, D. M., *Land and Water Use Characteristics in the Vicinity of the Savannah River Site*, Savannah River Site, Aiken, SC, March 1991.

WSRC-RP-92-1360, *Radiological Performance Assessment Report for the Z-Area Saltstone Disposal Facility at the Savannah River Site*, Savannah River Site, Aiken, SC, December 18, 1992.

WSRC-RP-92-225, *WSRC Quality Assurance Management Plan*, Savannah River Site, Aiken, SC, Rev. 22, March 31, 2009.

WSRC-RP-97-311_OUO, *Composite Analysis: E-Area Vaults and Saltstone Disposal Facilities*, Savannah River Site, Aiken, SC, Rev. 0, September 1997.

WSRC-RP-98-00156, Fowler, J. R., *Addendum to the Radiological Performance Assessment for the Z-Area Saltstone Disposal Facility at the Savannah River Site*, Savannah River Site, Aiken, SC, Rev. 0, April 30, 1998.

WSRC-SQP-A-00028, Collard, L. B., *Software Quality Assurance Plan for the PORFLOW Code*, Savannah River Site, Aiken, SC, Rev. 0, September 30, 2002.

WSRC-STI-2006-00123, Jannik, G. T., et al., *LADTAP-PA: A Spreadsheet for Estimating Dose Resulting from E-Area Groundwater Contamination at the Savannah River Site*, Savannah River Site, Aiken, SC, August 2006.

WSRC-STI-2006-00159, Crapse, K. P., et al., *Atmospheric Pathway Screening Analysis for the E-Area Low-Level Waste Facility*, Savannah River Site, Aiken, SC, September 5, 2006.

WSRC-STI-2006-00198, Phifer, M. A., et al., *Hydraulic Property Data Package for the E-Area and Z-Area Soils, Cementitious Materials, and Waste Zones*, Savannah River Site, Aiken, SC, Rev. 0, September 2006.

WSRC-STI-2007-00004, Lee, P. L., et al., *Baseline Parameter Update for Human Health Input and Transfer Factors for Radiological Performance Assessments at the Savannah River Site*, Savannah River Site, Aiken, SC, Rev. 4, June 13, 2008.

WSRC-STI-2007-00613, Kabela, E. D., and Weber, A. H., *Summary of Data Processing for the 2002-2006 SRS Meteorological Database*, Savannah River Site, Aiken, SC, December 13, 2007.

WSRC-STI-2007-00640, Kaplan, D. I., and Coates, J. M., *Partitioning of Dissolved Radionuclides to Concrete Under Scenarios Appropriate for Tank Closure Performance Assessments*, Savannah River Site, Aiken, SC, December 21, 2007.

WSRC-STI-2007-00649, Dixon, K., and Phifer, M. A., *Hydraulic and Physical Properties of MCU Saltstone*, Savannah River Site, Aiken, SC, Rev. 0, March 31, 2008.

WSRC-STI-2008-00057, Mamatey, A. R., *Savannah River Site Environmental Report for 2007*, Savannah River Site, Aiken, SC, 2007.

WSRC-STI-2008-00236, Denham, M. E., *Thermodynamic and Mass Balance Analysis of Expansive Phase Precipitation in Saltstone*, Savannah River Site, Aiken, SC, May 2008.

WSRC-STI-2008-00244, Jones, W. E., and Phifer, M. A., *Saltstone Disposal Facility Closure Cap Concept and Infiltration Estimates*, Savannah River Site, Aiken, SC, May 2008.

WSRC-TR-2000-00310, Cumbest, R. J., *Comparison of Cenozoic Faulting at the Savannah River Site to Fault Characteristics of the Atlantic Coast Fault Province: Implications for Fault Capability*, Savannah River Site, Aiken, SC, November 2000

WSRC-TR-2002-00456, Cook, J. R., et al., *Special Analysis: Reevaluation of the Inadvertent Intruder, Groundwater, Air, and Radon Analysis for the Saltstone Disposal Facility*, Savannah River Site, Aiken, SC, Rev. 0, October 23, 2002.

WSRC-TR-2003-00250, Hiergesell, R. A., et al., *An Updated Regional Water Table of the Savannah River Site and Related Coverages*, Savannah River Site, Aiken, SC, Rev. 0, December 2003.

WSRC-TR-2003-00436, Phifer, M. A., et al., *Saltstone Disposal Facility Closure Cap Configuration and Degradation Base Case: Institutional Control to Pine Forest Scenario*, Savannah River Site, Aiken, SC, Rev. 0, September 22, 2003.

WSRC-TR-2004-00106, Flach, G. P., *Groundwater Flow Model of the General Separations Area Using PORFLOW*, Savannah River Site, Aiken, SC, Rev. 0, July 15, 2004.

WSRC-TR-2004-00152, *Savannah River Site Groundwater Protection Program*, Savannah River Site, Aiken, SC, March 2004.

WSRC-TR-2005-00074, Cook, J. R., et al., *Special Analysis: Revision of Saltstone Vault 4 Disposal Limits*, Savannah River Site, Aiken, SC, Rev. 0, May 26, 2005.

WSRC-TR-2005-00131, Hiergesell, R. A., *Saltstone Disposal Facility: Determination of the Probable Maximum Water Table Elevation*, Savannah River Site, Aiken, SC, Rev. 0, April 2005.

WSRC-TR-2005-00201, Wike, L. D., et al., *SRS Ecology: Environmental Information Document*, Savannah River Site, Aiken, SC, March 2006.

WSRC-TR-2006-00004, Kaplan, D. I., *Geochemical Data Package for Performance Assessment Calculations Related to Savannah River Site*, Savannah River Site, Aiken, SC, Rev. 0, February 28, 2006.

WSRC-TR-2007-00118, Kabela, E. D., et al., *Savannah River Site Annual Meteorology Report for 2006*, Savannah River Site, Aiken, SC, April 20, 2007.

WSRC-TR-2007-00283, Millings, M. R., et al., *Hydrogeologic Data Summary in Support of the F-Area Tank Farm (FTF) Performance Assessment*, Savannah River Site, Aiken, SC, Rev. 0, July 2007.

WSRC-TR-2008-00090, Skidmore, T. E., and Billings, K. D., *Saltstone Vault #2 Interior Lining Review*, Savannah River Site, Aiken, SC, Rev. 0, May 2008.

WSRC-TR-95-0046, Denham, M. E., *SRS Geology & Hydrogeology Environmental Information Document*, Savannah River Site, Aiken, SC, June 1999.

WSRC-TR-96-0231, Friday, G. P., et al., *Radiological Bioconcentration Factors for Aquatic, Terrestrial, and Wetland Ecosystems at the Savannah River Site*, Savannah River Site, Aiken, SC, December 1996.

WSRC-TR-96-0399-Vol. 1, Flach, G. P., et al., *Integrated Hydrogeological Model of the General Separations Area, Vol. 1*, Savannah River Site, Aiken, SC, Rev. 0, August 1997.

WSRC-TR-96-0399-Vol. 2, Flach, G. P., et al., *Integrated Hydrogeological Model of the General Separations Area, Vol. 2*, Savannah River Site, Aiken, SC, Rev. 1, April 1999.

WSRC-TR-98-00045, Hiergesell, R. A., *The Regional Water Table of the Savannah River Site and Related Coverages*, Savannah River Site, Aiken, SC, September 1998.

WSRC-TR-99-00369, Chen, K. F., *Flood Hazard Recurrence Frequencies for C-, F-, E-, S-, H-, Y-, and Z-Areas*, Savannah River Site, Aiken, SC, September 30 1999.

www.acricfd.com/software/porflow/, *Computational Fluid Dynamics (CFD) Tool by Analytic & Computational Research, Inc.* (software demo download and purchasing information), Analytic & Computational Research, Inc., Bel Air, CA.

www.dutchlandinc.com/product_pages/circulair_5_lewistown.html, Image of proposed Saltstone storage tank, Dutchland Incorporated, Lancaster, PA.

www.epa.gov/radiation/heast, *Radionuclide Carcinogenicity Slope Factors: HEAST*, U.S. Environmental Protection Agency, Washington DC.

www.epa.gov/safewater/sdwa/index.html, *Safe Drinking Water Act (SDWA)*, U.S. Environmental Protection Agency, Washington DC.

www.epa.gov/superfund/policy/cercla.htm, *Comprehensive Environmental Response, Compensation, and Liability Act (CERCLA) of 1980*, Title 42, United States Code (U.S.C.) §§ 9601 et seq., as amended by the Superfund Amendments and Reauthorization Act of 1986, Pub. L. 99-499, U.S. Environmental Protection Agency, Washington DC.

www.epw.senate.gov/water.pdf, *Federal Water Pollution Control Act [As Amended Through P.L. 107-303, November 27, 2002]*, U.S. Senate Committee on Environment and Public Works, Washington DC, November 27, 2002.

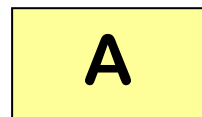
www.factfinder.census.gov, *Population Estimates*, American Fact Finder, U.S. Census Bureau, Washington DC, 2007.

www.goldsim.com, *Monte Carlo Simulation Software for Decision and Risk Analysis*, GoldSim Technology Group, Issaquah, WA.

X-ESR-Z-00007, Carpenter, S. A., *Linking Document Database (LDD) Environmental Permit Information for Saltstone (Z-Area)*, Savannah River Site, Aiken, SC, Rev. 0, April 1, 2009.

X-SD-Z-00001, *Waste Acceptance Criteria for Aqueous Waste Sent to the Z-Area Saltstone Production Facility*, Savannah River Site, Aiken, SC, Rev. 8, December 2008.

11.0 GLOSSARY



Absorption

Entering of particles of one phase into a different bulk phase by penetrating a surface.

Accuracy

Closeness of the result of a measurement to the true value of the quantity.

Actinide

Group of elements of atomic number 89 through 103. Laboratory analysis of actinides by alpha spectrometry generally refers to the elements plutonium, americium, uranium, and curium but may also include neptunium and thorium.

Adsorption

The enrichment or collection of particles on a surface or interface.

Air Pathway

Exposure pathway to radioactive material dispersed in the air in the form of dusts, fumes, particulates, mists, vapors, or gases.

ALARA

As Low As Reasonably Achievable - making every reasonable effort to maintain exposures to radiation as far below the dose limits as is practical and consistent with the purpose for which the licensed activity is undertaken, taking into account the state of technology, the economics of improvements in relation to state of technology, the economics of improvements in relation to benefits to the public health and safety, and other societal and socioeconomic considerations.

Ancillary Equipment

Above grade structures, utilities, equipment, etc., to be removed from the SDF and SPF area prior to installation of the closure cap (e.g., grout transfer lines, tanks, etc.).

Aquifer

Saturated, permeable geologic unit that can transmit significant quantities of water under ordinary hydraulic gradients.

Aquitard

Geologic unit that inhibits the flow of water.

Argillaceous

Containing, made of, or resembling clay; clayey.

**Atomic Energy
Commission**

Federal agency created in 1946 to manage the development, use, and control of nuclear energy for military and civilian application. It was abolished by the Energy Reorganization Act of 1974 and succeeded by the Energy Research and Development Administration. Functions of the Energy Research and Development Administration eventually were taken over by the U.S. Department of Energy and the U.S. Nuclear Regulatory Commission.

B

Background Radiation

Naturally occurring radiation, fallout, and cosmic radiation. Generally, the lowest level of radiation obtainable within the scope of an analytical measurement, i.e., a blank sample.

Base Case

Also known as Case A, the Base Case reflects the expected condition of the disposal unit during the period of performance.

Bioaccumulation Factor

Calculations that define parameters used to calculate contaminant concentrations via a variety of environmental mechanisms.

Biotic Transport

Amounts and rates of radionuclides transported by living components (i.e., animals, plants or bacterial life) of an ecosystem.

Bleed Water

Water that separates from the grout as the result of solids settling.

C

Cartesian coordinates

The set of numbers which locate a point in space with respect to a collection of mutually perpendicular axes.

Cell

For the SDF, cells refer to the individual disposal cells in existing Vaults 1 and 4, or to the unique FDCs.

Cementitious

Like or relevant to or having the properties of cement.

| | |
|---|--|
| Central Savannah River Area (CSRA) | Eighteen-county area in Georgia and South Carolina surrounding Augusta, Georgia. The Savannah River Site is included in the Central Savannah River Area. Counties are Richmond, Columbia, McDuffie, Burke, Emanuel, Glascock, Jenkins, Jefferson, Lincoln, Screven, Taliaferro, Warren, and Wilkes in Georgia and Aiken, Edgefield, Allendale, Barnwell, and McCormick in South Carolina. |
| Centroid | Geometric center of an object's shape. |
| CERCLA | Comprehensive Environmental Response, Compensation, and Liability Act (CERCLA), commonly known as Superfund, was enacted by Congress on December 11, 1980. This law provides to clean up uncontrolled or abandoned hazardous-waste sites as well as accidents, spills, and other emergency releases of pollutants and contaminants into the environment. Through the Act, EPA was given power to seek out those parties responsible for any release and assure their cooperation in the cleanup. |
| Citizens Advisory Board (CAB) | The Savannah River Site Citizens Advisory Board is composed of individuals from South Carolina and Georgia. The board members are chosen to reflect the cultural diversity of the population affected by SRS. The Board provides advice and recommendations to the U.S. Department of Energy (DOE) on environmental remediation, waste management and related issues. All meetings are open to the public and public participation is encouraged. Public comment periods are offered at various times throughout the meetings. |
| Clean Grout | Non-radioactive grout that is placed in the disposal unit upon completion of the saltstone filling process. |
| Clean Water Act | The Clean Water Act is the cornerstone of surface water quality protection in the United States. (The Act does not deal directly with groundwater or with water quantity issues.) The law employs a variety of regulatory and non-regulatory tools to sharply reduce direct pollutant discharges into waterways, finance municipal wastewater treatment facilities, and manage polluted runoff. |
| Closure Plan | Plan that presents the environmental regulatory standards and guidelines pertinent to the closure of the SDF. |
| Compressive Strength | Force per unit area required to break an unconfined grout or concrete sample. |
| Concentration | Amount (e.g., in grams or curies) per volume of a substance. |

| | |
|--|---|
| Cone Penetration Test | The cone penetration test (CPT) is an in-situ testing method used to determine the geotechnical engineering properties of soils and delineating soil stratigraphy. The CPT is one of the most used and accepted in-situ test methods for soil investigation. The test method consists of pushing an instrumented cone, tip first, into the ground at a controlled rate. |
| Consumption Rates | Physical human health exposure parameters used for evaluating pathway-specific dose. |
| Cretaceous | The geological time period between 140 and 65 million years ago. |
| Curie | A unit of radioactivity; the quantity of nuclear material that experiences $3.7\text{E}+10$ disintegrations per second. |
| D | |
| Darcy Velocity | Formula for measuring velocity and flow of groundwater. |
| Desorption | The opposite process to adsorption meaning the removal of aggregated particles from a surface. |
| Deterministic | When fixed parameters are used in calculations versus a distribution of values (probabilistic). |
| Diffusion/Diffusive Transfer | Movement of contaminants from an area of higher concentration to an area of lower concentration. |
| Diffusion Coefficient | The rate of diffusion of particles, depending on the particle size, viscosity and temperature. |
| Dispersivity | Equal to the dispersion coefficient divided by the velocity. |
| Distribution Coefficient (K_d) | The quantity of a solute absorbed by a solid, per unit weight of solid, divided by the quantity of the solute dissolved in the water per unit volume of water. |
| Disposal Unit | Global term used to describe any disposal structure (vault or FDC) located within the SDF. |
| Divalent cation | Cation with a net positive charge of +2. |

Dolomitic A magnesia-rich sedimentary rock resembling limestone.

Dose Conversion Factor A factor used to convert radionuclide concentrations in environmental media to doses. Factors are used for inhalation, ingestion, immersion and external exposure.

Dose Limits The permissible upper bounds of radiation doses.



Effective Diffusion Coefficient (D_e) The diffusion coefficient of a species through a saturated porous medium taken over the pore area of the medium through which diffusion occurs under steady-state conditions.

Effective Dose Equivalent The sum of the products of the dose equivalent to the organ or tissue (H_T) and the weighting factors (W_T) applicable to each of the body organs or tissues that are irradiated ($H_E = \sum W_T H_T$).

E_h The symbol for redox potential in millivolts.

Erosion Barrier The layer within a multi-part closure cap made of rock (riprap) and filler materials designed to prevent riprap movement during a Probable Maximum Precipitation event and therefore forms a barrier to further erosion and gully formation (i.e., provide closure cap physical stability). It will be used to maintain a minimum 10 ft of clean material above the disposal units to act as an intruder deterrent. It will also act to preclude burrowing animals from access to underlying closure cap layers. It also provides minimal water storage for the promotion of evapotranspiration.

Escarpment A steep slope or long cliff caused by erosion or faulting separating two level areas of differing heights.

Ettringite Ettringite is hexacalcium aluminate trisulfate hydrate. Ettringite is found in hydrated Portland cement system as a result of the reaction of calcium aluminate with calcium sulfate, both present in Portland cement.

Evaporator Steam-heated, water-cooled system installed in the tank farms to concentrate underground waste storage tank contents, in order to reduce the liquid waste volume.

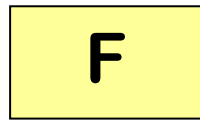
Evapotranspiration Evapotranspiration (ET) is a term used to describe the sum of evaporation and plant transpiration from the earth's land surface to atmosphere. Evaporation accounts for the movement of water to the air from sources such as the soil, canopy interception, and waterbodies.

Exposure Being exposed to ionizing radiation or to radioactive material.

Exposure Pathway The means by which humans are exposed to contaminants. The key exposure pathways are air and water, with most exposures via drinking water, crops, other foods, inhalation and direct radiation.

External Dose That portion of the dose equivalent received from radiation sources outside the body.

Extrapolated To infer (values of a variable in an unobserved interval) from values within an already observed interval.



Federal Facility Agreement (FFA) Agreement between EPA, DOE and SCDHEC that directs the comprehensive remediation of the Savannah River Site (SRS). It contains requirements for (1) site investigation and remediation of releases and potential releases of hazardous substances, and (2) interim status corrective action for releases of hazardous wastes or hazardous constituents.

Flux The time rate of change or concentration. For example, curies per year leaving the waste form.

Fly Ash Fly ash is a mineral admixture used in grout to enhance finishing characteristics, make the mix more economical, and to improve pumping. It is finer in consistency than cement, and its particles are round. These fine particles make the mix finish easier, and pump easier.

Future Disposal Cell The facilities that will be constructed in the future in coordination with disposal rates.

G

Gaussian plume equation

An equation that represents dispersion of a material from a release point.

General Separations Area

Centralized area of SRS including, E-, F-, H-, S- and Z-Areas that are the heavily industrialized areas of SRS.

Geosynthetic Clay Liner

A woven fabric-like material primarily used for the lining of landfills. It is a kind of geomembrane and Geosynthetic which incorporates a bentonite or other clay, which has a very low hydraulic conductivity.

GoldSim

A simulation software program designed to dynamically model the release and transport of radioactive constituents. The fundamental output consists of predicted mass fluxes at specified locations within a system, and predicted concentrations within environmental media (e.g., groundwater, soil, air).

Gradient Boosting Model

Modeling approach that utilizes binary recursive partitioning algorithms that deconstruct a response into the relative influence from a given set of explanatory variables (stochastic model input parameters).

Graham's Law

Grahams Law states that the rate of diffusion of a gas is inversely proportional to the square root of its molecular weight.

Groundwater Flow

The rate of groundwater movement through the subsurface.

H

Henry's Law

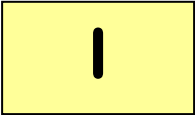
The concentration of a gas dissolved in a liquid at a given temperature is directly proportional to the partial pressure of the gas above the liquid.

Herpetofauna

Term used that refers to reptiles and amphibians, collectively.

Heterogeneous

Non-similar or non-uniform structure or composition throughout.

| | |
|---|--|
| Homogenous | Similar or uniform structure or composition throughout. |
| Hydraulic Conductivity | Velocity of water flow through saturated materials (e.g., concrete, grout, soil). |
| Hydrostatic Head | The force of pressure at a given point in a liquid at rest producing the same pressure or exerted force to a unit area surface due to the weight of the fluid above it. Hydrostatic Pressure. |
| Hydrostratigraphy | A geologic framework consisting of a body of rock having considerable lateral extent and composing a reasonably distinct hydrologic system. |
|  | |
| Igneous Rock | An aggregate of interlocking silicate minerals formed by cooling and solidification of magma or lava. Igneous rocks are formed by volcanic processes. |
| Indurated | Hard or thickened. |
| Institutional Control | A 100-year period in which DOE retains ownership and control of the SDF, such that facility maintenance and controls will be performed to prevent inadvertent intrusion and protect public health and the environment. |
| Interfluvial | The region of higher land between two rivers that are in the same drainage system. |
| Integrated Site Conceptual Model (ISCM) | The ISCM is the integration of all parts of the assumptions and understanding concerning the SDF behavior in the environment over time. |
| Internal Dose | That portion of the dose equivalent received from radioactive material taken into the body. |

J

Jurassic

The geological period between 210 and 140 million years ago.

L

Lacustrine Sediments

A type of deposit that comes from lakes which previously occupied the area. They are fine-grained soils that have settled through the water and accumulated on the lake bottom, typically leaving them in a soft condition.

Latin Hypercube Sampling

A form of sampling that can be applied to multiple variables. The method is commonly used to reduce the number of runs necessary for a Monte Carlo simulation to achieve a reasonably accurate random distribution.

Leaching

Leaching occurs when infiltrating water seeps into the closure system and transports contaminants out of the system.

Lithified Terrigenous Sediment

Sediments derived from the erosion of rocks on land.

Lithology

The description of rocks, especially in hand specimen and in outcrop, on the basis of such characteristics as color, mineralogical composition, and grain size.

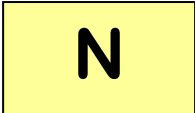
M

Macro Invertebrate

Any non-vertebrate organism that is large enough to be seen without the aid of a microscope.

Maximally Exposed Individual (MEI)

A hypothetical individual who, because of proximity, activities, or living habits, could potentially receive the maximum possible dose of radiation or of a hazardous chemical from a given event or process.

| | |
|---|---|
| Maximum Contaminant Level (MCL) | The highest level of a contaminant that is allowed in drinking water, below which there is no known or expected risk to health. MCLs are EPA enforceable standards. |
| Mesozoic | An area of geologic time, from the end of the Paleozoic to the beginning of the Cenozoic, or from about 225 million years to about 65 million years ago. |
| Metamorphosed Sedimentary Rock | Rock that is formed by the consolidation of sediment particles or of the remains of plants and animals. |
| Miocene-age | Middle of Tertiary Period, dating back 13-25 million years. |
| Molar | Relating to a solution that contains X moles of solute per liter of solution, where X is a number. |
| Monte Carlo Analysis | An analytical technique in which a large numbers of simulations are run using random quantities for uncertain variables and looking at the distribution of results to infer which values are most likely. |
| Montmorillonite Clay | Montmorillonite Clay: Very soft phyllosilicate mineral that typically forms in microscopic crystals, forming a clay. |
|  | |
| National Pollutant Discharge Elimination System | As authorized by the Clean Water Act, the National Pollutant Discharge Elimination System (NPDES) permit program controls water pollution by regulating point sources that discharge pollutants into waters of the United States. Point sources are discrete conveyances such as pipes or man-made ditches. |
| NDAA Section 3116 | The Ronald W. Reagan National Defense Authorization Act for Fiscal Year 2005 Section 3116 was passed by Congress on October 9, 2004 and signed by the President on October 28, 2004. Section 3116 of the NDAA specifies that the term “high-level radioactive waste” does not include radioactive waste that results from reprocessing spent nuclear fuel if the Secretary of Energy determines, in consultation with the NRC, that the waste meets certain criteria. |

O

Occupational Dose

The dose received by an individual in the course of employment in which the individual's assigned duties involve exposure to radiation or to radioactive material. Occupational dose does not include doses received from background radiation or from any medical administration the individual has received.

Official Use Only (OUO)

Information within the document is not approved for public release. A redacted version of these documents must be developed, removing sensitive information.

Operational Period

Period of time during which the SDF is in operation, the systems are grouted, and a closure cap is installed in accordance with FFA requirements.

Outcrop

Also referred to as seep line, it is the location where groundwater from the upper aquifers is discharged to the surface.

Oxidation Potential

The measure of a material to oxidize or lose electrons.

Oxidized

Combined with or having undergone a chemical reaction with oxygen.

P

Paleozoic

The geological period between 600 to 230 million years ago.

Par Pond

A lake constructed at Savannah River Site in 1958 to provide cooling water for P-Reactor and R-Reactor.

Perennial Stream

A perennial stream has flowing water year-round during a typical year. The water table is located above the stream bed for most of the year. Groundwater is the primary source of water for stream flow. Run-off from rainfall is a supplemental source of water for stream flow.

Permeability

Capability of a material to let pass other molecules or particles.

| | |
|-------------------------------|--|
| pH | A measure of the acidity or alkalinity of a solution, numerically equal to 7 for neutral solutions, increasing with increasing alkalinity and decreasing with increasing acidity. |
| Phosphatic | Pertaining to, or containing, phosphorus, phosphoric acid, or phosphates; as, phosphatic nodules. |
| Plume | A body of contaminated groundwater emanating from a specific source. |
| Pore | Hole in a material. |
| Pore Fluid | Fluid within material pores which for saltstone consists predominately of sodium, nitrate, and nitrite. The clean grout, made from process water, has a bulk composition similar to saltstone. |
| PORFLOW | A Comprehensive Fluid Dynamics (CFD) simulation software program developed to accurately solve problems involving transient or steady state fluid flow, heat, salinity and mass transport in multi-phase, variably saturated, porous or fractured media with dynamic phase change. The porous/fractured media may be anisotropic and heterogeneous, arbitrary sources (e.g., wells) may be present and chemical reactions or radioactive decay may take place. It accommodates alternate fluid and property relations and complex and arbitrary boundary conditions. |
| Porosity | Grout porosity is generally defined as the percentage of total volume of cured grout that is not occupied by the starting cementitious materials and the products that result from reaction of these cementitious materials with water. |
| Potable Water | Water that is safe for human consumption. |
| Power-Law Relationship | Special kind of mathematical relationship between two quantities. If one quantity is the frequency of an event, the relationship is a power-law distribution, and the frequencies decrease very slowly as the size of the event increases. |
| Pozzolan | A siliceous volcanic ash used to produce hydraulic cement. |
| Precambrian | An informal term to include all geologic time from the beginning of the Earth to the beginning of the Cambrian period 570 million years ago. |

Probabilistic

A model that assigns a likelihood to events or data within a population, as expressed by a ranked numerical value or an estimate of best case, worst case or most likely.

**Probable Maximum
Precipitation**

Theoretically, the greatest depth of precipitation for a given duration that is physically possible over a given size storm area at a particular geographical location at a certain time of the year.

Progeny

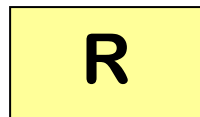
Decay products or descendants of specific radionuclides.

**Pseudo-Sorption
Coefficient**

The treatment of Tc-99 transport from the saltstone in a non-physical nature because the underlying process is not of sorption, but a K_d value is substituted.

Public Dose

The dose received by a member of the public from exposure to radiation from the disposal facility. Public dose does not include occupational dose or doses received from background radiation or from any medical administration the individual has received.



RCRA

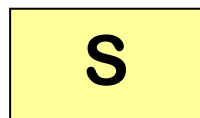
The Resource Conservation and Recovery Act (RCRA) is the public law that creates the framework for the proper management of hazardous and nonhazardous solid waste.

Redox

Redox (shorthand for oxidation/reduction reaction) describes all chemical reactions in which atoms have their oxidation number (oxidation state) changed.

Residual Radioactivity

Radioactivity in structures, materials, soils, groundwater, and other media at a site remaining after closure.



Saltcake

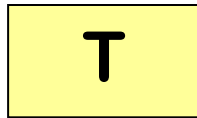
Saltcake located in waste tanks consists of crystallized salts with interstitial void space and entrained soluble solids (assumed to be partially sludge solids).

| | |
|--|--|
| Saltstone (grout) | Cementitious waste form made by mixing salt solution originating from liquid waste storage tanks in F- and H-Tank Farms of SRS with a dry mix containing blast furnace slag, fly ash, and cement or lime. |
| Saltstone Disposal Facility (SDF) | Consists of existing vaults (Vault 1 and Vault 4) and future disposal cells (FDCs) used for the final disposal of the solidified saltstone. |
| Saltstone Facilities | The Saltstone Facilities consists of two facility segments, one of which is the Saltstone Production Facility (SPF), which receives and treats salt solution to produce saltstone grout. The second facility segment is the Saltstone Disposal Facility (SDF), which consists of existing vaults (Vault 1 and Vault 4) and future disposal cells (FDCs) used for the final disposal of the solidified saltstone. |
| Saltstone Production Facility (SPF) | Receives and treats salt solution to produce saltstone grout. |
| Saturated zone | The saturated zone encompasses the area below ground in which all interconnected openings within the geologic medium are completely filled with water. |
| Sector | A logical division or grouping. |
| Seepage | Also referred to as outcrop or far field, it is the location where groundwater from the upper aquifers is discharged to the surface. |
| Sheet Drain | Device employed in the disposal units in order to facilitate the removal of excess water after saltstone disposal. |
| Shotcrete | Shotcrete is a substance applied via pressure hoses. Shotcrete is usually concrete conveyed through a hose and pneumatically projected at high velocity onto a surface. Shotcrete undergoes placement and compaction at the same time due to the force with which it is projected from the nozzle. Shotcrete will be used in the construction of the FDCs. |
| Shrinkage | Percent length change of grout samples cured at 73°F as a function of curing time in saturated and drying environments. |

| | |
|-------------------------------|---|
| Silica fume | Silica fume, also known as microsilica, is a byproduct of the reduction of high-purity quartz with coke in electric arc furnaces in the production of silicon and ferrosilicon alloys. Silica fume is used as an addition in Portland cement concretes to improve properties. It has been found that silica fume improves compressive strength, bond strength, and abrasion resistance. Addition of silica fume also reduces the permeability of concrete to chloride ions, which protects concrete's reinforcing steel from corrosion. |
| Slag | Vitreous by-product of the metal smelting process |
| Slug test | A slug test is a particular type of aquifer test where water is quickly added or removed from a groundwater well, and the change in hydraulic head is monitored through time, to determine the near-well aquifer characteristics. It is a method used by hydrogeologists to determine the transmissivity and storativity of the material the well is completed in. |
| Solubility | A property of a solid or liquid to dissolve into a homogeneous mixture with another liquid. |
| Source Term | The amount and type of radioactive material available for release into the environment. |
| Spalling | Destruction of a surface by frost, heat, corrosion, or mechanical causes. |
| Stabilized Contaminant | Grouted waste remaining in the Vaults or Future Disposal Cells after system closure. |
| STADIUM® | Proprietary modeling code developed by SIMCO Technologies, Inc. in collaboration with Laval University. |
| Stated Mean Sea Level | The reference point used as a standard for determining terrestrial and atmospheric elevation or ocean depths and is calculated as the average of hourly tide levels measured by mechanical tide gauges over extended periods of time. |
| Stochastic | A probabilistic distribution of parameters. |
| Stoichiometry | Calculation of the quantitative relationships between the amounts of reactants and products formed during a chemical reaction. |

Supernate

Liquid salt solution found above the sludge layer after settling of solids in waste tanks has occurred as a result of a liquid waste transfer to one of the waste processing facilities or receipt tanks.



Thermodynamic

The science of heat and temperature and of the laws governing the conversion of heat into mechanical, electrical, or chemical energy.

TNX

A designation code for one of the first facilities (T-Area) completed at SRS. Its use was primarily for technical support and development for Separations.

Tortuosity

The resistance to diffusion through a porous solid due to the influence of the pore structure.

**Total Effective Dose
Equivalent (TEDE)**

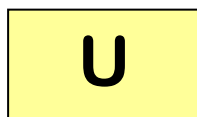
The sum of the deep-dose equivalent (for external exposures) and the committed EDE (for internal exposures).

Tracer

An amount of material introduced into a system model in order to follow the behavior of some component of that system.

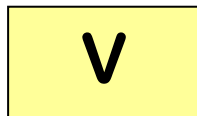
Triassic

The period of geological time between 248 and 213 million years ago.



Udorthents

Well drained soils that formed in heterogeneous materials, which are the spoil or refuse from excavations and major construction operations.



Vadose Zone

The unsaturated zone located between the ground surface and the water table or saturated zone.

Viscosity

Rheological quality of fluids describing the resistance to flow.

Volatilization

The transport of a liquid substance by vaporization.



**Waste Characterization
System**

SRS computer based system designed to integrate historical information, current sample data, and physical properties of constituents to develop predictions of concentrations and inventory.

Waste Inventory

Residual contaminants remaining in the radioactive waste tanks and associated ancillary equipment.



Young's Modulus

Young's modulus (E) is a measure of the stiffness of a given material. It is also known as the modulus of elasticity, elastic modulus or tensile modulus. It is defined as the ratio, for small strains, of the rate of change of stress with strain.

APPENDIX A.1

100-METER RADIOLOGICAL AND CHEMICAL CONCENTRATIONS AT THE UPPER THREE RUNS AQUIFER – UPPER ZONE

Appendix A.1 contains curves showing the 100 meter radiological and chemical concentrations for all of SDF (vault and FDC inventories) for the Base Case (Case A). 20,000 year concentration results are presented from the Upper Three Runs Aquifer-Upper Zone for Sectors A through L.

Graph heading example “CaseA All Ac-227 A-UA”

Key

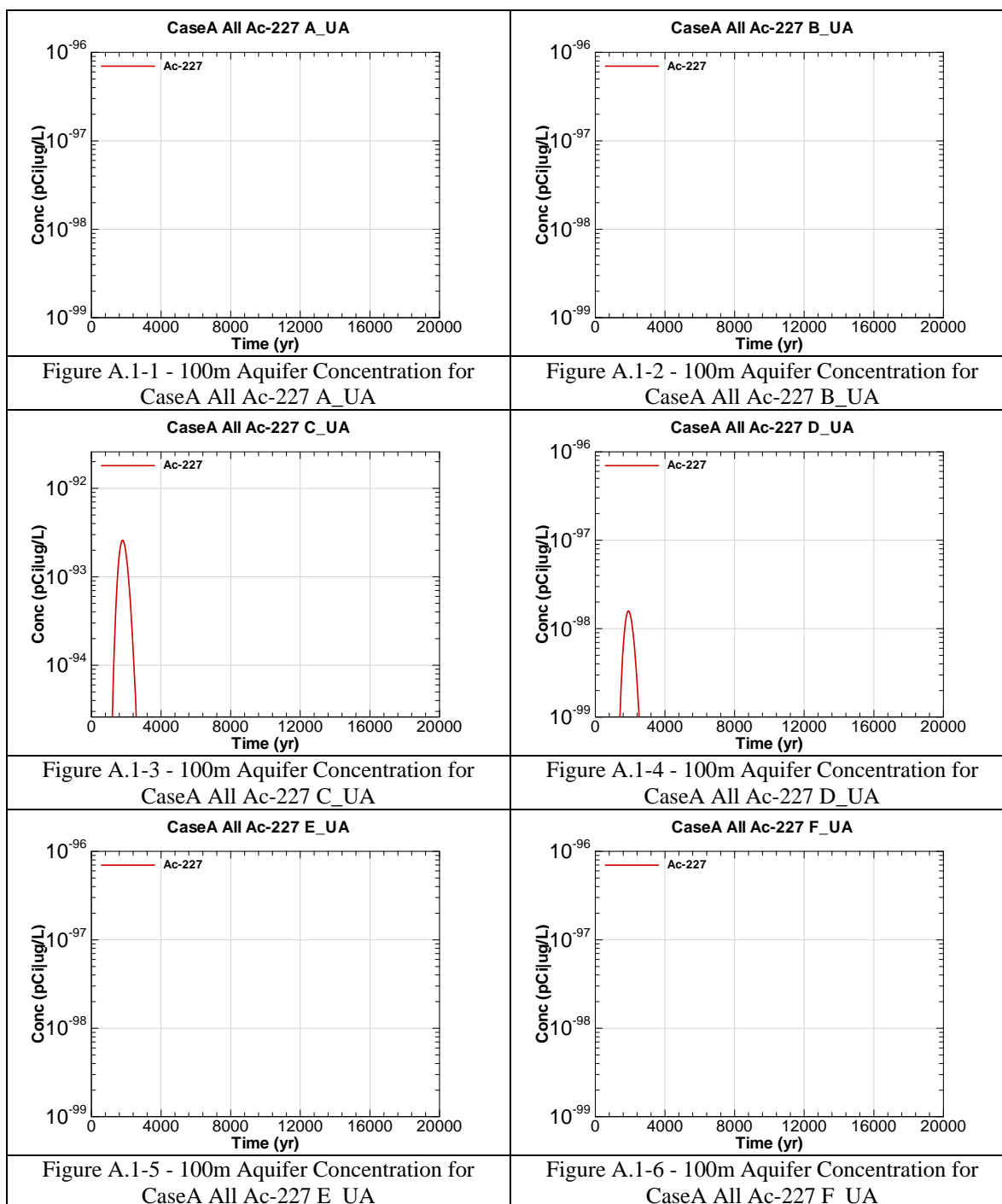
CaseA = Scenario case

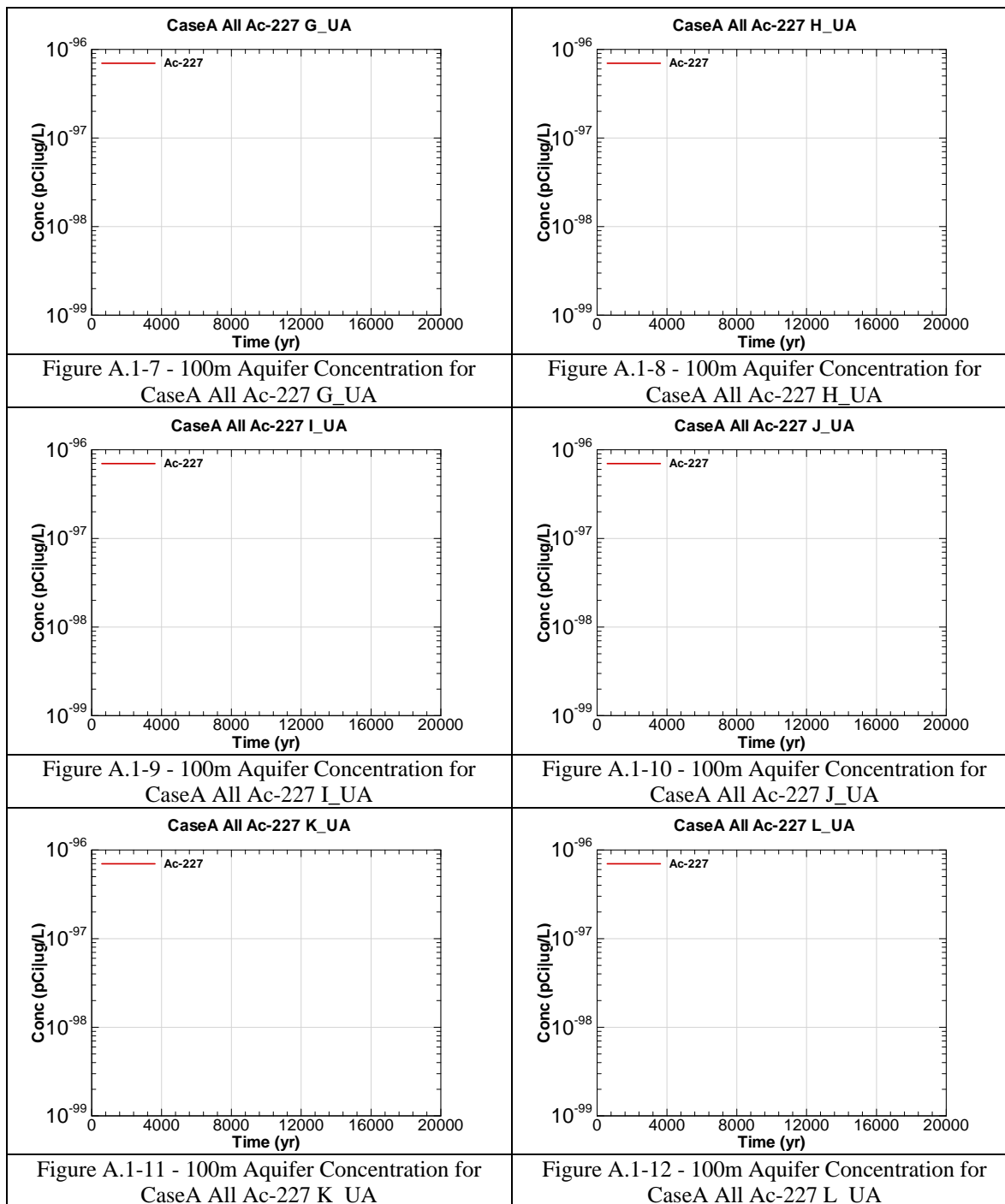
All = Inventory source is all disposal units

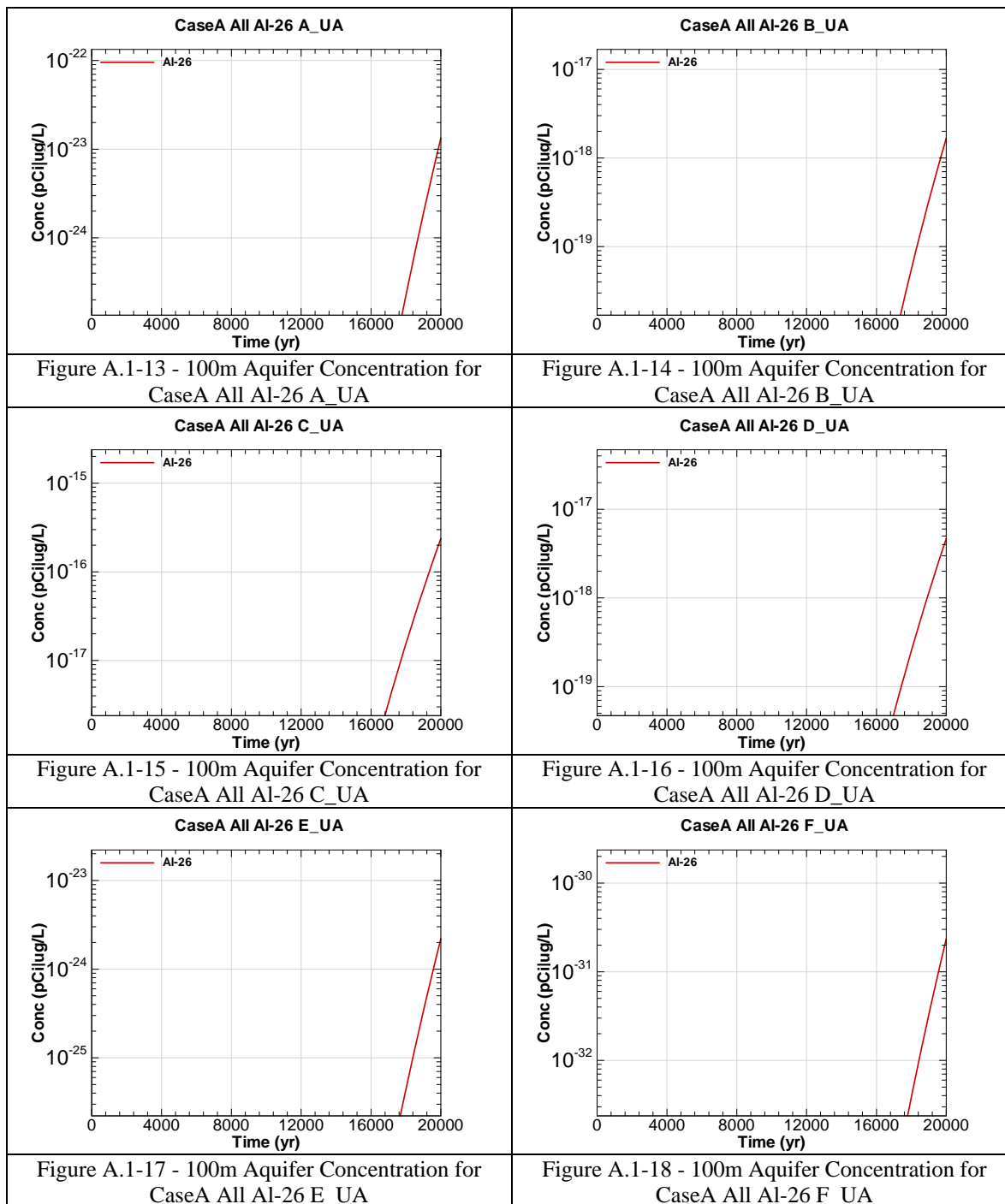
Ac-227 = Radionuclide or chemical of concern

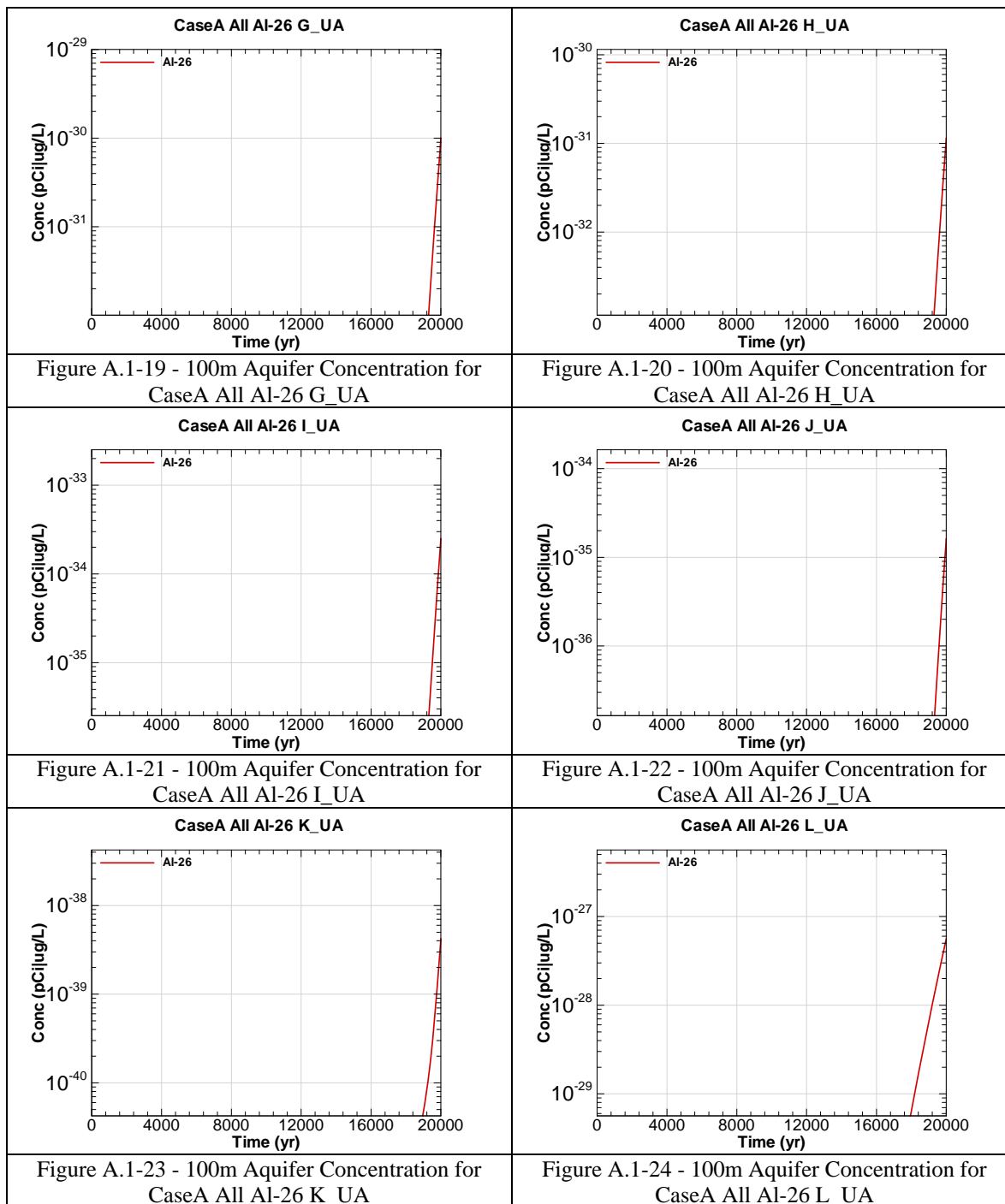
A = Evaluation sector of concern

UA = Aquifer of concern is Upper Three Runs Aquifer – Upper Zone









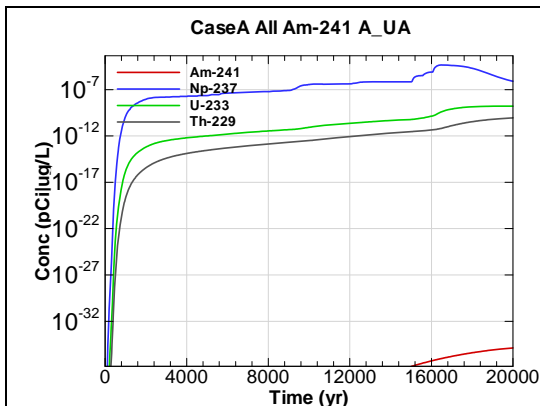


Figure A.1-25 - 100m Aquifer Concentration for CaseA All Am-241 A-UA

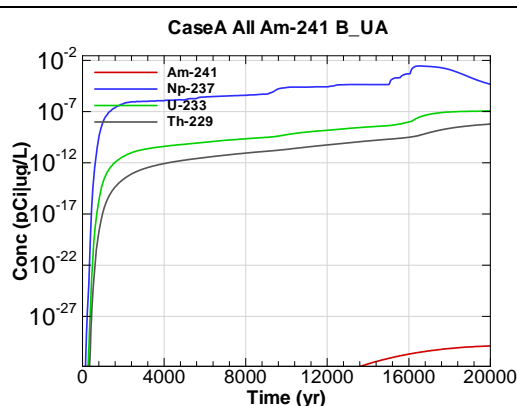


Figure A.1-26 - 100m Aquifer Concentration for CaseA All Am-241 B-UA

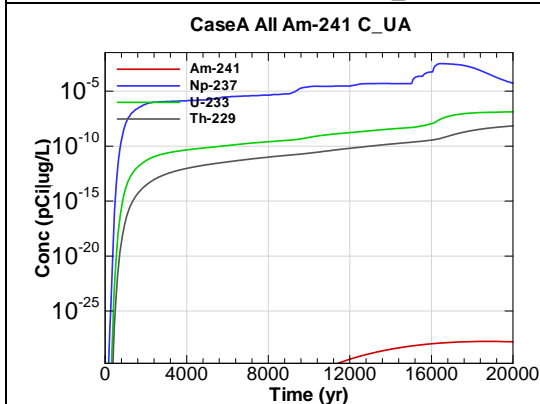


Figure A.1-27 - 100m Aquifer Concentration for CaseA All Am-241 C-UA

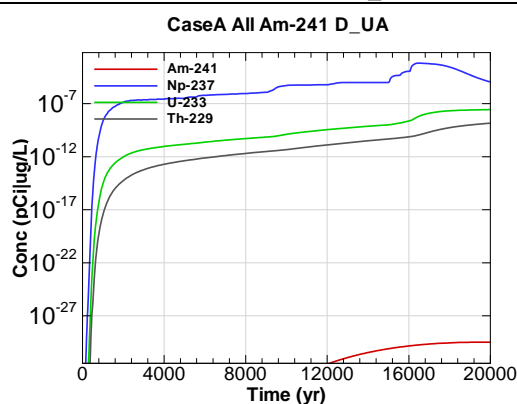


Figure A.1-28 - 100m Aquifer Concentration for CaseA All Am-241 D-UA

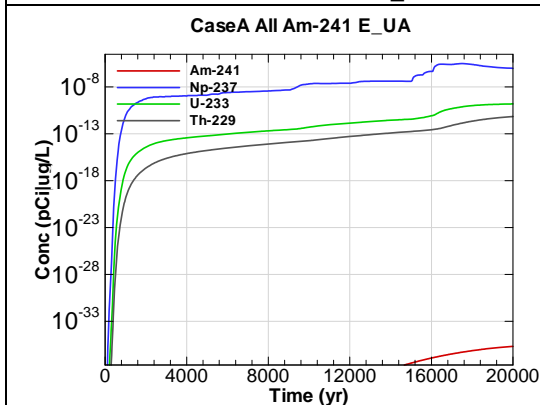


Figure A.1-29 - 100m Aquifer Concentration for CaseA All Am-241 E-UA

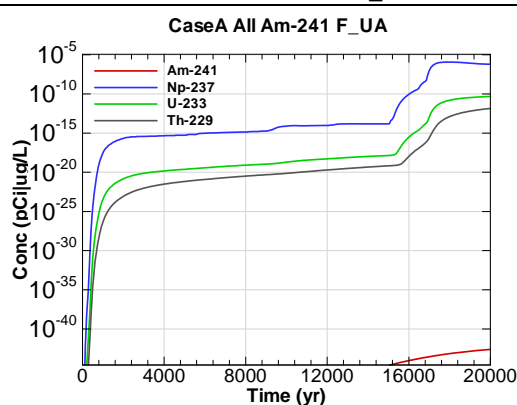


Figure A.1-30 - 100m Aquifer Concentration for CaseA All Am-241 F-UA

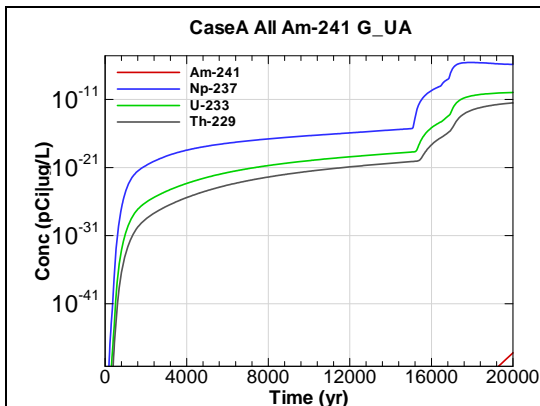


Figure A.1-31 - 100m Aquifer Concentration for CaseA All Am-241 G-UA

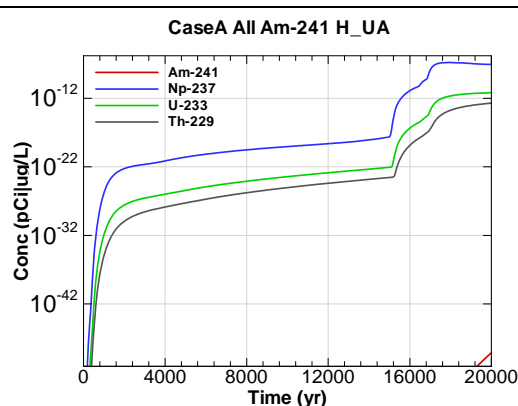


Figure A.1-32 - 100m Aquifer Concentration for CaseA All Am-241 H-UA

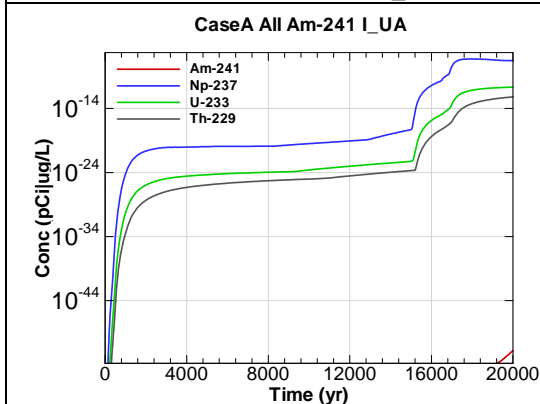


Figure A.1-33 - 100m Aquifer Concentration for CaseA All Am-241 I-UA

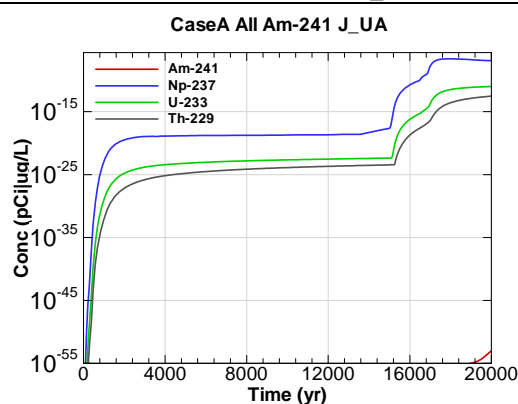


Figure A.1-34 - 100m Aquifer Concentration for CaseA All Am-241 J-UA

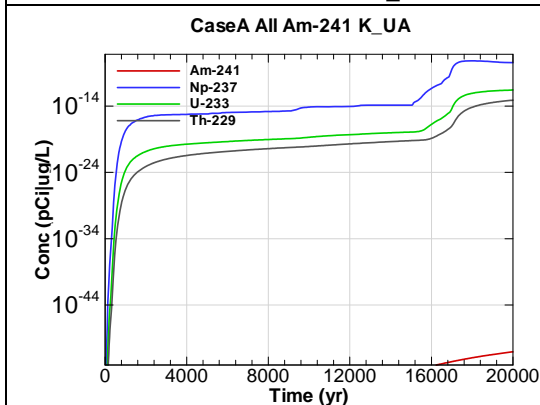


Figure A.1-35 - 100m Aquifer Concentration for CaseA All Am-241 K-UA

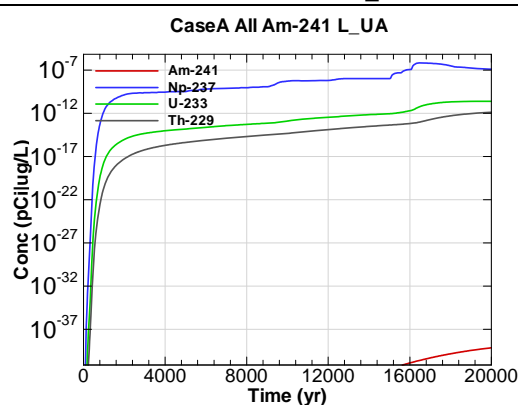


Figure A.1-36 - 100m Aquifer Concentration for CaseA All Am-241 L-UA

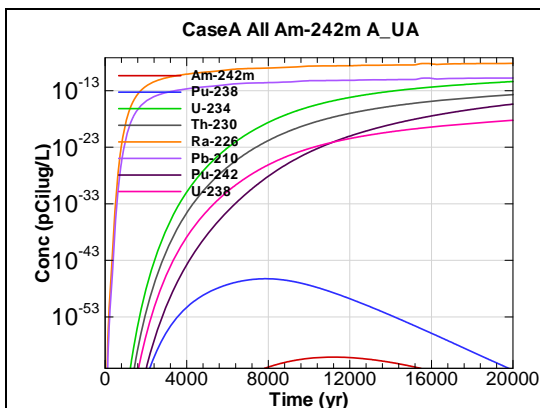


Figure A.1-37 - 100m Aquifer Concentration for
CaseA All Am-242m A_UA

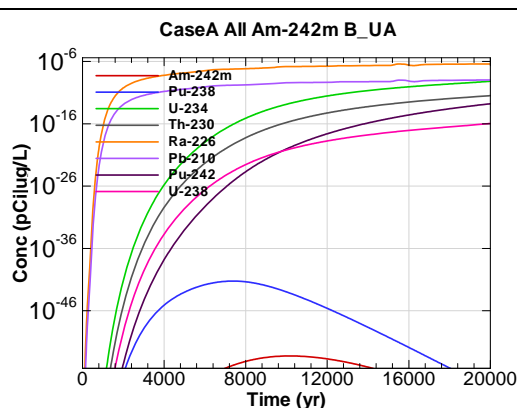


Figure A.1-38 - 100m Aquifer Concentration for
CaseA All Am-242m B_UA

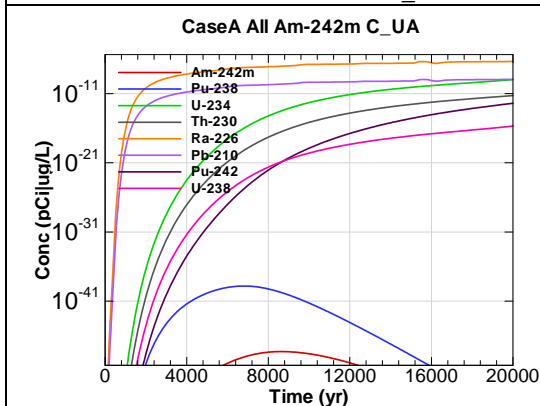


Figure A.1-39 - 100m Aquifer Concentration for
CaseA All Am-242m C_UA

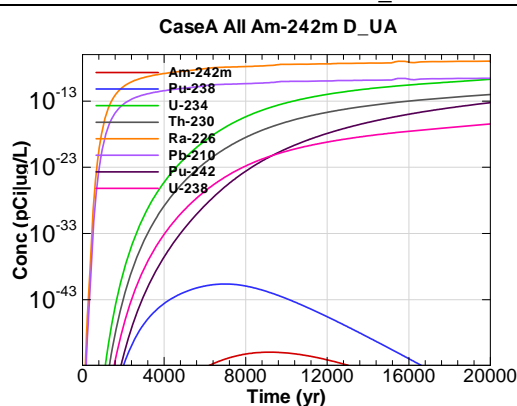


Figure A.1-40 - 100m Aquifer Concentration for
CaseA All Am-242m D_UA

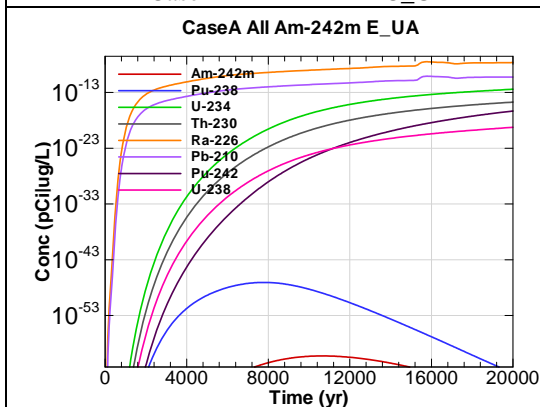


Figure A.1-41 - 100m Aquifer Concentration for
CaseA All Am-242m E_UA

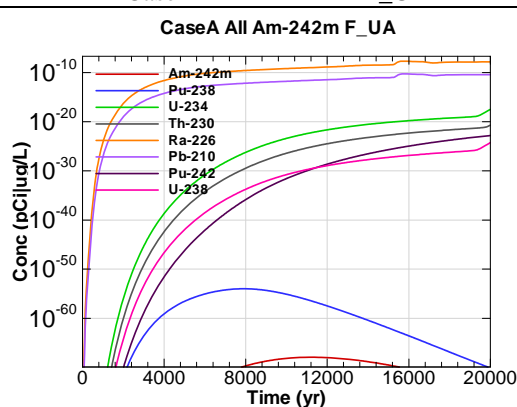


Figure A.1-42 - 100m Aquifer Concentration for
CaseA All Am-242m F_UA

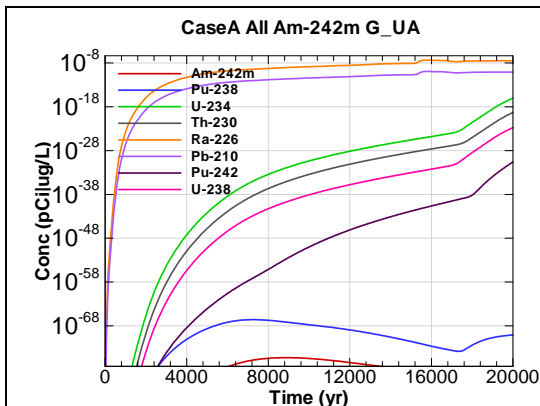


Figure A.1-43 - 100m Aquifer Concentration for CaseA All Am-242m G-UA

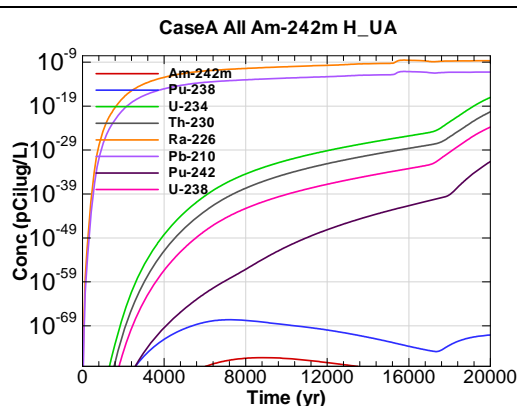


Figure A.1-44 - 100m Aquifer Concentration for CaseA All Am-242m H-UA

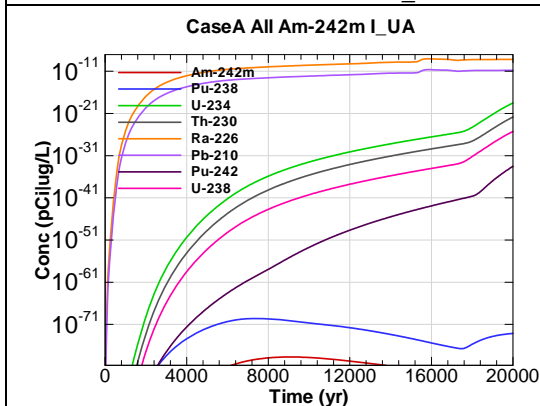


Figure A.1-45 - 100m Aquifer Concentration for CaseA All Am-242m I-UA

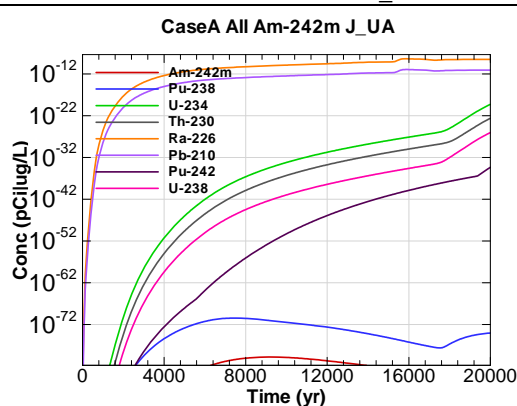


Figure A.1-46 - 100m Aquifer Concentration for CaseA All Am-242m J-UA

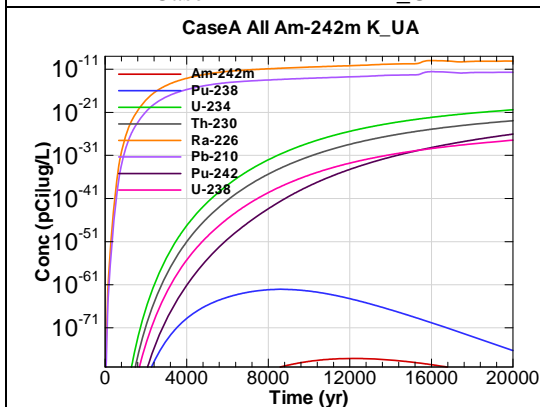


Figure A.1-47 - 100m Aquifer Concentration for CaseA All Am-242m K-UA

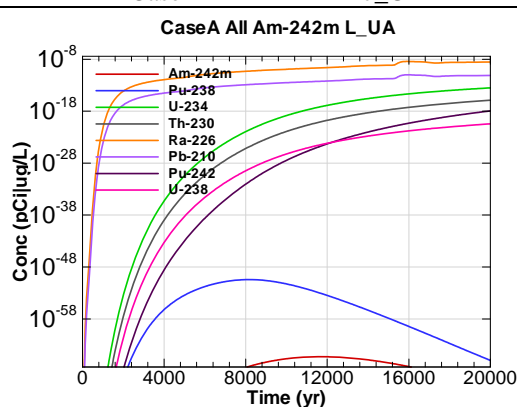


Figure A.1-48 - 100m Aquifer Concentration for CaseA All Am-242m L-UA

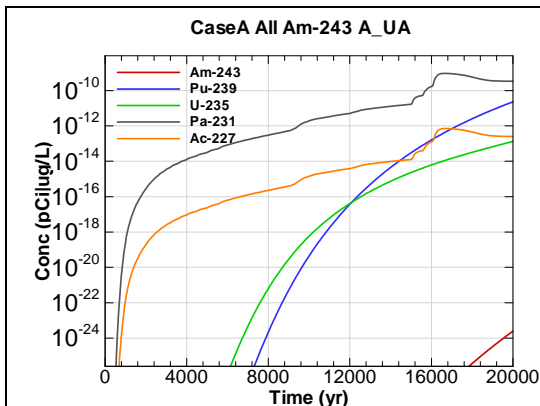


Figure A.1-49 - 100m Aquifer Concentration for
CaseA All Am-243 A_UA

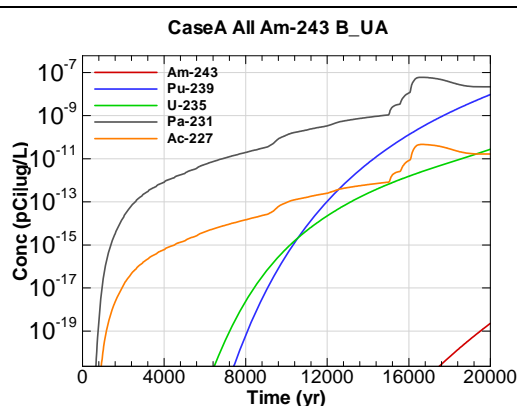


Figure A.1-50 - 100m Aquifer Concentration for
CaseA All Am-243 B_UA

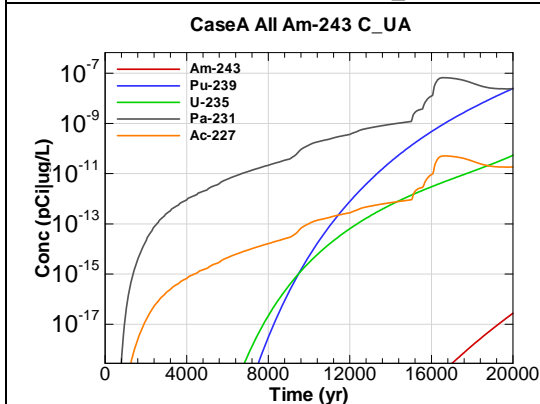


Figure A.1-51 - 100m Aquifer Concentration for
CaseA All Am-243 C_UA

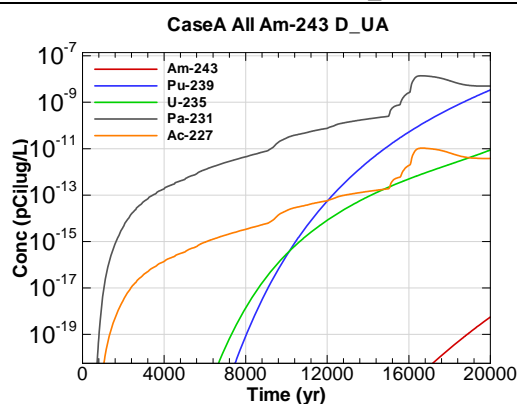


Figure A.1-52 - 100m Aquifer Concentration for
CaseA All Am-243 D_UA

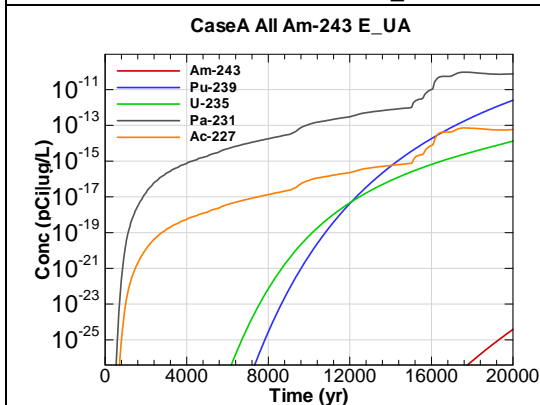


Figure A.1-53 - 100m Aquifer Concentration for
CaseA All Am-243 E_UA

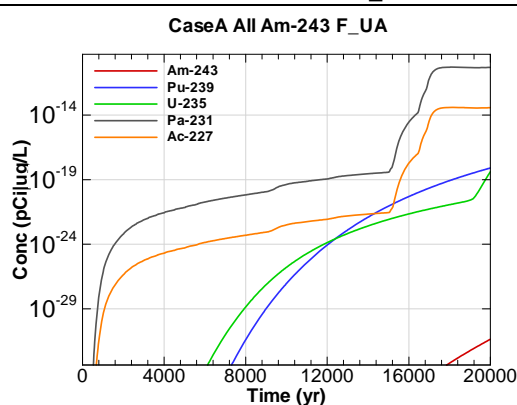


Figure A.1-54 - 100m Aquifer Concentration for
CaseA All Am-243 F_UA

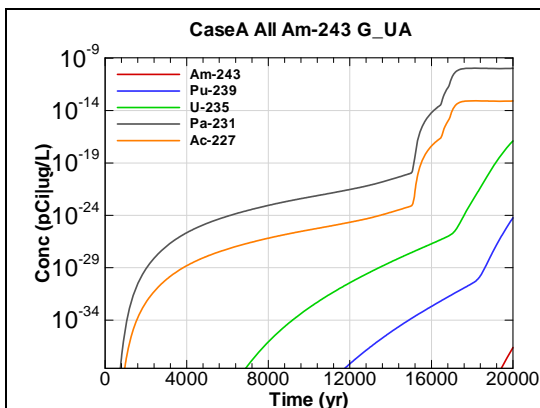


Figure A.1-55 - 100m Aquifer Concentration for
CaseA All Am-243 G-UA

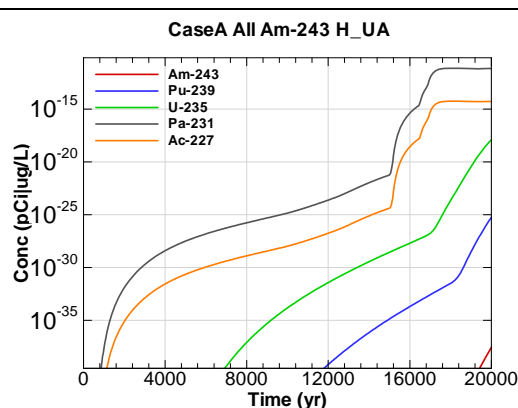


Figure A.1-56 - 100m Aquifer Concentration for
CaseA All Am-243 H-UA

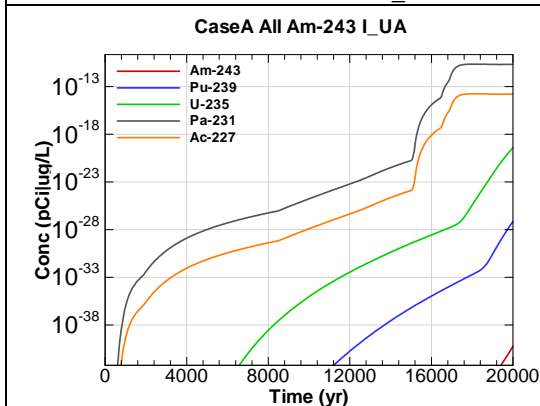


Figure A.1-57 - 100m Aquifer Concentration for
CaseA All Am-243 I-UA

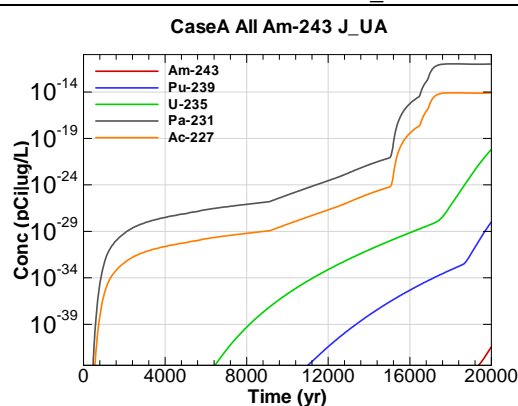


Figure A.1-58 - 100m Aquifer Concentration for
CaseA All Am-243 J-UA

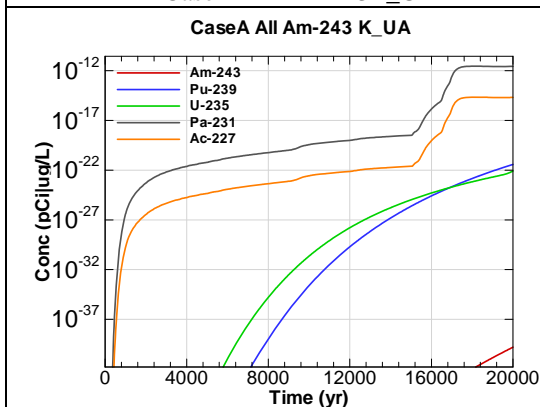


Figure A.1-59 - 100m Aquifer Concentration for
CaseA All Am-243 K-UA

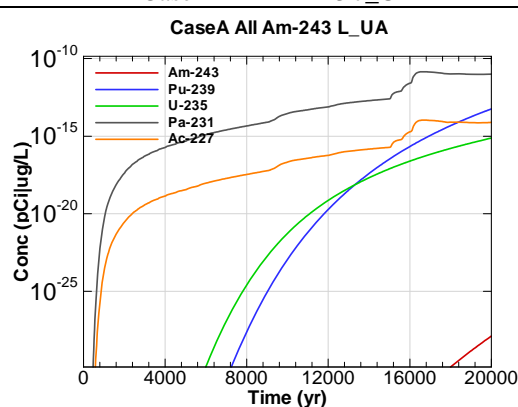
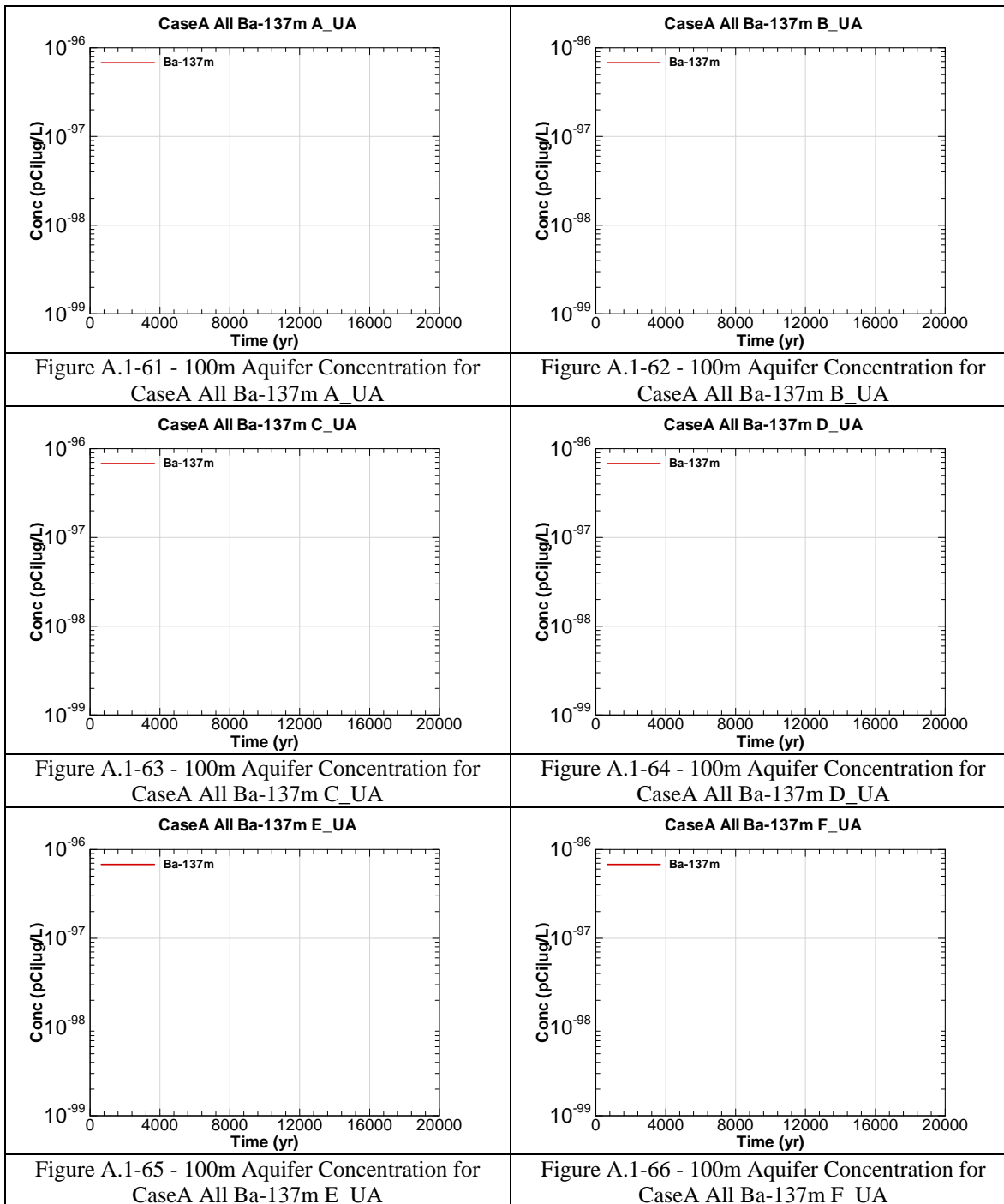
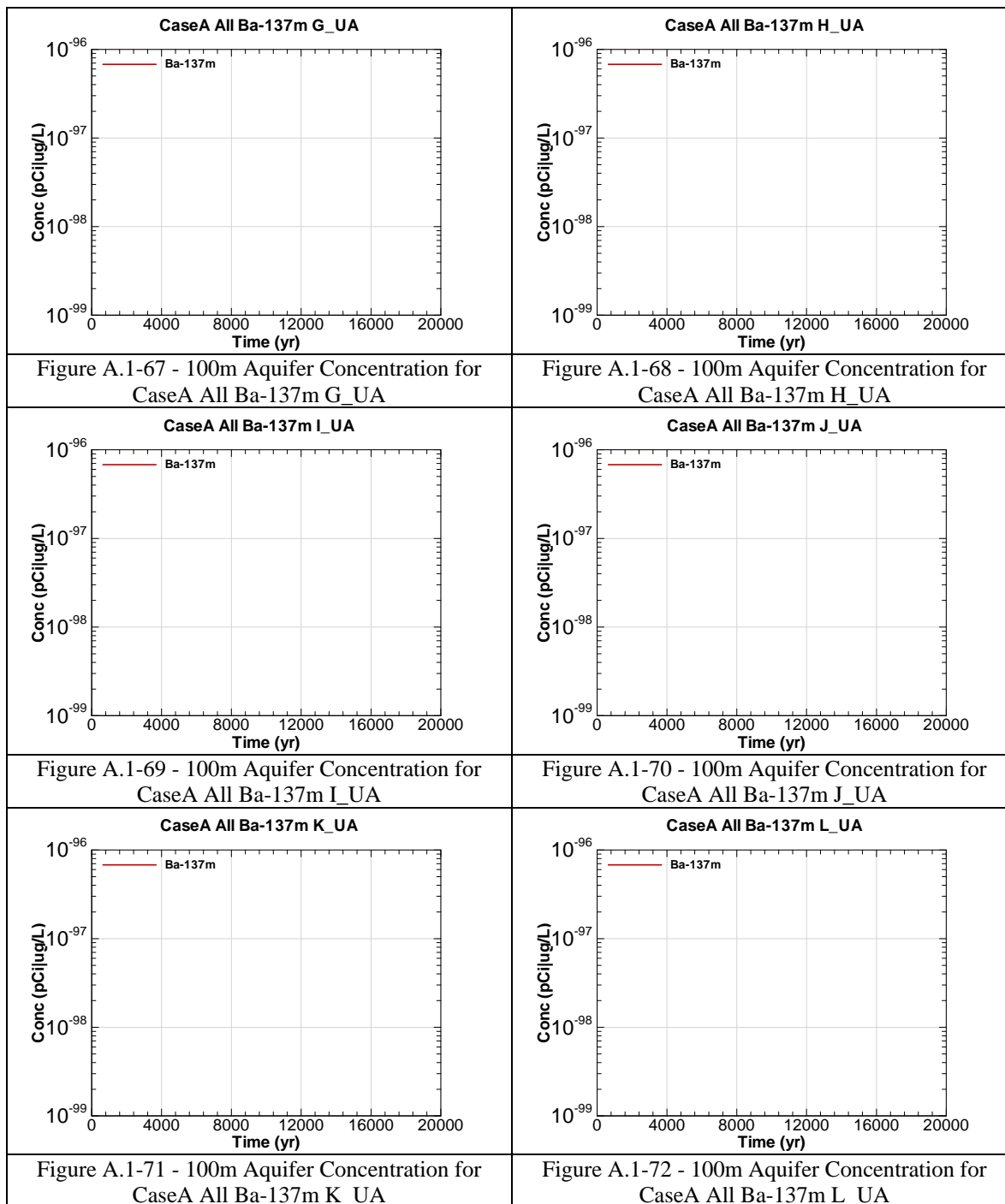


Figure A.1-60 - 100m Aquifer Concentration for
CaseA All Am-243 L-UA





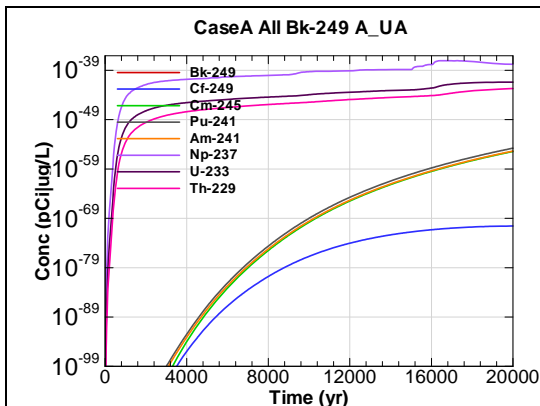


Figure A.1-73 - 100m Aquifer Concentration for
CaseA All Bk-249 A-UA

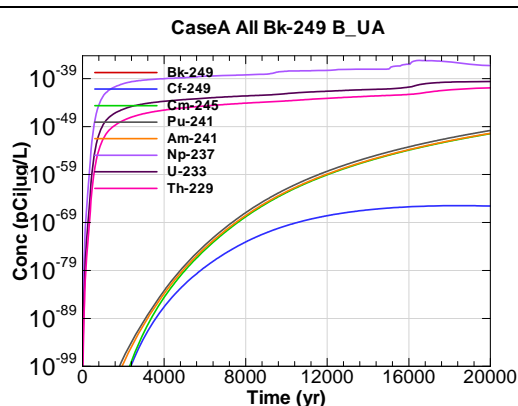


Figure A.1-74 - 100m Aquifer Concentration for
CaseA All Bk-249 B-UA

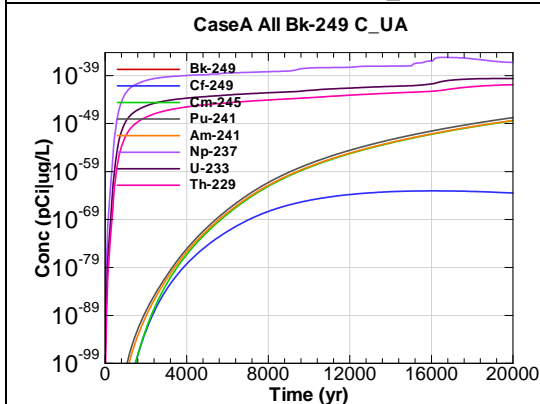


Figure A.1-75 - 100m Aquifer Concentration for
CaseA All Bk-249 C-UA

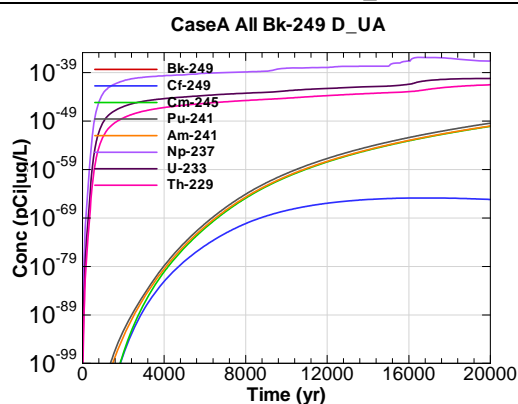


Figure A.1-76 - 100m Aquifer Concentration for
CaseA All Bk-249 D-UA

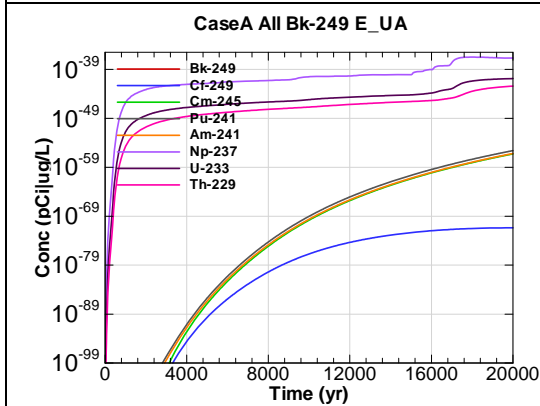


Figure A.1-77 - 100m Aquifer Concentration for
CaseA All Bk-249 E-UA

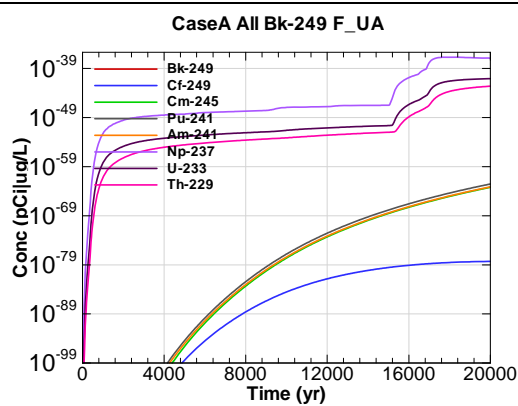


Figure A.1-78 - 100m Aquifer Concentration for
CaseA All Bk-249 F-UA

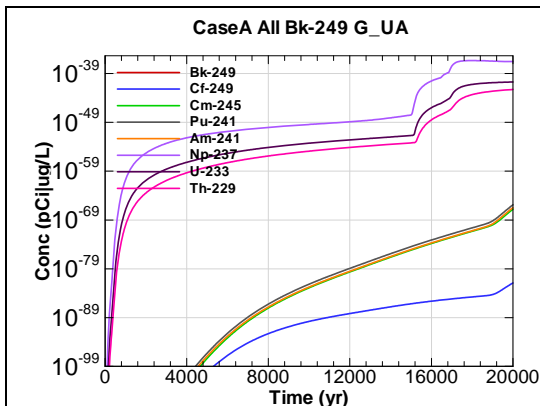


Figure A.1-79 - 100m Aquifer Concentration for
CaseA All Bk-249 G-UA

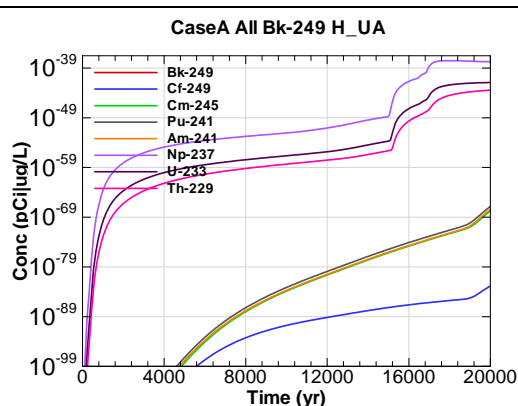


Figure A.1-80 - 100m Aquifer Concentration for
CaseA All Bk-249 H-UA

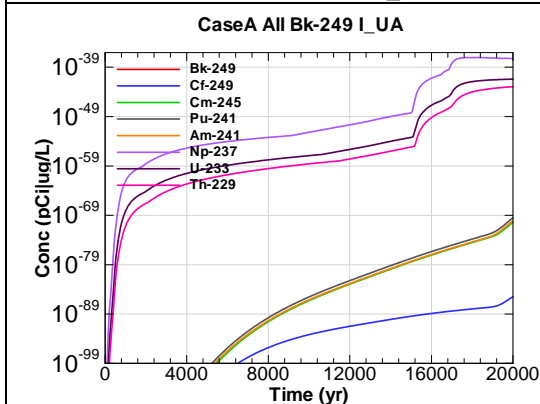


Figure A.1-81 - 100m Aquifer Concentration for
CaseA All Bk-249 I-UA

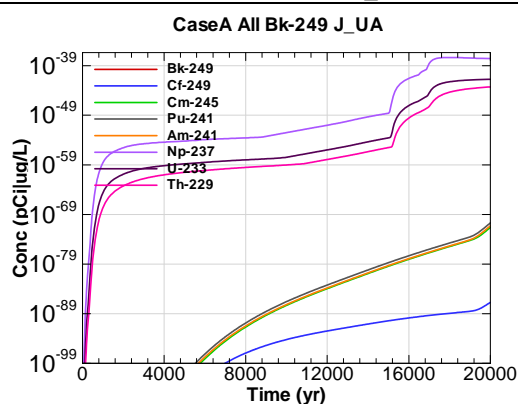


Figure A.1-82 - 100m Aquifer Concentration for
CaseA All Bk-249 J-UA

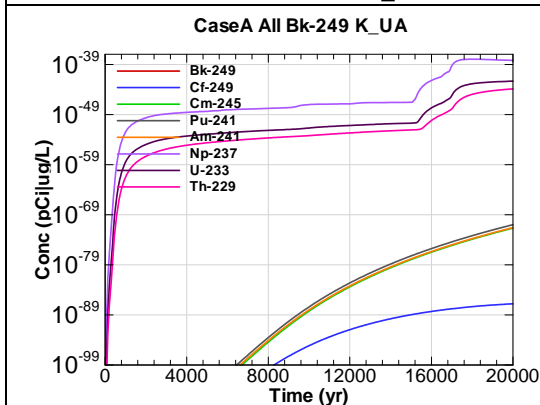


Figure A.1-83 - 100m Aquifer Concentration for
CaseA All Bk-249 K-UA

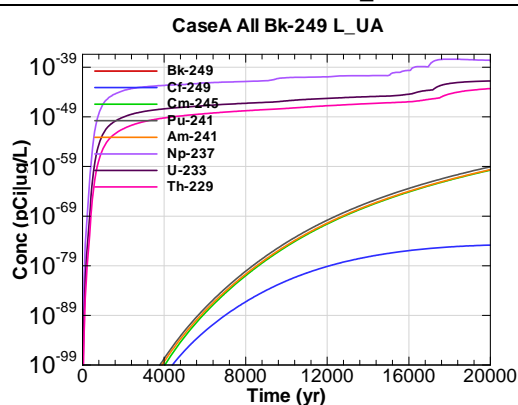
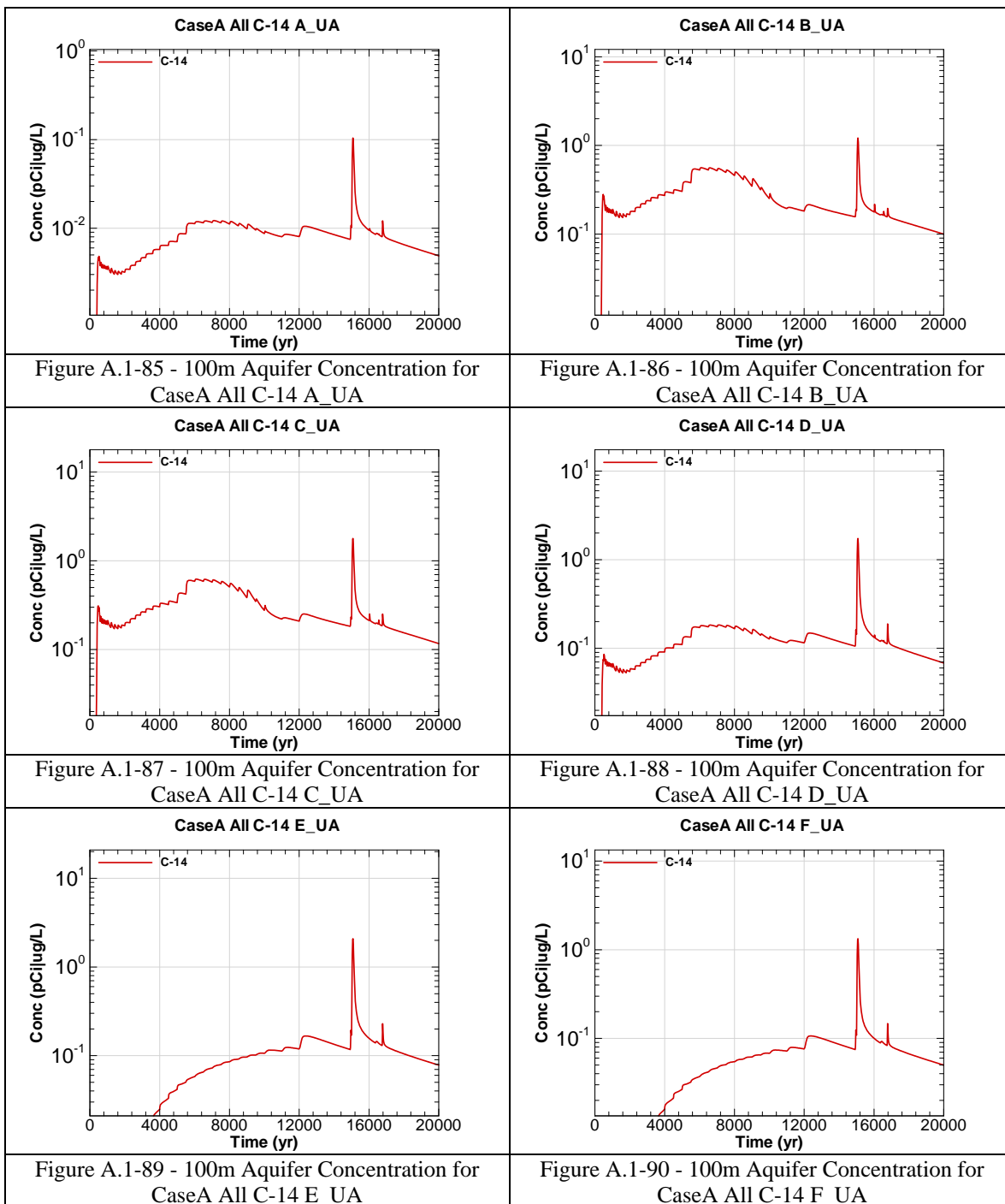
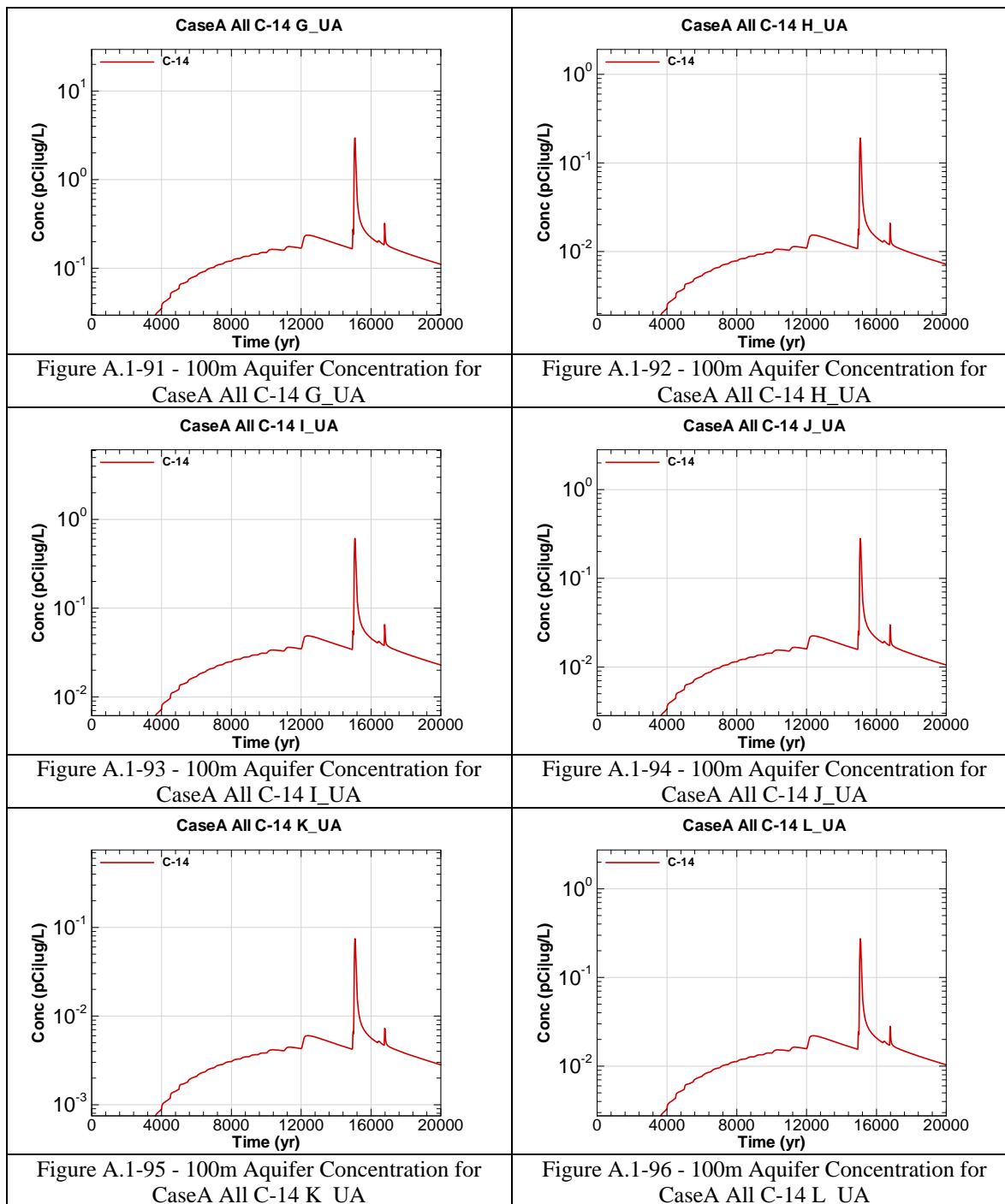
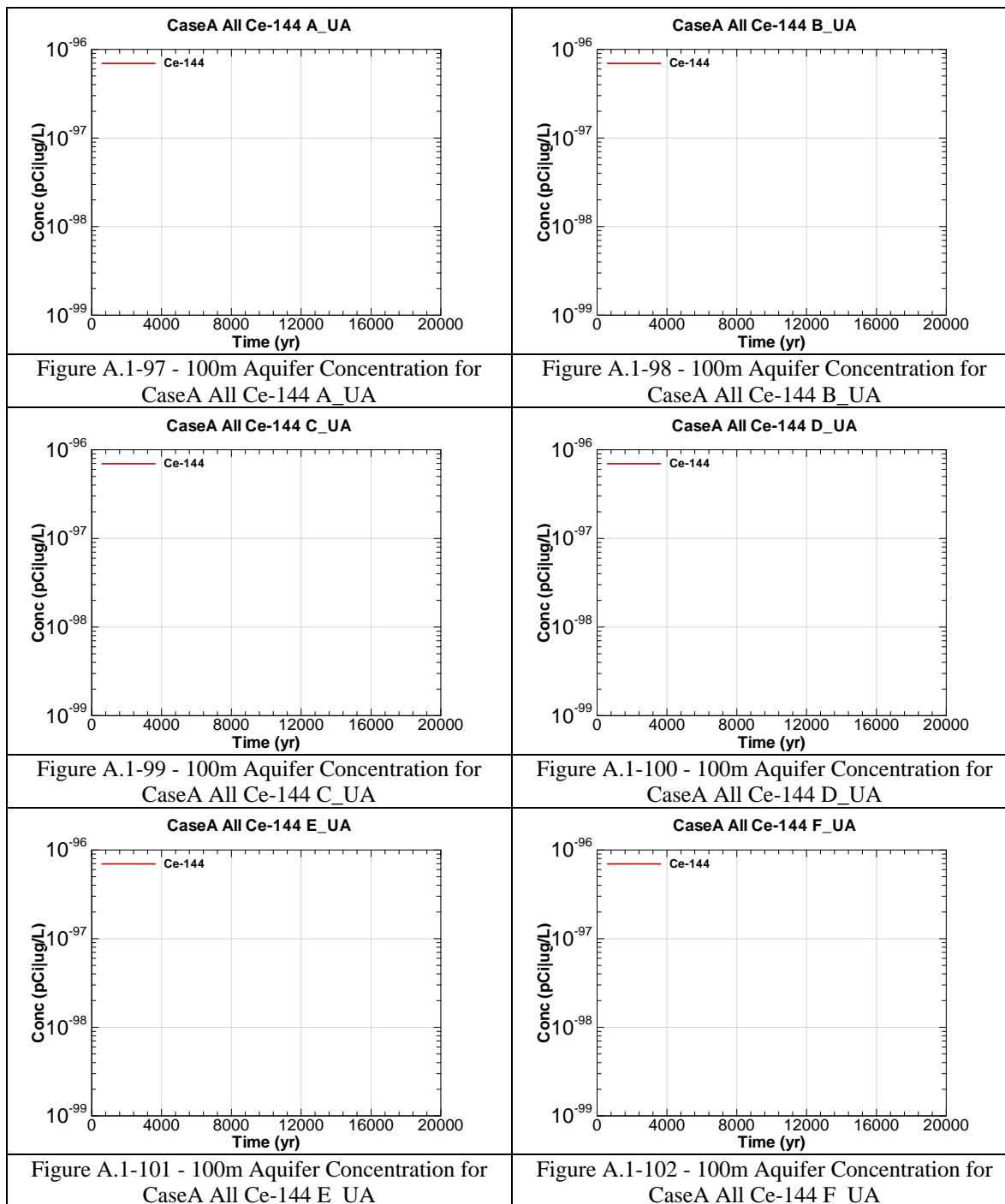
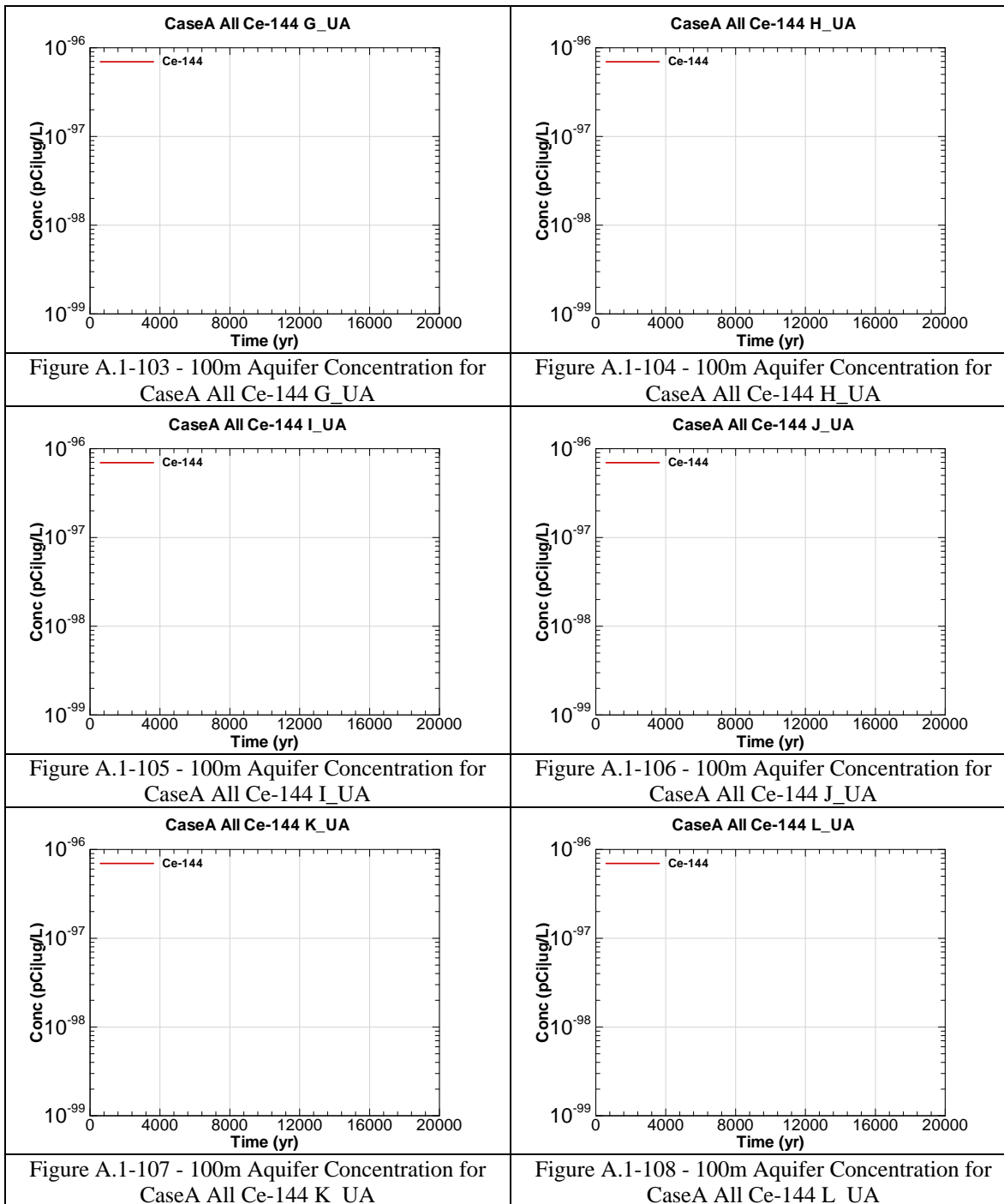


Figure A.1-84 - 100m Aquifer Concentration for
CaseA All Bk-249 L-UA









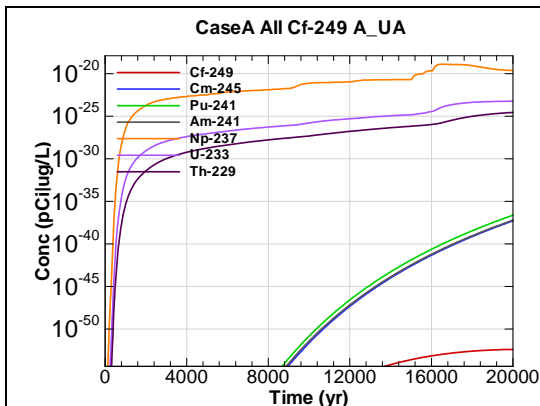


Figure A.1-109 - 100m Aquifer Concentration for
CaseA All Cf-249 A_UA

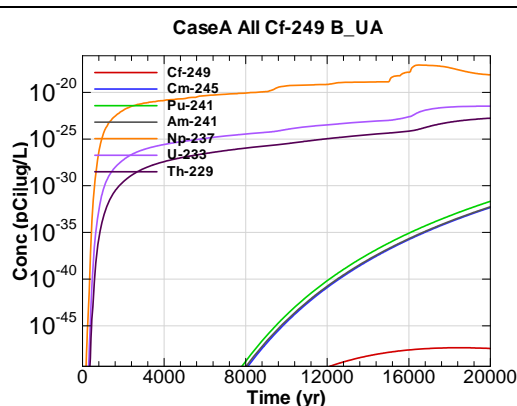


Figure A.1-110 - 100m Aquifer Concentration for
CaseA All Cf-249 B_UA

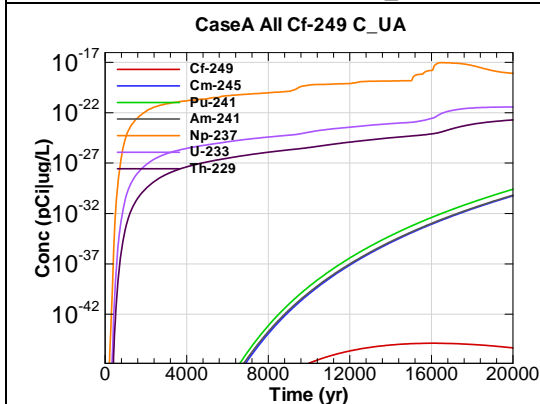


Figure A.1-111 - 100m Aquifer Concentration for
CaseA All Cf-249 C_UA

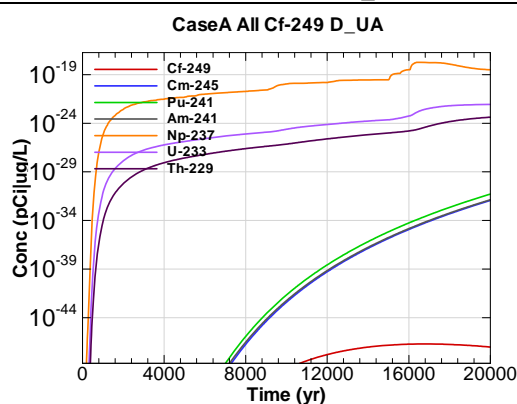


Figure A.1-112 - 100m Aquifer Concentration for
CaseA All Cf-249 D_UA

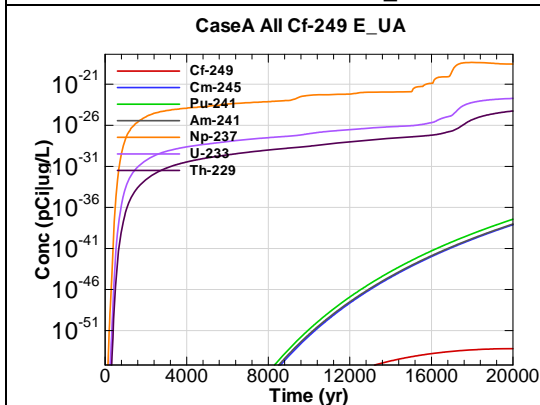


Figure A.1-113 - 100m Aquifer Concentration for
CaseA All Cf-249 E_UA

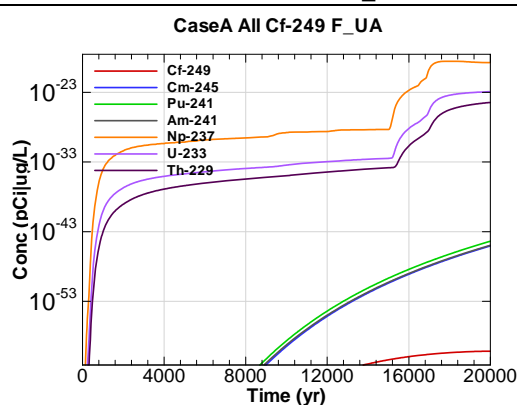


Figure A.1-114 - 100m Aquifer Concentration for
CaseA All Cf-249 F_UA

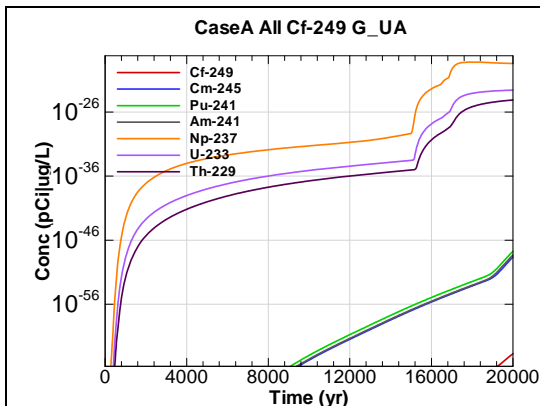


Figure A.1-115 - 100m Aquifer Concentration for
CaseA All Cf-249 G-UA

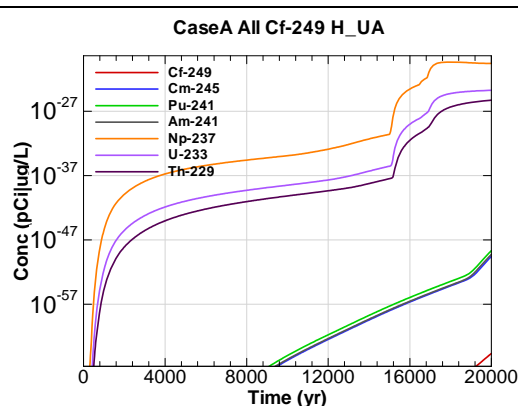


Figure A.1-116 - 100m Aquifer Concentration for
CaseA All Cf-249 H-UA

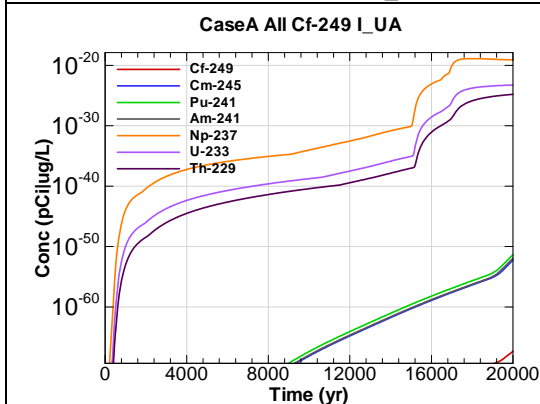


Figure A.1-117 - 100m Aquifer Concentration for
CaseA All Cf-249 I-UA

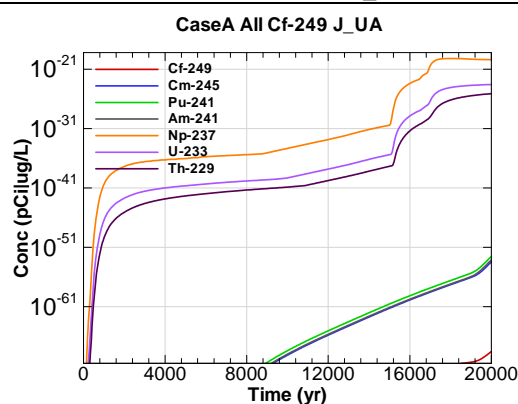


Figure A.1-118 - 100m Aquifer Concentration for
CaseA All Cf-249 J-UA

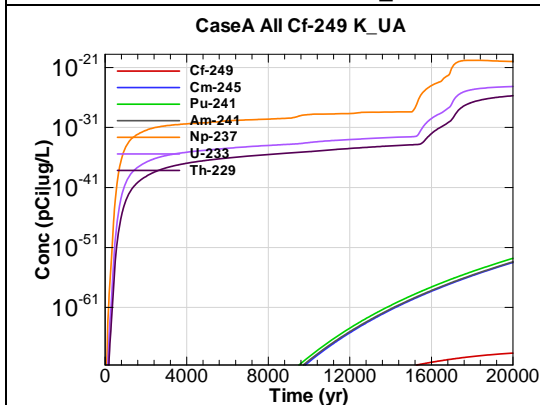


Figure A.1-119 - 100m Aquifer Concentration for
CaseA All Cf-249 K-UA

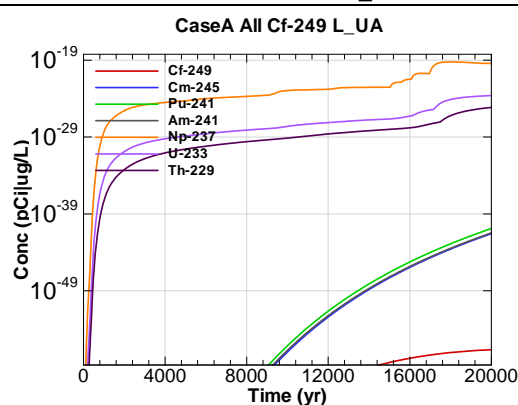


Figure A.1-120 - 100m Aquifer Concentration for
CaseA All Cf-249 L-UA

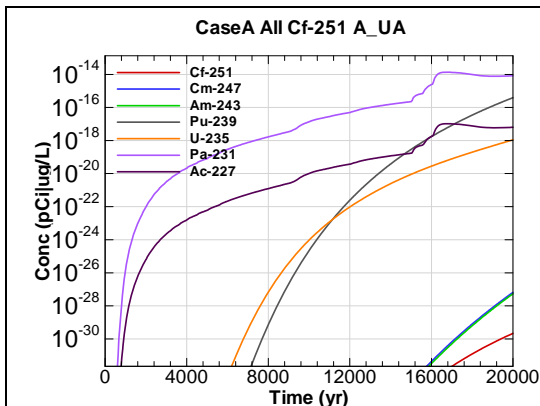


Figure A.1-121 - 100m Aquifer Concentration for
CaseA All Cf-251 A_UA

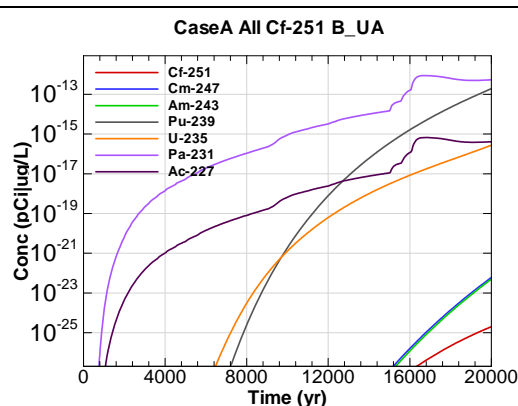


Figure A.1-122 - 100m Aquifer Concentration for
CaseA All Cf-251 B_UA

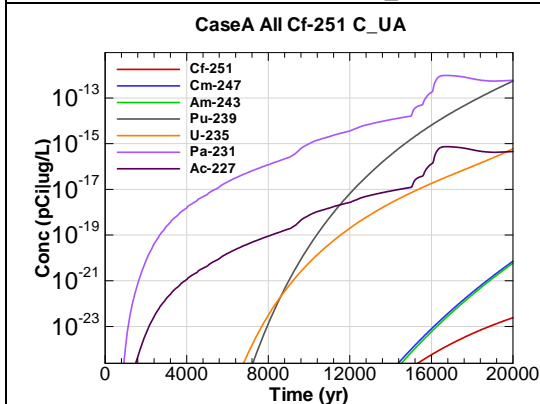


Figure A.1-123 - 100m Aquifer Concentration for
CaseA All Cf-251 C_UA

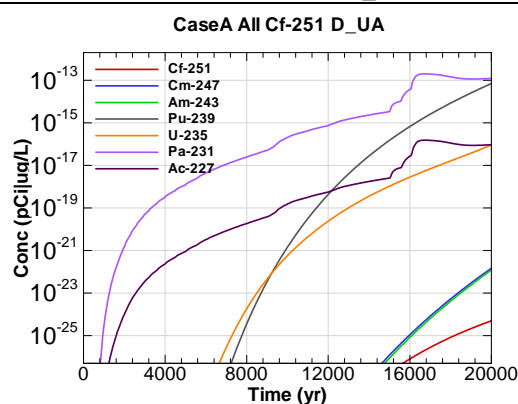


Figure A.1-124 - 100m Aquifer Concentration for
CaseA All Cf-251 D_UA

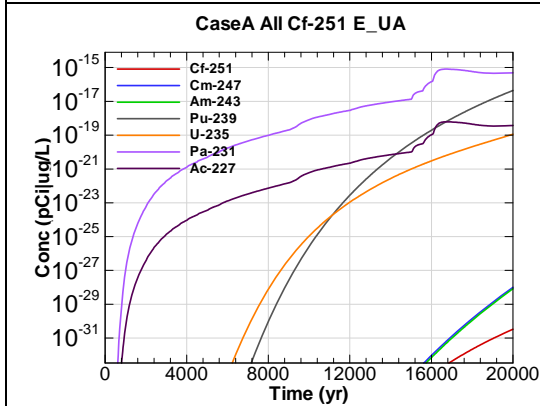


Figure A.1-125 - 100m Aquifer Concentration for
CaseA All Cf-251 E_UA

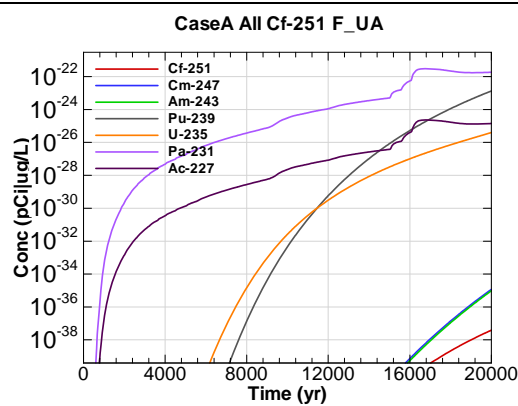


Figure A.1-126 - 100m Aquifer Concentration for
CaseA All Cf-251 F_UA

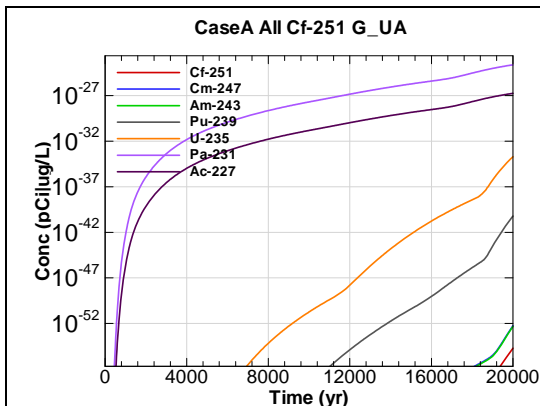


Figure A.1-127 - 100m Aquifer Concentration for
CaseA All Cf-251 G-UA

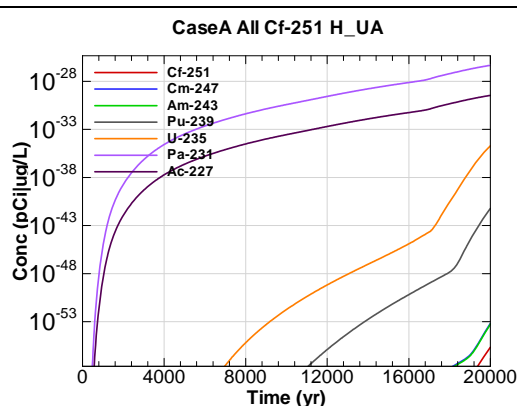


Figure A.1-128 - 100m Aquifer Concentration for
CaseA All Cf-251 H-UA

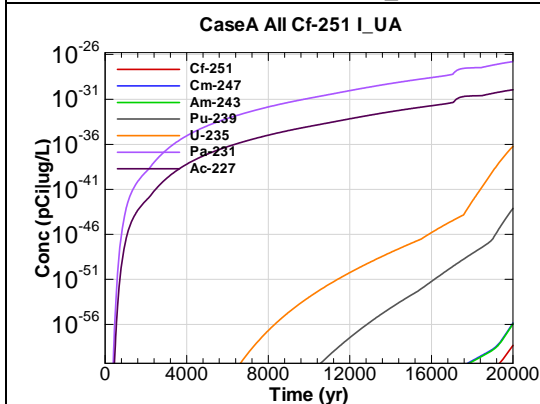


Figure A.1-129 - 100m Aquifer Concentration for
CaseA All Cf-251 I-UA

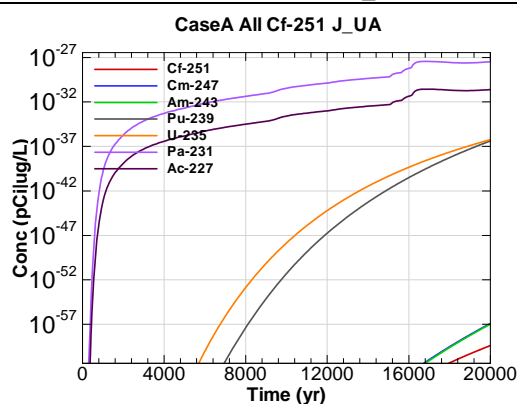


Figure A.1-130 - 100m Aquifer Concentration for
CaseA All Cf-251 J-UA

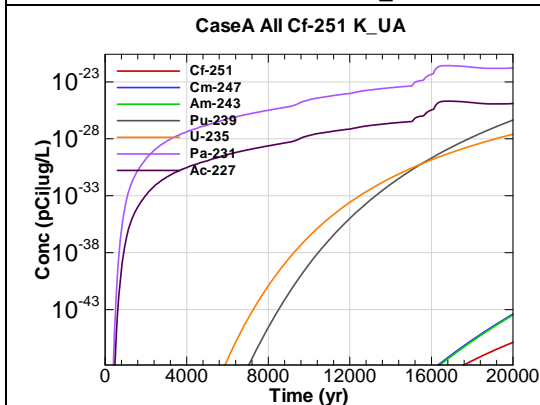


Figure A.1-131 - 100m Aquifer Concentration for
CaseA All Cf-251 K-UA

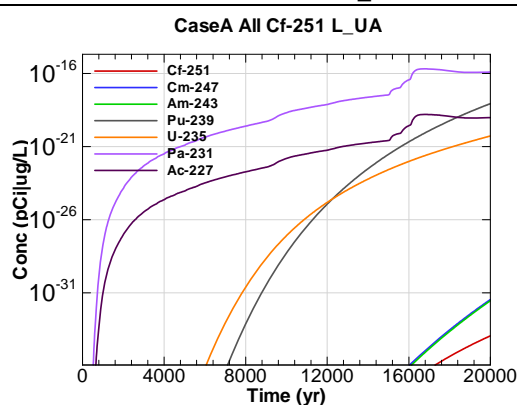


Figure A.1-132 - 100m Aquifer Concentration for
CaseA All Cf-251 L-UA

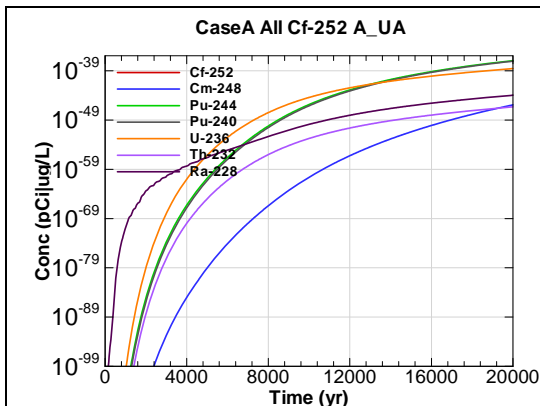


Figure A.1-133 - 100m Aquifer Concentration for
CaseA All Cf-252 A_UA

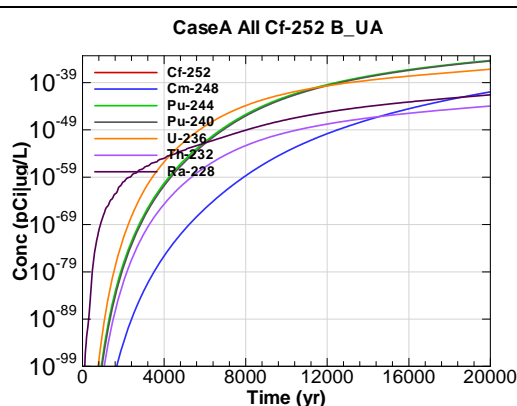


Figure A.1-134 - 100m Aquifer Concentration for
CaseA All Cf-252 B_UA

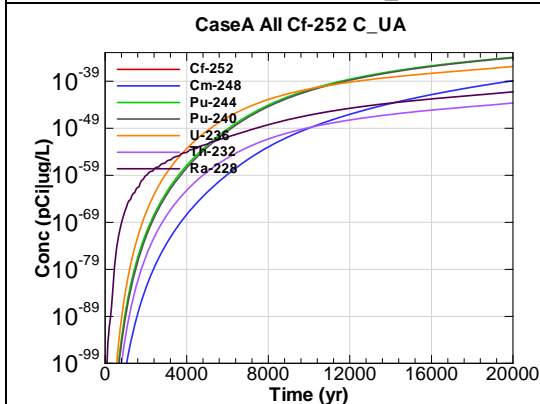


Figure A.1-135 - 100m Aquifer Concentration for
CaseA All Cf-252 C_UA

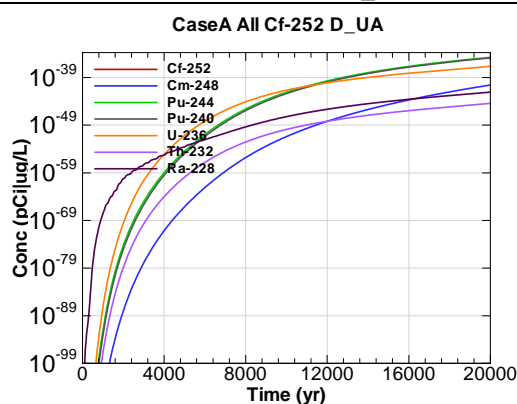


Figure A.1-136 - 100m Aquifer Concentration for
CaseA All Cf-252 D_UA

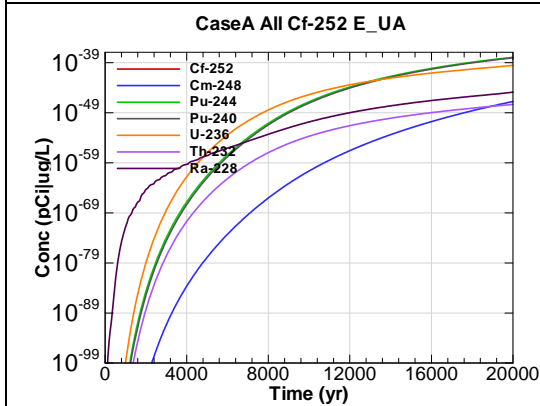


Figure A.1-137 - 100m Aquifer Concentration for
CaseA All Cf-252 E_UA

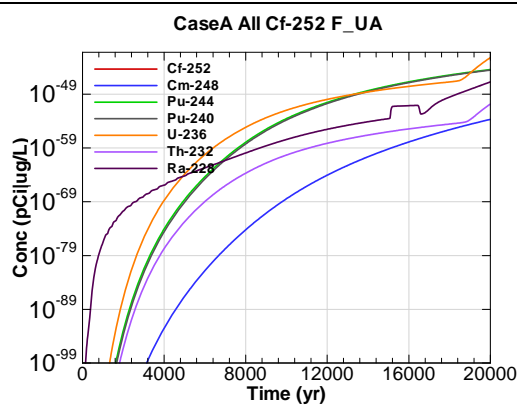


Figure A.1-138 - 100m Aquifer Concentration for
CaseA All Cf-252 F_UA

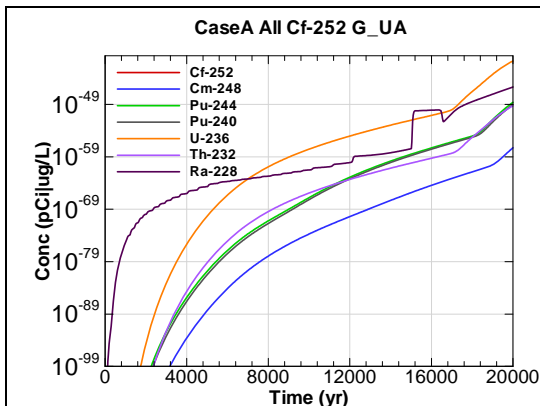


Figure A.1-139 - 100m Aquifer Concentration for
CaseA All Cf-252 G-UA

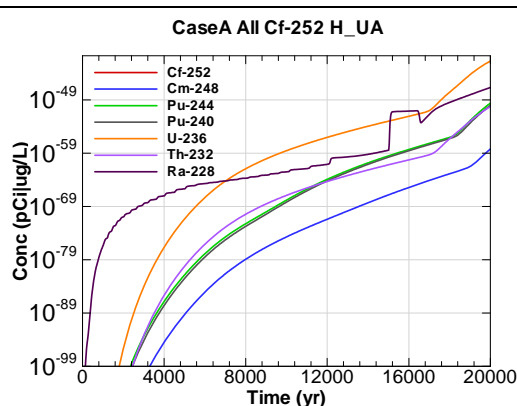


Figure A.1-140 - 100m Aquifer Concentration for
CaseA All Cf-252 H-UA

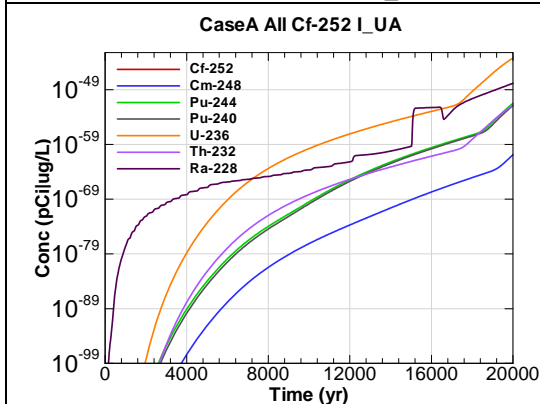


Figure A.1-141 - 100m Aquifer Concentration for
CaseA All Cf-252 I-UA

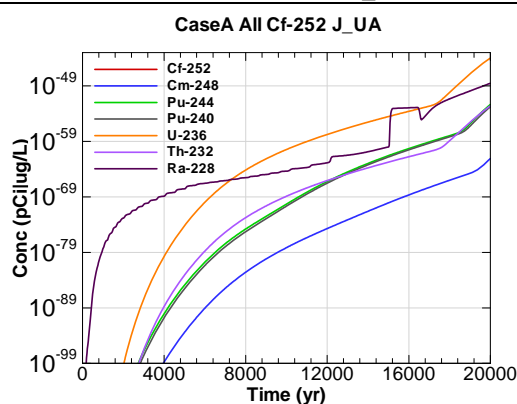


Figure A.1-142 - 100m Aquifer Concentration for
CaseA All Cf-252 J-UA

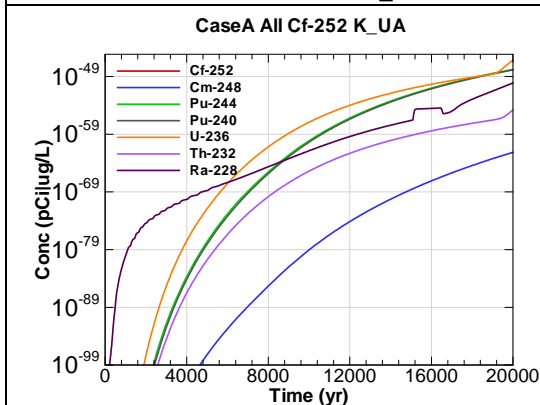


Figure A.1-143 - 100m Aquifer Concentration for
CaseA All Cf-252 K-UA

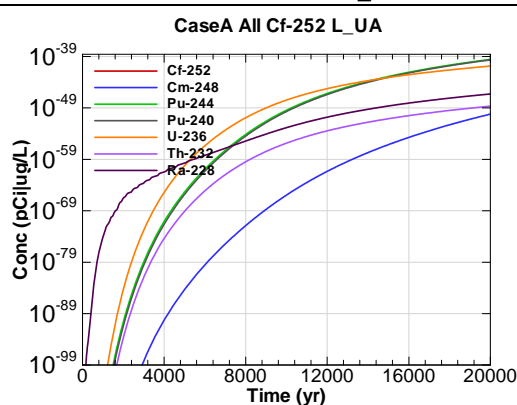
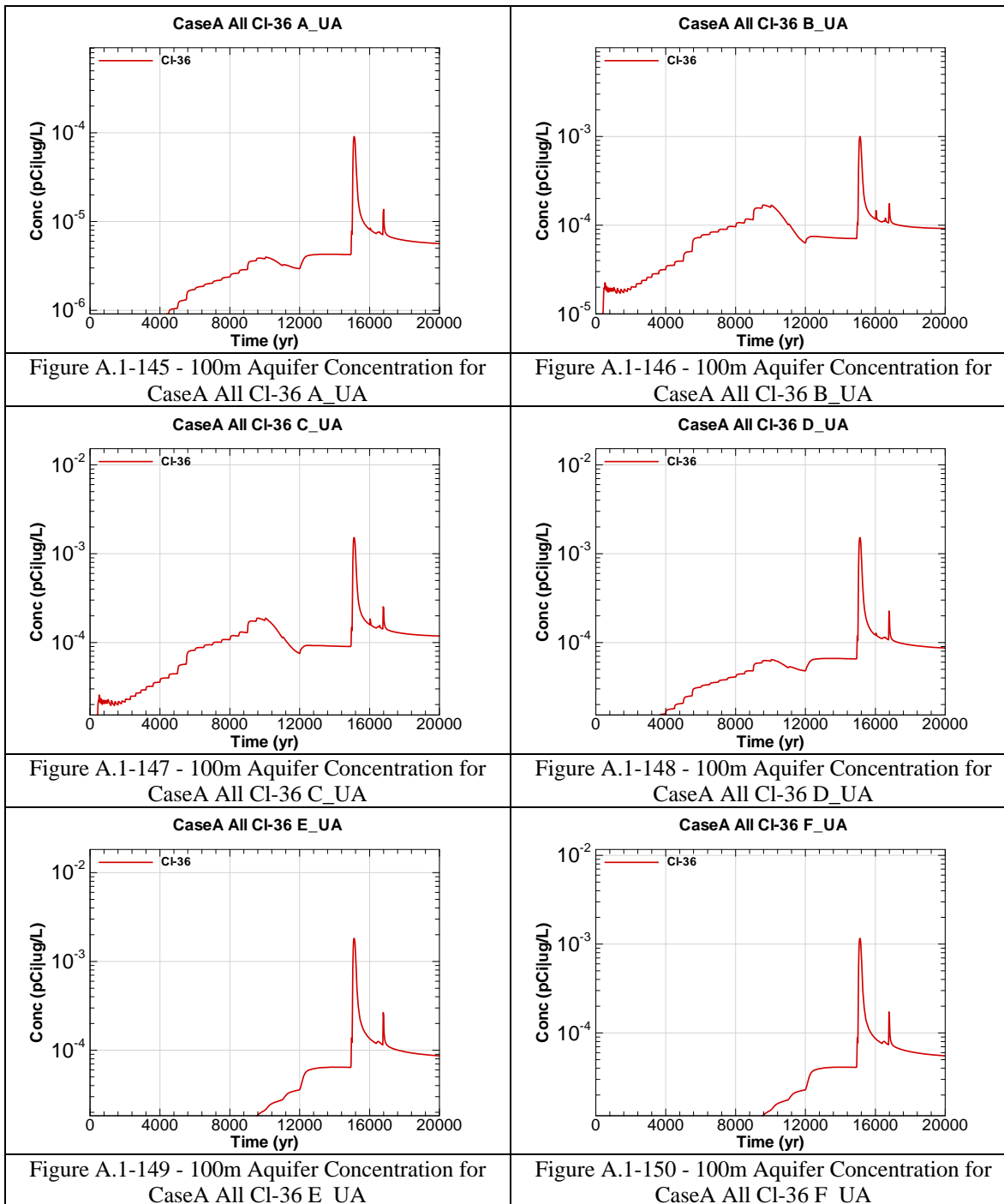
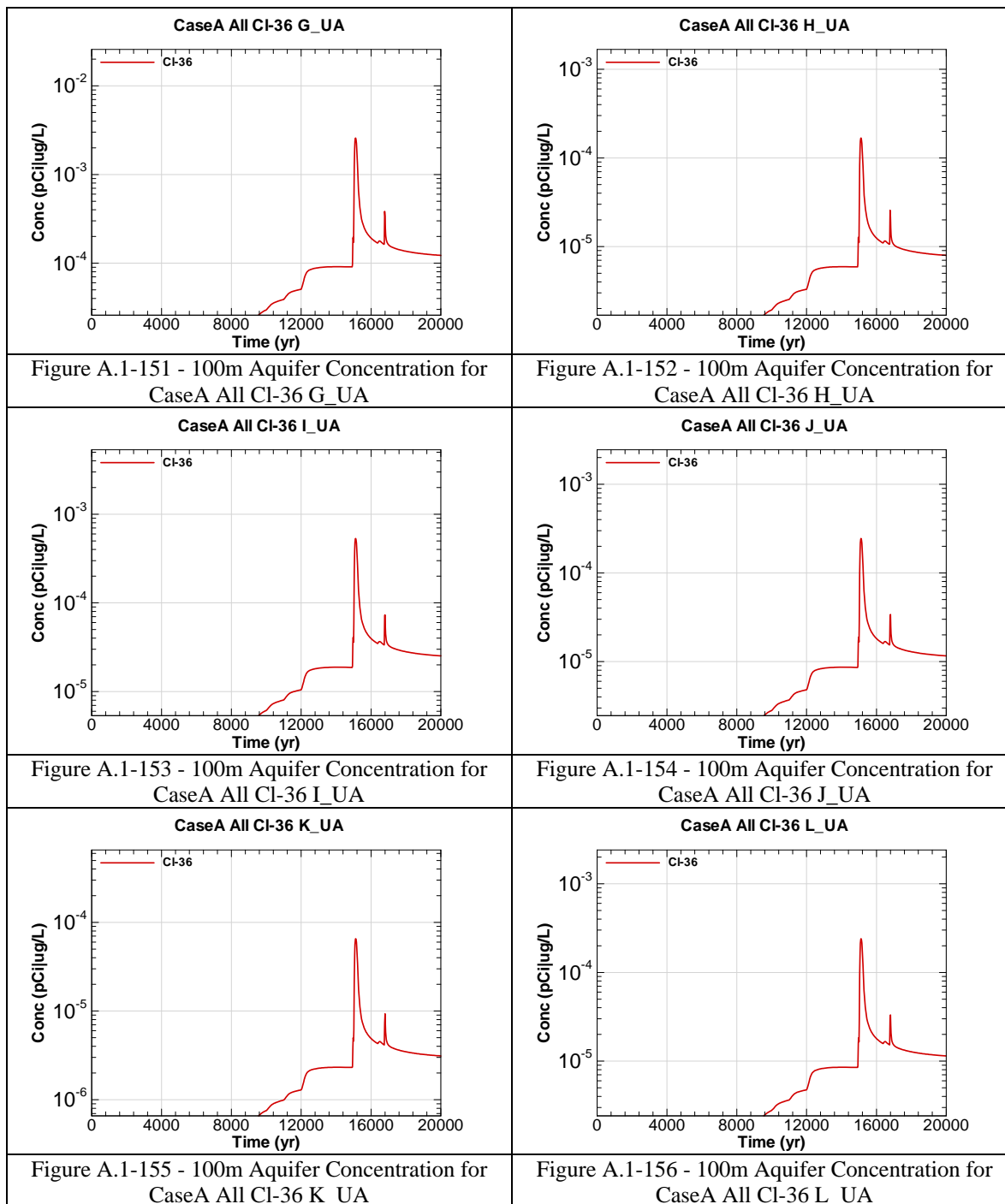


Figure A.1-144 - 100m Aquifer Concentration for
CaseA All Cf-252 L-UA





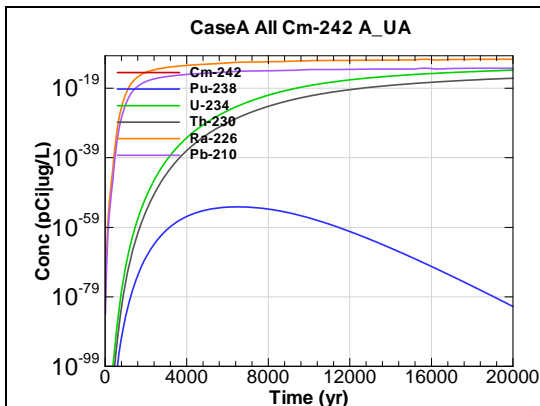


Figure A.1-157 - 100m Aquifer Concentration for
CaseA All Cm-242 A_UA

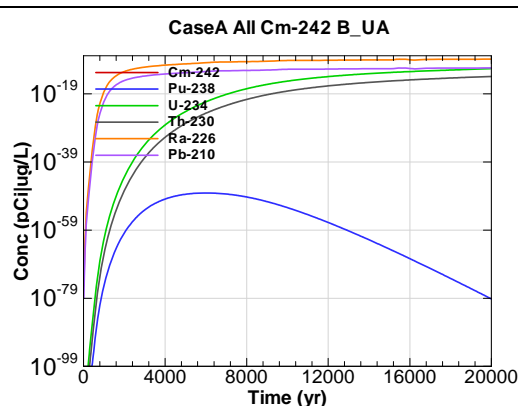


Figure A.1-158 - 100m Aquifer Concentration for
CaseA All Cm-242 B_UA

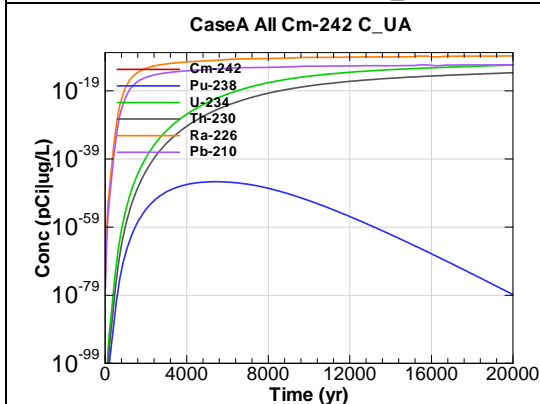


Figure A.1-159 - 100m Aquifer Concentration for
CaseA All Cm-242 C_UA

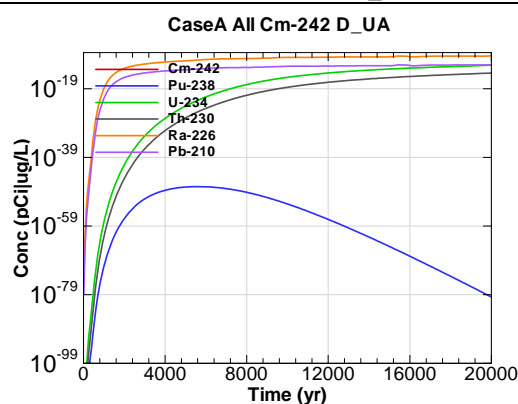


Figure A.1-160 - 100m Aquifer Concentration for
CaseA All Cm-242 D_UA

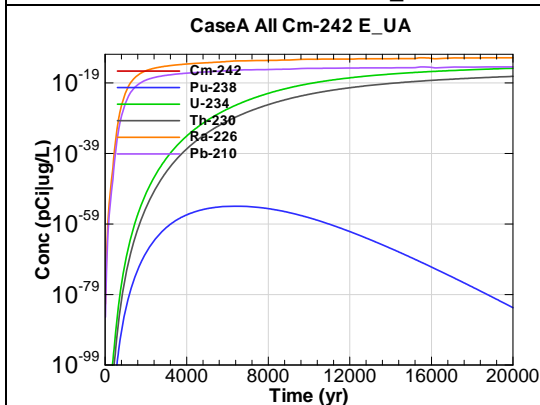


Figure A.1-161 - 100m Aquifer Concentration for
CaseA All Cm-242 E_UA

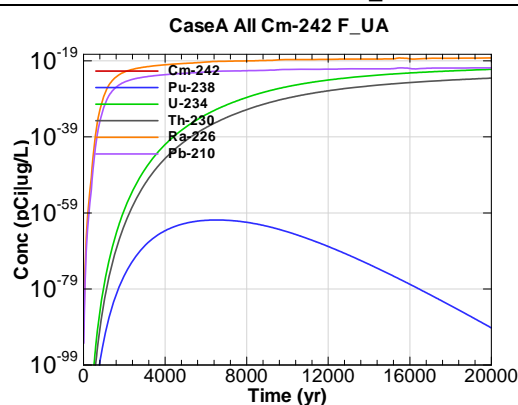


Figure A.1-162 - 100m Aquifer Concentration for
CaseA All Cm-242 F_UA

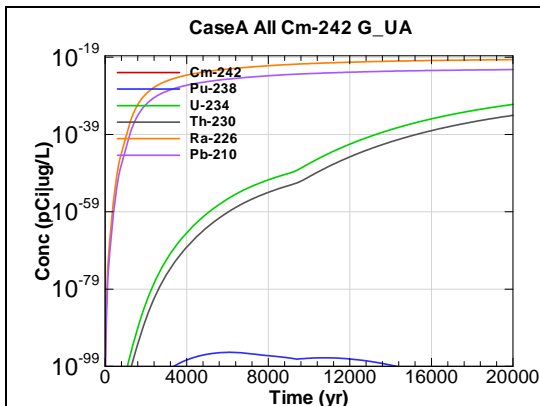


Figure A.1-163 - 100m Aquifer Concentration for CaseA All Cm-242 G-UA

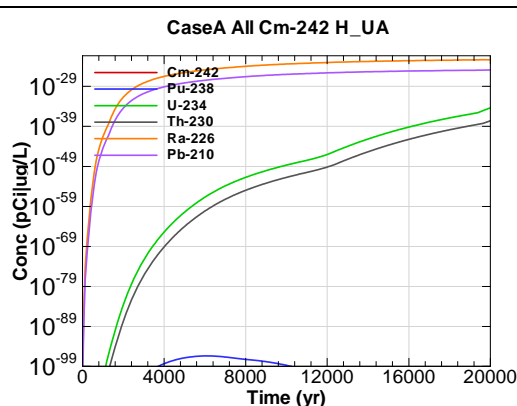


Figure A.1-164 - 100m Aquifer Concentration for CaseA All Cm-242 H-UA

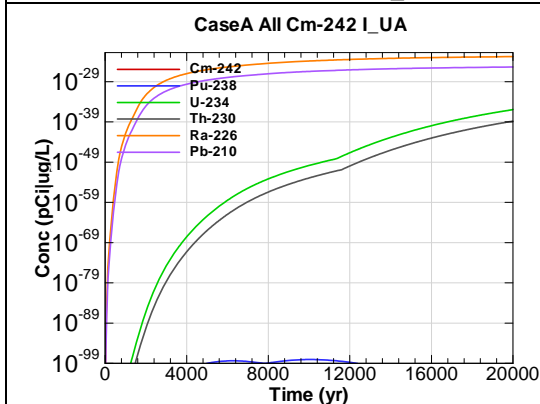


Figure A.1-165 - 100m Aquifer Concentration for CaseA All Cm-242 I-UA

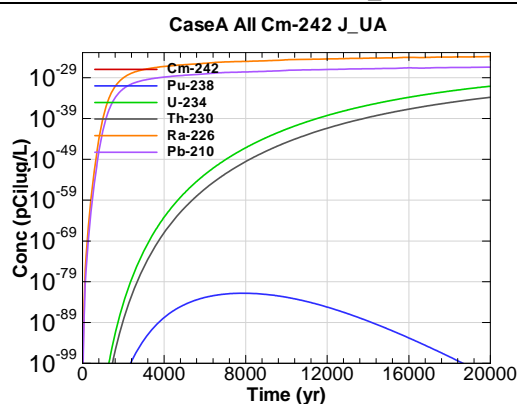


Figure A.1-166 - 100m Aquifer Concentration for CaseA All Cm-242 J-UA

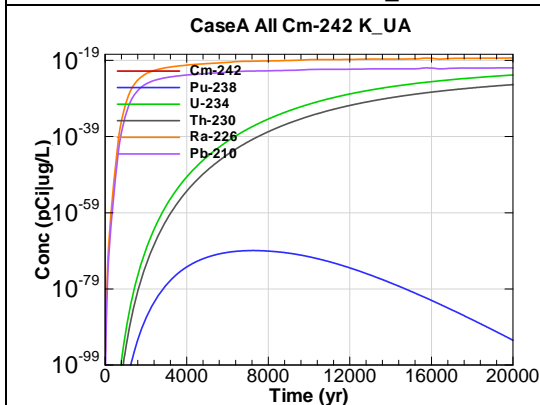


Figure A.1-167 - 100m Aquifer Concentration for CaseA All Cm-242 K-UA

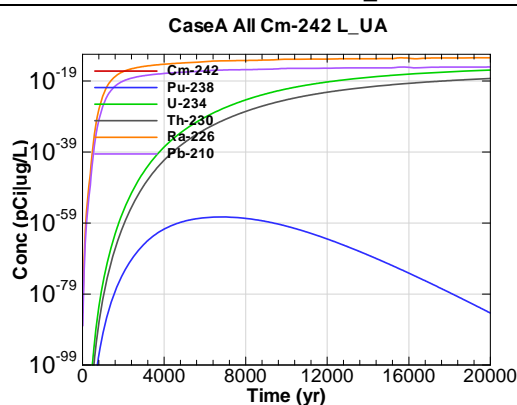


Figure A.1-168 - 100m Aquifer Concentration for CaseA All Cm-242 L-UA

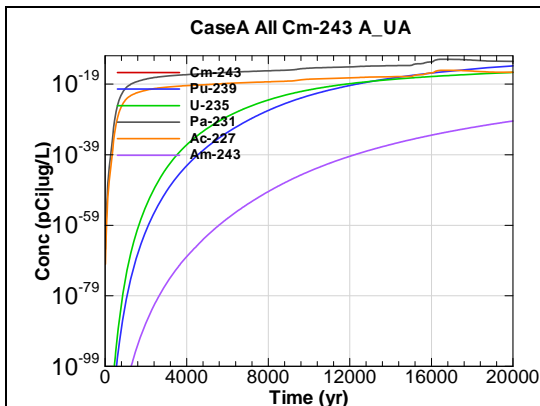


Figure A.1-169 - 100m Aquifer Concentration for CaseA All Cm-243 A_UA

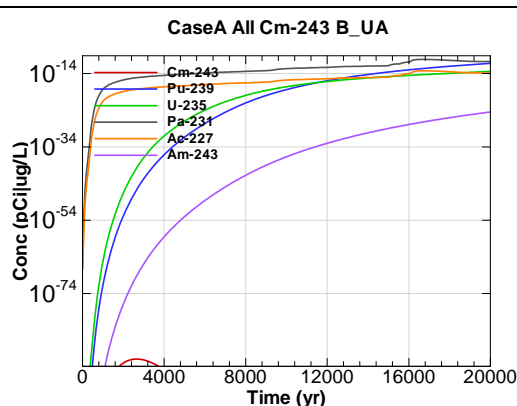


Figure A.1-170 - 100m Aquifer Concentration for CaseA All Cm-243 B_UA

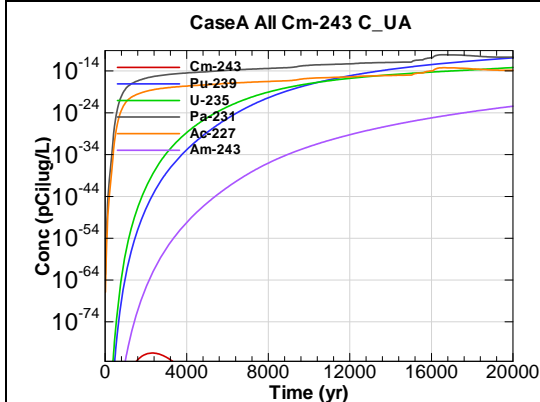


Figure A.1-171 - 100m Aquifer Concentration for CaseA All Cm-243 C_UA

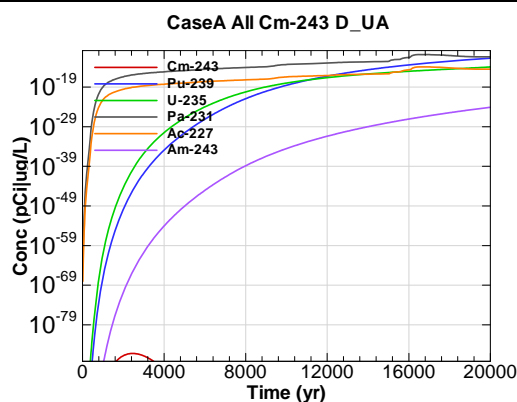


Figure A.1-172 - 100m Aquifer Concentration for CaseA All Cm-243 D_UA

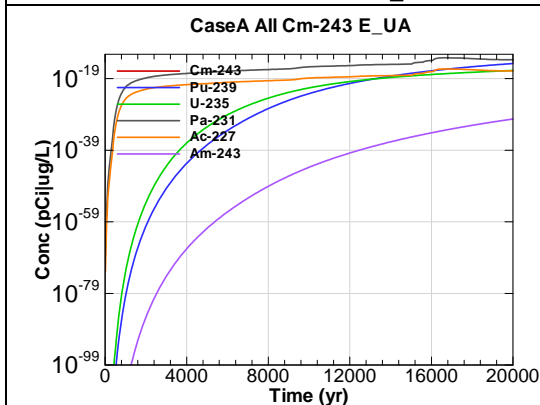


Figure A.1-173 - 100m Aquifer Concentration for CaseA All Cm-243 E_UA

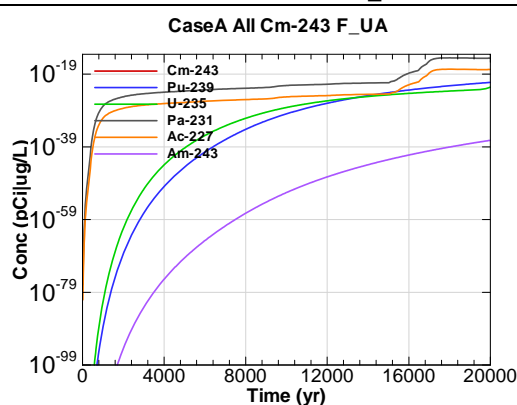


Figure A.1-174 - 100m Aquifer Concentration for CaseA All Cm-243 F_UA

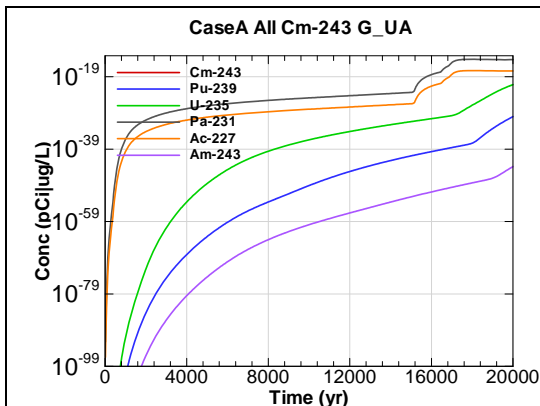


Figure A.1-175 - 100m Aquifer Concentration for
CaseA All Cm-243 G-UA

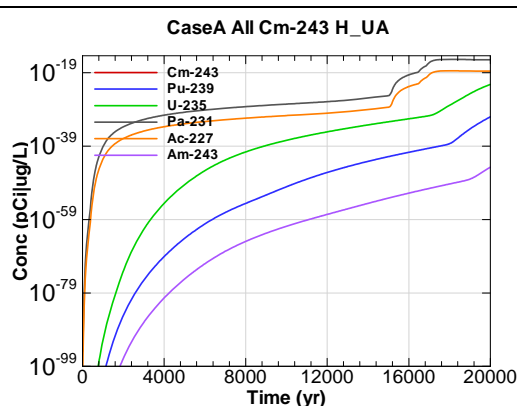


Figure A.1-176 - 100m Aquifer Concentration for
CaseA All Cm-243 H-UA

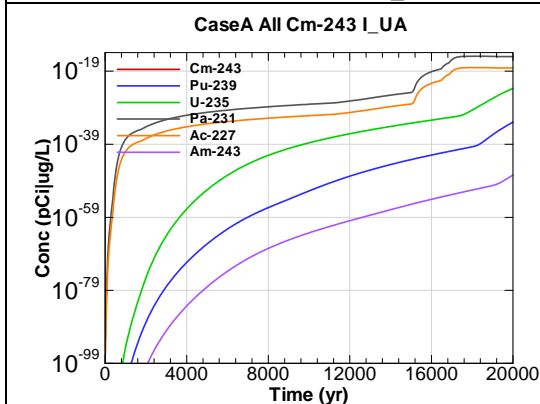


Figure A.1-177 - 100m Aquifer Concentration for
CaseA All Cm-243 I-UA

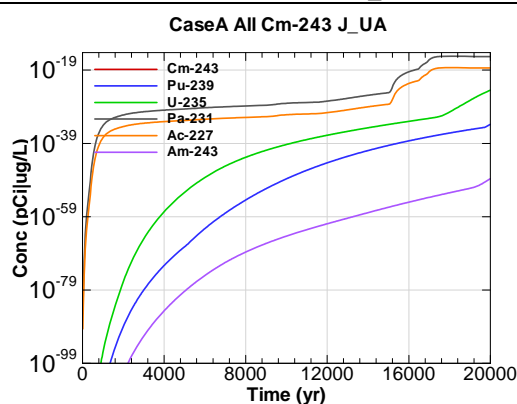


Figure A.1-178 - 100m Aquifer Concentration for
CaseA All Cm-243 J-UA

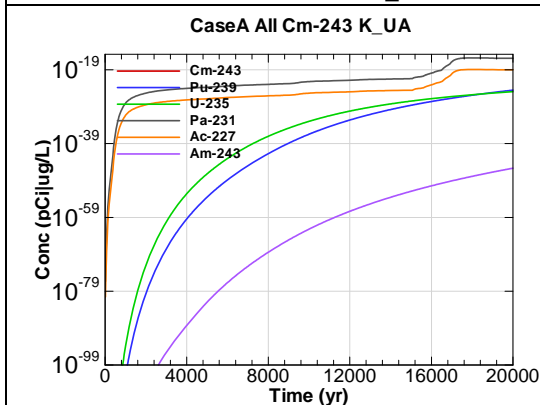


Figure A.1-179 - 100m Aquifer Concentration for
CaseA All Cm-243 K-UA

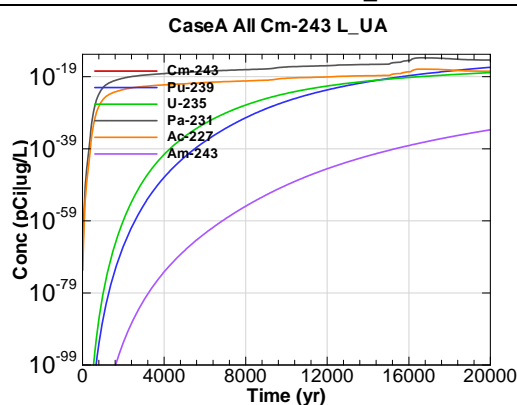
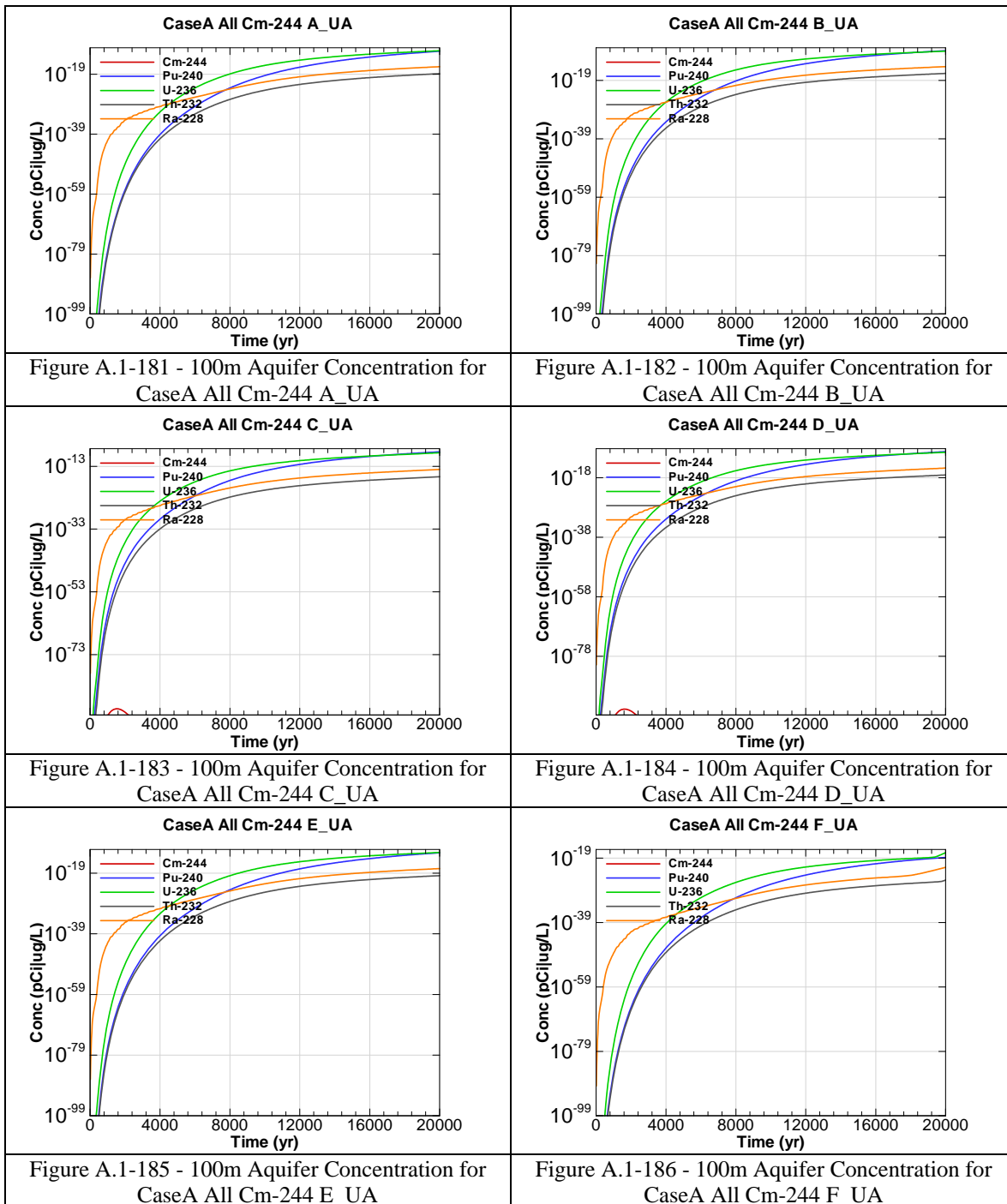


Figure A.1-180 - 100m Aquifer Concentration for
CaseA All Cm-243 L-UA



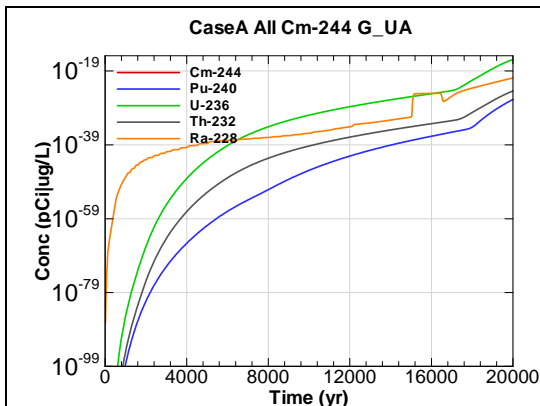


Figure A.1-187 - 100m Aquifer Concentration for CaseA All Cm-244 G-UA

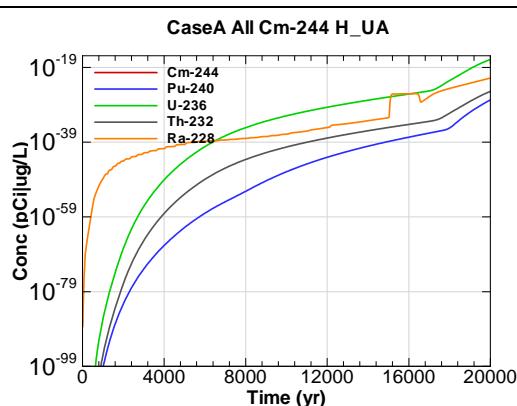


Figure A.1-188 - 100m Aquifer Concentration for CaseA All Cm-244 H-UA

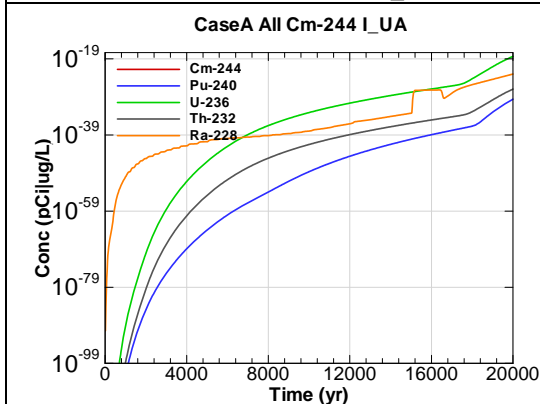


Figure A.1-189 - 100m Aquifer Concentration for CaseA All Cm-244 I-UA

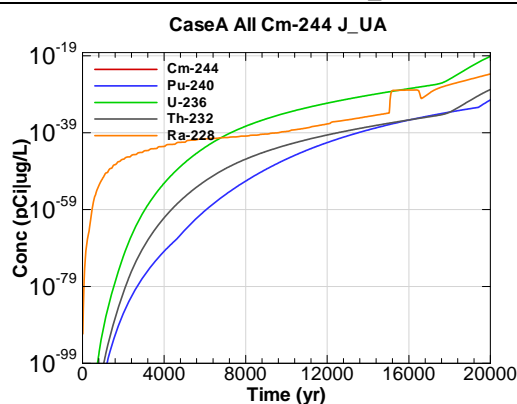


Figure A.1-190 - 100m Aquifer Concentration for CaseA All Cm-244 J-UA

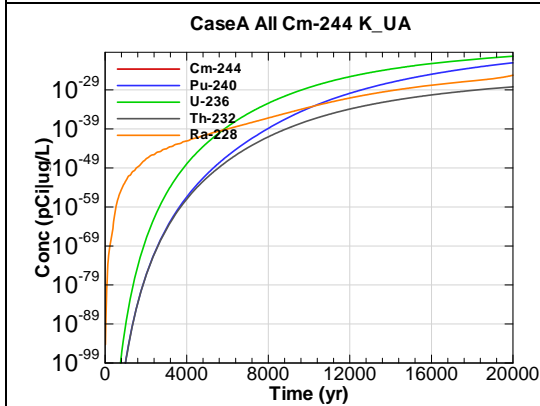


Figure A.1-191 - 100m Aquifer Concentration for CaseA All Cm-244 K-UA

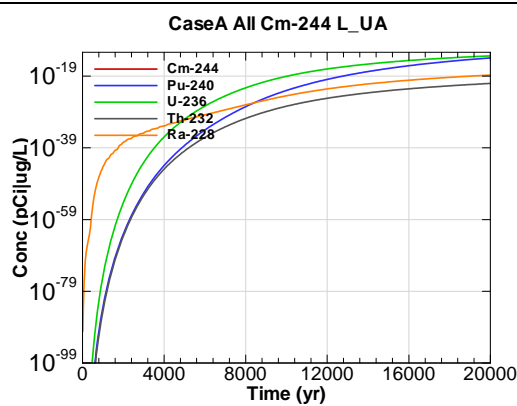


Figure A.1-192 - 100m Aquifer Concentration for CaseA All Cm-244 L-UA

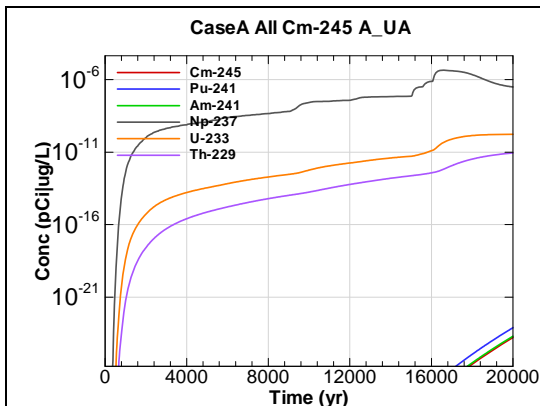


Figure A.1-193 - 100m Aquifer Concentration for
CaseA All Cm-245 A_UA

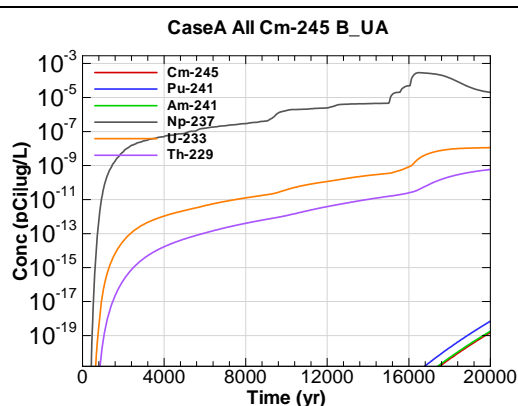


Figure A.1-194 - 100m Aquifer Concentration for
CaseA All Cm-245 B_UA

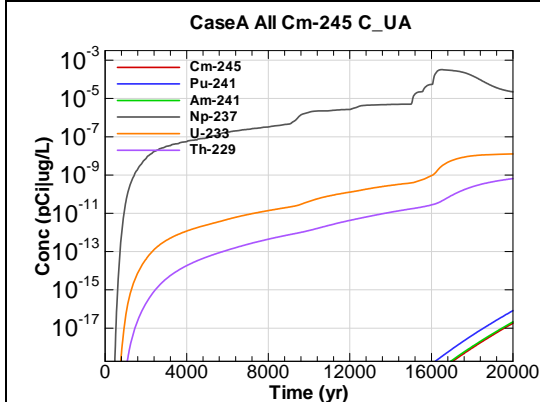


Figure A.1-195 - 100m Aquifer Concentration for
CaseA All Cm-245 C_UA

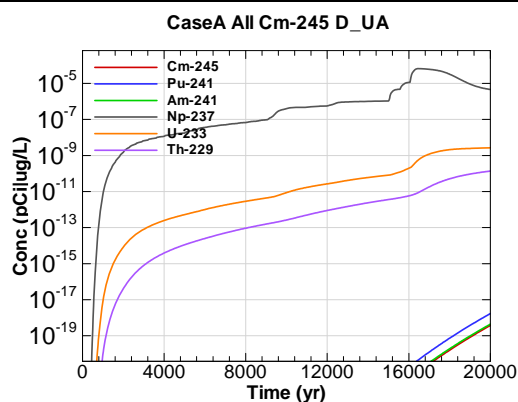


Figure A.1-196 - 100m Aquifer Concentration for
CaseA All Cm-245 D_UA

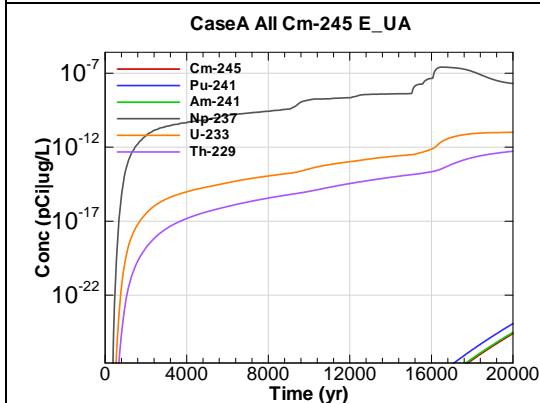


Figure A.1-197 - 100m Aquifer Concentration for
CaseA All Cm-245 E_UA

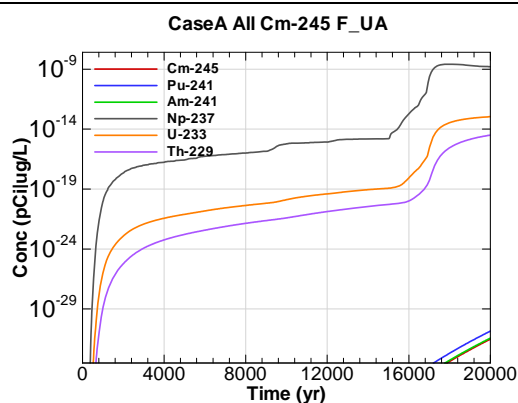
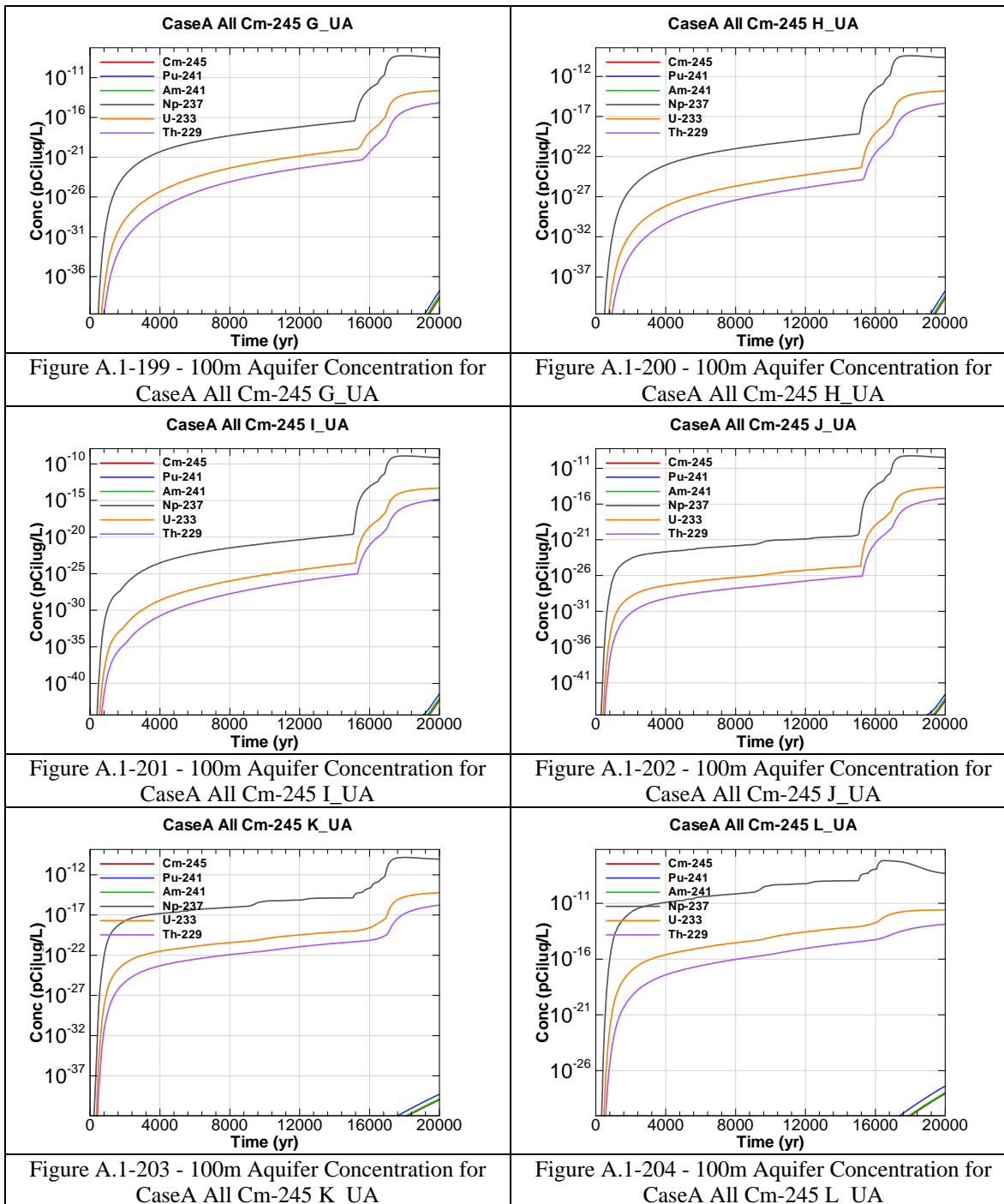


Figure A.1-198 - 100m Aquifer Concentration for
CaseA All Cm-245 F_UA



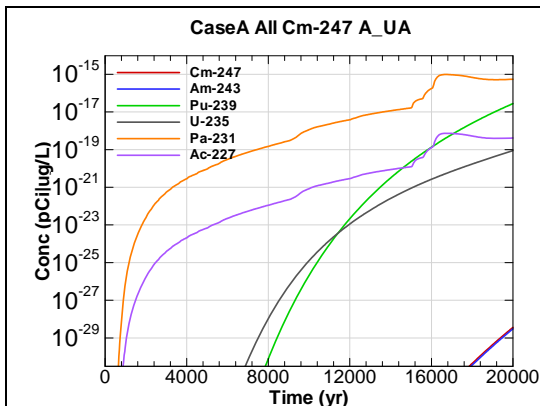


Figure A.1-205 - 100m Aquifer Concentration for CaseA All Cm-247 A-UA

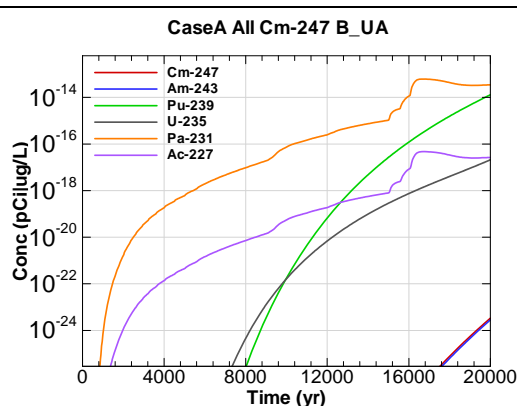


Figure A.1-206 - 100m Aquifer Concentration for CaseA All Cm-247 B-UA

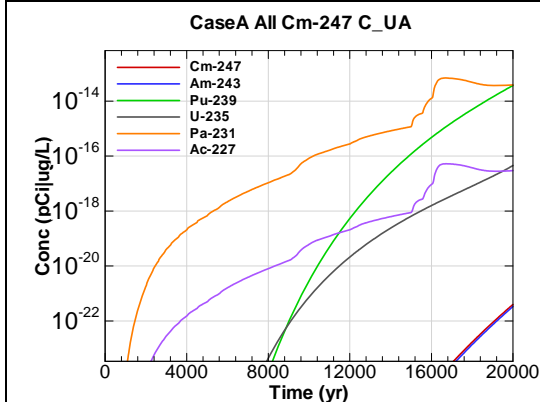


Figure A.1-207 - 100m Aquifer Concentration for CaseA All Cm-247 C-UA

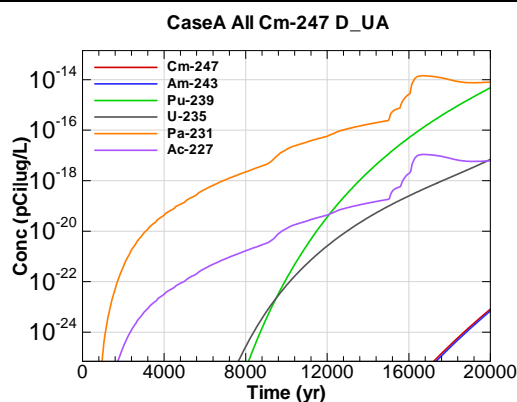


Figure A.1-208 - 100m Aquifer Concentration for CaseA All Cm-247 D-UA

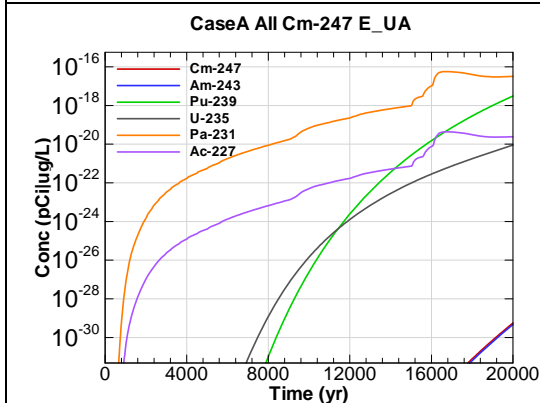


Figure A.1-209 - 100m Aquifer Concentration for CaseA All Cm-247 E-UA

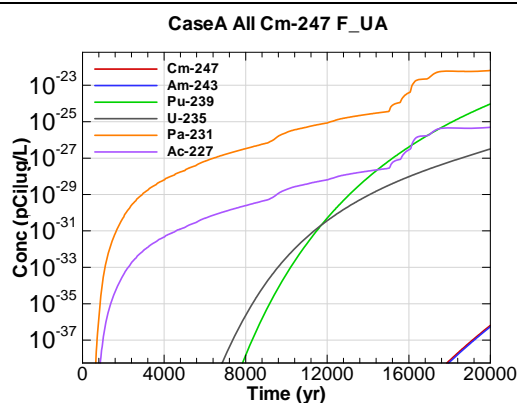


Figure A.1-210 - 100m Aquifer Concentration for CaseA All Cm-247 F-UA

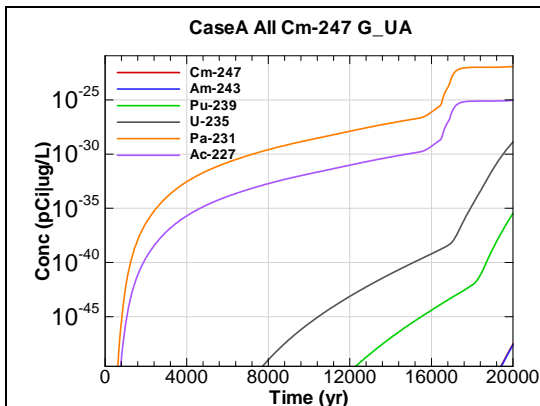


Figure A.1-211 - 100m Aquifer Concentration for CaseA All Cm-247 G-UA

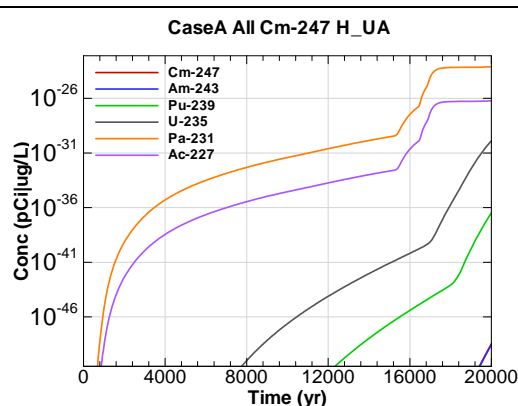


Figure A.1-212 - 100m Aquifer Concentration for CaseA All Cm-247 H-UA

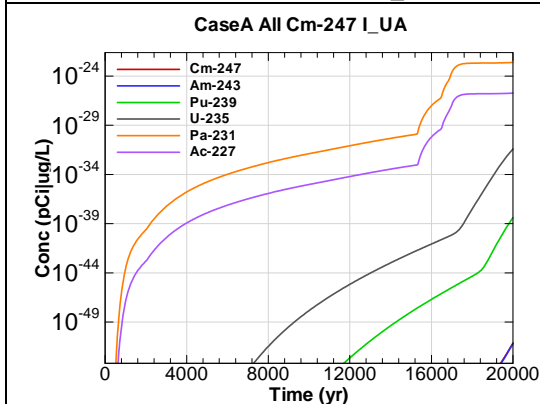


Figure A.1-213 - 100m Aquifer Concentration for CaseA All Cm-247 I-UA

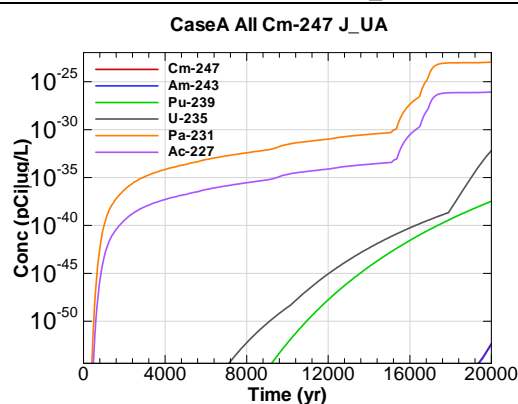


Figure A.1-214 - 100m Aquifer Concentration for CaseA All Cm-247 J-UA

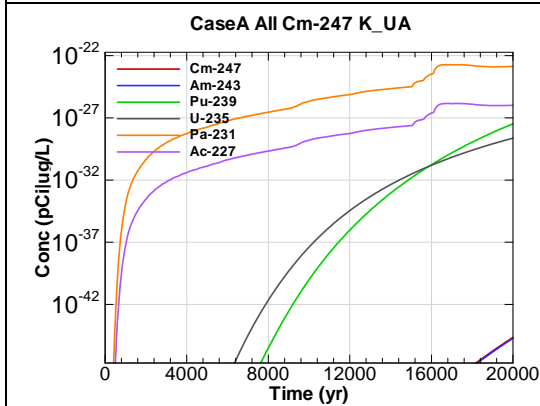


Figure A.1-215 - 100m Aquifer Concentration for CaseA All Cm-247 K-UA

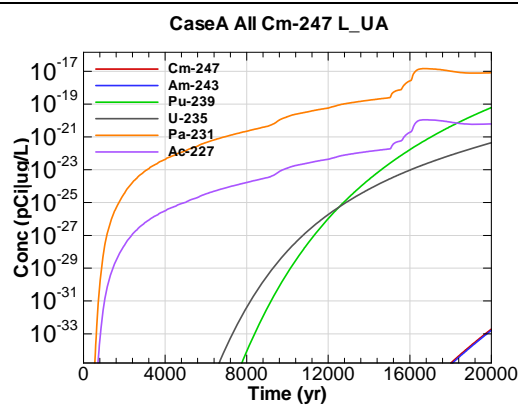


Figure A.1-216 - 100m Aquifer Concentration for CaseA All Cm-247 L-UA

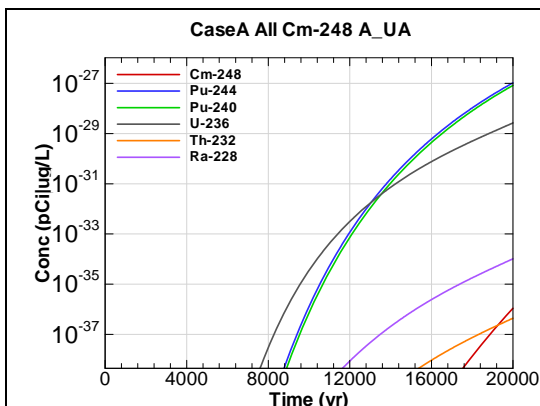


Figure A.1-217 - 100m Aquifer Concentration for CaseA All Cm-248 A_UA

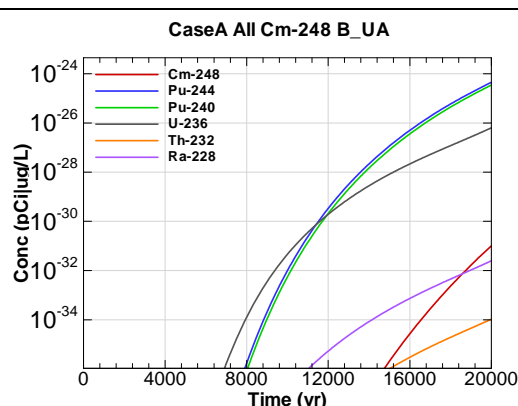


Figure A.1-218 - 100m Aquifer Concentration for CaseA All Cm-248 B_UA

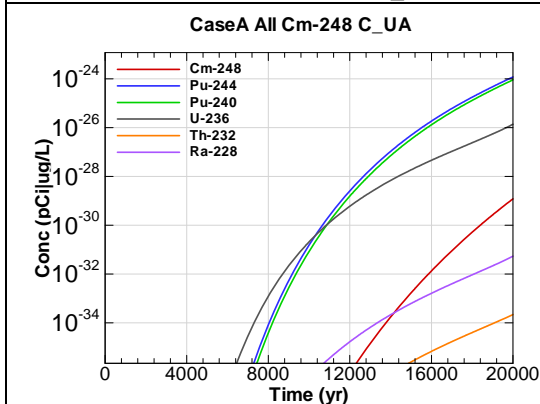


Figure A.1-219 - 100m Aquifer Concentration for CaseA All Cm-248 C_UA

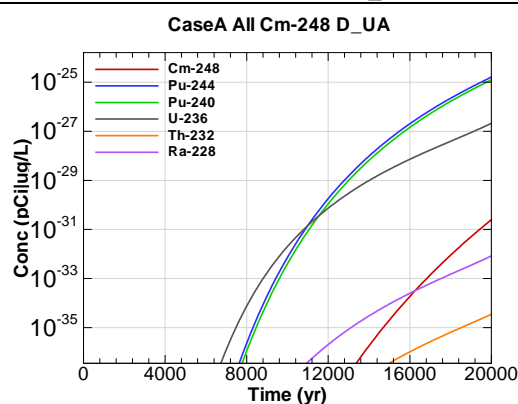


Figure A.1-220 - 100m Aquifer Concentration for CaseA All Cm-248 D_UA

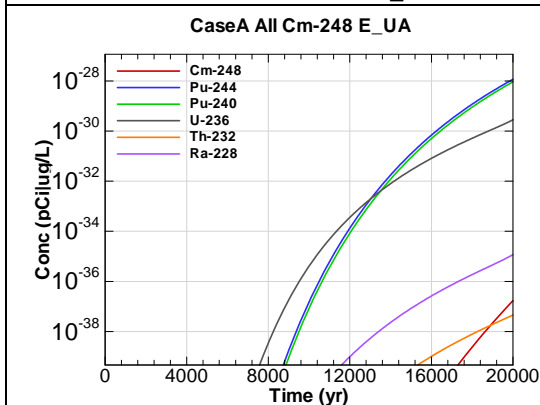


Figure A.1-221 - 100m Aquifer Concentration for CaseA All Cm-248 E_UA

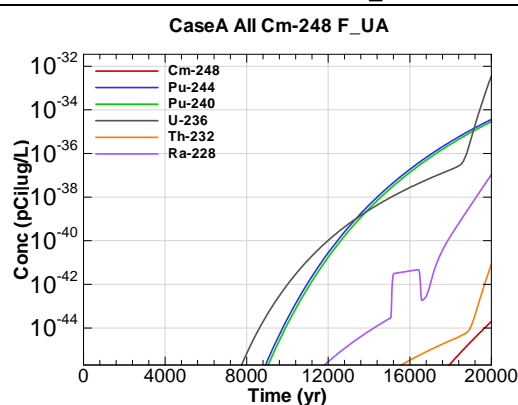
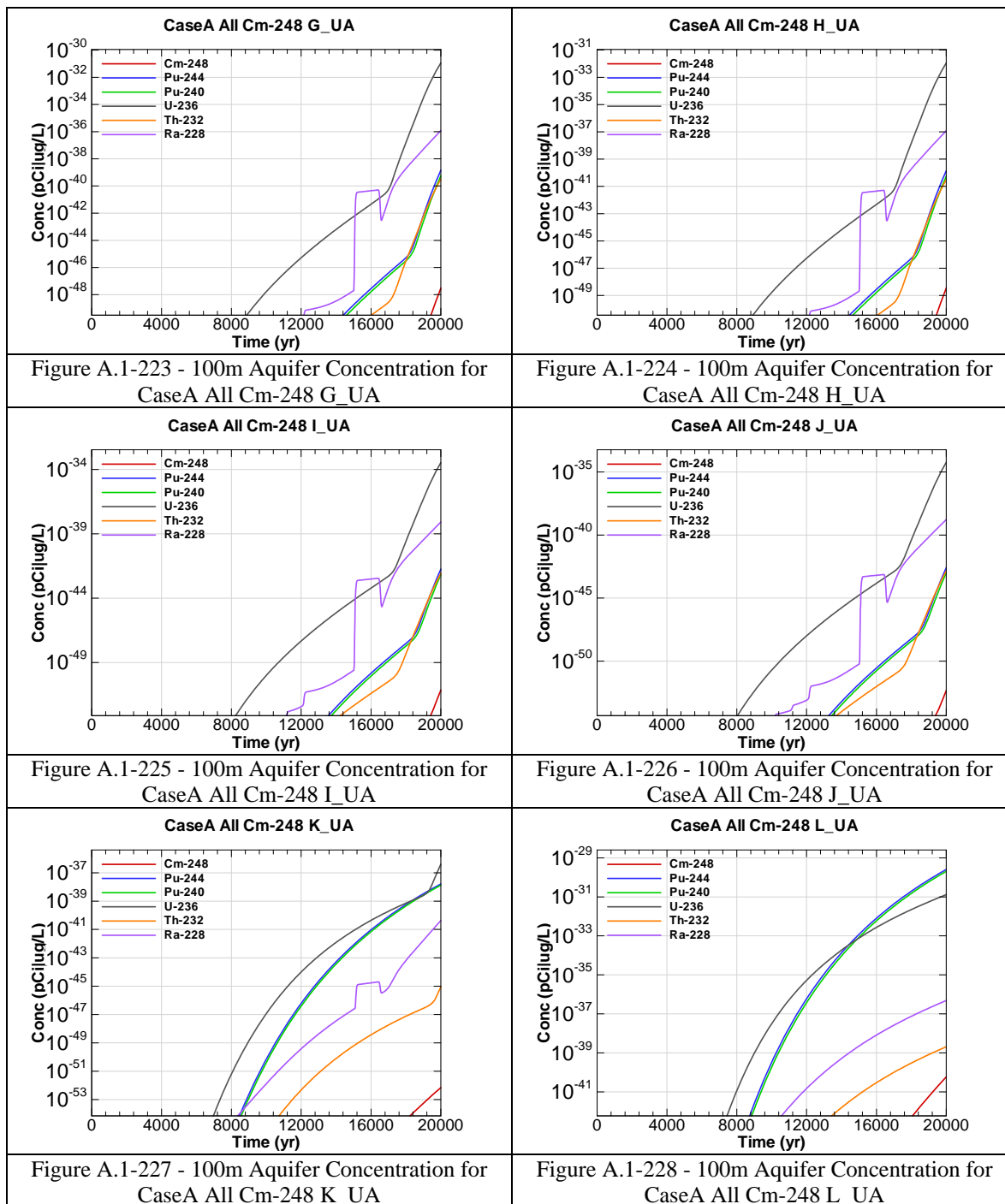
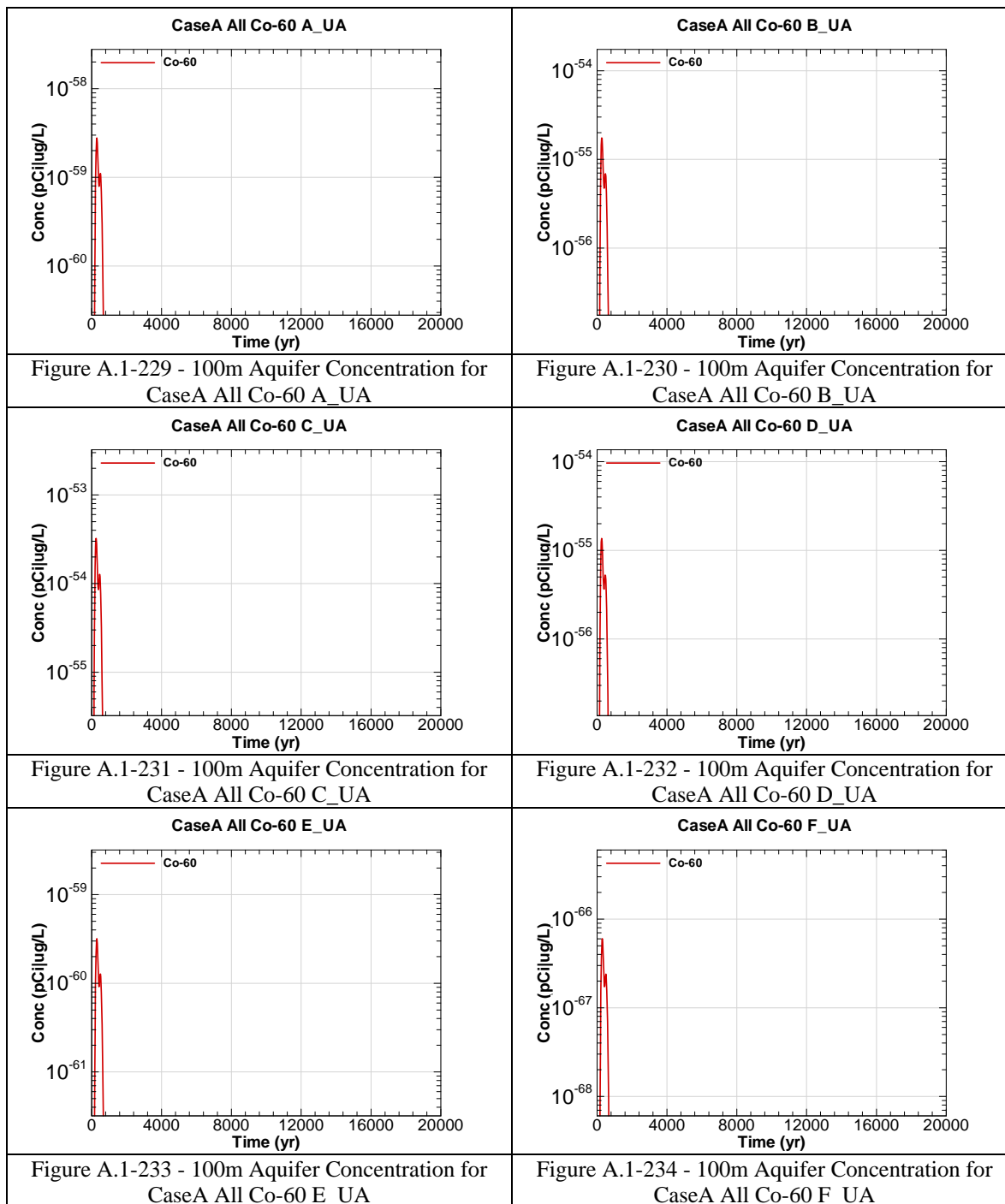
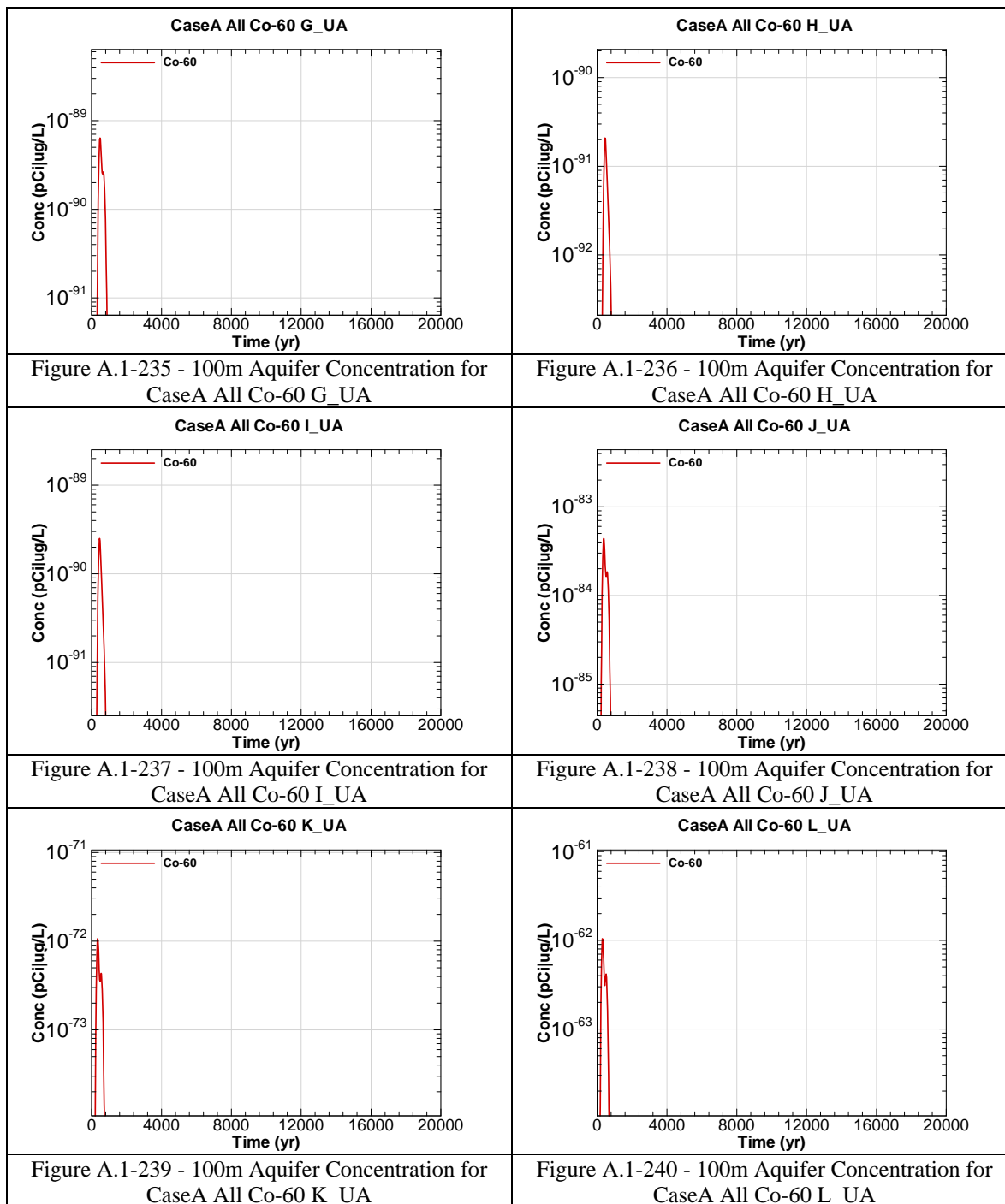
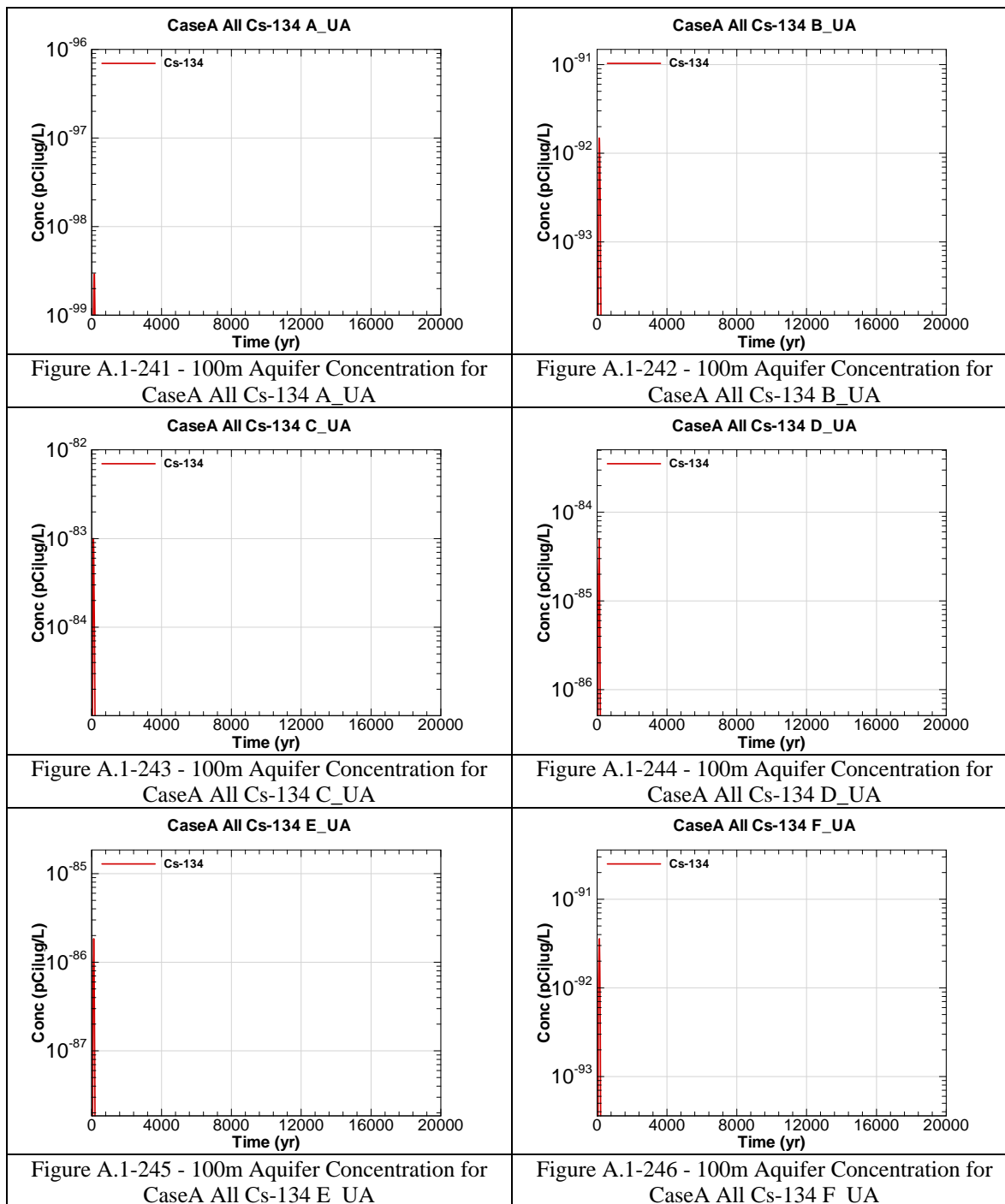


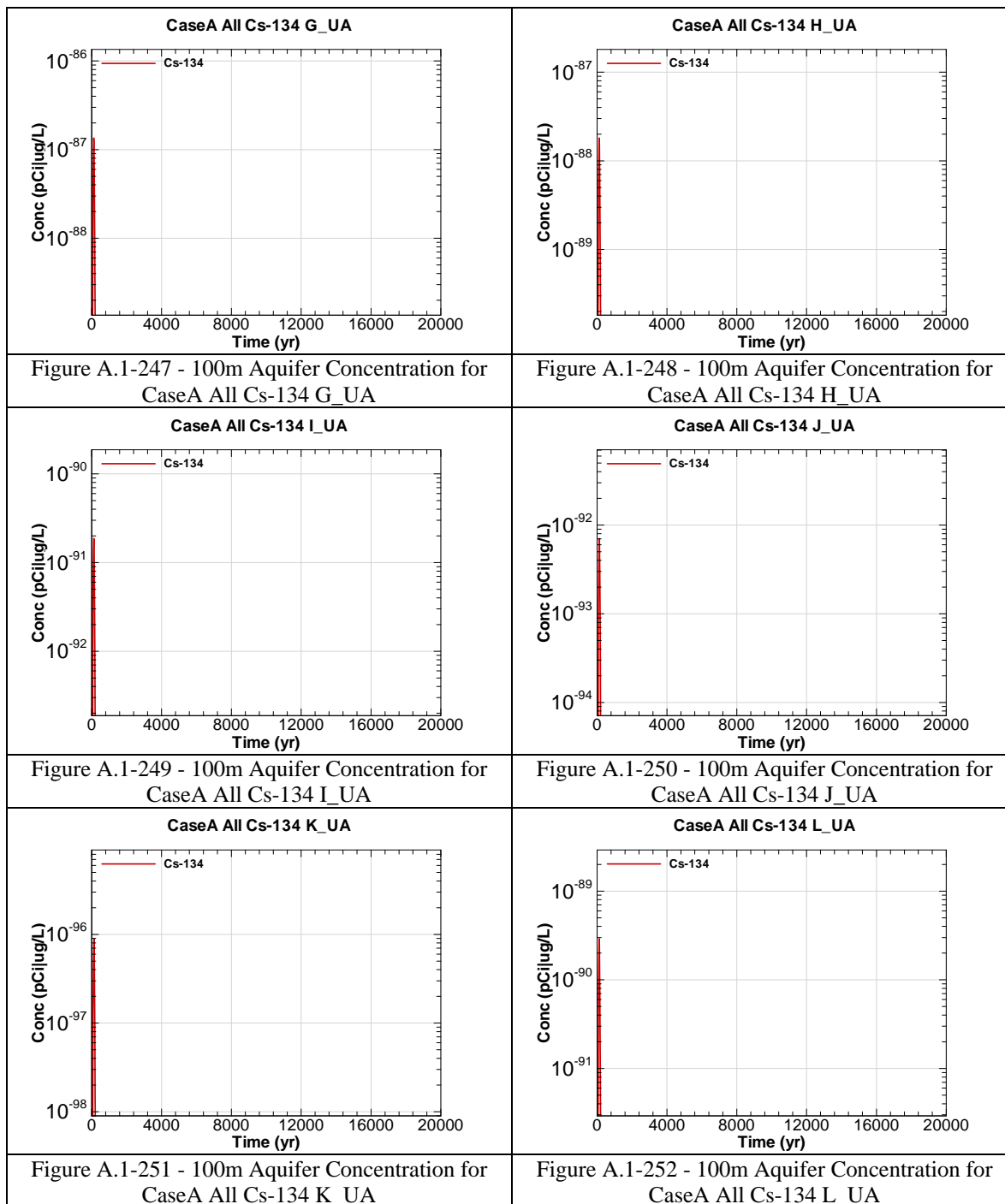
Figure A.1-222 - 100m Aquifer Concentration for CaseA All Cm-248 F_UA

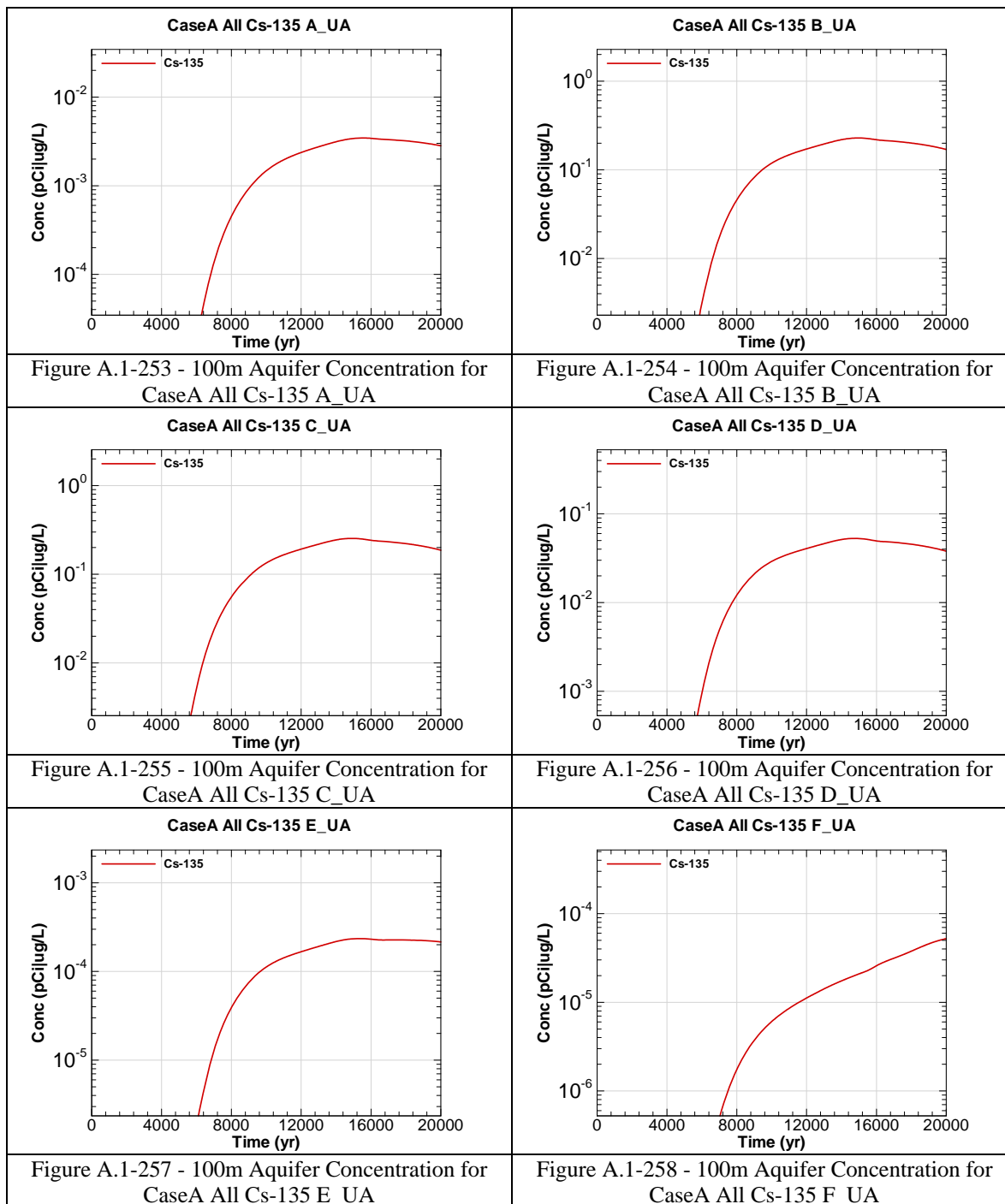


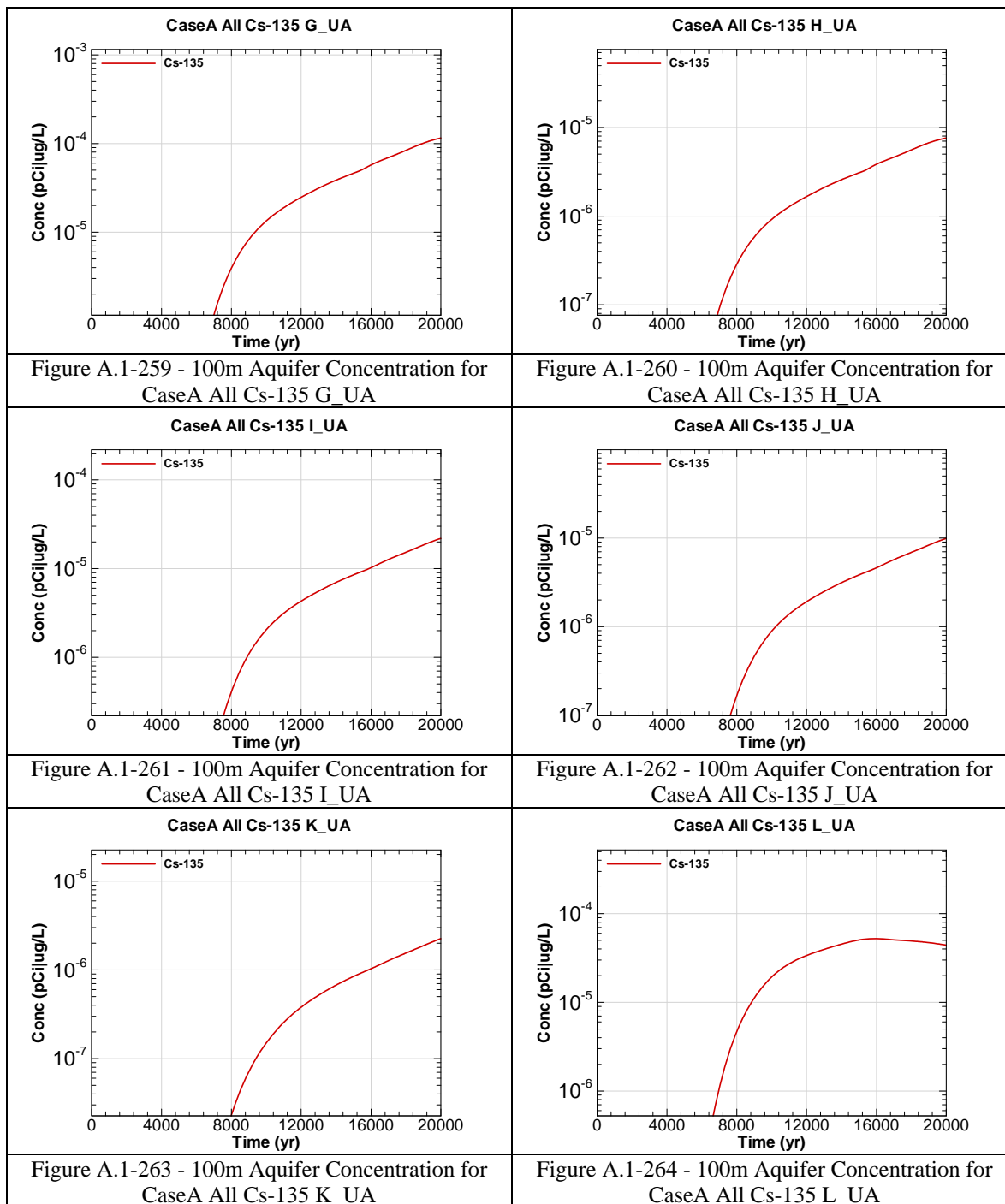


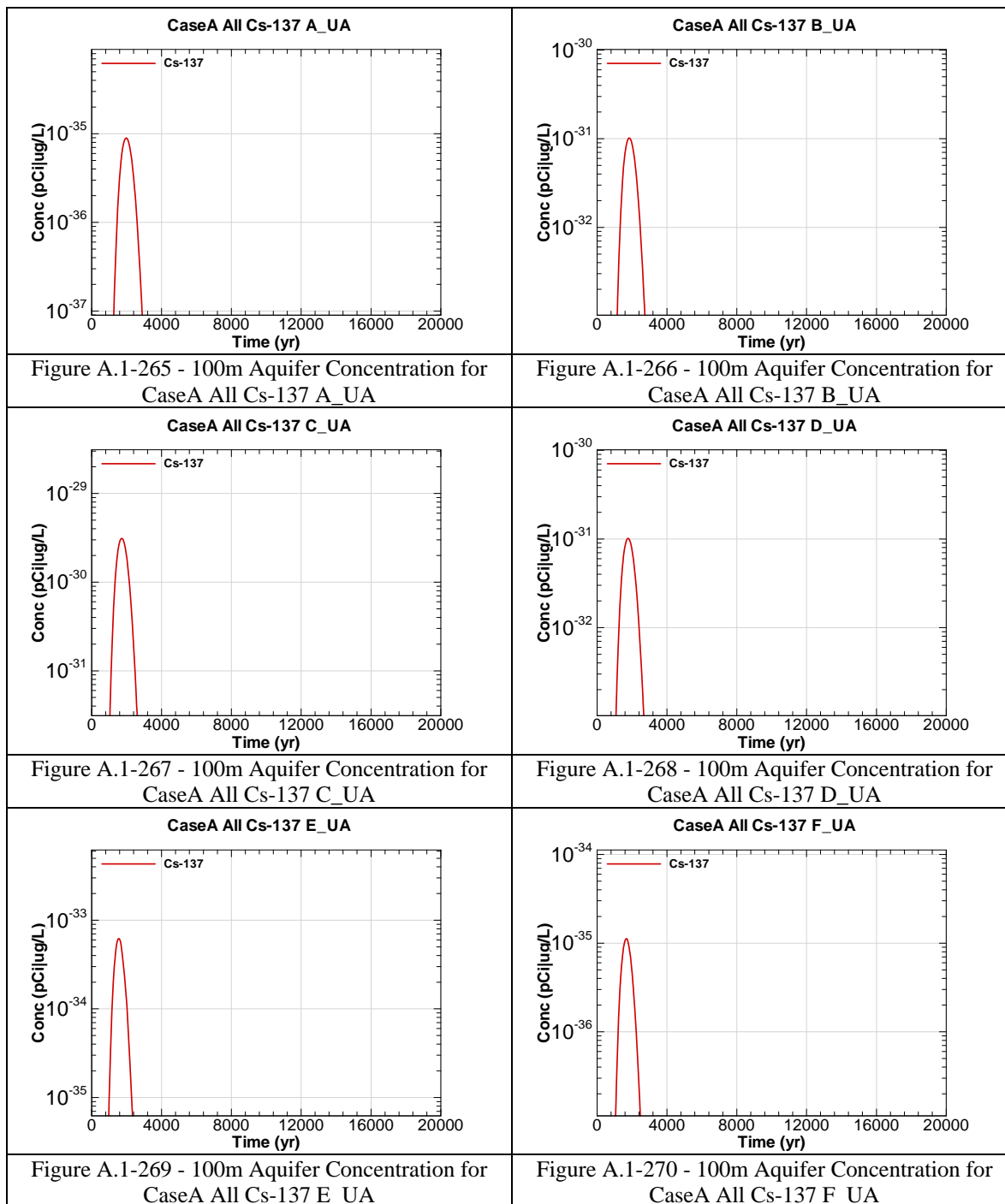


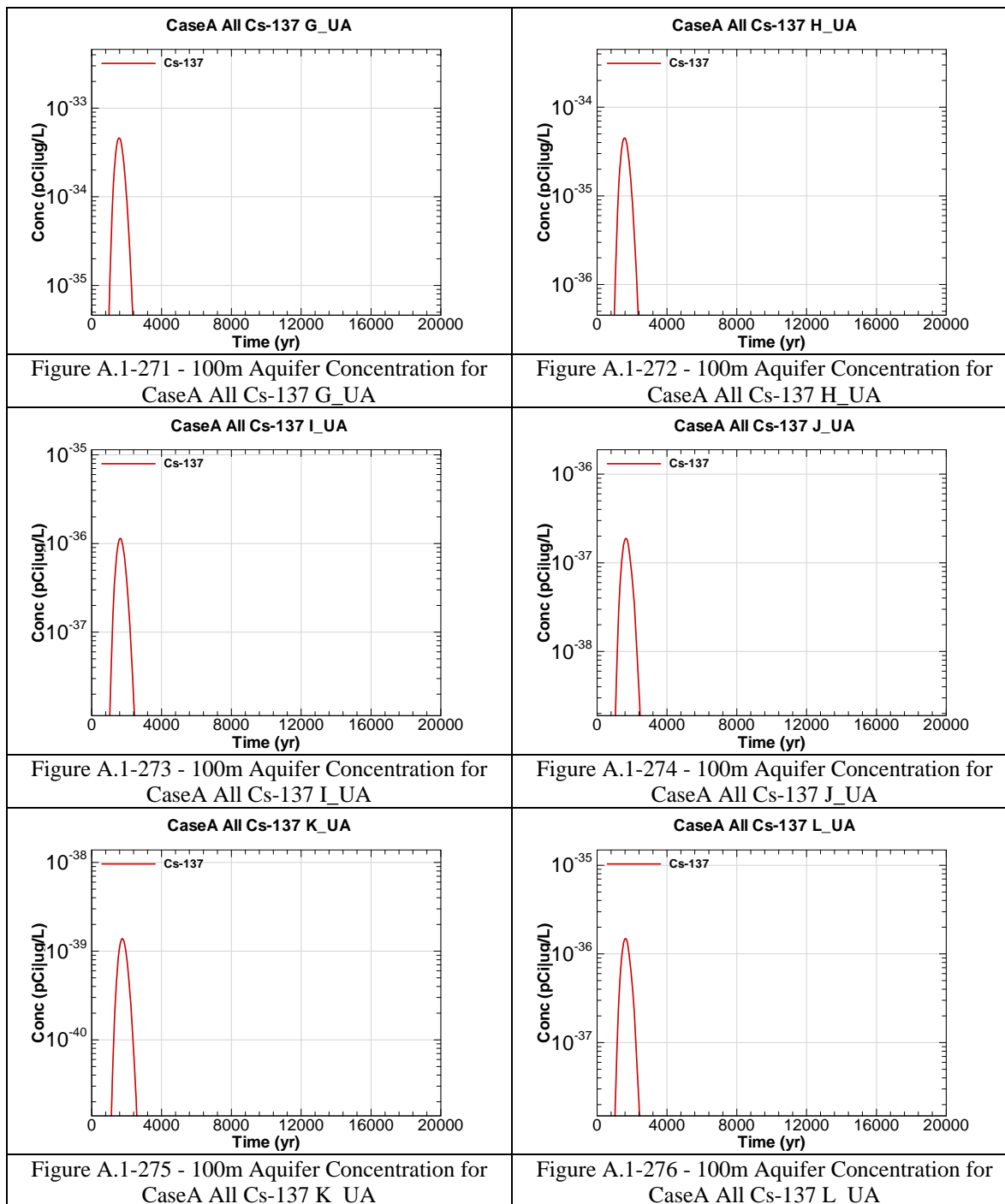


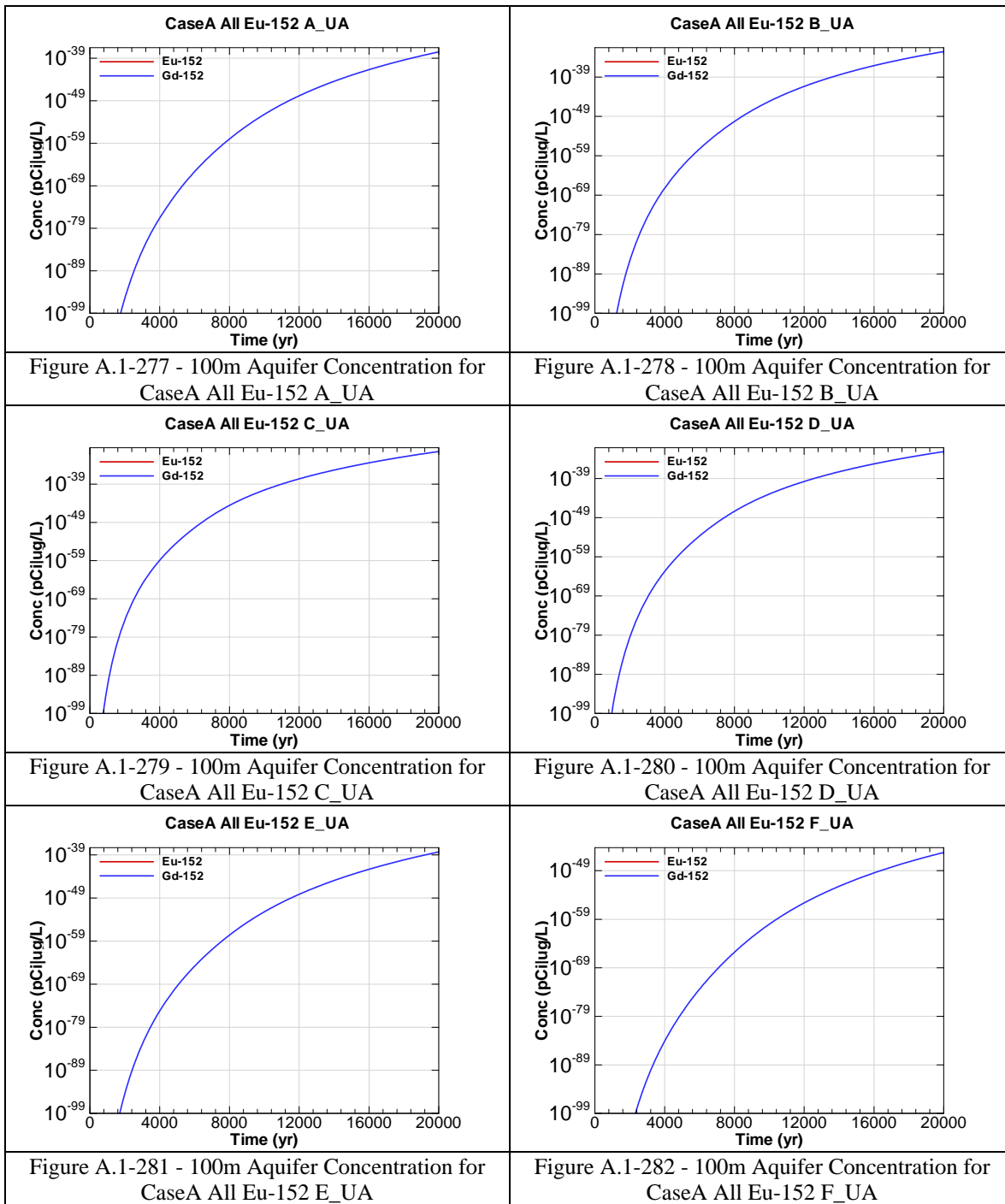


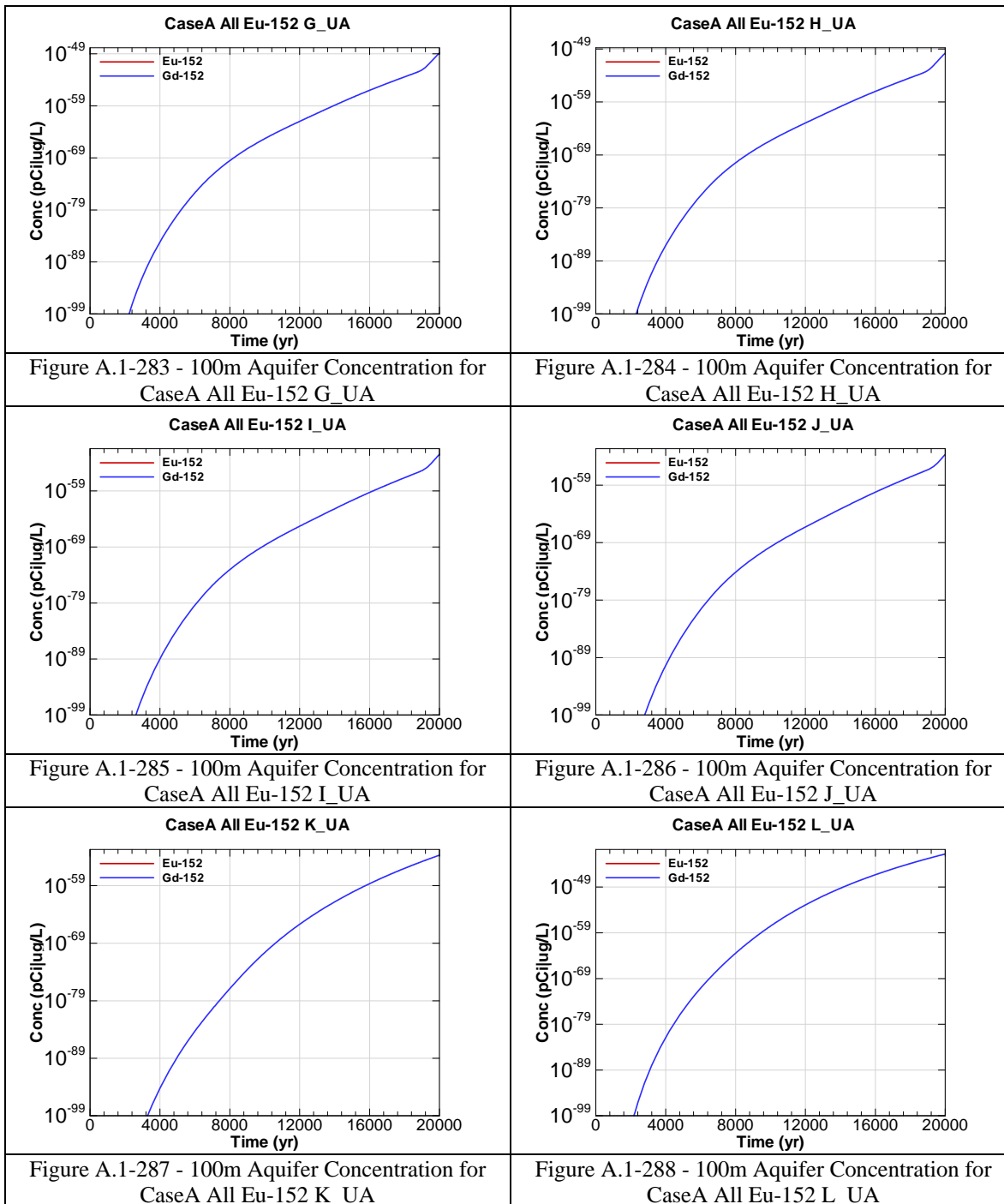


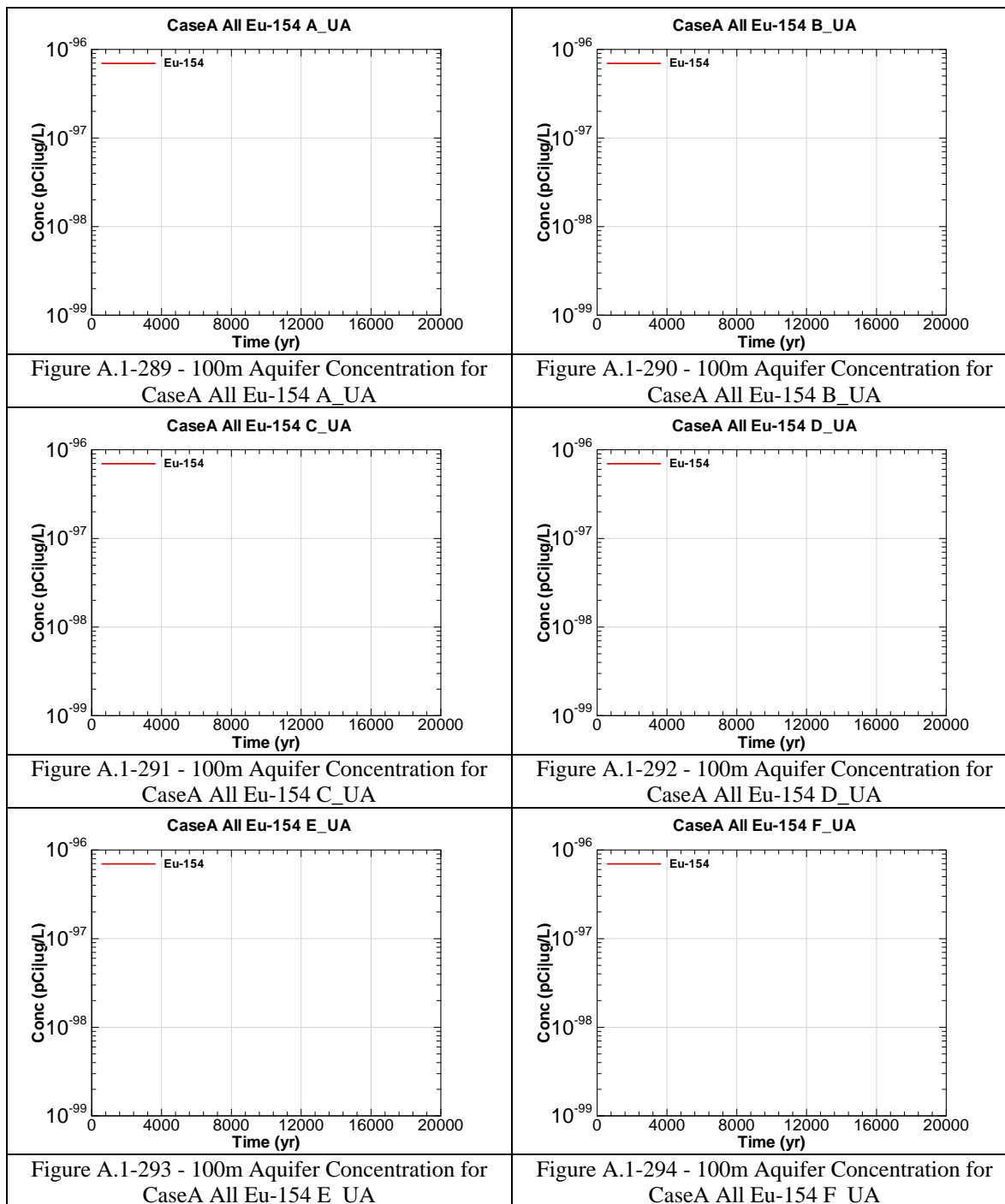


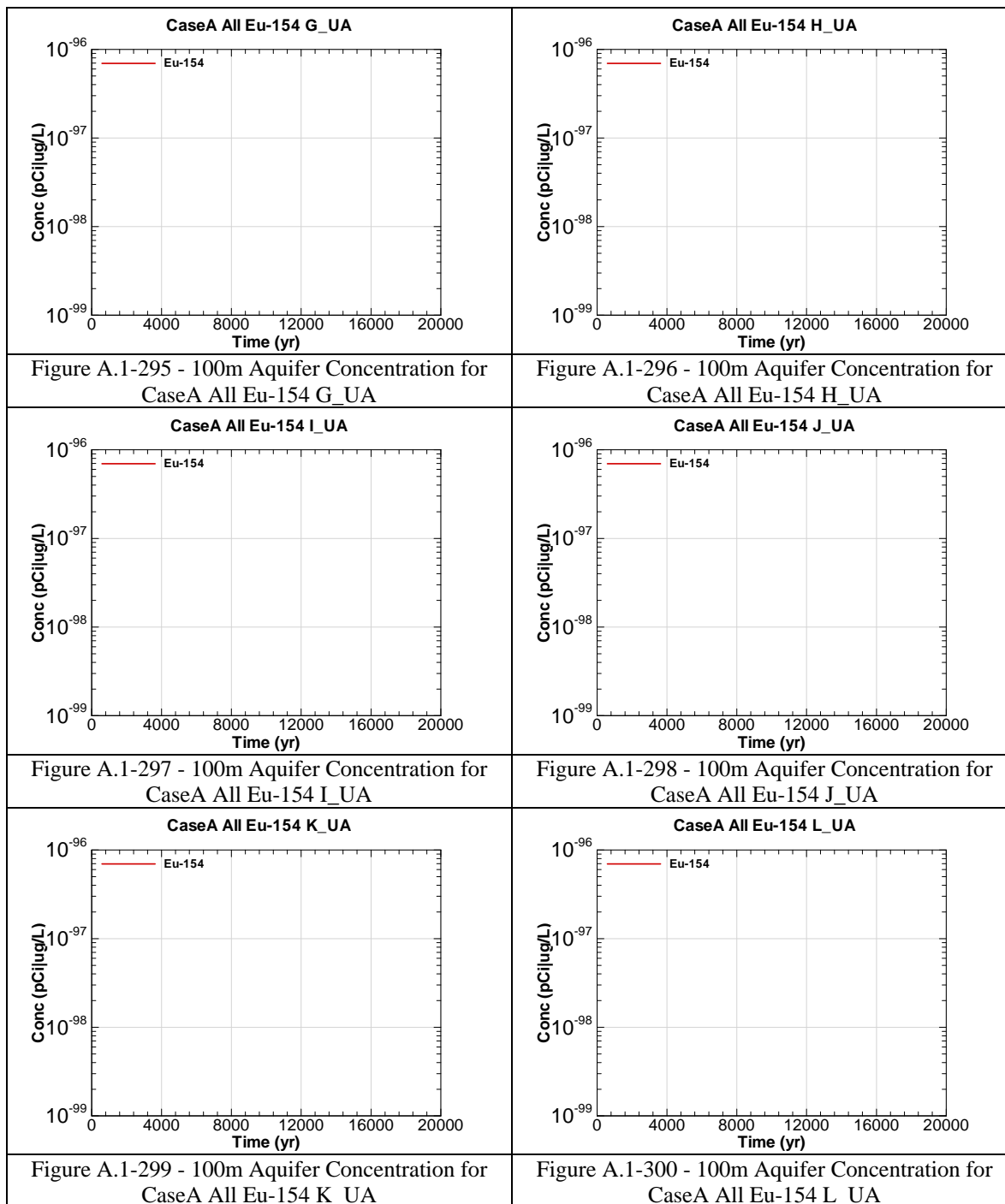


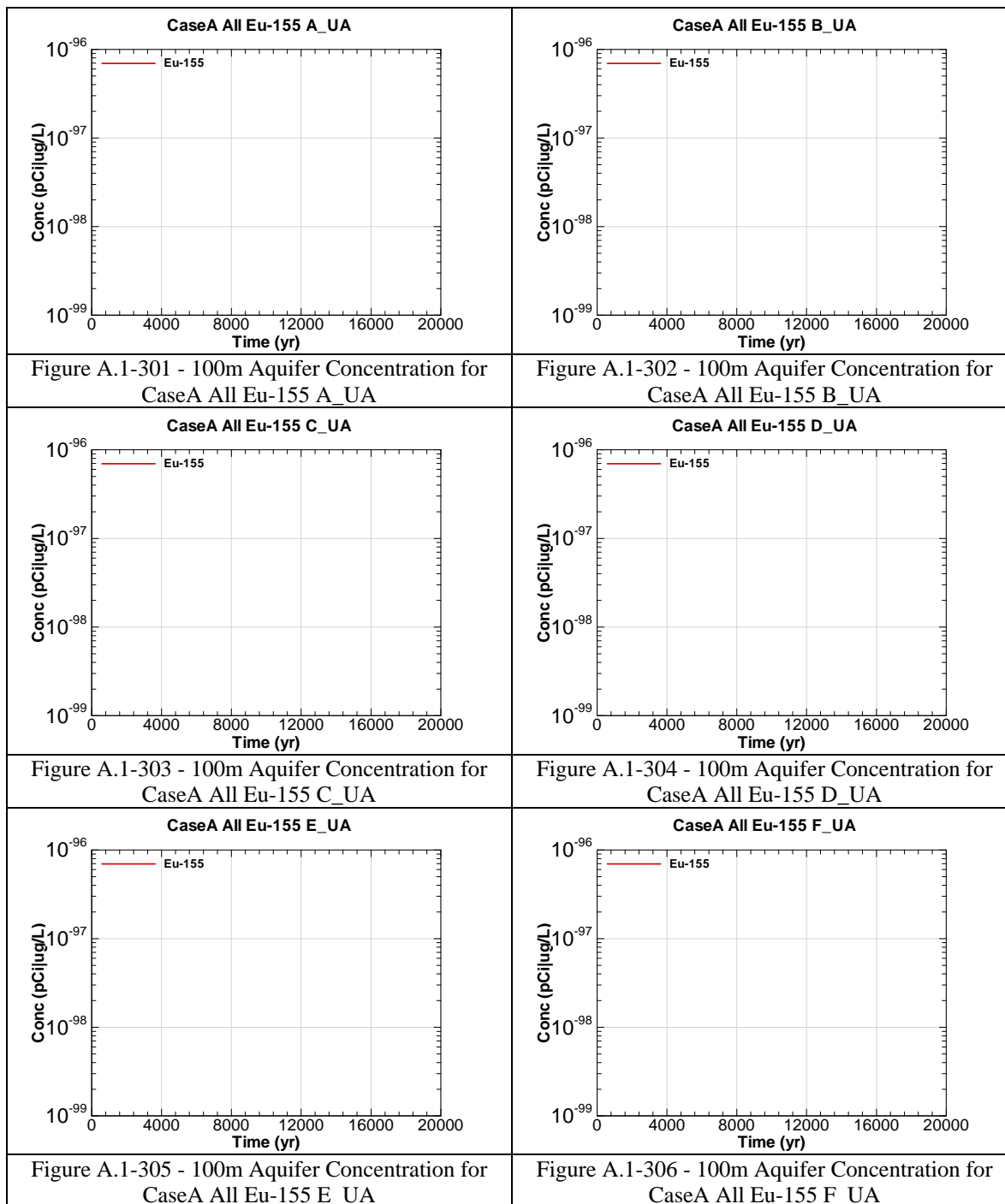


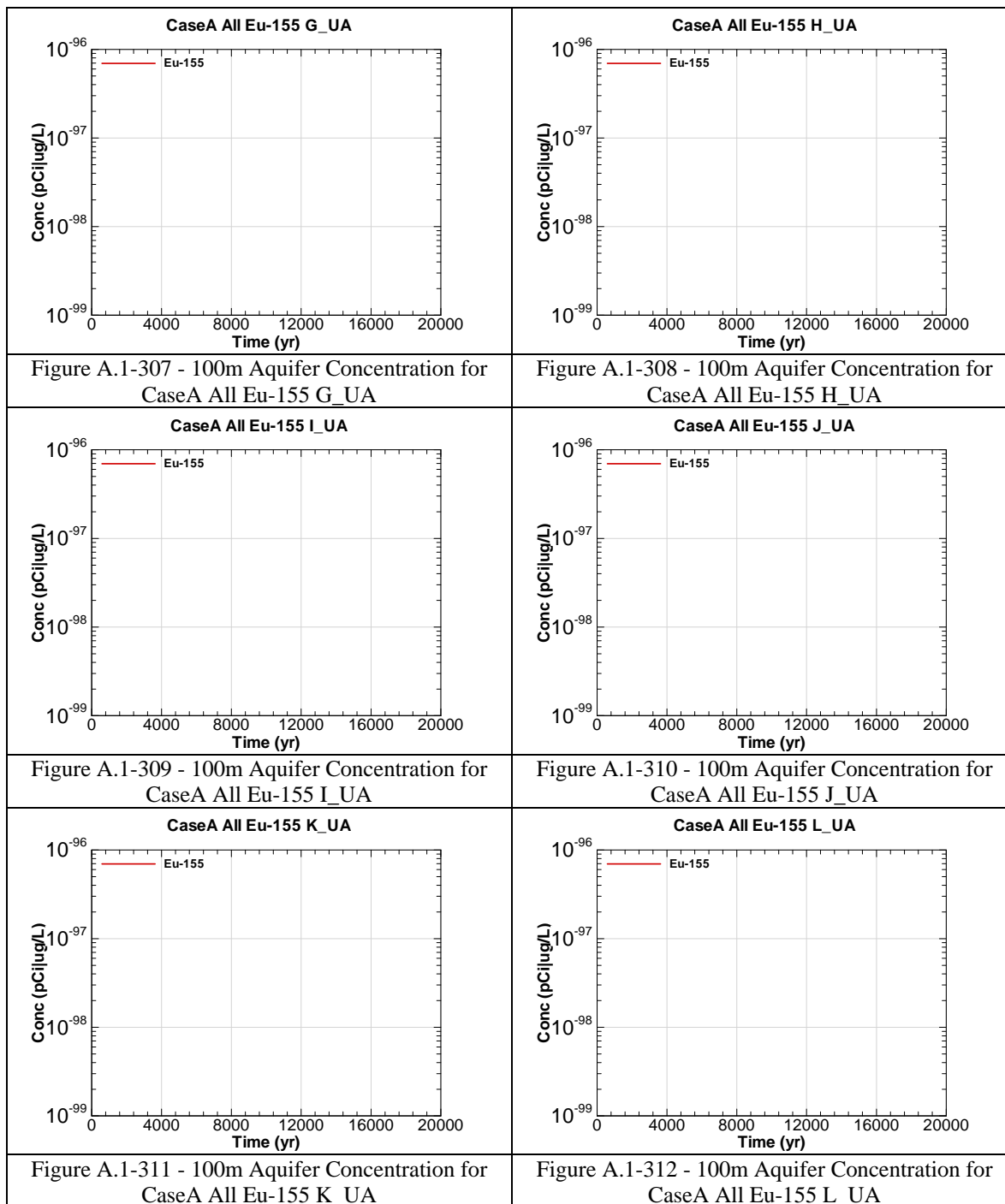


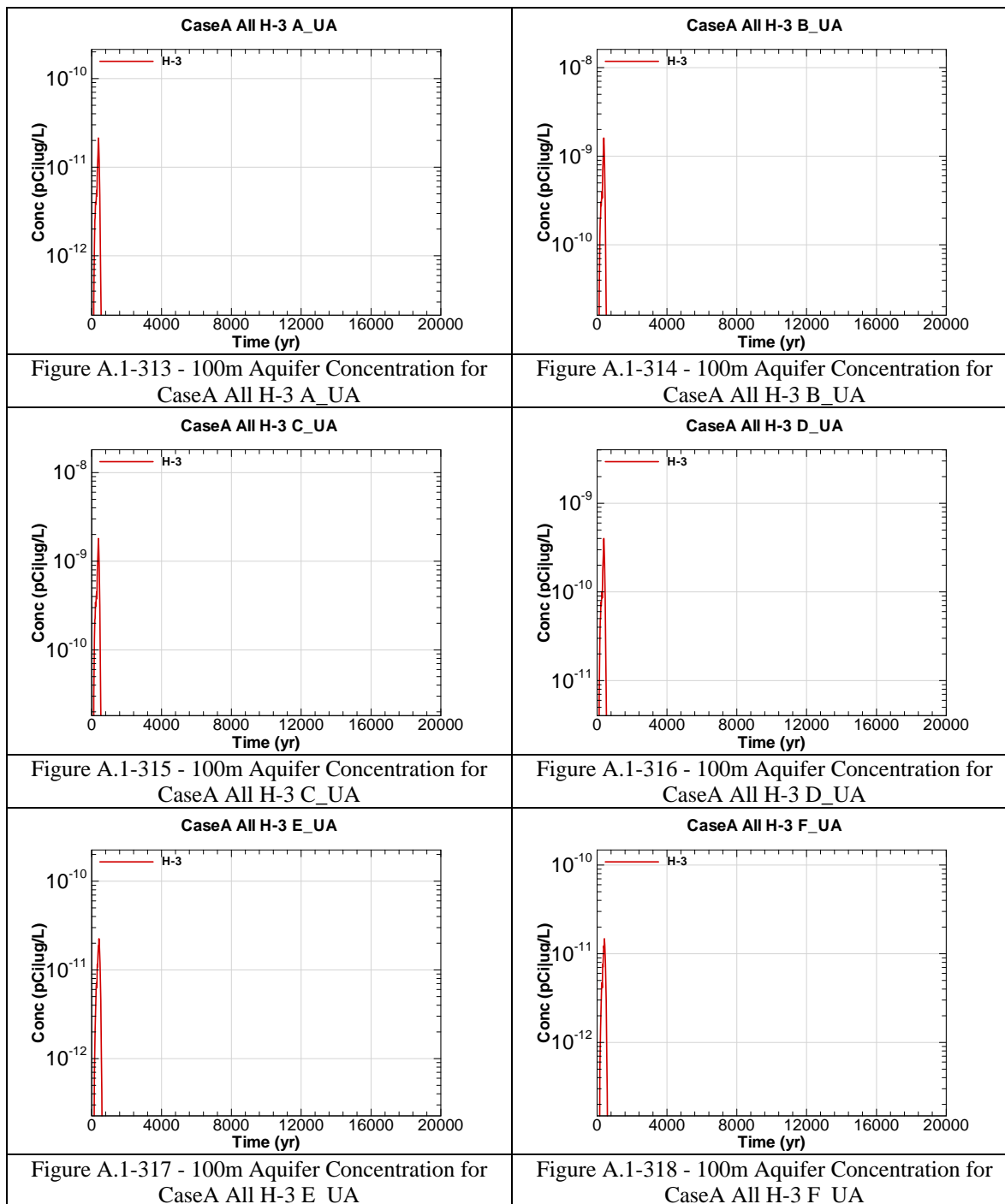


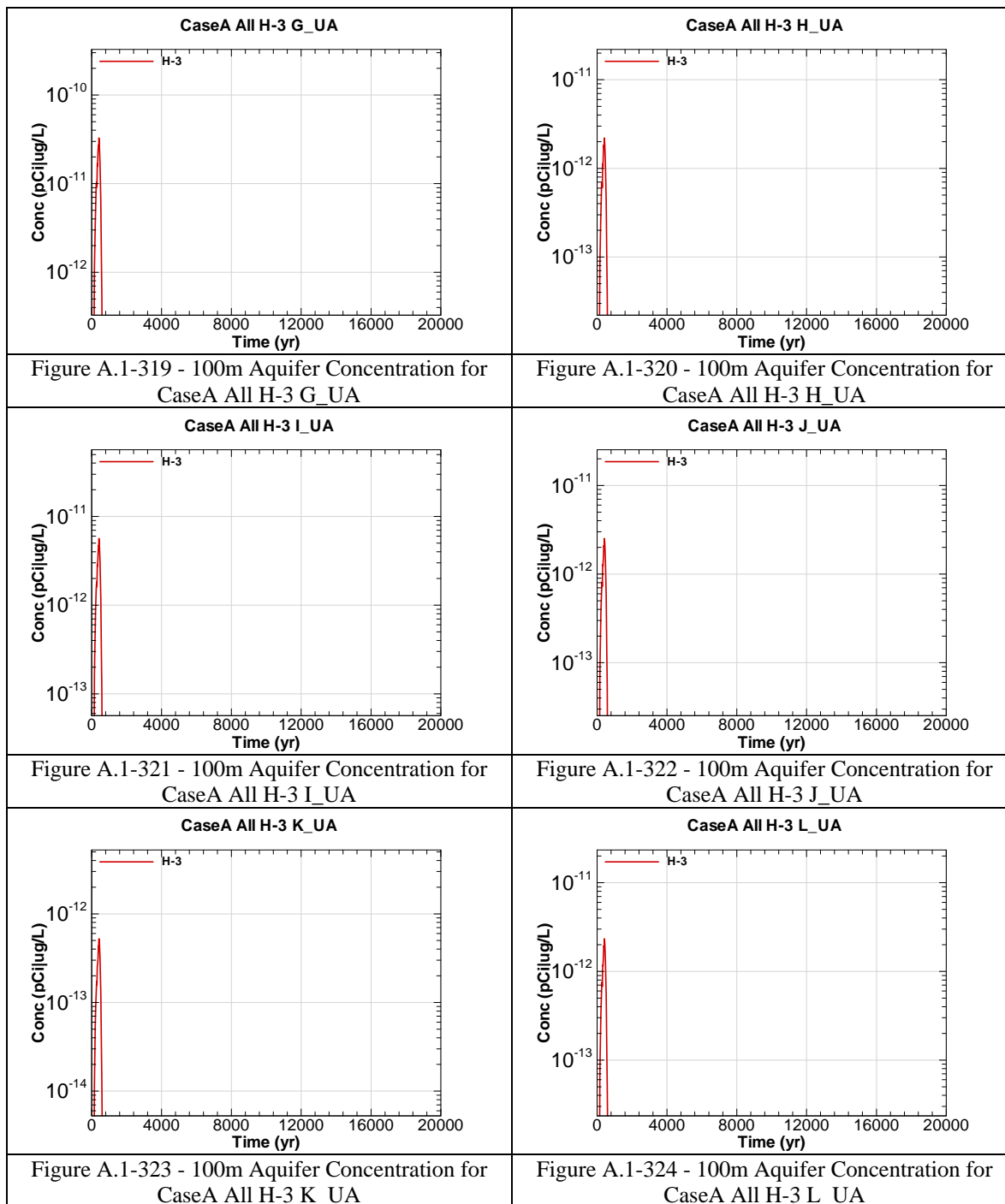


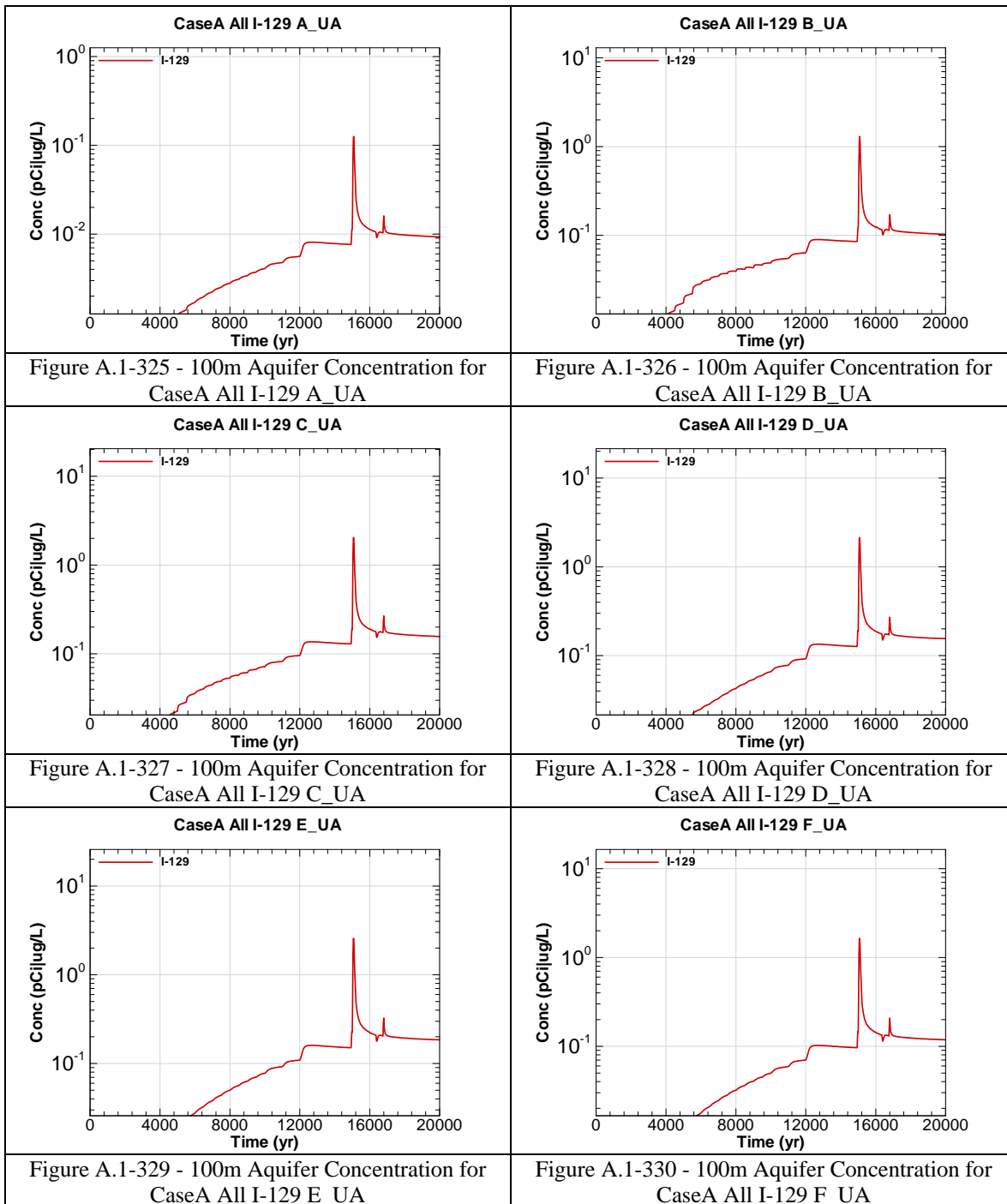


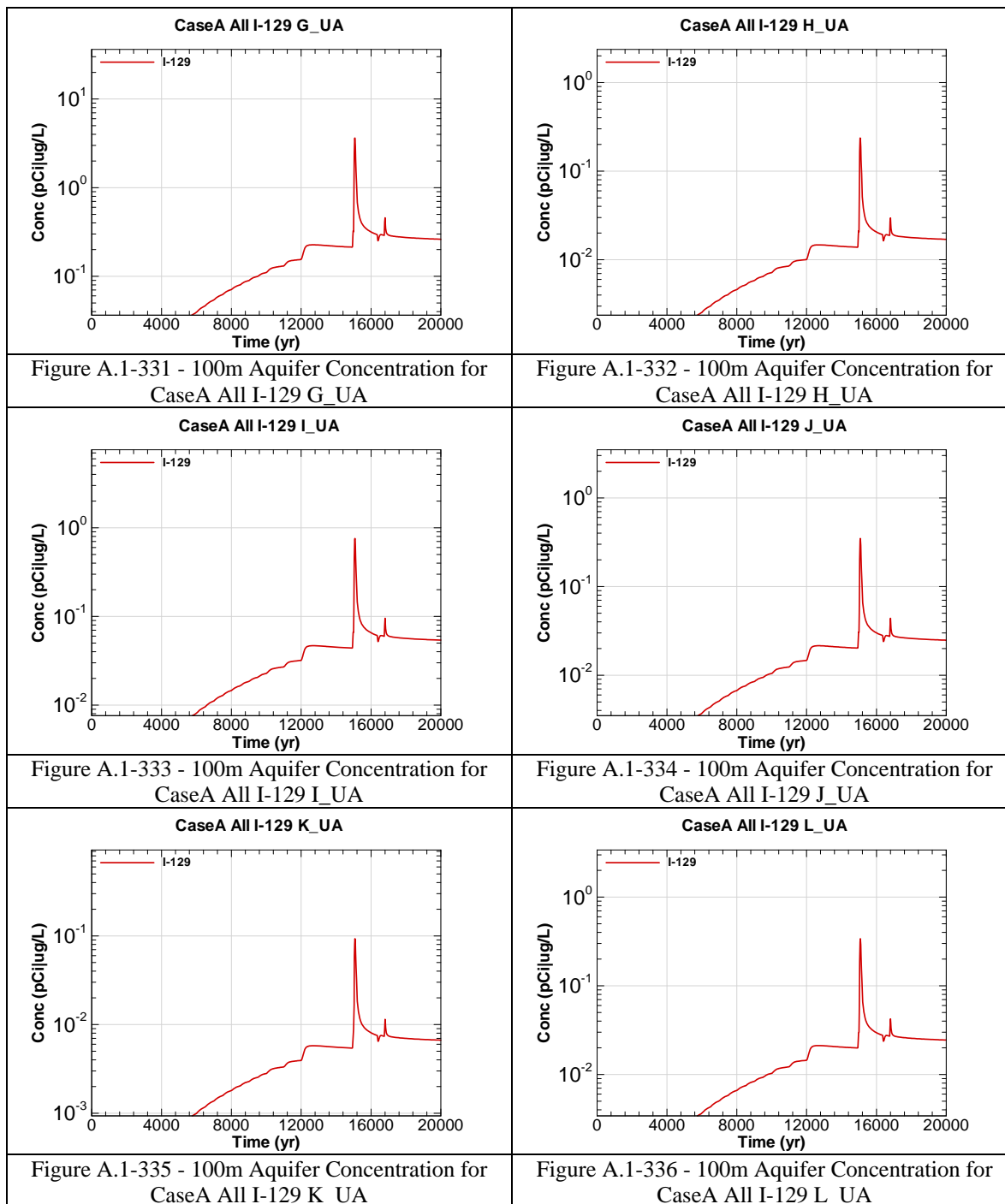


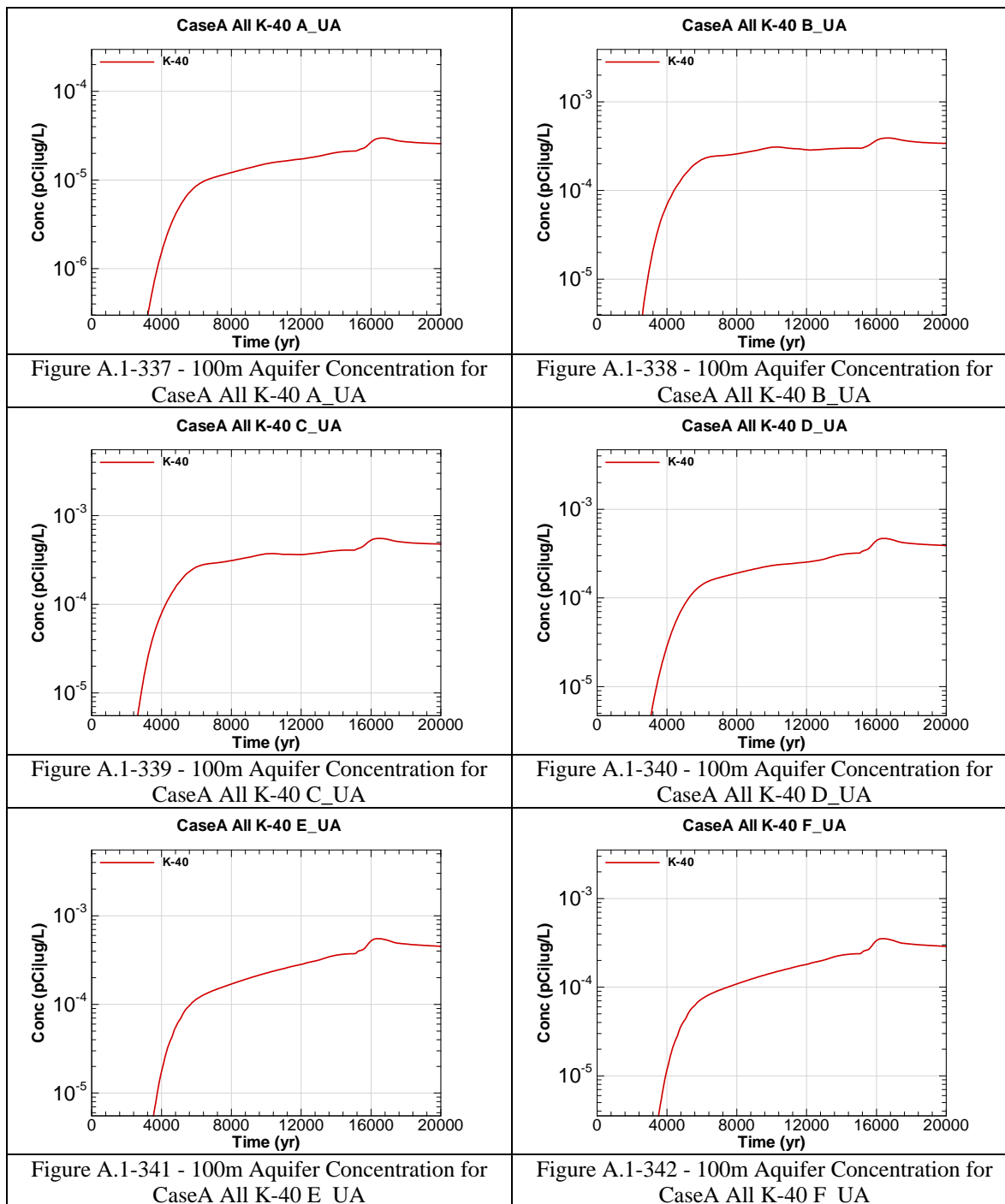


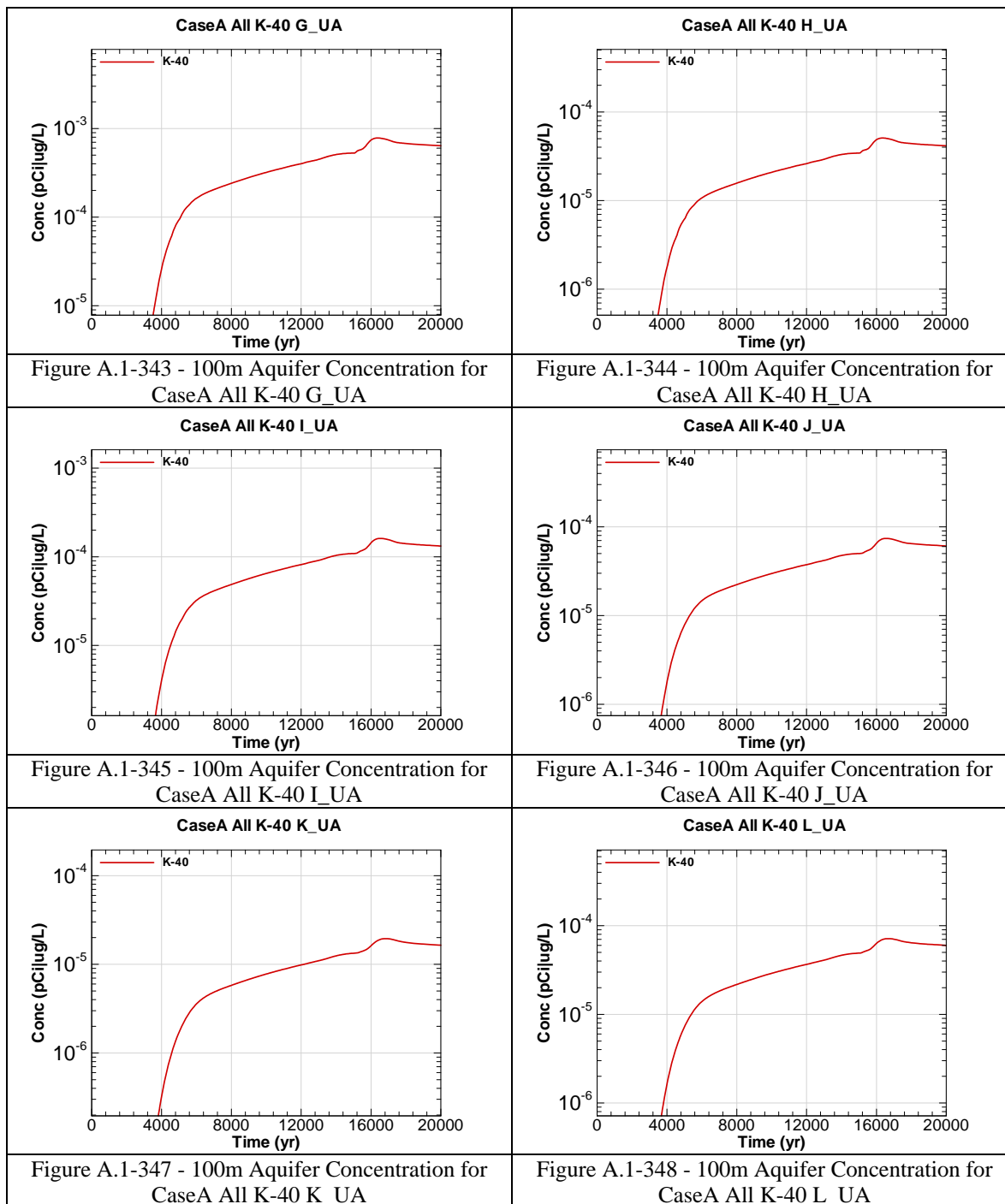


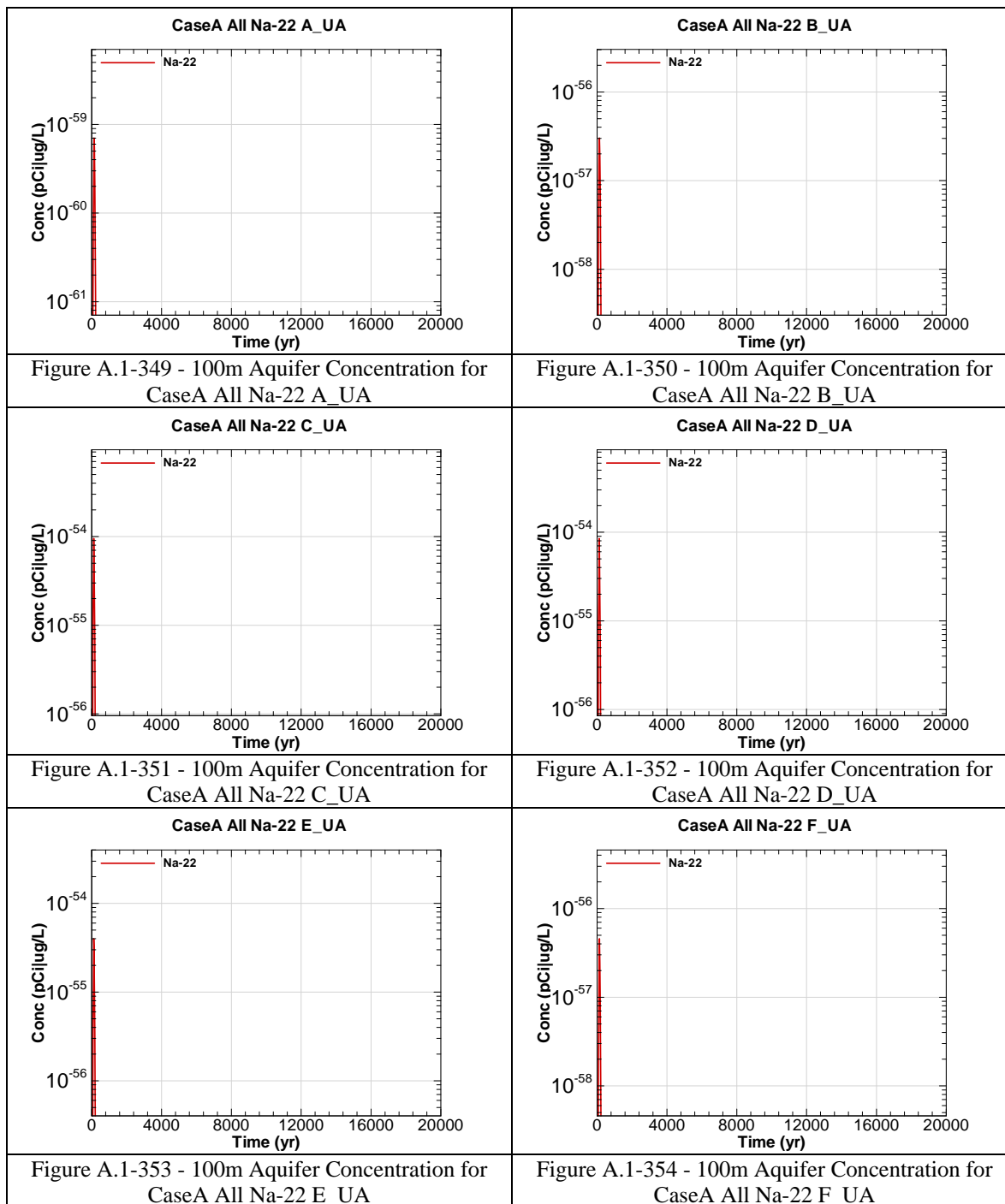


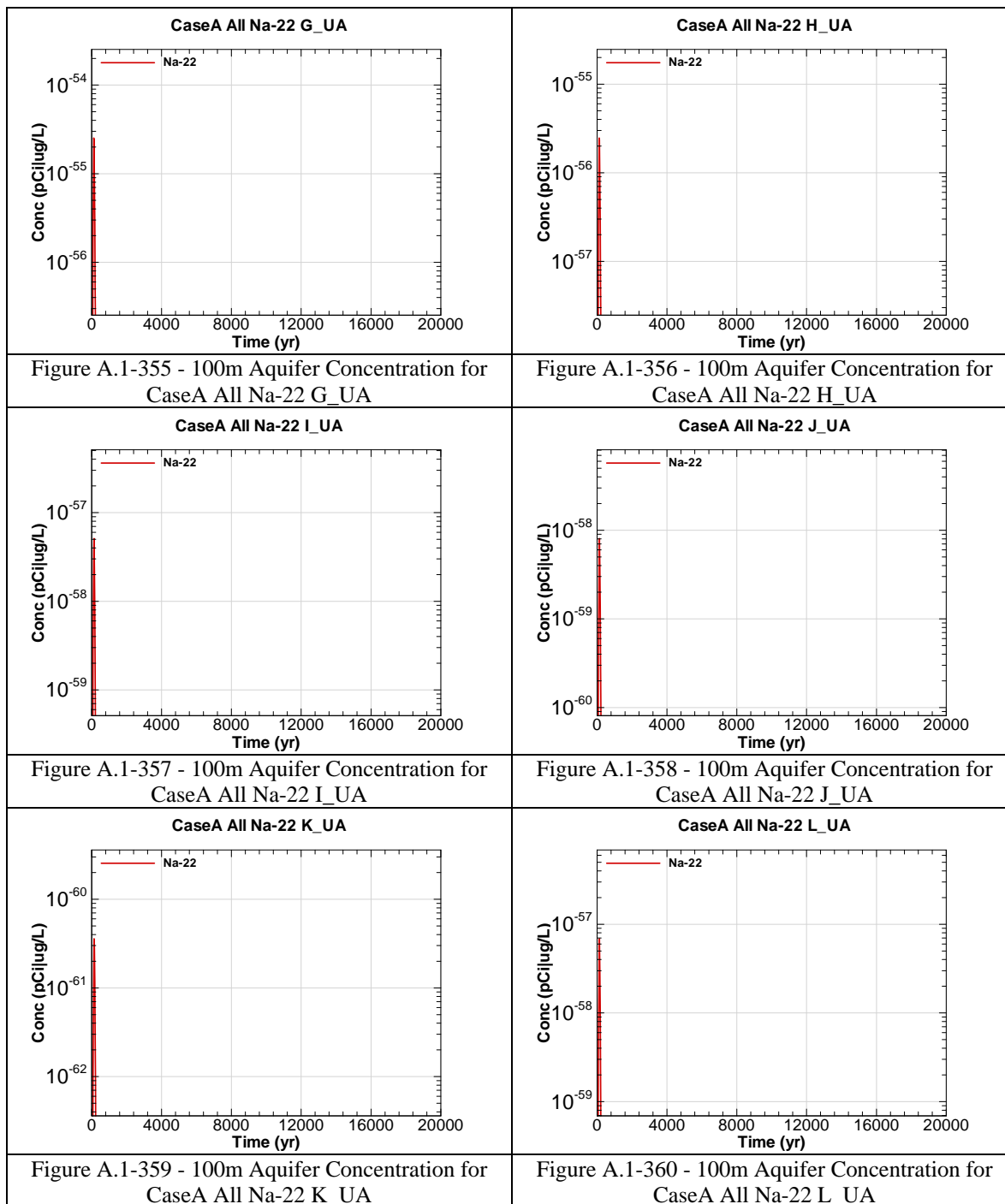


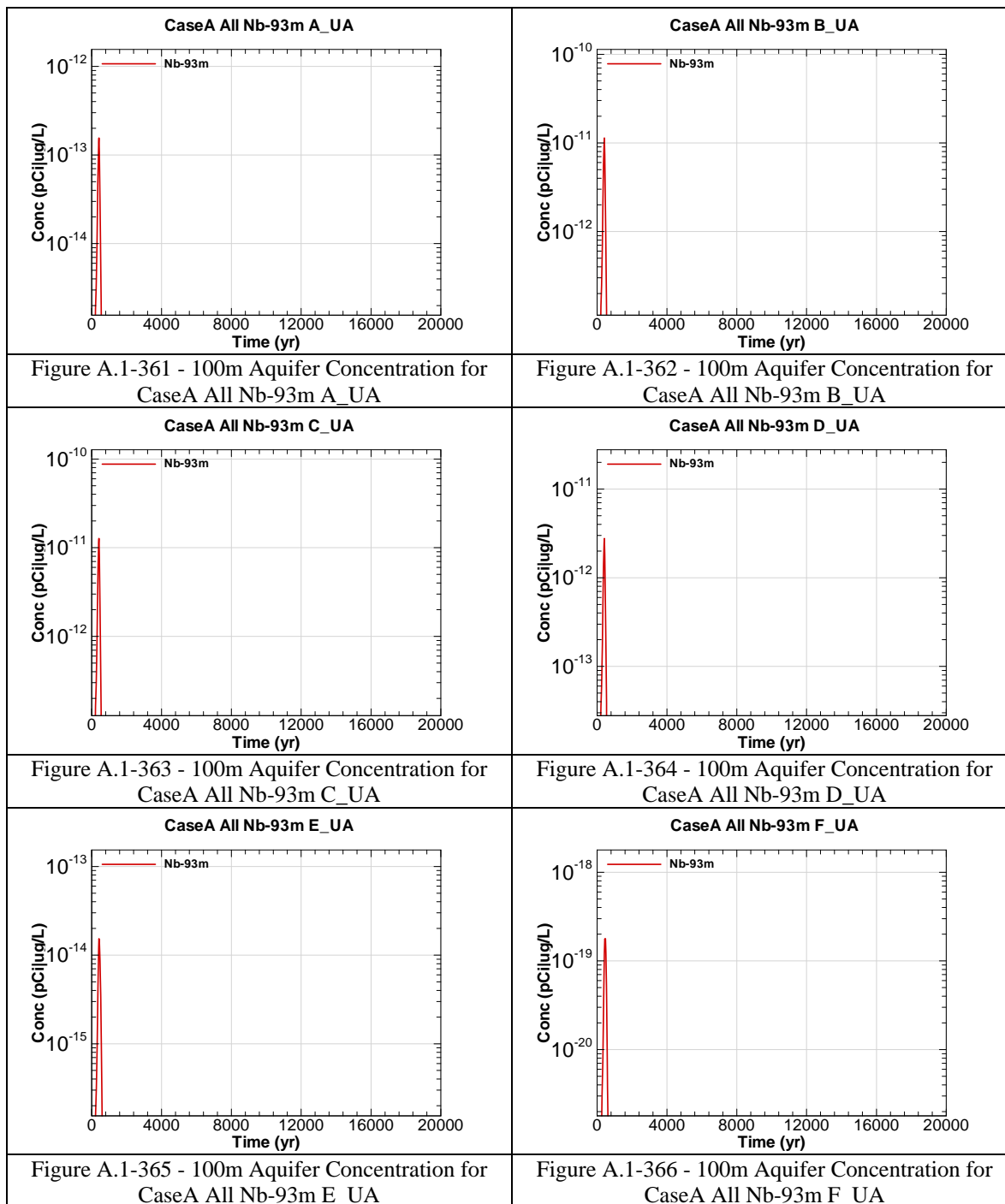


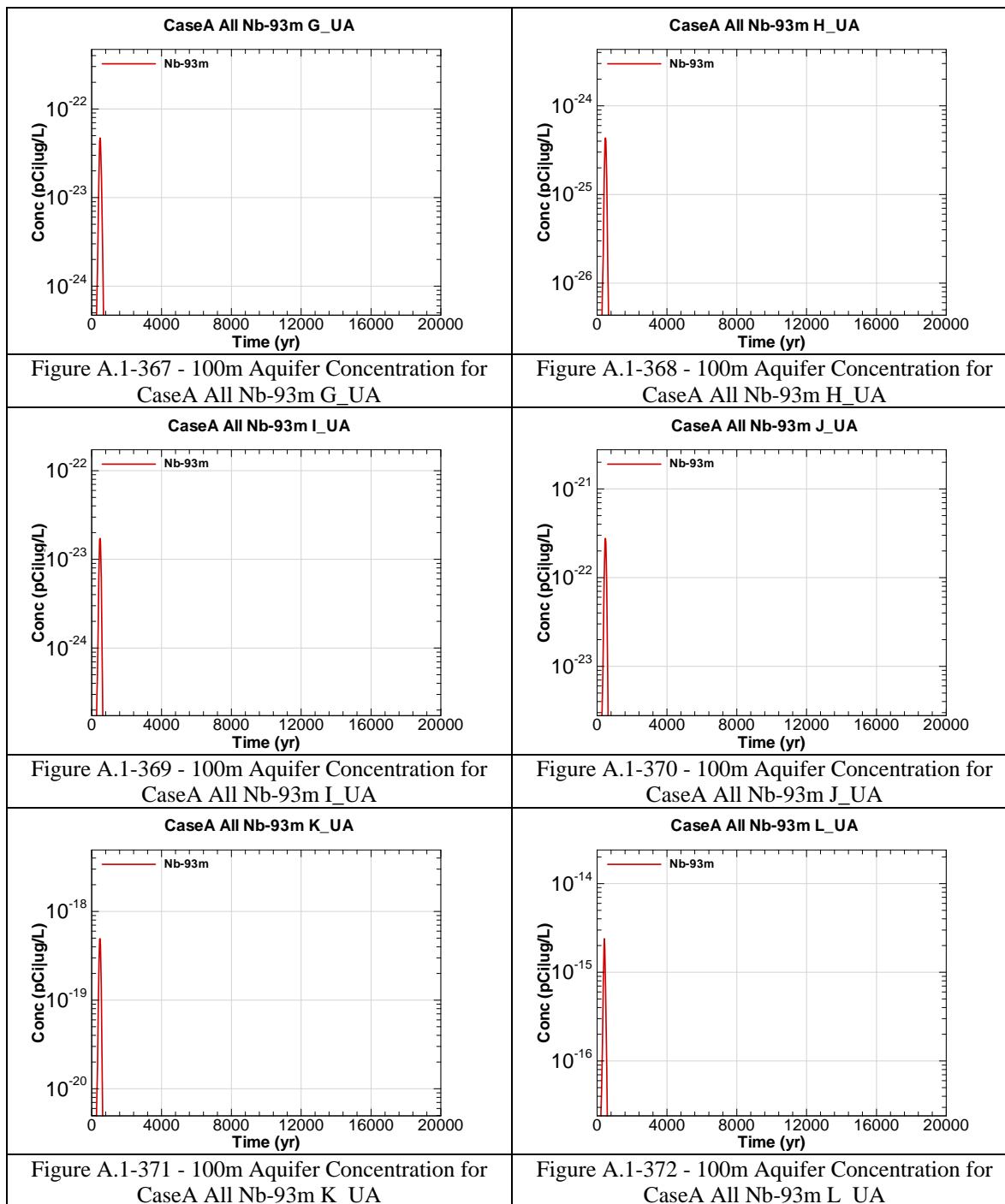


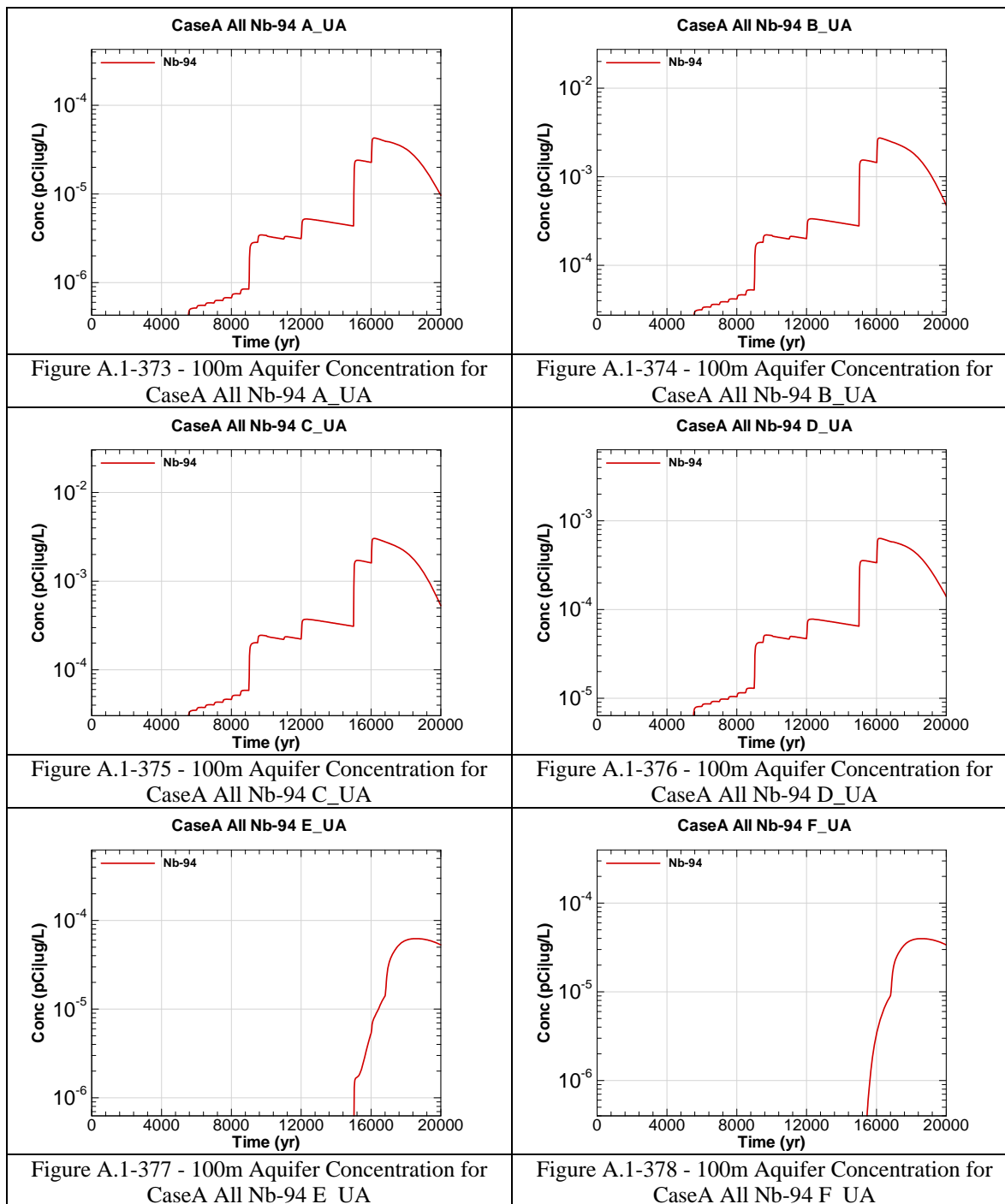


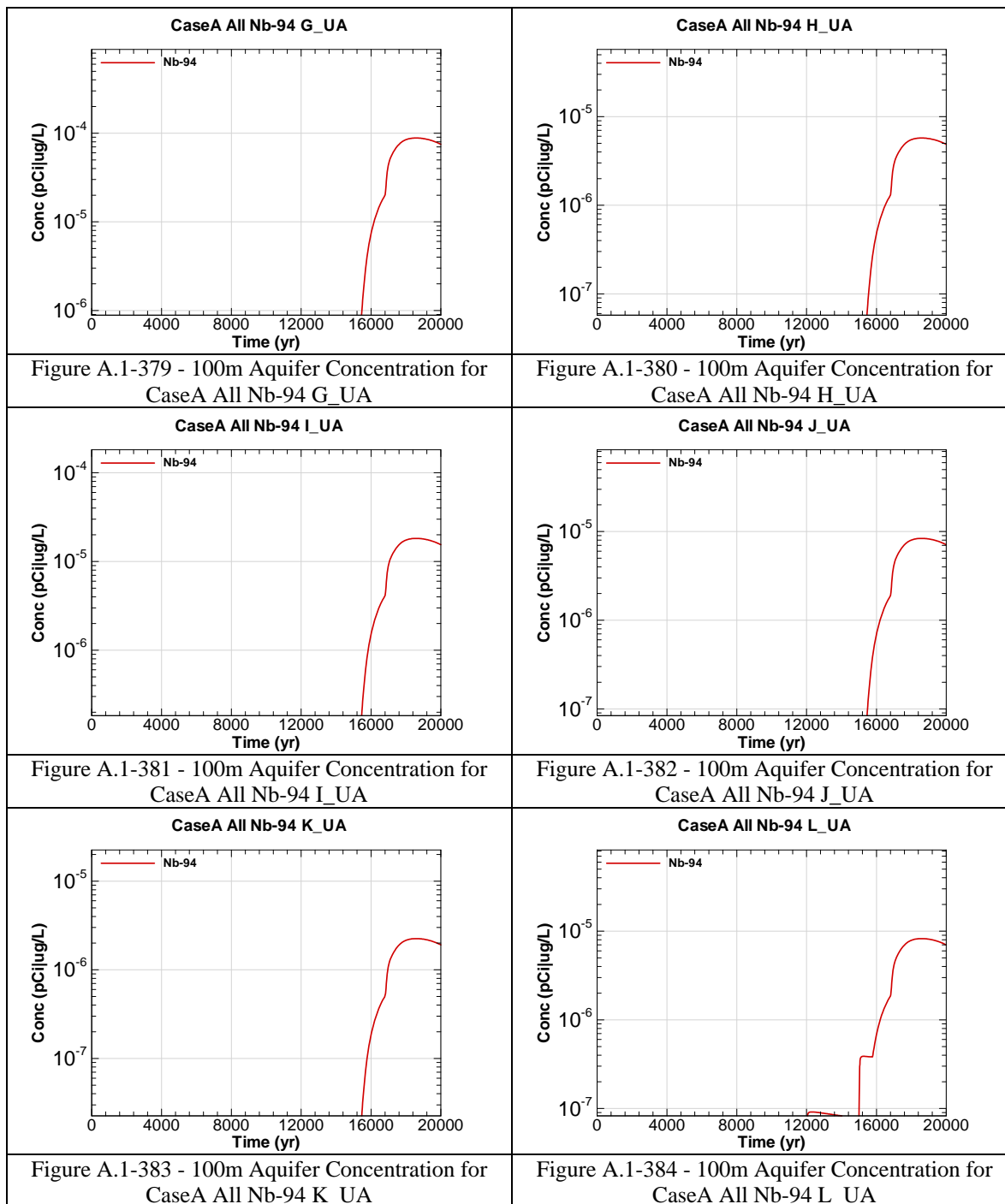


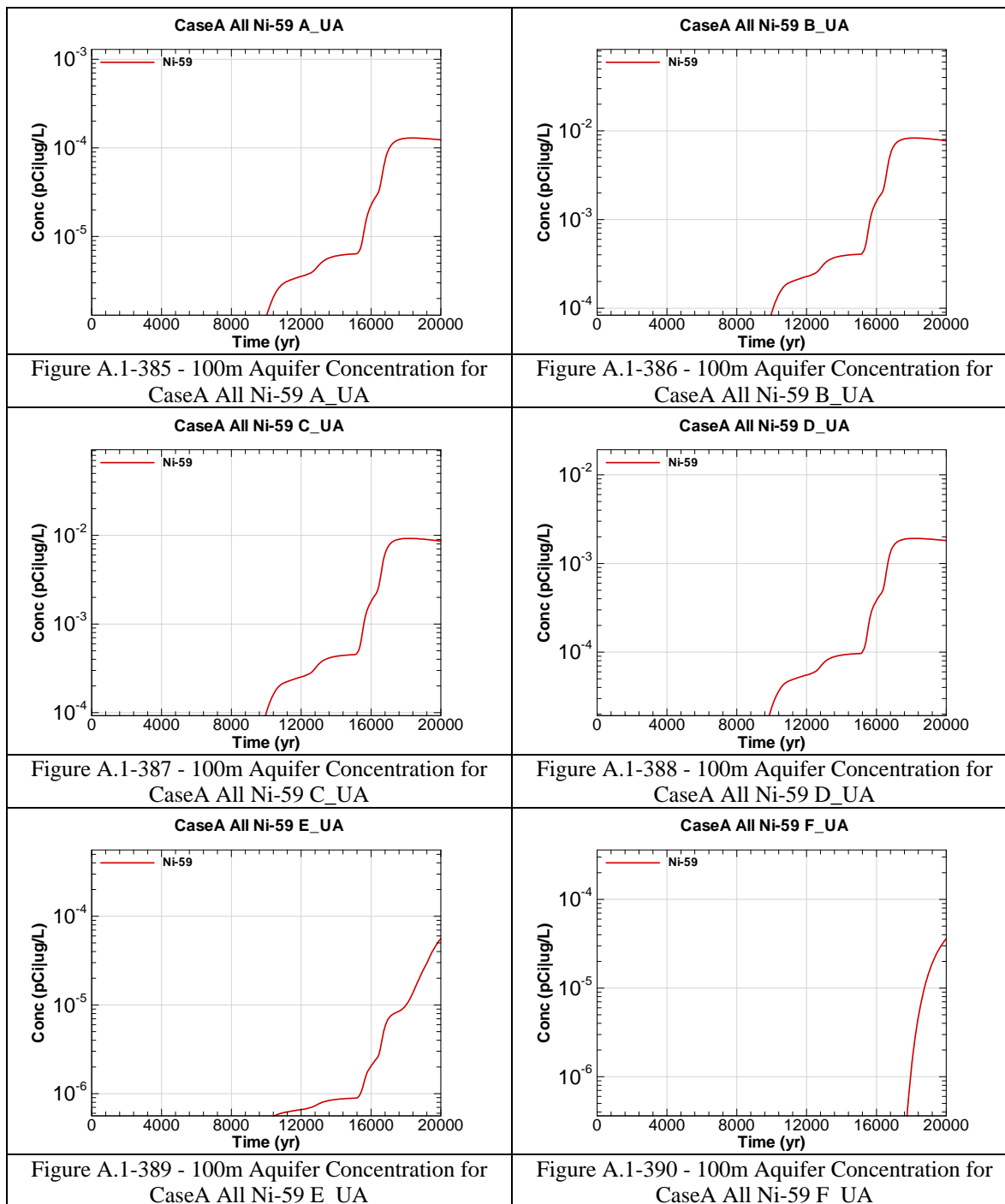


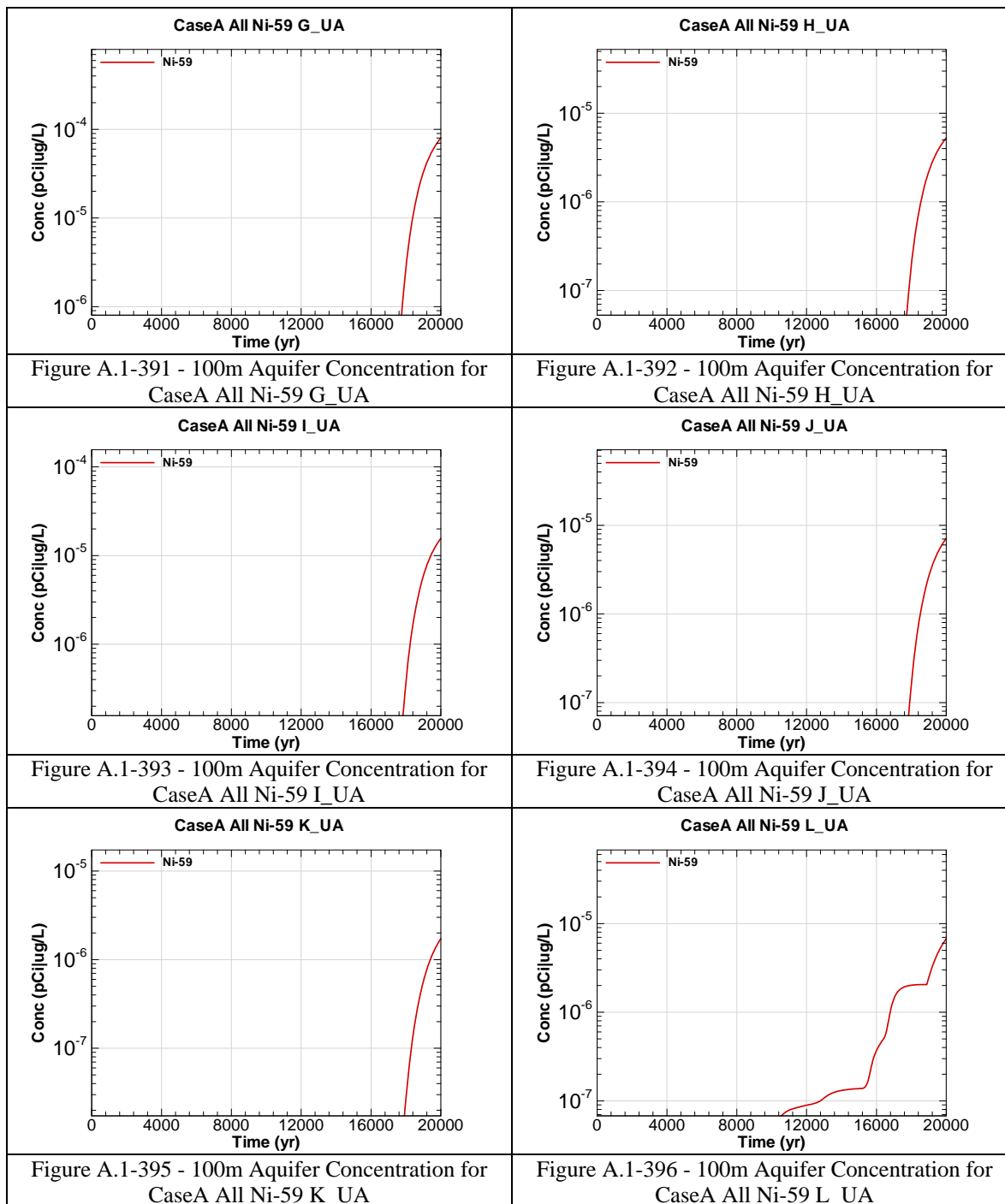


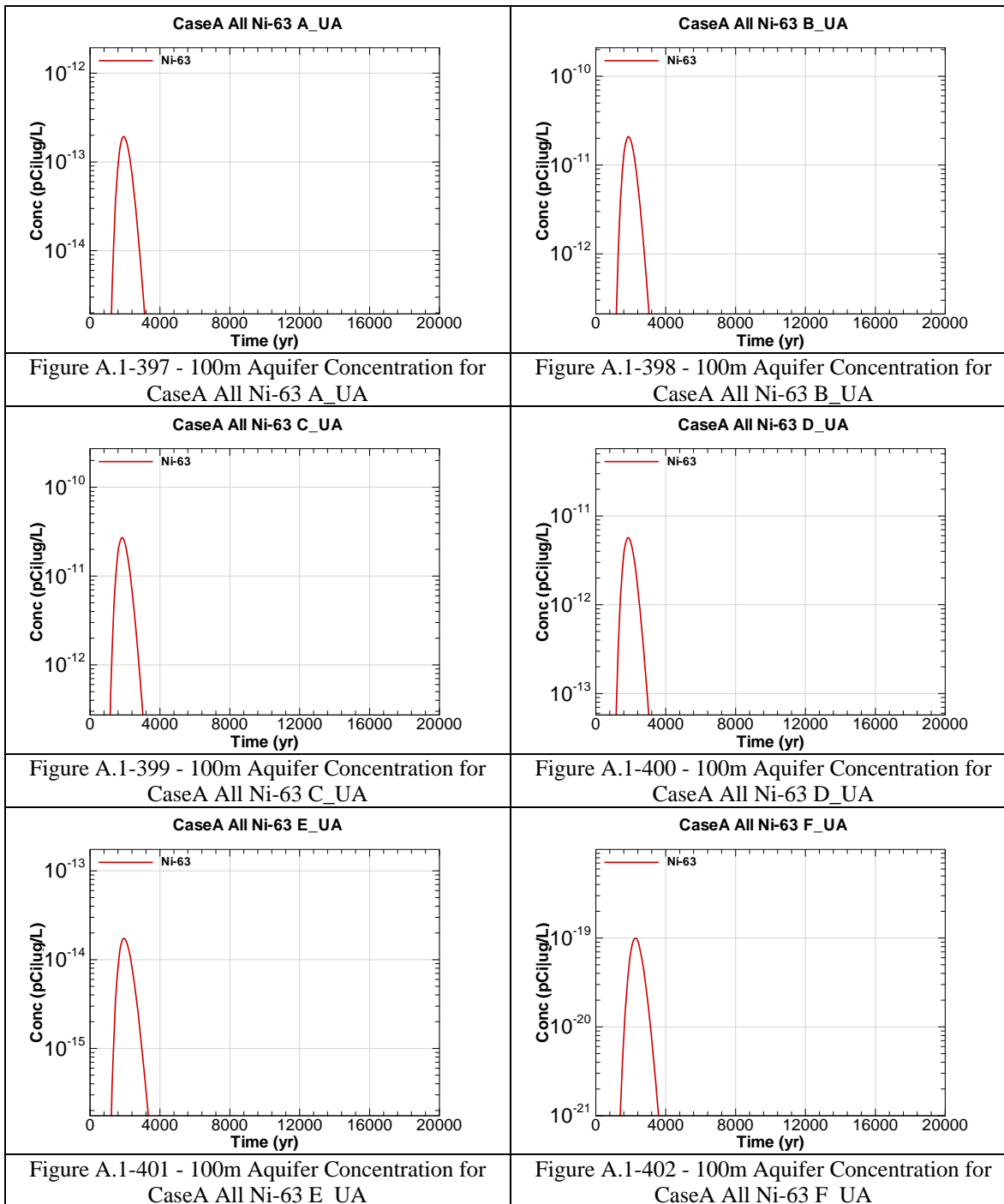


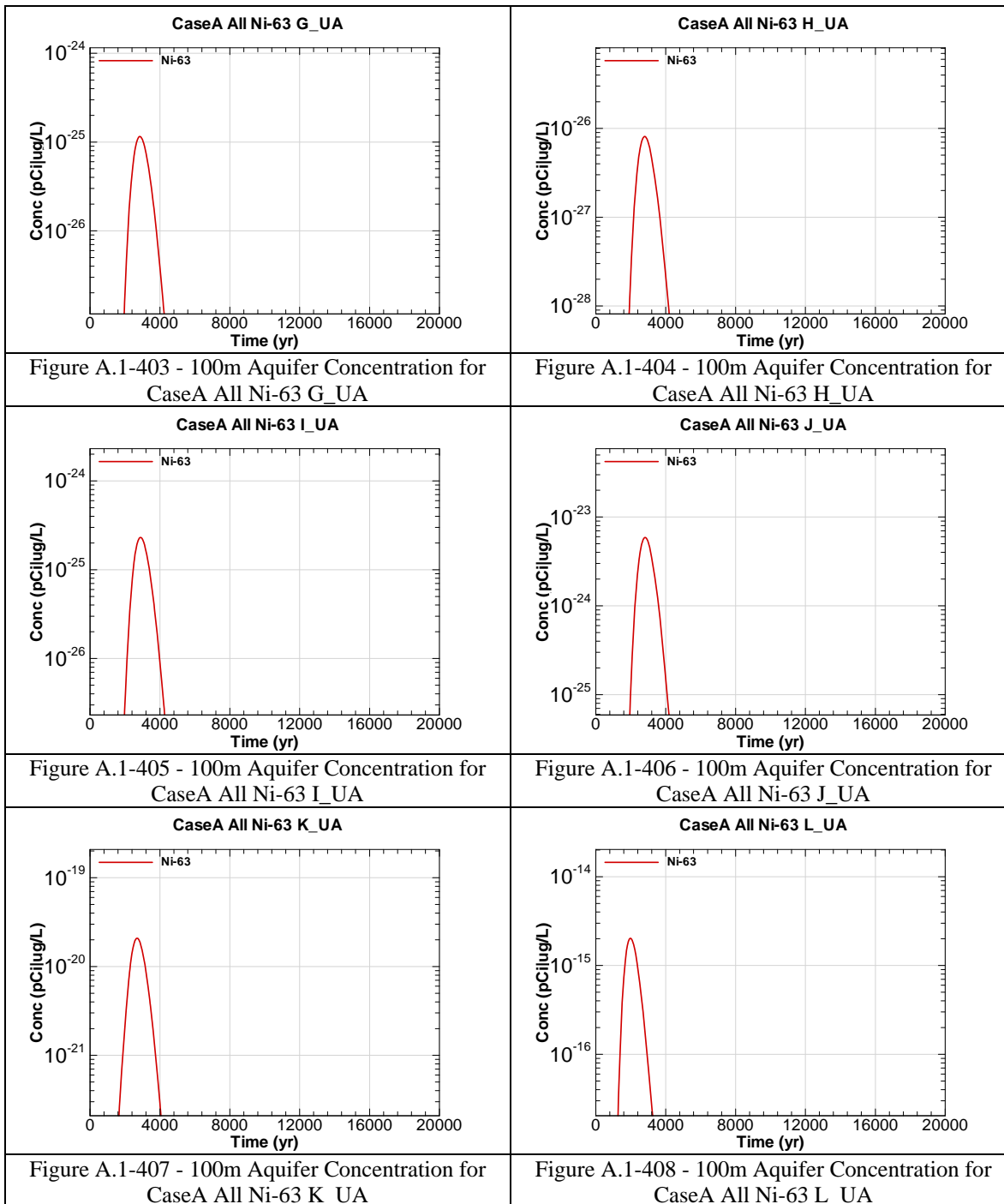












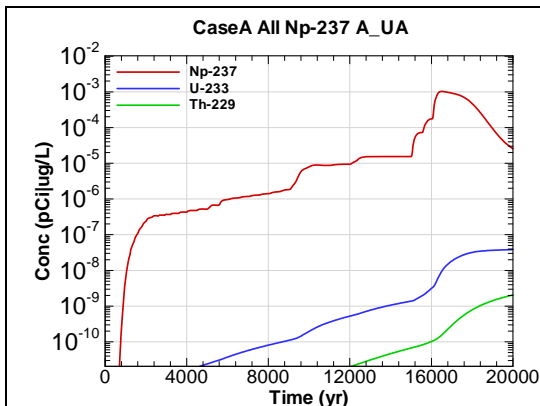


Figure A.1-409 - 100m Aquifer Concentration for CaseA All Np-237 A-UA

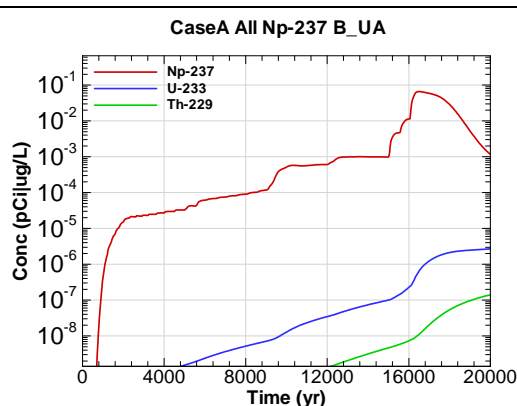


Figure A.1-410 - 100m Aquifer Concentration for CaseA All Np-237 B-UA

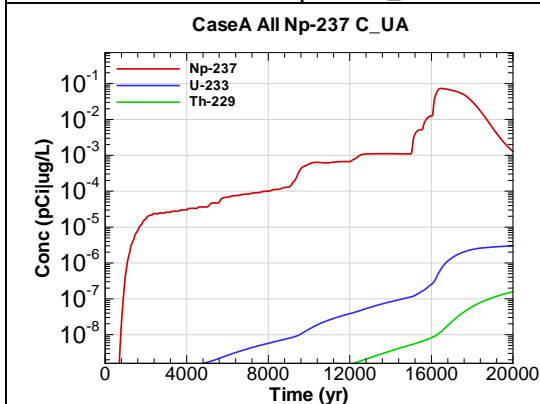


Figure A.1-411 - 100m Aquifer Concentration for CaseA All Np-237 C-UA

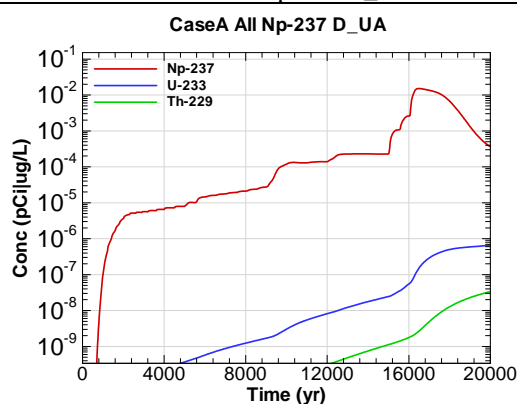


Figure A.1-412 - 100m Aquifer Concentration for CaseA All Np-237 D-UA

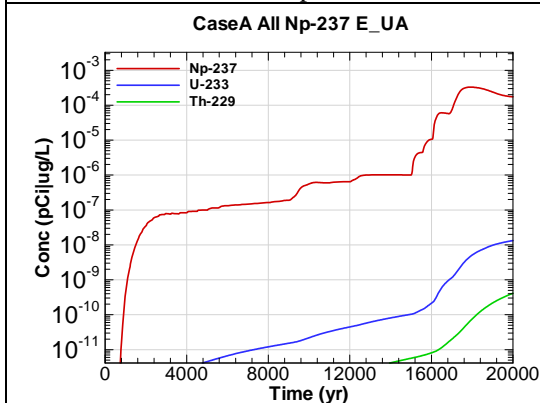


Figure A.1-413 - 100m Aquifer Concentration for CaseA All Np-237 E-UA

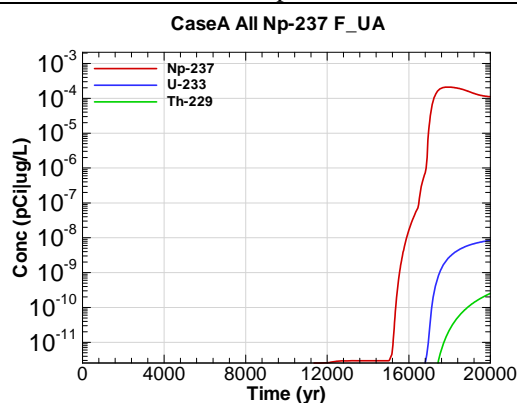
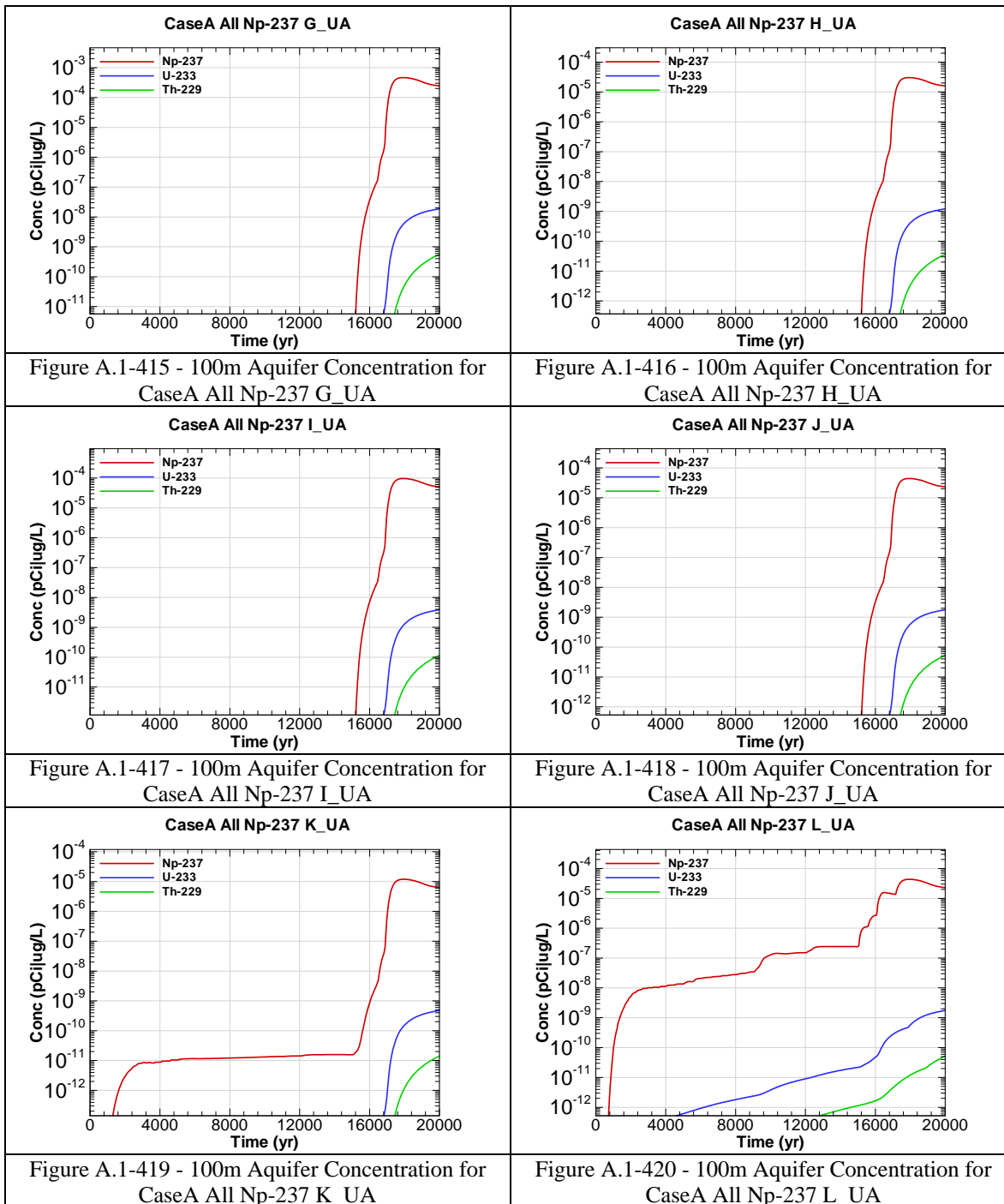


Figure A.1-414 - 100m Aquifer Concentration for CaseA All Np-237 F-UA



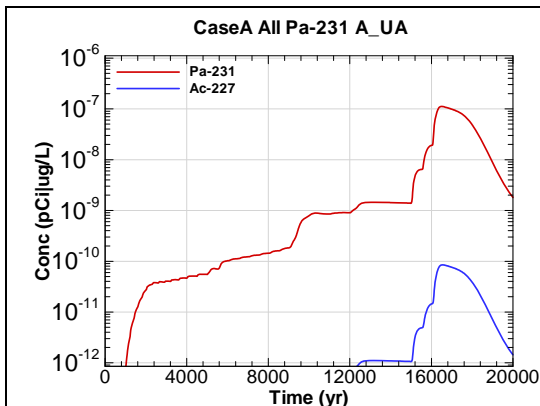


Figure A.1-421 - 100m Aquifer Concentration for
CaseA All Pa-231 A_UA

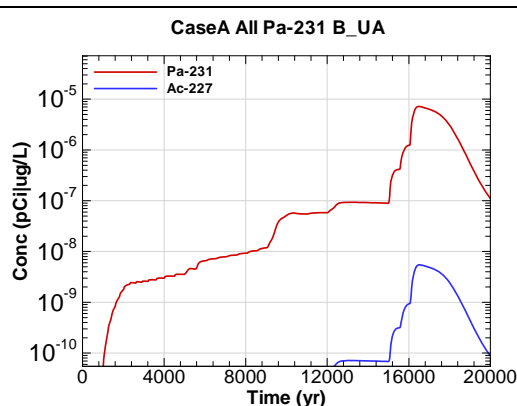


Figure A.1-422 - 100m Aquifer Concentration for
CaseA All Pa-231 B_UA

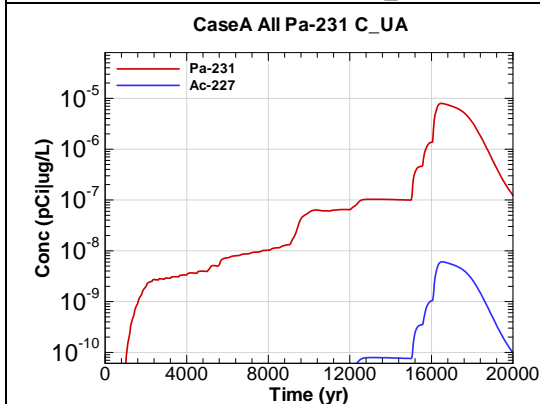


Figure A.1-423 - 100m Aquifer Concentration for
CaseA All Pa-231 C_UA

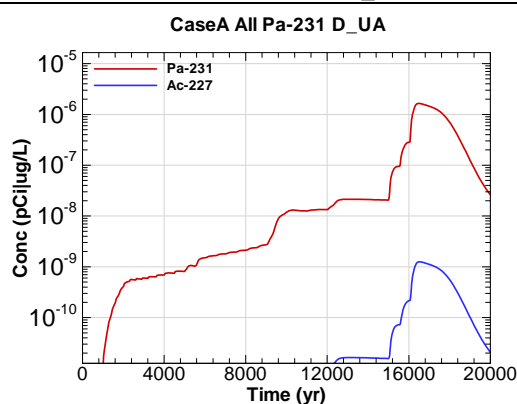


Figure A.1-424 - 100m Aquifer Concentration for
CaseA All Pa-231 D_UA

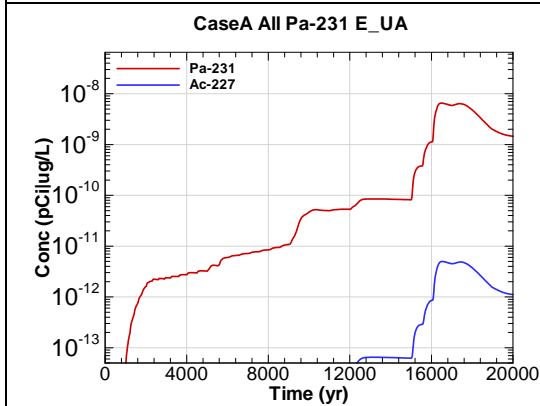


Figure A.1-425 - 100m Aquifer Concentration for
CaseA All Pa-231 E_UA

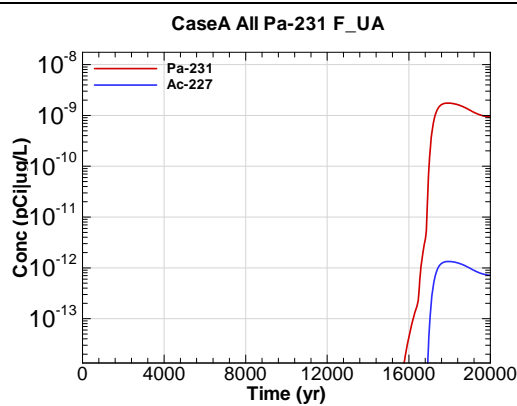
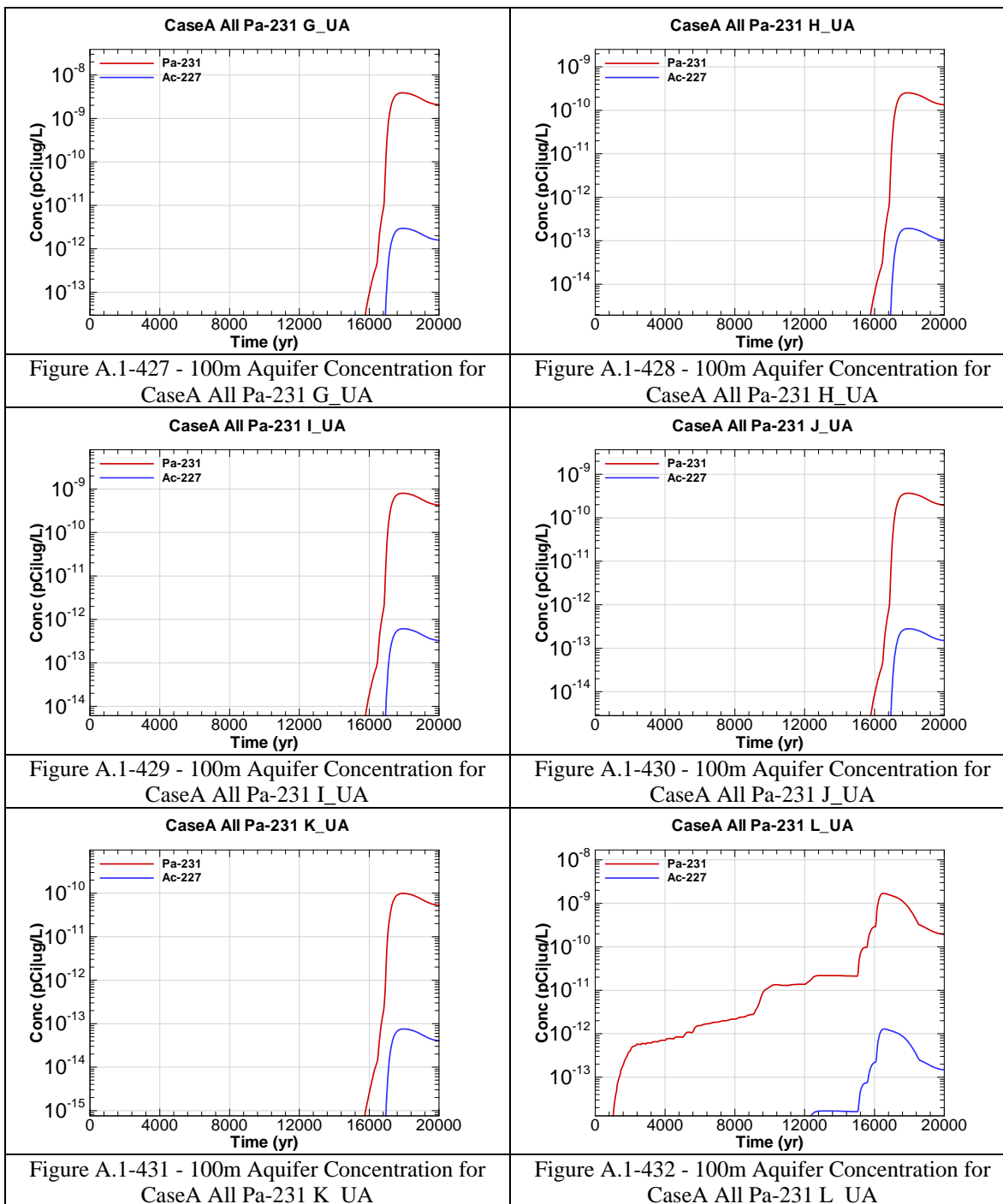
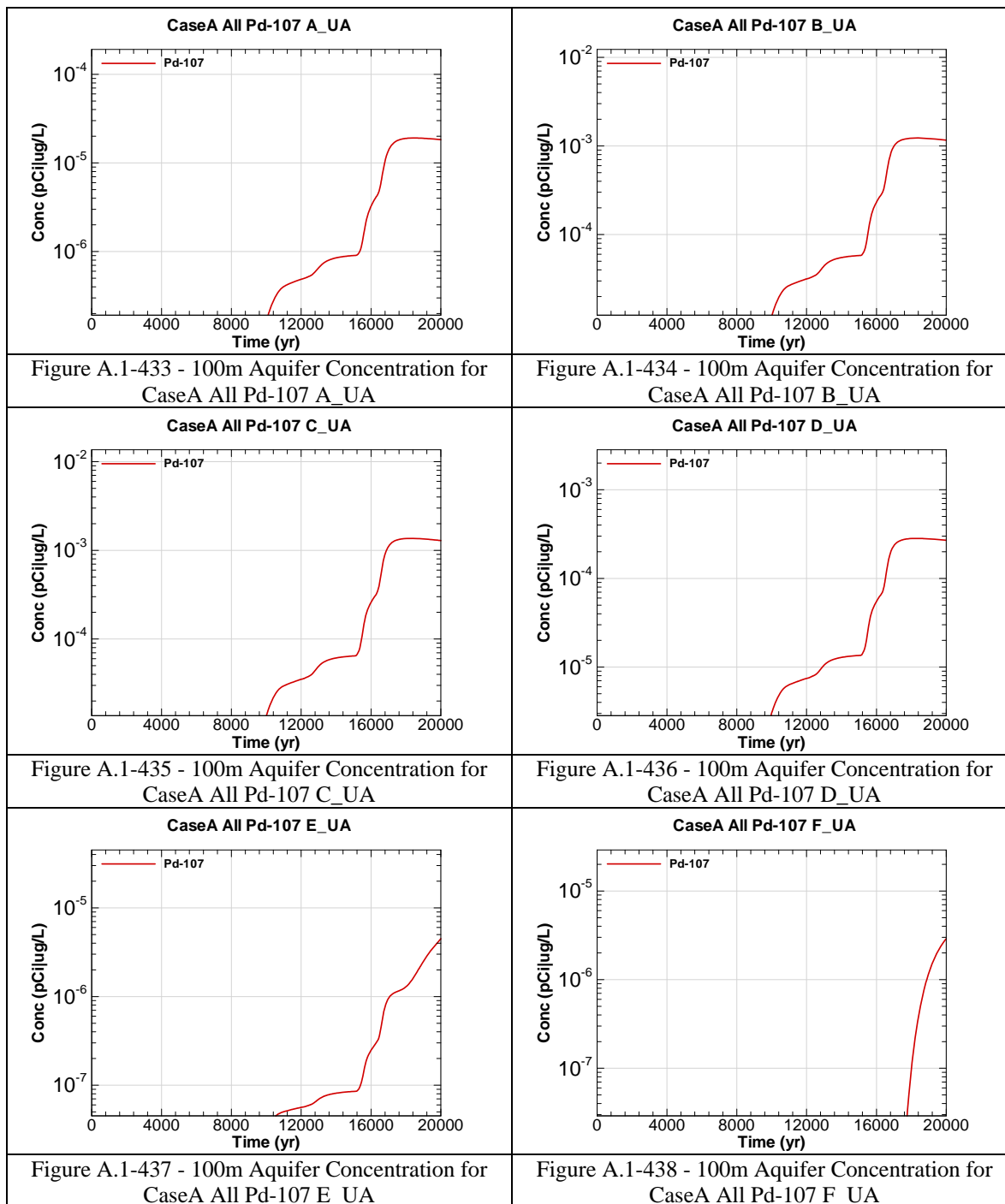
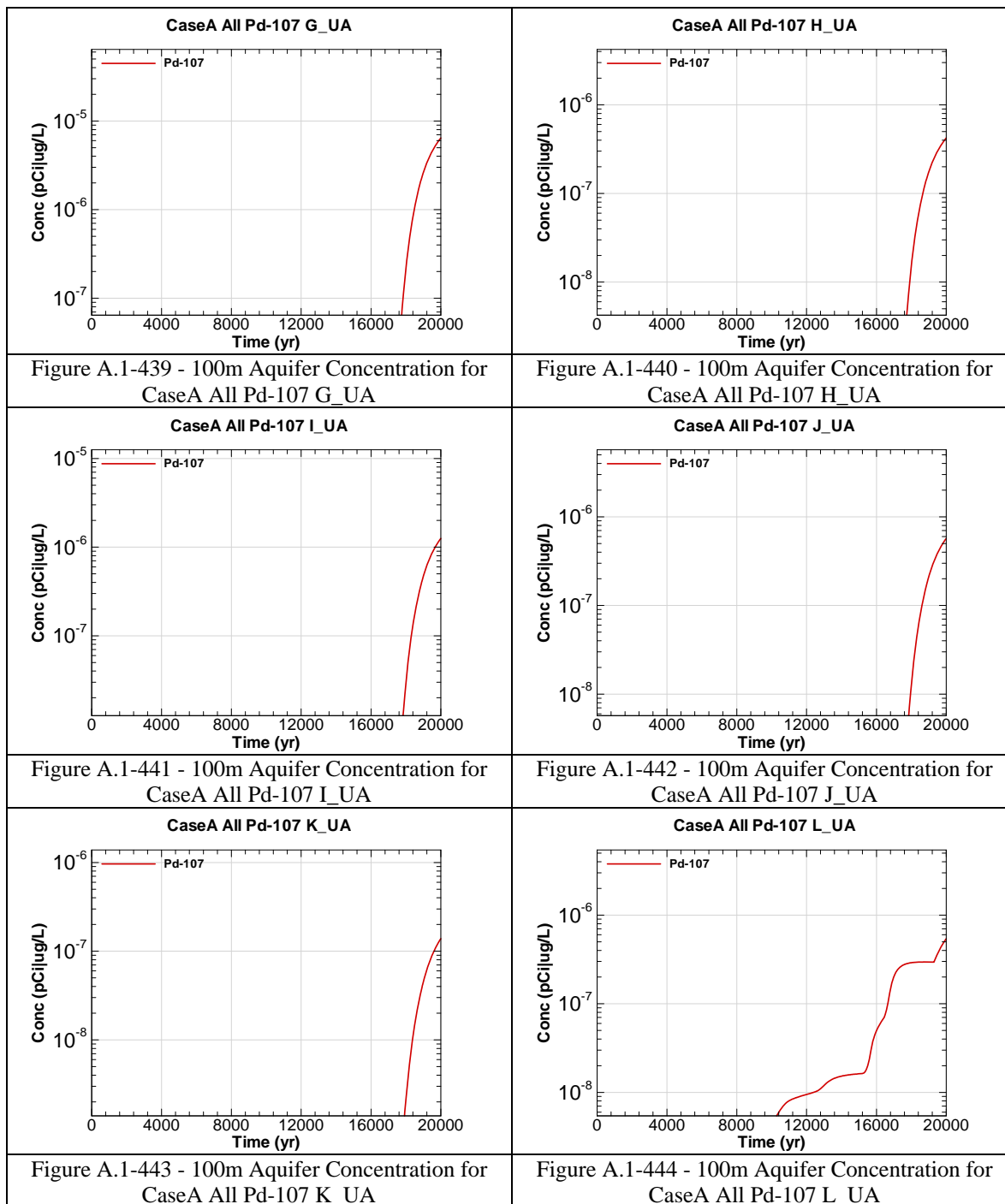
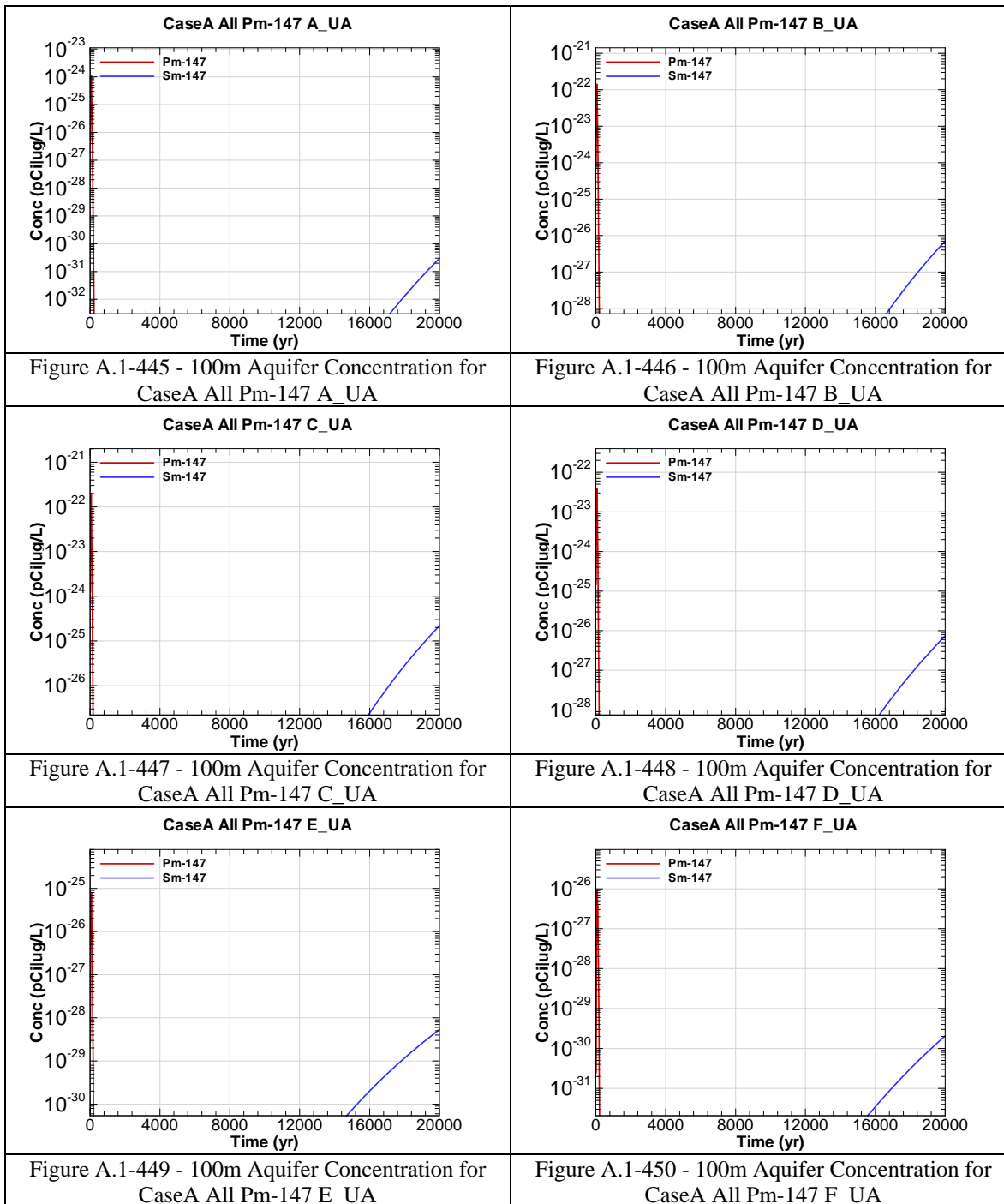


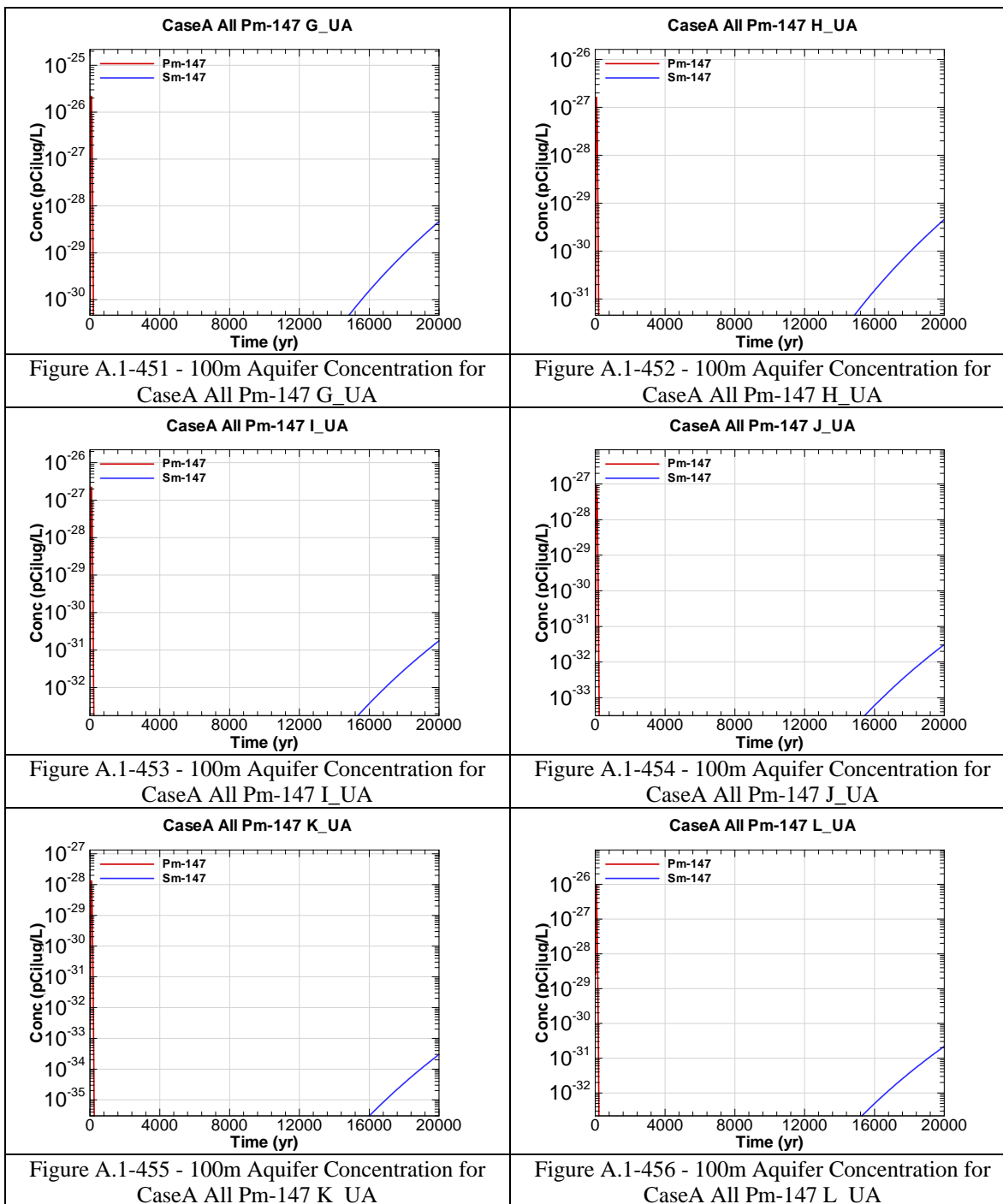
Figure A.1-426 - 100m Aquifer Concentration for
CaseA All Pa-231 F_UA

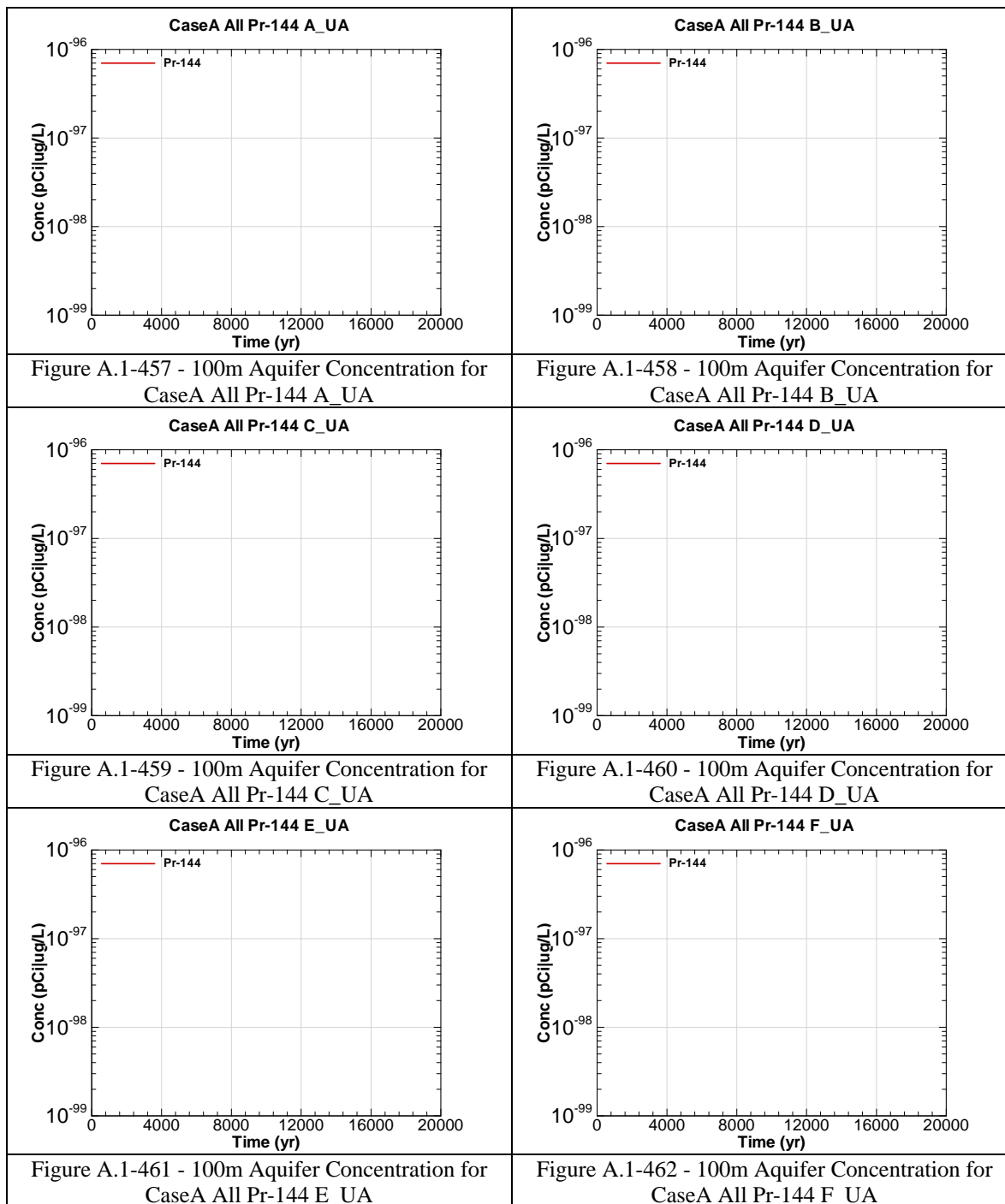


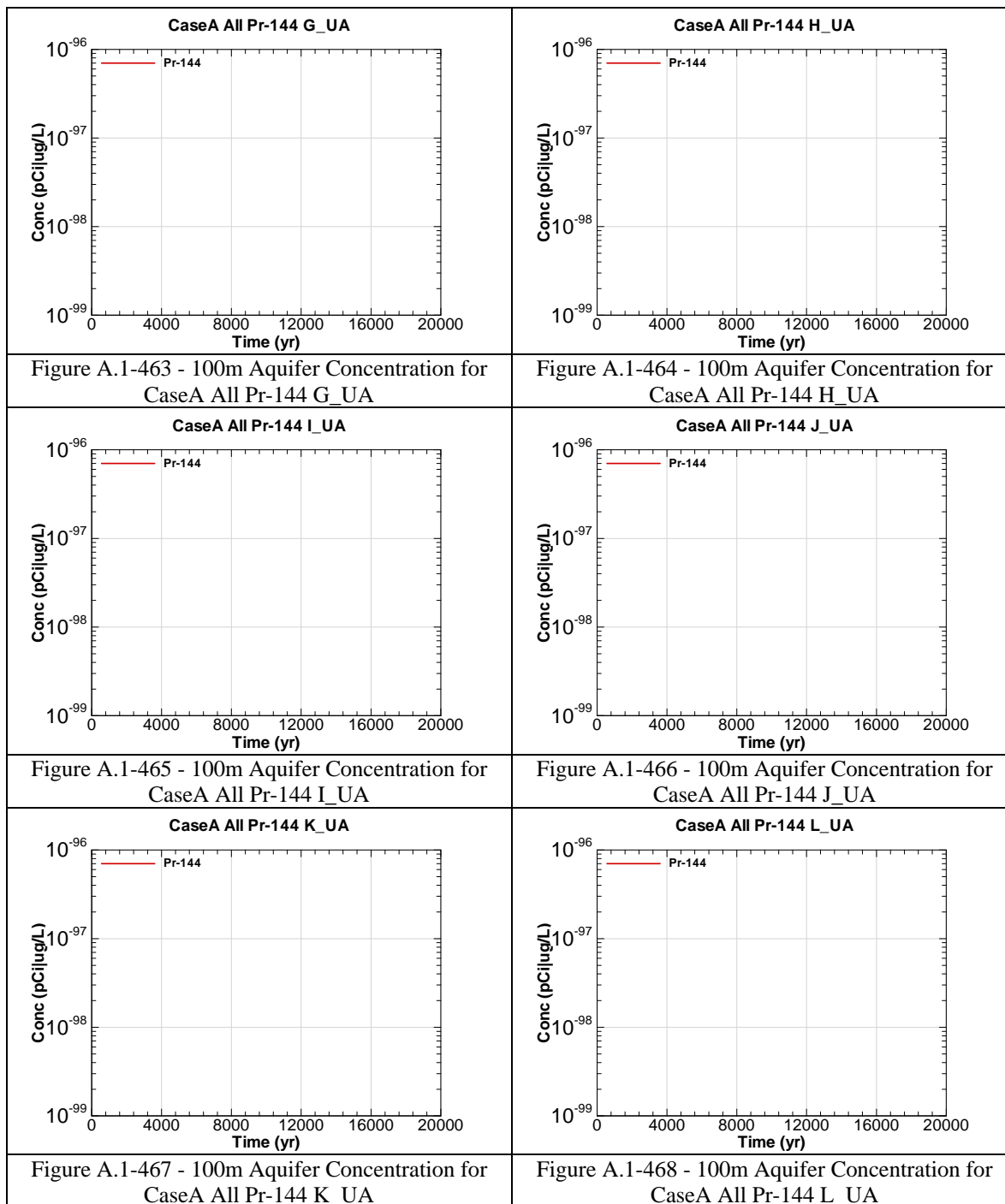


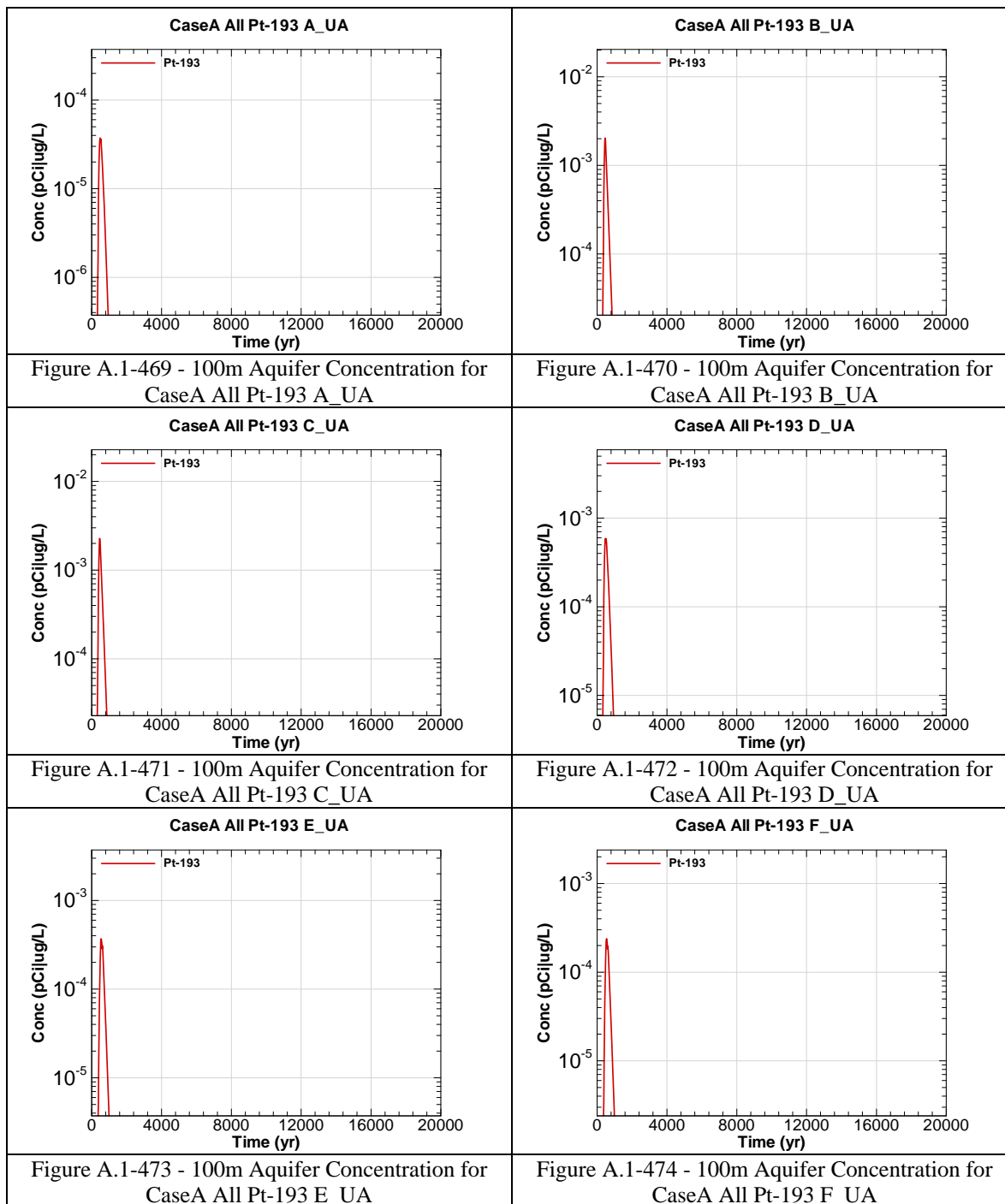


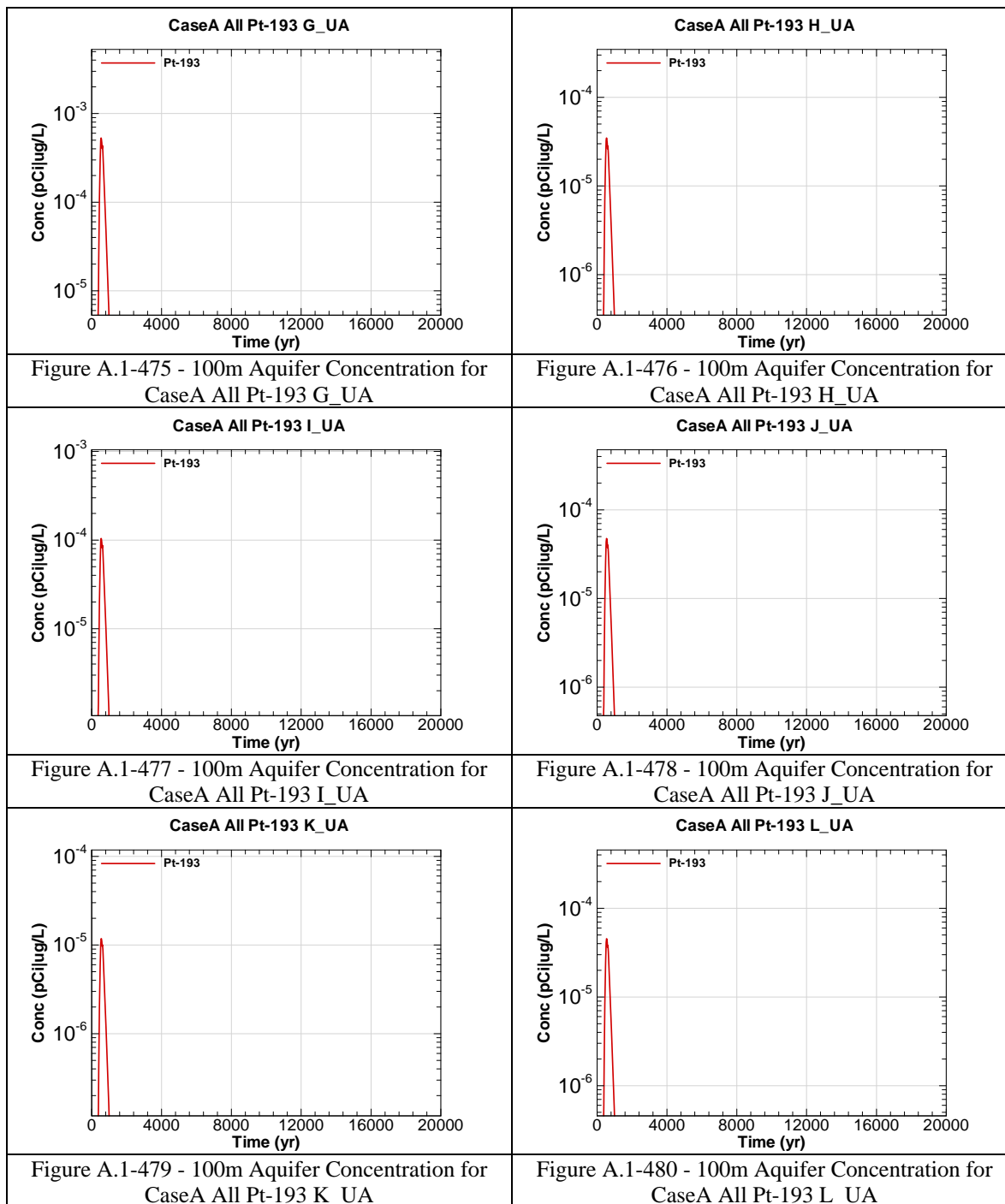












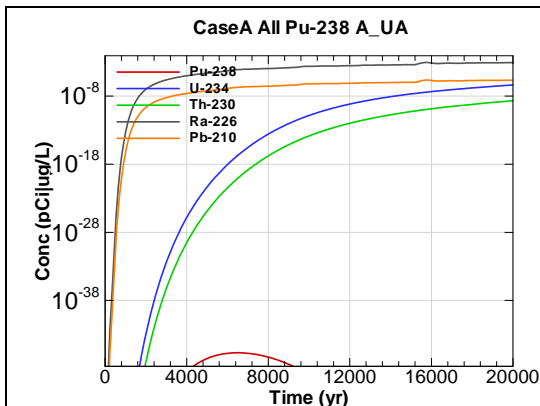


Figure A.1-481 - 100m Aquifer Concentration for
CaseA All Pu-238 A_UA

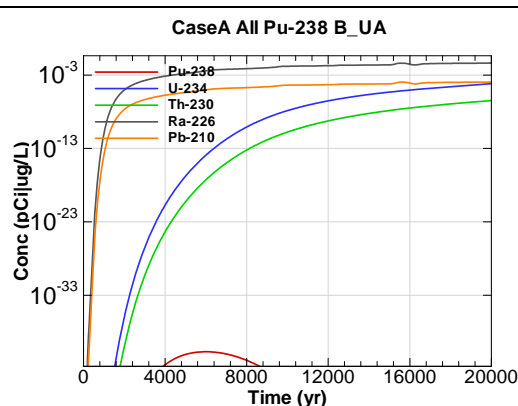


Figure A.1-482 - 100m Aquifer Concentration for
CaseA All Pu-238 B_UA

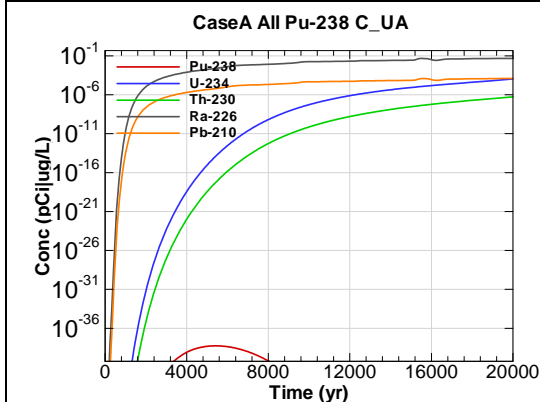


Figure A.1-483 - 100m Aquifer Concentration for
CaseA All Pu-238 C_UA

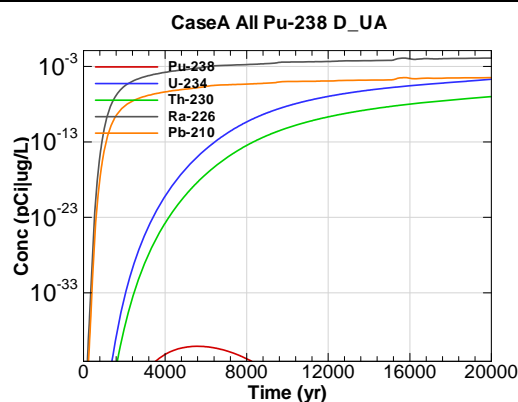


Figure A.1-484 - 100m Aquifer Concentration for
CaseA All Pu-238 D_UA

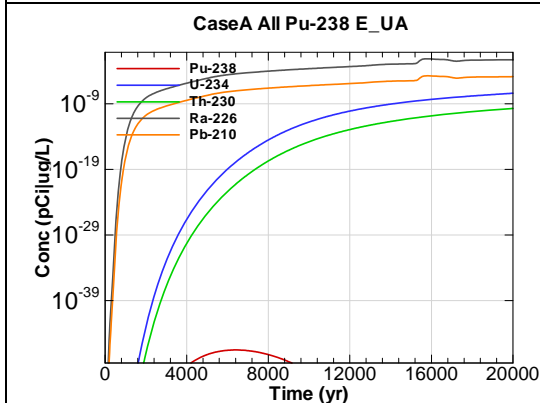


Figure A.1-485 - 100m Aquifer Concentration for
CaseA All Pu-238 E_UA

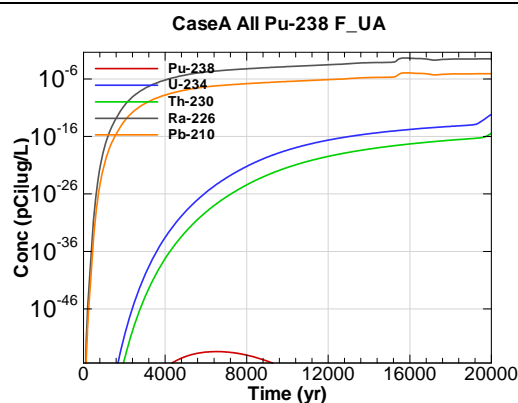


Figure A.1-486 - 100m Aquifer Concentration for
CaseA All Pu-238 F_UA

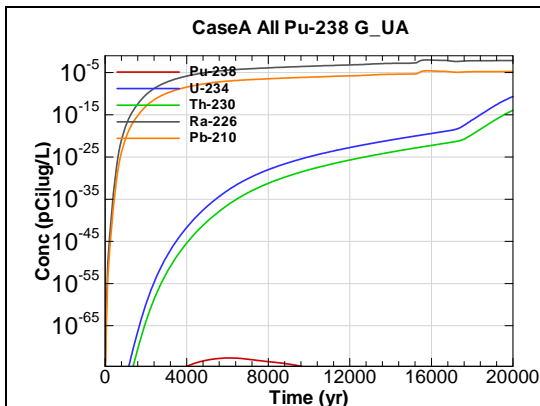


Figure A.1-487 - 100m Aquifer Concentration for
CaseA All Pu-238 G-UA

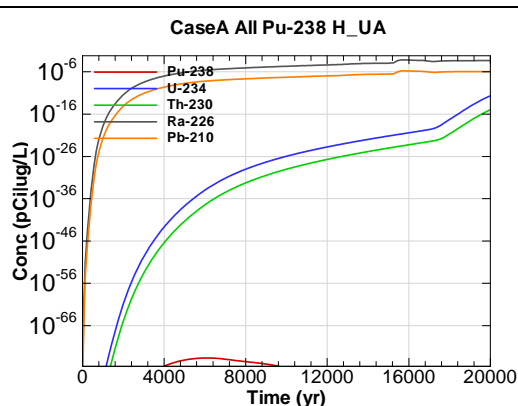


Figure A.1-488 - 100m Aquifer Concentration for
CaseA All Pu-238 H-UA

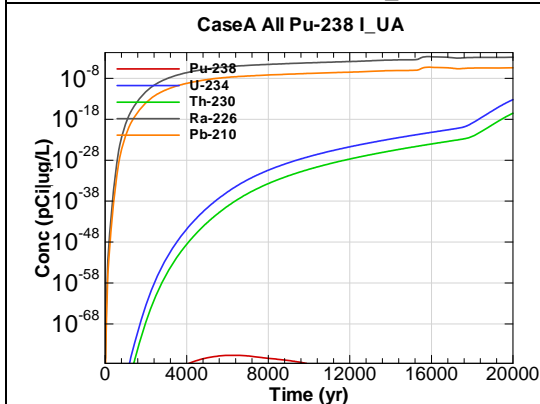


Figure A.1-489 - 100m Aquifer Concentration for
CaseA All Pu-238 I-UA

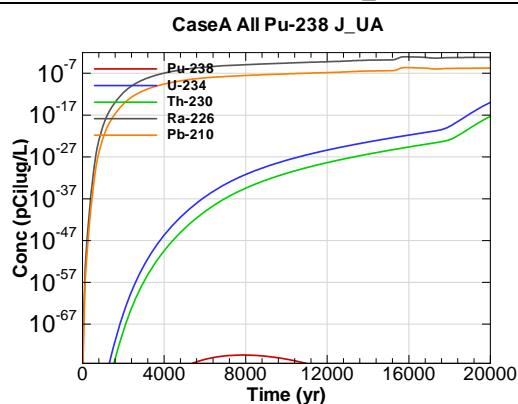


Figure A.1-490 - 100m Aquifer Concentration for
CaseA All Pu-238 J-UA

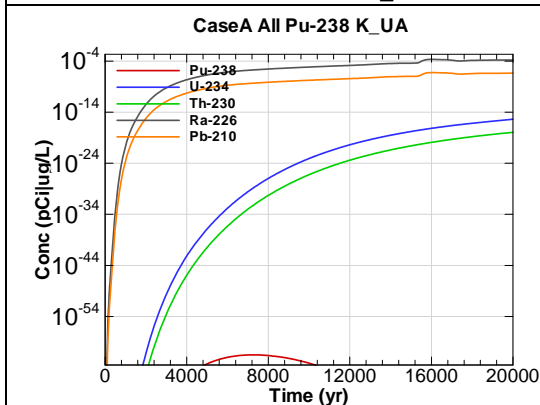


Figure A.1-491 - 100m Aquifer Concentration for
CaseA All Pu-238 K-UA

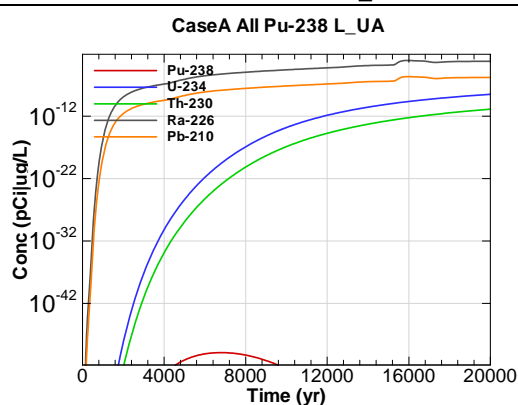


Figure A.1-492 - 100m Aquifer Concentration for
CaseA All Pu-238 L-UA

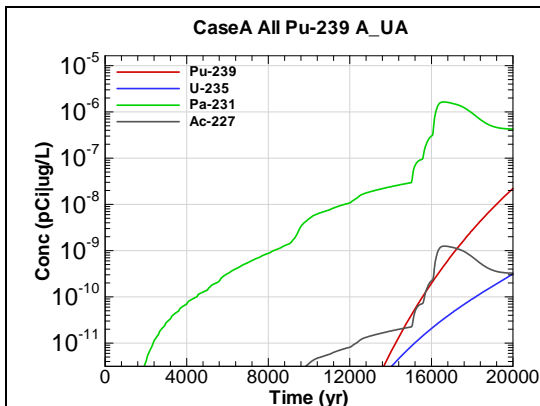


Figure A.1-493 - 100m Aquifer Concentration for
CaseA All Pu-239 A-UA

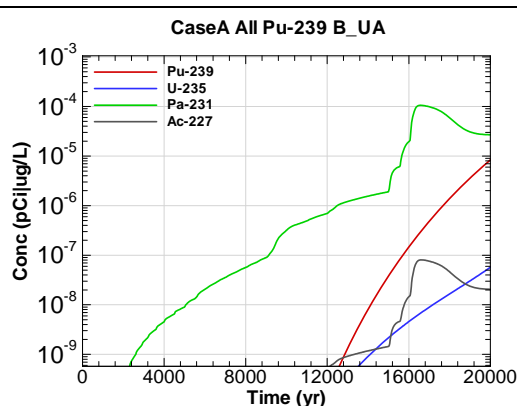


Figure A.1-494 - 100m Aquifer Concentration for
CaseA All Pu-239 B-UA

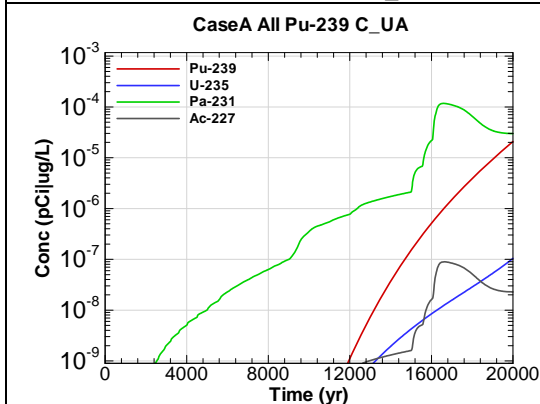


Figure A.1-495 - 100m Aquifer Concentration for
CaseA All Pu-239 C-UA

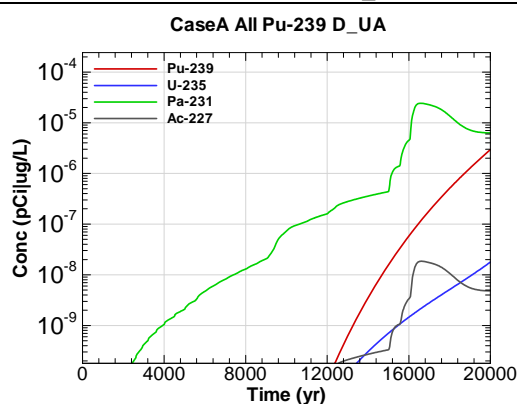


Figure A.1-496 - 100m Aquifer Concentration for
CaseA All Pu-239 D-UA

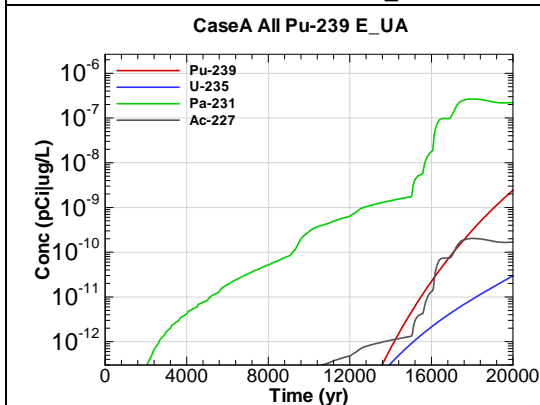


Figure A.1-497 - 100m Aquifer Concentration for
CaseA All Pu-239 E-UA

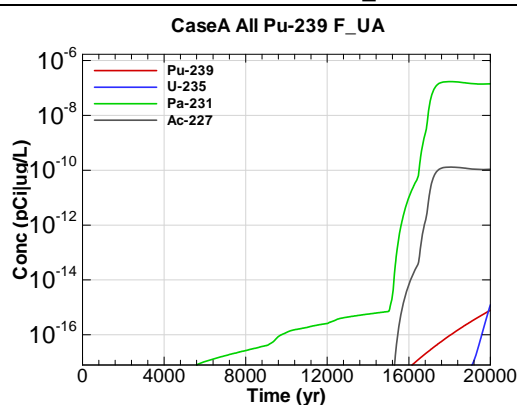
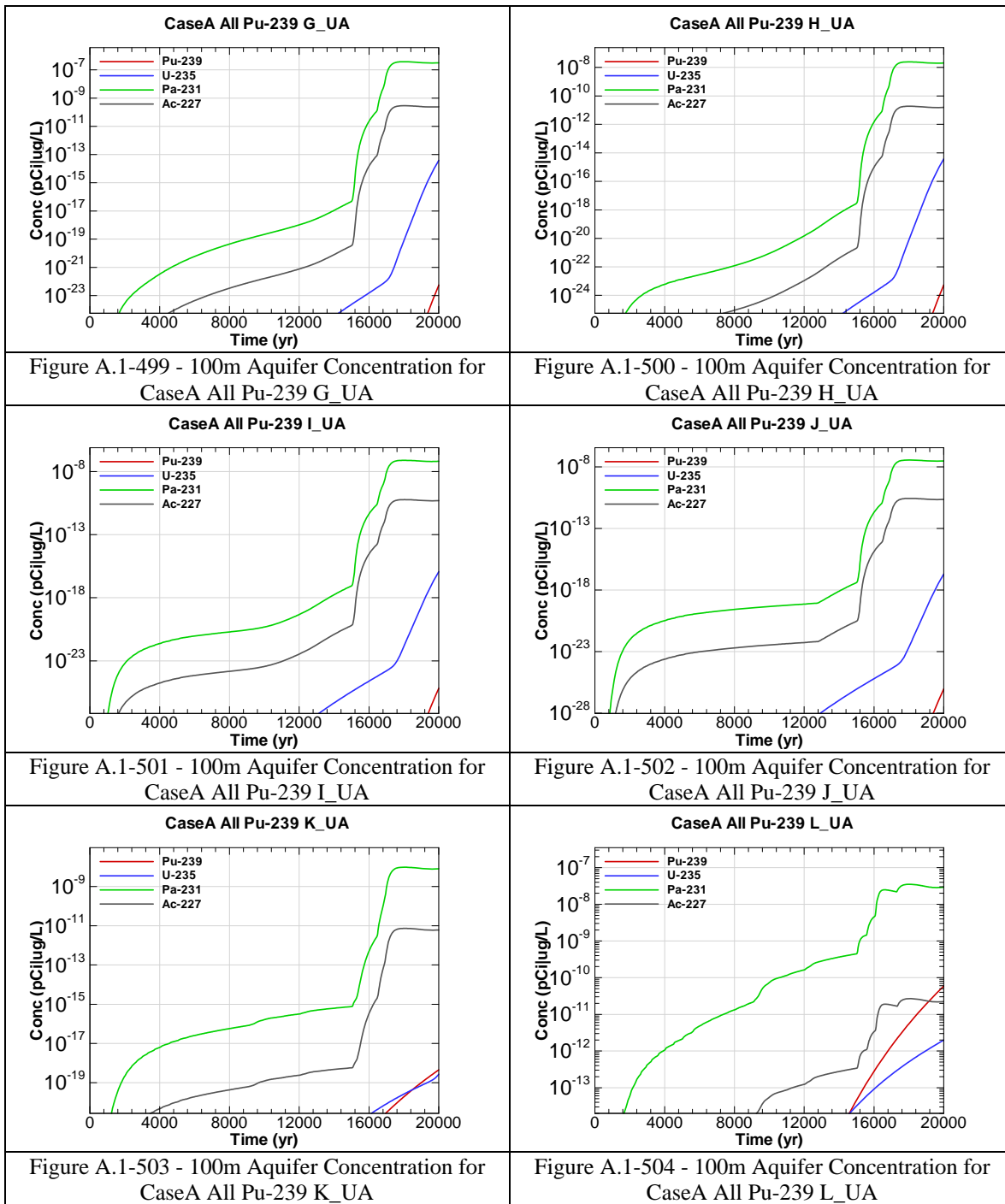
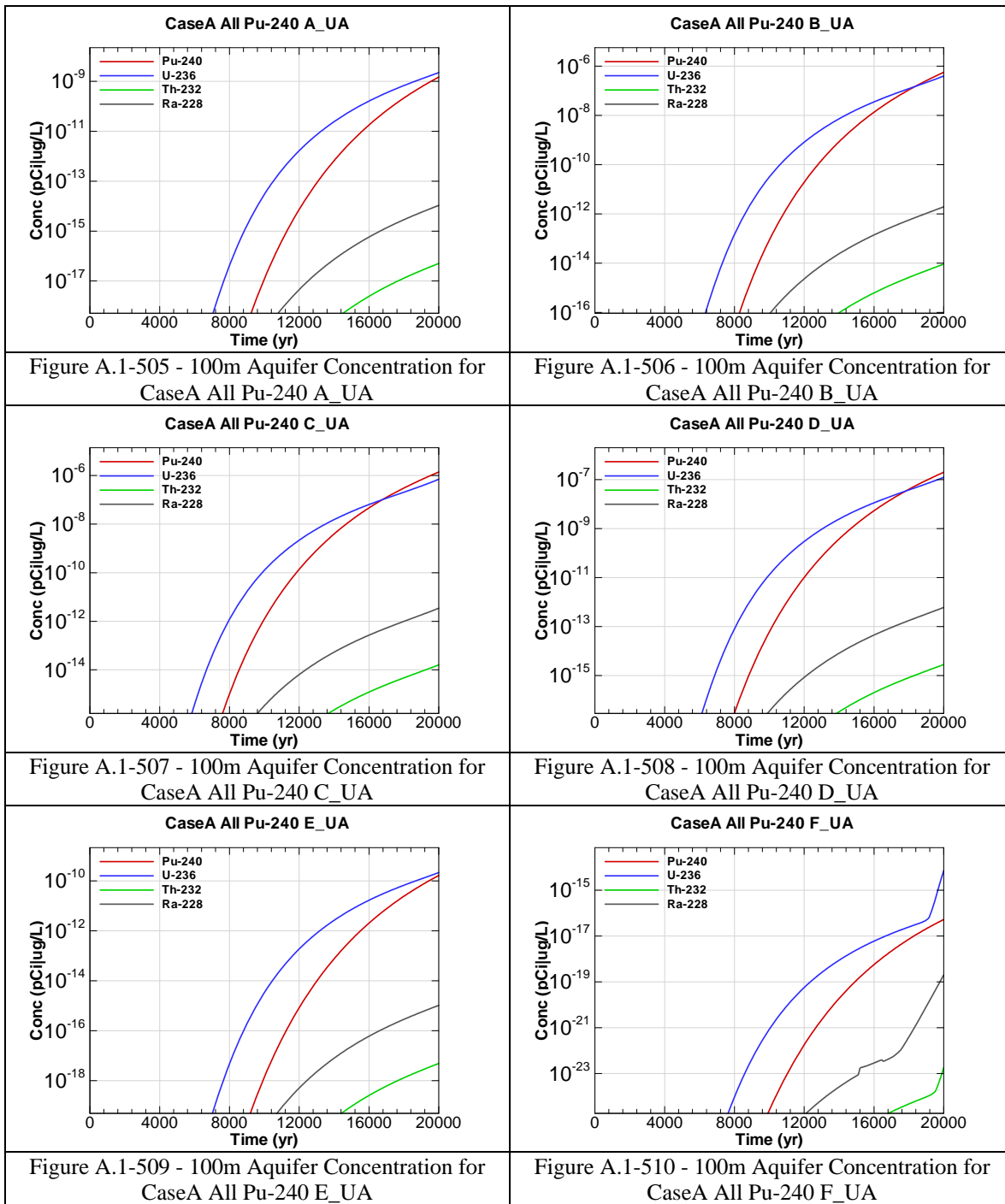
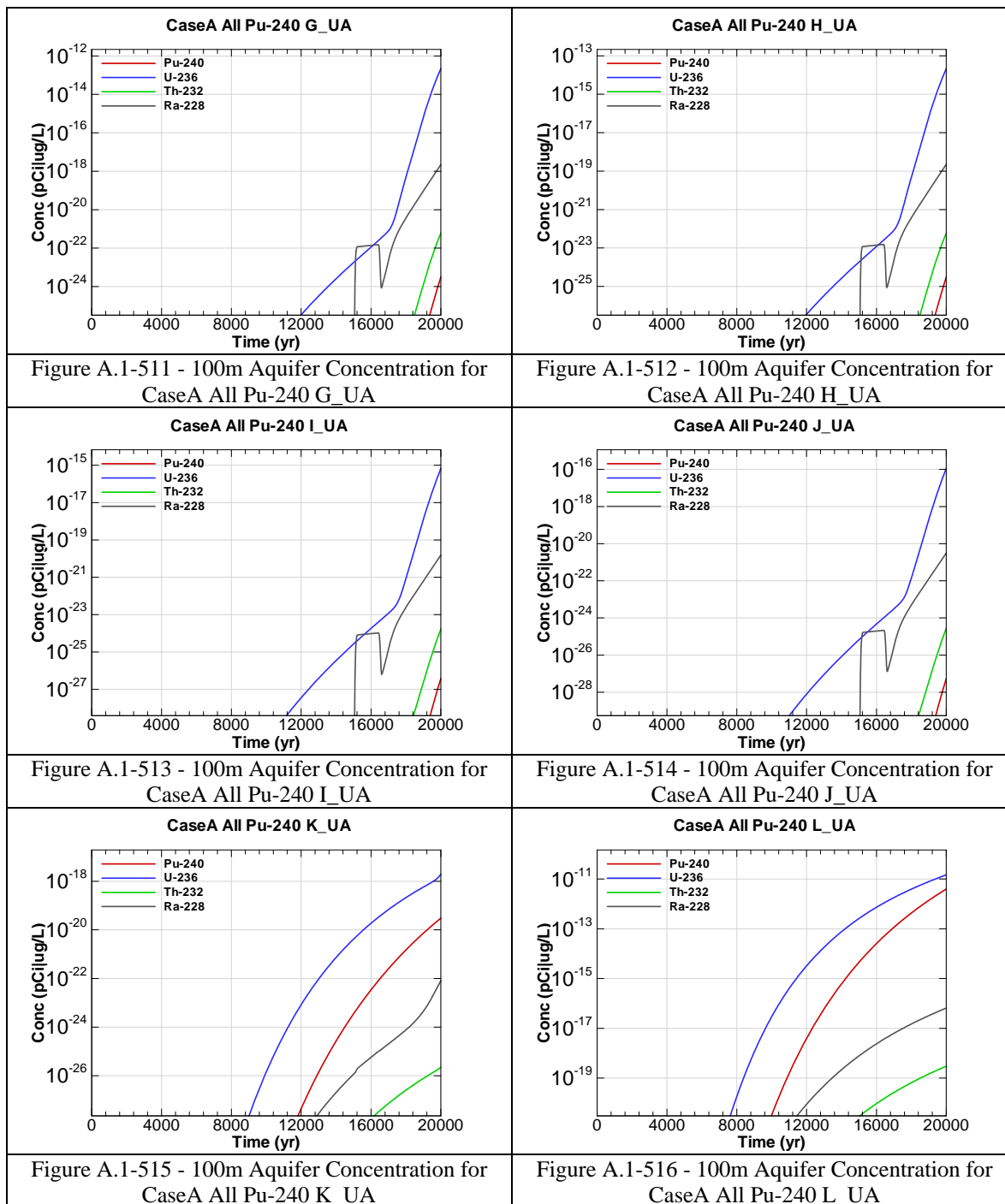


Figure A.1-498 - 100m Aquifer Concentration for
CaseA All Pu-239 F-UA







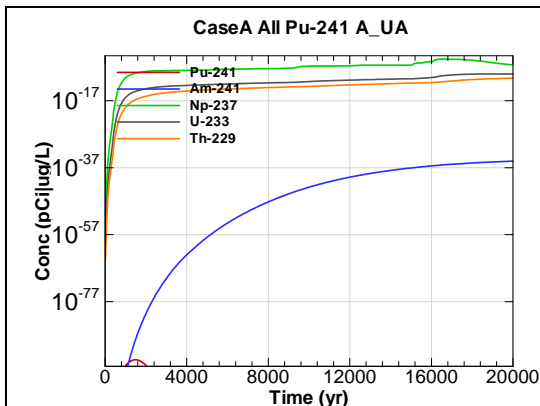


Figure A.1-517 - 100m Aquifer Concentration for
CaseA All Pu-241 A-UA

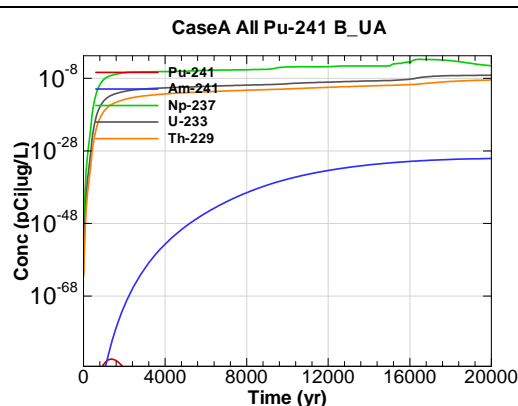


Figure A.1-518 - 100m Aquifer Concentration for
CaseA All Pu-241 B-UA

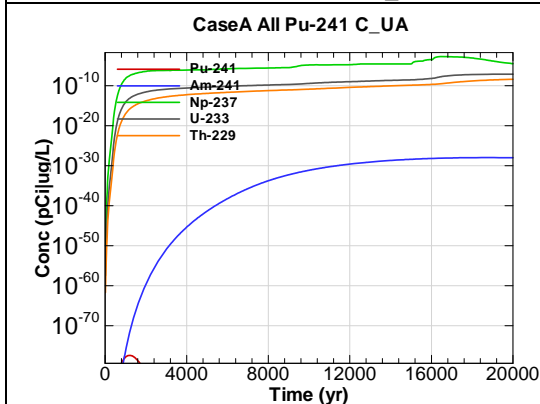


Figure A.1-519 - 100m Aquifer Concentration for
CaseA All Pu-241 C-UA

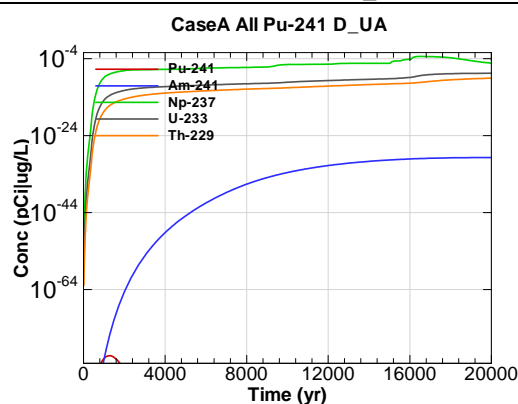


Figure A.1-520 - 100m Aquifer Concentration for
CaseA All Pu-241 D-UA

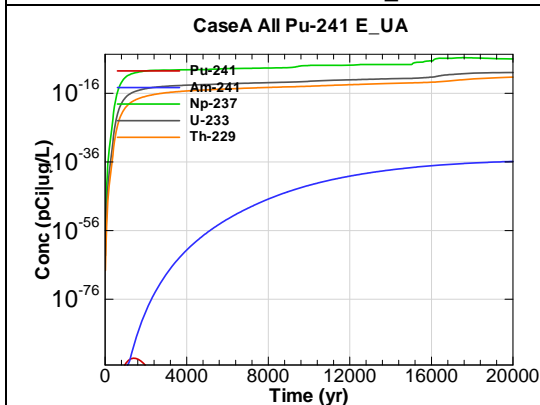


Figure A.1-521 - 100m Aquifer Concentration for
CaseA All Pu-241 E-UA

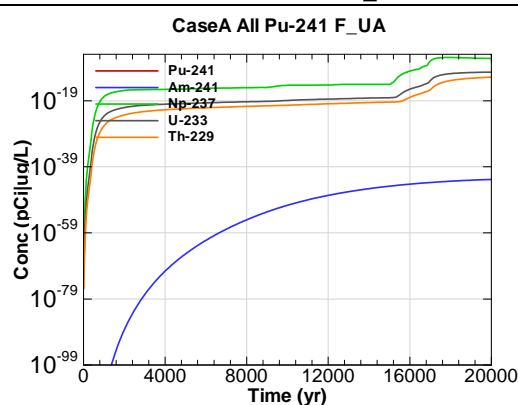
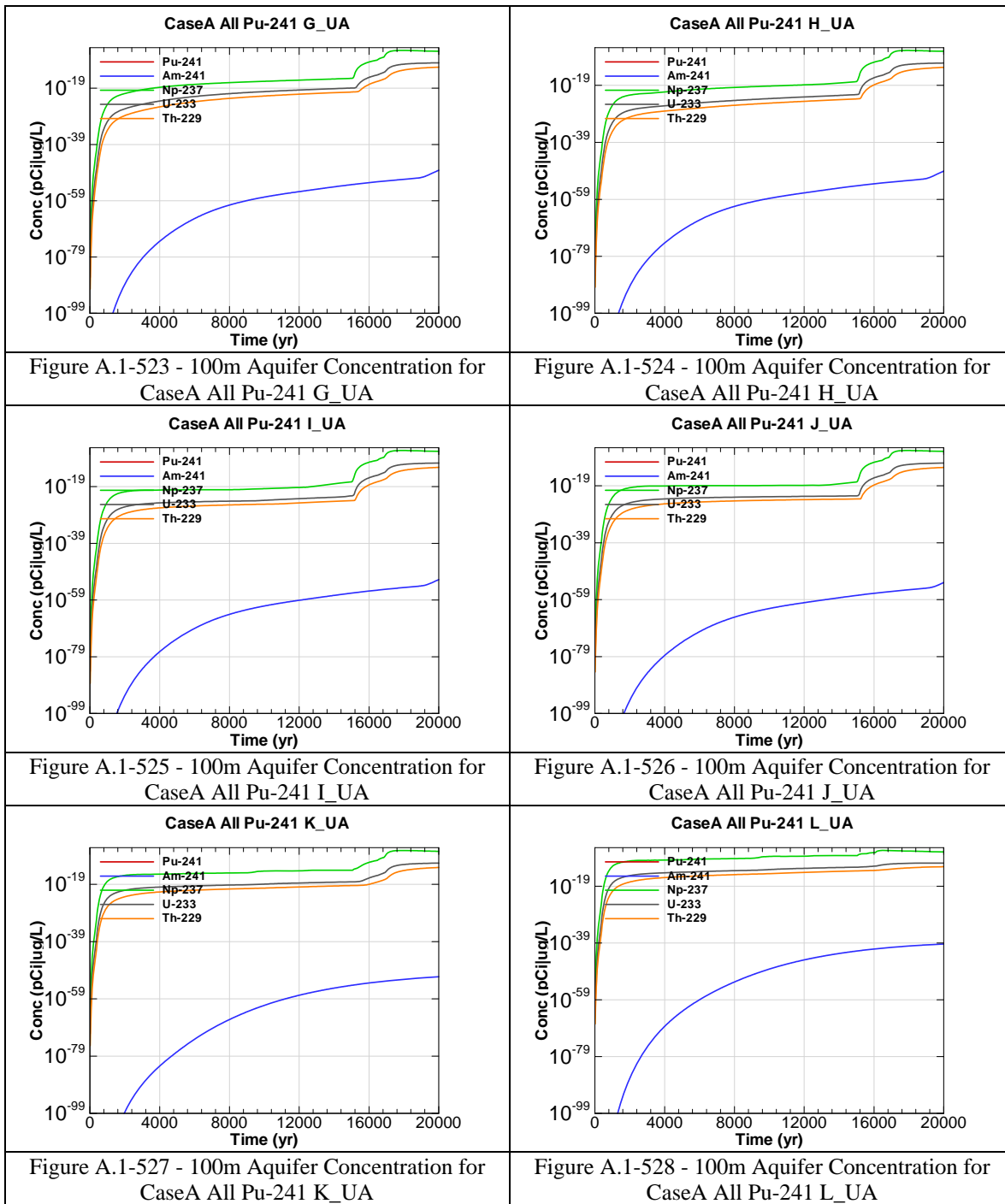


Figure A.1-522 - 100m Aquifer Concentration for
CaseA All Pu-241 F-UA



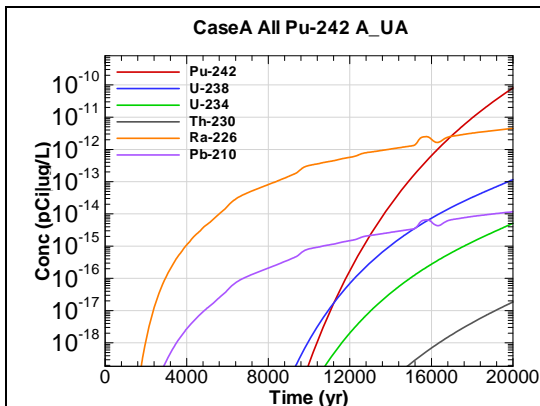


Figure A.1-529 - 100m Aquifer Concentration for
CaseA All Pu-242 A_UA

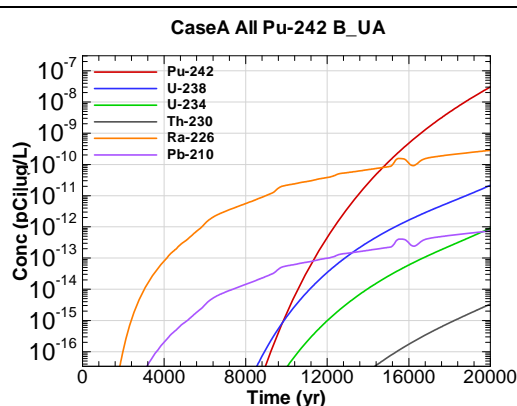


Figure A.1-530 - 100m Aquifer Concentration for
CaseA All Pu-242 B_UA

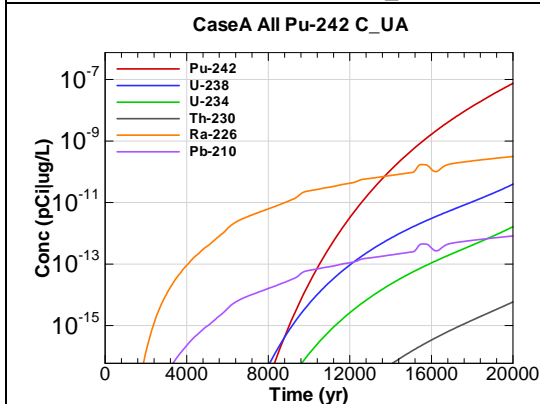


Figure A.1-531 - 100m Aquifer Concentration for
CaseA All Pu-242 C_UA

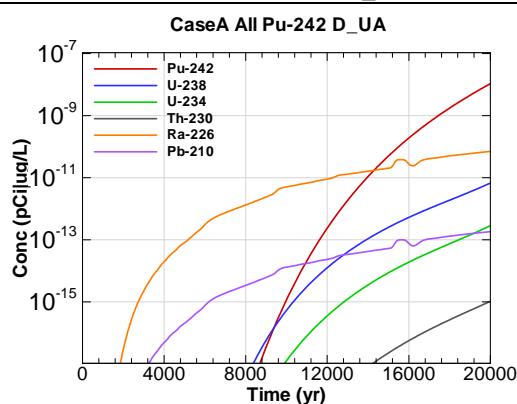


Figure A.1-532 - 100m Aquifer Concentration for
CaseA All Pu-242 D_UA

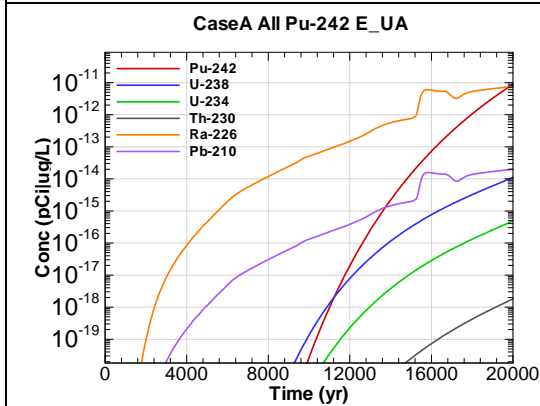


Figure A.1-533 - 100m Aquifer Concentration for
CaseA All Pu-242 E_UA

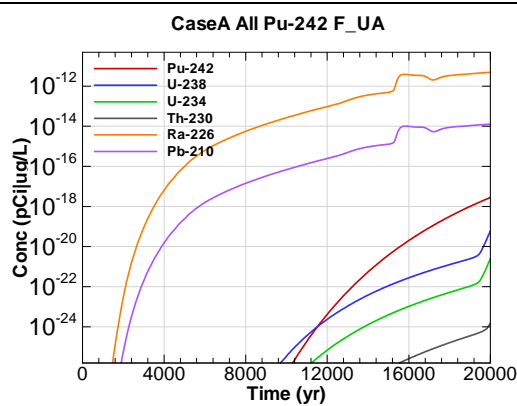


Figure A.1-534 - 100m Aquifer Concentration for
CaseA All Pu-242 F_UA

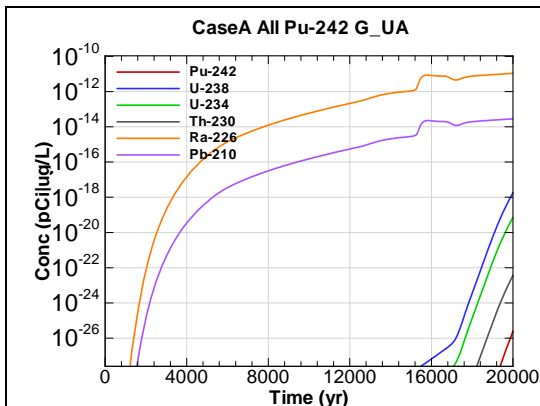


Figure A.1-535 - 100m Aquifer Concentration for
CaseA All Pu-242 G-UA

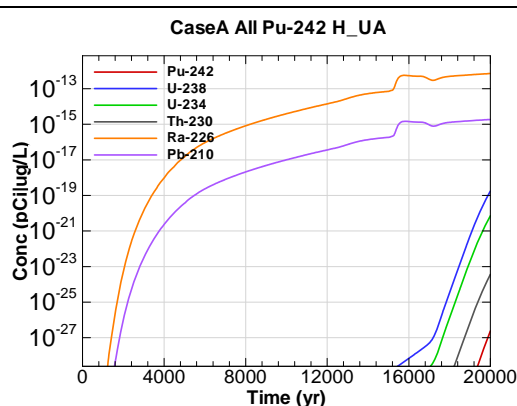


Figure A.1-536 - 100m Aquifer Concentration for
CaseA All Pu-242 H-UA

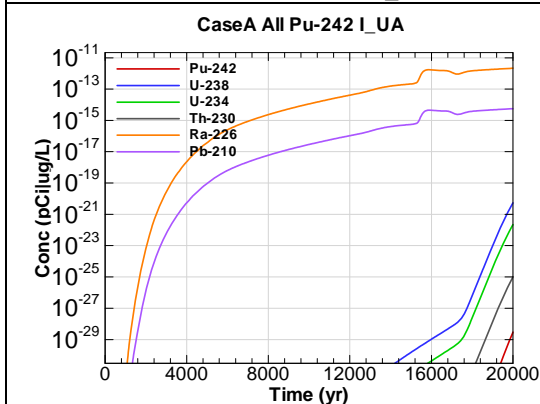


Figure A.1-537 - 100m Aquifer Concentration for
CaseA All Pu-242 I-UA

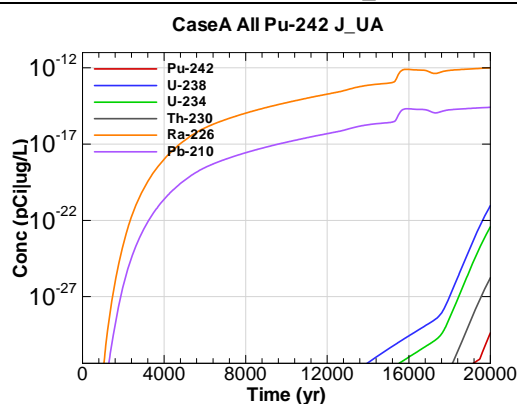


Figure A.1-538 - 100m Aquifer Concentration for
CaseA All Pu-242 J-UA

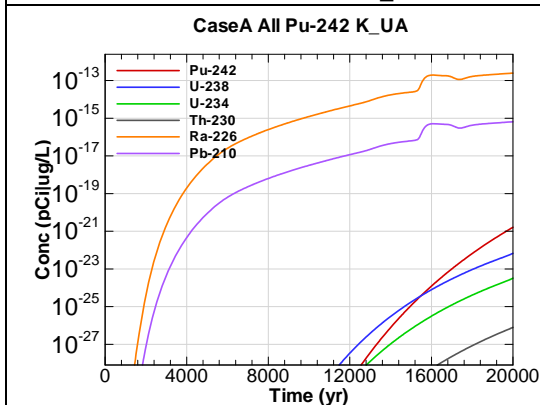


Figure A.1-539 - 100m Aquifer Concentration for
CaseA All Pu-242 K-UA

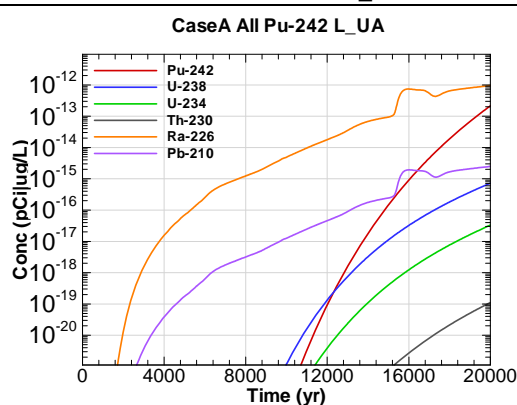


Figure A.1-540 - 100m Aquifer Concentration for
CaseA All Pu-242 L-UA

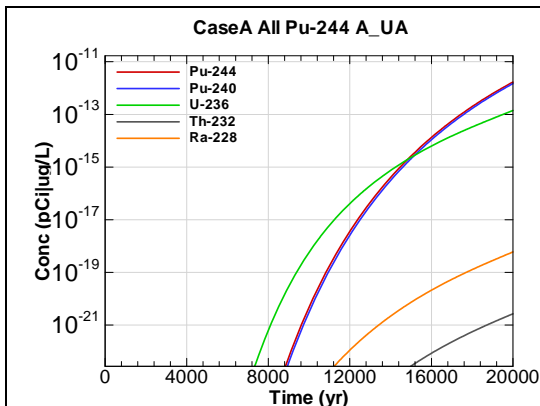


Figure A.1-541 - 100m Aquifer Concentration for
CaseA All Pu-244 A_UA

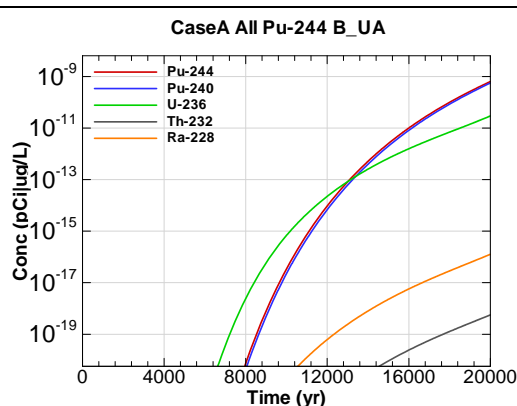


Figure A.1-542 - 100m Aquifer Concentration for
CaseA All Pu-244 B_UA

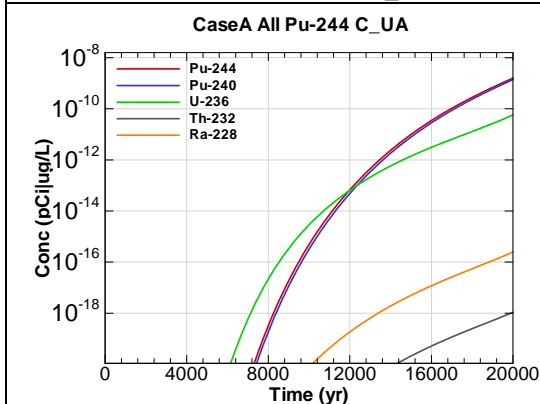


Figure A.1-543 - 100m Aquifer Concentration for
CaseA All Pu-244 C_UA

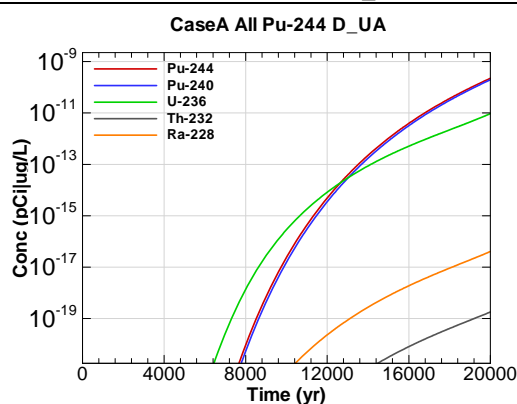


Figure A.1-544 - 100m Aquifer Concentration for
CaseA All Pu-244 D_UA

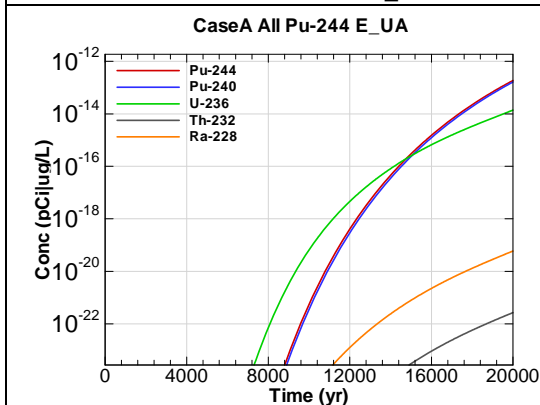


Figure A.1-545 - 100m Aquifer Concentration for
CaseA All Pu-244 E_UA

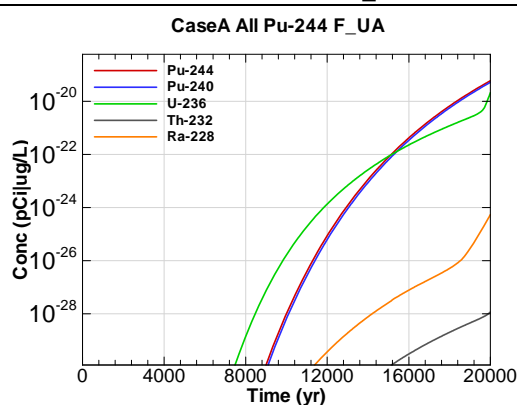


Figure A.1-546 - 100m Aquifer Concentration for
CaseA All Pu-244 F_UA

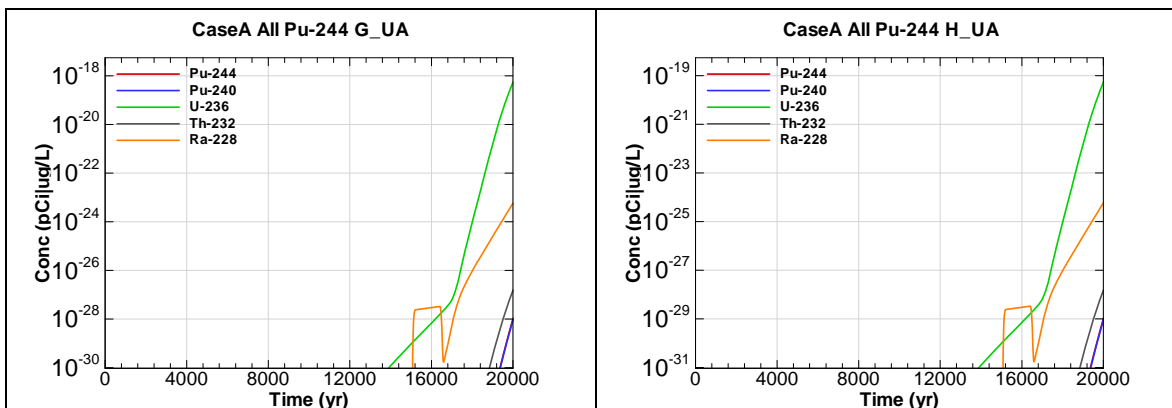


Figure A.1-547 - 100m Aquifer Concentration for
CaseA All Pu-244 G-UA

Figure A.1-548 - 100m Aquifer Concentration for
CaseA All Pu-244 H-UA

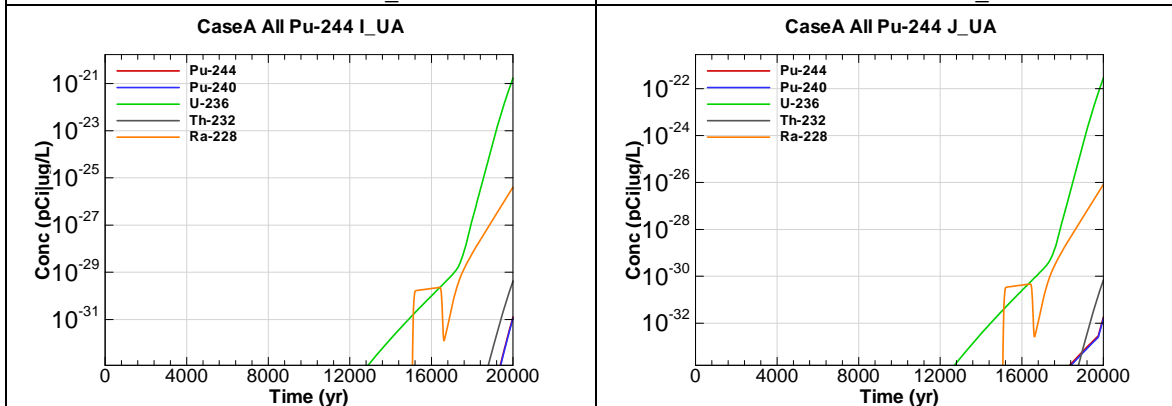


Figure A.1-549 - 100m Aquifer Concentration for
CaseA All Pu-244 I-UA

Figure A.1-550 - 100m Aquifer Concentration for
CaseA All Pu-244 J-UA

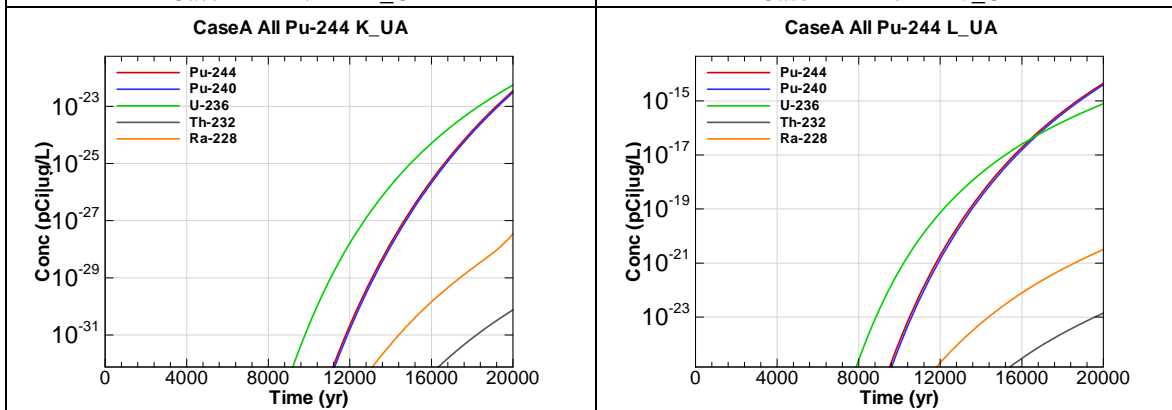


Figure A.1-551 - 100m Aquifer Concentration for
CaseA All Pu-244 K-UA

Figure A.1-552 - 100m Aquifer Concentration for
CaseA All Pu-244 L-UA

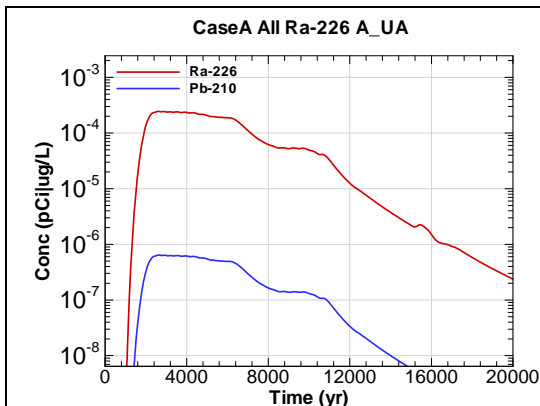


Figure A.1-553 - 100m Aquifer Concentration for
CaseA All Ra-226 A_UA

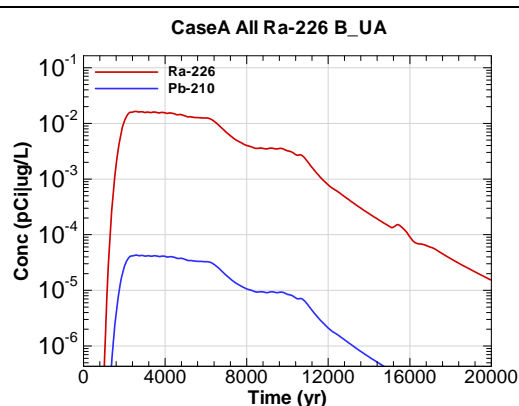


Figure A.1-554 - 100m Aquifer Concentration for
CaseA All Ra-226 B_UA

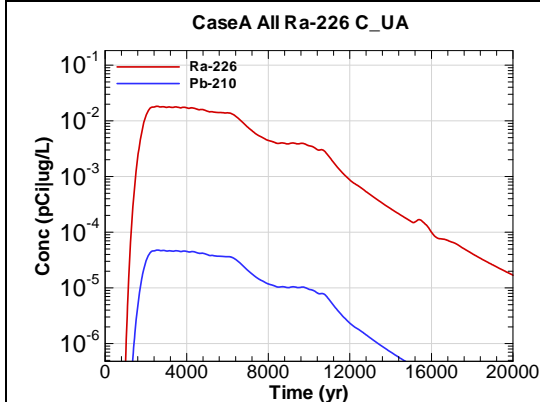


Figure A.1-555 - 100m Aquifer Concentration for
CaseA All Ra-226 C_UA

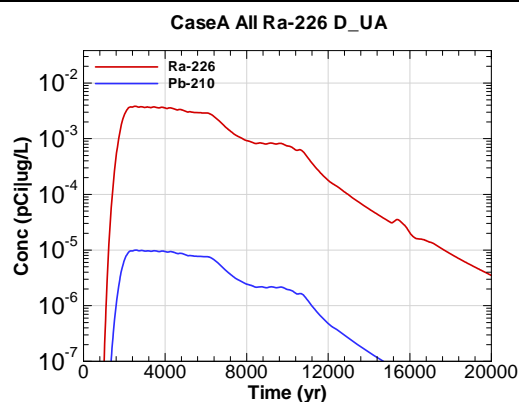


Figure A.1-556 - 100m Aquifer Concentration for
CaseA All Ra-226 D_UA

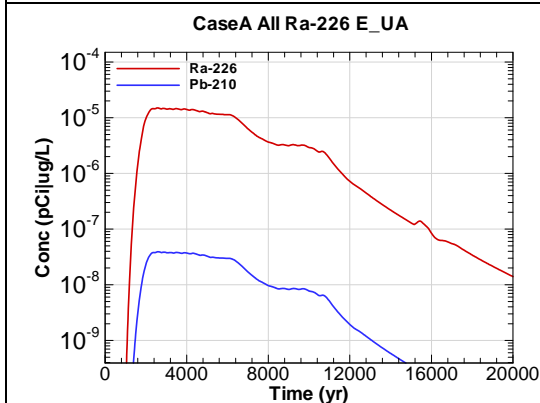


Figure A.1-557 - 100m Aquifer Concentration for
CaseA All Ra-226 E_UA

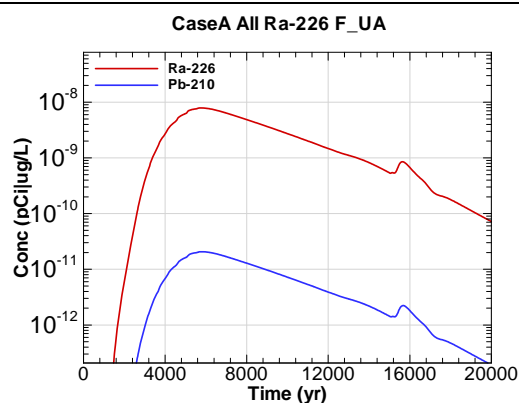


Figure A.1-558 - 100m Aquifer Concentration for
CaseA All Ra-226 F_UA

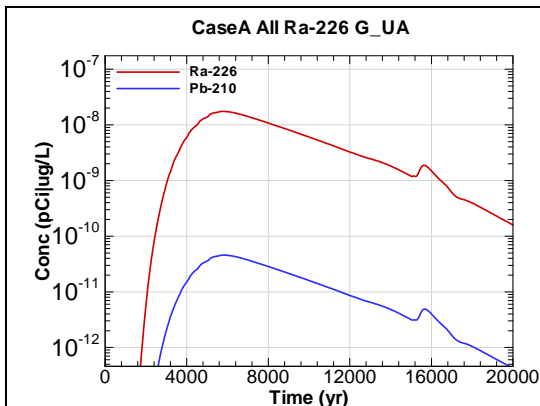


Figure A.1-559 - 100m Aquifer Concentration for
CaseA All Ra-226 G-UA

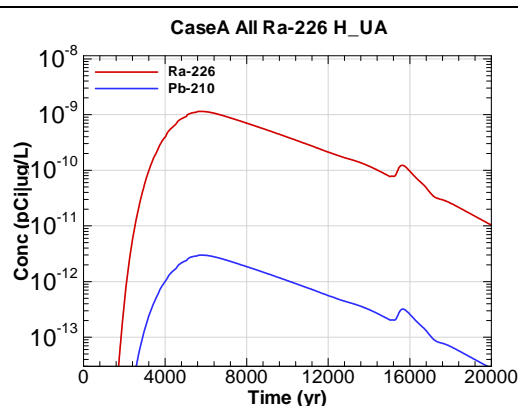


Figure A.1-560 - 100m Aquifer Concentration for
CaseA All Ra-226 H-UA

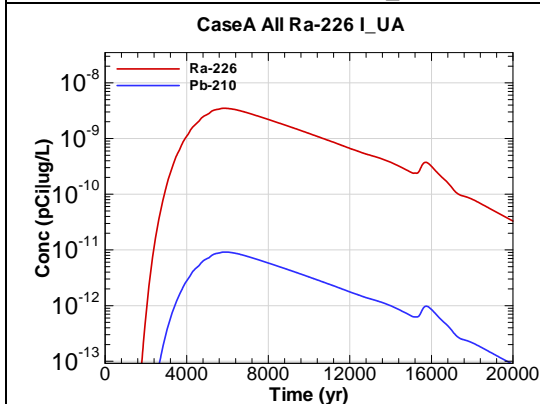


Figure A.1-561 - 100m Aquifer Concentration for
CaseA All Ra-226 I-UA

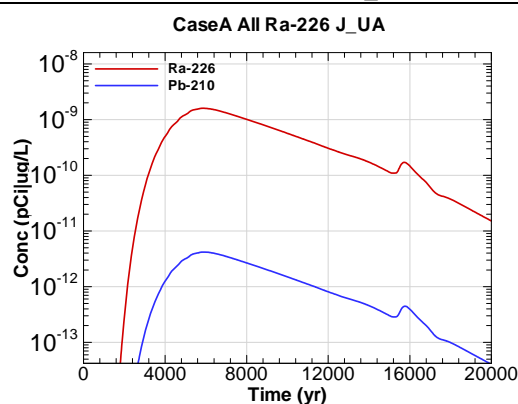


Figure A.1-562 - 100m Aquifer Concentration for
CaseA All Ra-226 J-UA

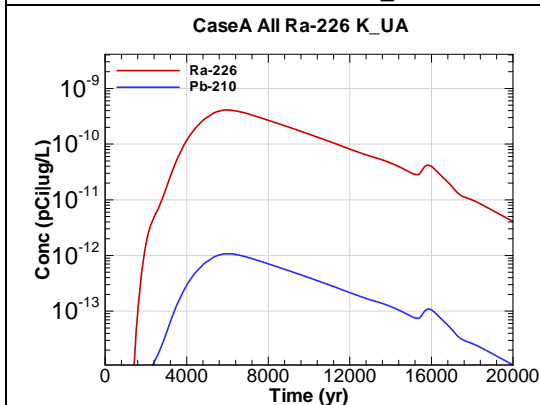


Figure A.1-563 - 100m Aquifer Concentration for
CaseA All Ra-226 K-UA

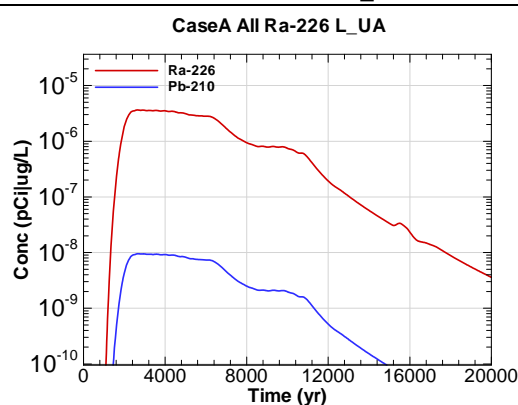
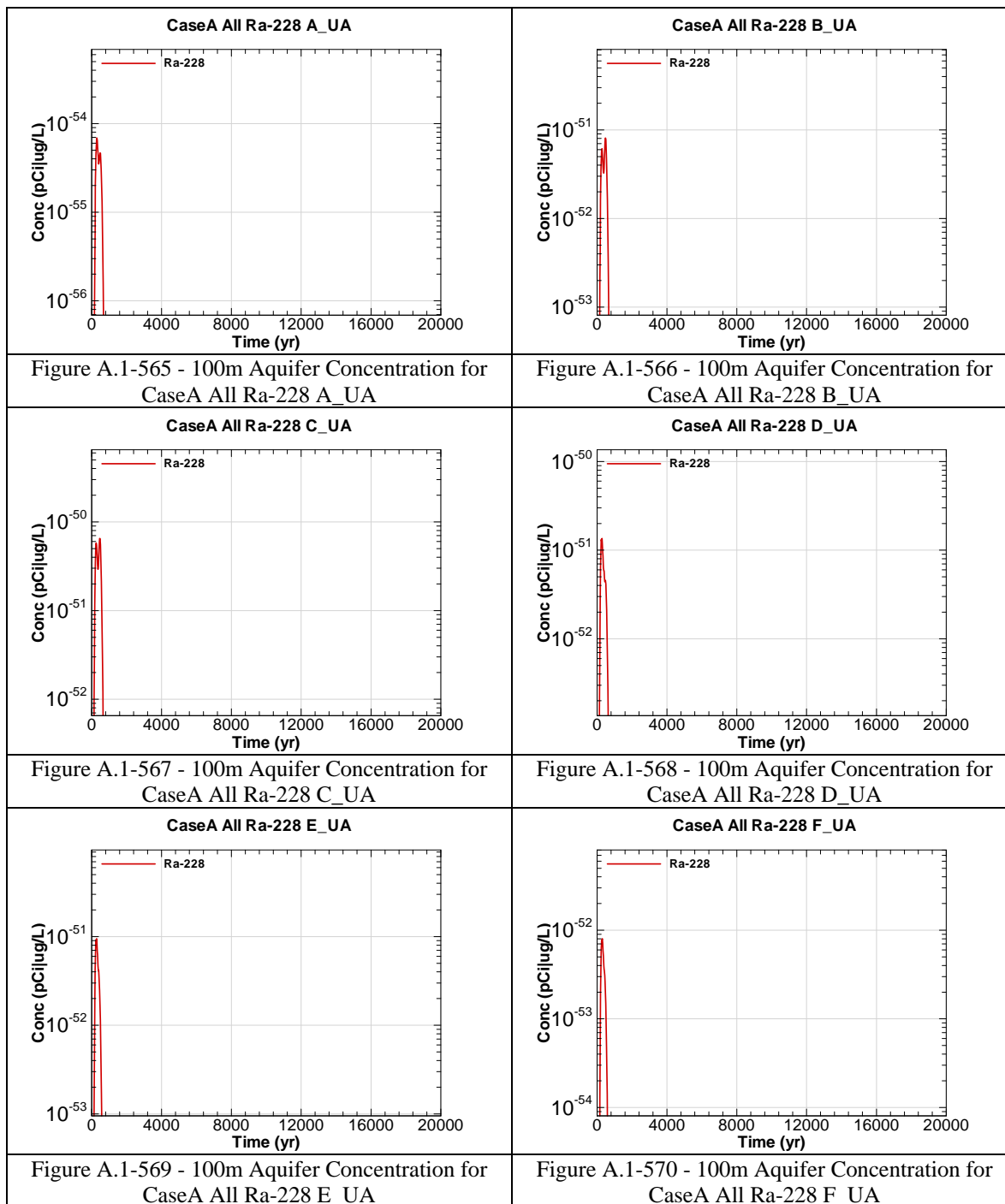
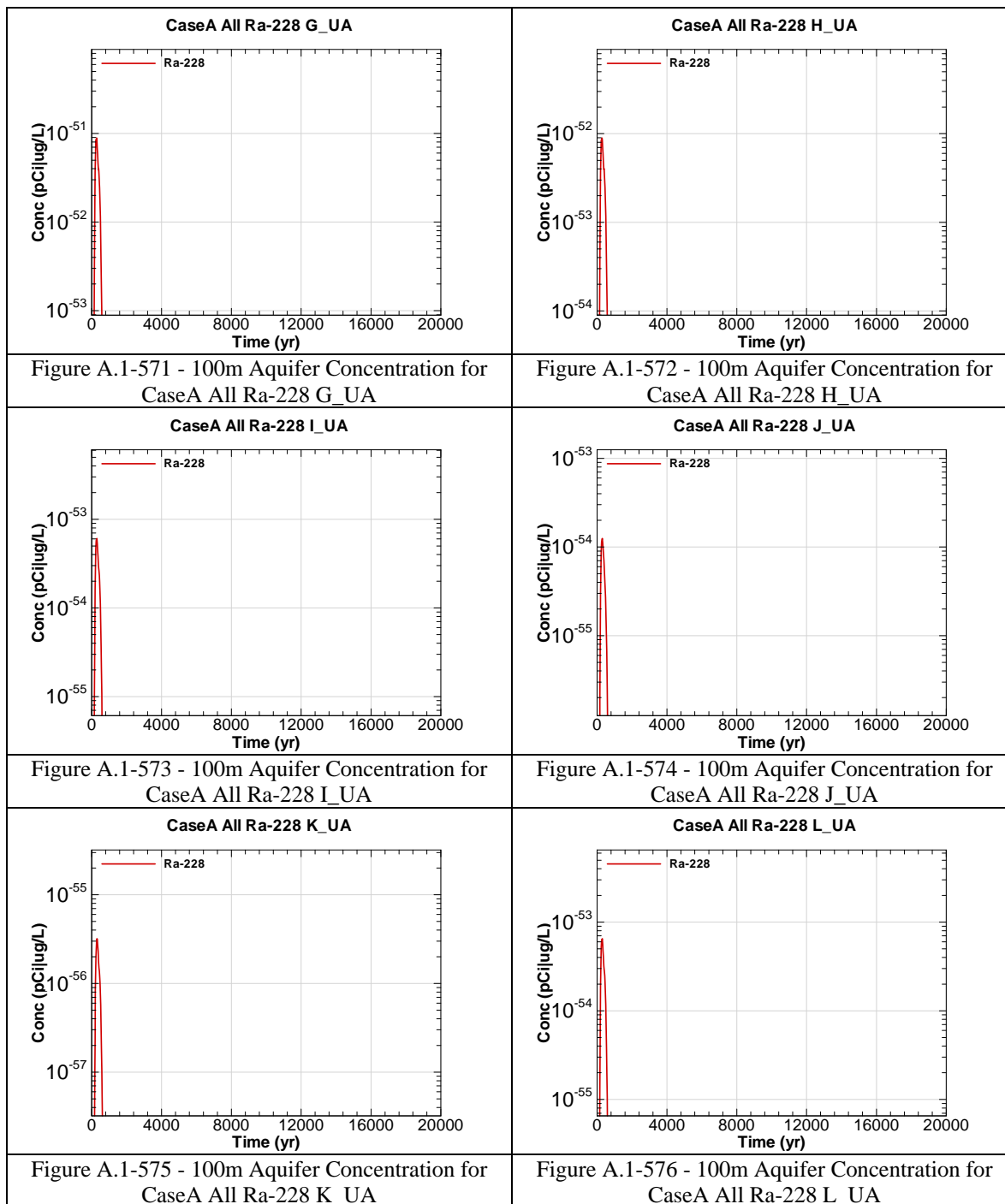
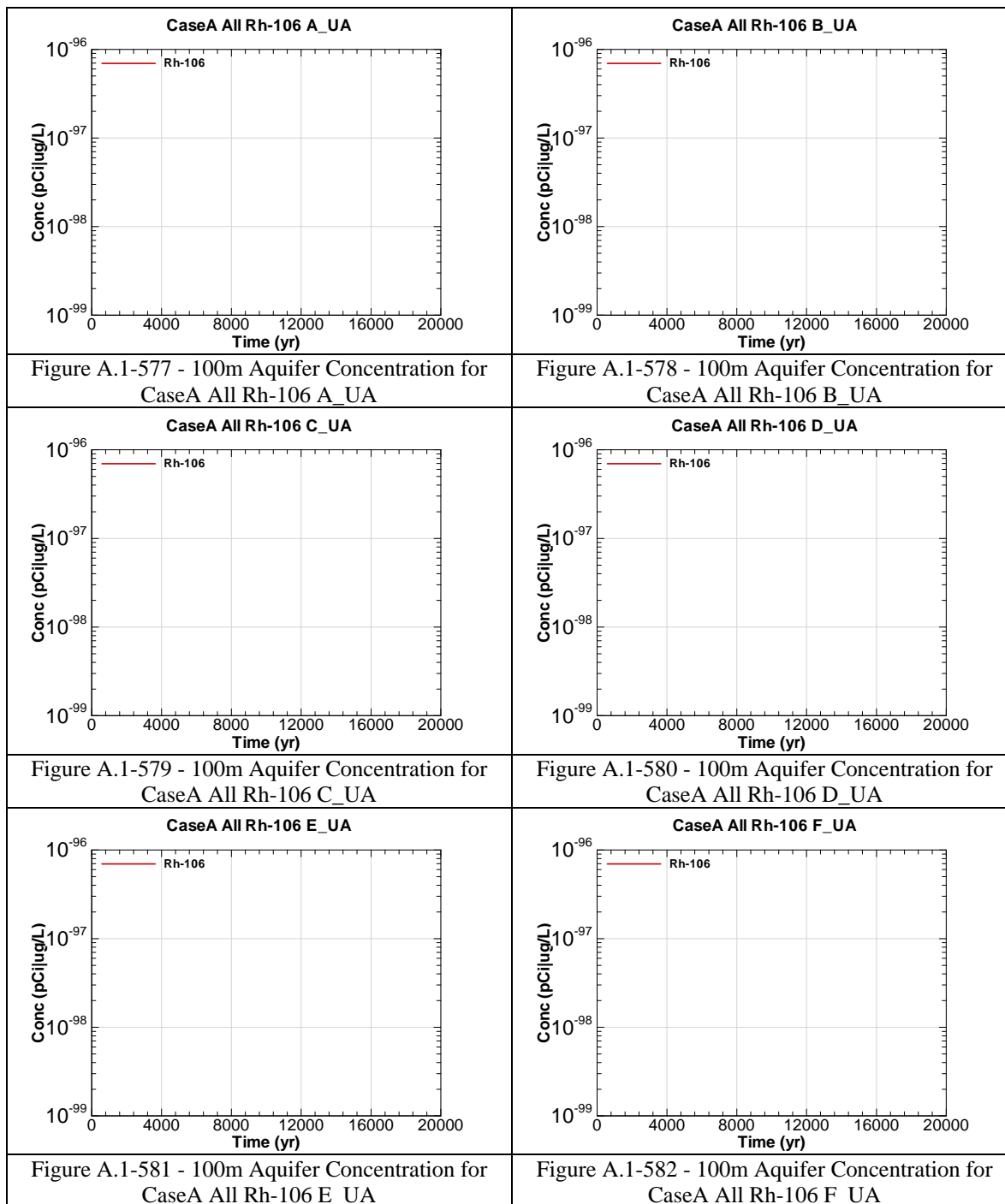
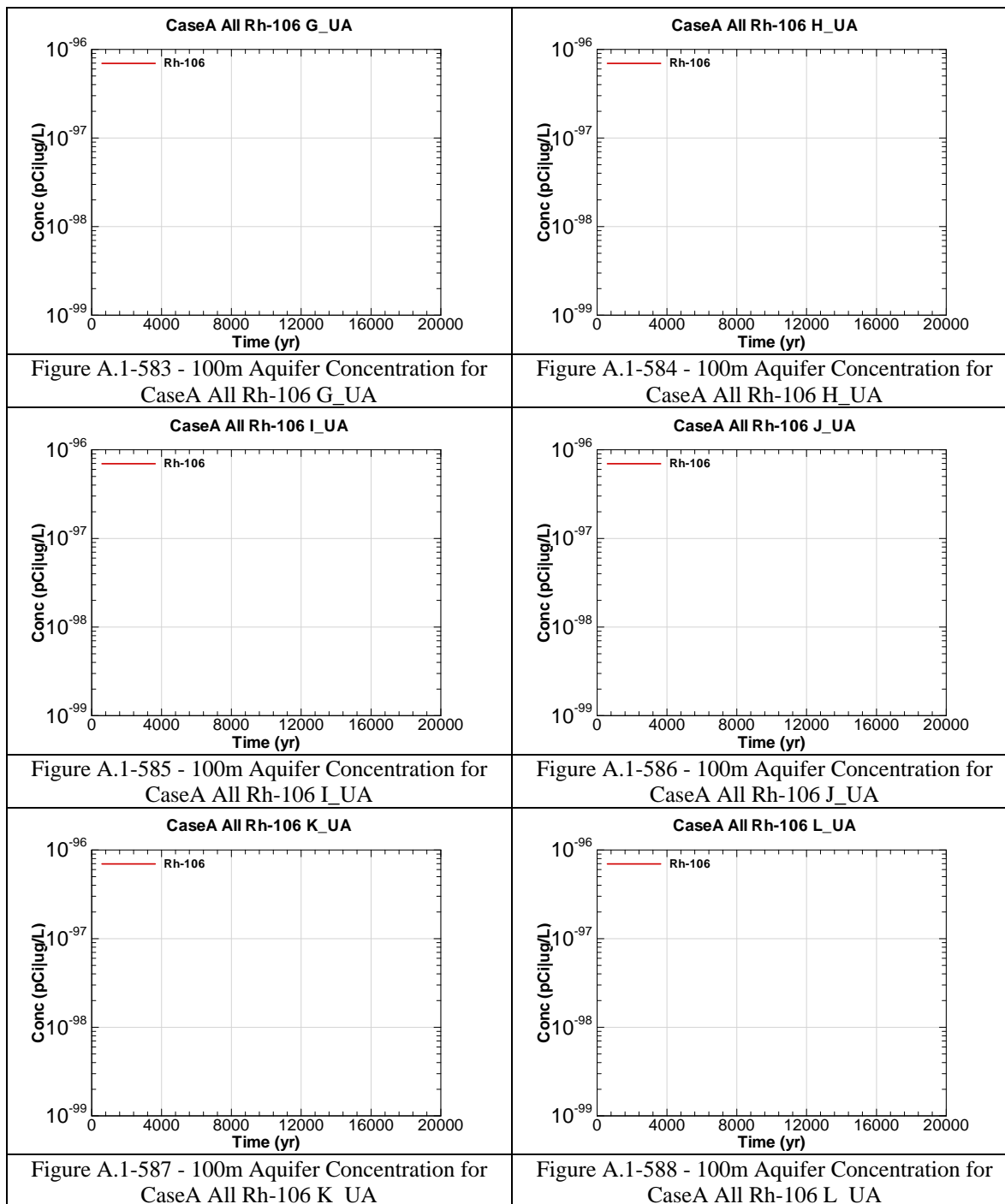


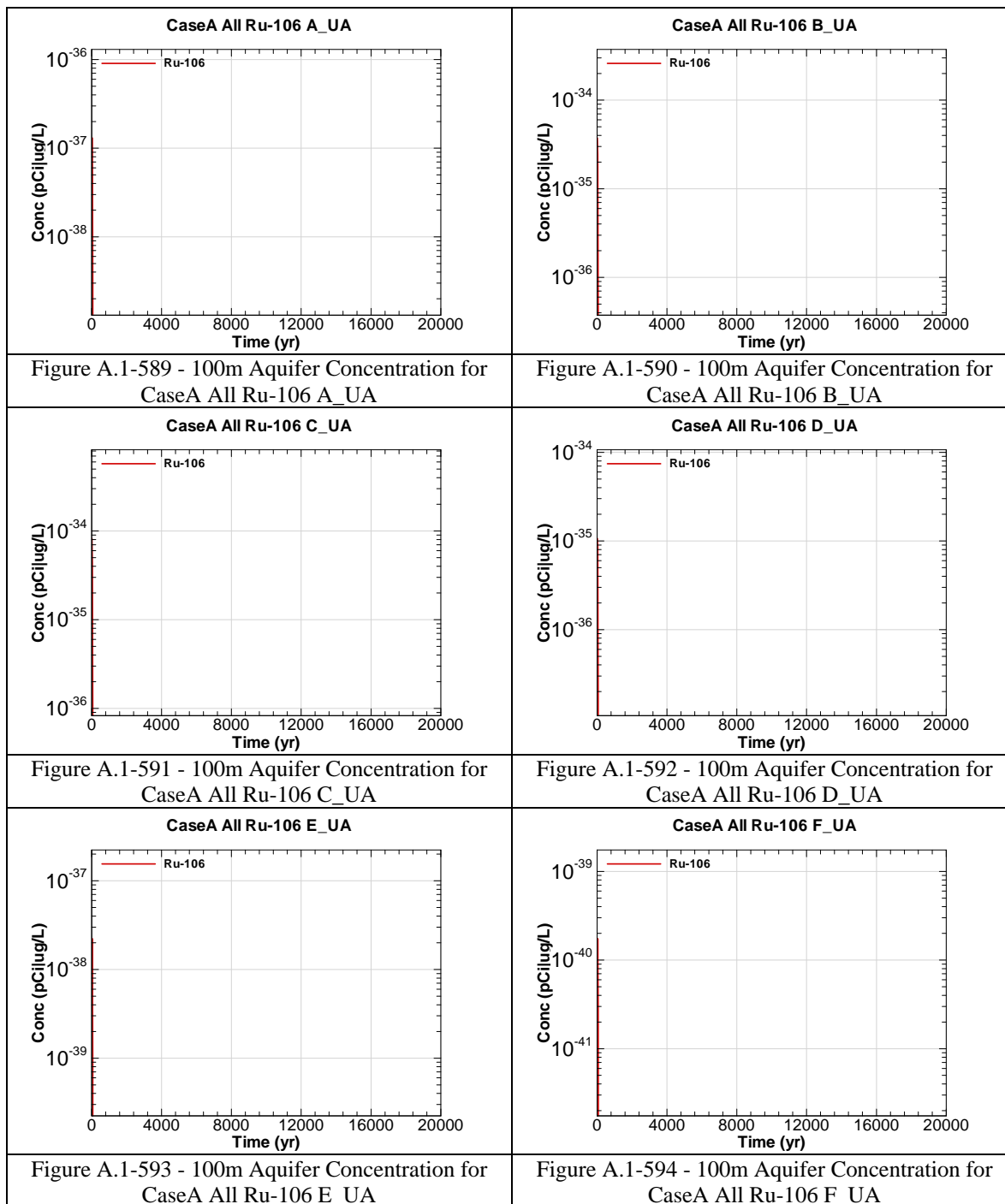
Figure A.1-564 - 100m Aquifer Concentration for
CaseA All Ra-226 L-UA

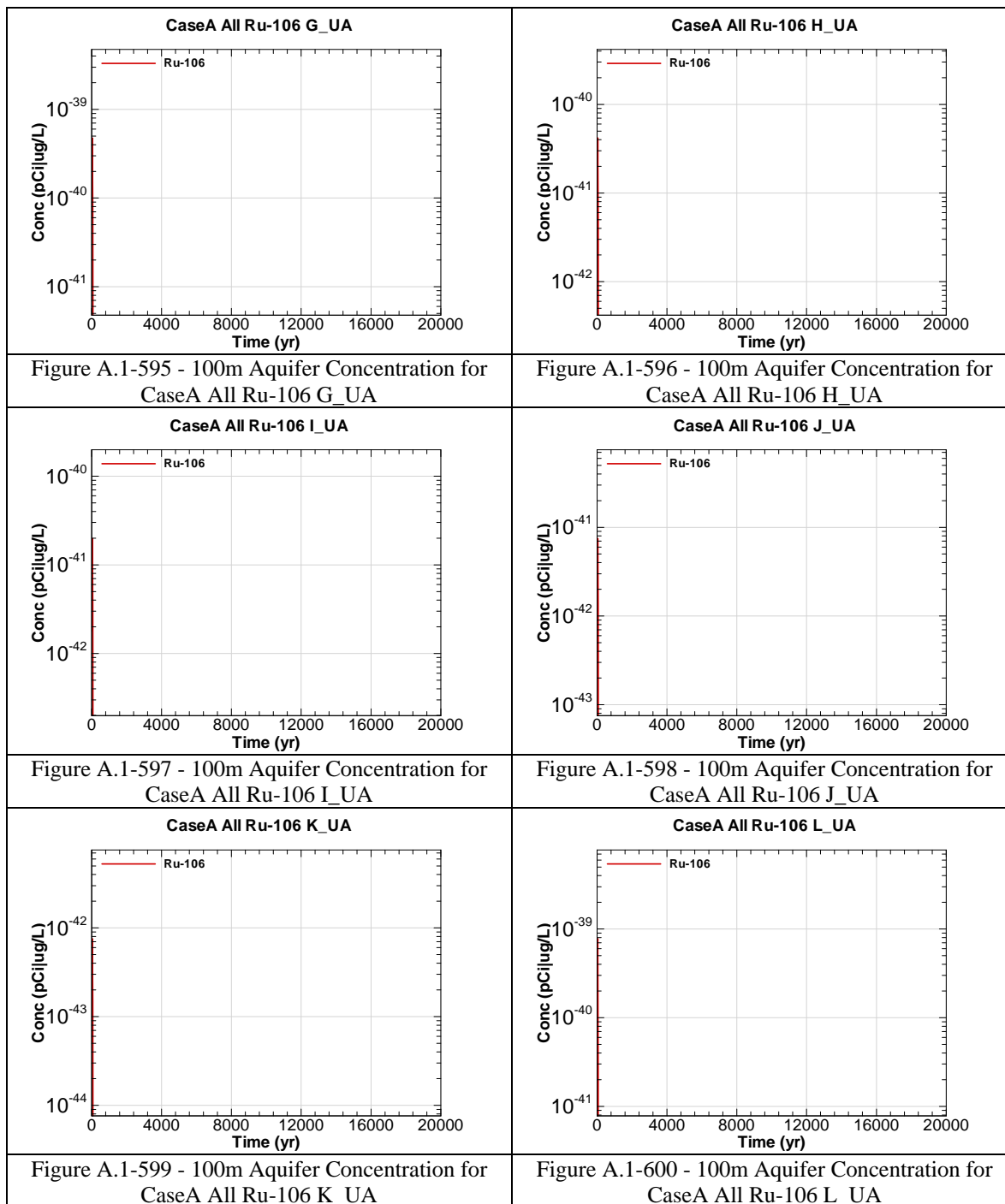


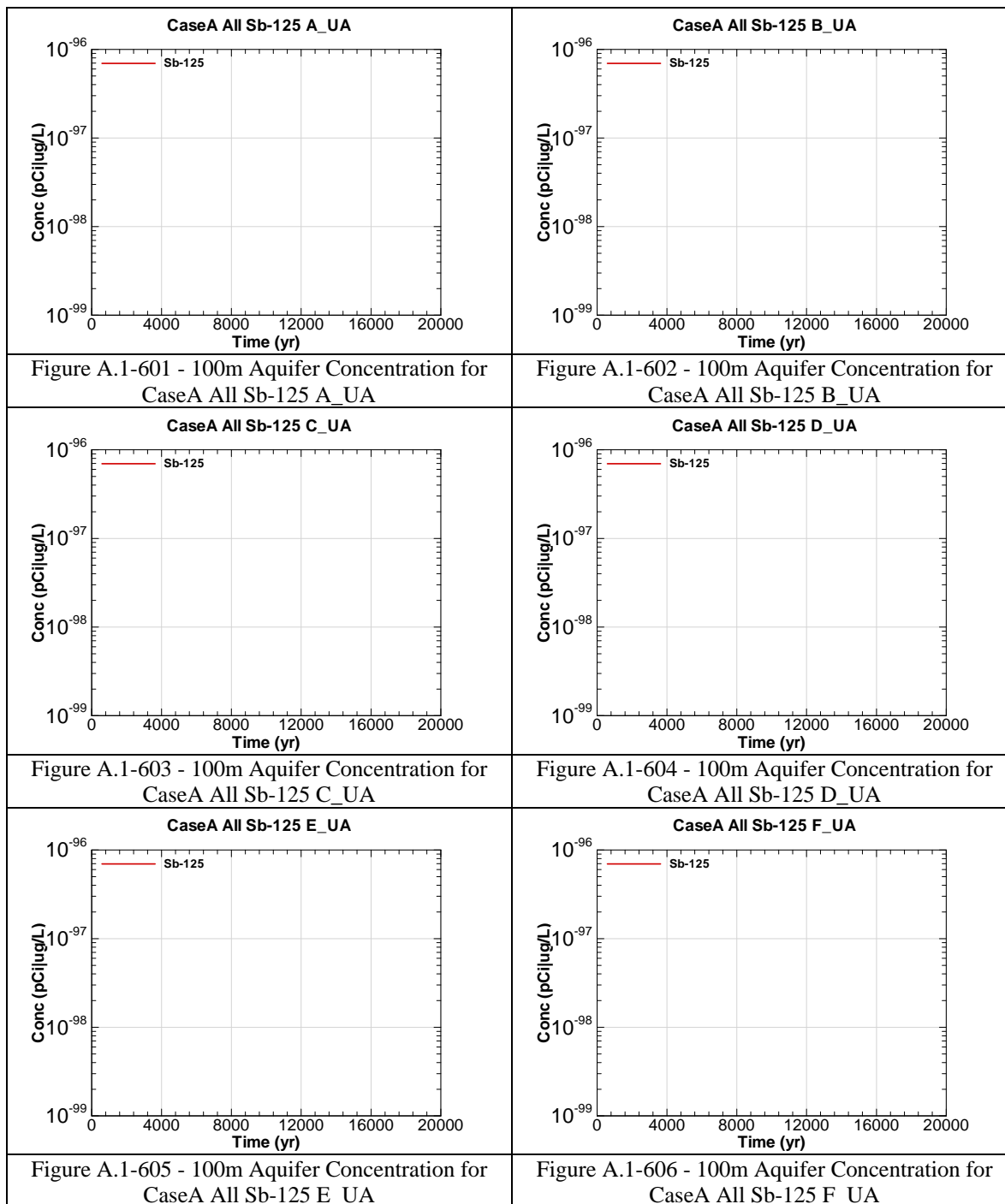


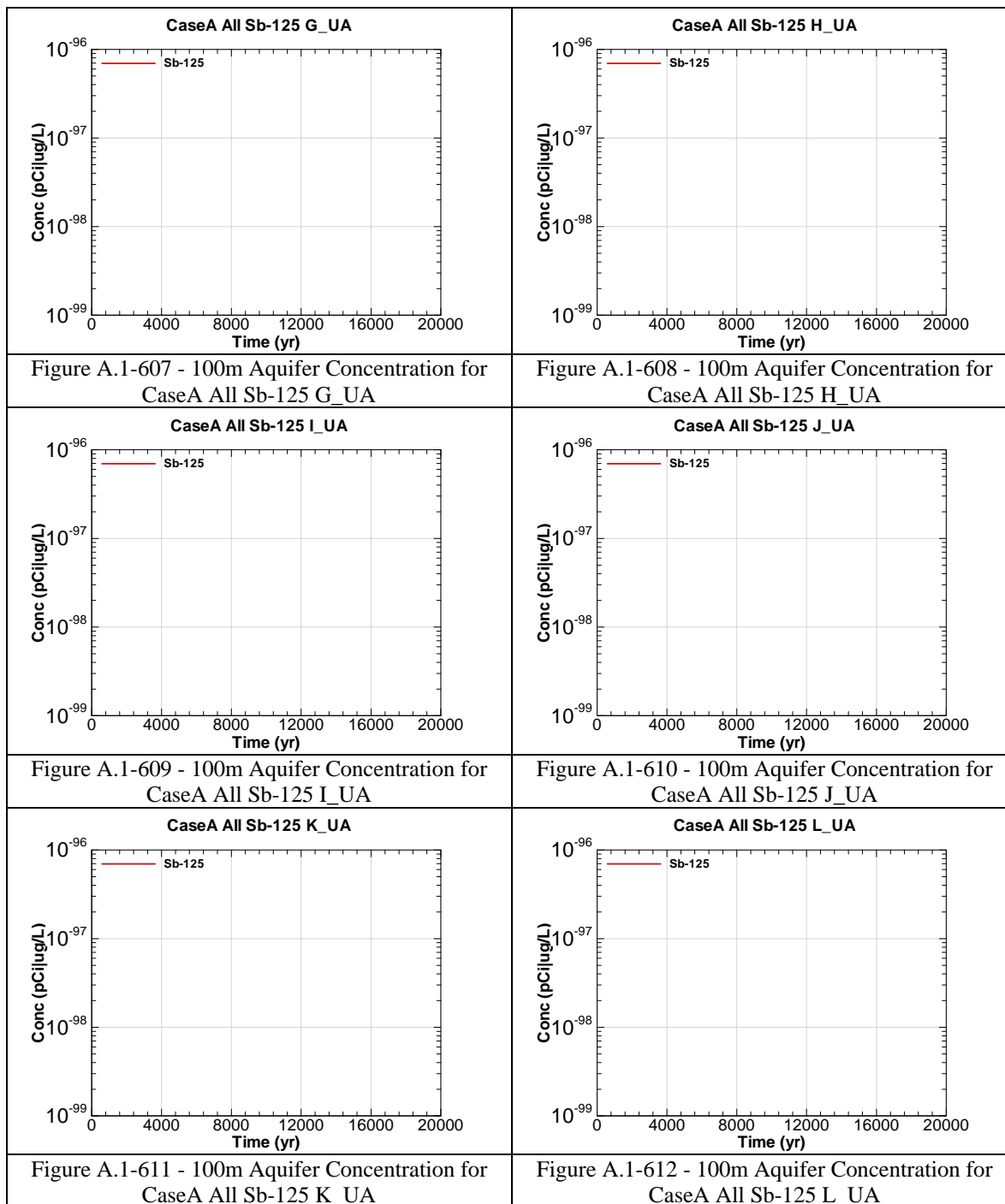


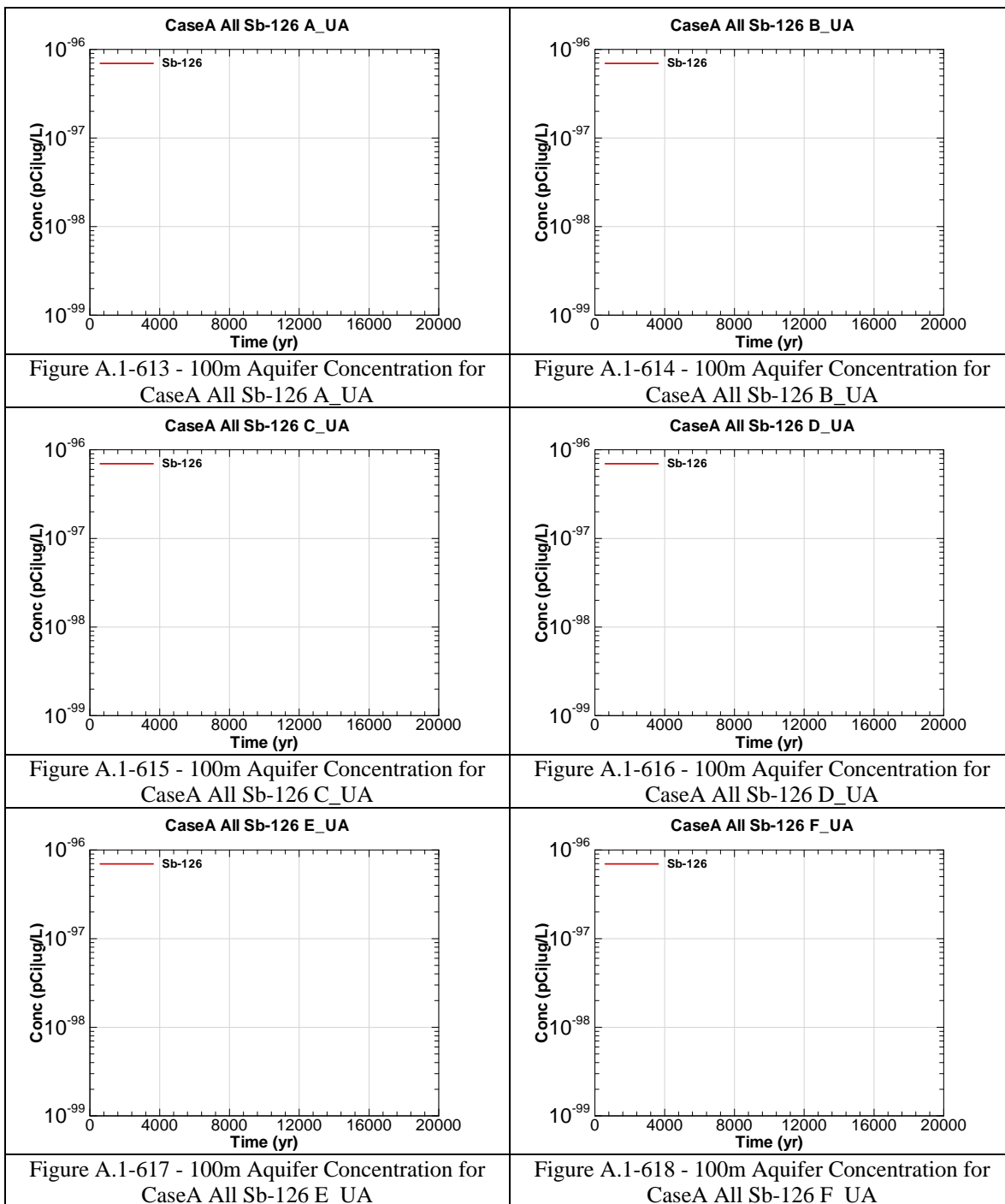


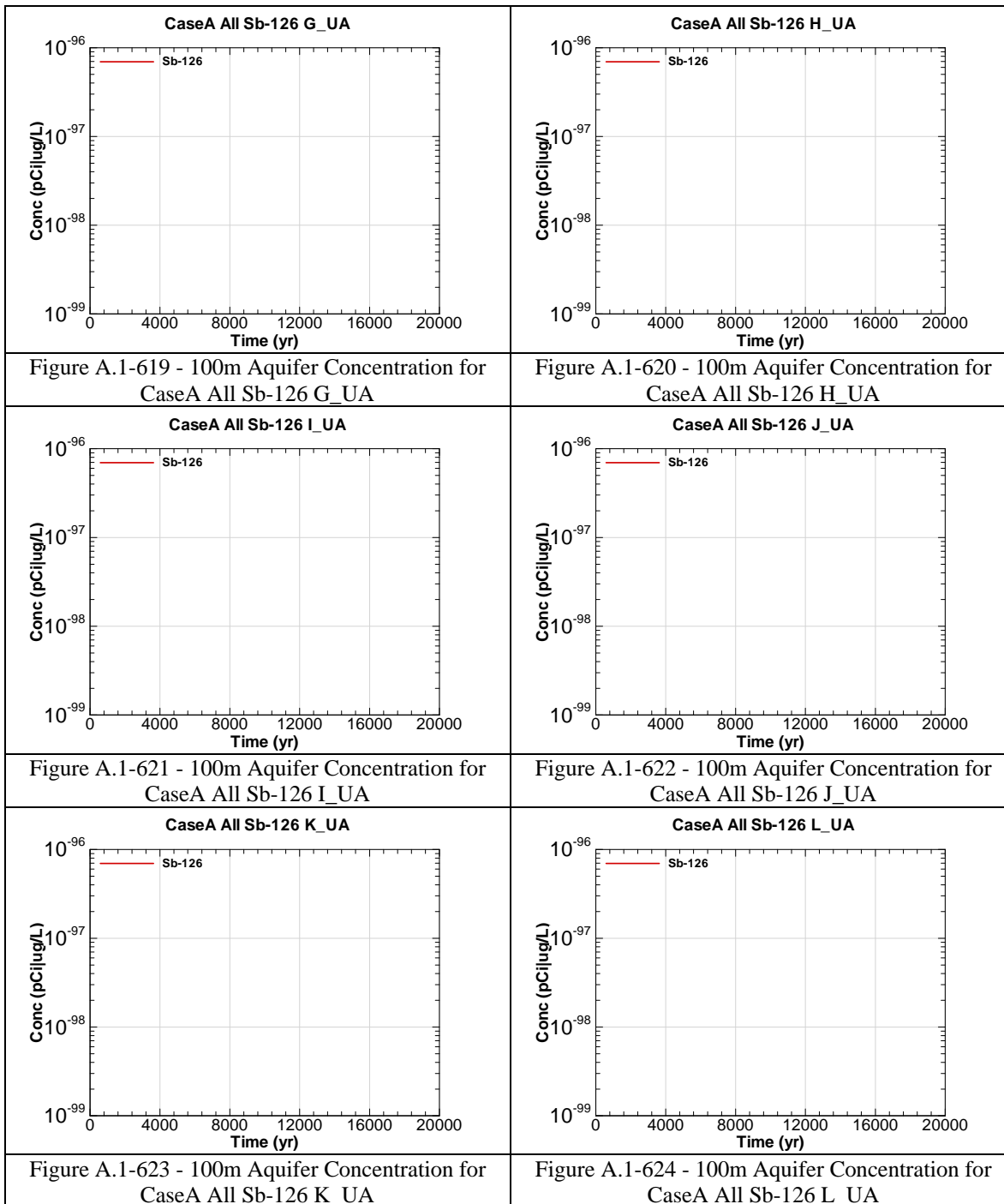


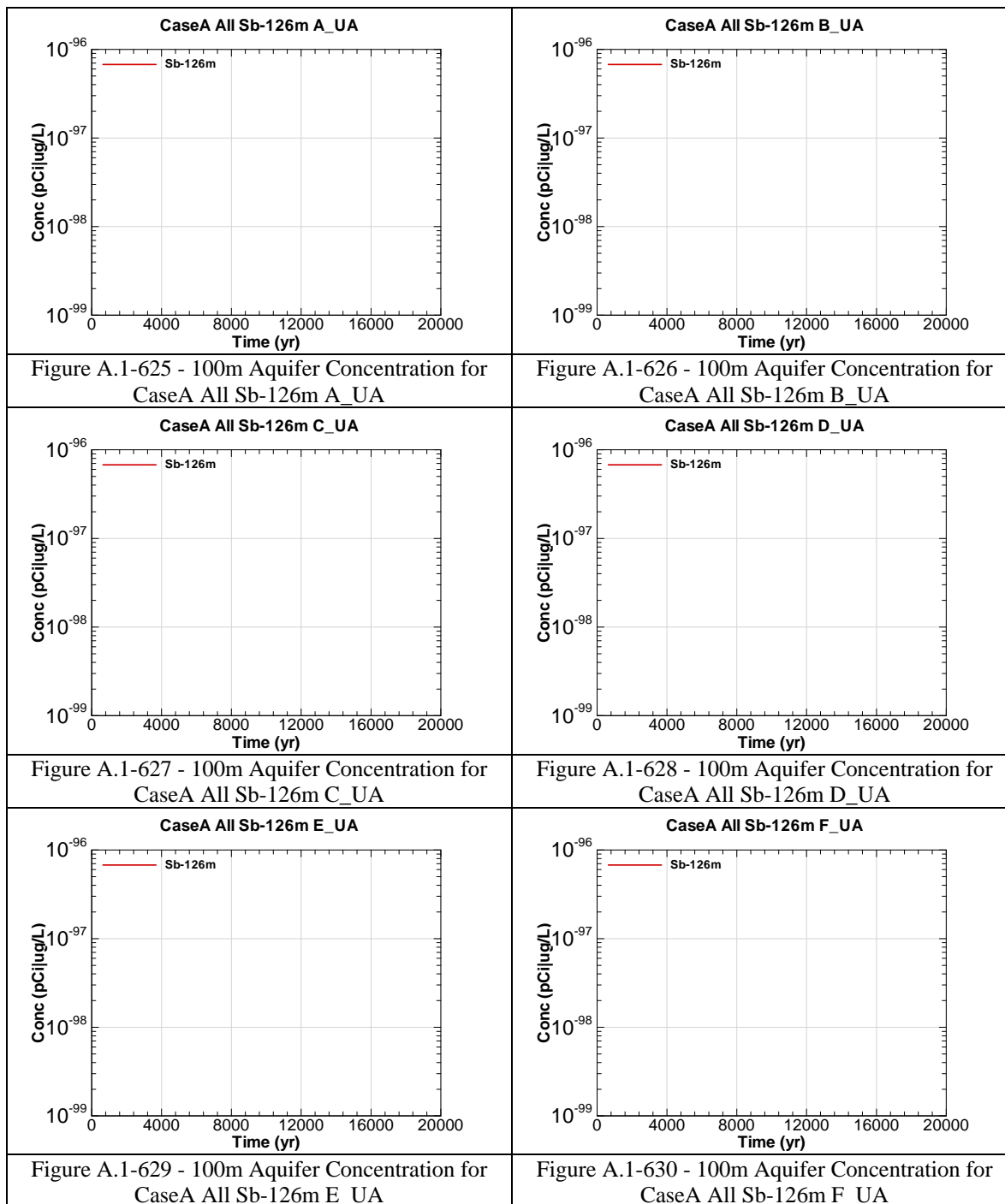


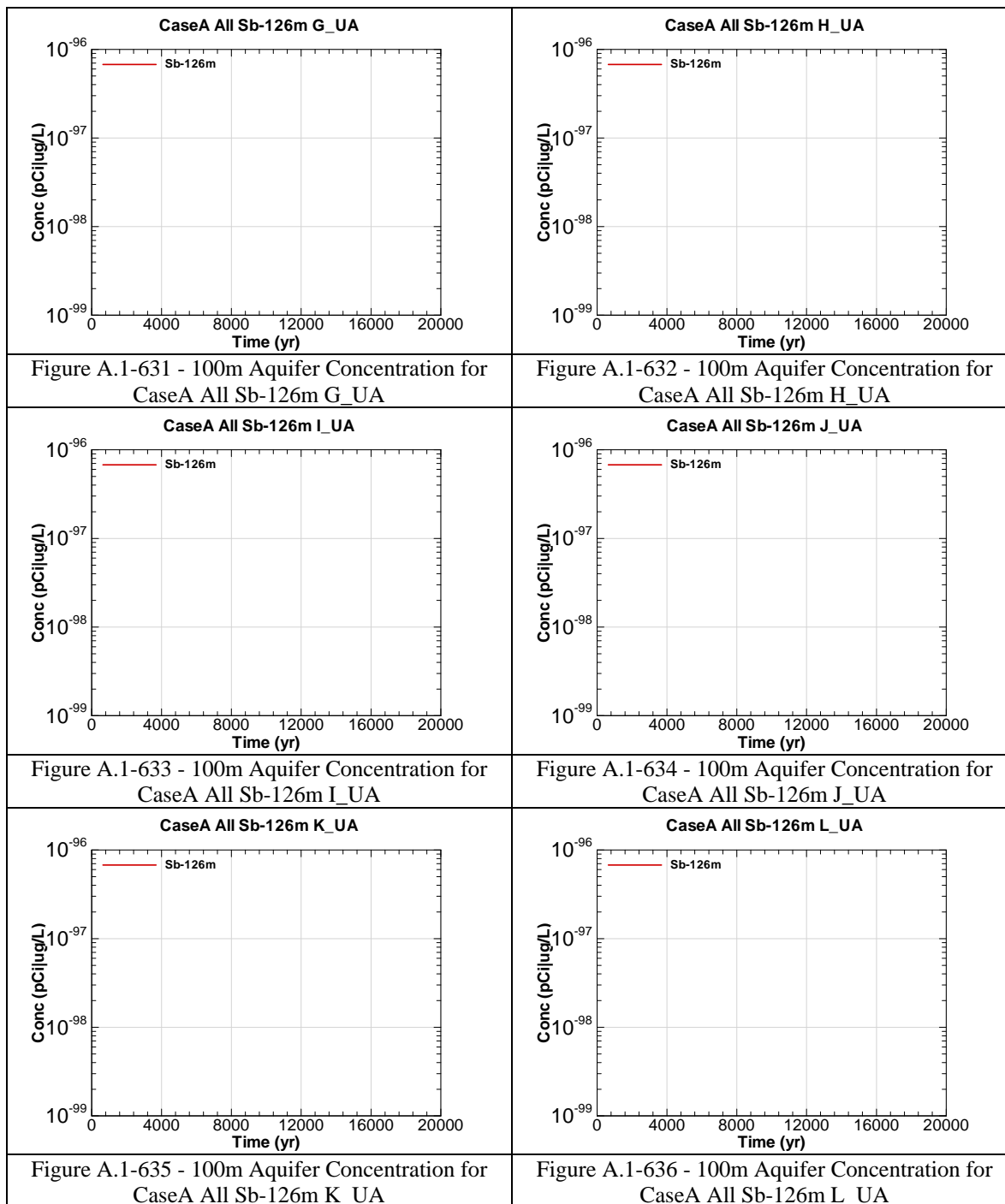


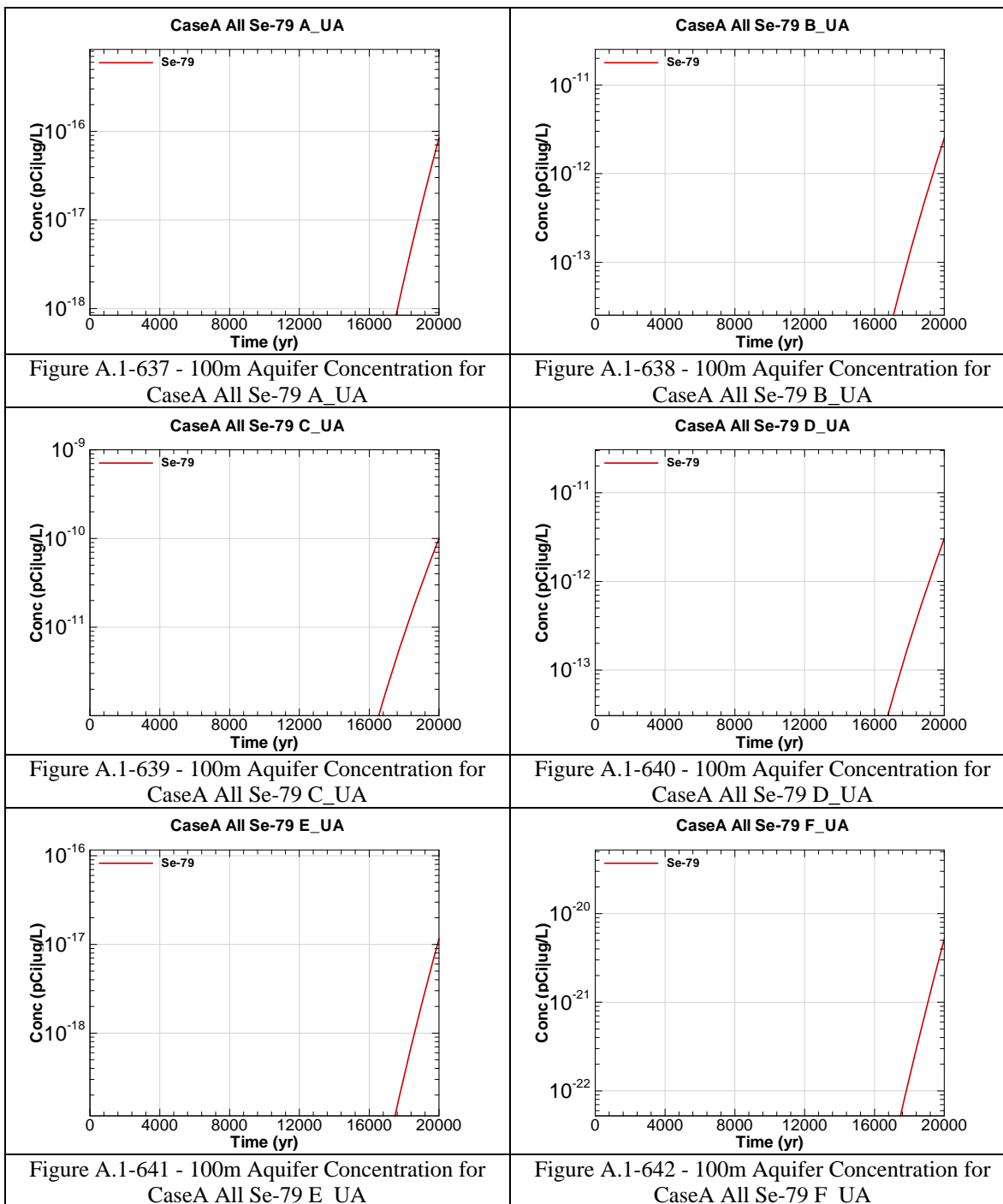


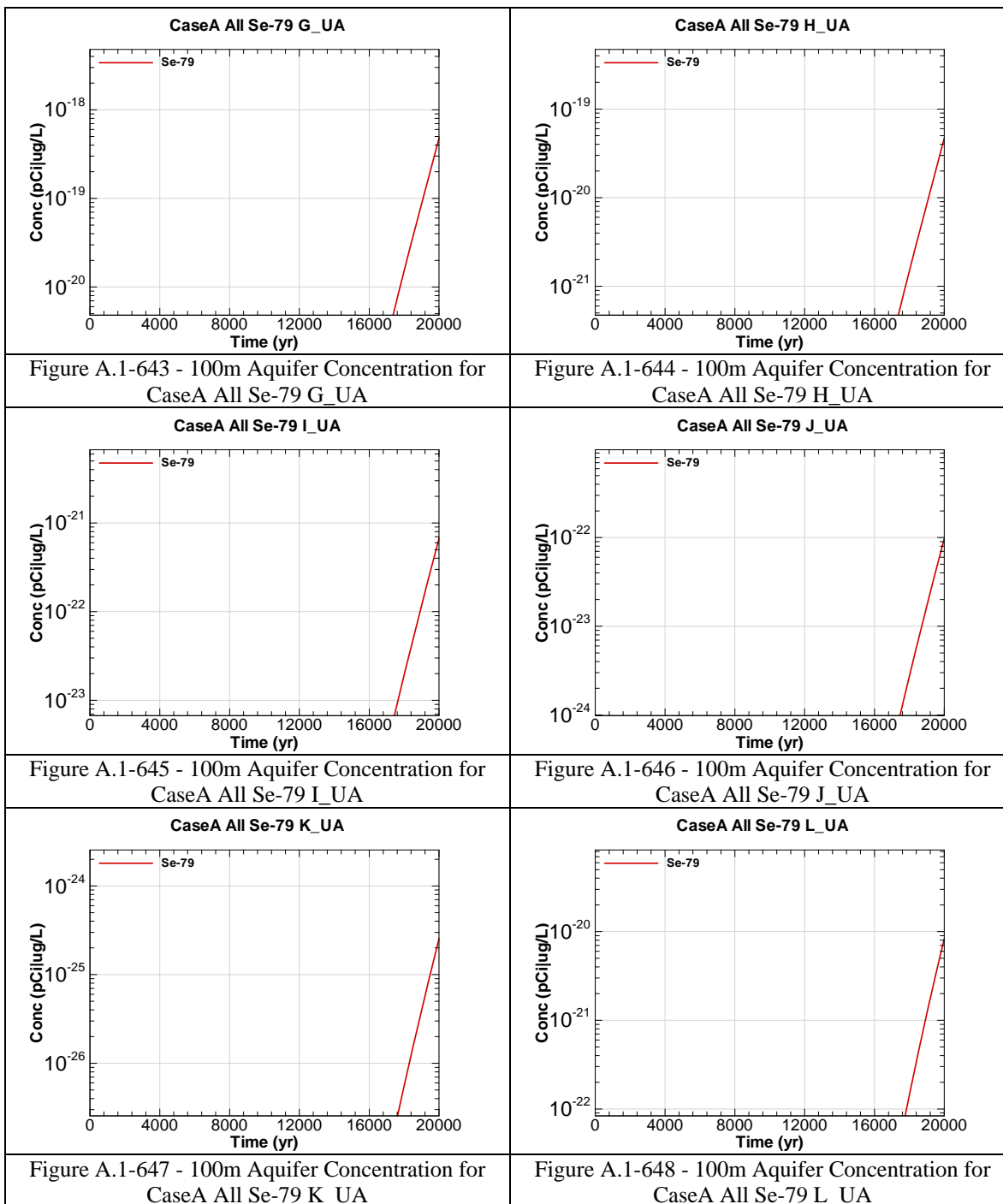


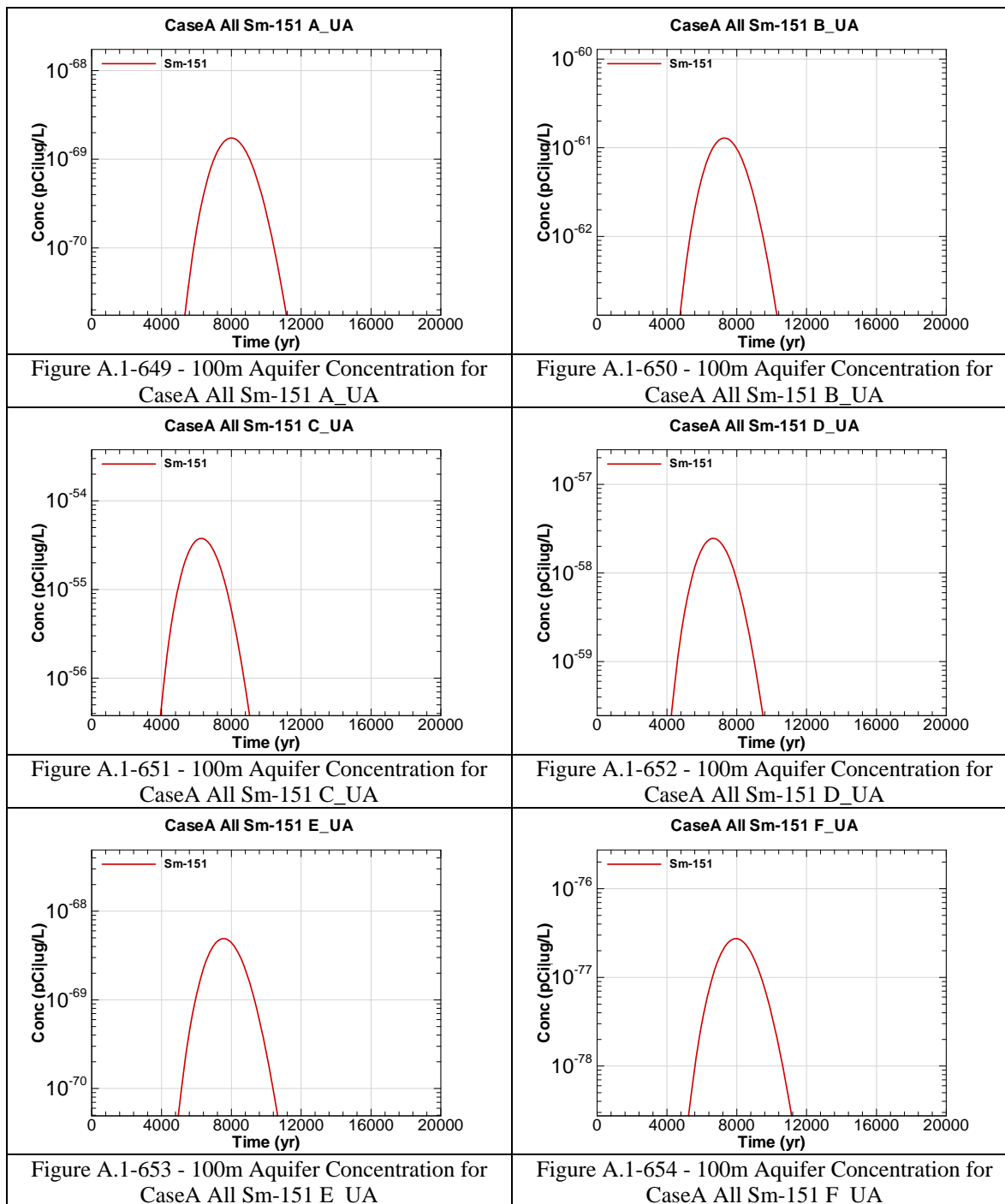


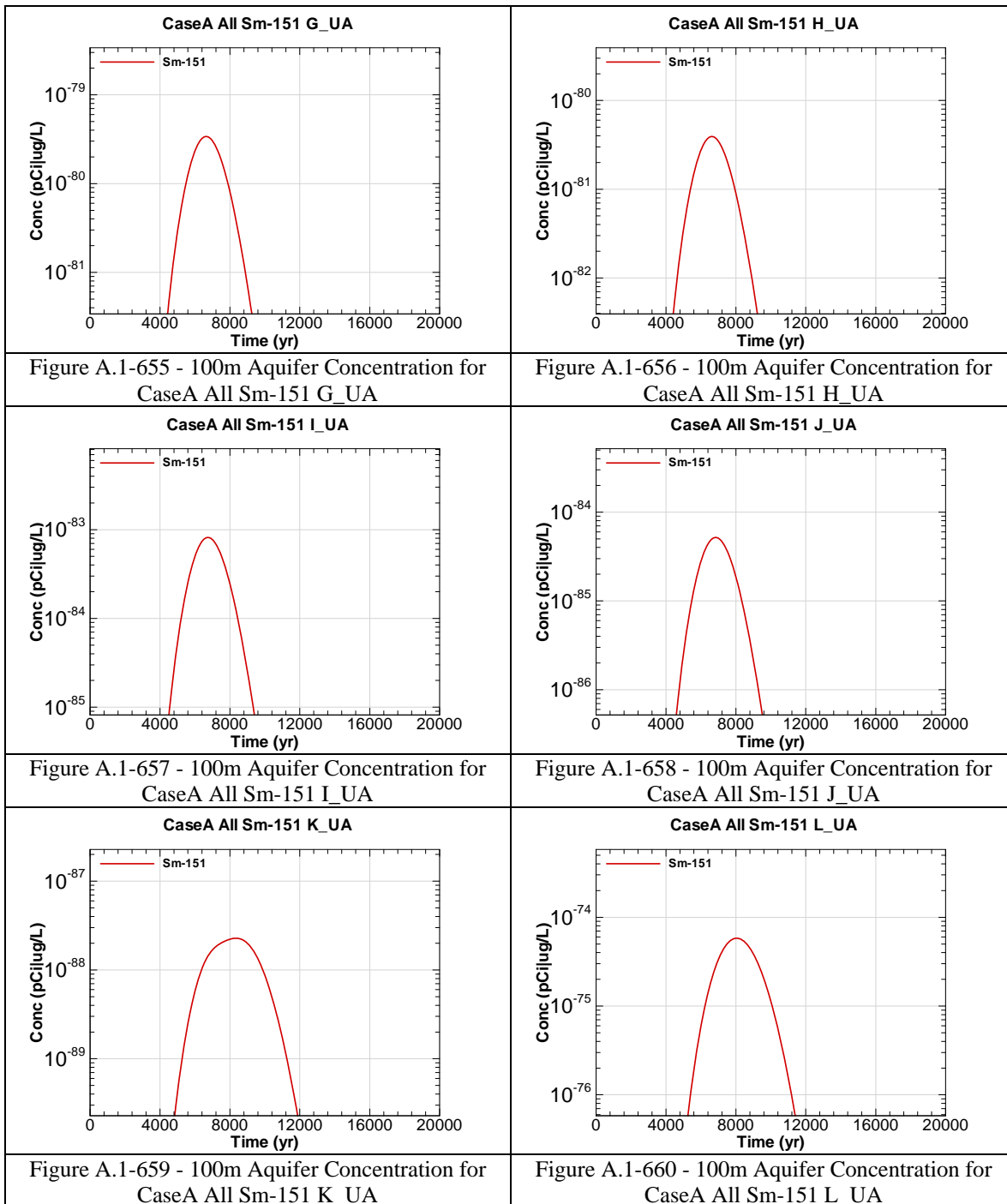


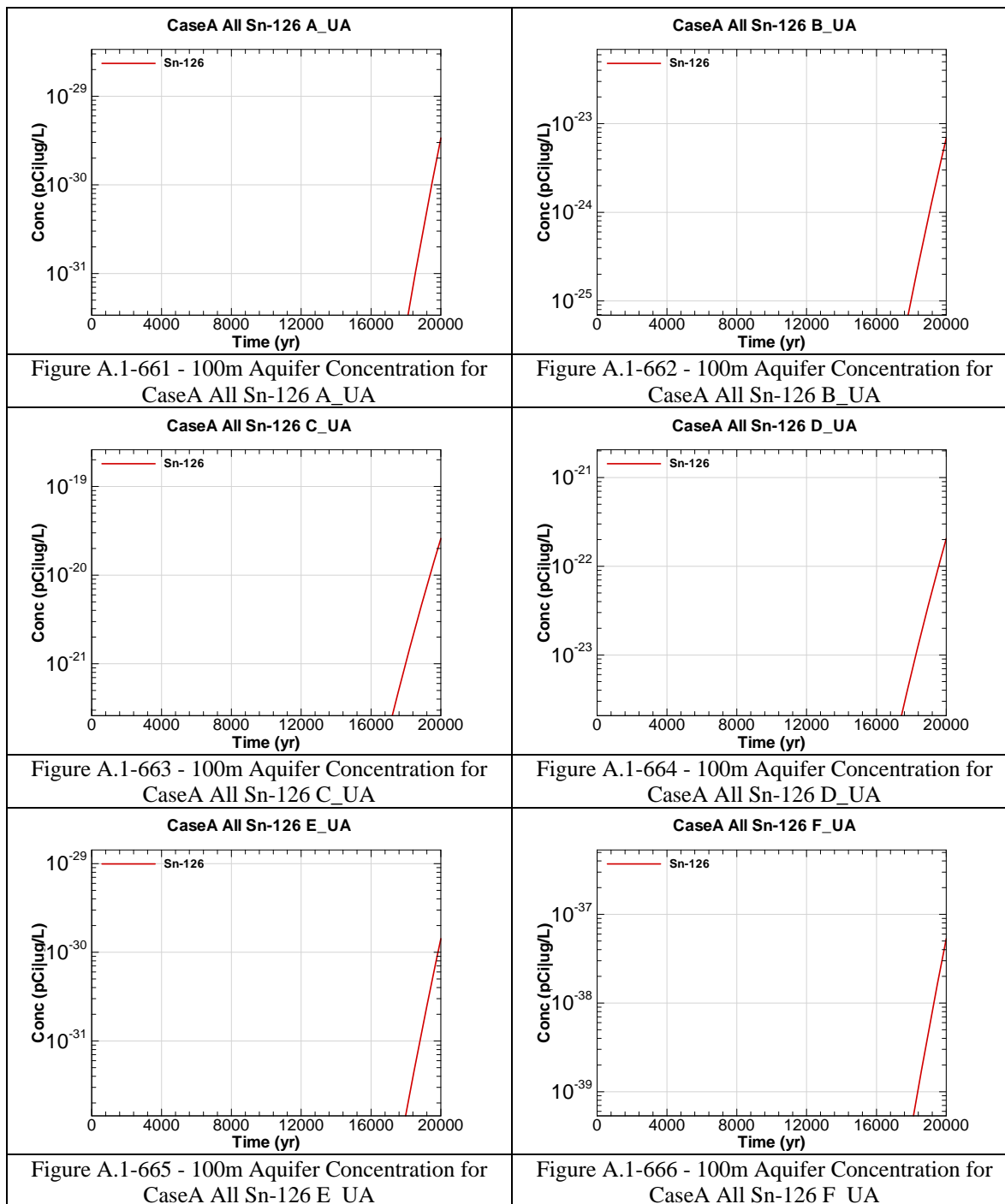


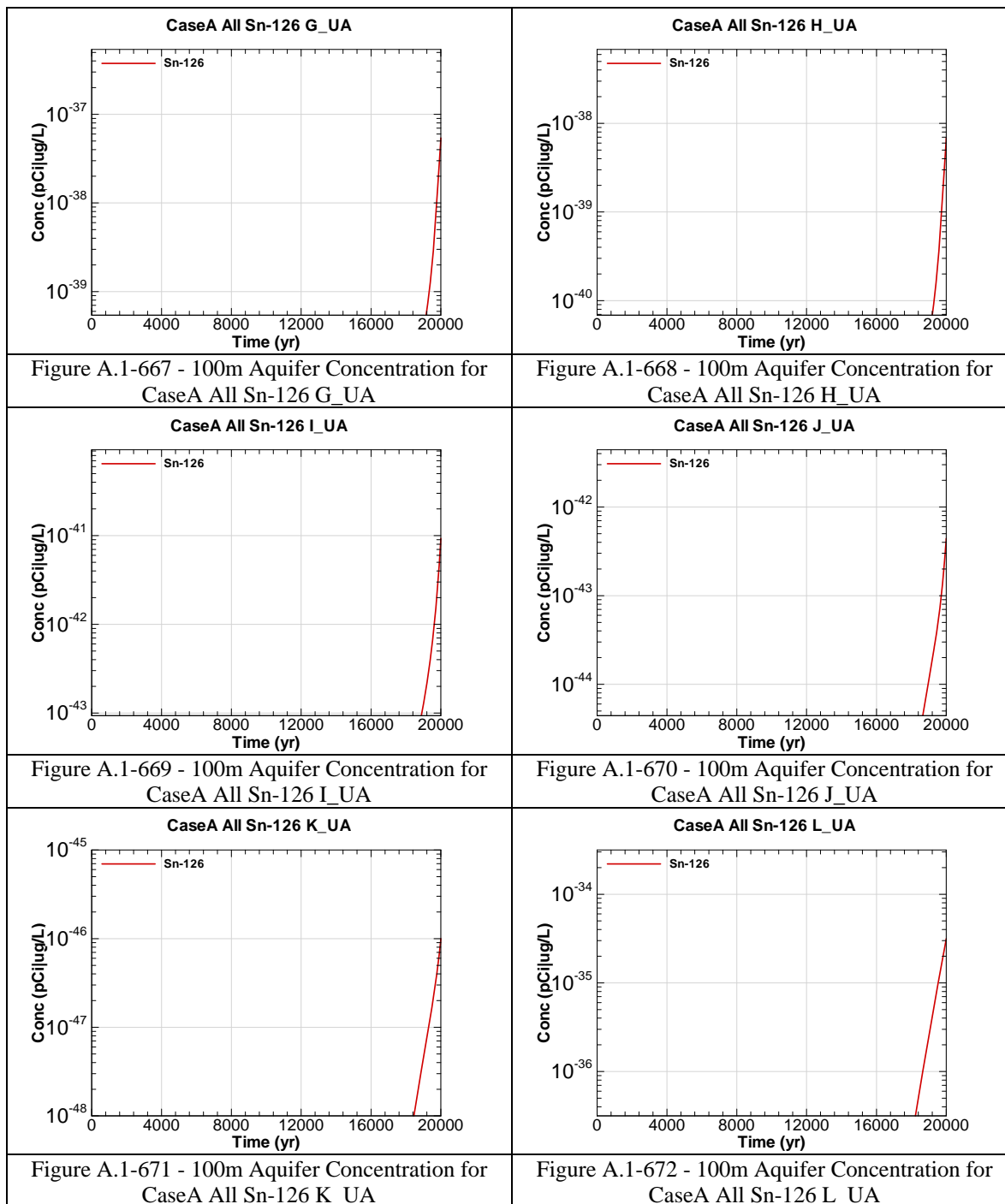


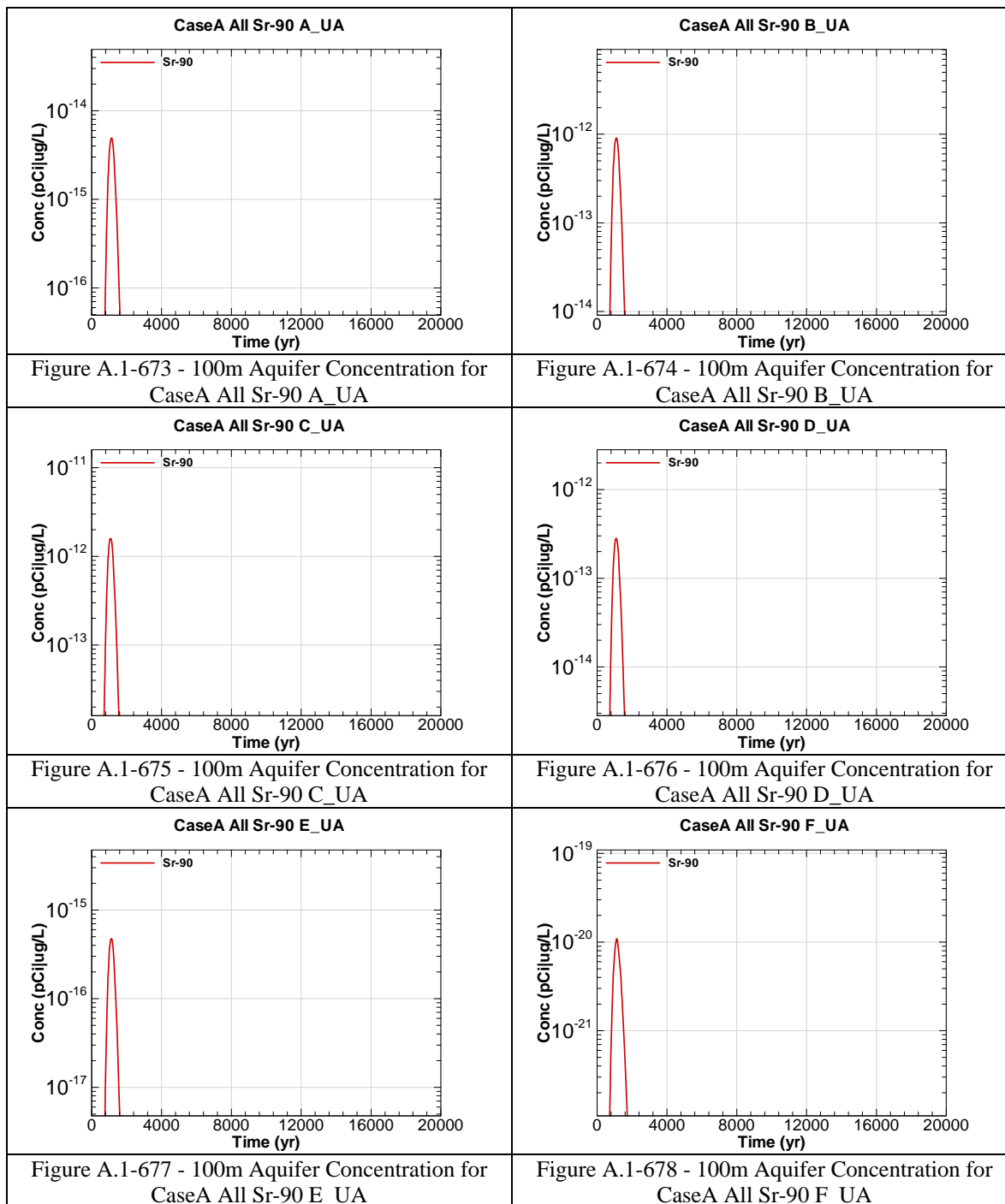


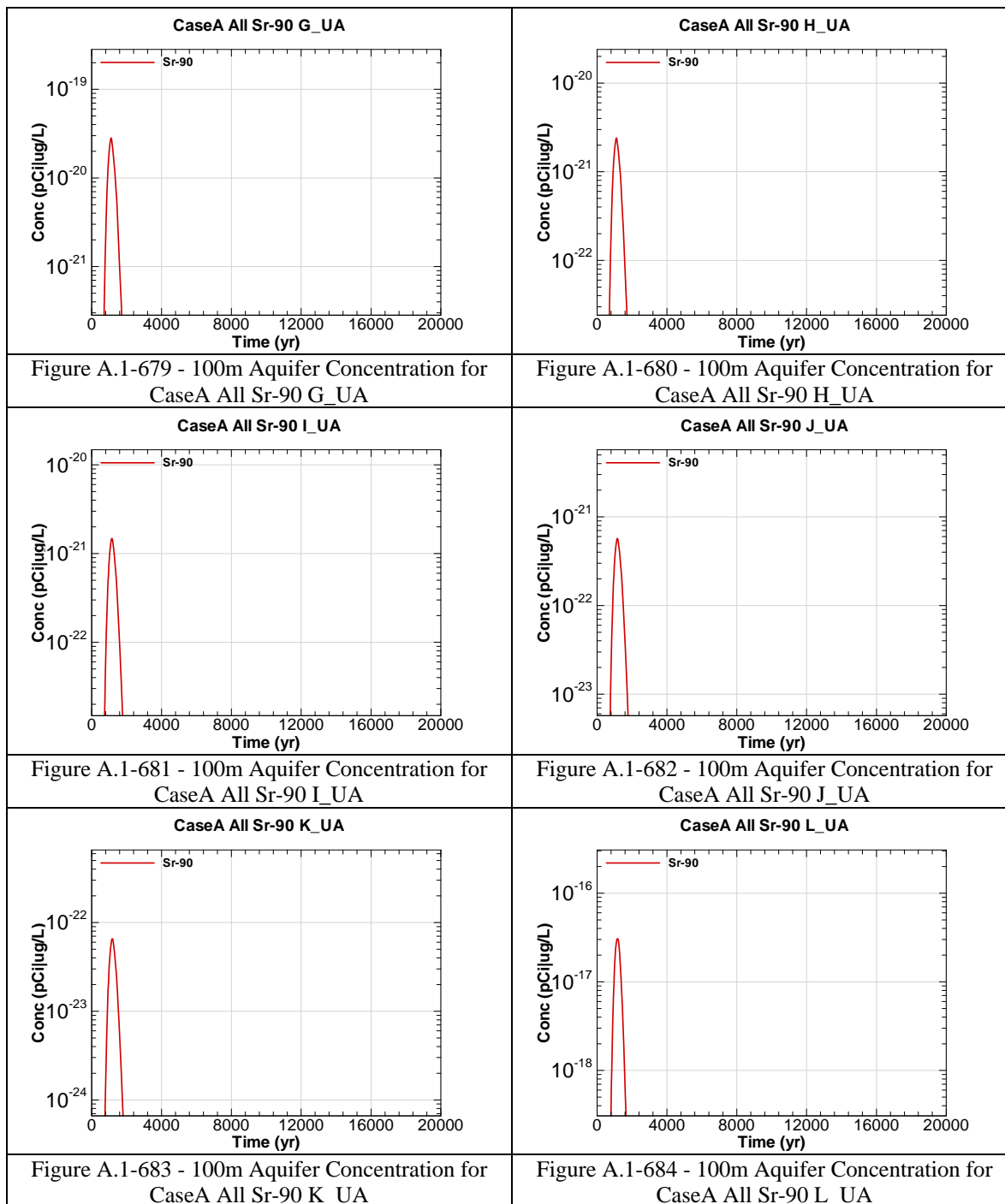


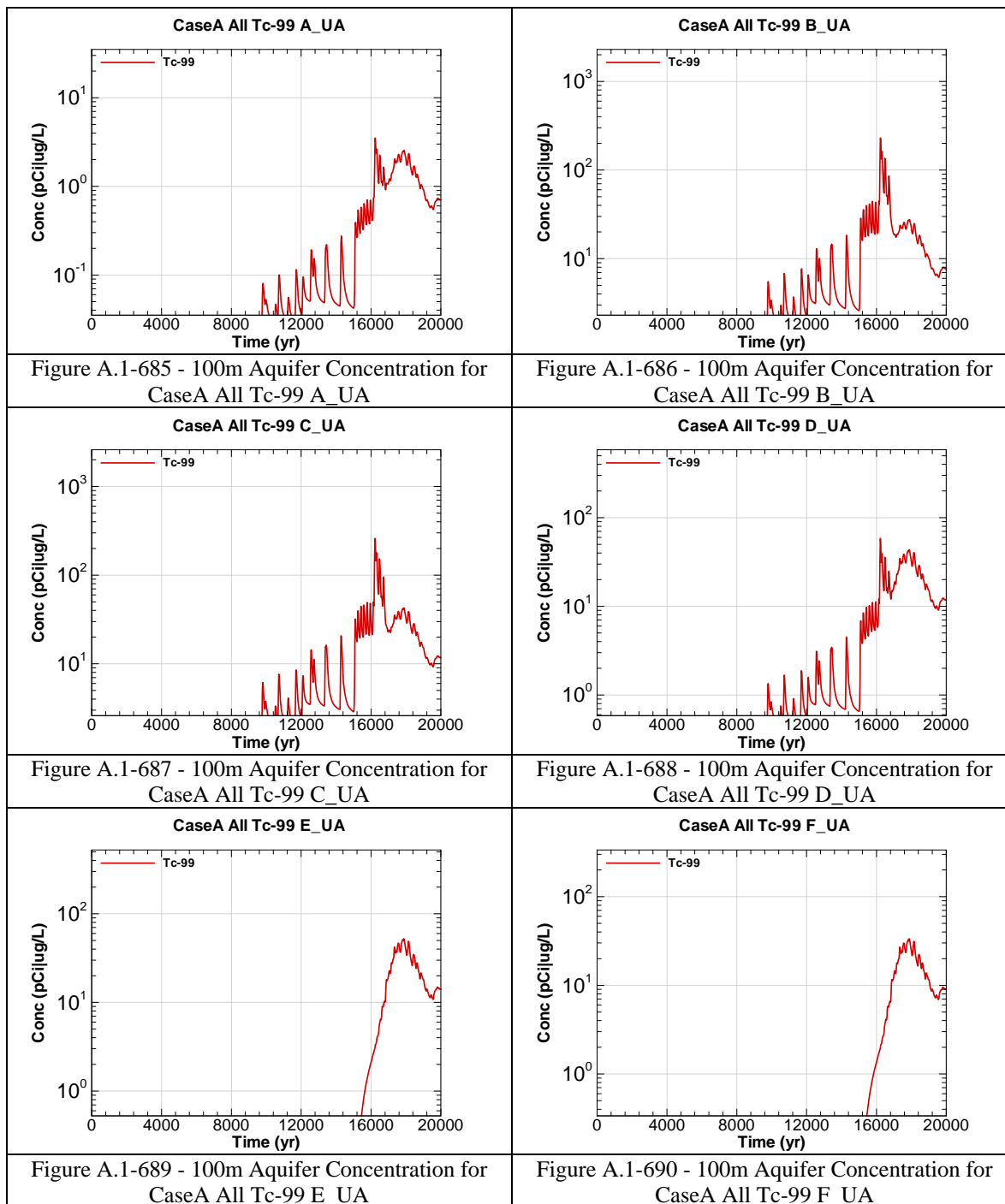


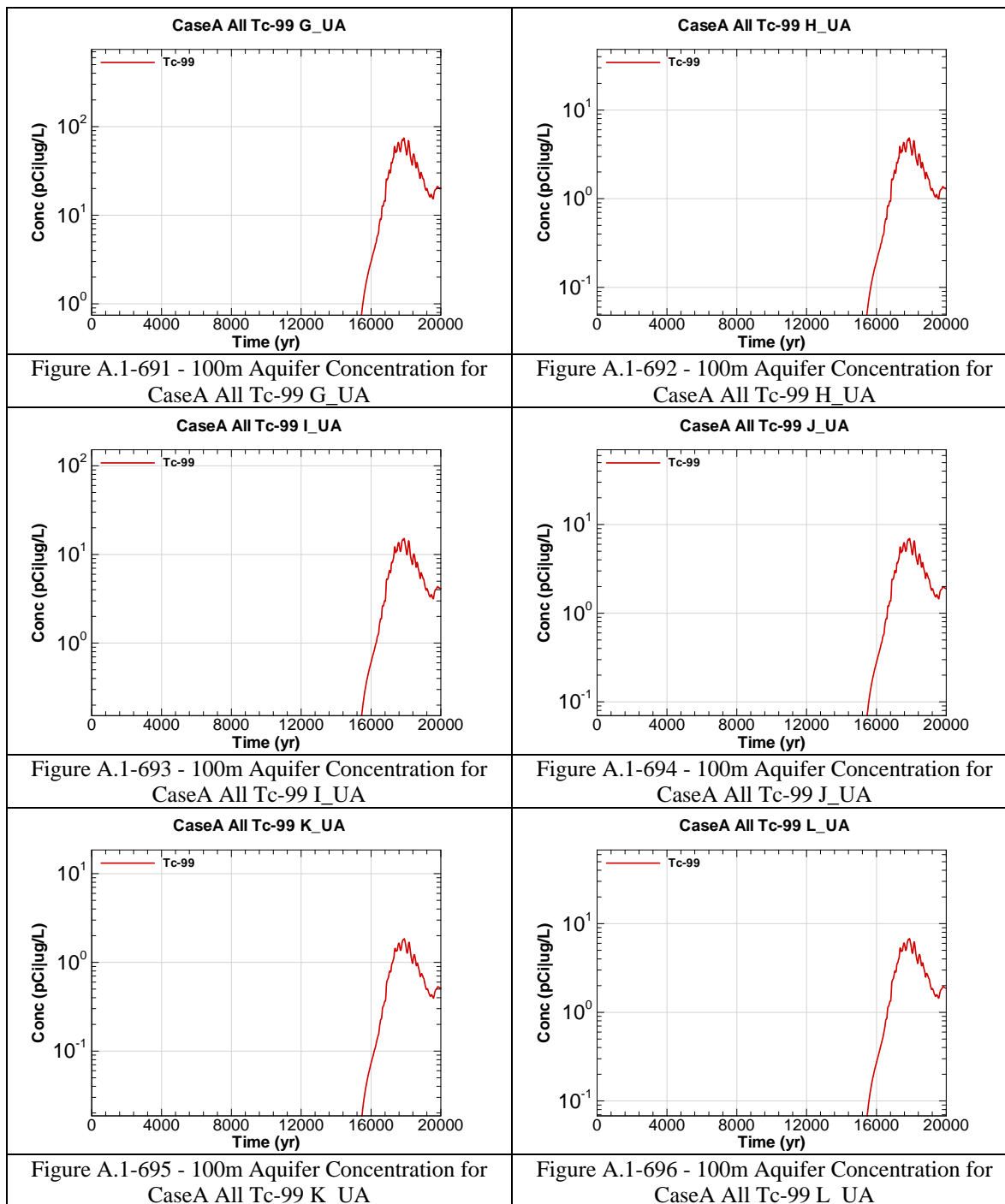


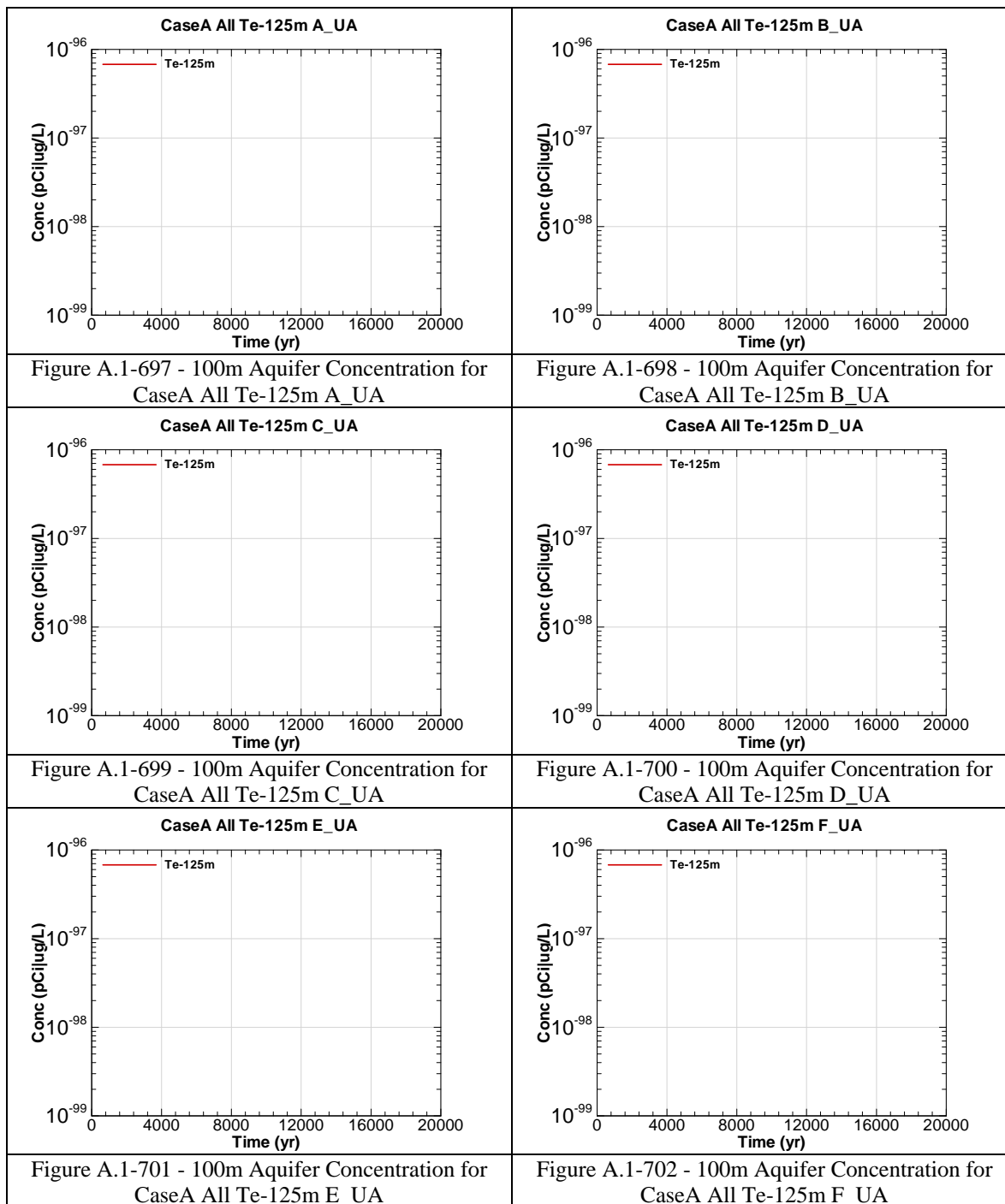


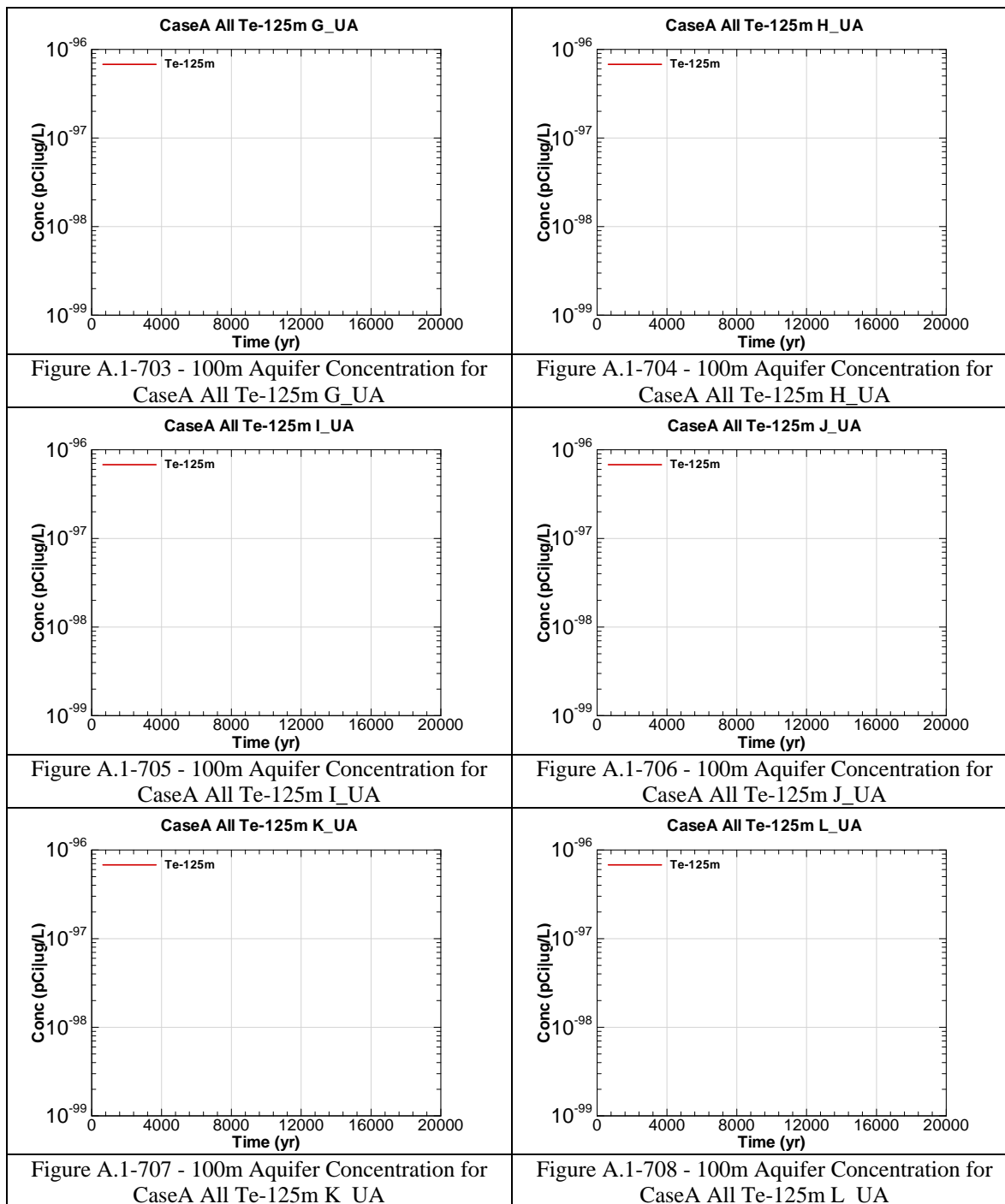


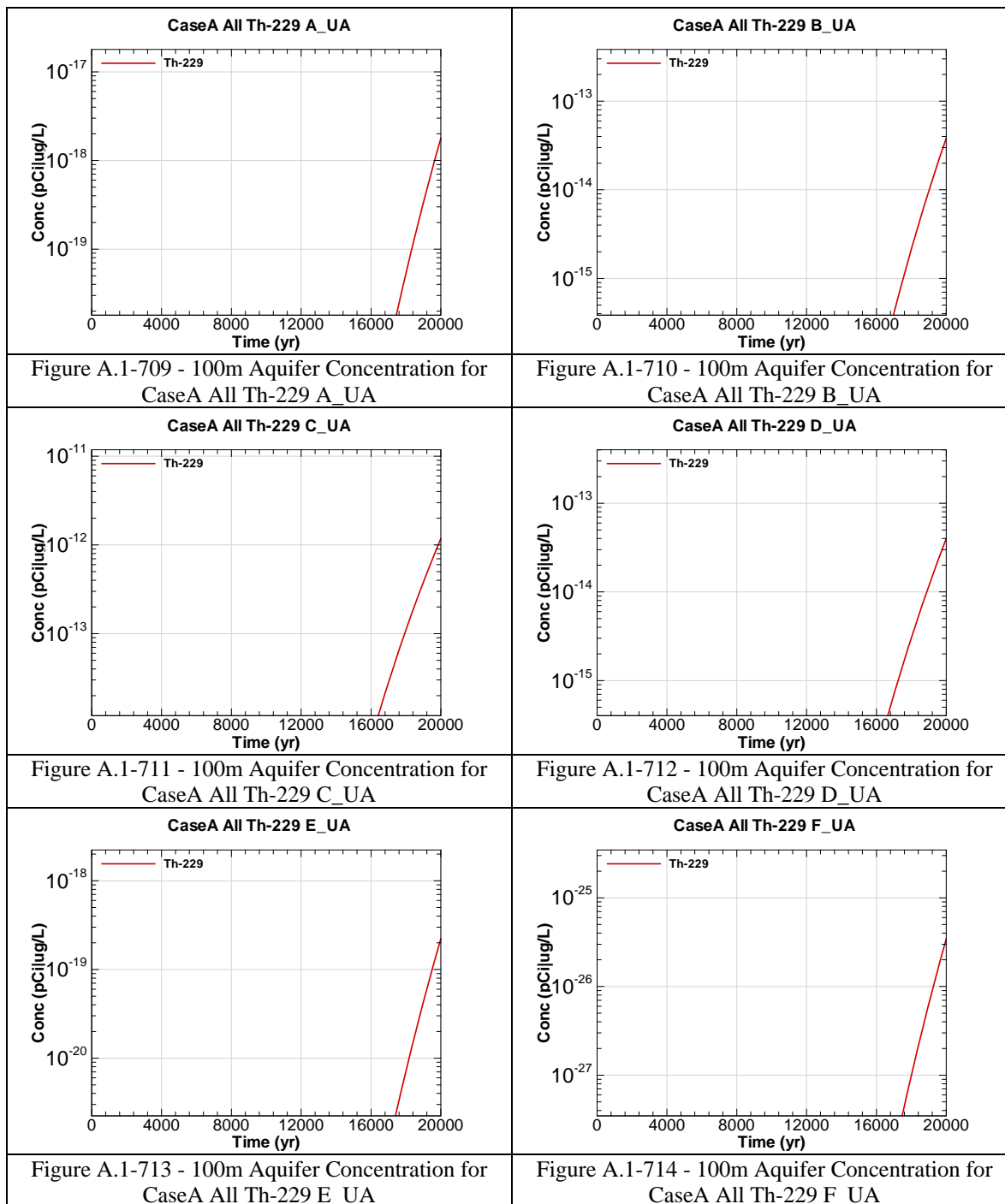


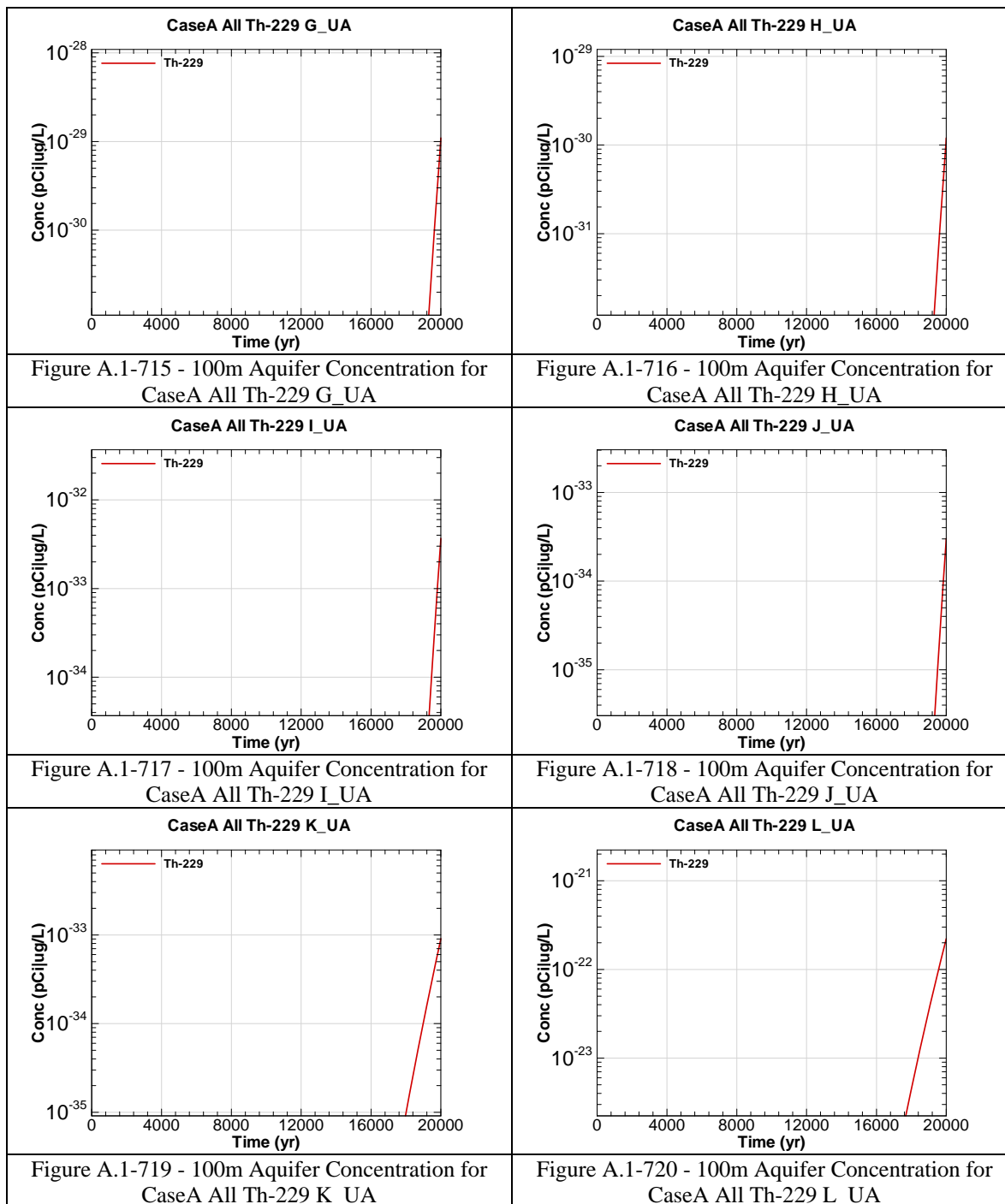


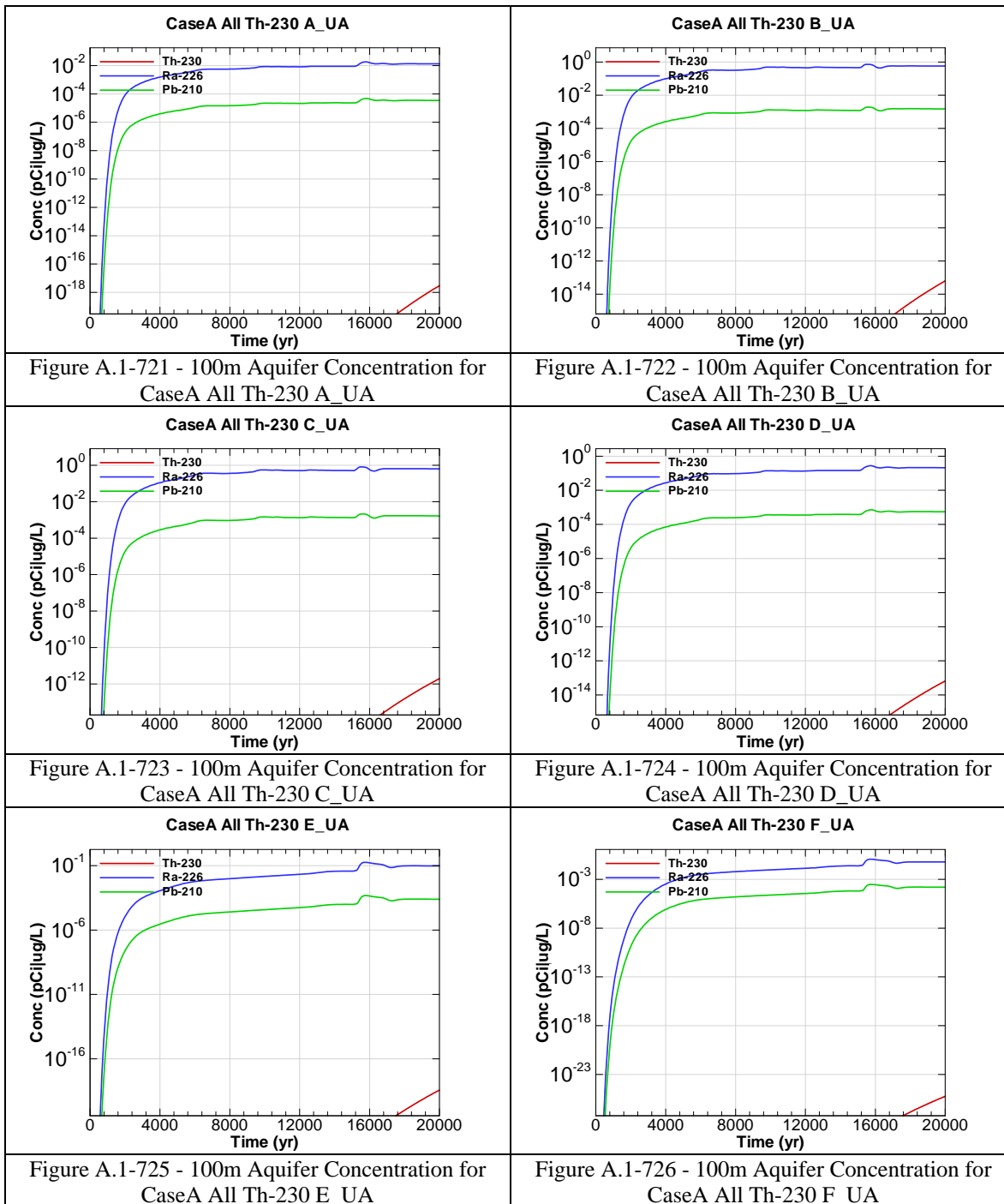












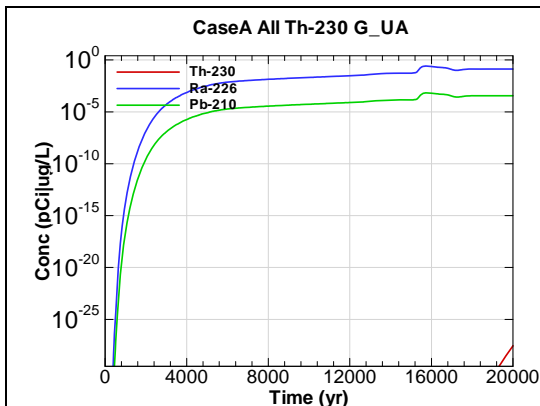


Figure A.1-727 - 100m Aquifer Concentration for
CaseA All Th-230 G-UA

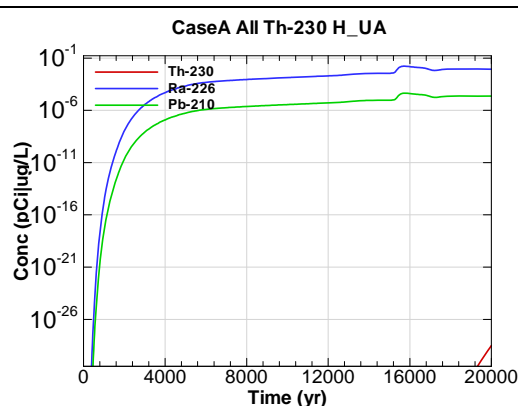


Figure A.1-728 - 100m Aquifer Concentration for
CaseA All Th-230 H-UA

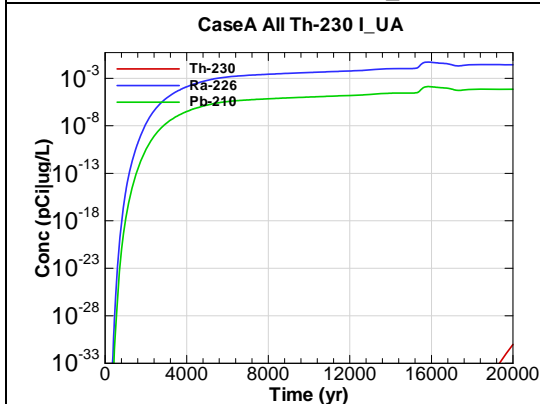


Figure A.1-729 - 100m Aquifer Concentration for
CaseA All Th-230 I-UA

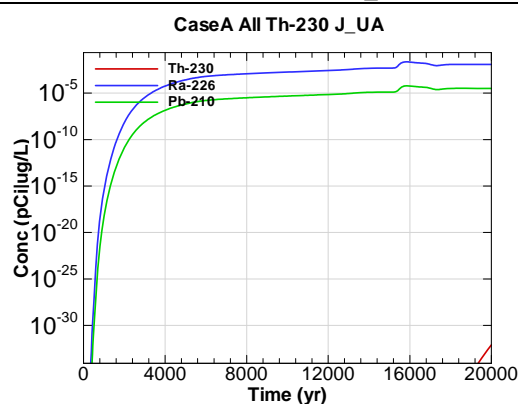


Figure A.1-730 - 100m Aquifer Concentration for
CaseA All Th-230 J-UA

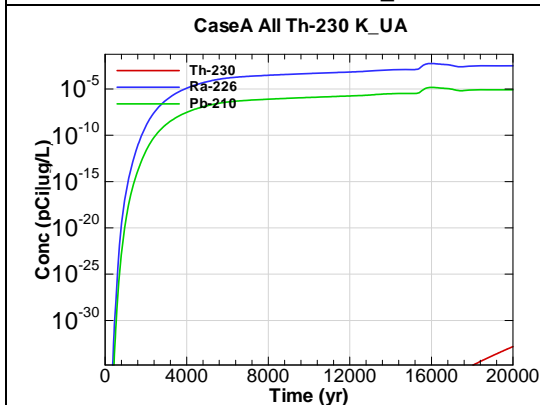


Figure A.1-731 - 100m Aquifer Concentration for
CaseA All Th-230 K-UA

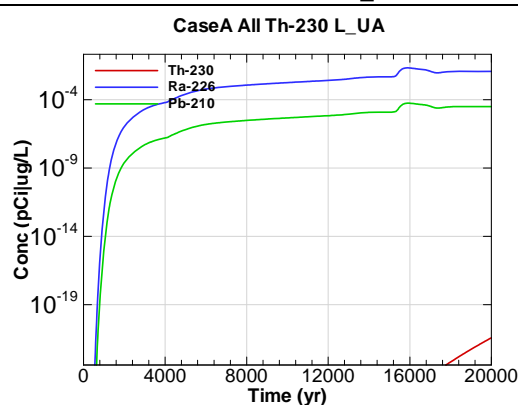


Figure A.1-732 - 100m Aquifer Concentration for
CaseA All Th-230 L-UA

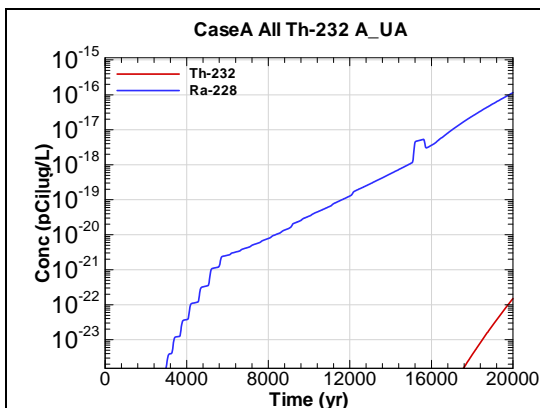


Figure A.1-733 - 100m Aquifer Concentration for CaseA All Th-232 A-UA

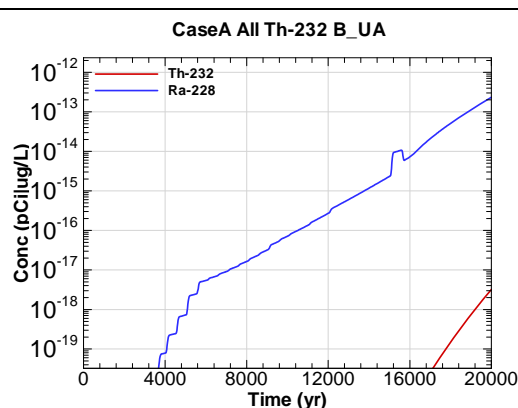


Figure A.1-734 - 100m Aquifer Concentration for CaseA All Th-232 B-UA

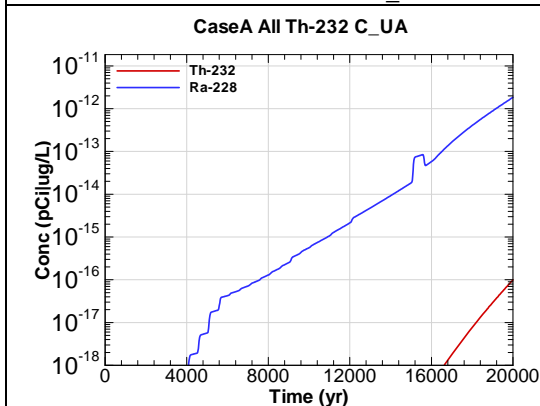


Figure A.1-735 - 100m Aquifer Concentration for CaseA All Th-232 C-UA

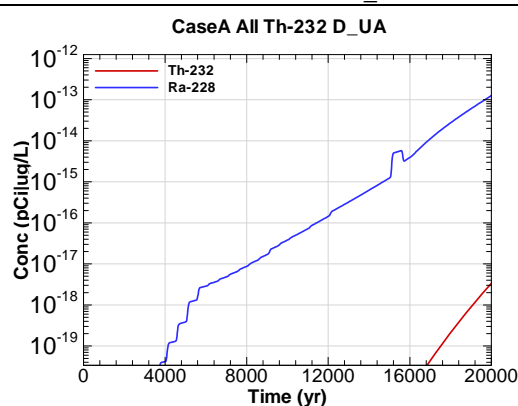


Figure A.1-736 - 100m Aquifer Concentration for CaseA All Th-232 D-UA

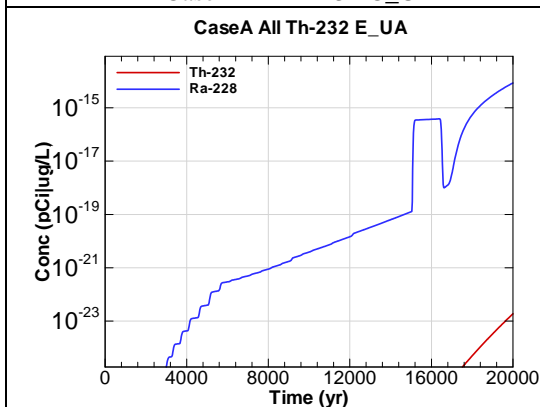


Figure A.1-737 - 100m Aquifer Concentration for CaseA All Th-232 E-UA

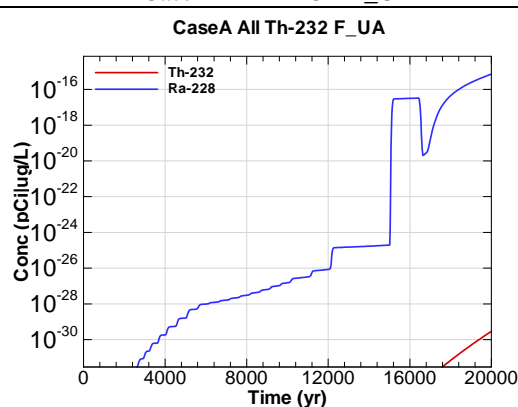
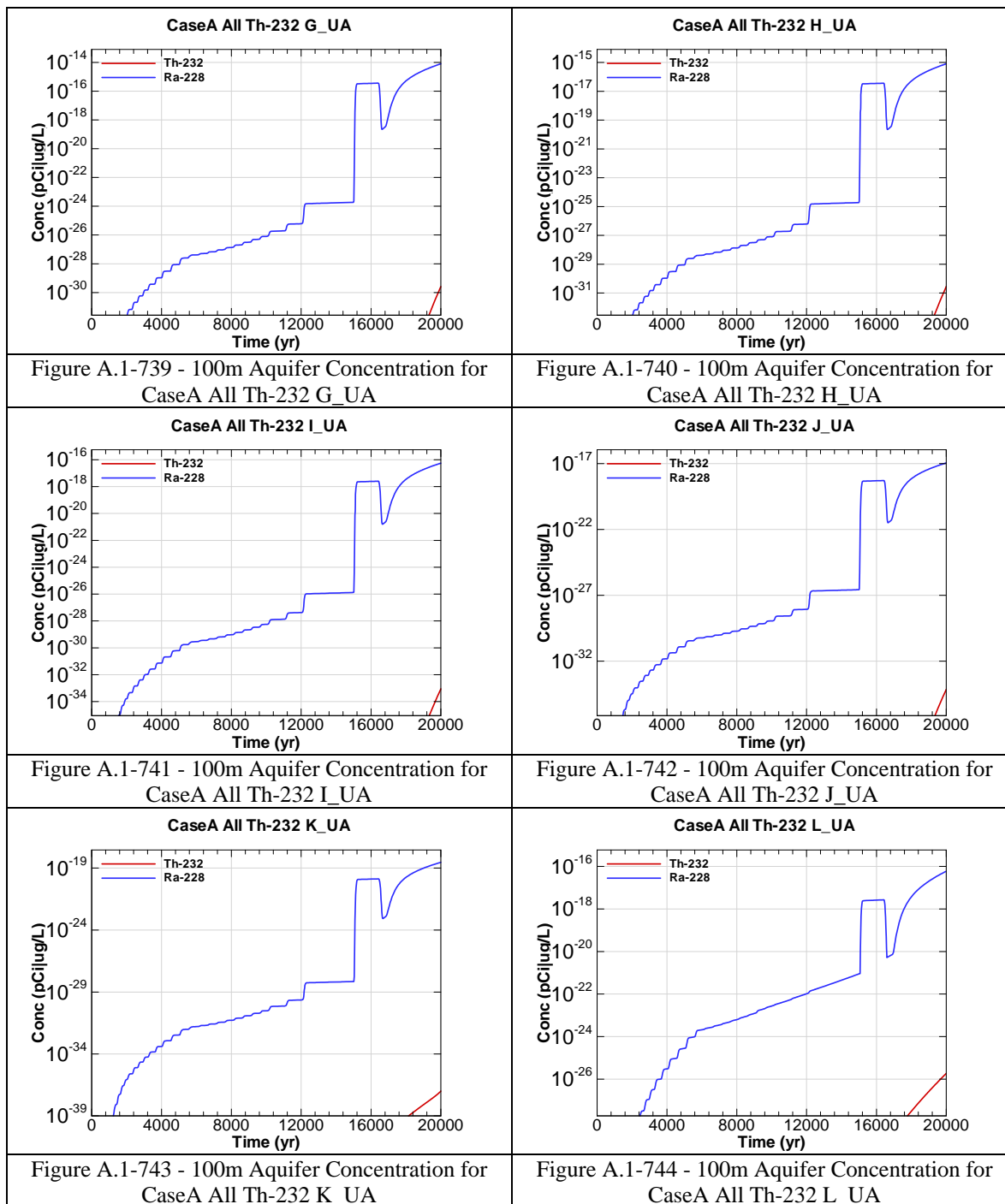
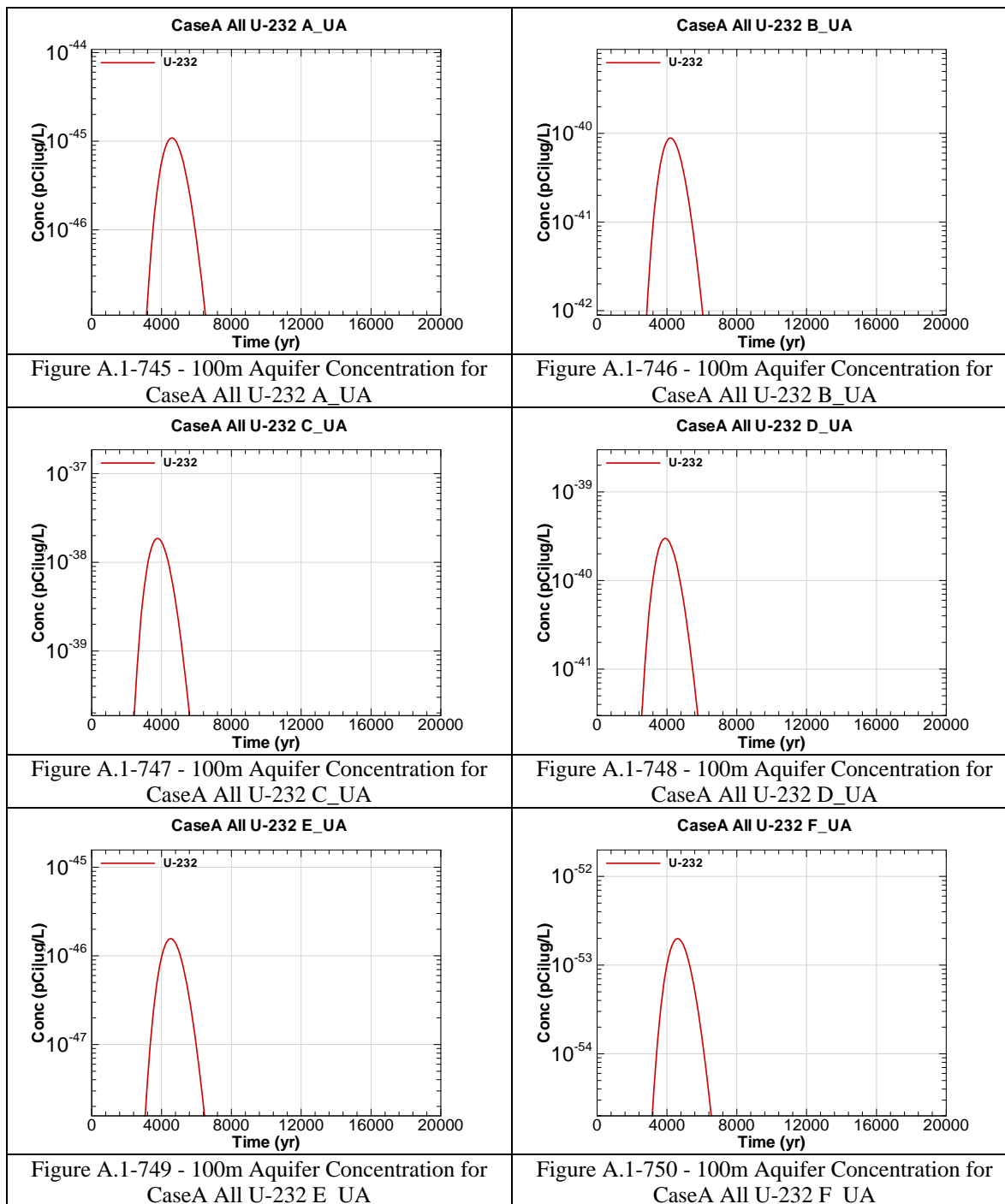
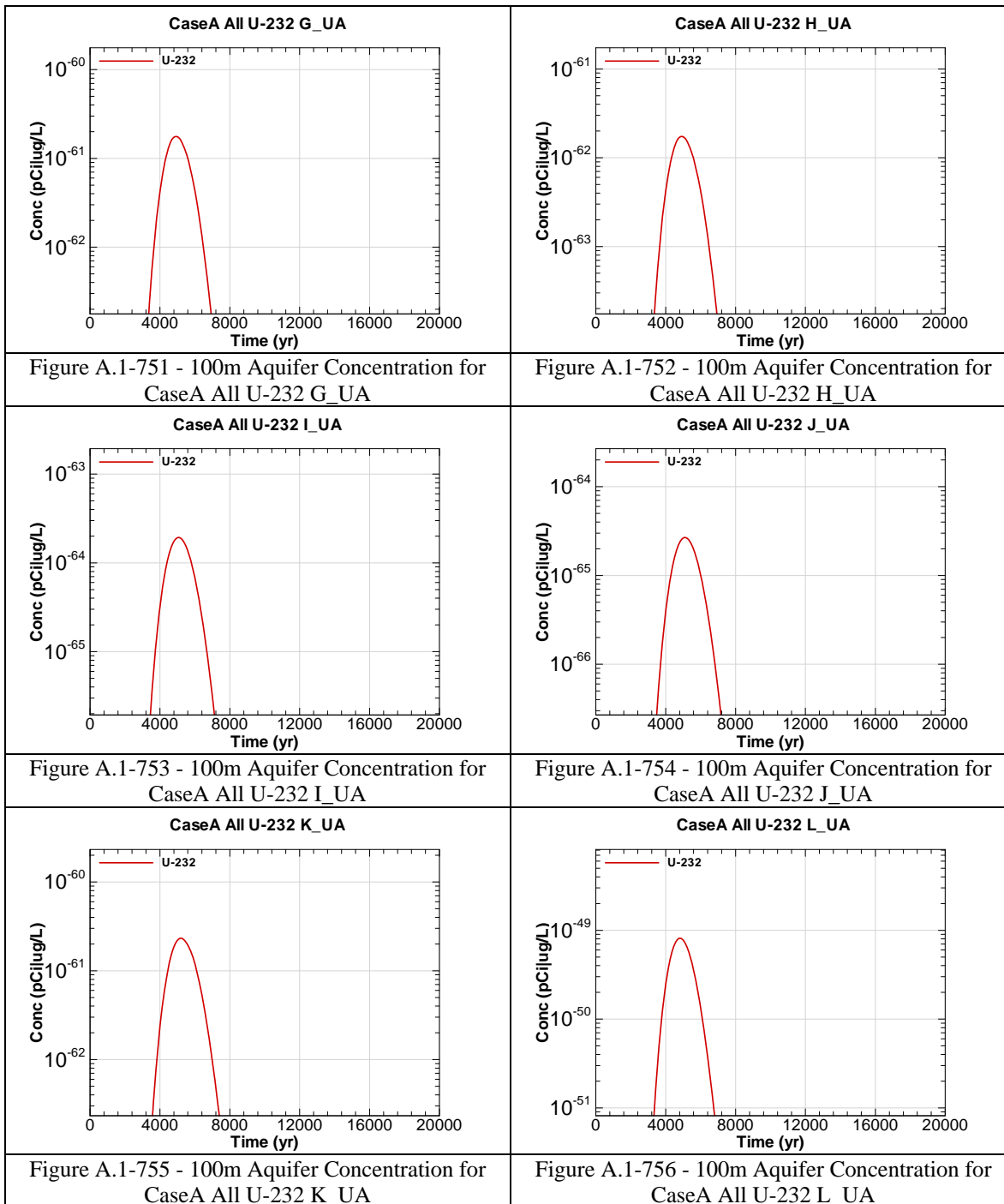
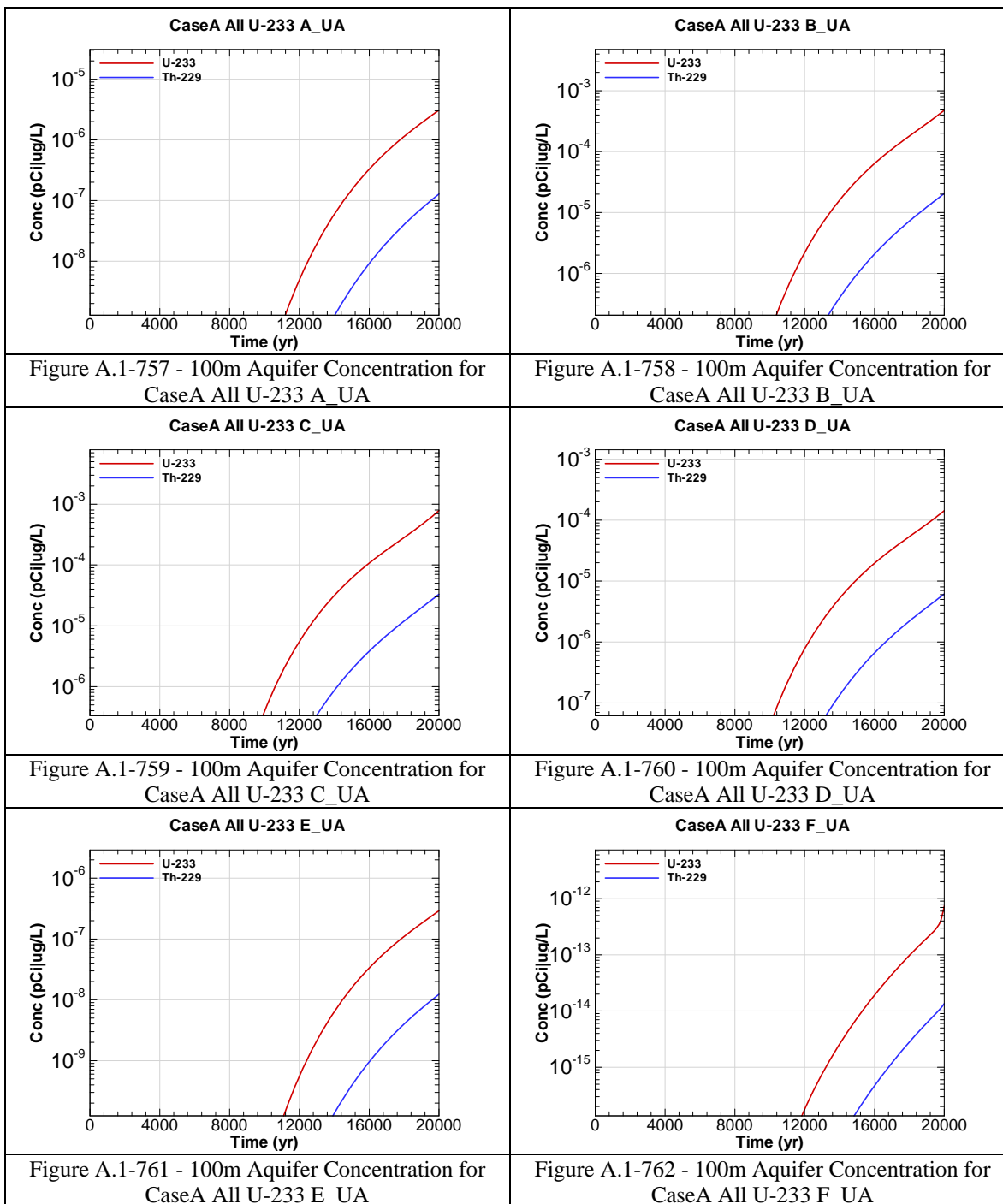


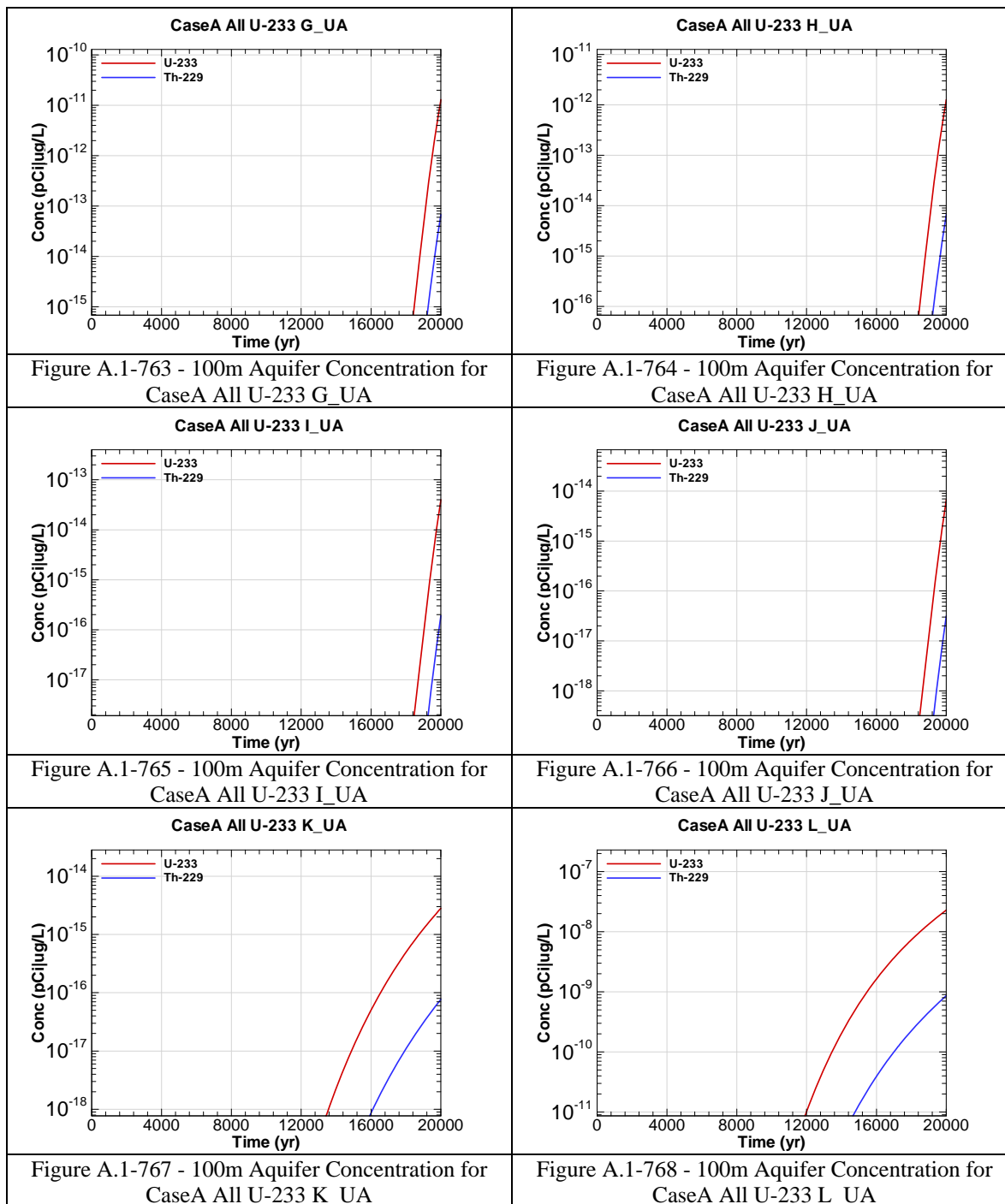
Figure A.1-738 - 100m Aquifer Concentration for CaseA All Th-232 F-UA











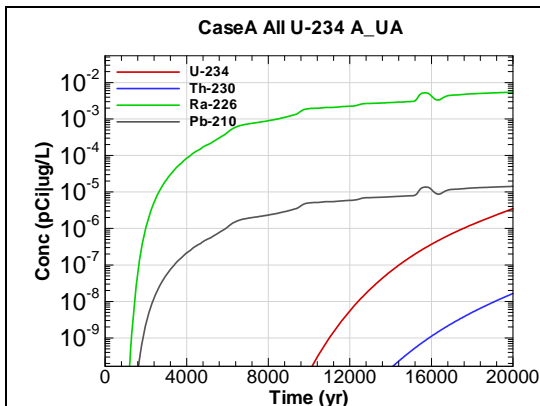


Figure A.1-769 - 100m Aquifer Concentration for
CaseA All U-234 A_UA

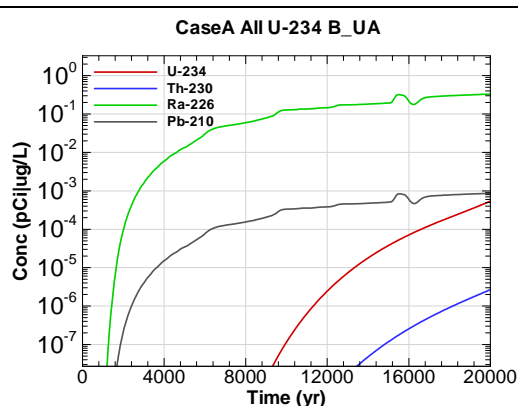


Figure A.1-770 - 100m Aquifer Concentration for
CaseA All U-234 B_UA

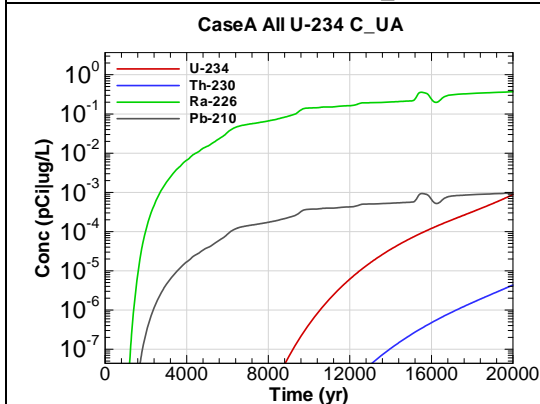


Figure A.1-771 - 100m Aquifer Concentration for
CaseA All U-234 C_UA

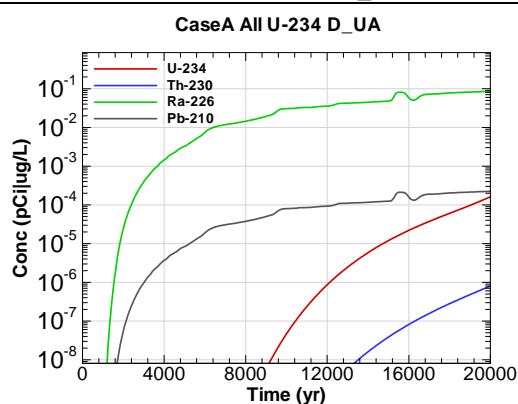


Figure A.1-772 - 100m Aquifer Concentration for
CaseA All U-234 D_UA

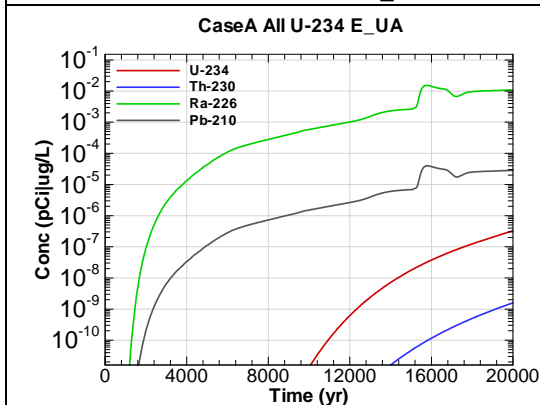


Figure A.1-773 - 100m Aquifer Concentration for
CaseA All U-234 E_UA

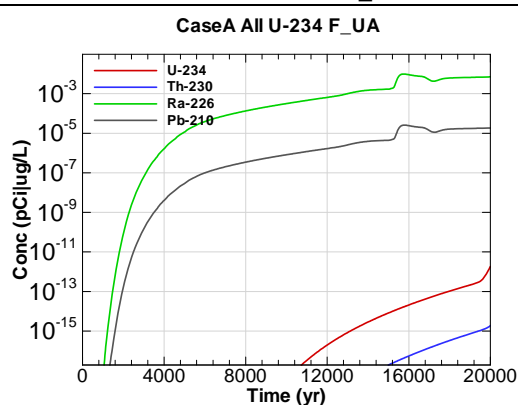
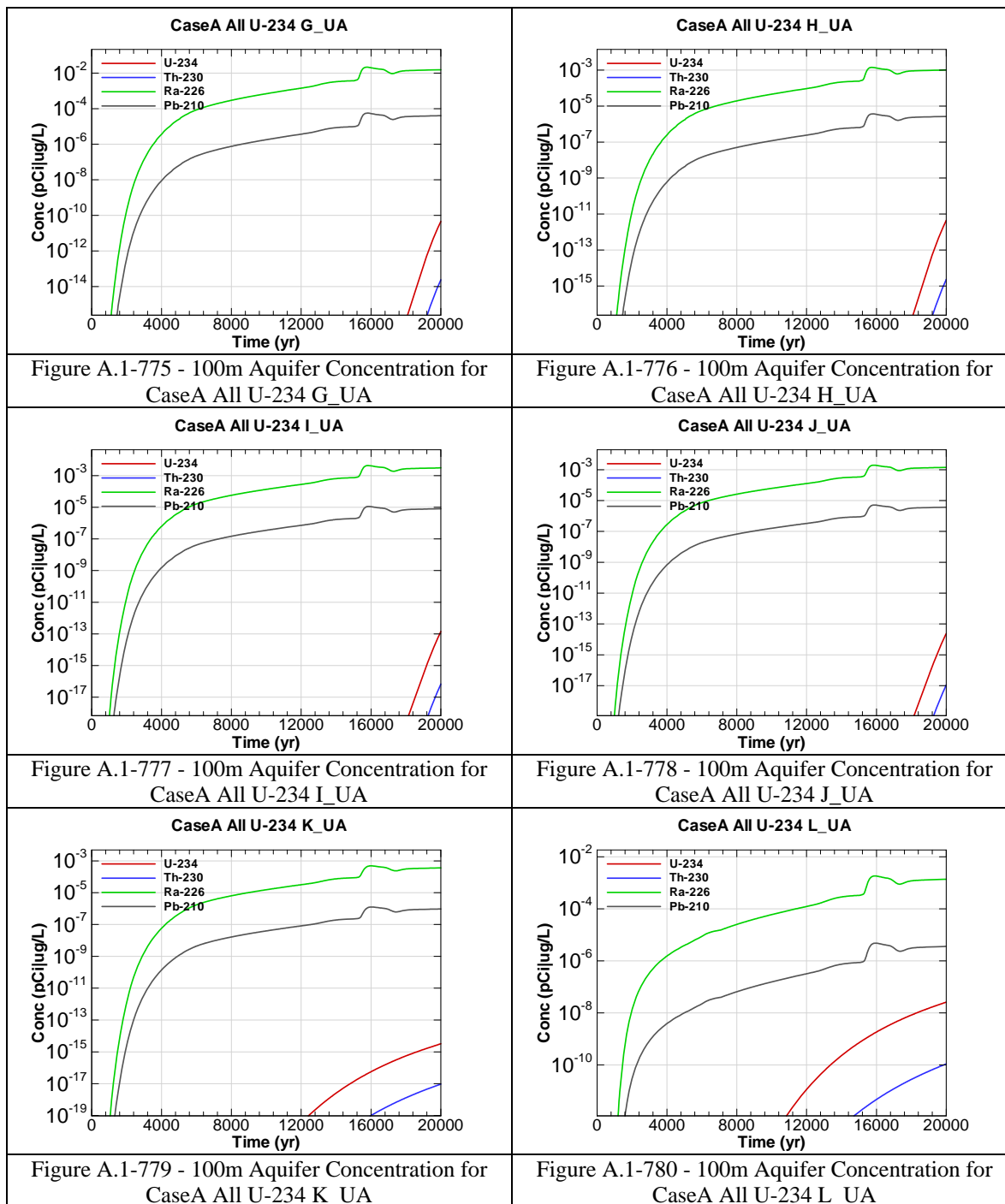
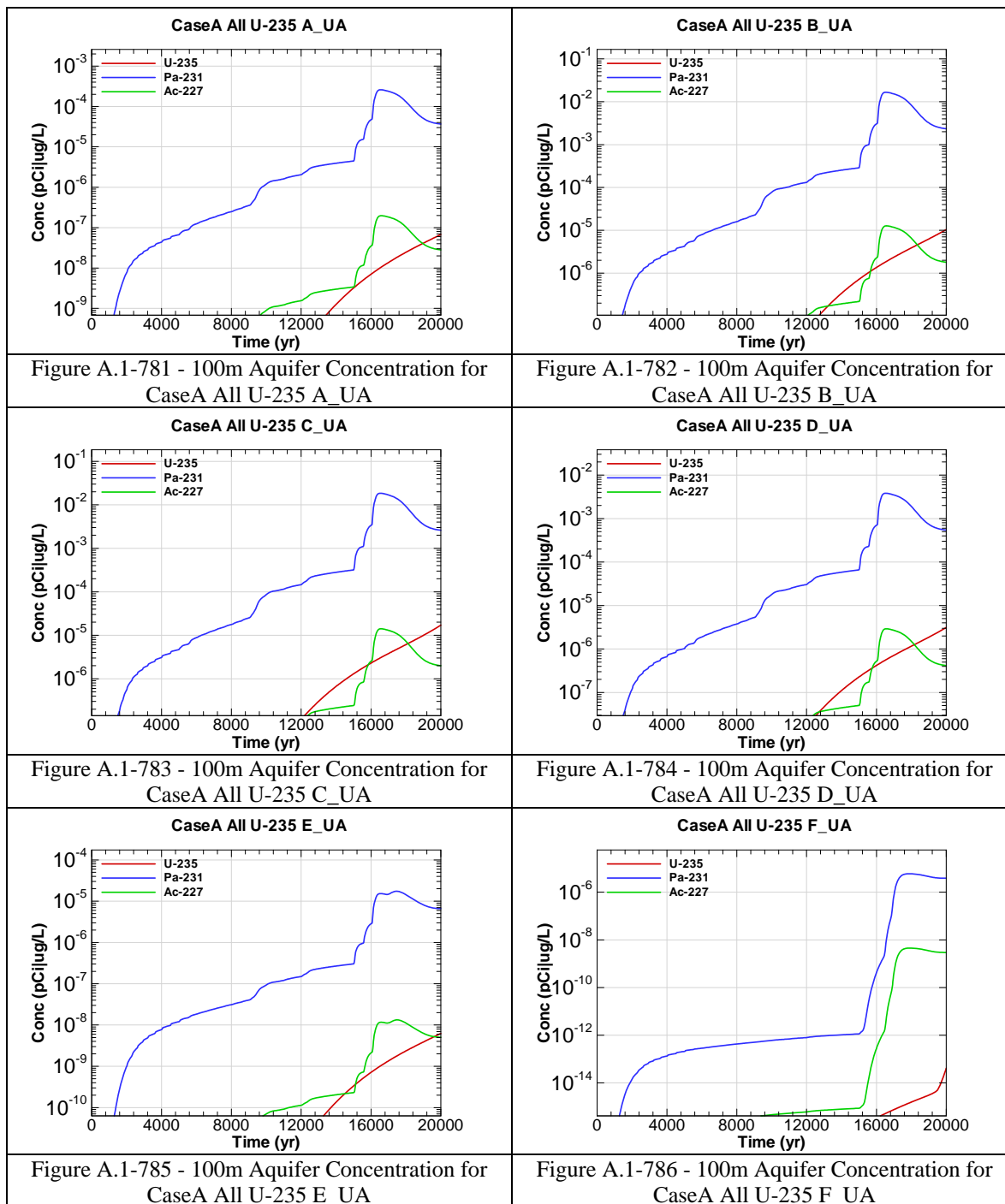
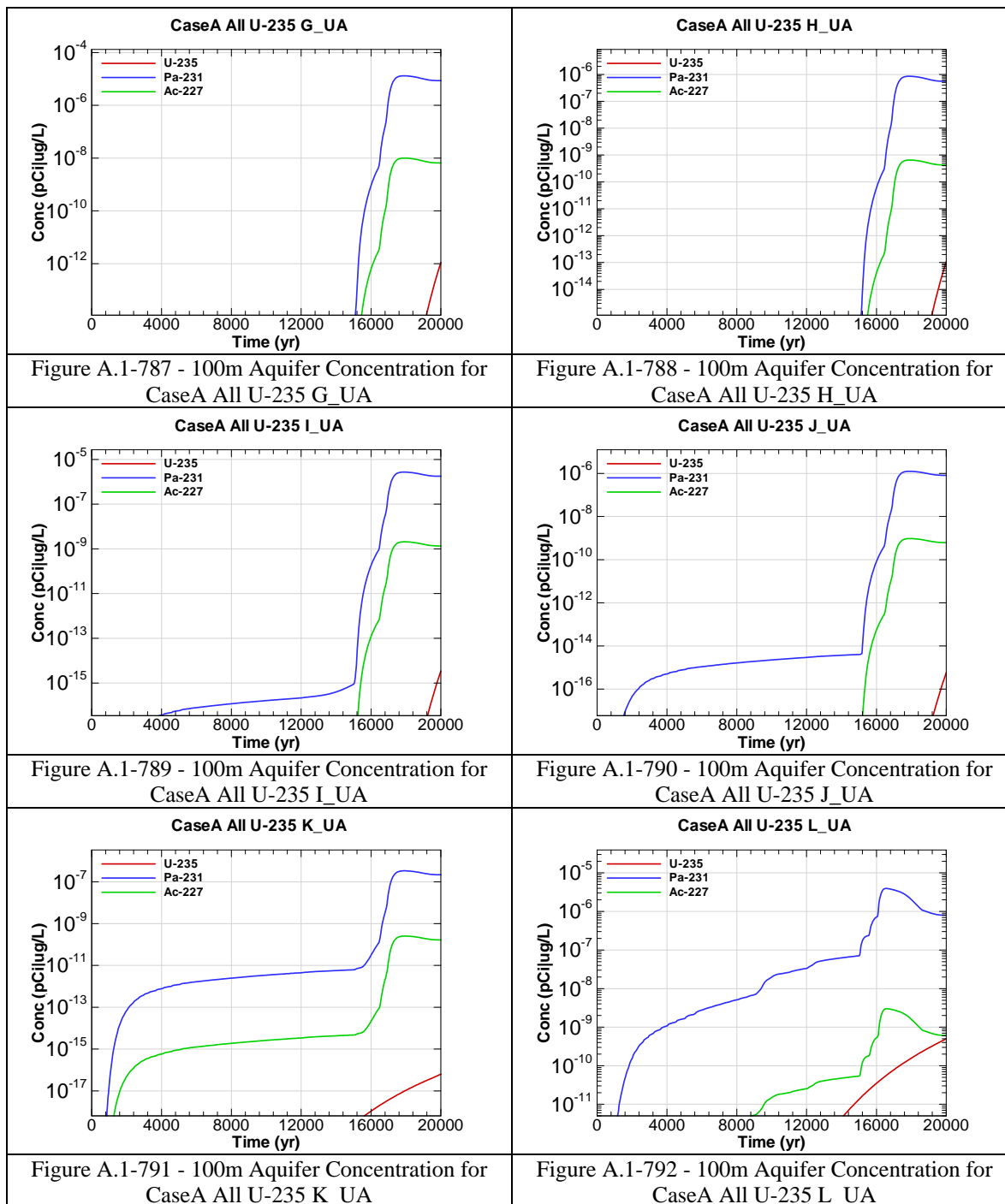
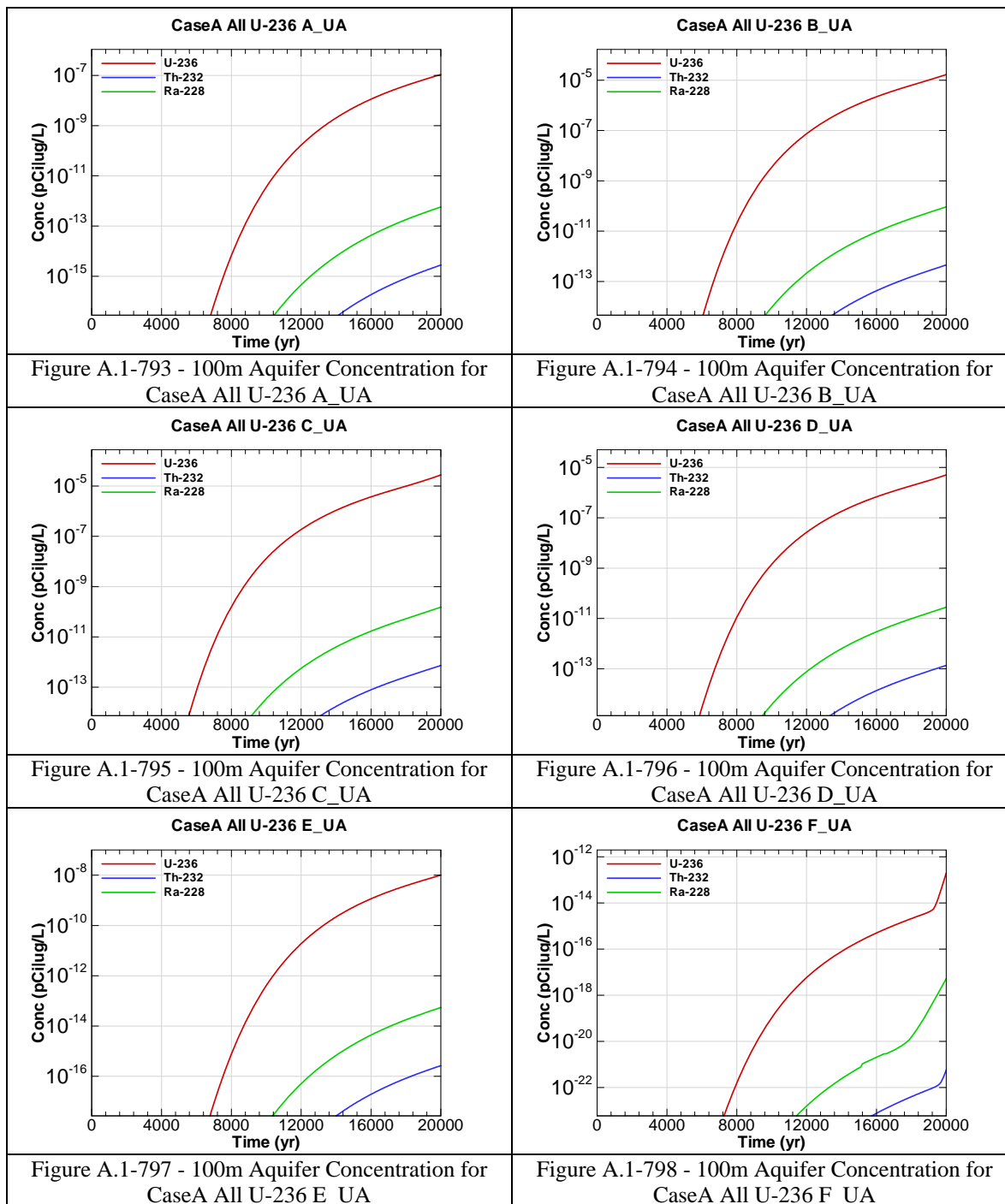


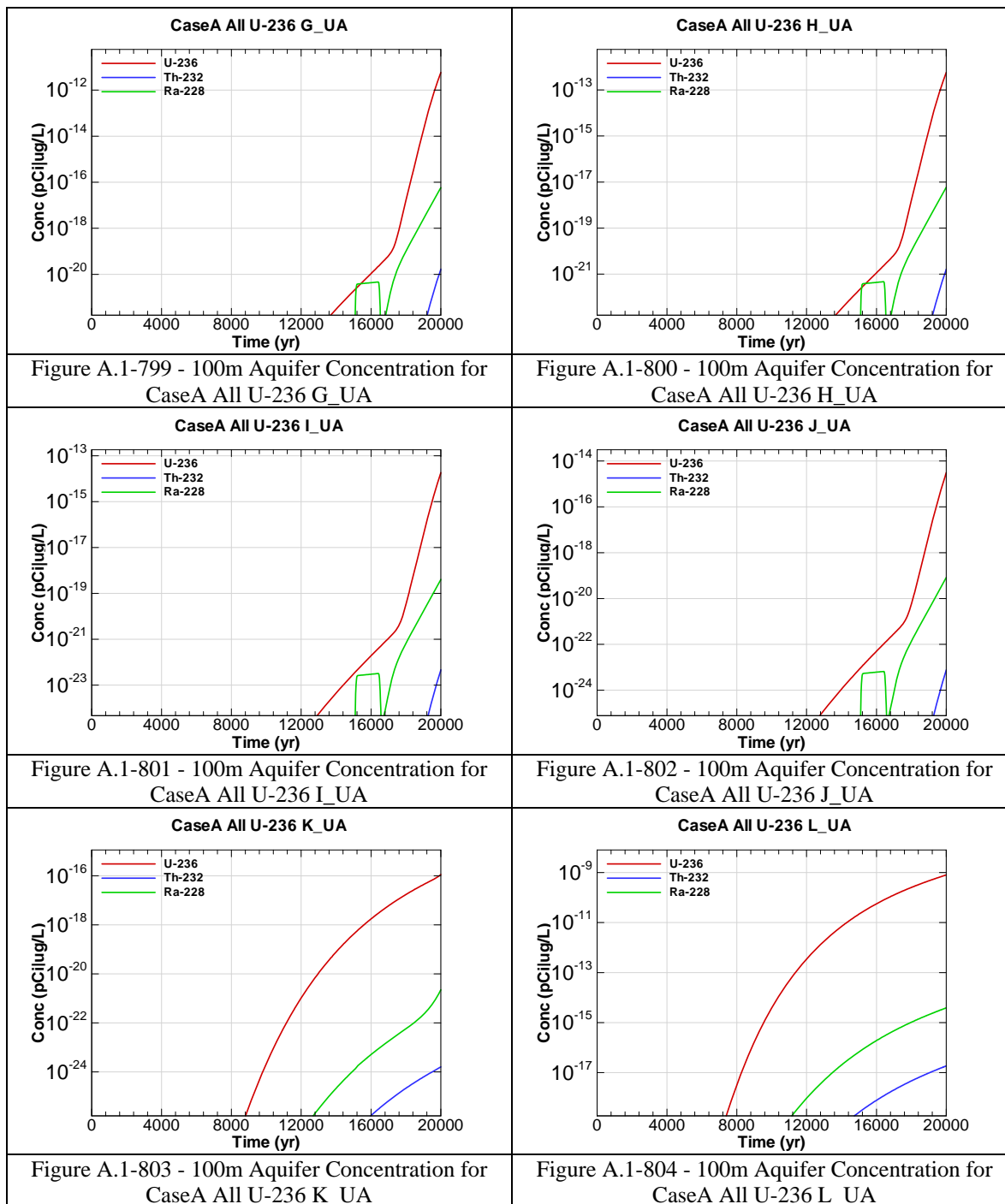
Figure A.1-774 - 100m Aquifer Concentration for
CaseA All U-234 F_UA











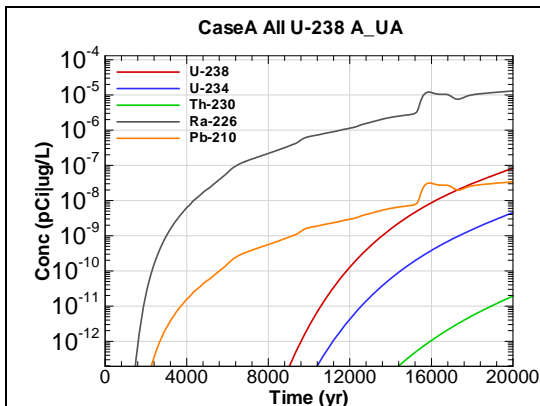


Figure A.1-805 - 100m Aquifer Concentration for
CaseA All U-238 A_UA

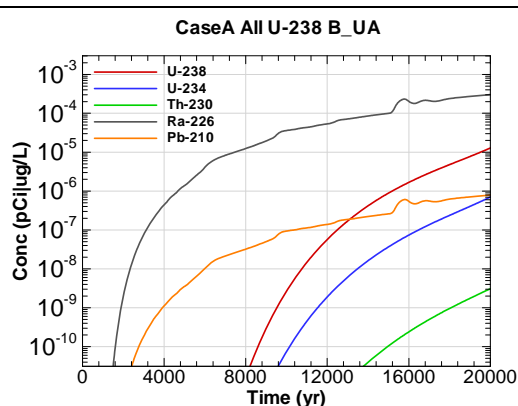


Figure A.1-806 - 100m Aquifer Concentration for
CaseA All U-238 B_UA

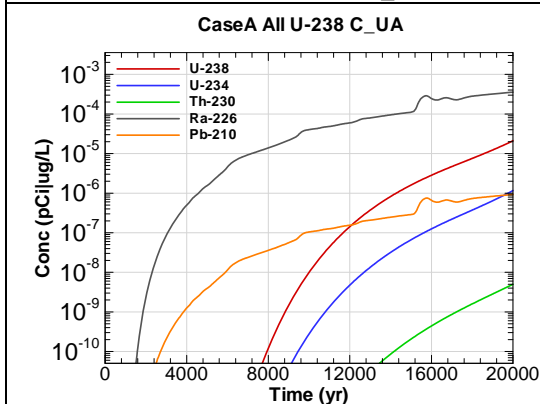


Figure A.1-807 - 100m Aquifer Concentration for
CaseA All U-238 C_UA

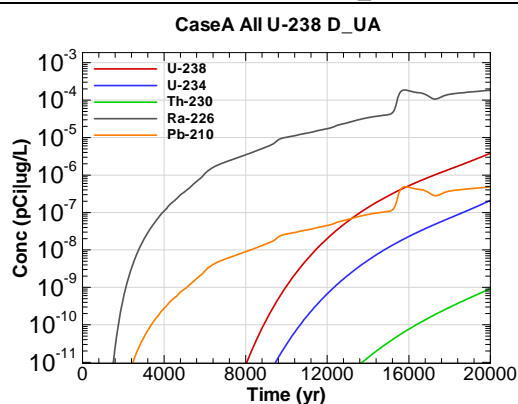


Figure A.1-808 - 100m Aquifer Concentration for
CaseA All U-238 D_UA

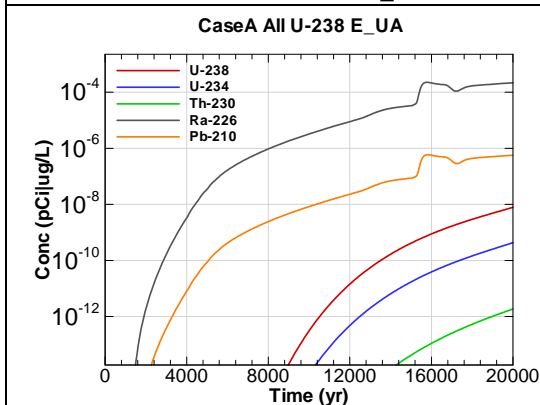


Figure A.1-809 - 100m Aquifer Concentration for
CaseA All U-238 E_UA

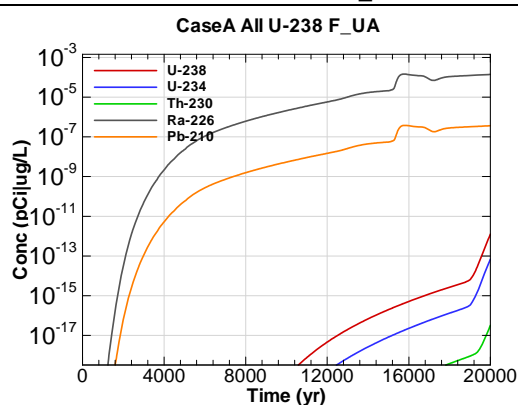
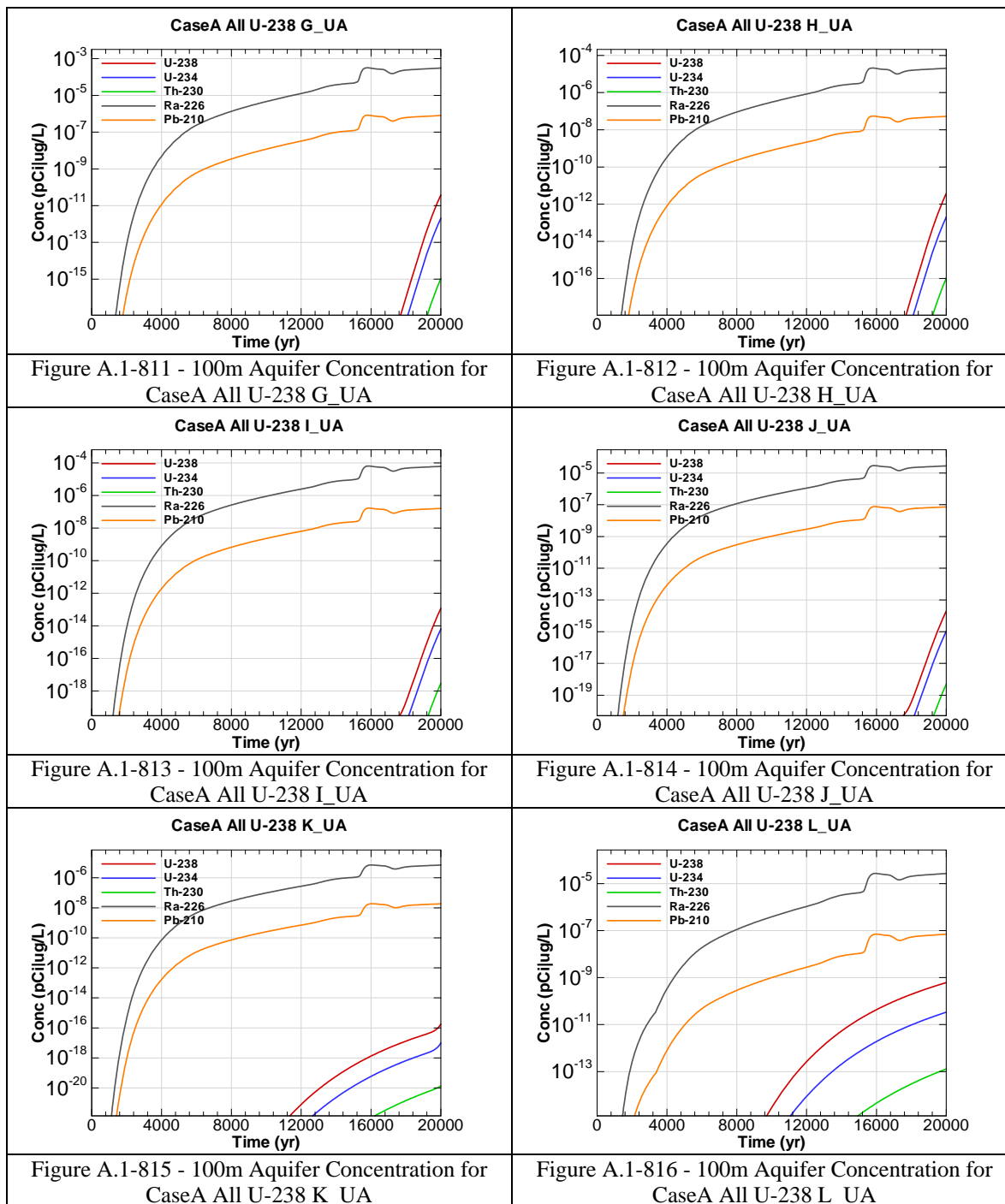
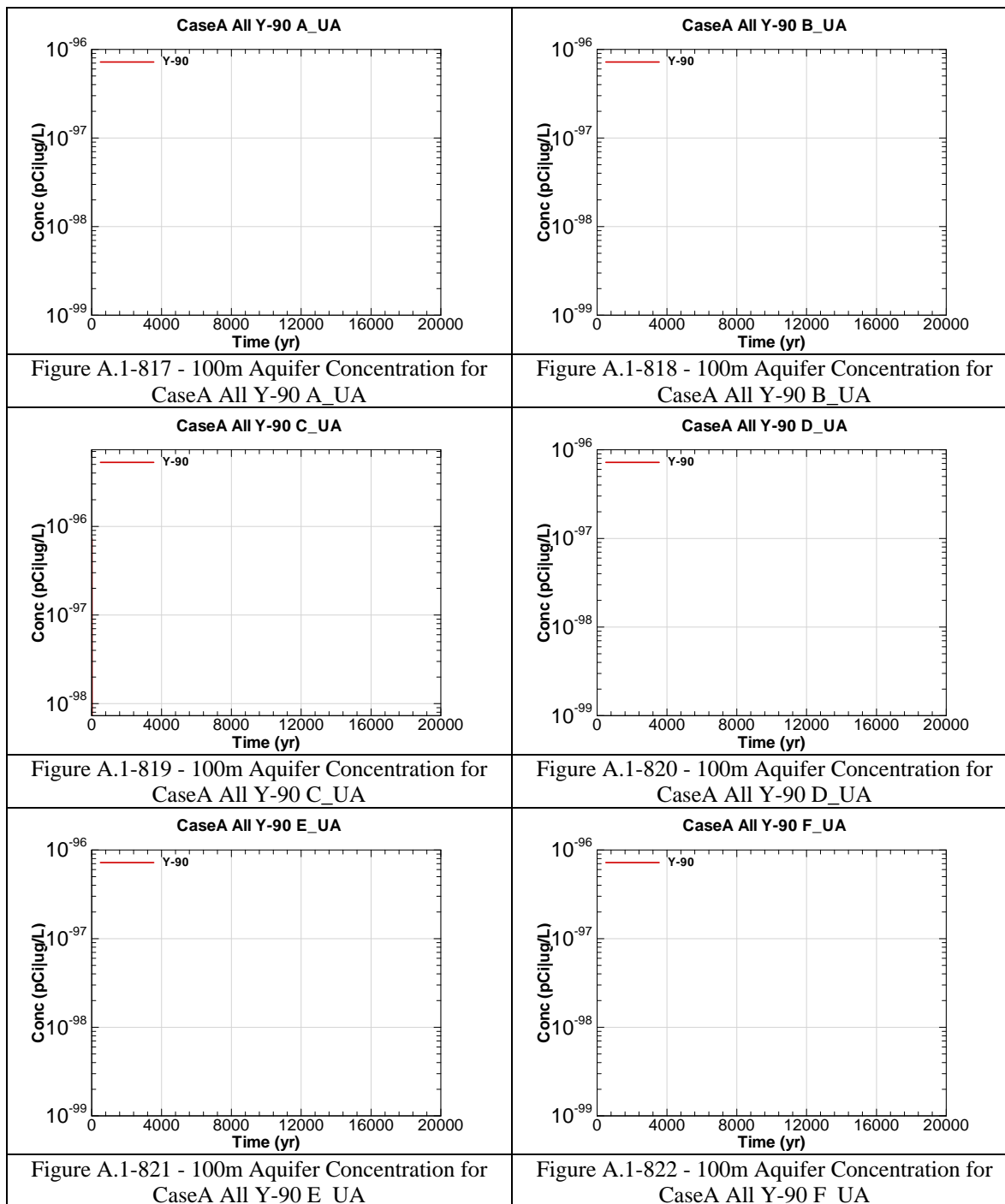
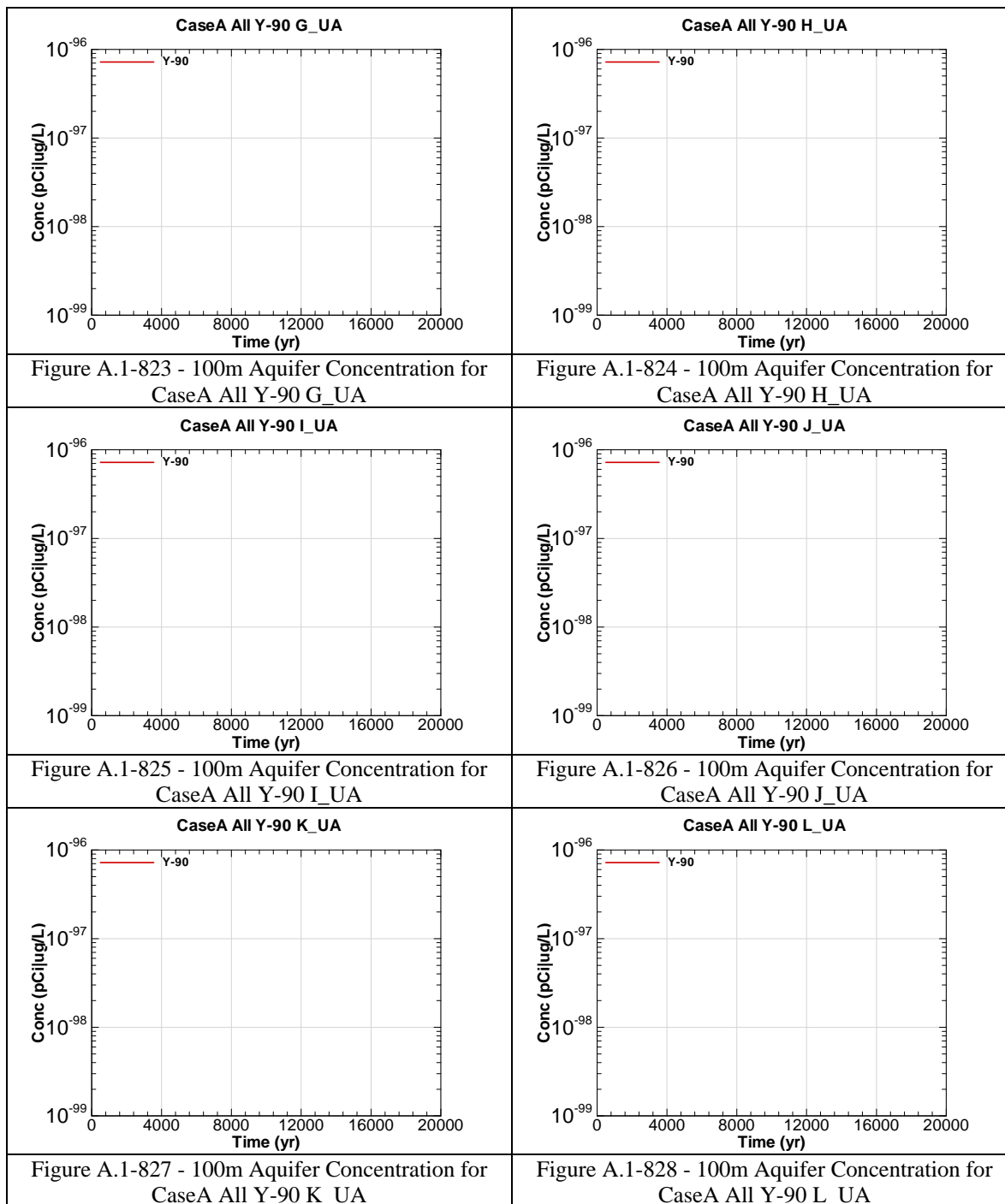
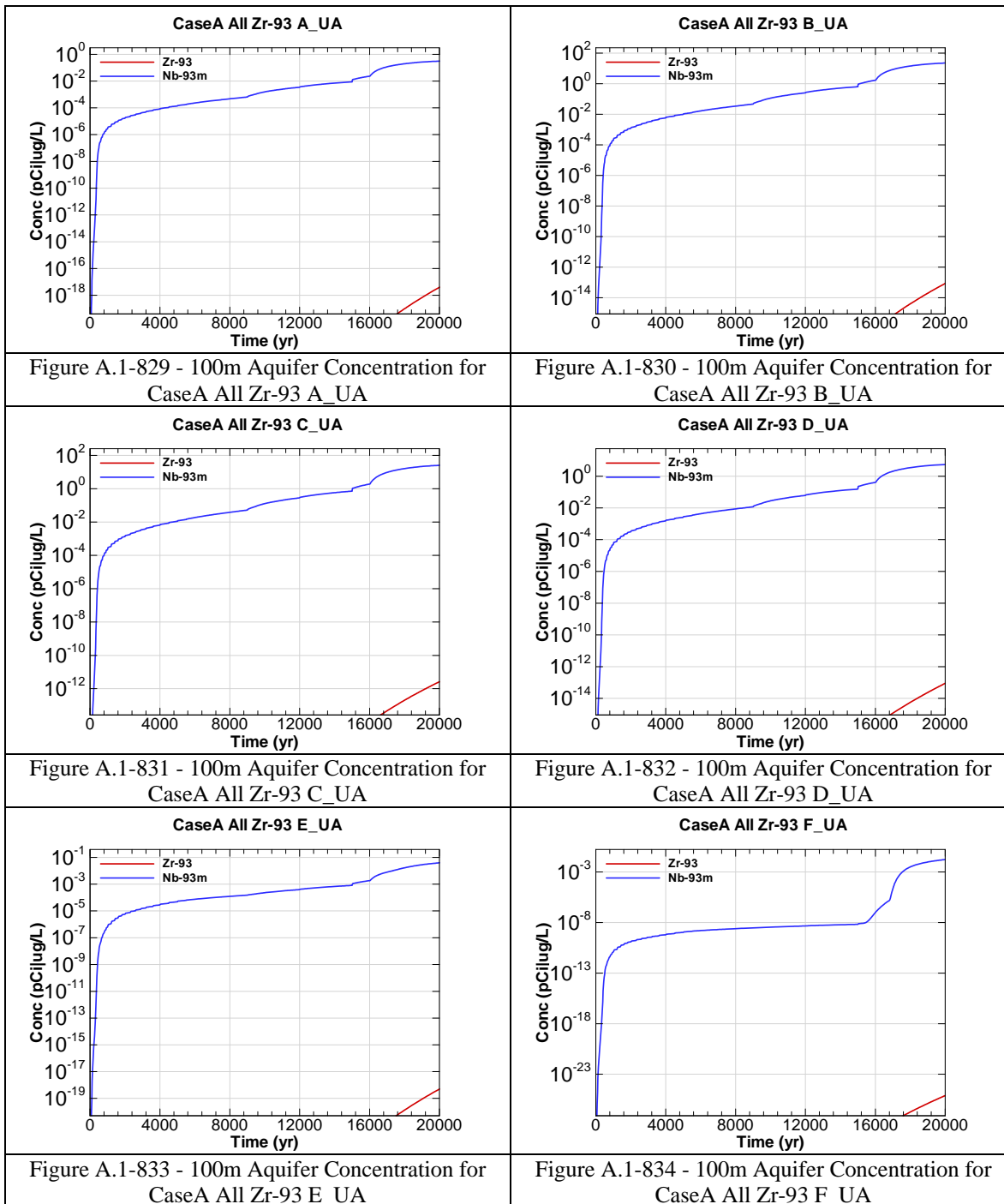


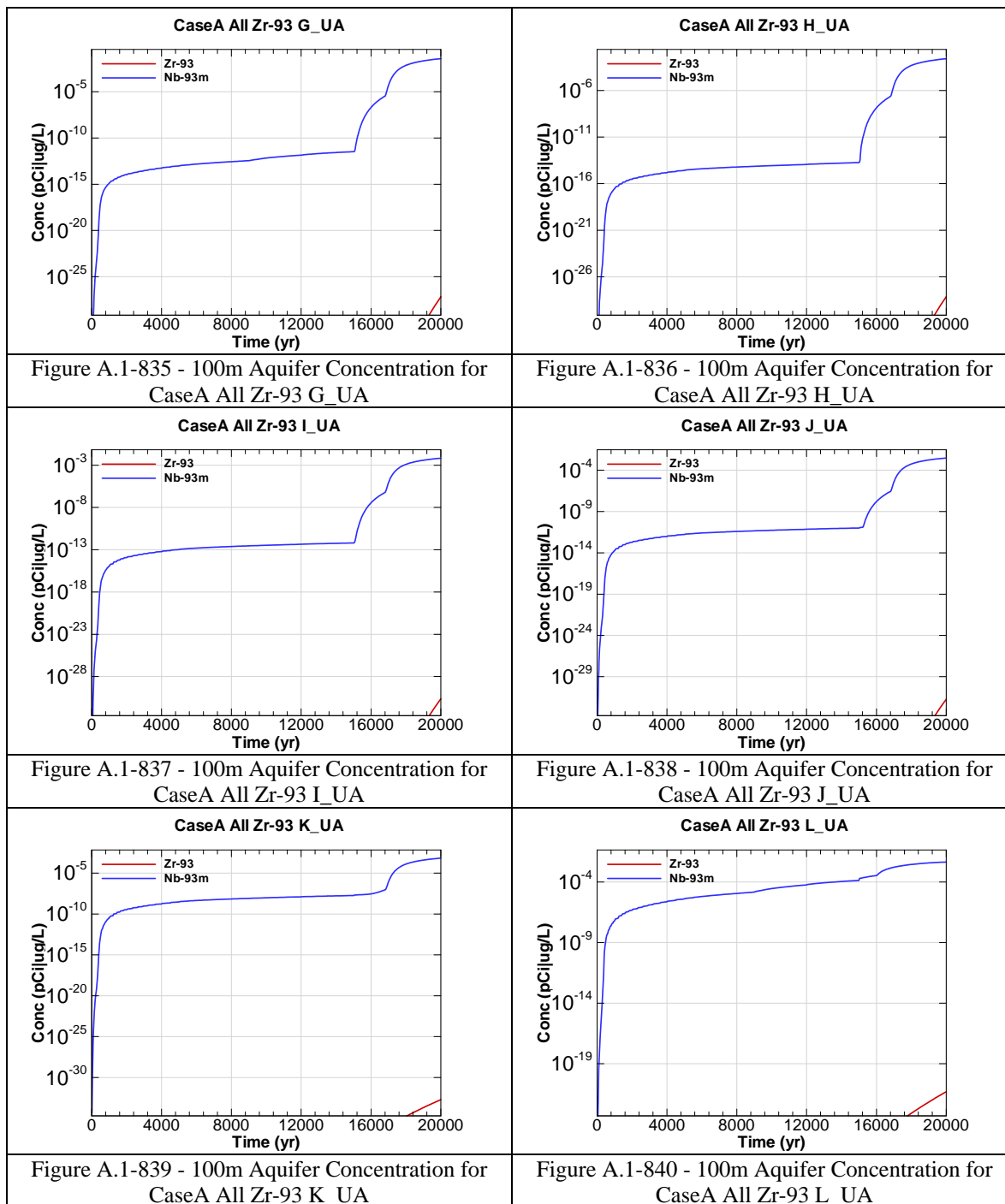
Figure A.1-810 - 100m Aquifer Concentration for
CaseA All U-238 F_UA





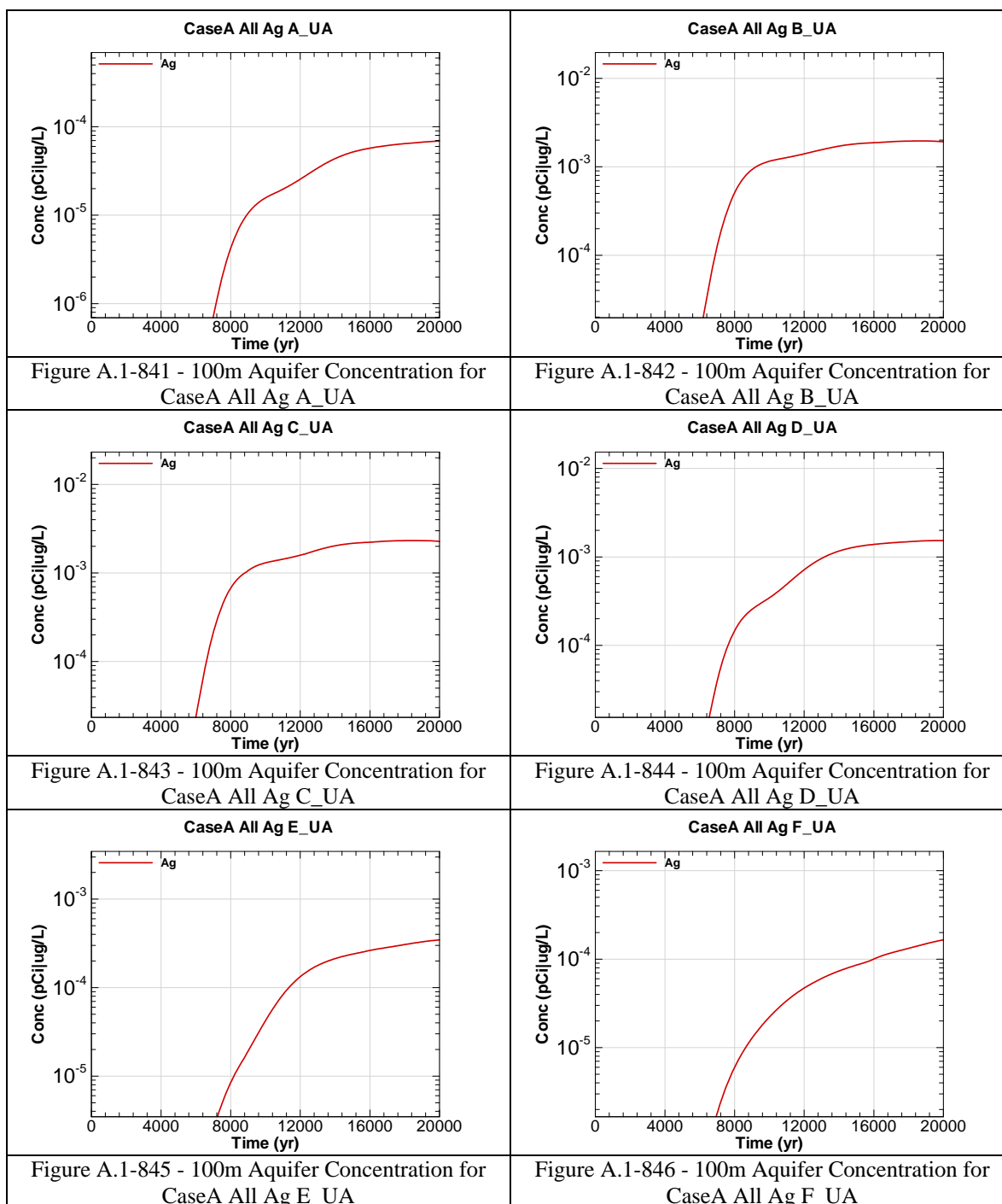


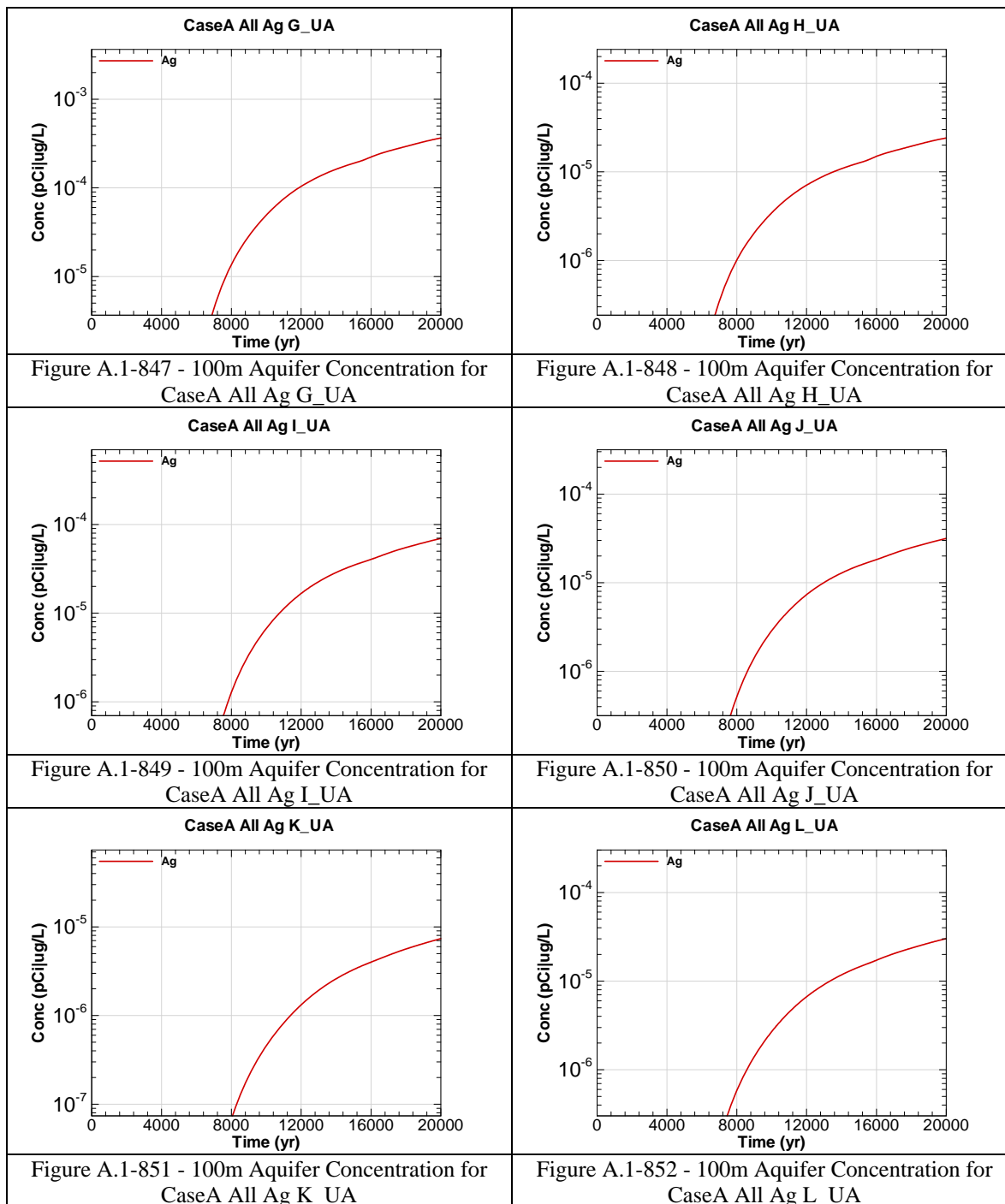


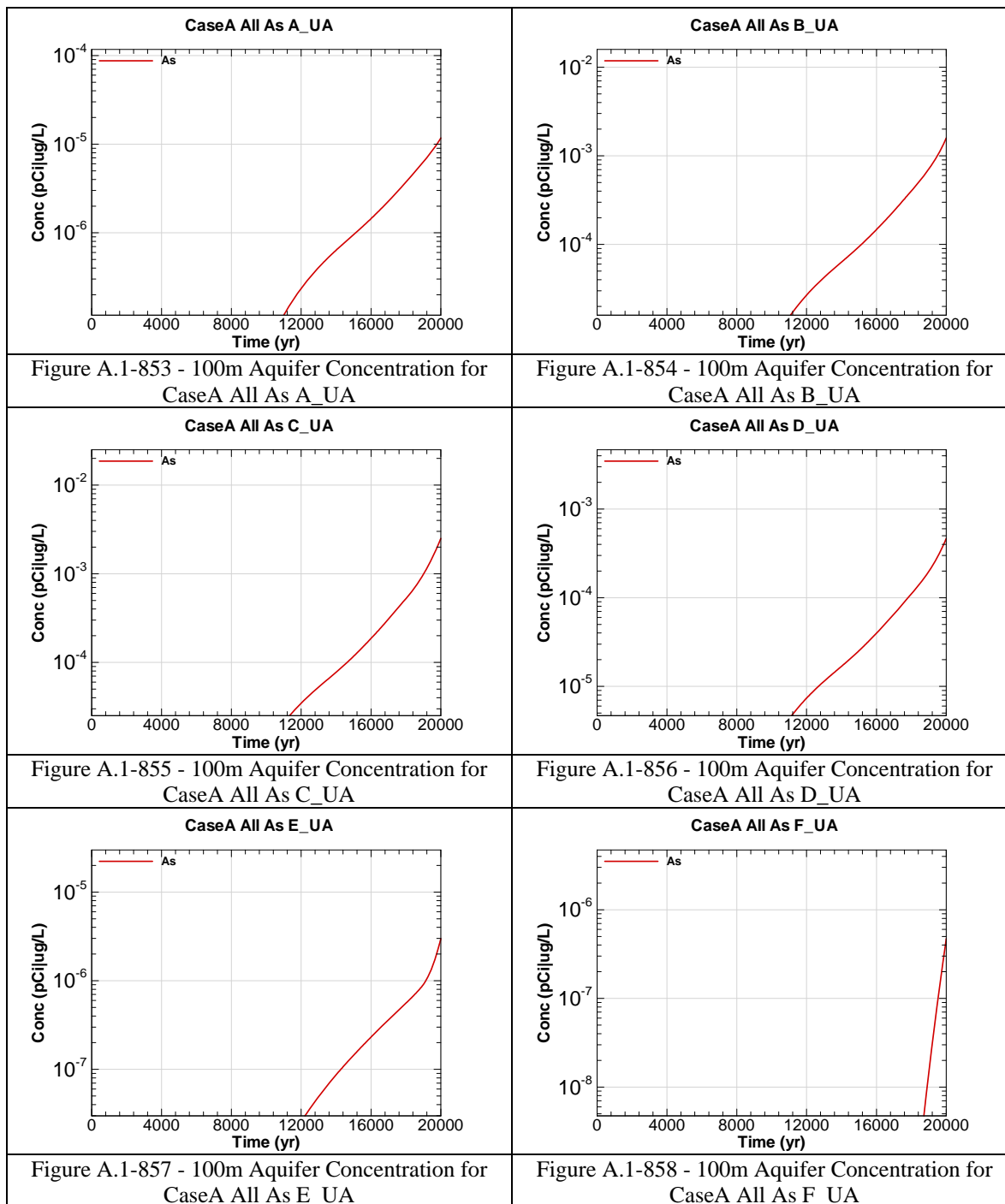


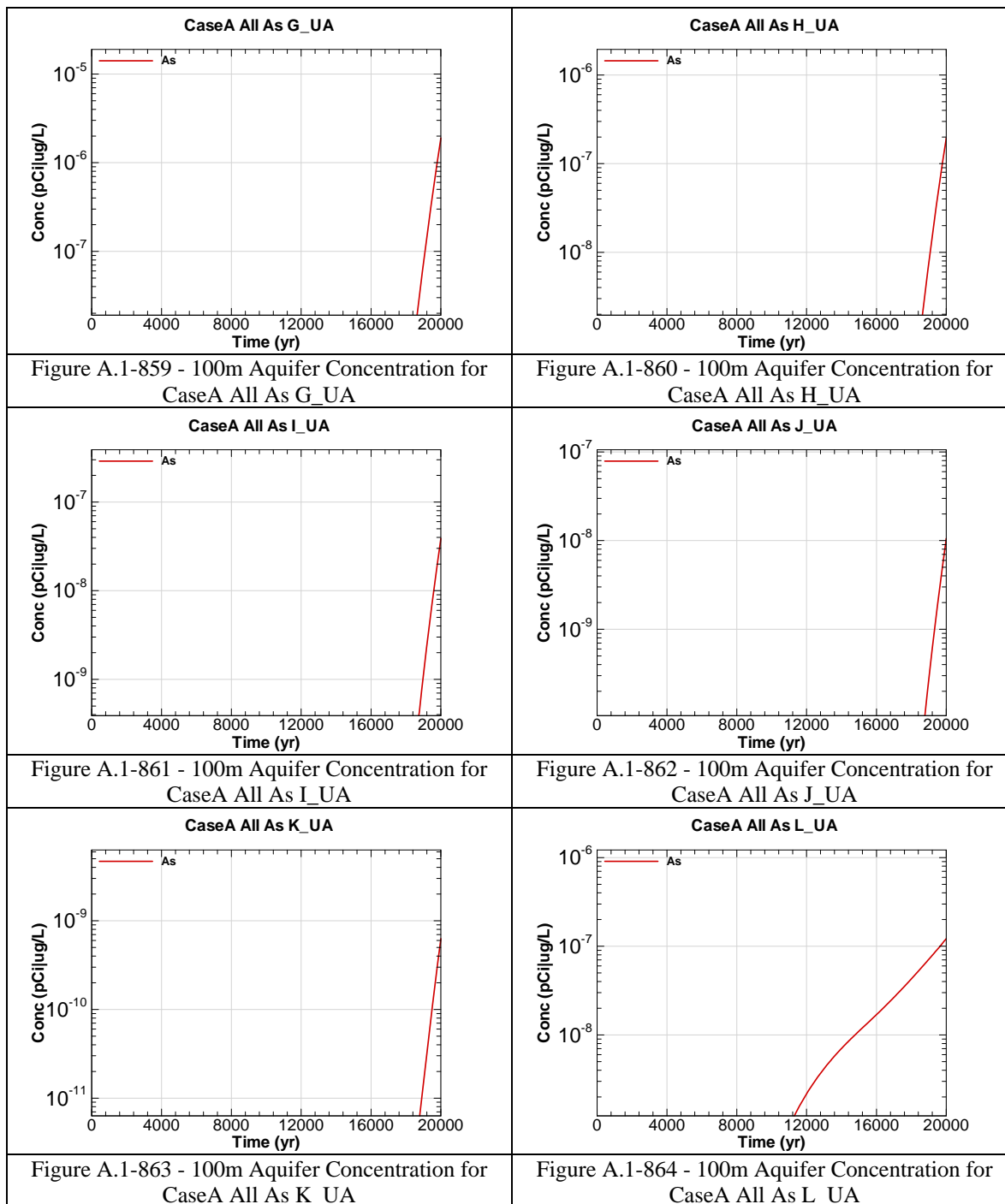
The chemical contaminants were modeled prior to the revision of the final closure inventory calculations presented in Table 3.3-8 for five chemical components: As, Cr, Cu, N and U. The figures that follow represent the concentrations calculated with an initial inventory input. The multipliers in the table below are to be used to determine the final concentrations with respect to time for the impacted chemicals as the inventory has a linear relationship with concentration in the Saltstone model. The groundwater concentration tables in Section 5 have been corrected using the multipliers.

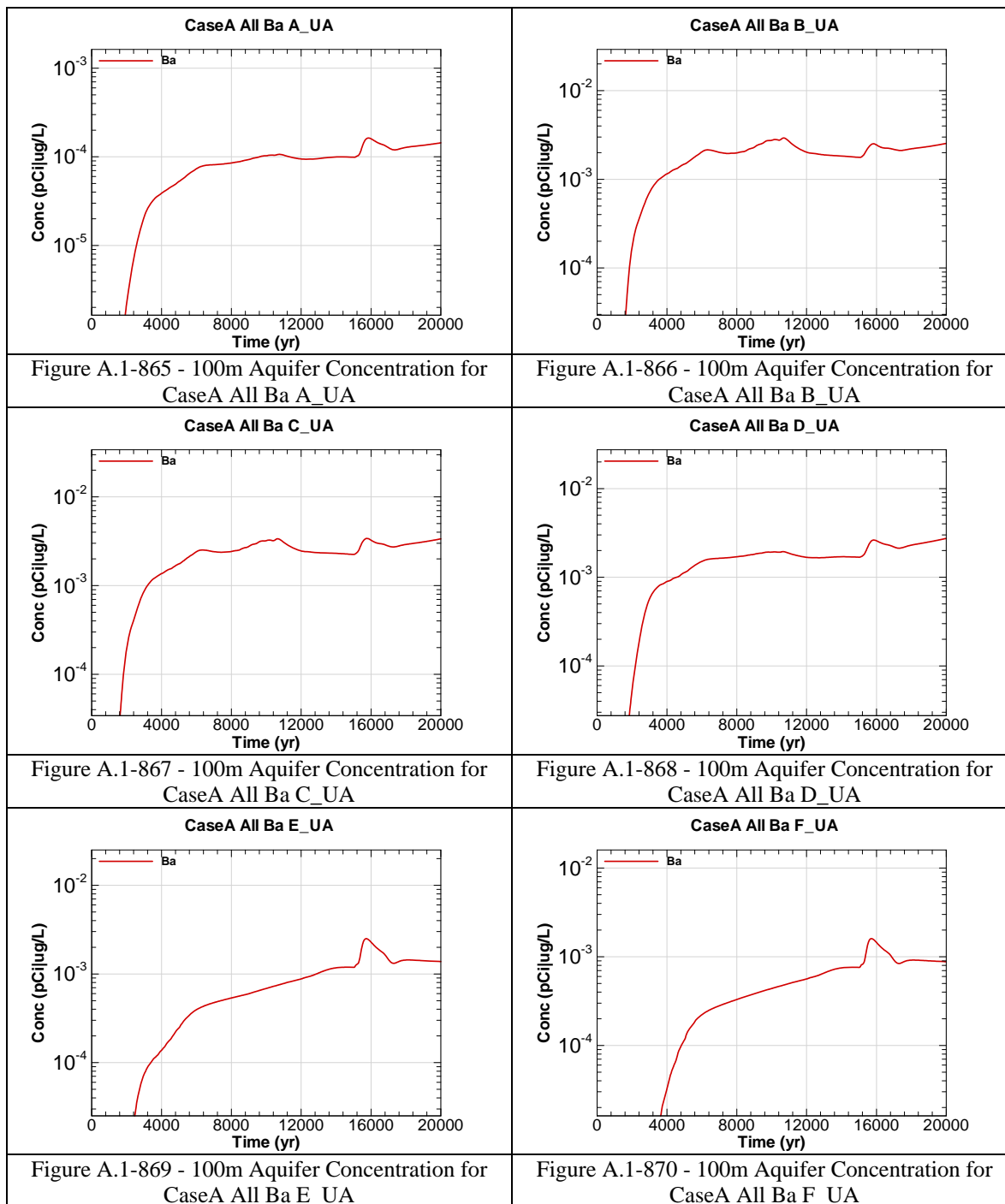
| Chemical Component | Modeled Inventory | Projected Inventory | Percent Increase | Multiplier |
|---------------------------|--------------------------|----------------------------|-------------------------|-------------------|
| Ag | 8.8E+01 | 8.8E+01 | 0.0% | None |
| As | 1.08E+04 | 1.1E+04 | 2.3% | 1.02E+00 |
| Ba | 1.7E+02 | 1.7E+02 | 0.0% | None |
| Cd | 1.3E+03 | 1.3E+03 | 0.0% | None |
| Cr | 2.9E+04 | 3.0E+04 | 1.4% | 1.01E+00 |
| Cu | 1.9E+04 | 1.9E+04 | 0.9% | 1.01E+00 |
| F | 1.7E+04 | 1.7E+04 | 0.0% | None |
| Fe | 2.9E+03 | 2.9E+03 | 0.0% | None |
| Hg | 1.1E+04 | 1.1E+04 | 0.0% | None |
| Mn | 7.3E+03 | 7.3E+03 | 0.0% | None |
| Ni | 1.5E+03 | 1.5E+03 | 0.0% | None |
| Total N | 2.2E+07 | 2.4E+07 | 5.8% | 1.06E+00 |
| Pb | 6.7E+03 | 6.7E+03 | 0.0% | None |
| Se | 4.0E+04 | 4.0E+04 | 0.0% | None |
| U | 8.2E+02 | 8.9E+02 | 8.9% | 1.10E+00 |
| Zn | 2.7E+04 | 2.7E+04 | 0.0% | None |

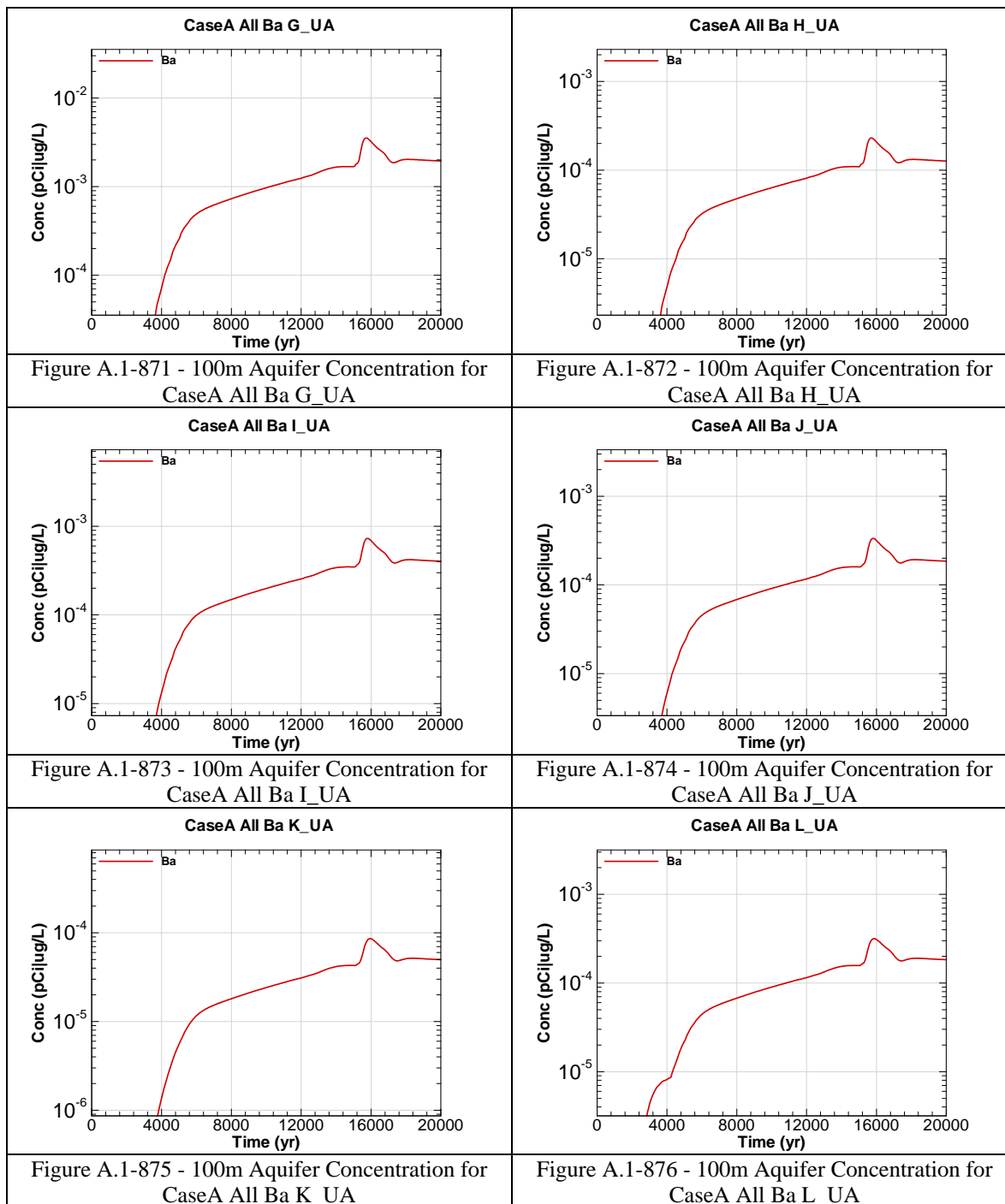


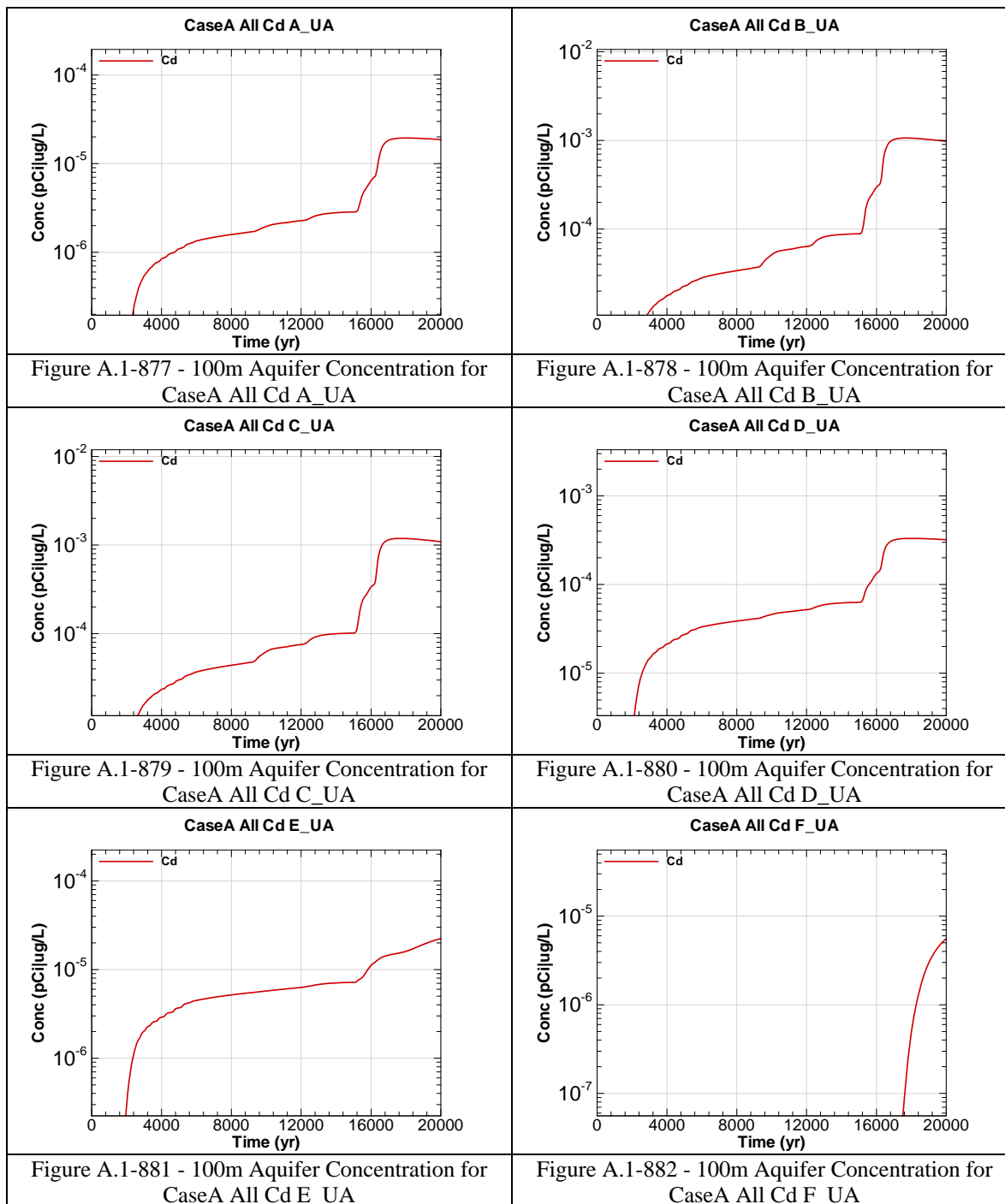


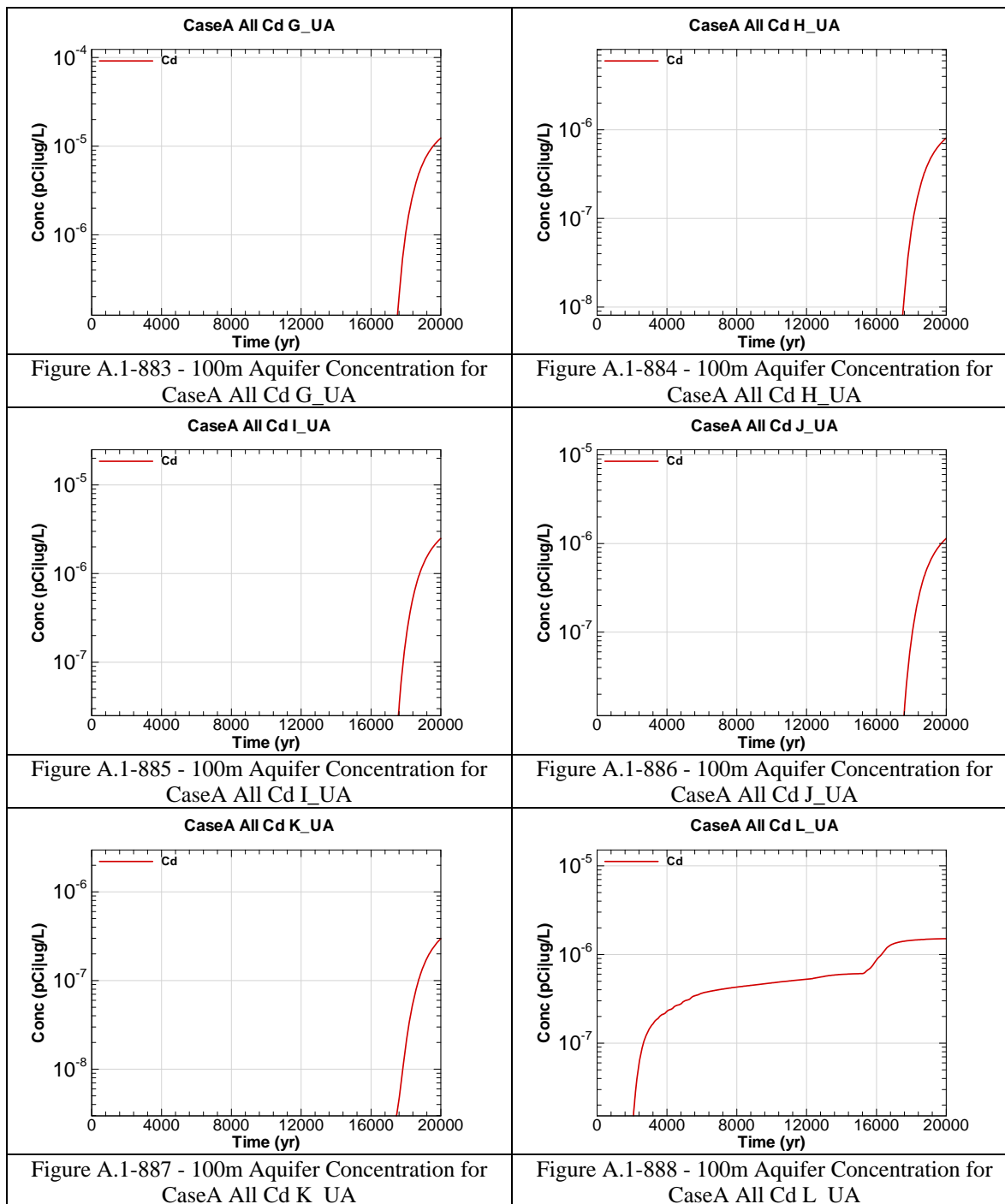


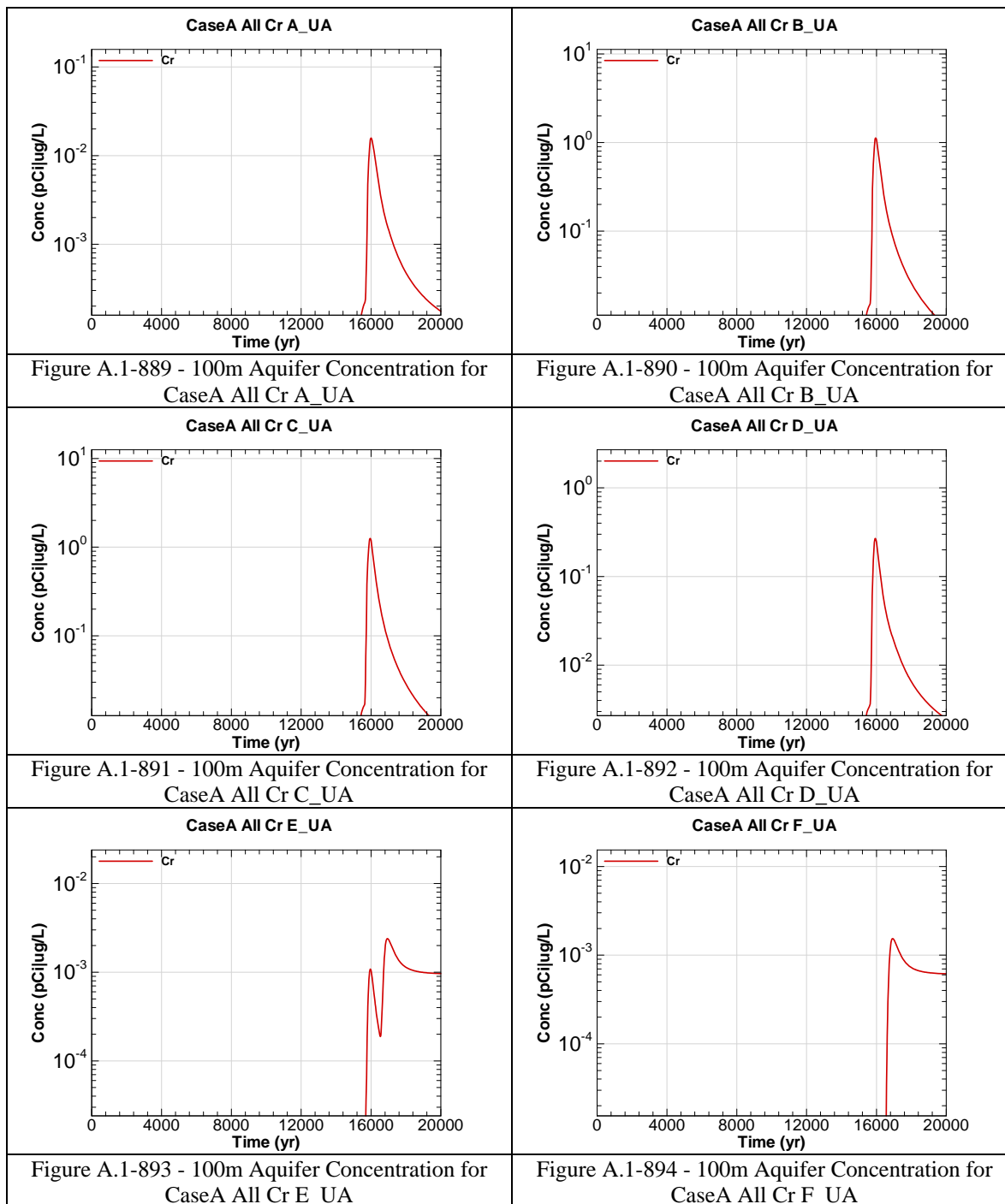


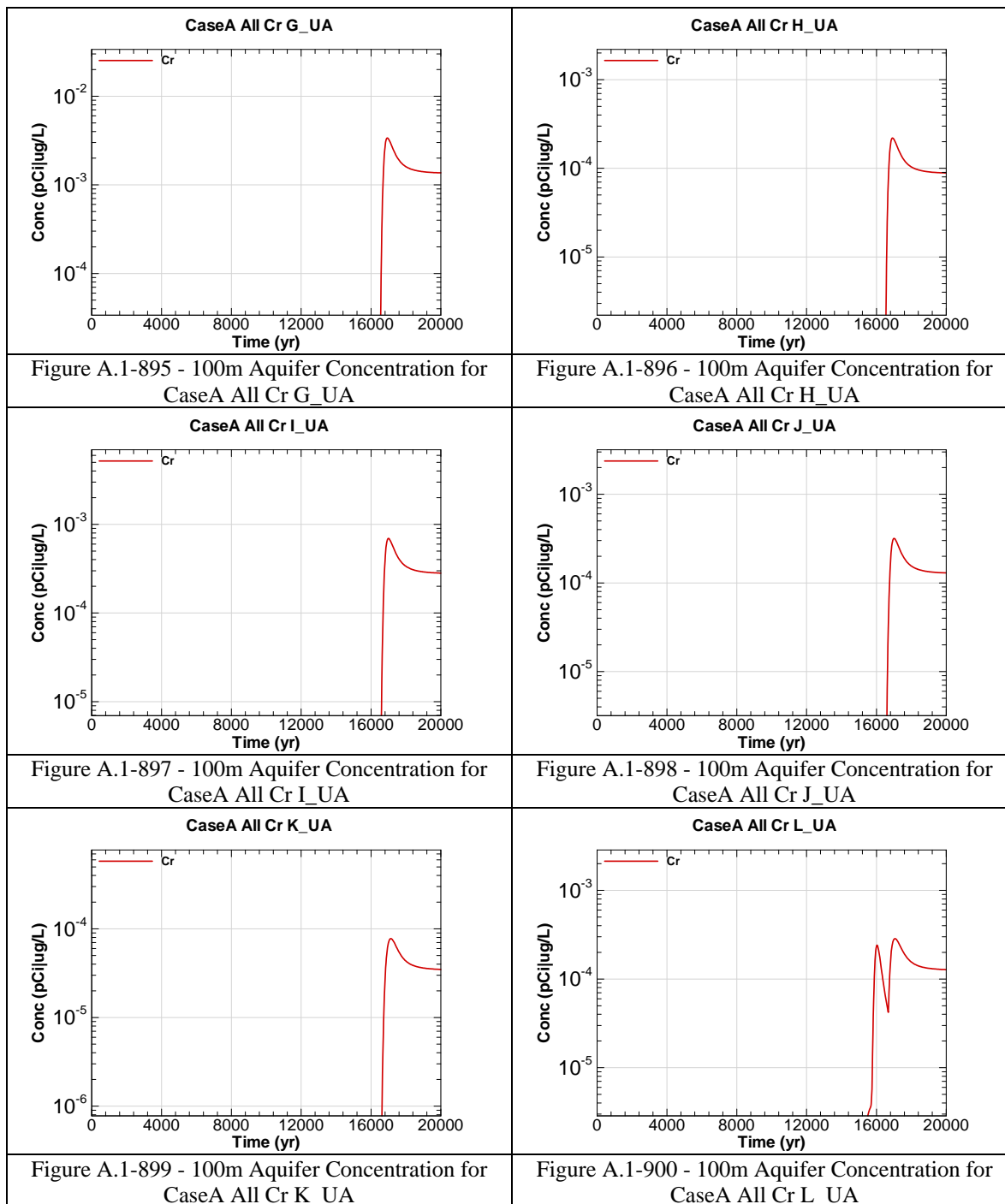


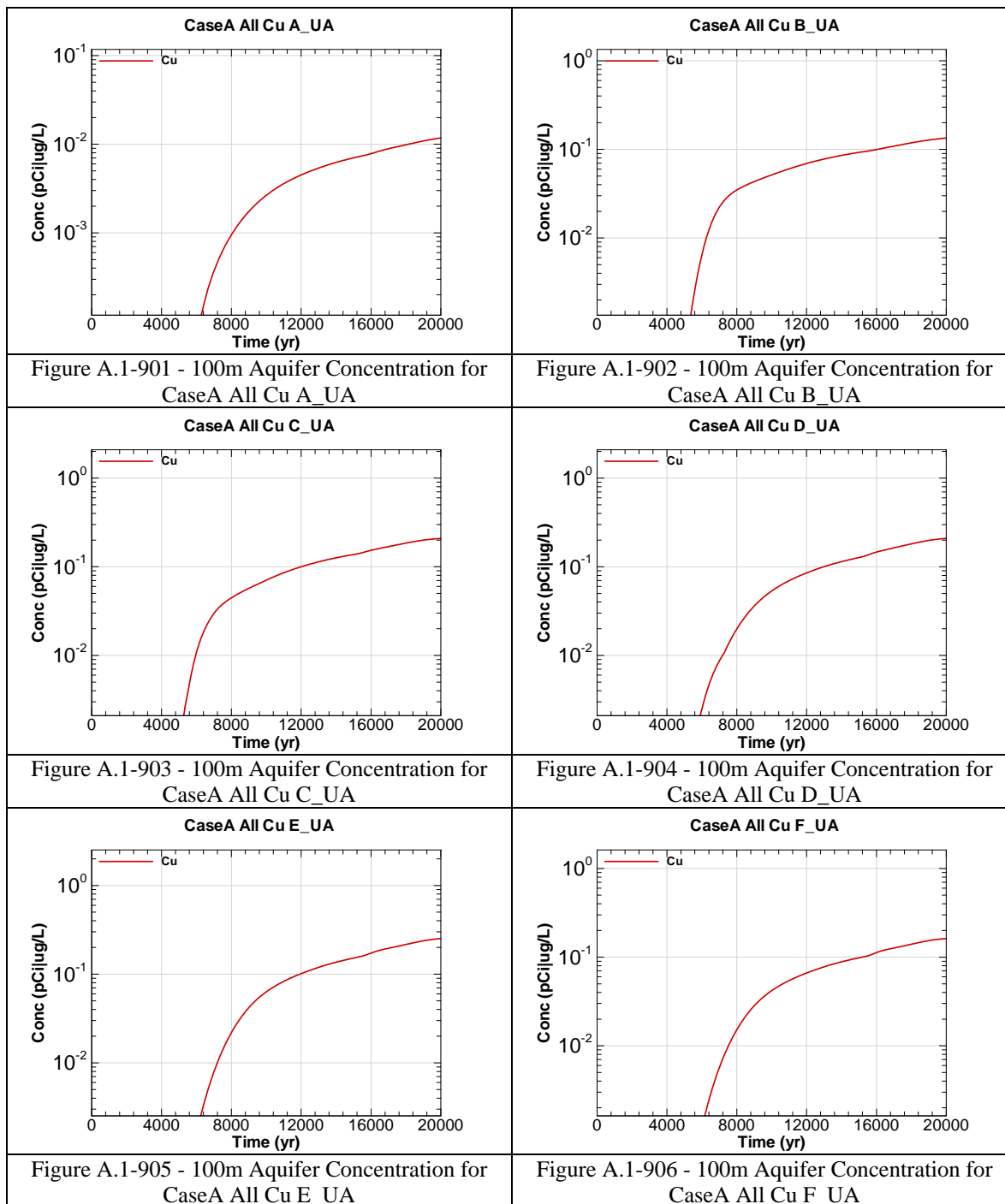


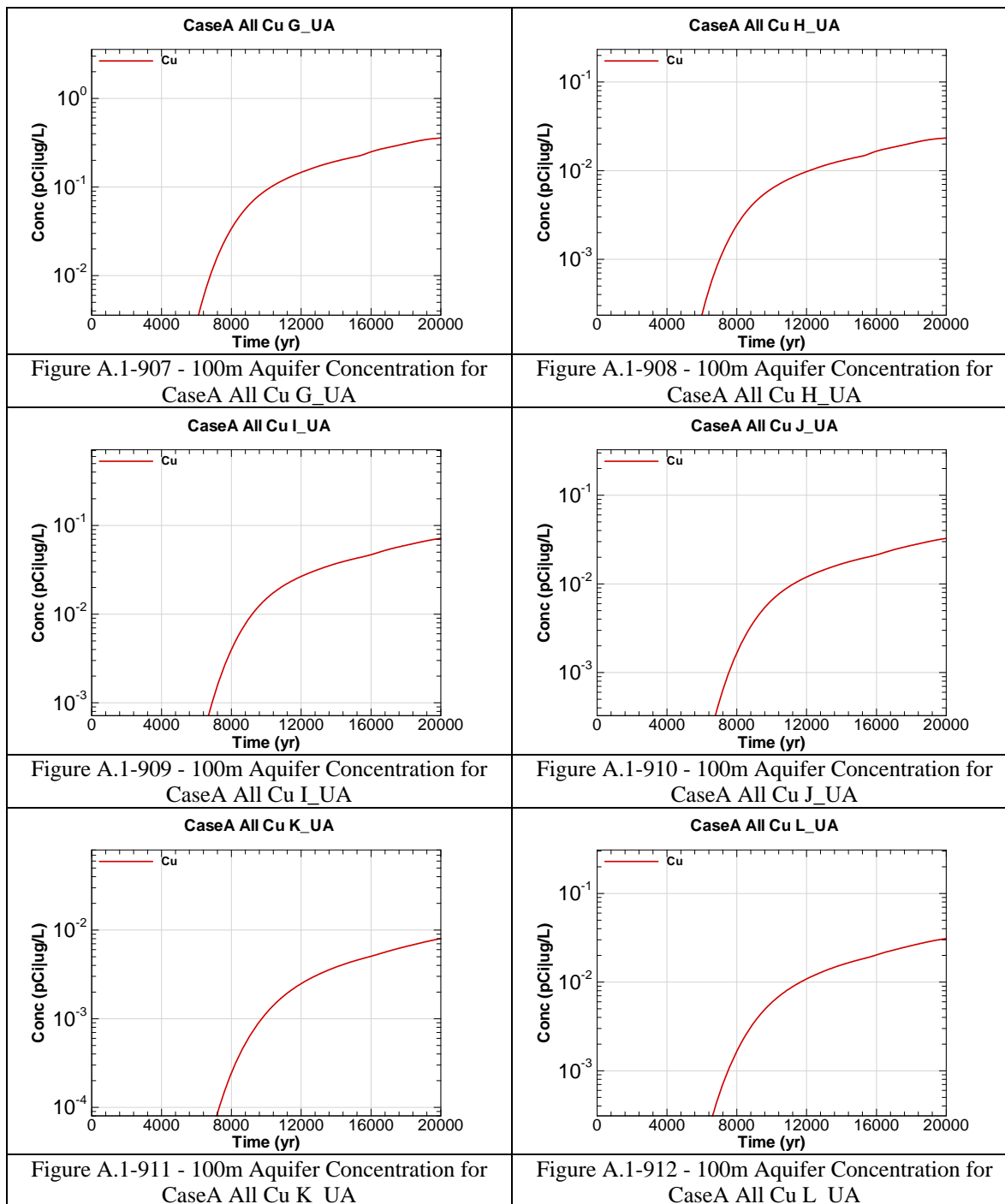


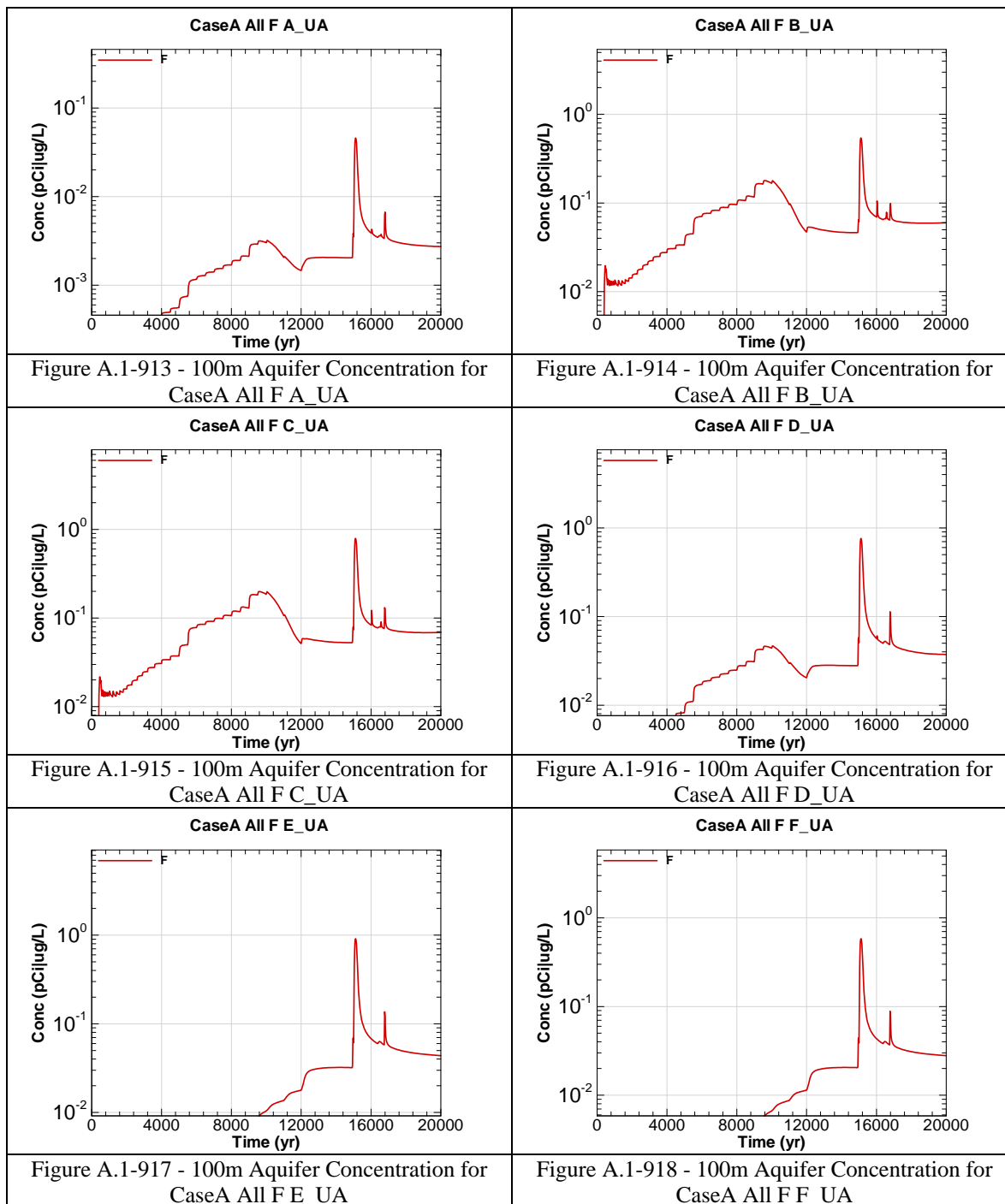


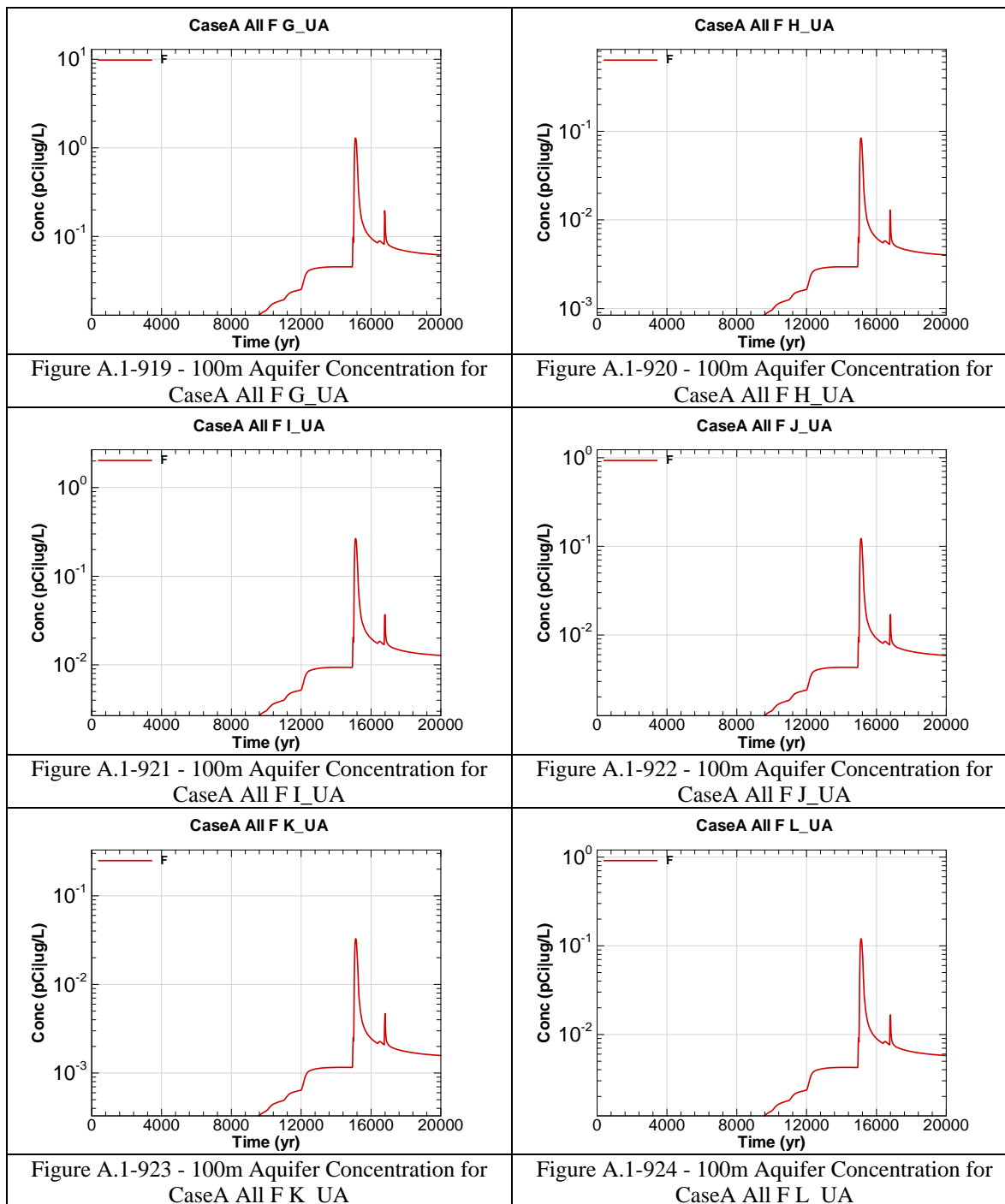


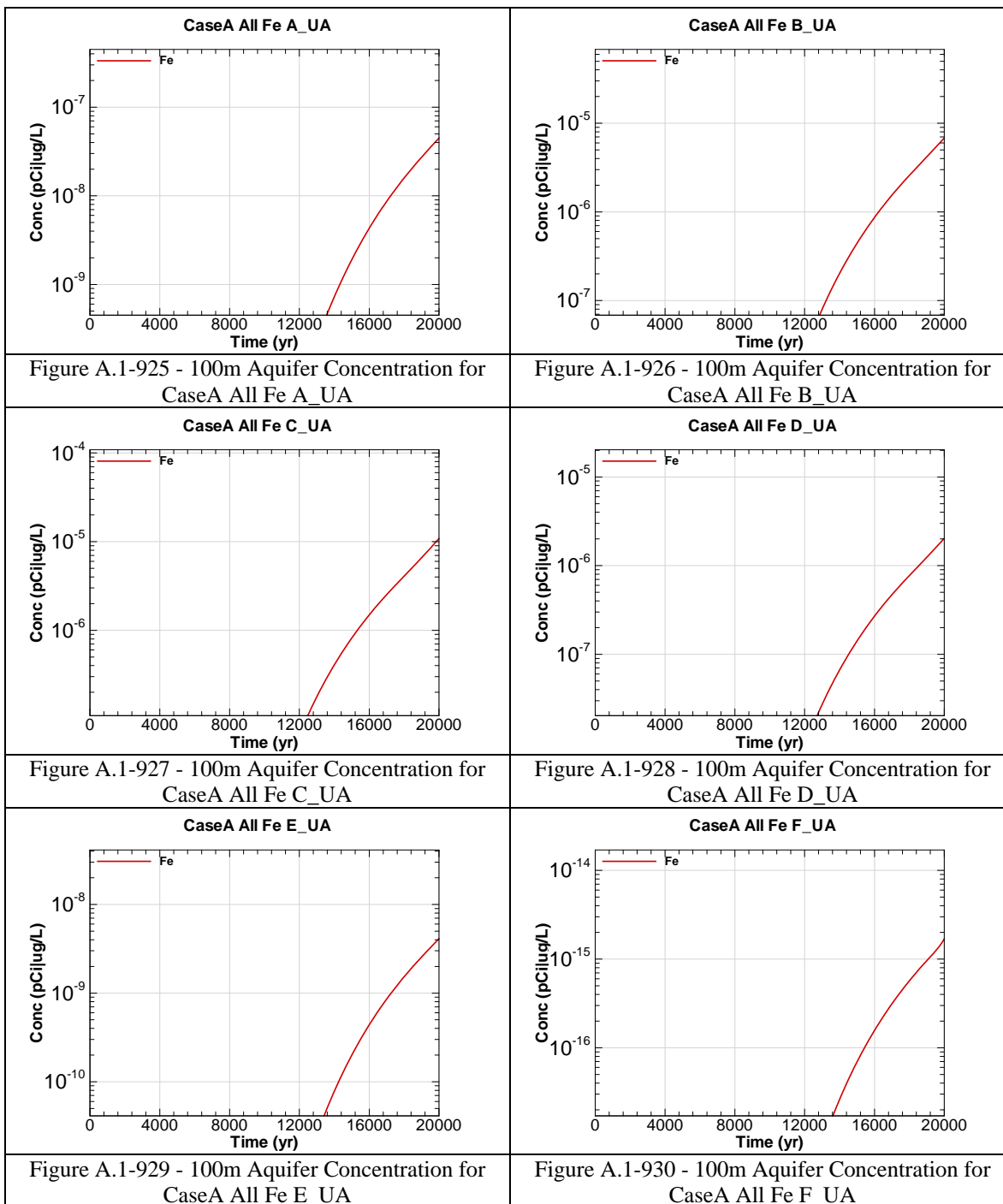


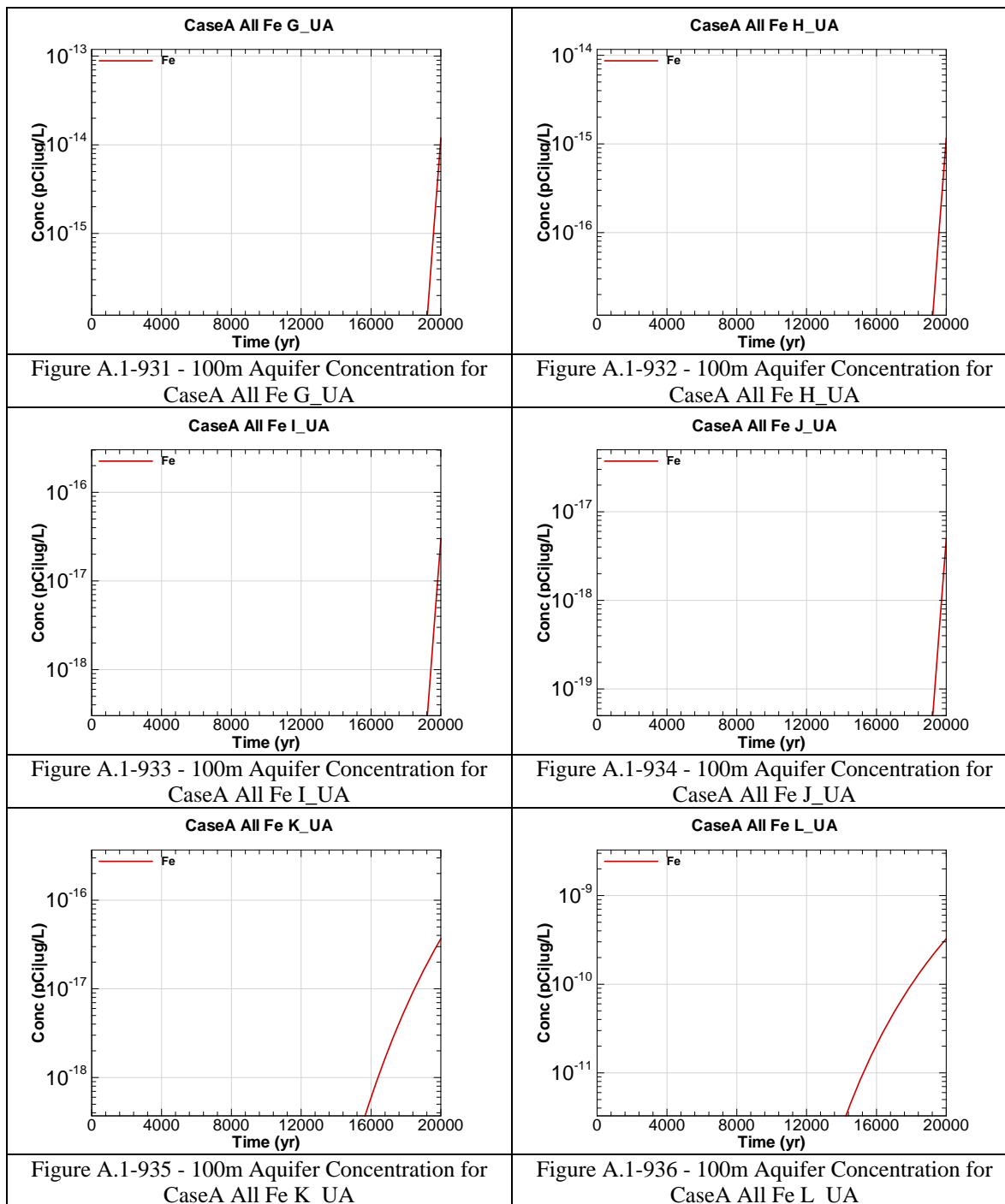


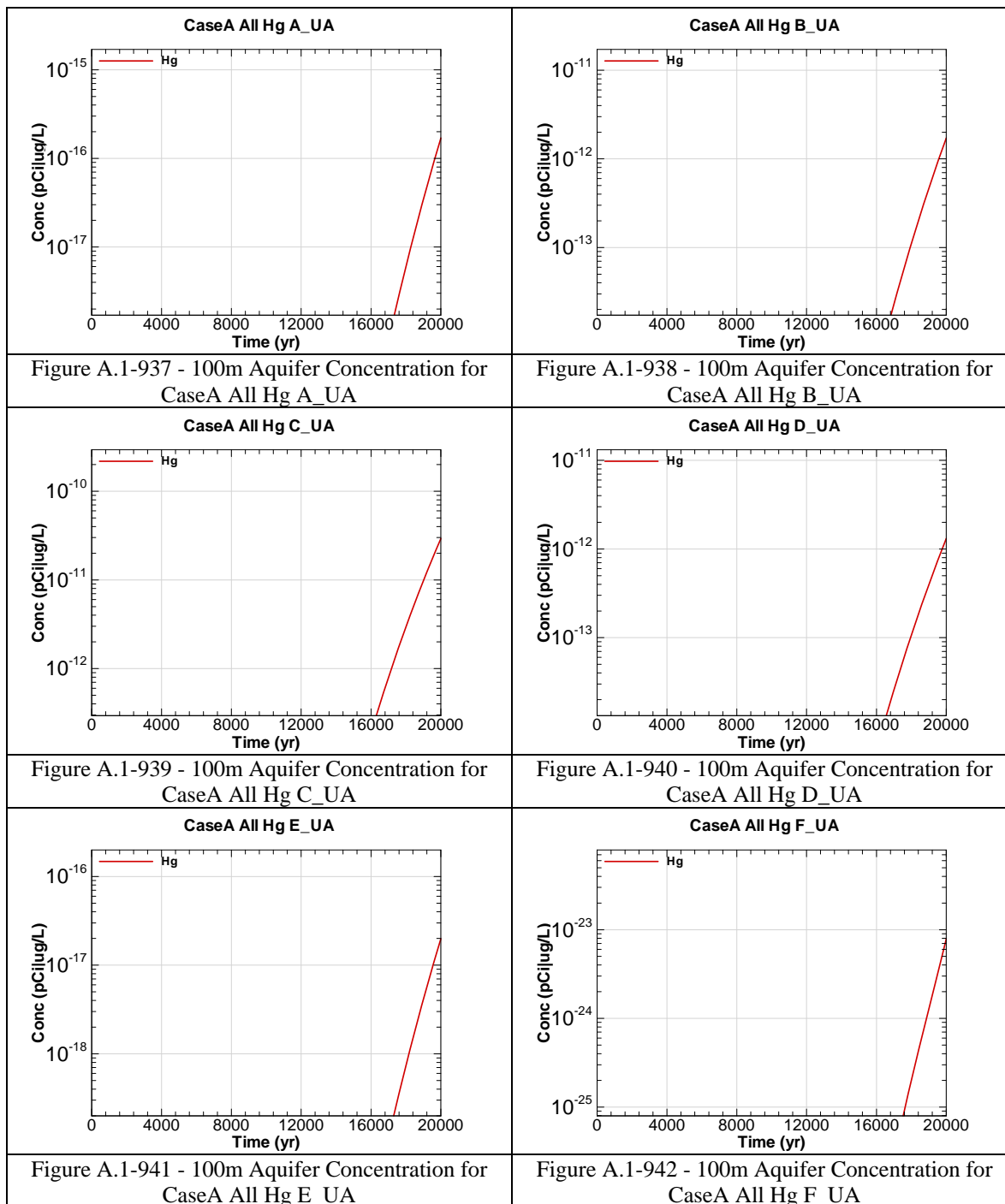


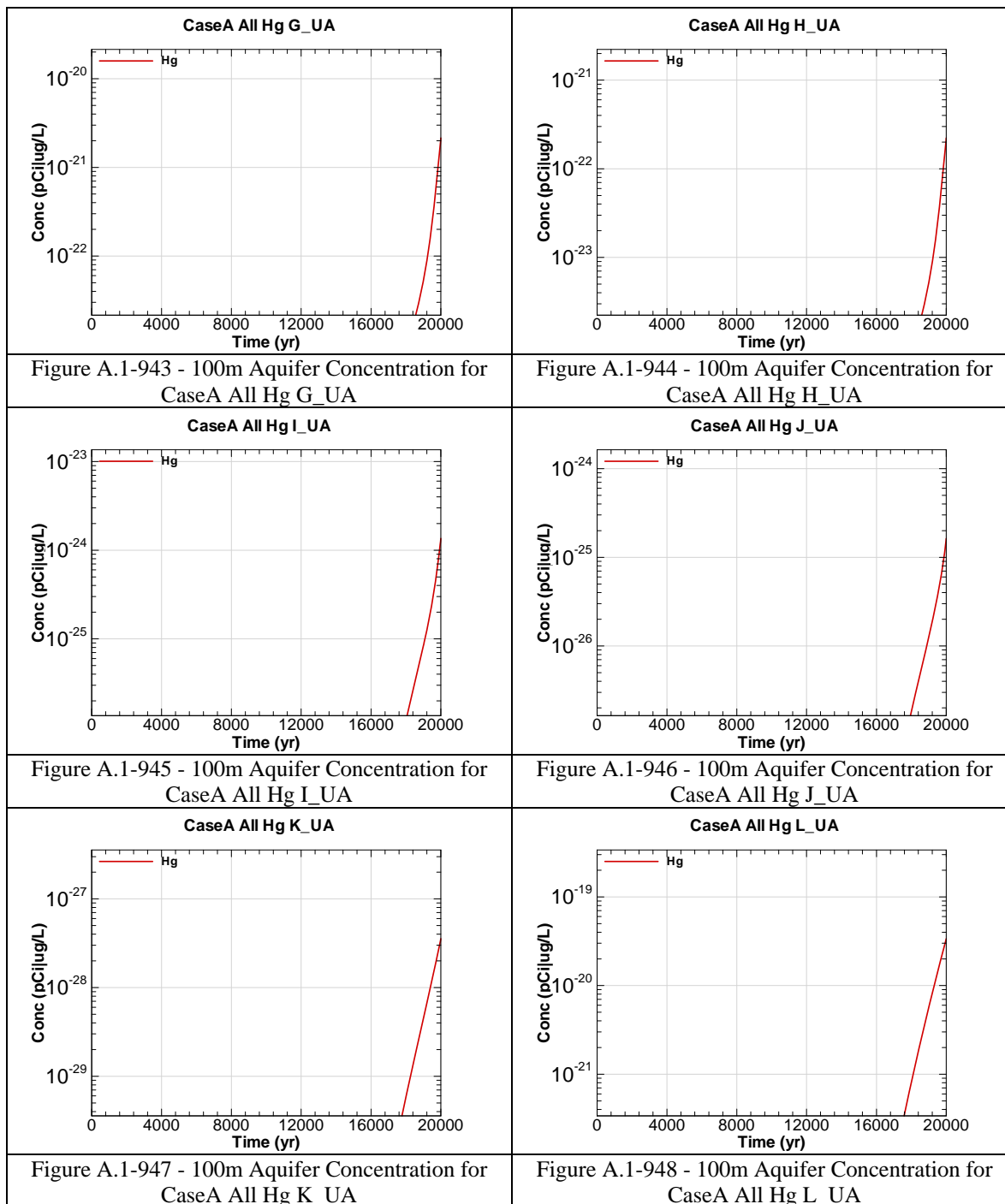


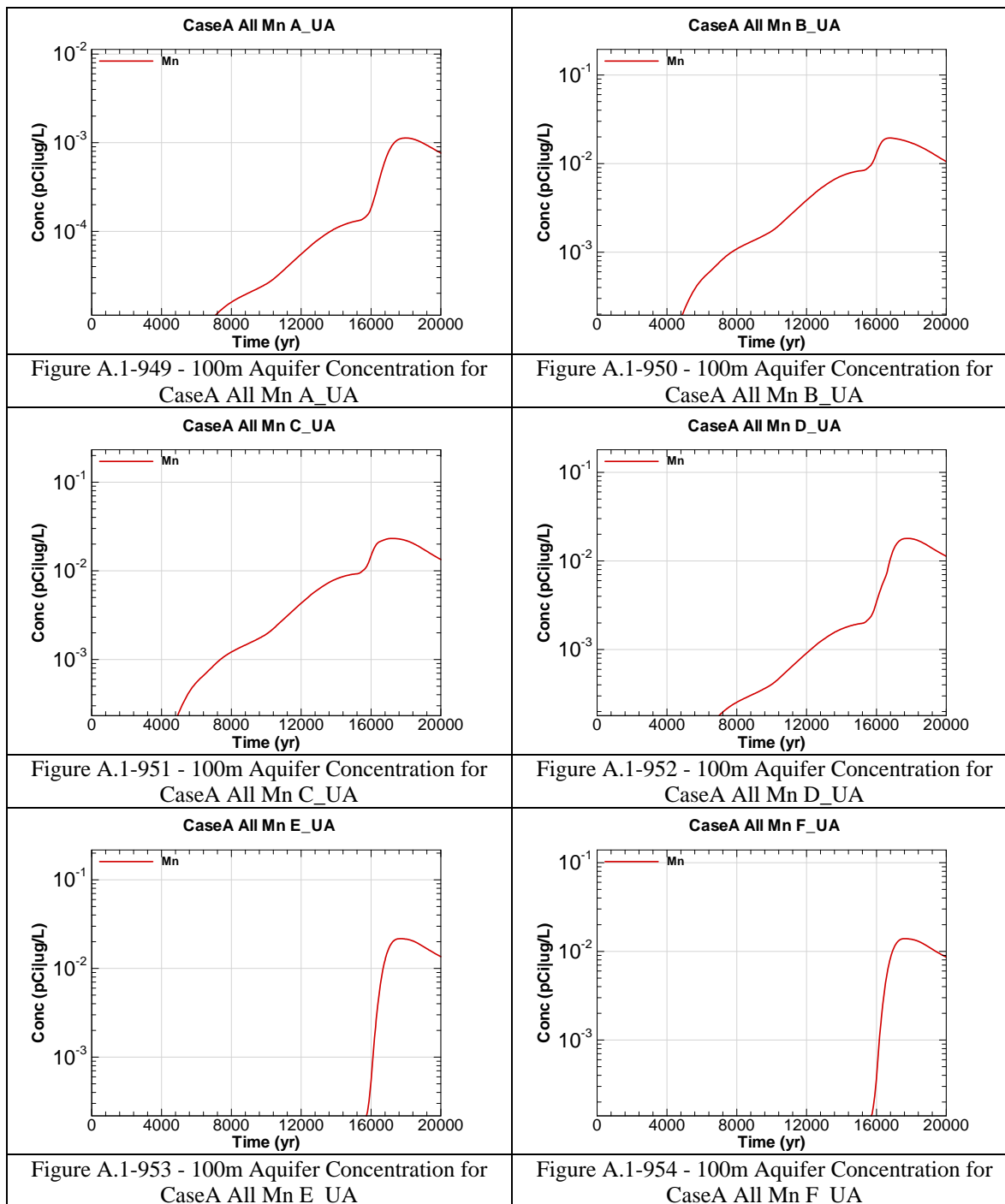


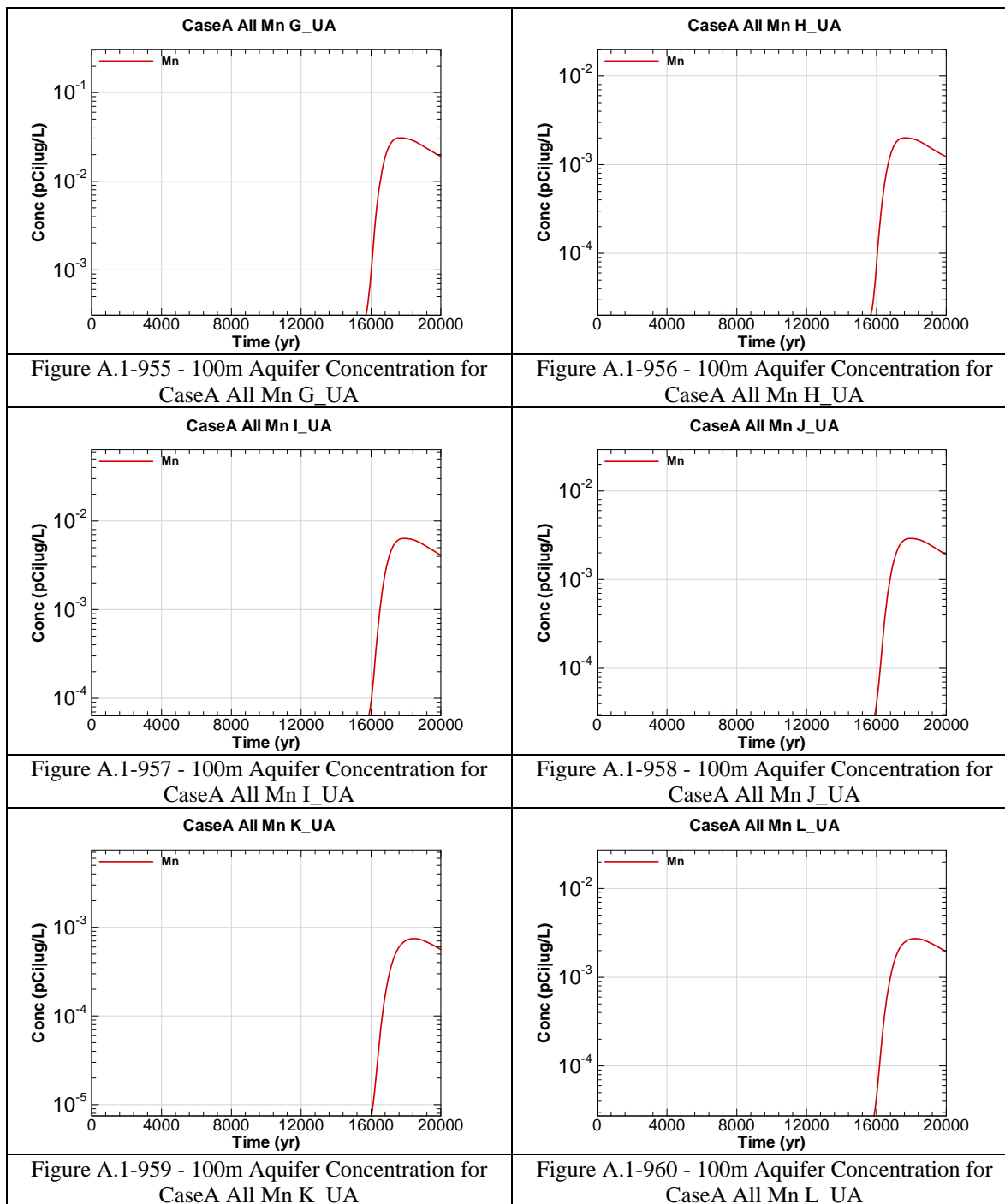


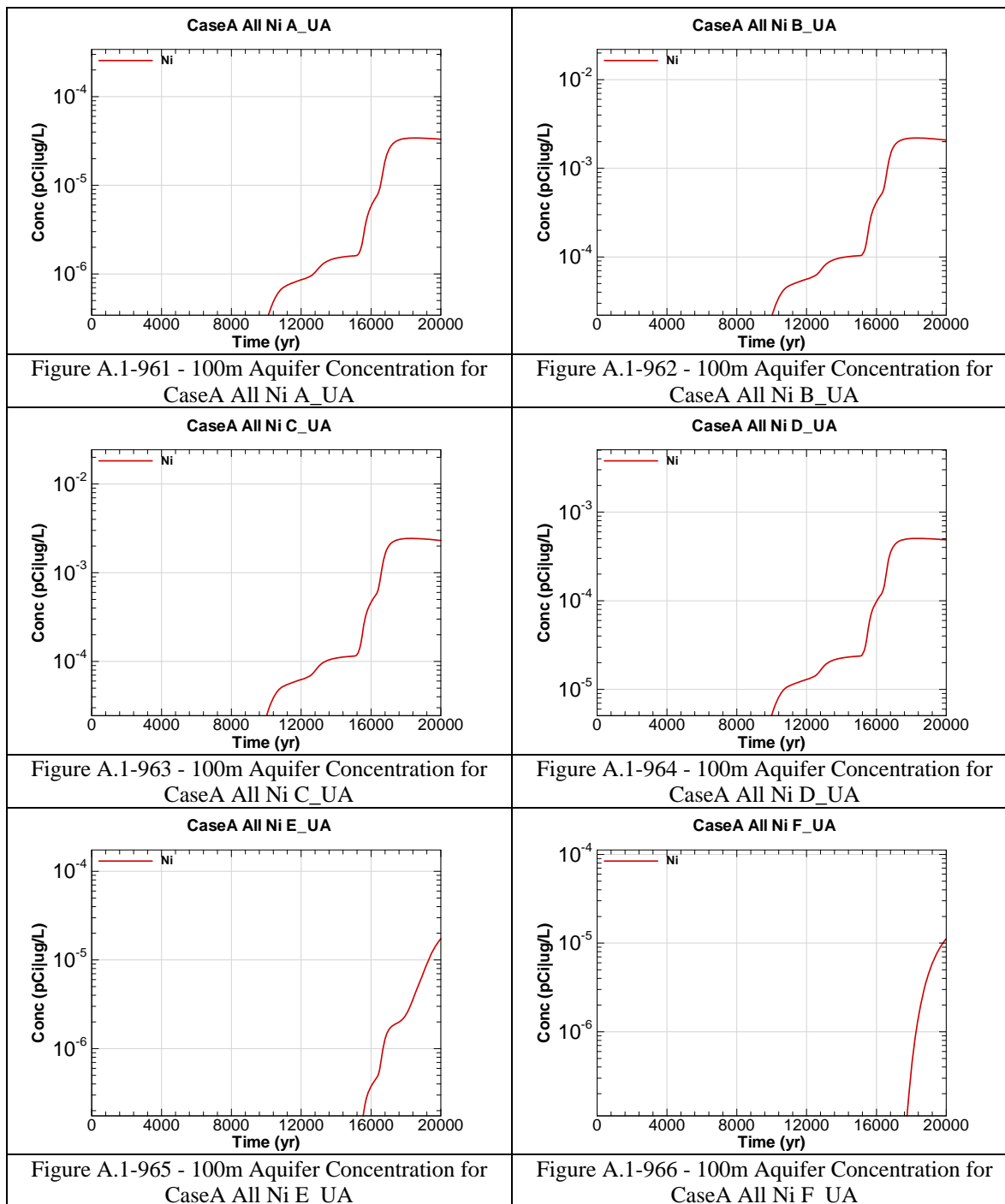


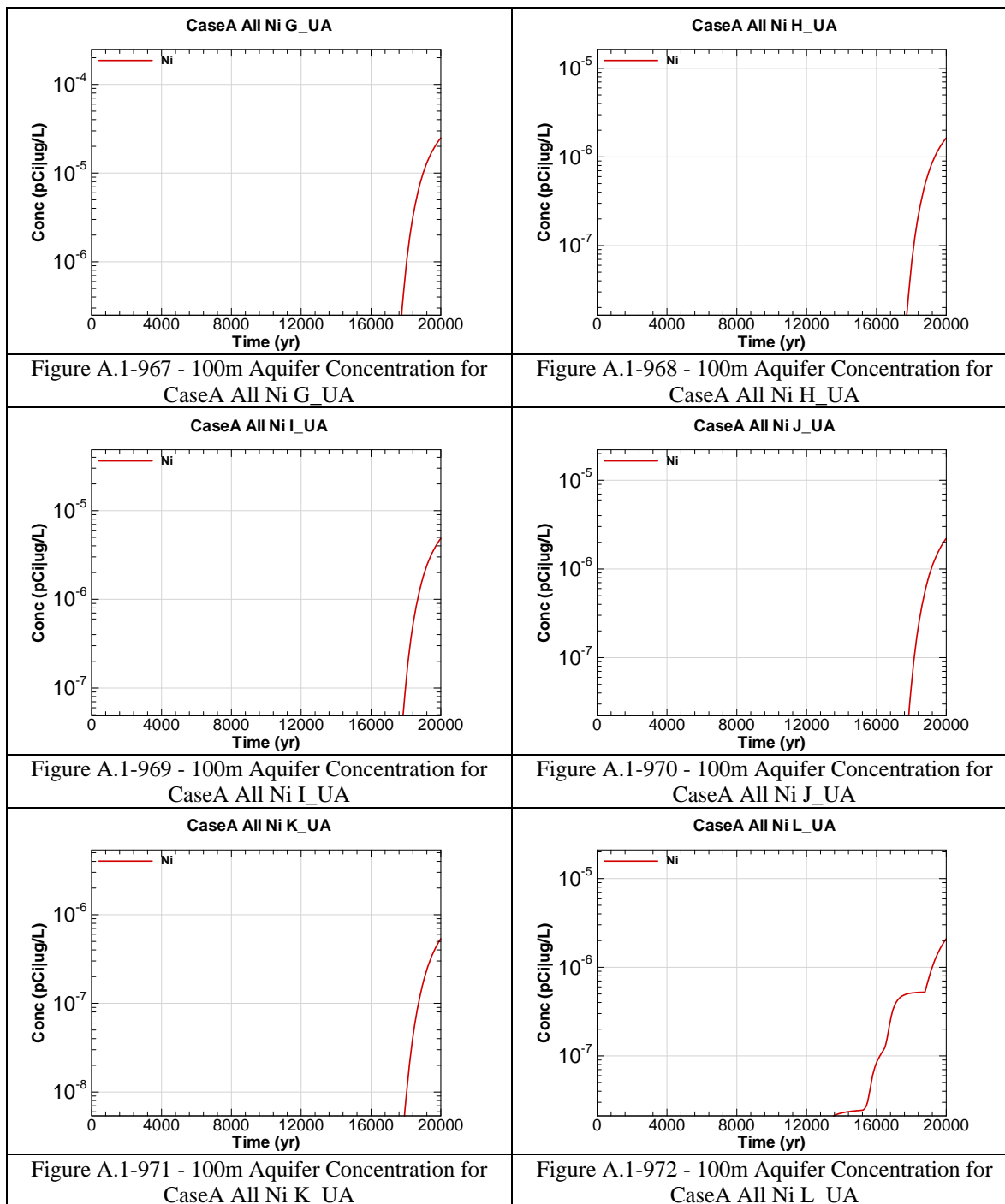


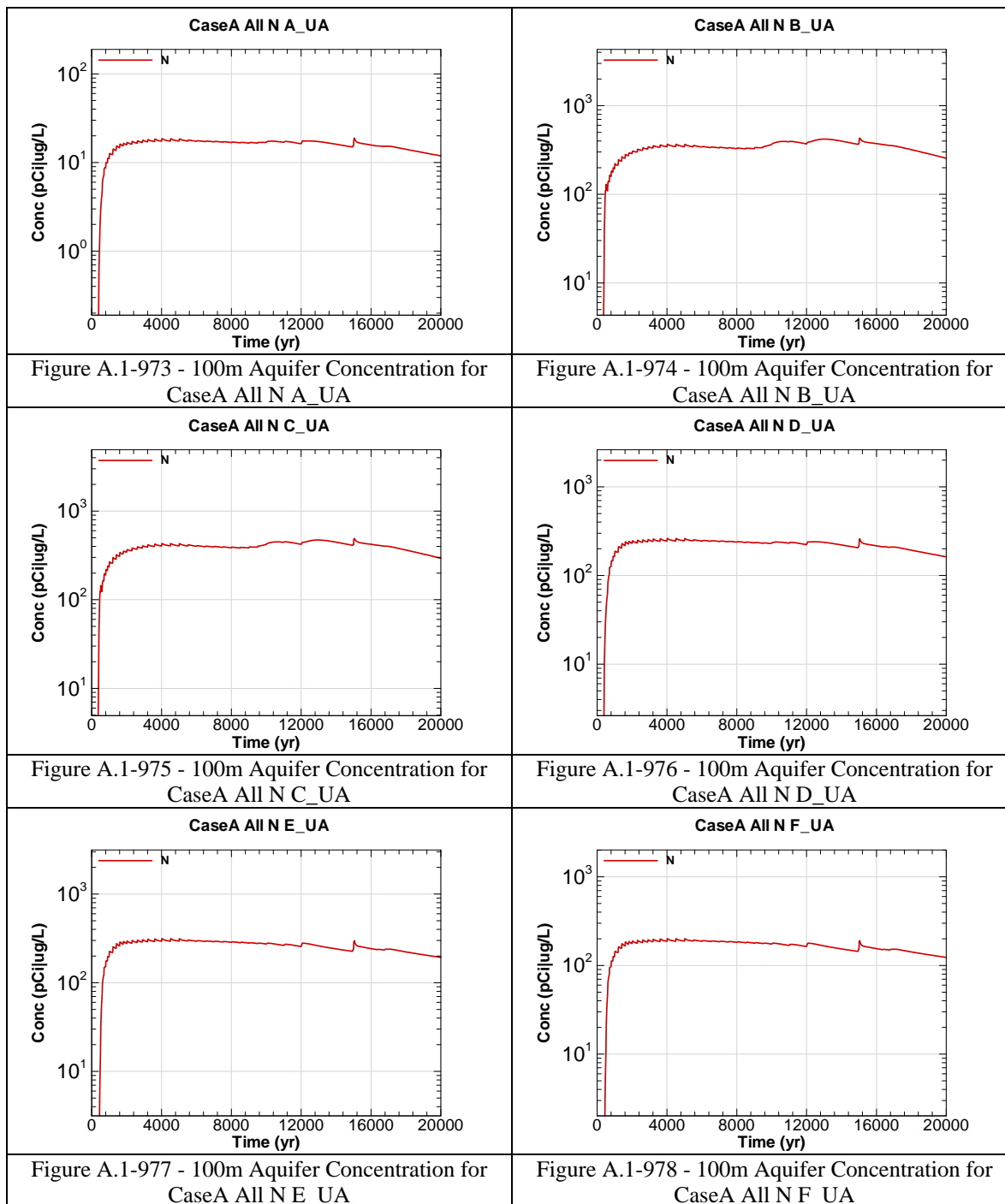


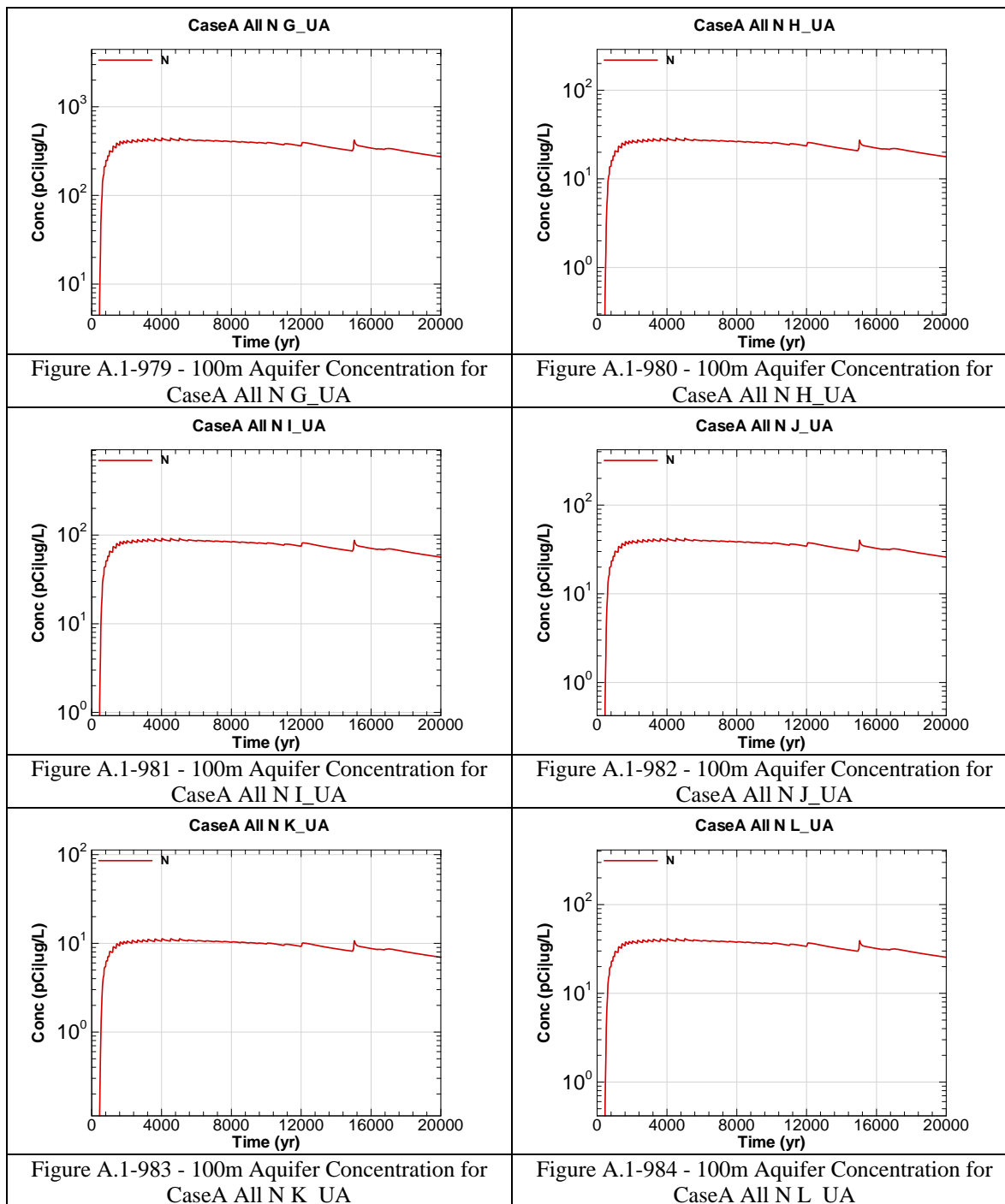


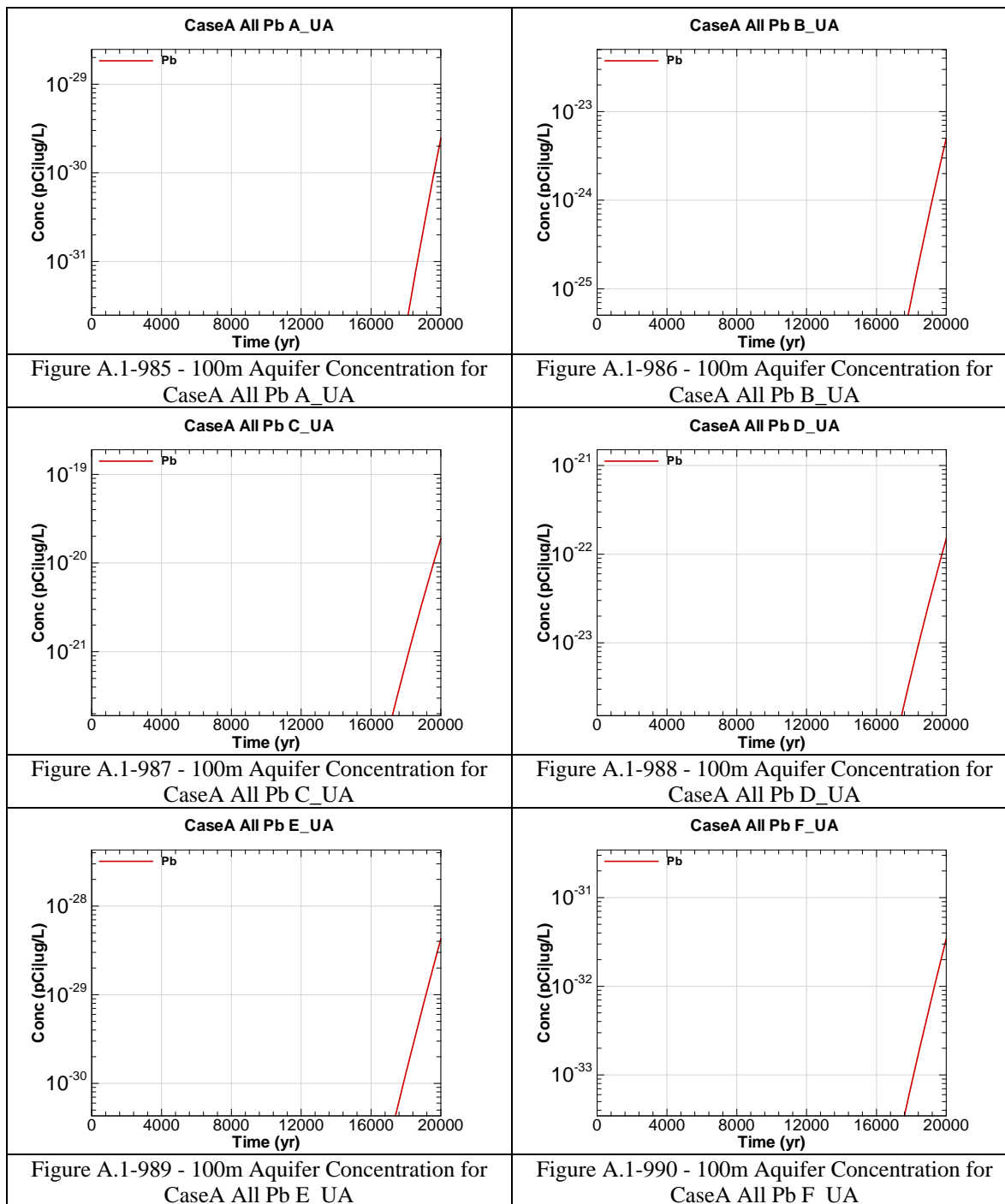


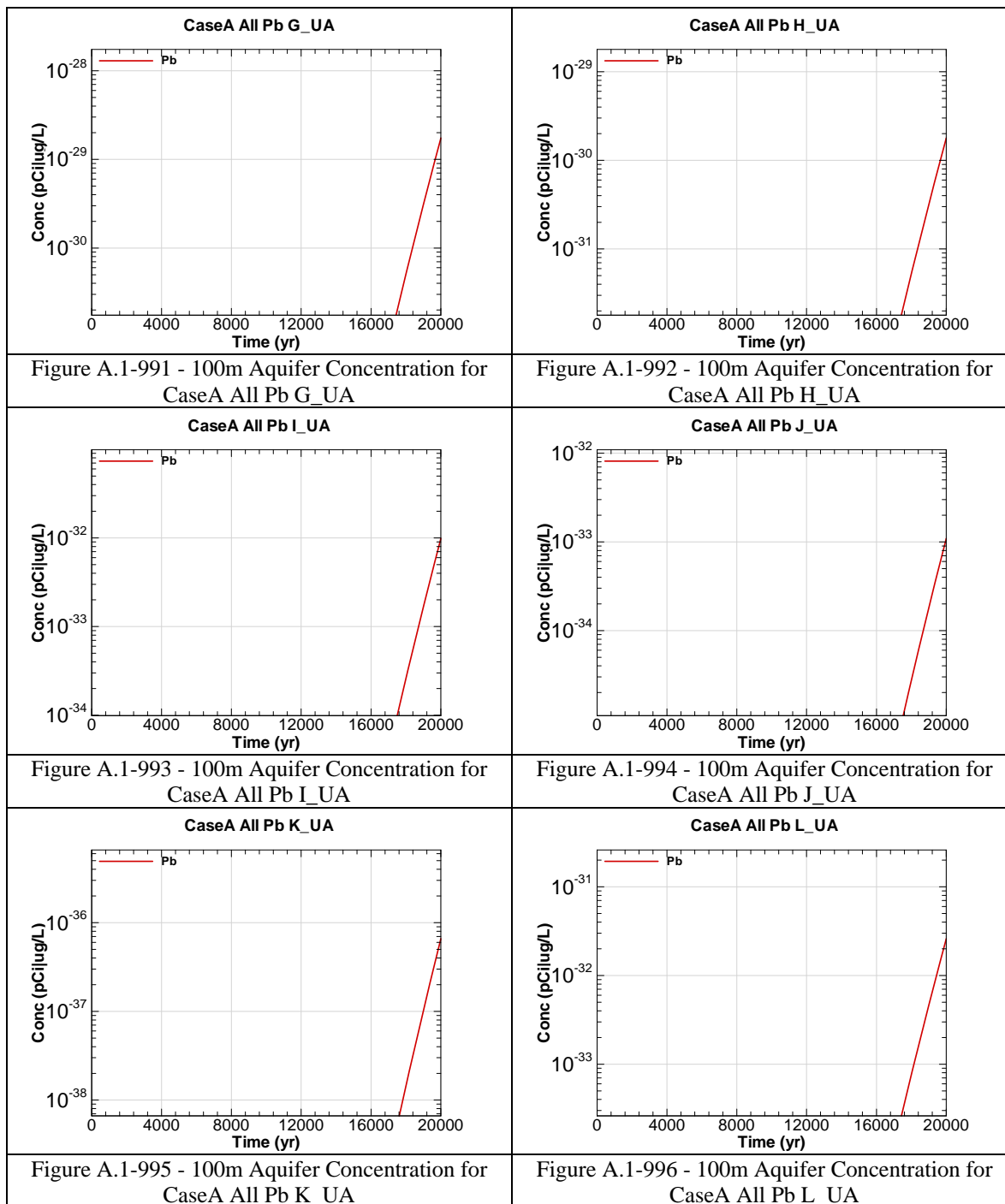


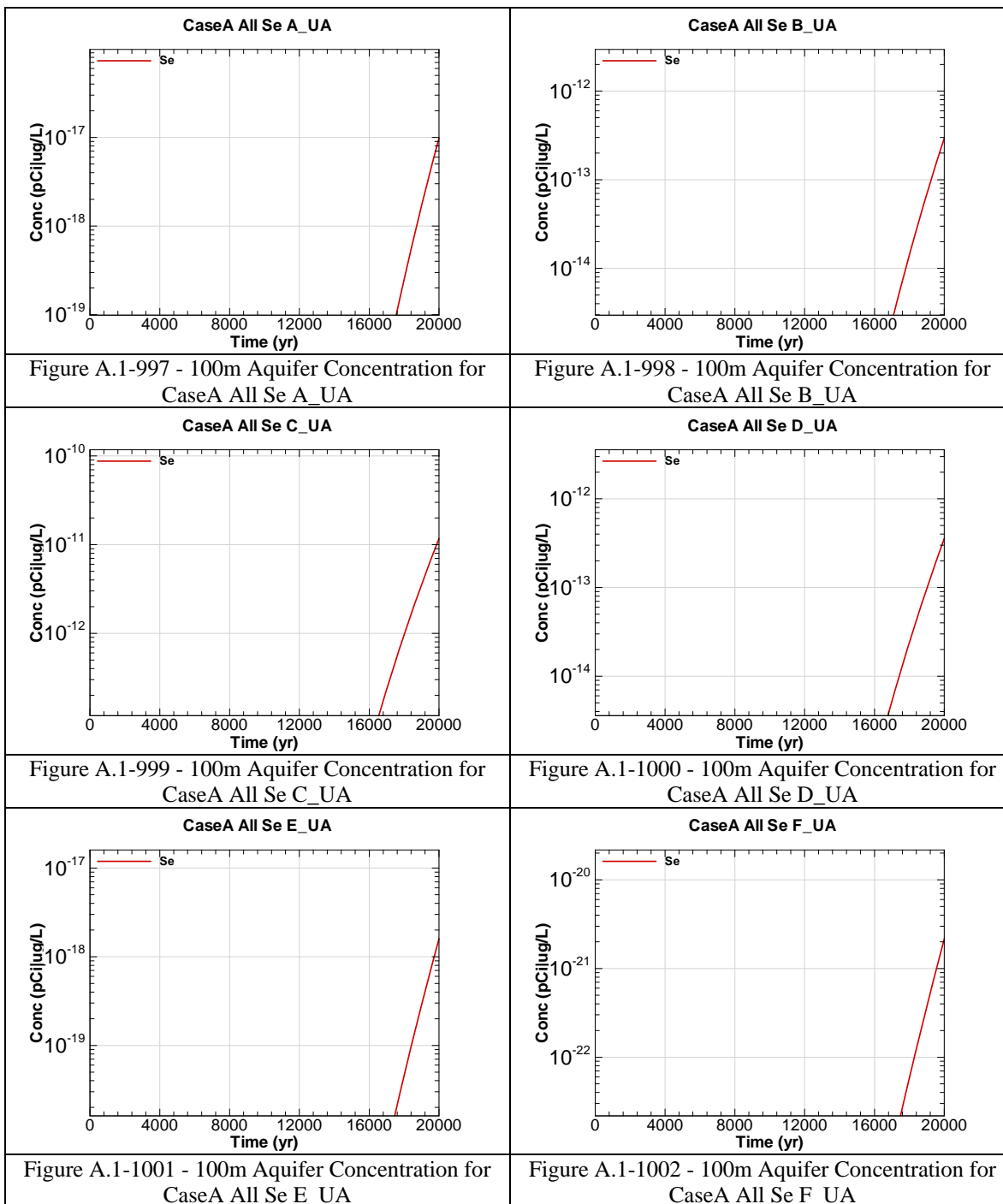


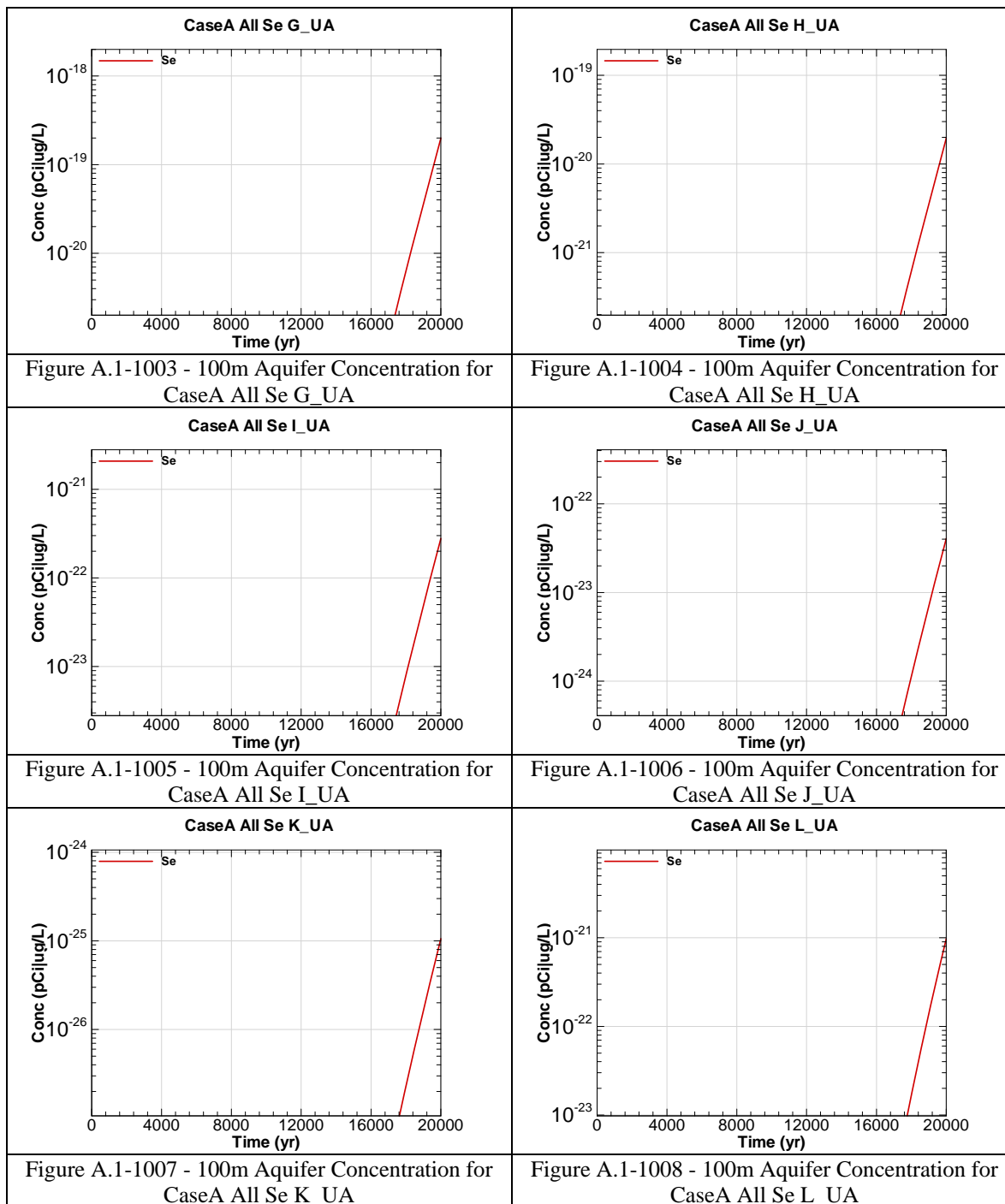


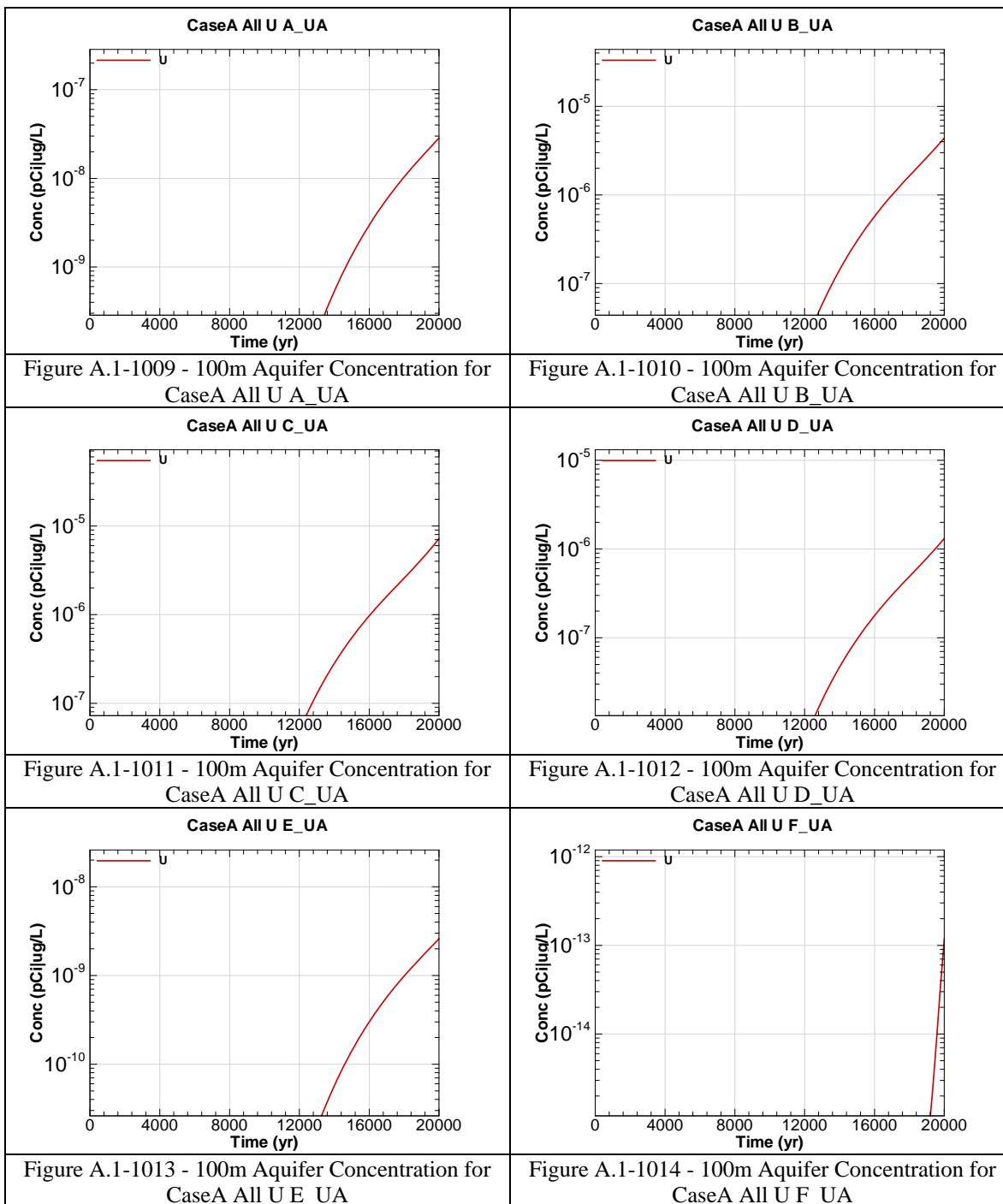


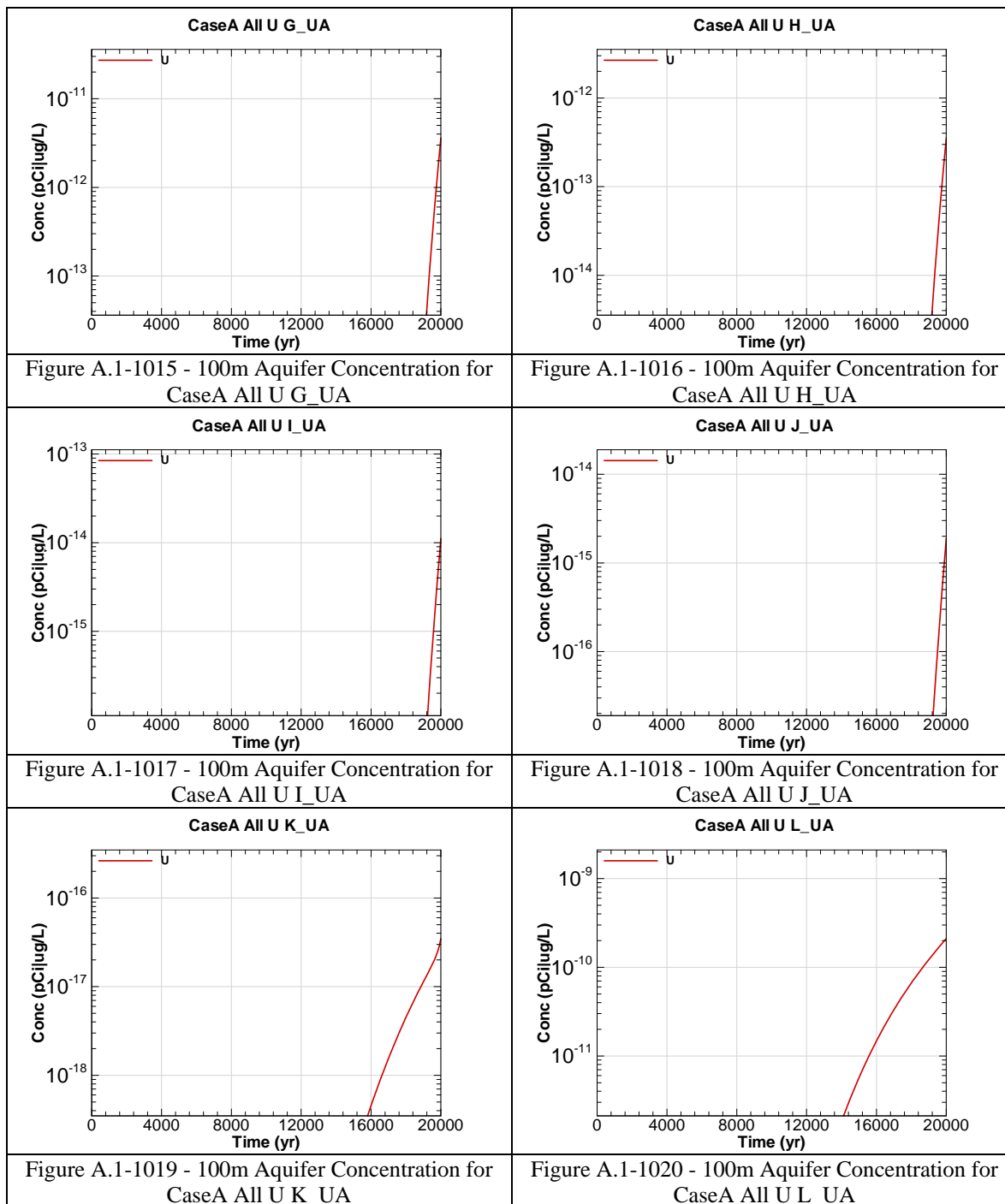


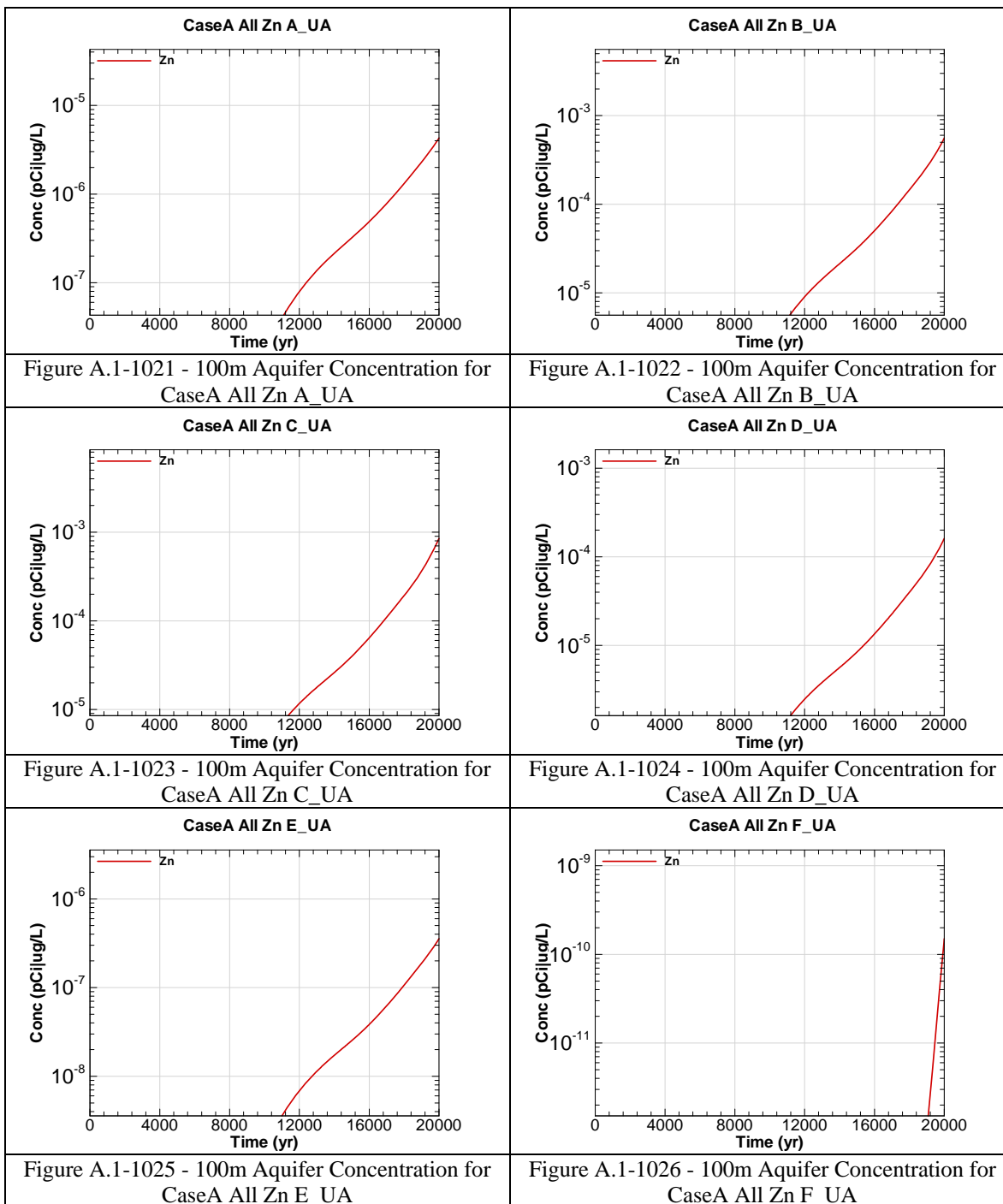


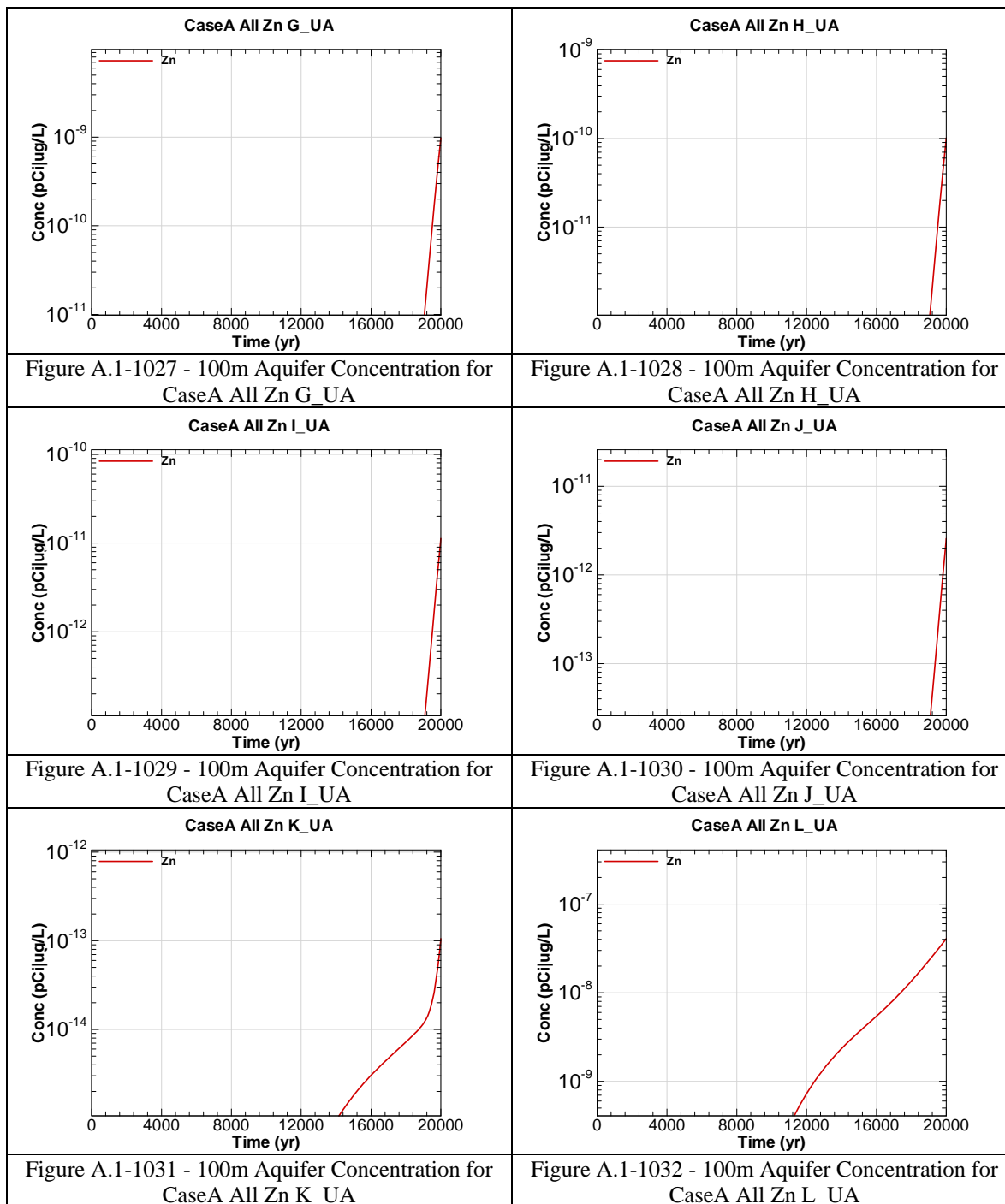












APPENDIX A.2

100-METER RADIOLOGICAL AND CHEMICAL CONCENTRATIONS AT THE UPPER THREE RUNS AQUIFER – LOWER ZONE

Appendix A.2 contains curves showing the 100 meter radiological and chemical concentrations for all of SDF (vault and FDC inventories) for the Base Case (Case A). 20,000 year concentration results are presented from the Upper Three Runs Aquifer- Lower Zone for Sectors A through L.

Graph heading example “CaseA All Ac-227 A_LA”

Key

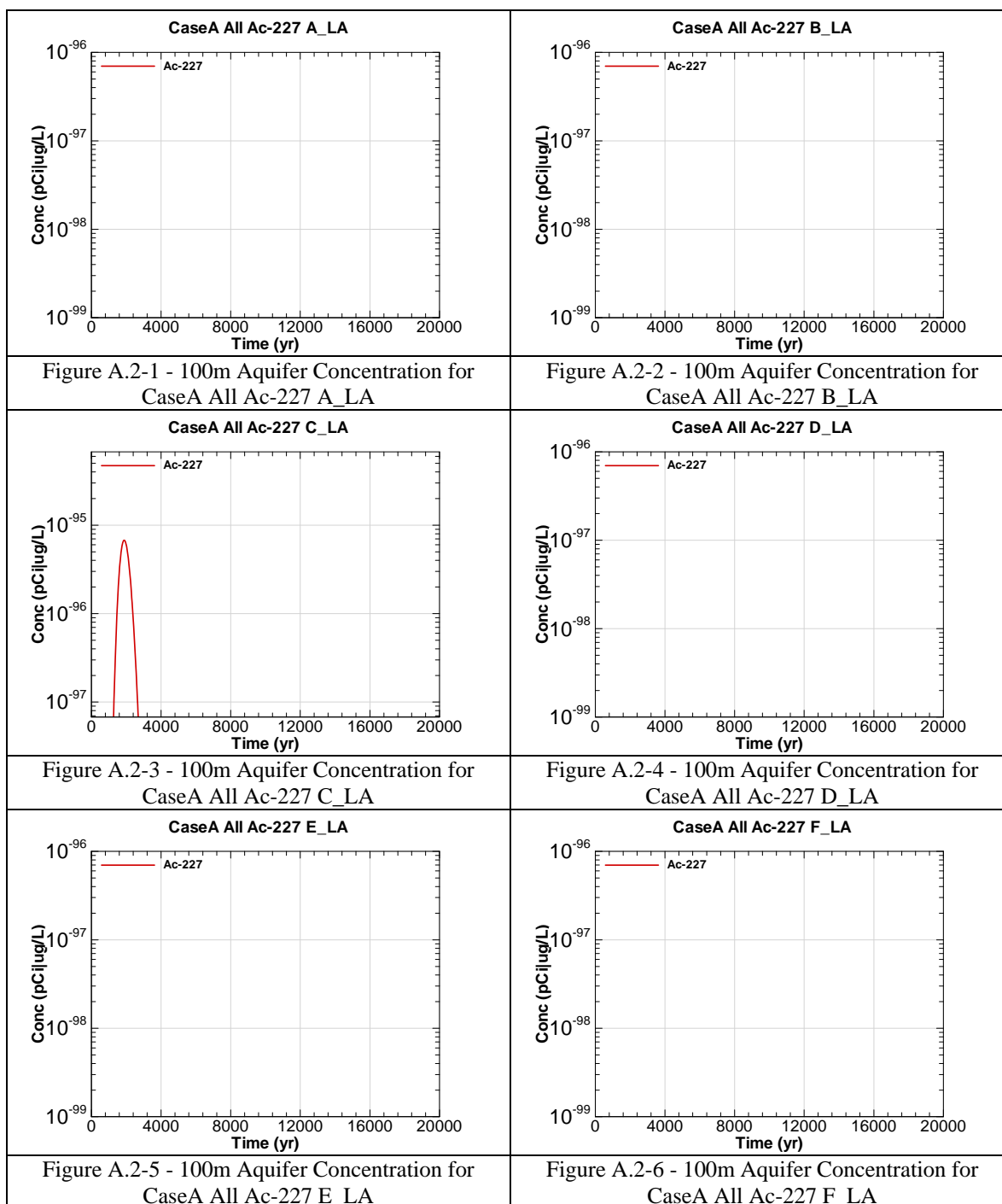
CaseA = Scenario case

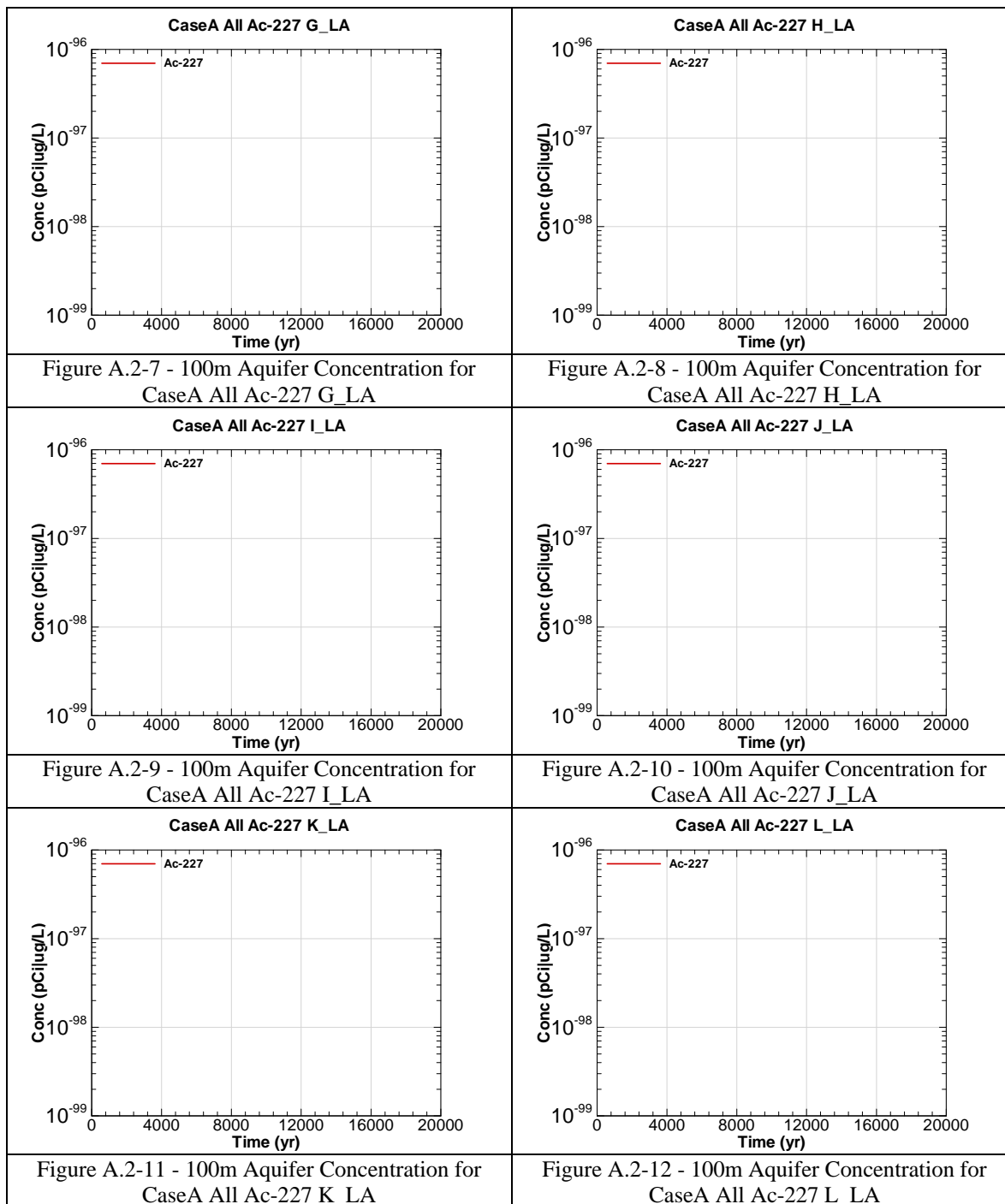
All = Inventory source is all disposal units

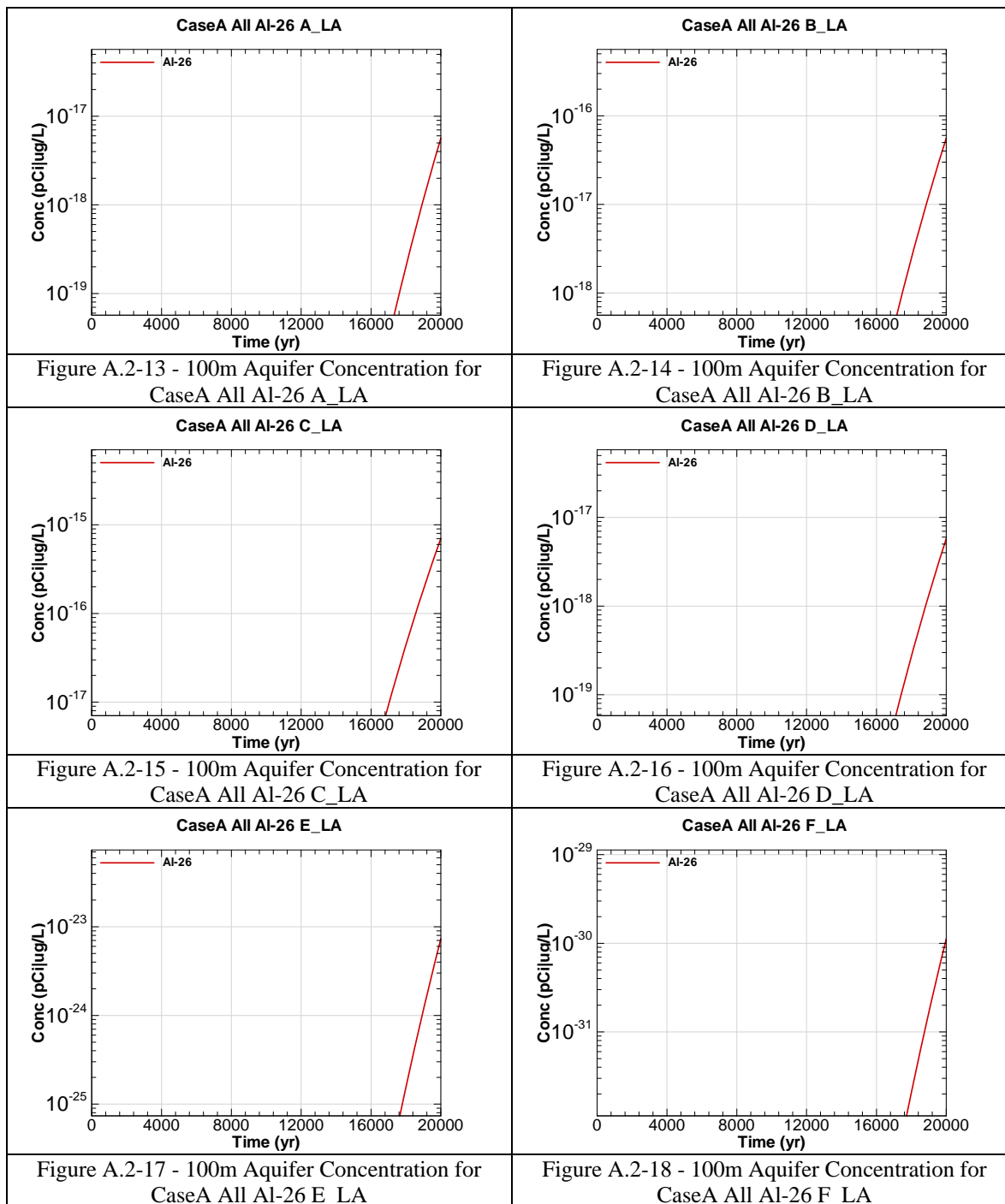
Ac-227 = Radionuclide or chemical of concern

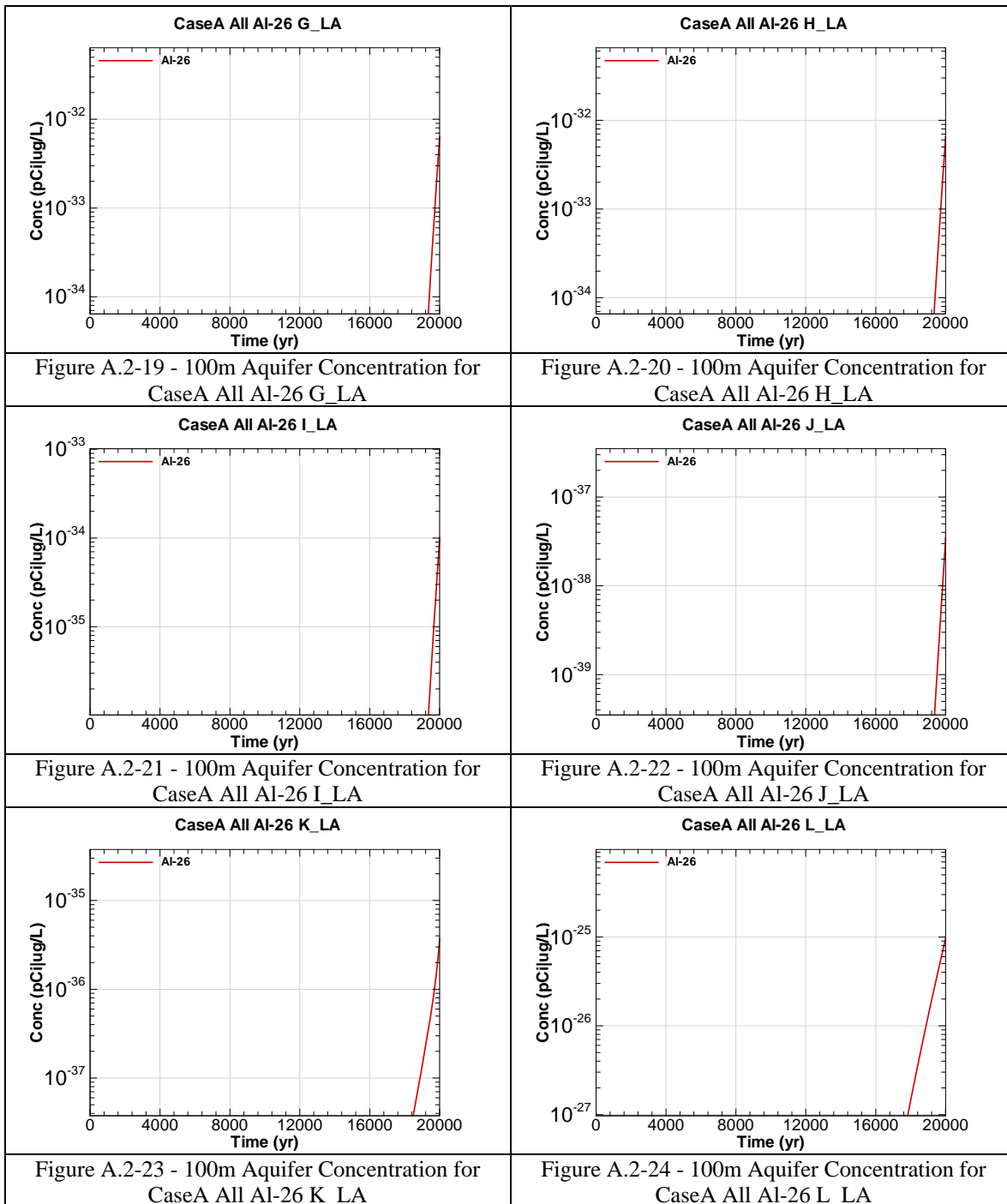
A = Evaluation sector of concern

UA = Aquifer of concern is Upper Three Runs Aquifer – Lower Zone









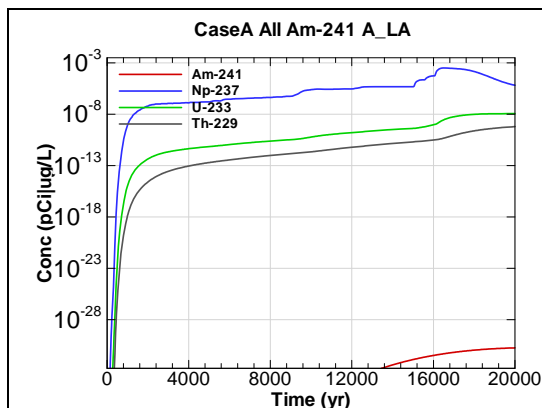


Figure A.2-25 - 100m Aquifer Concentration for CaseA All Am-241 A_LA

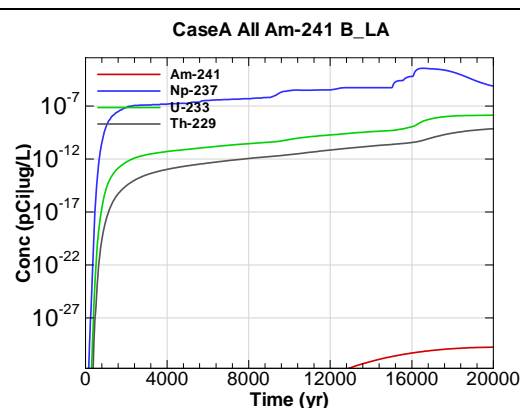


Figure A.2-26 - 100m Aquifer Concentration for CaseA All Am-241 B_LA

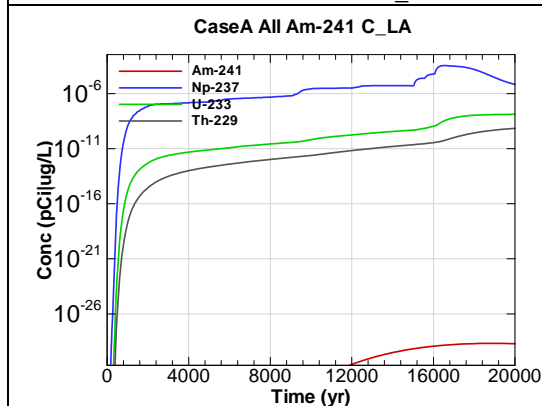


Figure A.2-27 - 100m Aquifer Concentration for CaseA All Am-241 C_LA

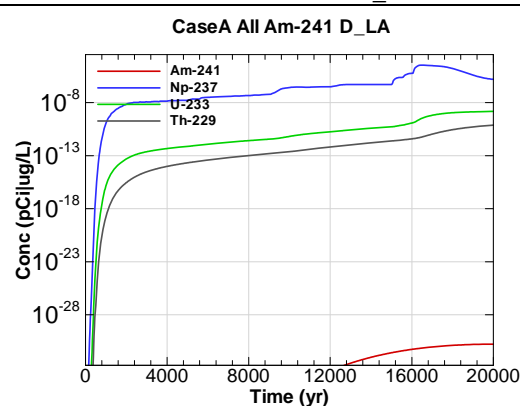


Figure A.2-28 - 100m Aquifer Concentration for CaseA All Am-241 D_LA

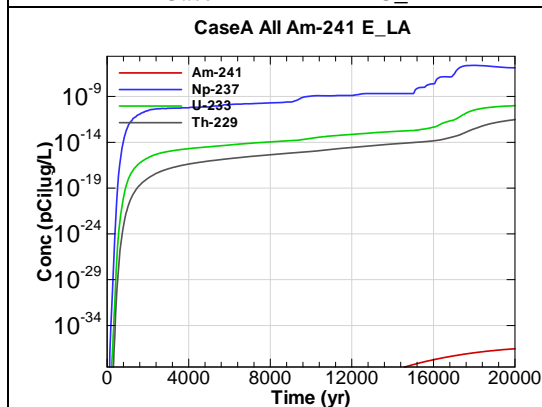


Figure A.2-29 - 100m Aquifer Concentration for CaseA All Am-241 E_LA

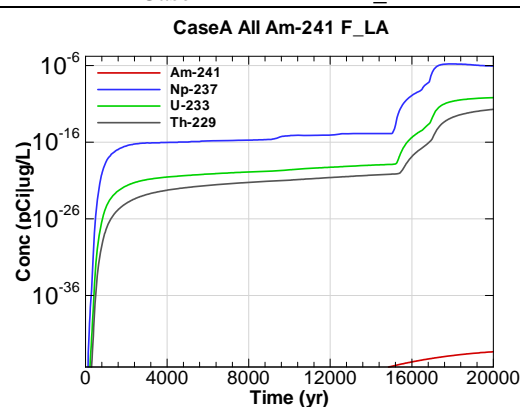


Figure A.2-30 - 100m Aquifer Concentration for CaseA All Am-241 F_LA

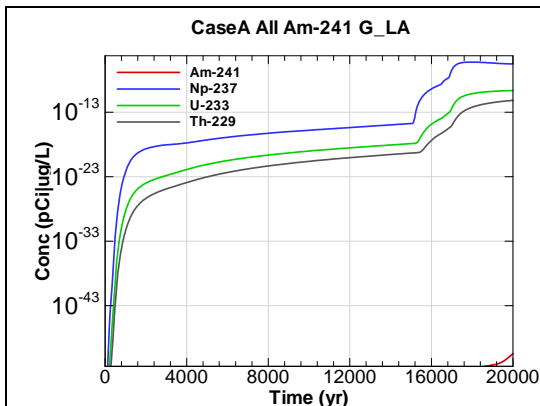


Figure A.2-31 - 100m Aquifer Concentration for
CaseA All Am-241 G_LA

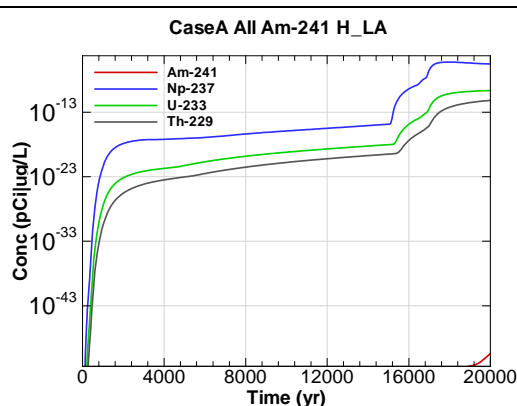


Figure A.2-32 - 100m Aquifer Concentration for
CaseA All Am-241 H_LA

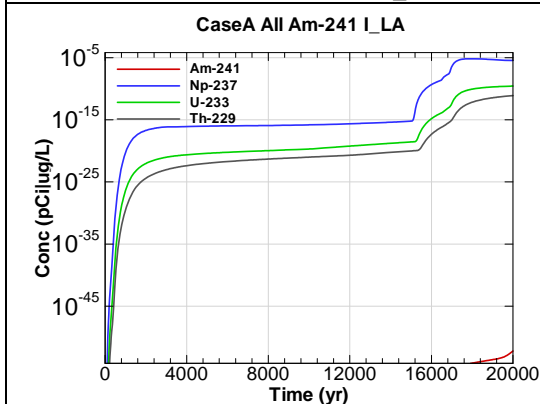


Figure A.2-33 - 100m Aquifer Concentration for
CaseA All Am-241 I_LA

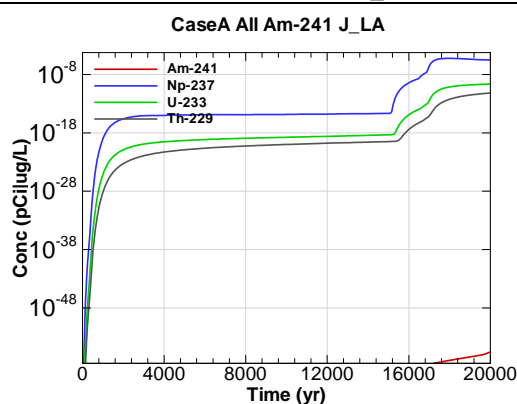


Figure A.2-34 - 100m Aquifer Concentration for
CaseA All Am-241 J_LA

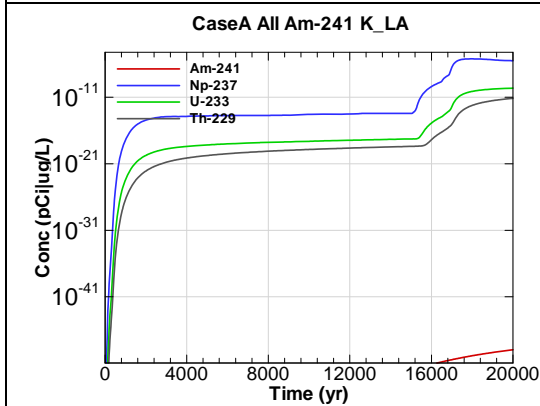


Figure A.2-35 - 100m Aquifer Concentration for
CaseA All Am-241 K_LA

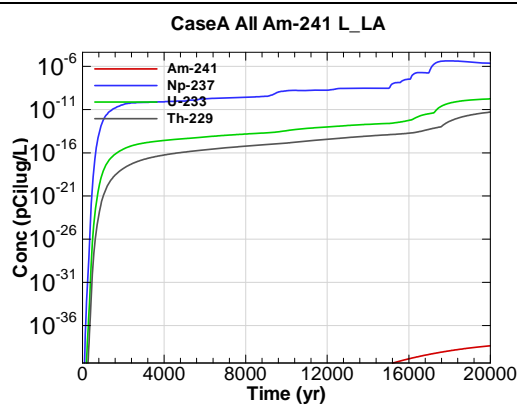


Figure A.2-36 - 100m Aquifer Concentration for
CaseA All Am-241 L_LA

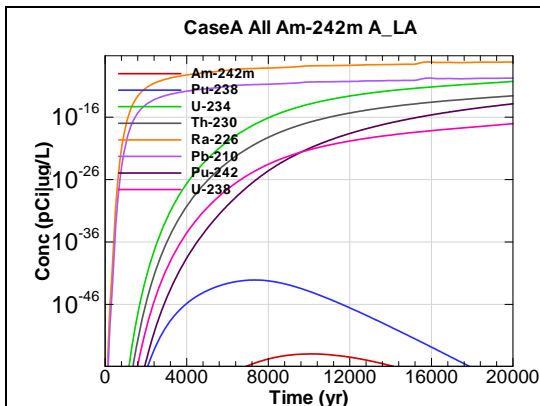


Figure A.2-37 - 100m Aquifer Concentration for CaseA All Am-242m A_LA

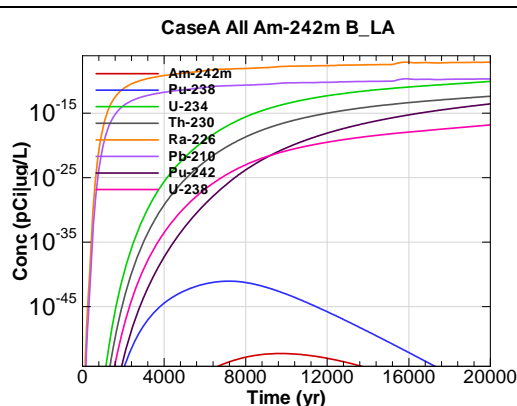


Figure A.2-38 - 100m Aquifer Concentration for CaseA All Am-242m B_LA

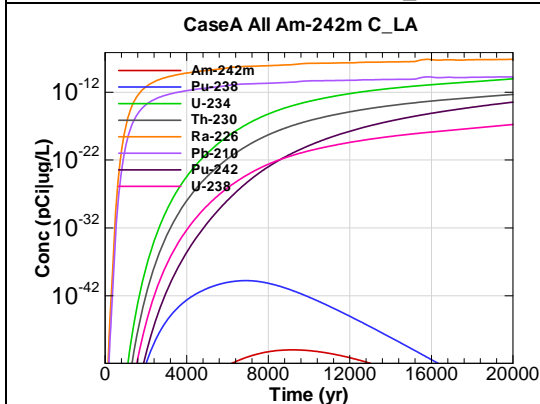


Figure A.2-39 - 100m Aquifer Concentration for CaseA All Am-242m C_LA

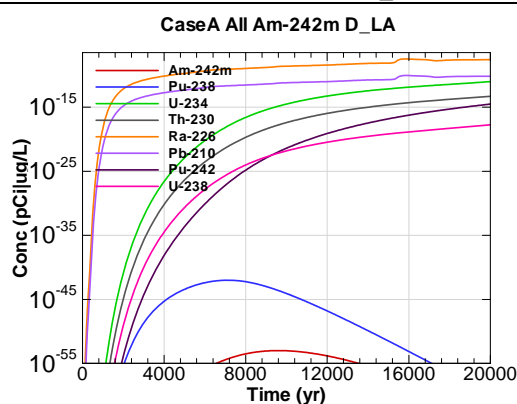


Figure A.2-40 - 100m Aquifer Concentration for CaseA All Am-242m D_LA

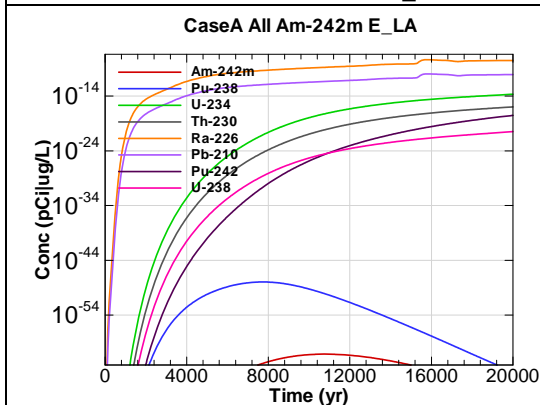


Figure A.2-41 - 100m Aquifer Concentration for CaseA All Am-242m E_LA

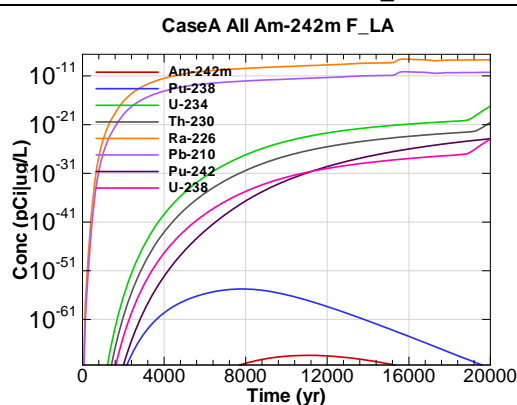


Figure A.2-42 - 100m Aquifer Concentration for CaseA All Am-242m F_LA

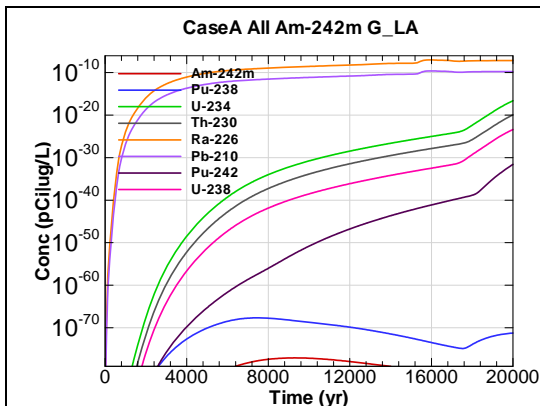


Figure A.2-43 - 100m Aquifer Concentration for CaseA All Am-242m G_LA

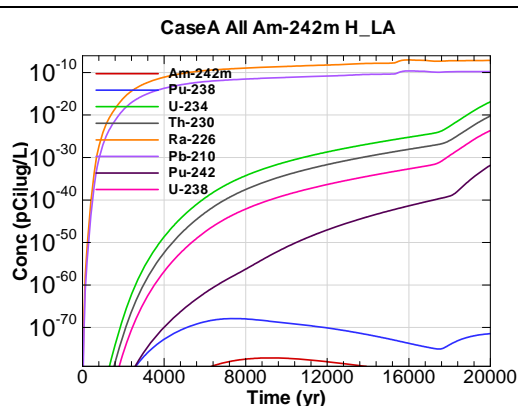


Figure A.2-44 - 100m Aquifer Concentration for CaseA All Am-242m H_LA

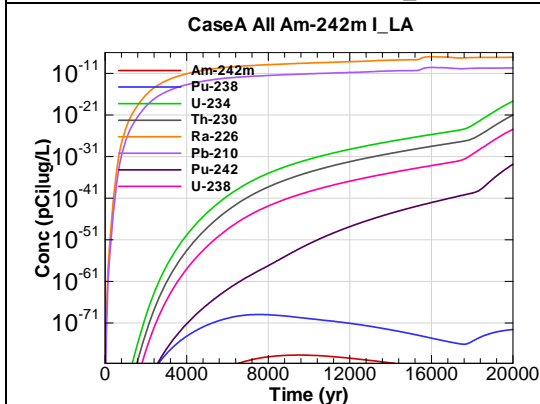


Figure A.2-45 - 100m Aquifer Concentration for CaseA All Am-242m I_LA

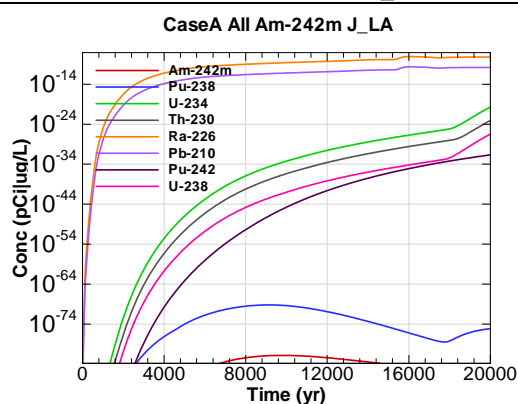


Figure A.2-46 - 100m Aquifer Concentration for CaseA All Am-242m J_LA

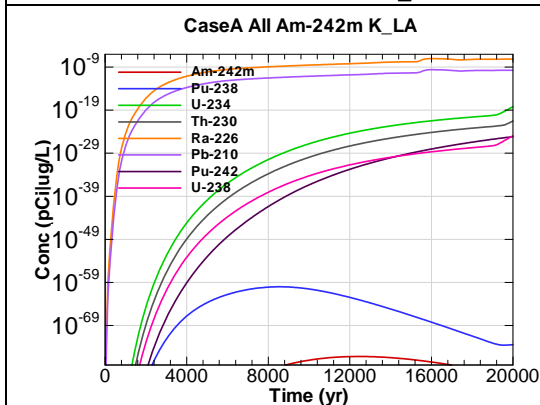


Figure A.2-47 - 100m Aquifer Concentration for CaseA All Am-242m K_LA

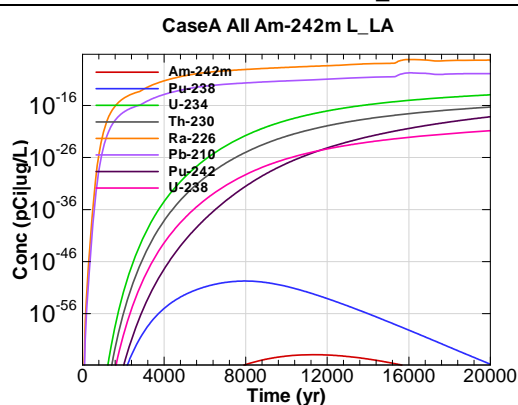


Figure A.2-48 - 100m Aquifer Concentration for CaseA All Am-242m L_LA

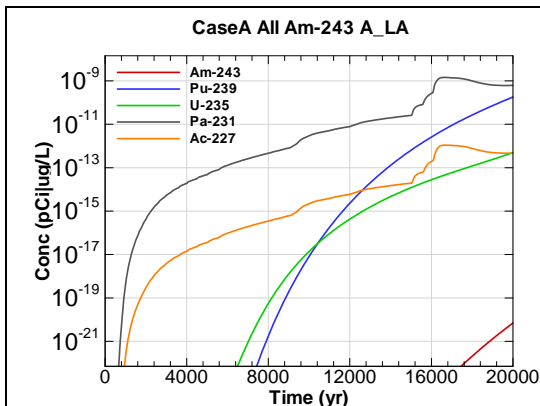


Figure A.2-49 - 100m Aquifer Concentration for
CaseA All Am-243 A_LA

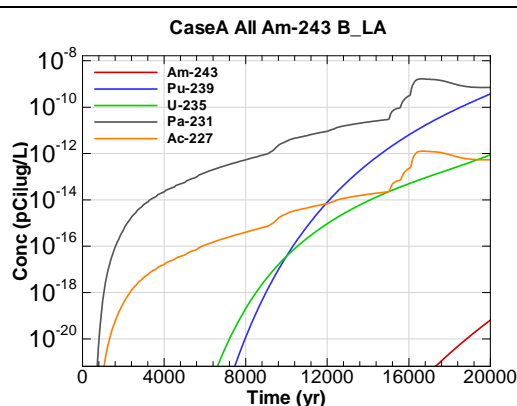


Figure A.2-50 - 100m Aquifer Concentration for
CaseA All Am-243 B_LA

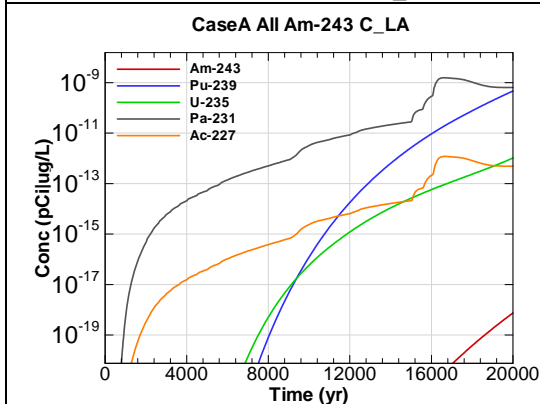


Figure A.2-51 - 100m Aquifer Concentration for
CaseA All Am-243 C_LA

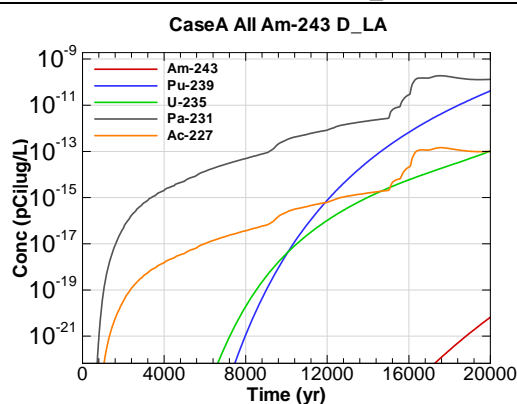


Figure A.2-52 - 100m Aquifer Concentration for
CaseA All Am-243 D_LA

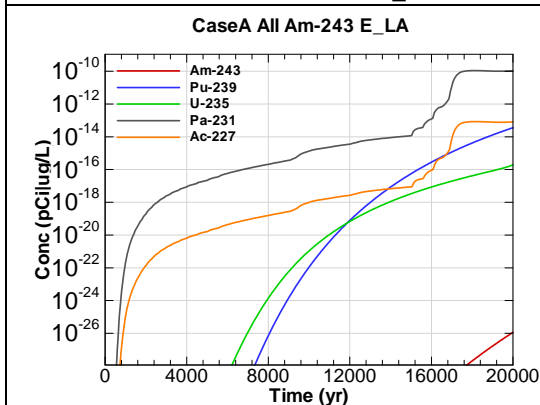


Figure A.2-53 - 100m Aquifer Concentration for
CaseA All Am-243 E_LA

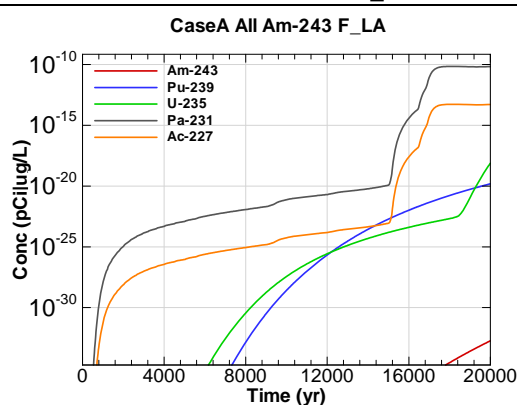


Figure A.2-54 - 100m Aquifer Concentration for
CaseA All Am-243 F_LA

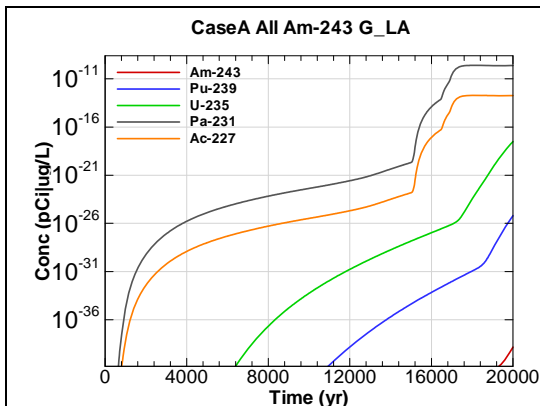


Figure A.2-55 - 100m Aquifer Concentration for
CaseA All Am-243 G_LA

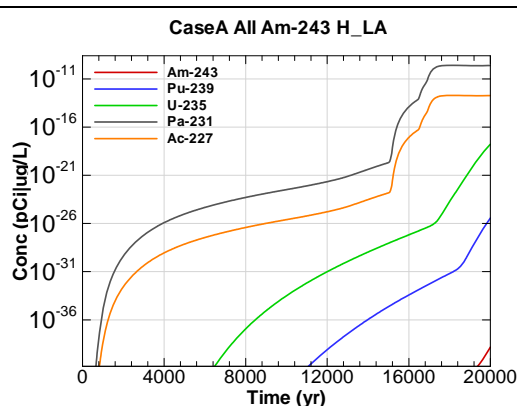


Figure A.2-56 - 100m Aquifer Concentration for
CaseA All Am-243 H_LA

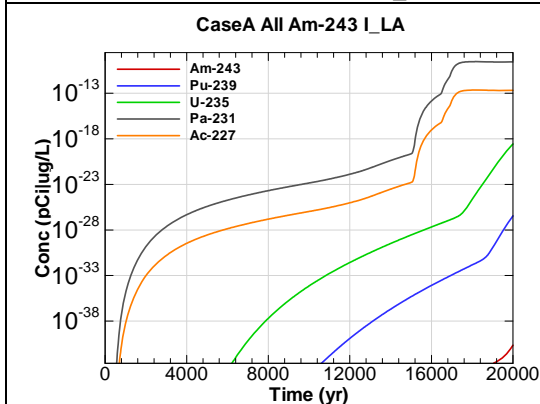


Figure A.2-57 - 100m Aquifer Concentration for
CaseA All Am-243 I_LA

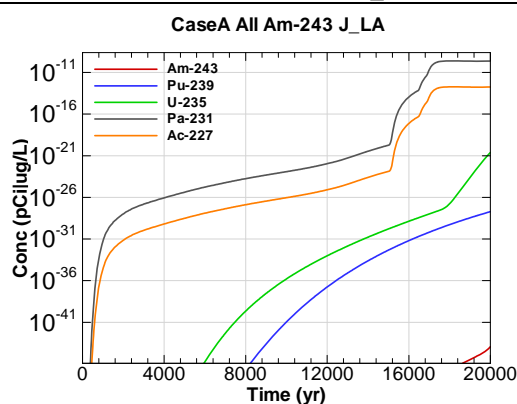


Figure A.2-58 - 100m Aquifer Concentration for
CaseA All Am-243 J_LA

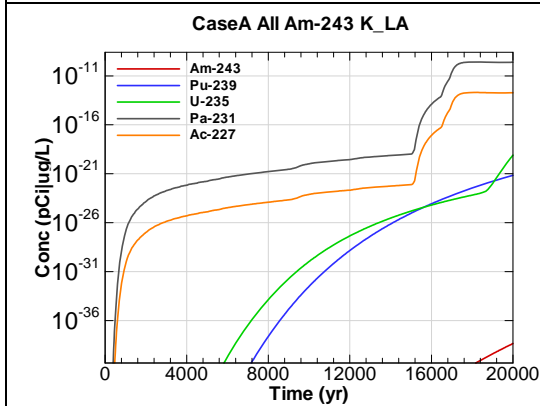


Figure A.2-59 - 100m Aquifer Concentration for
CaseA All Am-243 K_LA

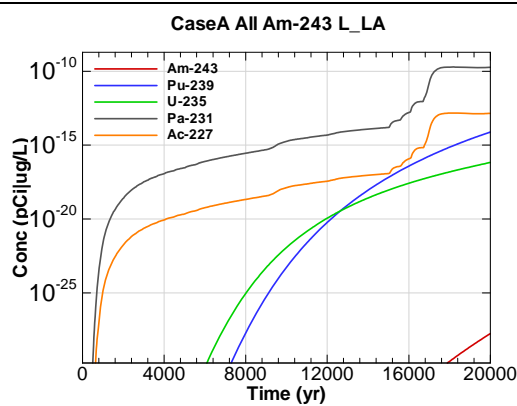
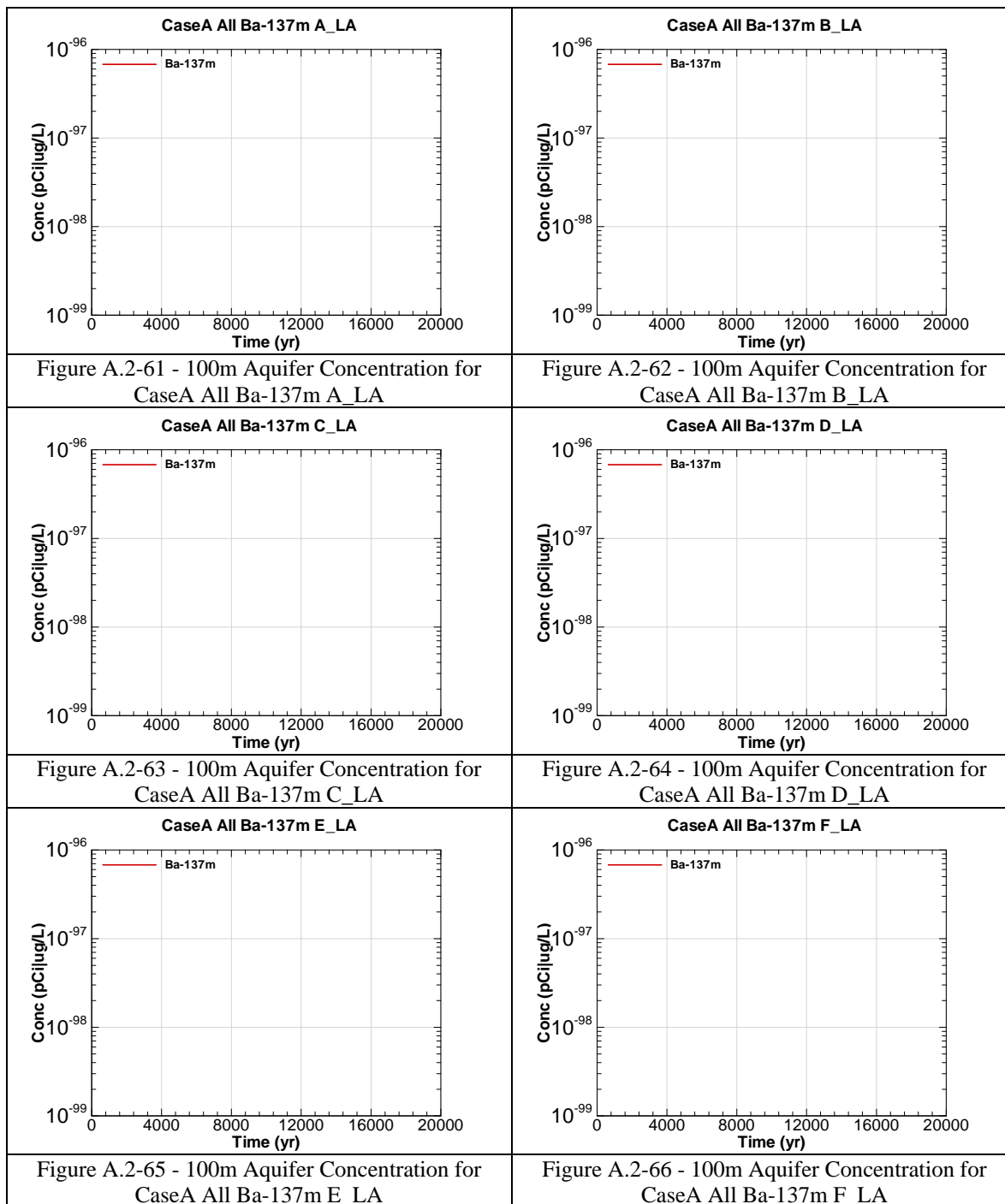
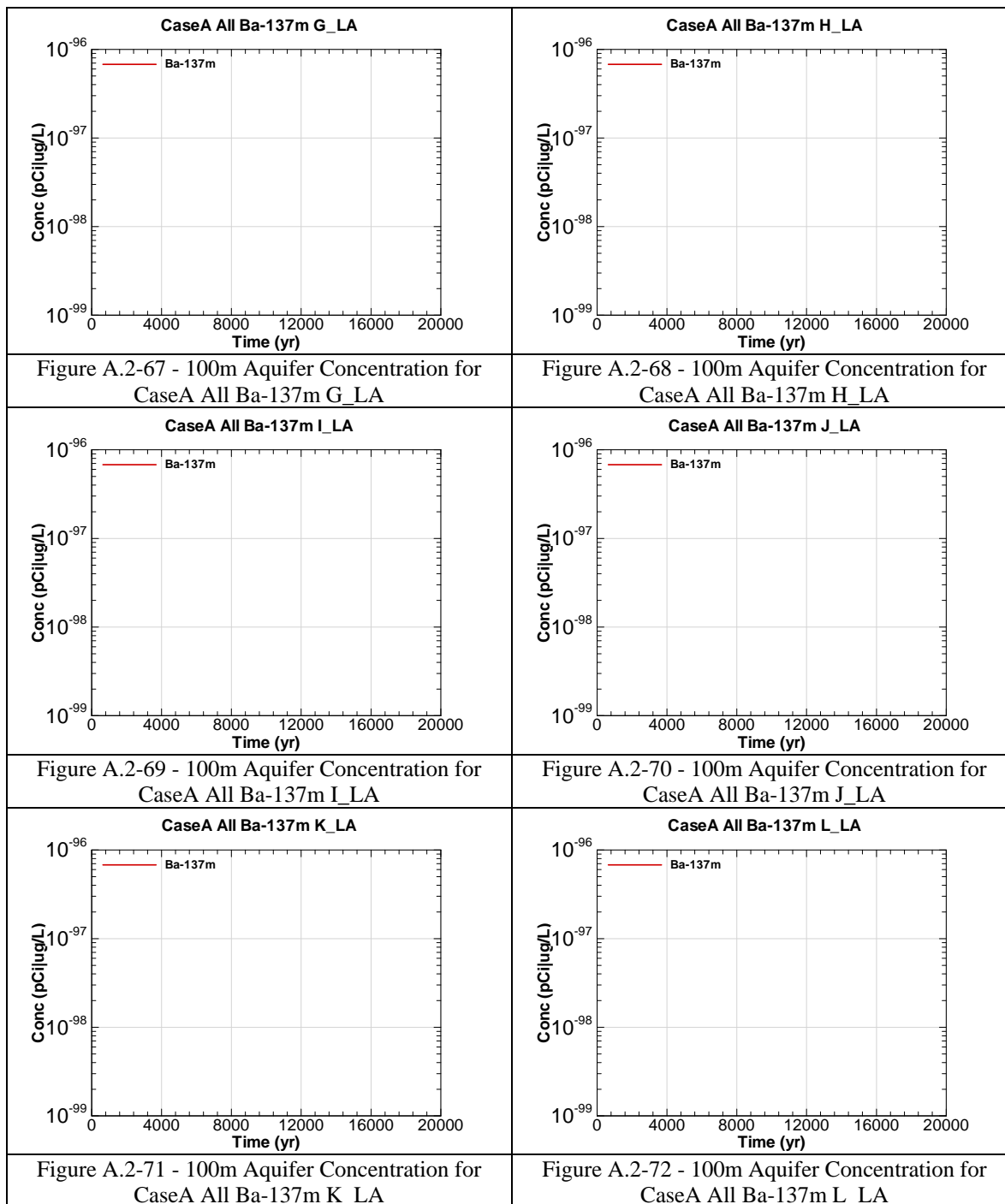


Figure A.2-60 - 100m Aquifer Concentration for
CaseA All Am-243 L_LA





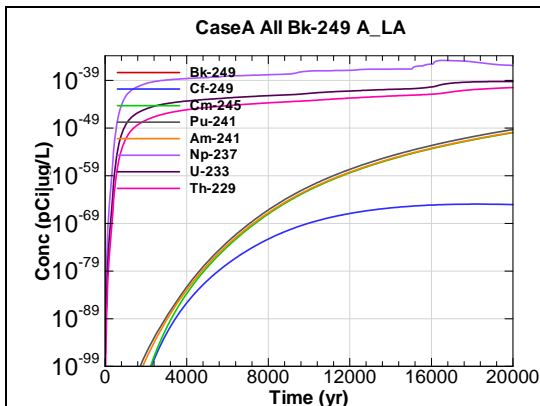


Figure A.2-73 - 100m Aquifer Concentration for
CaseA All Bk-249 A_LA

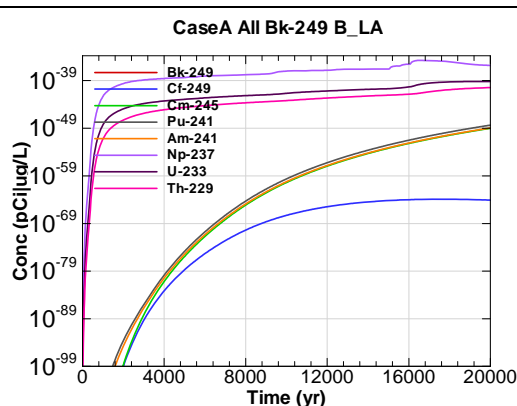


Figure A.2-74 - 100m Aquifer Concentration for
CaseA All Bk-249 B_LA

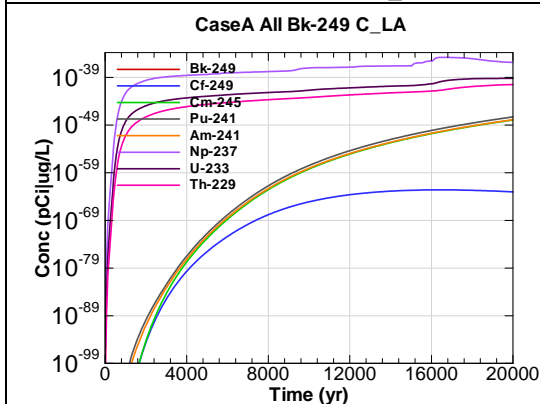


Figure A.2-75 - 100m Aquifer Concentration for
CaseA All Bk-249 C_LA

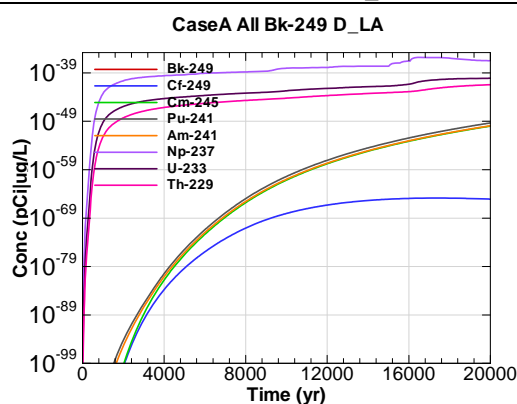


Figure A.2-76 - 100m Aquifer Concentration for
CaseA All Bk-249 D_LA

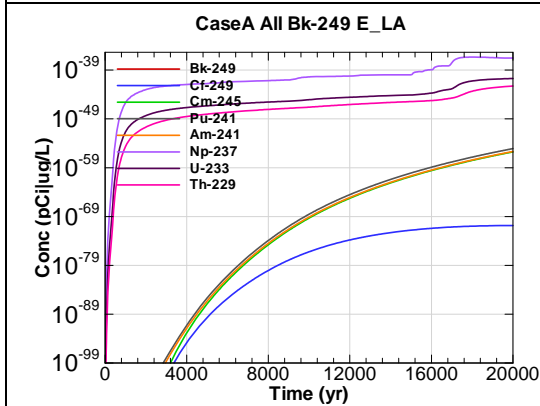


Figure A.2-77 - 100m Aquifer Concentration for
CaseA All Bk-249 E_LA

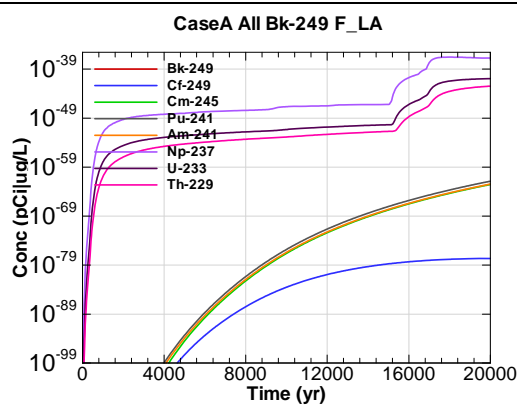


Figure A.2-78 - 100m Aquifer Concentration for
CaseA All Bk-249 F_LA

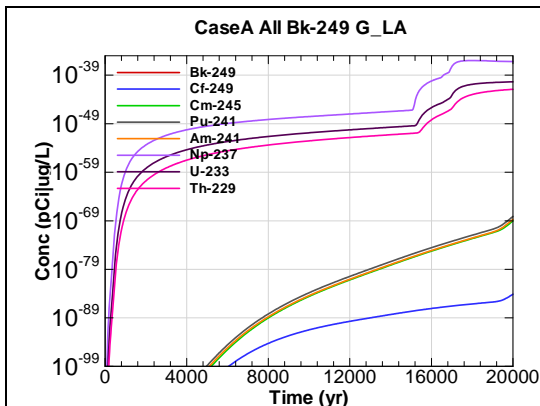


Figure A.2-79 - 100m Aquifer Concentration for
CaseA All Bk-249 G_LA

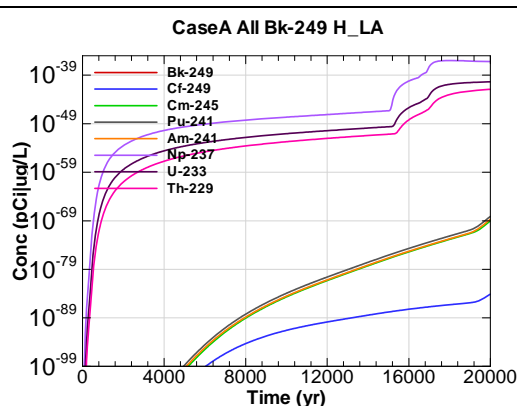


Figure A.2-80 - 100m Aquifer Concentration for
CaseA All Bk-249 H_LA

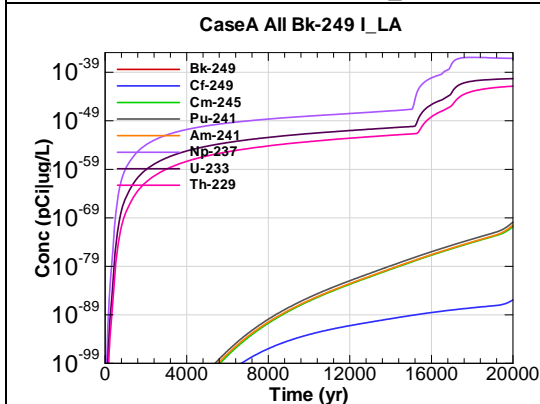


Figure A.2-81 - 100m Aquifer Concentration for
CaseA All Bk-249 I_LA

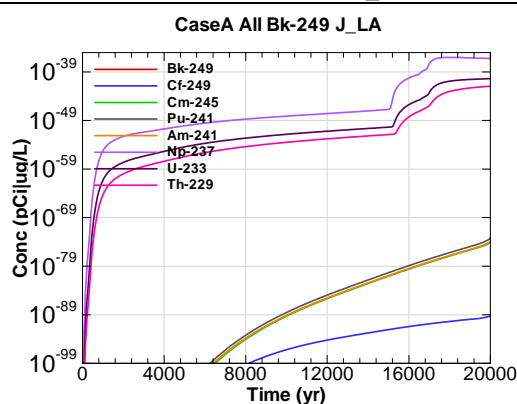


Figure A.2-82 - 100m Aquifer Concentration for
CaseA All Bk-249 J_LA

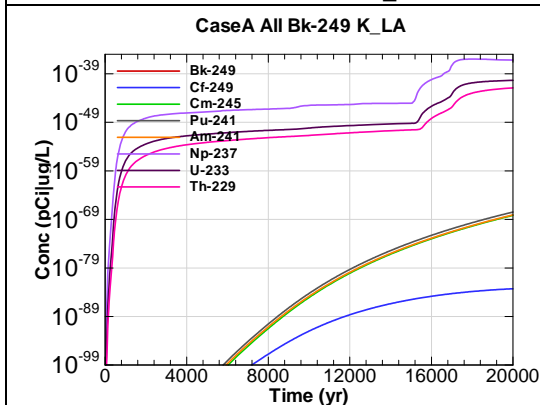


Figure A.2-83 - 100m Aquifer Concentration for
CaseA All Bk-249 K_LA

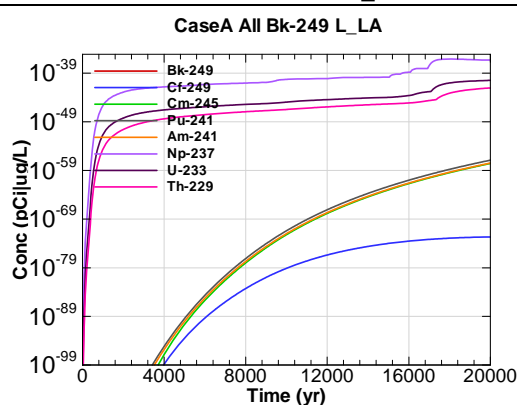


Figure A.2-84 - 100m Aquifer Concentration for
CaseA All Bk-249 L_LA

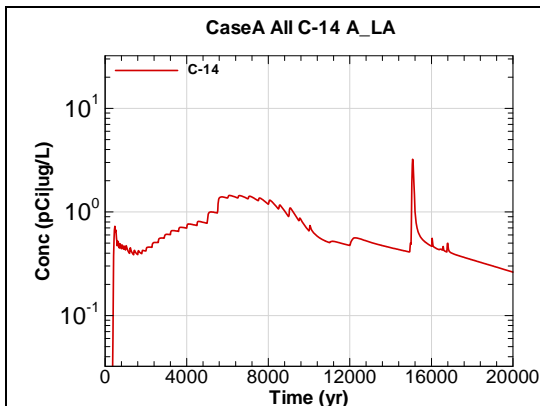


Figure A.2-85 - 100m Aquifer Concentration for
CaseA All C-14 A_LA

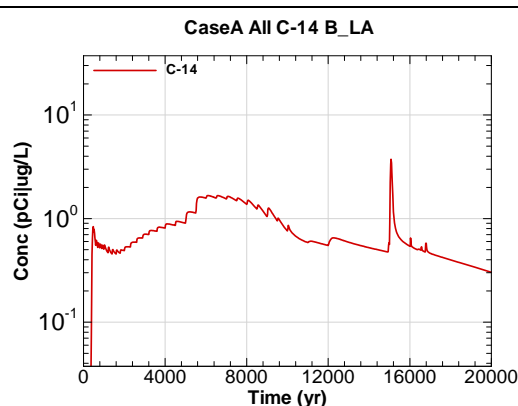


Figure A.2-86 - 100m Aquifer Concentration for
CaseA All C-14 B_LA

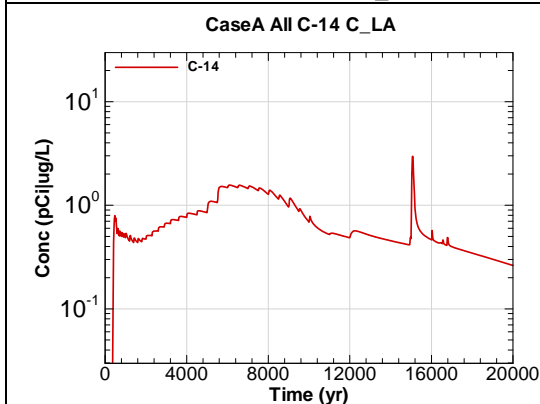


Figure A.2-87 - 100m Aquifer Concentration for
CaseA All C-14 C_LA

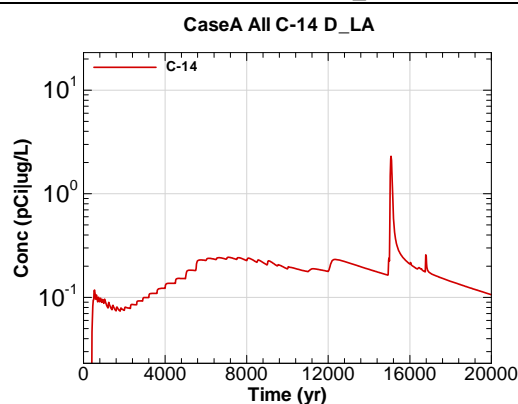


Figure A.2-88 - 100m Aquifer Concentration for
CaseA All C-14 D_LA

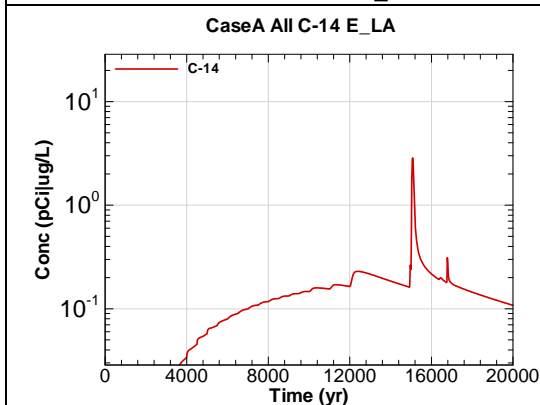


Figure A.2-89 - 100m Aquifer Concentration for
CaseA All C-14 E_LA

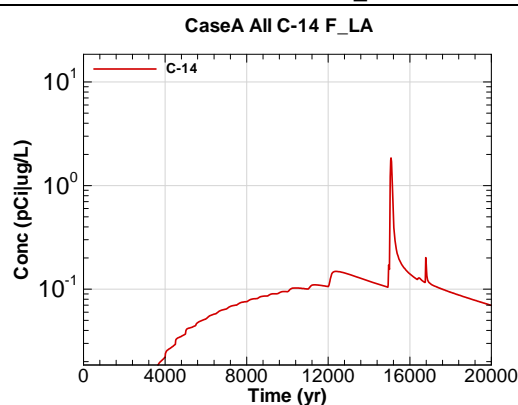
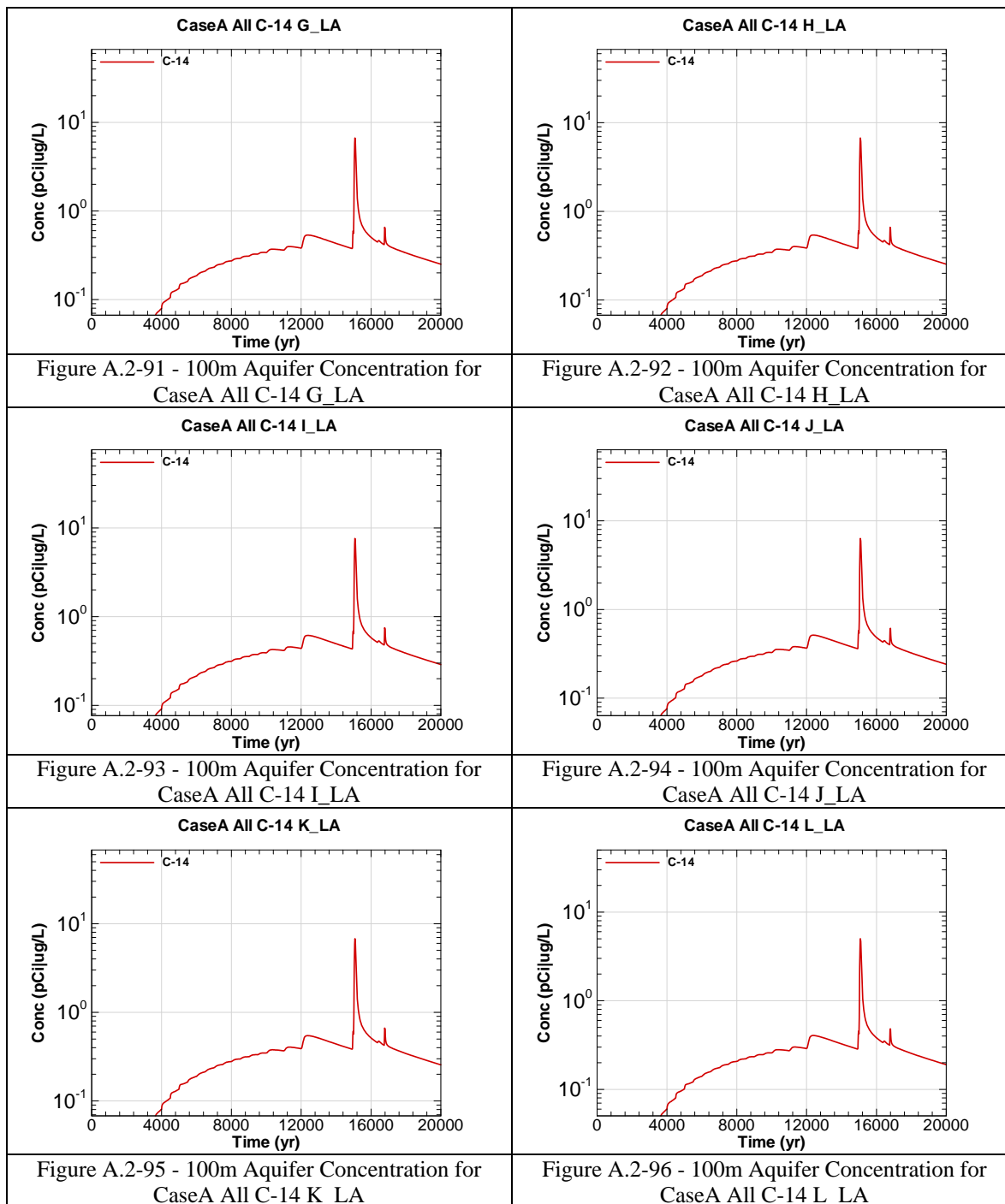
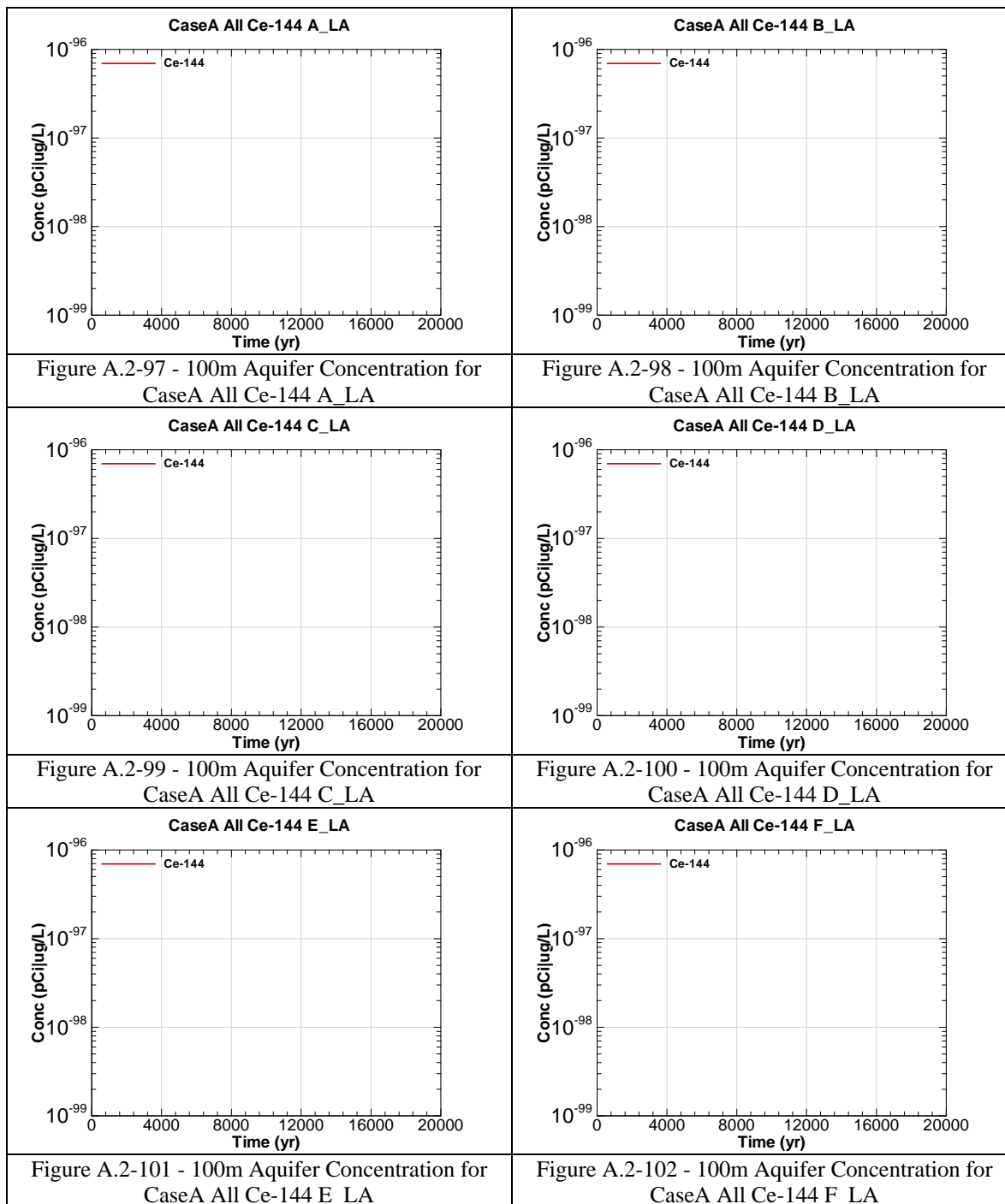
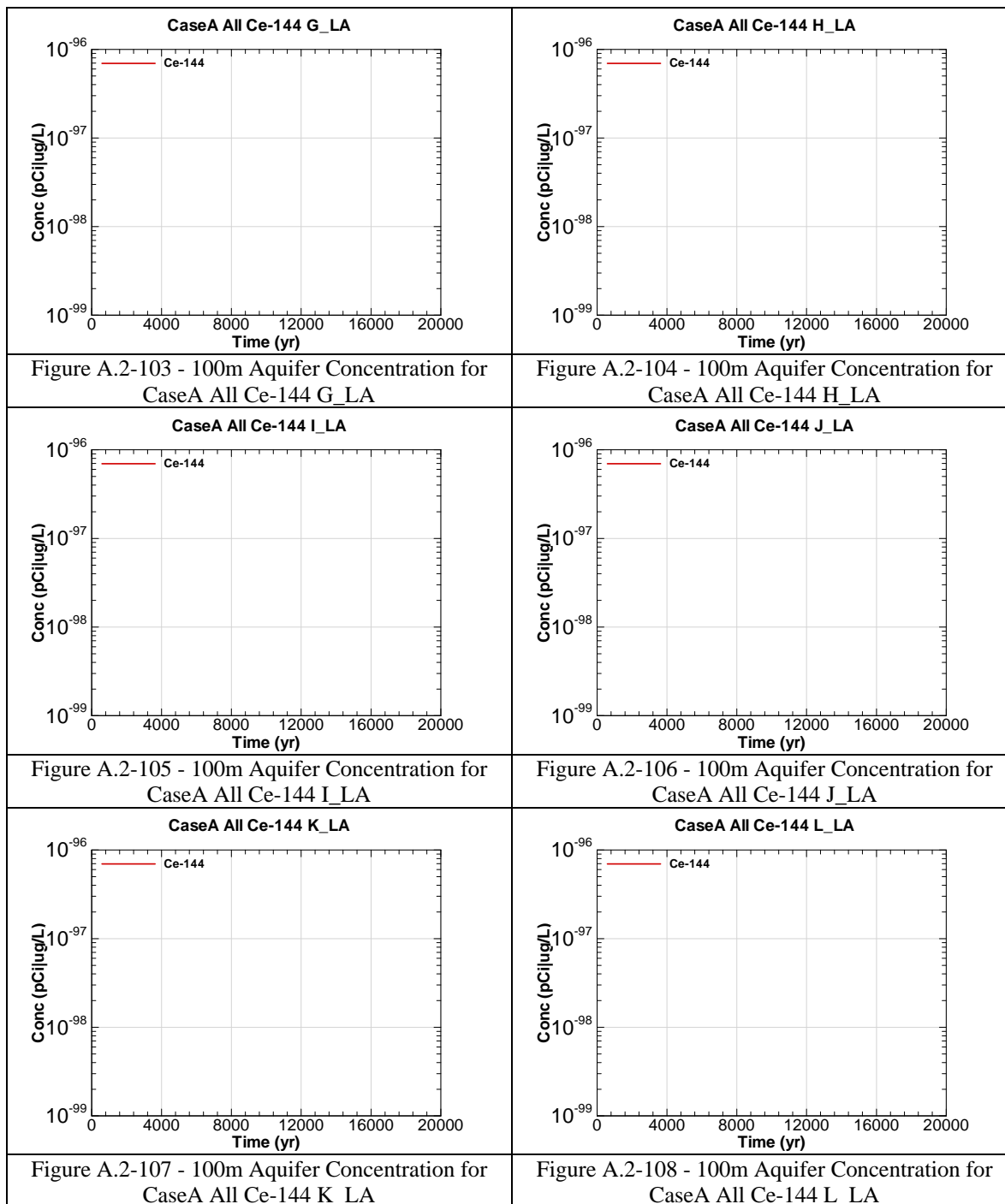


Figure A.2-90 - 100m Aquifer Concentration for
CaseA All C-14 F_LA







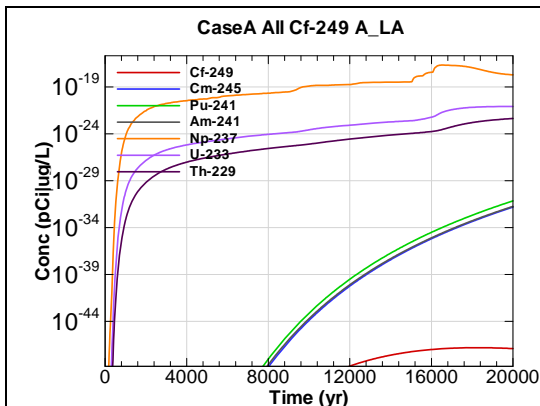


Figure A.2-109 - 100m Aquifer Concentration for
CaseA All Cf-249 A_LA

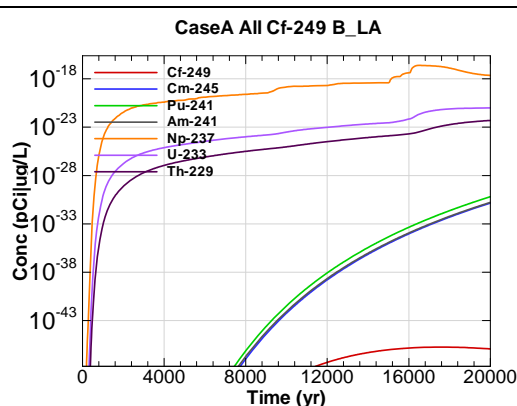


Figure A.2-110 - 100m Aquifer Concentration for
CaseA All Cf-249 B_LA

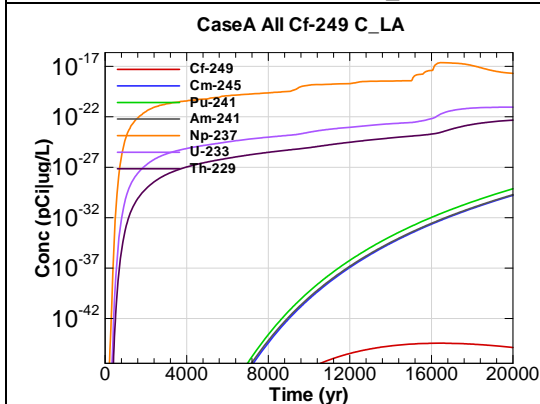


Figure A.2-111 - 100m Aquifer Concentration for
CaseA All Cf-249 C_LA

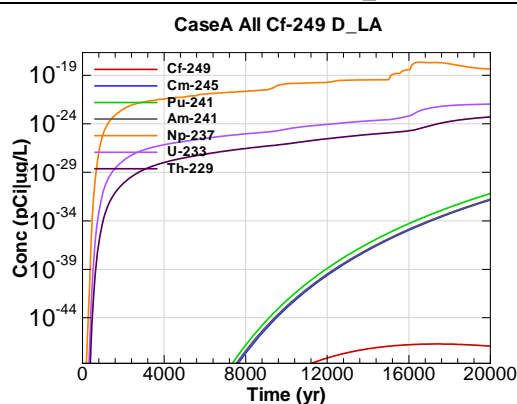


Figure A.2-112 - 100m Aquifer Concentration for
CaseA All Cf-249 D_LA

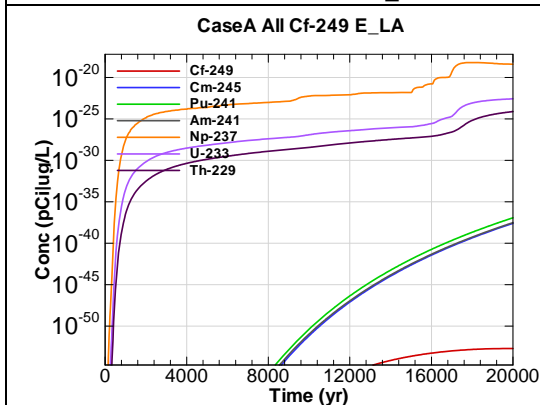


Figure A.2-113 - 100m Aquifer Concentration for
CaseA All Cf-249 E_LA

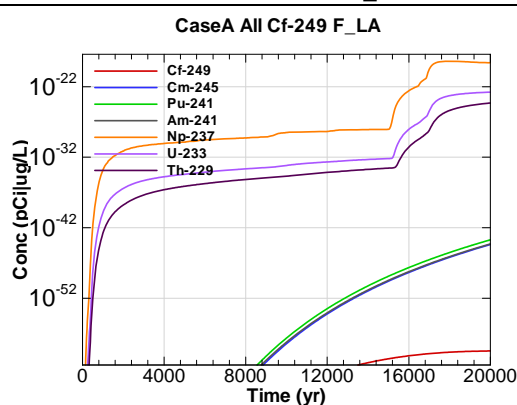


Figure A.2-114 - 100m Aquifer Concentration for
CaseA All Cf-249 F_LA

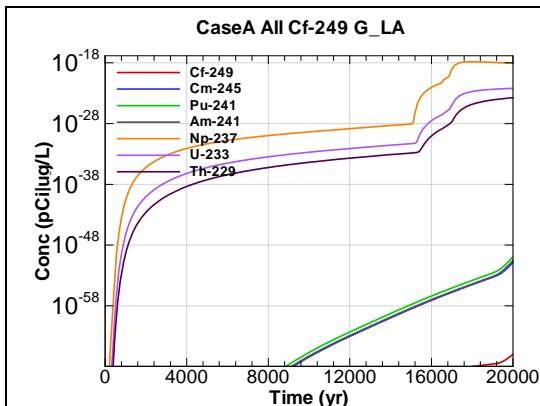


Figure A.2-115 - 100m Aquifer Concentration for CaseA All Cf-249 G_LA

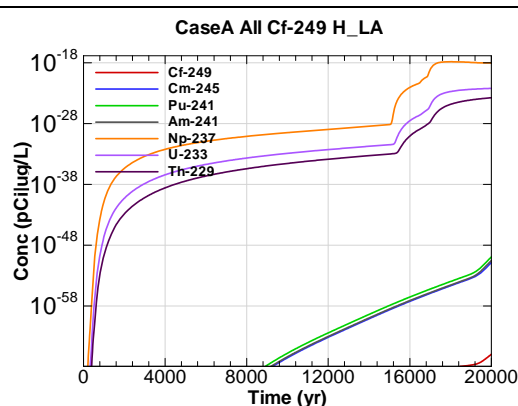


Figure A.2-116 - 100m Aquifer Concentration for CaseA All Cf-249 H_LA

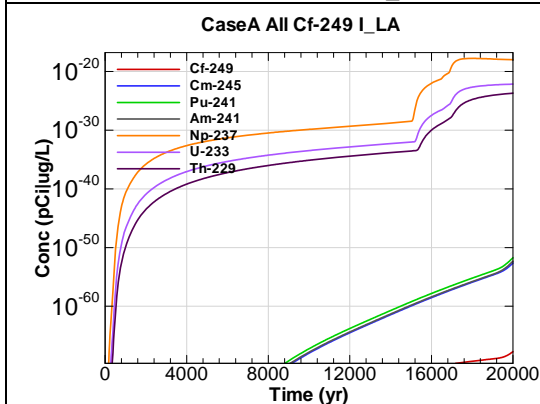


Figure A.2-117 - 100m Aquifer Concentration for CaseA All Cf-249 I_LA

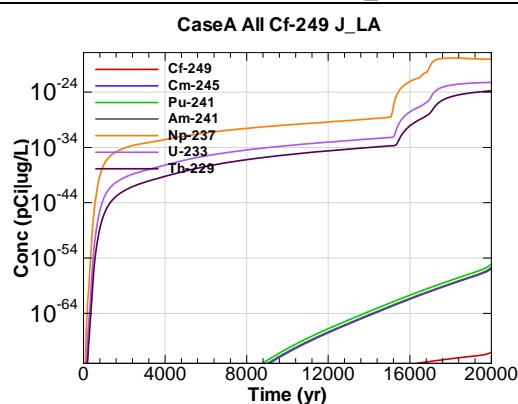


Figure A.2-118 - 100m Aquifer Concentration for CaseA All Cf-249 J_LA

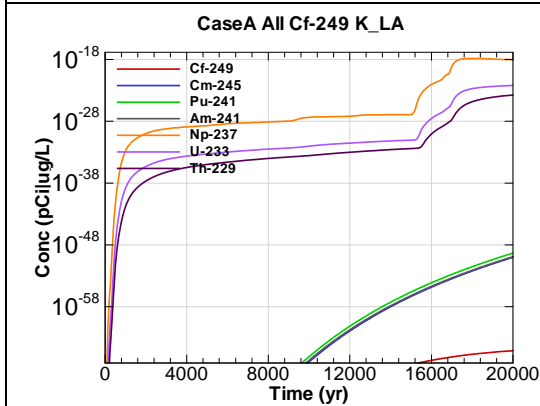


Figure A.2-119 - 100m Aquifer Concentration for CaseA All Cf-249 K_LA

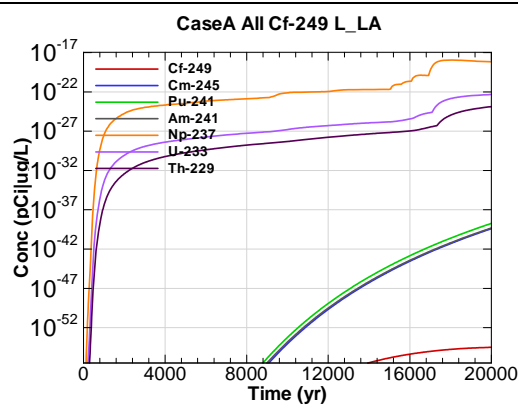


Figure A.2-120 - 100m Aquifer Concentration for CaseA All Cf-249 L_LA

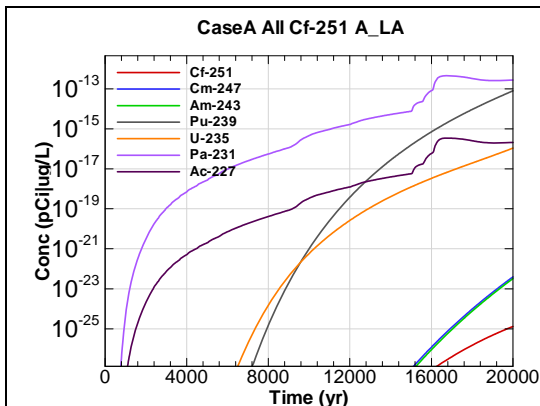


Figure A.2-121 - 100m Aquifer Concentration for
CaseA All Cf-251 A_LA

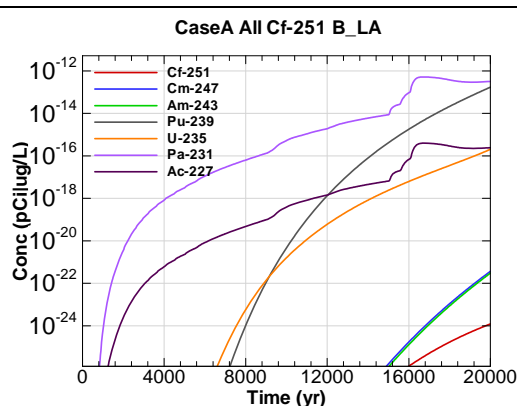


Figure A.2-122 - 100m Aquifer Concentration for
CaseA All Cf-251 B_LA

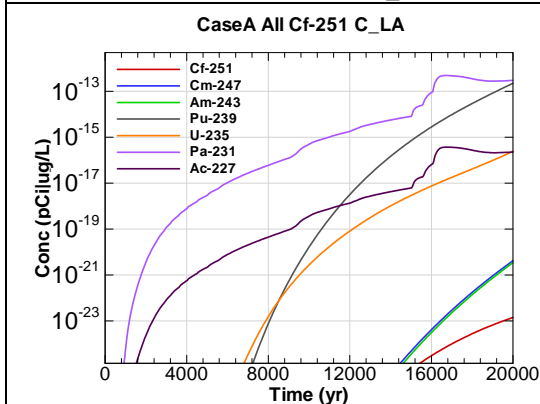


Figure A.2-123 - 100m Aquifer Concentration for
CaseA All Cf-251 C_LA

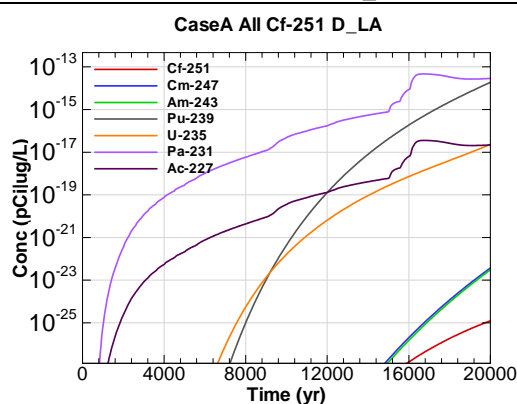


Figure A.2-124 - 100m Aquifer Concentration for
CaseA All Cf-251 D_LA

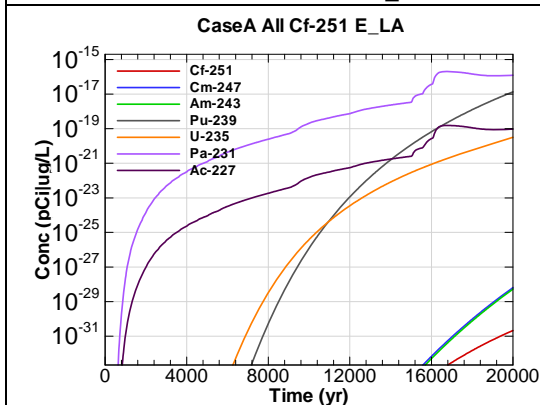


Figure A.2-125 - 100m Aquifer Concentration for
CaseA All Cf-251 E_LA

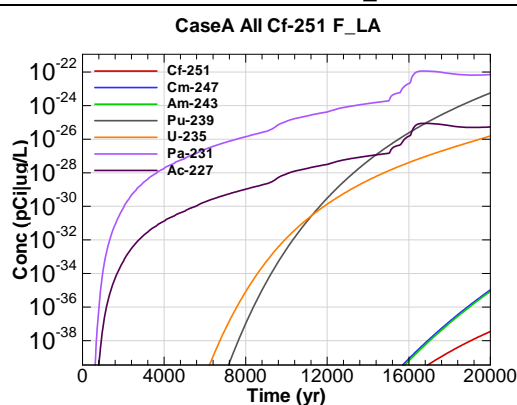


Figure A.2-126 - 100m Aquifer Concentration for
CaseA All Cf-251 F_LA

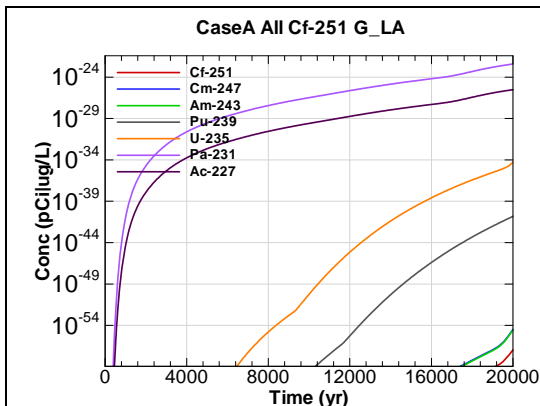


Figure A.2-127 - 100m Aquifer Concentration for CaseA All Cf-251 G_LA

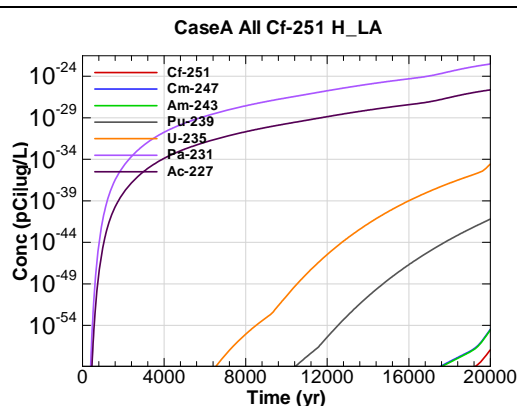


Figure A.2-128 - 100m Aquifer Concentration for CaseA All Cf-251 H_LA

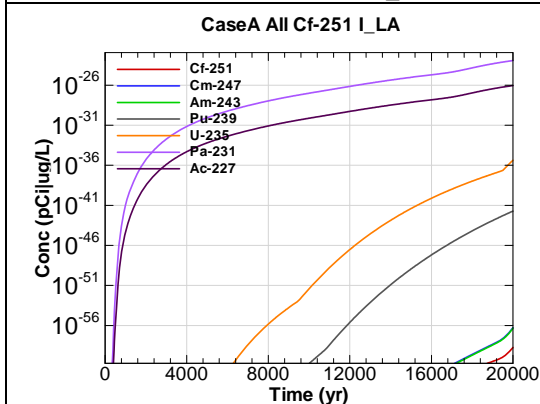


Figure A.2-129 - 100m Aquifer Concentration for CaseA All Cf-251 I_LA

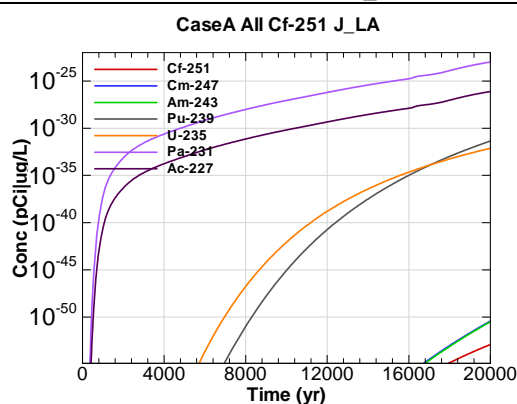


Figure A.2-130 - 100m Aquifer Concentration for CaseA All Cf-251 J_LA

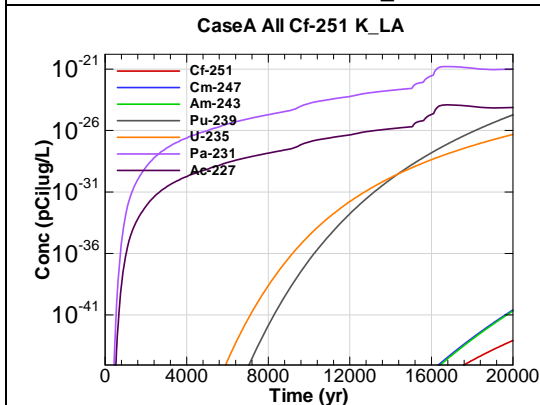


Figure A.2-131 - 100m Aquifer Concentration for CaseA All Cf-251 K_LA

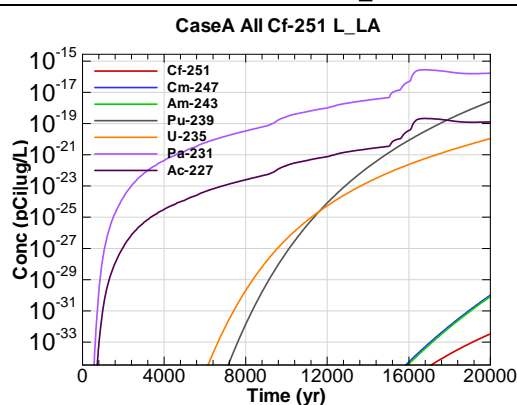


Figure A.2-132 - 100m Aquifer Concentration for CaseA All Cf-251 L_LA

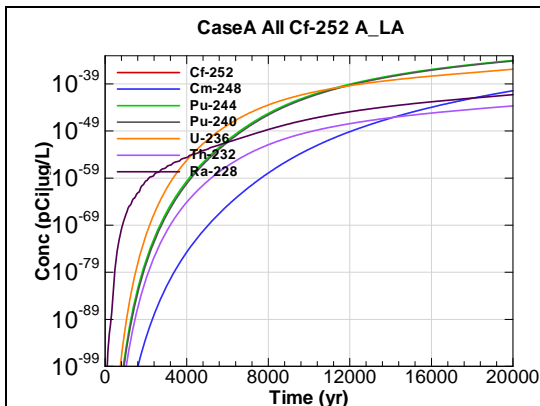


Figure A.2-133 - 100m Aquifer Concentration for
CaseA All Cf-252 A_LA

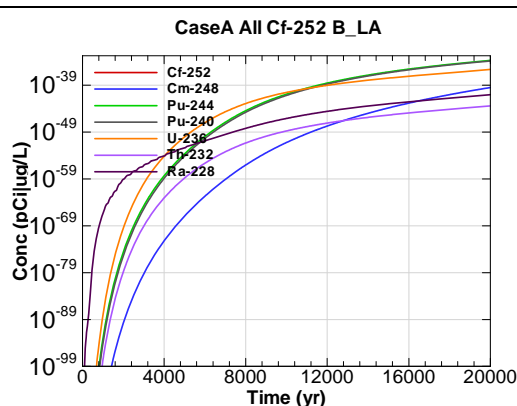


Figure A.2-134 - 100m Aquifer Concentration for
CaseA All Cf-252 B_LA

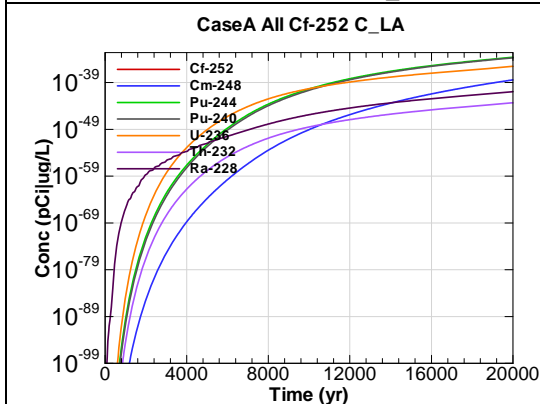


Figure A.2-135 - 100m Aquifer Concentration for
CaseA All Cf-252 C_LA

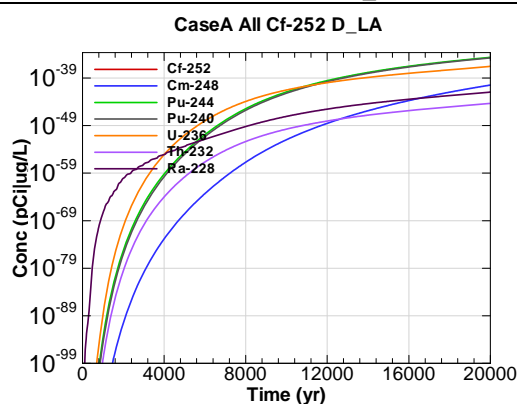


Figure A.2-136 - 100m Aquifer Concentration for
CaseA All Cf-252 D_LA

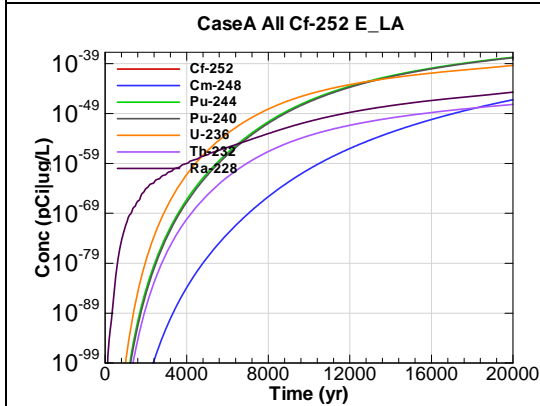


Figure A.2-137 - 100m Aquifer Concentration for
CaseA All Cf-252 E_LA

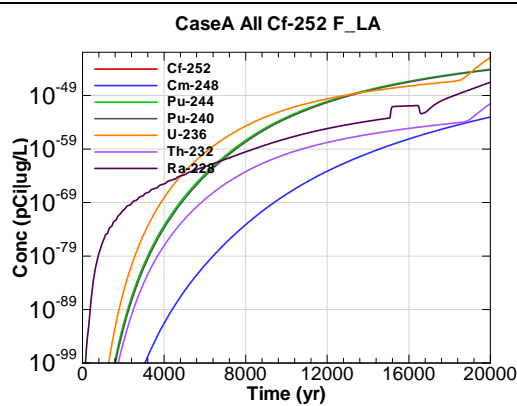


Figure A.2-138 - 100m Aquifer Concentration for
CaseA All Cf-252 F_LA

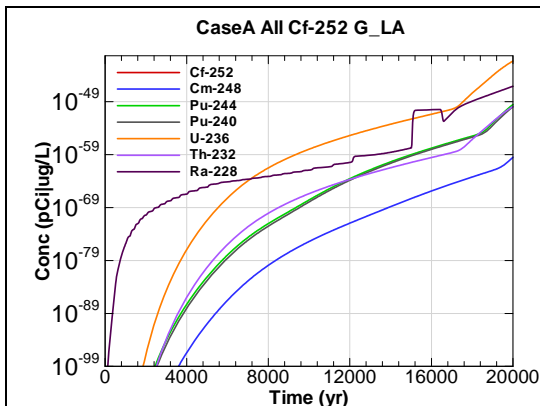


Figure A.2-139 - 100m Aquifer Concentration for
CaseA All Cf-252 G_LA

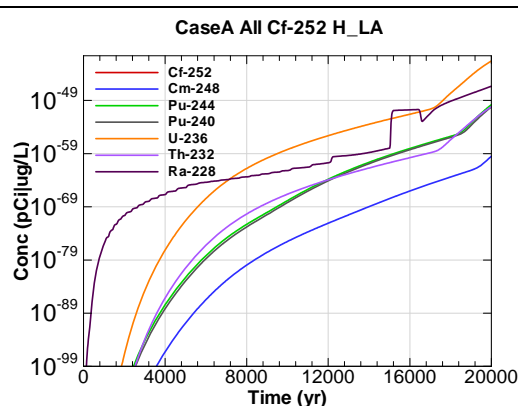


Figure A.2-140 - 100m Aquifer Concentration for
CaseA All Cf-252 H_LA

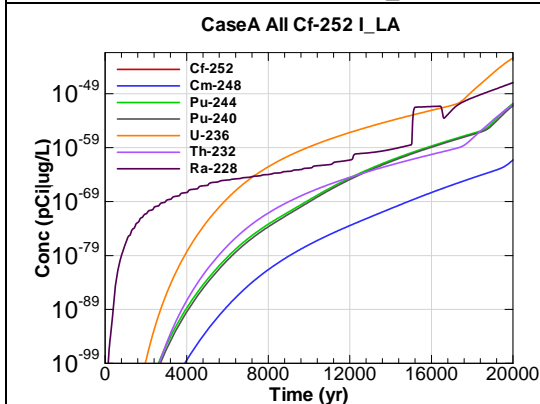


Figure A.2-141 - 100m Aquifer Concentration for
CaseA All Cf-252 I_LA

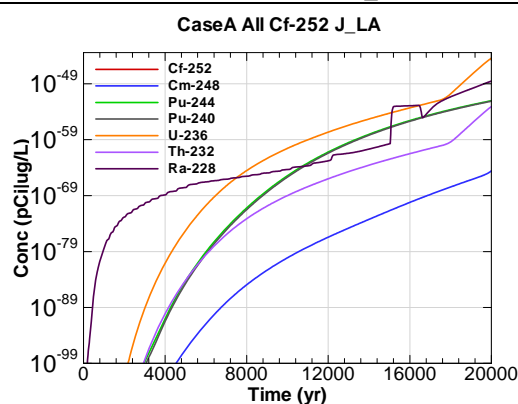


Figure A.2-142 - 100m Aquifer Concentration for
CaseA All Cf-252 J_LA

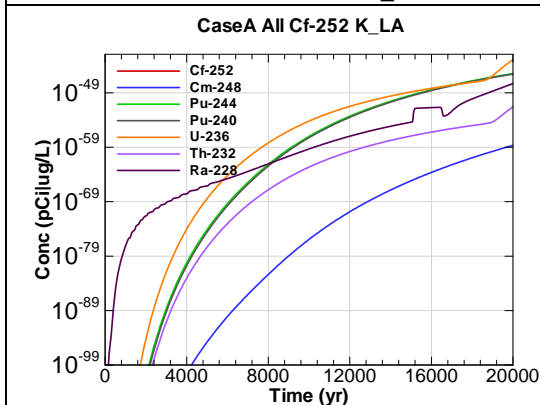


Figure A.2-143 - 100m Aquifer Concentration for
CaseA All Cf-252 K_LA

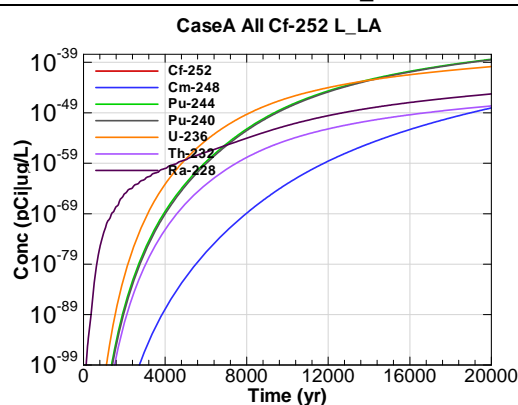
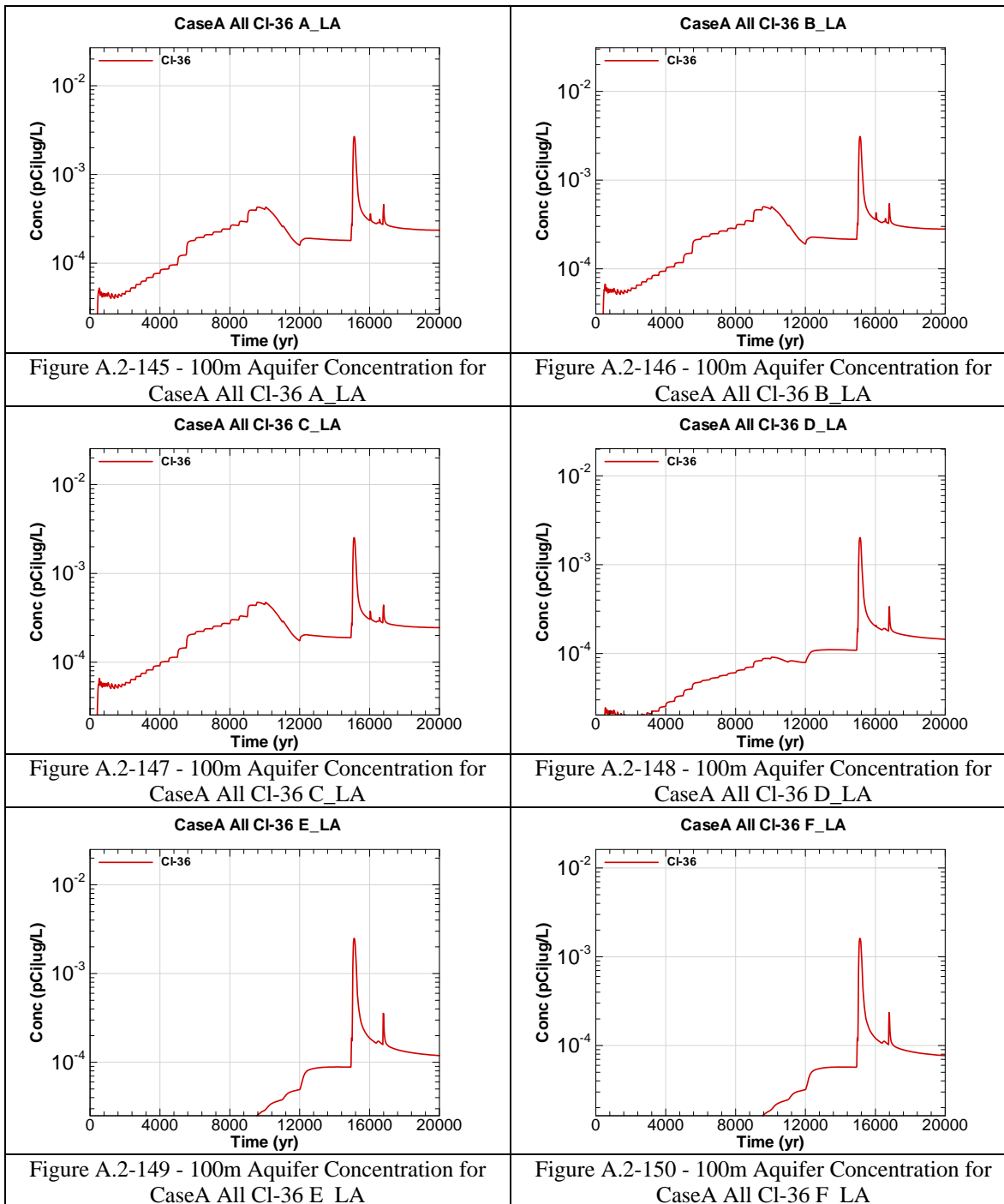
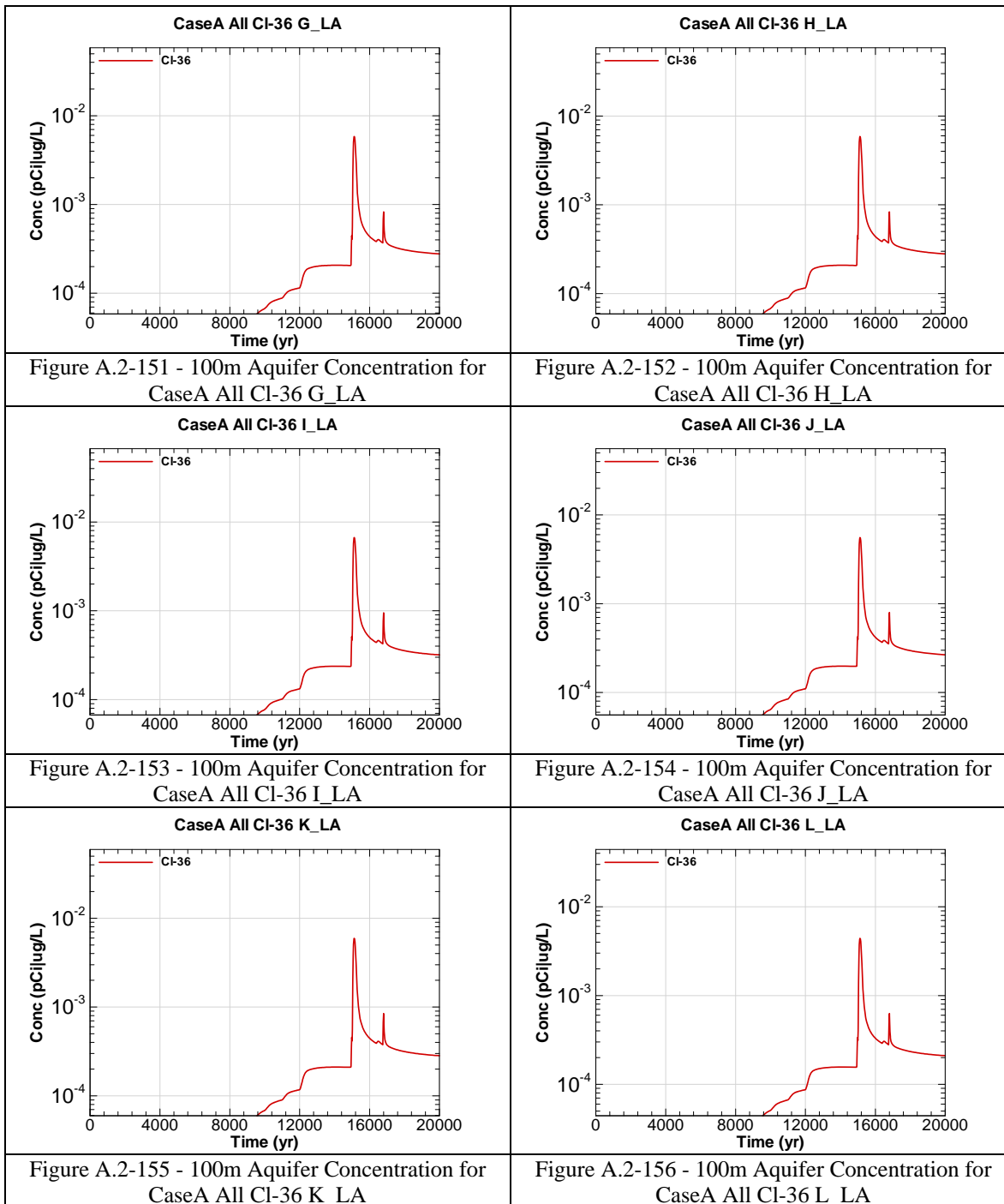


Figure A.2-144 - 100m Aquifer Concentration for
CaseA All Cf-252 L_LA





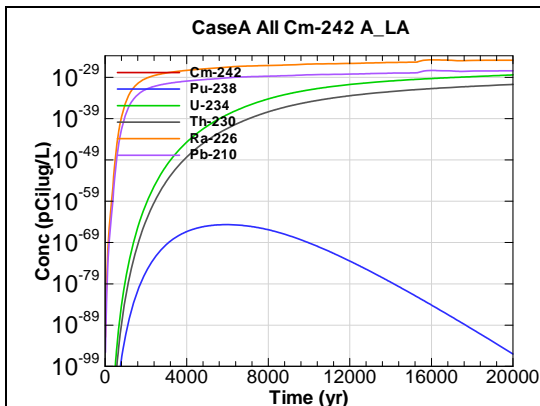


Figure A.2-157 - 100m Aquifer Concentration for
CaseA All Cm-242 A_LA

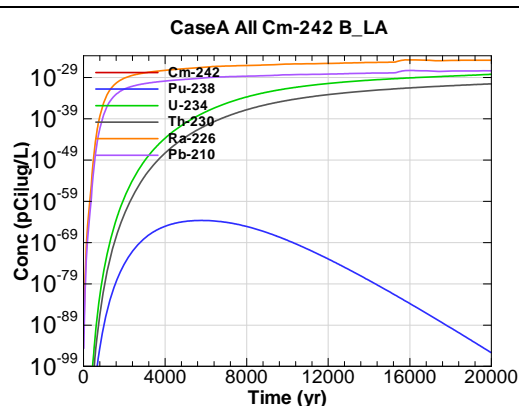


Figure A.2-158 - 100m Aquifer Concentration for
CaseA All Cm-242 B_LA

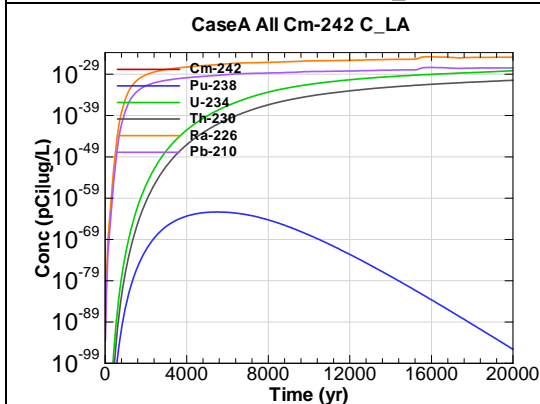


Figure A.2-159 - 100m Aquifer Concentration for
CaseA All Cm-242 C_LA

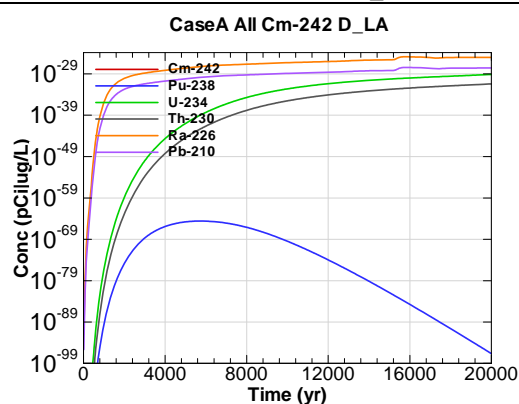


Figure A.2-160 - 100m Aquifer Concentration for
CaseA All Cm-242 D_LA

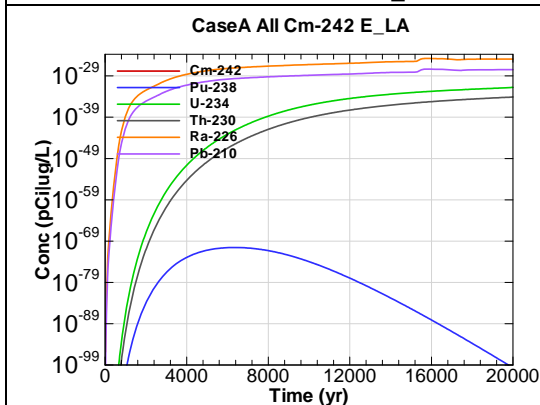


Figure A.2-161 - 100m Aquifer Concentration for
CaseA All Cm-242 E_LA

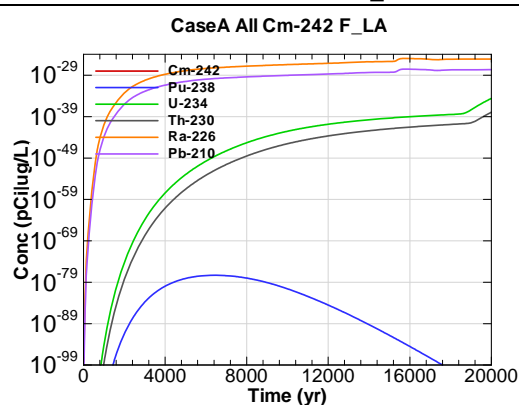


Figure A.2-162 - 100m Aquifer Concentration for
CaseA All Cm-242 F_LA

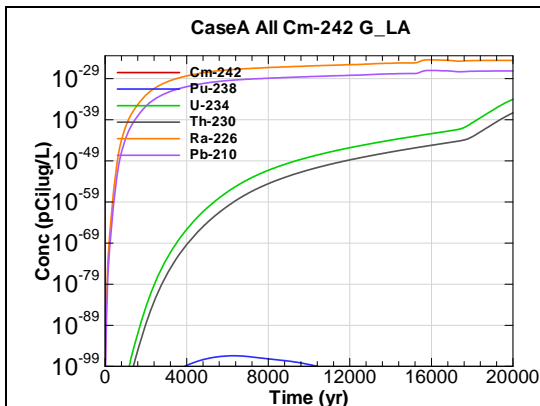


Figure A.2-163 - 100m Aquifer Concentration for
CaseA All Cm-242 G_LA

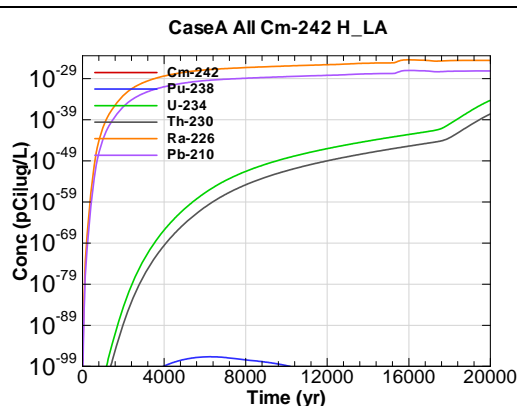


Figure A.2-164 - 100m Aquifer Concentration for
CaseA All Cm-242 H_LA

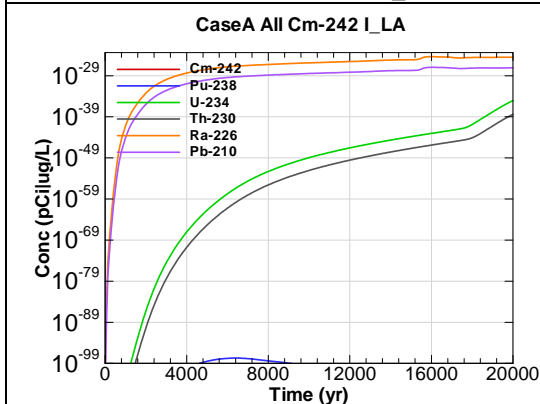


Figure A.2-165 - 100m Aquifer Concentration for
CaseA All Cm-242 I_LA

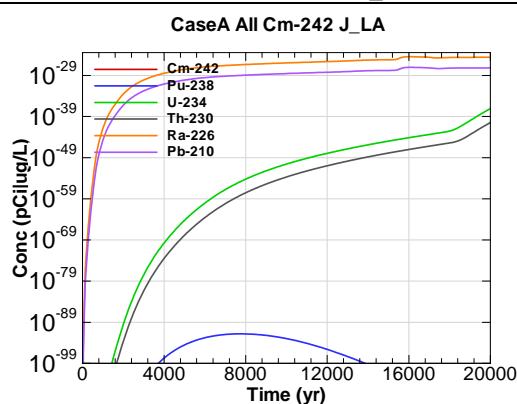


Figure A.2-166 - 100m Aquifer Concentration for
CaseA All Cm-242 J_LA

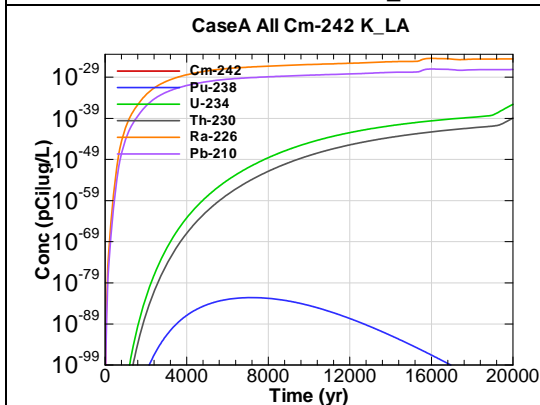


Figure A.2-167 - 100m Aquifer Concentration for
CaseA All Cm-242 K_LA

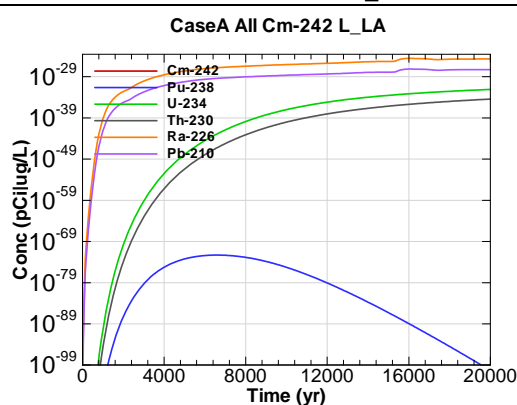


Figure A.2-168 - 100m Aquifer Concentration for
CaseA All Cm-242 L_LA

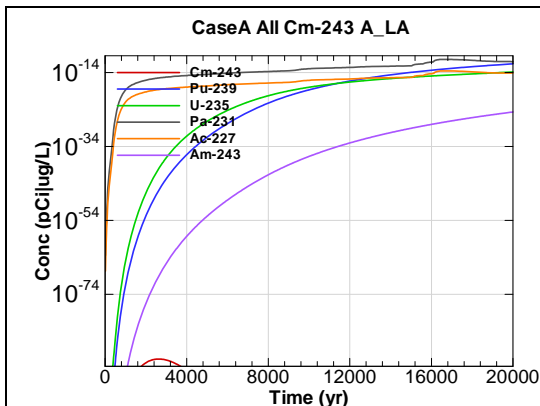


Figure A.2-169 - 100m Aquifer Concentration for CaseA All Cm-243 A_LA

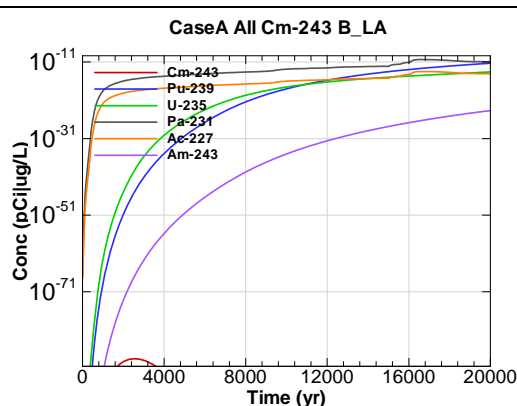


Figure A.2-170 - 100m Aquifer Concentration for CaseA All Cm-243 B_LA

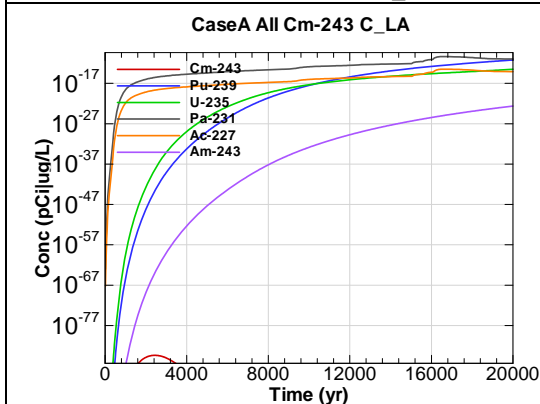


Figure A.2-171 - 100m Aquifer Concentration for CaseA All Cm-243 C_LA

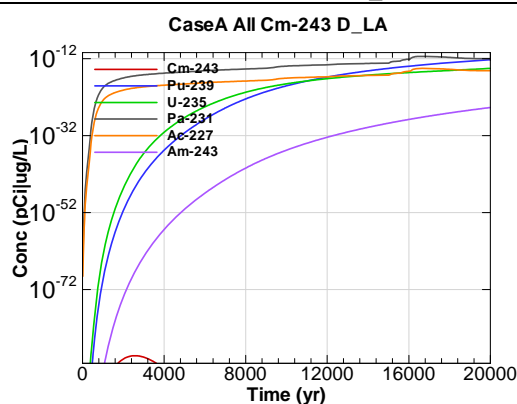


Figure A.2-172 - 100m Aquifer Concentration for CaseA All Cm-243 D_LA

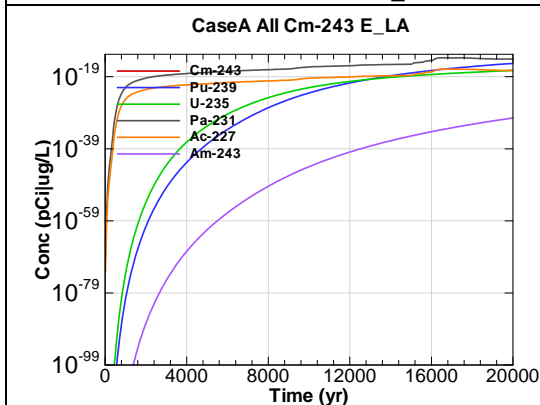


Figure A.2-173 - 100m Aquifer Concentration for CaseA All Cm-243 E_LA

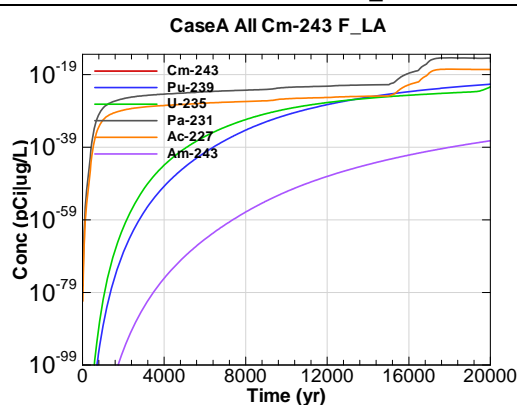


Figure A.2-174 - 100m Aquifer Concentration for CaseA All Cm-243 F_LA

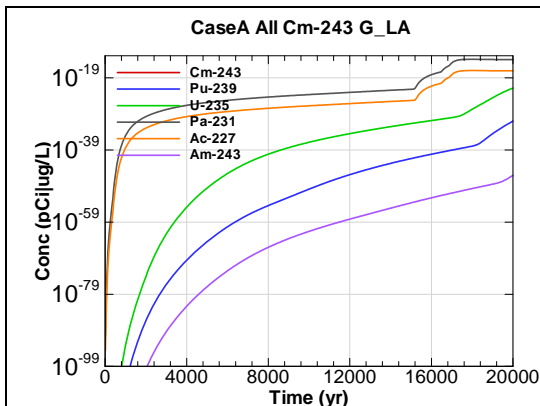


Figure A.2-175 - 100m Aquifer Concentration for
CaseA All Cm-243 G_LA

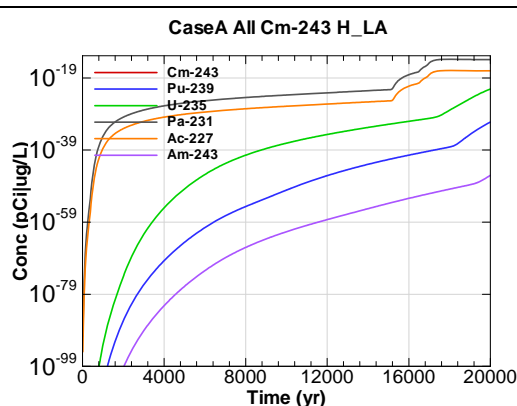


Figure A.2-176 - 100m Aquifer Concentration for
CaseA All Cm-243 H_LA

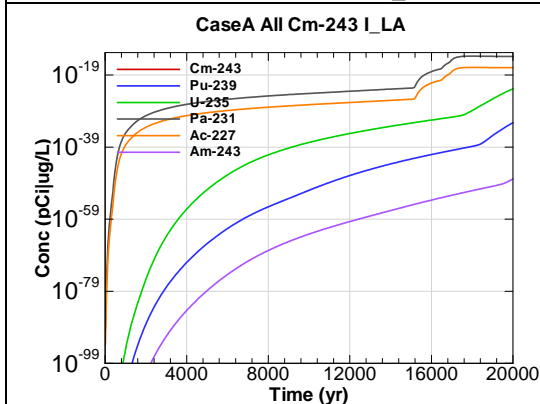


Figure A.2-177 - 100m Aquifer Concentration for
CaseA All Cm-243 I_LA

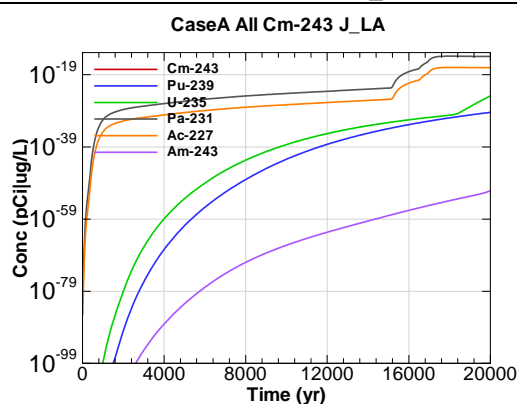


Figure A.2-178 - 100m Aquifer Concentration for
CaseA All Cm-243 J_LA

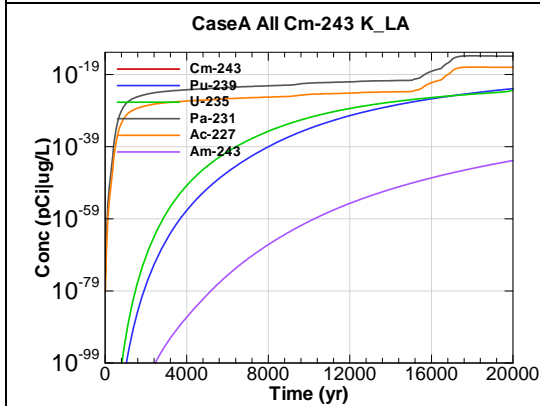


Figure A.2-179 - 100m Aquifer Concentration for
CaseA All Cm-243 K_LA

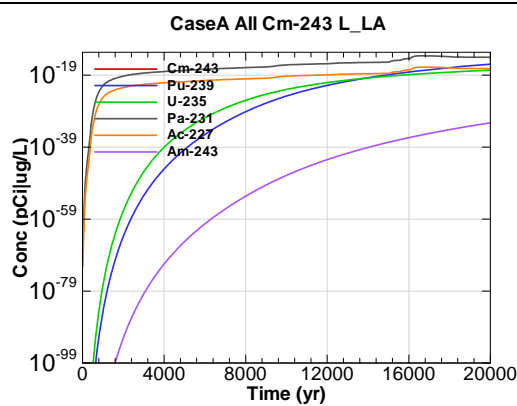


Figure A.2-180 - 100m Aquifer Concentration for
CaseA All Cm-243 L_LA

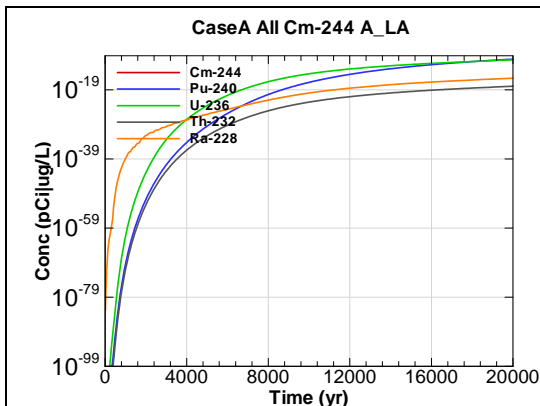


Figure A.2-181 - 100m Aquifer Concentration for
CaseA All Cm-244 A_LA

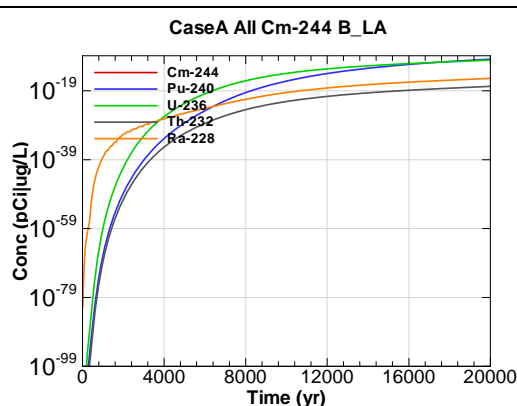


Figure A.2-182 - 100m Aquifer Concentration for
CaseA All Cm-244 B_LA

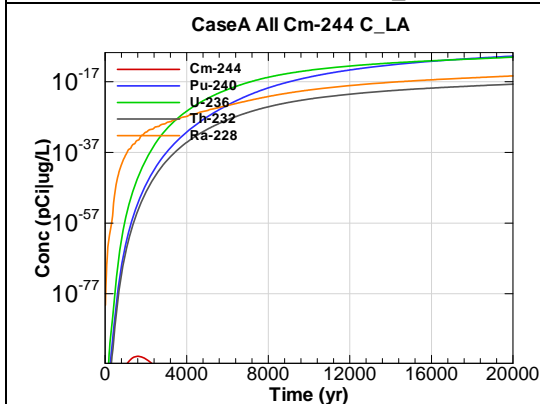


Figure A.2-183 - 100m Aquifer Concentration for
CaseA All Cm-244 C_LA

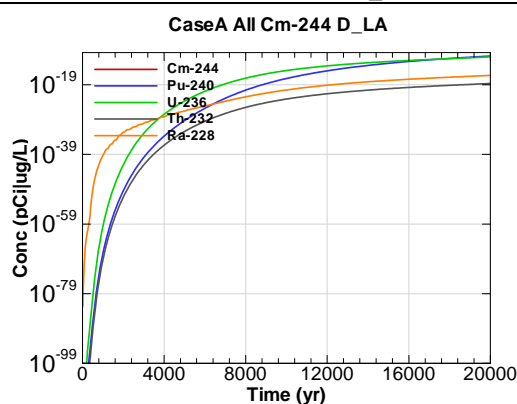


Figure A.2-184 - 100m Aquifer Concentration for
CaseA All Cm-244 D_LA

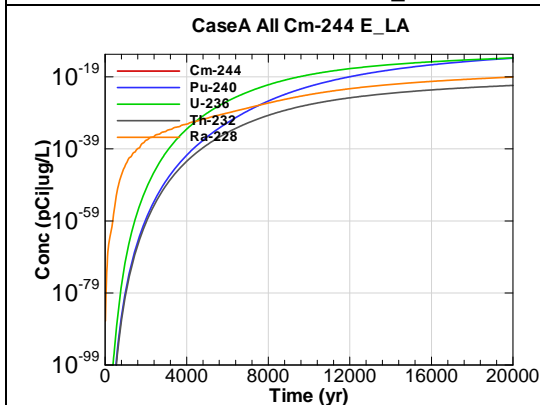


Figure A.2-185 - 100m Aquifer Concentration for
CaseA All Cm-244 E_LA

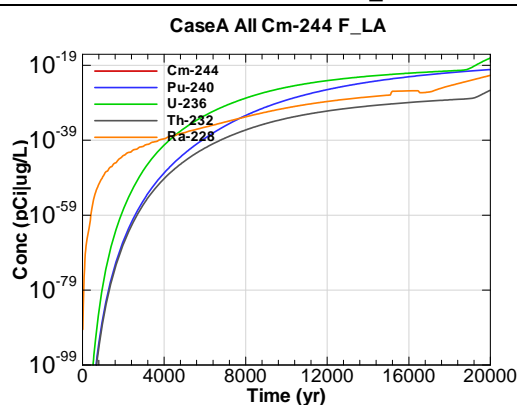


Figure A.2-186 - 100m Aquifer Concentration for
CaseA All Cm-244 F_LA

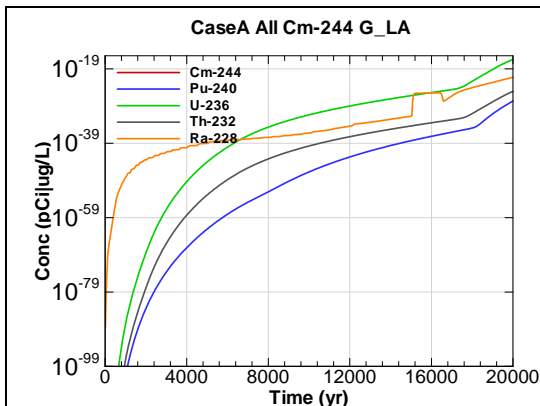


Figure A.2-187 - 100m Aquifer Concentration for CaseA All Cm-244 G_LA

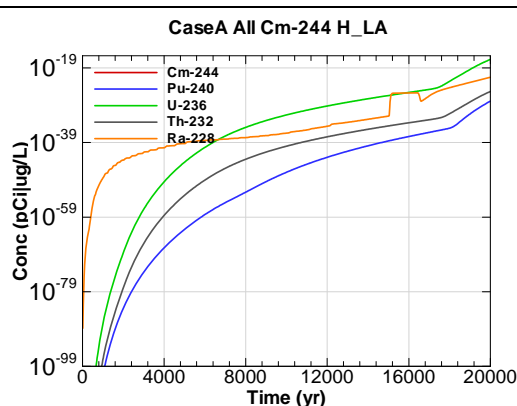


Figure A.2-188 - 100m Aquifer Concentration for CaseA All Cm-244 H_LA

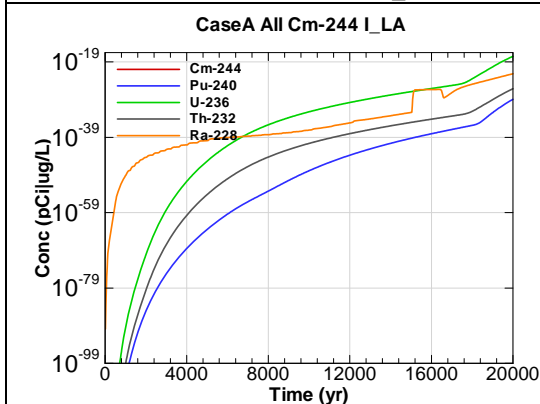


Figure A.2-189 - 100m Aquifer Concentration for CaseA All Cm-244 I_LA

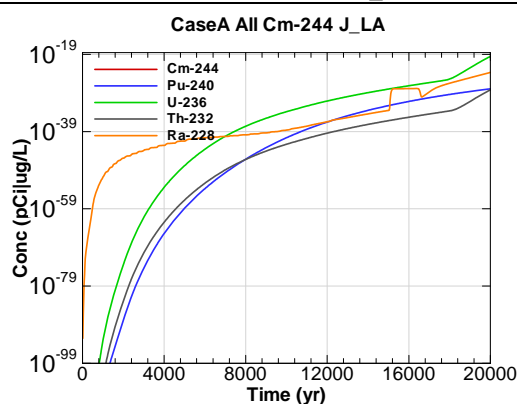


Figure A.2-190 - 100m Aquifer Concentration for CaseA All Cm-244 J_LA

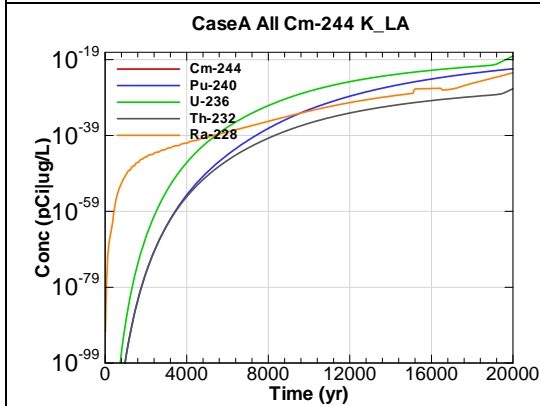


Figure A.2-191 - 100m Aquifer Concentration for CaseA All Cm-244 K_LA

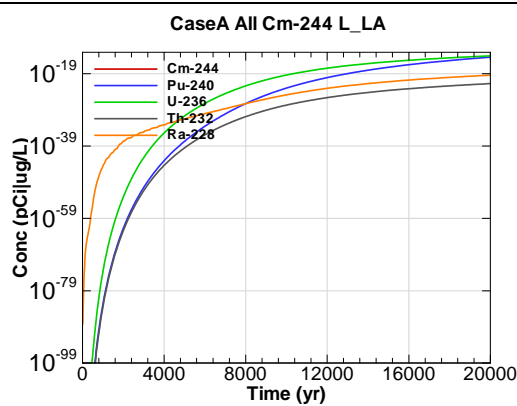


Figure A.2-192 - 100m Aquifer Concentration for CaseA All Cm-244 L_LA

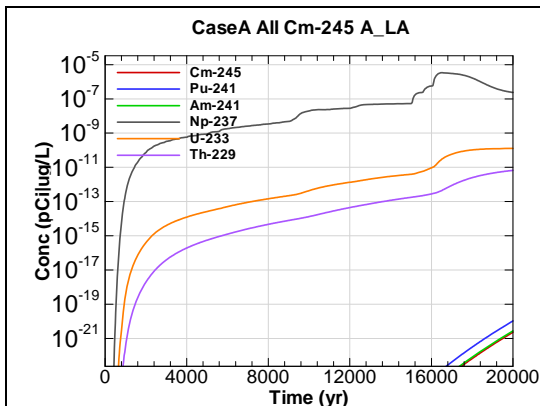


Figure A.2-193 - 100m Aquifer Concentration for
CaseA All Cm-245 A_LA

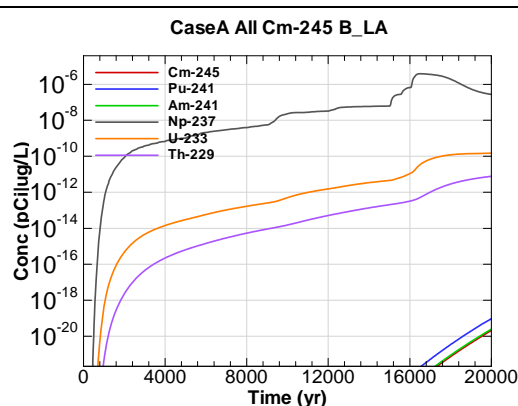


Figure A.2-194 - 100m Aquifer Concentration for
CaseA All Cm-245 B_LA

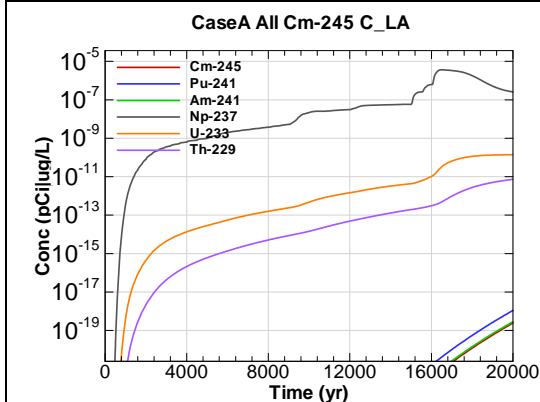


Figure A.2-195 - 100m Aquifer Concentration for
CaseA All Cm-245 C_LA

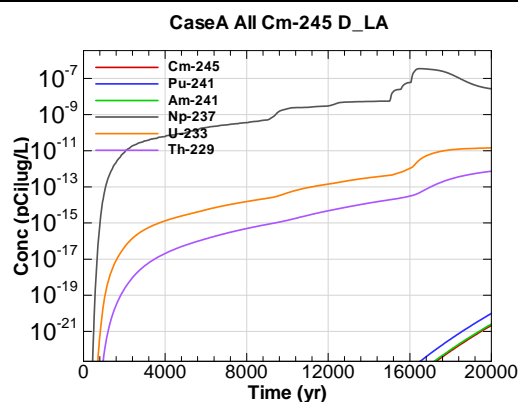


Figure A.2-196 - 100m Aquifer Concentration for
CaseA All Cm-245 D_LA

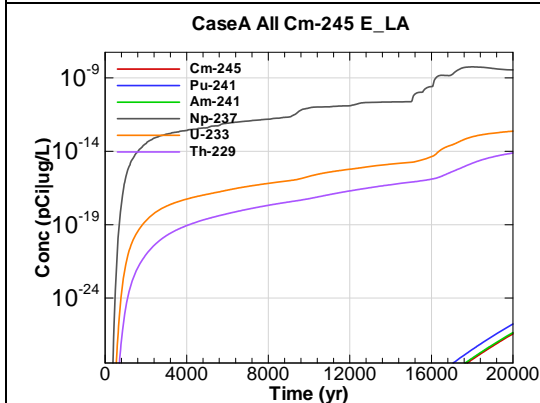


Figure A.2-197 - 100m Aquifer Concentration for
CaseA All Cm-245 E_LA

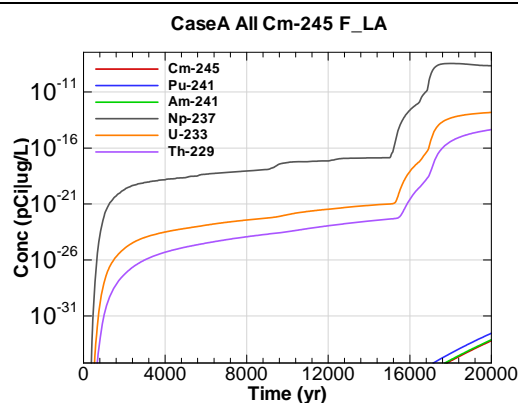


Figure A.2-198 - 100m Aquifer Concentration for
CaseA All Cm-245 F_LA

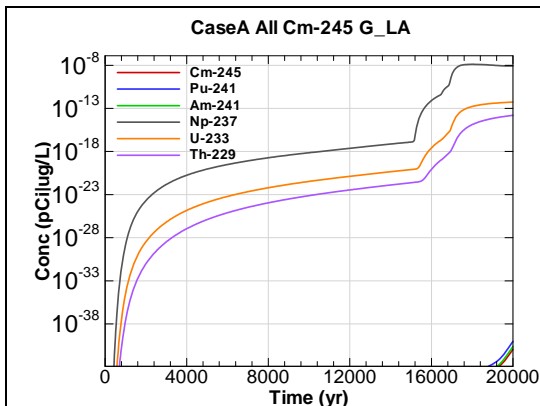


Figure A.2-199 - 100m Aquifer Concentration for CaseA All Cm-245 G_LA

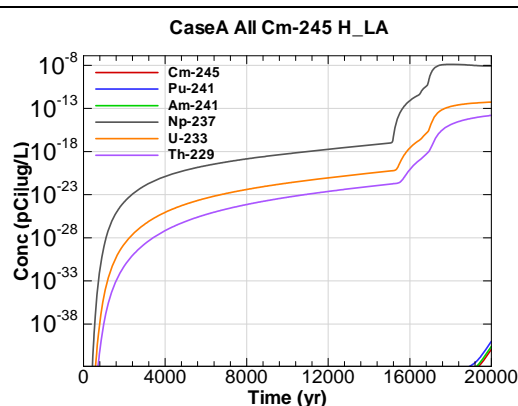


Figure A.2-200 - 100m Aquifer Concentration for CaseA All Cm-245 H_LA

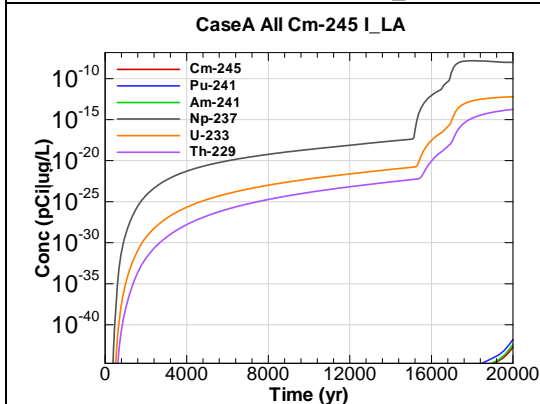


Figure A.2-201 - 100m Aquifer Concentration for CaseA All Cm-245 I_LA

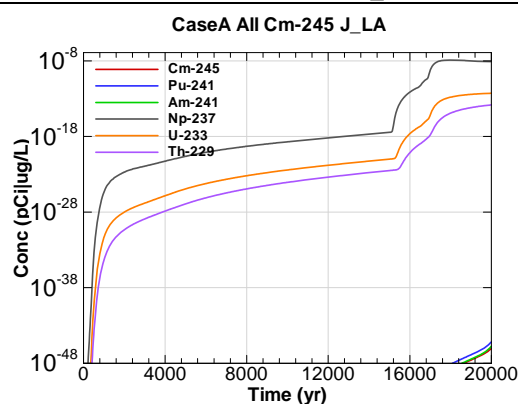


Figure A.2-202 - 100m Aquifer Concentration for CaseA All Cm-245 J_LA

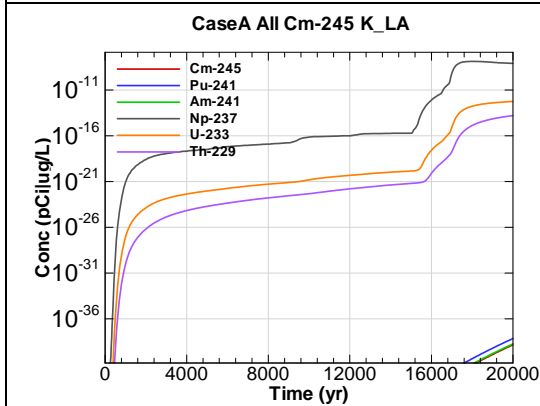


Figure A.2-203 - 100m Aquifer Concentration for CaseA All Cm-245 K_LA

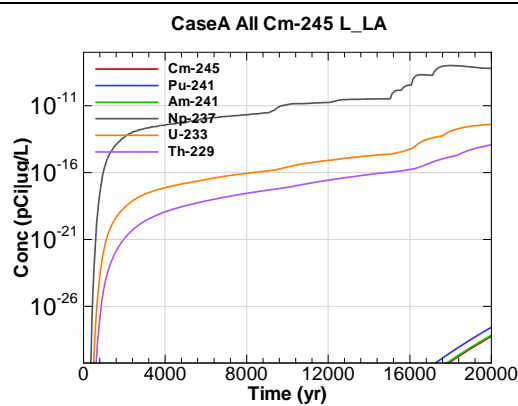


Figure A.2-204 - 100m Aquifer Concentration for CaseA All Cm-245 L_LA

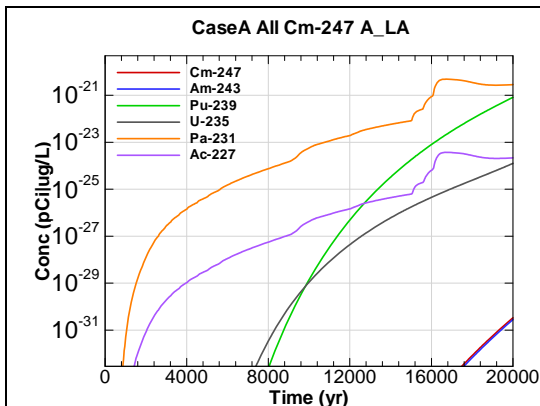


Figure A.2-205 - 100m Aquifer Concentration for
CaseA All Cm-247 A_LA

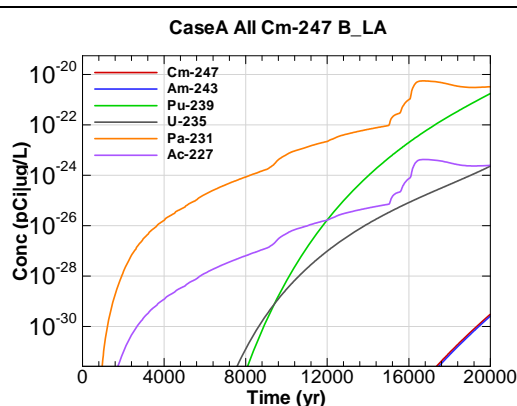


Figure A.2-206 - 100m Aquifer Concentration for
CaseA All Cm-247 B_LA

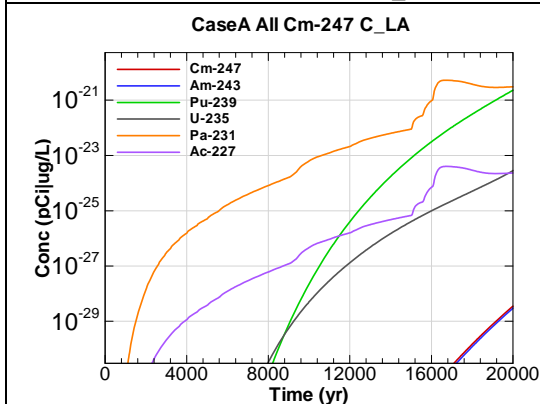


Figure A.2-207 - 100m Aquifer Concentration for
CaseA All Cm-247 C_LA

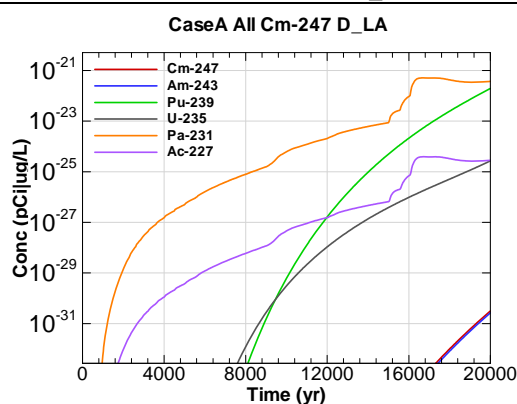


Figure A.2-208 - 100m Aquifer Concentration for
CaseA All Cm-247 D_LA

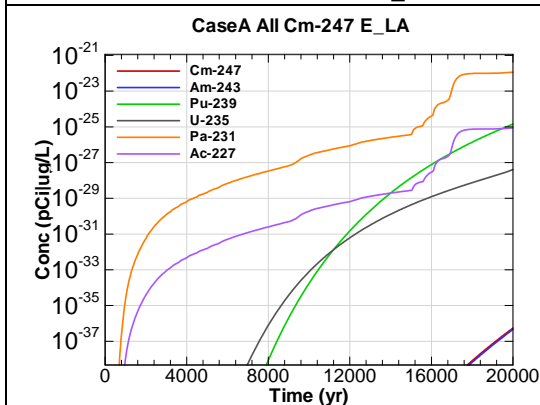


Figure A.2-209 - 100m Aquifer Concentration for
CaseA All Cm-247 E_LA

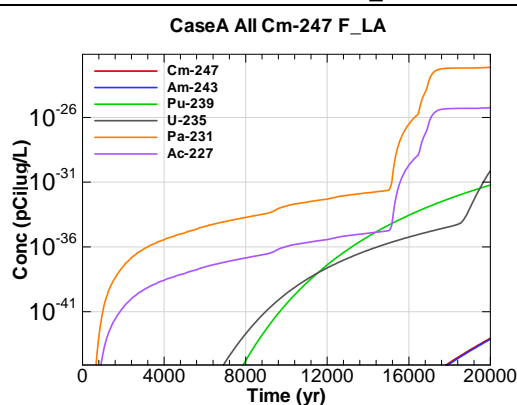


Figure A.2-210 - 100m Aquifer Concentration for
CaseA All Cm-247 F_LA

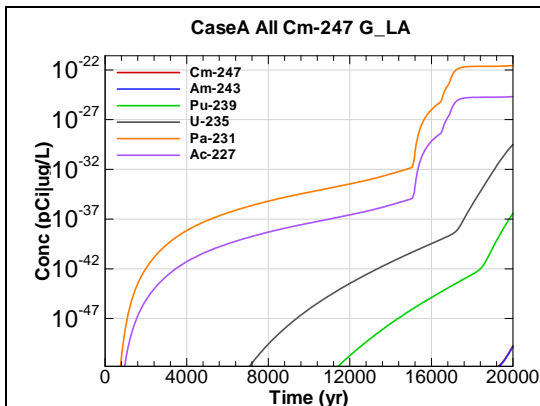


Figure A.2-211 - 100m Aquifer Concentration for CaseA All Cm-247 G_LA

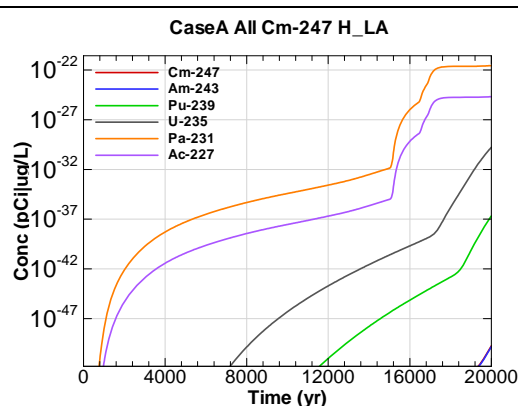


Figure A.2-212 - 100m Aquifer Concentration for CaseA All Cm-247 H_LA

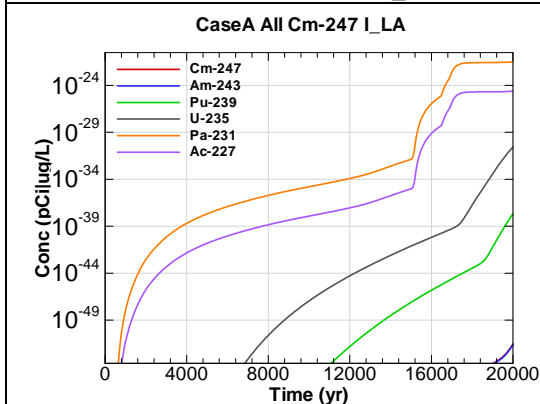


Figure A.2-213 - 100m Aquifer Concentration for CaseA All Cm-247 I_LA

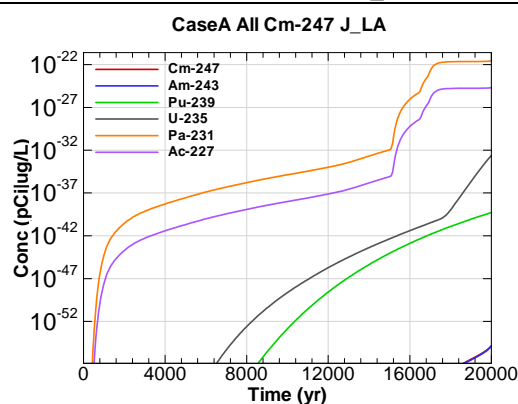


Figure A.2-214 - 100m Aquifer Concentration for CaseA All Cm-247 J_LA

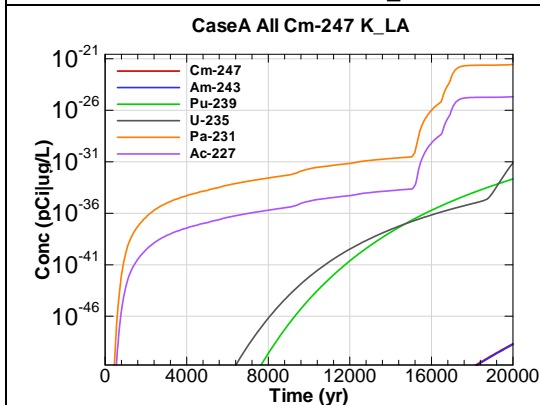


Figure A.2-215 - 100m Aquifer Concentration for CaseA All Cm-247 K_LA

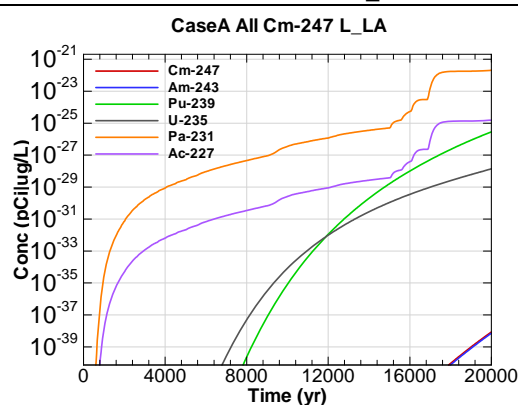
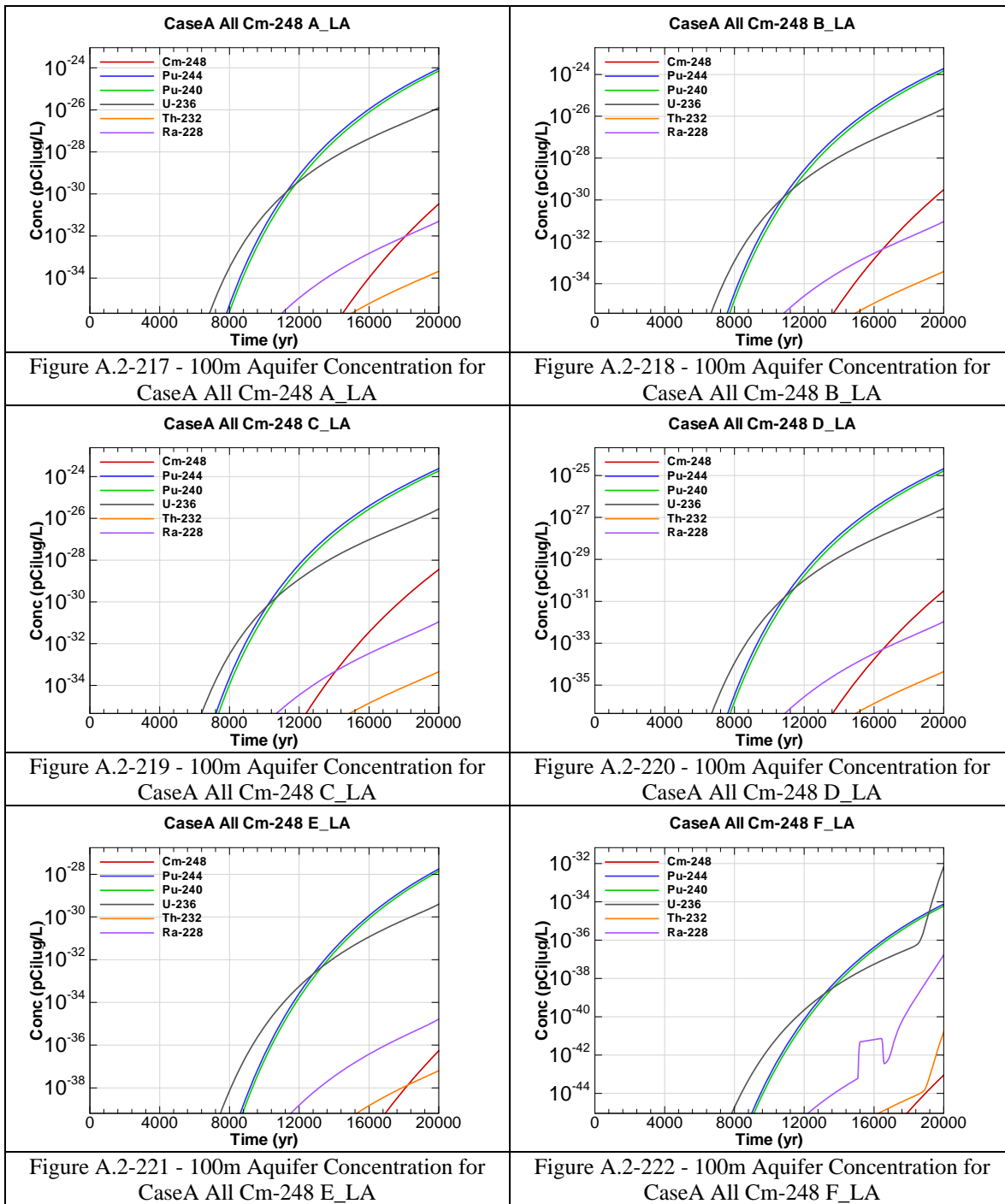


Figure A.2-216 - 100m Aquifer Concentration for CaseA All Cm-247 L_LA



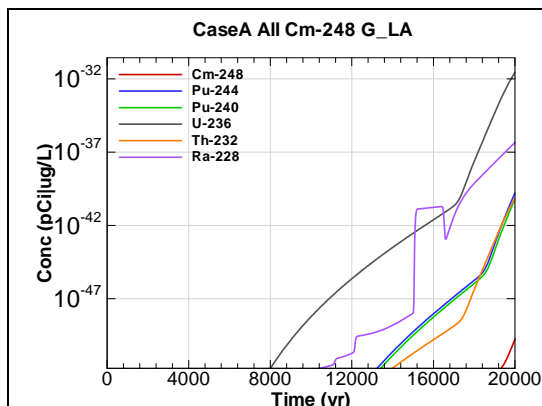


Figure A.2-223 - 100m Aquifer Concentration for
CaseA All Cm-248 G_LA

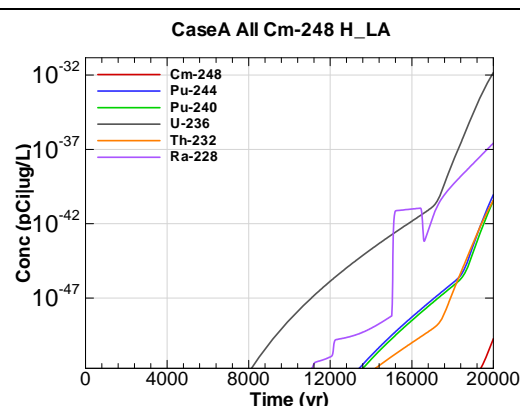


Figure A.2-224 - 100m Aquifer Concentration for
CaseA All Cm-248 H_LA

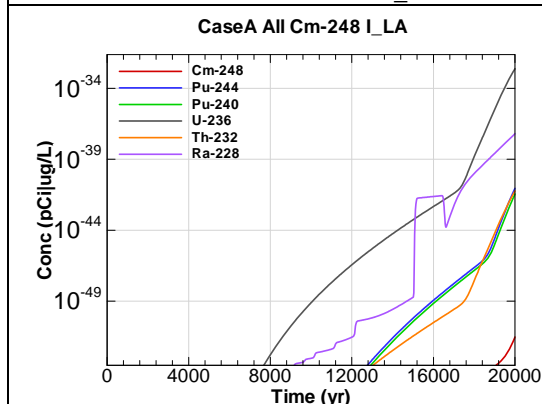


Figure A.2-225 - 100m Aquifer Concentration for
CaseA All Cm-248 I_LA

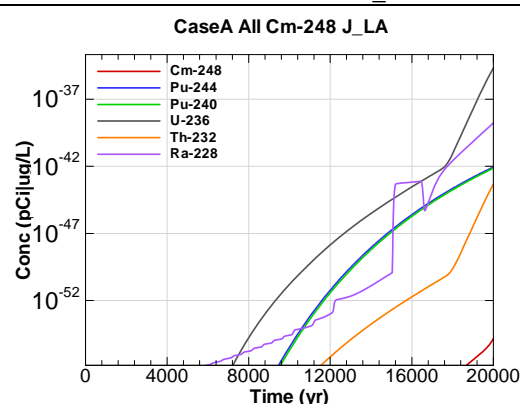


Figure A.2-226 - 100m Aquifer Concentration for
CaseA All Cm-248 J_LA

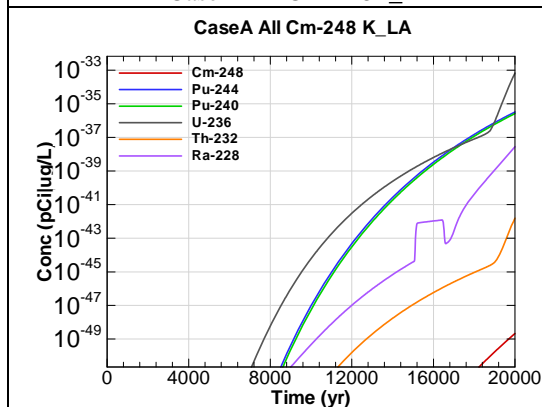


Figure A.2-227 - 100m Aquifer Concentration for
CaseA All Cm-248 K_LA

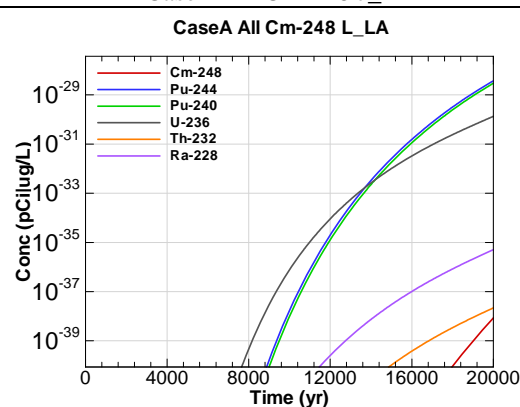
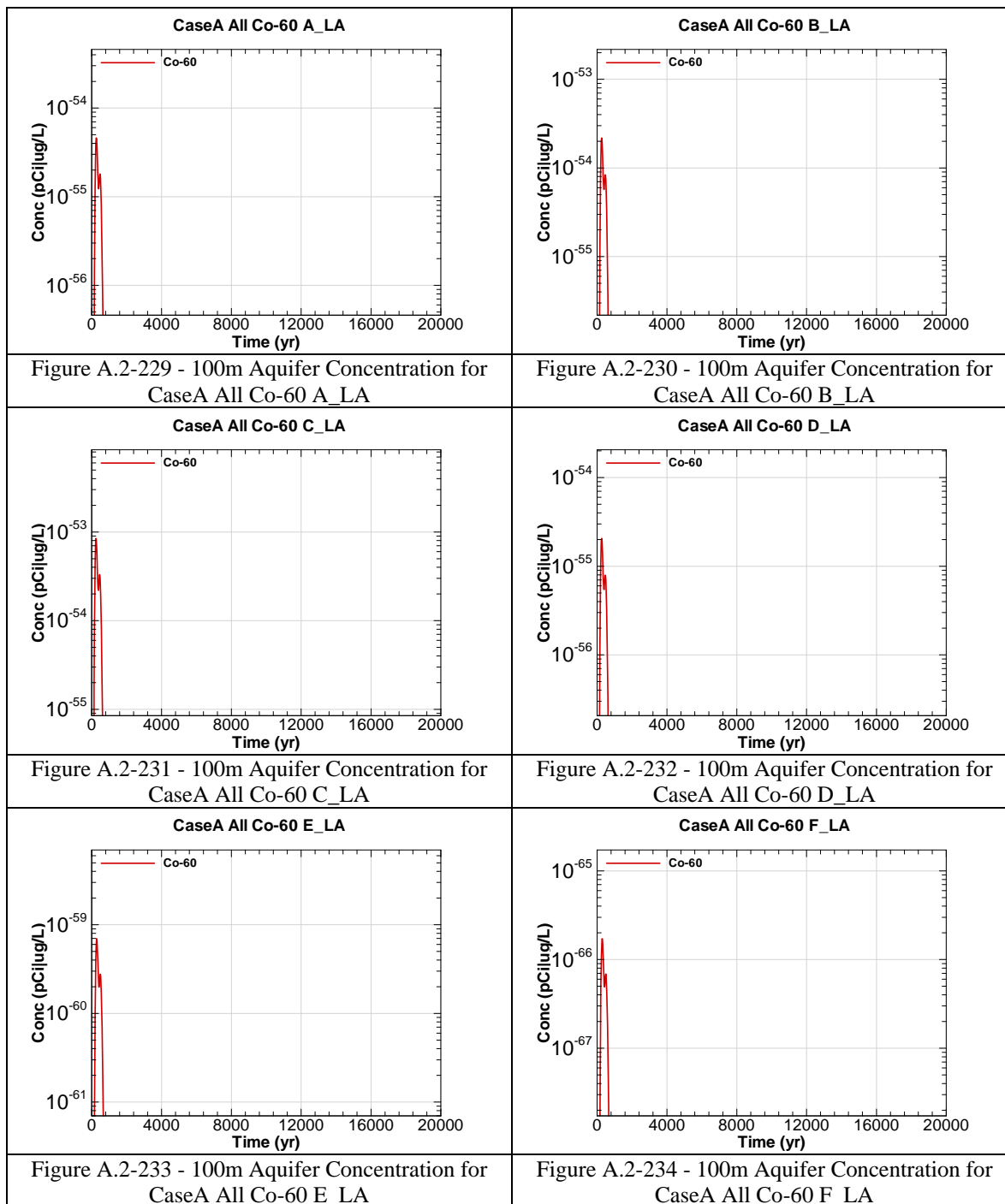
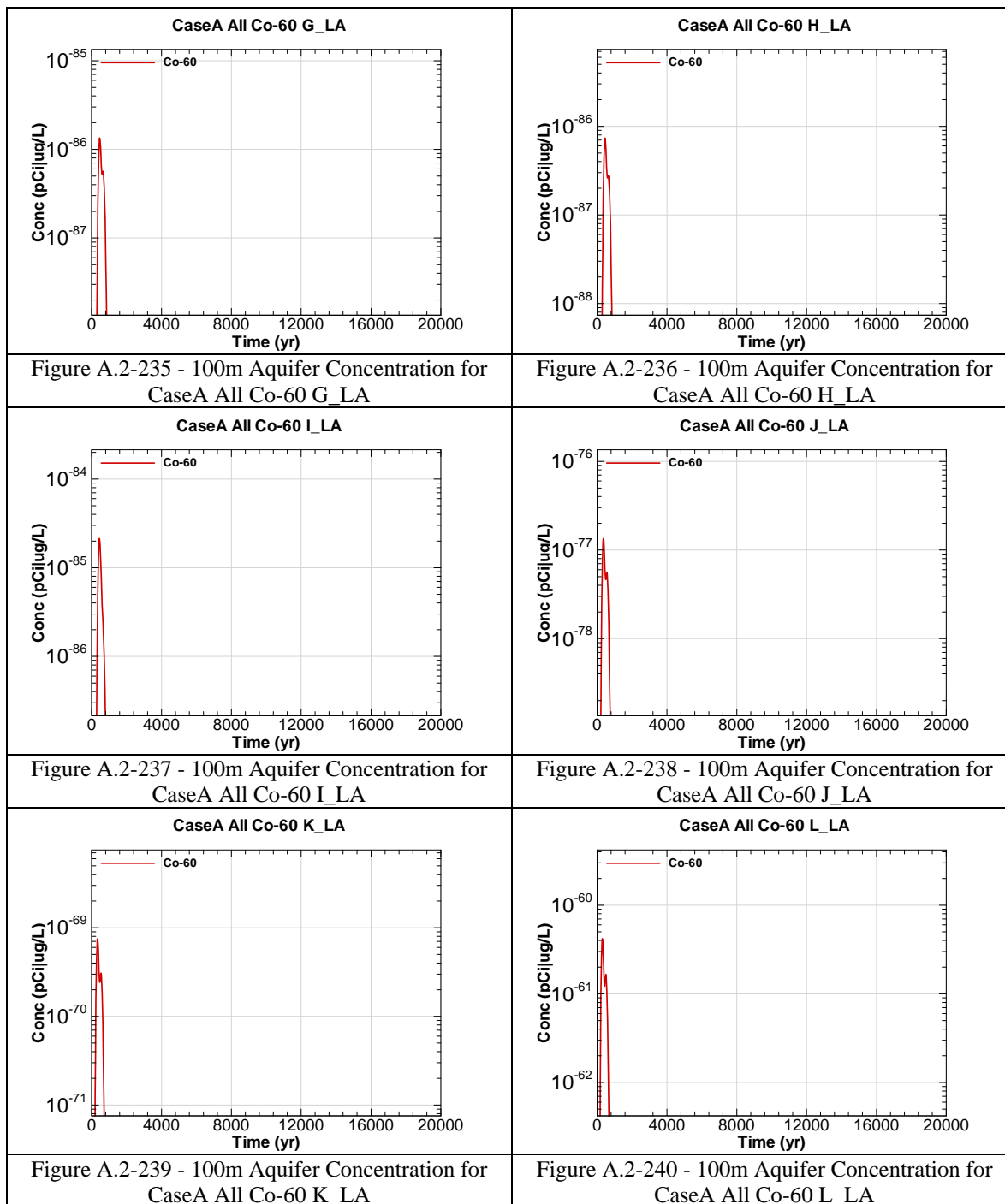
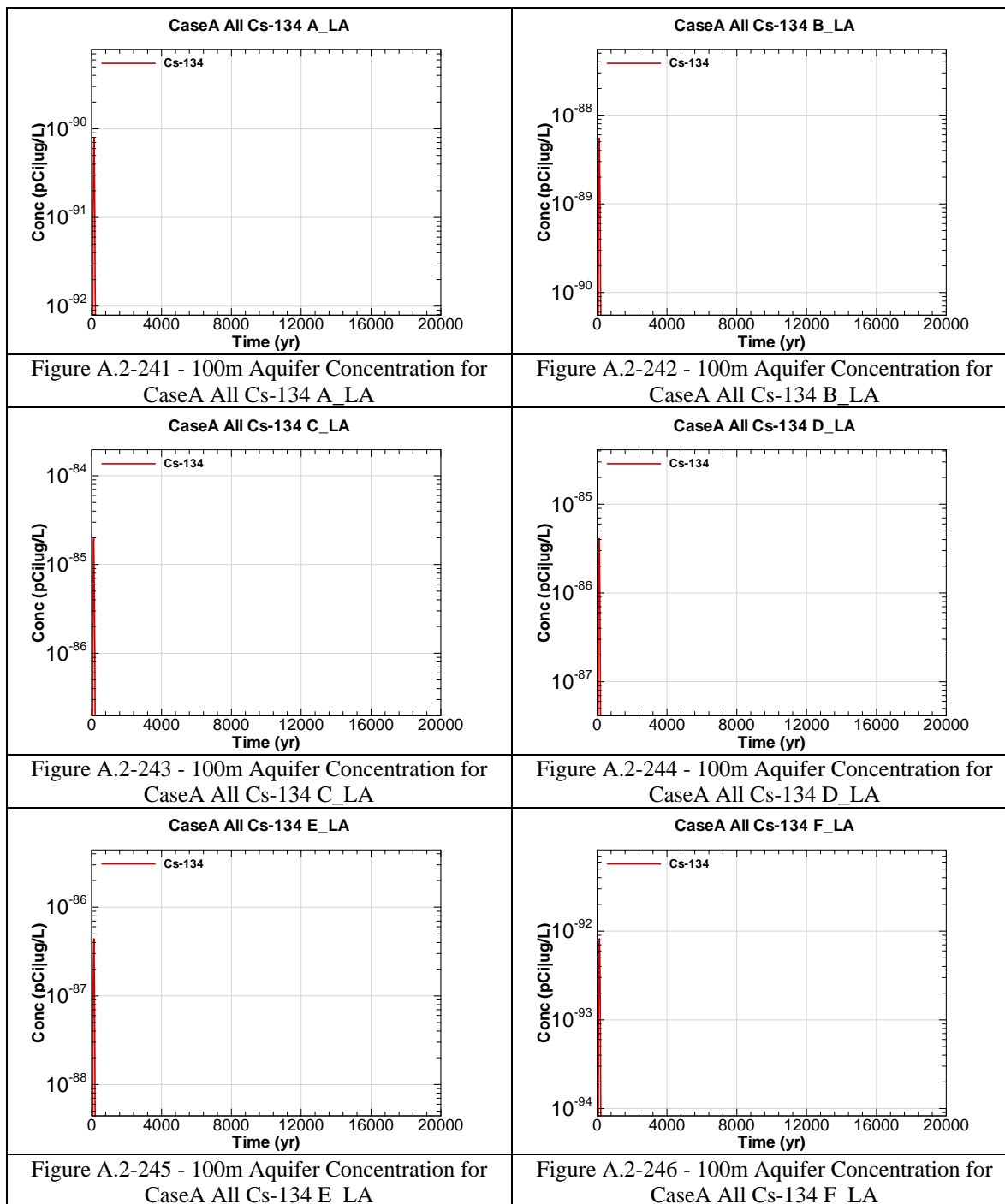
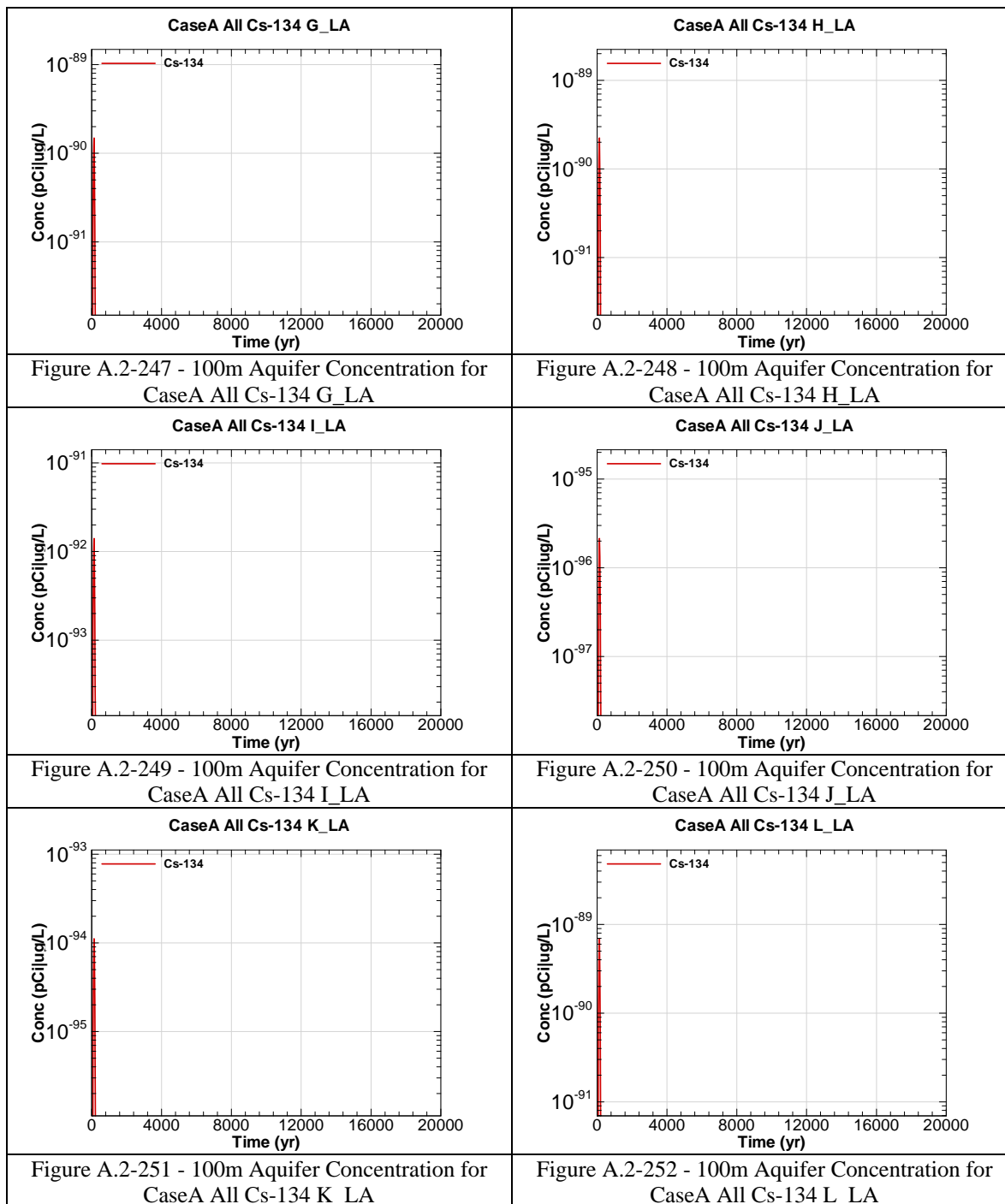


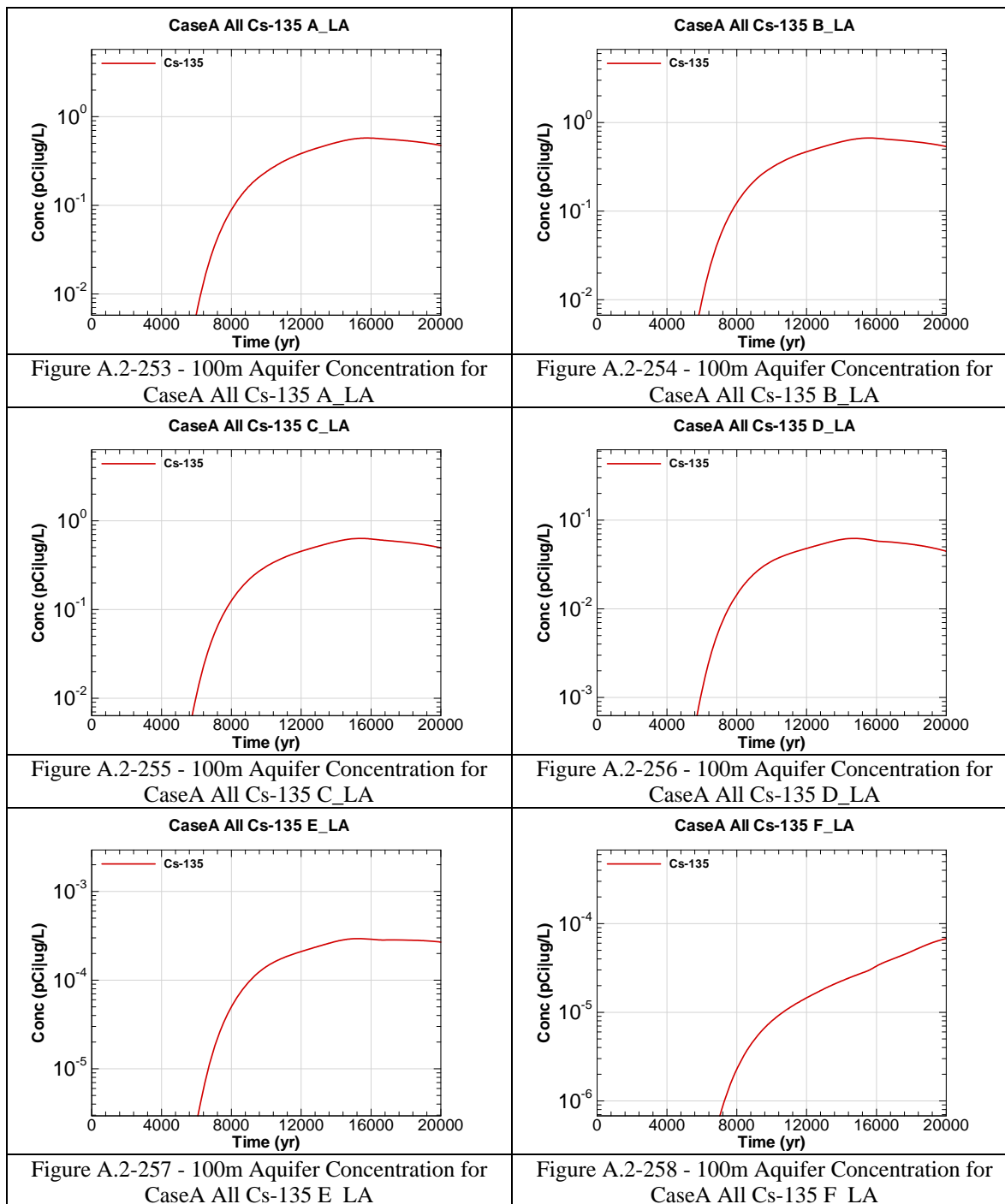
Figure A.2-228 - 100m Aquifer Concentration for
CaseA All Cm-248 L_LA

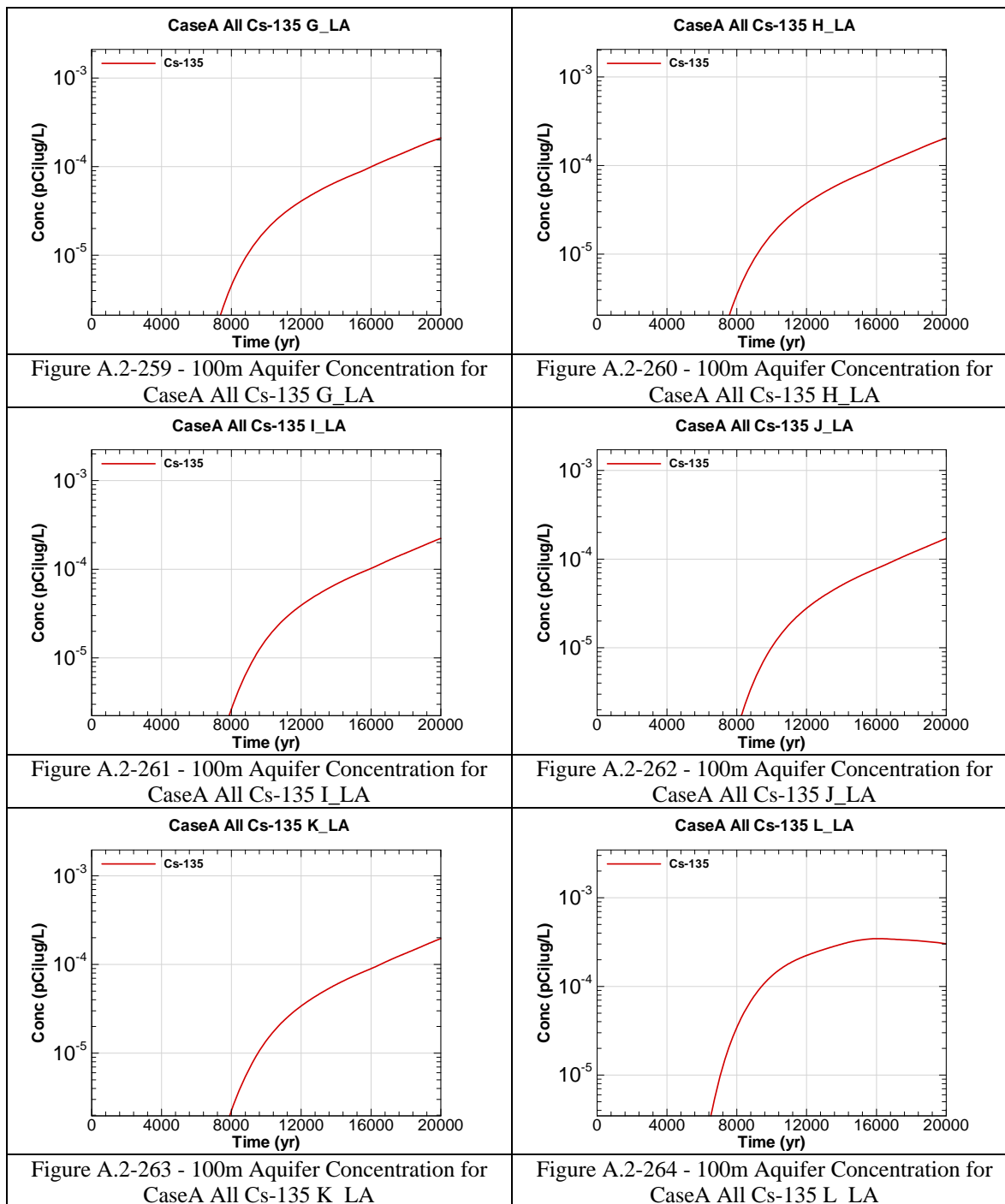


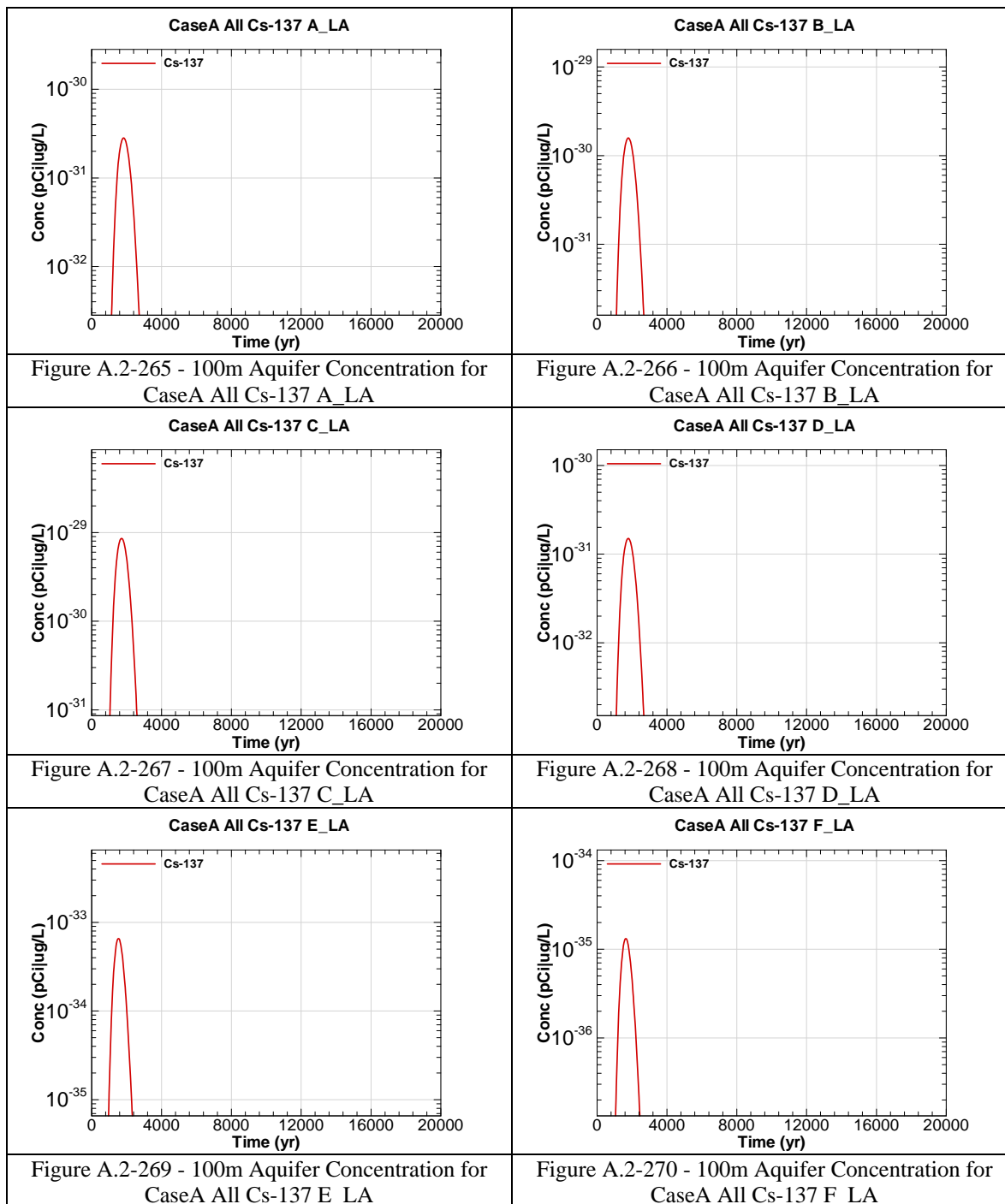


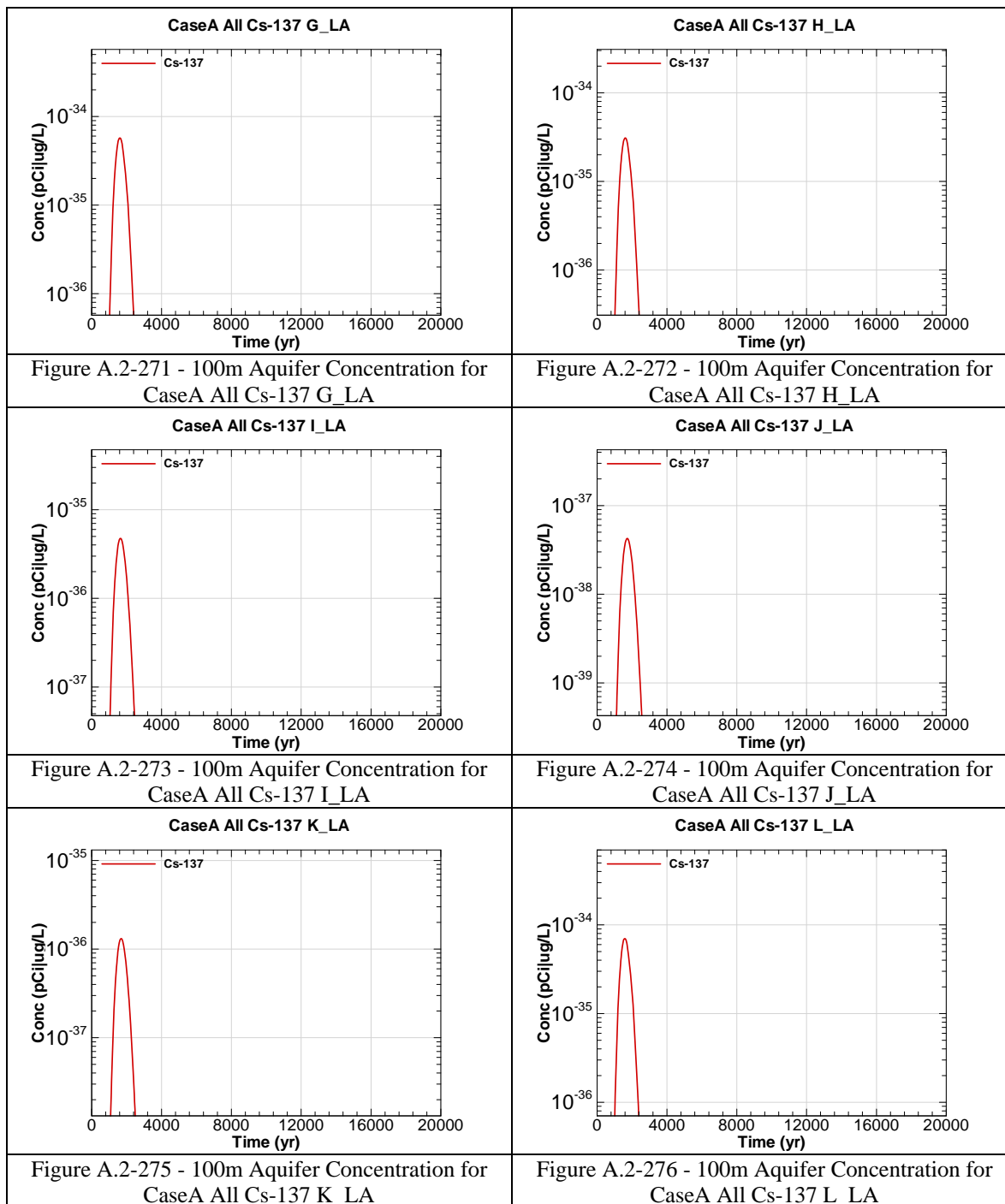


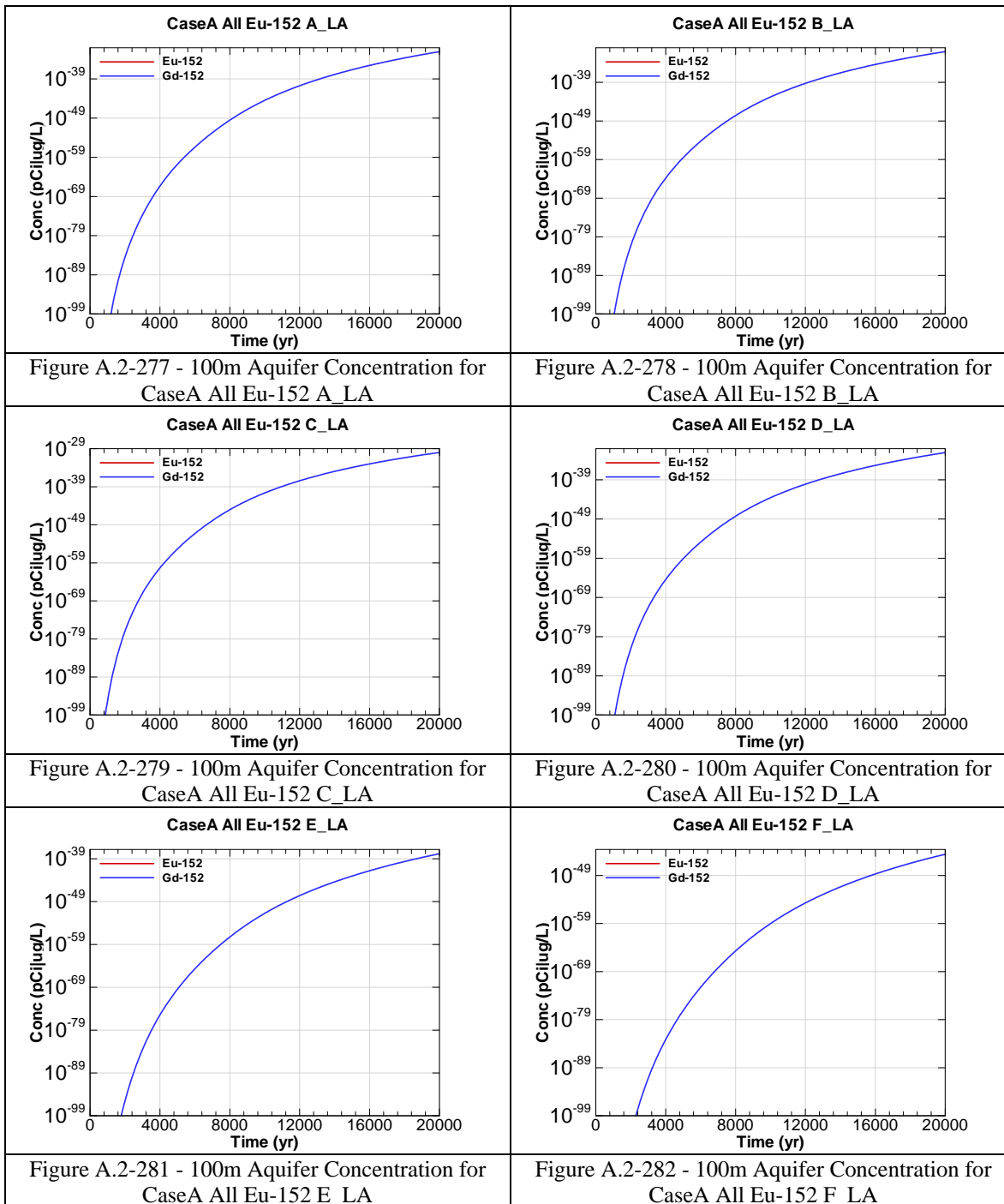


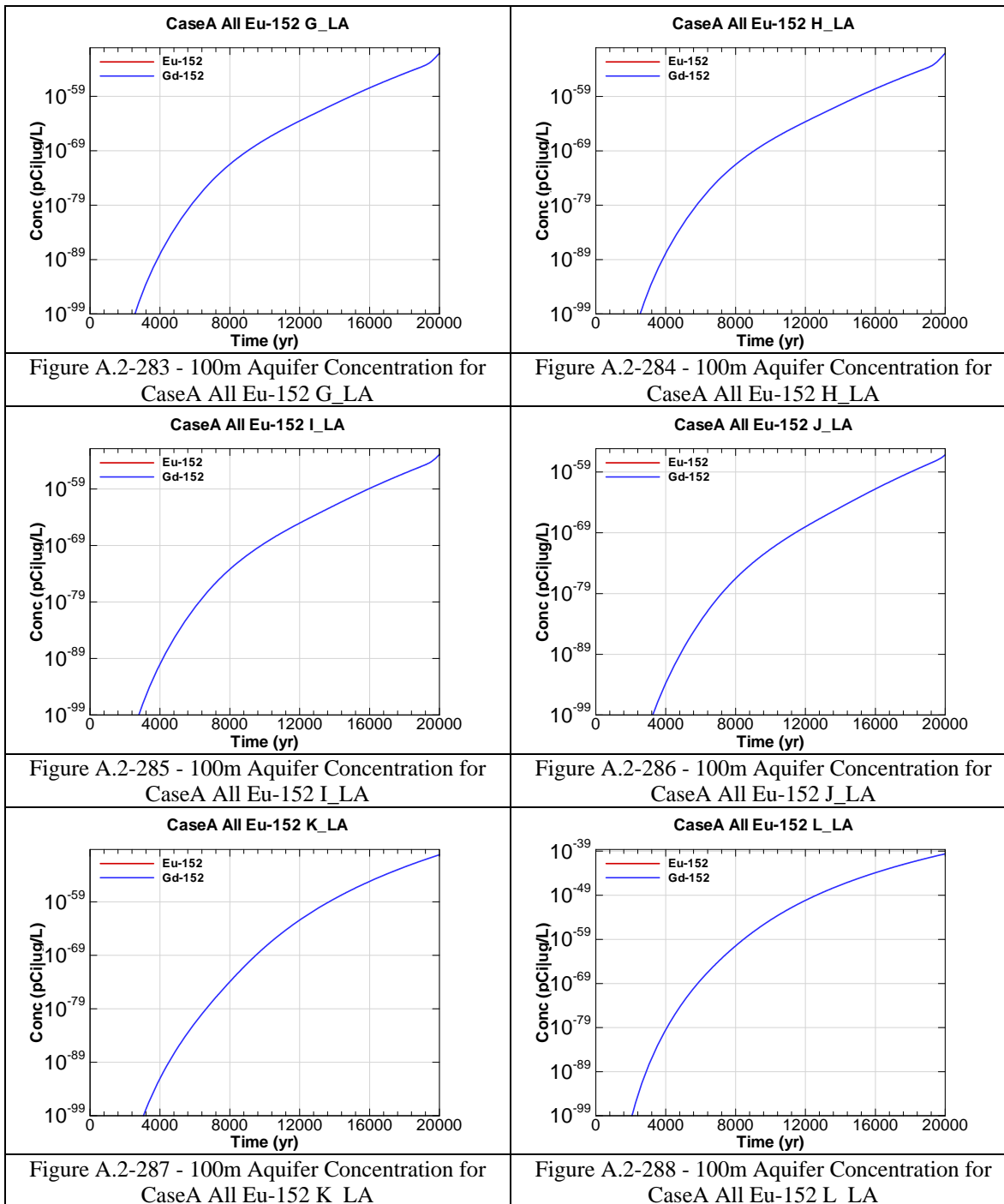


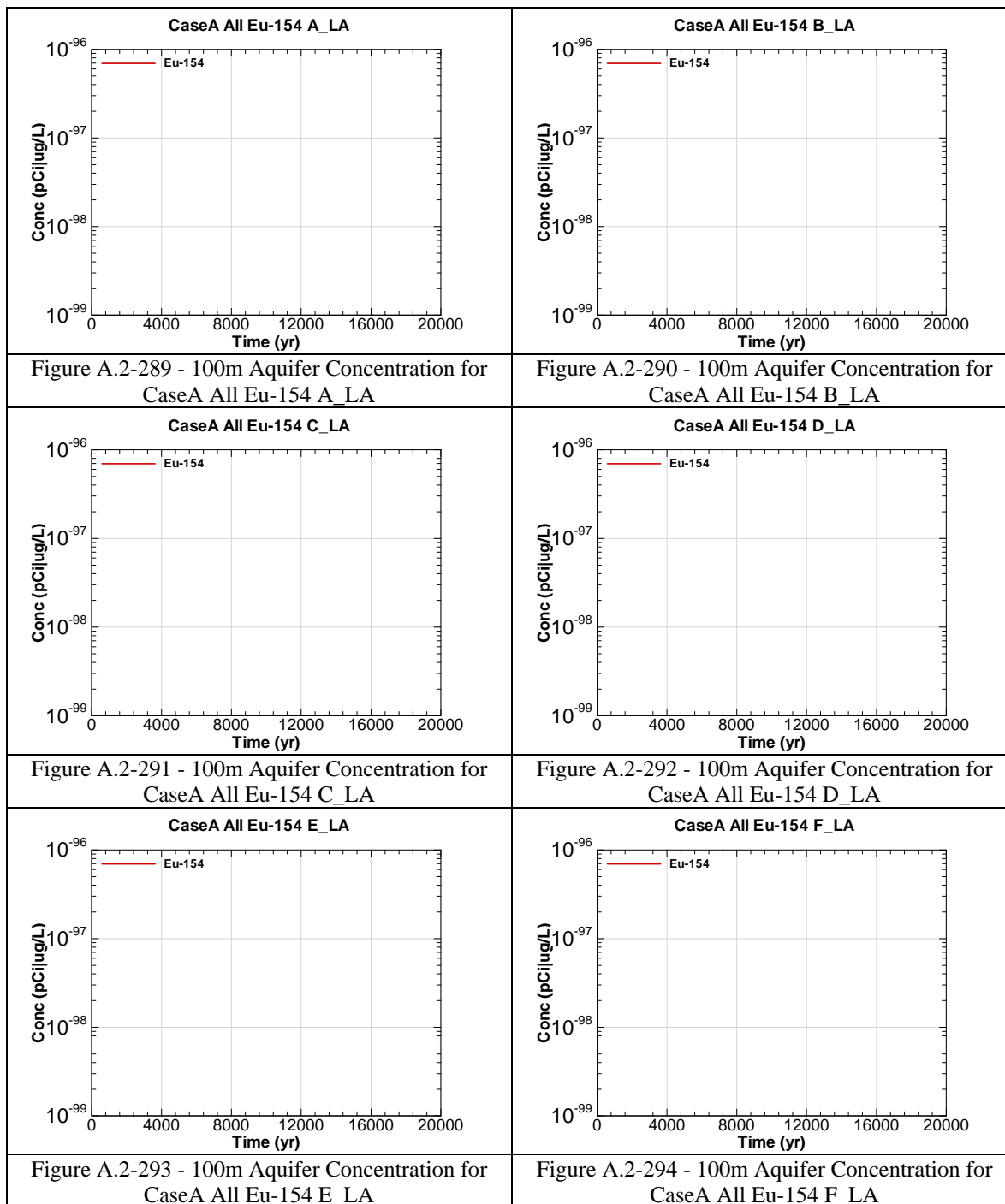


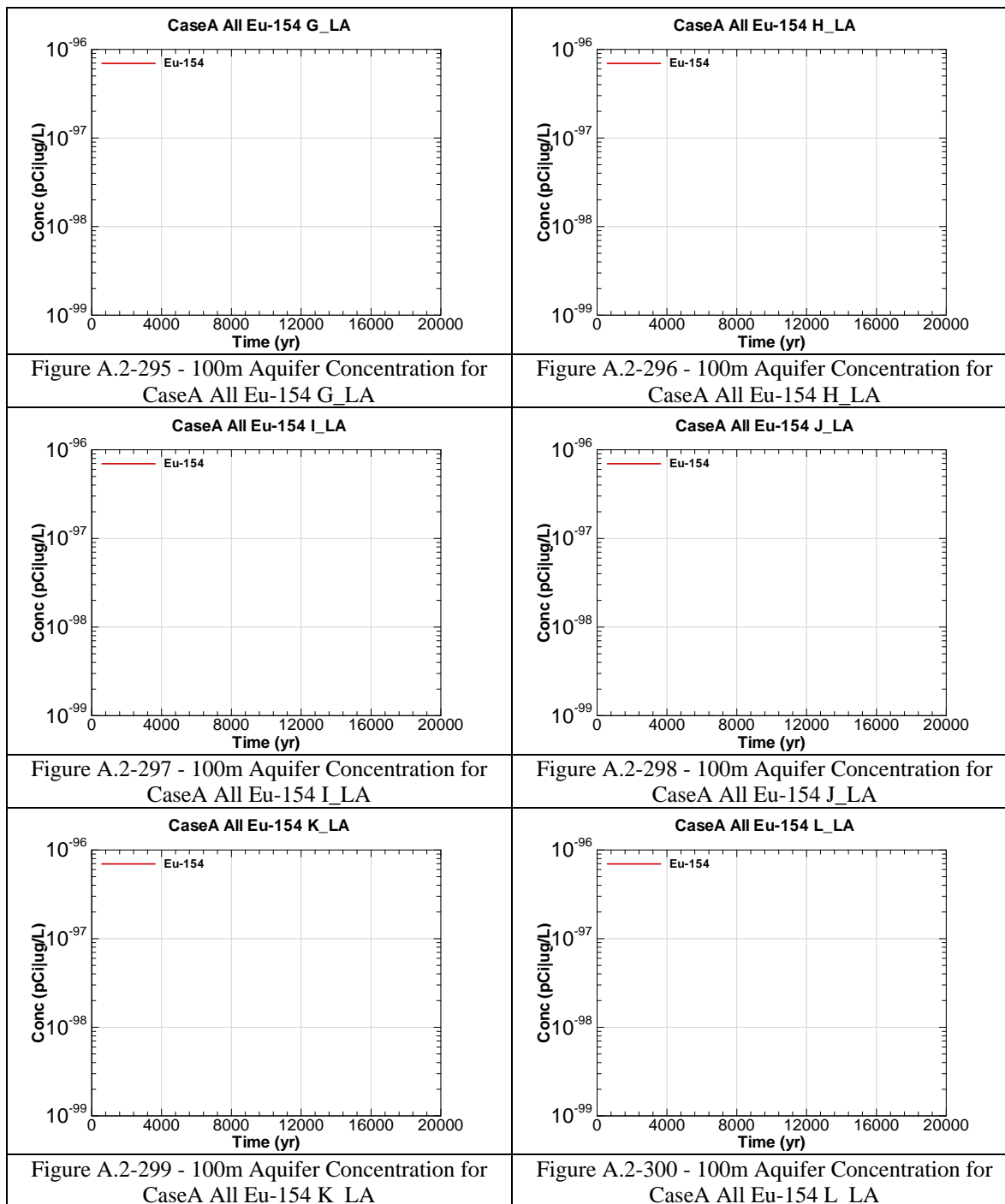


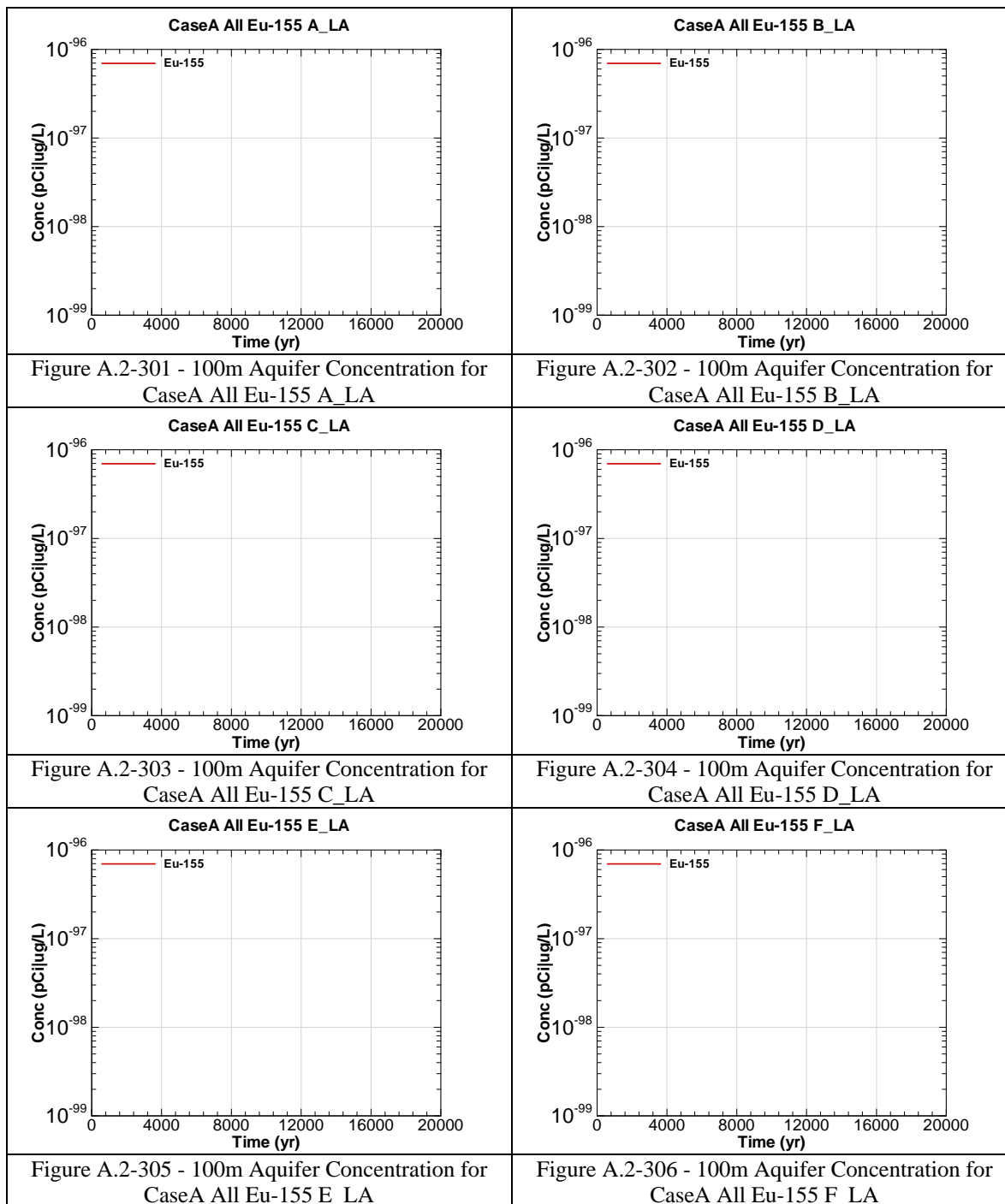


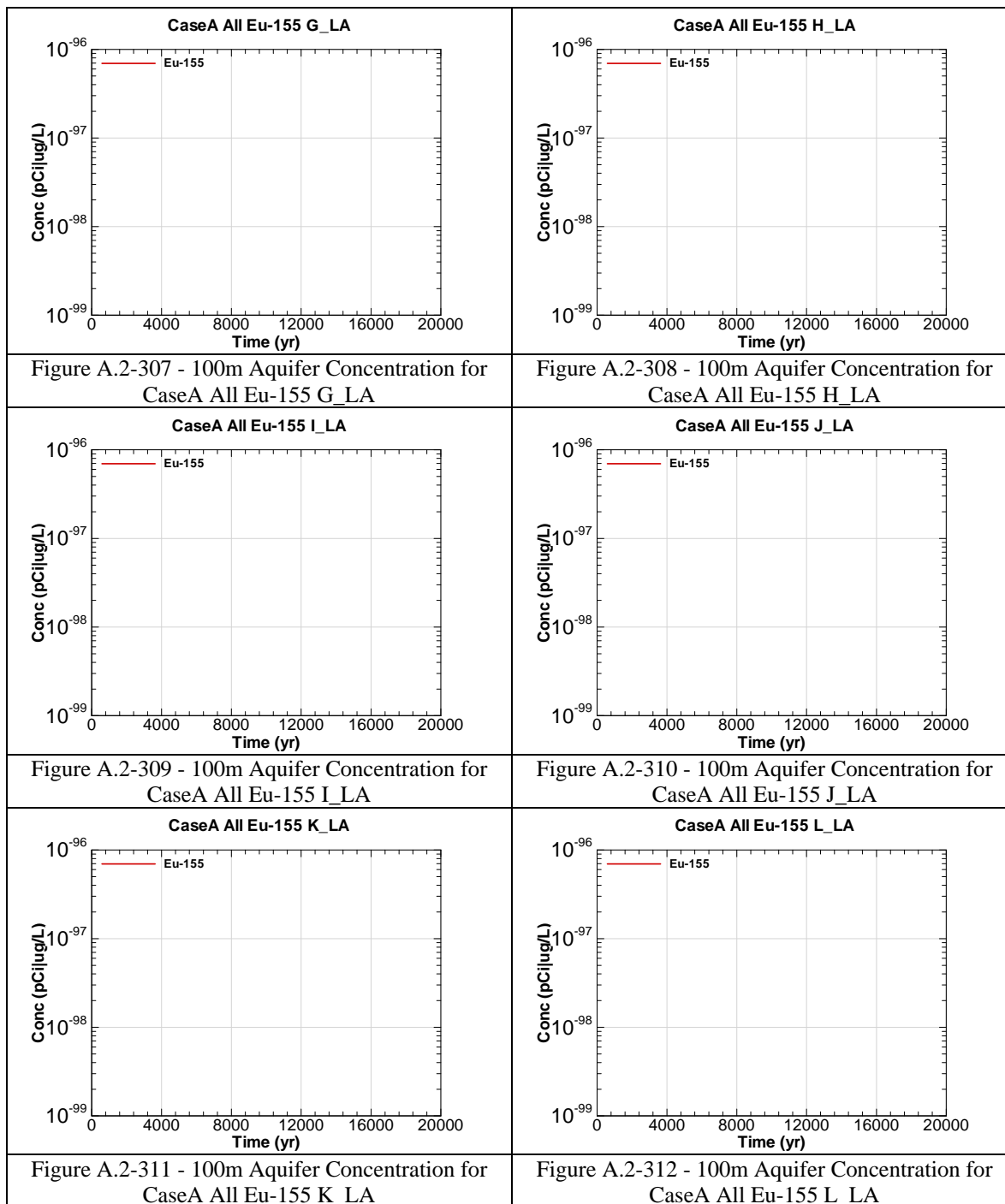


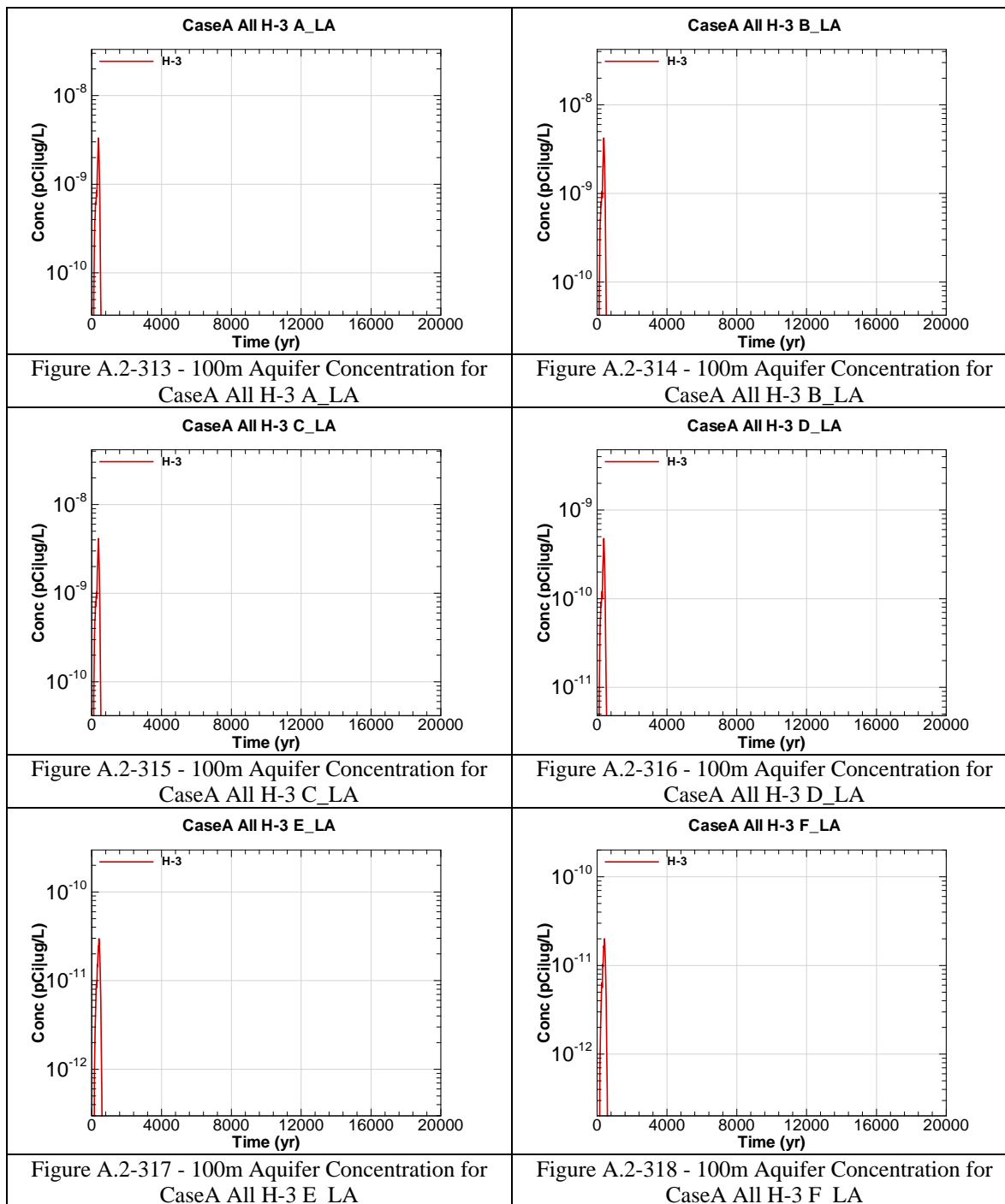


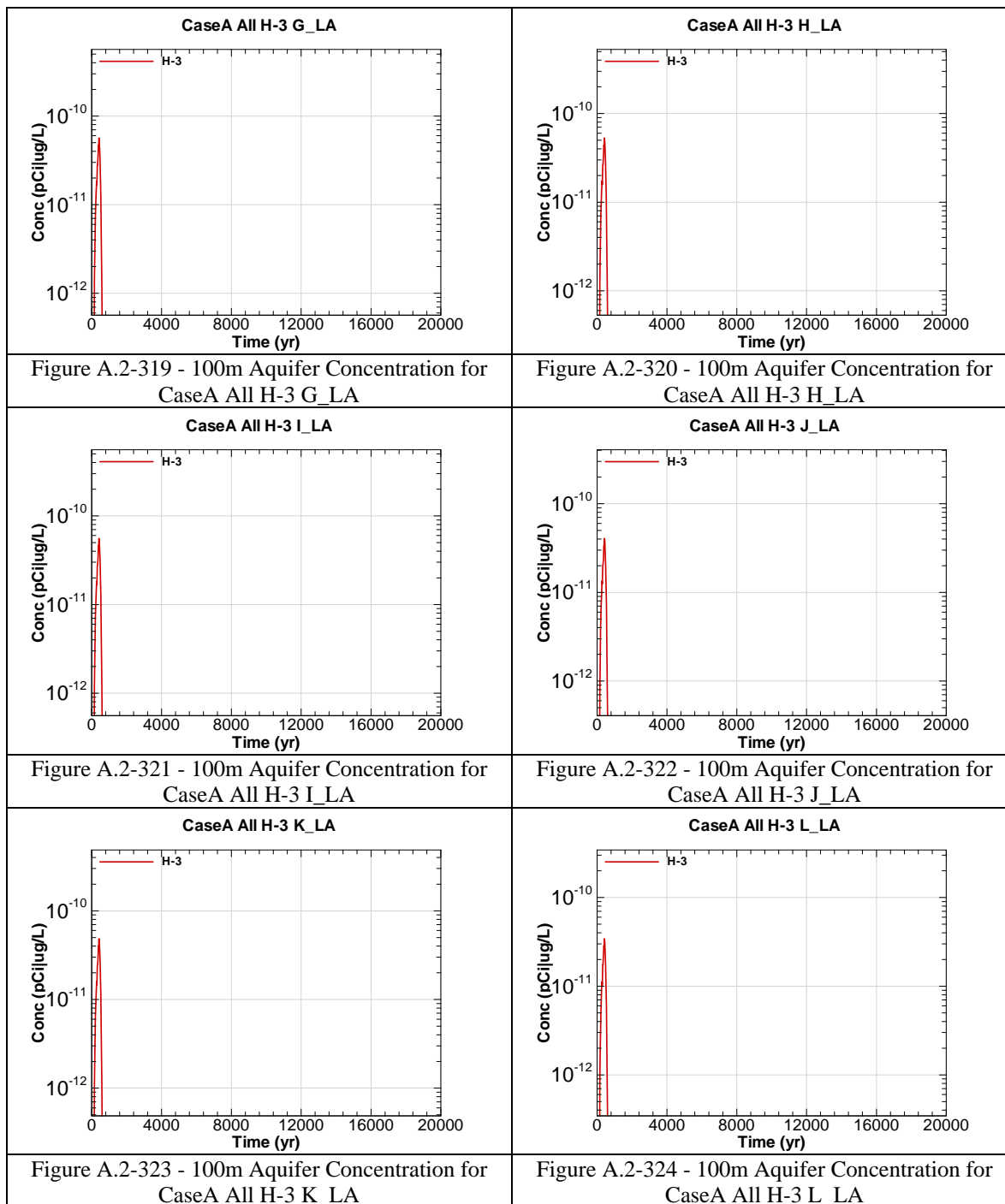


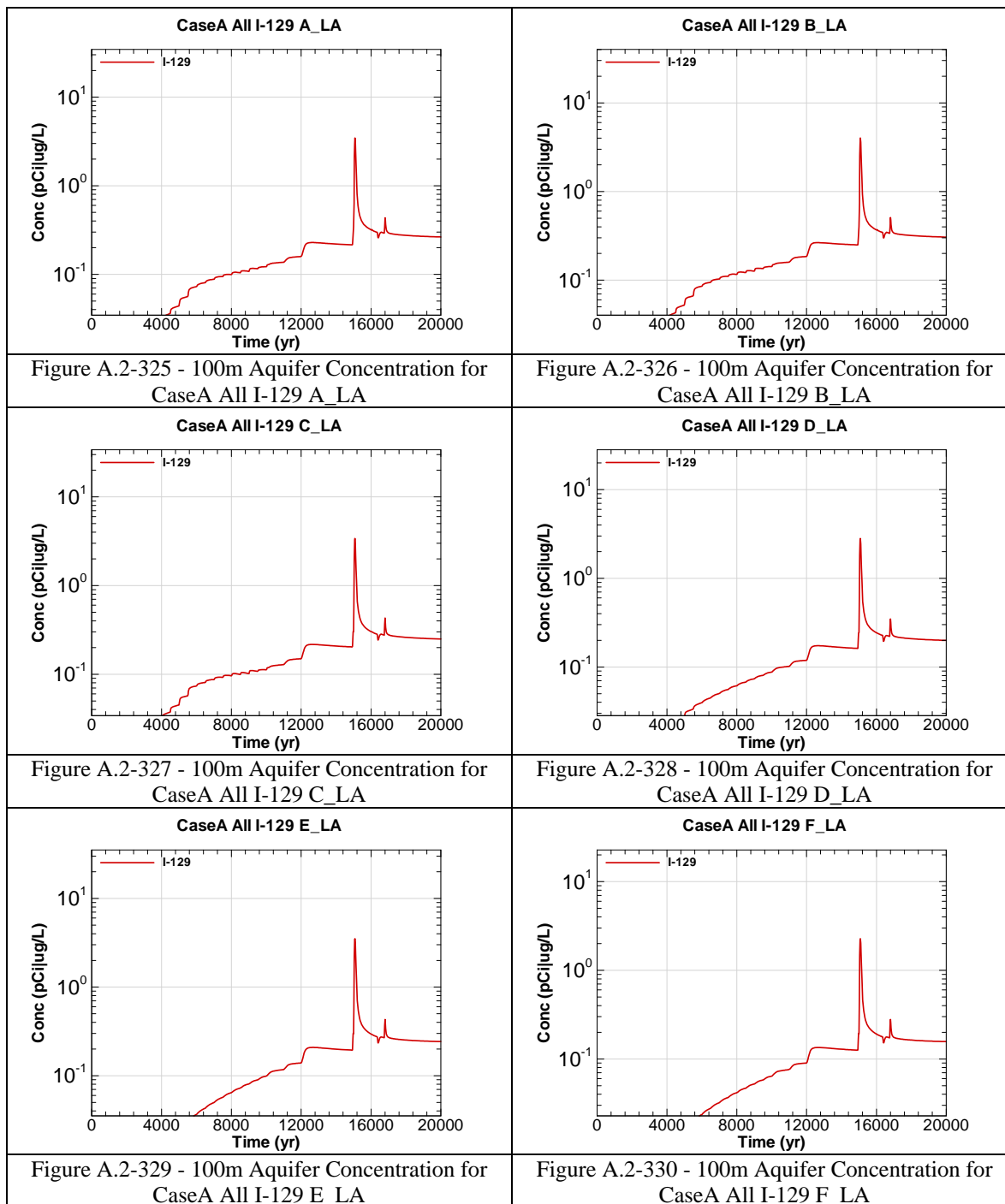


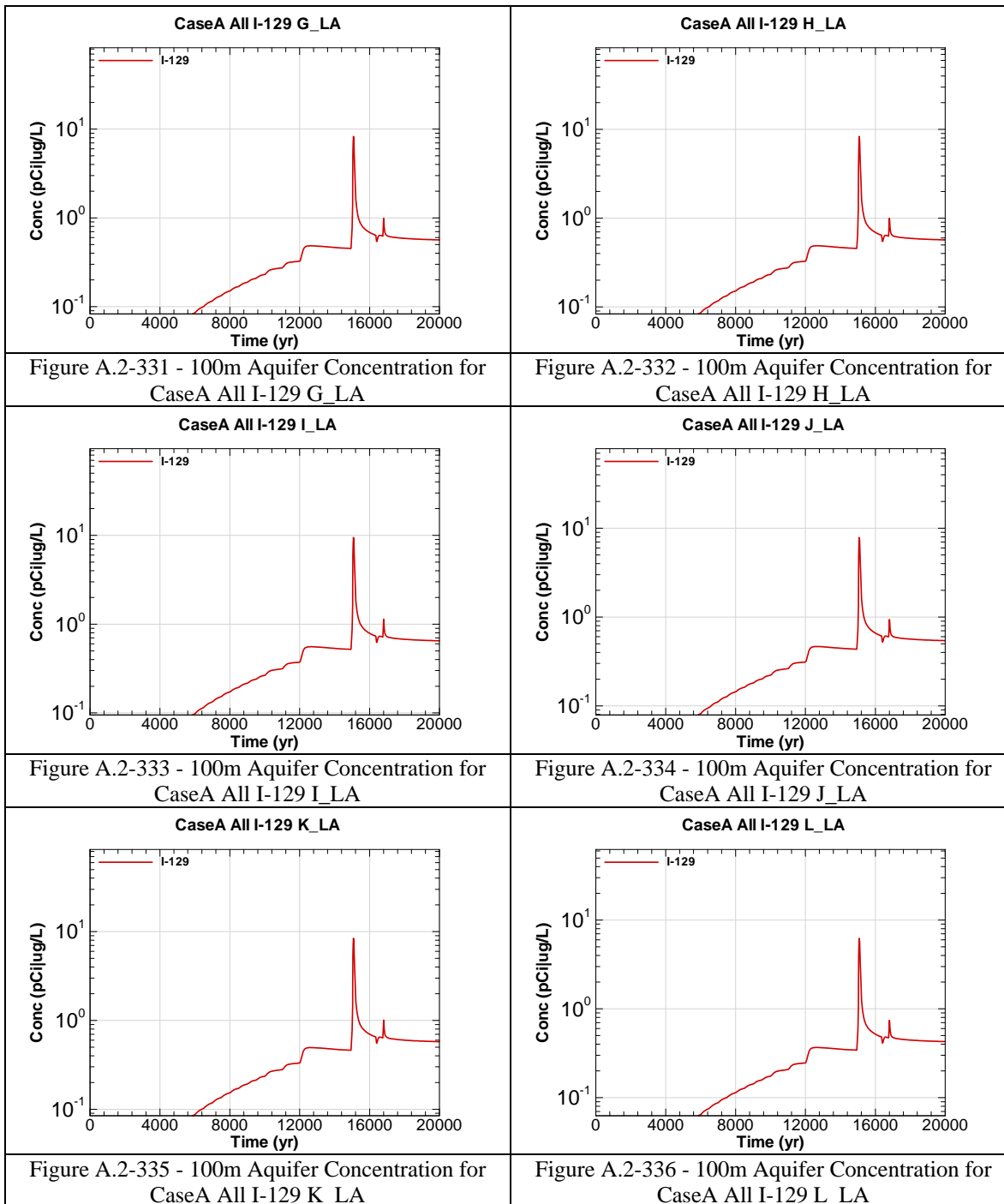


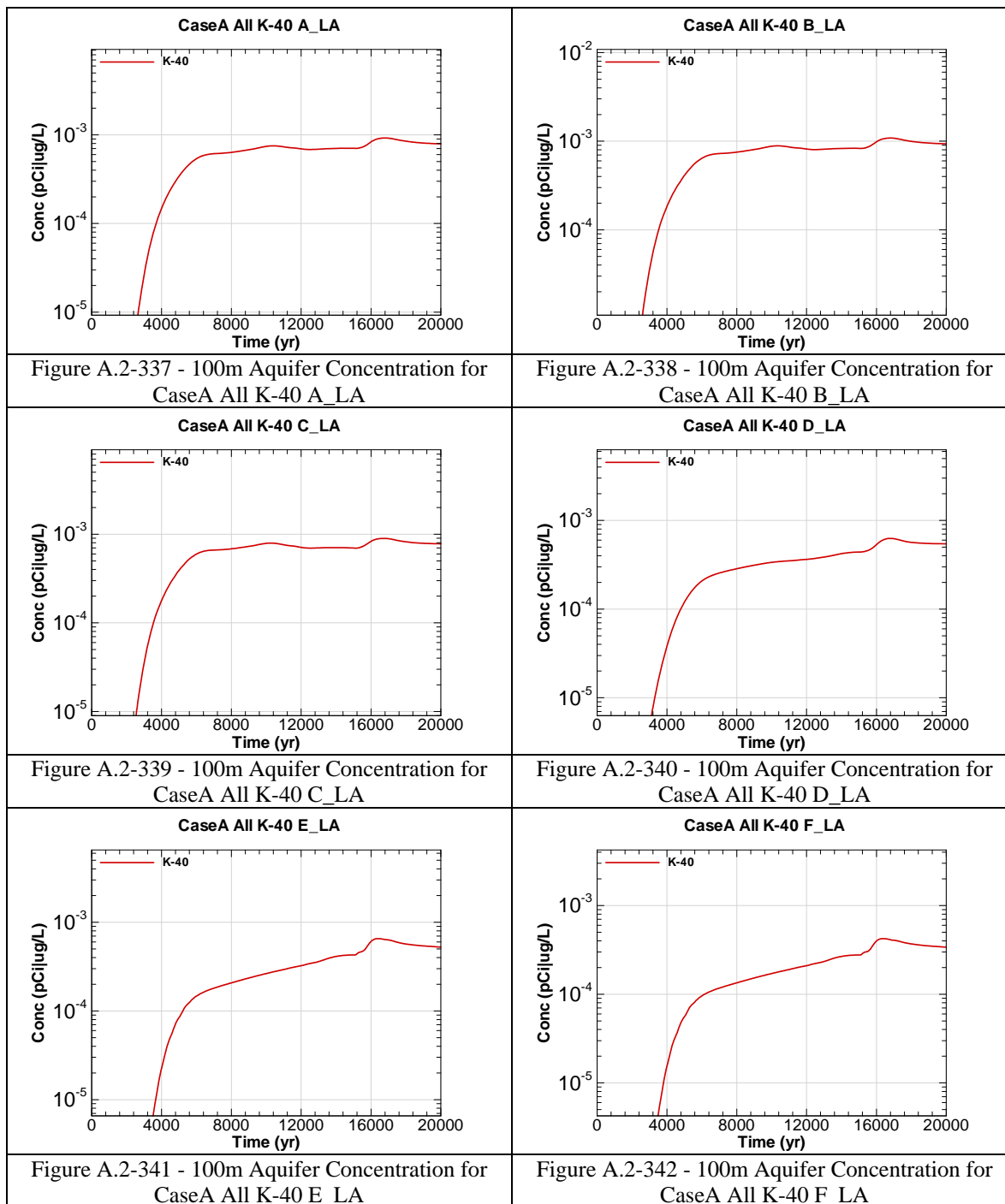


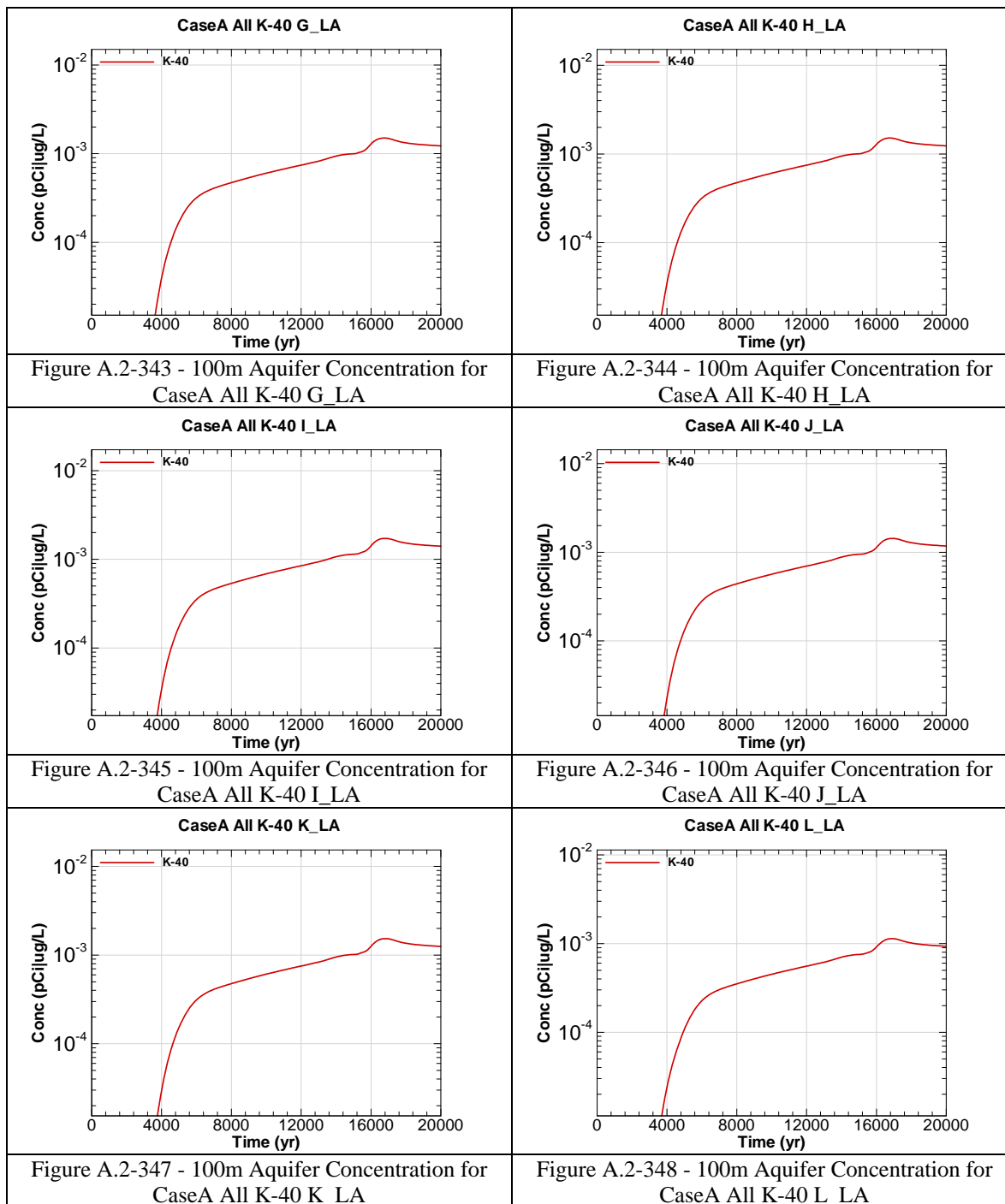


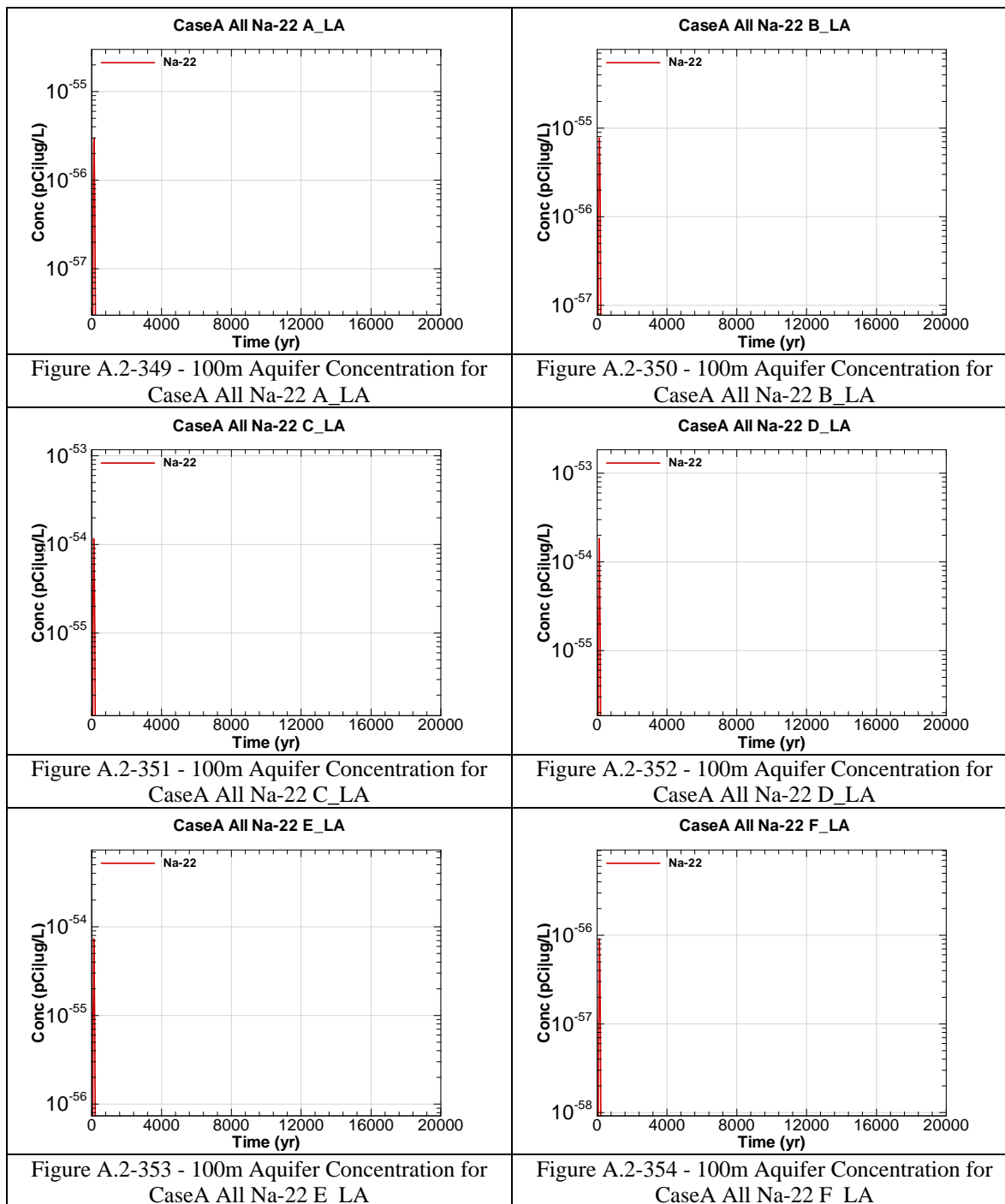


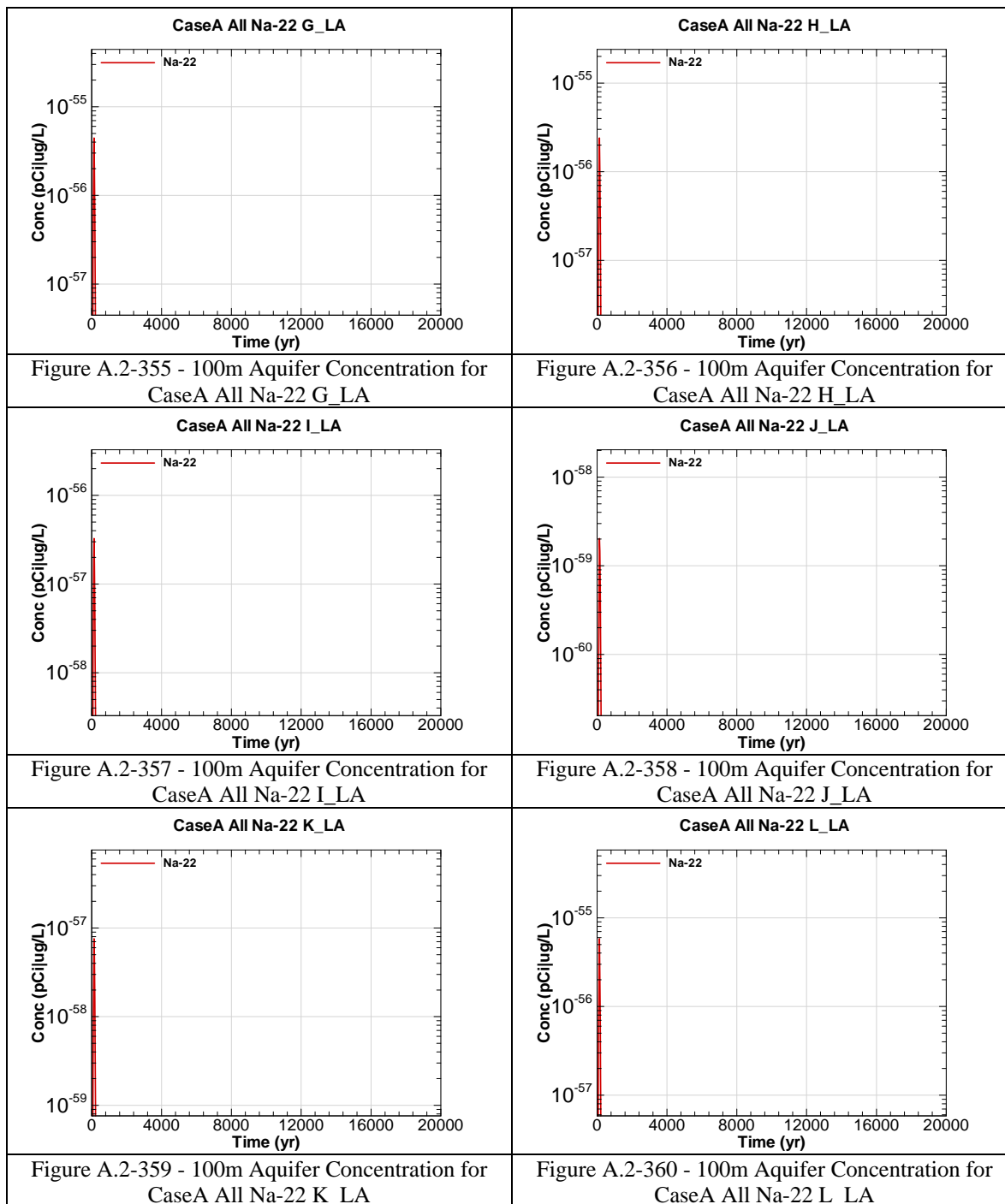


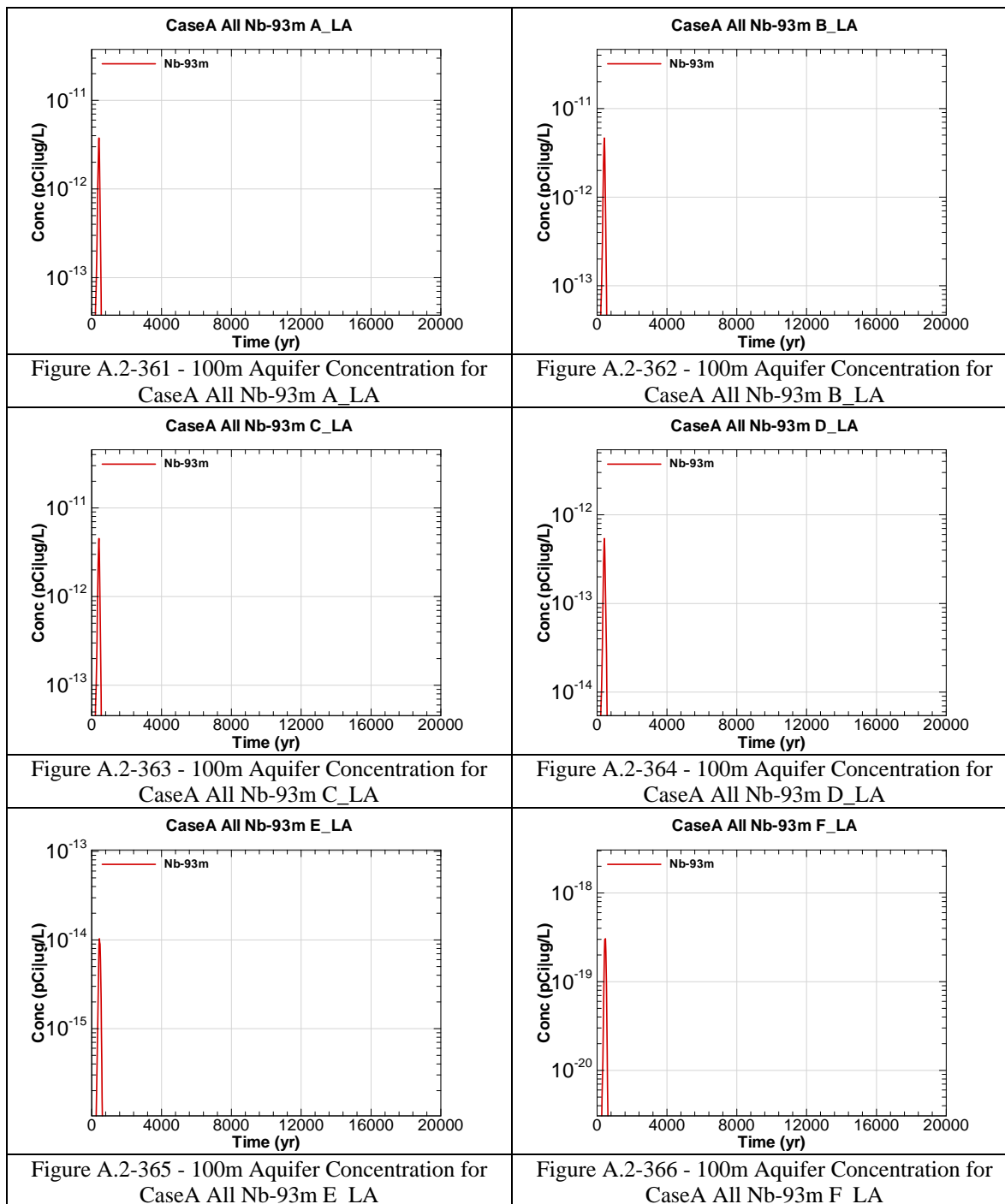


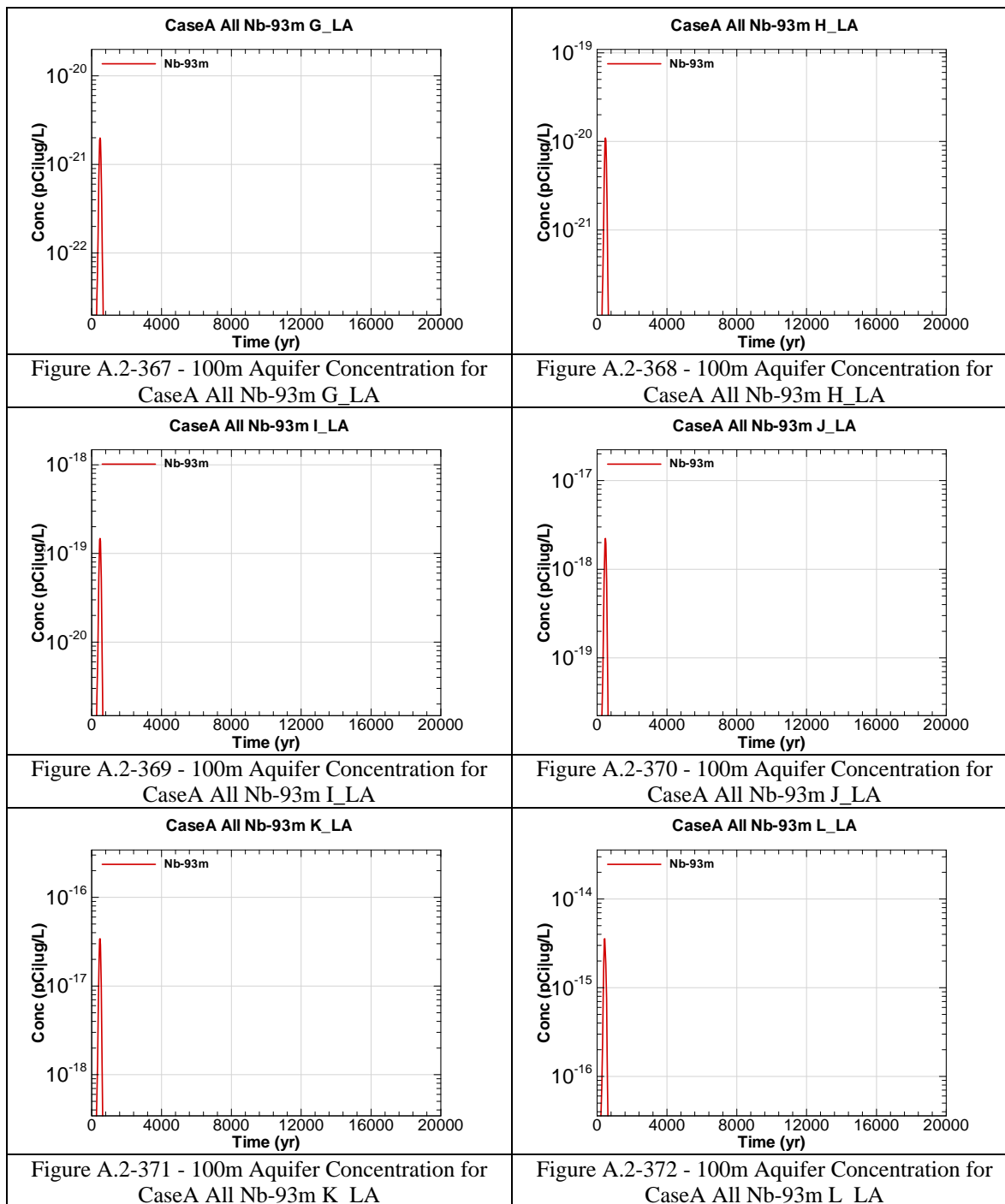


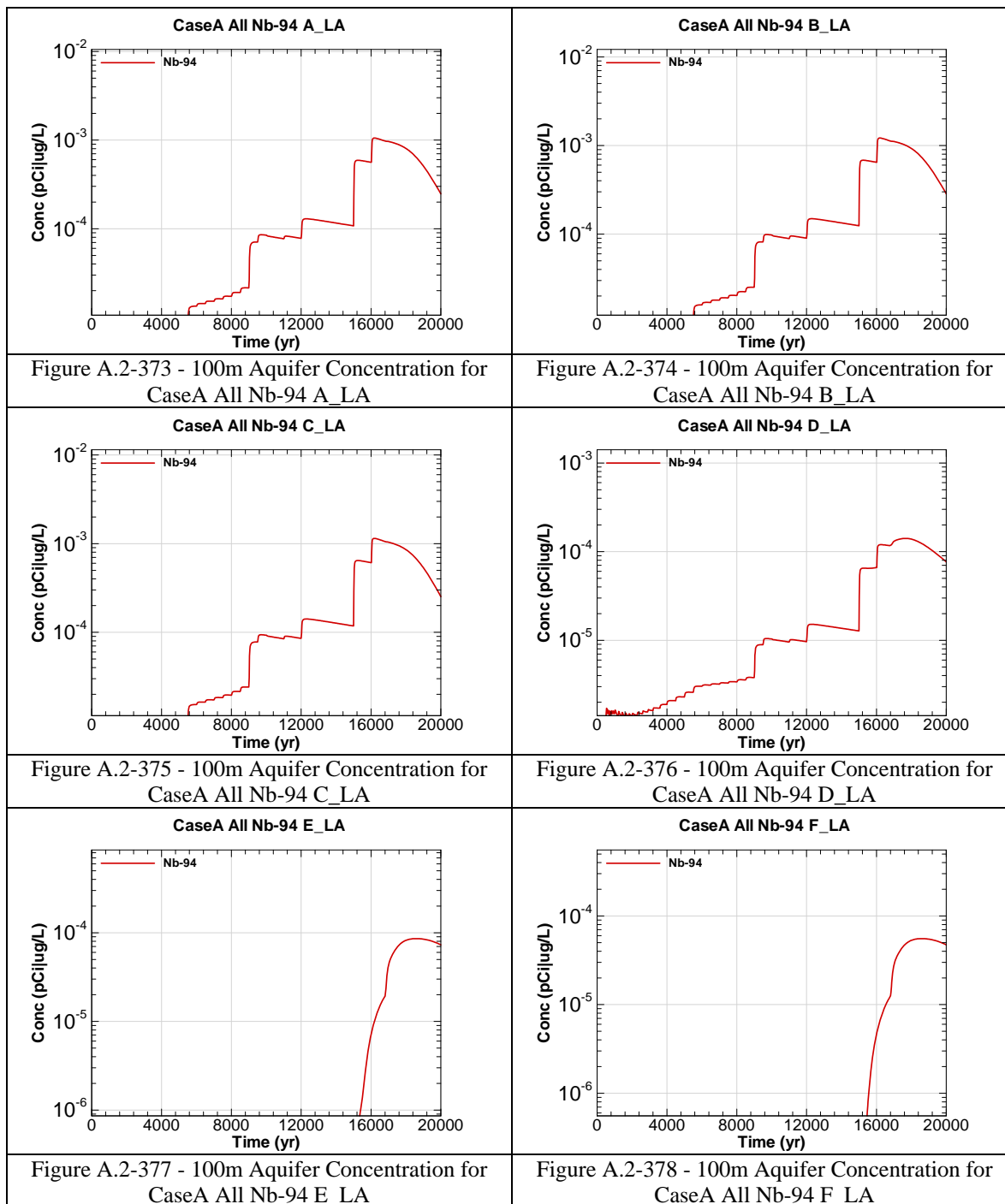


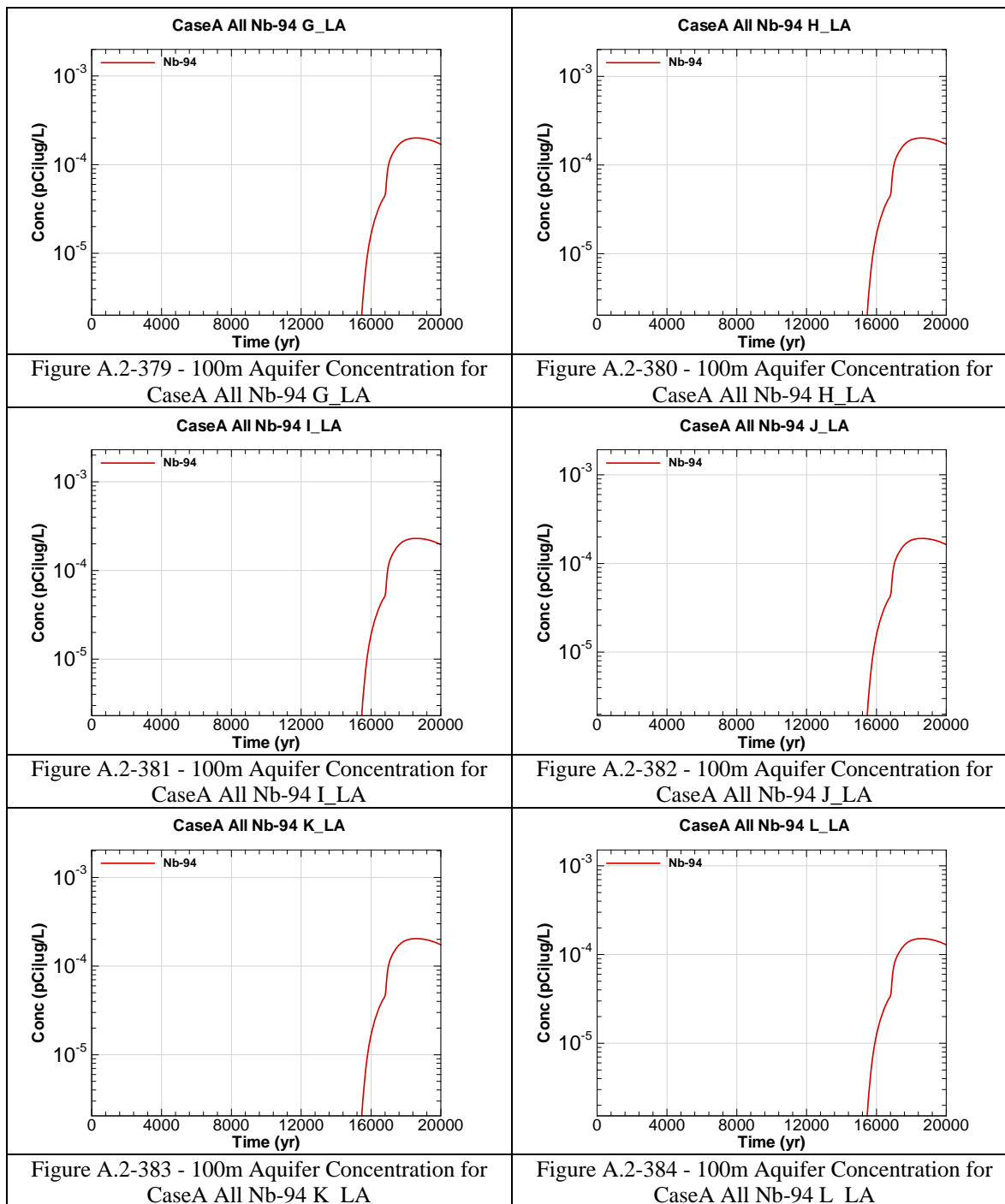


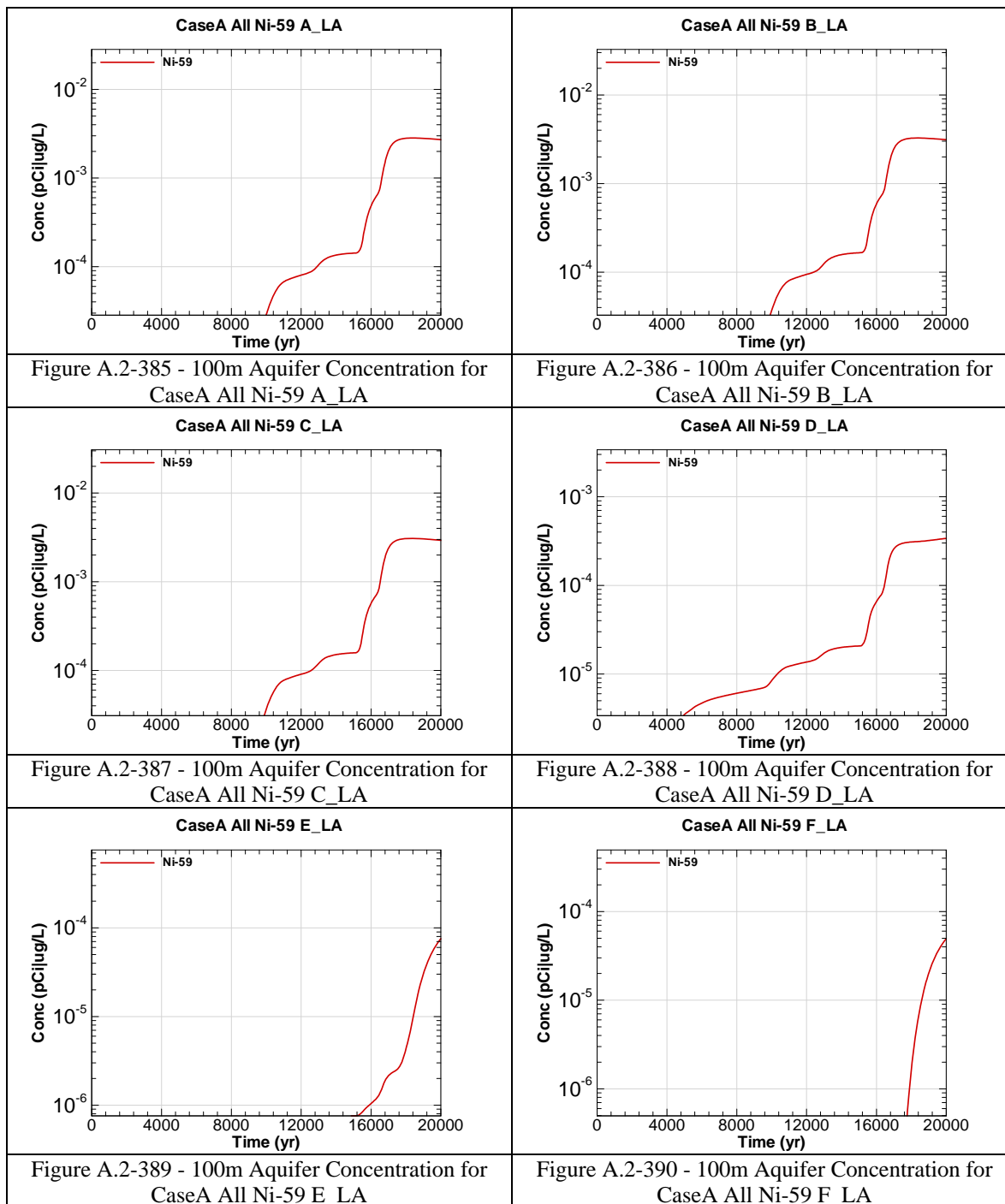


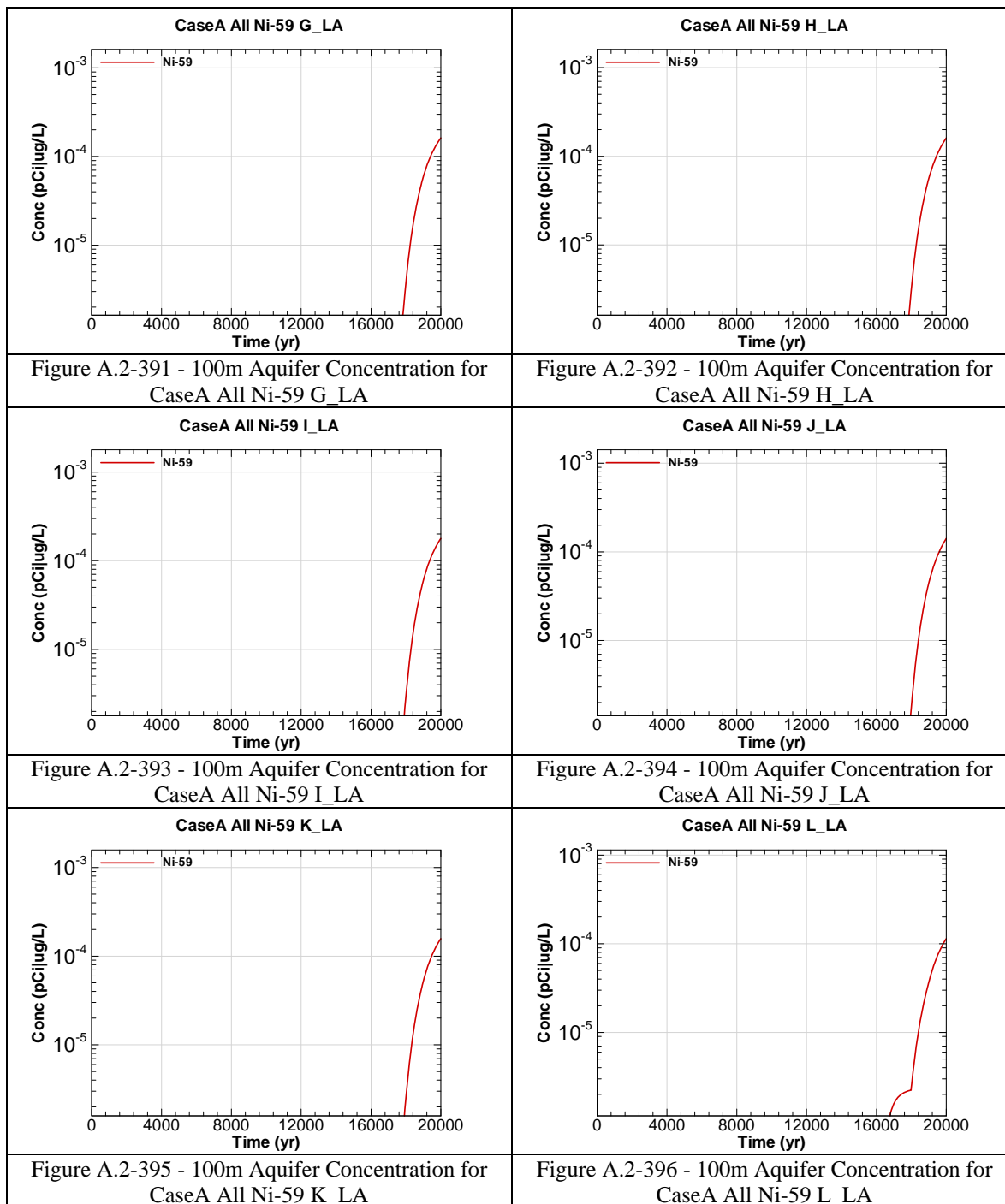


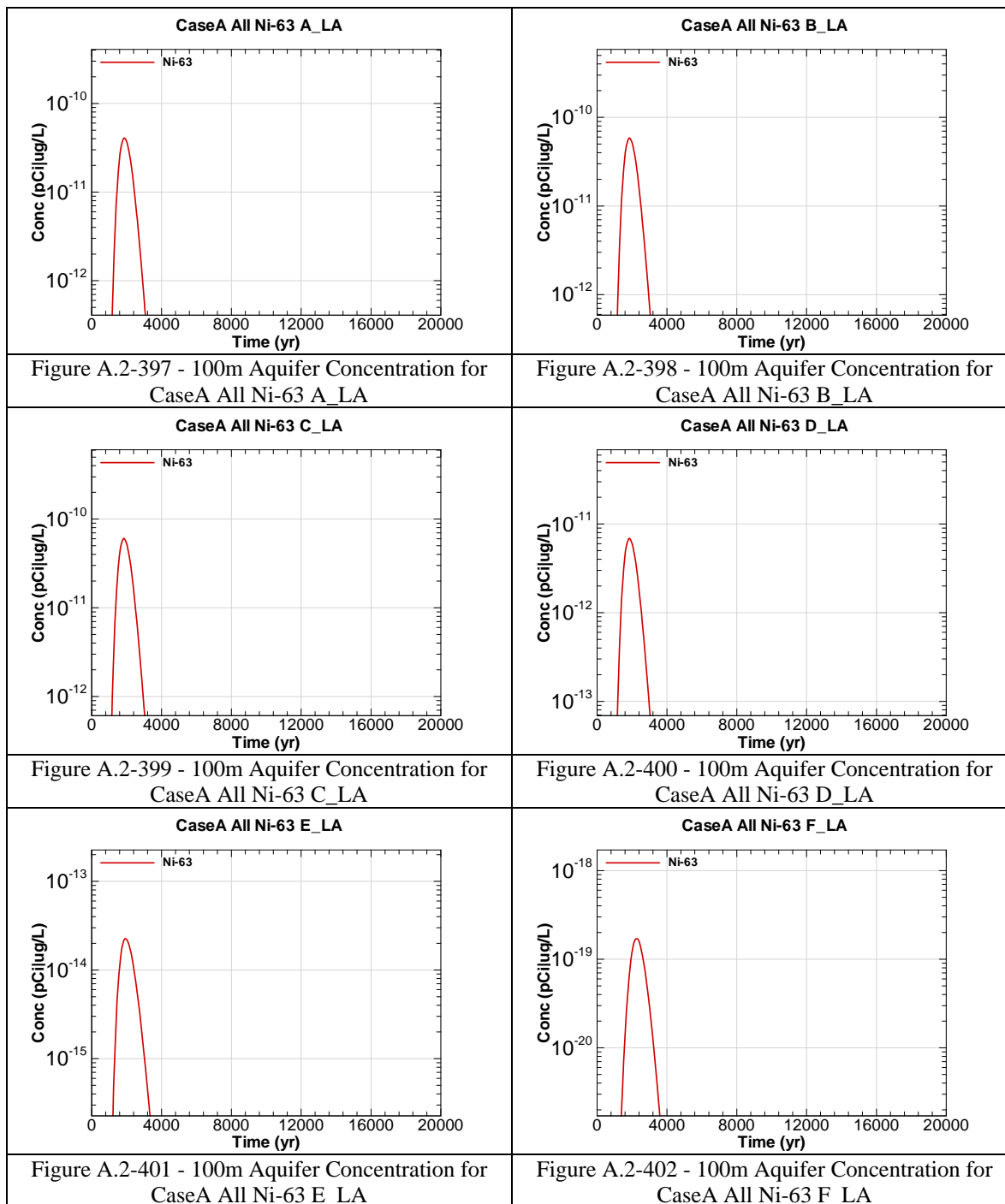


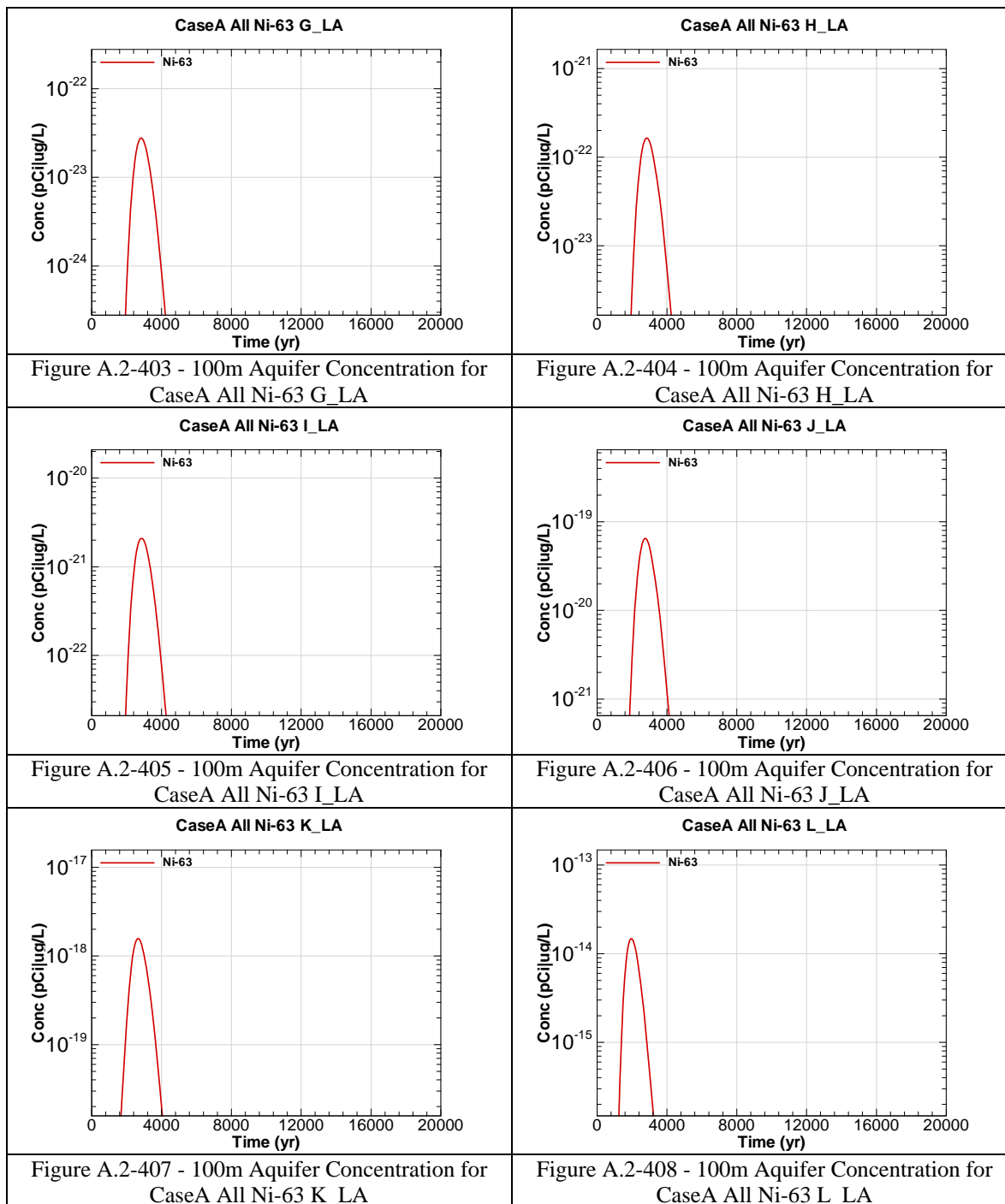












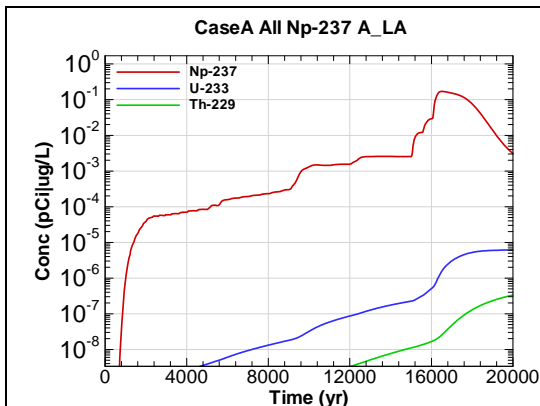


Figure A.2-409 - 100m Aquifer Concentration for
CaseA All Np-237 A_LA

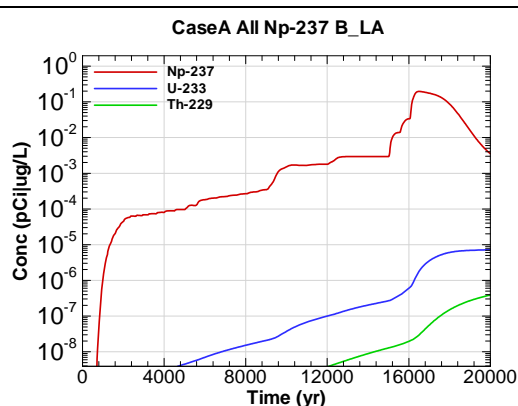


Figure A.2-410 - 100m Aquifer Concentration for
CaseA All Np-237 B_LA

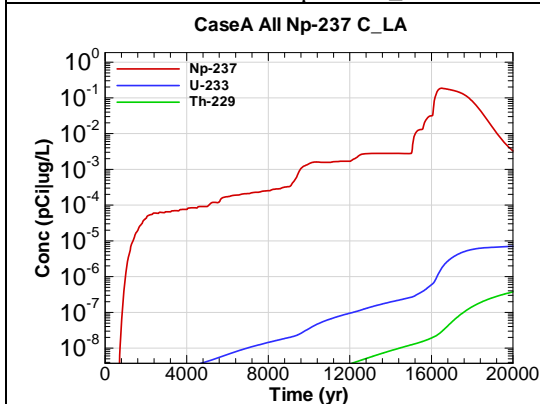


Figure A.2-411 - 100m Aquifer Concentration for
CaseA All Np-237 C_LA

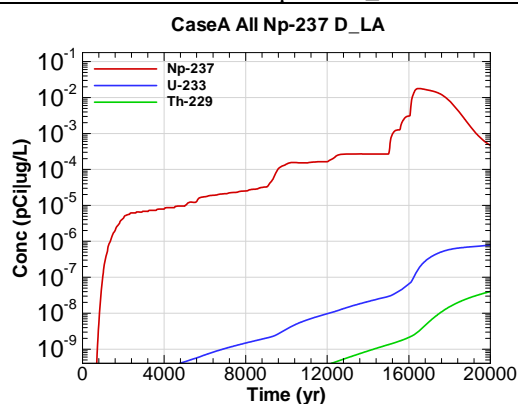


Figure A.2-412 - 100m Aquifer Concentration for
CaseA All Np-237 D_LA

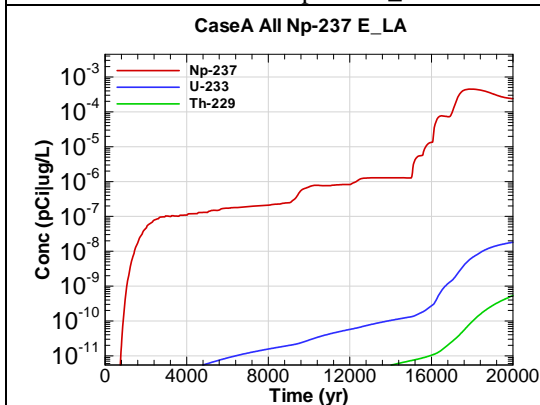


Figure A.2-413 - 100m Aquifer Concentration for
CaseA All Np-237 E_LA

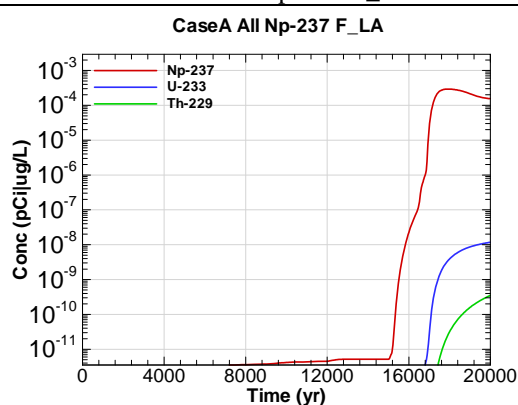
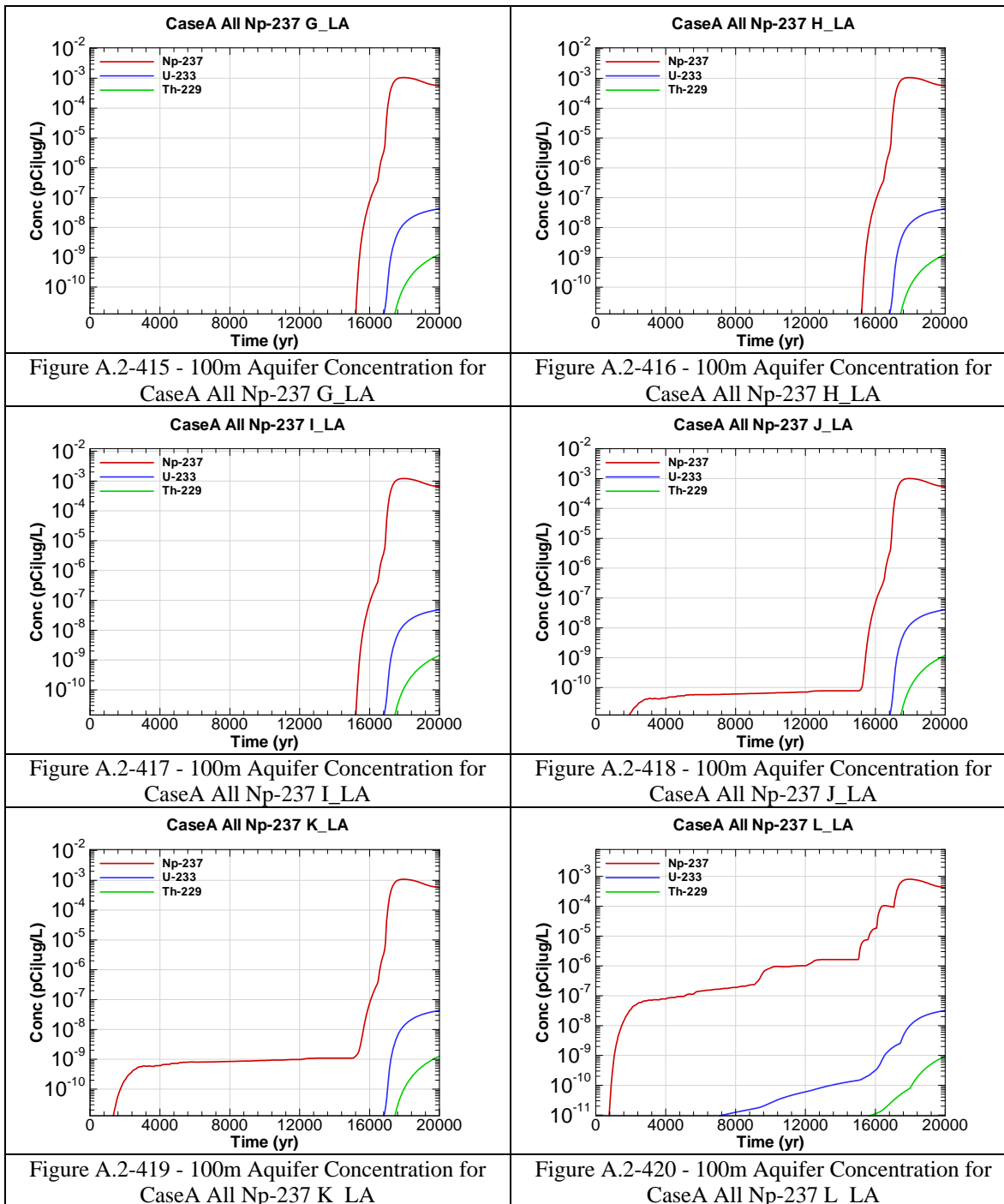
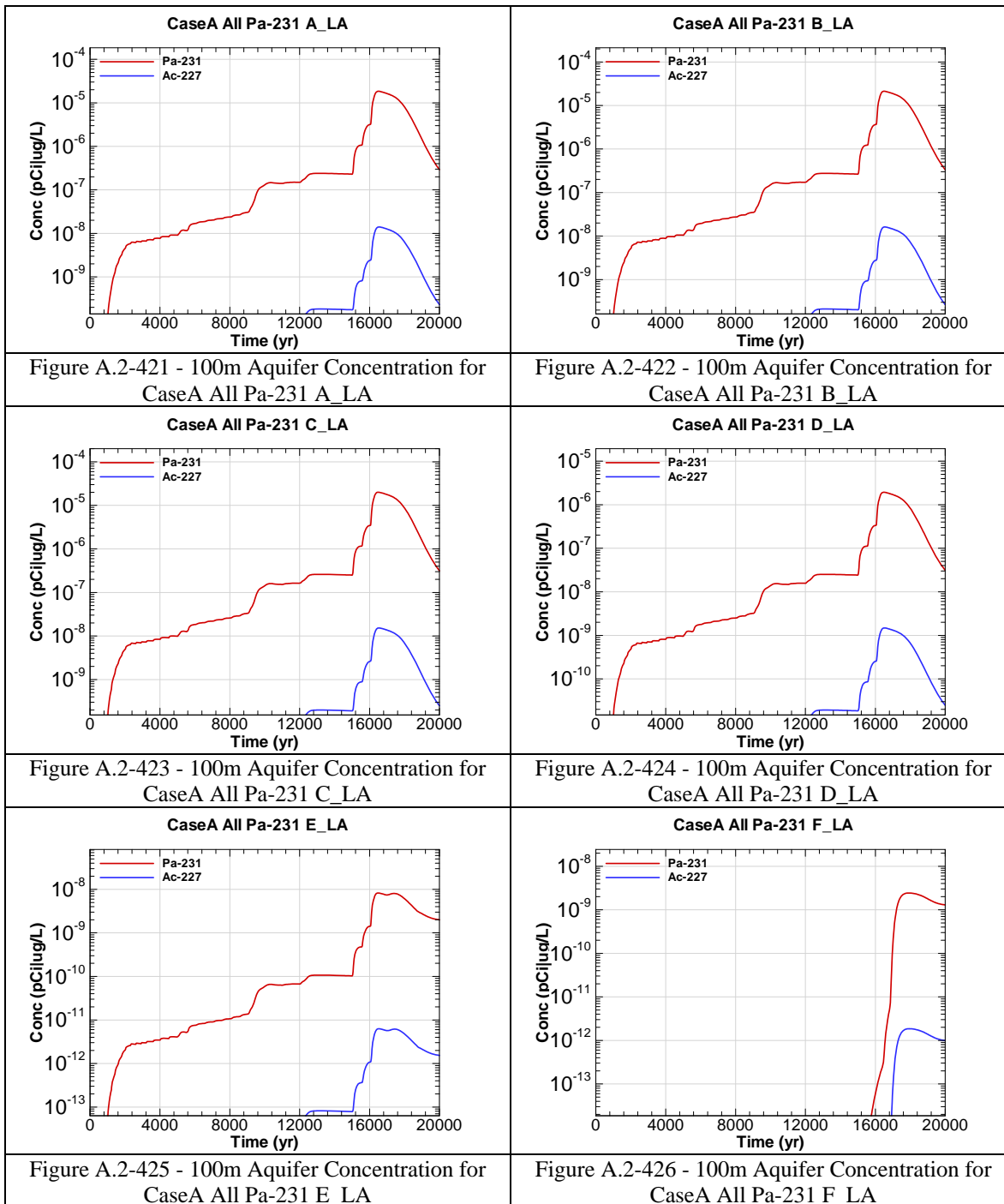
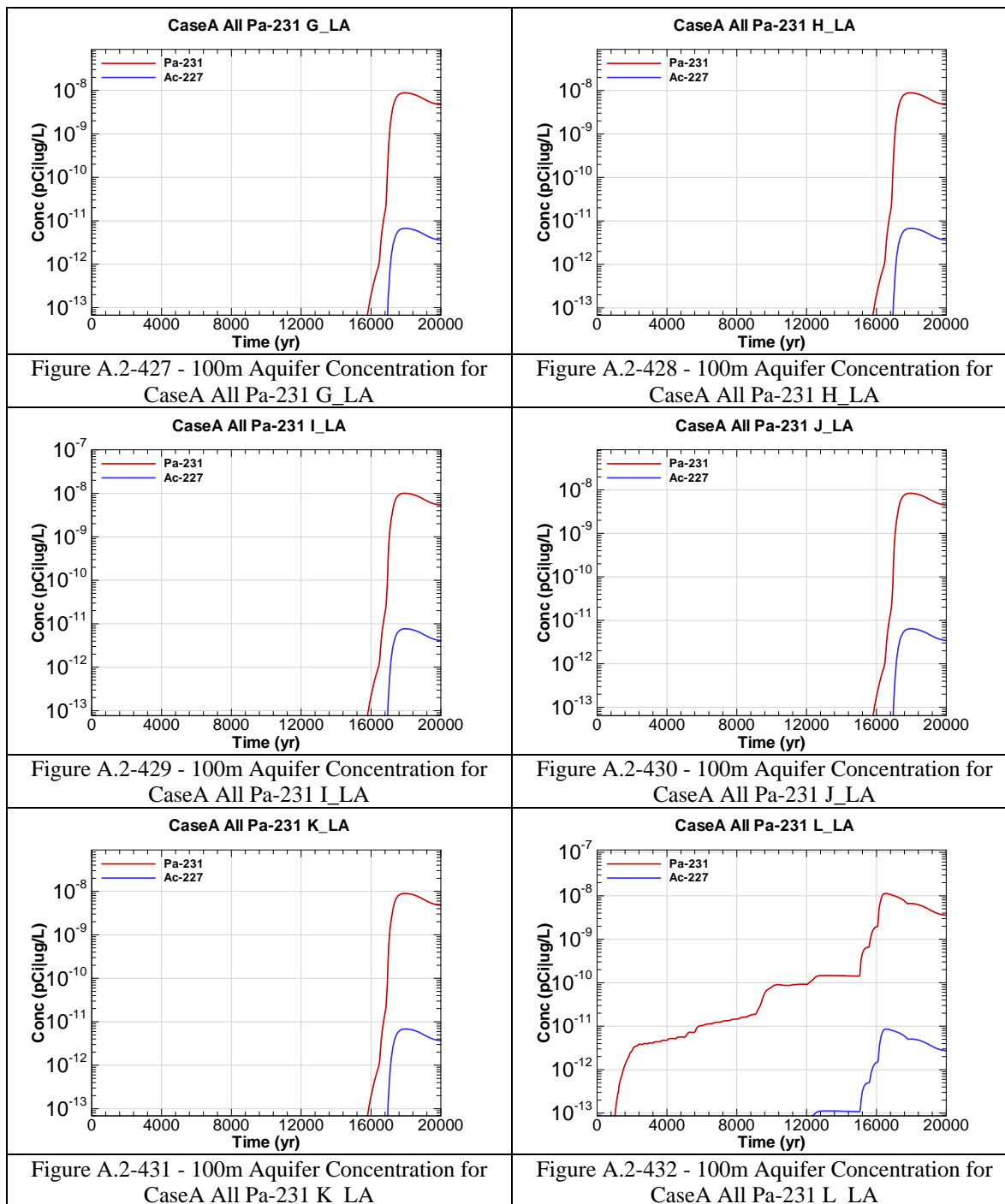
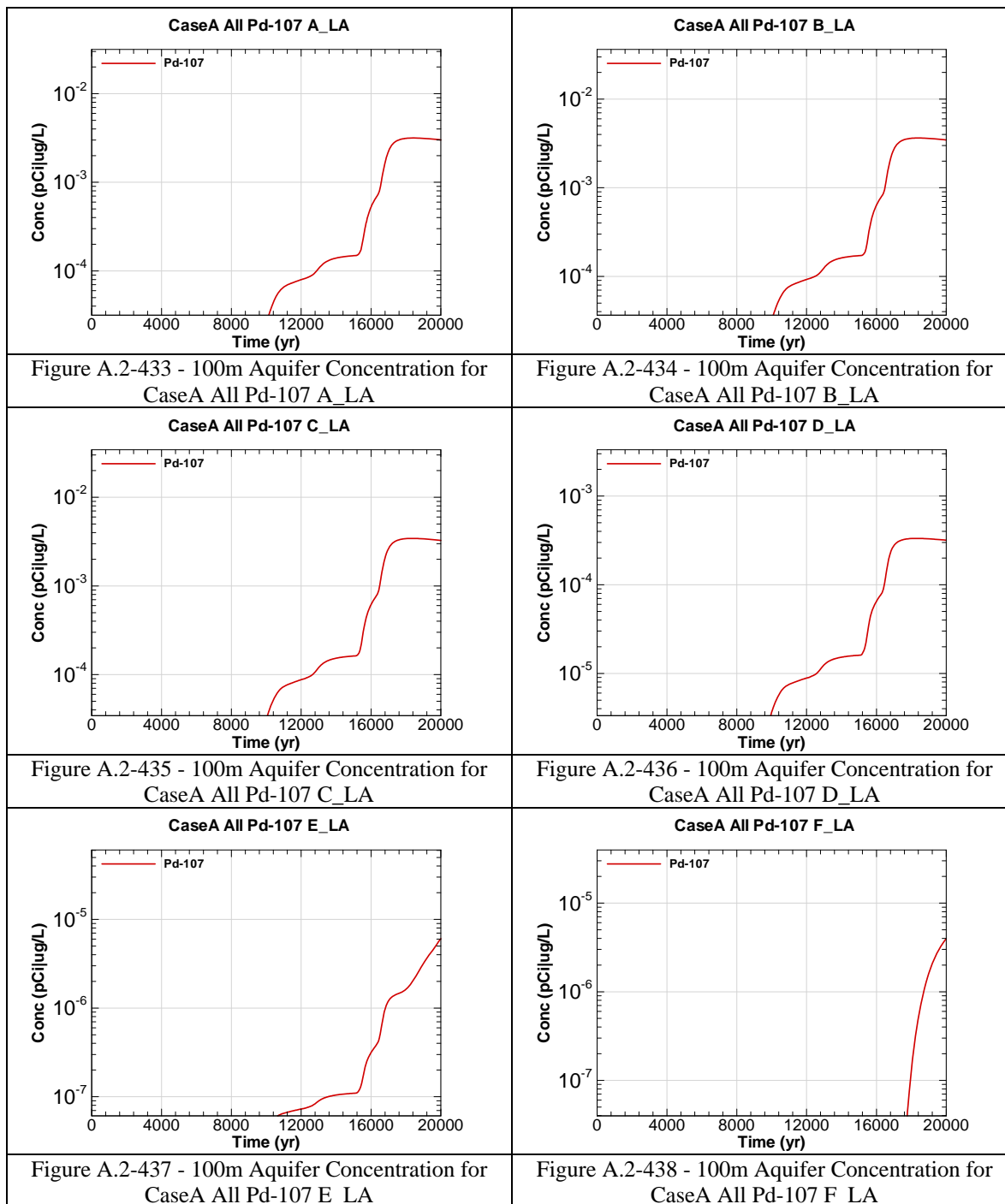


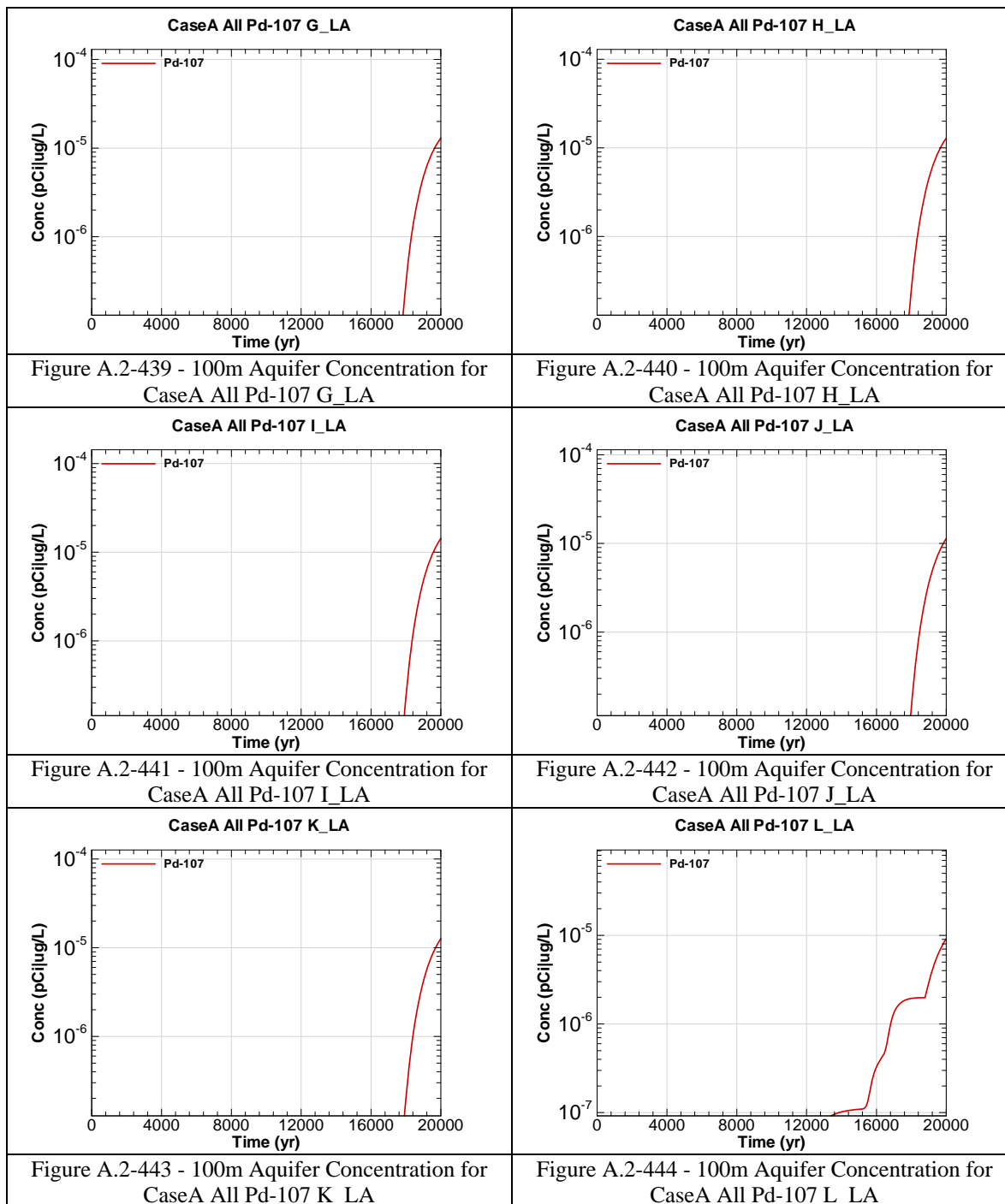
Figure A.2-414 - 100m Aquifer Concentration for
CaseA All Np-237 F_LA

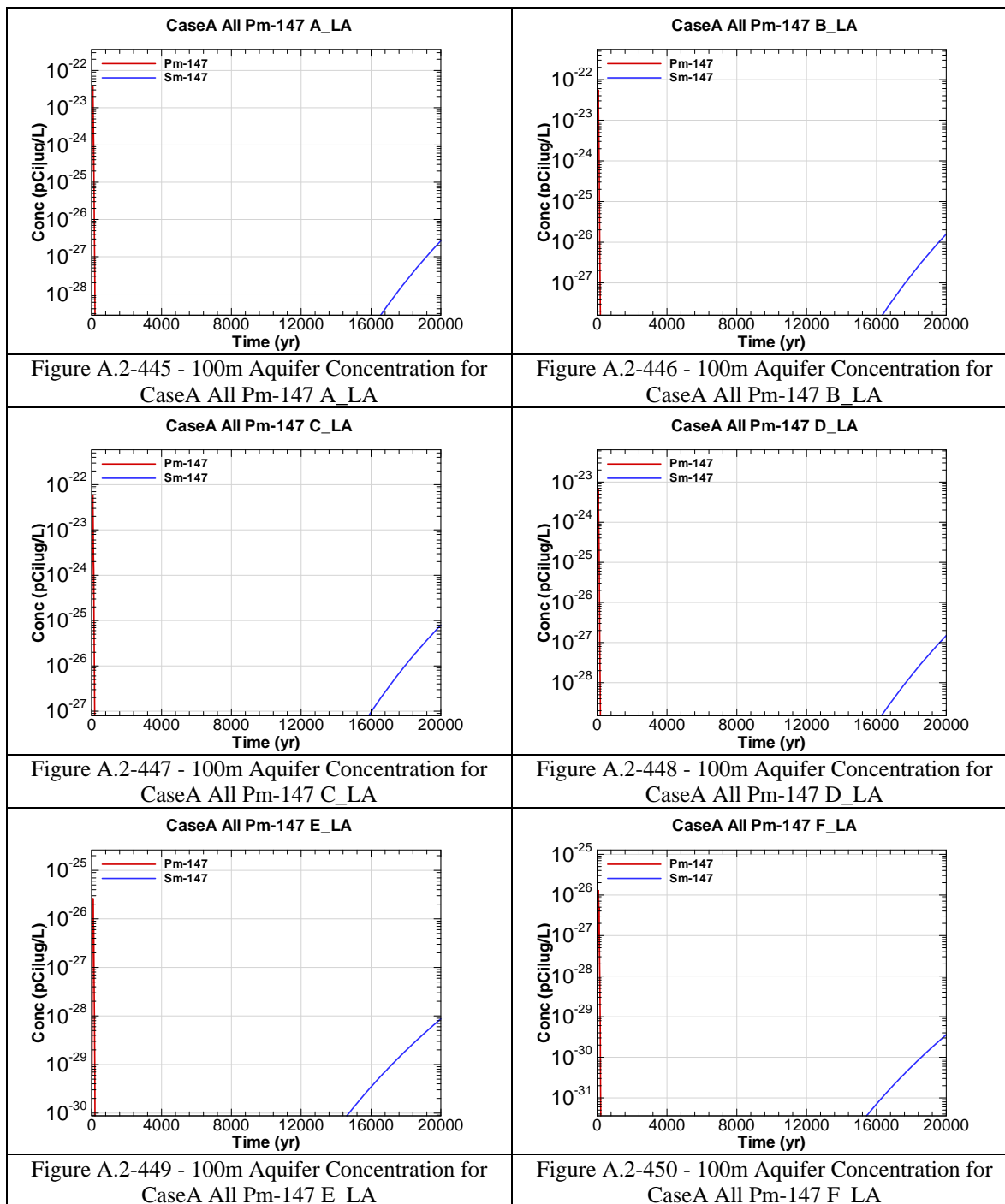


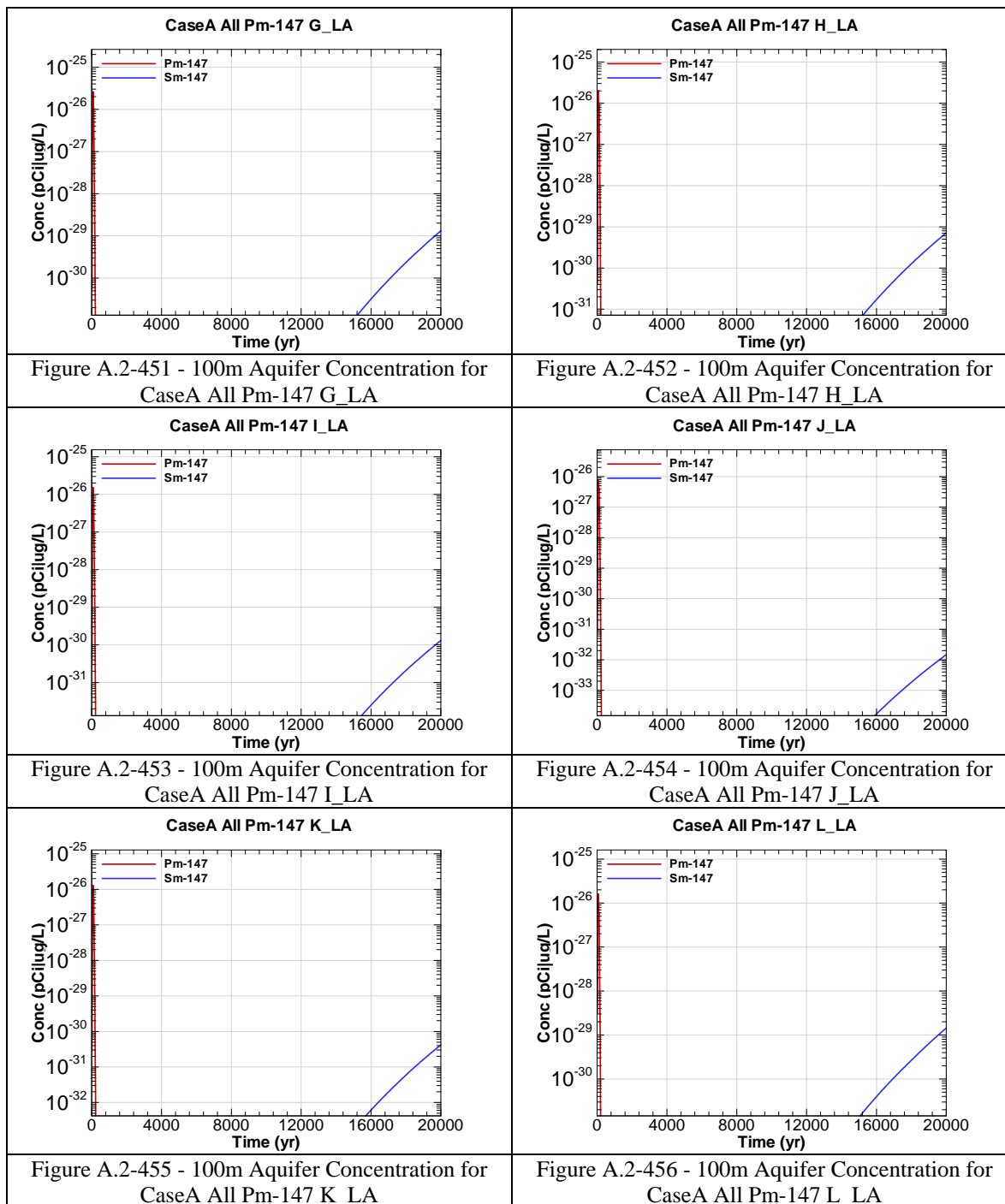


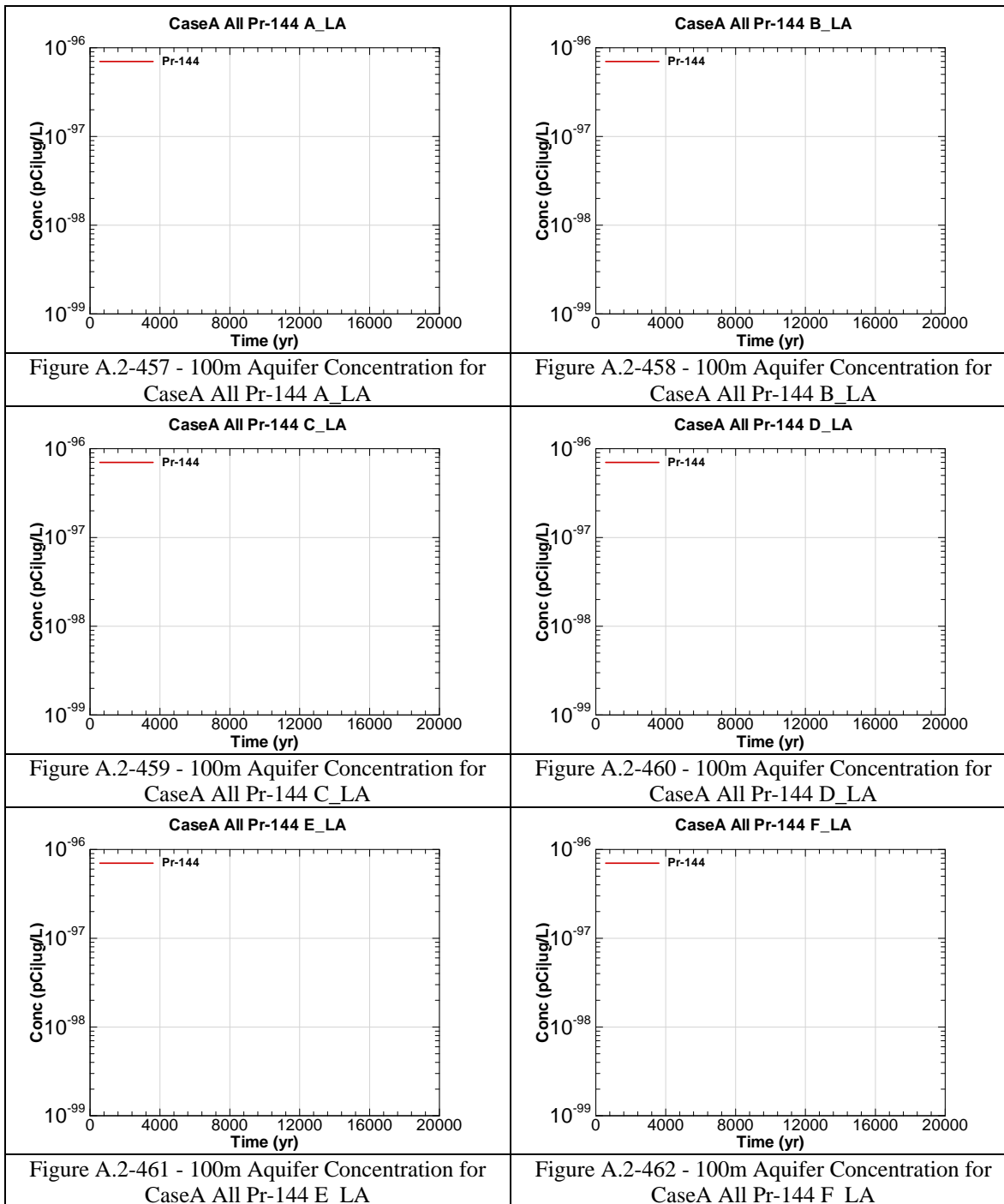


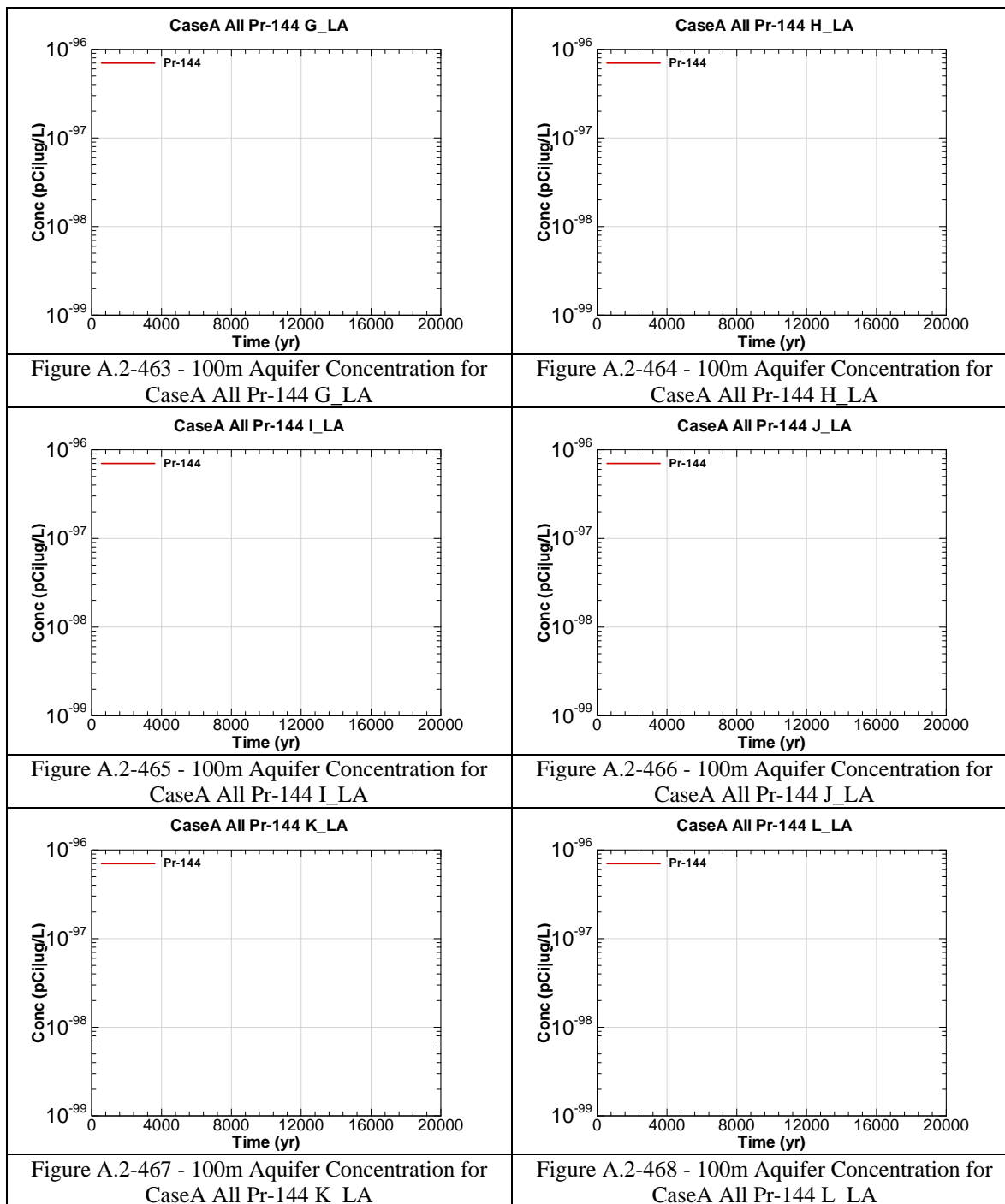


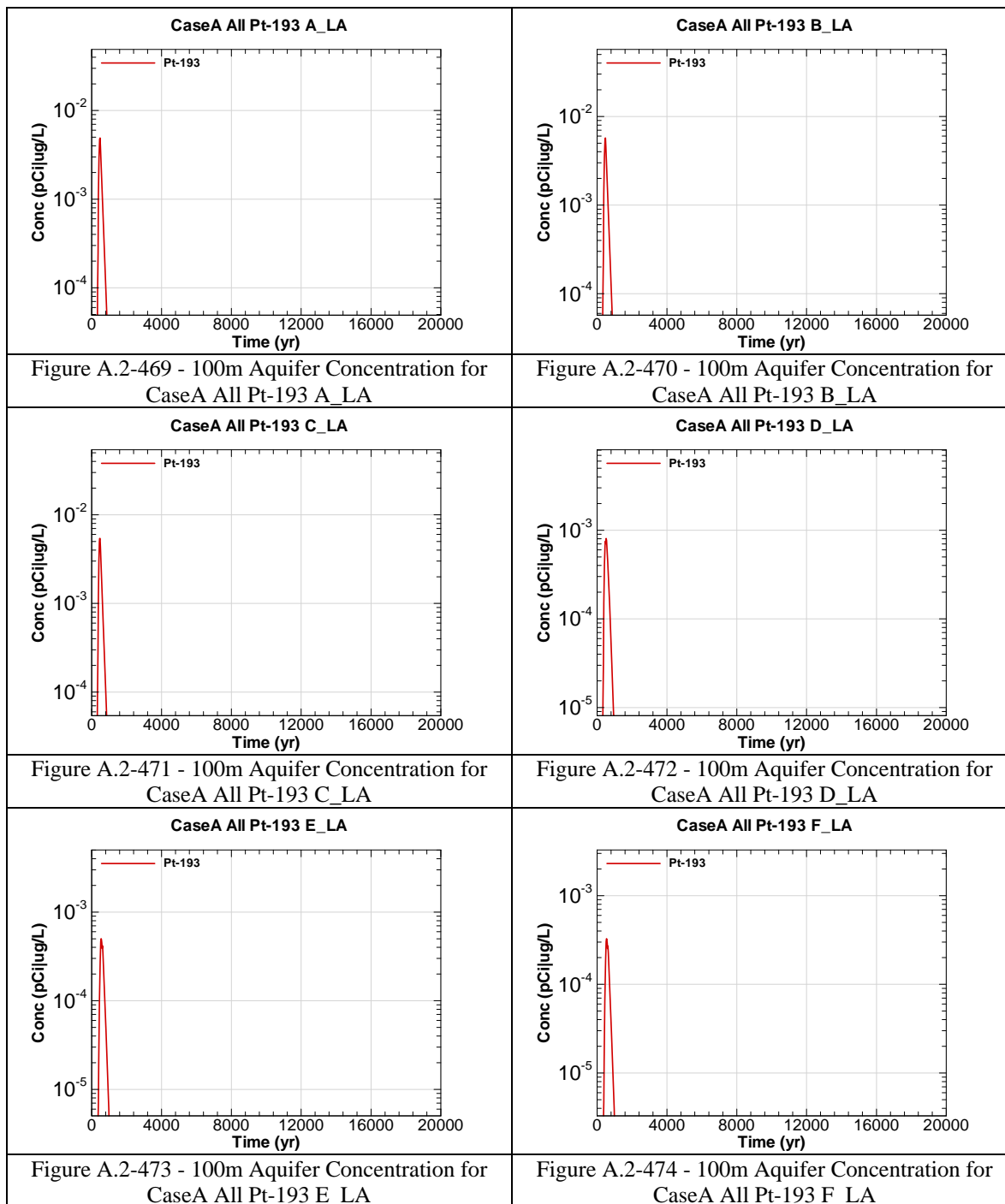


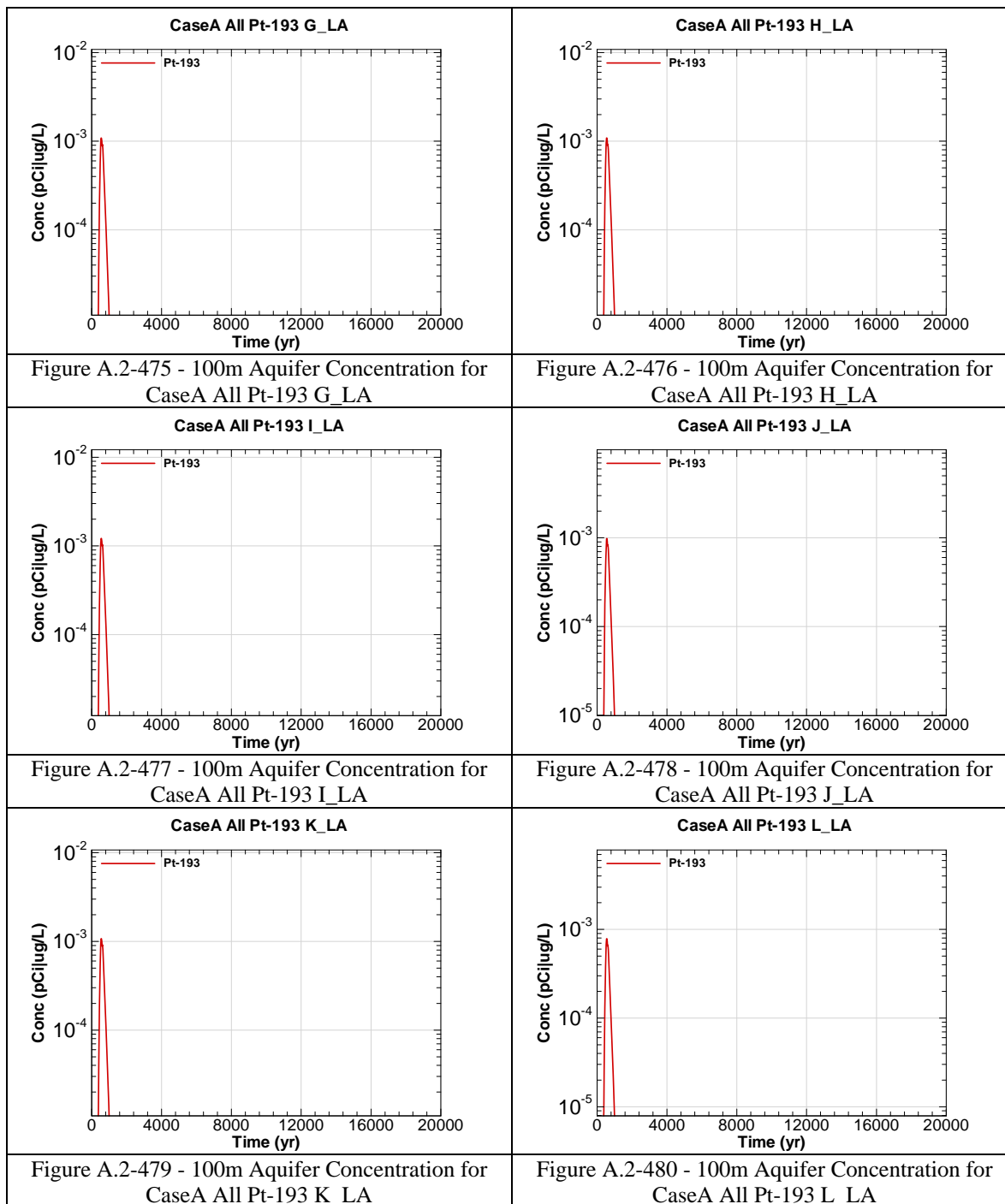












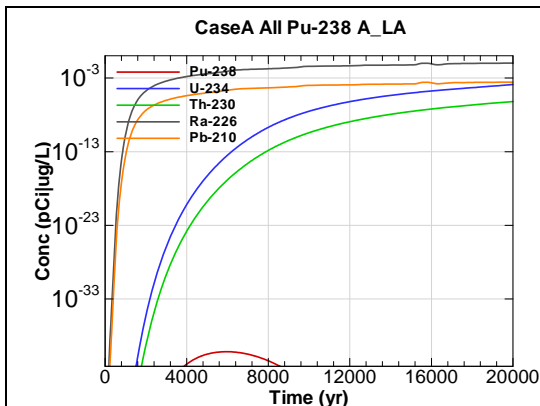


Figure A.2-481 - 100m Aquifer Concentration for
CaseA All Pu-238 A_LA

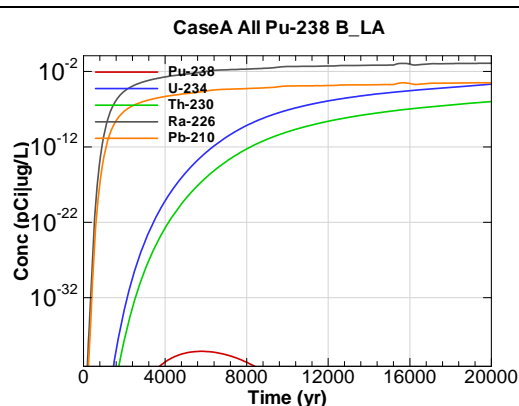


Figure A.2-482 - 100m Aquifer Concentration for
CaseA All Pu-238 B_LA

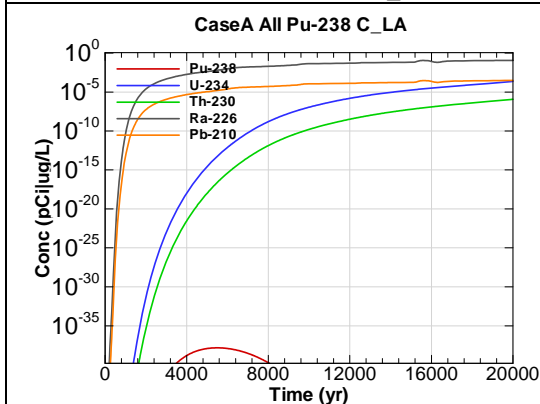


Figure A.2-483 - 100m Aquifer Concentration for
CaseA All Pu-238 C_LA

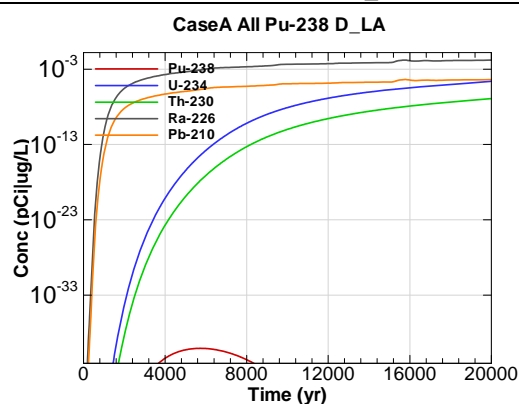


Figure A.2-484 - 100m Aquifer Concentration for
CaseA All Pu-238 D_LA

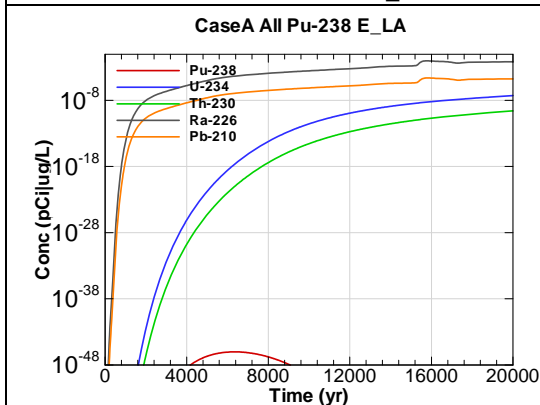


Figure A.2-485 - 100m Aquifer Concentration for
CaseA All Pu-238 E_LA

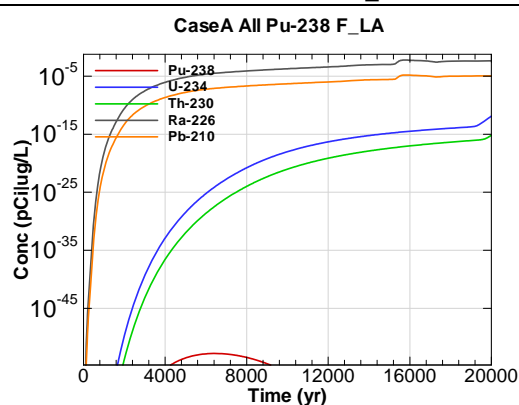


Figure A.2-486 - 100m Aquifer Concentration for
CaseA All Pu-238 F_LA

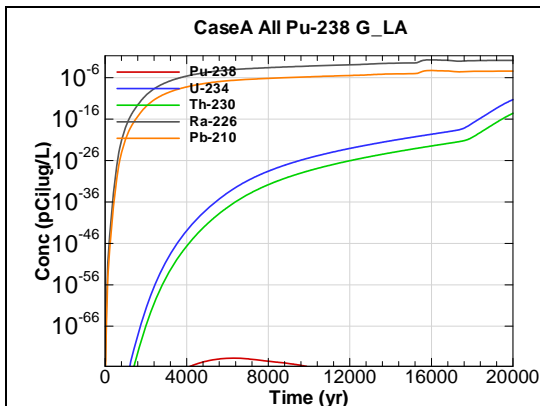


Figure A.2-487 - 100m Aquifer Concentration for
CaseA All Pu-238 G_LA

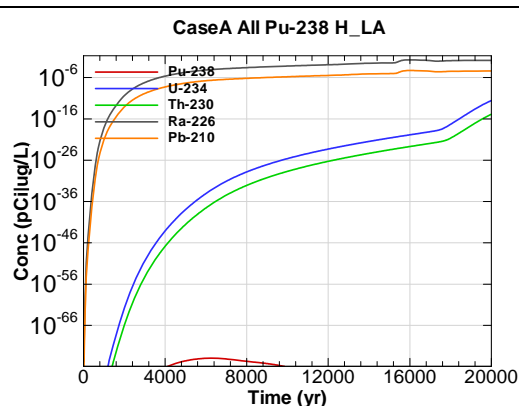


Figure A.2-488 - 100m Aquifer Concentration for
CaseA All Pu-238 H_LA

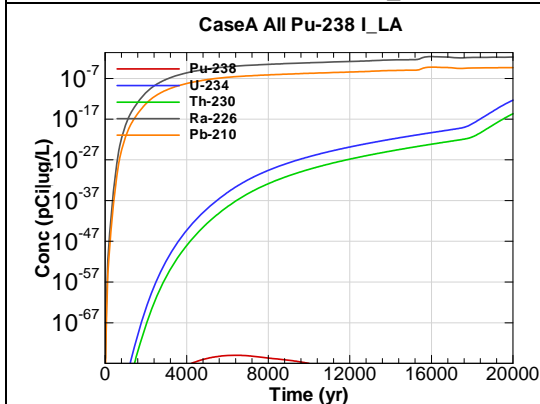


Figure A.2-489 - 100m Aquifer Concentration for
CaseA All Pu-238 I_LA

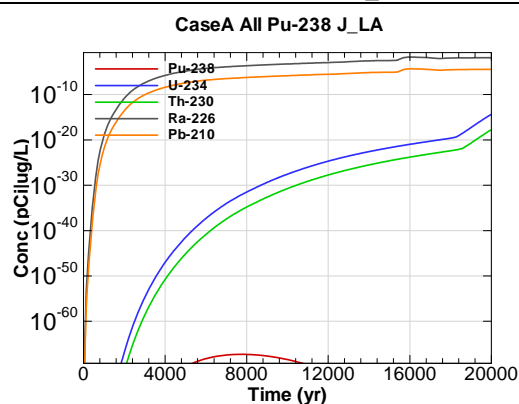


Figure A.2-490 - 100m Aquifer Concentration for
CaseA All Pu-238 J_LA

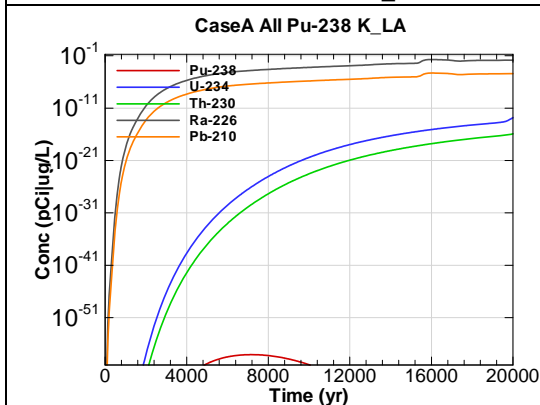


Figure A.2-491 - 100m Aquifer Concentration for
CaseA All Pu-238 K_LA

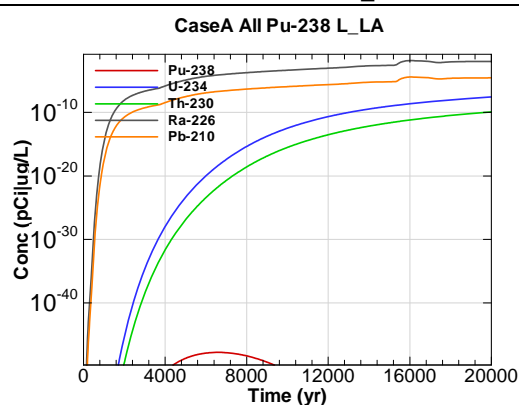


Figure A.2-492 - 100m Aquifer Concentration for
CaseA All Pu-238 L_LA

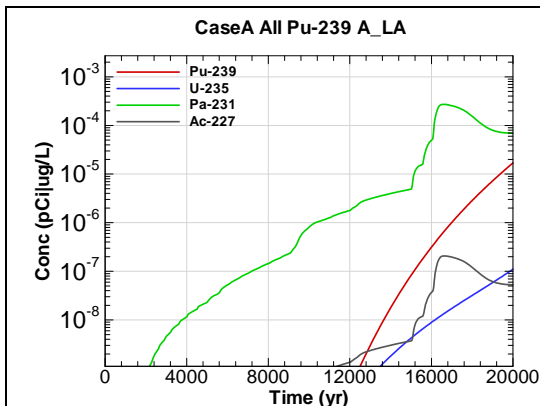


Figure A.2-493 - 100m Aquifer Concentration for
CaseA All Pu-239 A_LA

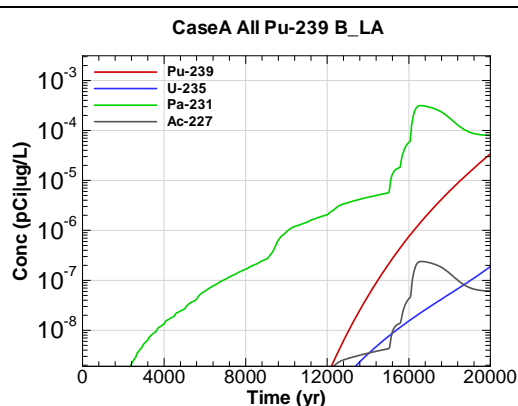


Figure A.2-494 - 100m Aquifer Concentration for
CaseA All Pu-239 B_LA

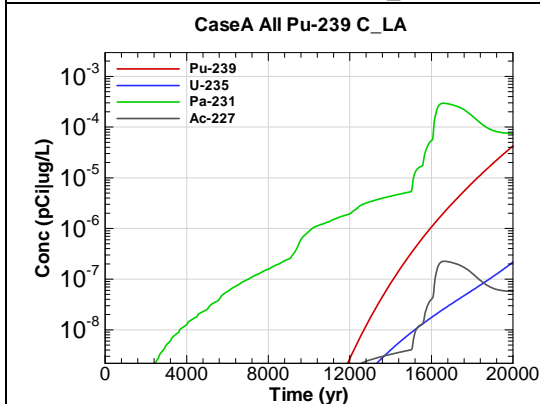


Figure A.2-495 - 100m Aquifer Concentration for
CaseA All Pu-239 C_LA

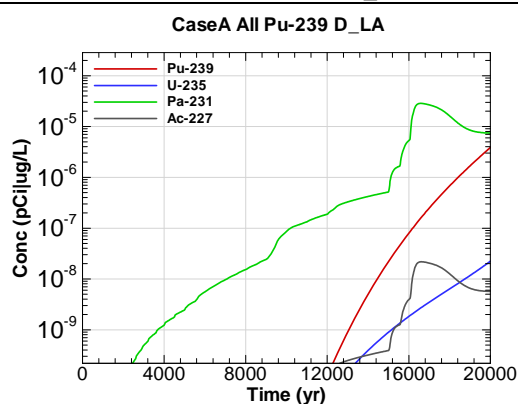


Figure A.2-496 - 100m Aquifer Concentration for
CaseA All Pu-239 D_LA

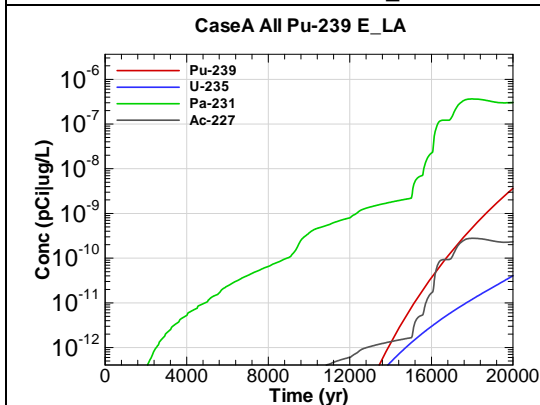


Figure A.2-497 - 100m Aquifer Concentration for
CaseA All Pu-239 E_LA

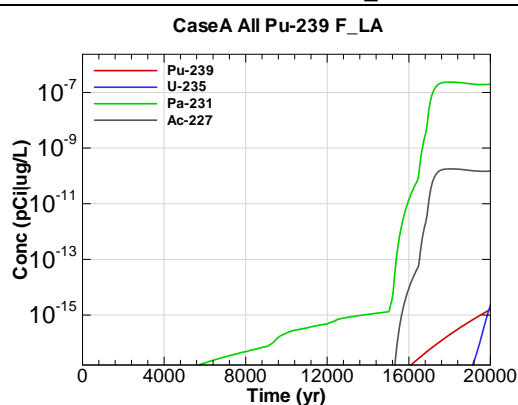


Figure A.2-498 - 100m Aquifer Concentration for
CaseA All Pu-239 F_LA

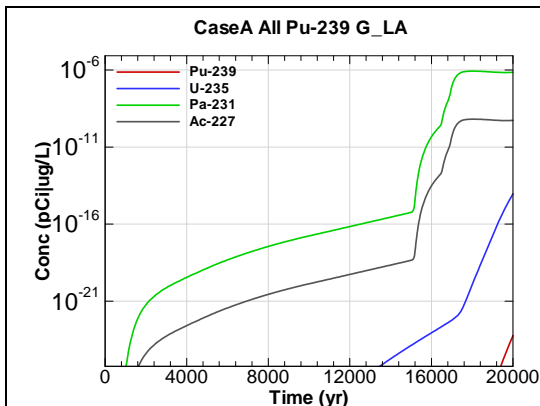


Figure A.2-499 - 100m Aquifer Concentration for
CaseA All Pu-239 G_LA

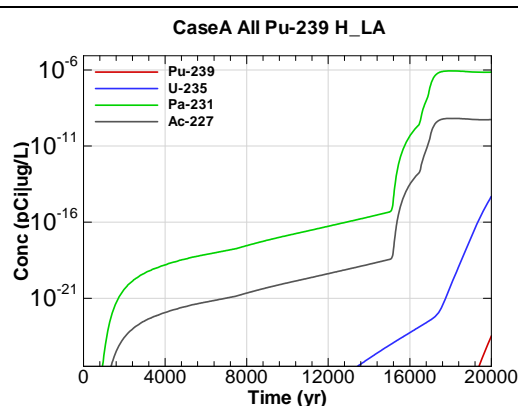


Figure A.2-500 - 100m Aquifer Concentration for
CaseA All Pu-239 H_LA

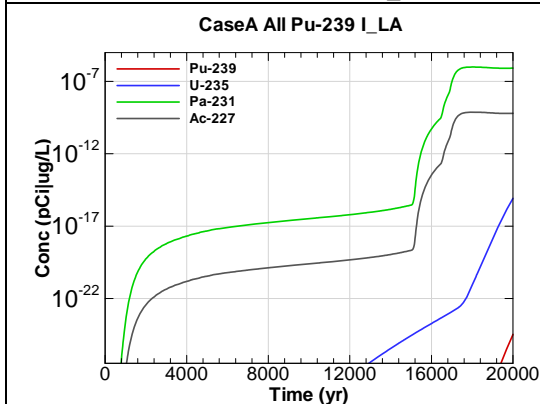


Figure A.2-501 - 100m Aquifer Concentration for
CaseA All Pu-239 I_LA

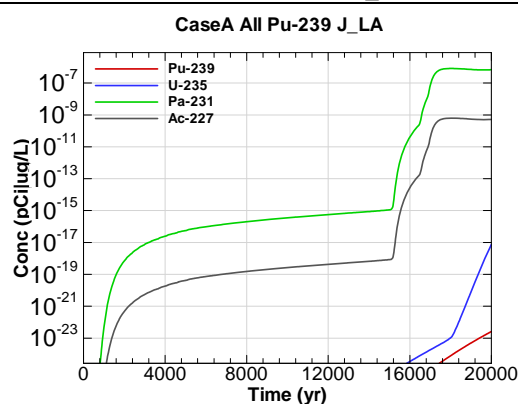


Figure A.2-502 - 100m Aquifer Concentration for
CaseA All Pu-239 J_LA

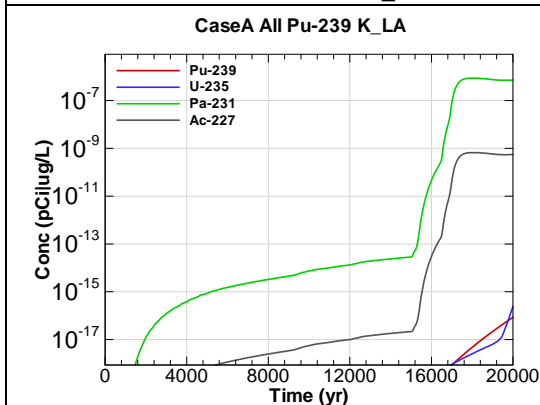


Figure A.2-503 - 100m Aquifer Concentration for
CaseA All Pu-239 K_LA

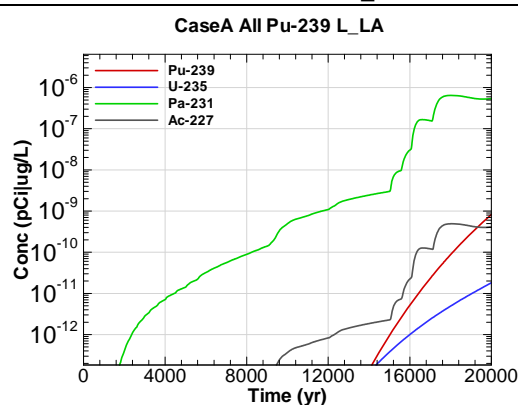


Figure A.2-504 - 100m Aquifer Concentration for
CaseA All Pu-239 L_LA

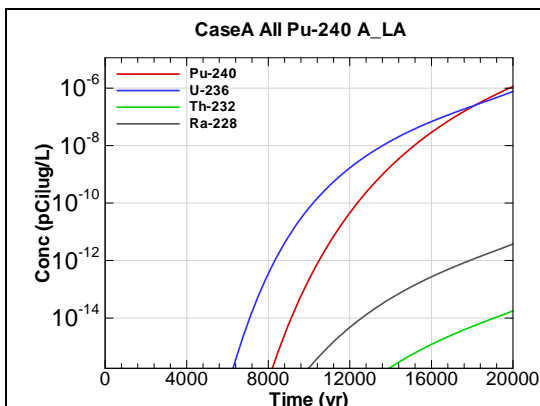


Figure A.2-505 - 100m Aquifer Concentration for
CaseA All Pu-240 A_LA

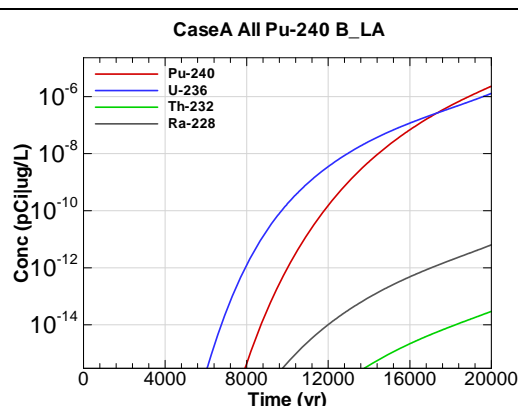


Figure A.2-506 - 100m Aquifer Concentration for
CaseA All Pu-240 B_LA

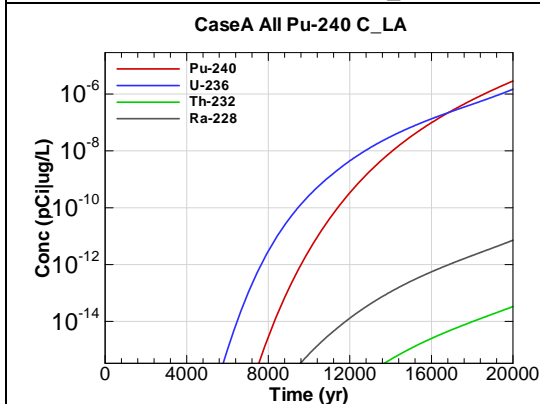


Figure A.2-507 - 100m Aquifer Concentration for
CaseA All Pu-240 C_LA

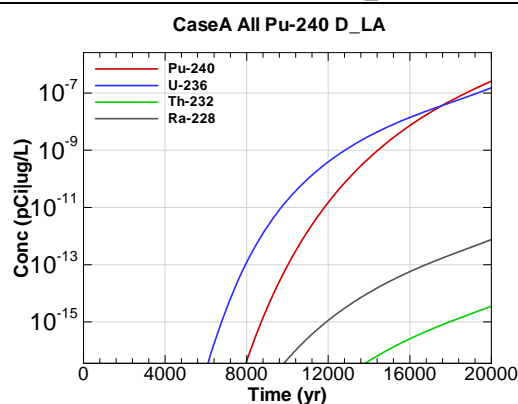


Figure A.2-508 - 100m Aquifer Concentration for
CaseA All Pu-240 D_LA

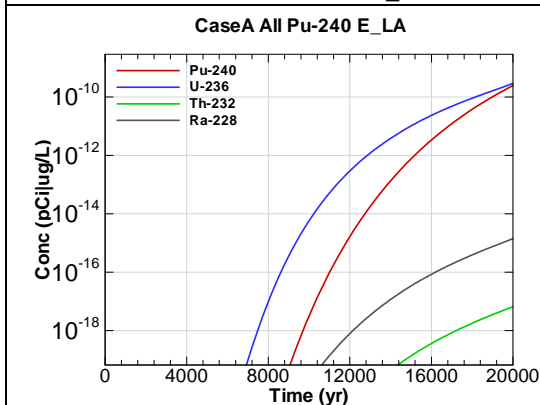


Figure A.2-509 - 100m Aquifer Concentration for
CaseA All Pu-240 E_LA

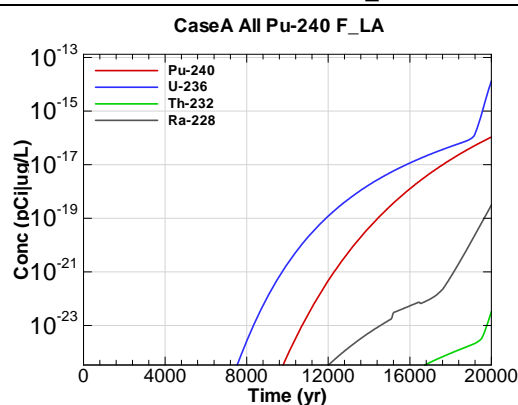
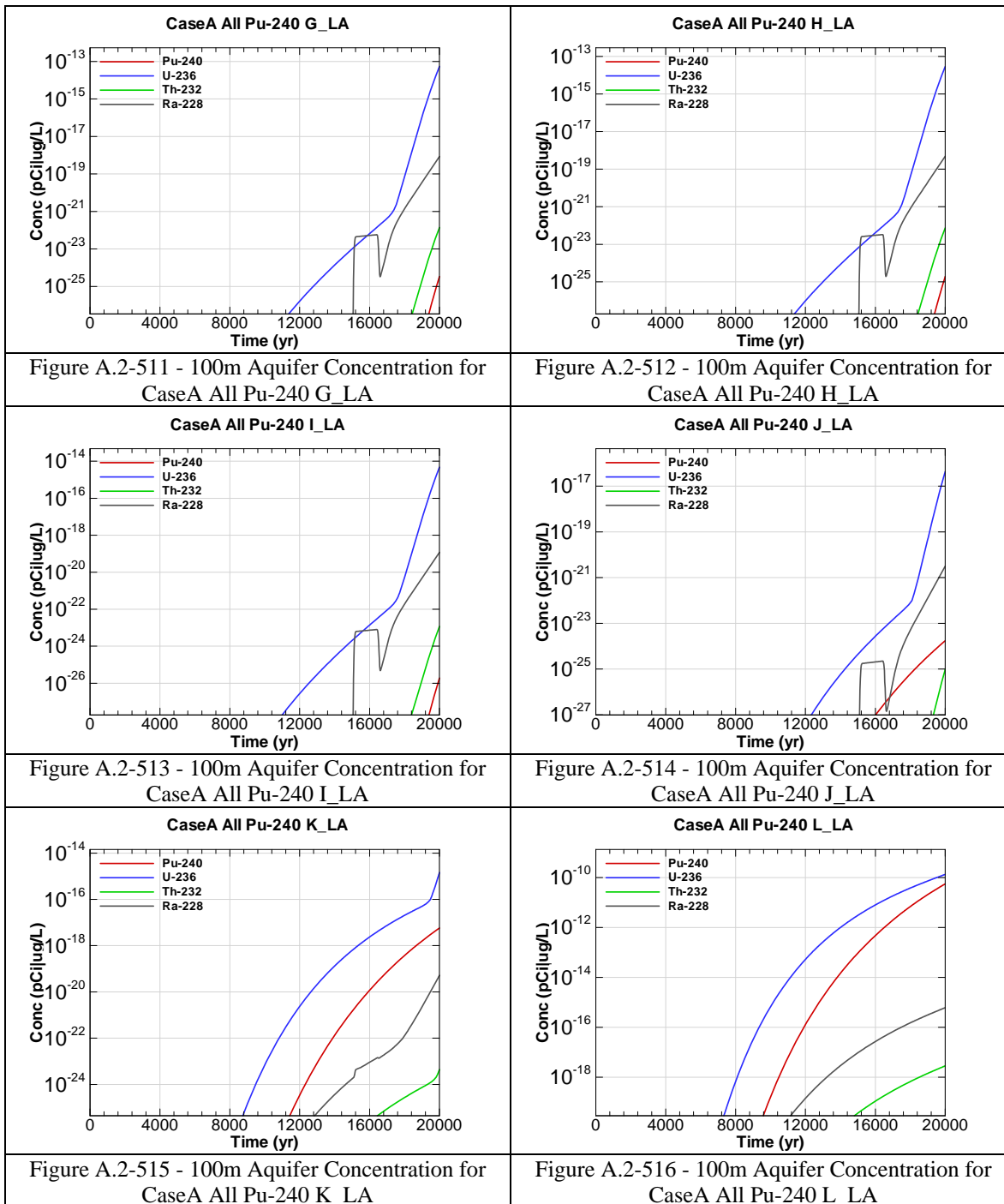


Figure A.2-510 - 100m Aquifer Concentration for
CaseA All Pu-240 F_LA



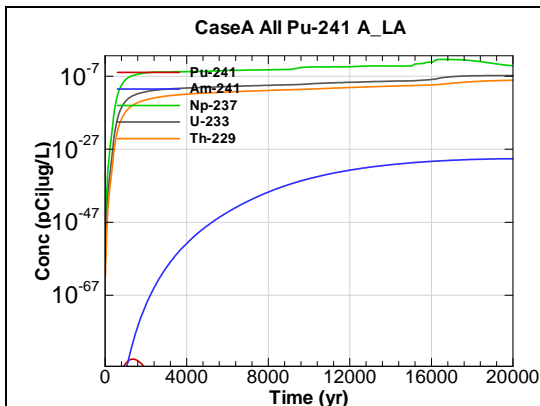


Figure A.2-517 - 100m Aquifer Concentration for
CaseA All Pu-241 A_LA

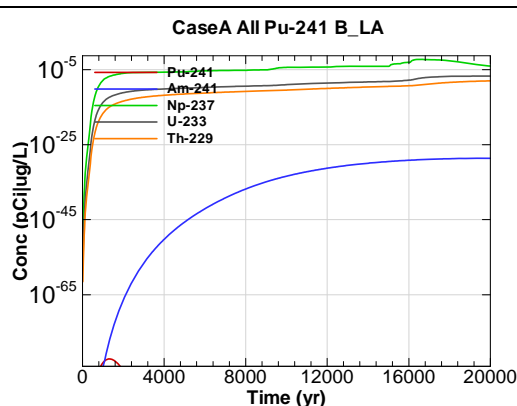


Figure A.2-518 - 100m Aquifer Concentration for
CaseA All Pu-241 B_LA

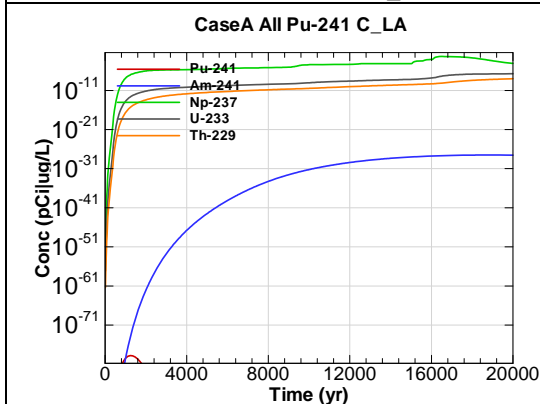


Figure A.2-519 - 100m Aquifer Concentration for
CaseA All Pu-241 C_LA

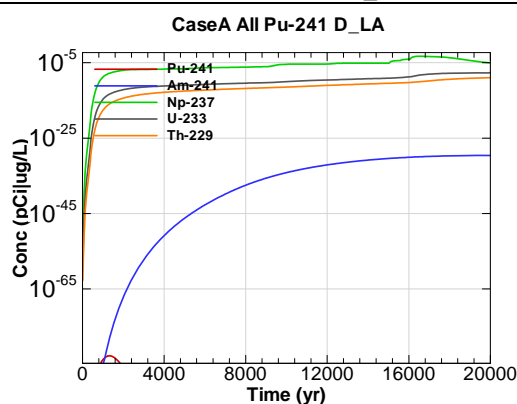


Figure A.2-520 - 100m Aquifer Concentration for
CaseA All Pu-241 D_LA

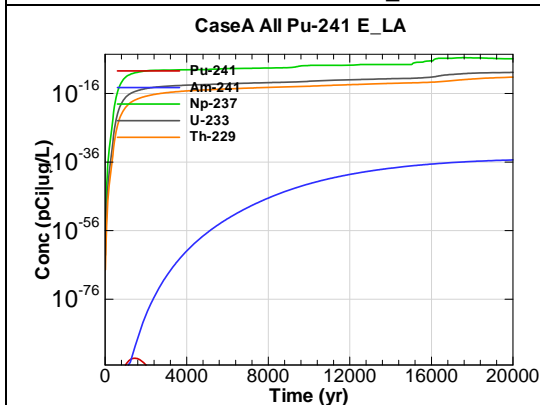


Figure A.2-521 - 100m Aquifer Concentration for
CaseA All Pu-241 E_LA

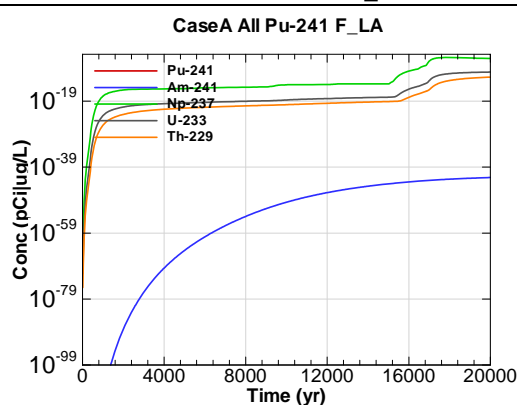


Figure A.2-522 - 100m Aquifer Concentration for
CaseA All Pu-241 F_LA

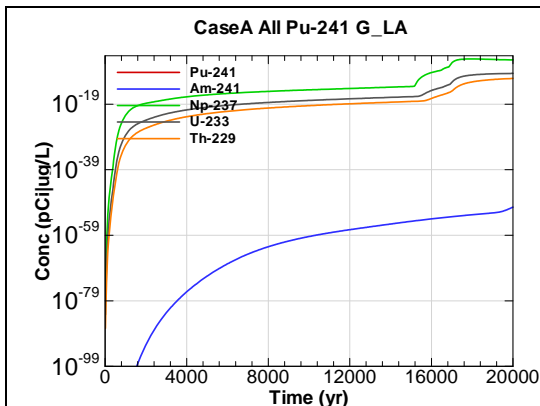


Figure A.2-523 - 100m Aquifer Concentration for
CaseA All Pu-241 G_LA

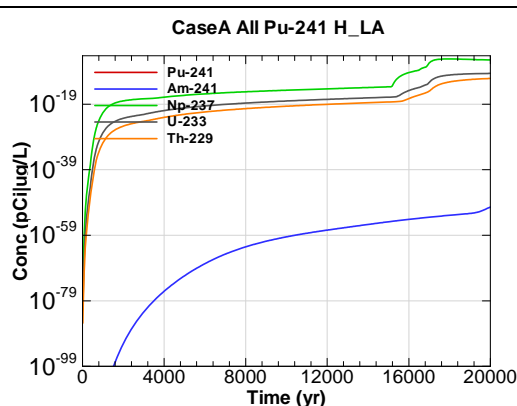


Figure A.2-524 - 100m Aquifer Concentration for
CaseA All Pu-241 H_LA

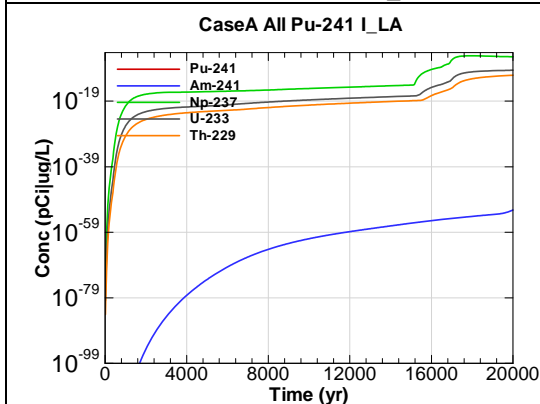


Figure A.2-525 - 100m Aquifer Concentration for
CaseA All Pu-241 I_LA

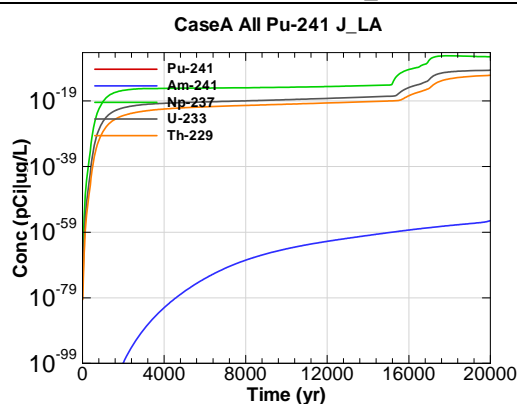


Figure A.2-526 - 100m Aquifer Concentration for
CaseA All Pu-241 J_LA

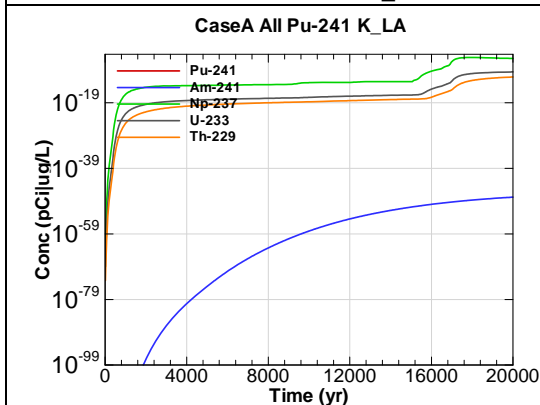


Figure A.2-527 - 100m Aquifer Concentration for
CaseA All Pu-241 K_LA

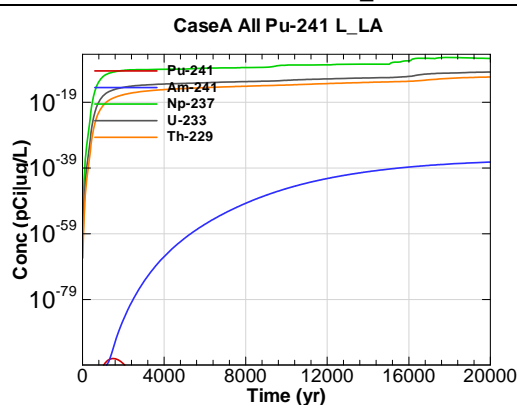


Figure A.2-528 - 100m Aquifer Concentration for
CaseA All Pu-241 L_LA

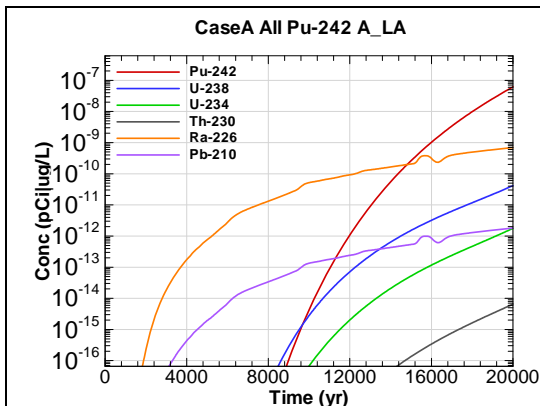


Figure A.2-529 - 100m Aquifer Concentration for
CaseA All Pu-242 A_LA

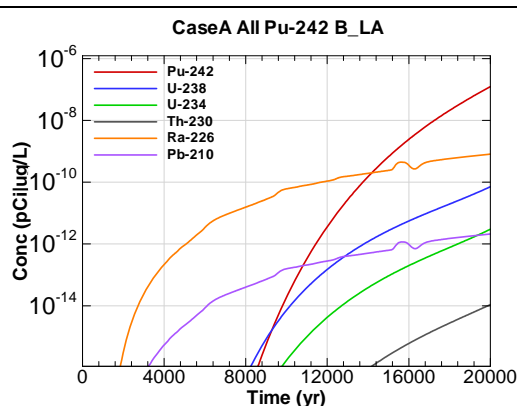


Figure A.2-530 - 100m Aquifer Concentration for
CaseA All Pu-242 B_LA

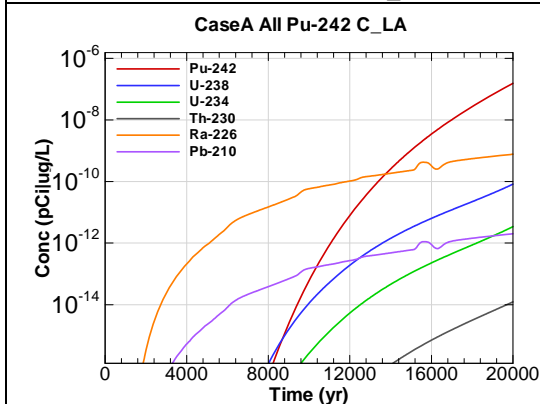


Figure A.2-531 - 100m Aquifer Concentration for
CaseA All Pu-242 C_LA

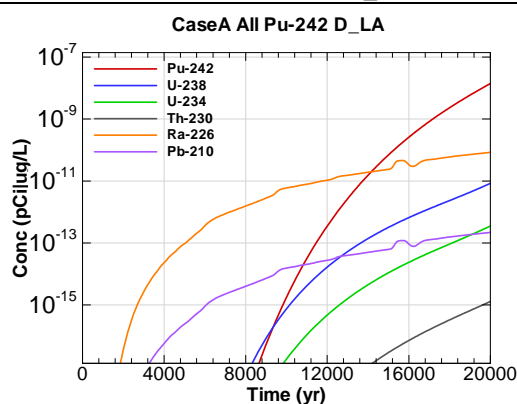


Figure A.2-532 - 100m Aquifer Concentration for
CaseA All Pu-242 D_LA

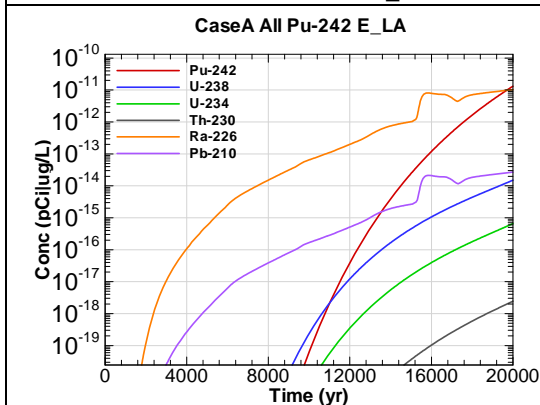


Figure A.2-533 - 100m Aquifer Concentration for
CaseA All Pu-242 E_LA

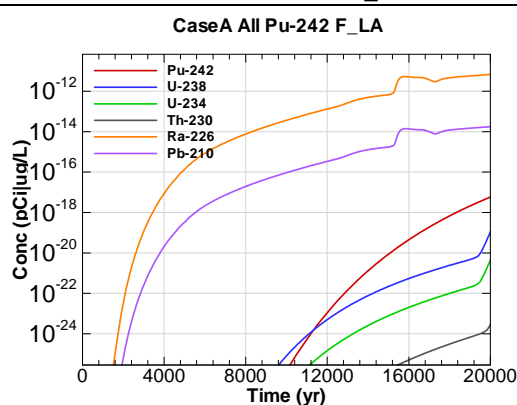


Figure A.2-534 - 100m Aquifer Concentration for
CaseA All Pu-242 F_LA

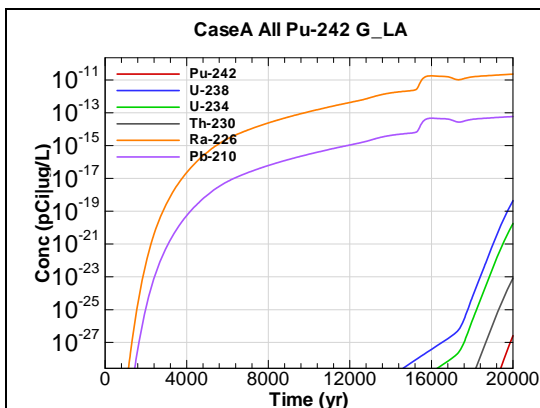


Figure A.2-535 - 100m Aquifer Concentration for
CaseA All Pu-242 G_LA

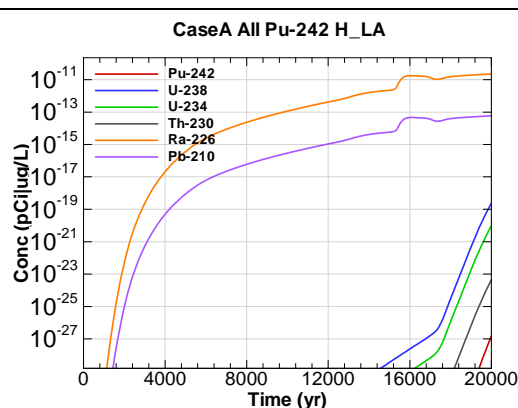


Figure A.2-536 - 100m Aquifer Concentration for
CaseA All Pu-242 H_LA

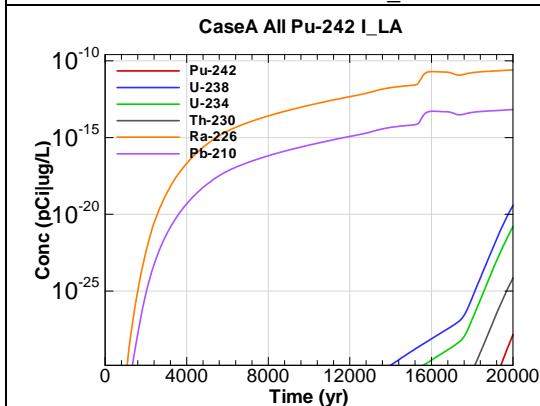


Figure A.2-537 - 100m Aquifer Concentration for
CaseA All Pu-242 I_LA

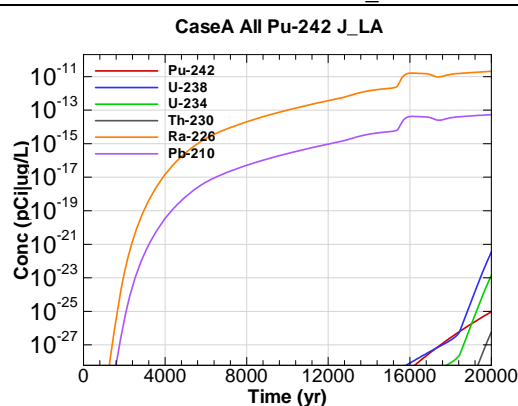


Figure A.2-538 - 100m Aquifer Concentration for
CaseA All Pu-242 J_LA

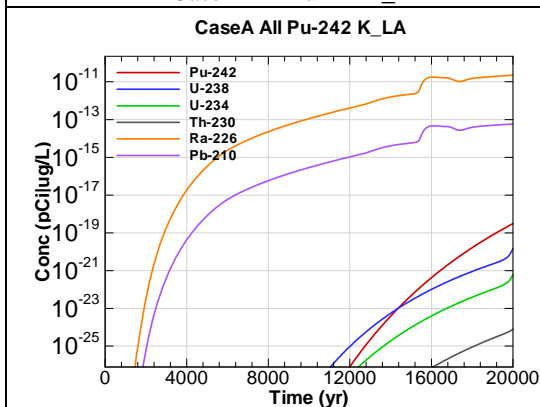


Figure A.2-539 - 100m Aquifer Concentration for
CaseA All Pu-242 K_LA

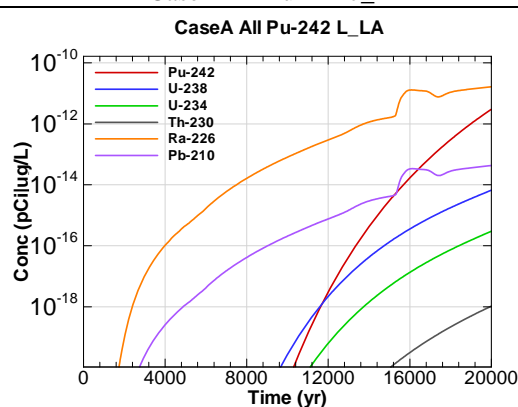


Figure A.2-540 - 100m Aquifer Concentration for
CaseA All Pu-242 L_LA

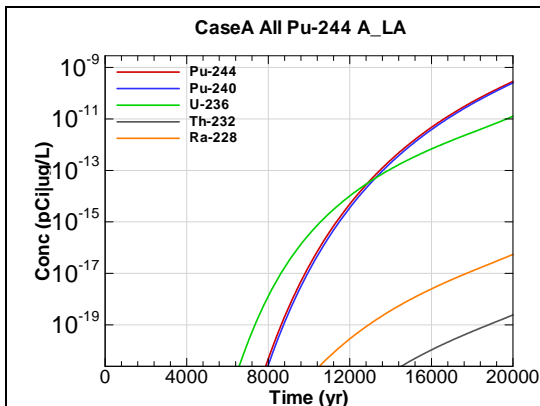


Figure A.2-541 - 100m Aquifer Concentration for
CaseA All Pu-244 A_LA

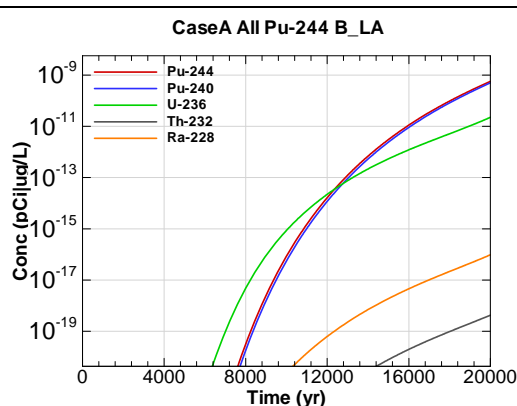


Figure A.2-542 - 100m Aquifer Concentration for
CaseA All Pu-244 B_LA

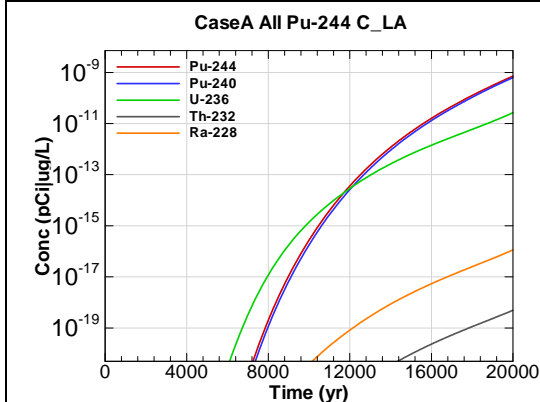


Figure A.2-543 - 100m Aquifer Concentration for
CaseA All Pu-244 C_LA

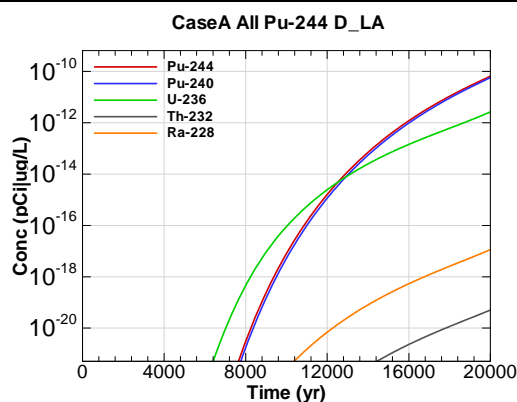


Figure A.2-544 - 100m Aquifer Concentration for
CaseA All Pu-244 D_LA

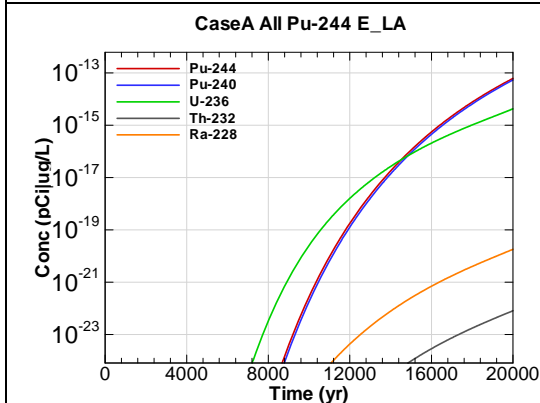


Figure A.2-545 - 100m Aquifer Concentration for
CaseA All Pu-244 E_LA

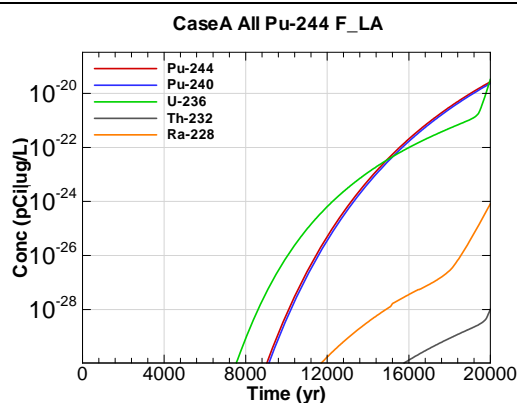
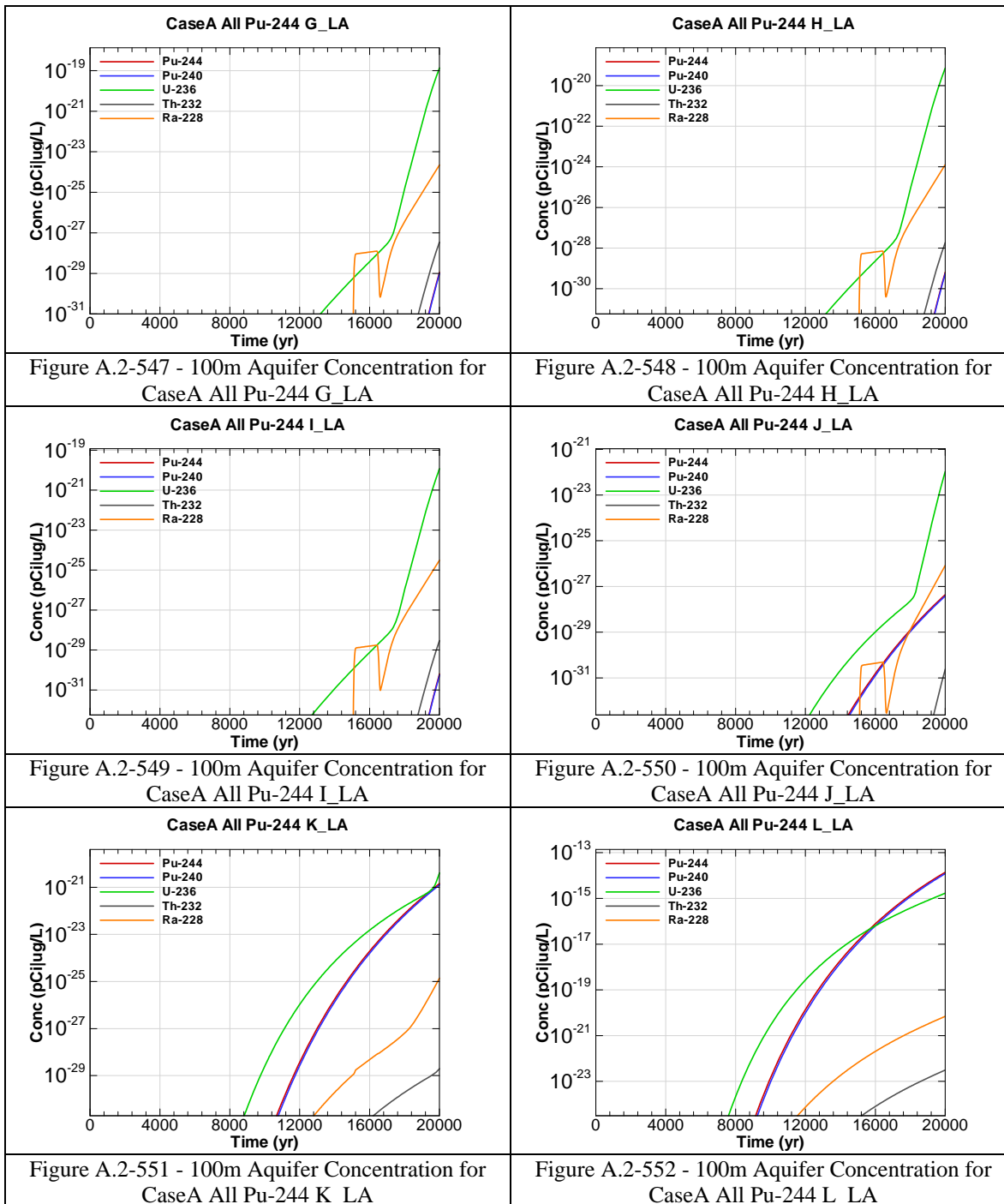
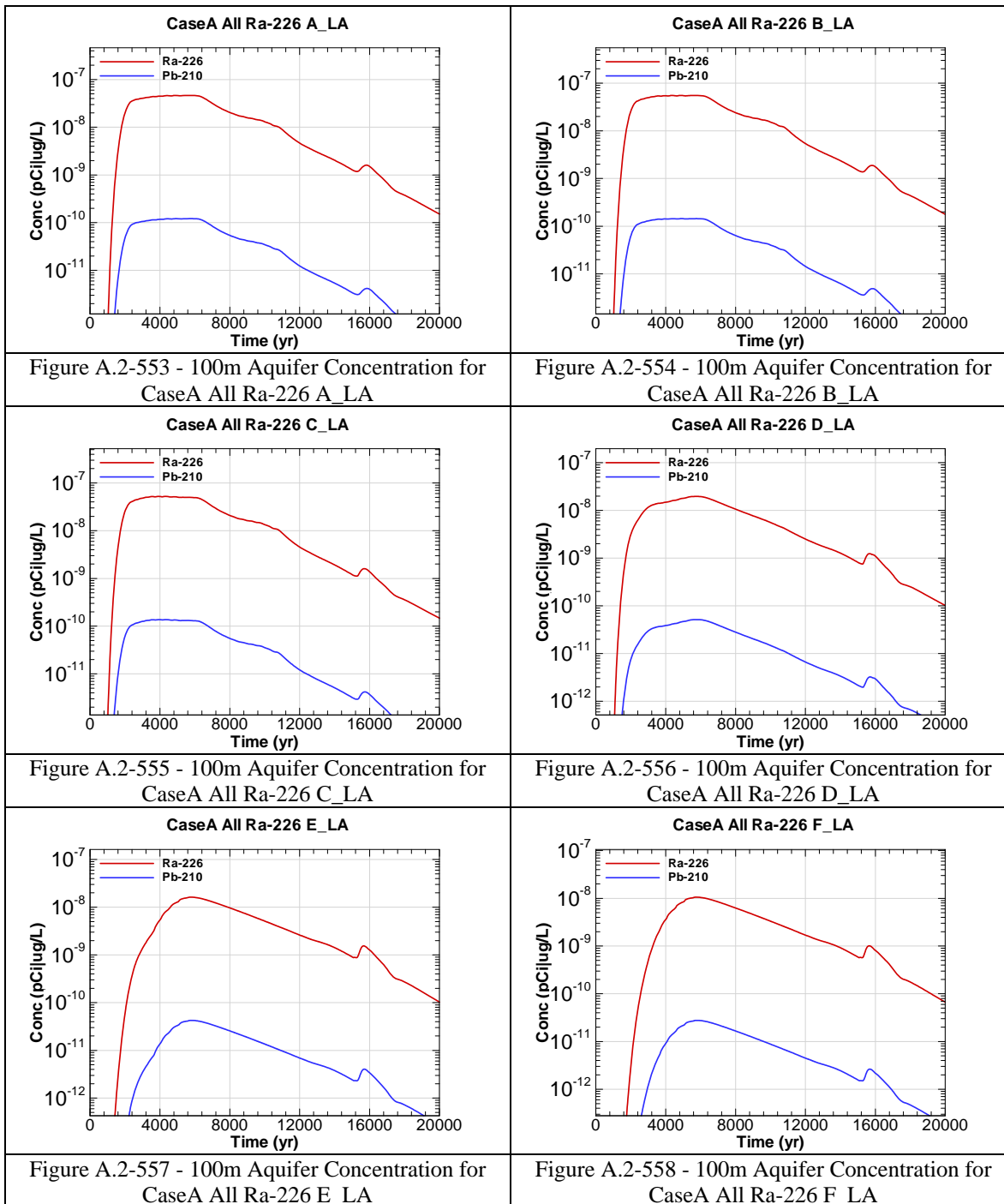
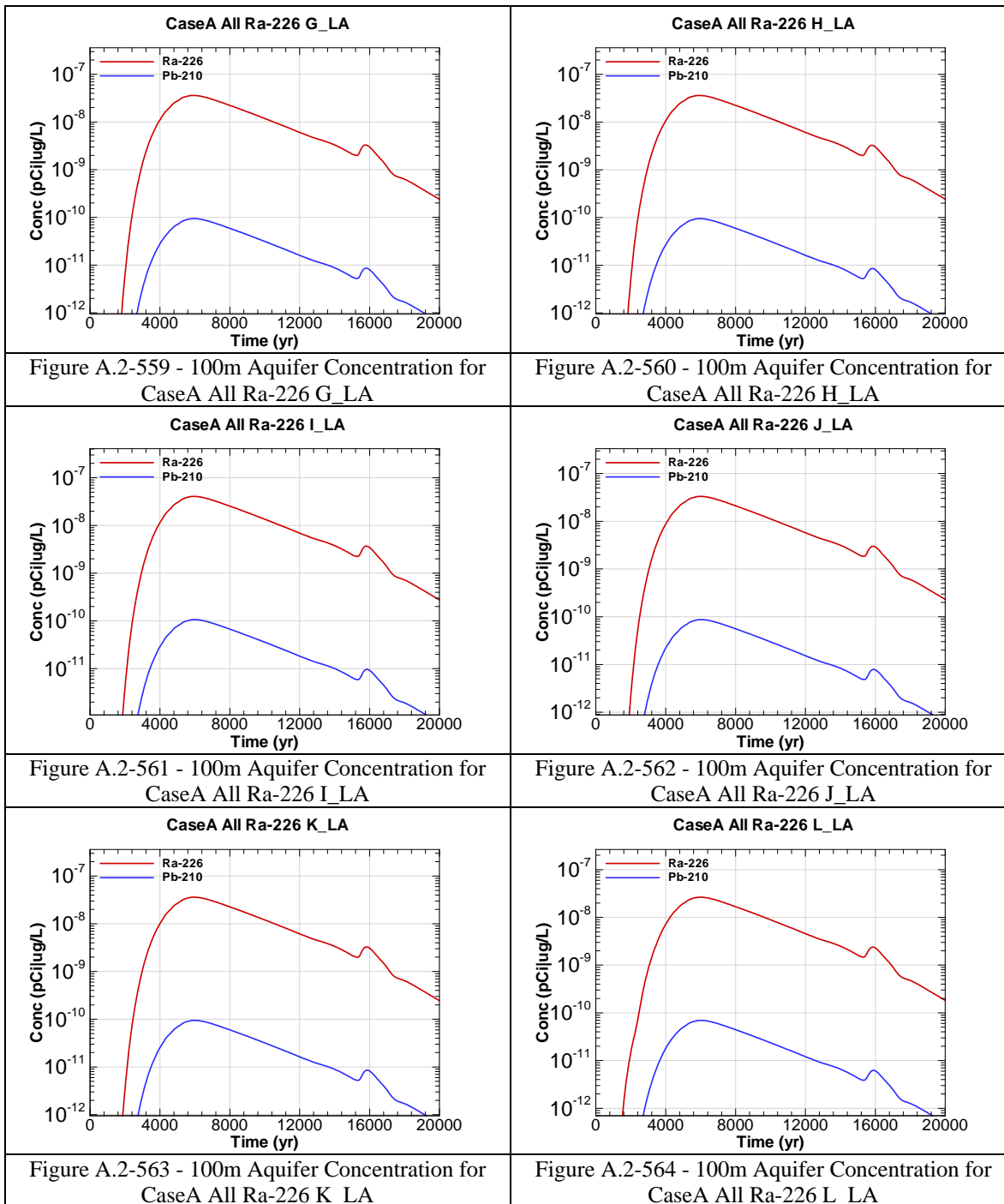
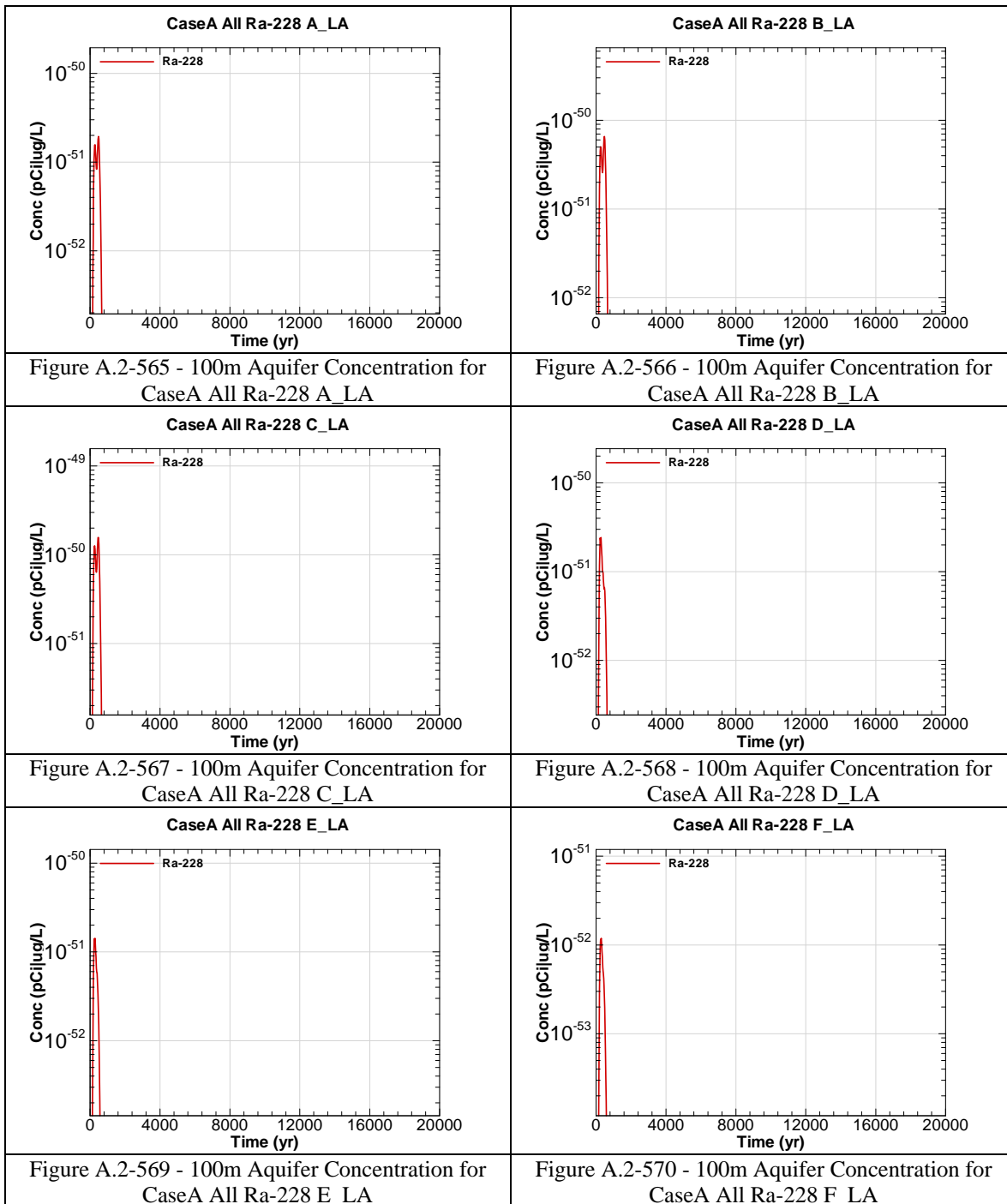


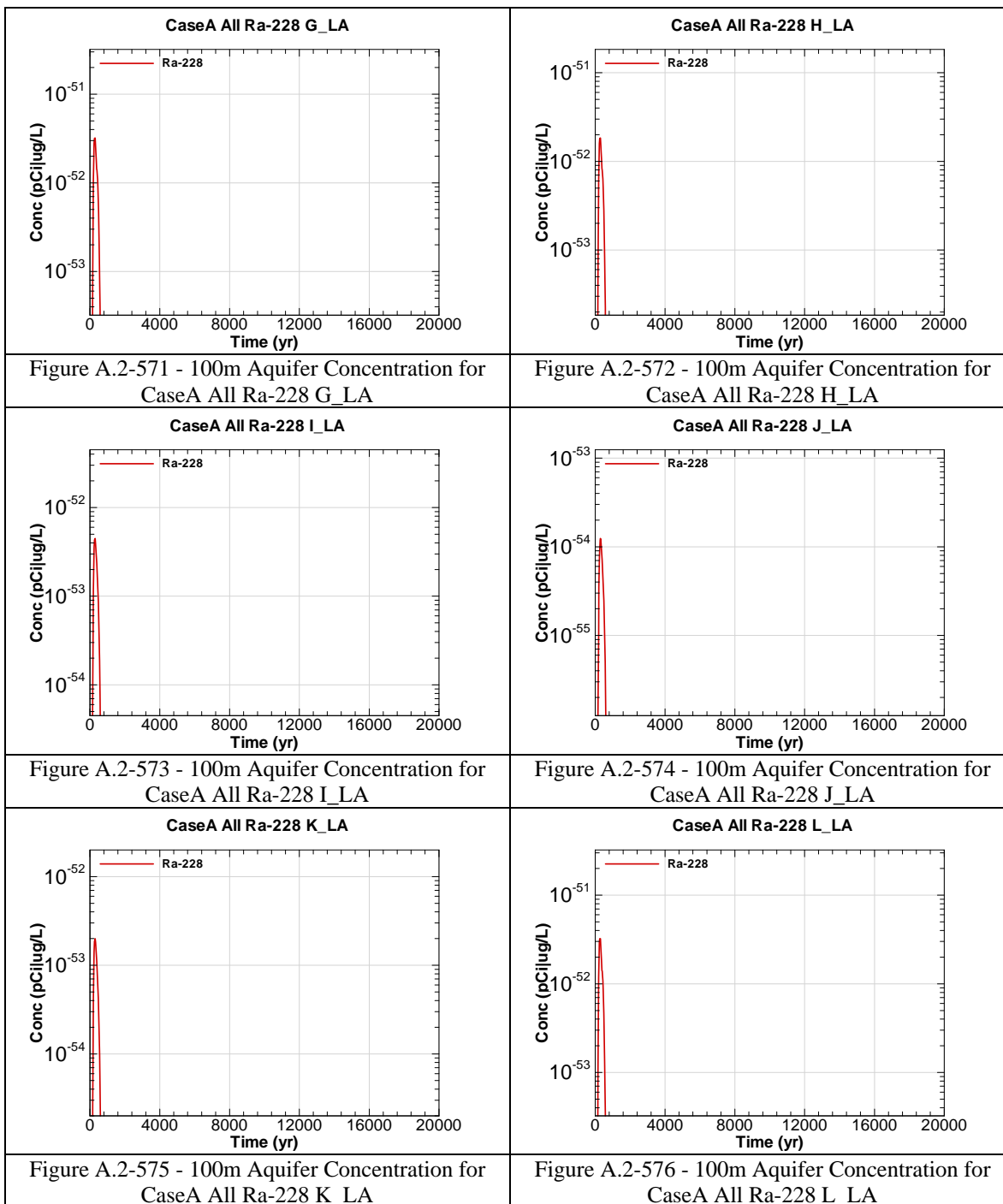
Figure A.2-546 - 100m Aquifer Concentration for
CaseA All Pu-244 F_LA

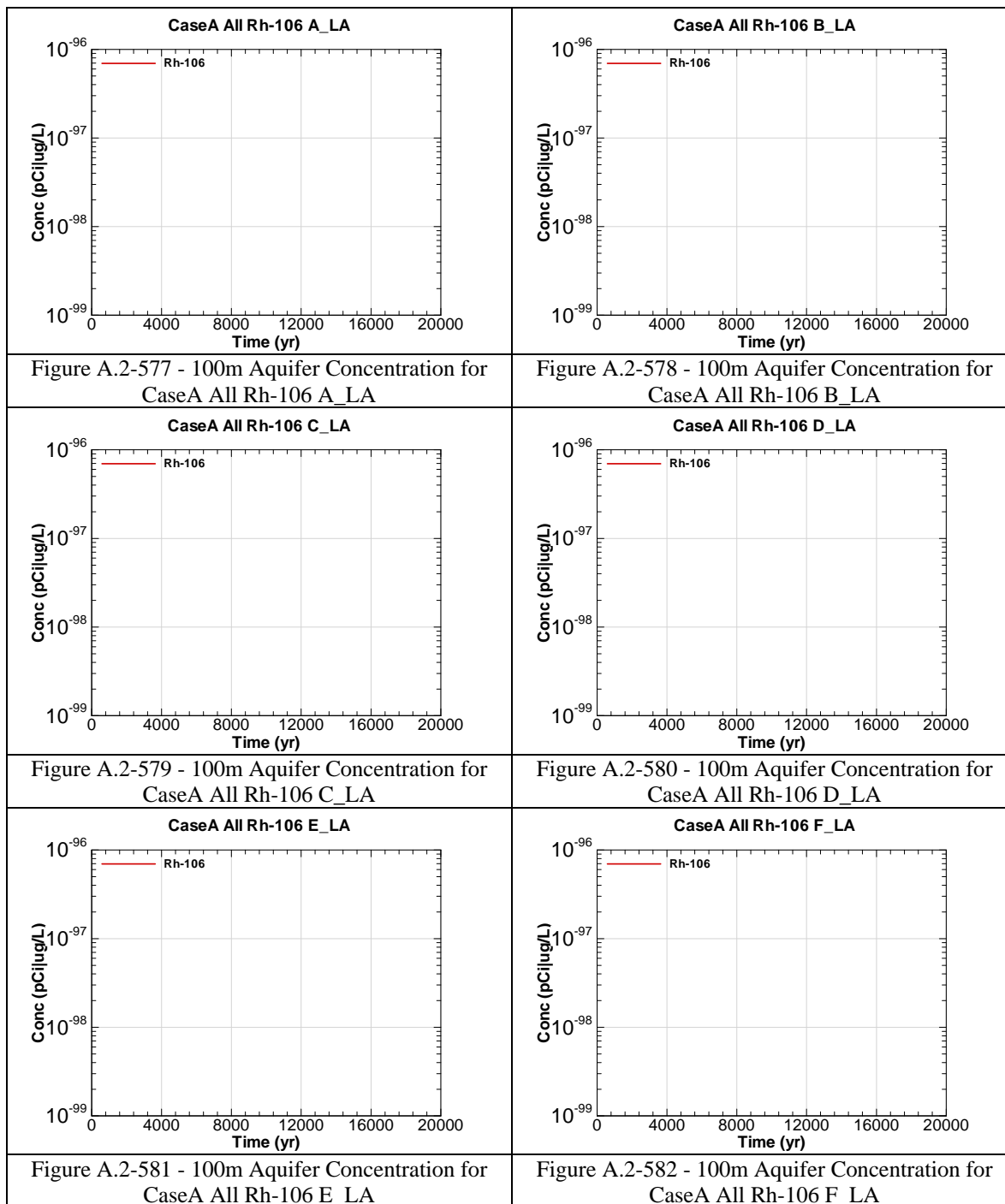


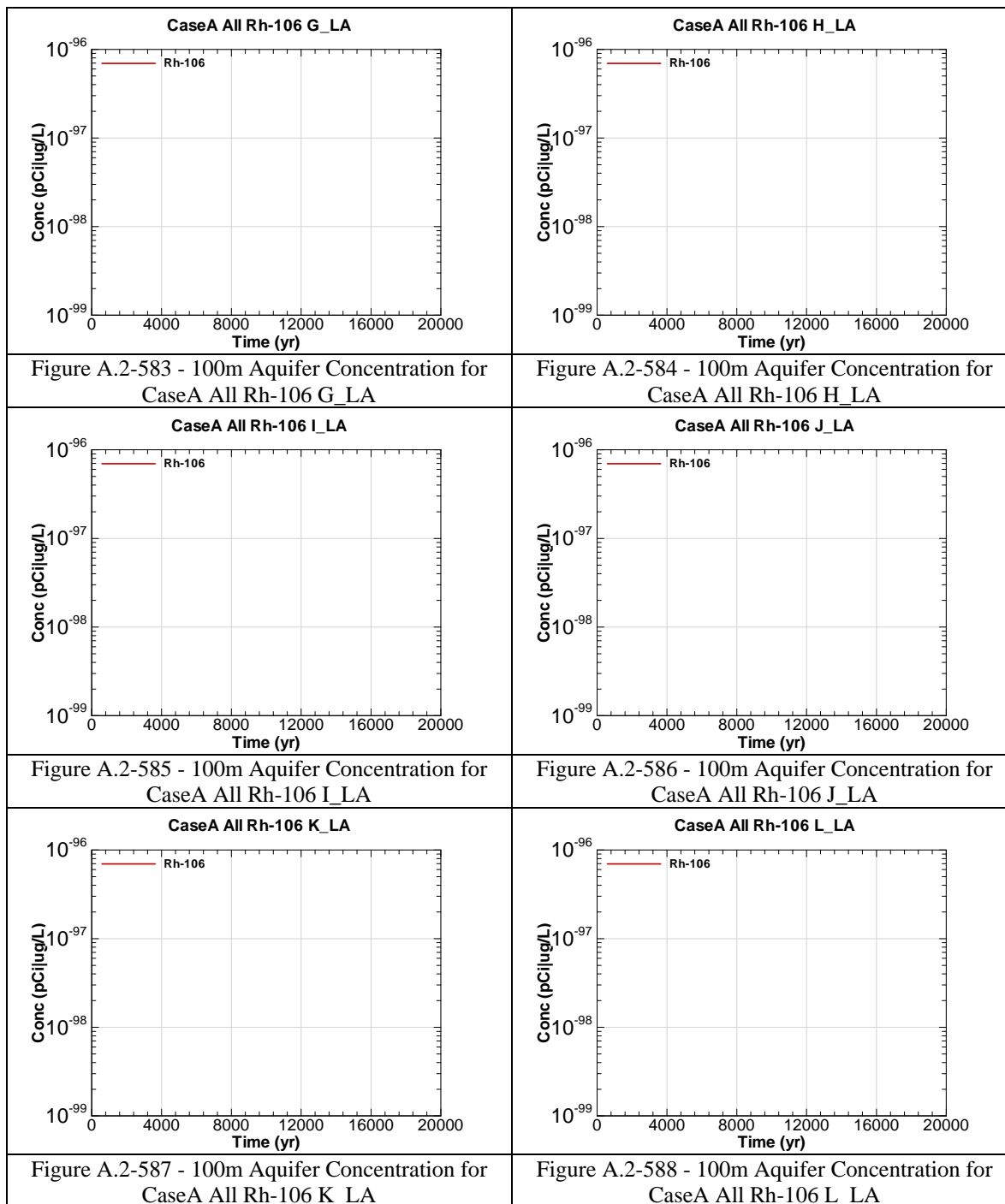


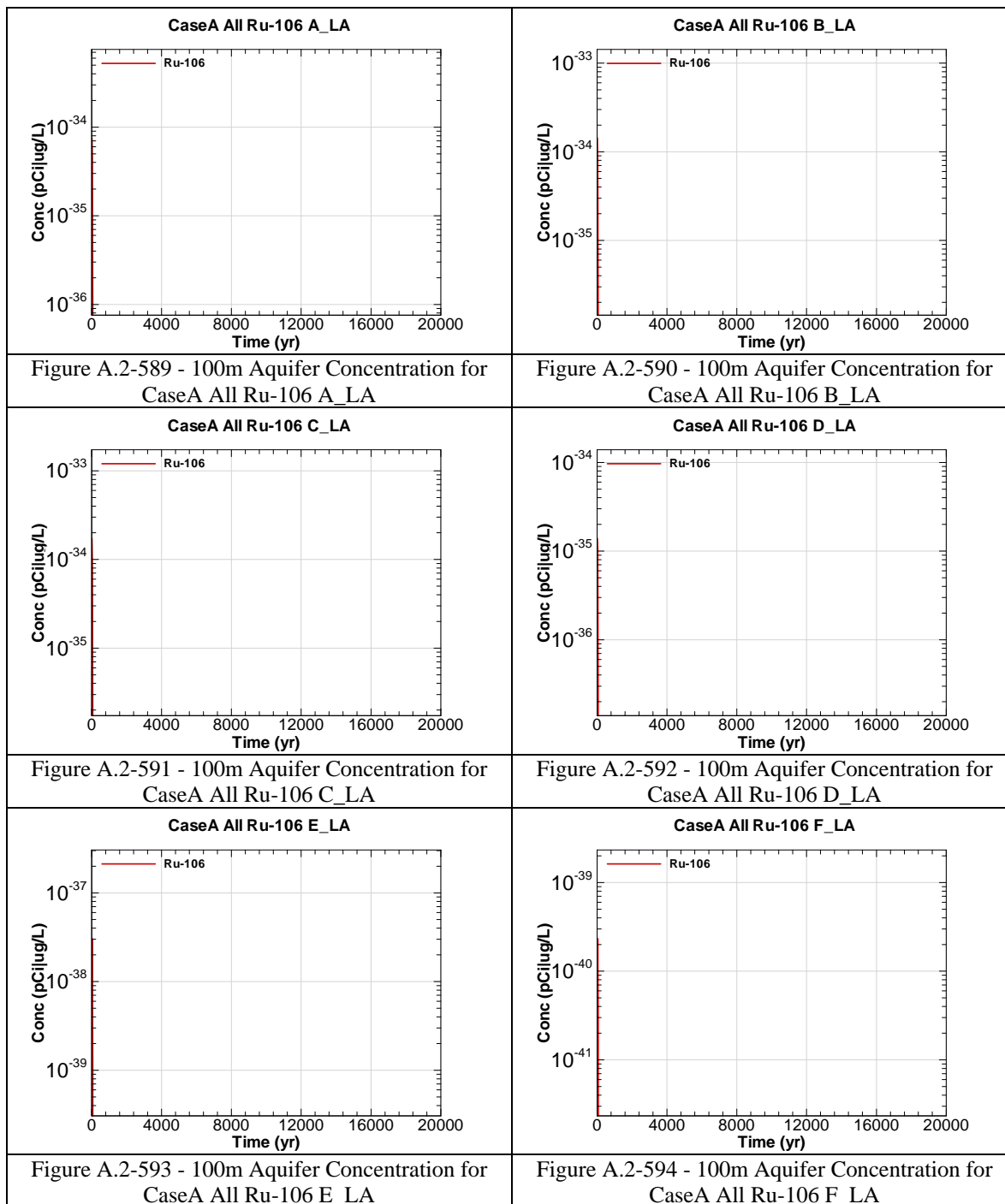


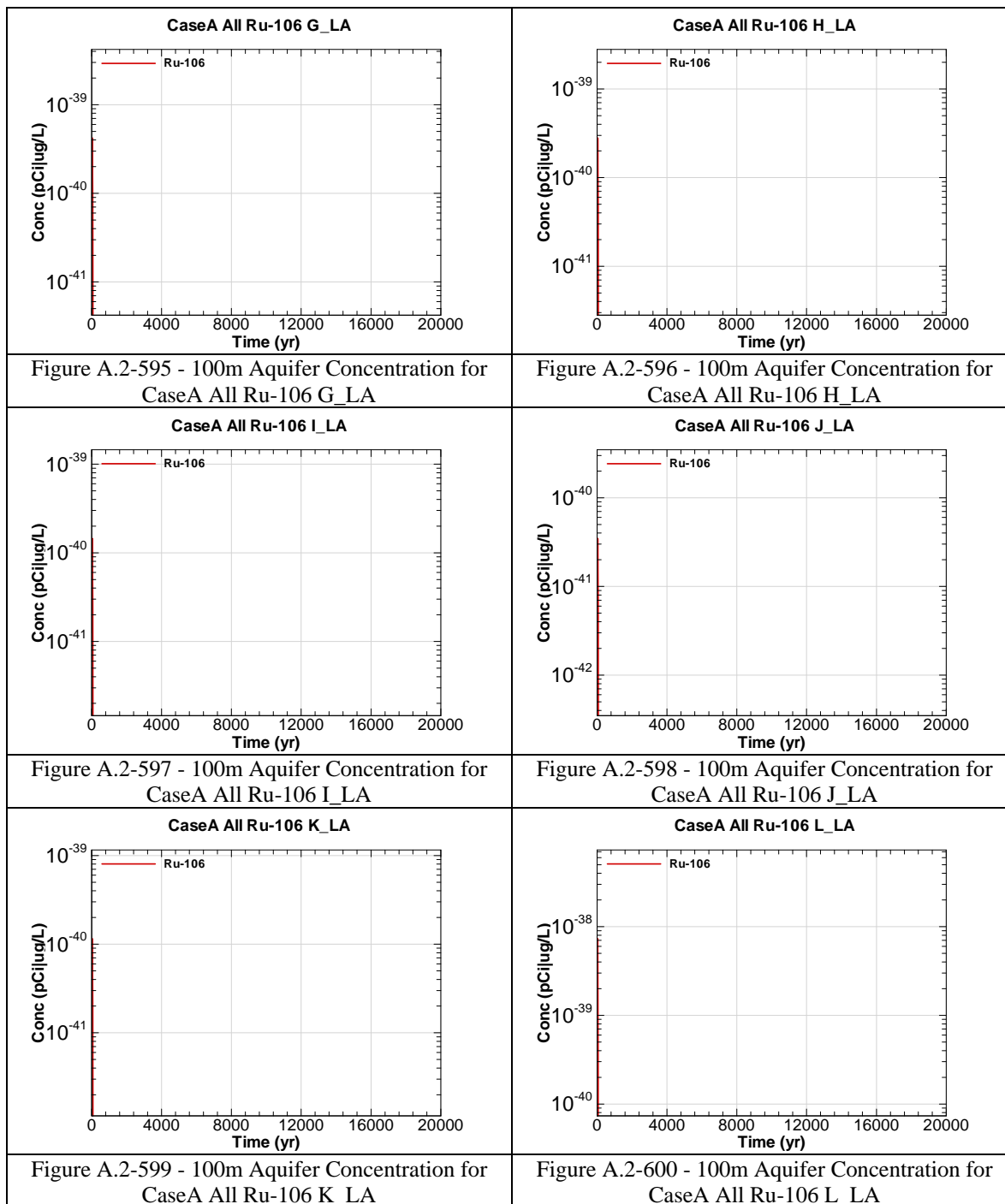


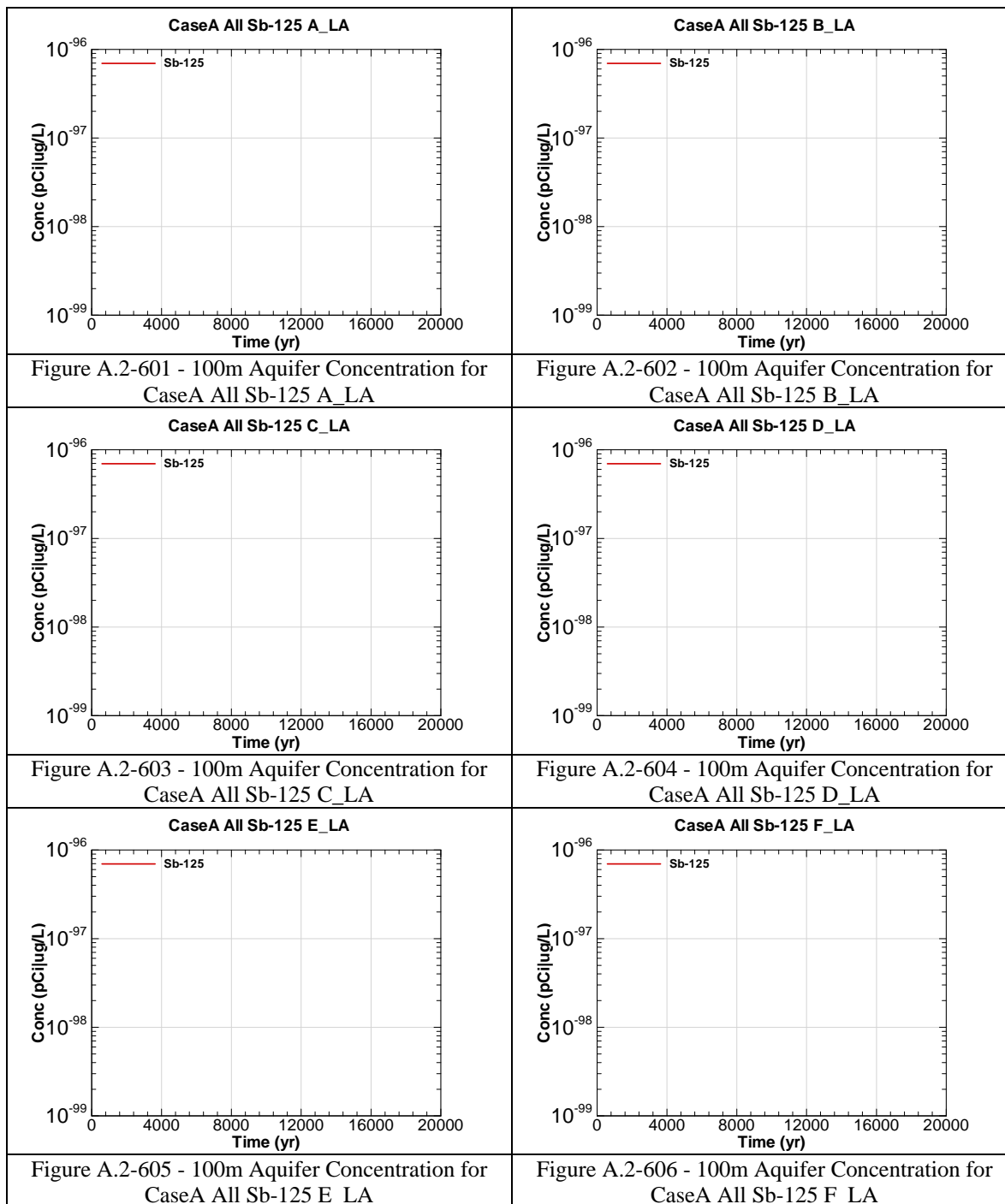


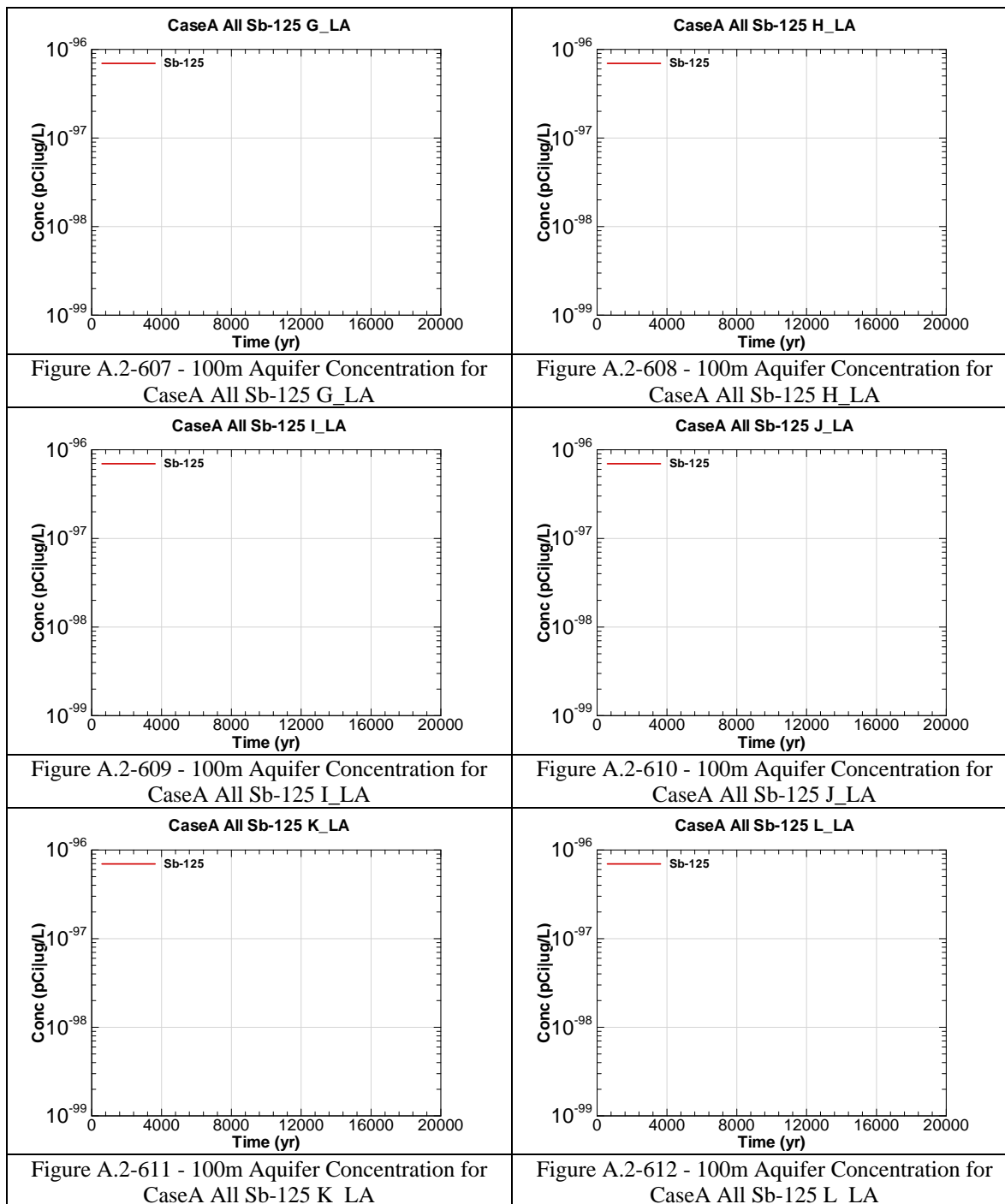


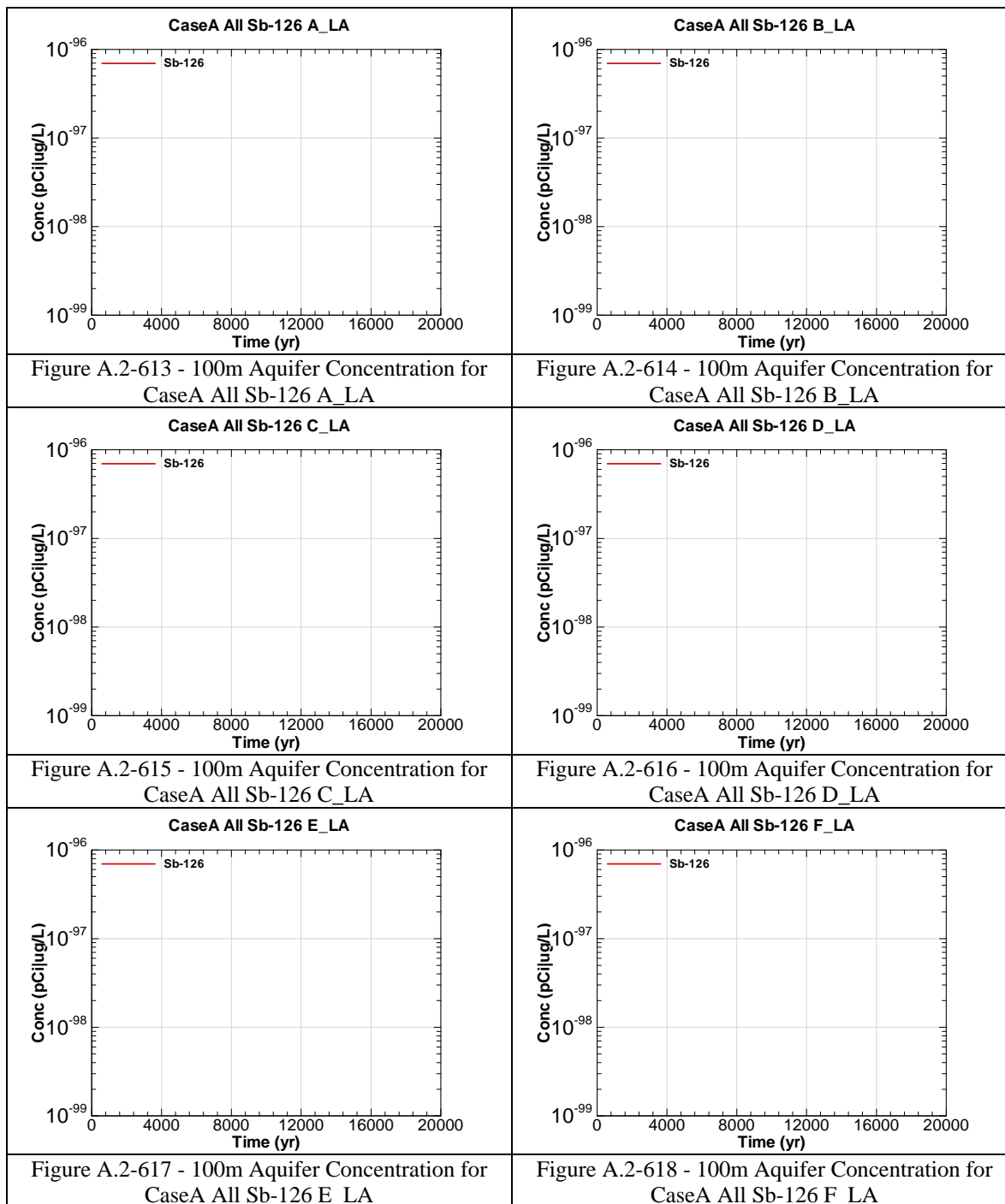


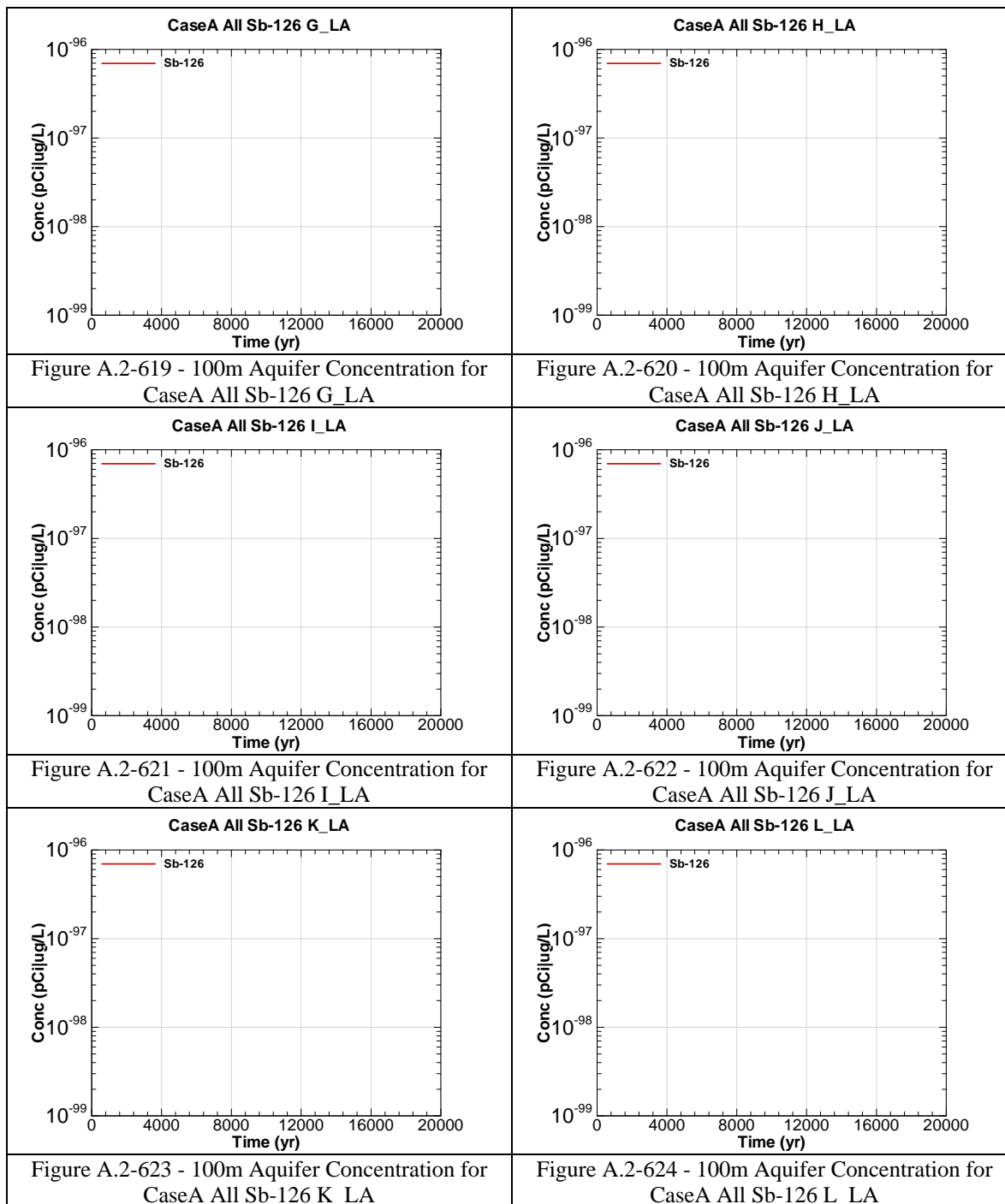


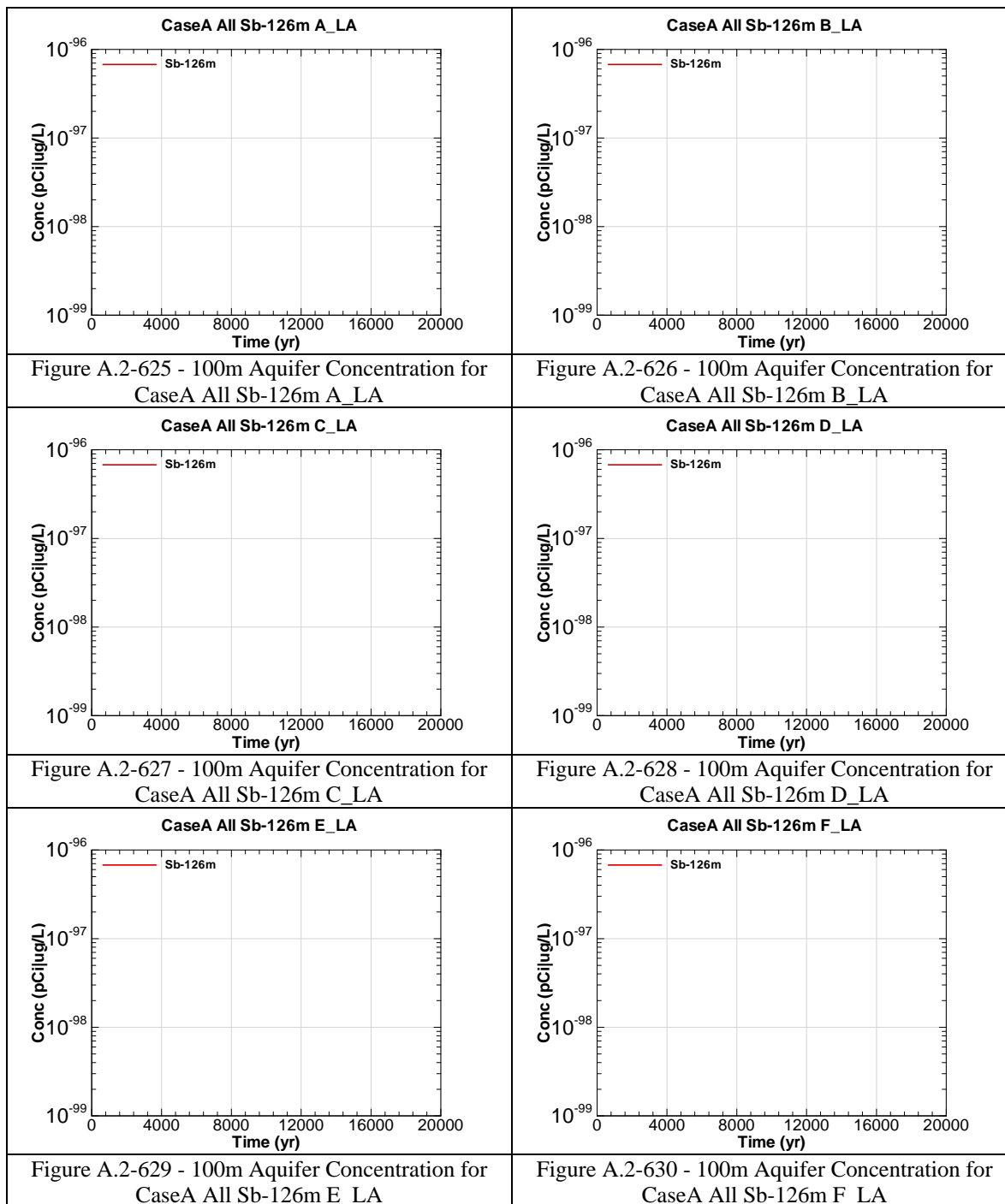


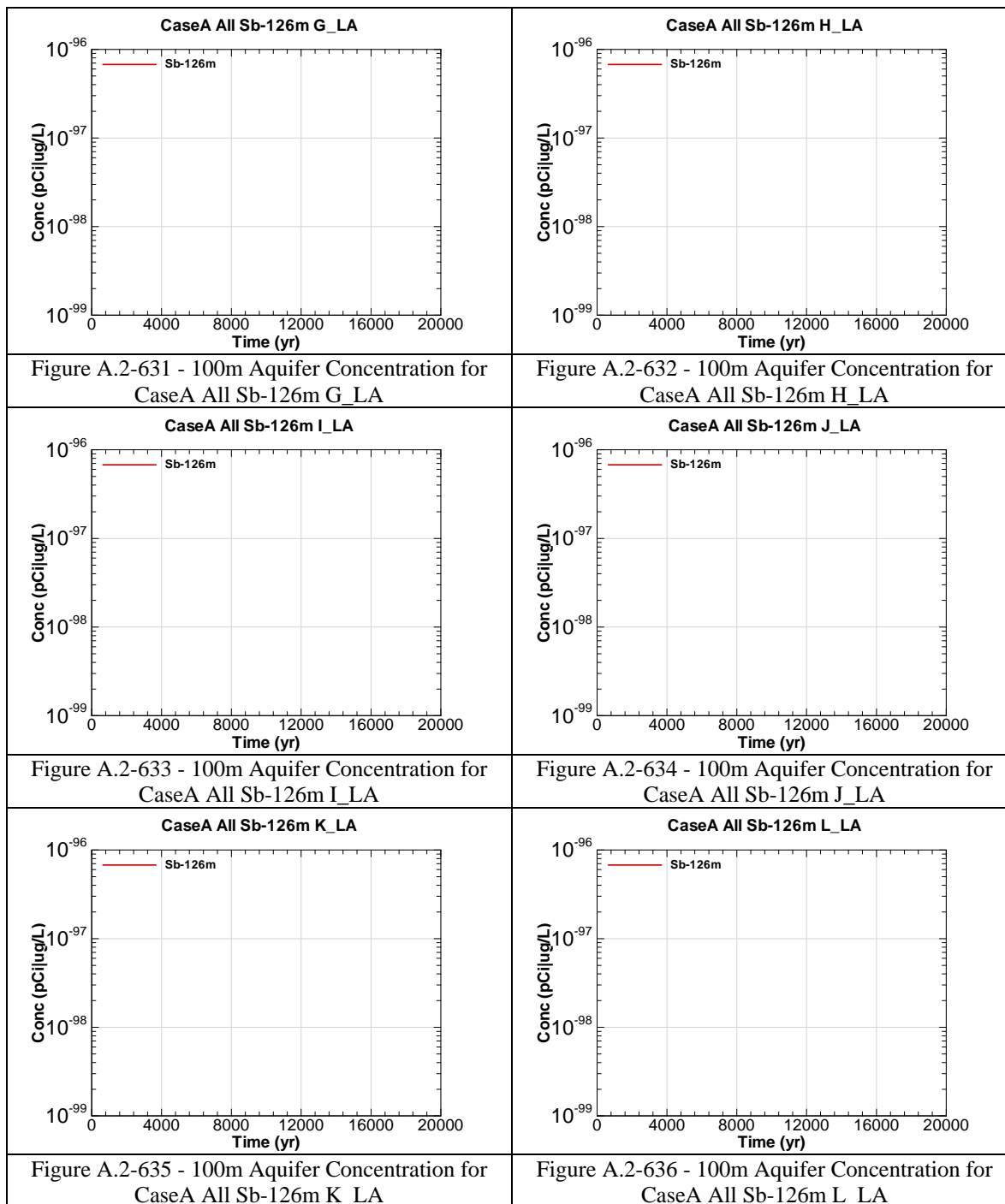


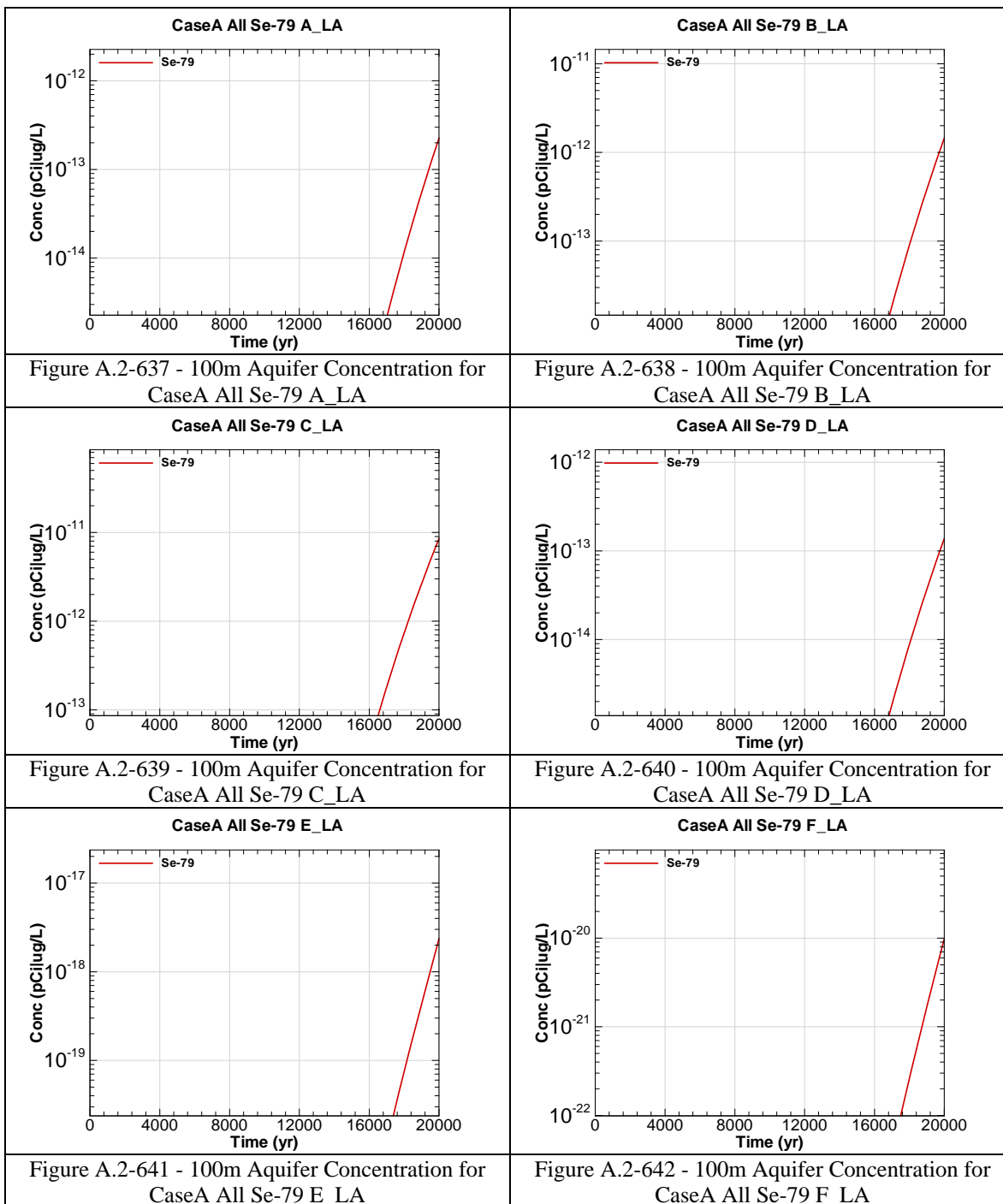


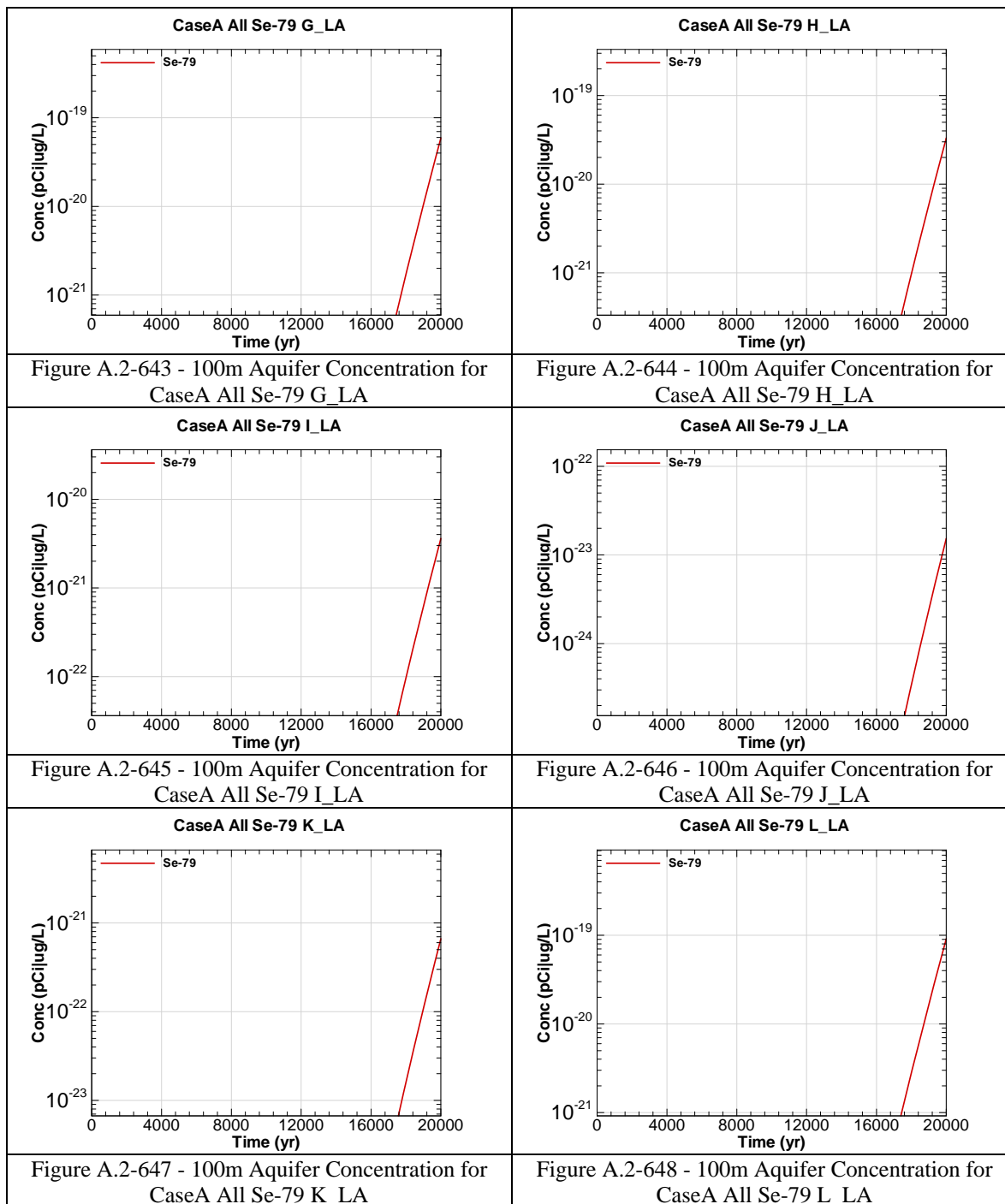


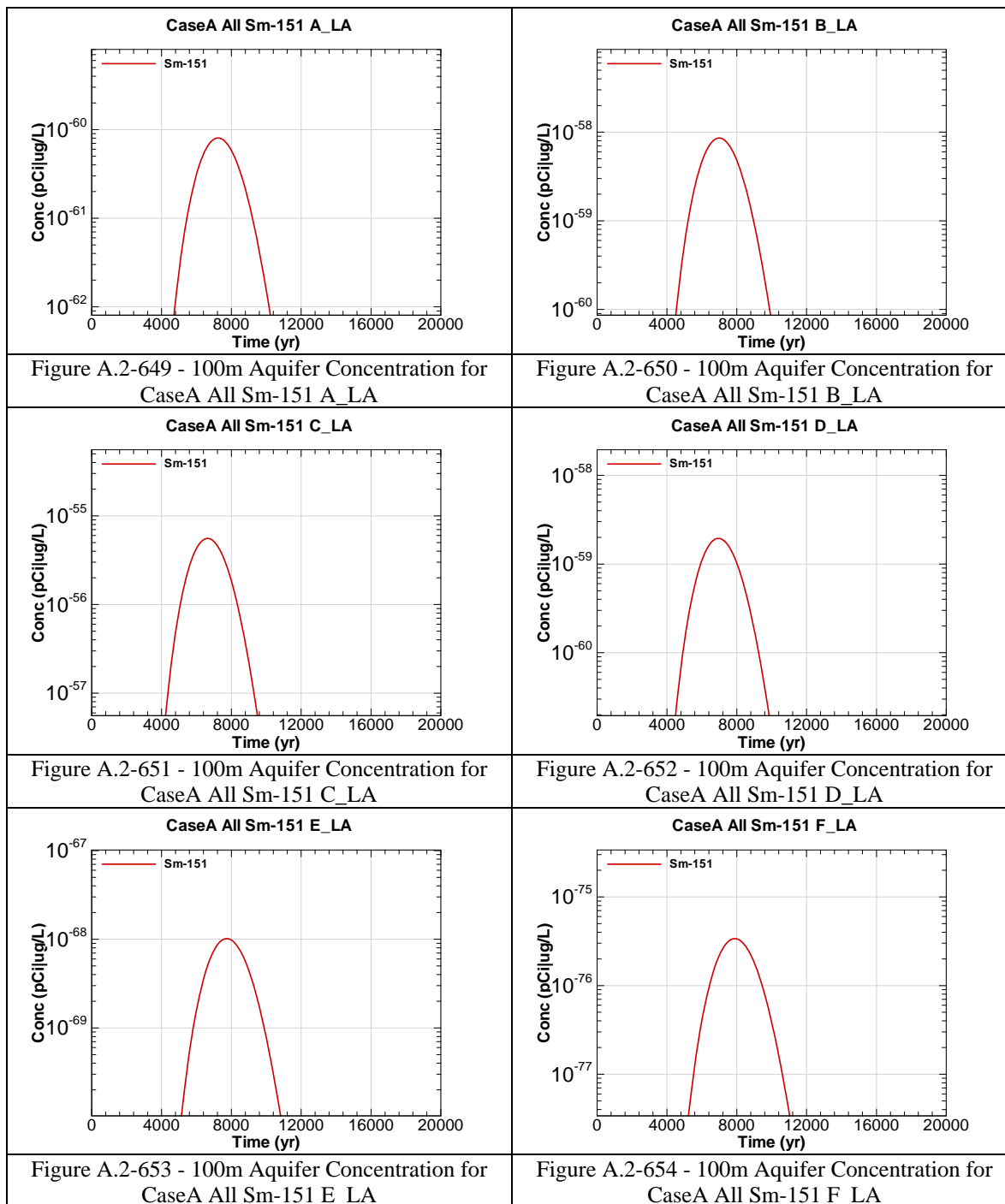


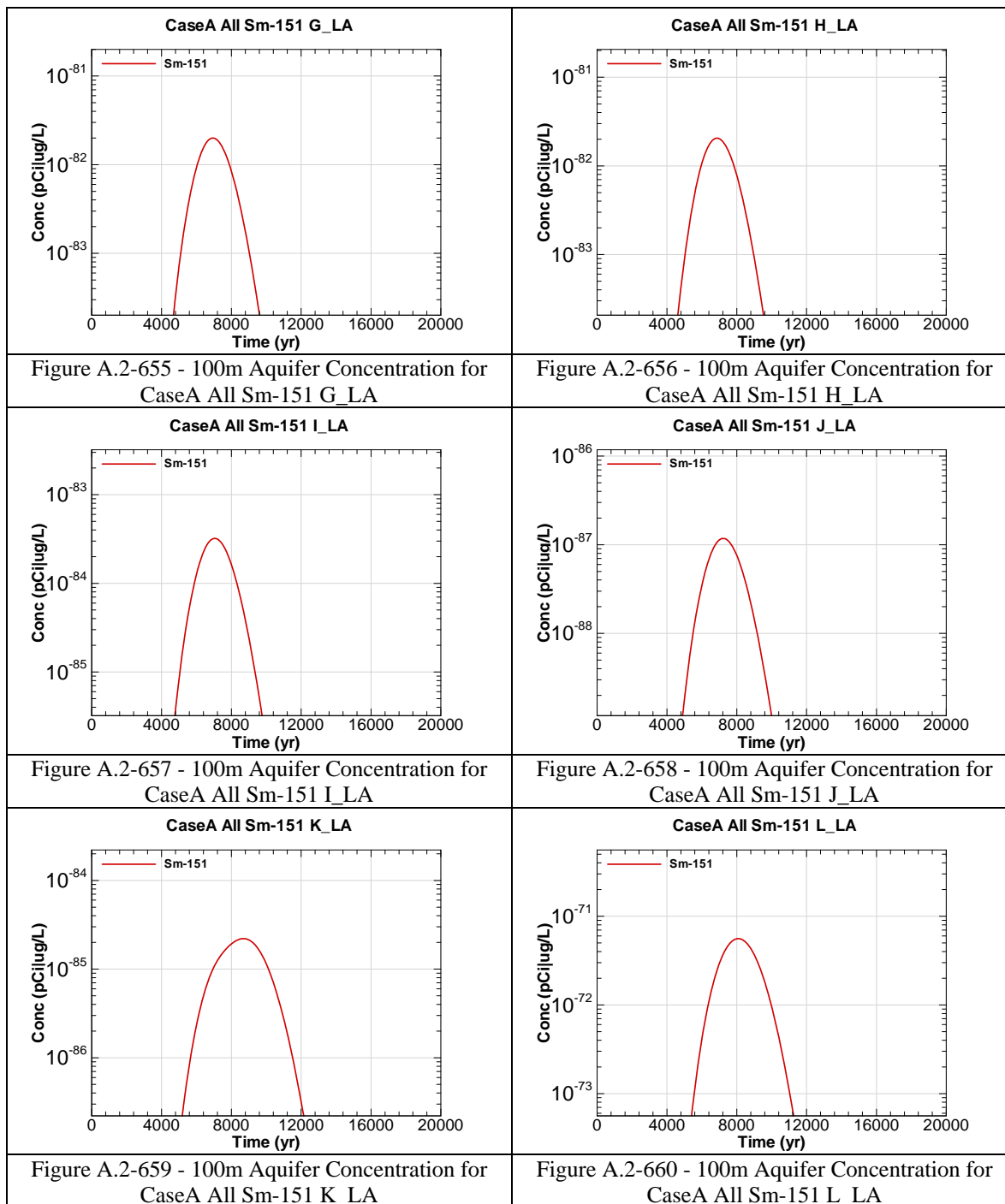


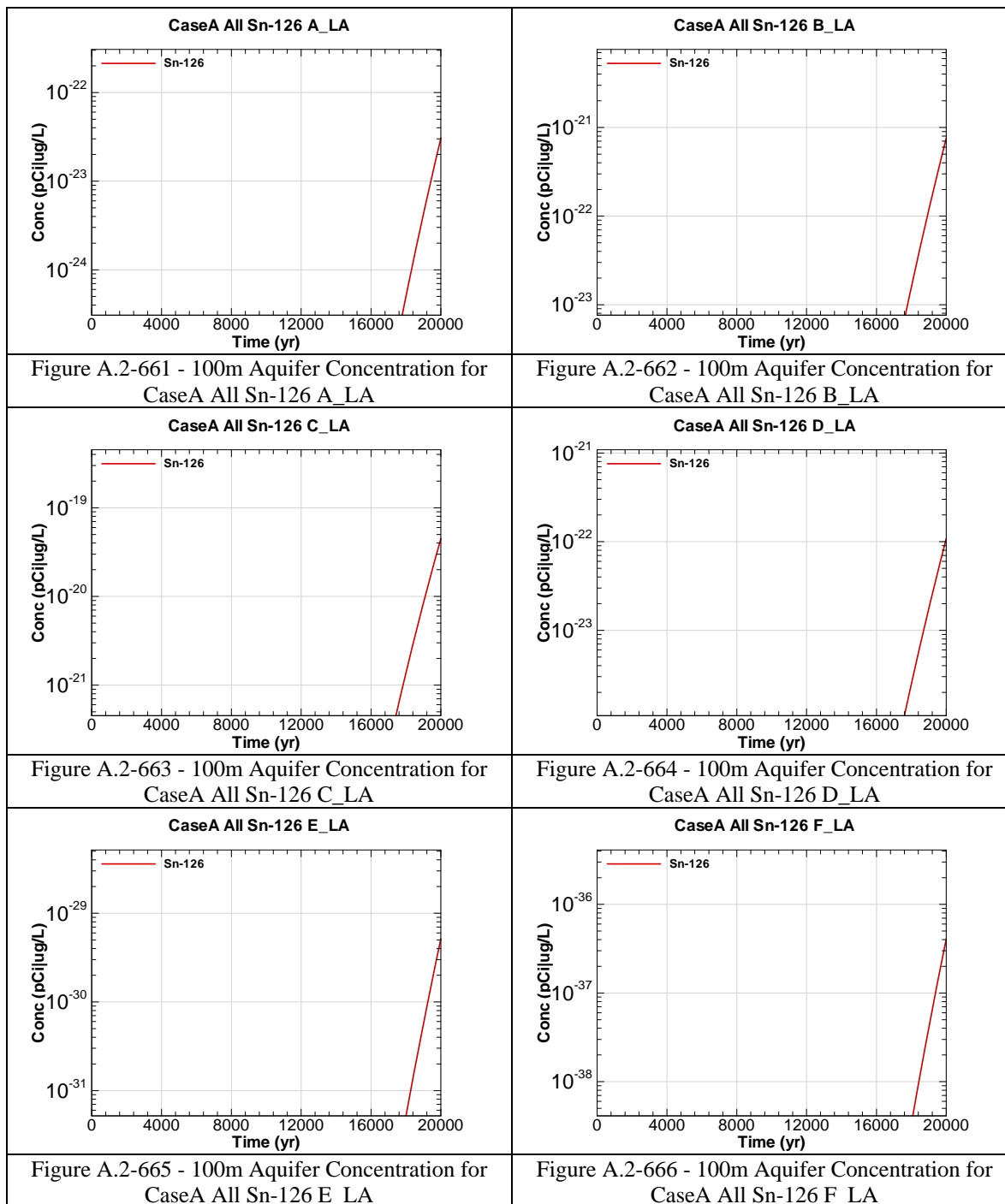


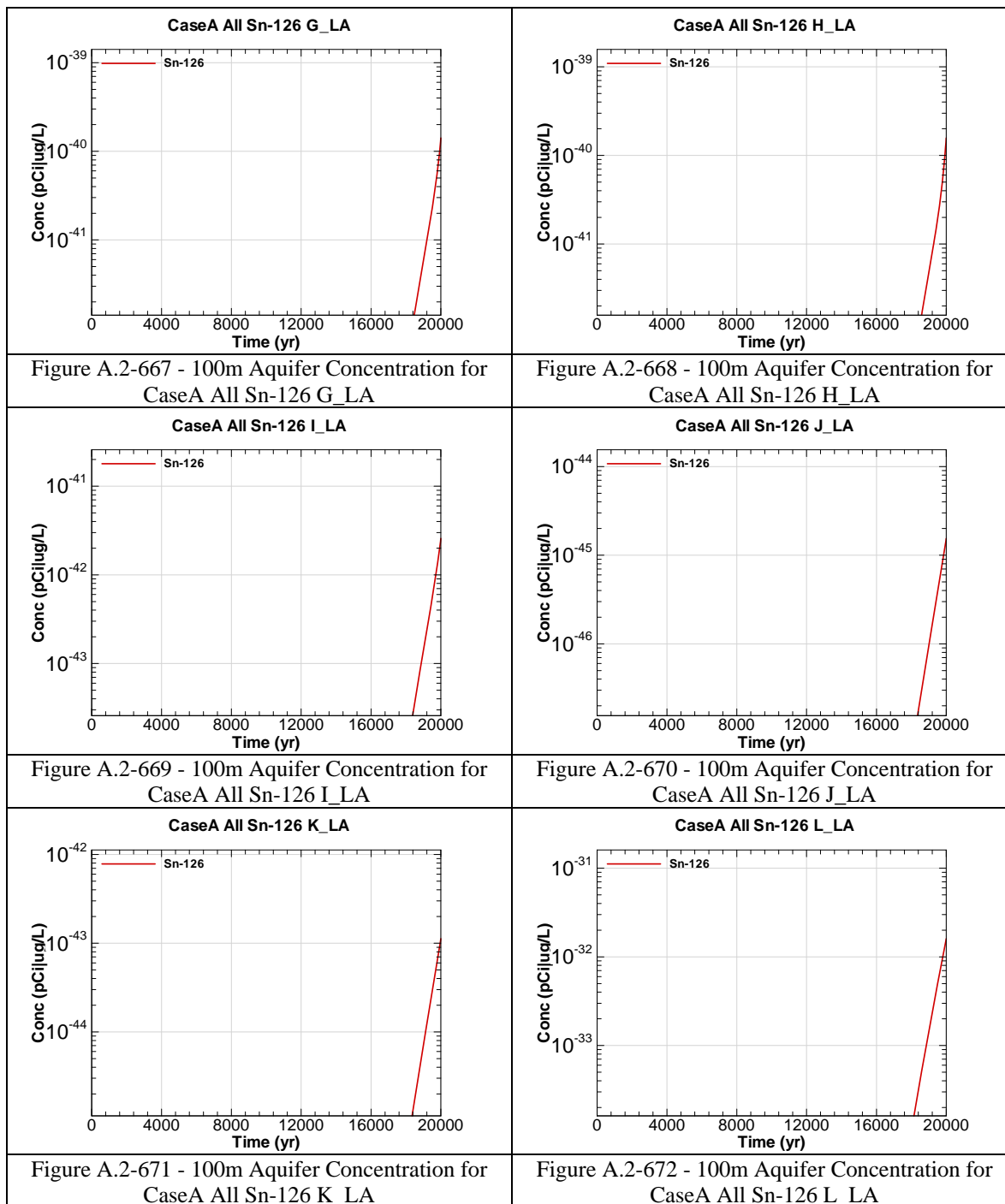


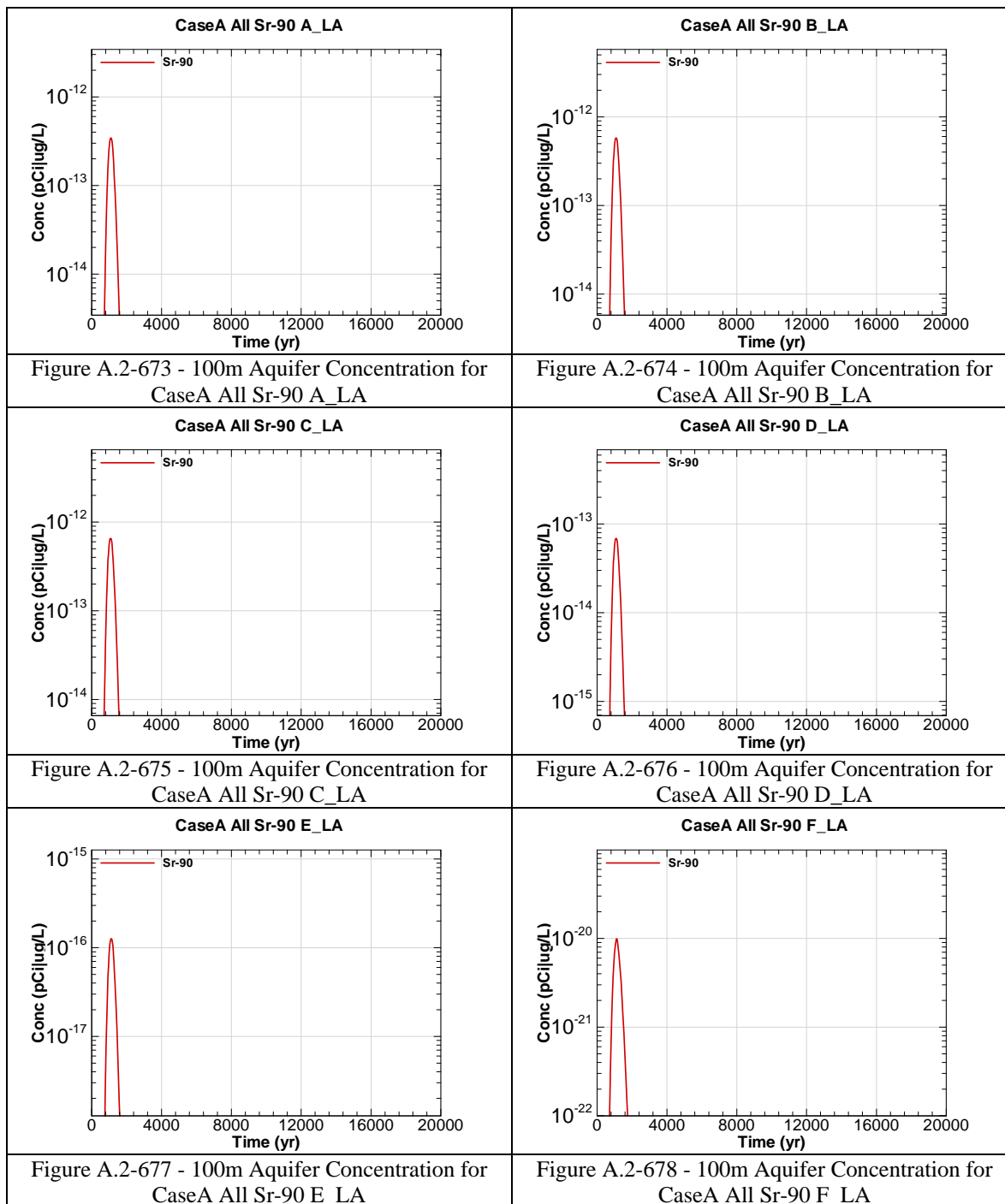


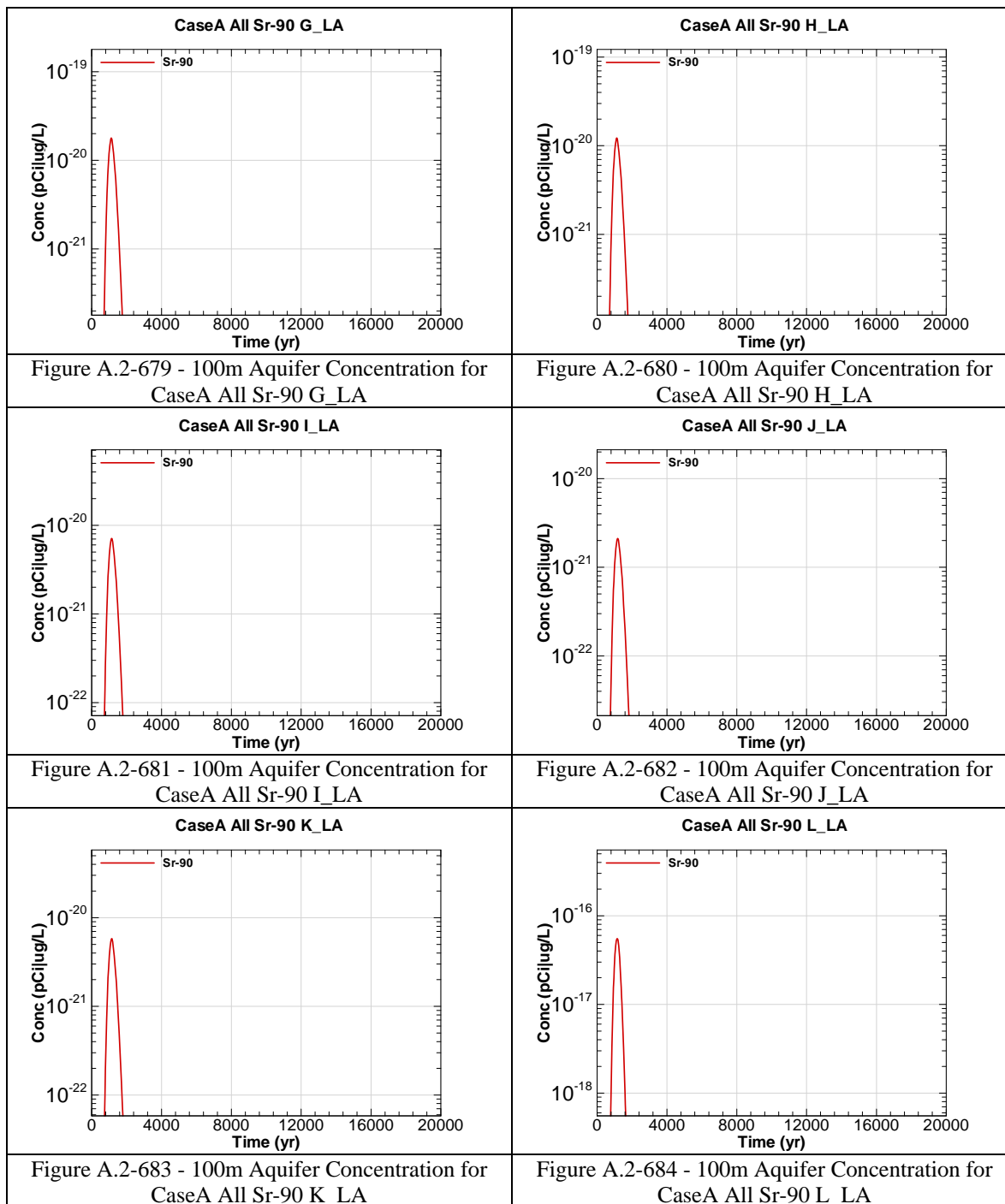


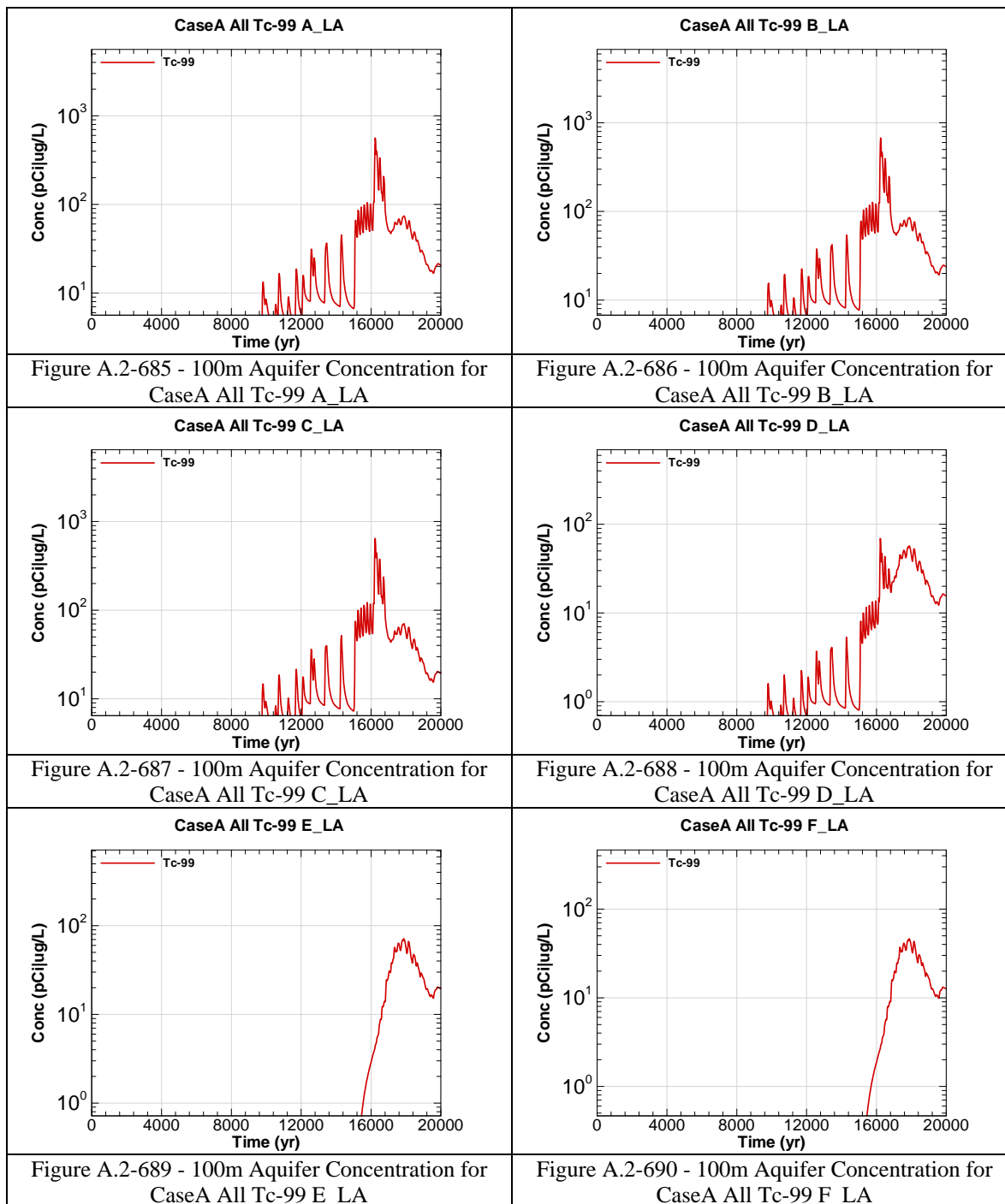


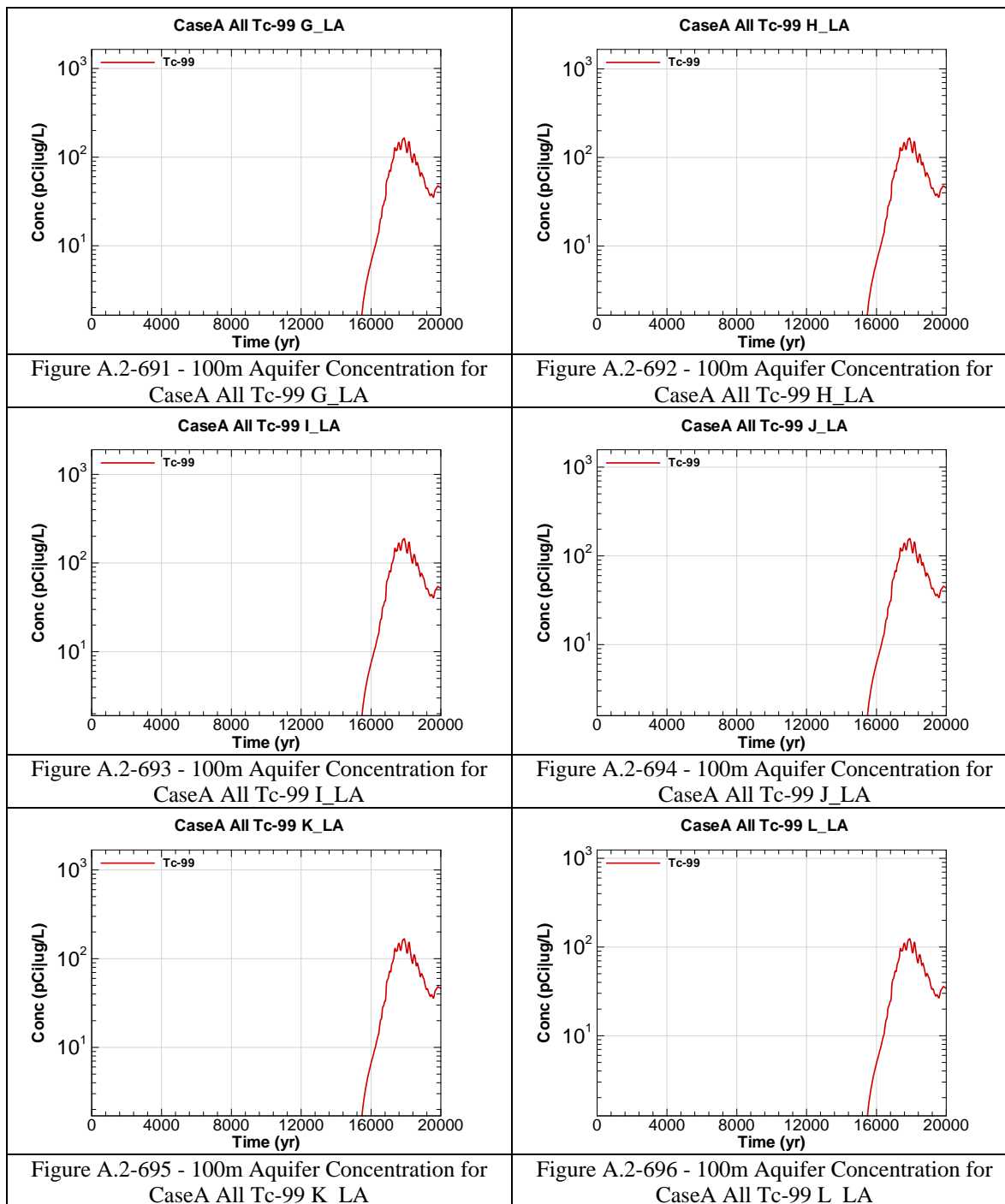


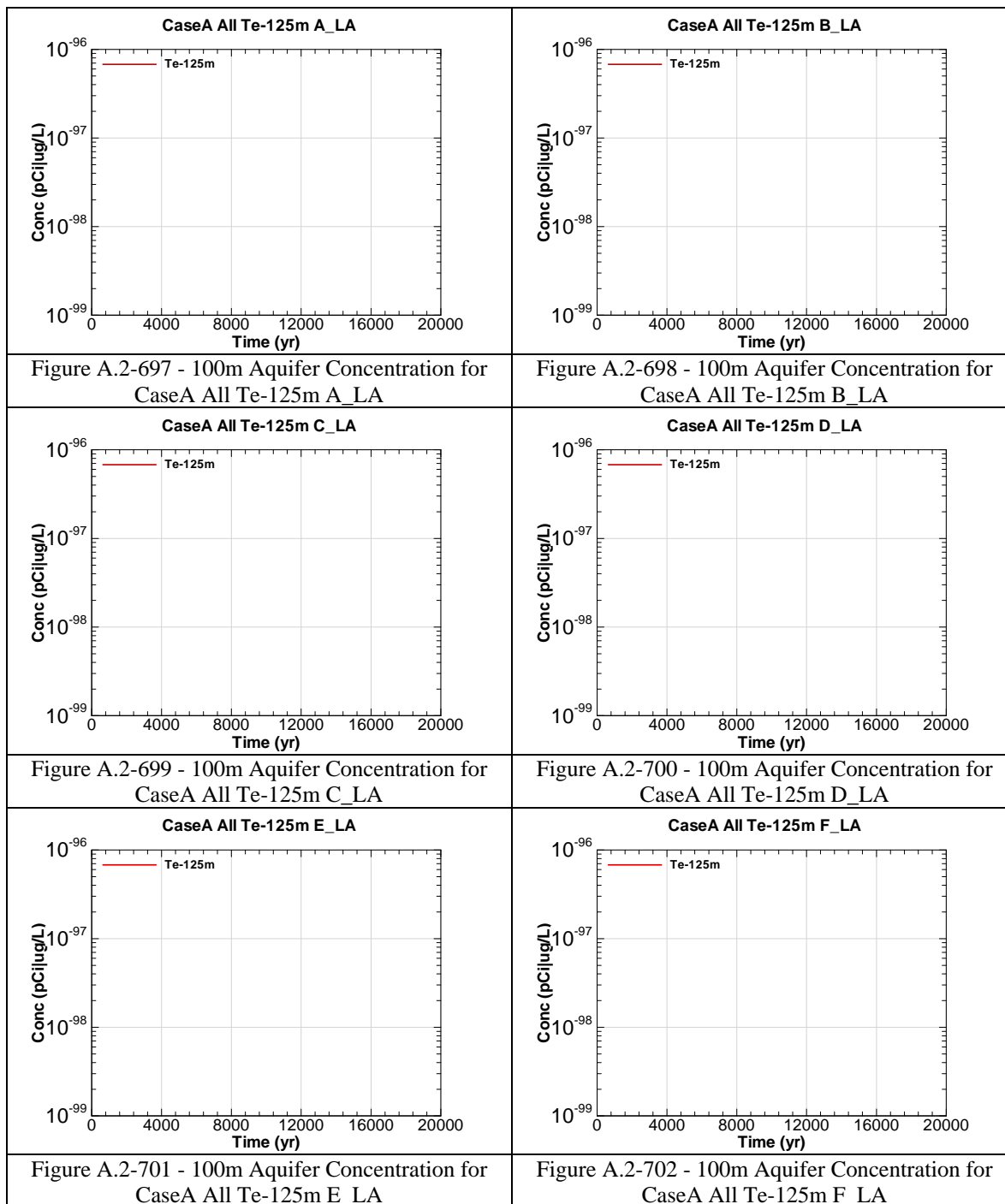


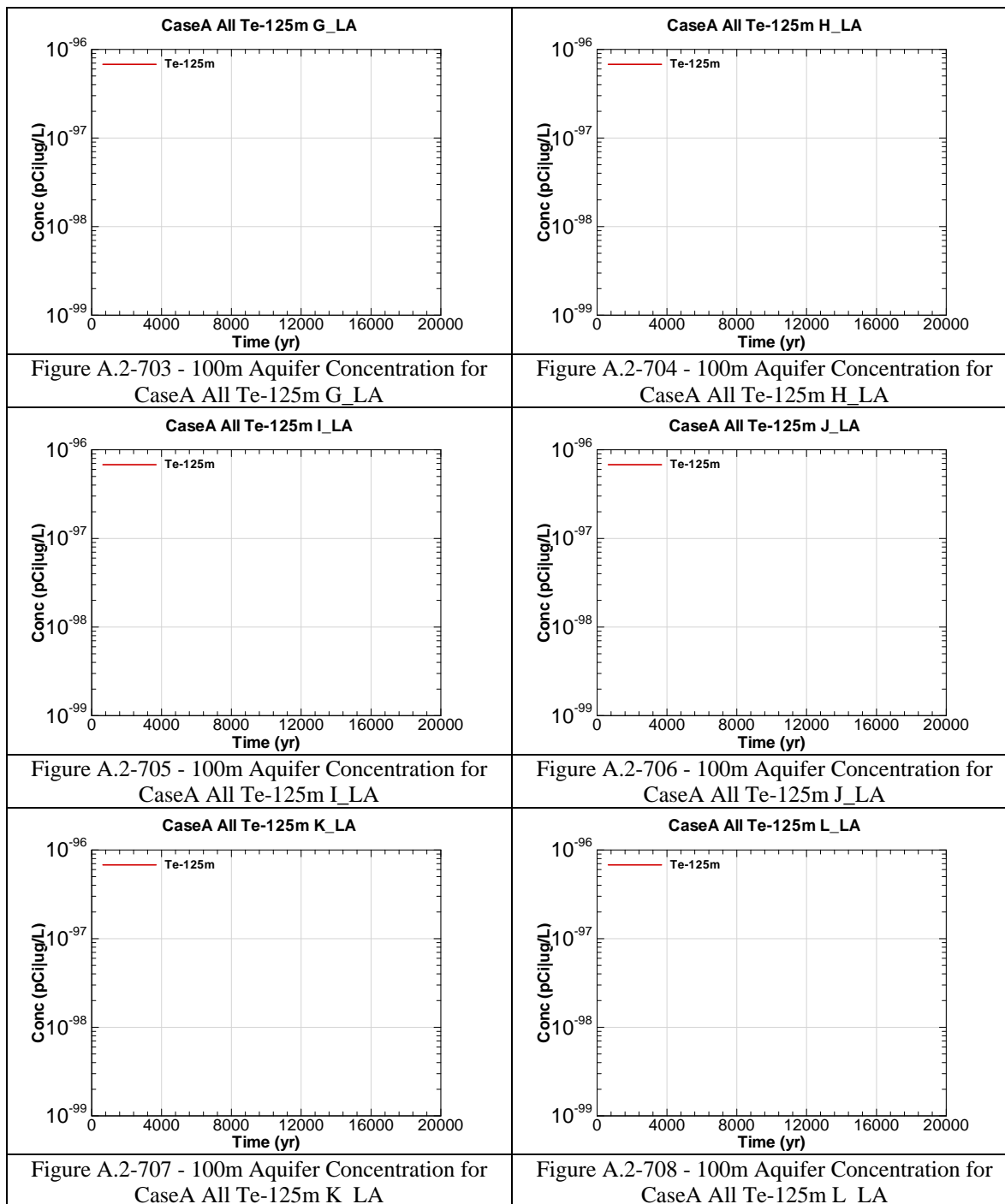


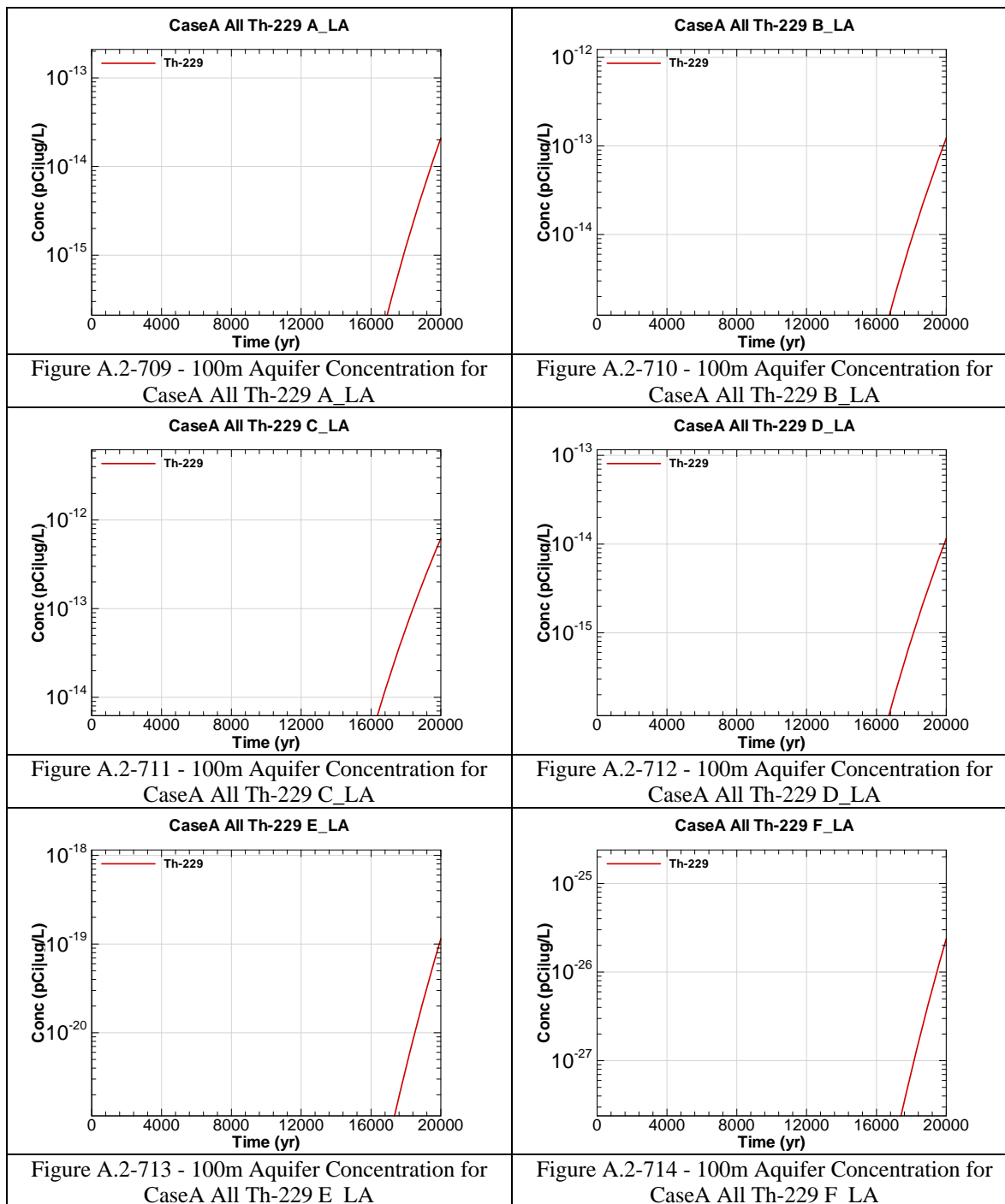


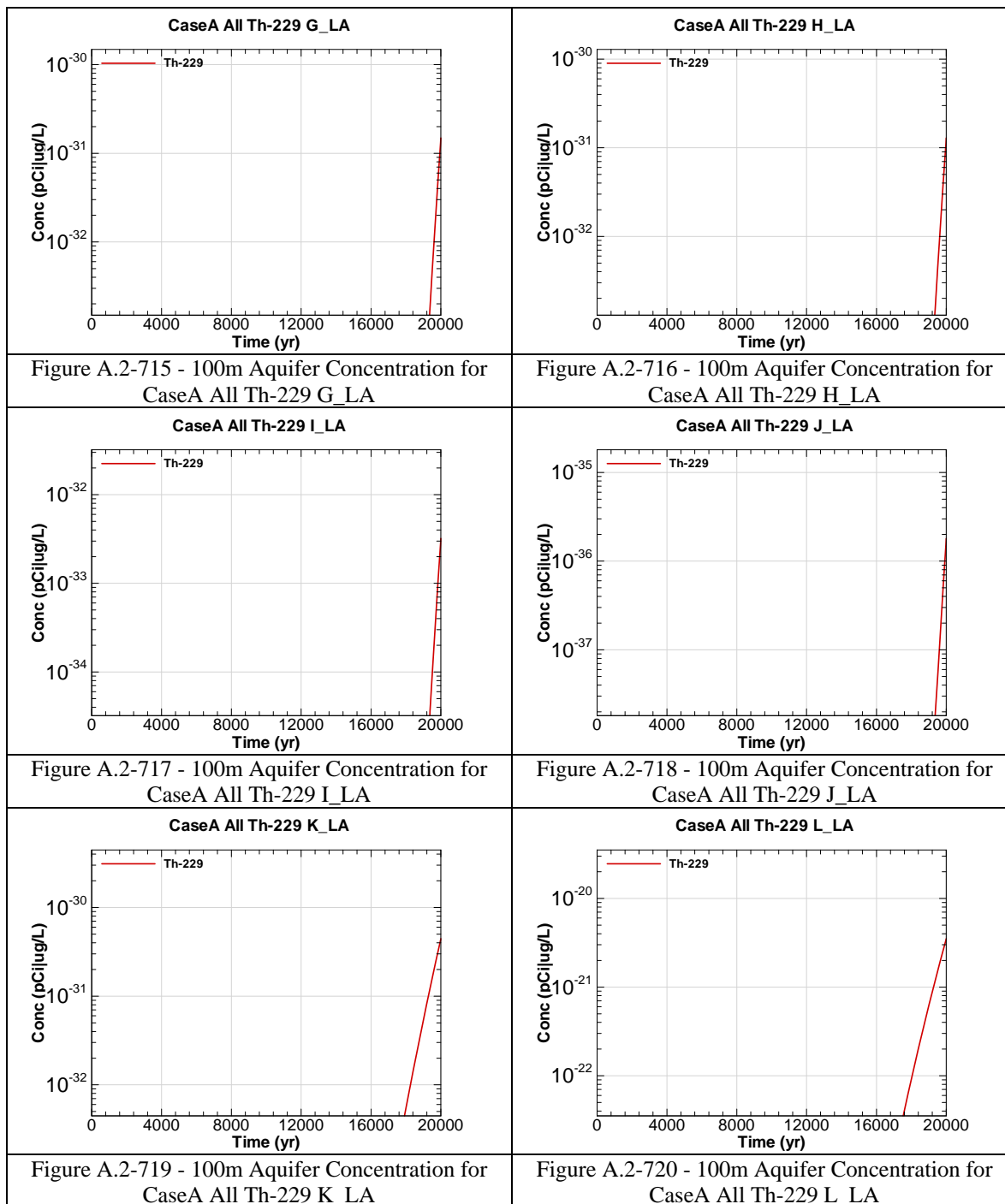












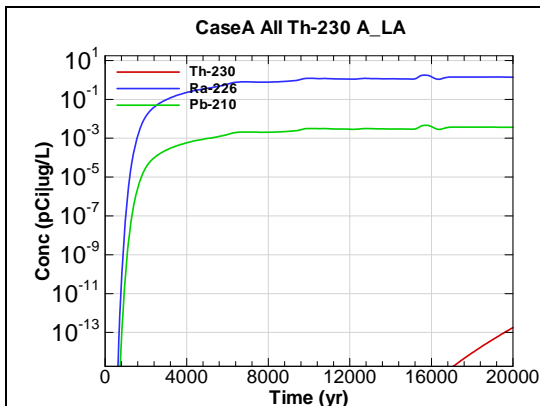


Figure A.2-721 - 100m Aquifer Concentration for
CaseA All Th-230 A_LA

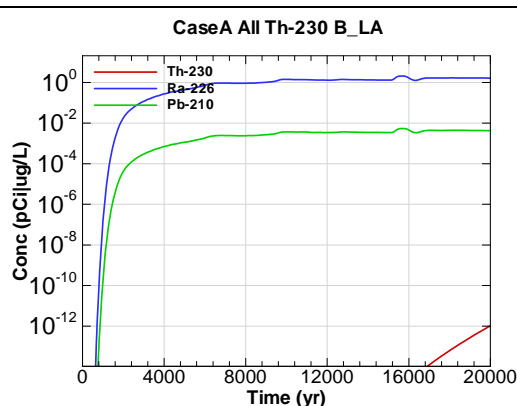


Figure A.2-722 - 100m Aquifer Concentration for
CaseA All Th-230 B_LA

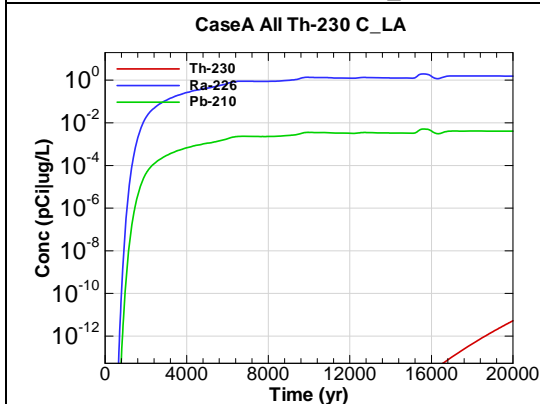


Figure A.2-723 - 100m Aquifer Concentration for
CaseA All Th-230 C_LA

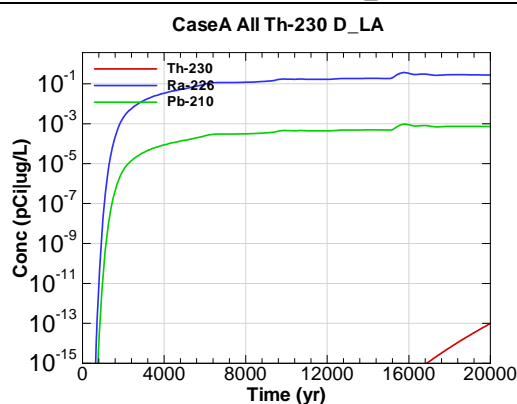


Figure A.2-724 - 100m Aquifer Concentration for
CaseA All Th-230 D_LA

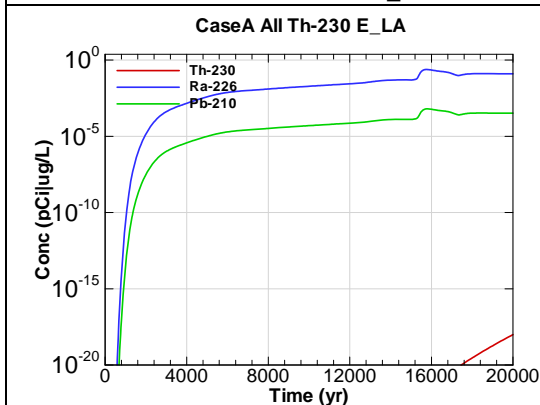


Figure A.2-725 - 100m Aquifer Concentration for
CaseA All Th-230 E_LA

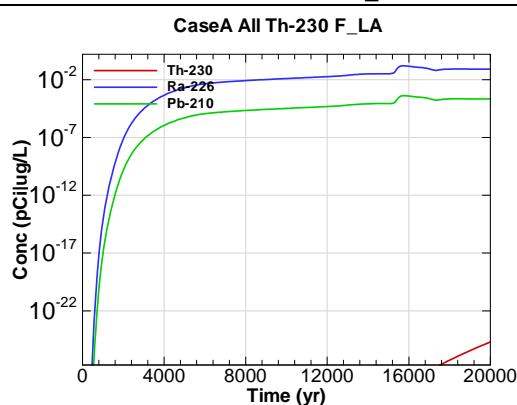


Figure A.2-726 - 100m Aquifer Concentration for
CaseA All Th-230 F_LA

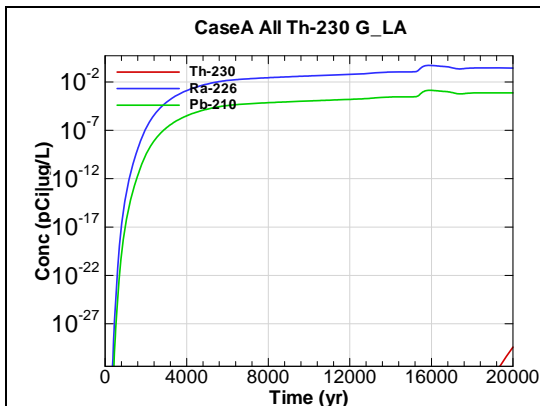


Figure A.2-727 - 100m Aquifer Concentration for
CaseA All Th-230 G_LA

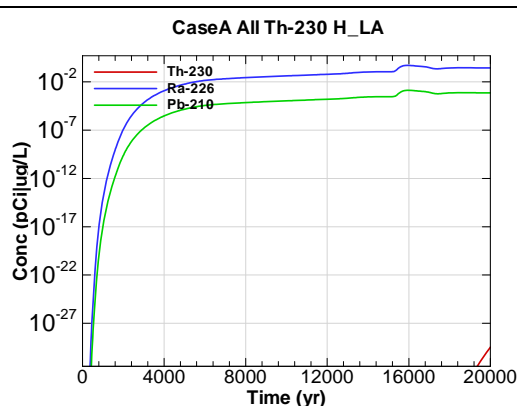


Figure A.2-728 - 100m Aquifer Concentration for
CaseA All Th-230 H_LA

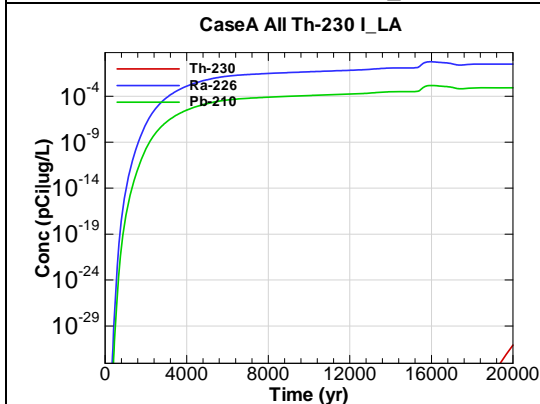


Figure A.2-729 - 100m Aquifer Concentration for
CaseA All Th-230 I_LA

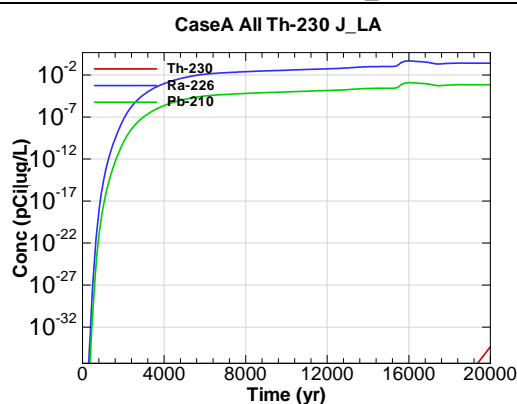


Figure A.2-730 - 100m Aquifer Concentration for
CaseA All Th-230 J_LA

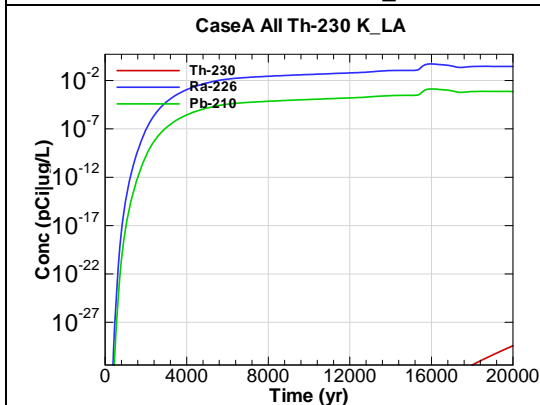


Figure A.2-731 - 100m Aquifer Concentration for
CaseA All Th-230 K_LA

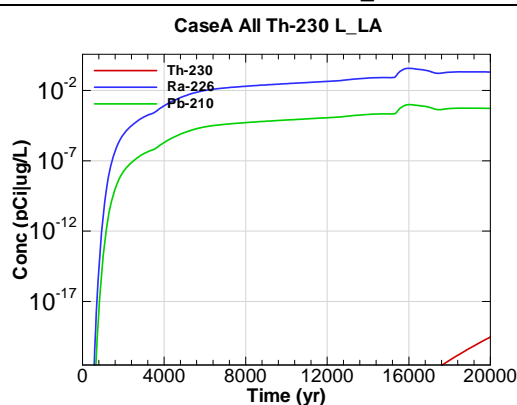
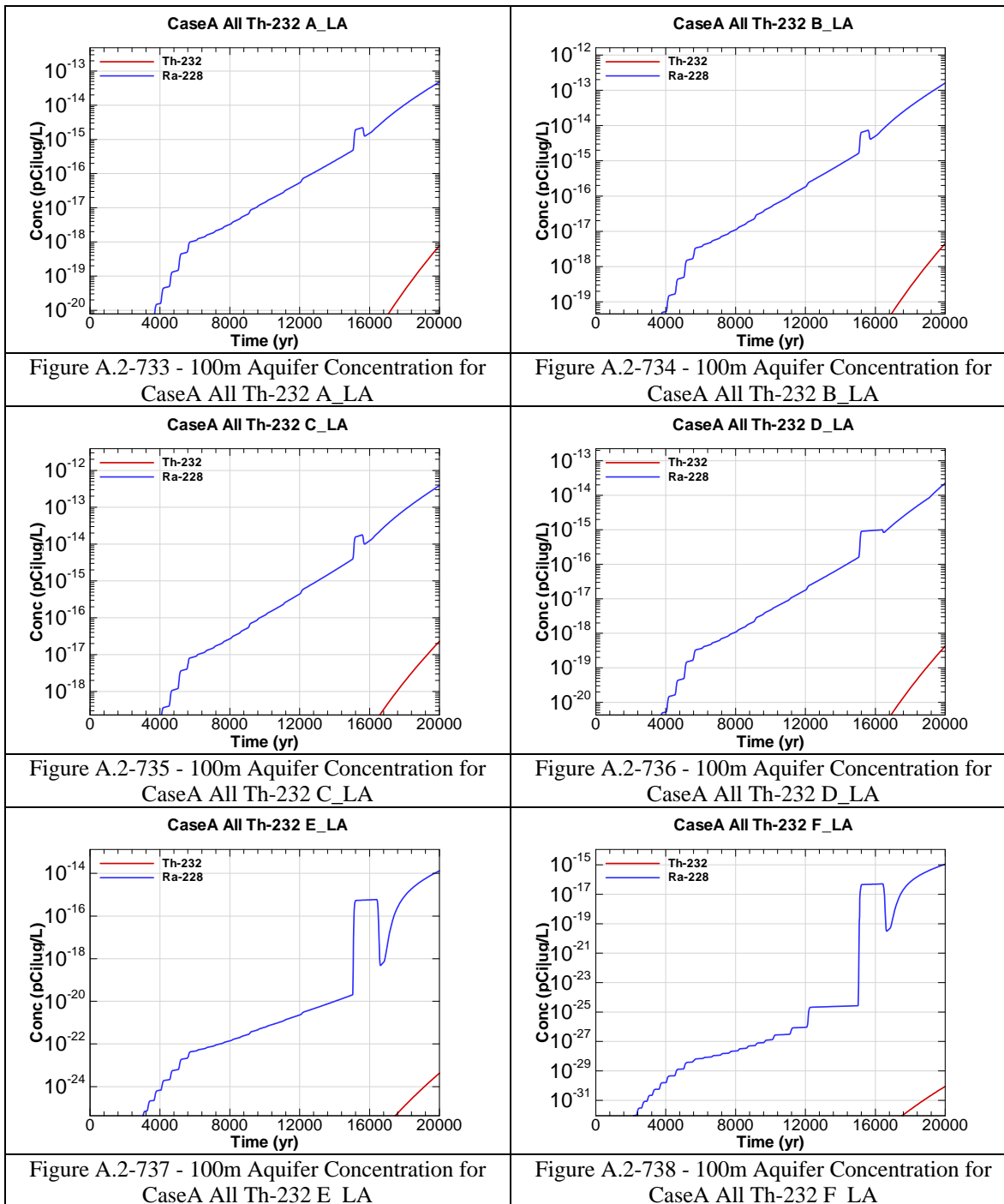
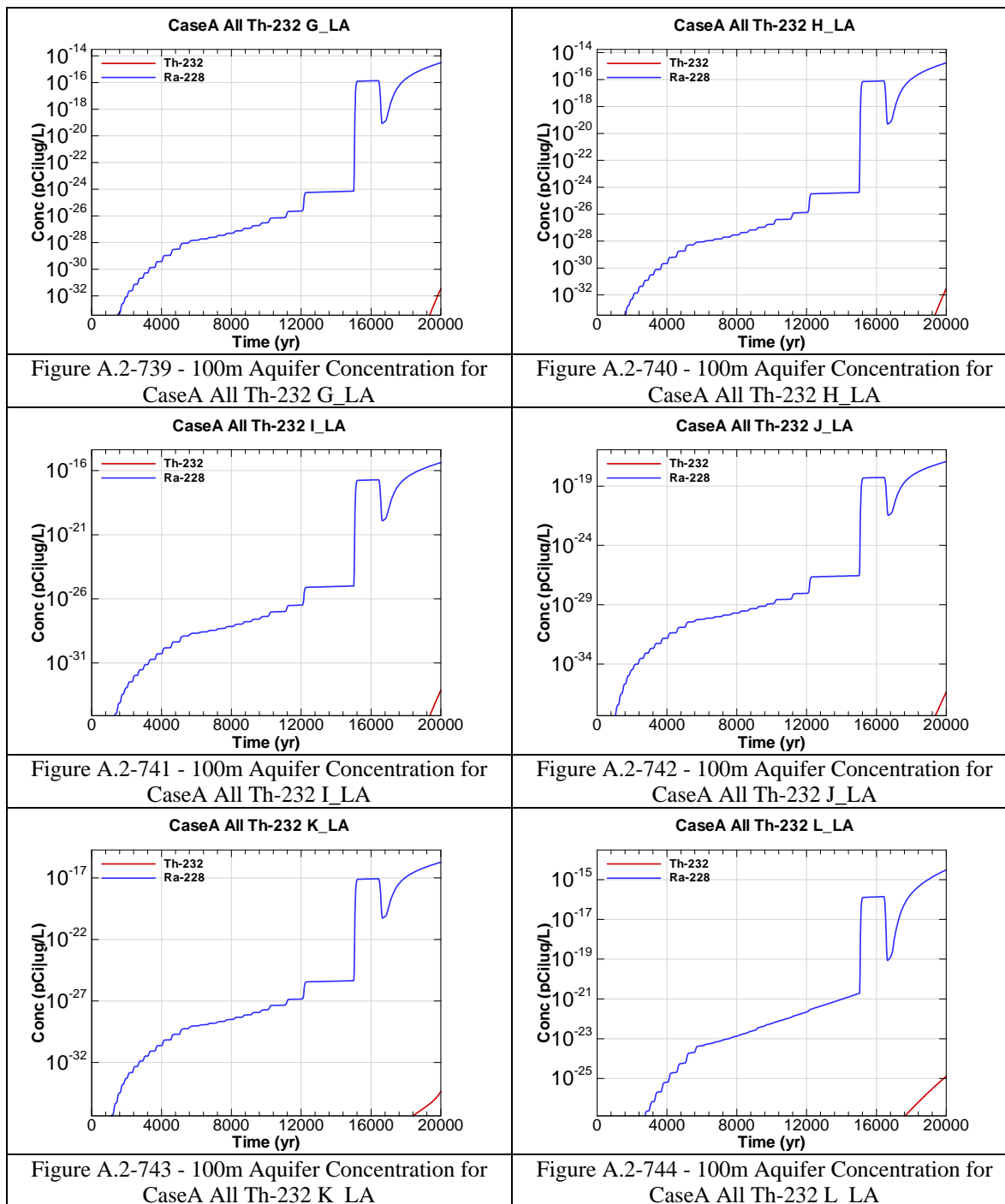
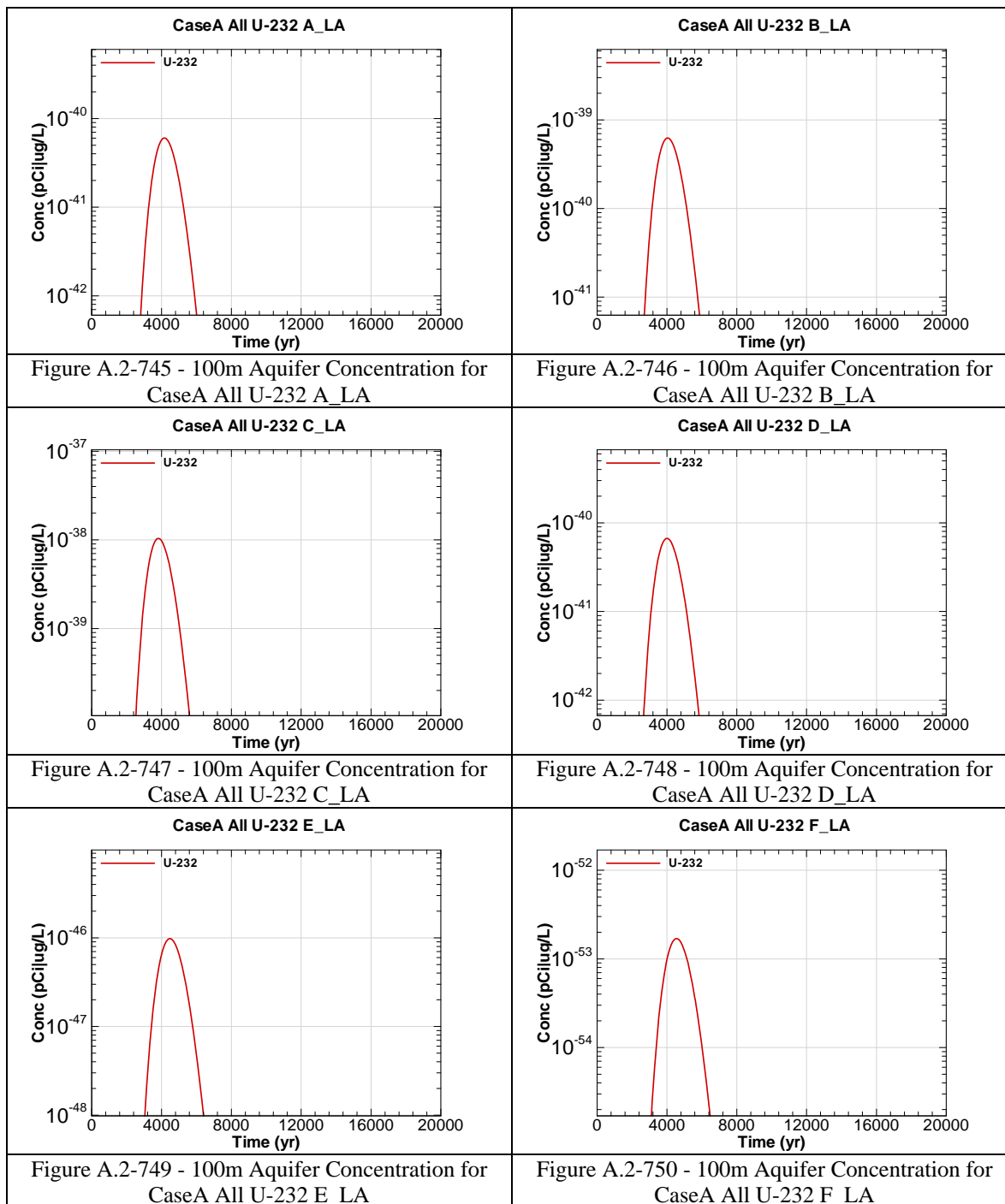
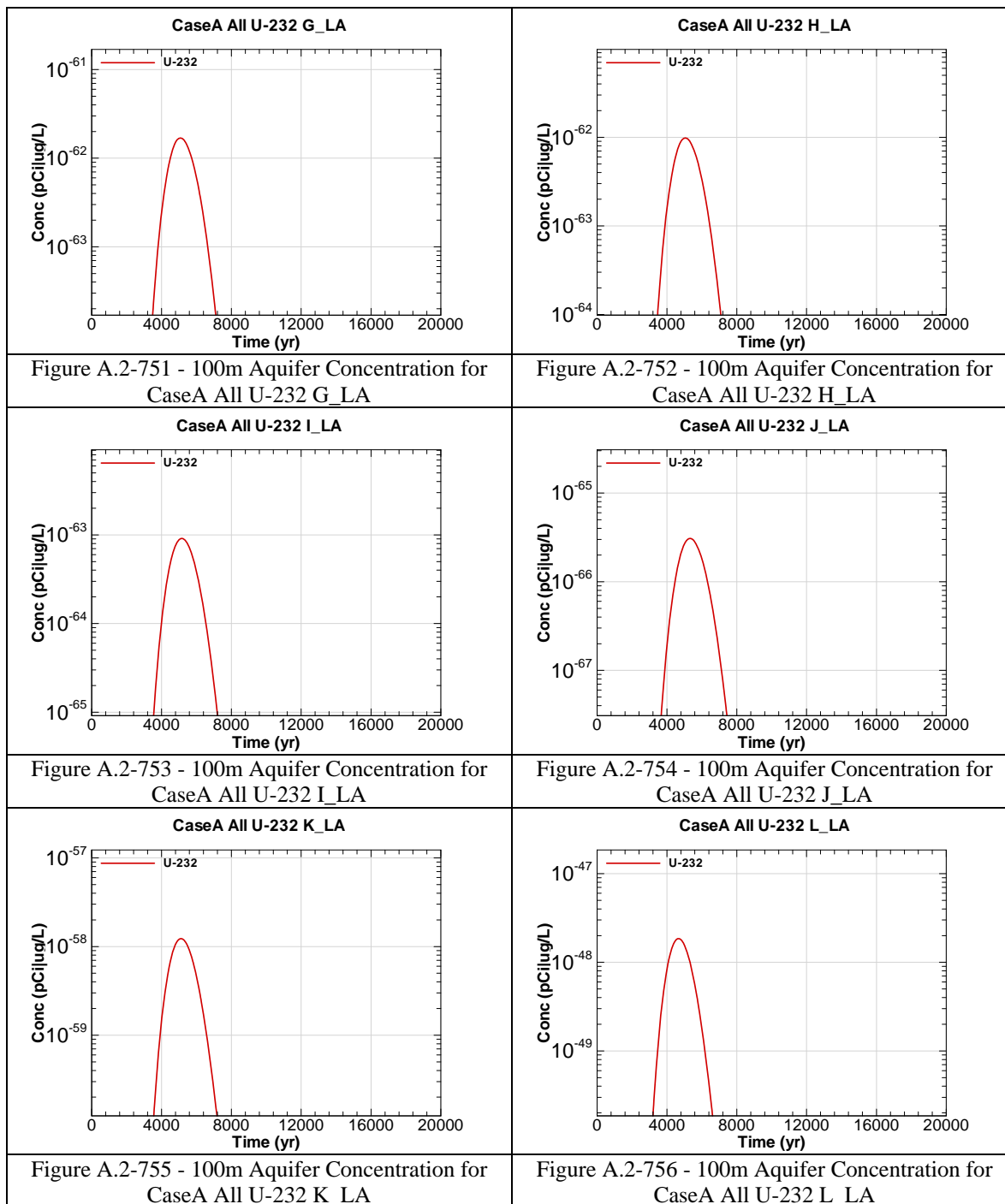


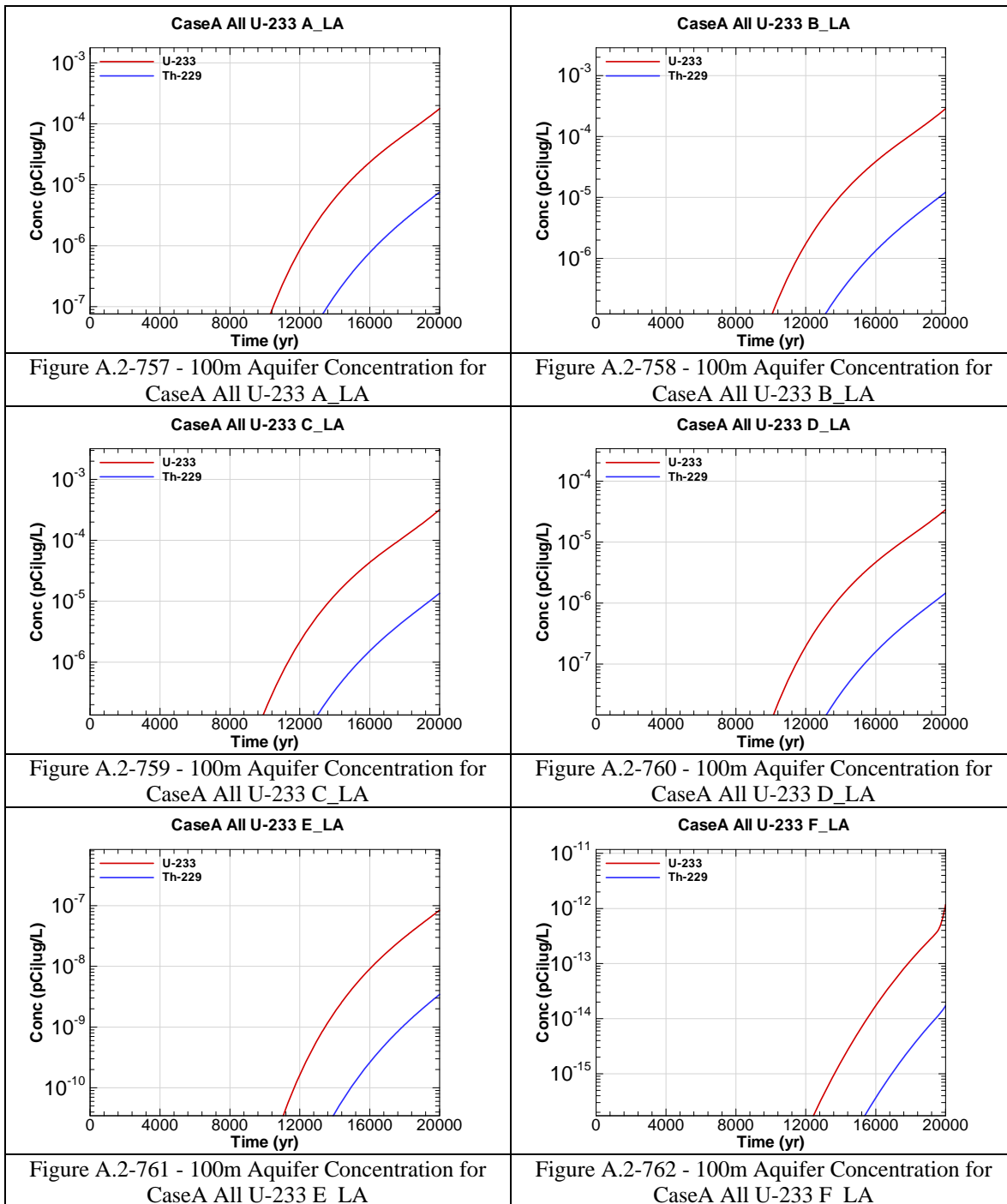
Figure A.2-732 - 100m Aquifer Concentration for
CaseA All Th-230 L_LA

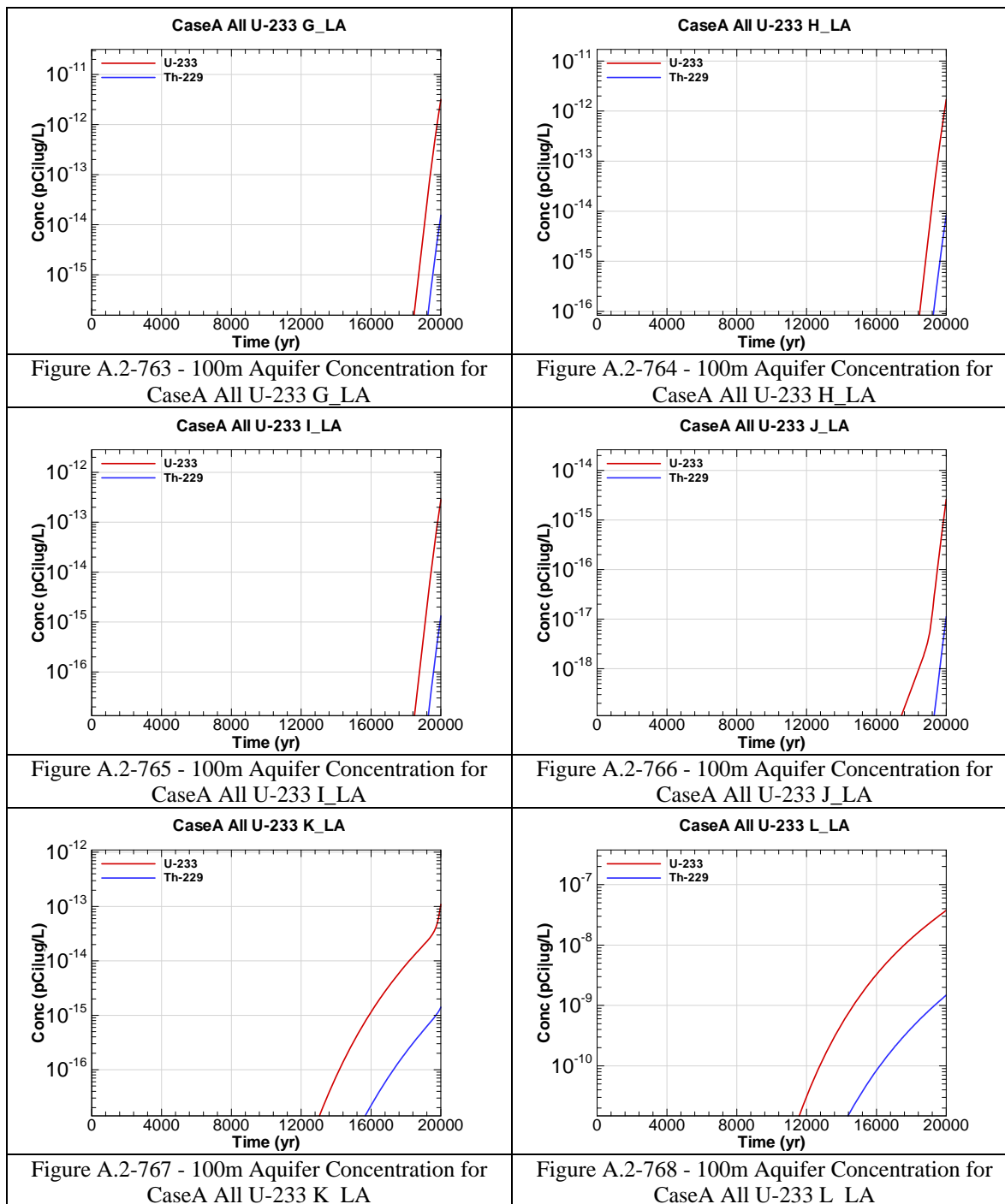


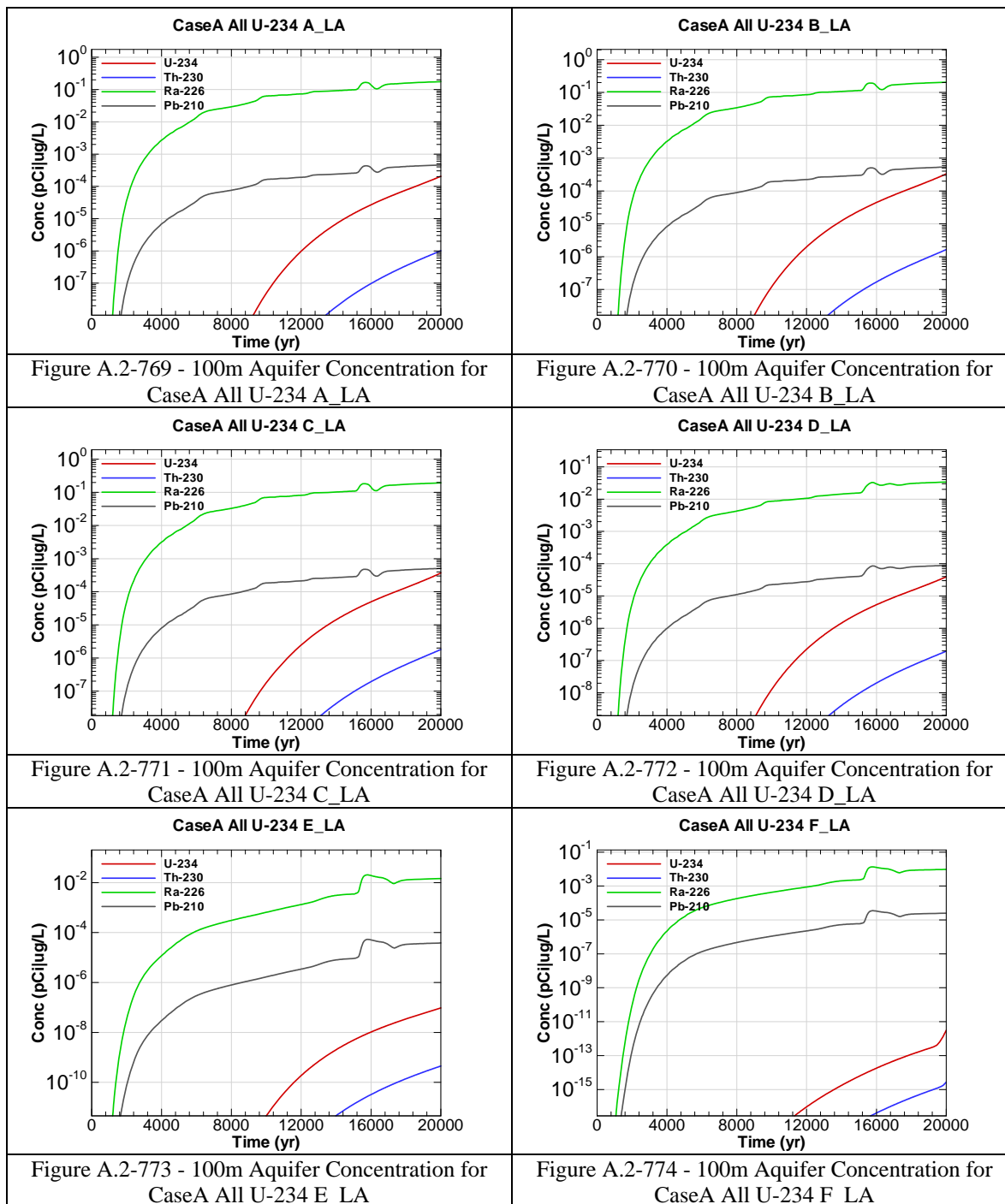












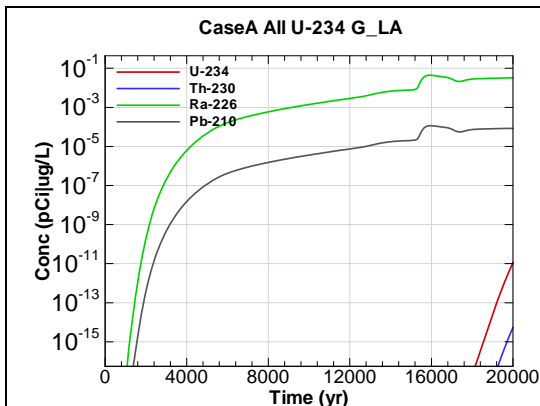


Figure A.2-775 - 100m Aquifer Concentration for
CaseA All U-234 G_LA

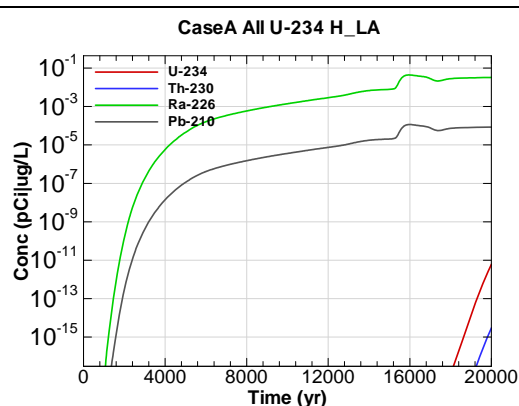


Figure A.2-776 - 100m Aquifer Concentration for
CaseA All U-234 H_LA

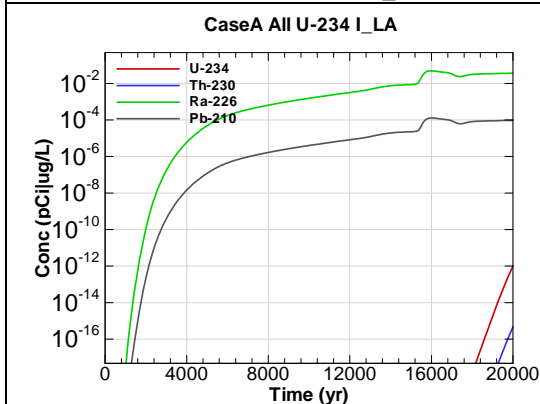


Figure A.2-777 - 100m Aquifer Concentration for
CaseA All U-234 I_LA

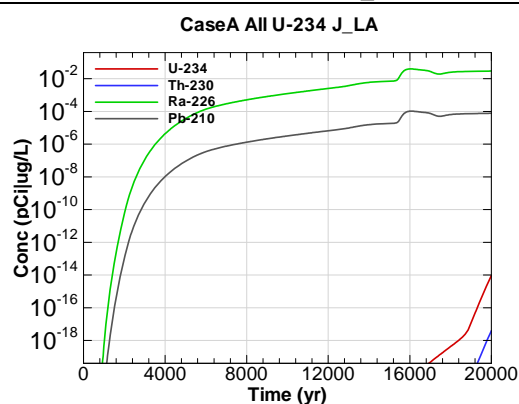


Figure A.2-778 - 100m Aquifer Concentration for
CaseA All U-234 J_LA

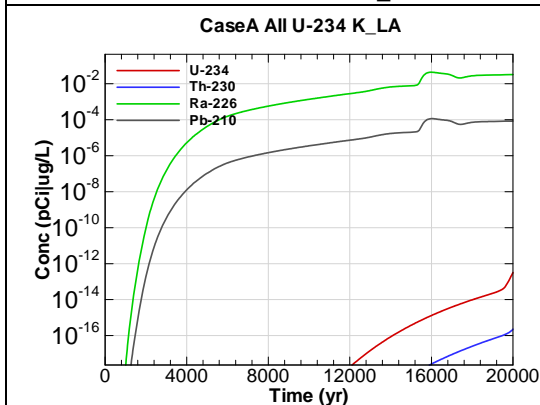


Figure A.2-779 - 100m Aquifer Concentration for
CaseA All U-234 K_LA

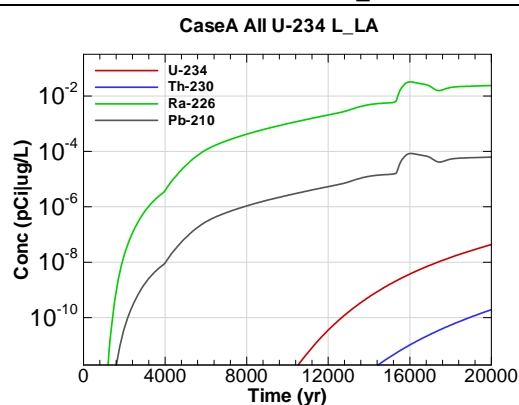
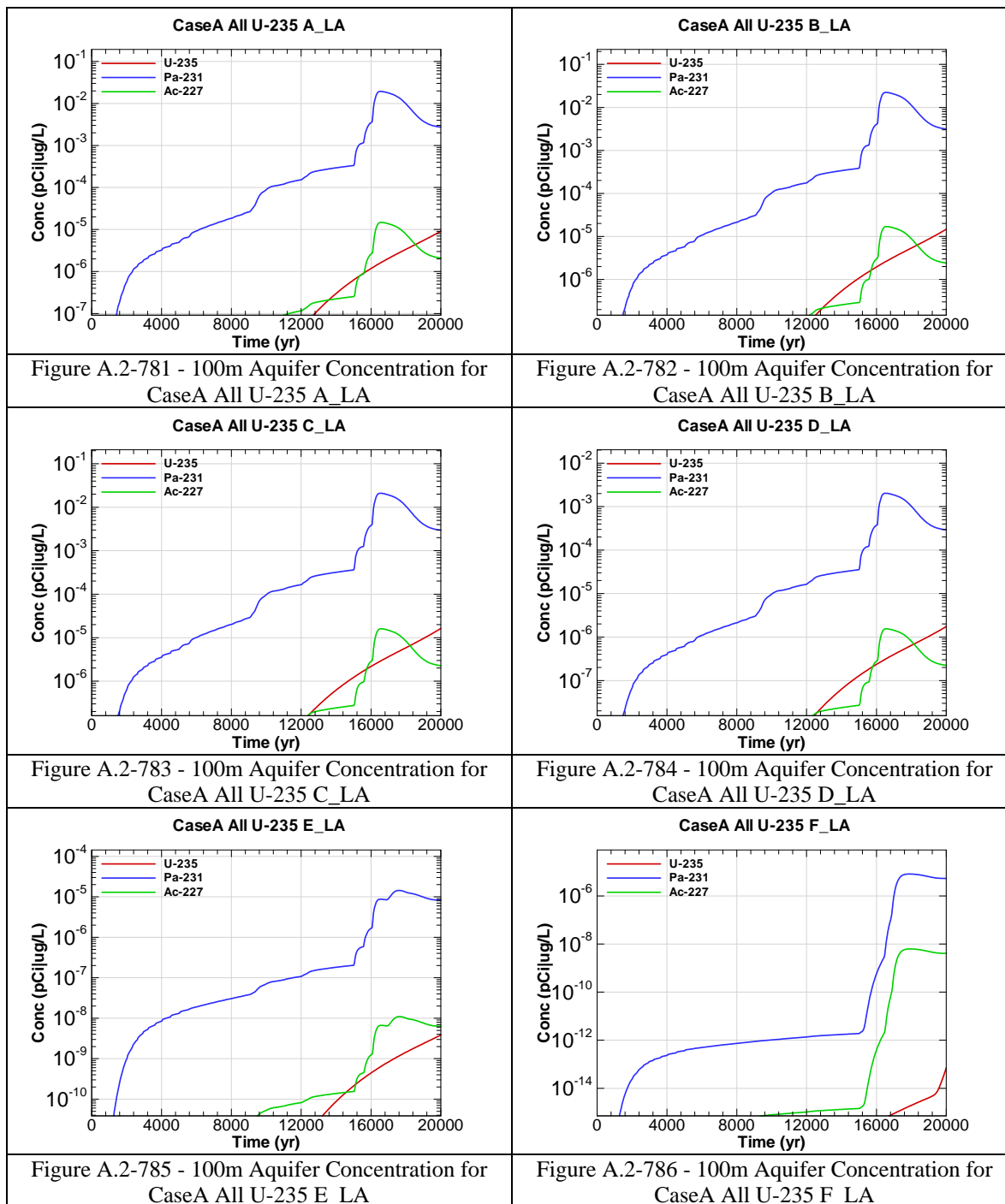
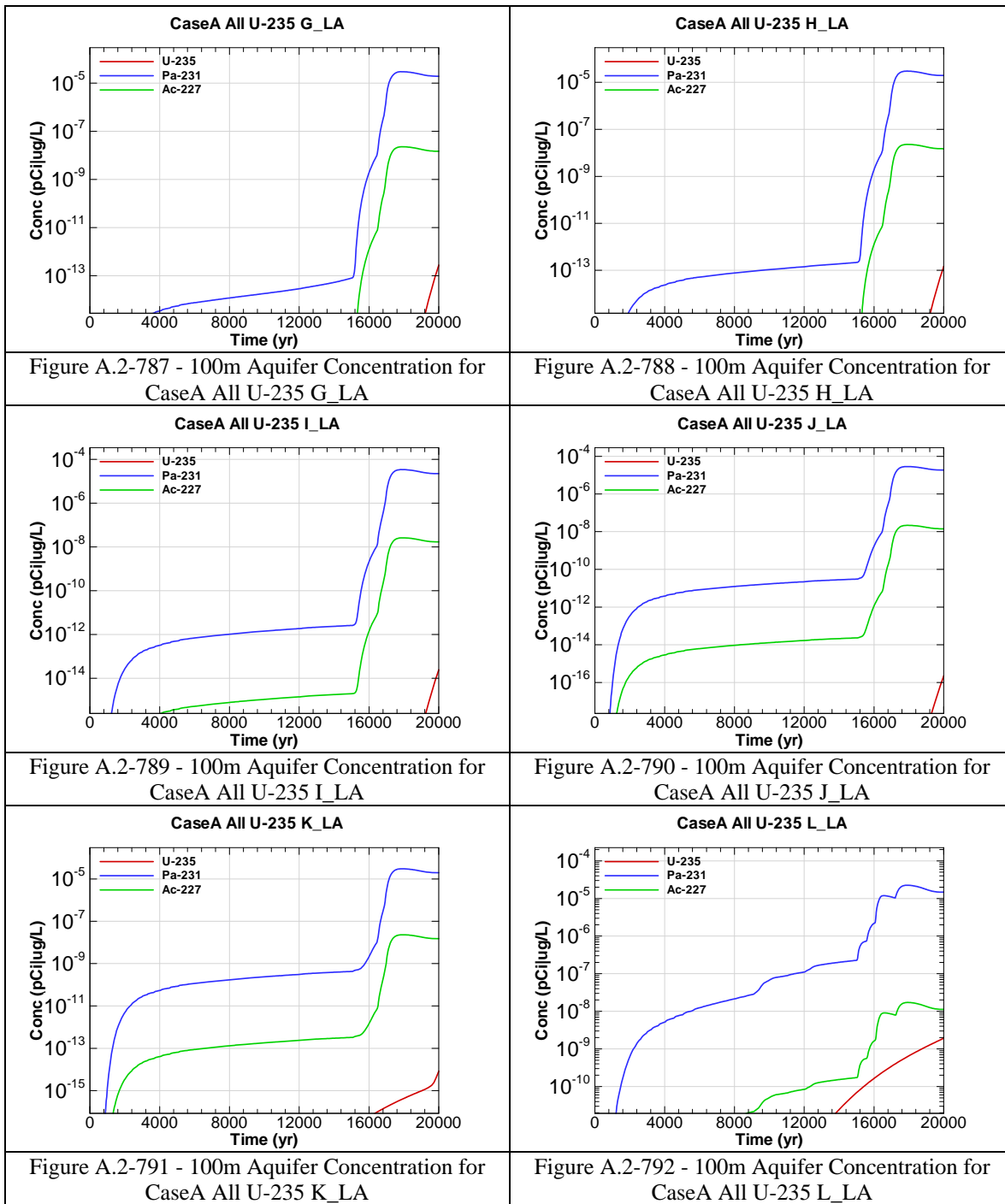
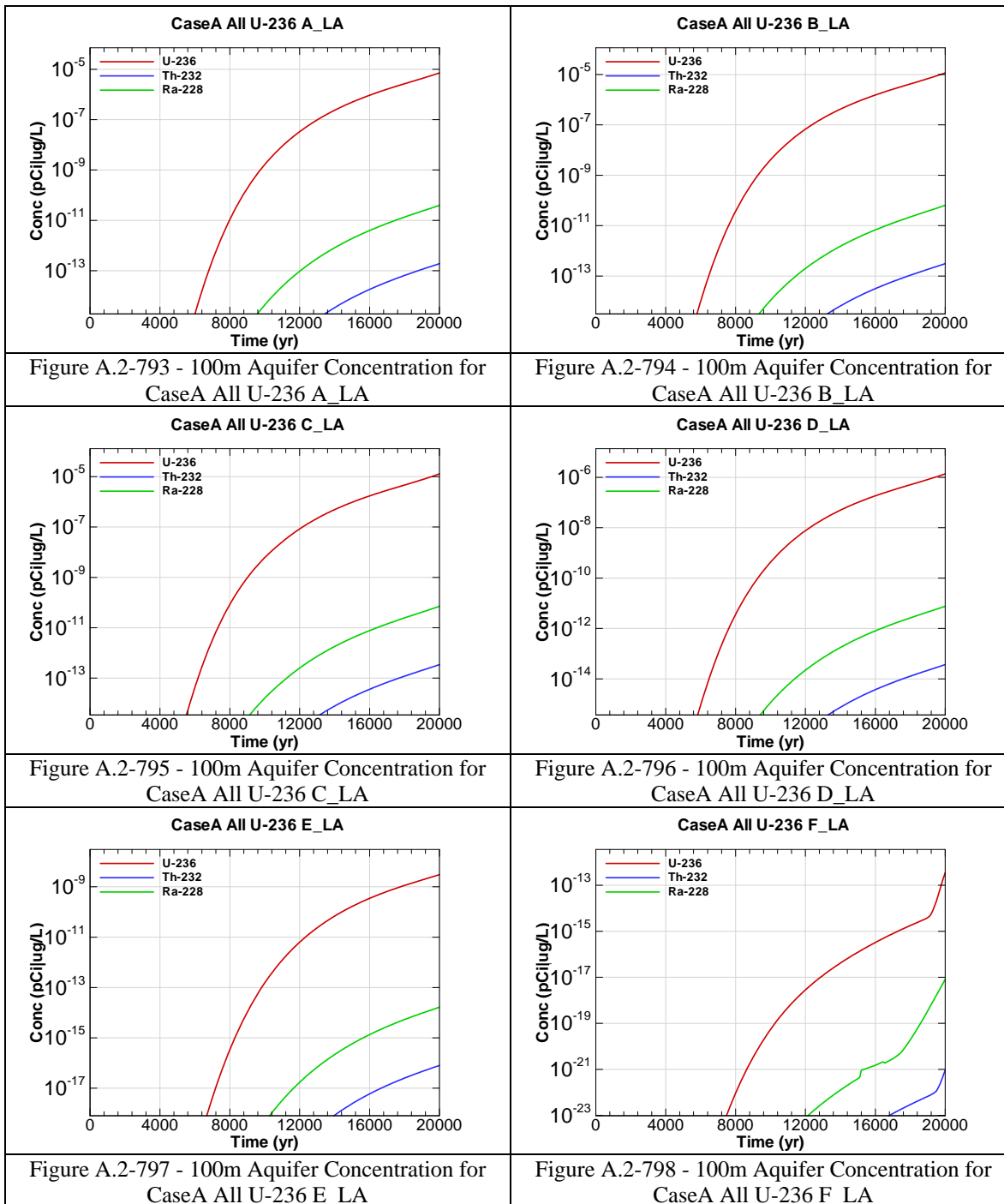
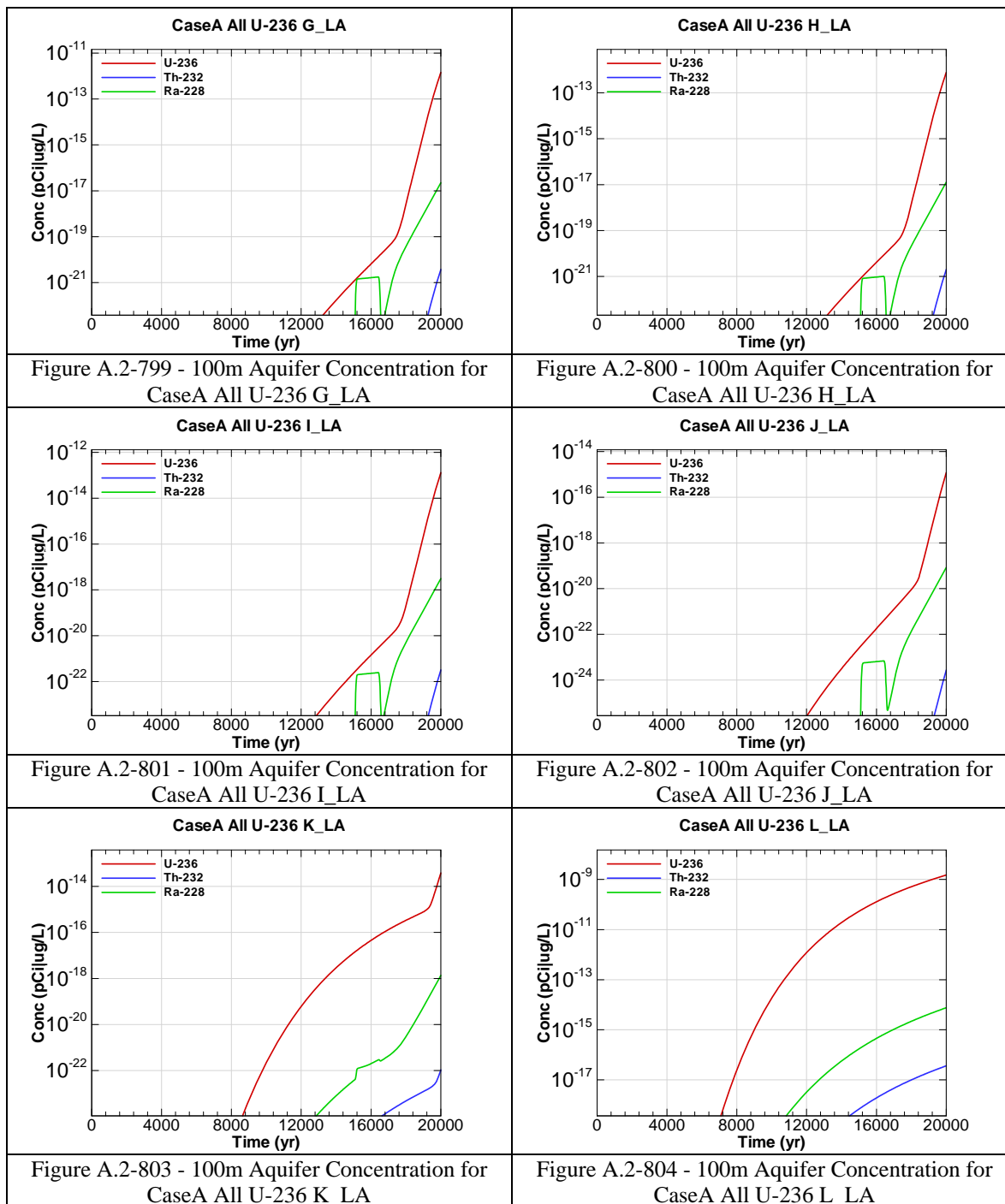


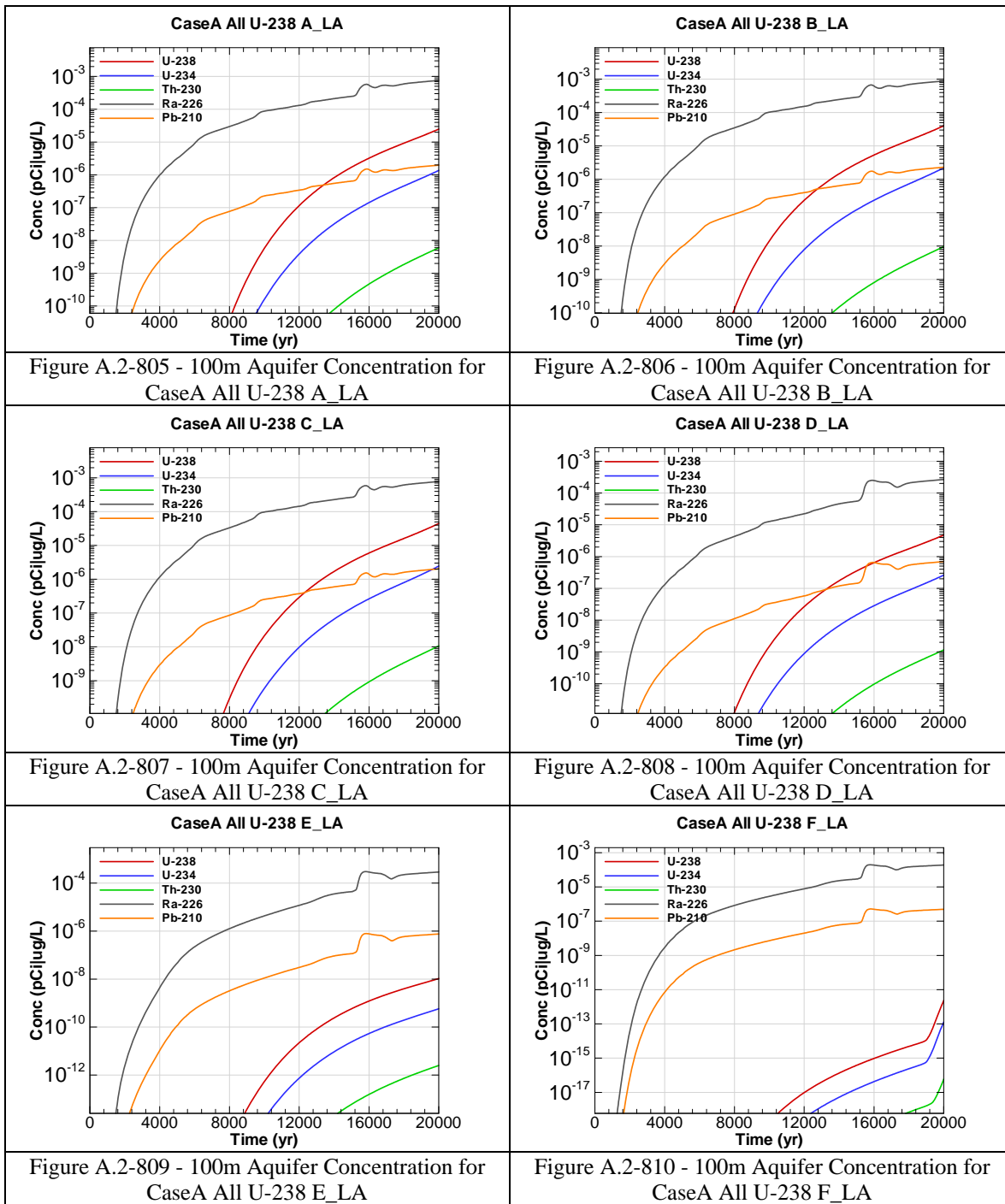
Figure A.2-780 - 100m Aquifer Concentration for
CaseA All U-234 L_LA

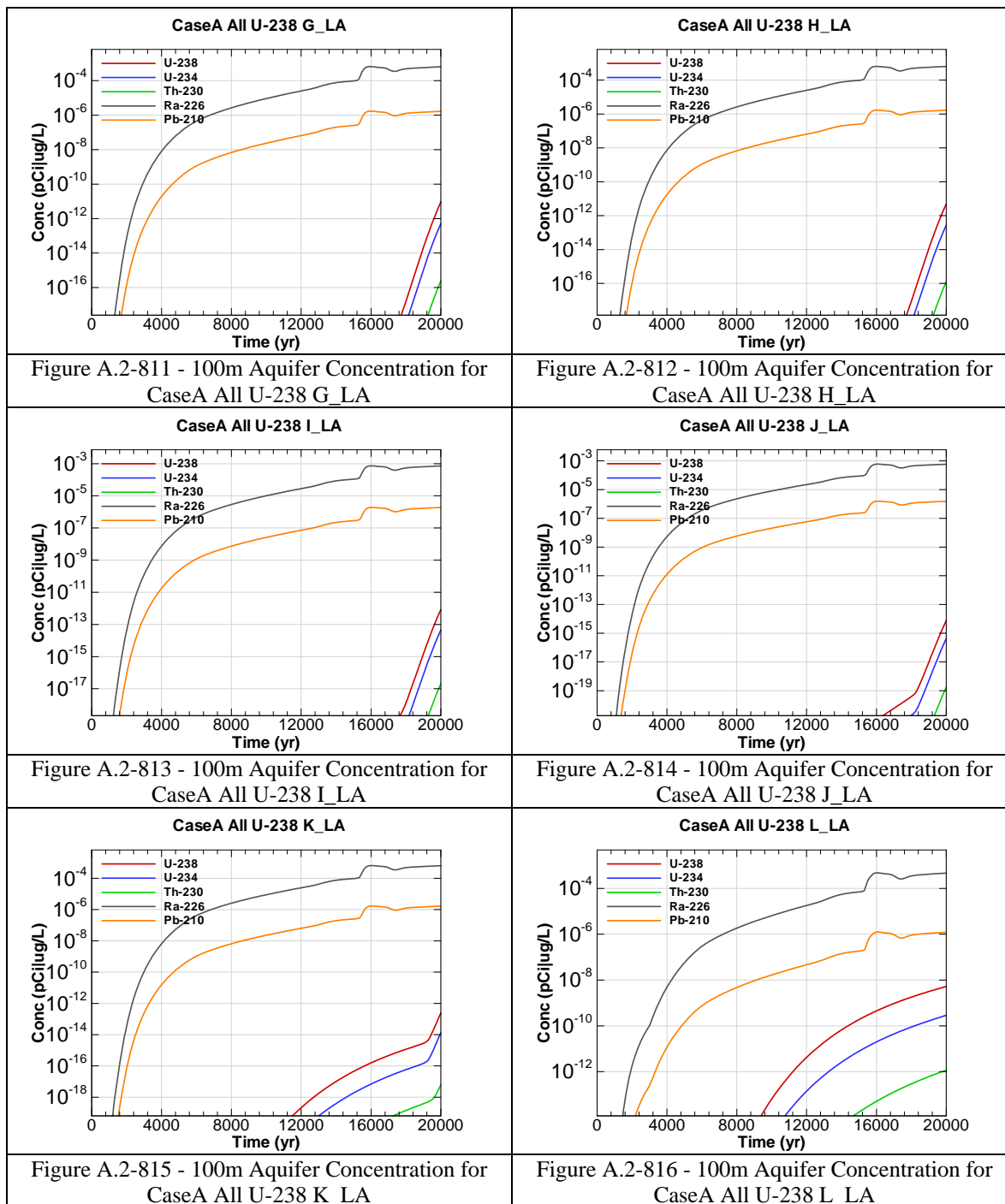


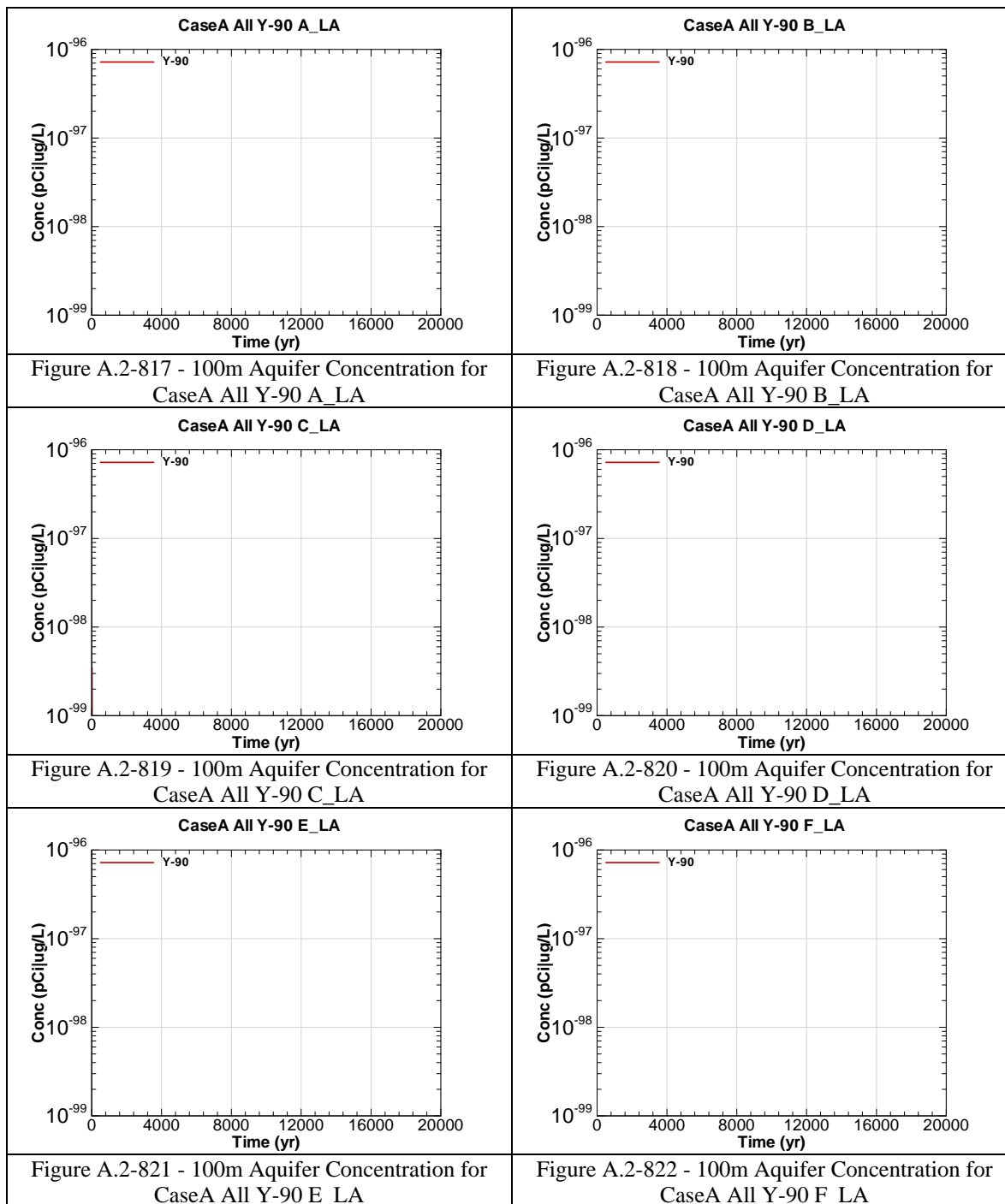


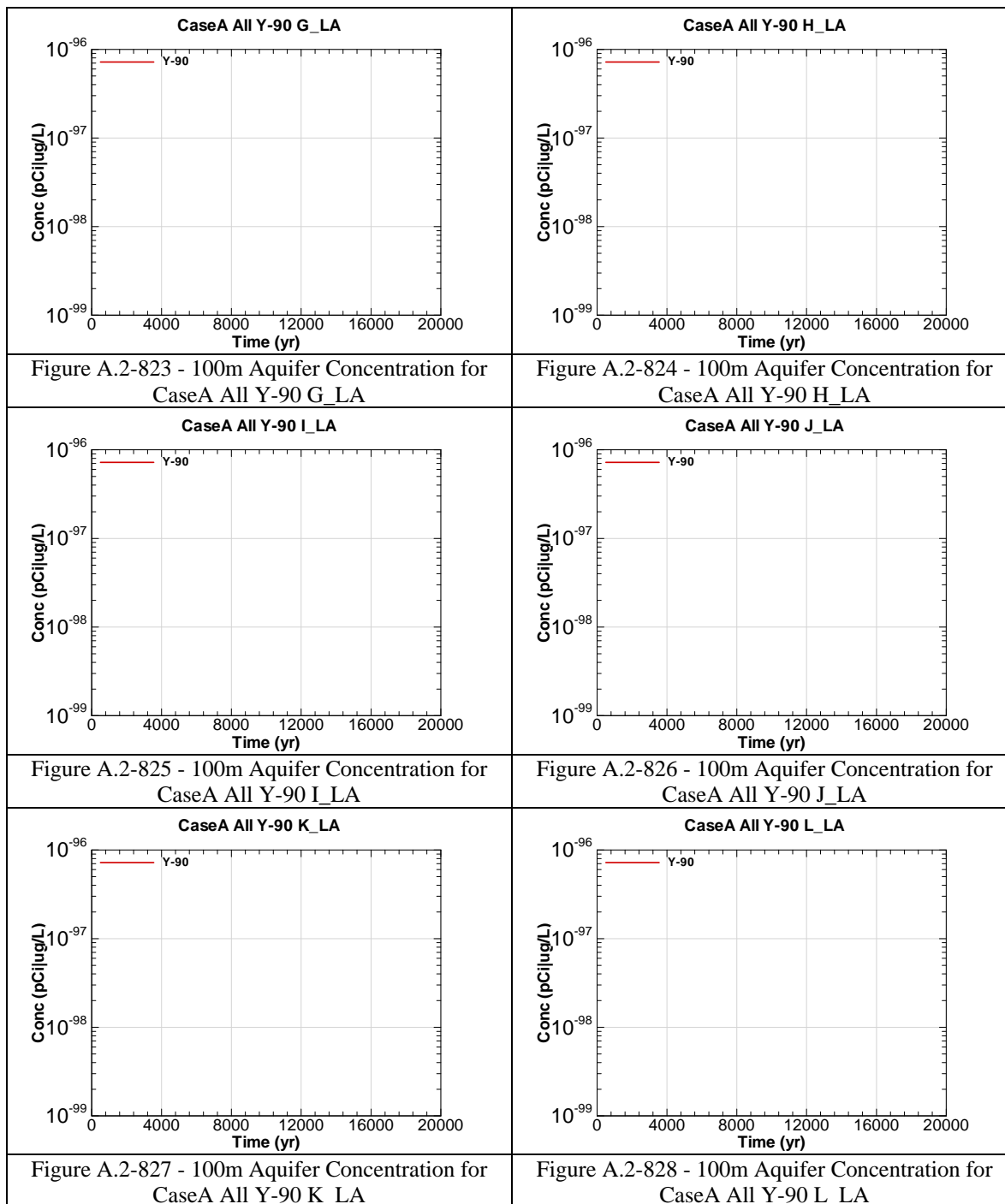


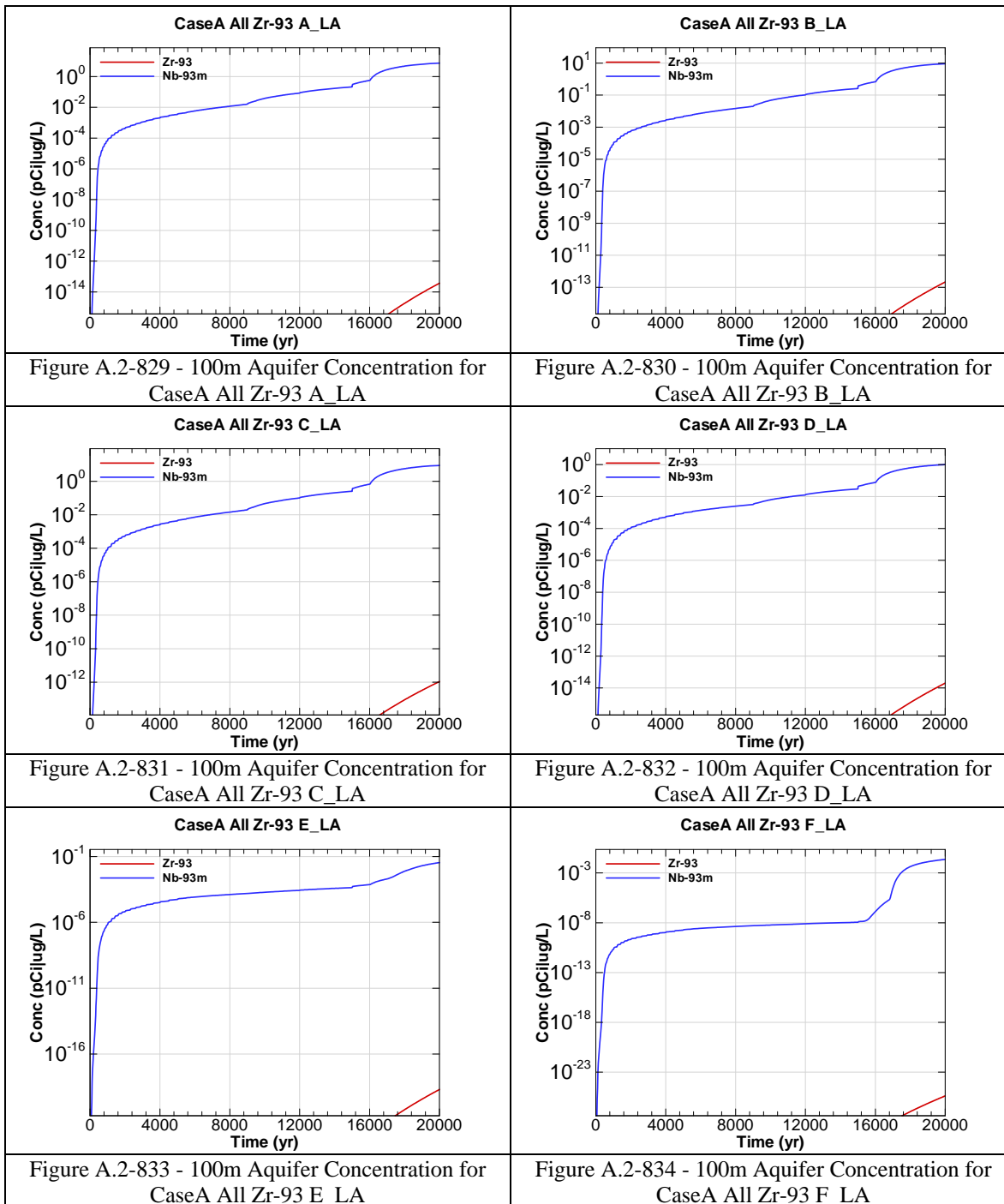


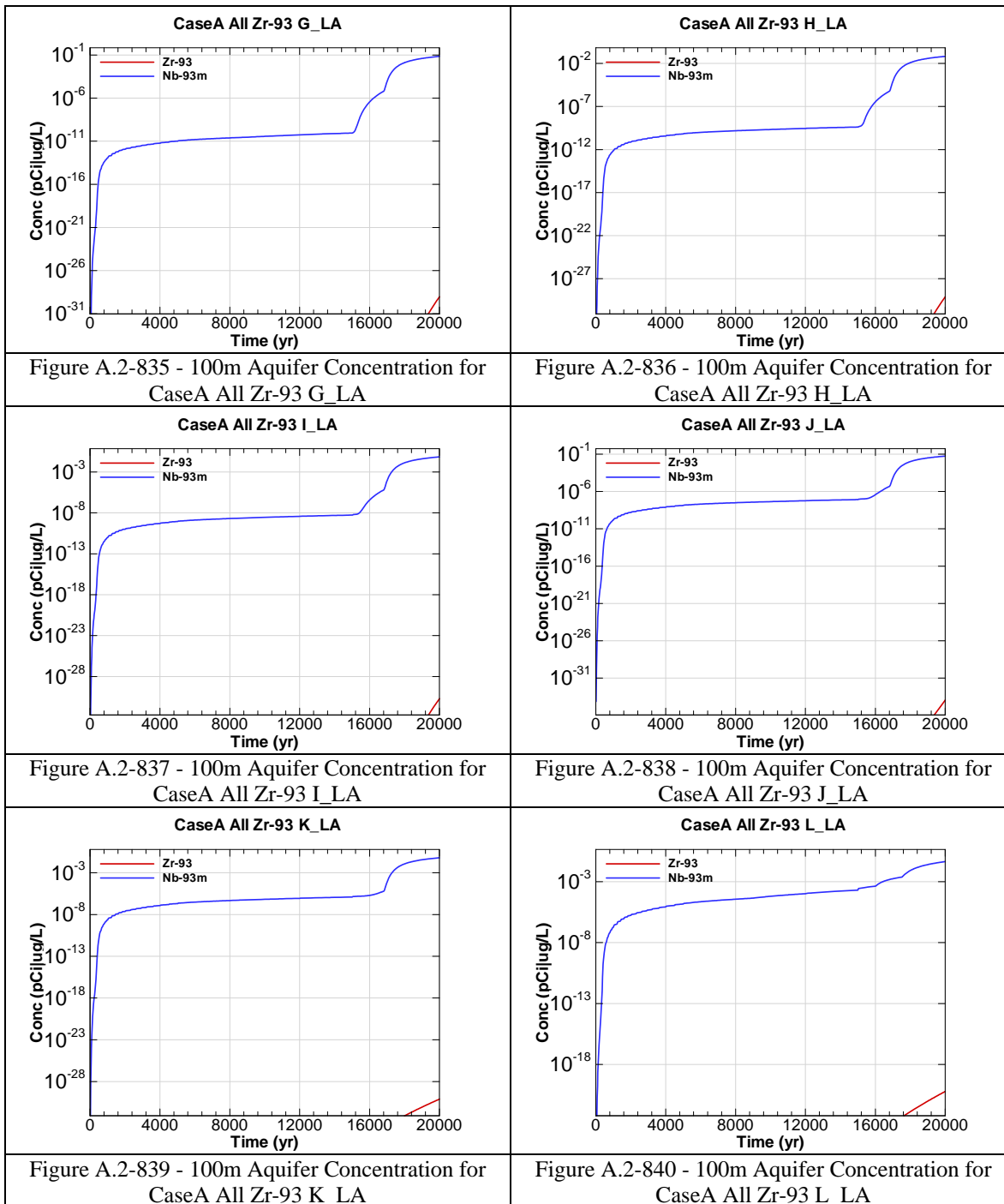






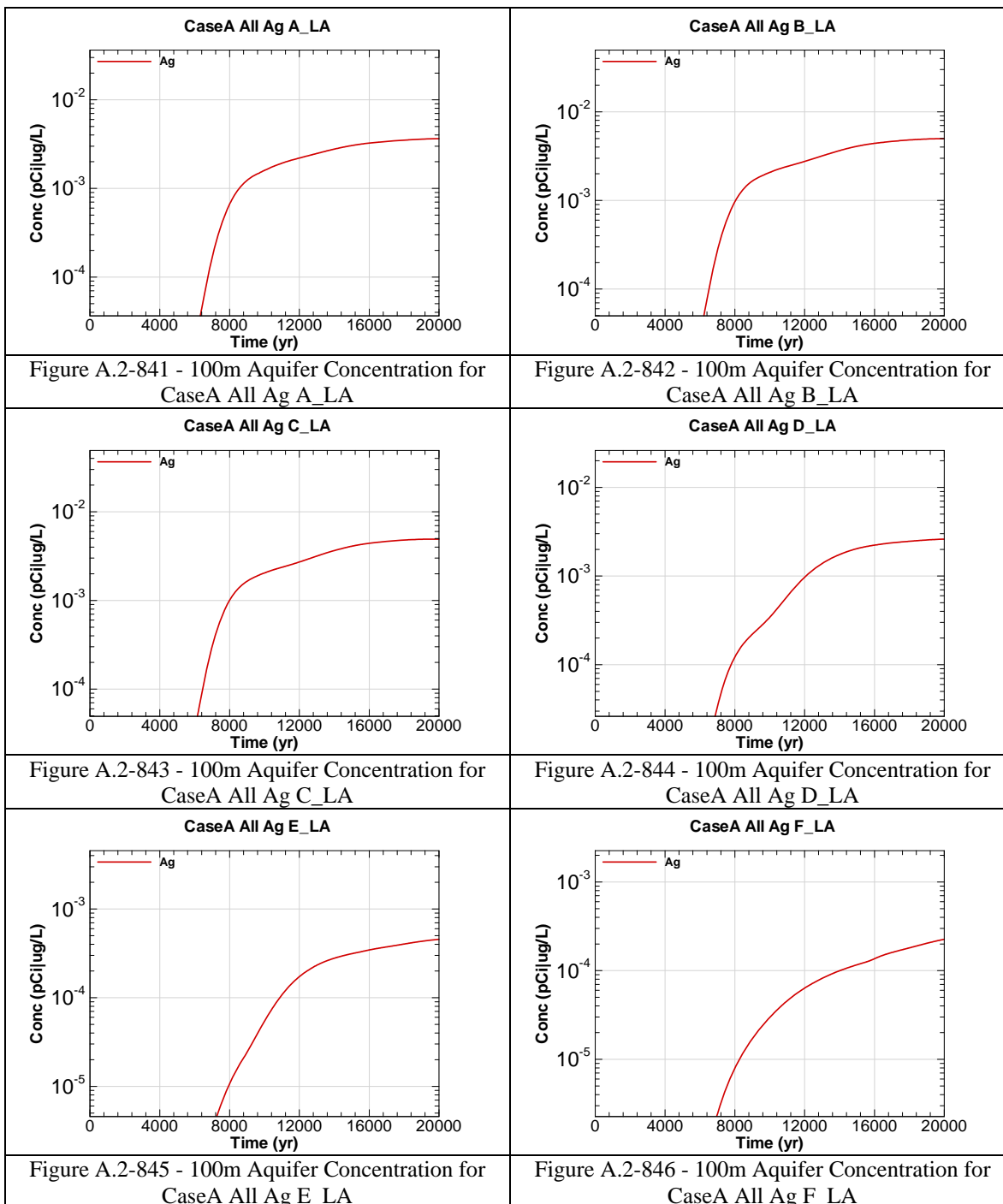


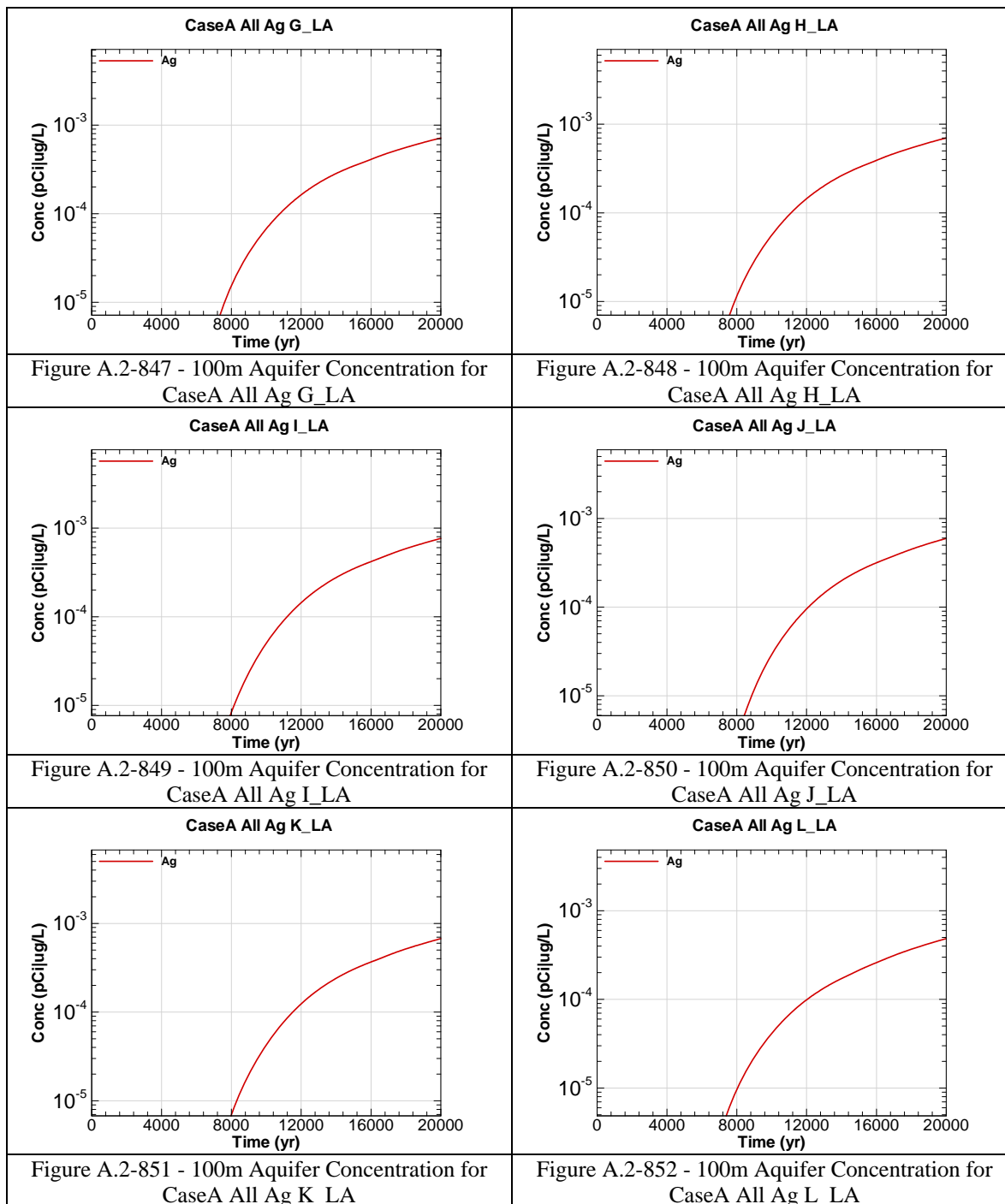


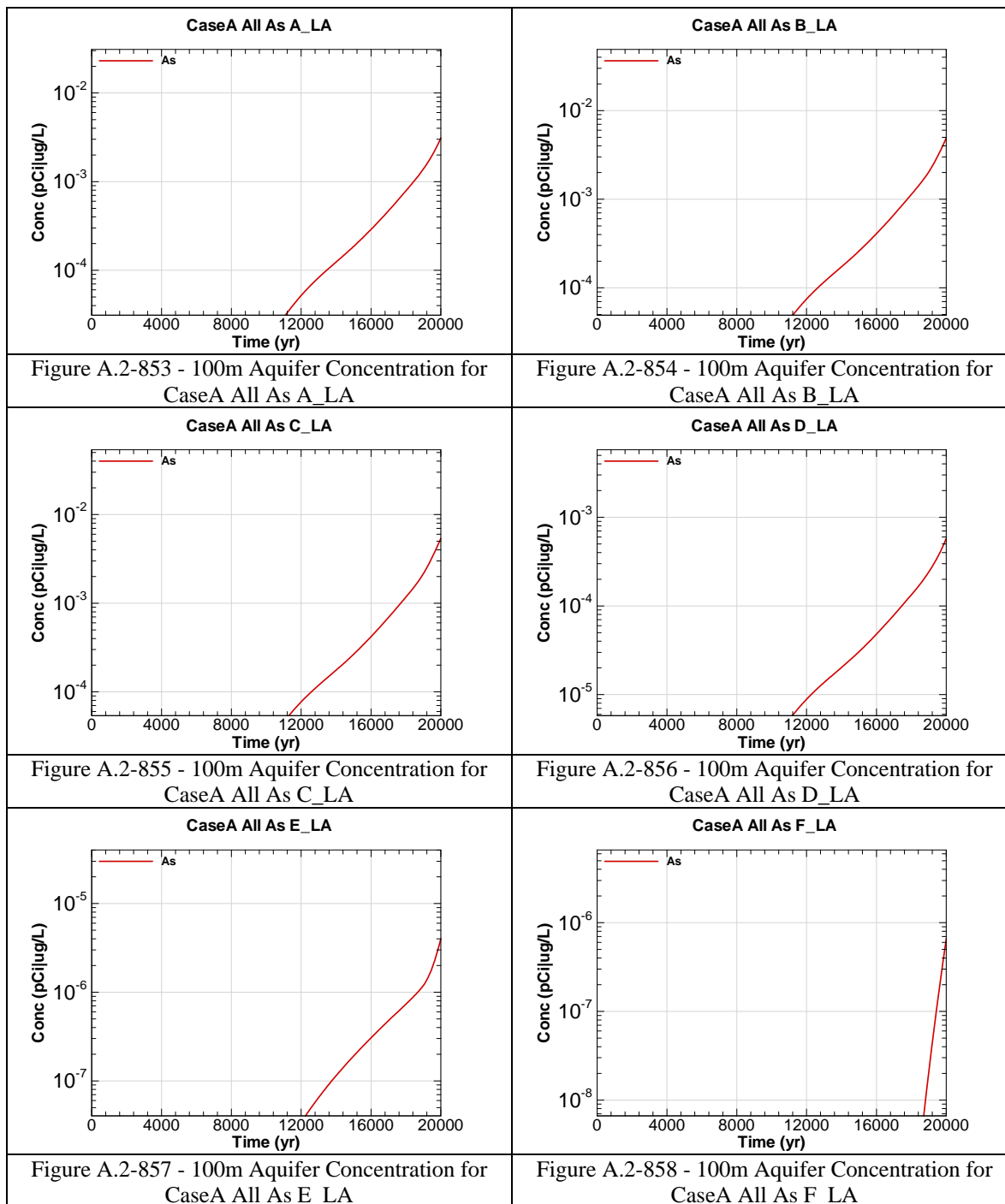


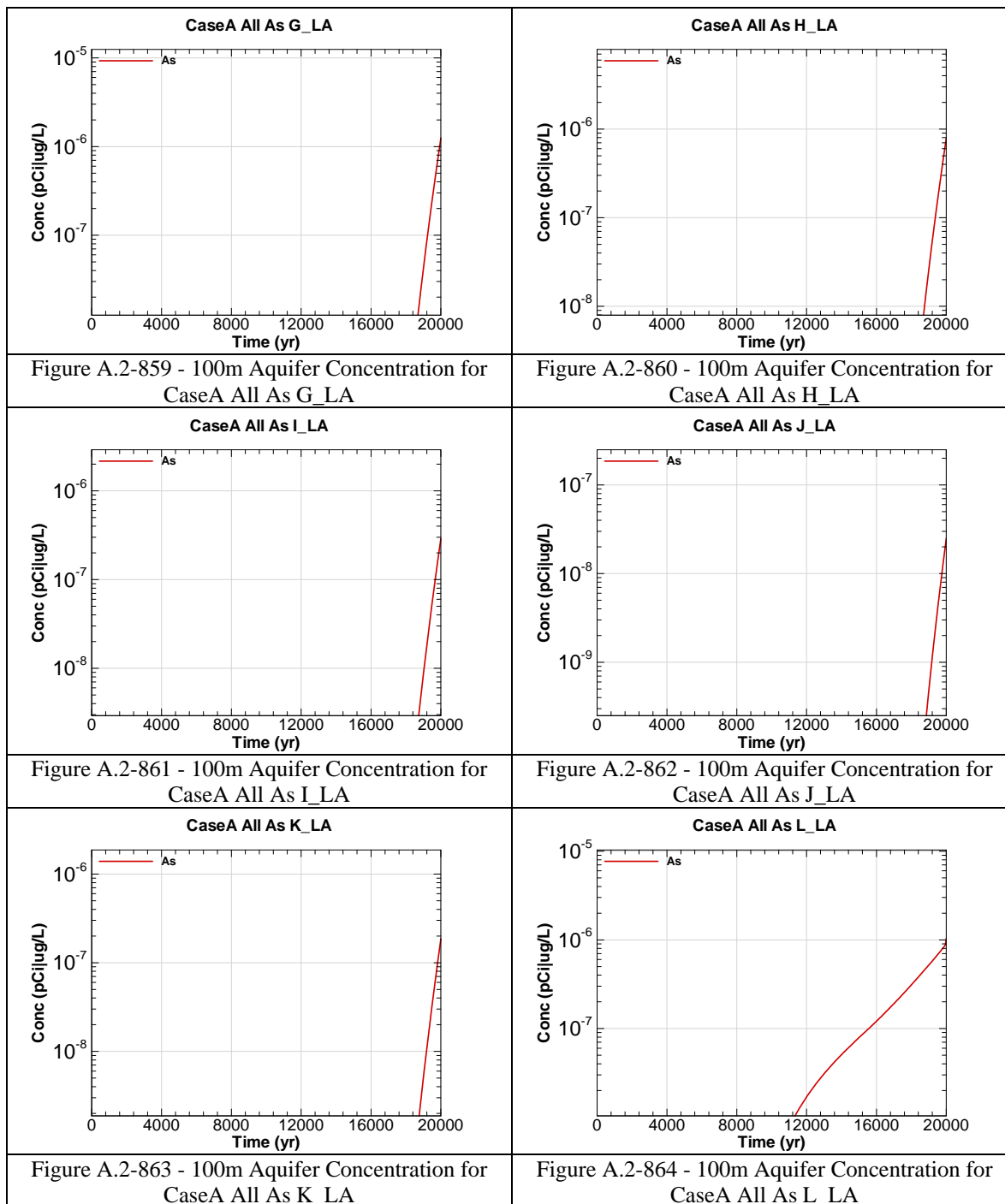
The chemical contaminants were modeled prior to the revision of the final closure inventory calculations presented in Table 3.3-8 for five chemical components: As, Cr, Cu, N and U. The figures that follow represent the concentrations calculated with an initial inventory input. The multipliers in the table below are to be used to determine the final concentrations with respect to time for the impacted chemicals as the inventory has a linear relationship with concentration in the Saltstone model. The groundwater concentration tables in Section 5 have been corrected using the multipliers.

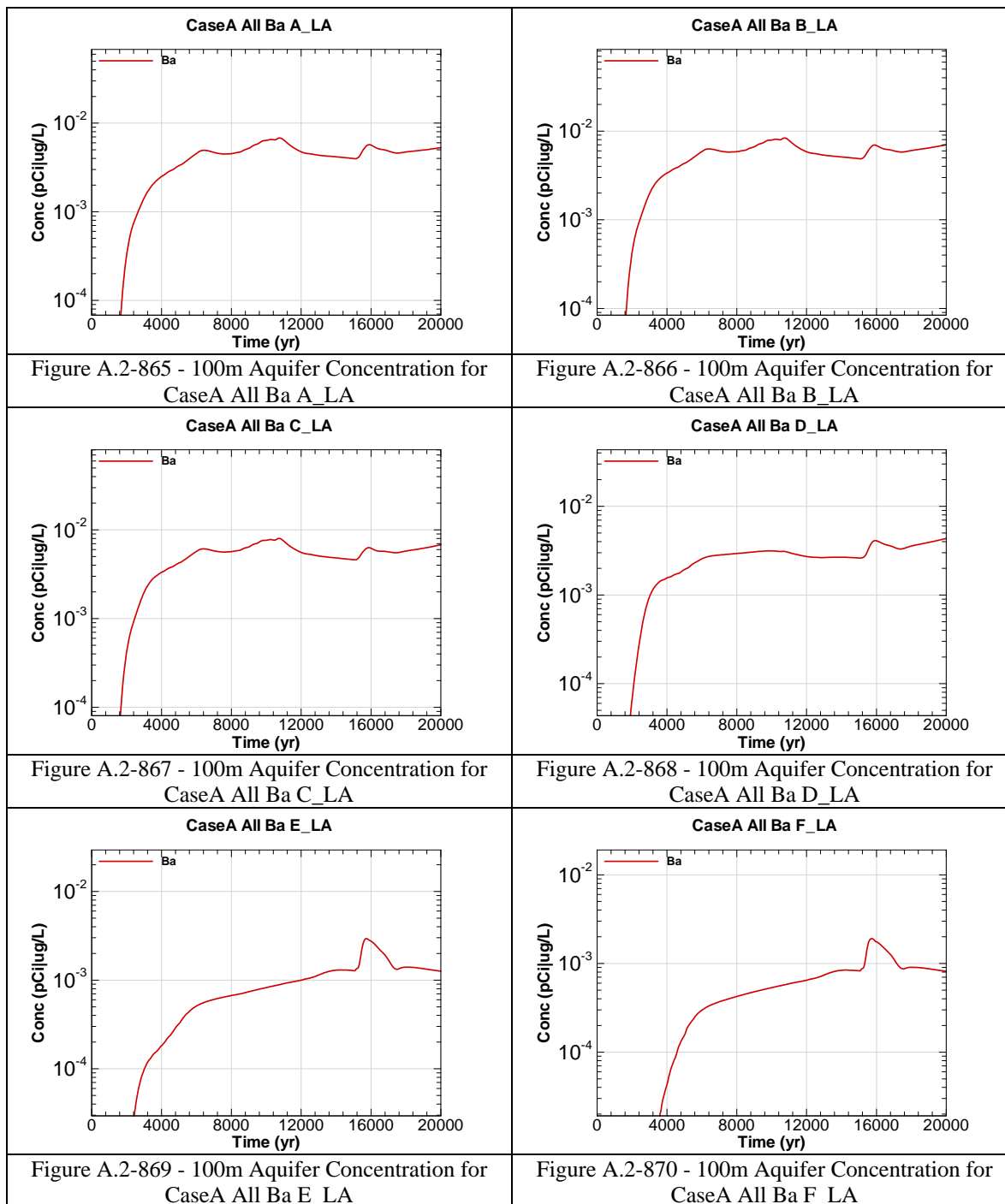
| Chemical Component | Modeled Inventory | Projected Inventory | Percent Increase | Multiplier |
|---------------------------|--------------------------|----------------------------|-------------------------|-------------------|
| Ag | 8.8E+01 | 8.8E+01 | 0.0% | None |
| As | 1.08E+04 | 1.1E+04 | 2.3% | 1.02E+00 |
| Ba | 1.7E+02 | 1.7E+02 | 0.0% | None |
| Cd | 1.3E+03 | 1.3E+03 | 0.0% | None |
| Cr | 2.9E+04 | 3.0E+04 | 1.4% | 1.01E+00 |
| Cu | 1.9E+04 | 1.9E+04 | 0.9% | 1.01E+00 |
| F | 1.7E+04 | 1.7E+04 | 0.0% | None |
| Fe | 2.9E+03 | 2.9E+03 | 0.0% | None |
| Hg | 1.1E+04 | 1.1E+04 | 0.0% | None |
| Mn | 7.3E+03 | 7.3E+03 | 0.0% | None |
| Ni | 1.5E+03 | 1.5E+03 | 0.0% | None |
| Total N | 2.2E+07 | 2.4E+07 | 5.8% | 1.06E+00 |
| Pb | 6.7E+03 | 6.7E+03 | 0.0% | None |
| Se | 4.0E+04 | 4.0E+04 | 0.0% | None |
| U | 8.2E+02 | 8.9E+02 | 8.9% | 1.10E+00 |
| Zn | 2.7E+04 | 2.7E+04 | 0.0% | None |

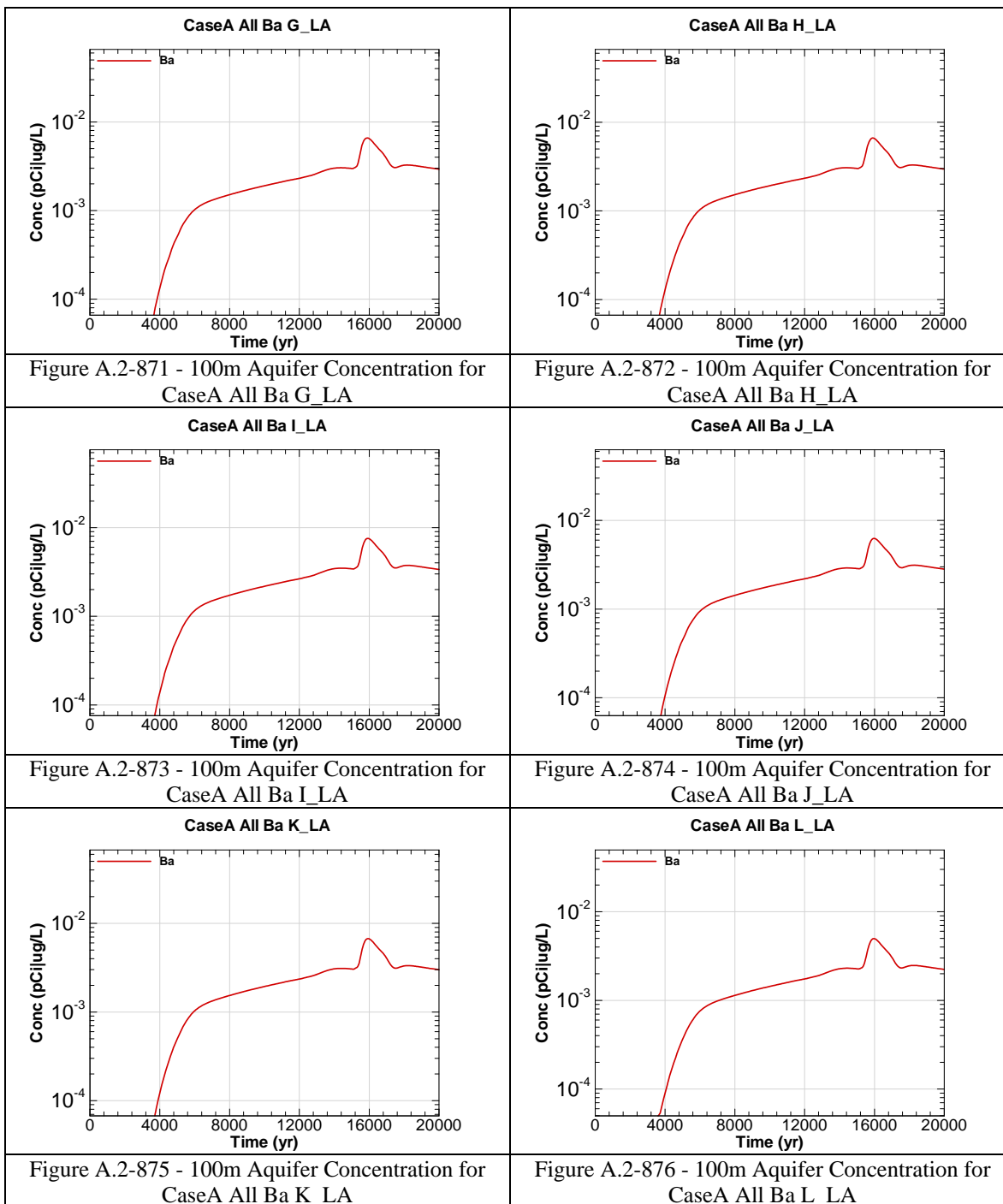


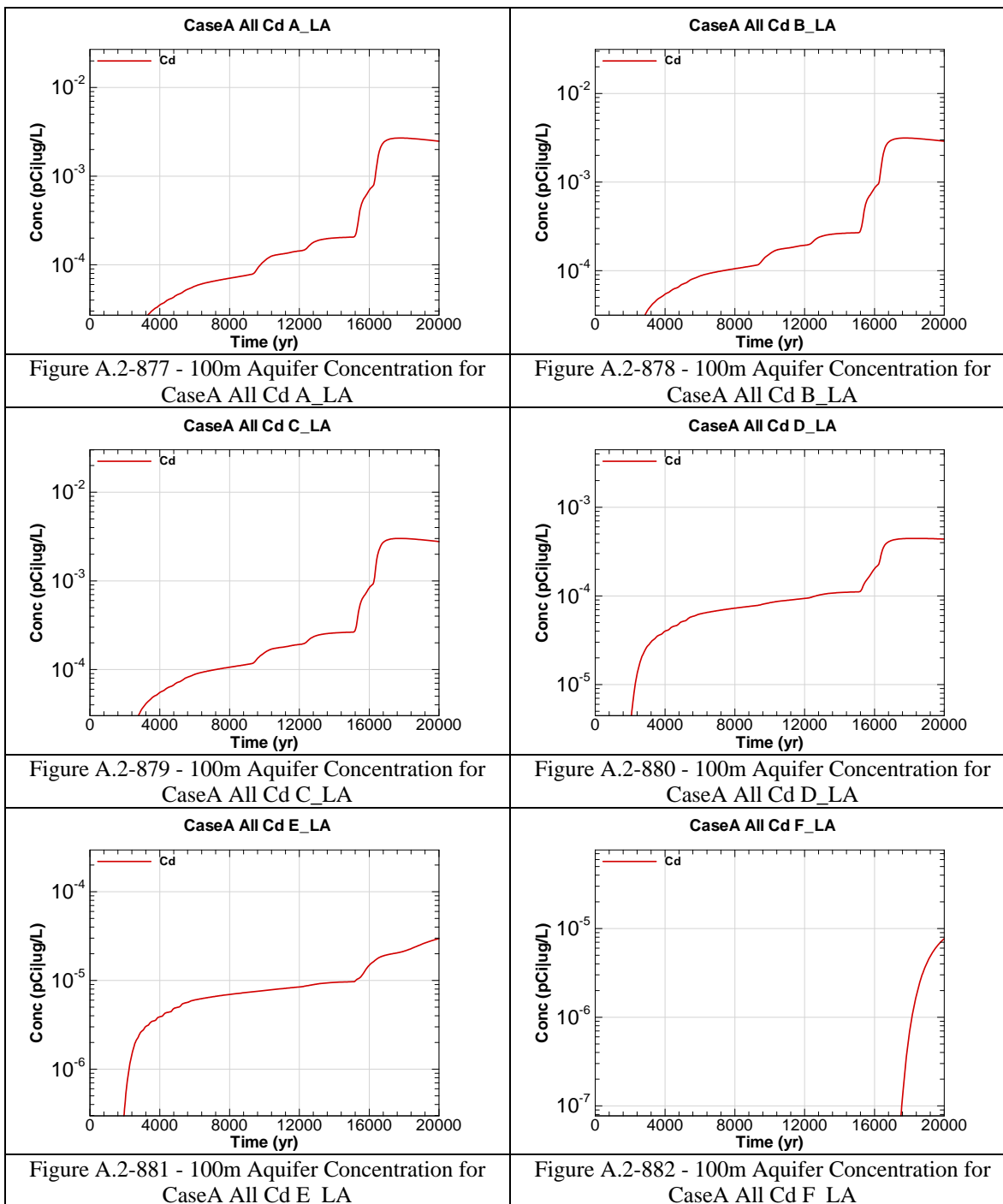


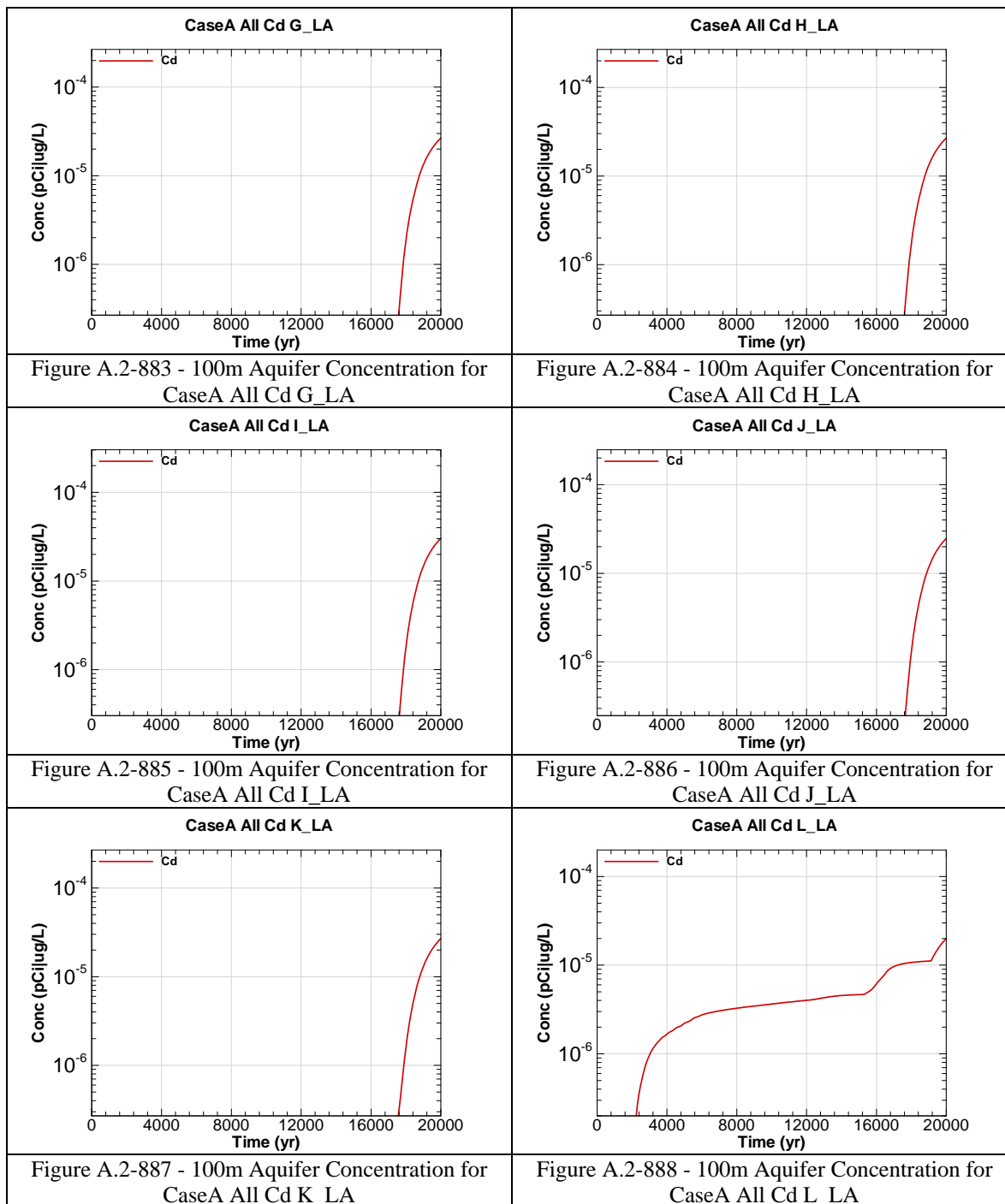


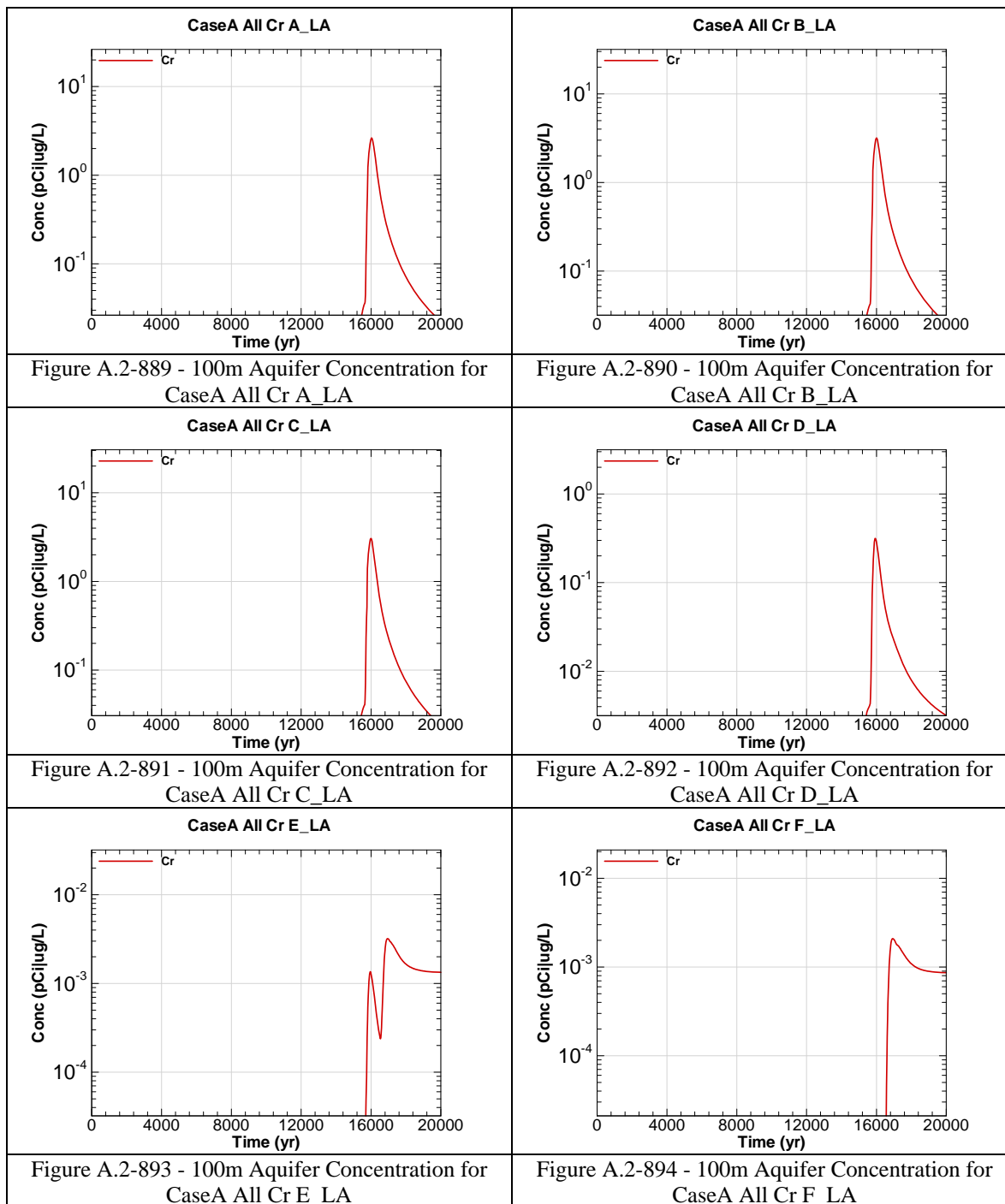


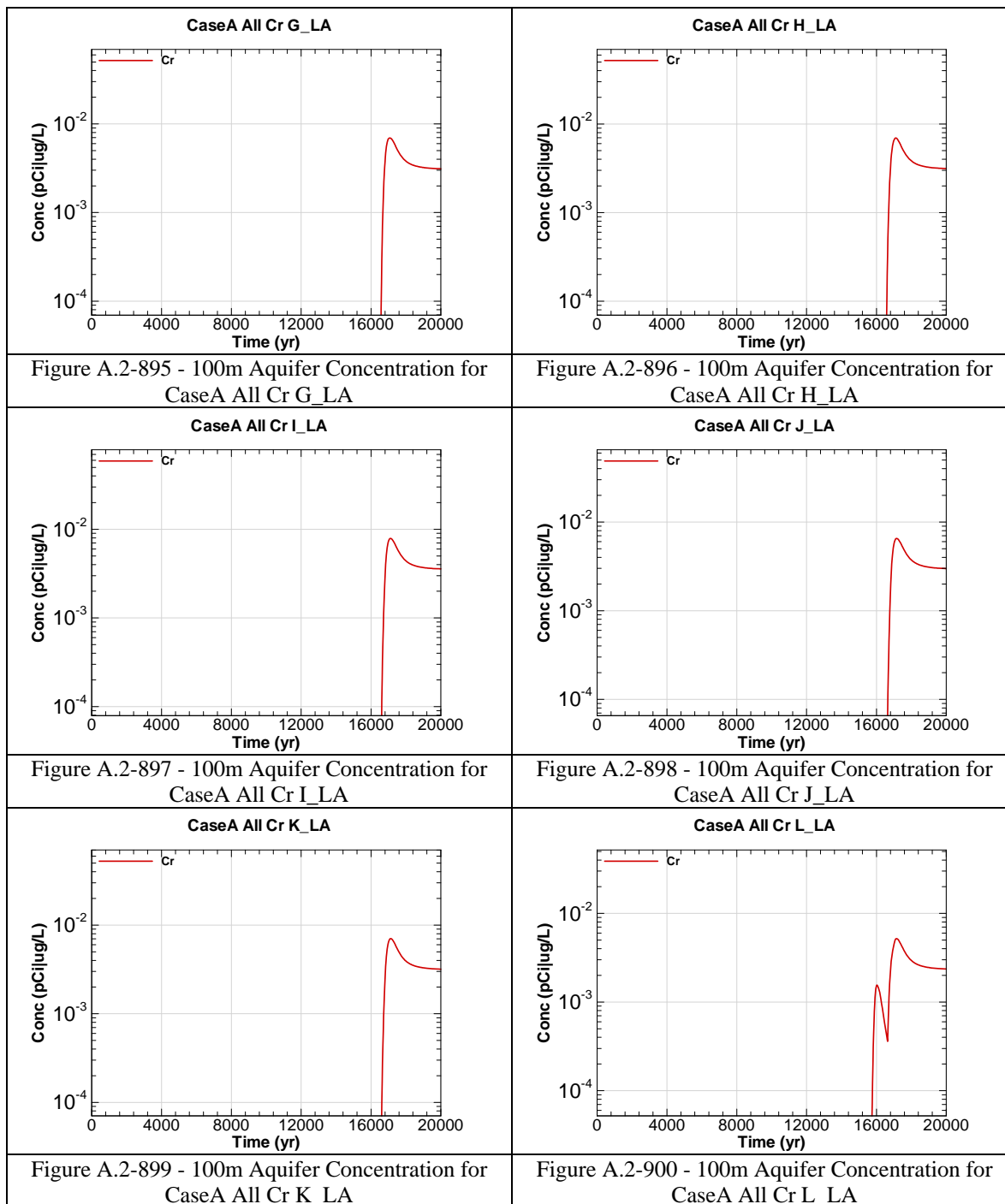


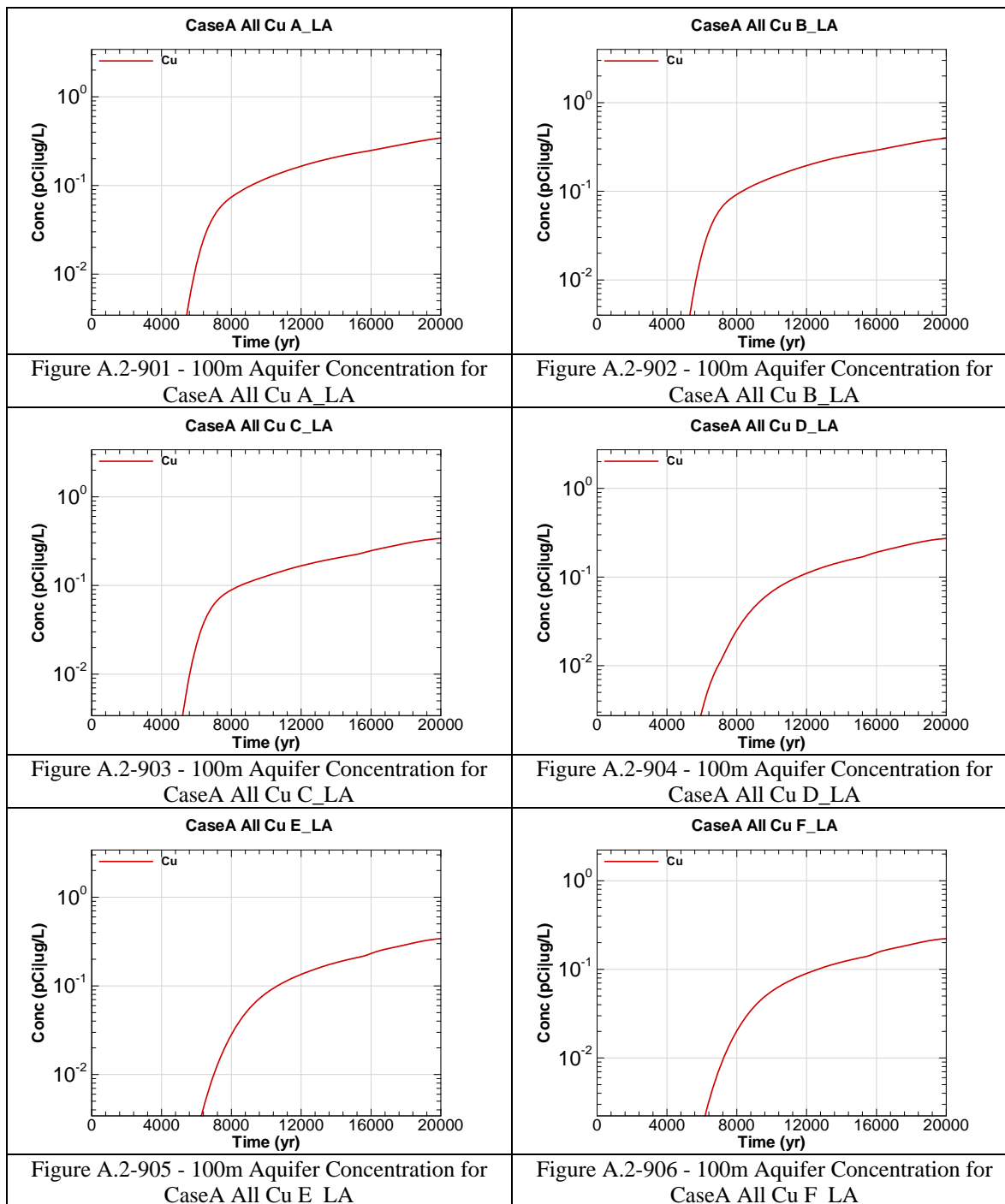


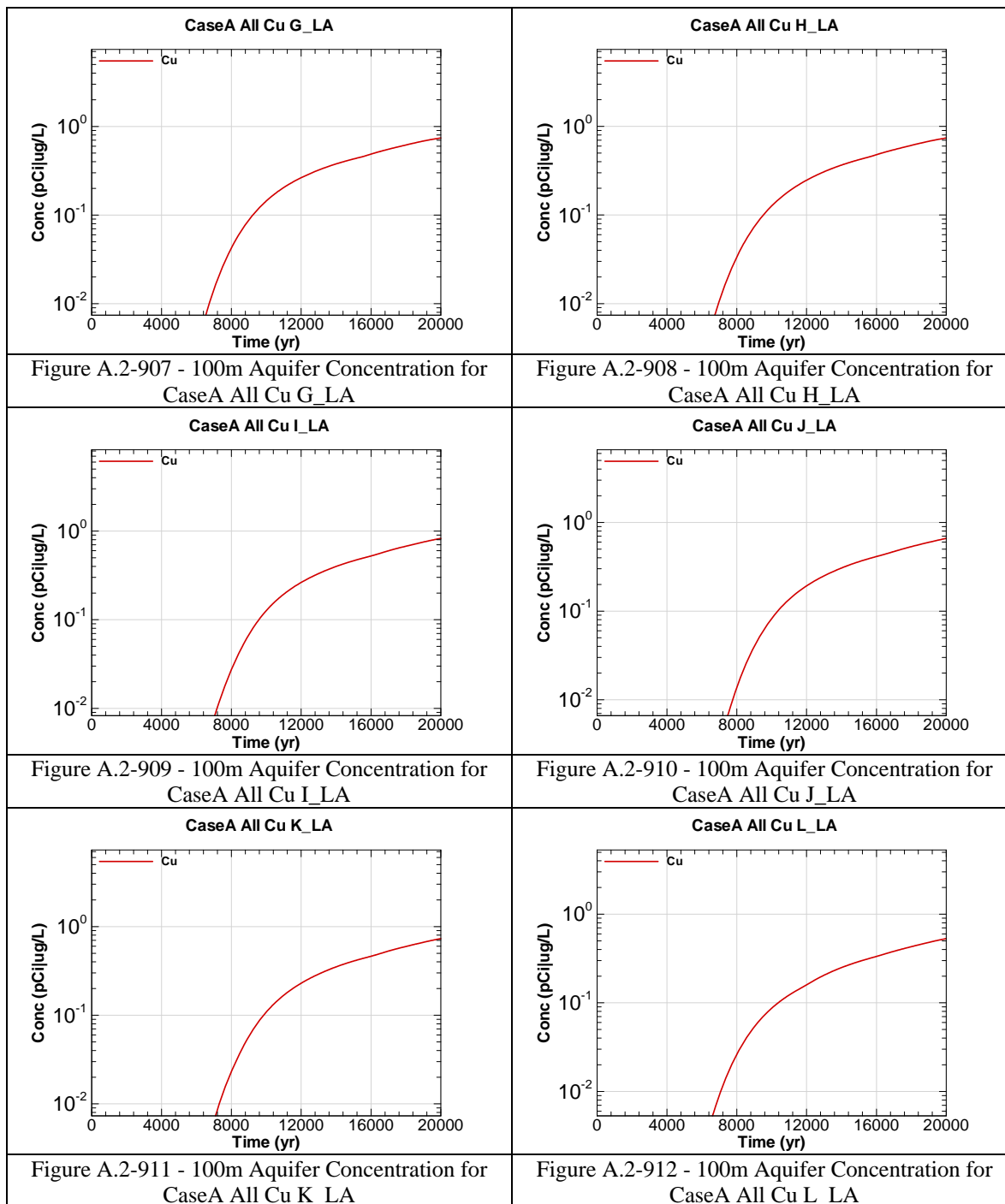


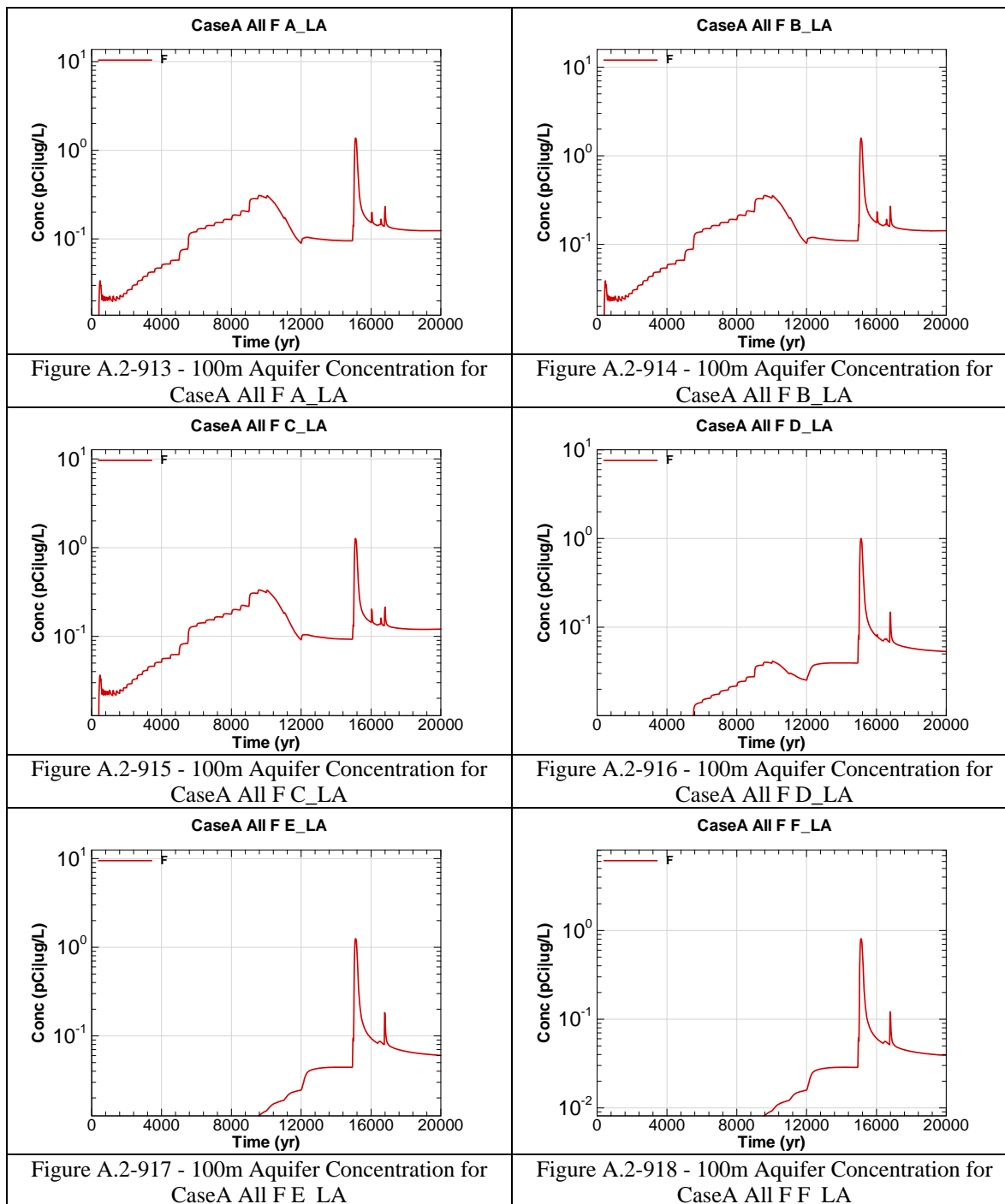


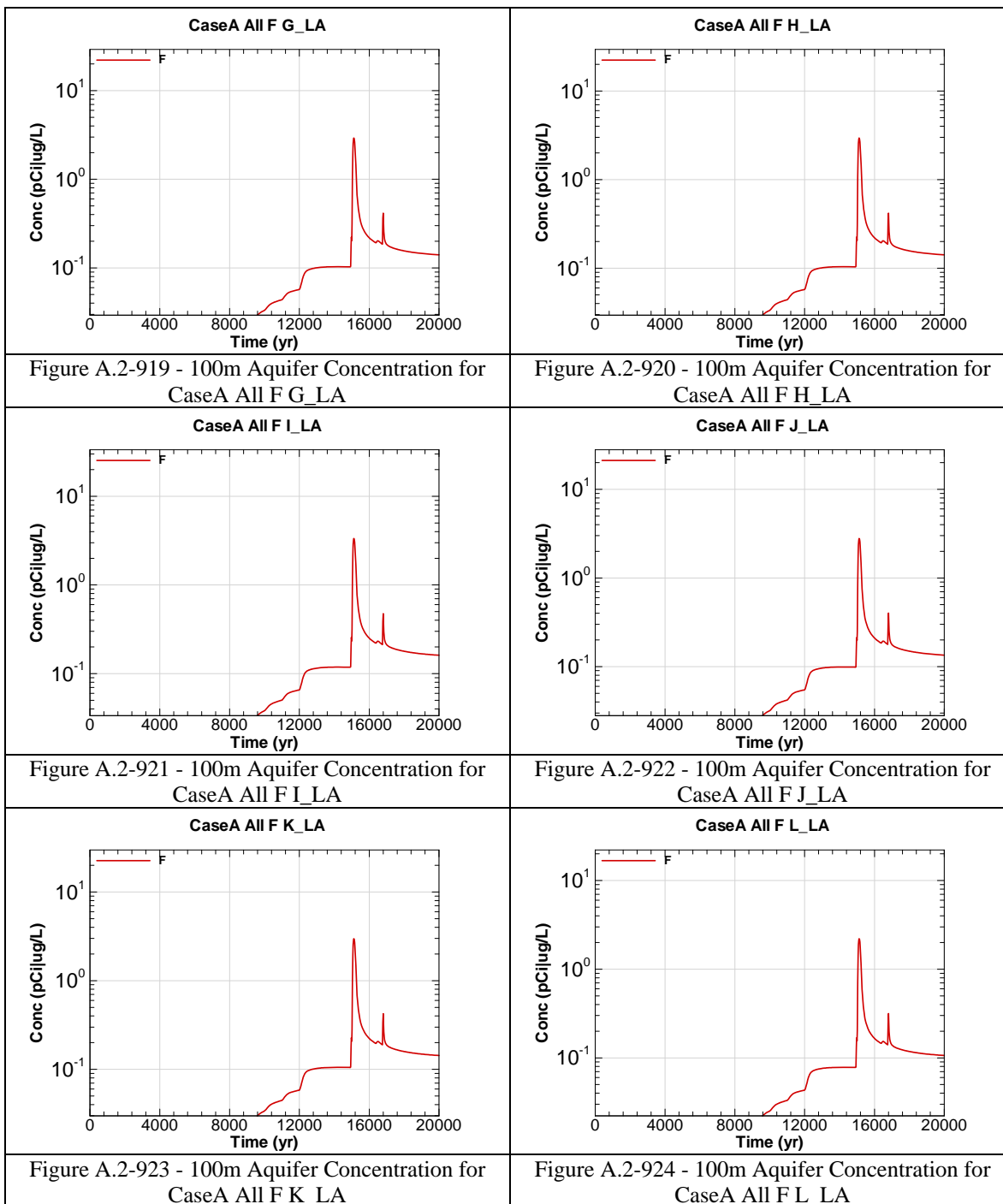


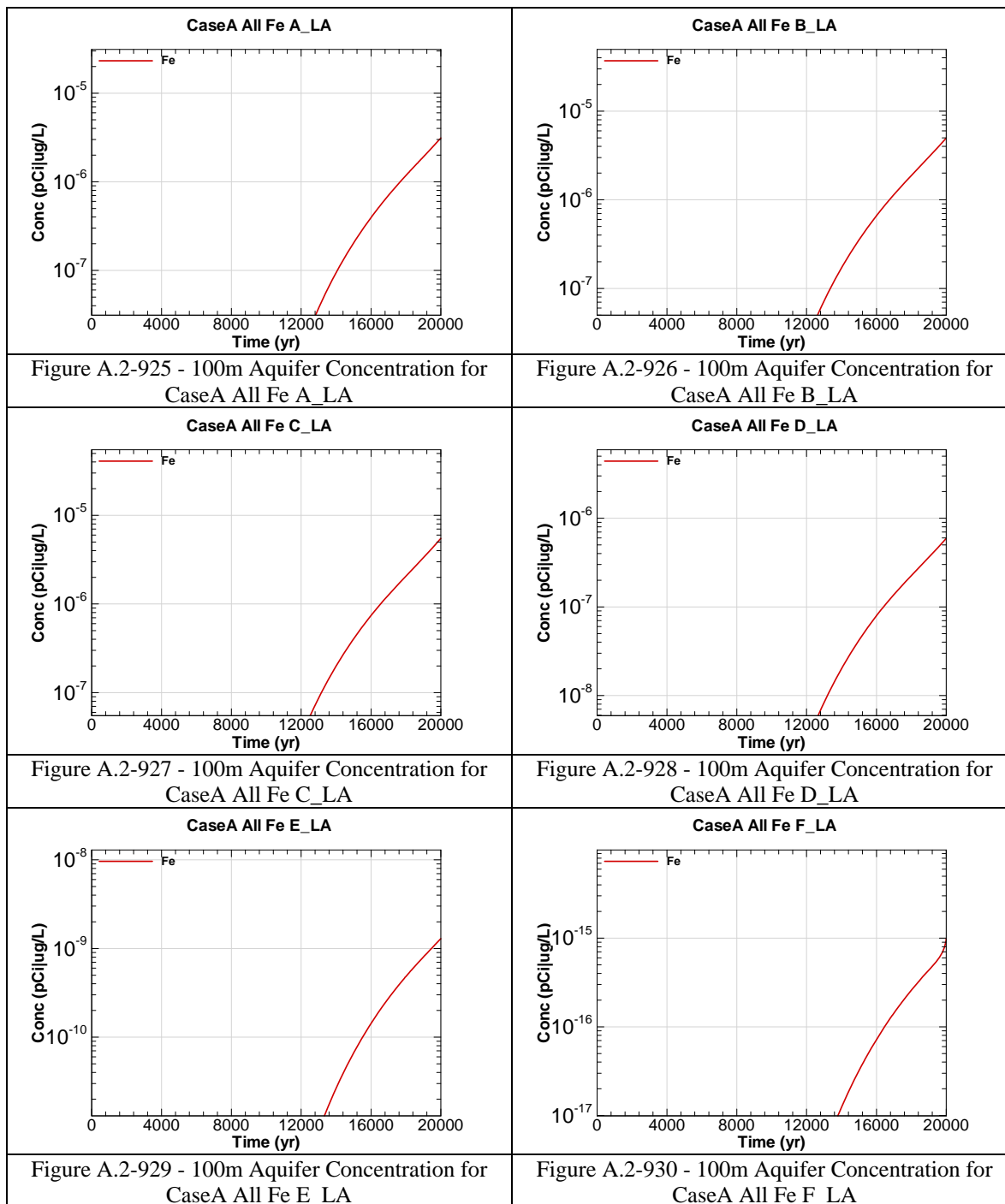


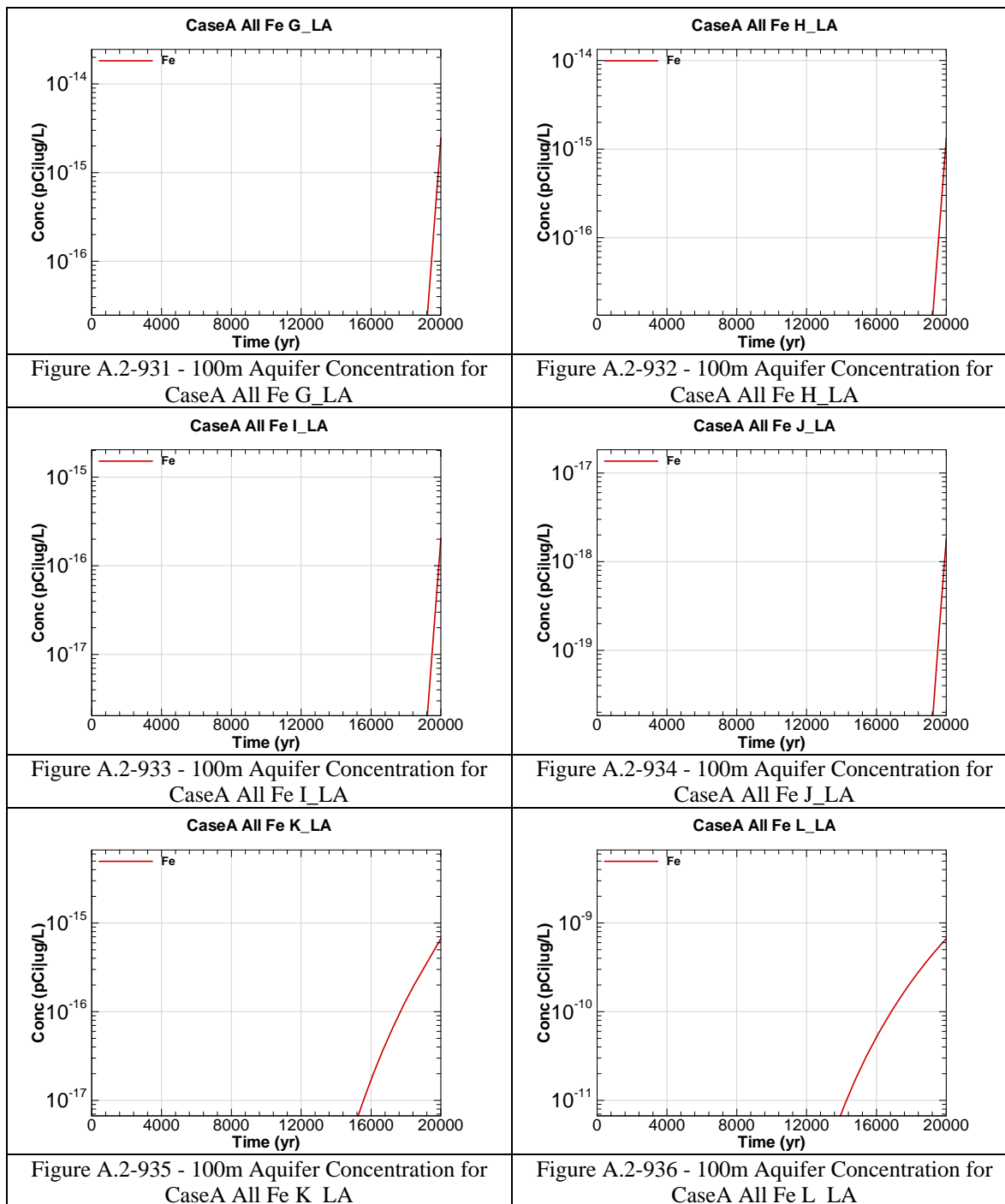


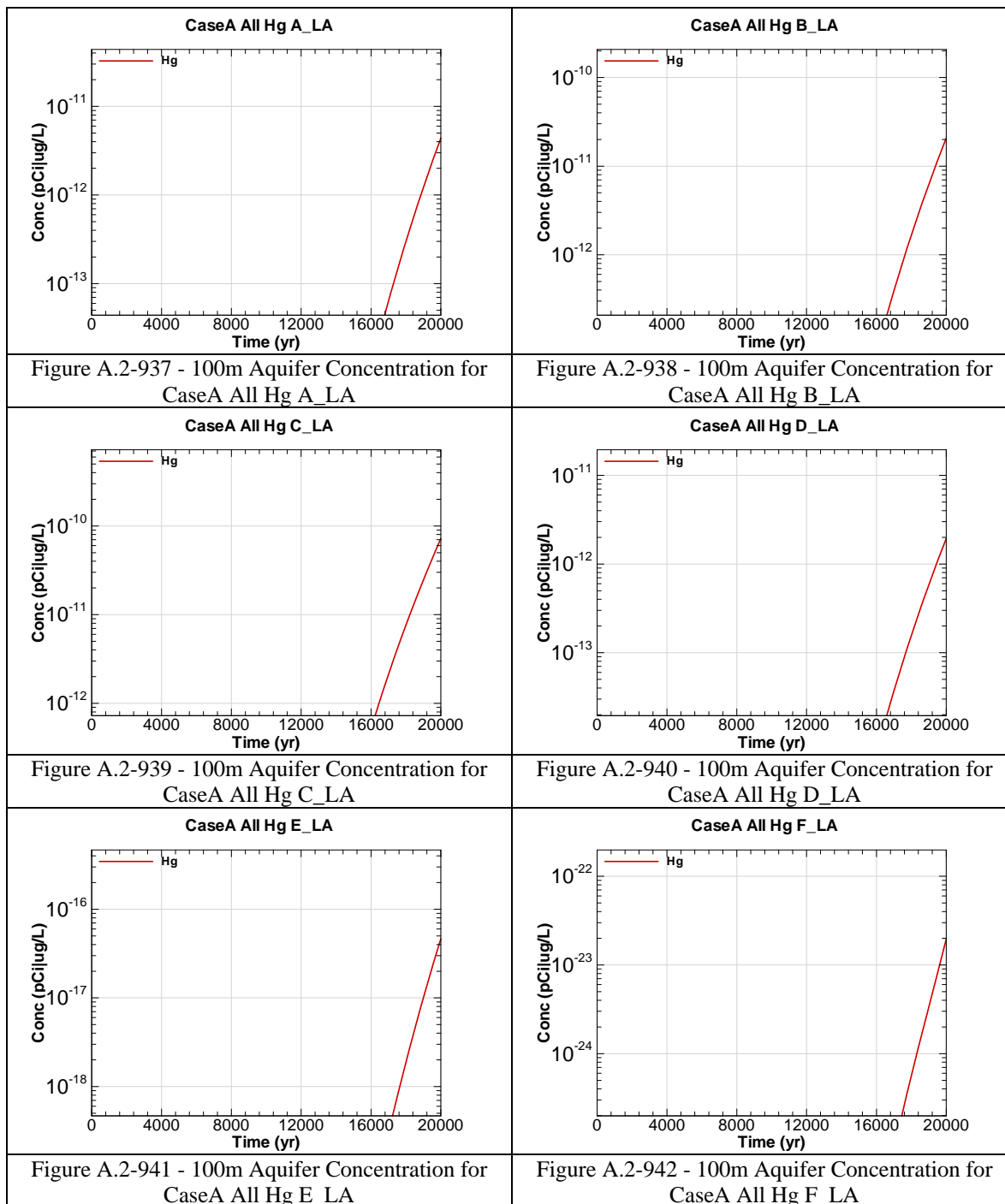


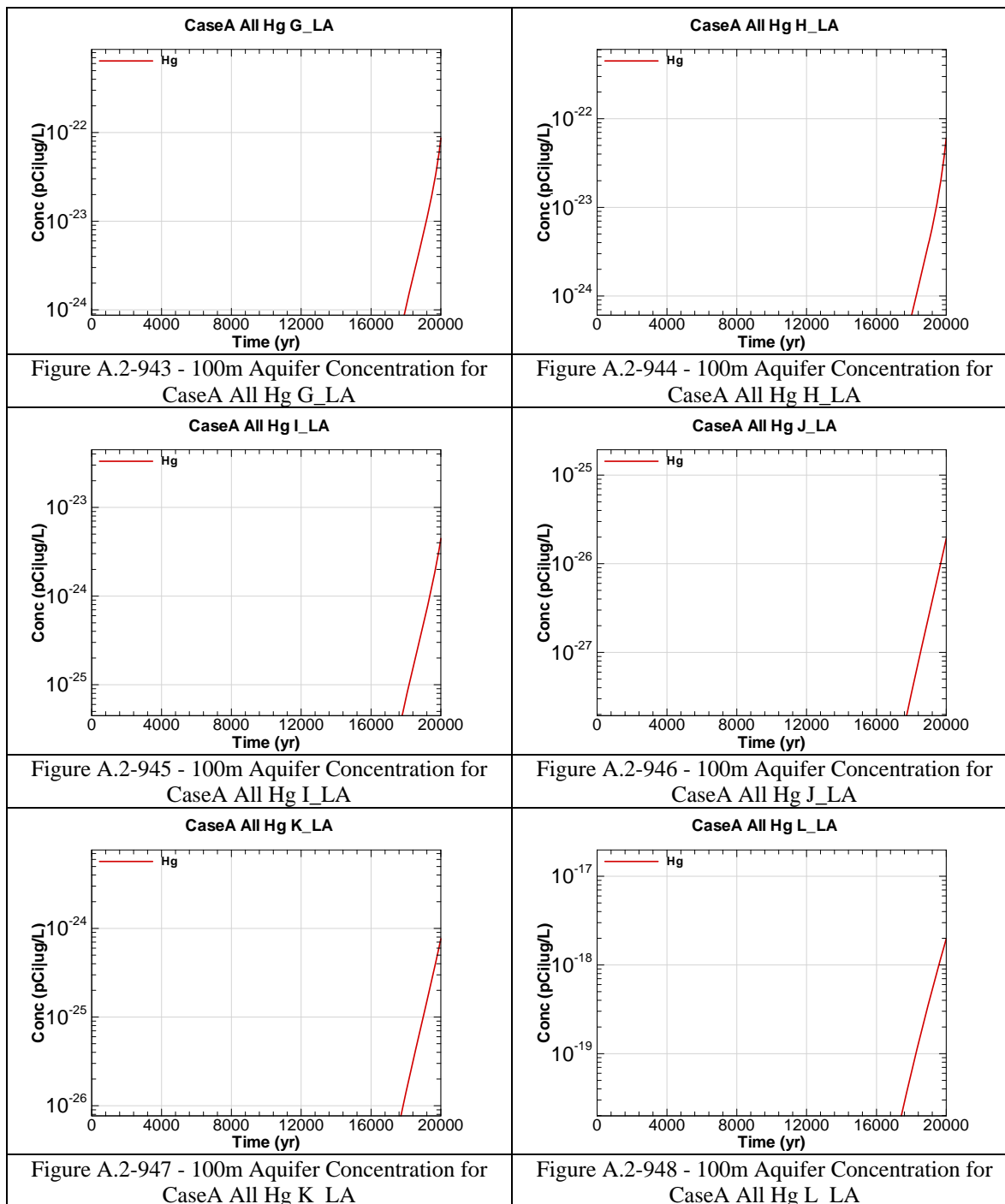


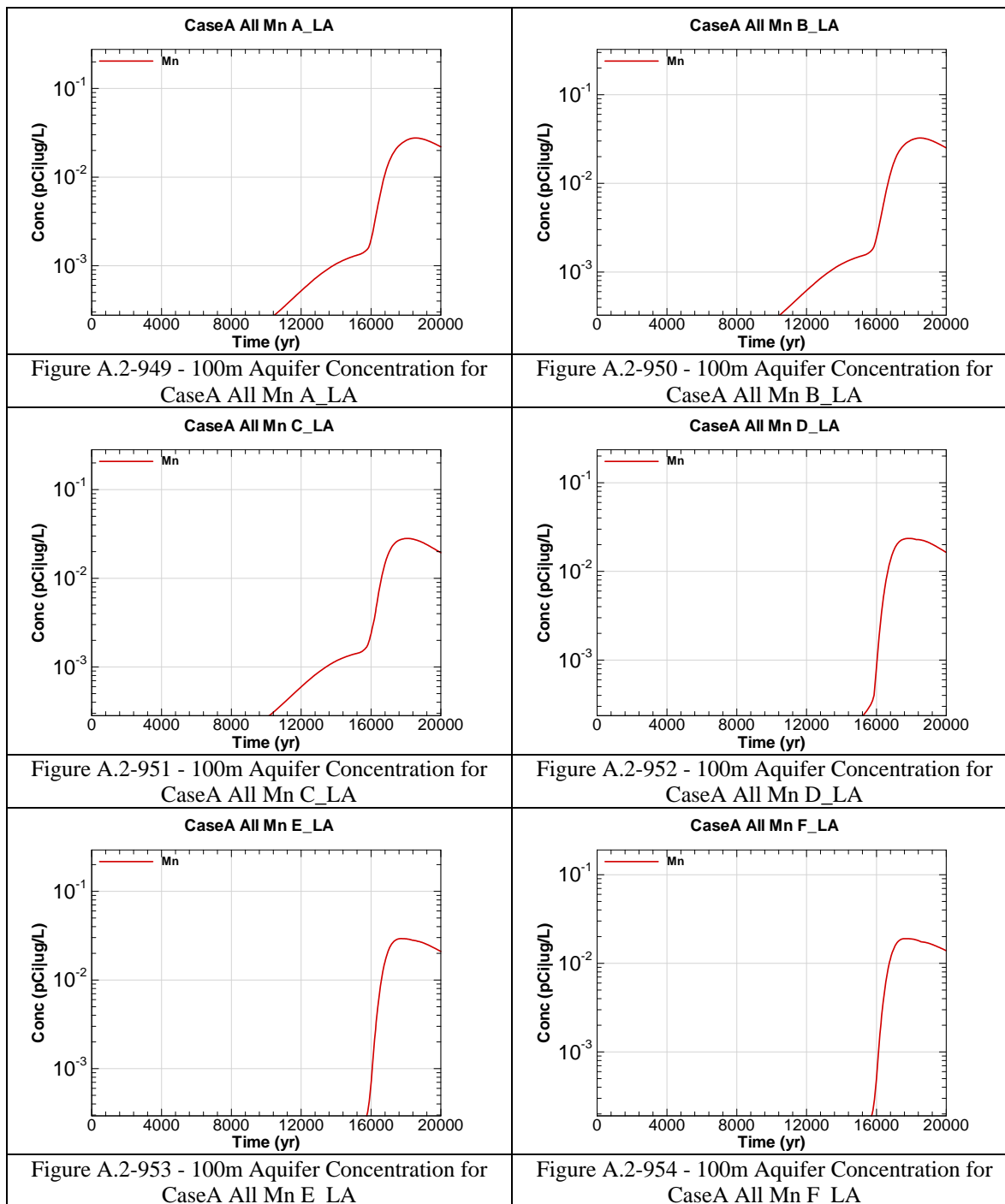


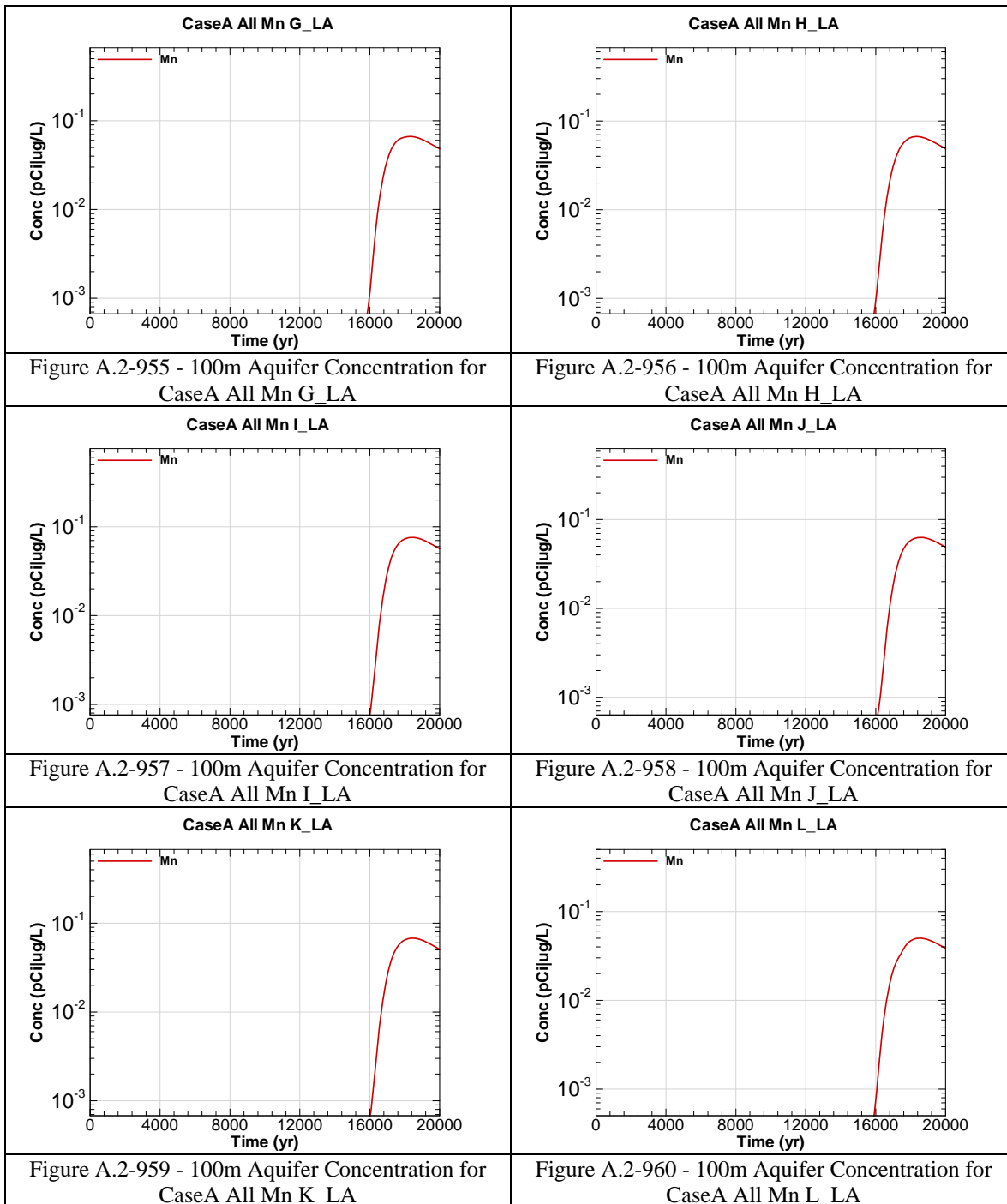


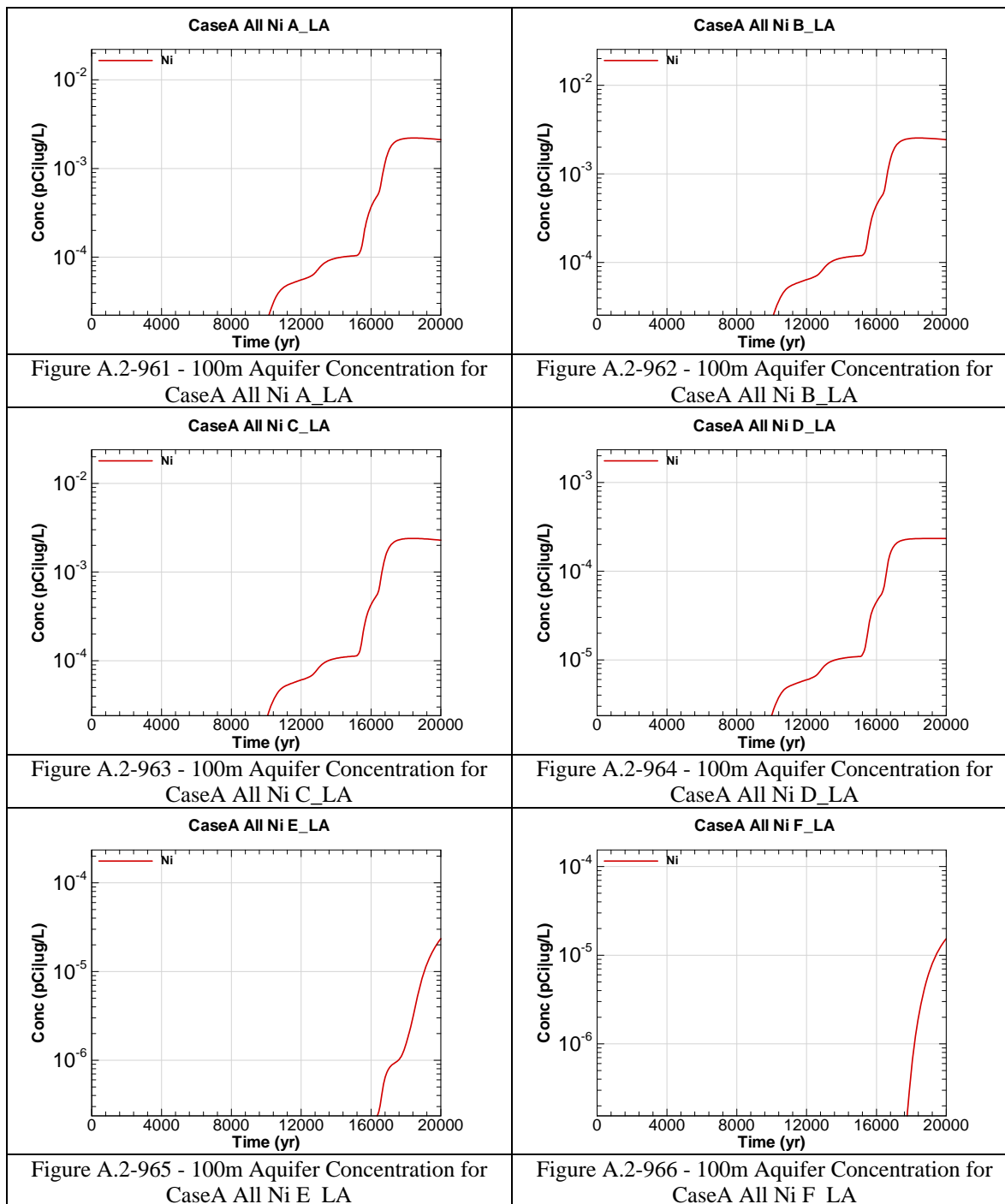


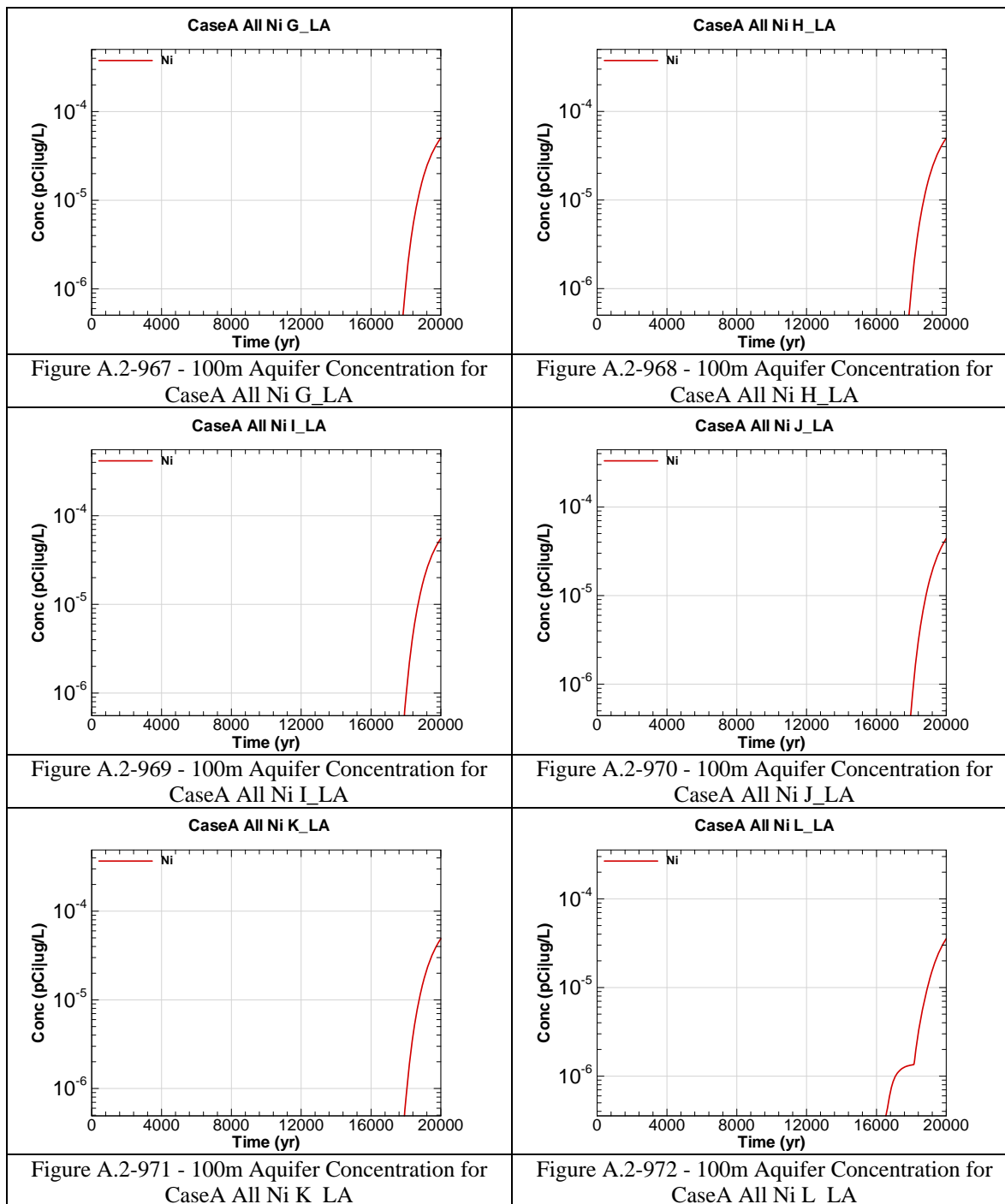


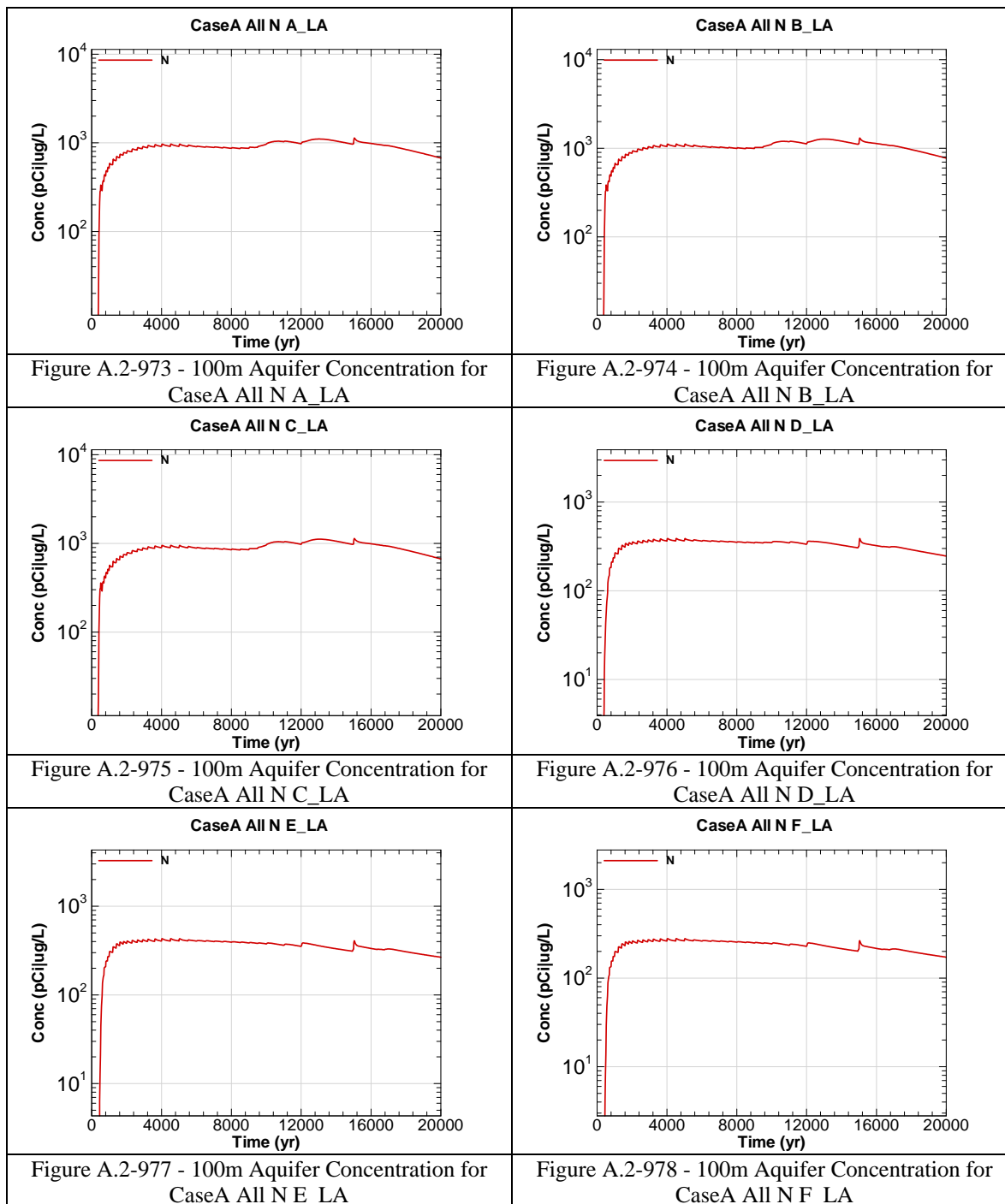


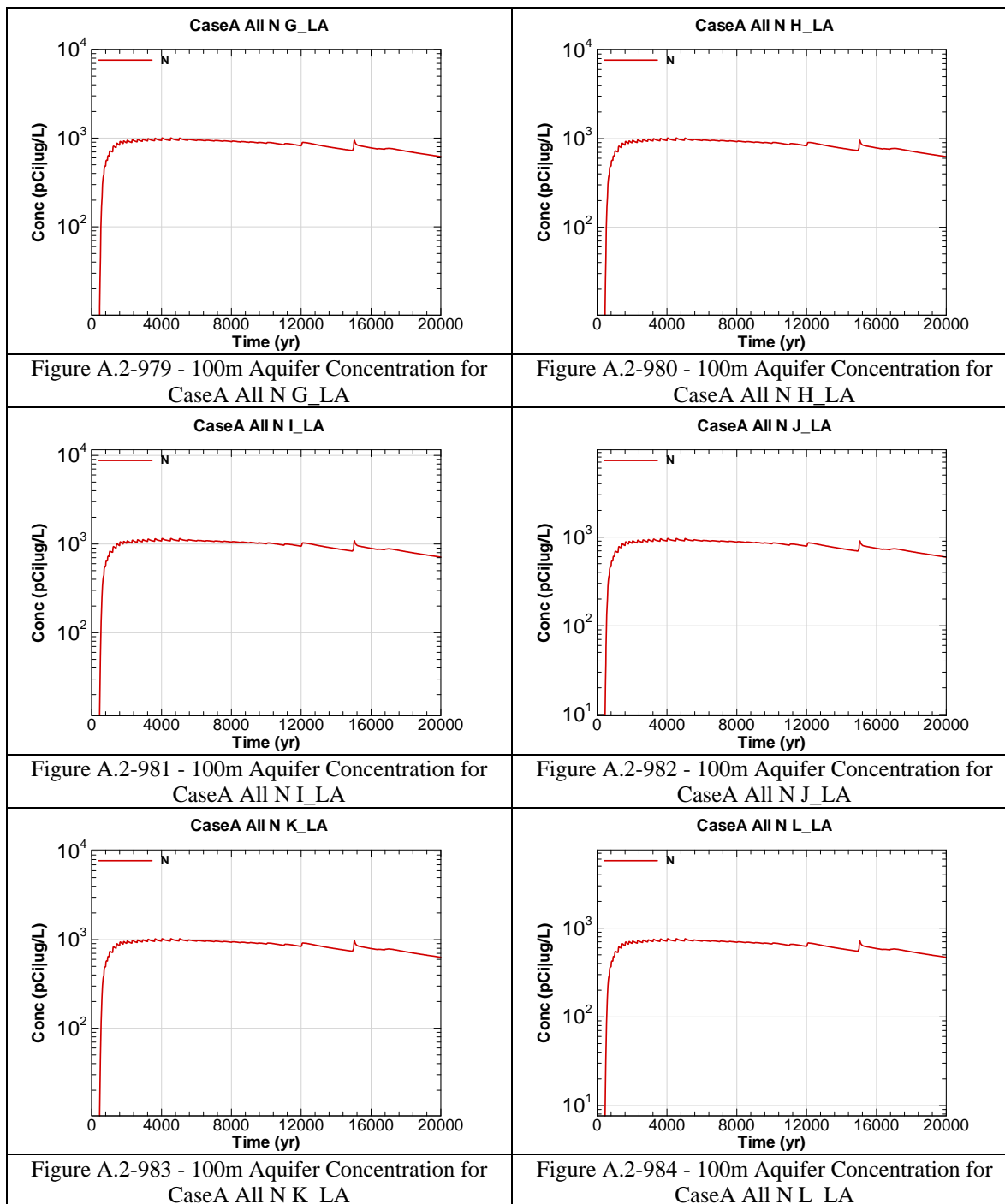


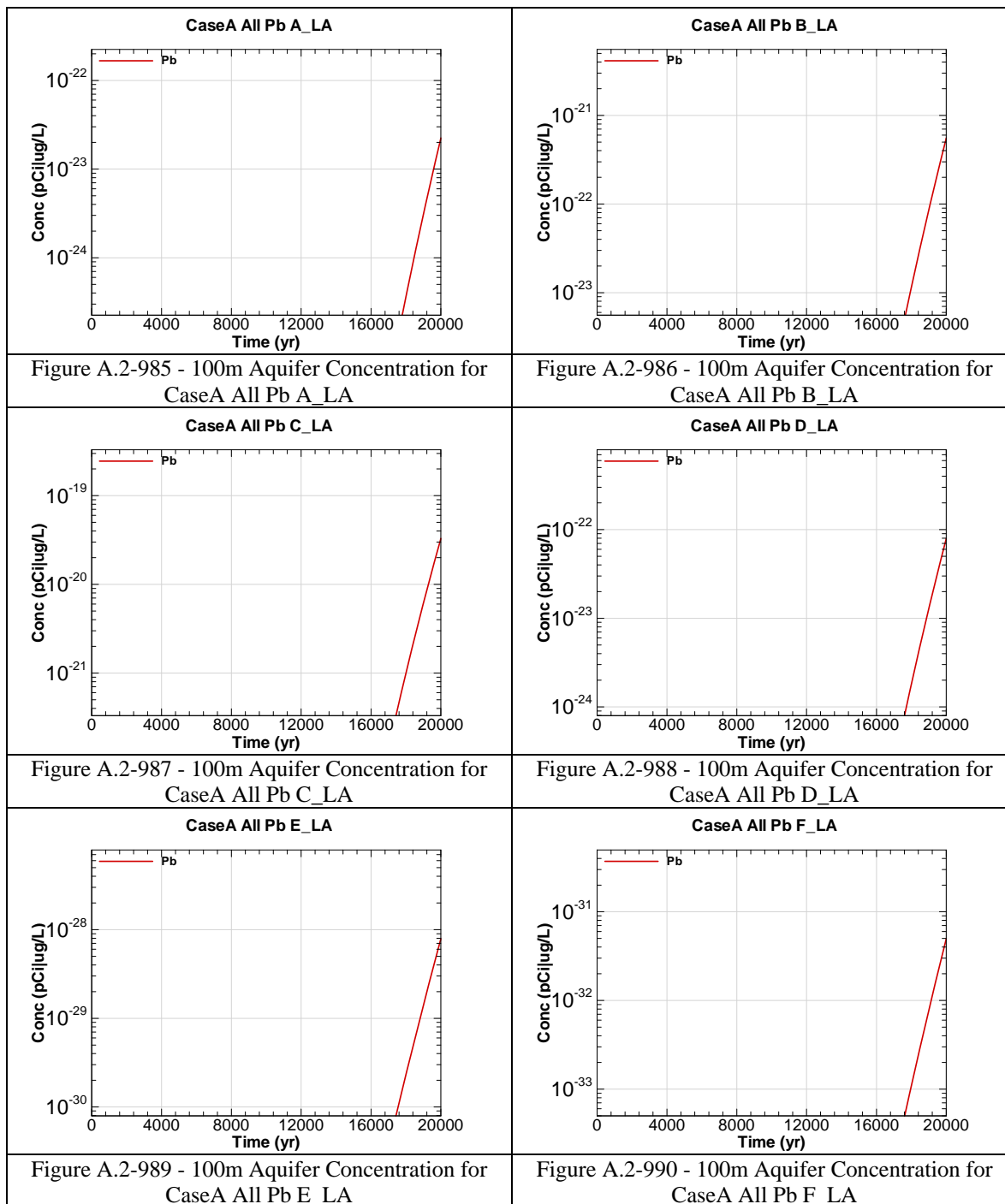


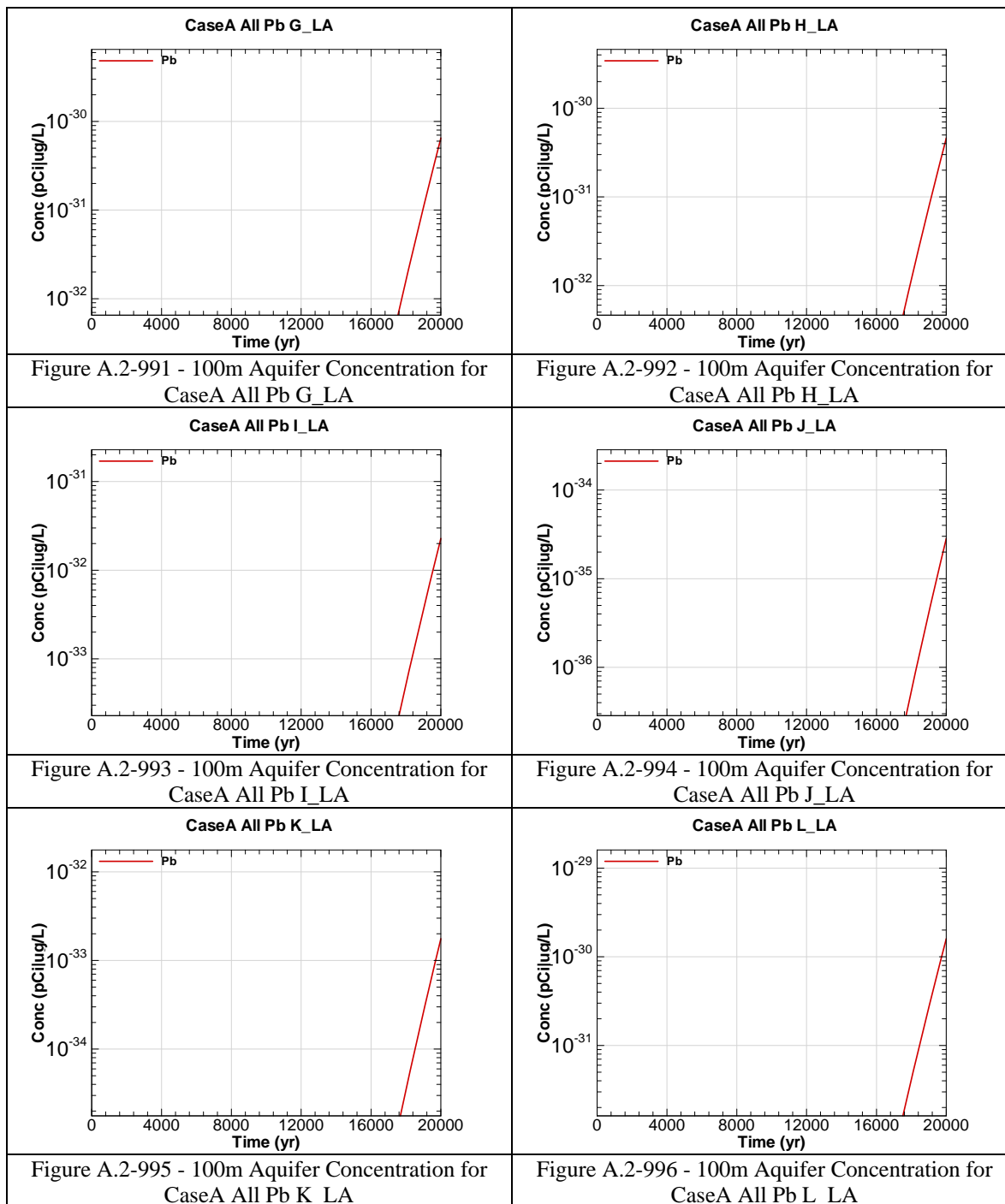


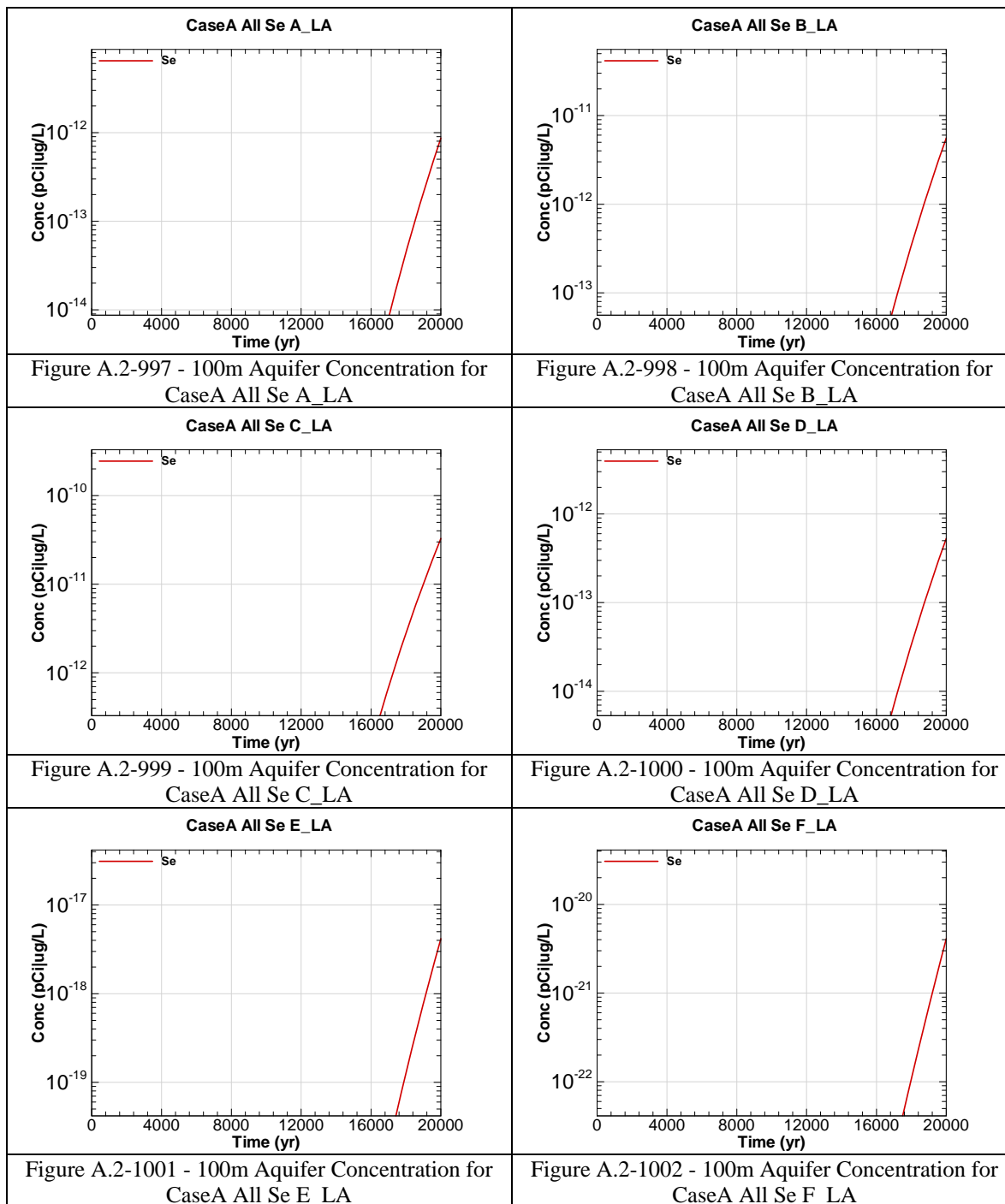


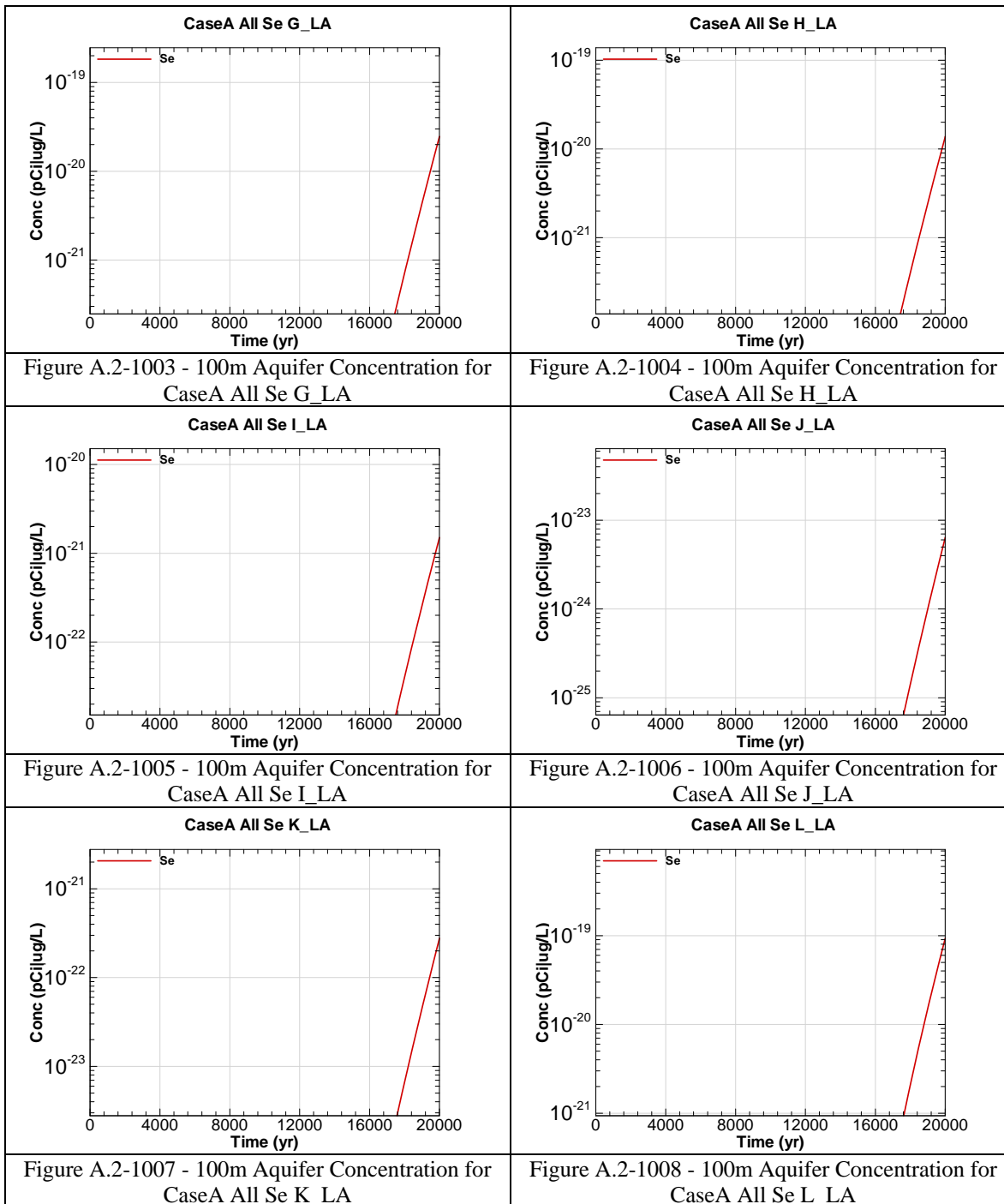


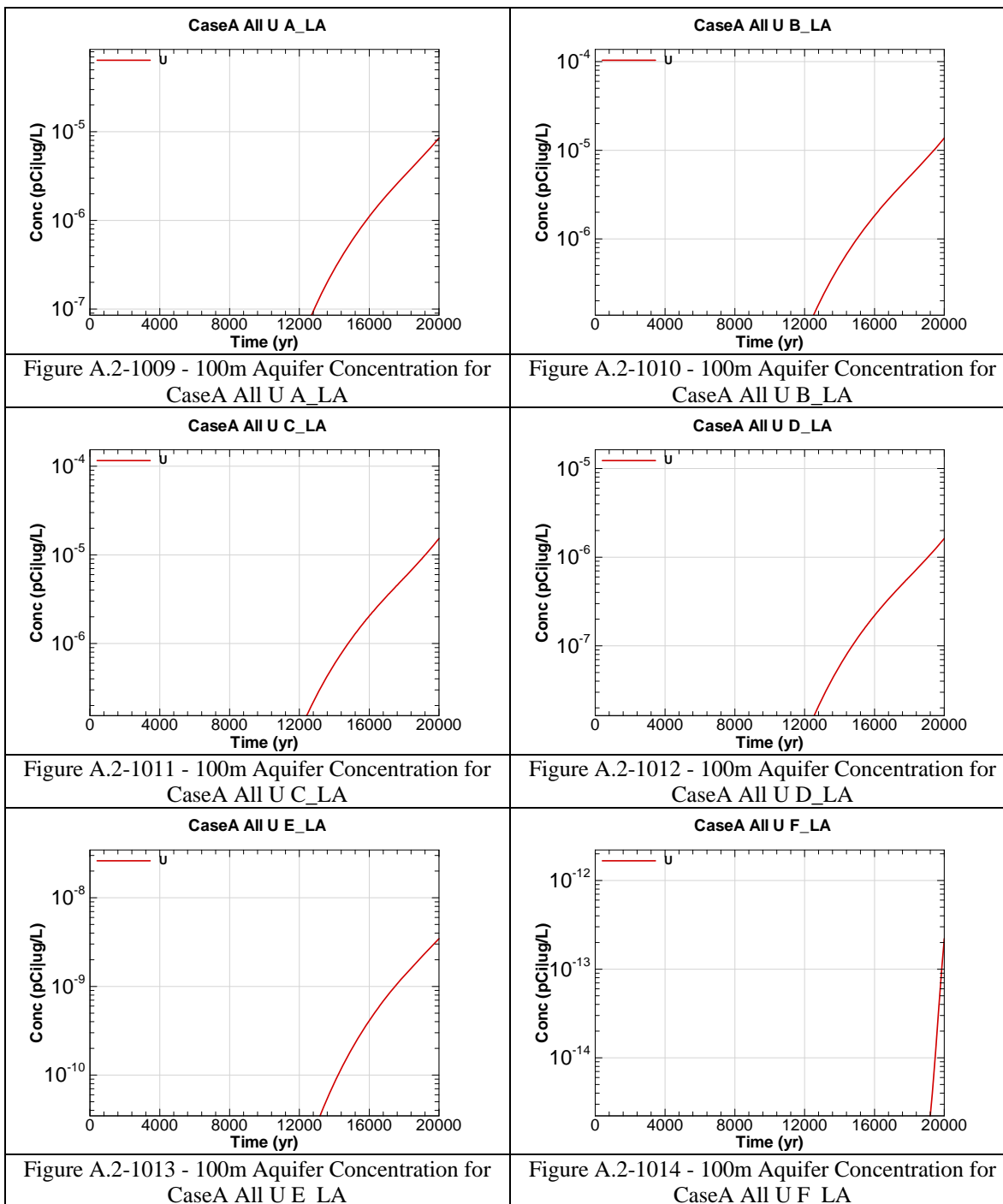


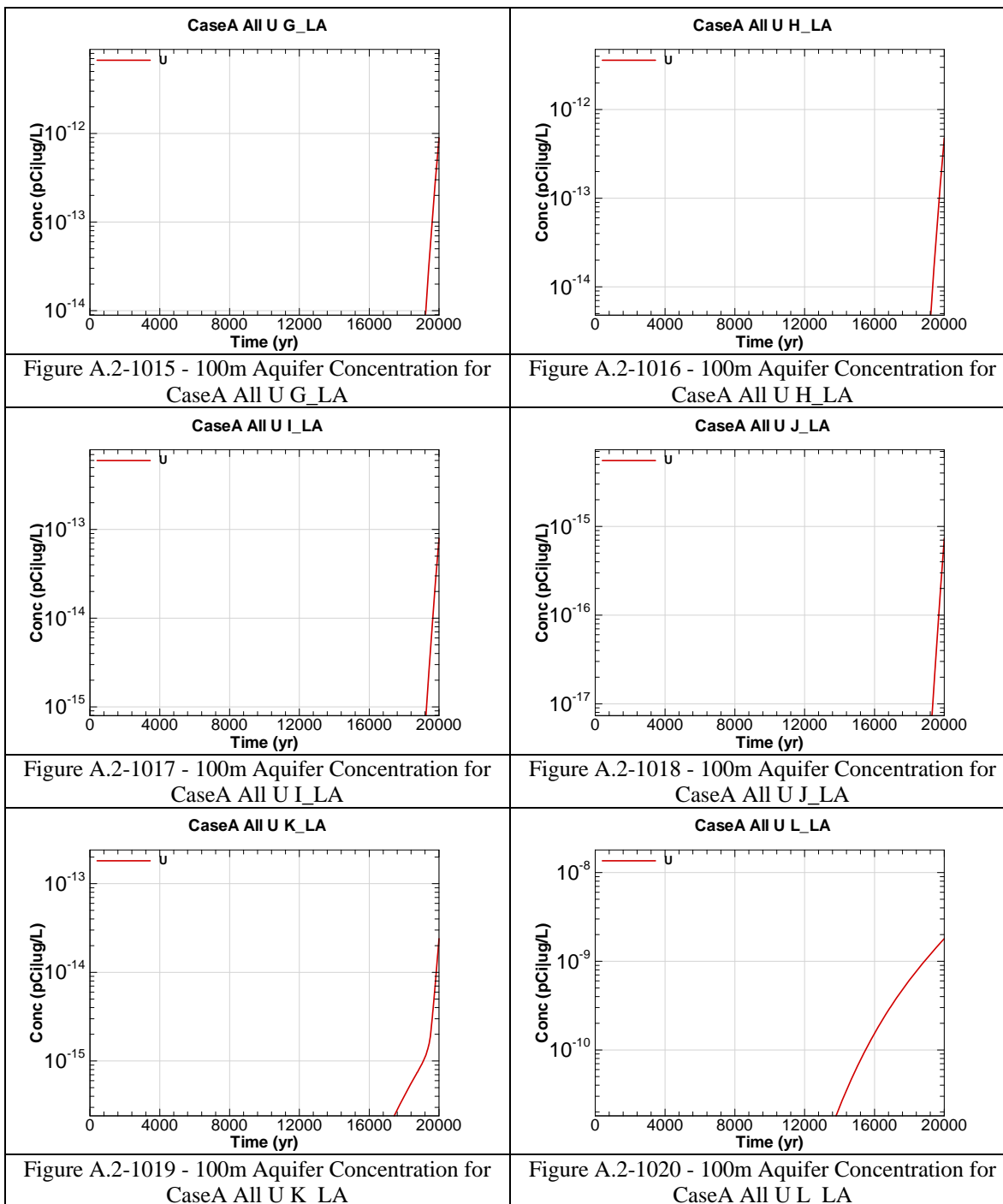


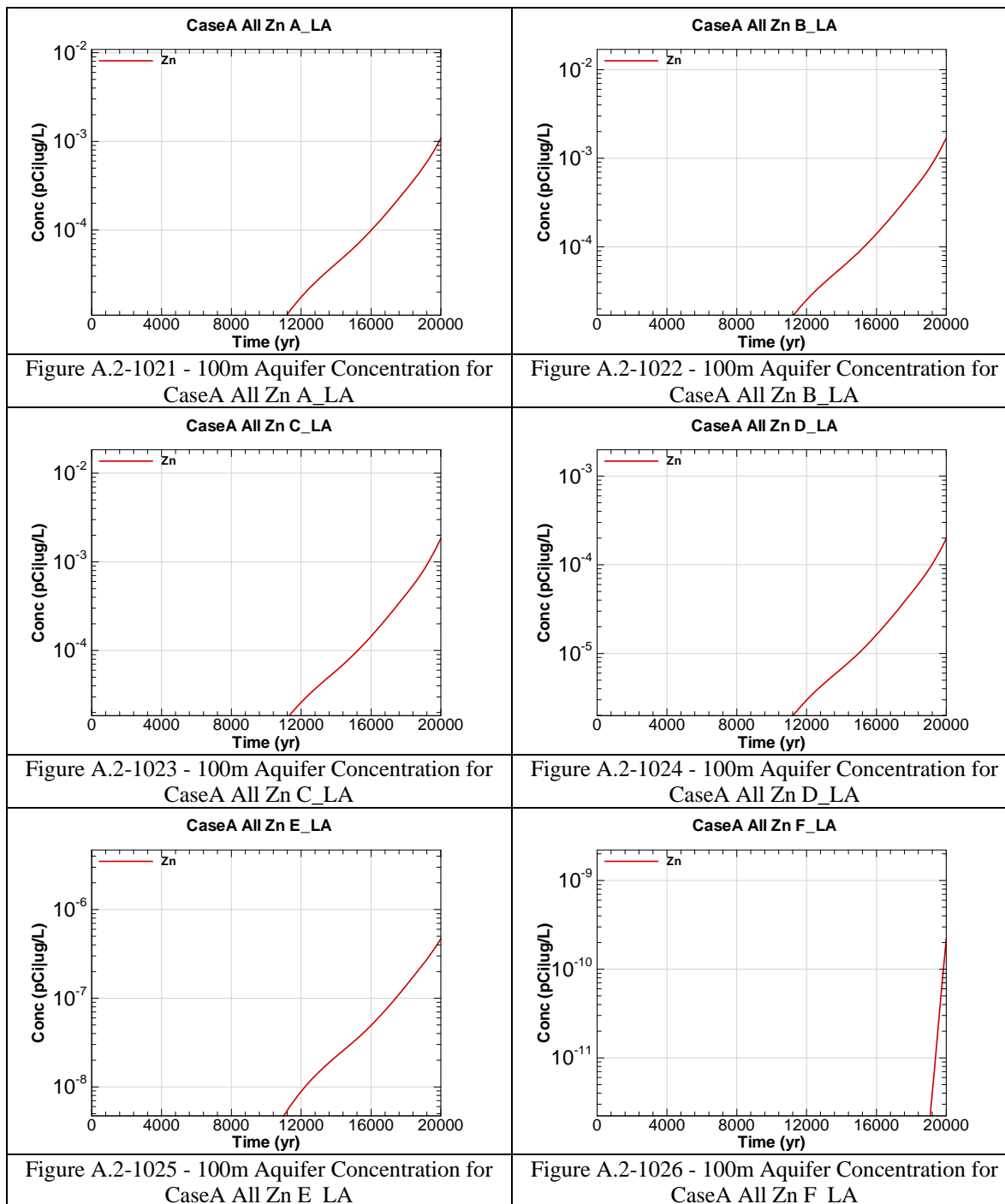


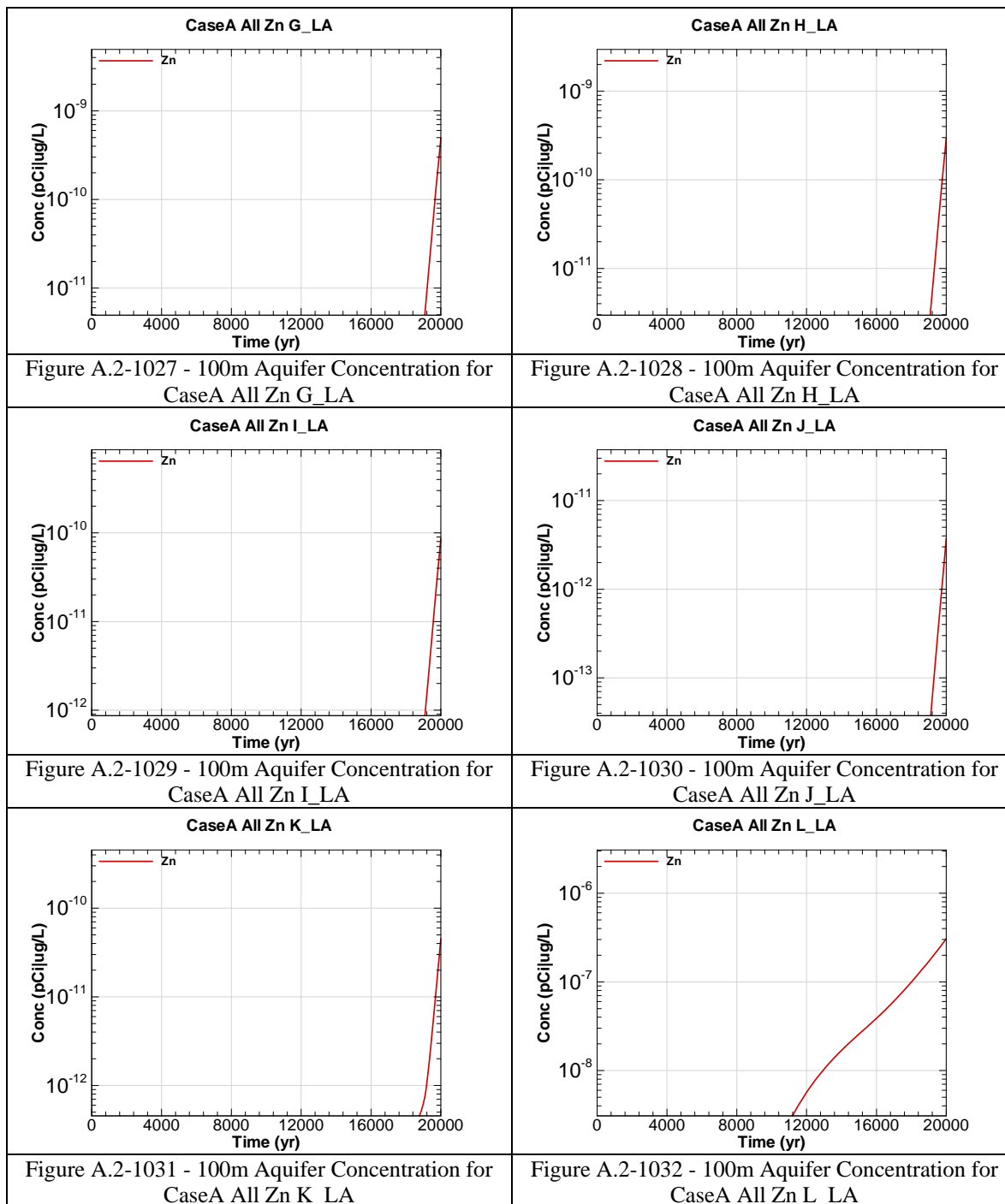












APPENDIX A.3

100-METER RADIOLOGICAL AND CHEMICAL CONCENTRATIONS AT THE GORDON AQUIFER

Appendix A.3 contains curves showing the 100 meter radiological and chemical concentrations for all of SDF (vault and FDC inventories) for the Base Case (Case A). 20,000 year concentration results are presented from the Gordon Aquifer for Sectors A through L.

Graph heading example "CaseA All Ac-227 A_GA"

Key

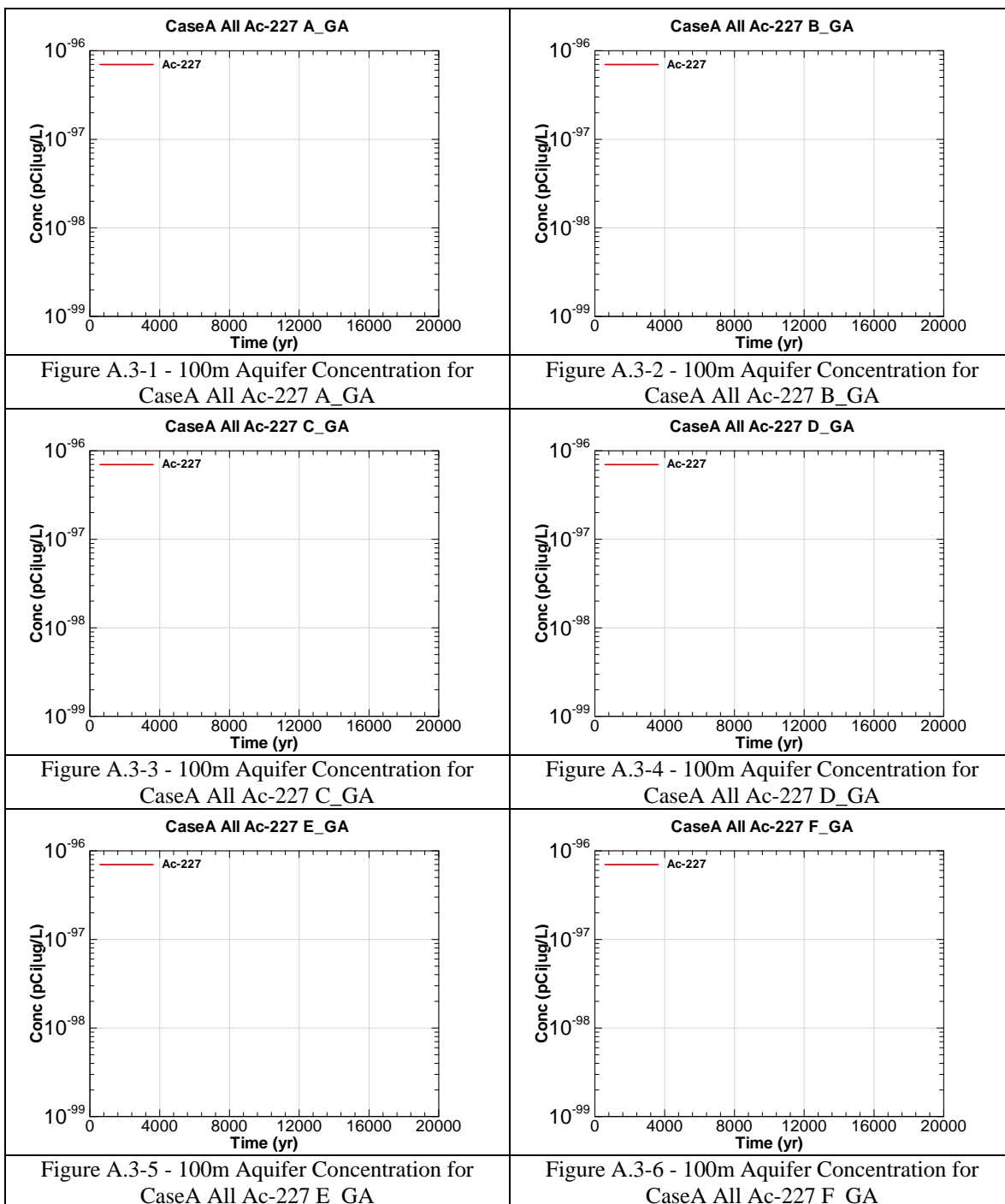
CaseA = Scenario case

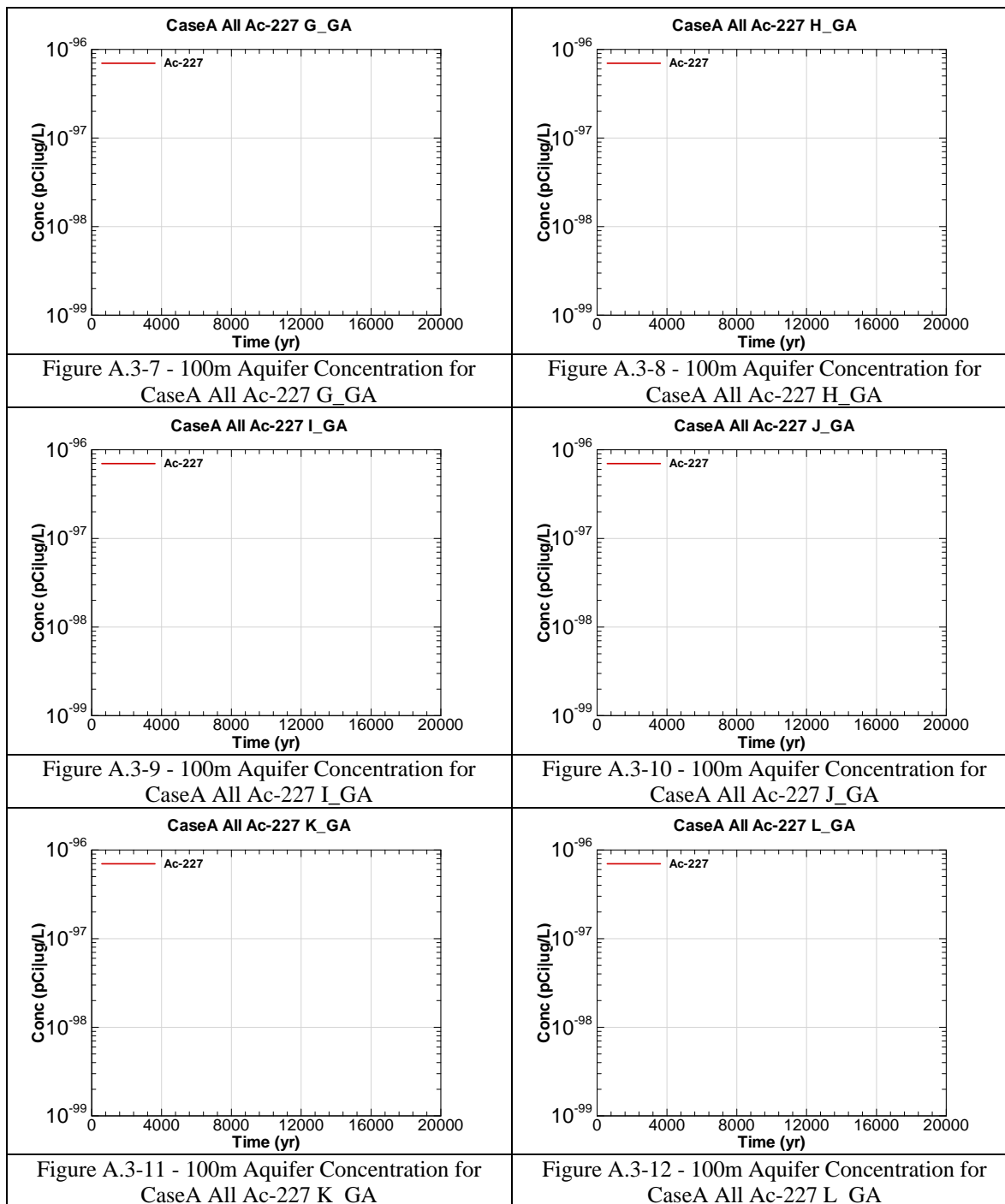
All = Inventory source is all disposal units

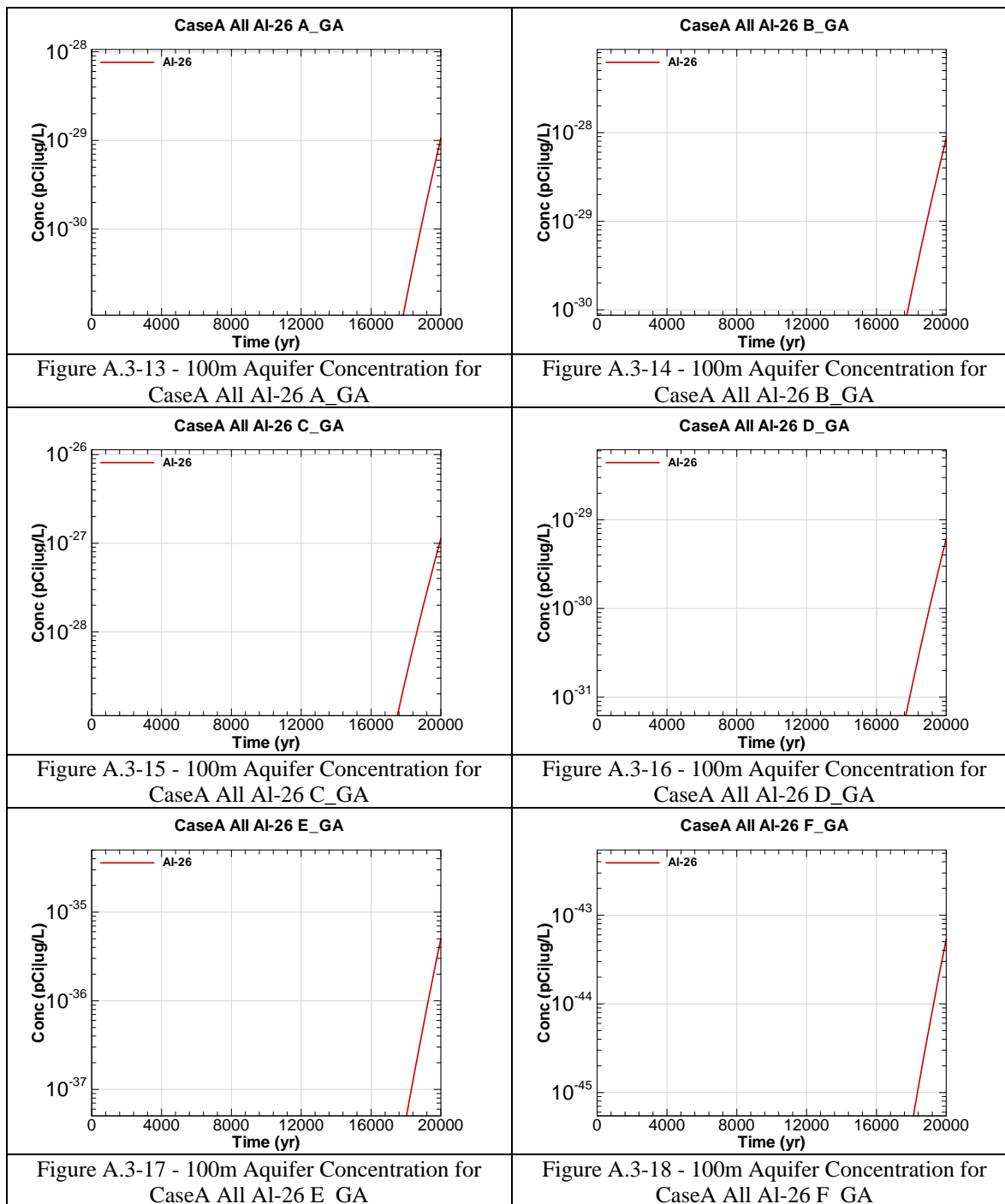
Ac-227 = Radionuclide or chemical of concern

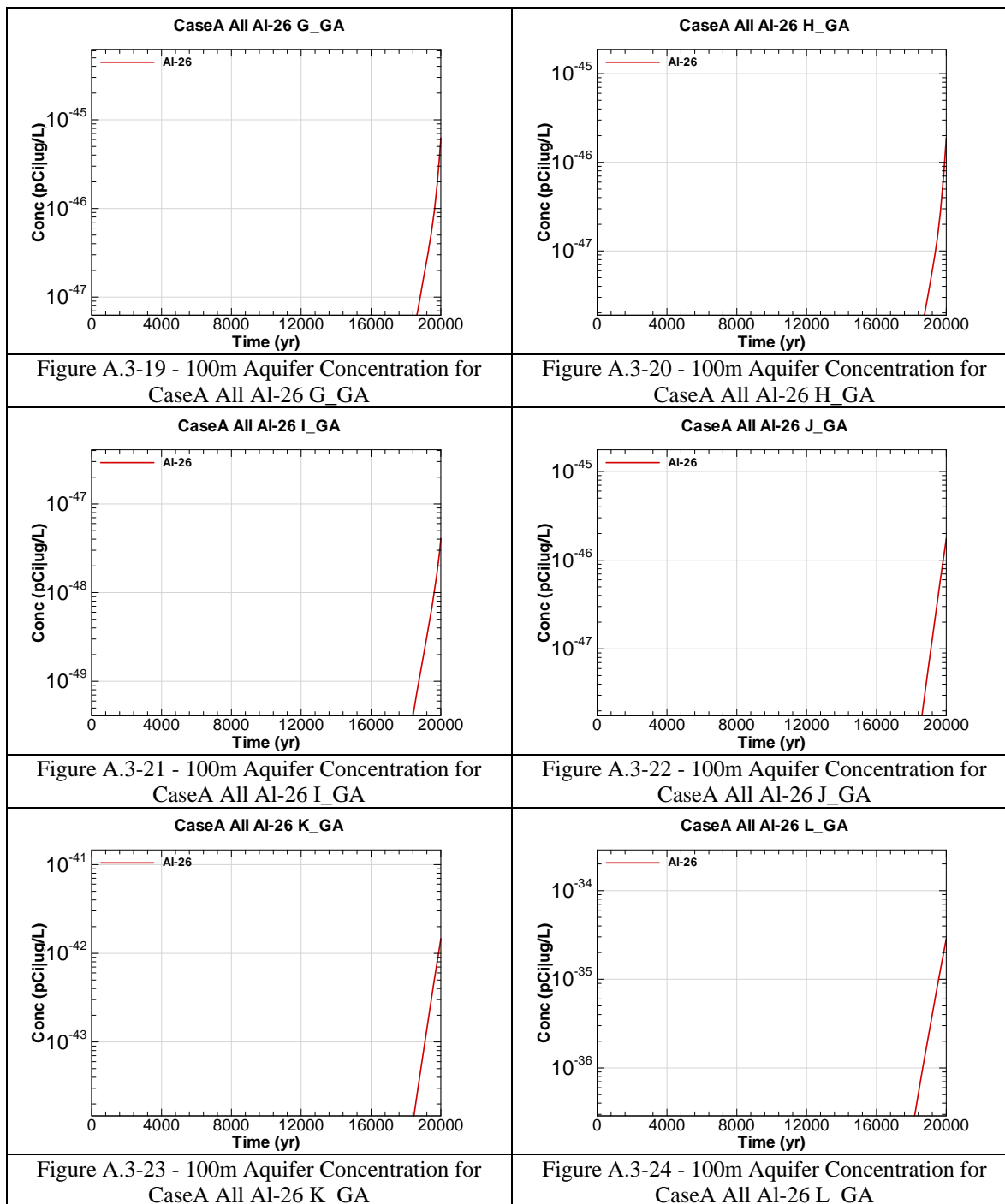
A = Evaluation sector of concern

GA = Aquifer of concern is Gordon Aquifer









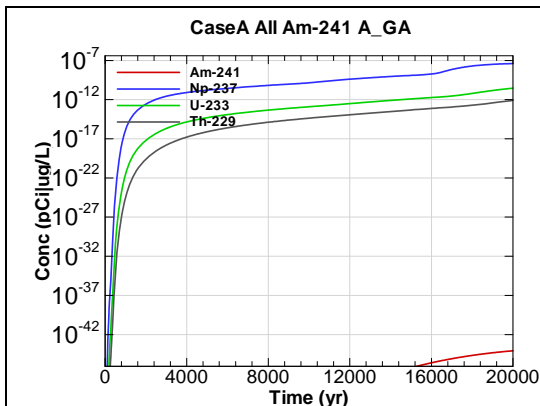


Figure A.3-25 - 100m Aquifer Concentration for CaseA All Am-241 A_GA

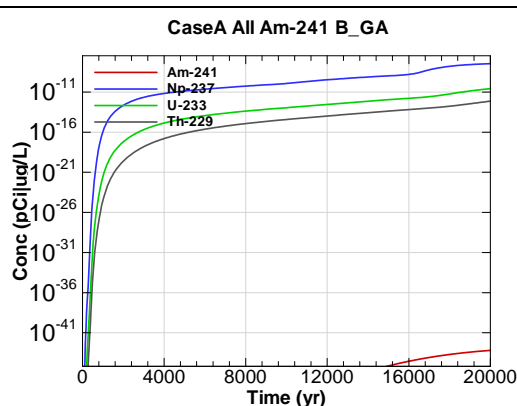


Figure A.3-26 - 100m Aquifer Concentration for CaseA All Am-241 B_GA

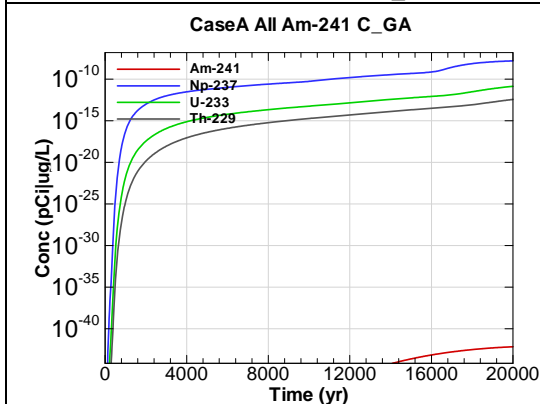


Figure A.3-27 - 100m Aquifer Concentration for CaseA All Am-241 C_GA

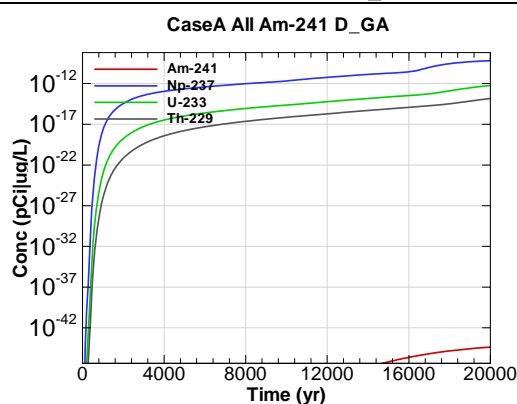


Figure A.3-28 - 100m Aquifer Concentration for CaseA All Am-241 D_GA

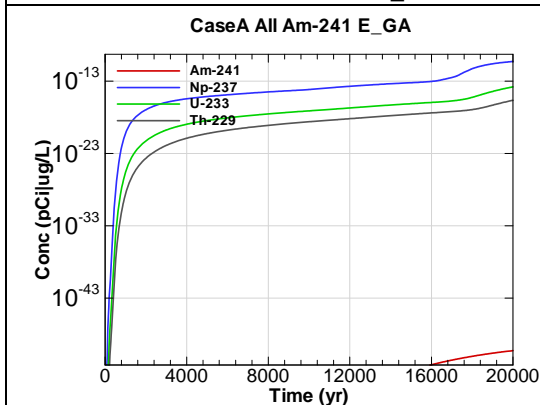


Figure A.3-29 - 100m Aquifer Concentration for CaseA All Am-241 E_GA

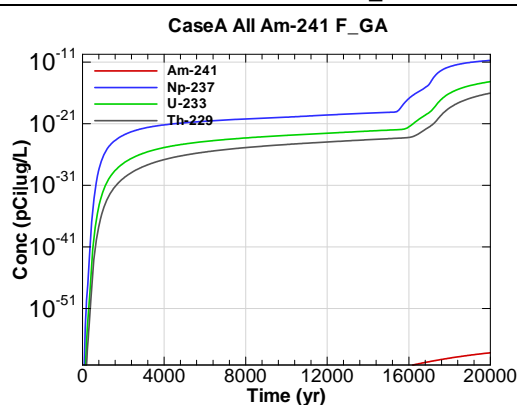


Figure A.3-30 - 100m Aquifer Concentration for CaseA All Am-241 F_GA

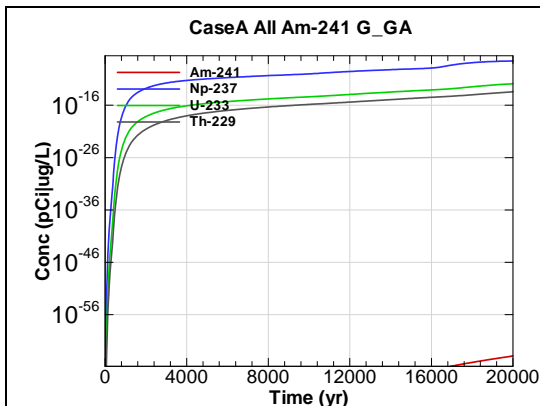


Figure A.3-31 - 100m Aquifer Concentration for CaseA All Am-241 G_GA

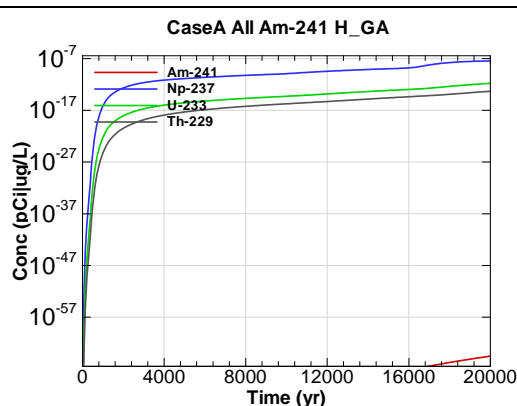


Figure A.3-32 - 100m Aquifer Concentration for CaseA All Am-241 H_GA

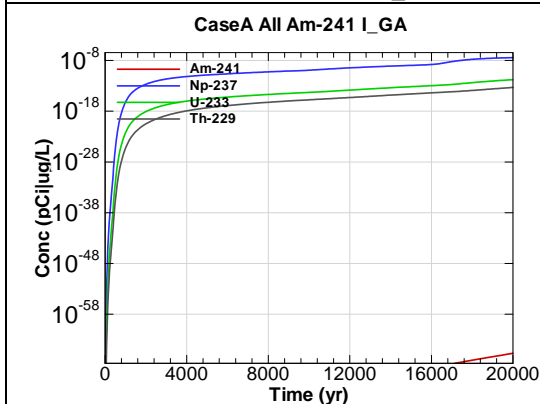


Figure A.3-33 - 100m Aquifer Concentration for CaseA All Am-241 I_GA

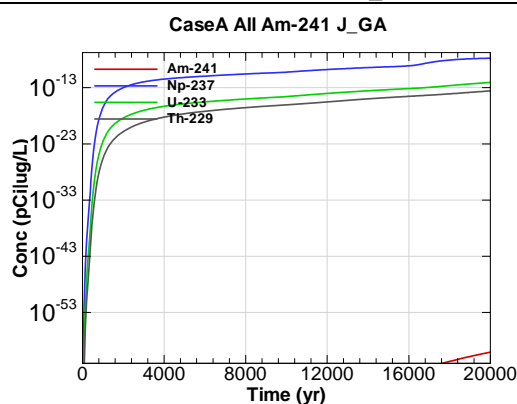


Figure A.3-34 - 100m Aquifer Concentration for CaseA All Am-241 J_GA

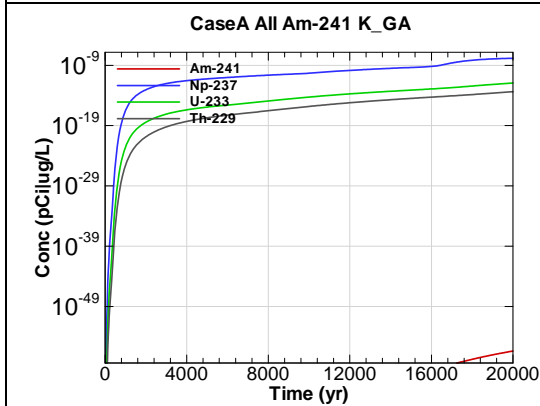


Figure A.3-35 - 100m Aquifer Concentration for CaseA All Am-241 K_GA

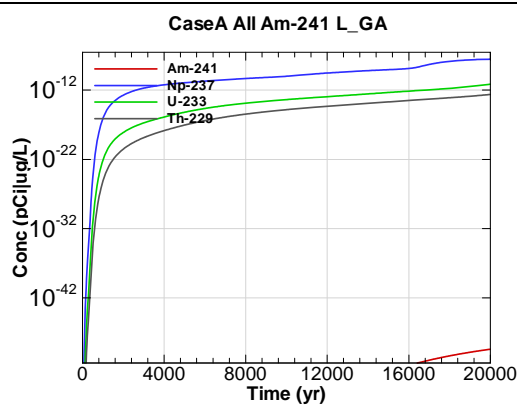


Figure A.3-36 - 100m Aquifer Concentration for CaseA All Am-241 L_GA

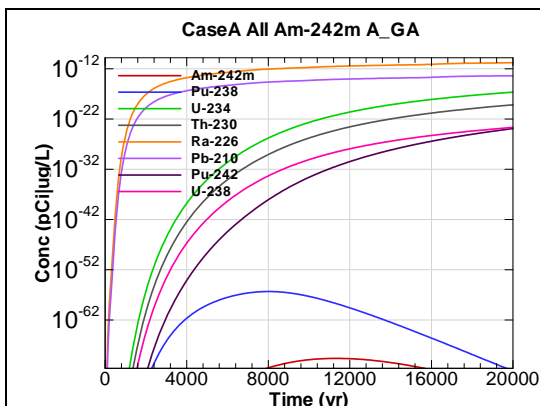


Figure A.3-37 - 100m Aquifer Concentration for
CaseA All Am-242m A_GA

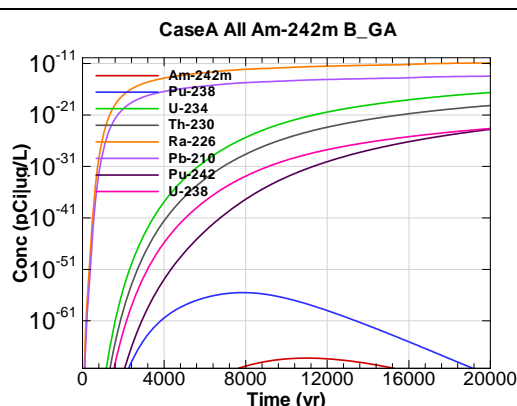


Figure A.3-38 - 100m Aquifer Concentration for
CaseA All Am-242m B_GA

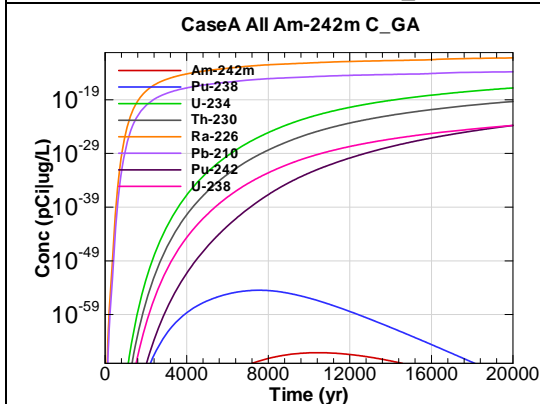


Figure A.3-39 - 100m Aquifer Concentration for
CaseA All Am-242m C_GA

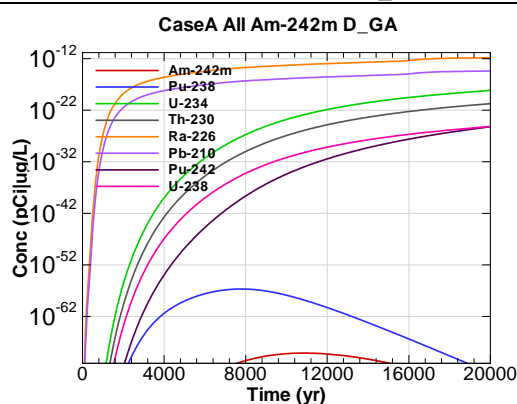


Figure A.3-40 - 100m Aquifer Concentration for
CaseA All Am-242m D_GA

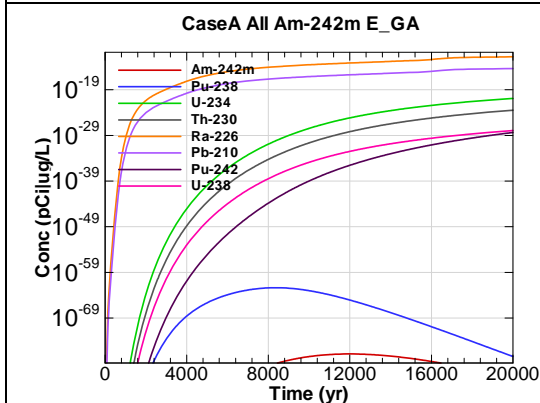


Figure A.3-41 - 100m Aquifer Concentration for
CaseA All Am-242m E_GA

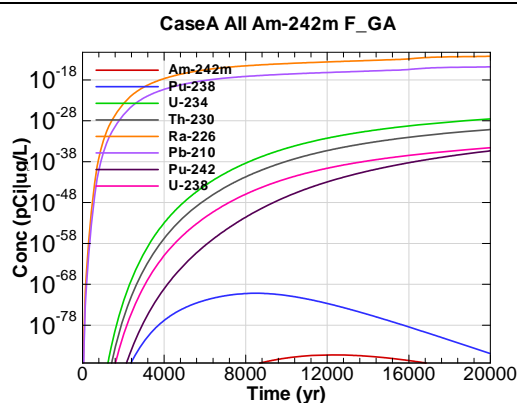


Figure A.3-42 - 100m Aquifer Concentration for
CaseA All Am-242m F_GA

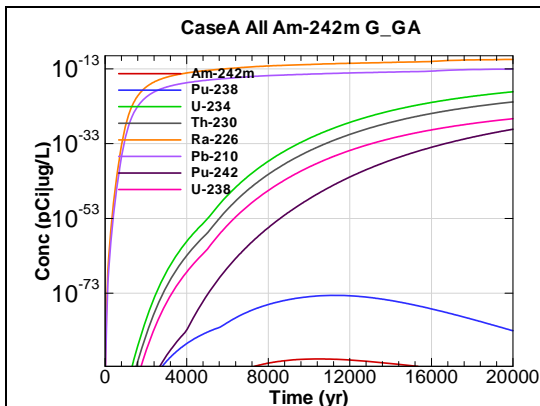


Figure A.3-43 - 100m Aquifer Concentration for
CaseA All Am-242m G_GA

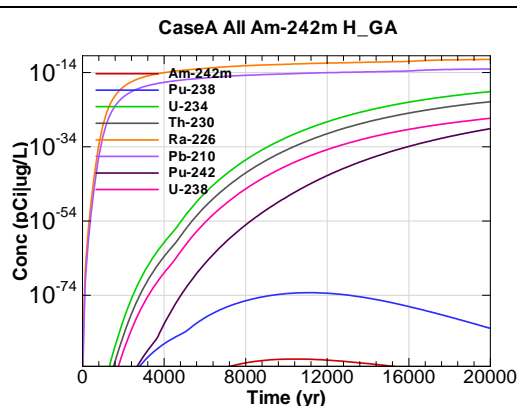


Figure A.3-44 - 100m Aquifer Concentration for
CaseA All Am-242m H_GA

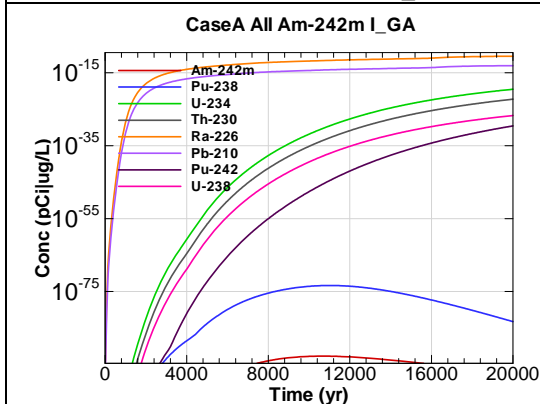


Figure A.3-45 - 100m Aquifer Concentration for
CaseA All Am-242m I_GA

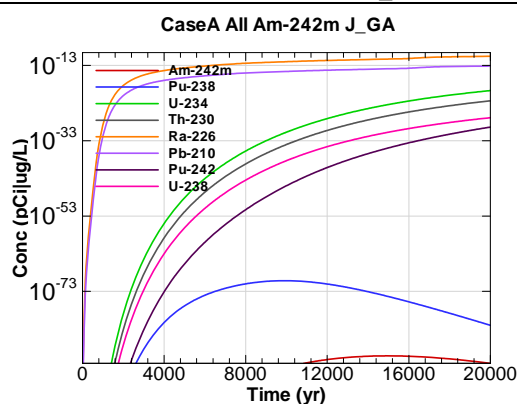


Figure A.3-46 - 100m Aquifer Concentration for
CaseA All Am-242m J_GA

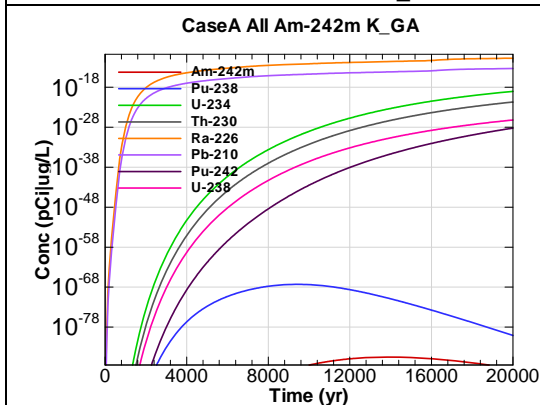


Figure A.3-47 - 100m Aquifer Concentration for
CaseA All Am-242m K_GA

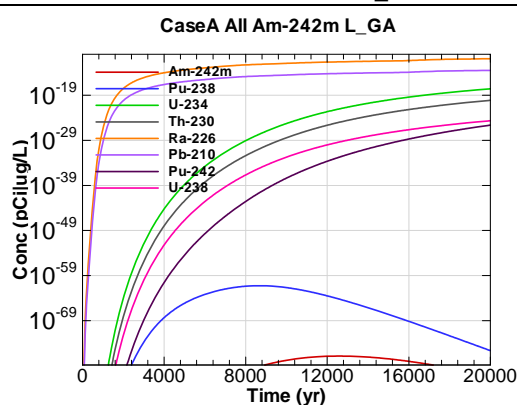


Figure A.3-48 - 100m Aquifer Concentration for
CaseA All Am-242m L_GA

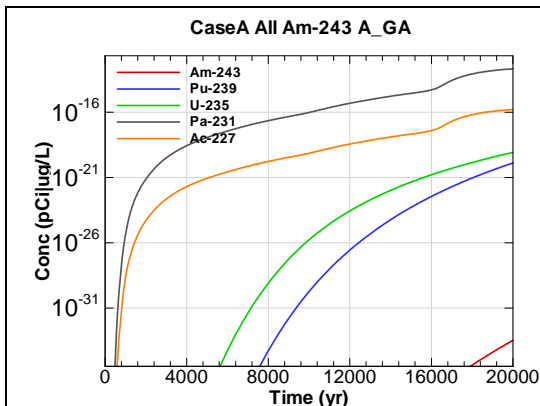


Figure A.3-49 - 100m Aquifer Concentration for
CaseA All Am-243 A_GA

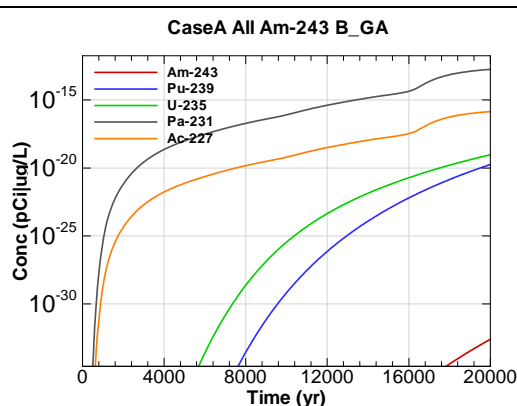


Figure A.3-50 - 100m Aquifer Concentration for
CaseA All Am-243 B_GA

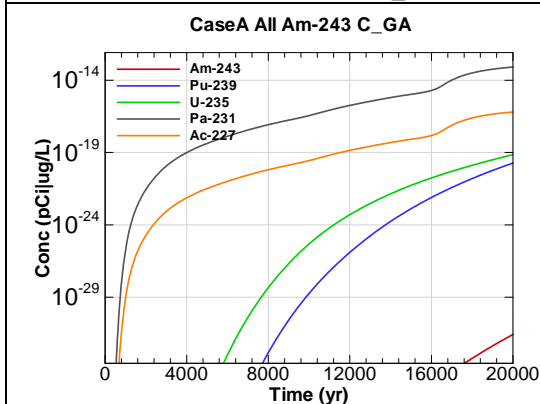


Figure A.3-51 - 100m Aquifer Concentration for
CaseA All Am-243 C_GA

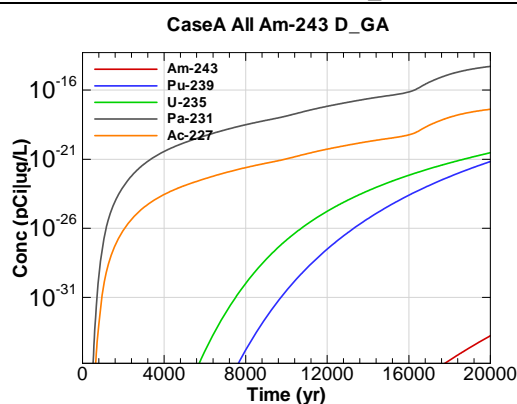


Figure A.3-52 - 100m Aquifer Concentration for
CaseA All Am-243 D_GA

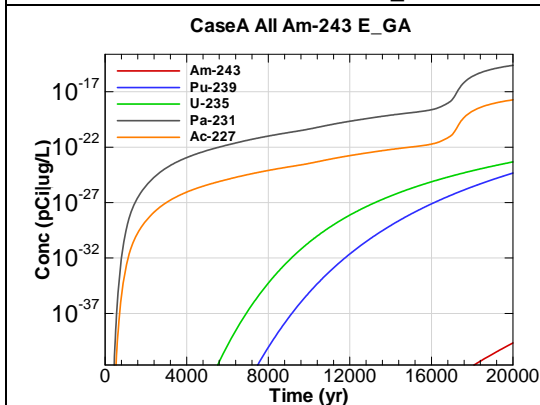


Figure A.3-53 - 100m Aquifer Concentration for
CaseA All Am-243 E_GA

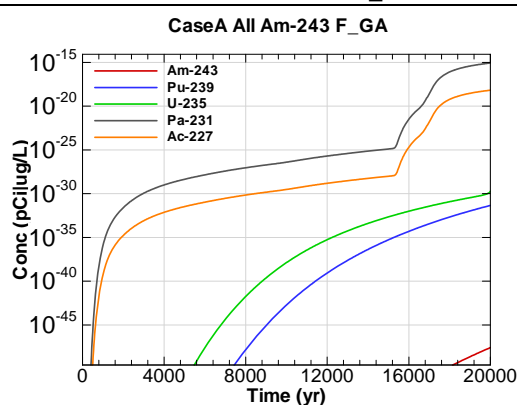


Figure A.3-54 - 100m Aquifer Concentration for
CaseA All Am-243 F_GA

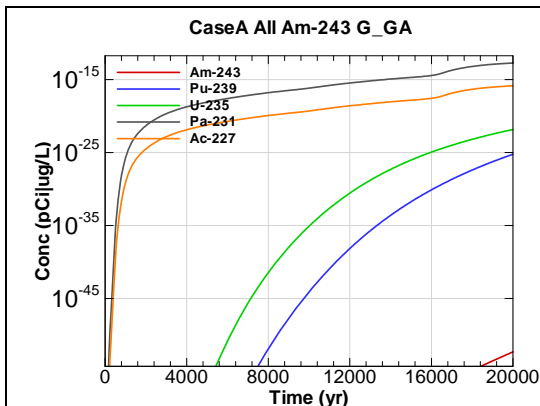


Figure A.3-55 - 100m Aquifer Concentration for
CaseA All Am-243 G_GA

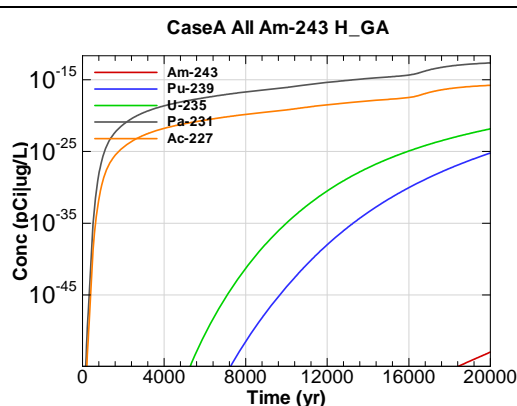


Figure A.3-56 - 100m Aquifer Concentration for
CaseA All Am-243 H_GA

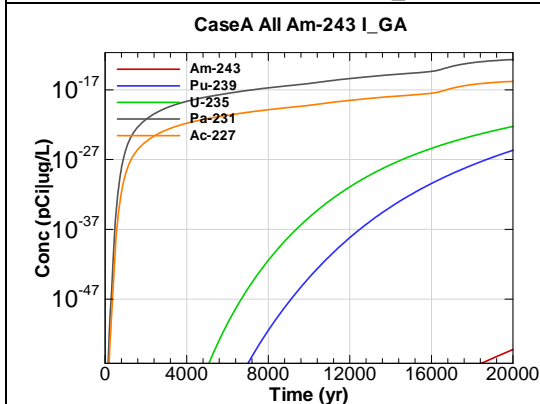


Figure A.3-57 - 100m Aquifer Concentration for
CaseA All Am-243 I_GA

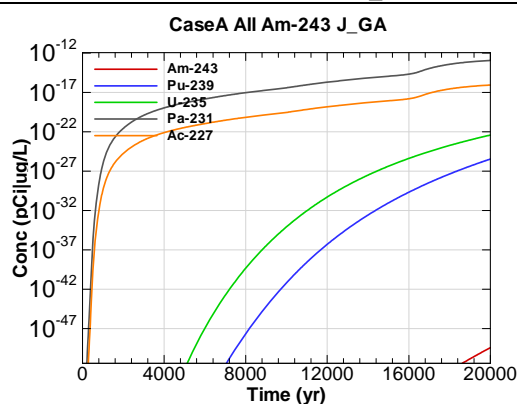


Figure A.3-58 - 100m Aquifer Concentration for
CaseA All Am-243 J_GA

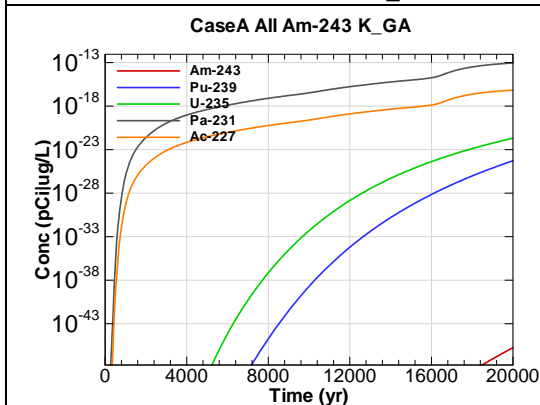


Figure A.3-59 - 100m Aquifer Concentration for
CaseA All Am-243 K_GA

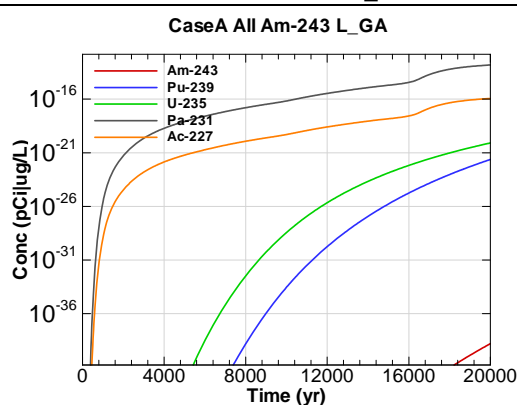
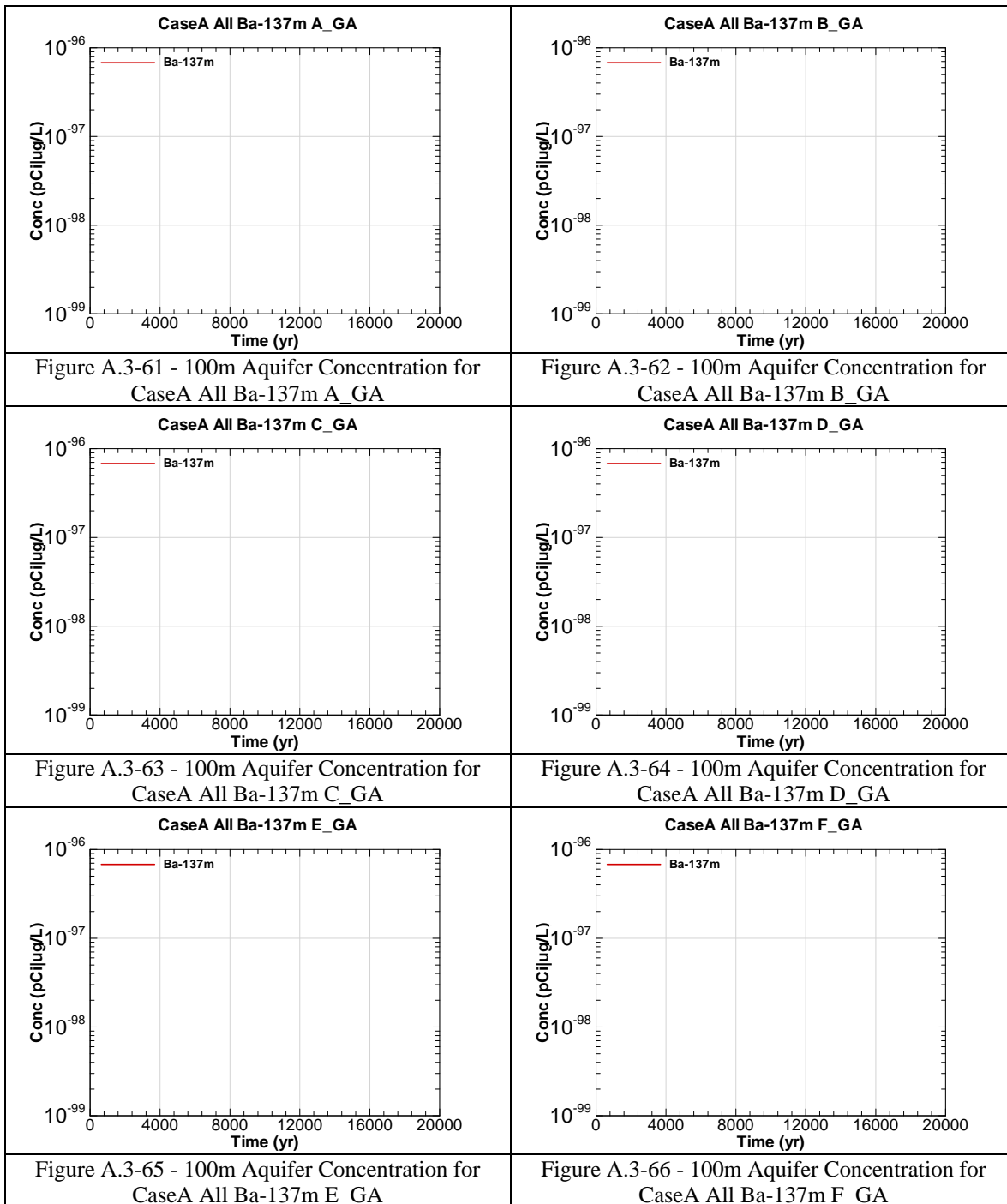
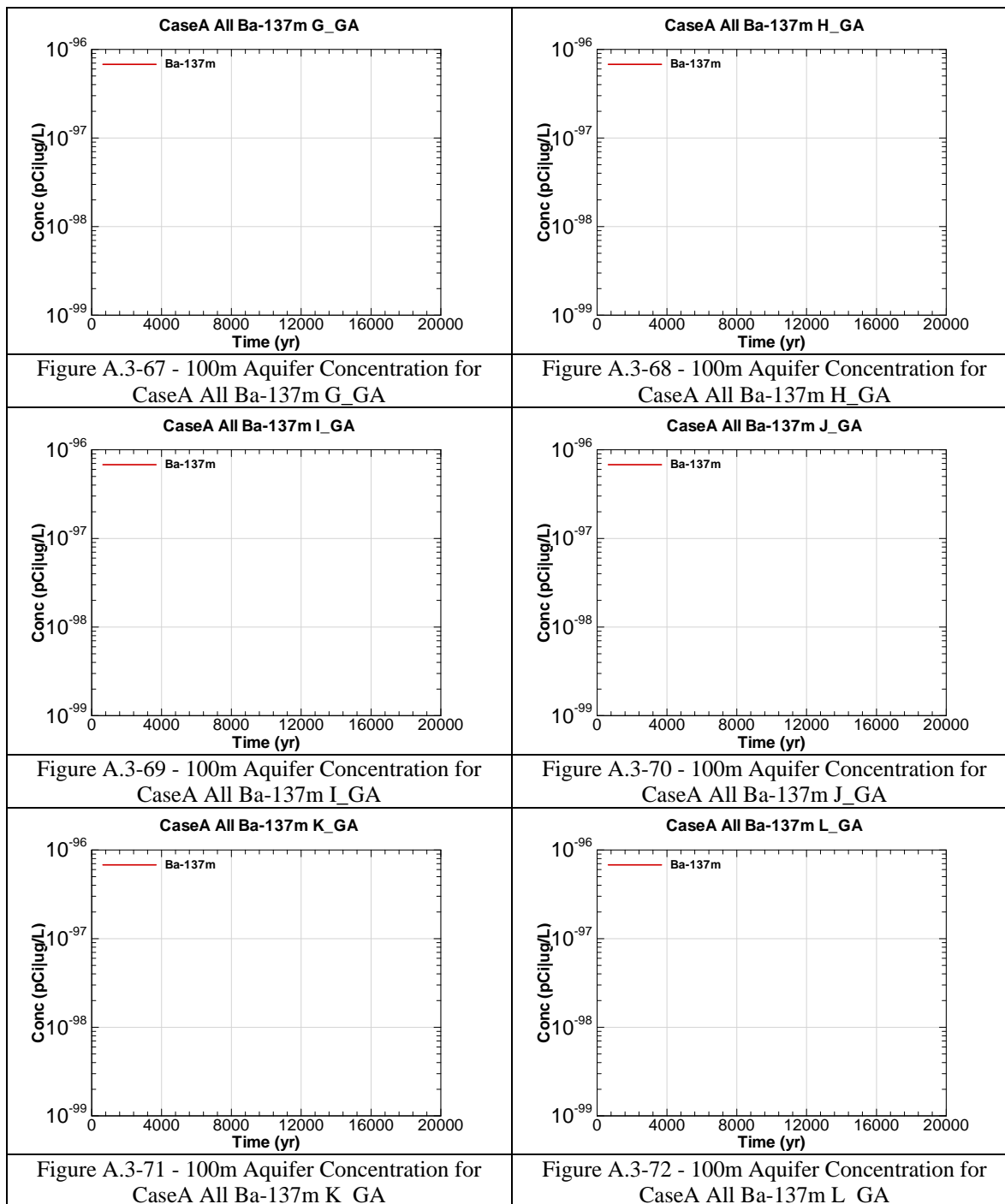


Figure A.3-60 - 100m Aquifer Concentration for
CaseA All Am-243 L_GA





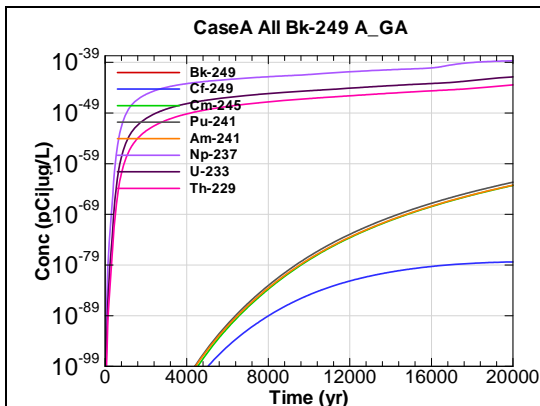


Figure A.3-73 - 100m Aquifer Concentration for
CaseA All Bk-249 A_GA

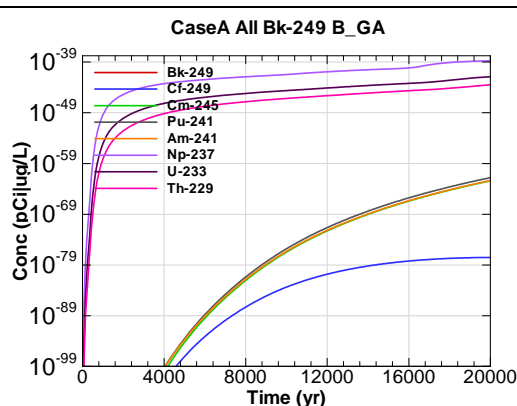


Figure A.3-74 - 100m Aquifer Concentration for
CaseA All Bk-249 B_GA

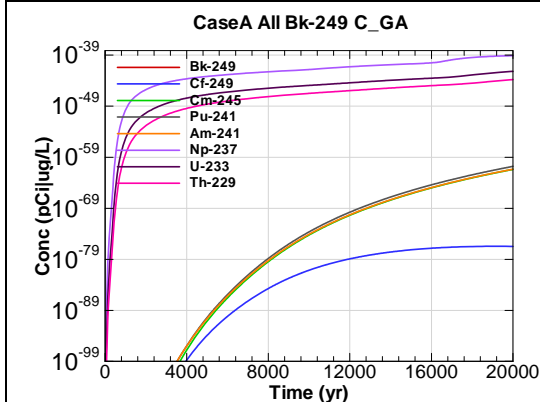


Figure A.3-75 - 100m Aquifer Concentration for
CaseA All Bk-249 C_GA

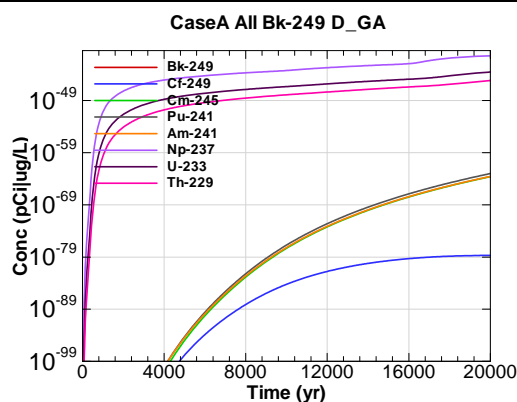


Figure A.3-76 - 100m Aquifer Concentration for
CaseA All Bk-249 D_GA

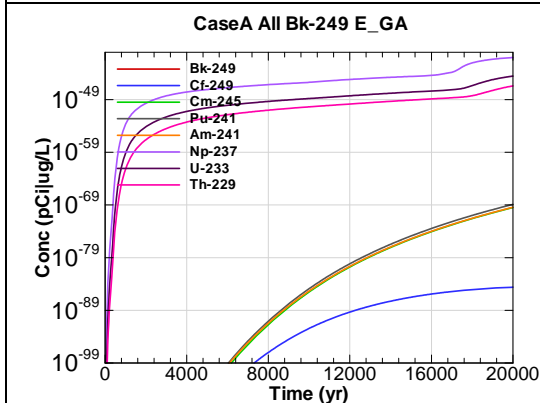


Figure A.3-77 - 100m Aquifer Concentration for
CaseA All Bk-249 E_GA

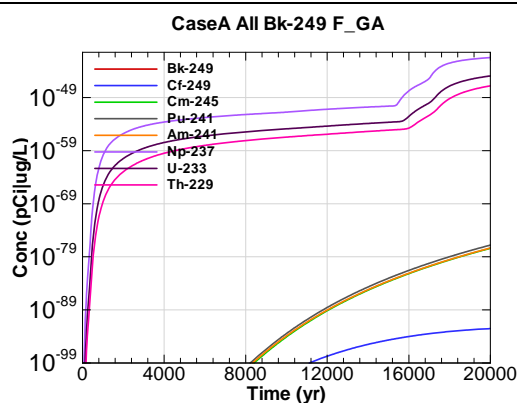


Figure A.3-78 - 100m Aquifer Concentration for
CaseA All Bk-249 F_GA

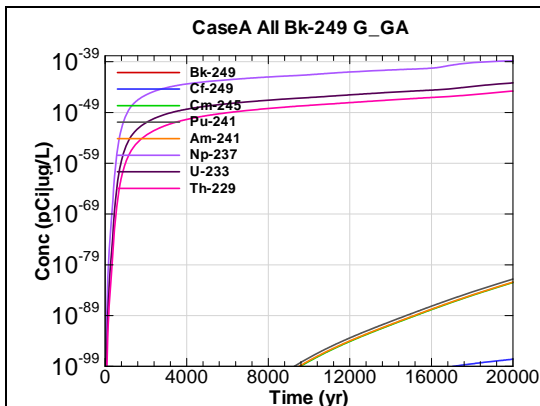


Figure A.3-79 - 100m Aquifer Concentration for
CaseA All Bk-249 G_GA

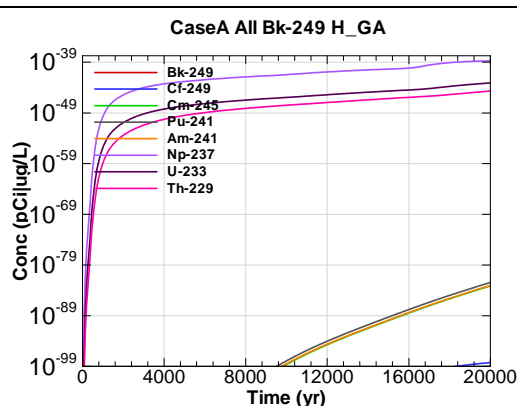


Figure A.3-80 - 100m Aquifer Concentration for
CaseA All Bk-249 H_GA

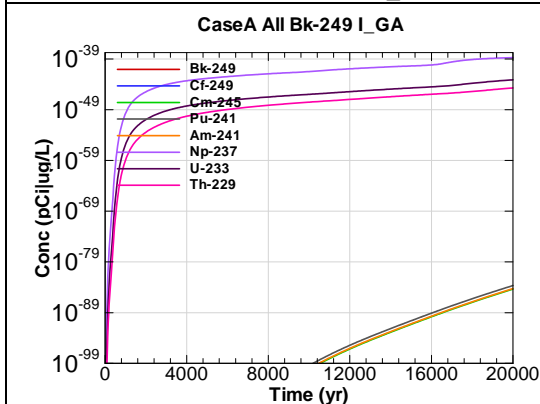


Figure A.3-81 - 100m Aquifer Concentration for
CaseA All Bk-249 I_GA

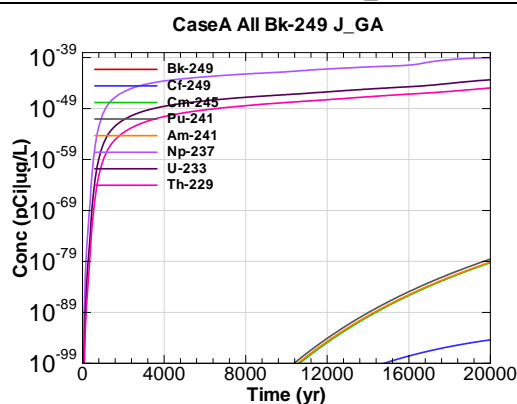


Figure A.3-82 - 100m Aquifer Concentration for
CaseA All Bk-249 J_GA

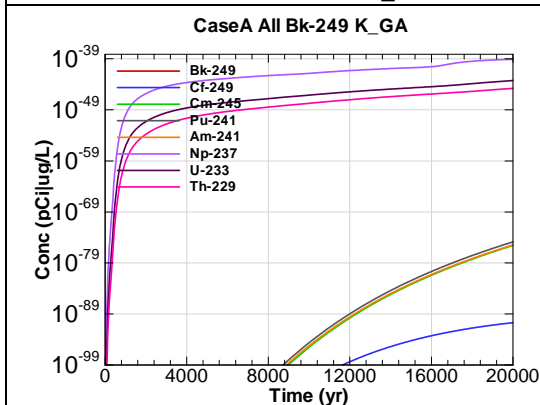


Figure A.3-83 - 100m Aquifer Concentration for
CaseA All Bk-249 K_GA

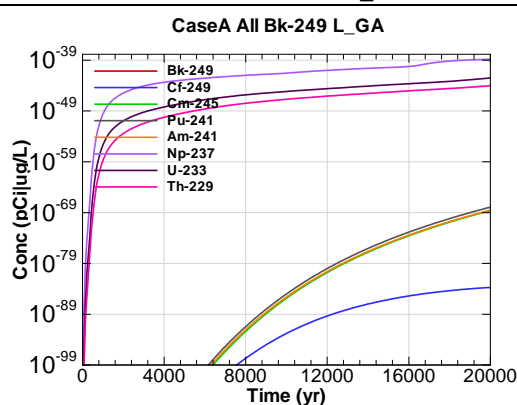
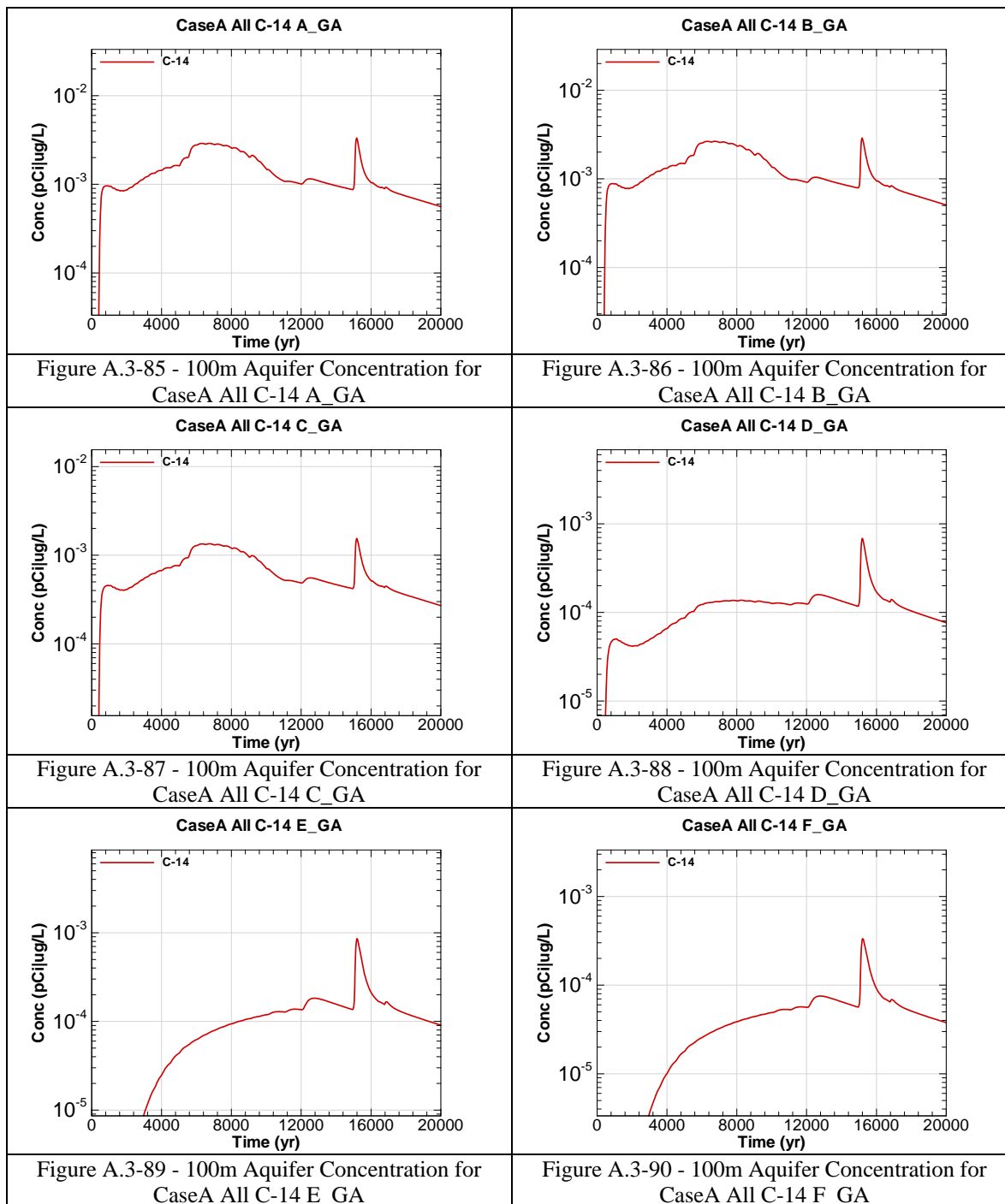
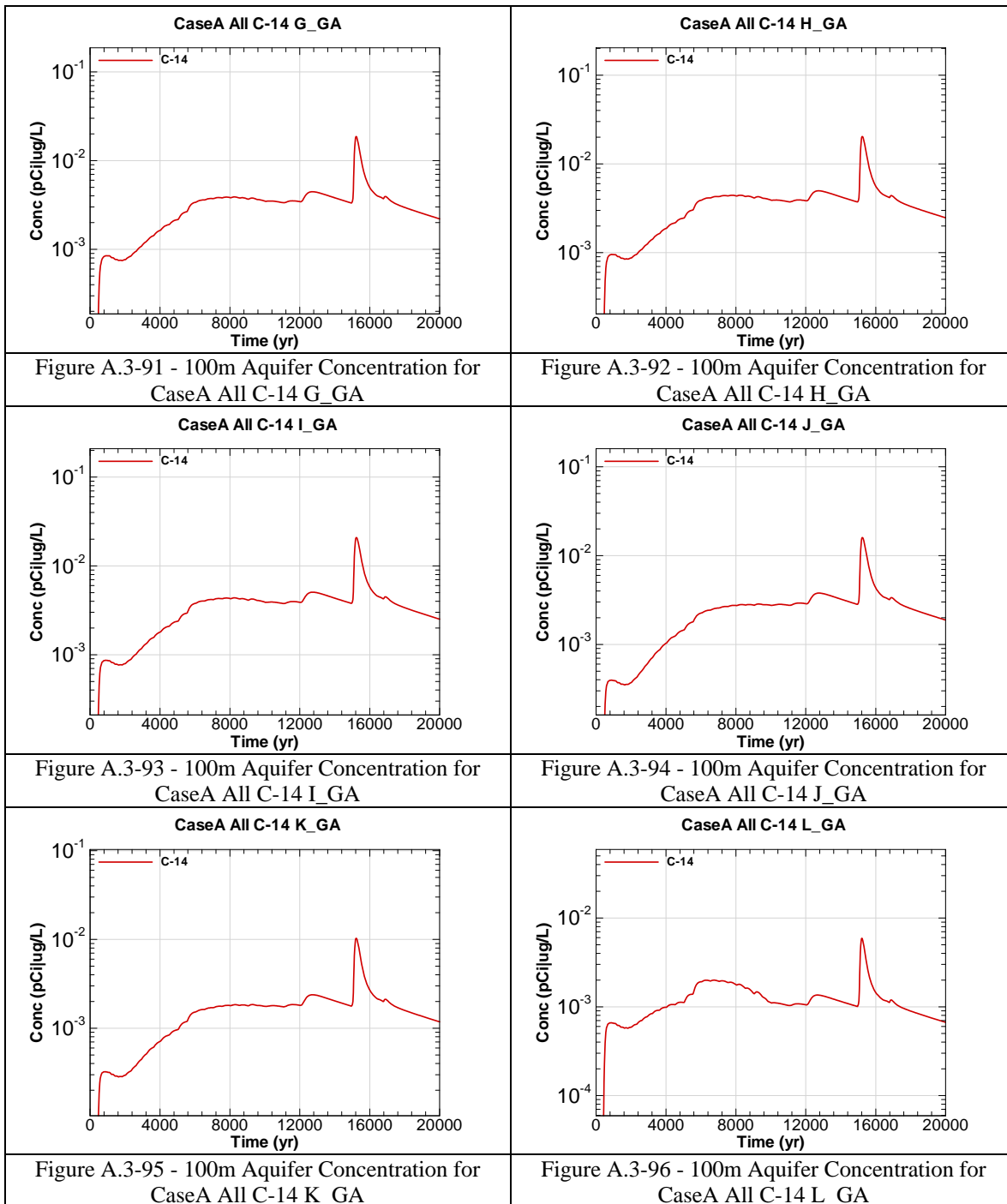
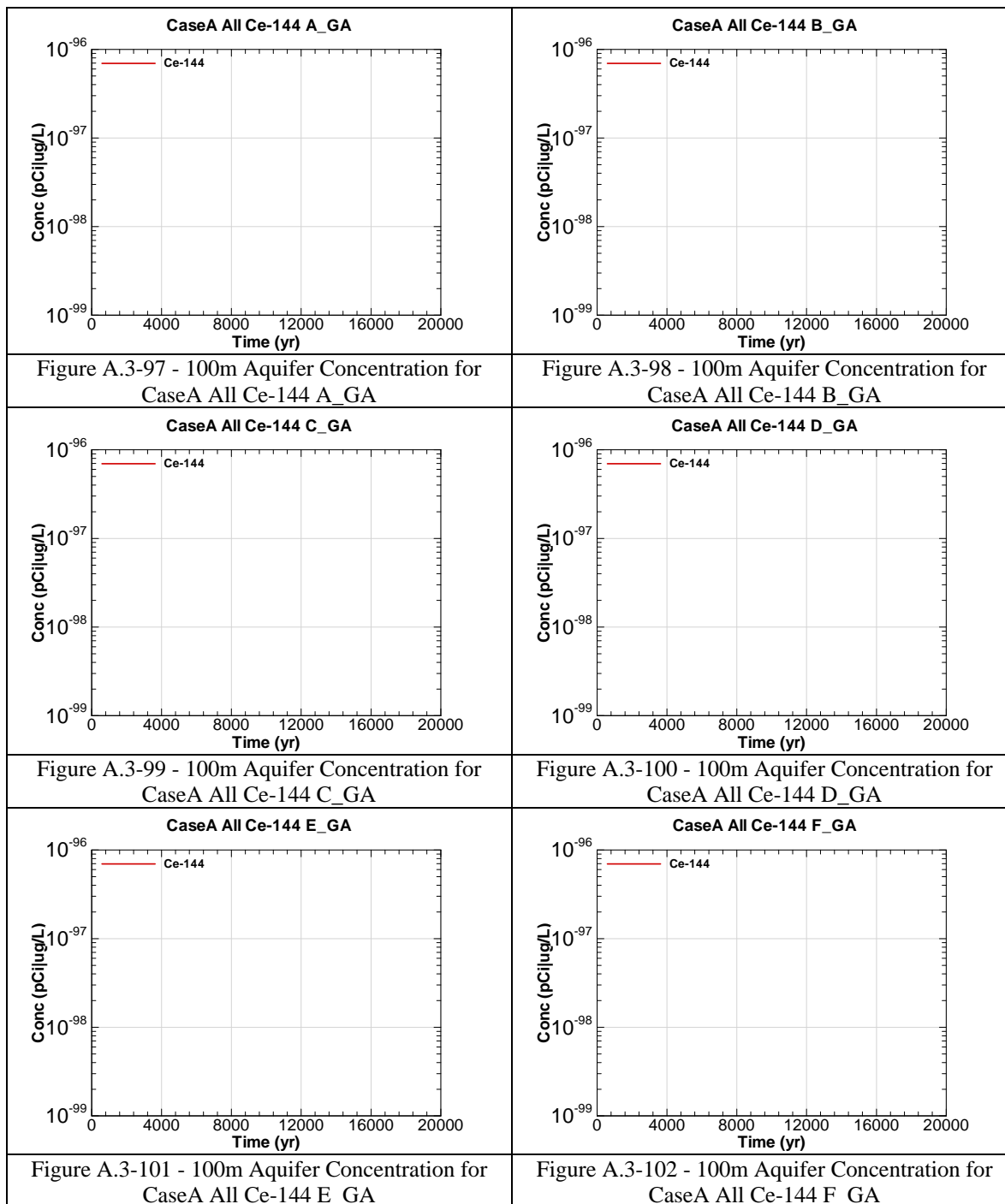
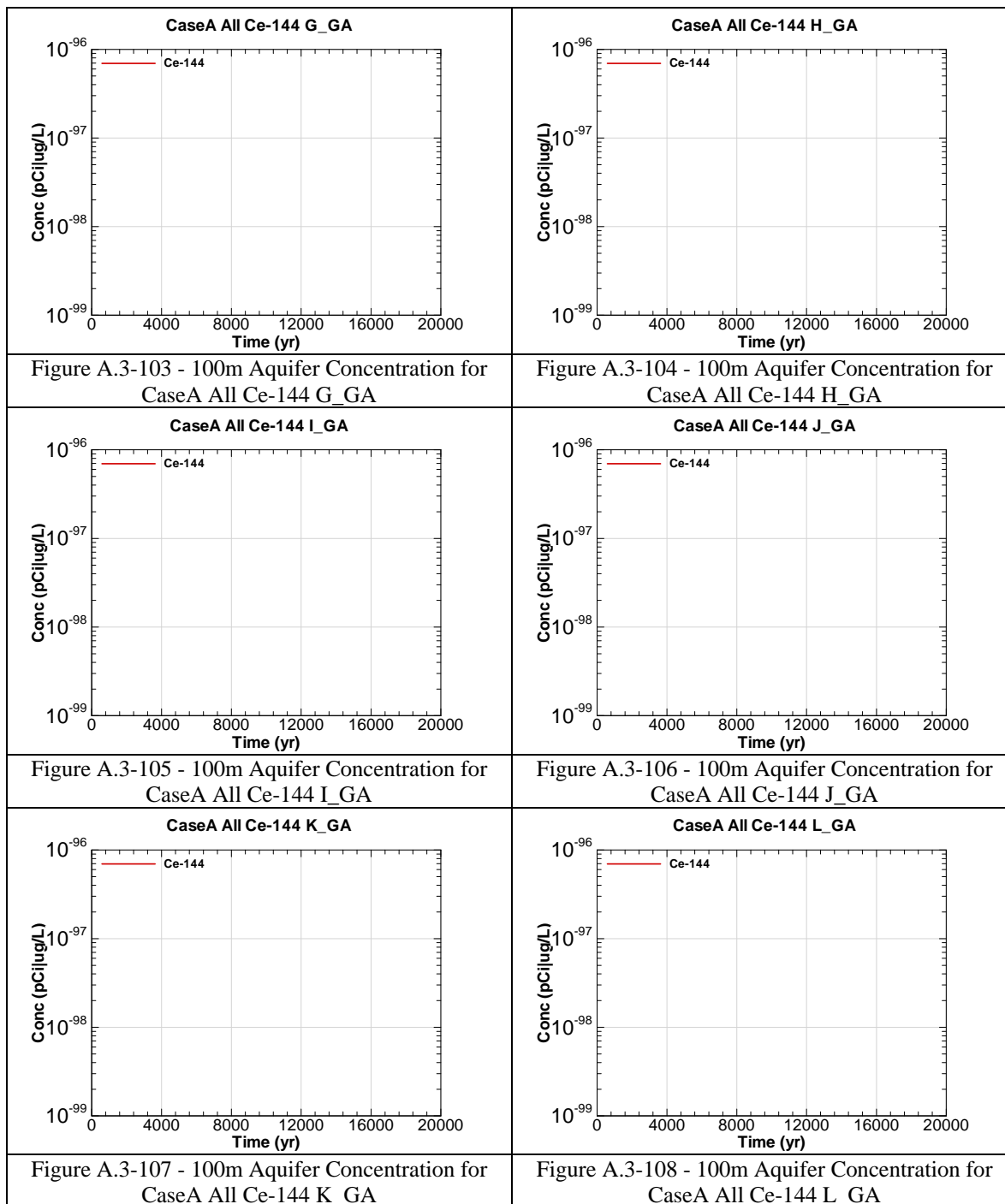


Figure A.3-84 - 100m Aquifer Concentration for
CaseA All Bk-249 L_GA









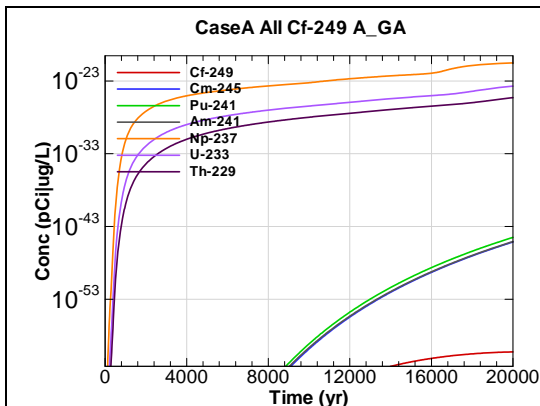


Figure A.3-109 - 100m Aquifer Concentration for
CaseA All Cf-249 A_GA

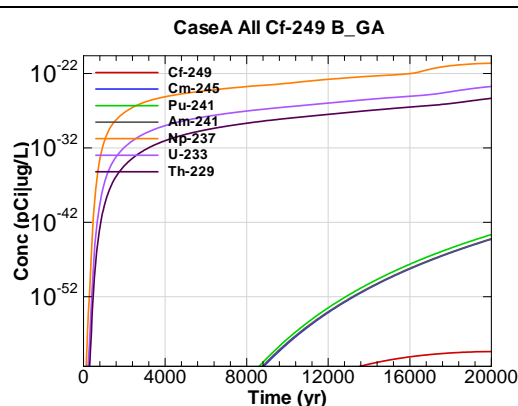


Figure A.3-110 - 100m Aquifer Concentration for
CaseA All Cf-249 B_GA

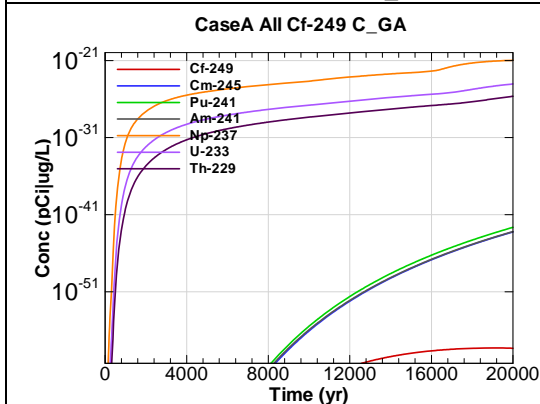


Figure A.3-111 - 100m Aquifer Concentration for
CaseA All Cf-249 C_GA

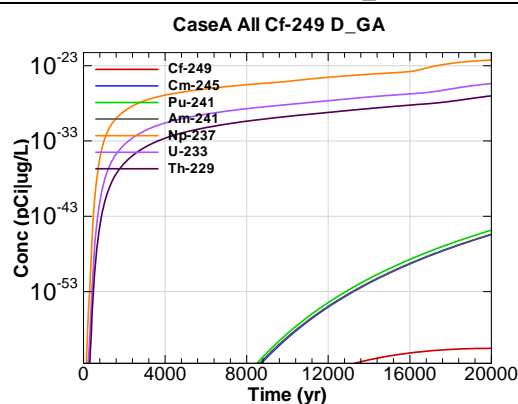


Figure A.3-112 - 100m Aquifer Concentration for
CaseA All Cf-249 D_GA

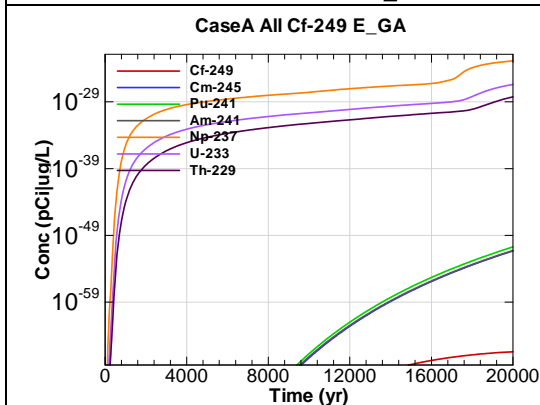


Figure A.3-113 - 100m Aquifer Concentration for
CaseA All Cf-249 E_GA

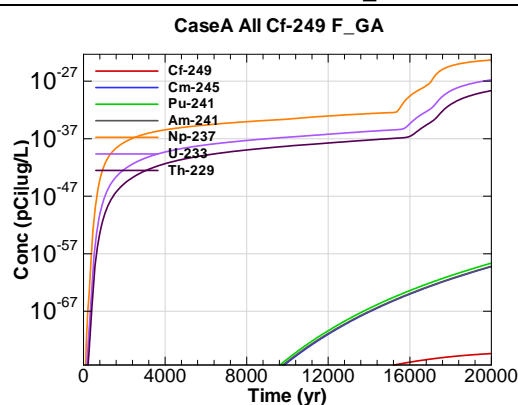


Figure A.3-114 - 100m Aquifer Concentration for
CaseA All Cf-249 F_GA

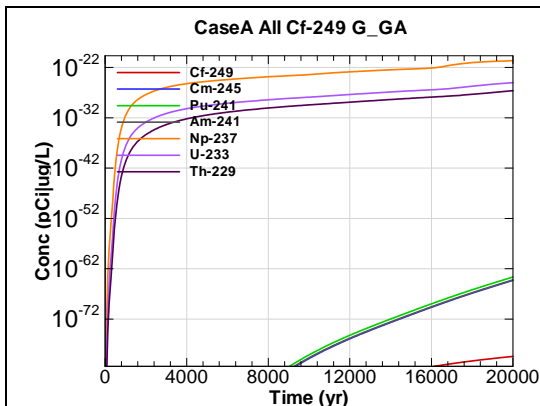


Figure A.3-115 - 100m Aquifer Concentration for
CaseA All Cf-249 G_GA

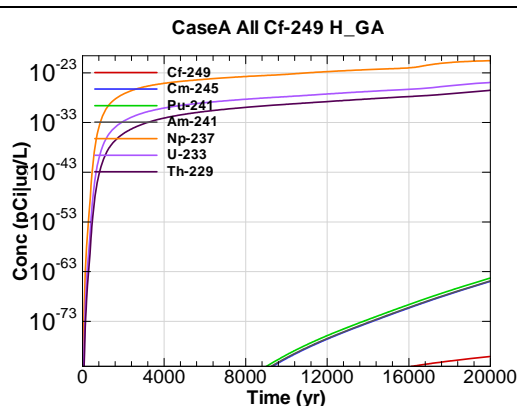


Figure A.3-116 - 100m Aquifer Concentration for
CaseA All Cf-249 H_GA

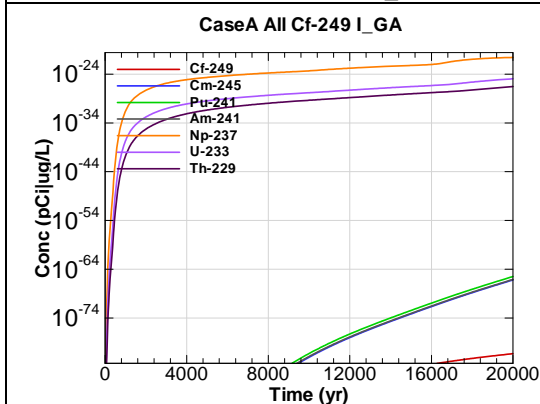


Figure A.3-117 - 100m Aquifer Concentration for
CaseA All Cf-249 I_GA

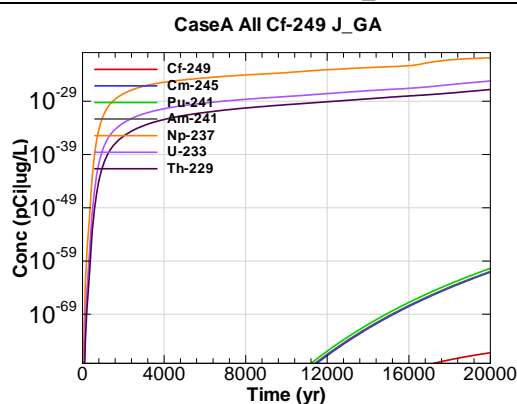


Figure A.3-118 - 100m Aquifer Concentration for
CaseA All Cf-249 J_GA

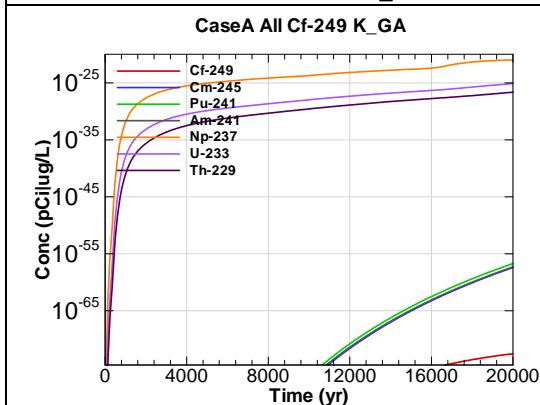


Figure A.3-119 - 100m Aquifer Concentration for
CaseA All Cf-249 K_GA

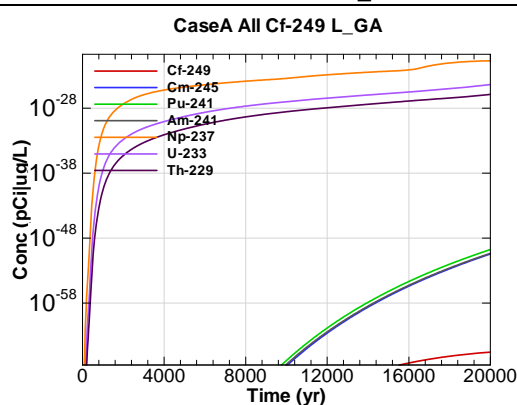


Figure A.3-120 - 100m Aquifer Concentration for
CaseA All Cf-249 L_GA

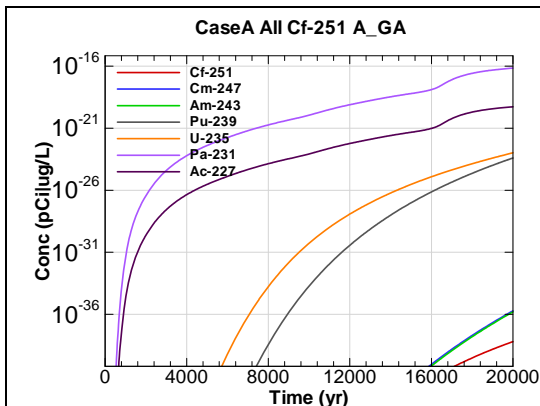


Figure A.3-121 - 100m Aquifer Concentration for
CaseA All Cf-251 A_GA

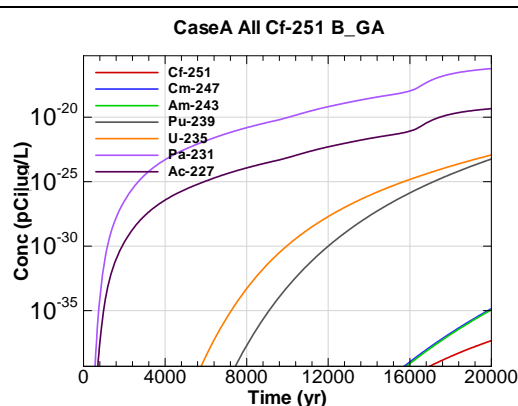


Figure A.3-122 - 100m Aquifer Concentration for
CaseA All Cf-251 B_GA

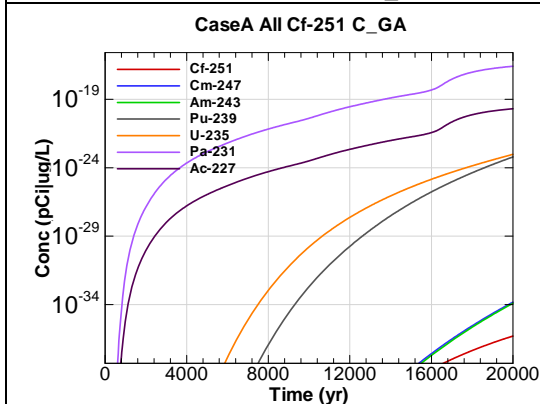


Figure A.3-123 - 100m Aquifer Concentration for
CaseA All Cf-251 C_GA

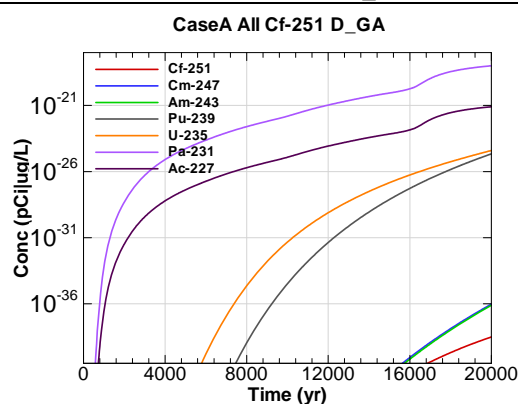


Figure A.3-124 - 100m Aquifer Concentration for
CaseA All Cf-251 D_GA

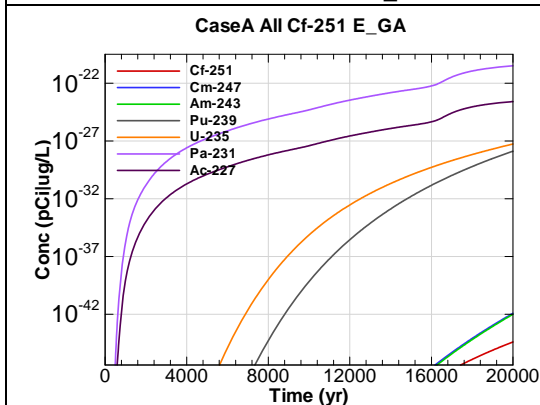


Figure A.3-125 - 100m Aquifer Concentration for
CaseA All Cf-251 E_GA

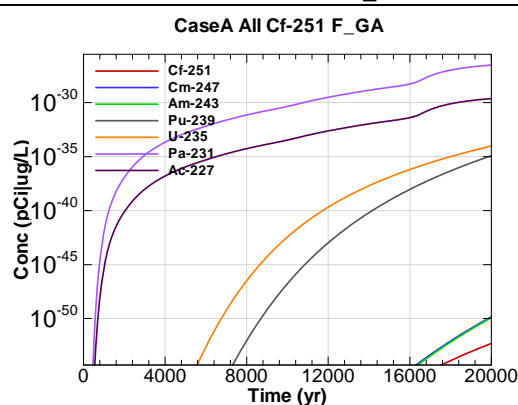


Figure A.3-126 - 100m Aquifer Concentration for
CaseA All Cf-251 F_GA

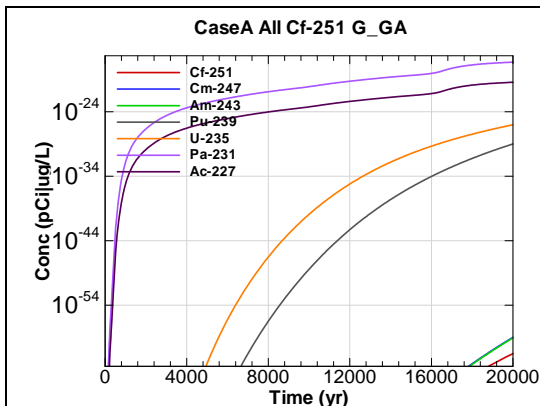


Figure A.3-127 - 100m Aquifer Concentration for
CaseA All Cf-251 G_GA

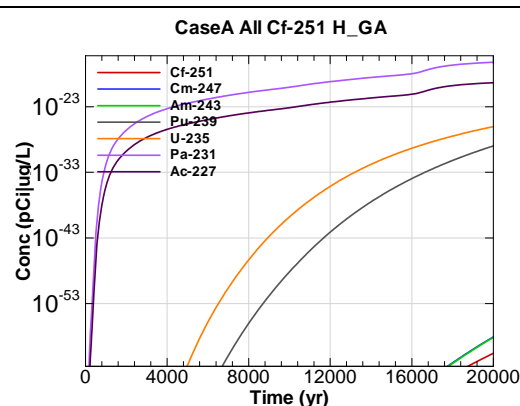


Figure A.3-128 - 100m Aquifer Concentration for
CaseA All Cf-251 H_GA

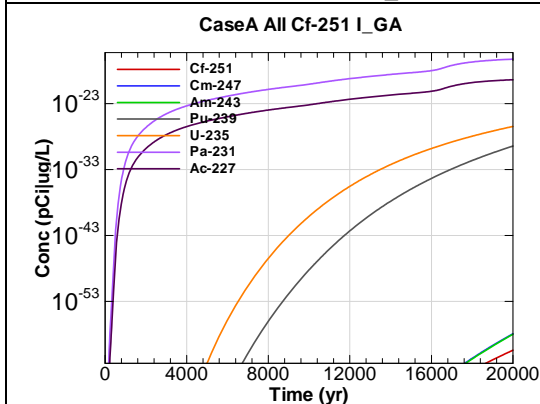


Figure A.3-129 - 100m Aquifer Concentration for
CaseA All Cf-251 I_GA

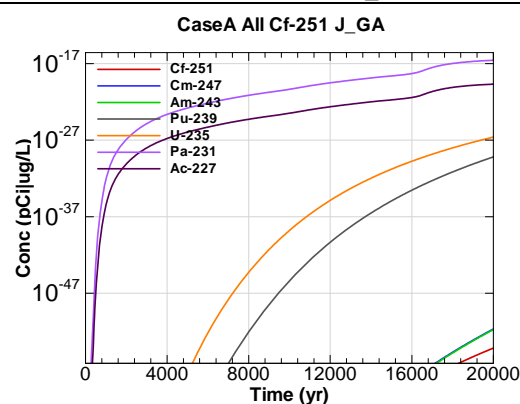


Figure A.3-130 - 100m Aquifer Concentration for
CaseA All Cf-251 J_GA

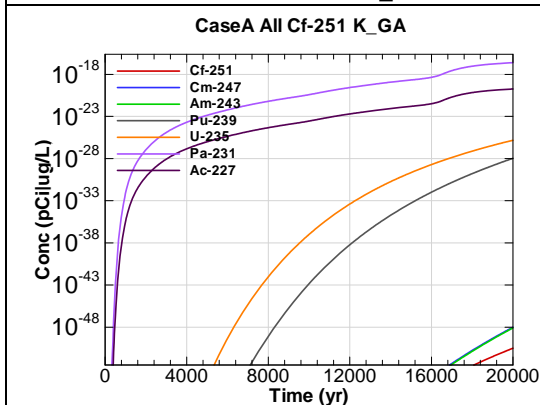


Figure A.3-131 - 100m Aquifer Concentration for
CaseA All Cf-251 K_GA

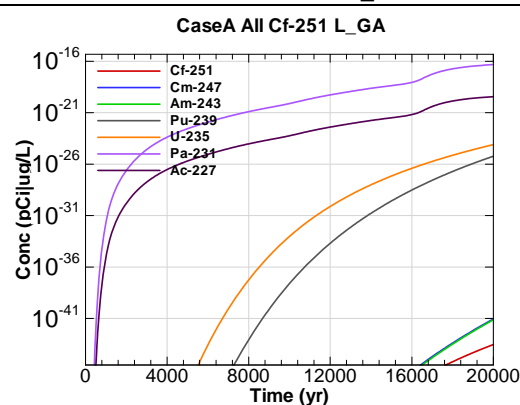


Figure A.3-132 - 100m Aquifer Concentration for
CaseA All Cf-251 L_GA

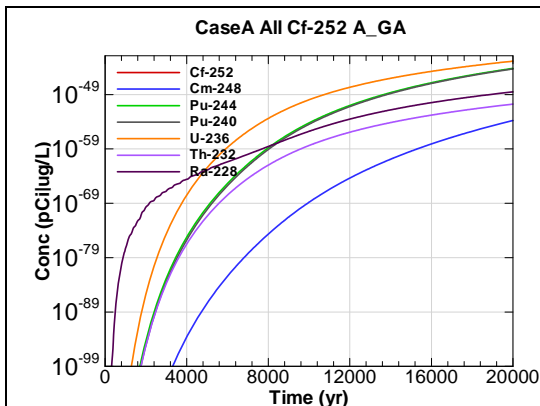


Figure A.3-133 - 100m Aquifer Concentration for
CaseA All Cf-252 A_GA

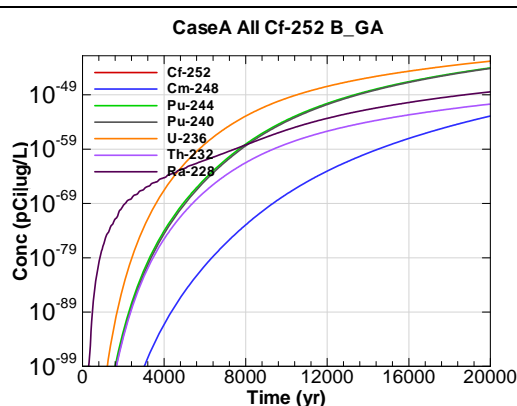


Figure A.3-134 - 100m Aquifer Concentration for
CaseA All Cf-252 B_GA

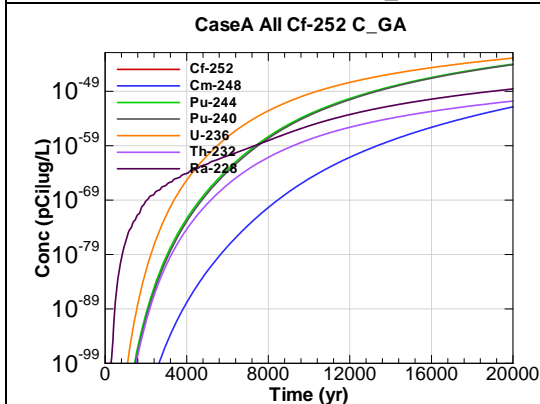


Figure A.3-135 - 100m Aquifer Concentration for
CaseA All Cf-252 C_GA

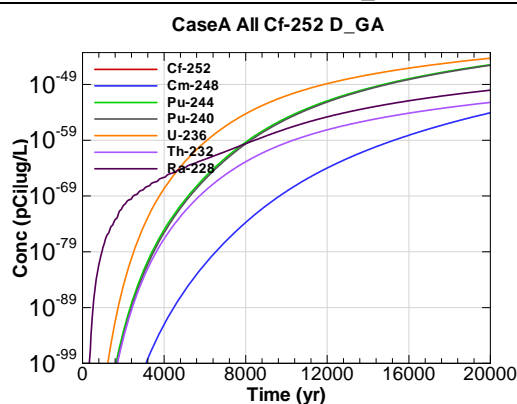


Figure A.3-136 - 100m Aquifer Concentration for
CaseA All Cf-252 D_GA

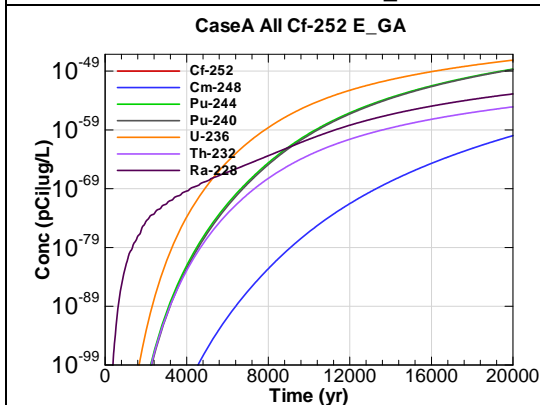


Figure A.3-137 - 100m Aquifer Concentration for
CaseA All Cf-252 E_GA

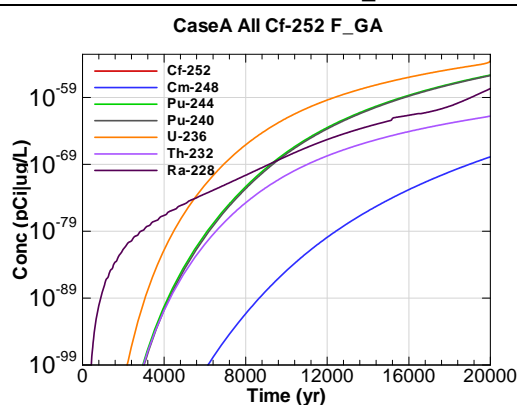


Figure A.3-138 - 100m Aquifer Concentration for
CaseA All Cf-252 F_GA

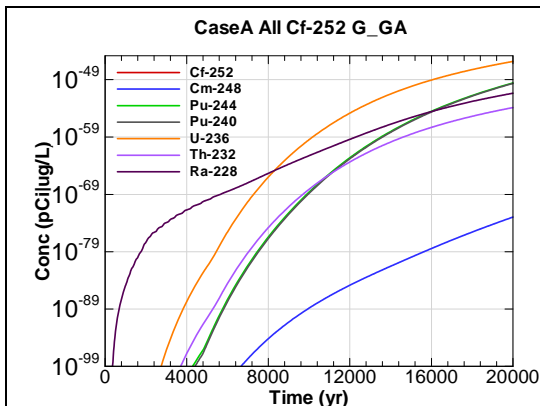


Figure A.3-139 - 100m Aquifer Concentration for
CaseA All Cf-252 G_GA

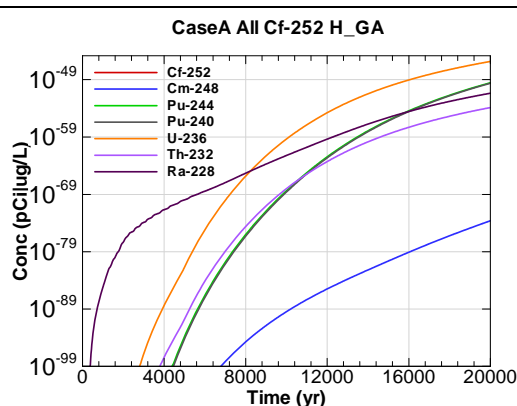


Figure A.3-140 - 100m Aquifer Concentration for
CaseA All Cf-252 H_GA

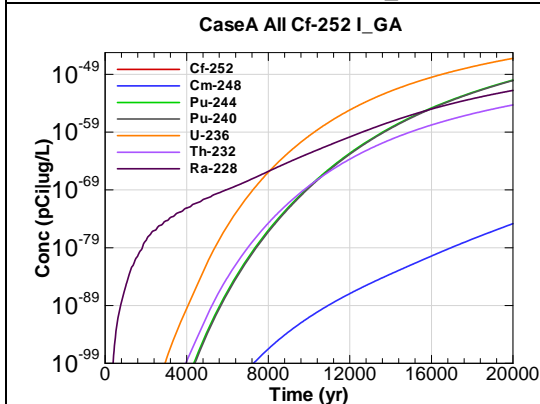


Figure A.3-141 - 100m Aquifer Concentration for
CaseA All Cf-252 I_GA

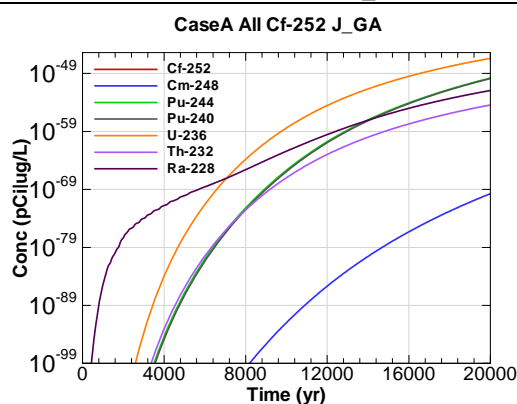


Figure A.3-142 - 100m Aquifer Concentration for
CaseA All Cf-252 J_GA

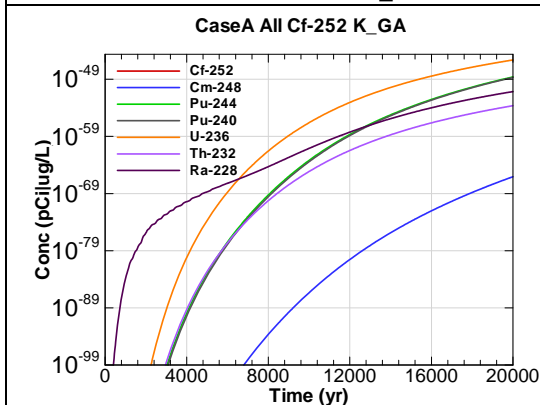


Figure A.3-143 - 100m Aquifer Concentration for
CaseA All Cf-252 K_GA

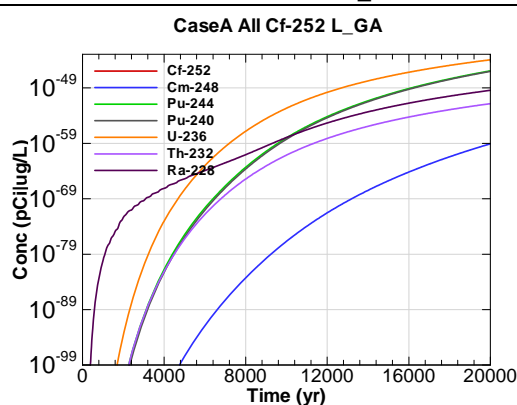
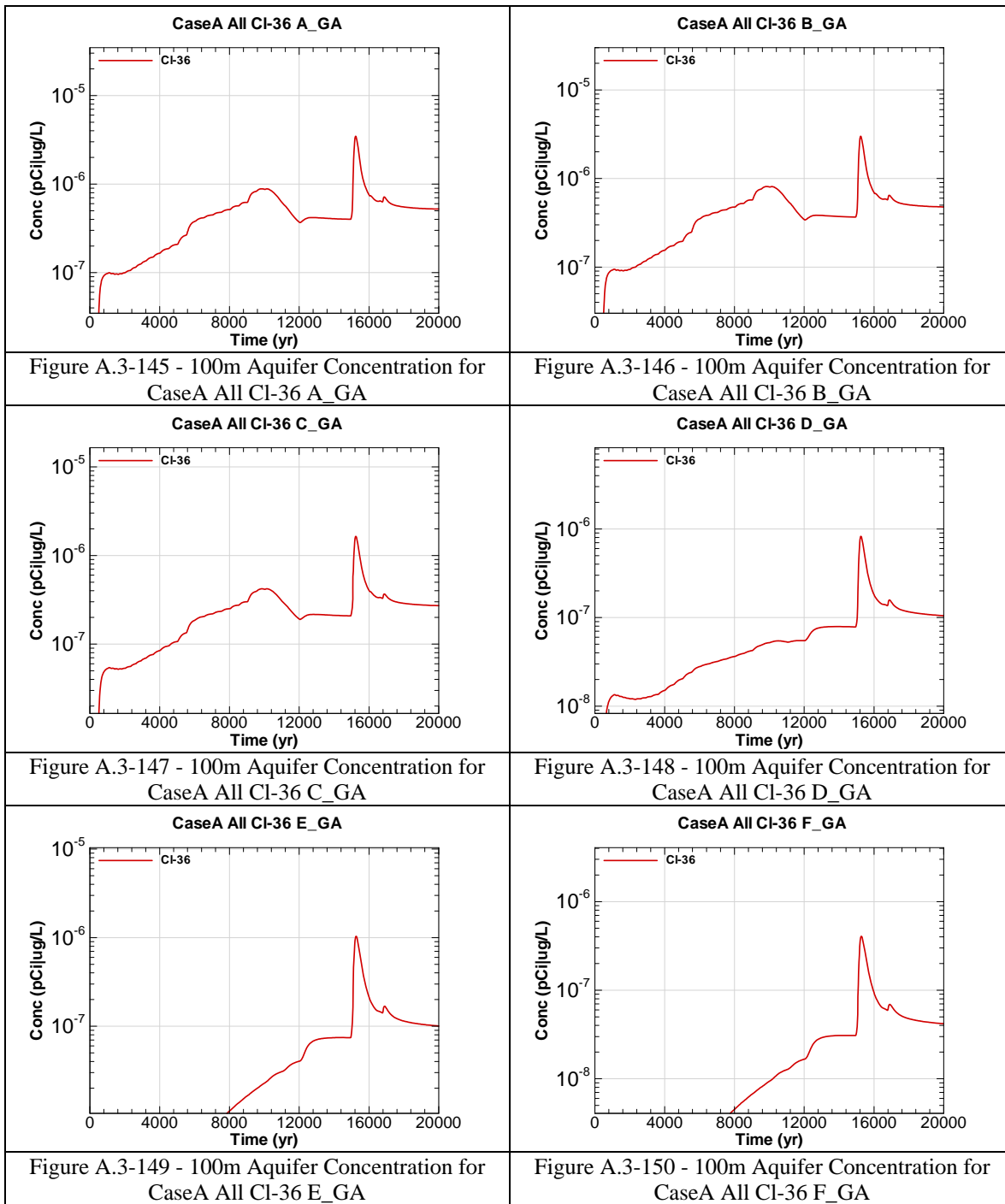
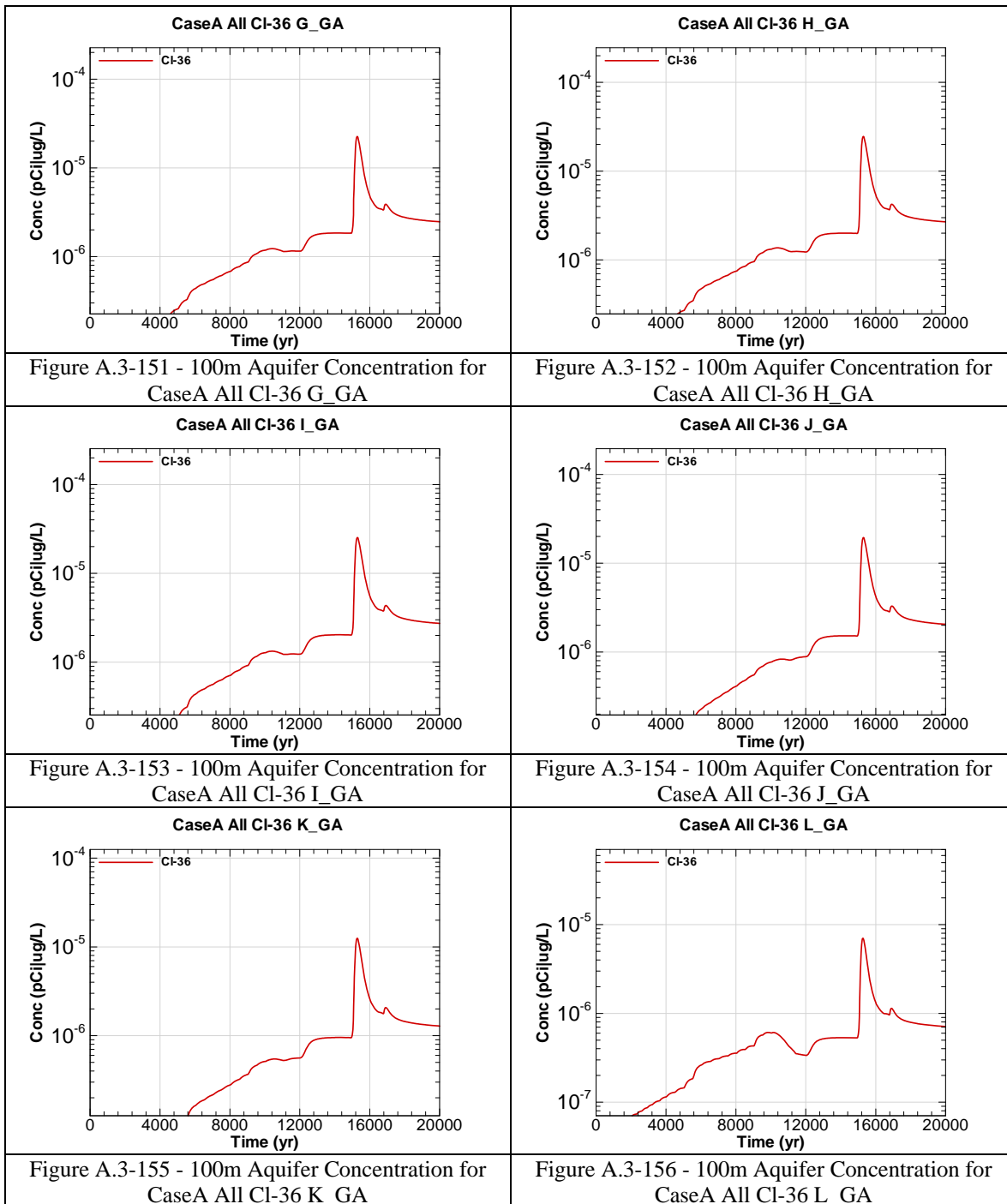


Figure A.3-144 - 100m Aquifer Concentration for
CaseA All Cf-252 L_GA





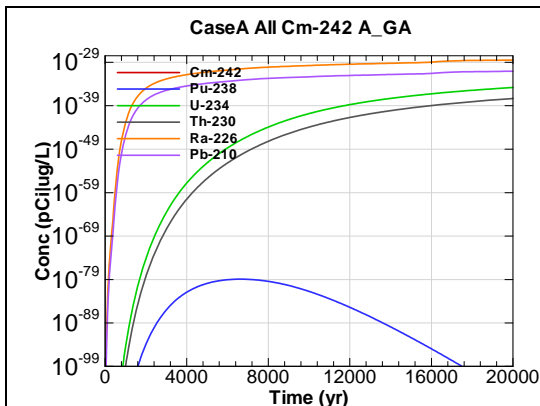


Figure A.3-157 - 100m Aquifer Concentration for
CaseA All Cm-242 A_GA

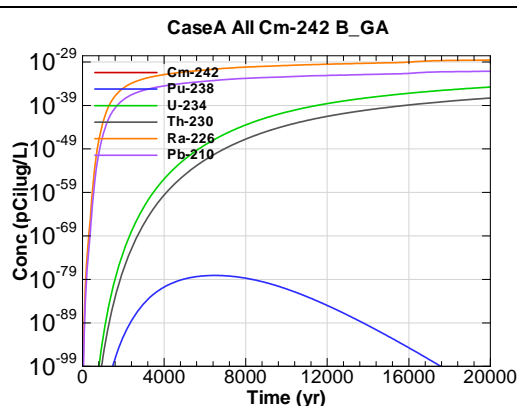


Figure A.3-158 - 100m Aquifer Concentration for
CaseA All Cm-242 B_GA

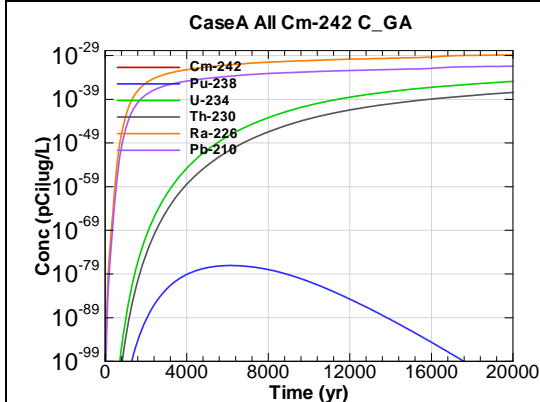


Figure A.3-159 - 100m Aquifer Concentration for
CaseA All Cm-242 C_GA

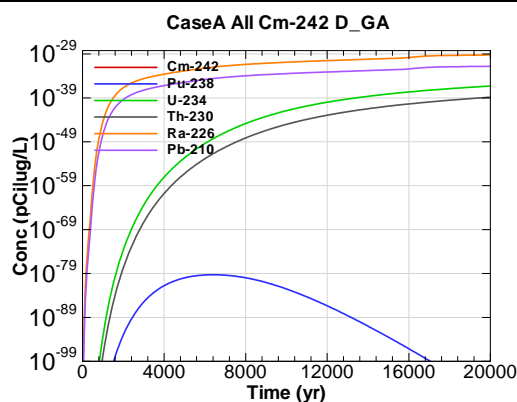


Figure A.3-160 - 100m Aquifer Concentration for
CaseA All Cm-242 D_GA

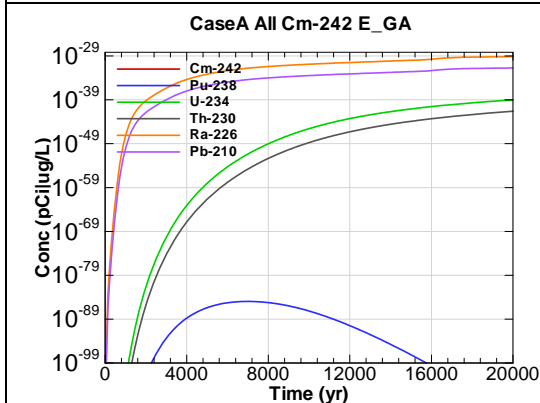


Figure A.3-161 - 100m Aquifer Concentration for
CaseA All Cm-242 E_GA

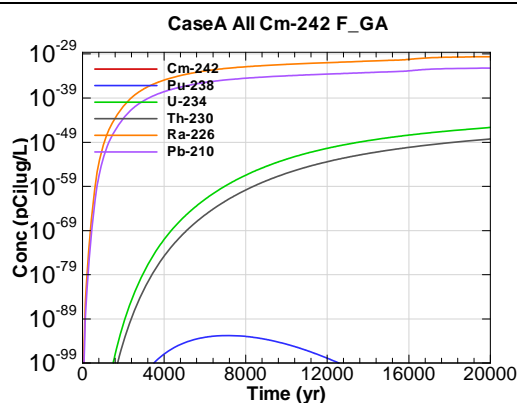


Figure A.3-162 - 100m Aquifer Concentration for
CaseA All Cm-242 F_GA

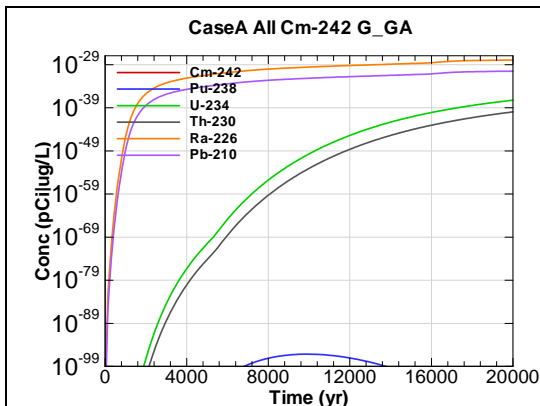


Figure A.3-163 - 100m Aquifer Concentration for
CaseA All Cm-242 G_GA

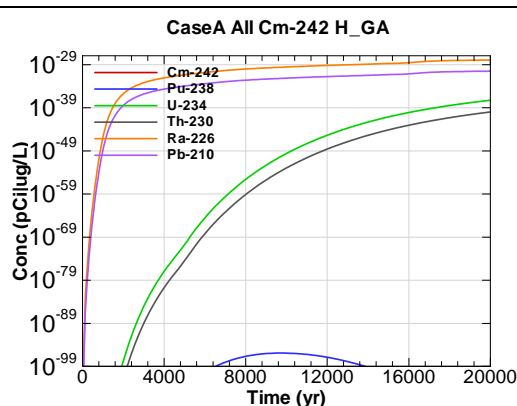


Figure A.3-164 - 100m Aquifer Concentration for
CaseA All Cm-242 H_GA

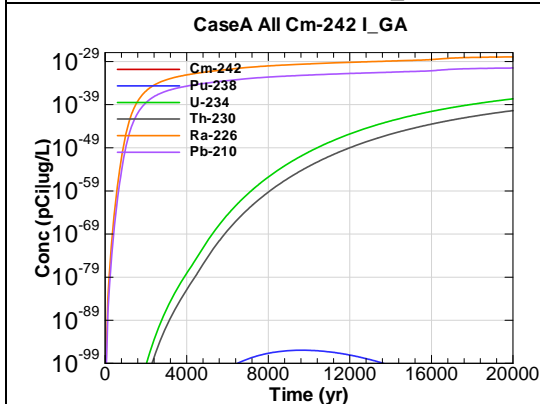


Figure A.3-165 - 100m Aquifer Concentration for
CaseA All Cm-242 I_GA

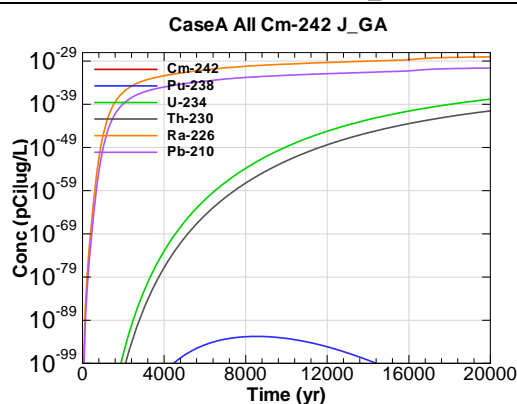


Figure A.3-166 - 100m Aquifer Concentration for
CaseA All Cm-242 J_GA

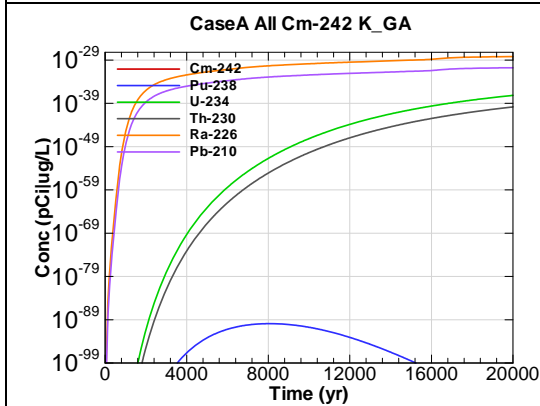


Figure A.3-167 - 100m Aquifer Concentration for
CaseA All Cm-242 K_GA

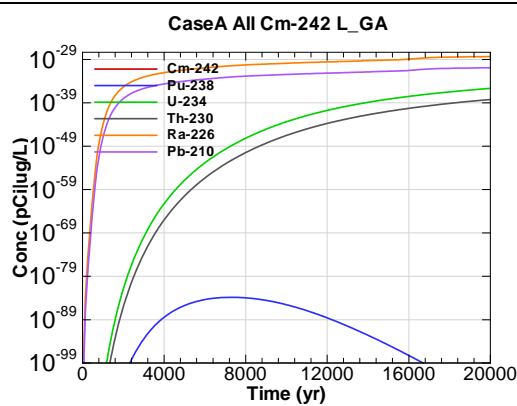
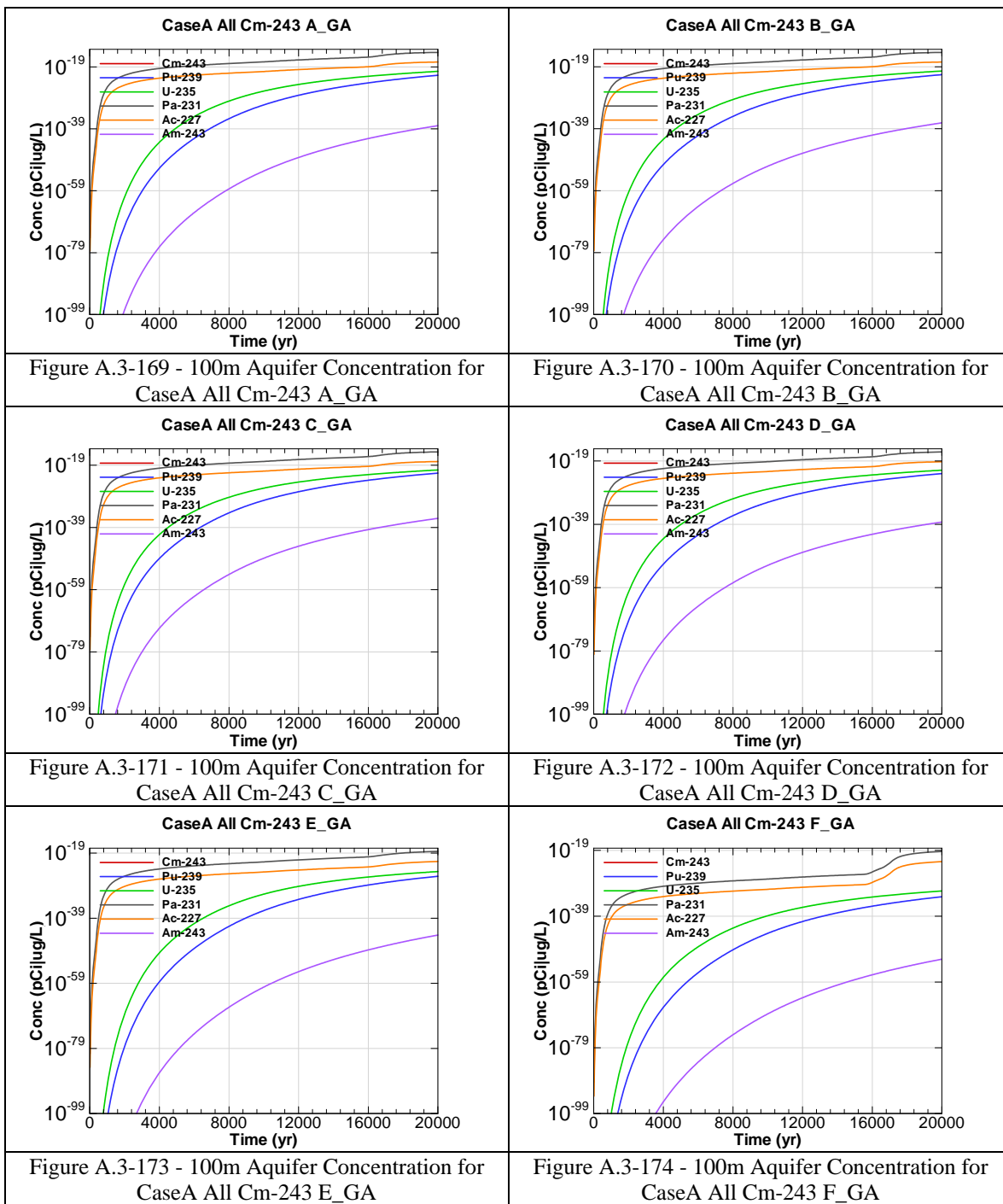


Figure A.3-168 - 100m Aquifer Concentration for
CaseA All Cm-242 L_GA



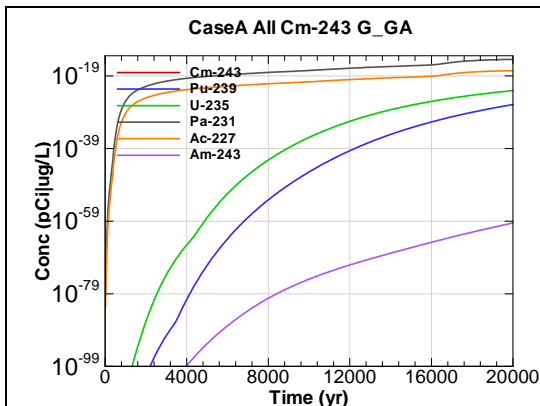


Figure A.3-175 - 100m Aquifer Concentration for
CaseA All Cm-243 G_GA

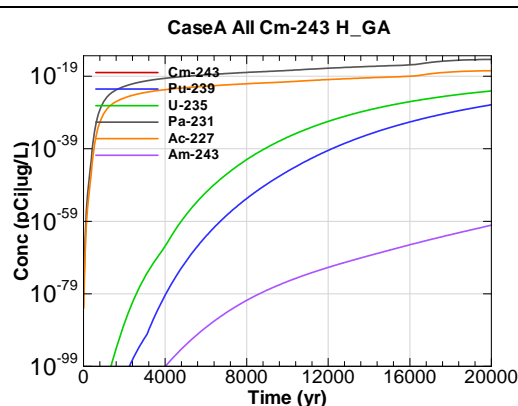


Figure A.3-176 - 100m Aquifer Concentration for
CaseA All Cm-243 H_GA

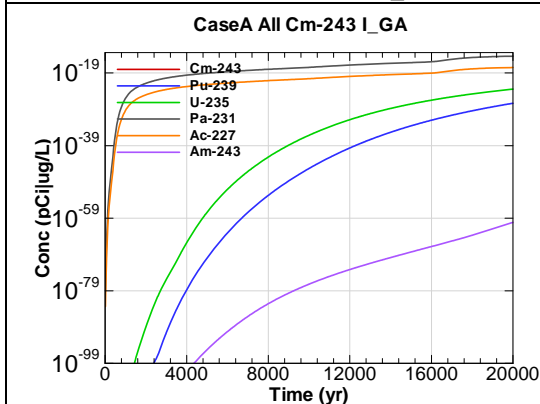


Figure A.3-177 - 100m Aquifer Concentration for
CaseA All Cm-243 I_GA

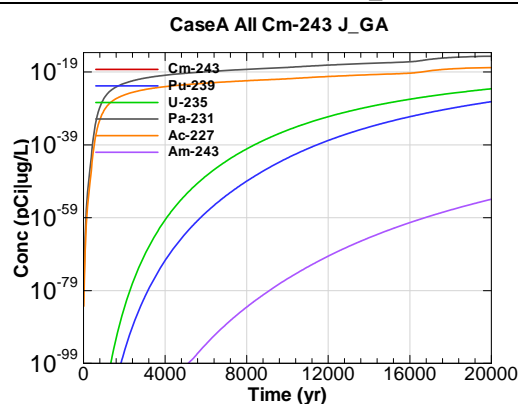


Figure A.3-178 - 100m Aquifer Concentration for
CaseA All Cm-243 J_GA

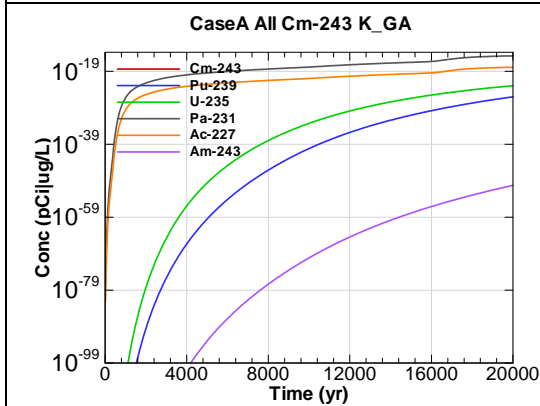


Figure A.3-179 - 100m Aquifer Concentration for
CaseA All Cm-243 K_GA

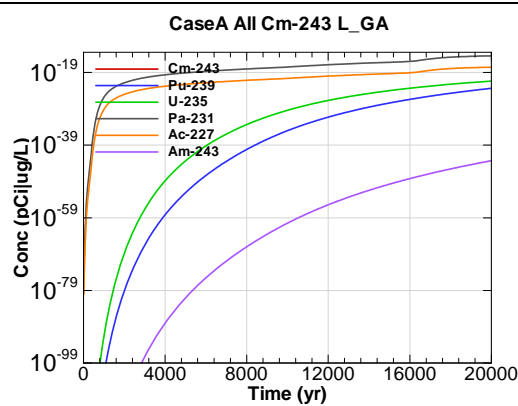
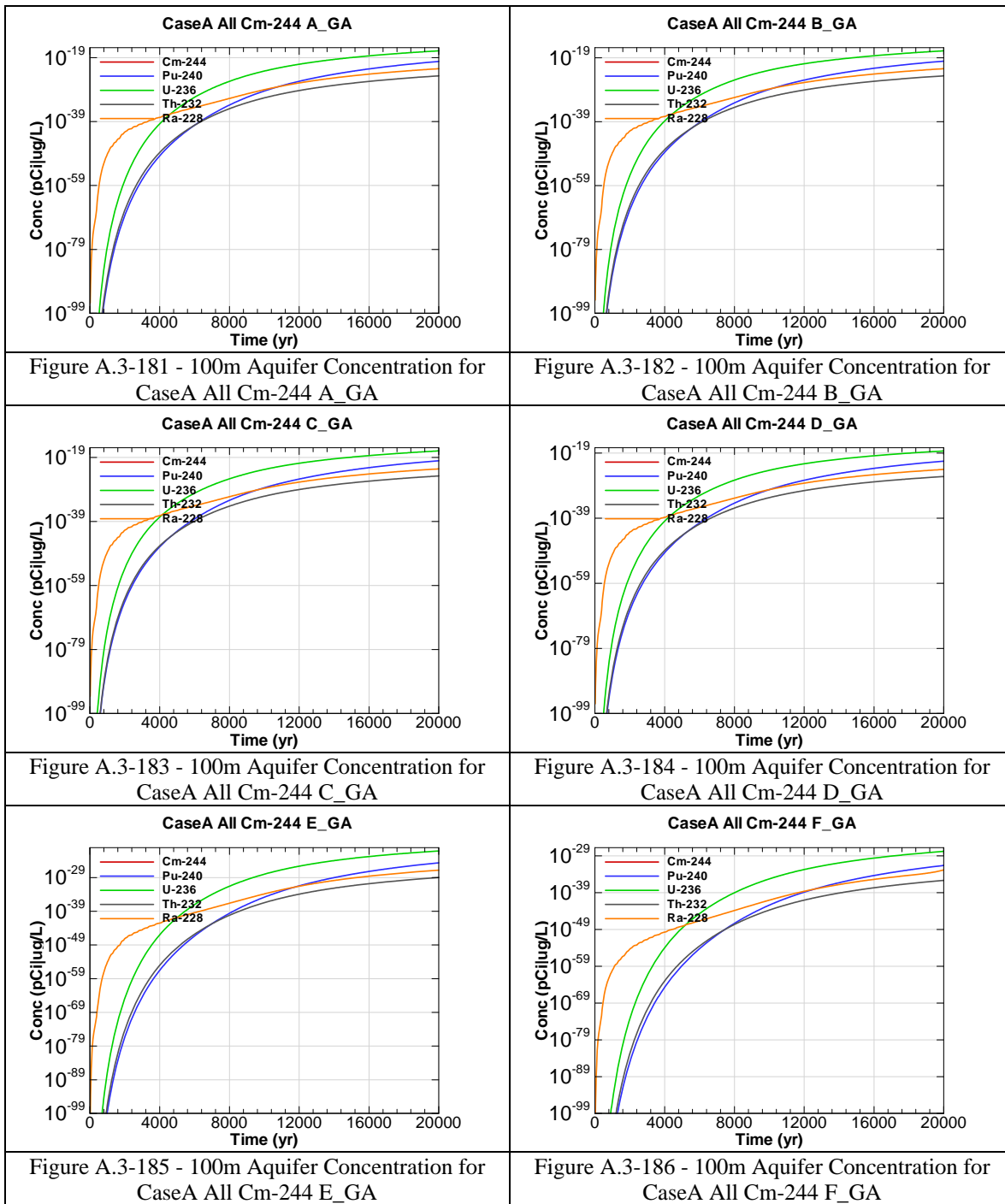


Figure A.3-180 - 100m Aquifer Concentration for
CaseA All Cm-243 L_GA



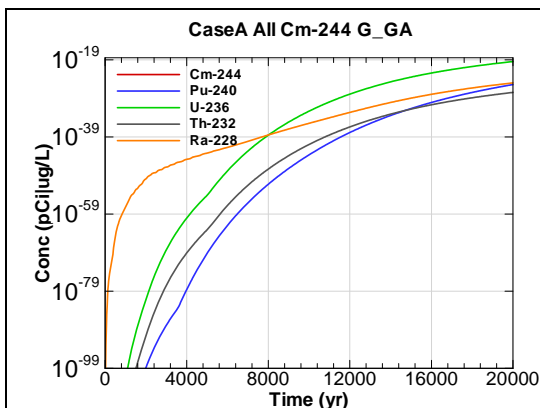


Figure A.3-187 - 100m Aquifer Concentration for CaseA All Cm-244 G_GA

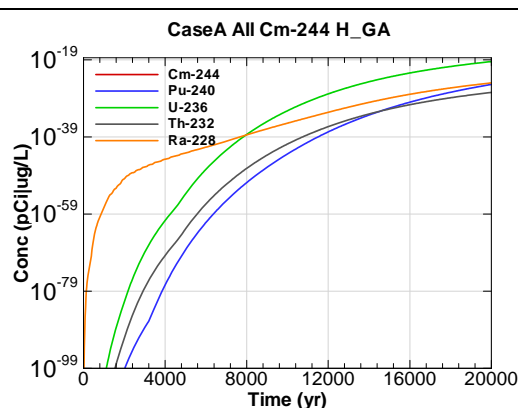


Figure A.3-188 - 100m Aquifer Concentration for CaseA All Cm-244 H_GA

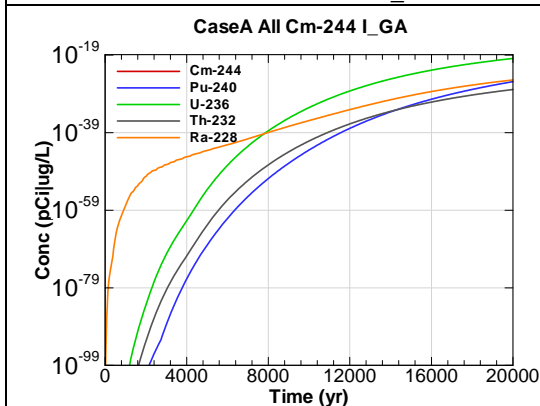


Figure A.3-189 - 100m Aquifer Concentration for CaseA All Cm-244 I_GA

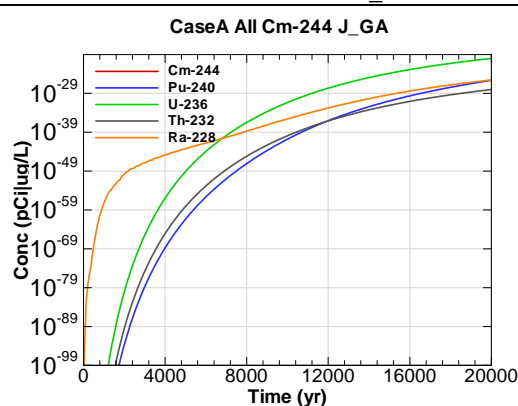


Figure A.3-190 - 100m Aquifer Concentration for CaseA All Cm-244 J_GA

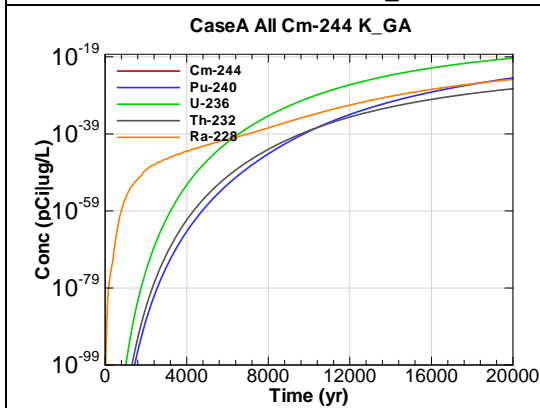


Figure A.3-191 - 100m Aquifer Concentration for CaseA All Cm-244 K_GA

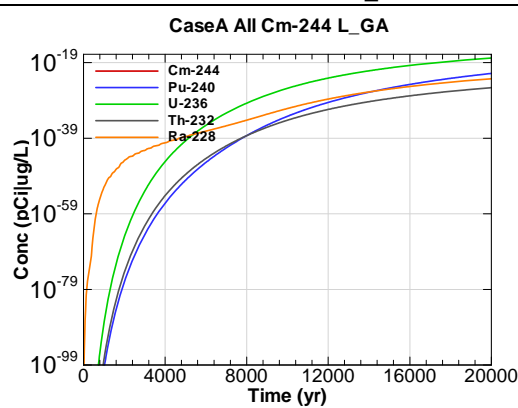
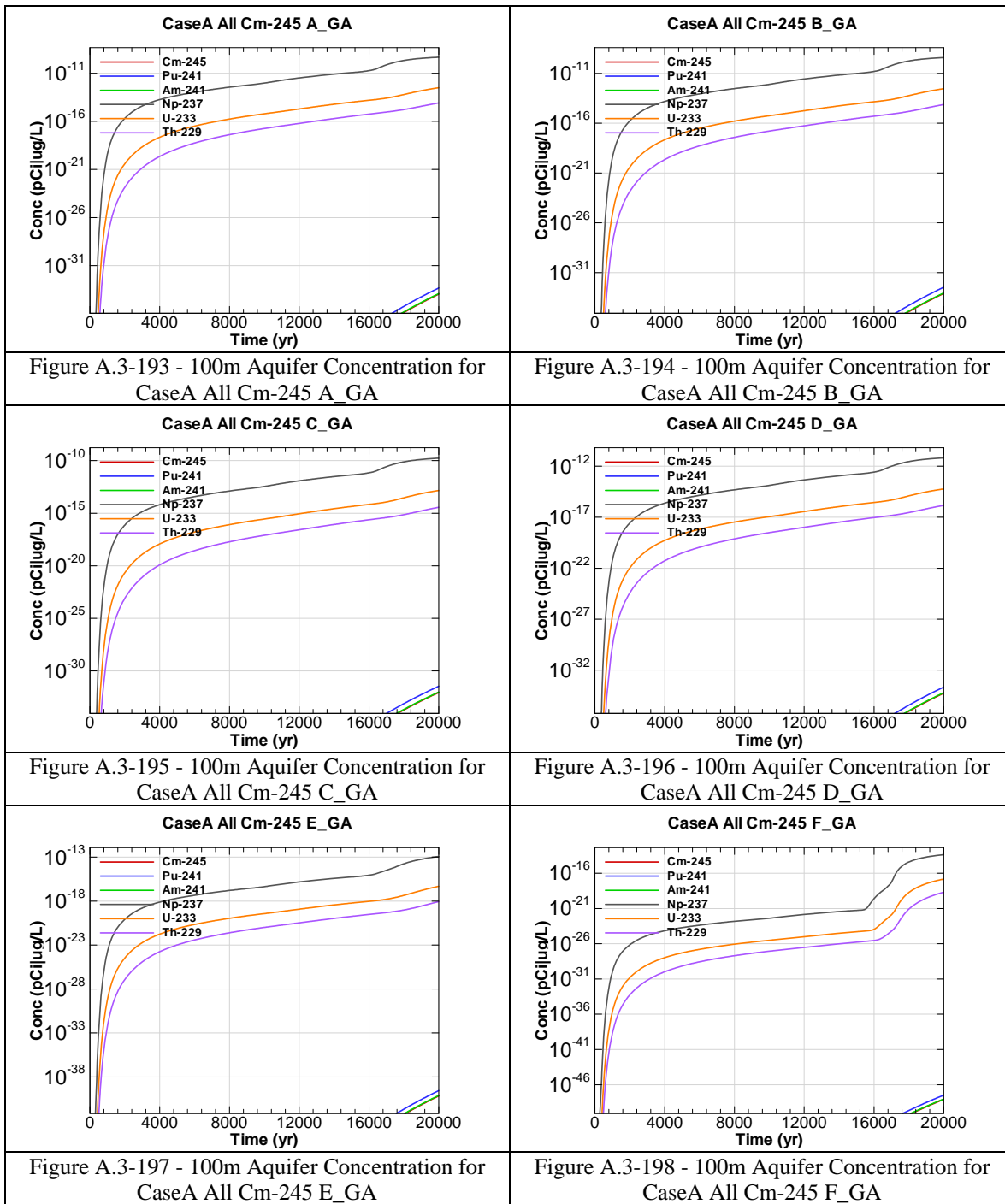
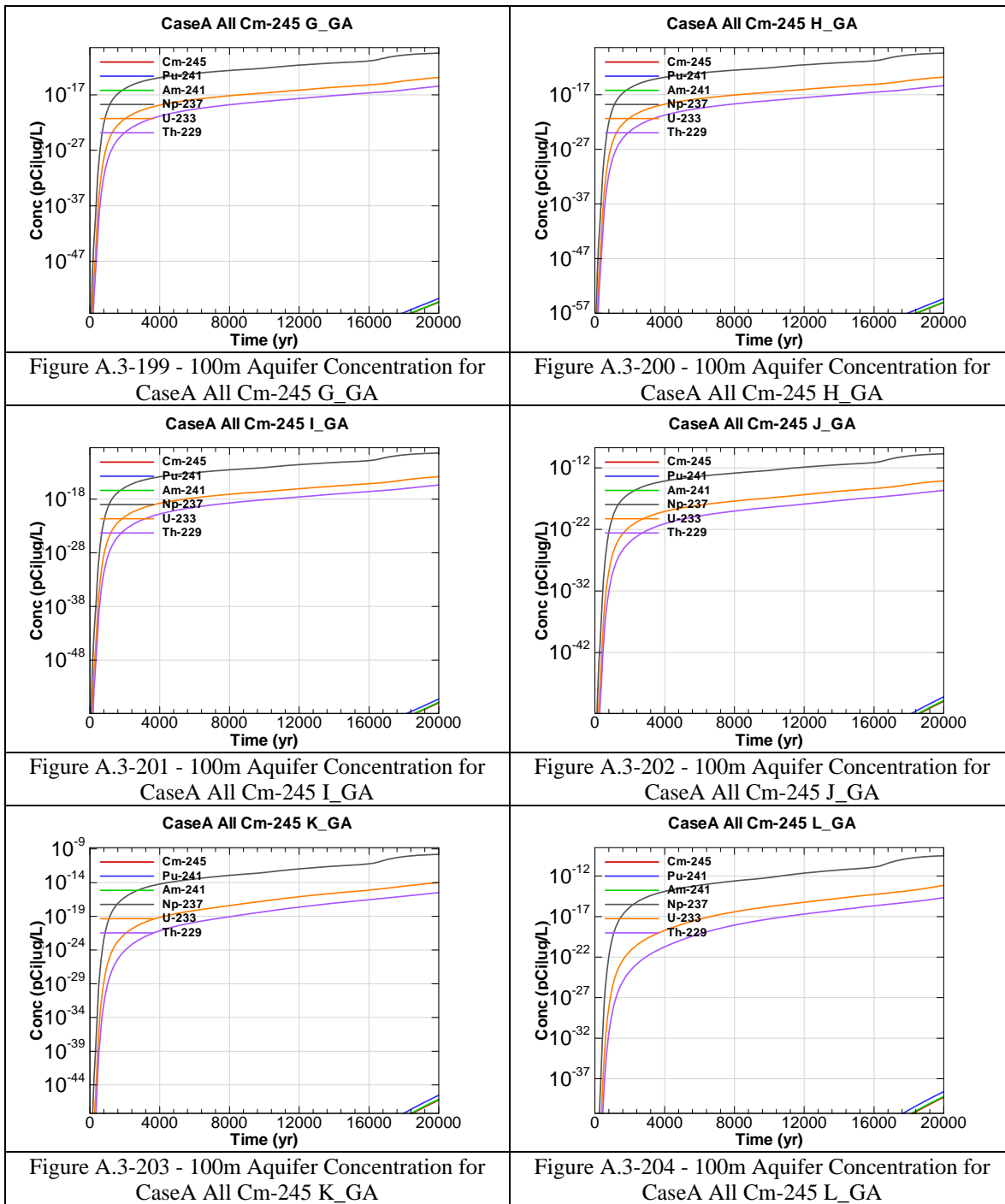


Figure A.3-192 - 100m Aquifer Concentration for CaseA All Cm-244 L_GA





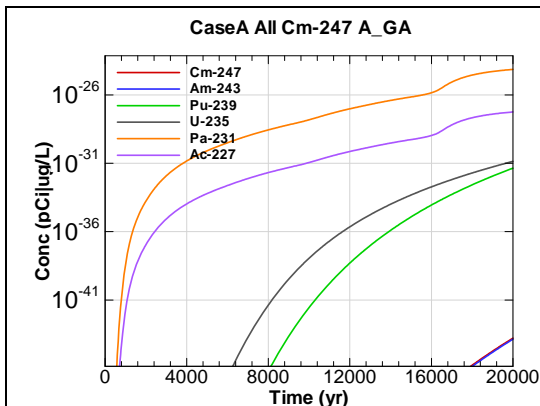


Figure A.3-205 - 100m Aquifer Concentration for CaseA All Cm-247 A_GA

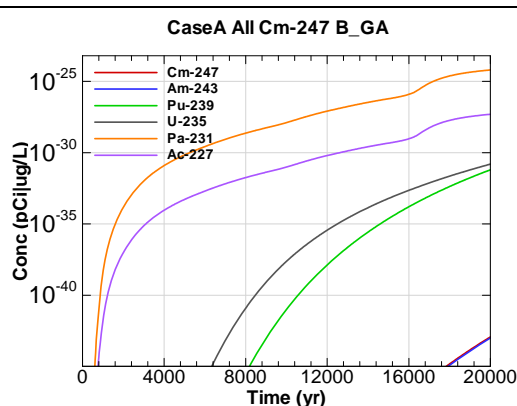


Figure A.3-206 - 100m Aquifer Concentration for CaseA All Cm-247 B_GA

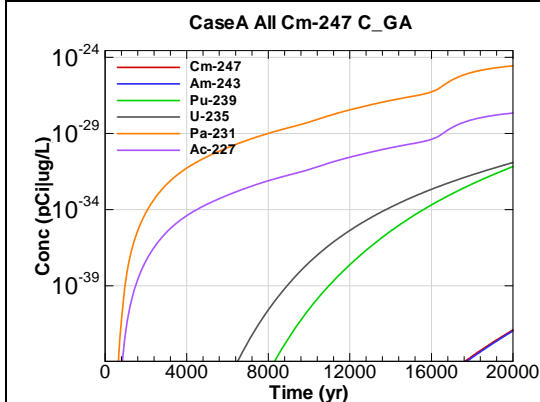


Figure A.3-207 - 100m Aquifer Concentration for CaseA All Cm-247 C_GA

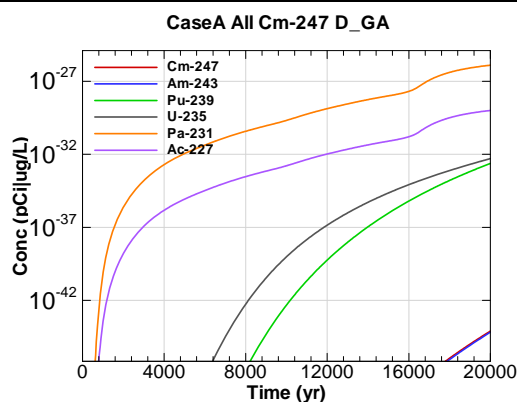


Figure A.3-208 - 100m Aquifer Concentration for CaseA All Cm-247 D_GA

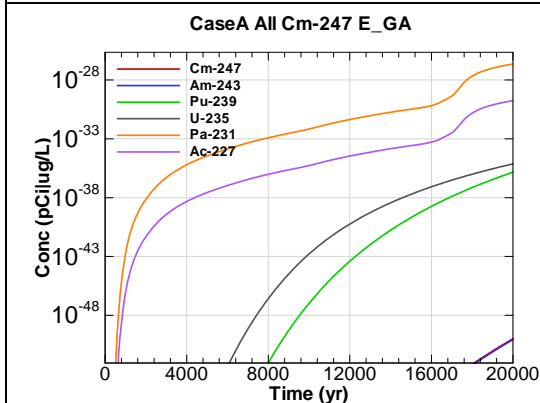


Figure A.3-209 - 100m Aquifer Concentration for CaseA All Cm-247 E_GA

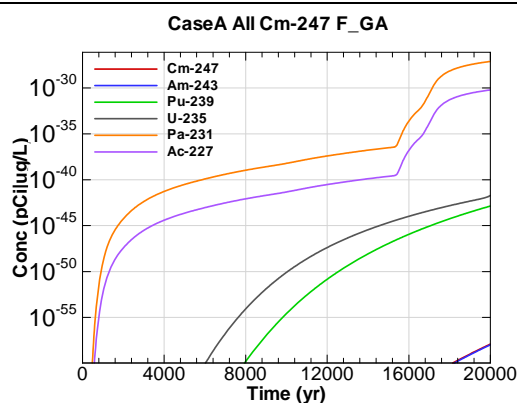


Figure A.3-210 - 100m Aquifer Concentration for CaseA All Cm-247 F_GA

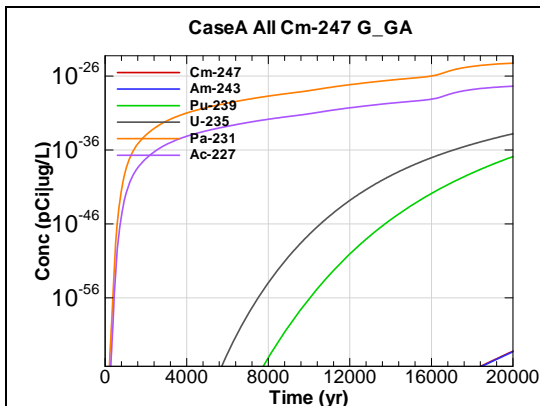


Figure A.3-211 - 100m Aquifer Concentration for CaseA All Cm-247 G_GA

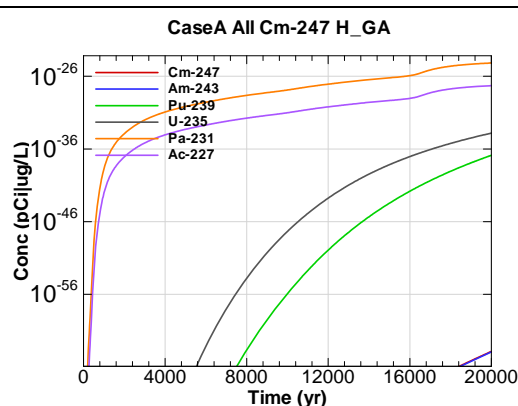


Figure A.3-212 - 100m Aquifer Concentration for CaseA All Cm-247 H_GA

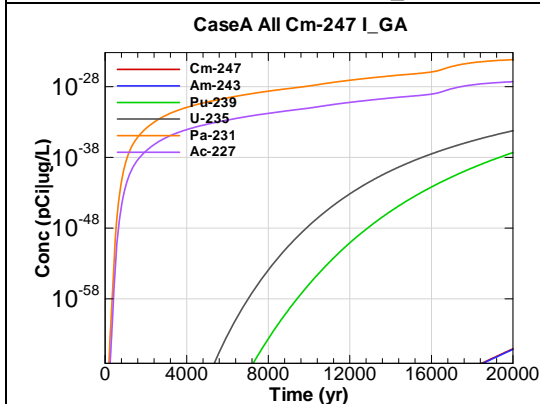


Figure A.3-213 - 100m Aquifer Concentration for CaseA All Cm-247 I_GA

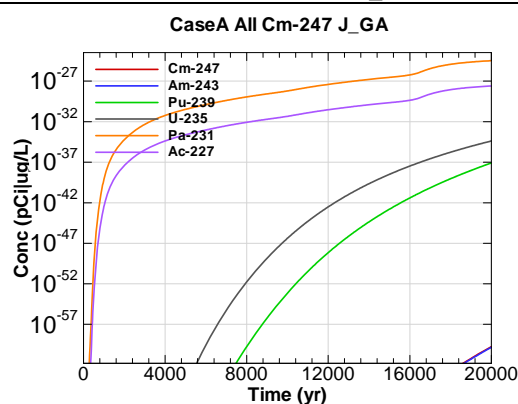


Figure A.3-214 - 100m Aquifer Concentration for CaseA All Cm-247 J_GA

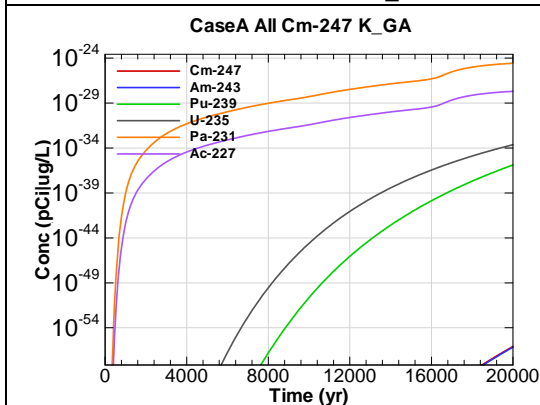


Figure A.3-215 - 100m Aquifer Concentration for CaseA All Cm-247 K_GA

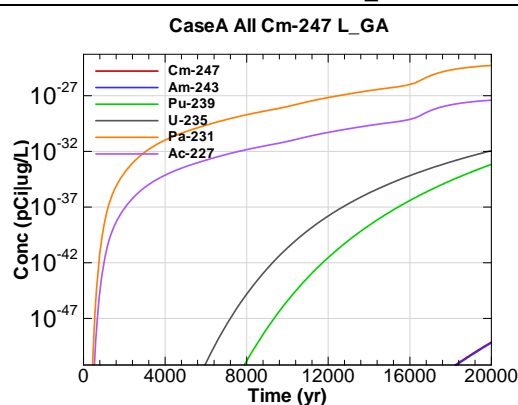


Figure A.3-216 - 100m Aquifer Concentration for CaseA All Cm-247 L_GA

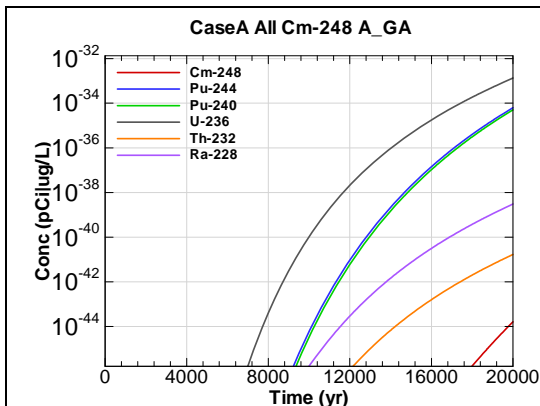


Figure A.3-217 - 100m Aquifer Concentration for CaseA All Cm-248 A_GA

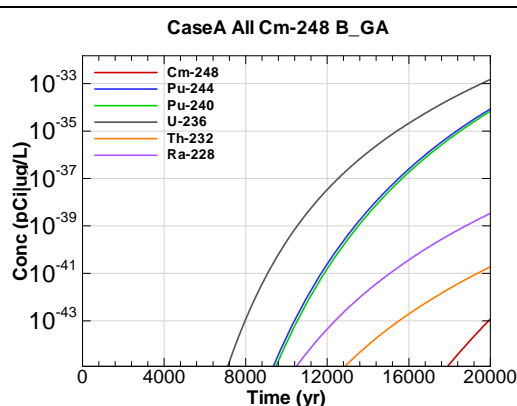


Figure A.3-218 - 100m Aquifer Concentration for CaseA All Cm-248 B_GA

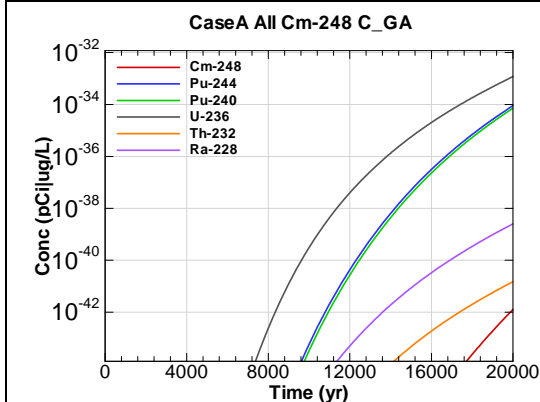


Figure A.3-219 - 100m Aquifer Concentration for CaseA All Cm-248 C_GA

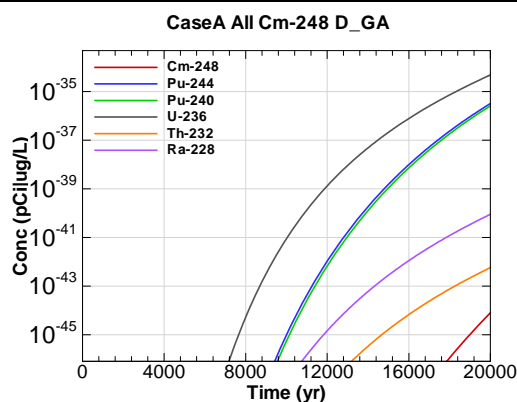


Figure A.3-220 - 100m Aquifer Concentration for CaseA All Cm-248 D_GA

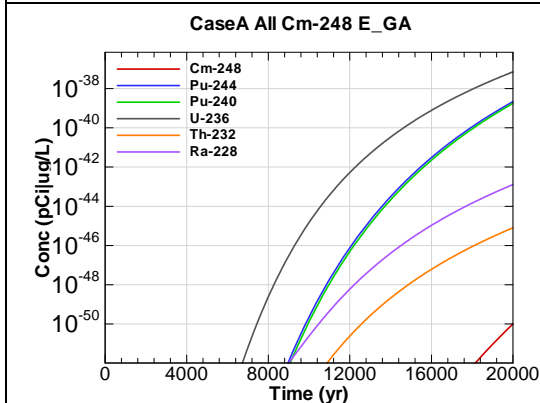


Figure A.3-221 - 100m Aquifer Concentration for CaseA All Cm-248 E_GA

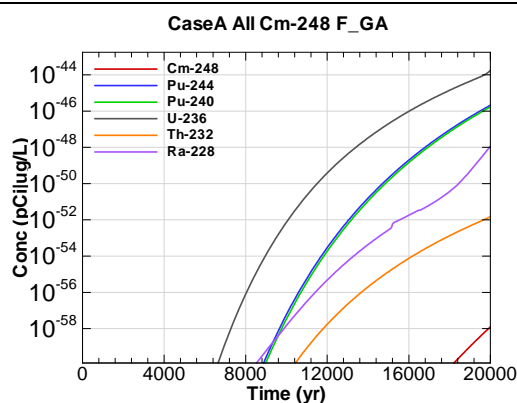


Figure A.3-222 - 100m Aquifer Concentration for CaseA All Cm-248 F_GA

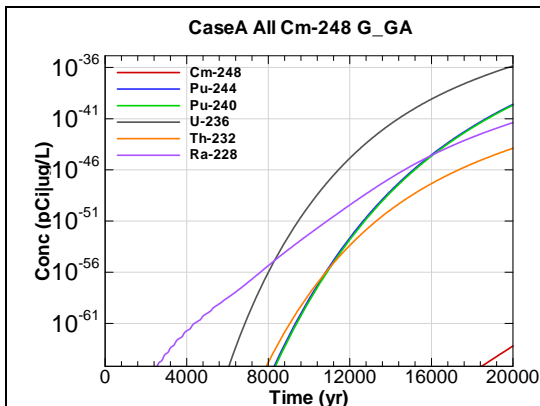


Figure A.3-223 - 100m Aquifer Concentration for CaseA All Cm-248 G_GA

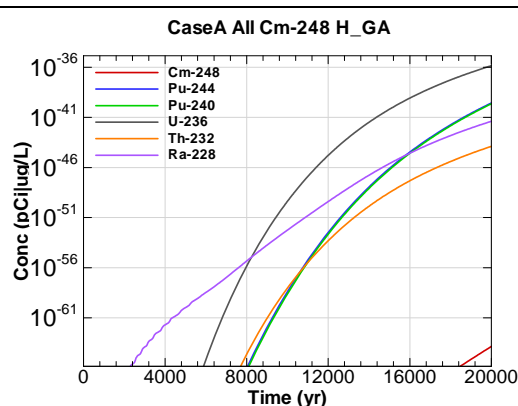


Figure A.3-224 - 100m Aquifer Concentration for CaseA All Cm-248 H_GA

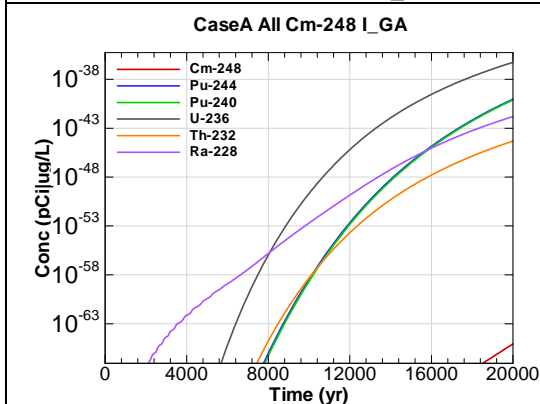


Figure A.3-225 - 100m Aquifer Concentration for CaseA All Cm-248 I_GA

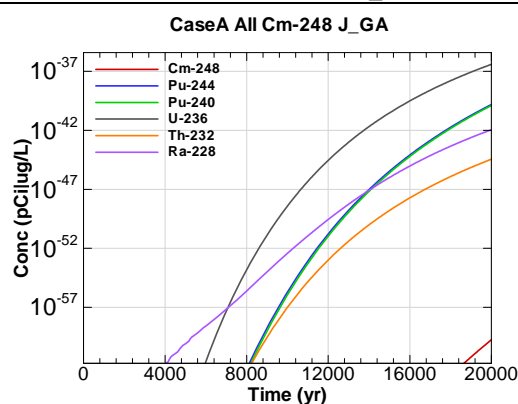


Figure A.3-226 - 100m Aquifer Concentration for CaseA All Cm-248 J_GA

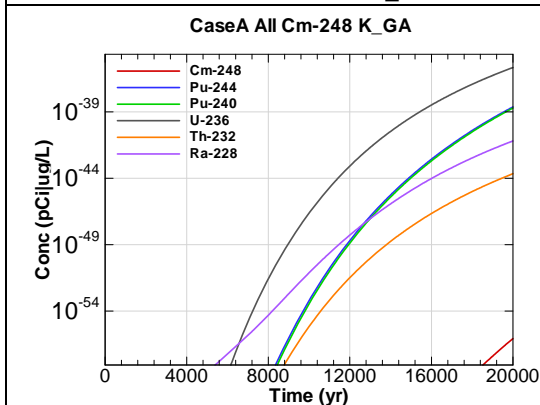


Figure A.3-227 - 100m Aquifer Concentration for CaseA All Cm-248 K_GA

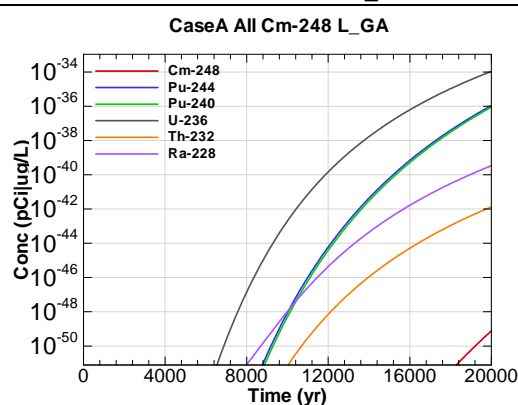
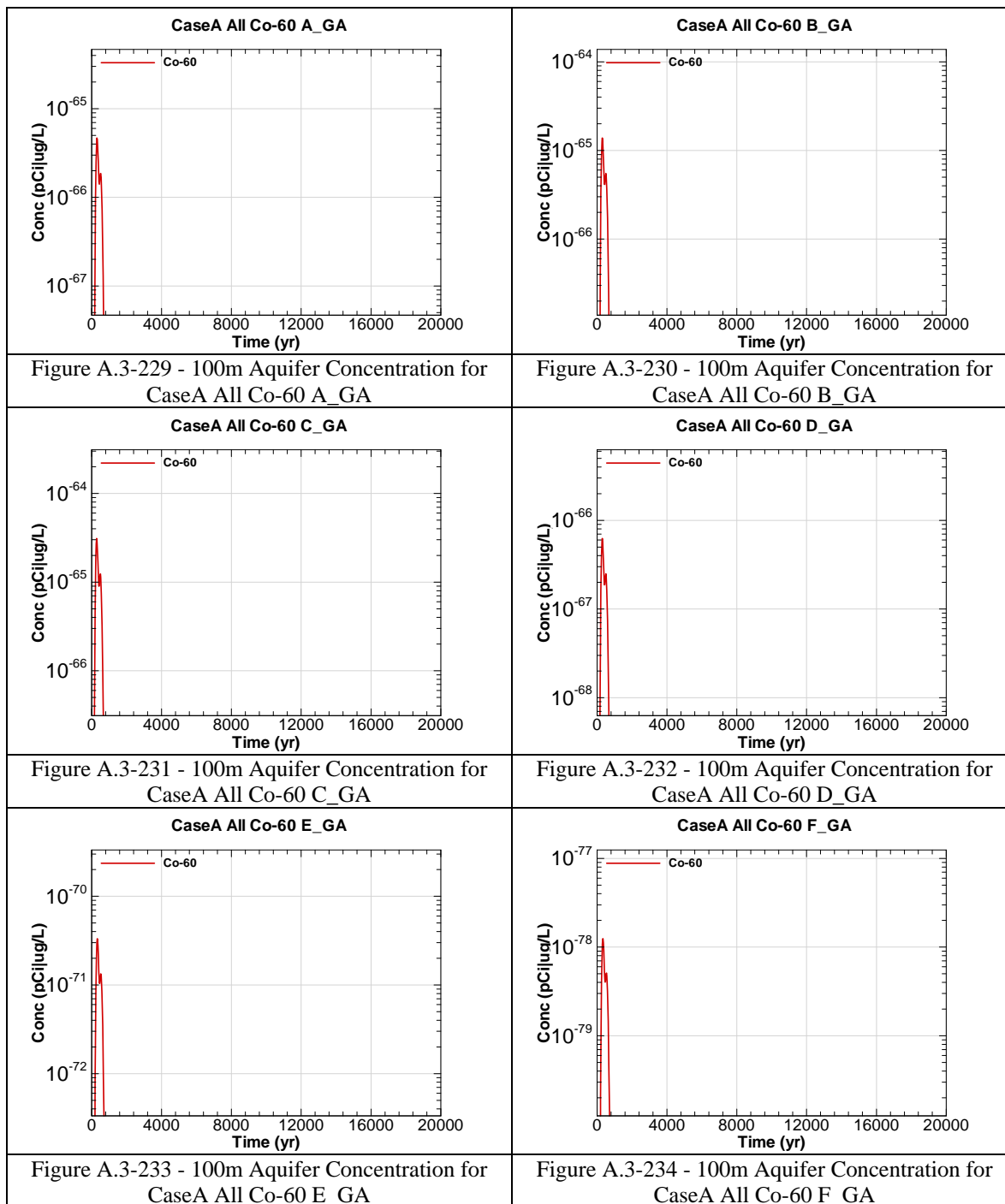
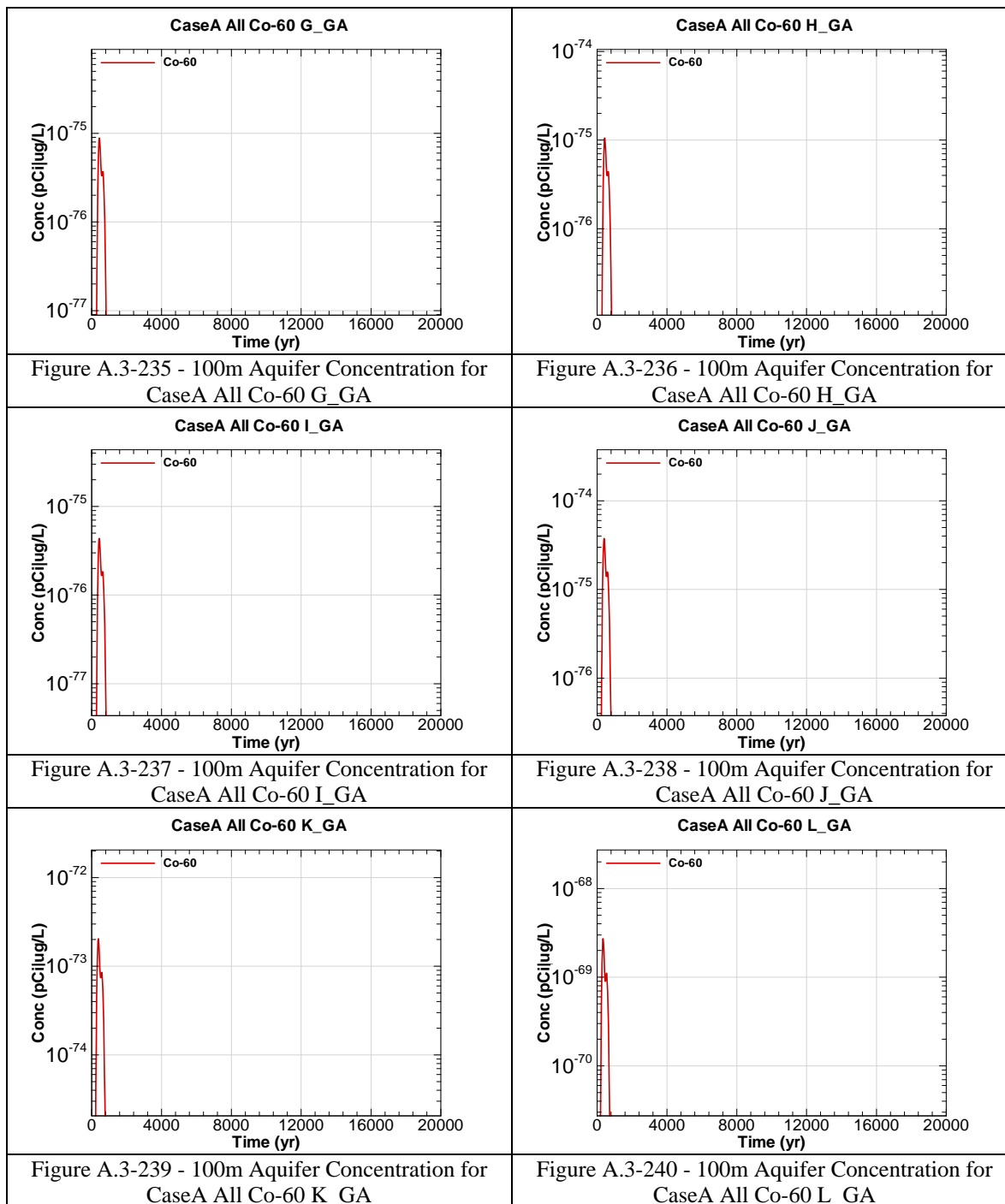
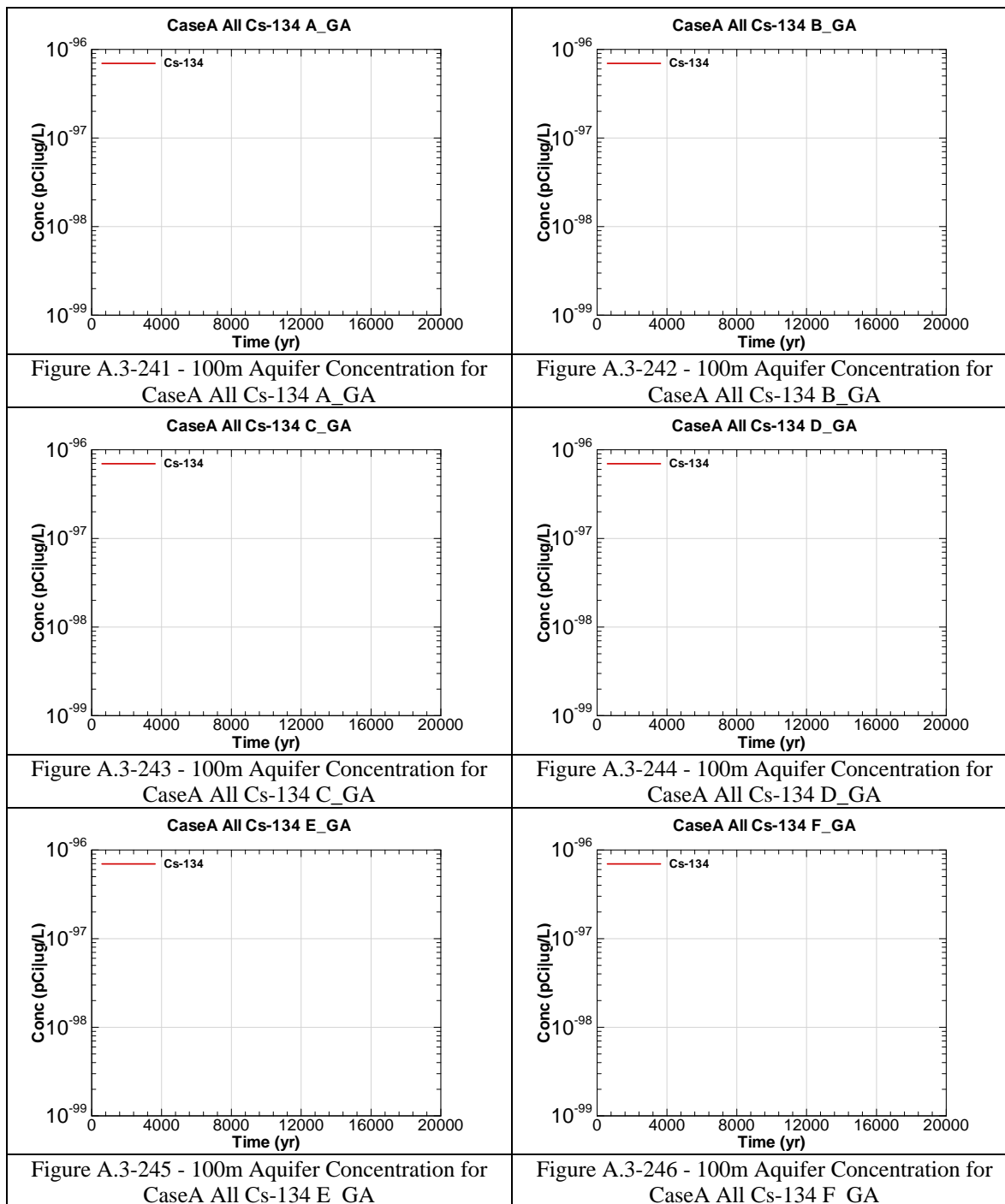
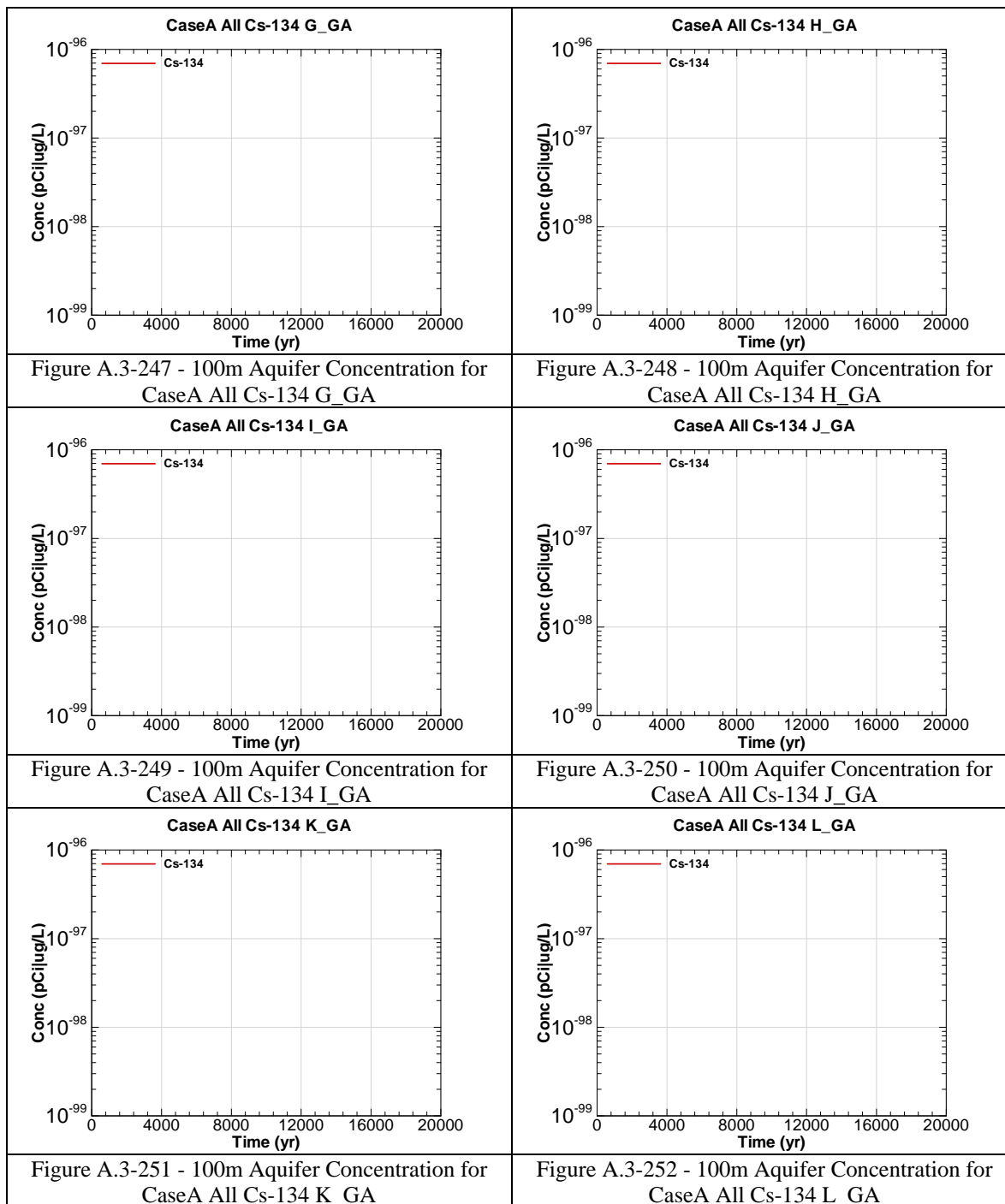


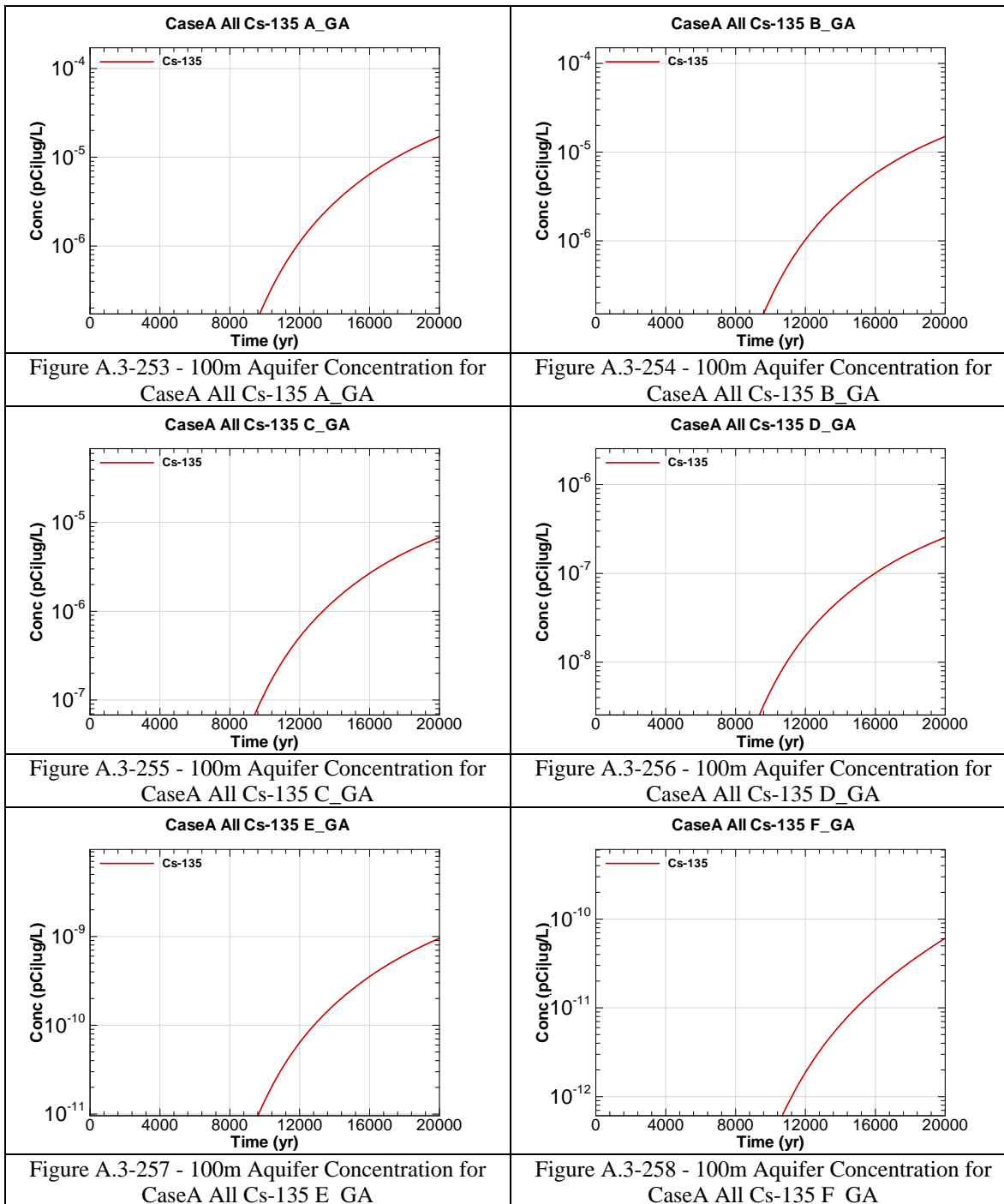
Figure A.3-228 - 100m Aquifer Concentration for CaseA All Cm-248 L_GA

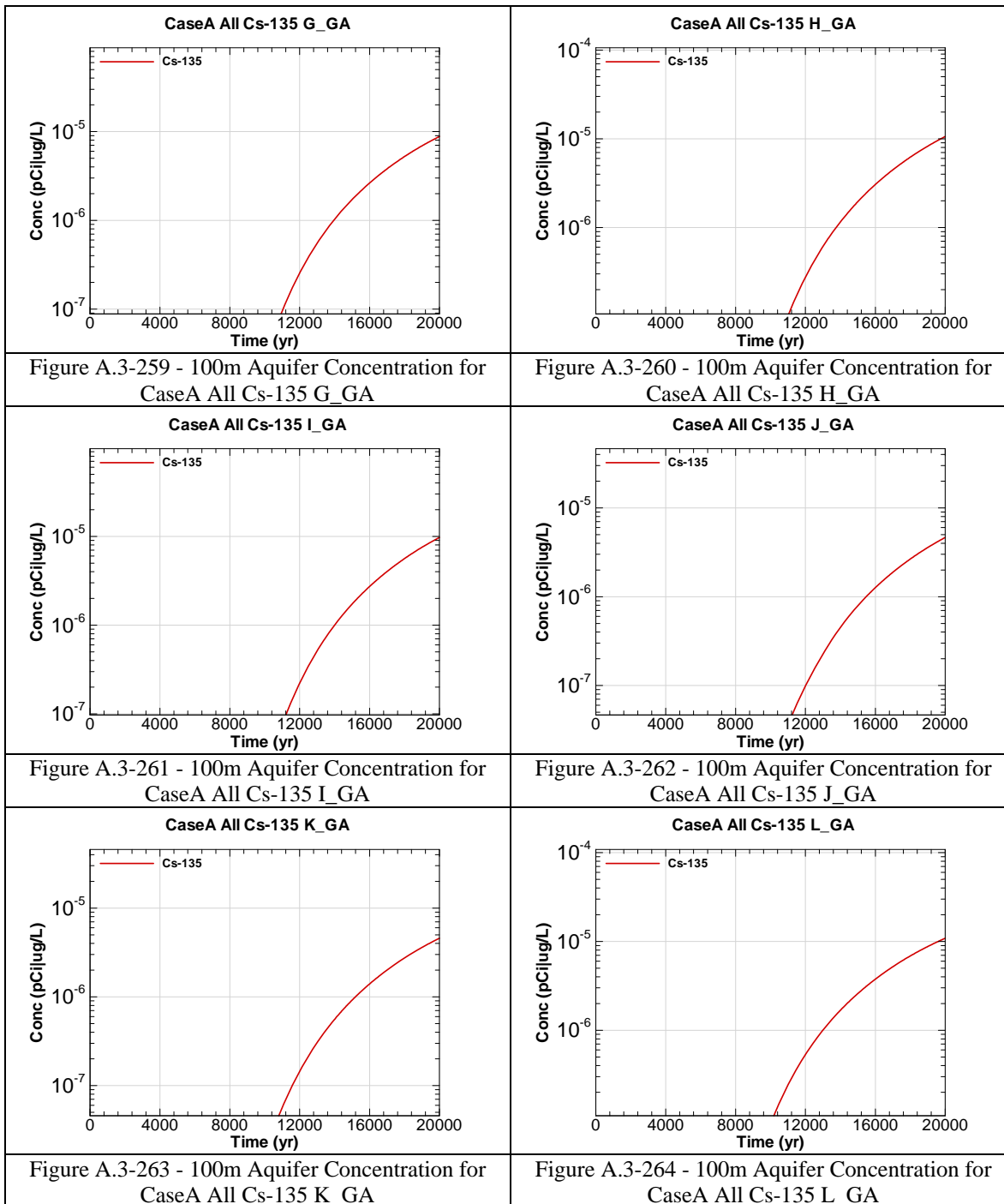


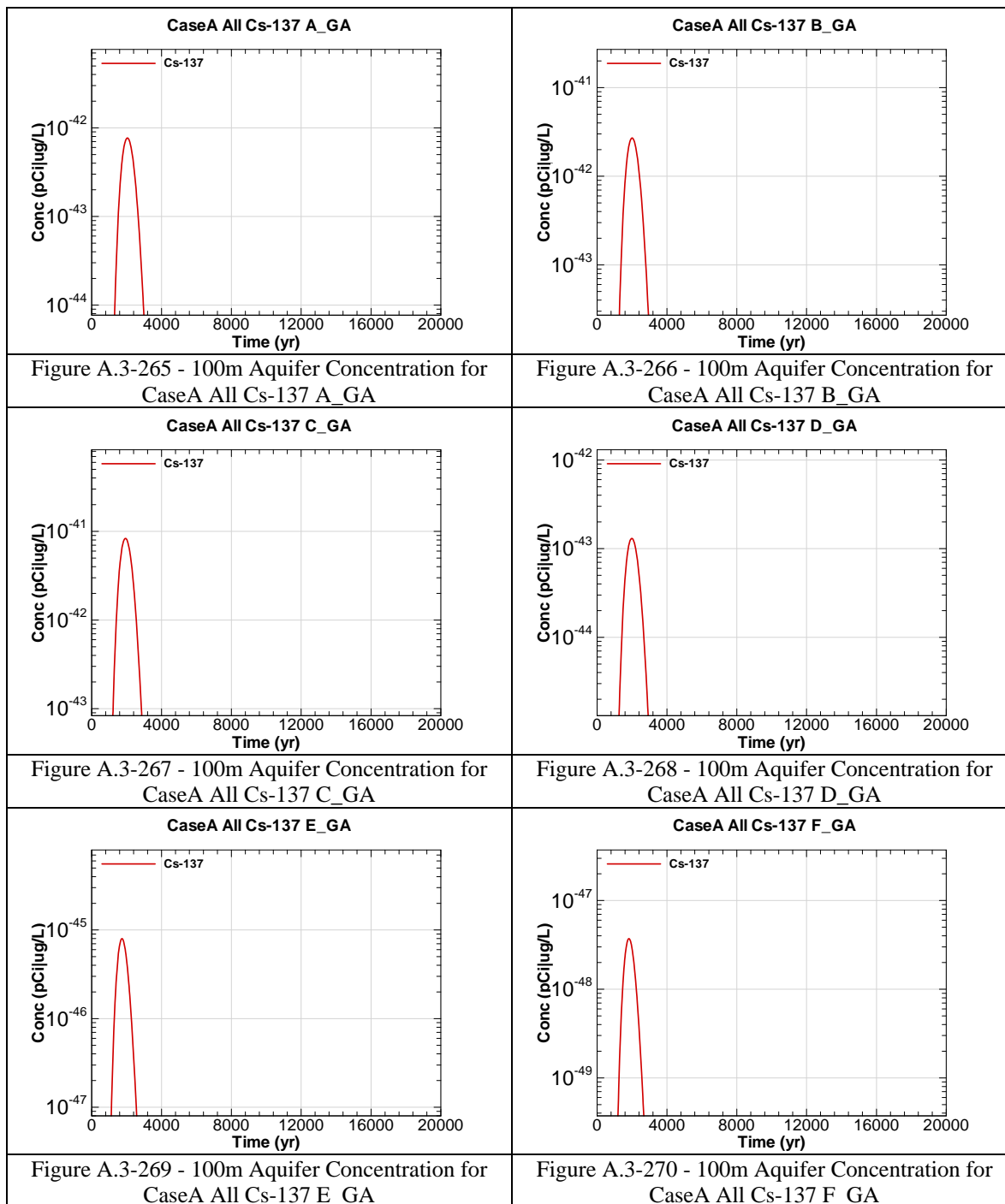


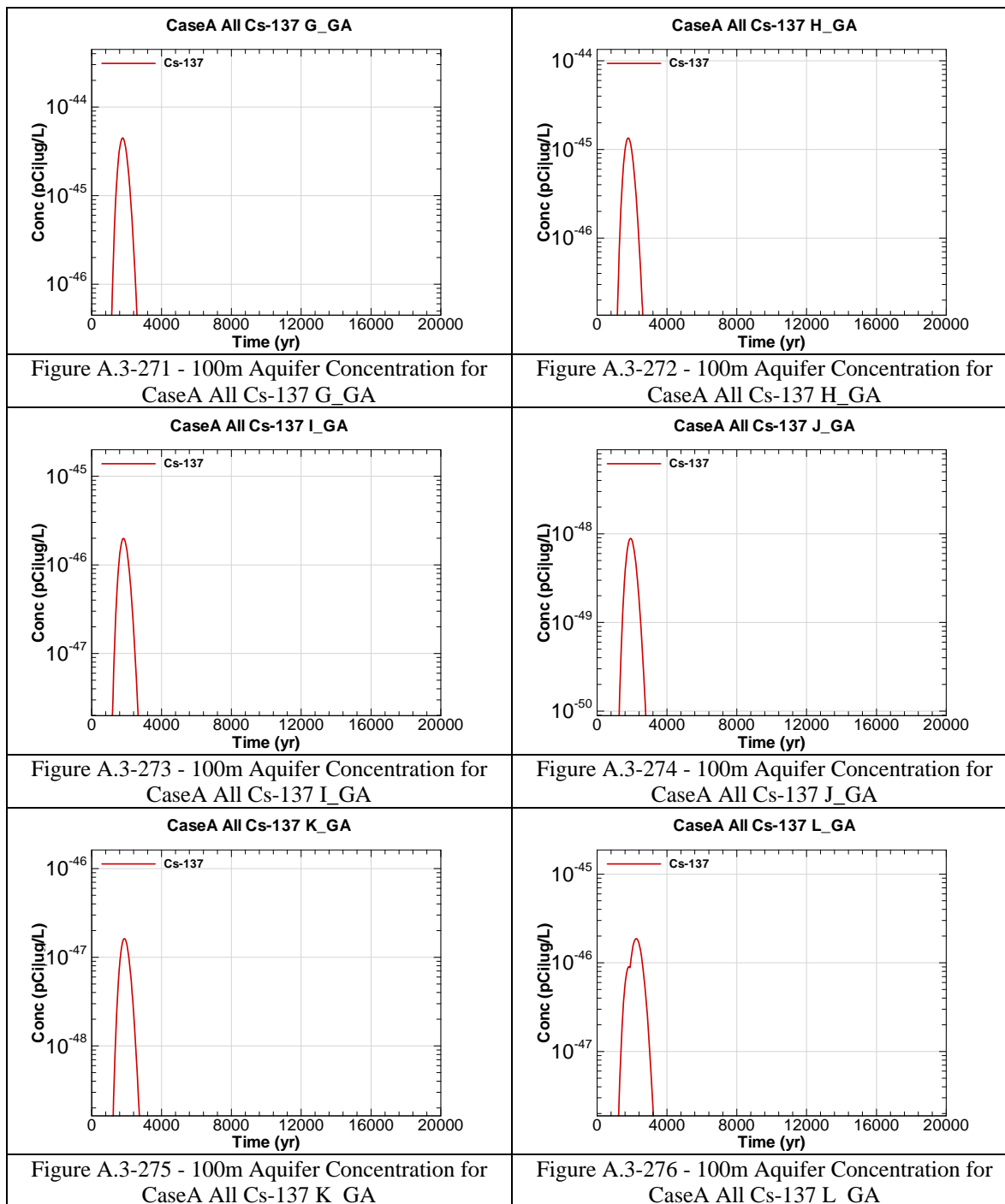


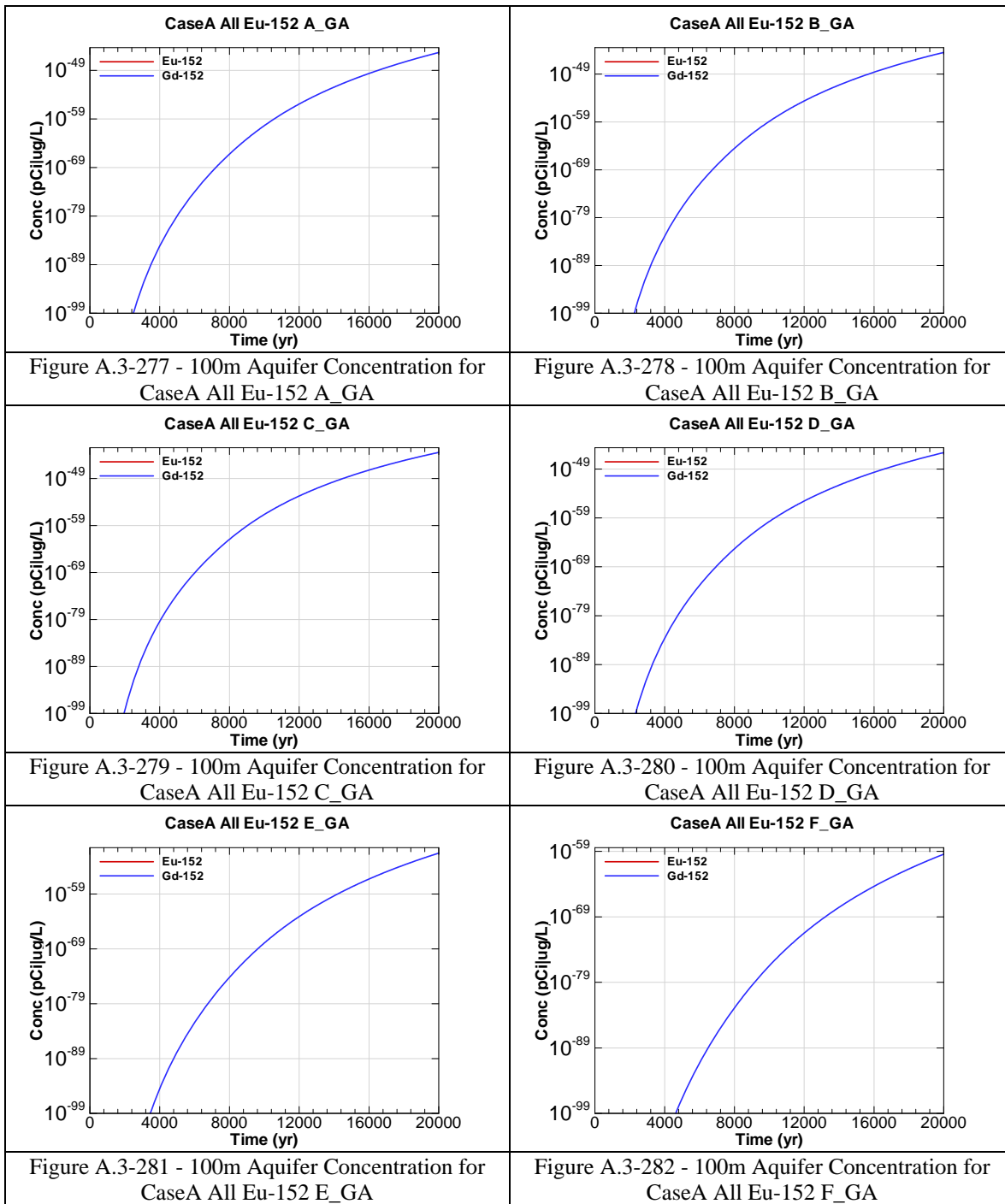


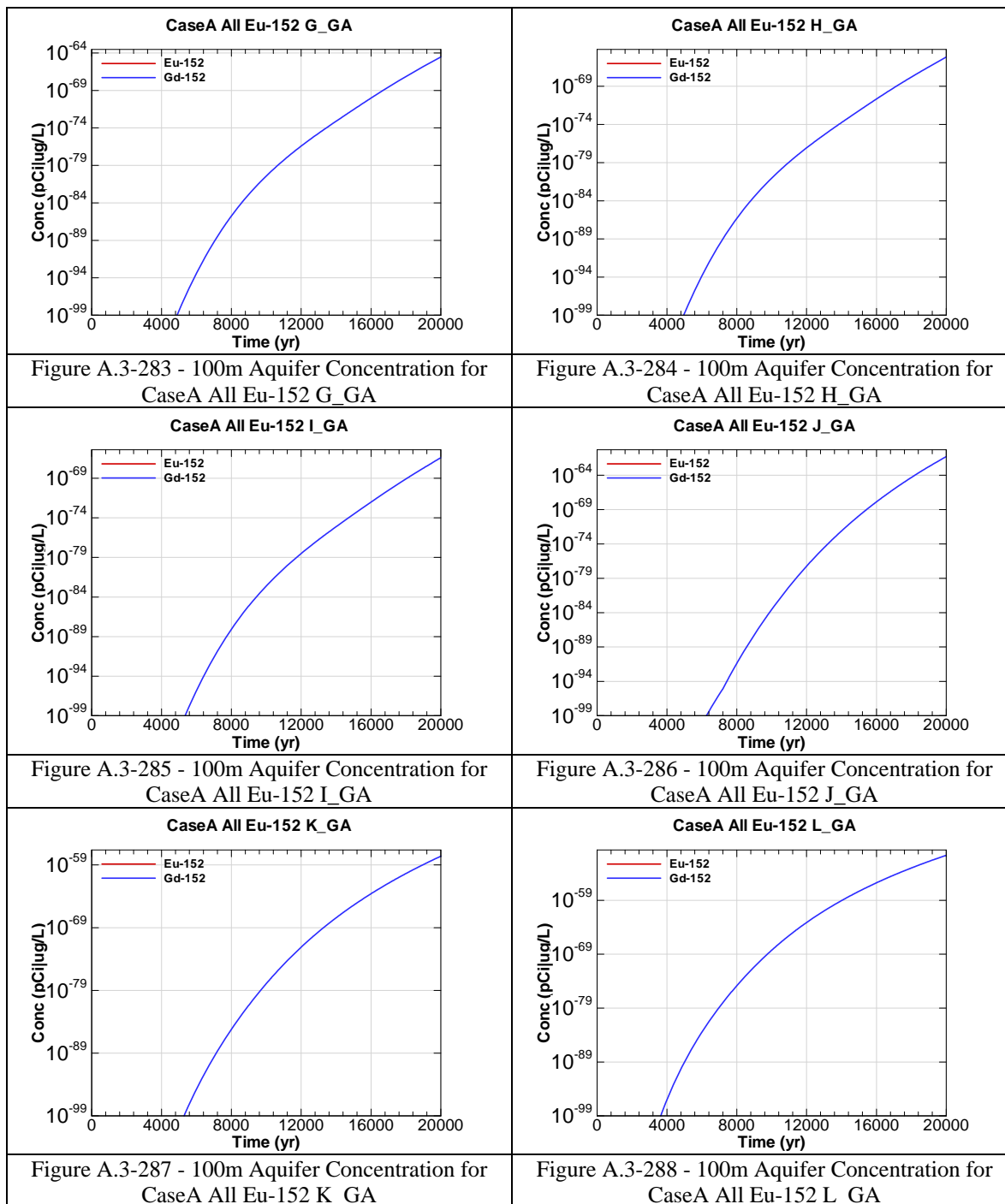


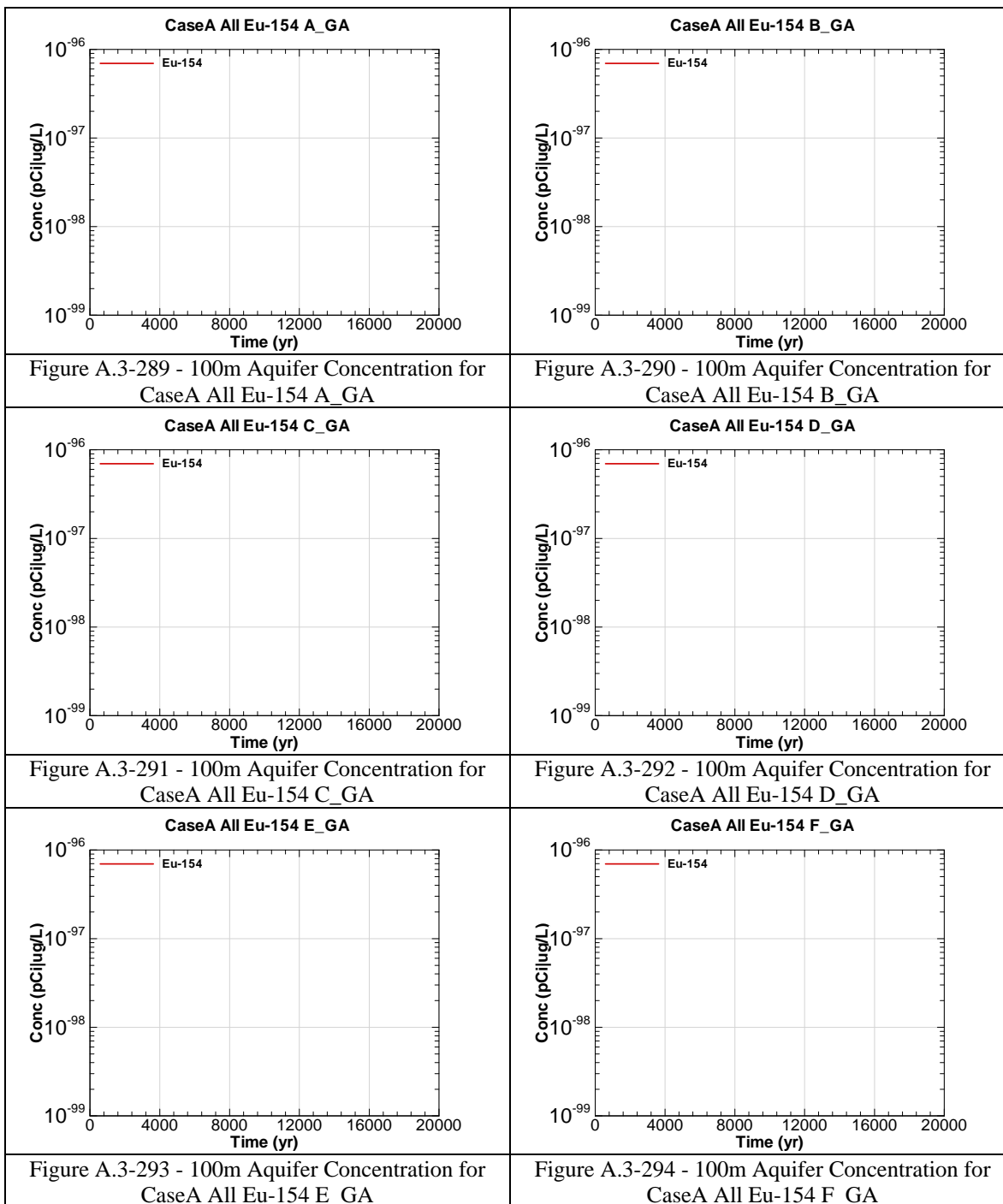


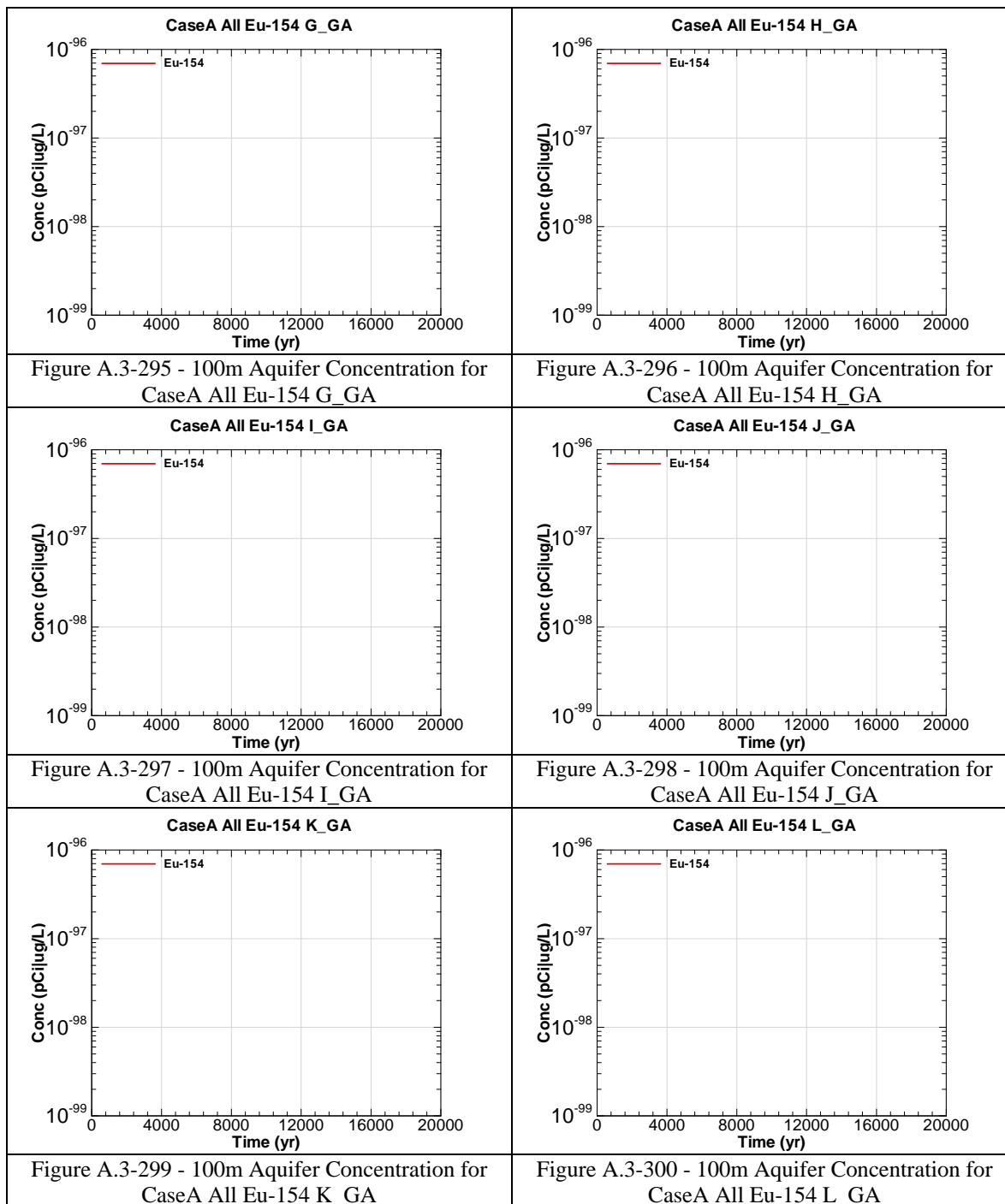


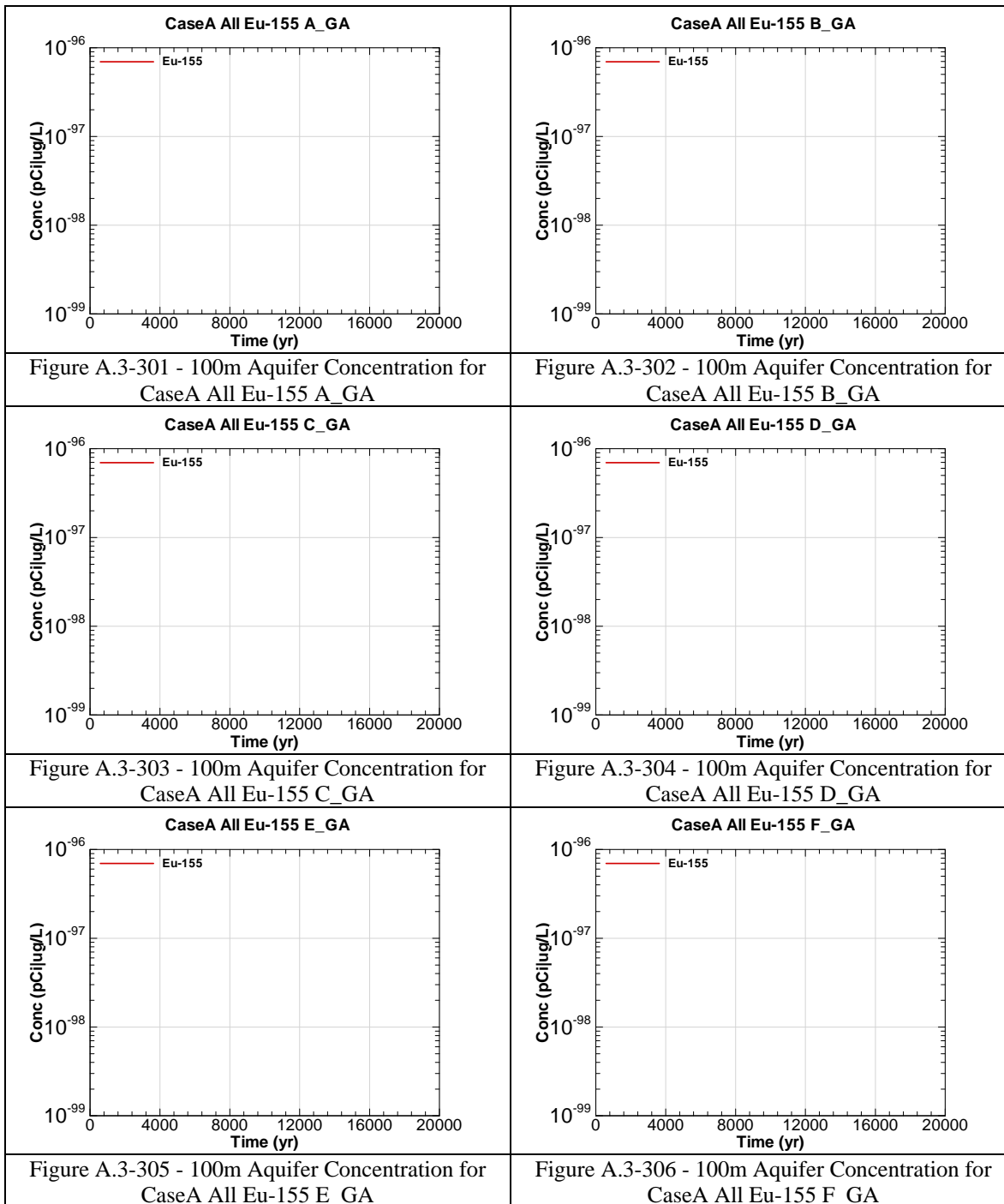


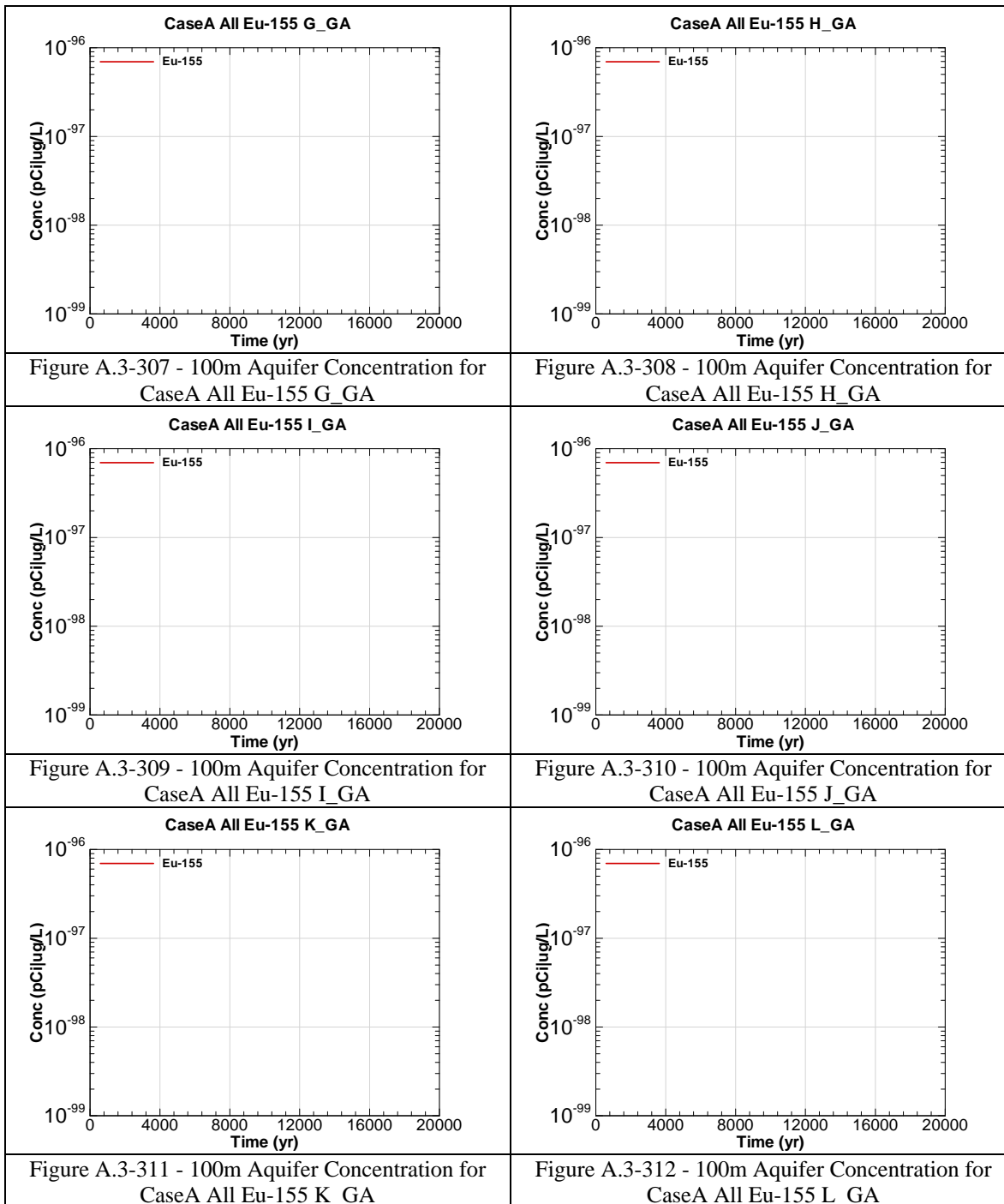


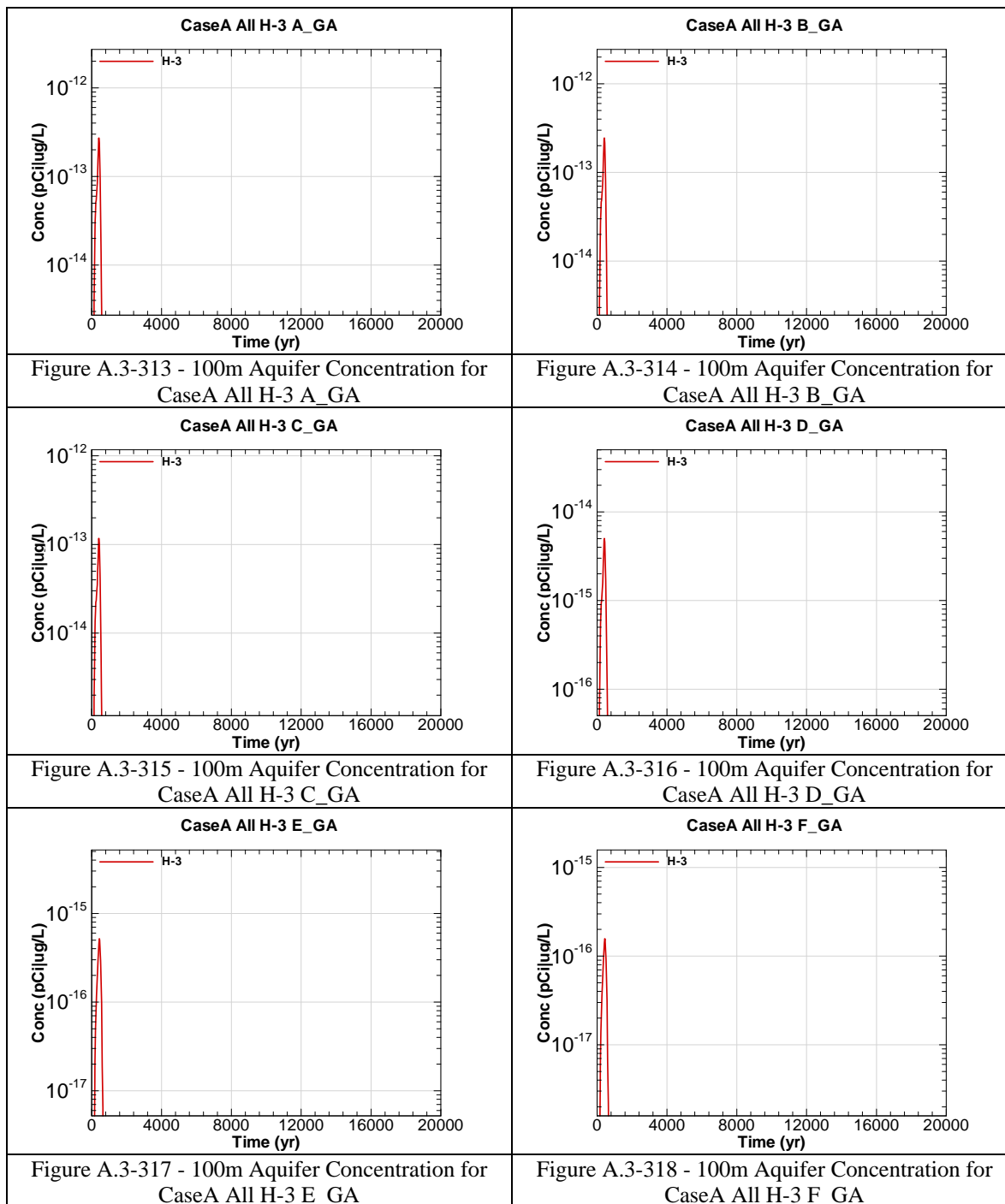


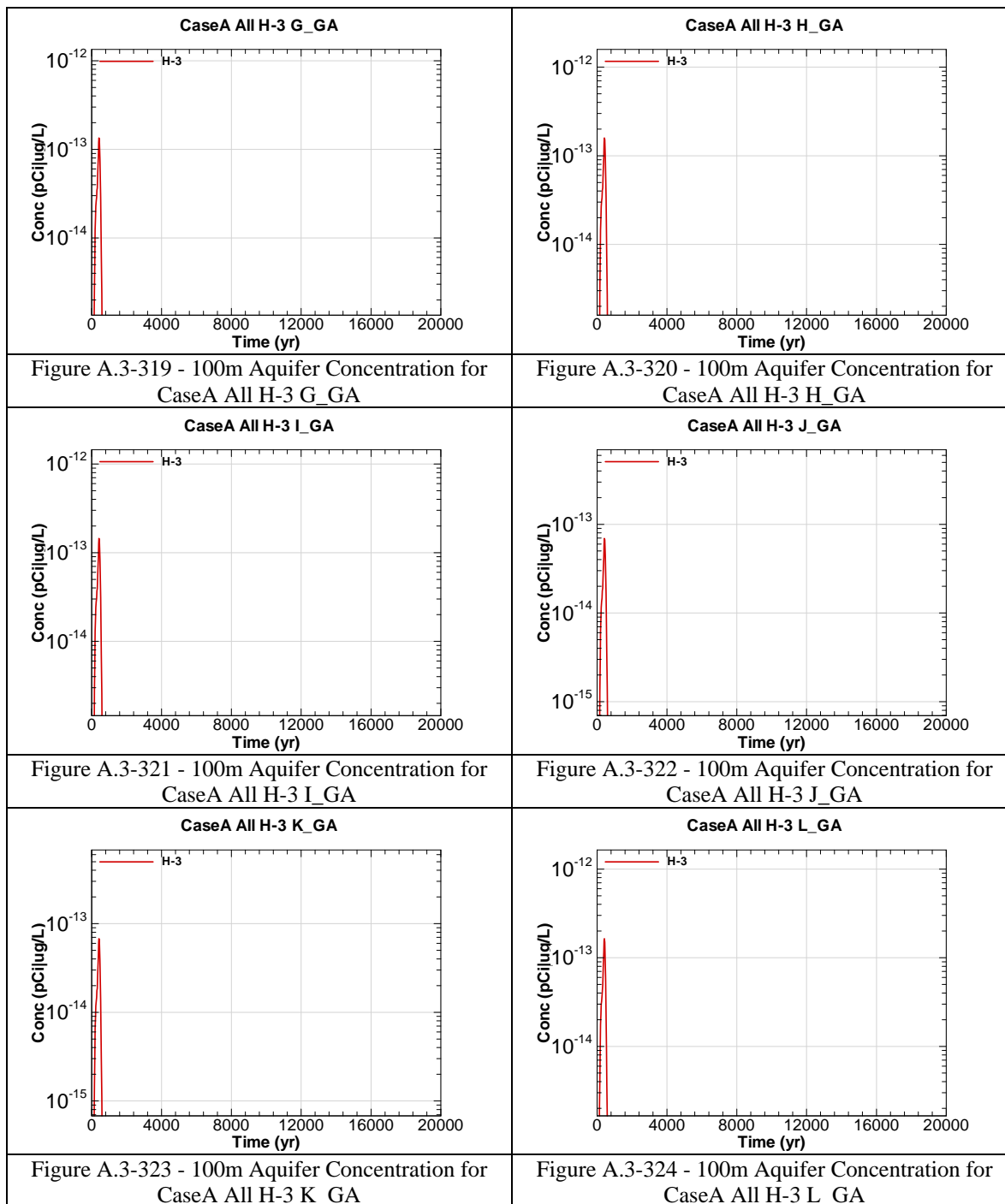


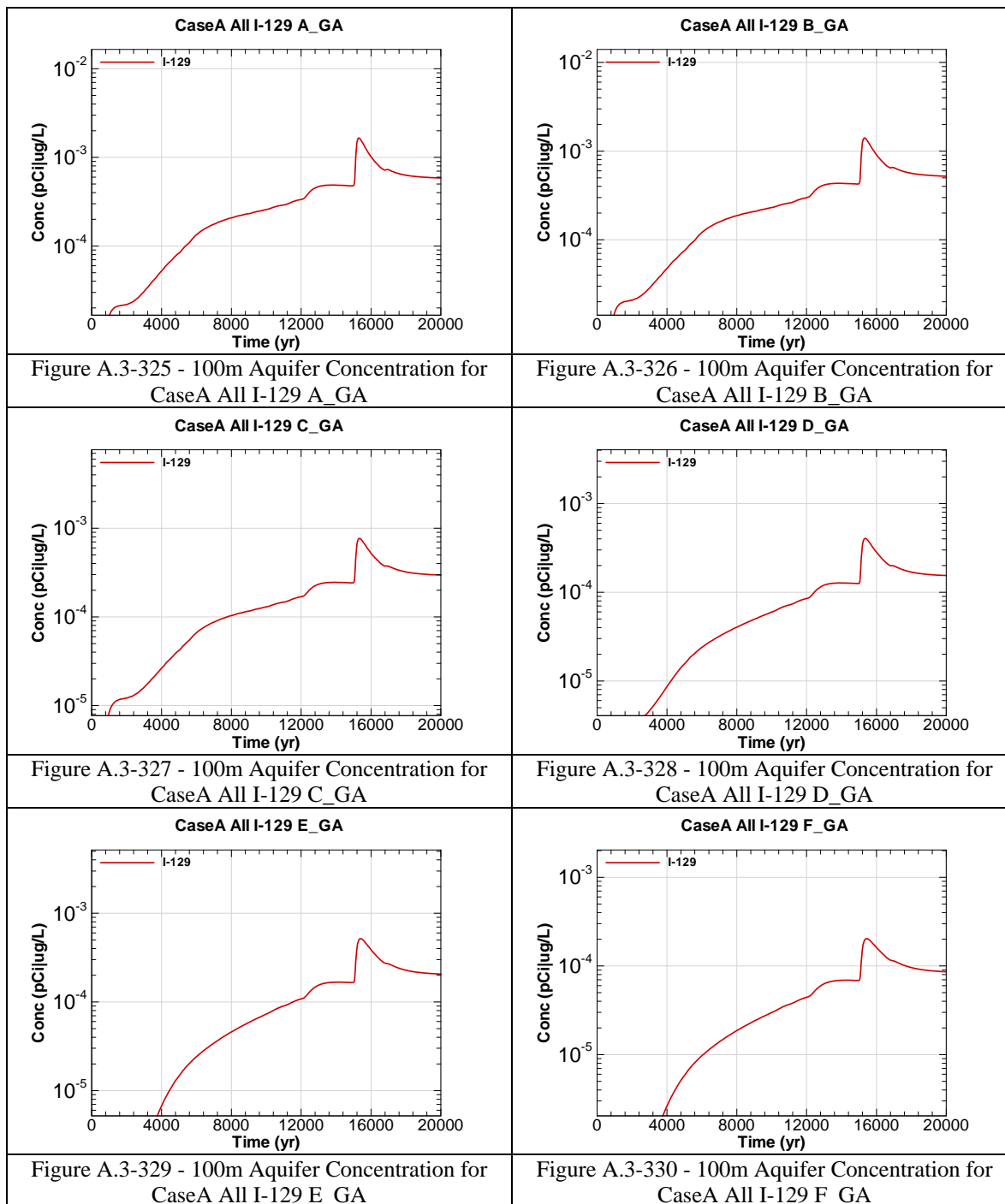


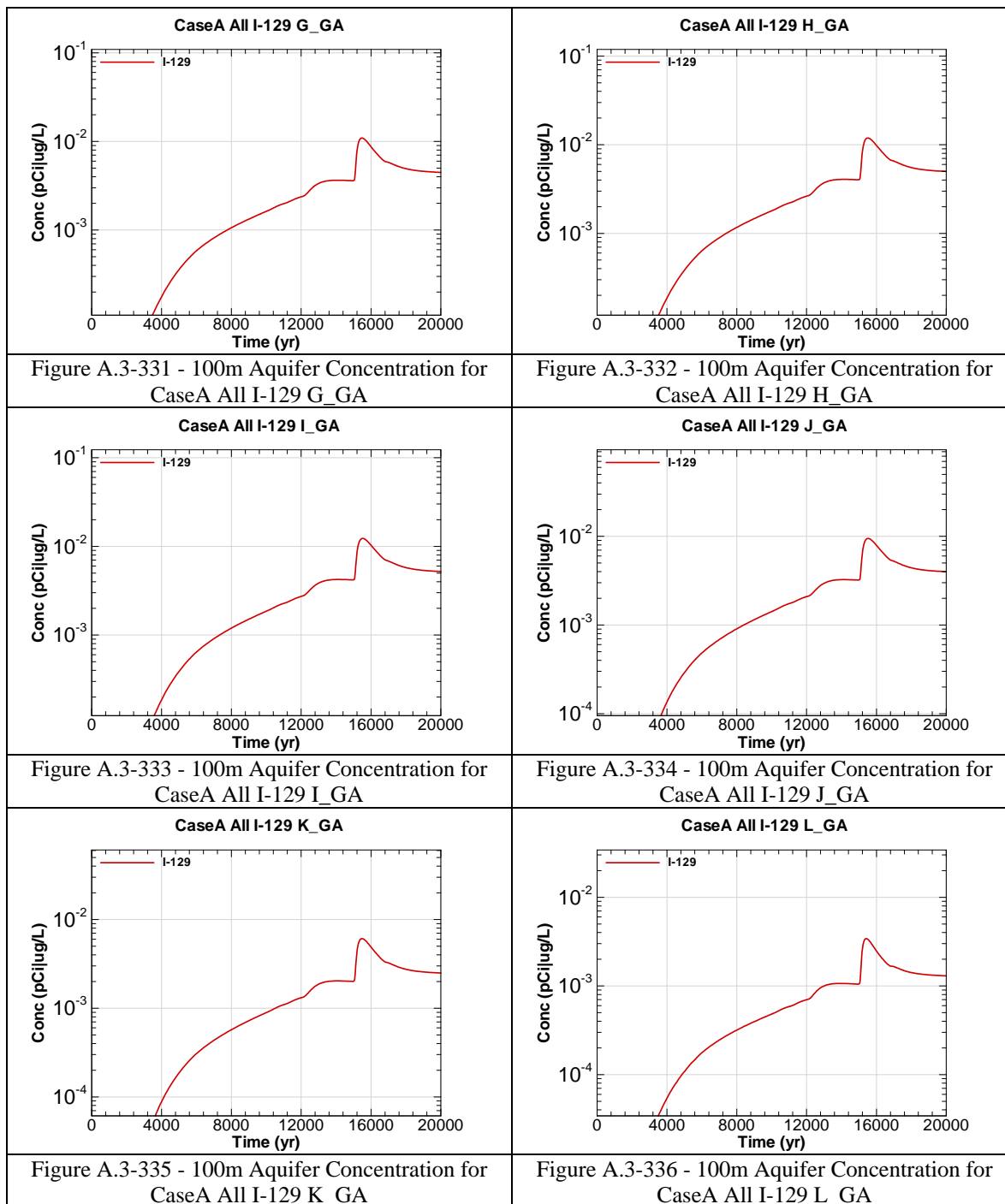


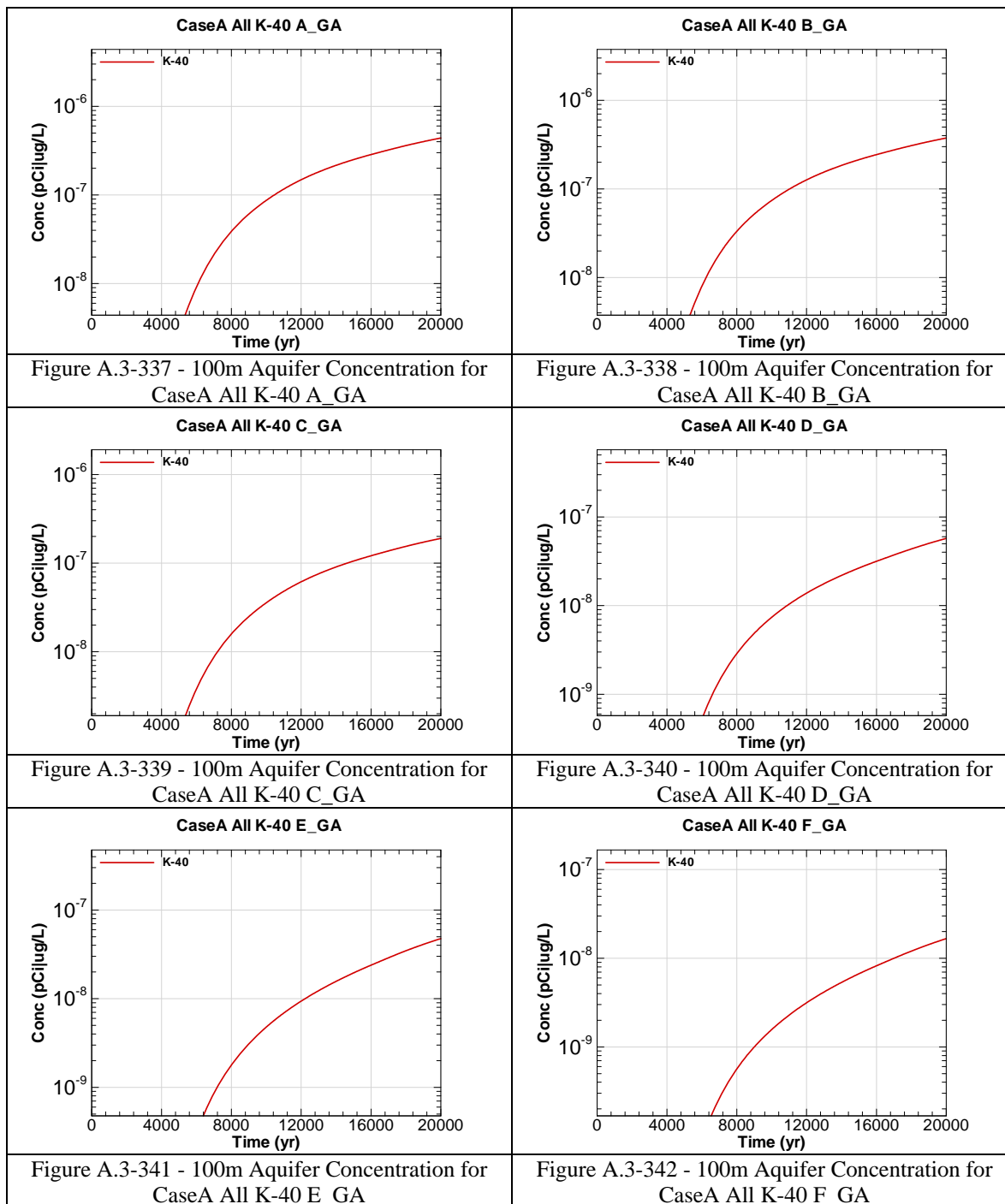


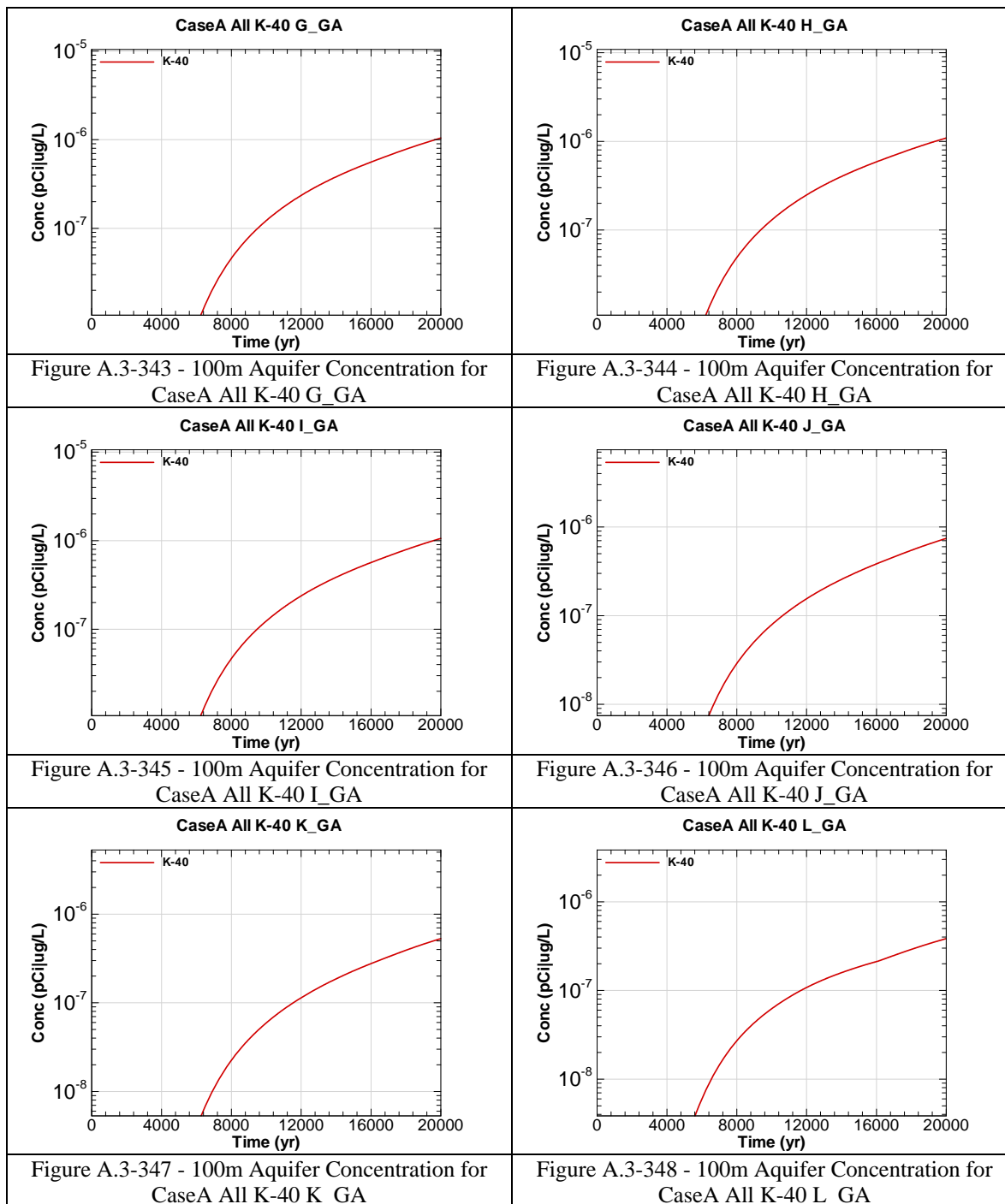


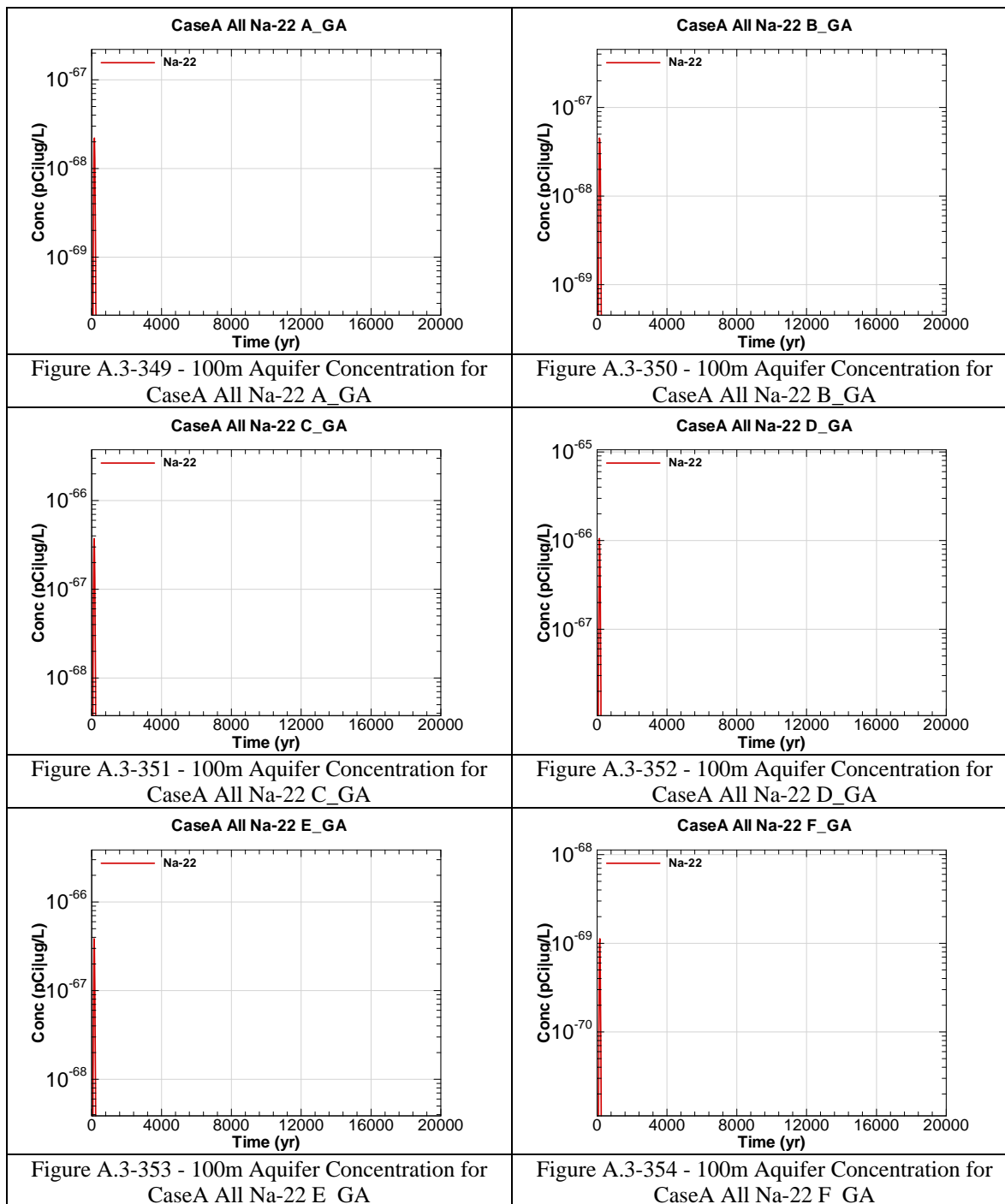


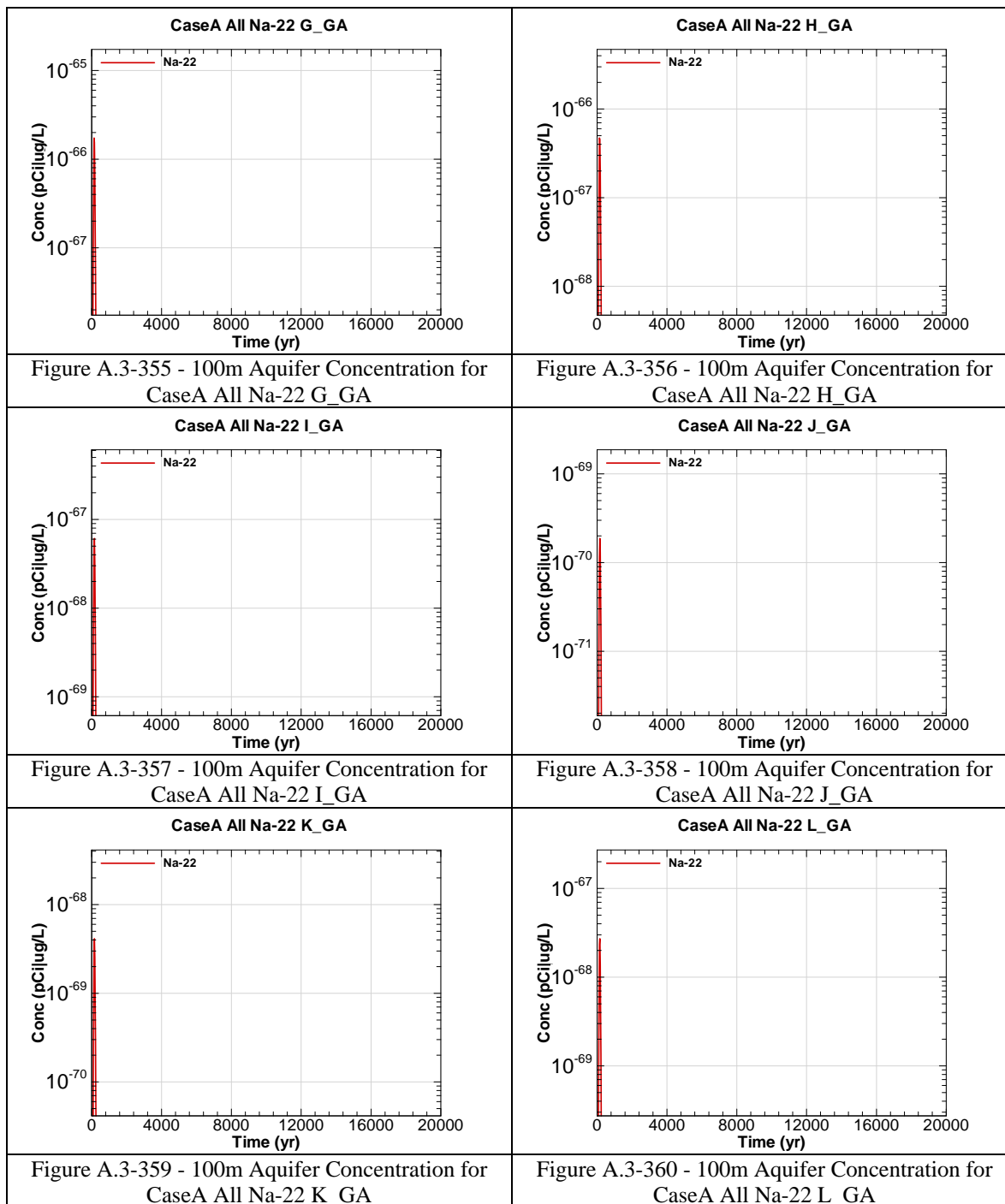


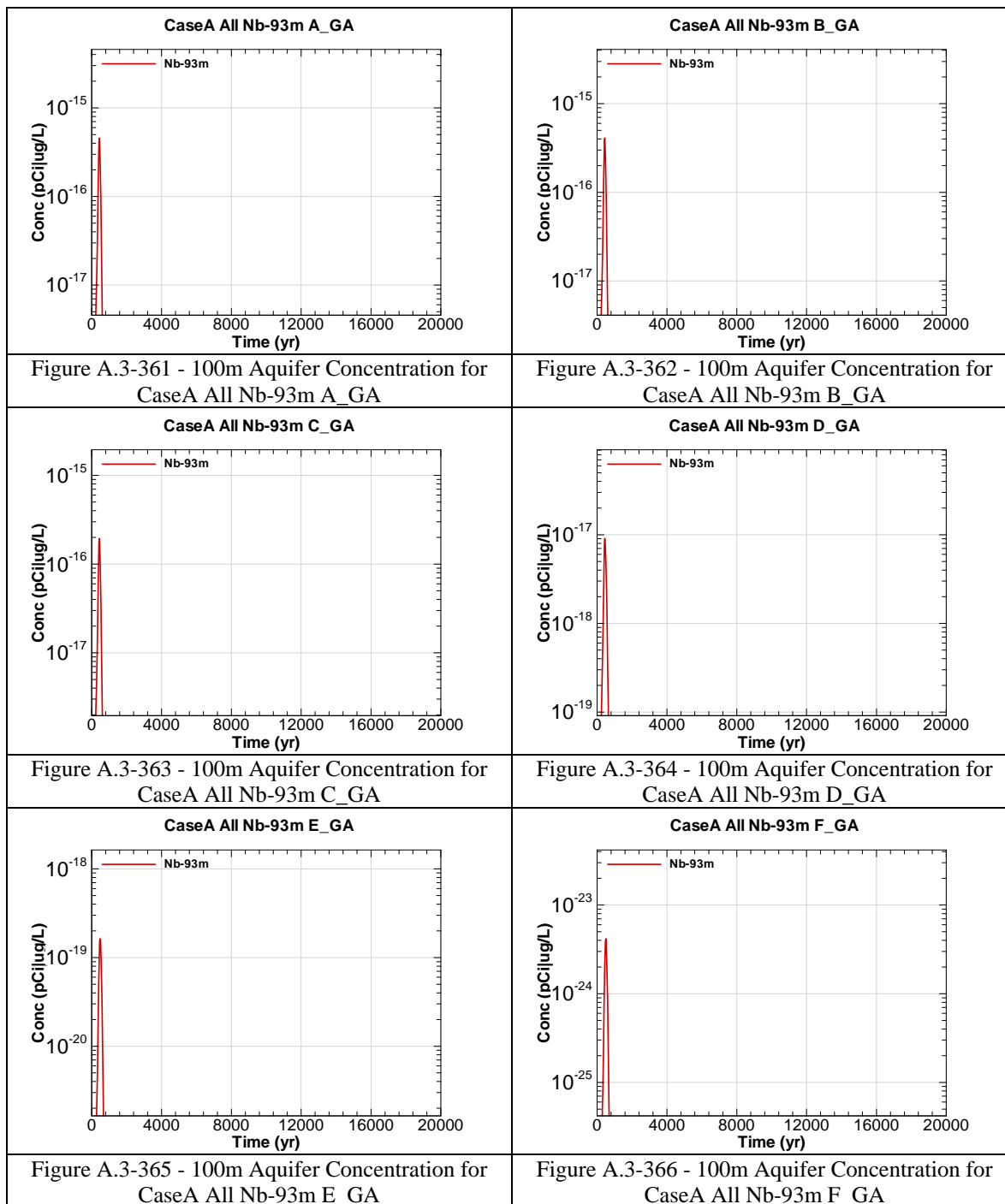


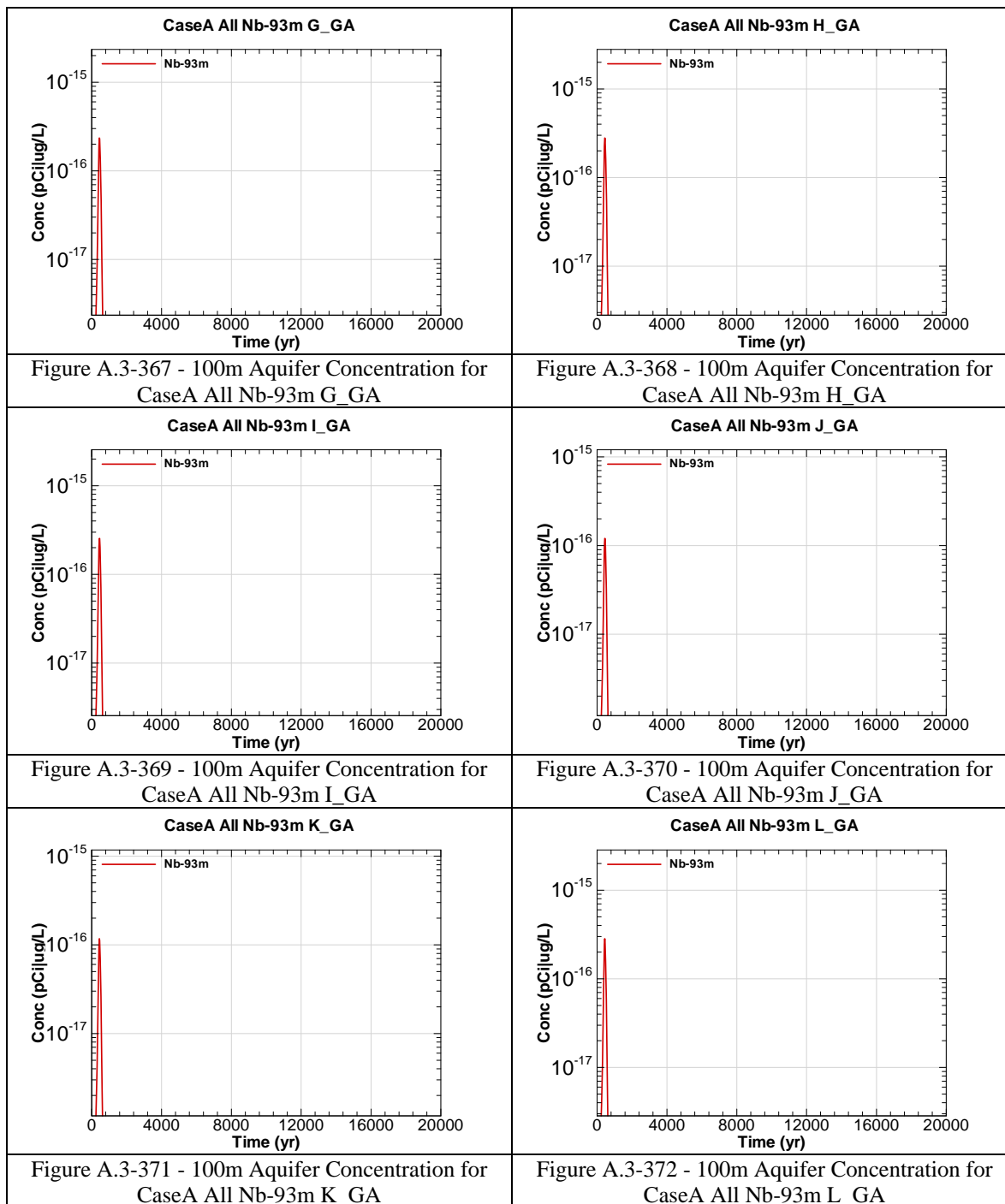


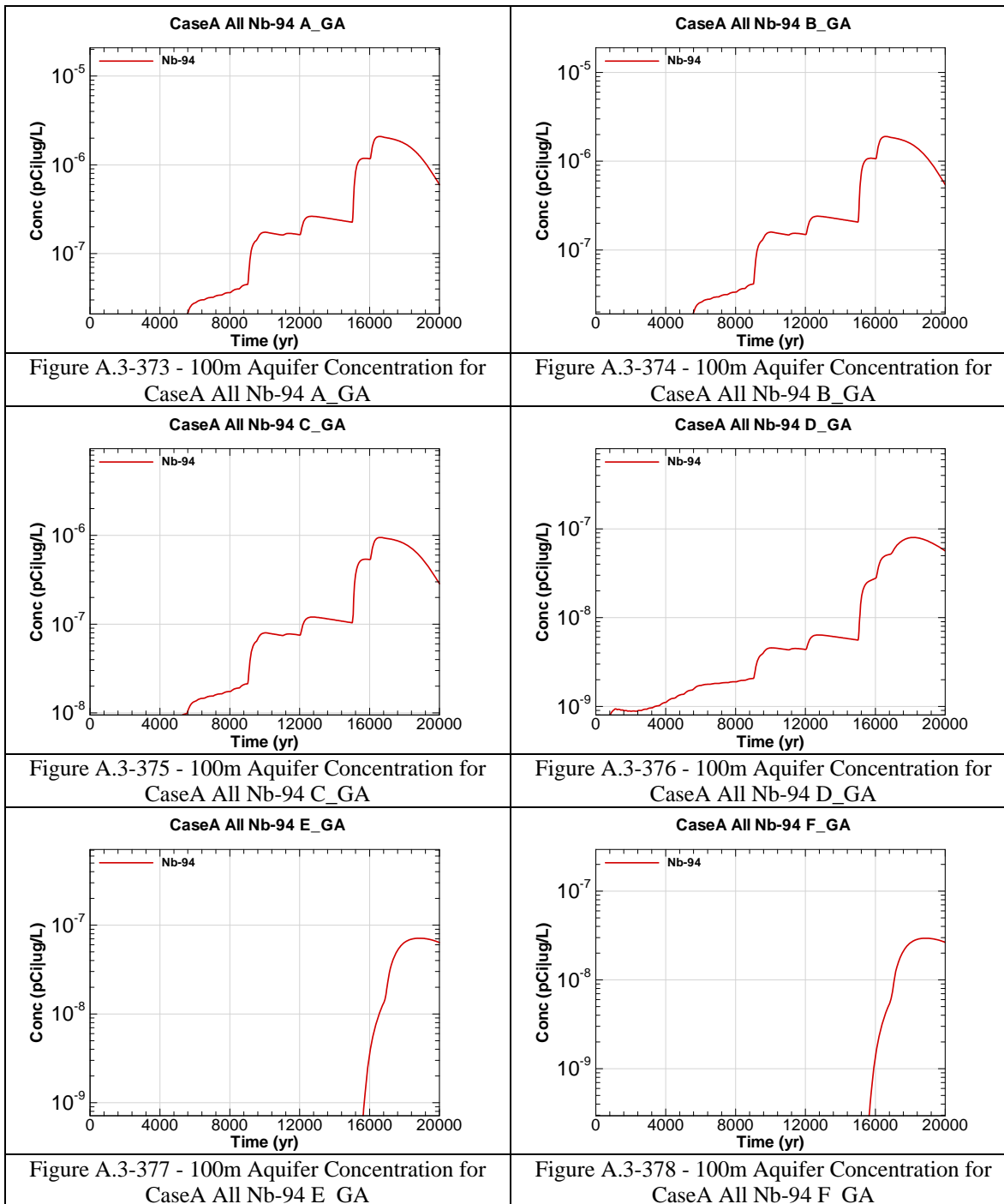


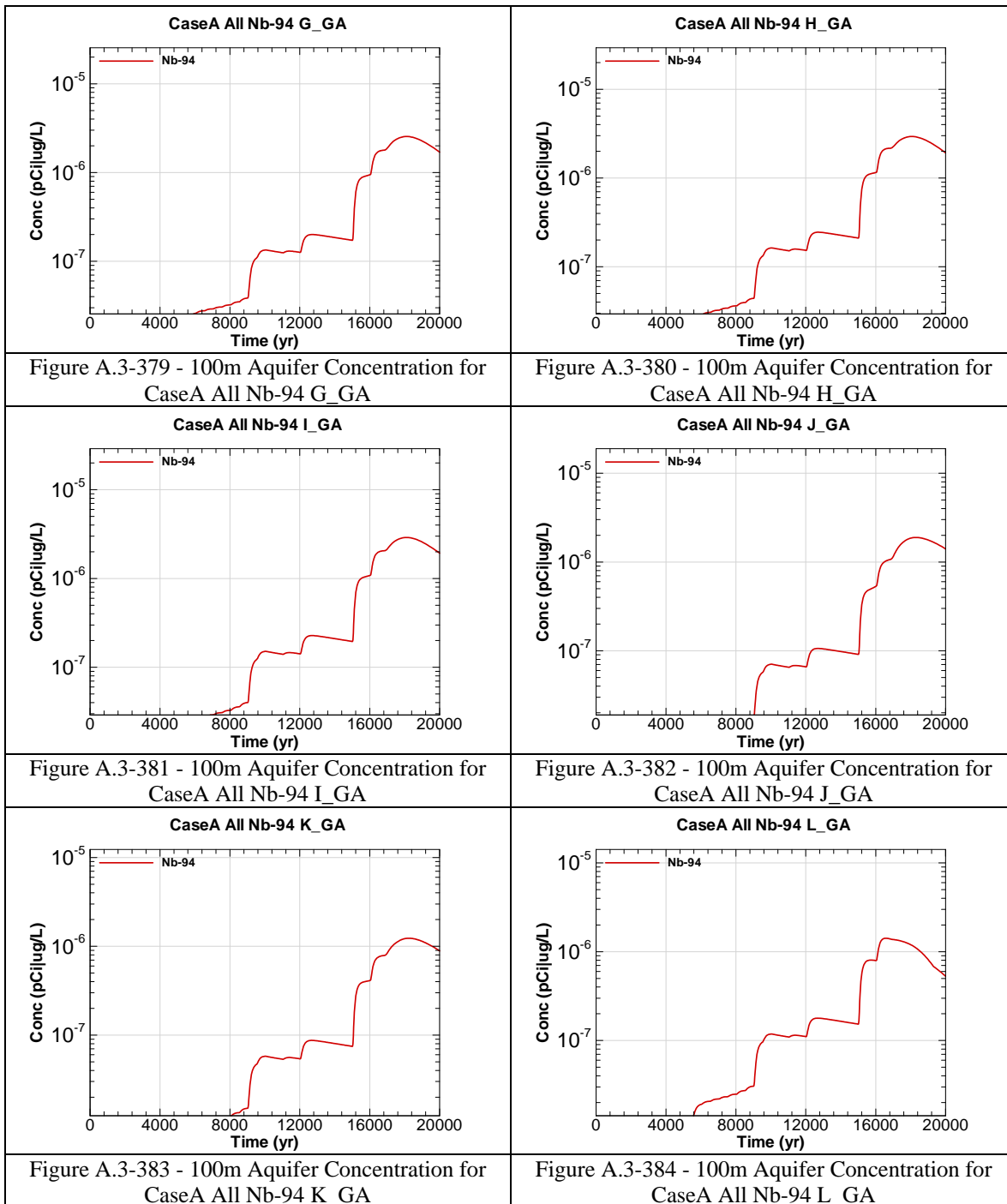


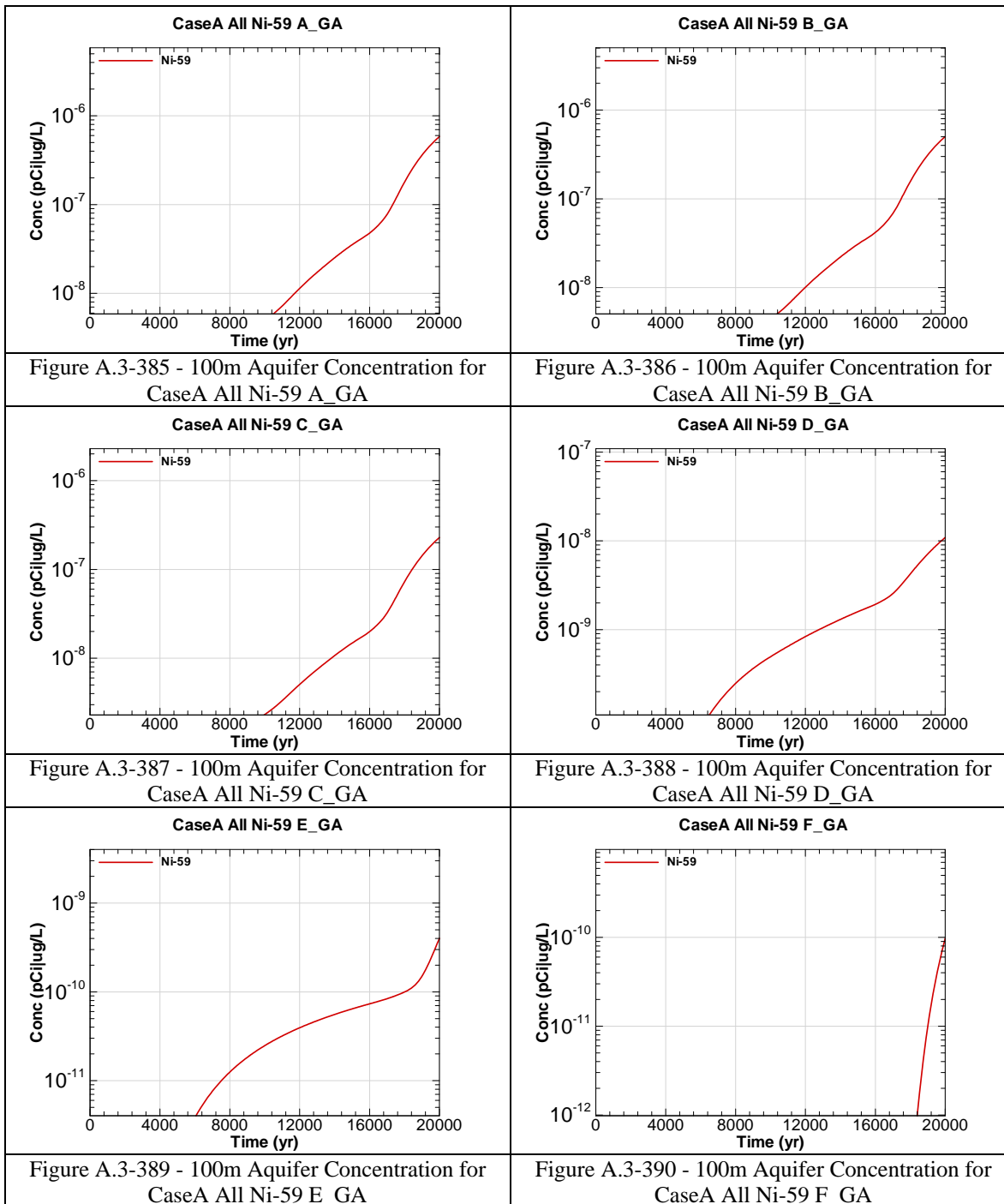


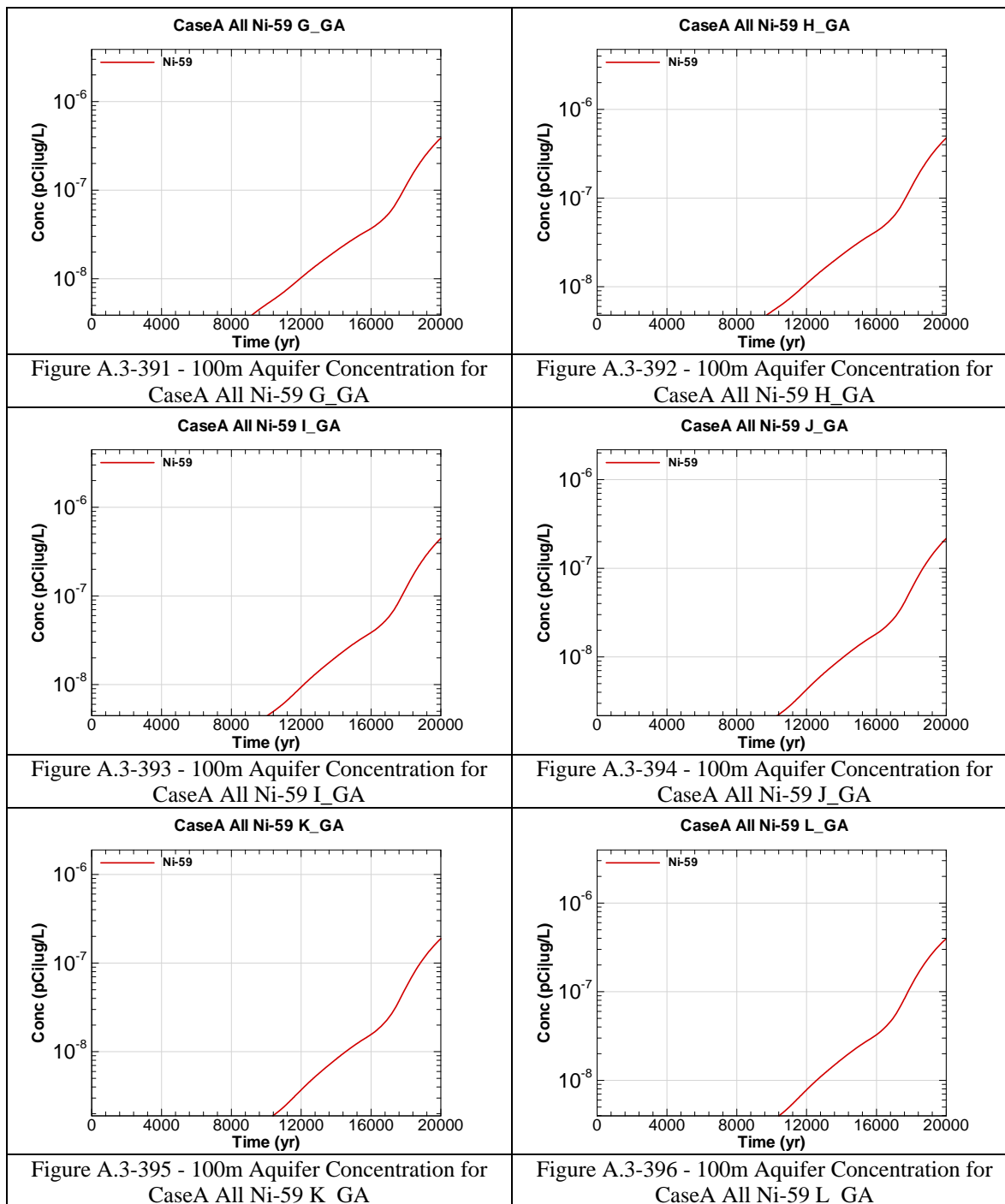


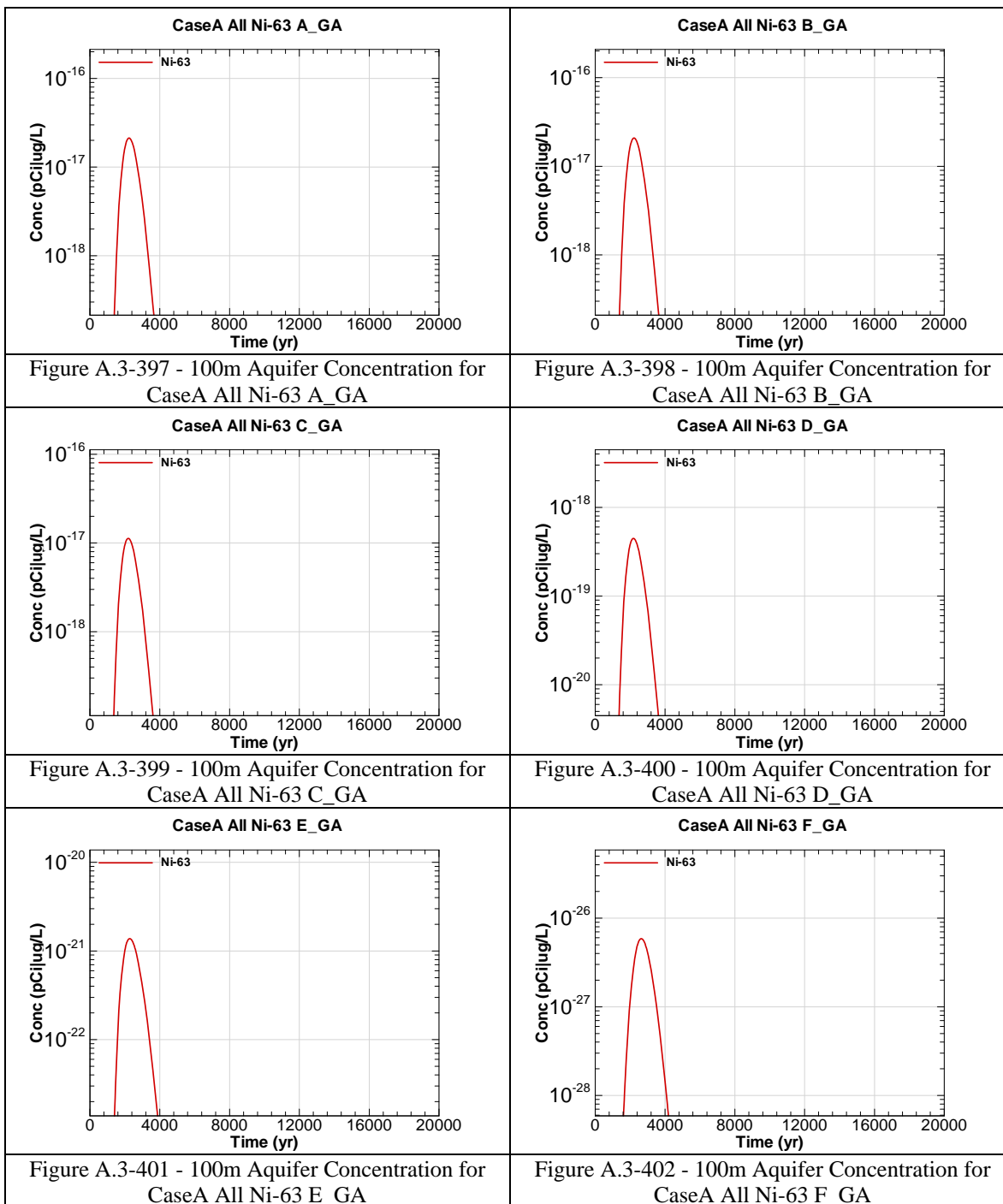


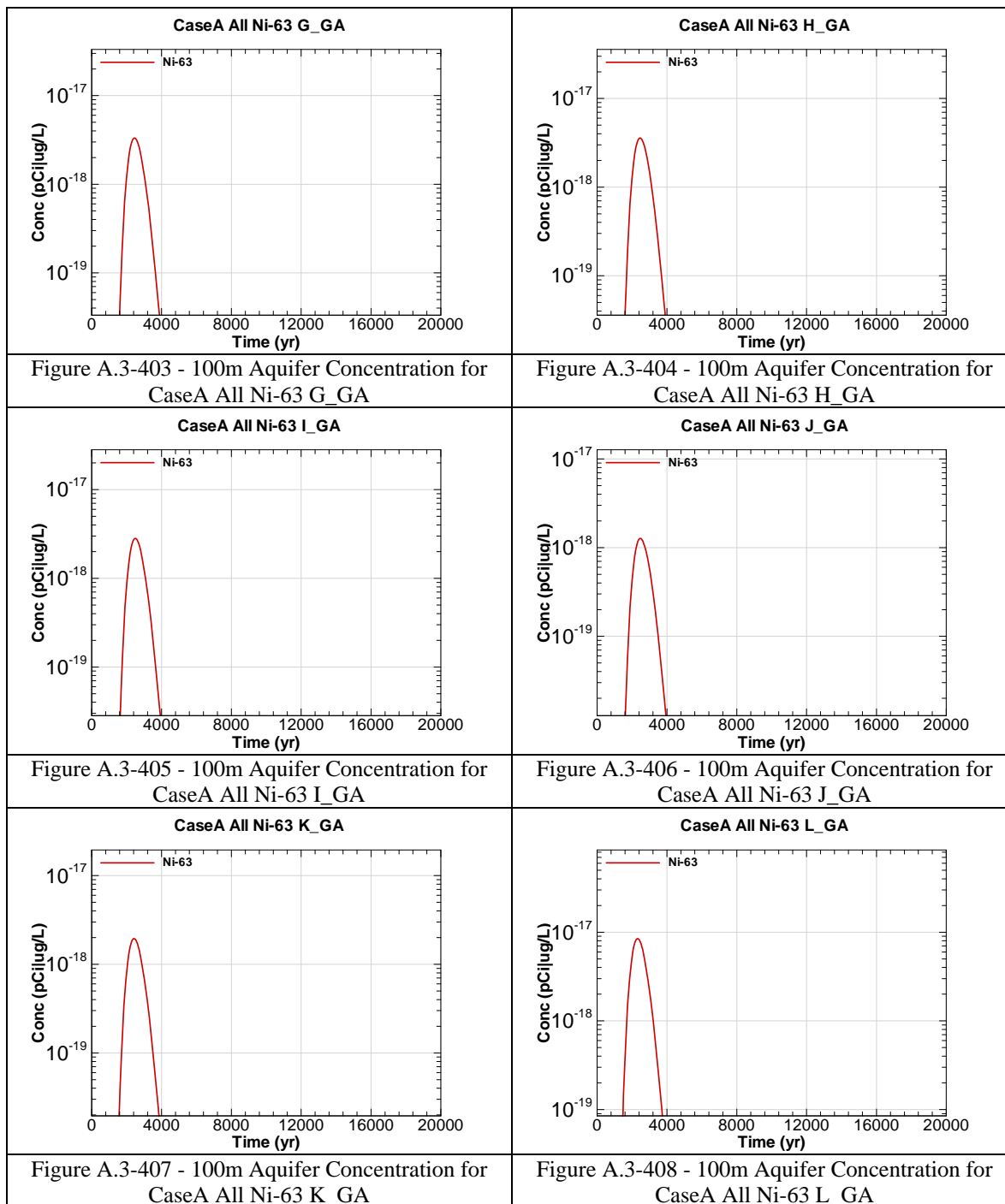


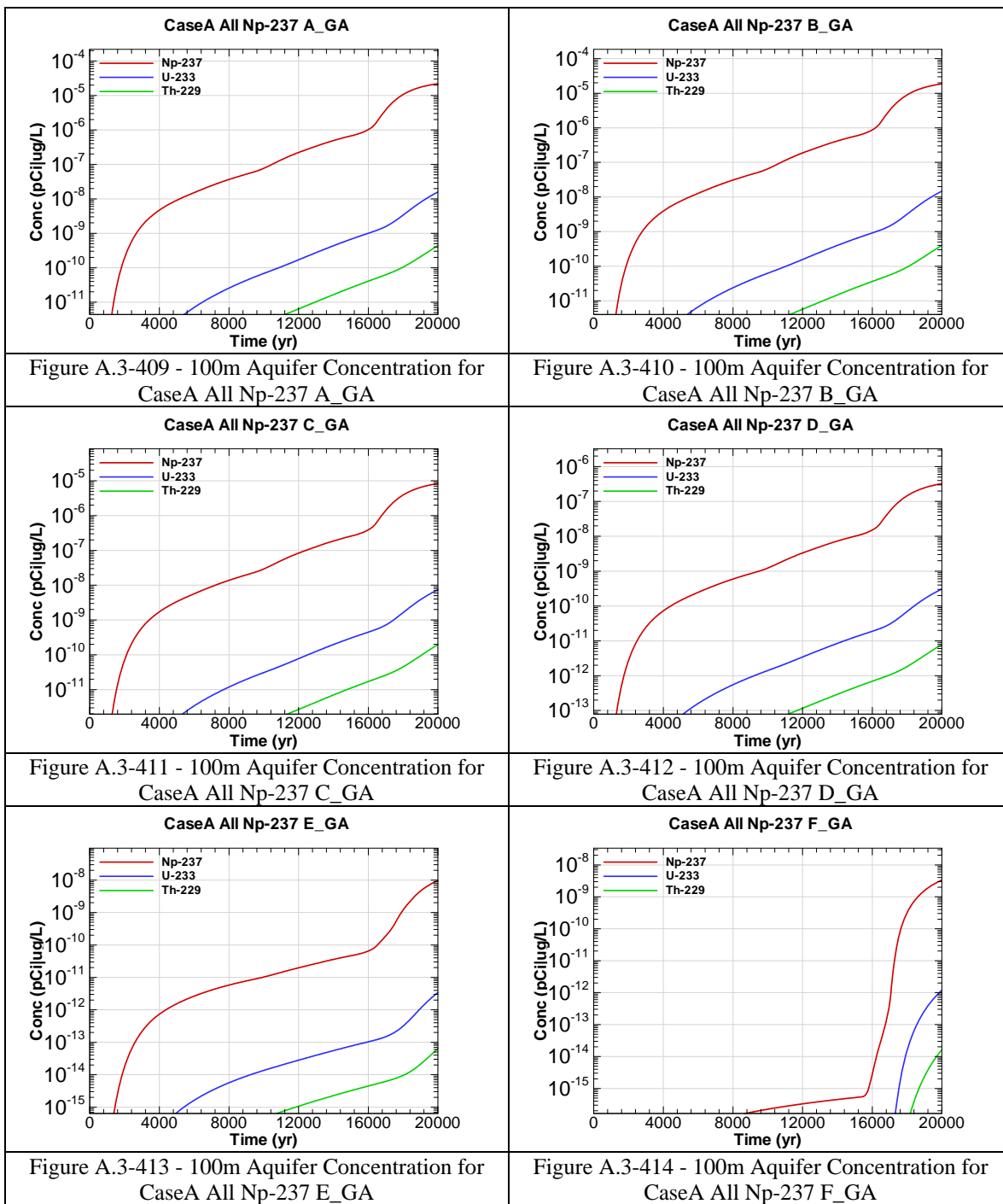












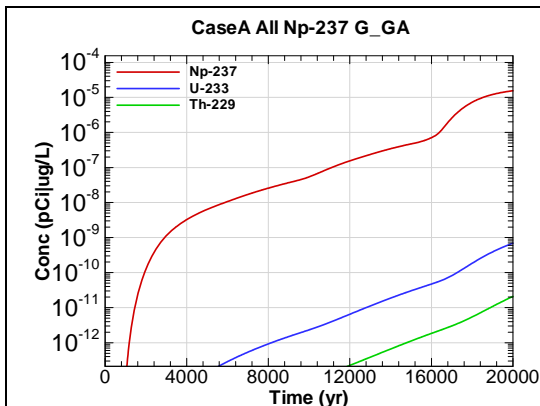


Figure A.3-415 - 100m Aquifer Concentration for
CaseA All Np-237 G_GA

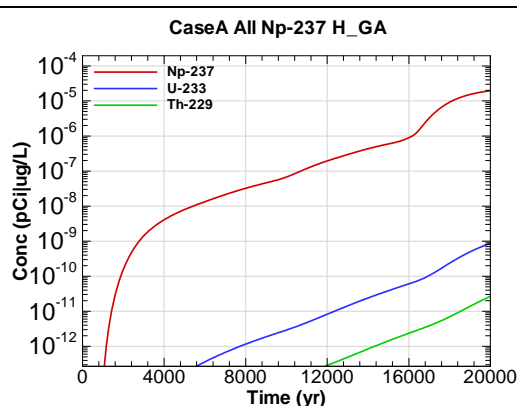


Figure A.3-416 - 100m Aquifer Concentration for
CaseA All Np-237 H_GA

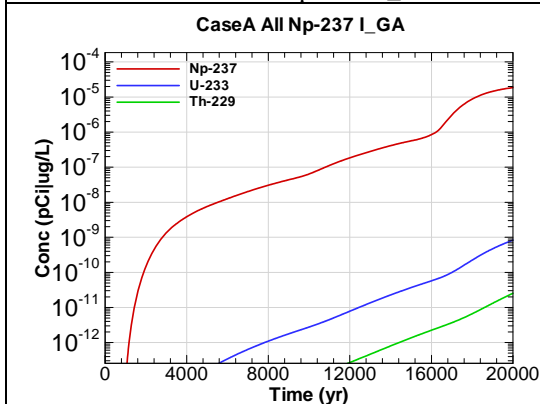


Figure A.3-417 - 100m Aquifer Concentration for
CaseA All Np-237 I_GA

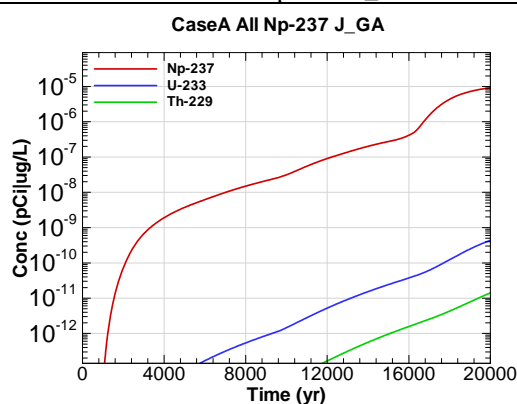


Figure A.3-418 - 100m Aquifer Concentration for
CaseA All Np-237 J_GA

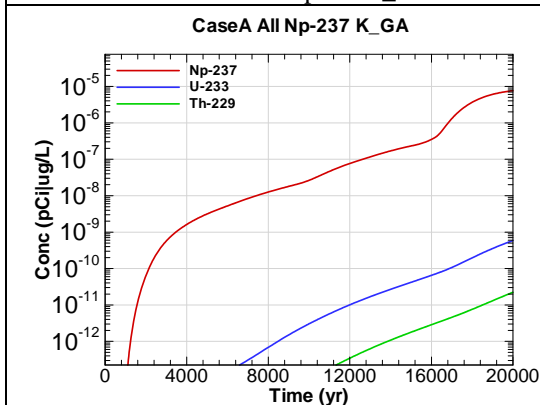


Figure A.3-419 - 100m Aquifer Concentration for
CaseA All Np-237 K_GA

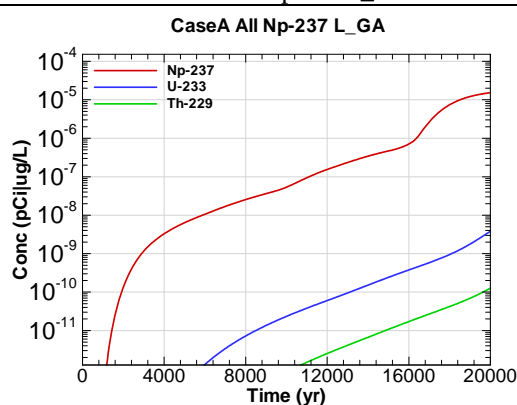
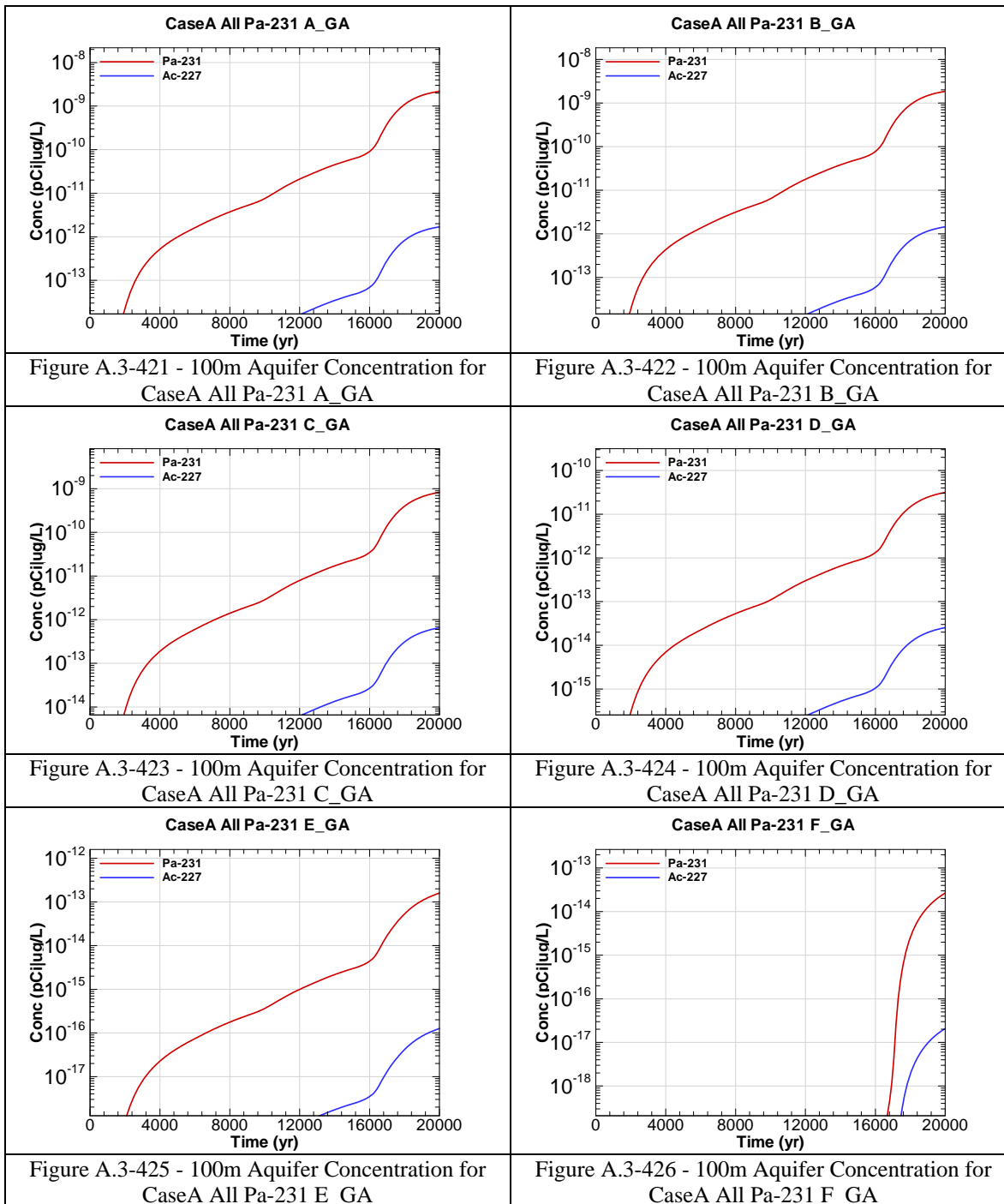
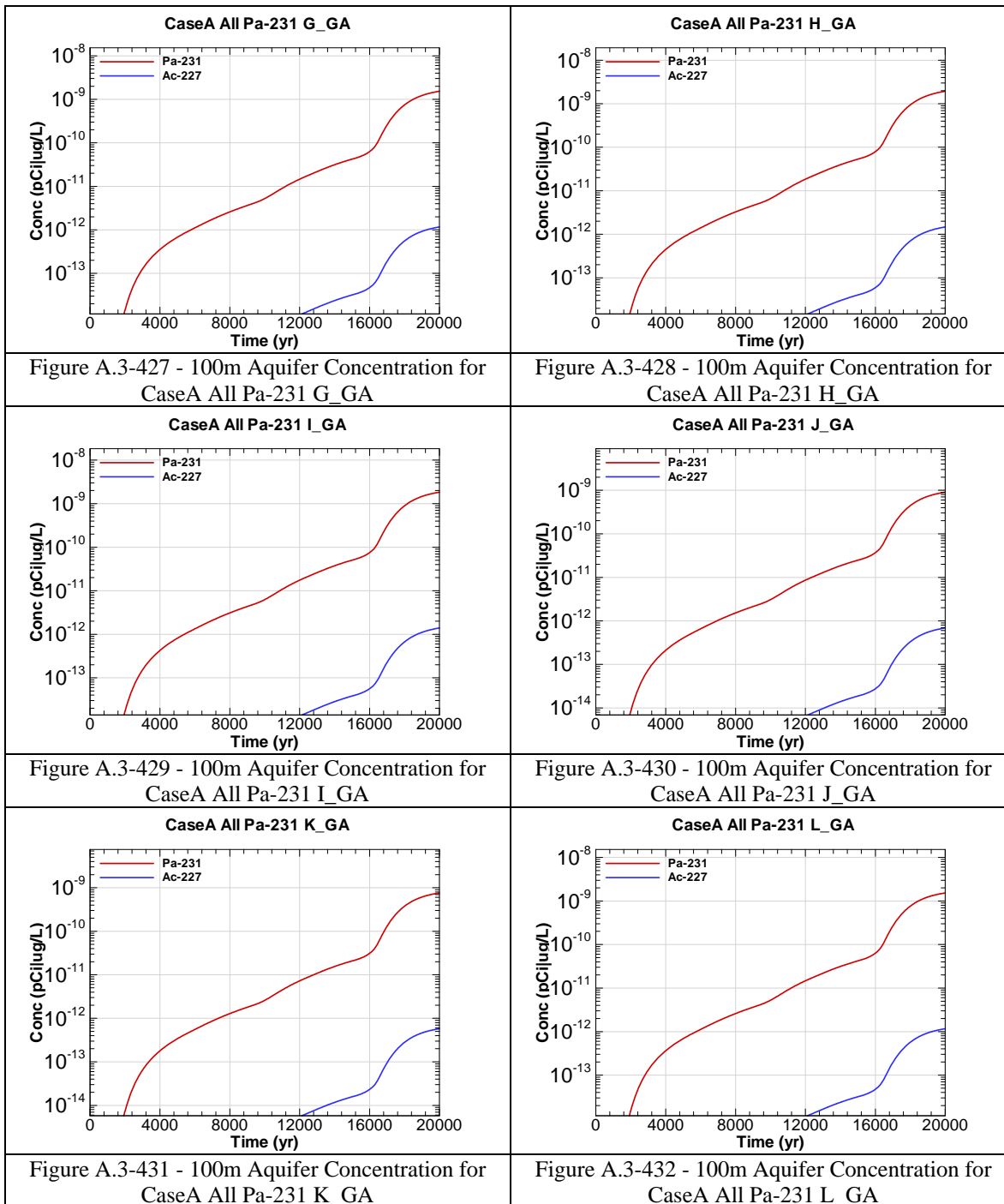
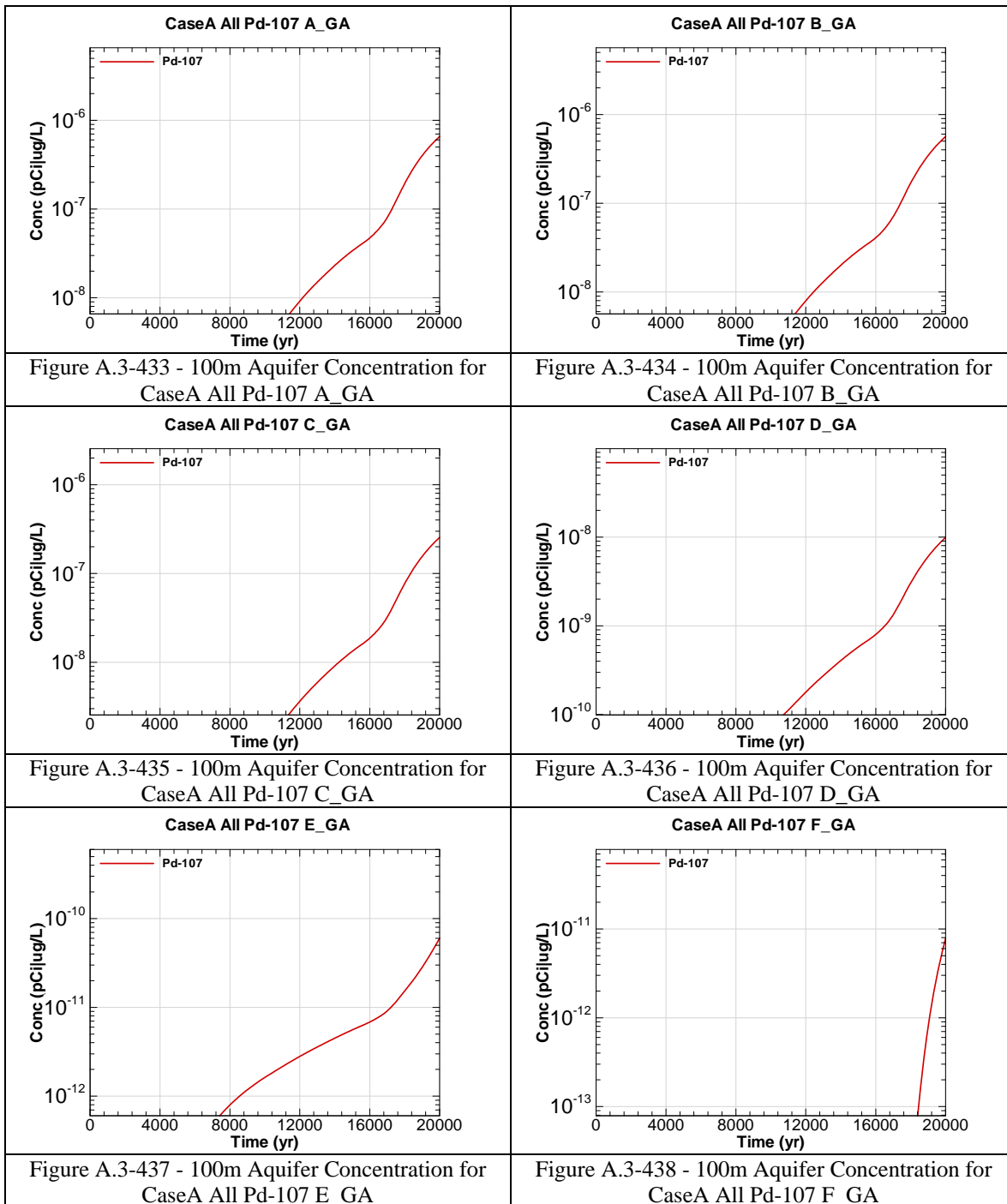
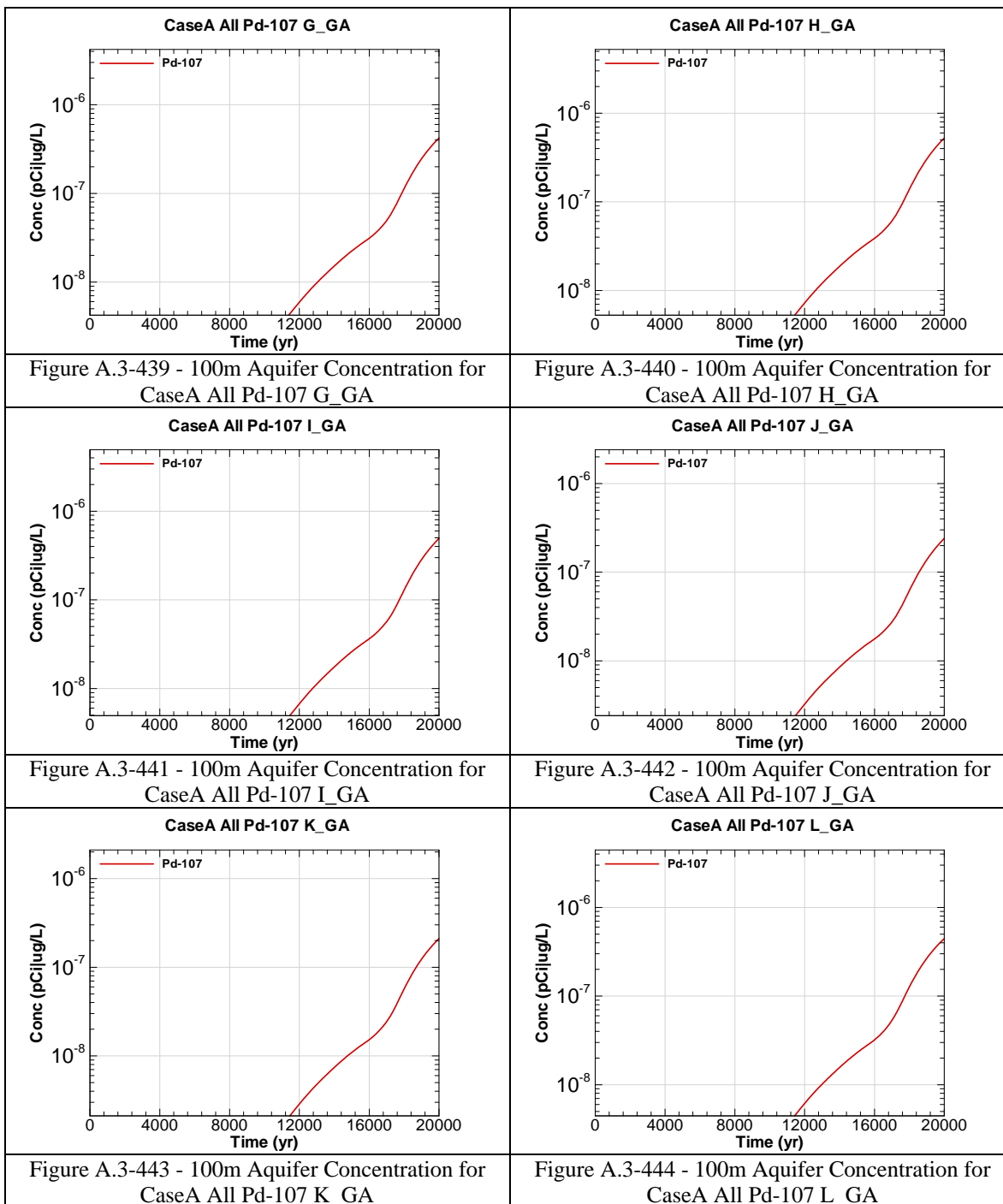


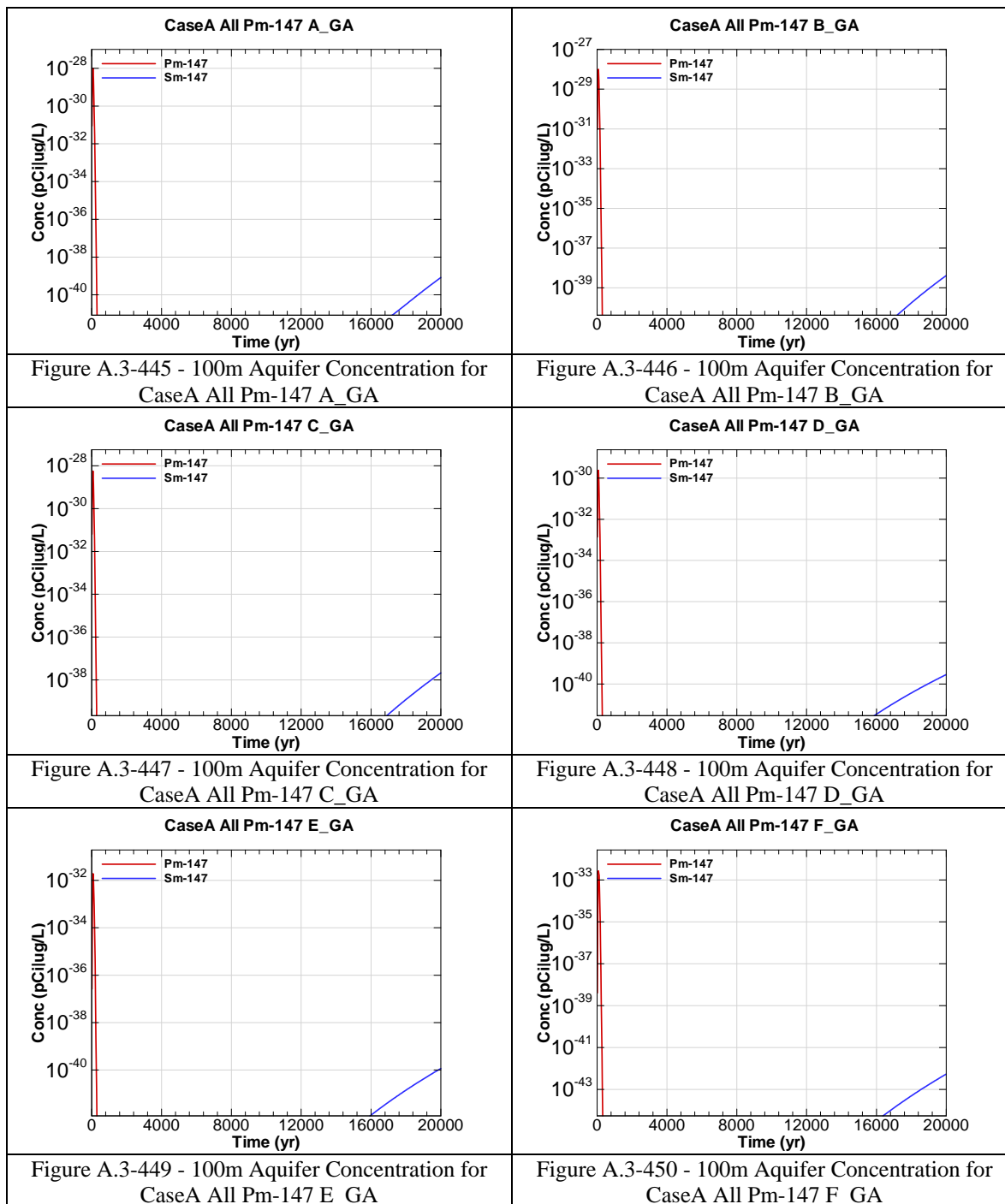
Figure A.3-420 - 100m Aquifer Concentration for
CaseA All Np-237 L_GA

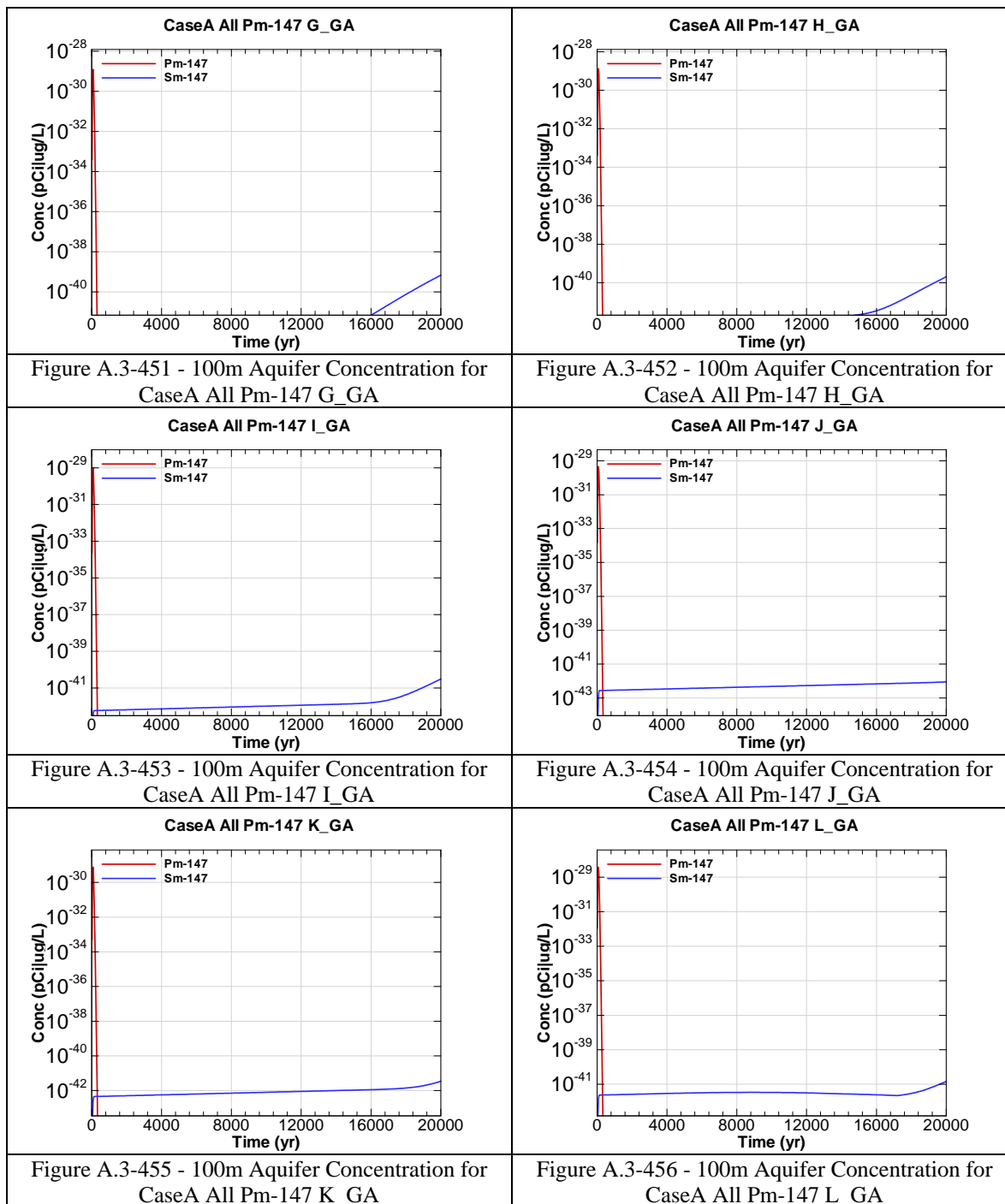


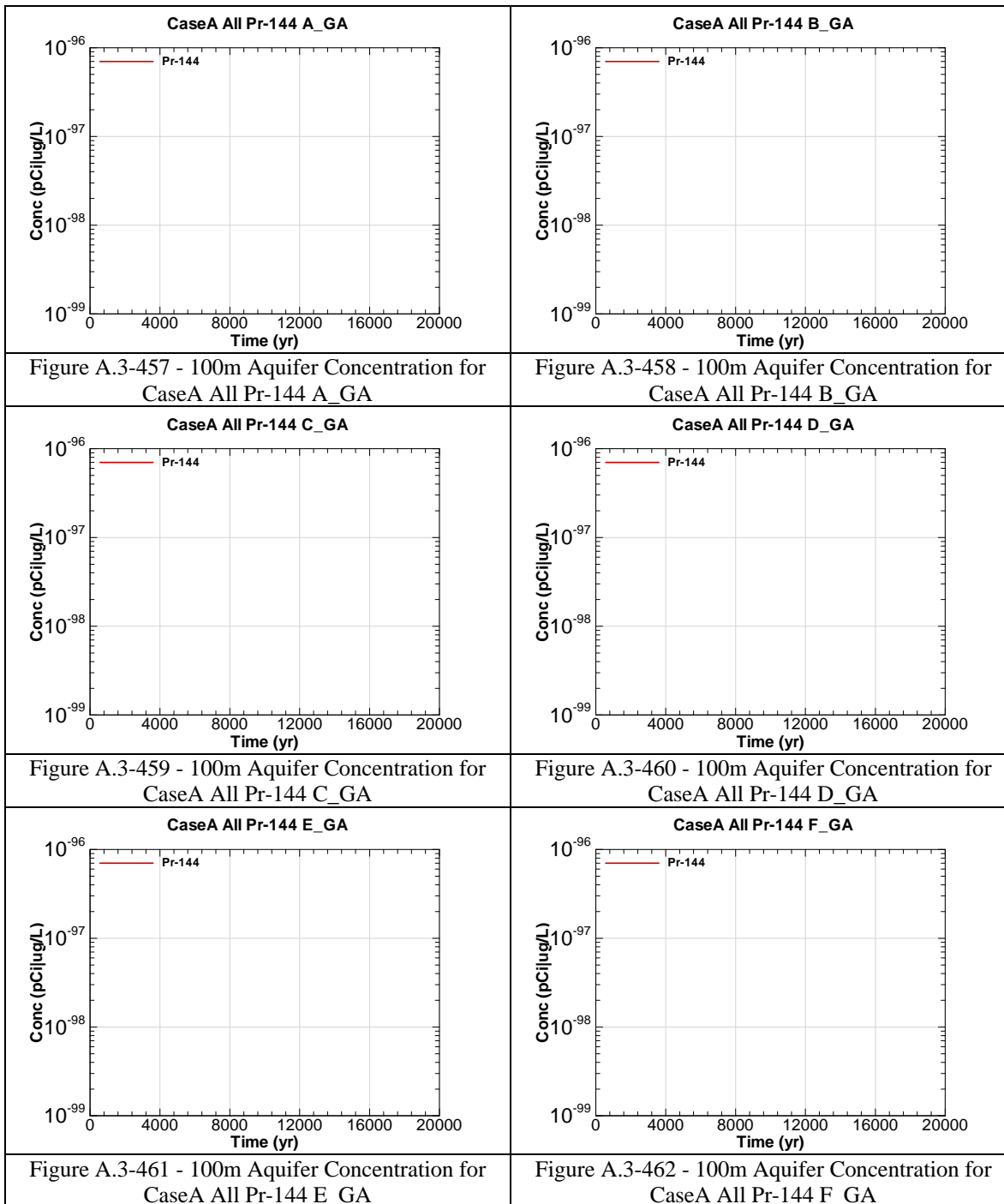


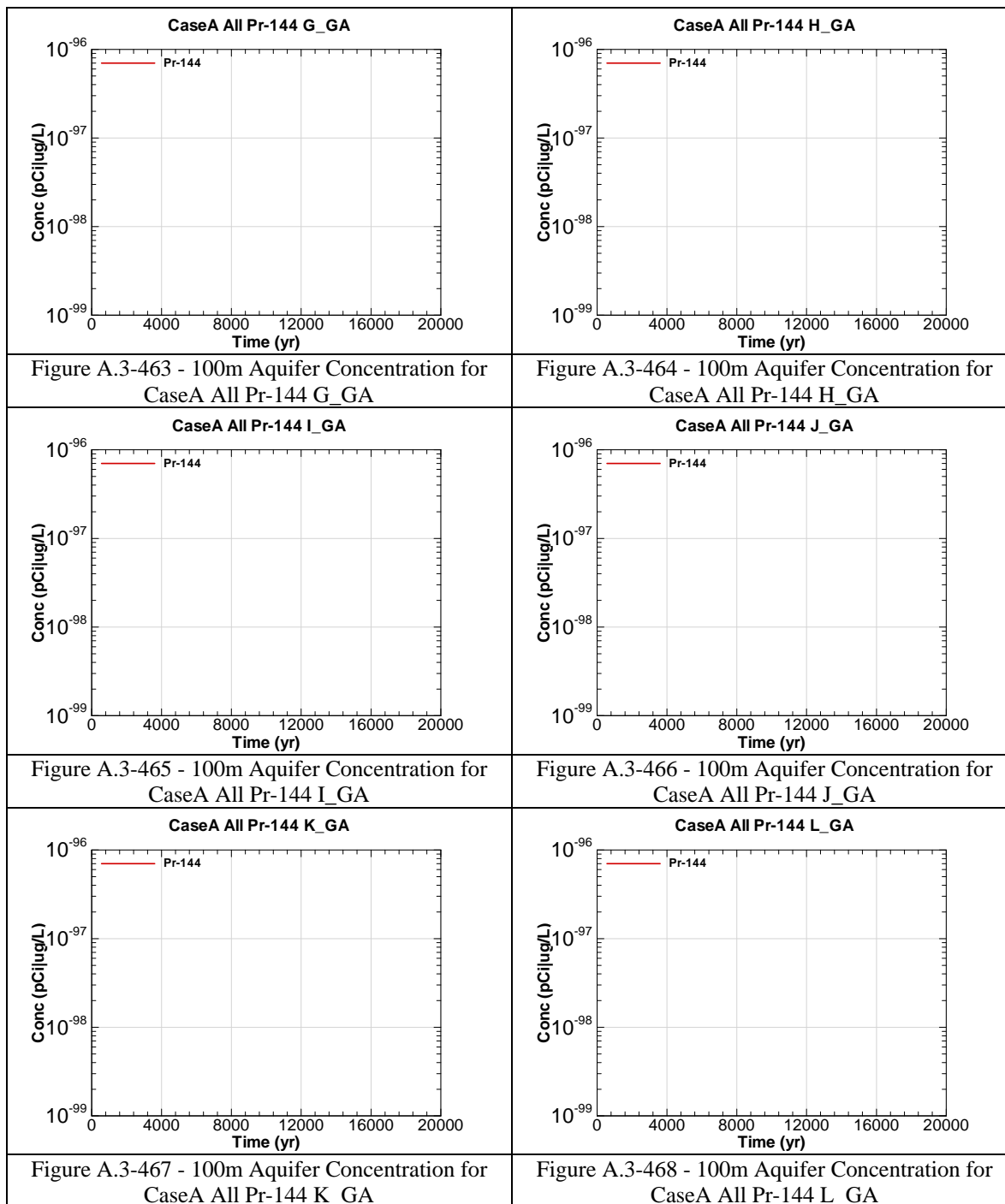


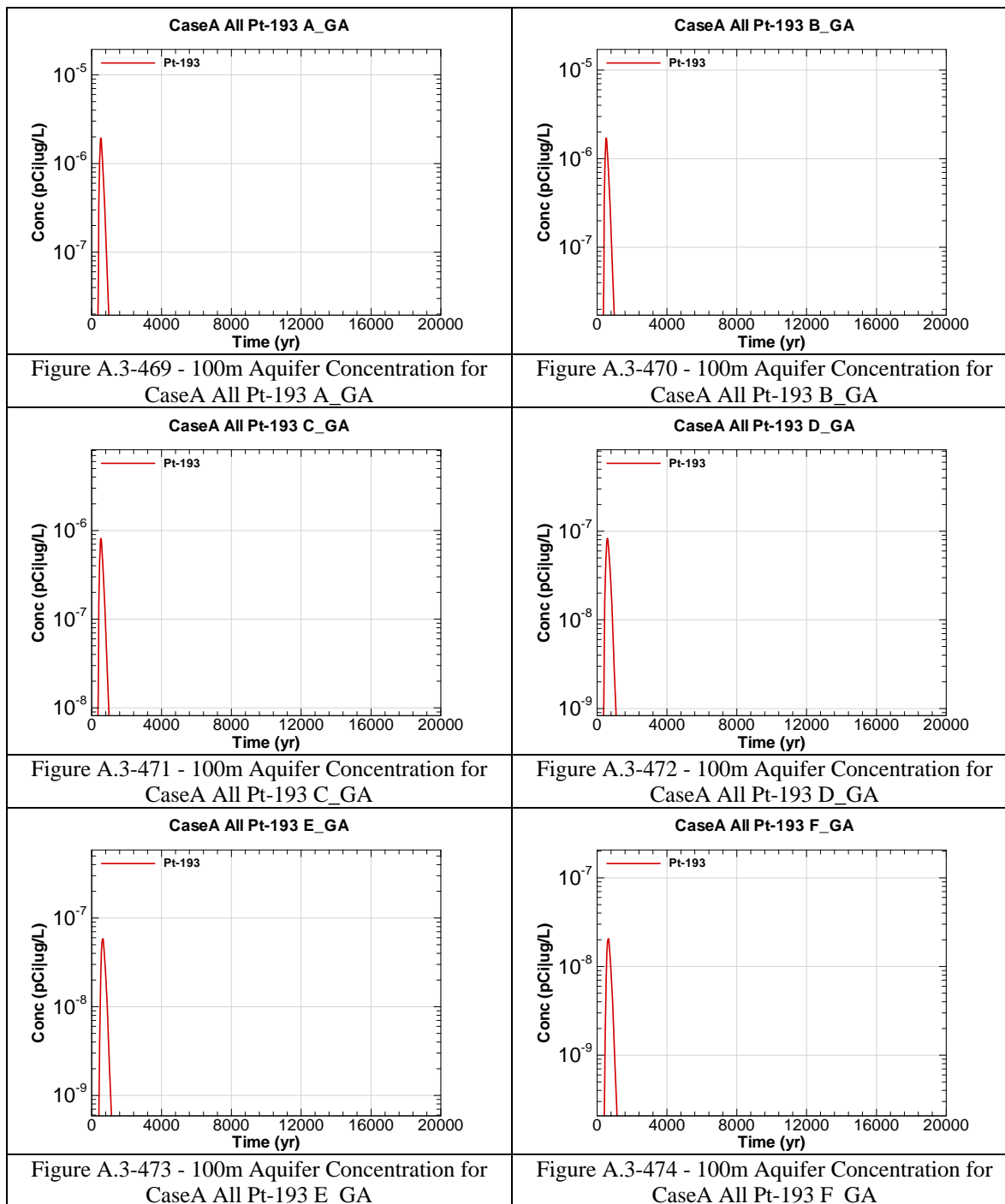


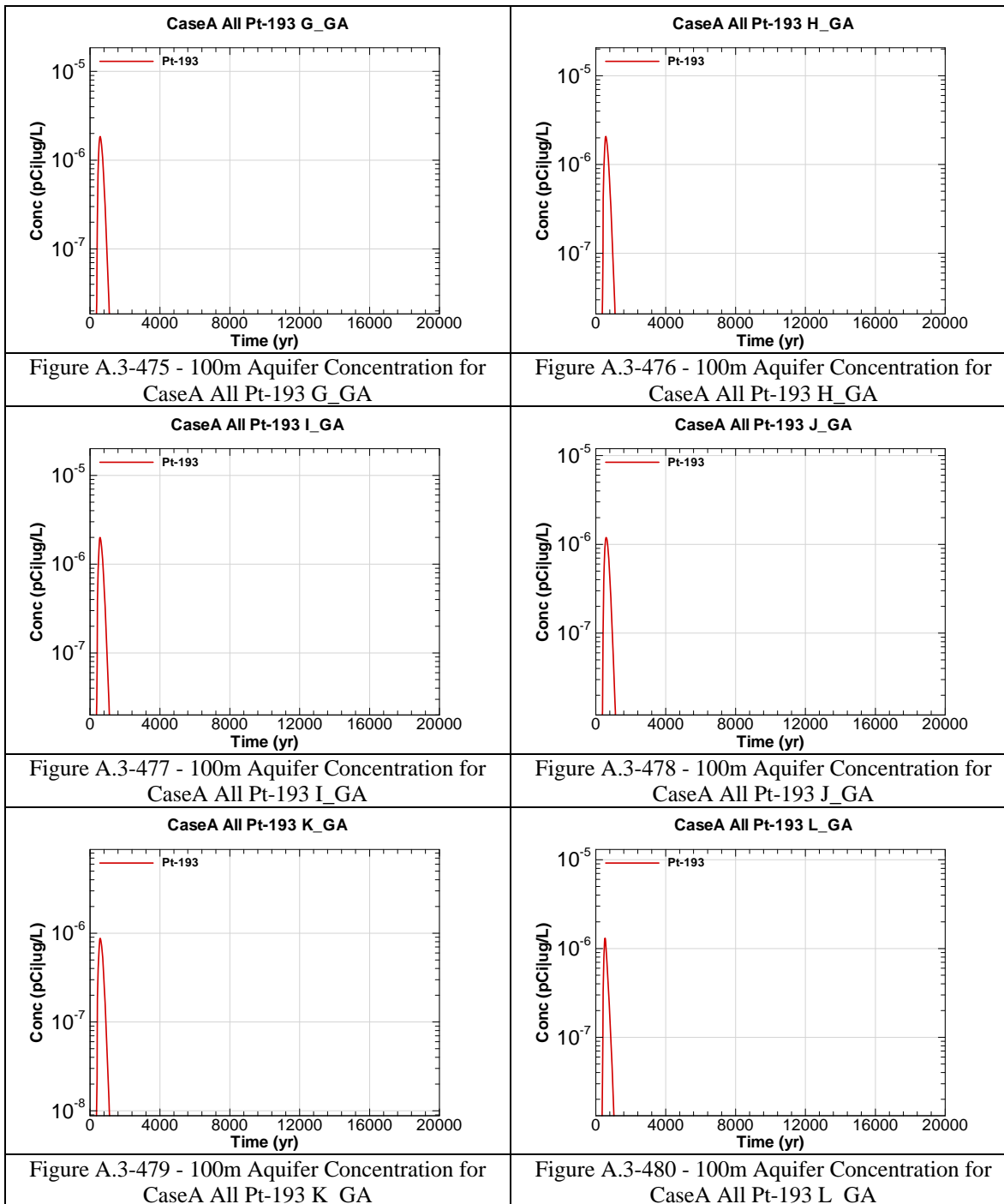












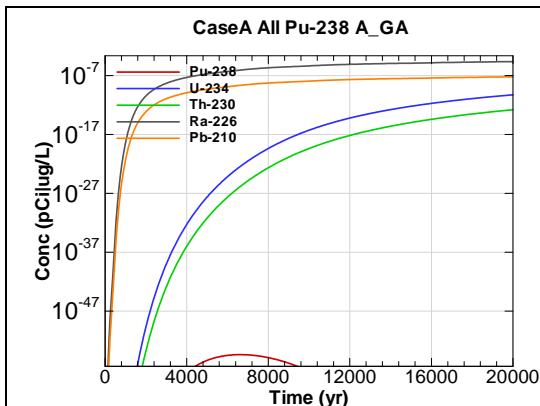


Figure A.3-481 - 100m Aquifer Concentration for
CaseA All Pu-238 A_GA

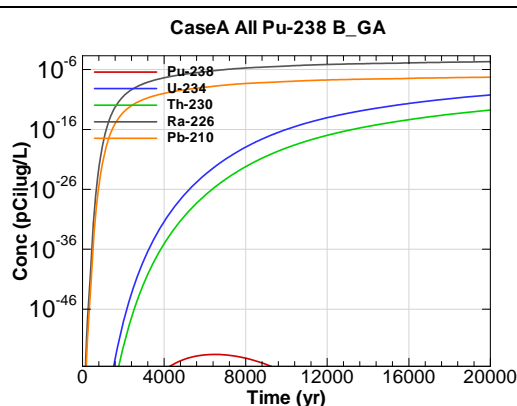


Figure A.3-482 - 100m Aquifer Concentration for
CaseA All Pu-238 B_GA

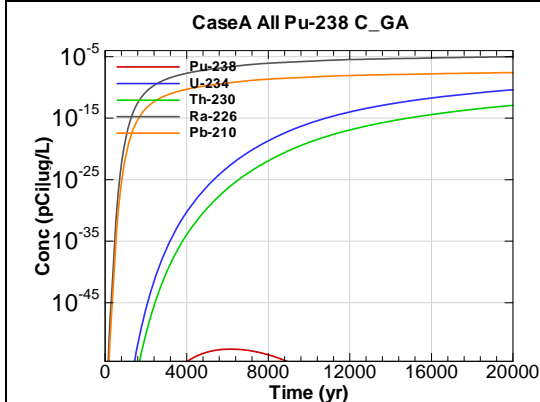


Figure A.3-483 - 100m Aquifer Concentration for
CaseA All Pu-238 C_GA

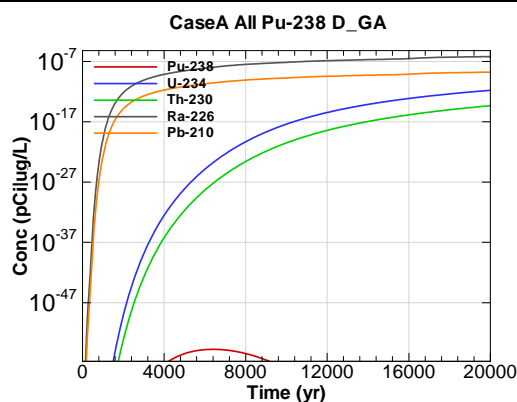


Figure A.3-484 - 100m Aquifer Concentration for
CaseA All Pu-238 D_GA

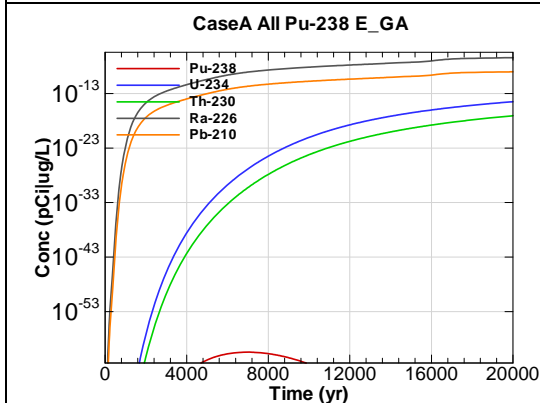


Figure A.3-485 - 100m Aquifer Concentration for
CaseA All Pu-238 E_GA

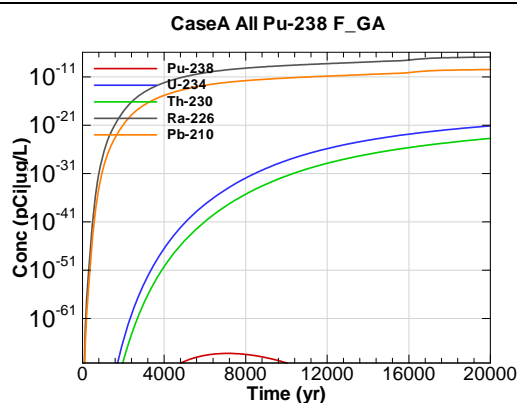


Figure A.3-486 - 100m Aquifer Concentration for
CaseA All Pu-238 F_GA

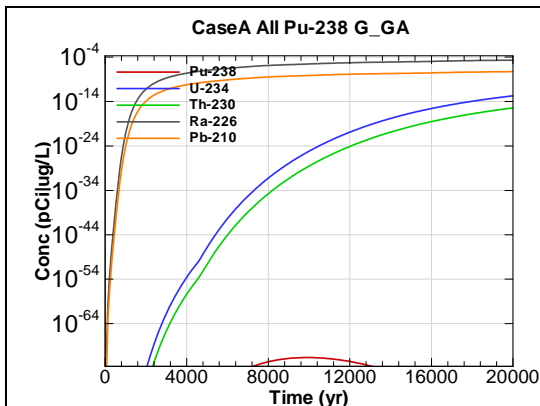


Figure A.3-487 - 100m Aquifer Concentration for
CaseA All Pu-238 G_GA

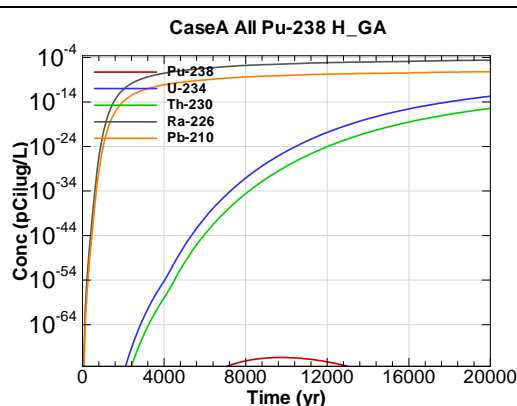


Figure A.3-488 - 100m Aquifer Concentration for
CaseA All Pu-238 H_GA

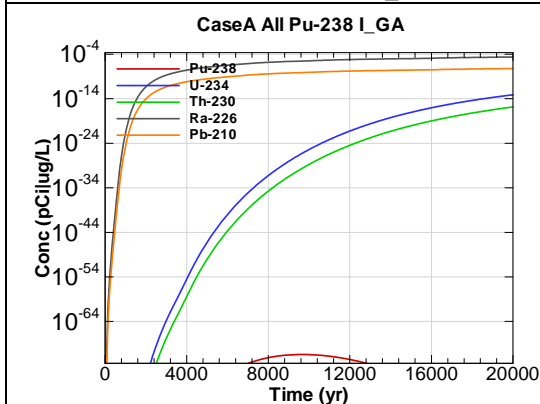


Figure A.3-489 - 100m Aquifer Concentration for
CaseA All Pu-238 I_GA

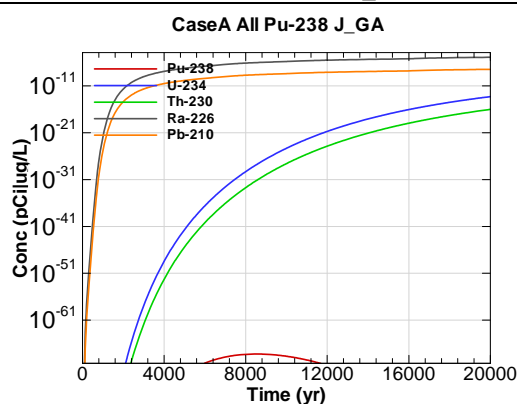


Figure A.3-490 - 100m Aquifer Concentration for
CaseA All Pu-238 J_GA

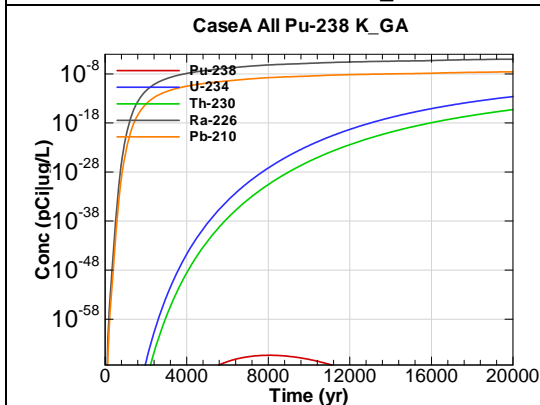


Figure A.3-491 - 100m Aquifer Concentration for
CaseA All Pu-238 K_GA

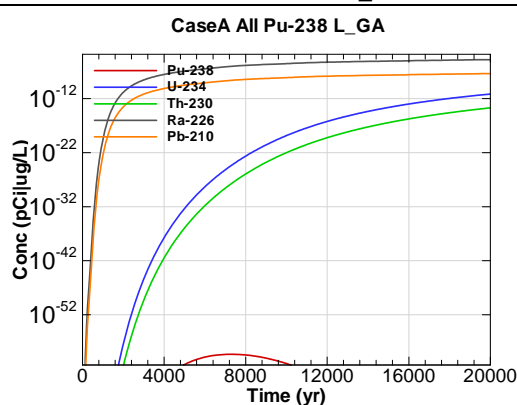
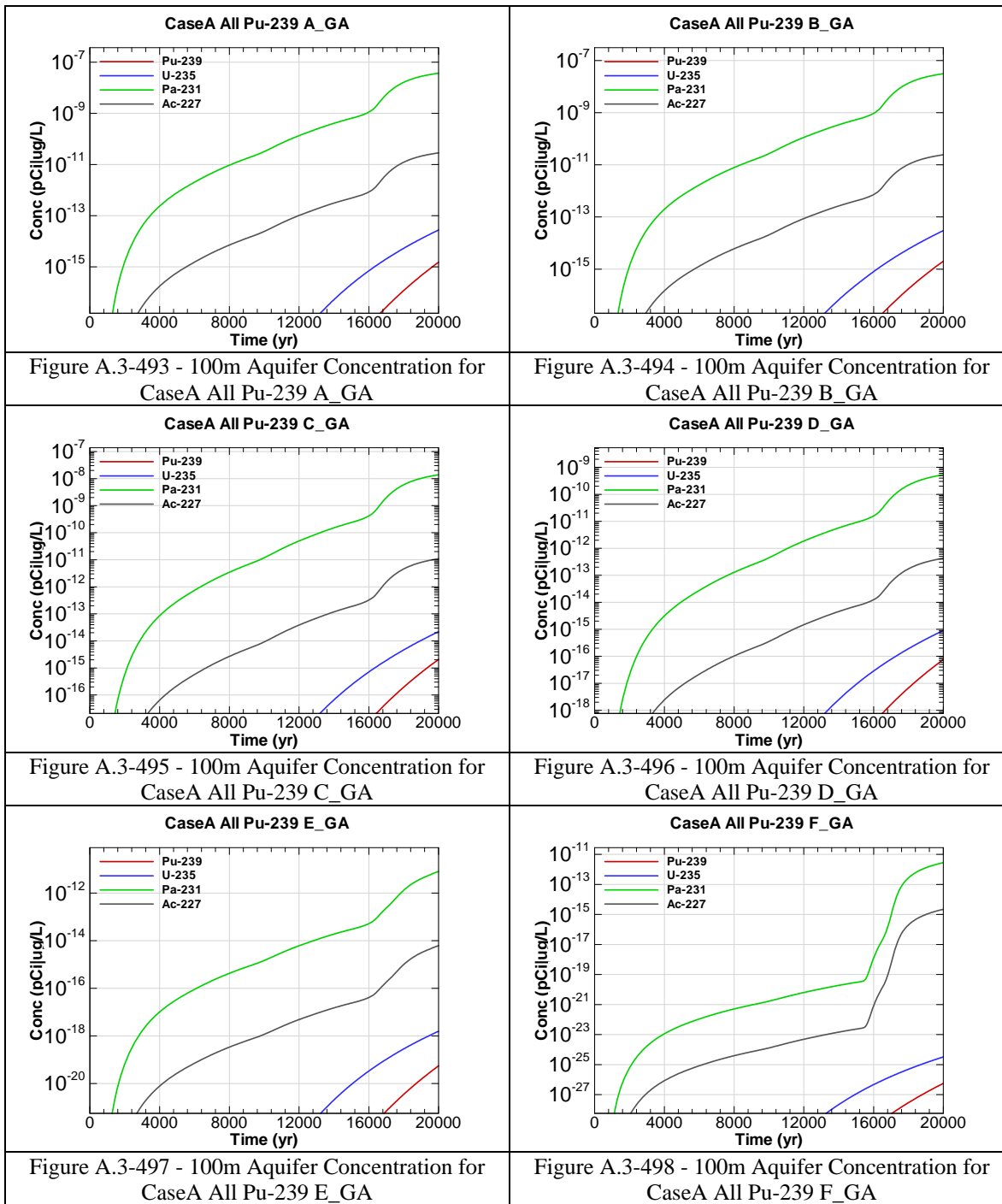
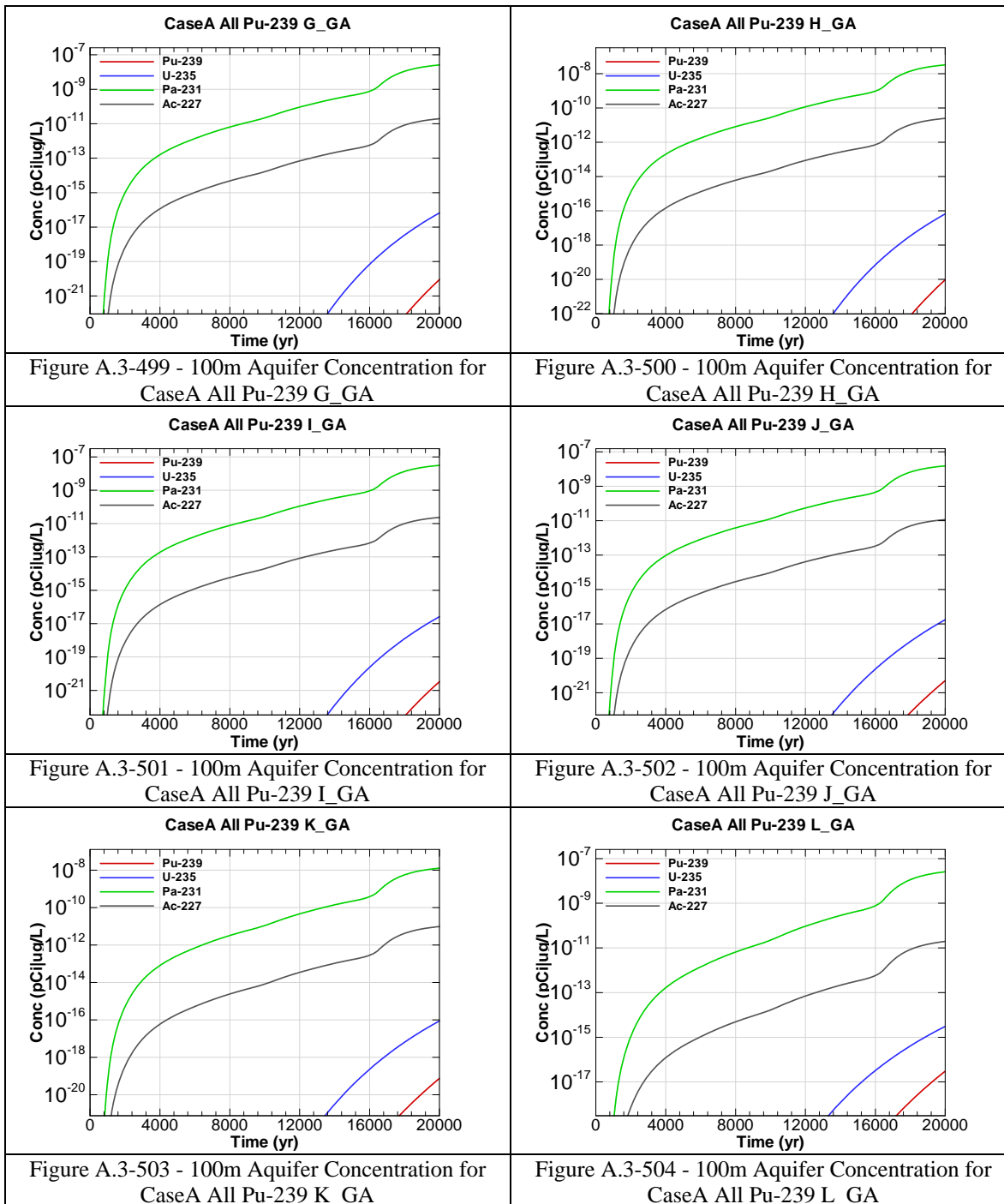
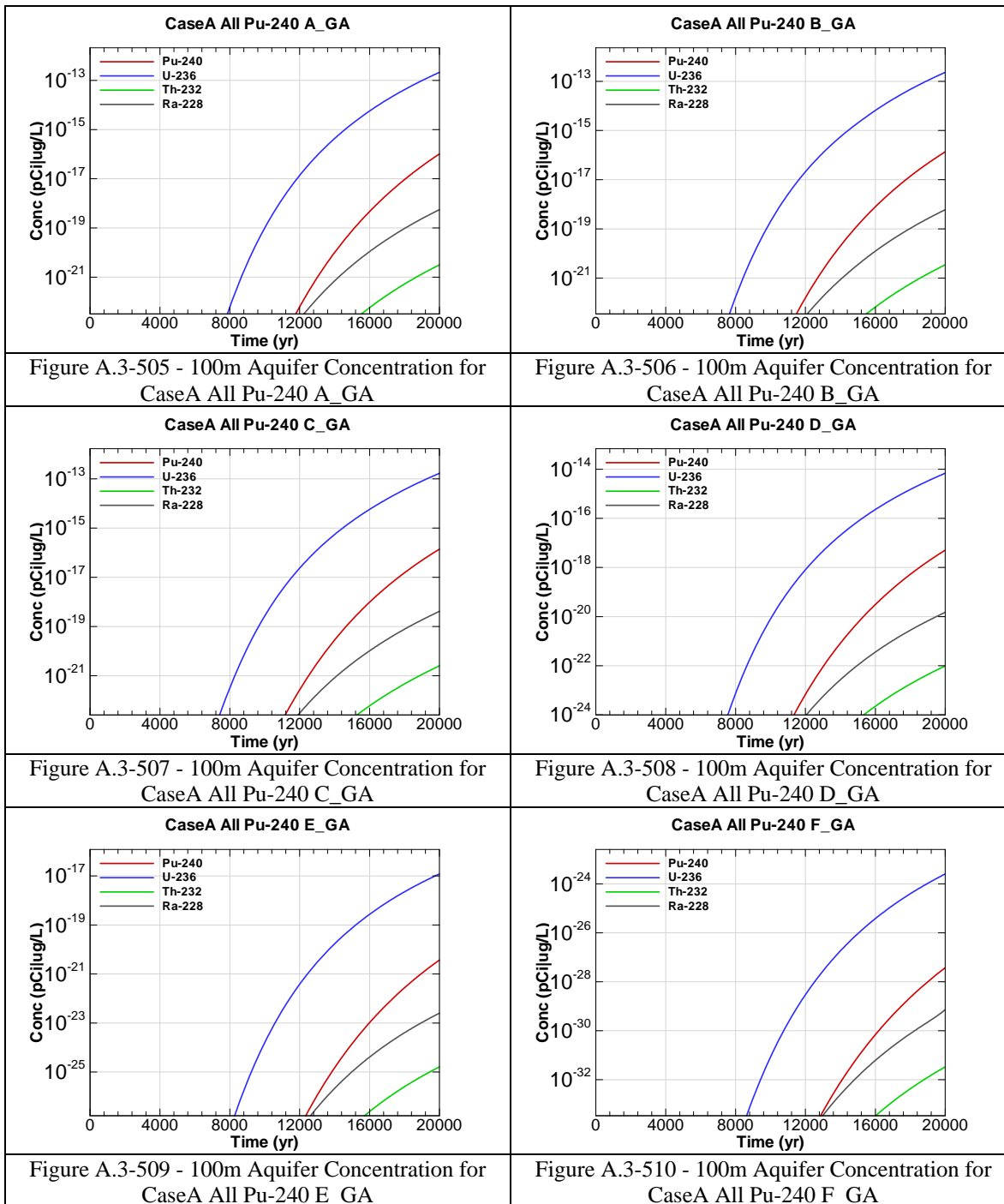
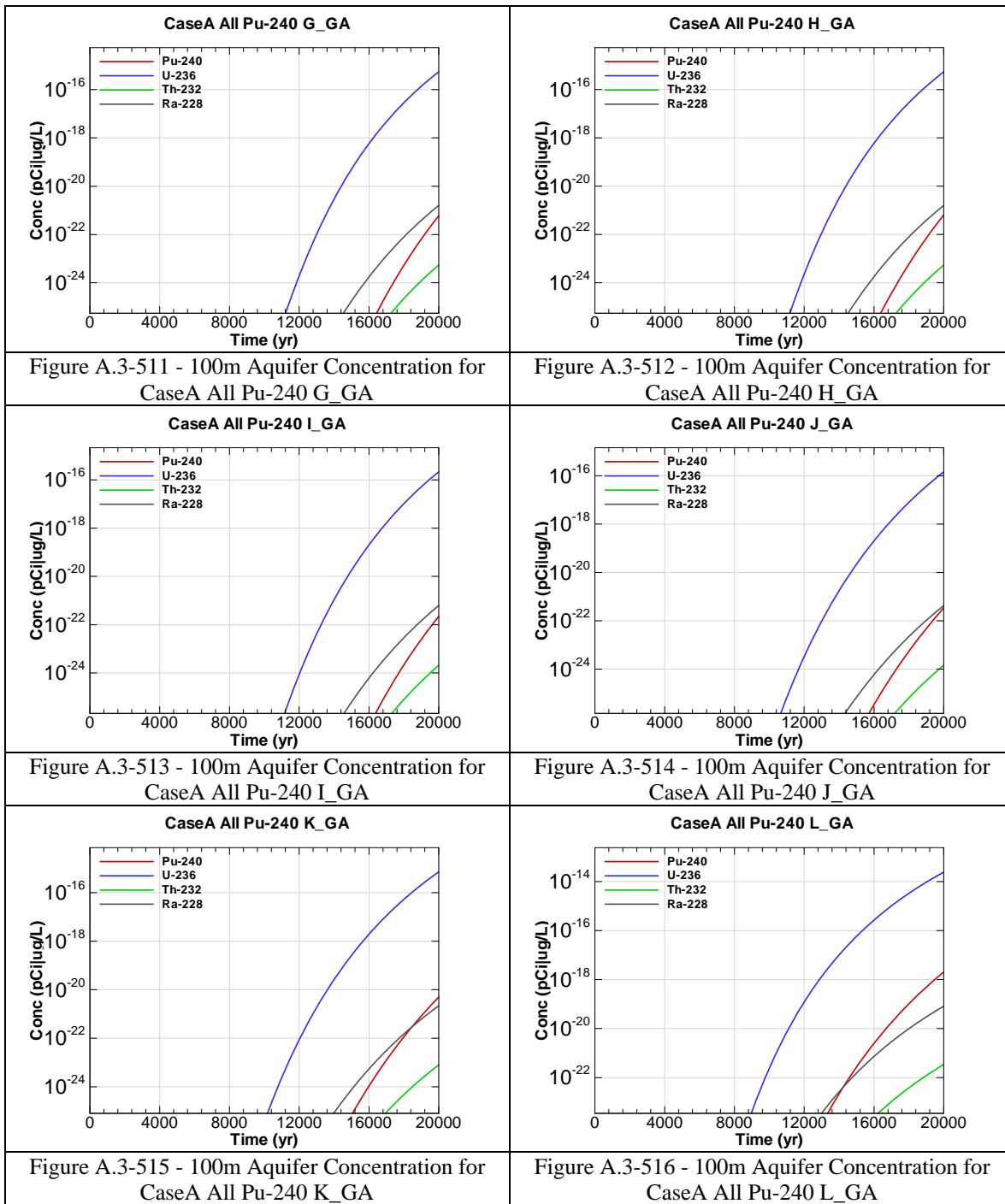


Figure A.3-492 - 100m Aquifer Concentration for
CaseA All Pu-238 L_GA









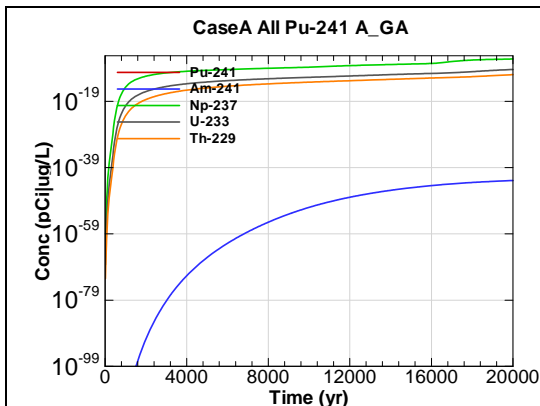


Figure A.3-517 - 100m Aquifer Concentration for
CaseA All Pu-241 A_GA

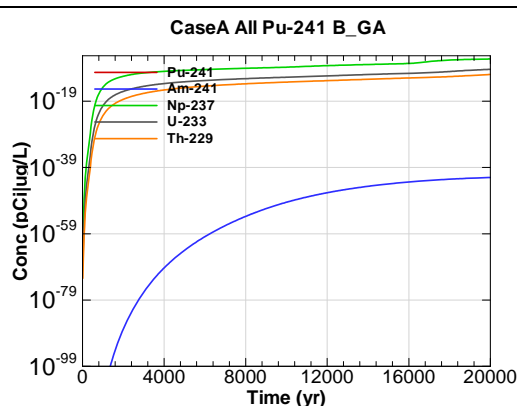


Figure A.3-518 - 100m Aquifer Concentration for
CaseA All Pu-241 B_GA

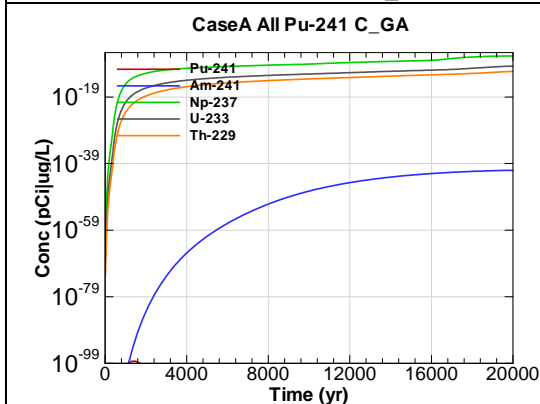


Figure A.3-519 - 100m Aquifer Concentration for
CaseA All Pu-241 C_GA

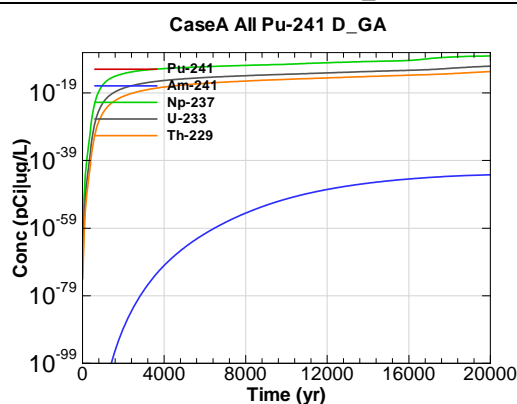


Figure A.3-520 - 100m Aquifer Concentration for
CaseA All Pu-241 D_GA

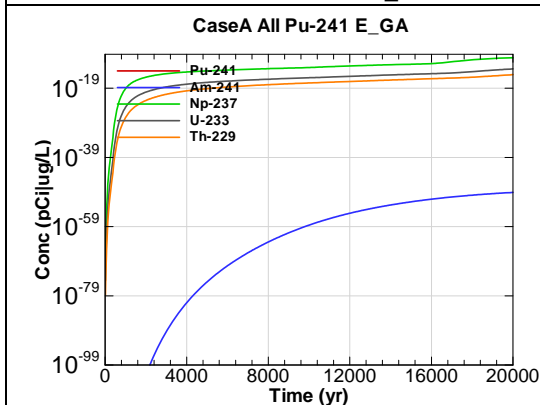


Figure A.3-521 - 100m Aquifer Concentration for
CaseA All Pu-241 E_GA

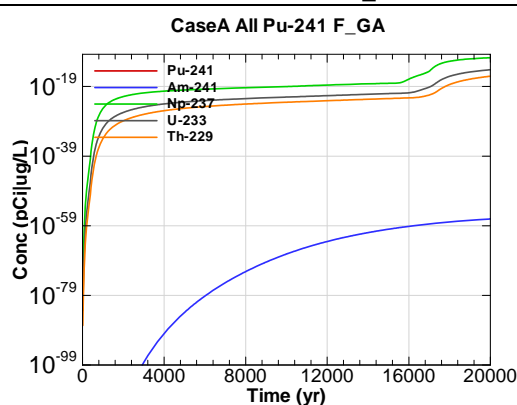
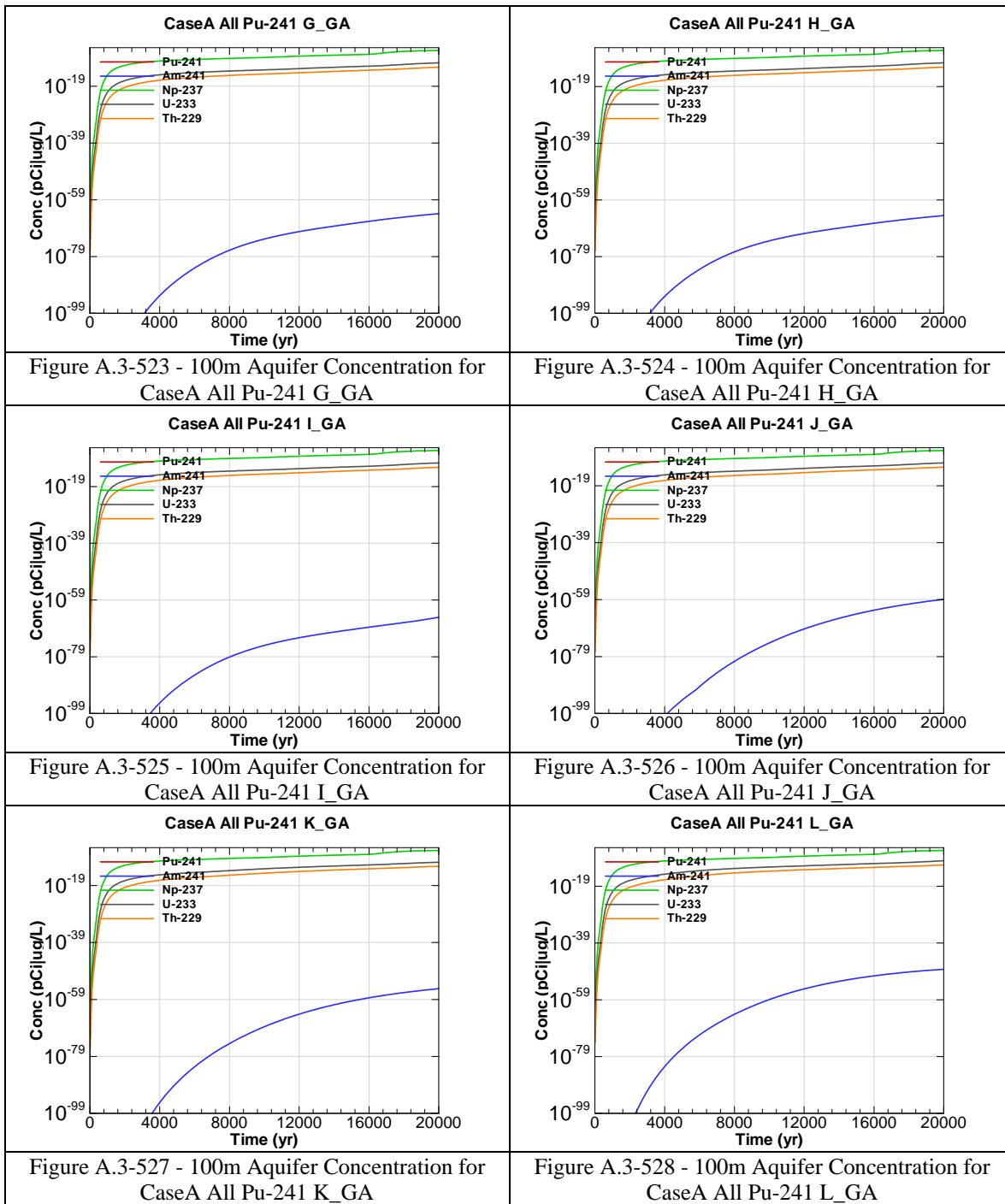


Figure A.3-522 - 100m Aquifer Concentration for
CaseA All Pu-241 F_GA



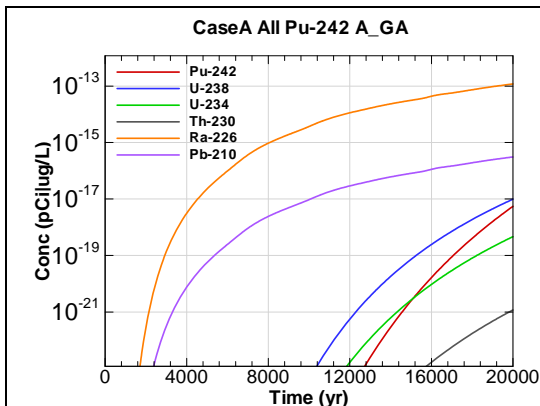


Figure A.3-529 - 100m Aquifer Concentration for
CaseA All Pu-242 A_GA

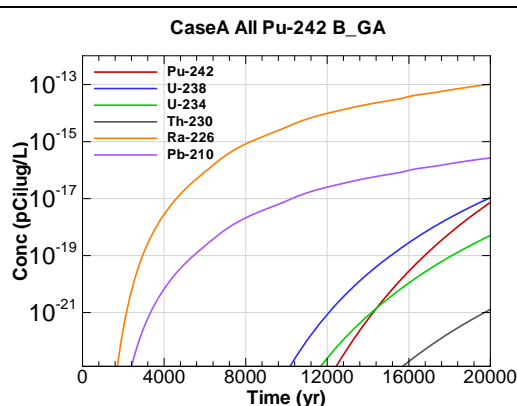


Figure A.3-530 - 100m Aquifer Concentration for
CaseA All Pu-242 B_GA

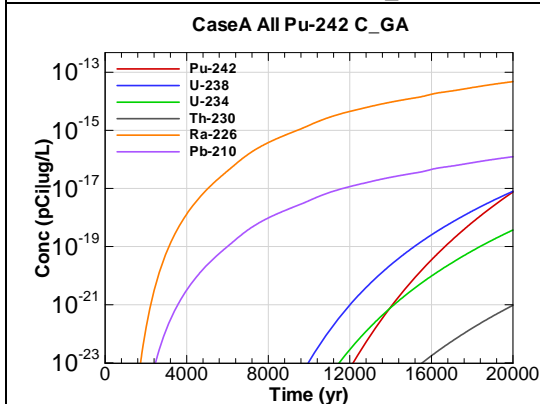


Figure A.3-531 - 100m Aquifer Concentration for
CaseA All Pu-242 C_GA

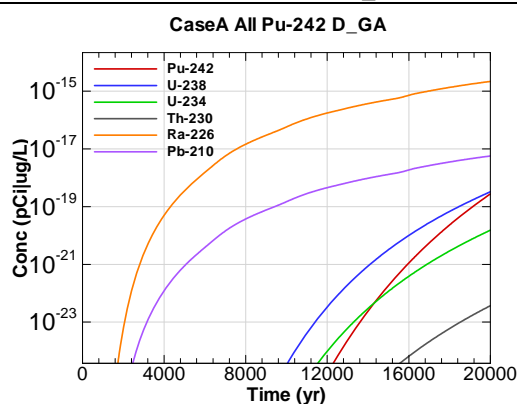


Figure A.3-532 - 100m Aquifer Concentration for
CaseA All Pu-242 D_GA

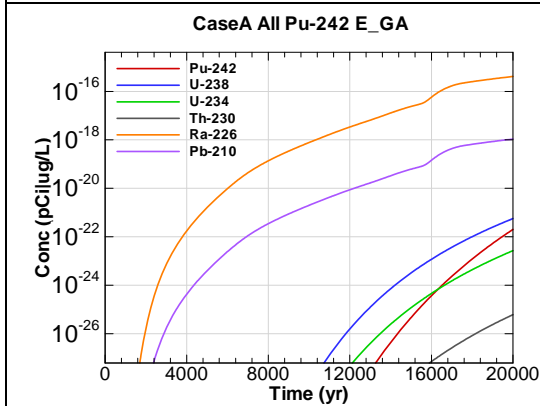


Figure A.3-533 - 100m Aquifer Concentration for
CaseA All Pu-242 E_GA

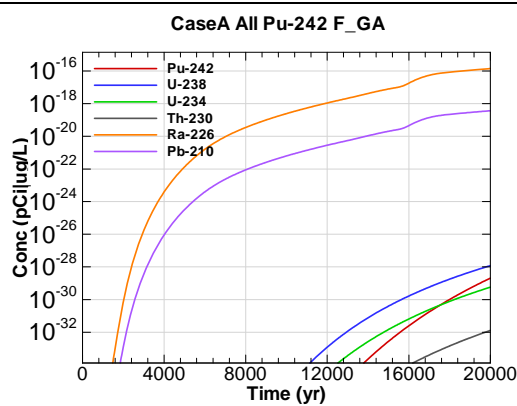


Figure A.3-534 - 100m Aquifer Concentration for
CaseA All Pu-242 F_GA

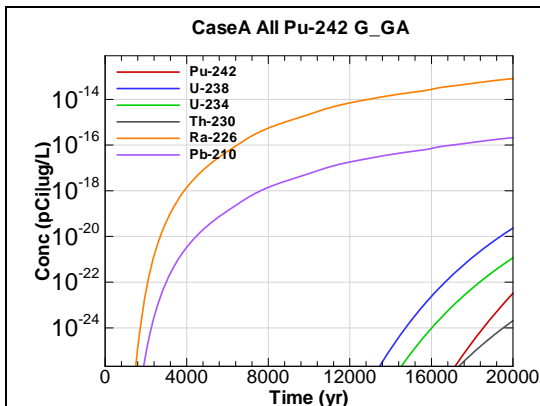


Figure A.3-535 - 100m Aquifer Concentration for
CaseA All Pu-242 G_GA

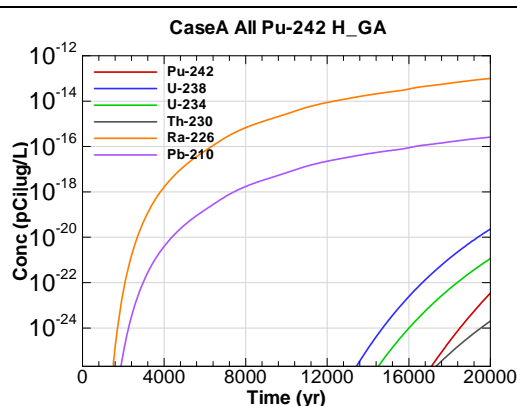


Figure A.3-536 - 100m Aquifer Concentration for
CaseA All Pu-242 H_GA

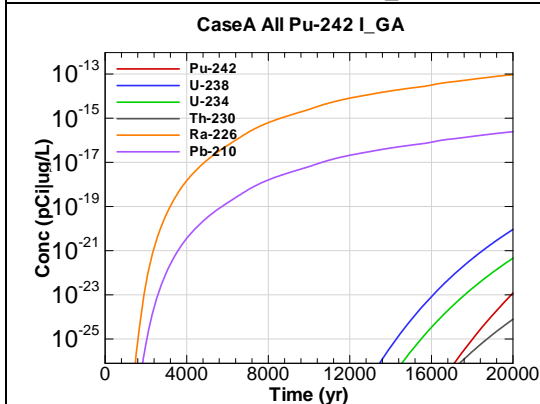


Figure A.3-537 - 100m Aquifer Concentration for
CaseA All Pu-242 I_GA

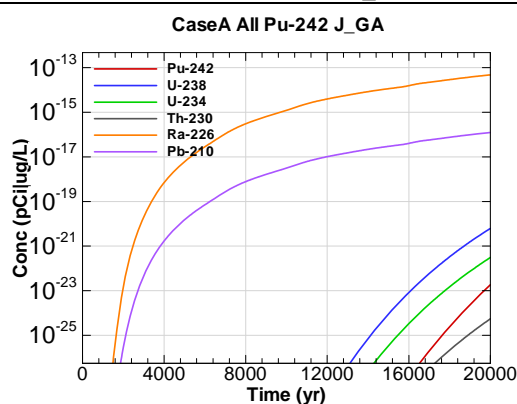


Figure A.3-538 - 100m Aquifer Concentration for
CaseA All Pu-242 J_GA

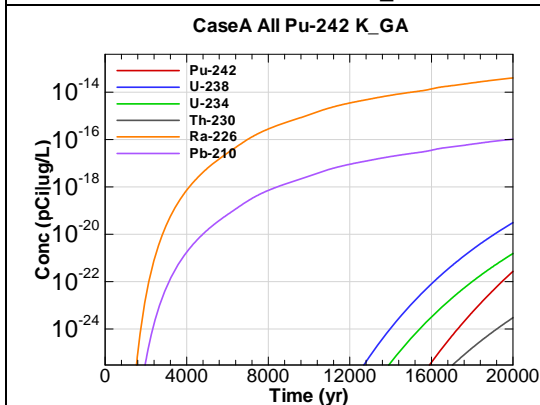


Figure A.3-539 - 100m Aquifer Concentration for
CaseA All Pu-242 K_GA

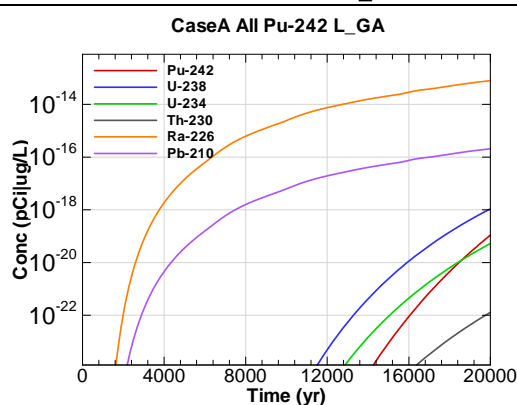
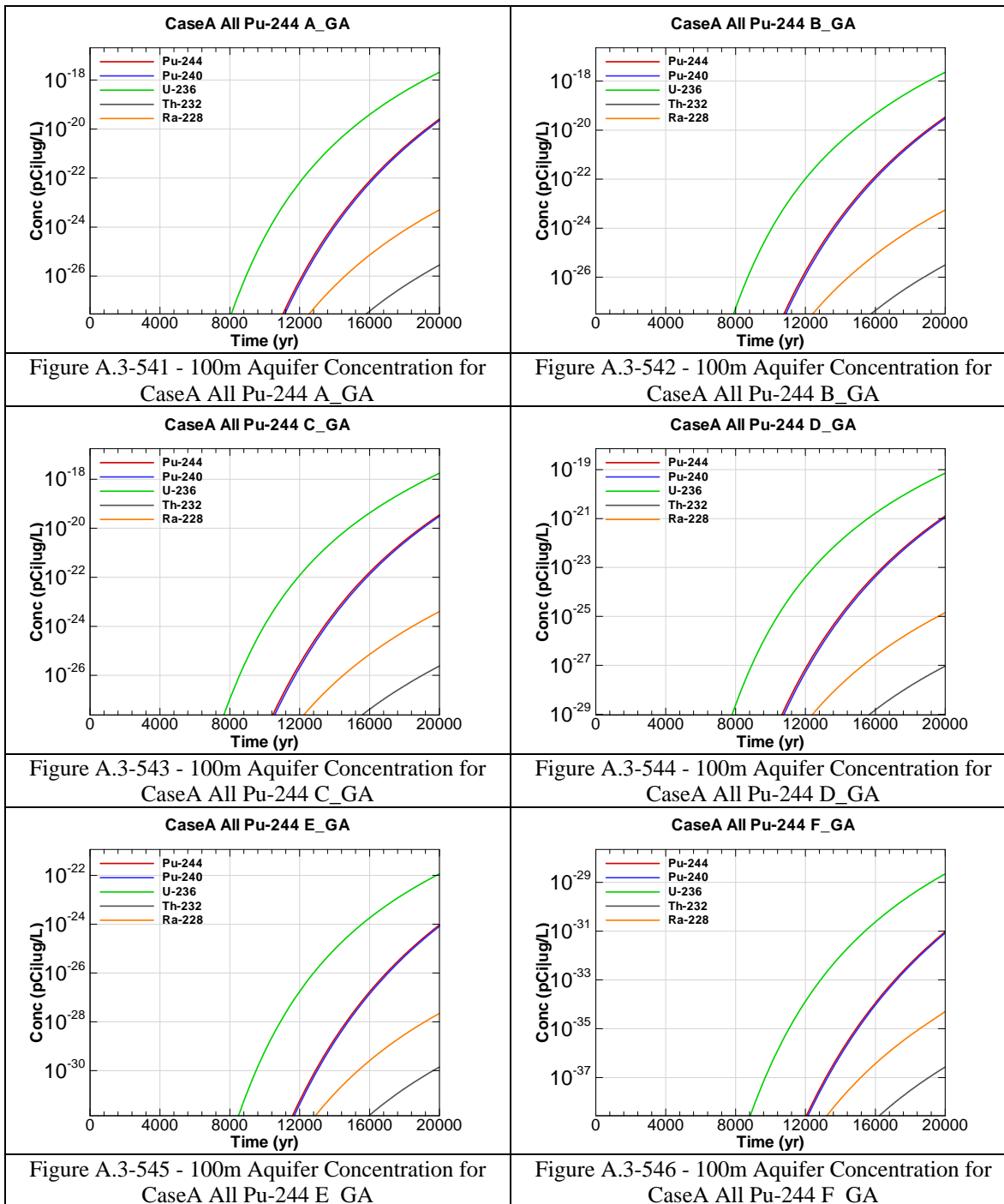


Figure A.3-540 - 100m Aquifer Concentration for
CaseA All Pu-242 L_GA



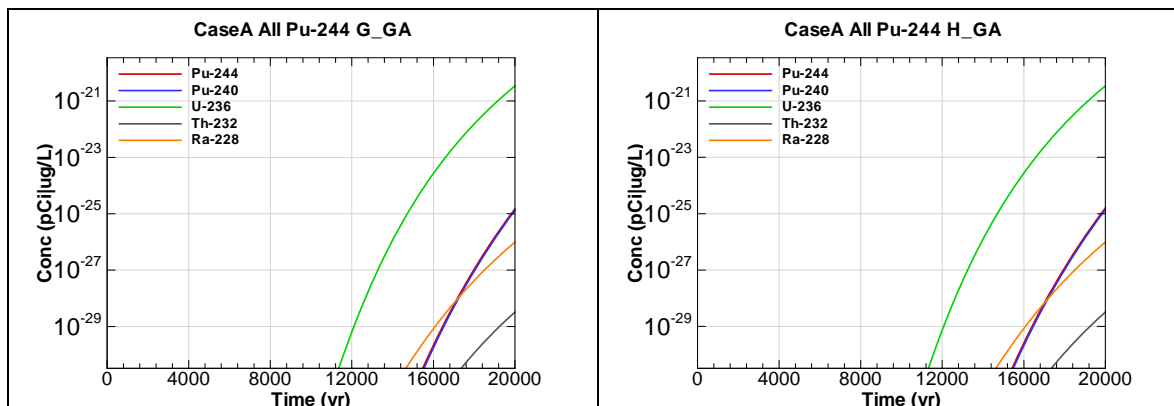


Figure A.3-547 - 100m Aquifer Concentration for
CaseA All Pu-244 G_GA

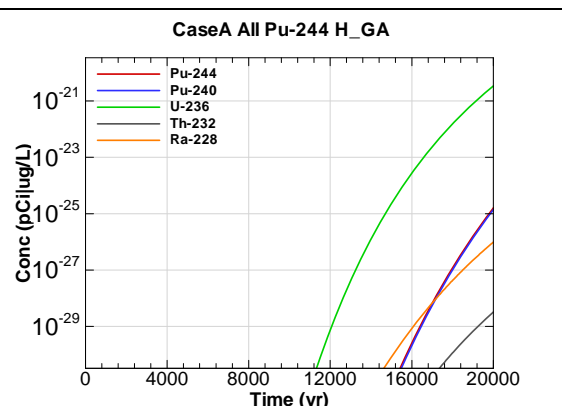


Figure A.3-548 - 100m Aquifer Concentration for
CaseA All Pu-244 H_GA

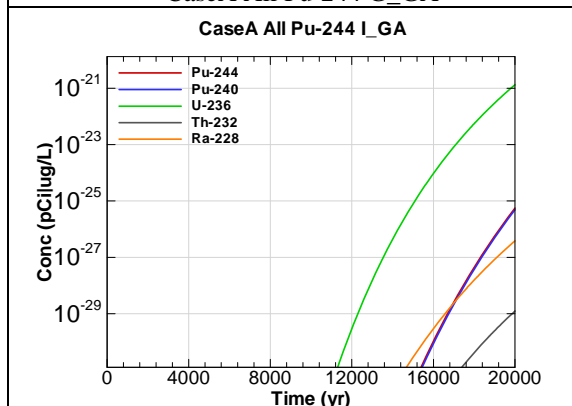


Figure A.3-549 - 100m Aquifer Concentration for
CaseA All Pu-244 I_GA

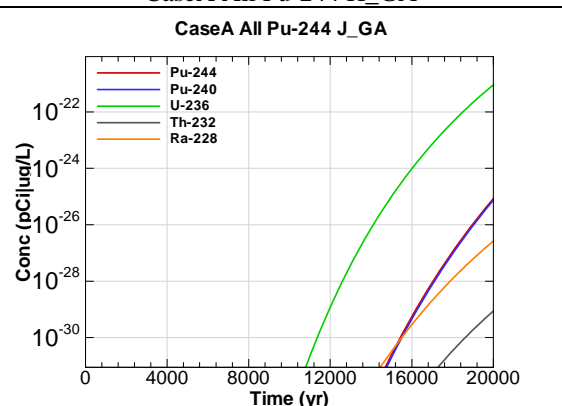


Figure A.3-550 - 100m Aquifer Concentration for
CaseA All Pu-244 J_GA

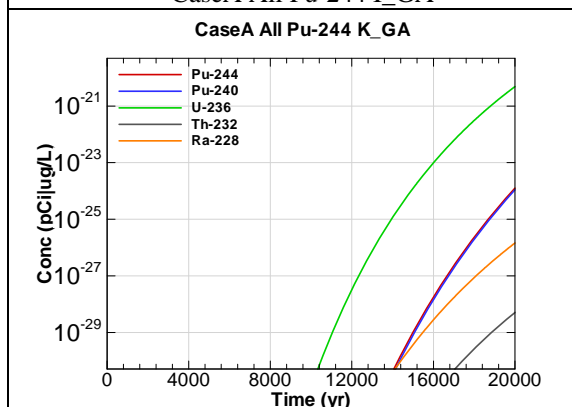


Figure A.3-551 - 100m Aquifer Concentration for
CaseA All Pu-244 K_GA

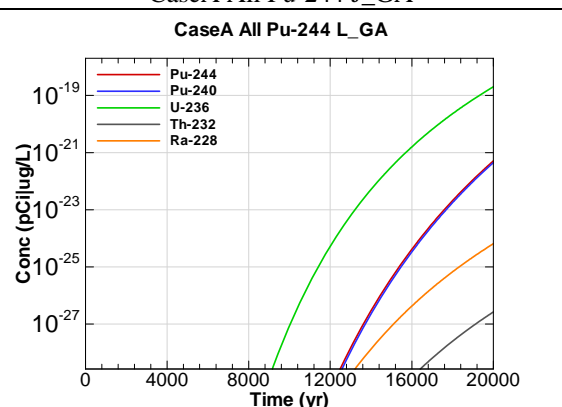


Figure A.3-552 - 100m Aquifer Concentration for
CaseA All Pu-244 L_GA

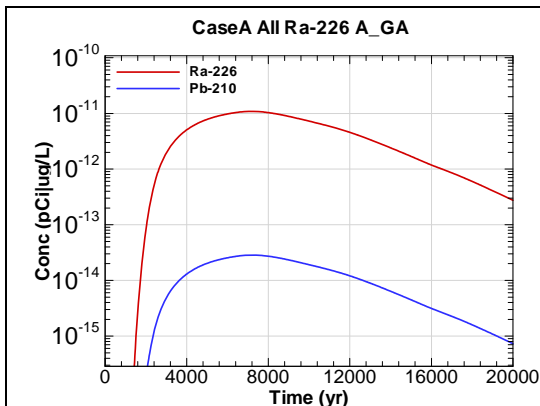


Figure A.3-553 - 100m Aquifer Concentration for
CaseA All Ra-226 A_GA

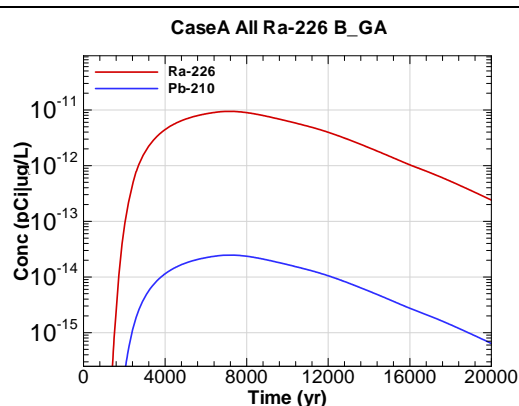


Figure A.3-554 - 100m Aquifer Concentration for
CaseA All Ra-226 B_GA

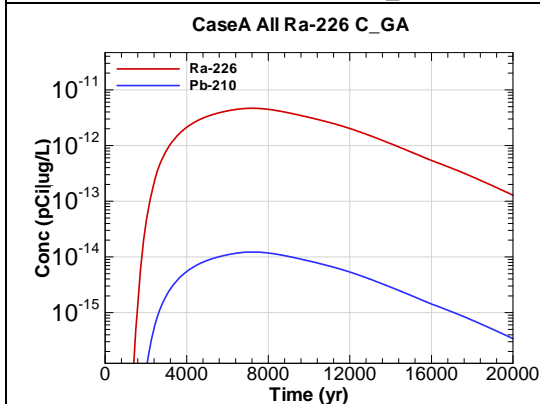


Figure A.3-555 - 100m Aquifer Concentration for
CaseA All Ra-226 C_GA

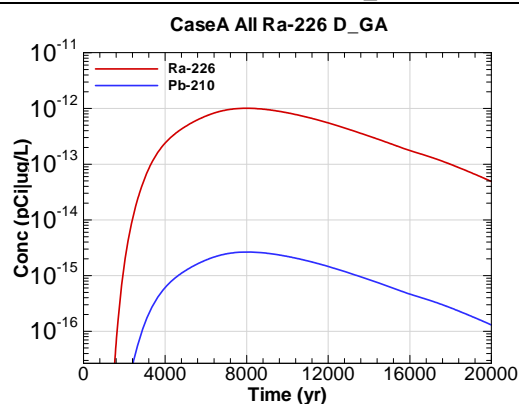


Figure A.3-556 - 100m Aquifer Concentration for
CaseA All Ra-226 D_GA

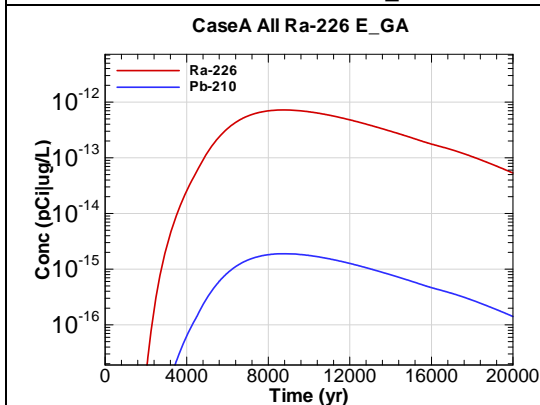


Figure A.3-557 - 100m Aquifer Concentration for
CaseA All Ra-226 E_GA

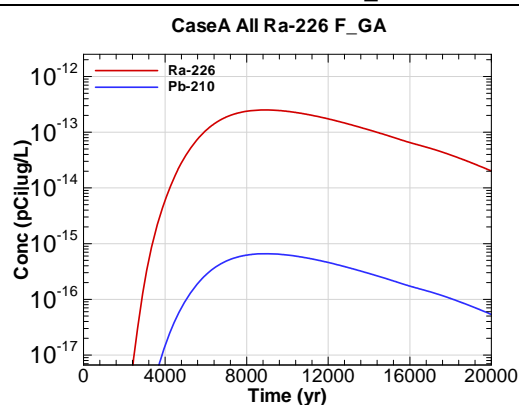


Figure A.3-558 - 100m Aquifer Concentration for
CaseA All Ra-226 F_GA

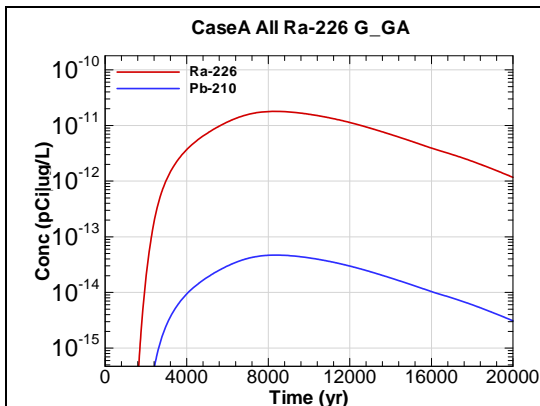


Figure A.3-559 - 100m Aquifer Concentration for
CaseA All Ra-226 G_GA

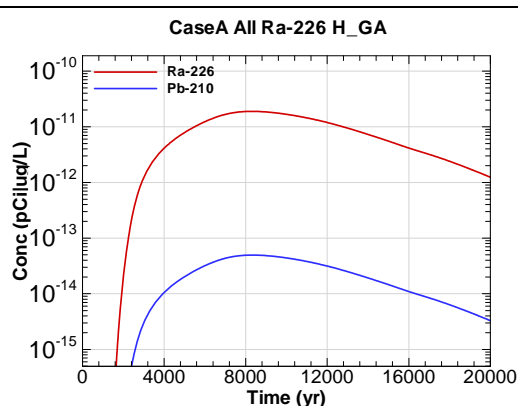


Figure A.3-560 - 100m Aquifer Concentration for
CaseA All Ra-226 H_GA

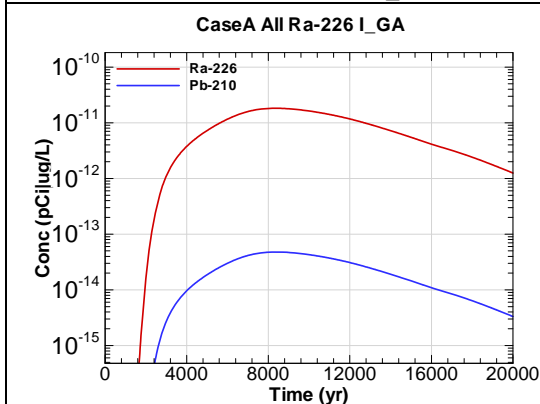


Figure A.3-561 - 100m Aquifer Concentration for
CaseA All Ra-226 I_GA

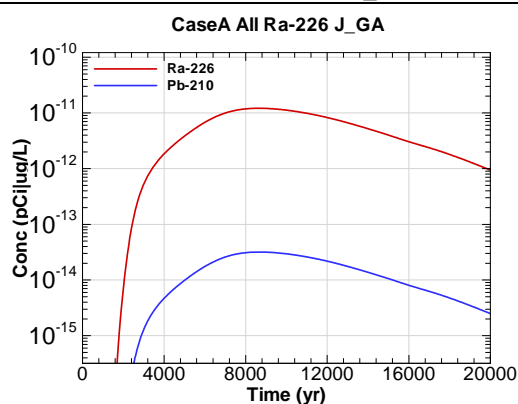


Figure A.3-562 - 100m Aquifer Concentration for
CaseA All Ra-226 J_GA

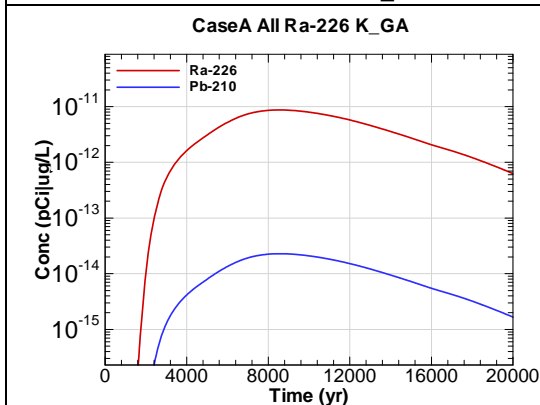


Figure A.3-563 - 100m Aquifer Concentration for
CaseA All Ra-226 K_GA

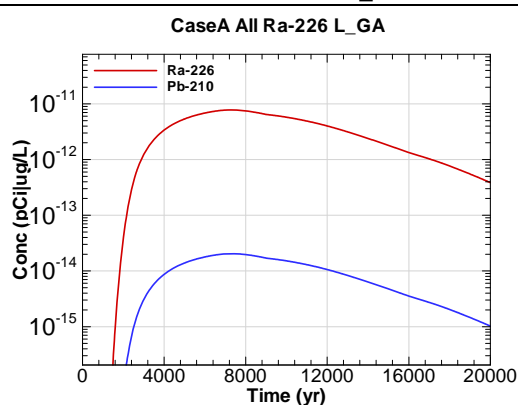
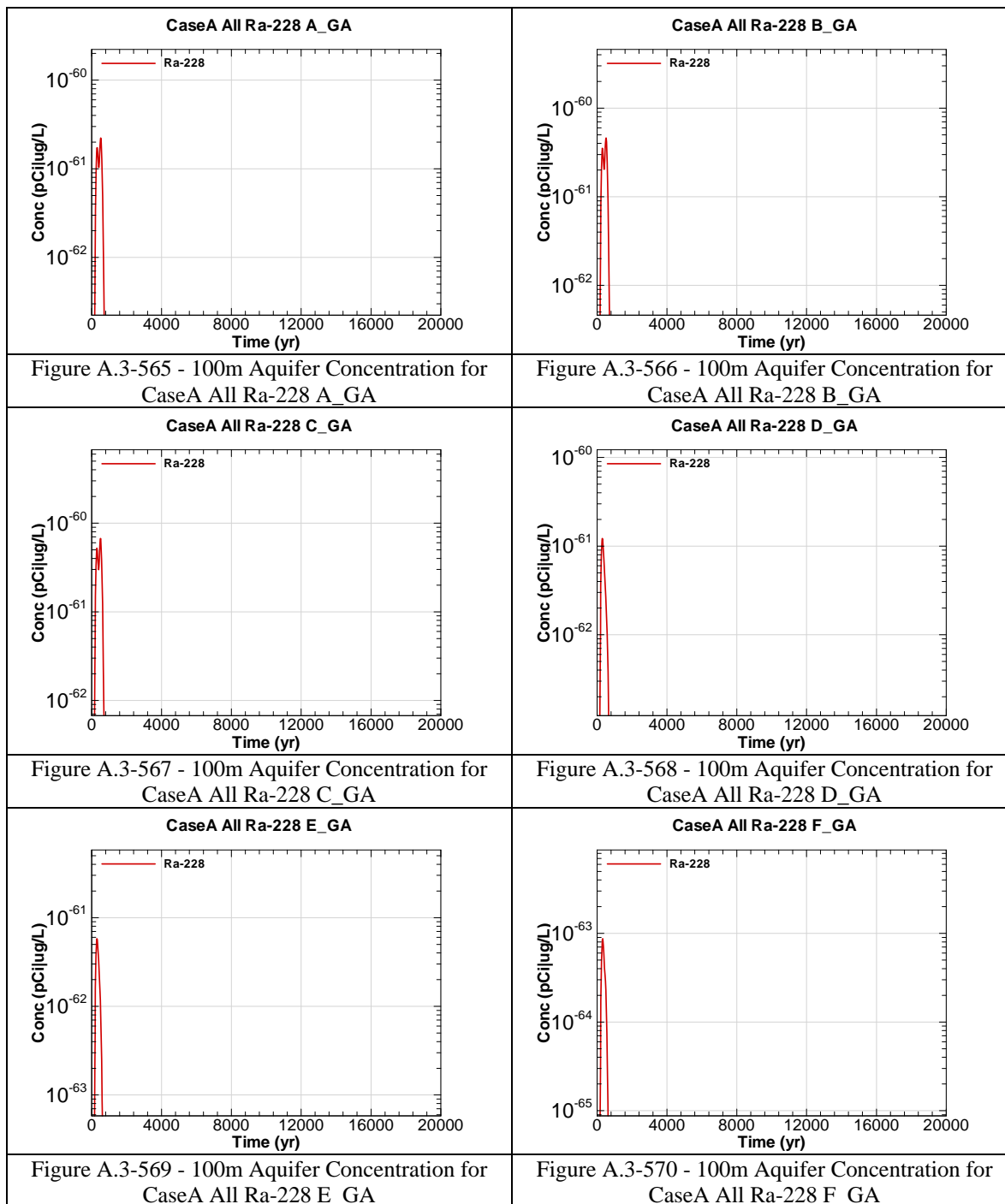
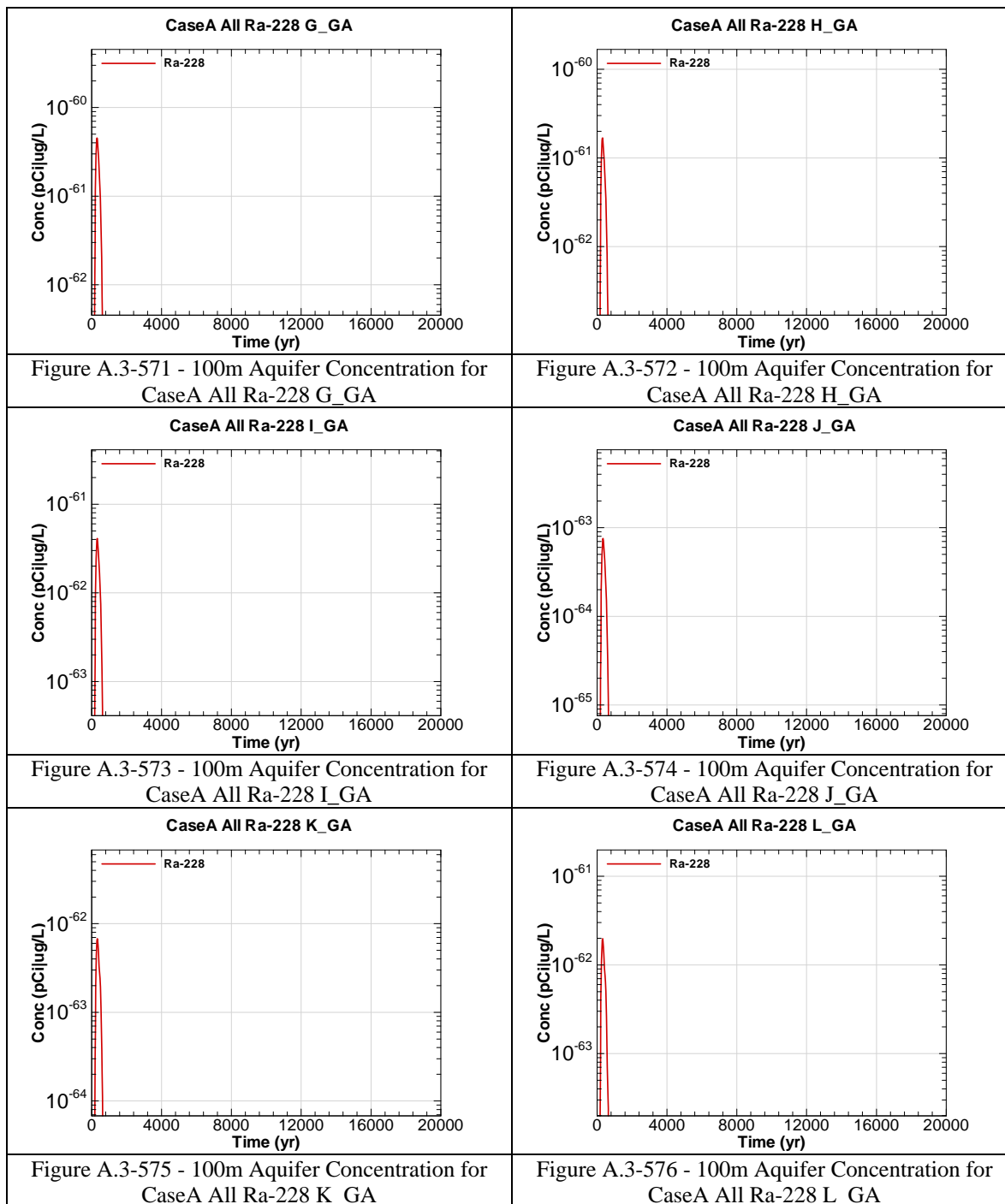
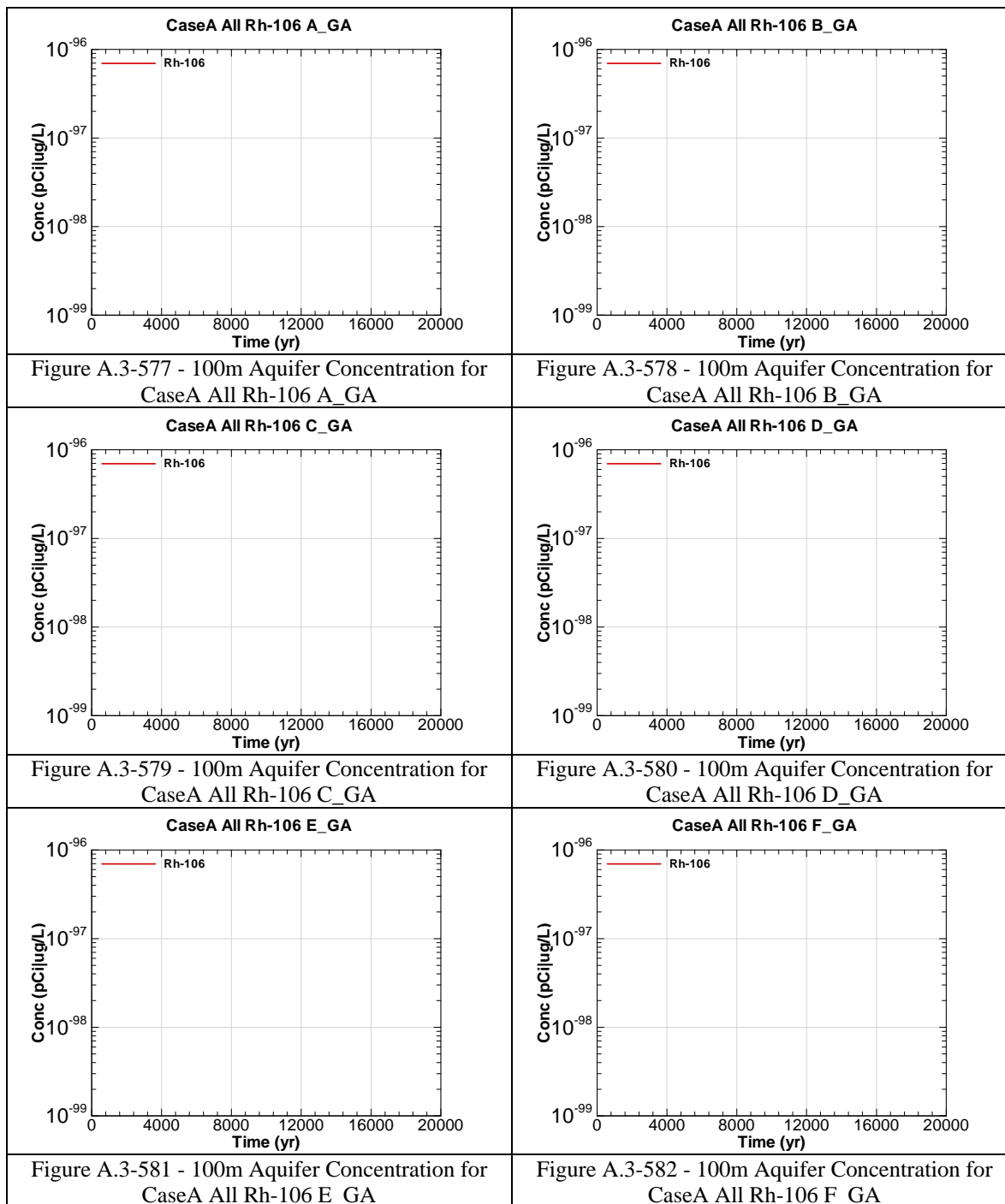
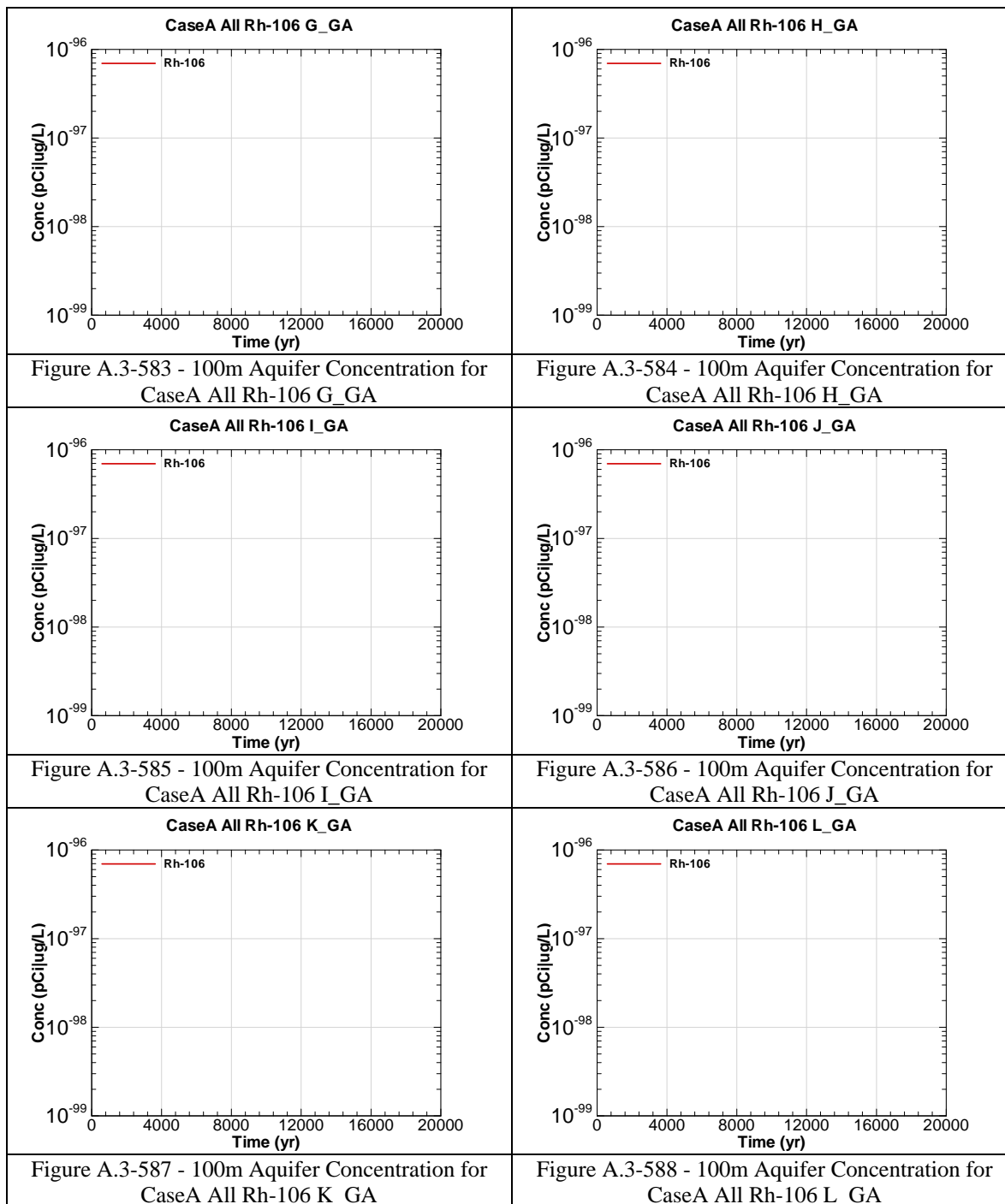


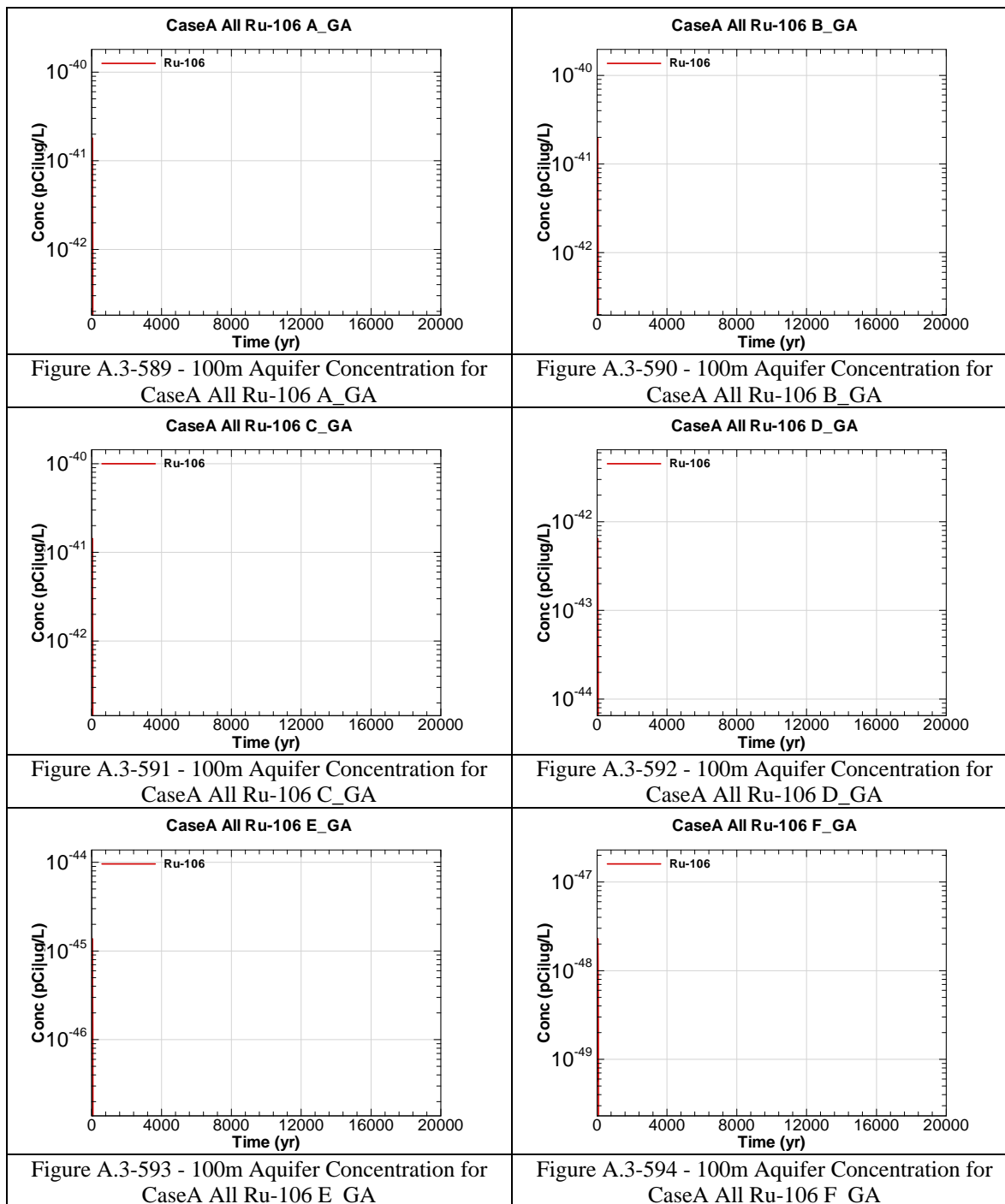
Figure A.3-564 - 100m Aquifer Concentration for
CaseA All Ra-226 L_GA

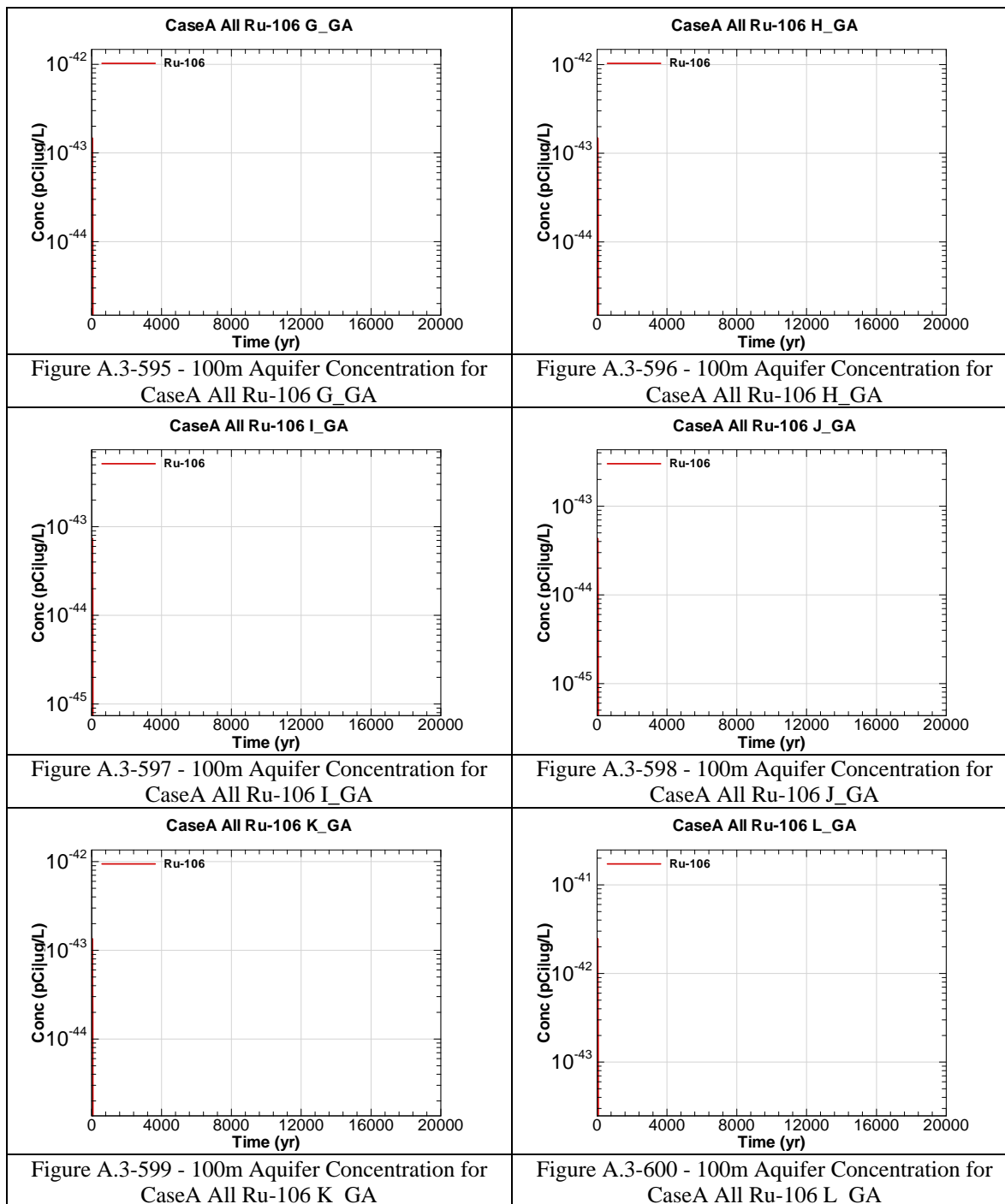


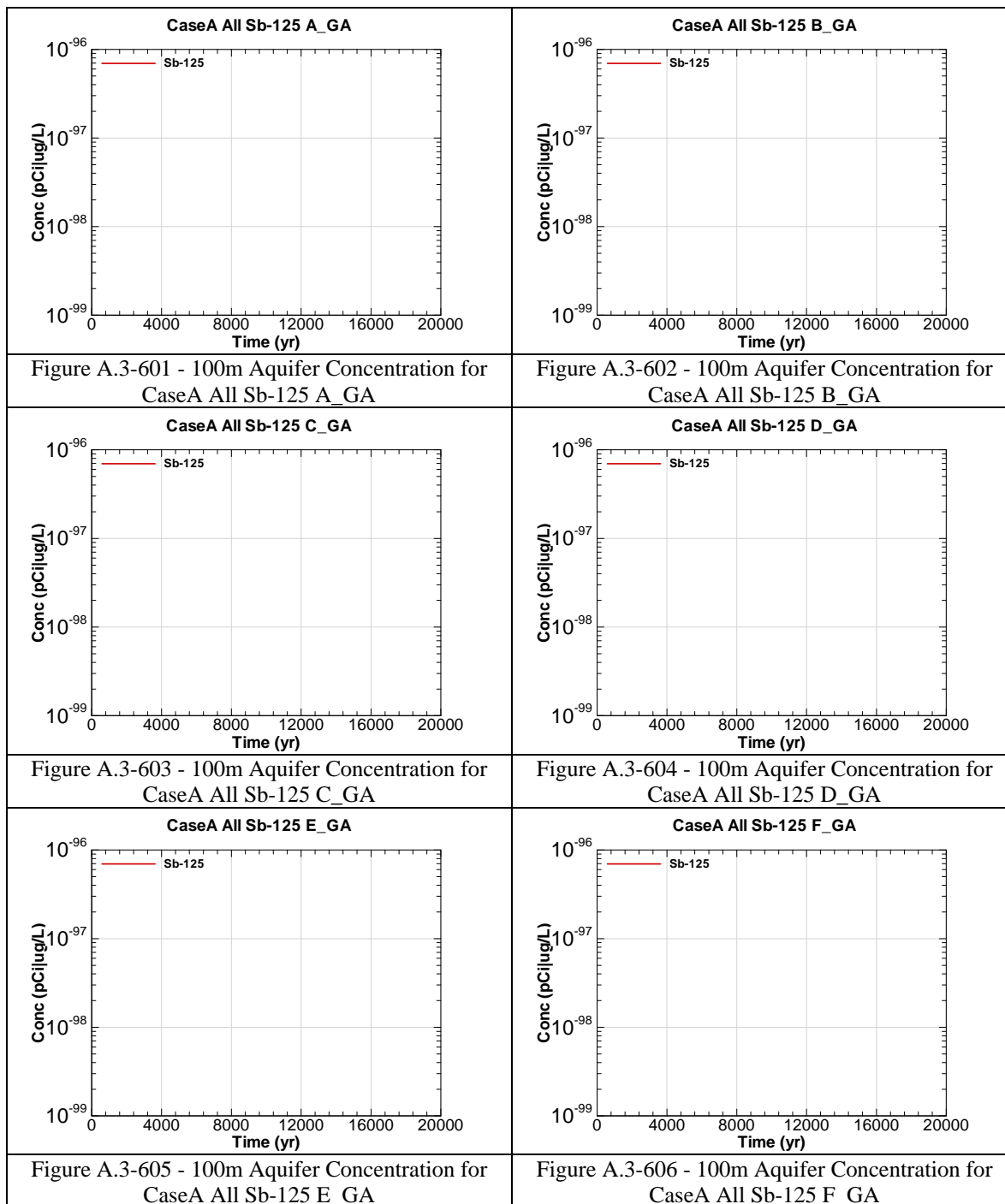


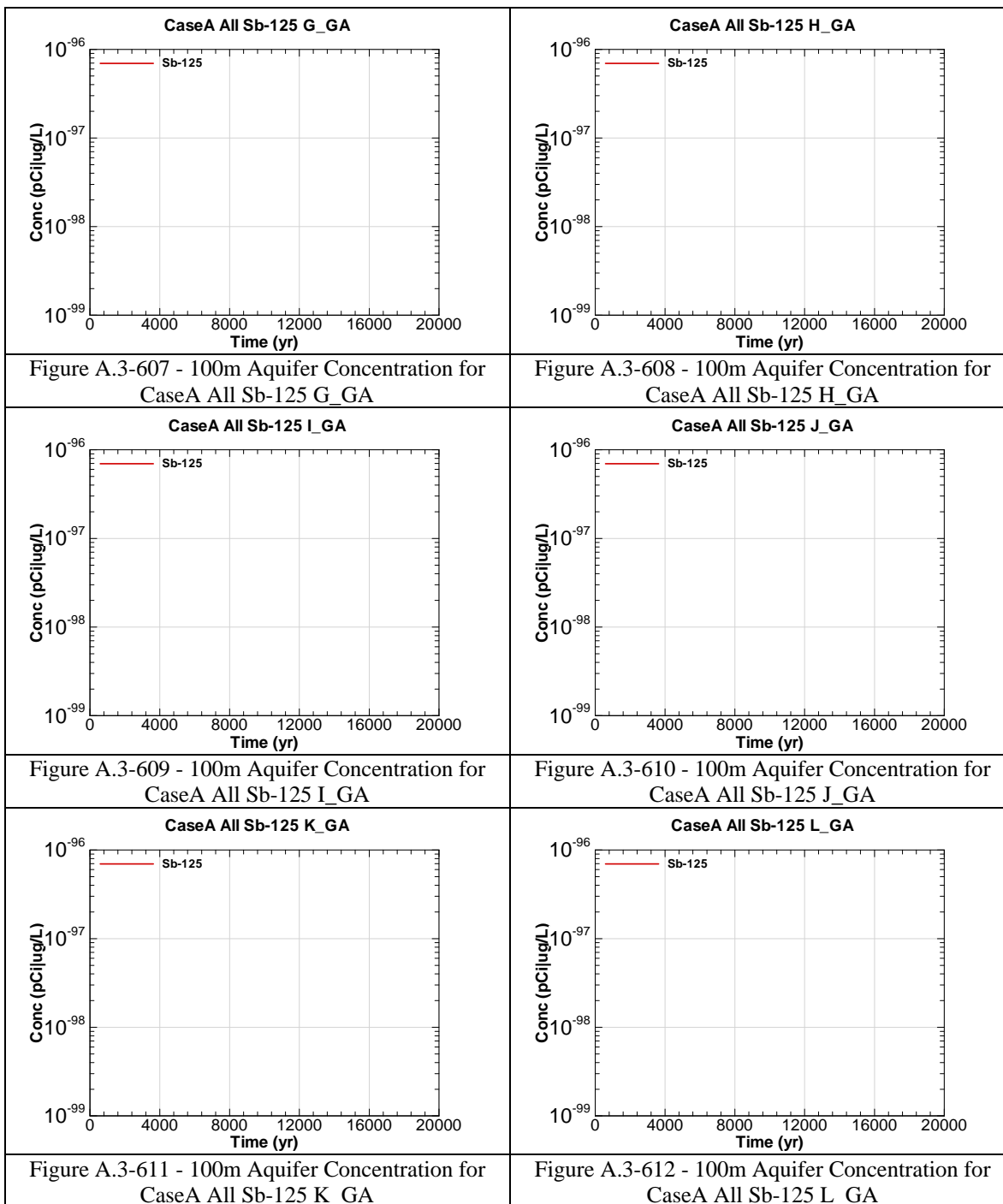


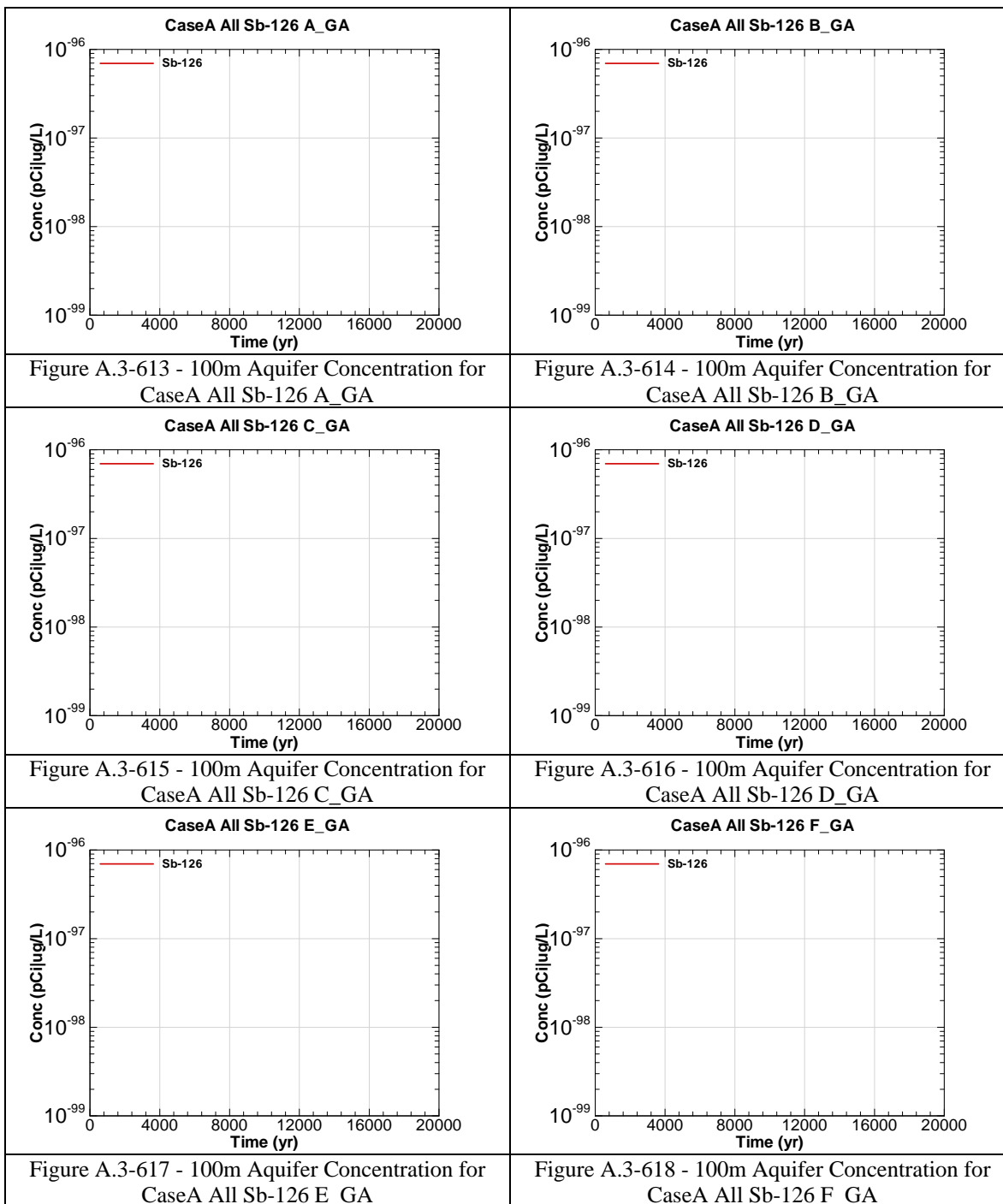


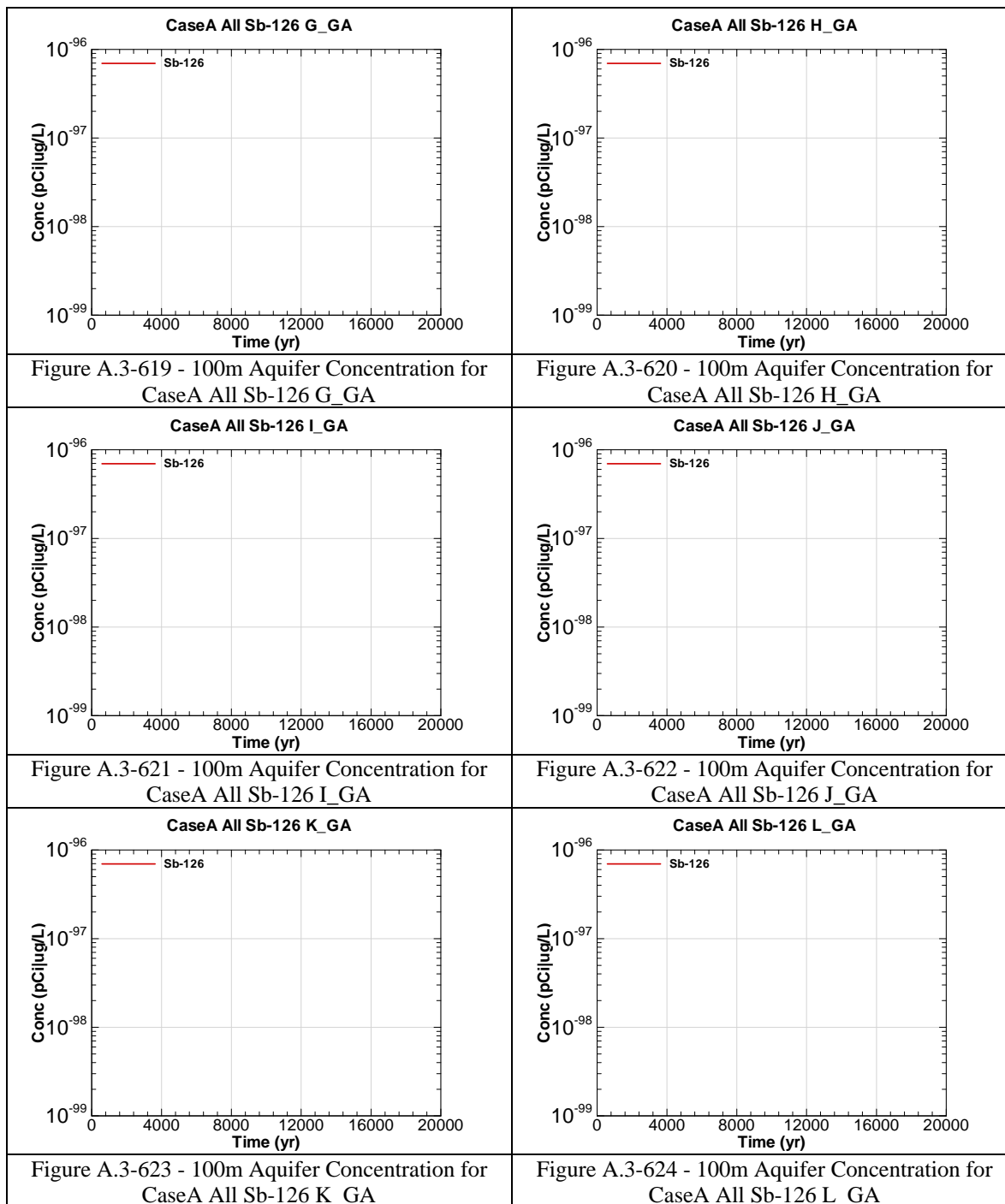


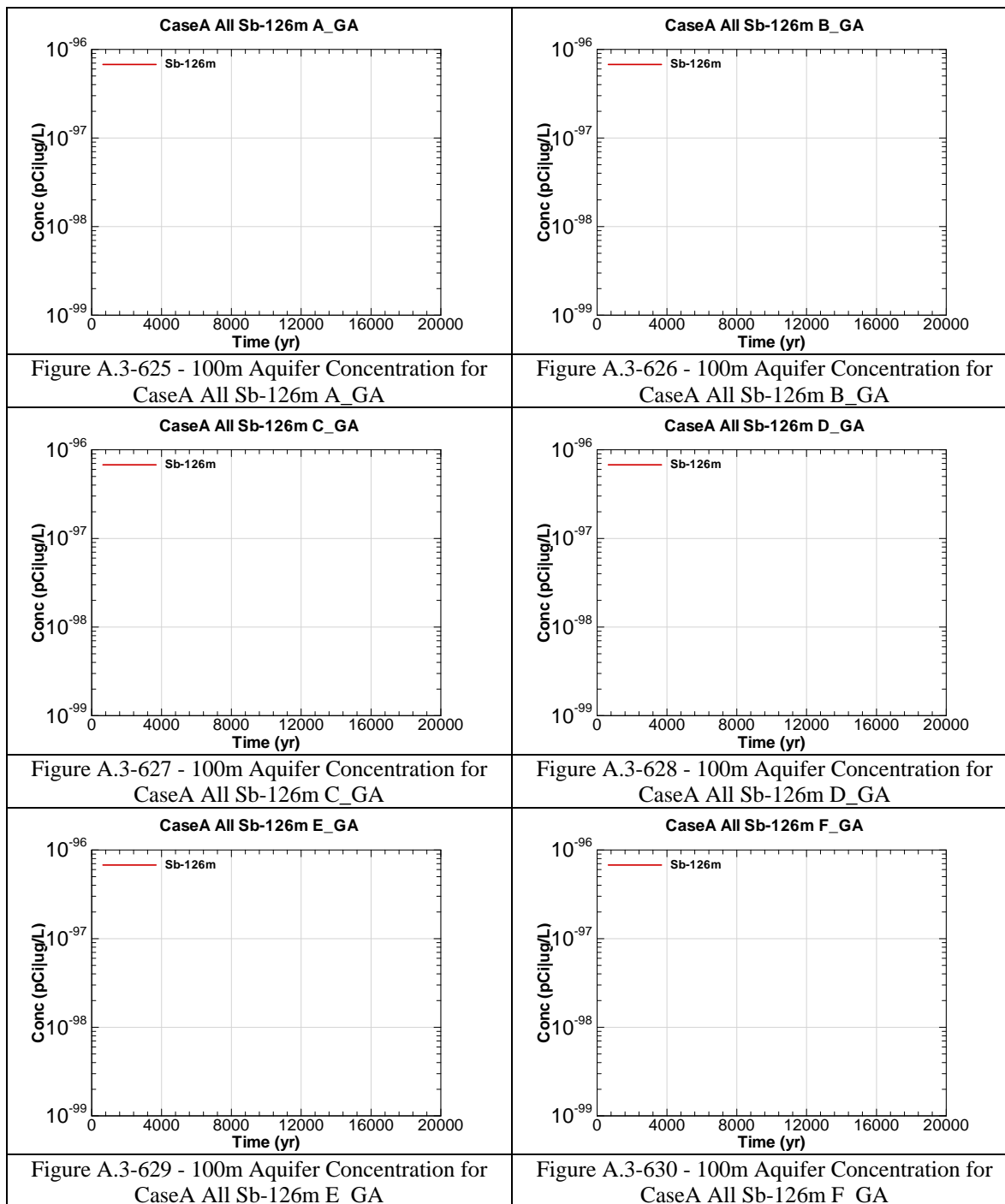


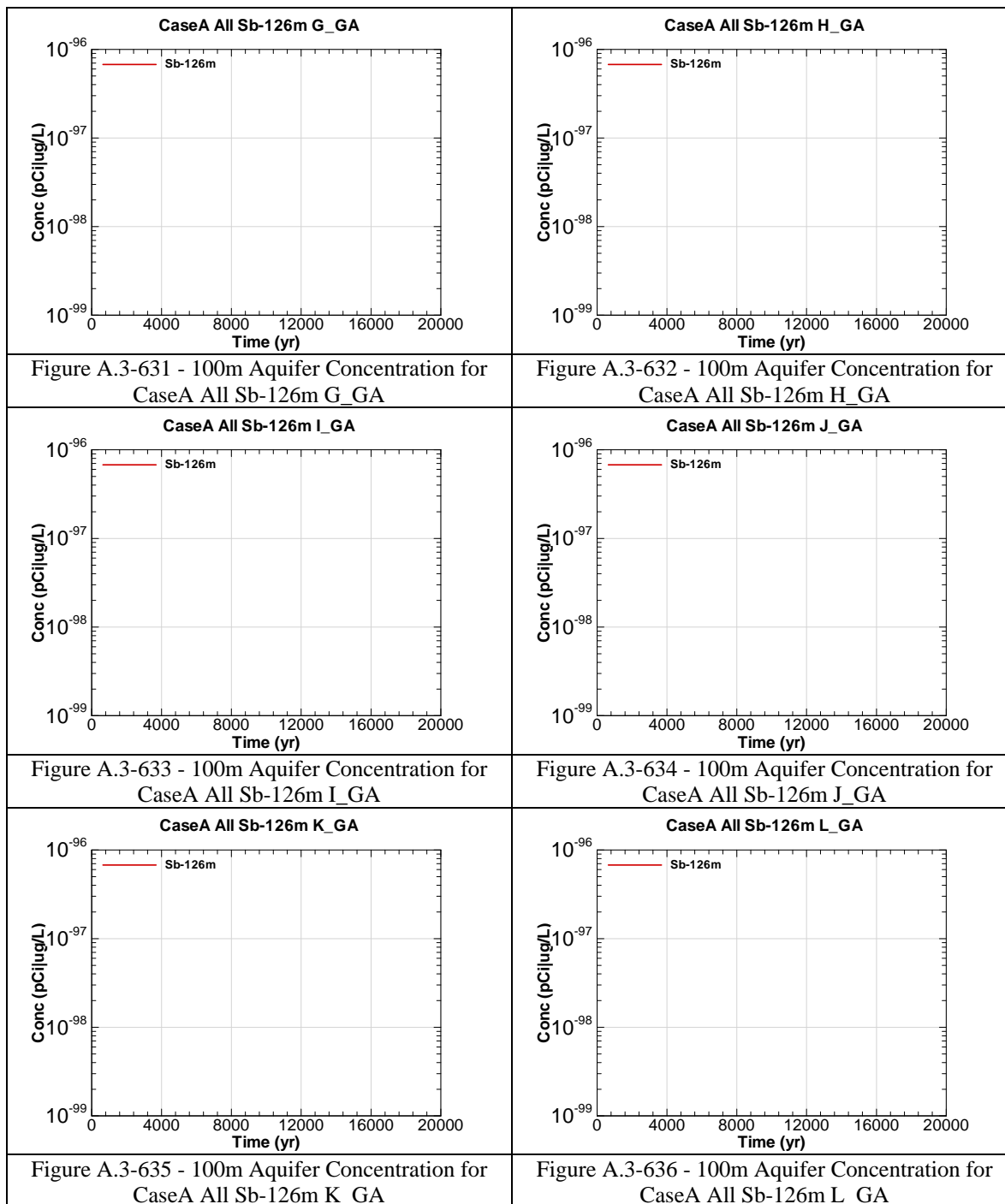


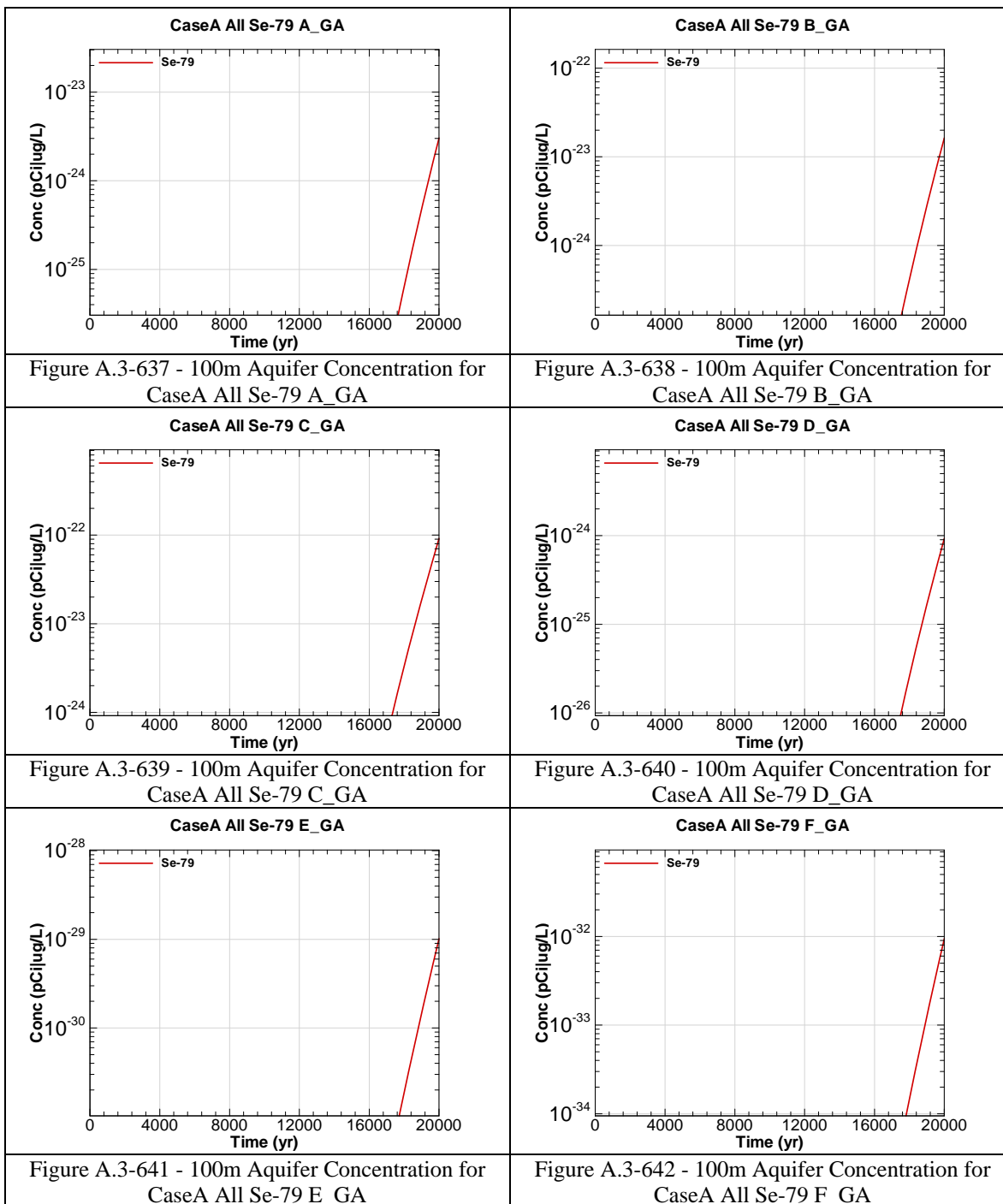


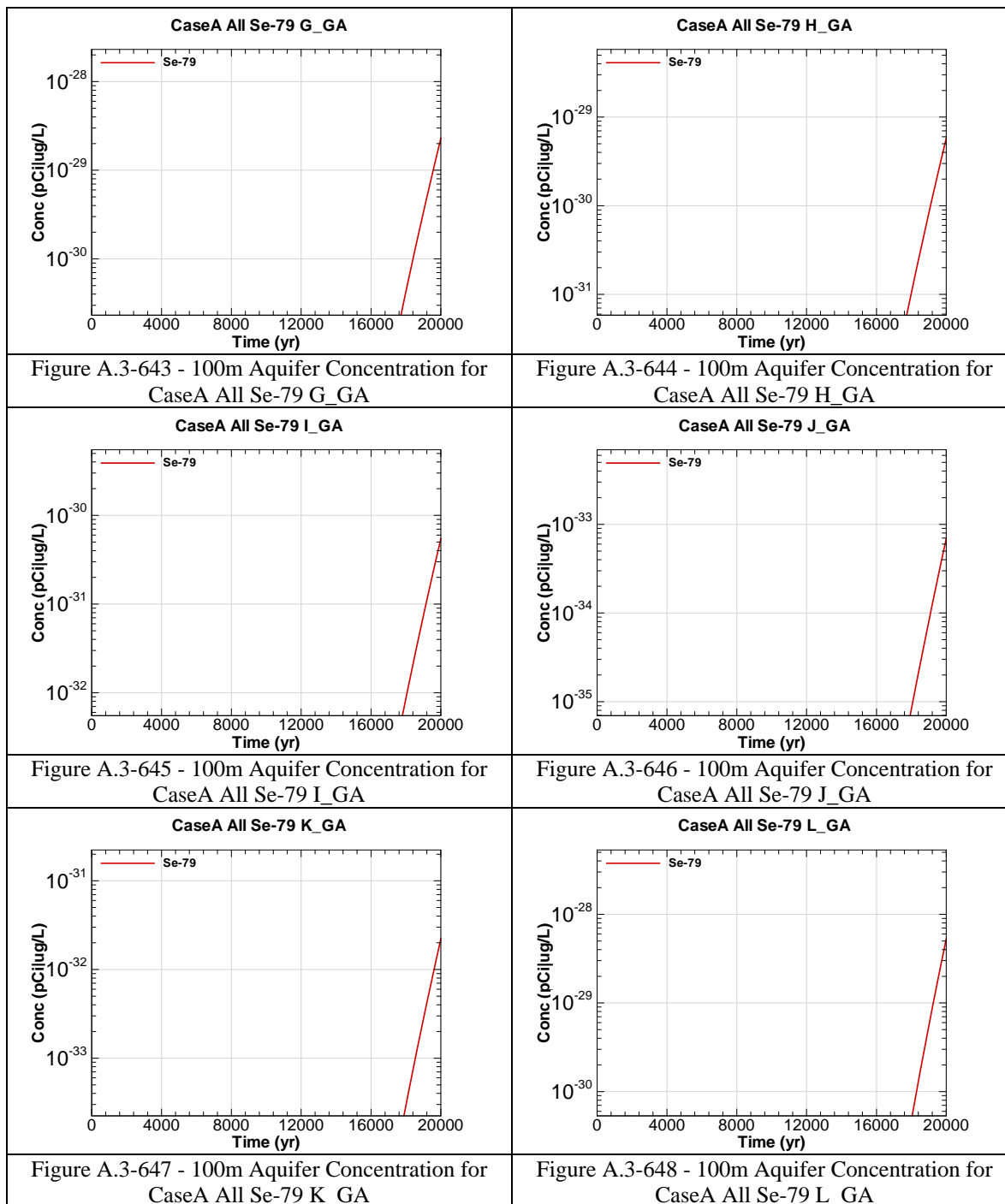


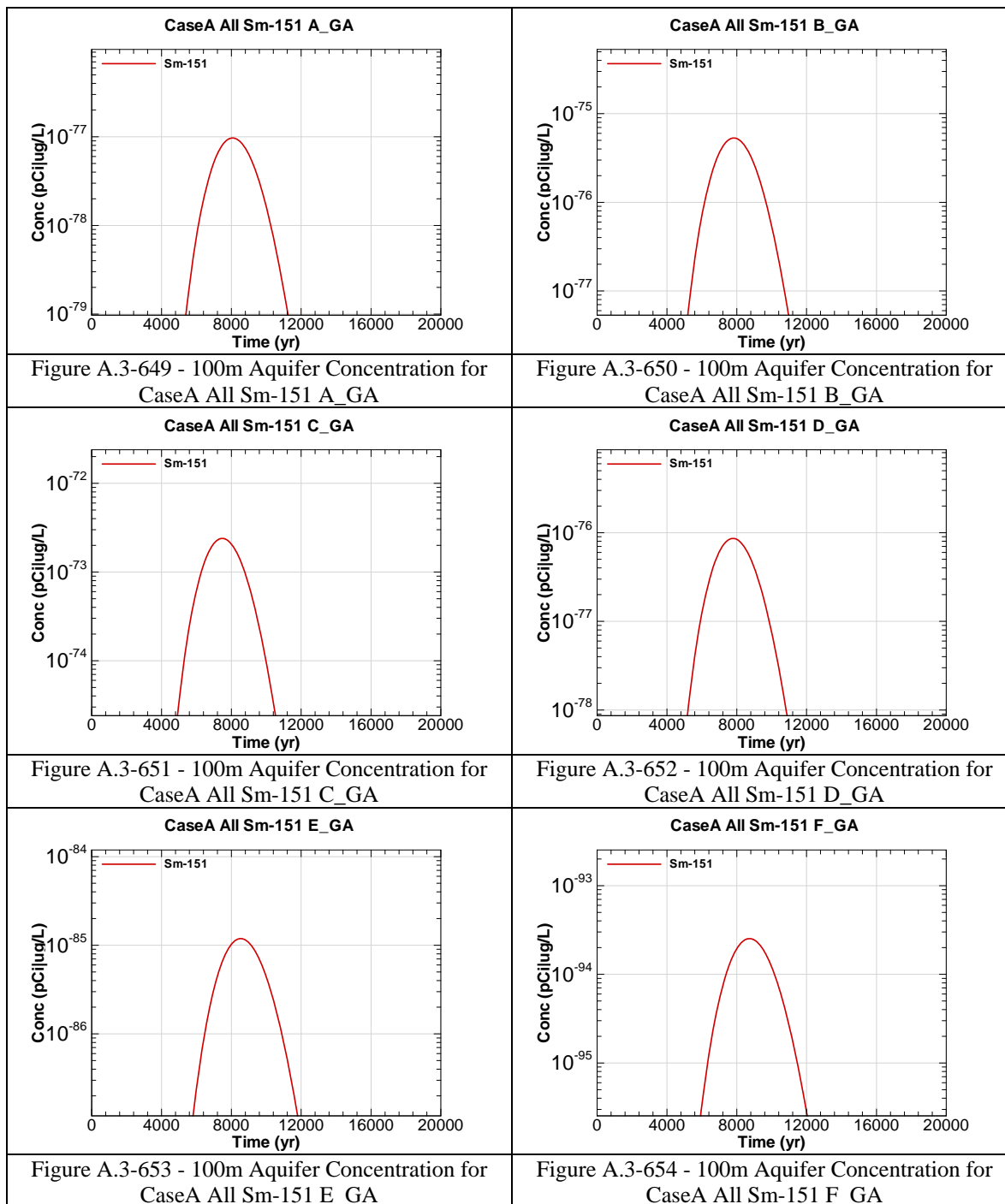


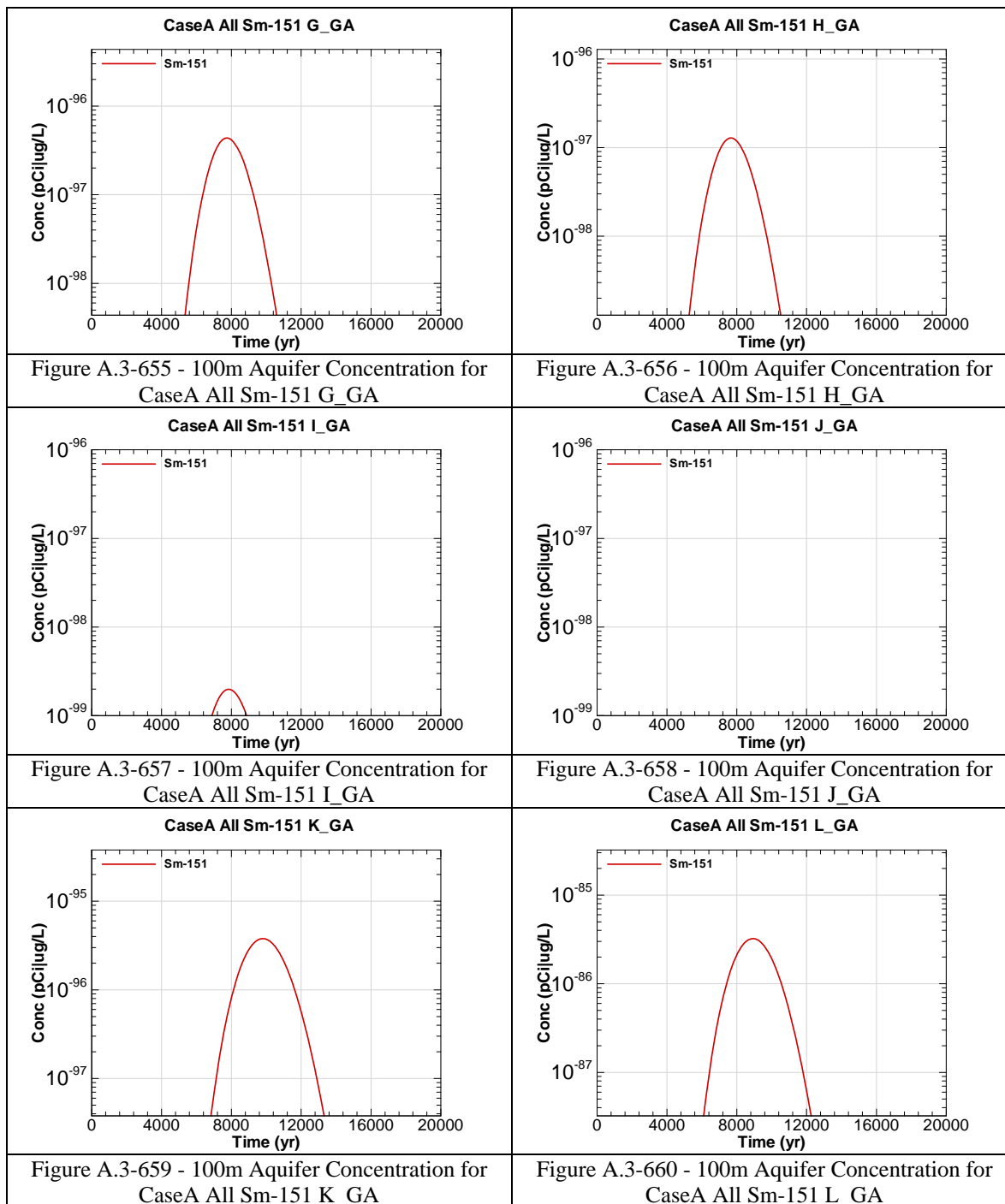


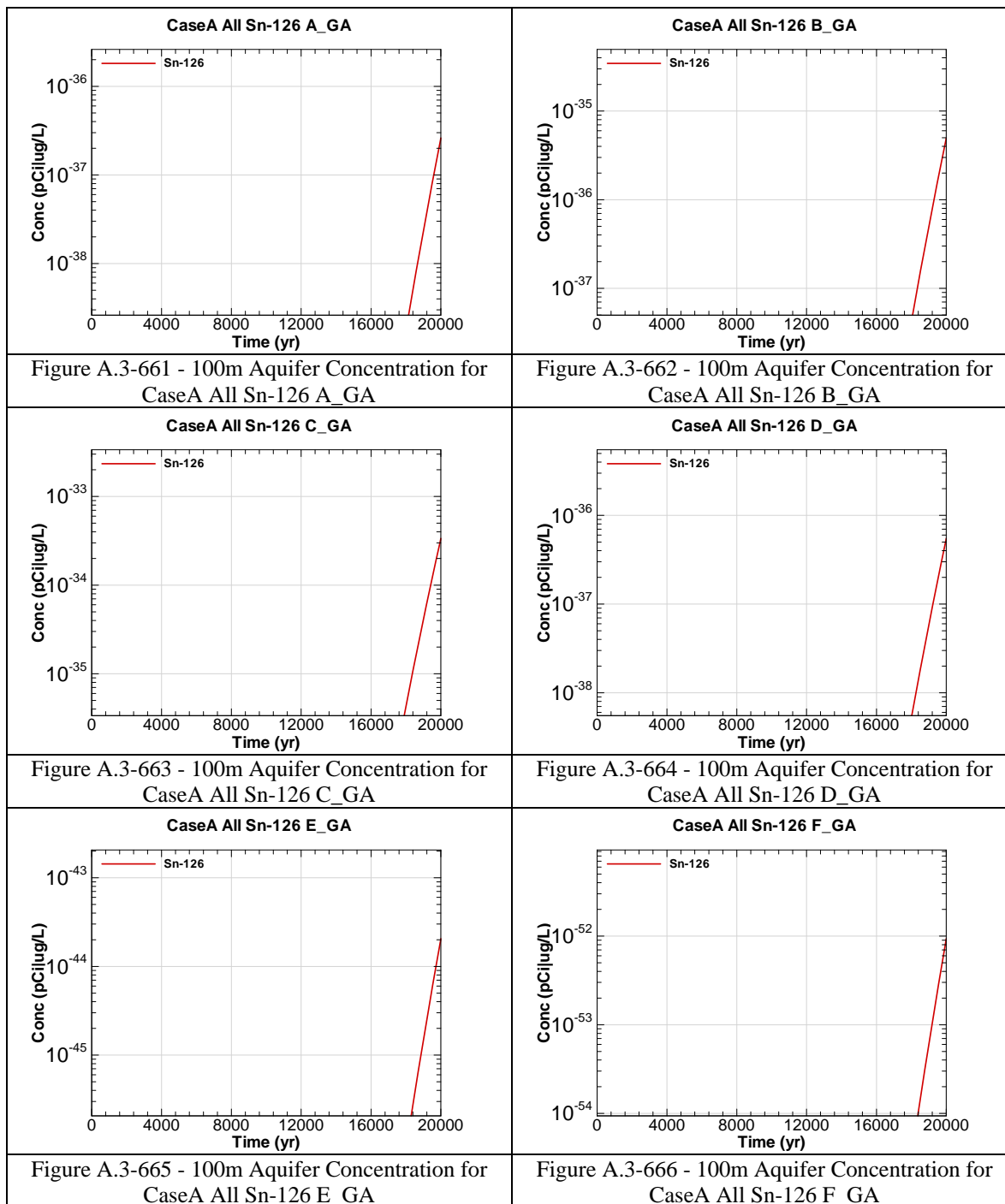


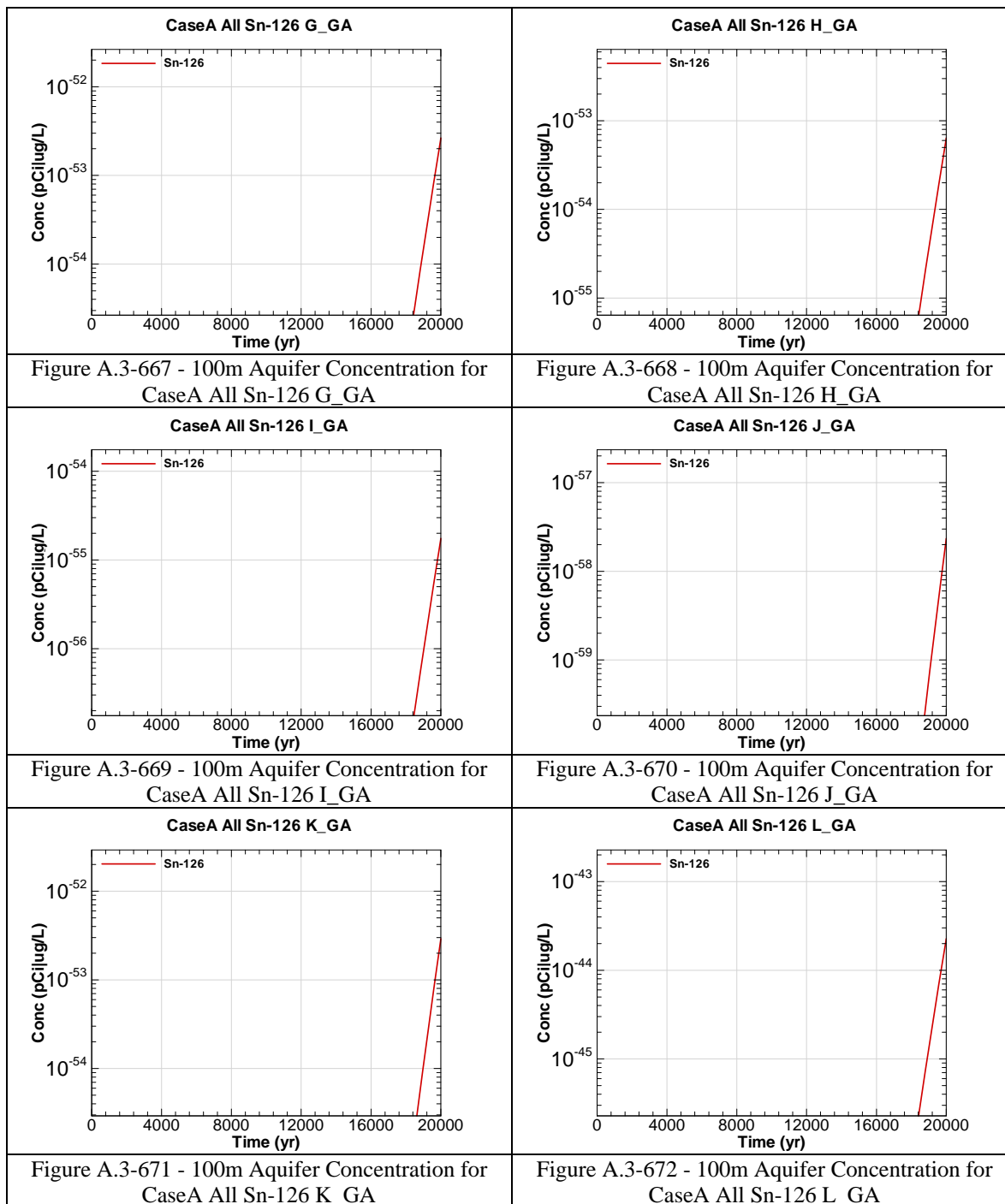


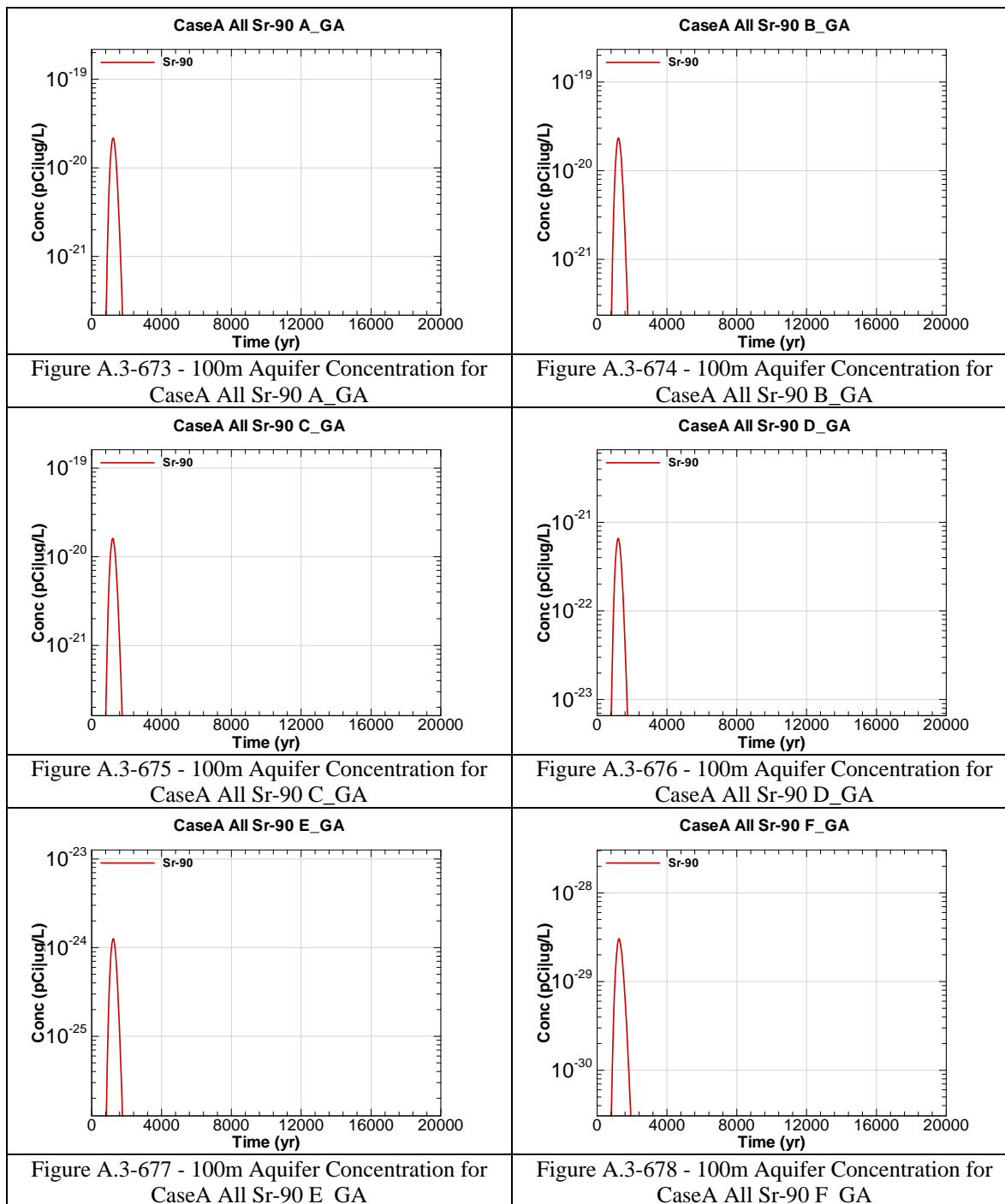


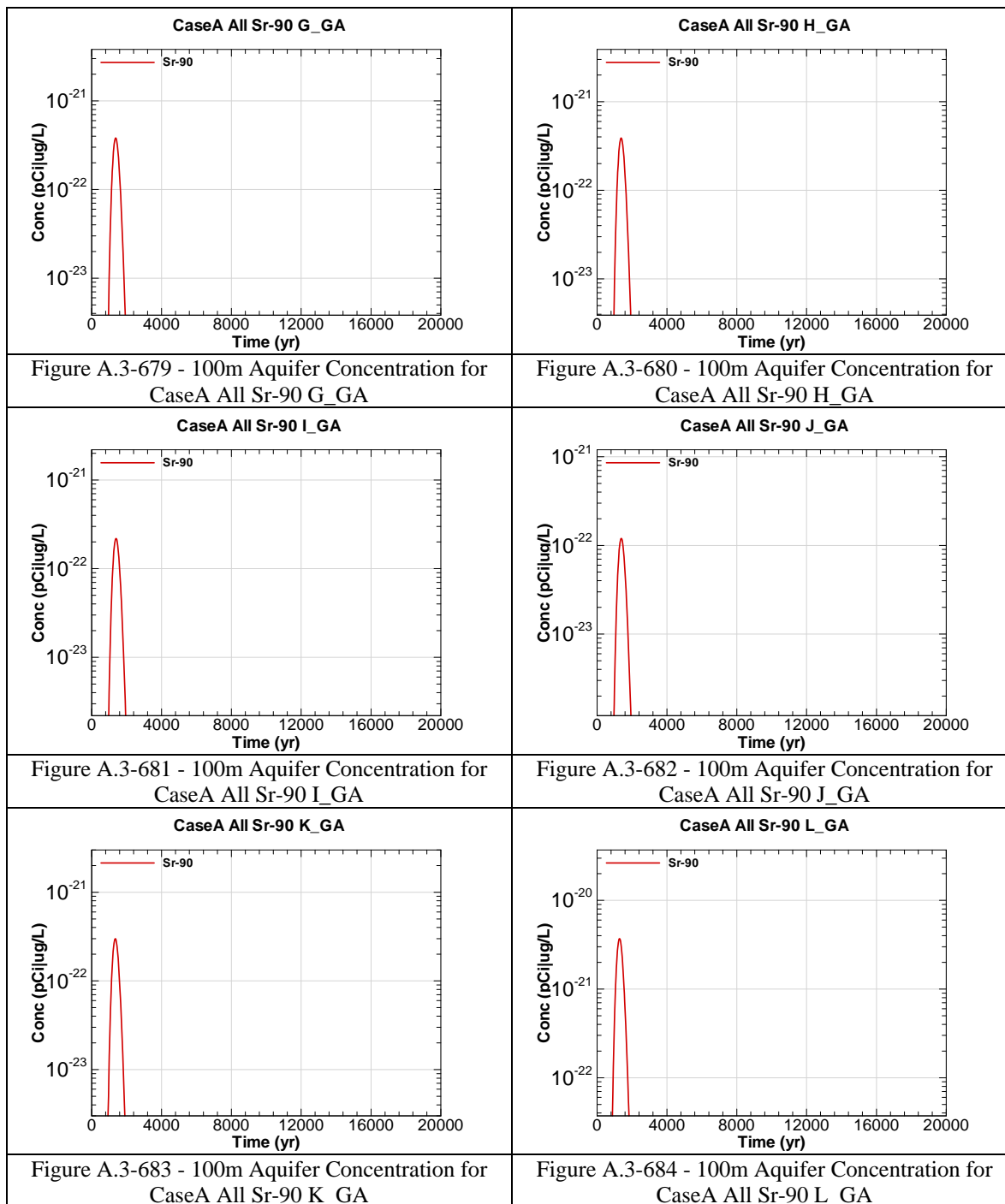


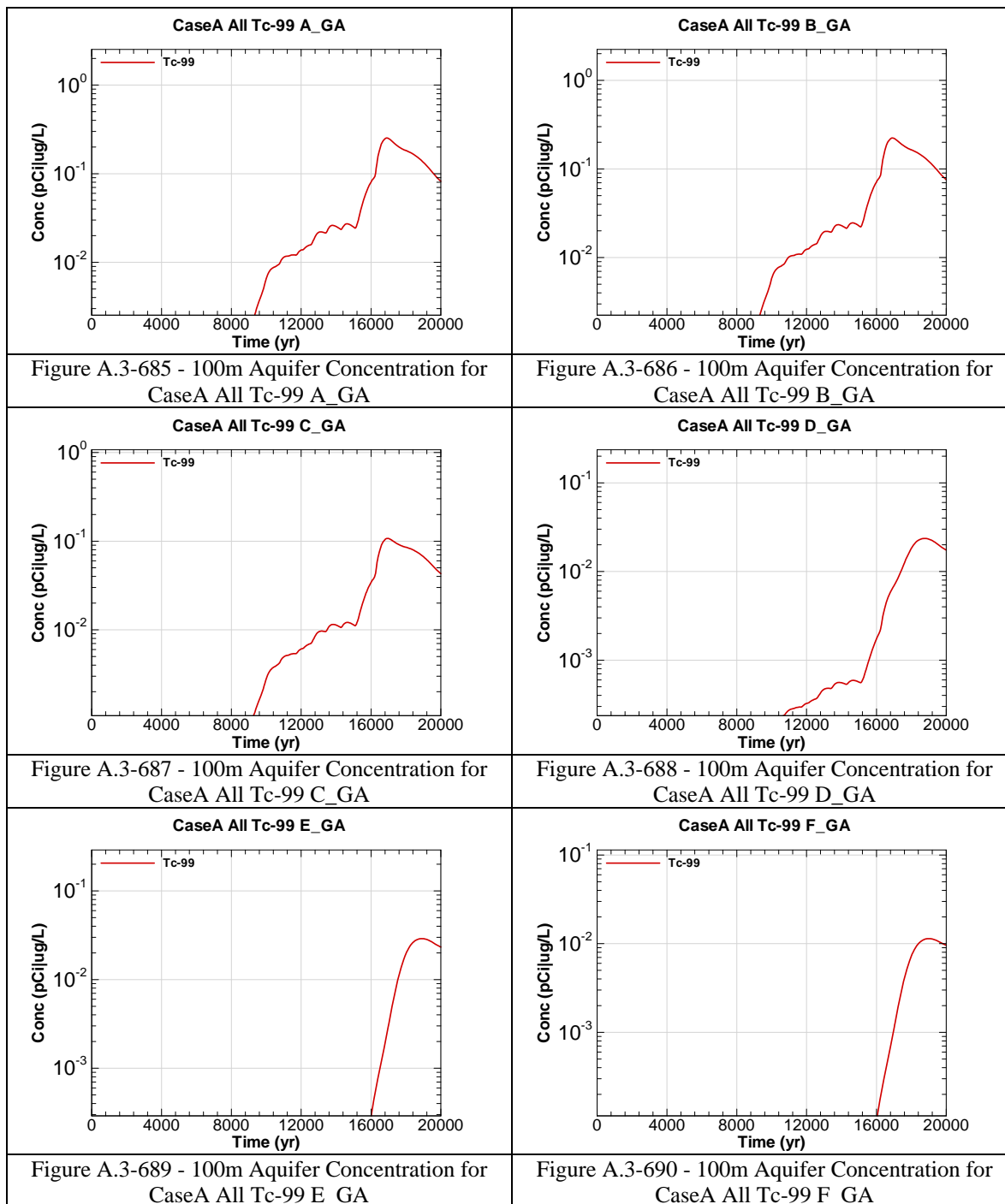


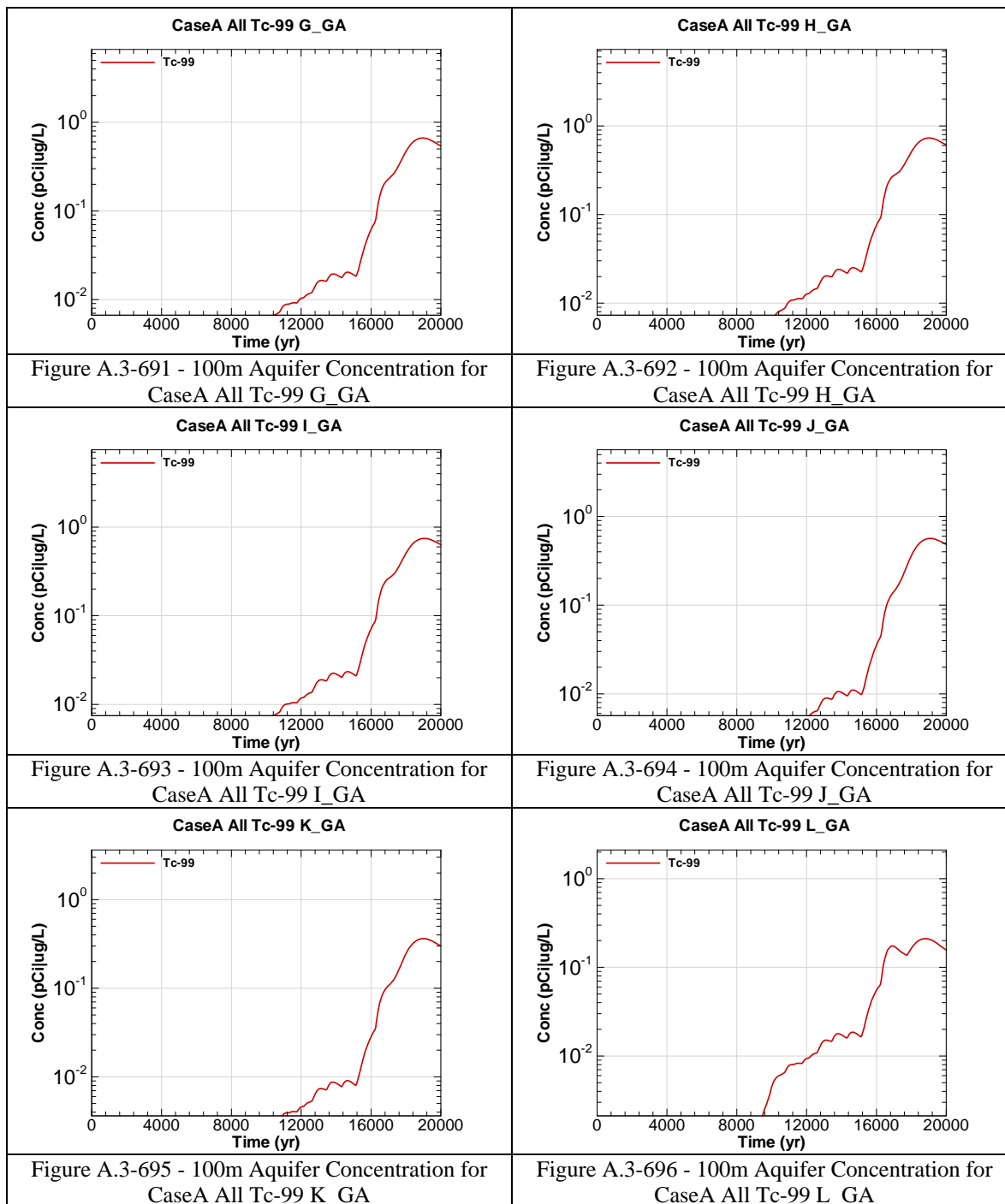


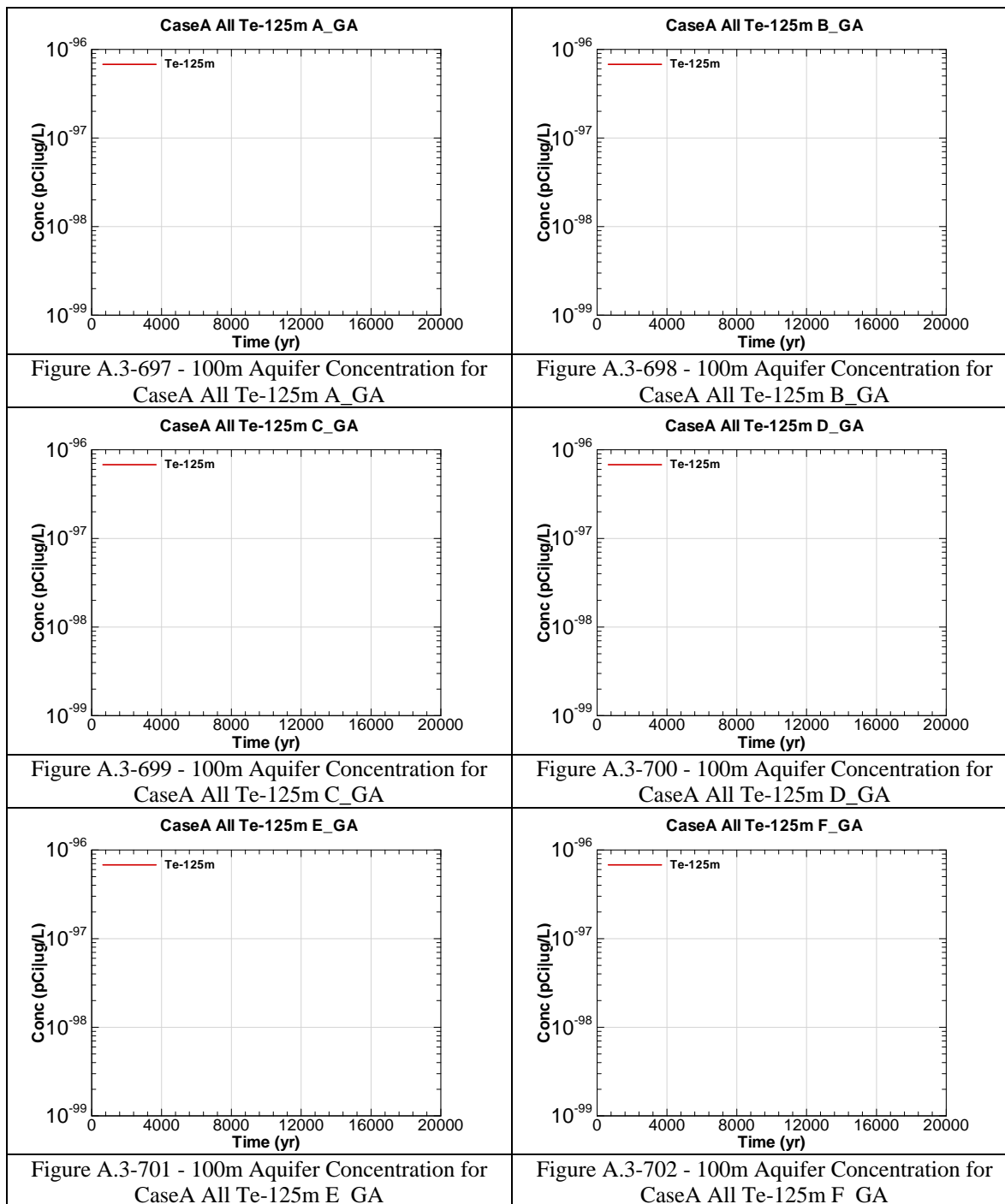


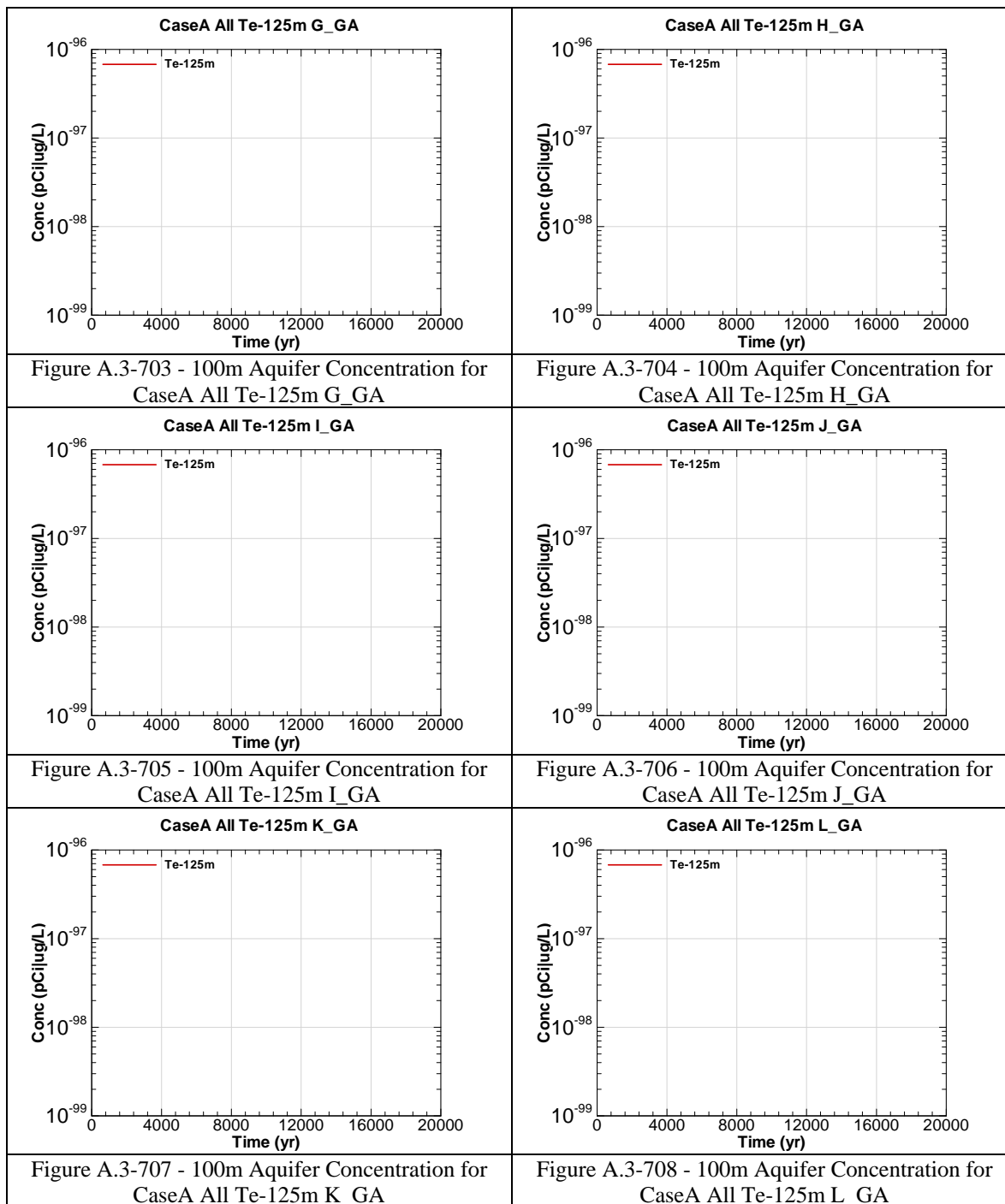


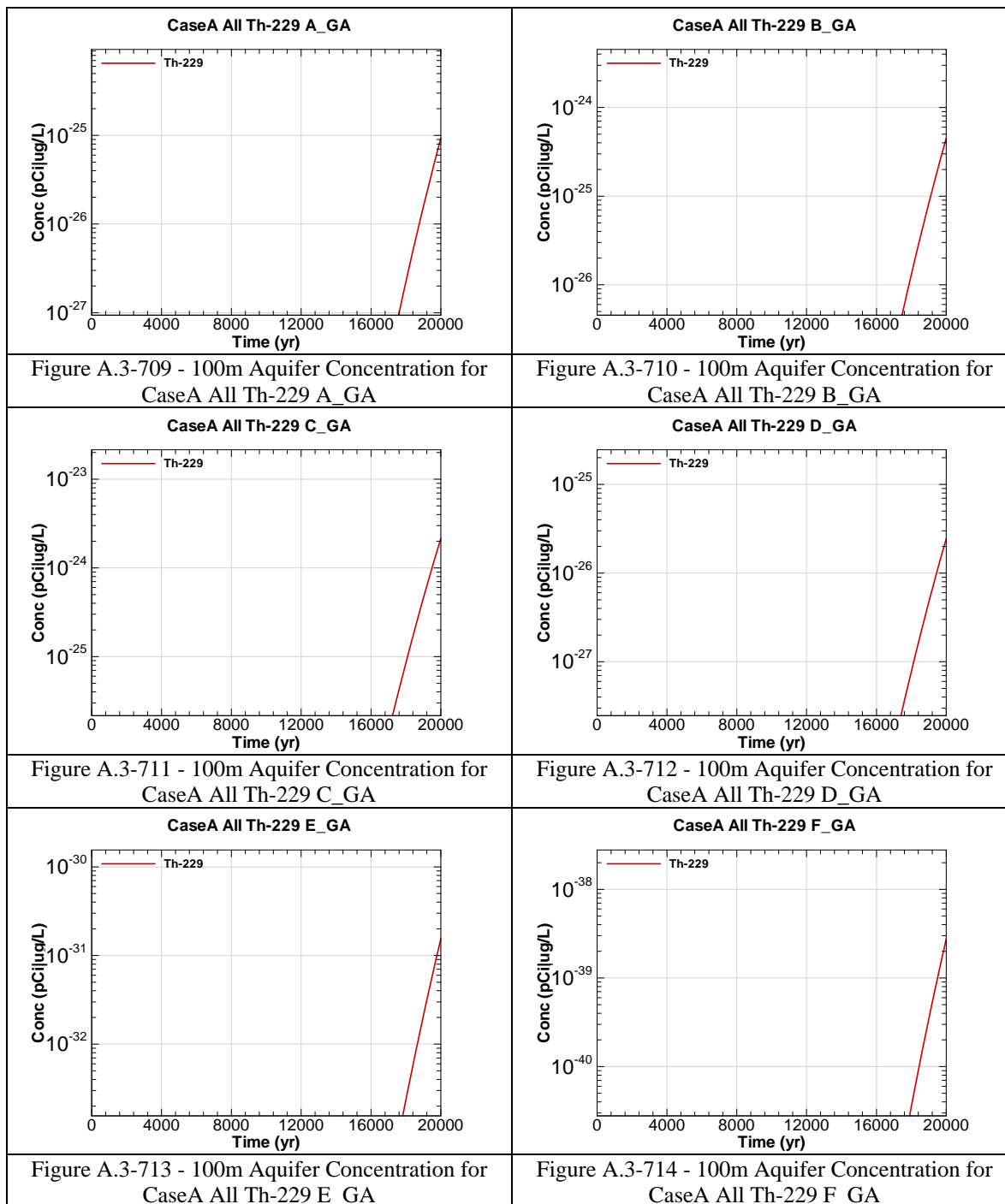


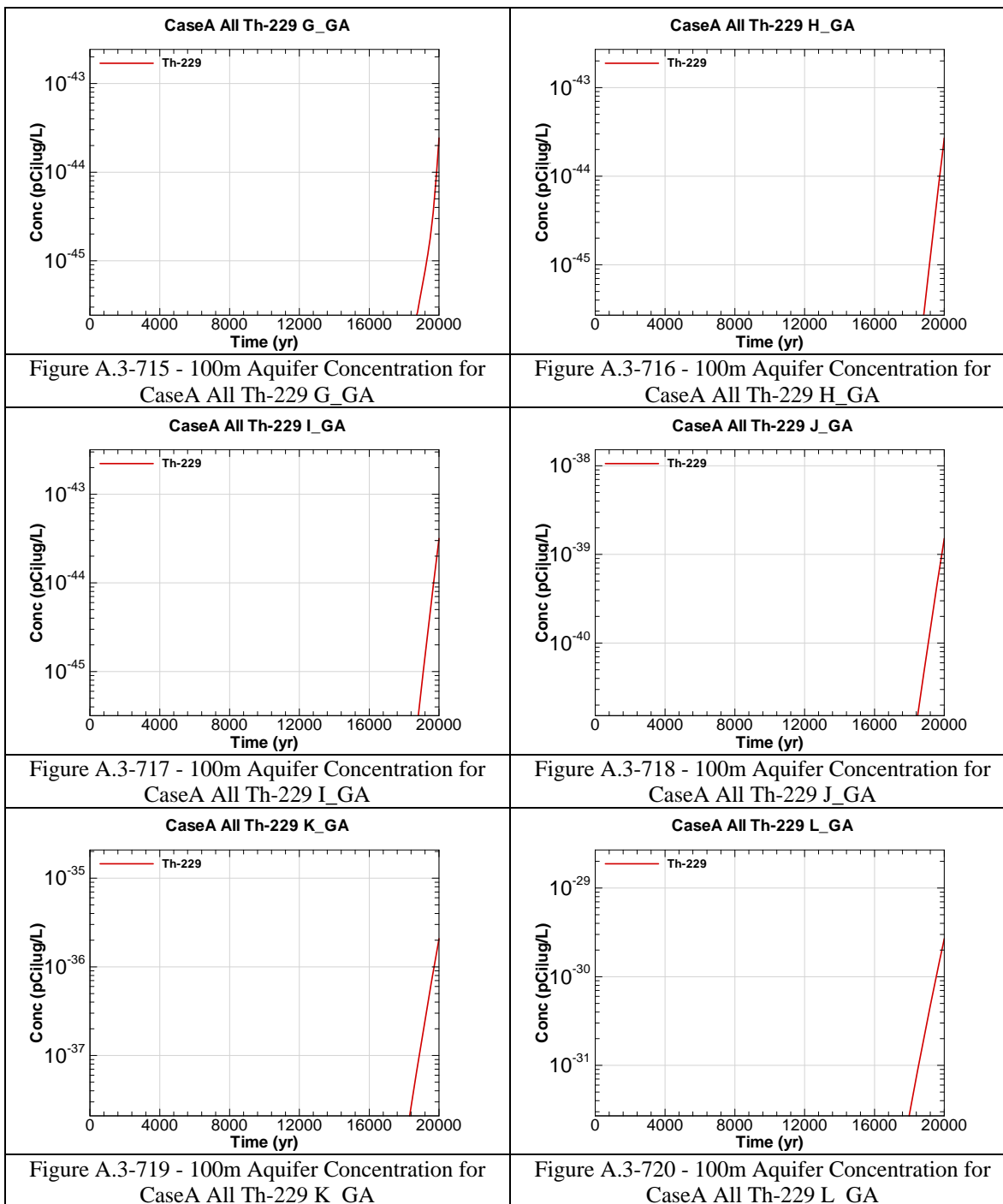


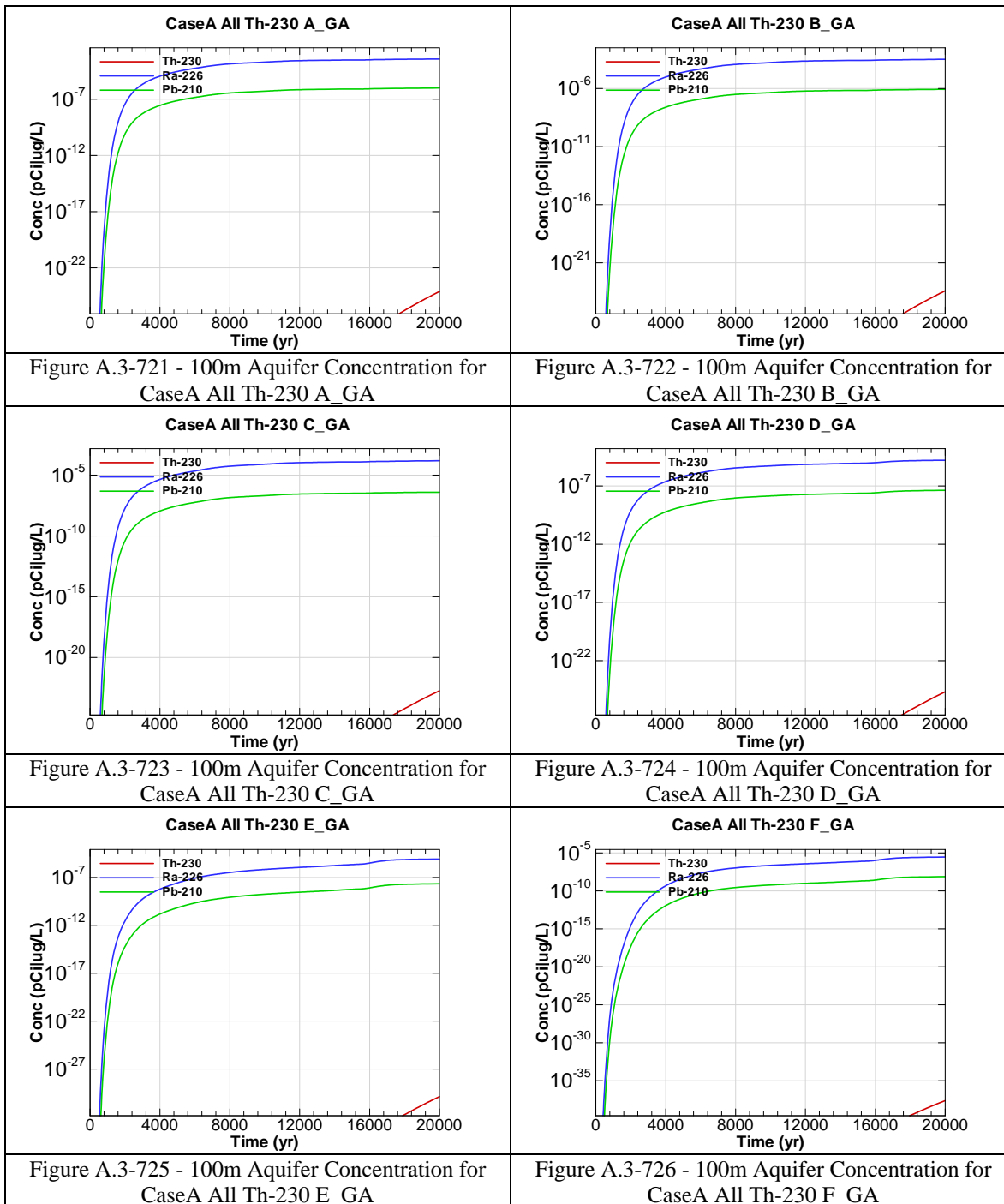


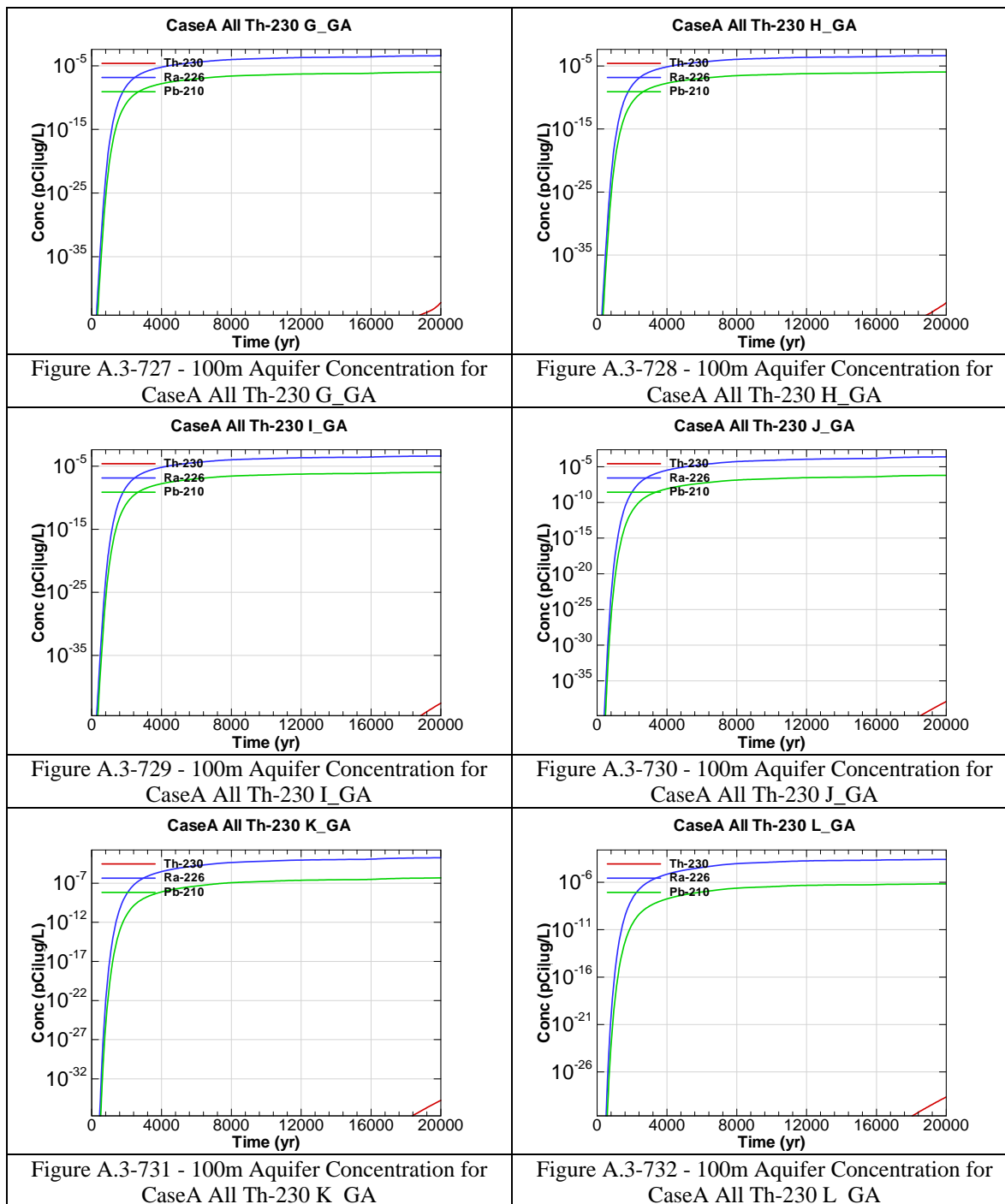












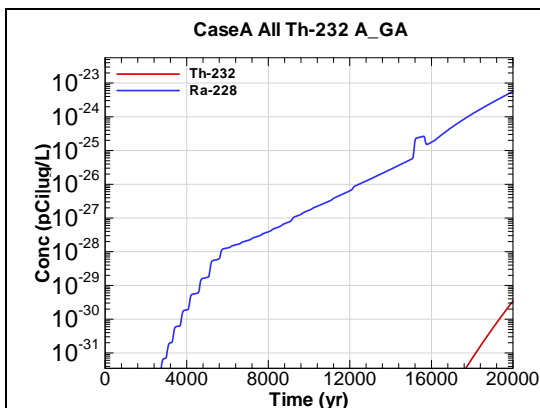


Figure A.3-733 - 100m Aquifer Concentration for CaseA All Th-232 A_GA

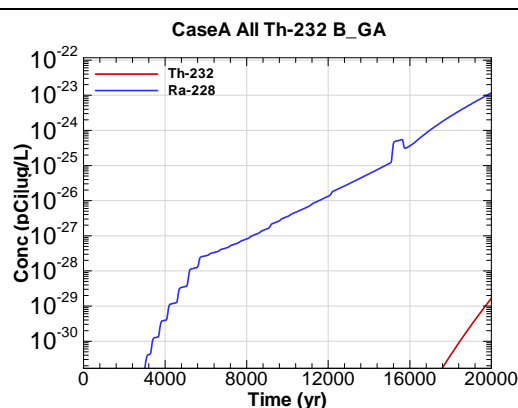


Figure A.3-734 - 100m Aquifer Concentration for CaseA All Th-232 B_GA

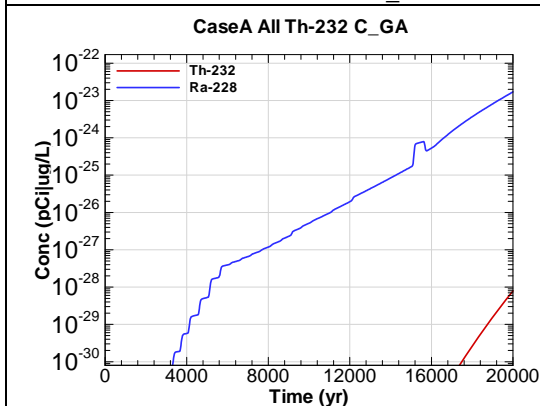


Figure A.3-735 - 100m Aquifer Concentration for CaseA All Th-232 C_GA

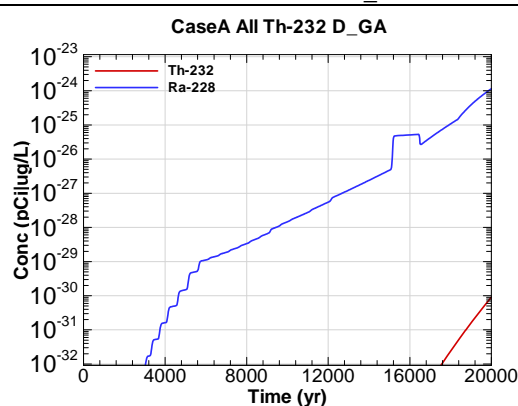


Figure A.3-736 - 100m Aquifer Concentration for CaseA All Th-232 D_GA

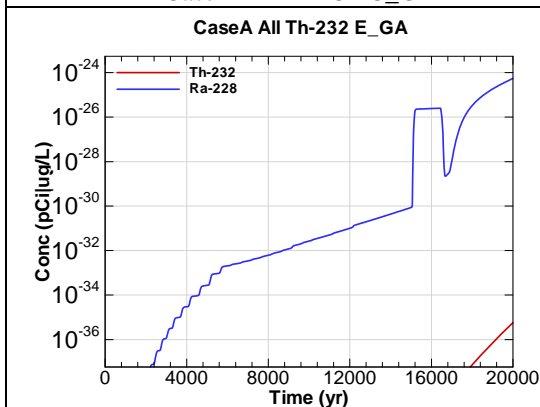


Figure A.3-737 - 100m Aquifer Concentration for CaseA All Th-232 E_GA

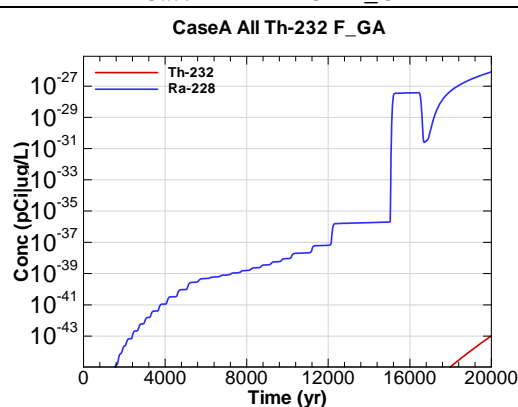
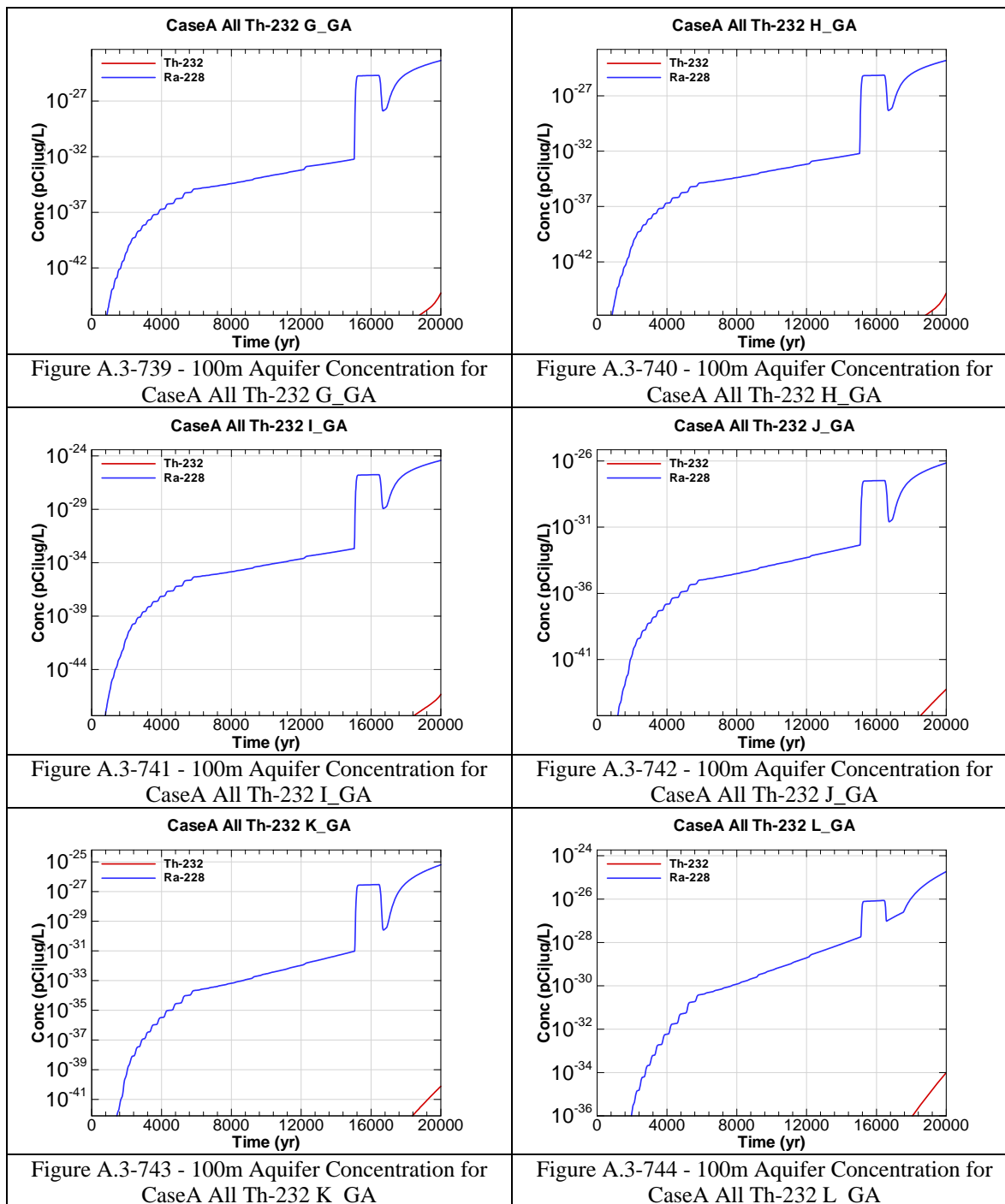
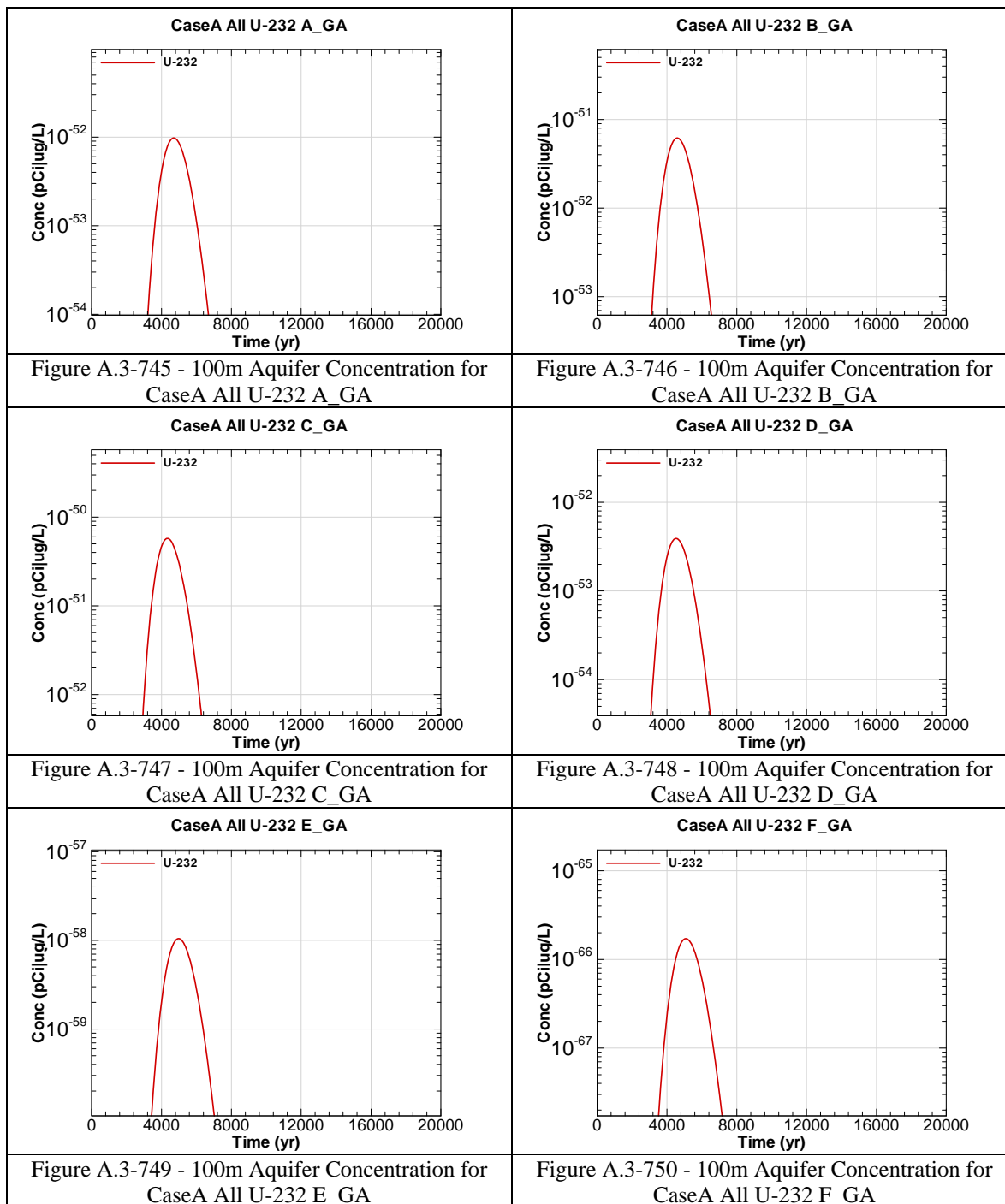
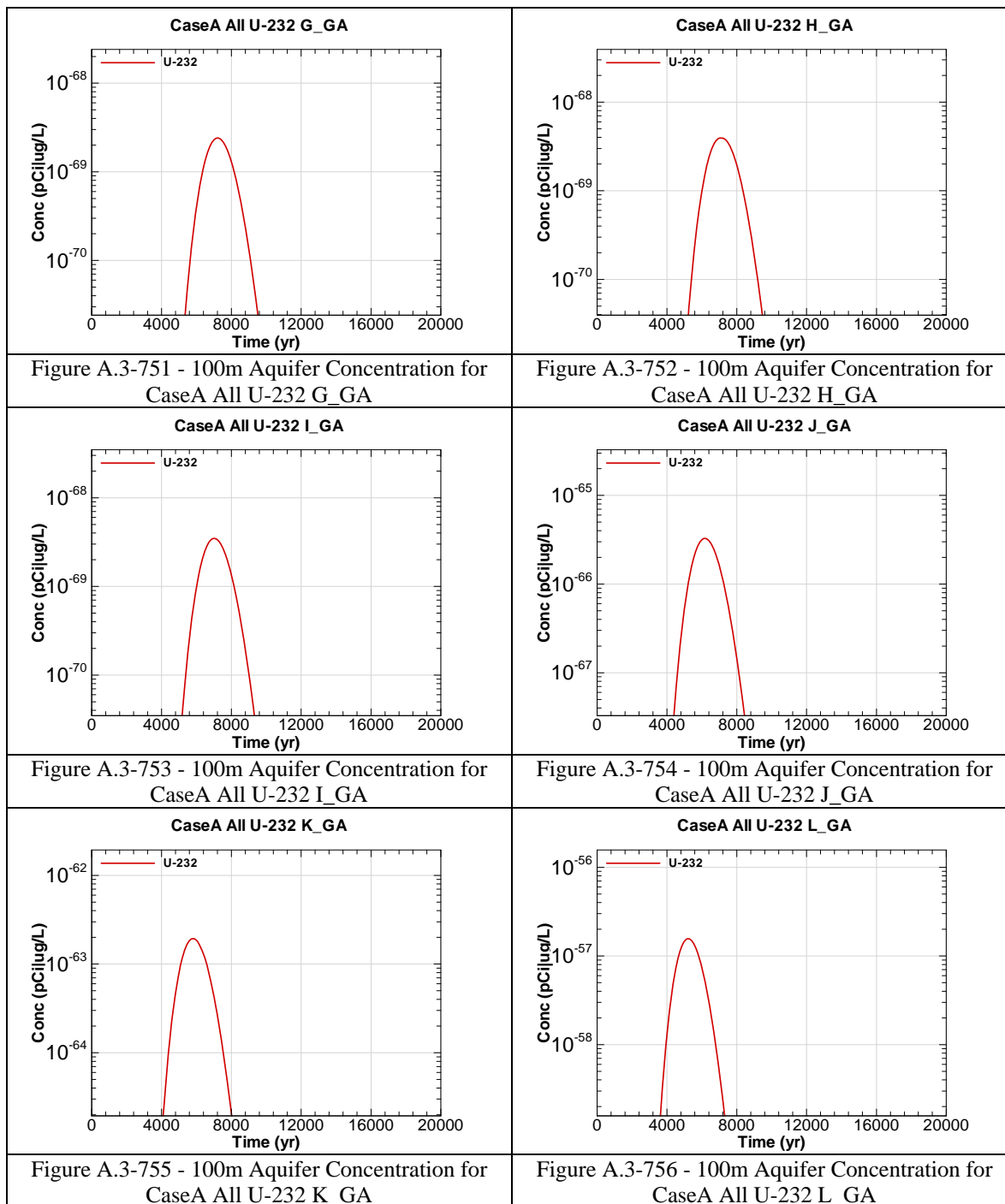
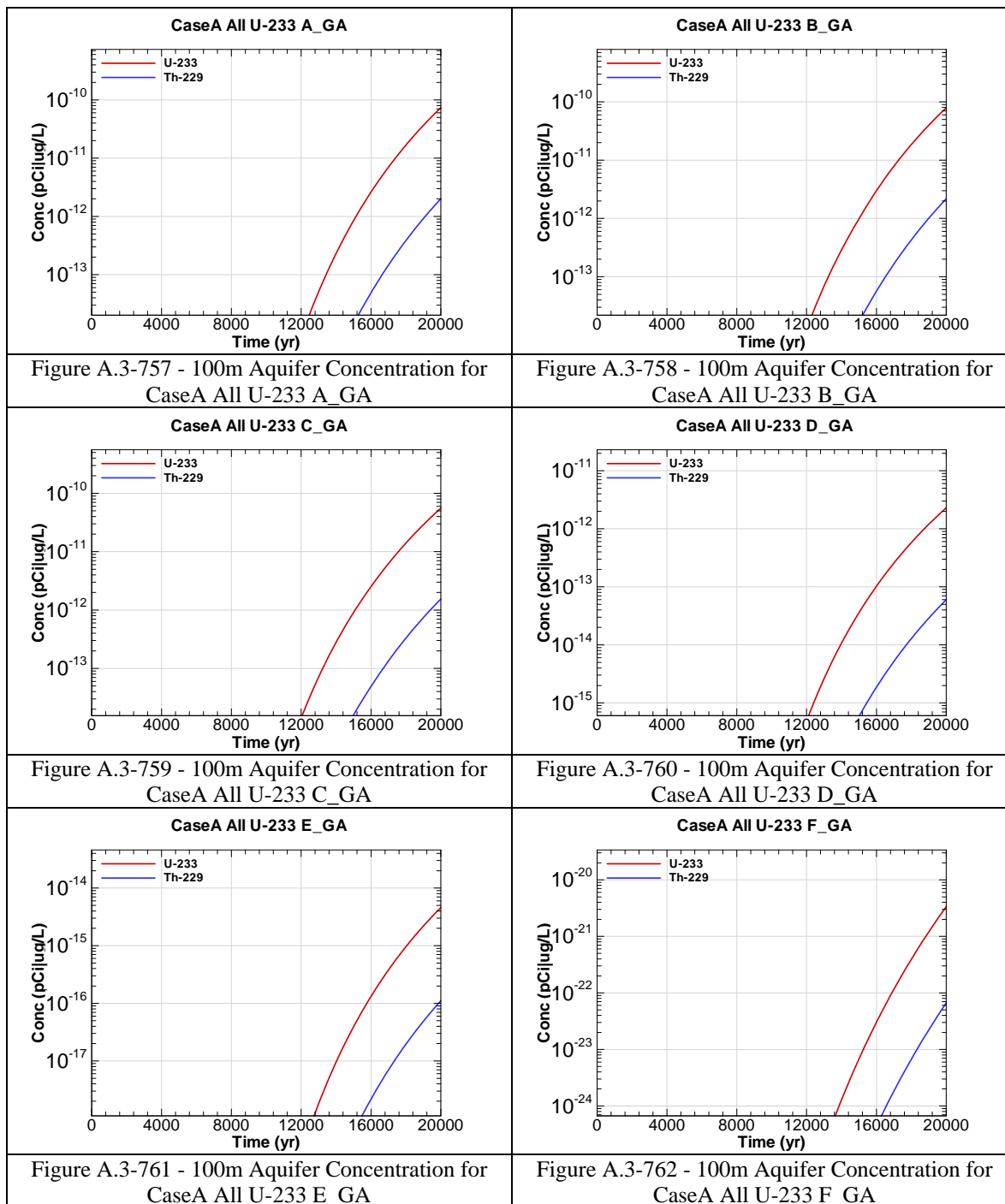


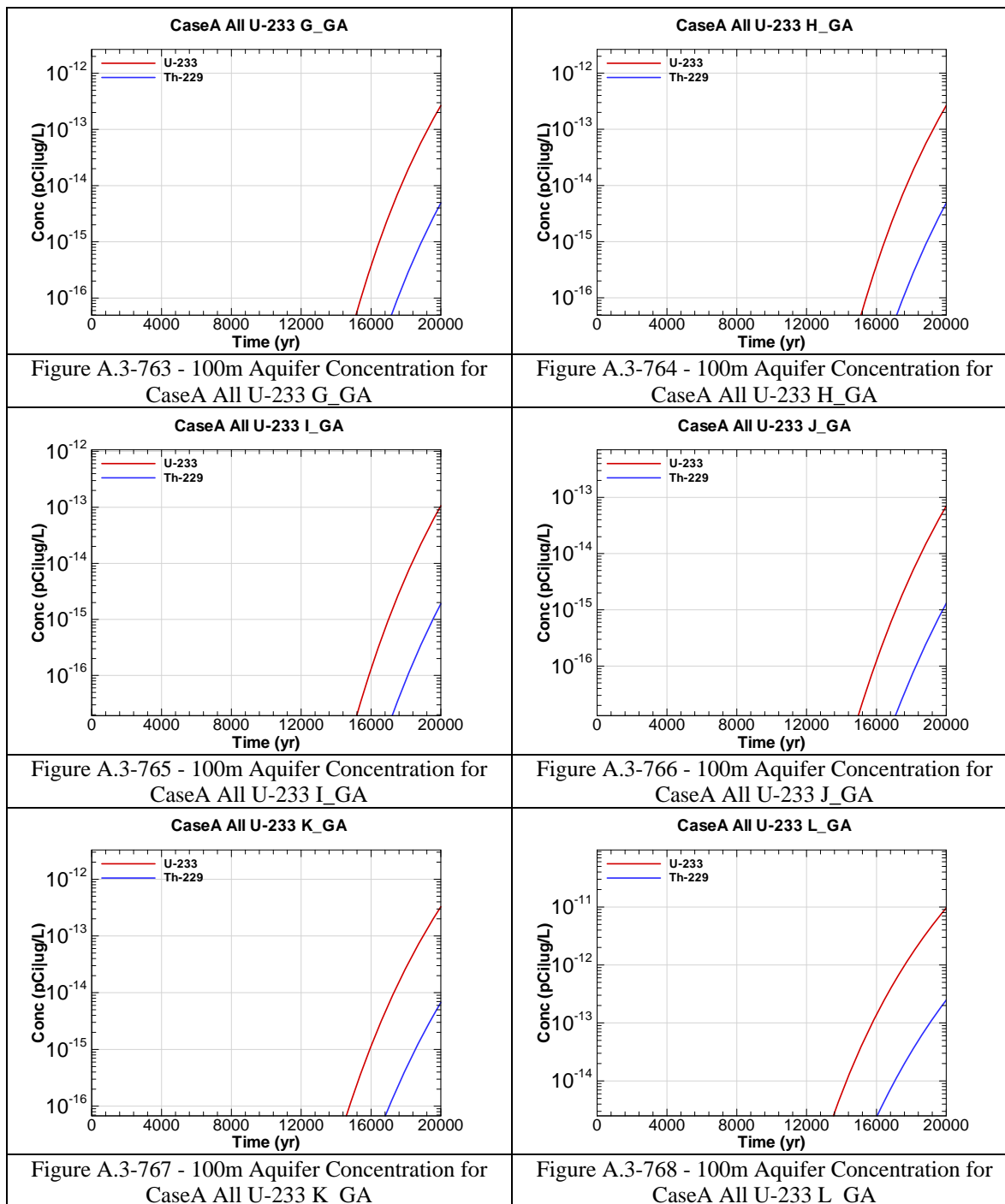
Figure A.3-738 - 100m Aquifer Concentration for CaseA All Th-232 F_GA

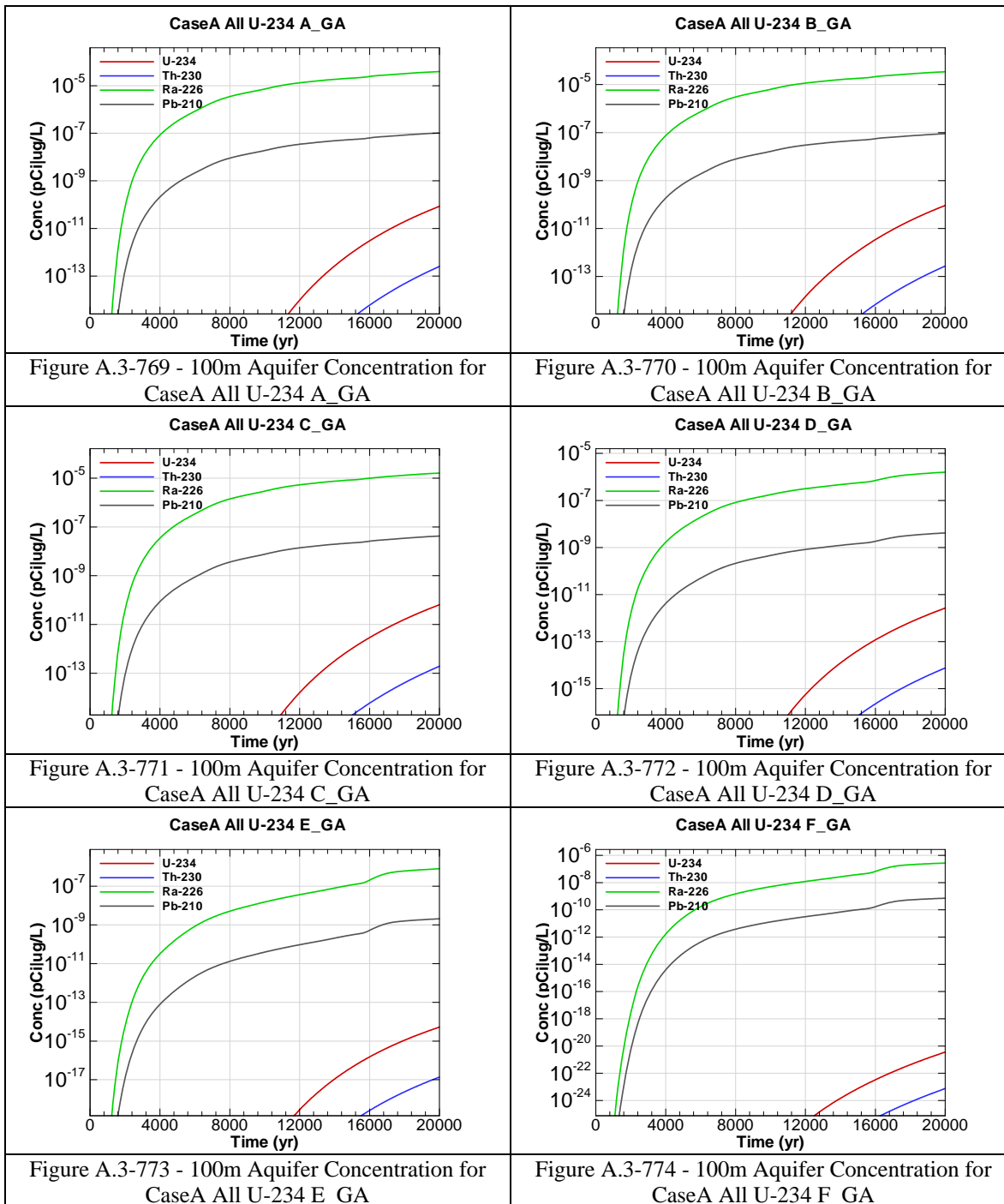


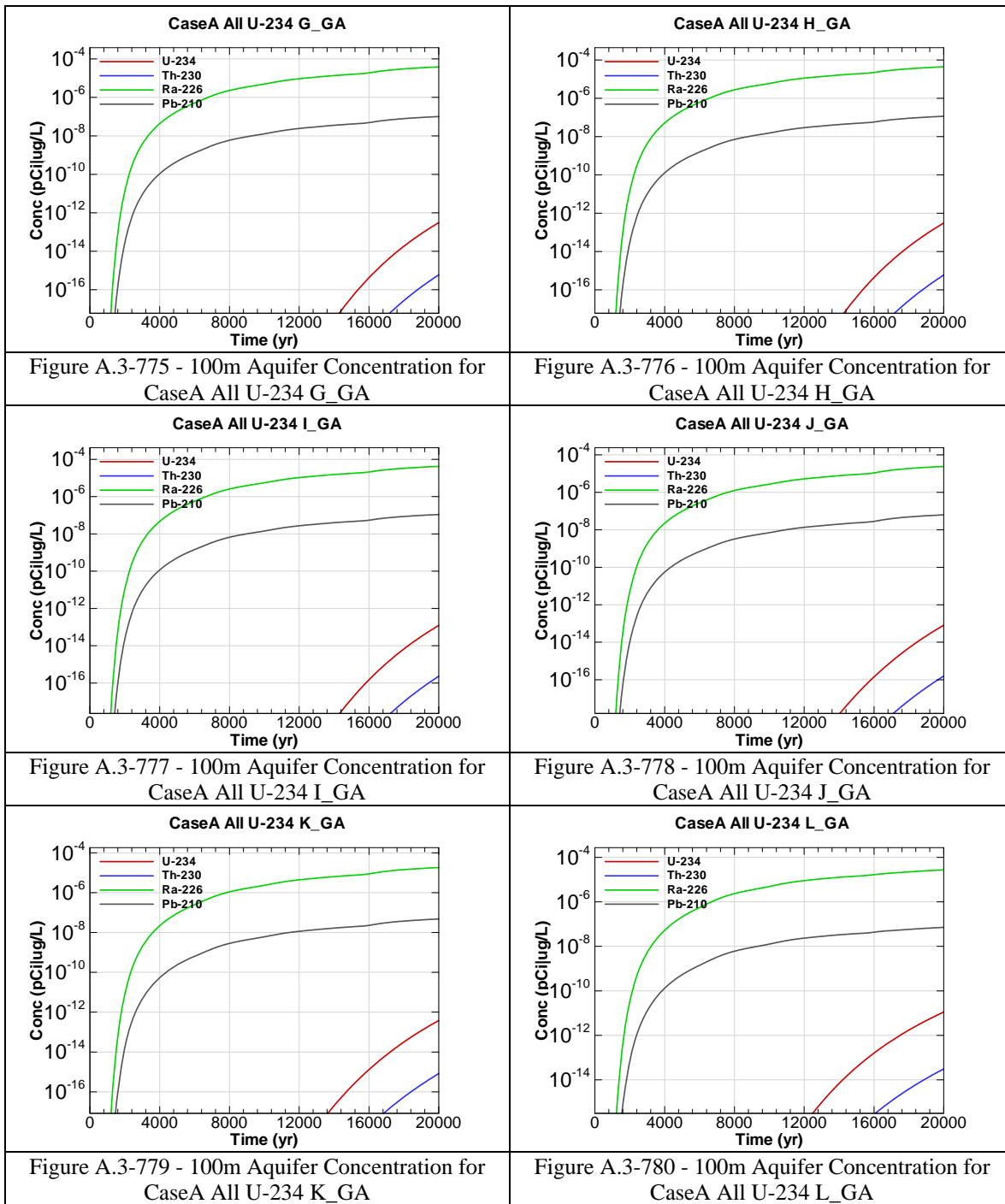


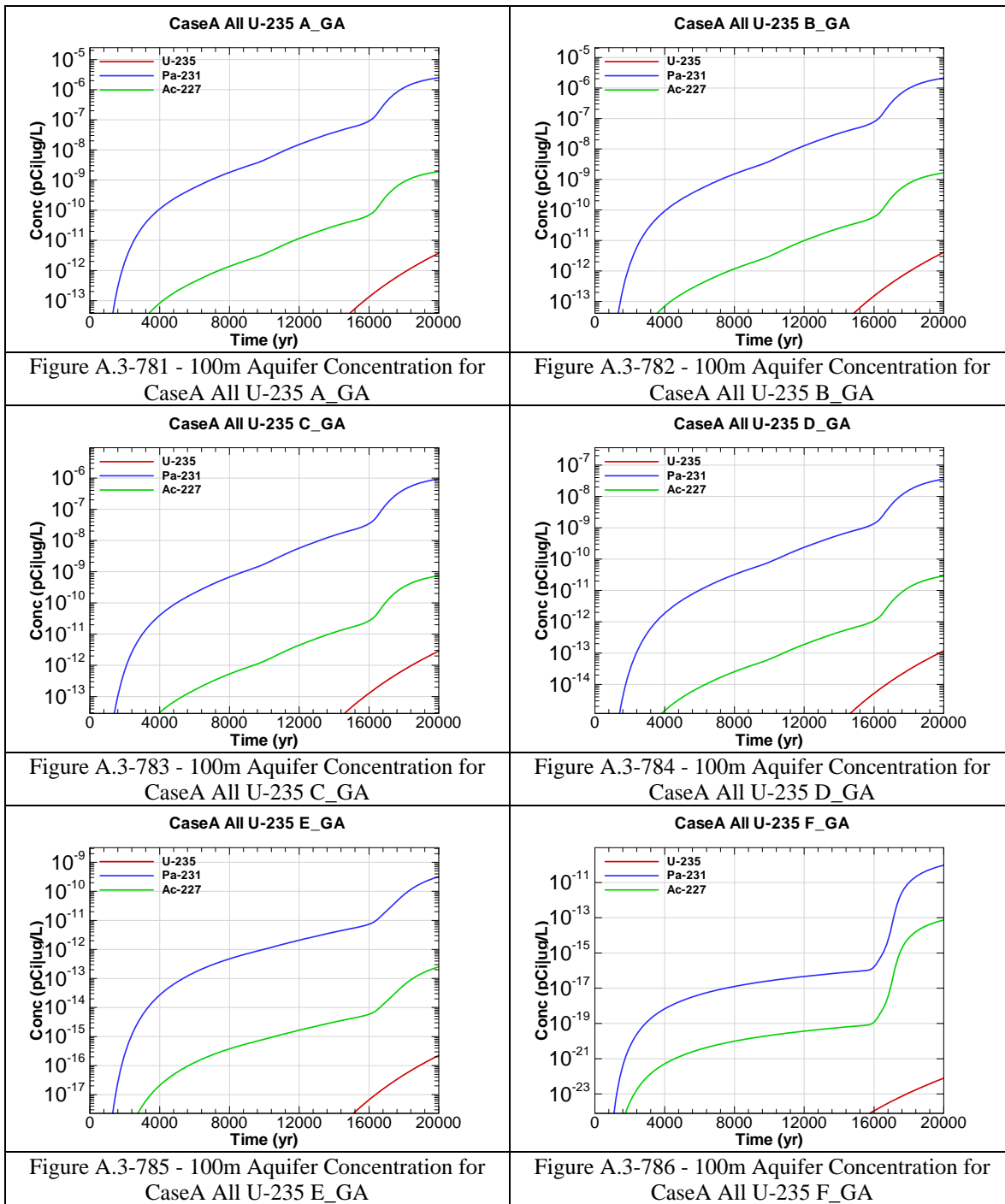


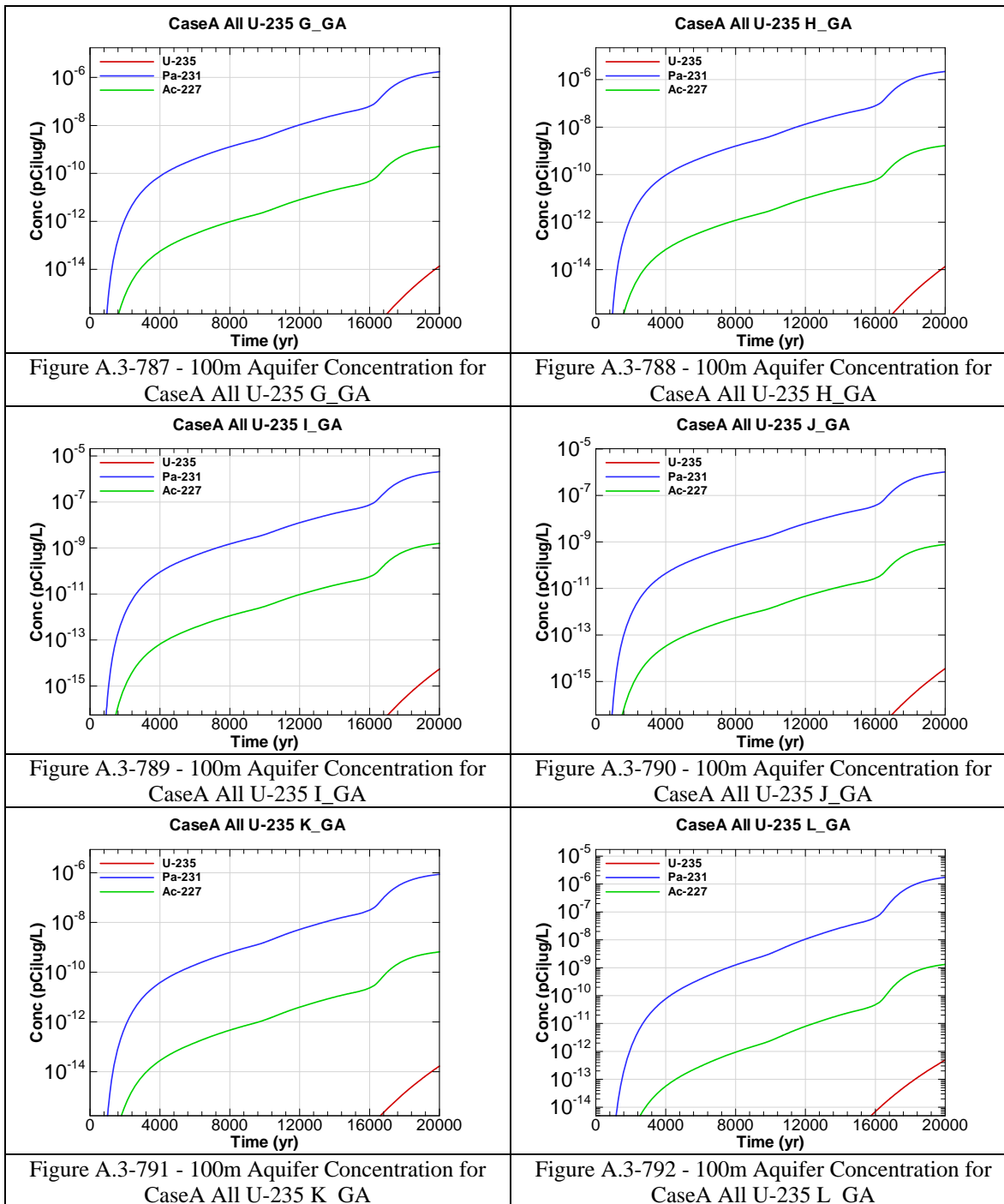


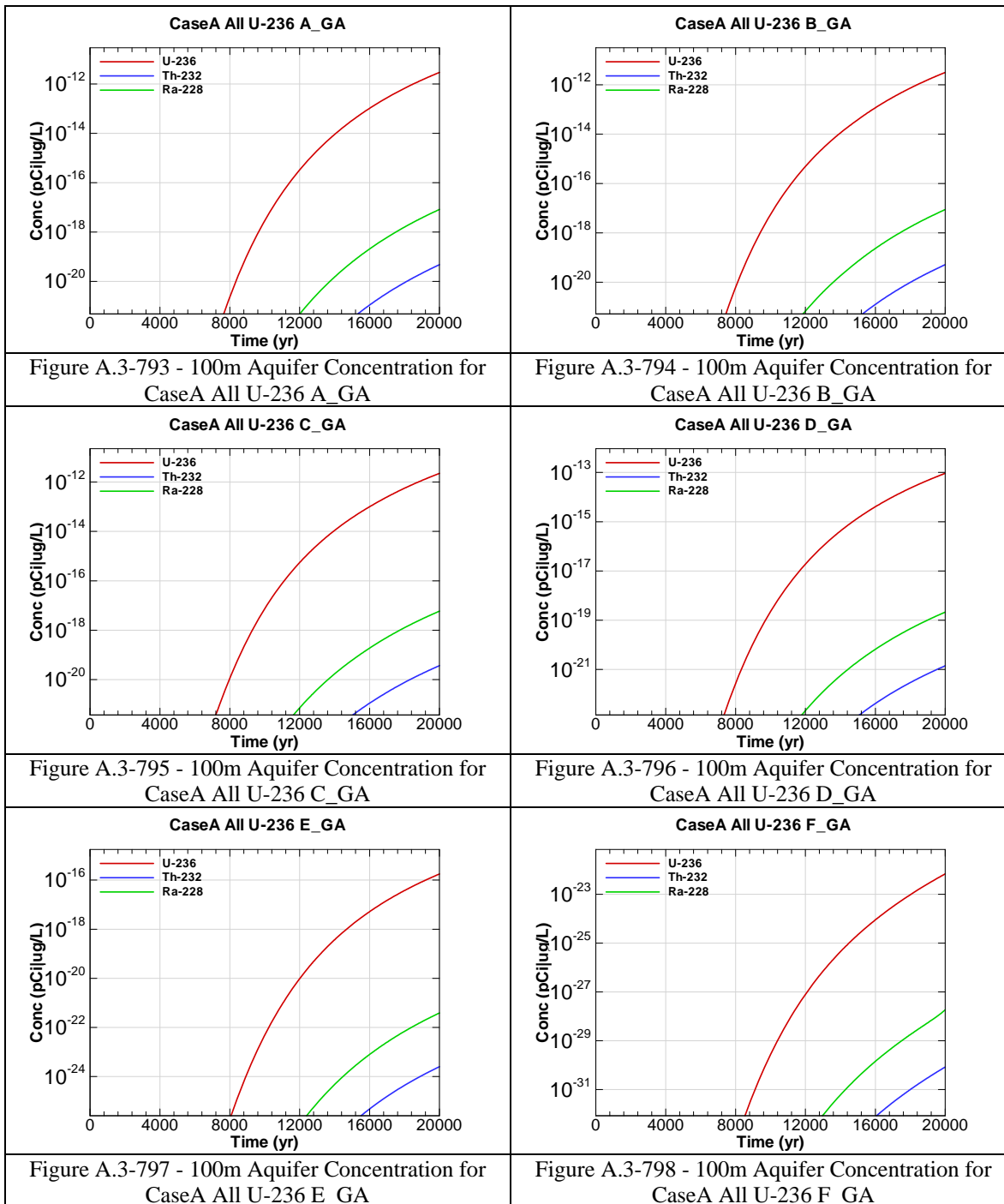


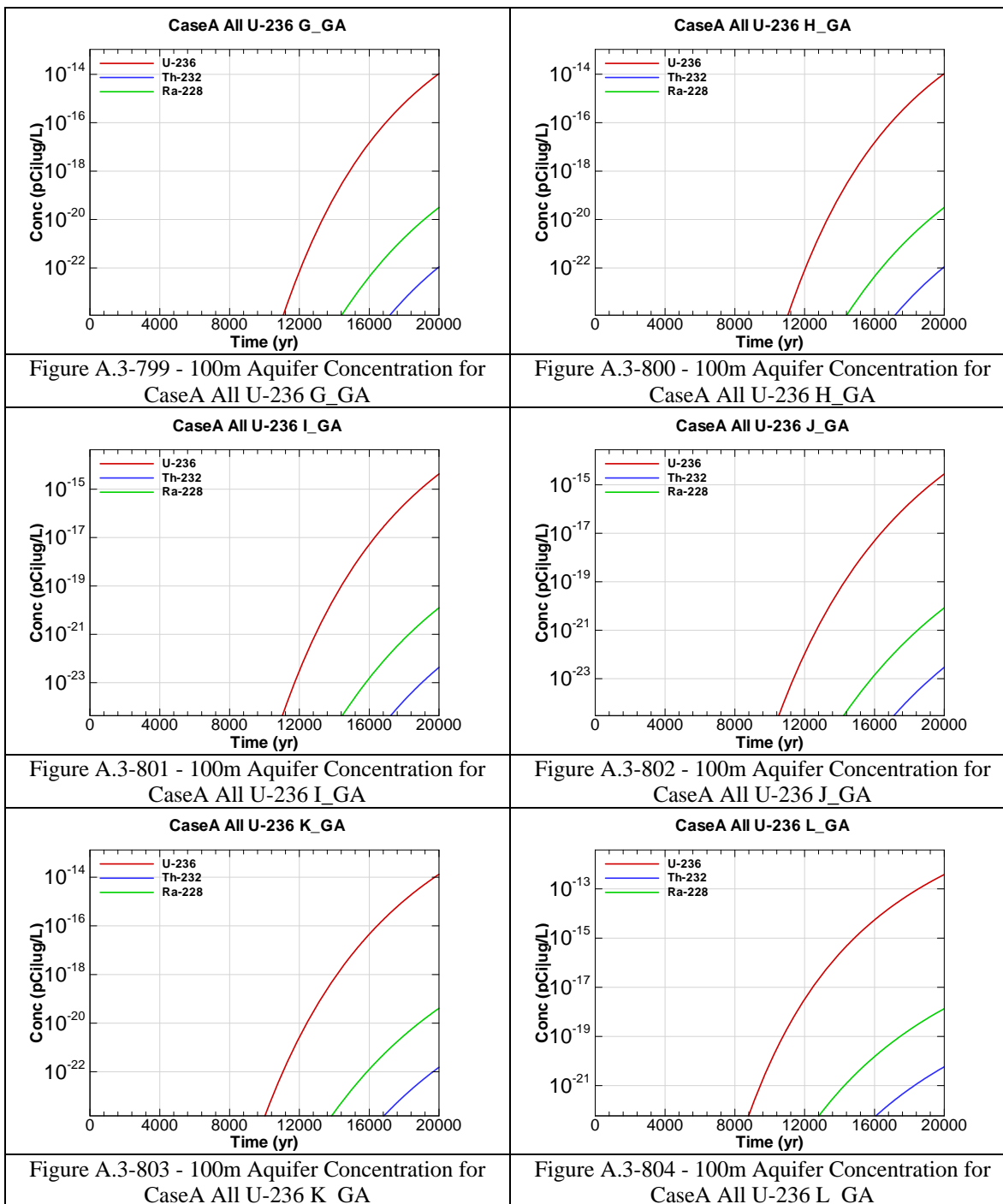












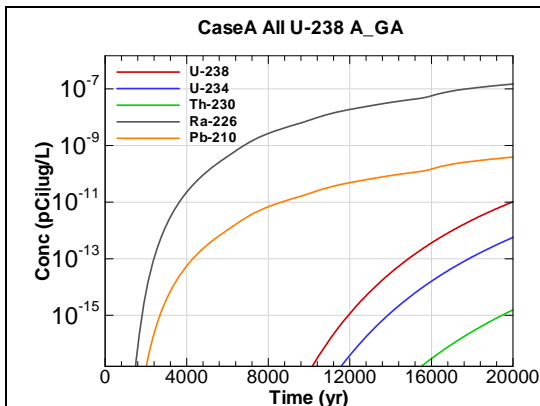


Figure A.3-805 - 100m Aquifer Concentration for
CaseA All U-238 A_GA

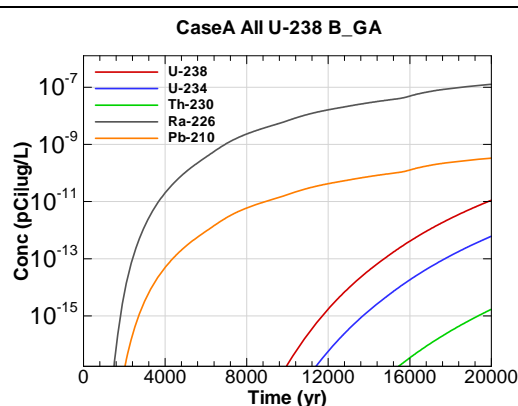


Figure A.3-806 - 100m Aquifer Concentration for
CaseA All U-238 B_GA

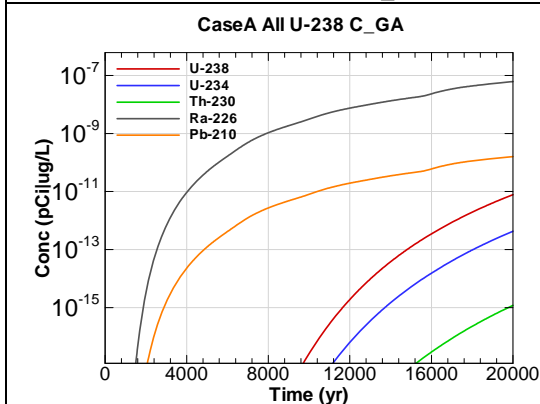


Figure A.3-807 - 100m Aquifer Concentration for
CaseA All U-238 C_GA

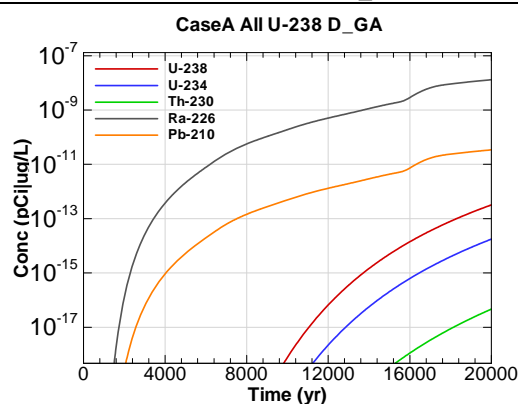


Figure A.3-808 - 100m Aquifer Concentration for
CaseA All U-238 D_GA

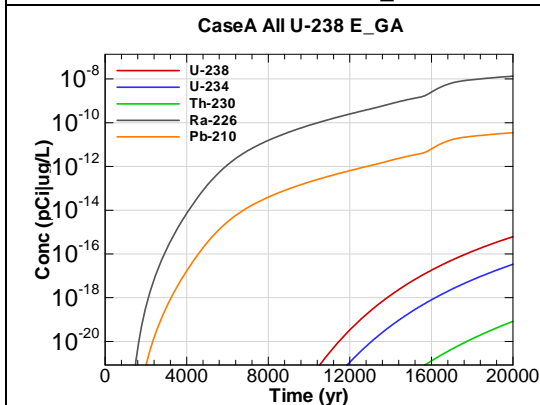


Figure A.3-809 - 100m Aquifer Concentration for
CaseA All U-238 E_GA

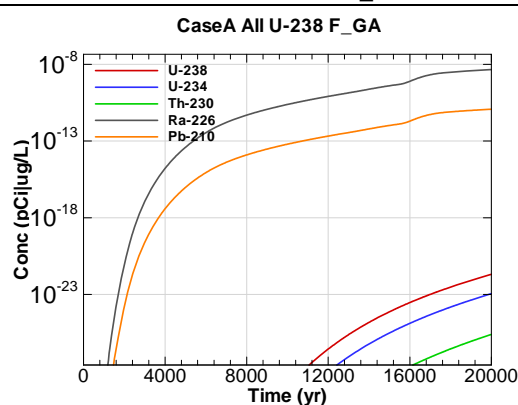


Figure A.3-810 - 100m Aquifer Concentration for
CaseA All U-238 F_GA

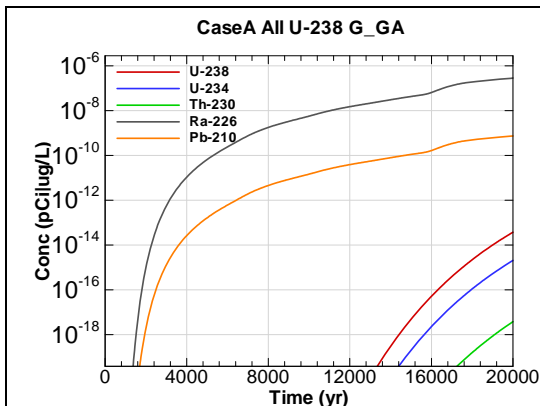


Figure A.3-811 - 100m Aquifer Concentration for
CaseA All U-238 G_GA

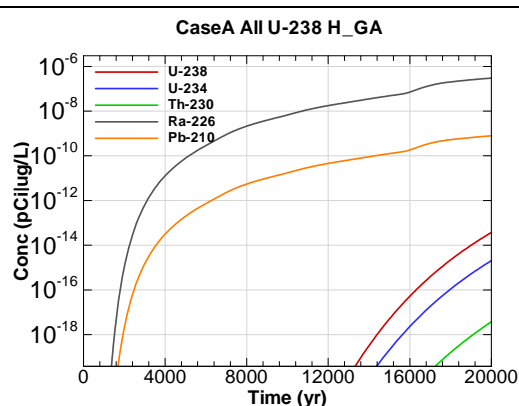


Figure A.3-812 - 100m Aquifer Concentration for
CaseA All U-238 H_GA

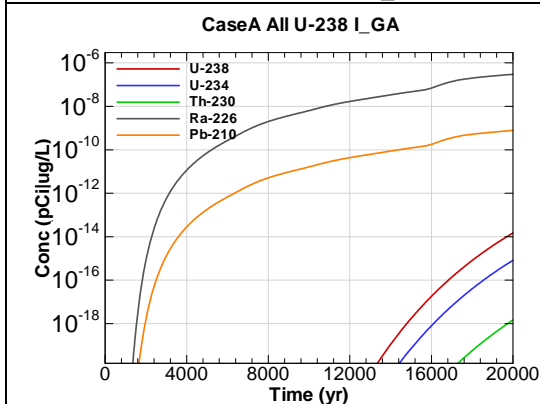


Figure A.3-813 - 100m Aquifer Concentration for
CaseA All U-238 I_GA

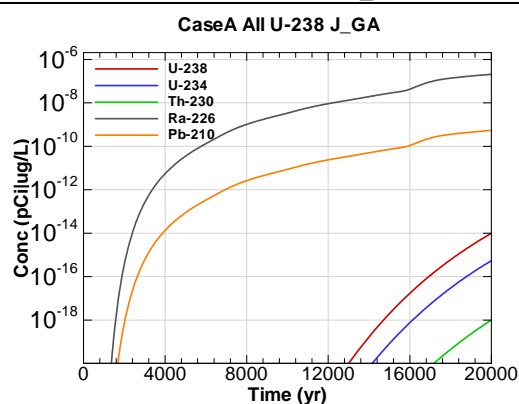


Figure A.3-814 - 100m Aquifer Concentration for
CaseA All U-238 J_GA

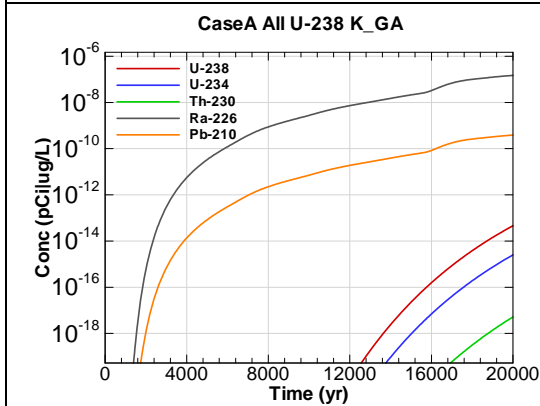


Figure A.3-815 - 100m Aquifer Concentration for
CaseA All U-238 K_GA

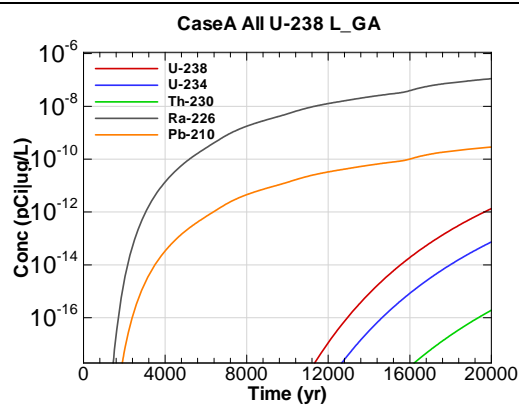
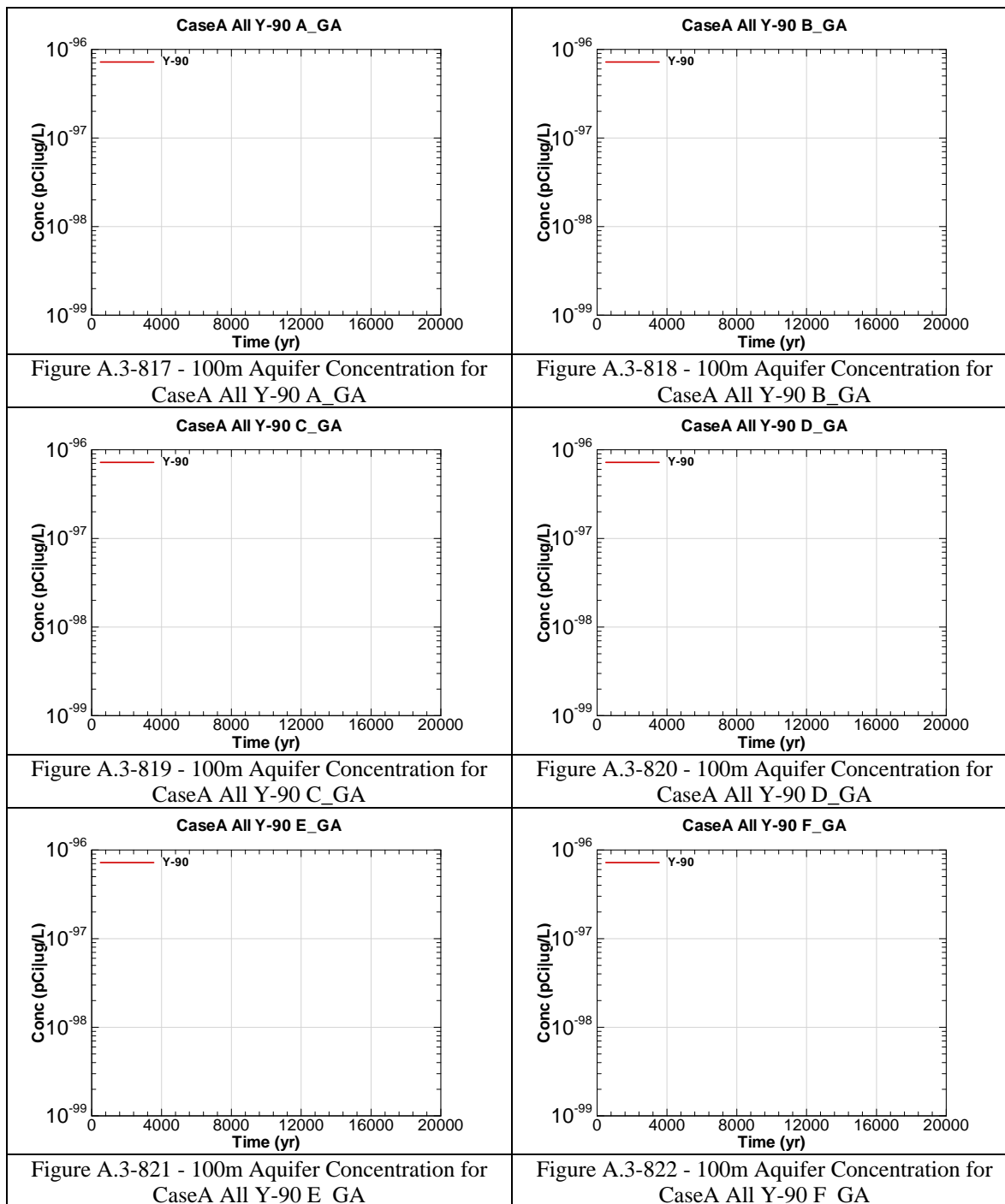
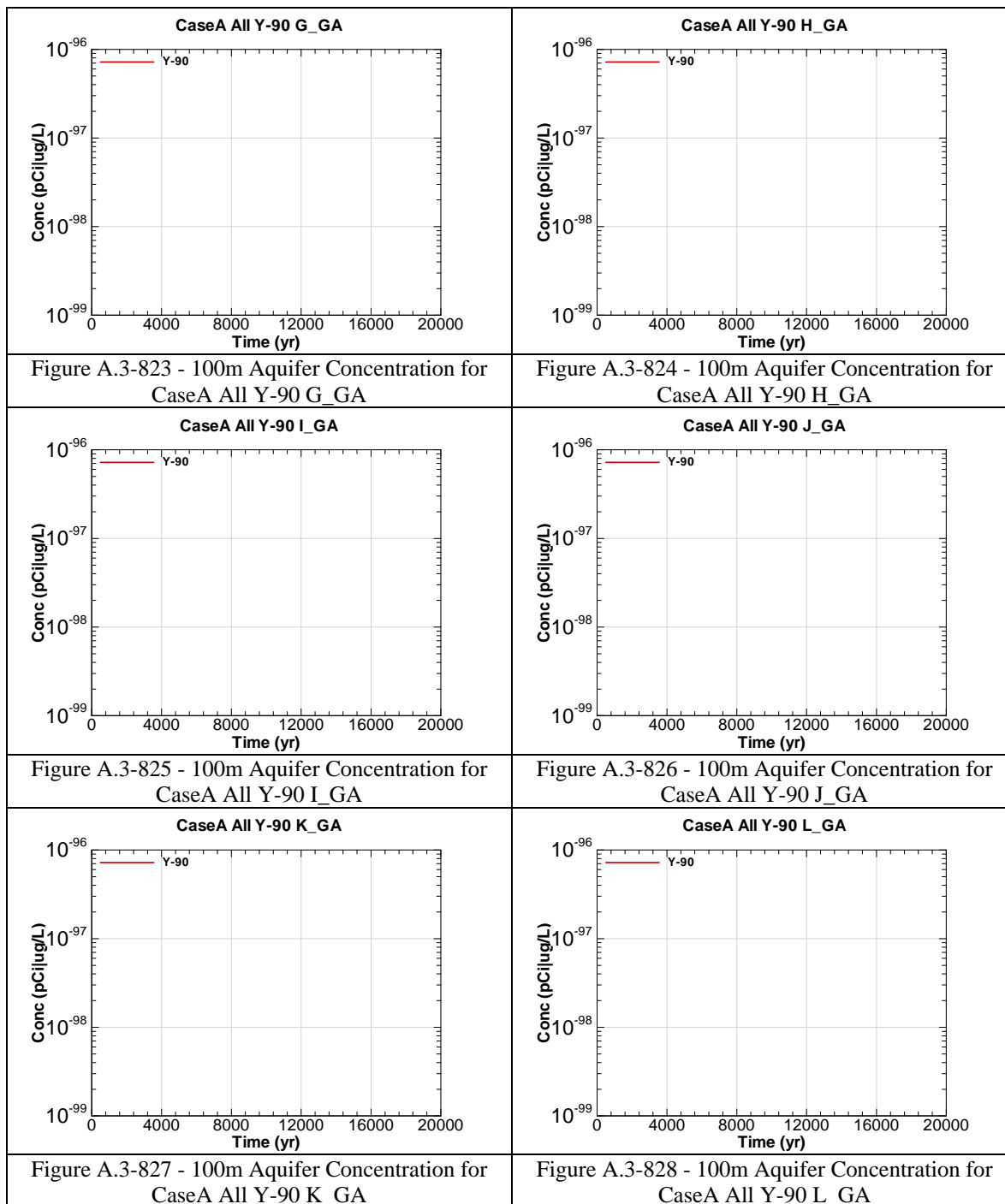
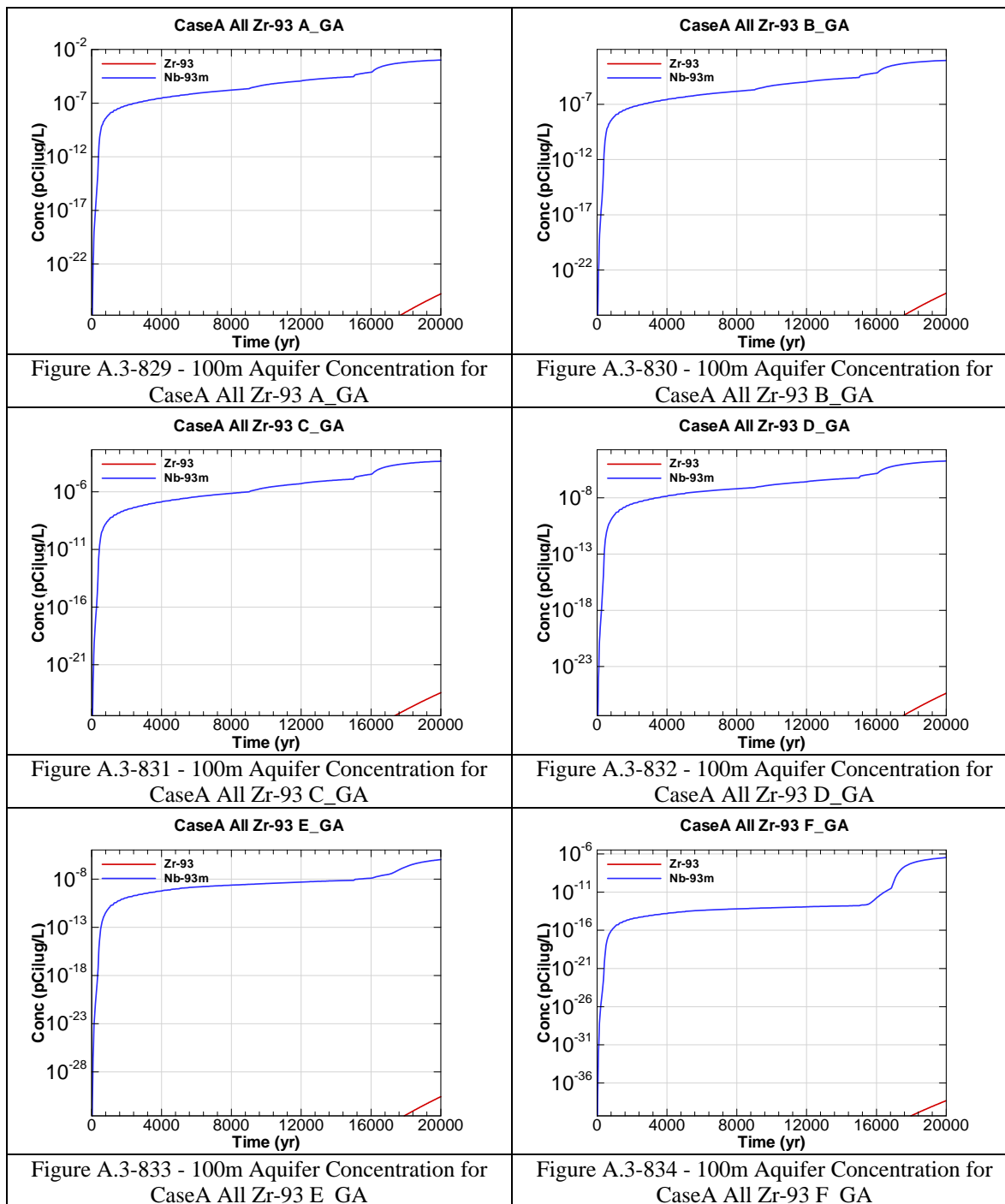
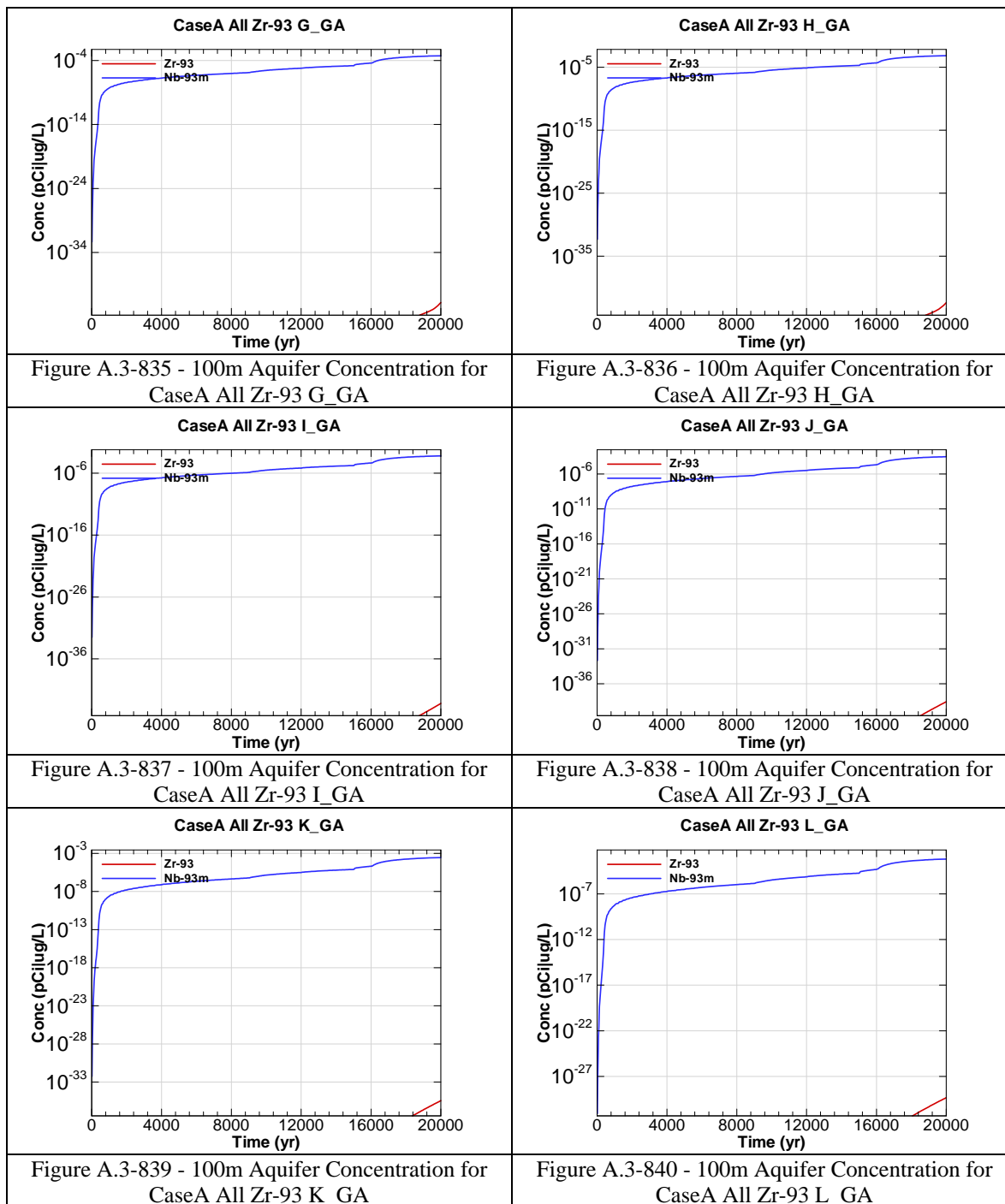


Figure A.3-816 - 100m Aquifer Concentration for
CaseA All U-238 L_GA



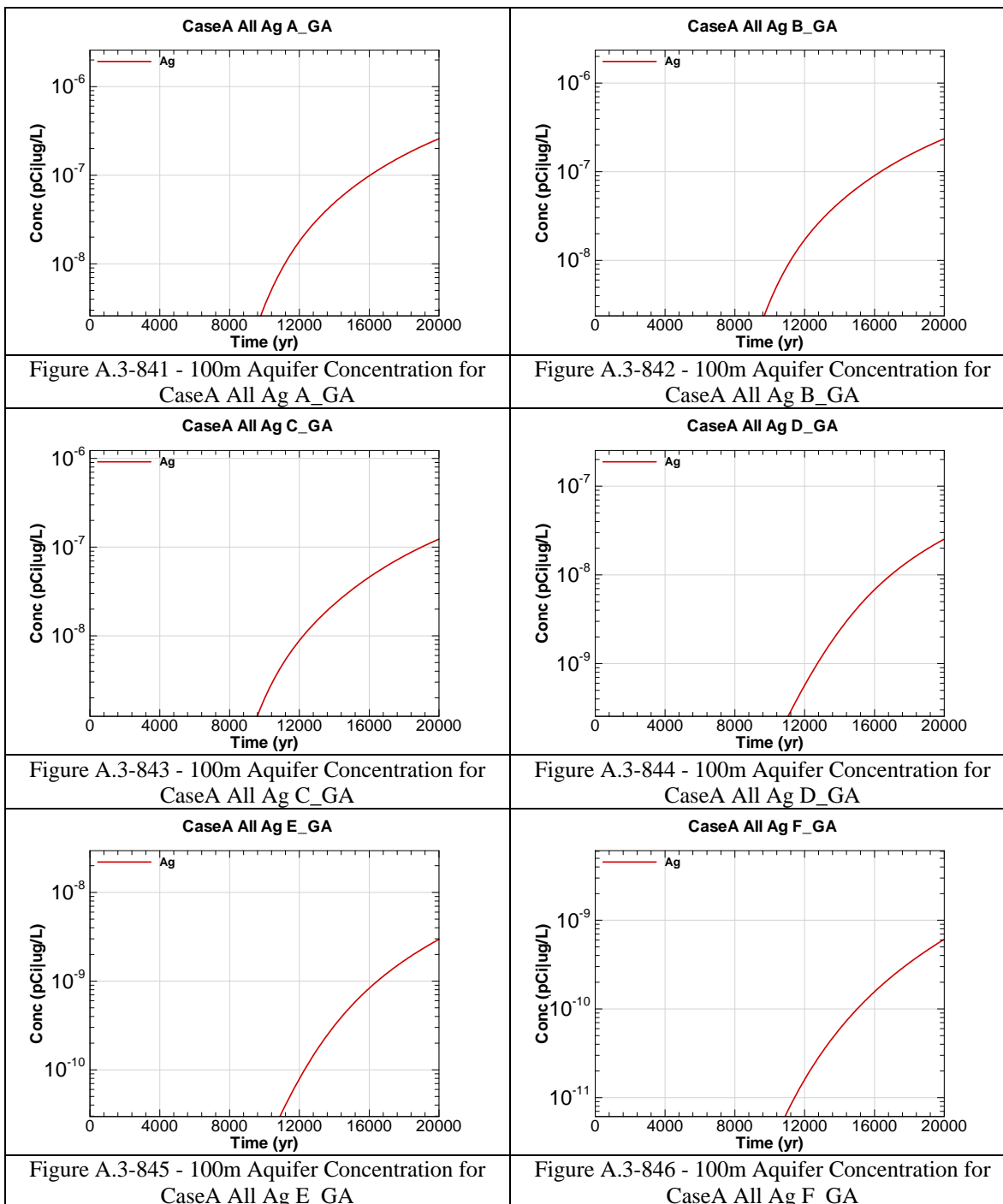


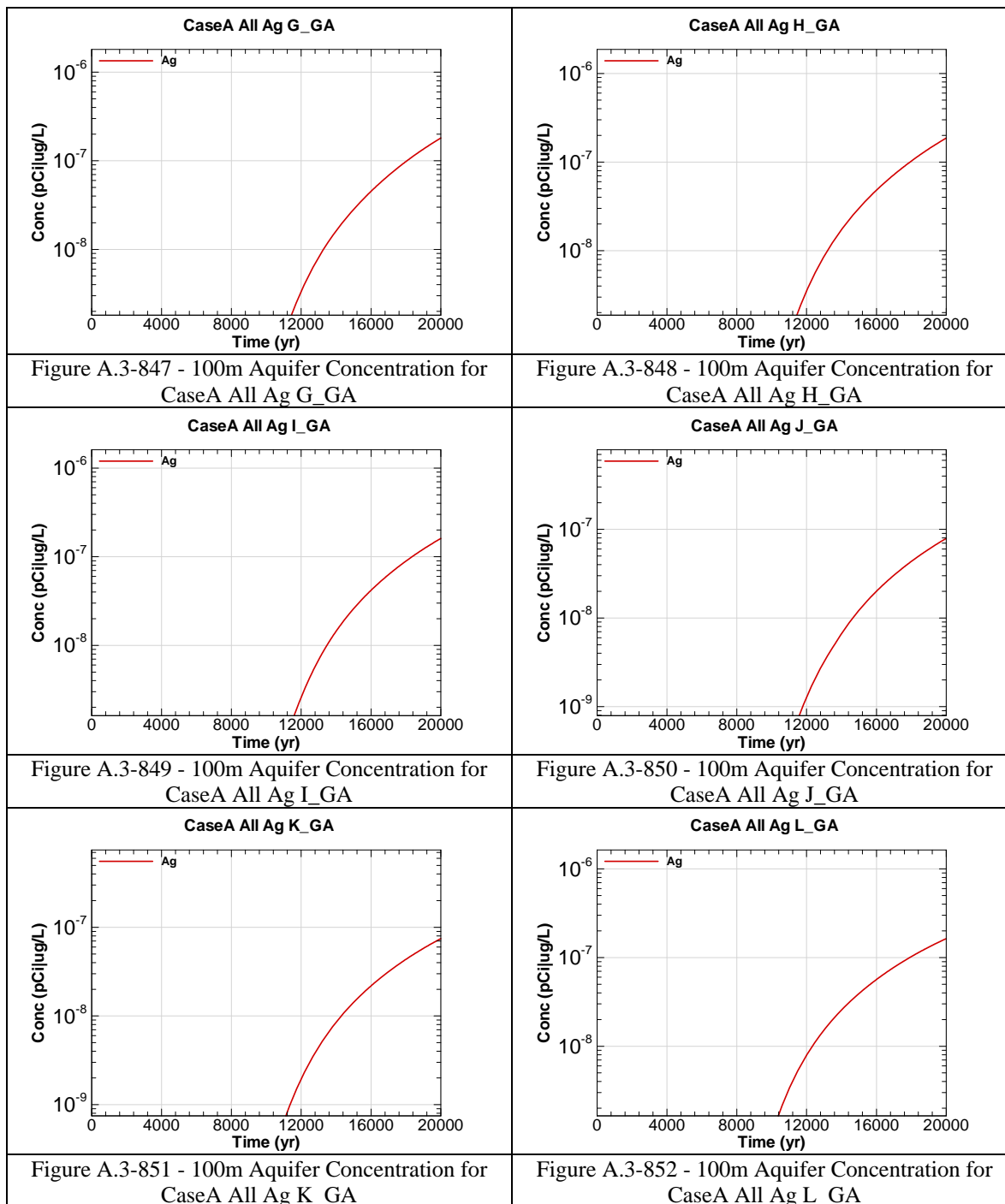


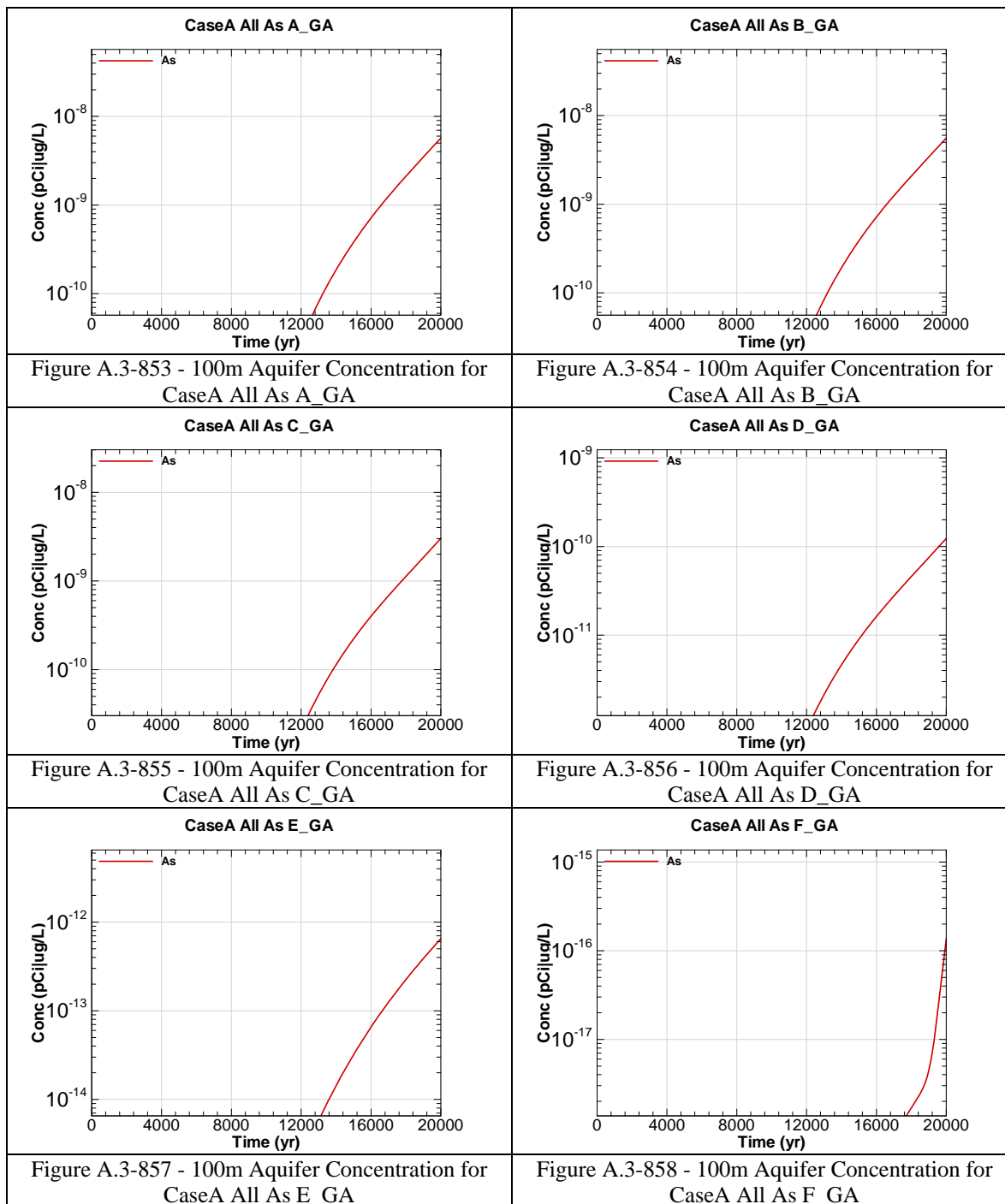


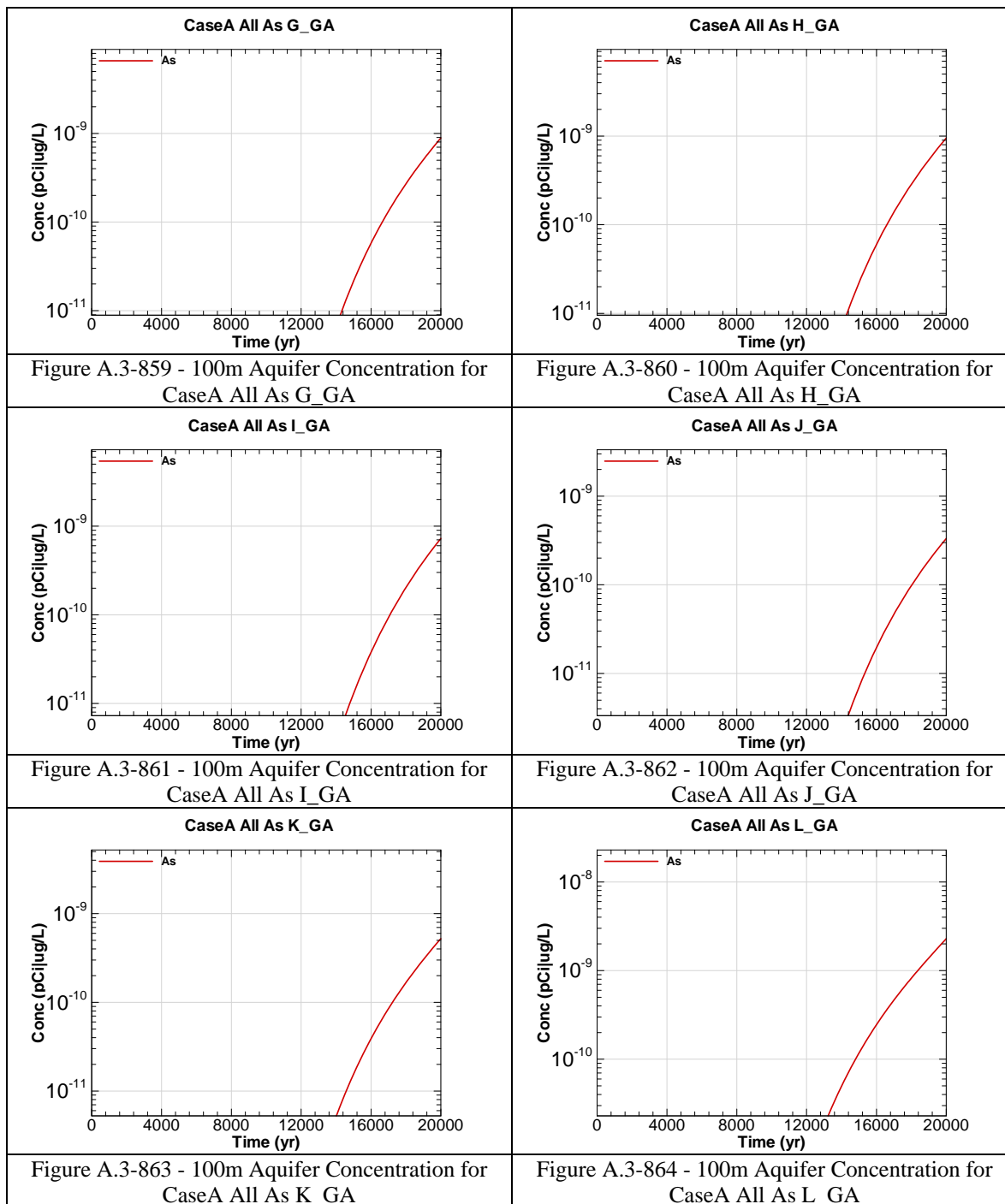
The chemical contaminants were modeled prior to the revision of the final closure inventory calculations presented in Table 3.3-8 for five chemical components: As, Cr, Cu, N and U. The figures that follow represent the concentrations calculated with an initial inventory input. The multipliers in the table below are to be used to determine the final concentrations with respect to time for the impacted chemicals as the inventory has a linear relationship with concentration in the Saltstone model. The groundwater concentration tables in Section 5 have been corrected using the multipliers.

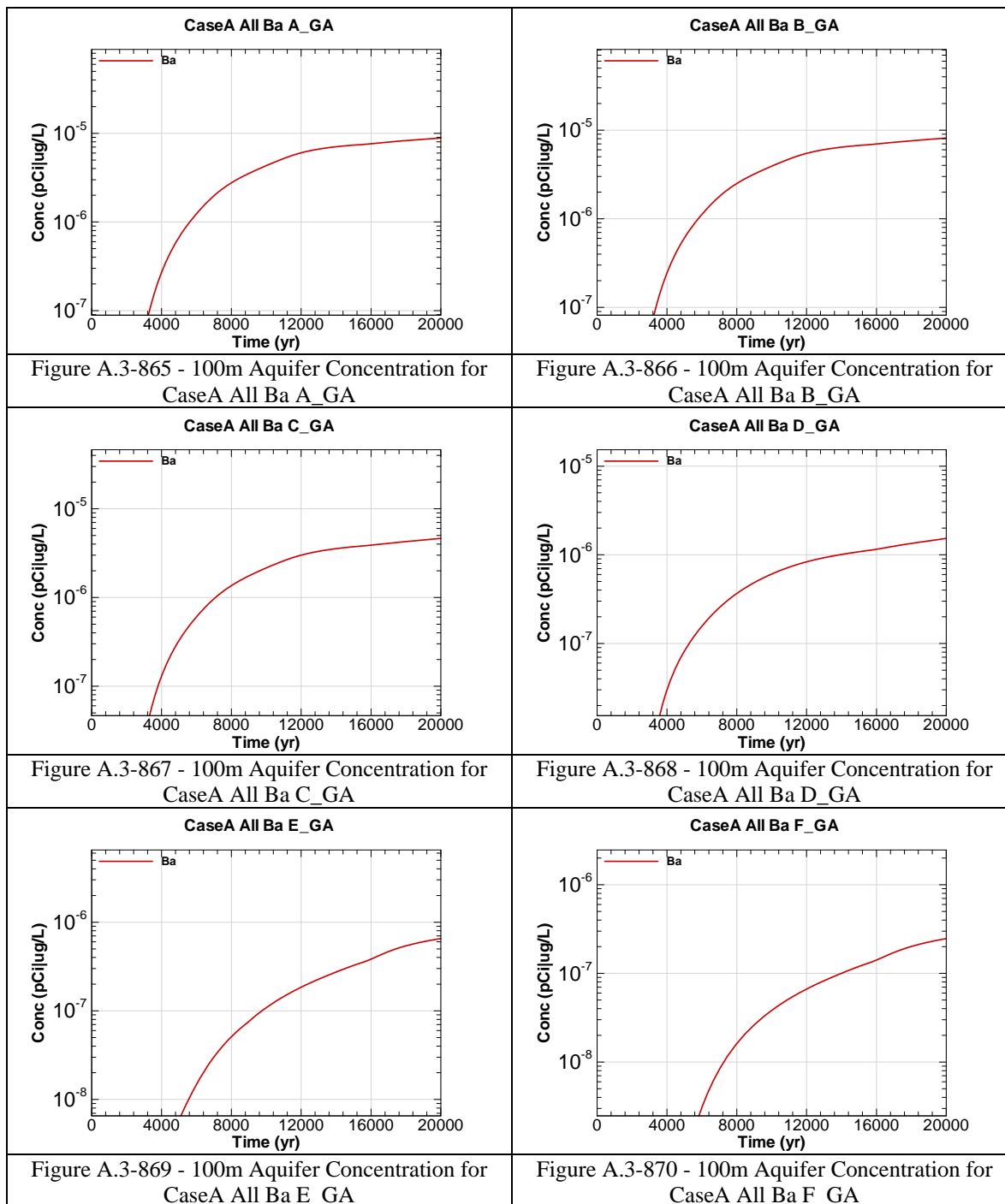
| Chemical Component | Modeled Inventory | Projected Inventory | Percent Increase | Multiplier |
|--------------------|-------------------|---------------------|------------------|------------|
| Ag | 8.8E+01 | 8.8E+01 | 0.0% | None |
| As | 1.08E+04 | 1.1E+04 | 2.3% | 1.02E+00 |
| Ba | 1.7E+02 | 1.7E+02 | 0.0% | None |
| Cd | 1.3E+03 | 1.3E+03 | 0.0% | None |
| Cr | 2.9E+04 | 3.0E+04 | 1.4% | 1.01E+00 |
| Cu | 1.9E+04 | 1.9E+04 | 0.9% | 1.01E+00 |
| F | 1.7E+04 | 1.7E+04 | 0.0% | None |
| Fe | 2.9E+03 | 2.9E+03 | 0.0% | None |
| Hg | 1.1E+04 | 1.1E+04 | 0.0% | None |
| Mn | 7.3E+03 | 7.3E+03 | 0.0% | None |
| Ni | 1.5E+03 | 1.5E+03 | 0.0% | None |
| Total N | 2.2E+07 | 2.4E+07 | 5.8% | 1.06E+00 |
| Pb | 6.7E+03 | 6.7E+03 | 0.0% | None |
| Se | 4.0E+04 | 4.0E+04 | 0.0% | None |
| U | 8.2E+02 | 8.9E+02 | 8.9% | 1.10E+00 |
| Zn | 2.7E+04 | 2.7E+04 | 0.0% | None |

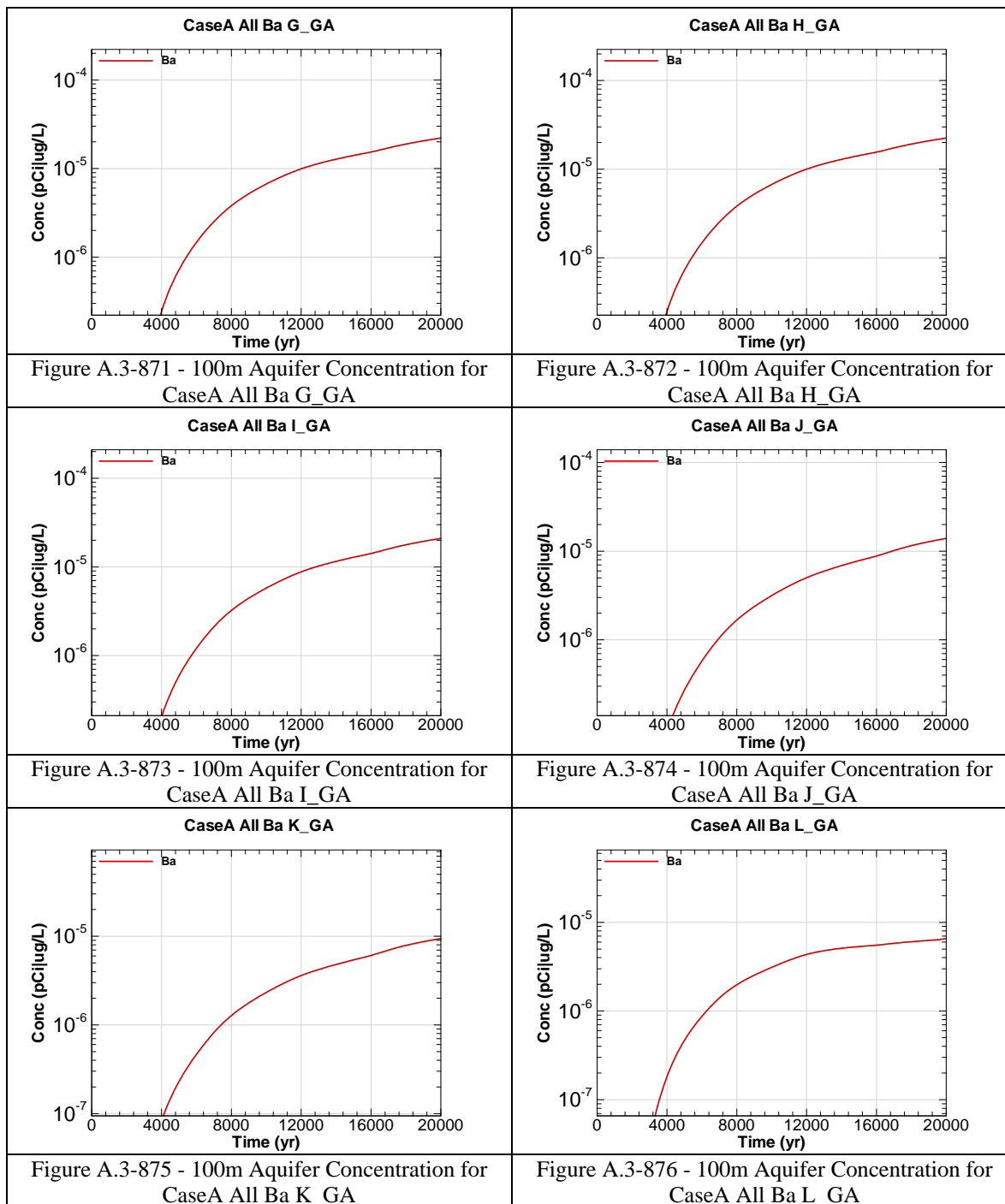


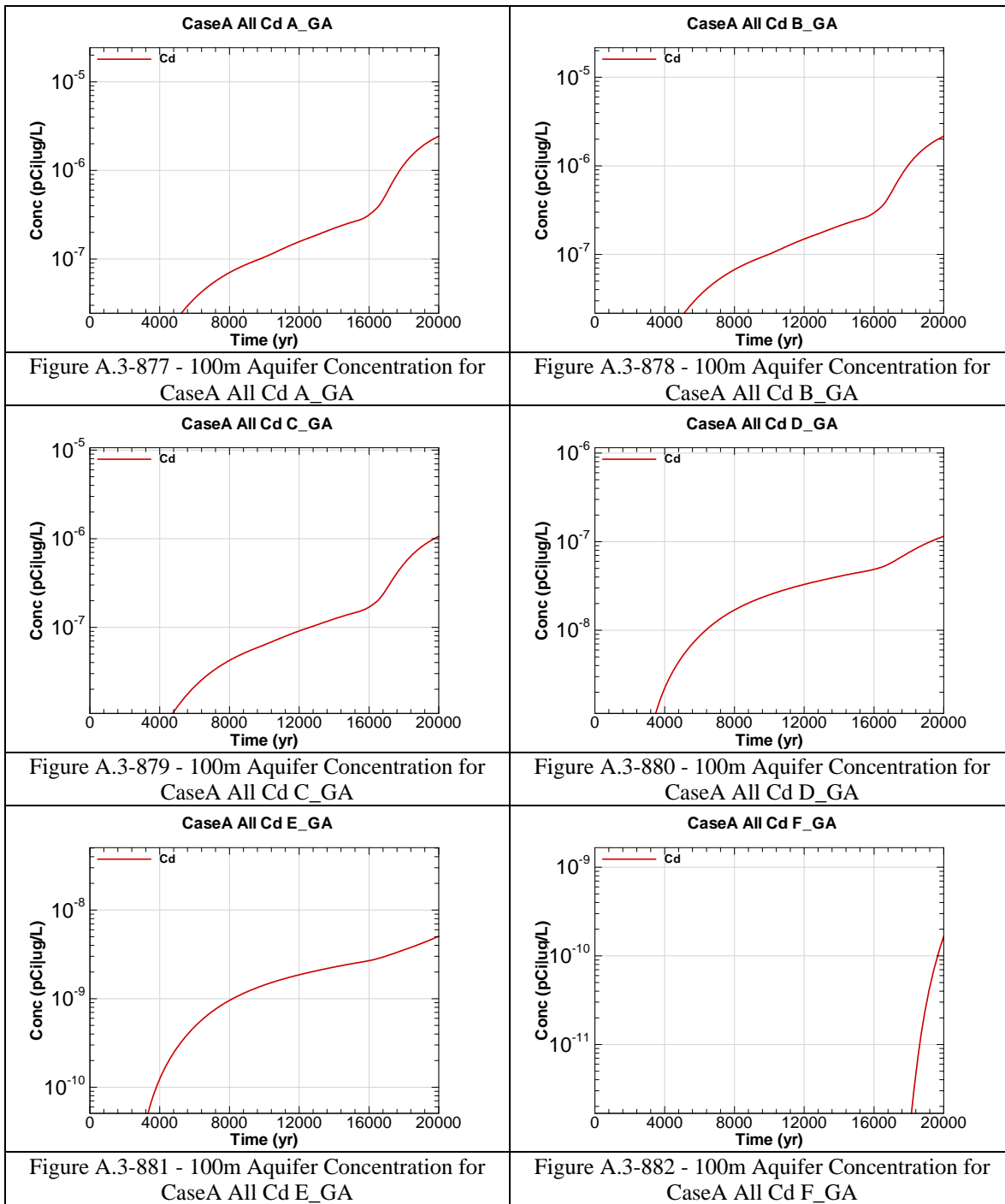


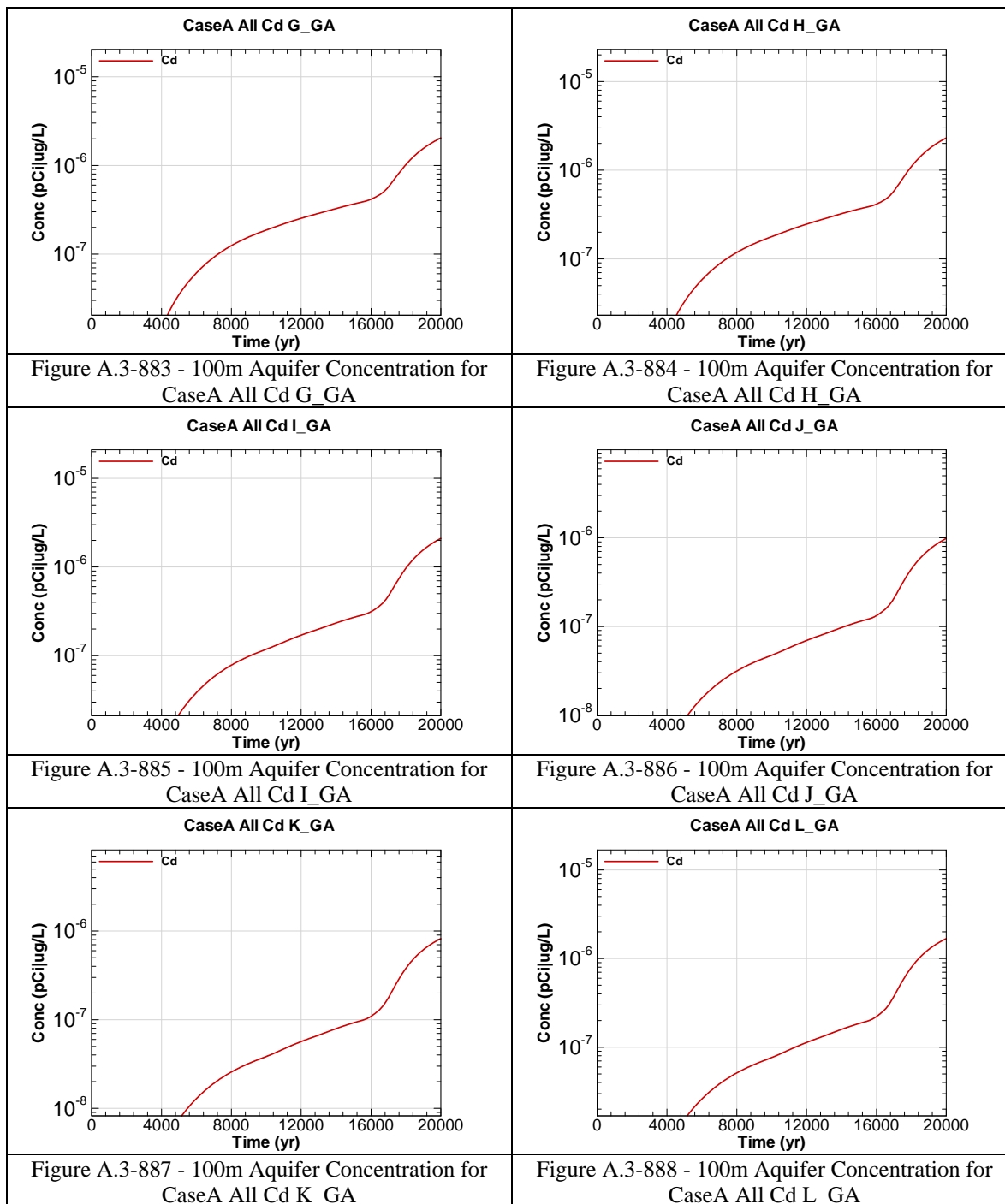


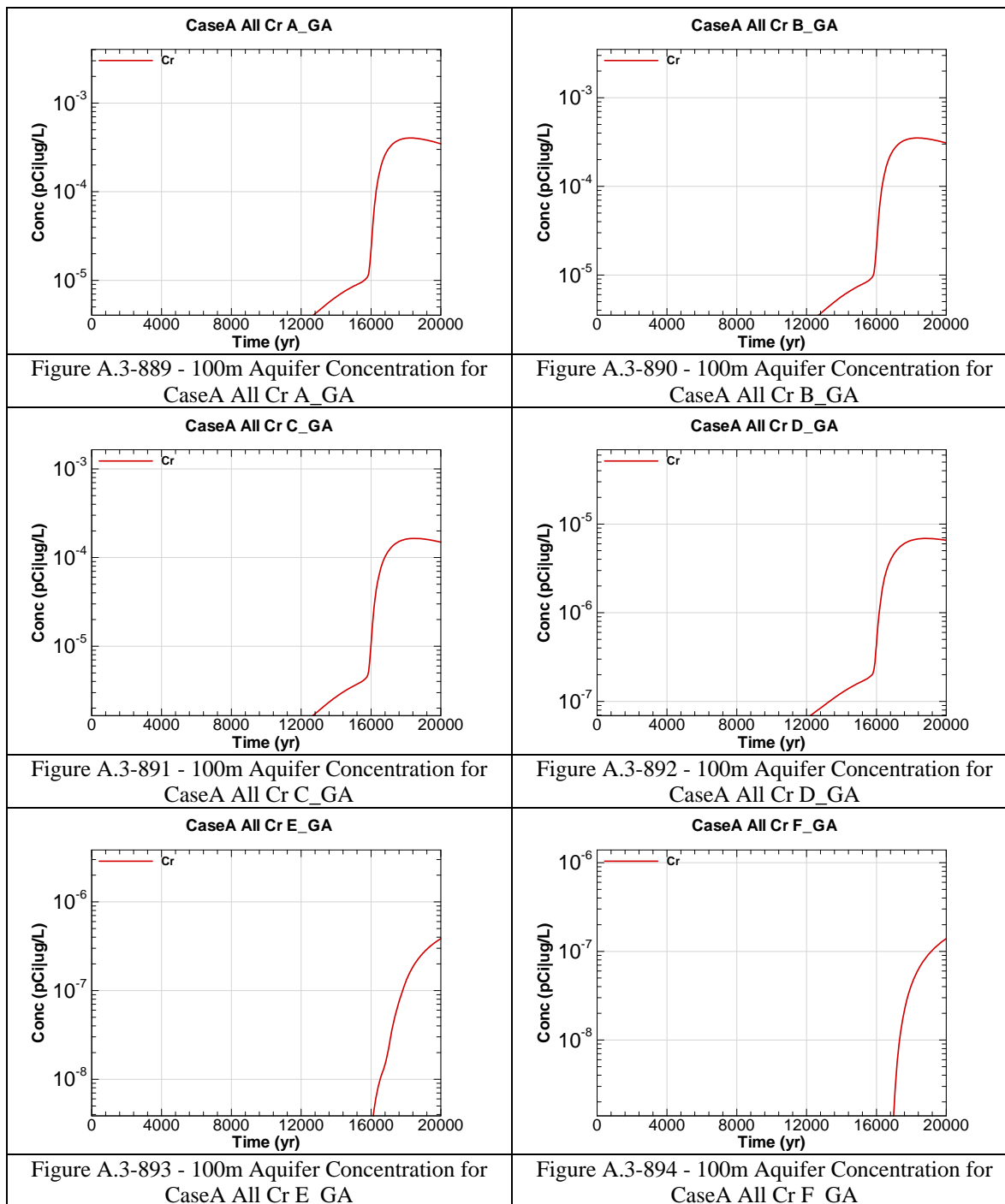


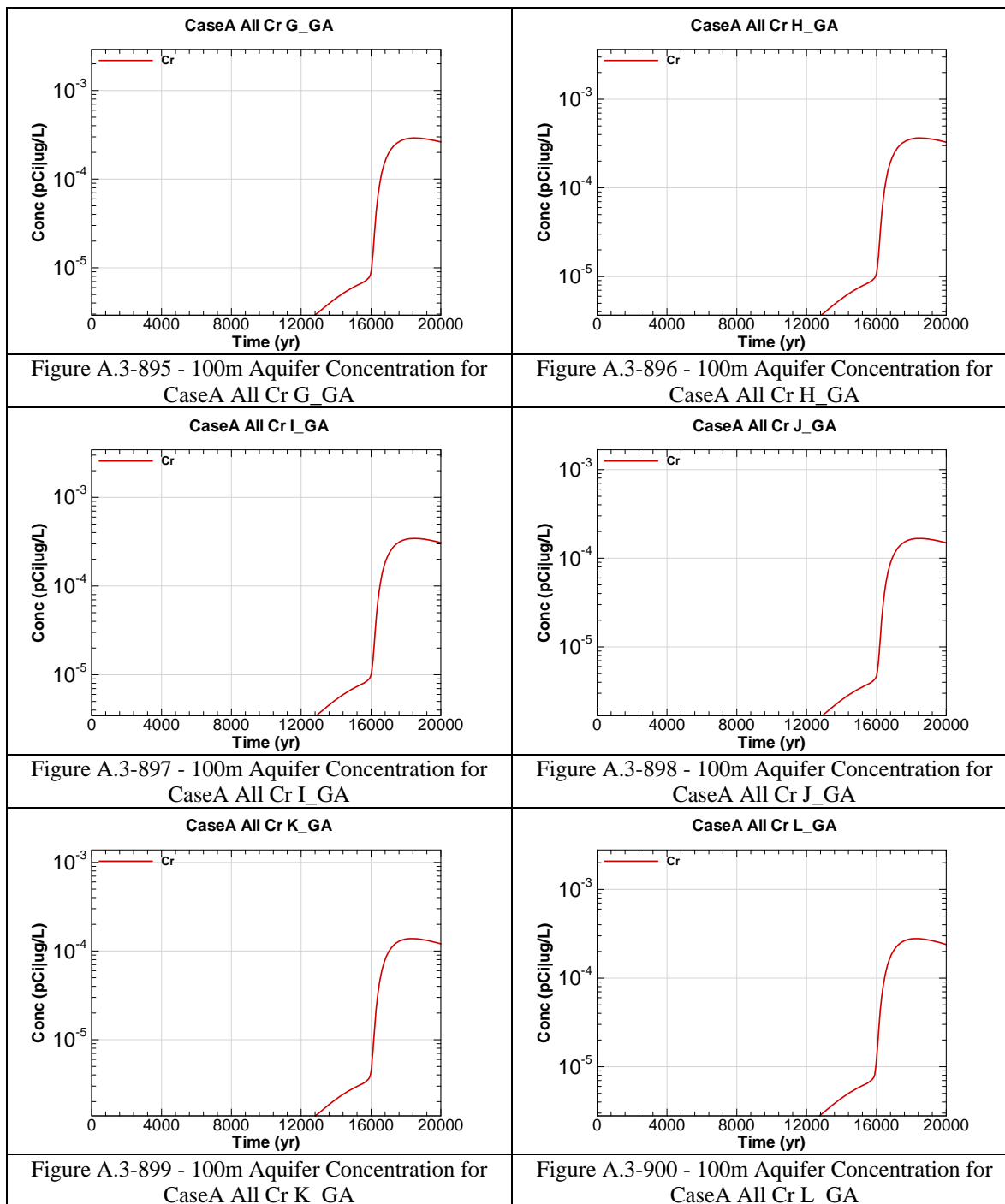


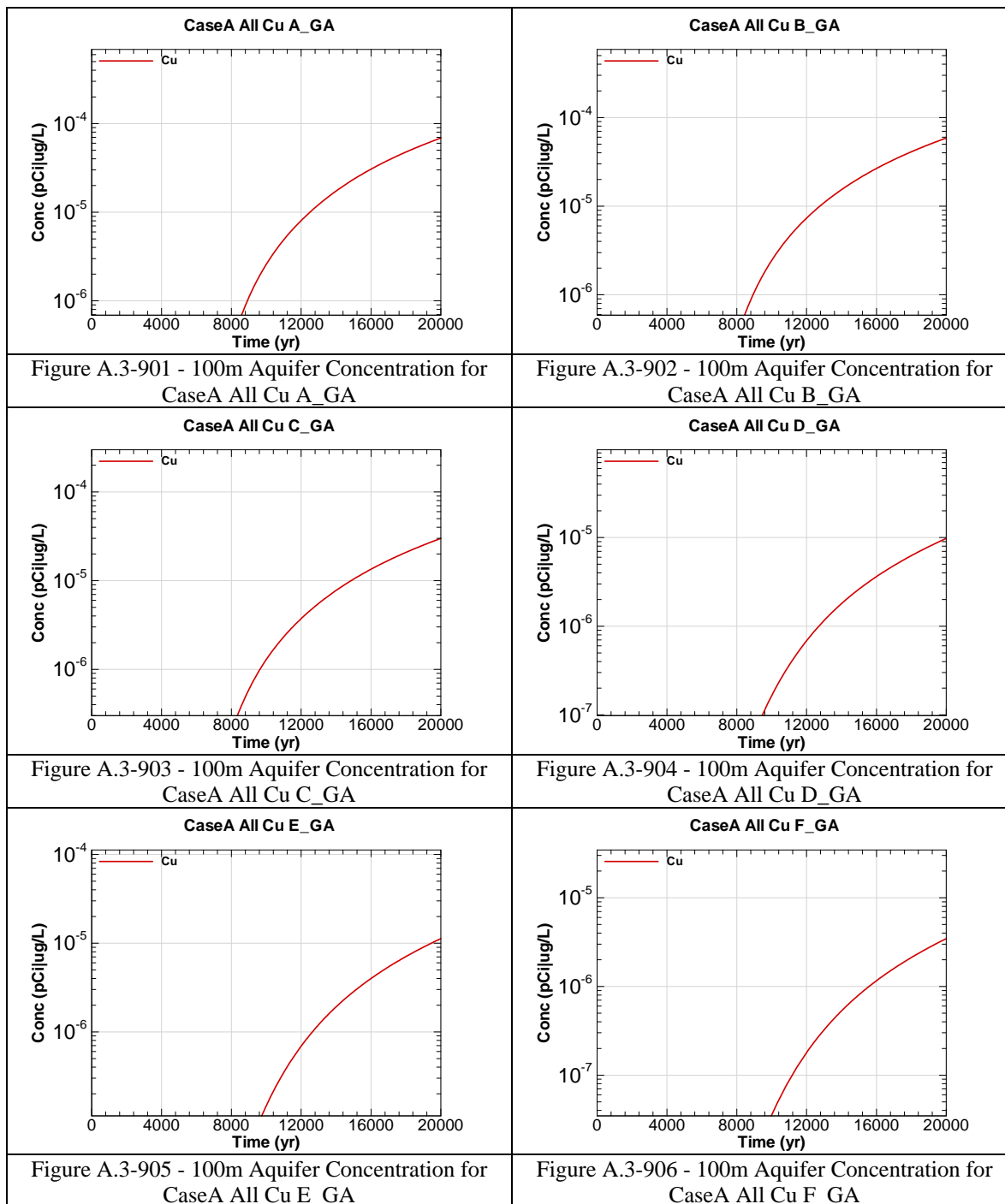


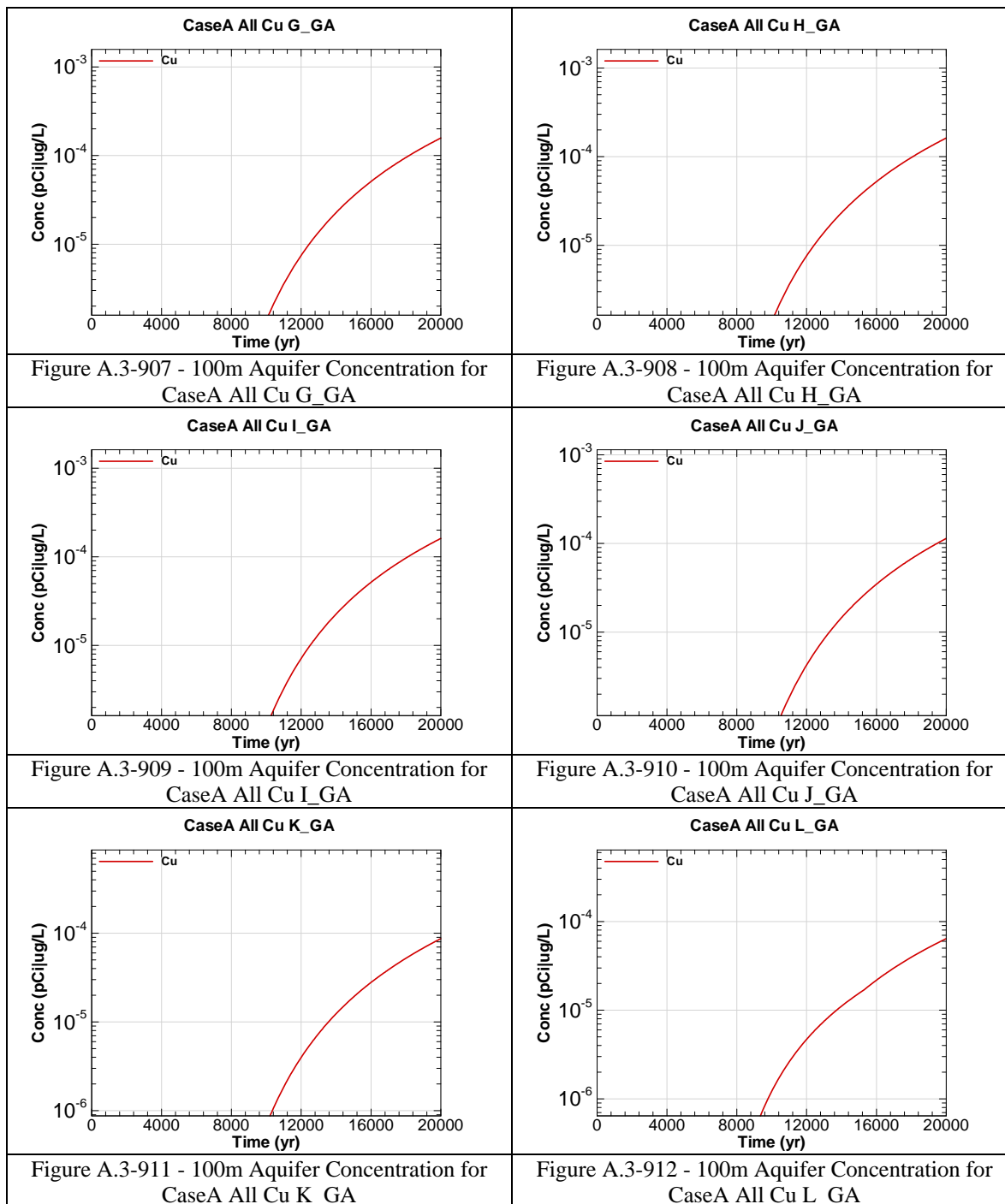


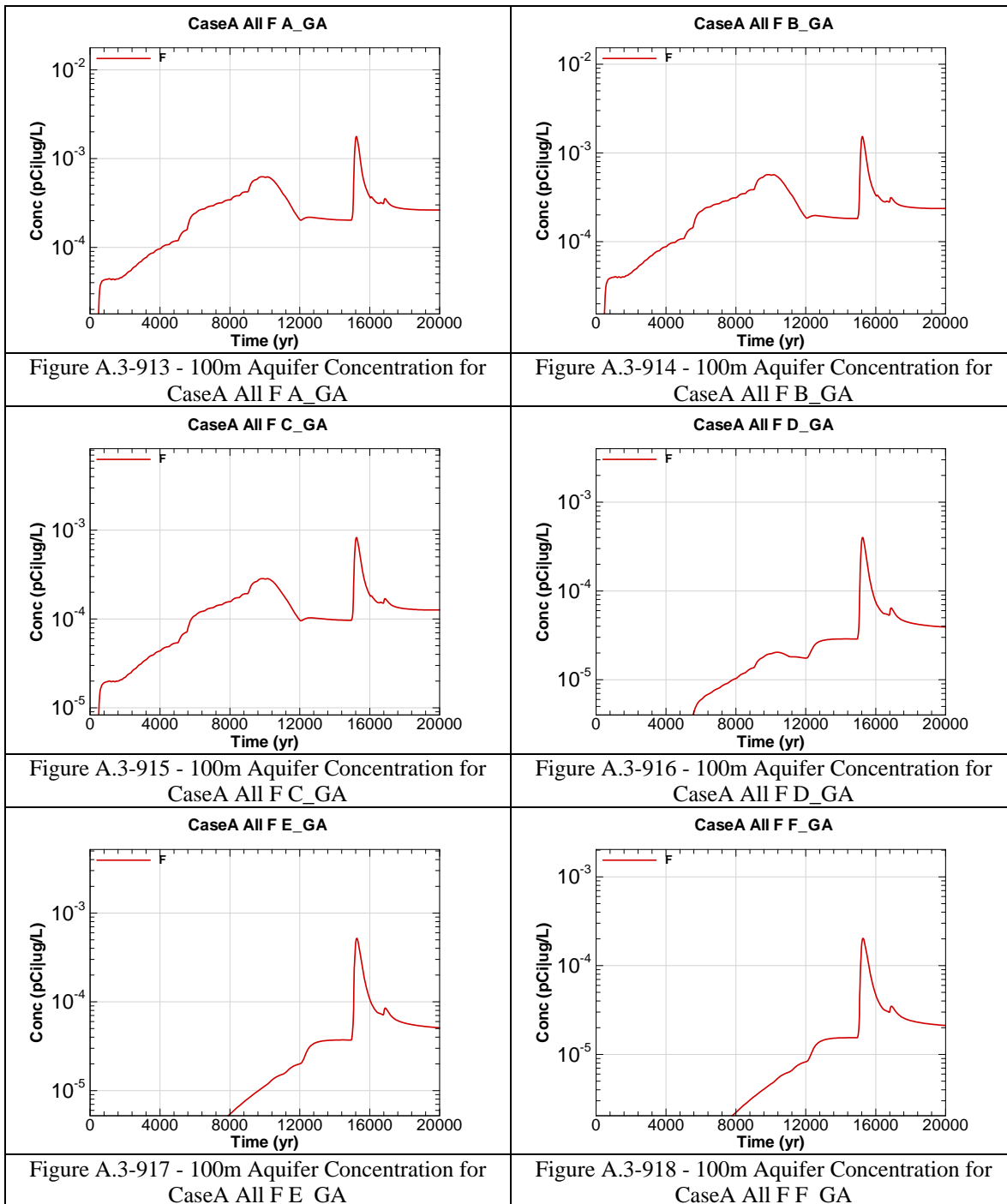


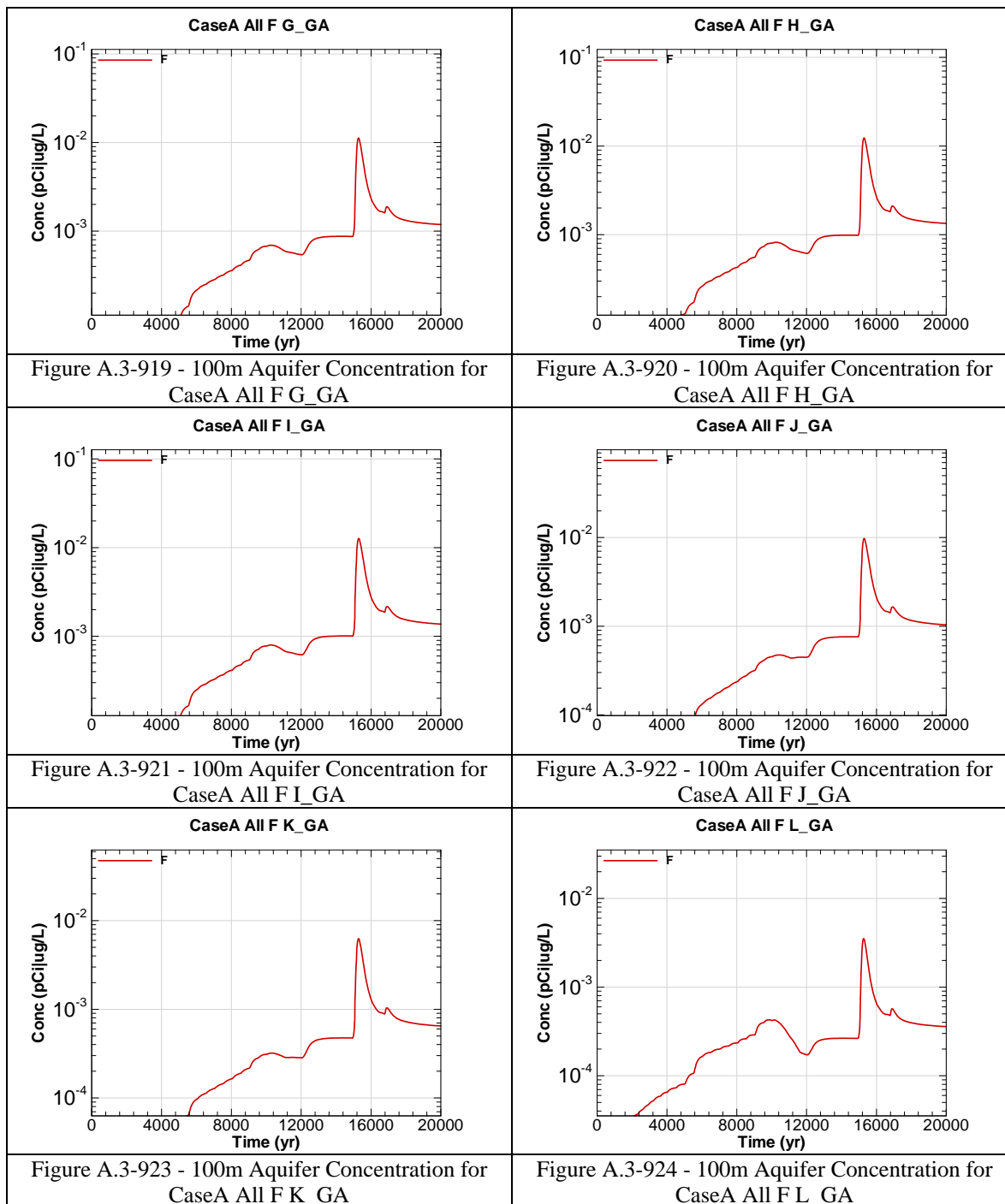


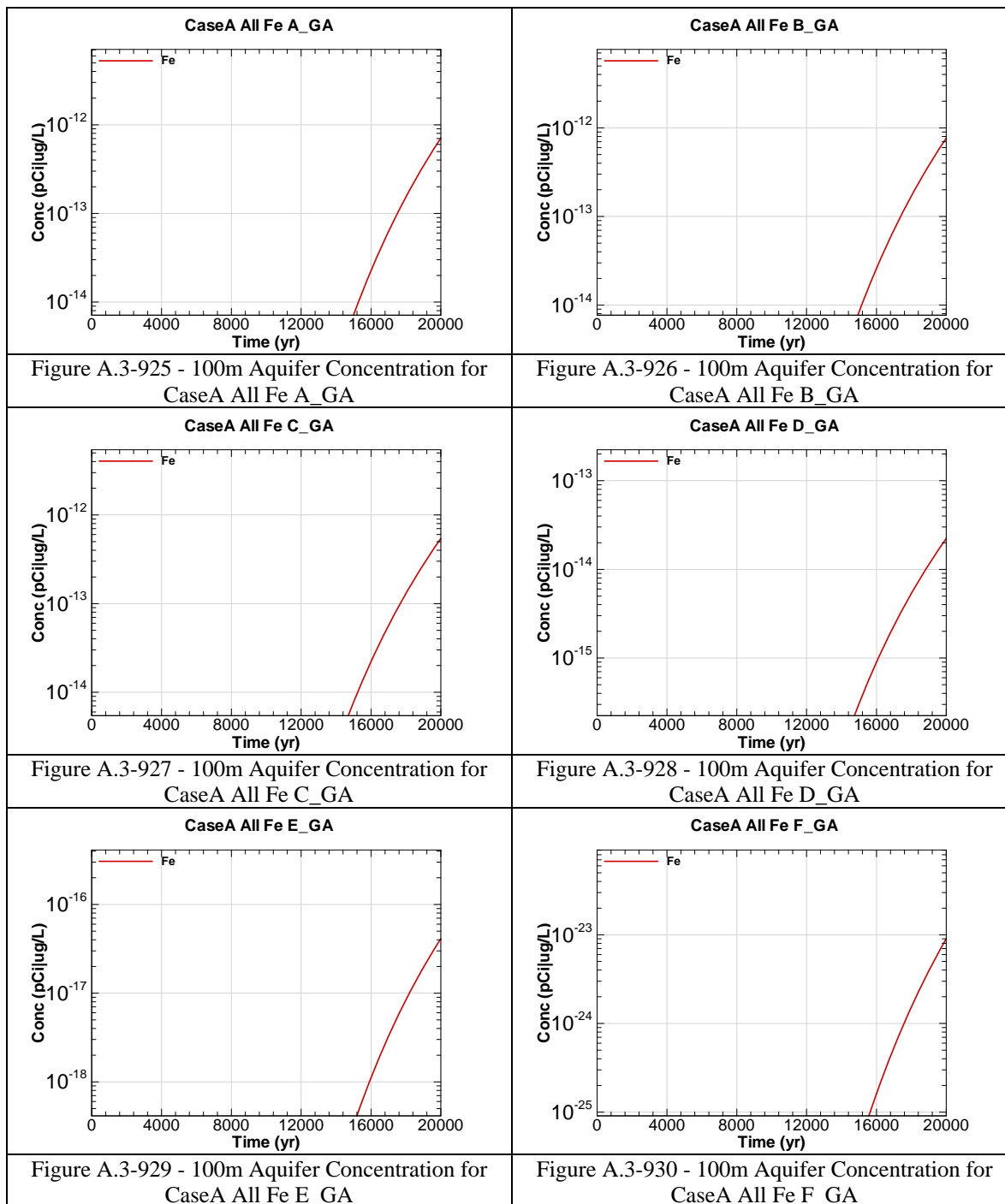


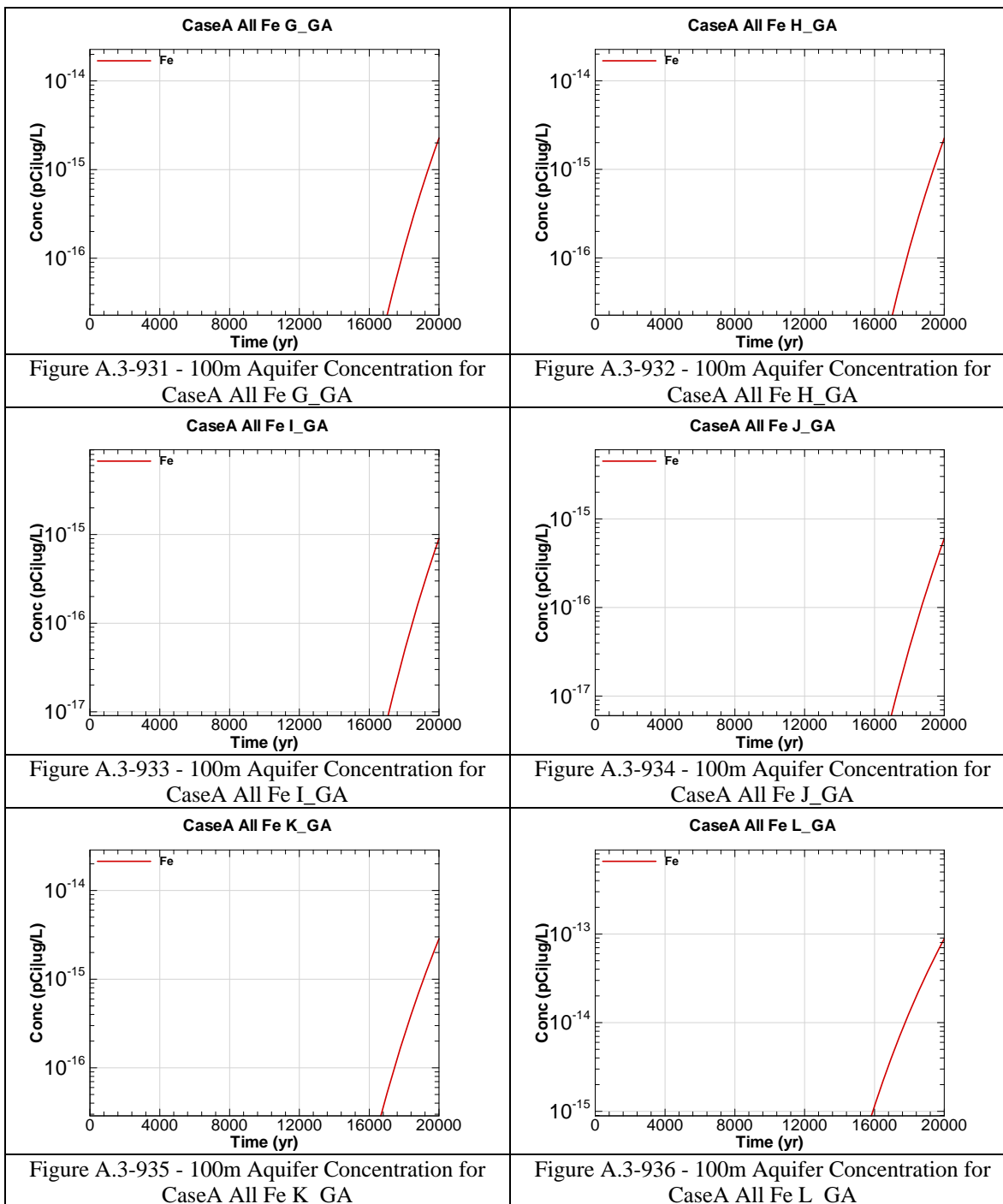


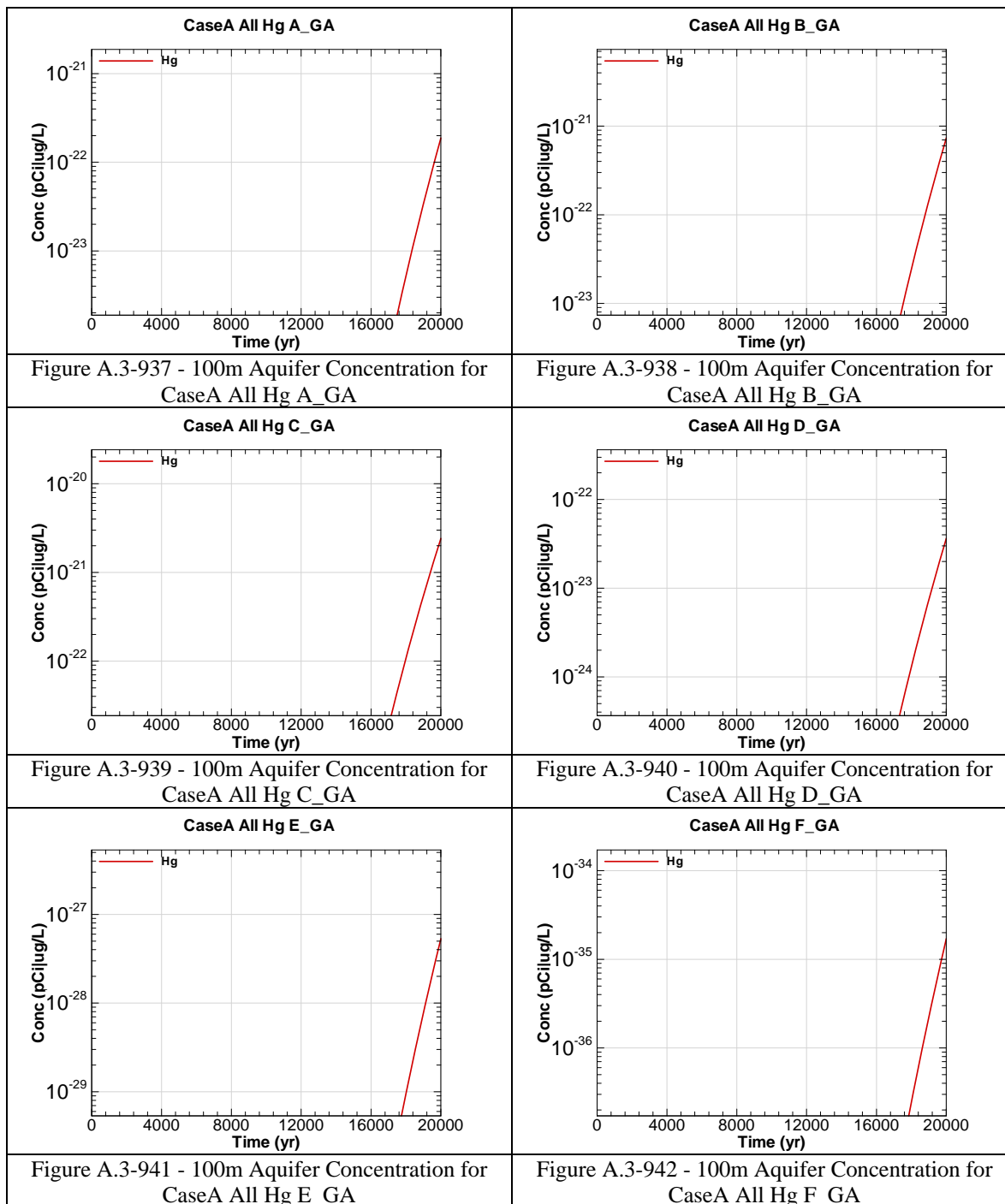


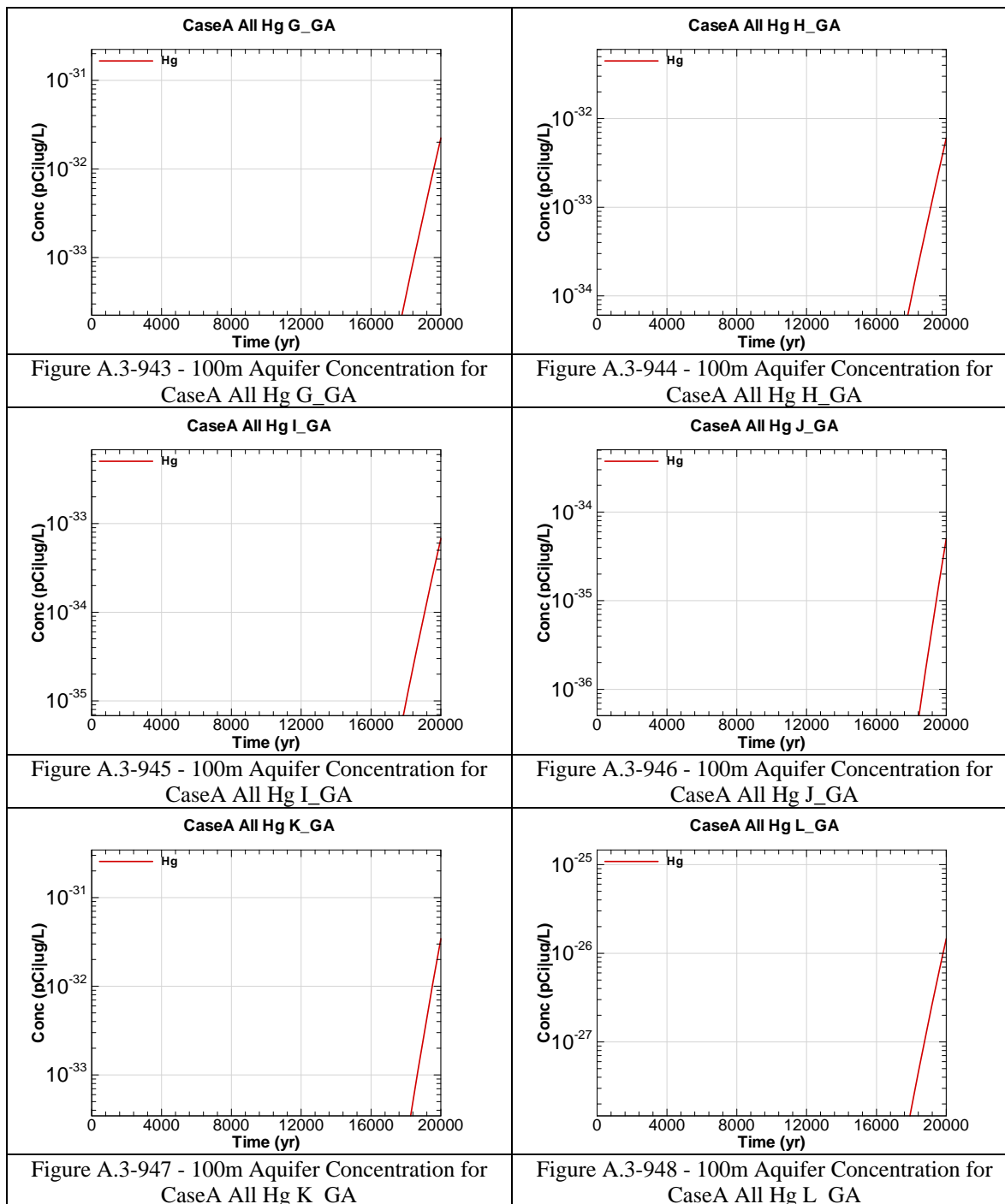


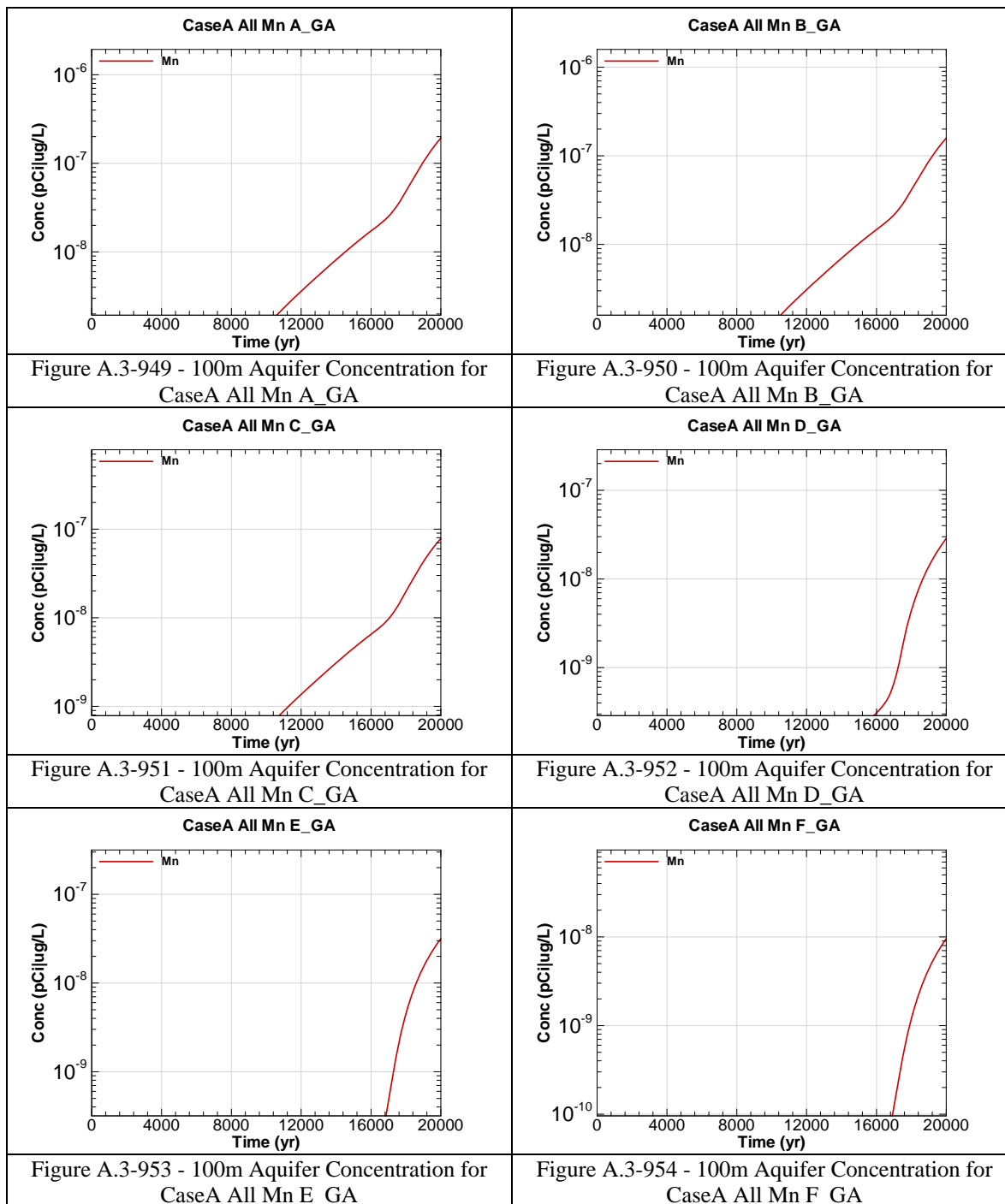


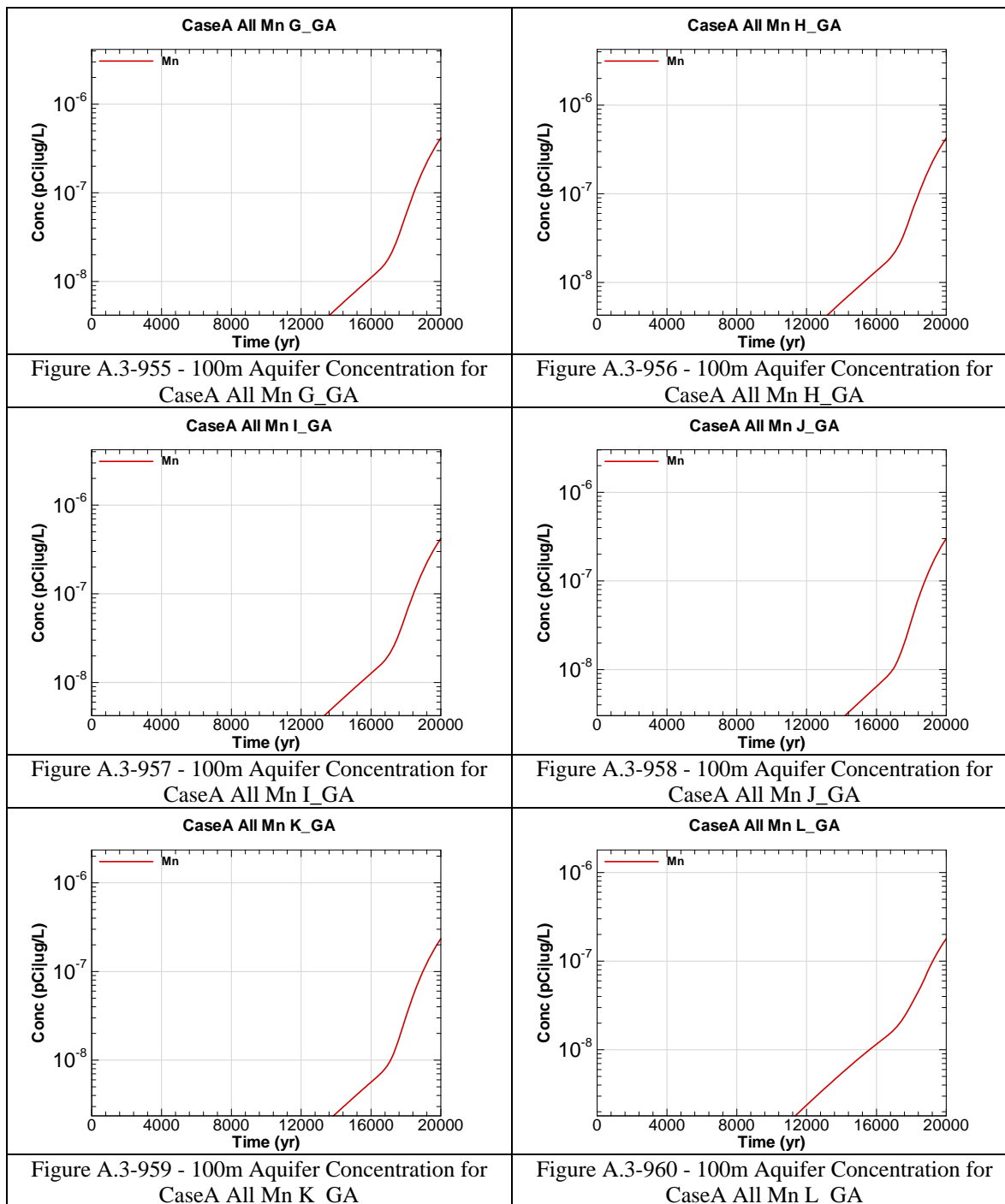


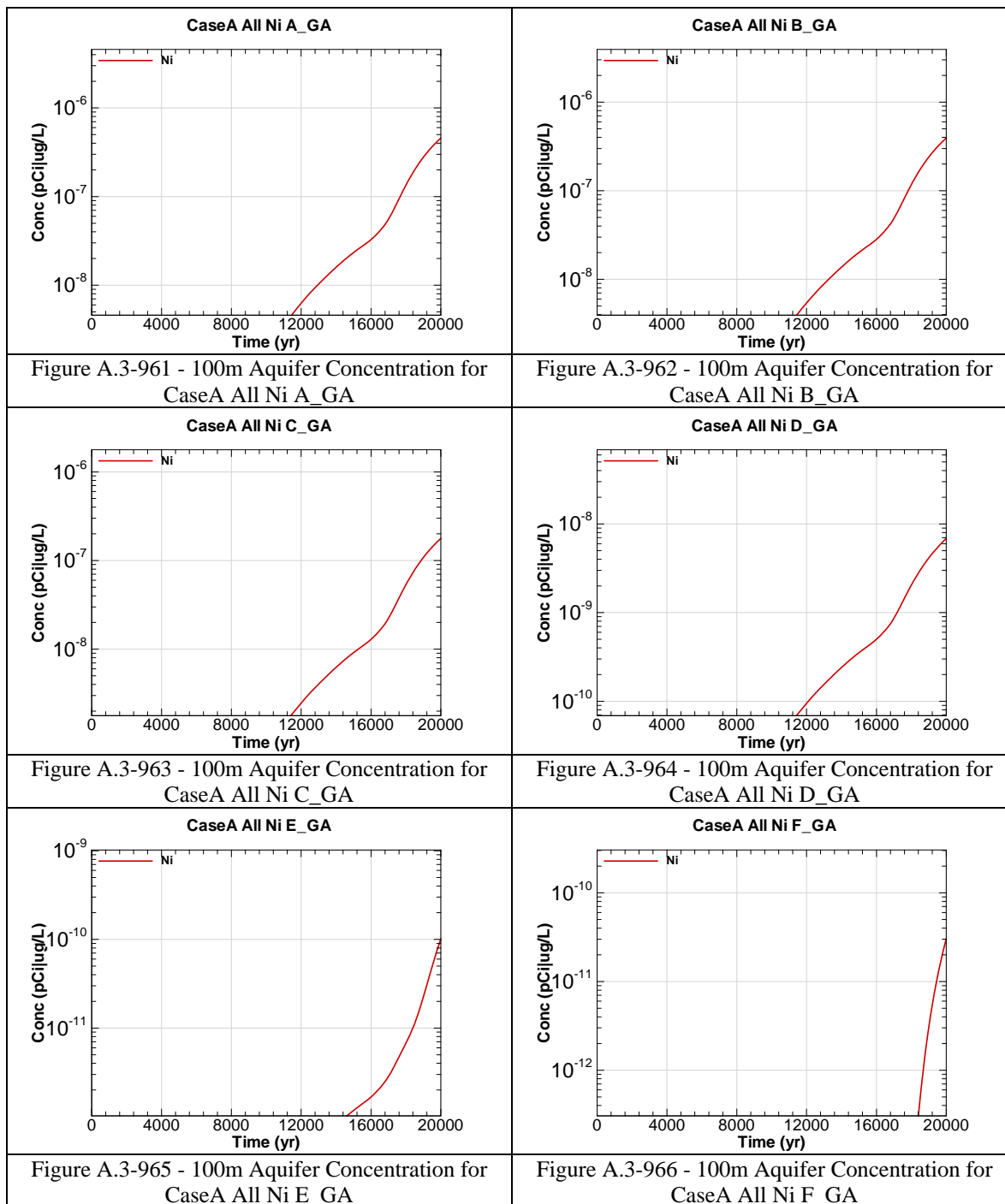


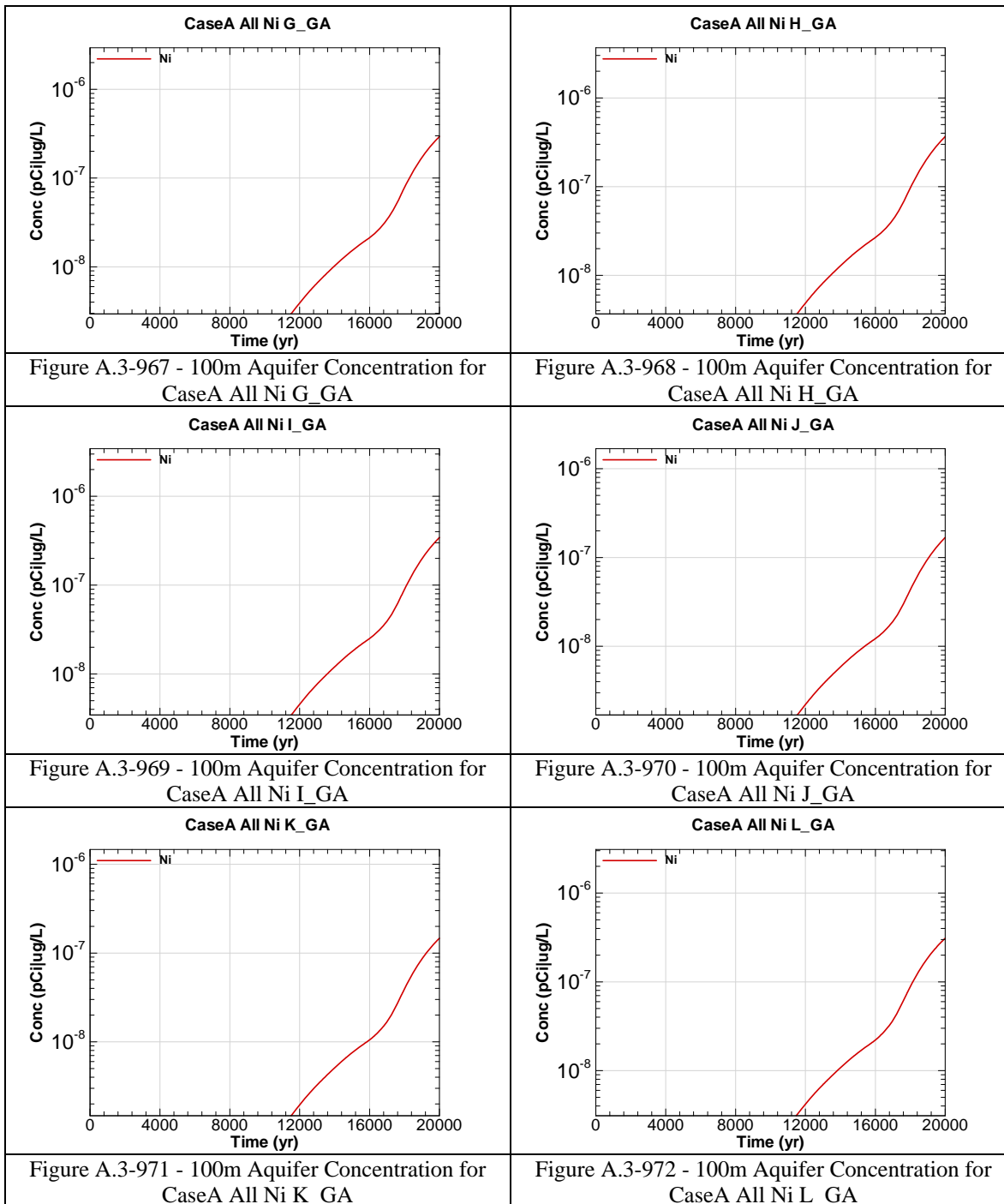


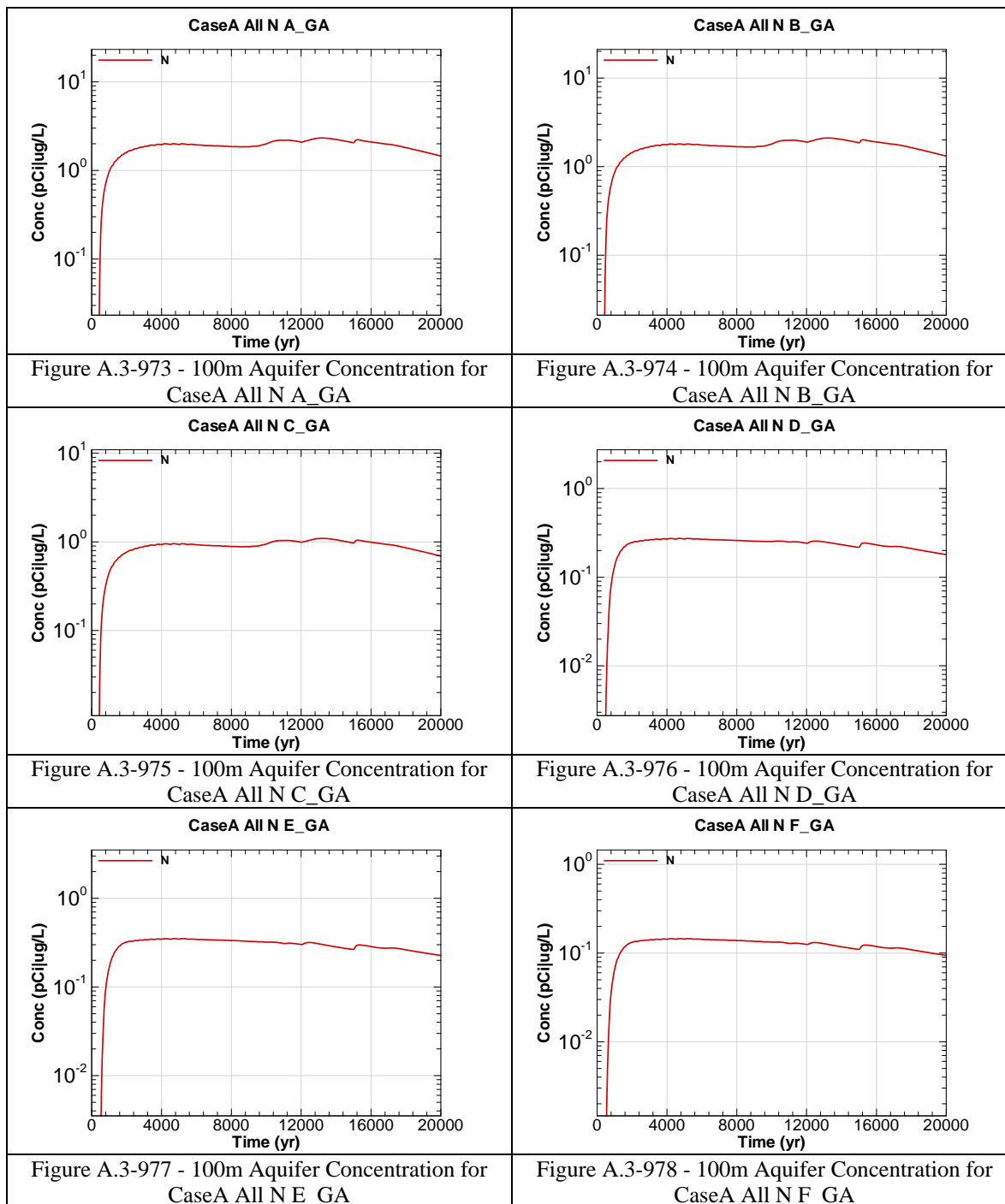


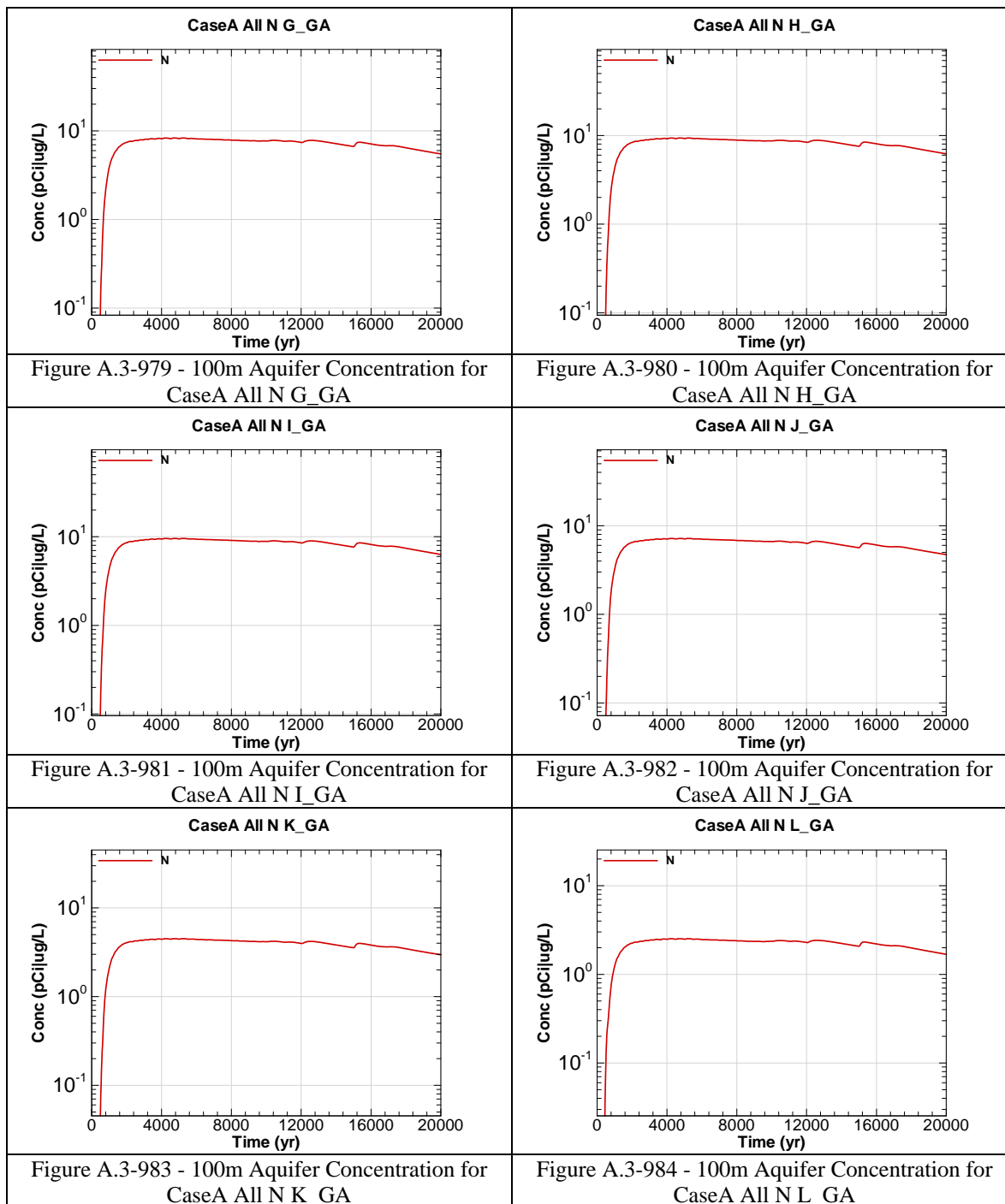


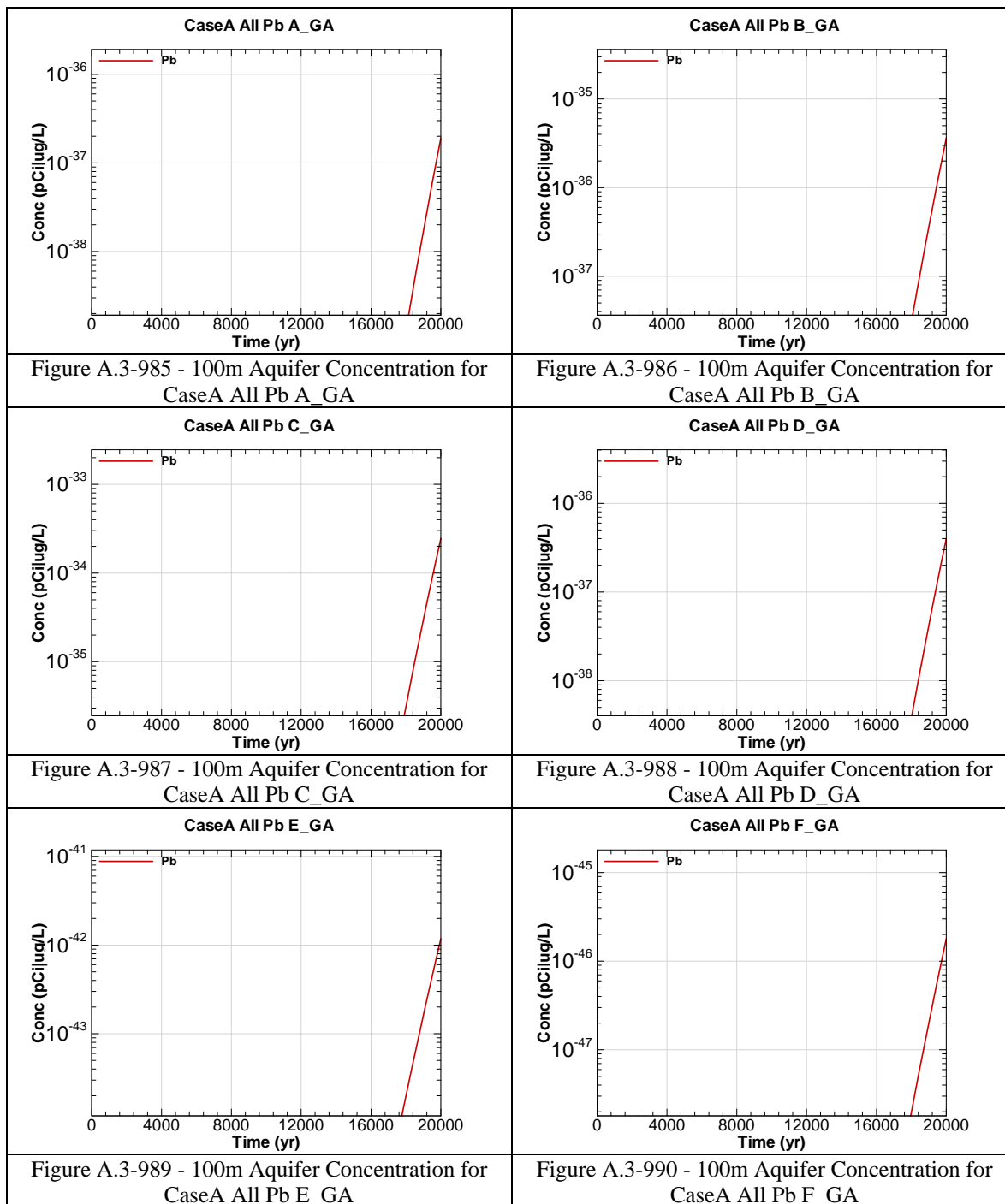


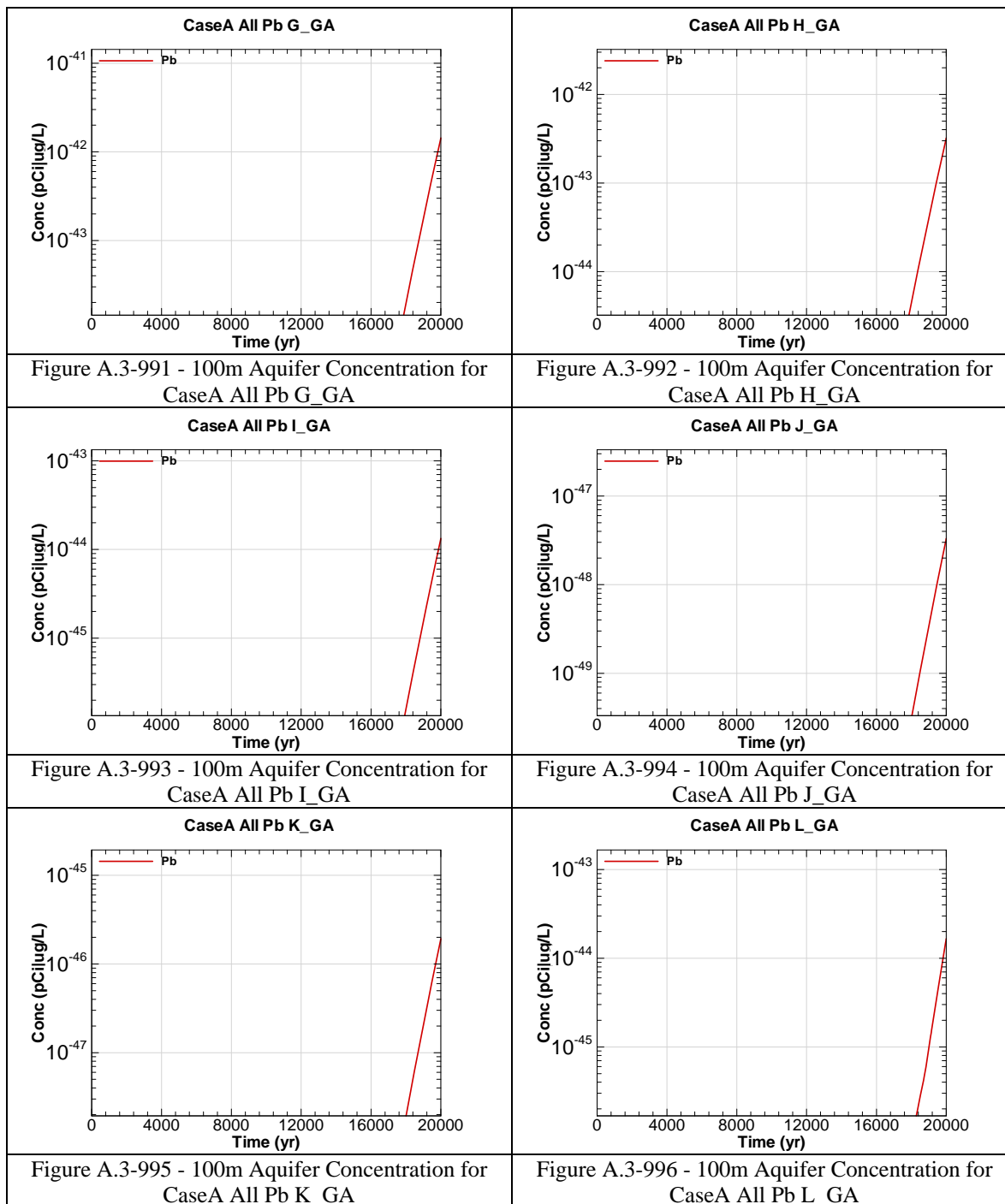


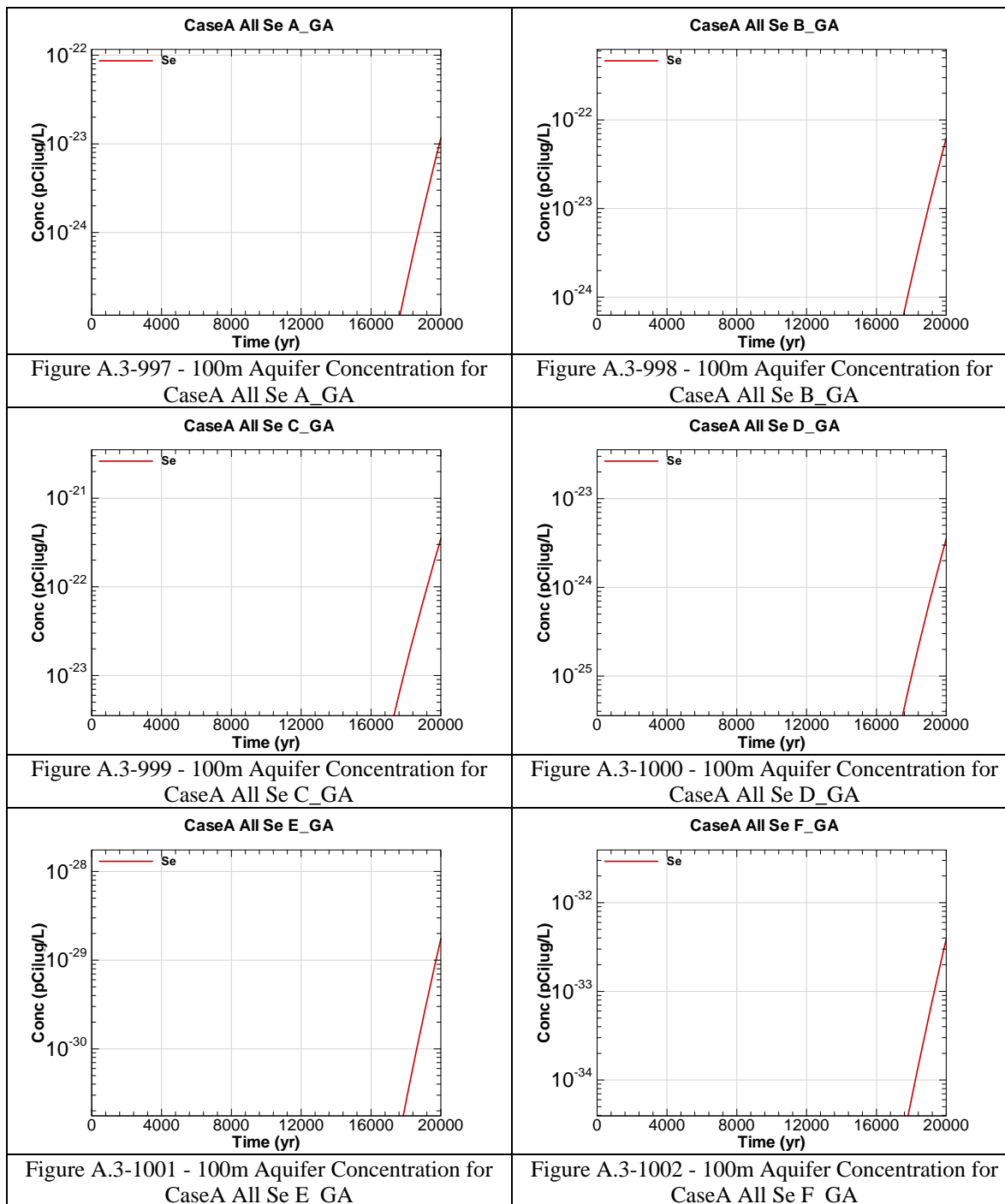


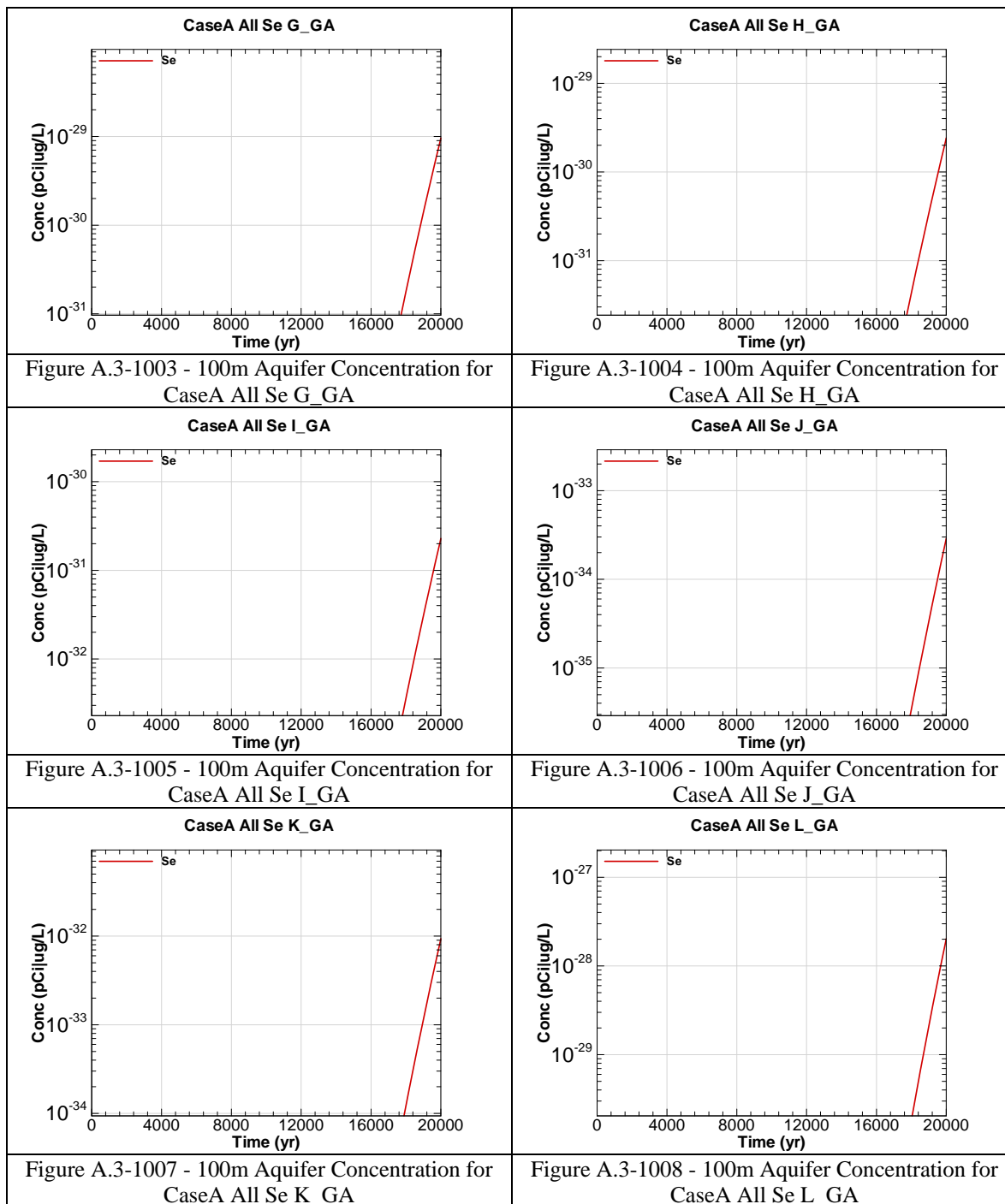


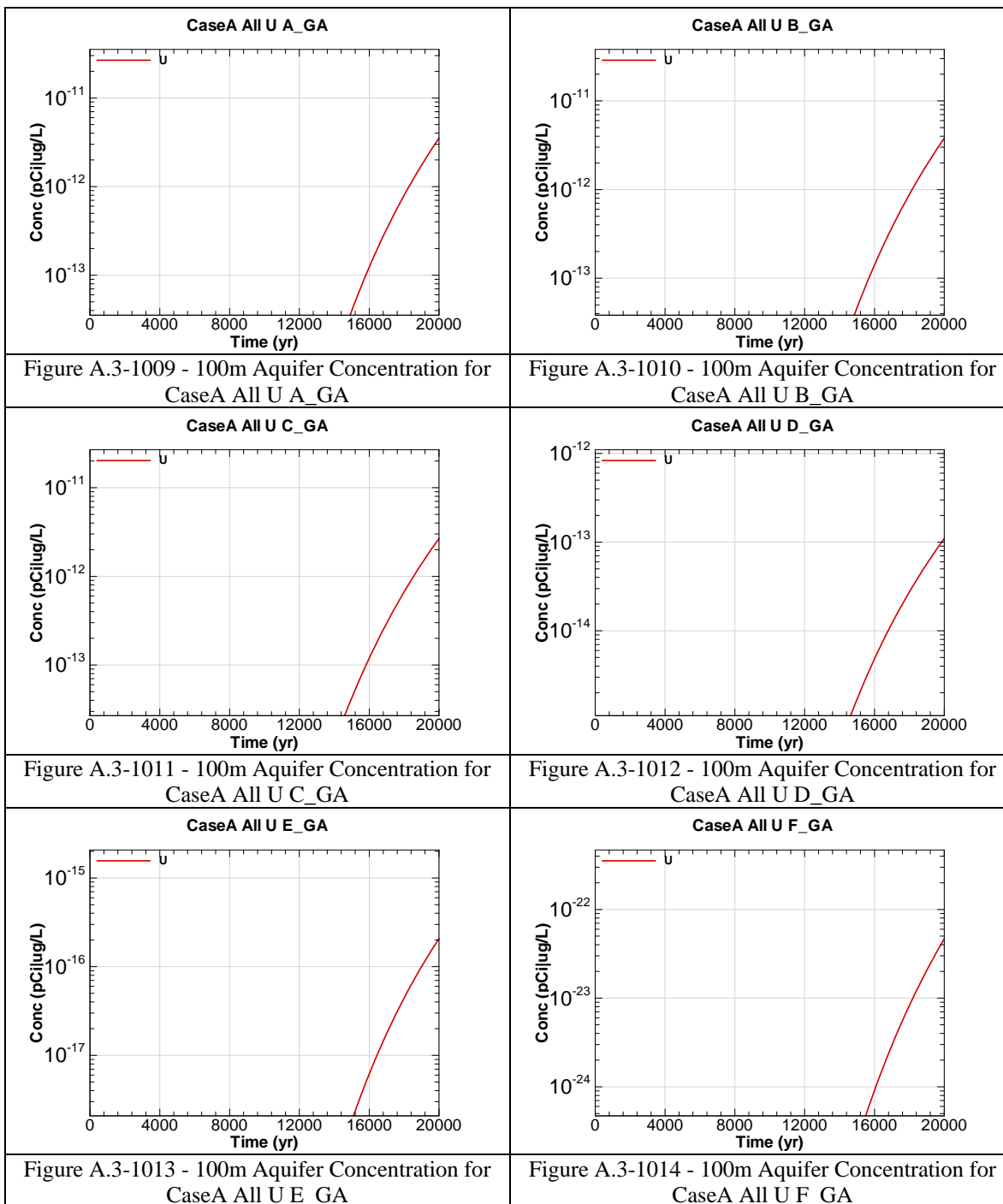


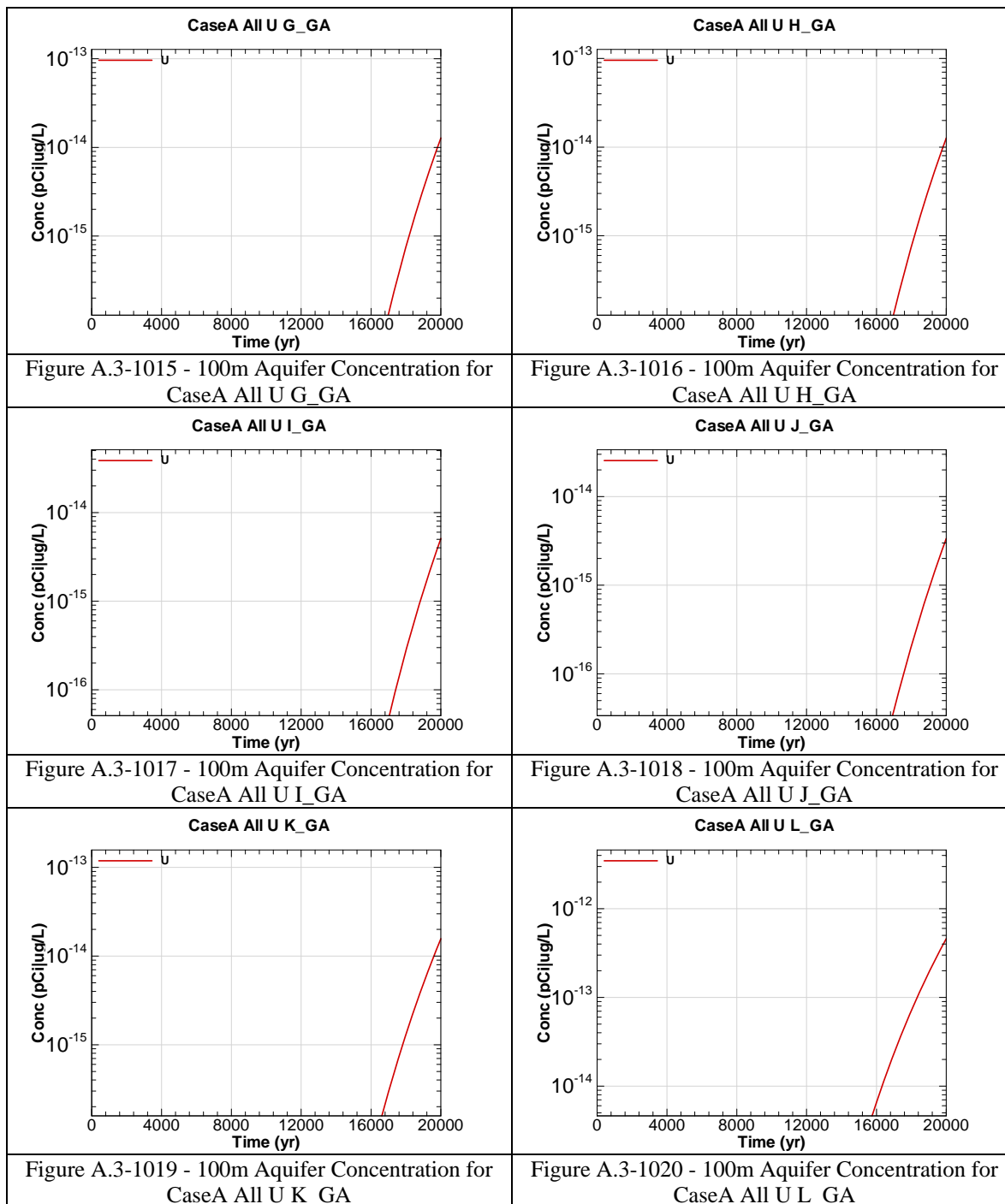


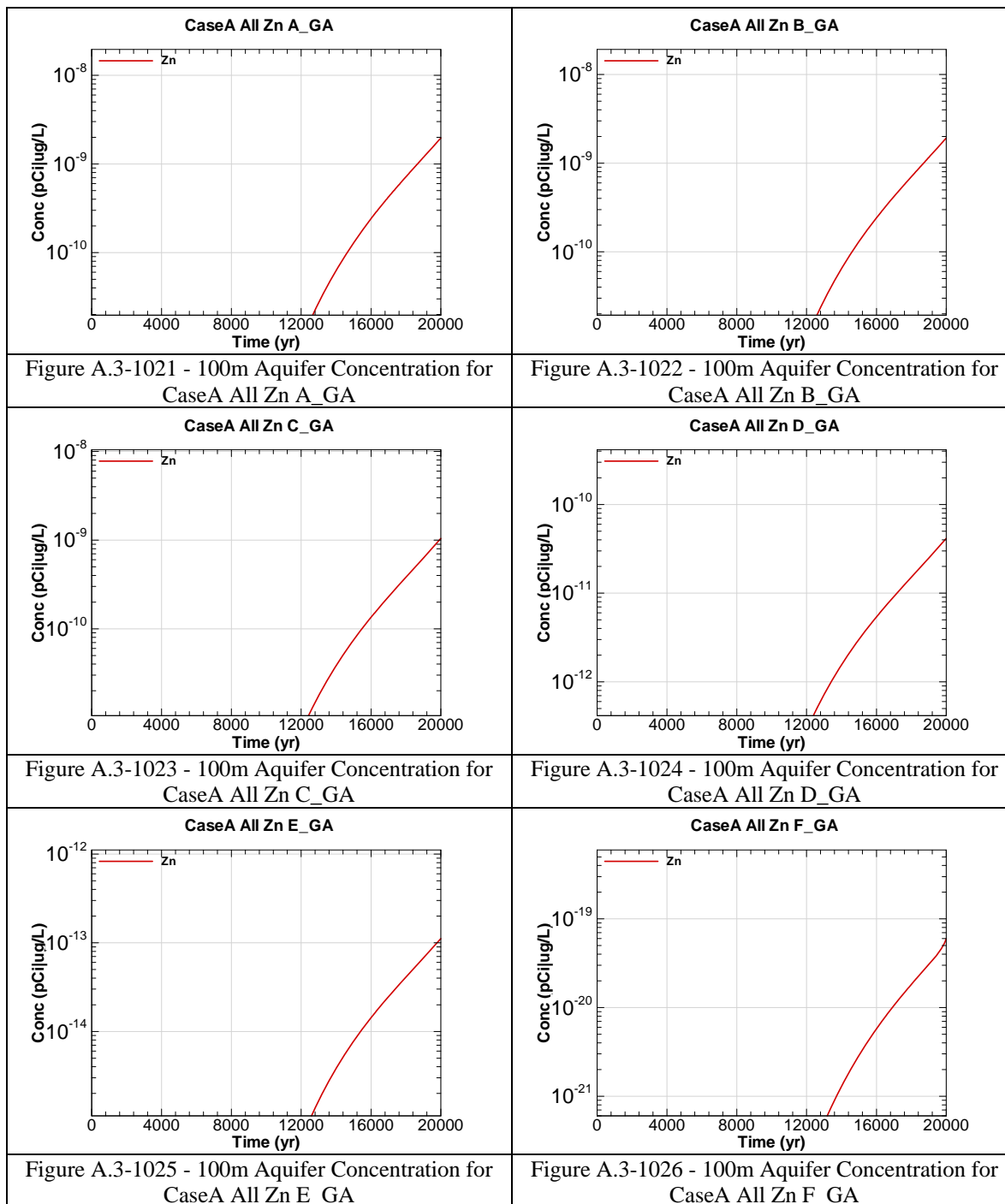


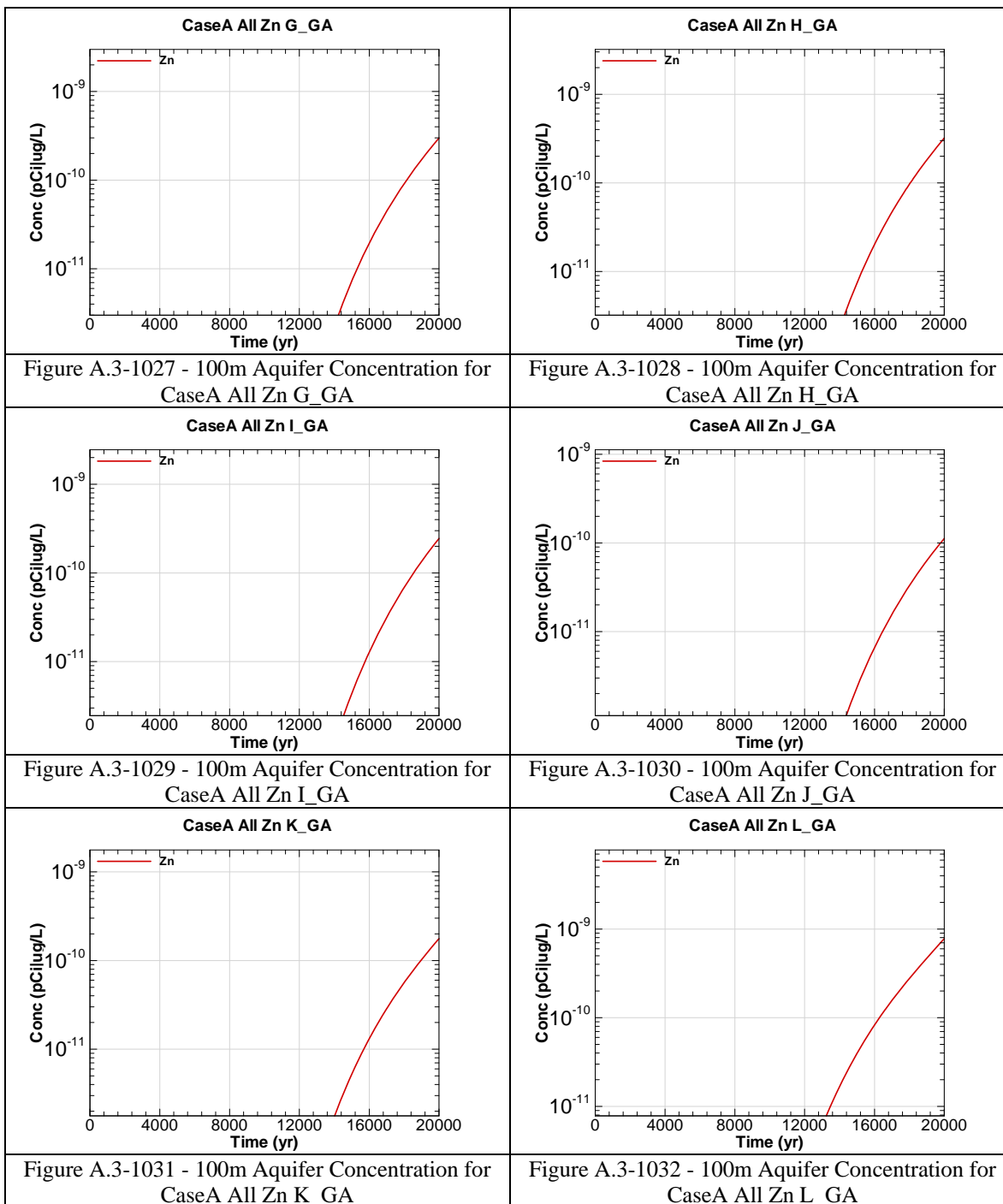












APPENDIX A.4

100-METER RADIOLOGICAL AND CHEMICAL CONCENTRATIONS – CASE B

Appendix A.4 contains curves showing the 100 meter key radiological and chemical concentrations for all of SDF (vault and FDC inventories) for Case B. 20,000 year concentration results are presented for Sectors A through L for the peak concentration per sector regardless of aquifer.

Graph heading example “CaseB All I-129 A”

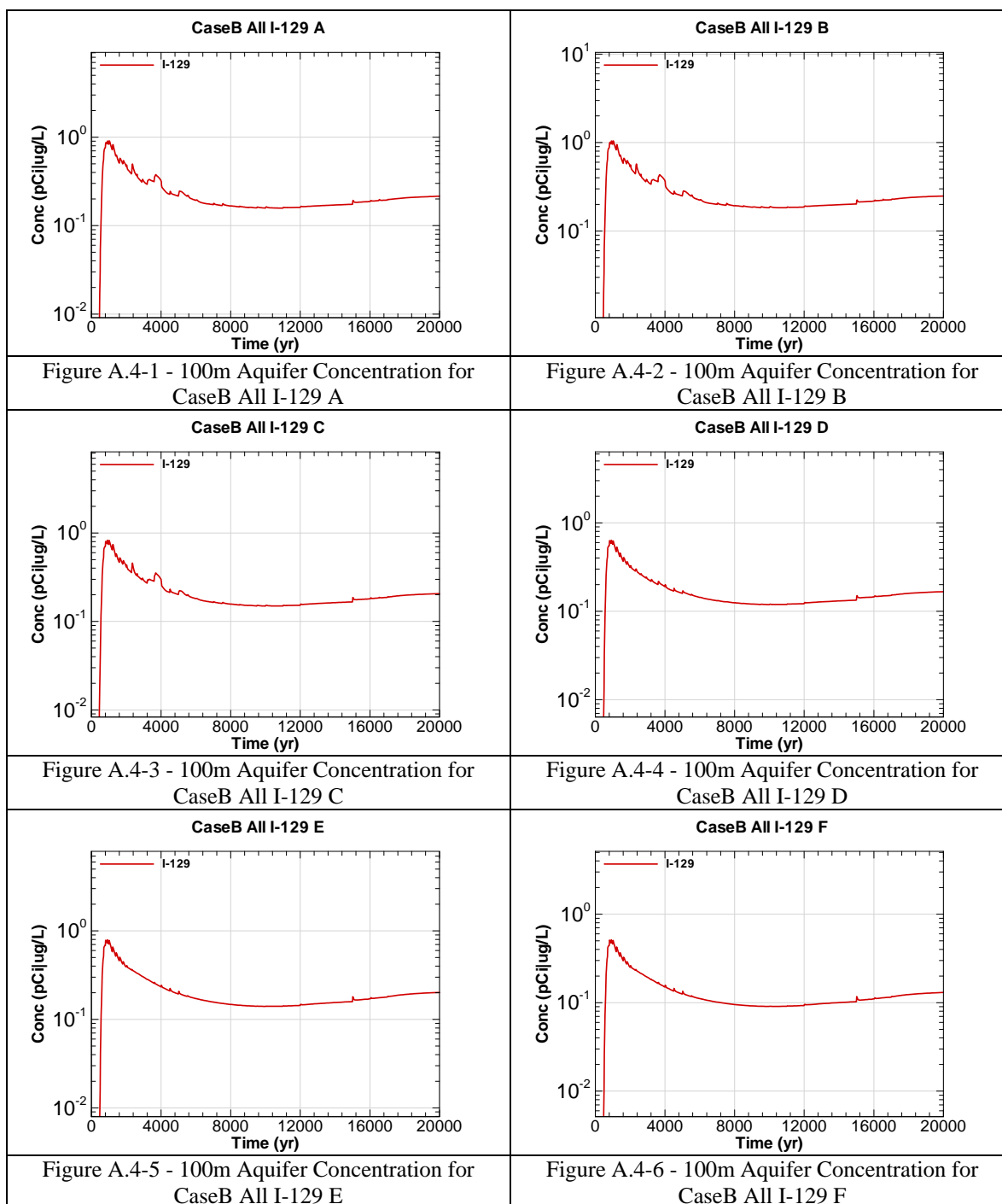
Key

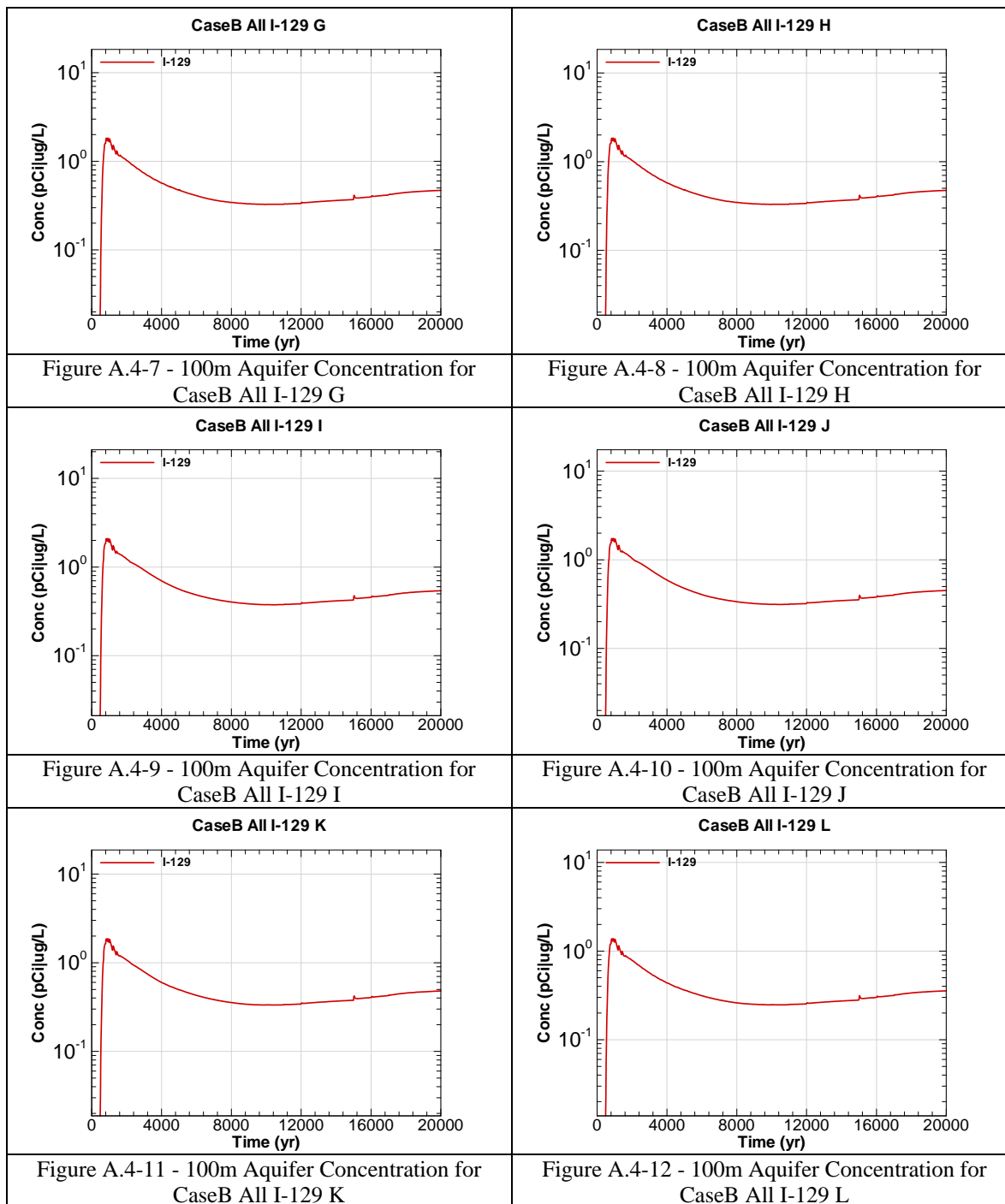
CaseB = Scenario case

All = Inventory source is all disposal units

I-129 = Radionuclide or chemical of concern

A = Evaluation sector of concern





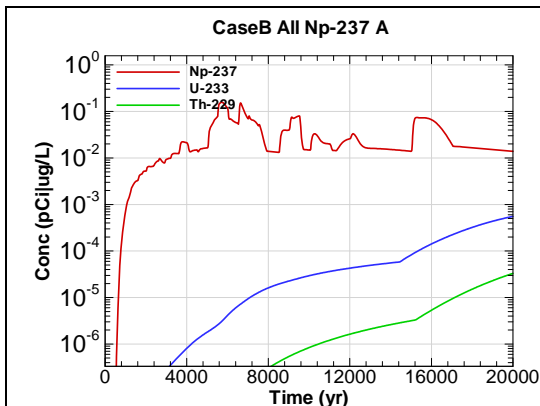


Figure A.4-13 - 100m Aquifer Concentration for
CaseB All Np-237 A

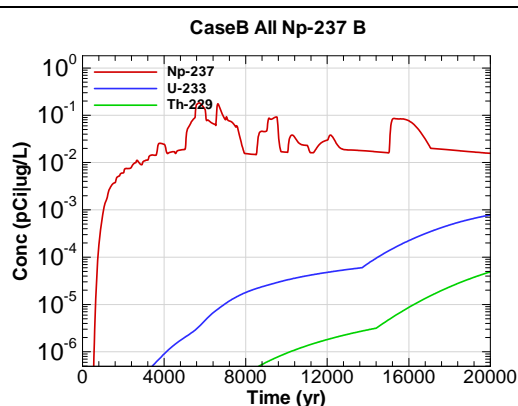


Figure A.4-14 - 100m Aquifer Concentration for
CaseB All Np-237 B

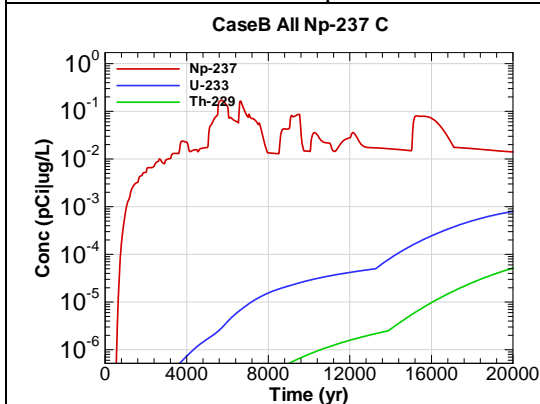


Figure A.4-15 - 100m Aquifer Concentration for
CaseB All Np-237 C

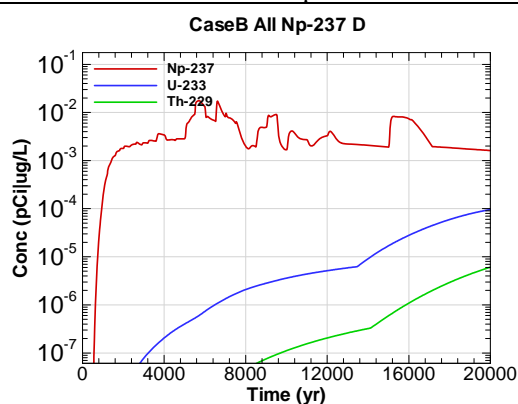


Figure A.4-16 - 100m Aquifer Concentration for
CaseB All Np-237 D

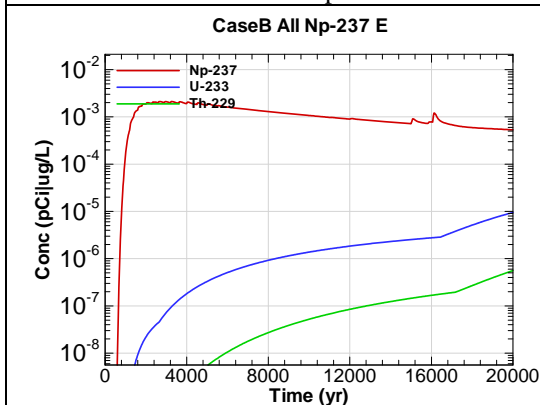


Figure A.4-17 - 100m Aquifer Concentration for
CaseB All Np-237 E

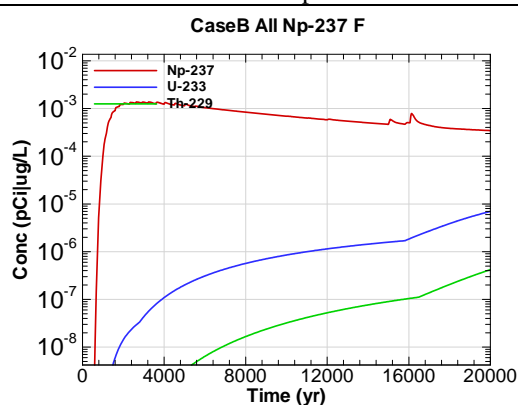


Figure A.4-18 - 100m Aquifer Concentration for
CaseB All Np-237 F

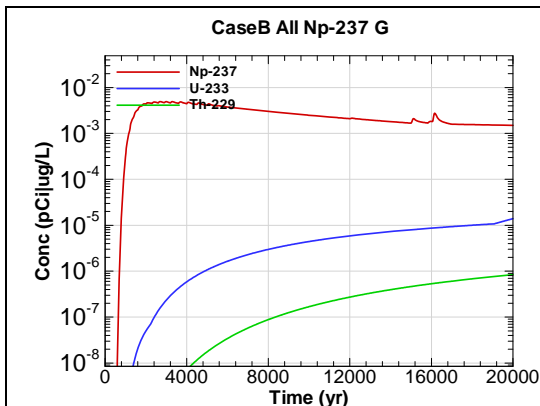


Figure A.4-19 - 100m Aquifer Concentration for
CaseB All Np-237 G

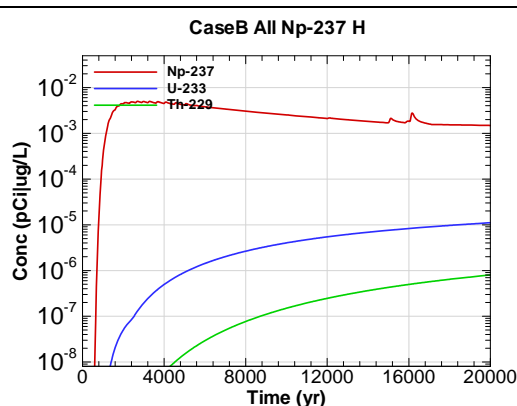


Figure A.4-20 - 100m Aquifer Concentration for
CaseB All Np-237 H

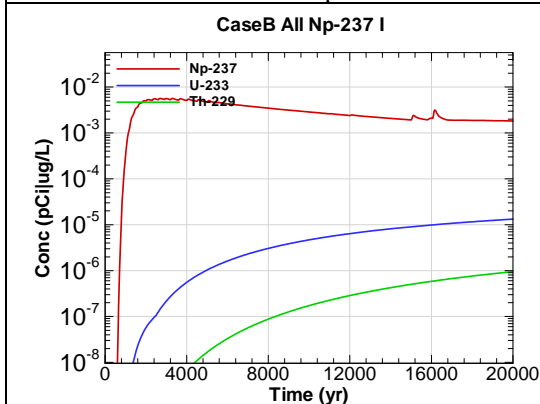


Figure A.4-21 - 100m Aquifer Concentration for
CaseB All Np-237 I

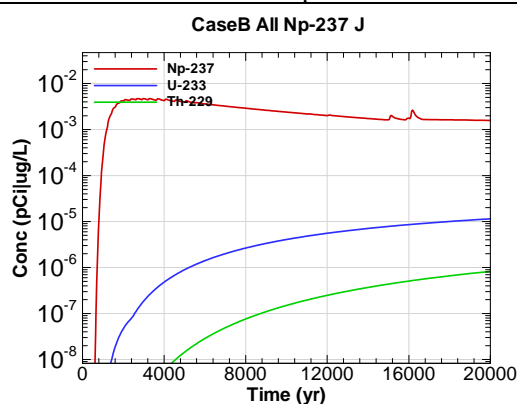


Figure A.4-22 - 100m Aquifer Concentration for
CaseB All Np-237 J

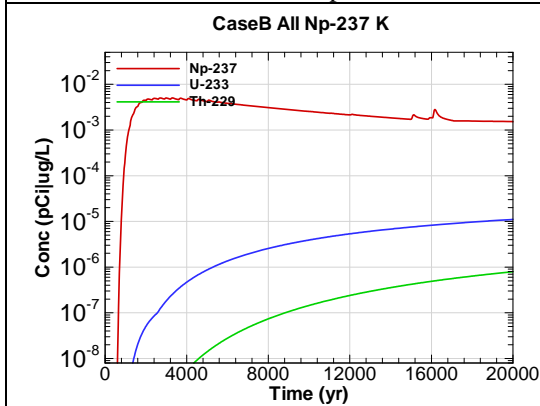


Figure A.4-23 - 100m Aquifer Concentration for
CaseB All Np-237 K

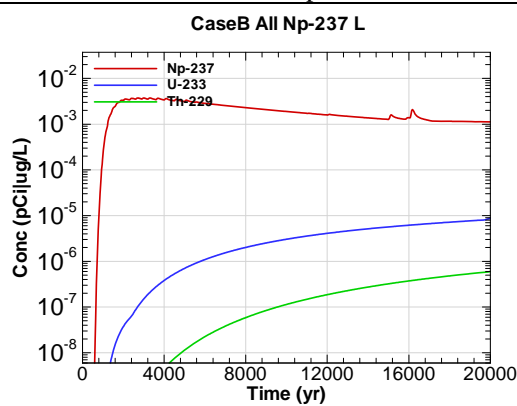


Figure A.4-24 - 100m Aquifer Concentration for
CaseB All Np-237 L

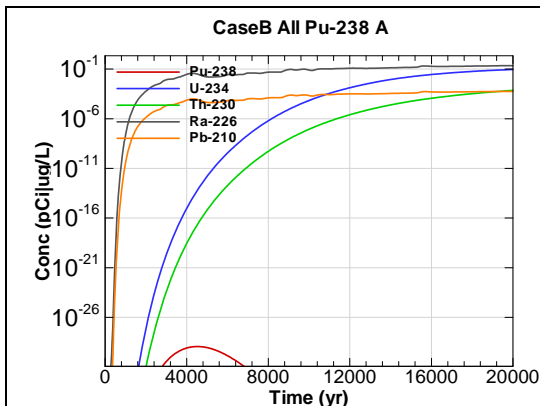


Figure A.4-25 - 100m Aquifer Concentration for
CaseB All Pu-238 A

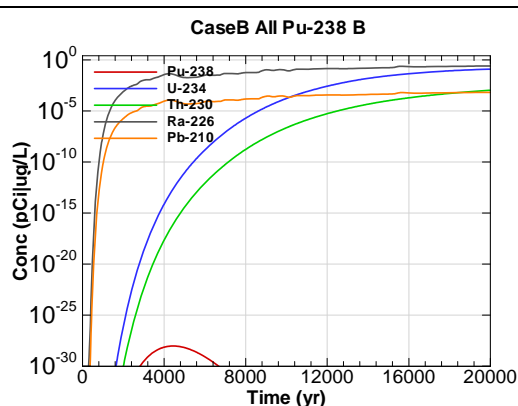


Figure A.4-26 - 100m Aquifer Concentration for
CaseB All Pu-238 B

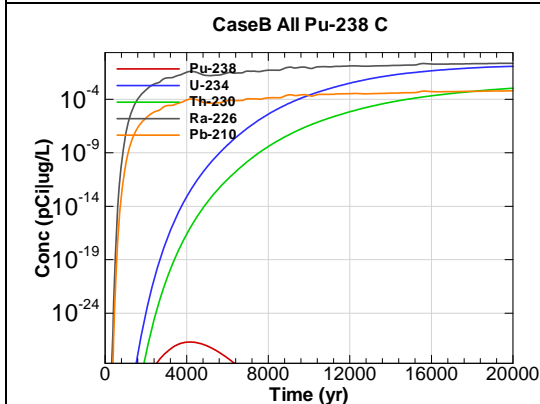


Figure A.4-27 - 100m Aquifer Concentration for
CaseB All Pu-238 C

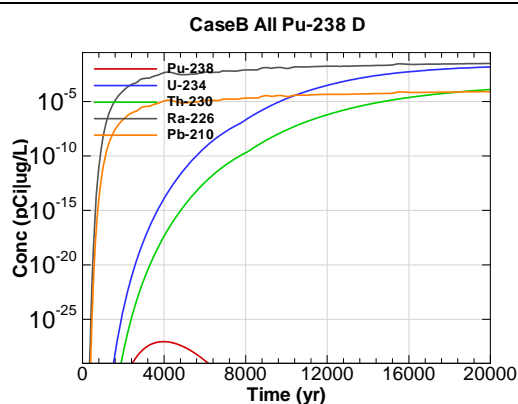


Figure A.4-28 - 100m Aquifer Concentration for
CaseB All Pu-238 D

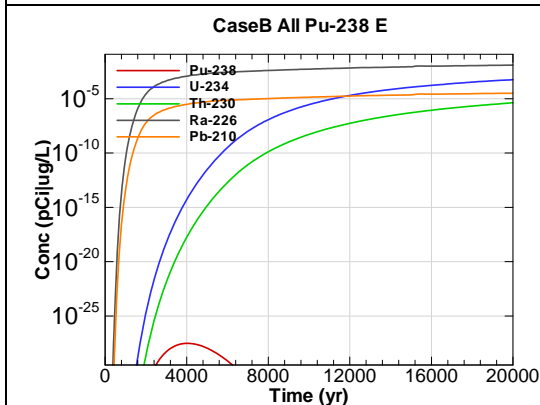


Figure A.4-29 - 100m Aquifer Concentration for
CaseB All Pu-238 E

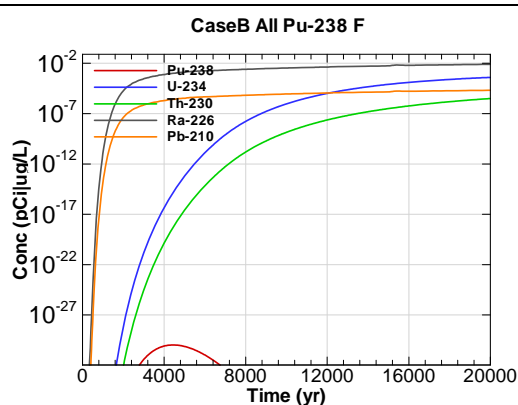


Figure A.4-30 - 100m Aquifer Concentration for
CaseB All Pu-238 F

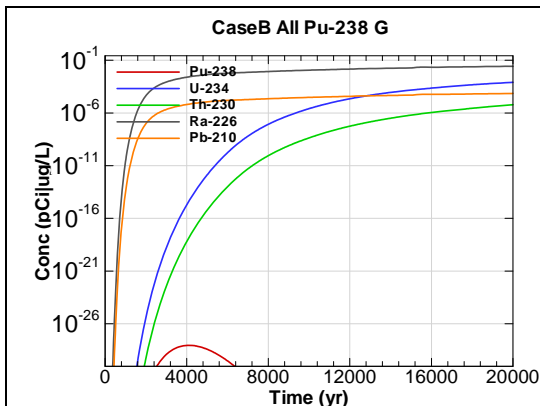


Figure A.4-31 - 100m Aquifer Concentration for
CaseB All Pu-238 G

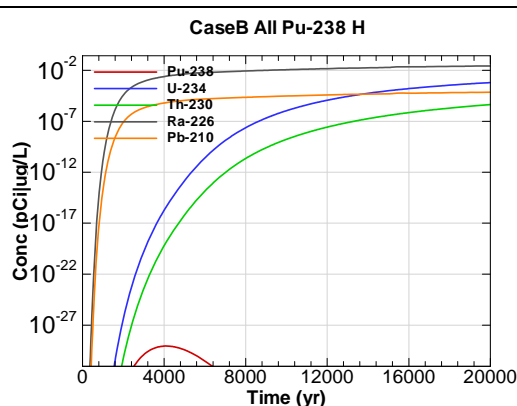


Figure A.4-32 - 100m Aquifer Concentration for
CaseB All Pu-238 H

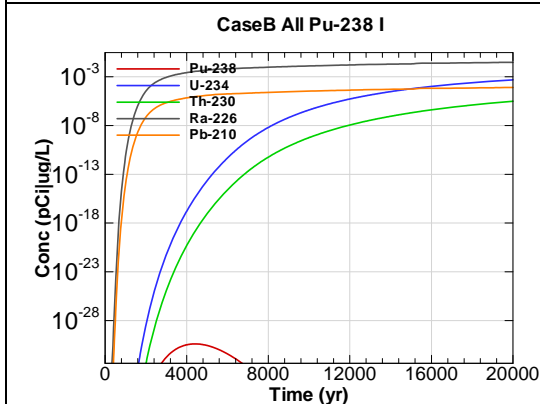


Figure A.4-33 - 100m Aquifer Concentration for
CaseB All Pu-238 I

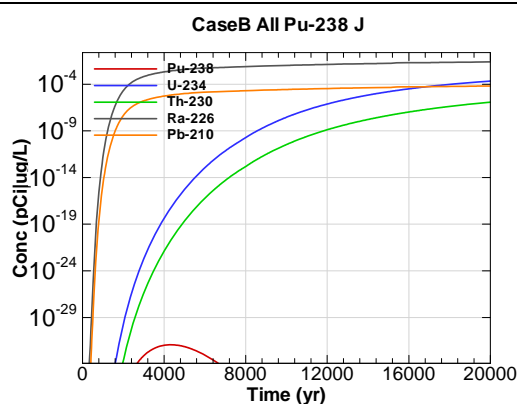


Figure A.4-34 - 100m Aquifer Concentration for
CaseB All Pu-238 J

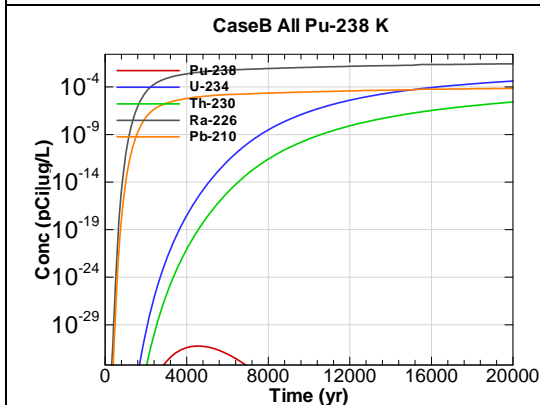


Figure A.4-35 - 100m Aquifer Concentration for
CaseB All Pu-238 K

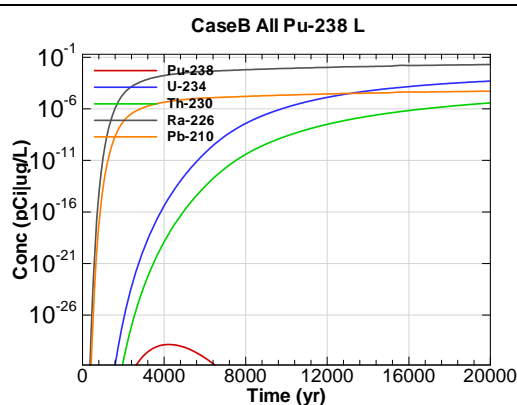
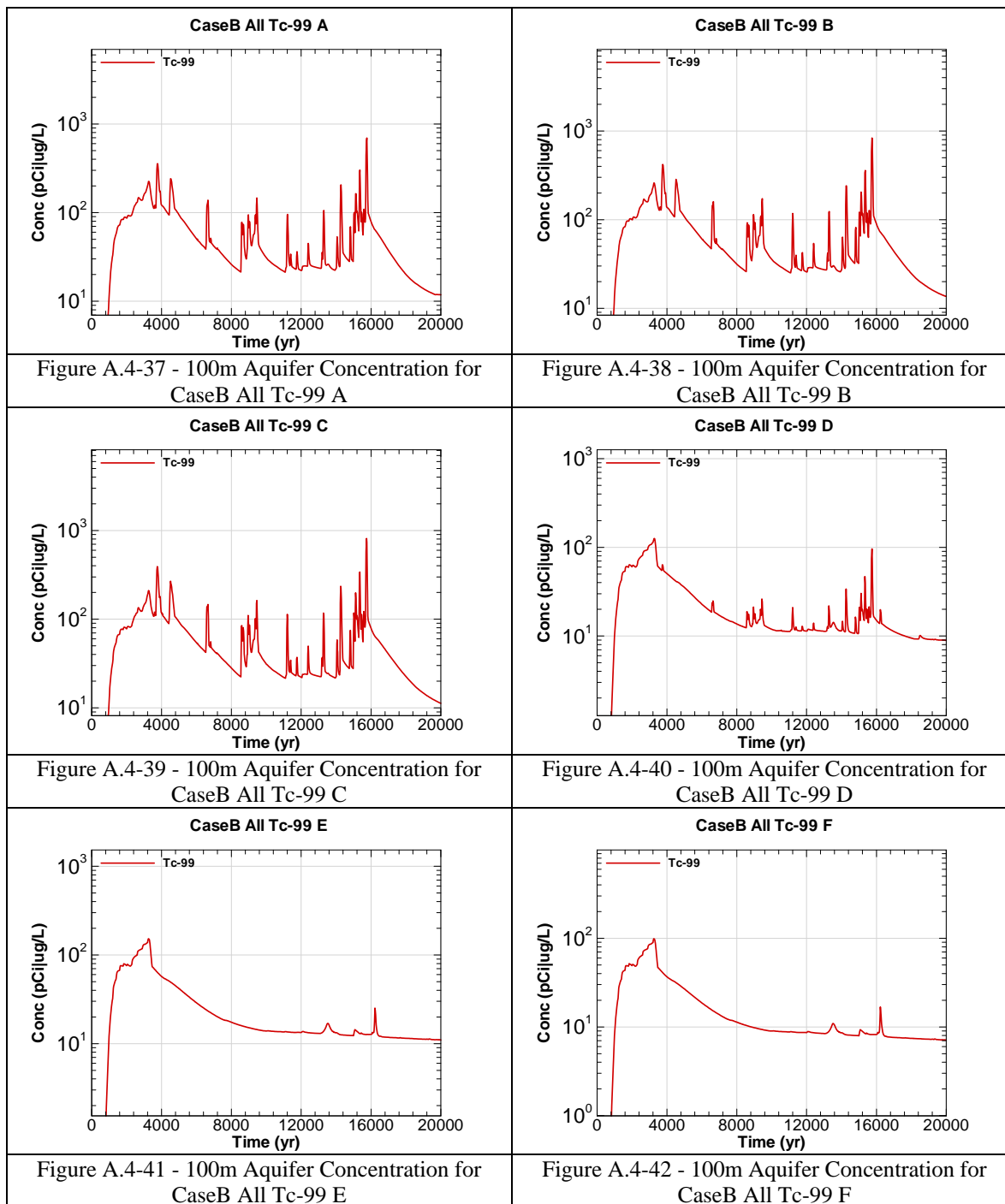
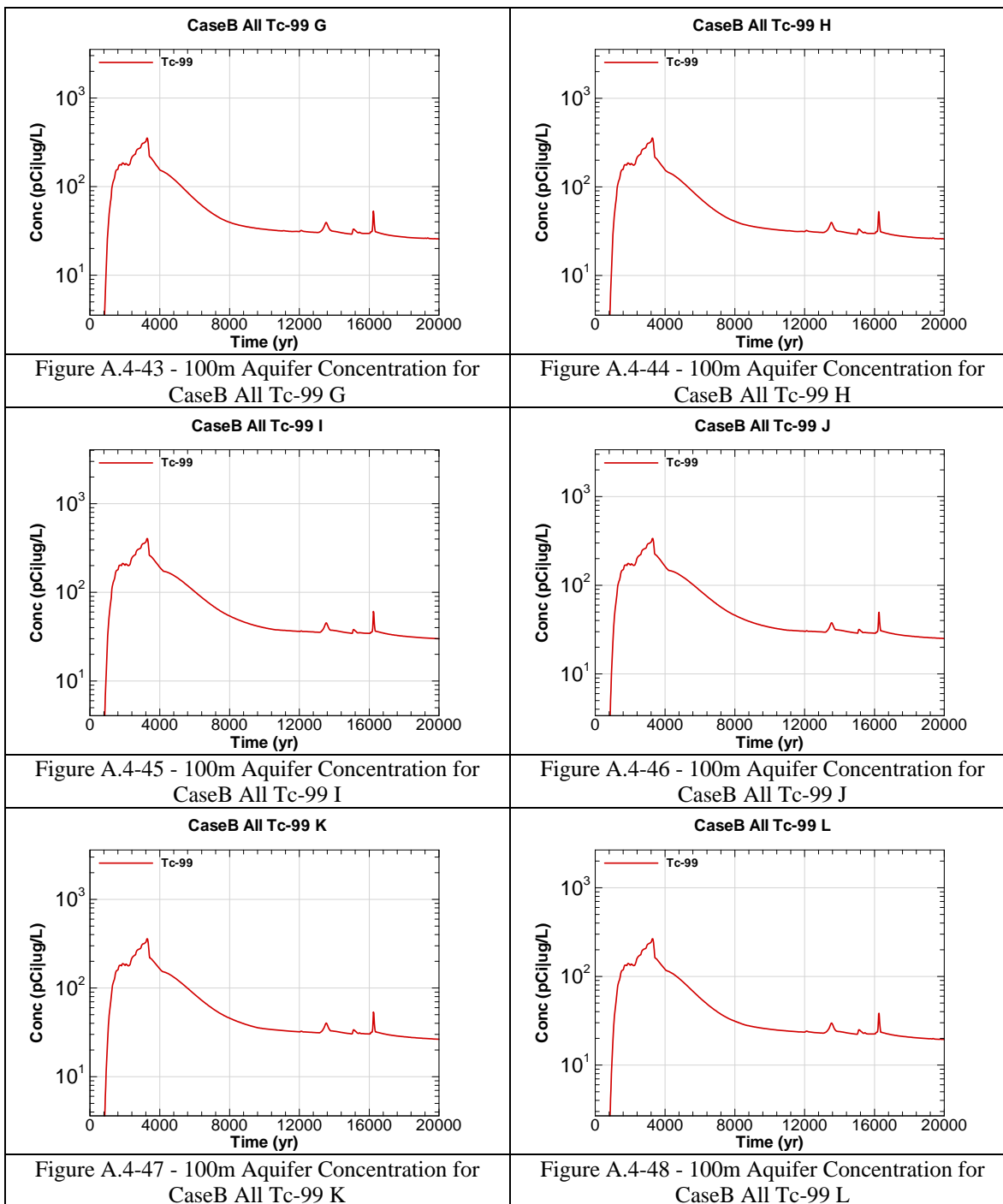


Figure A.4-36 - 100m Aquifer Concentration for
CaseB All Pu-238 L





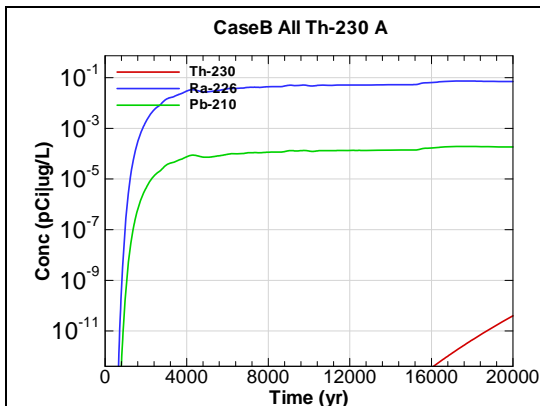


Figure A.4-49 - 100m Aquifer Concentration for CaseB All Th-230 A

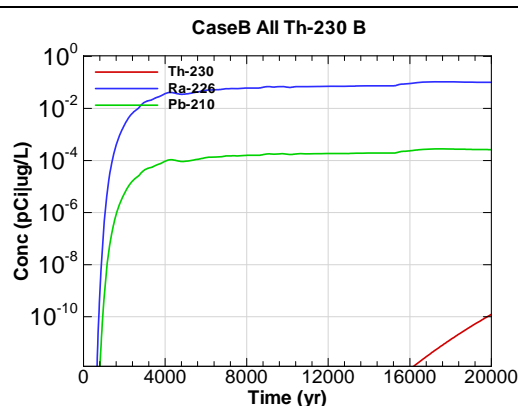


Figure A.4-50 - 100m Aquifer Concentration for CaseB All Th-230 B

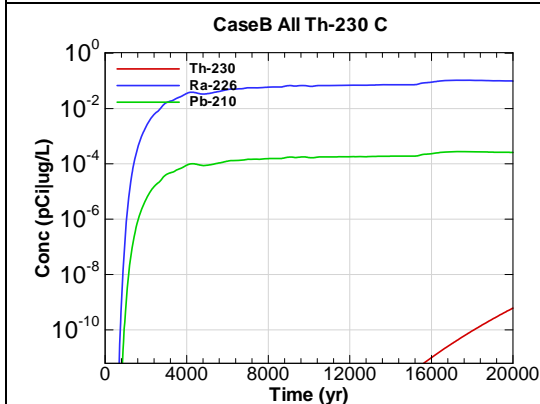


Figure A.4-51 - 100m Aquifer Concentration for CaseB All Th-230 C

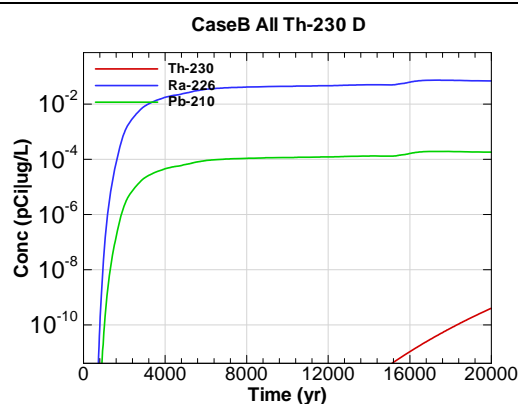


Figure A.4-52 - 100m Aquifer Concentration for CaseB All Th-230 D

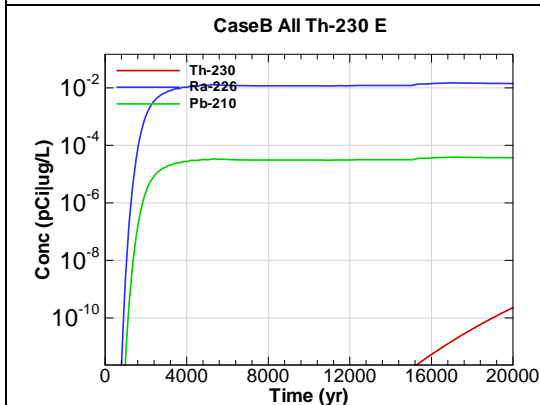


Figure A.4-53 - 100m Aquifer Concentration for CaseB All Th-230 E

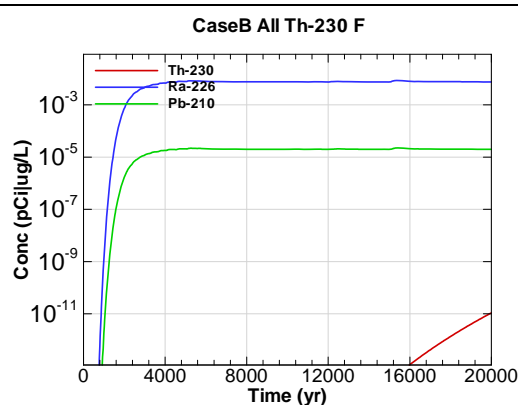


Figure A.4-54 - 100m Aquifer Concentration for CaseB All Th-230 F

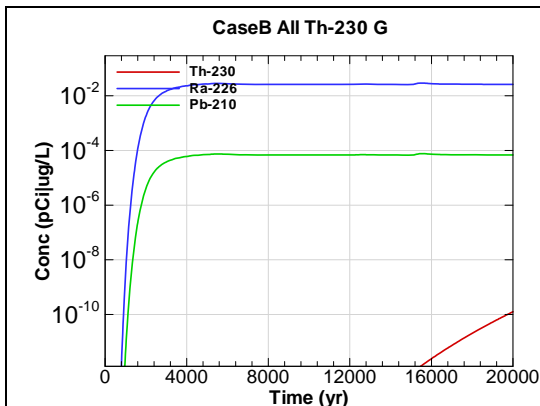


Figure A.4-55 - 100m Aquifer Concentration for
CaseB All Th-230 G

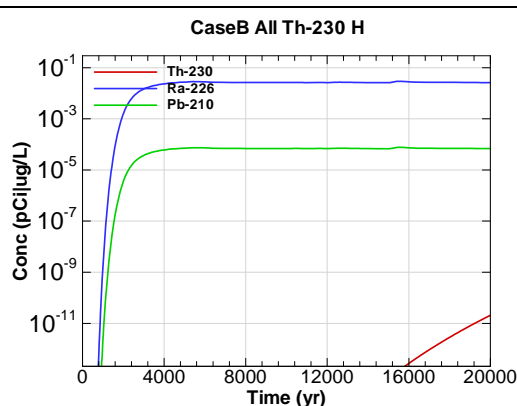


Figure A.4-56 - 100m Aquifer Concentration for
CaseB All Th-230 H

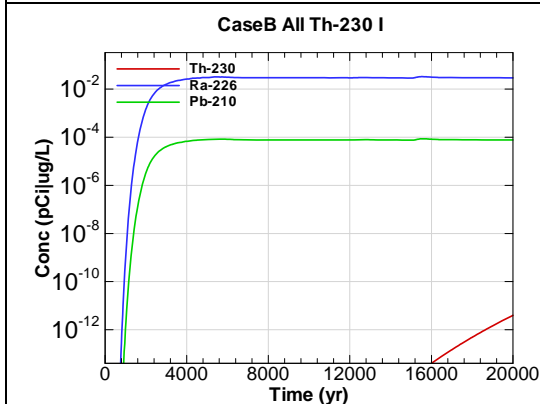


Figure A.4-57 - 100m Aquifer Concentration for
CaseB All Th-230 I

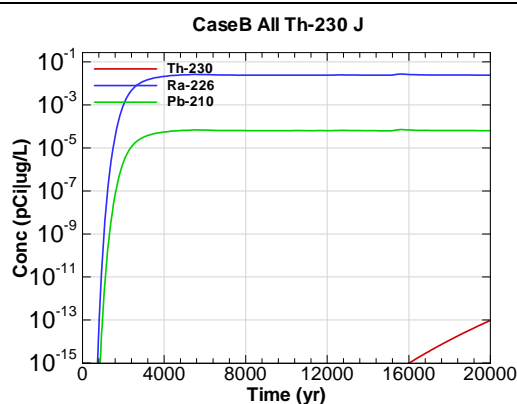


Figure A.4-58 - 100m Aquifer Concentration for
CaseB All Th-230 J

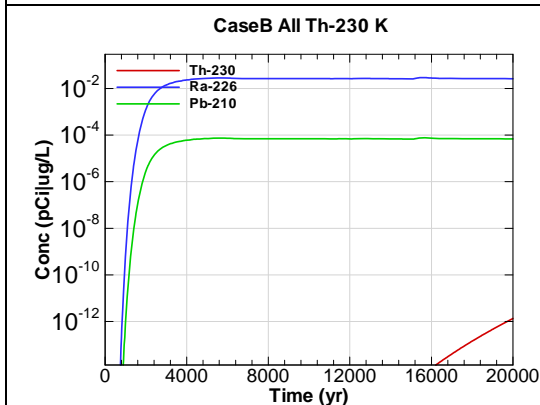


Figure A.4-59 - 100m Aquifer Concentration for
CaseB All Th-230 K

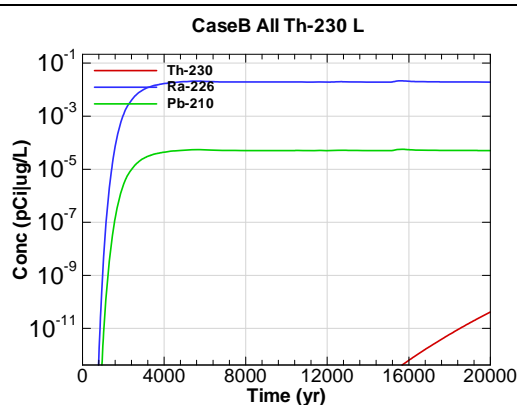


Figure A.4-60 - 100m Aquifer Concentration for
CaseB All Th-230 L

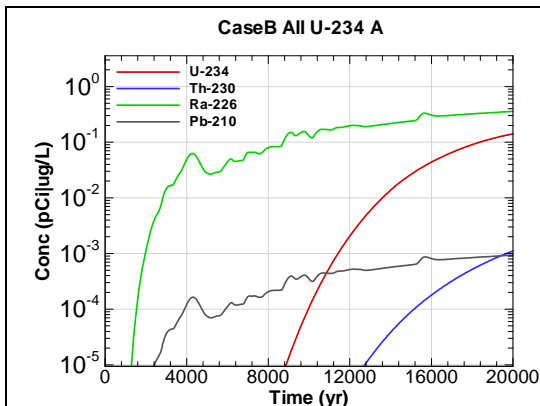


Figure A.4-61 - 100m Aquifer Concentration for
CaseB All U-234 A

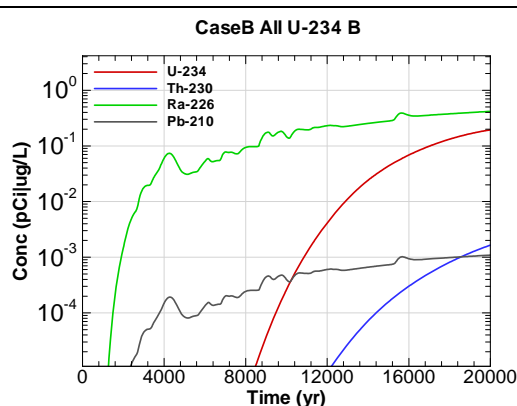


Figure A.4-62 - 100m Aquifer Concentration for
CaseB All U-234 B

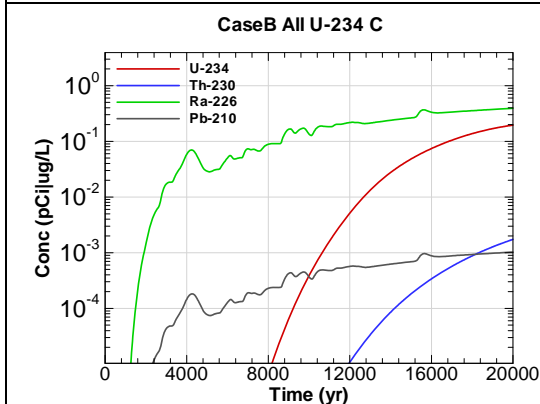


Figure A.4-63 - 100m Aquifer Concentration for
CaseB All U-234 C

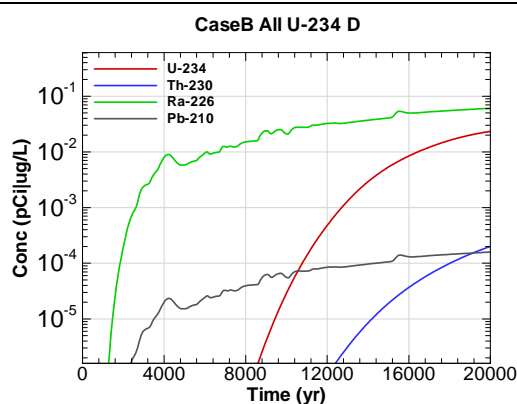


Figure A.4-64 - 100m Aquifer Concentration for
CaseB All U-234 D

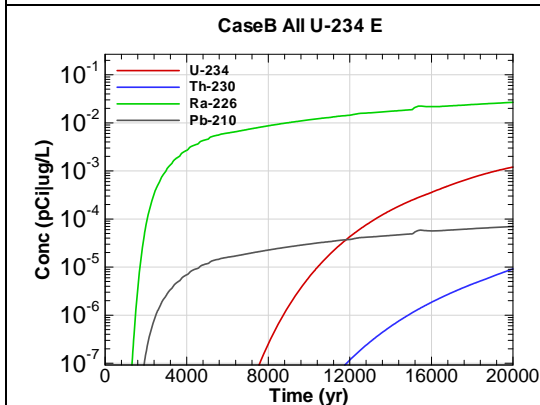


Figure A.4-65 - 100m Aquifer Concentration for
CaseB All U-234 E

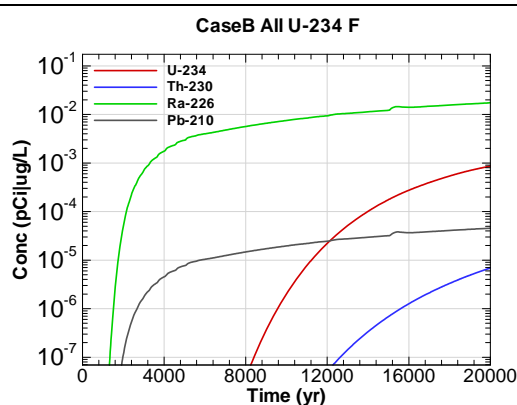


Figure A.4-66 - 100m Aquifer Concentration for
CaseB All U-234 F

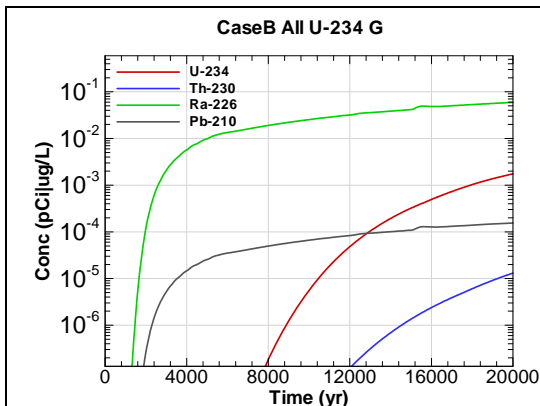


Figure A.4-67 - 100m Aquifer Concentration for
CaseB All U-234 G

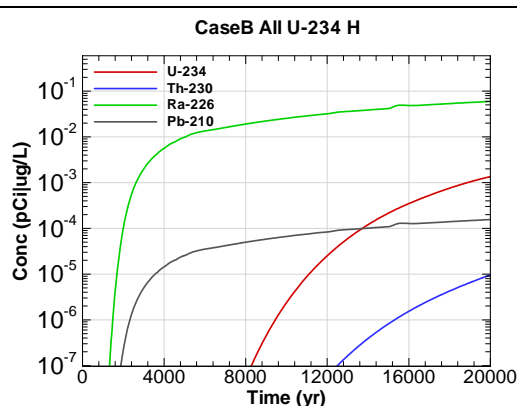


Figure A.4-68 - 100m Aquifer Concentration for
CaseB All U-234 H

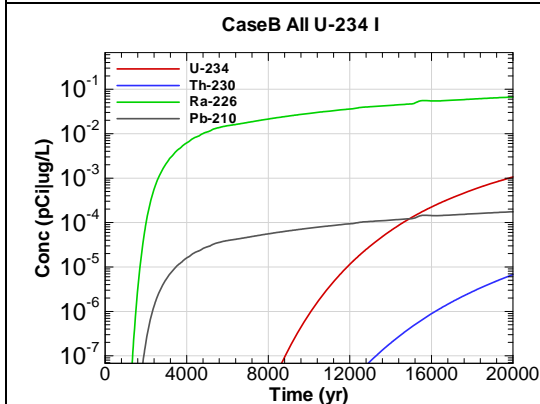


Figure A.4-69 - 100m Aquifer Concentration for
CaseB All U-234 I

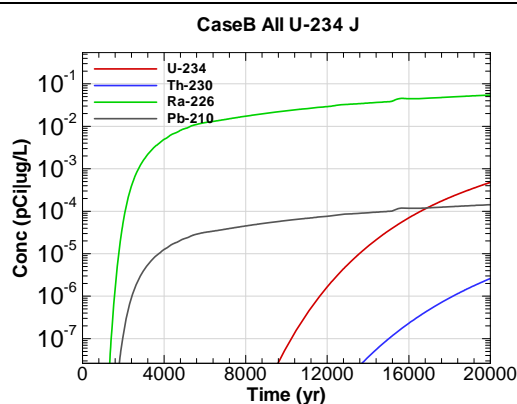


Figure A.4-70 - 100m Aquifer Concentration for
CaseB All U-234 J

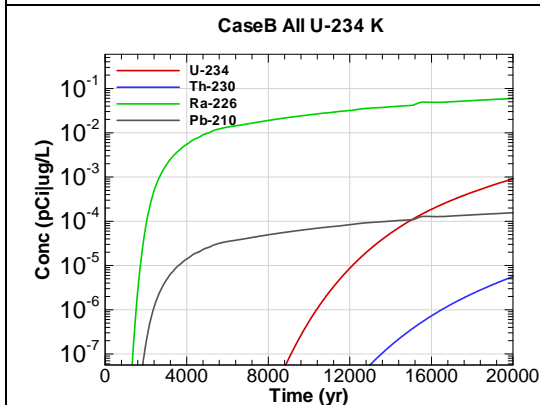


Figure A.4-71 - 100m Aquifer Concentration for
CaseB All U-234 K

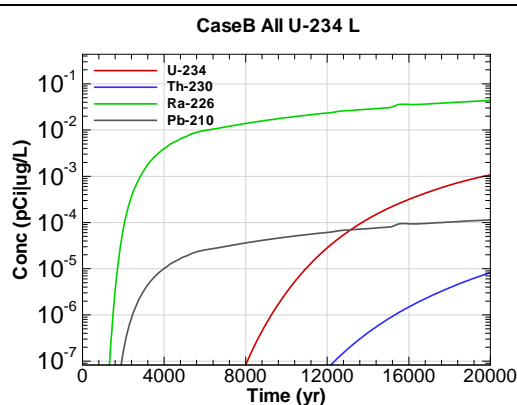


Figure A.4-72 - 100m Aquifer Concentration for
CaseB All U-234 L

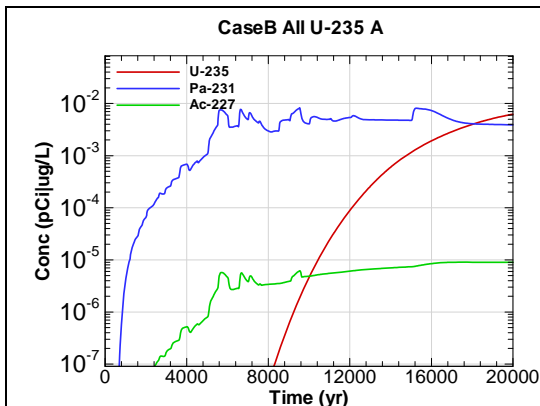


Figure A.4-73 - 100m Aquifer Concentration for
CaseB All U-235 A

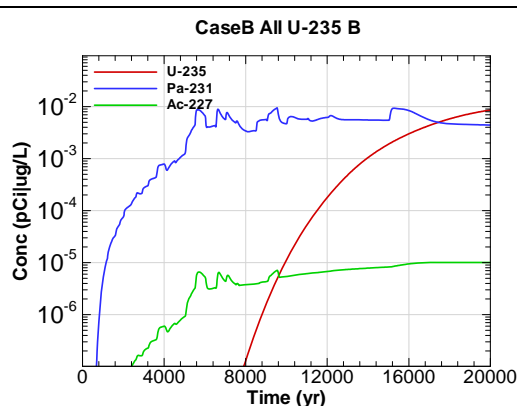


Figure A.4-74 - 100m Aquifer Concentration for
CaseB All U-235 B

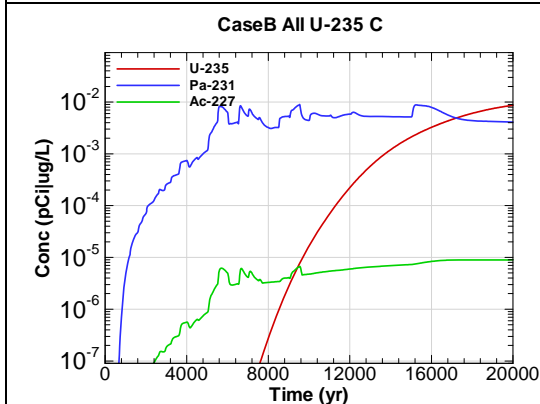


Figure A.4-75 - 100m Aquifer Concentration for
CaseB All U-235 C

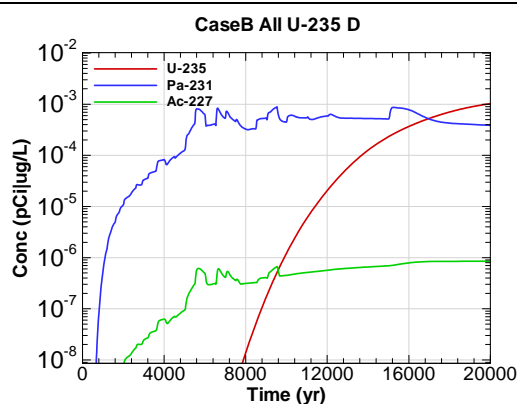


Figure A.4-76 - 100m Aquifer Concentration for
CaseB All U-235 D

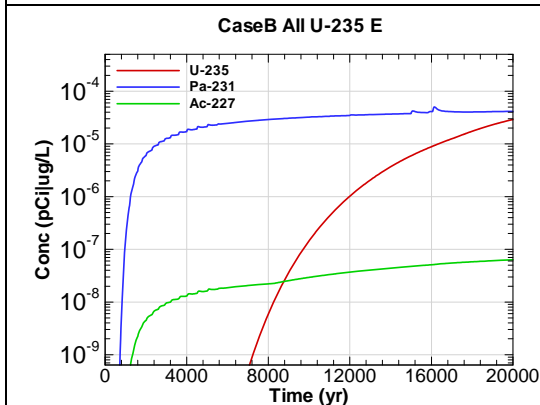


Figure A.4-77 - 100m Aquifer Concentration for
CaseB All U-235 E

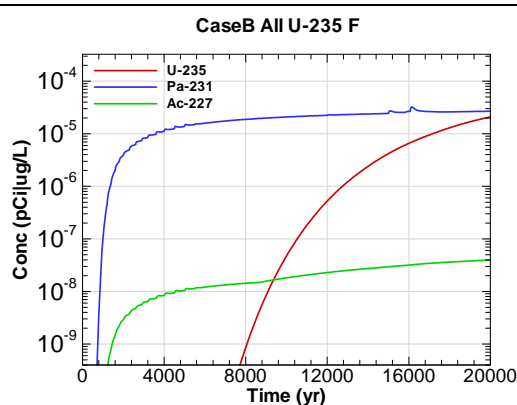


Figure A.4-78 - 100m Aquifer Concentration for
CaseB All U-235 F

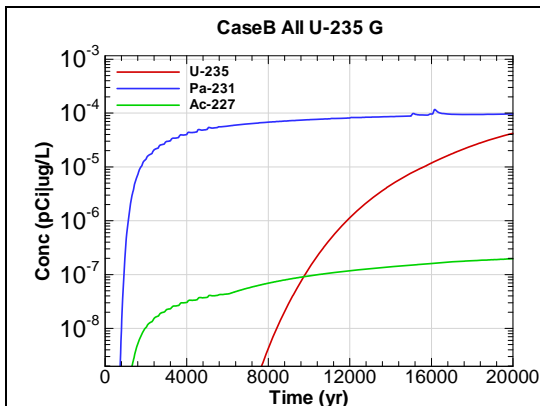


Figure A.4-79 - 100m Aquifer Concentration for
CaseB All U-235 G

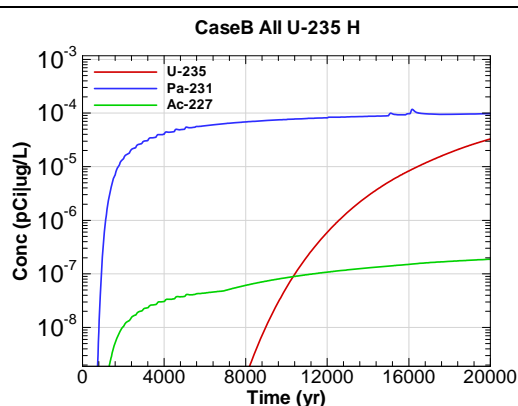


Figure A.4-80 - 100m Aquifer Concentration for
CaseB All U-235 H

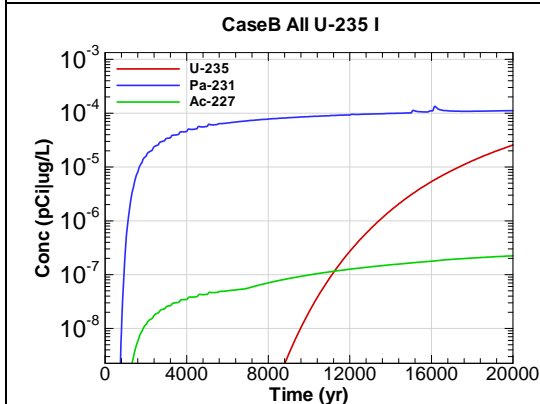


Figure A.4-81 - 100m Aquifer Concentration for
CaseB All U-235 I

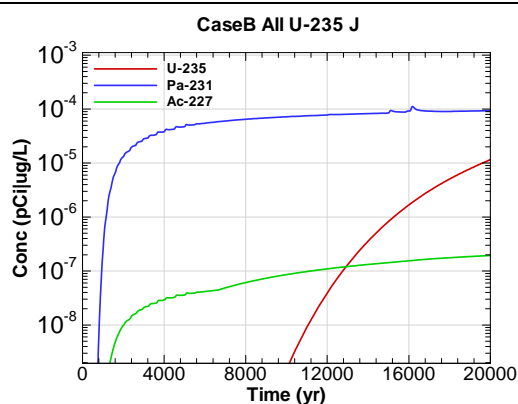


Figure A.4-82 - 100m Aquifer Concentration for
CaseB All U-235 J

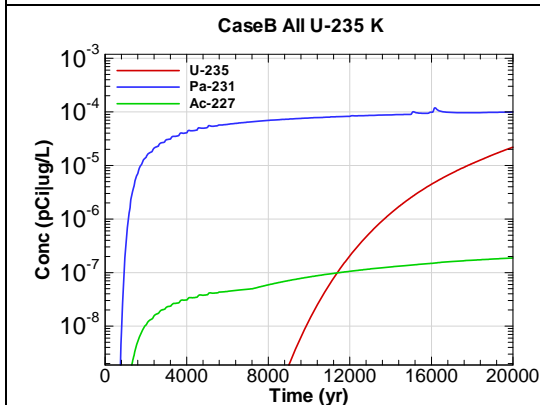


Figure A.4-83 - 100m Aquifer Concentration for
CaseB All U-235 K

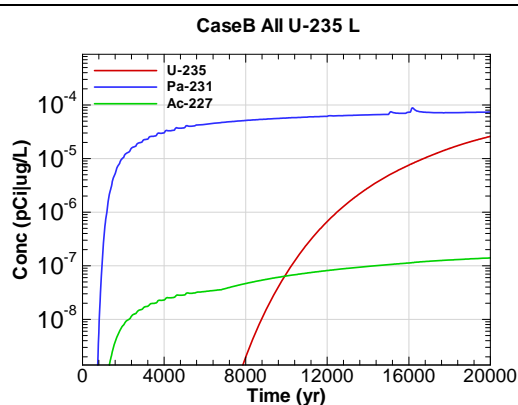
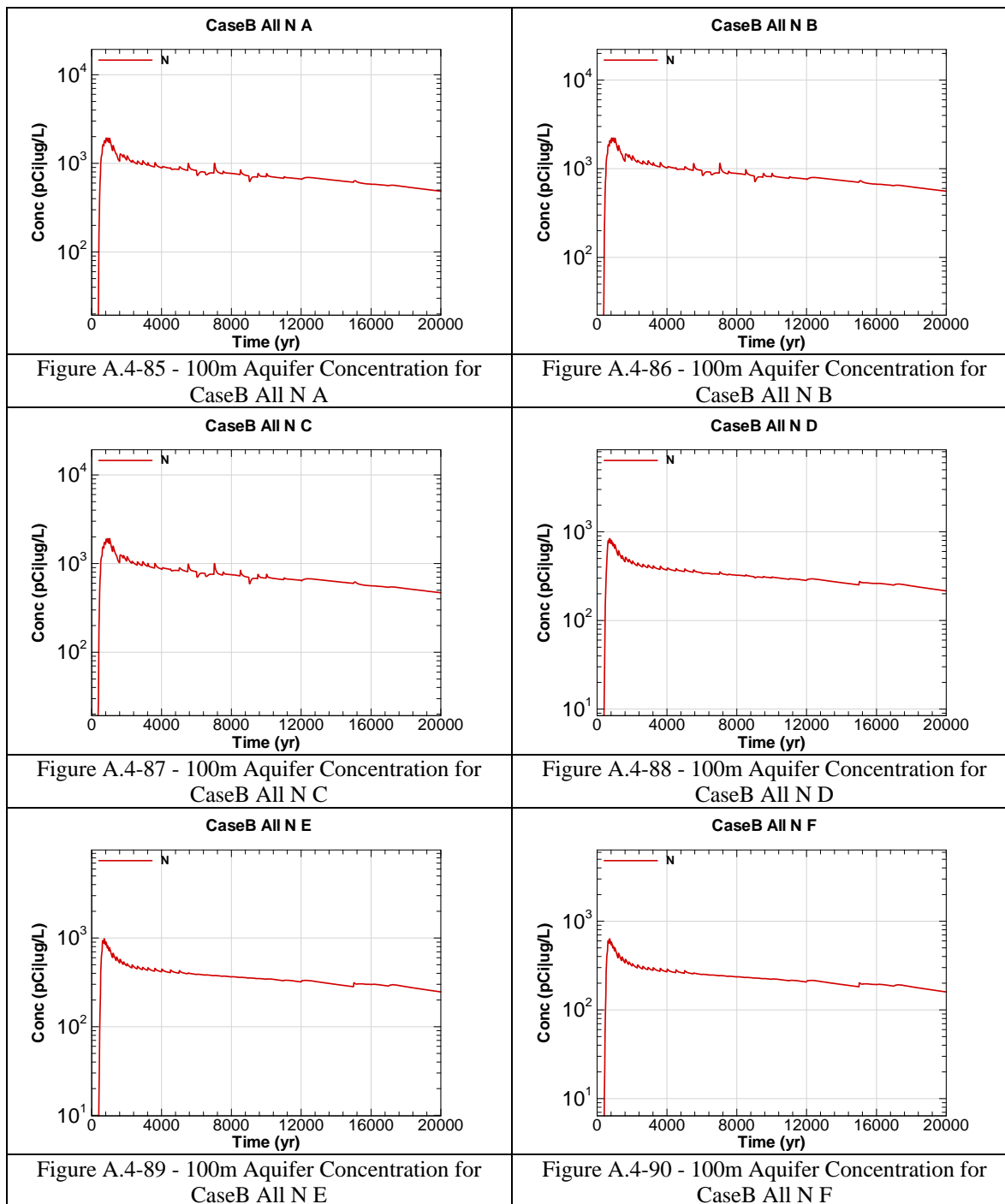
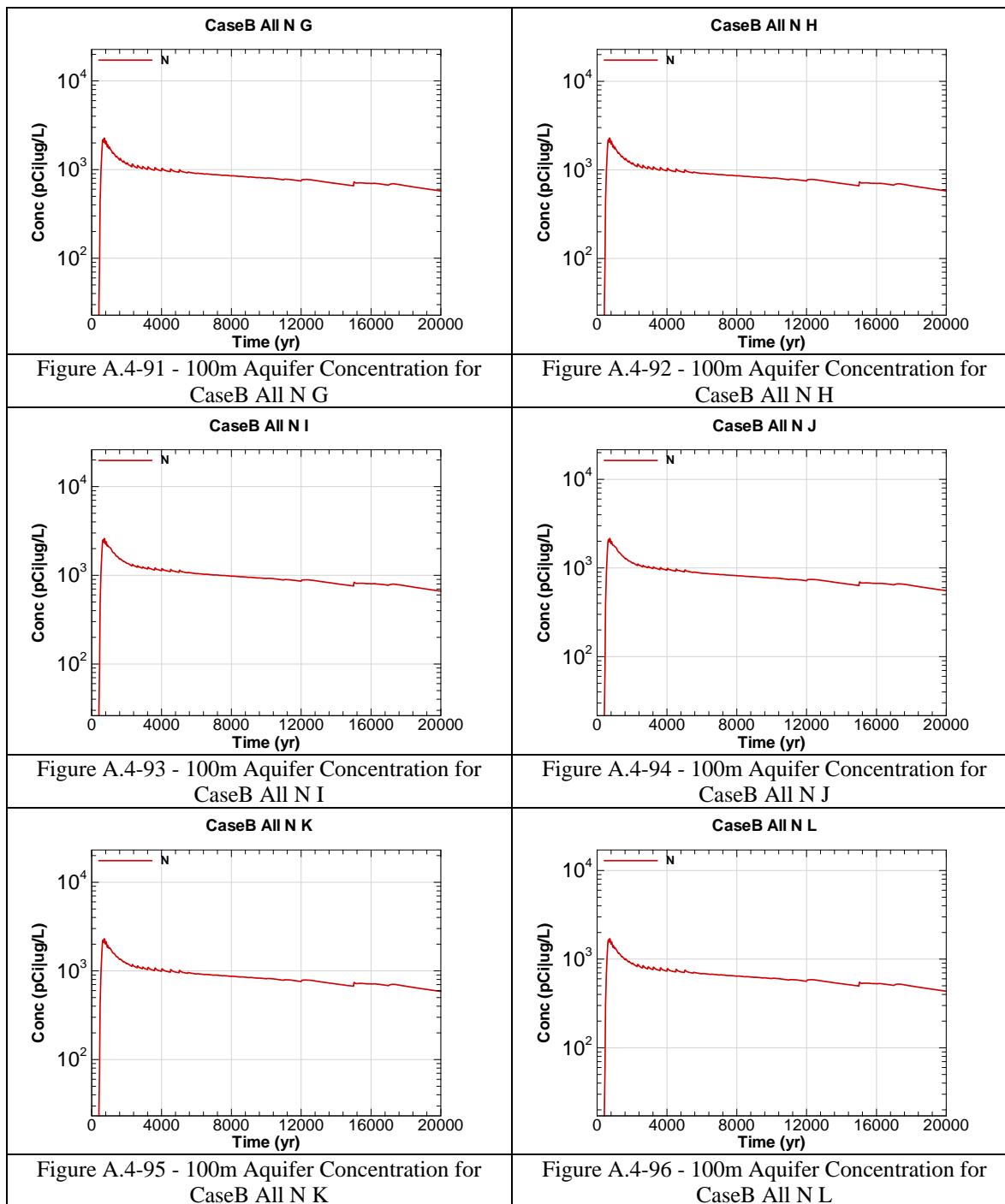


Figure A.4-84 - 100m Aquifer Concentration for
CaseB All U-235 L





This page intentionally left blank

APPENDIX A.5

100-METER RADIOLOGICAL AND CHEMICAL CONCENTRATIONS – CASE C

Appendix A.5 contains curves showing the 100 meter key radiological and chemical concentrations for all of SDF (vault and FDC inventories) for Case C. 20,000 year concentration results are presented for Sectors A through L for the peak concentration per sector regardless of aquifer.

Graph heading example “CaseC All I-129 A”

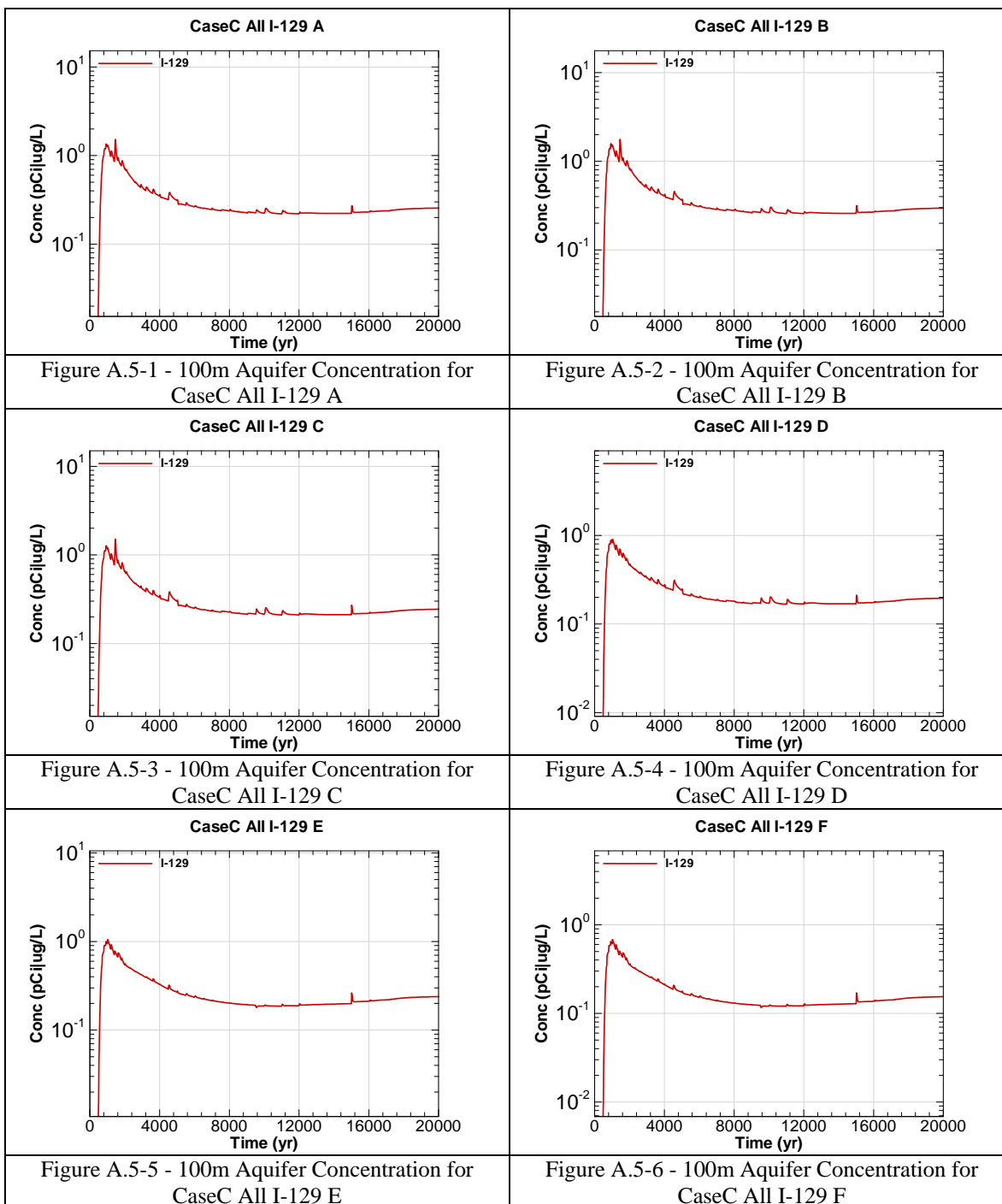
Key

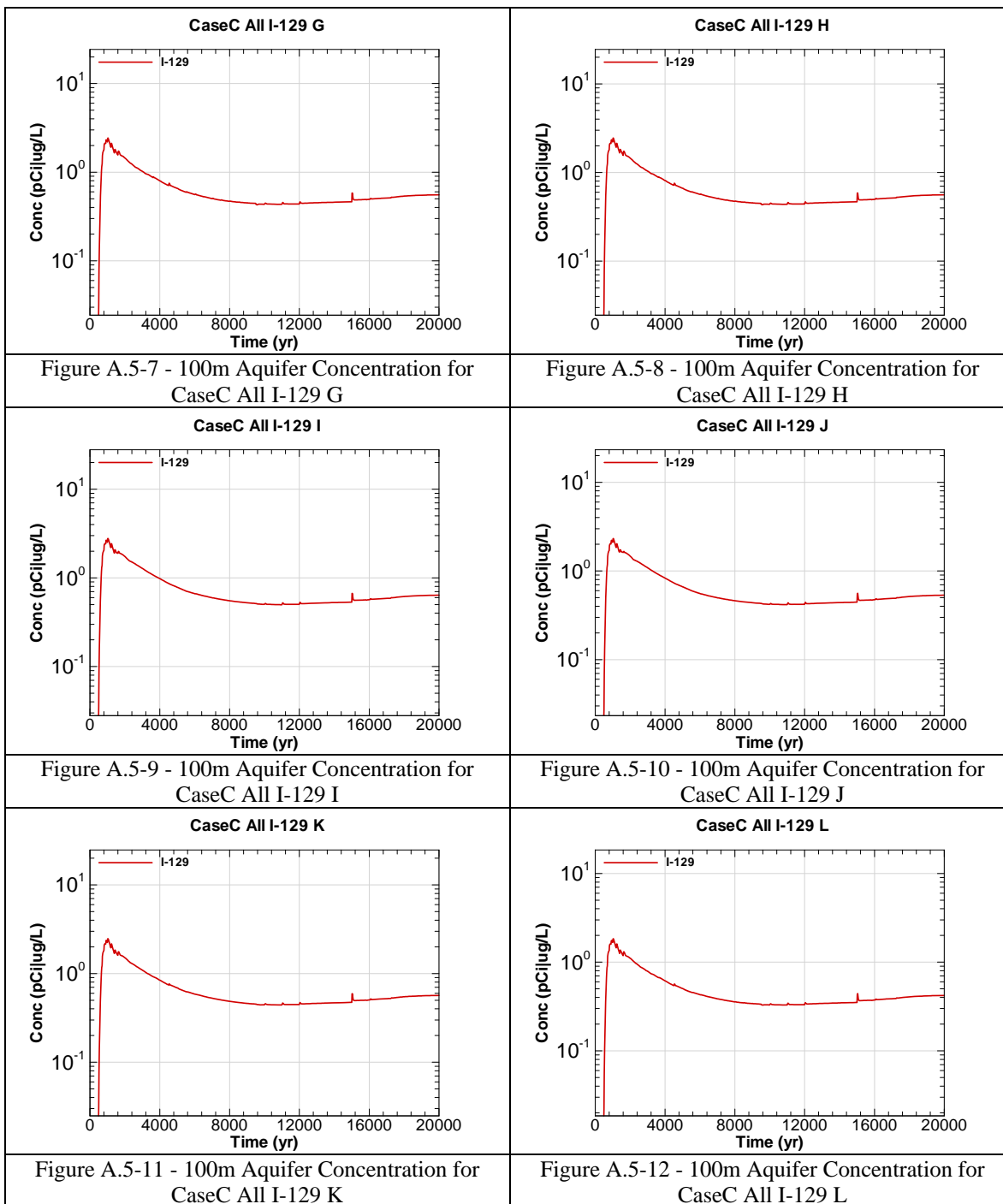
CaseC = Scenario case

All = Inventory source is all disposal units

I-129 = Radionuclide or chemical of concern

A = Evaluation sector of concern





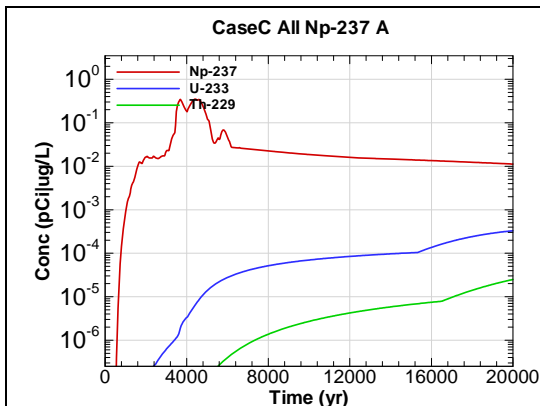


Figure A.5-13 - 100m Aquifer Concentration for
CaseC All Np-237 A

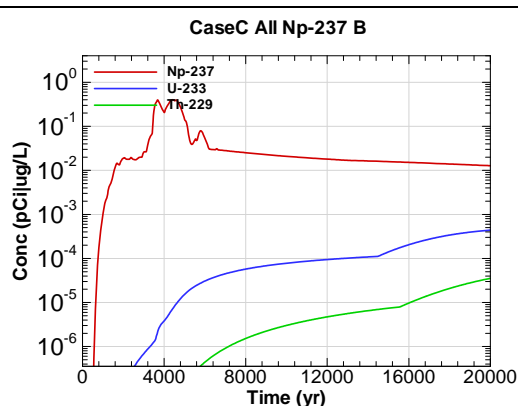


Figure A.5-14 - 100m Aquifer Concentration for
CaseC All Np-237 B

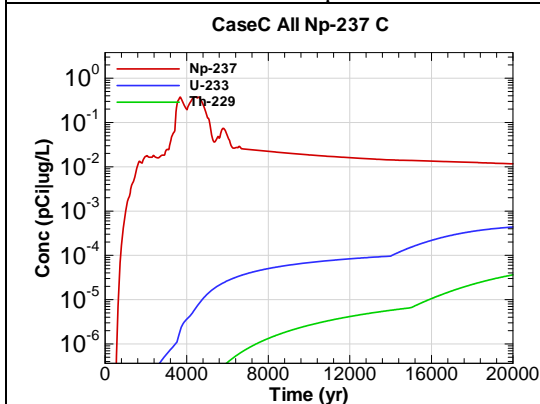


Figure A.5-15 - 100m Aquifer Concentration for
CaseC All Np-237 C

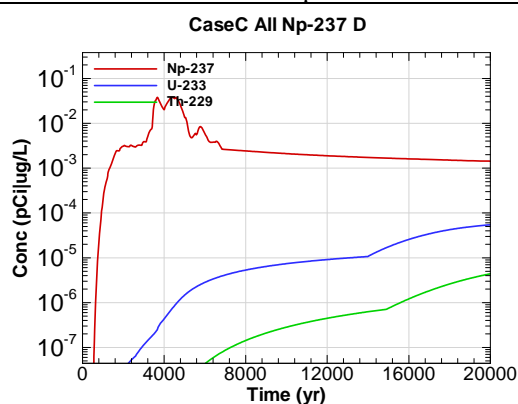


Figure A.5-16 - 100m Aquifer Concentration for
CaseC All Np-237 D

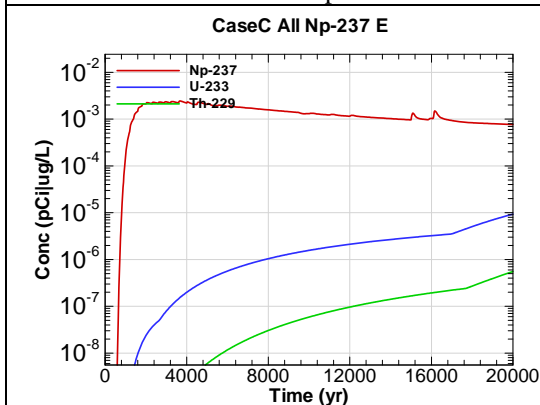


Figure A.5-17 - 100m Aquifer Concentration for
CaseC All Np-237 E

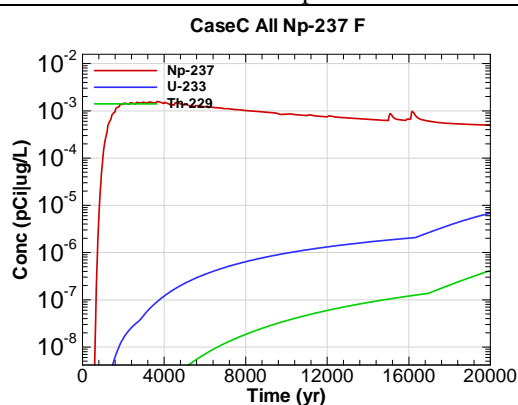


Figure A.5-18 - 100m Aquifer Concentration for
CaseC All Np-237 F

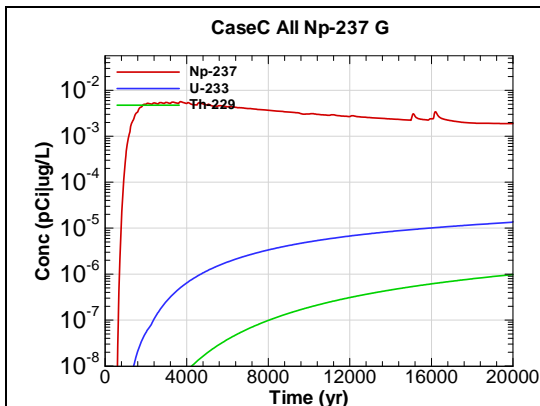


Figure A.5-19 - 100m Aquifer Concentration for
CaseC All Np-237 G

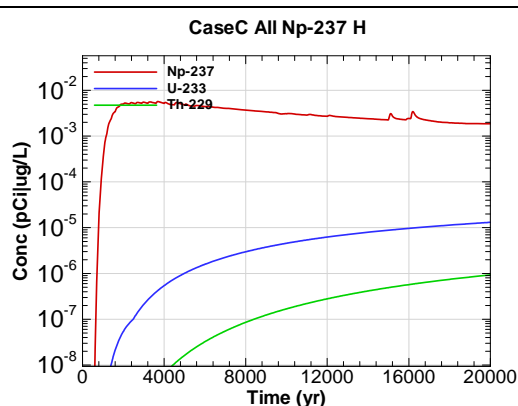


Figure A.5-20 - 100m Aquifer Concentration for
CaseC All Np-237 H

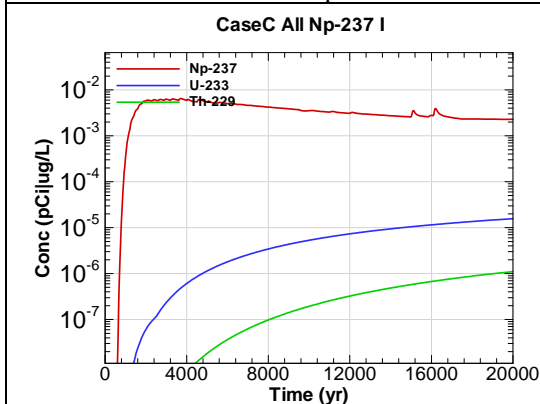


Figure A.5-21 - 100m Aquifer Concentration for
CaseC All Np-237 I

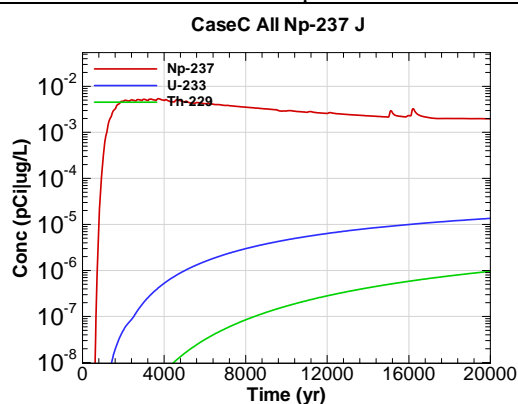


Figure A.5-22 - 100m Aquifer Concentration for
CaseC All Np-237 J

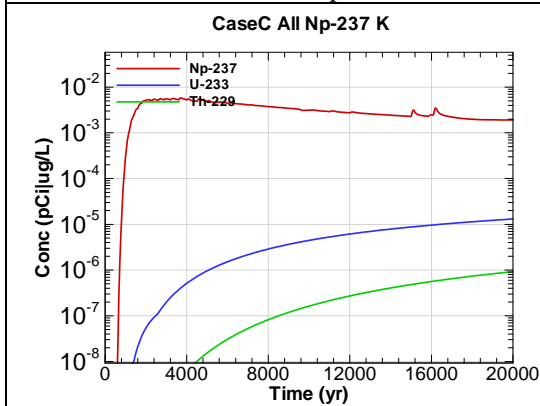


Figure A.5-23 - 100m Aquifer Concentration for
CaseC All Np-237 K

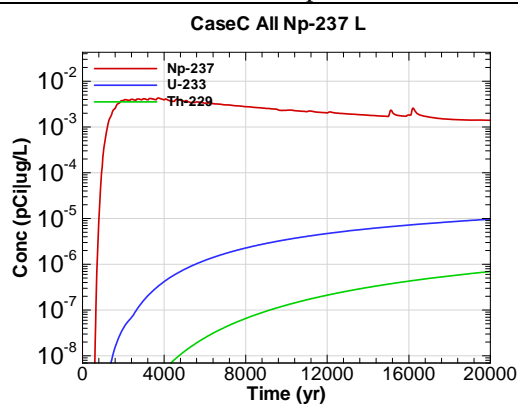


Figure A.5-24 - 100m Aquifer Concentration for
CaseC All Np-237 L

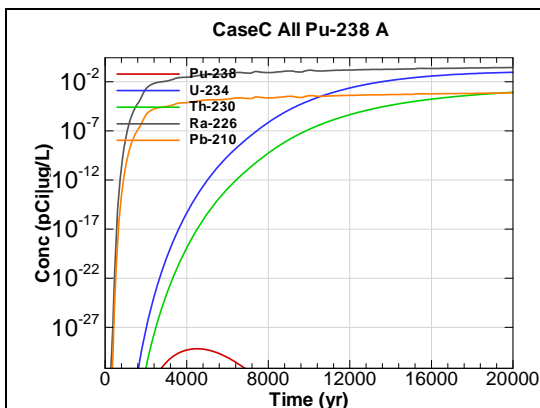


Figure A.5-25 - 100m Aquifer Concentration for
CaseC All Pu-238 A

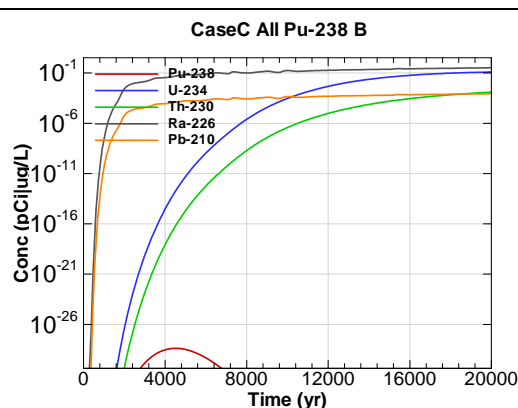


Figure A.5-26 - 100m Aquifer Concentration for
CaseC All Pu-238 B

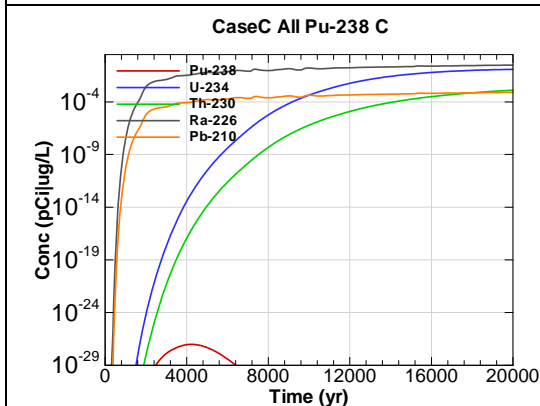


Figure A.5-27 - 100m Aquifer Concentration for
CaseC All Pu-238 C

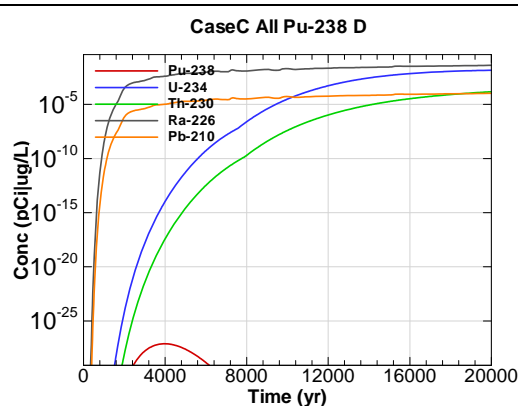


Figure A.5-28 - 100m Aquifer Concentration for
CaseC All Pu-238 D

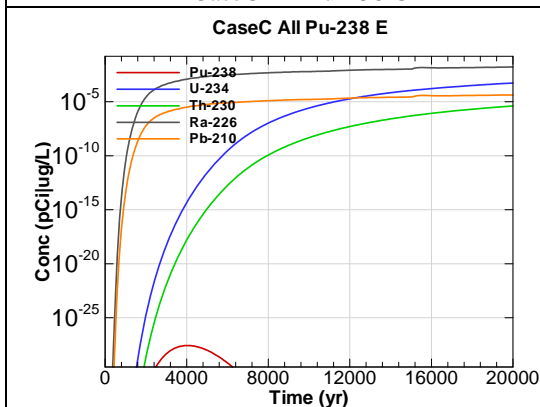


Figure A.5-29 - 100m Aquifer Concentration for
CaseC All Pu-238 E

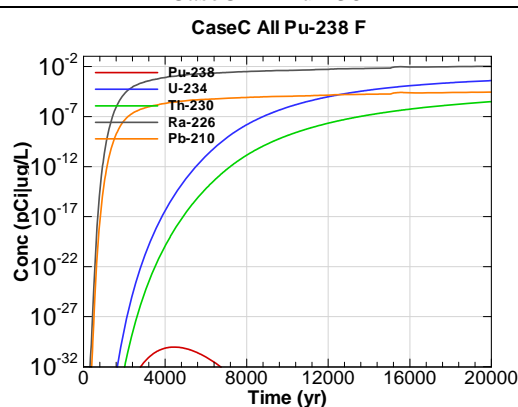


Figure A.5-30 - 100m Aquifer Concentration for
CaseC All Pu-238 F

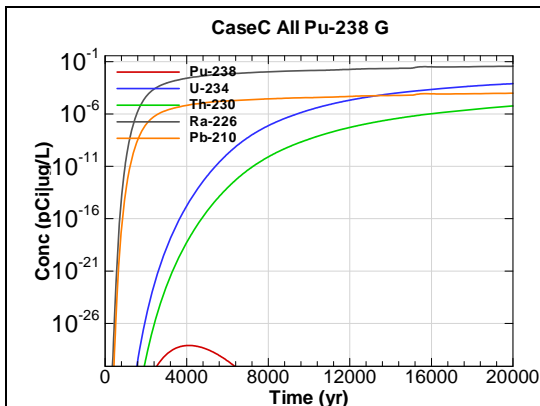


Figure A.5-31 - 100m Aquifer Concentration for
CaseC All Pu-238 G

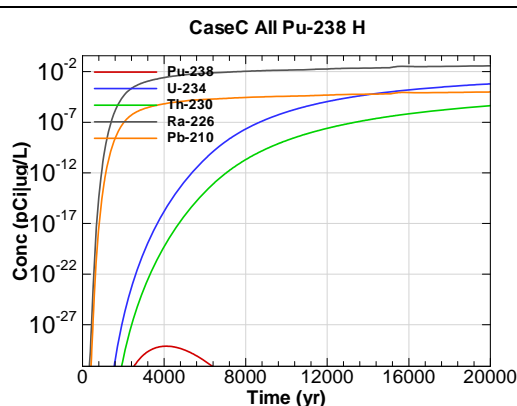


Figure A.5-32 - 100m Aquifer Concentration for
CaseC All Pu-238 H

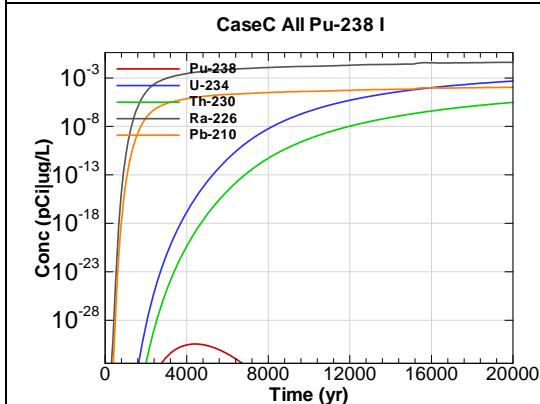


Figure A.5-33 - 100m Aquifer Concentration for
CaseC All Pu-238 I

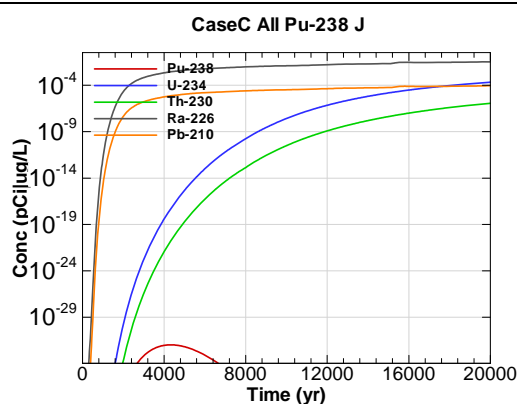


Figure A.5-34 - 100m Aquifer Concentration for
CaseC All Pu-238 J

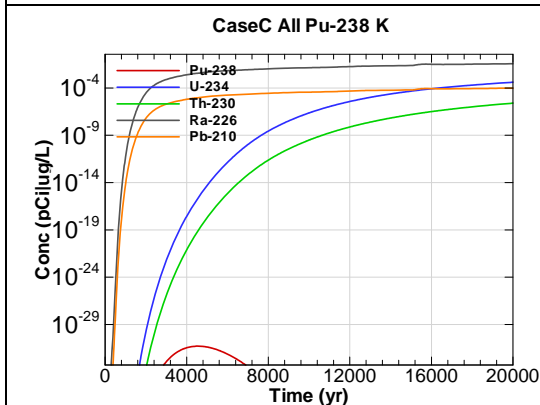


Figure A.5-35 - 100m Aquifer Concentration for
CaseC All Pu-238 K

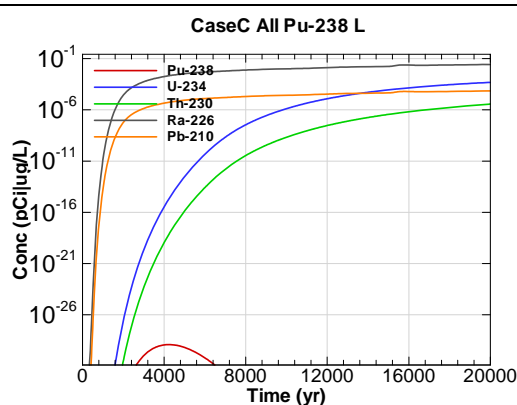
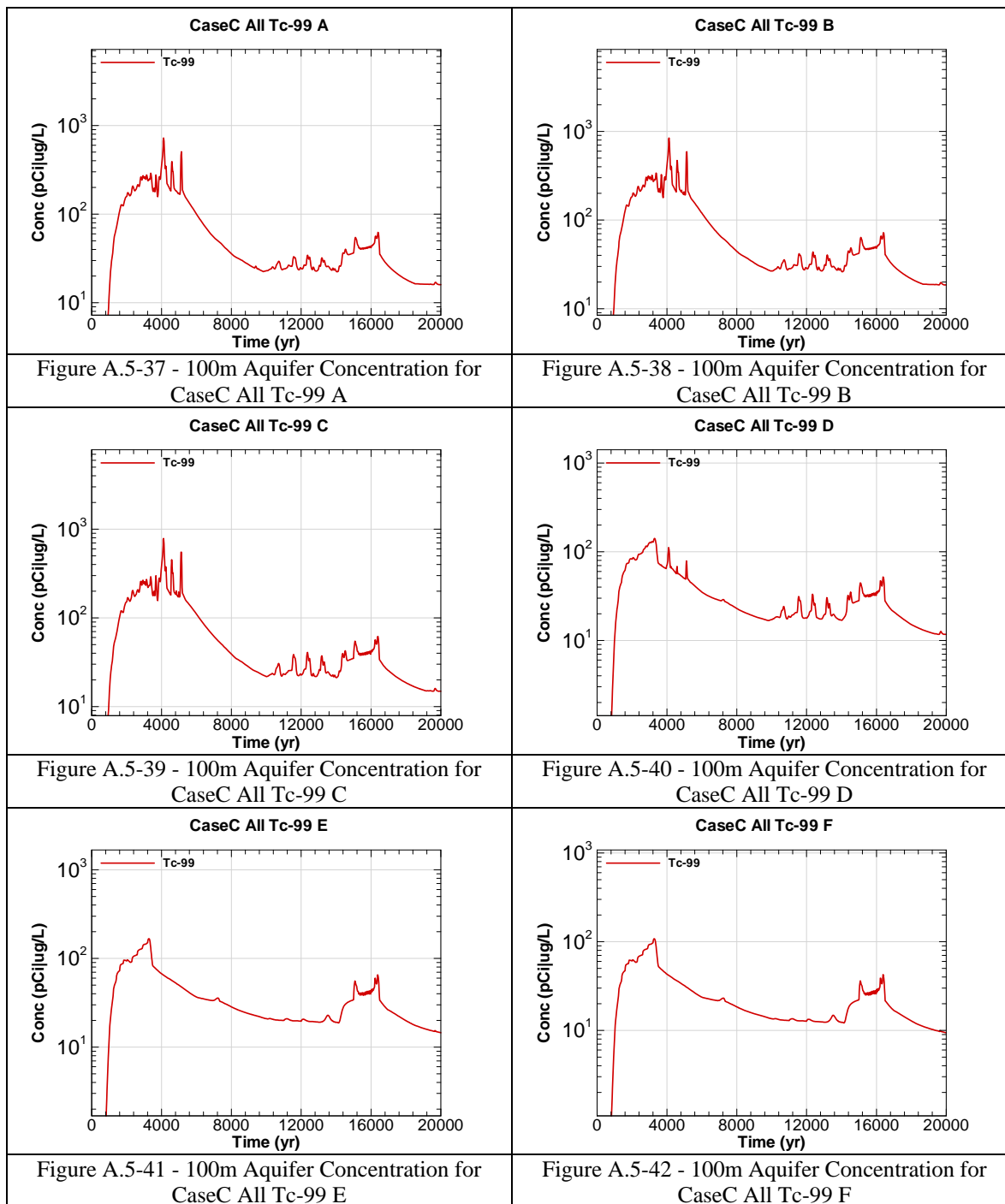
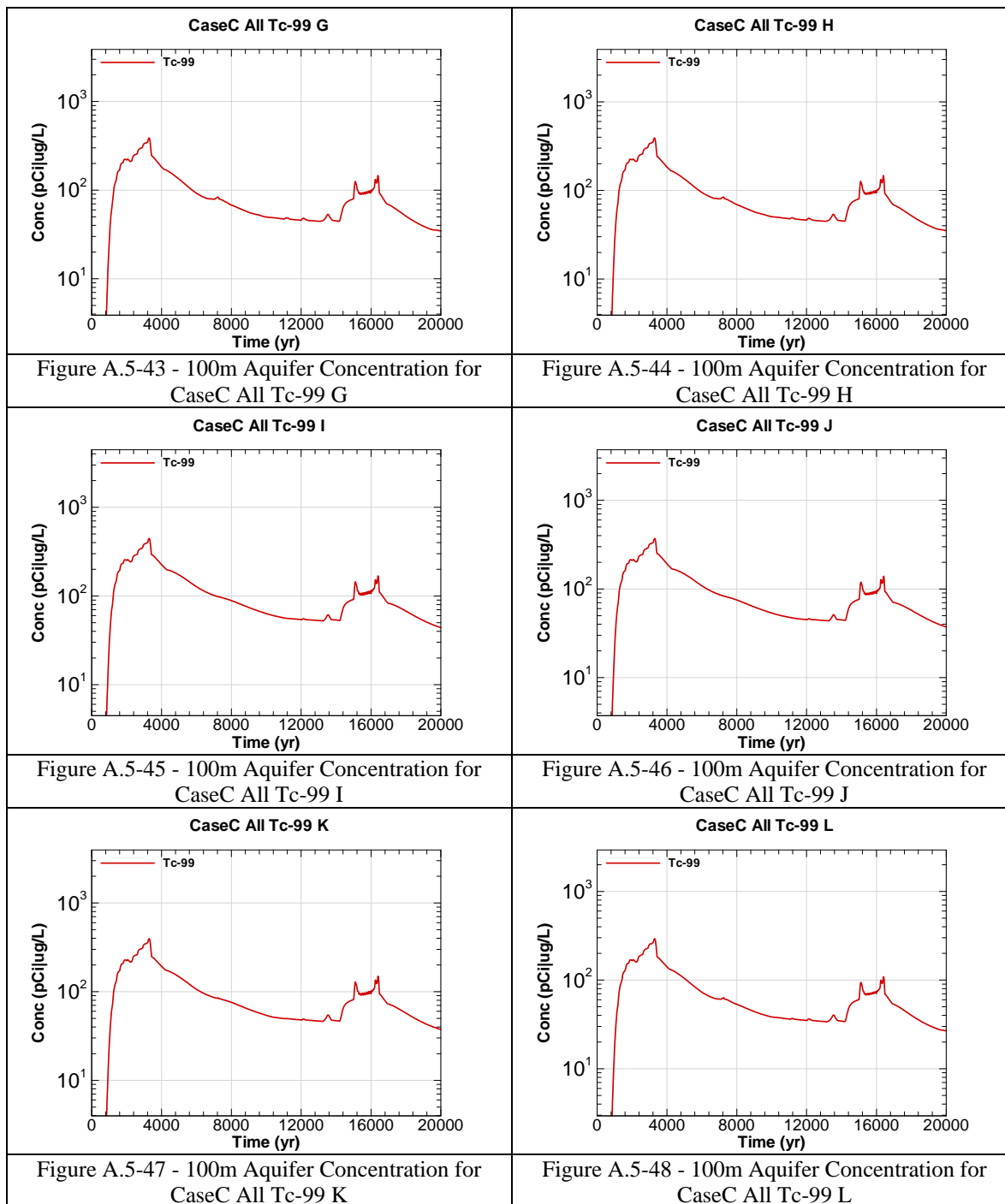


Figure A.5-36 - 100m Aquifer Concentration for
CaseC All Pu-238 L





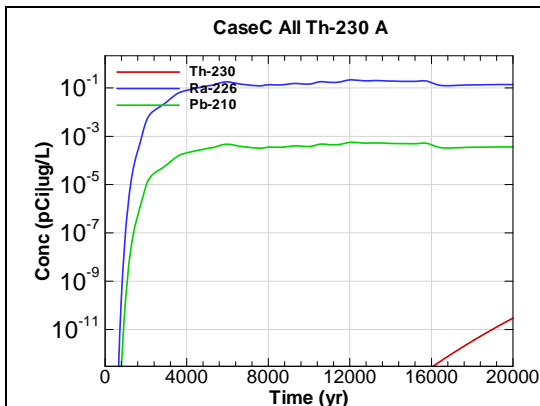


Figure A.5-49 - 100m Aquifer Concentration for
CaseC All Th-230 A

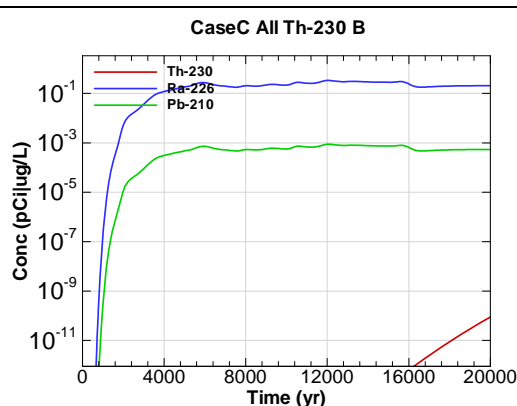


Figure A.5-50 - 100m Aquifer Concentration for
CaseC All Th-230 B

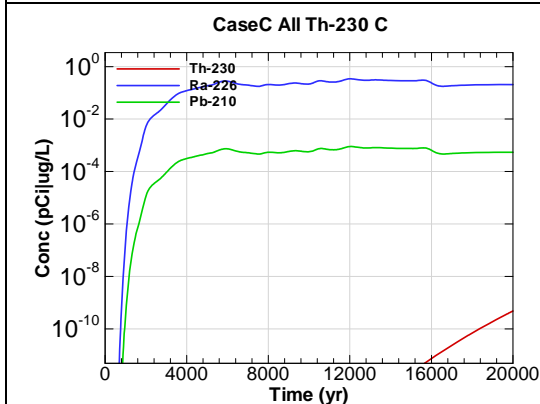


Figure A.5-51 - 100m Aquifer Concentration for
CaseC All Th-230 C

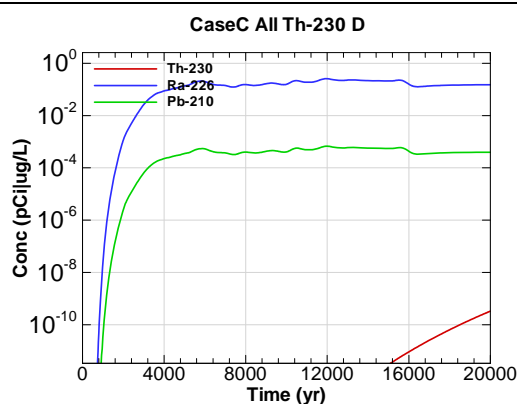


Figure A.5-52 - 100m Aquifer Concentration for
CaseC All Th-230 D

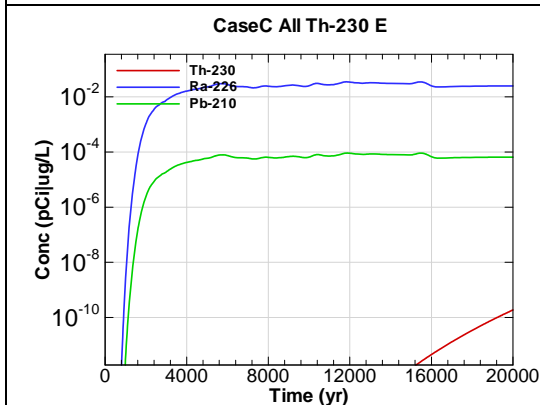


Figure A.5-53 - 100m Aquifer Concentration for
CaseC All Th-230 E

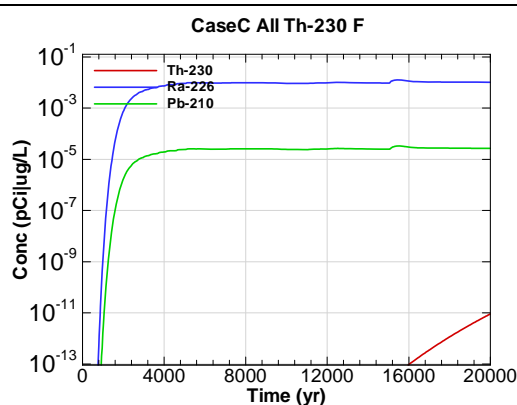


Figure A.5-54 - 100m Aquifer Concentration for
CaseC All Th-230 F

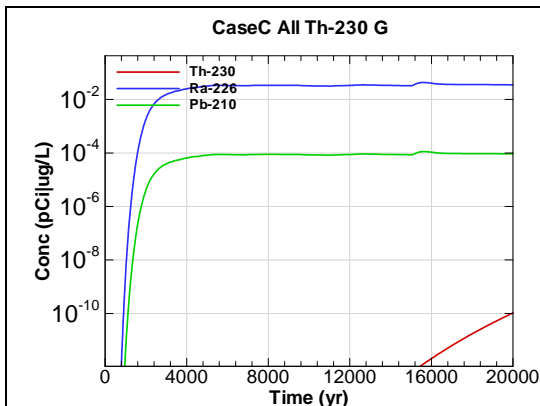


Figure A.5-55 - 100m Aquifer Concentration for
CaseC All Th-230 G

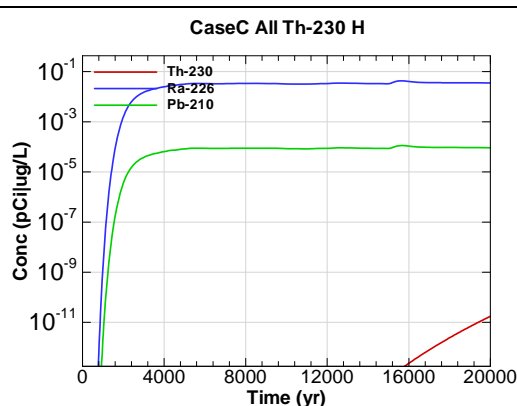


Figure A.5-56 - 100m Aquifer Concentration for
CaseC All Th-230 H

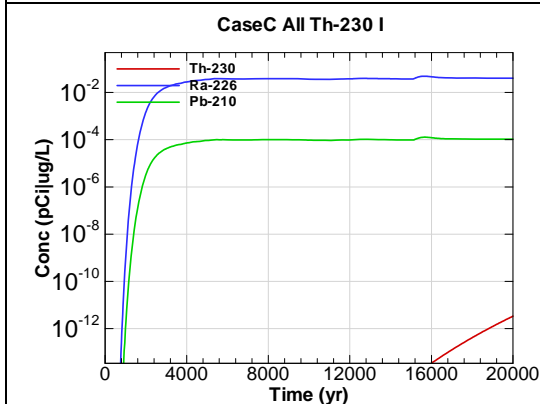


Figure A.5-57 - 100m Aquifer Concentration for
CaseC All Th-230 I

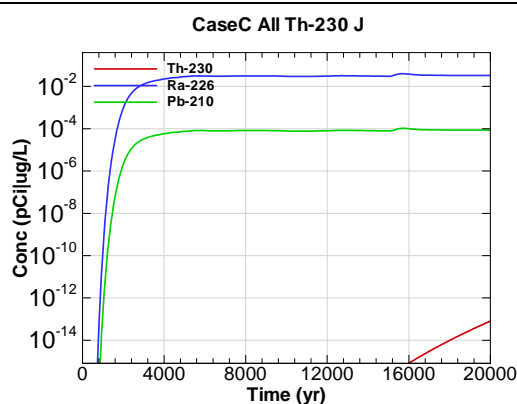


Figure A.5-58 - 100m Aquifer Concentration for
CaseC All Th-230 J

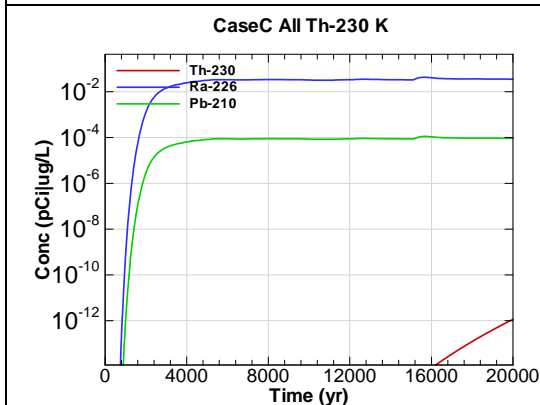


Figure A.5-59 - 100m Aquifer Concentration for
CaseC All Th-230 K

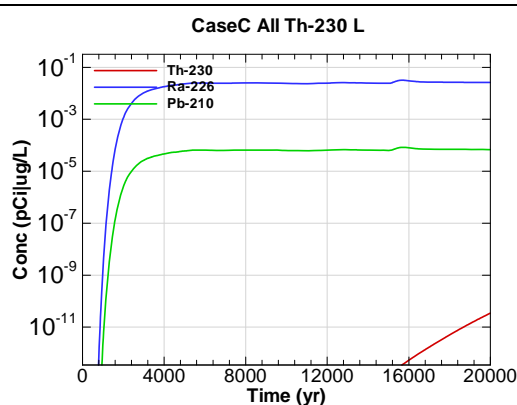
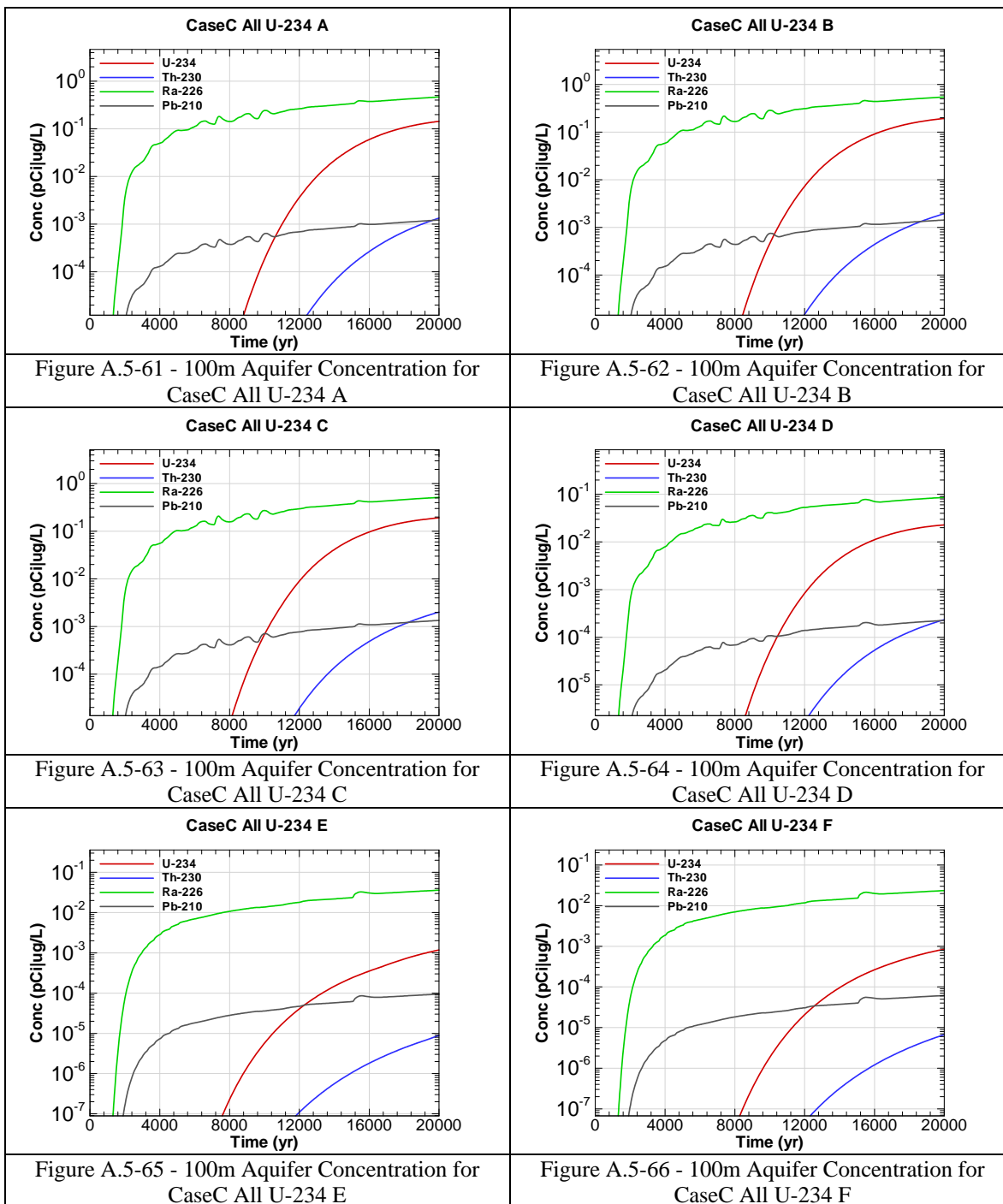


Figure A.5-60 - 100m Aquifer Concentration for
CaseC All Th-230 L



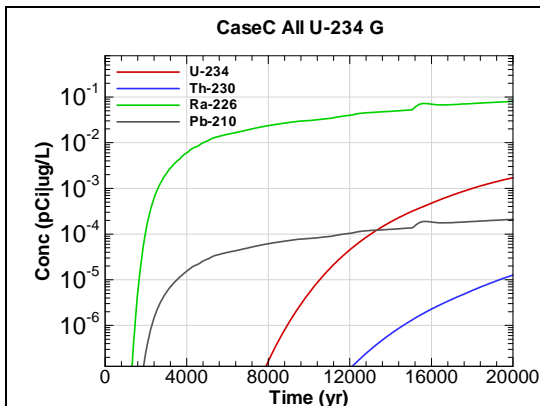


Figure A.5-67 - 100m Aquifer Concentration for
CaseC All U-234 G

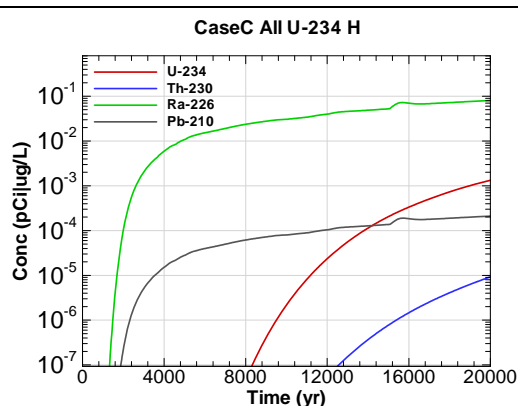


Figure A.5-68 - 100m Aquifer Concentration for
CaseC All U-234 H

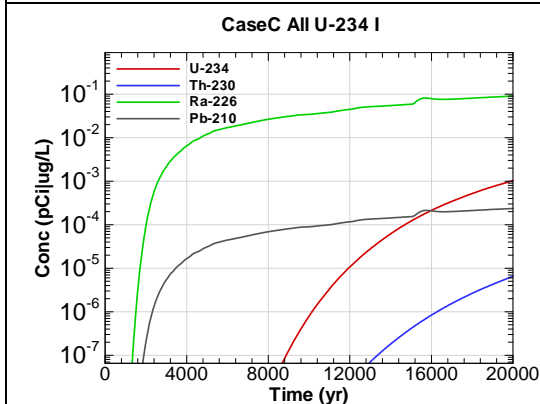


Figure A.5-69 - 100m Aquifer Concentration for
CaseC All U-234 I

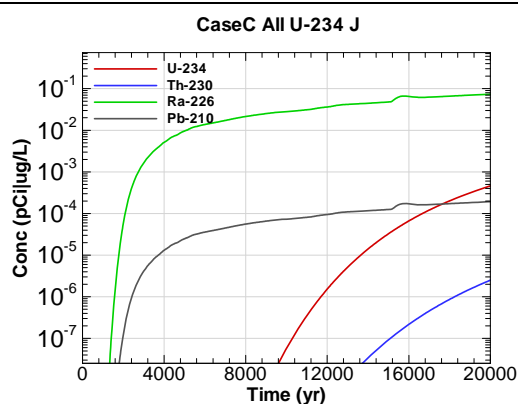


Figure A.5-70 - 100m Aquifer Concentration for
CaseC All U-234 J

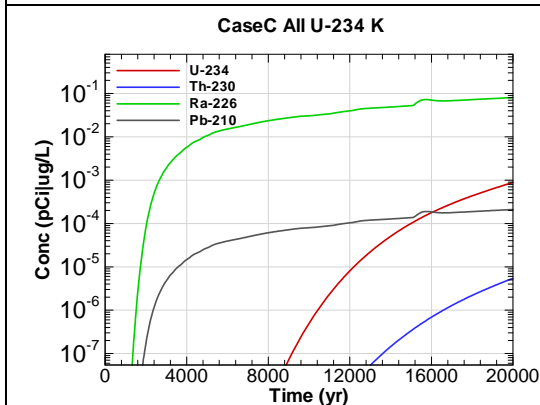


Figure A.5-71 - 100m Aquifer Concentration for
CaseC All U-234 K

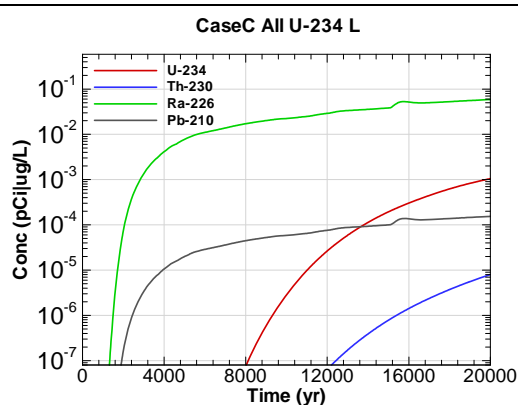


Figure A.5-72 - 100m Aquifer Concentration for
CaseC All U-234 L

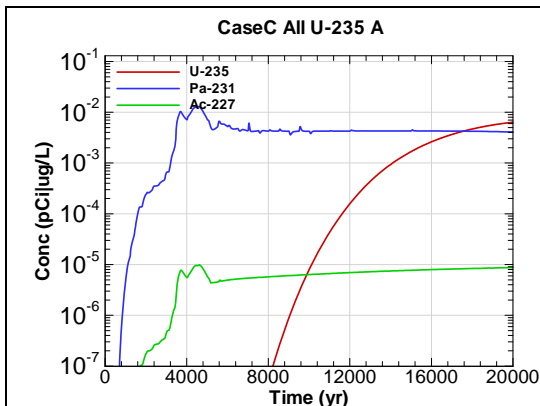


Figure A.5-73 - 100m Aquifer Concentration for
CaseC All U-235 A

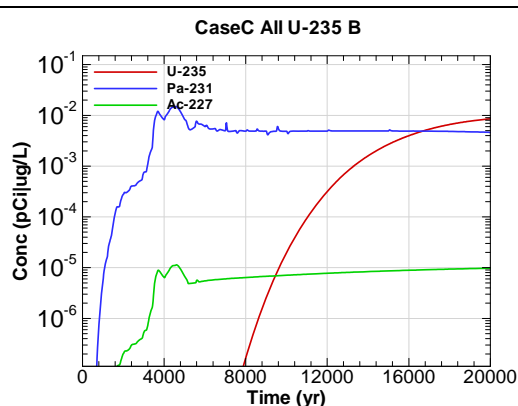


Figure A.5-74 - 100m Aquifer Concentration for
CaseC All U-235 B

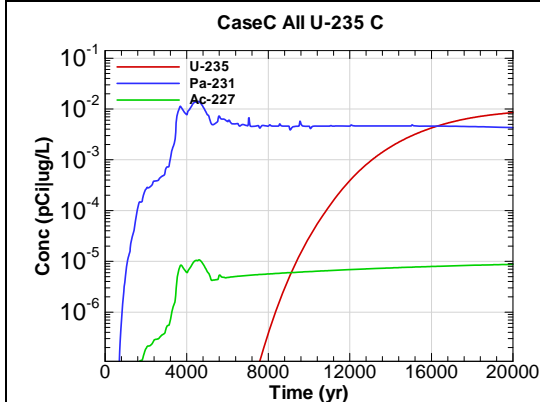


Figure A.5-75 - 100m Aquifer Concentration for
CaseC All U-235 C

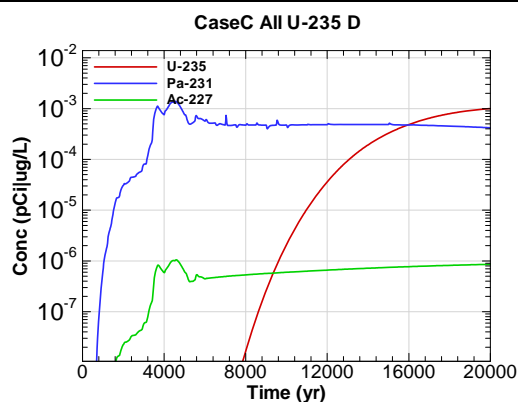


Figure A.5-76 - 100m Aquifer Concentration for
CaseC All U-235 D

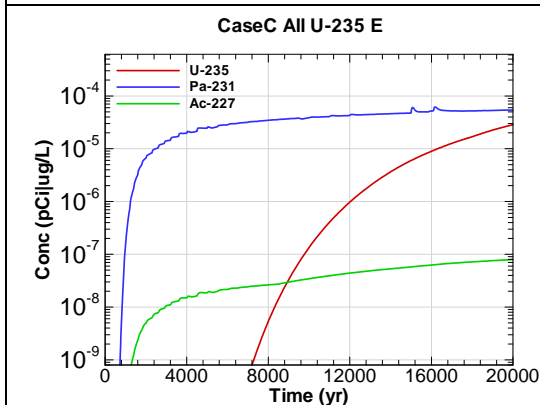


Figure A.5-77 - 100m Aquifer Concentration for
CaseC All U-235 E

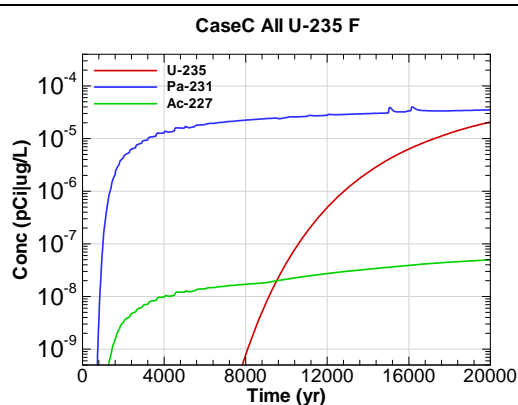


Figure A.5-78 - 100m Aquifer Concentration for
CaseC All U-235 F

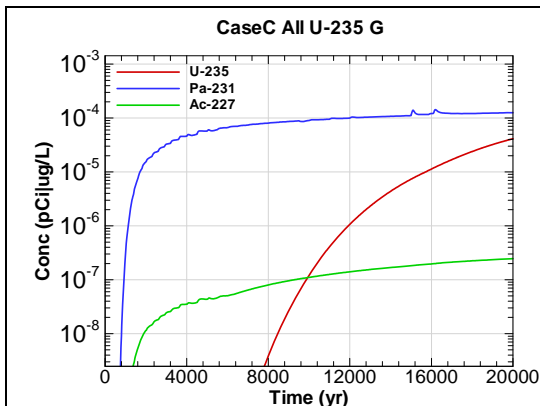


Figure A.5-79 - 100m Aquifer Concentration for
CaseC All U-235 G

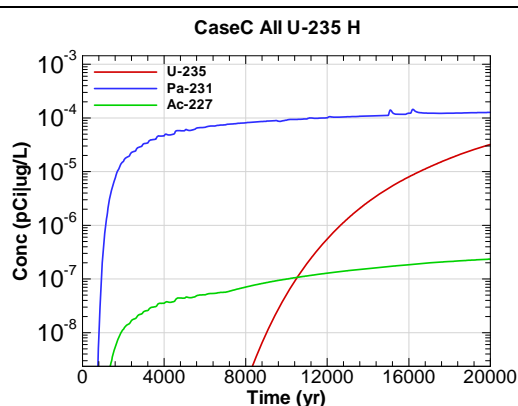


Figure A.5-80 - 100m Aquifer Concentration for
CaseC All U-235 H

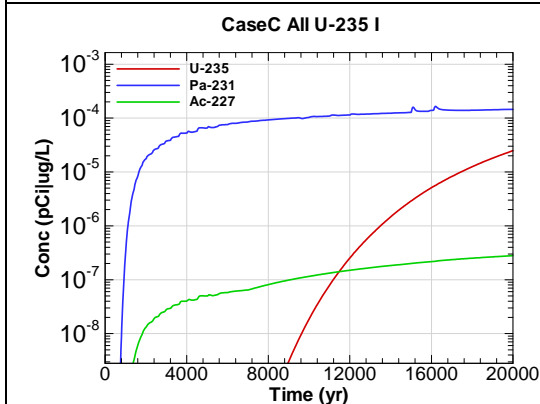


Figure A.5-81 - 100m Aquifer Concentration for
CaseC All U-235 I

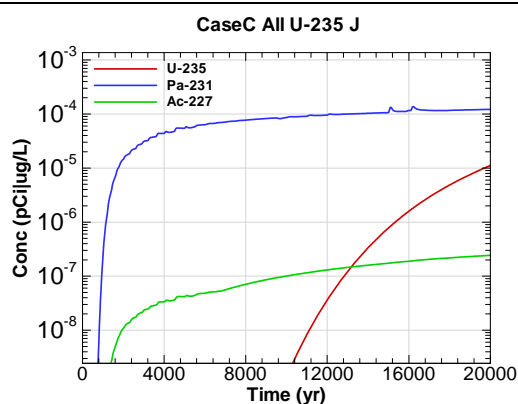


Figure A.5-82 - 100m Aquifer Concentration for
CaseC All U-235 J

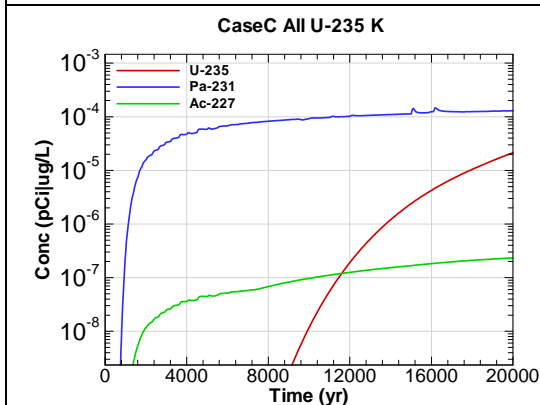


Figure A.5-83 - 100m Aquifer Concentration for
CaseC All U-235 K

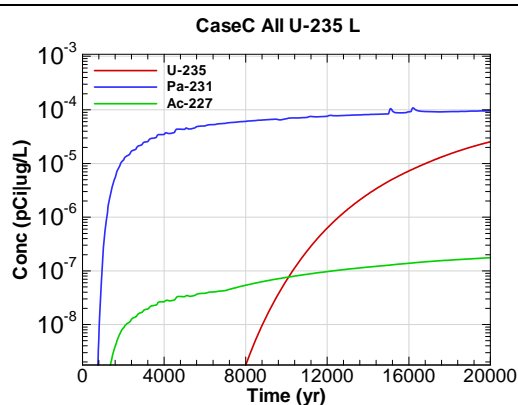
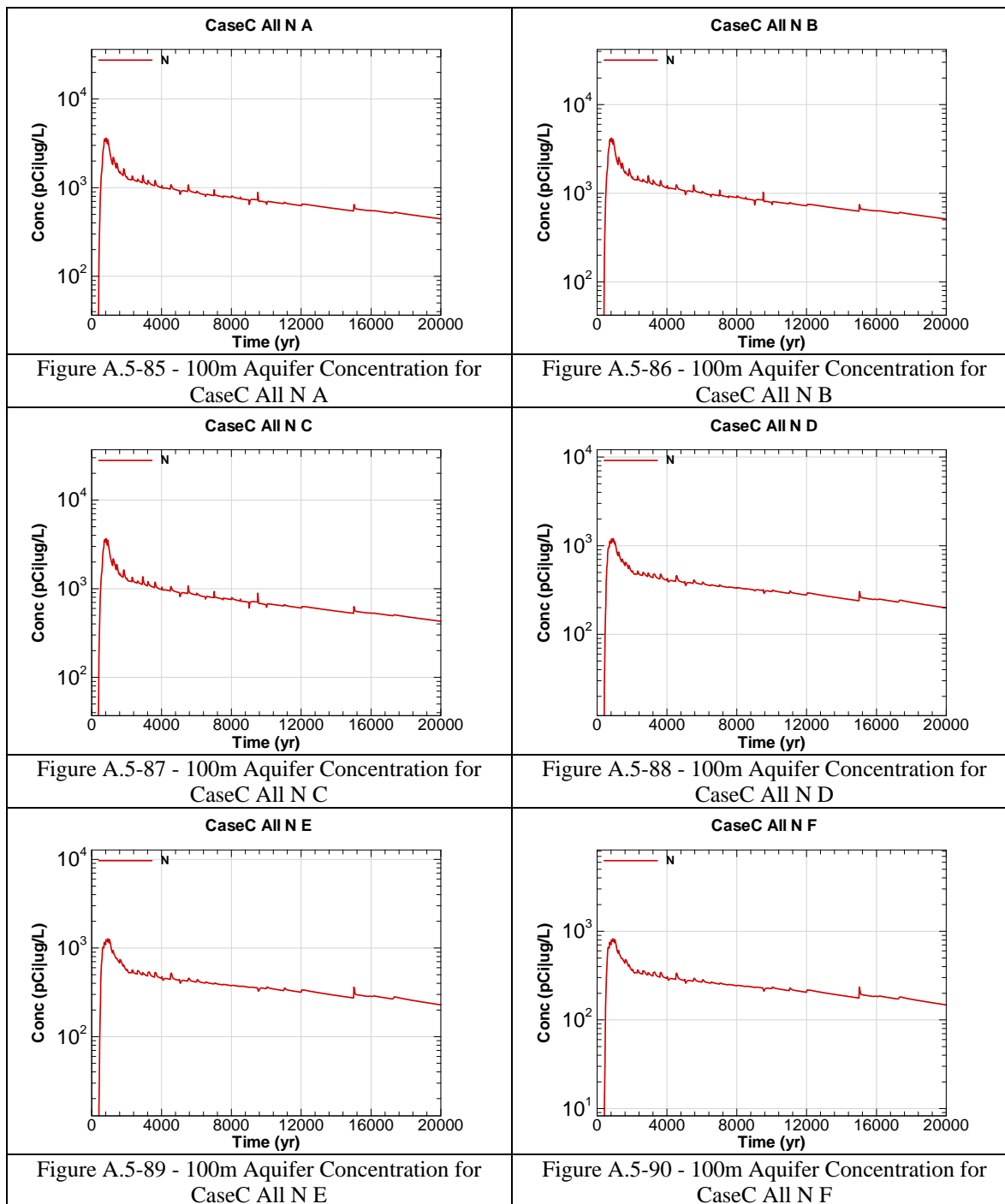
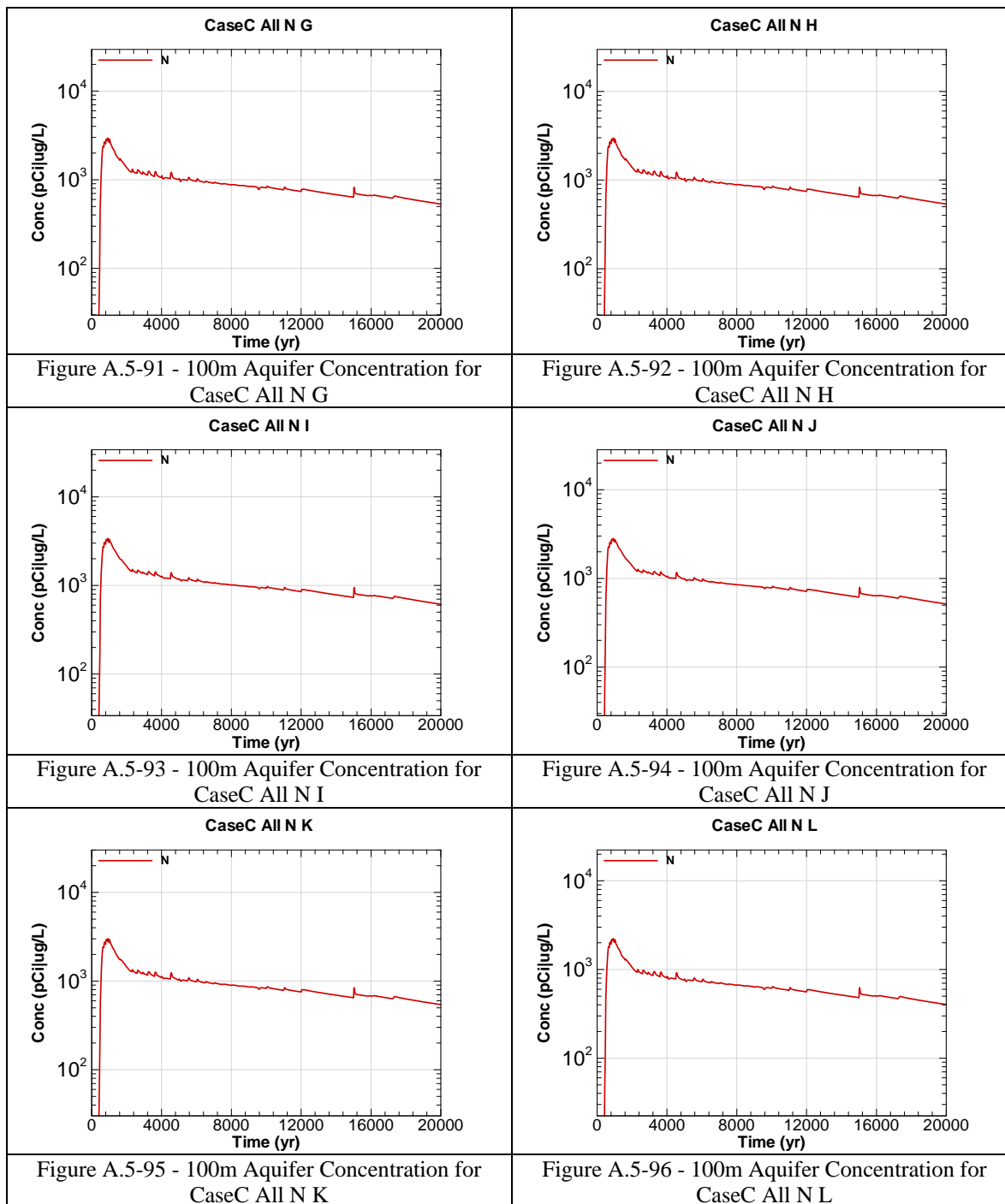


Figure A.5-84 - 100m Aquifer Concentration for
CaseC All U-235 L





This page intentionally left blank

APPENDIX A.6

100-METER RADIOLOGICAL AND CHEMICAL CONCENTRATIONS – CASE D

Appendix A.6 contains curves showing the 100 meter key radiological and chemical concentrations for all of SDF (vault and FDC inventories) for Case D. 20,000 year concentration results are presented for Sectors A through L for the peak concentration per sector regardless of aquifer.

Graph heading example “CaseD All I-129 A”

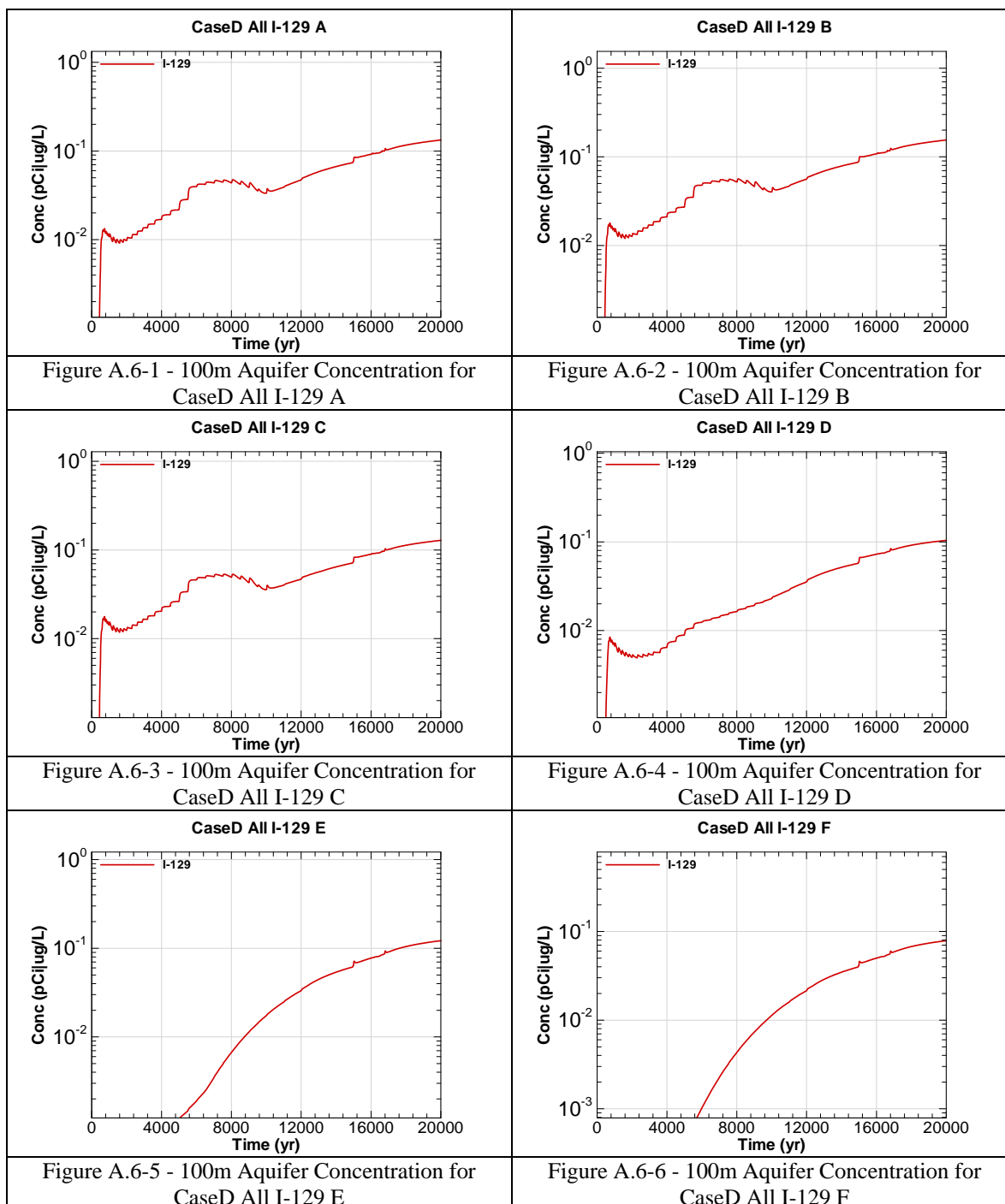
Key

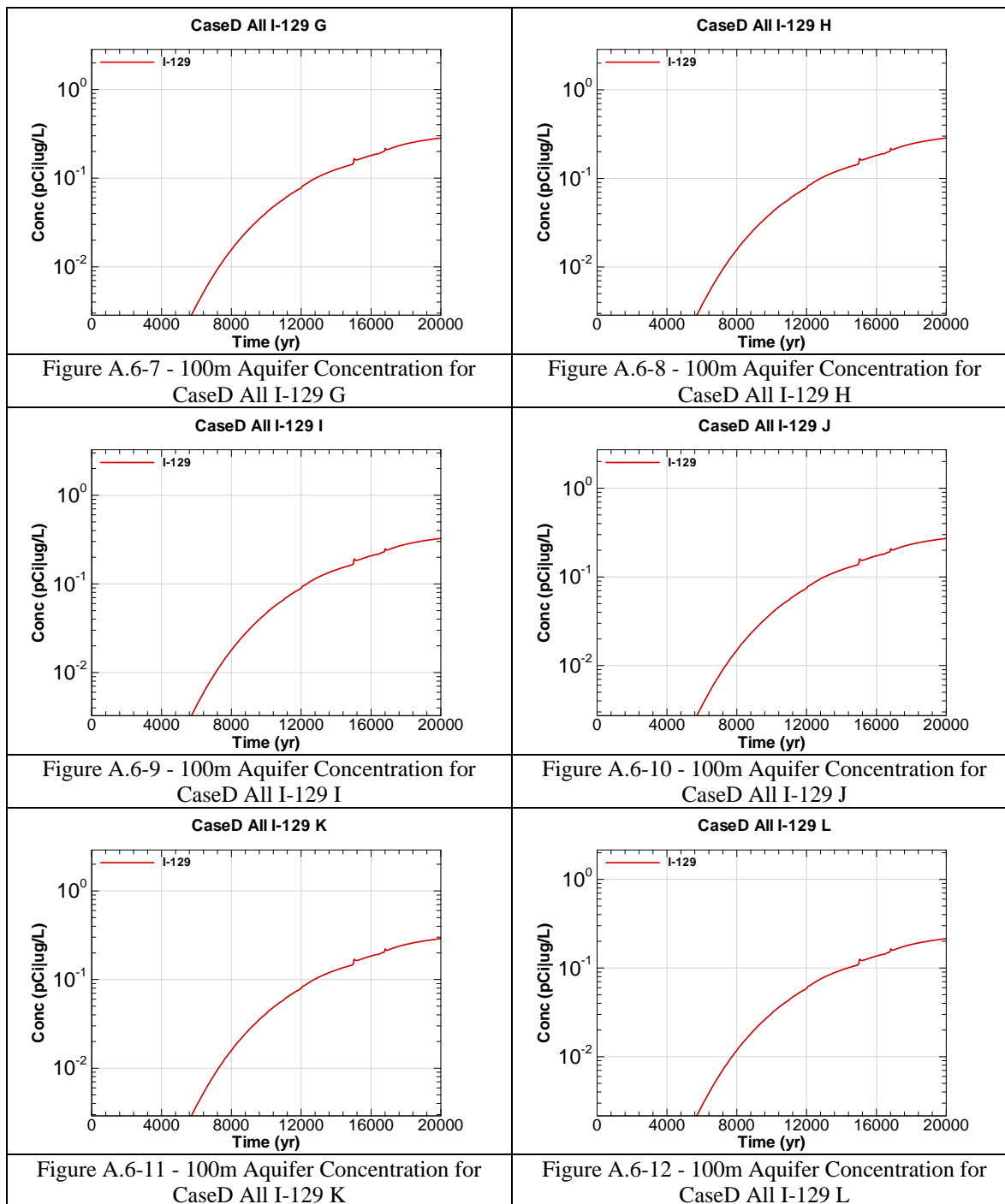
CaseD = Scenario case

All = Inventory source is all disposal units

I-129 = Radionuclide or chemical of concern

A = Evaluation sector of concern





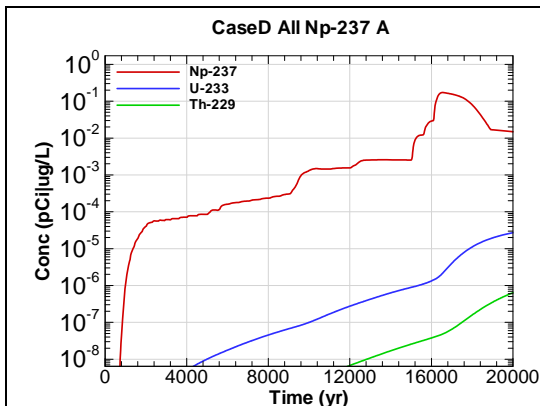


Figure A.6-13 - 100m Aquifer Concentration for CaseD All Np-237 A

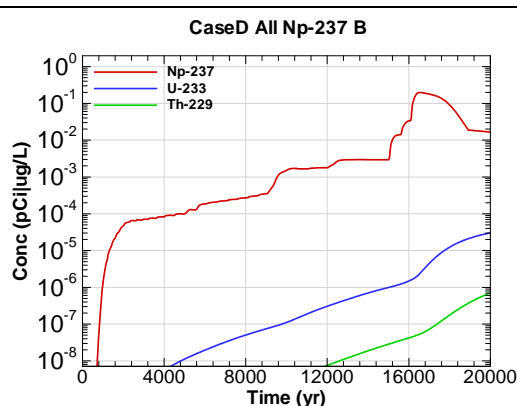


Figure A.6-14 - 100m Aquifer Concentration for CaseD All Np-237 B

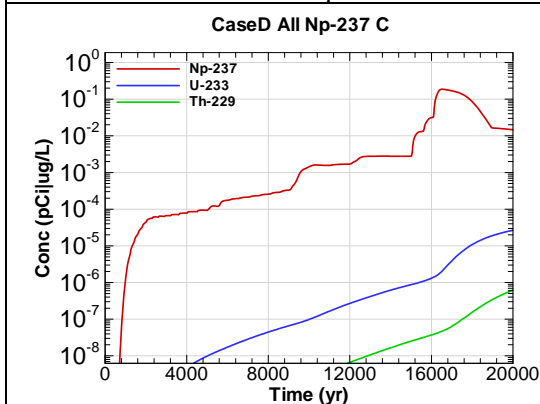


Figure A.6-15 - 100m Aquifer Concentration for CaseD All Np-237 C

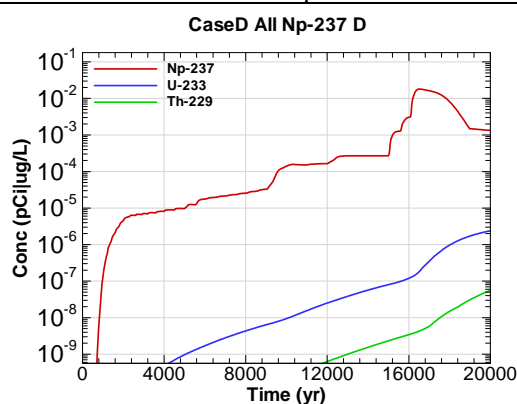


Figure A.6-16 - 100m Aquifer Concentration for CaseD All Np-237 D

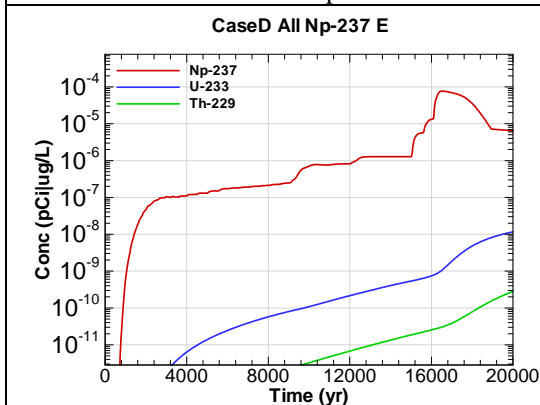


Figure A.6-17 - 100m Aquifer Concentration for CaseD All Np-237 E

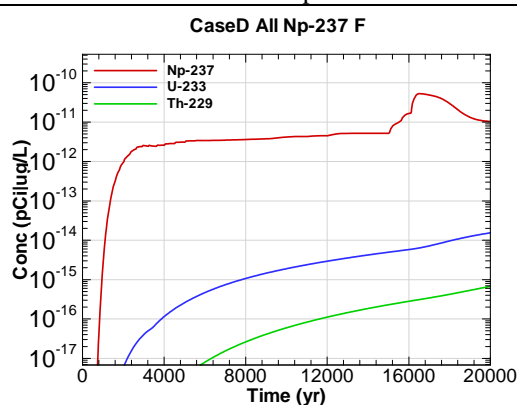


Figure A.6-18 - 100m Aquifer Concentration for CaseD All Np-237 F

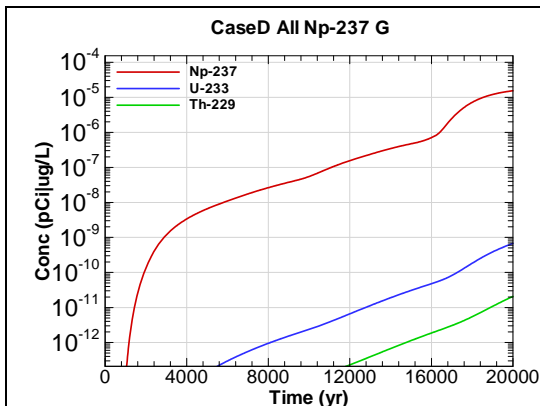


Figure A.6-19 - 100m Aquifer Concentration for
CaseD All Np-237 G

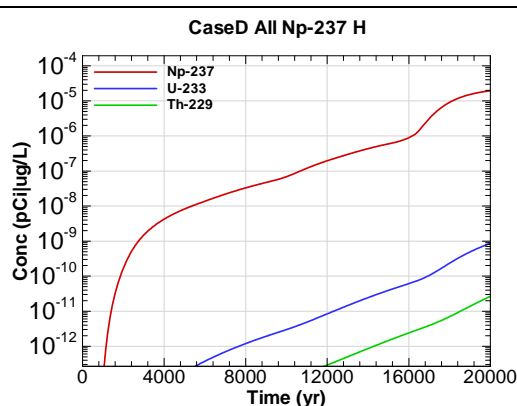


Figure A.6-20 - 100m Aquifer Concentration for
CaseD All Np-237 H

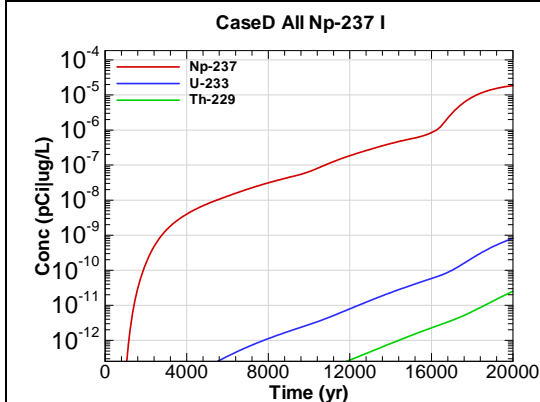


Figure A.6-21 - 100m Aquifer Concentration for
CaseD All Np-237 I

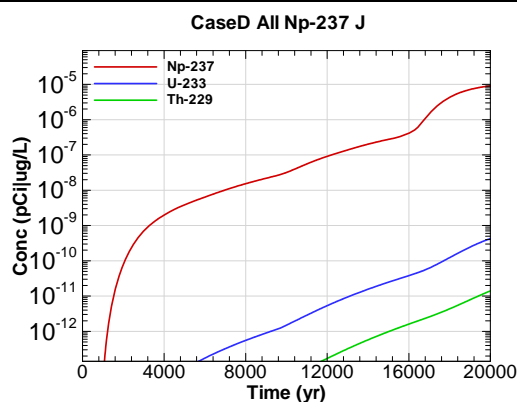


Figure A.6-22 - 100m Aquifer Concentration for
CaseD All Np-237 J

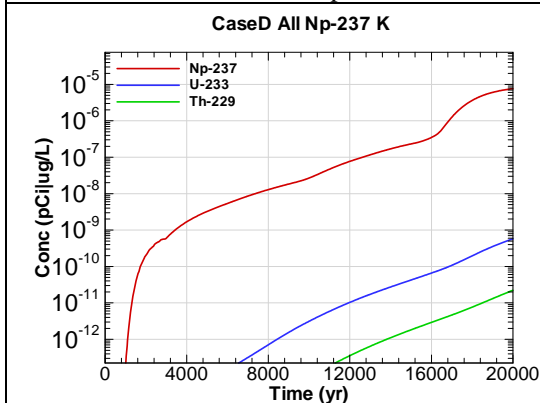


Figure A.6-23 - 100m Aquifer Concentration for
CaseD All Np-237 K

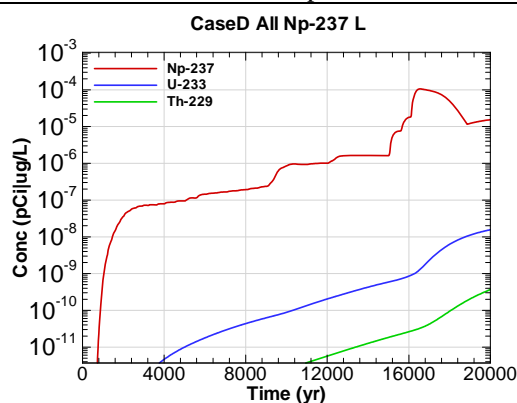


Figure A.6-24 - 100m Aquifer Concentration for
CaseD All Np-237 L

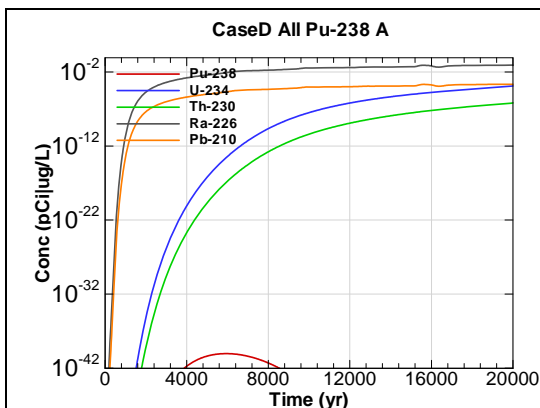


Figure A.6-25 - 100m Aquifer Concentration for CaseD All Pu-238 A

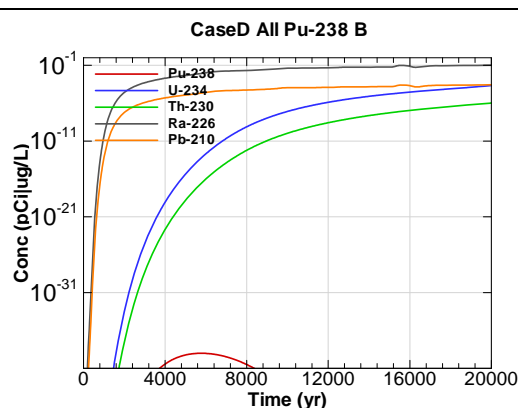


Figure A.6-26 - 100m Aquifer Concentration for CaseD All Pu-238 B

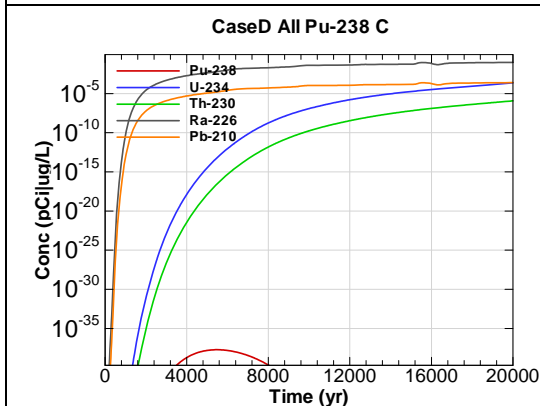


Figure A.6-27 - 100m Aquifer Concentration for CaseD All Pu-238 C

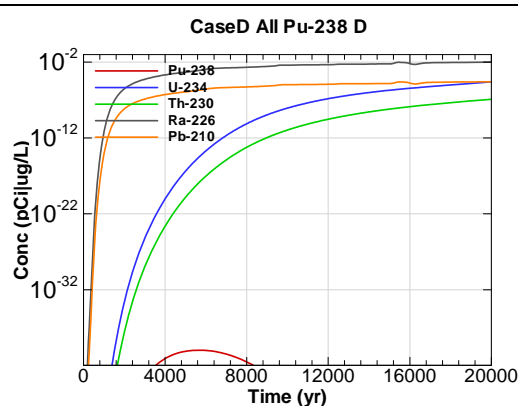


Figure A.6-28 - 100m Aquifer Concentration for CaseD All Pu-238 D

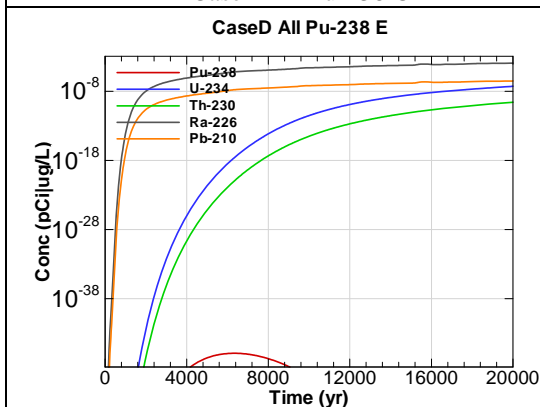


Figure A.6-29 - 100m Aquifer Concentration for CaseD All Pu-238 E

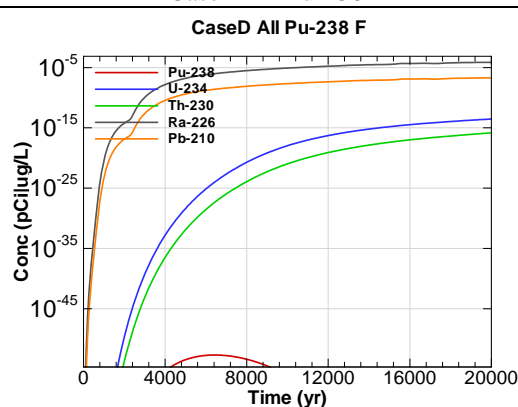


Figure A.6-30 - 100m Aquifer Concentration for CaseD All Pu-238 F

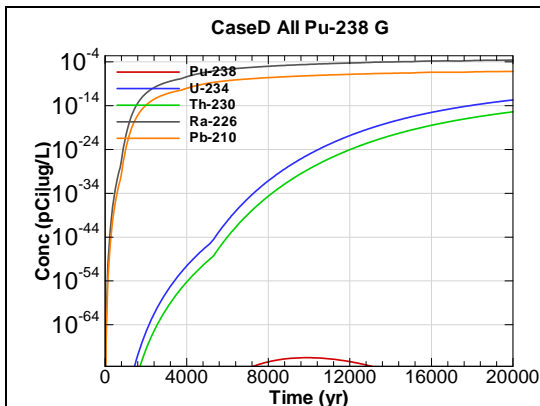


Figure A.6-31 - 100m Aquifer Concentration for CaseD All Pu-238 G

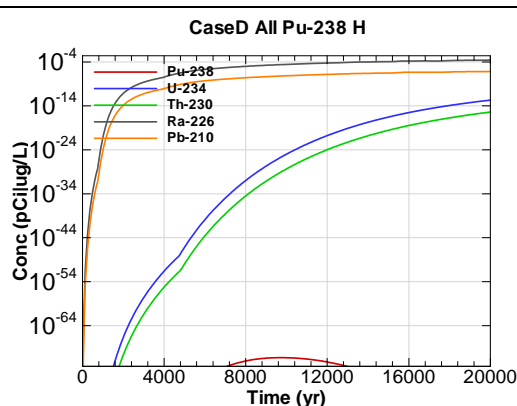


Figure A.6-32 - 100m Aquifer Concentration for CaseD All Pu-238 H

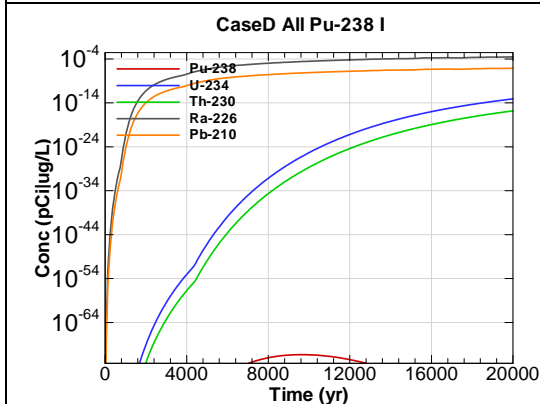


Figure A.6-33 - 100m Aquifer Concentration for CaseD All Pu-238 I

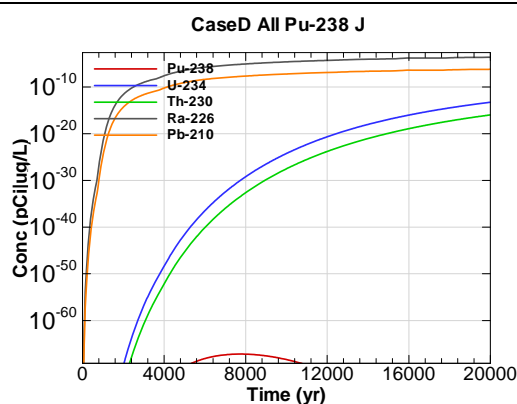


Figure A.6-34 - 100m Aquifer Concentration for CaseD All Pu-238 J

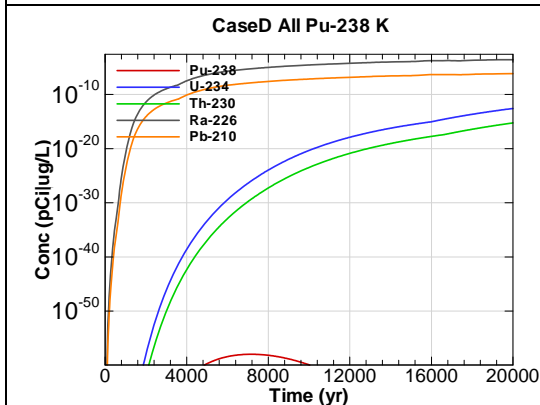


Figure A.6-35 - 100m Aquifer Concentration for CaseD All Pu-238 K

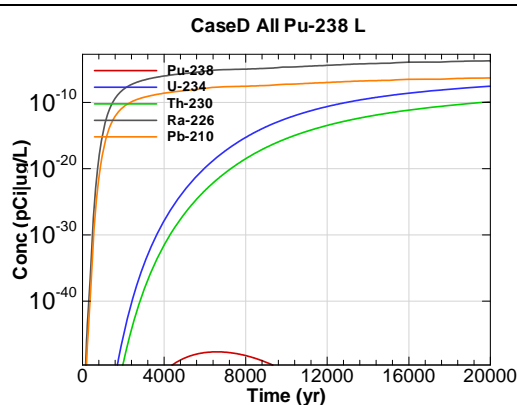
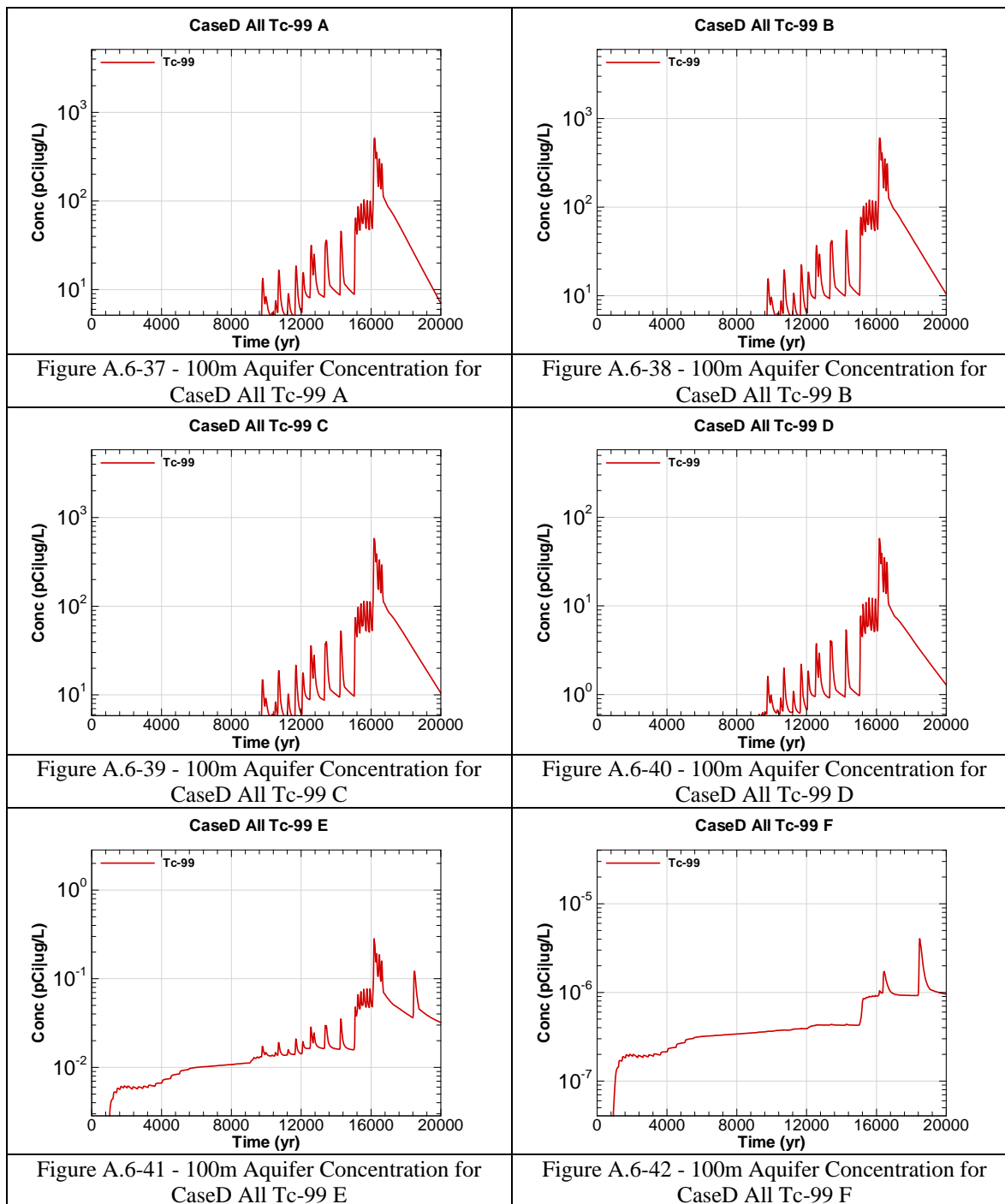
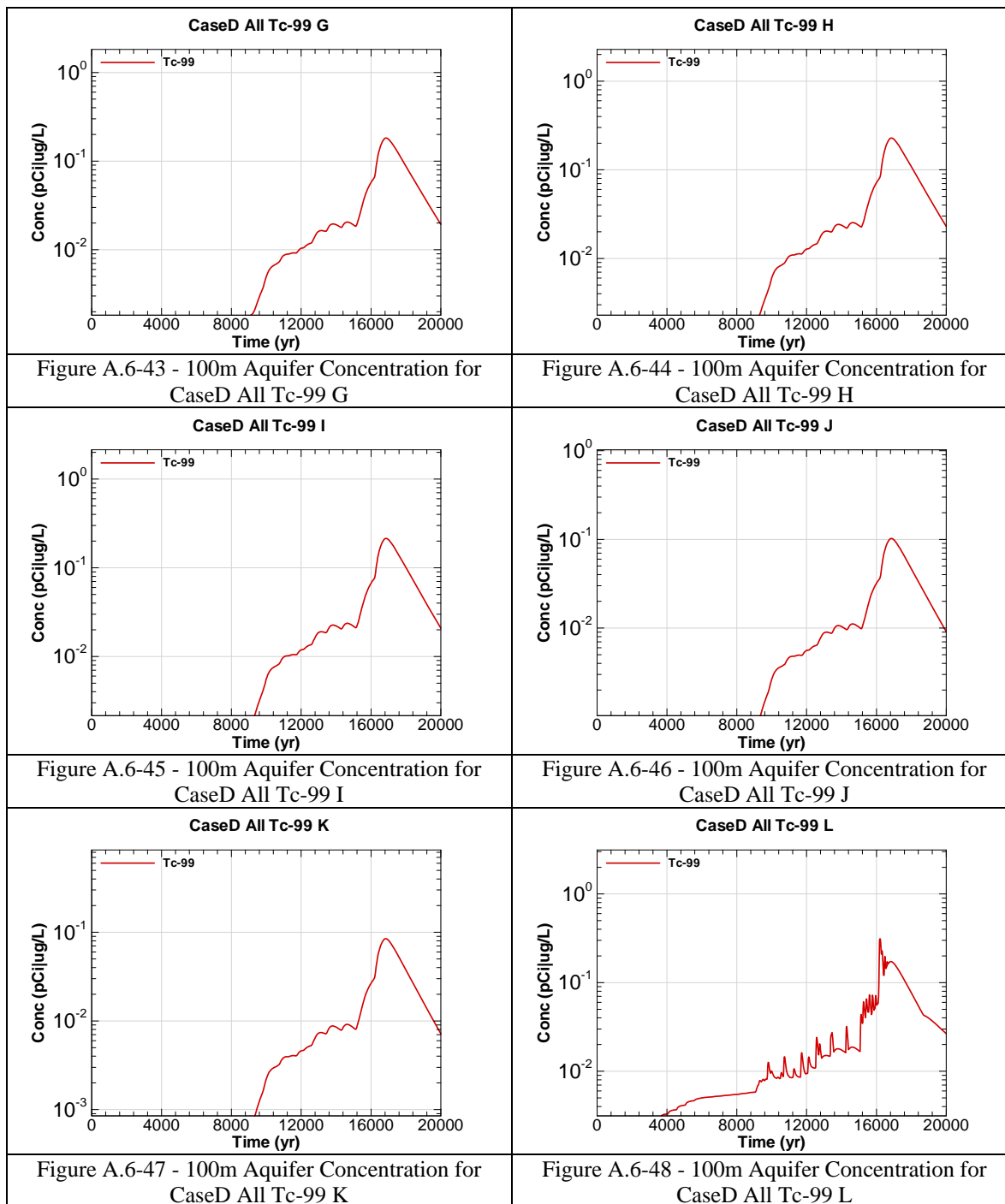


Figure A.6-36 - 100m Aquifer Concentration for CaseD All Pu-238 L





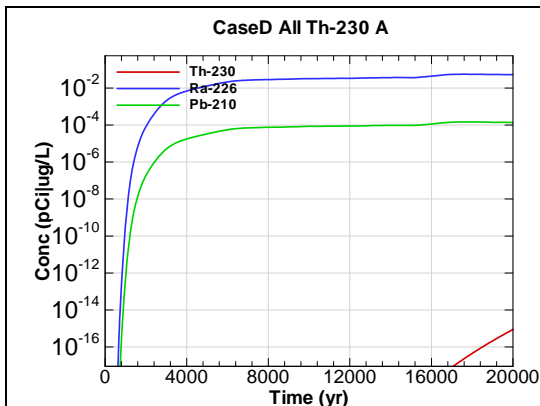


Figure A.6-49 - 100m Aquifer Concentration for CaseD All Th-230 A

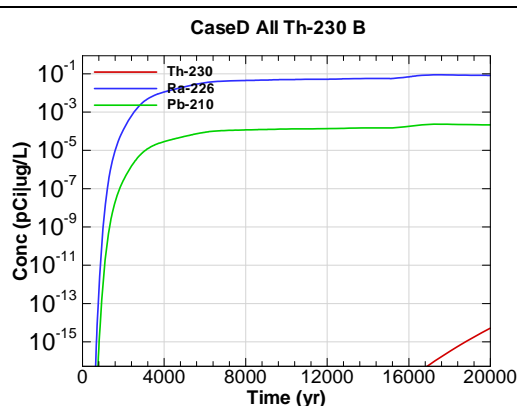


Figure A.6-50 - 100m Aquifer Concentration for CaseD All Th-230 B

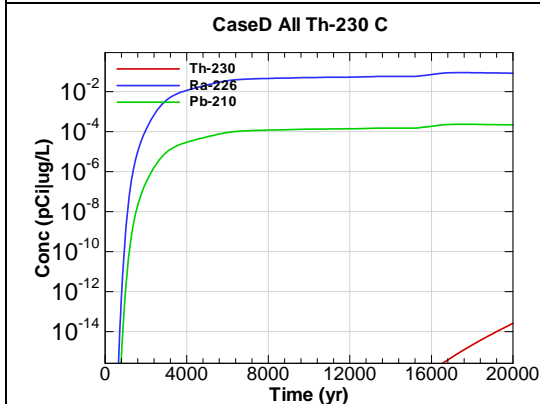


Figure A.6-51 - 100m Aquifer Concentration for CaseD All Th-230 C

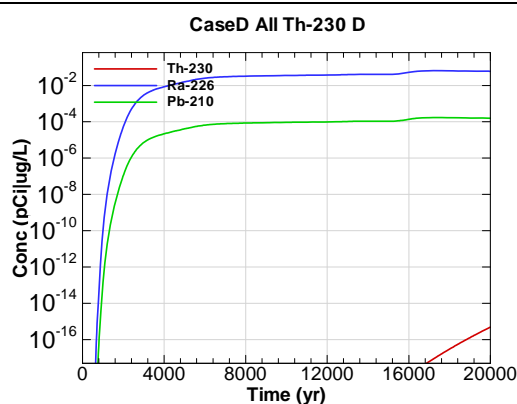


Figure A.6-52 - 100m Aquifer Concentration for CaseD All Th-230 D

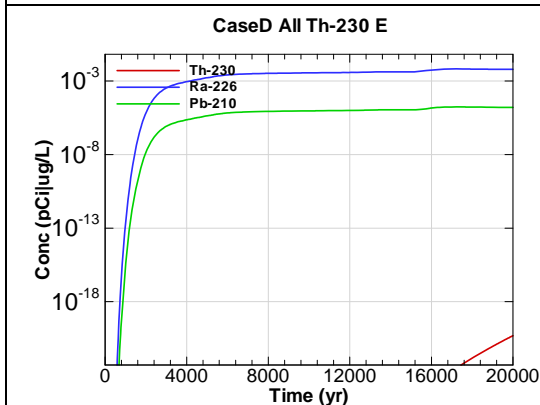


Figure A.6-53 - 100m Aquifer Concentration for CaseD All Th-230 E

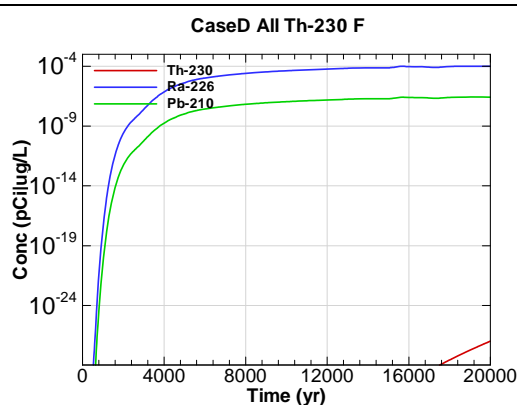


Figure A.6-54 - 100m Aquifer Concentration for CaseD All Th-230 F

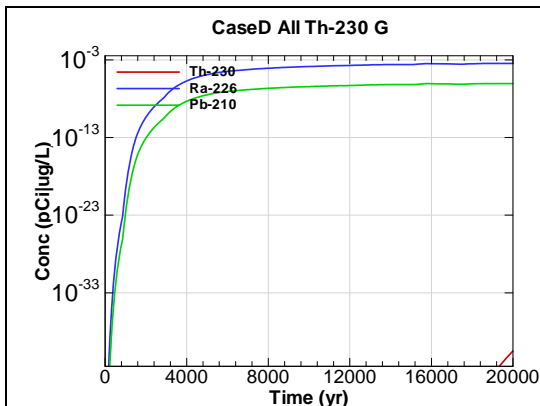


Figure A.6-55 - 100m Aquifer Concentration for CaseD All Th-230 G

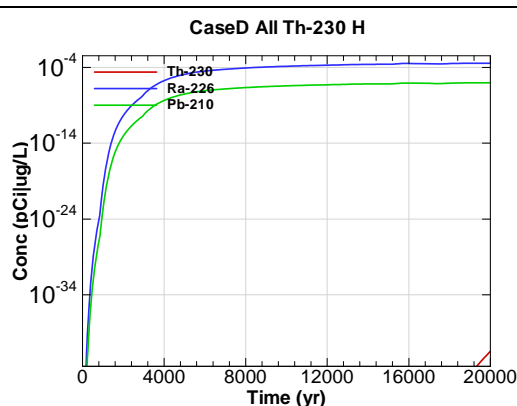


Figure A.6-56 - 100m Aquifer Concentration for CaseD All Th-230 H

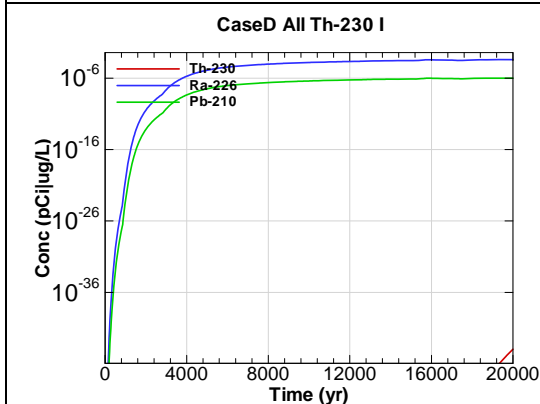


Figure A.6-57 - 100m Aquifer Concentration for CaseD All Th-230 I

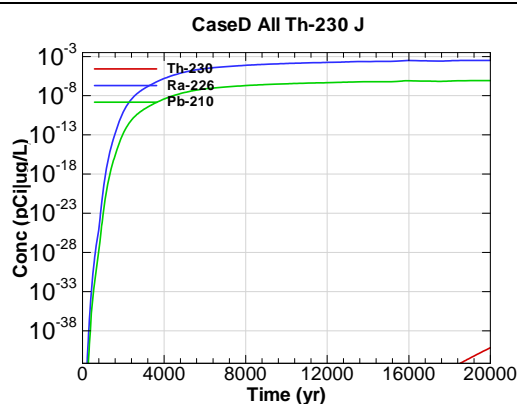


Figure A.6-58 - 100m Aquifer Concentration for CaseD All Th-230 J

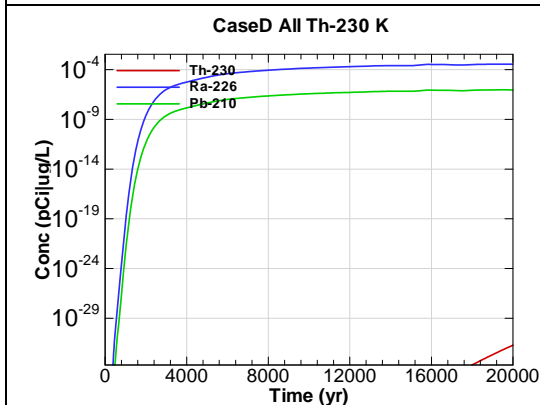


Figure A.6-59 - 100m Aquifer Concentration for CaseD All Th-230 K

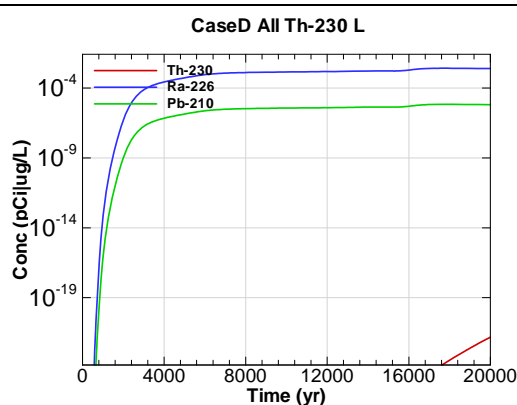


Figure A.6-60 - 100m Aquifer Concentration for CaseD All Th-230 L

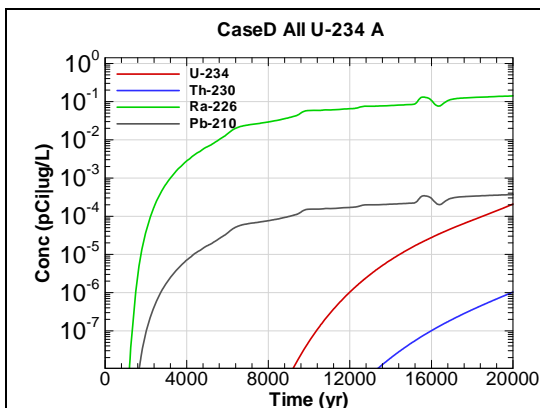


Figure A.6-61 - 100m Aquifer Concentration for CaseD All U-234 A

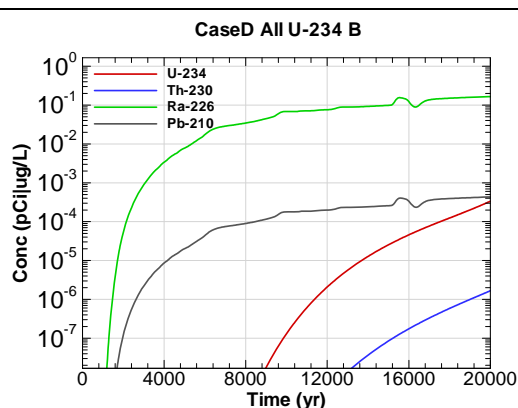


Figure A.6-62 - 100m Aquifer Concentration for CaseD All U-234 B

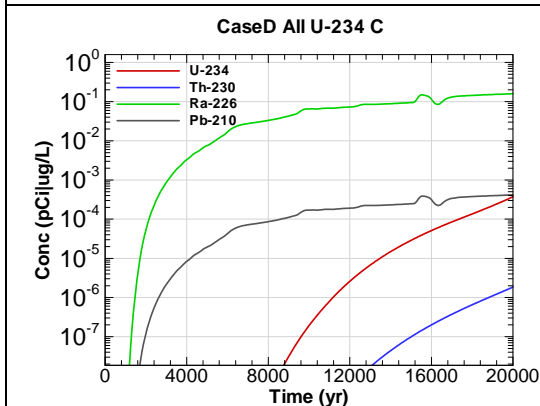


Figure A.6-63 - 100m Aquifer Concentration for CaseD All U-234 C

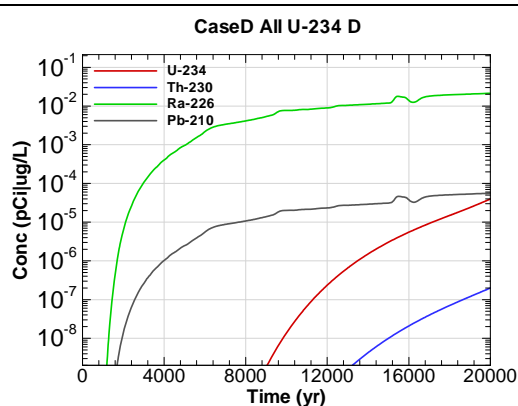


Figure A.6-64 - 100m Aquifer Concentration for CaseD All U-234 D

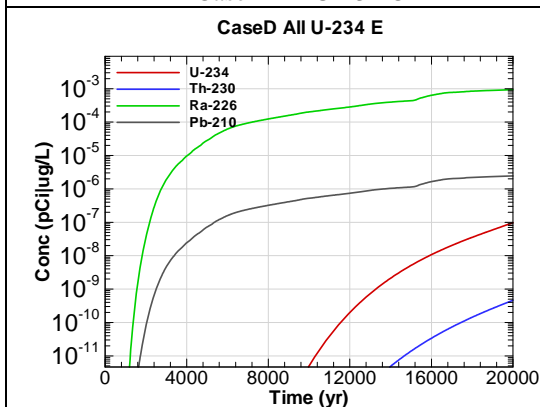


Figure A.6-65 - 100m Aquifer Concentration for CaseD All U-234 E

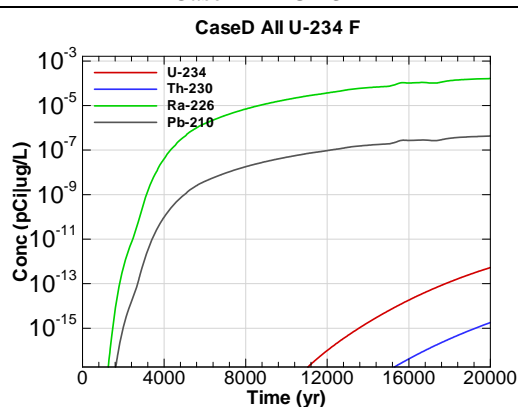


Figure A.6-66 - 100m Aquifer Concentration for CaseD All U-234 F

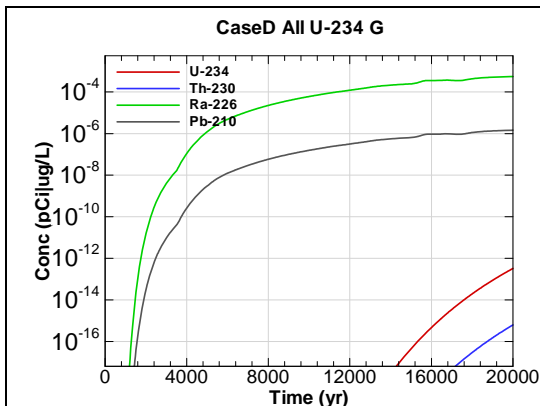


Figure A.6-67 - 100m Aquifer Concentration for CaseD All U-234 G

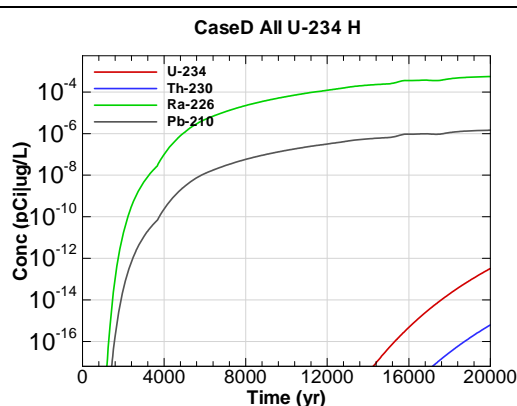


Figure A.6-68 - 100m Aquifer Concentration for CaseD All U-234 H

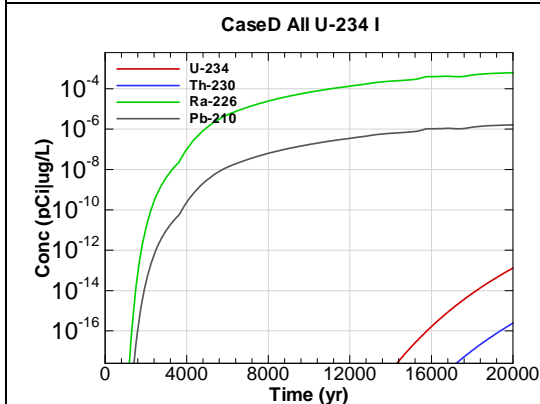


Figure A.6-69 - 100m Aquifer Concentration for CaseD All U-234 I

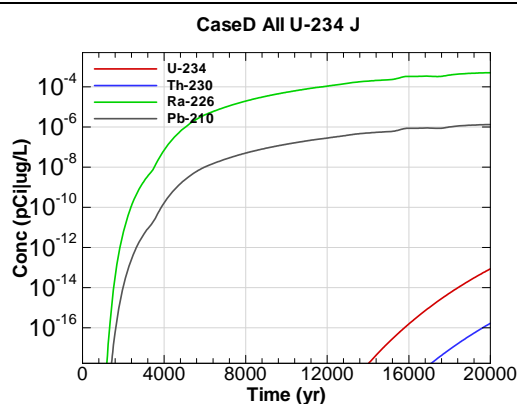


Figure A.6-70 - 100m Aquifer Concentration for CaseD All U-234 J

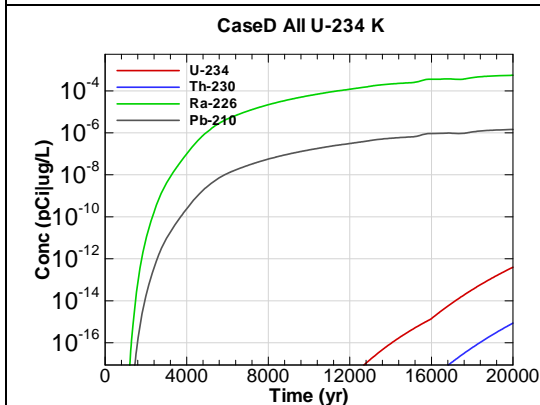


Figure A.6-71 - 100m Aquifer Concentration for CaseD All U-234 K

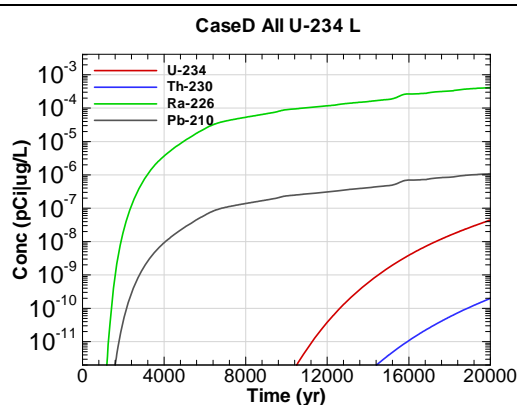
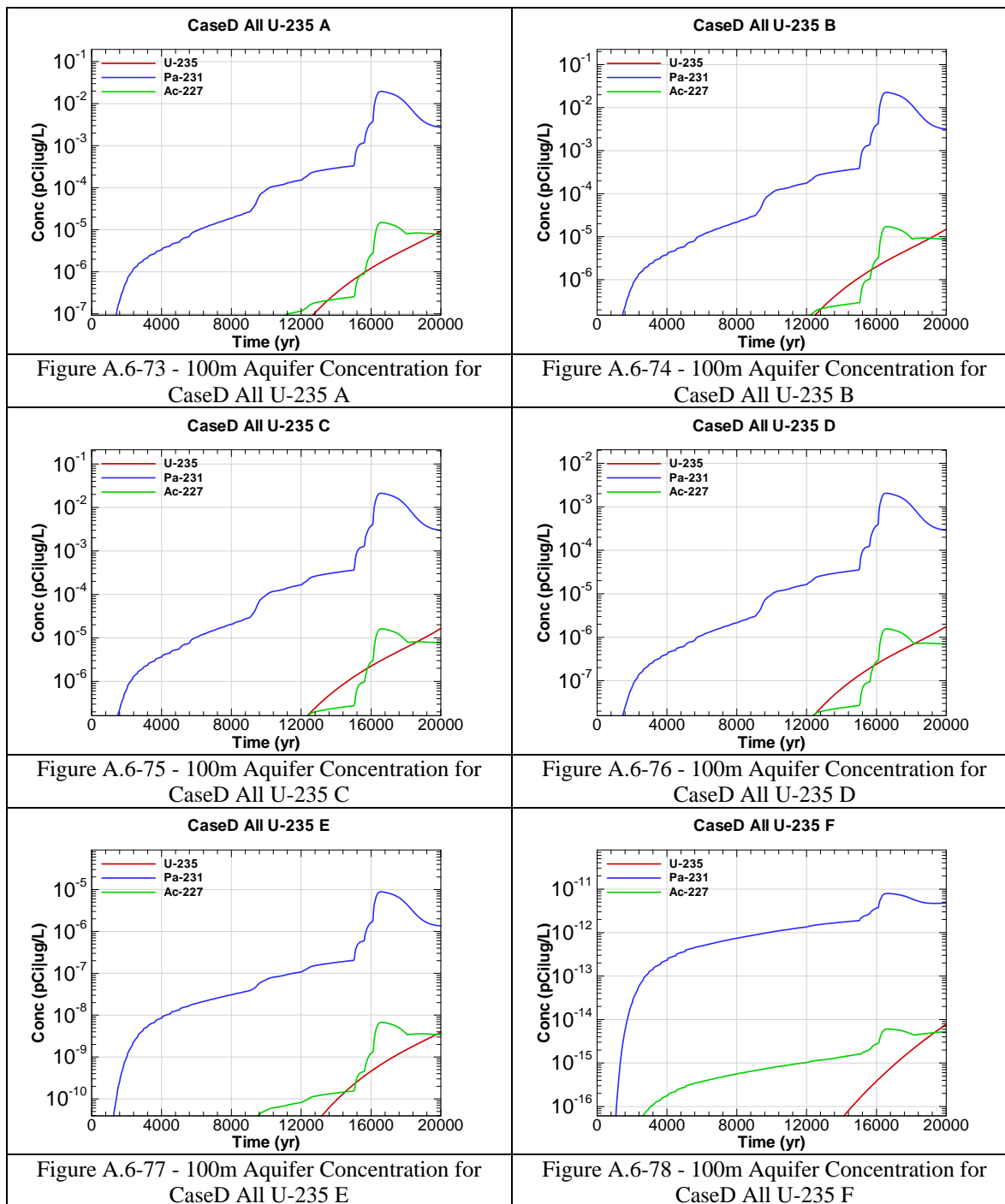


Figure A.6-72 - 100m Aquifer Concentration for CaseD All U-234 L



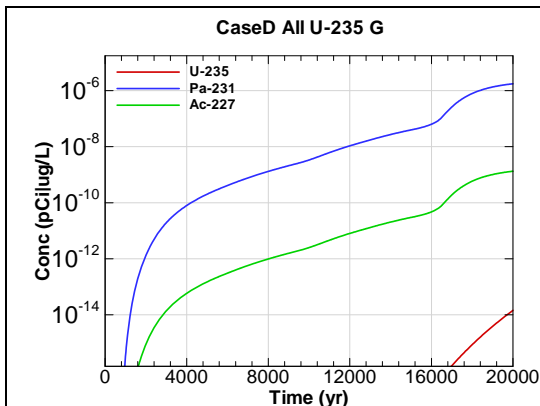


Figure A.6-79 - 100m Aquifer Concentration for
CaseD All U-235 G

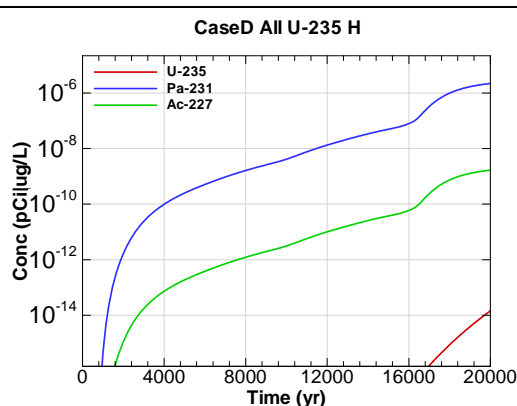


Figure A.6-80 - 100m Aquifer Concentration for
CaseD All U-235 H

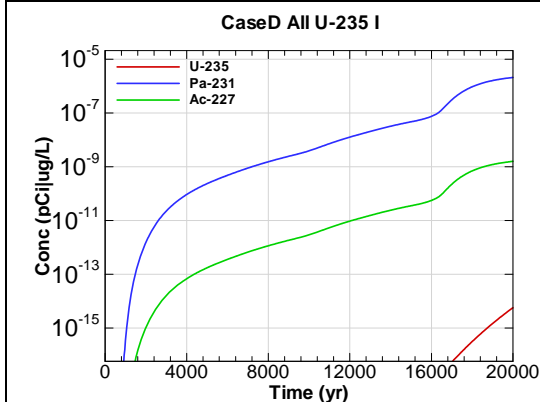


Figure A.6-81 - 100m Aquifer Concentration for
CaseD All U-235 I

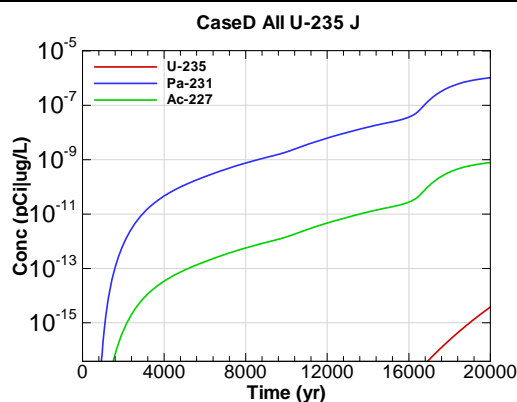


Figure A.6-82 - 100m Aquifer Concentration for
CaseD All U-235 J

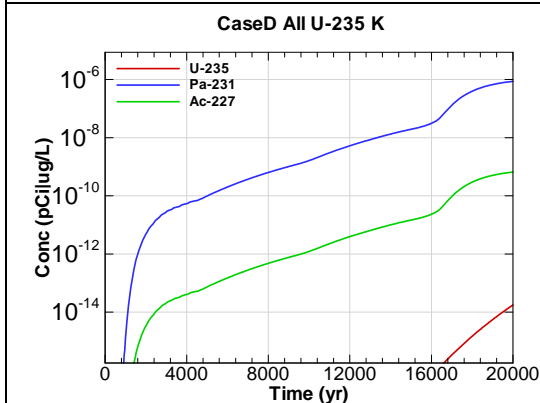


Figure A.6-83 - 100m Aquifer Concentration for
CaseD All U-235 K

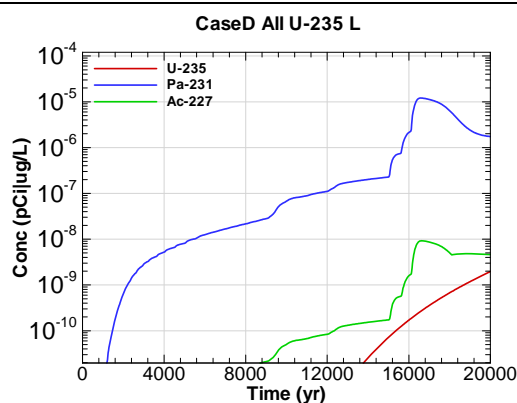
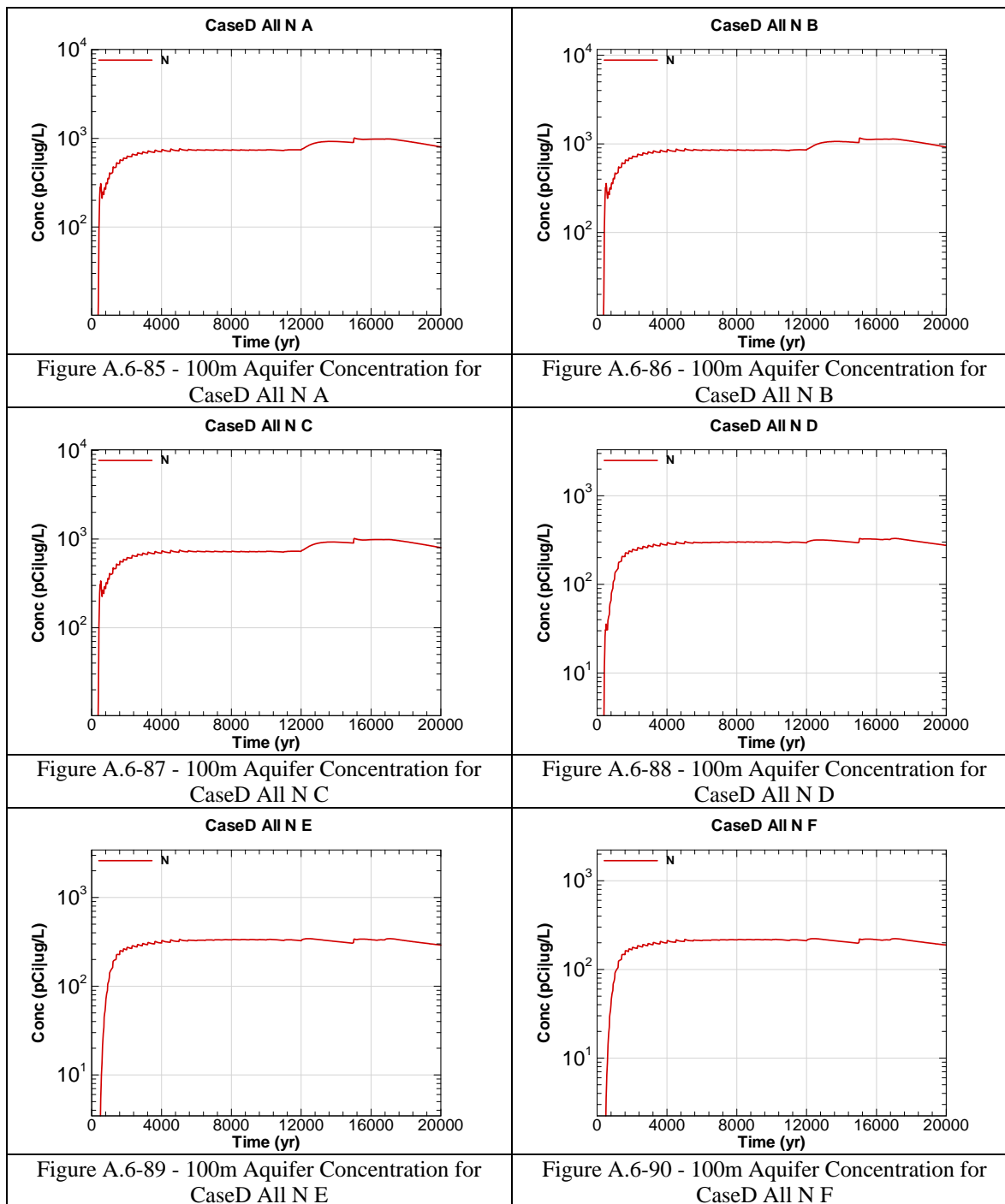
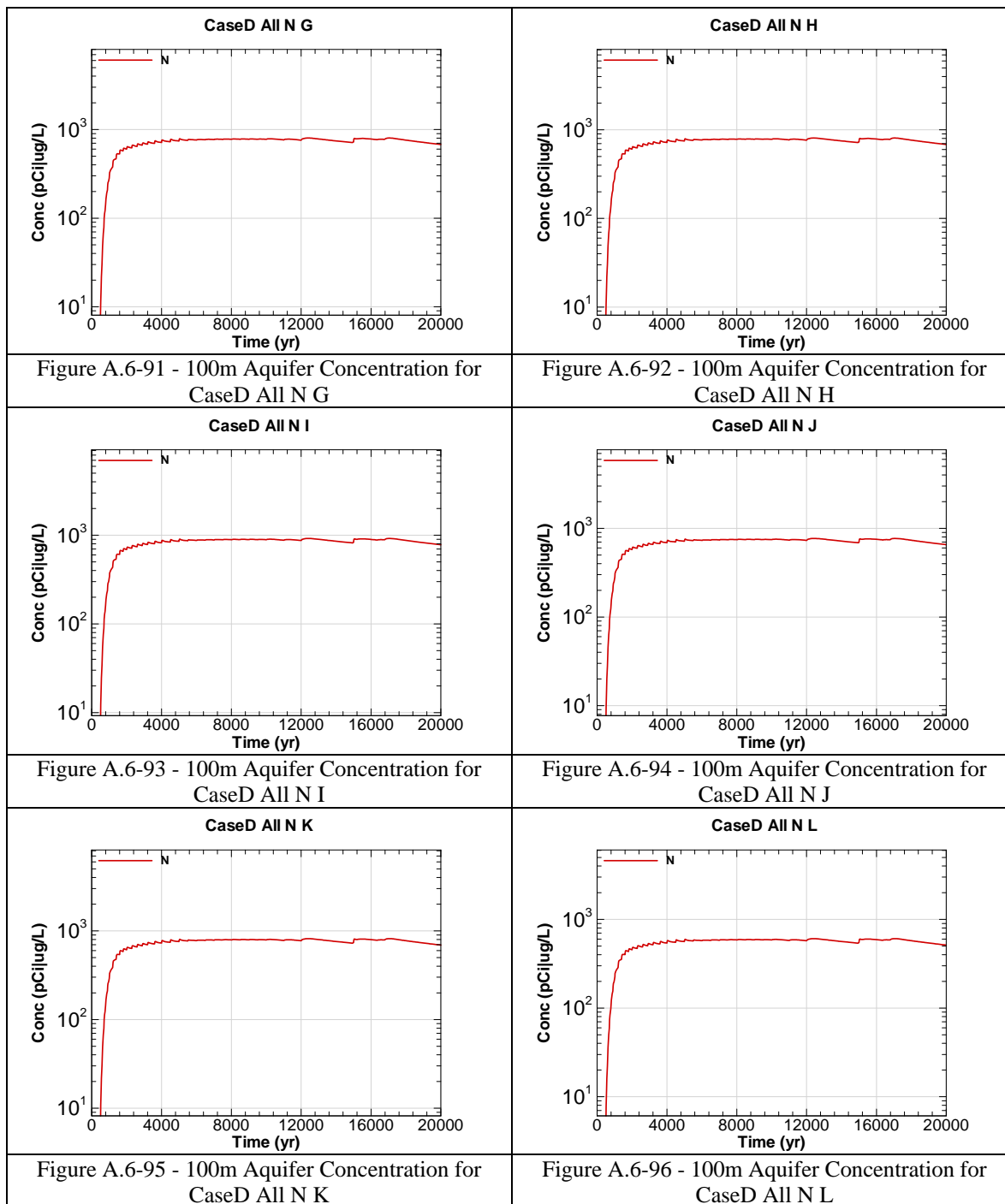


Figure A.6-84 - 100m Aquifer Concentration for
CaseD All U-235 L





This page intentionally left blank

APPENDIX A.7

100-METER RADIOLOGICAL AND CHEMICAL CONCENTRATIONS – CASE E

Appendix A.7 contains curves showing the 100 meter key radiological and chemical concentrations for all of SDF (vault and FDC inventories) for Case E. 20,000 year concentration results are presented for Sectors A through L for the peak concentration per sector regardless of aquifer.

Graph heading example “CaseE All I-129 A”

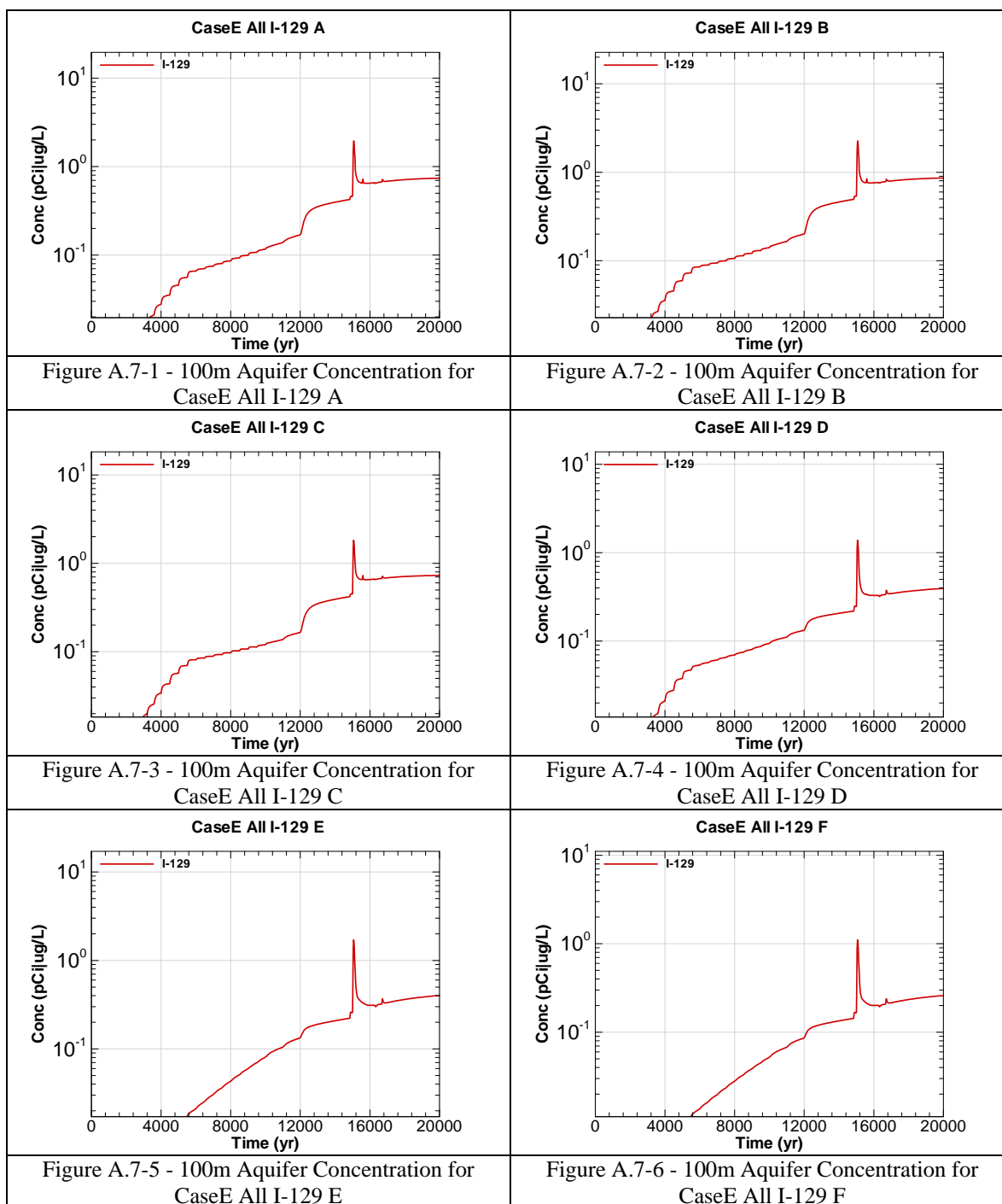
Key

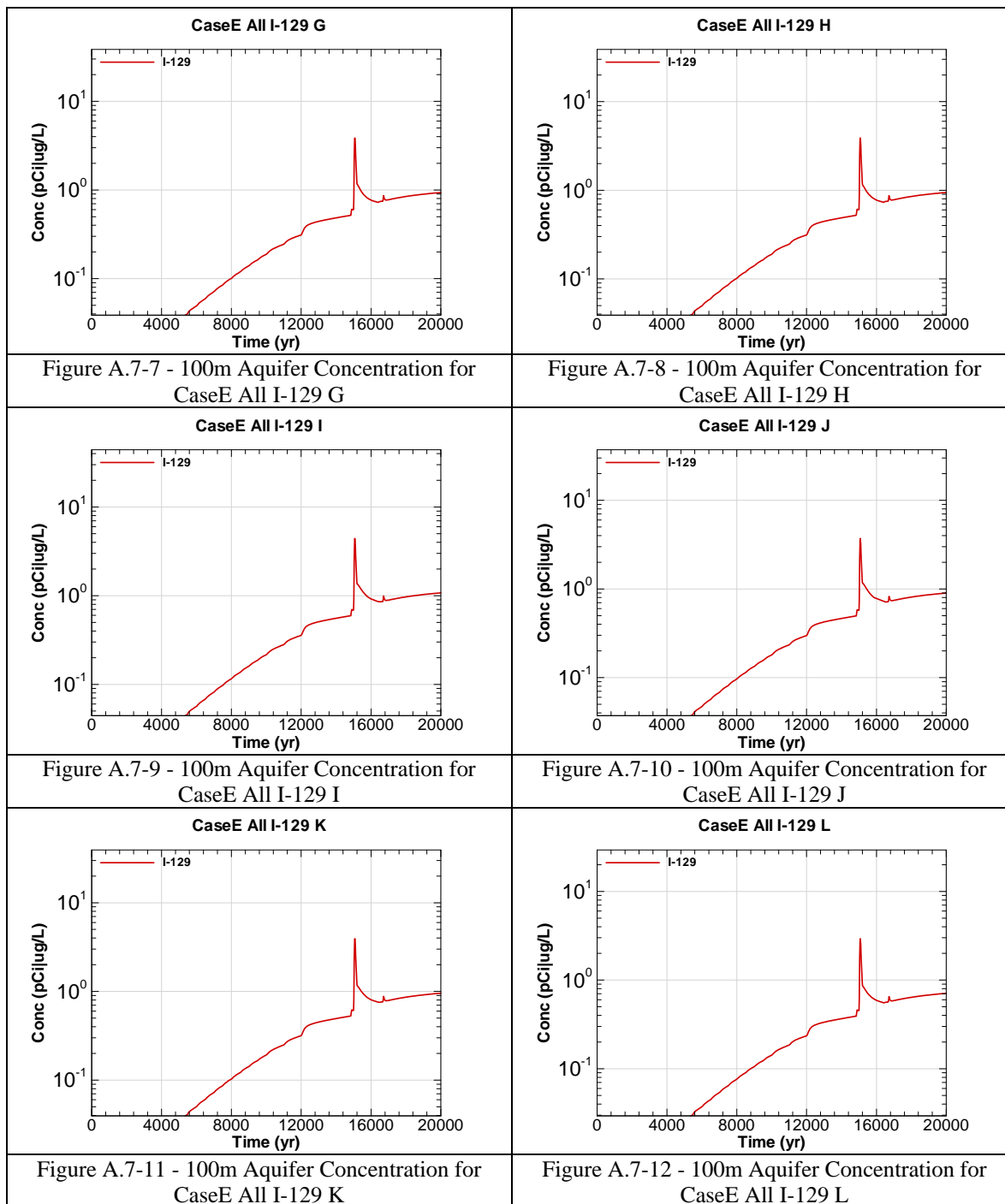
CaseE = Scenario case

All = Inventory source is all disposal units

I-129 = Radionuclide or chemical of concern

A = Evaluation sector of concern





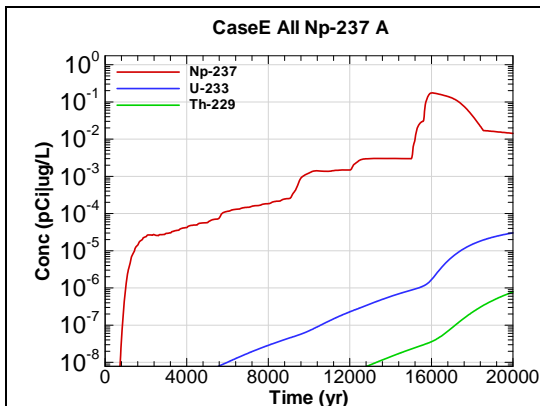


Figure A.7-13 - 100m Aquifer Concentration for CaseE All Np-237 A

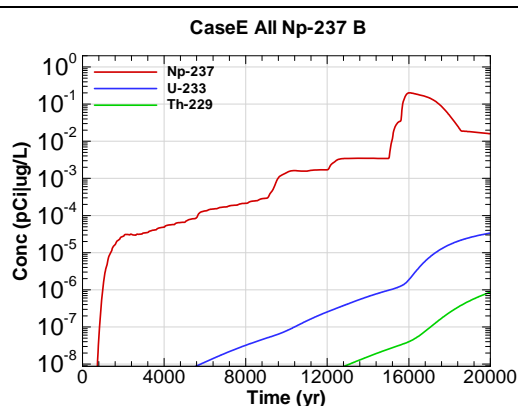


Figure A.7-14 - 100m Aquifer Concentration for CaseE All Np-237 B

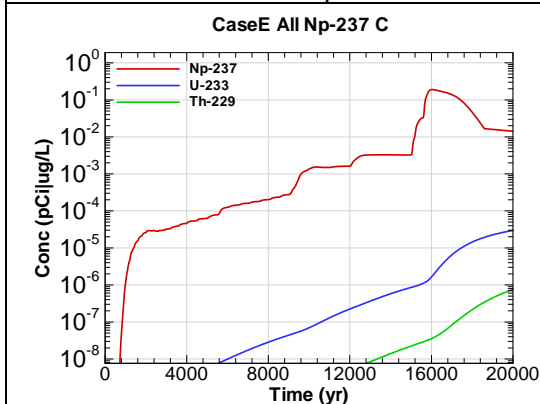


Figure A.7-15 - 100m Aquifer Concentration for CaseE All Np-237 C

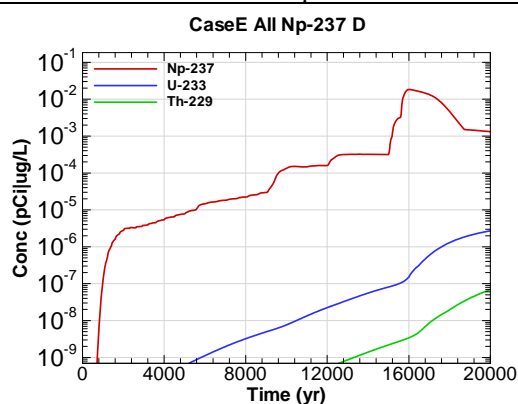


Figure A.7-16 - 100m Aquifer Concentration for CaseE All Np-237 D

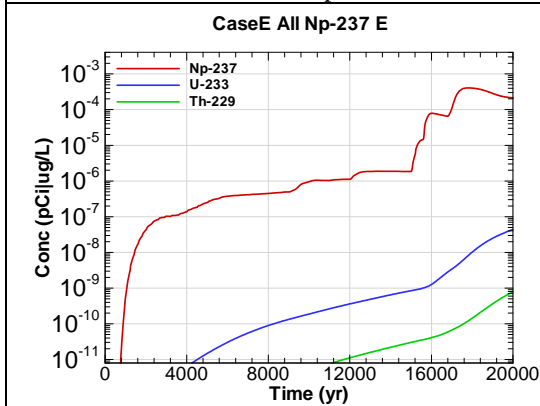


Figure A.7-17 - 100m Aquifer Concentration for CaseE All Np-237 E

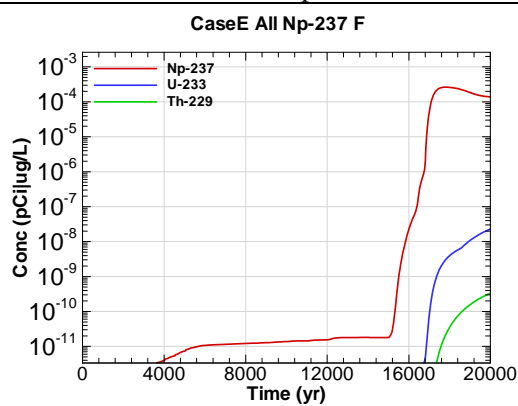


Figure A.7-18 - 100m Aquifer Concentration for CaseE All Np-237 F

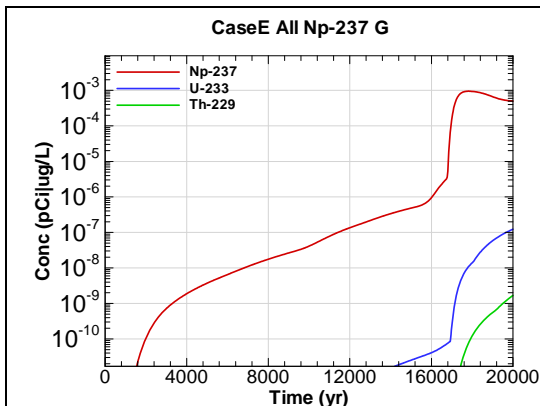


Figure A.7-19 - 100m Aquifer Concentration for CaseE All Np-237 G

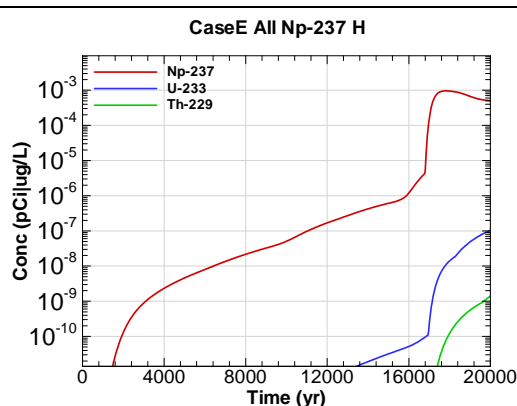


Figure A.7-20 - 100m Aquifer Concentration for CaseE All Np-237 H

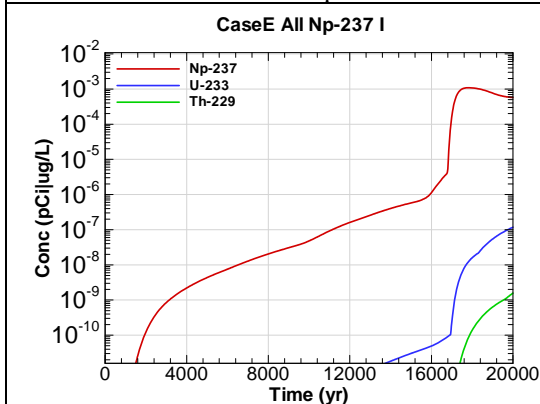


Figure A.7-21 - 100m Aquifer Concentration for CaseE All Np-237 I

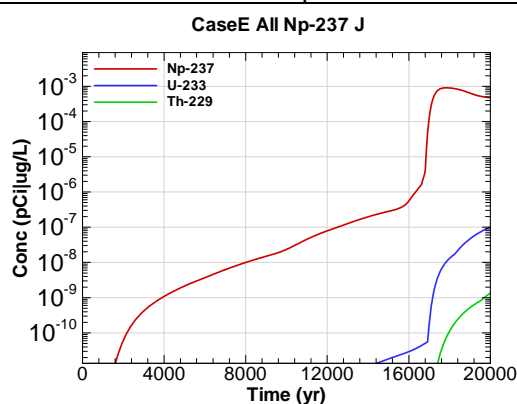


Figure A.7-22 - 100m Aquifer Concentration for CaseE All Np-237 J

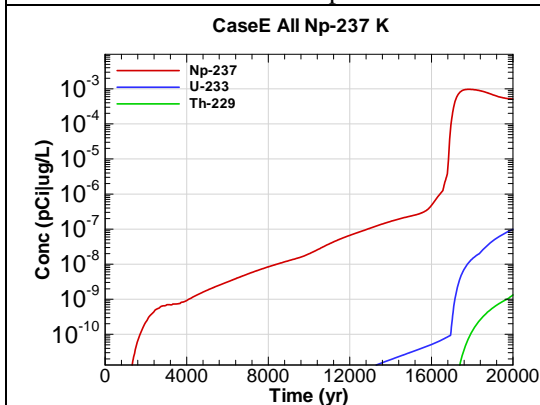


Figure A.7-23 - 100m Aquifer Concentration for CaseE All Np-237 K

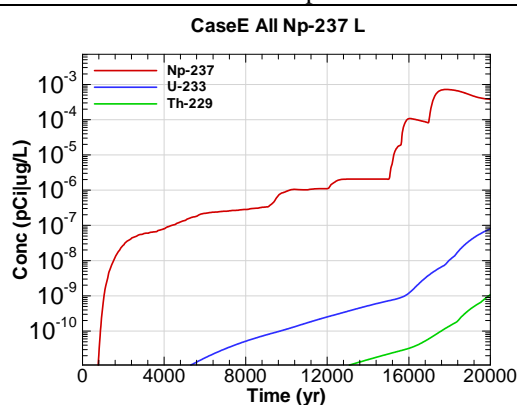


Figure A.7-24 - 100m Aquifer Concentration for CaseE All Np-237 L

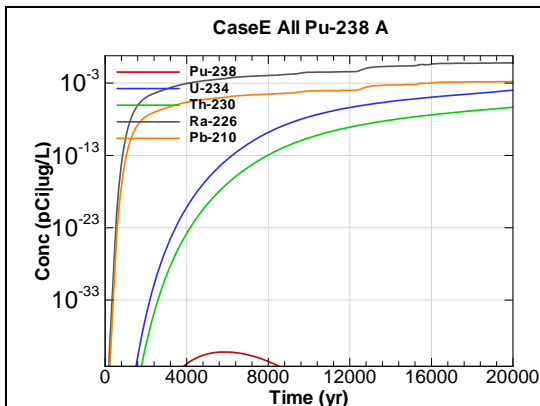


Figure A.7-25 - 100m Aquifer Concentration for
CaseE All Pu-238 A

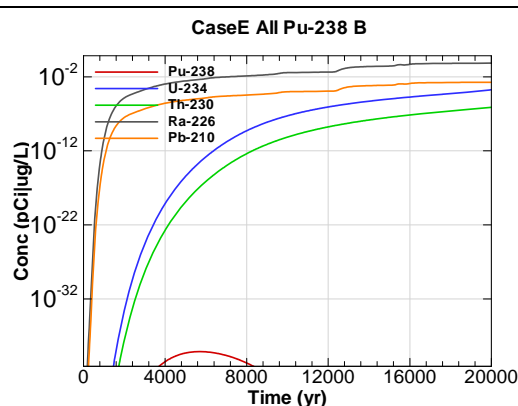


Figure A.7-26 - 100m Aquifer Concentration for
CaseE All Pu-238 B

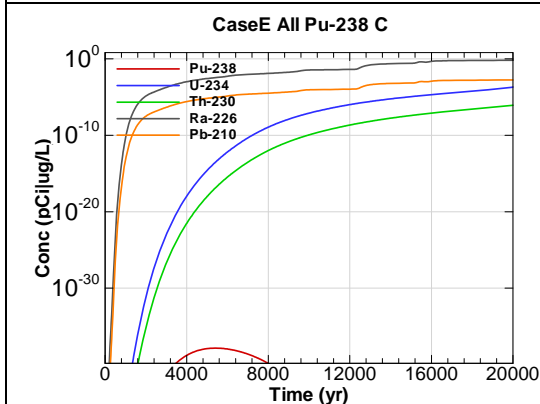


Figure A.7-27 - 100m Aquifer Concentration for
CaseE All Pu-238 C

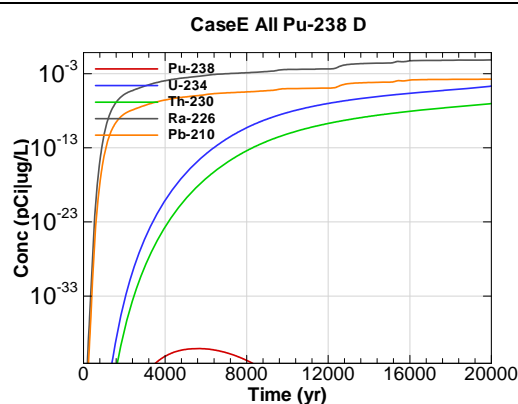


Figure A.7-28 - 100m Aquifer Concentration for
CaseE All Pu-238 D

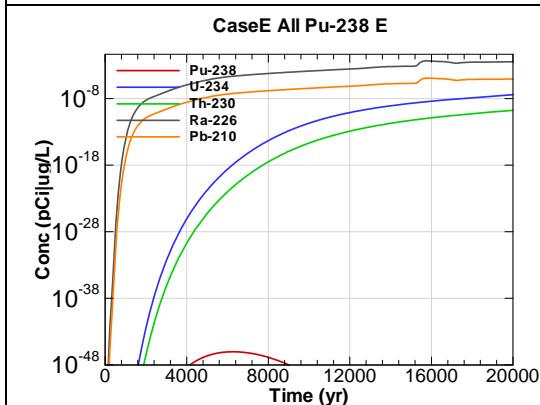


Figure A.7-29 - 100m Aquifer Concentration for
CaseE All Pu-238 E

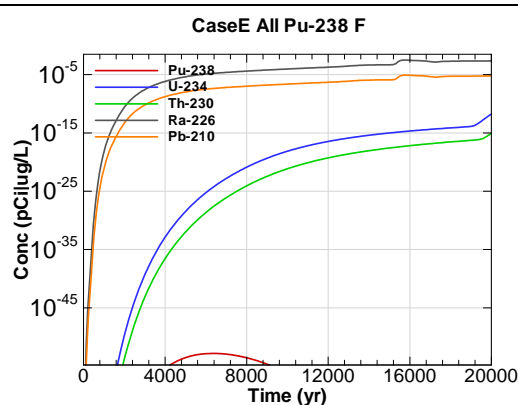


Figure A.7-30 - 100m Aquifer Concentration for
CaseE All Pu-238 F

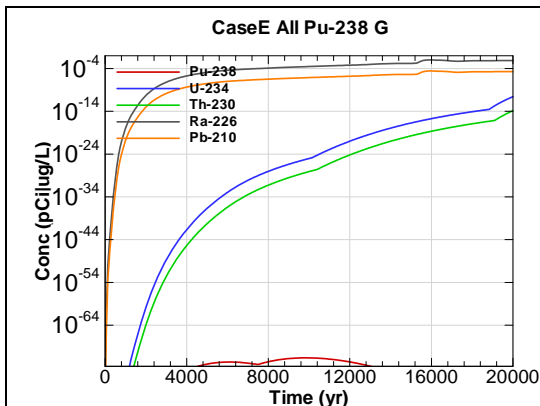


Figure A.7-31 - 100m Aquifer Concentration for
CaseE All Pu-238 G

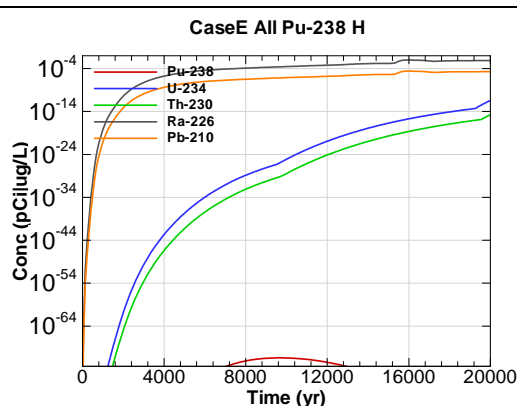


Figure A.7-32 - 100m Aquifer Concentration for
CaseE All Pu-238 H

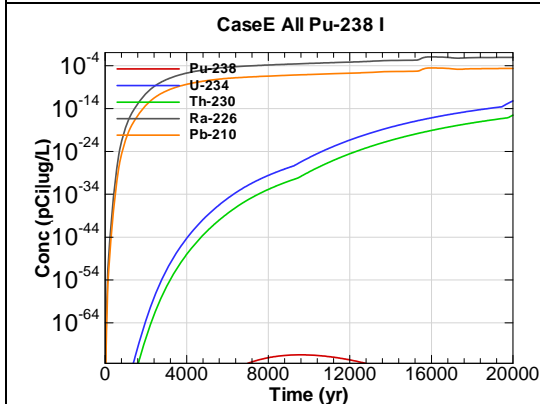


Figure A.7-33 - 100m Aquifer Concentration for
CaseE All Pu-238 I

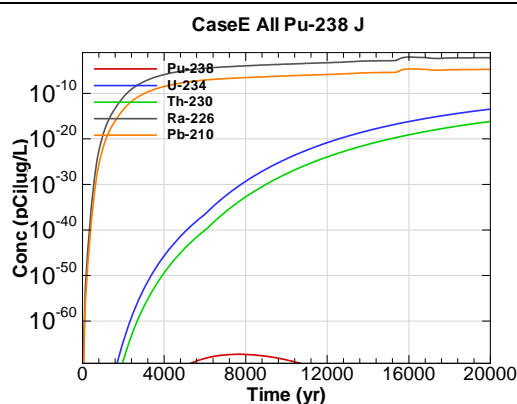


Figure A.7-34 - 100m Aquifer Concentration for
CaseE All Pu-238 J

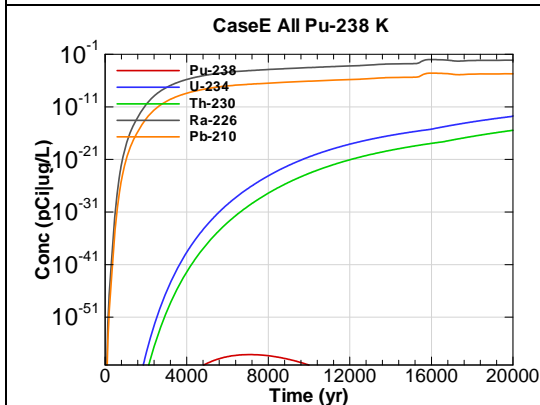


Figure A.7-35 - 100m Aquifer Concentration for
CaseE All Pu-238 K

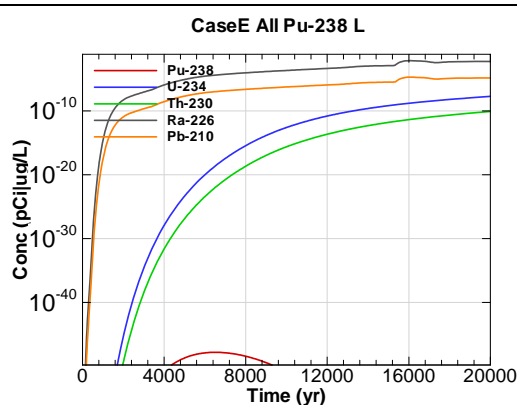
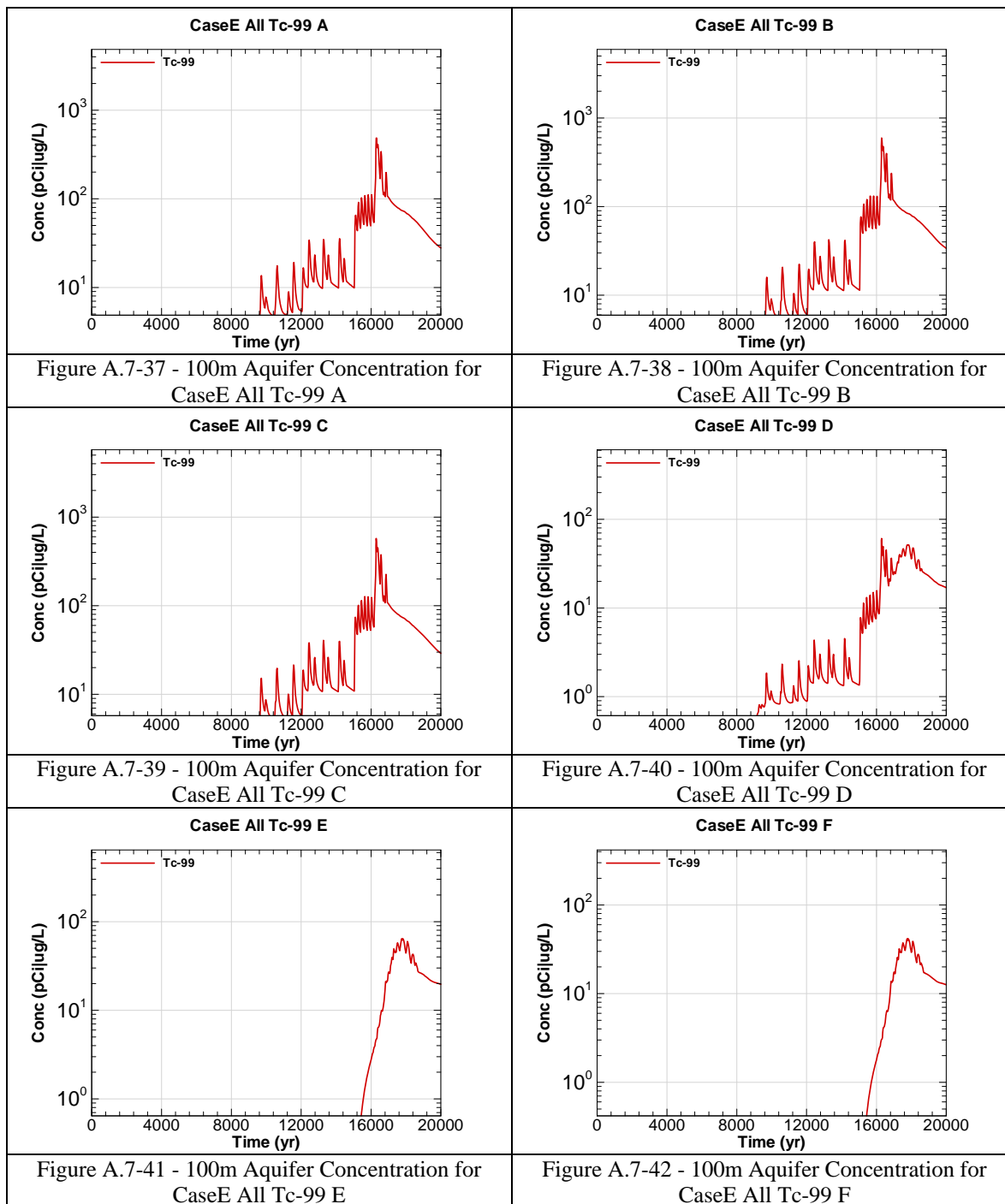
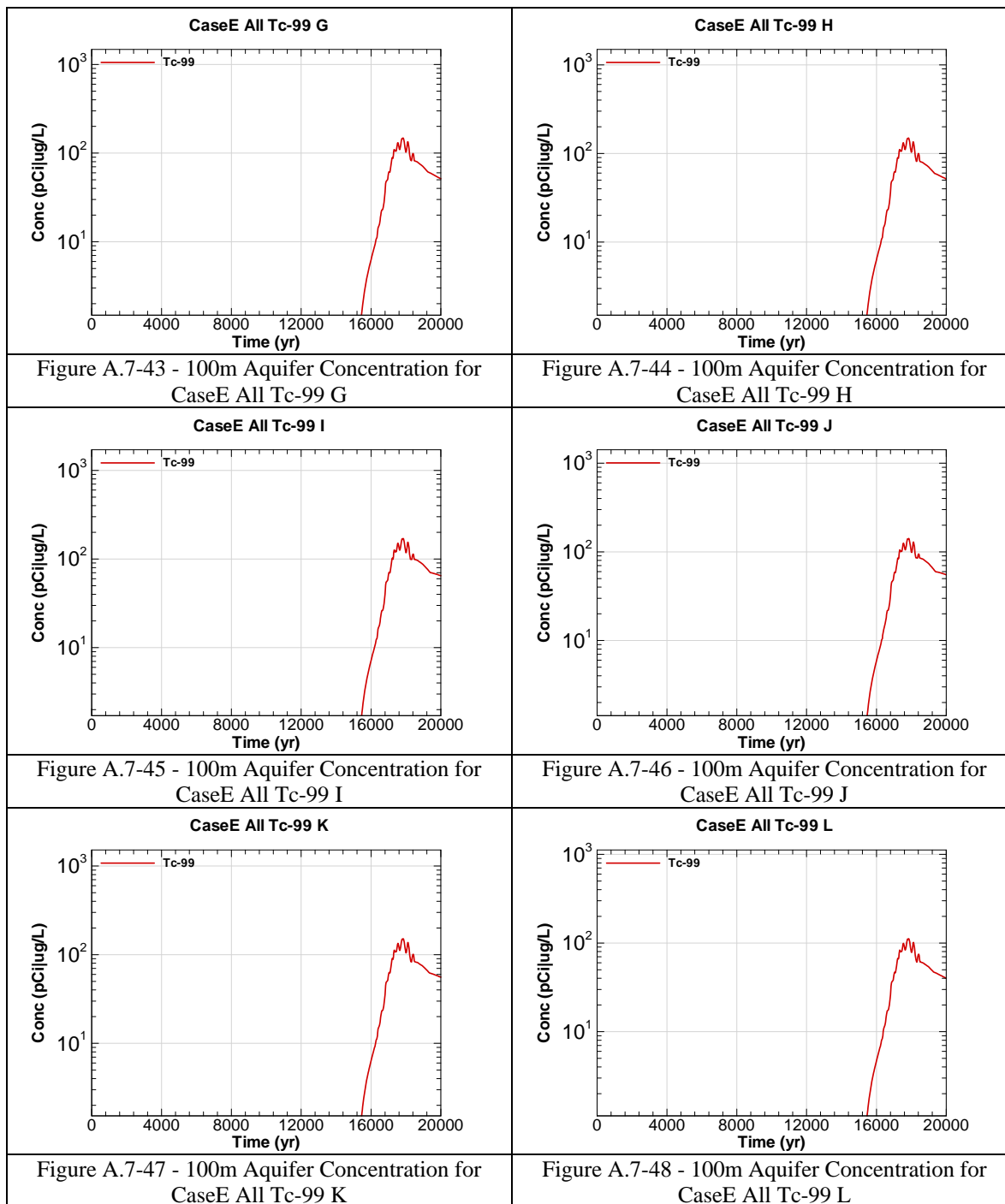


Figure A.7-36 - 100m Aquifer Concentration for
CaseE All Pu-238 L





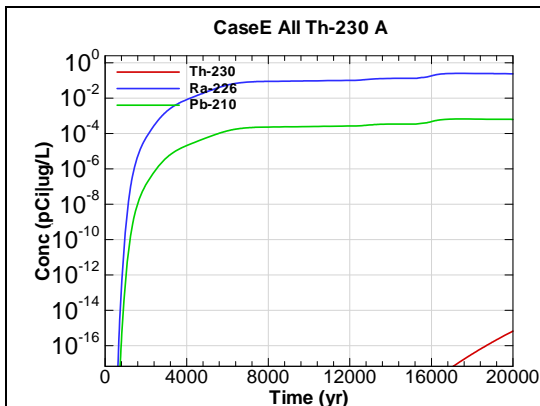


Figure A.7-49 - 100m Aquifer Concentration for CaseE All Th-230 A

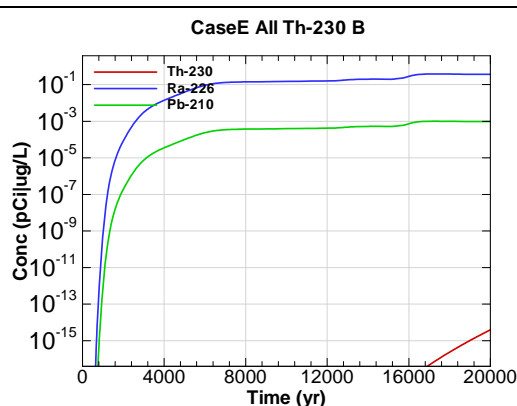


Figure A.7-50 - 100m Aquifer Concentration for CaseE All Th-230 B

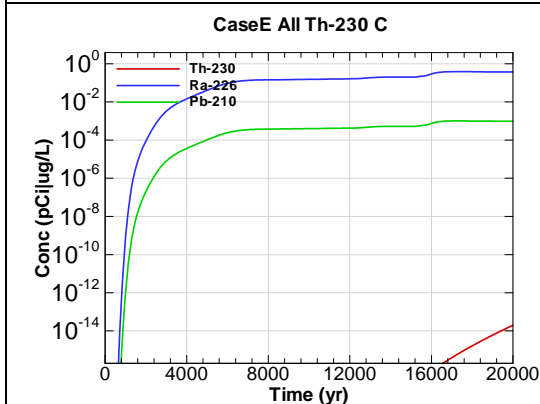


Figure A.7-51 - 100m Aquifer Concentration for CaseE All Th-230 C

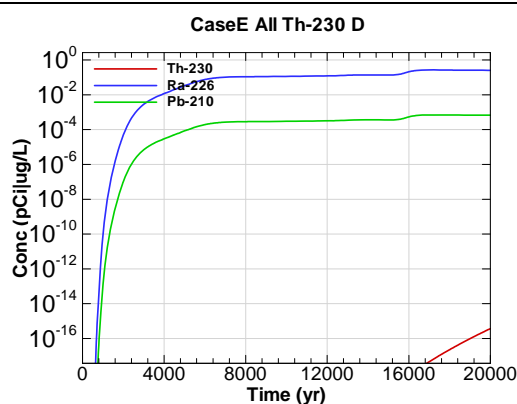


Figure A.7-52 - 100m Aquifer Concentration for CaseE All Th-230 D

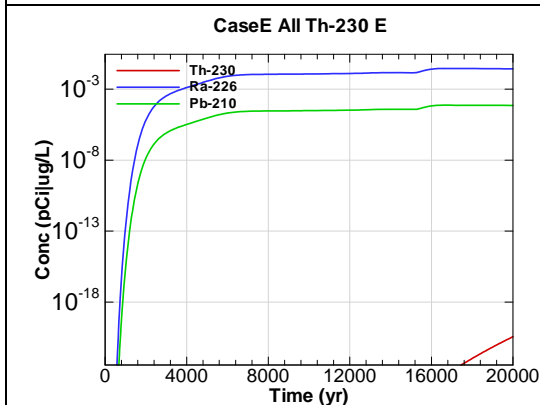


Figure A.7-53 - 100m Aquifer Concentration for CaseE All Th-230 E

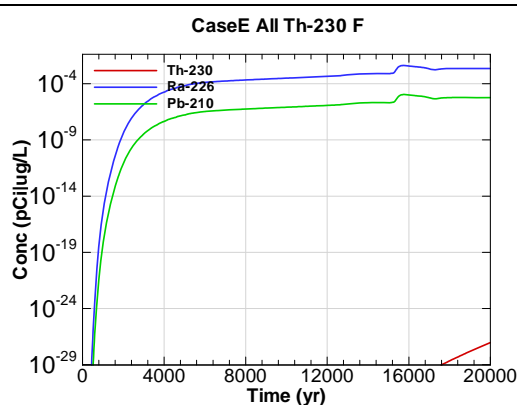
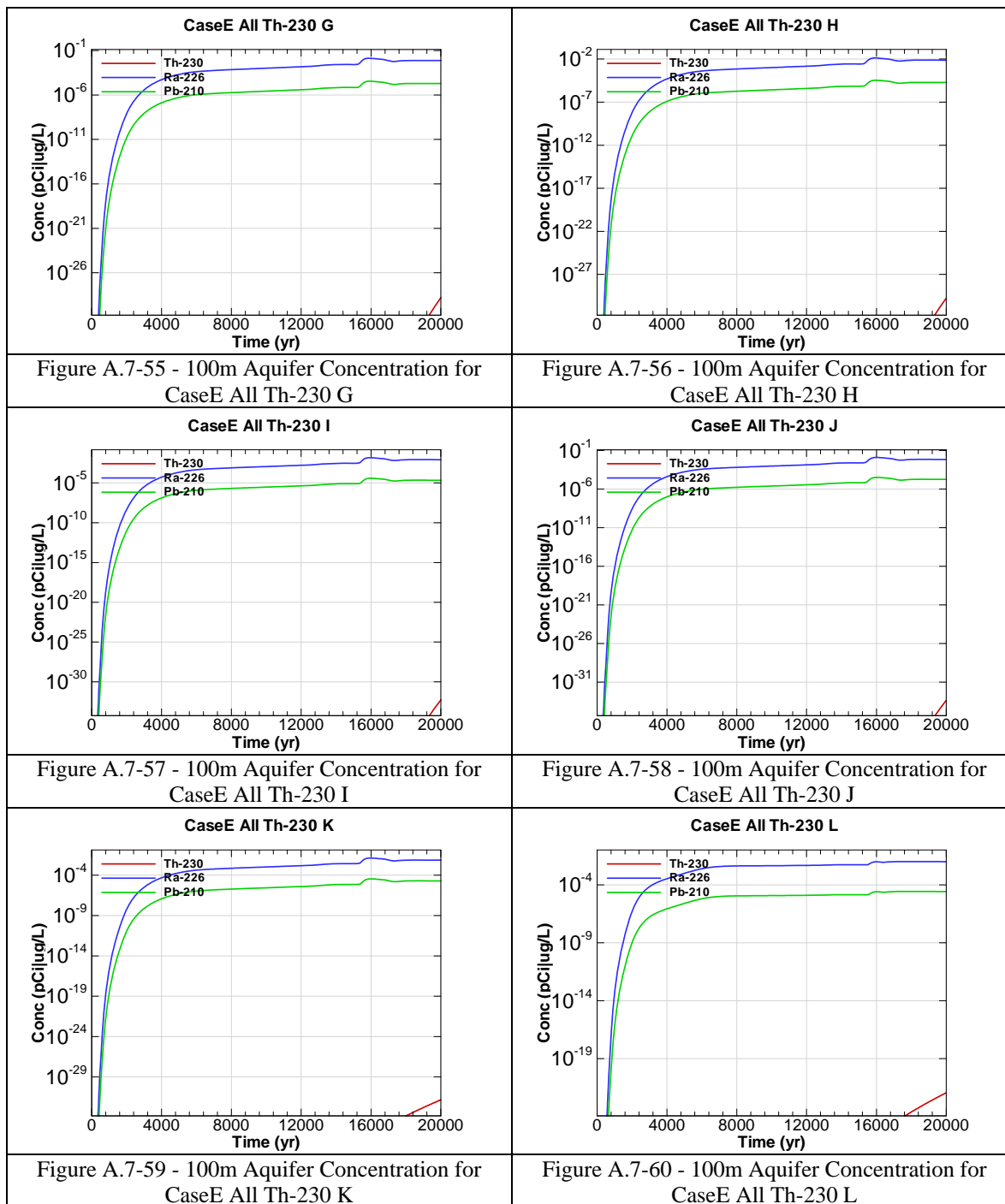


Figure A.7-54 - 100m Aquifer Concentration for CaseE All Th-230 F



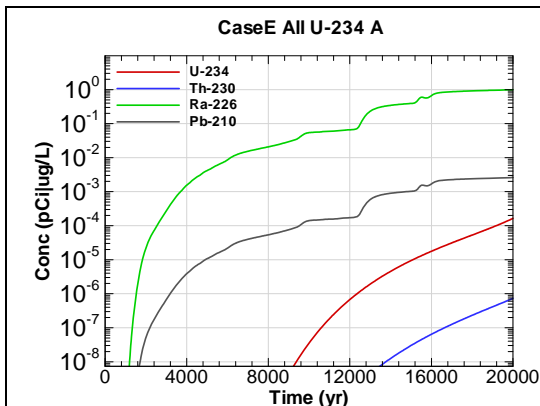


Figure A.7-61 - 100m Aquifer Concentration for
CaseE All U-234 A

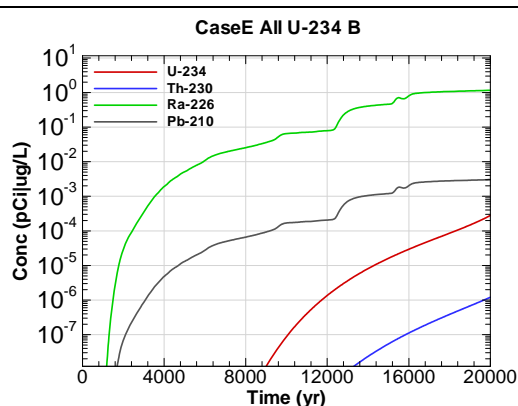


Figure A.7-62 - 100m Aquifer Concentration for
CaseE All U-234 B

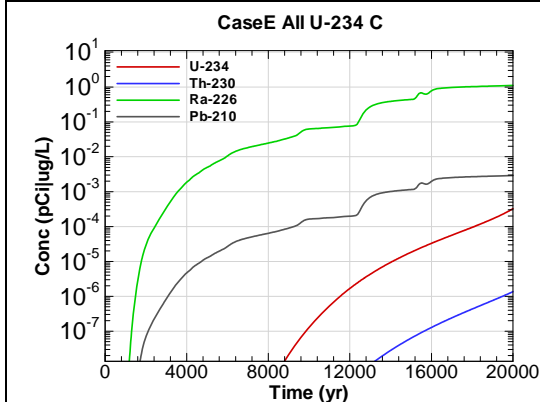


Figure A.7-63 - 100m Aquifer Concentration for
CaseE All U-234 C

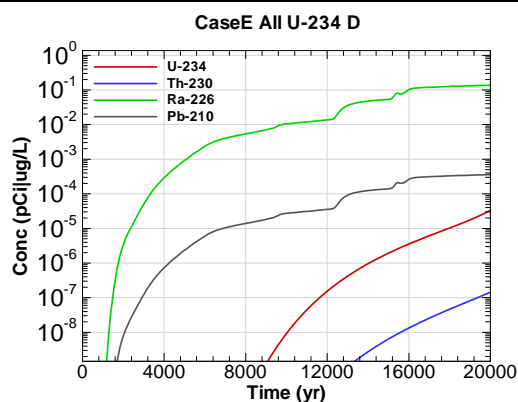


Figure A.7-64 - 100m Aquifer Concentration for
CaseE All U-234 D

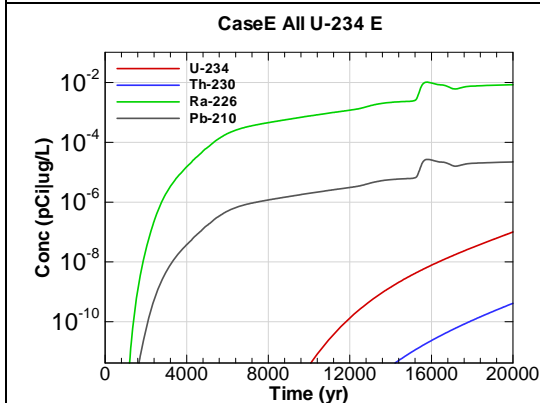


Figure A.7-65 - 100m Aquifer Concentration for
CaseE All U-234 E

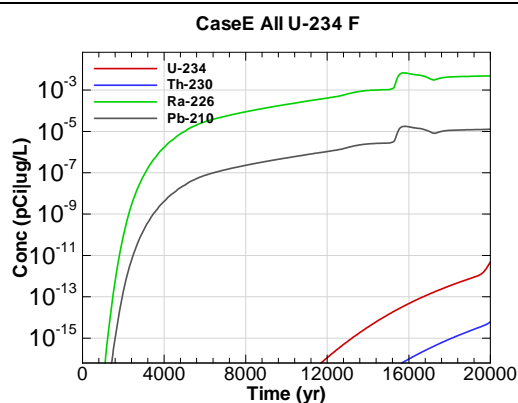


Figure A.7-66 - 100m Aquifer Concentration for
CaseE All U-234 F

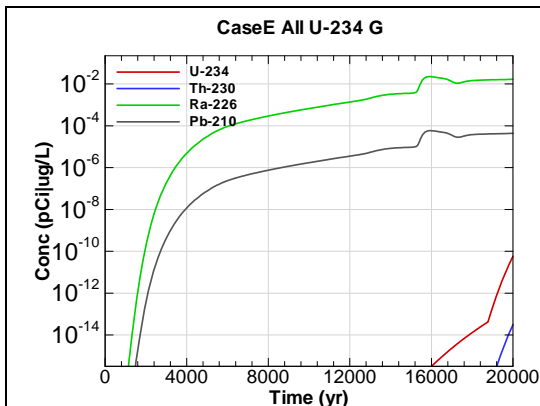


Figure A.7-67 - 100m Aquifer Concentration for
CaseE All U-234 G

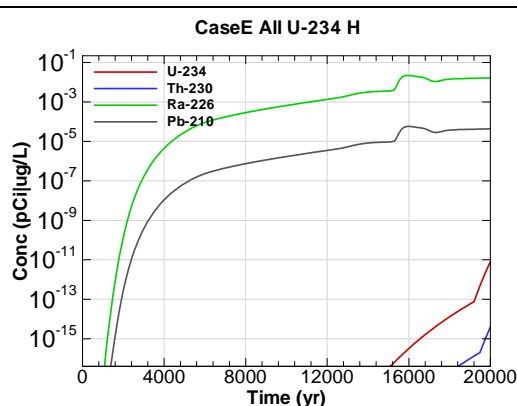


Figure A.7-68 - 100m Aquifer Concentration for
CaseE All U-234 H

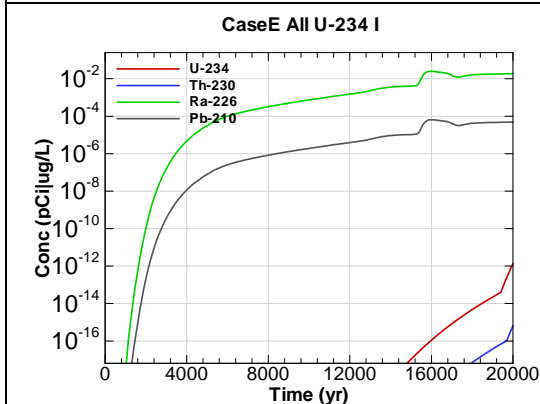


Figure A.7-69 - 100m Aquifer Concentration for
CaseE All U-234 I

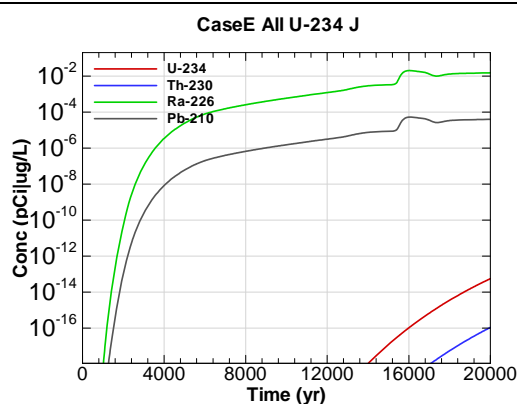


Figure A.7-70 - 100m Aquifer Concentration for
CaseE All U-234 J

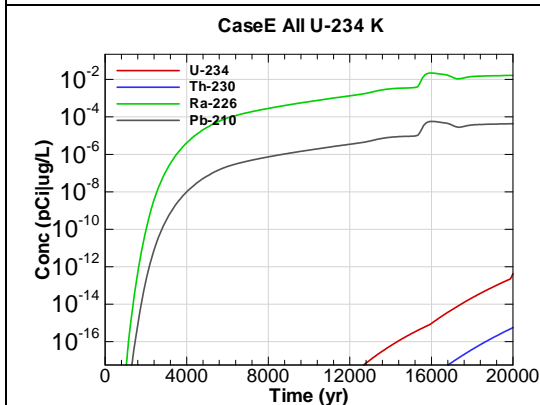


Figure A.7-71 - 100m Aquifer Concentration for
CaseE All U-234 K

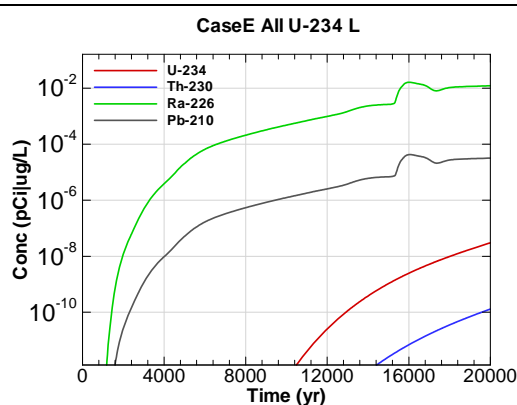


Figure A.7-72 - 100m Aquifer Concentration for
CaseE All U-234 L

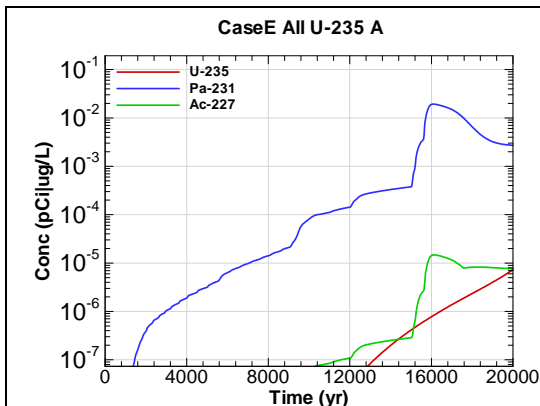


Figure A.7-73 - 100m Aquifer Concentration for
CaseE All U-235 A

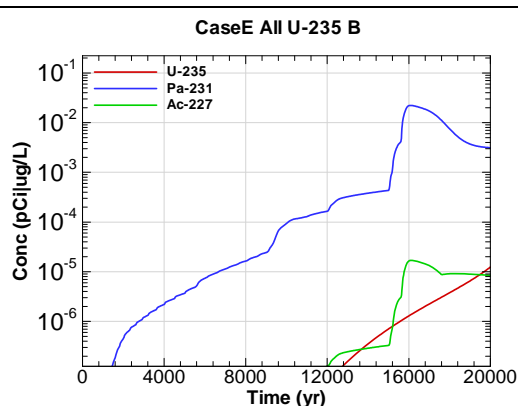


Figure A.7-74 - 100m Aquifer Concentration for
CaseE All U-235 B

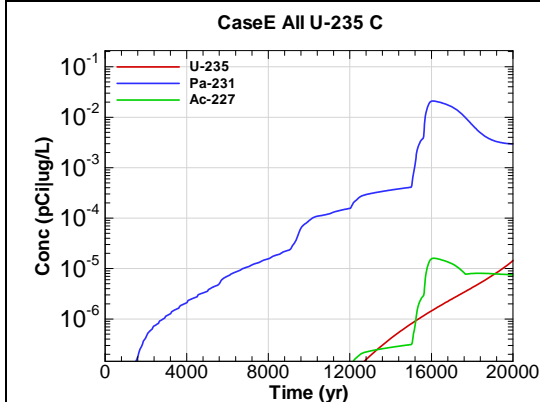


Figure A.7-75 - 100m Aquifer Concentration for
CaseE All U-235 C

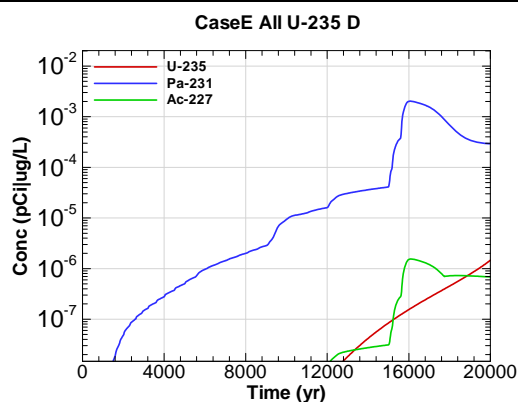


Figure A.7-76 - 100m Aquifer Concentration for
CaseE All U-235 D

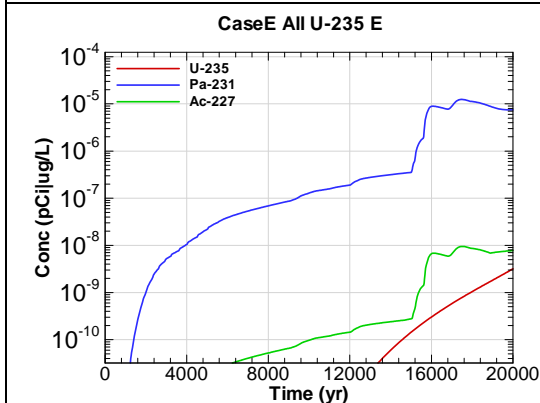


Figure A.7-77 - 100m Aquifer Concentration for
CaseE All U-235 E

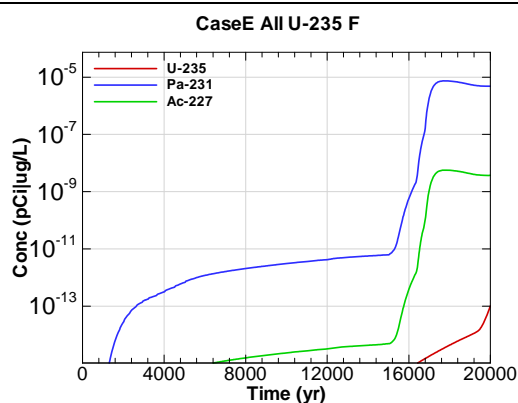
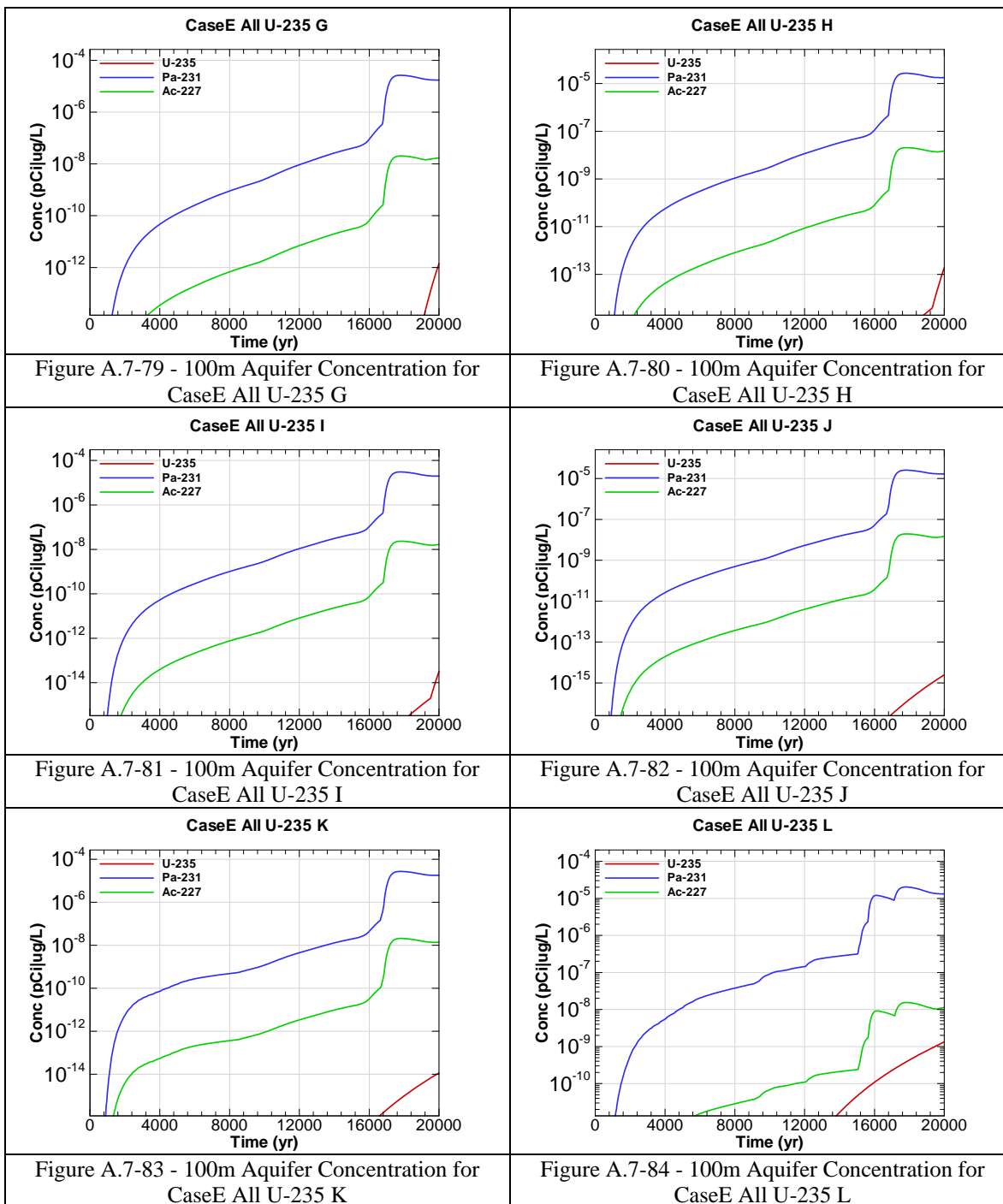
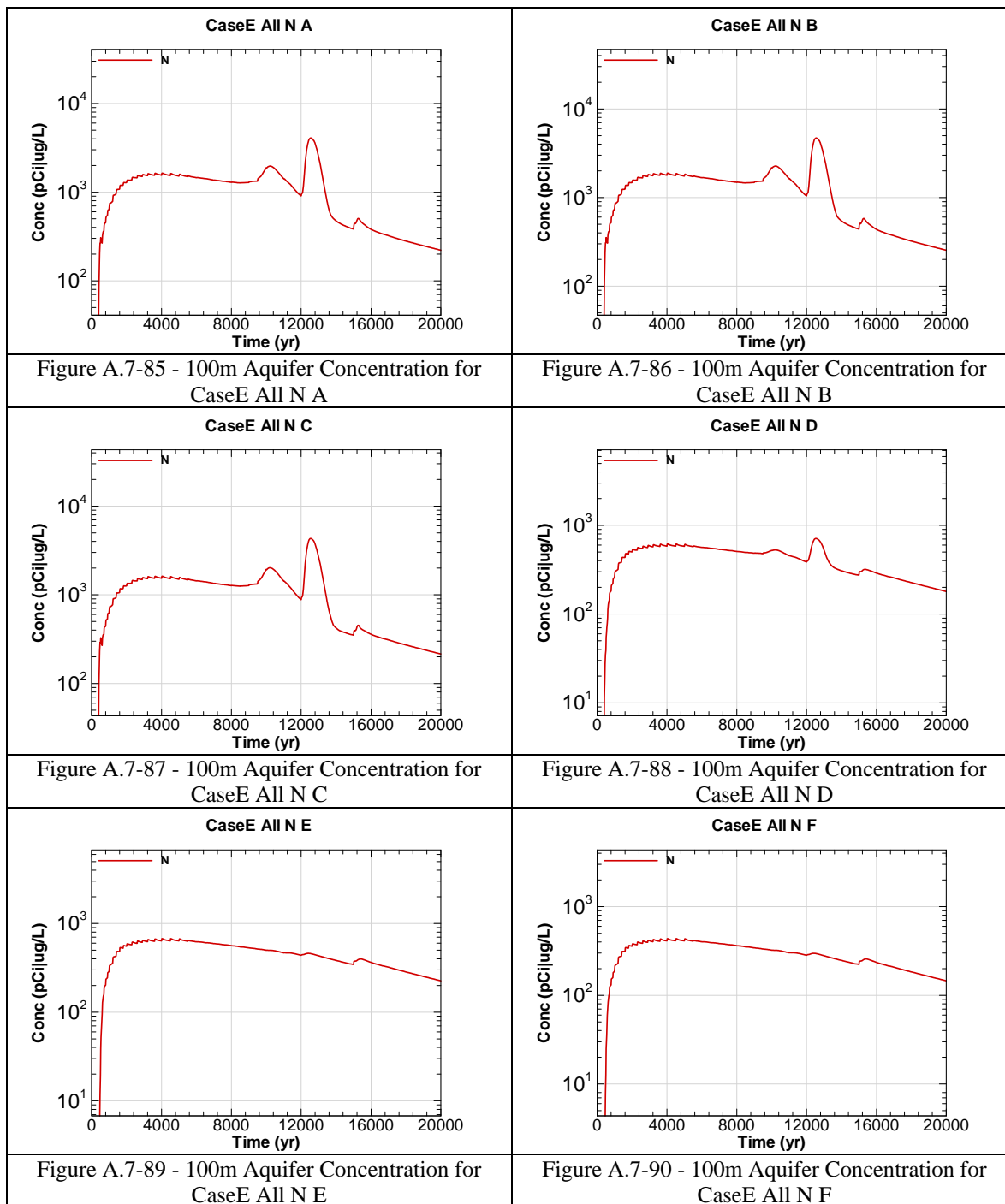
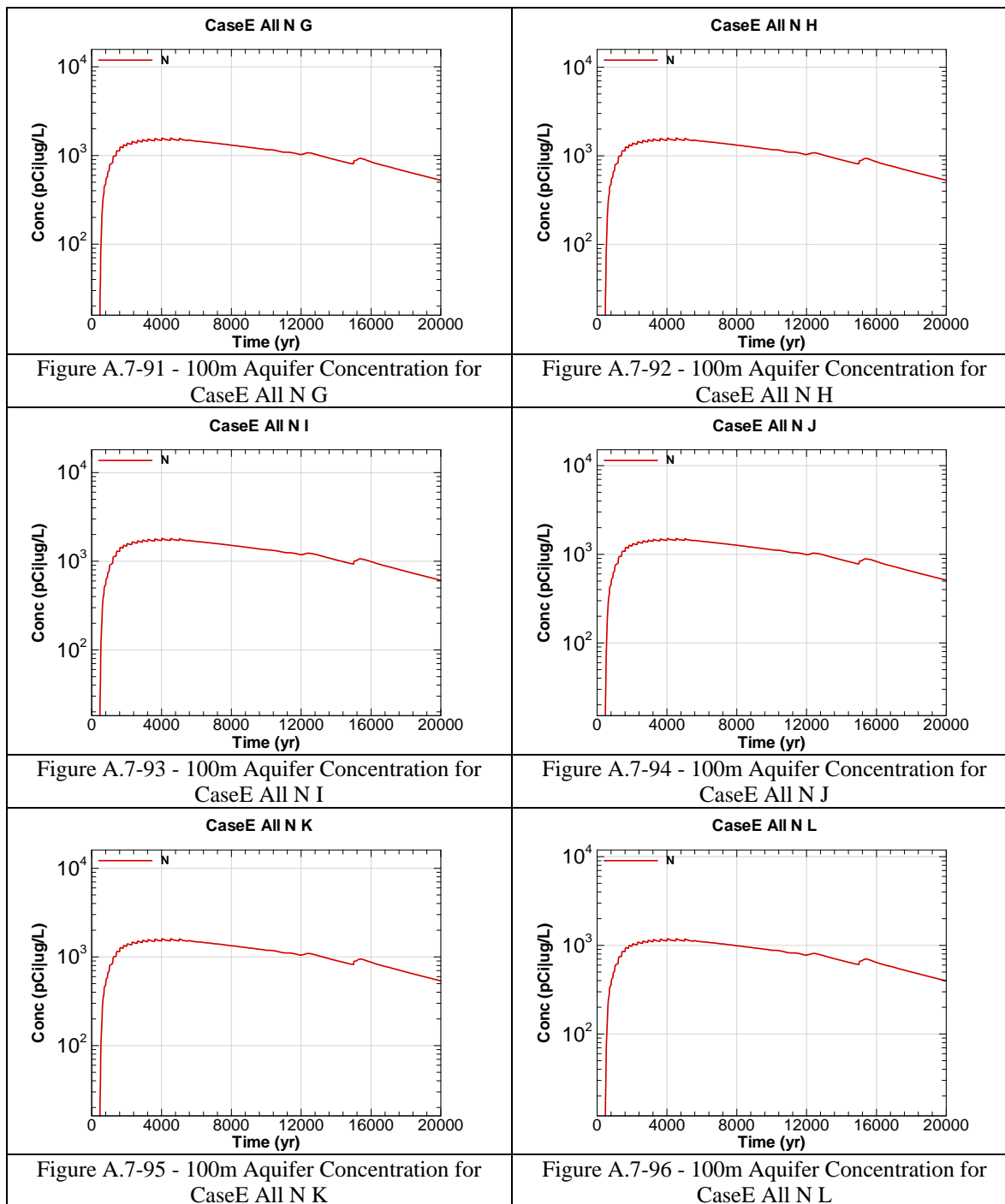


Figure A.7-78 - 100m Aquifer Concentration for
CaseE All U-235 F







This page intentionally left blank

APPENDIX B

SEEPLINE KEY RADIONUCLIDE AND CHEMICAL CONCENTRATIONS

Appendix B contains curves showing the far field (i.e., seepline) radiological concentrations (key radionuclides only) for all of SDF (vault and FDC inventories) for the Base Case (Case A). 20,000 year peak concentration results are presented for Upper Three Runs and McQueen Branch.

Graph heading example “CaseA All I-129 UTR”

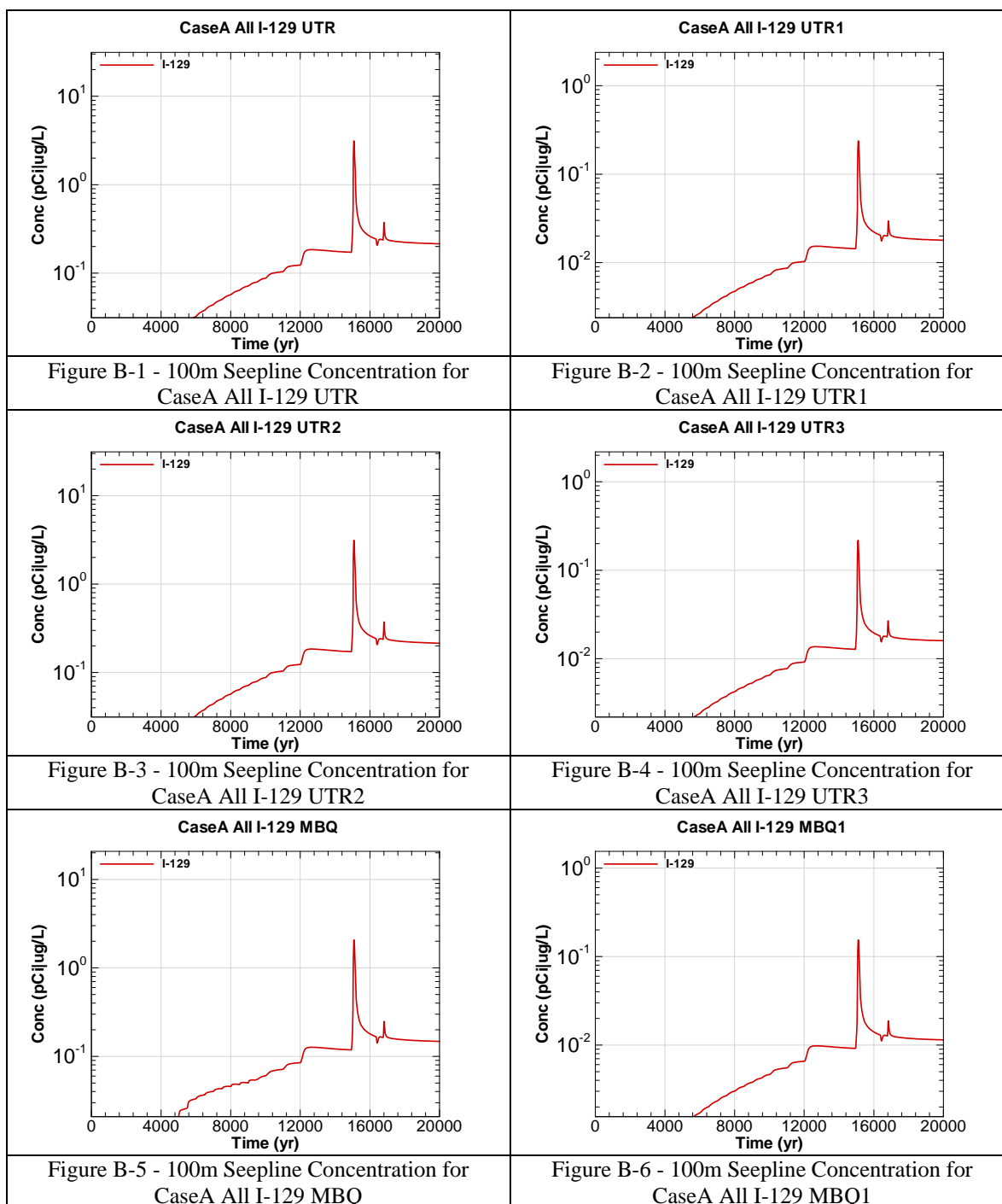
Key

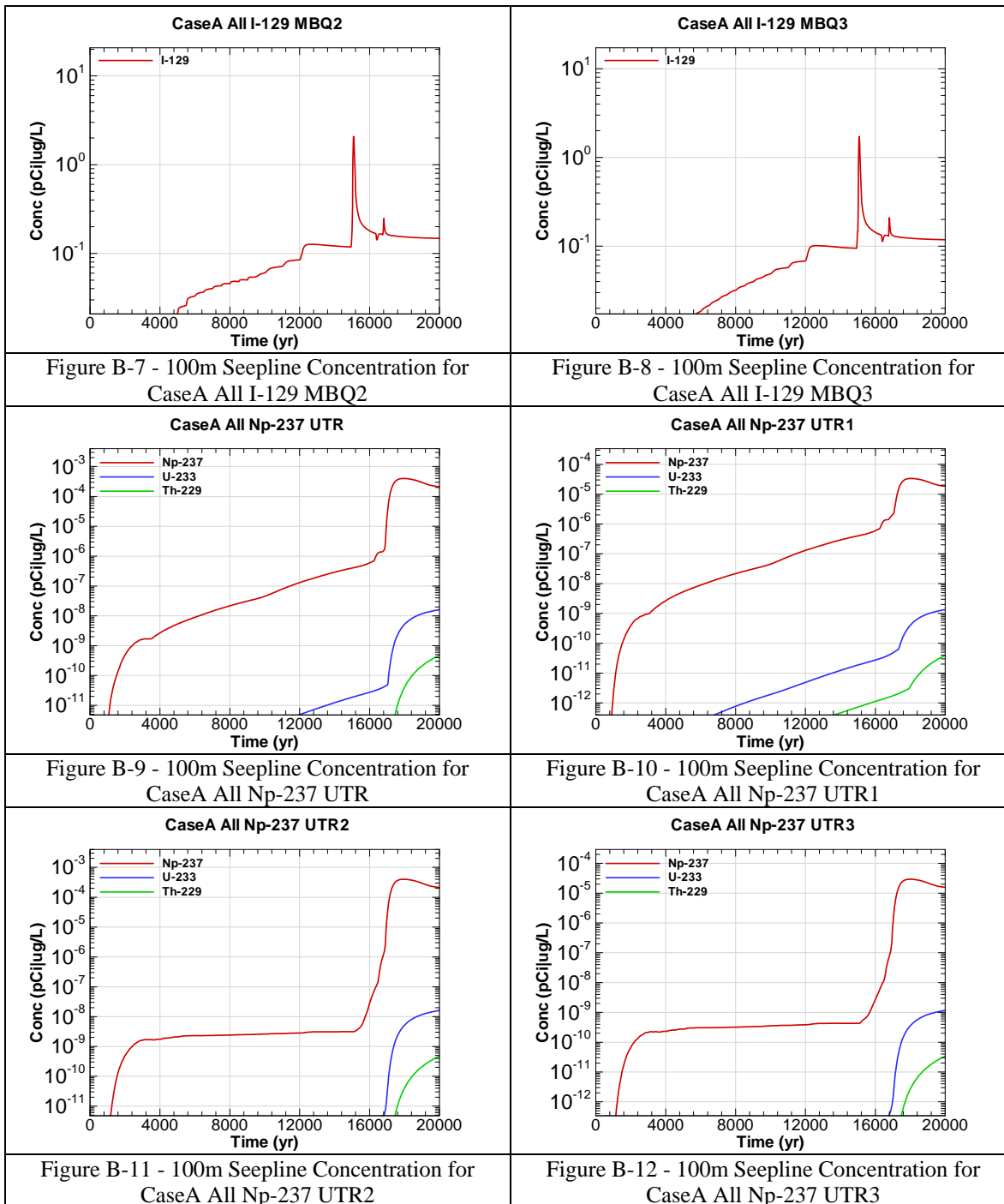
CaseA = Scenario case

All = Inventory source is all disposal units

I-129 = Radionuclide or chemical of concern

UTR = Evaluation seepline of concern (UTR = maximum UTR concentration regardless of location; UTR1 = individual seepline concentration)





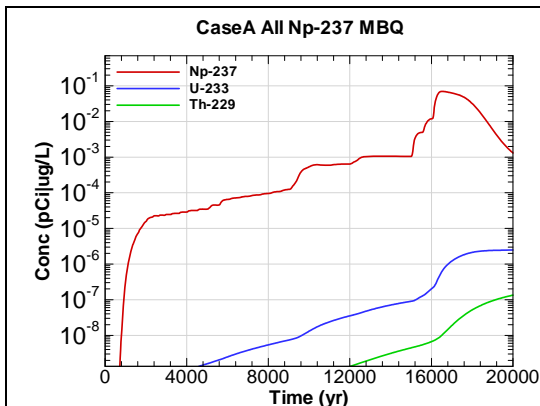


Figure B-13 - 100m Seepage Concentration for
CaseA All Np-237 MBQ

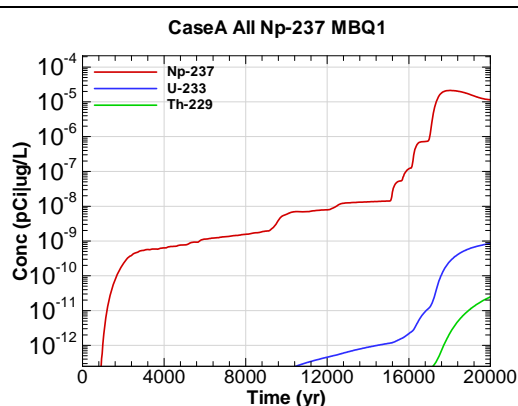


Figure B-14 - 100m Seepage Concentration for
CaseA All Np-237 MBQ1

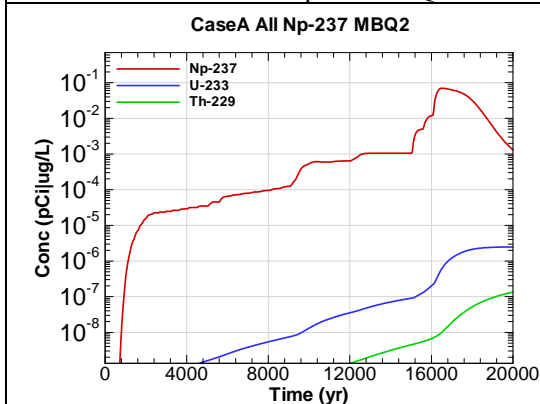


Figure B-15 - 100m Seepage Concentration for
CaseA All Np-237 MBQ2

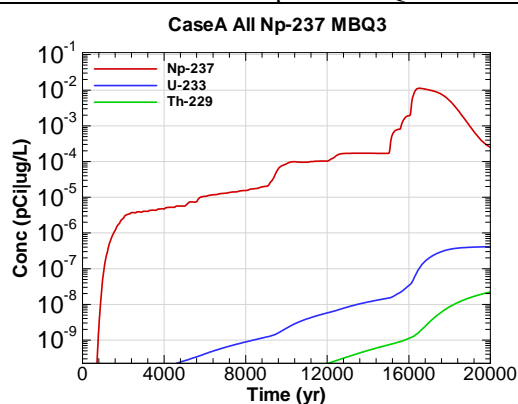


Figure B-16 - 100m Seepage Concentration for
CaseA All Np-237 MBQ3

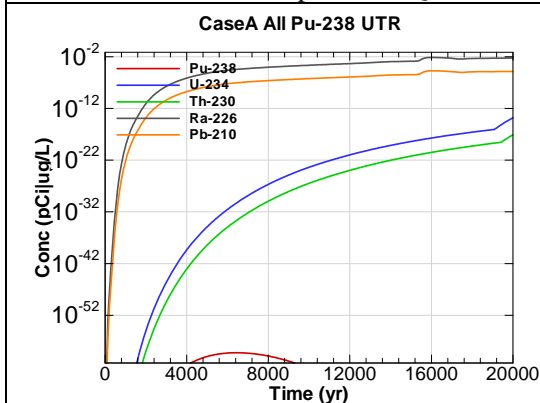


Figure B-17 - 100m Seepage Concentration for
CaseA All Pu-238 UTR

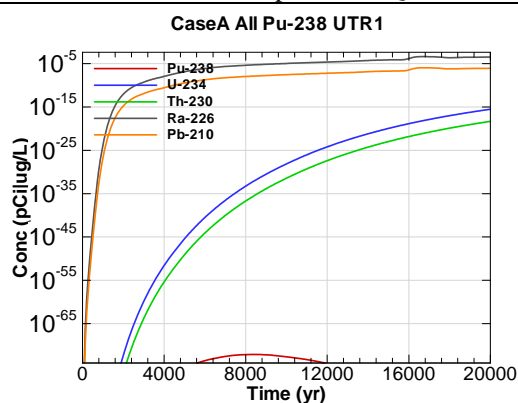


Figure B-18 - 100m Seepage Concentration for
CaseA All Pu-238 UTR1

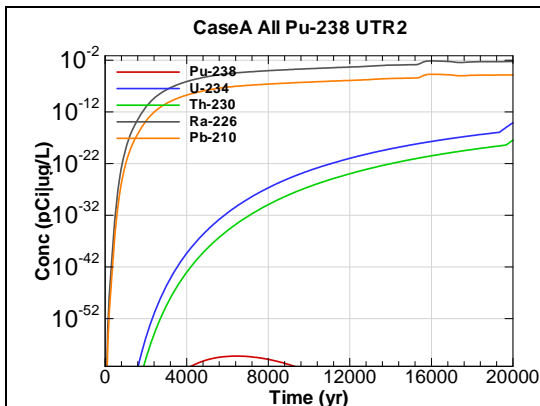


Figure B-19 - 100m Seepage Concentration for
CaseA All Pu-238 UTR2

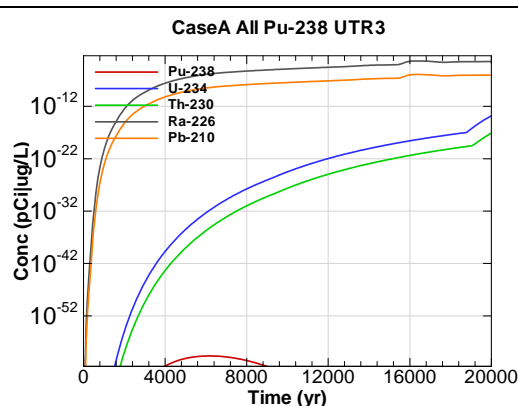


Figure B-20 - 100m Seepage Concentration for
CaseA All Pu-238 UTR3

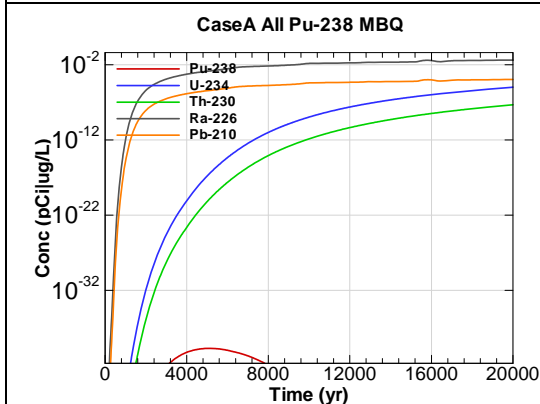


Figure B-21 - 100m Seepage Concentration for
CaseA All Pu-238 MBQ

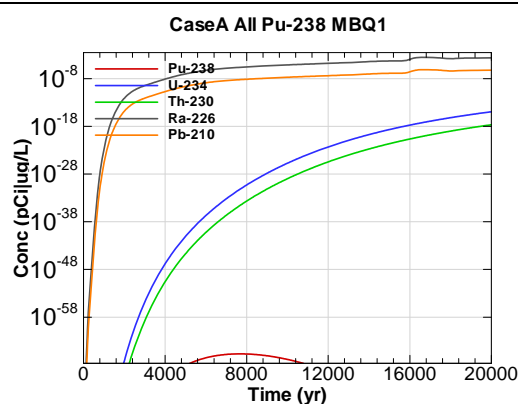


Figure B-22 - 100m Seepage Concentration for
CaseA All Pu-238 MBQ1

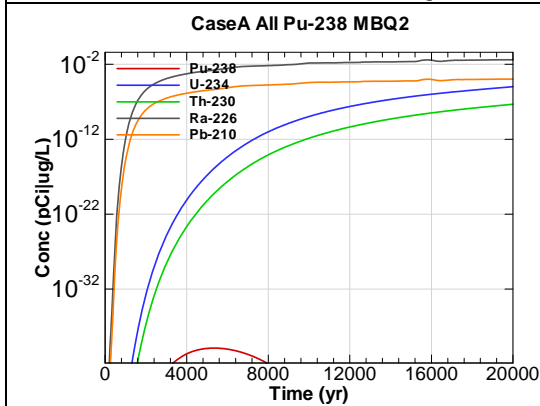


Figure B-23 - 100m Seepage Concentration for
CaseA All Pu-238 MBQ2

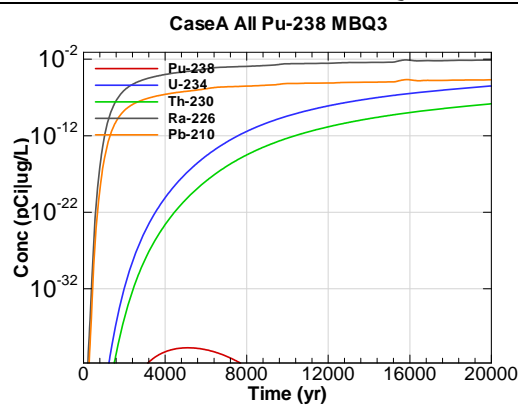
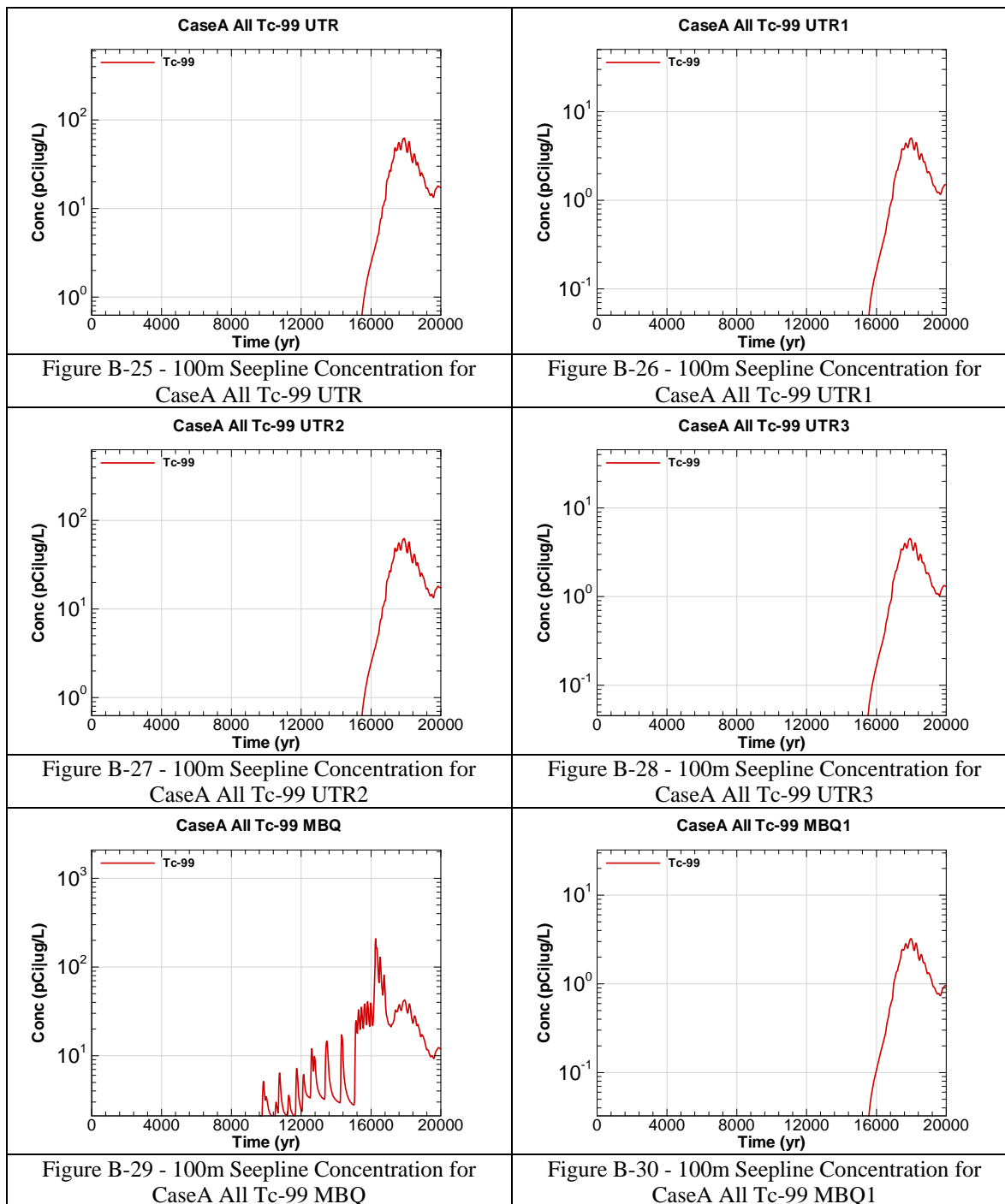


Figure B-24 - 100m Seepage Concentration for
CaseA All Pu-238 MBQ3



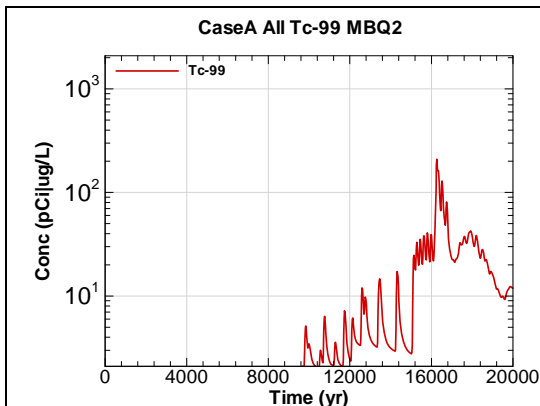


Figure B-31 - 100m Seepage Concentration for
CaseA All Tc-99 MBQ2

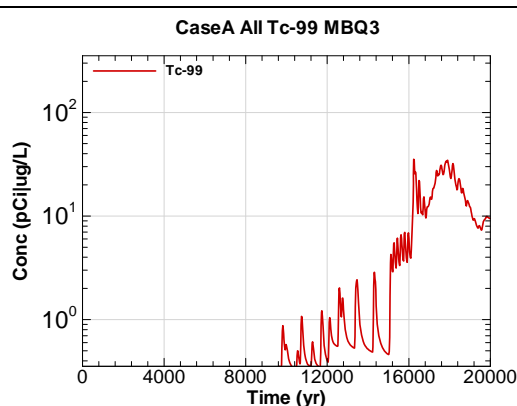


Figure B-32 - 100m Seepage Concentration for
CaseA All Tc-99 MBQ3

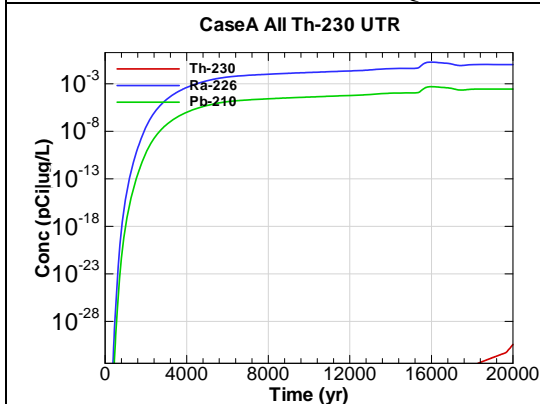


Figure B-33 - 100m Seepage Concentration for
CaseA All Th-230 UTR

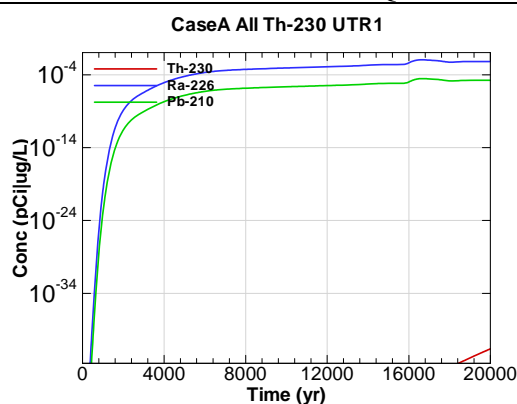


Figure B-34 - 100m Seepage Concentration for
CaseA All Th-230 UTR1

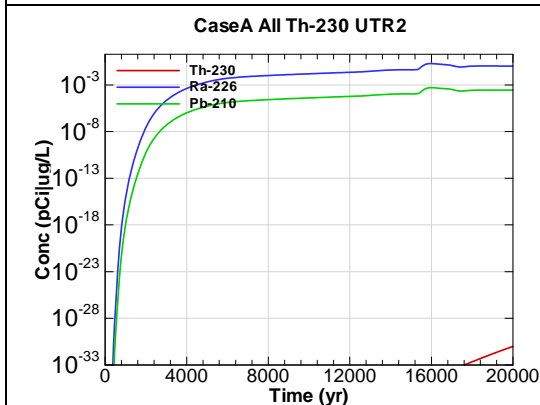


Figure B-35 - 100m Seepage Concentration for
CaseA All Th-230 UTR2

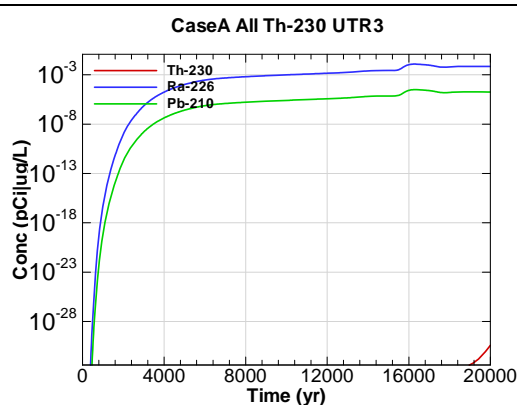
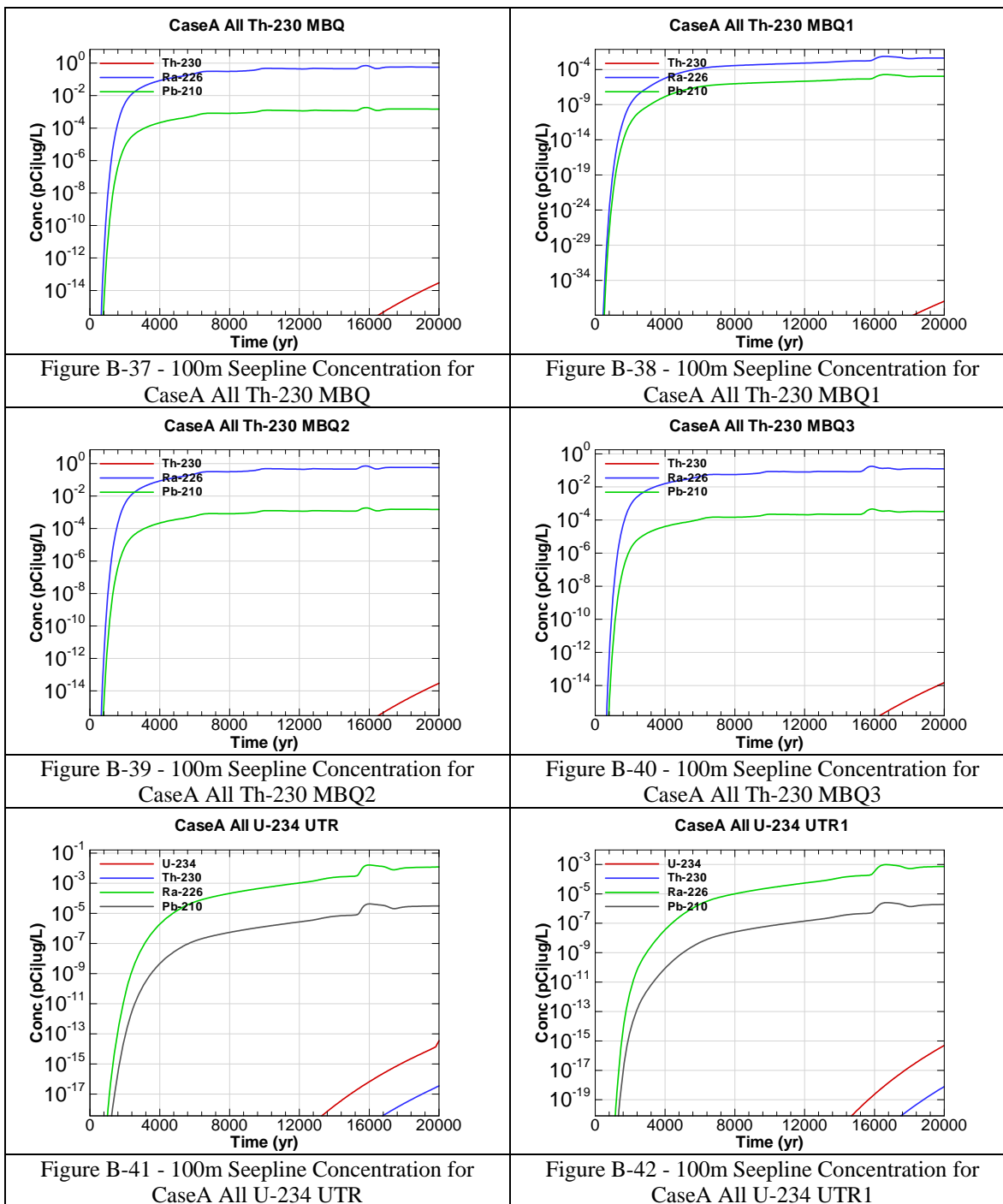


Figure B-36 - 100m Seepage Concentration for
CaseA All Th-230 UTR3



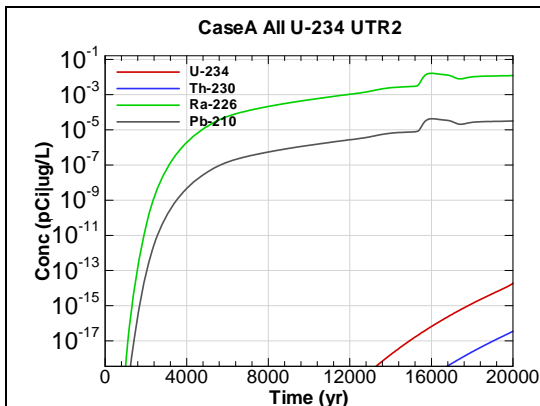


Figure B-43 - 100m Seepline Concentration for
CaseA All U-234 UTR2

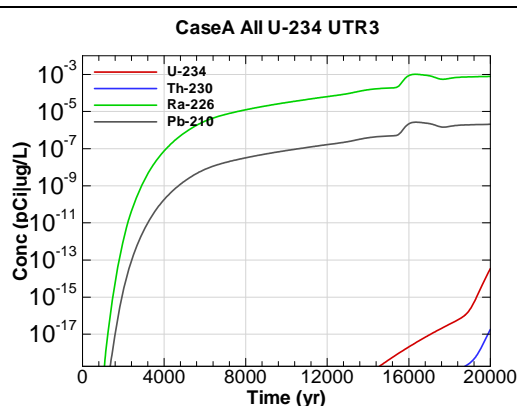


Figure B-44 - 100m Seepline Concentration for
CaseA All U-234 UTR3

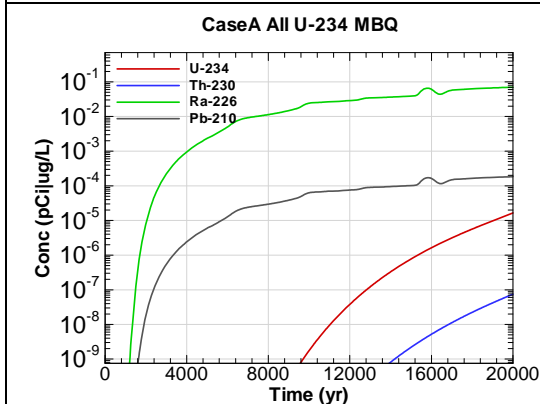


Figure B-45 - 100m Seepline Concentration for
CaseA All U-234 MBQ

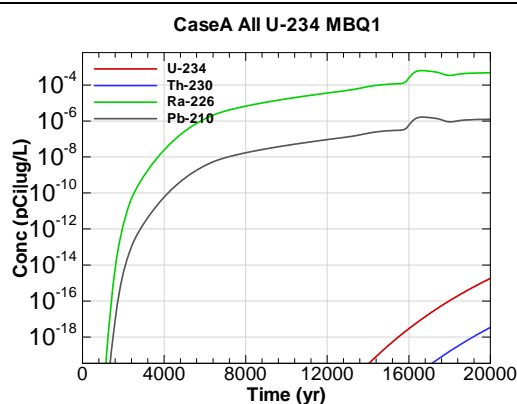


Figure B-46 - 100m Seepline Concentration for
CaseA All U-234 MBQ1

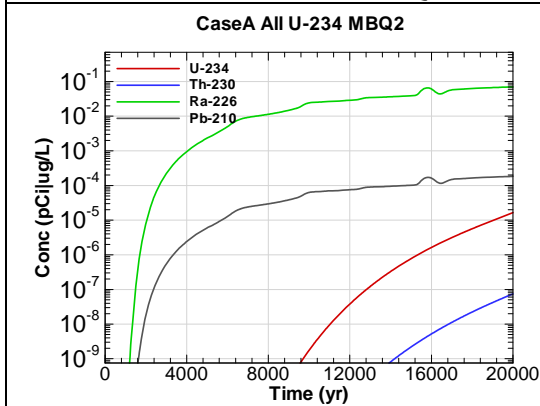


Figure B-47 - 100m Seepline Concentration for
CaseA All U-234 MBQ2

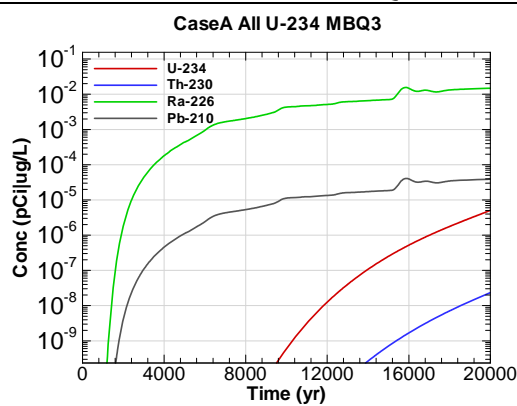


Figure B-48 - 100m Seepline Concentration for
CaseA All U-234 MBQ3

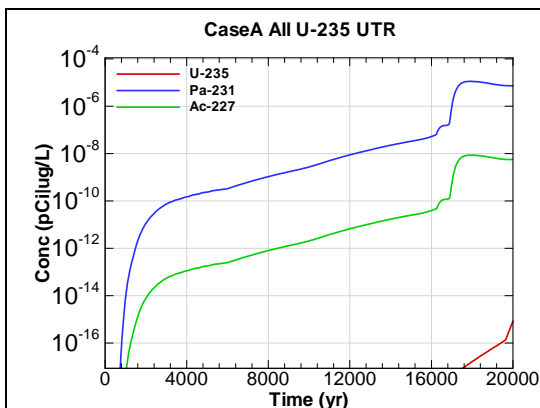


Figure B-49 - 100m Seepline Concentration for CaseA All U-235 UTR

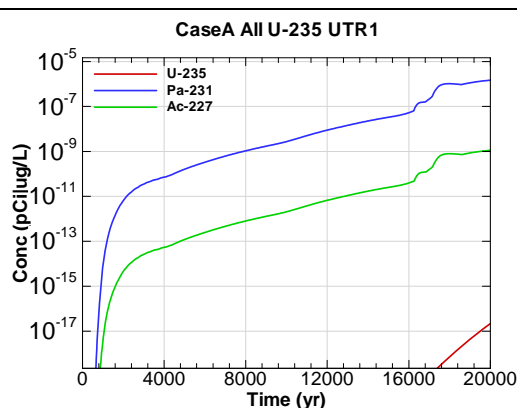


Figure B-50 - 100m Seepline Concentration for CaseA All U-235 UTR1

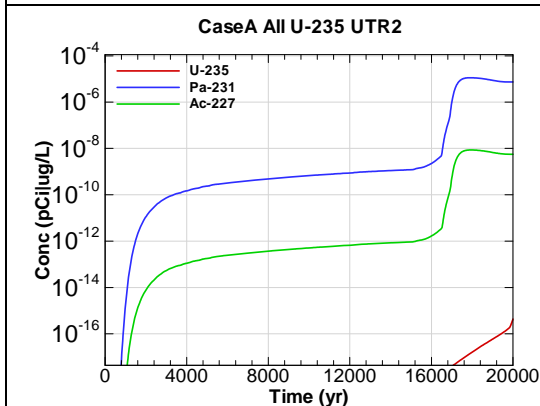


Figure B-51 - 100m Seepline Concentration for CaseA All U-235 UTR2

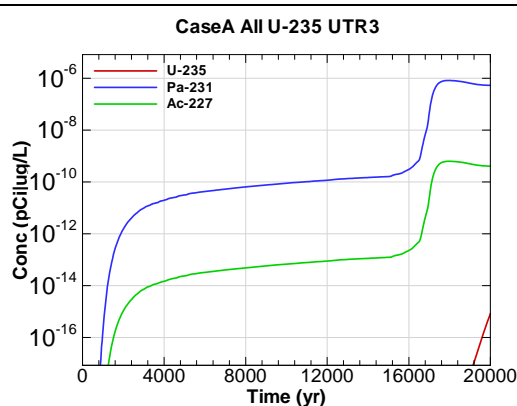


Figure B-52 - 100m Seepline Concentration for CaseA All U-235 UTR3

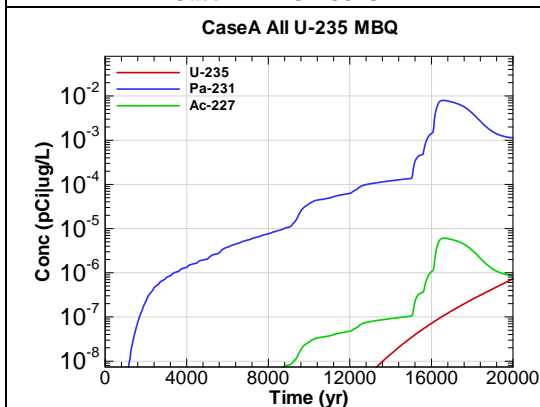


Figure B-53 - 100m Seepline Concentration for CaseA All U-235 MBQ

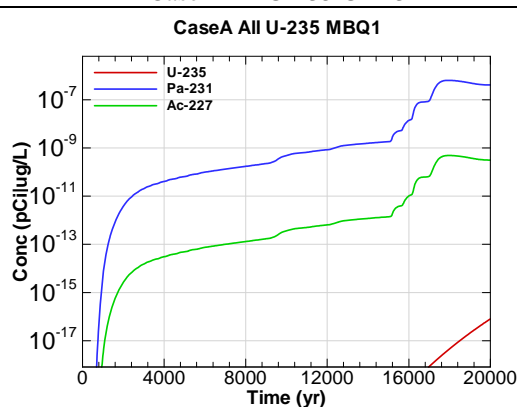
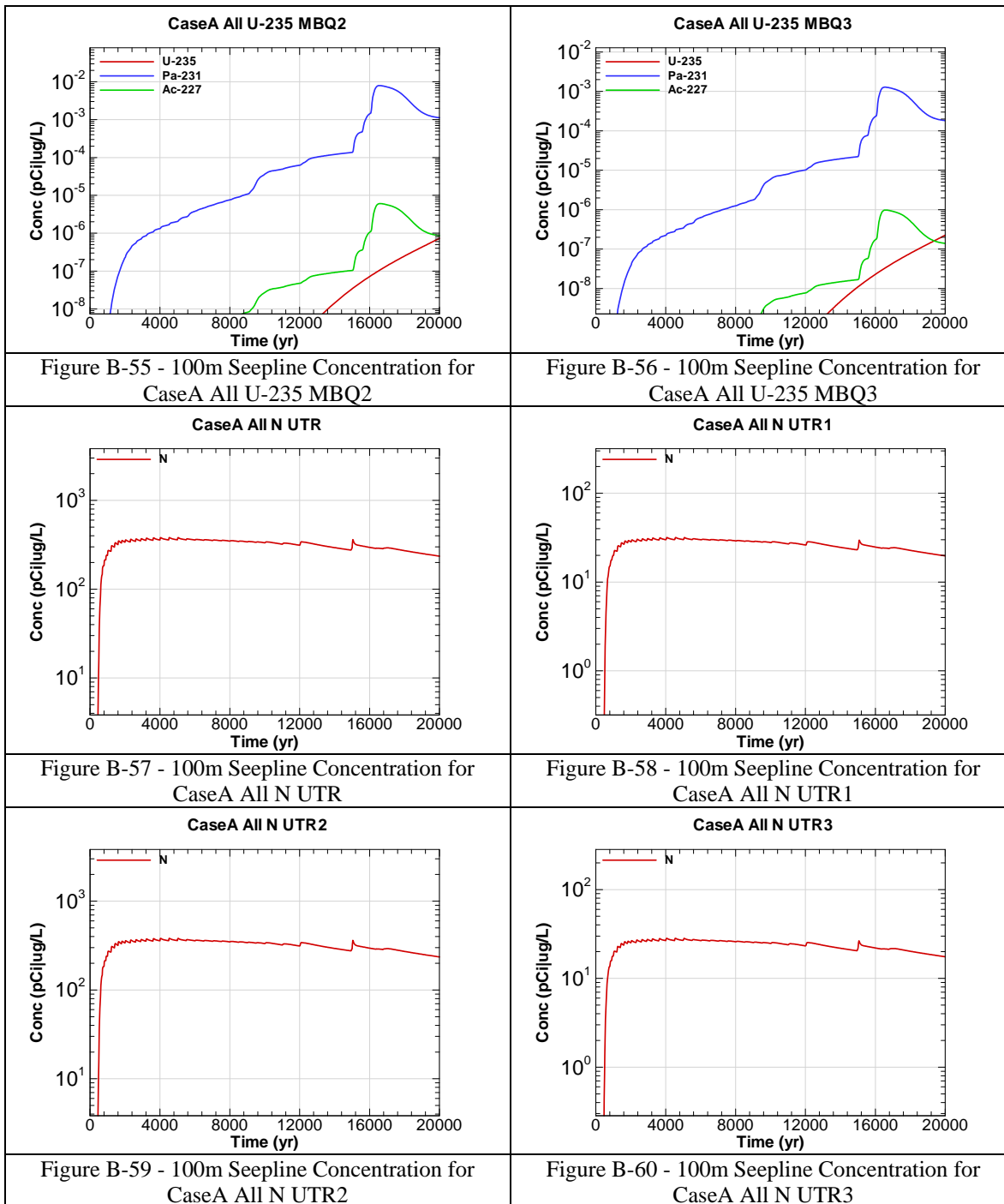
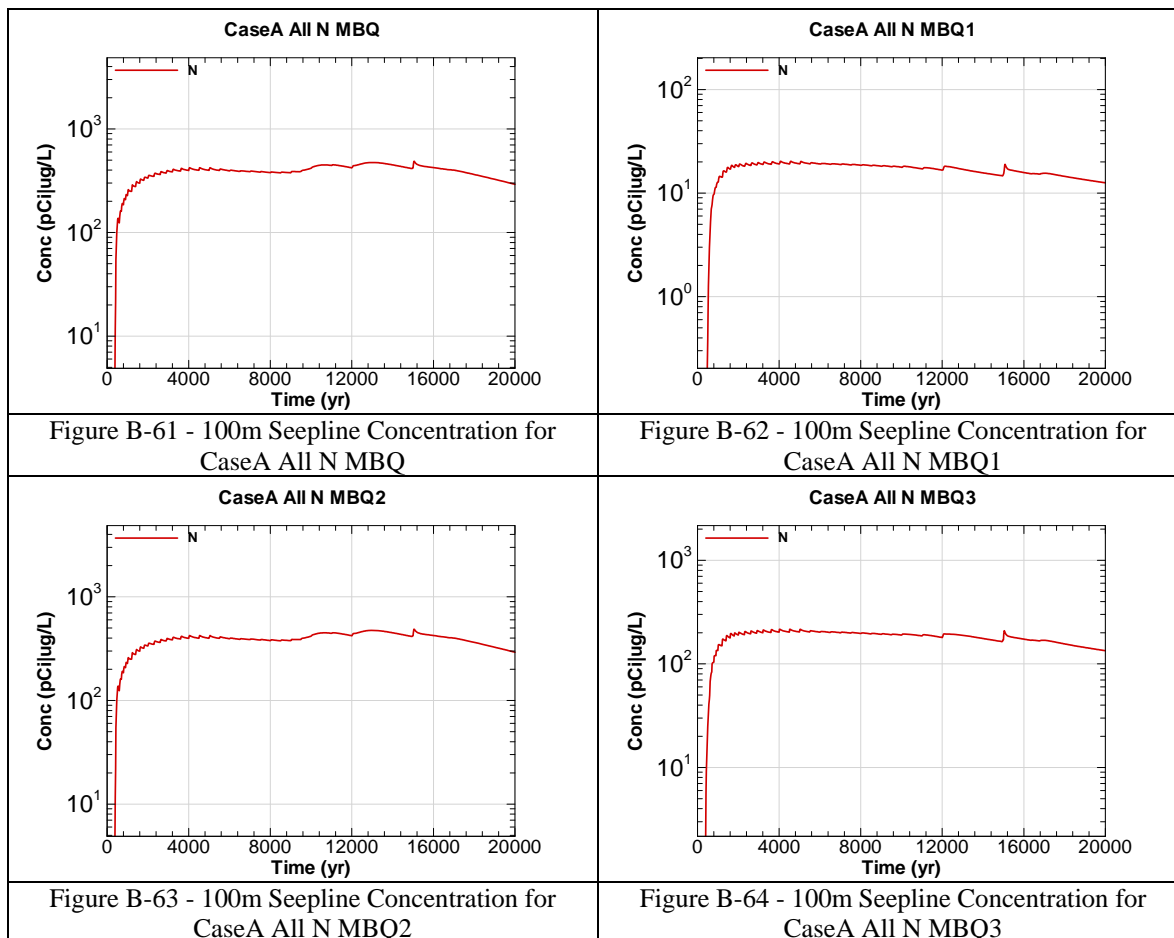


Figure B-54 - 100m Seepline Concentration for CaseA All U-235 MBQ1





APPENDIX C

100-METER KEY RADIONUCLIDE CONCENTRATIONS FOR 40,000 YEARS

Appendix C contains curves showing the 100 meter radiological concentrations (key radionuclides only) for all of SDF (vault and FDC inventories) for the Base Case (Case A). 40,000 year concentration results are for Sectors A through L for the peak concentration per sector regardless of aquifer.

Graph heading example "CaseA_40k All I-129 A"

Key

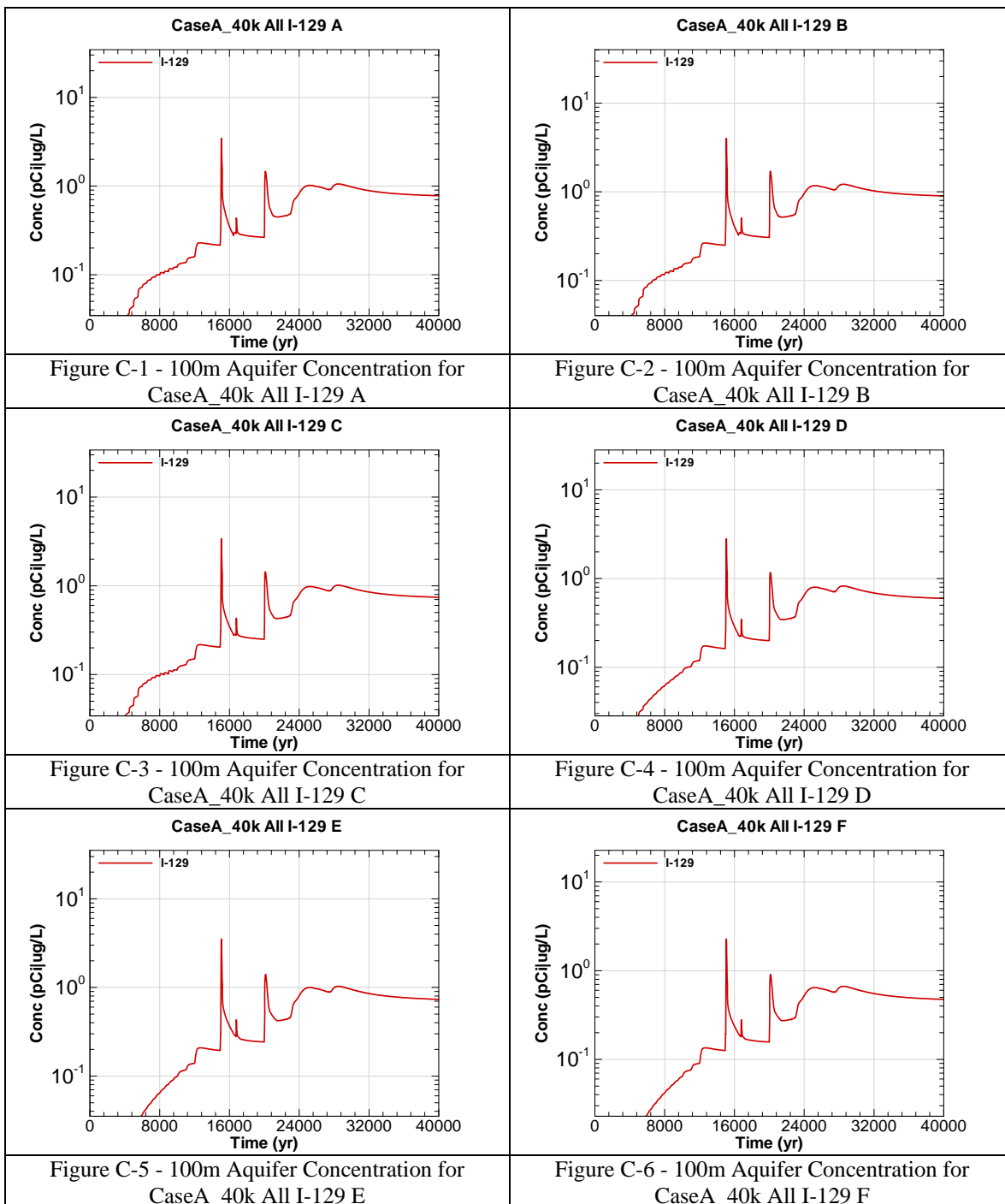
CaseA = Scenario case

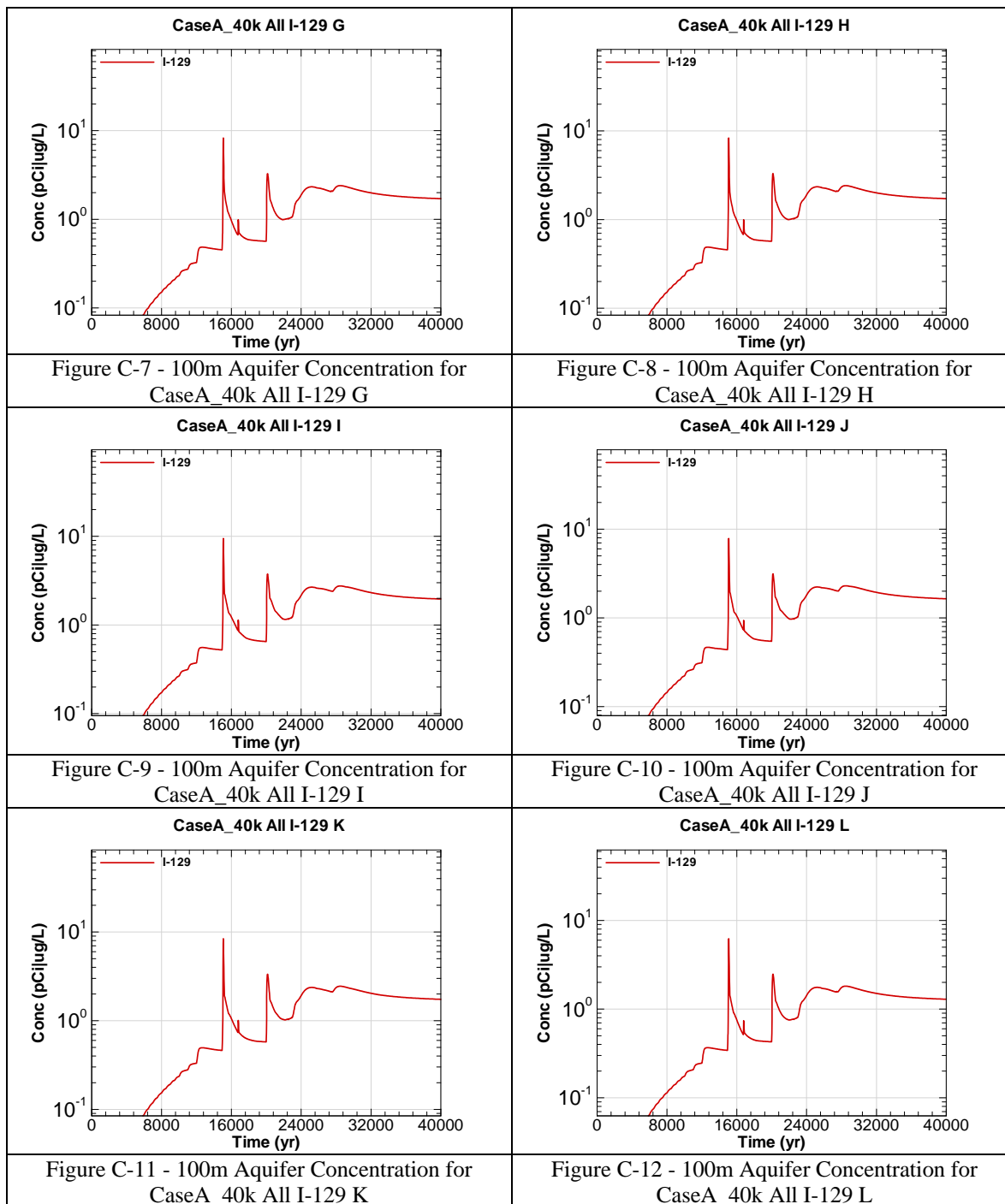
40k = 40,000 year run

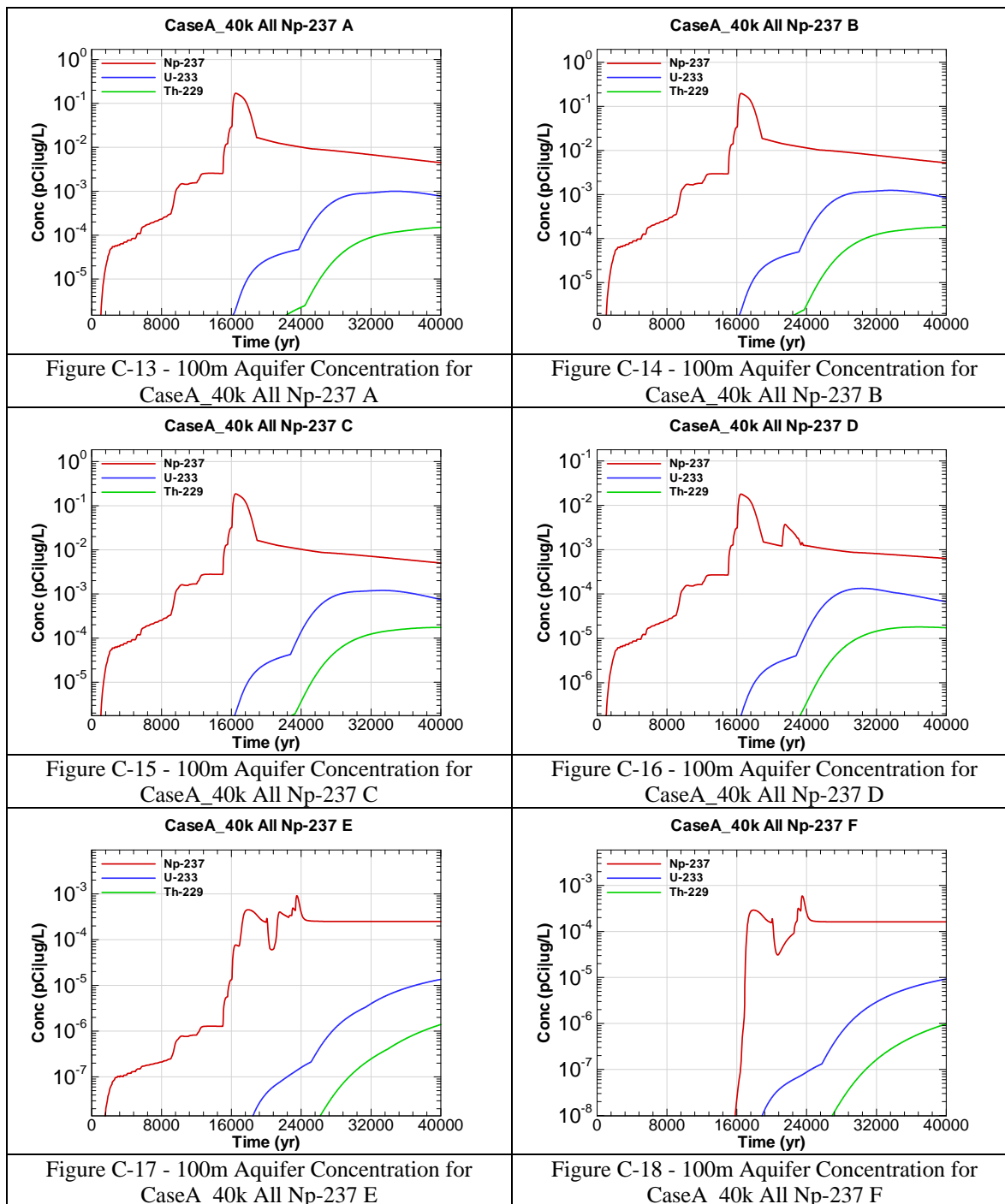
All = Inventory source is all disposal units

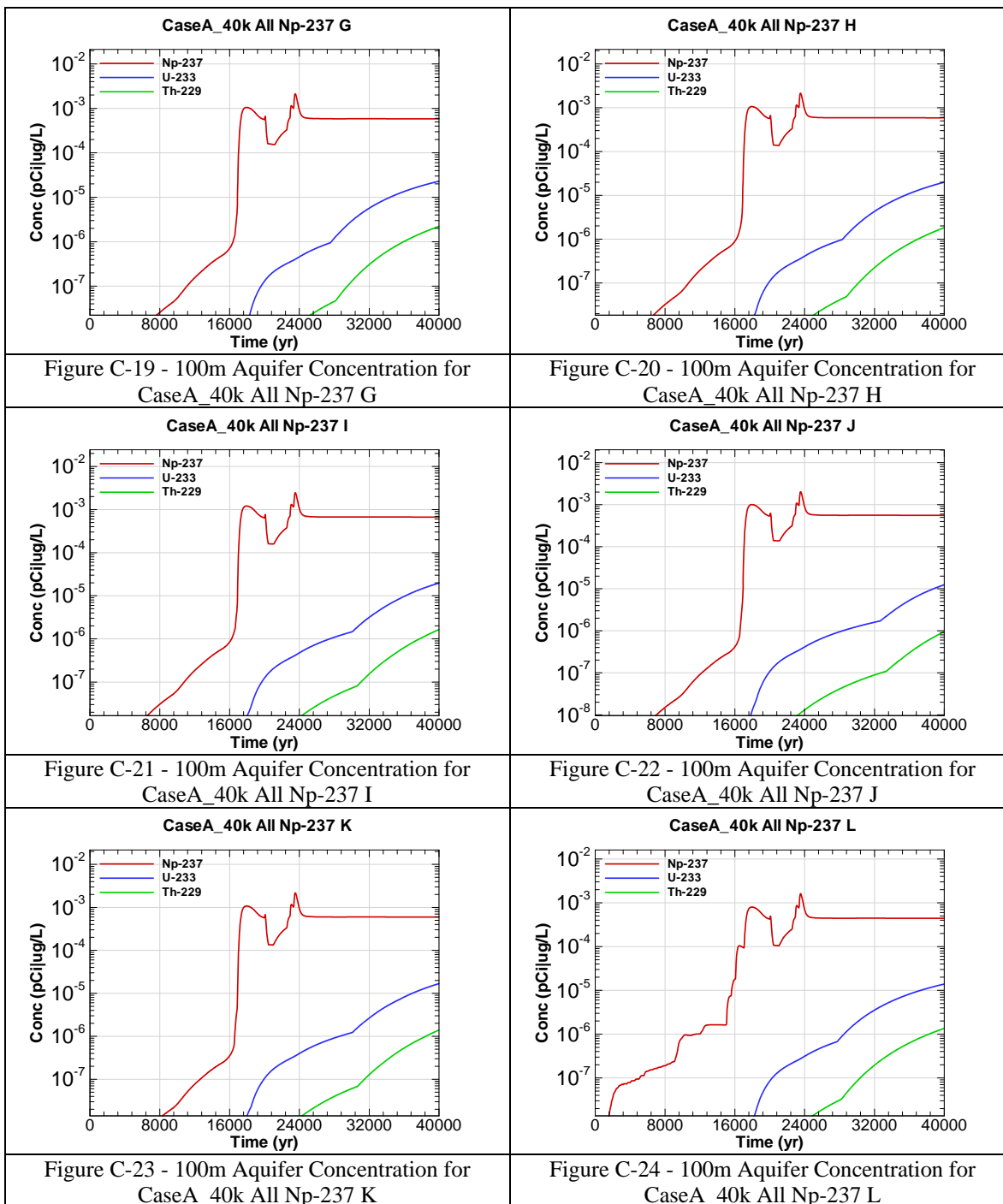
I-129 = Radionuclide or chemical of concern

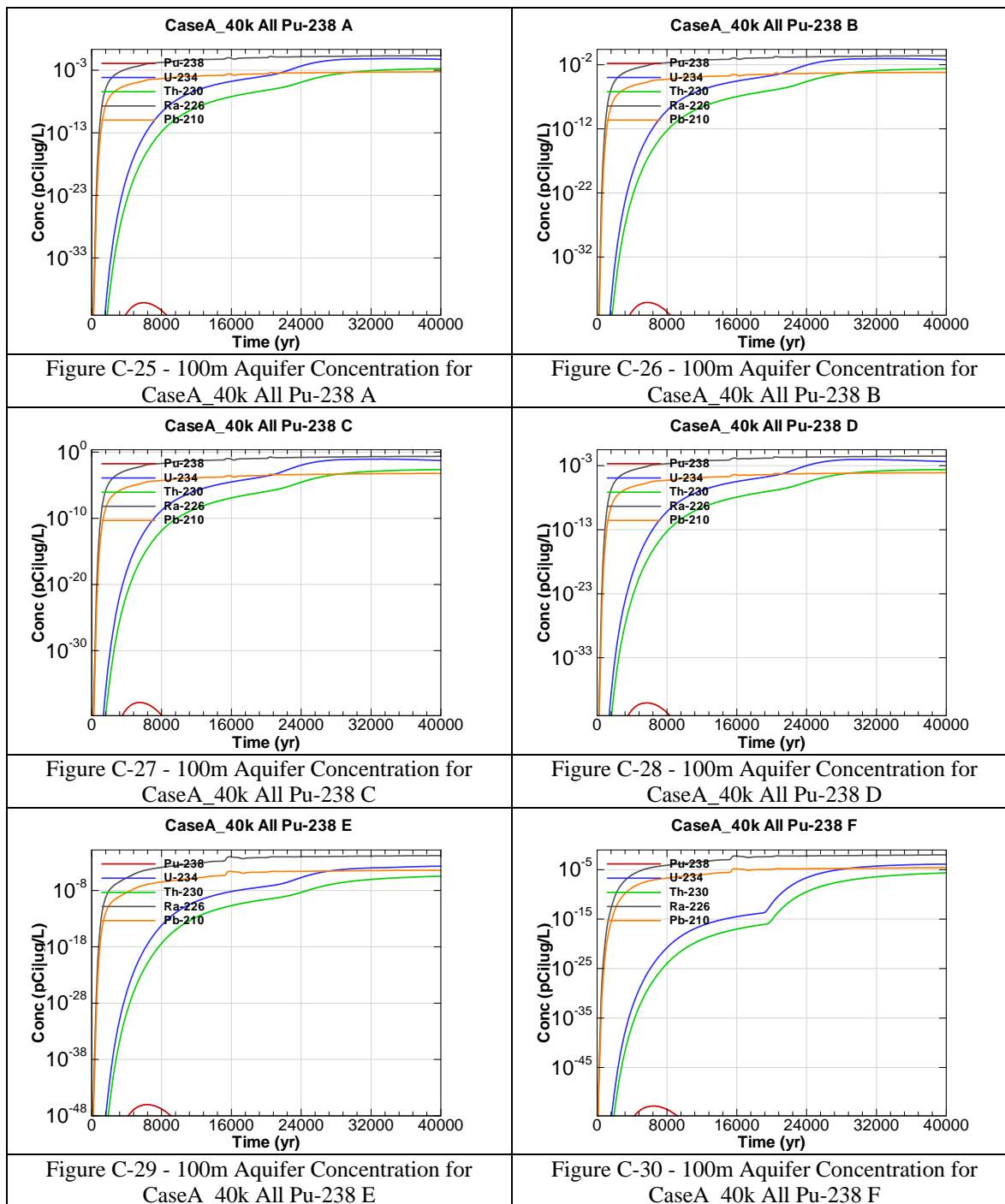
A = Evaluation sector of concern











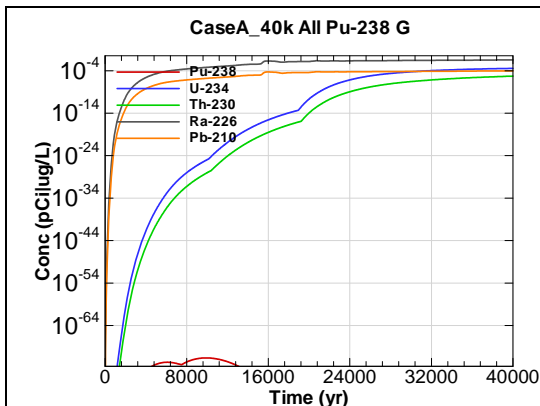


Figure C-31 - 100m Aquifer Concentration for
CaseA_40k All Pu-238 G

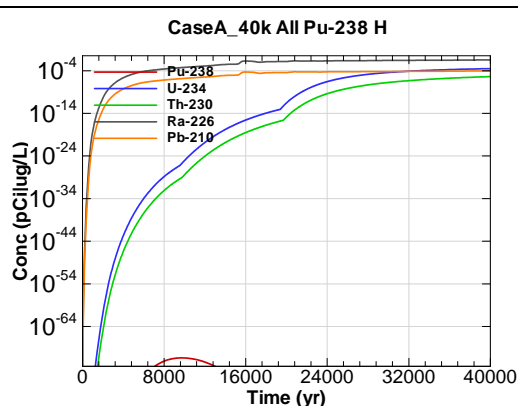


Figure C-32 - 100m Aquifer Concentration for
CaseA_40k All Pu-238 H

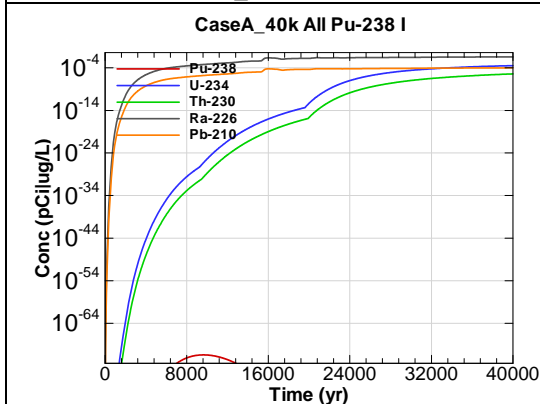


Figure C-33 - 100m Aquifer Concentration for
CaseA_40k All Pu-238 I

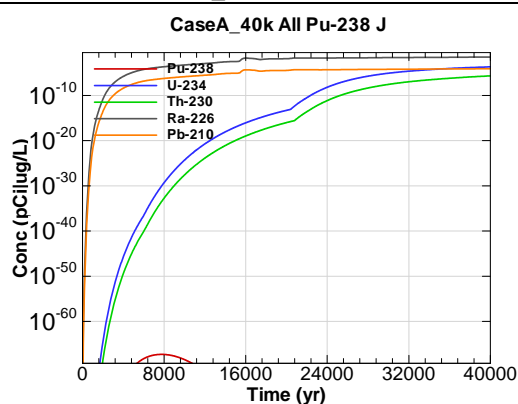


Figure C-34 - 100m Aquifer Concentration for
CaseA_40k All Pu-238 J

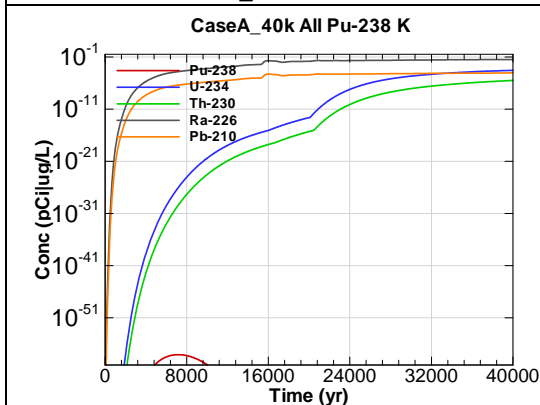


Figure C-35 - 100m Aquifer Concentration for
CaseA_40k All Pu-238 K

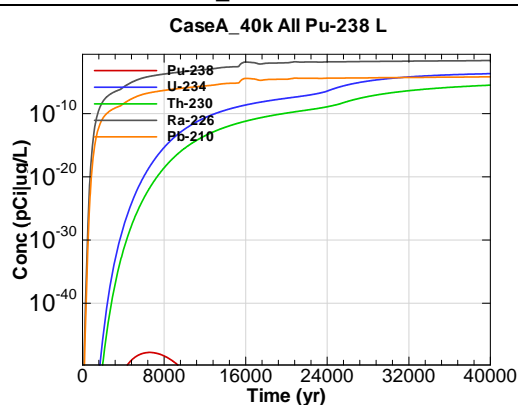
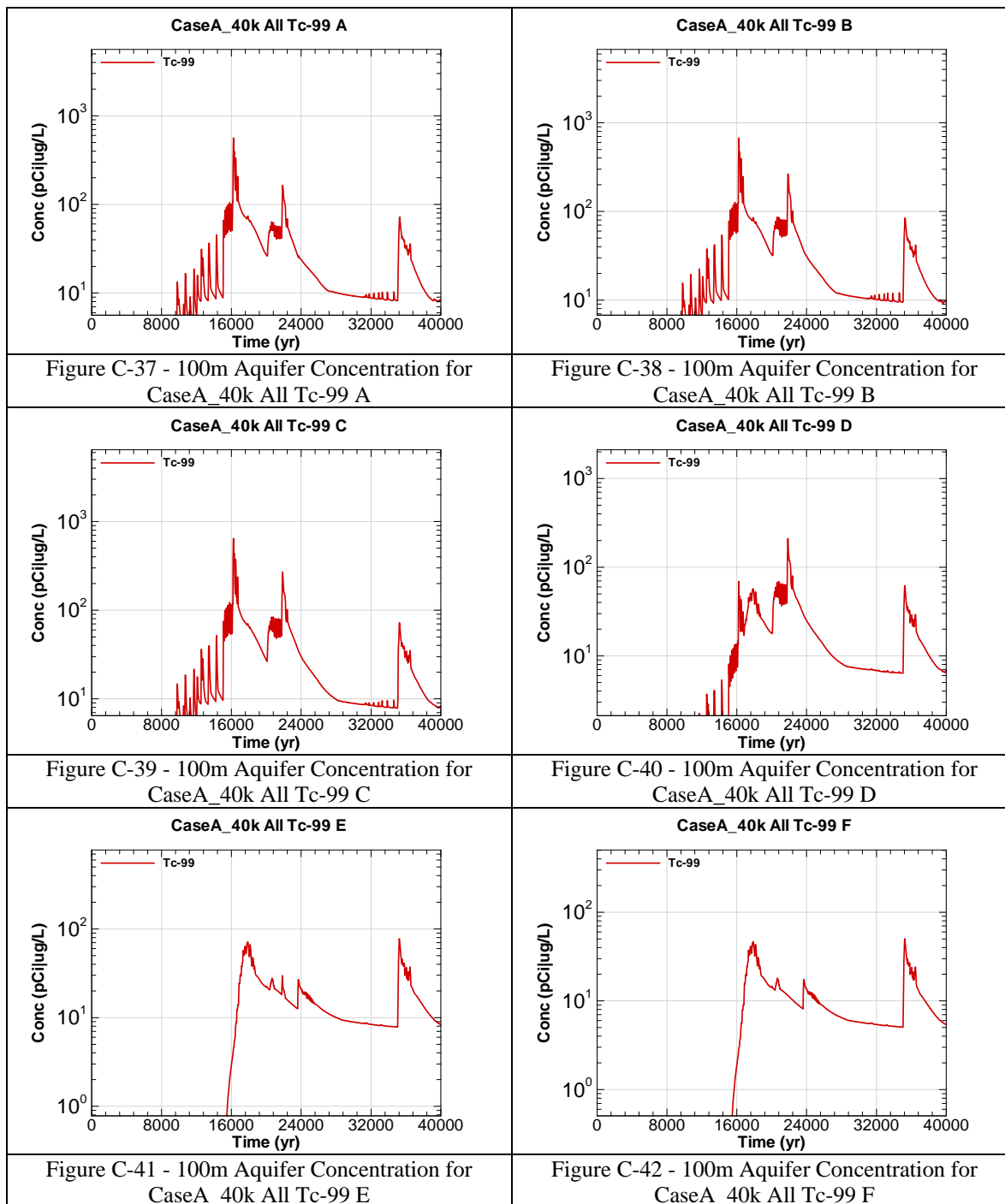
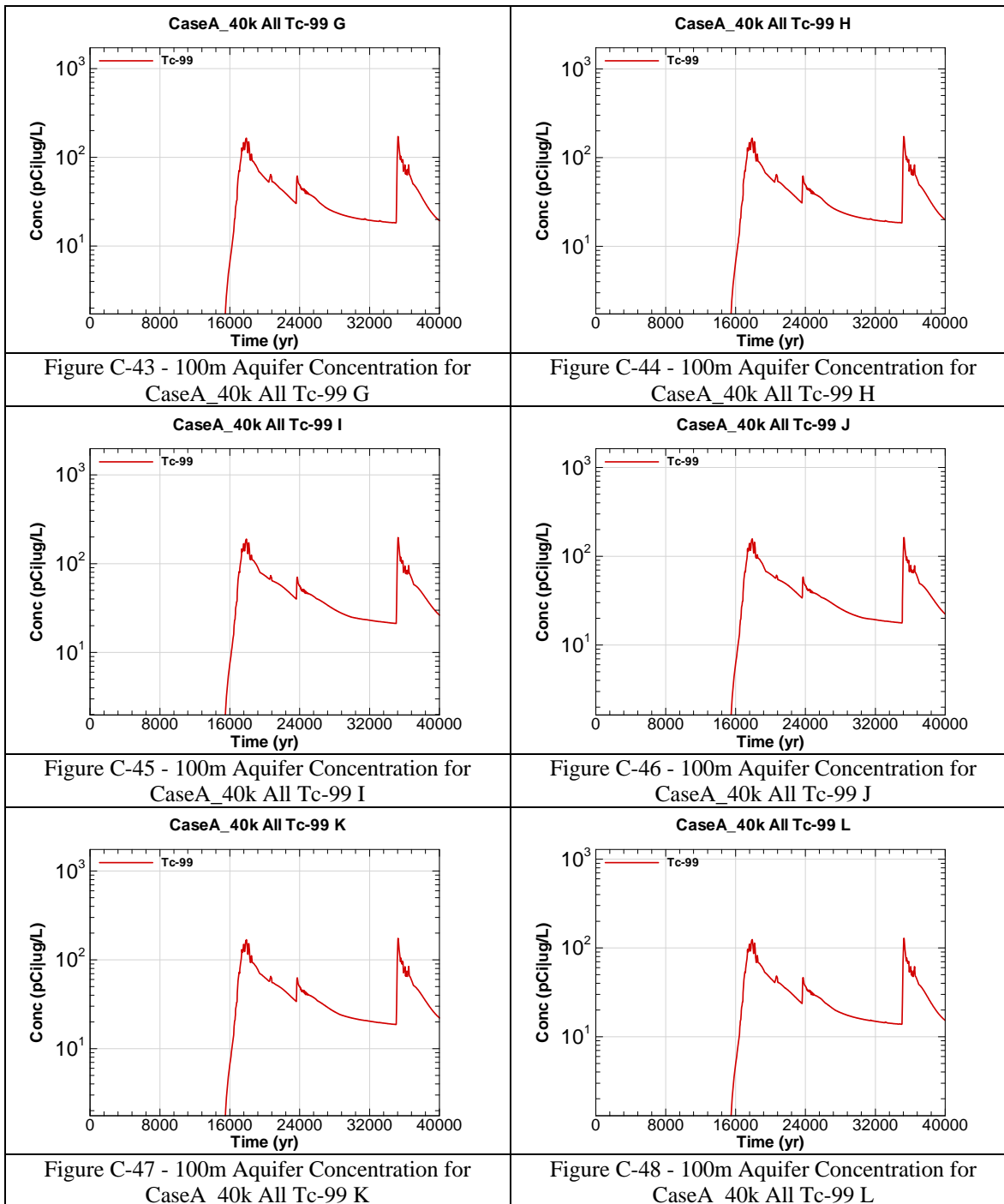
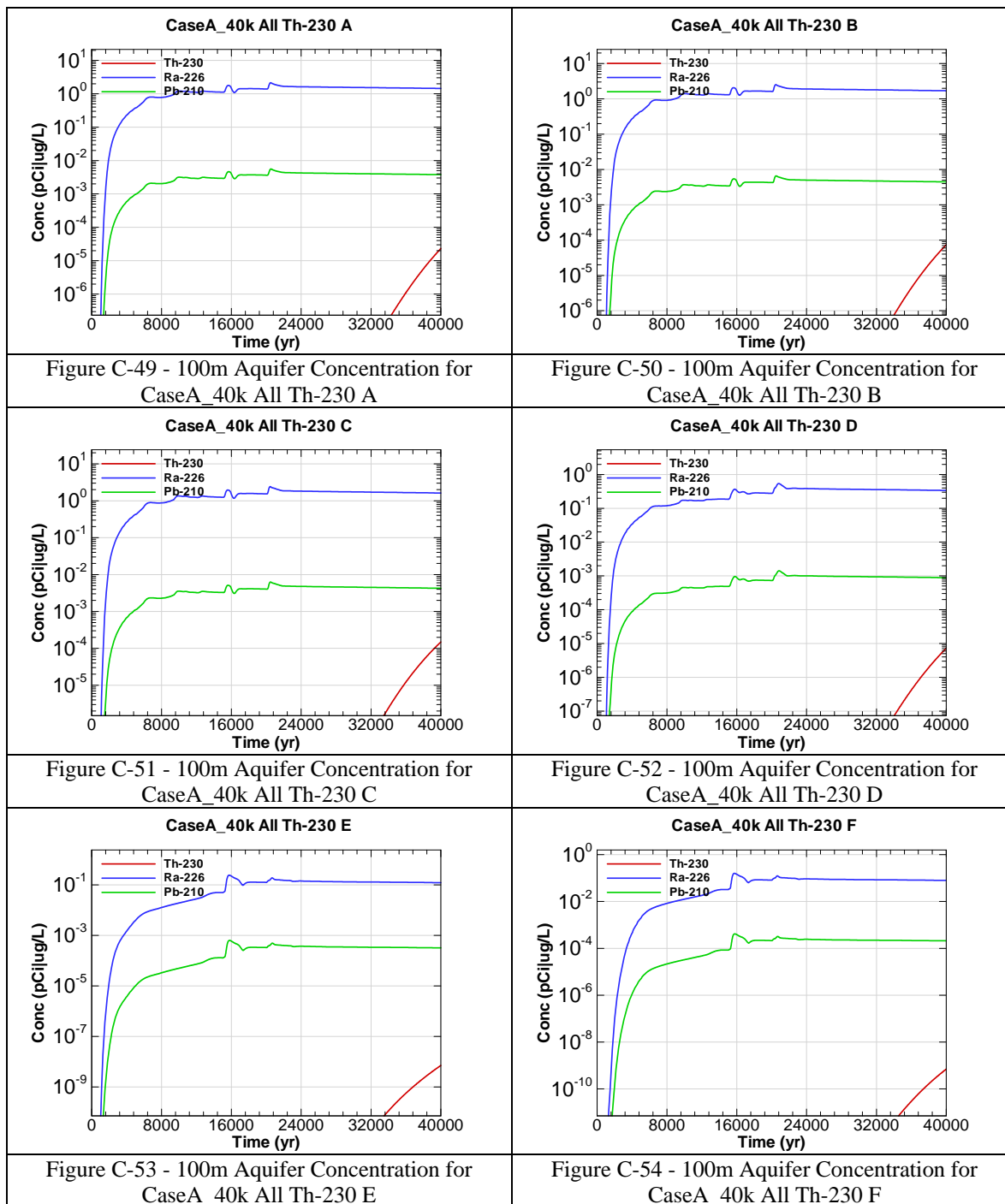
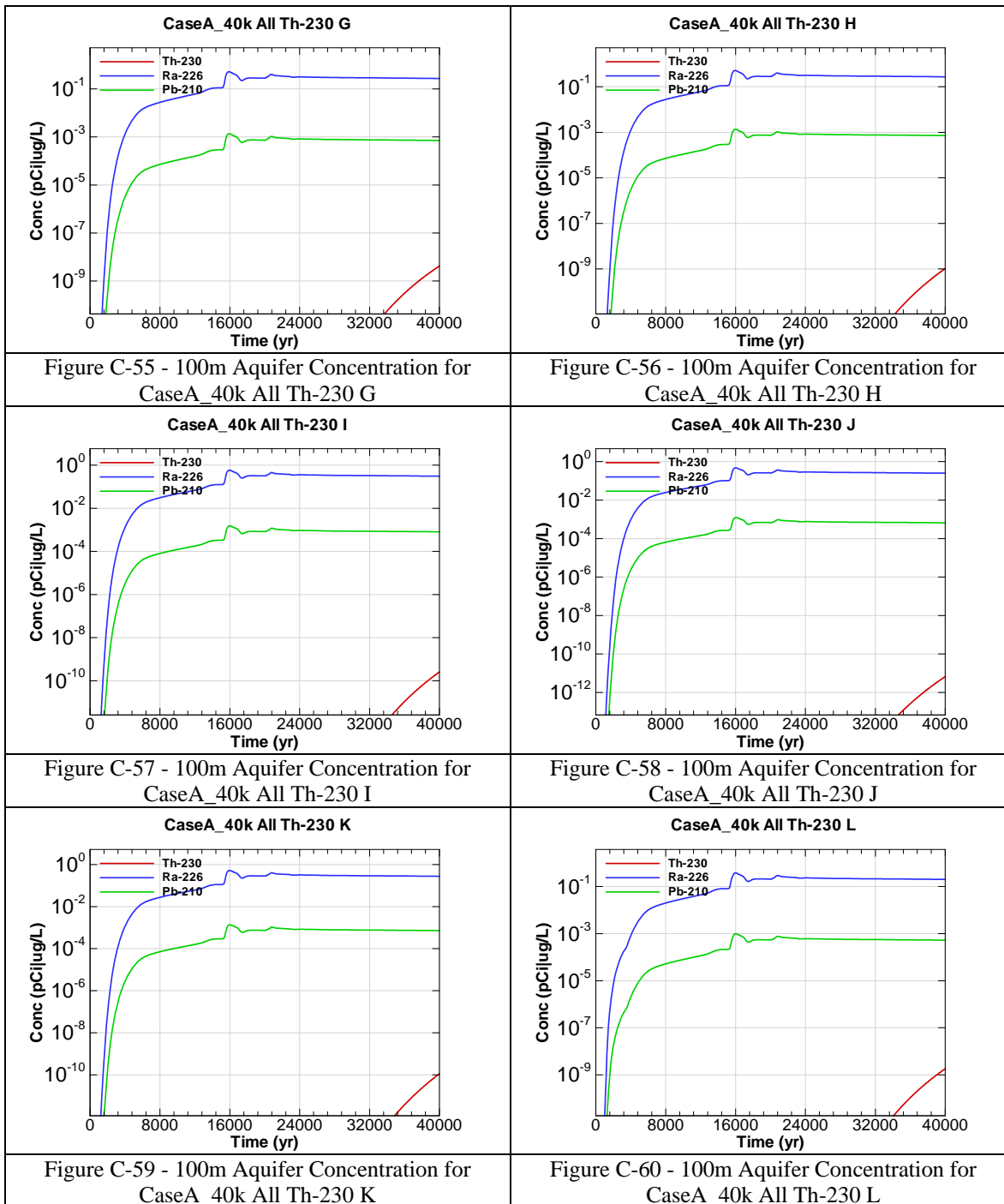


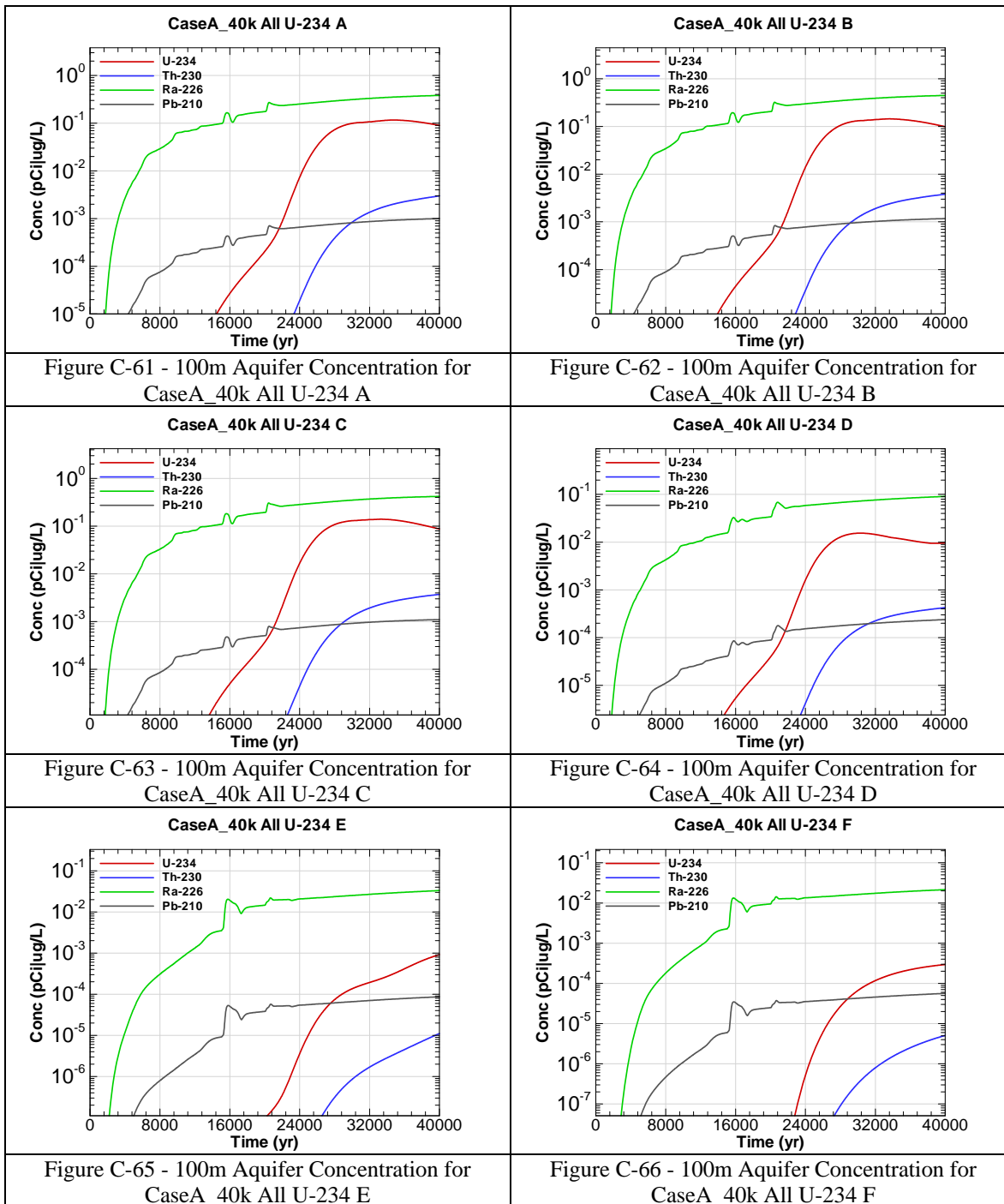
Figure C-36 - 100m Aquifer Concentration for
CaseA_40k All Pu-238 L

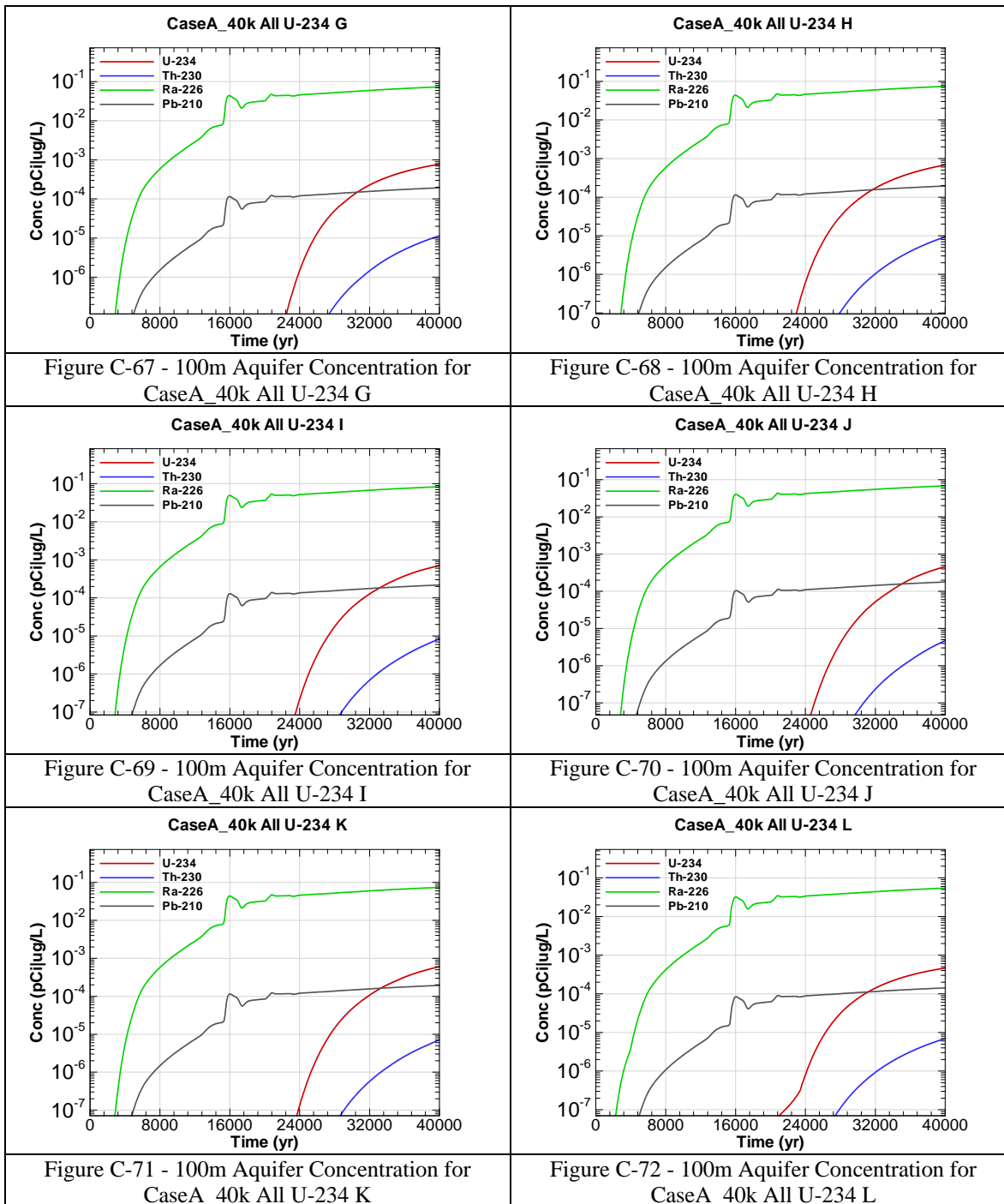


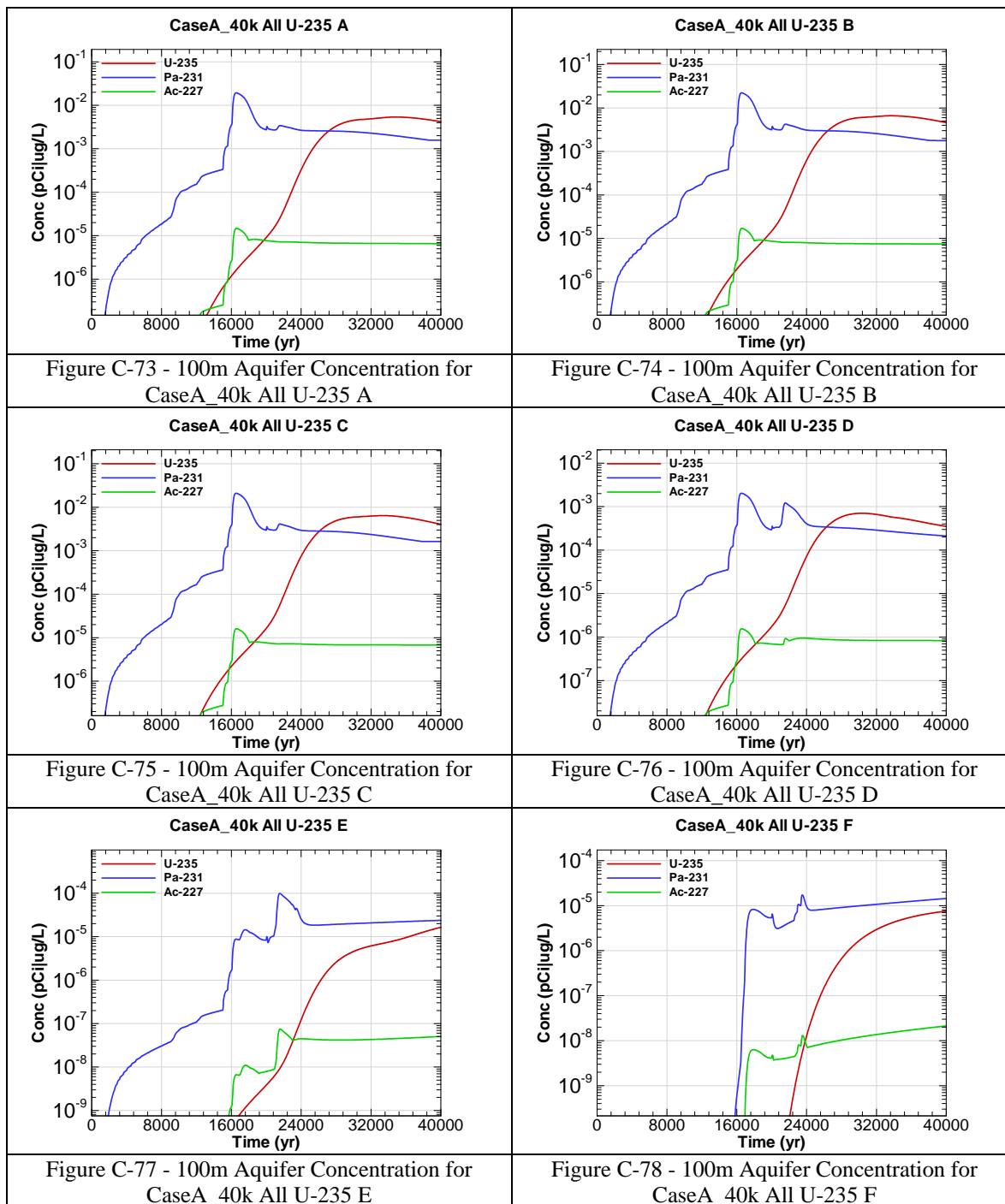


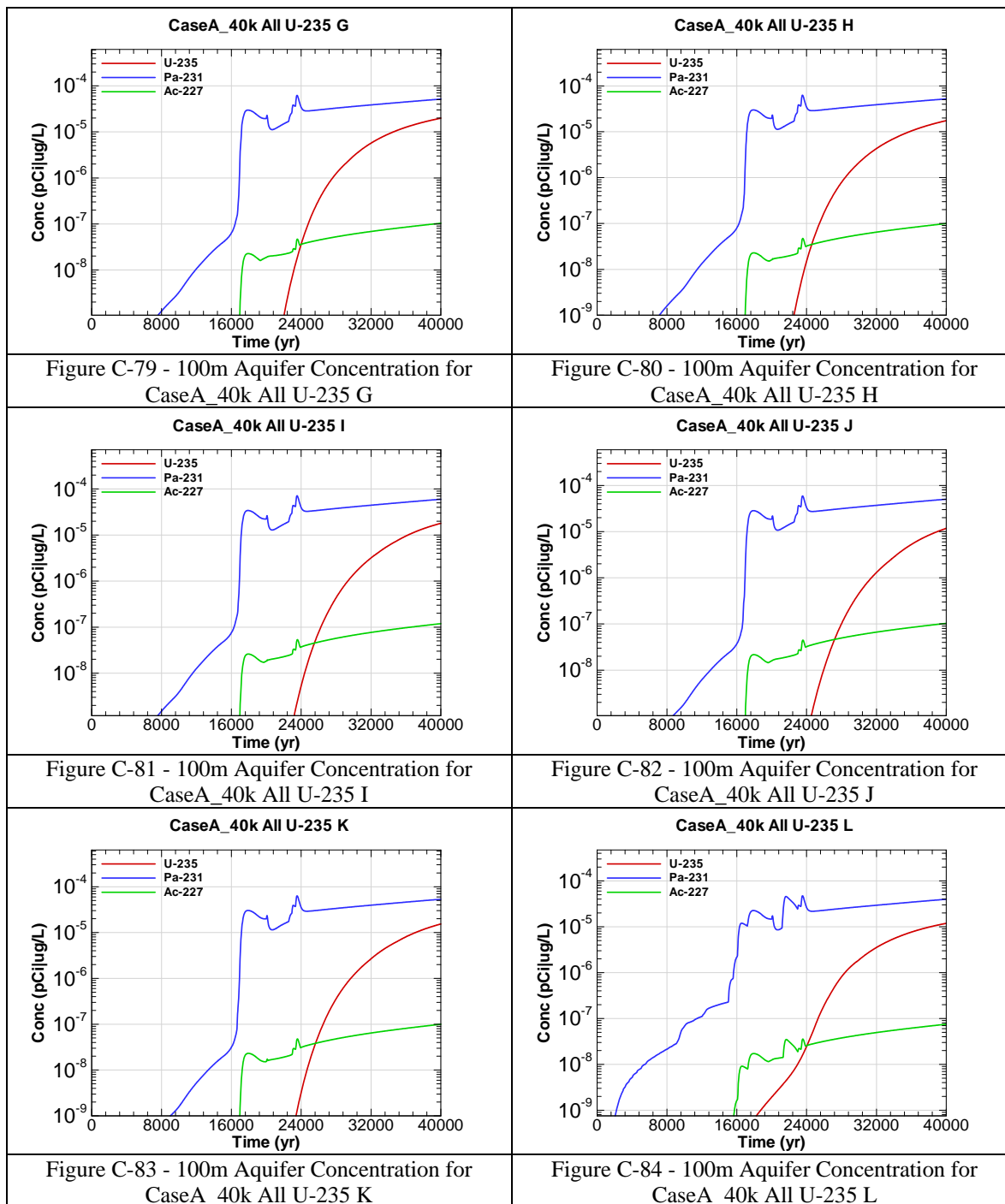


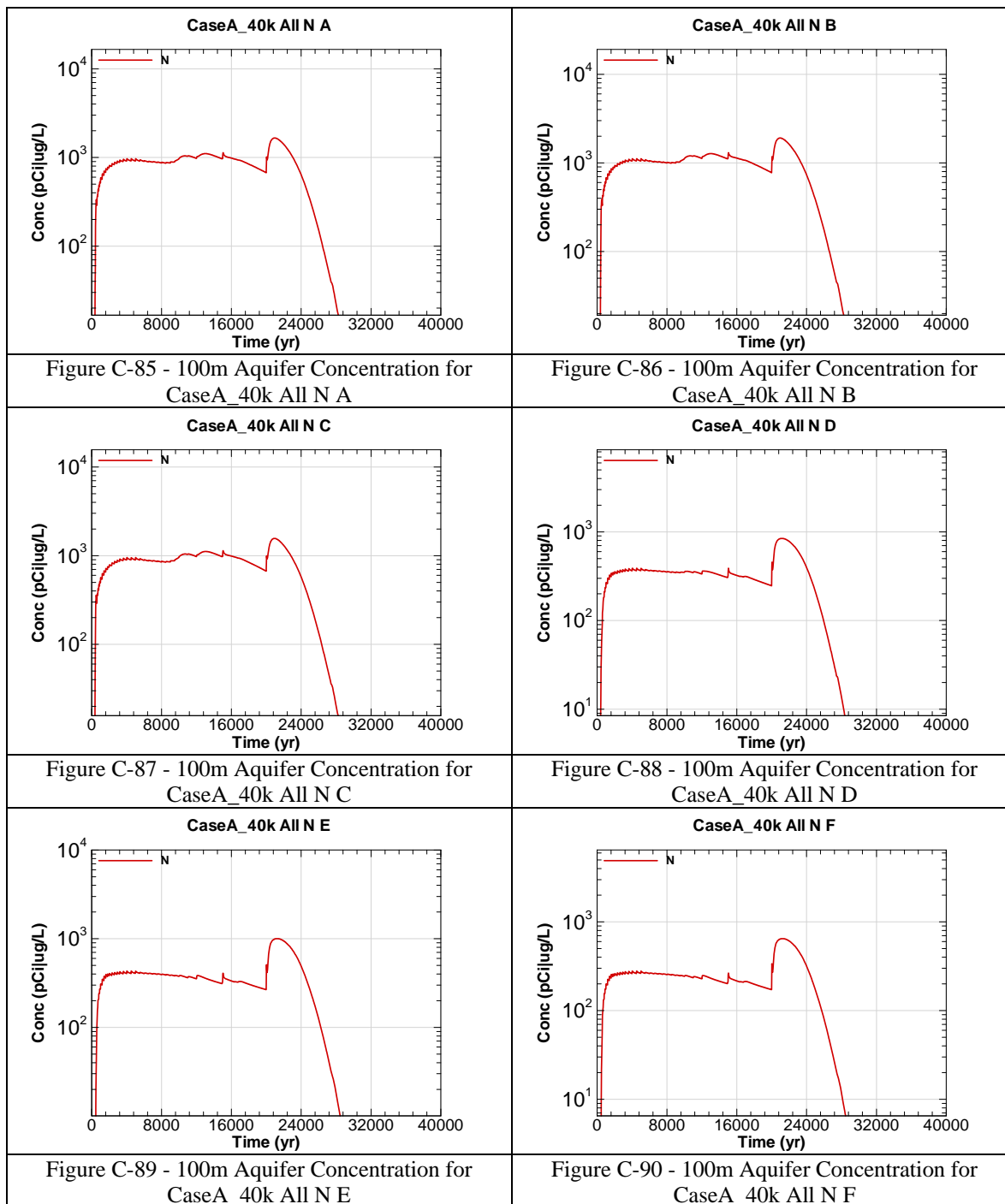


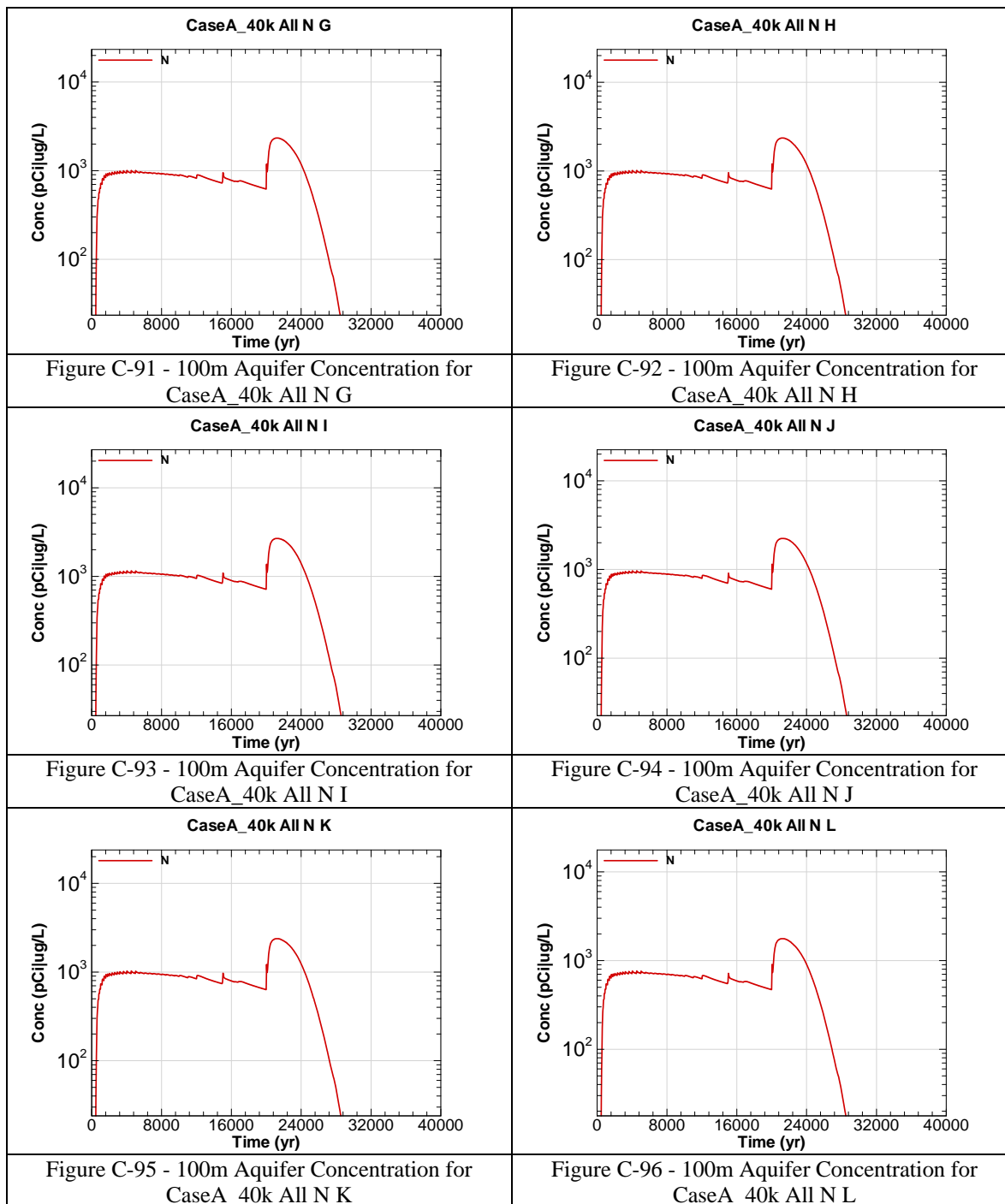












This page intentionally left blank

APPENDIX D

100-METER KEY RADIONUCLIDE AND CHEMICAL CONCENTRATIONS FOR SELECTED SOURCES

Appendix D contains curves showing the 100 meter radiological concentrations (key radionuclides only) for selected SDF sources (V1, V4, FDC0207A, and FDC all) for the Base Case (Case A). 20,000 year concentration results are presented for Sectors A through L for the peak concentration per sector regardless of aquifer.

Graph heading example "CaseA V1 I-129 A"

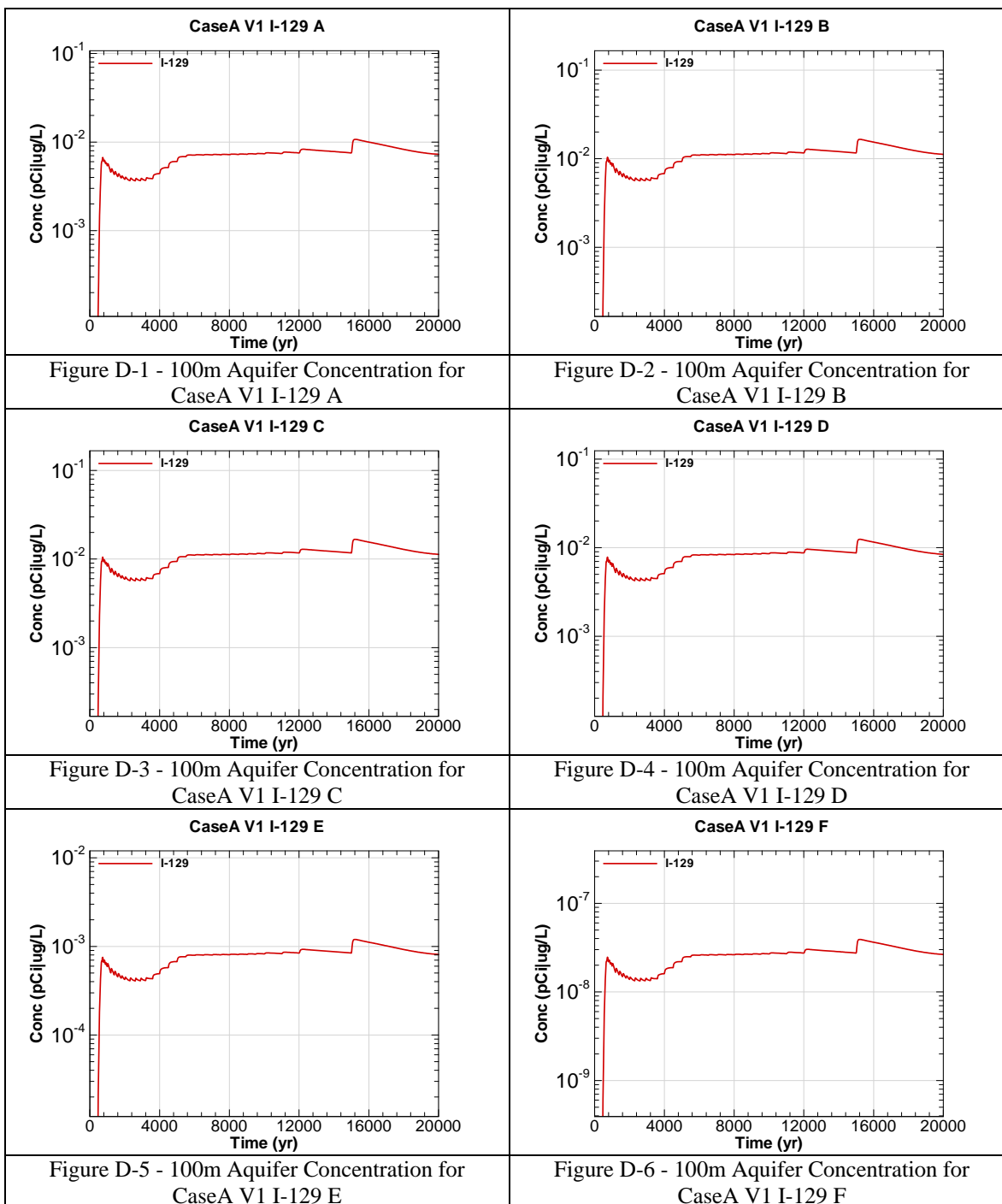
Key

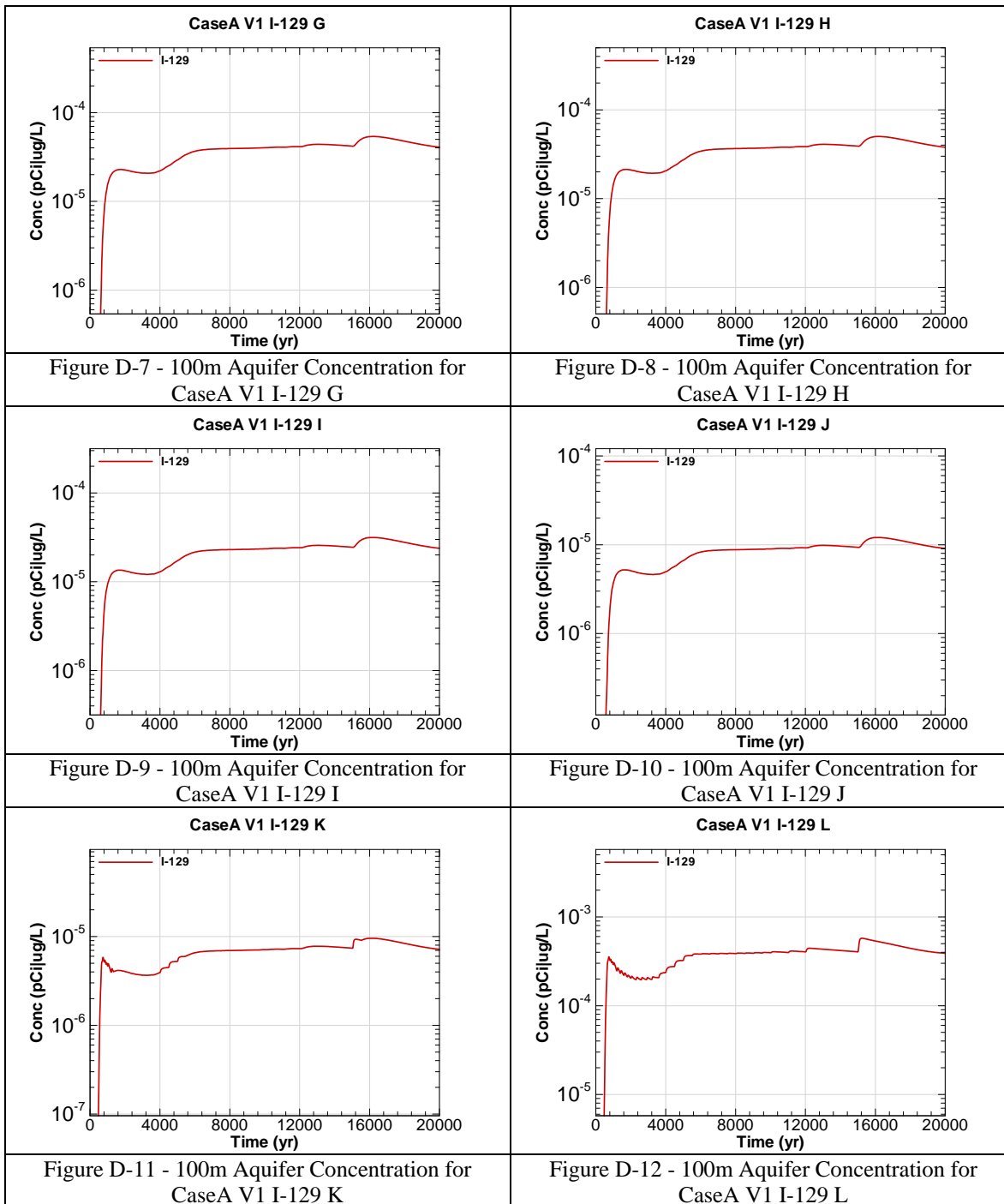
CaseA = Scenario case

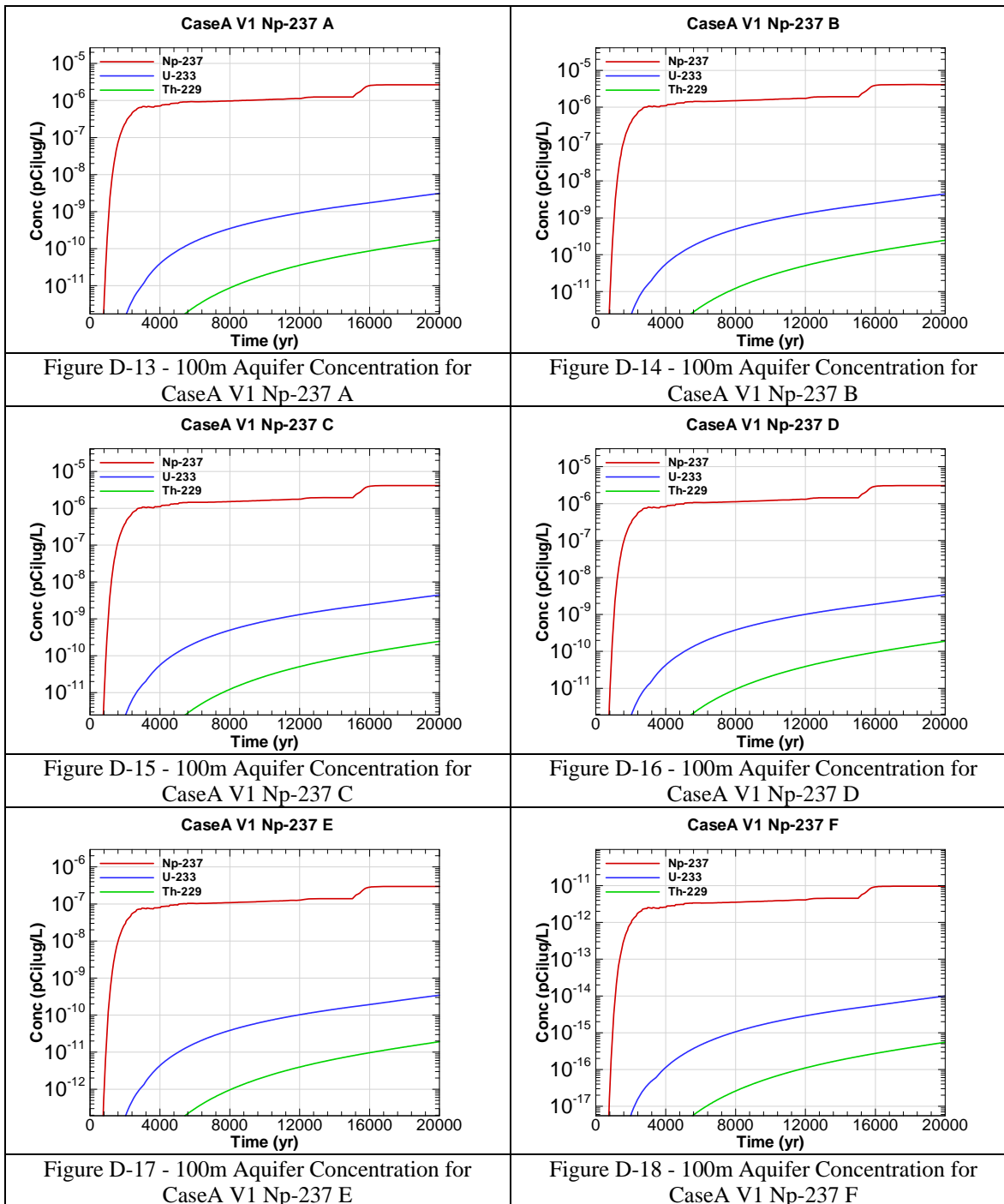
V1 = Inventory source of concern (V1=Vault 1, V4=Vault 4, FDC=All future disposal cells,
FDC0207A=One FDC in Sector I)

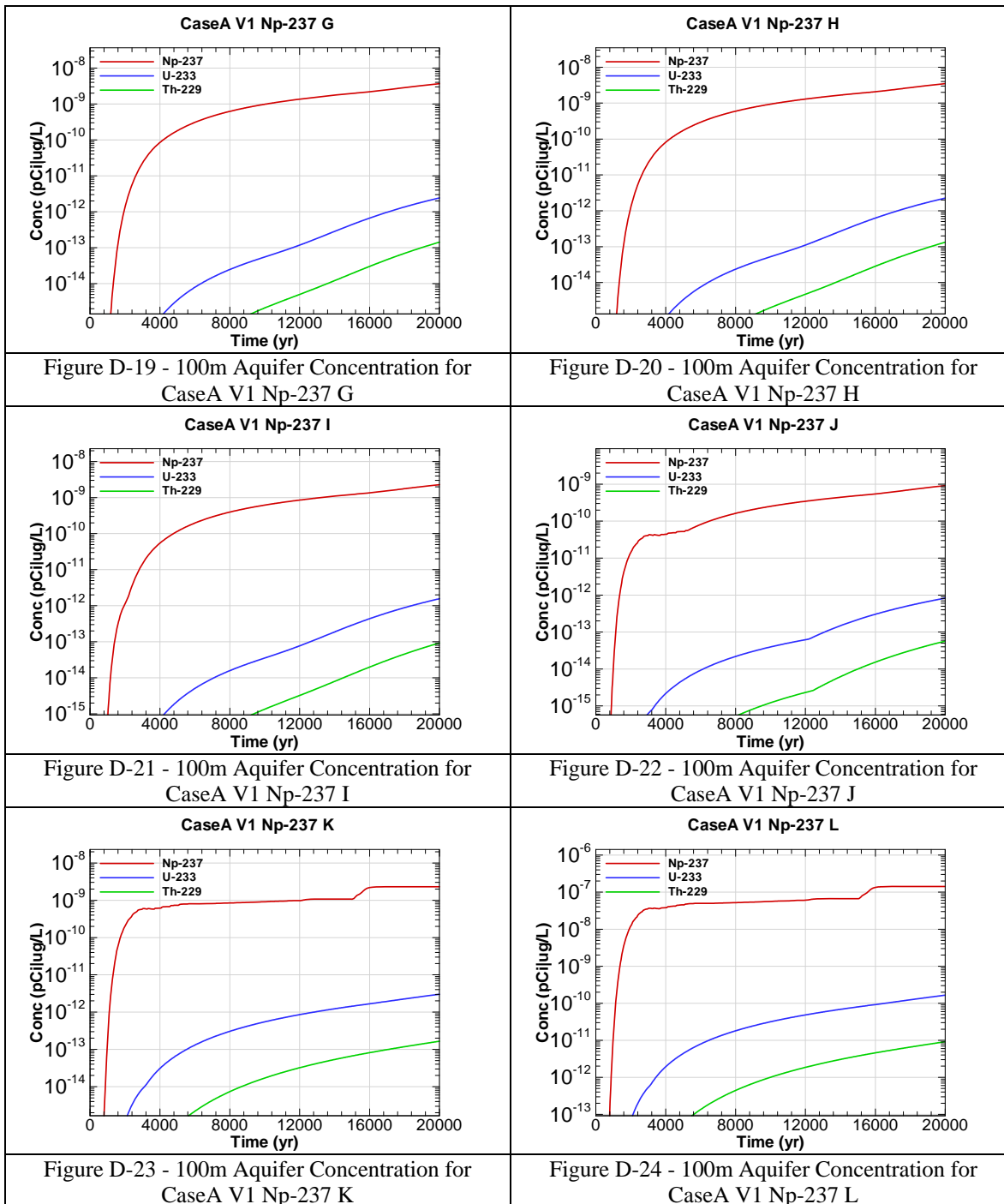
I-129 = Radionuclide or chemical of concern

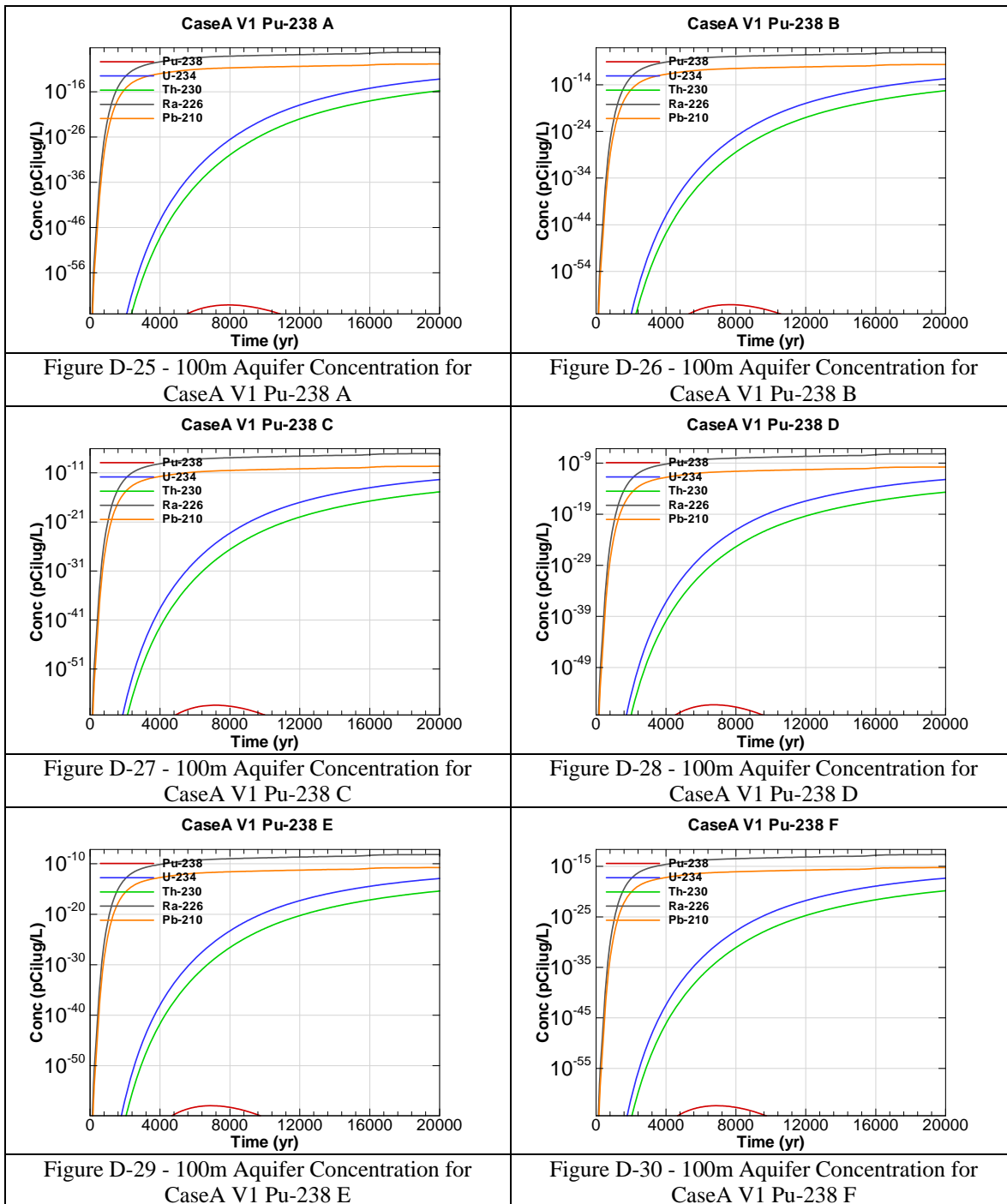
A = Evaluation sector of concern











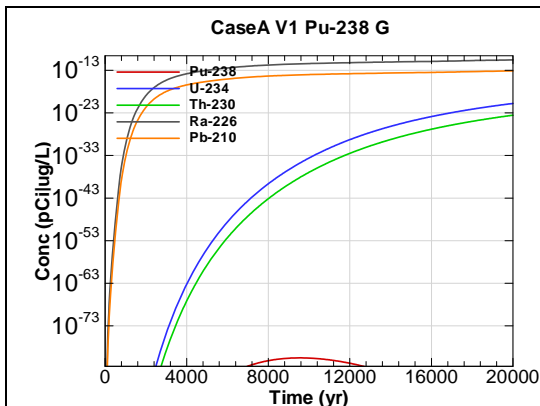


Figure D-31 - 100m Aquifer Concentration for
CaseA V1 Pu-238 G

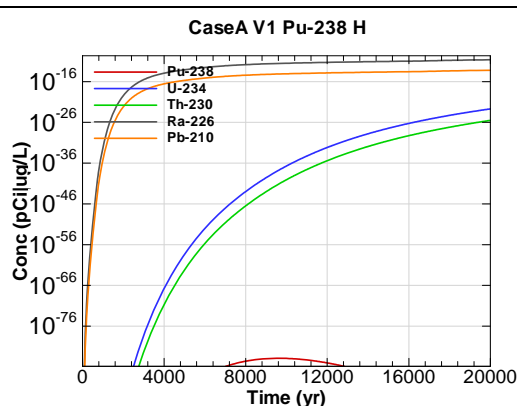


Figure D-32 - 100m Aquifer Concentration for
CaseA V1 Pu-238 H

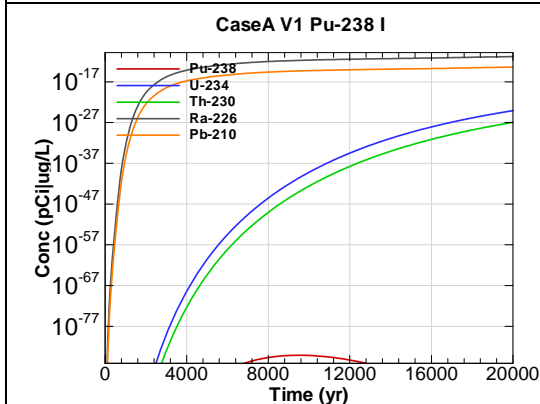


Figure D-33 - 100m Aquifer Concentration for
CaseA V1 Pu-238 I

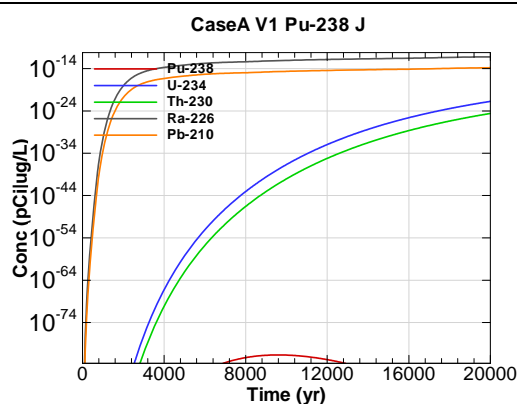


Figure D-34 - 100m Aquifer Concentration for
CaseA V1 Pu-238 J

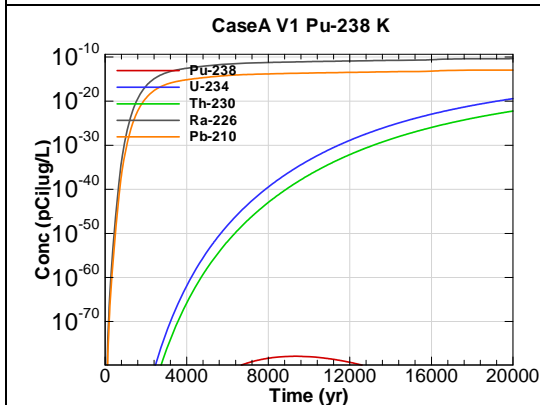


Figure D-35 - 100m Aquifer Concentration for
CaseA V1 Pu-238 K

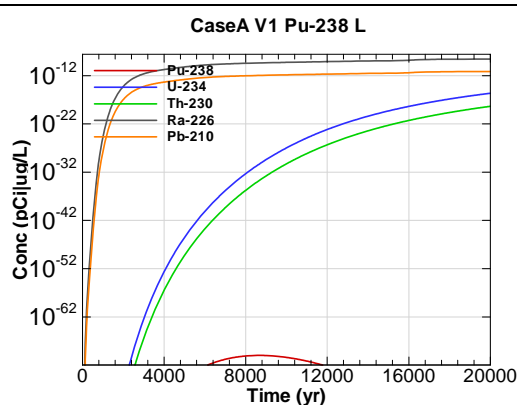
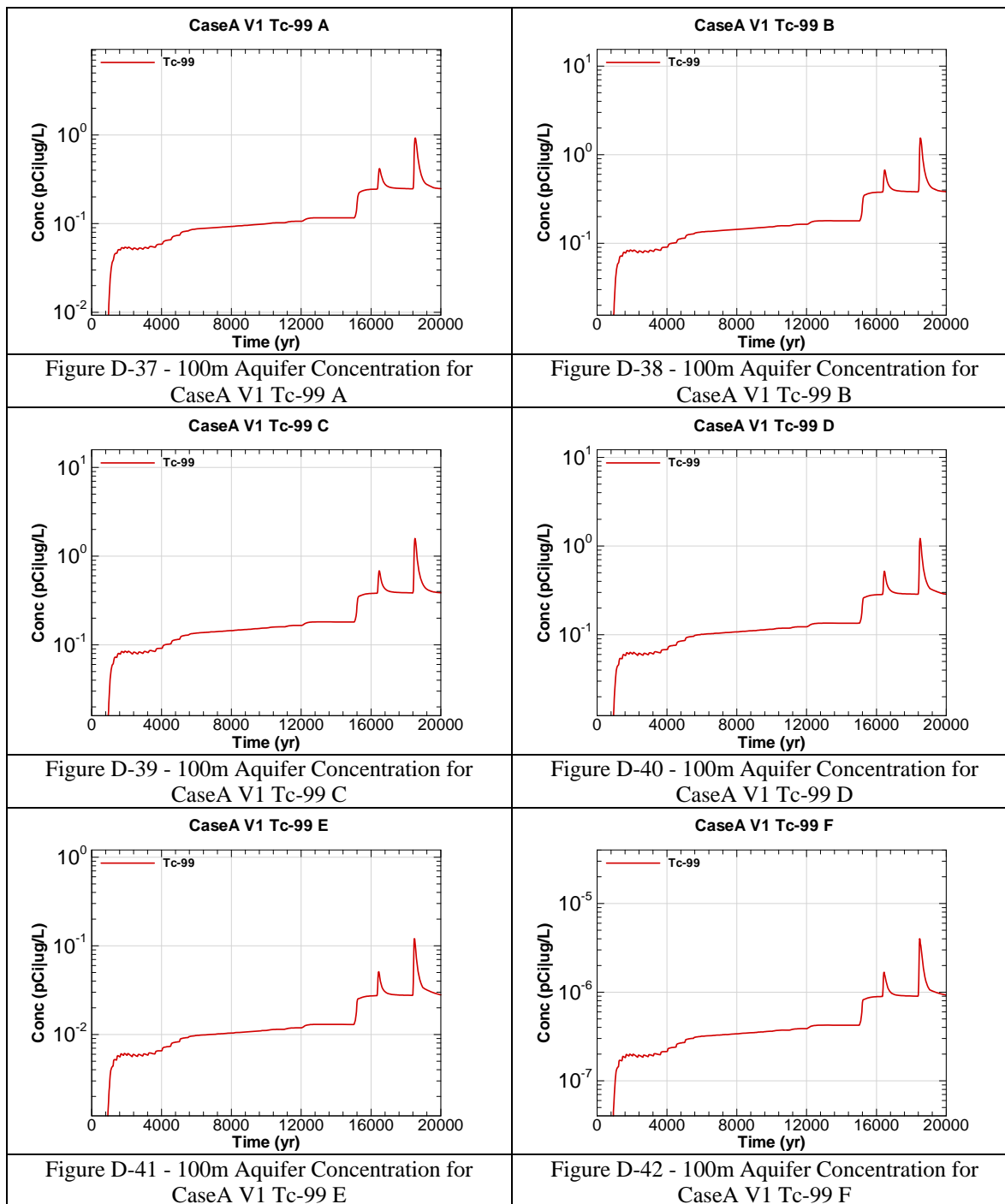
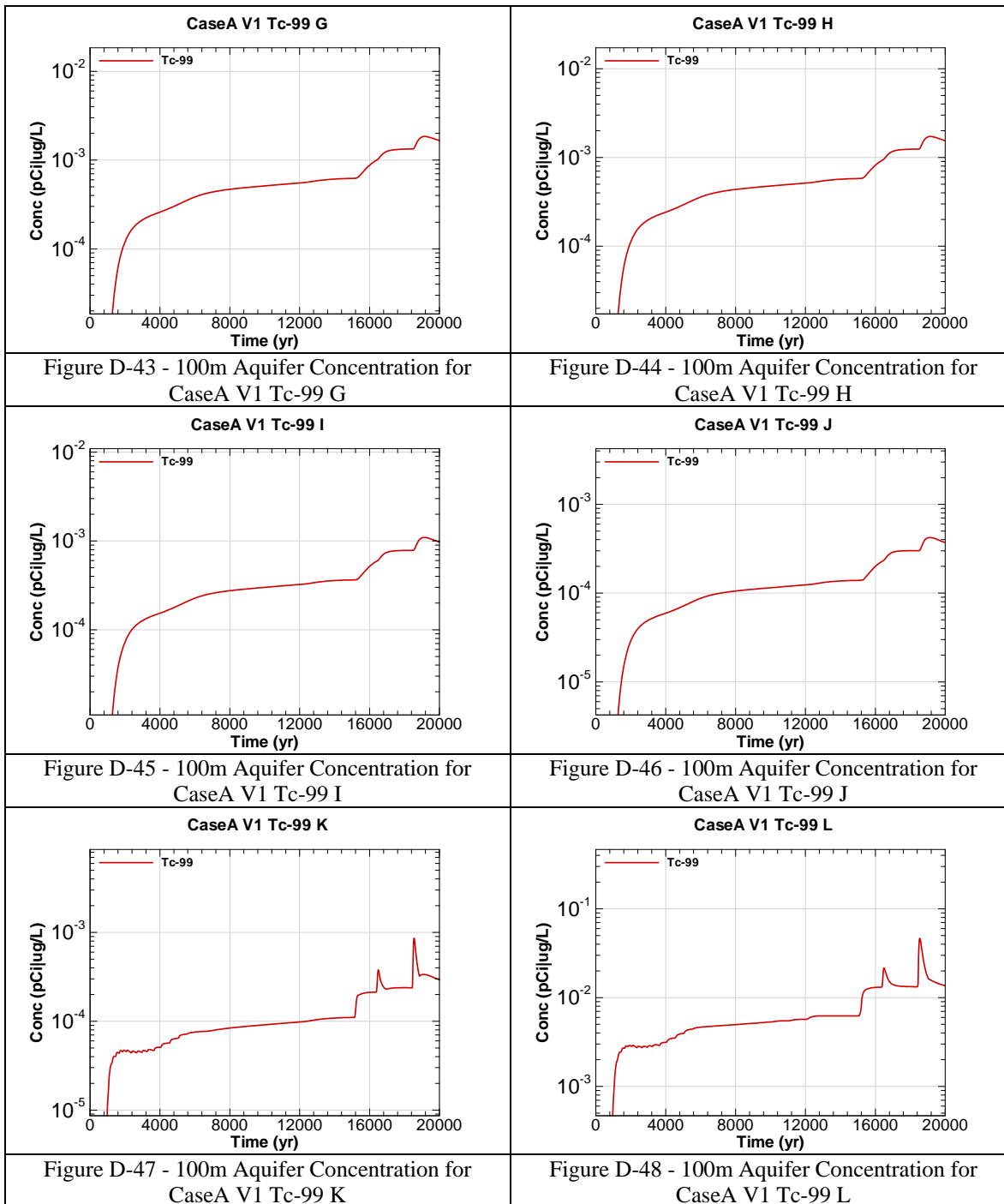
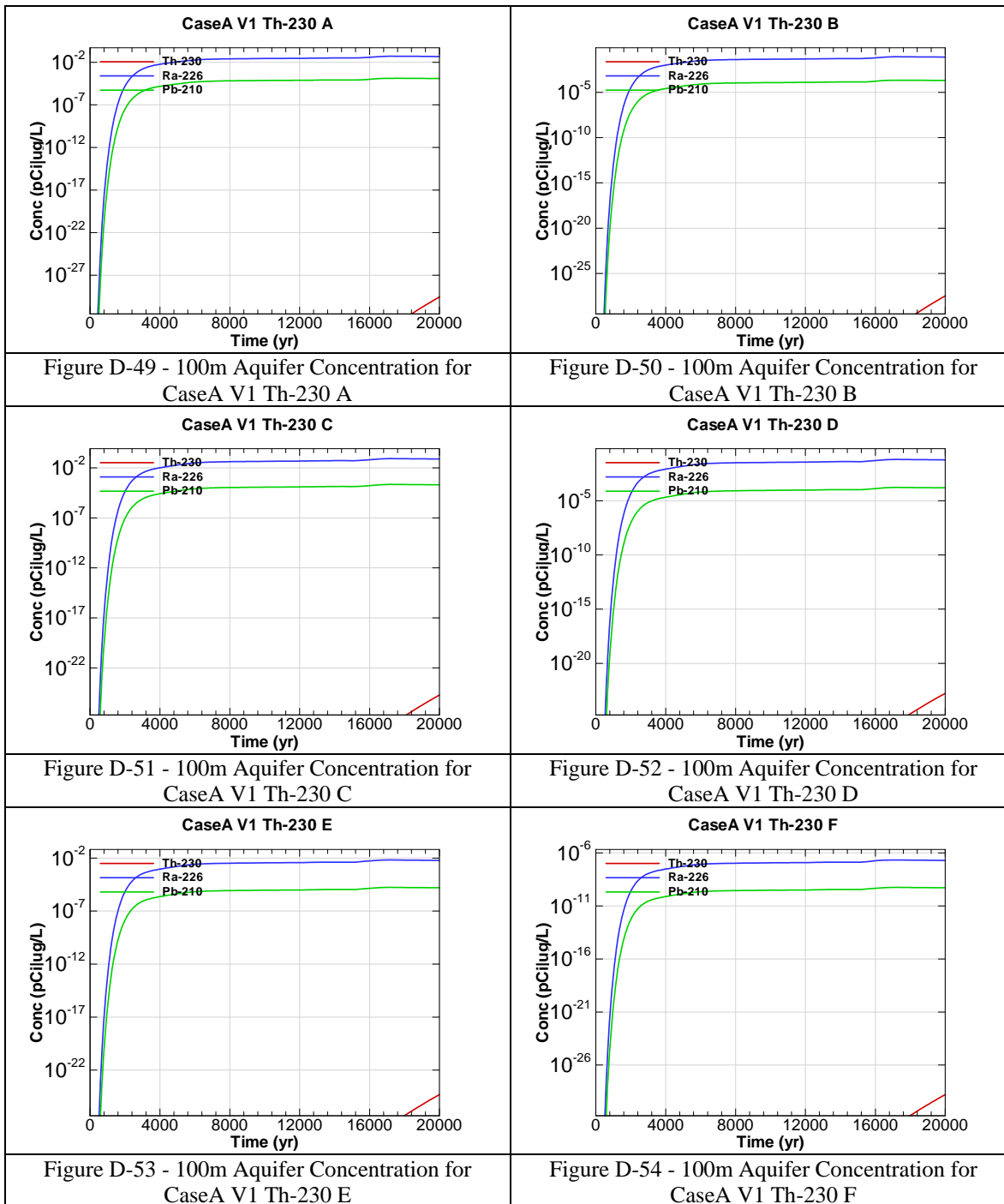
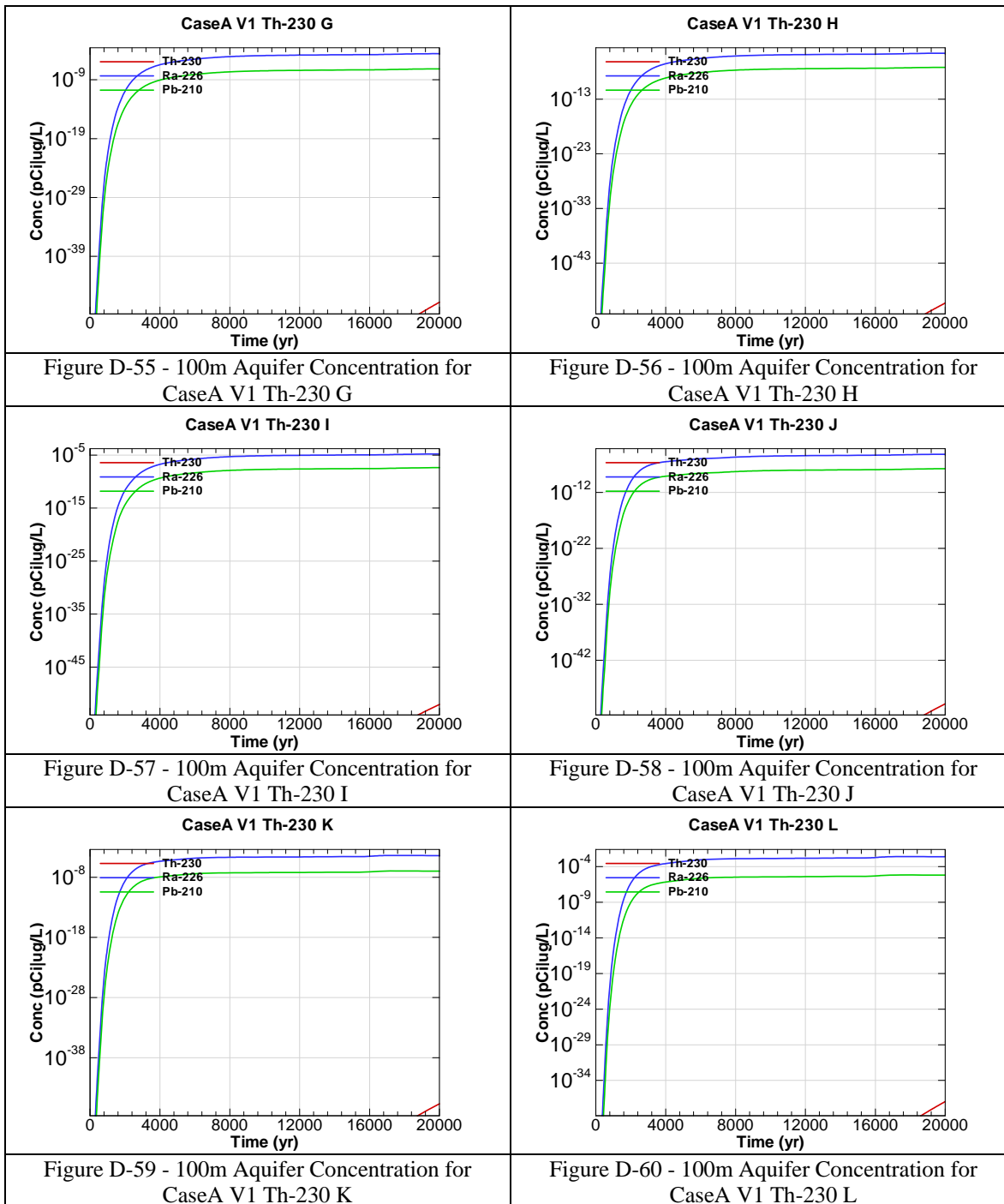


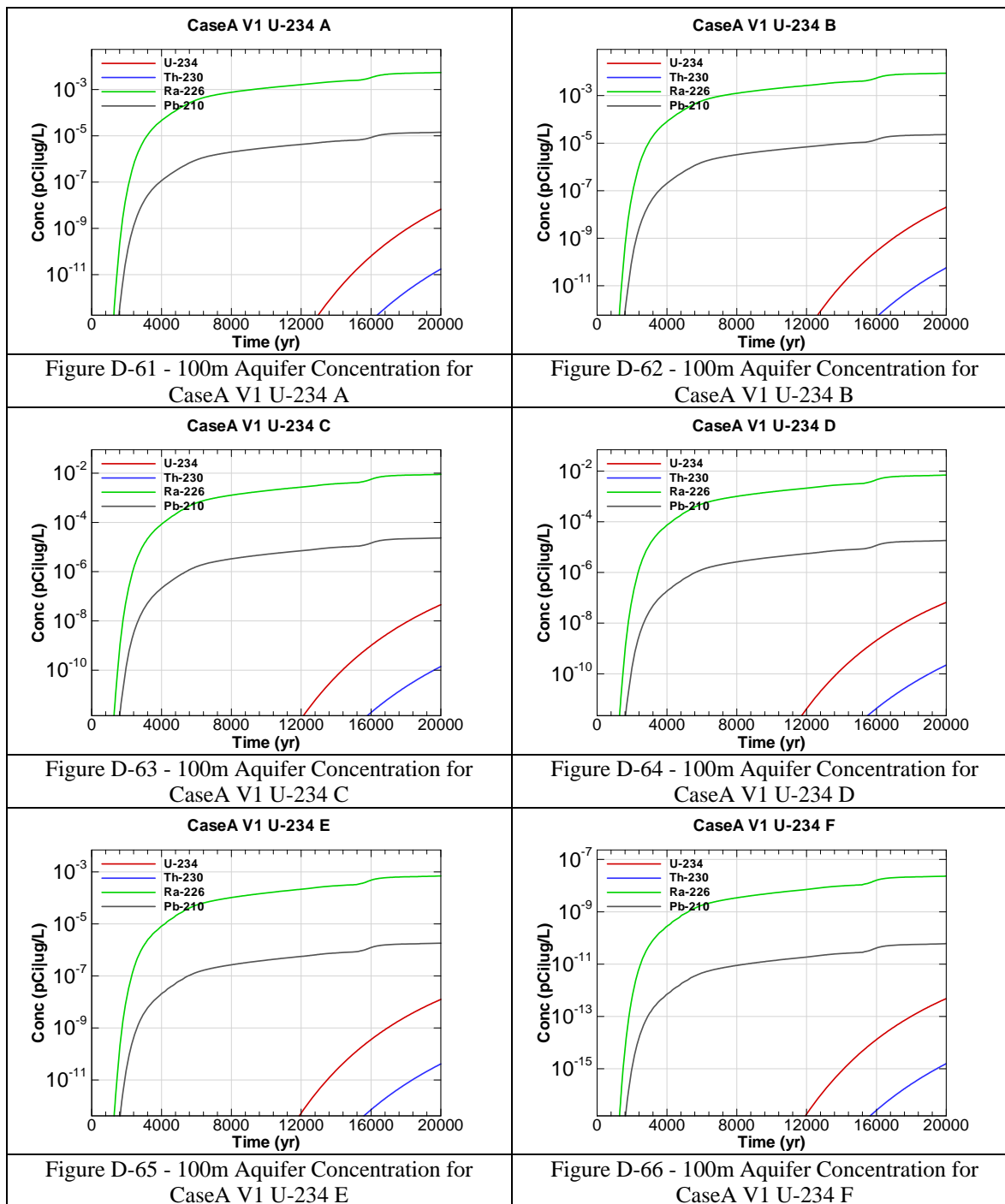
Figure D-36 - 100m Aquifer Concentration for
CaseA V1 Pu-238 L

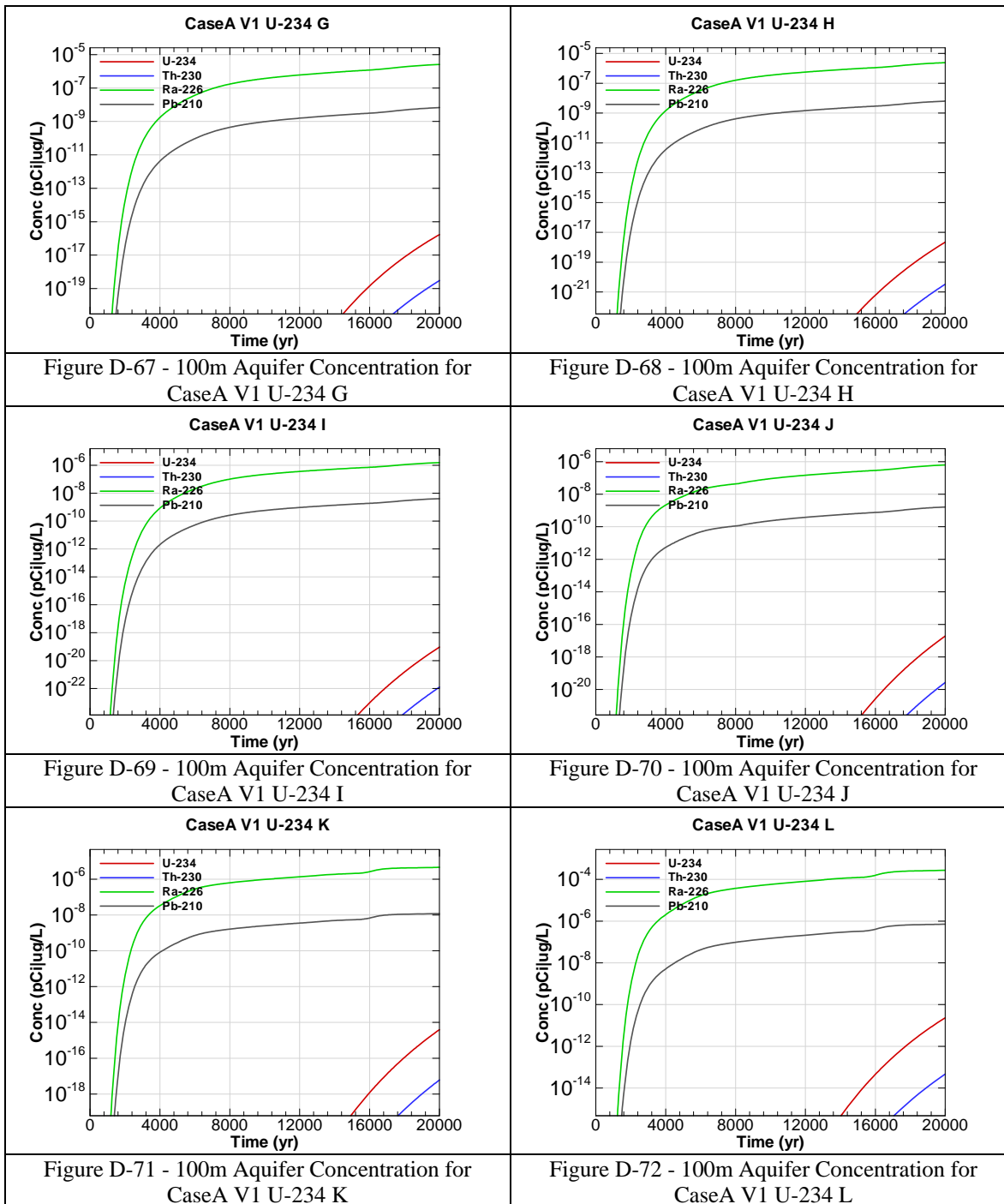


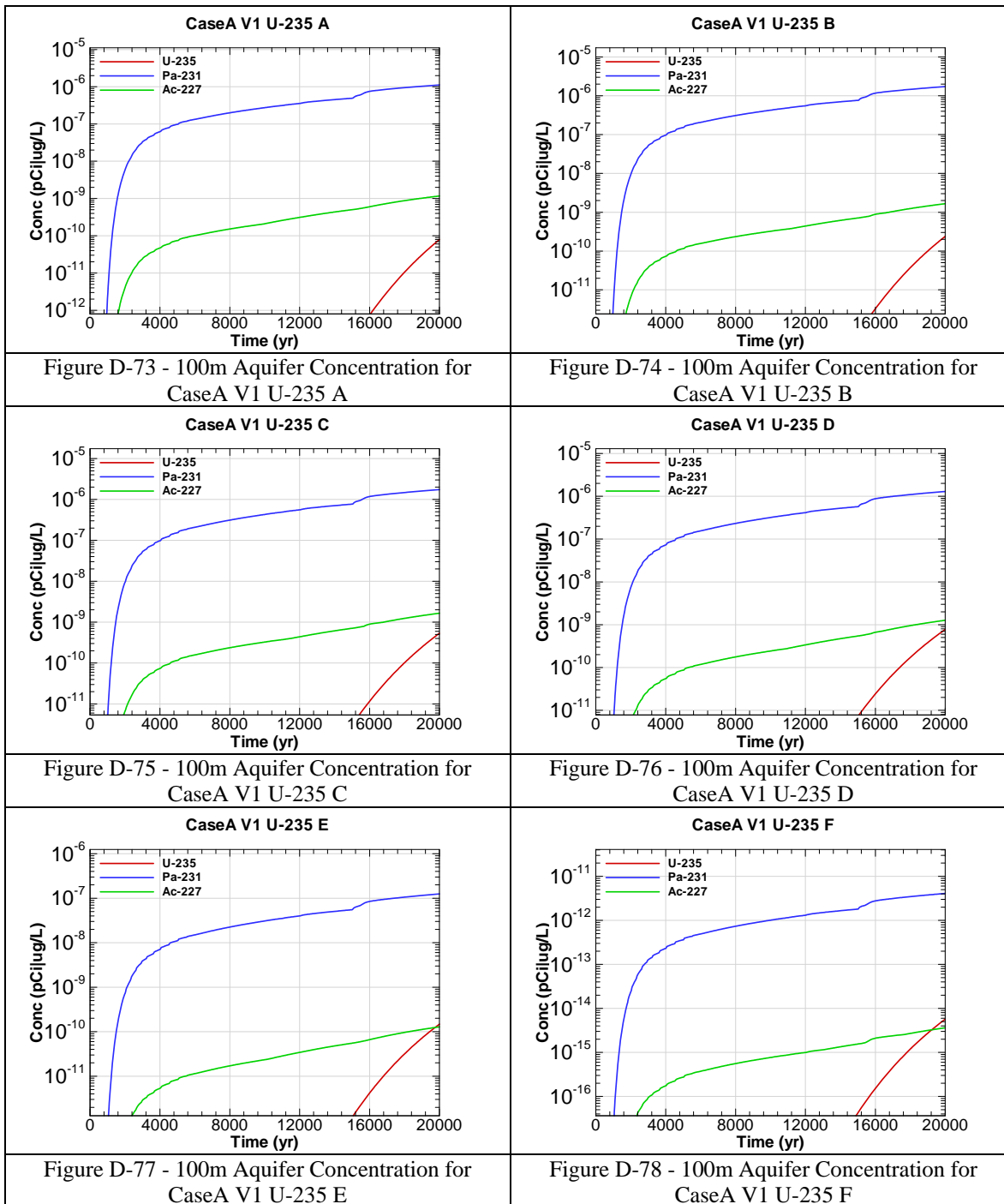


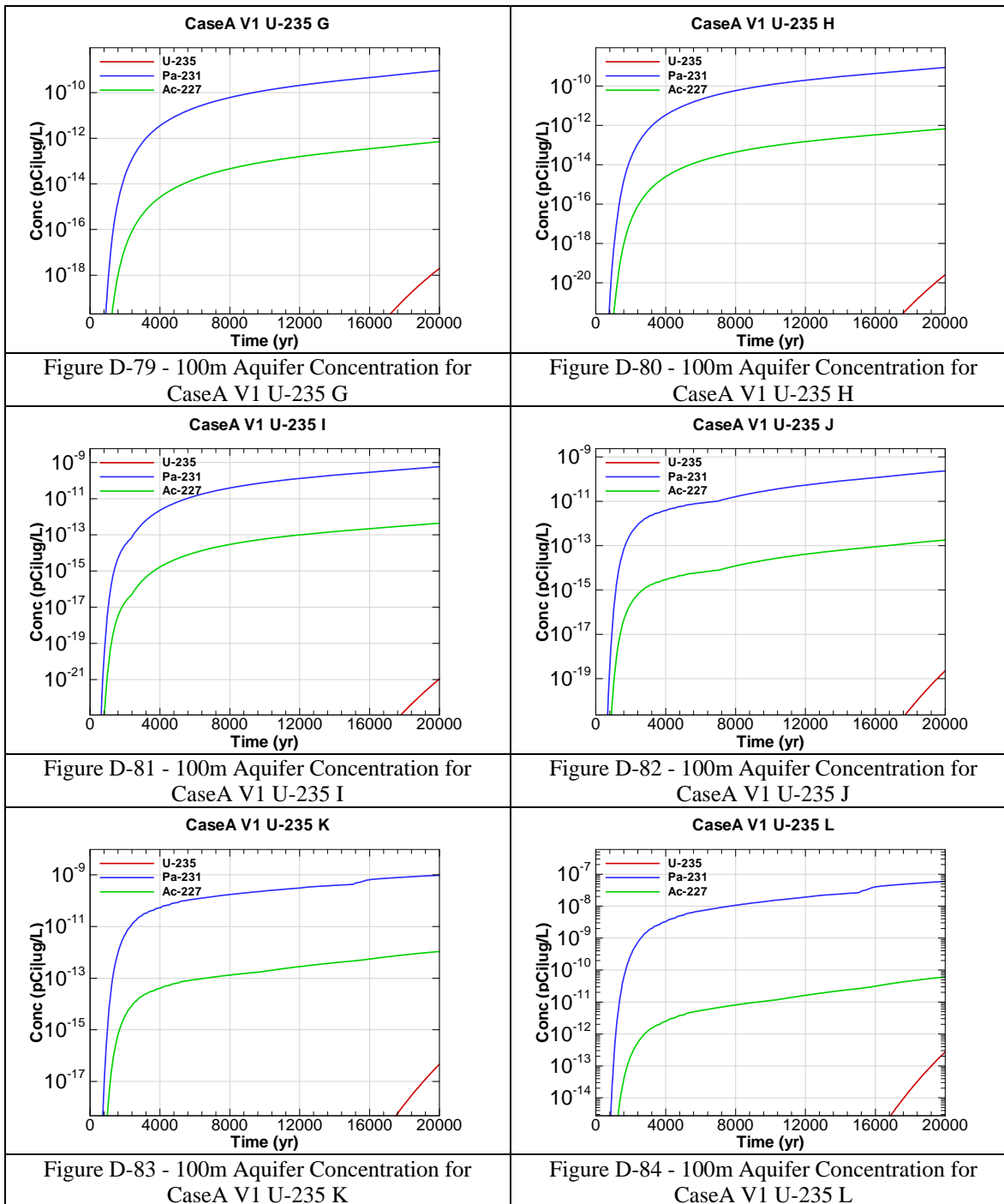


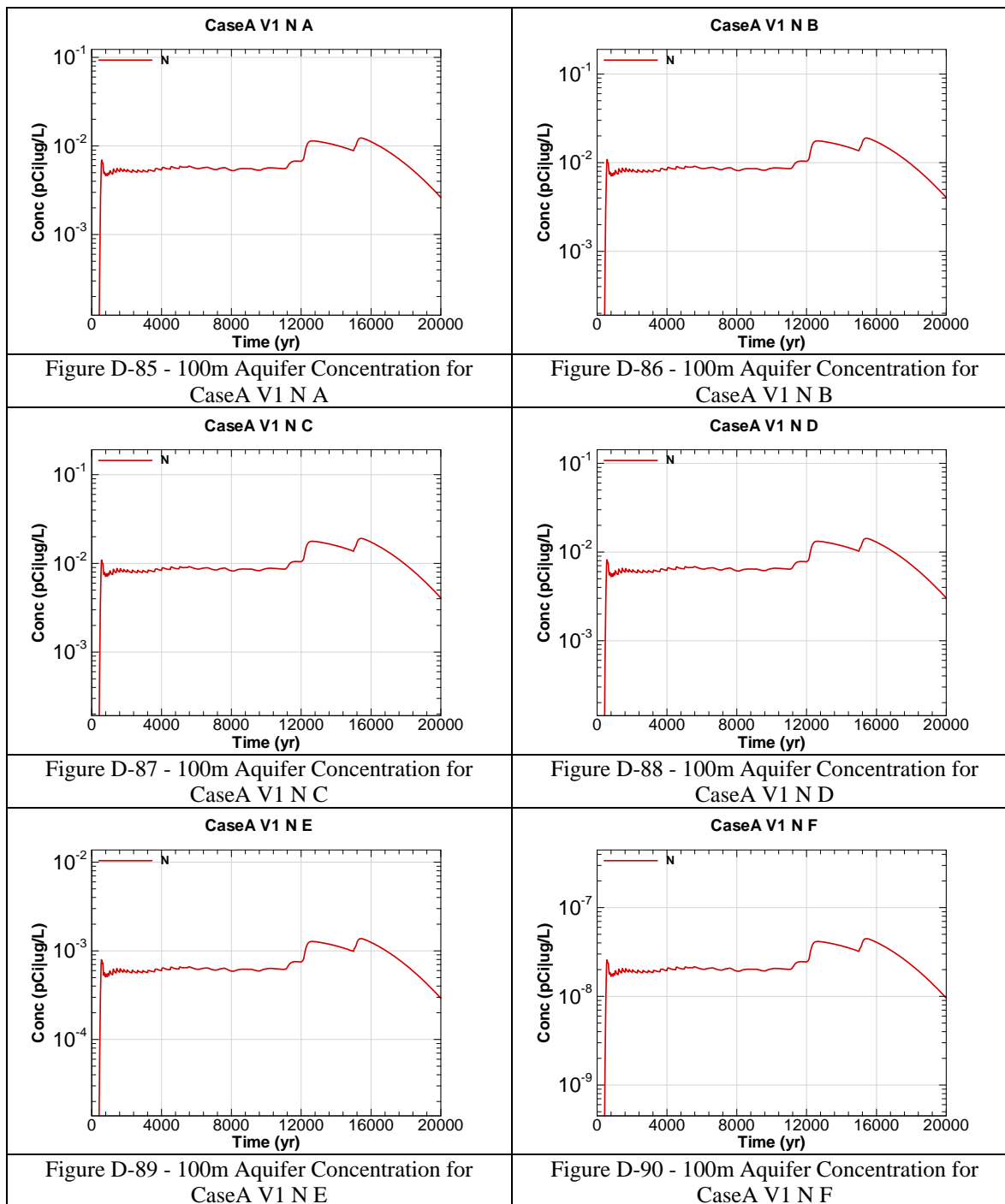


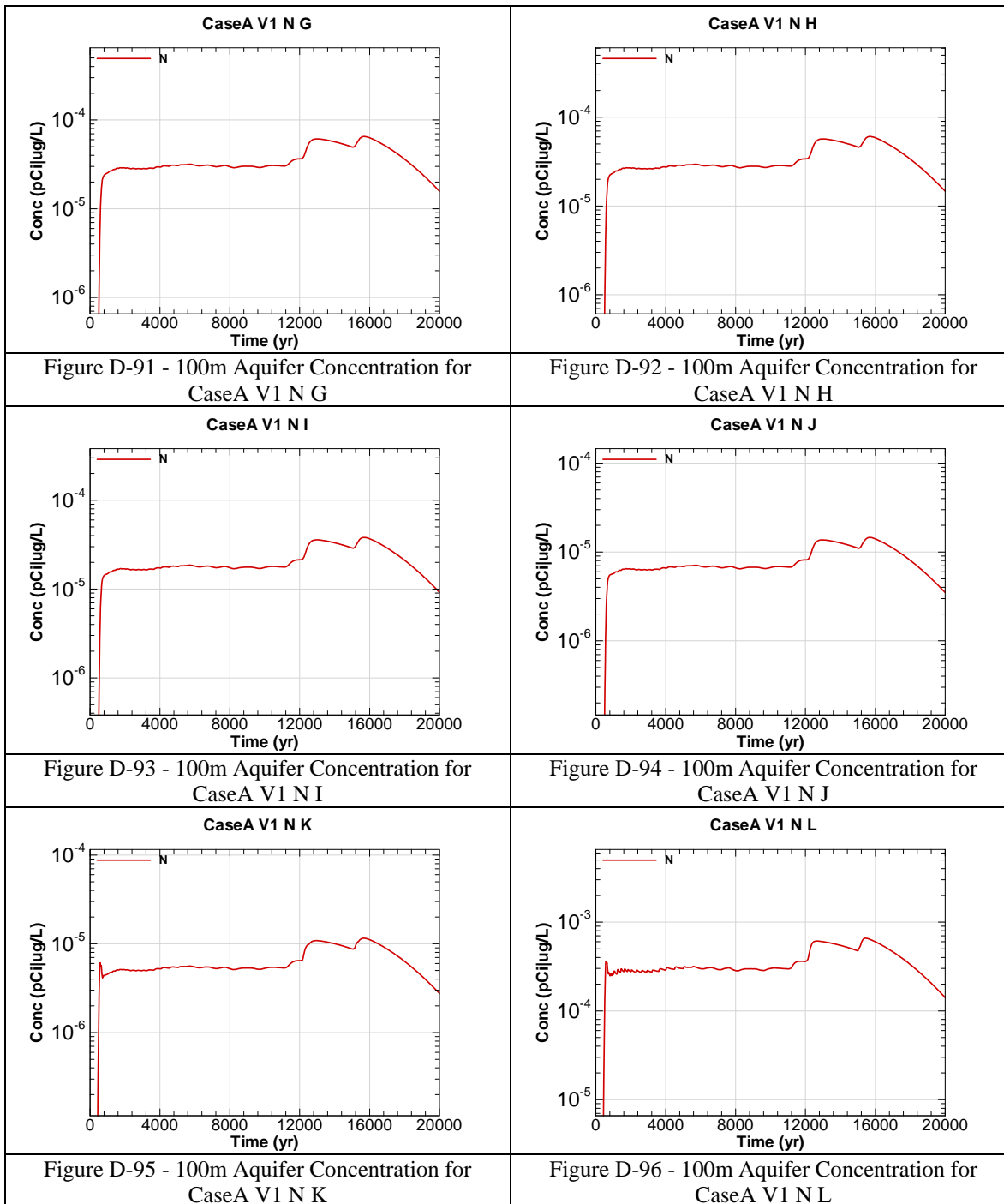


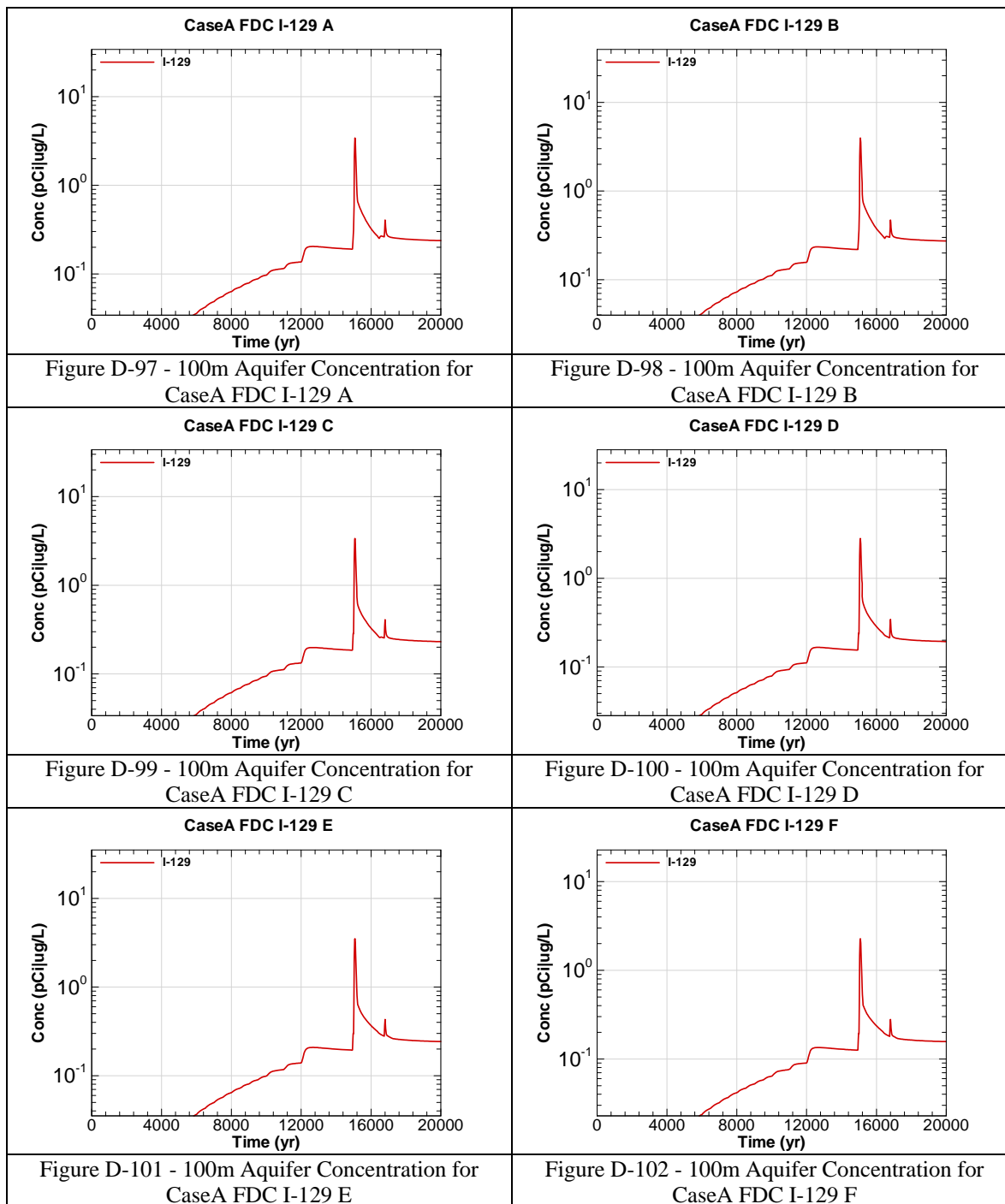


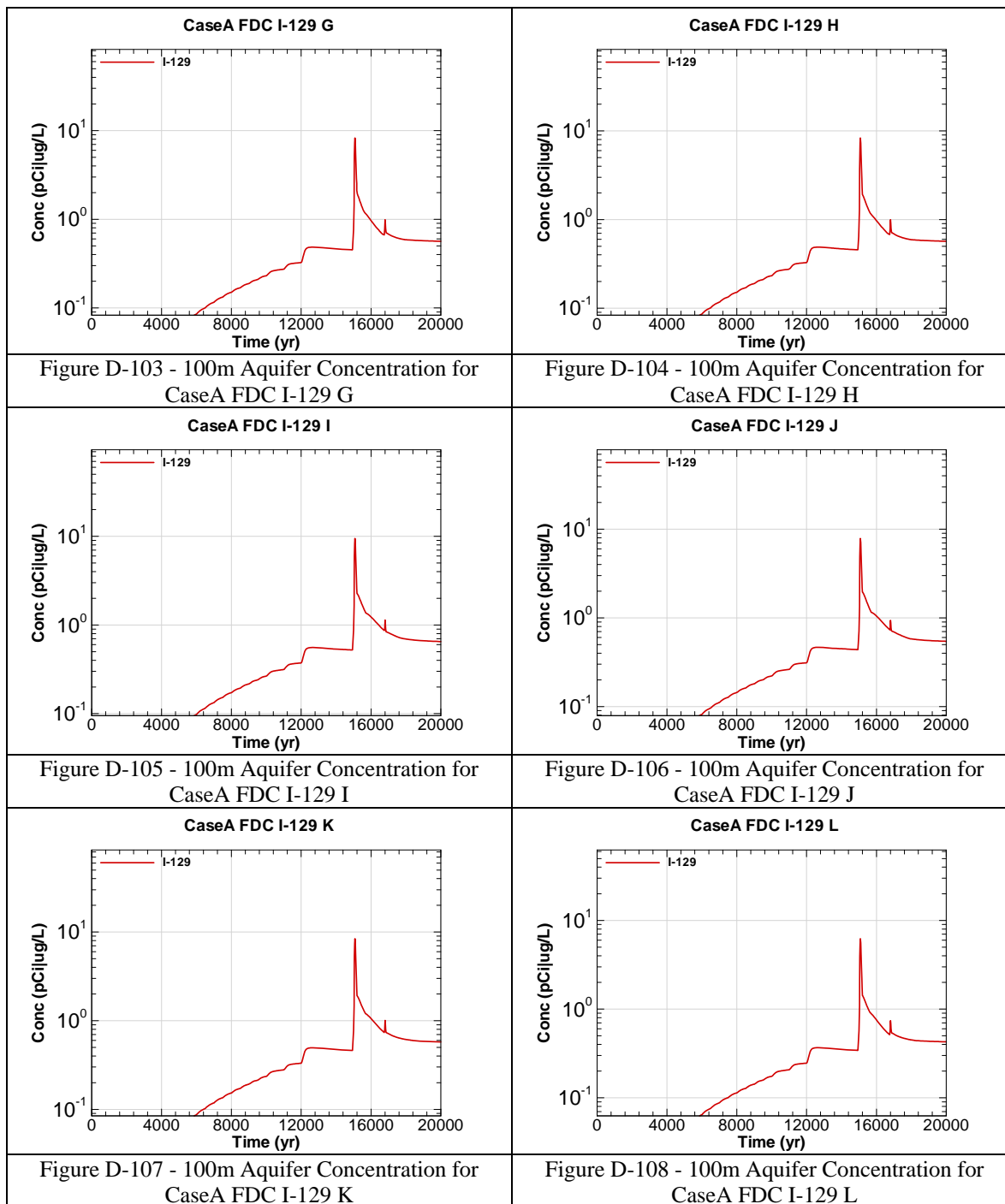


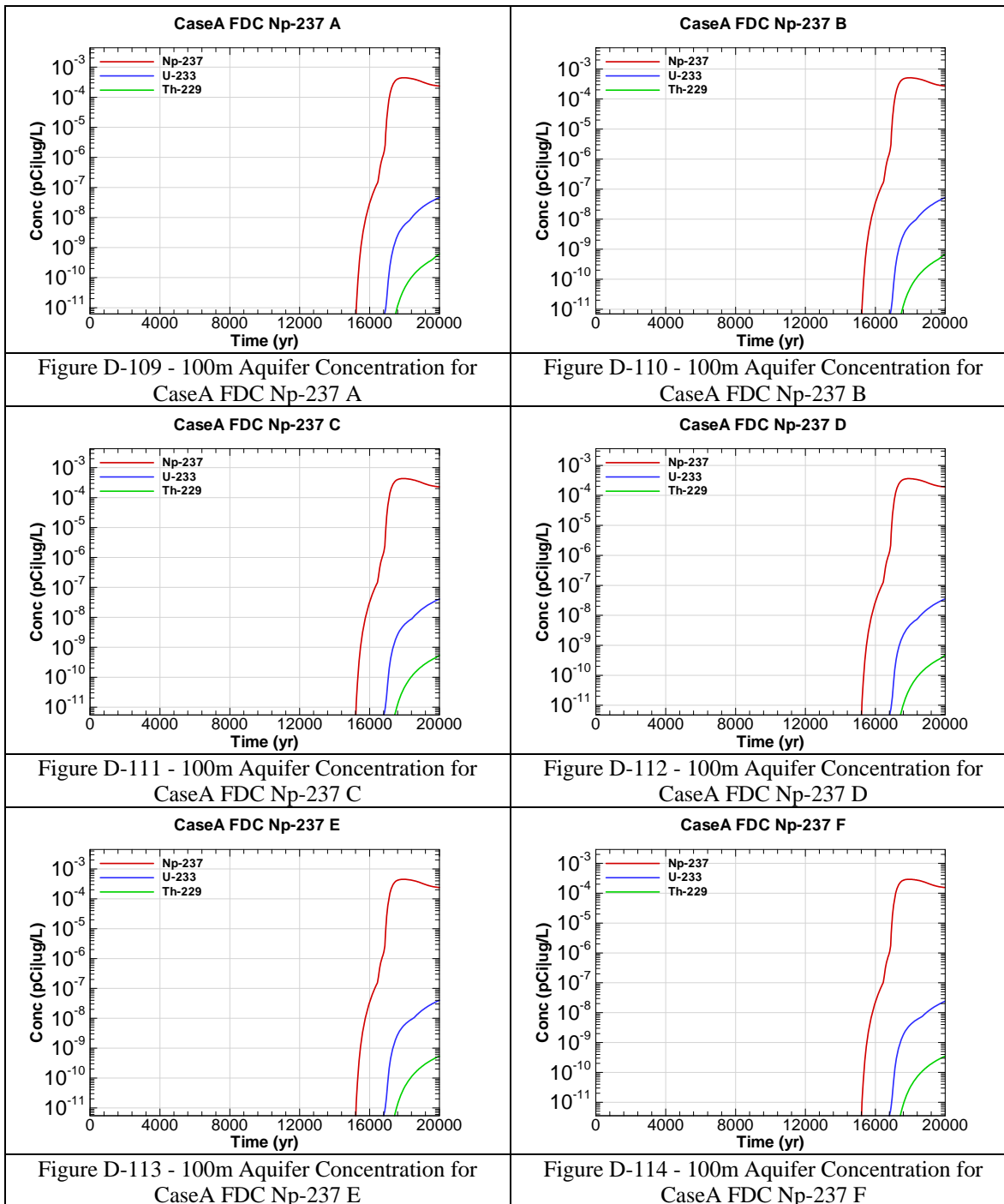


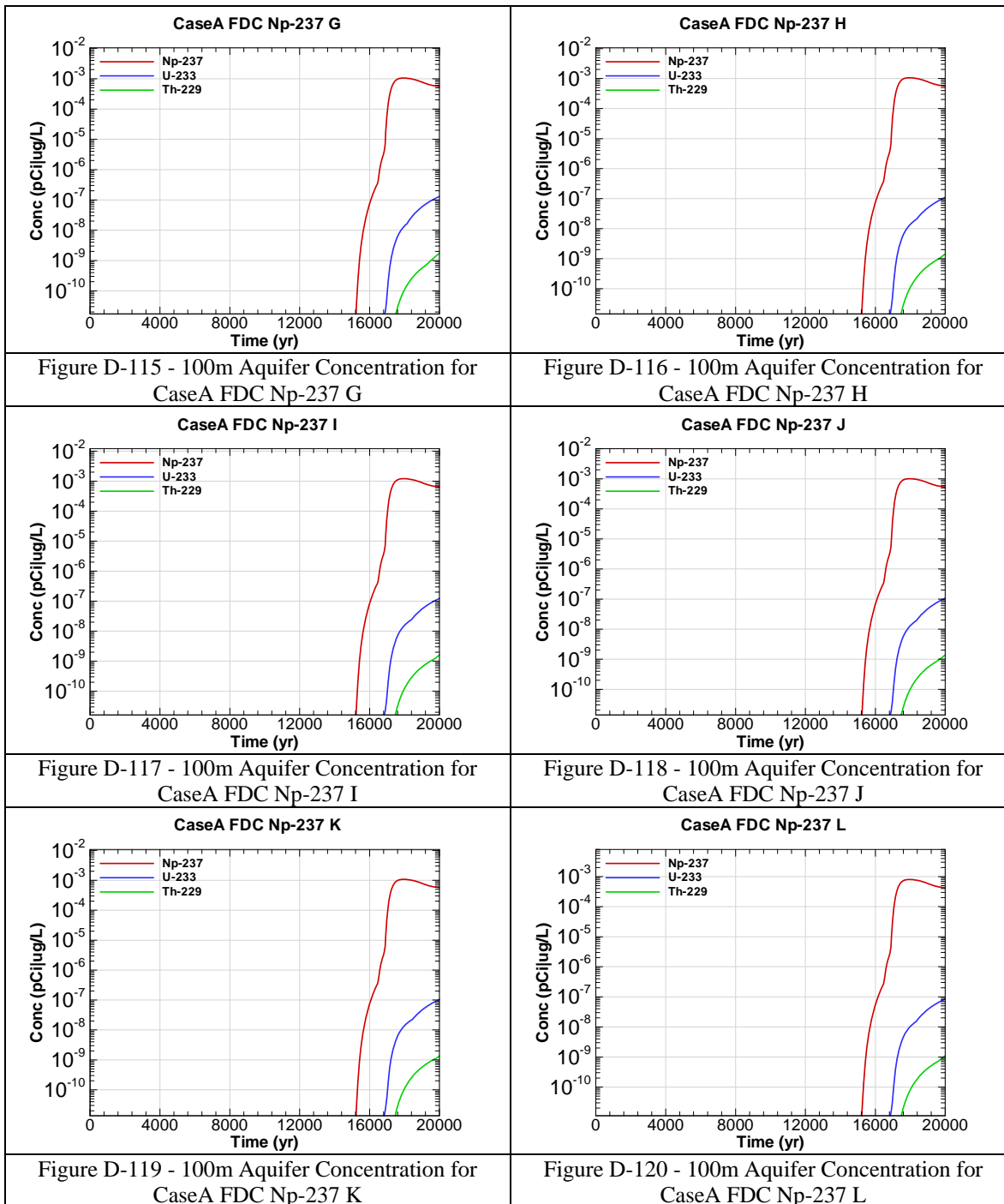


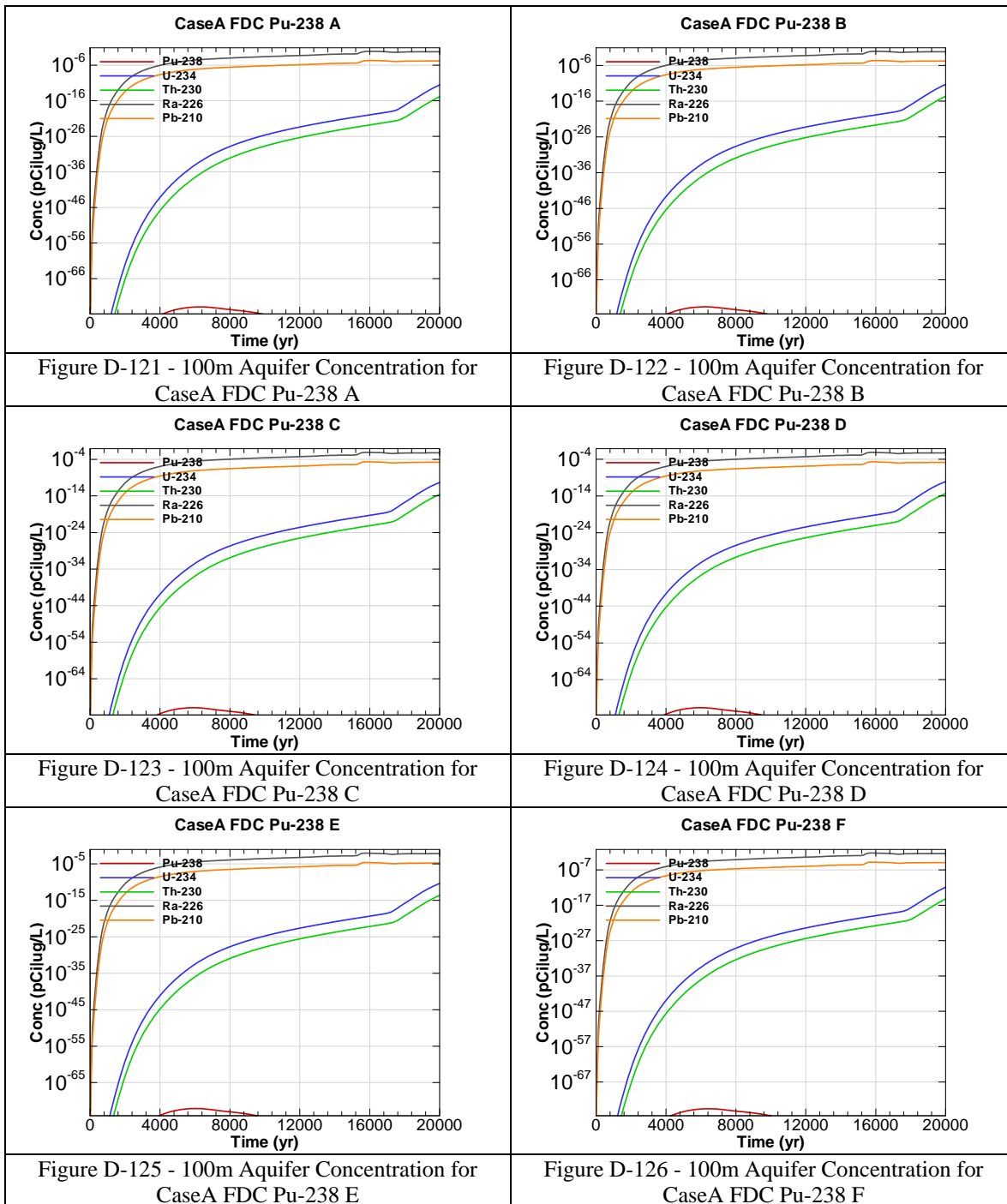












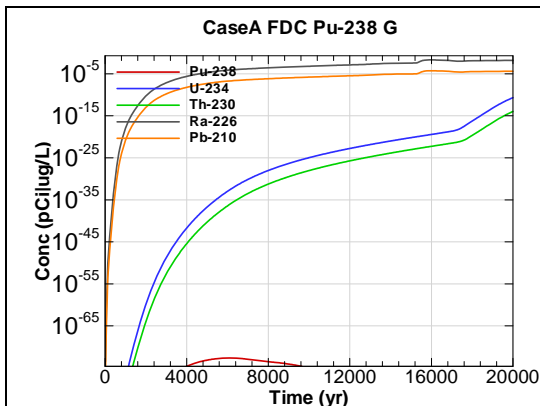


Figure D-127 - 100m Aquifer Concentration for
CaseA FDC Pu-238 G

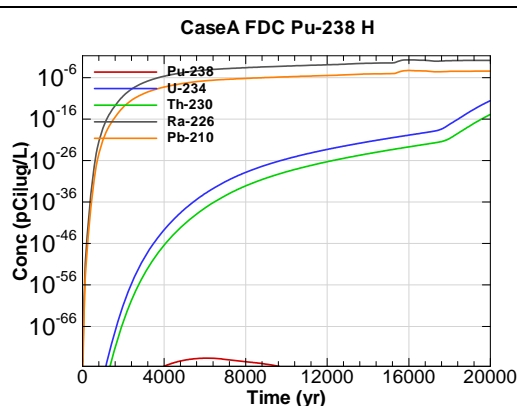


Figure D-128 - 100m Aquifer Concentration for
CaseA FDC Pu-238 H

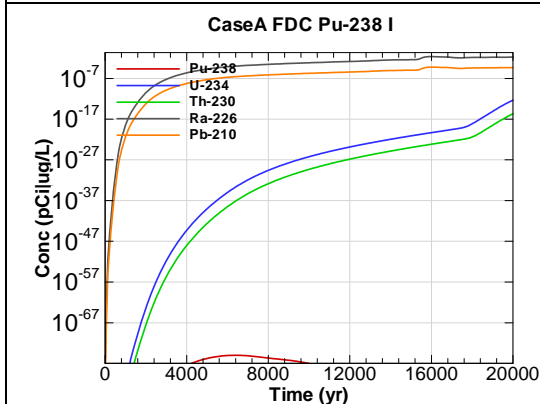


Figure D-129 - 100m Aquifer Concentration for
CaseA FDC Pu-238 I

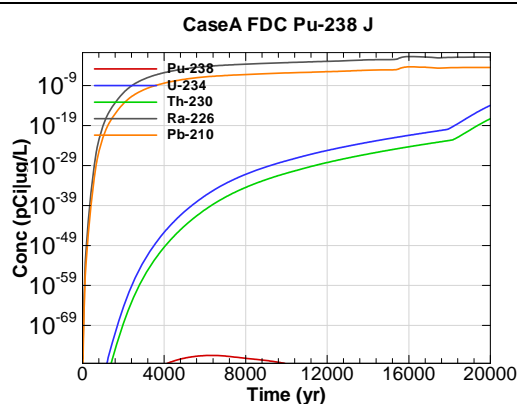


Figure D-130 - 100m Aquifer Concentration for
CaseA FDC Pu-238 J

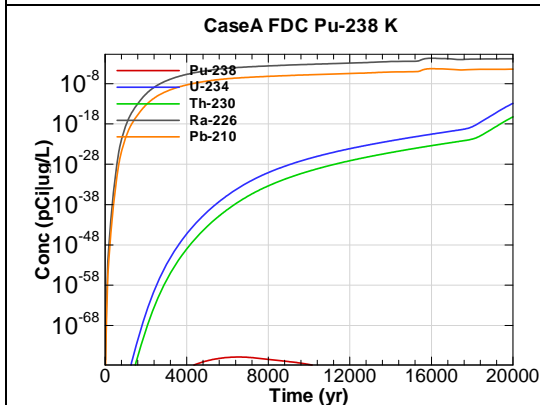


Figure D-131 - 100m Aquifer Concentration for
CaseA FDC Pu-238 K

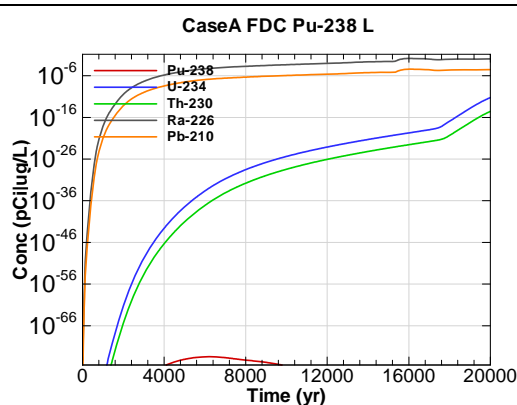
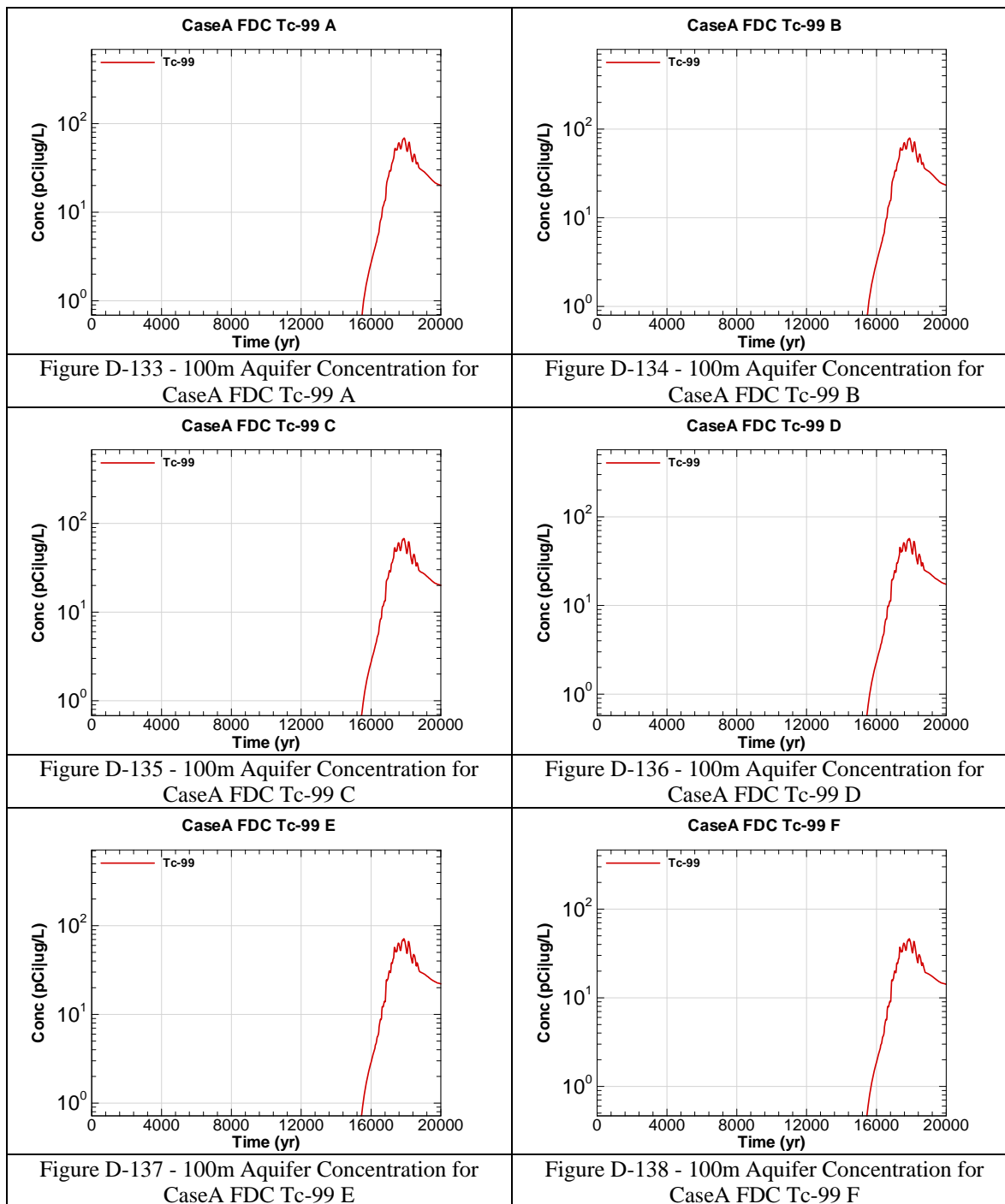
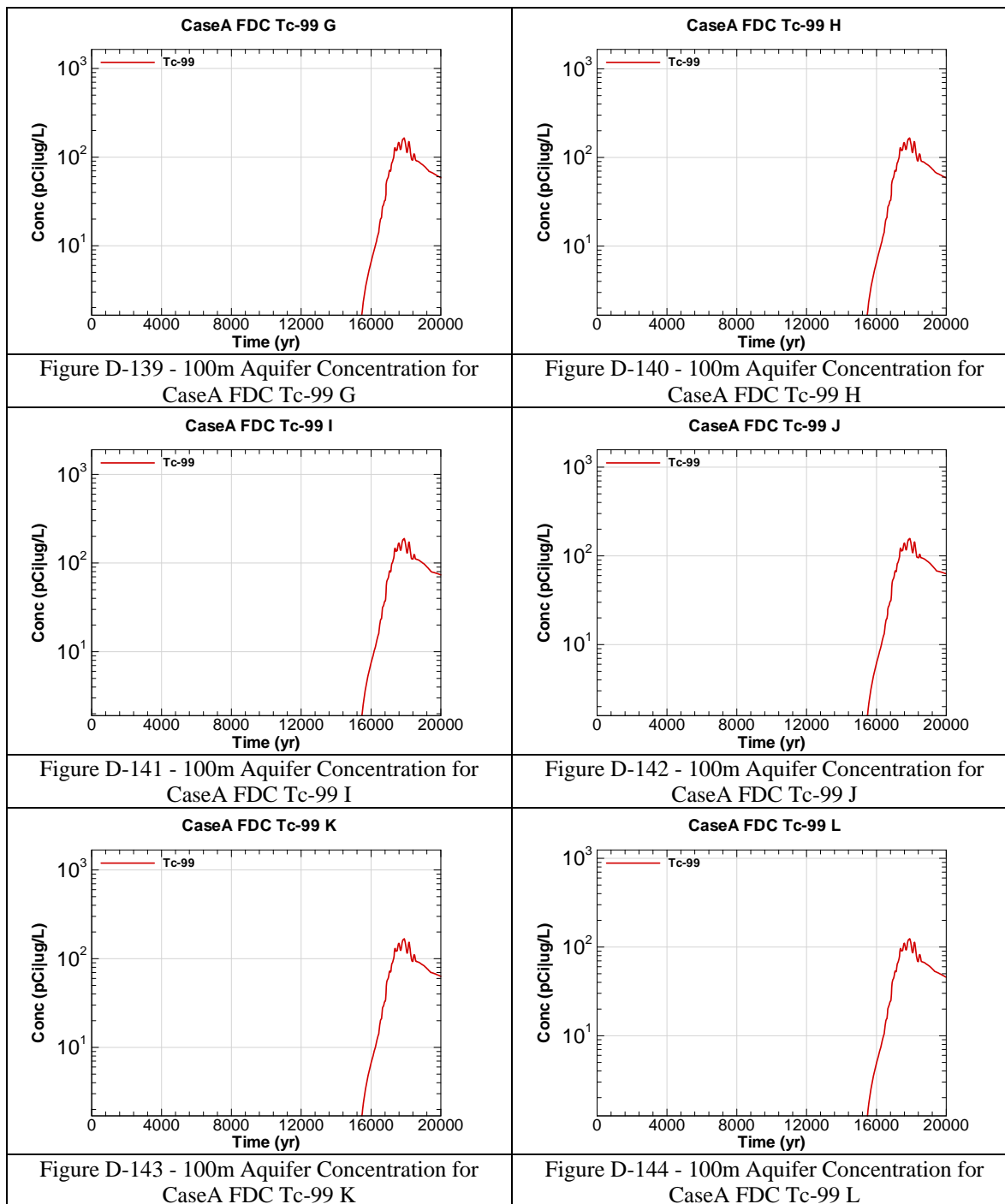
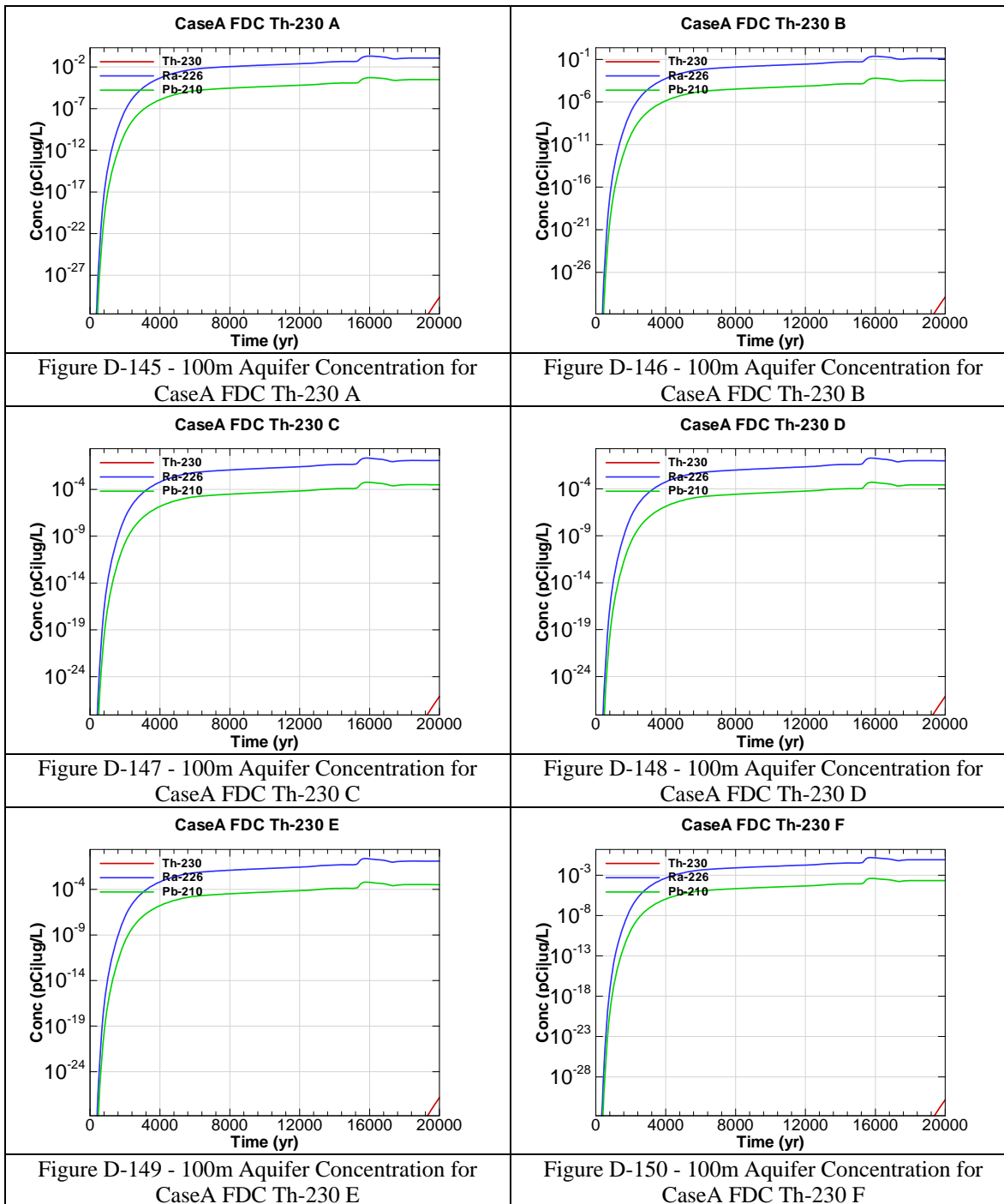


Figure D-132 - 100m Aquifer Concentration for
CaseA FDC Pu-238 L







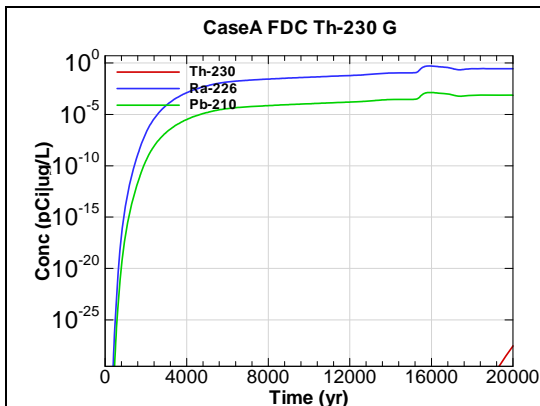


Figure D-151 - 100m Aquifer Concentration for
CaseA FDC Th-230 G

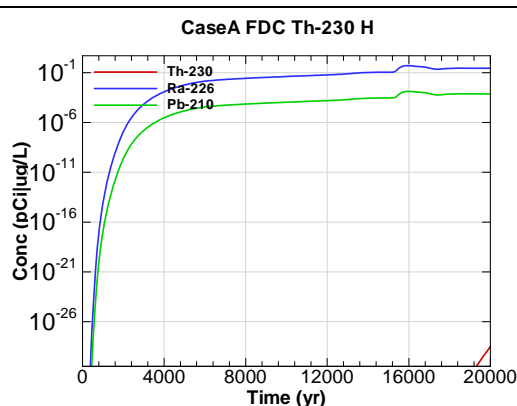


Figure D-152 - 100m Aquifer Concentration for
CaseA FDC Th-230 H

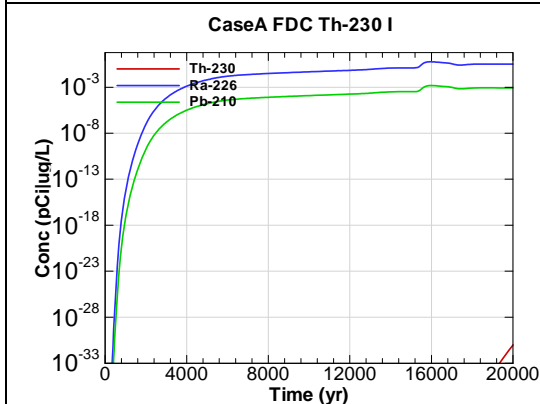


Figure D-153 - 100m Aquifer Concentration for
CaseA FDC Th-230 I

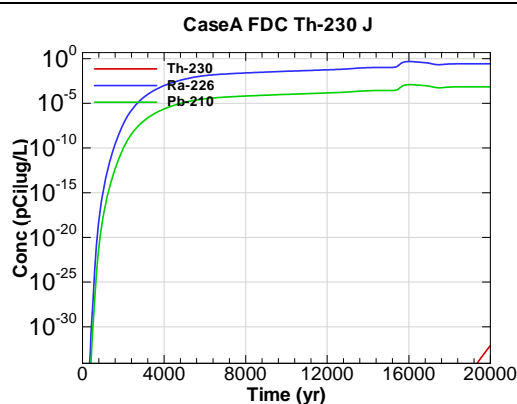


Figure D-154 - 100m Aquifer Concentration for
CaseA FDC Th-230 J

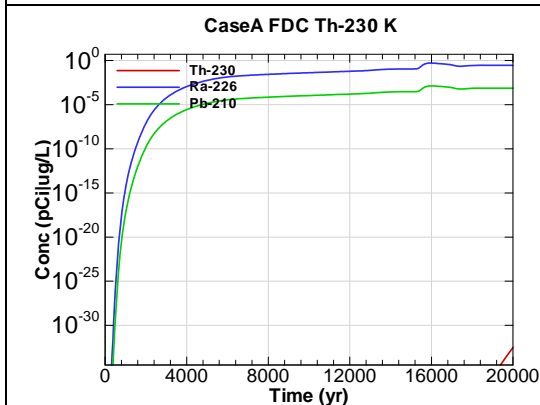


Figure D-155 - 100m Aquifer Concentration for
CaseA FDC Th-230 K

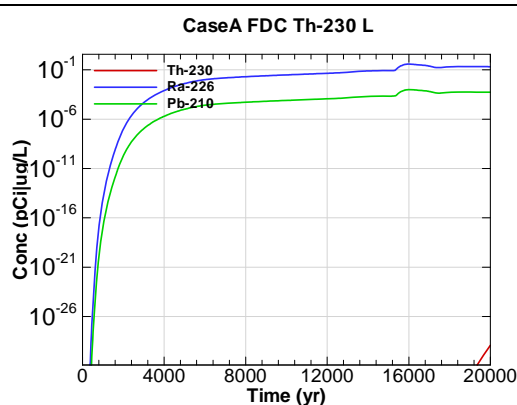
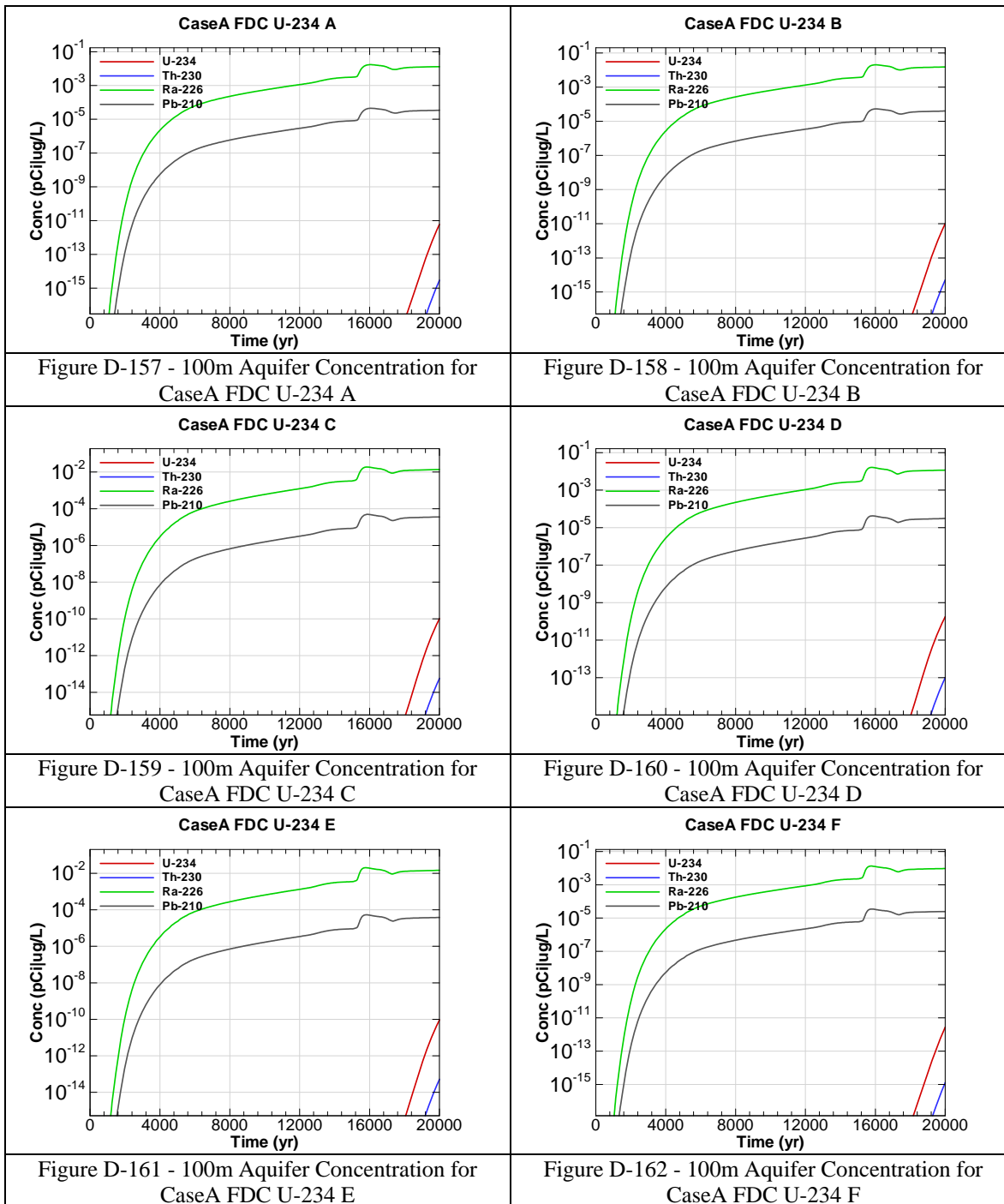
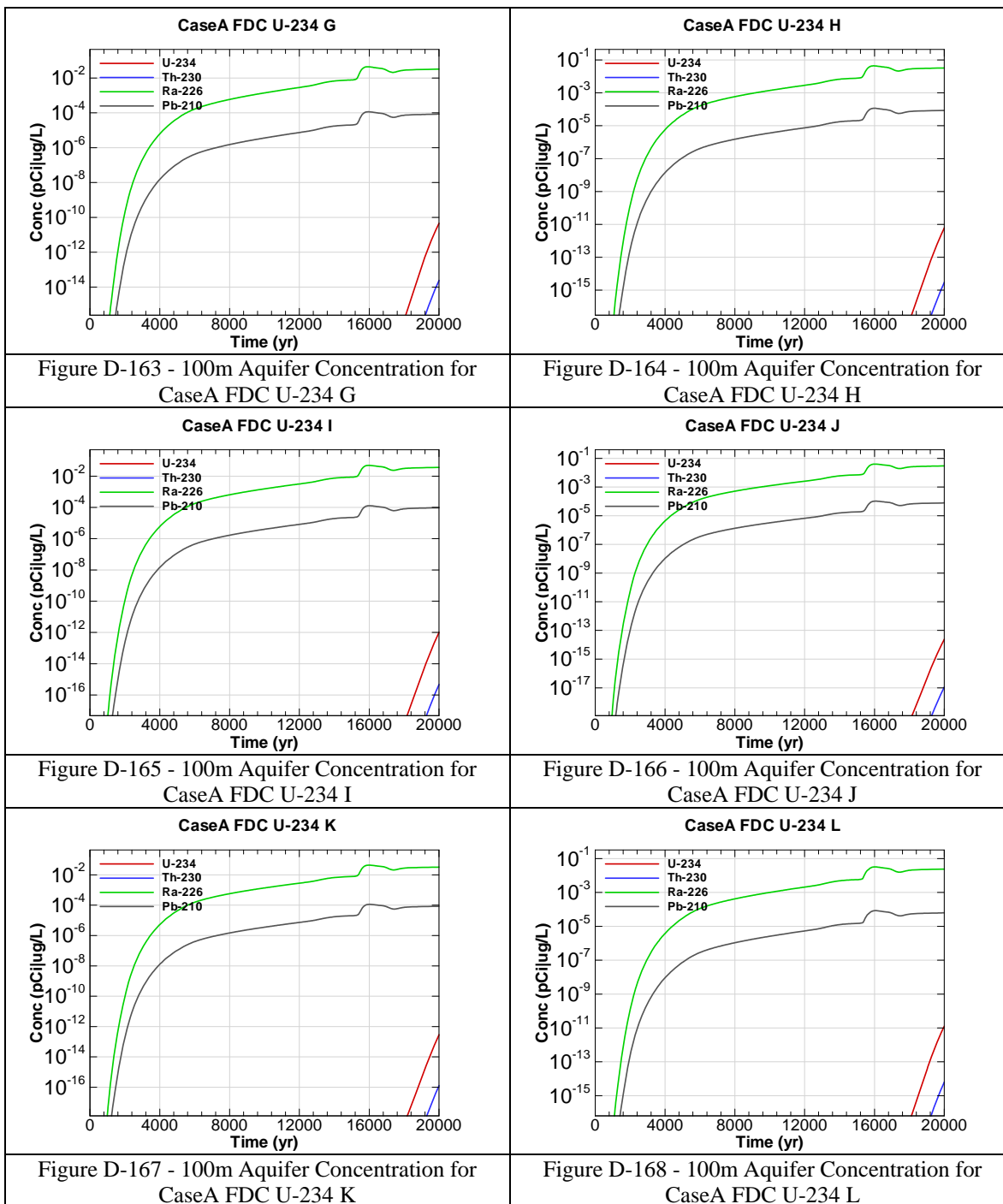
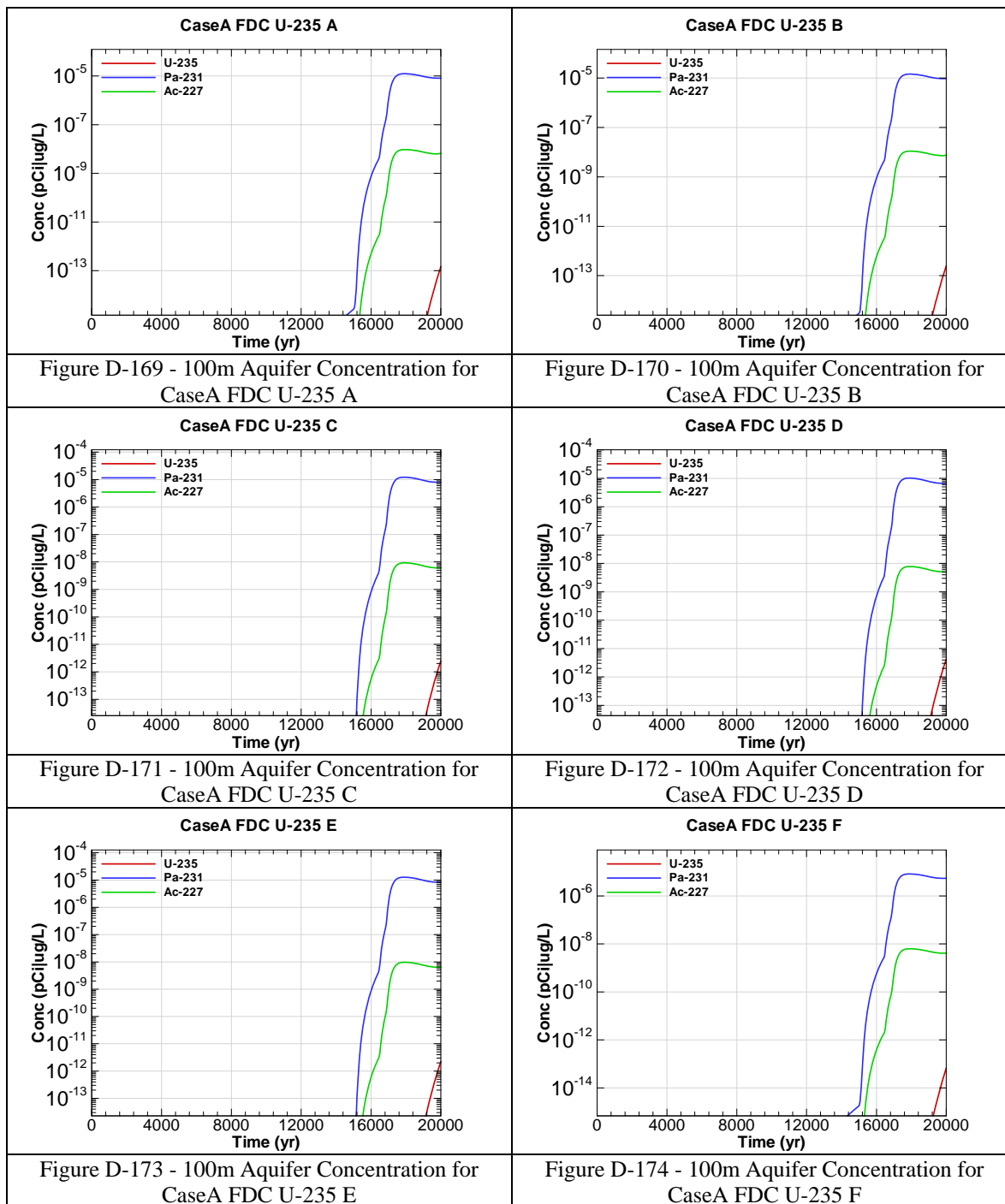
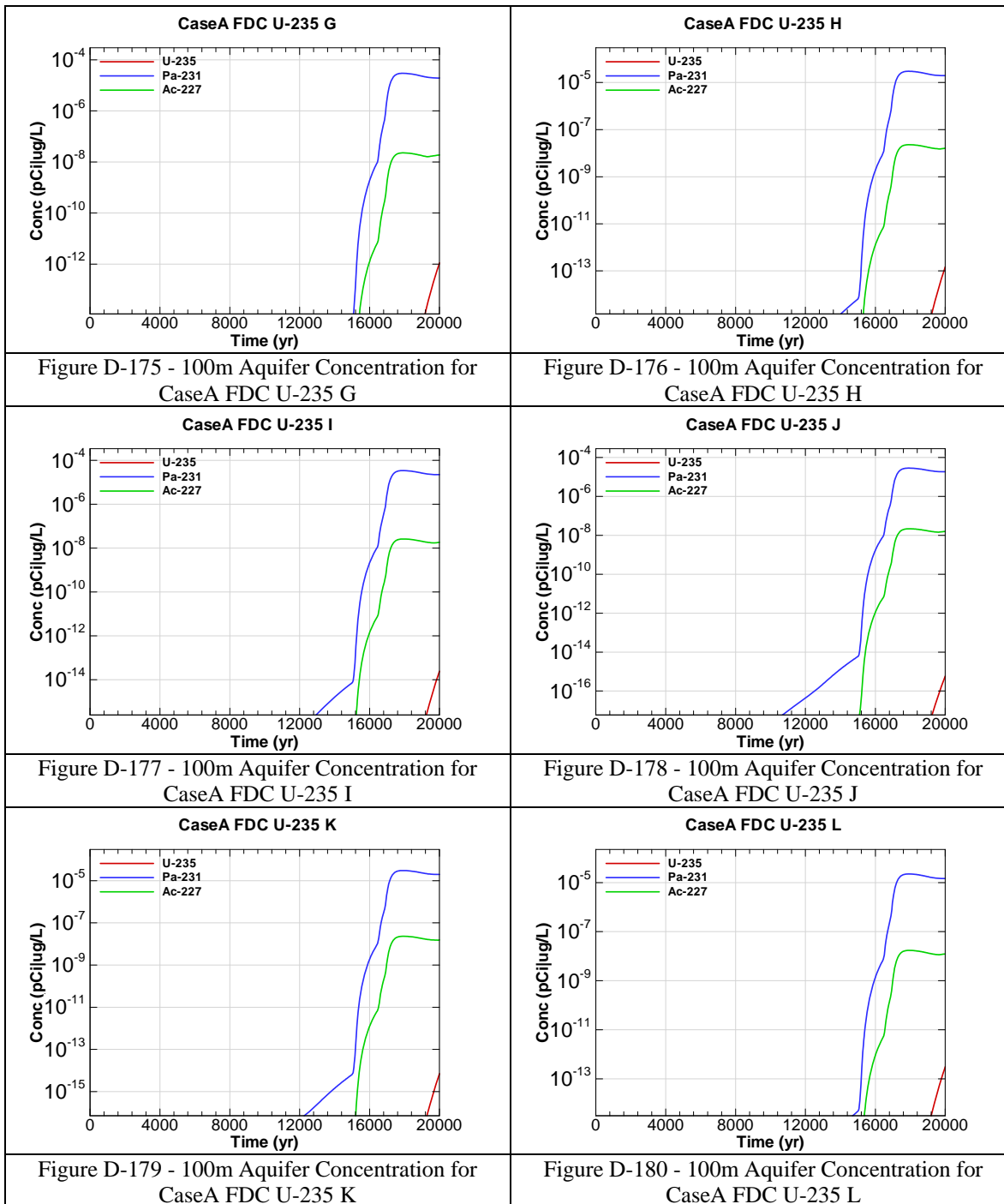


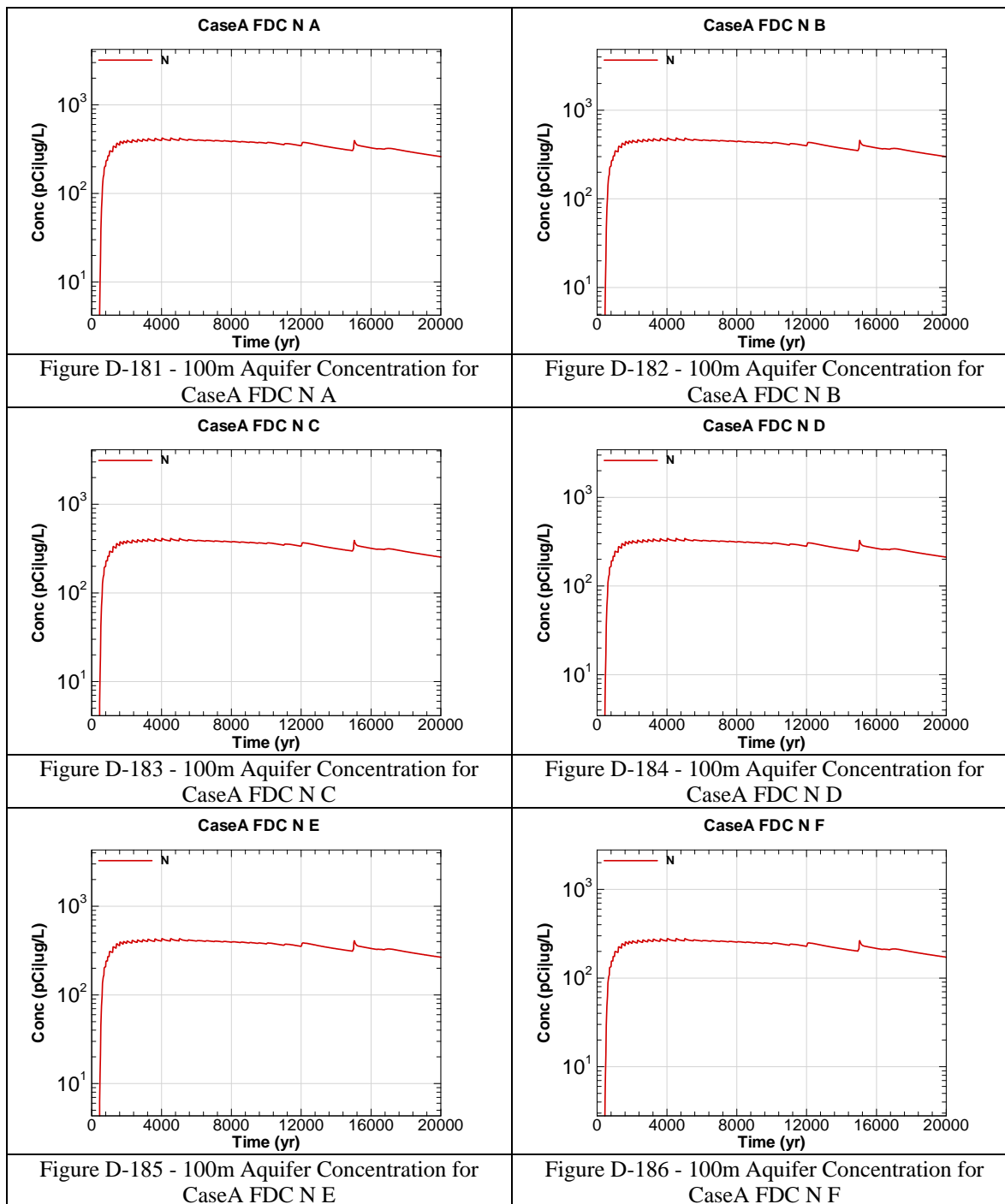
Figure D-156 - 100m Aquifer Concentration for
CaseA FDC Th-230 L

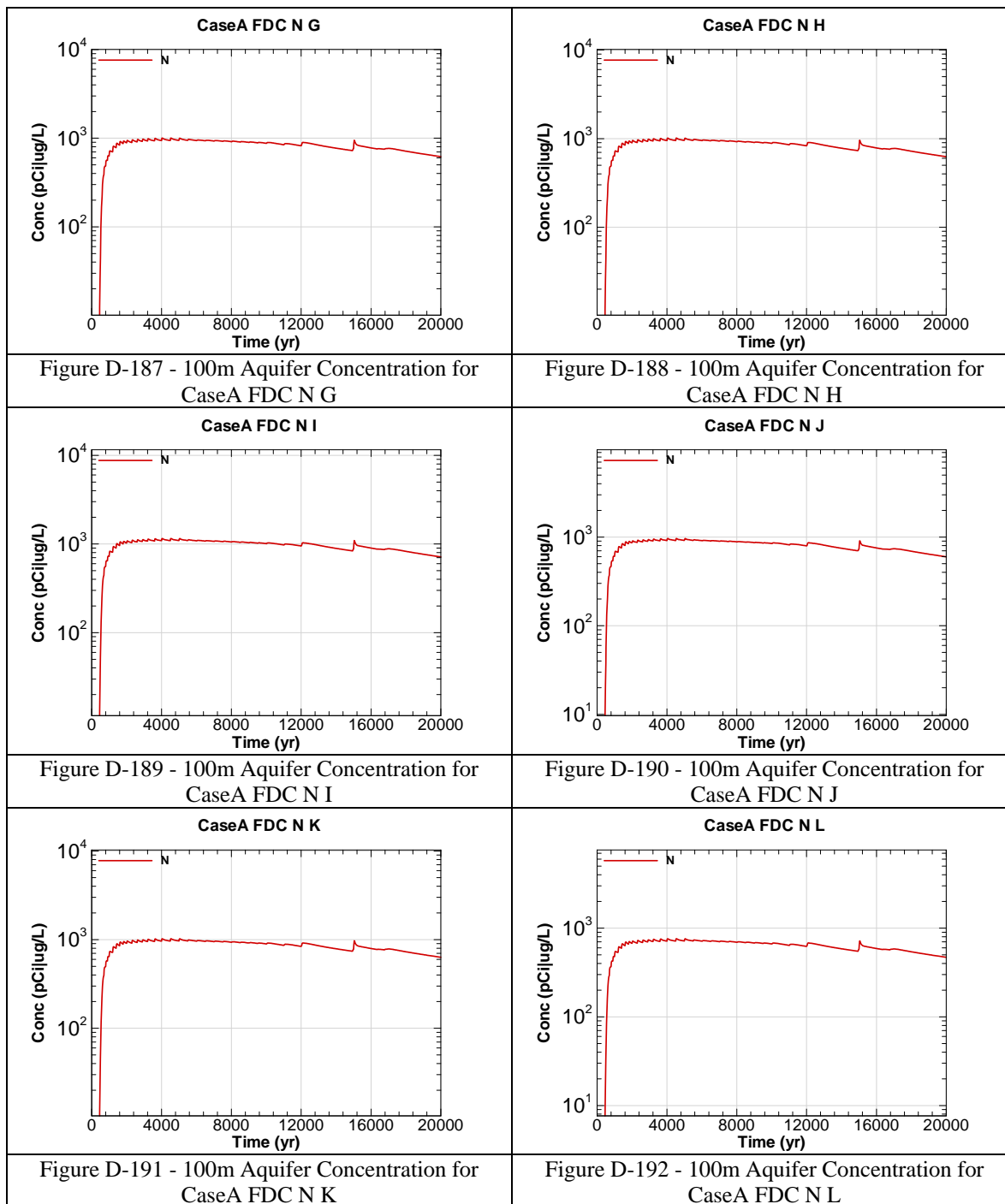


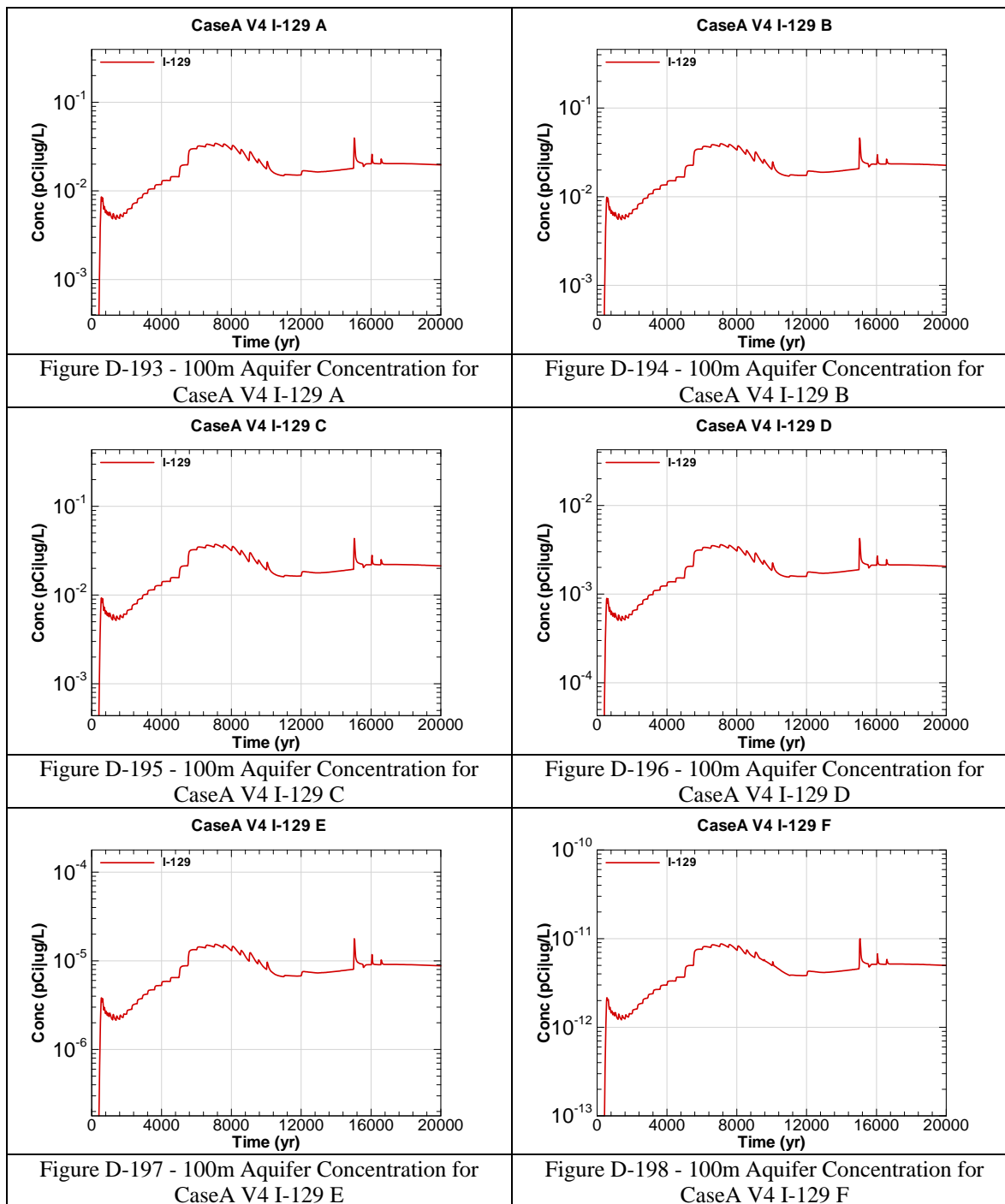


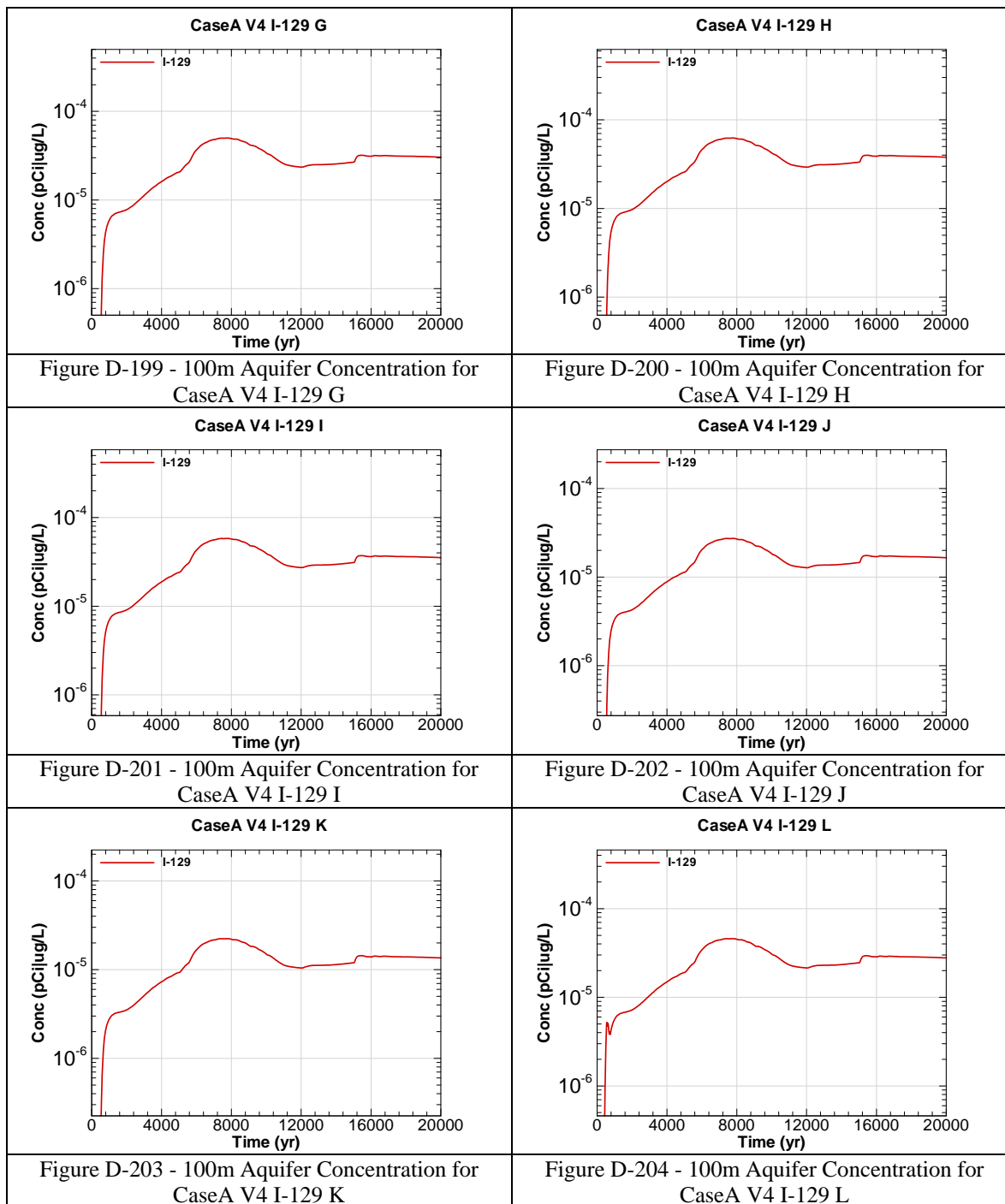


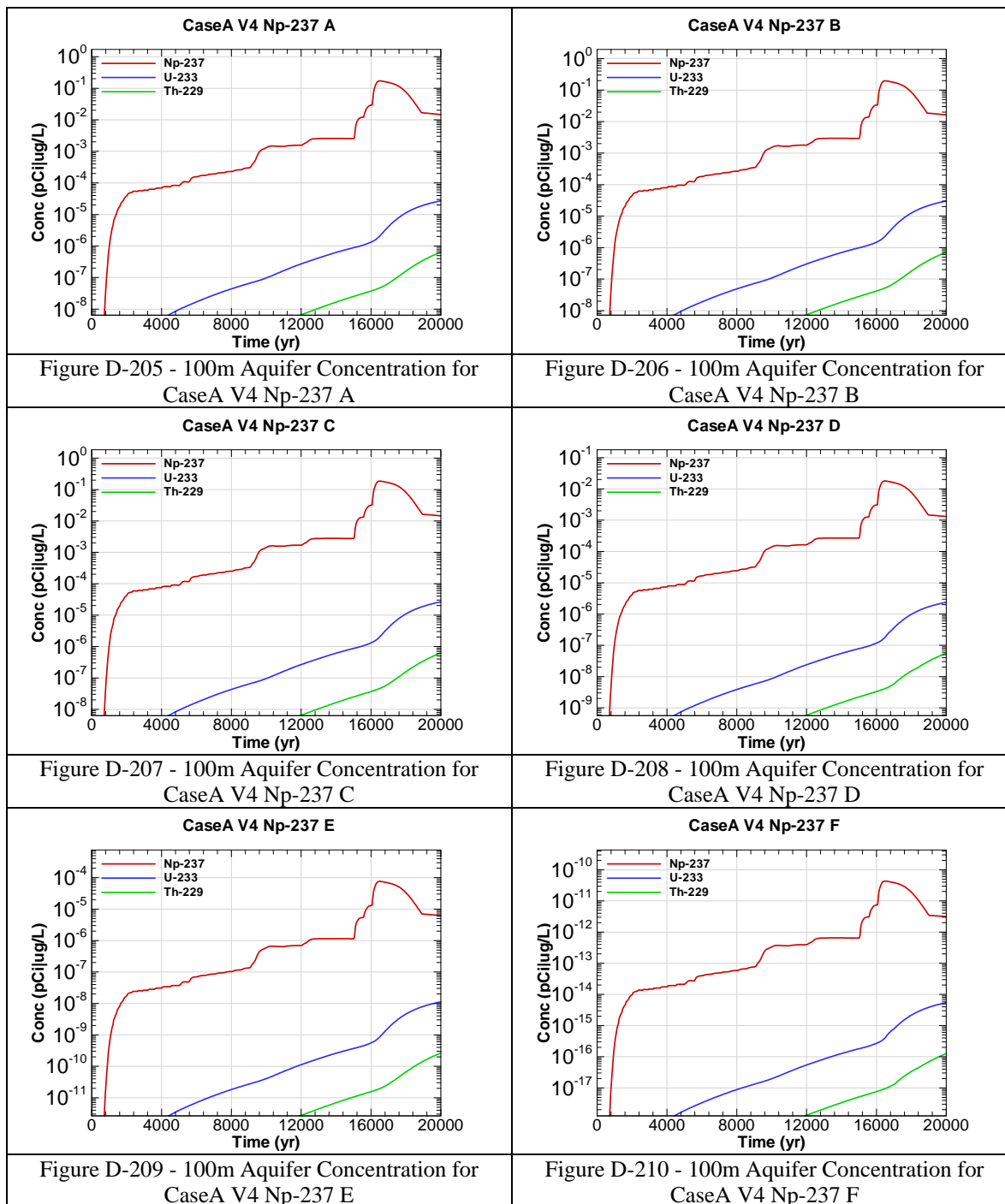












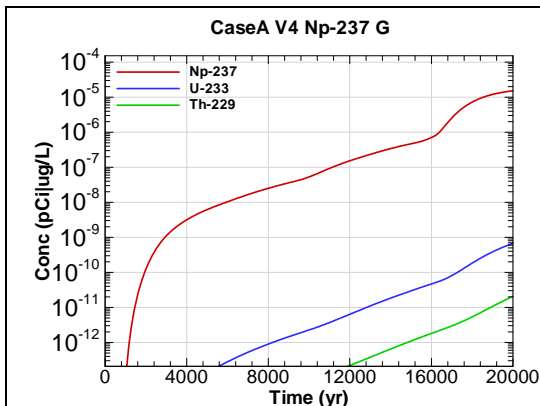


Figure D-211 - 100m Aquifer Concentration for
CaseA V4 Np-237 G

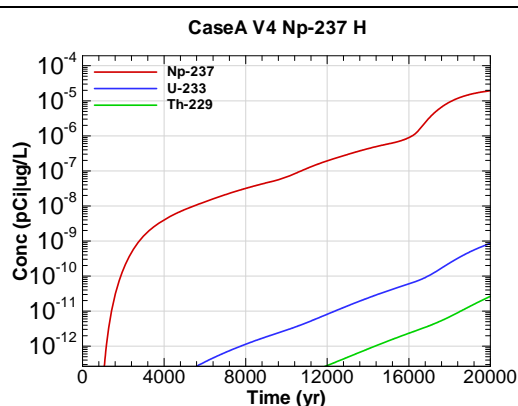


Figure D-212 - 100m Aquifer Concentration for
CaseA V4 Np-237 H

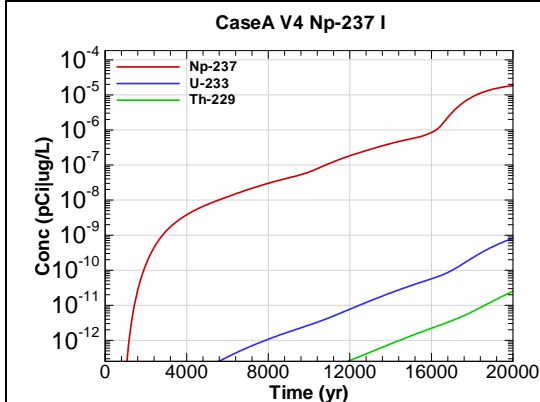


Figure D-213 - 100m Aquifer Concentration for
CaseA V4 Np-237 I

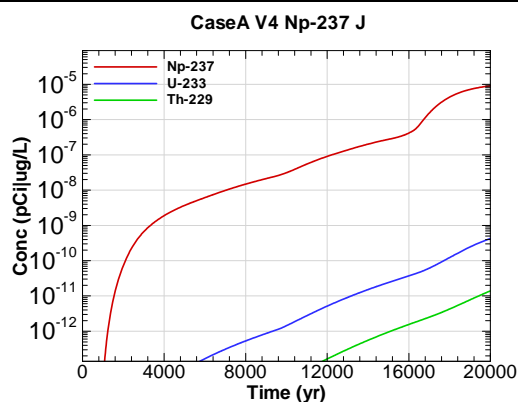


Figure D-214 - 100m Aquifer Concentration for
CaseA V4 Np-237 J

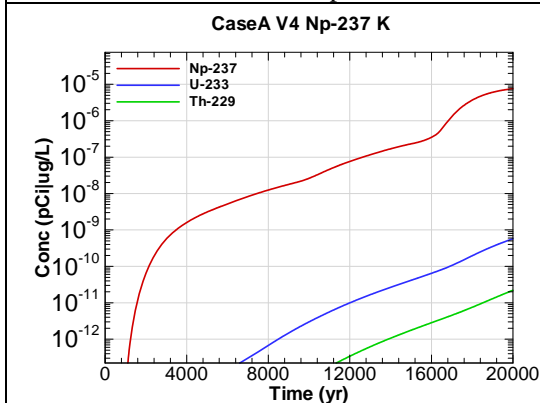


Figure D-215 - 100m Aquifer Concentration for
CaseA V4 Np-237 K

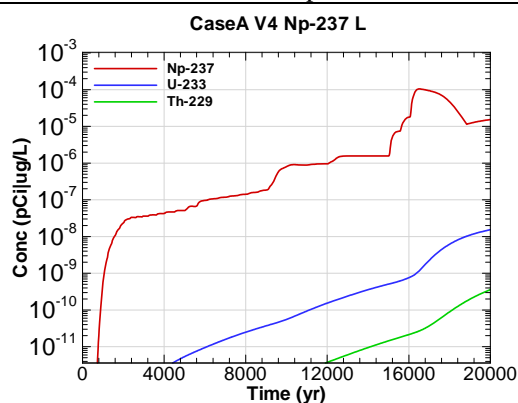


Figure D-216 - 100m Aquifer Concentration for
CaseA V4 Np-237 L

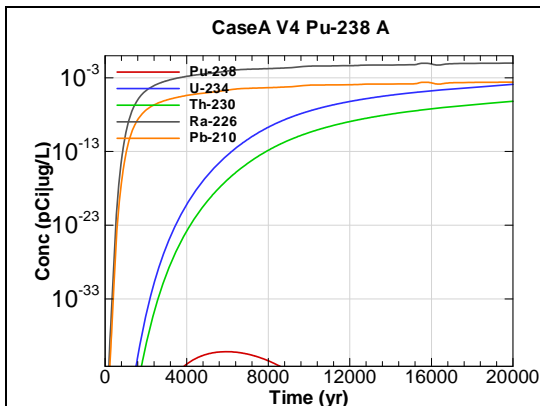


Figure D-217 - 100m Aquifer Concentration for
CaseA V4 Pu-238 A

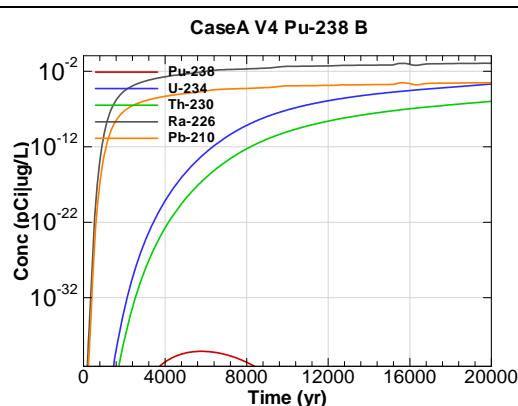


Figure D-218 - 100m Aquifer Concentration for
CaseA V4 Pu-238 B

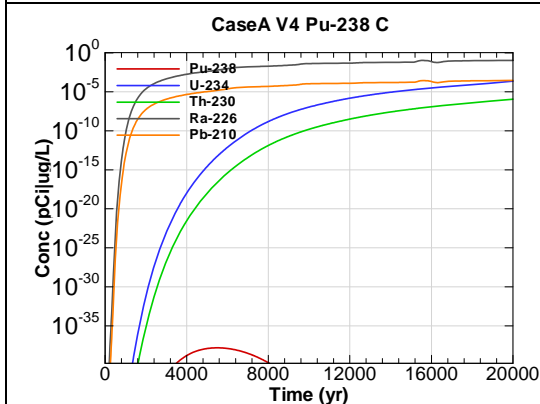


Figure D-219 - 100m Aquifer Concentration for
CaseA V4 Pu-238 C

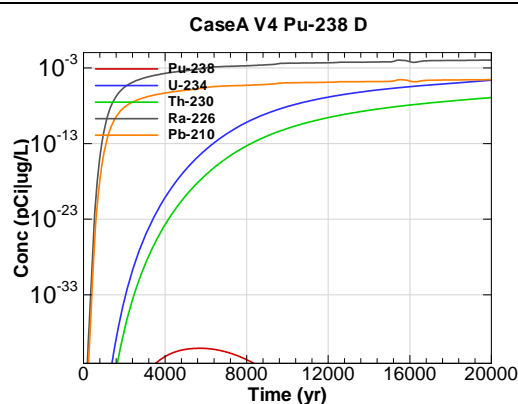


Figure D-220 - 100m Aquifer Concentration for
CaseA V4 Pu-238 D

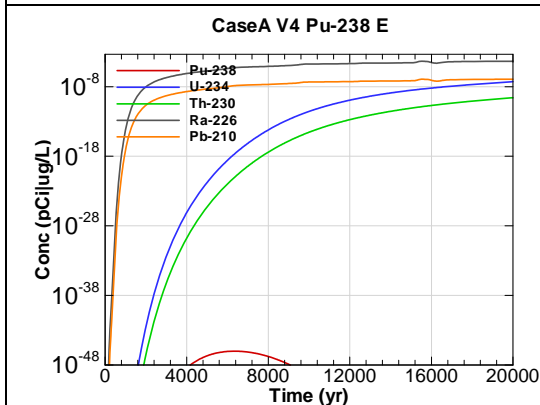


Figure D-221 - 100m Aquifer Concentration for
CaseA V4 Pu-238 E

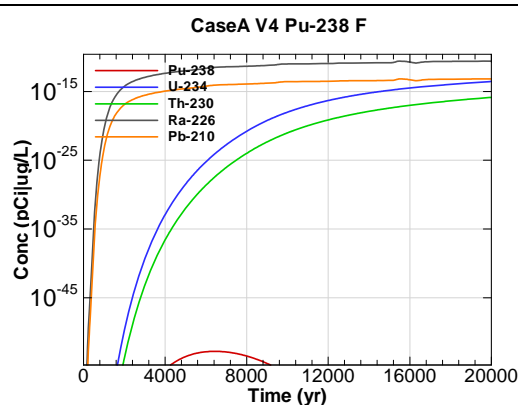


Figure D-222 - 100m Aquifer Concentration for
CaseA V4 Pu-238 F

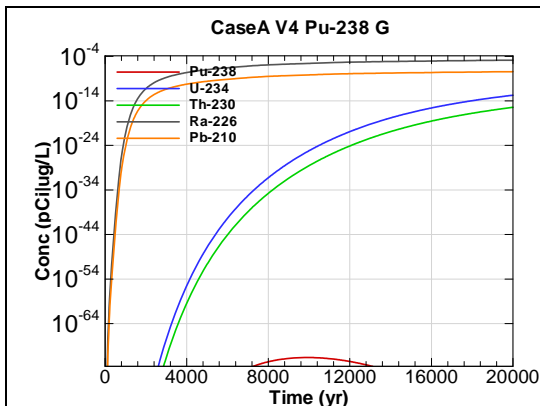


Figure D-223 - 100m Aquifer Concentration for
CaseA V4 Pu-238 G

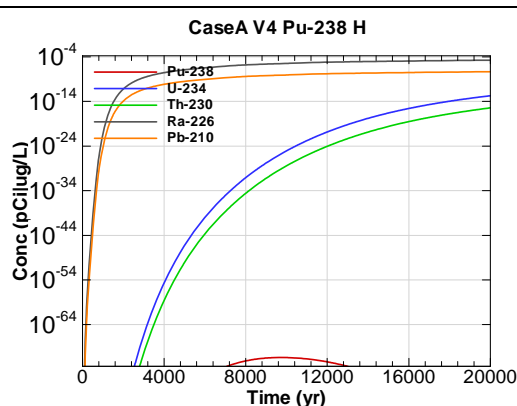


Figure D-224 - 100m Aquifer Concentration for
CaseA V4 Pu-238 H

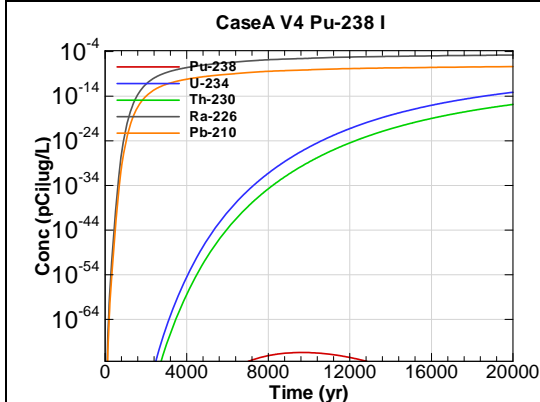


Figure D-225 - 100m Aquifer Concentration for
CaseA V4 Pu-238 I

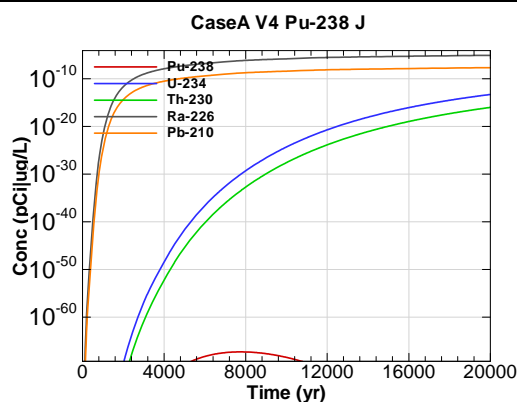


Figure D-226 - 100m Aquifer Concentration for
CaseA V4 Pu-238 J

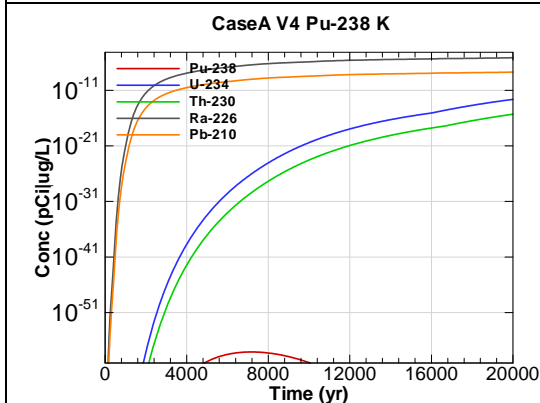


Figure D-227 - 100m Aquifer Concentration for
CaseA V4 Pu-238 K

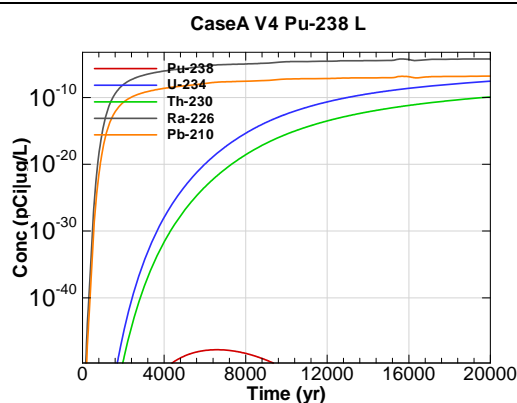
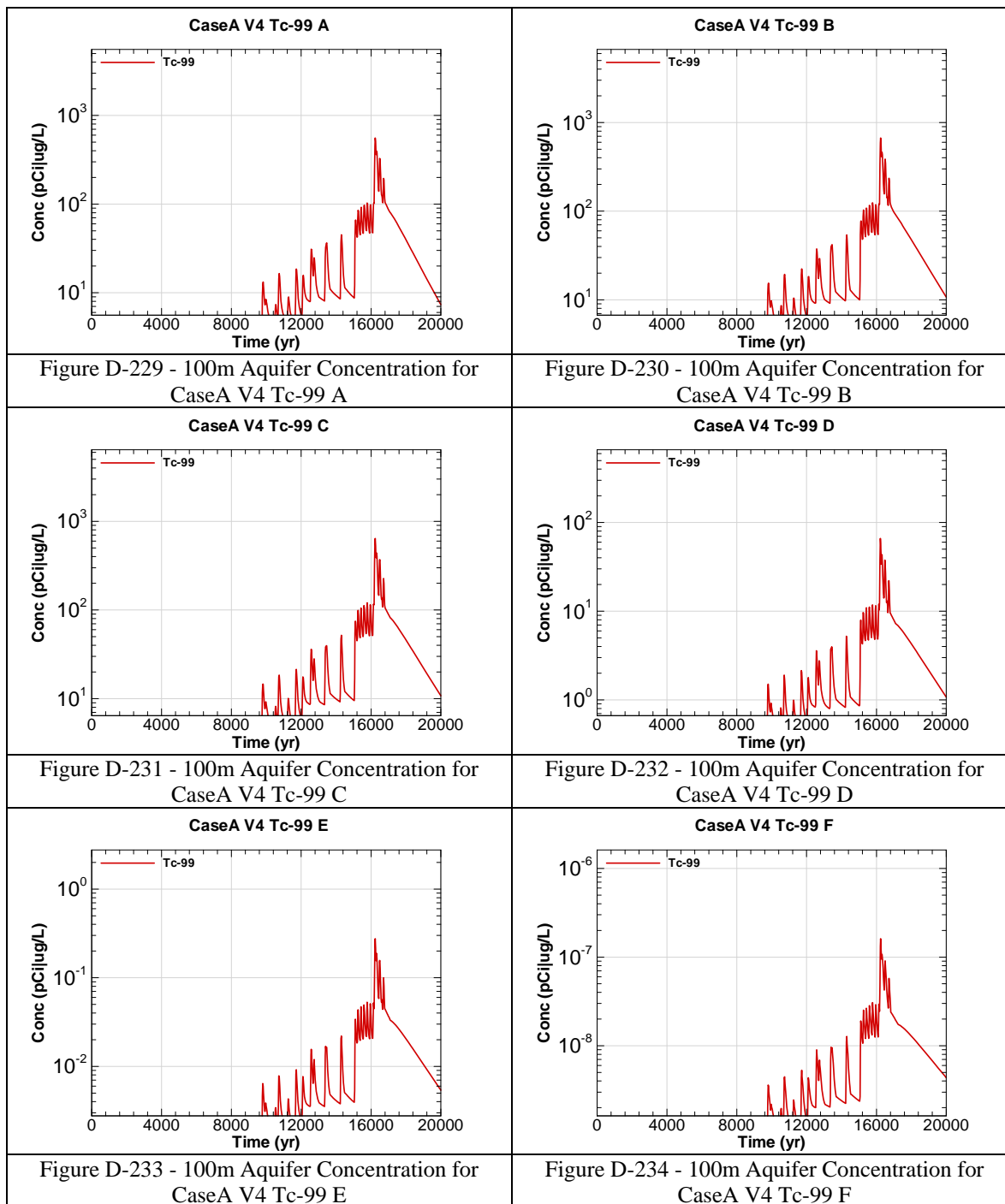
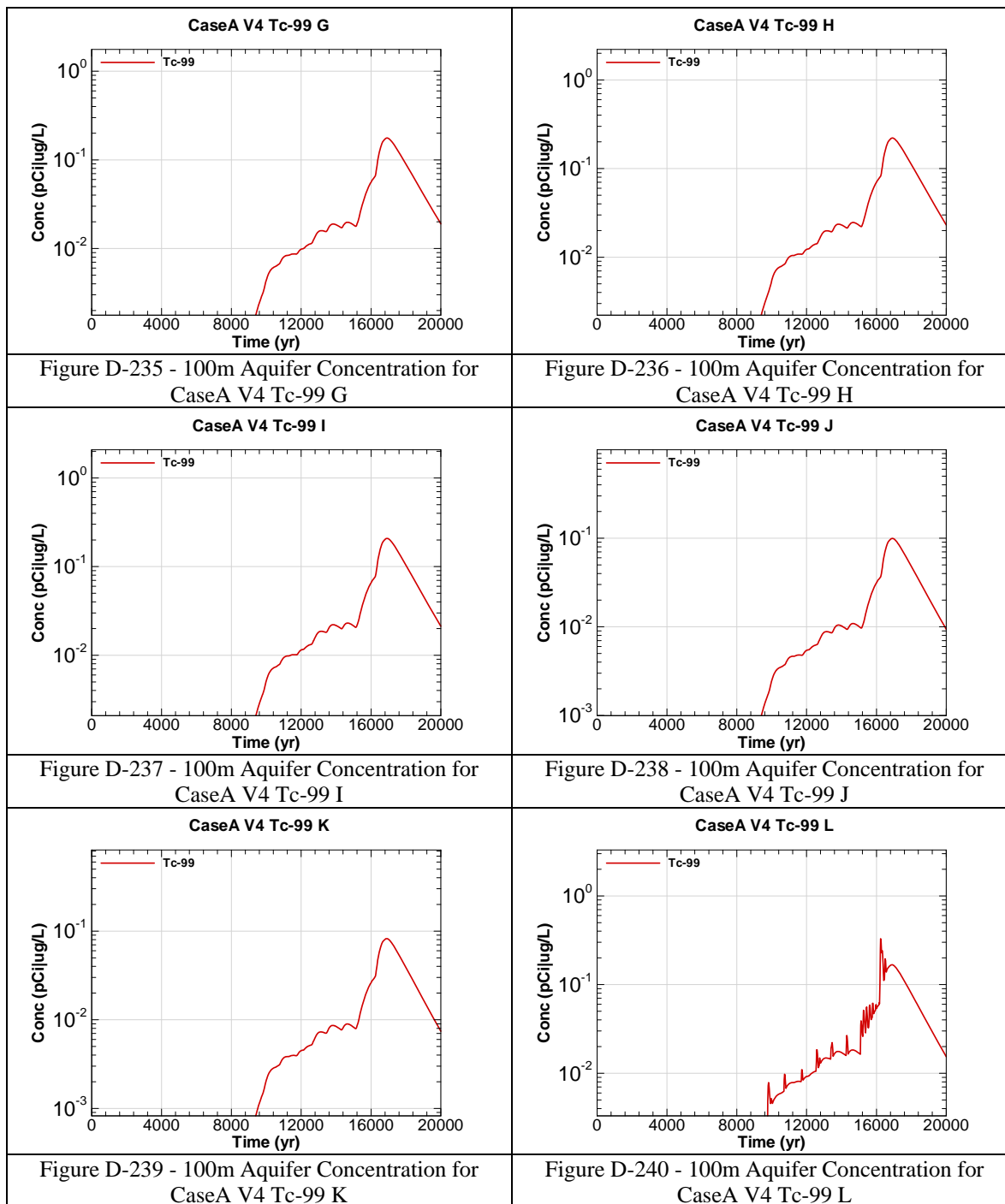
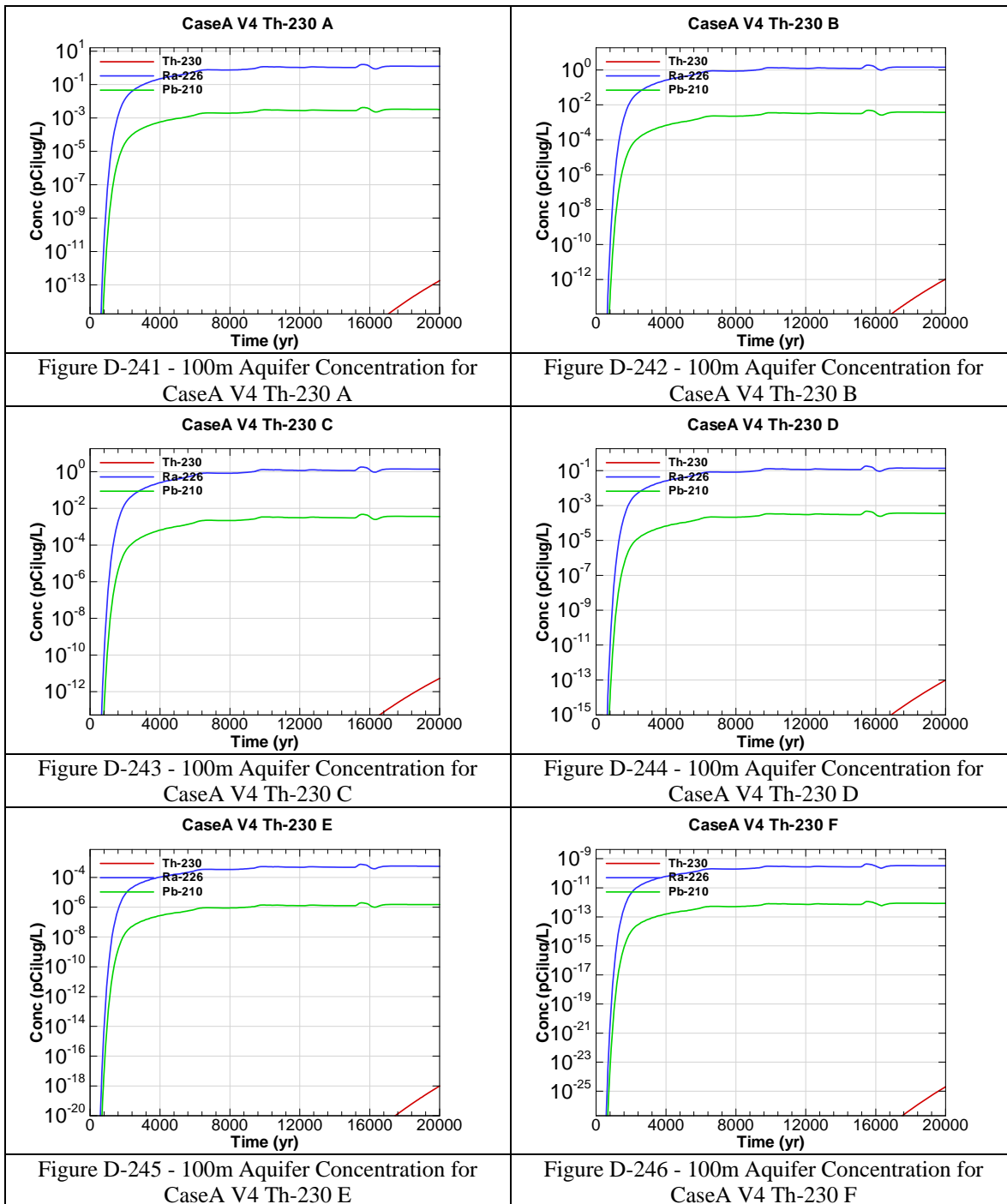


Figure D-228 - 100m Aquifer Concentration for
CaseA V4 Pu-238 L







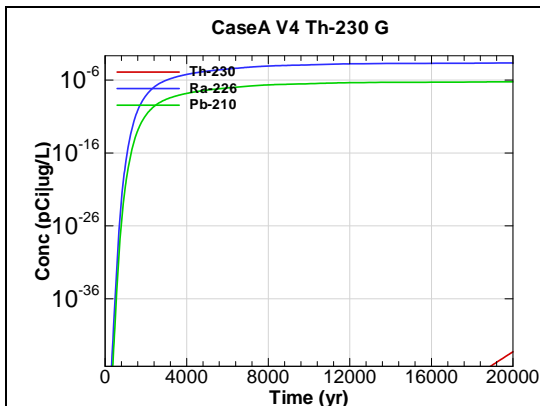


Figure D-247 - 100m Aquifer Concentration for CaseA V4 Th-230 G

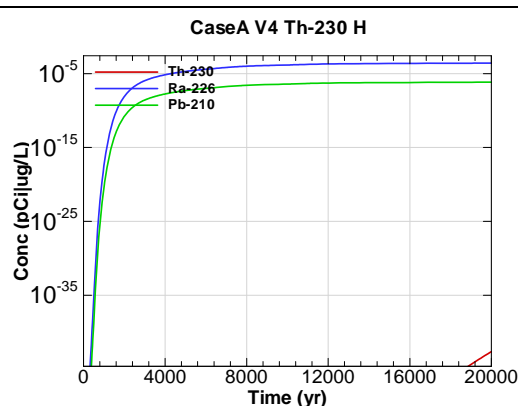


Figure D-248 - 100m Aquifer Concentration for CaseA V4 Th-230 H

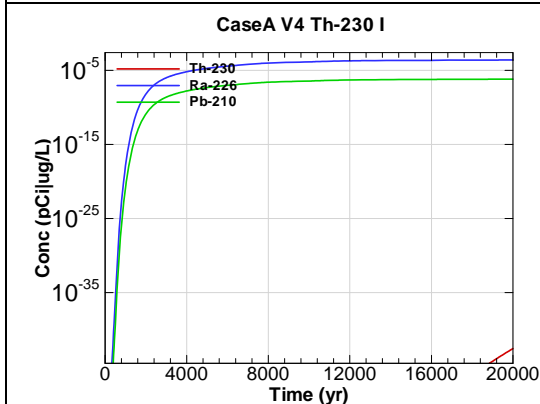


Figure D-249 - 100m Aquifer Concentration for CaseA V4 Th-230 I

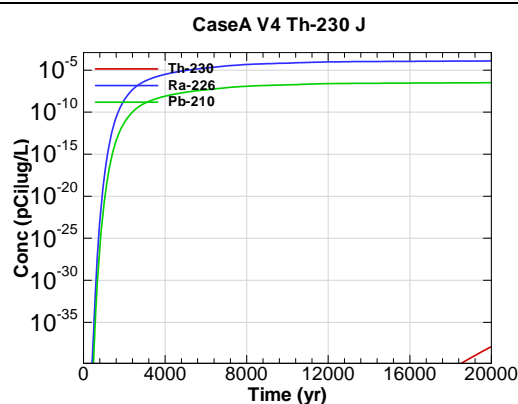


Figure D-250 - 100m Aquifer Concentration for CaseA V4 Th-230 J

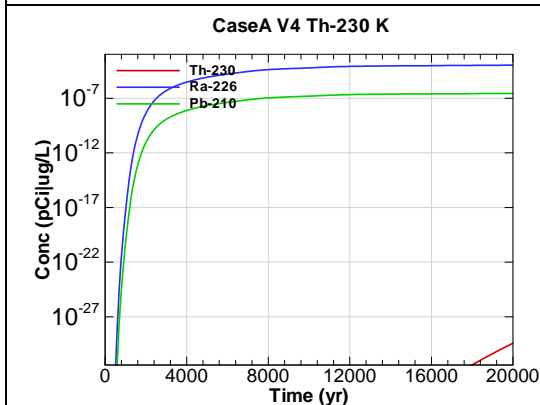


Figure D-251 - 100m Aquifer Concentration for CaseA V4 Th-230 K

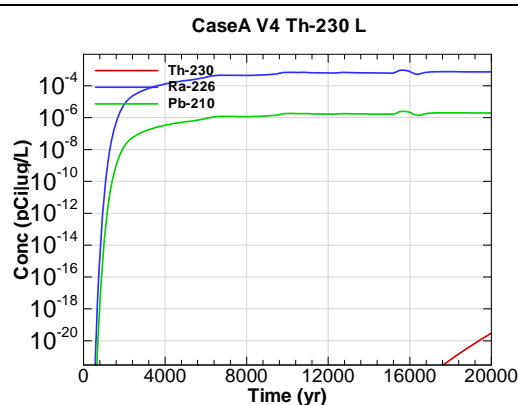


Figure D-252 - 100m Aquifer Concentration for CaseA V4 Th-230 L

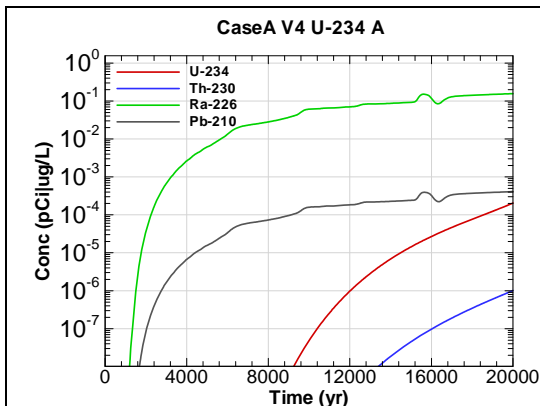


Figure D-253 - 100m Aquifer Concentration for
CaseA V4 U-234 A

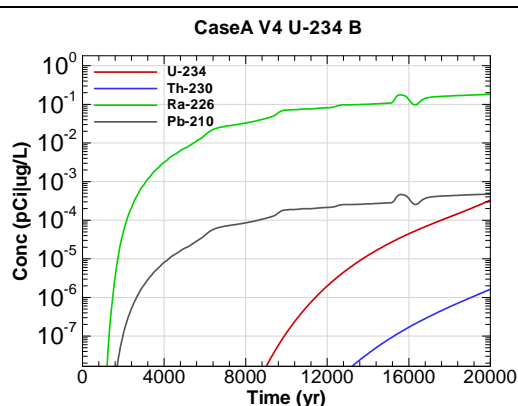


Figure D-254 - 100m Aquifer Concentration for
CaseA V4 U-234 B

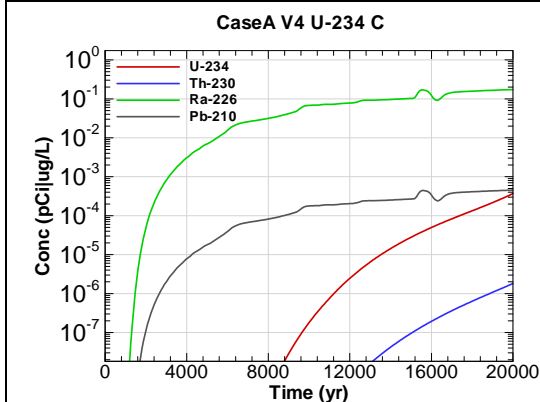


Figure D-255 - 100m Aquifer Concentration for
CaseA V4 U-234 C

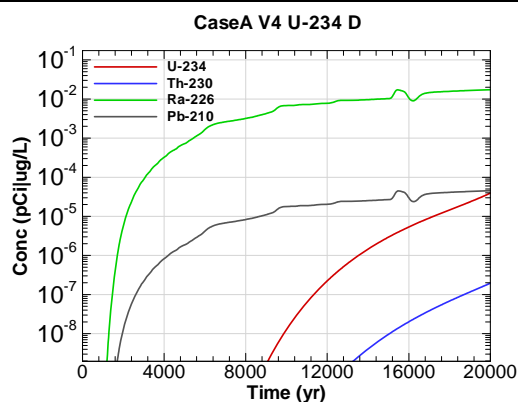


Figure D-256 - 100m Aquifer Concentration for
CaseA V4 U-234 D

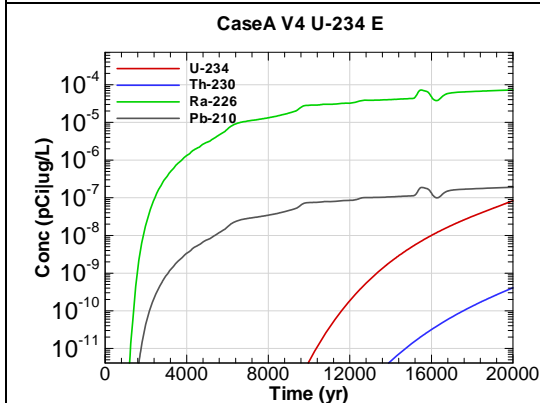


Figure D-257 - 100m Aquifer Concentration for
CaseA V4 U-234 E

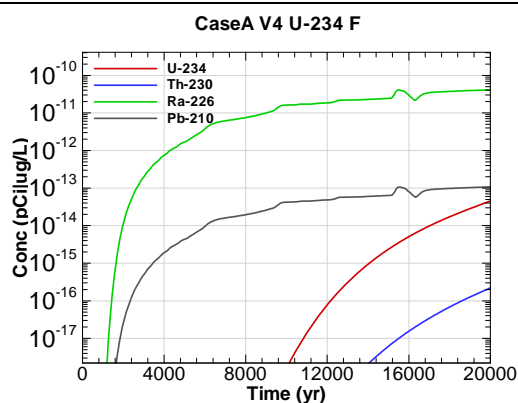


Figure D-258 - 100m Aquifer Concentration for
CaseA V4 U-234 F

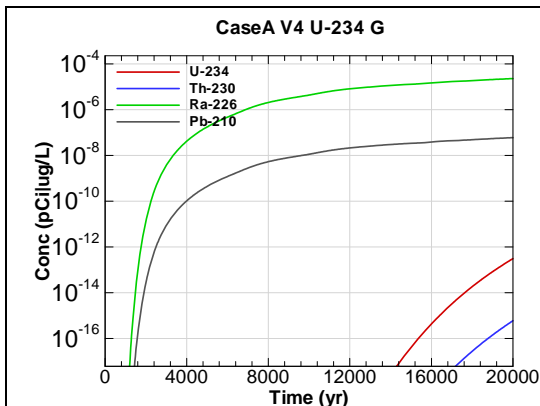


Figure D-259 - 100m Aquifer Concentration for
CaseA V4 U-234 G

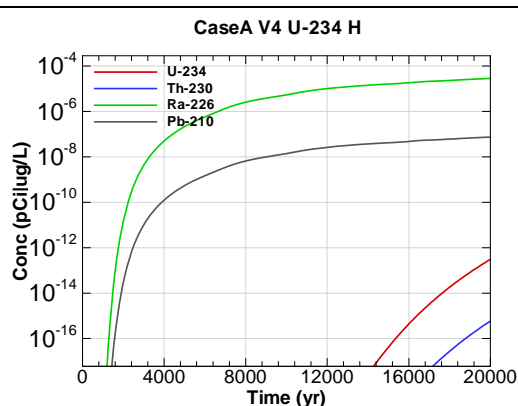


Figure D-260 - 100m Aquifer Concentration for
CaseA V4 U-234 H

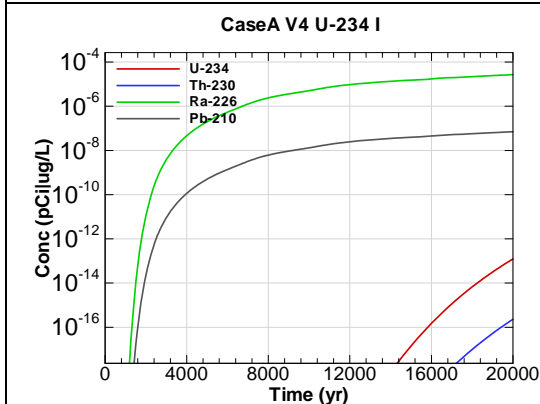


Figure D-261 - 100m Aquifer Concentration for
CaseA V4 U-234 I

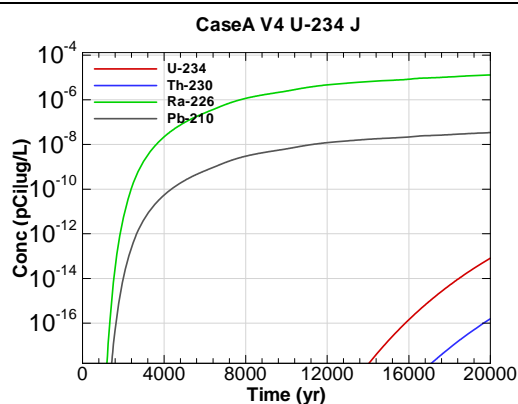


Figure D-262 - 100m Aquifer Concentration for
CaseA V4 U-234 J

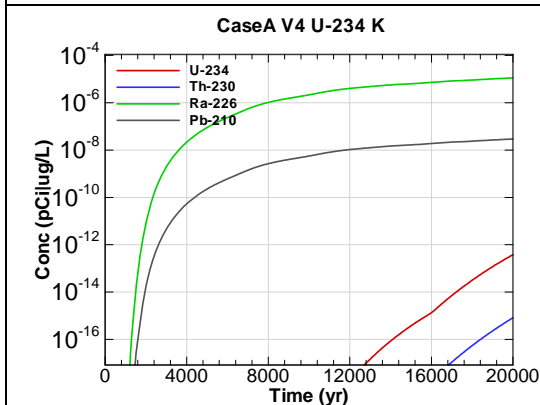


Figure D-263 - 100m Aquifer Concentration for
CaseA V4 U-234 K

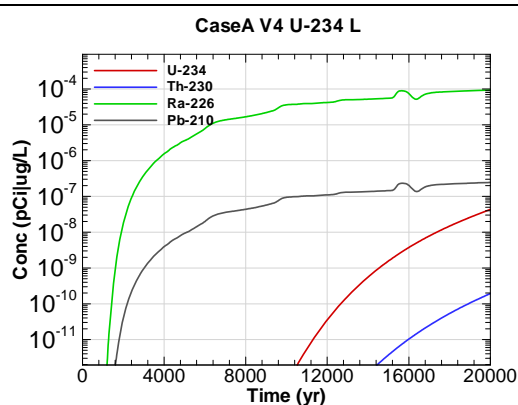
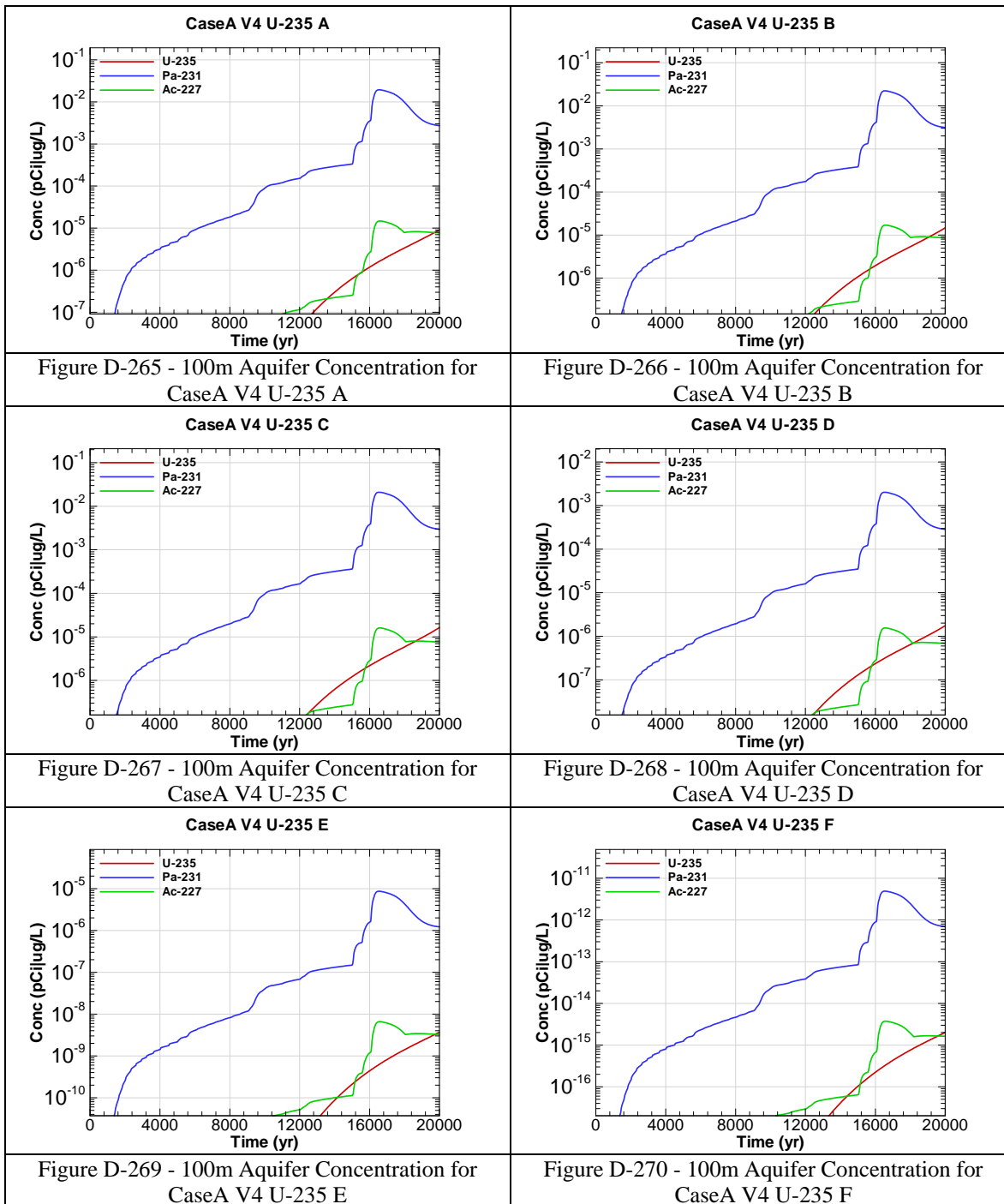
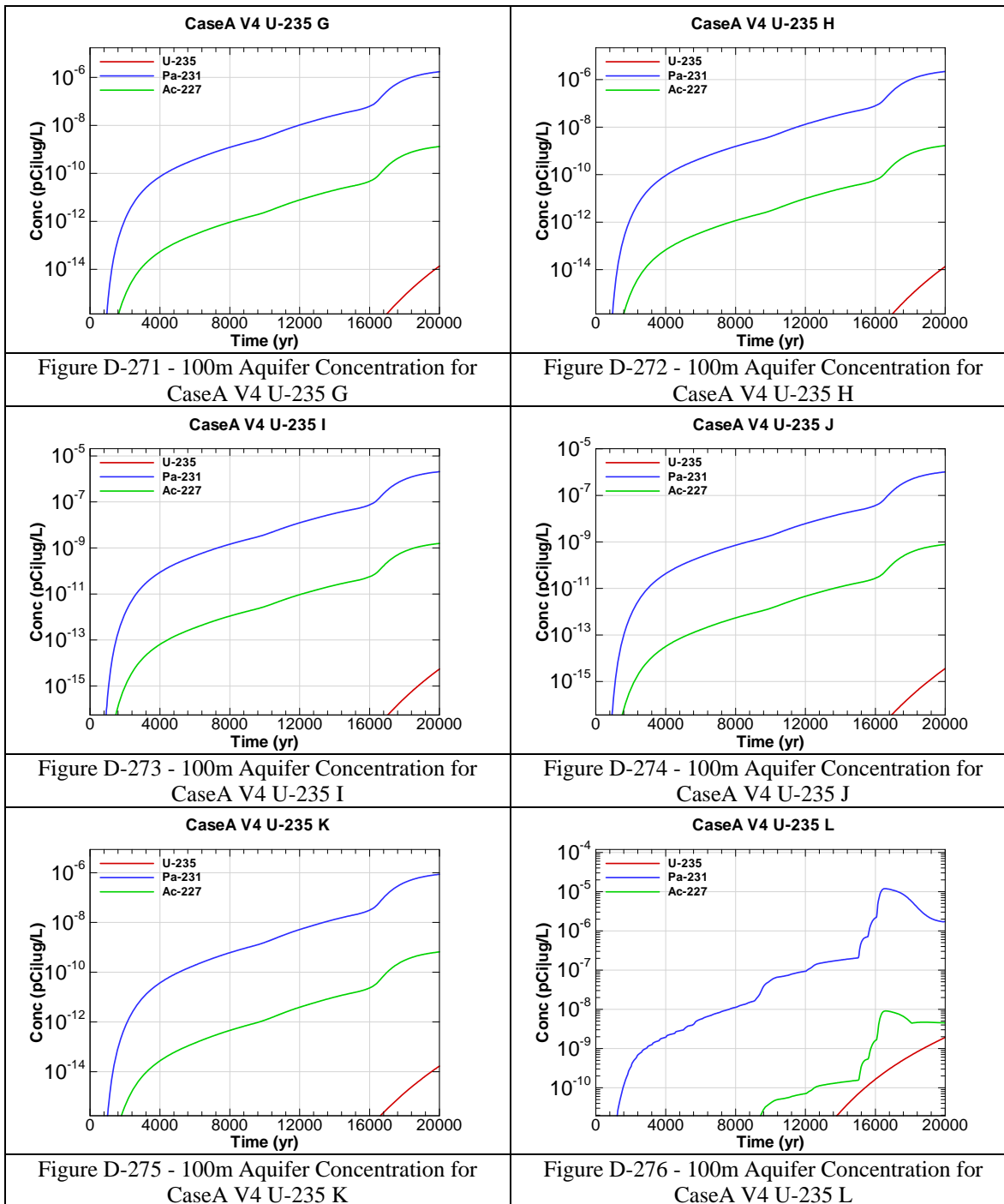
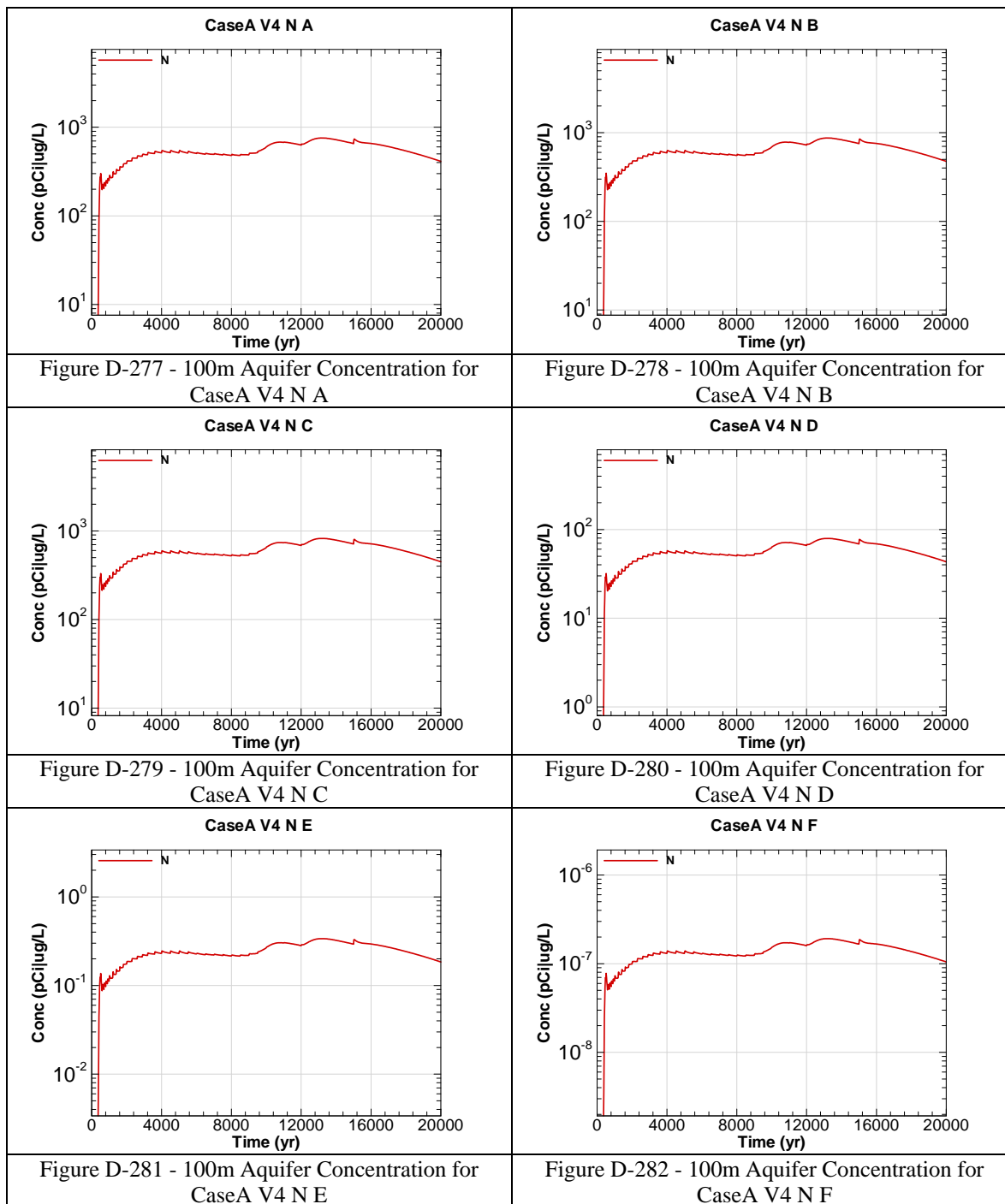
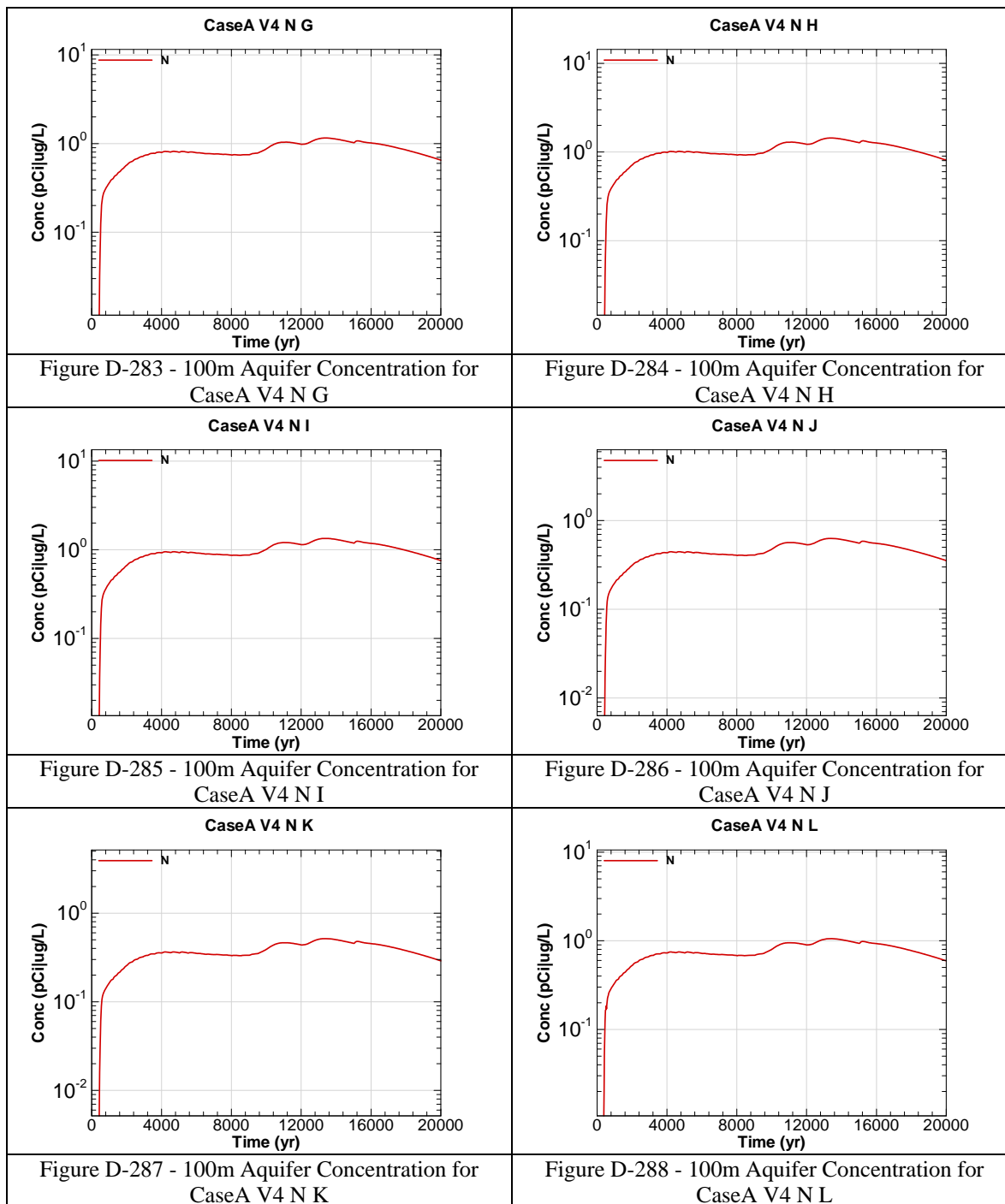


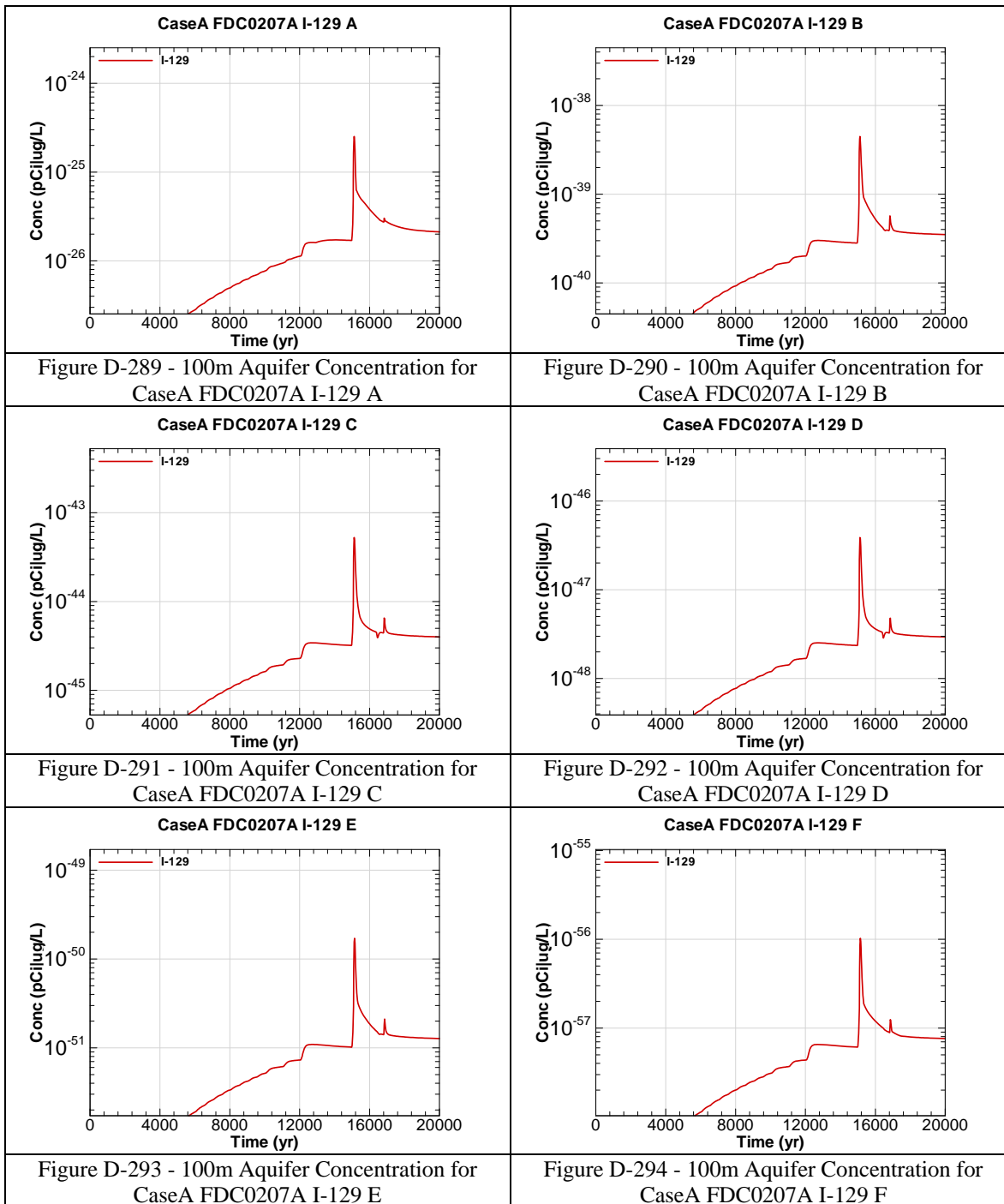
Figure D-264 - 100m Aquifer Concentration for
CaseA V4 U-234 L

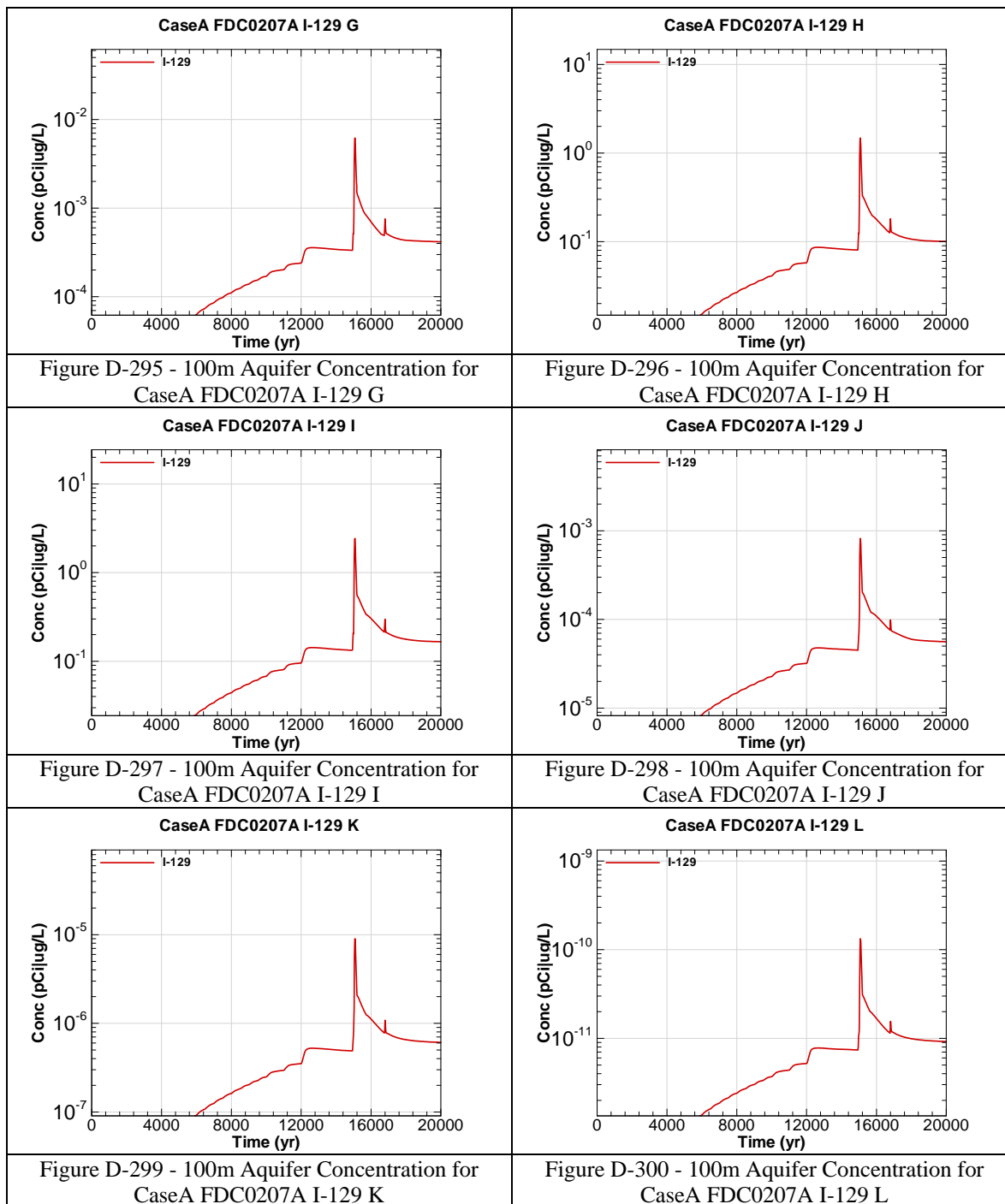


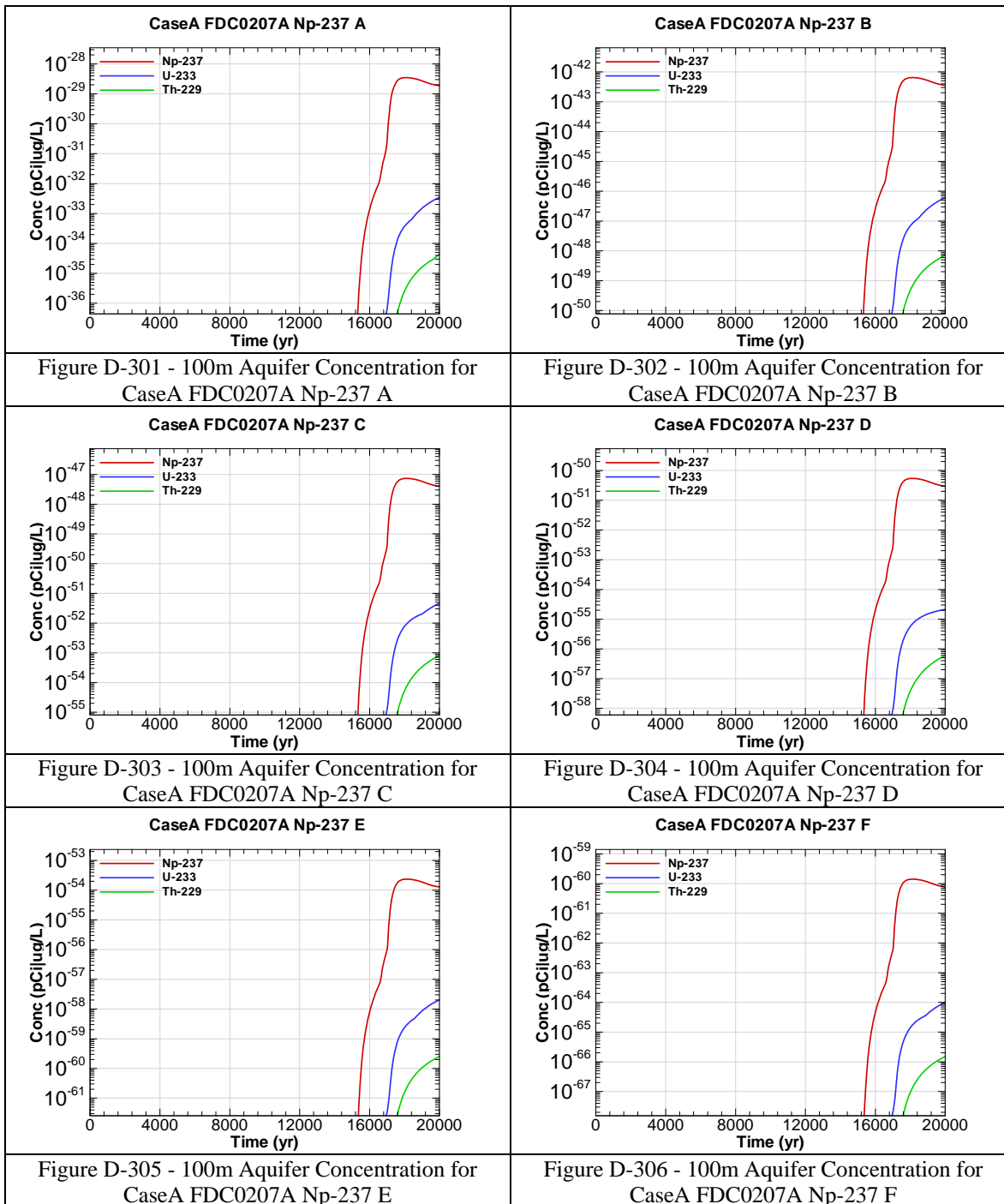


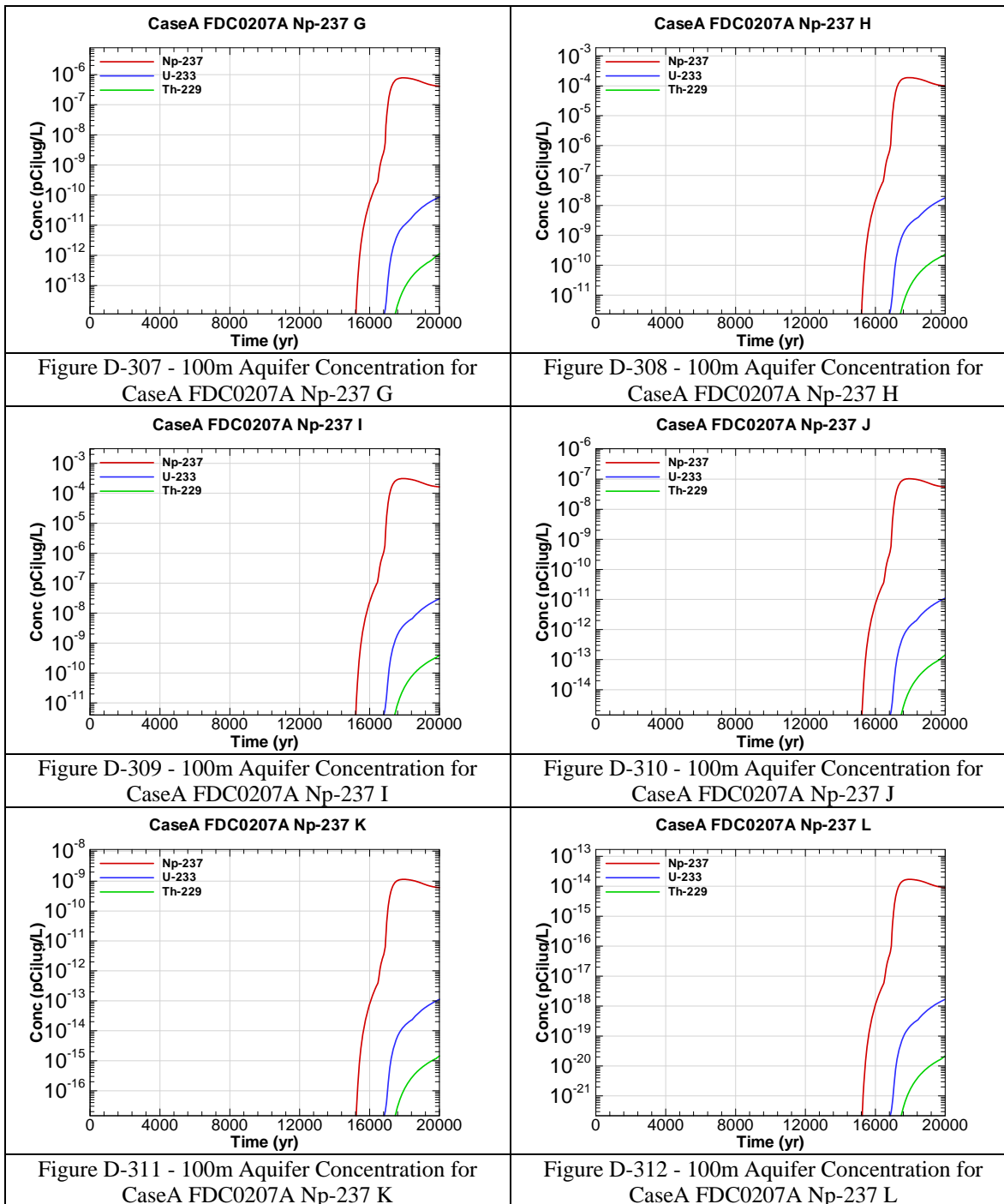


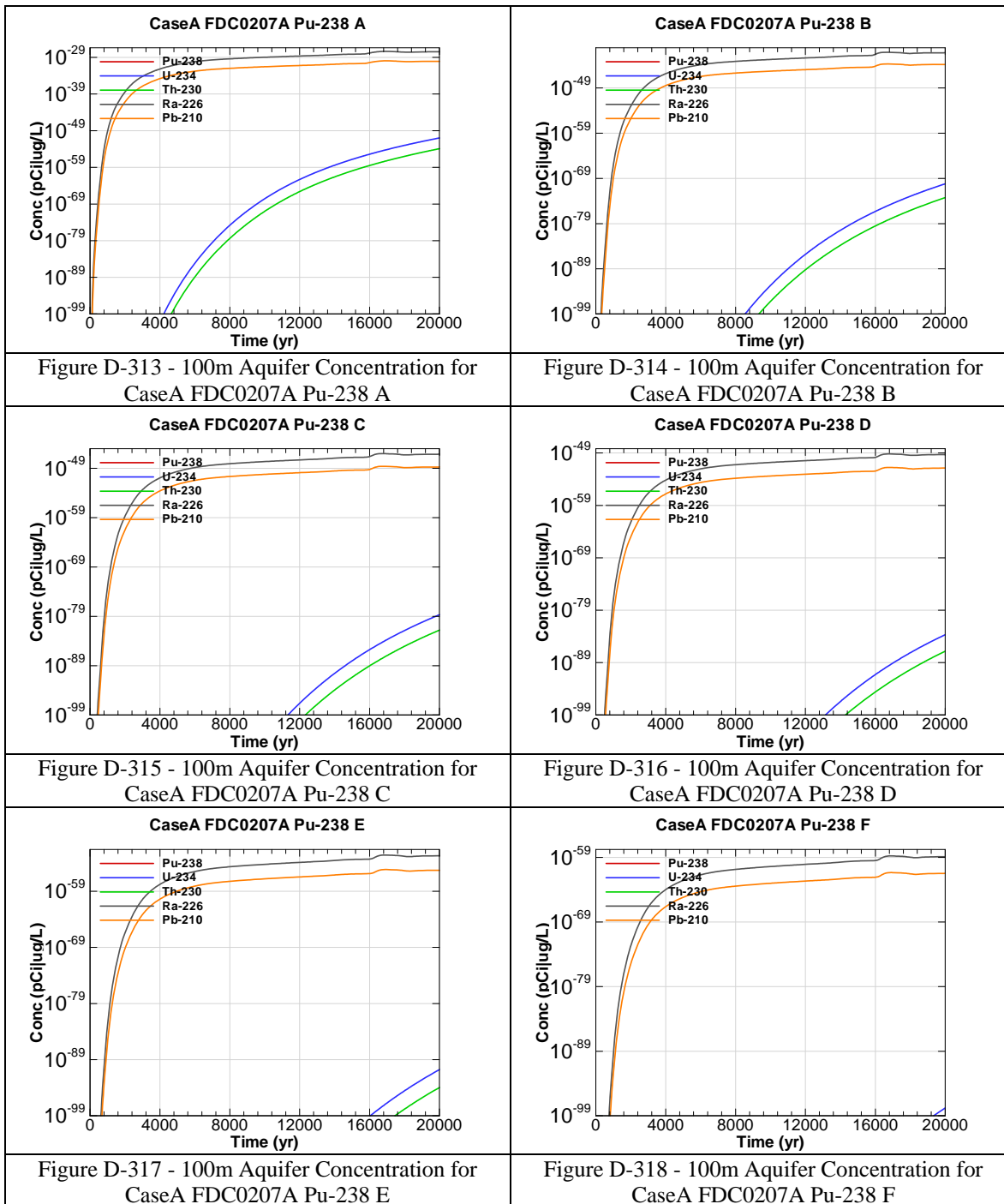


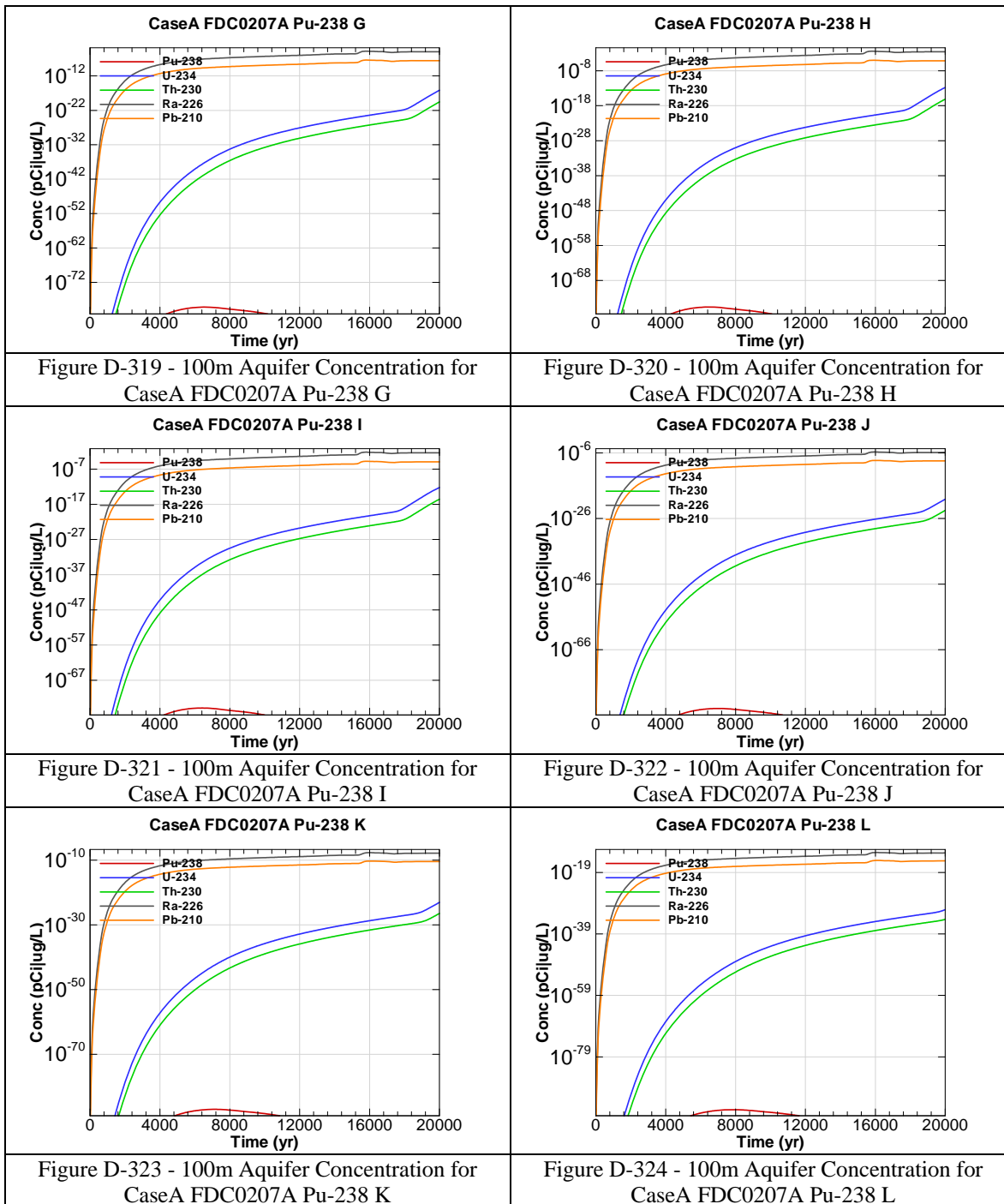


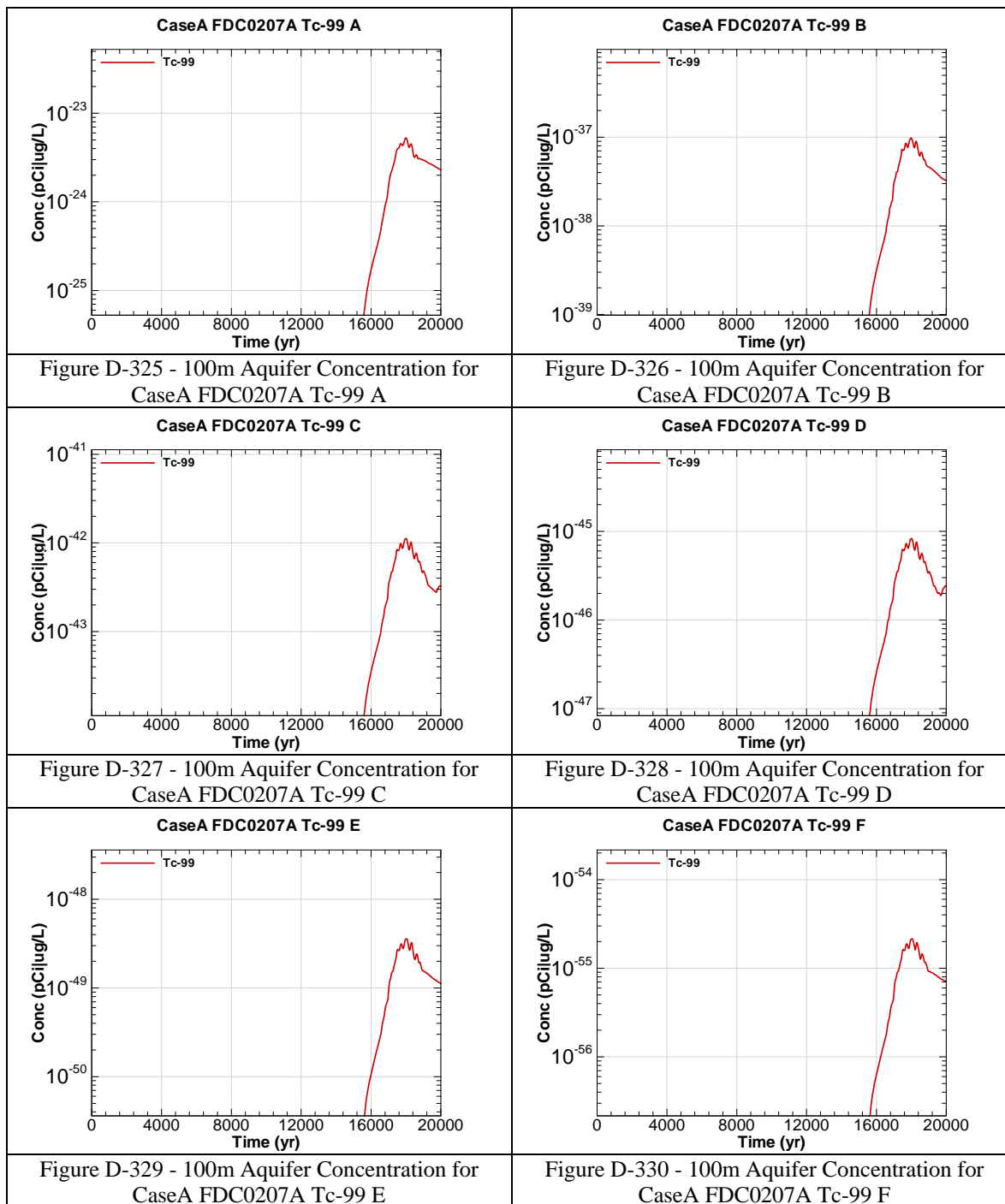


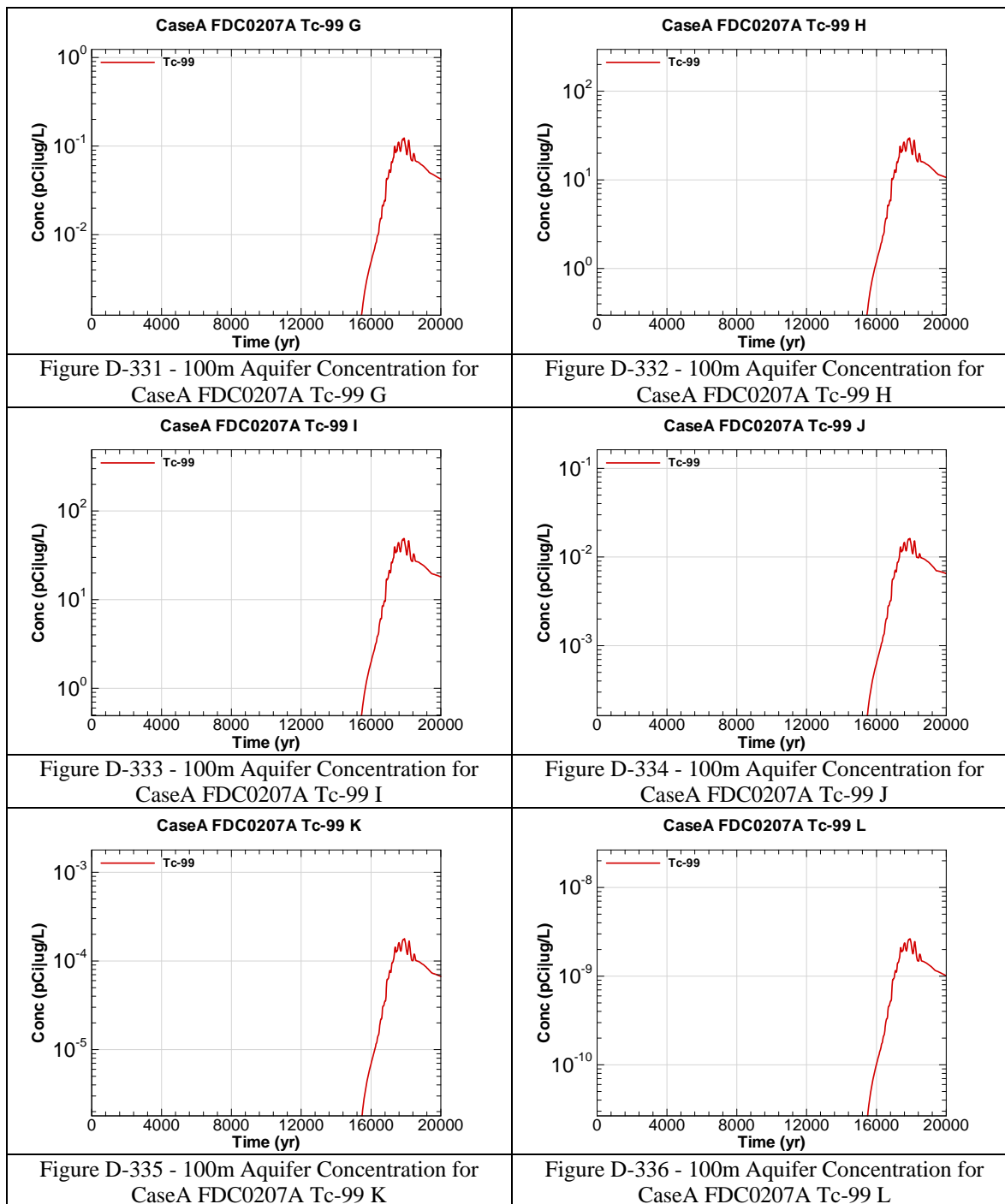












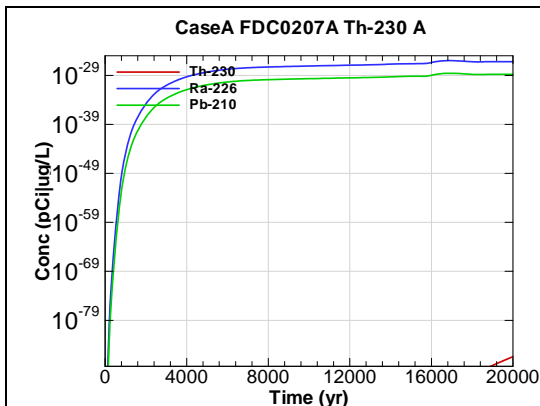


Figure D-337 - 100m Aquifer Concentration for
CaseA FDC0207A Th-230 A

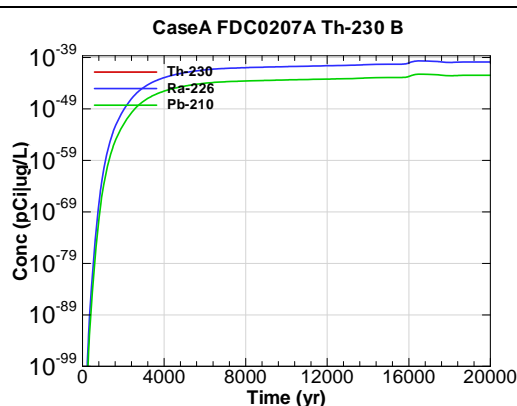


Figure D-338 - 100m Aquifer Concentration for
CaseA FDC0207A Th-230 B

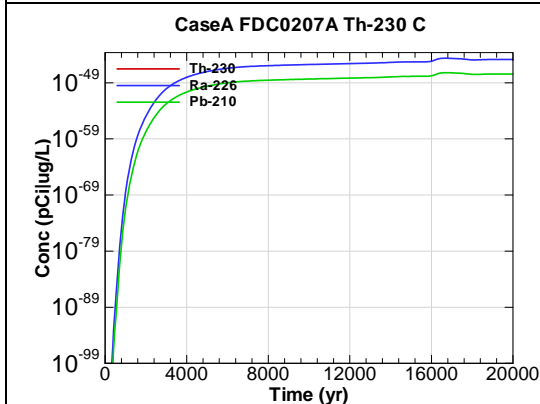


Figure D-339 - 100m Aquifer Concentration for
CaseA FDC0207A Th-230 C

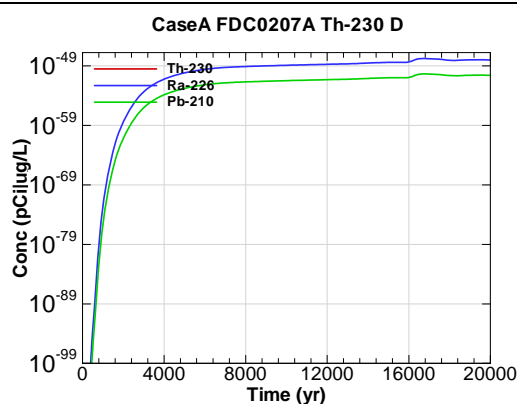


Figure D-340 - 100m Aquifer Concentration for
CaseA FDC0207A Th-230 D

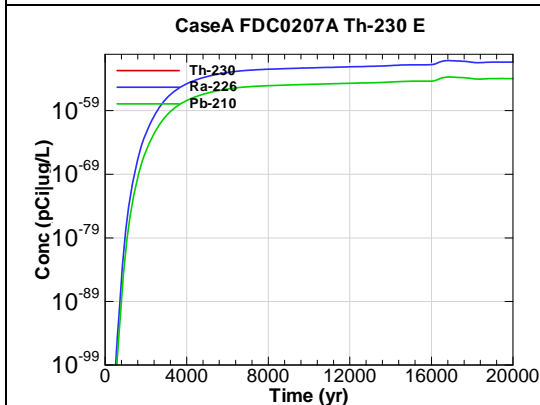


Figure D-341 - 100m Aquifer Concentration for
CaseA FDC0207A Th-230 E

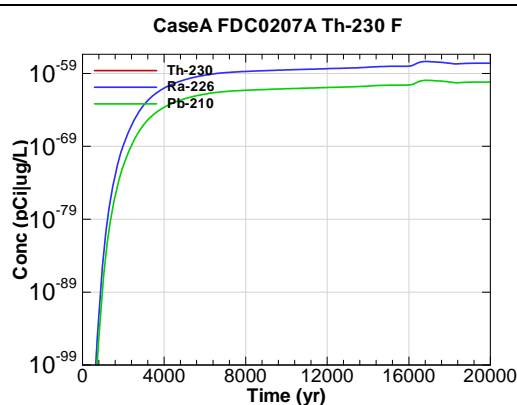
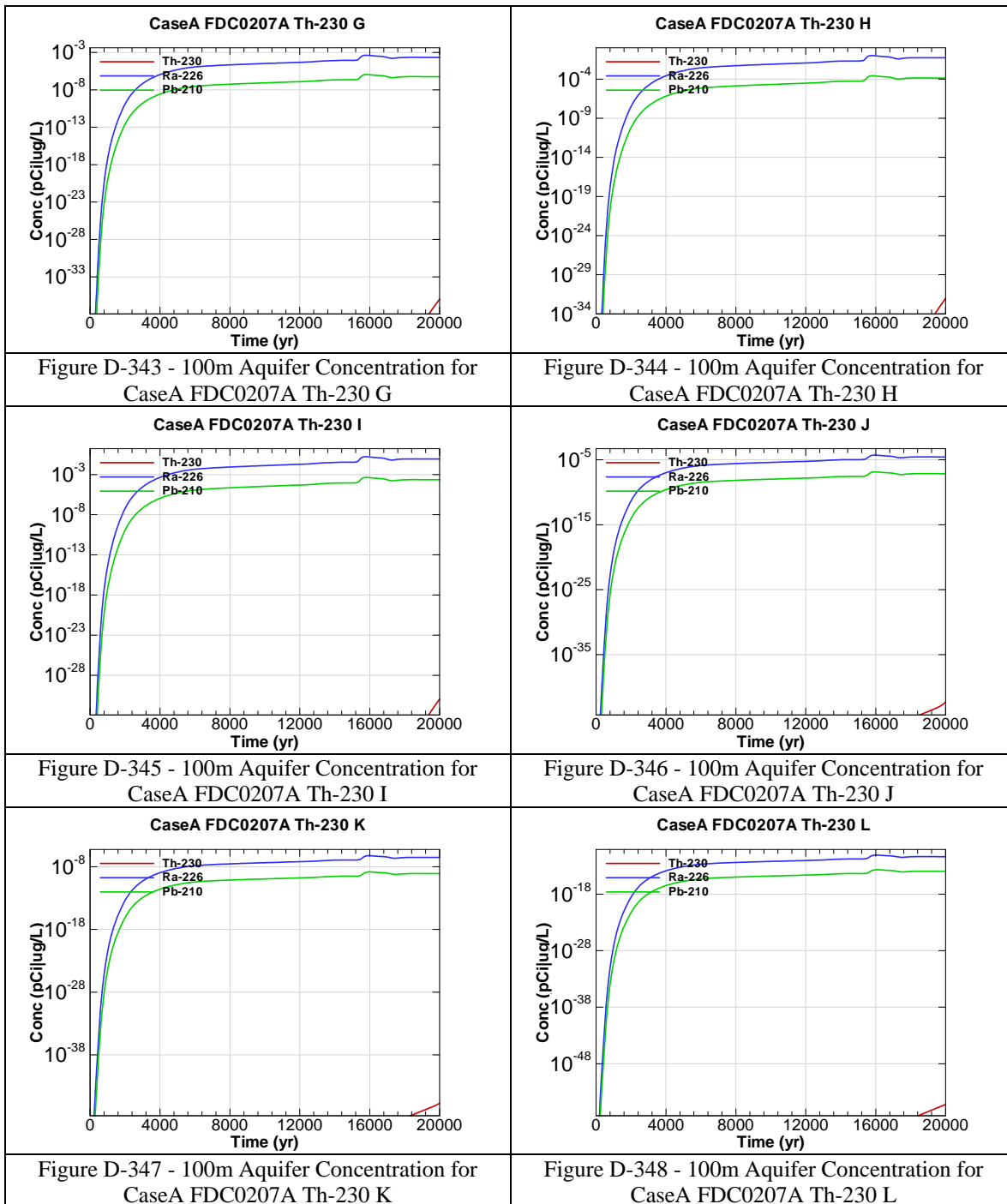
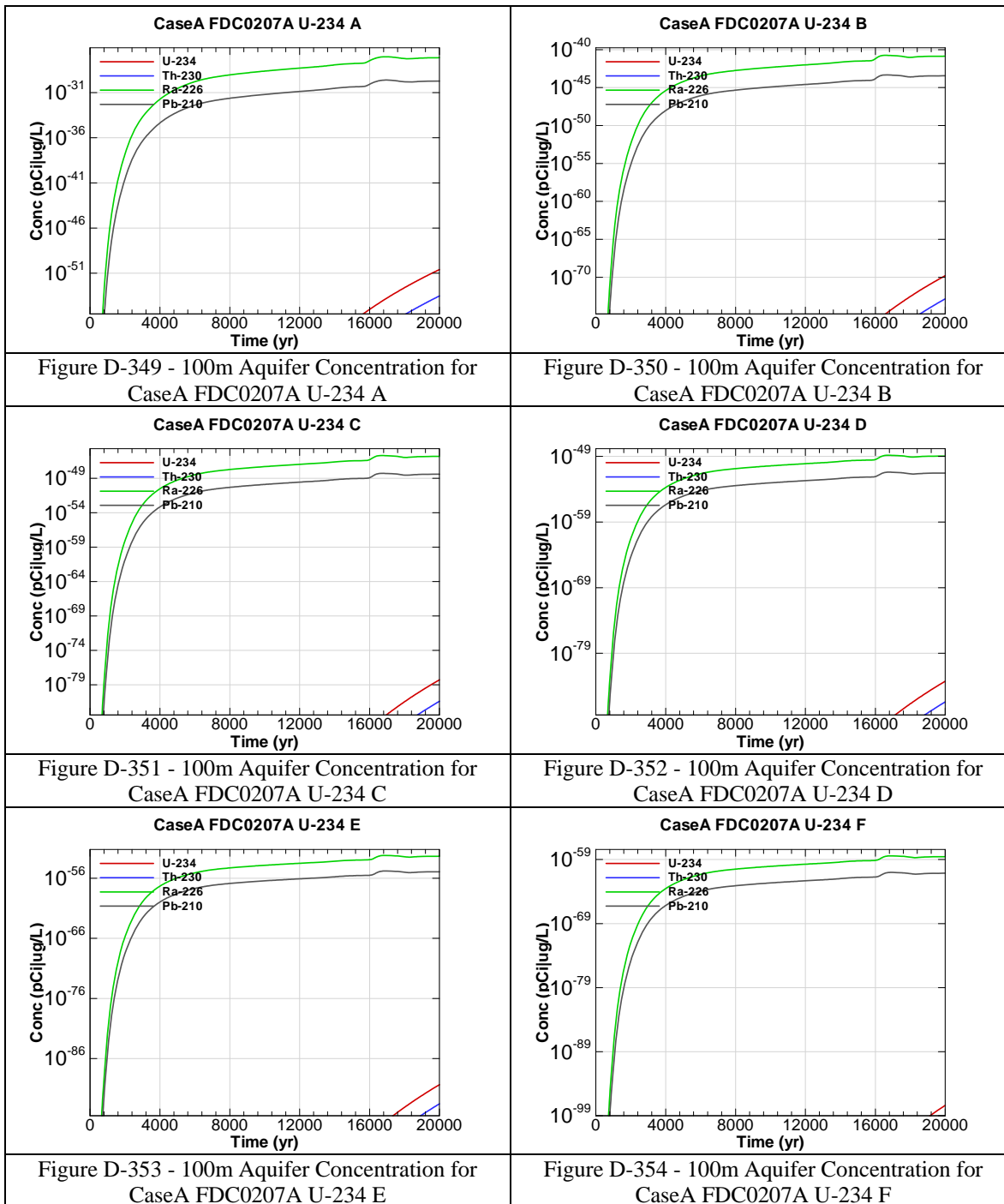
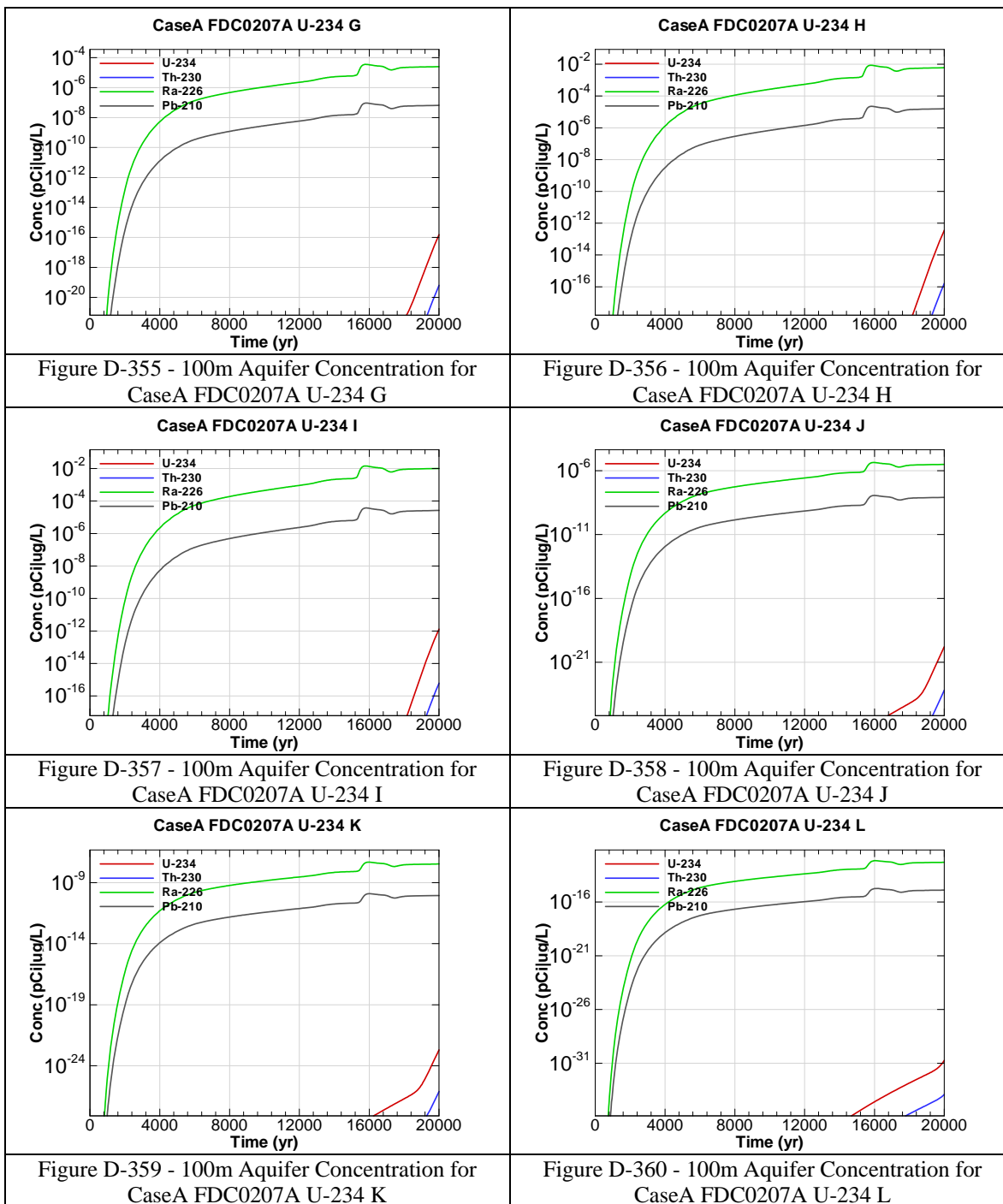
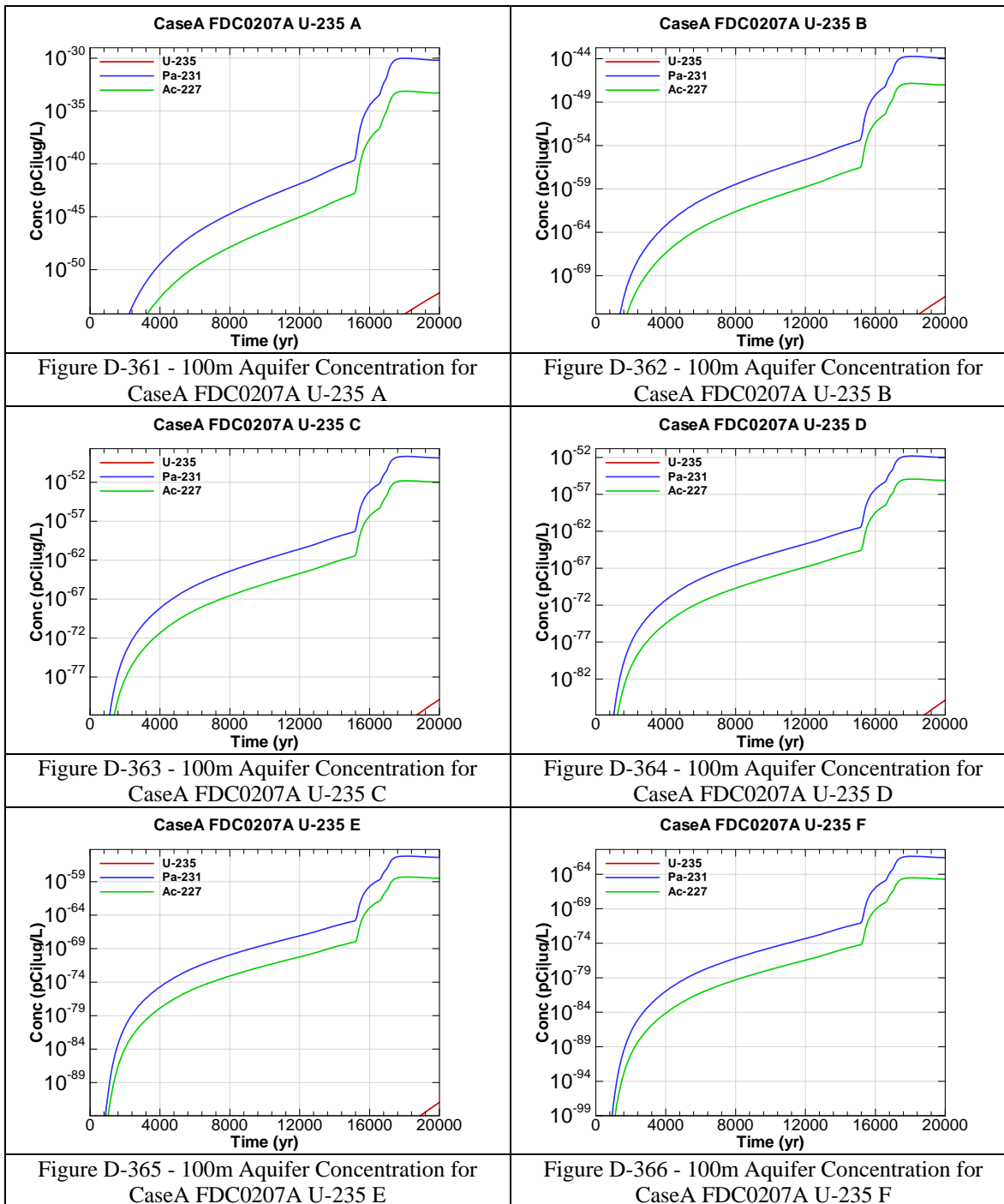


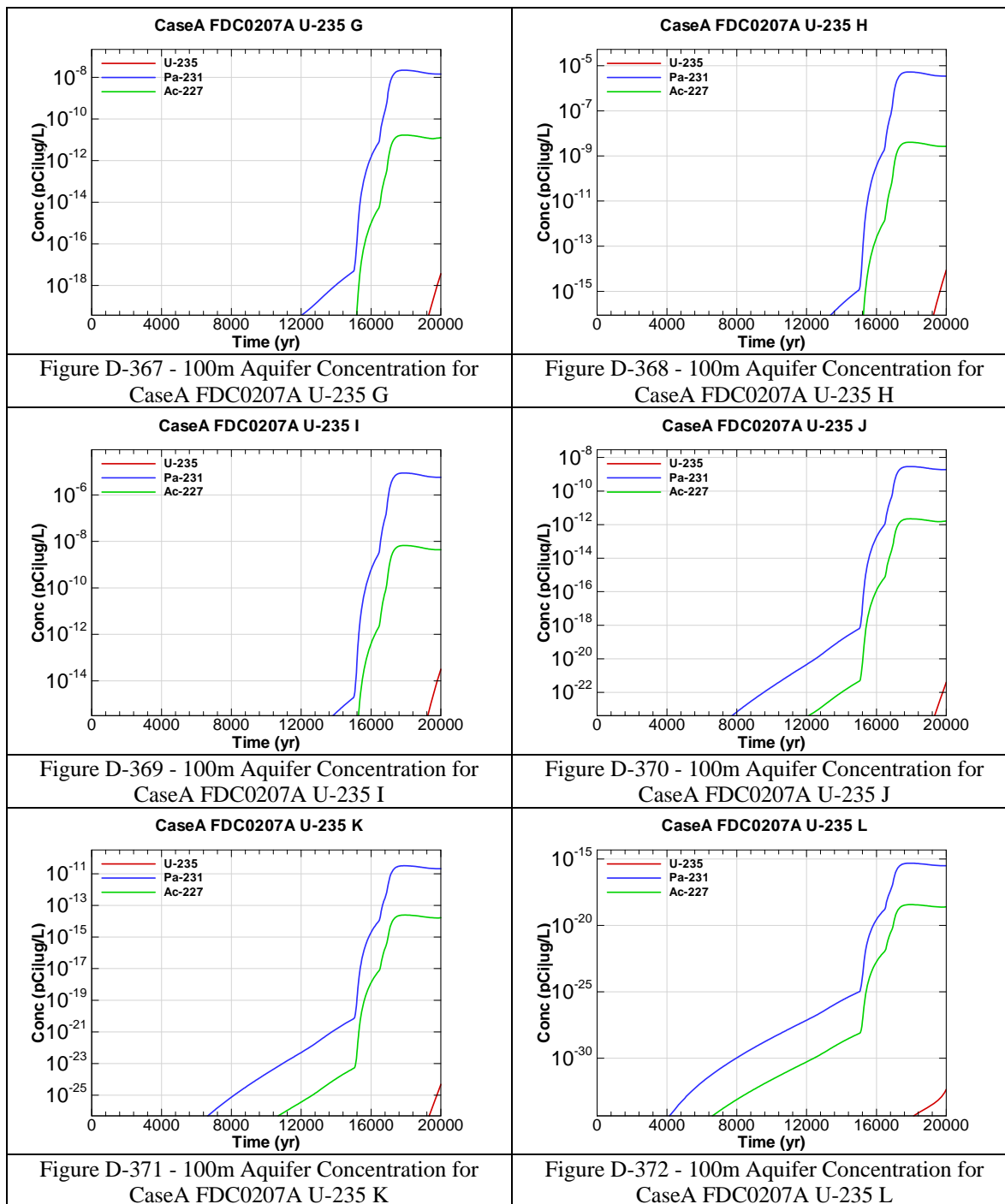
Figure D-342 - 100m Aquifer Concentration for
CaseA FDC0207A Th-230 F

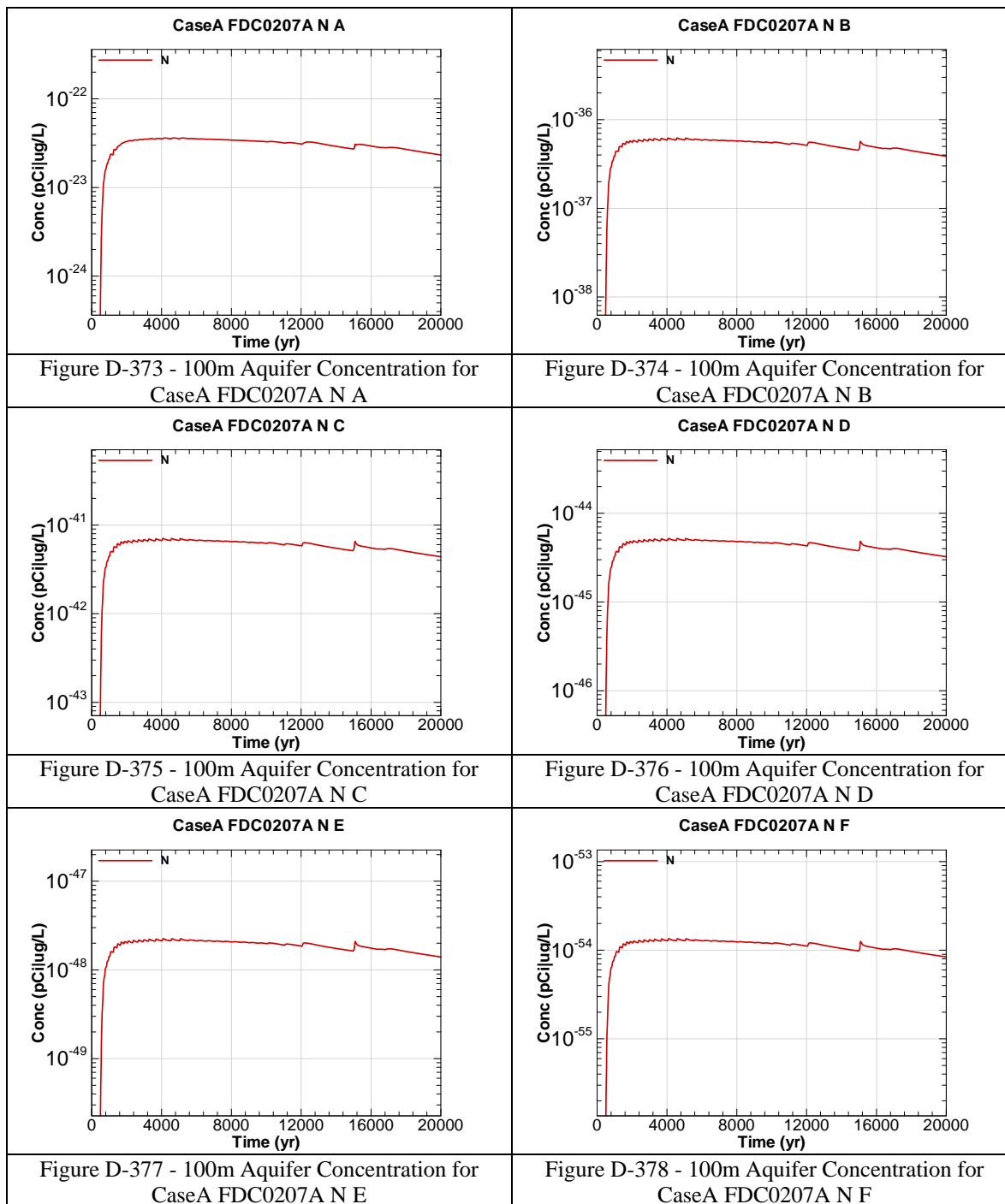


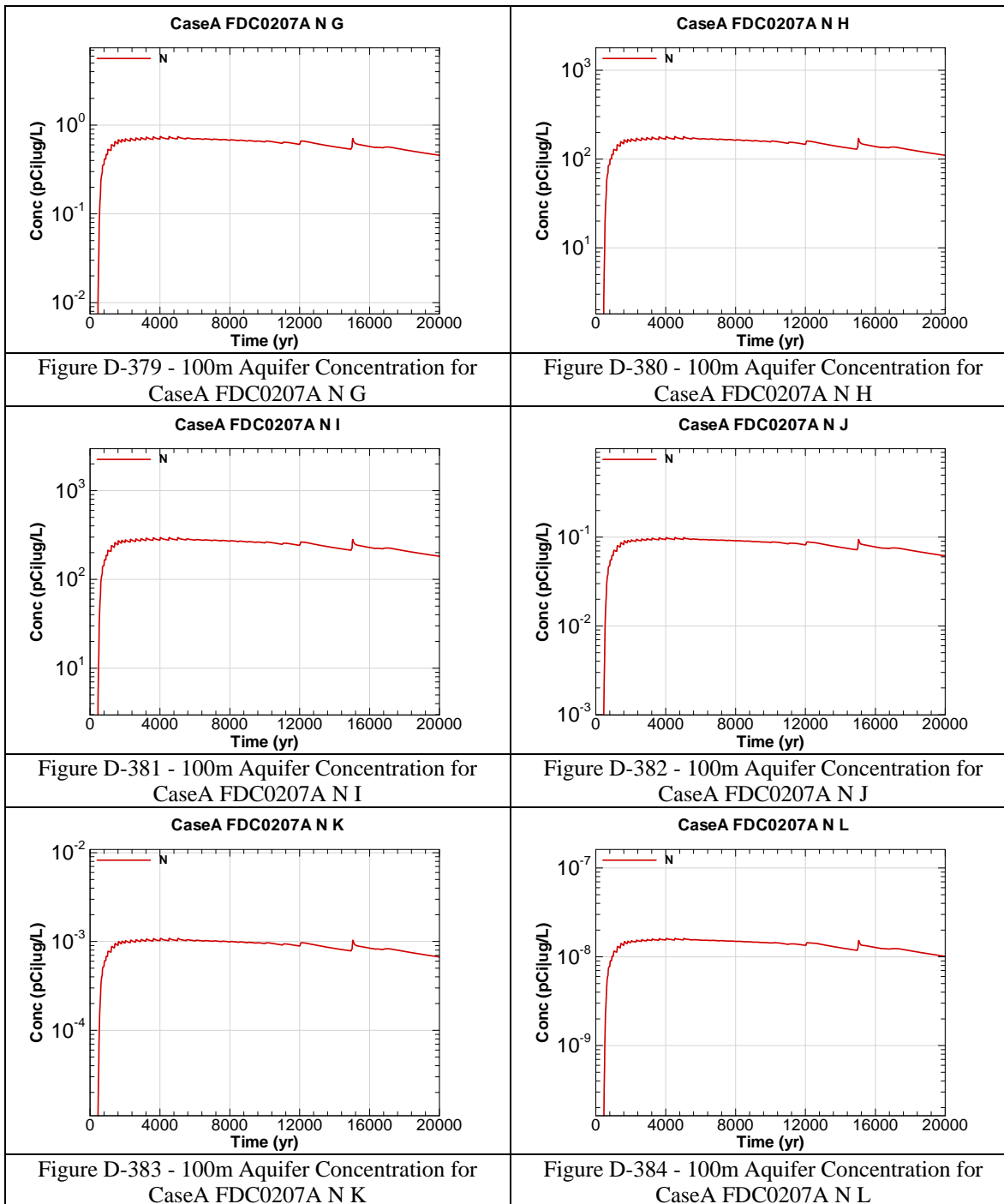












This page intentionally left blank

APPENDIX E.1

CONCENTRATIONS OF KEY RADIONUCLIDES AT 100-METERS AND THE SEEPLINE

Appendix E.1 is a comparison of key radionuclide peak concentrations at 100 meters to seepline concentrations. The concentrations are for the Base Case (Case A), at the peak sector.

Table E.1-1 – Key Radionuclide Peak Seepage and 100 Meter Concentrations for Sectors A - L

| Radionuclide | 20,000 Years Peak Seepage Concentration (pCi/L) | 20,000 Years Peak 100M Concentration (pCi/L) | | | | | |
|--------------|---|--|----------|----------|----------|----------|----------|
| | | Sector A | Sector B | Sector C | Sector D | Sector E | Sector F |
| I-129 | 3.1E+00 | 3.5E+00 | 4.0E+00 | 3.4E+00 | 2.8E+00 | 3.5E+00 | 2.3E+00 |
| Np-237 | 7.0E-02 | 1.8E-01 | 2.1E-01 | 2.0E-01 | 1.9E-02 | 4.6E-04 | 2.9E-04 |
| Pa-231 | 1.8E-02 | 4.3E-02 | 5.0E-02 | 4.7E-02 | 4.5E-03 | 2.2E-05 | 8.5E-06 |
| Ra-226 | 1.1E+00 | 2.7E+00 | 3.1E+00 | 3.0E+00 | 4.9E-01 | 2.7E-01 | 1.8E-01 |
| Tc-99 | 2.1E+02 | 5.6E+02 | 6.7E+02 | 6.5E+02 | 6.9E+01 | 7.2E+01 | 4.7E+01 |

| Radionuclide | 20,000 Years Peak Seepage Concentration (pCi/L) | 20,000 Years Peak 100M Concentration (pCi/L) | | | | | |
|--------------|---|--|----------|----------|----------|----------|----------|
| | | Sector G | Sector H | Sector I | Sector J | Sector K | Sector L |
| I-129 | 3.1E+00 | 8.3E+00 | 8.4E+00 | 9.5E+00 | 7.9E+00 | 8.5E+00 | 6.3E+00 |
| Np-237 | 7.0E-02 | 1.1E-03 | 1.1E-03 | 1.2E-03 | 1.0E-03 | 1.1E-03 | 8.1E-04 |
| Pa-231 | 1.8E-02 | 3.1E-05 | 3.1E-05 | 3.5E-05 | 2.9E-05 | 3.1E-05 | 2.7E-05 |
| Ra-226 | 1.1E+00 | 5.9E-01 | 5.9E-01 | 6.6E-01 | 5.4E-01 | 5.9E-01 | 4.3E-01 |
| Tc-99 | 2.1E+02 | 1.6E+02 | 1.7E+02 | 1.9E+02 | 1.6E+02 | 1.7E+02 | 1.2E+02 |

Table E.1-2 – Comparisons of Peak Seepage and 100 Meter Concentrations

| Radionuclide | 20,000 Years Peak Seepage Concentration (pCi/L) | 20,000 Years Peak 100M Concentration (pCi/L) | Ratio Peak Seepage to Peak 100M Concentration |
|--------------|---|--|---|
| I-129 | 3.1E+00 | 9.5E+00 | 33% |
| Np-237 | 7.0E-02 | 2.1E-01 | 33% |
| Pa-231 | 1.8E-02 | 5.0E-02 | 35% |
| Ra-226 | 1.1E+00 | 3.1E+00 | 34% |
| Tc-99 | 2.1E+02 | 6.7E+02 | 31% |

APPENDIX E.2

COMPARISON OF 100-METER CONCENTRATIONS PER AQUIFER

Appendix E.2 is a comparison of key radionuclide peak concentrations at 100 meters. The concentrations are for the Base Case (Case A) for the 3 aquifers, at each sector.

Key

UTR-U= Upper Three Runs – Upper Zone
UTR-L = Upper Three Runs – Lower Zone

Table E.2-1: Key Radionuclide Peak Concentrations Aquifer Comparisons, Sector A

| Nuclide | UTR-Upper | UTR-Lower | Gordon | UTR-U/UTR-L | Gordon/UTR-L |
|---------|-----------|-----------|----------|-------------|--------------|
| | (pCi/L) | (pCi/L) | (pCi/L) | | |
| I-129 | 3.80E-03 | 1.20E-01 | 2.60E-04 | 3.2% | 0.2% |
| Np-237 | 8.18E-06 | 1.40E-03 | 7.90E-08 | 0.6% | < 0.1% |
| Pa-231 | 5.47E-07 | 9.00E-05 | 4.70E-09 | 0.6% | < 0.1% |
| Ra226 | 9.00E-03 | 1.30E+00 | 2.10E-04 | 0.7% | < 0.1% |
| Tc-99 | 8.00E-02 | 1.30E+01 | 6.60E-03 | 0.6% | < 0.1% |

Table E.2-2: Key Radionuclide Peak Concentrations Aquifer Comparisons, Sector B

| Nuclide | UTR-Upper | UTR-Lower | Gordon | UTR-U/UTR-L | Gordon/UTR-L |
|---------|-----------|-----------|----------|-------------|--------------|
| | (pCi/L) | (pCi/L) | (pCi/L) | | |
| I-129 | 4.60E-02 | 1.40E-01 | 2.30E-04 | 32.9% | 0.2% |
| Np-237 | 5.29E-04 | 1.60E-03 | 6.70E-08 | 33.1% | < 0.1% |
| Pa-231 | 3.54E-05 | 1.00E-04 | 4.00E-09 | 35.4% | < 0.1% |
| Ra226 | 5.30E-01 | 1.50E+00 | 1.80E-04 | 35.3% | < 0.1% |
| Tc-99 | 5.50E+00 | 1.60E+01 | 5.80E-03 | 34.4% | < 0.1% |

Table E.2-3: Key Radionuclide Peak Concentrations Aquifer Comparisons, Sector C

| Nuclide | UTR-Upper | UTR-Lower | Gordon | UTR-U/UTR-L | Gordon/UTR-L |
|---------|-----------|-----------|----------|-------------|--------------|
| | (pCi/L) | (pCi/L) | (pCi/L) | | |
| I-129 | 6.70E-02 | 1.10E-01 | 1.30E-04 | 60.9% | 0.1% |
| Np-237 | 5.88E-04 | 1.50E-03 | 3.00E-08 | 39.2% | < 0.1% |
| Pa-231 | 3.93E-05 | 9.80E-05 | 1.80E-09 | 40.1% | < 0.1% |
| Ra226 | 6.00E-01 | 1.50E+00 | 8.40E-05 | 40.0% | < 0.1% |
| Tc-99 | 6.10E+00 | 1.50E+01 | 2.80E-03 | 40.7% | < 0.1% |

Table E.2-4: Key Radionuclide Peak Concentrations Aquifer Comparisons, Sector D

| Nuclide | UTR-Upper | UTR-Lower | Gordon | UTR-U/UTR-L | Gordon/UTR-L |
|---------|-----------|-----------|----------|-------------|--------------|
| | (pCi/L) | (pCi/L) | (pCi/L) | | |
| I-129 | 6.10E-02 | 8.70E-02 | 6.00E-05 | 70.1% | 0.1% |
| Np-237 | 1.22E-04 | 1.40E-04 | 1.30E-09 | 87.4% | < 0.1% |
| Pa-231 | 8.28E-06 | 9.80E-06 | 8.10E-11 | 84.5% | < 0.1% |
| Ra226 | 1.50E-01 | 1.90E-01 | 5.60E-06 | 78.9% | < 0.1% |
| Tc-99 | 1.30E+00 | 1.60E+00 | 1.80E-04 | 81.3% | < 0.1% |

Table E.2-5: Key Radionuclide Peak Concentrations Aquifer Comparisons, Sector E

| Nuclide | UTR-Upper | UTR-Lower | Gordon | UTR-U/UTR-L | Gordon/UTR-L |
|---------|-----------|-----------|----------|-------------|--------------|
| | (pCi/L) | (pCi/L) | (pCi/L) | | |
| I-129 | 7.20E-02 | 9.90E-02 | 7.30E-05 | 72.7% | 0.1% |
| Np-237 | 5.69E-07 | 7.20E-07 | 1.00E-11 | 79.0% | < 0.1% |
| Pa-231 | 5.50E-08 | 7.10E-08 | 1.00E-12 | 77.5% | < 0.1% |
| Ra226 | 1.50E-02 | 2.00E-02 | 7.10E-07 | 75.0% | < 0.1% |
| Tc-99 | 1.30E-02 | 1.70E-02 | 4.60E-06 | 76.5% | < 0.1% |

Table E.2-6: Key Radionuclide Peak Concentrations Aquifer Comparisons, Sector F

| Nuclide | UTR-Upper | UTR-Lower | Gordon | UTR-U/UTR-L | Gordon/UTR-L |
|---------|-----------|-----------|----------|-------------|--------------|
| | (pCi/L) | (pCi/L) | (pCi/L) | | |
| I-129 | 4.60E-02 | 6.40E-02 | 3.00E-05 | 71.9% | < 0.1% |
| Np-237 | 2.38E-12 | 4.20E-12 | 2.20E-16 | 56.6% | < 0.1% |
| Pa-231 | 5.91E-13 | 1.00E-12 | 2.60E-17 | 59.1% | < 0.1% |
| Ra226 | 9.50E-03 | 1.30E-02 | 2.40E-07 | 73.1% | < 0.1% |
| Tc-99 | 4.50E-07 | 7.10E-07 | 2.30E-10 | 63.4% | < 0.1% |

Table E.2-7: Key Radionuclide Peak Concentrations Aquifer Comparisons, Sector G

| Nuclide | UTR-Upper | UTR-Lower | Gordon | UTR-U/UTR-L | Gordon/UTR-L |
|---------|-----------|-----------|----------|-------------|--------------|
| | (pCi/L) | (pCi/L) | (pCi/L) | | |
| I-129 | 1.00E-01 | 2.30E-01 | 1.60E-03 | 43.5% | 0.7% |
| Np-237 | 1.48E-15 | 1.30E-13 | 5.50E-08 | 1.1% | > 100% |
| Pa-231 | 1.24E-16 | 1.80E-14 | 3.30E-09 | 0.7% | > 100% |
| Ra226 | 2.10E-02 | 4.40E-02 | 1.50E-04 | 47.7% | 0.3% |
| Tc-99 | 5.60E-07 | 1.40E-06 | 4.90E-03 | 40.0% | > 100% |

Table E.2-8: Key Radionuclide Peak Concentrations Aquifer Comparisons, Sector H

| Nuclide | UTR-Upper | UTR-Lower | Gordon | UTR-U/UTR-L | Gordon/UTR-L |
|---------|-----------|-----------|----------|-------------|--------------|
| | (pCi/L) | (pCi/L) | (pCi/L) | | |
| I-129 | 6.60E-03 | 2.30E-01 | 1.80E-03 | 2.9% | 0.8% |
| Np-237 | 1.62E-17 | 4.40E-13 | 7.00E-08 | < 0.1% | > 100% |
| Pa-231 | 4.13E-18 | 1.10E-13 | 4.10E-09 | < 0.1% | > 100% |
| Ra226 | 1.40E-03 | 4.40E-02 | 1.80E-04 | 3.2% | 0.4% |
| Tc-99 | 3.60E-08 | 1.40E-06 | 5.90E-03 | 2.6% | > 100% |

Table E.2-9: Key Radionuclide Peak Concentrations Aquifer Comparisons, Sector I

| Nuclide | UTR-Upper | UTR-Lower | Gordon | UTR-U/UTR-L | Gordon/UTR-L |
|---------|-----------|-----------|----------|-------------|--------------|
| | (pCi/L) | (pCi/L) | (pCi/L) | | |
| I-129 | 2.10E-02 | 2.60E-01 | 1.90E-03 | 8.1% | 0.7% |
| Np-237 | 6.27E-16 | 5.50E-12 | 6.60E-08 | < 0.1% | > 100% |
| Pa-231 | 1.63E-16 | 1.40E-12 | 3.90E-09 | < 0.1% | > 100% |
| Ra226 | 4.20E-03 | 4.90E-02 | 1.70E-04 | 8.6% | 0.3% |
| Tc-99 | 1.10E-07 | 1.80E-06 | 5.40E-03 | 6.1% | > 100% |

Table E.2-10: Key Radionuclide Peak Concentrations Aquifer Comparisons, Sector J

| Nuclide | UTR-Upper | UTR-Lower | Gordon | UTR-U/UTR-L | Gordon/UTR-L |
|---------|-----------|-----------|----------|-------------|--------------|
| | (pCi/L) | (pCi/L) | (pCi/L) | | |
| I-129 | 9.70E-03 | 2.20E-01 | 1.40E-03 | 4.4% | 0.6% |
| Np-237 | 8.62E-15 | 6.50E-11 | 3.20E-08 | < 0.1% | > 100% |
| Pa-231 | 2.25E-15 | 1.70E-11 | 1.90E-09 | < 0.1% | > 100% |
| Ra226 | 1.90E-03 | 4.00E-02 | 8.30E-05 | 4.8% | 0.2% |
| Tc-99 | 5.20E-08 | 7.30E-06 | 2.60E-03 | 0.7% | > 100% |

Table E.2-11: Key Radionuclide Peak Concentrations Aquifer Comparisons, Sector K

| Nuclide | UTR-Upper | UTR-Lower | Gordon | UTR-U/UTR-L | Gordon/UTR-L |
|---------|-----------|-----------|----------|-------------|--------------|
| | (pCi/L) | (pCi/L) | (pCi/L) | | |
| I-129 | 2.60E-03 | 2.40E-01 | 8.90E-04 | 1.1% | 0.4% |
| Np-237 | 1.32E-11 | 9.20E-10 | 2.70E-08 | 1.4% | > 100% |
| Pa-231 | 3.42E-12 | 2.40E-10 | 1.60E-09 | 1.4% | > 100% |
| Ra226 | 4.80E-04 | 4.40E-02 | 7.00E-05 | 1.1% | 0.2% |
| Tc-99 | 1.20E-06 | 8.70E-05 | 2.20E-03 | 1.4% | > 100% |

Table E.2-12: Key Radionuclide Peak Concentrations Aquifer Comparisons, Sector L

| Nuclide | UTR-Upper | UTR-Lower | Gordon | UTR-U/UTR-L | Gordon/UTR-L |
|---------|-----------|-----------|----------|-------------|--------------|
| | (pCi/L) | (pCi/L) | (pCi/L) | | |
| I-129 | 9.50E-03 | 1.70E-01 | 4.80E-04 | 5.6% | 0.3% |
| Np-237 | 1.30E-07 | 8.70E-07 | 5.50E-08 | 15.0% | 6.3% |
| Pa-231 | 1.01E-08 | 6.80E-08 | 3.30E-09 | 14.8% | 4.9% |
| Ra226 | 1.80E-03 | 3.20E-02 | 1.40E-04 | 5.6% | 0.4% |
| Tc-99 | 1.90E-03 | 1.30E-02 | 4.50E-03 | 14.6% | 34.6% |

This page intentionally left blank

APPENDIX F.1

1-METER RADIOLOGICAL AND CHEMICAL CONCENTRATIONS AT THE UPPER THREE RUNS AQUIFER - UPPER ZONE

Appendix F.1 contains curves showing the 1 meter radiological and chemical concentrations for all of SDF (vault and FDC inventories) for the Base Case (Case A). 20,000 year concentration results are presented from the Upper Three Runs Aquifer-Upper Zone for Sectors A through L

Graph heading example “CaseA All Ac-227 1A_UA”

Key

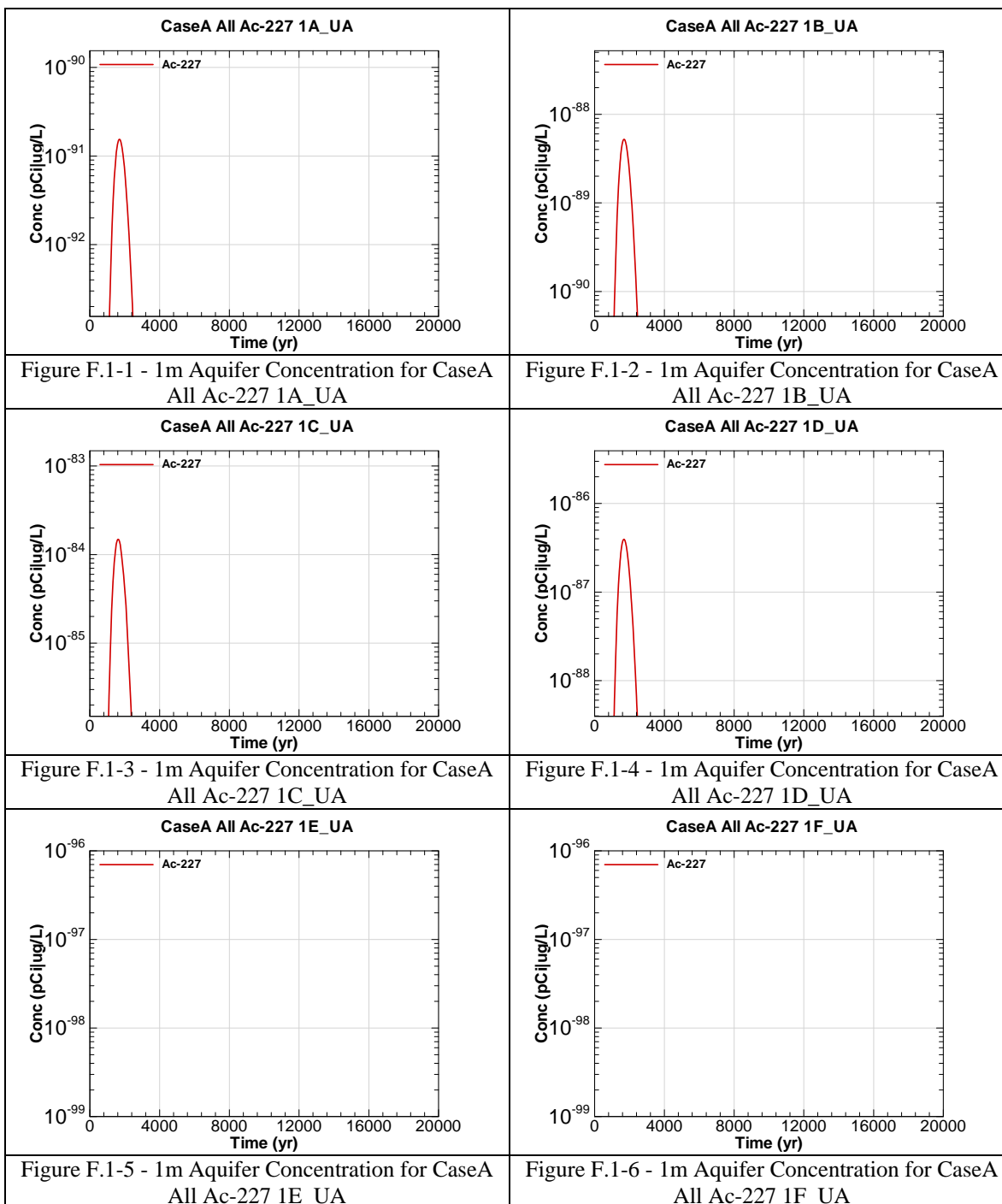
CaseA = Scenario case

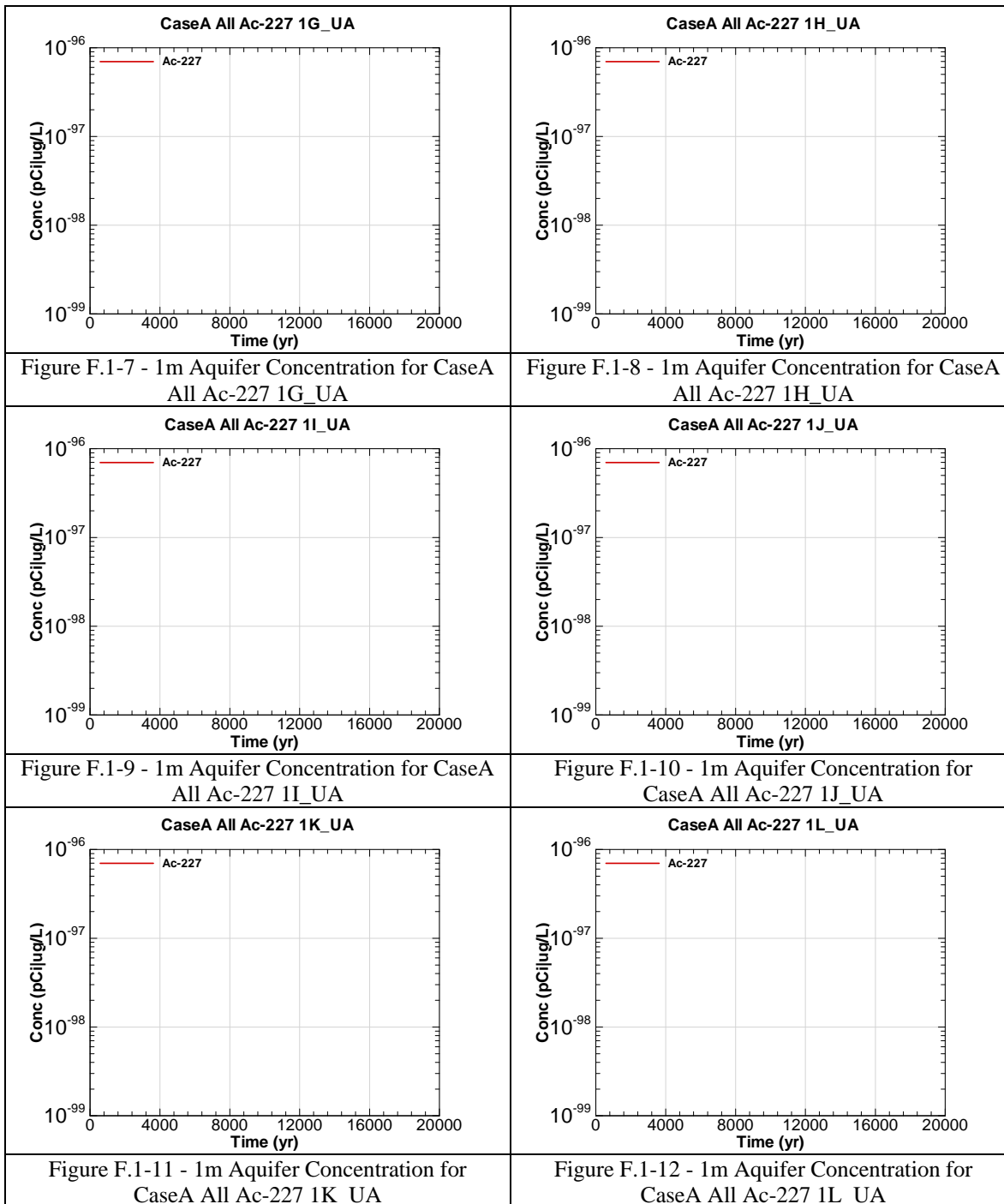
All = Inventory source is all disposal units

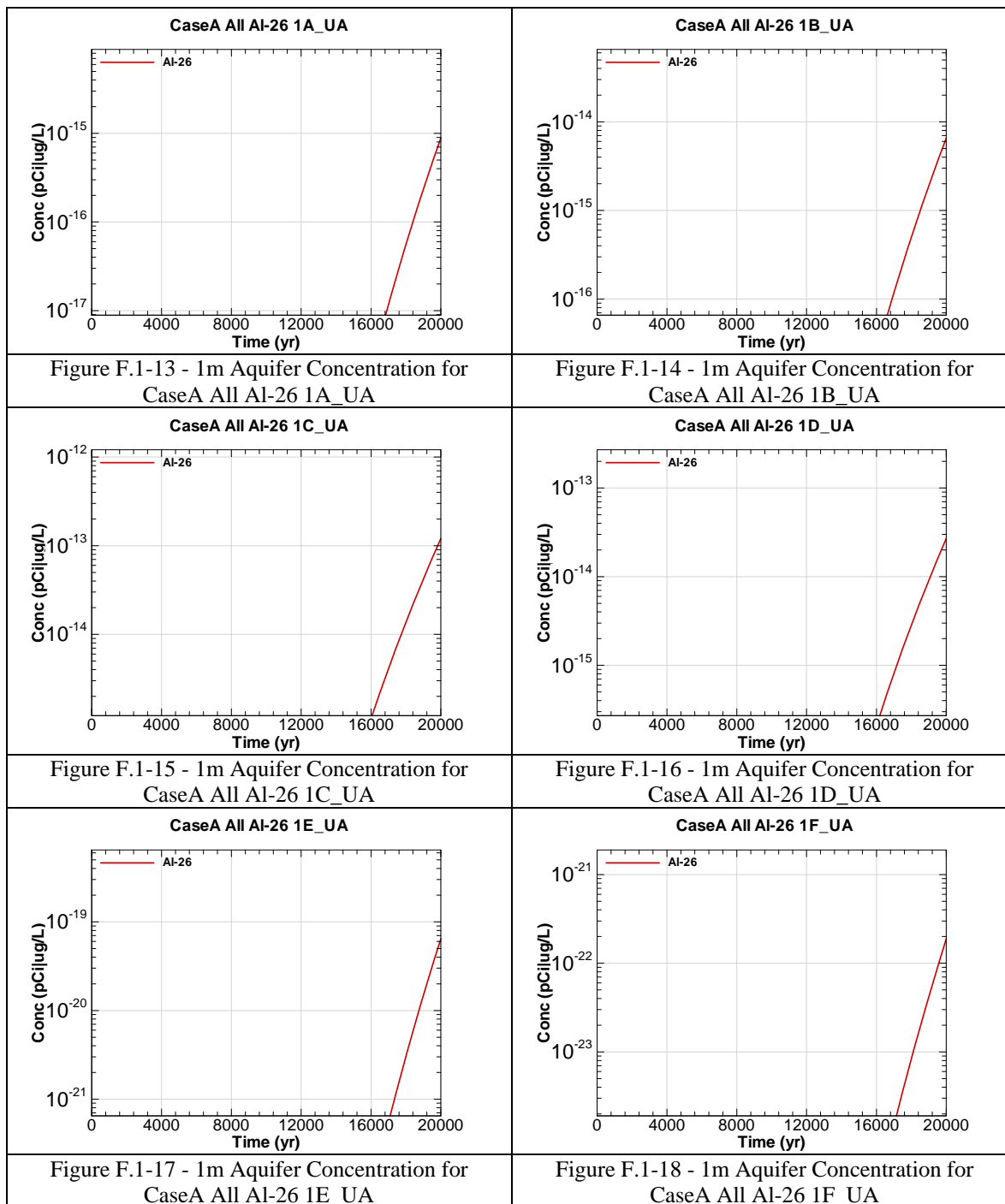
Ac-227 = Radionuclide or chemical of concern

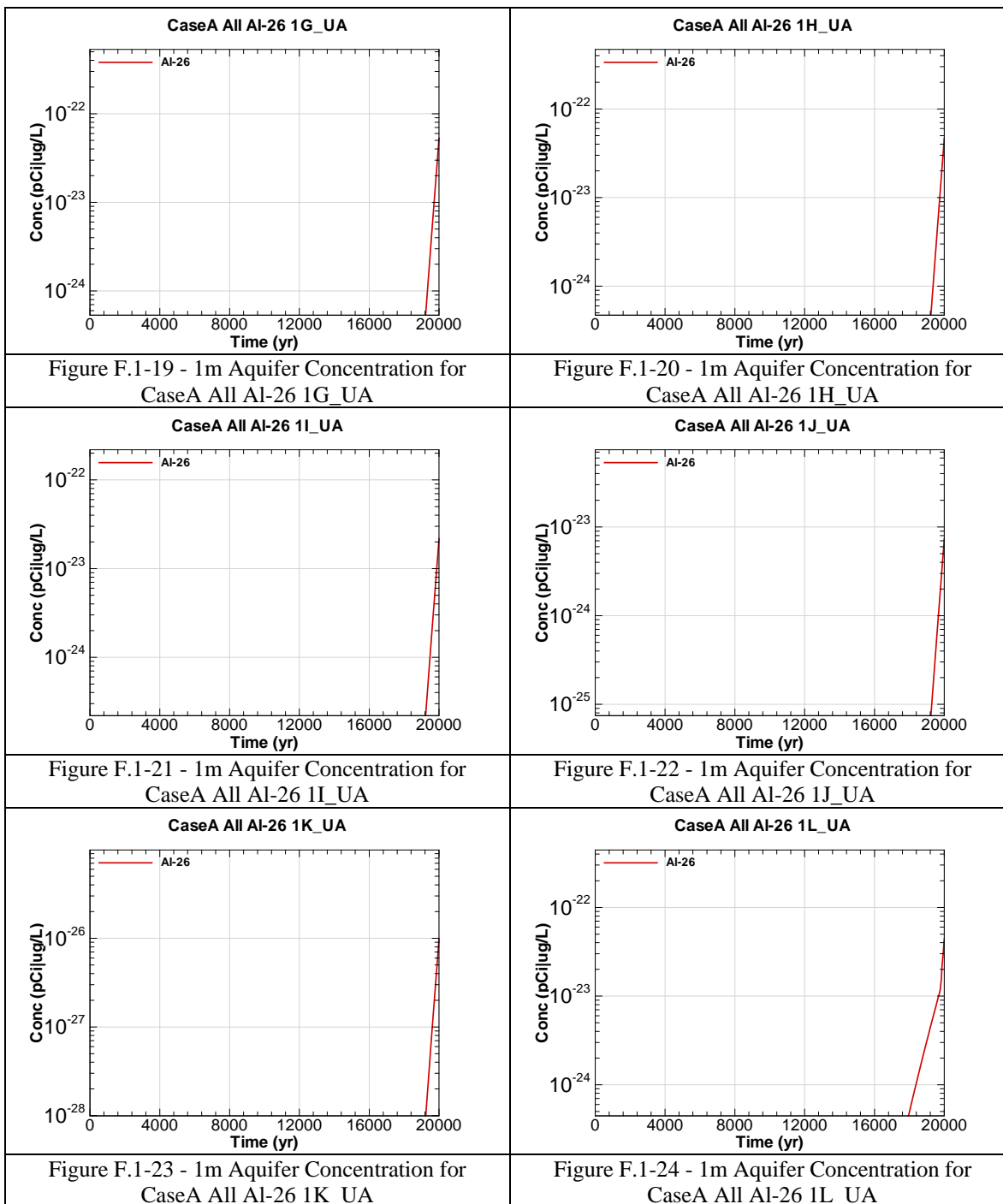
1A = 1 meter evaluation sector of concern

UA = Aquifer of concern is Upper Three Runs Aquifer – Upper Zone









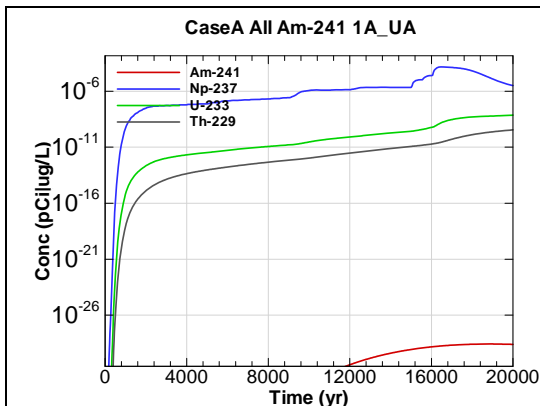


Figure F.1-25 - 1m Aquifer Concentration for
CaseA All Am-241 1A_UA

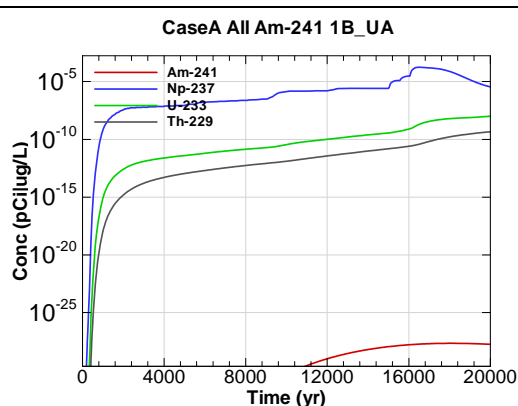


Figure F.1-26 - 1m Aquifer Concentration for
CaseA All Am-241 1B_UA

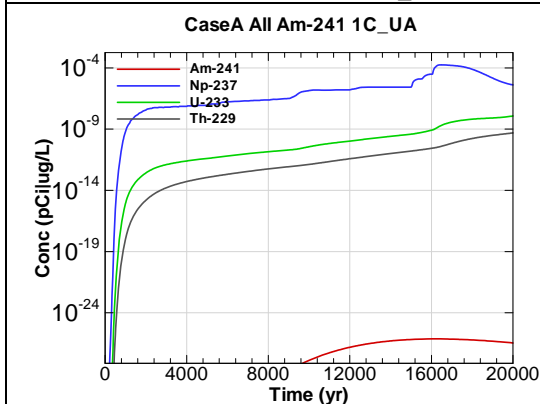


Figure F.1-27 - 1m Aquifer Concentration for
CaseA All Am-241 1C_UA

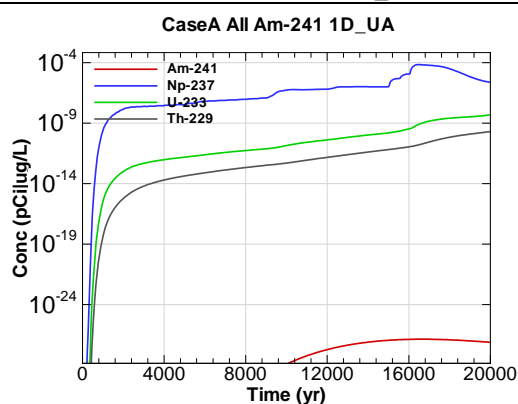


Figure F.1-28 - 1m Aquifer Concentration for
CaseA All Am-241 1D_UA

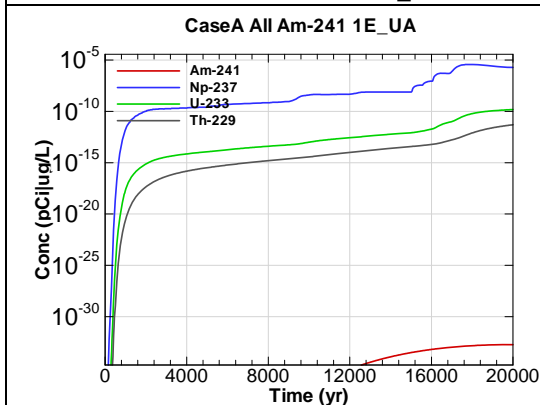


Figure F.1-29 - 1m Aquifer Concentration for
CaseA All Am-241 1E_UA

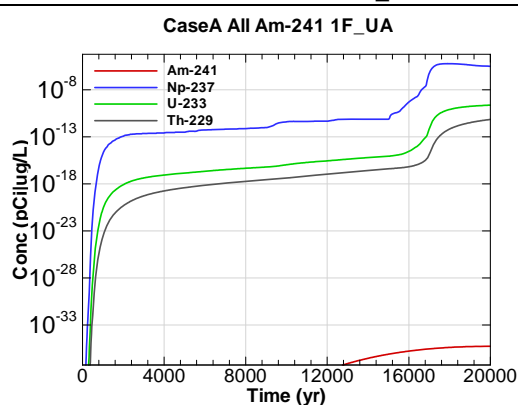
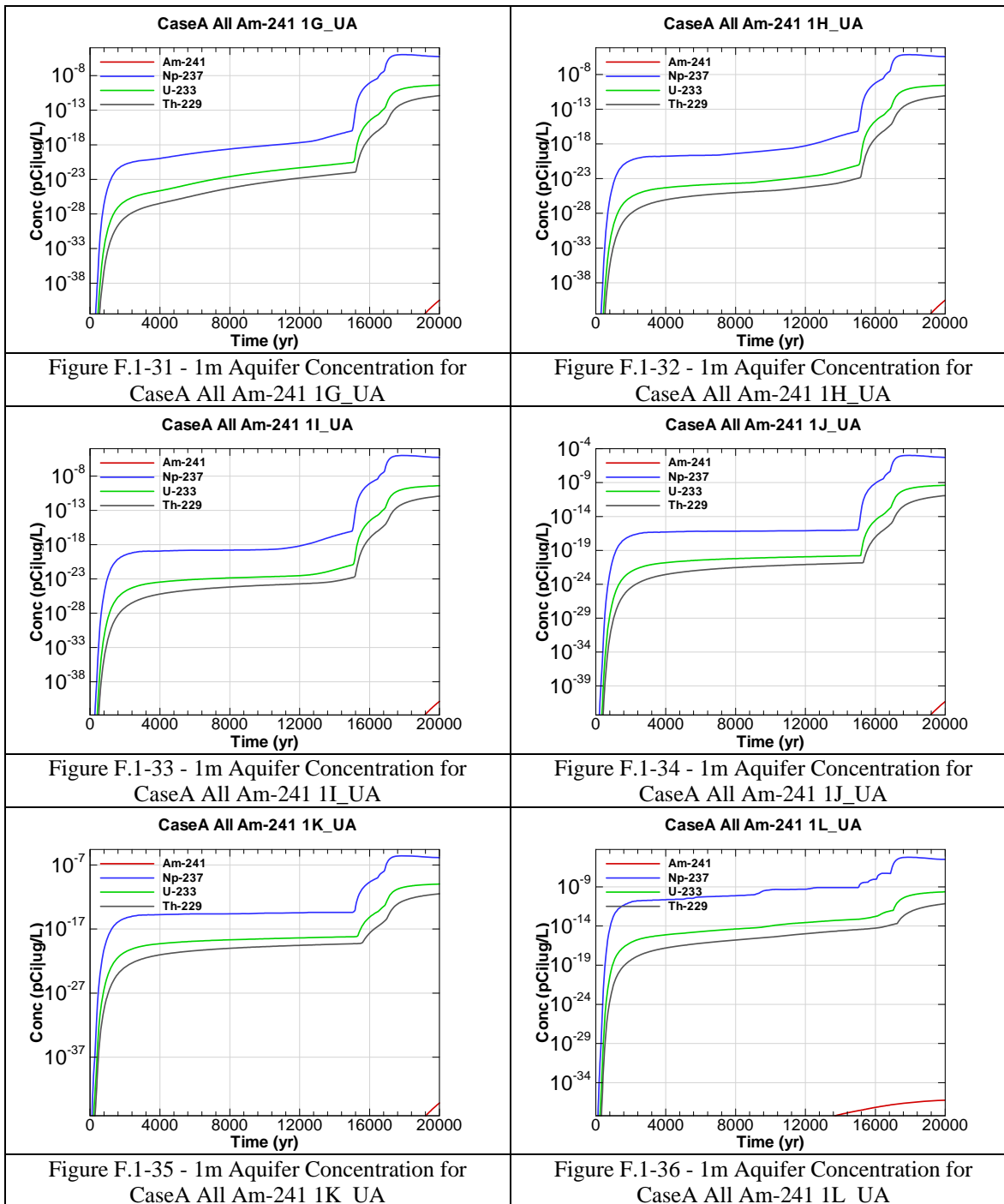


Figure F.1-30 - 1m Aquifer Concentration for
CaseA All Am-241 1F_UA



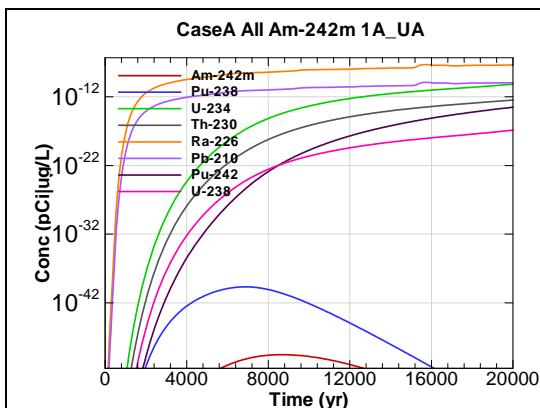


Figure F.1-37 - 1m Aquifer Concentration for
CaseA All Am-242m 1A_UA

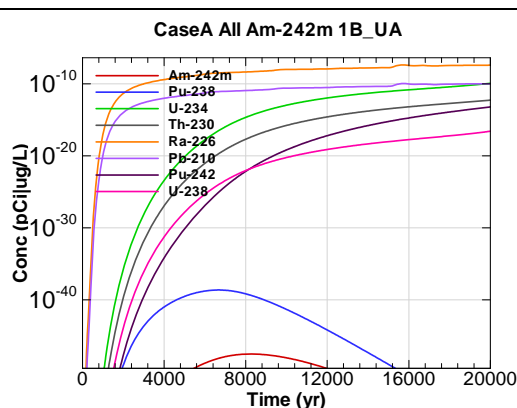


Figure F.1-38 - 1m Aquifer Concentration for
CaseA All Am-242m 1B_UA

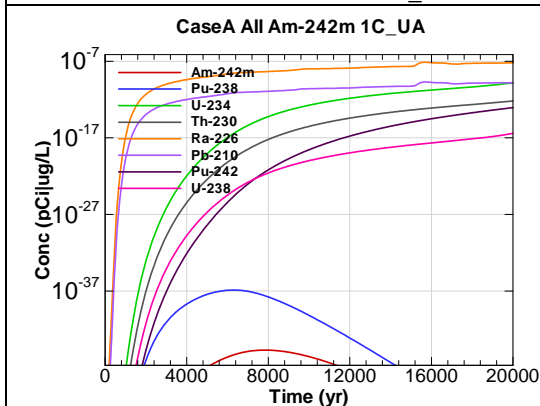


Figure F.1-39 - 1m Aquifer Concentration for
CaseA All Am-242m 1C_UA

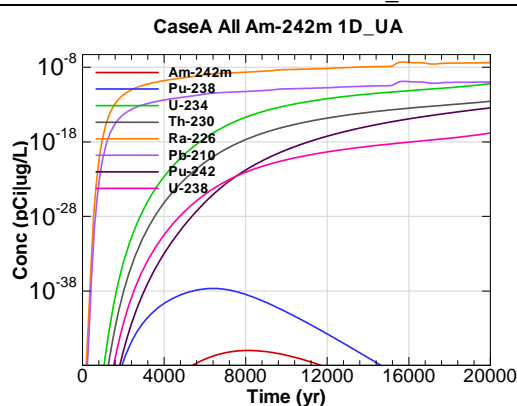


Figure F.1-40 - 1m Aquifer Concentration for
CaseA All Am-242m 1D_UA

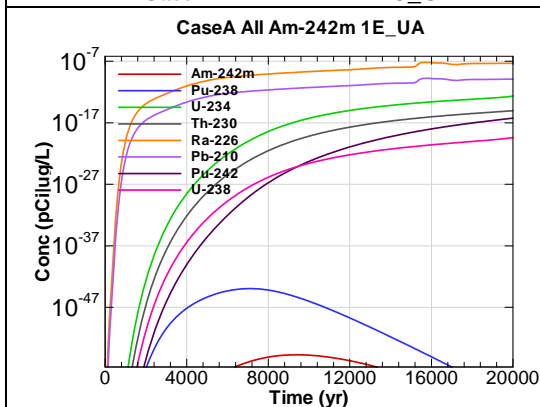


Figure F.1-41 - 1m Aquifer Concentration for
CaseA All Am-242m 1E_UA

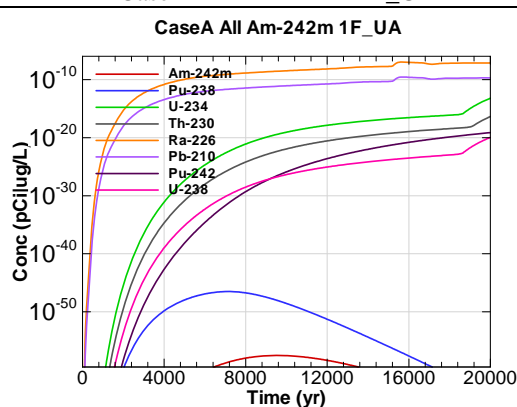


Figure F.1-42 - 1m Aquifer Concentration for
CaseA All Am-242m 1F_UA

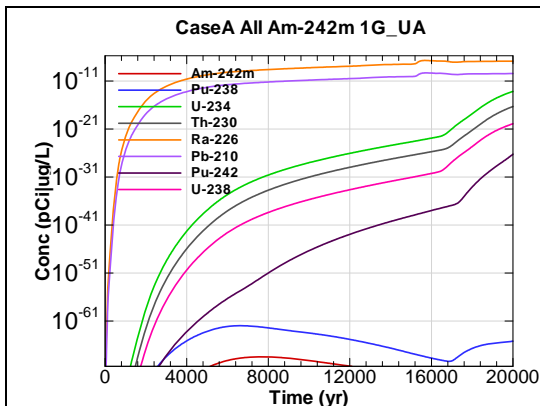


Figure F.1-43 - 1m Aquifer Concentration for
CaseA All Am-242m 1G_UA

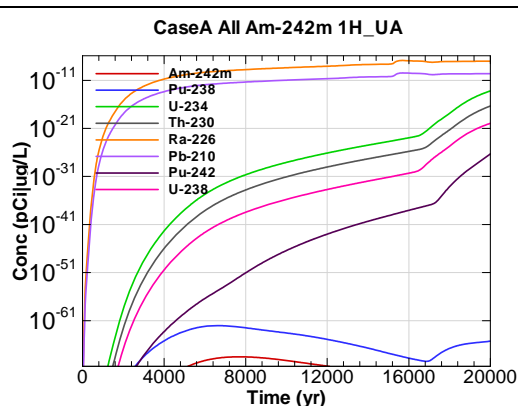


Figure F.1-44 - 1m Aquifer Concentration for
CaseA All Am-242m 1H_UA

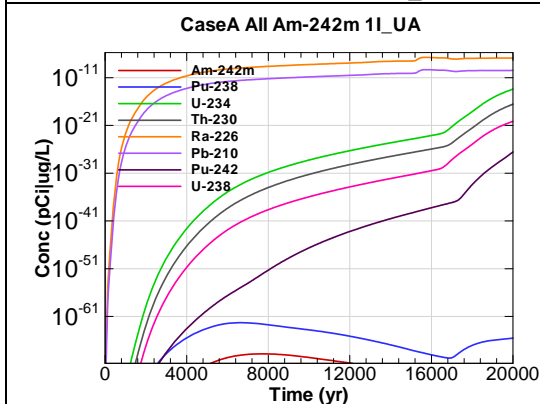


Figure F.1-45 - 1m Aquifer Concentration for
CaseA All Am-242m 1I_UA

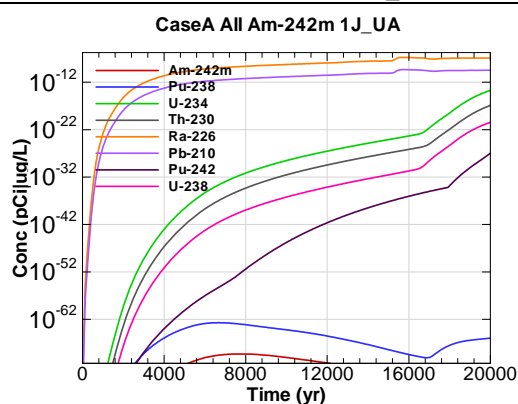


Figure F.1-46 - 1m Aquifer Concentration for
CaseA All Am-242m 1J_UA

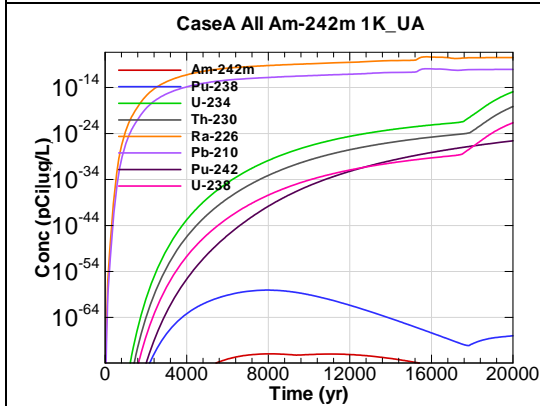


Figure F.1-47 - 1m Aquifer Concentration for
CaseA All Am-242m 1K_UA

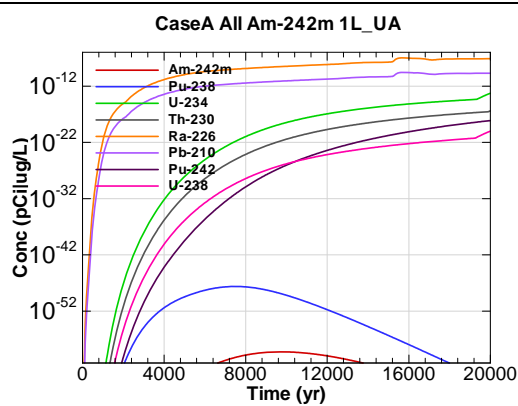


Figure F.1-48 - 1m Aquifer Concentration for
CaseA All Am-242m 1L_UA

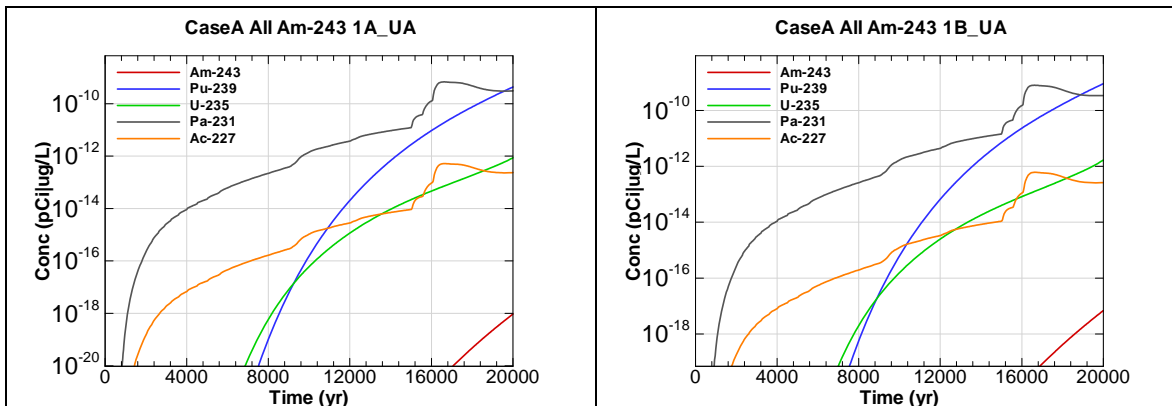


Figure F.1-49 - 1m Aquifer Concentration for
CaseA All Am-243 1A_UA

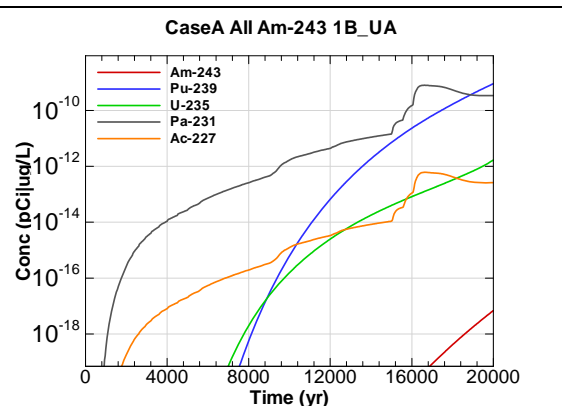


Figure F.1-50 - 1m Aquifer Concentration for
CaseA All Am-243 1B_UA

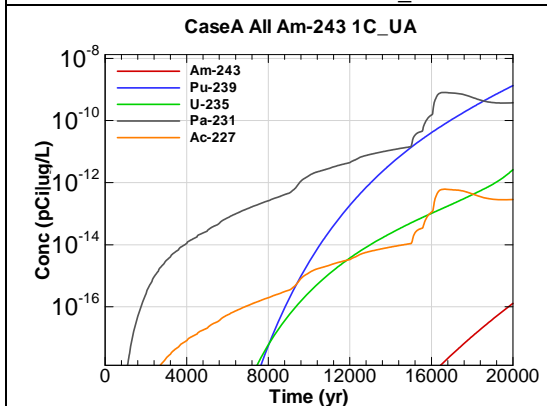


Figure F.1-51 - 1m Aquifer Concentration for
CaseA All Am-243 1C_UA

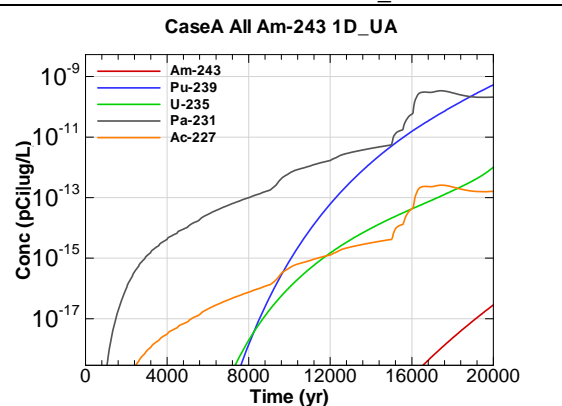


Figure F.1-52 - 1m Aquifer Concentration for
CaseA All Am-243 1D_UA

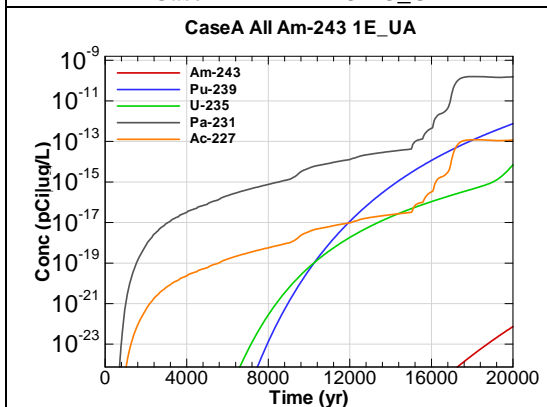


Figure F.1-53 - 1m Aquifer Concentration for
CaseA All Am-243 1E_UA

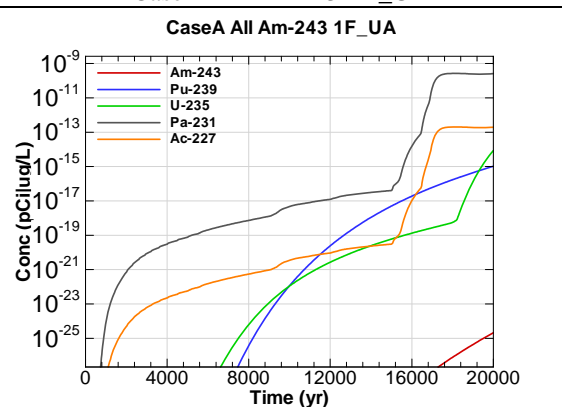
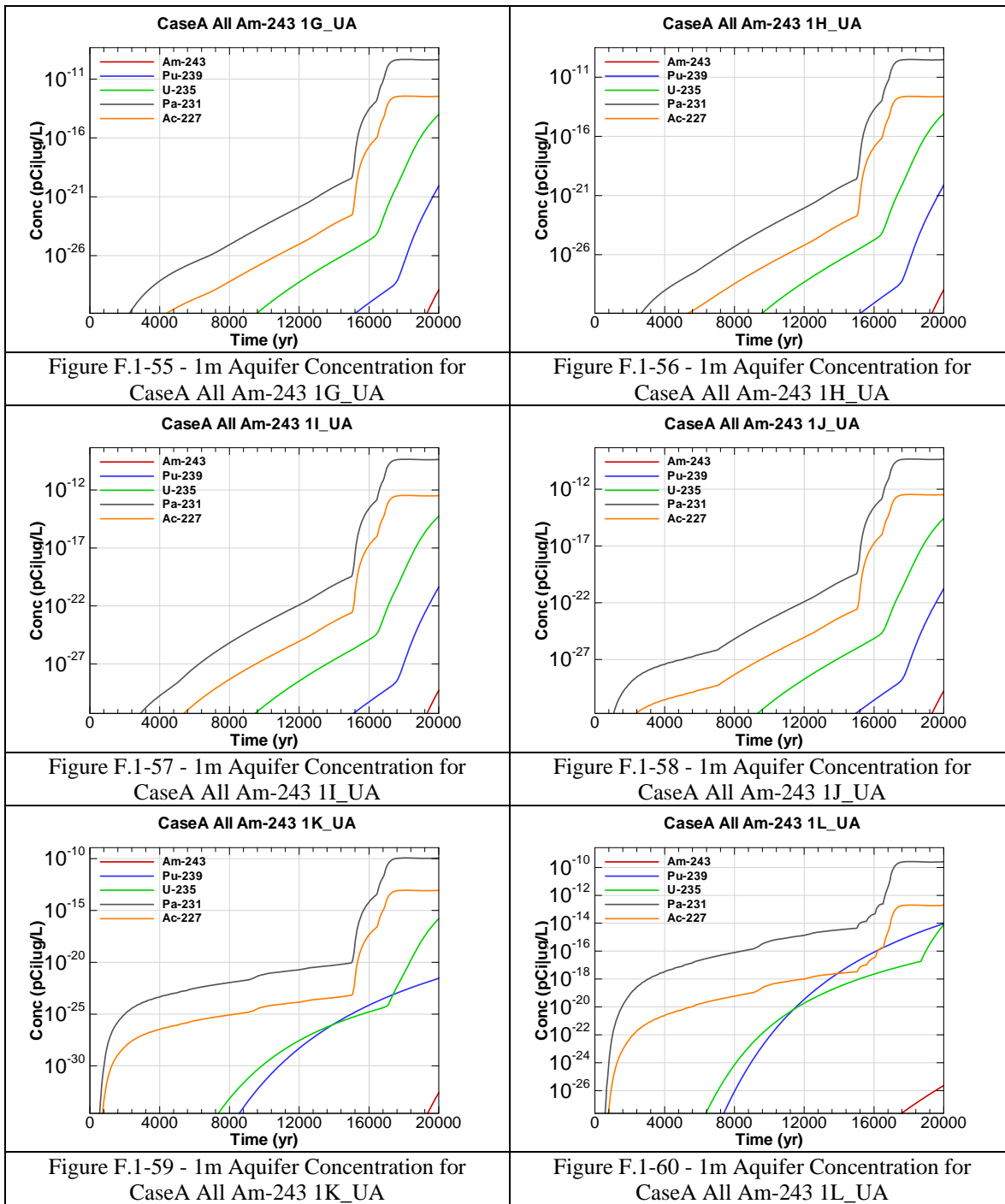
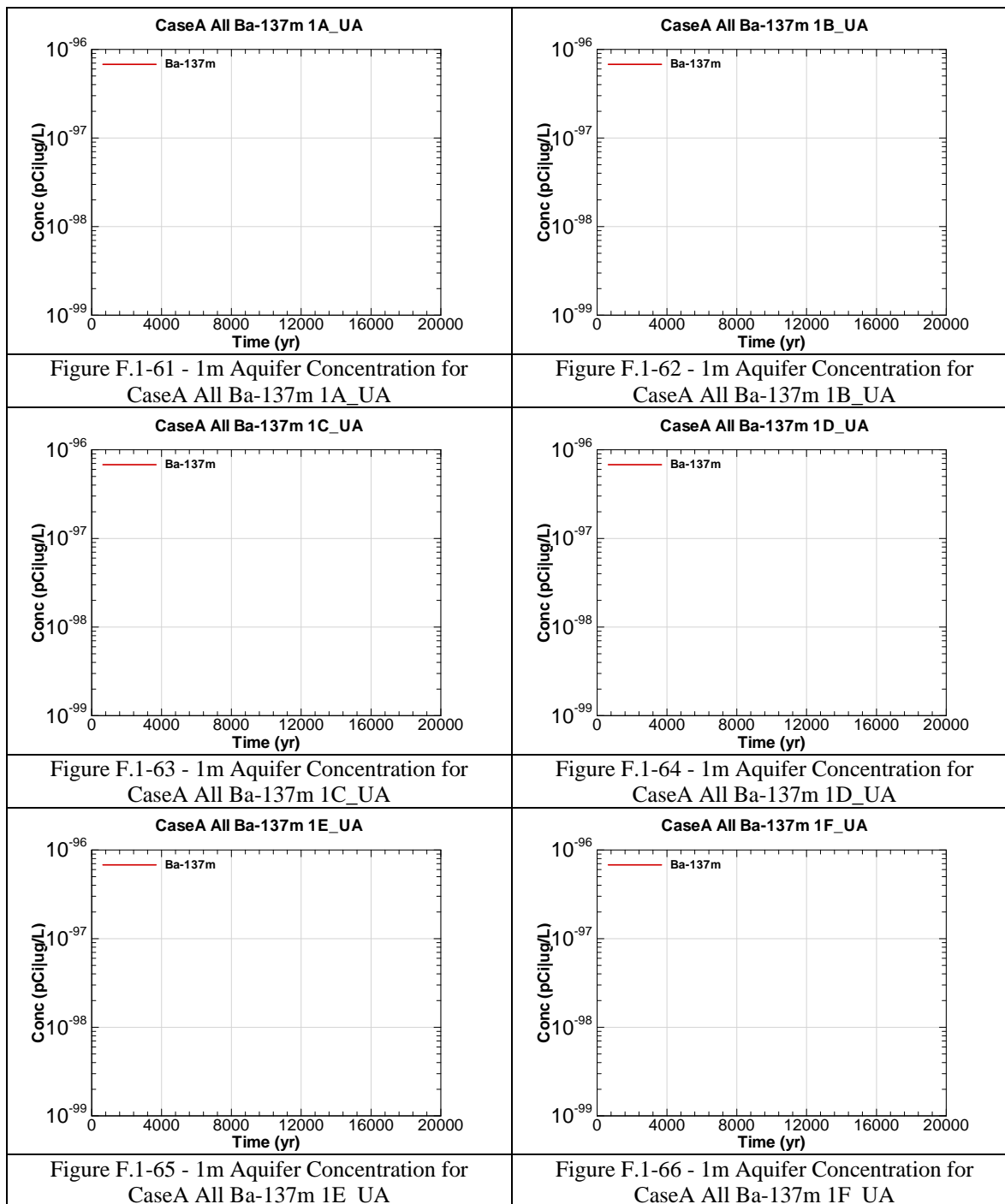
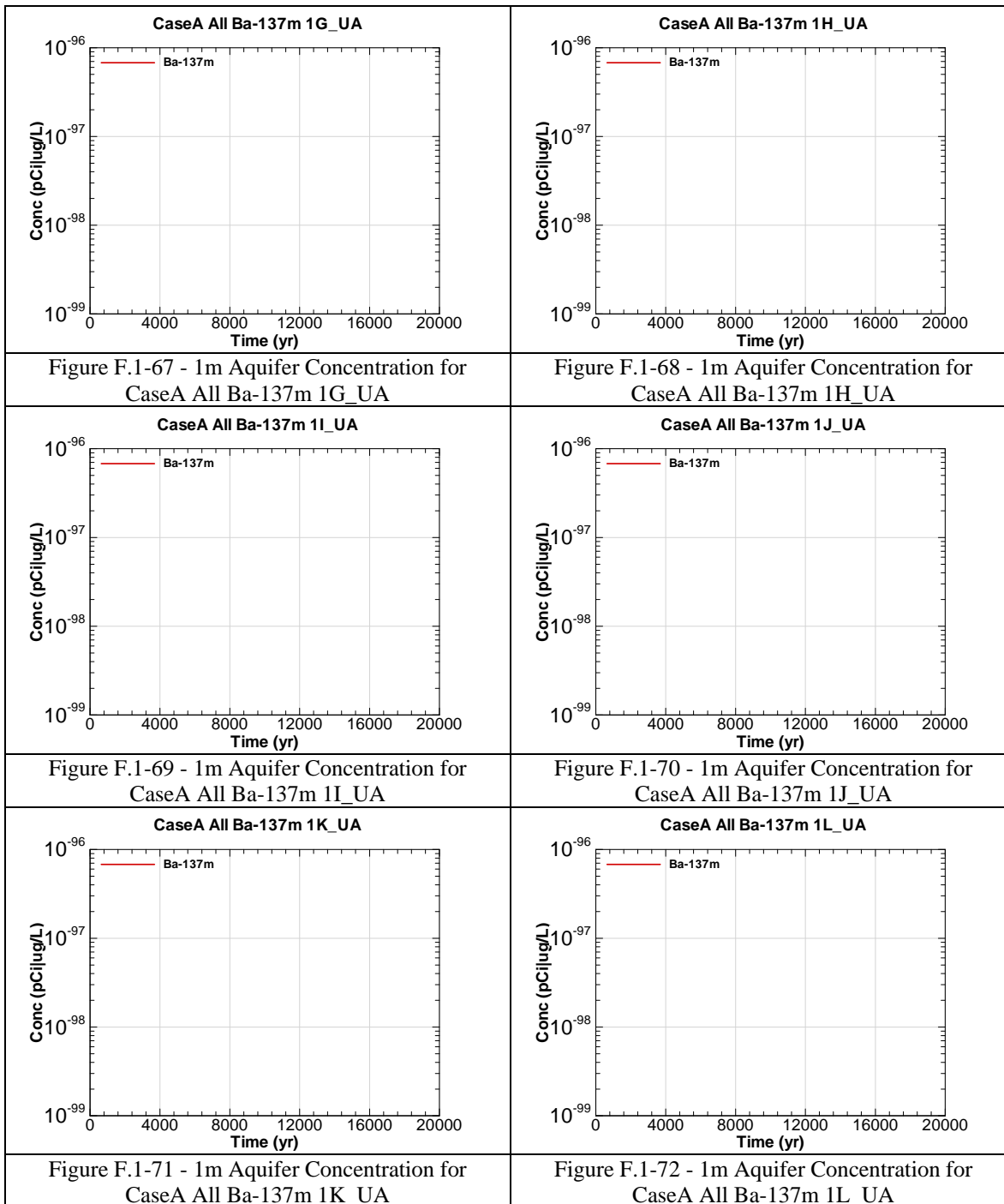


Figure F.1-54 - 1m Aquifer Concentration for
CaseA All Am-243 1F_UA







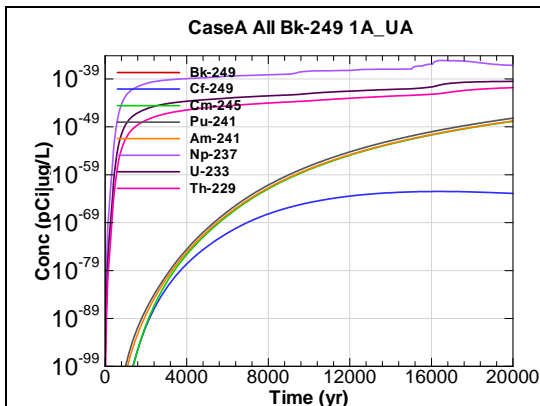


Figure F.1-73 - 1m Aquifer Concentration for
CaseA All Bk-249 1A_UA

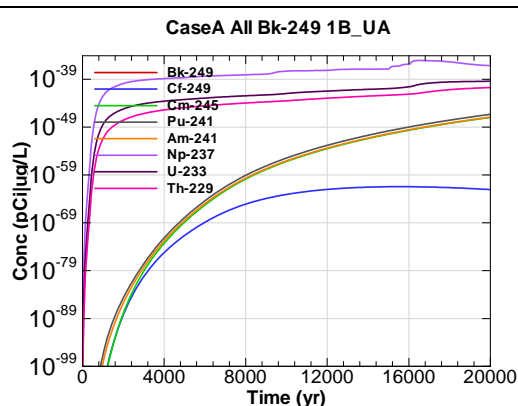


Figure F.1-74 - 1m Aquifer Concentration for
CaseA All Bk-249 1B_UA

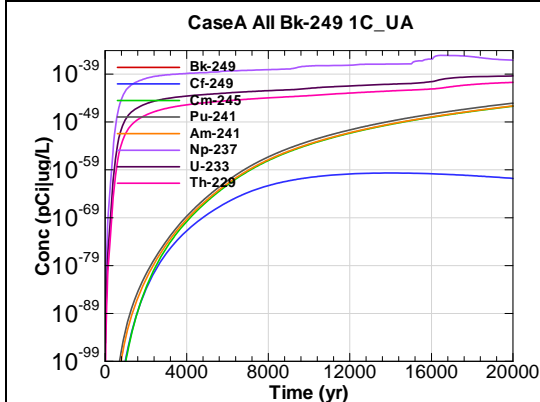


Figure F.1-75 - 1m Aquifer Concentration for
CaseA All Bk-249 1C_UA

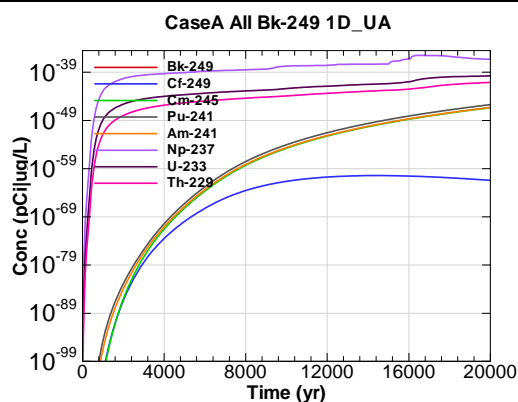


Figure F.1-76 - 1m Aquifer Concentration for
CaseA All Bk-249 1D_UA

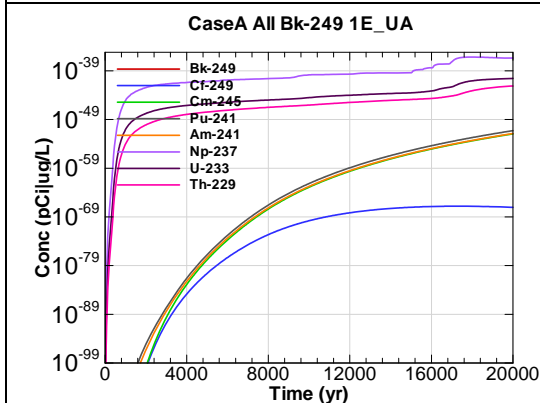


Figure F.1-77 - 1m Aquifer Concentration for
CaseA All Bk-249 1E_UA

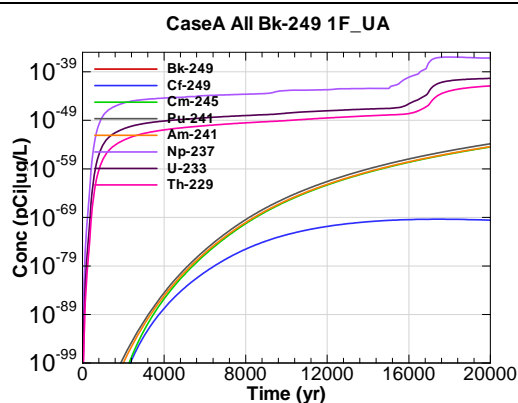


Figure F.1-78 - 1m Aquifer Concentration for
CaseA All Bk-249 1F_UA

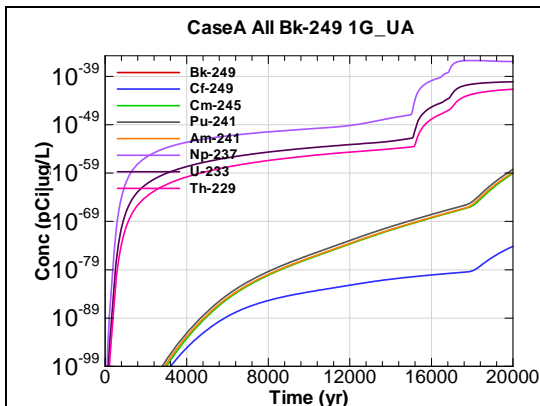


Figure F.1-79 - 1m Aquifer Concentration for
CaseA All Bk-249 1G_UA

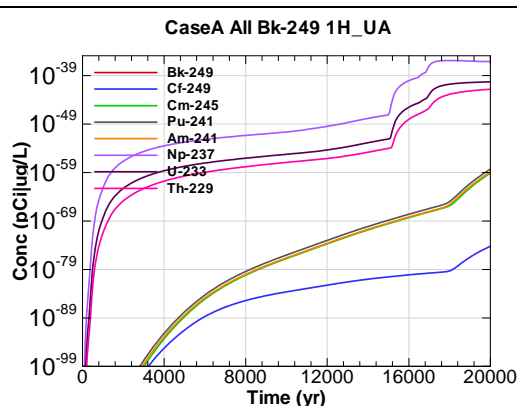


Figure F.1-80 - 1m Aquifer Concentration for
CaseA All Bk-249 1H_UA

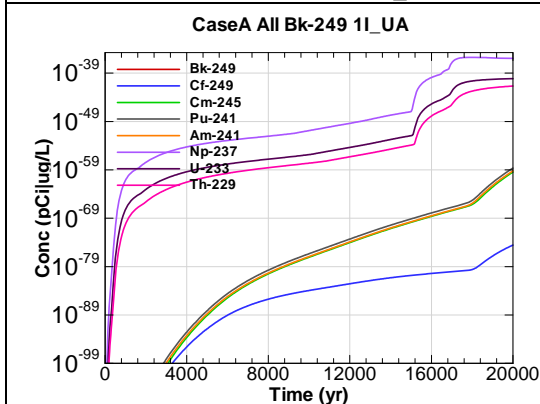


Figure F.1-81 - 1m Aquifer Concentration for
CaseA All Bk-249 1I_UA

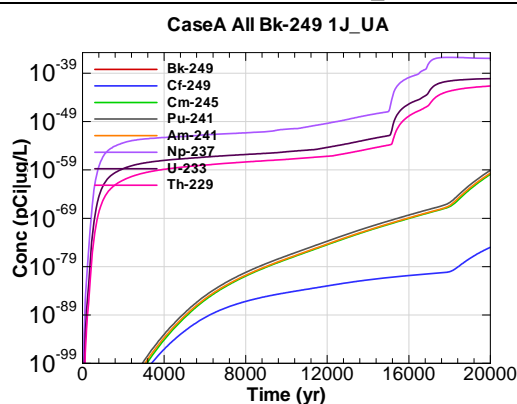


Figure F.1-82 - 1m Aquifer Concentration for
CaseA All Bk-249 1J_UA

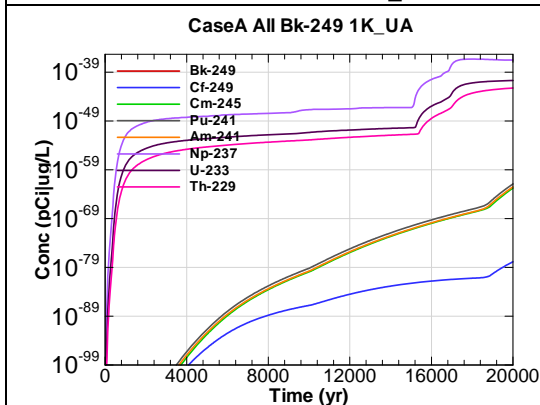


Figure F.1-83 - 1m Aquifer Concentration for
CaseA All Bk-249 1K_UA

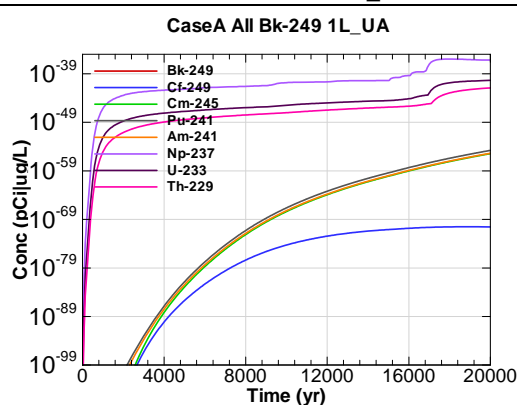
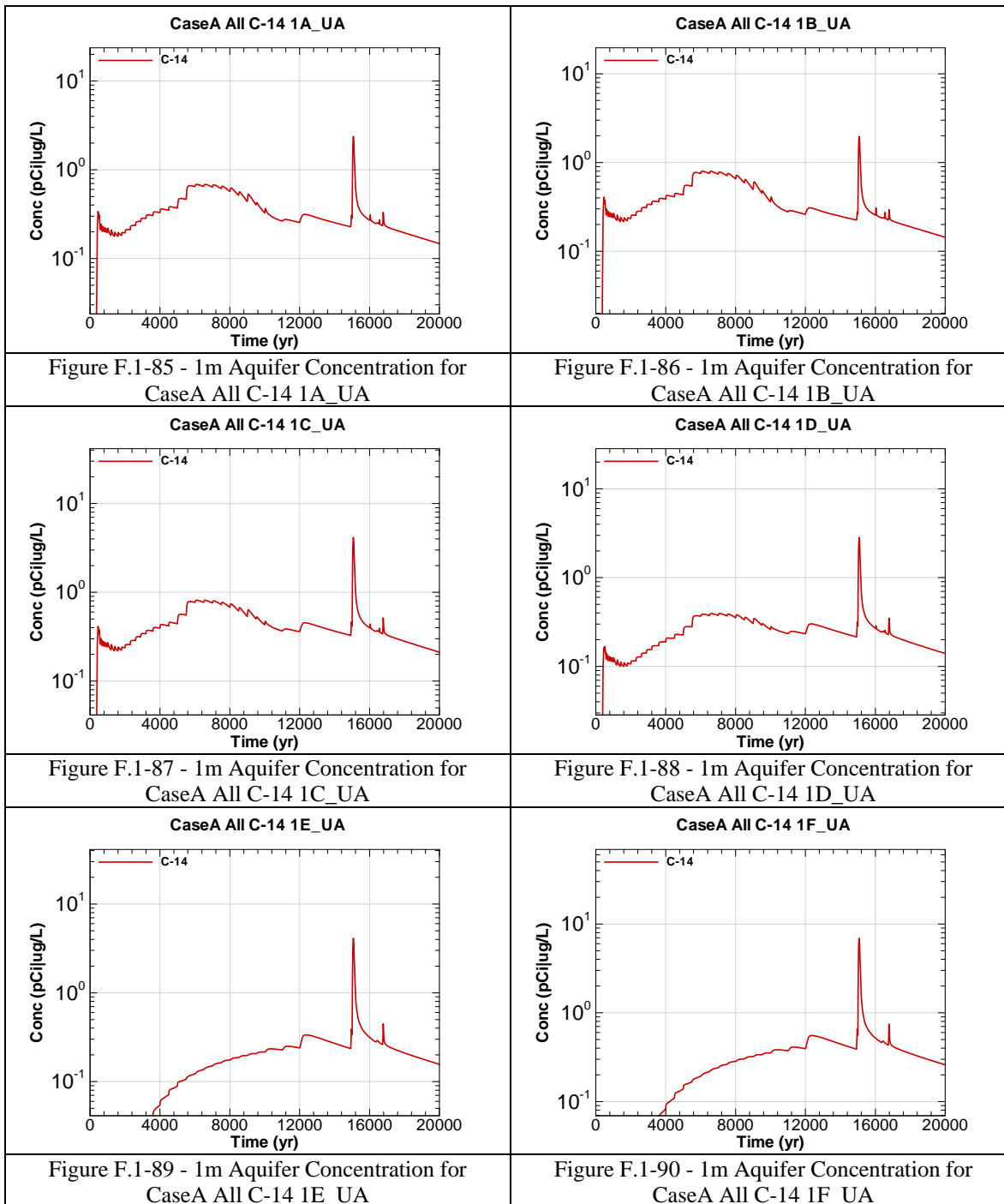
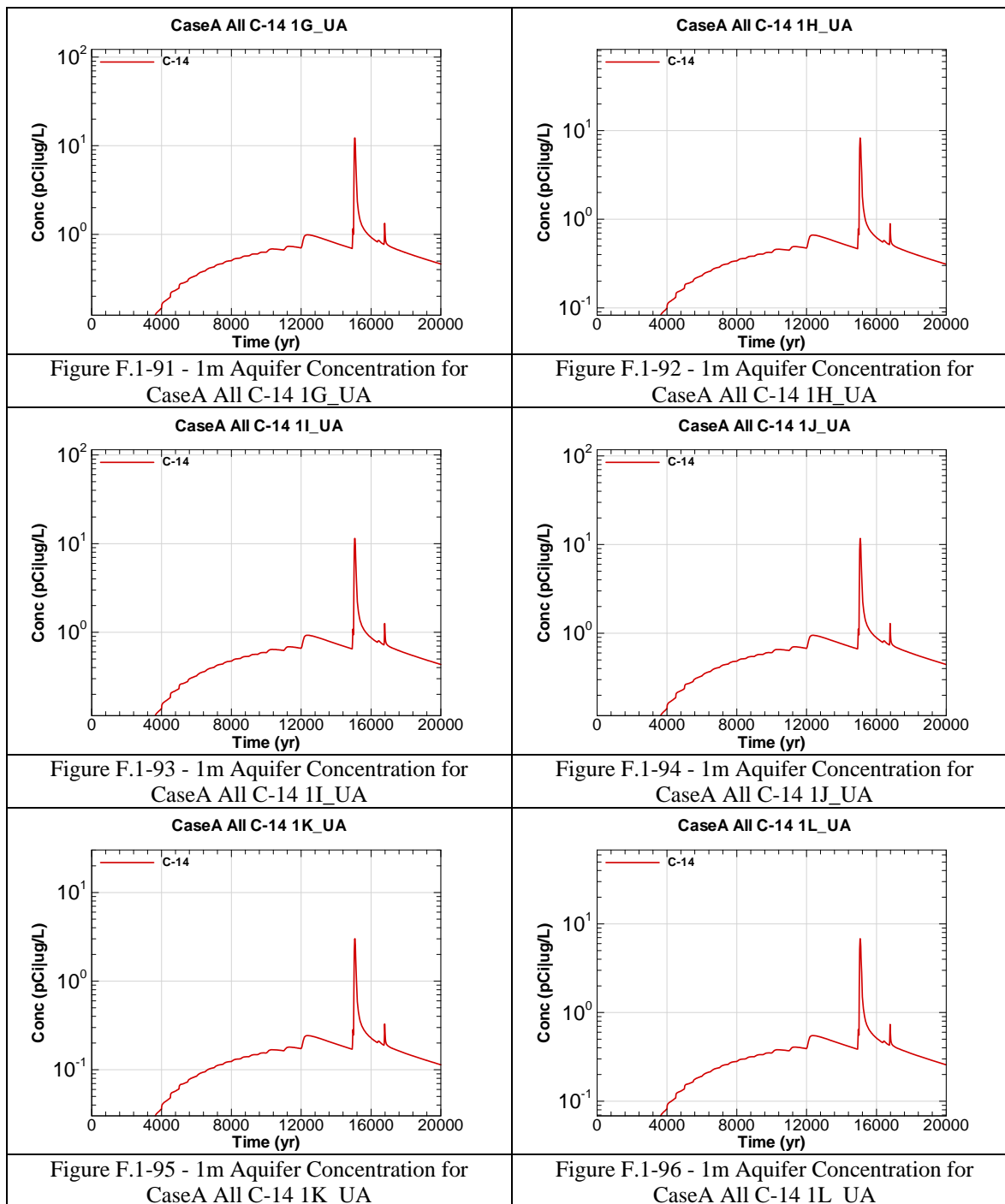
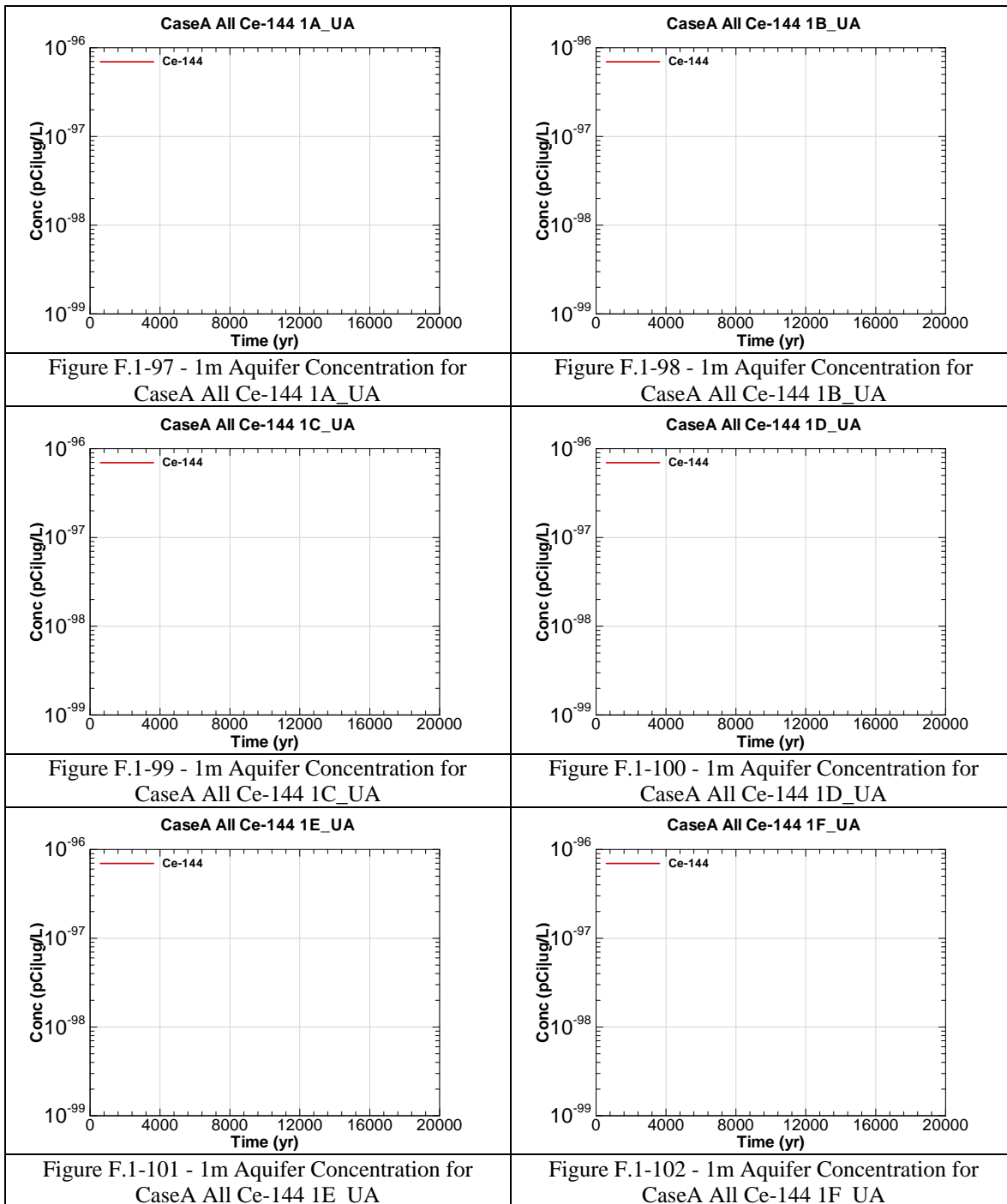
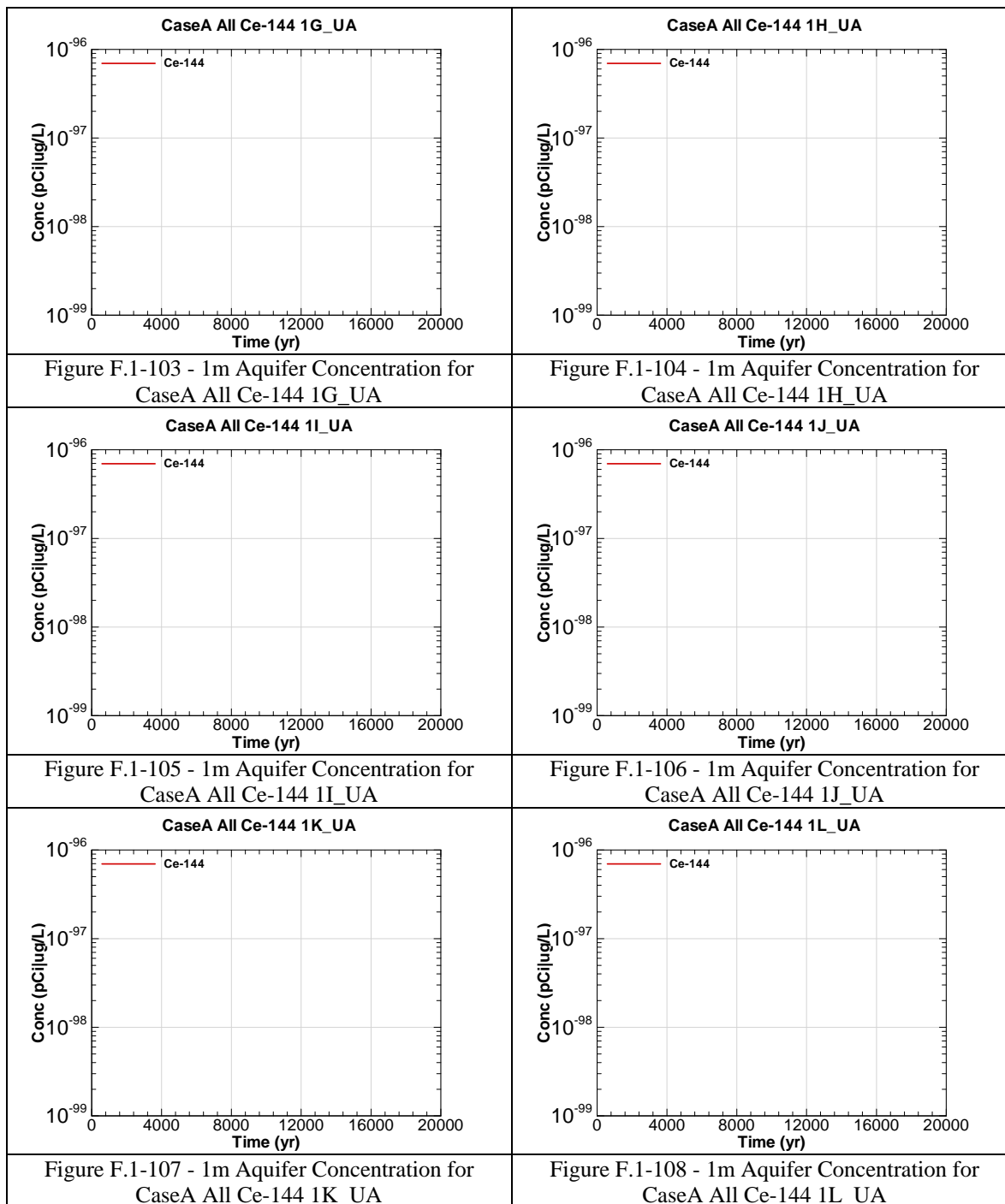


Figure F.1-84 - 1m Aquifer Concentration for
CaseA All Bk-249 1L_UA









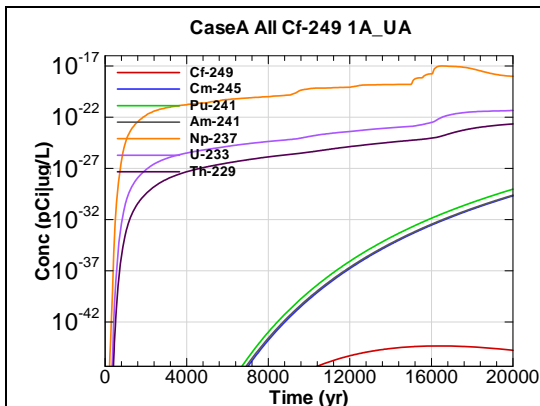


Figure F.1-109 - 1m Aquifer Concentration for
CaseA All Cf-249 1A_UA

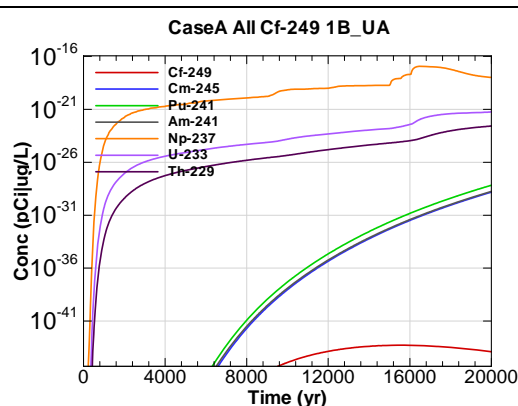


Figure F.1-110 - 1m Aquifer Concentration for
CaseA All Cf-249 1B_UA

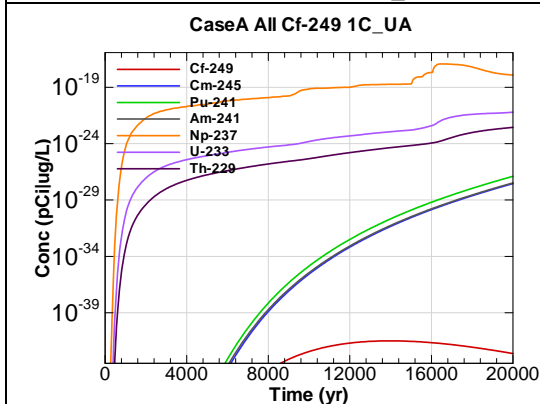


Figure F.1-111 - 1m Aquifer Concentration for
CaseA All Cf-249 1C_UA

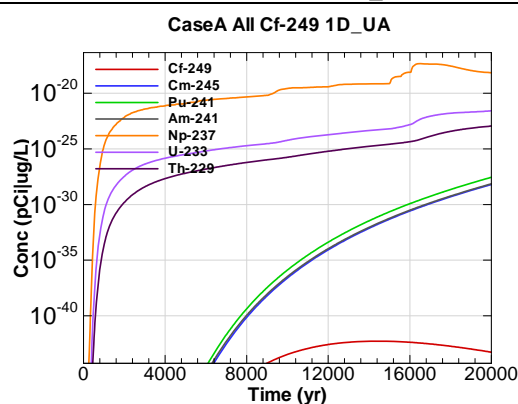


Figure F.1-112 - 1m Aquifer Concentration for
CaseA All Cf-249 1D_UA

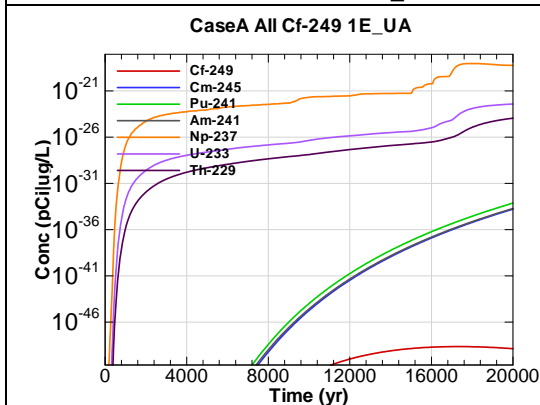


Figure F.1-113 - 1m Aquifer Concentration for
CaseA All Cf-249 1E_UA

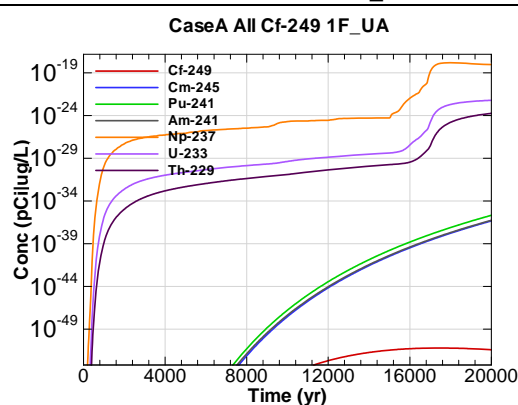


Figure F.1-114 - 1m Aquifer Concentration for
CaseA All Cf-249 1F_UA

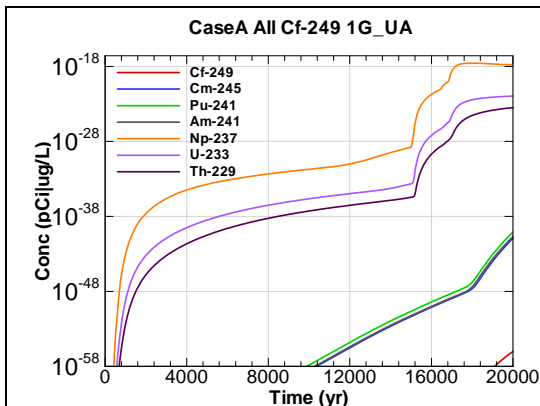


Figure F.1-115 - 1m Aquifer Concentration for
CaseA All Cf-249 1G_UA

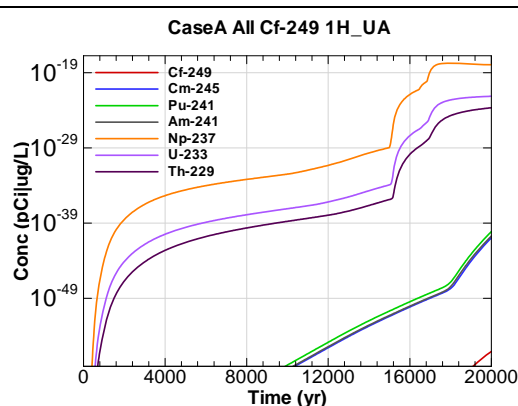


Figure F.1-116 - 1m Aquifer Concentration for
CaseA All Cf-249 1H_UA

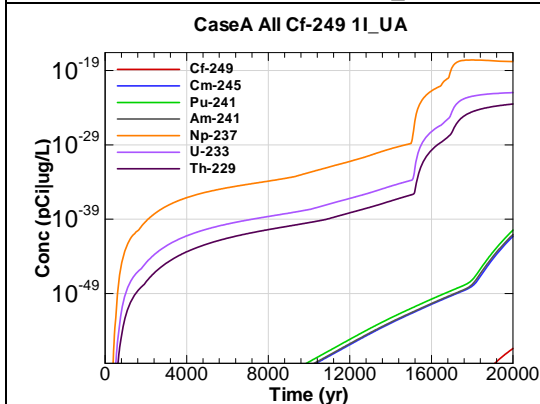


Figure F.1-117 - 1m Aquifer Concentration for
CaseA All Cf-249 1I_UA

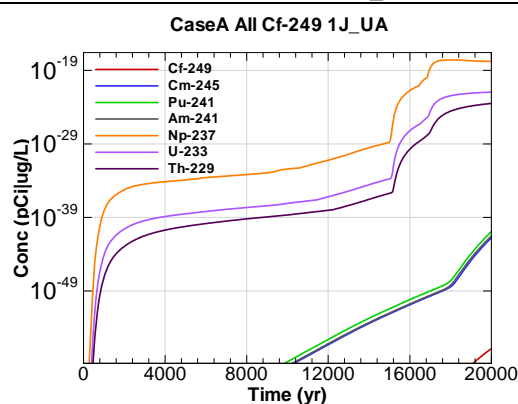


Figure F.1-118 - 1m Aquifer Concentration for
CaseA All Cf-249 1J_UA

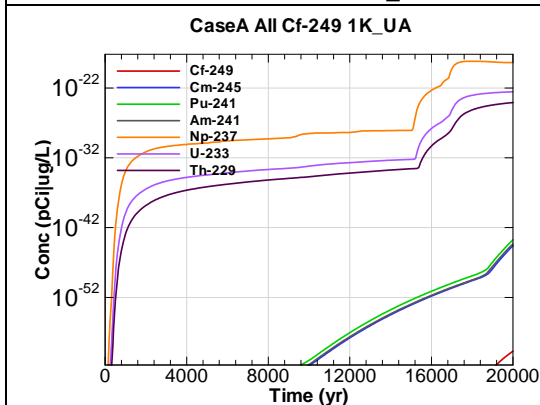


Figure F.1-119 - 1m Aquifer Concentration for
CaseA All Cf-249 1K_UA

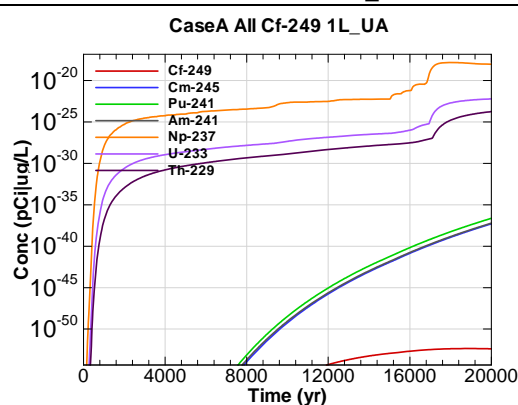
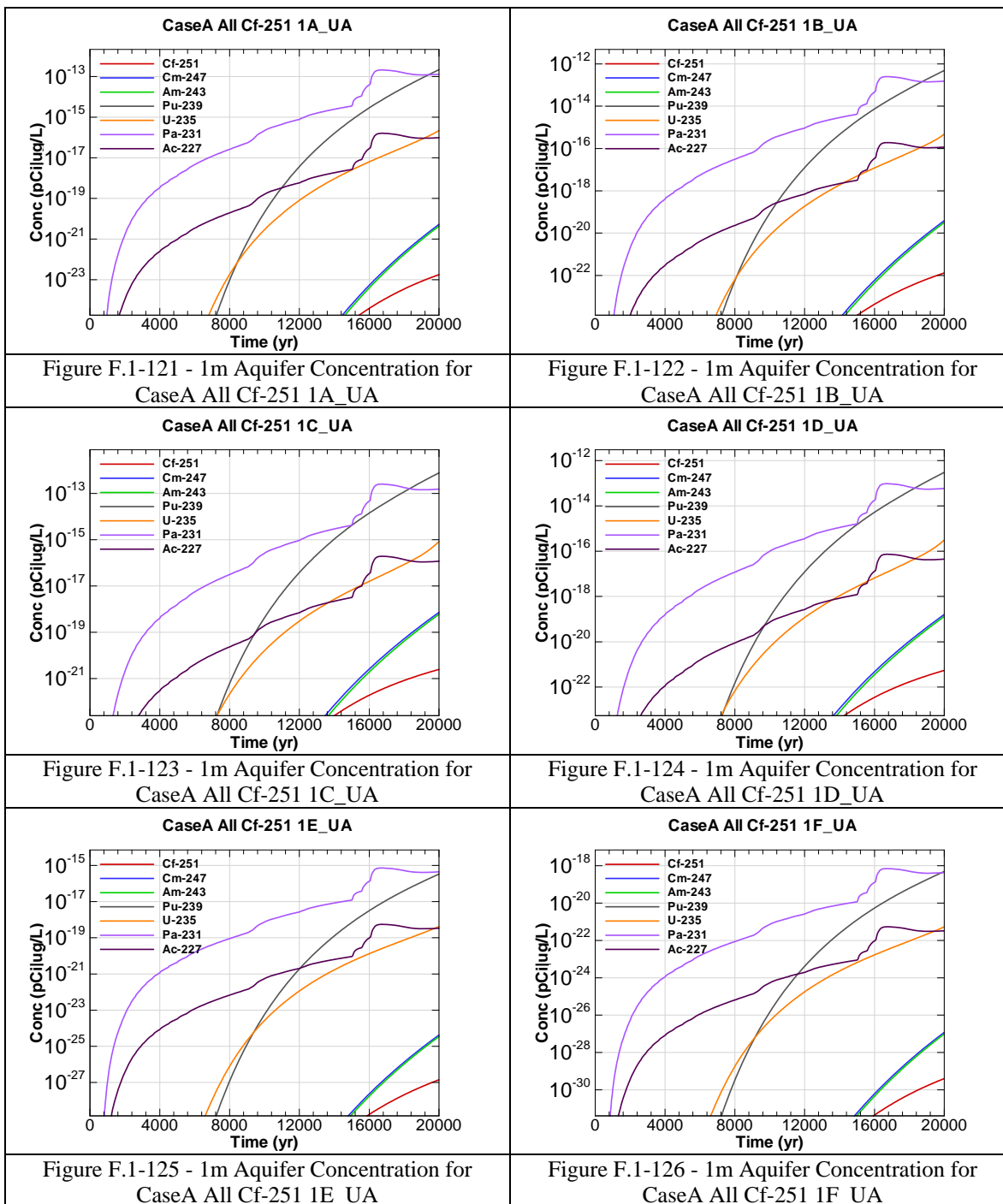


Figure F.1-120 - 1m Aquifer Concentration for
CaseA All Cf-249 1L_UA



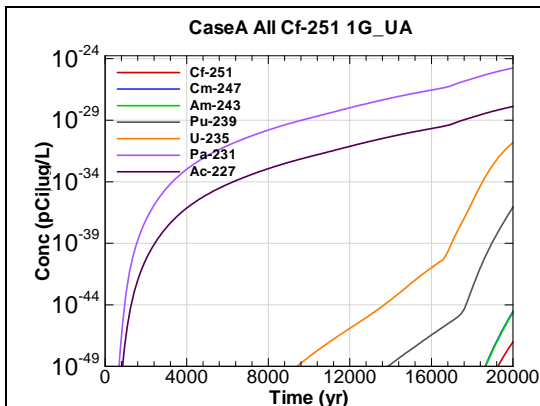


Figure F.1-127 - 1m Aquifer Concentration for
CaseA All Cf-251 1G_UA

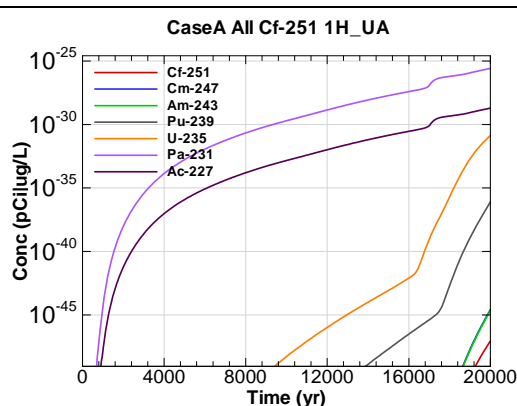


Figure F.1-128 - 1m Aquifer Concentration for
CaseA All Cf-251 1H_UA

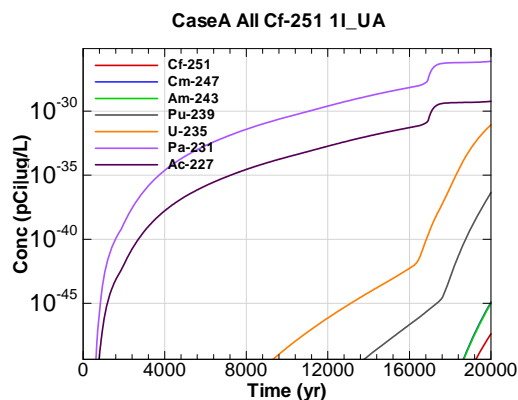


Figure F.1-129 - 1m Aquifer Concentration for
CaseA All Cf-251 1I_UA

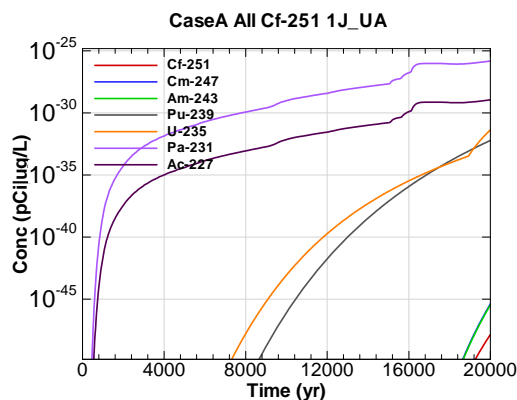


Figure F.1-130 - 1m Aquifer Concentration for
CaseA All Cf-251 1J_UA

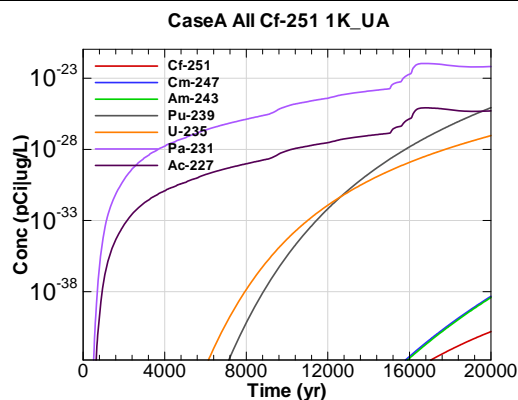


Figure F.1-131 - 1m Aquifer Concentration for
CaseA All Cf-251 1K_UA

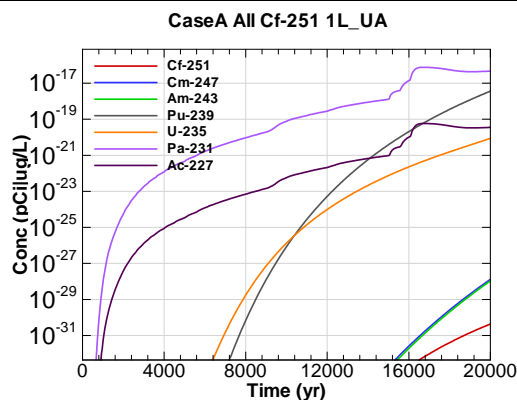
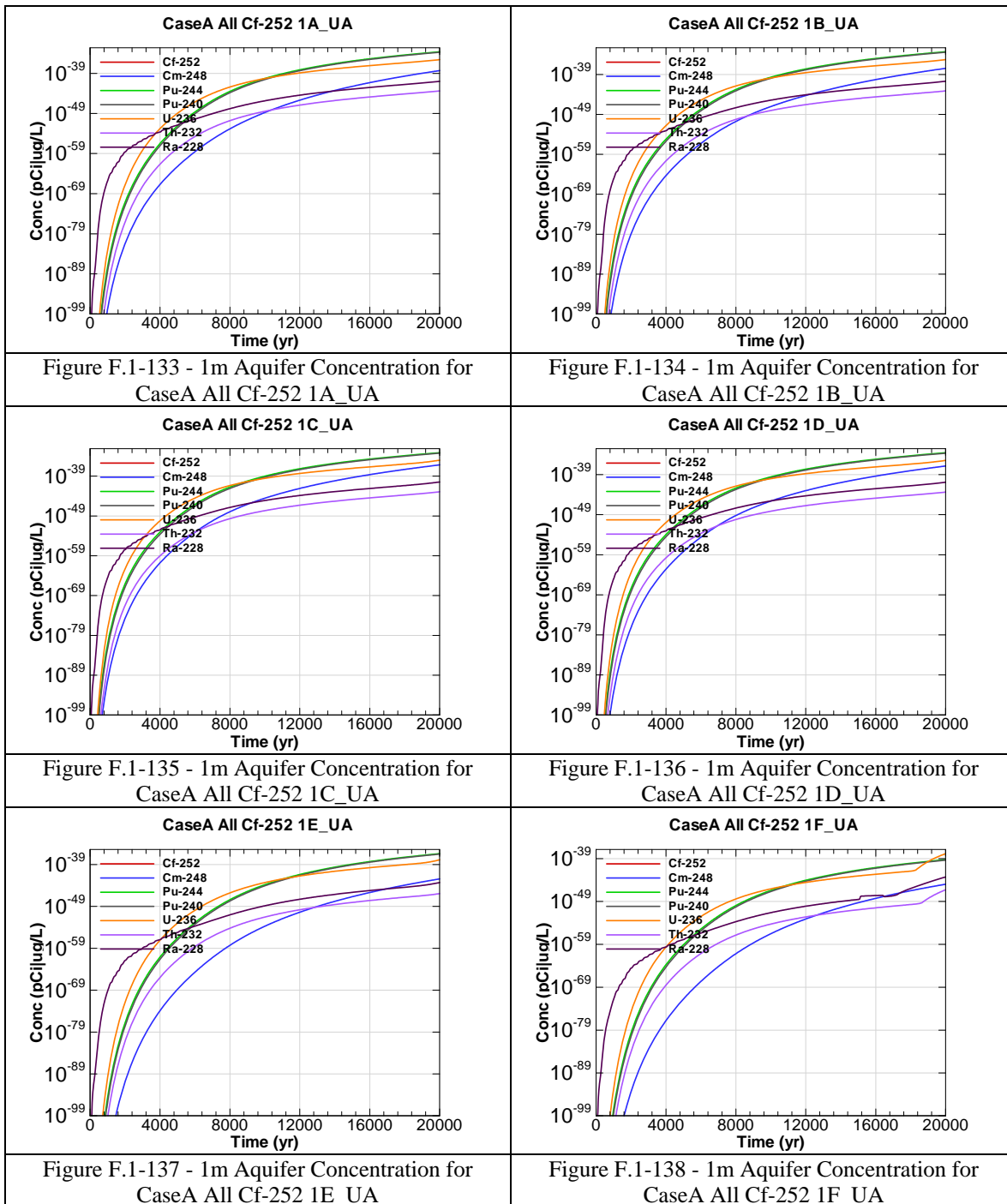


Figure F.1-132 - 1m Aquifer Concentration for
CaseA All Cf-251 1L_UA



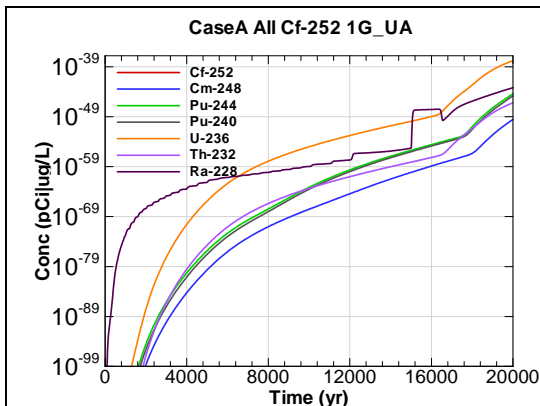


Figure F.1-139 - 1m Aquifer Concentration for
CaseA All Cf-252 1G_UA

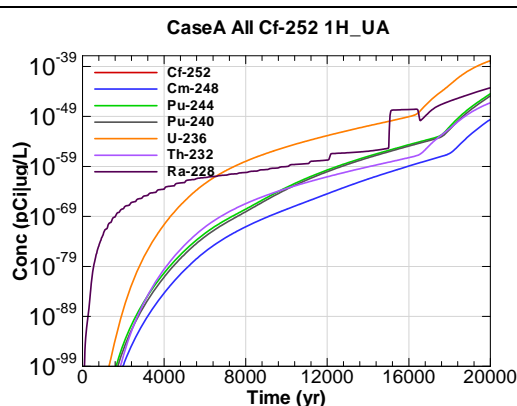


Figure F.1-140 - 1m Aquifer Concentration for
CaseA All Cf-252 1H_UA

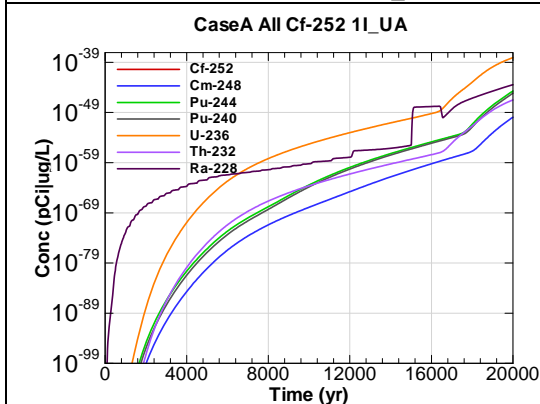


Figure F.1-141 - 1m Aquifer Concentration for
CaseA All Cf-252 1I_UA

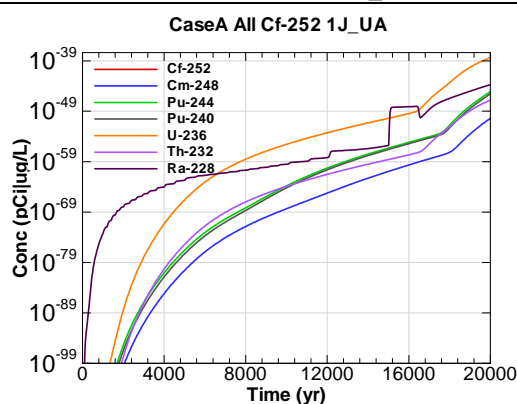


Figure F.1-142 - 1m Aquifer Concentration for
CaseA All Cf-252 1J_UA

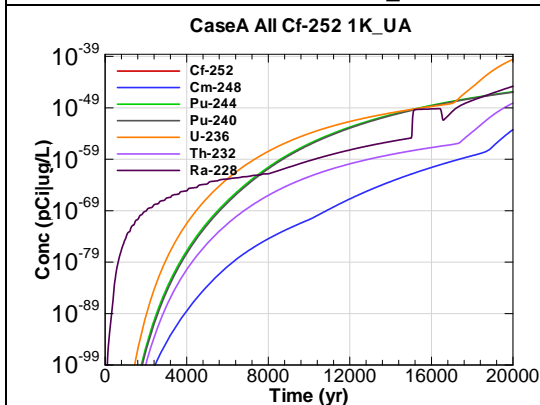


Figure F.1-143 - 1m Aquifer Concentration for
CaseA All Cf-252 1K_UA

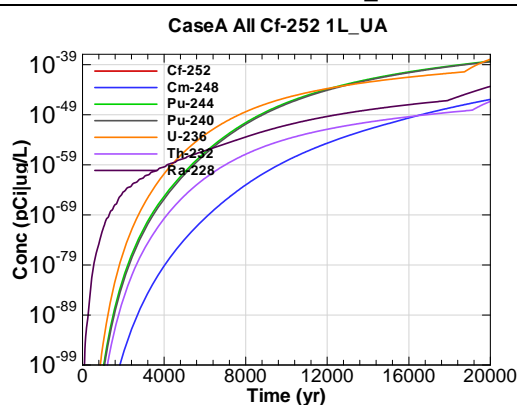
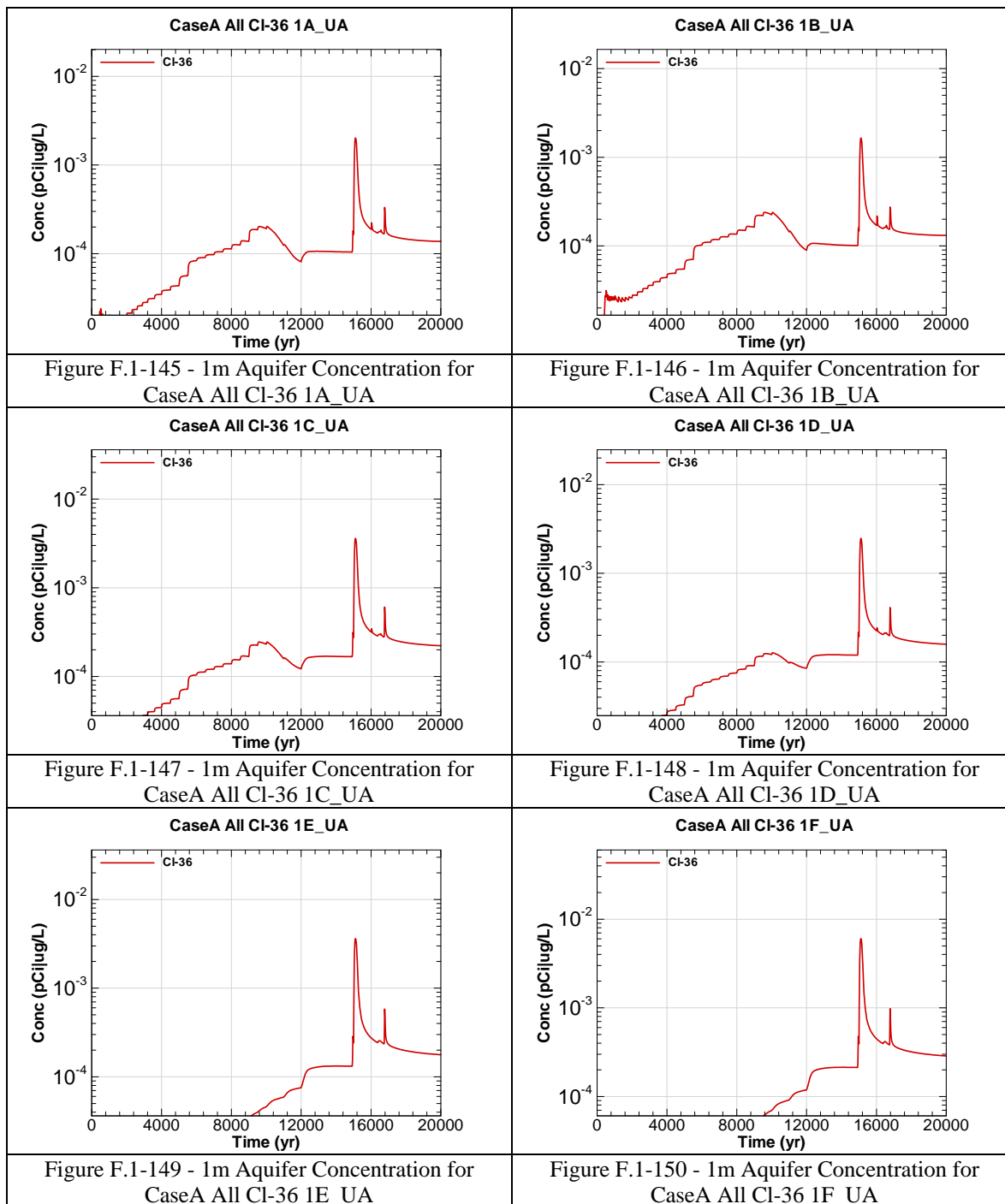
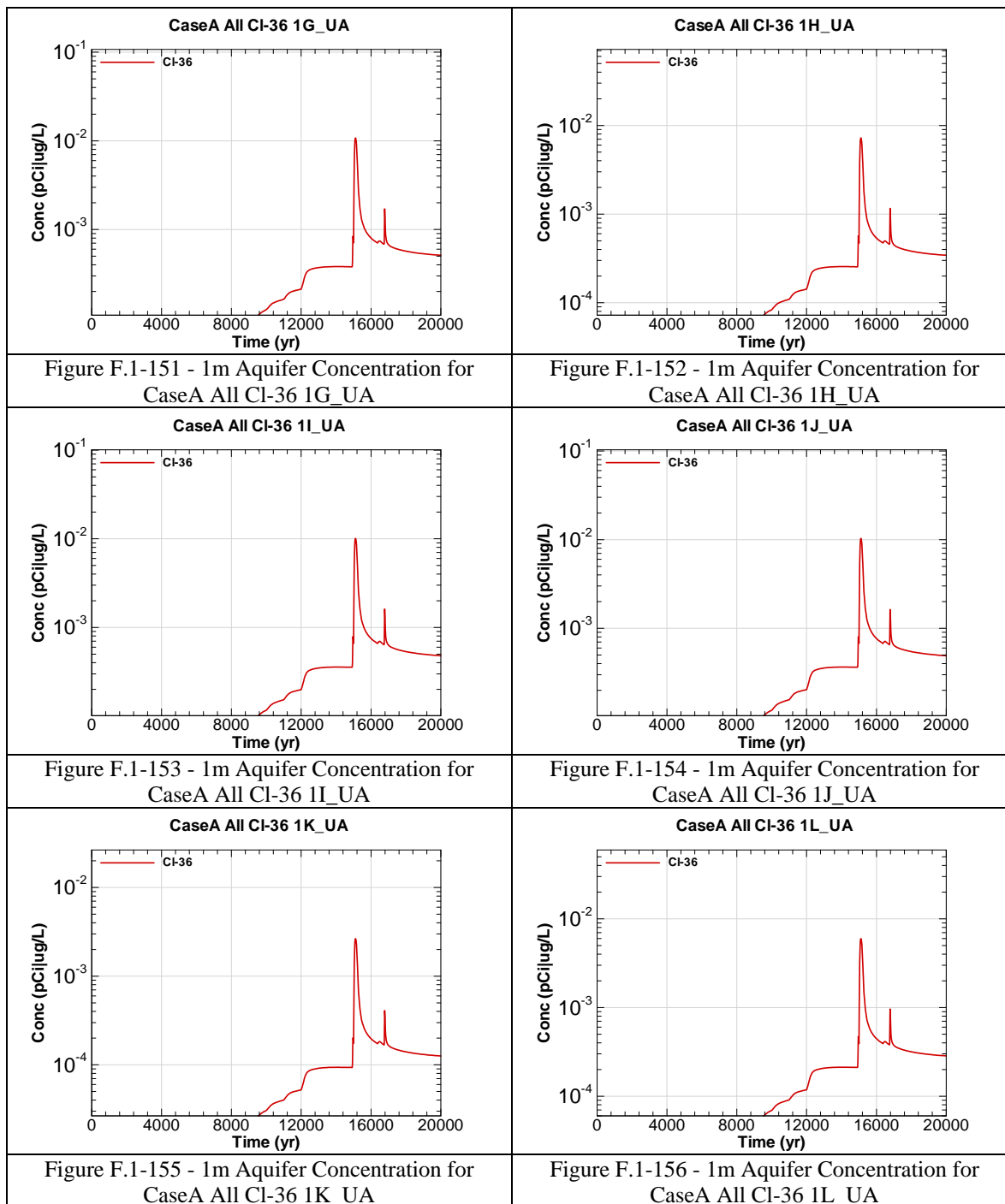
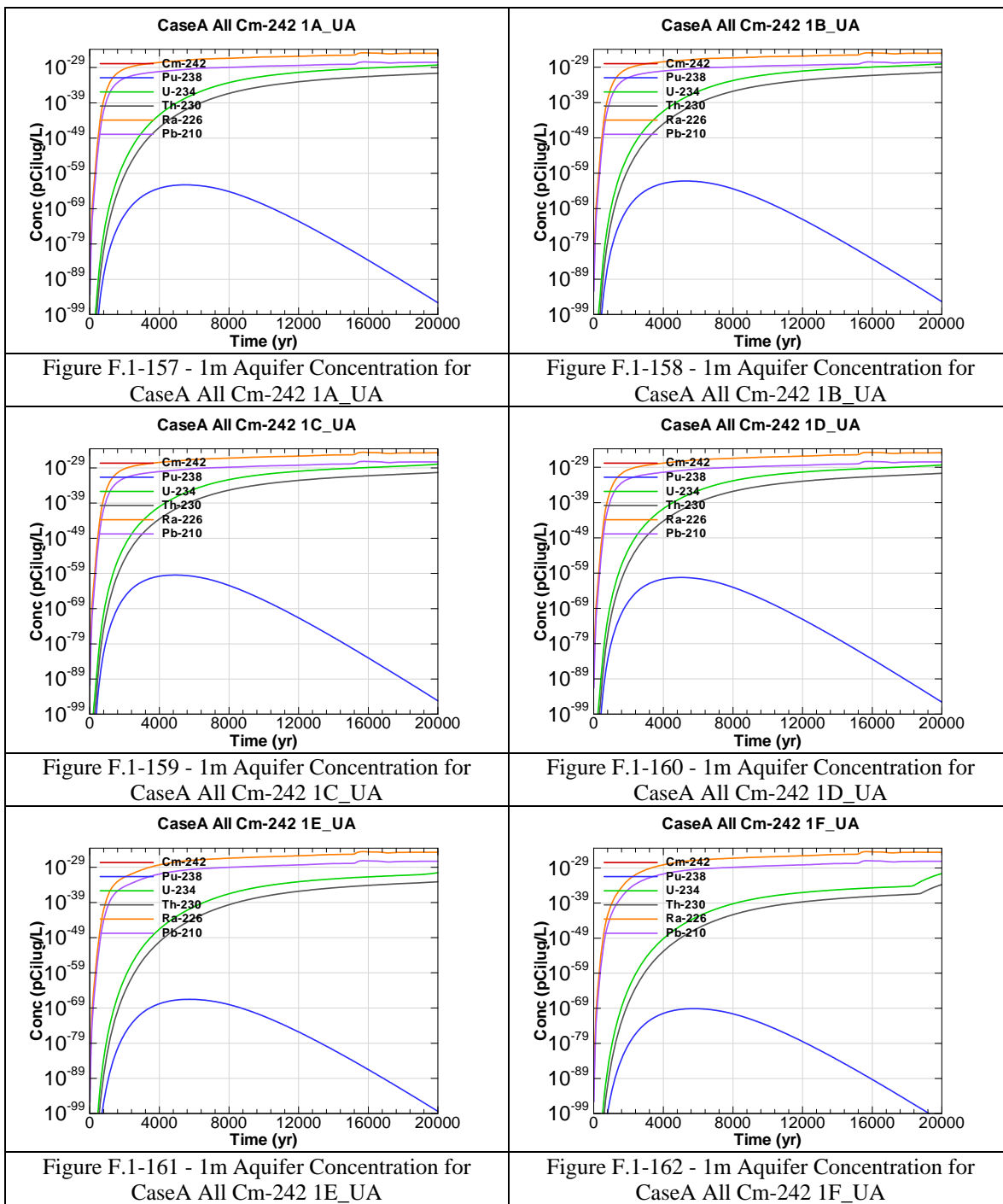
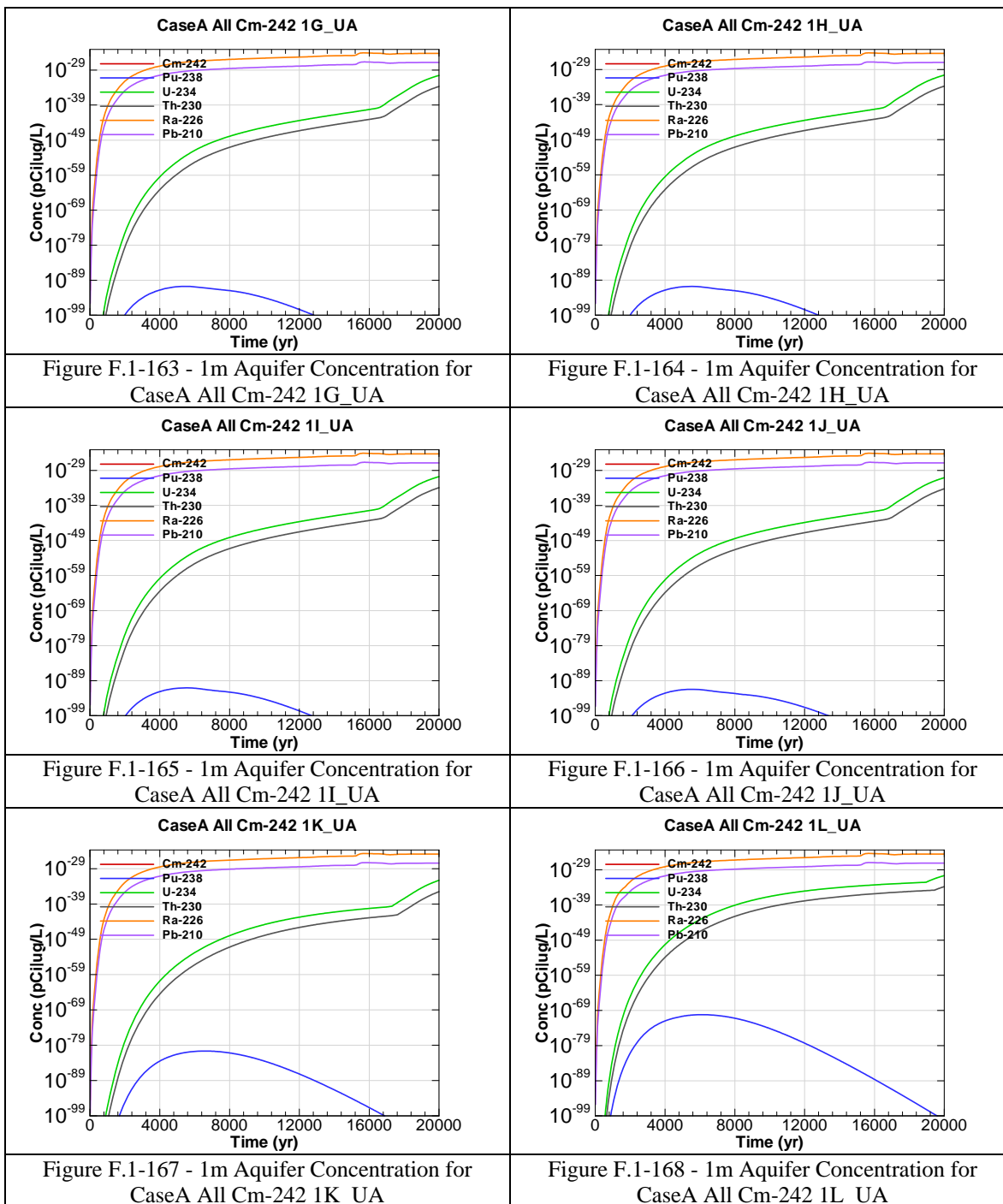


Figure F.1-144 - 1m Aquifer Concentration for
CaseA All Cf-252 1L_UA









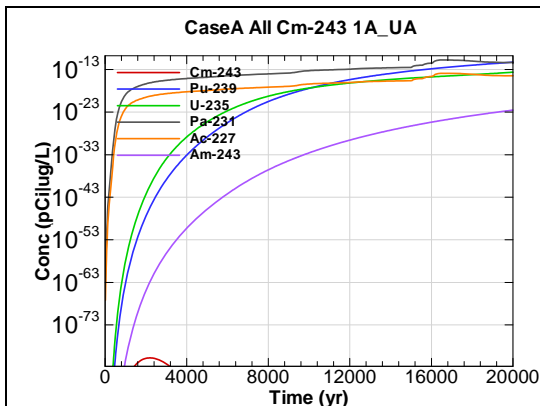


Figure F.1-169 - 1m Aquifer Concentration for
CaseA All Cm-243 1A_UA

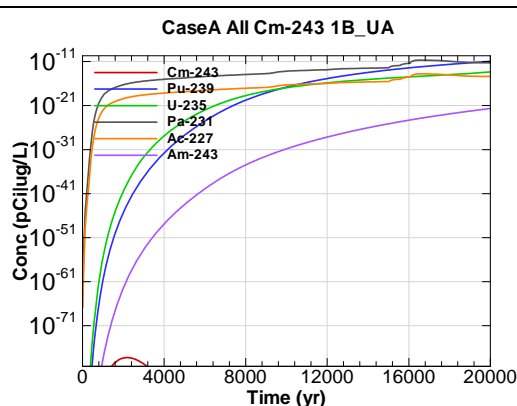


Figure F.1-170 - 1m Aquifer Concentration for
CaseA All Cm-243 1B_UA

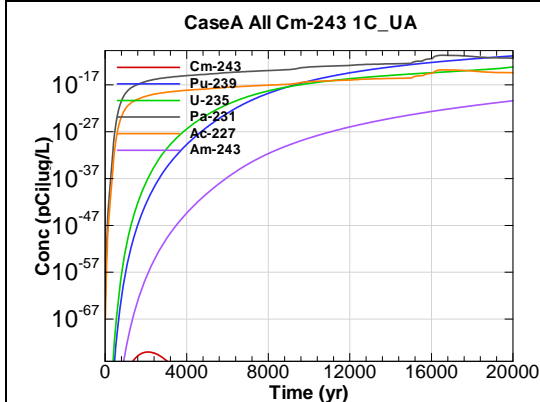


Figure F.1-171 - 1m Aquifer Concentration for
CaseA All Cm-243 1C_UA

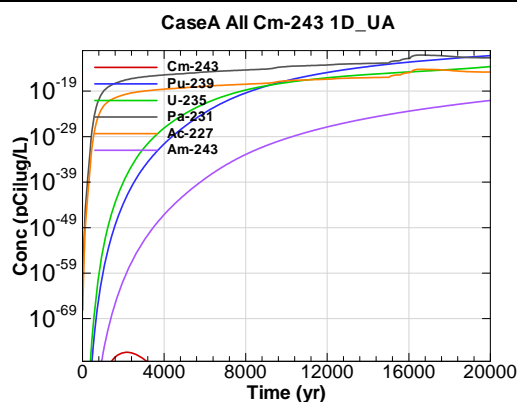


Figure F.1-172 - 1m Aquifer Concentration for
CaseA All Cm-243 1D_UA

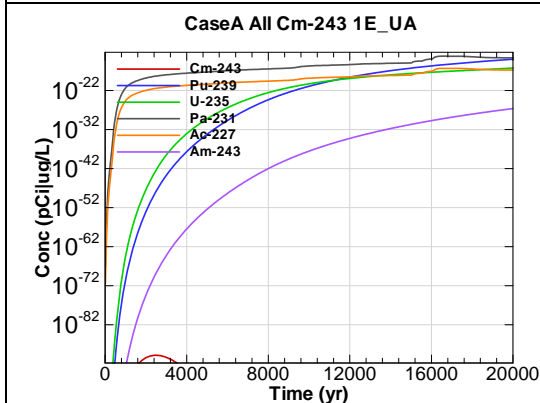


Figure F.1-173 - 1m Aquifer Concentration for
CaseA All Cm-243 1E_UA

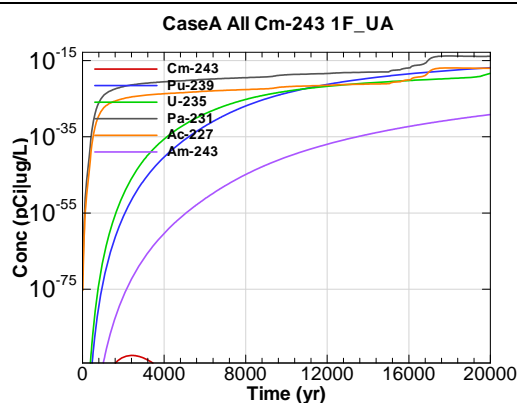


Figure F.1-174 - 1m Aquifer Concentration for
CaseA All Cm-243 1F_UA

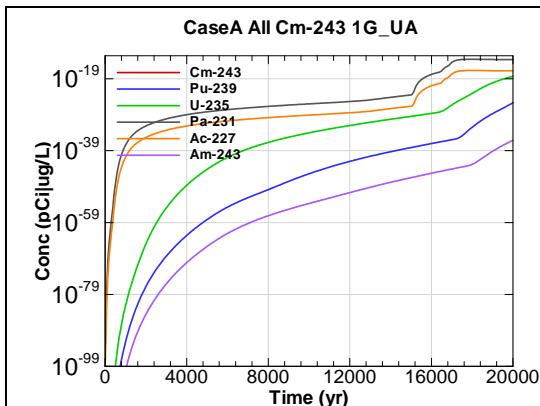


Figure F.1-175 - 1m Aquifer Concentration for
CaseA All Cm-243 1G_UA

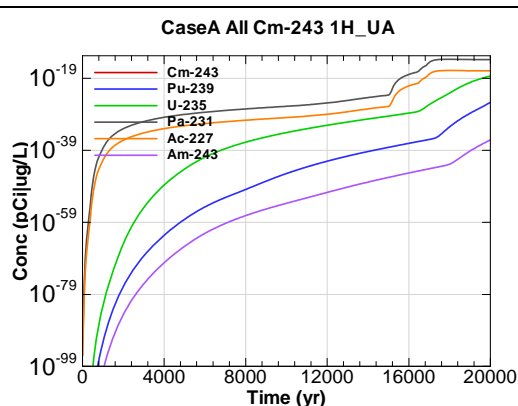


Figure F.1-176 - 1m Aquifer Concentration for
CaseA All Cm-243 1H_UA

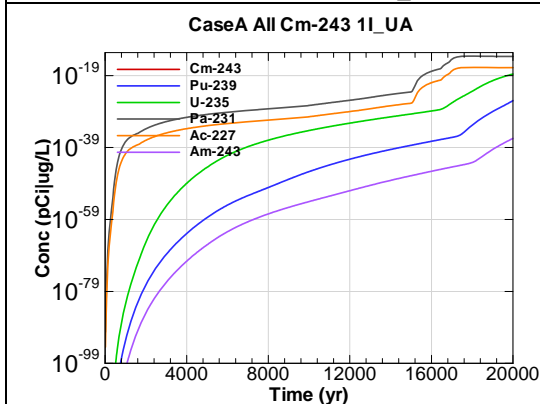


Figure F.1-177 - 1m Aquifer Concentration for
CaseA All Cm-243 1I_UA

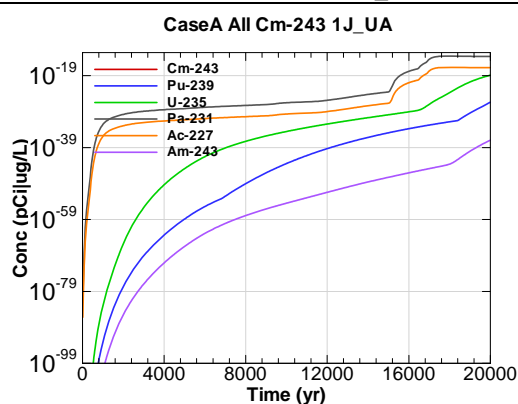


Figure F.1-178 - 1m Aquifer Concentration for
CaseA All Cm-243 1J_UA

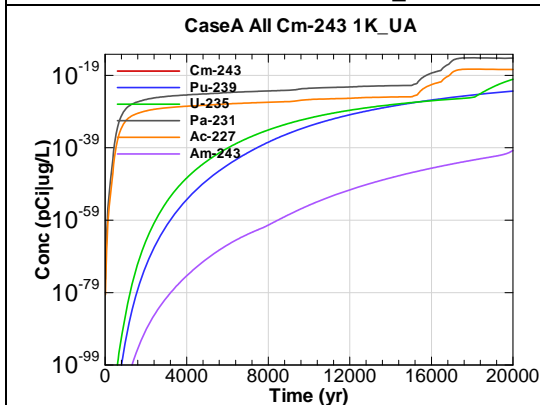


Figure F.1-179 - 1m Aquifer Concentration for
CaseA All Cm-243 1K_UA

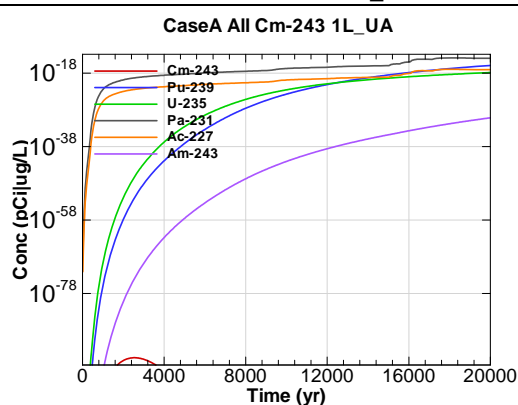
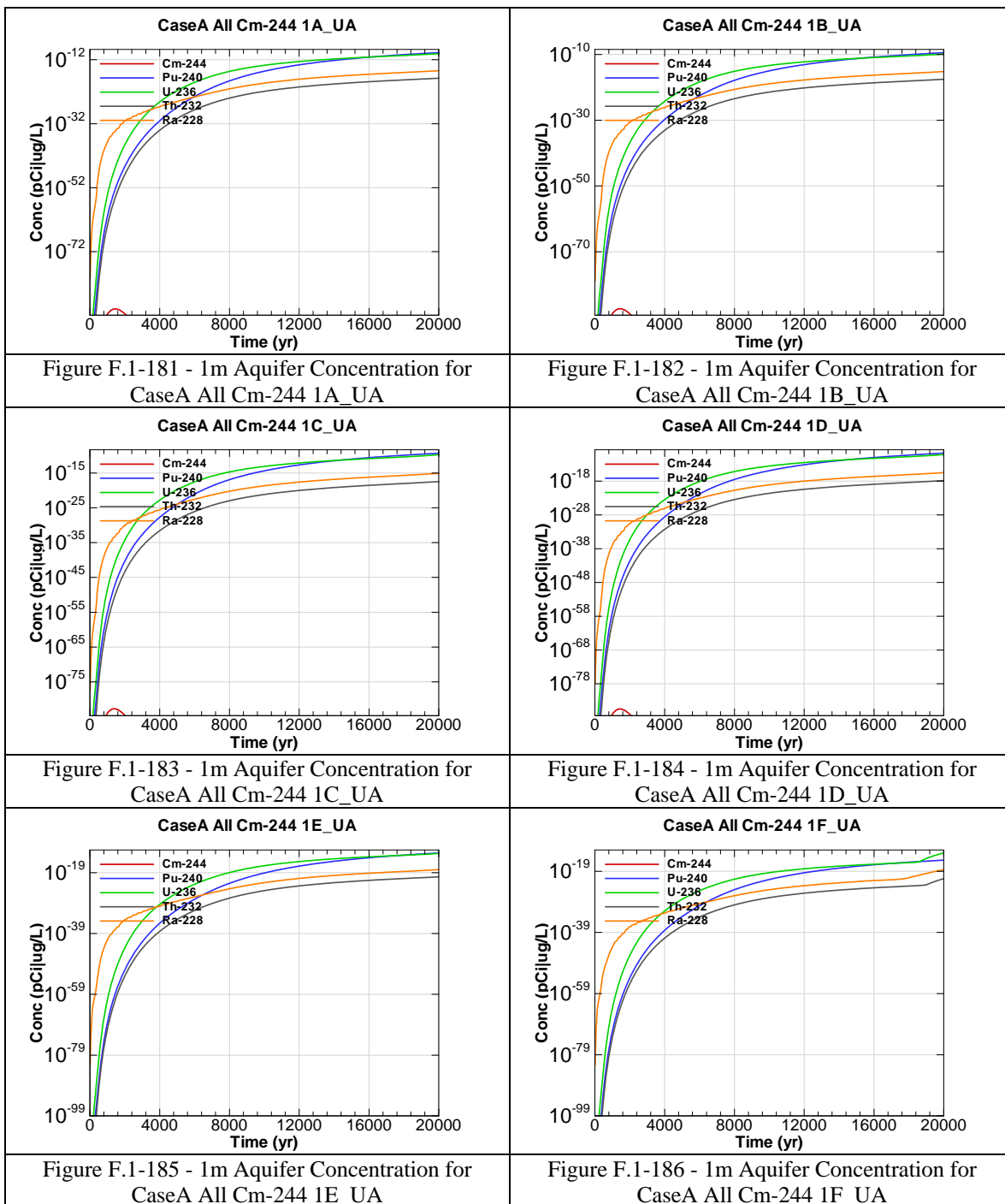


Figure F.1-180 - 1m Aquifer Concentration for
CaseA All Cm-243 1L_UA



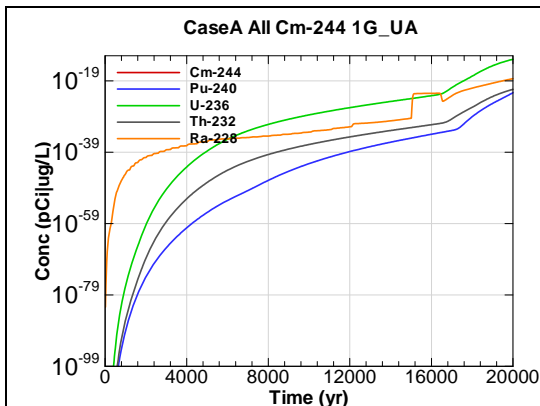


Figure F.1-187 - 1m Aquifer Concentration for
CaseA All Cm-244 1G_UA

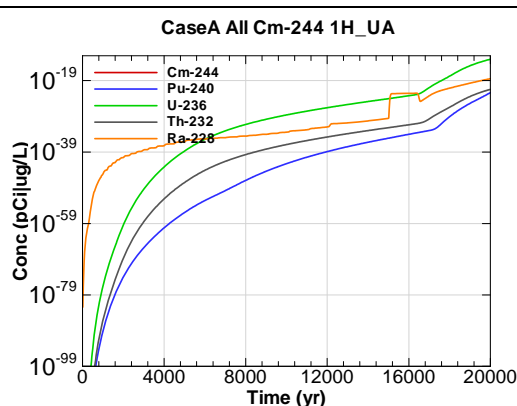


Figure F.1-188 - 1m Aquifer Concentration for
CaseA All Cm-244 1H_UA

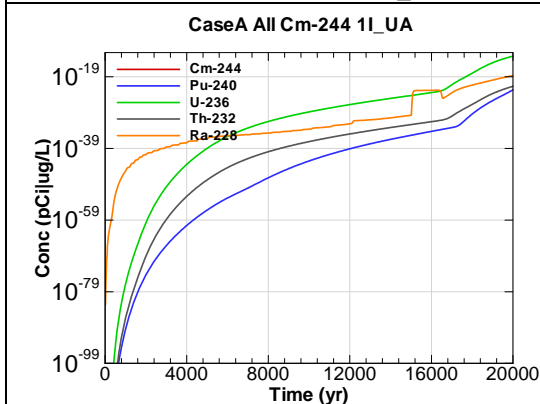


Figure F.1-189 - 1m Aquifer Concentration for
CaseA All Cm-244 1I_UA

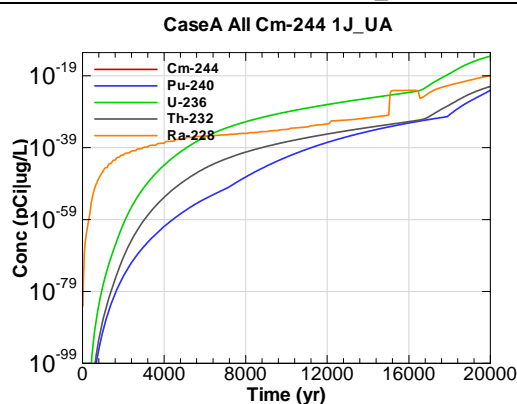


Figure F.1-190 - 1m Aquifer Concentration for
CaseA All Cm-244 1J_UA

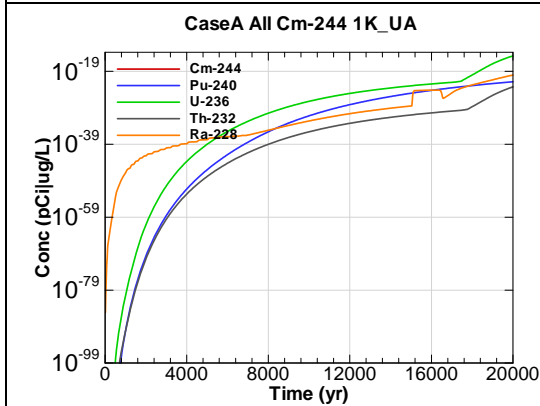


Figure F.1-191 - 1m Aquifer Concentration for
CaseA All Cm-244 1K_UA

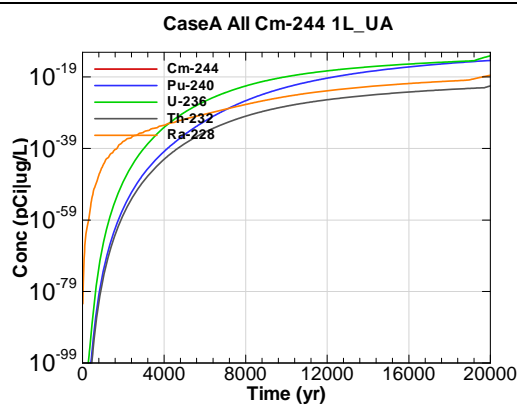
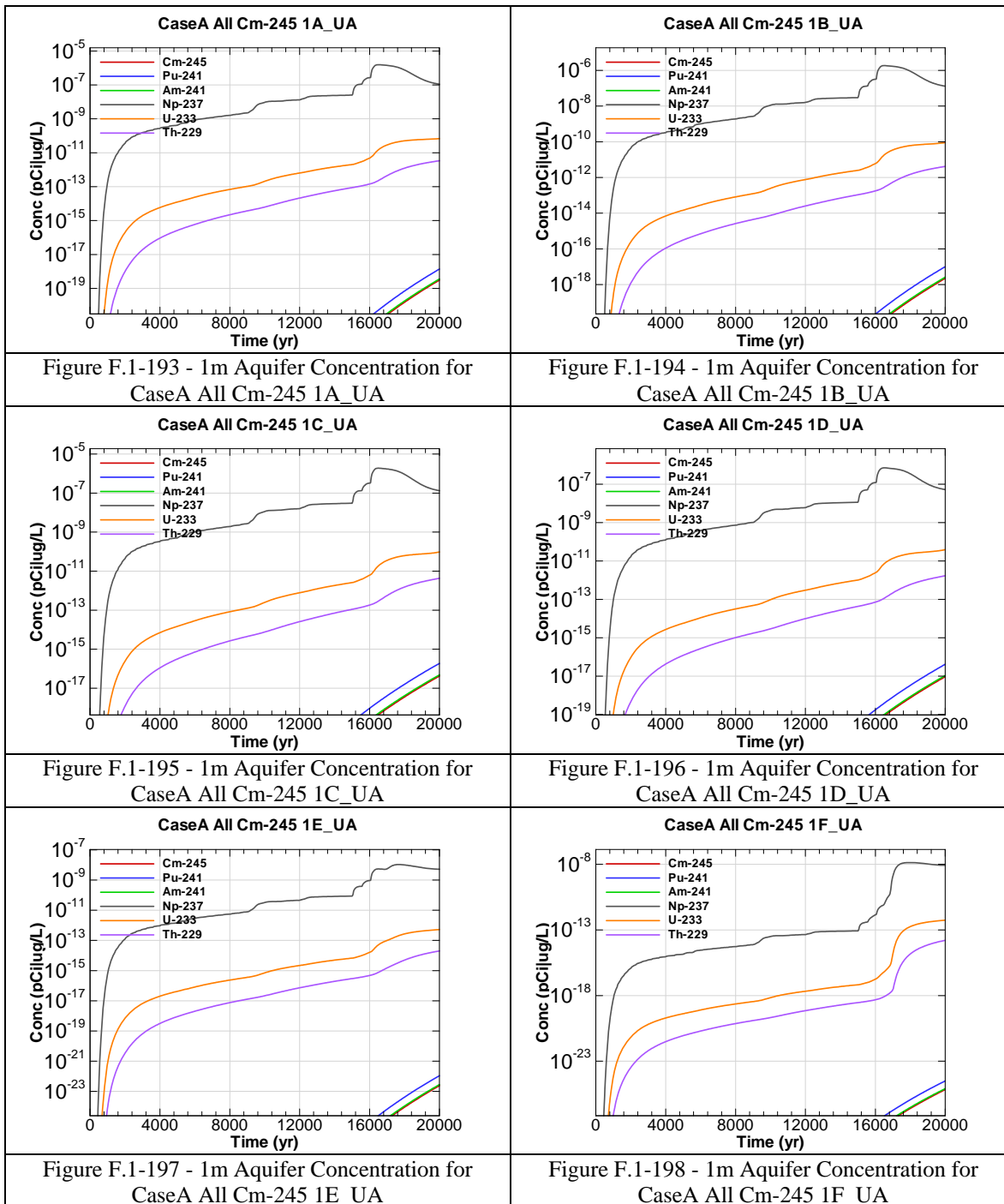
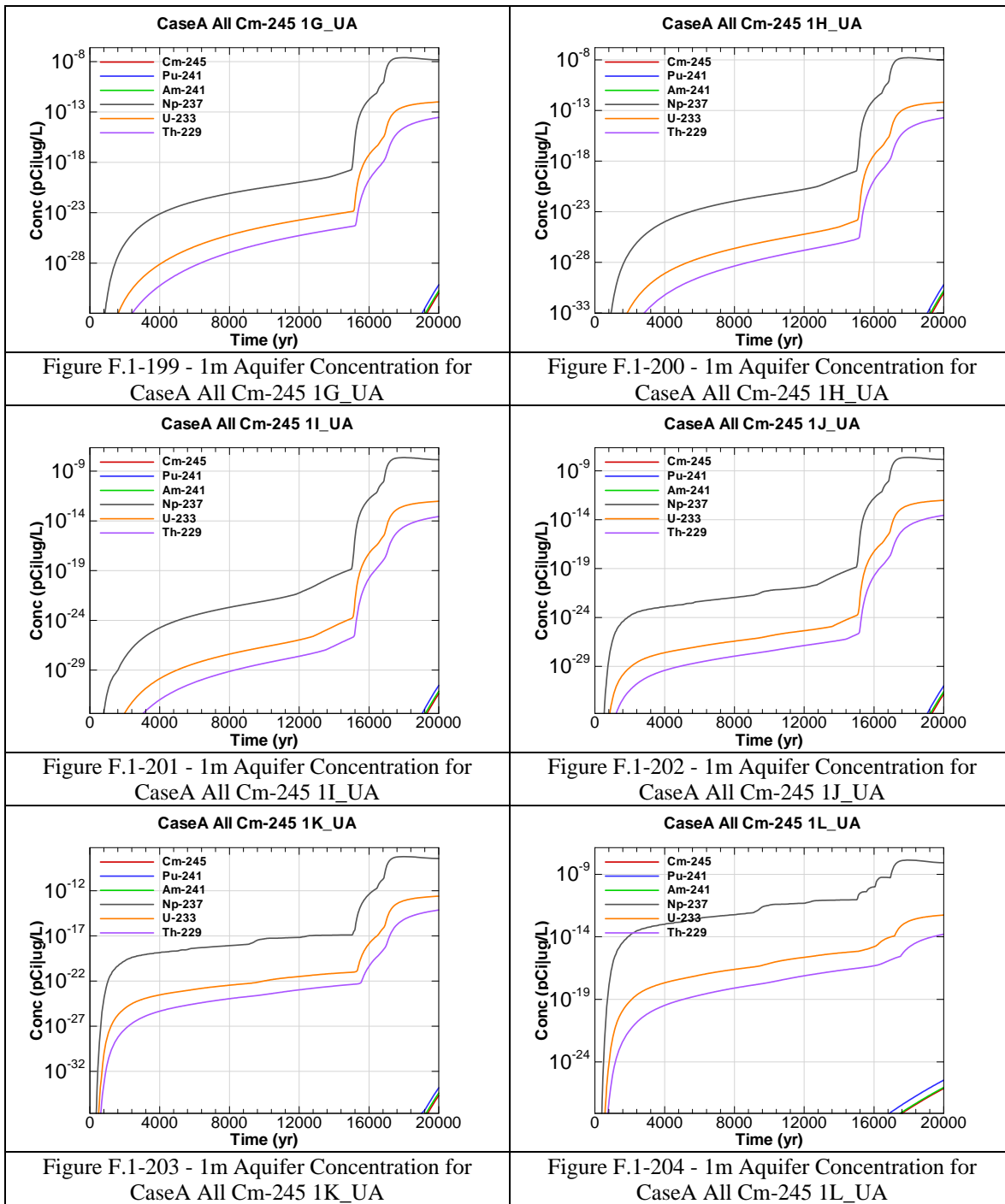


Figure F.1-192 - 1m Aquifer Concentration for
CaseA All Cm-244 1L_UA





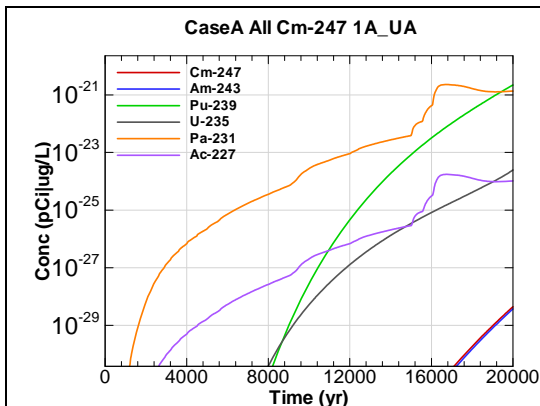


Figure F.1-205 - 1m Aquifer Concentration for
CaseA All Cm-247 1A_UA

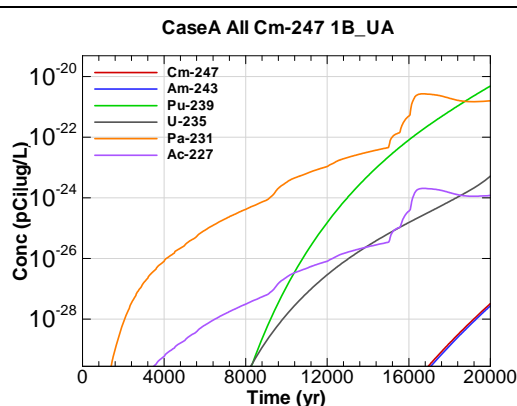


Figure F.1-206 - 1m Aquifer Concentration for
CaseA All Cm-247 1B_UA

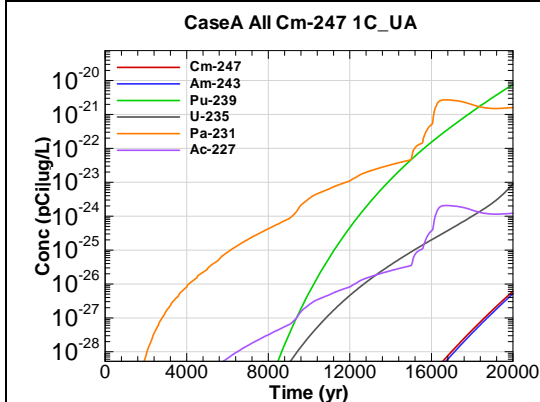


Figure F.1-207 - 1m Aquifer Concentration for
CaseA All Cm-247 1C_UA

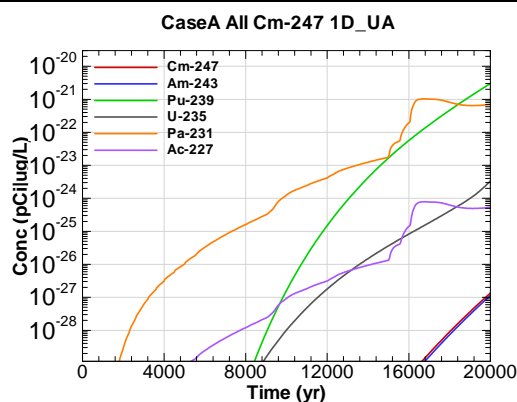


Figure F.1-208 - 1m Aquifer Concentration for
CaseA All Cm-247 1D_UA

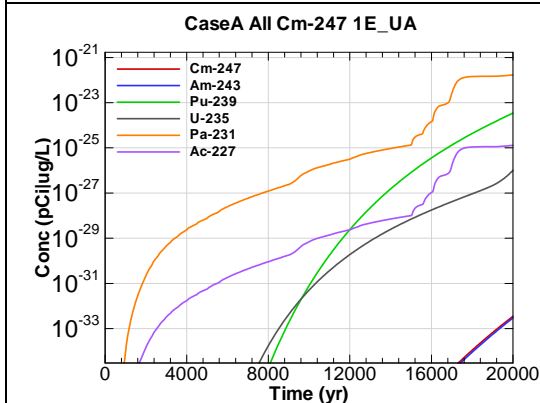


Figure F.1-209 - 1m Aquifer Concentration for
CaseA All Cm-247 1E_UA

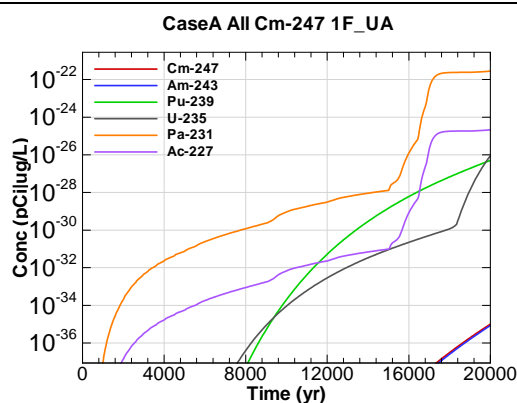
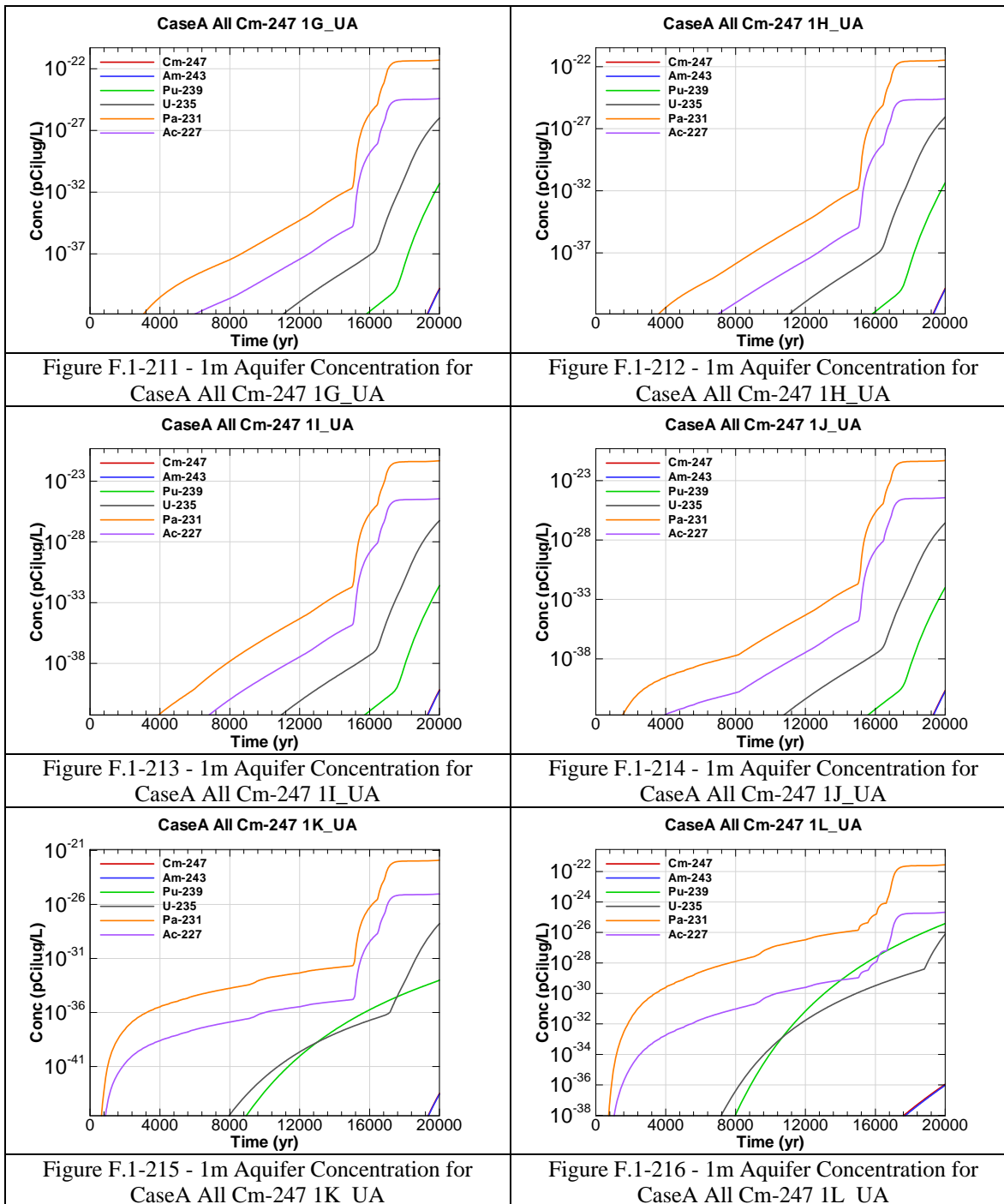


Figure F.1-210 - 1m Aquifer Concentration for
CaseA All Cm-247 1F_UA



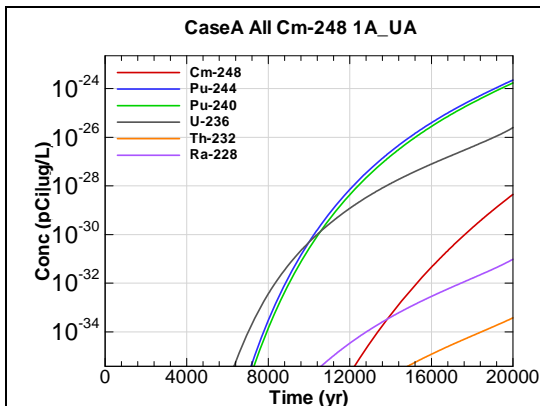


Figure F.1-217 - 1m Aquifer Concentration for
CaseA All Cm-248 1A_UA

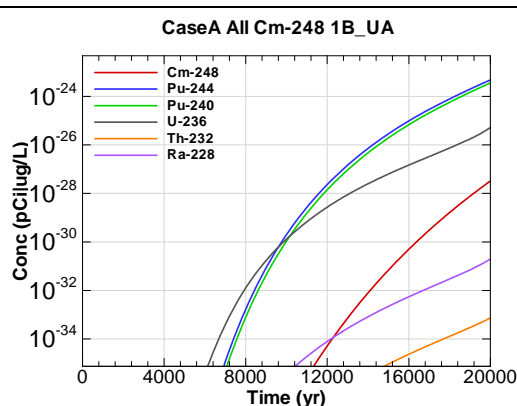


Figure F.1-218 - 1m Aquifer Concentration for
CaseA All Cm-248 1B_UA

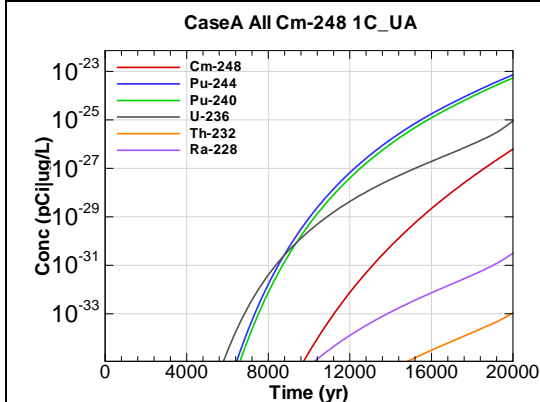


Figure F.1-219 - 1m Aquifer Concentration for
CaseA All Cm-248 1C_UA

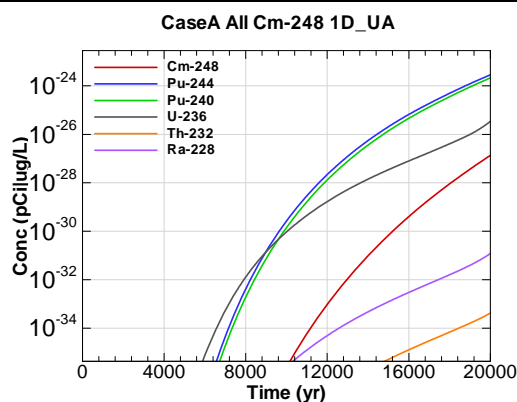


Figure F.1-220 - 1m Aquifer Concentration for
CaseA All Cm-248 1D_UA

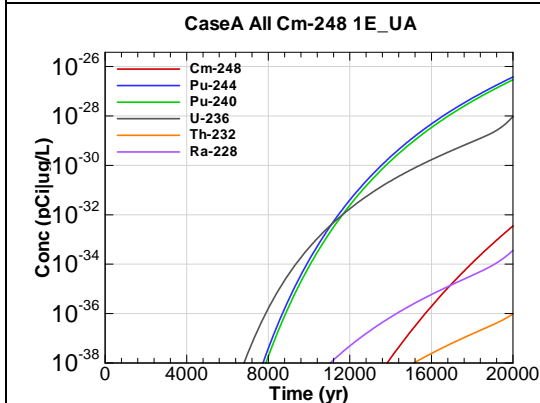


Figure F.1-221 - 1m Aquifer Concentration for
CaseA All Cm-248 1E_UA

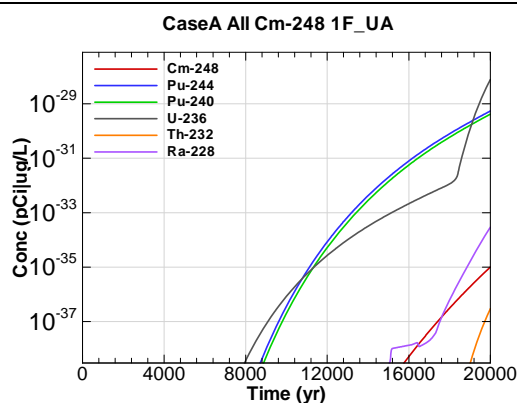


Figure F.1-222 - 1m Aquifer Concentration for
CaseA All Cm-248 1F_UA

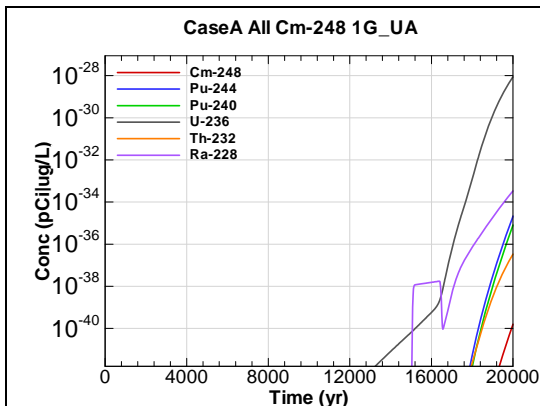


Figure F.1-223 - 1m Aquifer Concentration for
CaseA All Cm-248 1G_UA

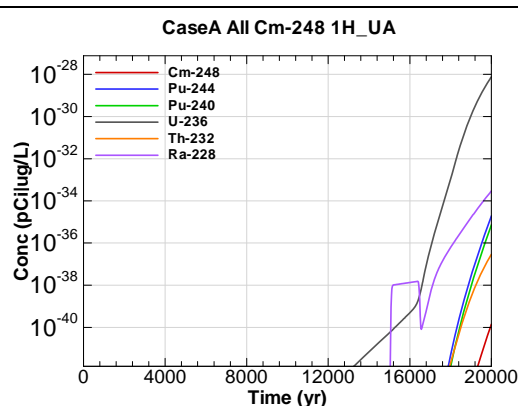


Figure F.1-224 - 1m Aquifer Concentration for
CaseA All Cm-248 1H_UA

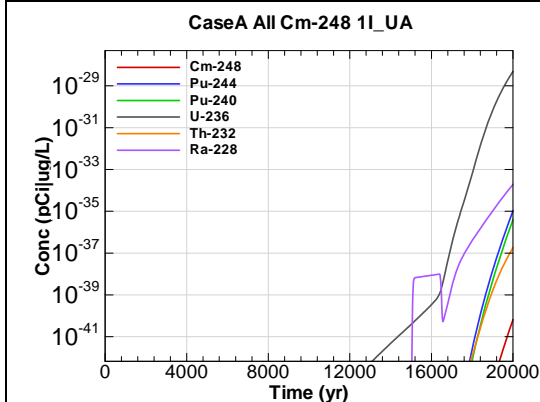


Figure F.1-225 - 1m Aquifer Concentration for
CaseA All Cm-248 1I_UA

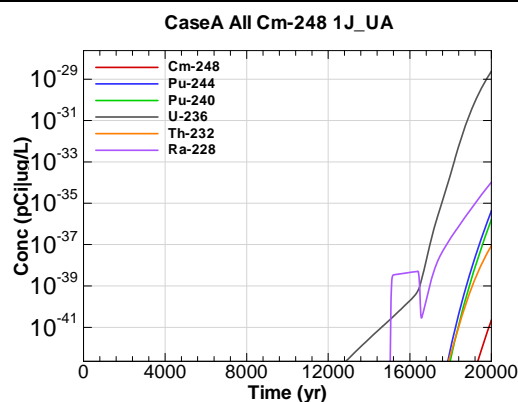


Figure F.1-226 - 1m Aquifer Concentration for
CaseA All Cm-248 1J_UA

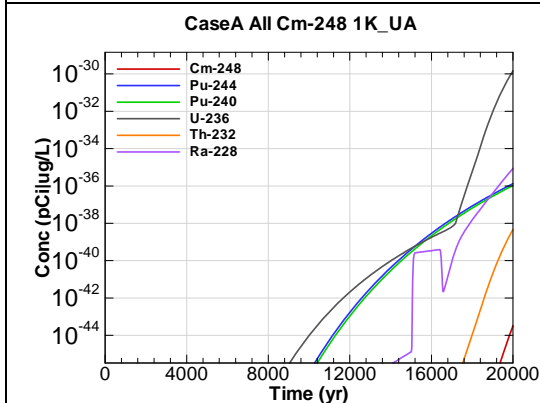


Figure F.1-227 - 1m Aquifer Concentration for
CaseA All Cm-248 1K_UA

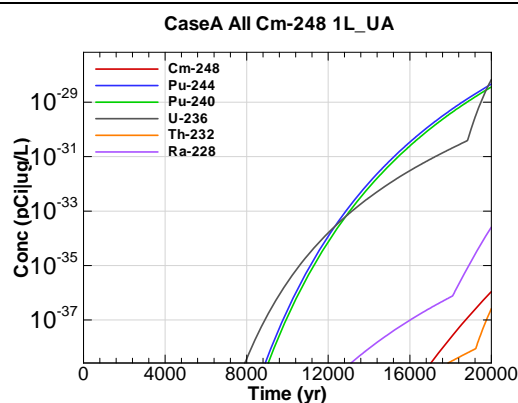
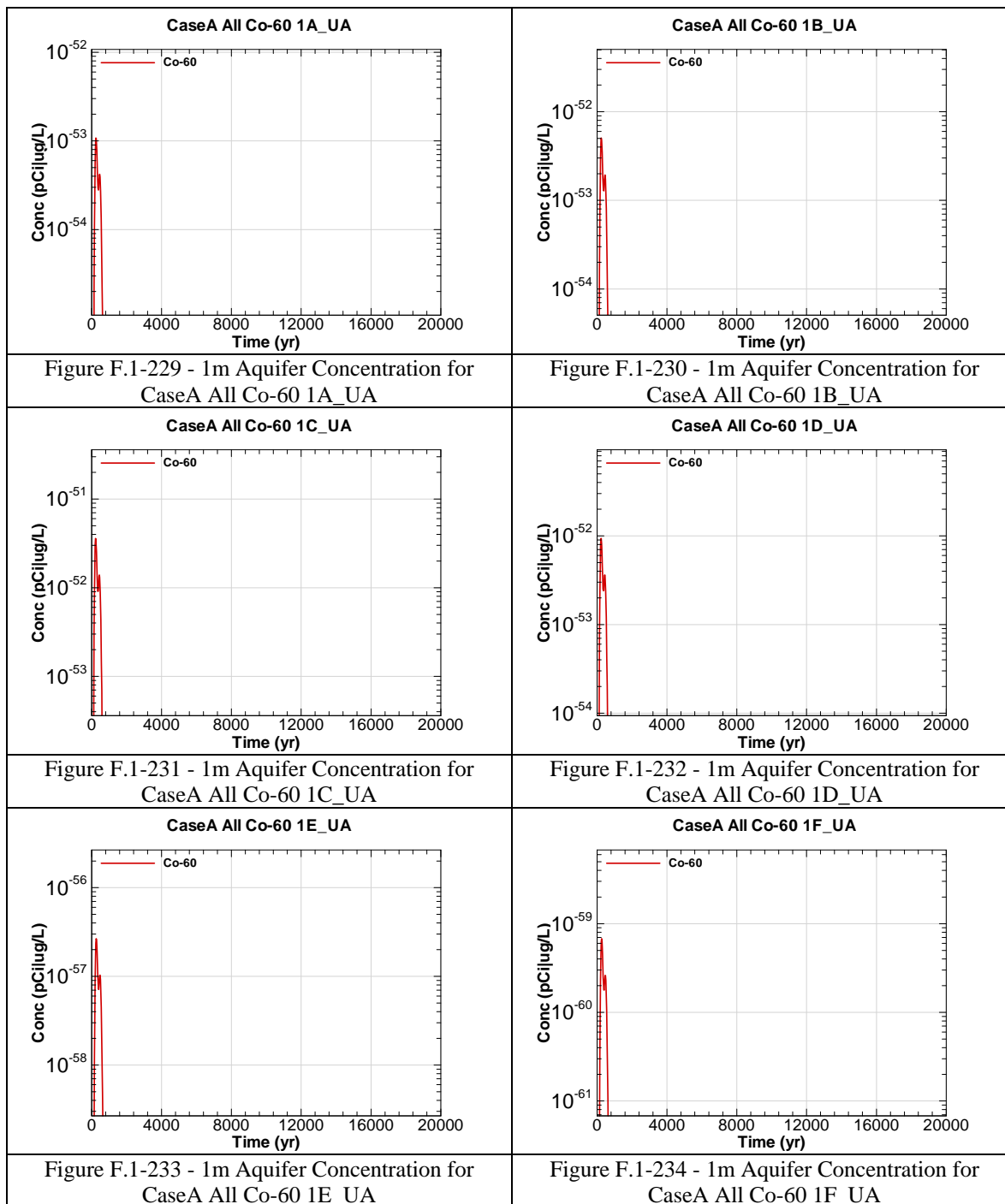
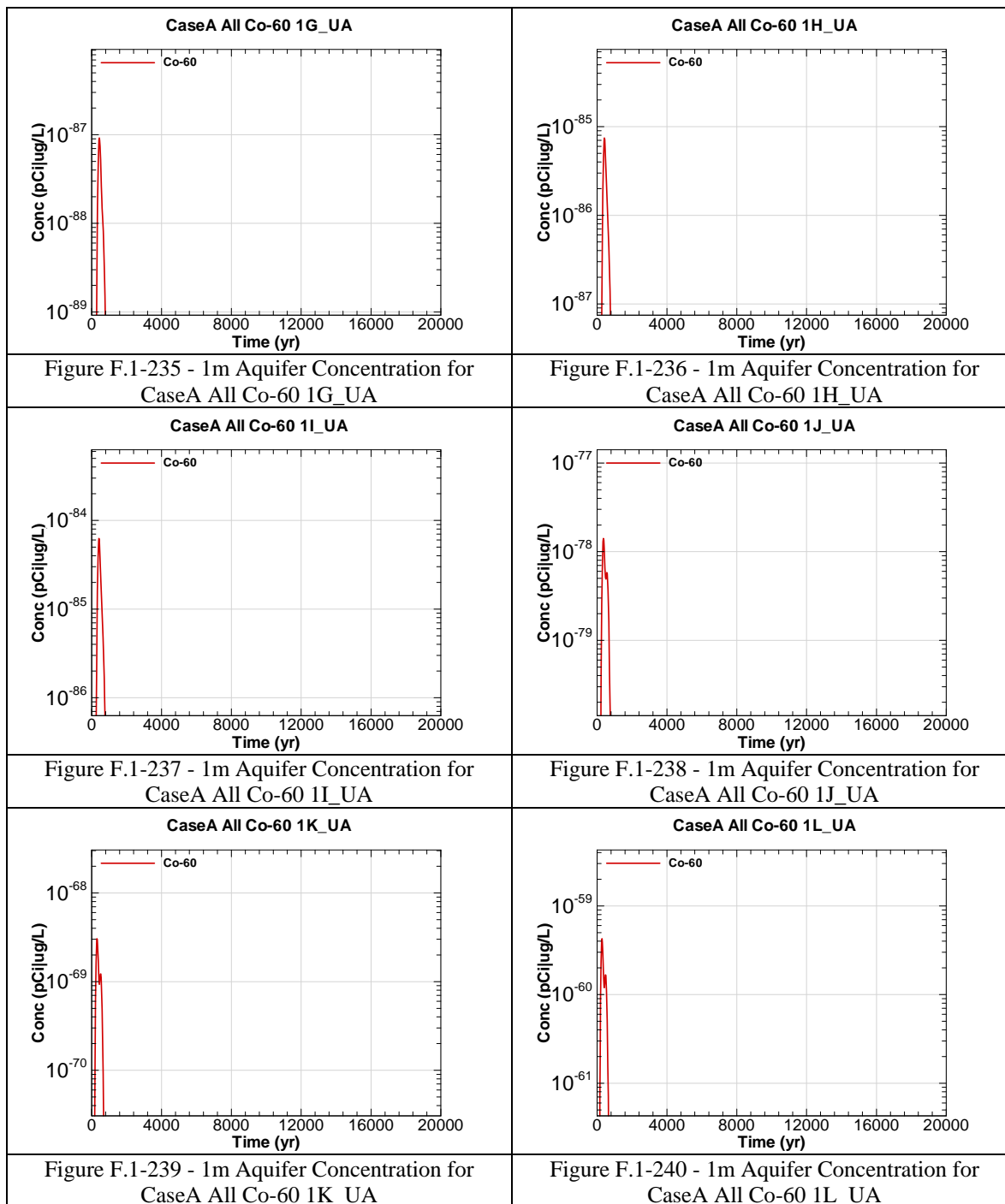
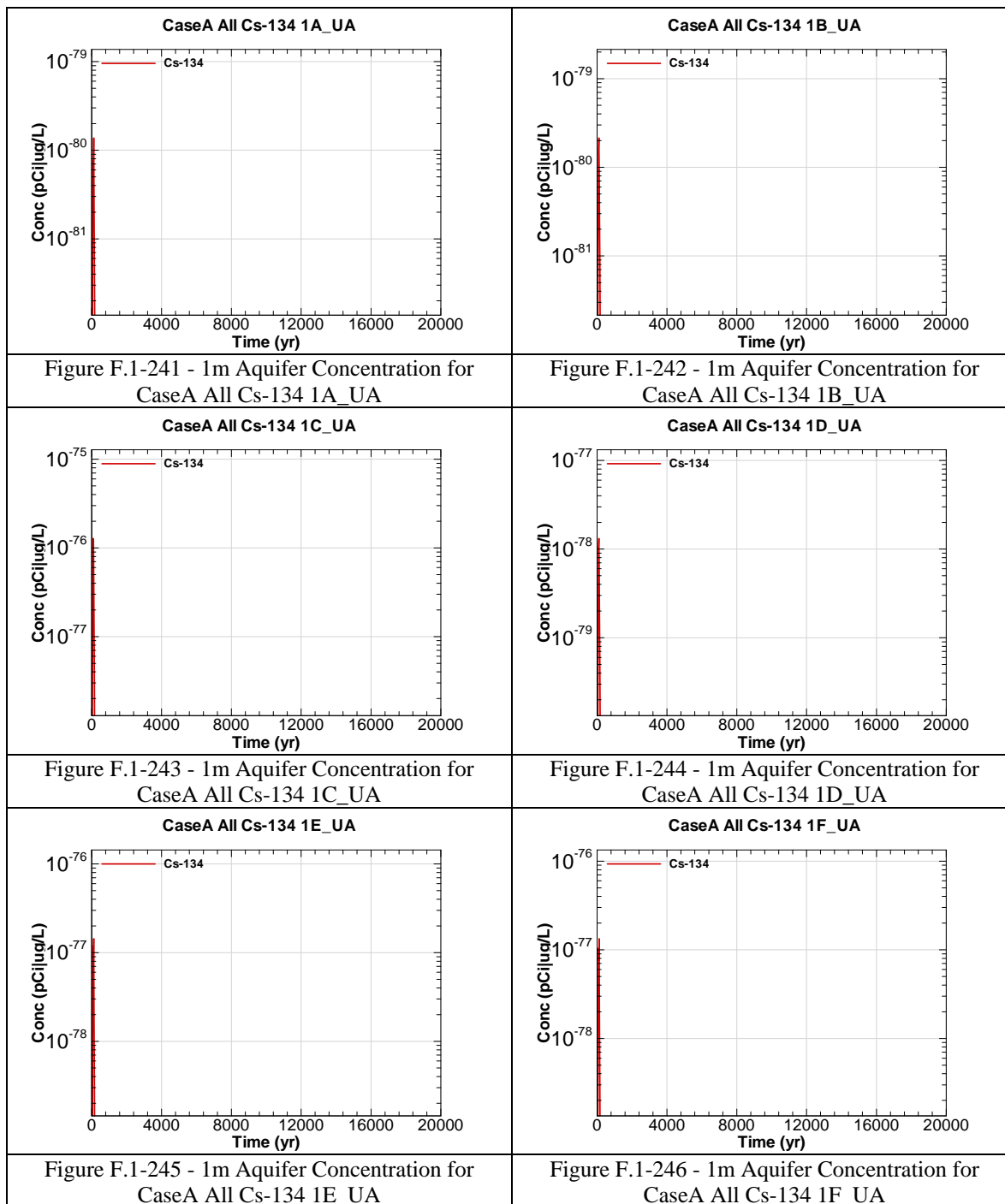
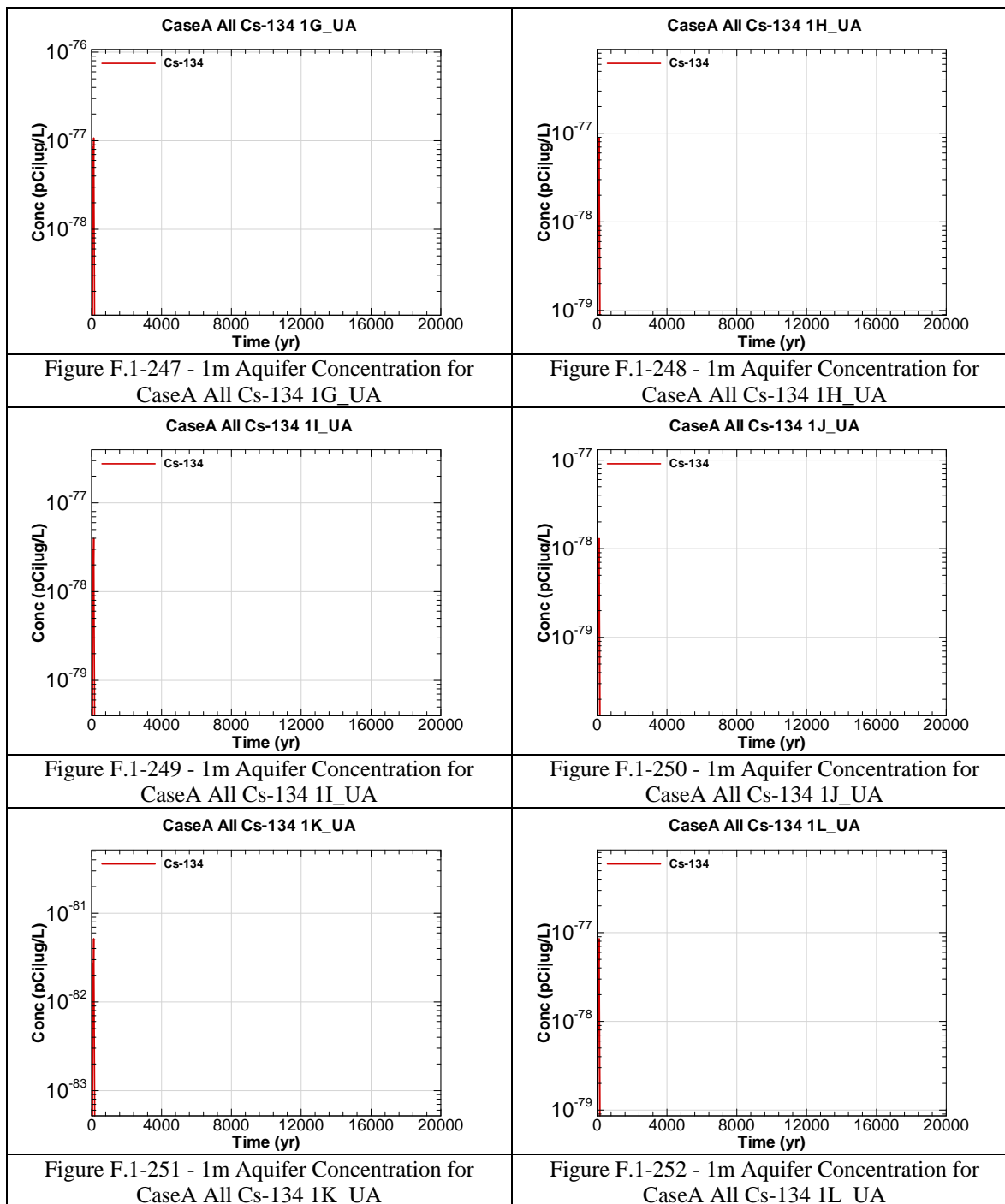


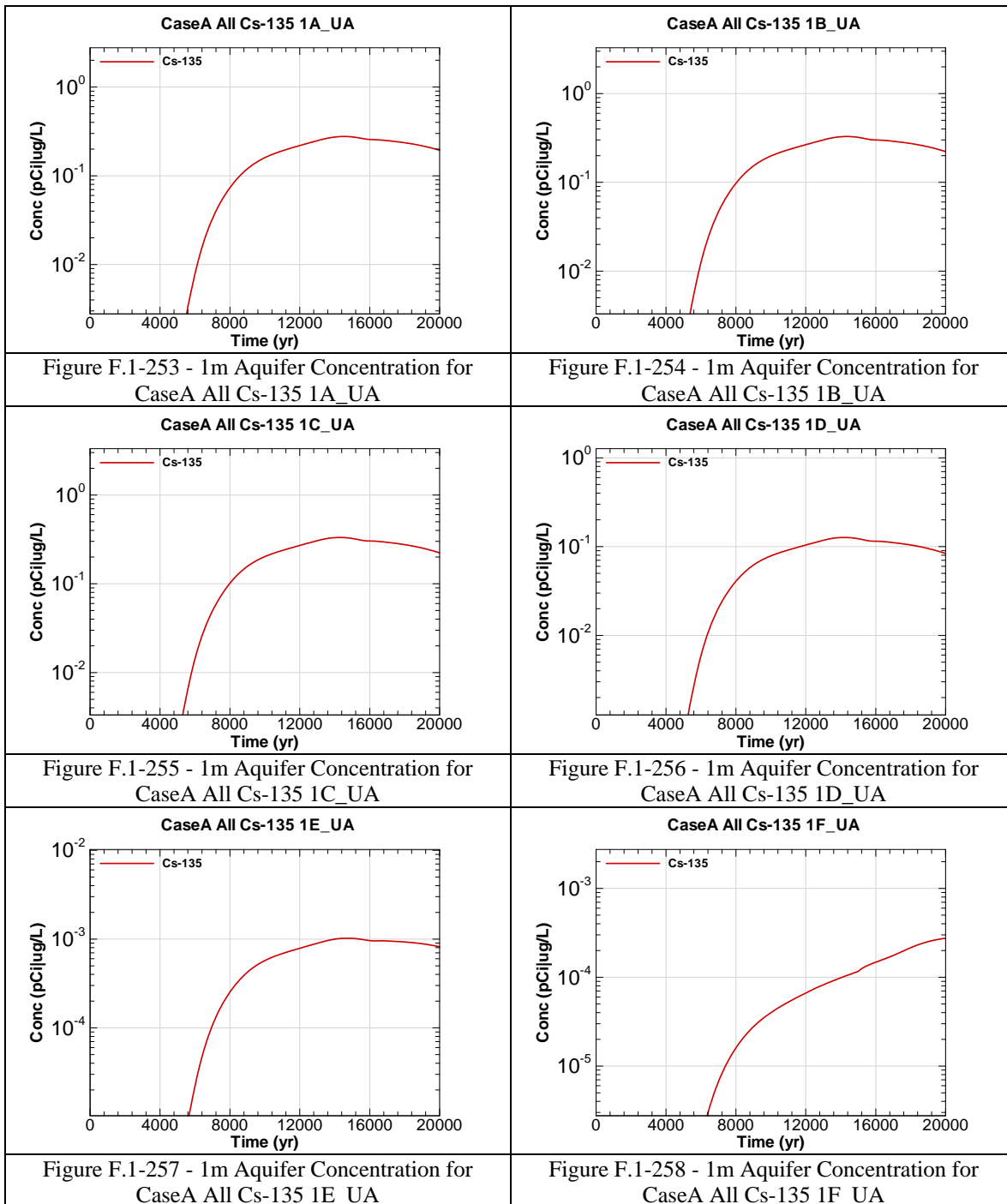
Figure F.1-228 - 1m Aquifer Concentration for
CaseA All Cm-248 1L_UA

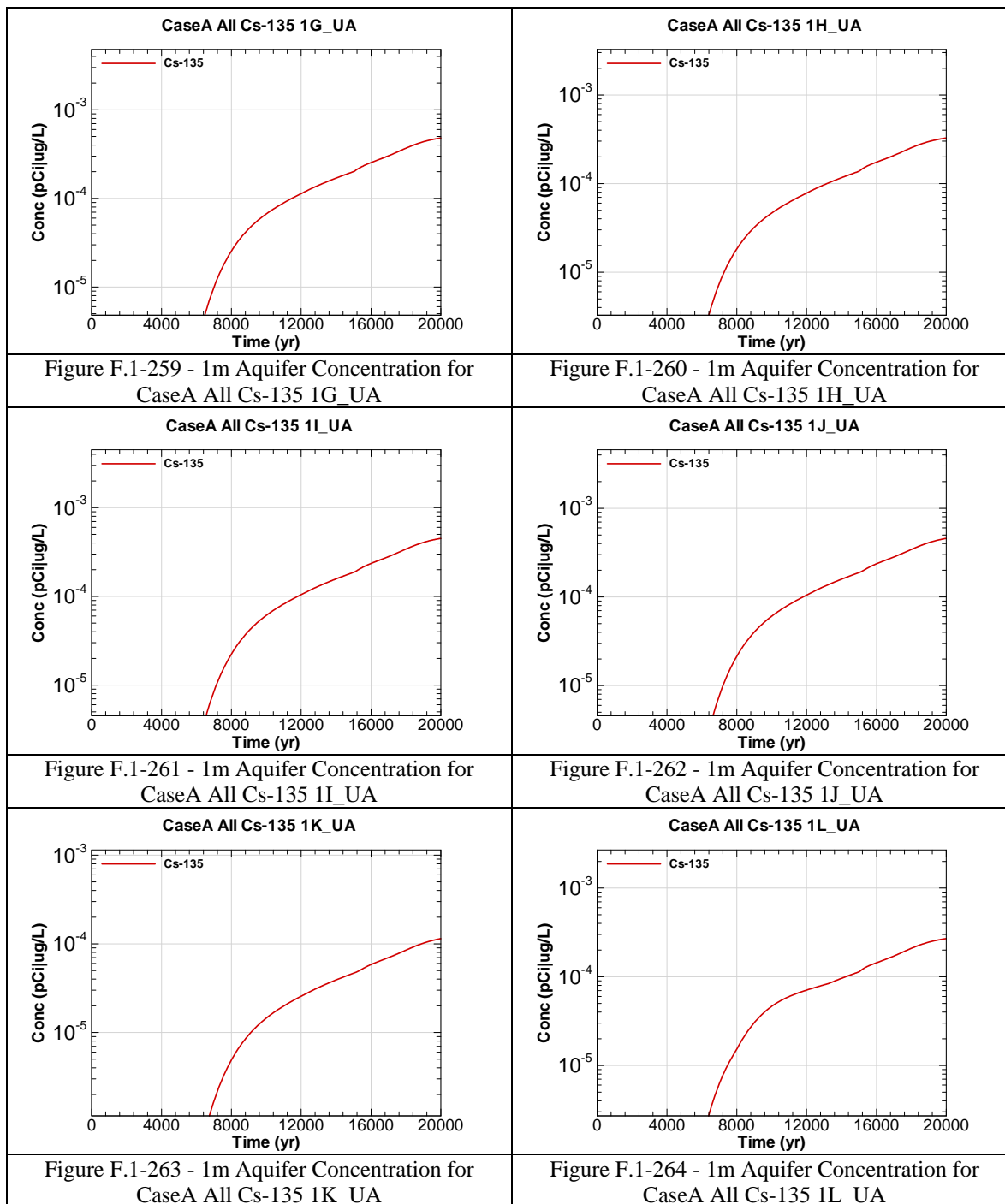


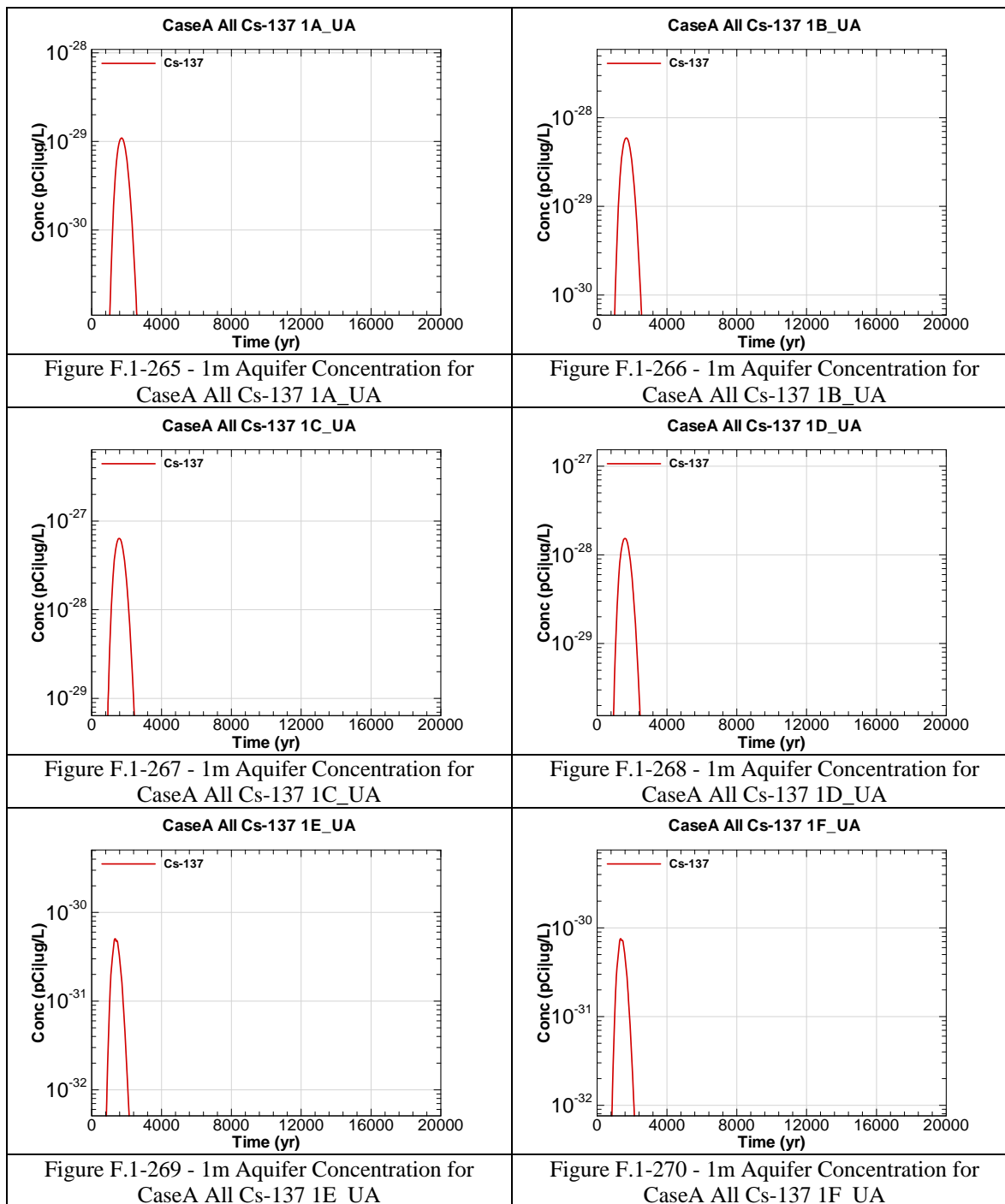


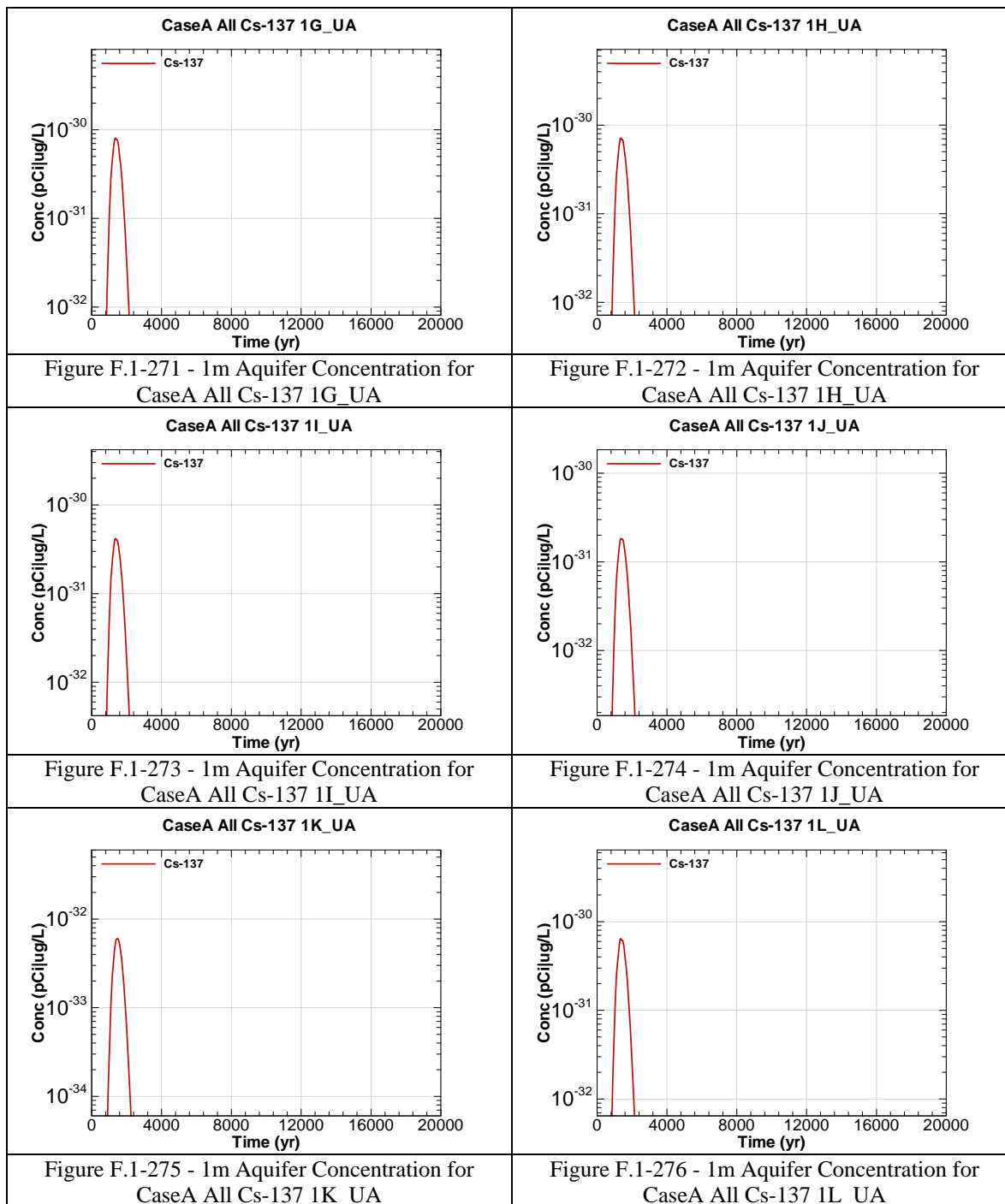


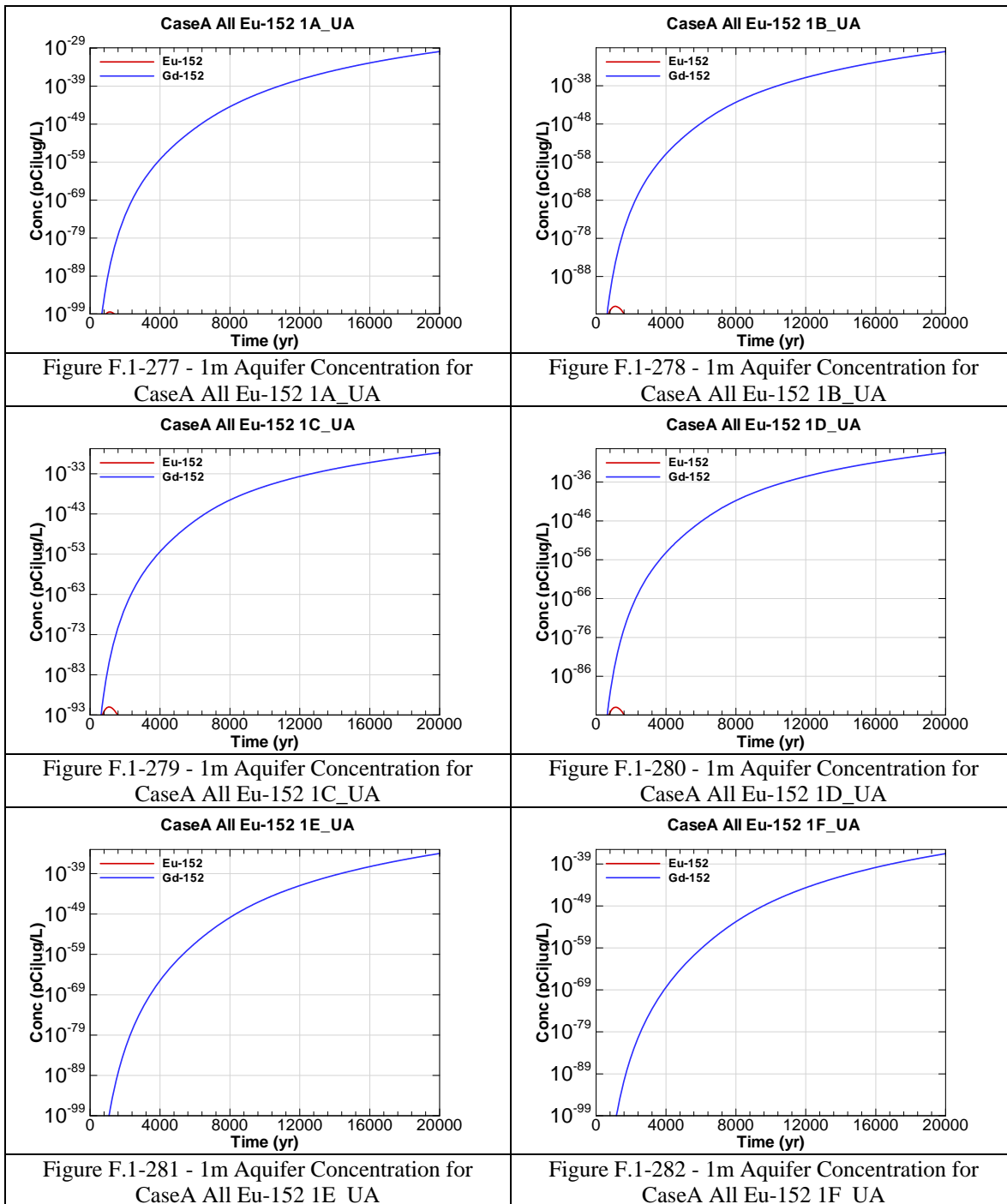


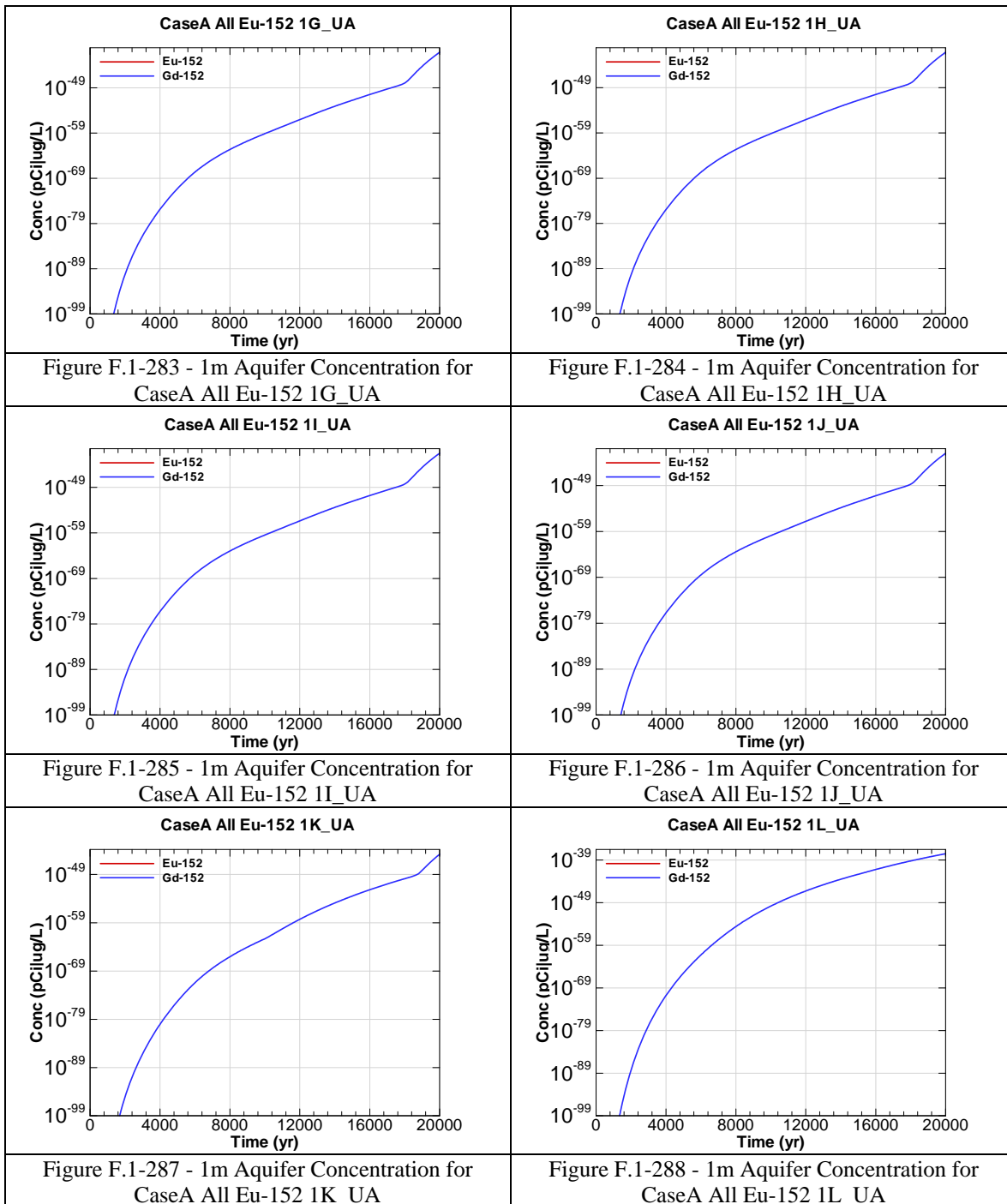


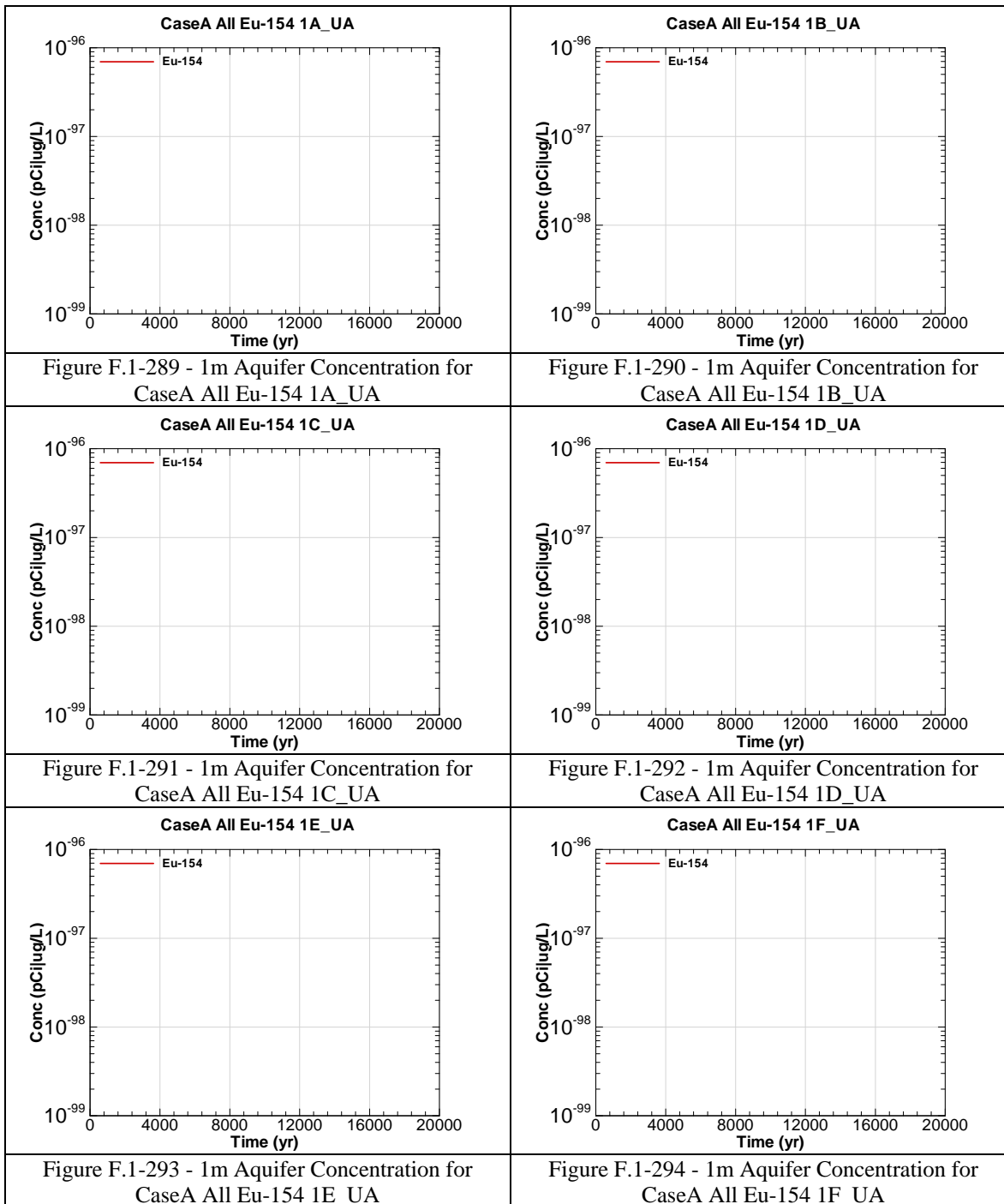


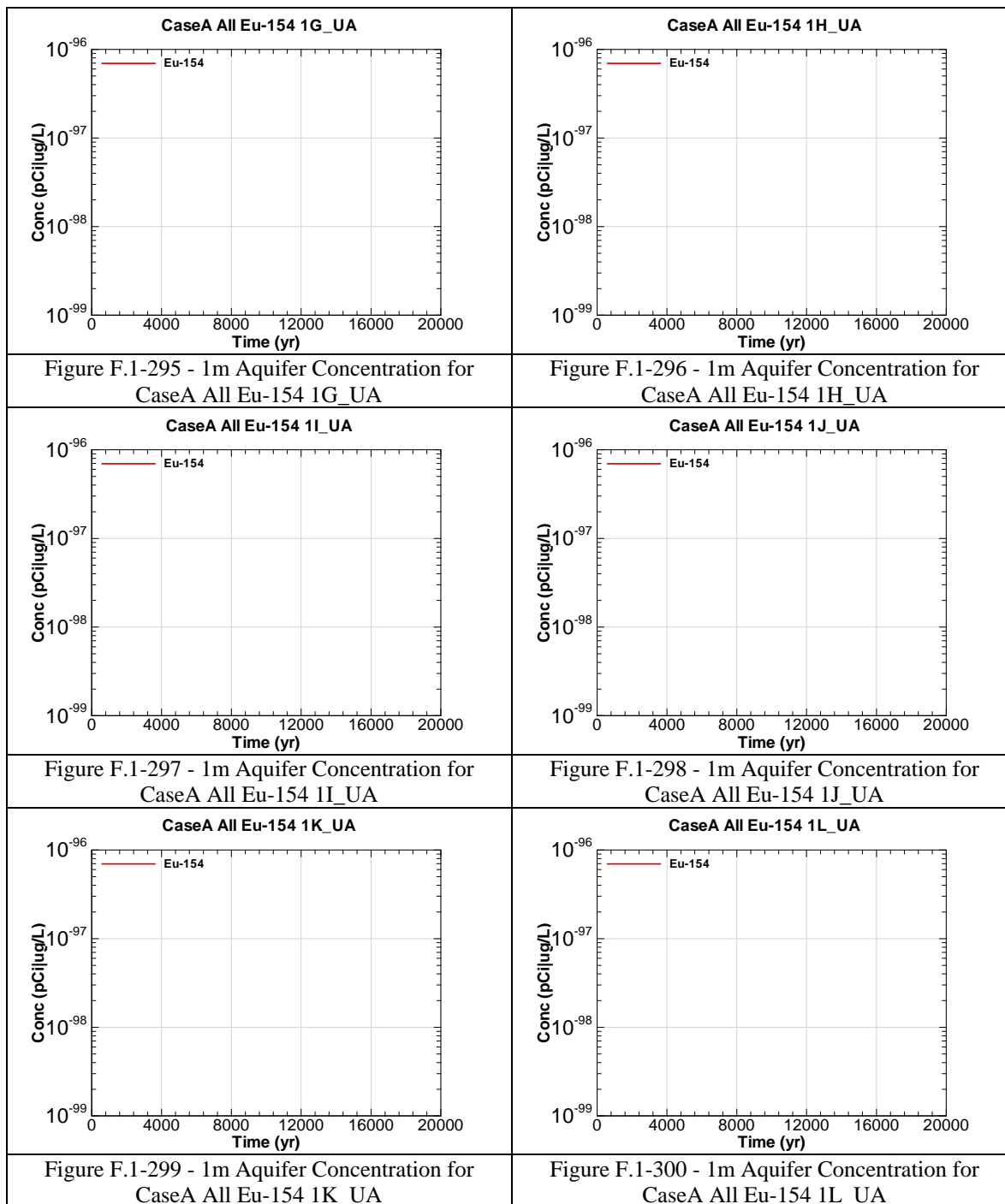


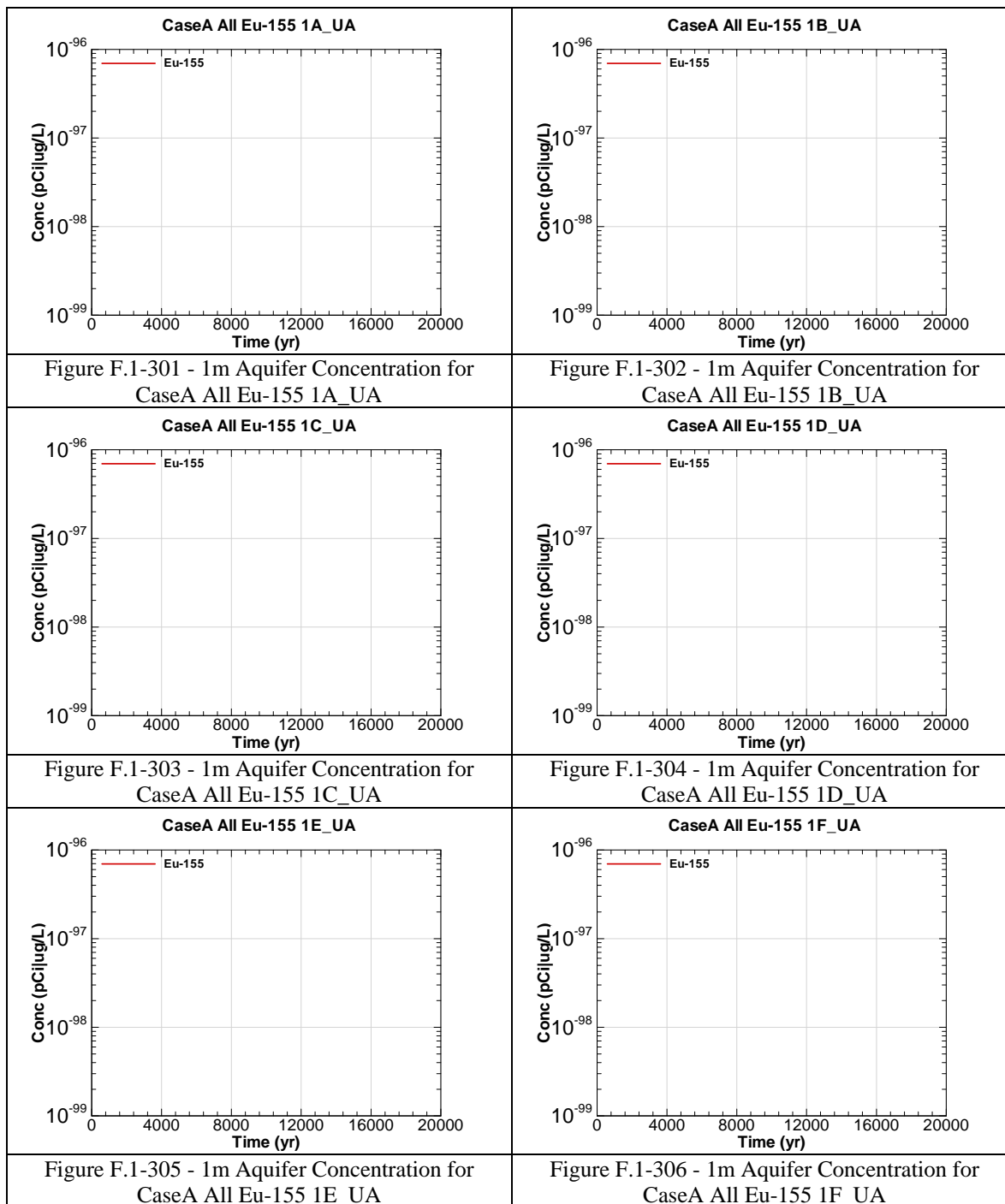


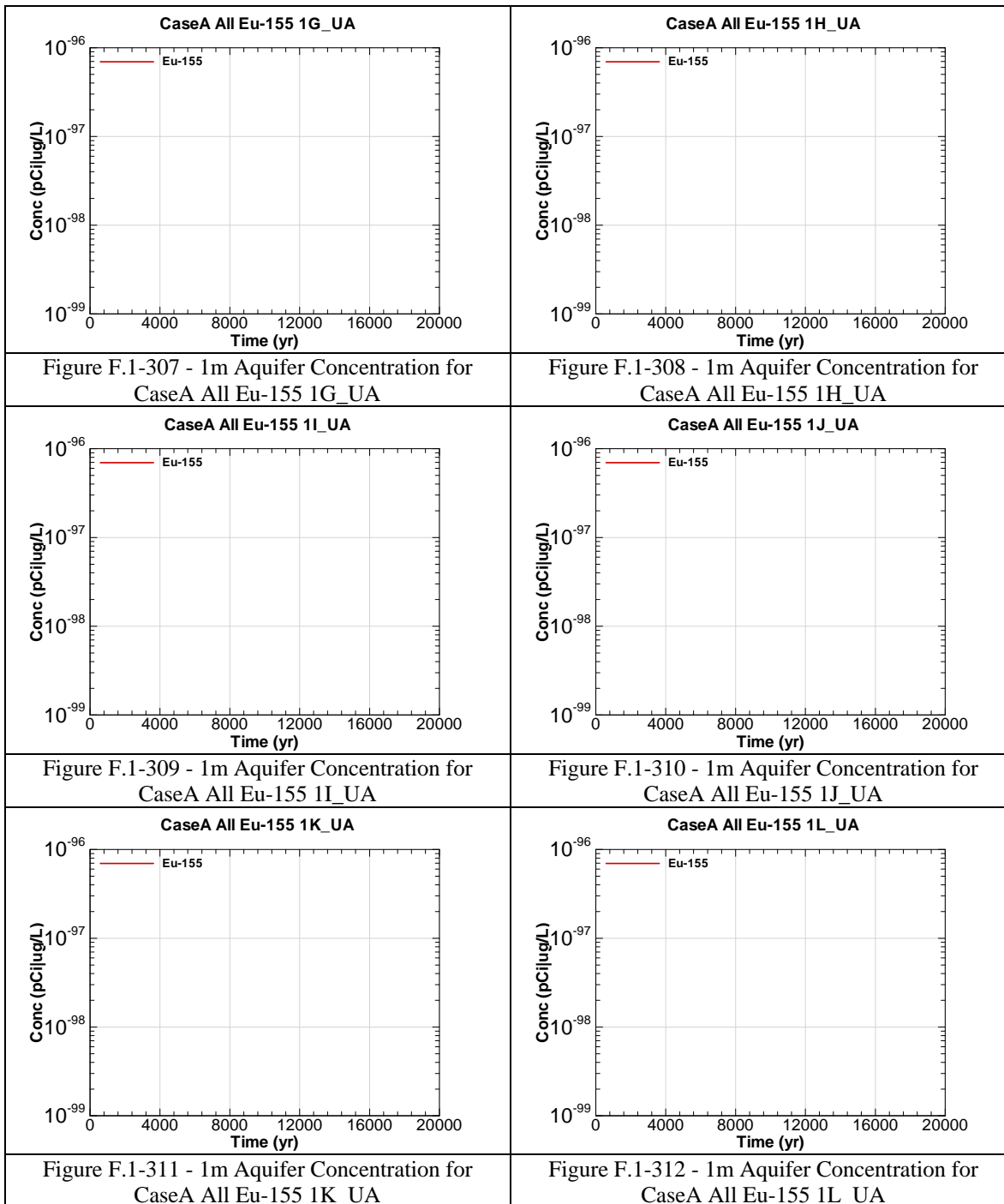


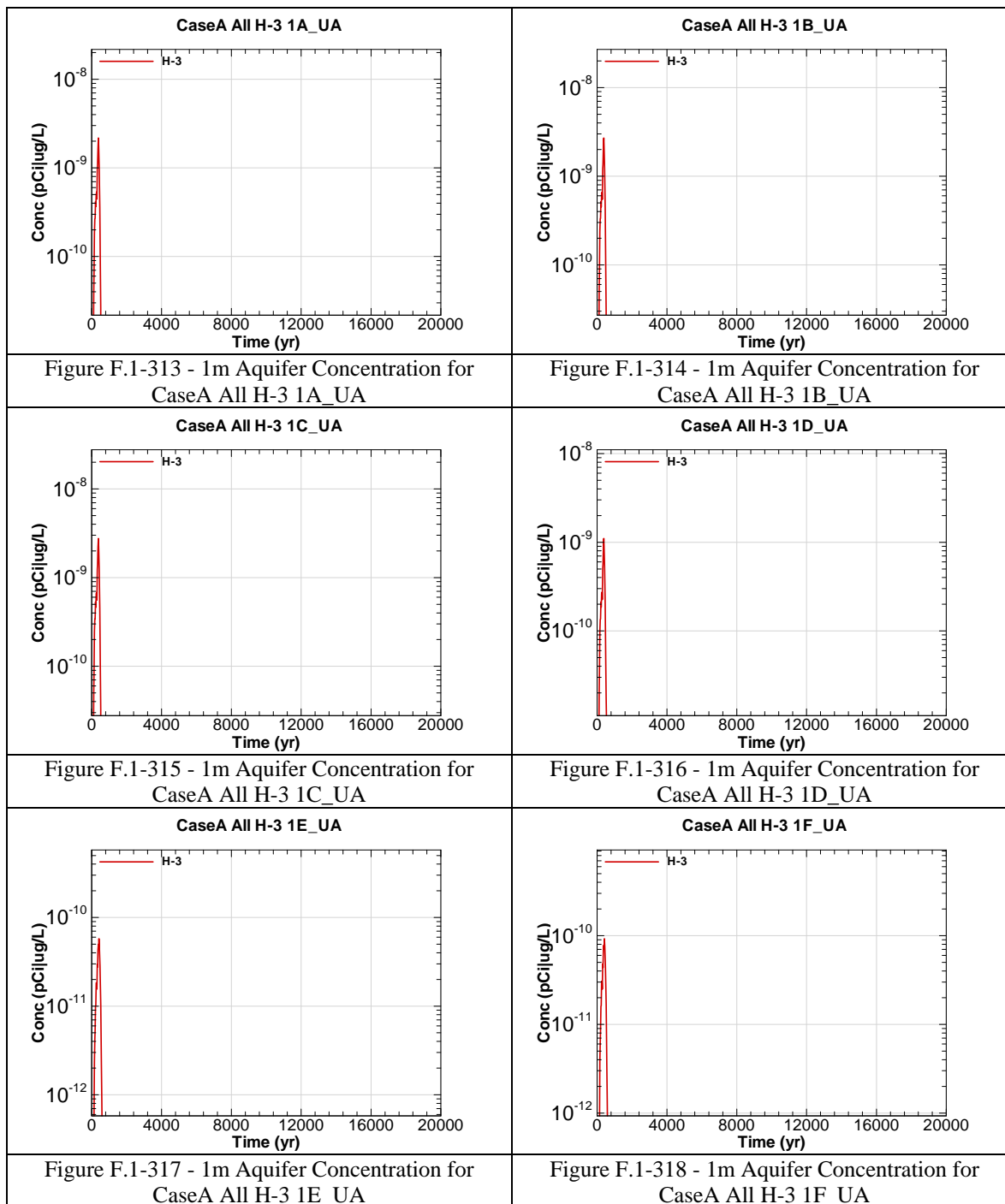


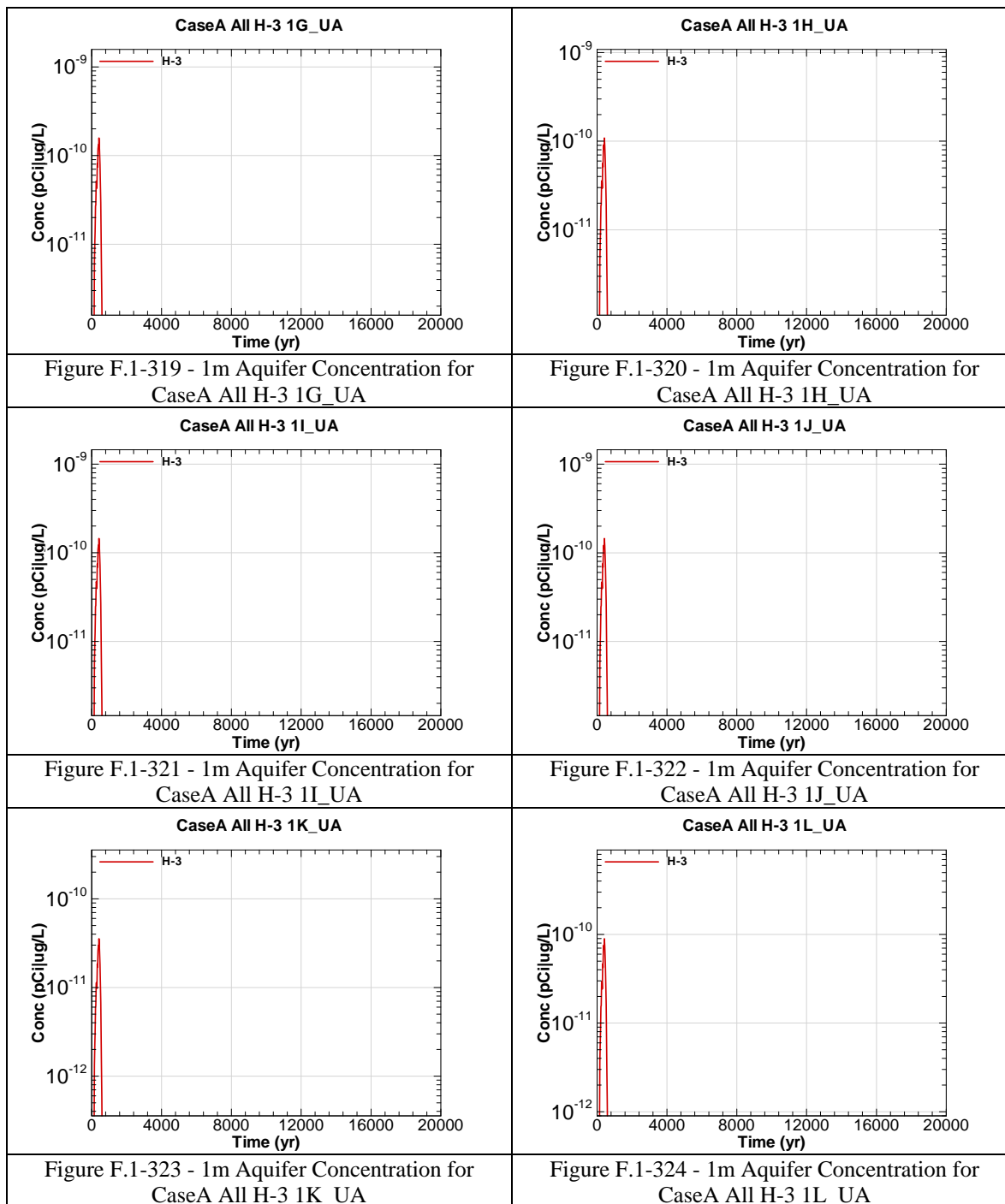


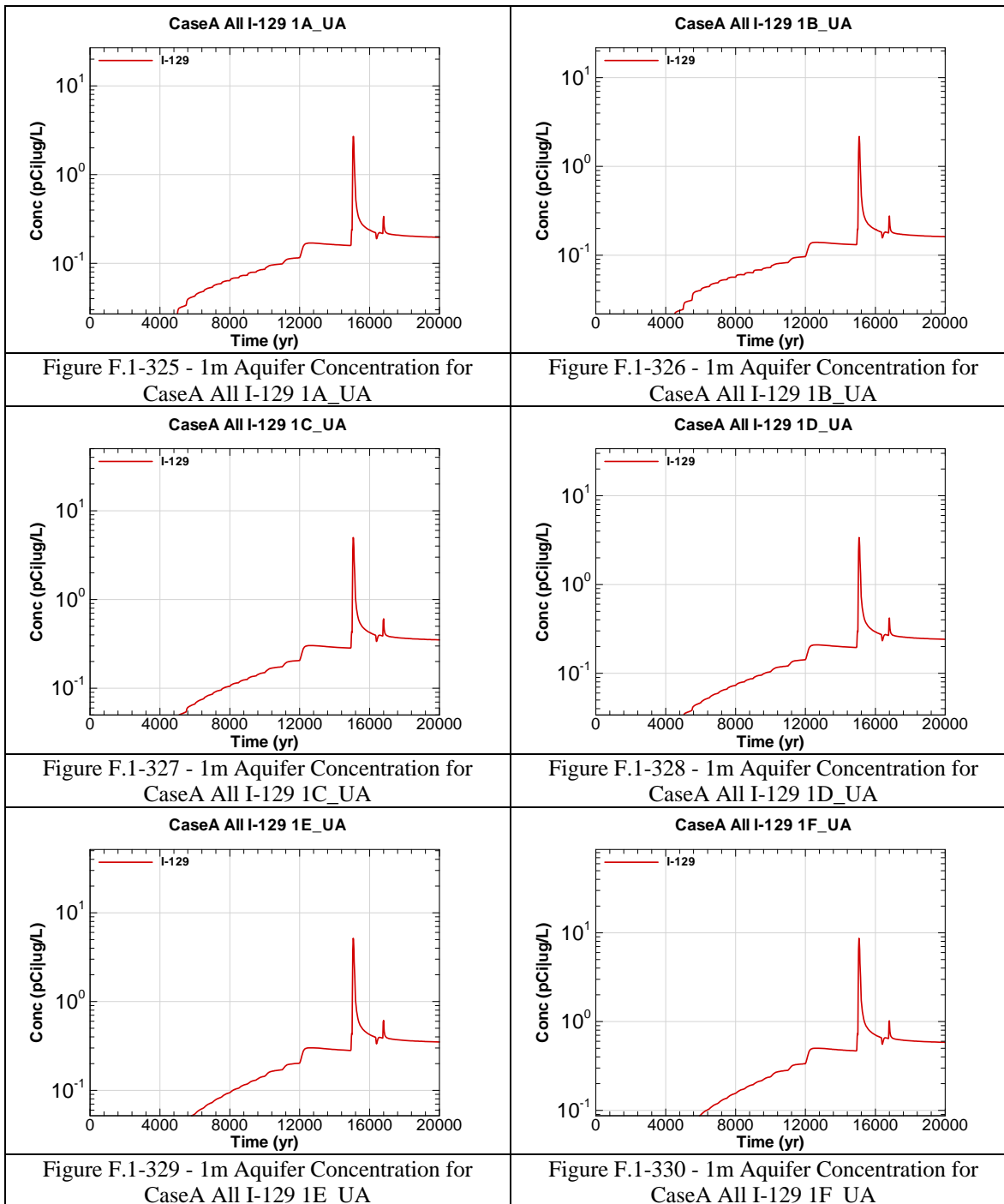


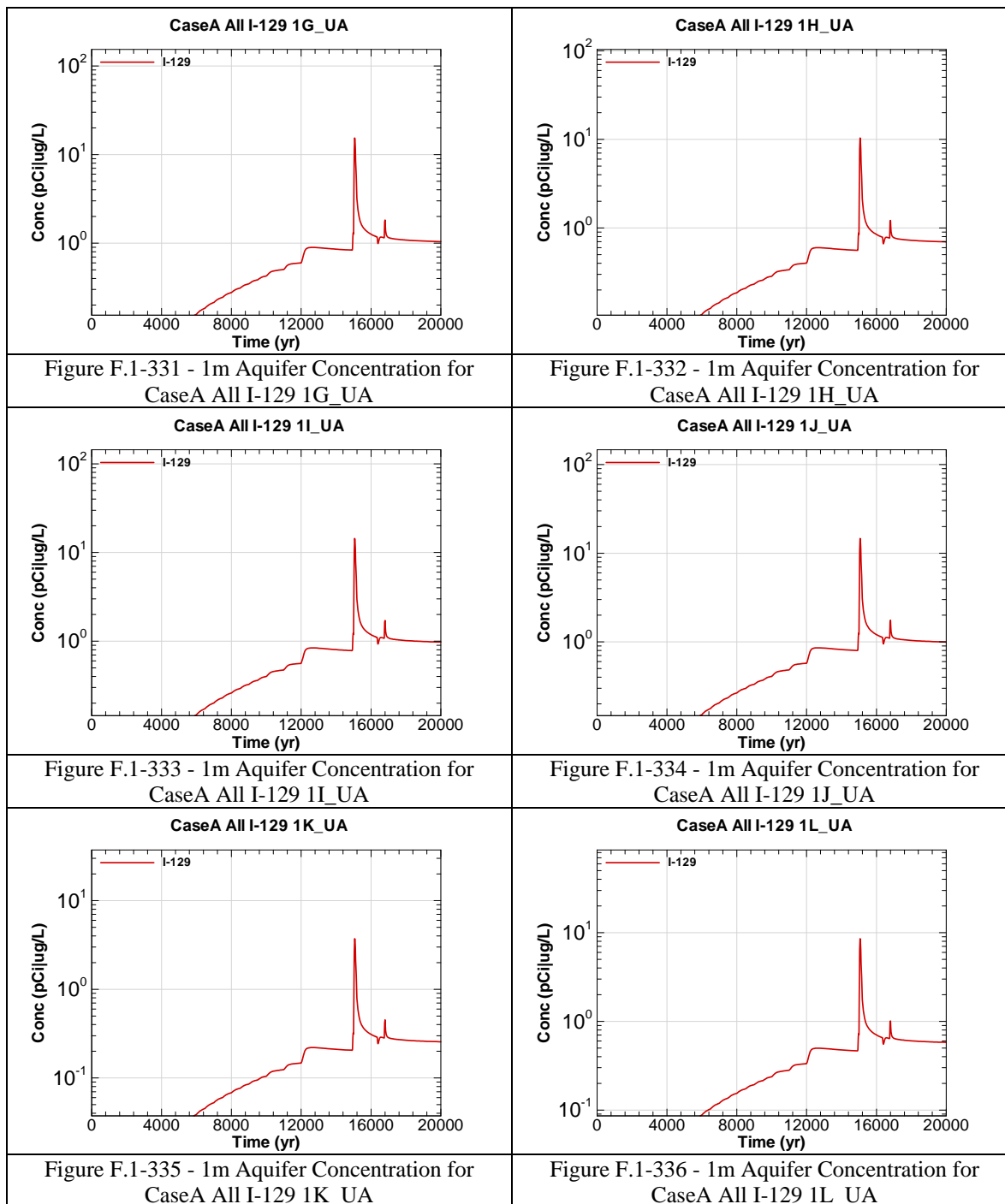


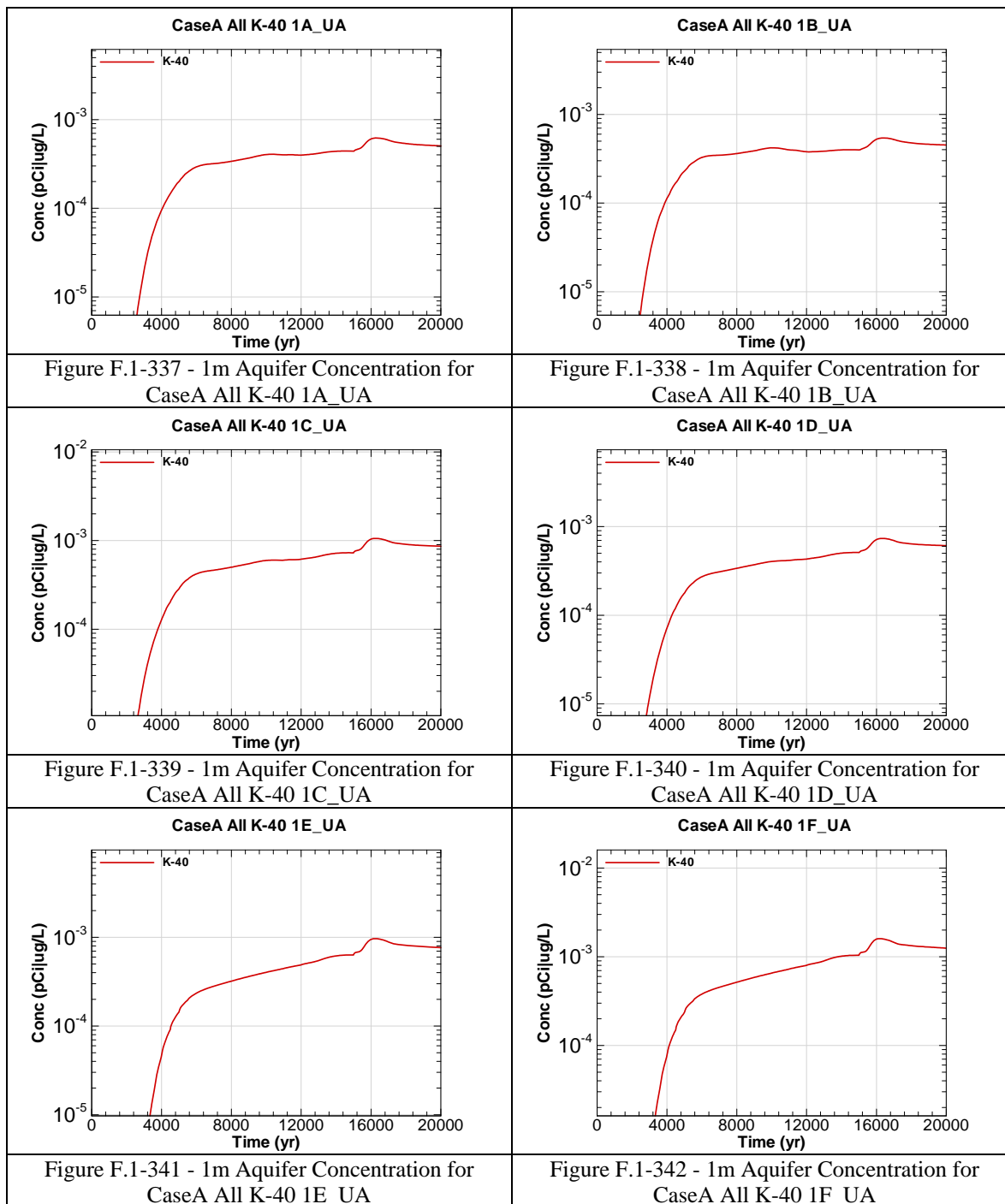


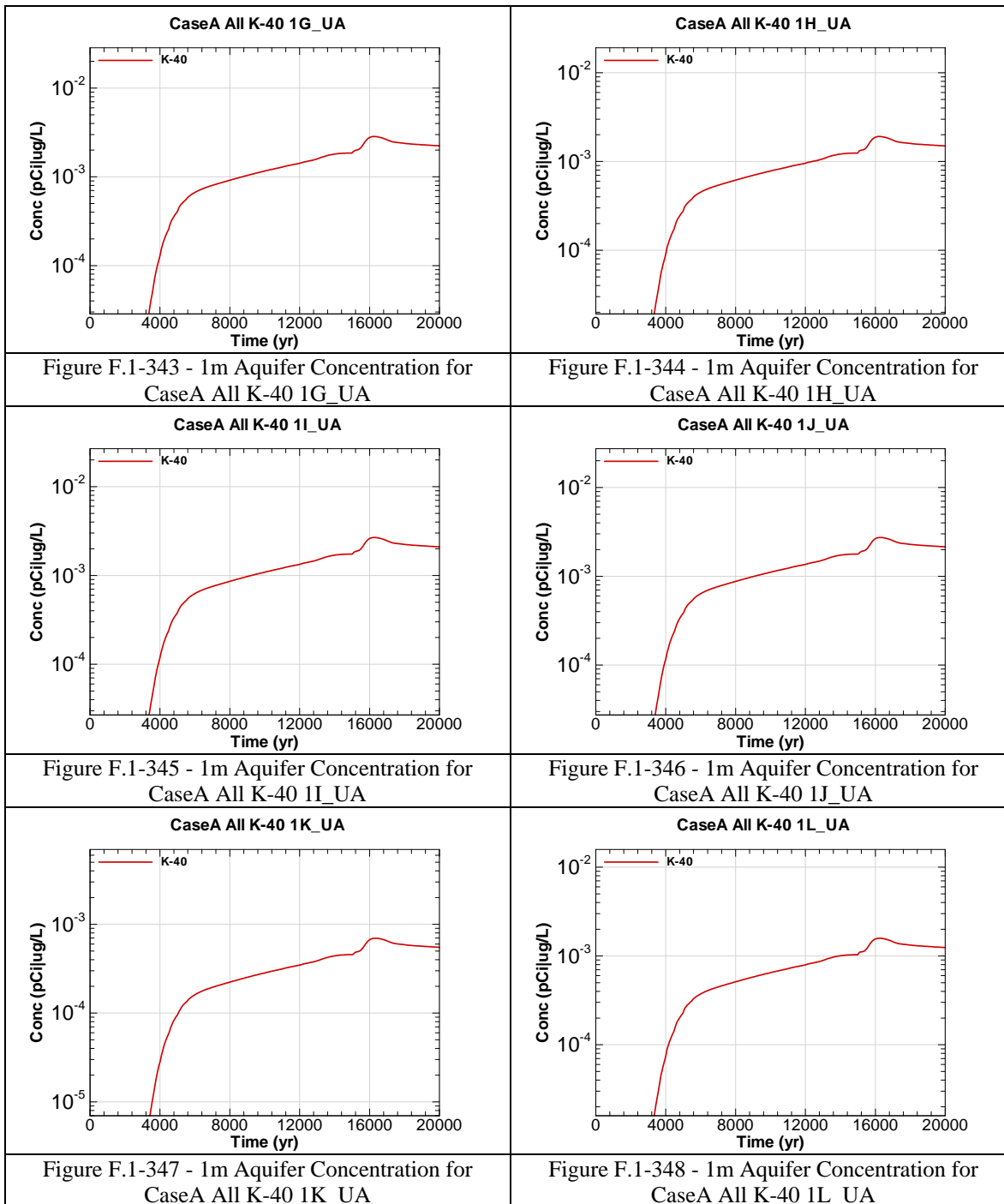


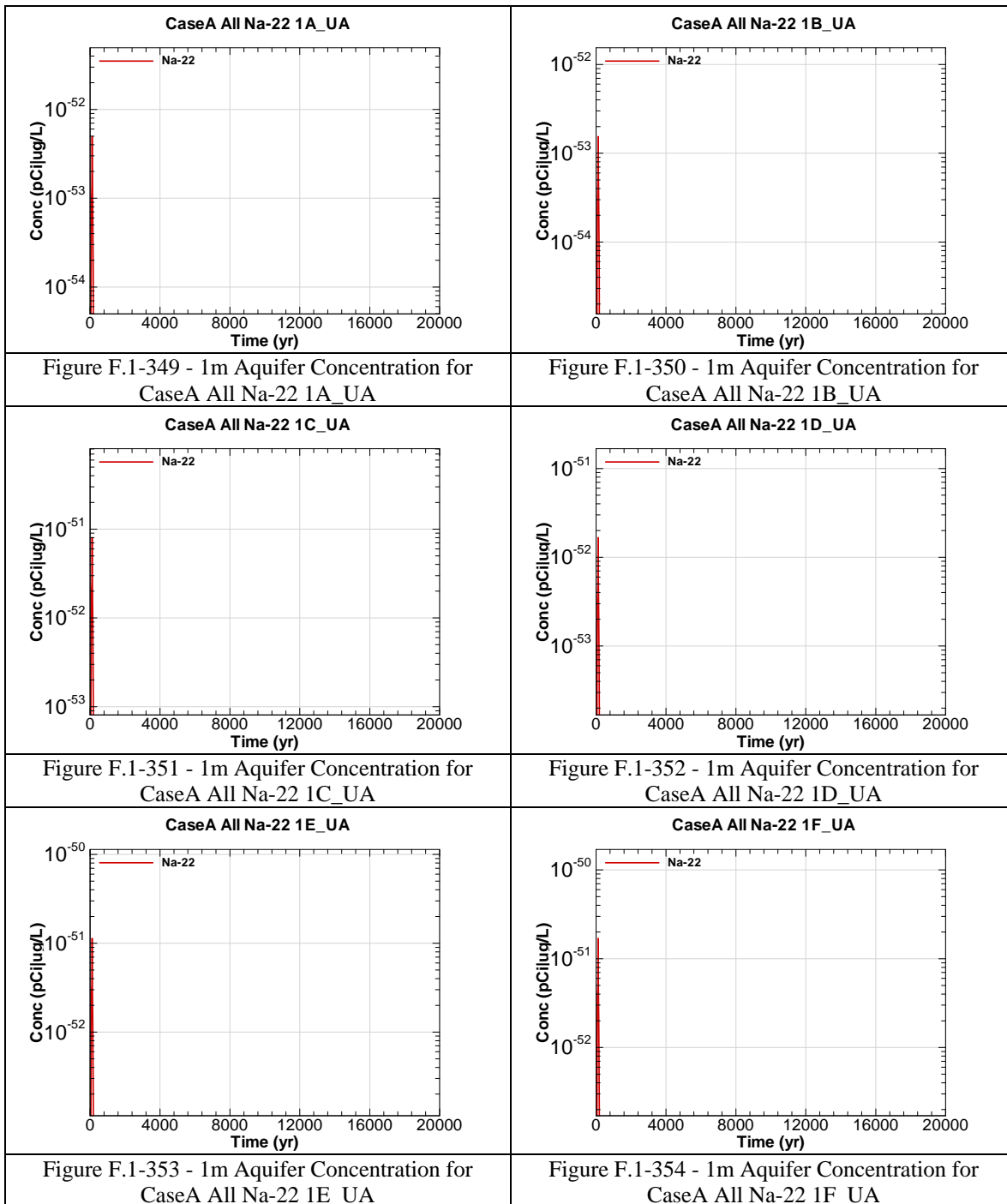


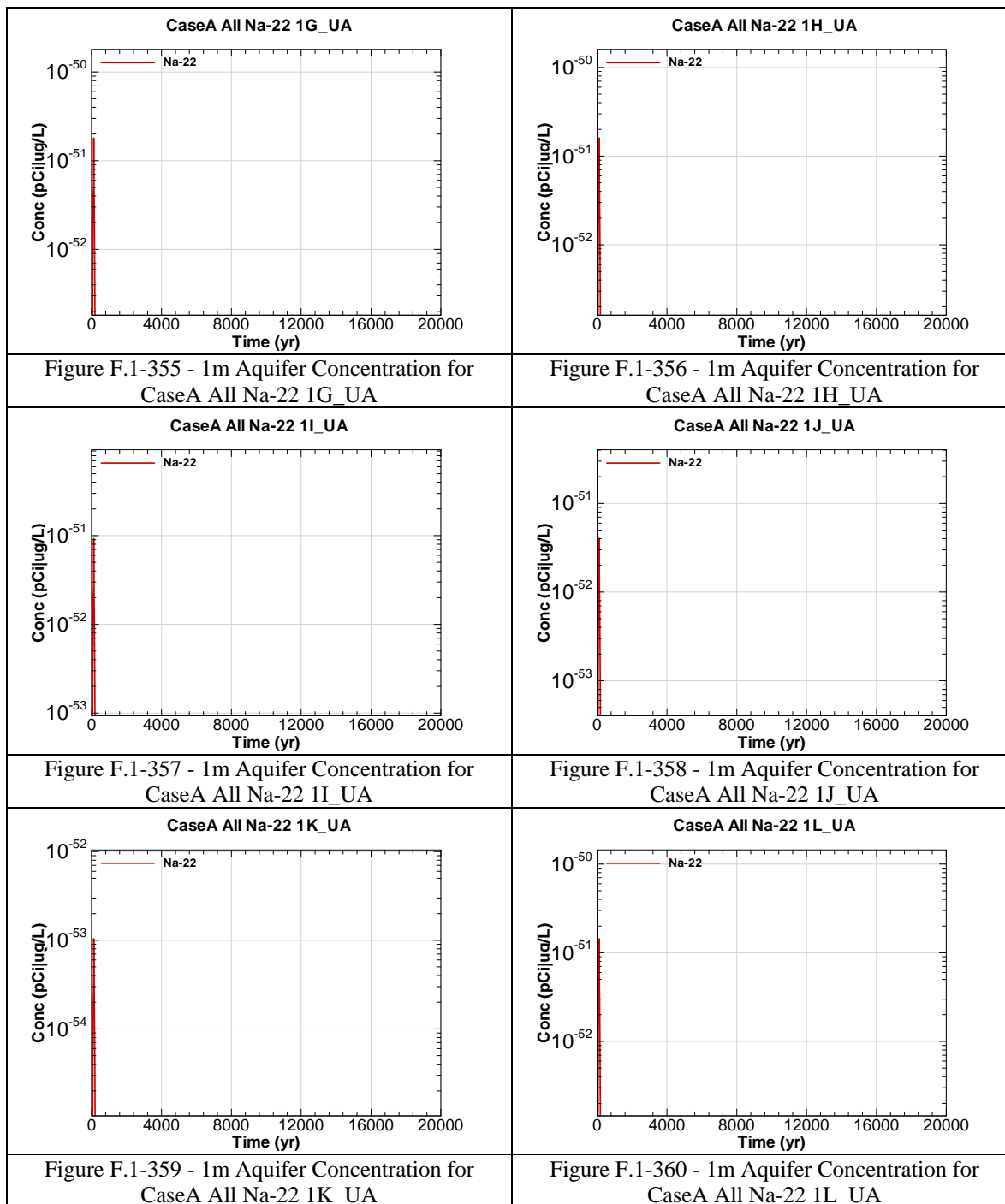


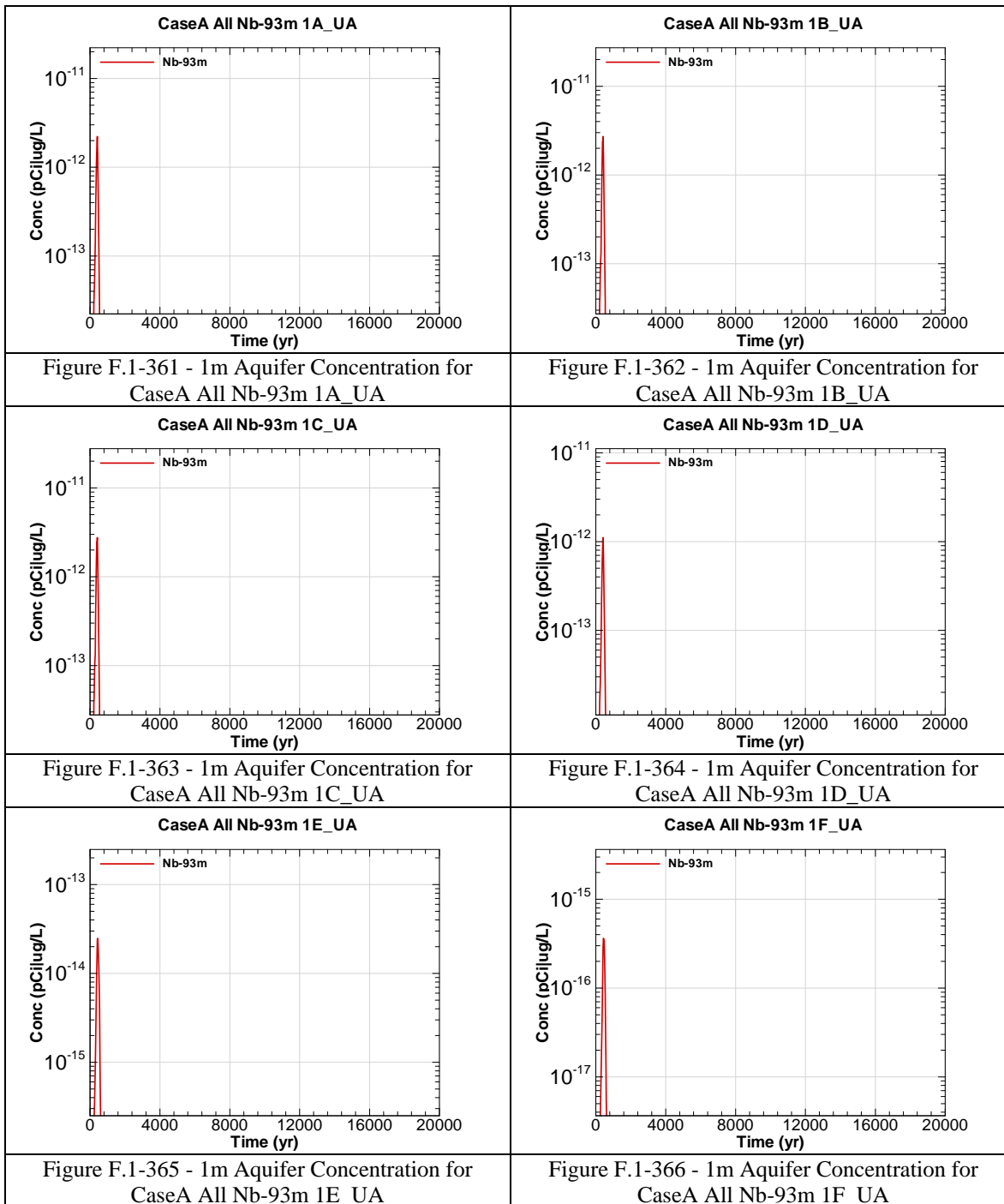


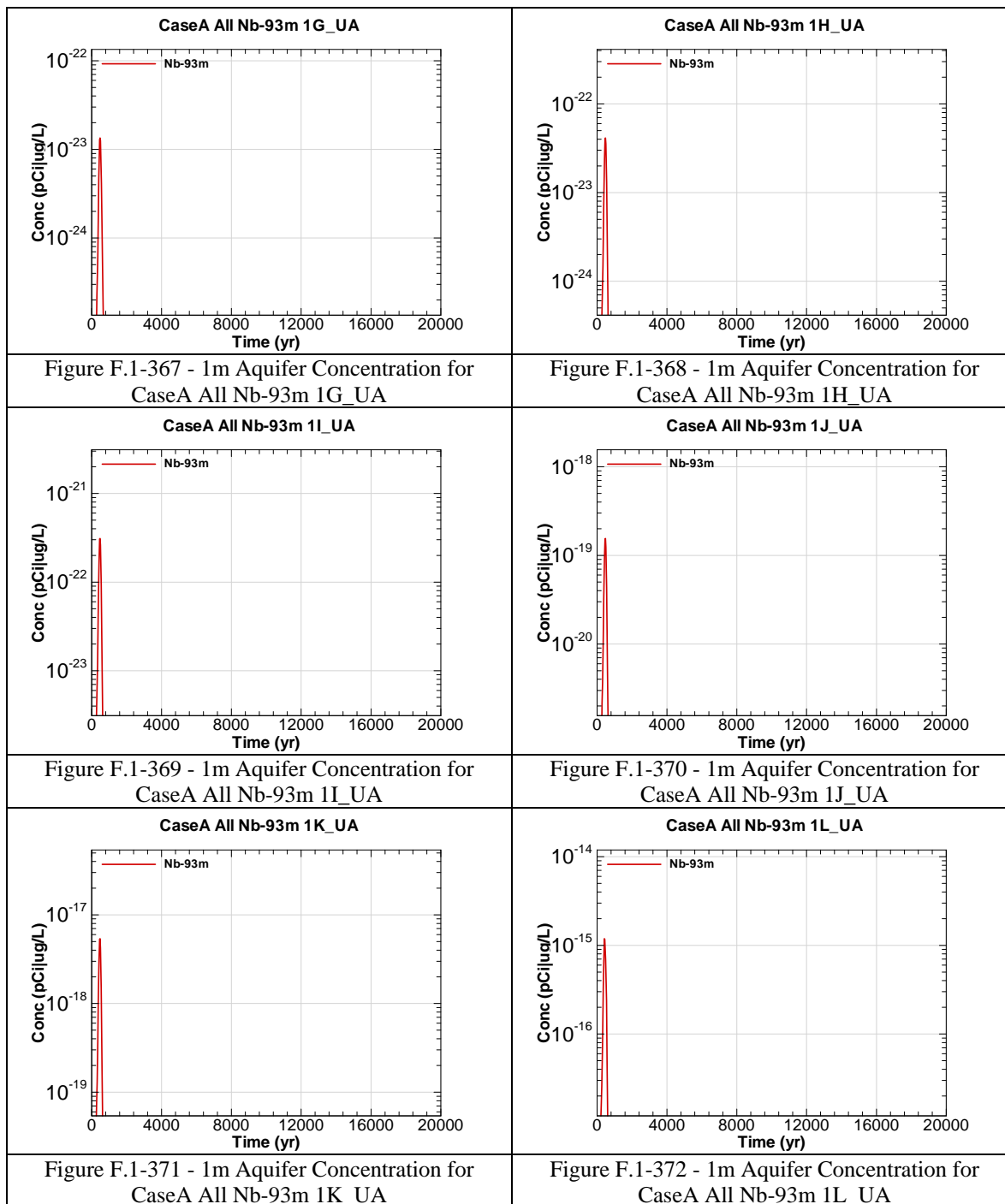


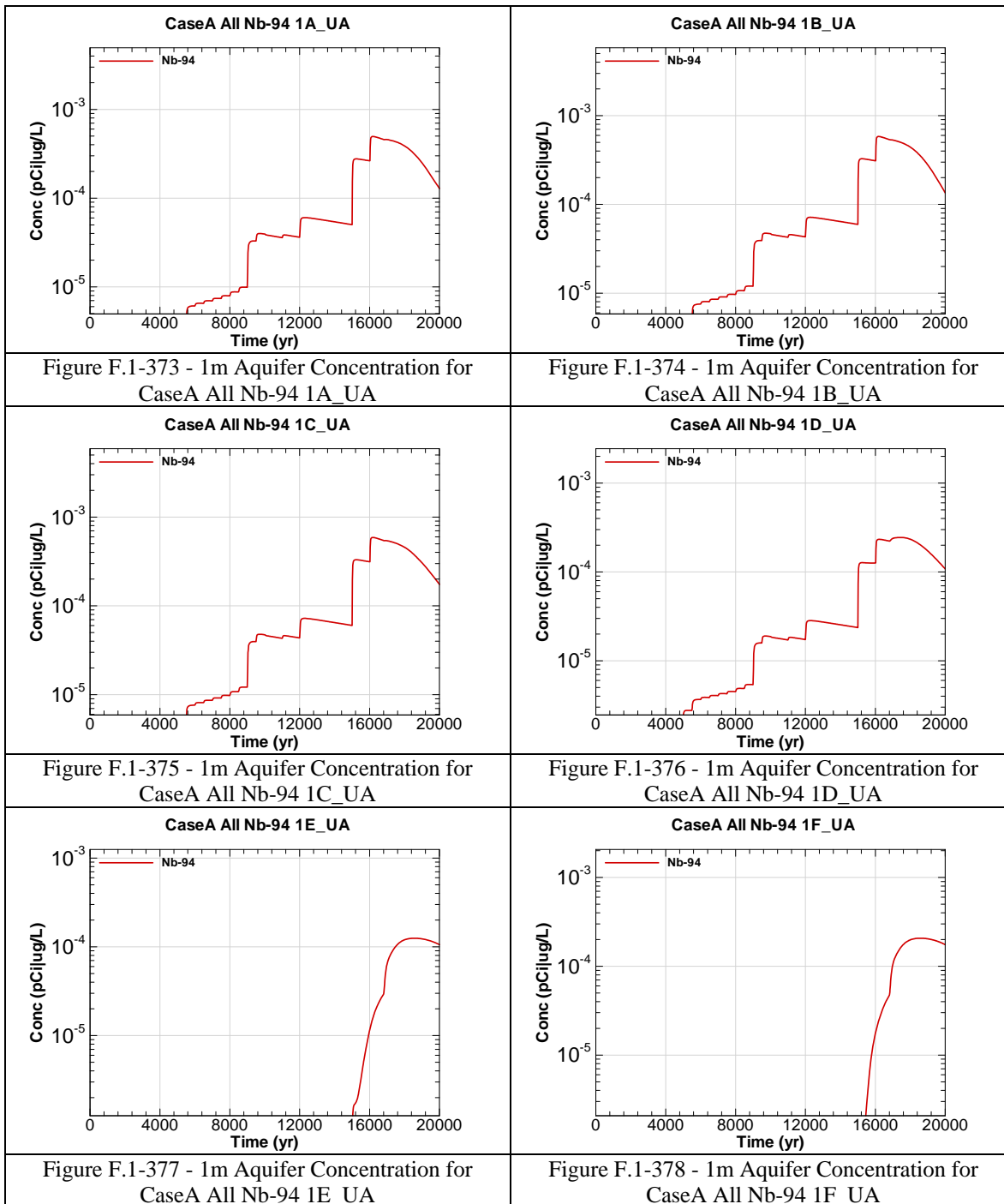


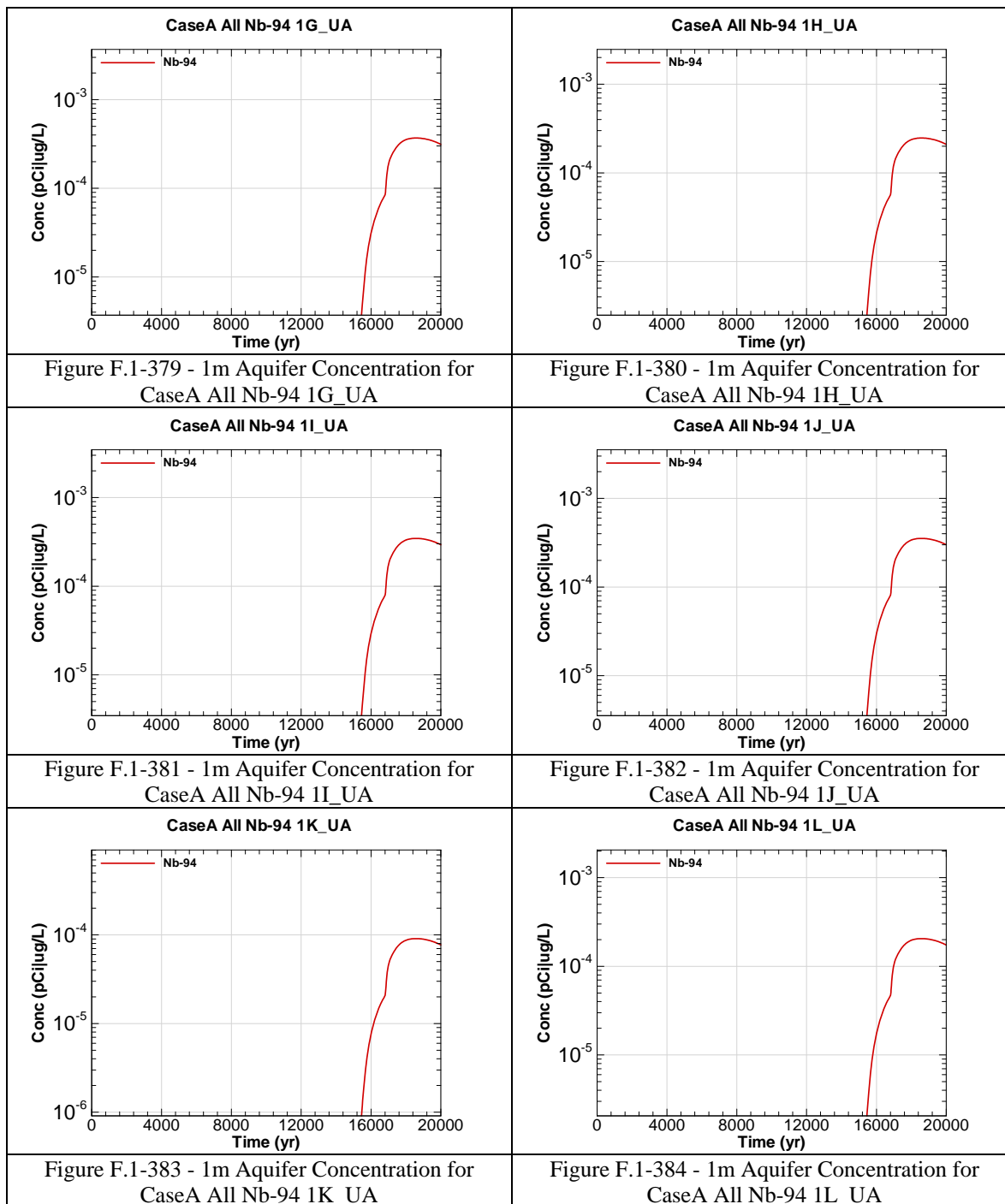


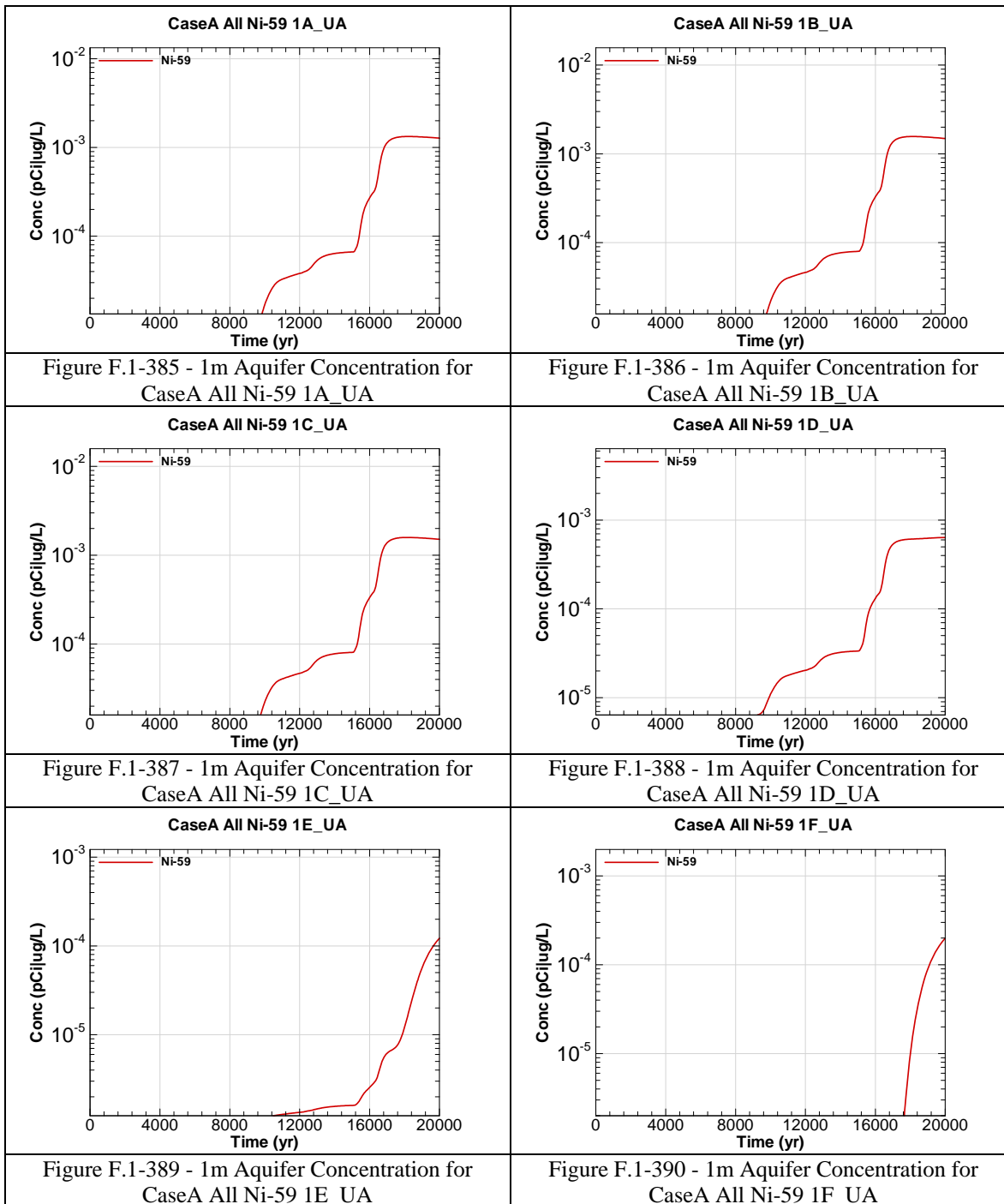


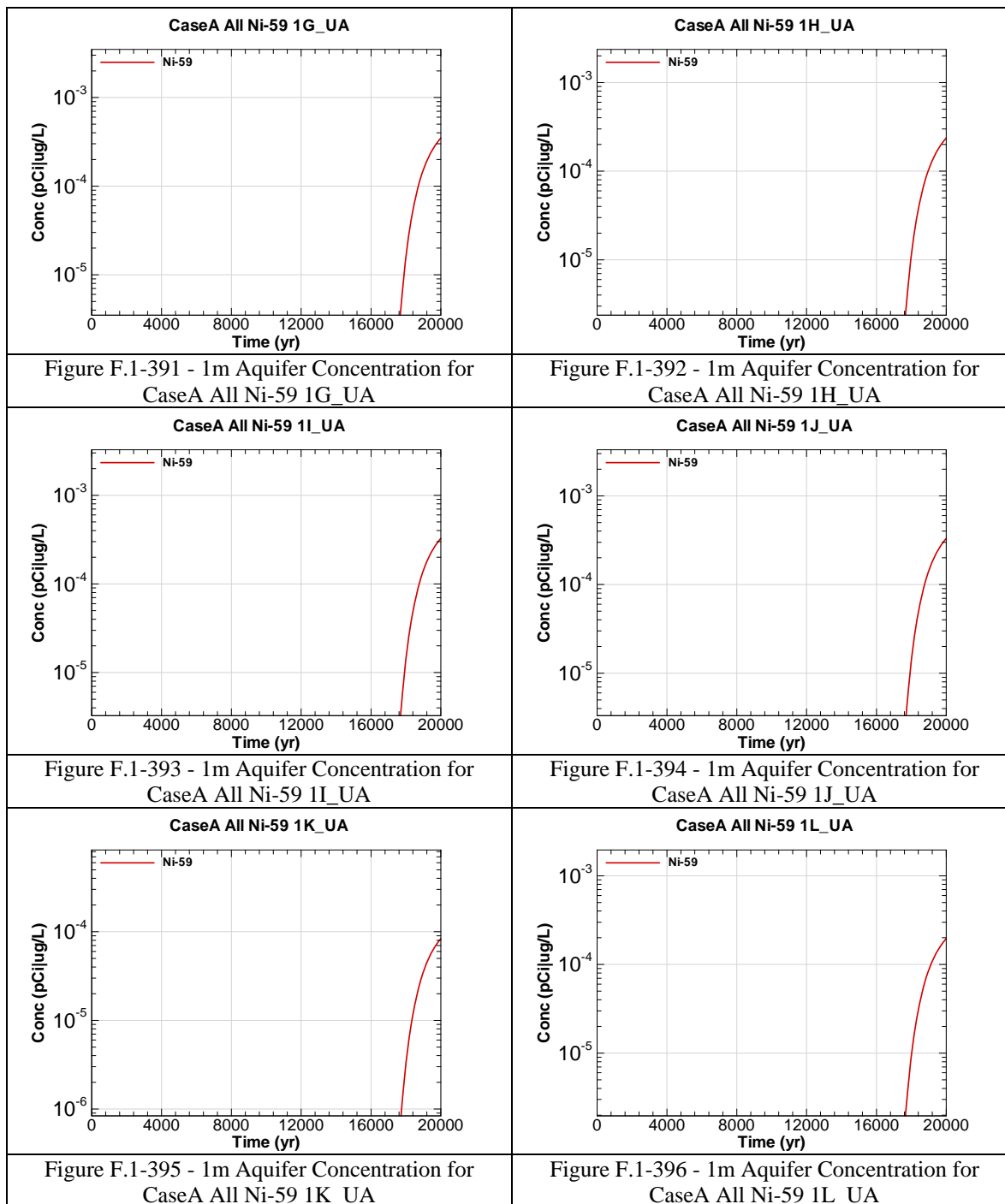


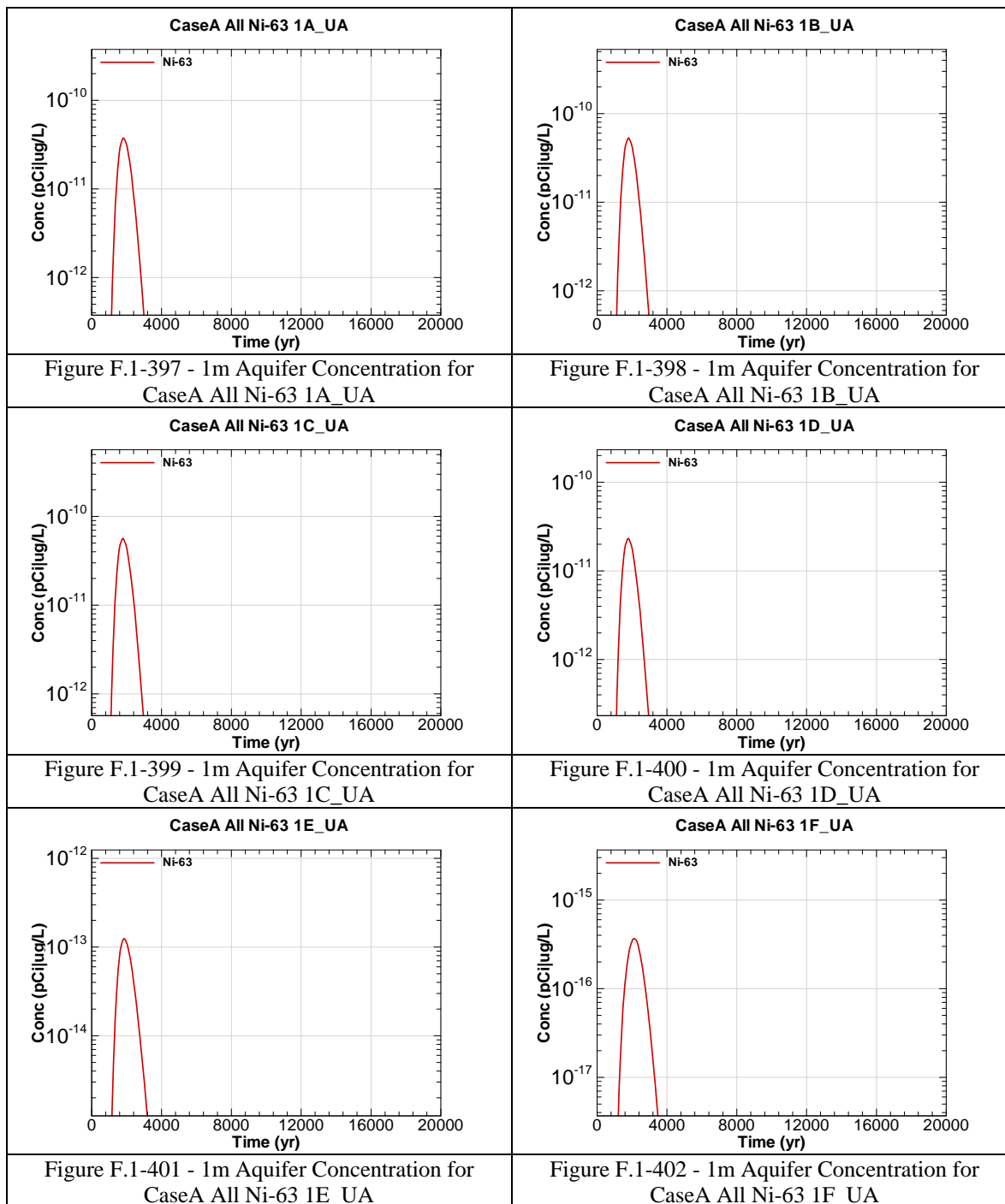


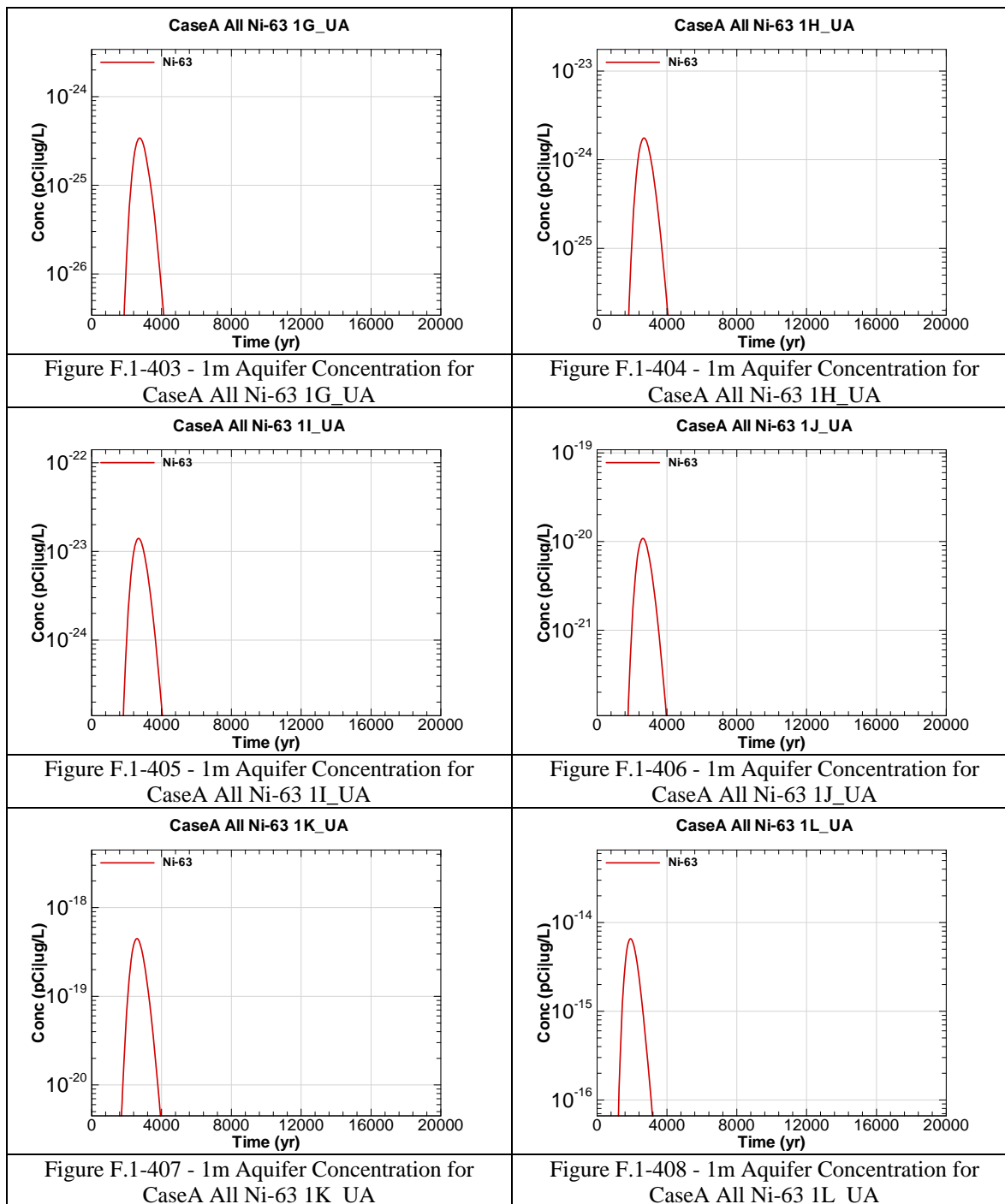












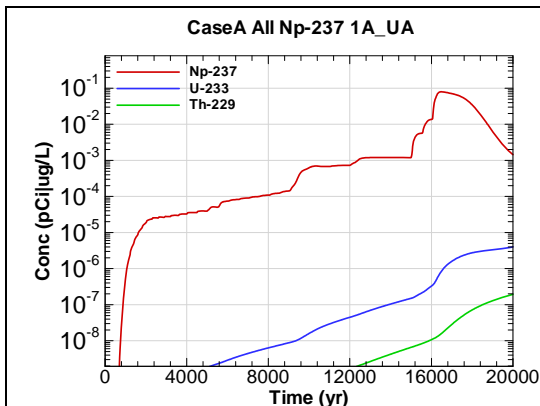


Figure F.1-409 - 1m Aquifer Concentration for
CaseA All Np-237 1A_UA

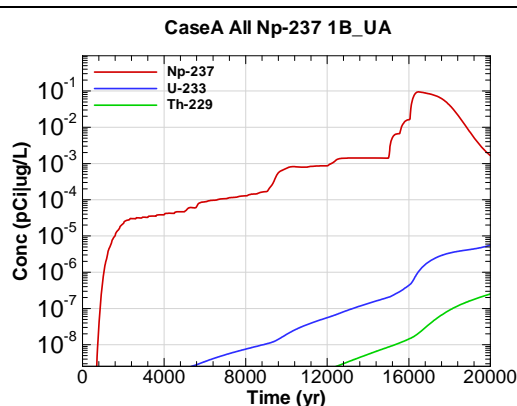


Figure F.1-410 - 1m Aquifer Concentration for
CaseA All Np-237 1B_UA

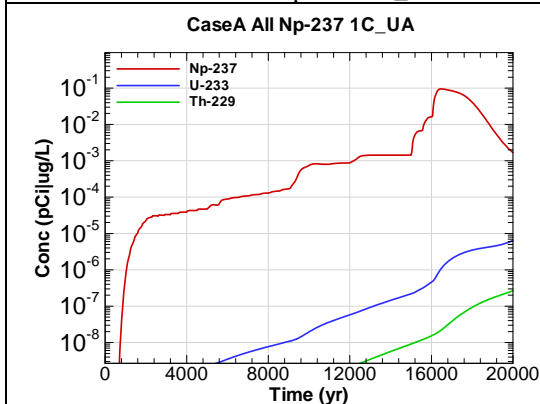


Figure F.1-411 - 1m Aquifer Concentration for
CaseA All Np-237 1C_UA

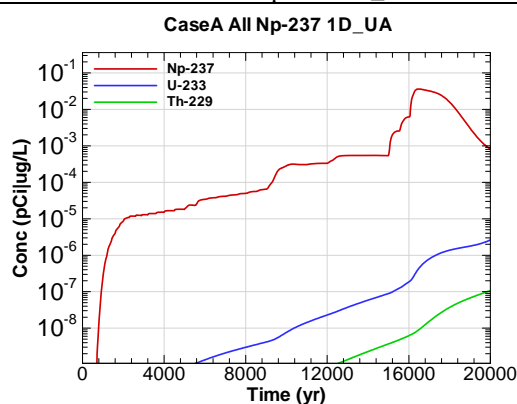


Figure F.1-412 - 1m Aquifer Concentration for
CaseA All Np-237 1D_UA

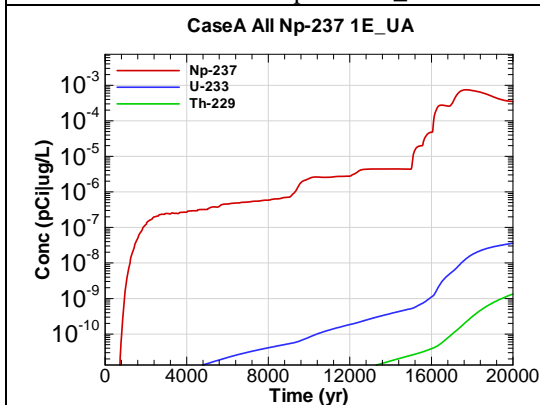


Figure F.1-413 - 1m Aquifer Concentration for
CaseA All Np-237 1E_UA

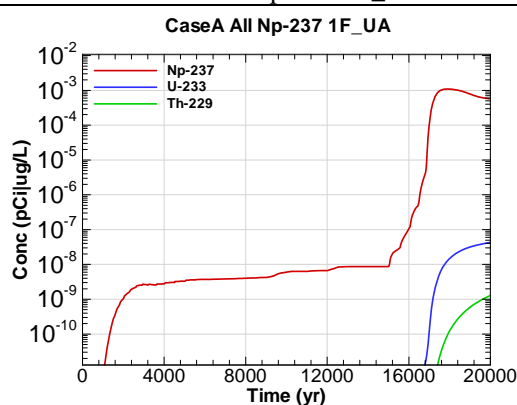
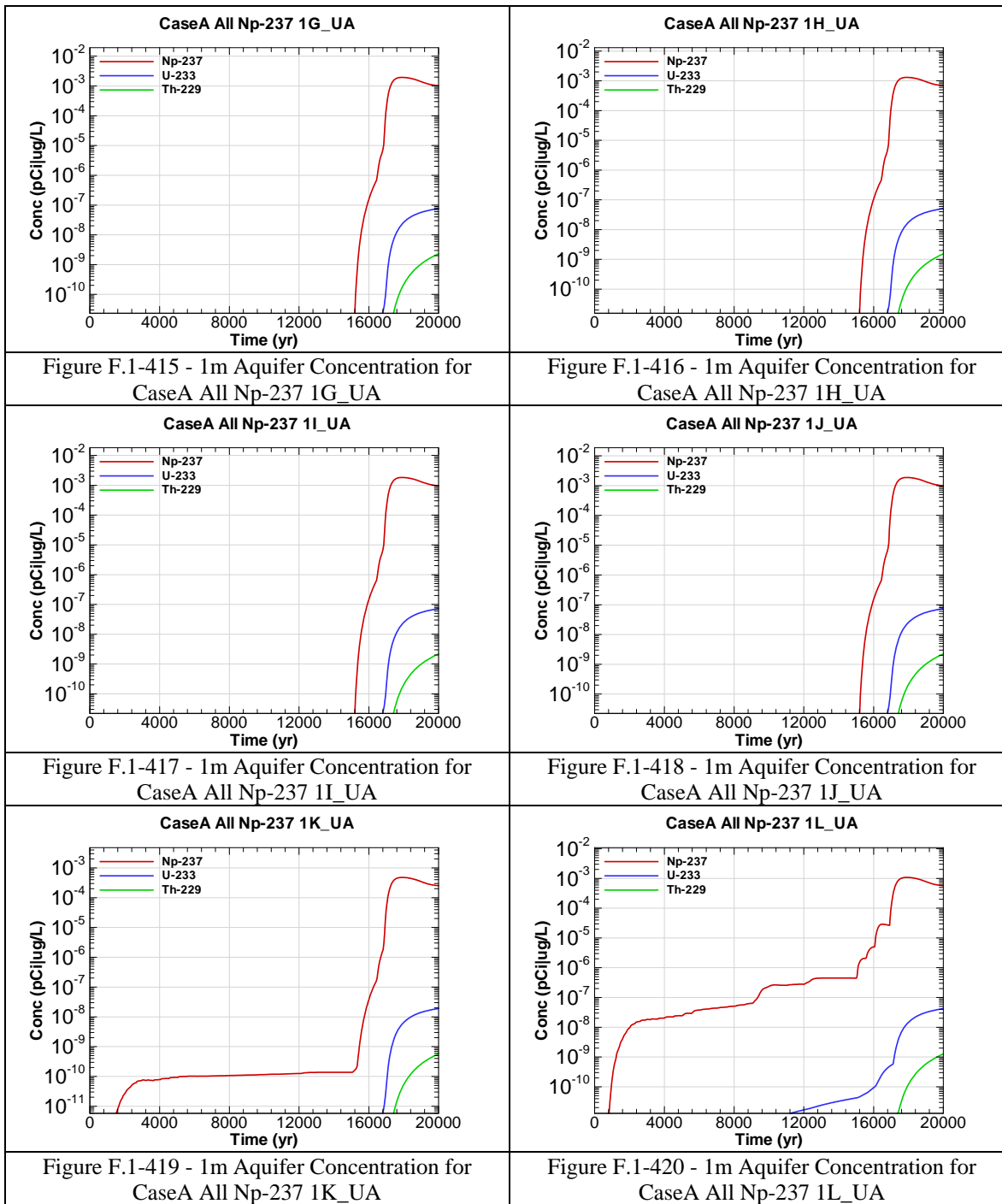
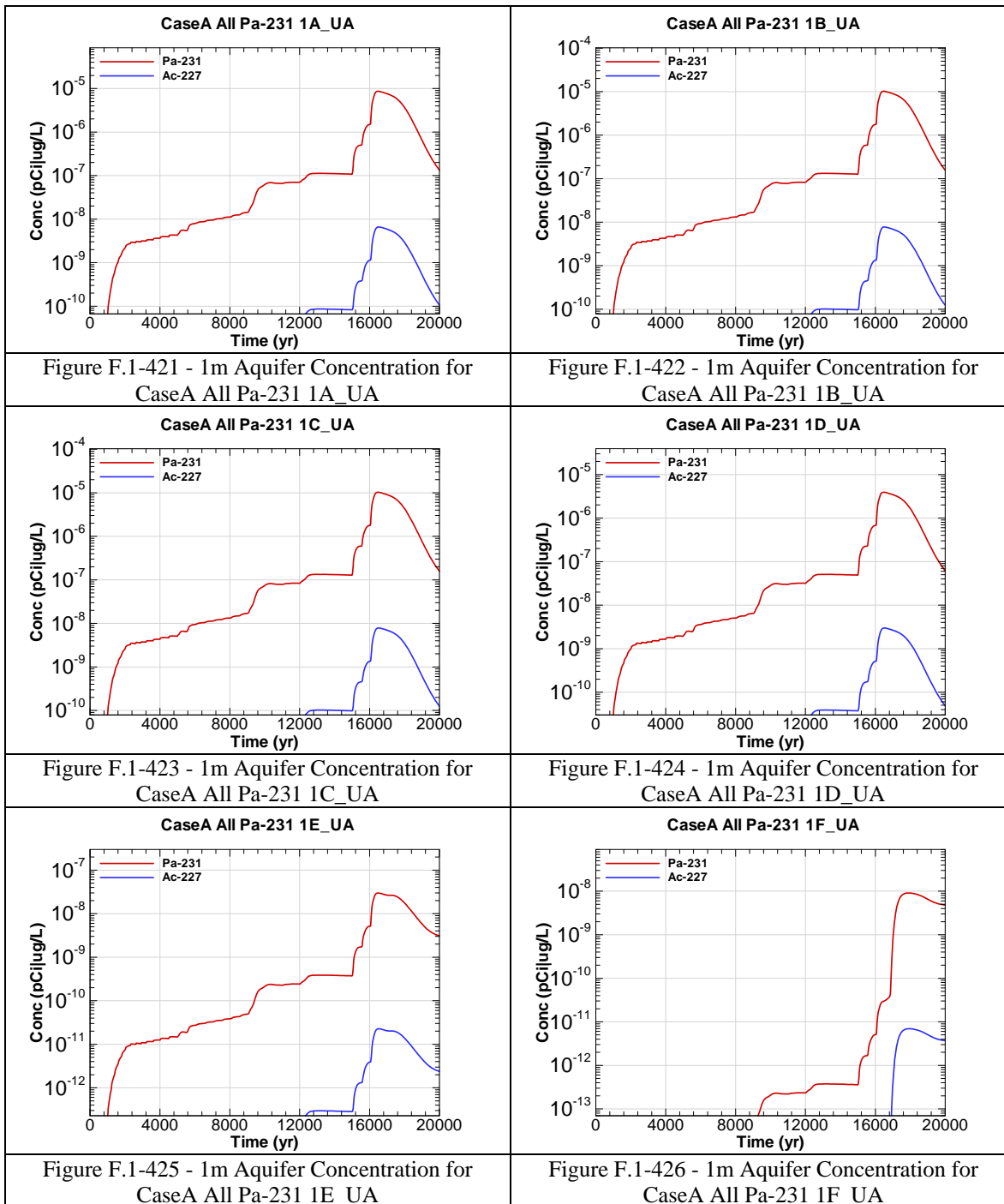
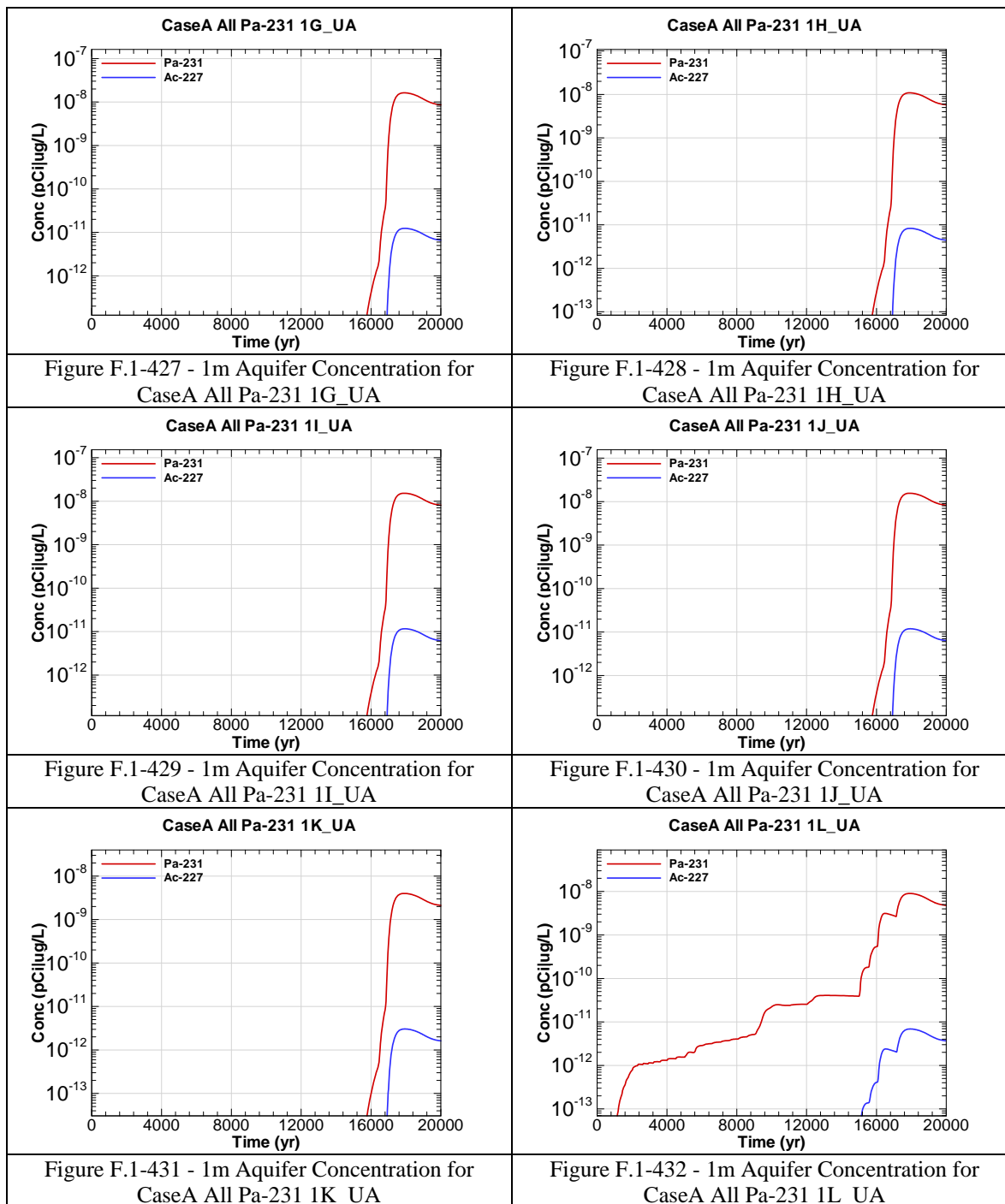
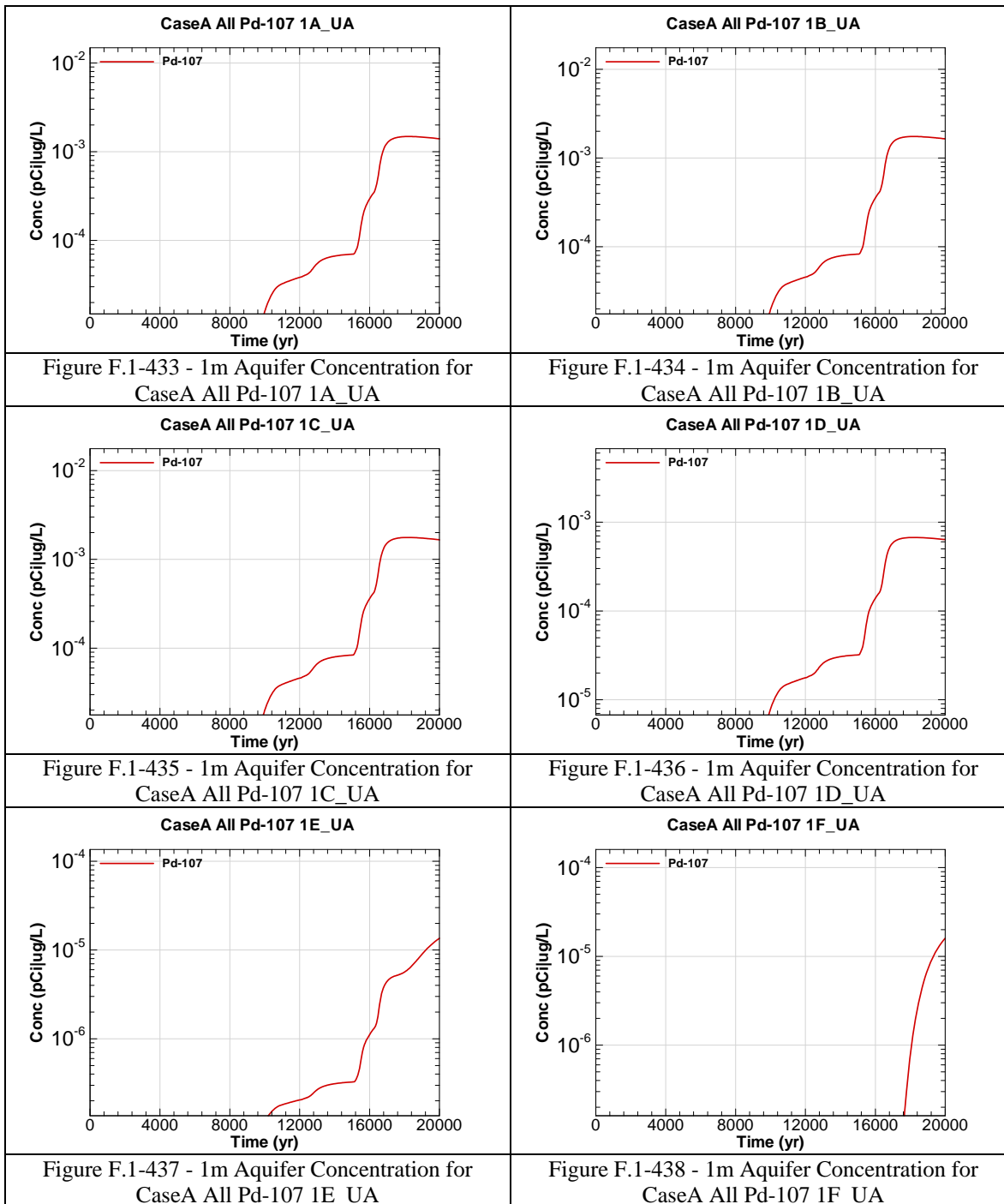


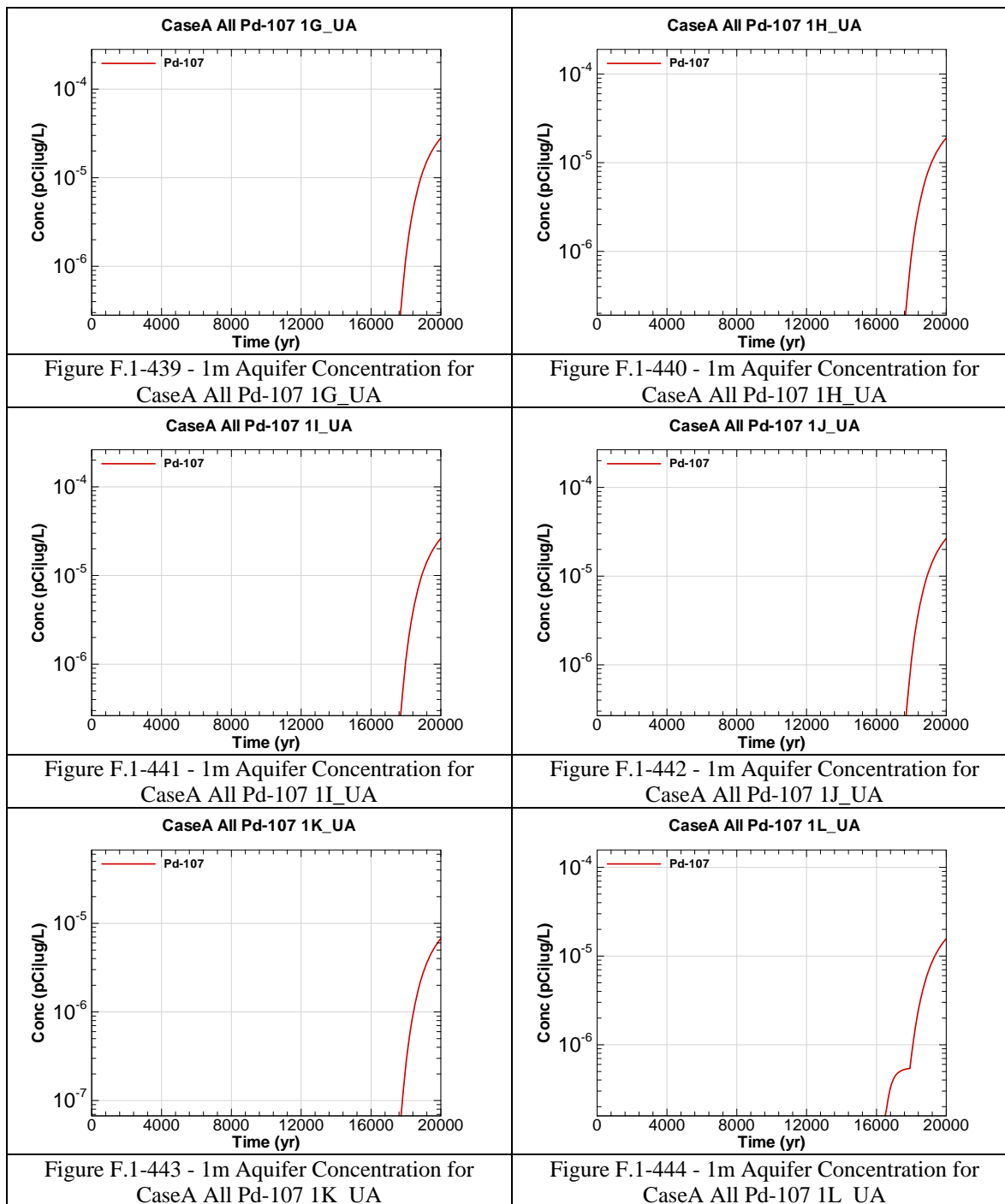
Figure F.1-414 - 1m Aquifer Concentration for
CaseA All Np-237 1F_UA

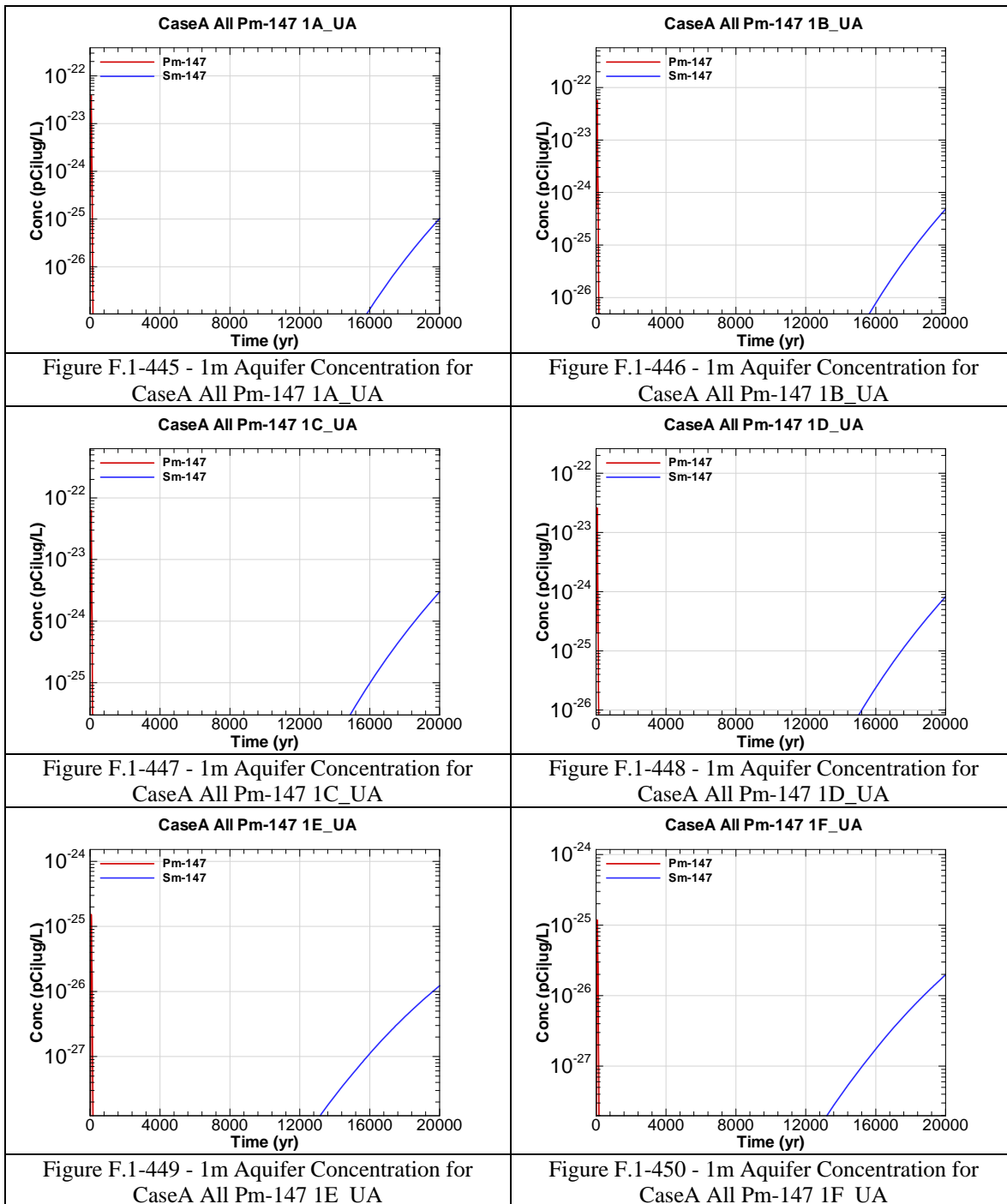


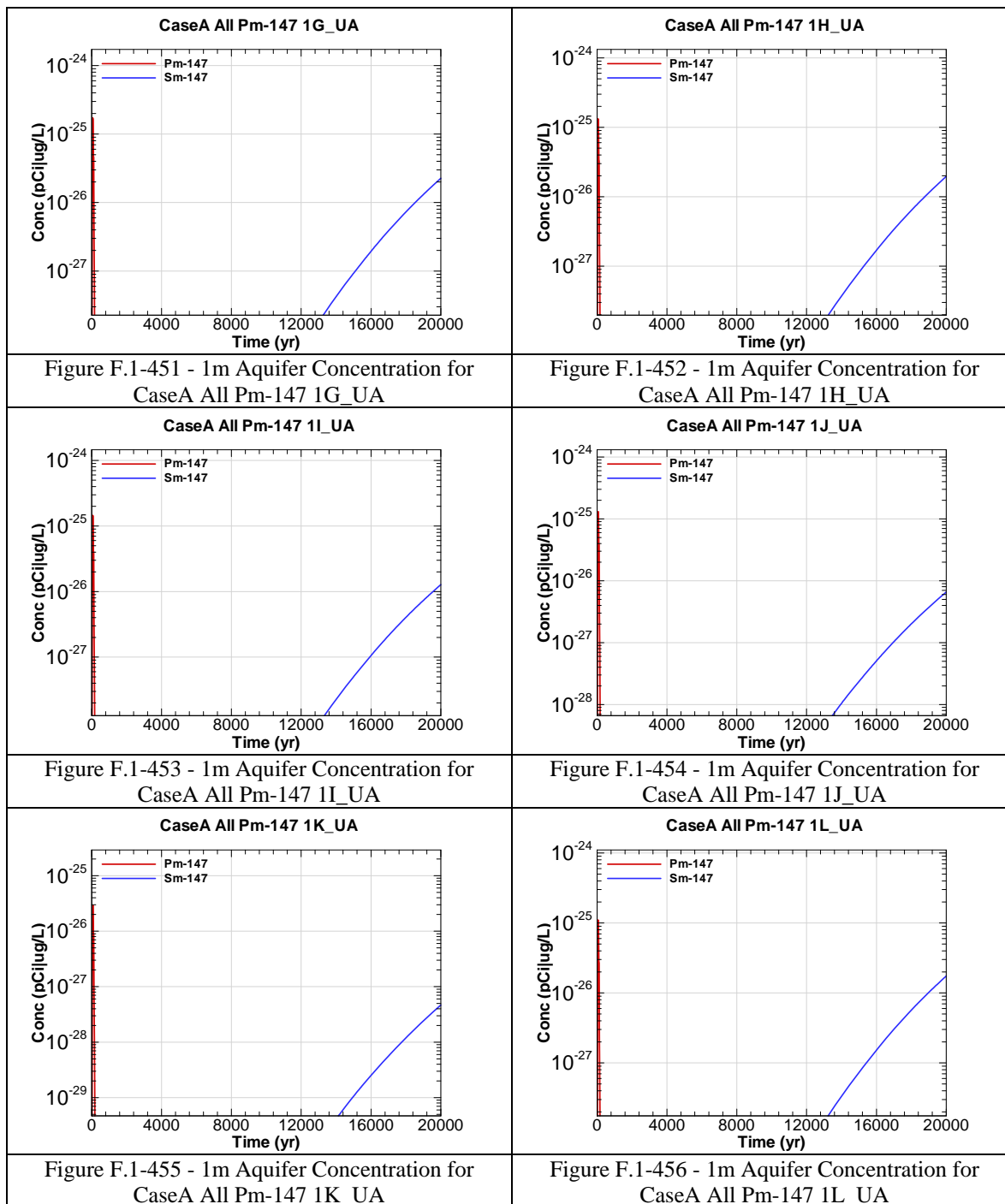


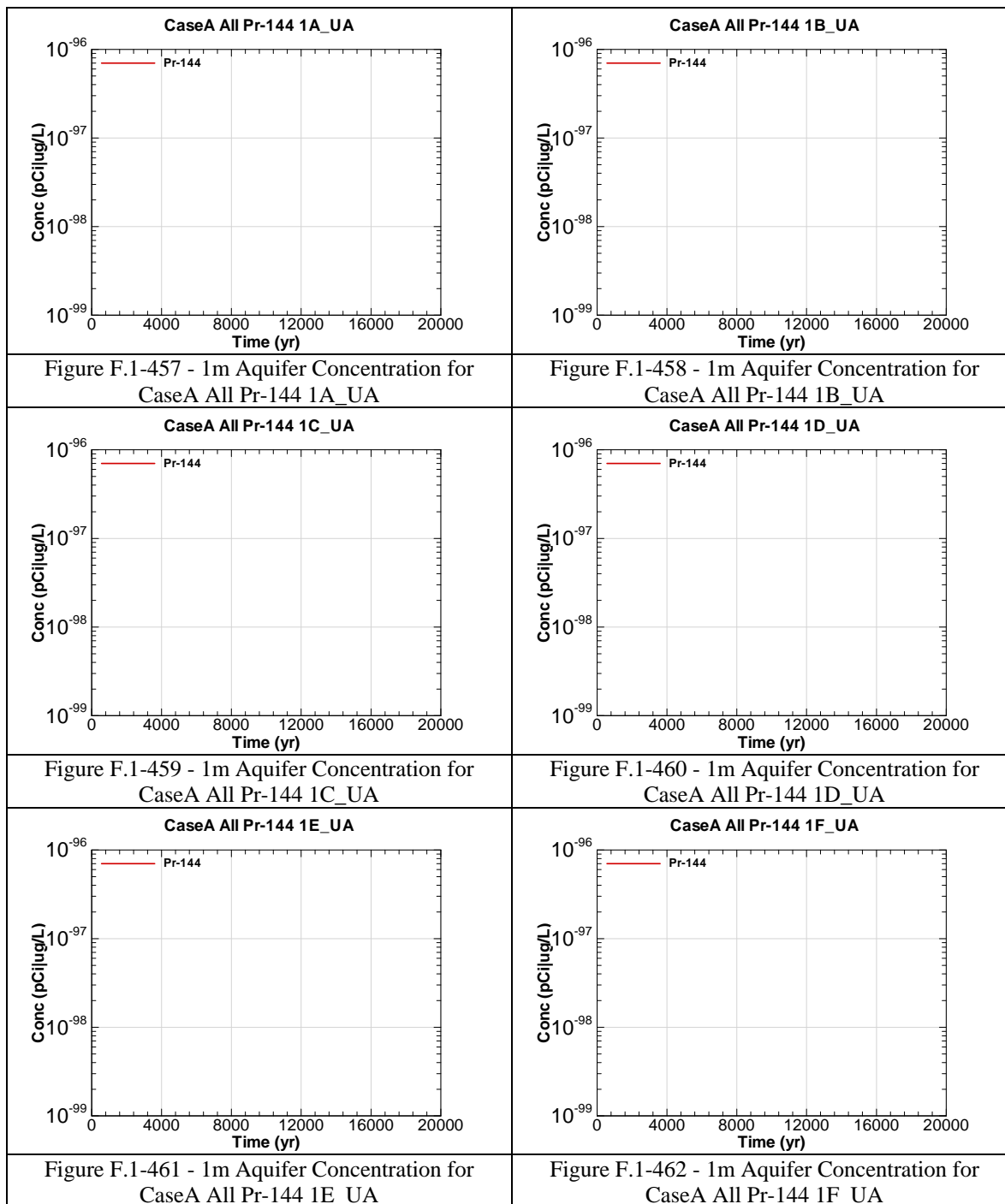


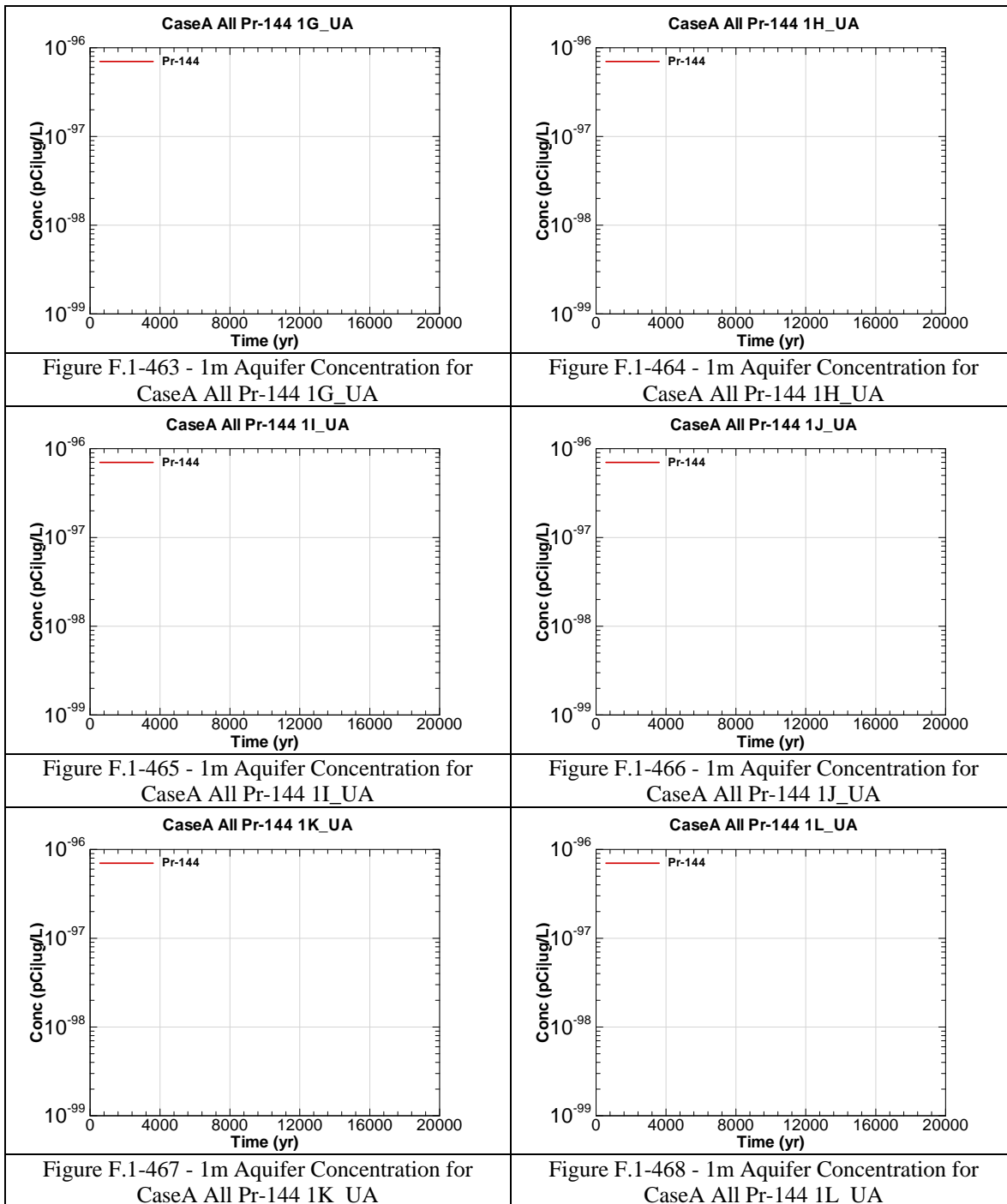


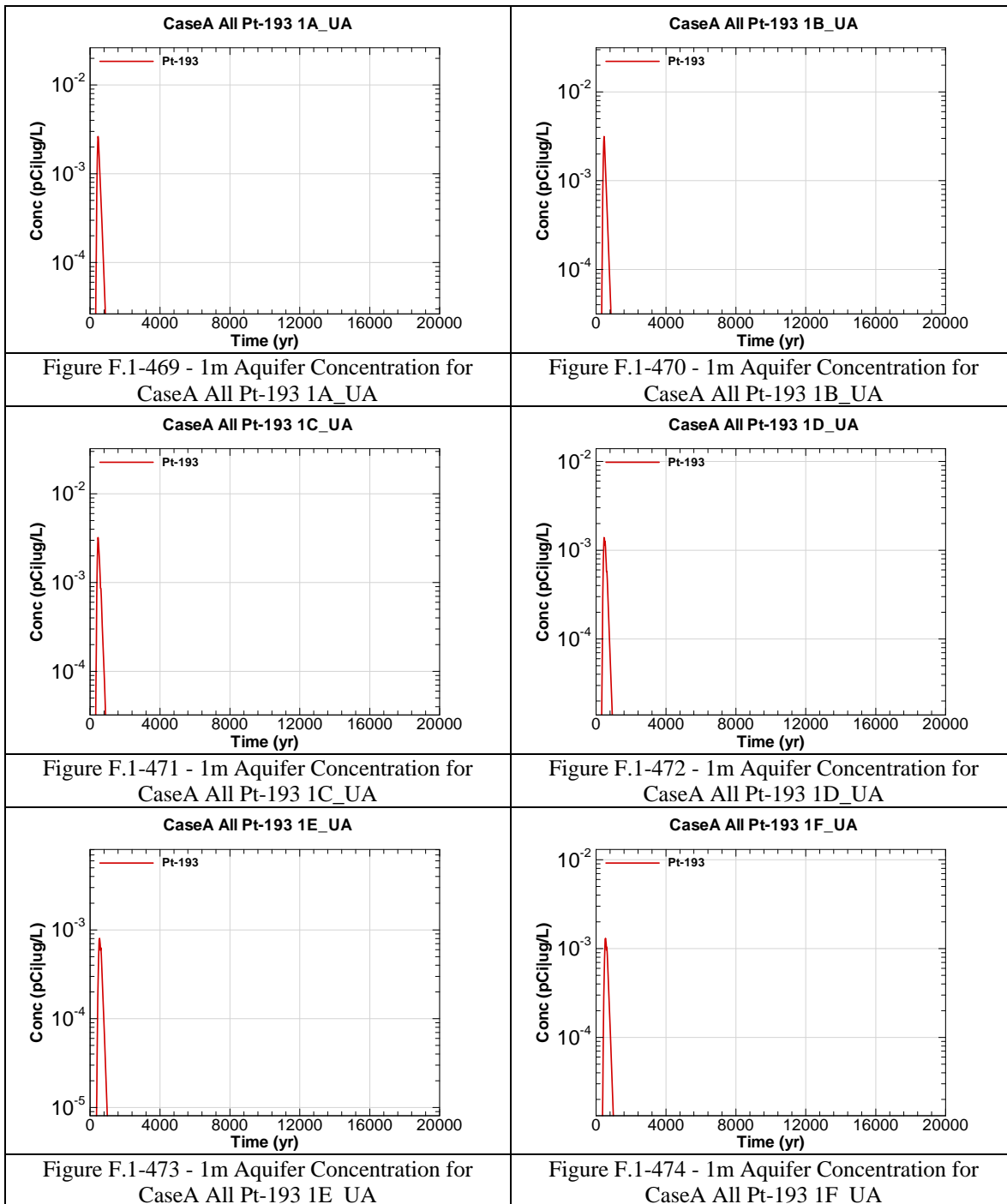


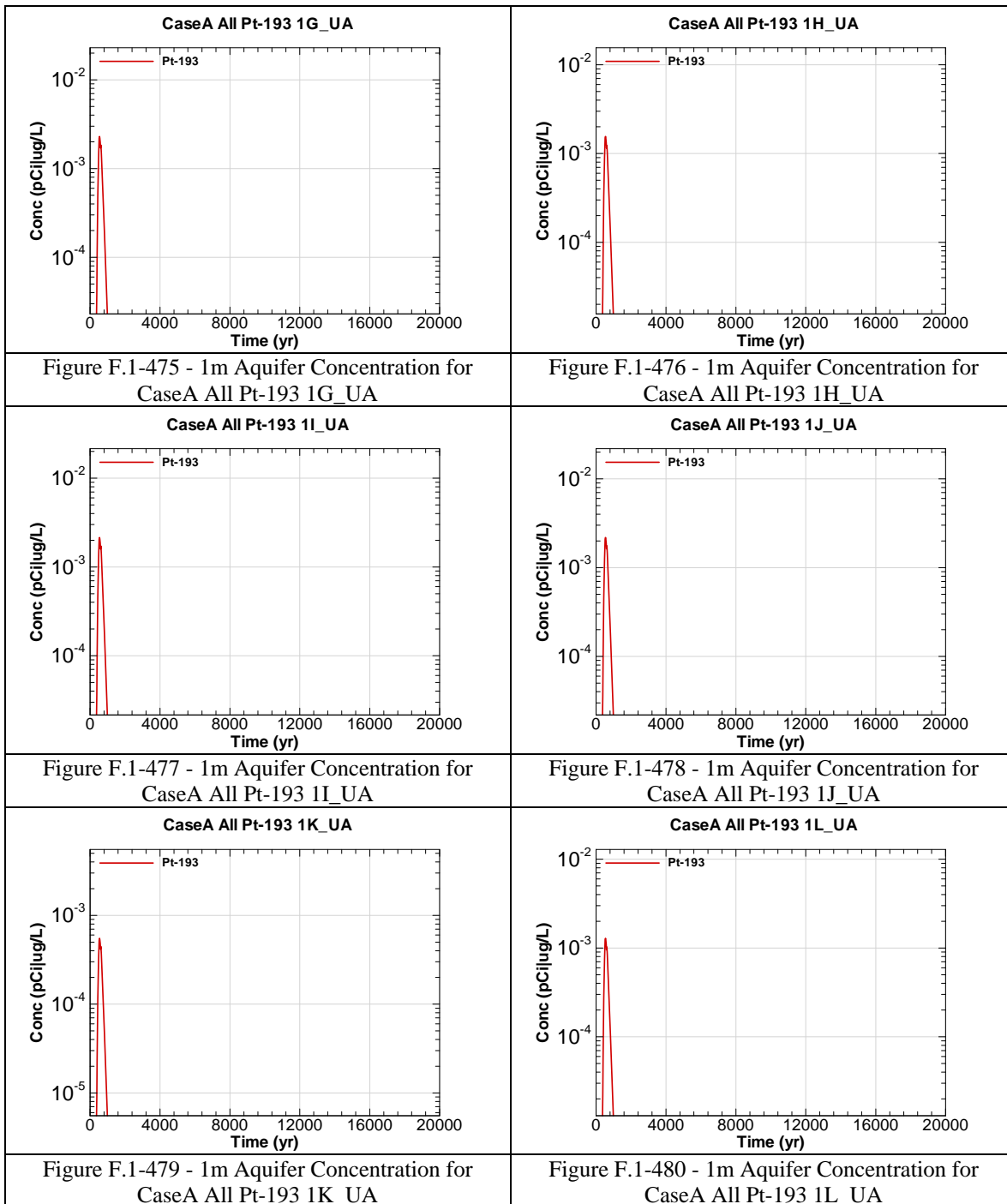


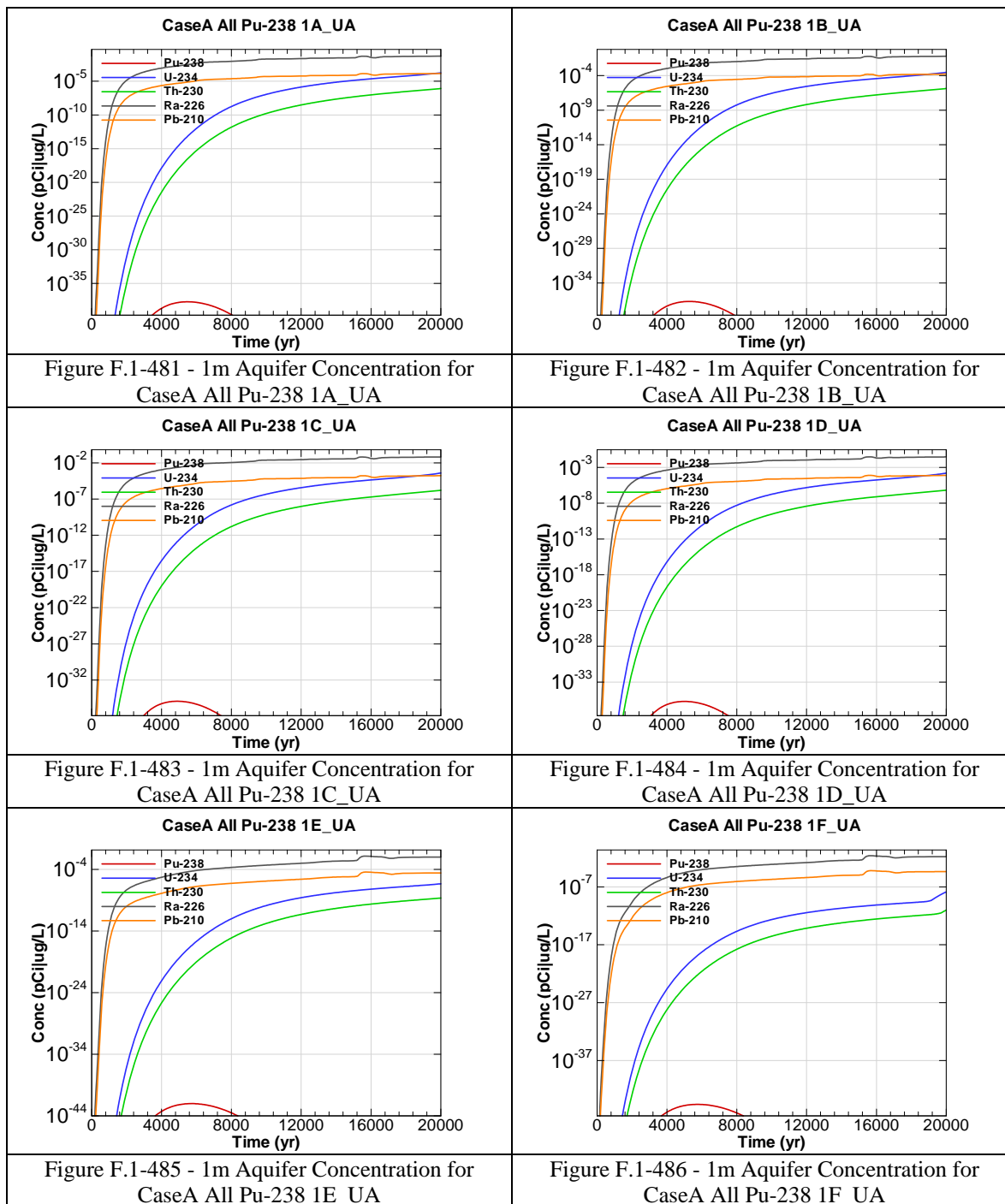


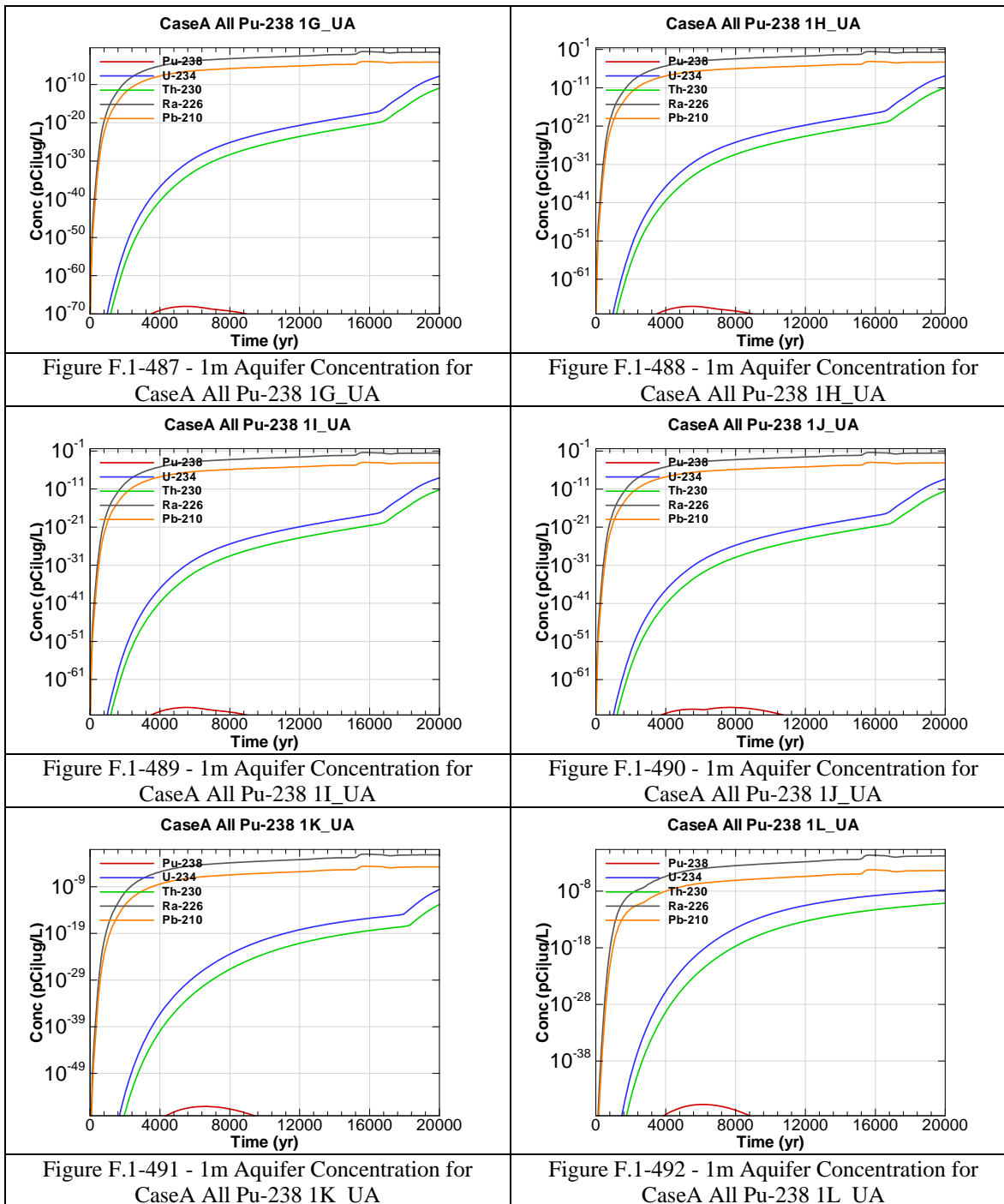












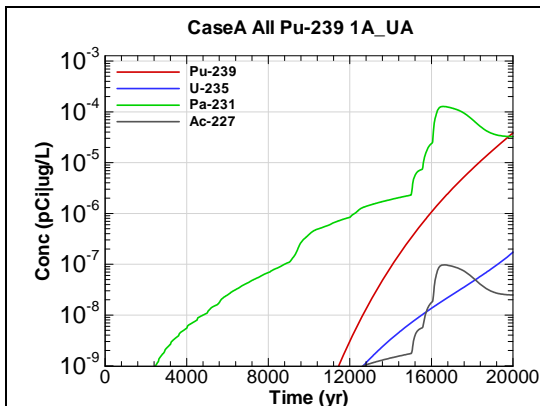


Figure F.1-493 - 1m Aquifer Concentration for
CaseA All Pu-239 1A_UA

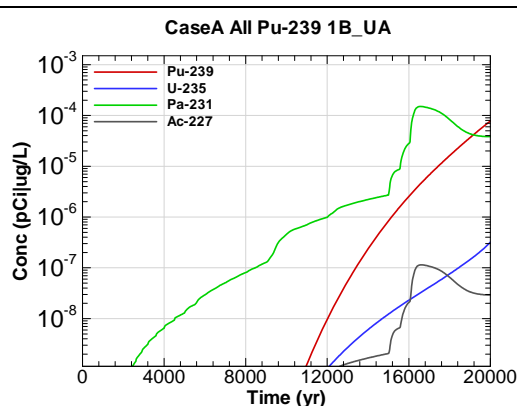


Figure F.1-494 - 1m Aquifer Concentration for
CaseA All Pu-239 1B_UA

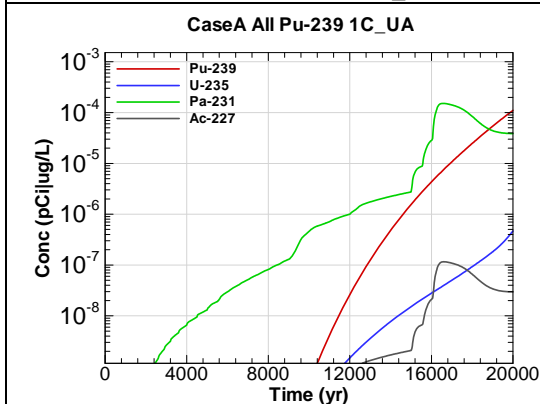


Figure F.1-495 - 1m Aquifer Concentration for
CaseA All Pu-239 1C_UA

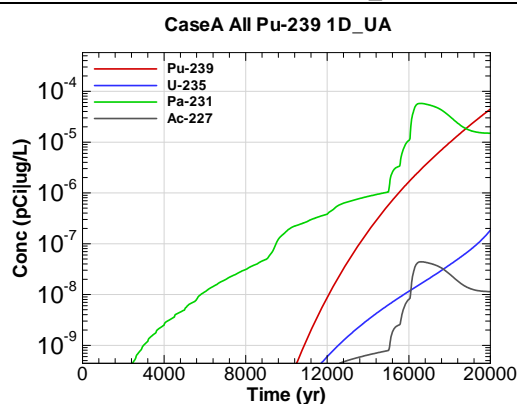


Figure F.1-496 - 1m Aquifer Concentration for
CaseA All Pu-239 1D_UA

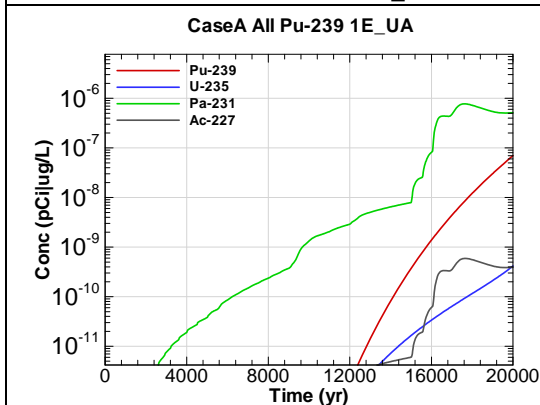


Figure F.1-497 - 1m Aquifer Concentration for
CaseA All Pu-239 1E_UA

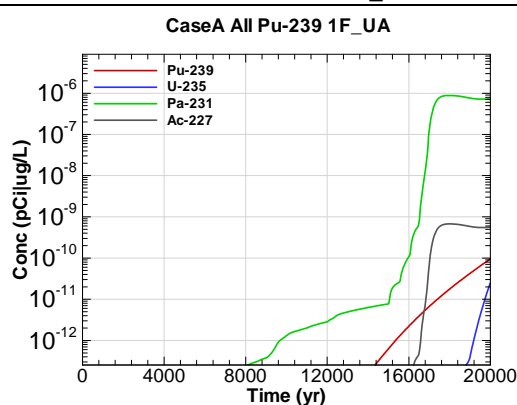
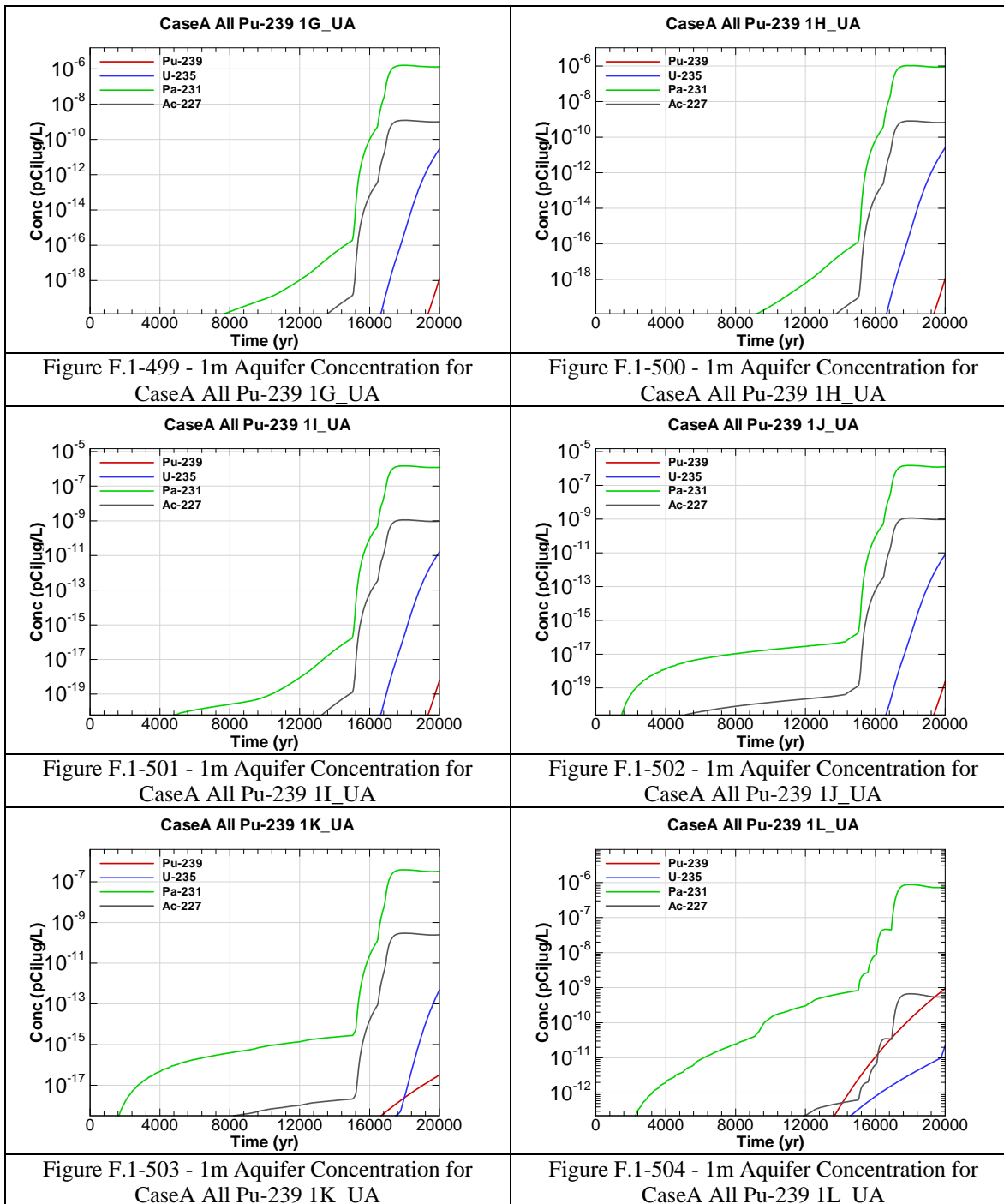
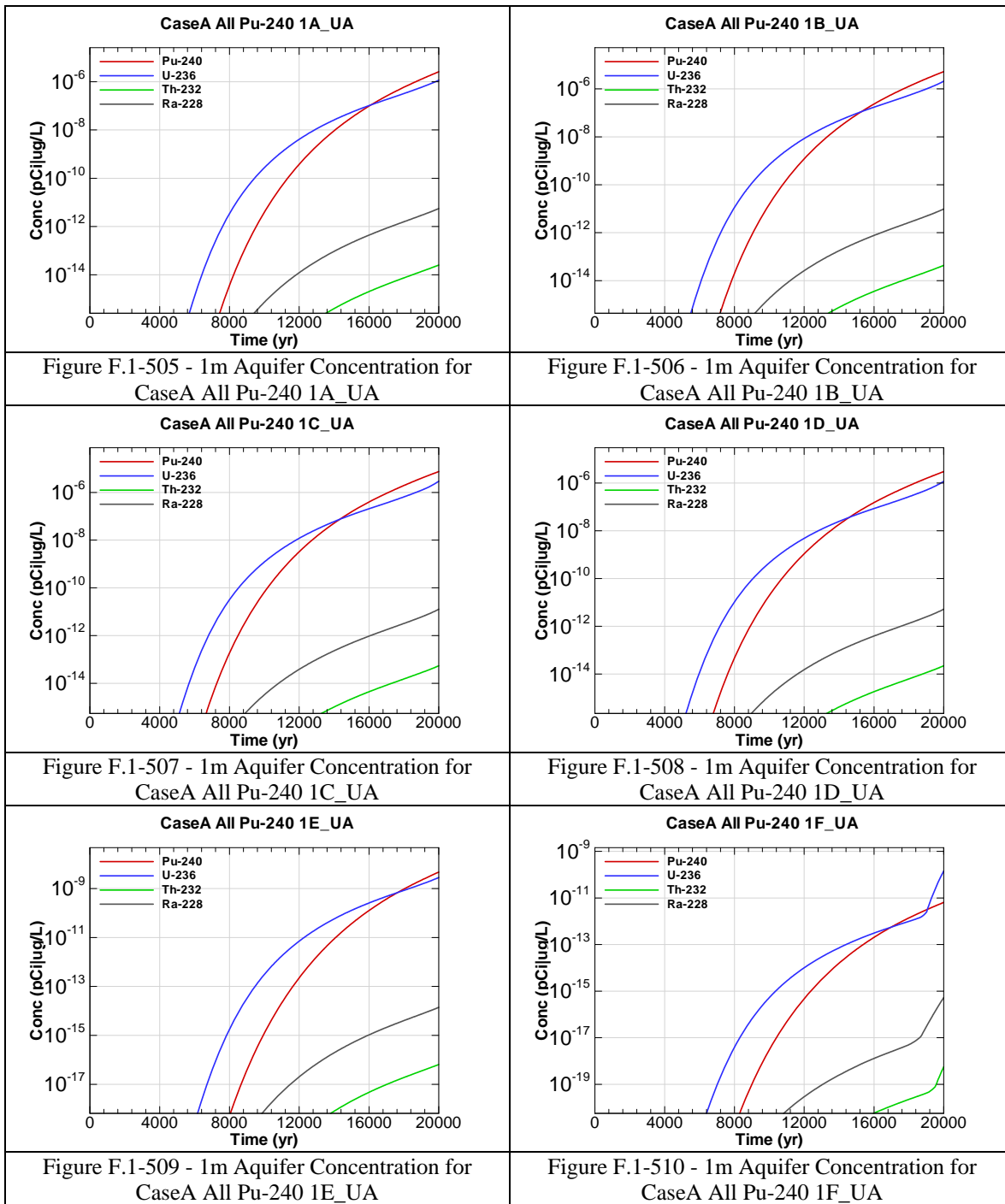
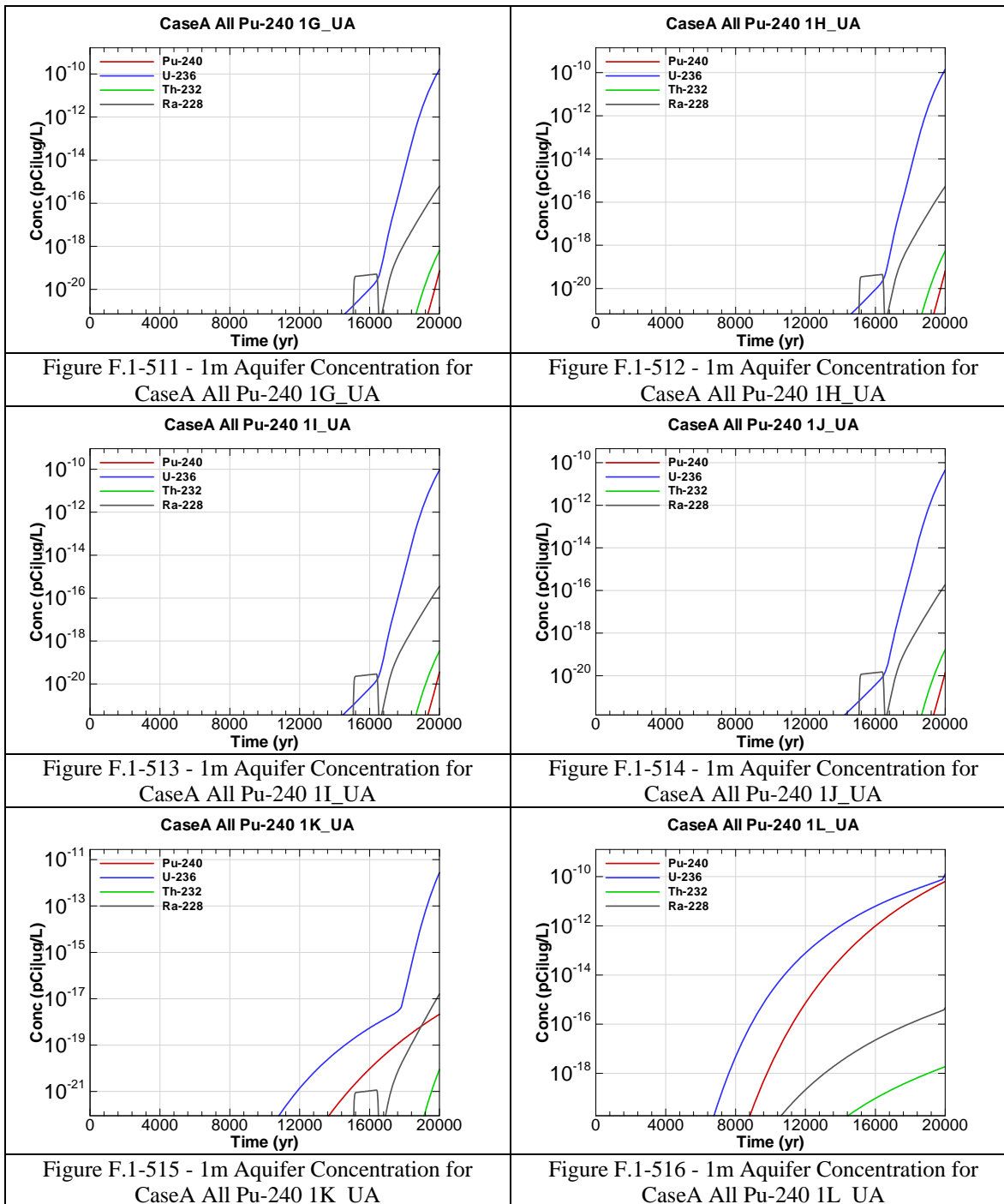


Figure F.1-498 - 1m Aquifer Concentration for
CaseA All Pu-239 1F_UA







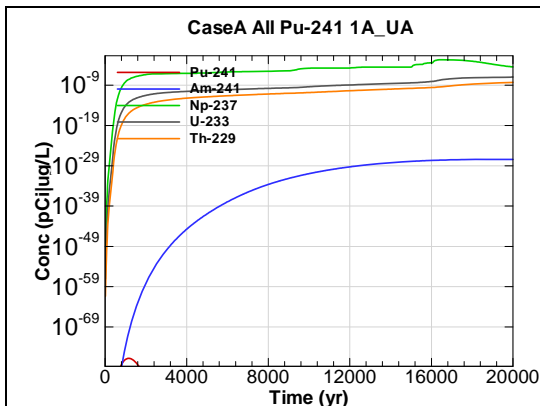


Figure F.1-517 - 1m Aquifer Concentration for
CaseA All Pu-241 1A_UA

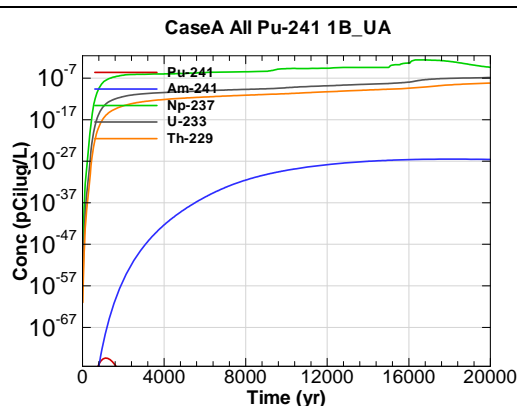


Figure F.1-518 - 1m Aquifer Concentration for
CaseA All Pu-241 1B_UA

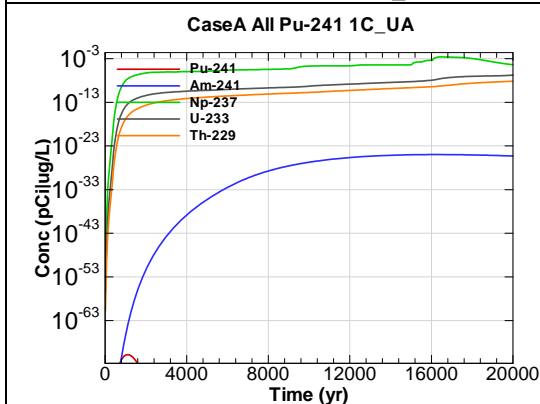


Figure F.1-519 - 1m Aquifer Concentration for
CaseA All Pu-241 1C_UA

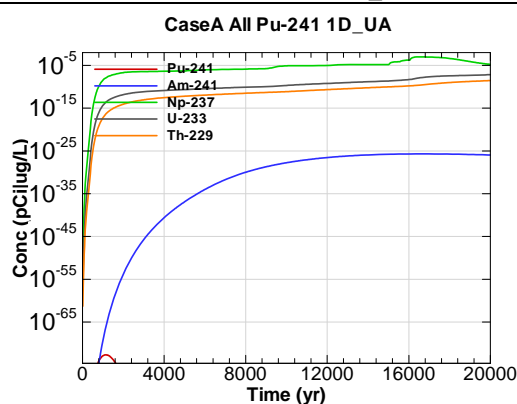


Figure F.1-520 - 1m Aquifer Concentration for
CaseA All Pu-241 1D_UA

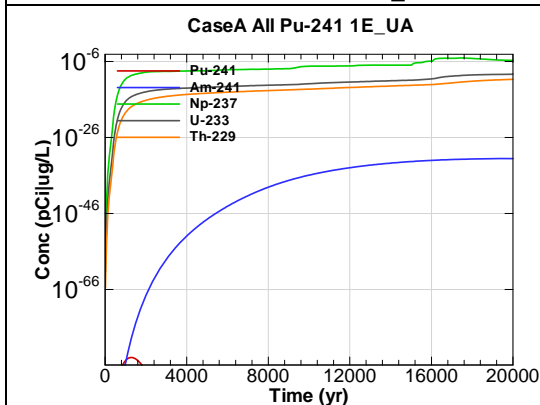


Figure F.1-521 - 1m Aquifer Concentration for
CaseA All Pu-241 1E_UA

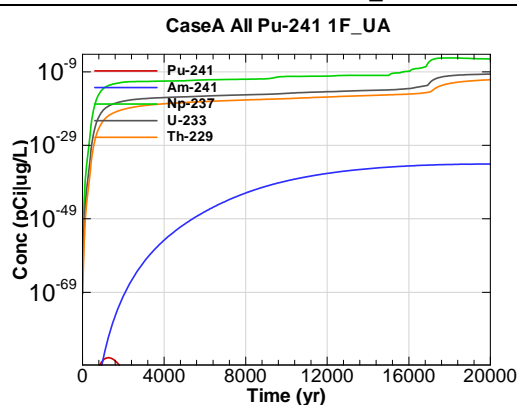
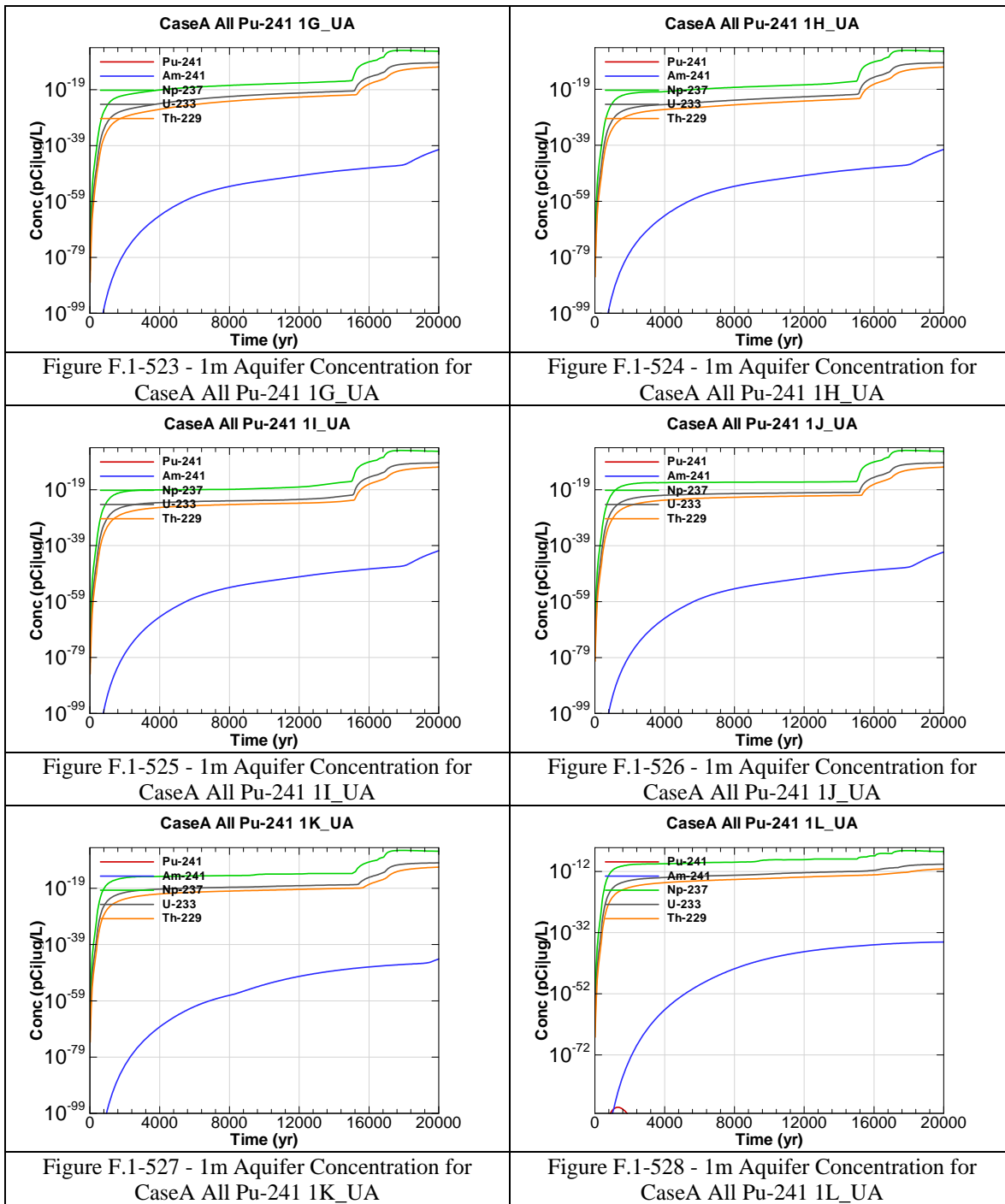


Figure F.1-522 - 1m Aquifer Concentration for
CaseA All Pu-241 1F_UA



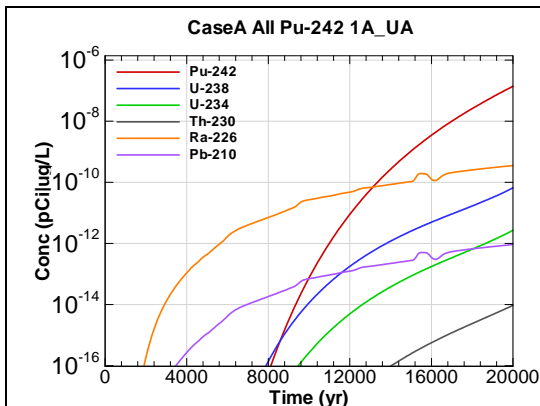


Figure F.1-529 - 1m Aquifer Concentration for
CaseA All Pu-242 1A_UA

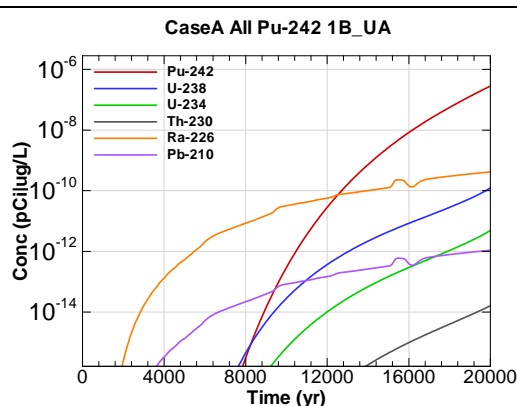


Figure F.1-530 - 1m Aquifer Concentration for
CaseA All Pu-242 1B_UA

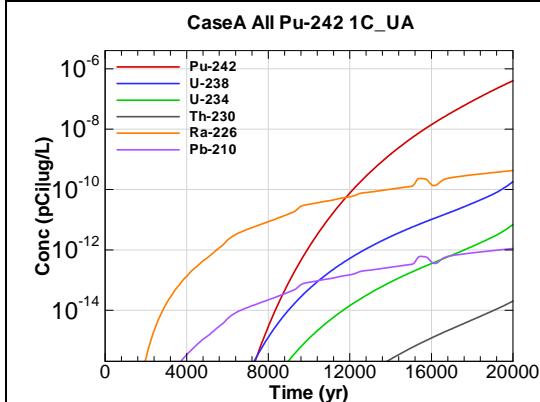


Figure F.1-531 - 1m Aquifer Concentration for
CaseA All Pu-242 1C_UA

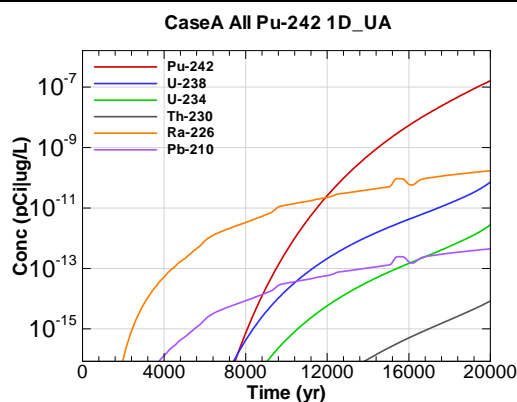


Figure F.1-532 - 1m Aquifer Concentration for
CaseA All Pu-242 1D_UA

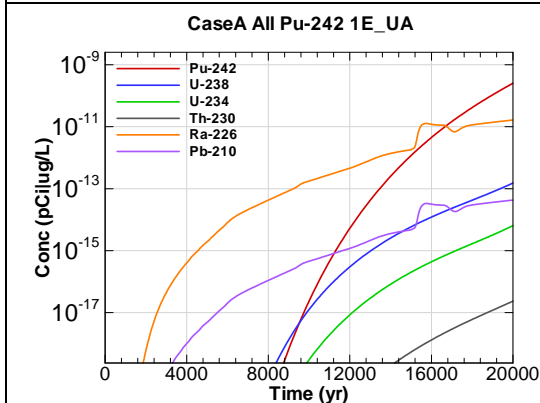


Figure F.1-533 - 1m Aquifer Concentration for
CaseA All Pu-242 1E_UA

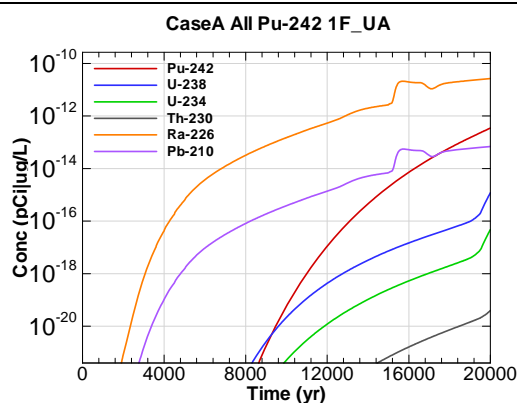
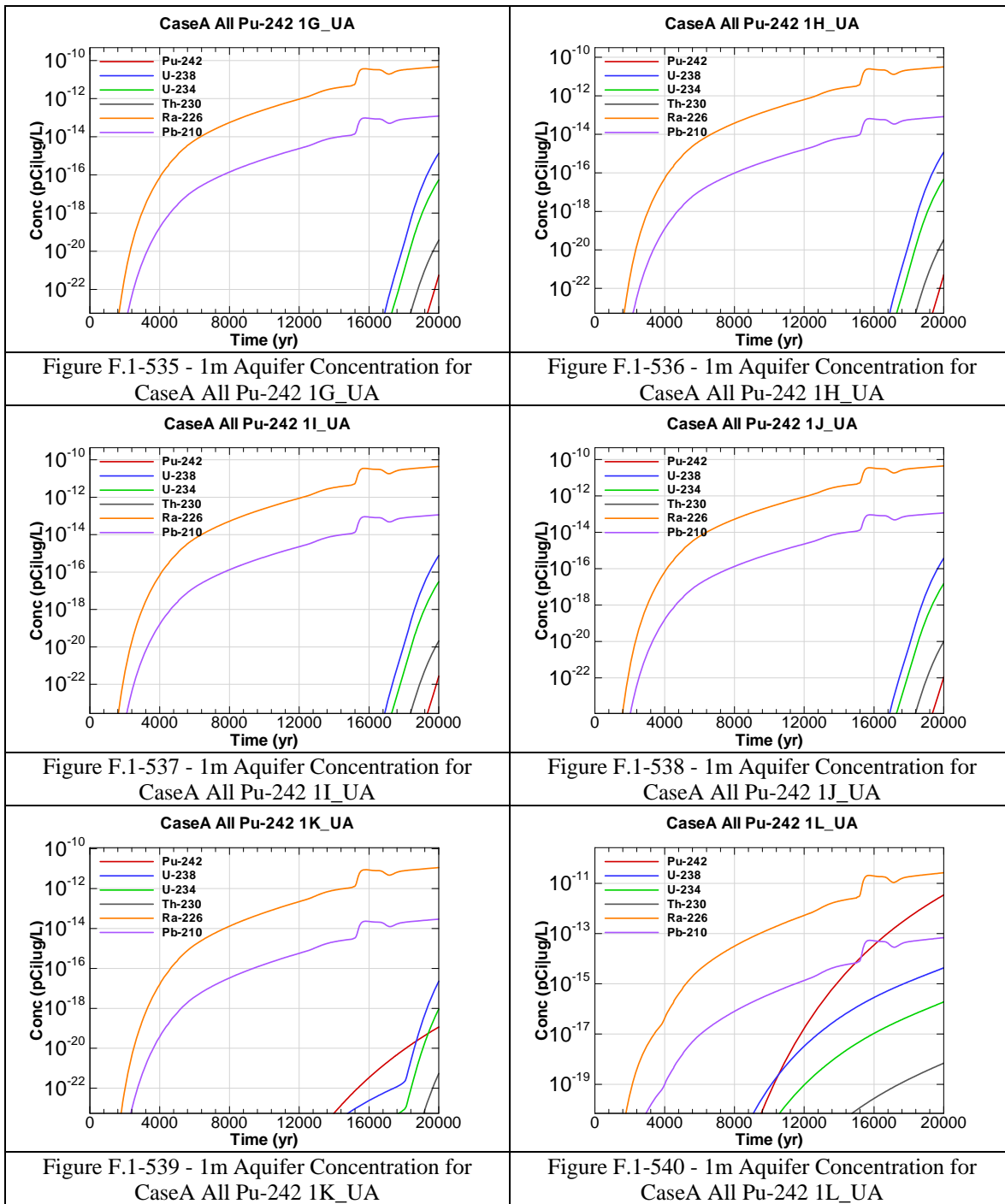
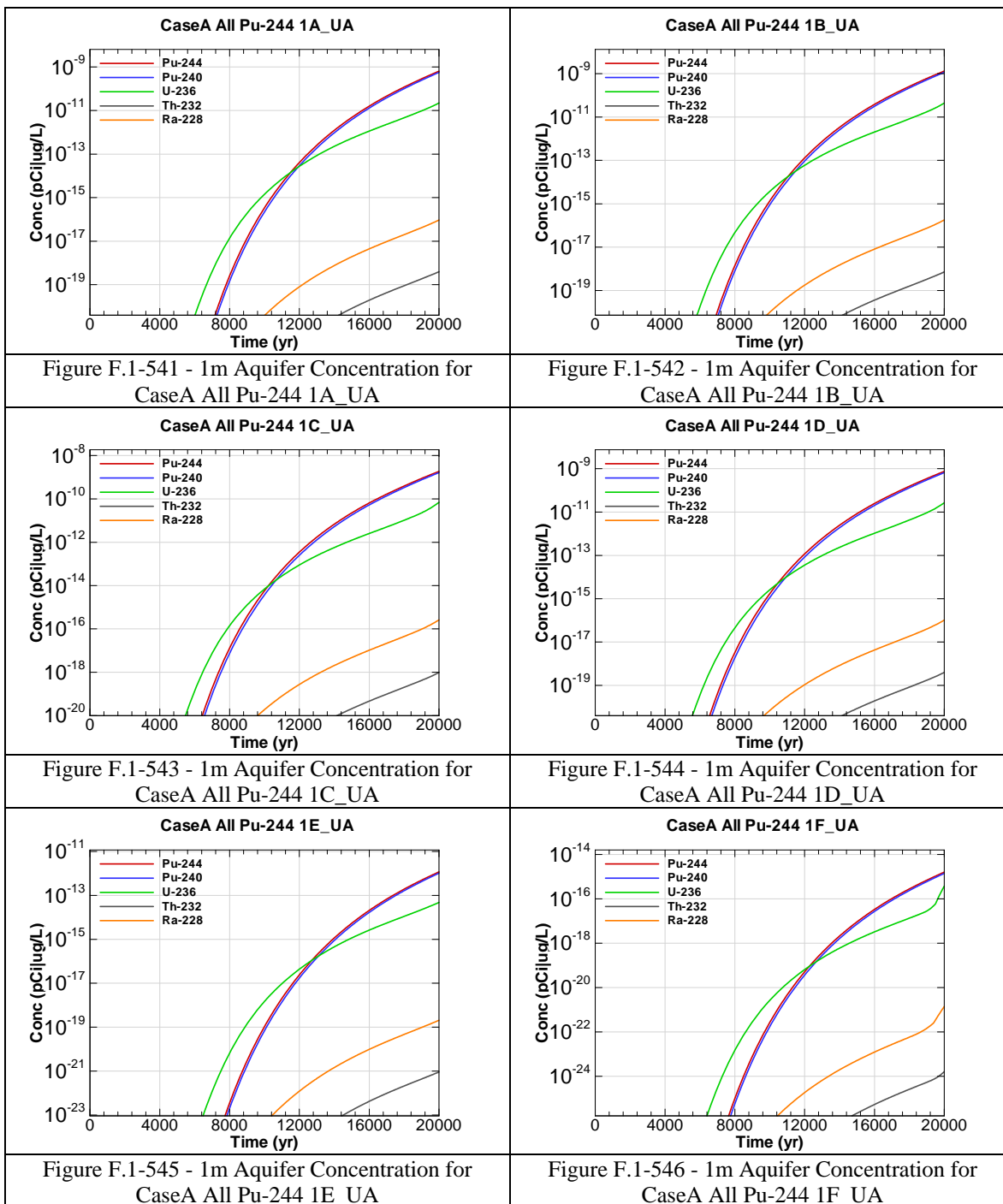
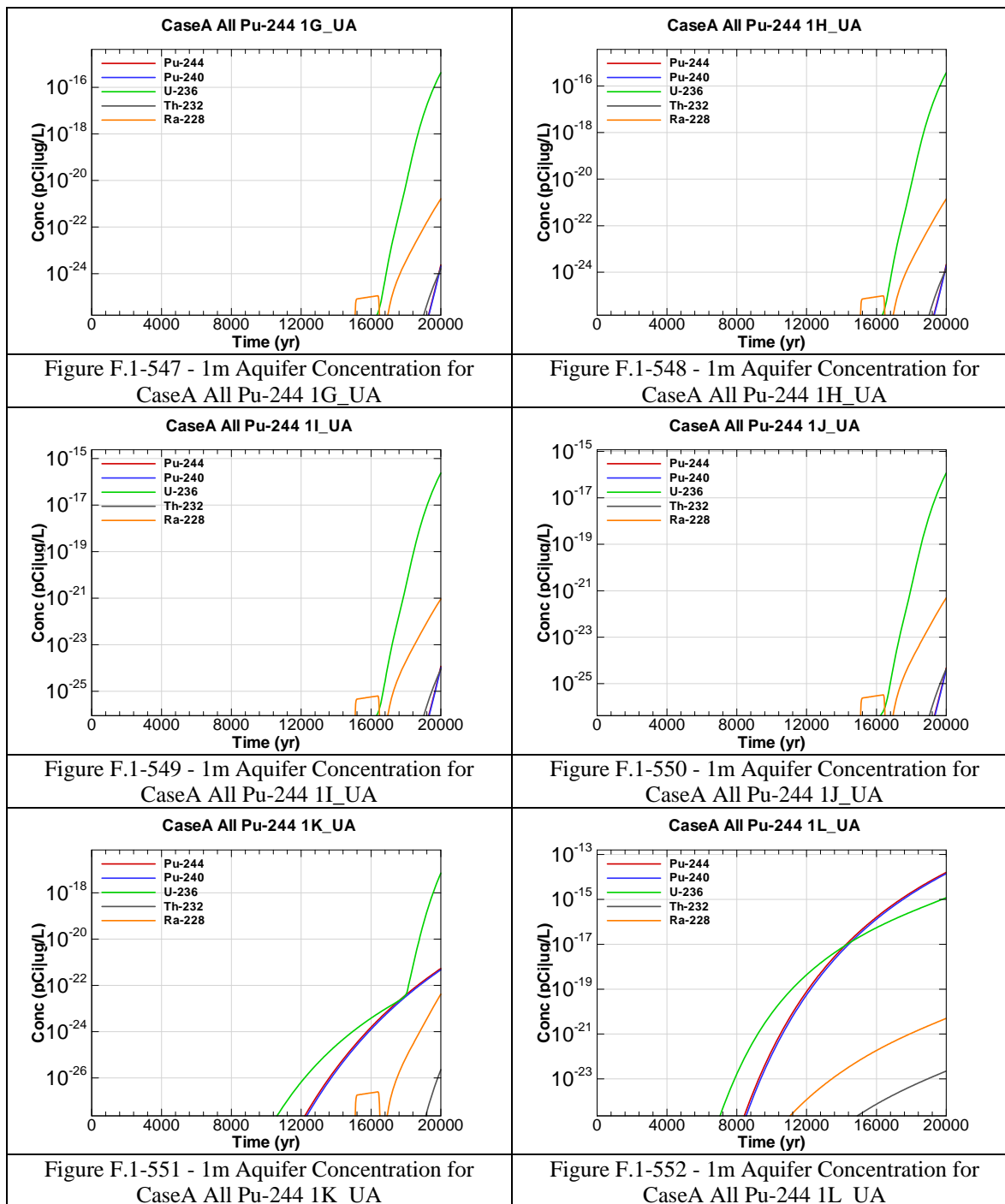
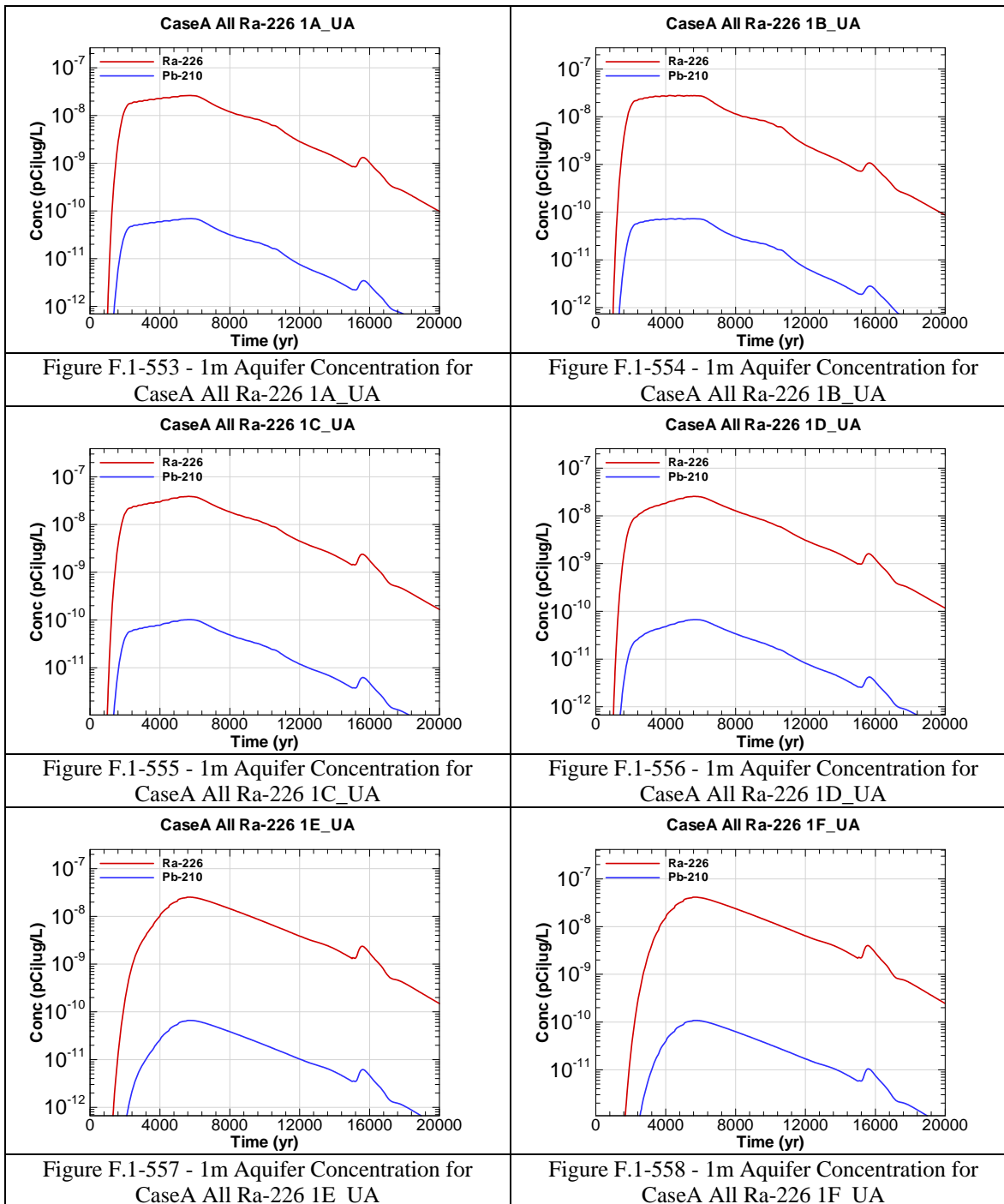


Figure F.1-534 - 1m Aquifer Concentration for
CaseA All Pu-242 1F_UA









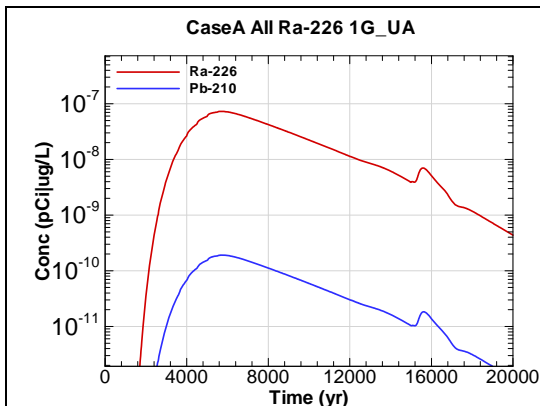


Figure F.1-559 - 1m Aquifer Concentration for
CaseA All Ra-226 1G_UA

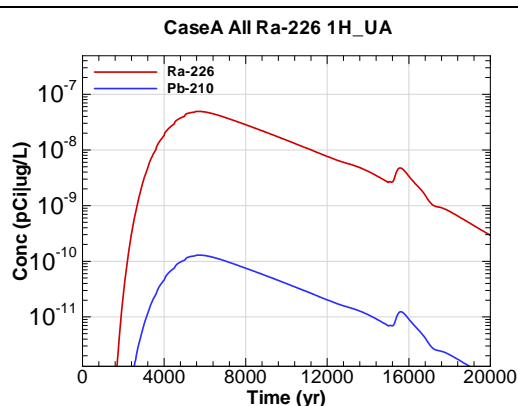


Figure F.1-560 - 1m Aquifer Concentration for
CaseA All Ra-226 1H_UA

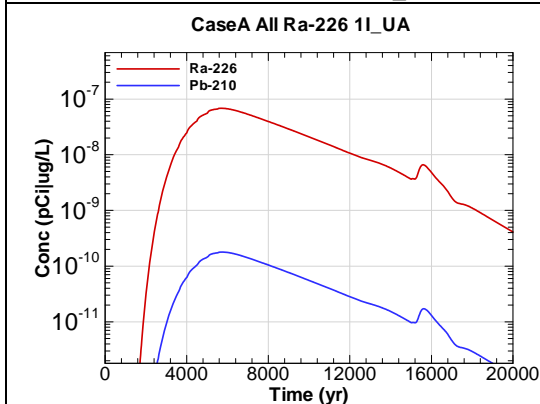


Figure F.1-561 - 1m Aquifer Concentration for
CaseA All Ra-226 1I_UA

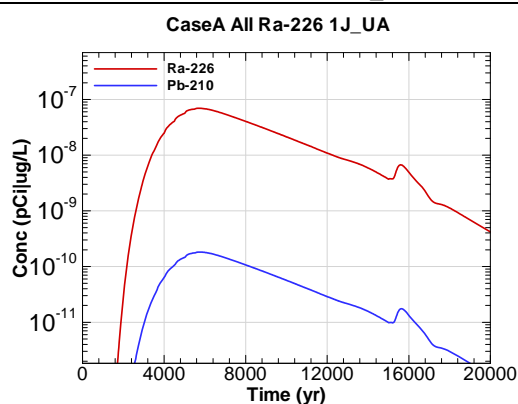


Figure F.1-562 - 1m Aquifer Concentration for
CaseA All Ra-226 1J_UA

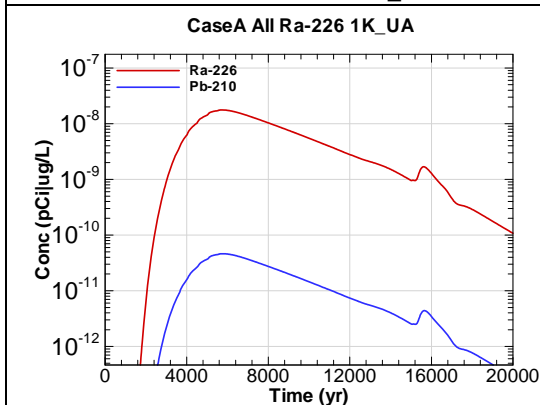


Figure F.1-563 - 1m Aquifer Concentration for
CaseA All Ra-226 1K_UA

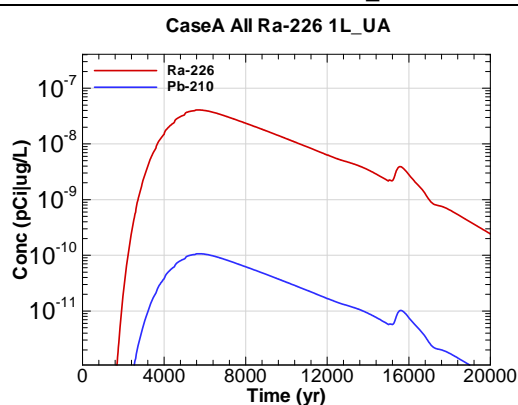
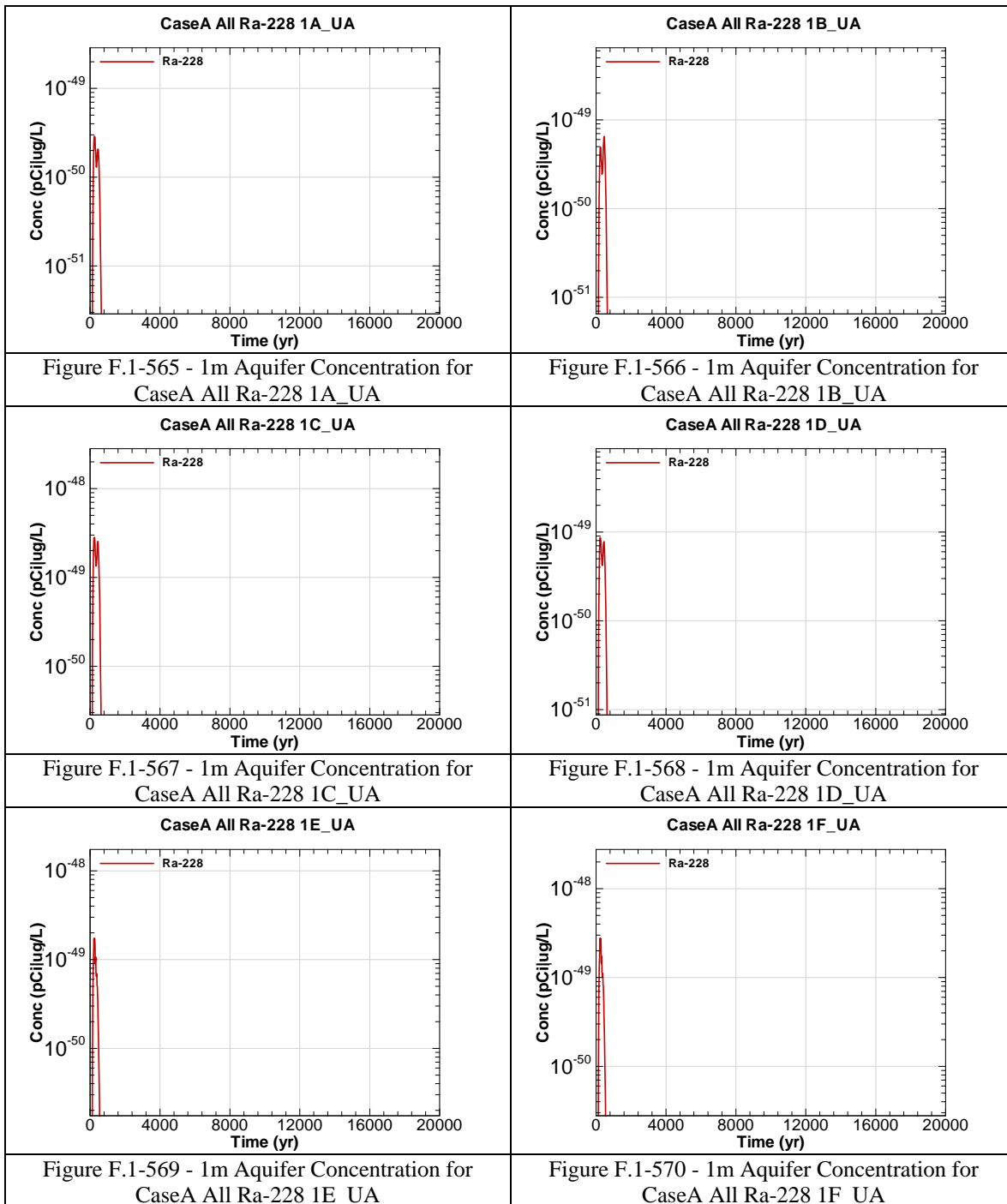
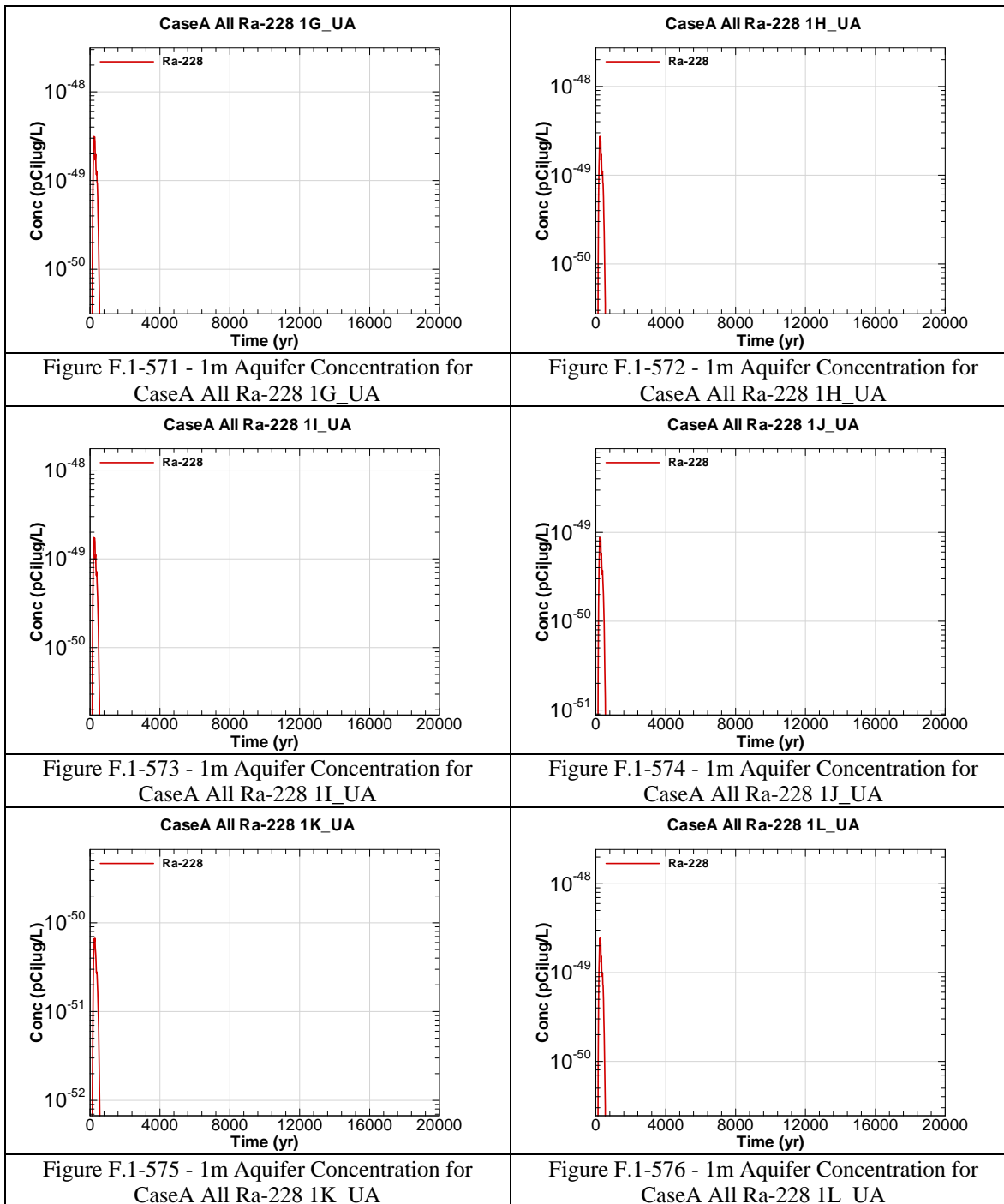
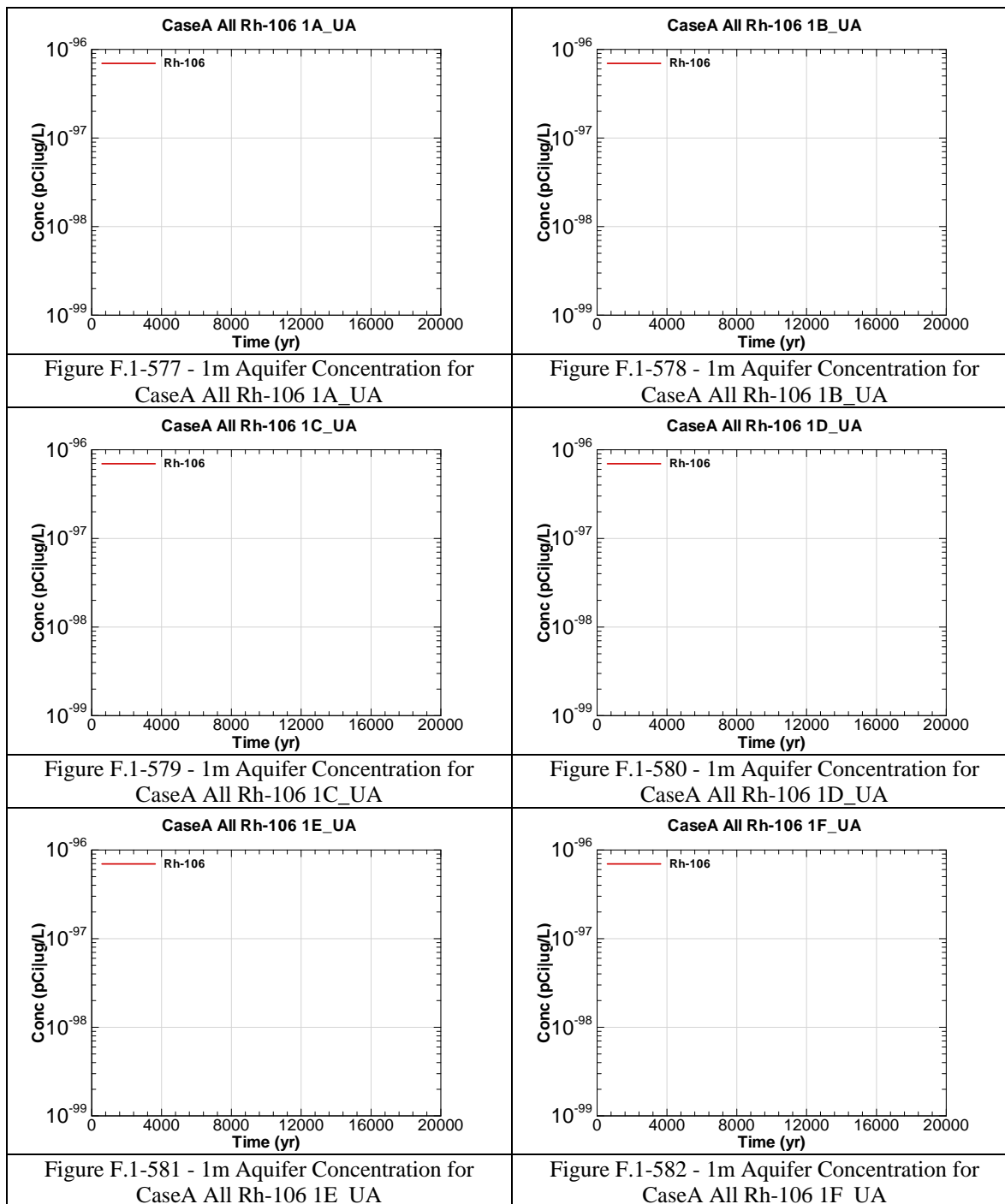
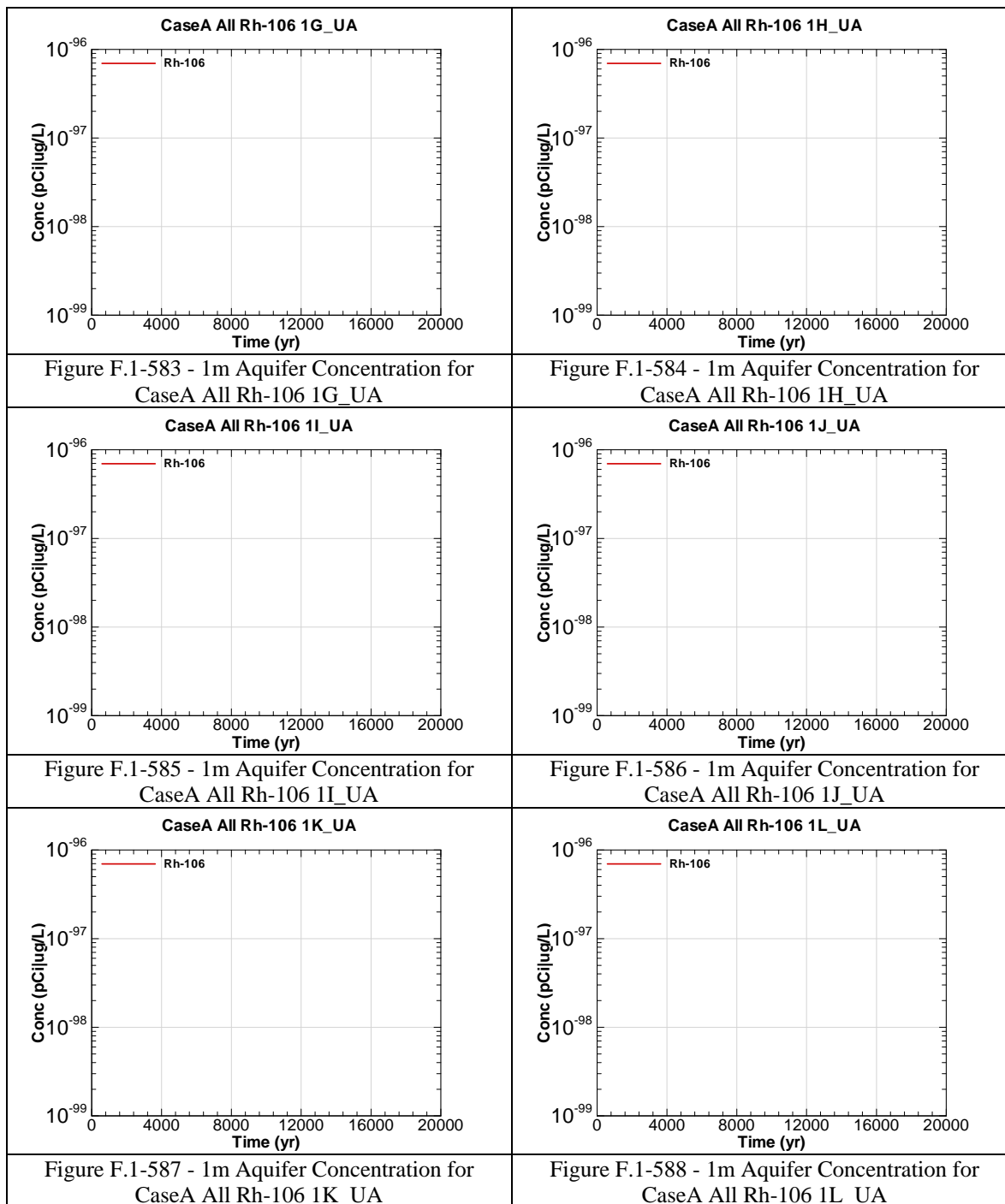


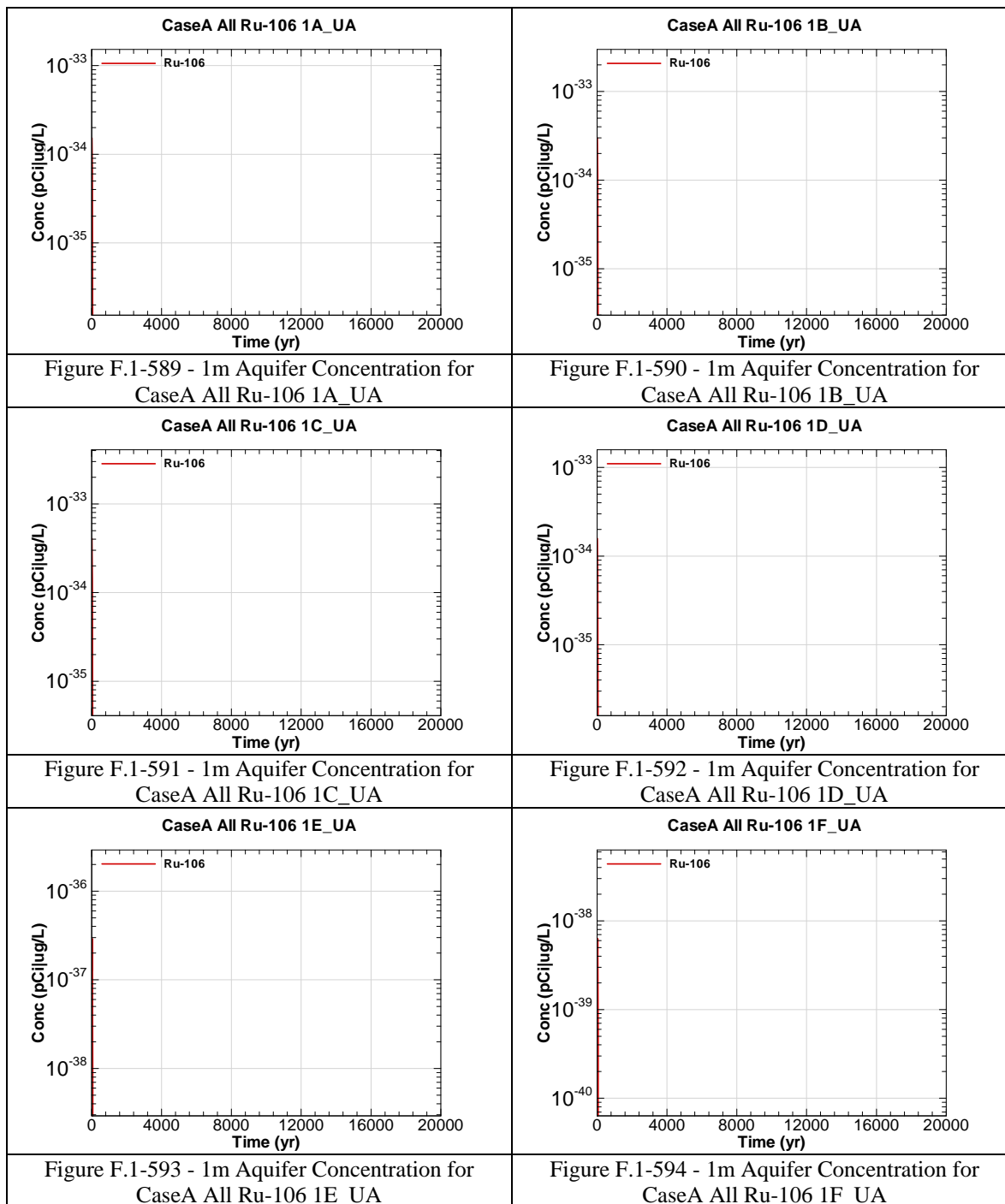
Figure F.1-564 - 1m Aquifer Concentration for
CaseA All Ra-226 1L_UA

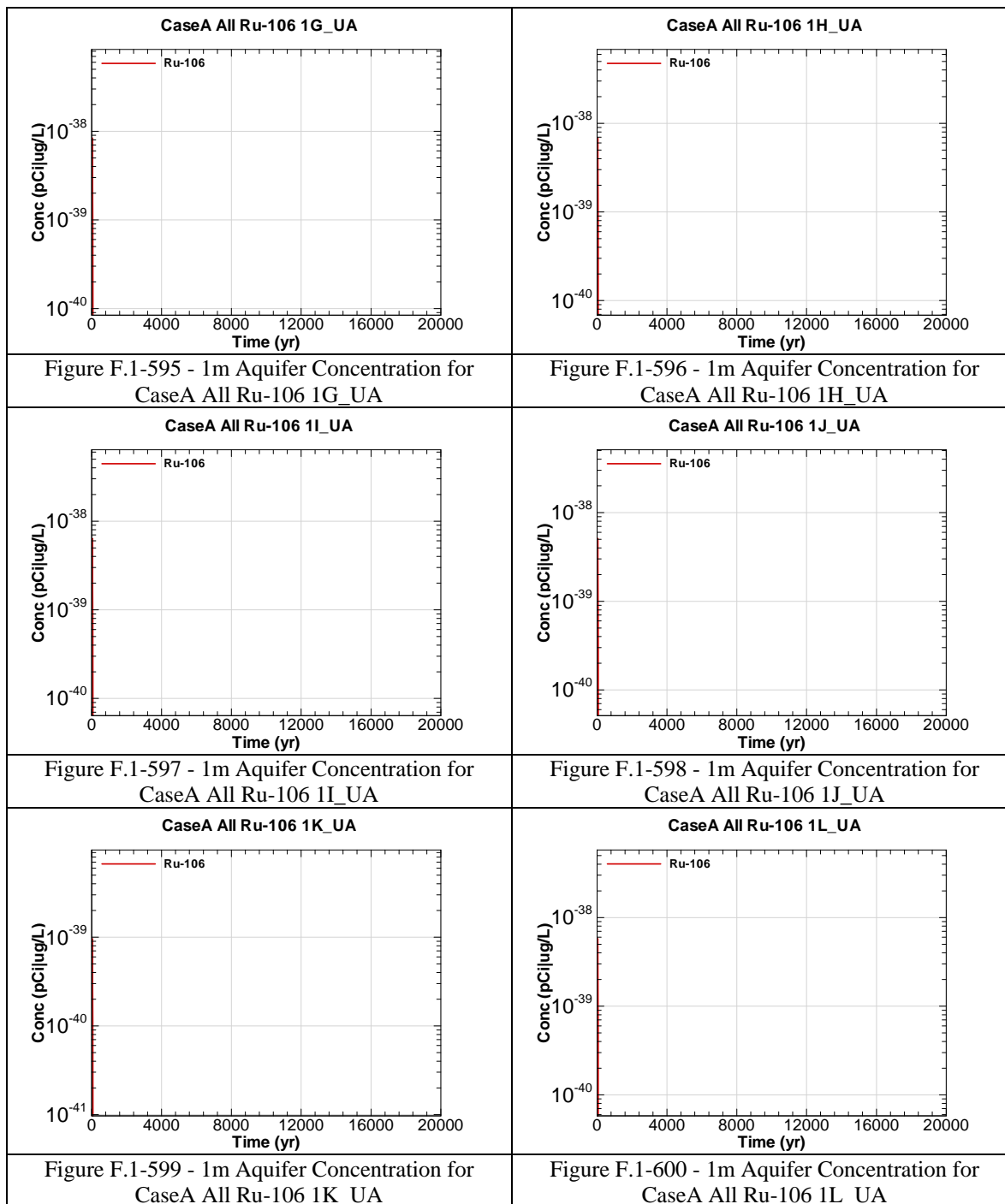


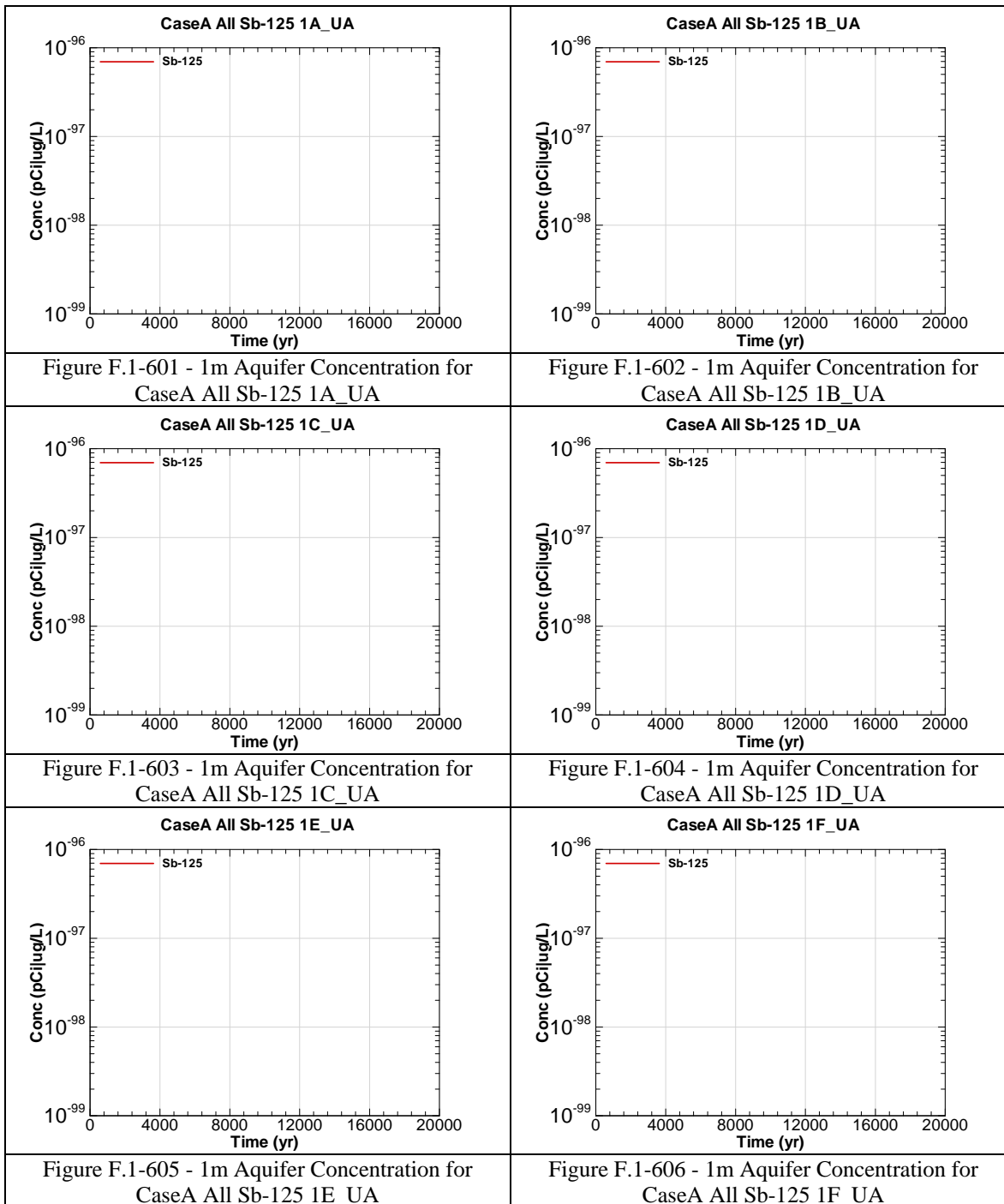


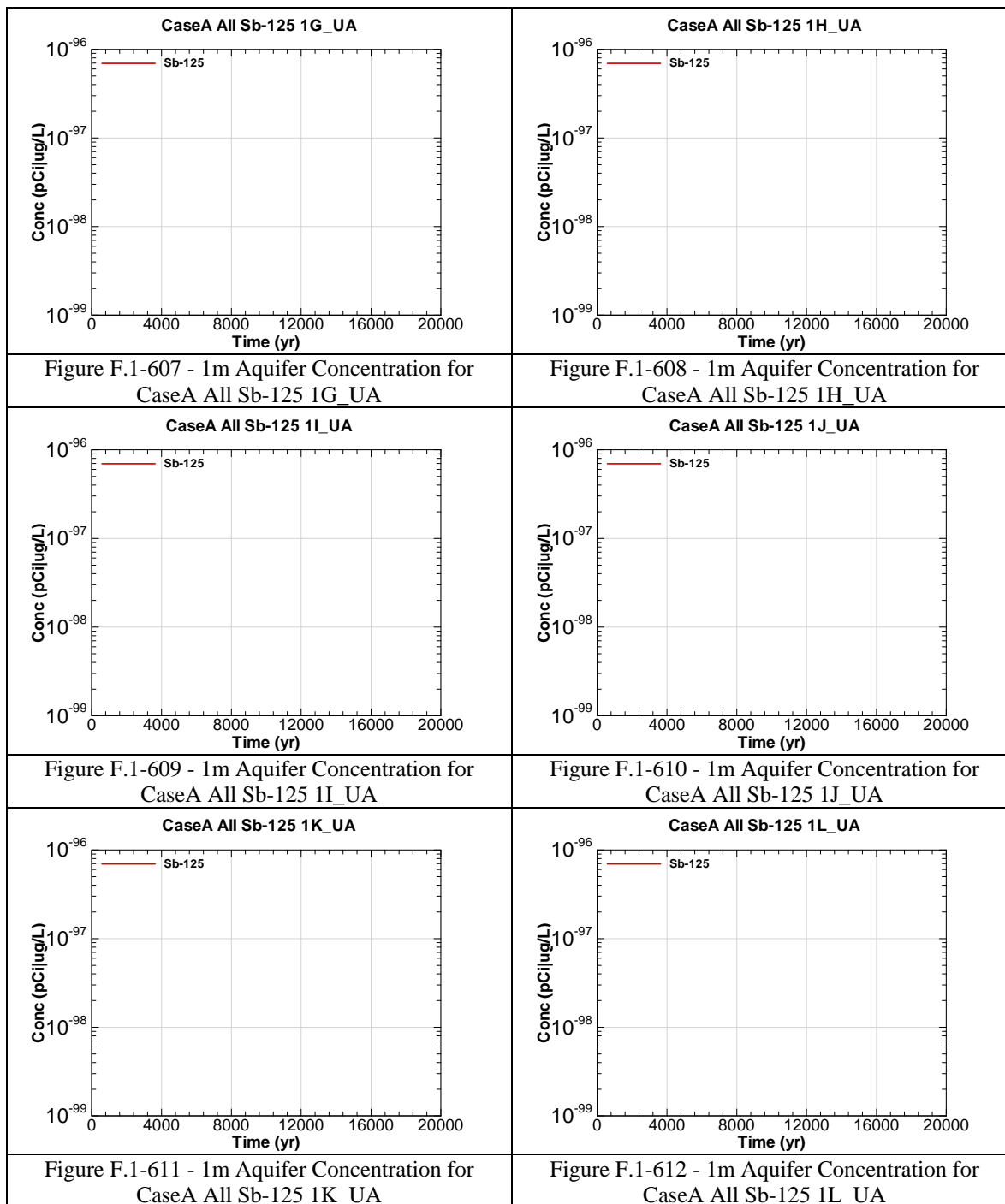


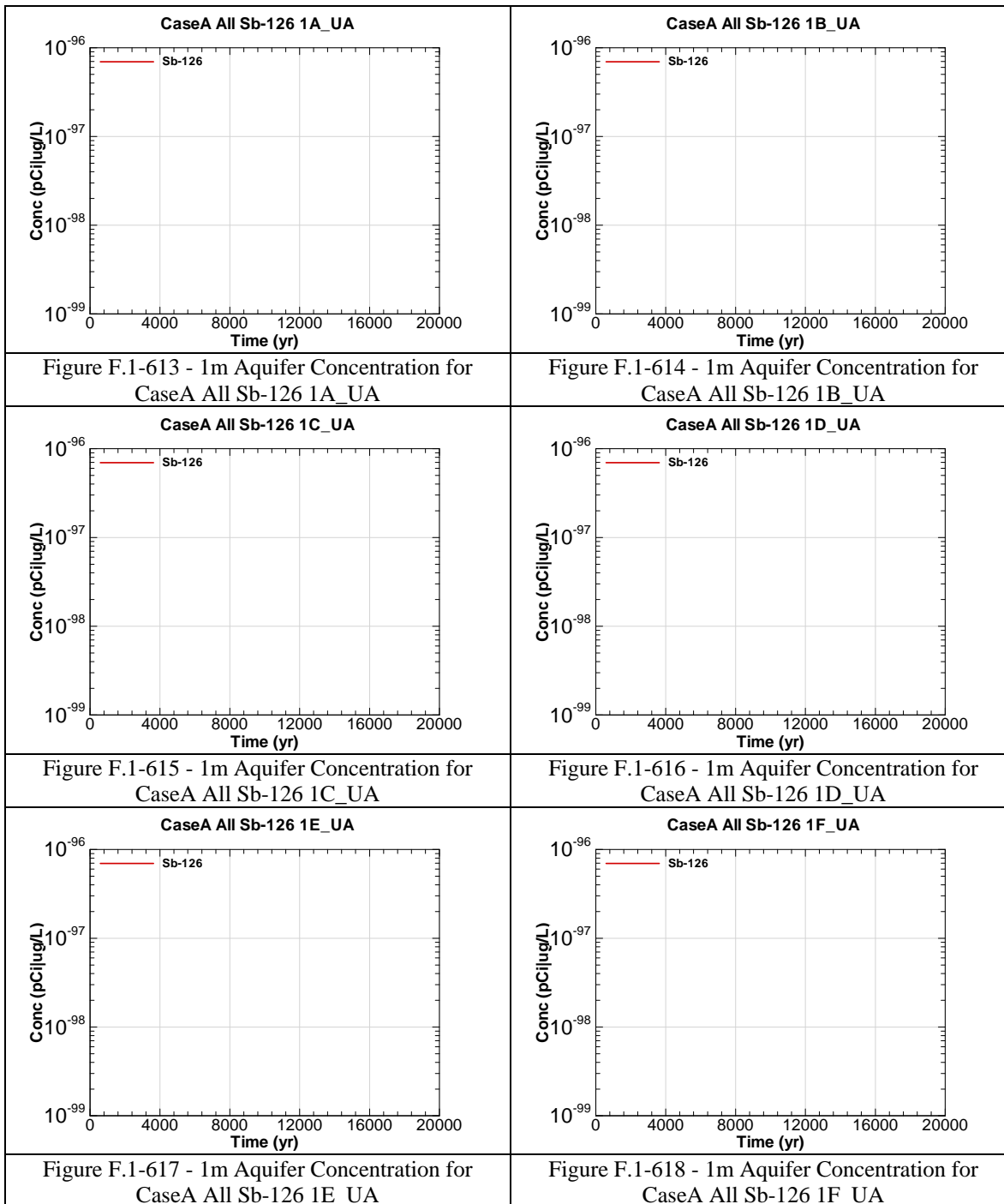


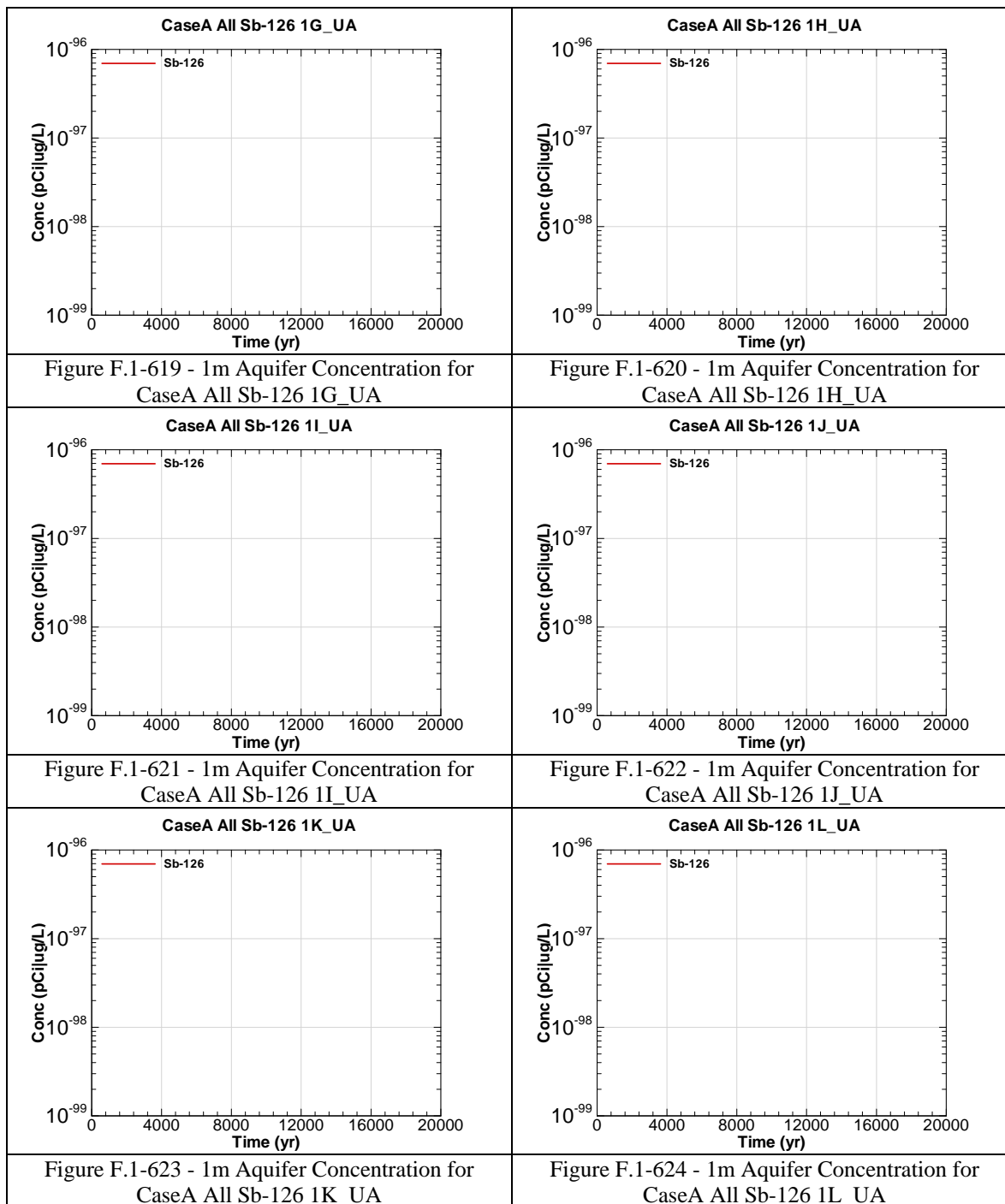


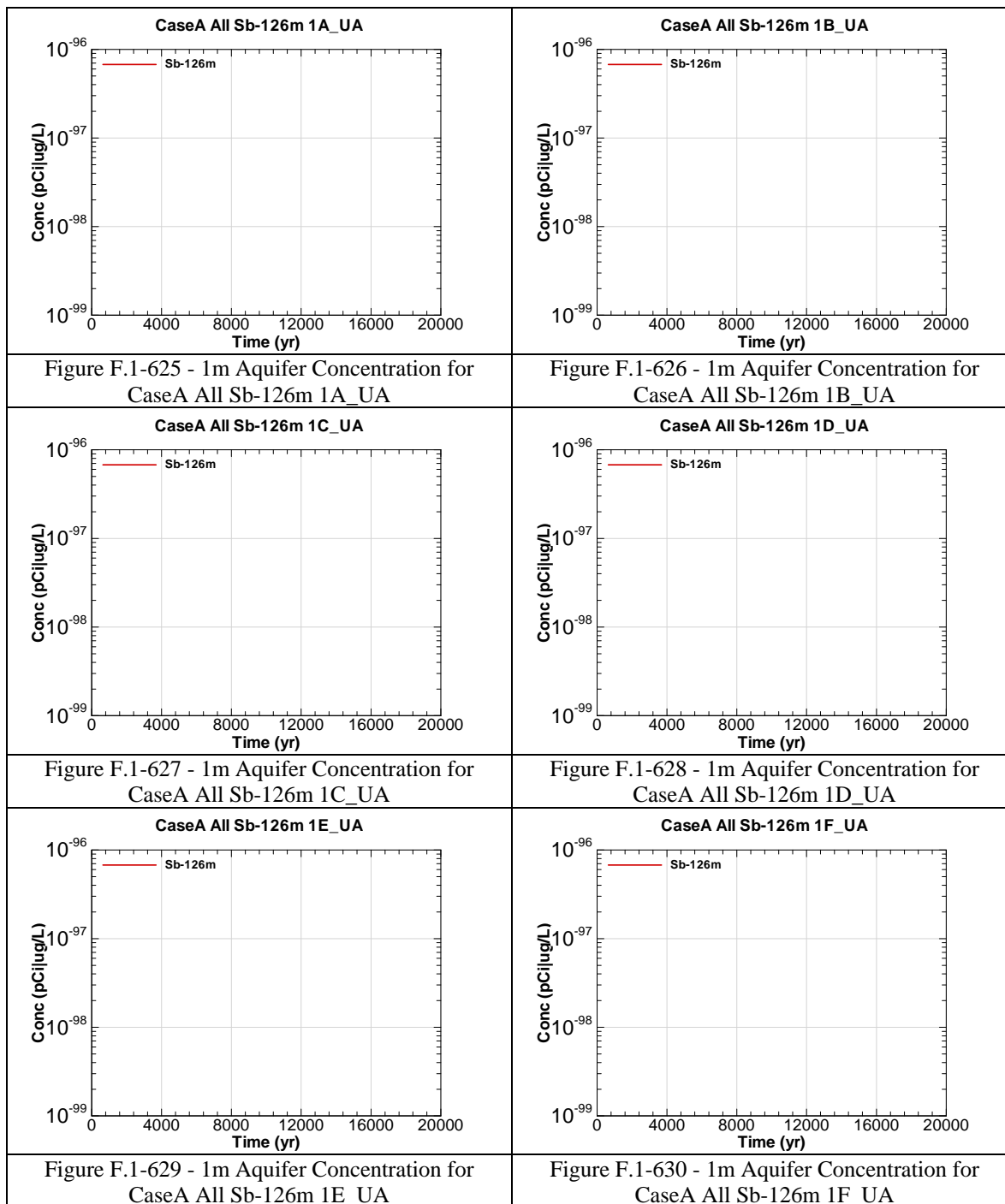


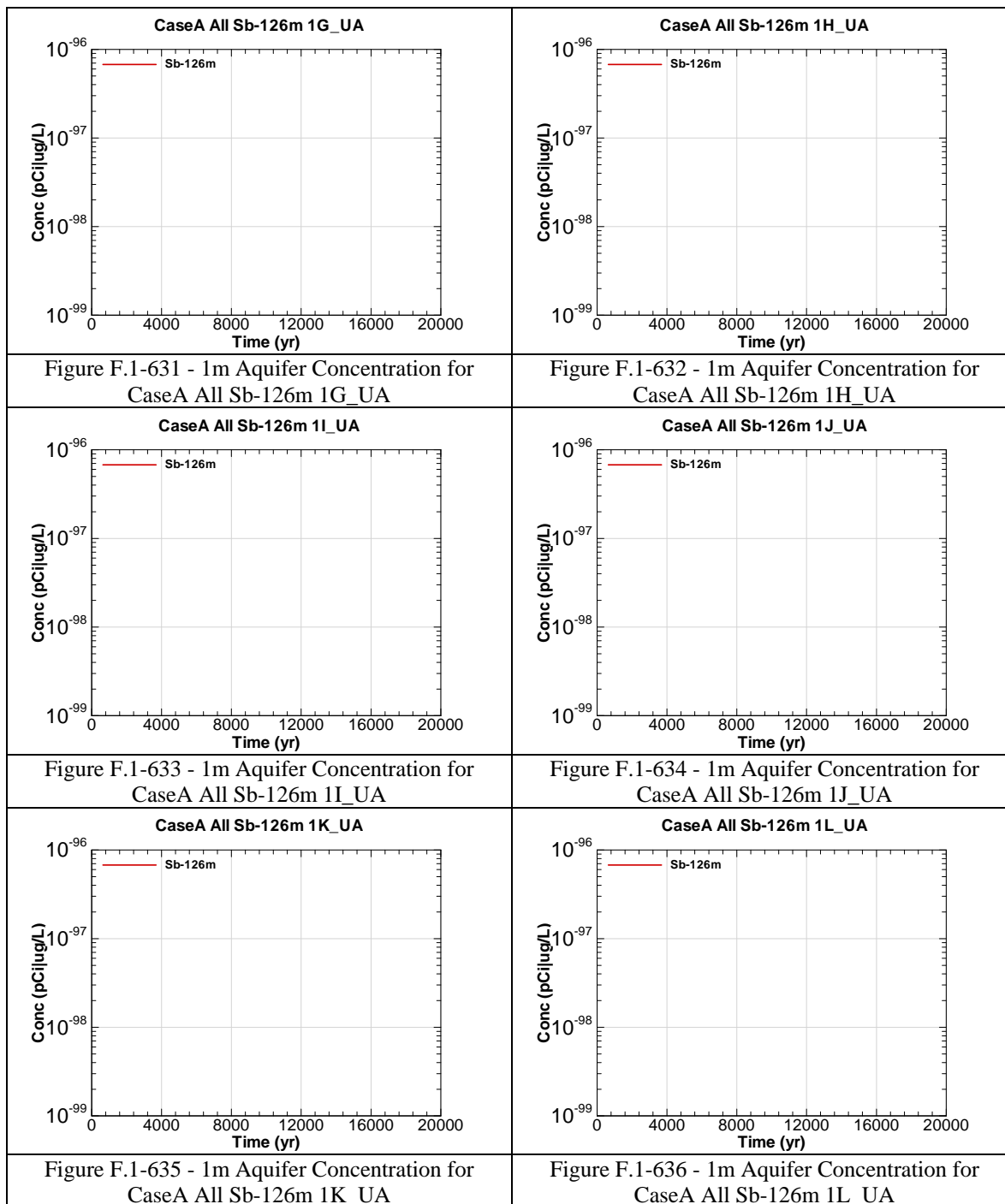


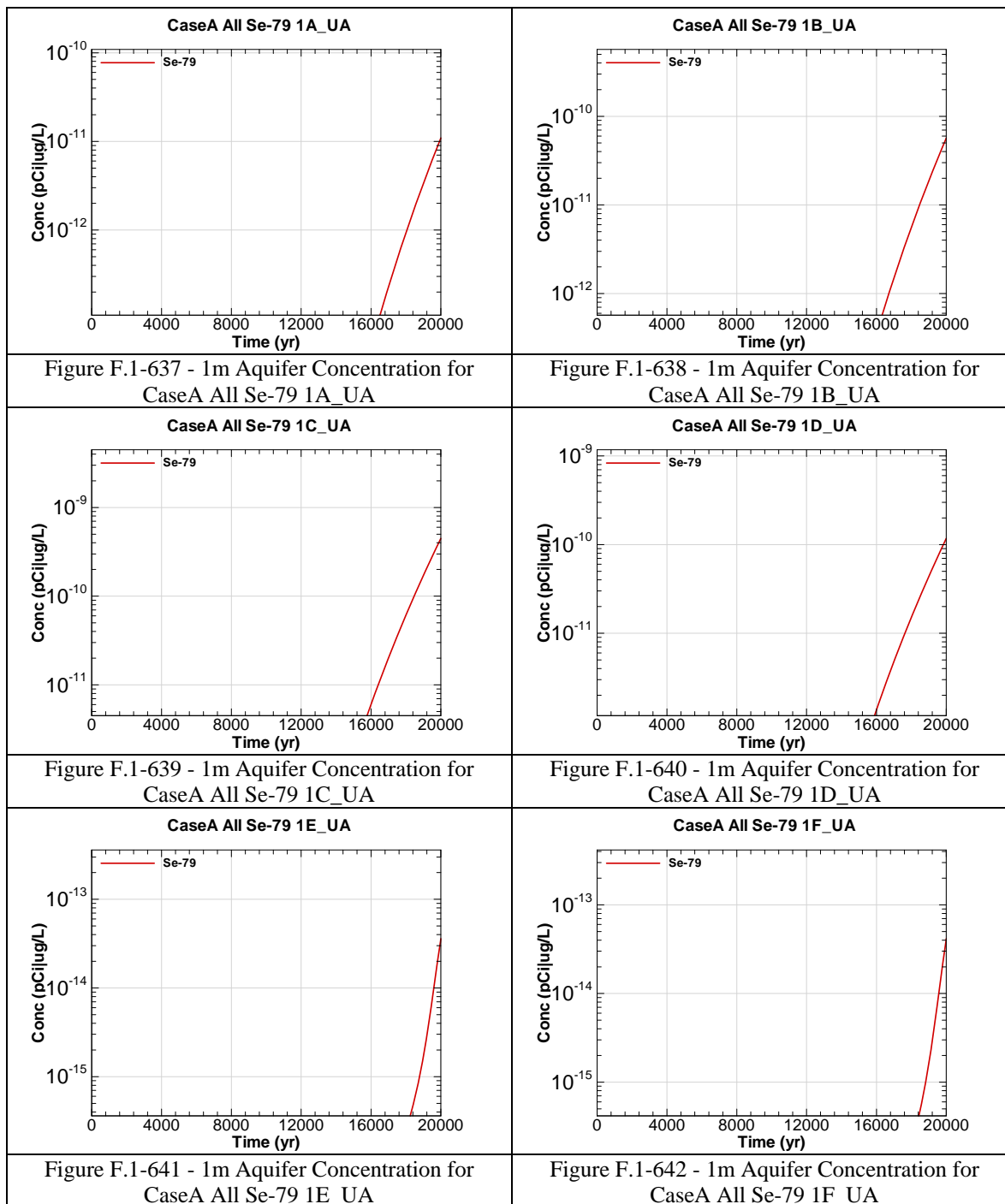


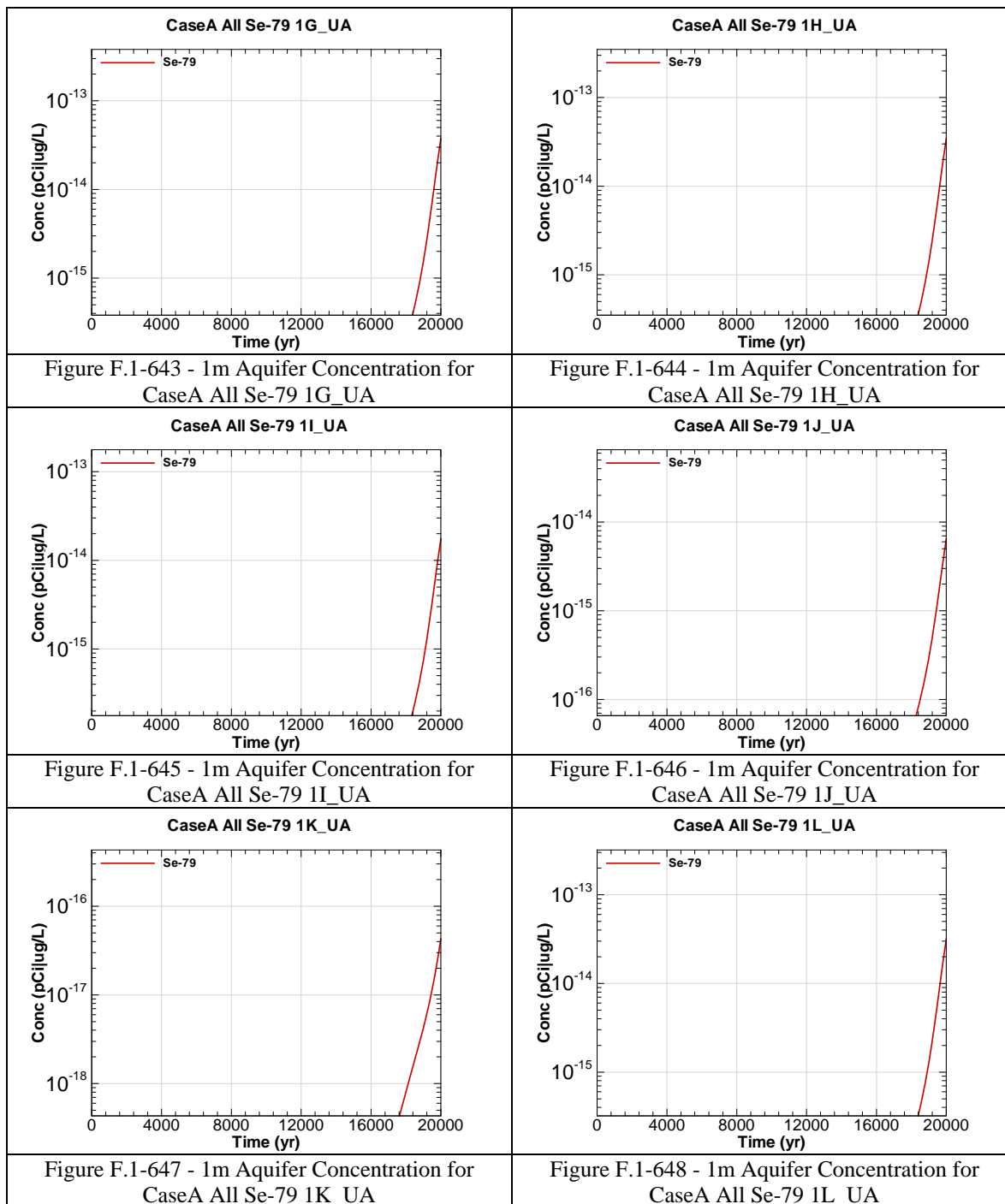


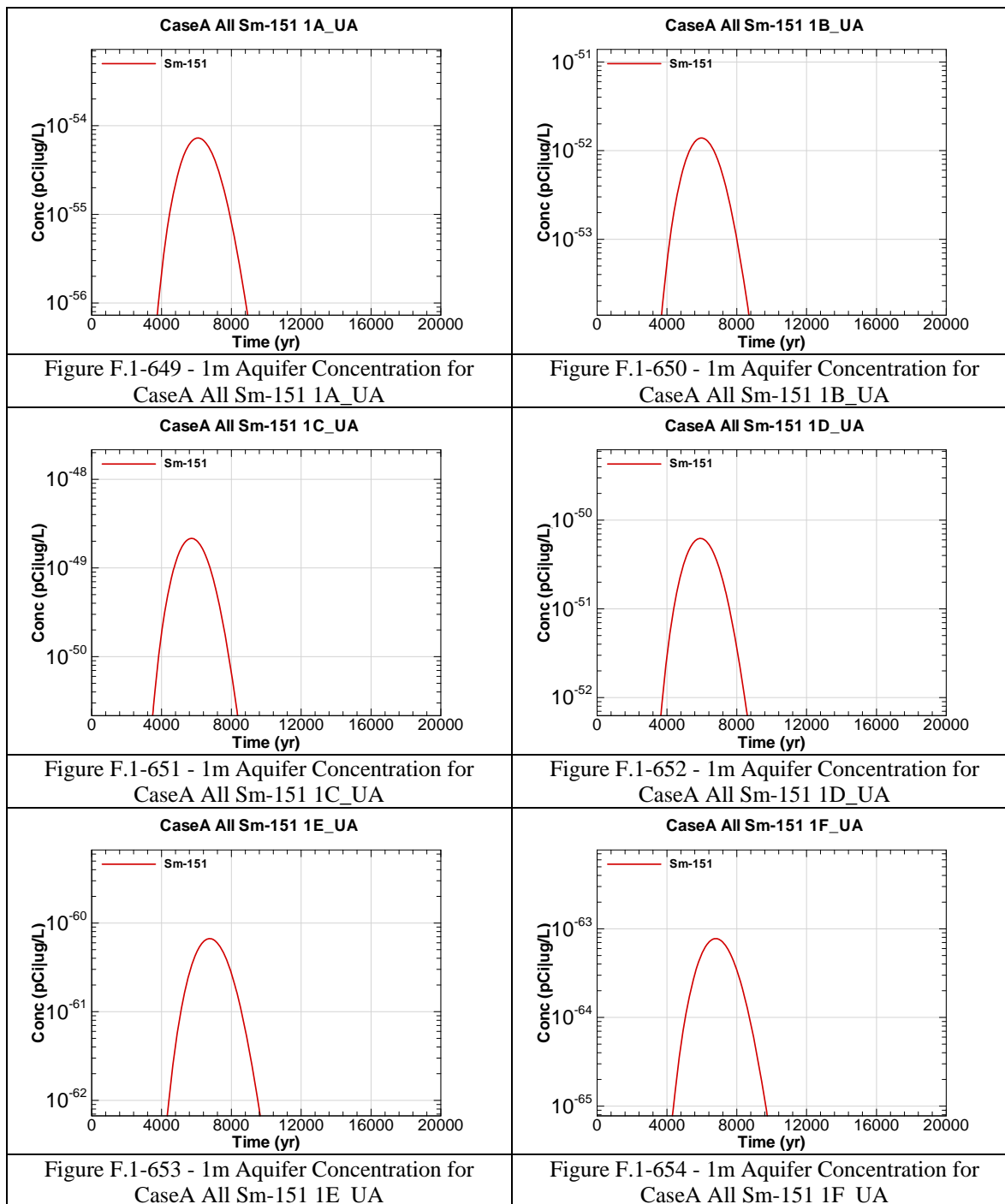


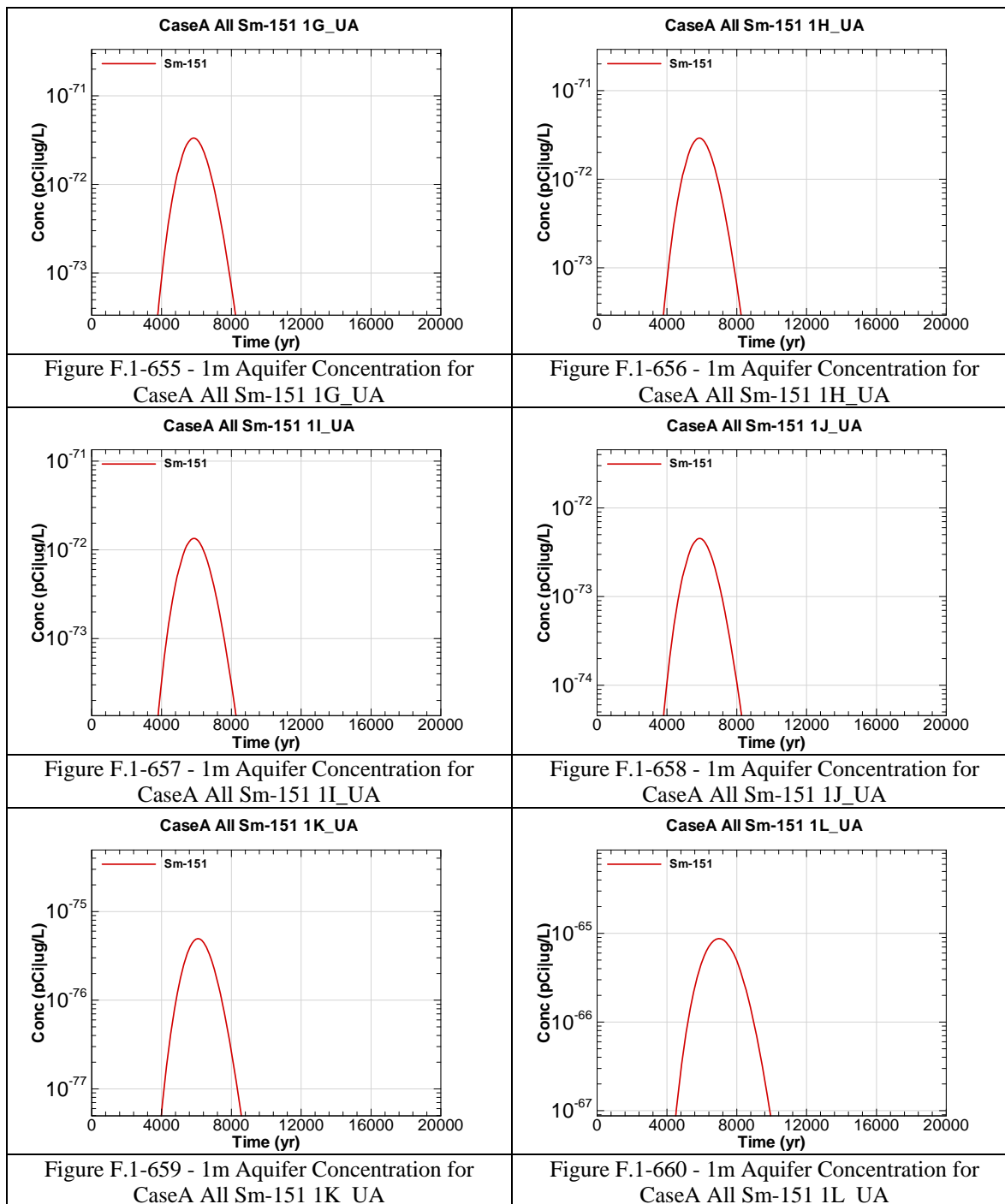


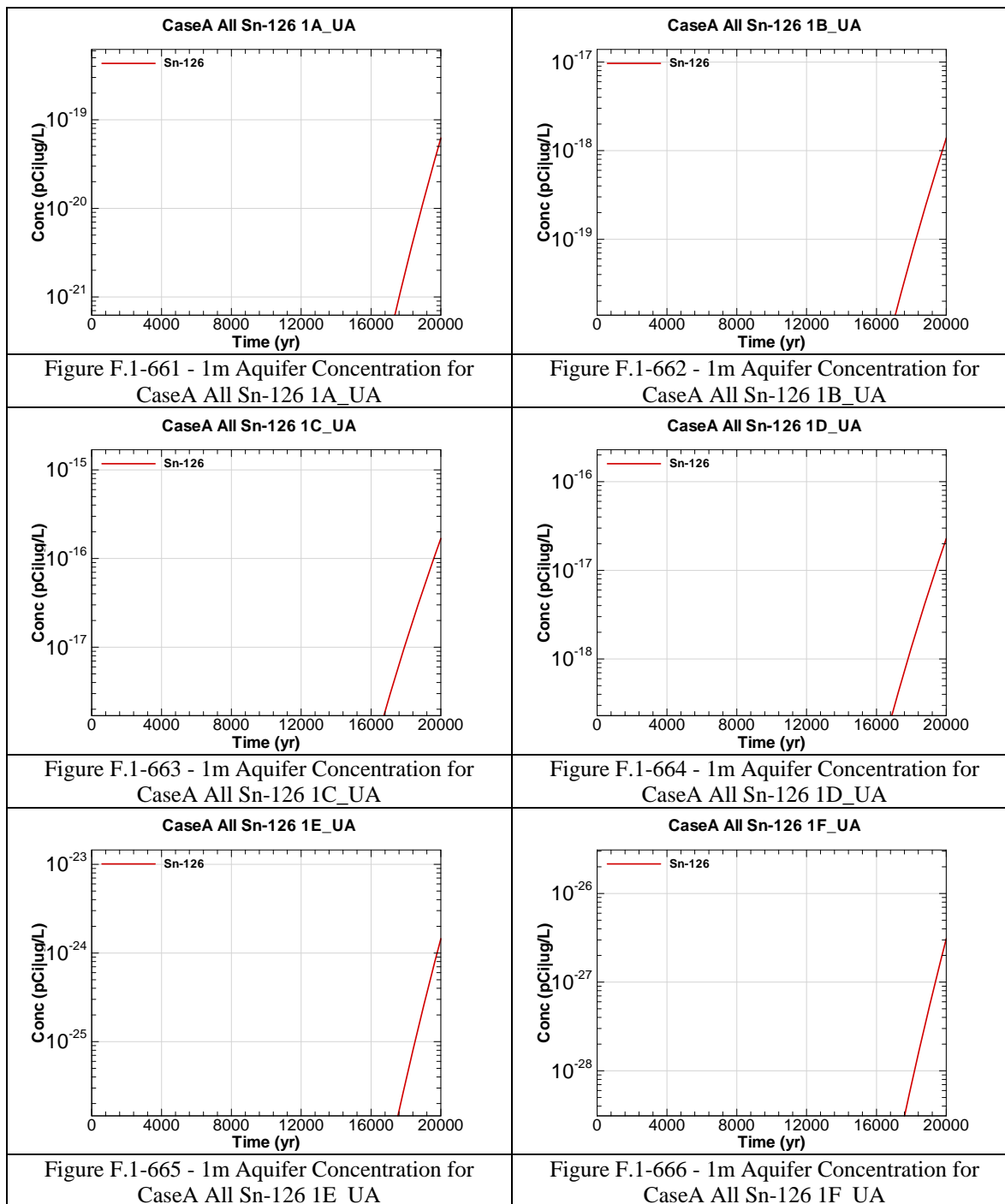


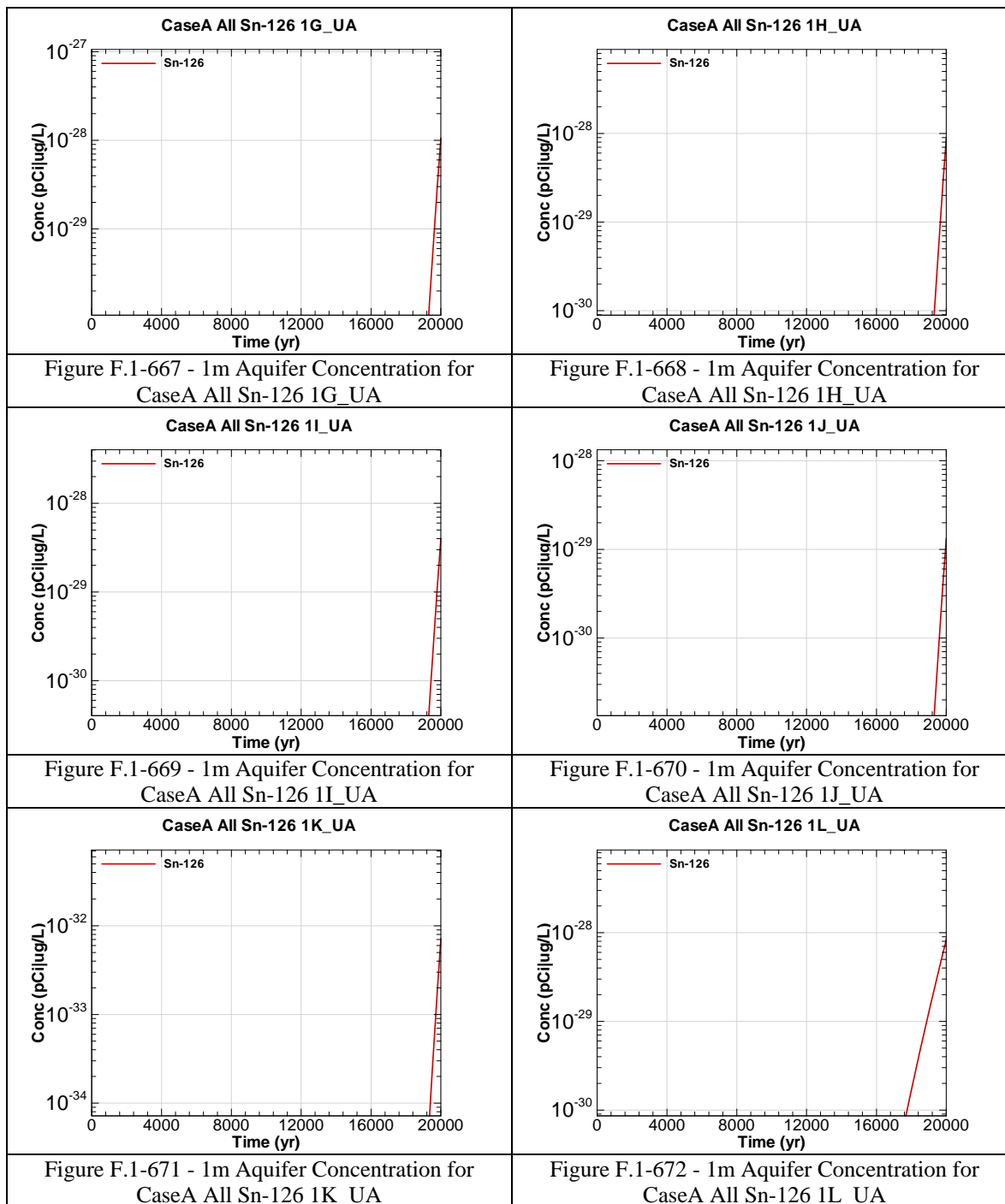


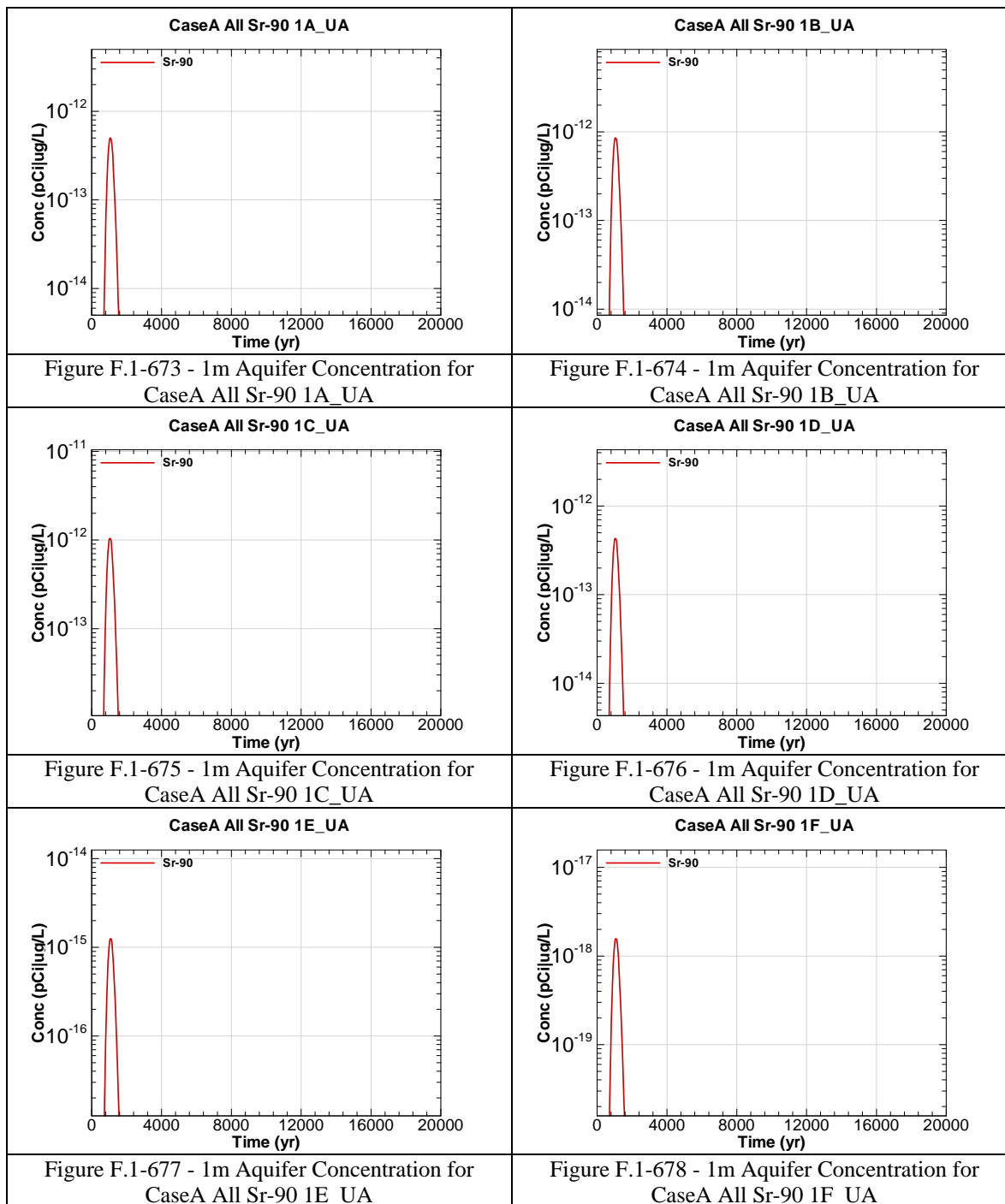


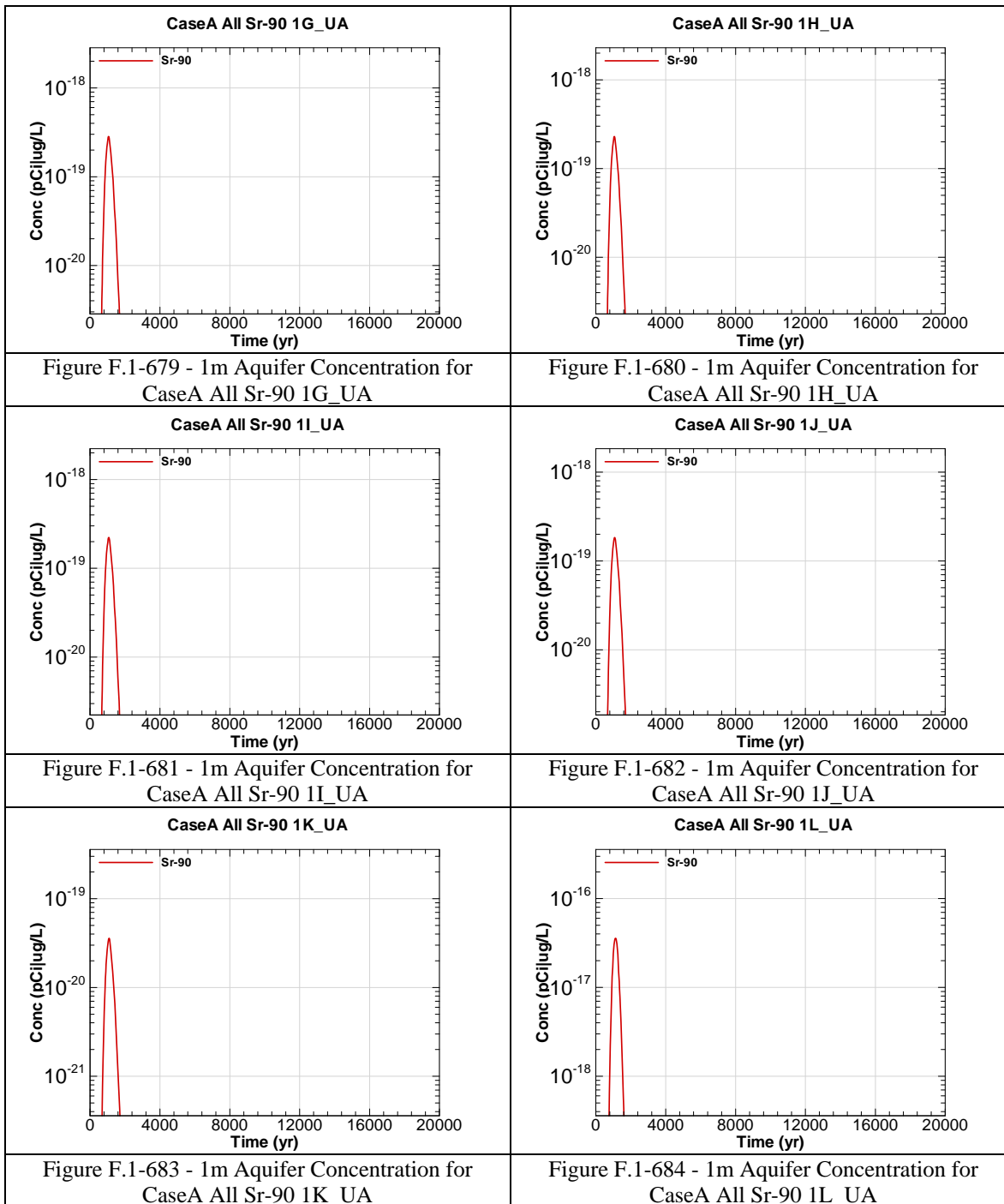


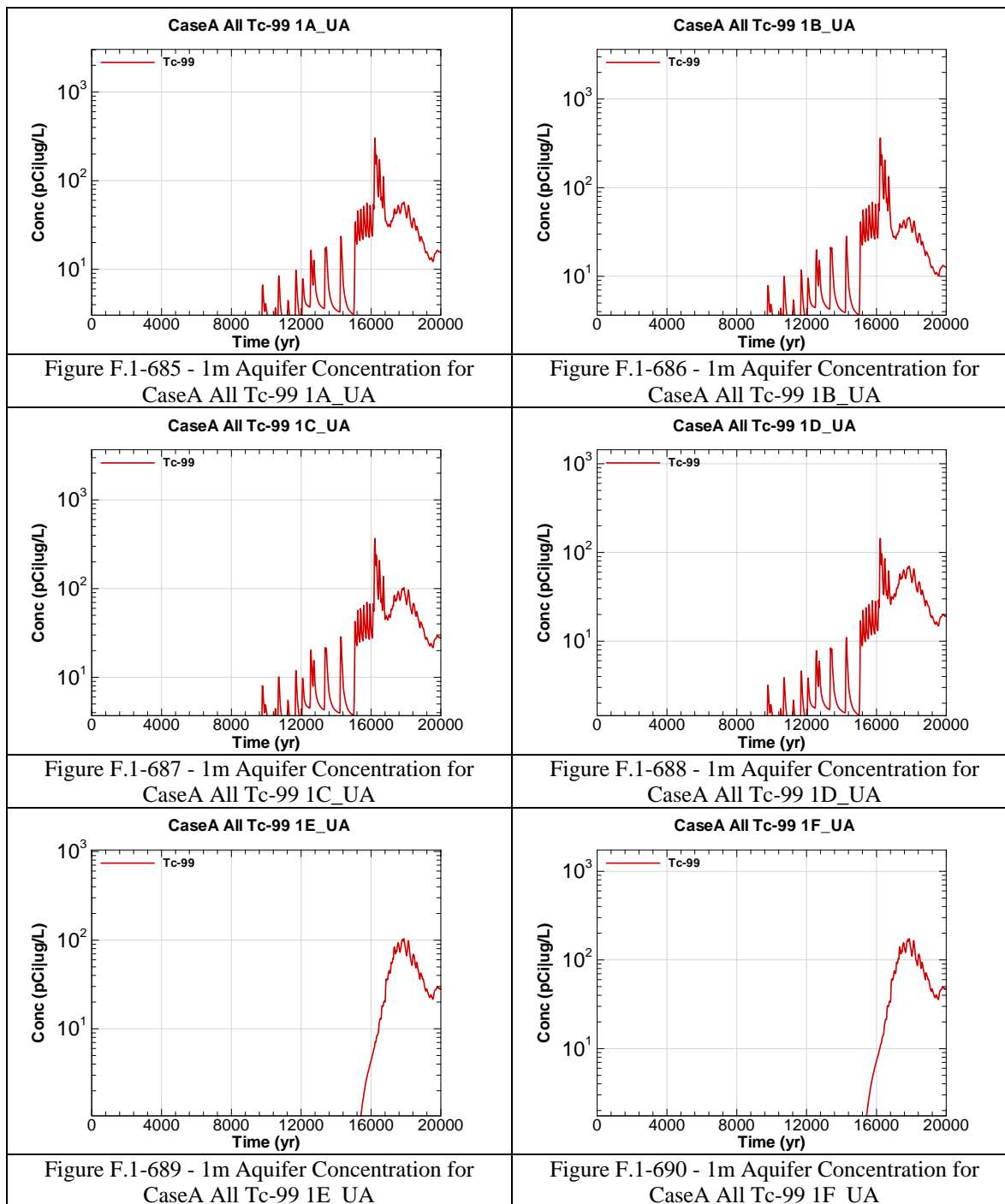


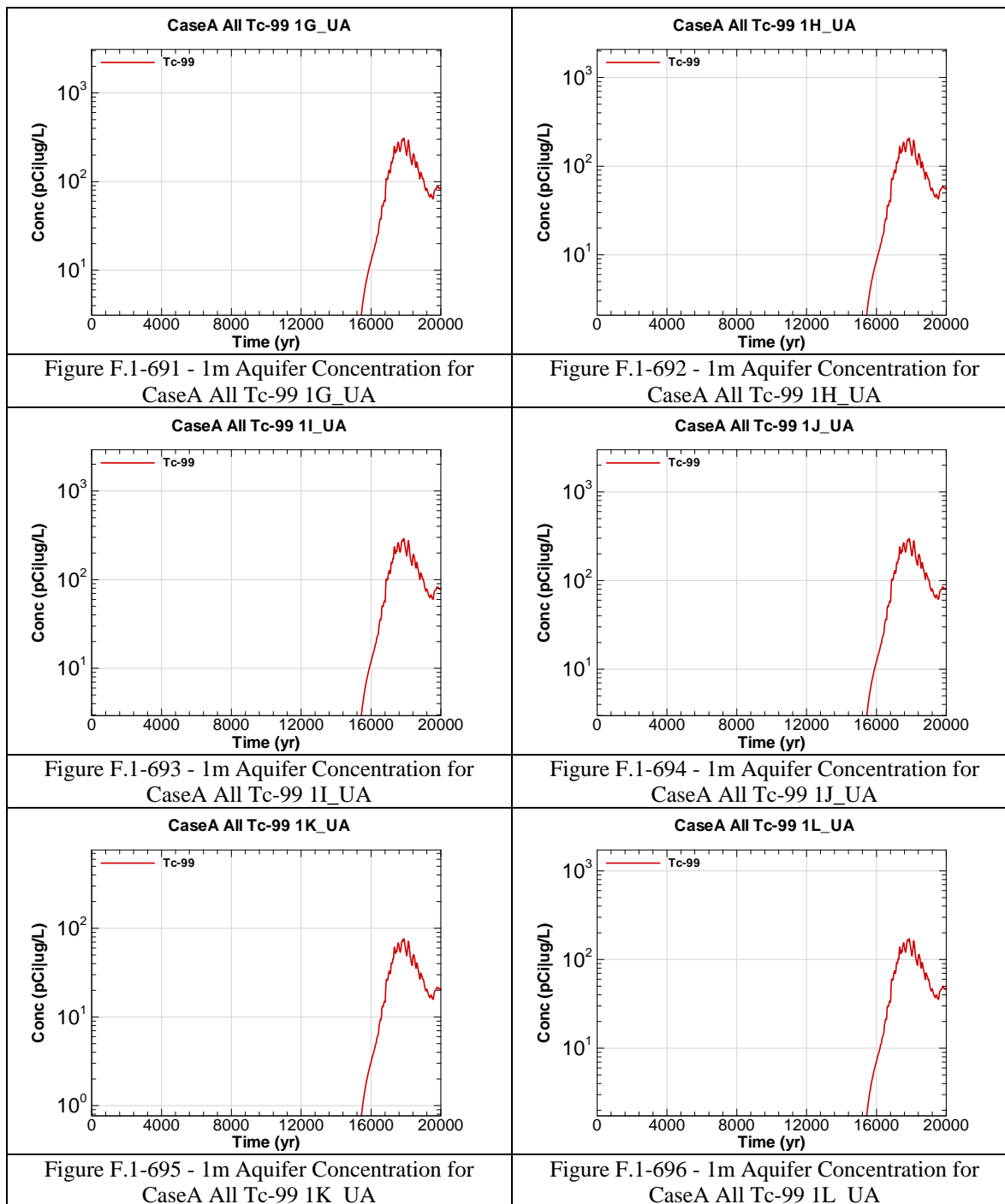


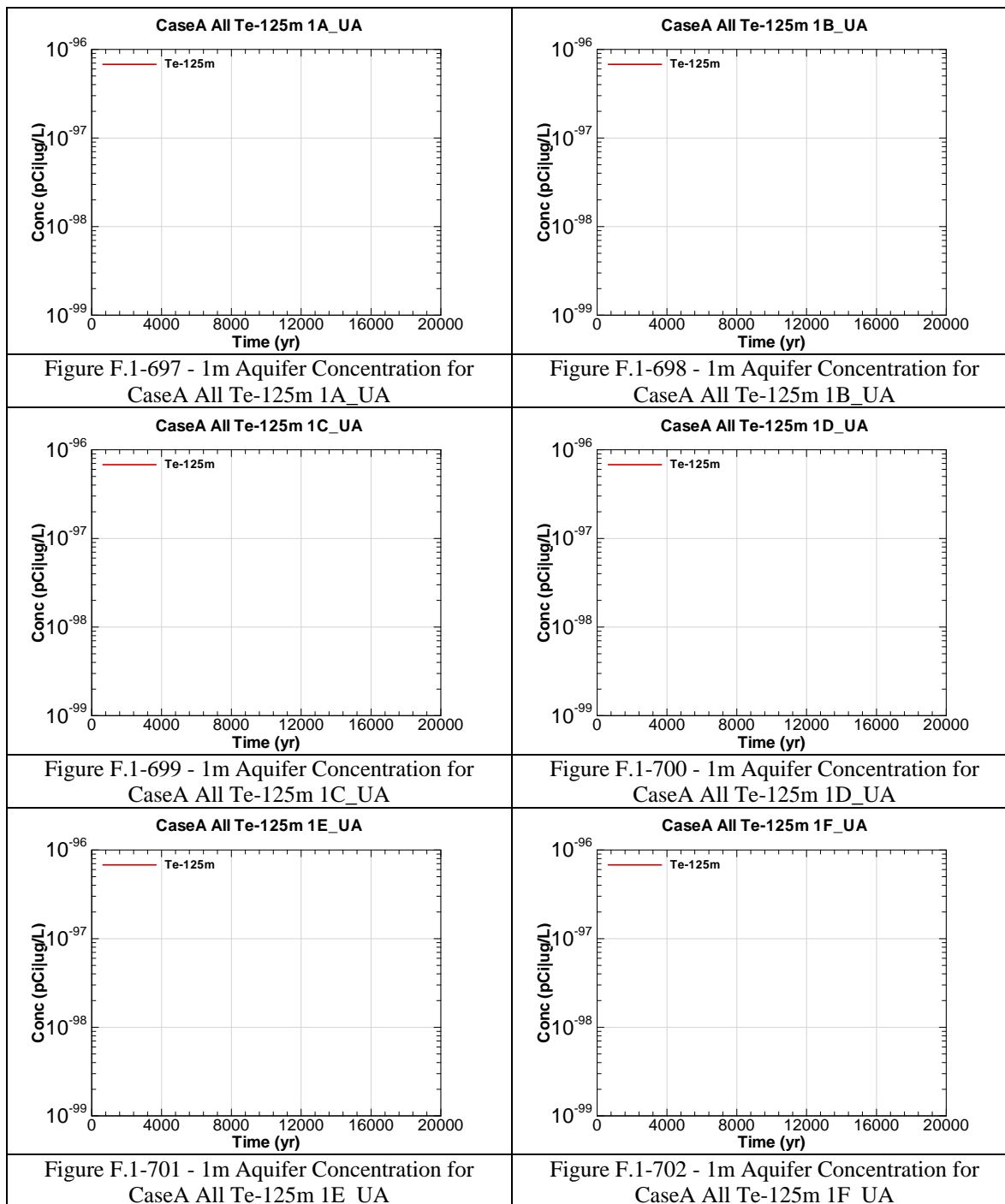


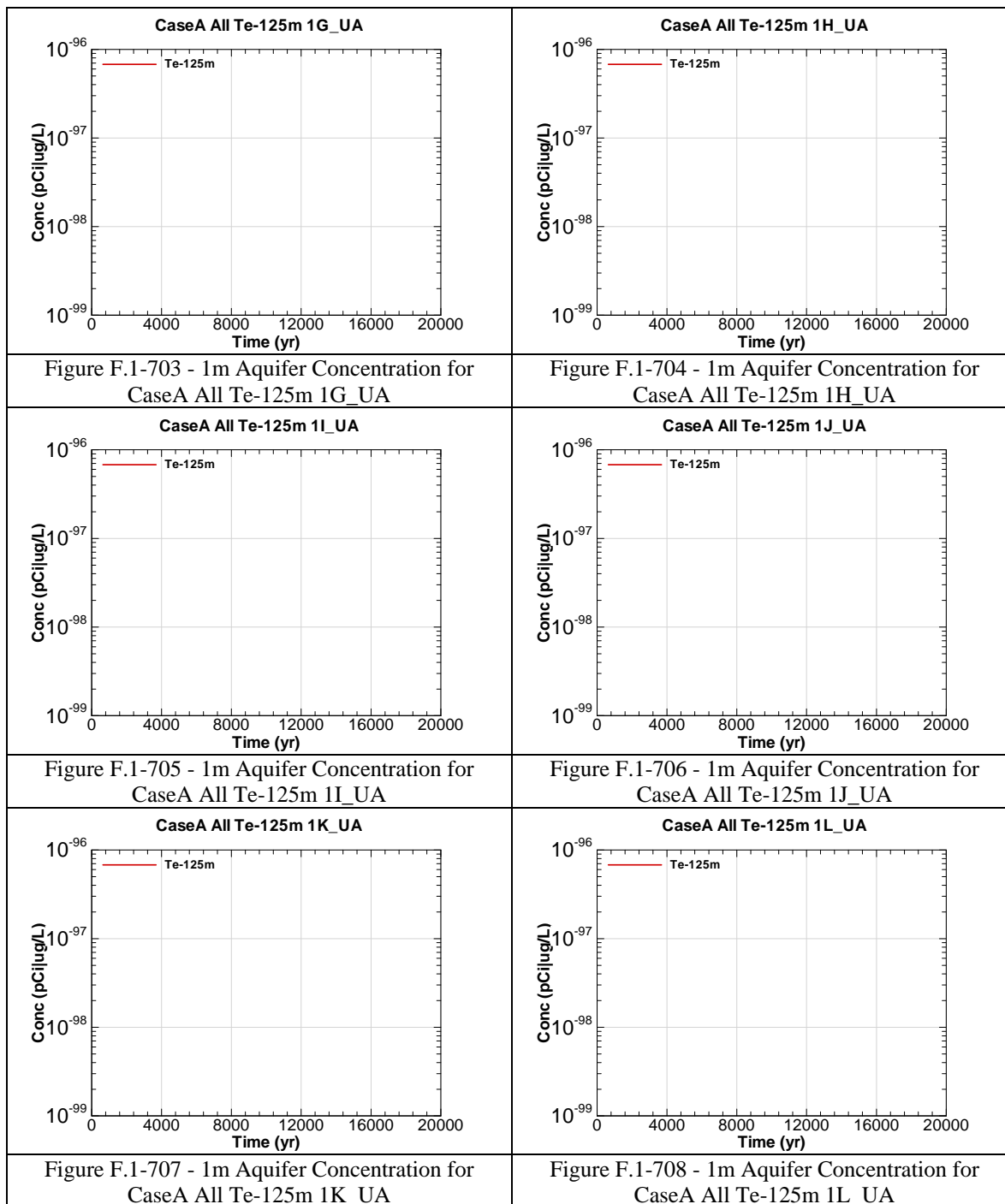


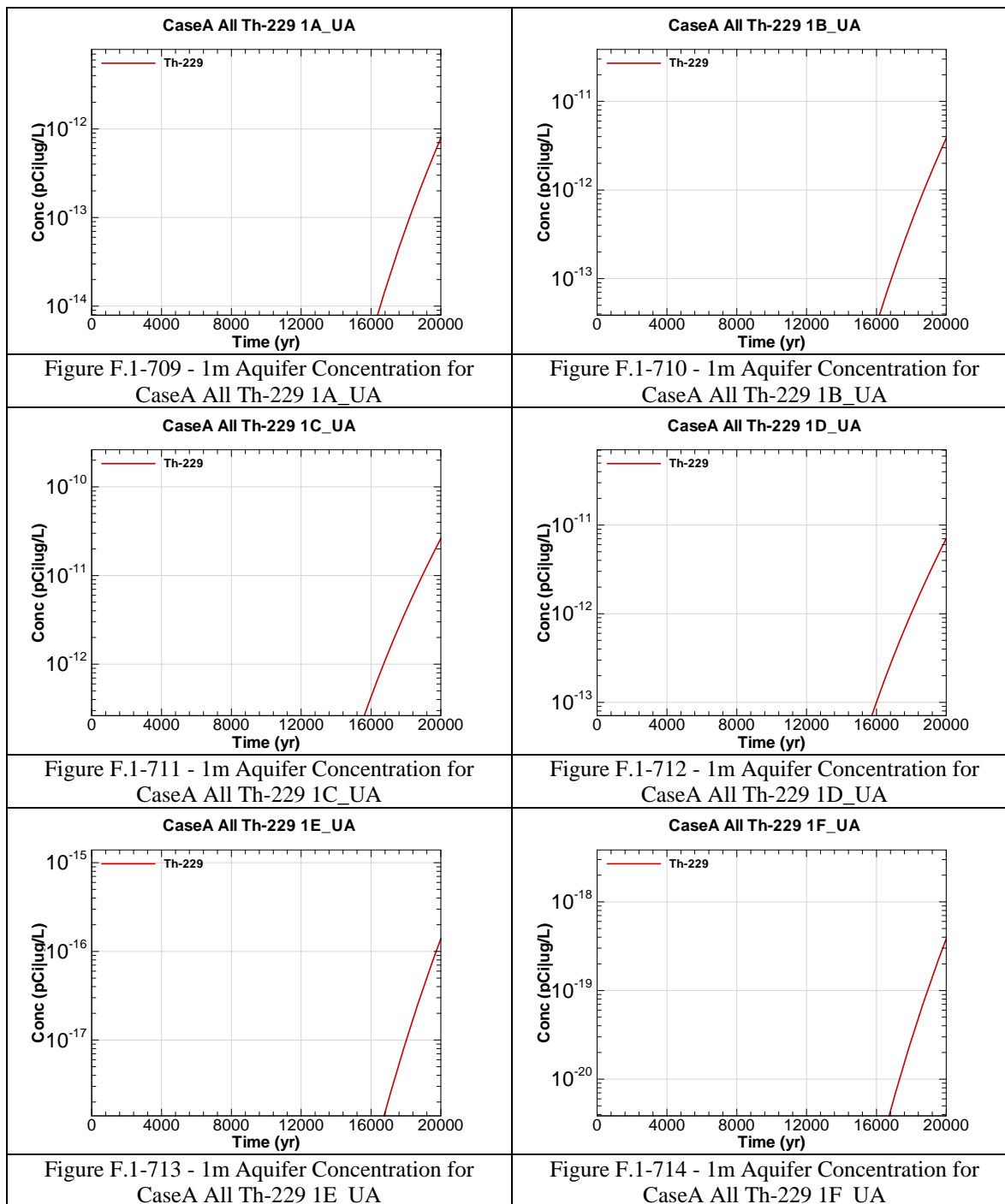


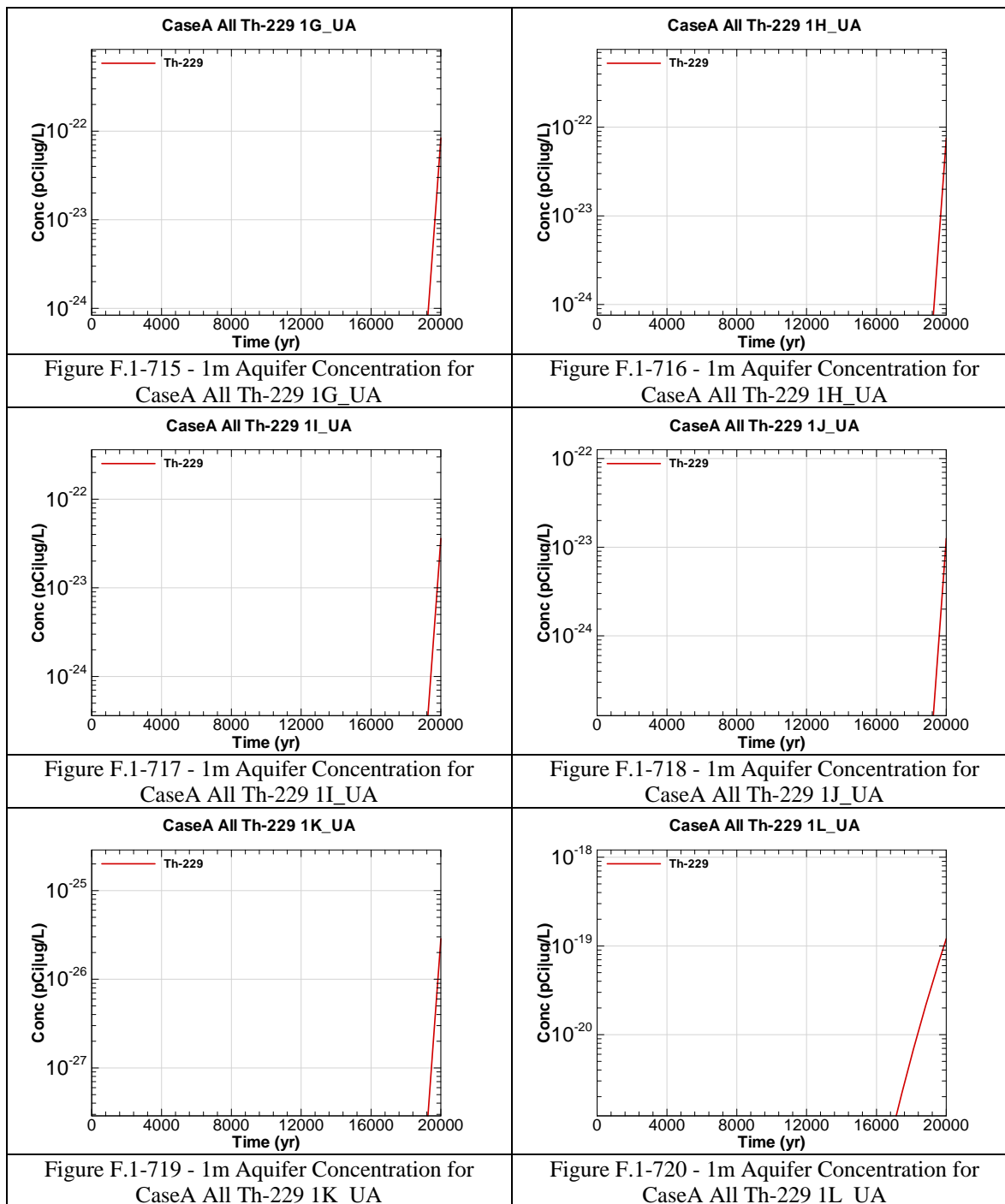


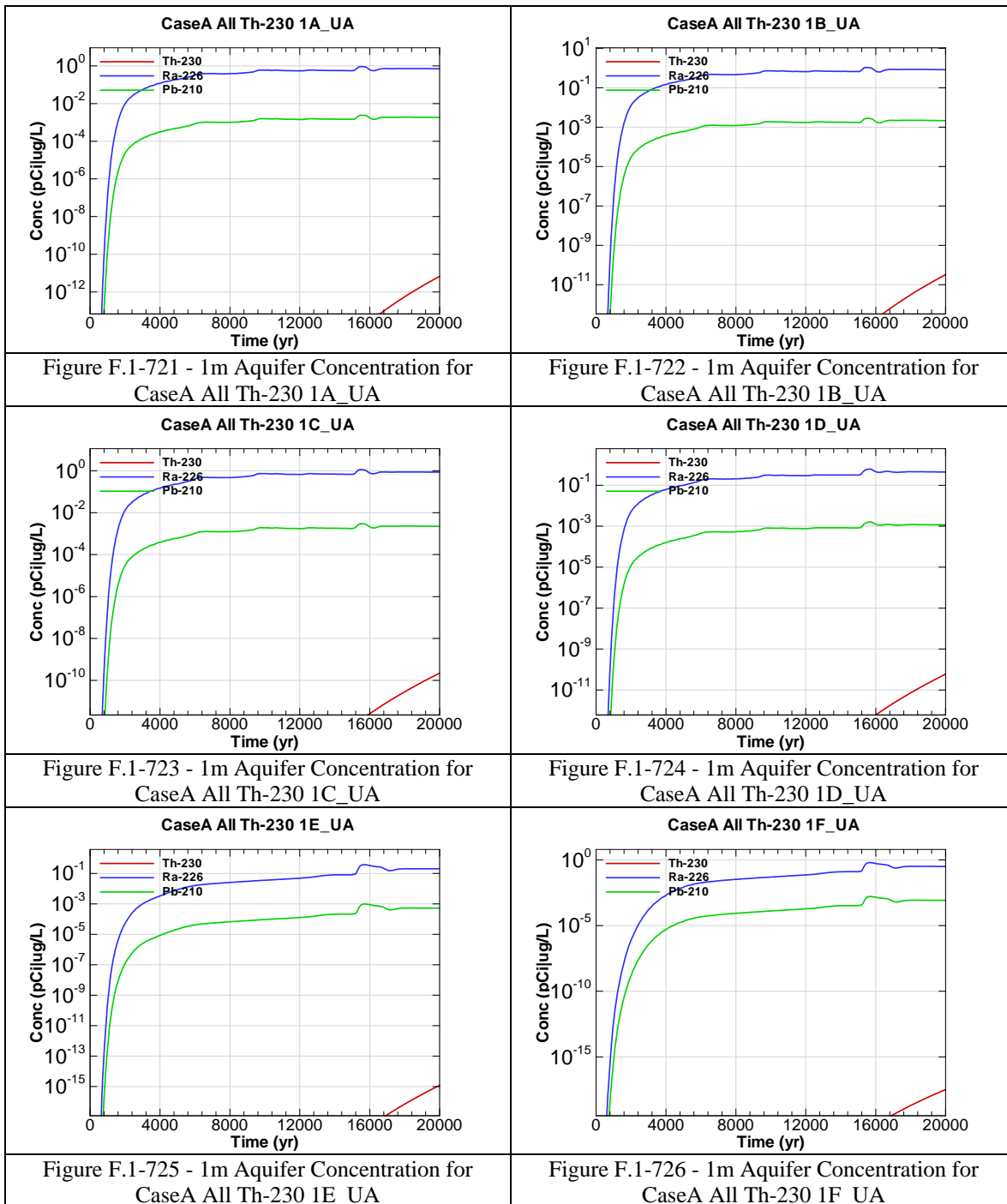


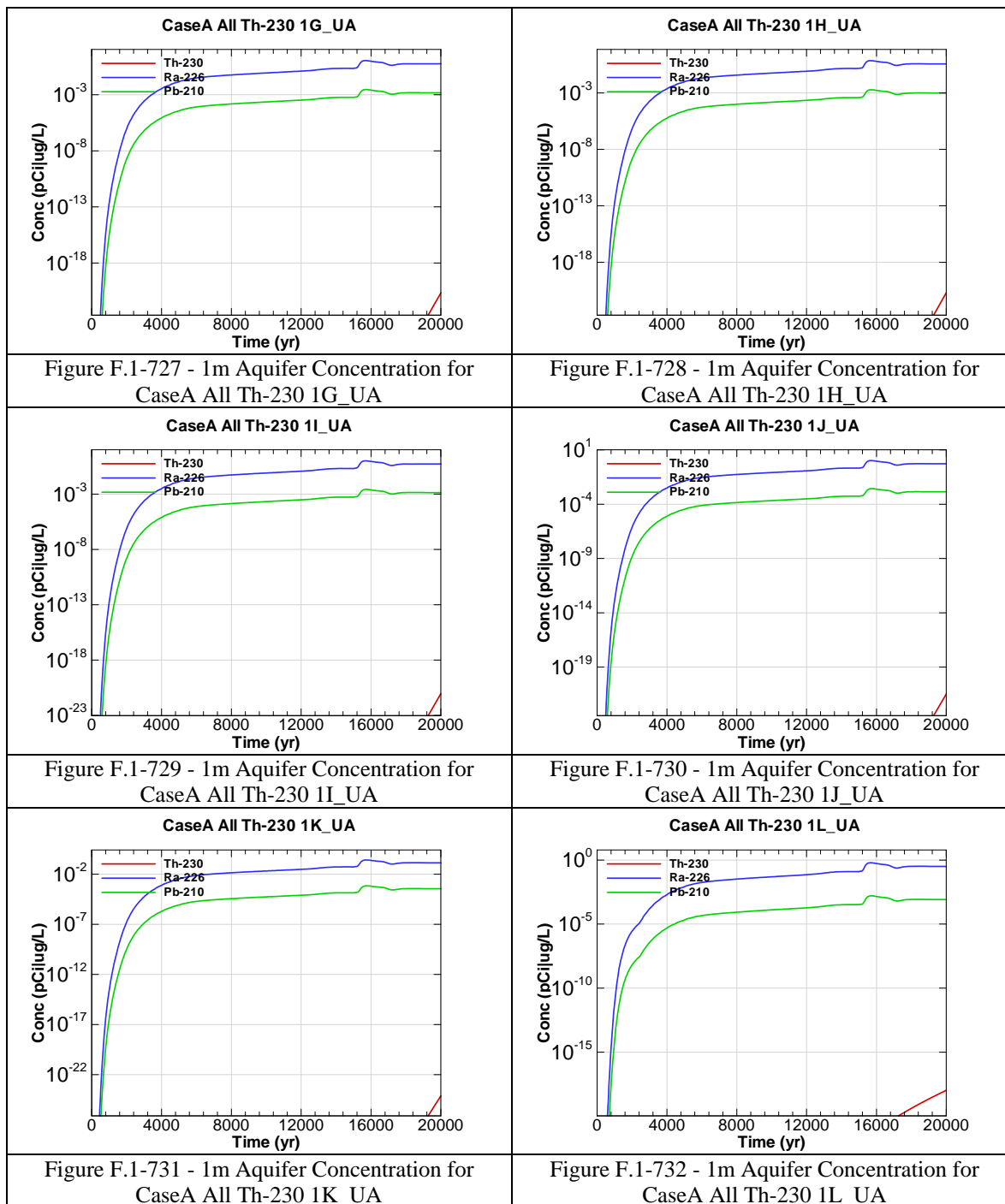


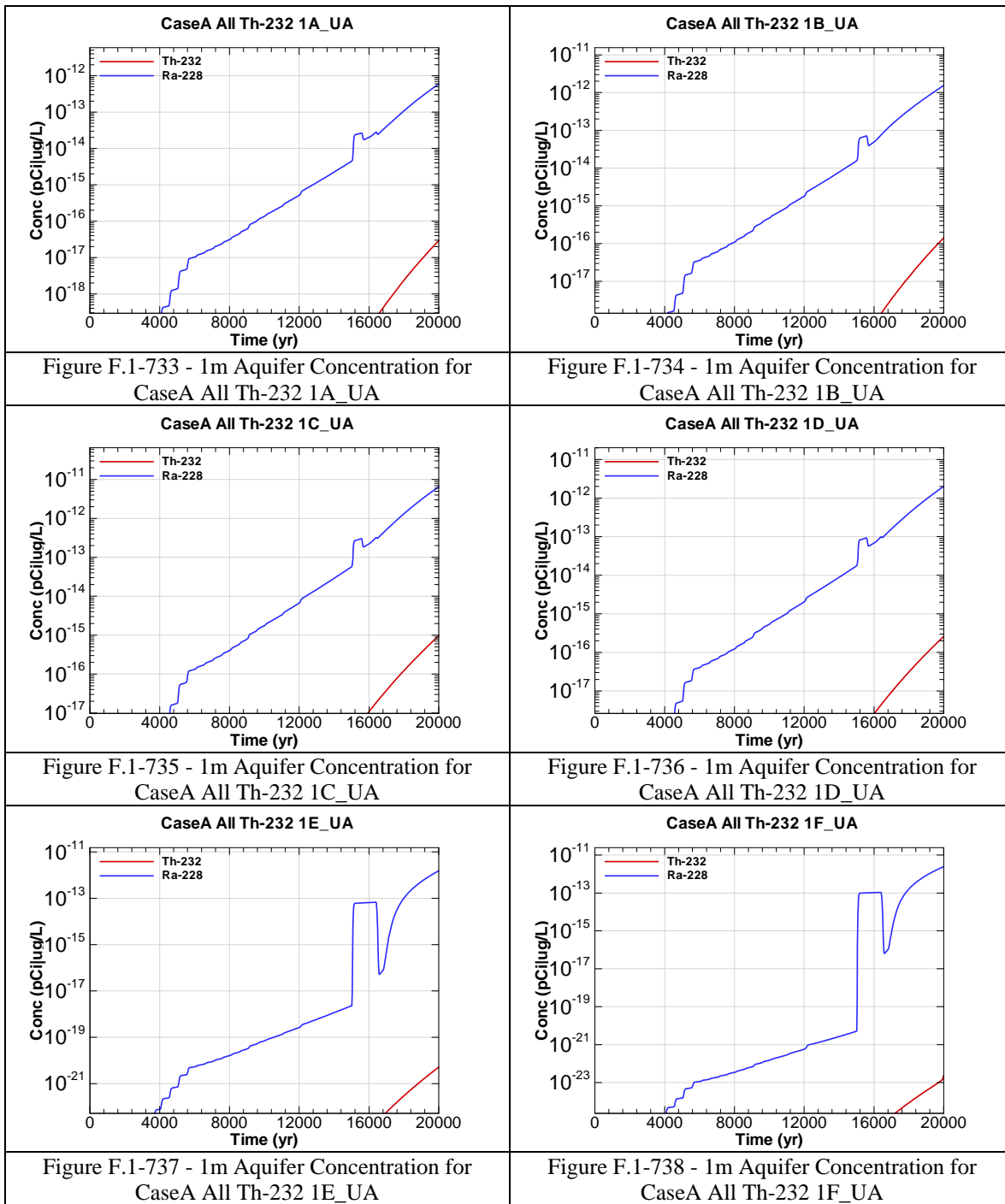


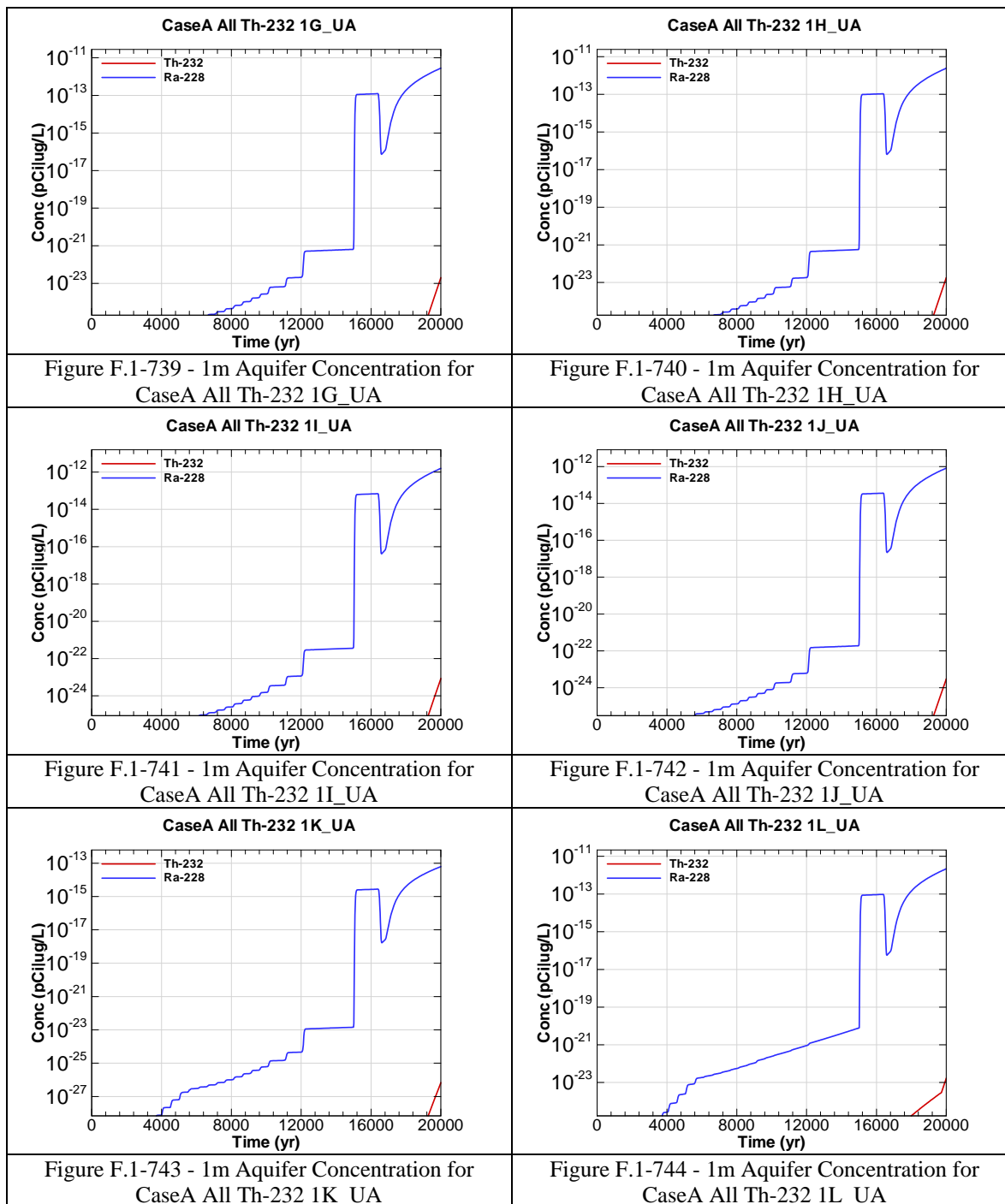


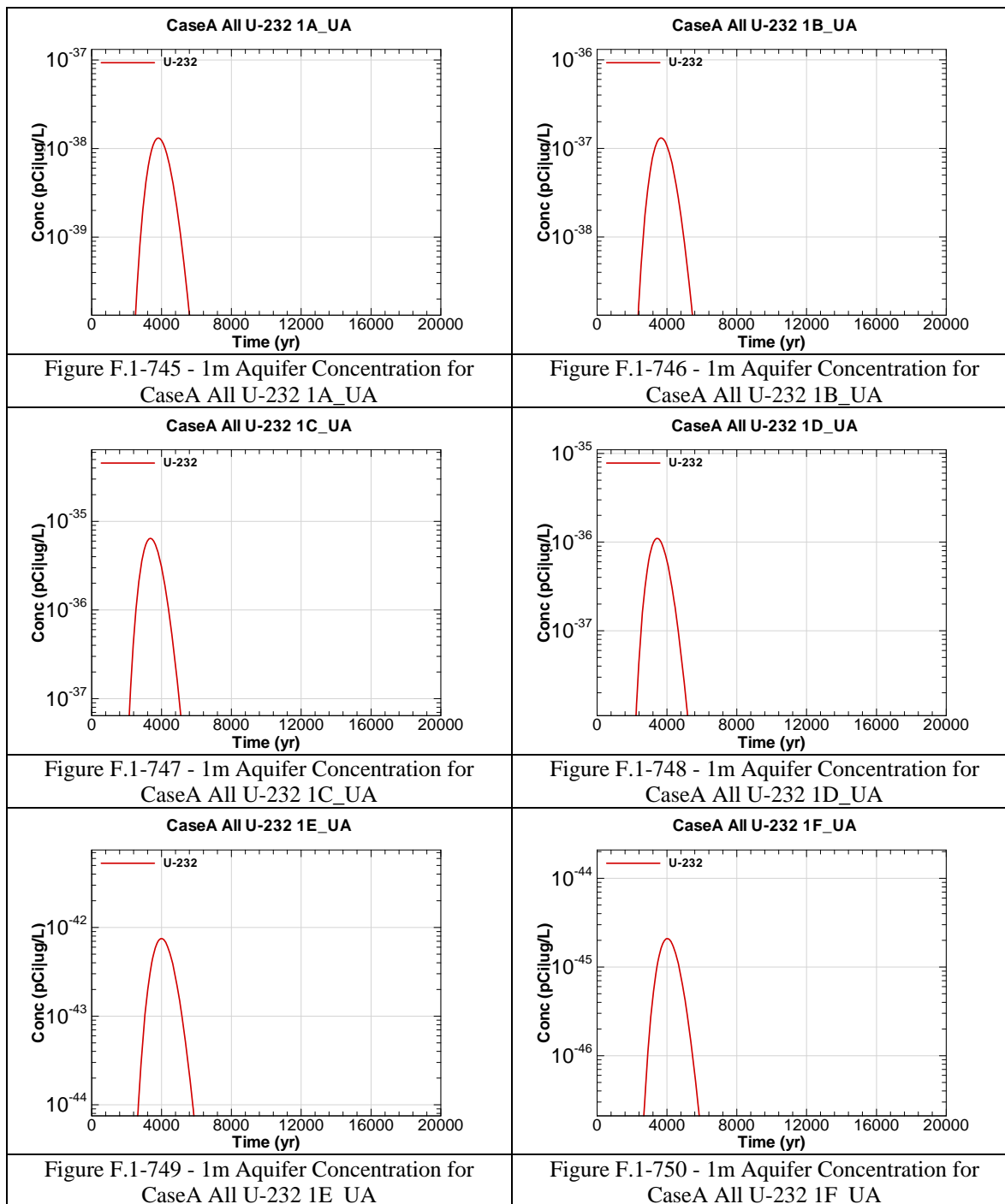


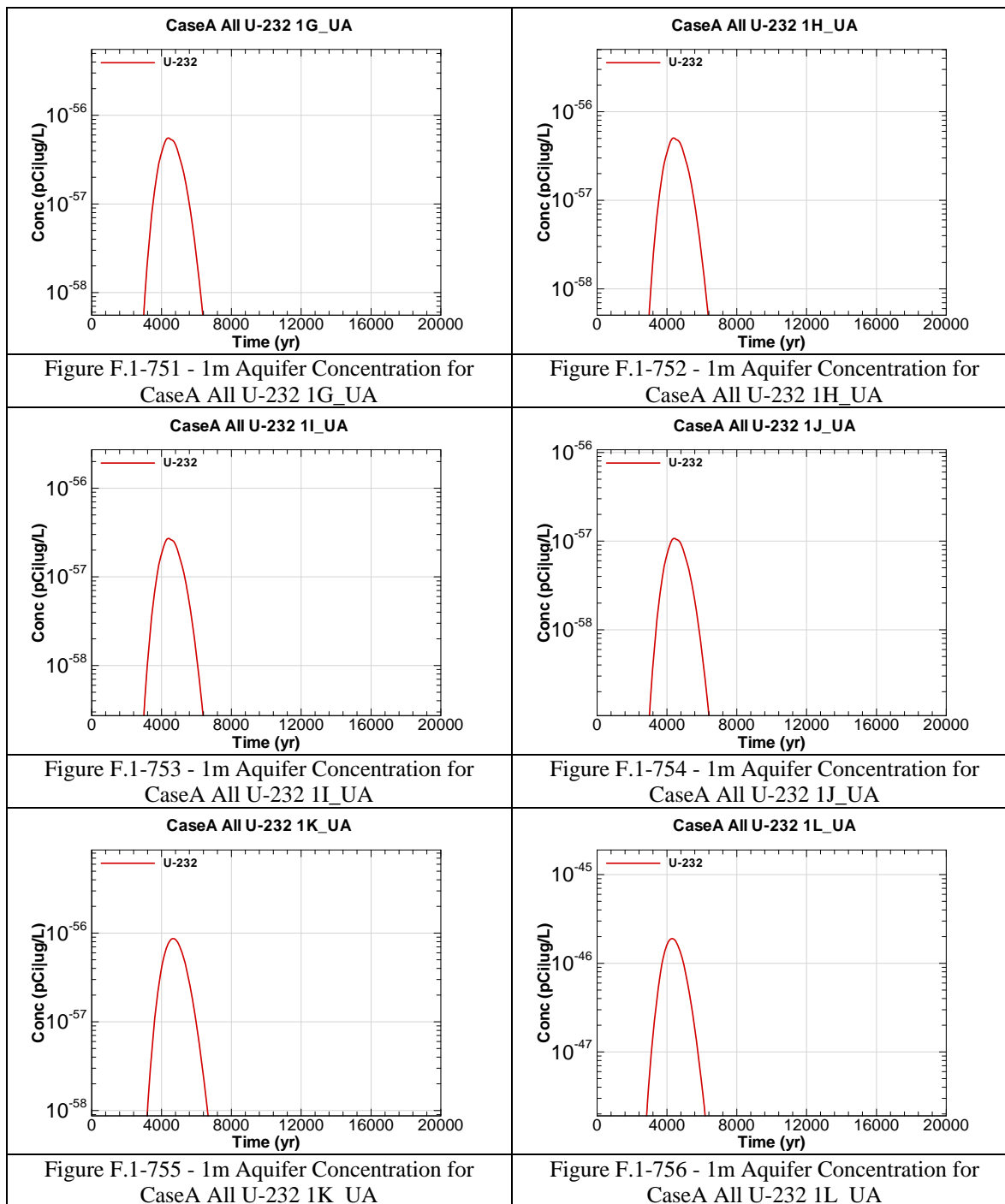


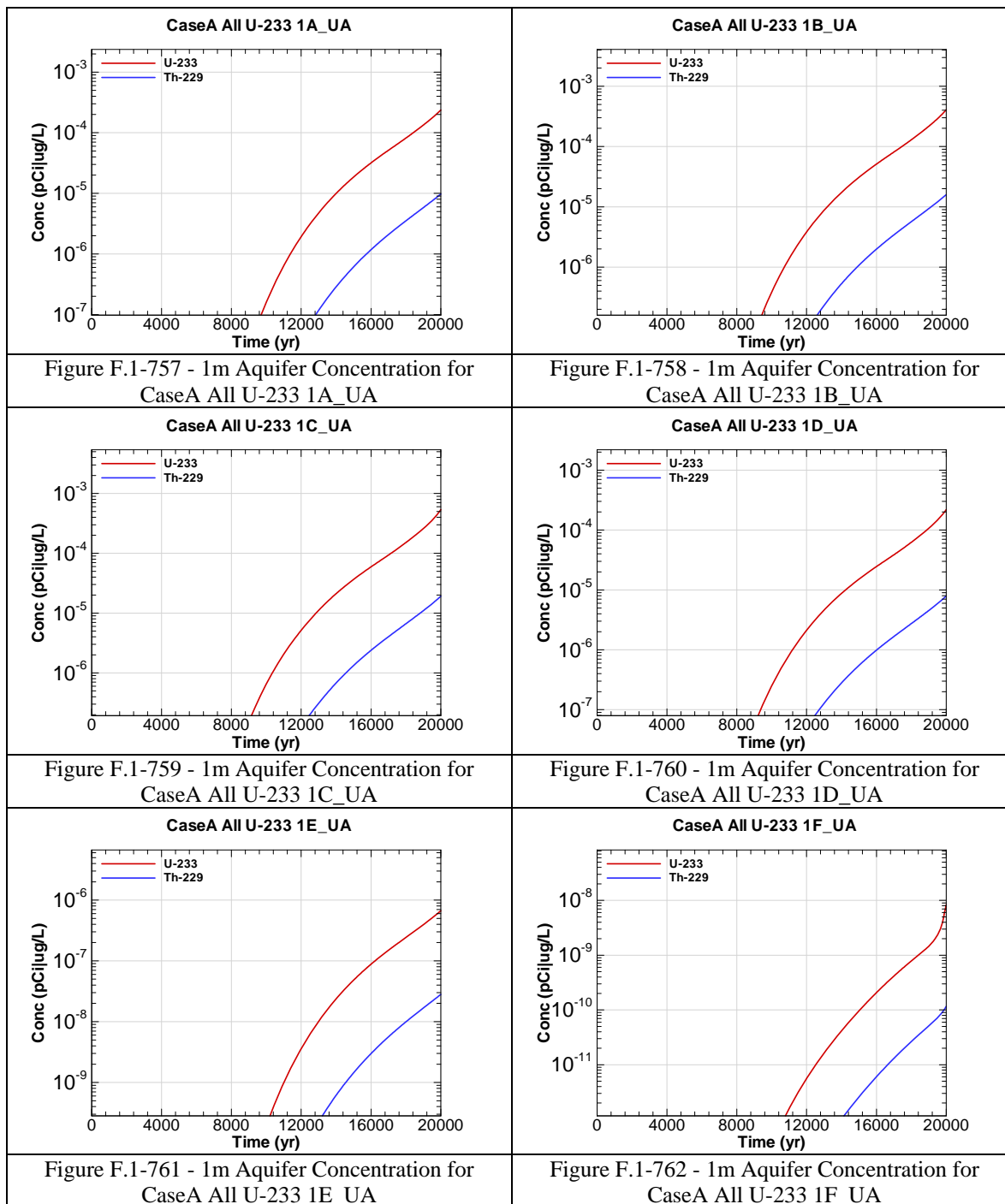


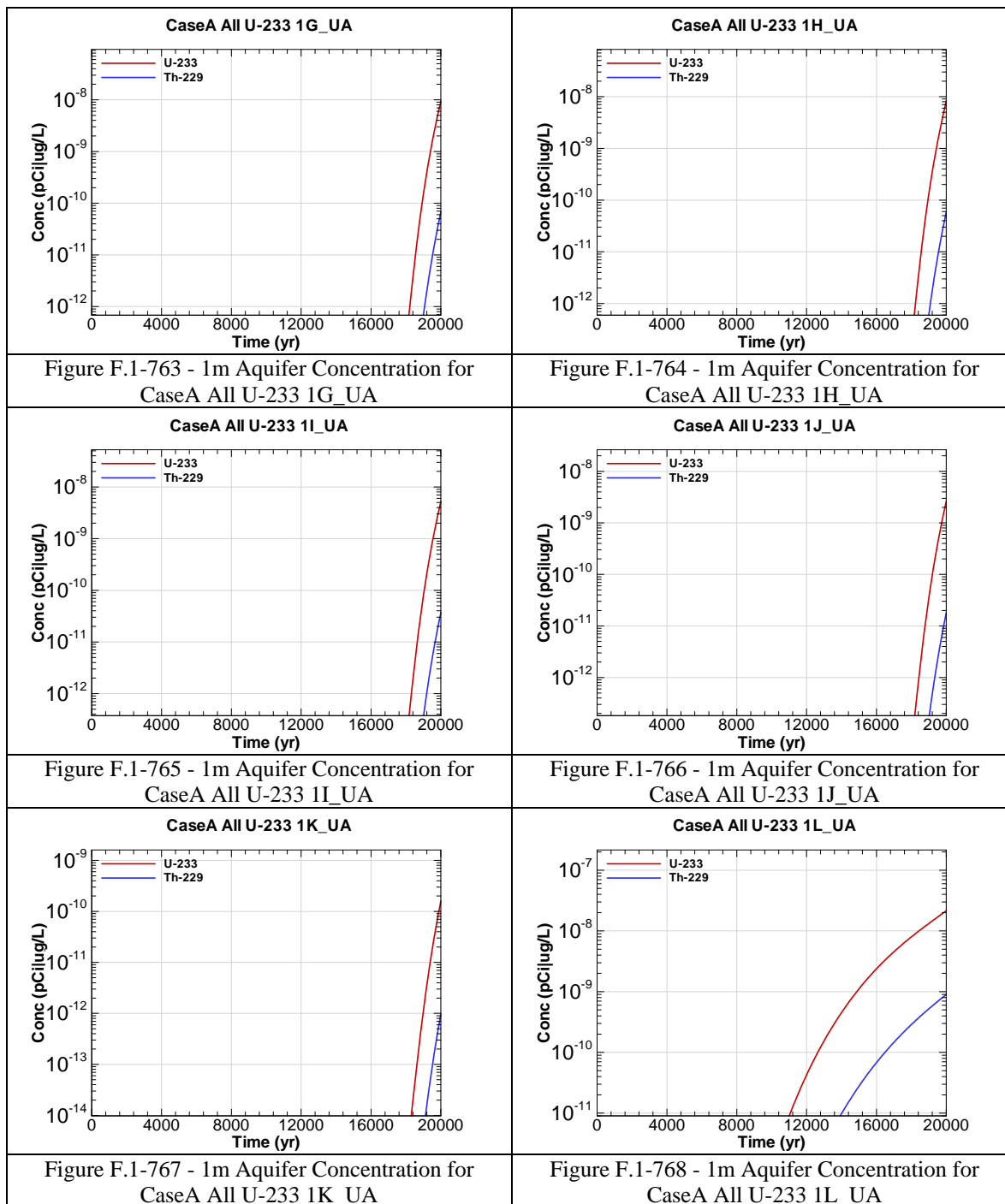


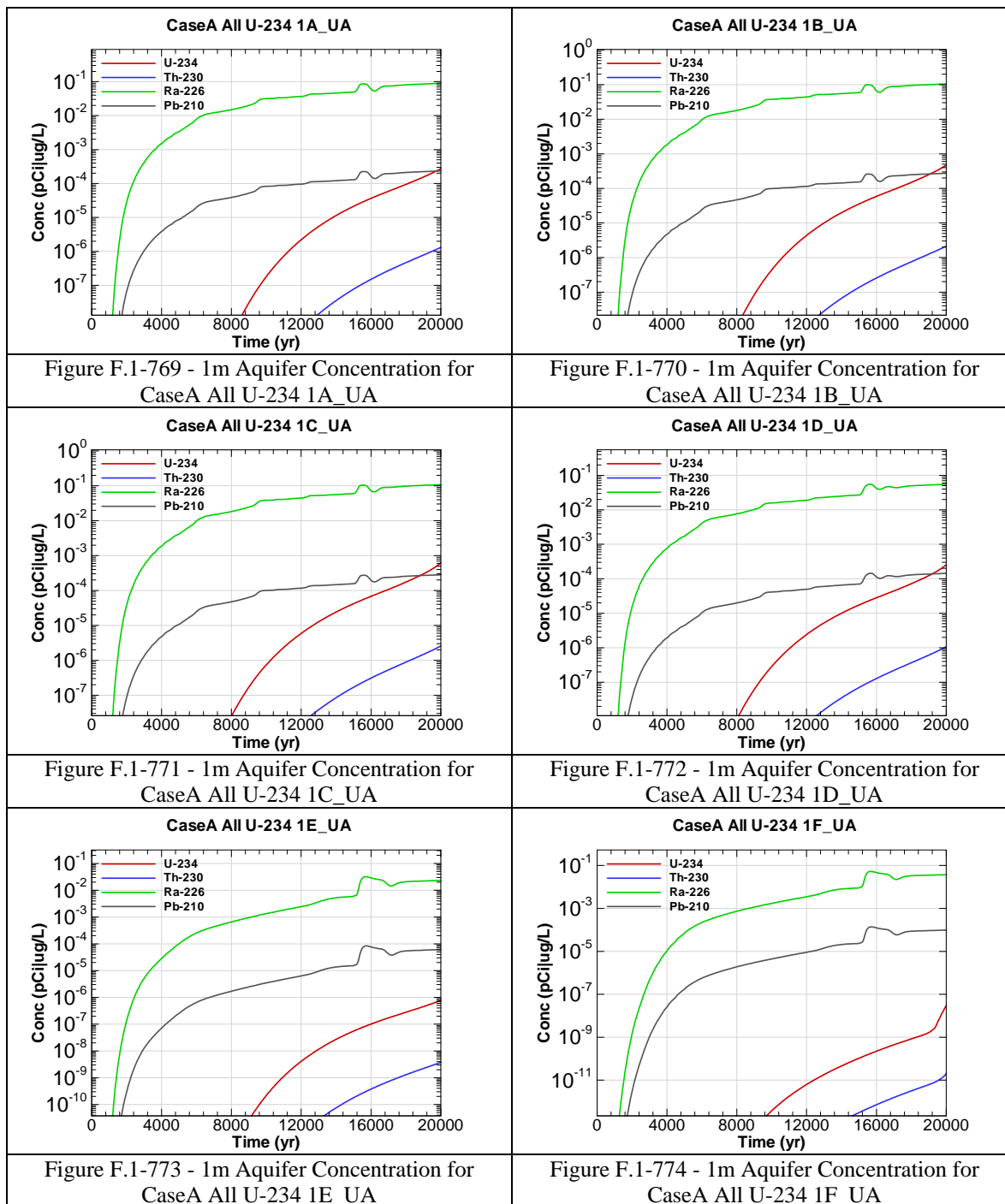


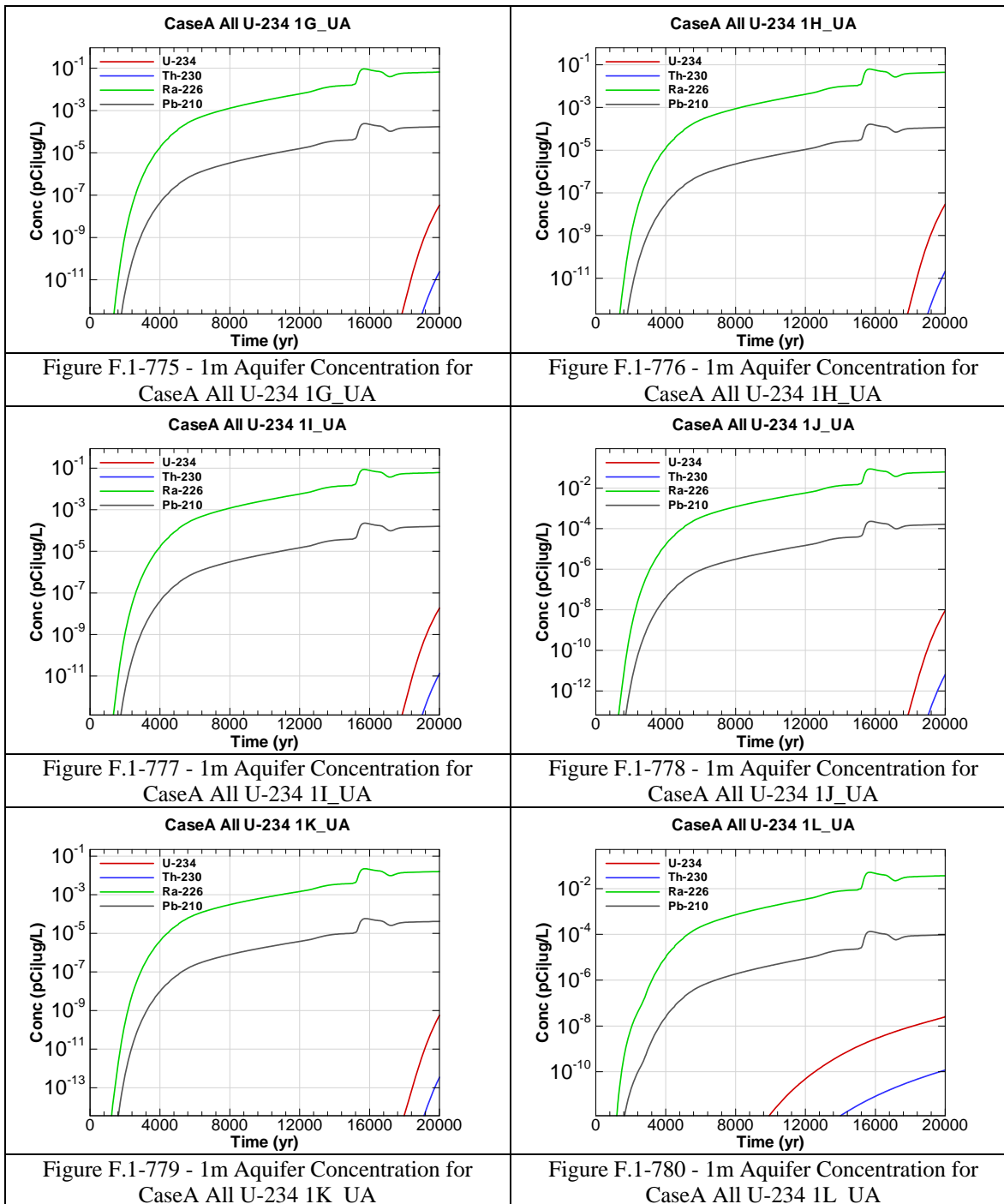


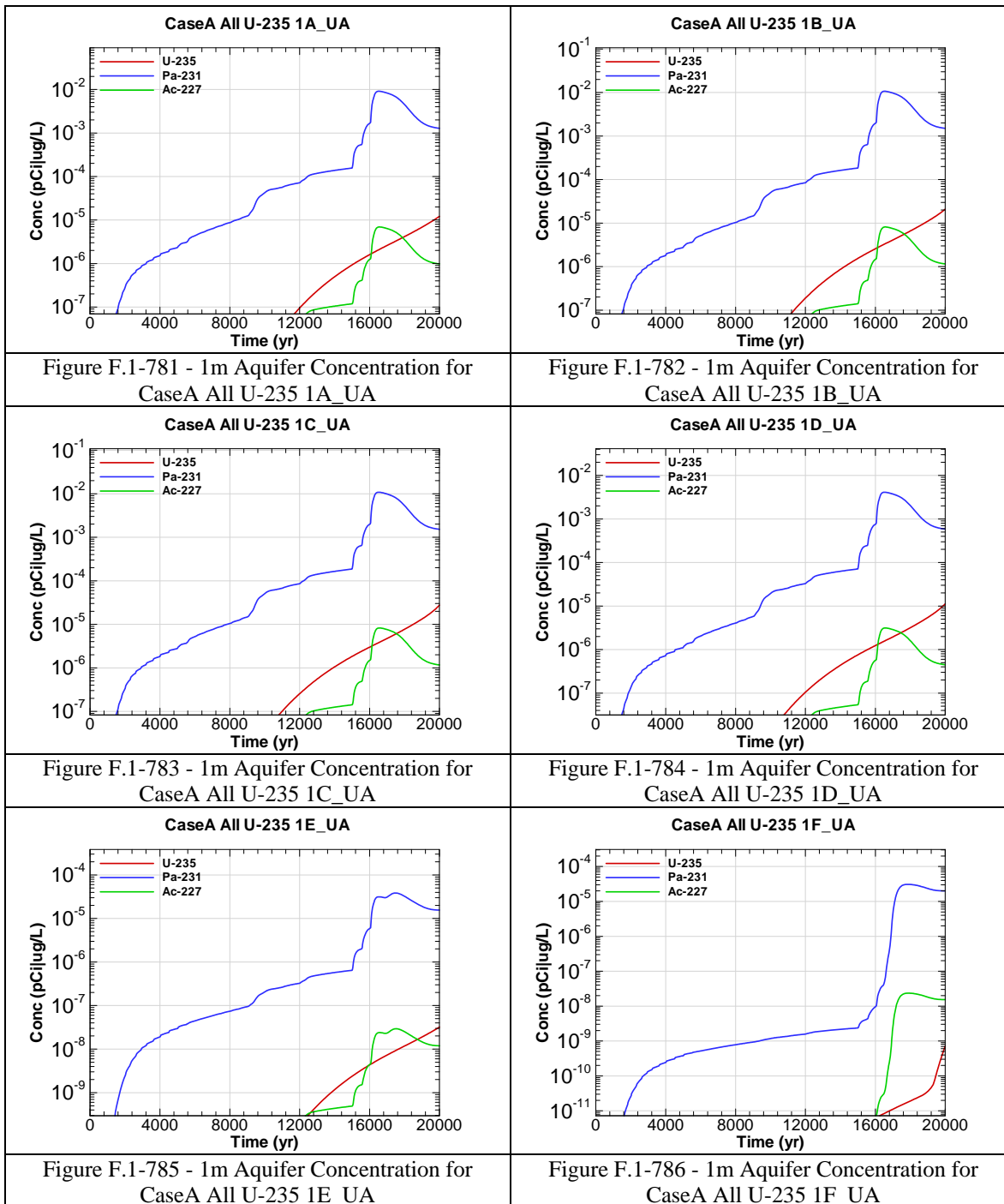


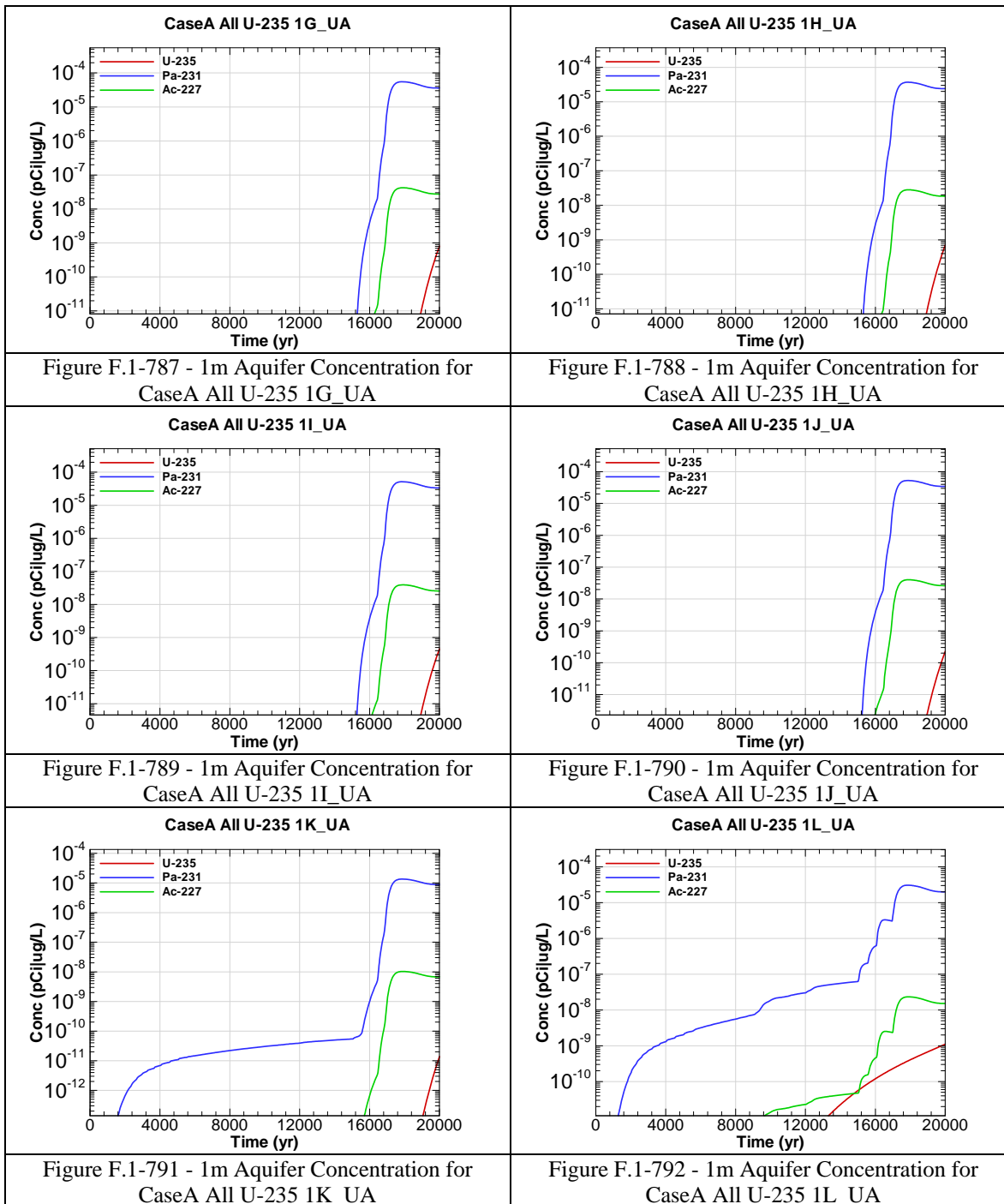


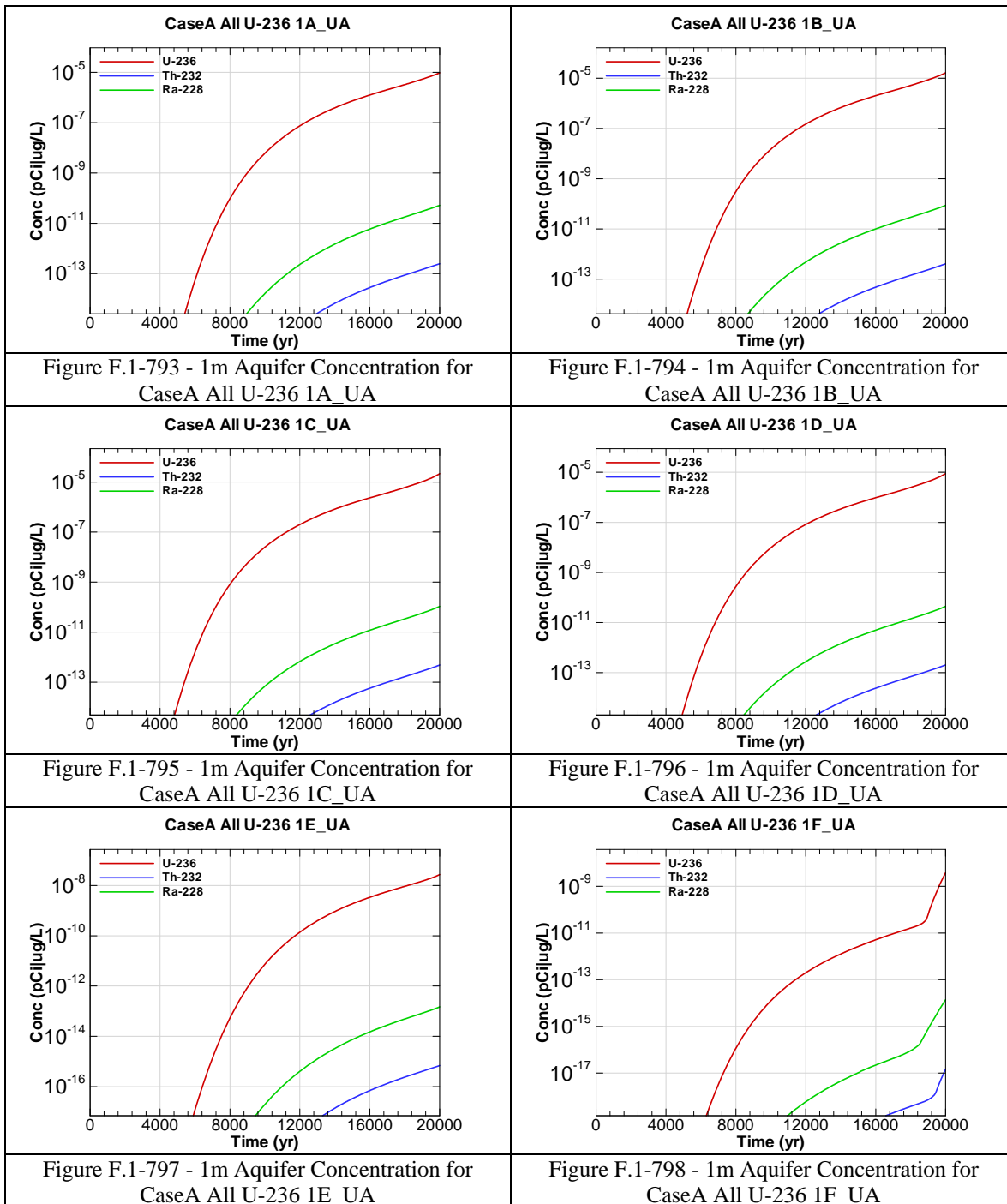


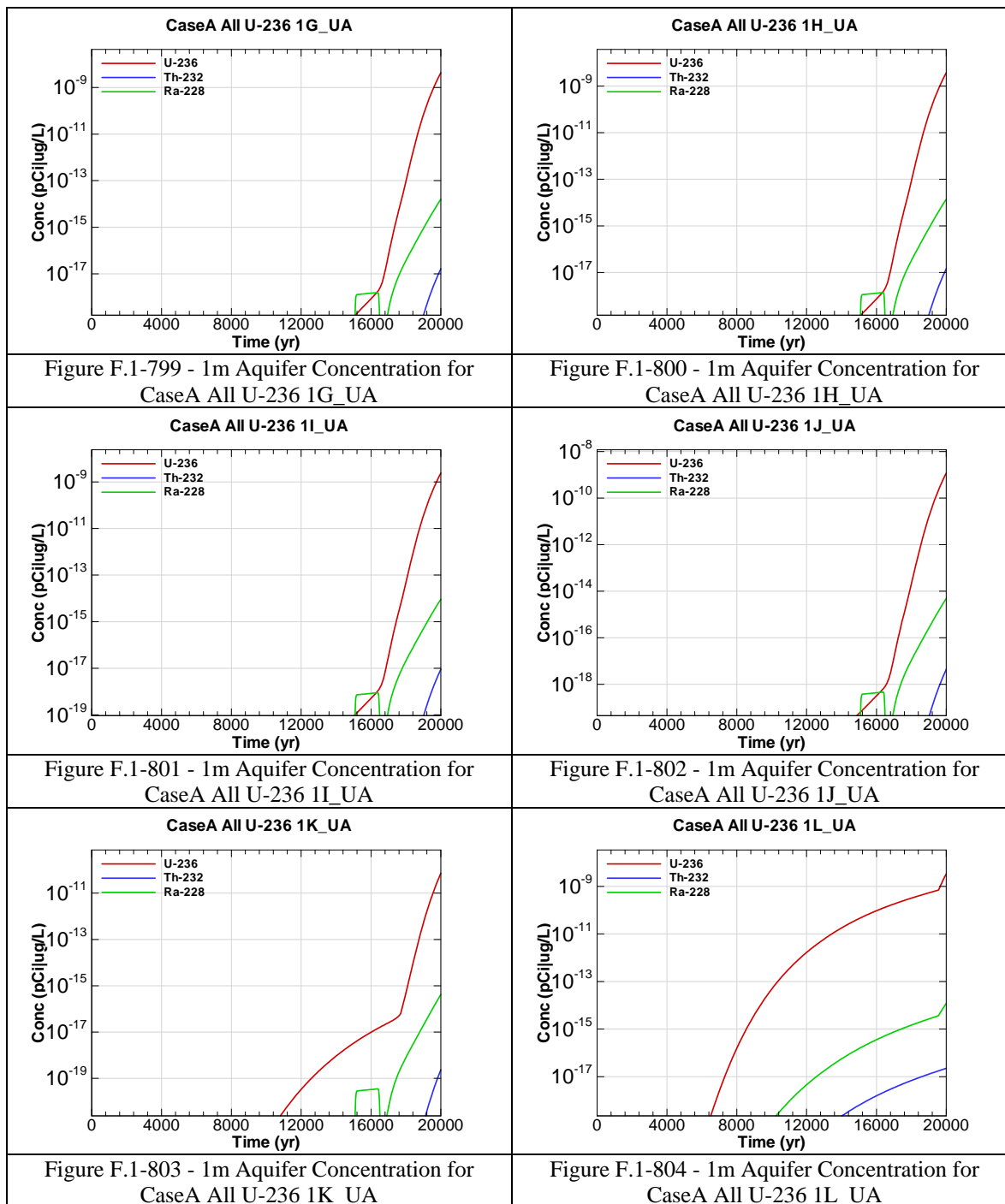


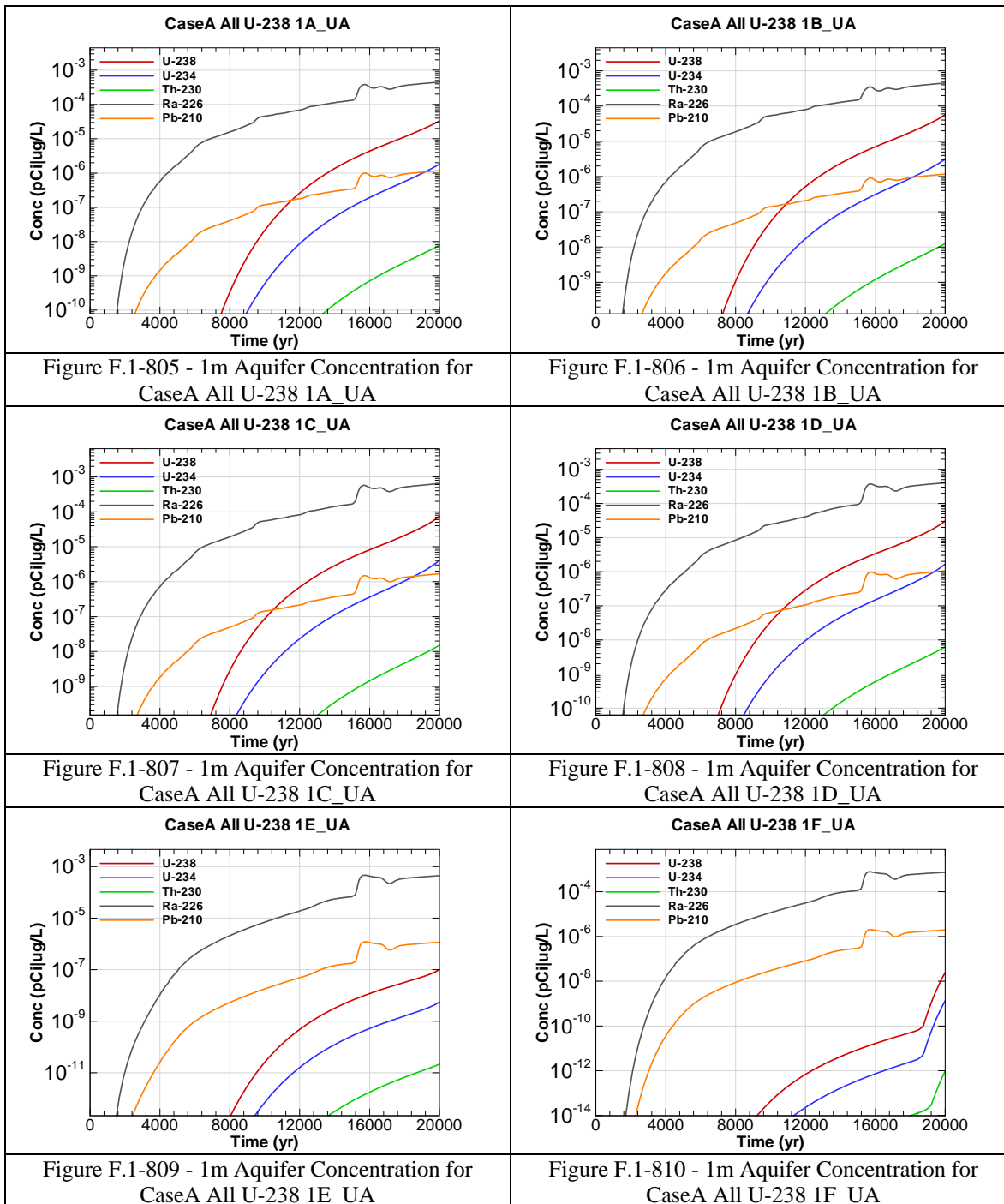


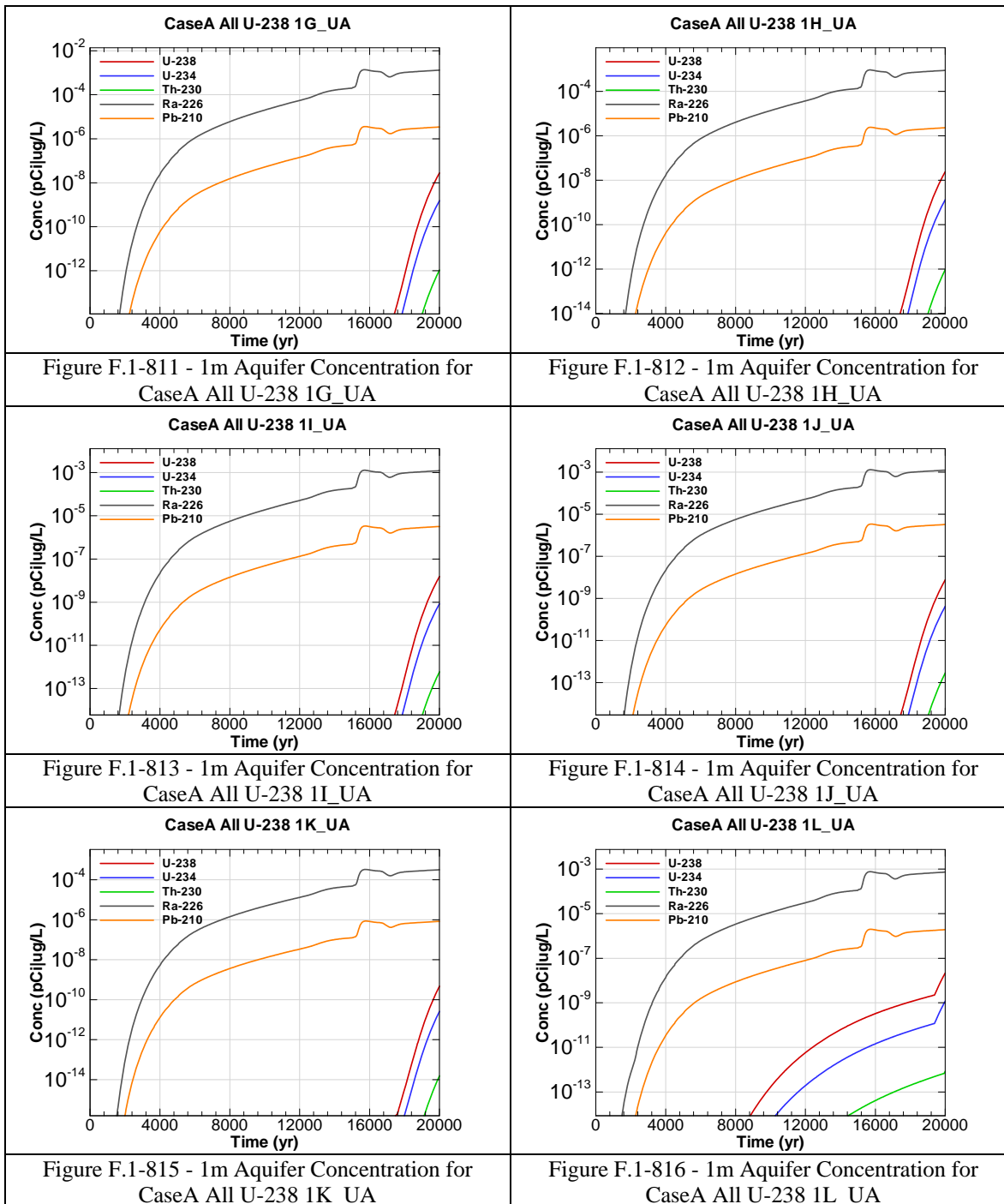


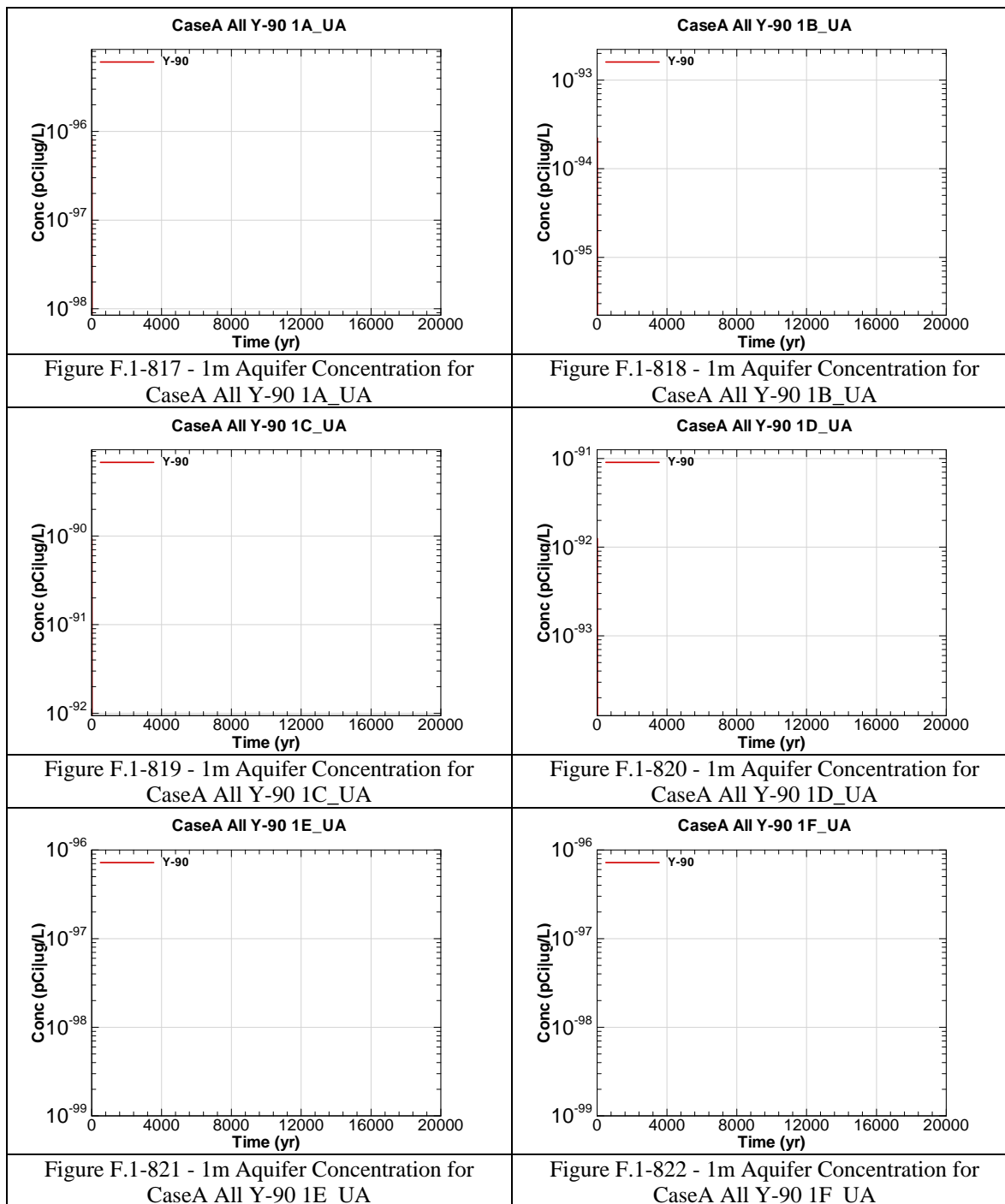


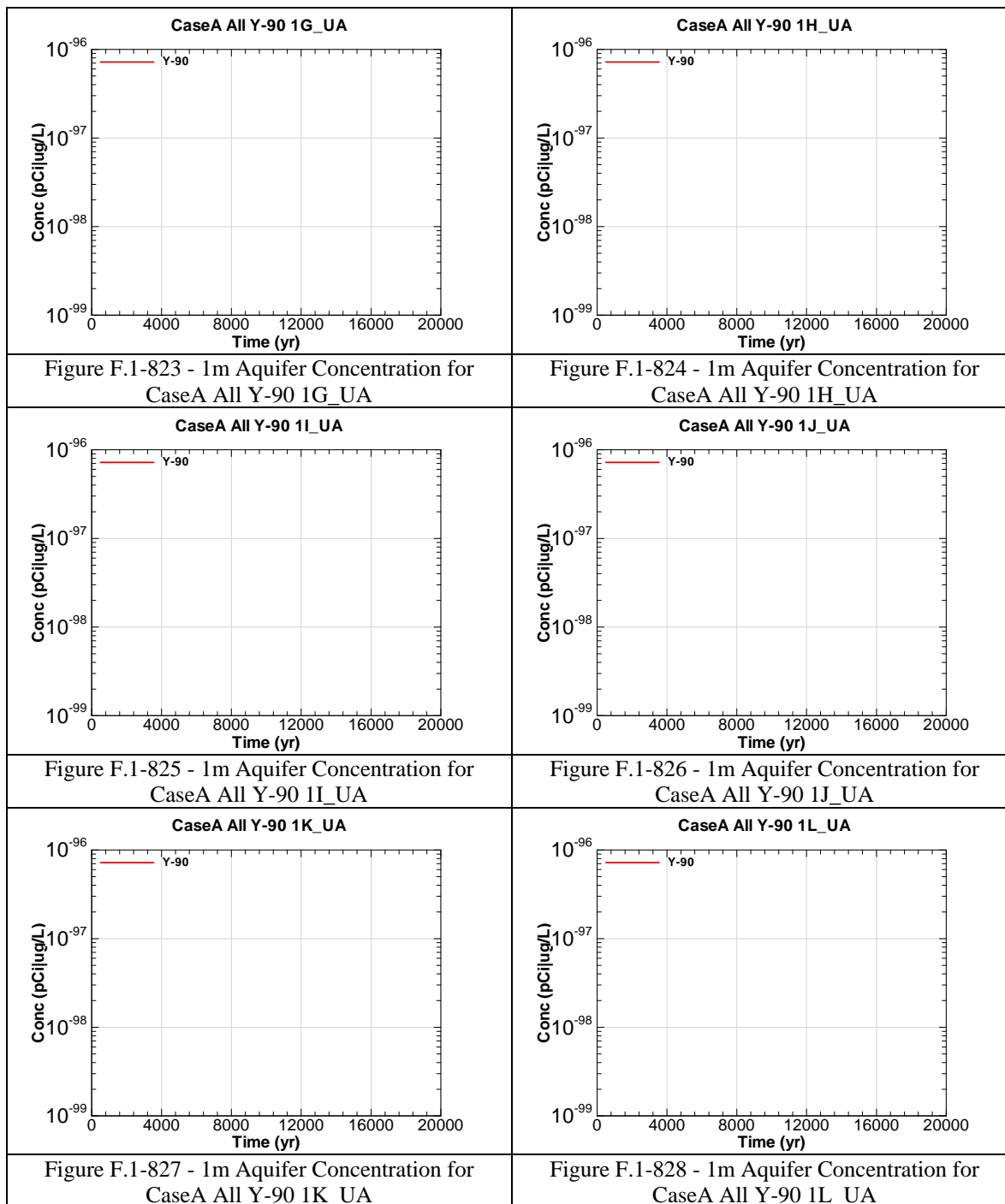


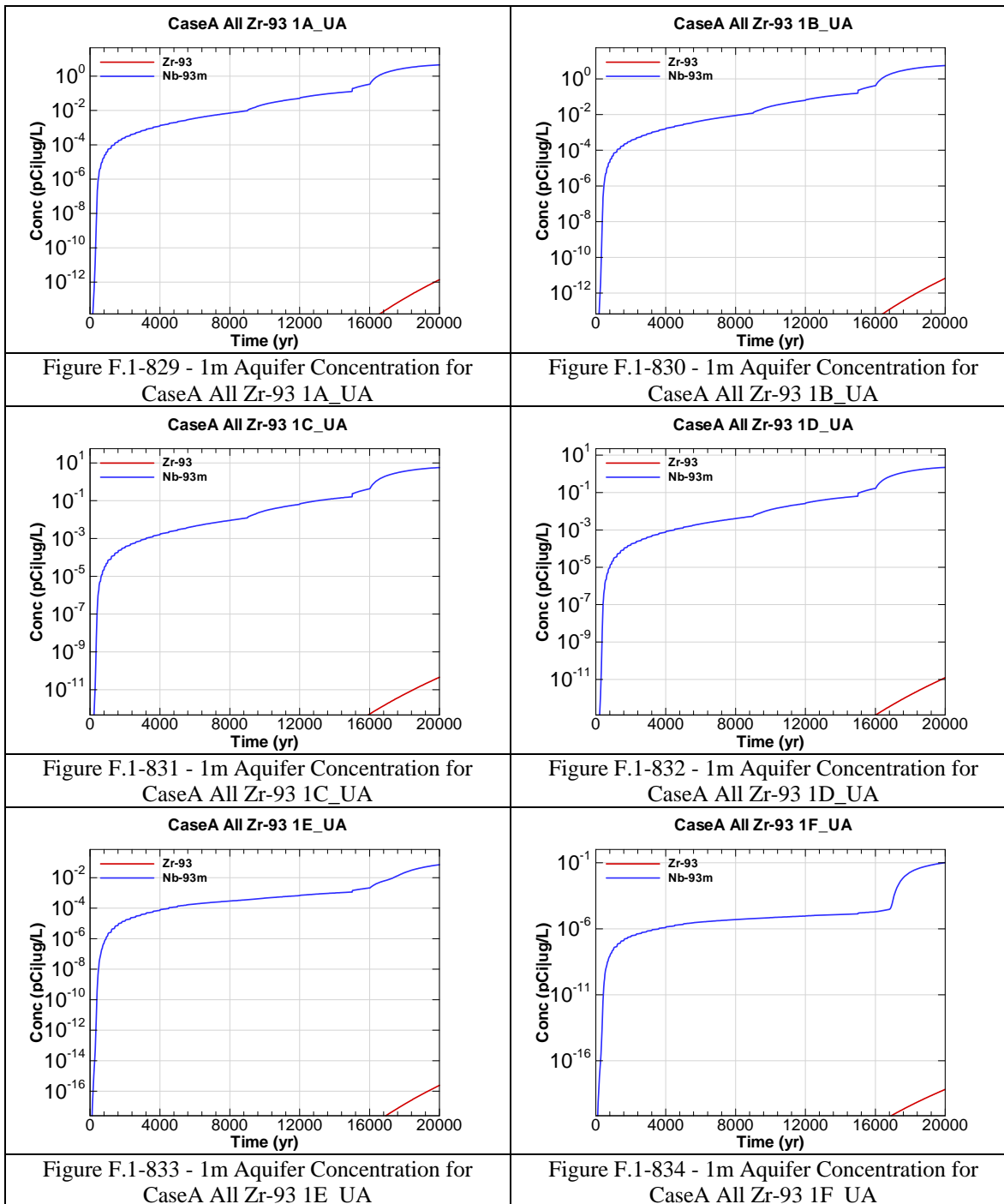


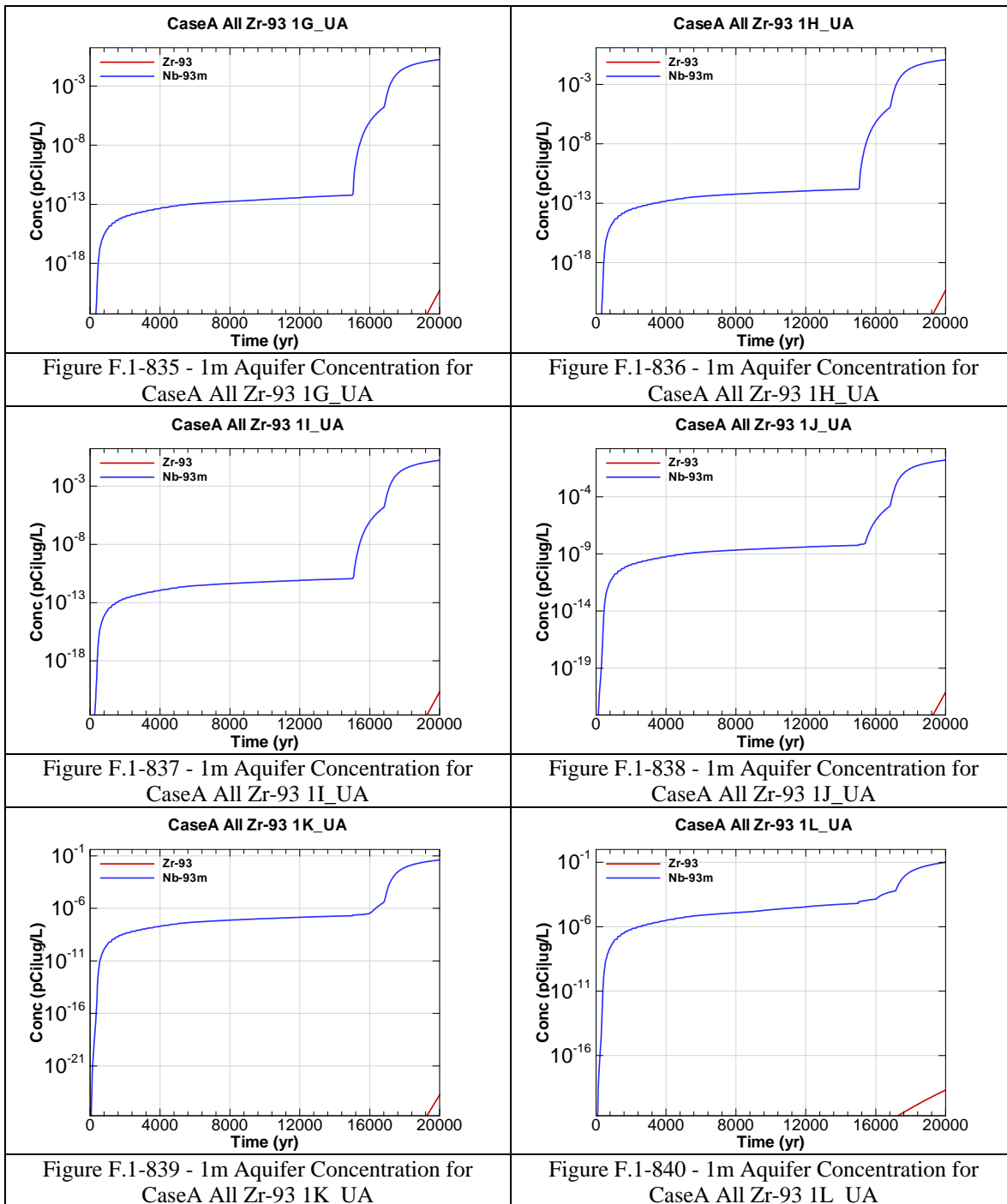






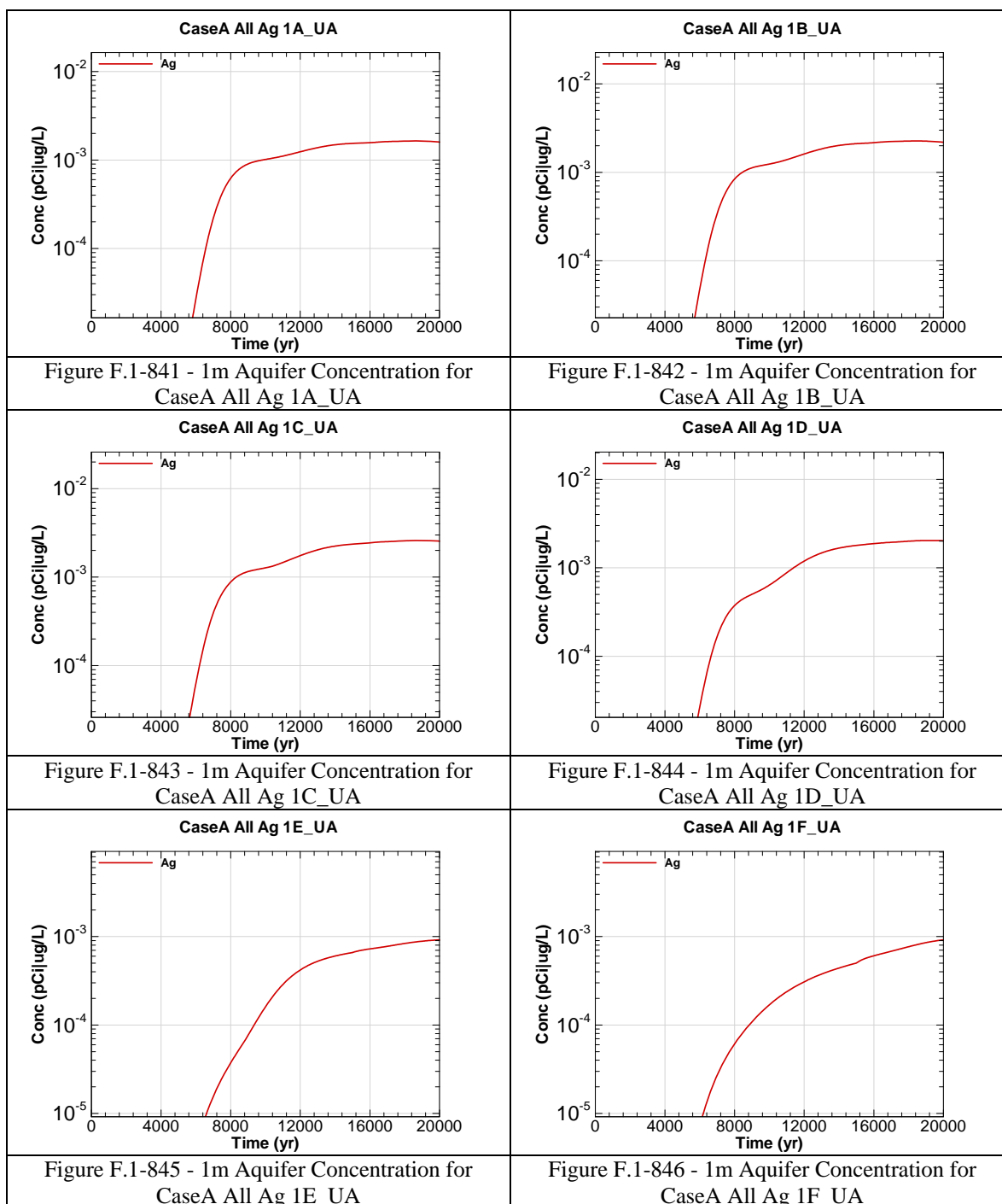


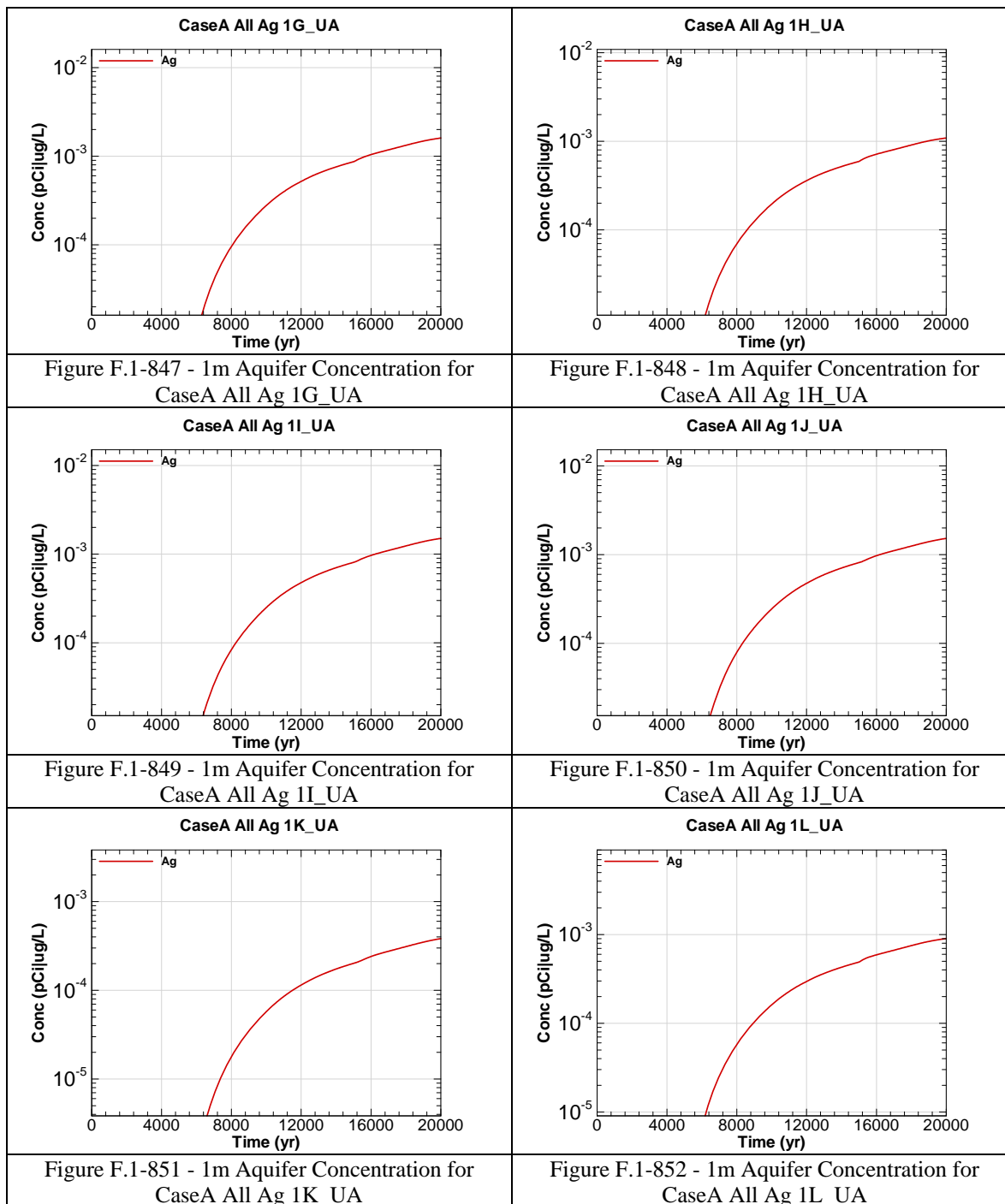


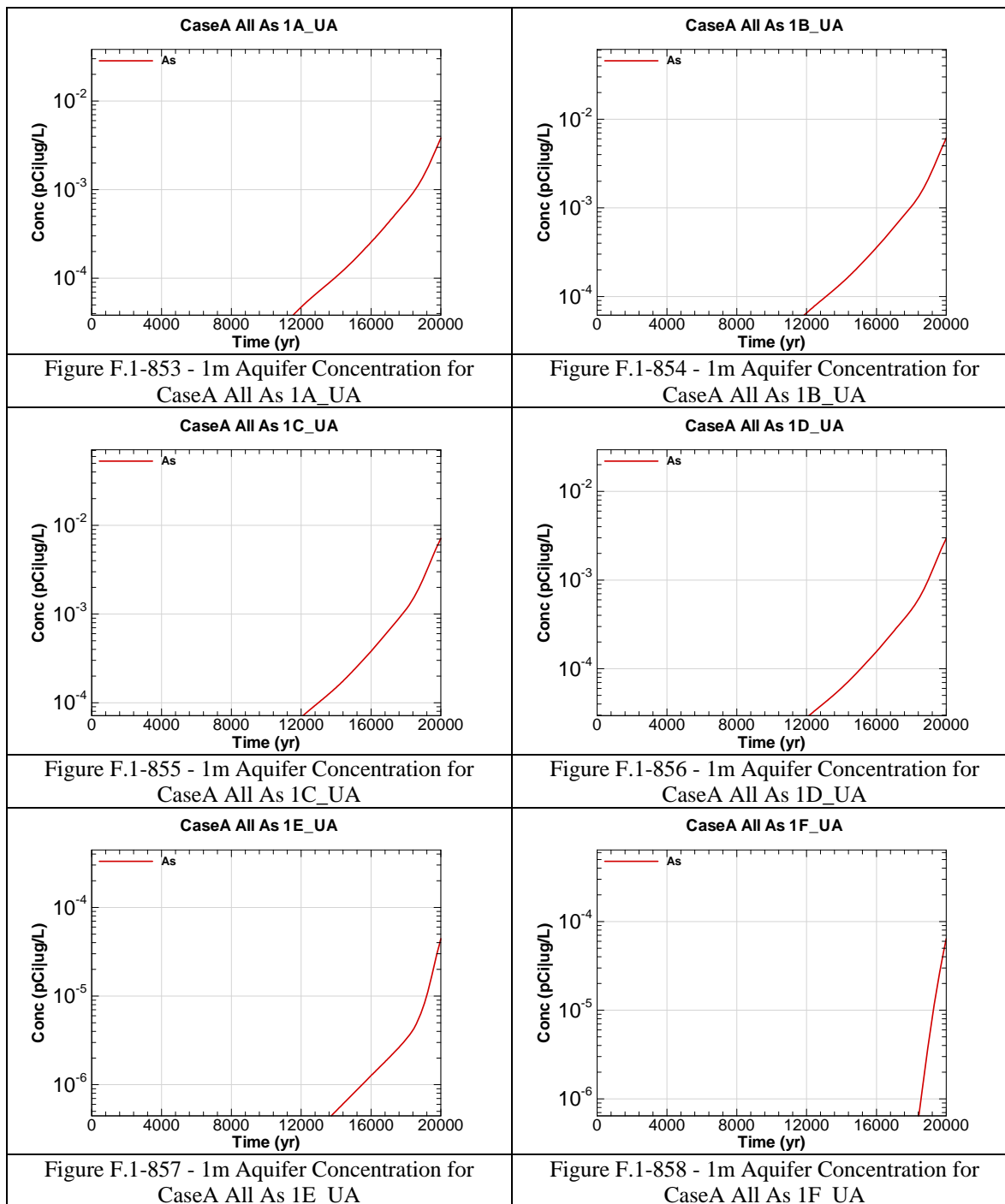


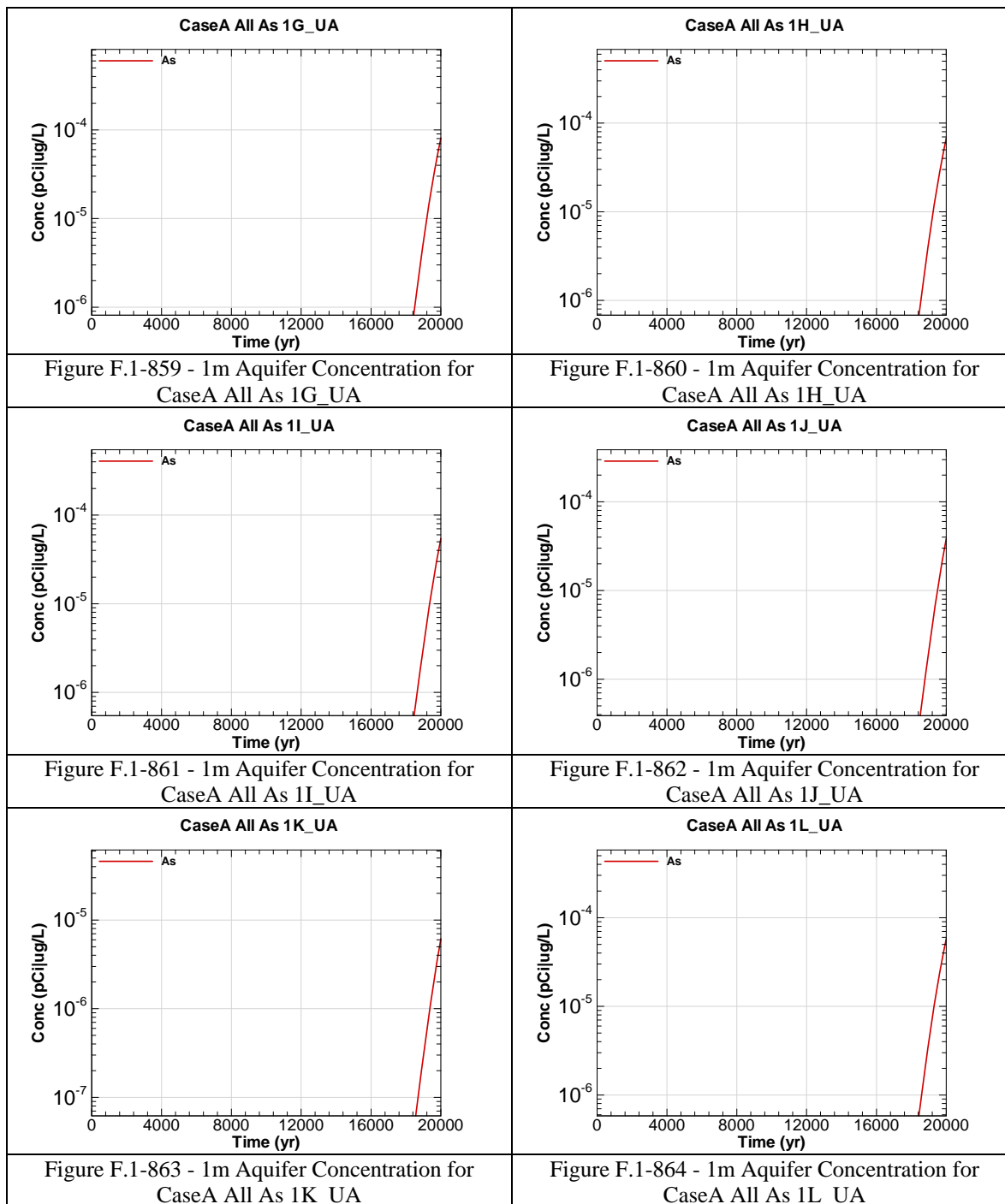
The chemical contaminants were modeled prior to the revision of the final closure inventory calculations presented in Table 3.3-8 for five chemical components: As, Cr, Cu, N and U. The figures that follow represent the concentrations calculated with an initial inventory input. The multipliers in the table below are to be used to determine the final concentrations with respect to time for the impacted chemicals as the inventory has a linear relationship with concentration in the Saltstone model. The groundwater concentration tables in Section 5 have been corrected using the multipliers.

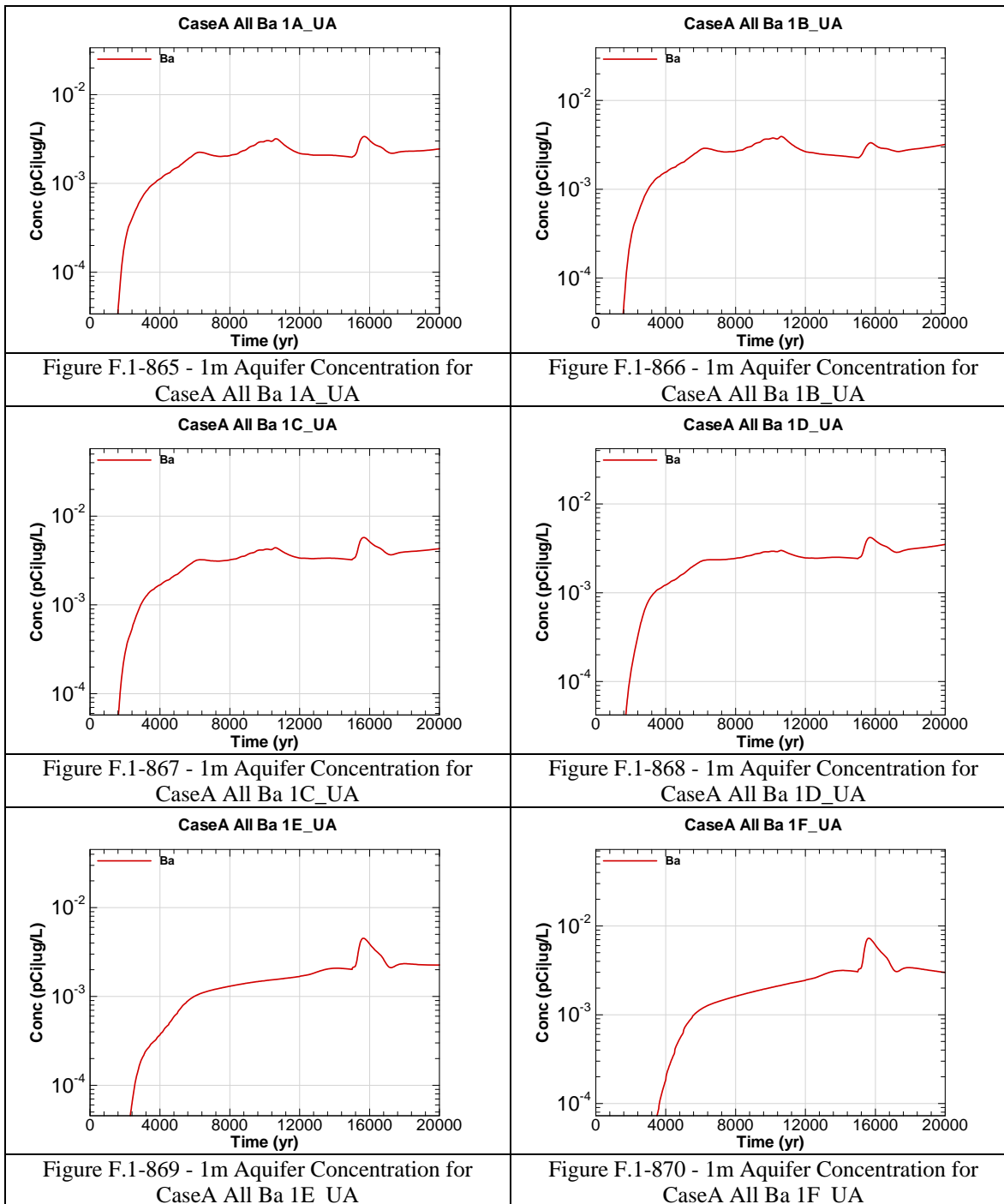
| Chemical Component | Modeled Inventory | Projected Inventory | Percent Increase | Multiplier |
|---------------------------|--------------------------|----------------------------|-------------------------|-------------------|
| Ag | 8.8E+01 | 8.8E+01 | 0.0% | None |
| As | 1.08E+04 | 1.1E+04 | 2.3% | 1.02E+00 |
| Ba | 1.7E+02 | 1.7E+02 | 0.0% | None |
| Cd | 1.3E+03 | 1.3E+03 | 0.0% | None |
| Cr | 2.9E+04 | 3.0E+04 | 1.4% | 1.01E+00 |
| Cu | 1.9E+04 | 1.9E+04 | 0.9% | 1.01E+00 |
| F | 1.7E+04 | 1.7E+04 | 0.0% | None |
| Fe | 2.9E+03 | 2.9E+03 | 0.0% | None |
| Hg | 1.1E+04 | 1.1E+04 | 0.0% | None |
| Mn | 7.3E+03 | 7.3E+03 | 0.0% | None |
| Ni | 1.5E+03 | 1.5E+03 | 0.0% | None |
| Total N | 2.2E+07 | 2.4E+07 | 5.8% | 1.06E+00 |
| Pb | 6.7E+03 | 6.7E+03 | 0.0% | None |
| Se | 4.0E+04 | 4.0E+04 | 0.0% | None |
| U | 8.2E+02 | 8.9E+02 | 8.9% | 1.10E+00 |
| Zn | 2.7E+04 | 2.7E+04 | 0.0% | None |

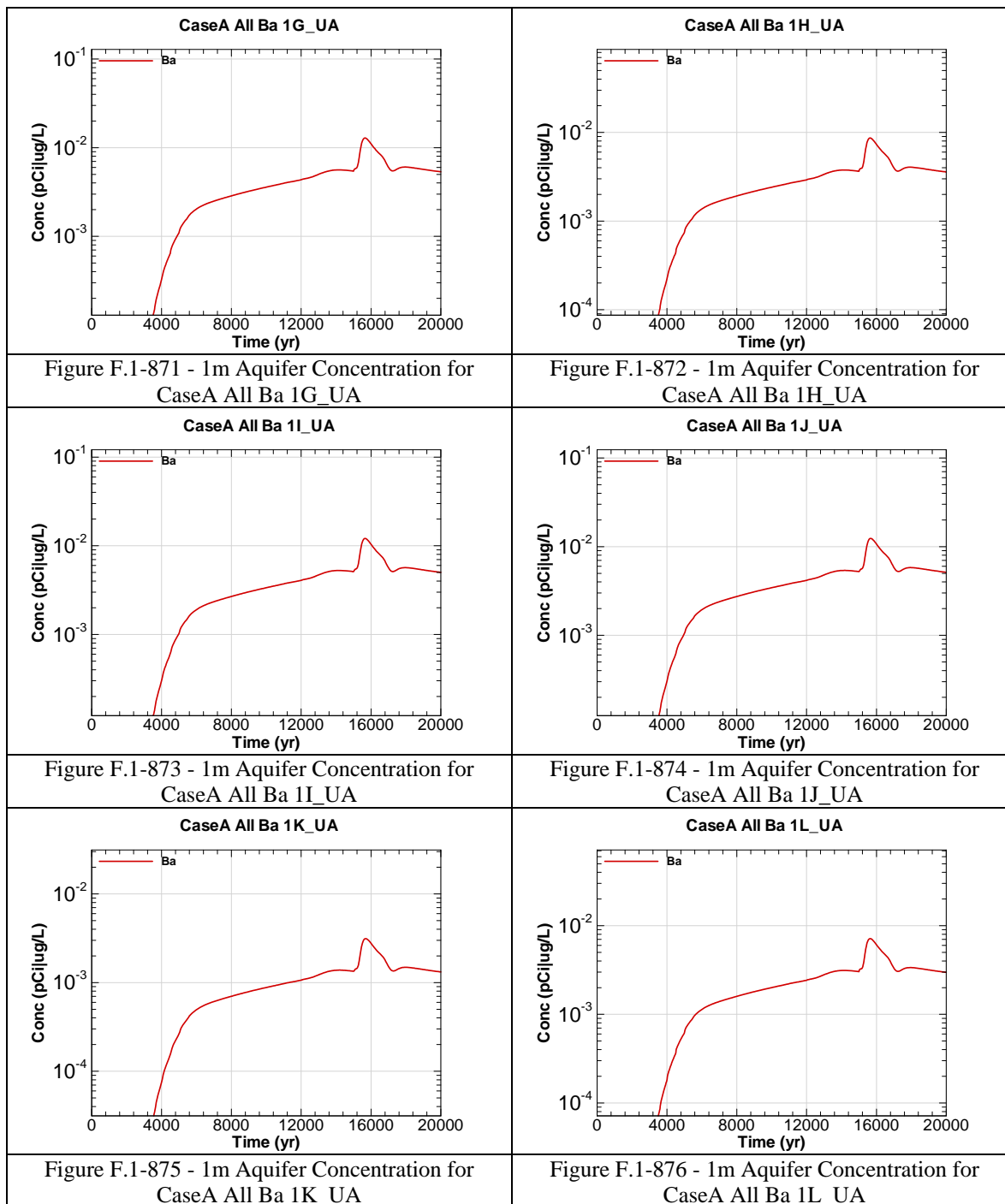


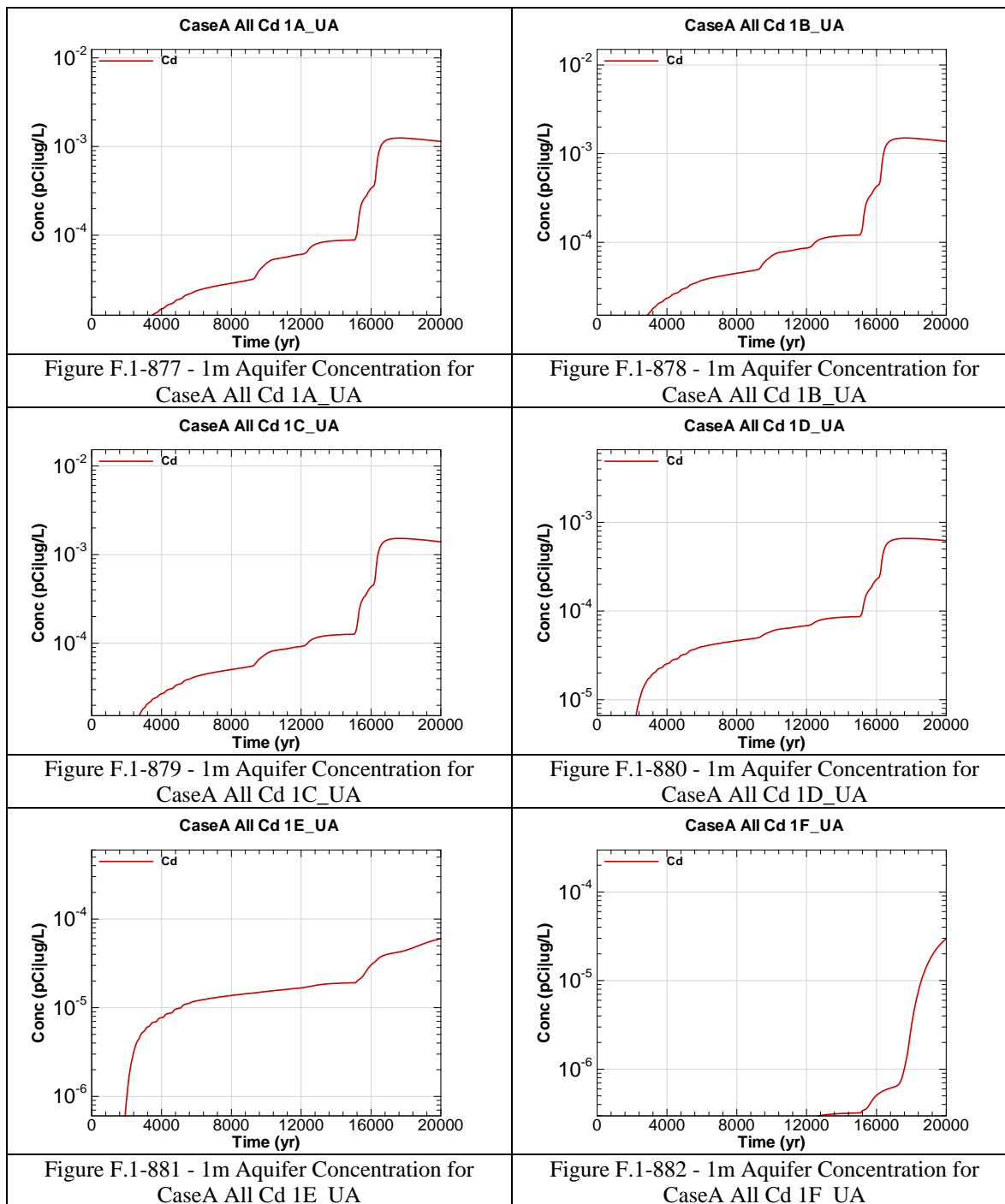


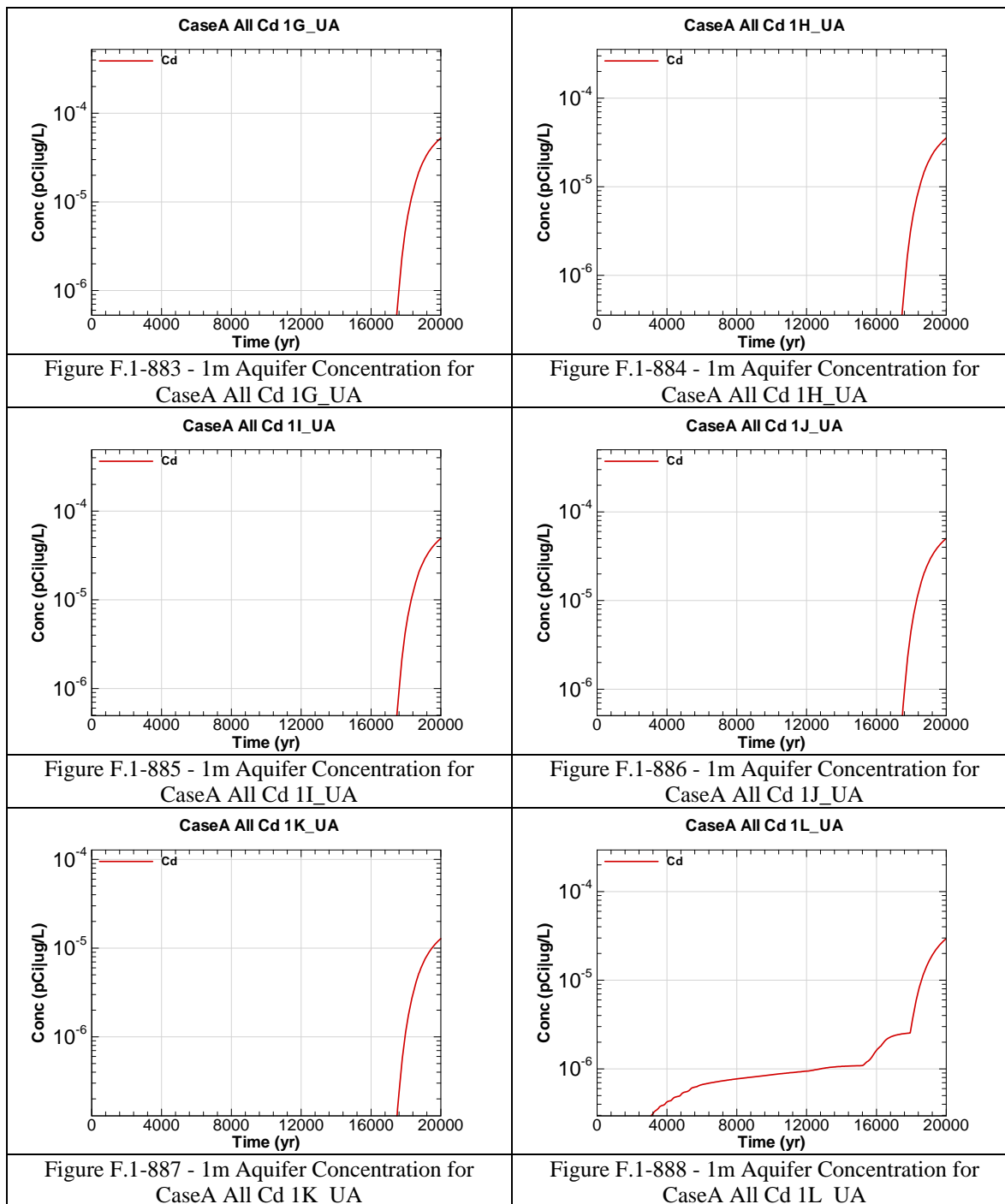


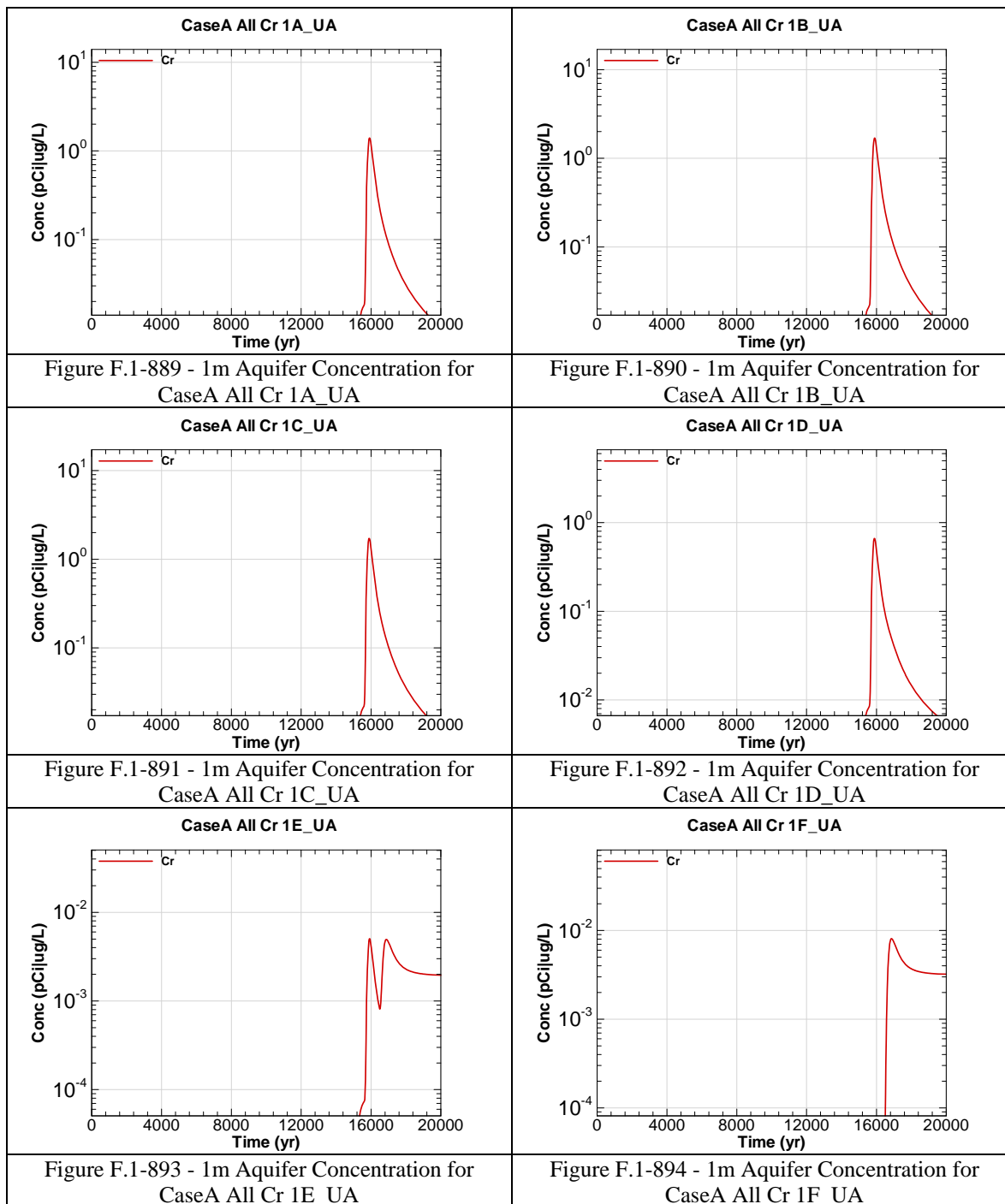


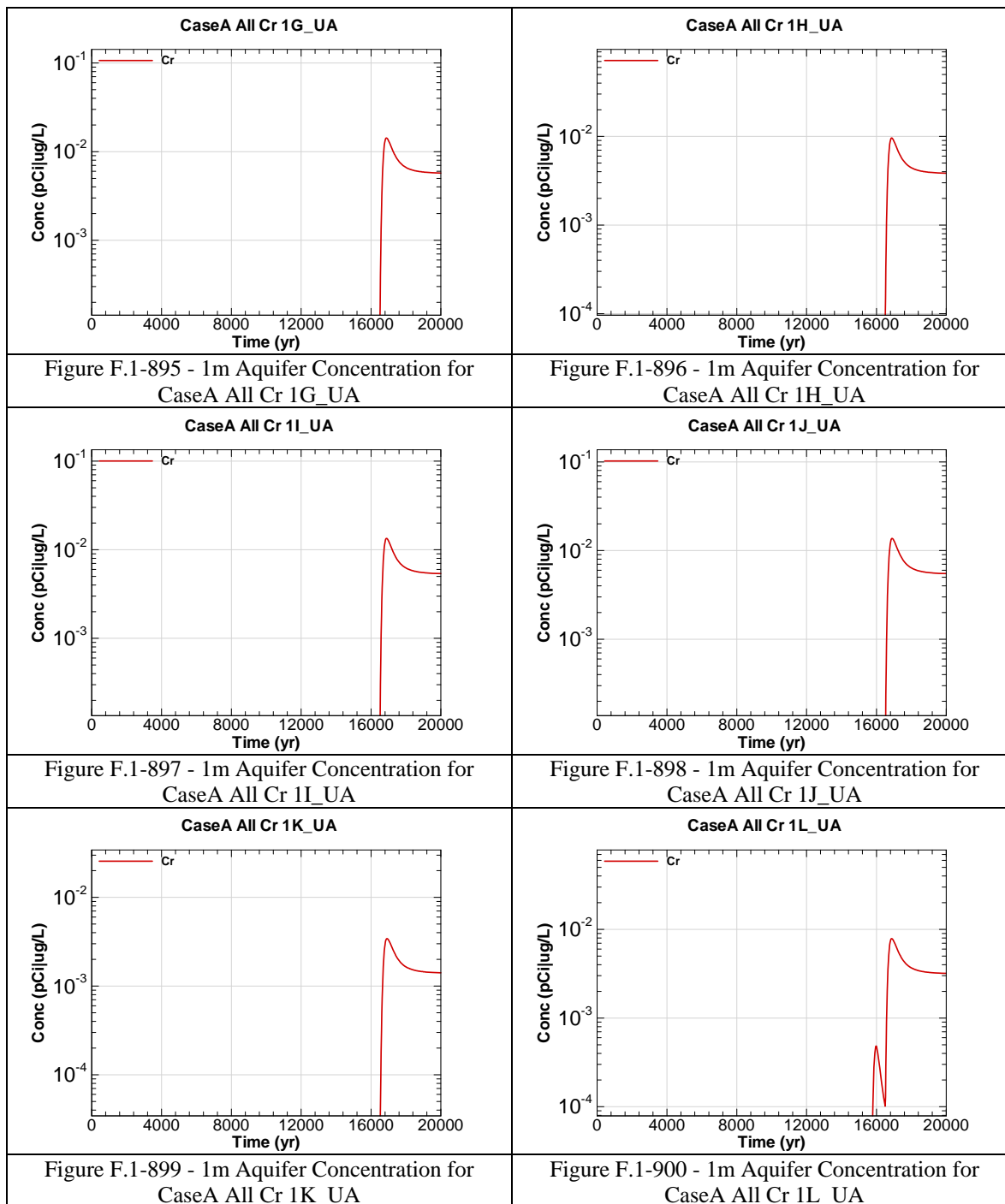


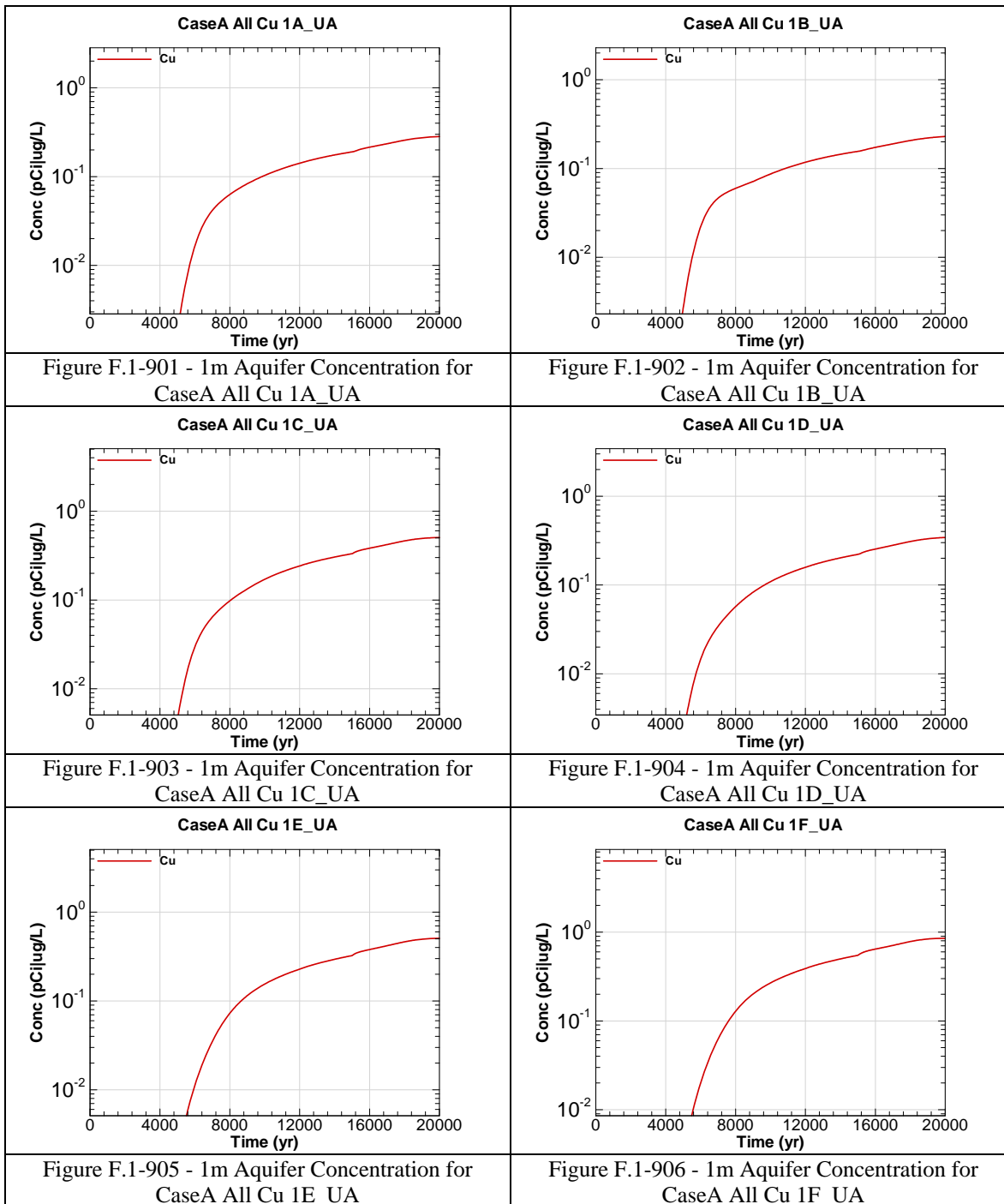


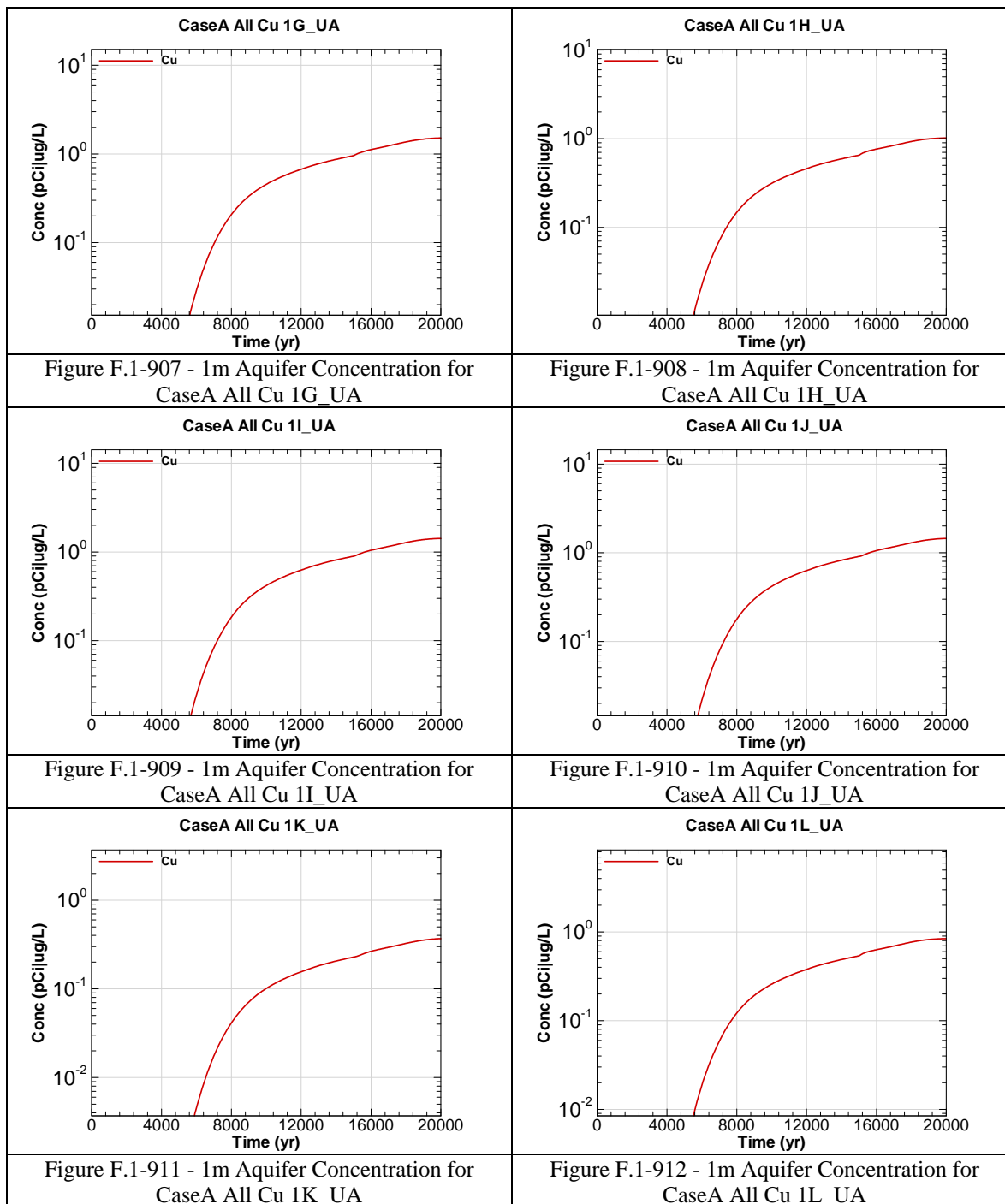


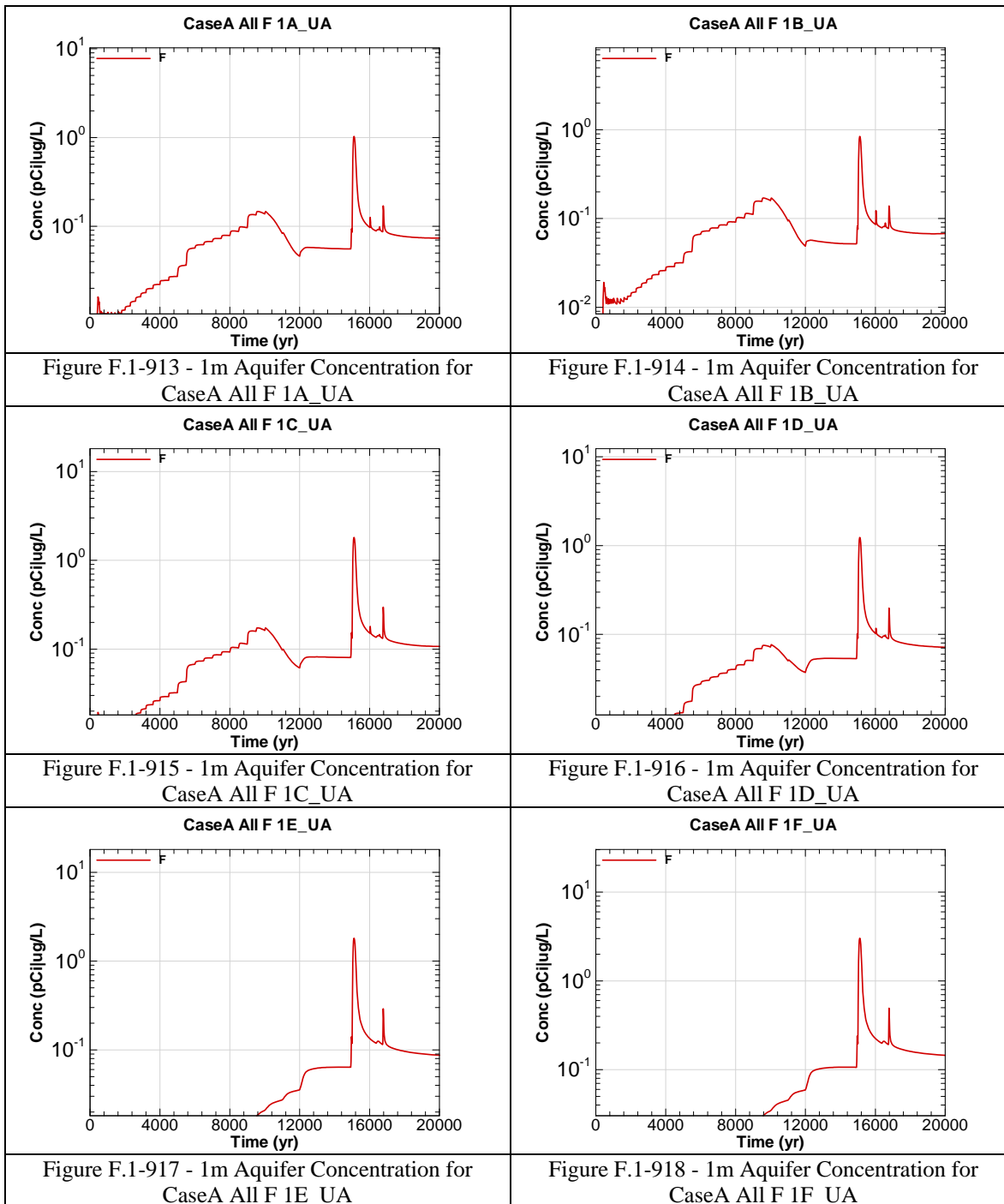


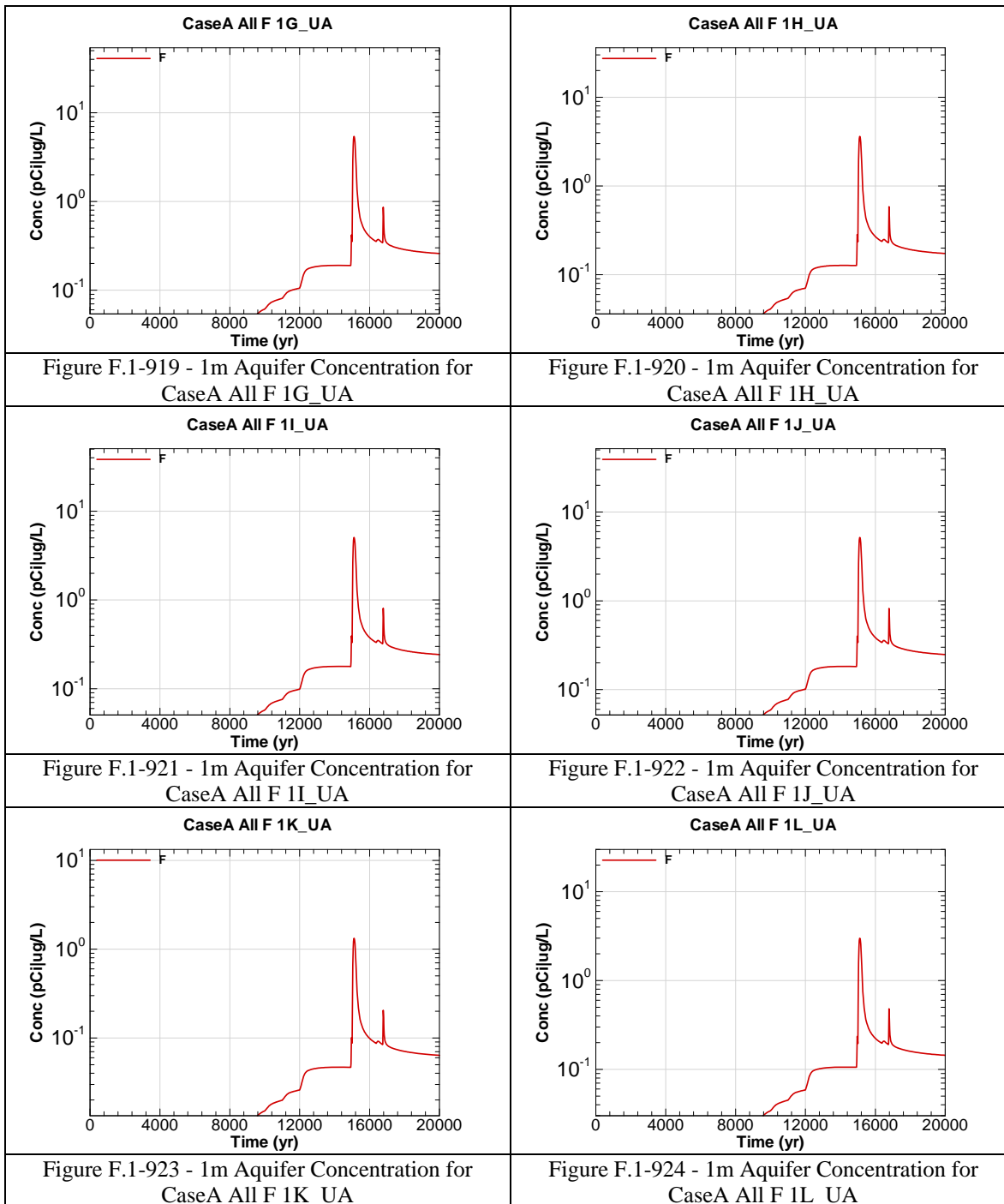


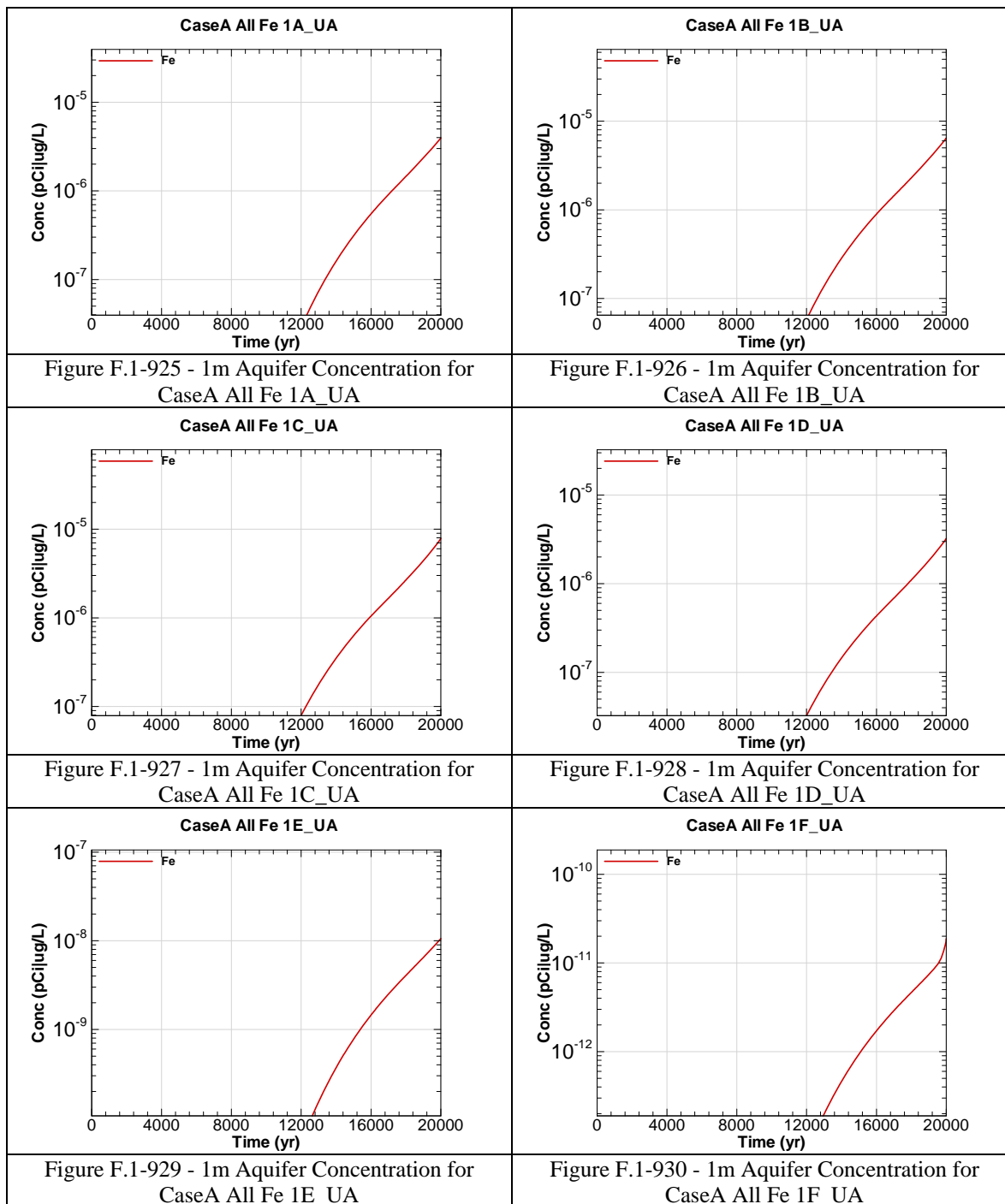


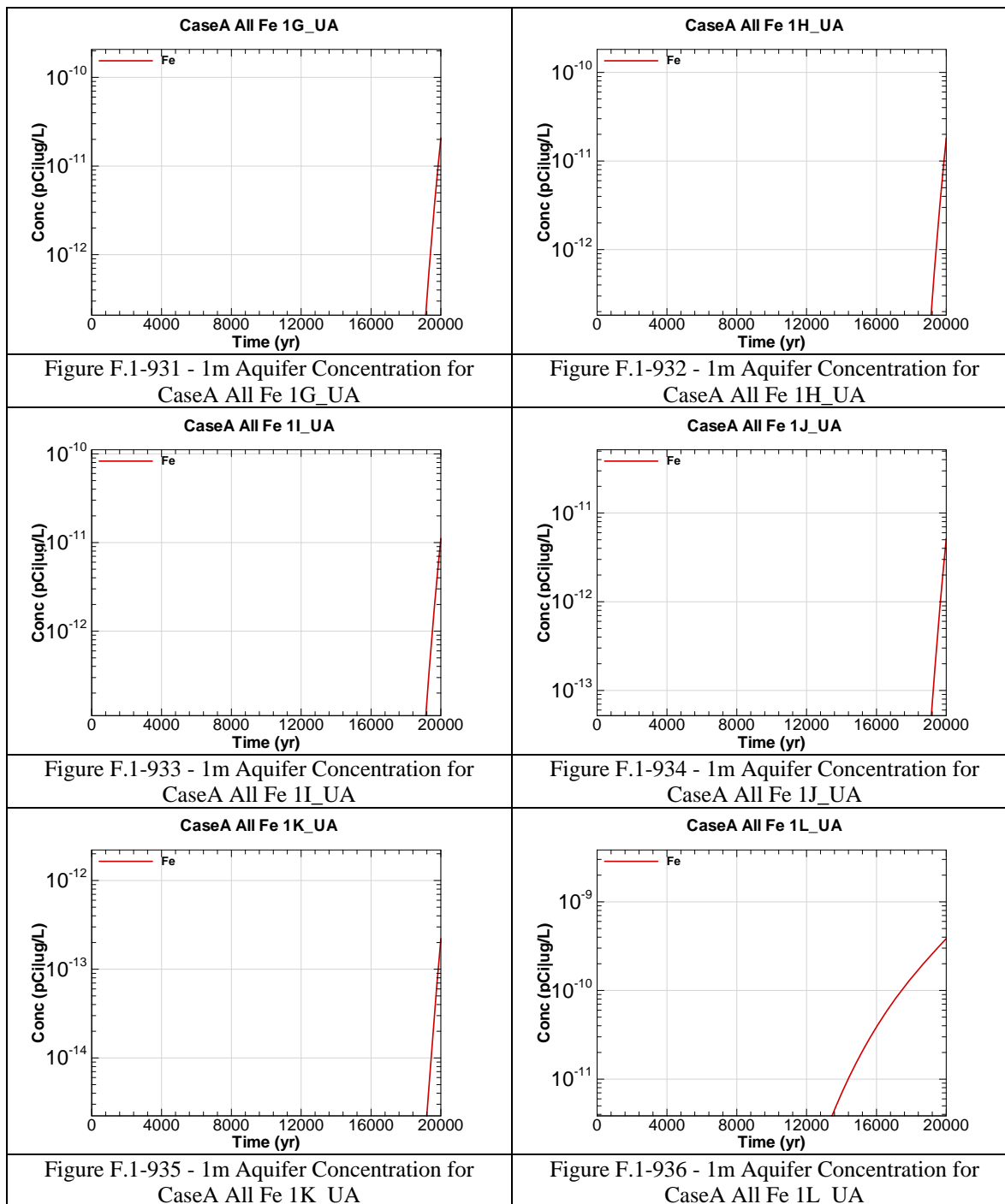


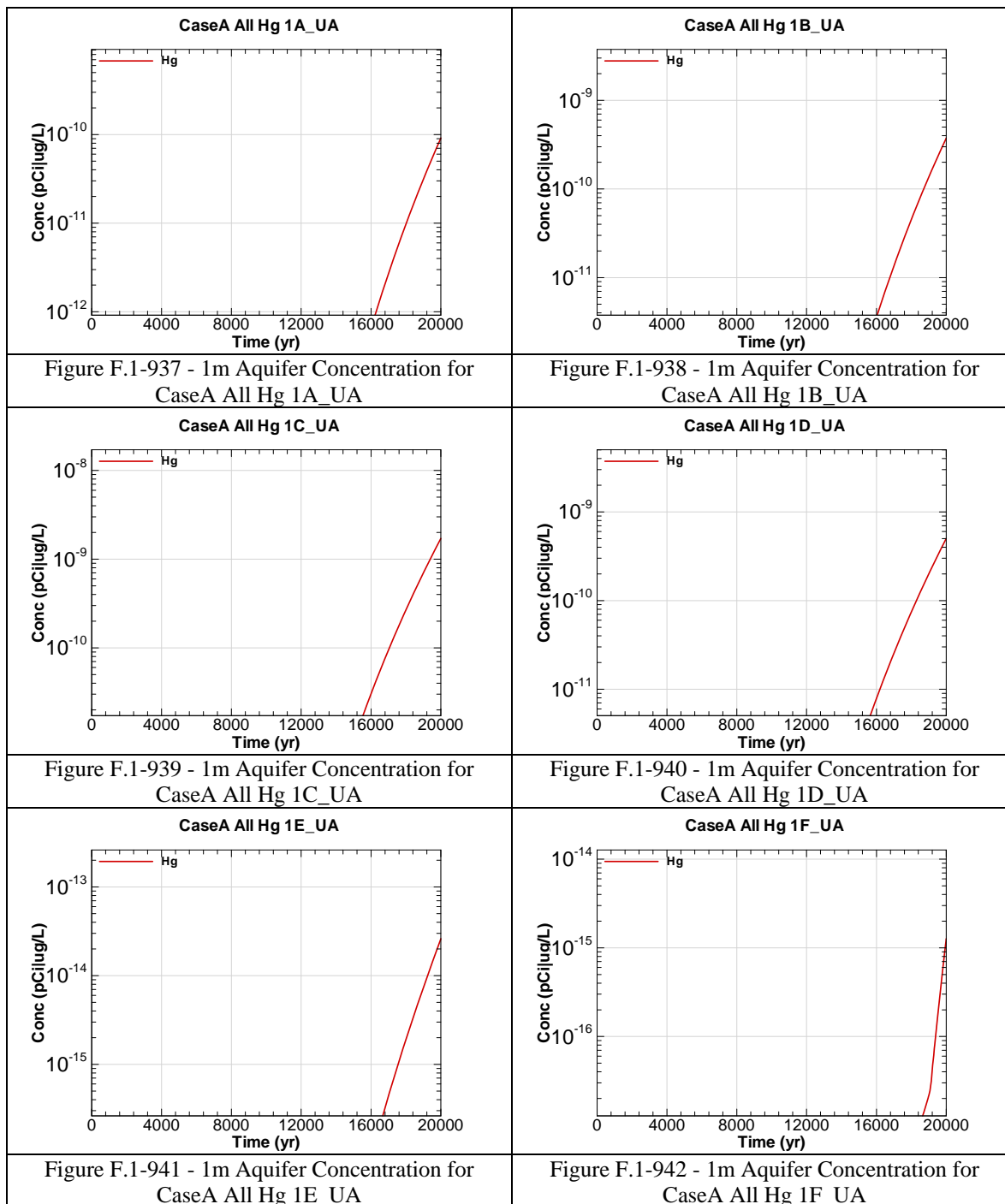


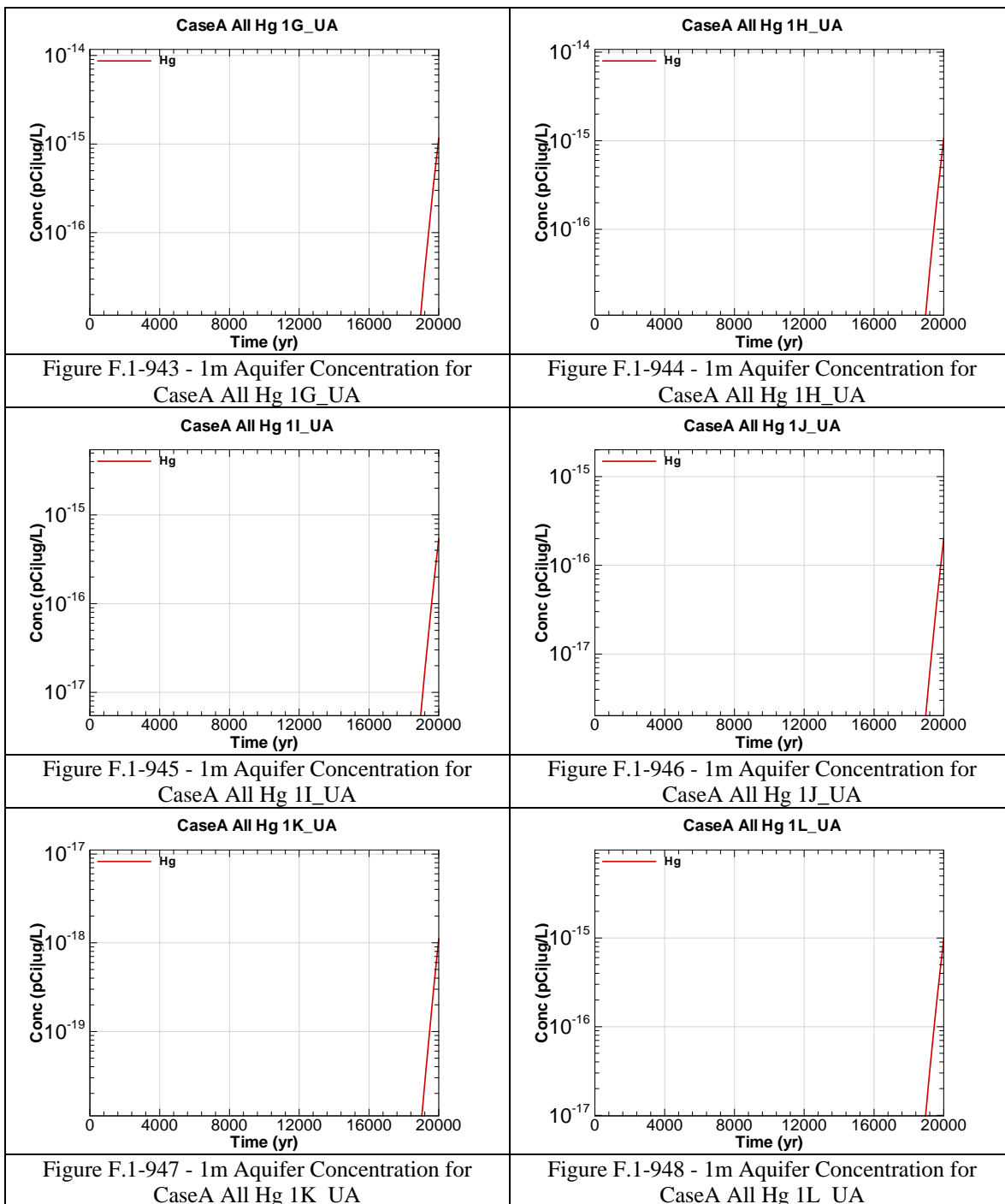


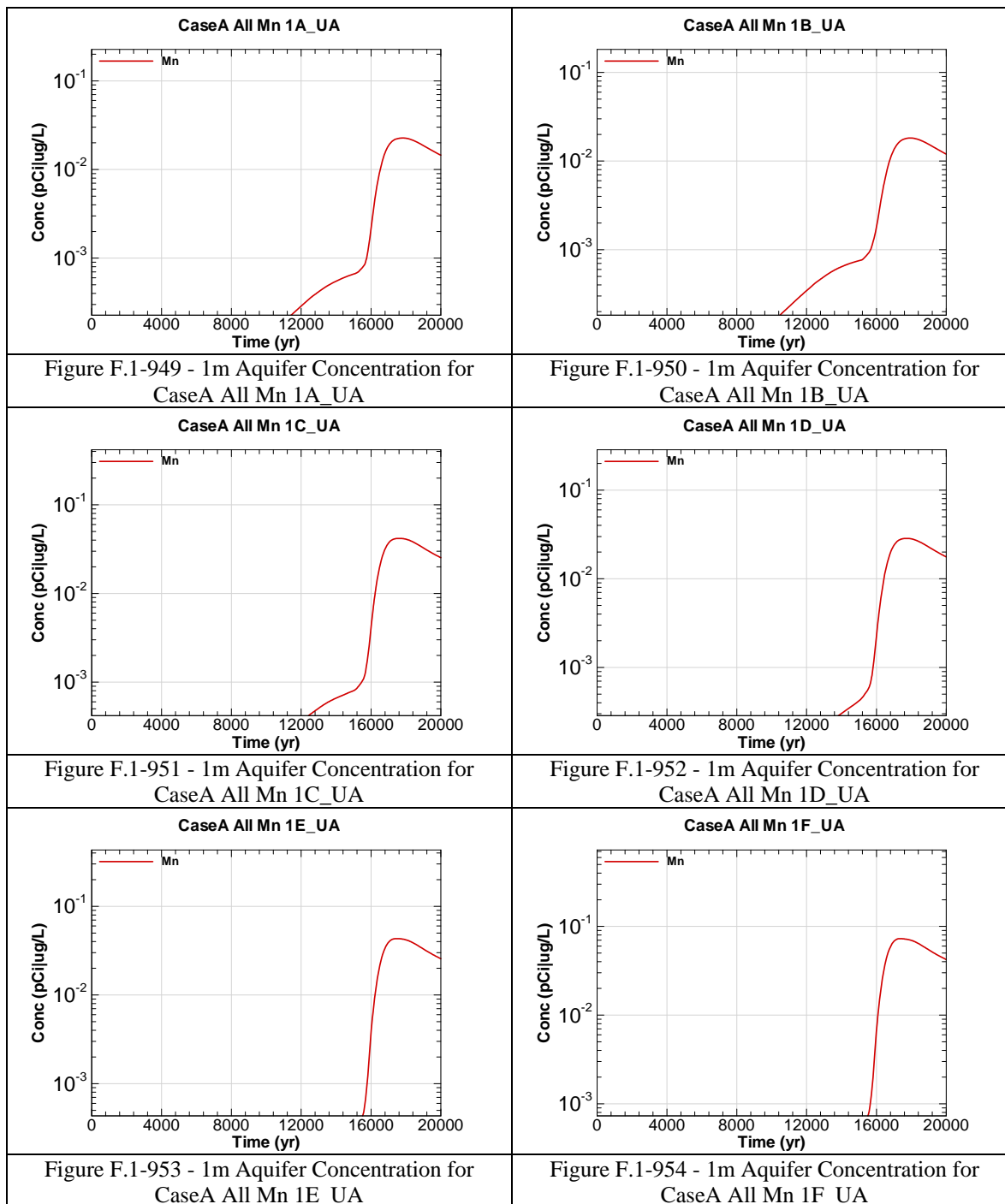


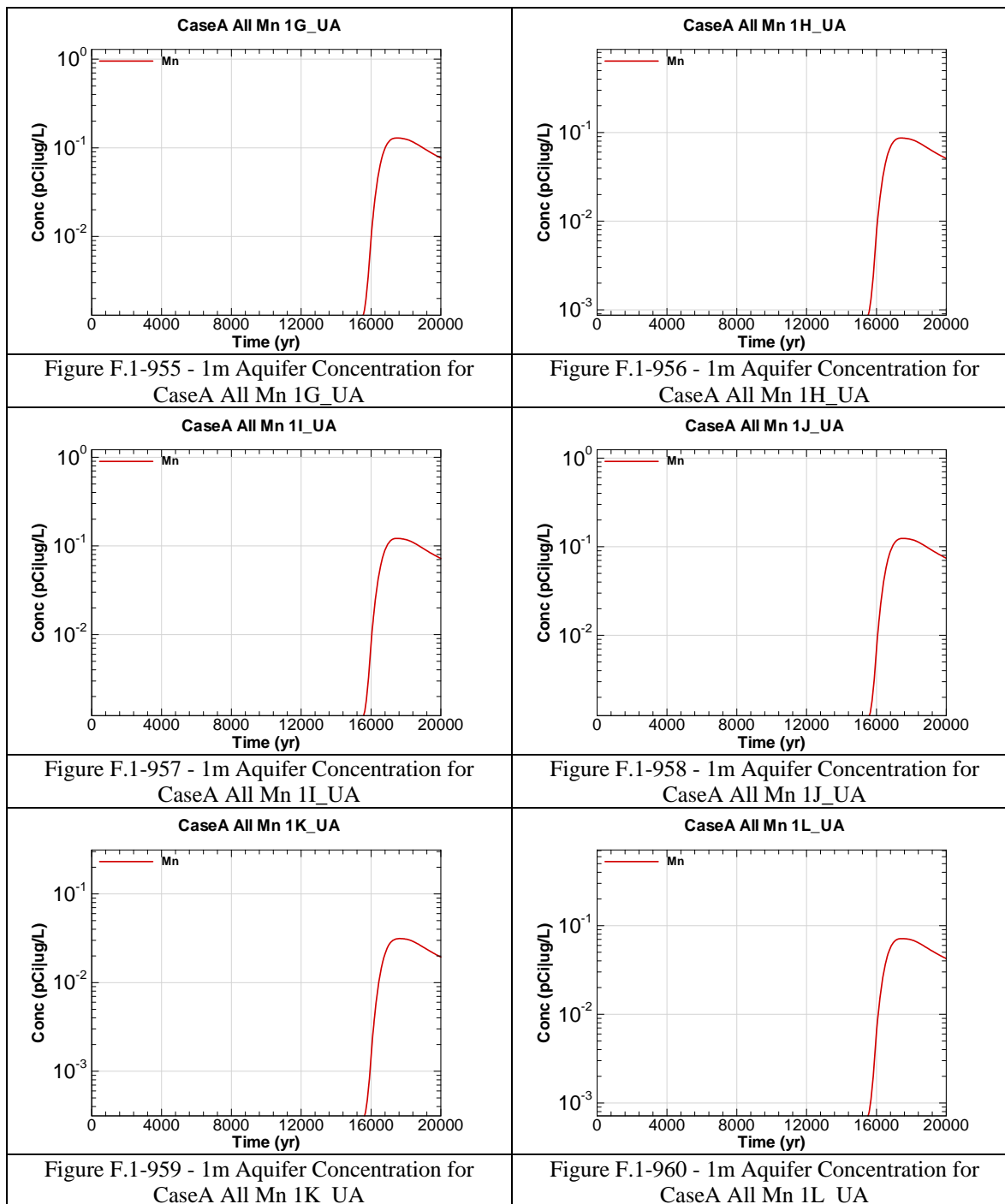


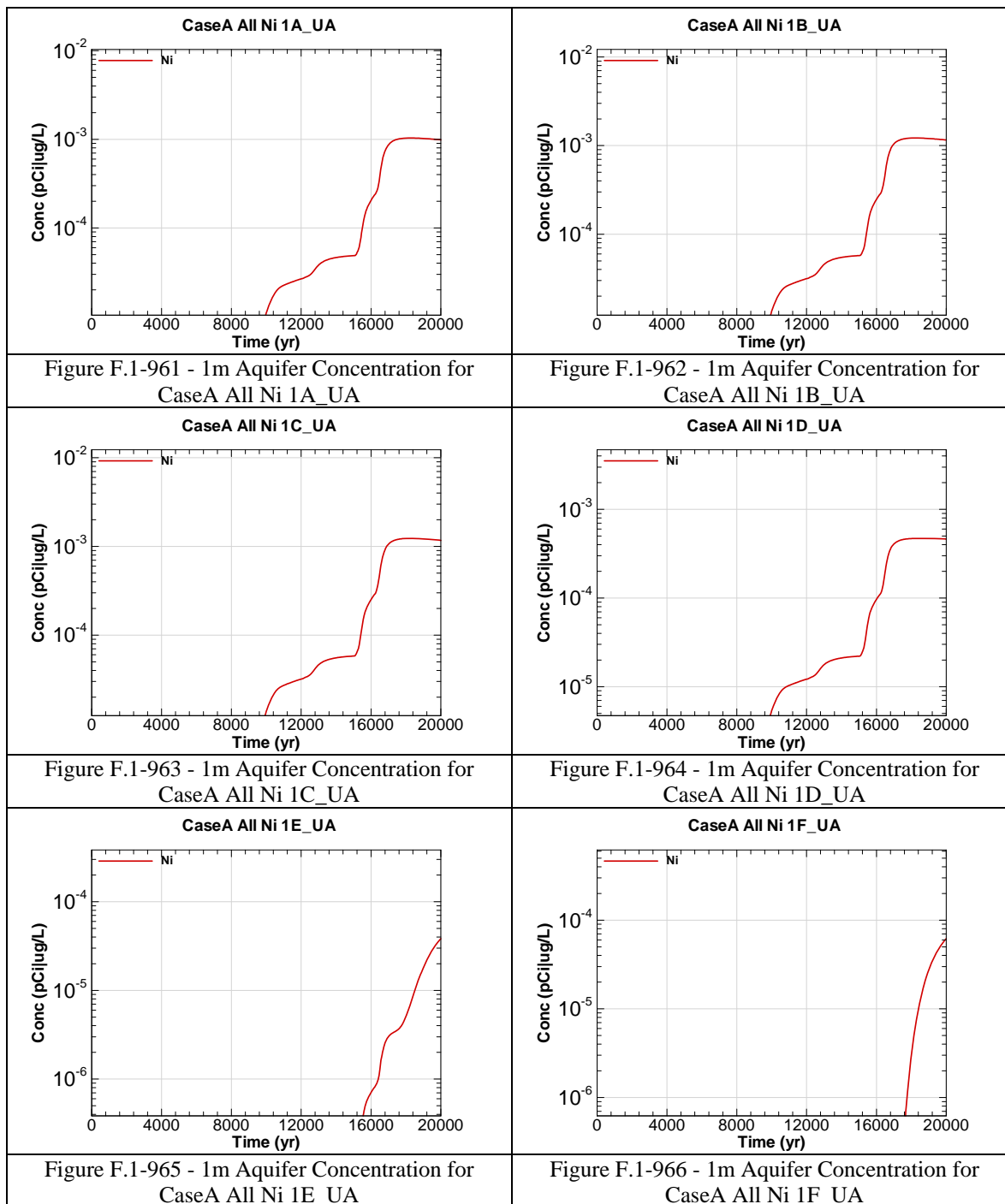


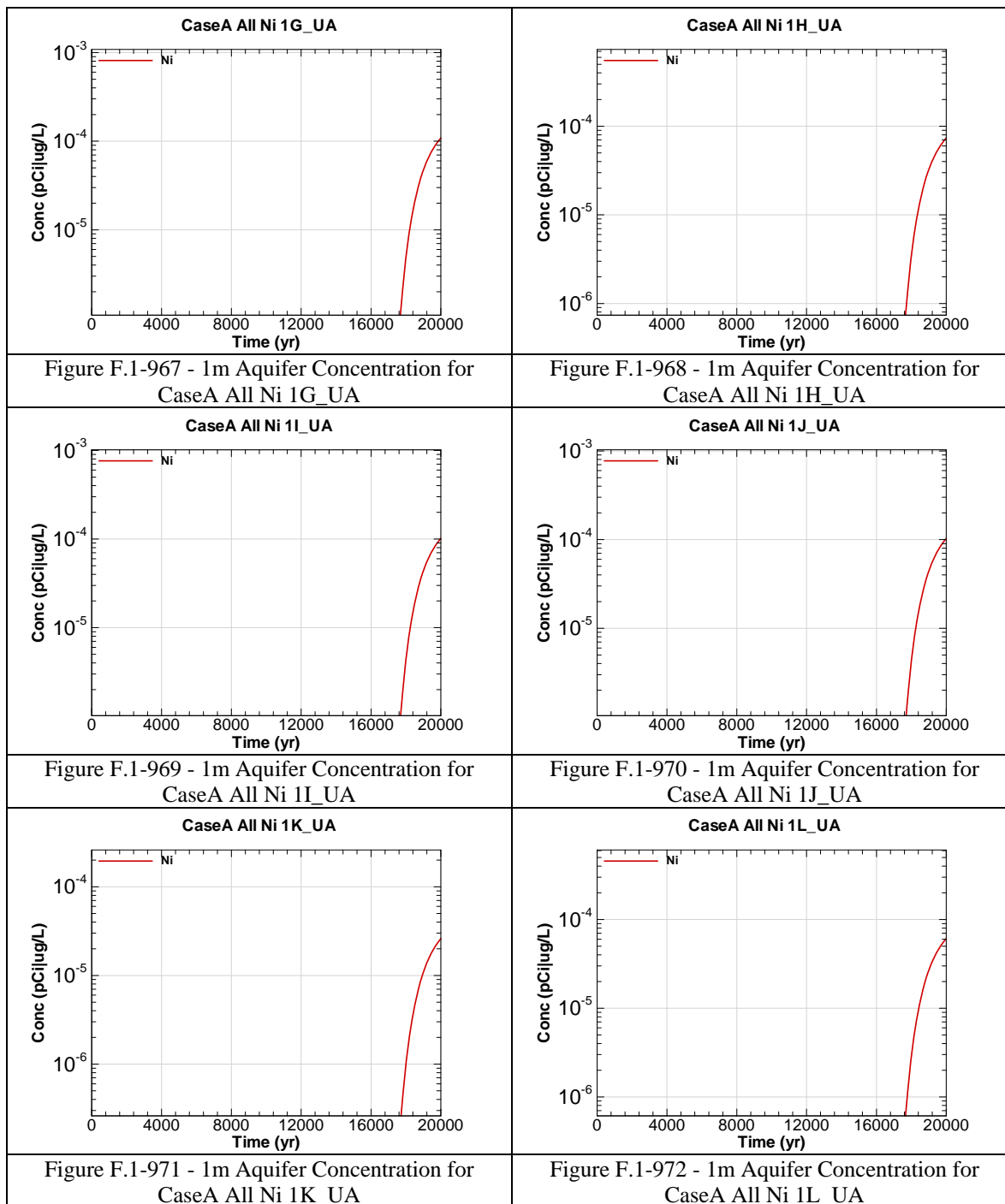


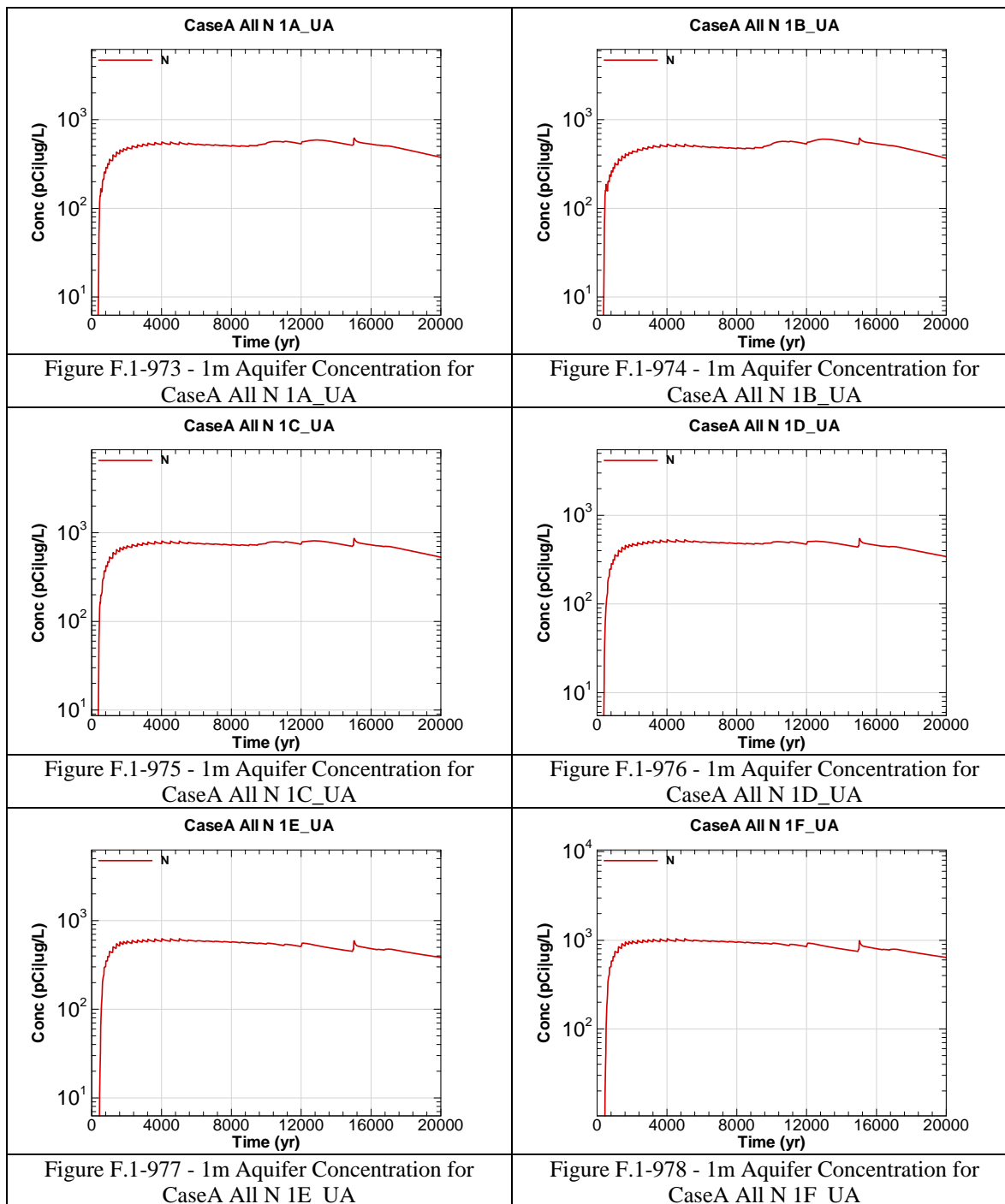


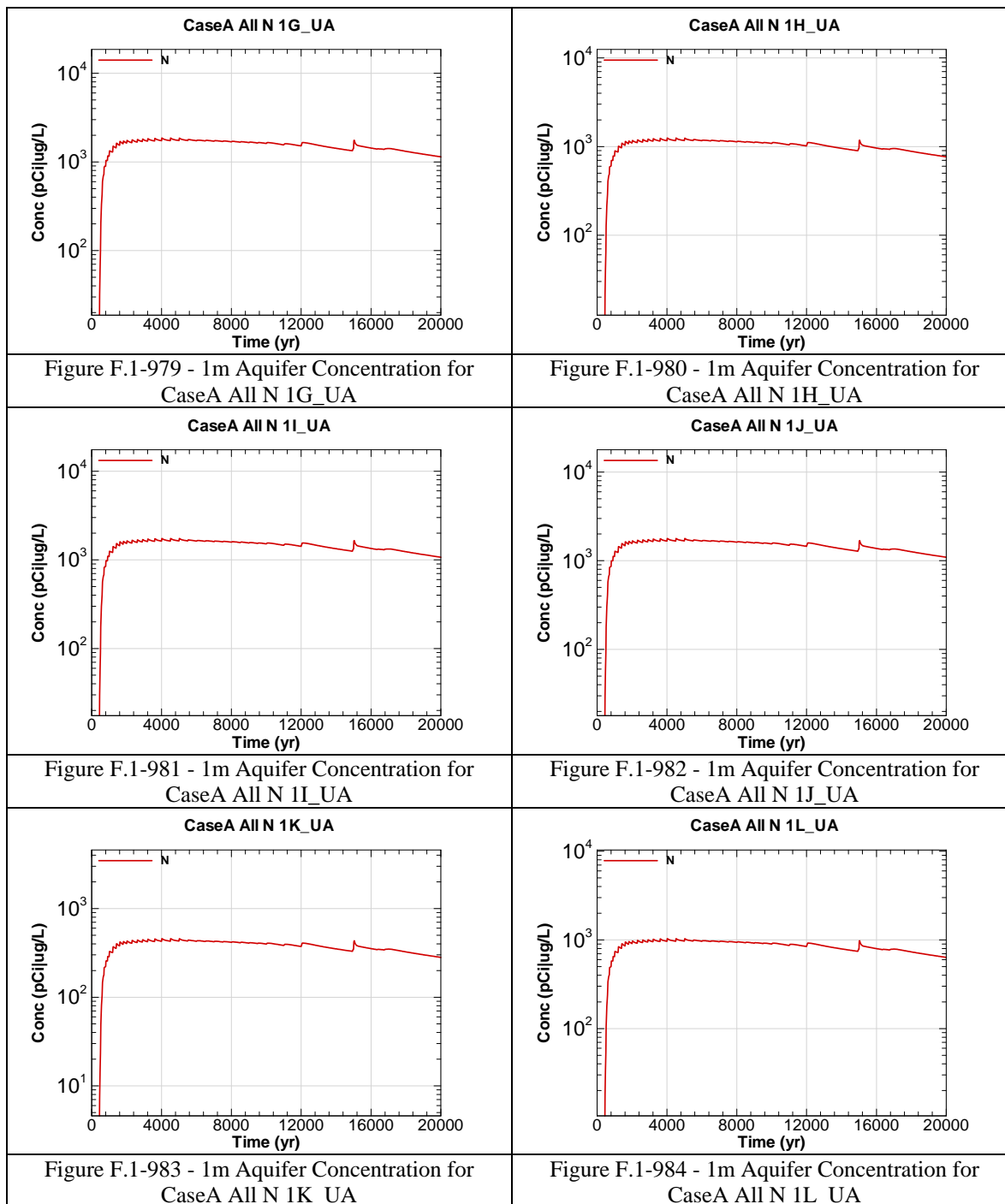


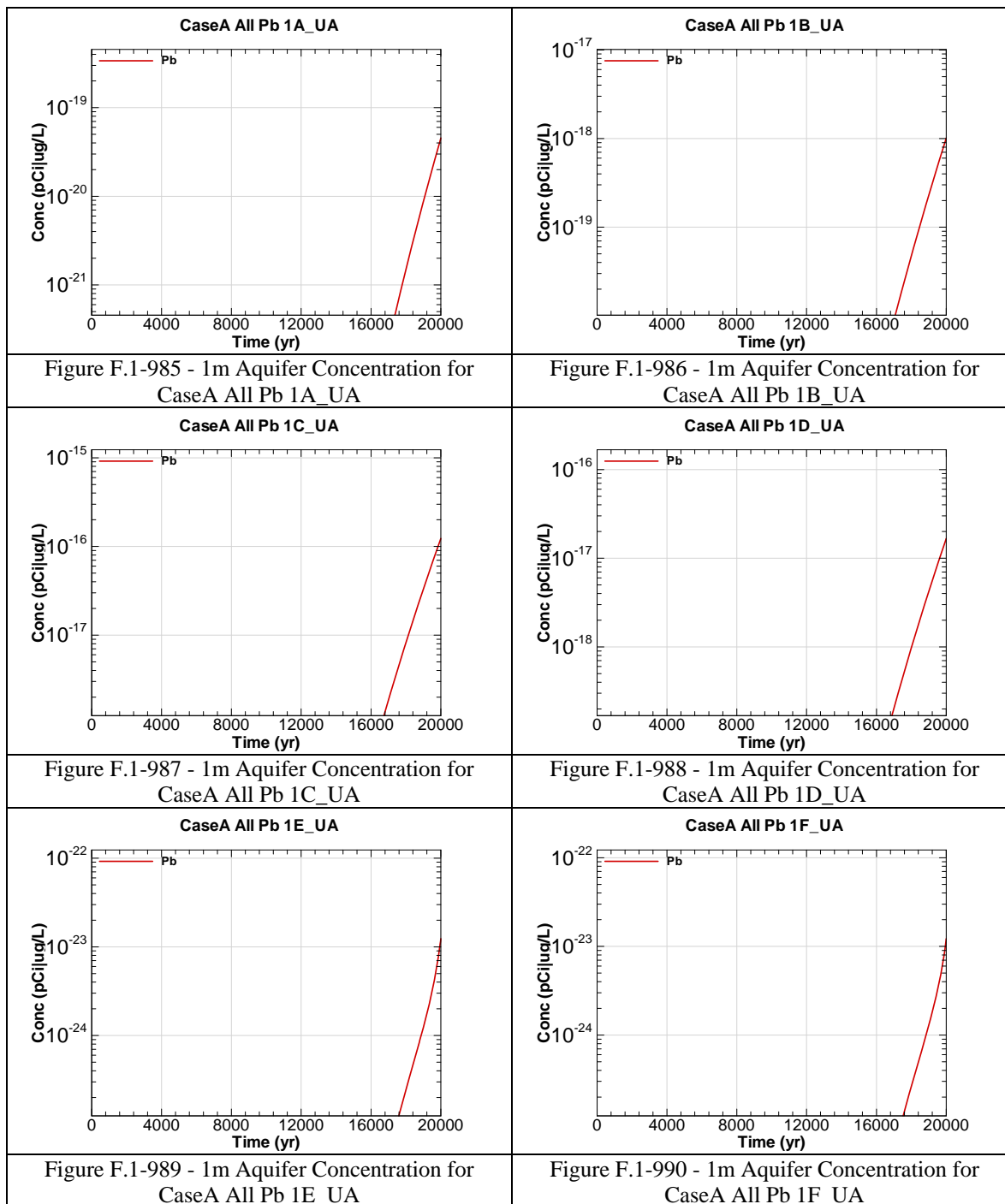


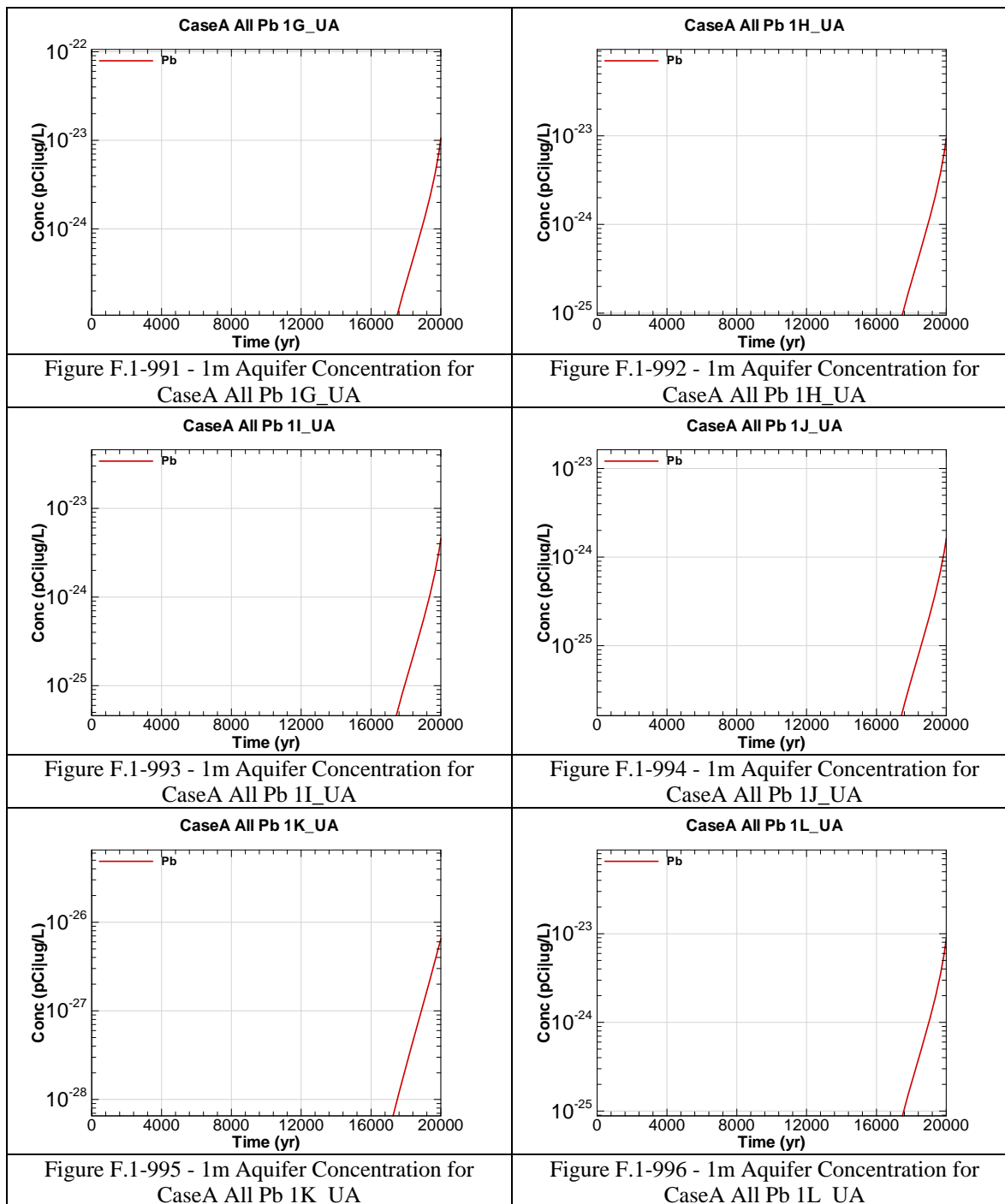


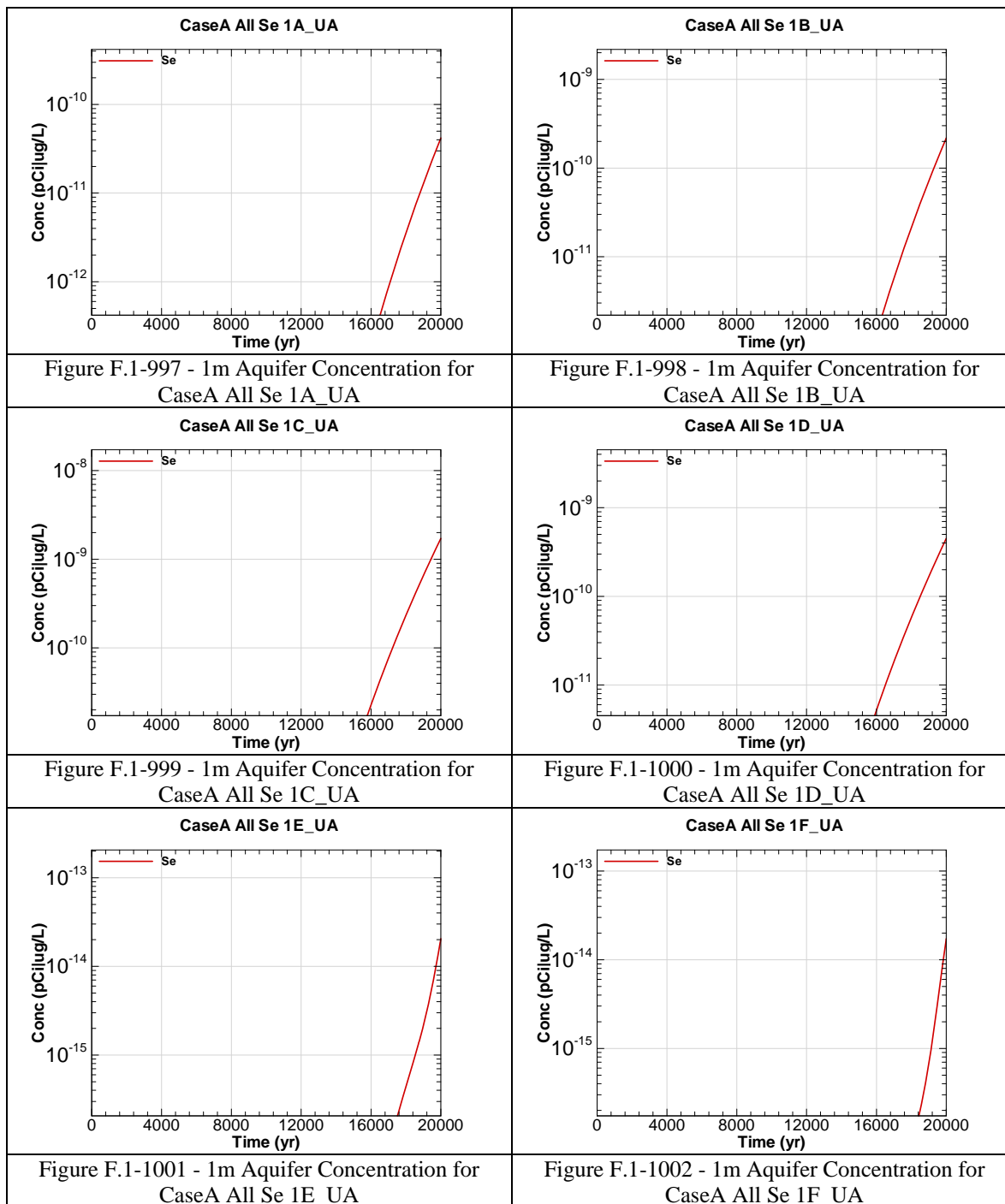


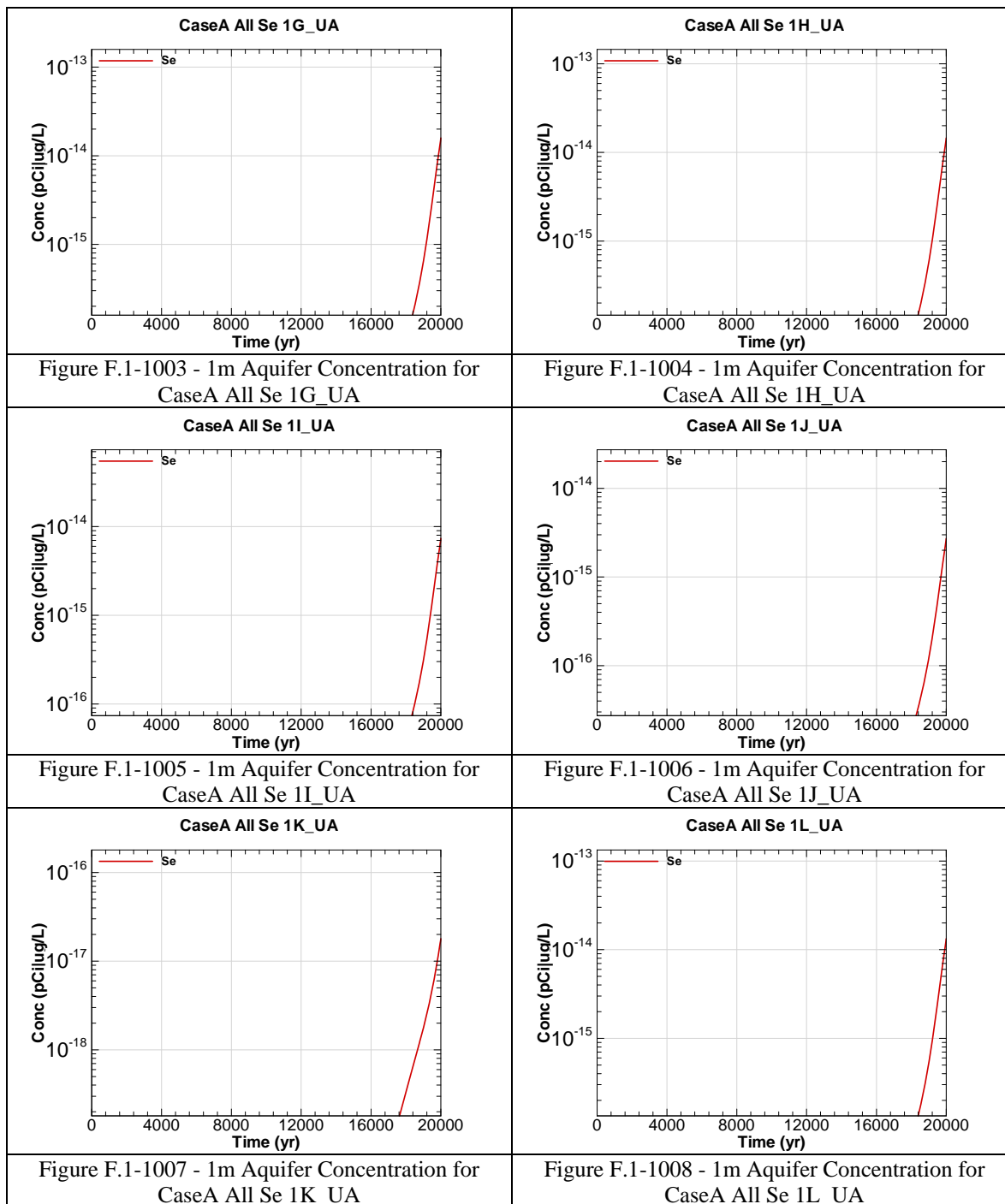


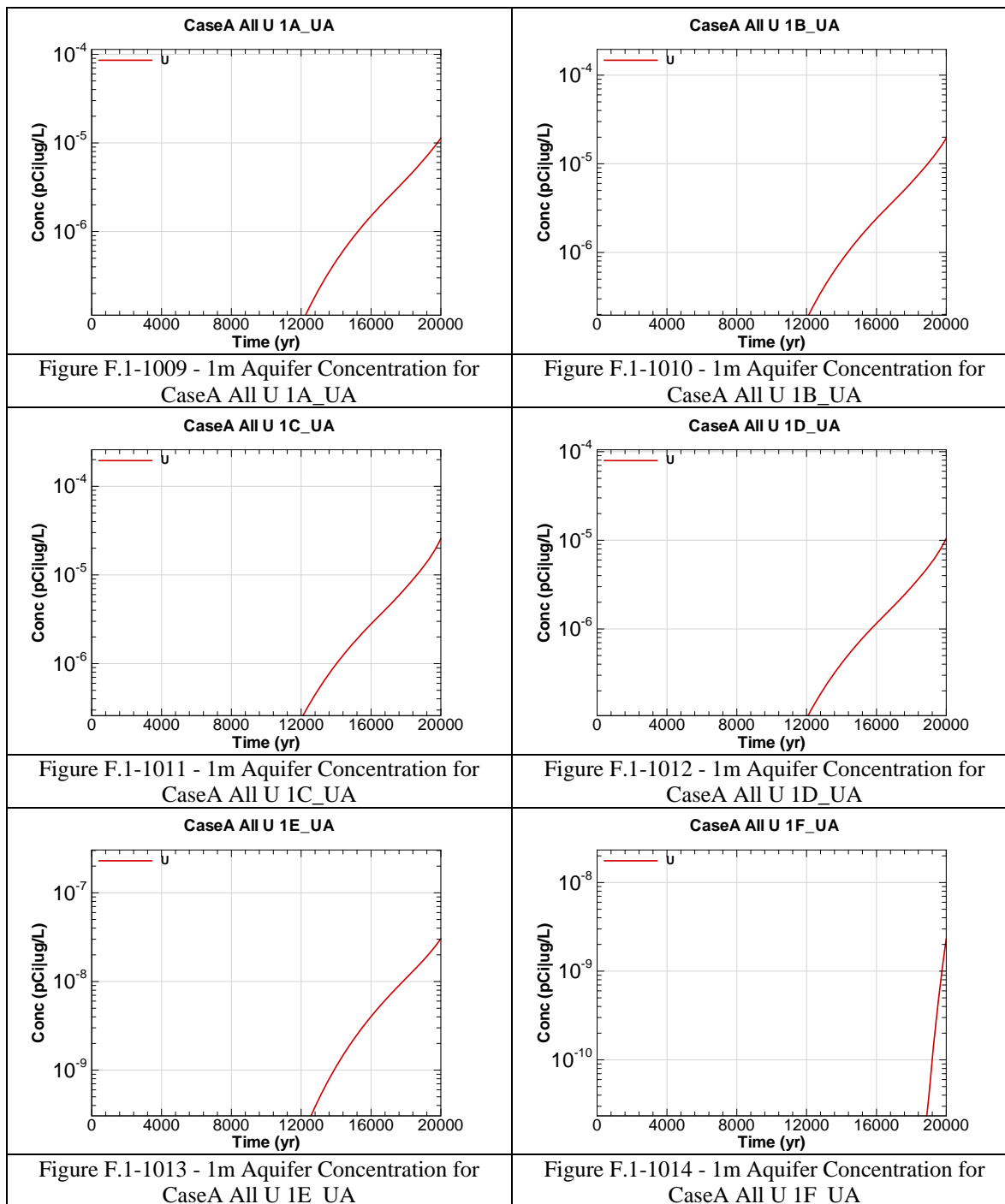


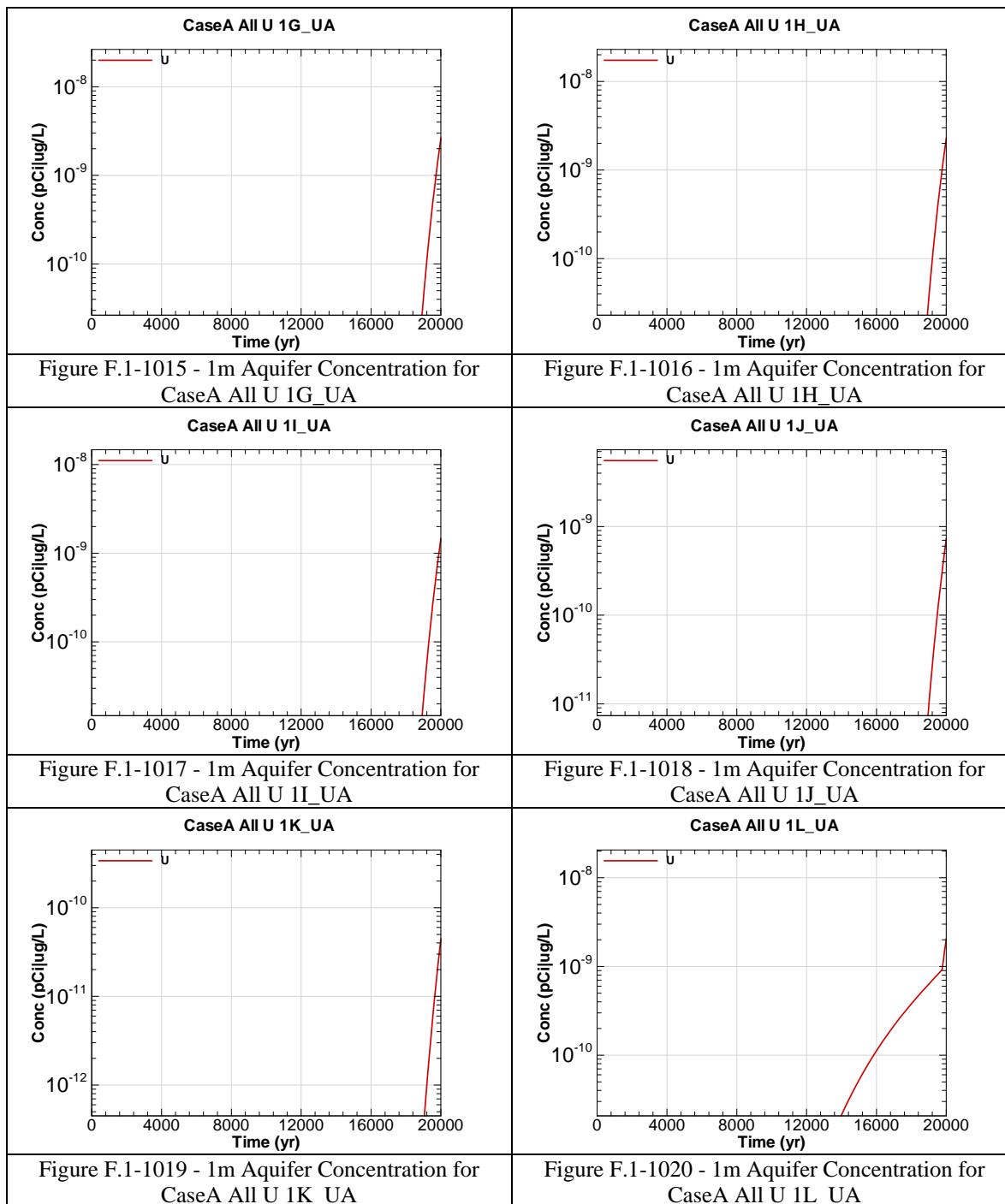


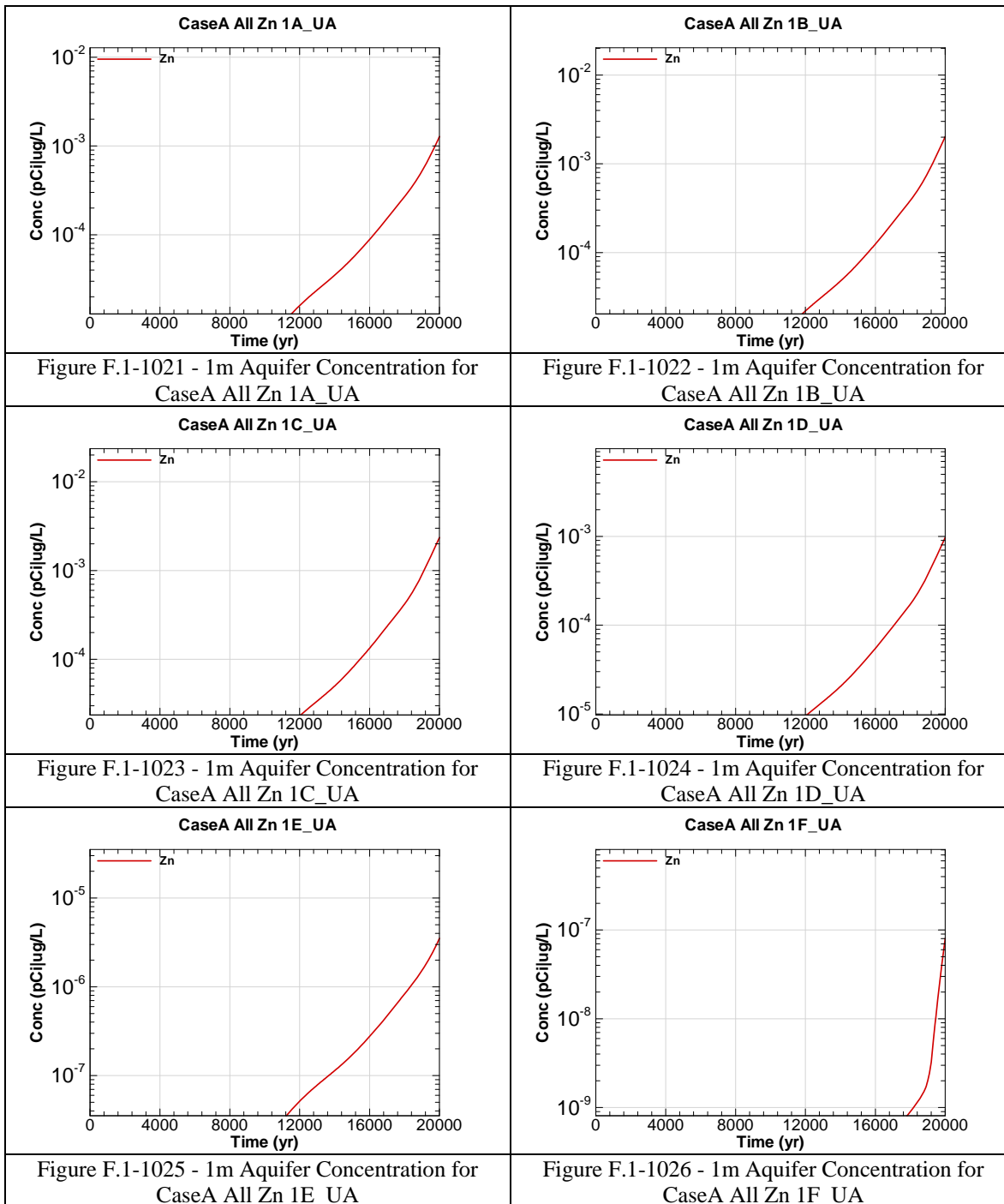


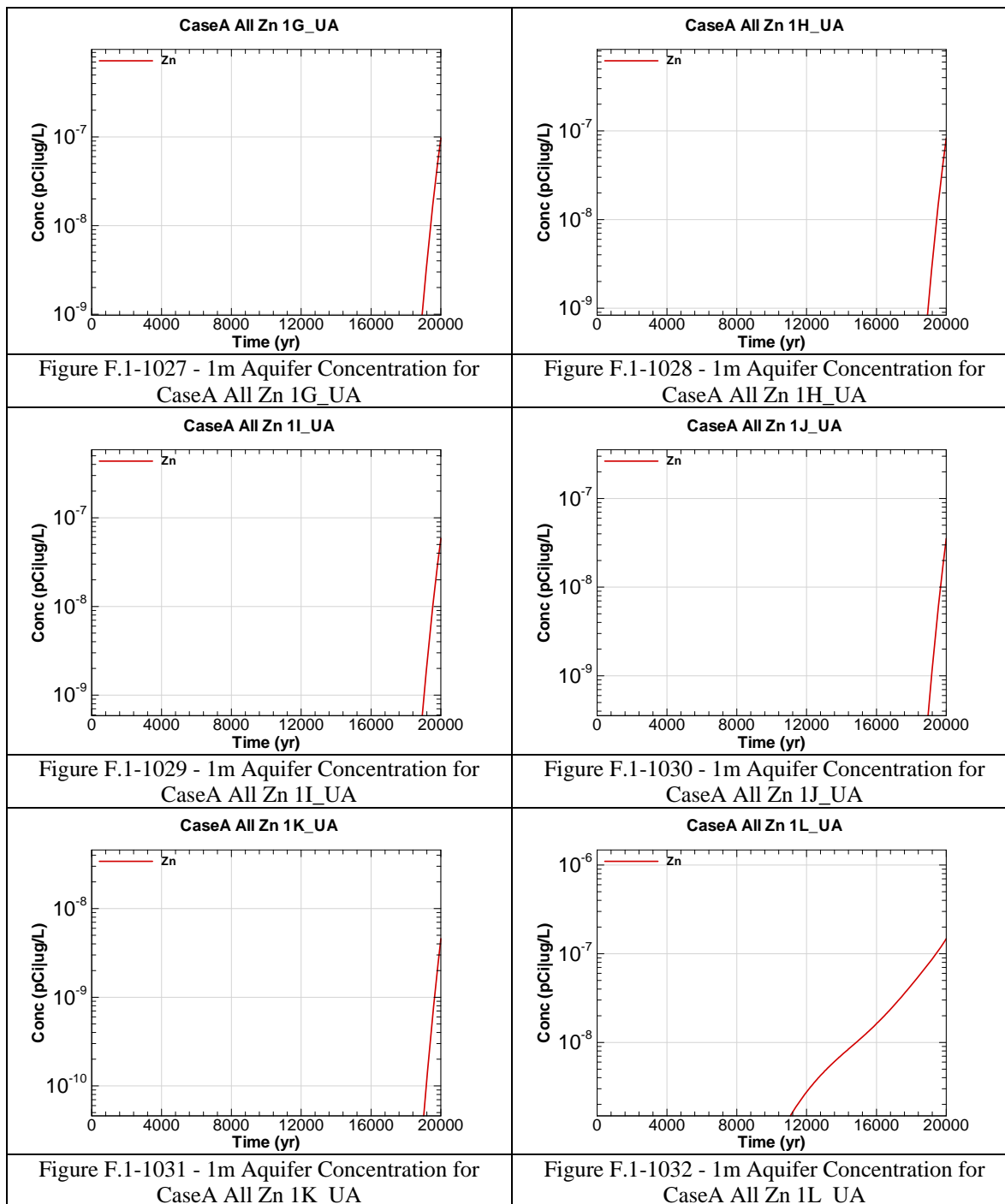












APPENDIX F.2

1-METER RADIOLOGICAL AND CHEMICAL CONCENTRATIONS AT THE UPPER THREE RUNS AQUIFER – LOWER ZONE

Appendix F.2 contains curves showing the 1 meter radiological and chemical concentrations for all SDF (vault and FDC inventories) for the Base Case (Case A). 20,000 year concentration results are presented from the Upper Three Runs Aquifer- Lower Zone for Sectors A through L

Graph heading example “CaseA All Ac-227 1A_LA”

Key

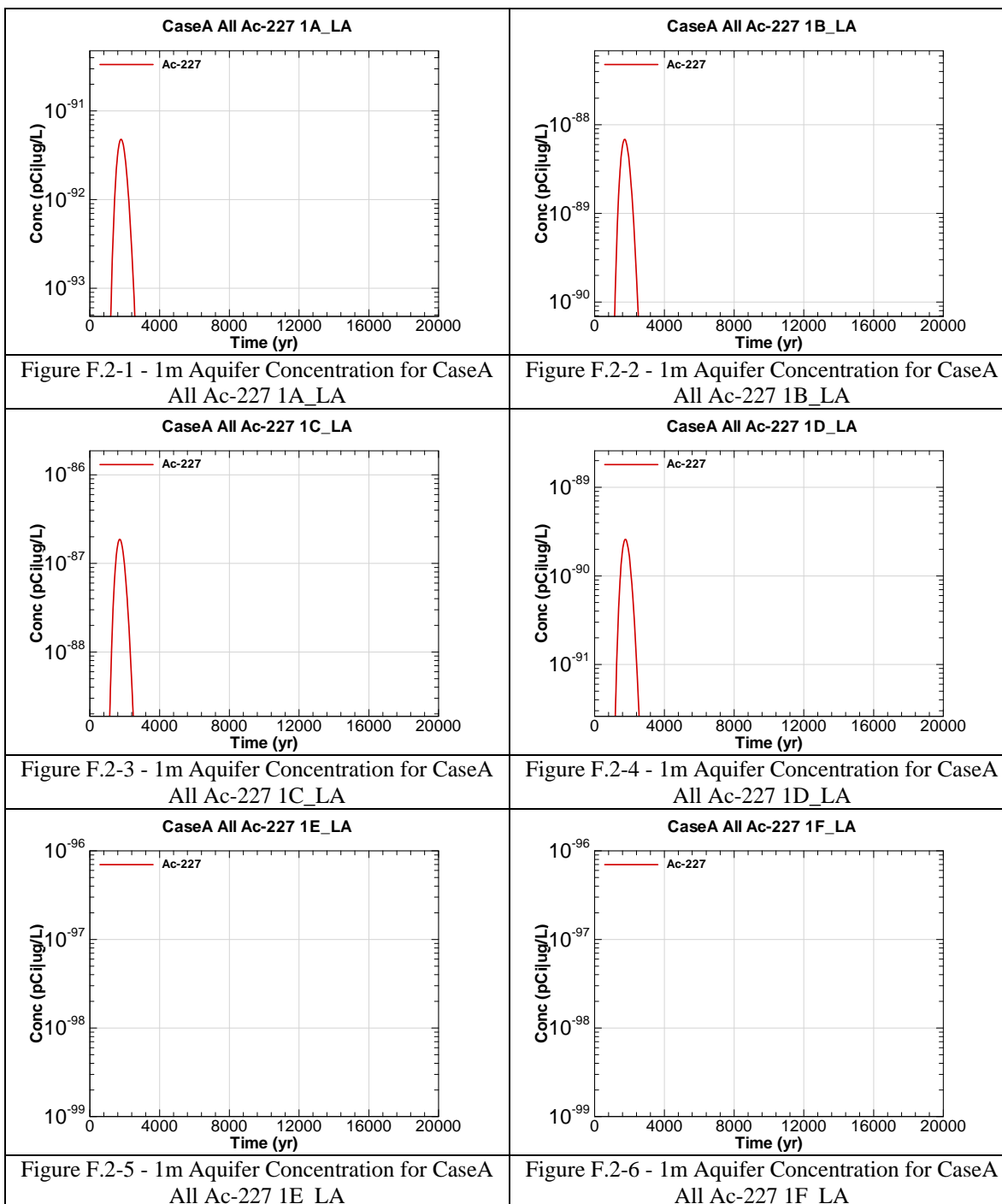
CaseA = Scenario case

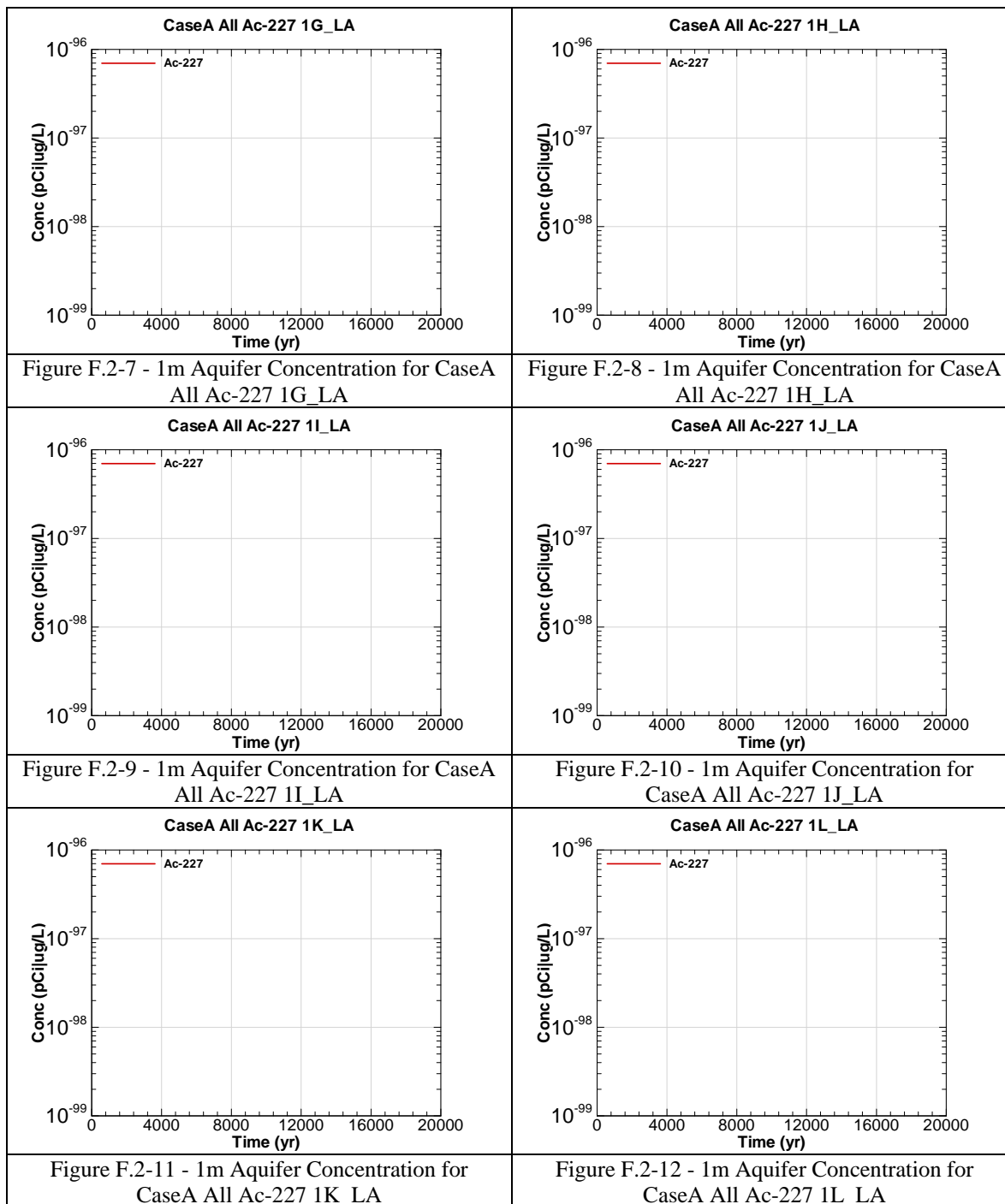
All = Inventory source is all disposal units

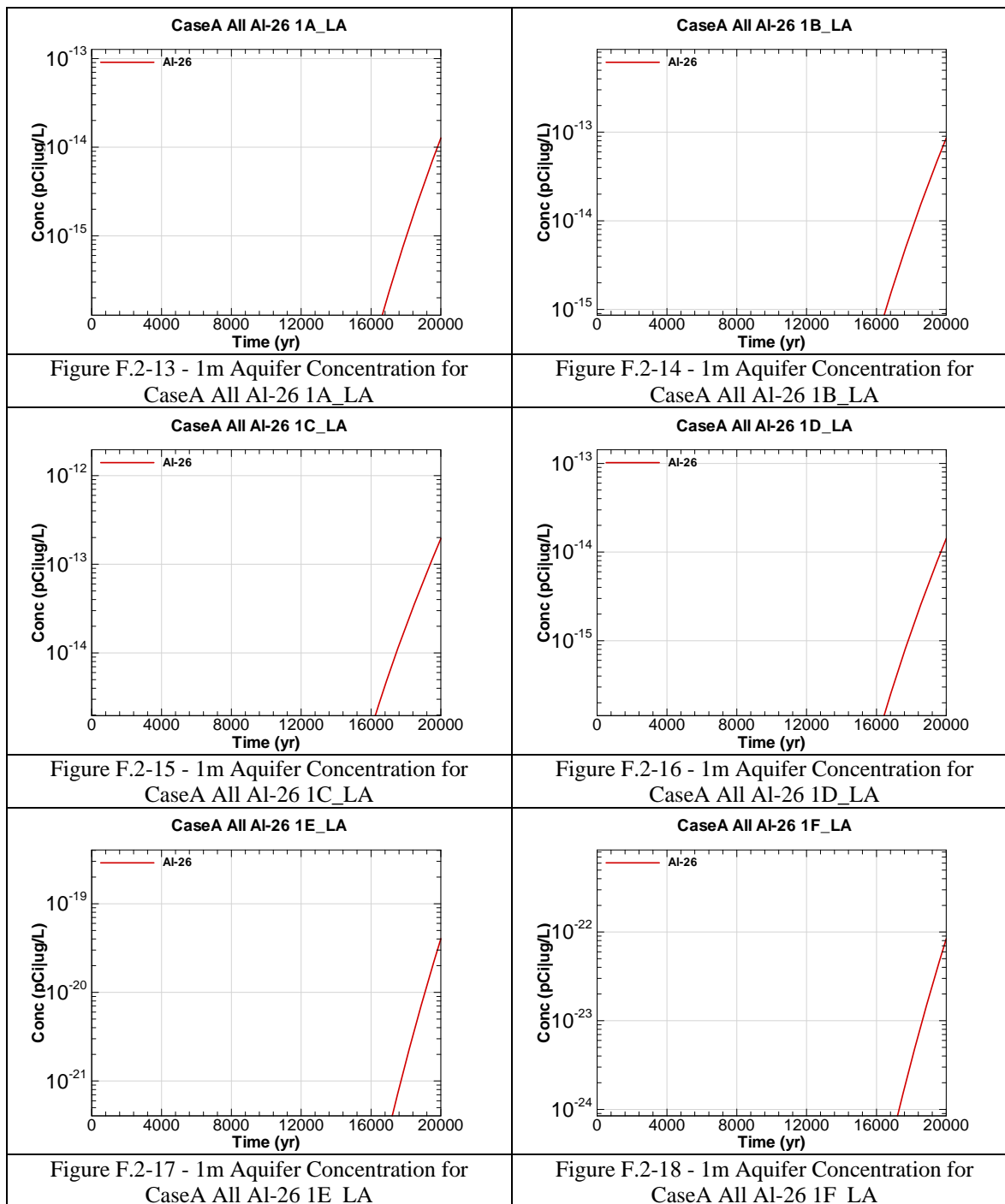
Ac-227 = Radionuclide or chemical of concern

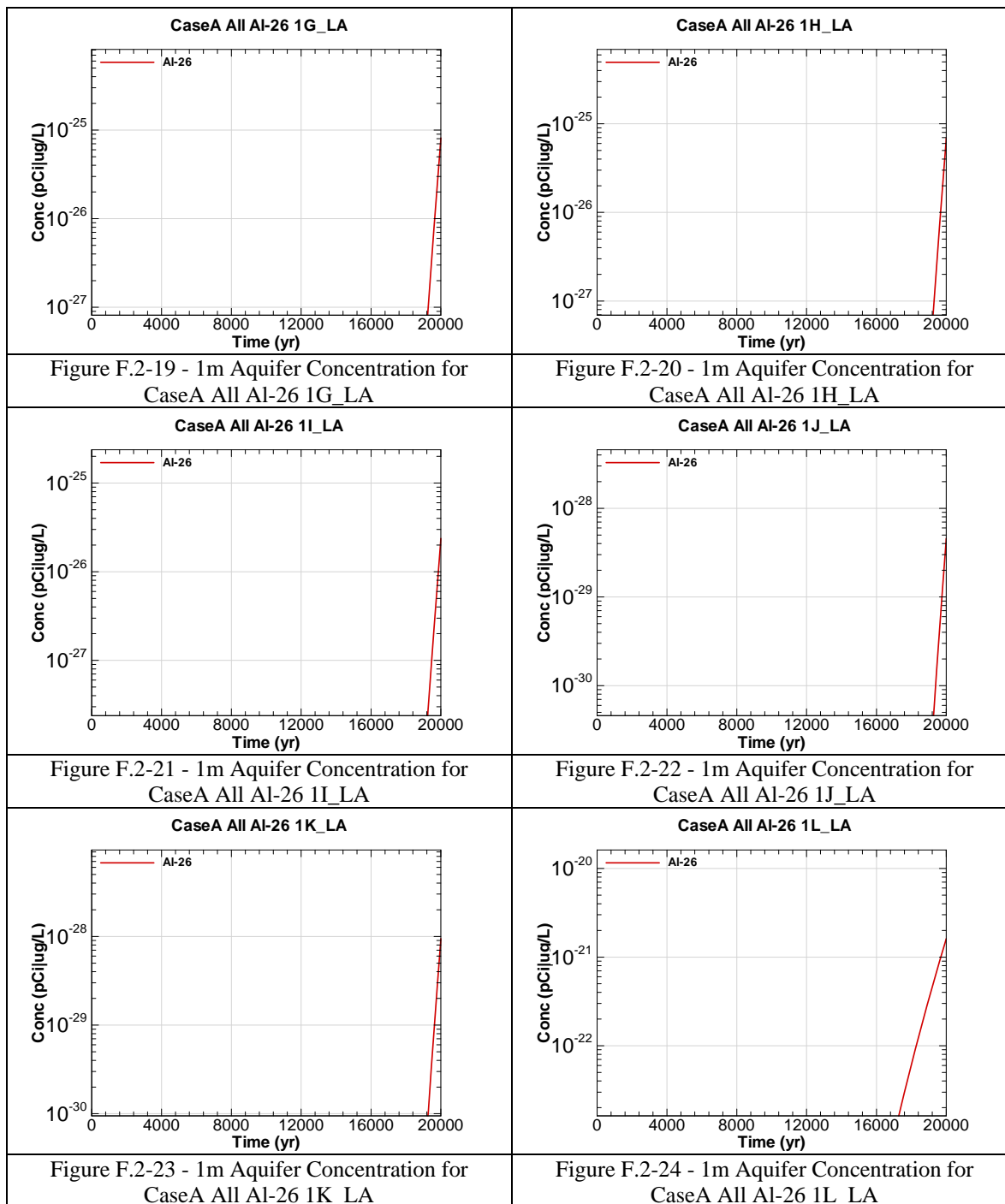
1A = 1 meter evaluation sector of concern

LA = Aquifer of concern is Upper Three Runs Aquifer – Lower Zone









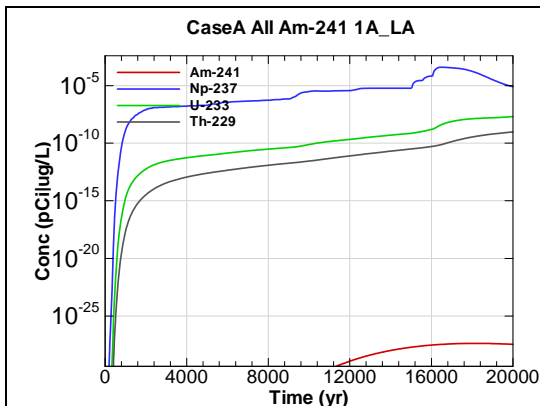


Figure F.2-25 - 1m Aquifer Concentration for CaseA All Am-241 1A_LA

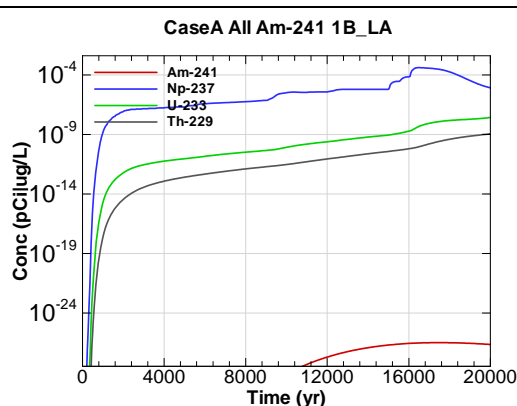


Figure F.2-26 - 1m Aquifer Concentration for CaseA All Am-241 1B_LA

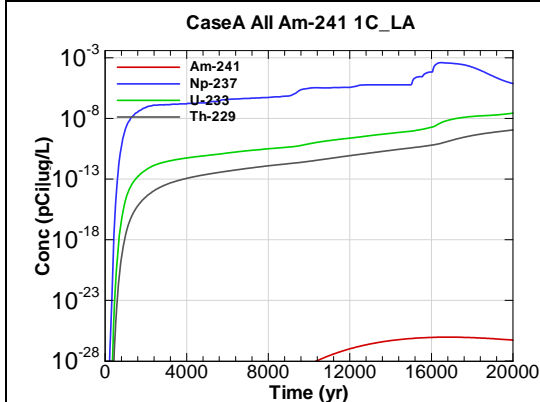


Figure F.2-27 - 1m Aquifer Concentration for CaseA All Am-241 1C_LA

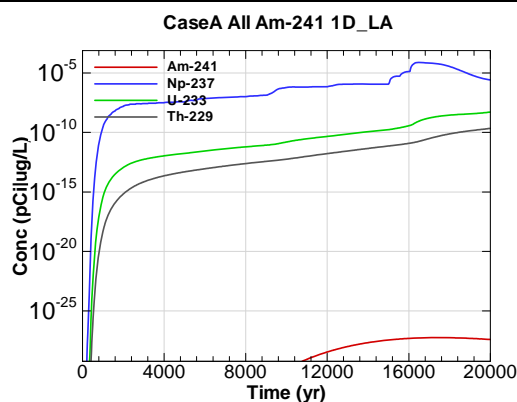


Figure F.2-28 - 1m Aquifer Concentration for CaseA All Am-241 1D_LA

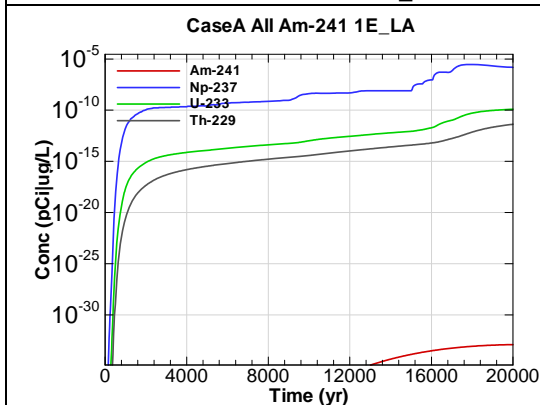


Figure F.2-29 - 1m Aquifer Concentration for CaseA All Am-241 1E_LA

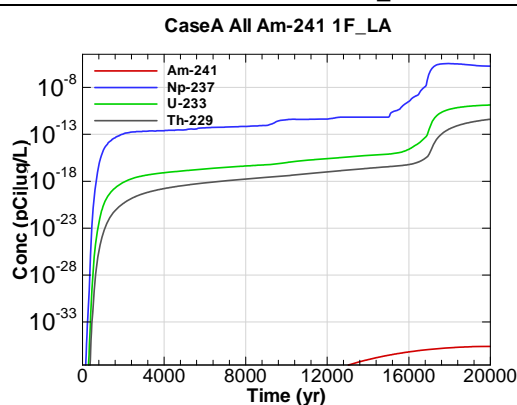


Figure F.2-30 - 1m Aquifer Concentration for CaseA All Am-241 1F_LA

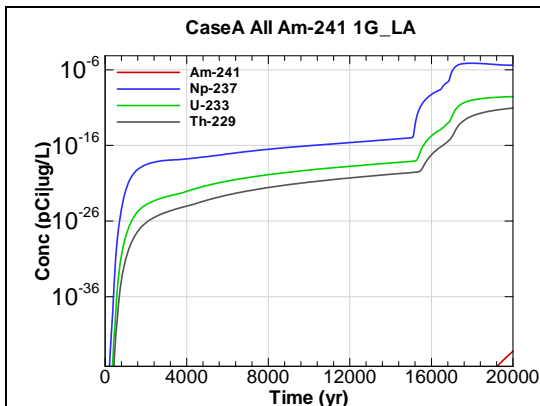


Figure F.2-31 - 1m Aquifer Concentration for
CaseA All Am-241 1G_LA

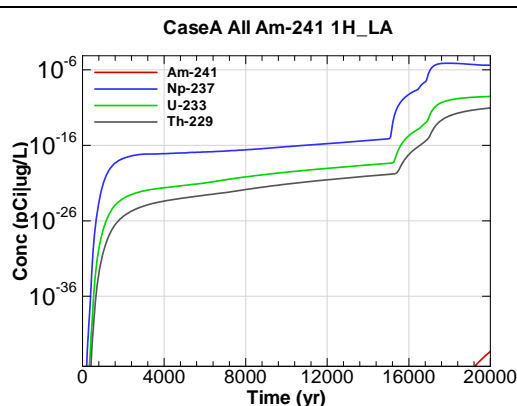


Figure F.2-32 - 1m Aquifer Concentration for
CaseA All Am-241 1H_LA

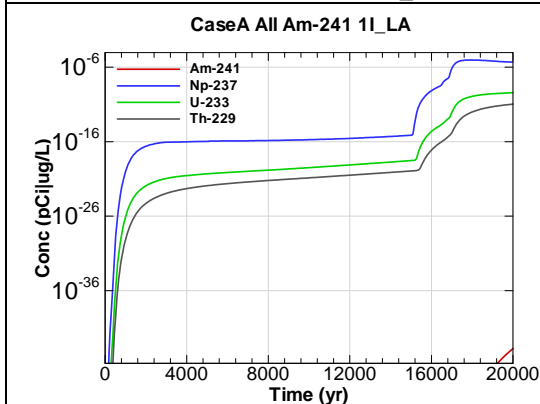


Figure F.2-33 - 1m Aquifer Concentration for
CaseA All Am-241 1I_LA

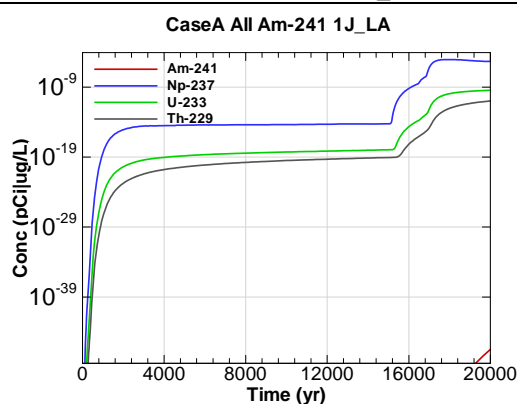


Figure F.2-34 - 1m Aquifer Concentration for
CaseA All Am-241 1J_LA

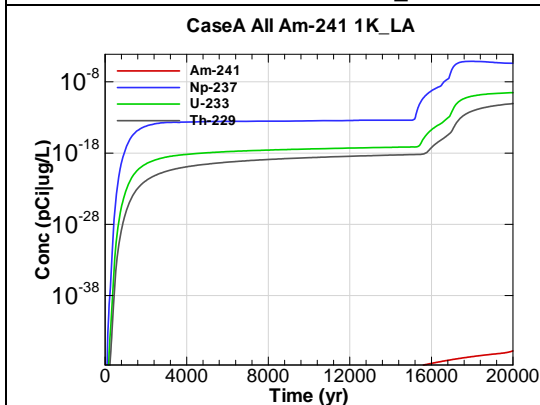


Figure F.2-35 - 1m Aquifer Concentration for
CaseA All Am-241 1K_LA

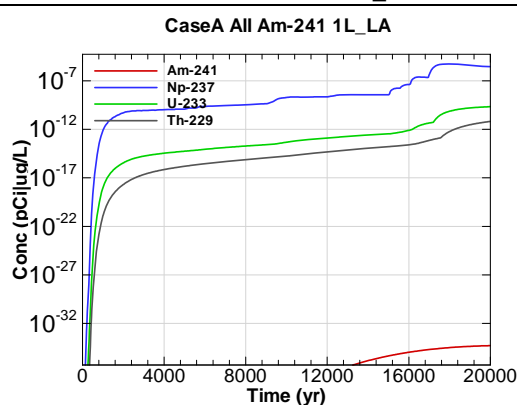


Figure F.2-36 - 1m Aquifer Concentration for
CaseA All Am-241 1L_LA

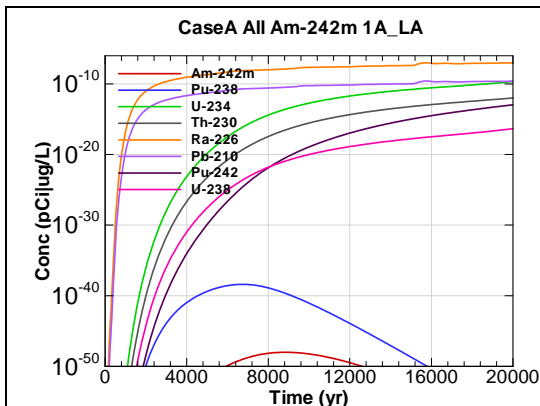


Figure F.2-37 - 1m Aquifer Concentration for
CaseA All Am-242m 1A_LA

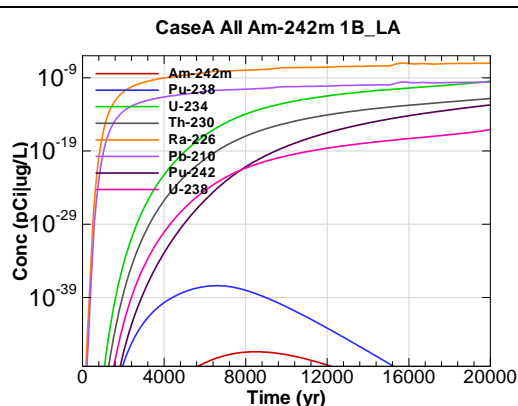


Figure F.2-38 - 1m Aquifer Concentration for
CaseA All Am-242m 1B_LA

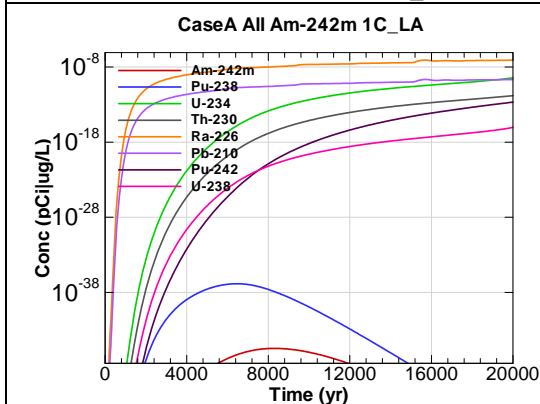


Figure F.2-39 - 1m Aquifer Concentration for
CaseA All Am-242m 1C_LA

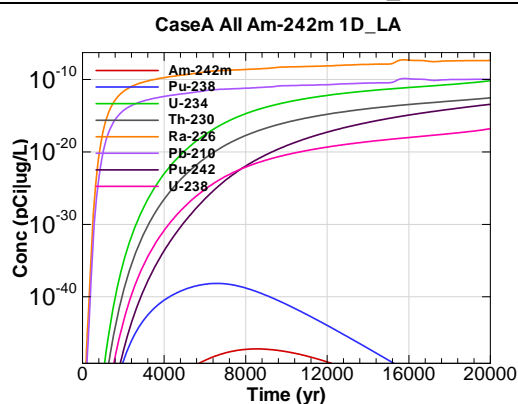


Figure F.2-40 - 1m Aquifer Concentration for
CaseA All Am-242m 1D_LA

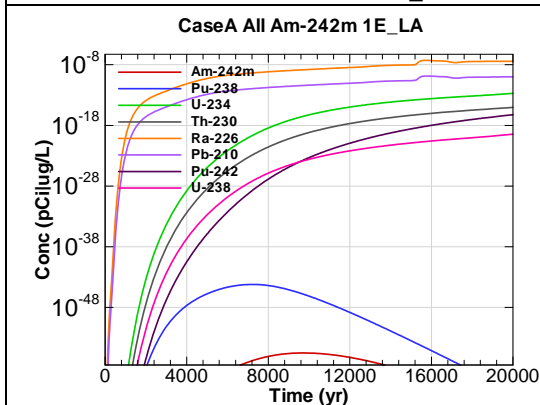


Figure F.2-41 - 1m Aquifer Concentration for
CaseA All Am-242m 1E_LA

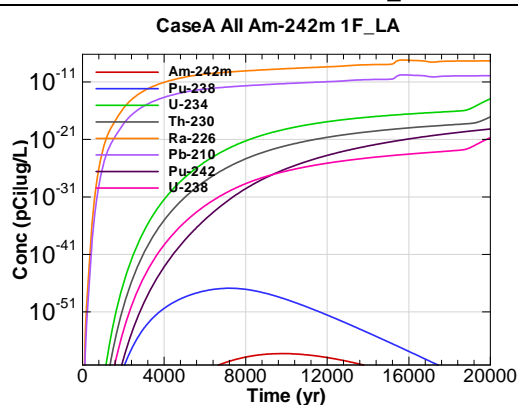


Figure F.2-42 - 1m Aquifer Concentration for
CaseA All Am-242m 1F_LA

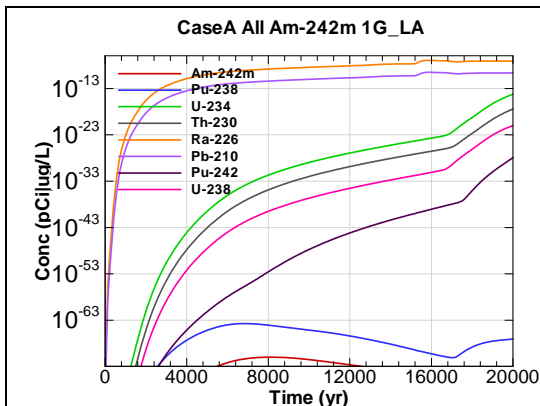


Figure F.2-43 - 1m Aquifer Concentration for
CaseA All Am-242m 1G_LA

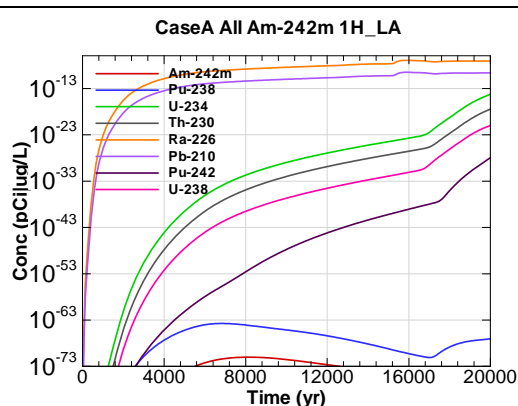


Figure F.2-44 - 1m Aquifer Concentration for
CaseA All Am-242m 1H_LA

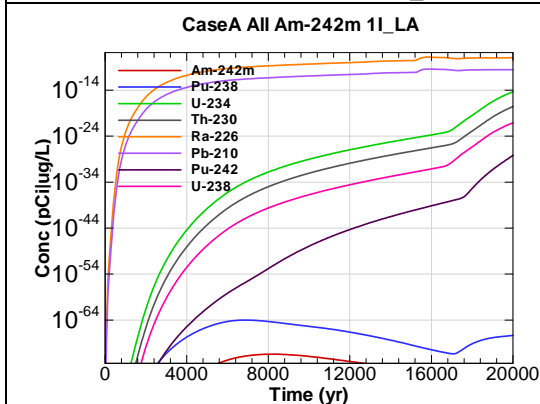


Figure F.2-45 - 1m Aquifer Concentration for
CaseA All Am-242m 1I_LA

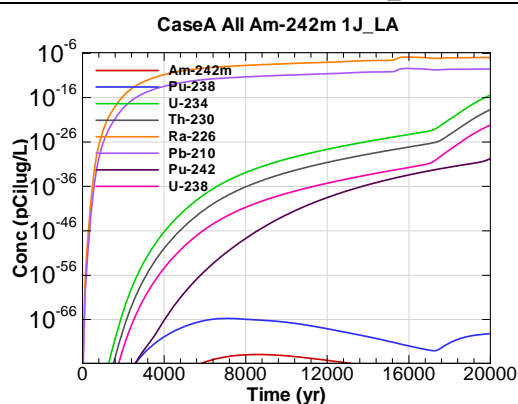


Figure F.2-46 - 1m Aquifer Concentration for
CaseA All Am-242m 1J_LA

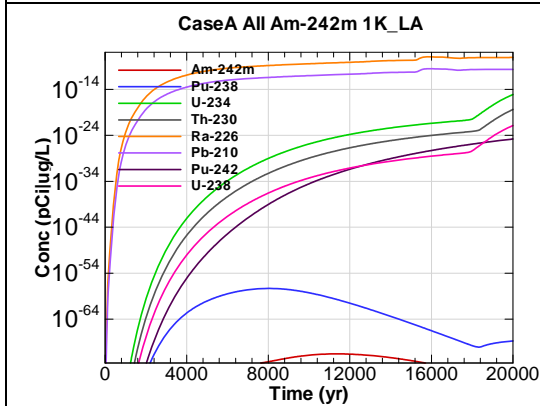


Figure F.2-47 - 1m Aquifer Concentration for
CaseA All Am-242m 1K_LA

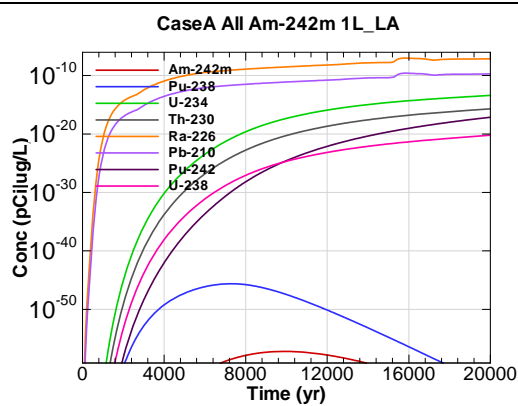


Figure F.2-48 - 1m Aquifer Concentration for
CaseA All Am-242m 1L_LA

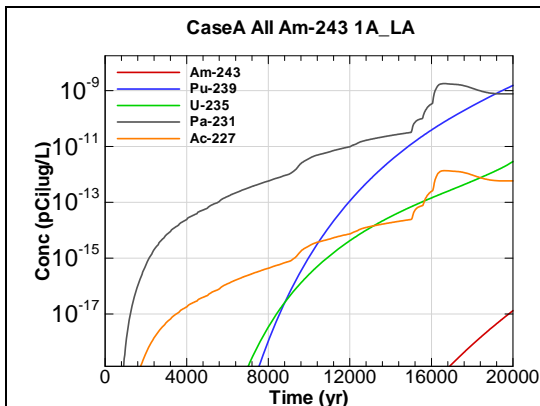


Figure F.2-49 - 1m Aquifer Concentration for
CaseA All Am-243 1A_LA

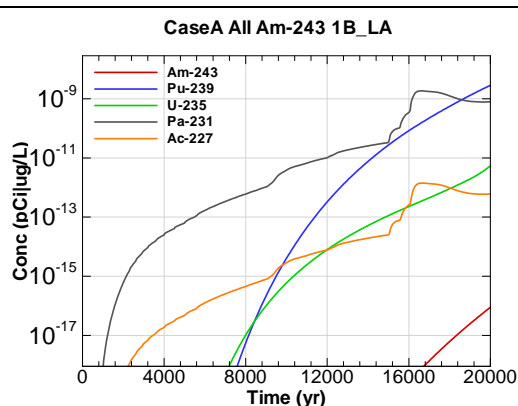


Figure F.2-50 - 1m Aquifer Concentration for
CaseA All Am-243 1B_LA

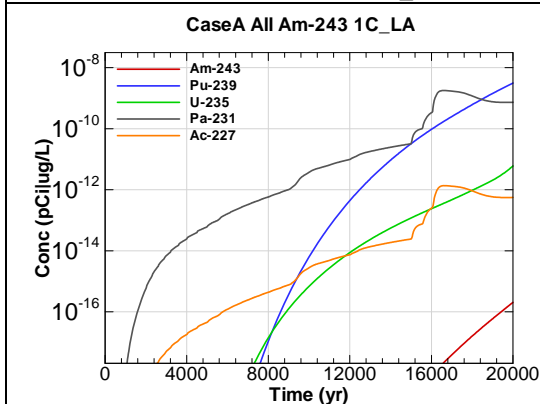


Figure F.2-51 - 1m Aquifer Concentration for
CaseA All Am-243 1C_LA

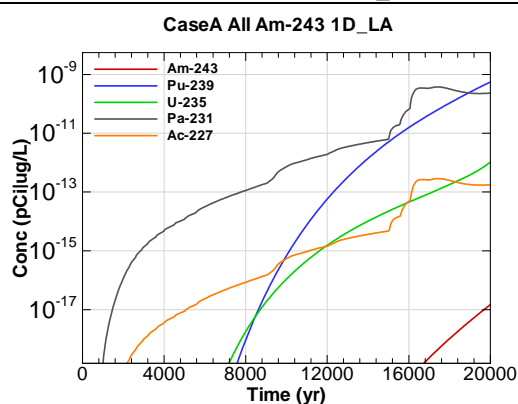


Figure F.2-52 - 1m Aquifer Concentration for
CaseA All Am-243 1D_LA

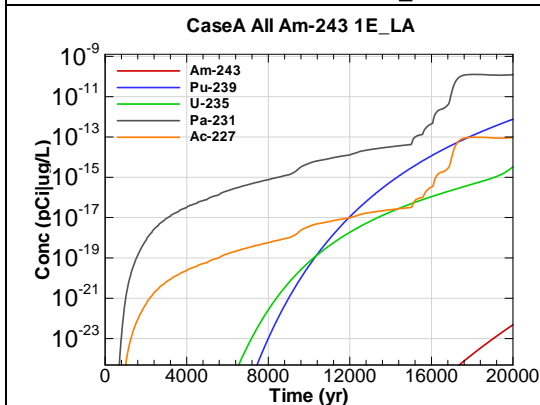


Figure F.2-53 - 1m Aquifer Concentration for
CaseA All Am-243 1E_LA

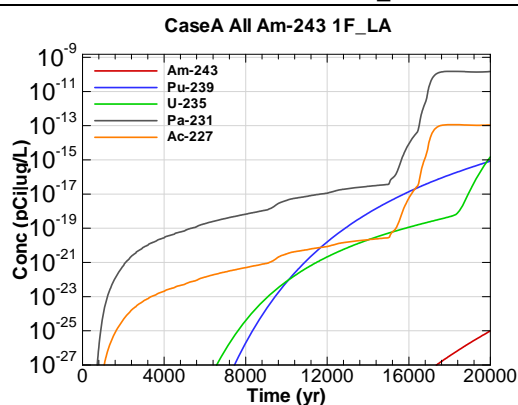


Figure F.2-54 - 1m Aquifer Concentration for
CaseA All Am-243 1F_LA

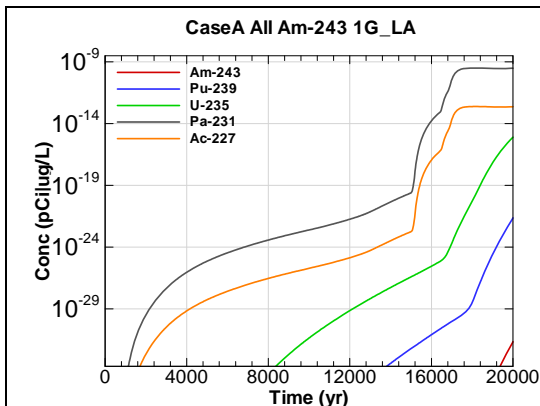


Figure F.2-55 - 1m Aquifer Concentration for
CaseA All Am-243 1G_LA

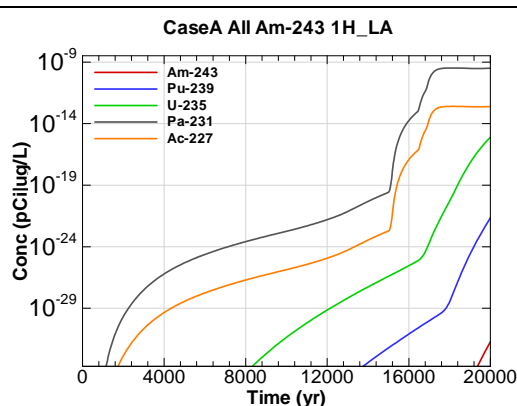


Figure F.2-56 - 1m Aquifer Concentration for
CaseA All Am-243 1H_LA

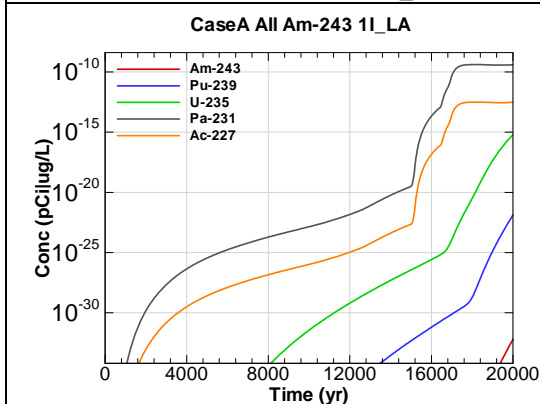


Figure F.2-57 - 1m Aquifer Concentration for
CaseA All Am-243 1I_LA

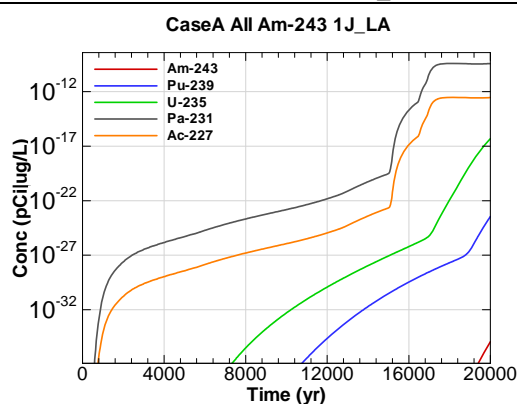


Figure F.2-58 - 1m Aquifer Concentration for
CaseA All Am-243 1J_LA

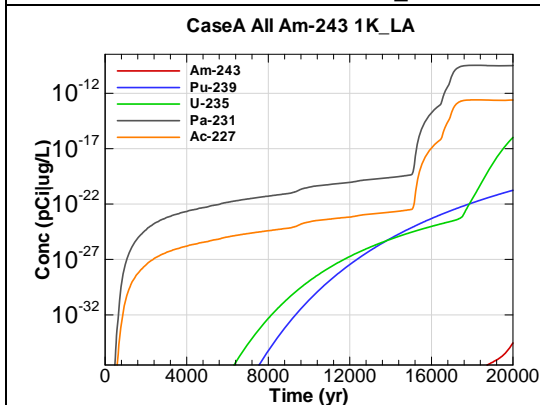


Figure F.2-59 - 1m Aquifer Concentration for
CaseA All Am-243 1K_LA

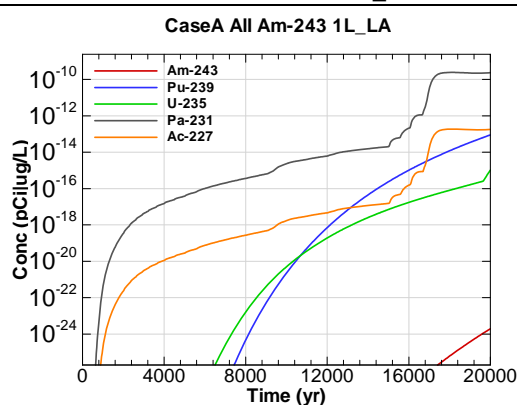
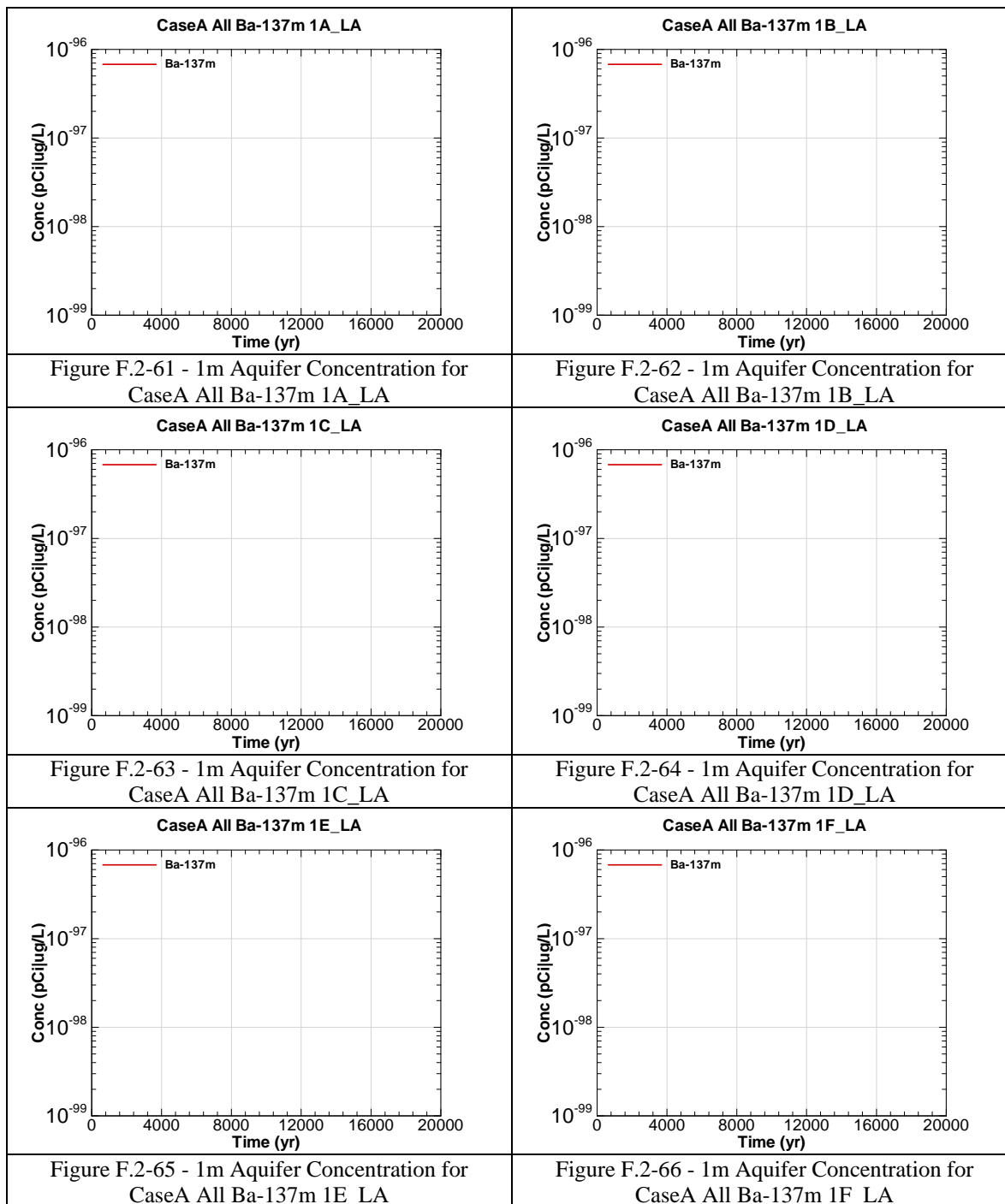
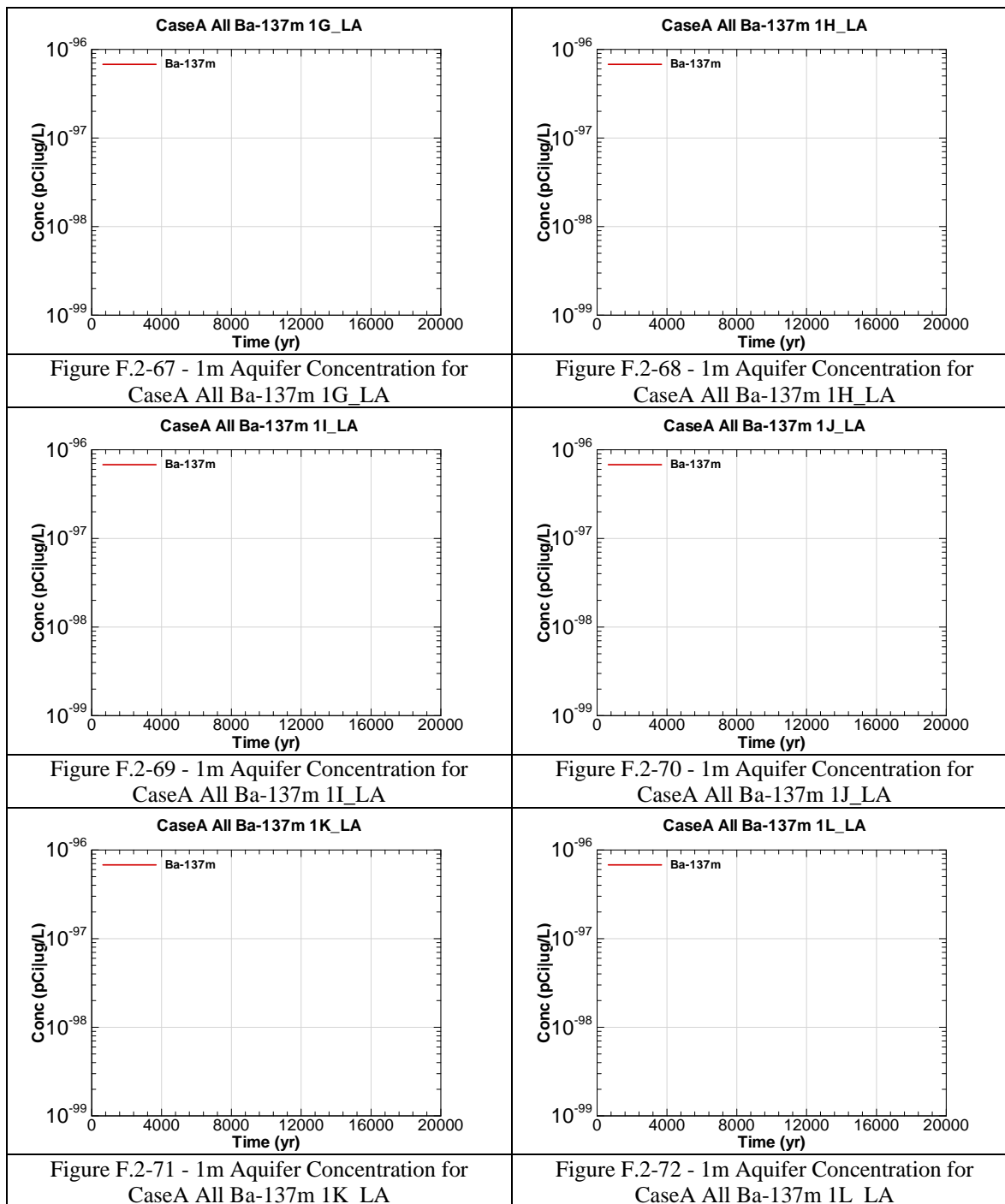


Figure F.2-60 - 1m Aquifer Concentration for
CaseA All Am-243 1L_LA





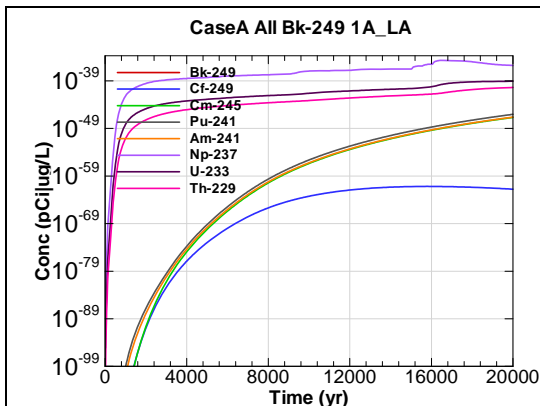


Figure F.2-73 - 1m Aquifer Concentration for
CaseA All Bk-249 1A_LA

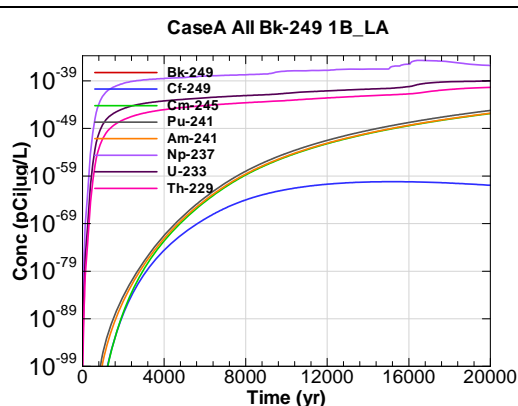


Figure F.2-74 - 1m Aquifer Concentration for
CaseA All Bk-249 1B_LA

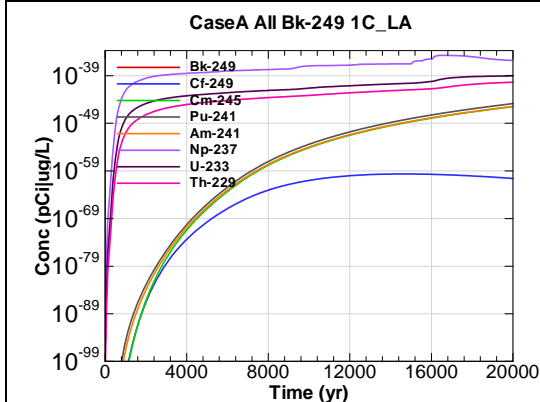


Figure F.2-75 - 1m Aquifer Concentration for
CaseA All Bk-249 1C_LA

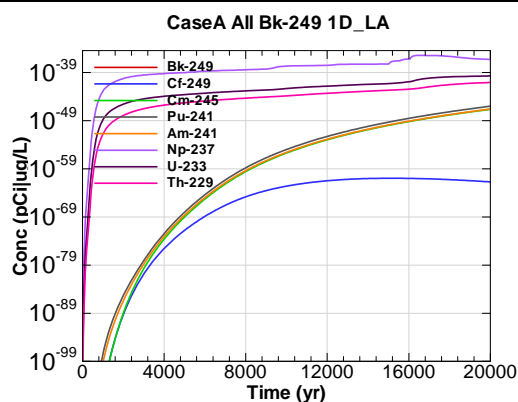


Figure F.2-76 - 1m Aquifer Concentration for
CaseA All Bk-249 1D_LA

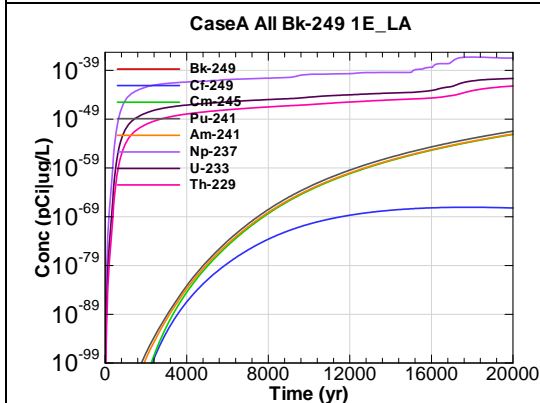


Figure F.2-77 - 1m Aquifer Concentration for
CaseA All Bk-249 1E_LA

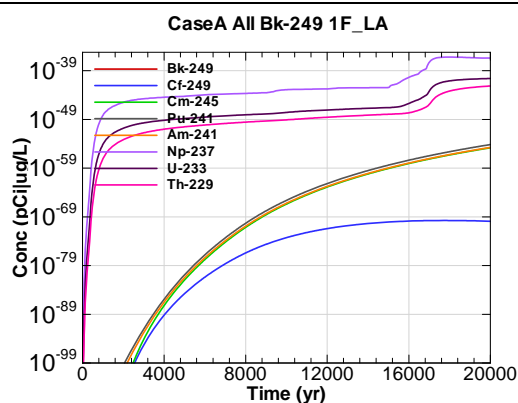


Figure F.2-78 - 1m Aquifer Concentration for
CaseA All Bk-249 1F_LA

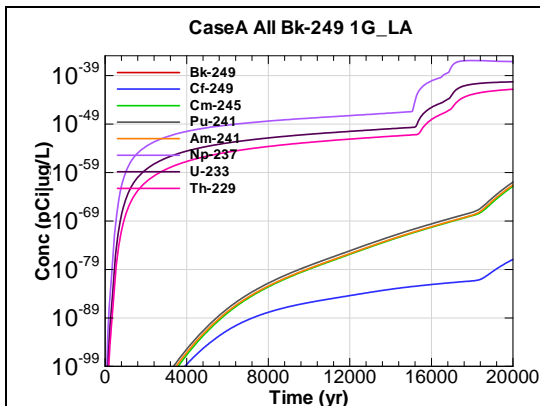


Figure F.2-79 - 1m Aquifer Concentration for
CaseA All Bk-249 1G_LA

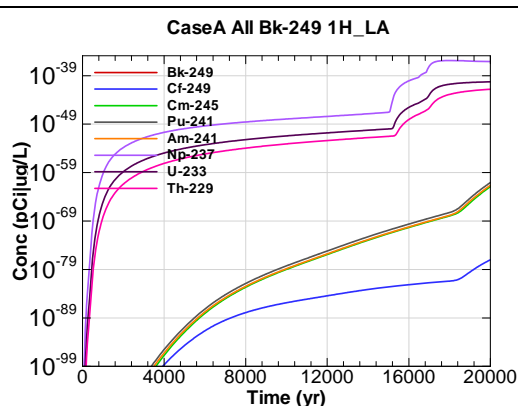


Figure F.2-80 - 1m Aquifer Concentration for
CaseA All Bk-249 1H_LA

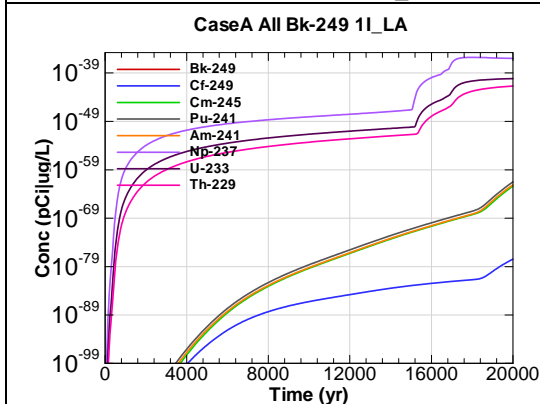


Figure F.2-81 - 1m Aquifer Concentration for
CaseA All Bk-249 1I_LA

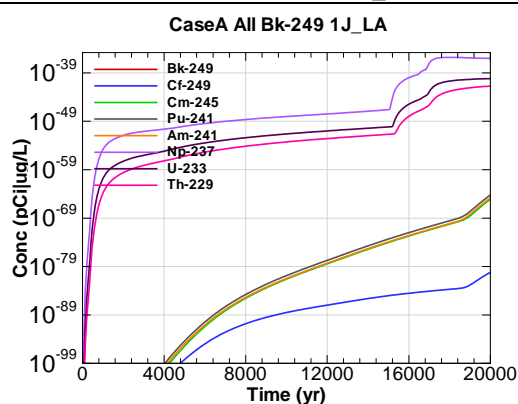


Figure F.2-82 - 1m Aquifer Concentration for
CaseA All Bk-249 1J_LA

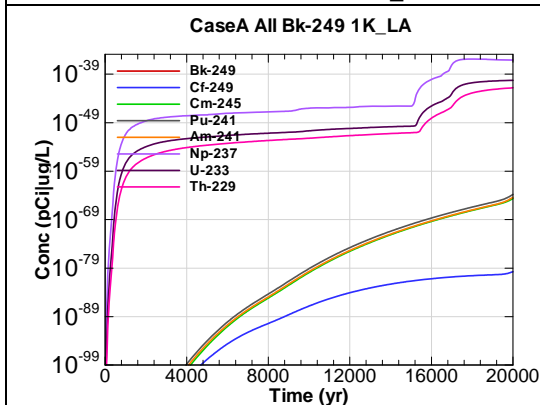


Figure F.2-83 - 1m Aquifer Concentration for
CaseA All Bk-249 1K_LA

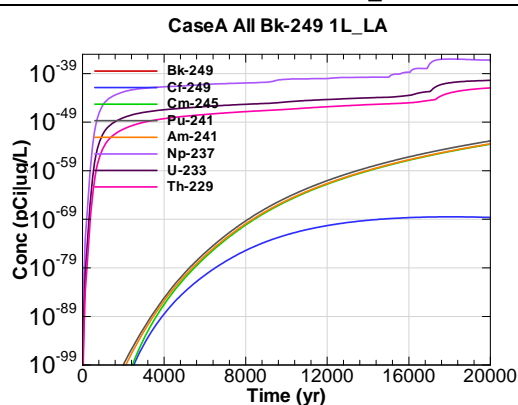
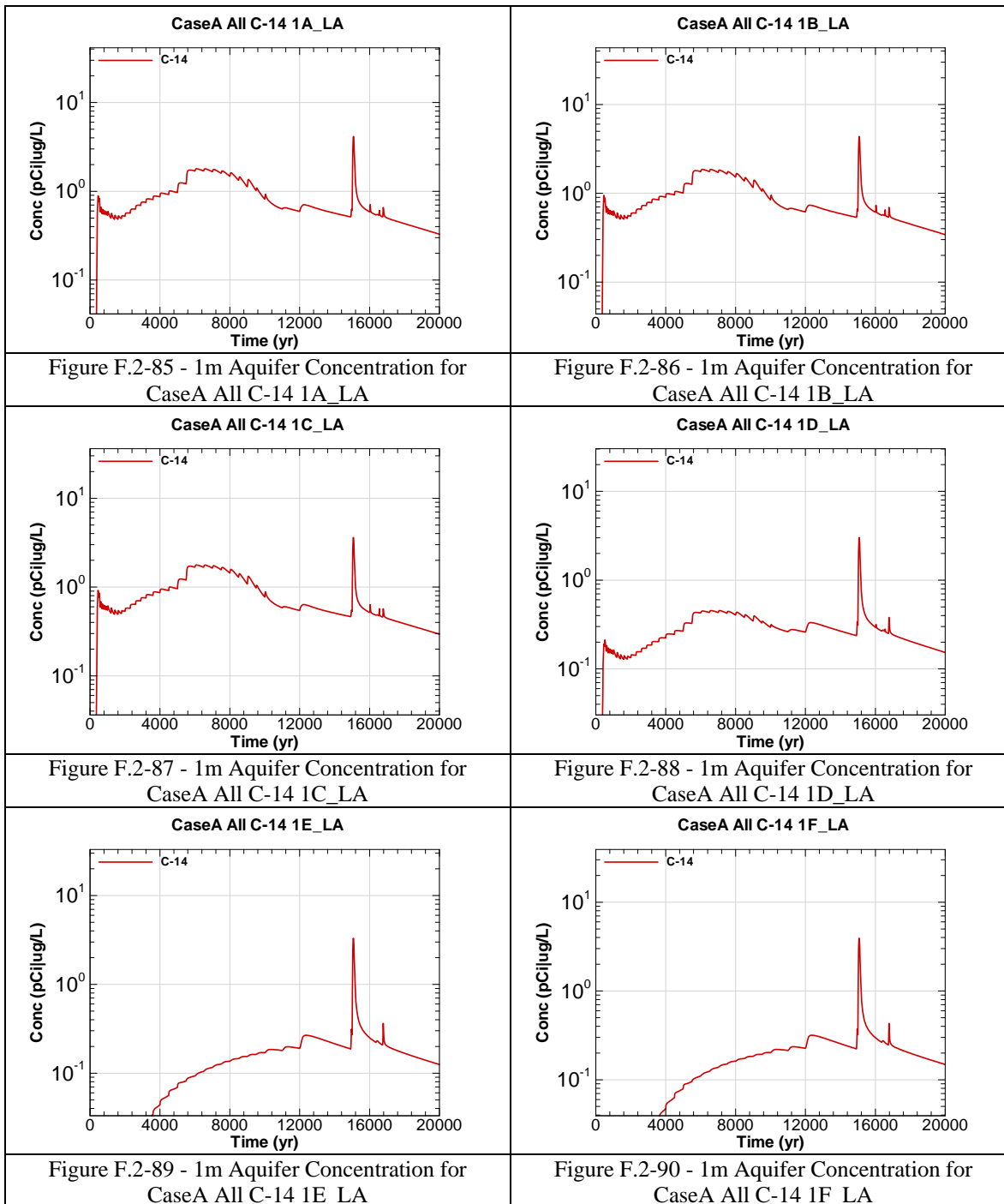
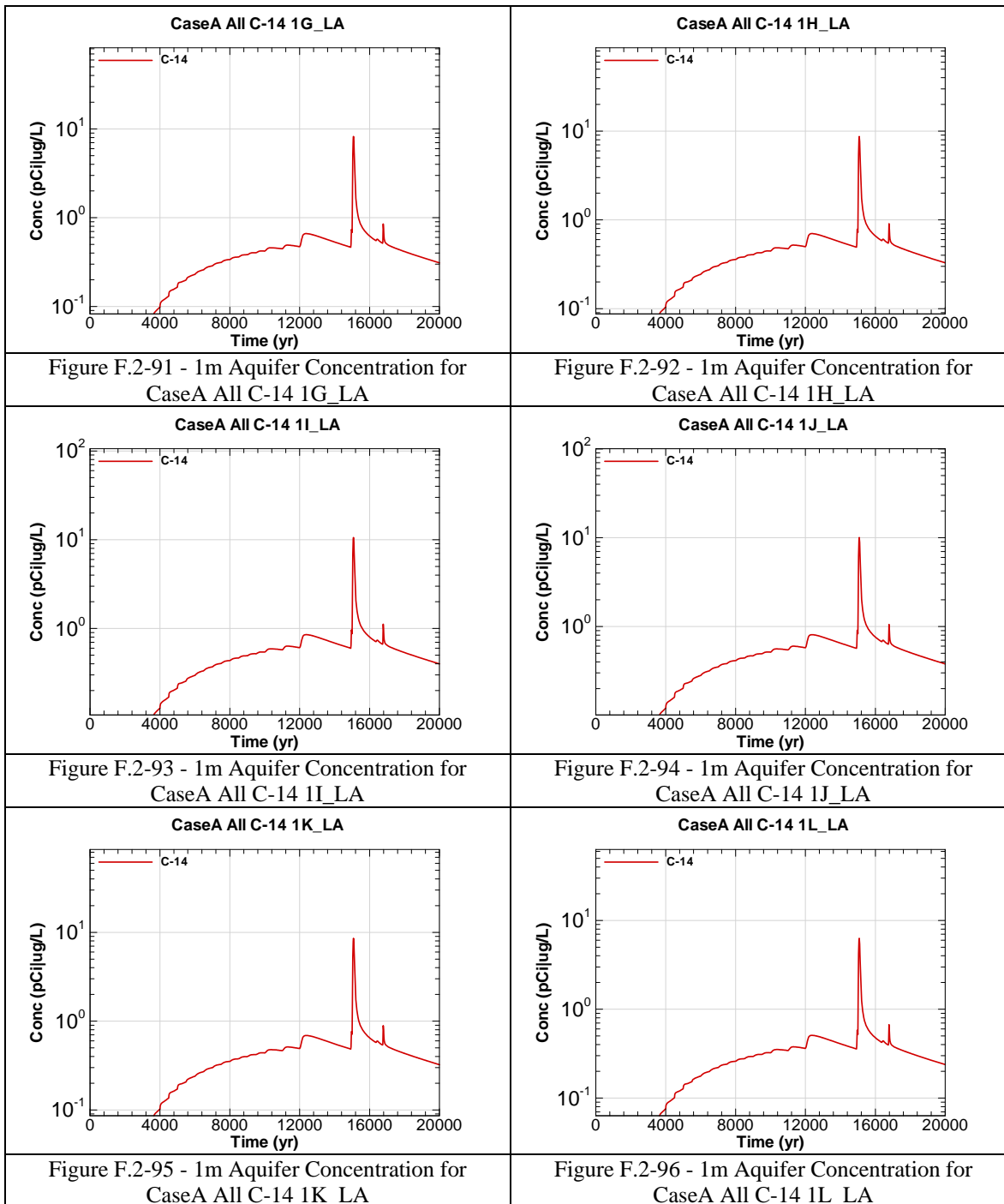
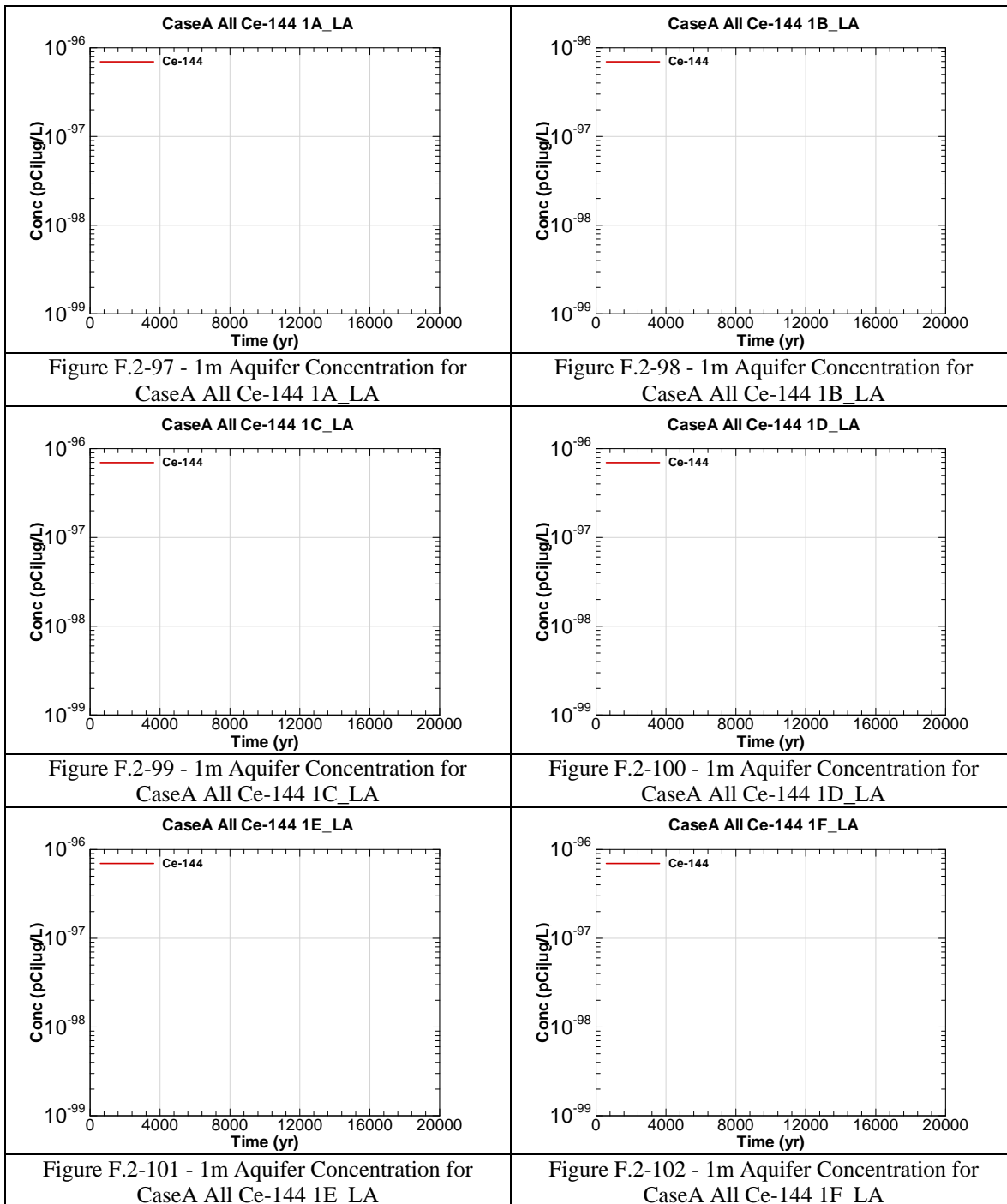
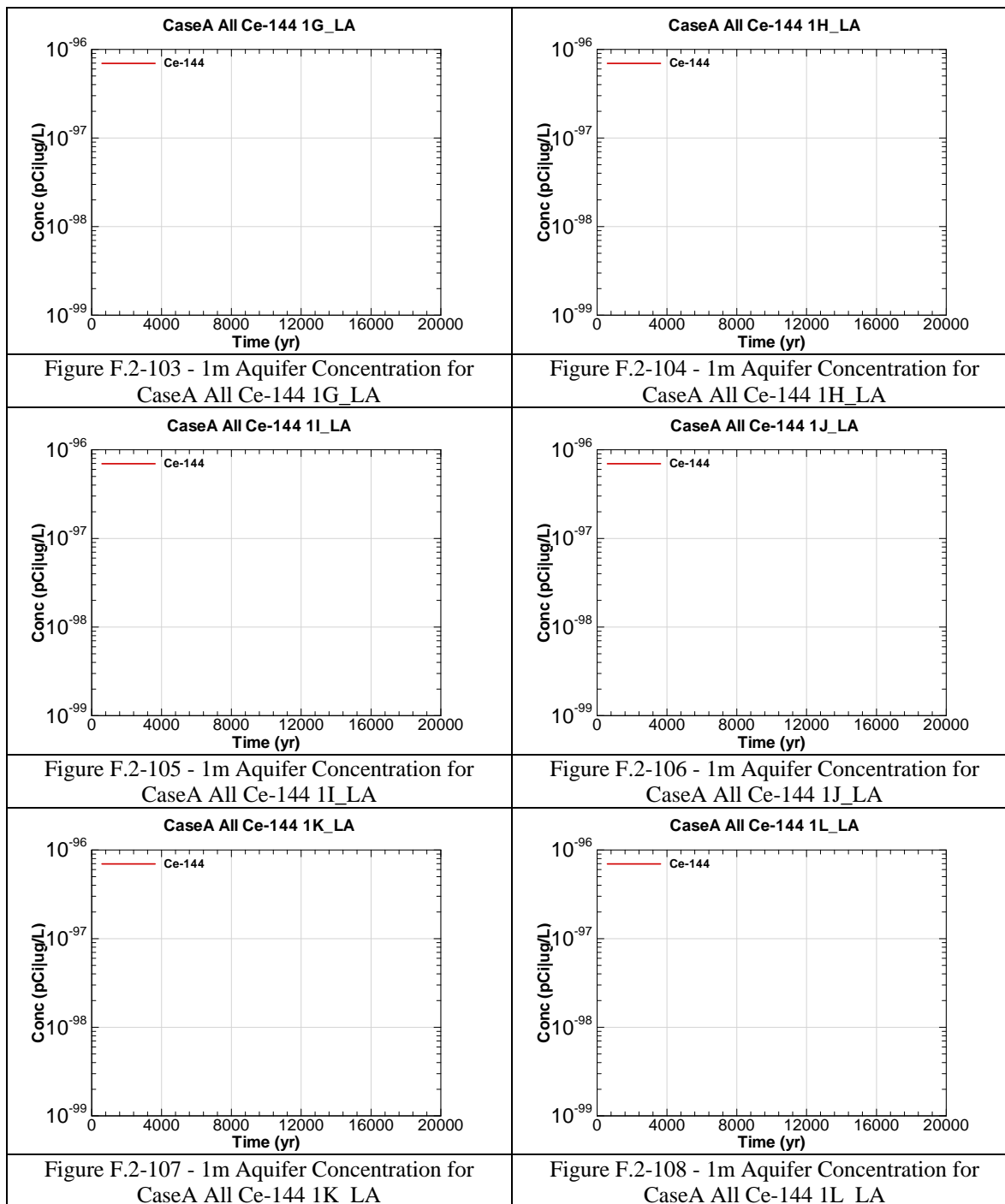


Figure F.2-84 - 1m Aquifer Concentration for
CaseA All Bk-249 1L_LA









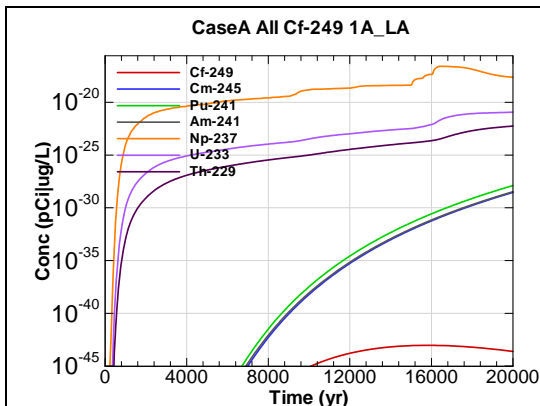


Figure F.2-109 - 1m Aquifer Concentration for
CaseA All Cf-249 1A_LA

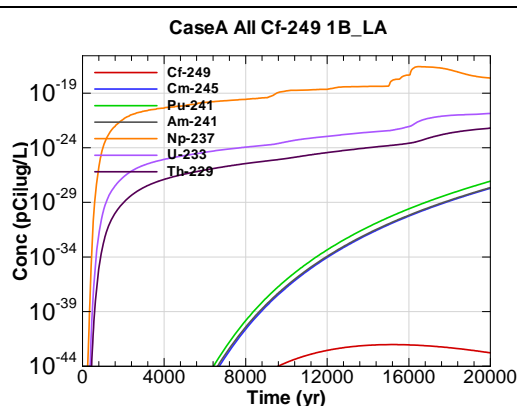


Figure F.2-110 - 1m Aquifer Concentration for
CaseA All Cf-249 1B_LA

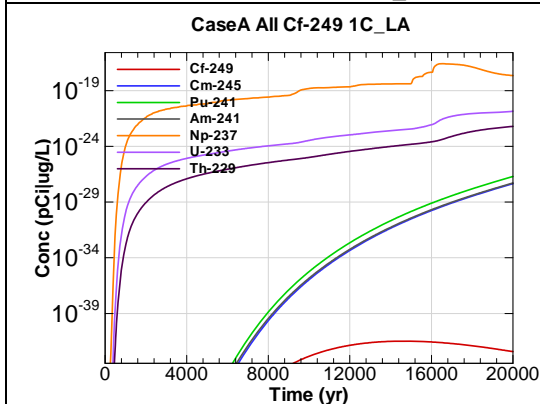


Figure F.2-111 - 1m Aquifer Concentration for
CaseA All Cf-249 1C_LA

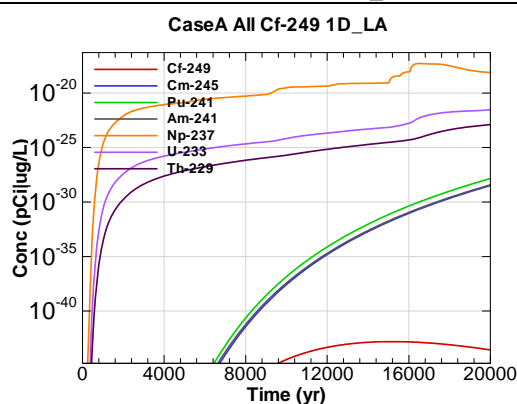


Figure F.2-112 - 1m Aquifer Concentration for
CaseA All Cf-249 1D_LA

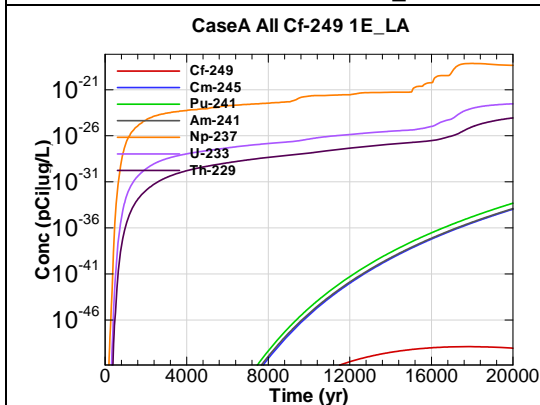


Figure F.2-113 - 1m Aquifer Concentration for
CaseA All Cf-249 1E_LA

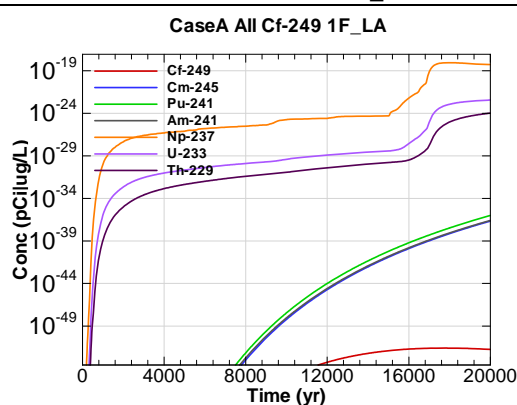


Figure F.2-114 - 1m Aquifer Concentration for
CaseA All Cf-249 1F_LA

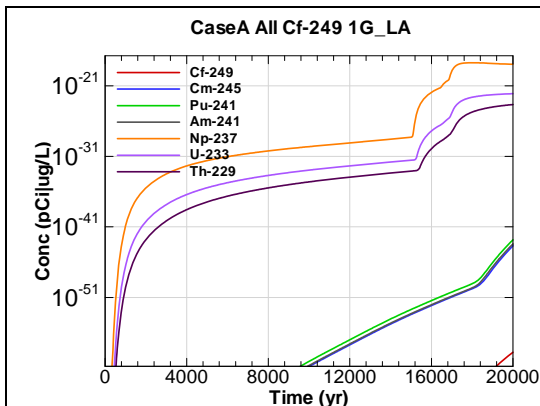


Figure F.2-115 - 1m Aquifer Concentration for
CaseA All Cf-249 1G_LA

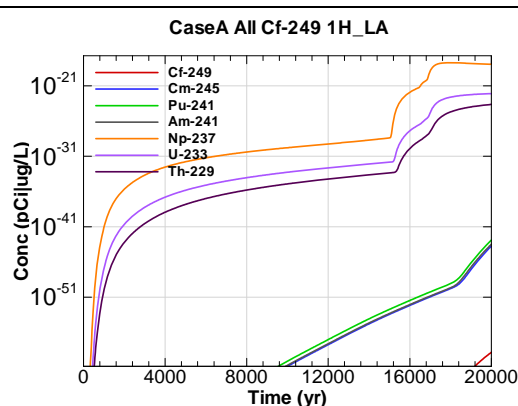


Figure F.2-116 - 1m Aquifer Concentration for
CaseA All Cf-249 1H_LA

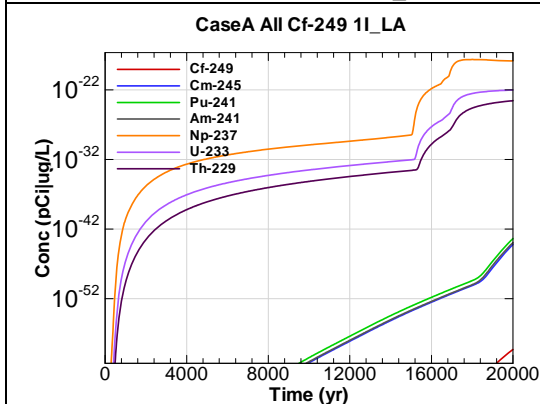


Figure F.2-117 - 1m Aquifer Concentration for
CaseA All Cf-249 1I_LA

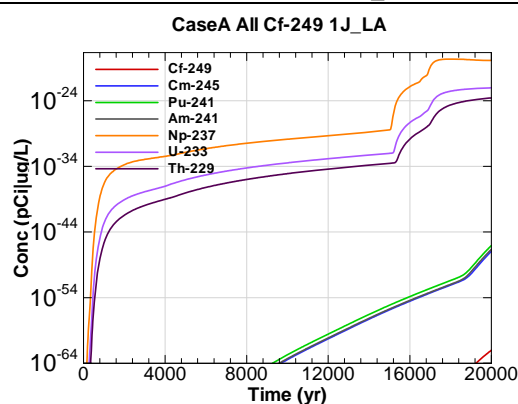


Figure F.2-118 - 1m Aquifer Concentration for
CaseA All Cf-249 1J_LA

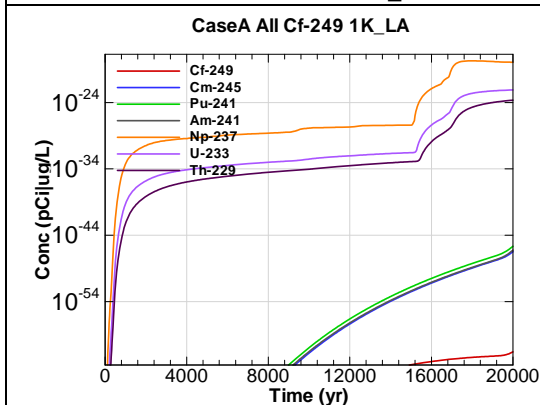


Figure F.2-119 - 1m Aquifer Concentration for
CaseA All Cf-249 1K_LA

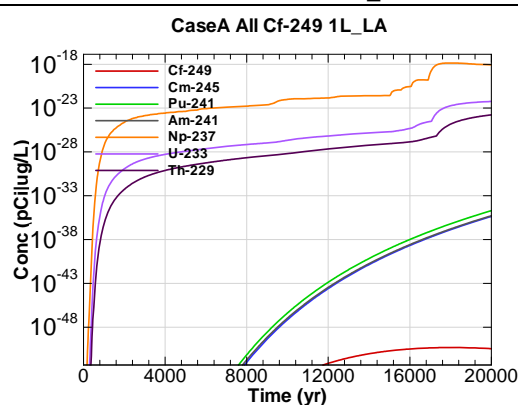


Figure F.2-120 - 1m Aquifer Concentration for
CaseA All Cf-249 1L_LA

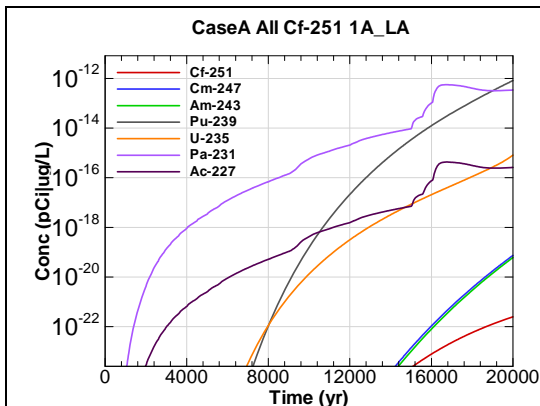


Figure F.2-121 - 1m Aquifer Concentration for
CaseA All Cf-251 1A_LA

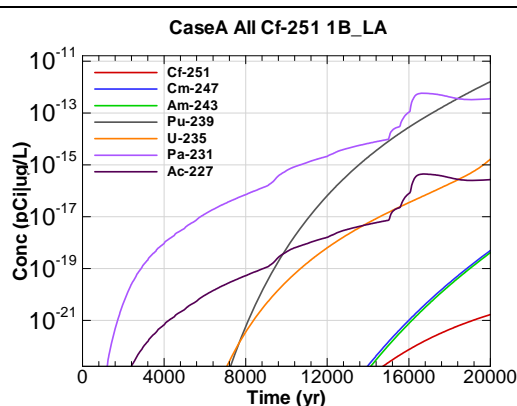


Figure F.2-122 - 1m Aquifer Concentration for
CaseA All Cf-251 1B_LA

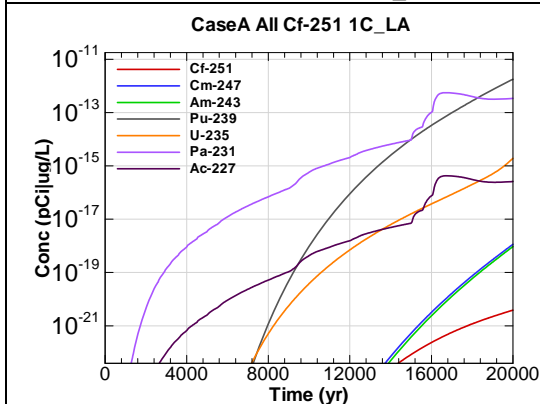


Figure F.2-123 - 1m Aquifer Concentration for
CaseA All Cf-251 1C_LA

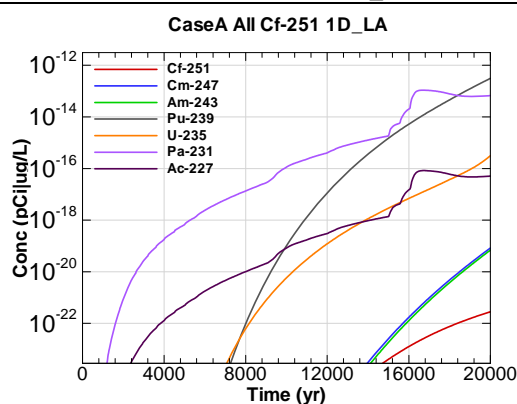


Figure F.2-124 - 1m Aquifer Concentration for
CaseA All Cf-251 1D_LA

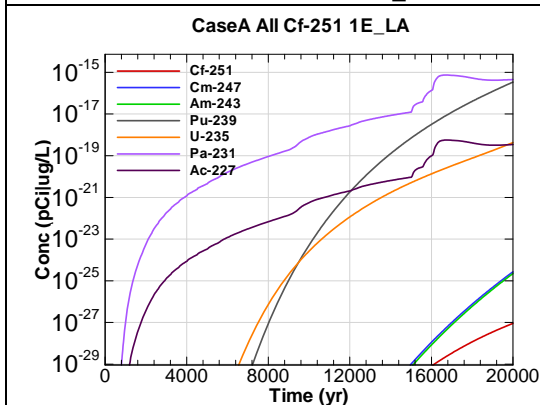


Figure F.2-125 - 1m Aquifer Concentration for
CaseA All Cf-251 1E_LA

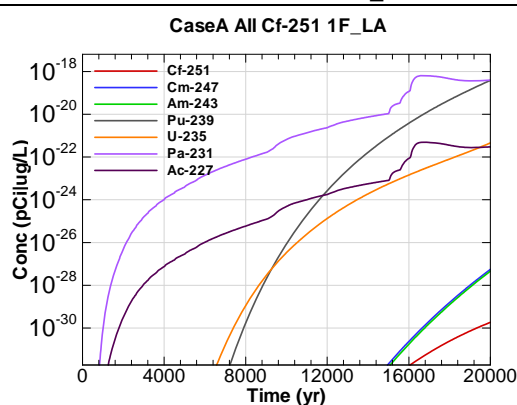


Figure F.2-126 - 1m Aquifer Concentration for
CaseA All Cf-251 1F_LA

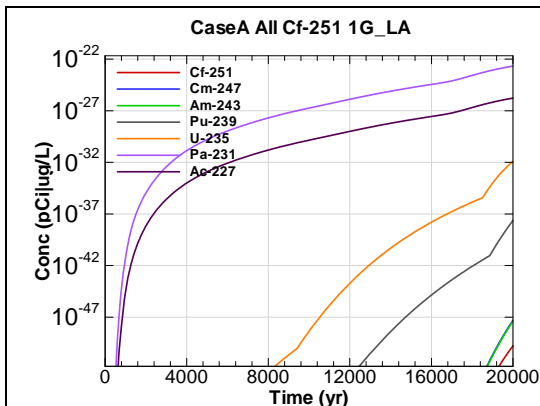


Figure F.2-127 - 1m Aquifer Concentration for
CaseA All Cf-251 1G_LA

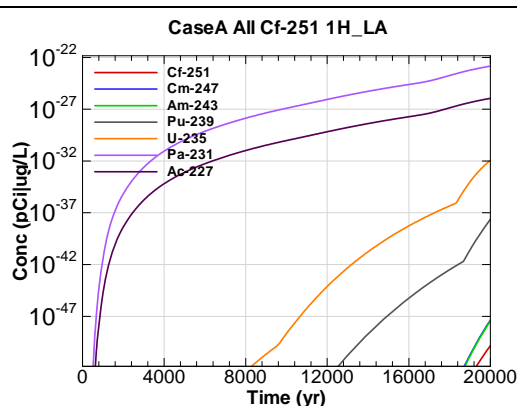


Figure F.2-128 - 1m Aquifer Concentration for
CaseA All Cf-251 1H_LA

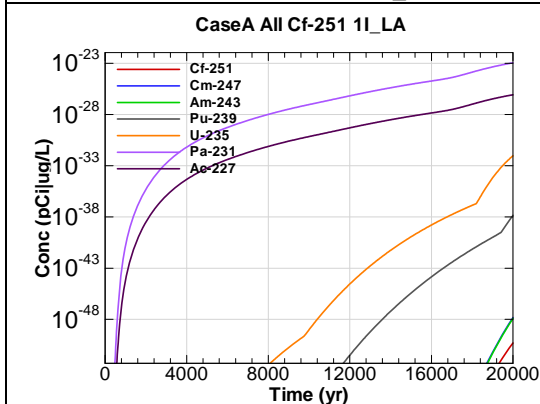


Figure F.2-129 - 1m Aquifer Concentration for
CaseA All Cf-251 1I_LA

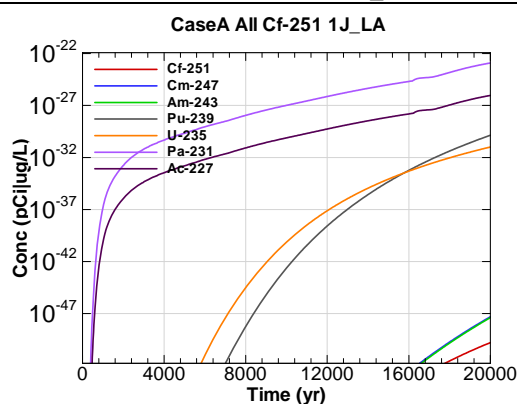


Figure F.2-130 - 1m Aquifer Concentration for
CaseA All Cf-251 1J_LA

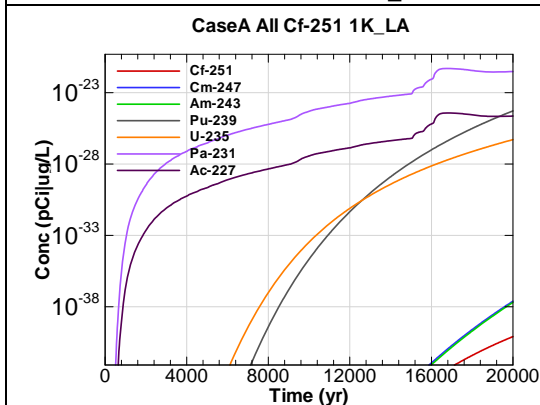


Figure F.2-131 - 1m Aquifer Concentration for
CaseA All Cf-251 1K_LA

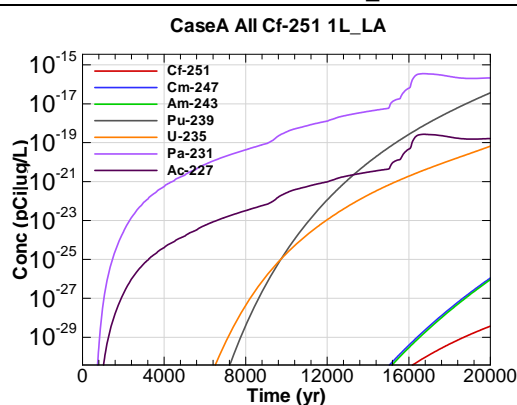


Figure F.2-132 - 1m Aquifer Concentration for
CaseA All Cf-251 1L_LA

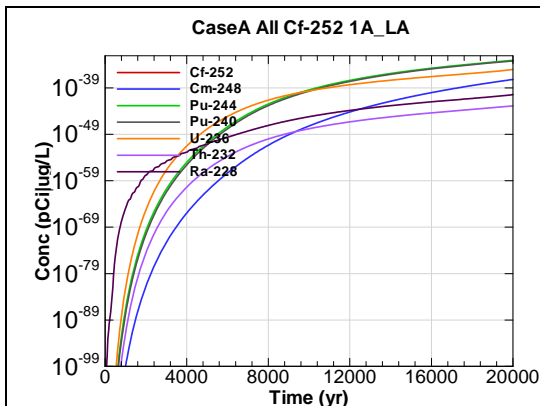


Figure F.2-133 - 1m Aquifer Concentration for
CaseA All Cf-252 1A_LA

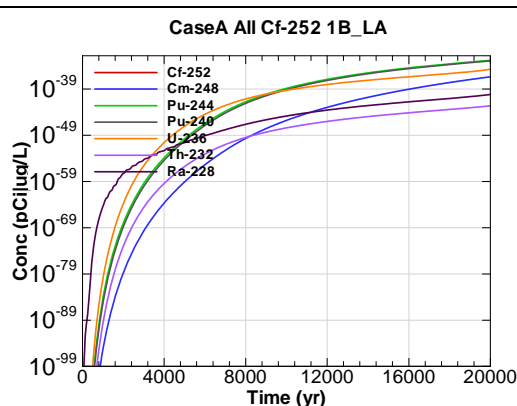


Figure F.2-134 - 1m Aquifer Concentration for
CaseA All Cf-252 1B_LA

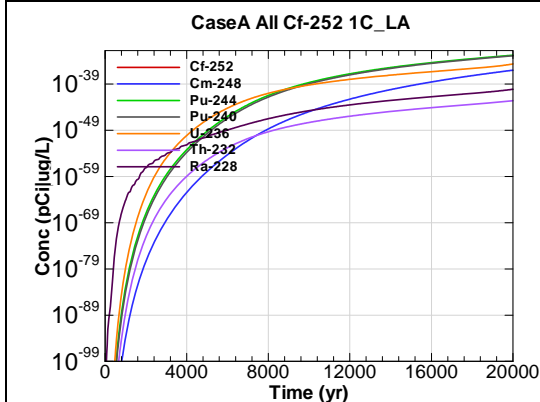


Figure F.2-135 - 1m Aquifer Concentration for
CaseA All Cf-252 1C_LA

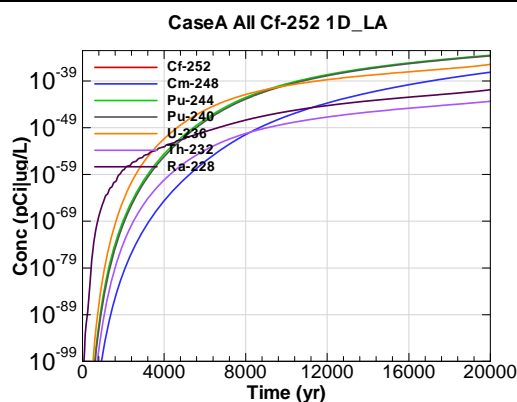


Figure F.2-136 - 1m Aquifer Concentration for
CaseA All Cf-252 1D_LA

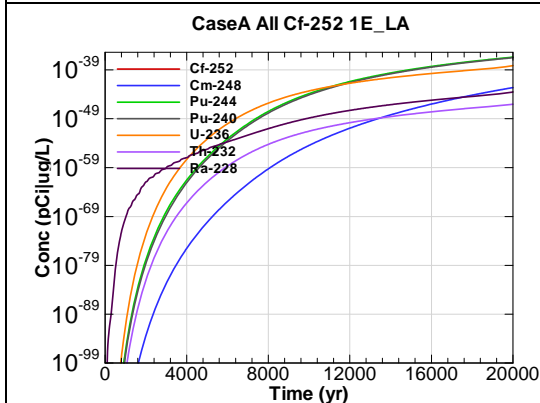


Figure F.2-137 - 1m Aquifer Concentration for
CaseA All Cf-252 1E_LA

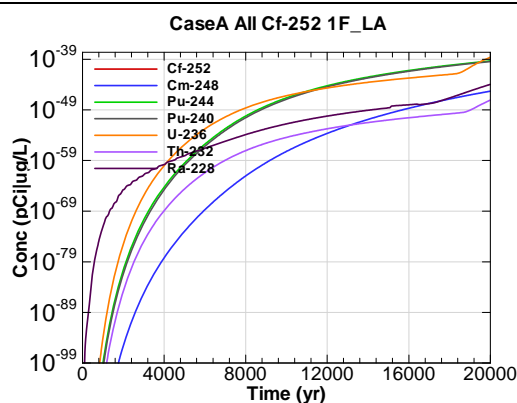


Figure F.2-138 - 1m Aquifer Concentration for
CaseA All Cf-252 1F_LA

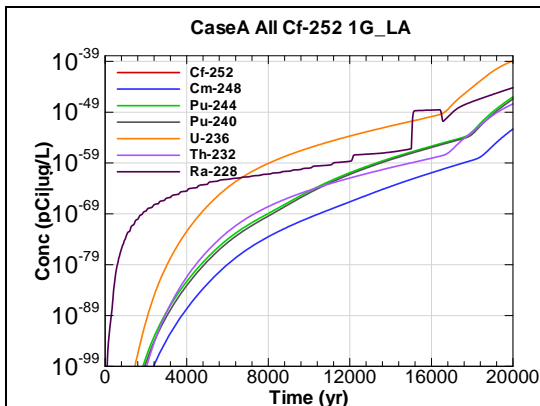


Figure F.2-139 - 1m Aquifer Concentration for
CaseA All Cf-252 1G_LA

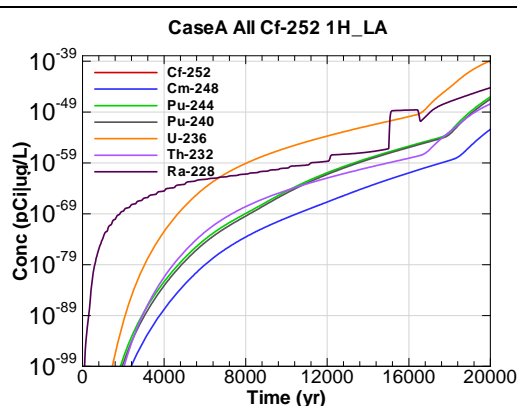


Figure F.2-140 - 1m Aquifer Concentration for
CaseA All Cf-252 1H_LA

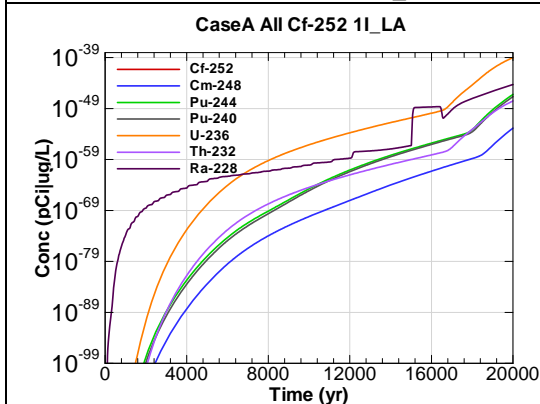


Figure F.2-141 - 1m Aquifer Concentration for
CaseA All Cf-252 1I_LA

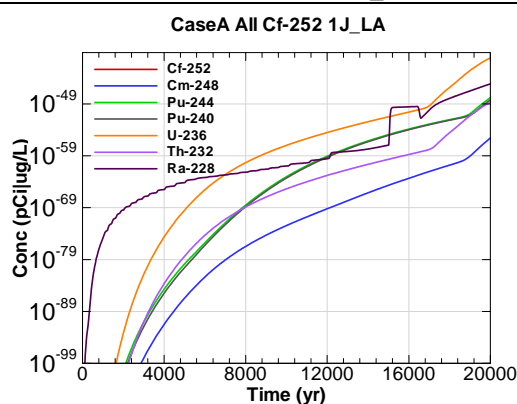


Figure F.2-142 - 1m Aquifer Concentration for
CaseA All Cf-252 1J_LA

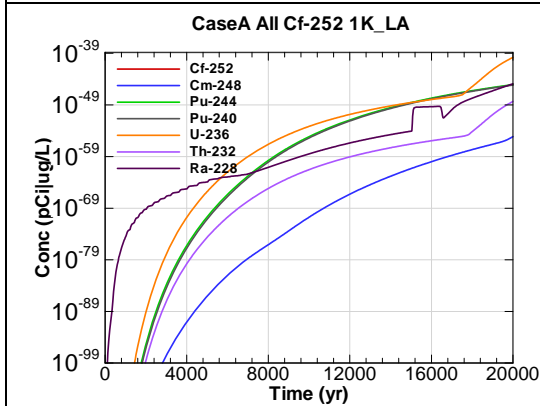


Figure F.2-143 - 1m Aquifer Concentration for
CaseA All Cf-252 1K_LA

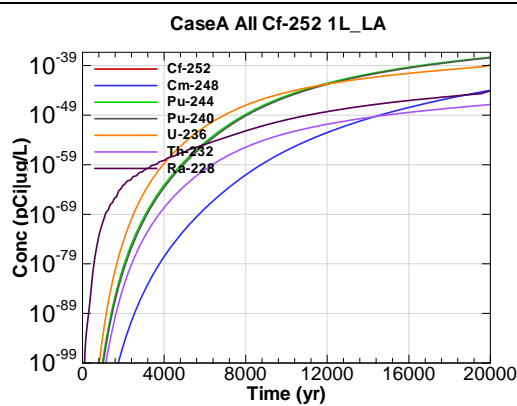
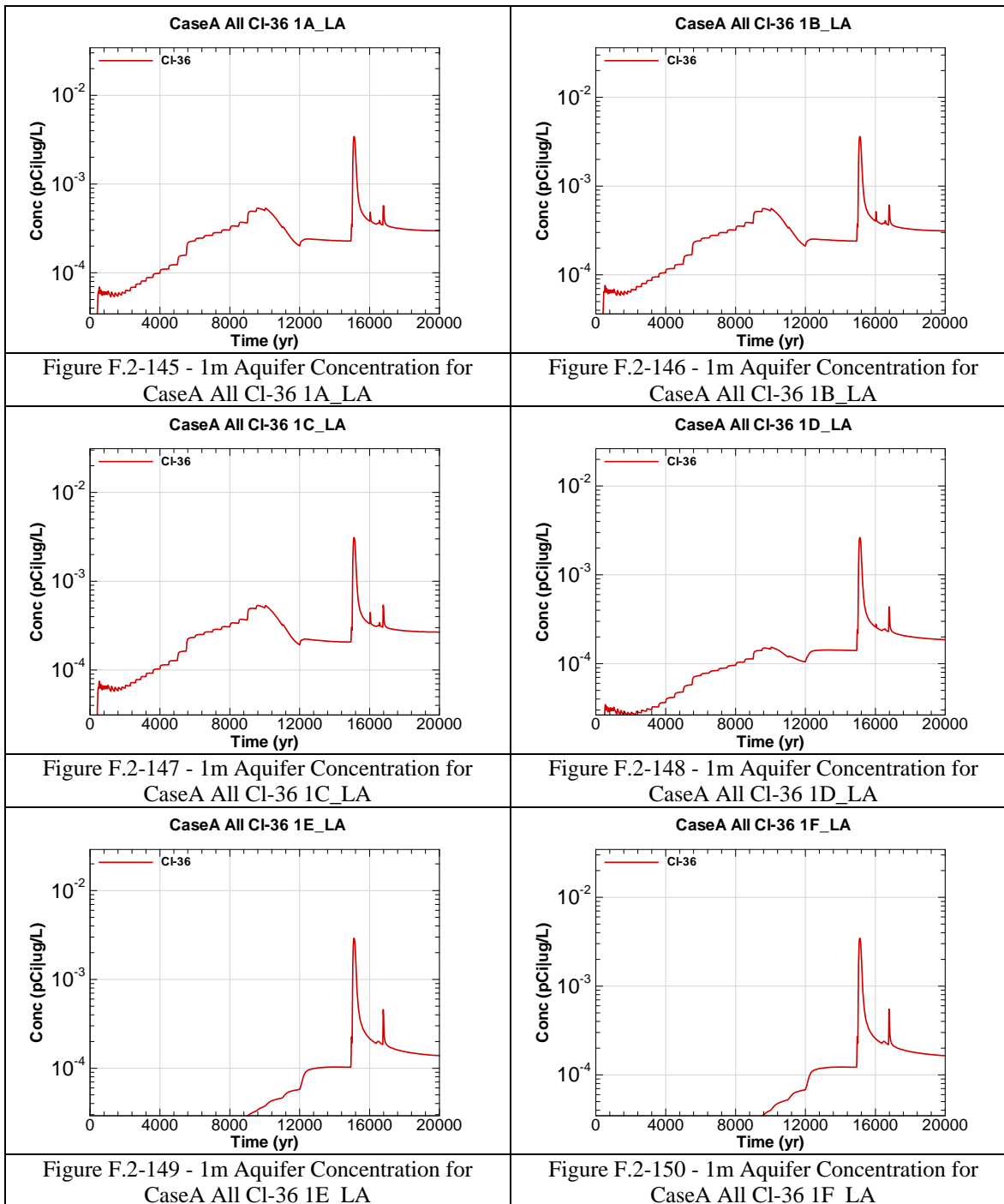
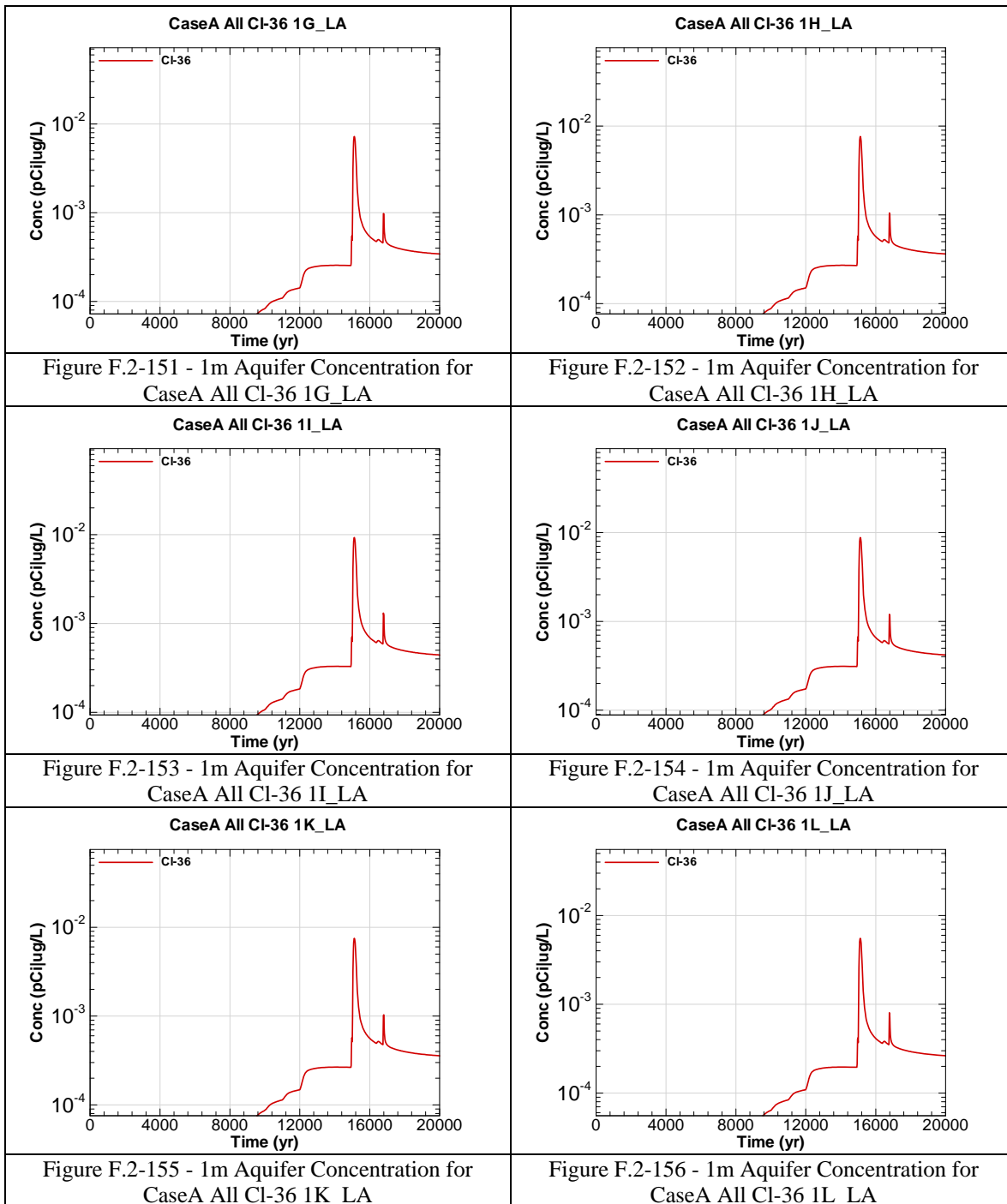


Figure F.2-144 - 1m Aquifer Concentration for
CaseA All Cf-252 1L_LA





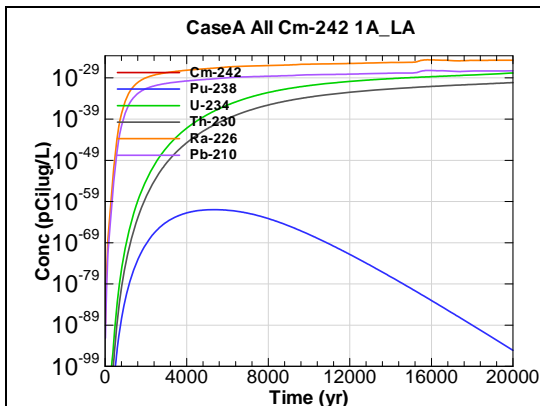


Figure F.2-157 - 1m Aquifer Concentration for
CaseA All Cm-242 1A_LA

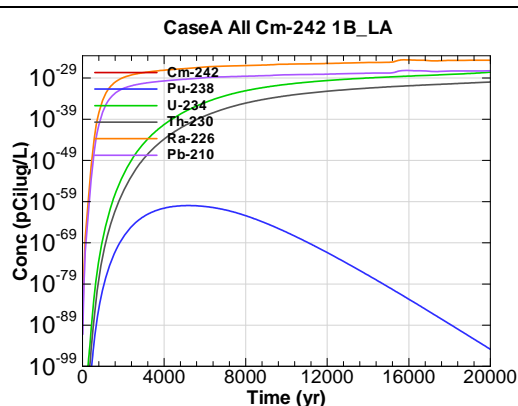


Figure F.2-158 - 1m Aquifer Concentration for
CaseA All Cm-242 1B_LA

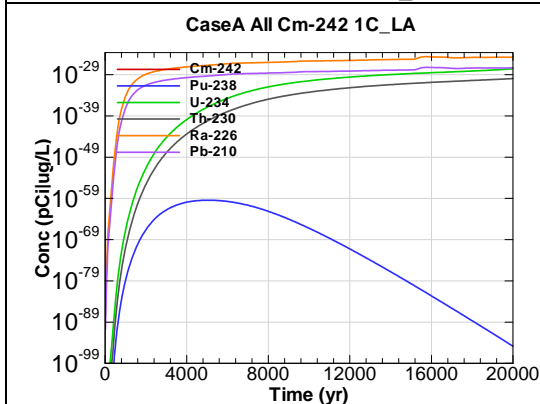


Figure F.2-159 - 1m Aquifer Concentration for
CaseA All Cm-242 1C_LA

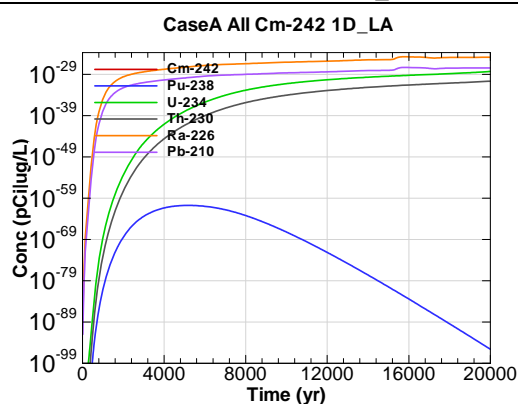


Figure F.2-160 - 1m Aquifer Concentration for
CaseA All Cm-242 1D_LA

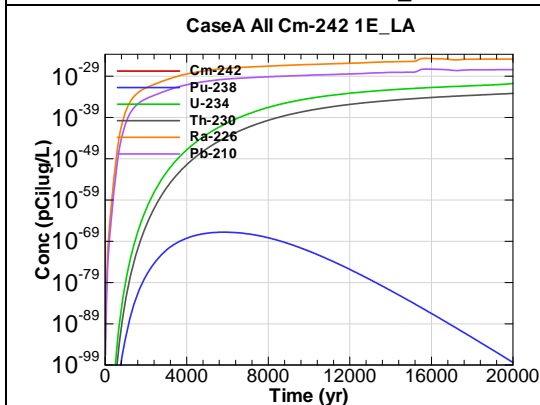


Figure F.2-161 - 1m Aquifer Concentration for
CaseA All Cm-242 1E_LA

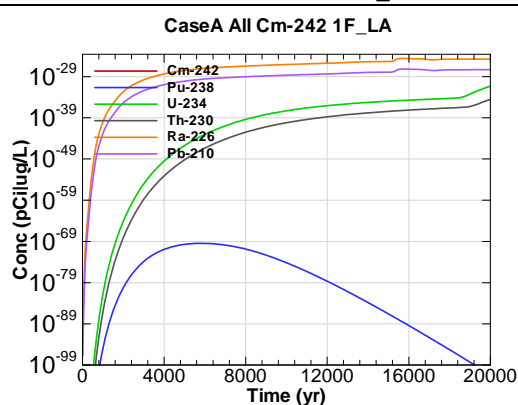


Figure F.2-162 - 1m Aquifer Concentration for
CaseA All Cm-242 1F_LA

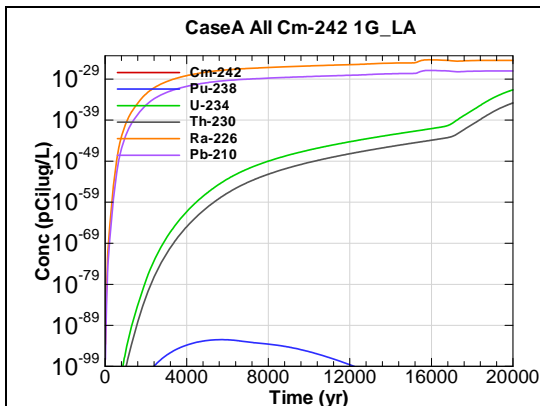


Figure F.2-163 - 1m Aquifer Concentration for
CaseA All Cm-242 1G_LA

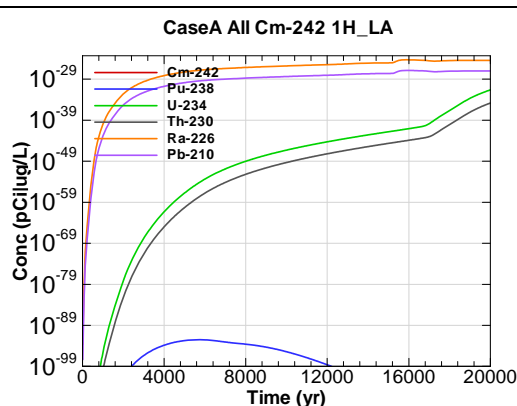


Figure F.2-164 - 1m Aquifer Concentration for
CaseA All Cm-242 1H_LA

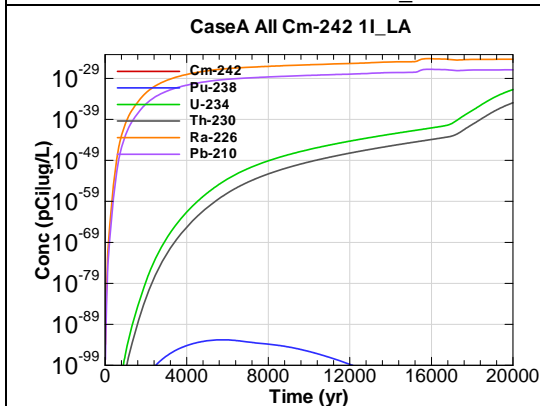


Figure F.2-165 - 1m Aquifer Concentration for
CaseA All Cm-242 1I_LA

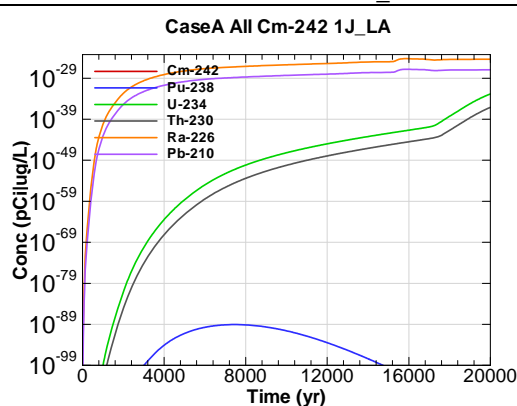


Figure F.2-166 - 1m Aquifer Concentration for
CaseA All Cm-242 1J_LA

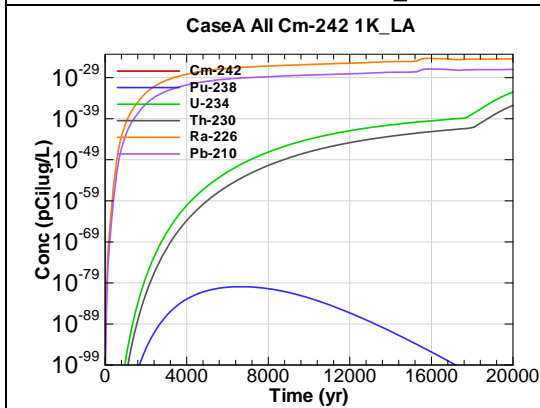


Figure F.2-167 - 1m Aquifer Concentration for
CaseA All Cm-242 1K_LA

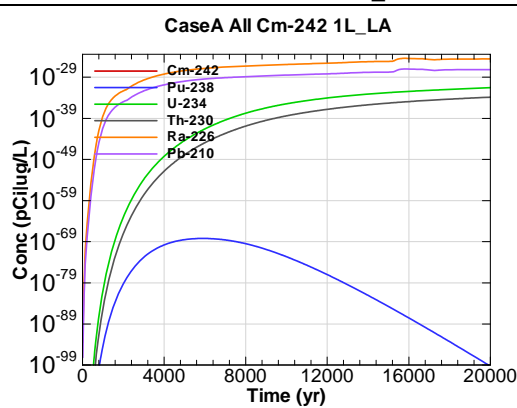


Figure F.2-168 - 1m Aquifer Concentration for
CaseA All Cm-242 1L_LA

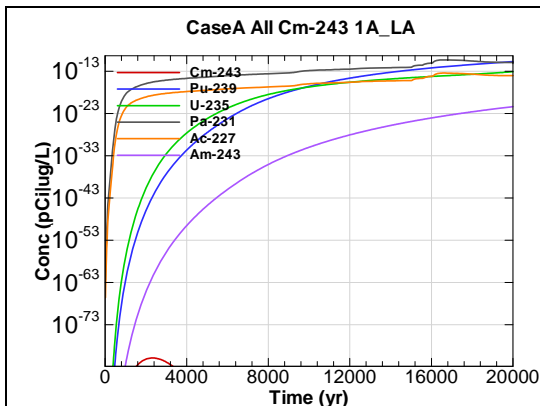


Figure F.2-169 - 1m Aquifer Concentration for
CaseA All Cm-243 1A_LA

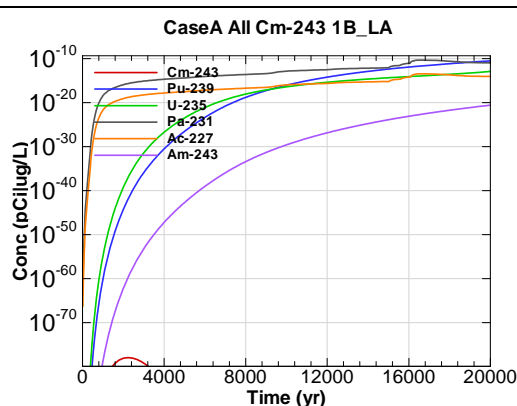


Figure F.2-170 - 1m Aquifer Concentration for
CaseA All Cm-243 1B_LA

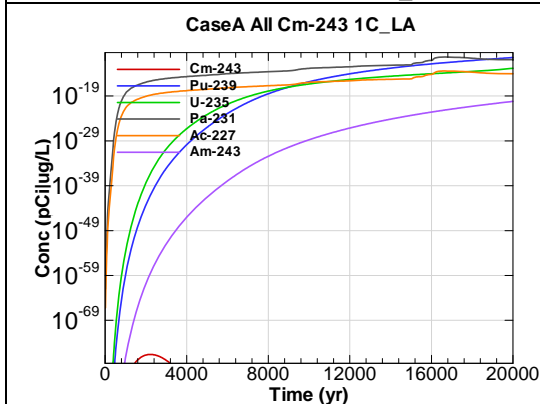


Figure F.2-171 - 1m Aquifer Concentration for
CaseA All Cm-243 1C_LA

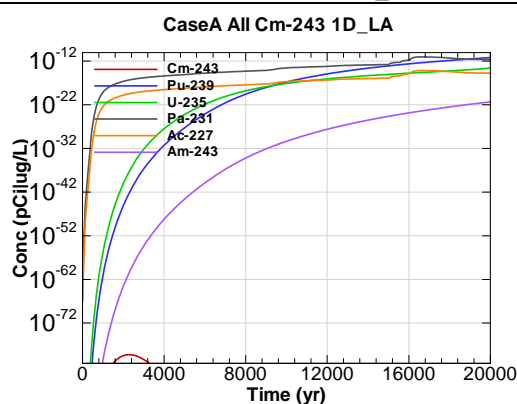


Figure F.2-172 - 1m Aquifer Concentration for
CaseA All Cm-243 1D_LA

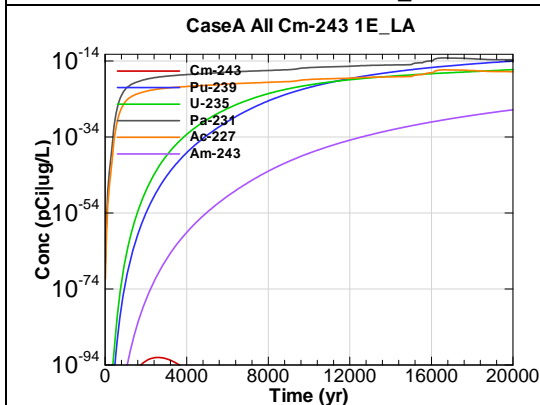


Figure F.2-173 - 1m Aquifer Concentration for
CaseA All Cm-243 1E_LA

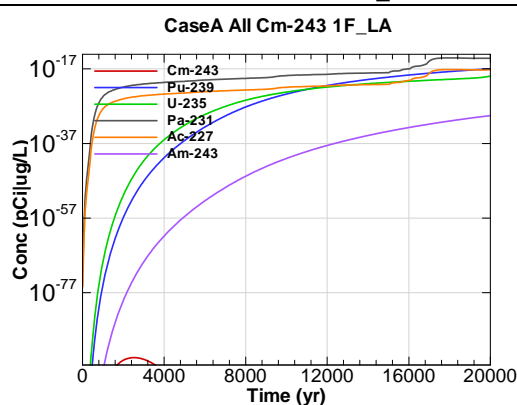


Figure F.2-174 - 1m Aquifer Concentration for
CaseA All Cm-243 1F_LA

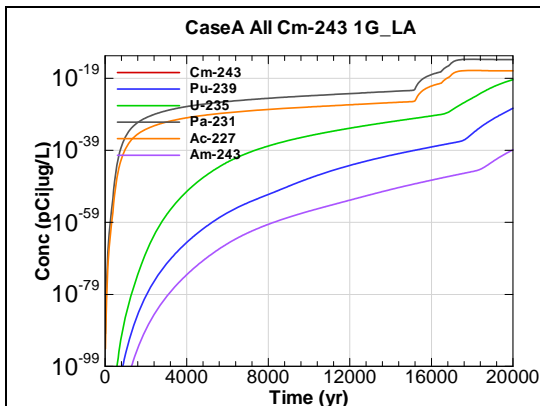


Figure F.2-175 - 1m Aquifer Concentration for
CaseA All Cm-243 1G_LA

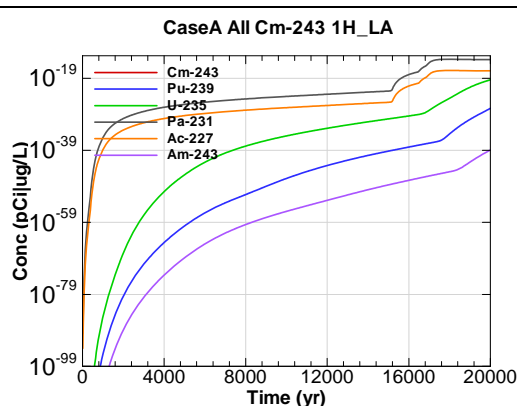


Figure F.2-176 - 1m Aquifer Concentration for
CaseA All Cm-243 1H_LA

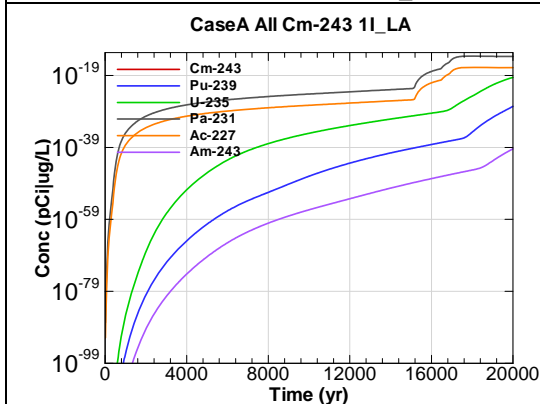


Figure F.2-177 - 1m Aquifer Concentration for
CaseA All Cm-243 1I_LA

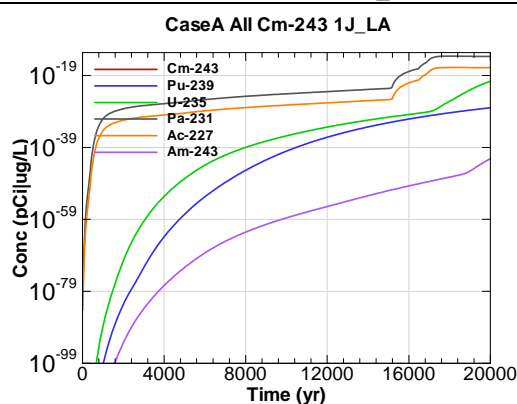


Figure F.2-178 - 1m Aquifer Concentration for
CaseA All Cm-243 1J_LA

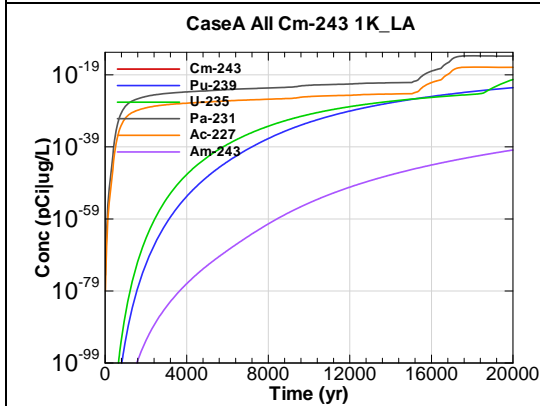


Figure F.2-179 - 1m Aquifer Concentration for
CaseA All Cm-243 1K_LA

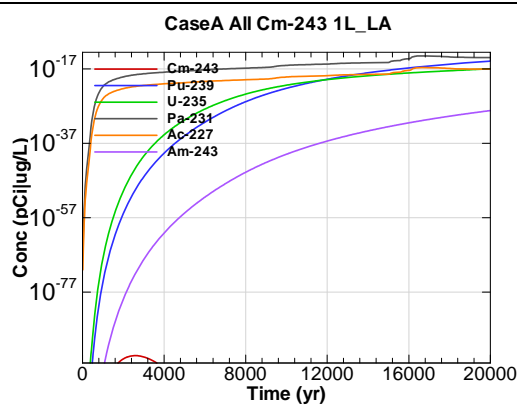


Figure F.2-180 - 1m Aquifer Concentration for
CaseA All Cm-243 1L_LA

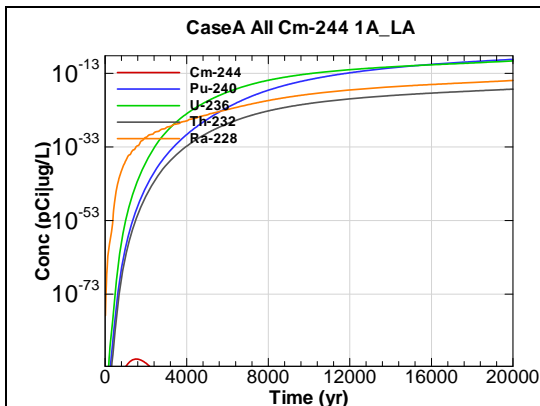


Figure F.2-181 - 1m Aquifer Concentration for
CaseA All Cm-244 1A_LA

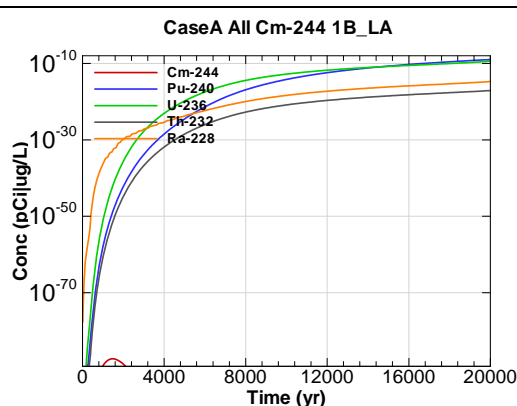


Figure F.2-182 - 1m Aquifer Concentration for
CaseA All Cm-244 1B_LA

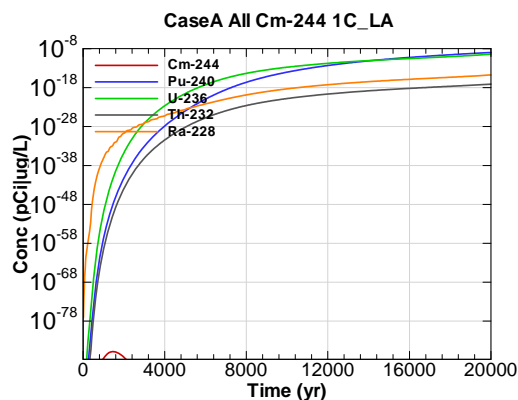


Figure F.2-183 - 1m Aquifer Concentration for
CaseA All Cm-244 1C_LA

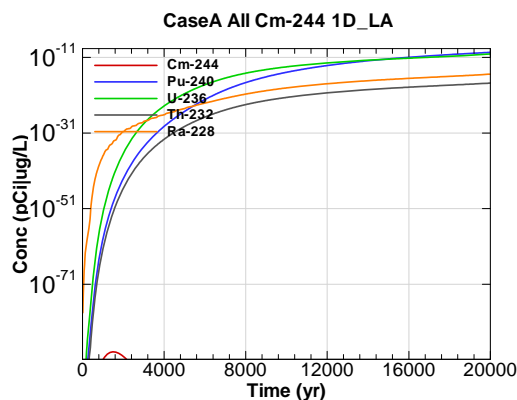


Figure F.2-184 - 1m Aquifer Concentration for
CaseA All Cm-244 1D_LA

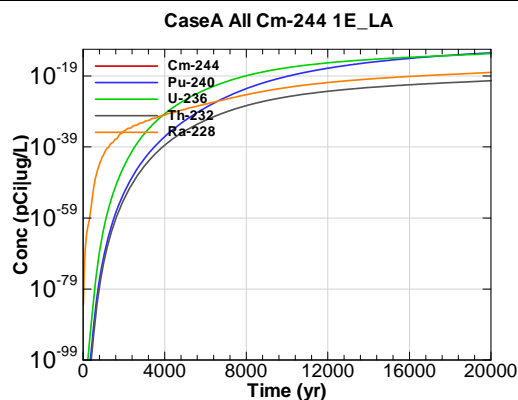


Figure F.2-185 - 1m Aquifer Concentration for
CaseA All Cm-244 1E_LA

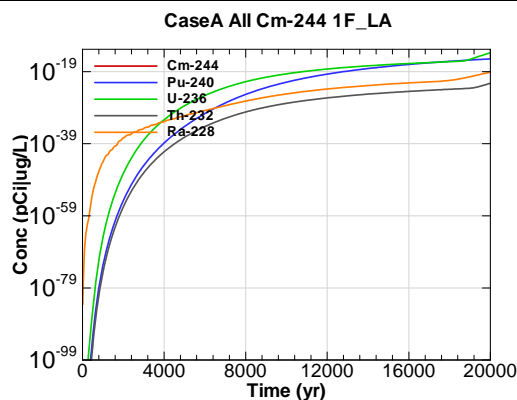


Figure F.2-186 - 1m Aquifer Concentration for
CaseA All Cm-244 1F_LA

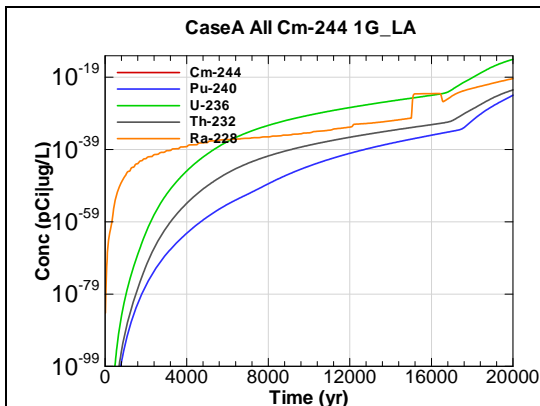


Figure F.2-187 - 1m Aquifer Concentration for
CaseA All Cm-244 1G_LA

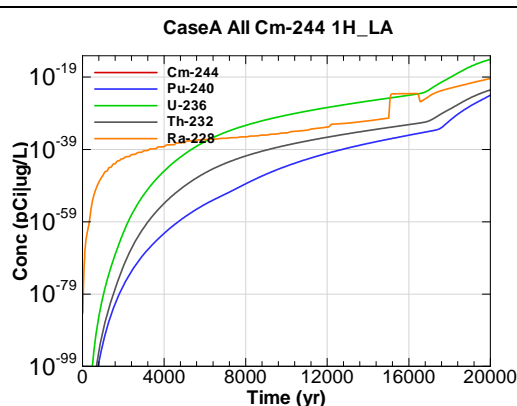


Figure F.2-188 - 1m Aquifer Concentration for
CaseA All Cm-244 1H_LA

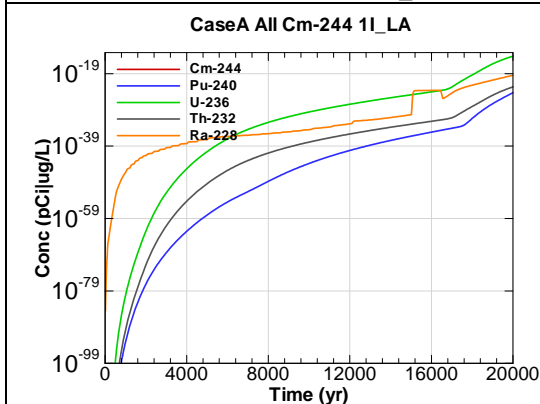


Figure F.2-189 - 1m Aquifer Concentration for
CaseA All Cm-244 1I_LA

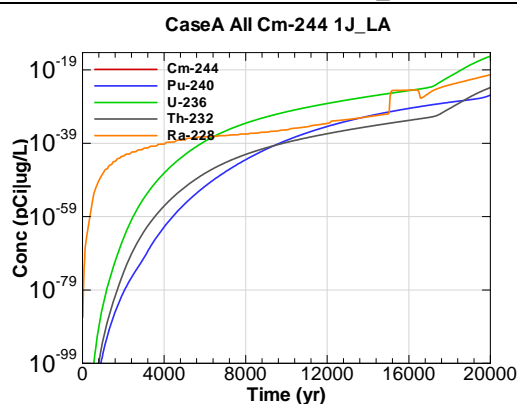


Figure F.2-190 - 1m Aquifer Concentration for
CaseA All Cm-244 1J_LA

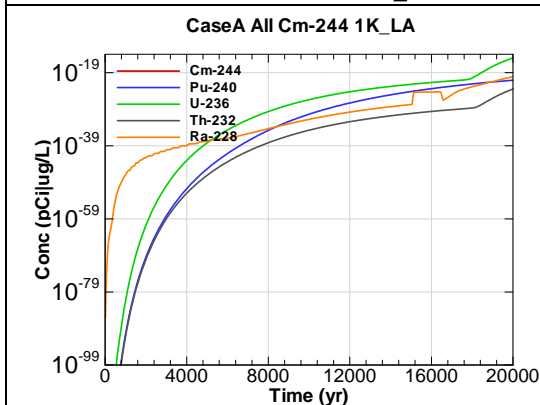


Figure F.2-191 - 1m Aquifer Concentration for
CaseA All Cm-244 1K_LA

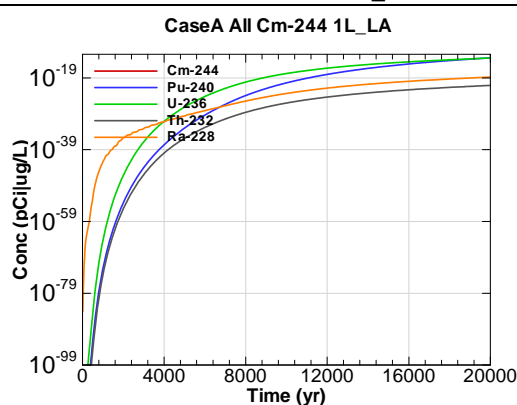
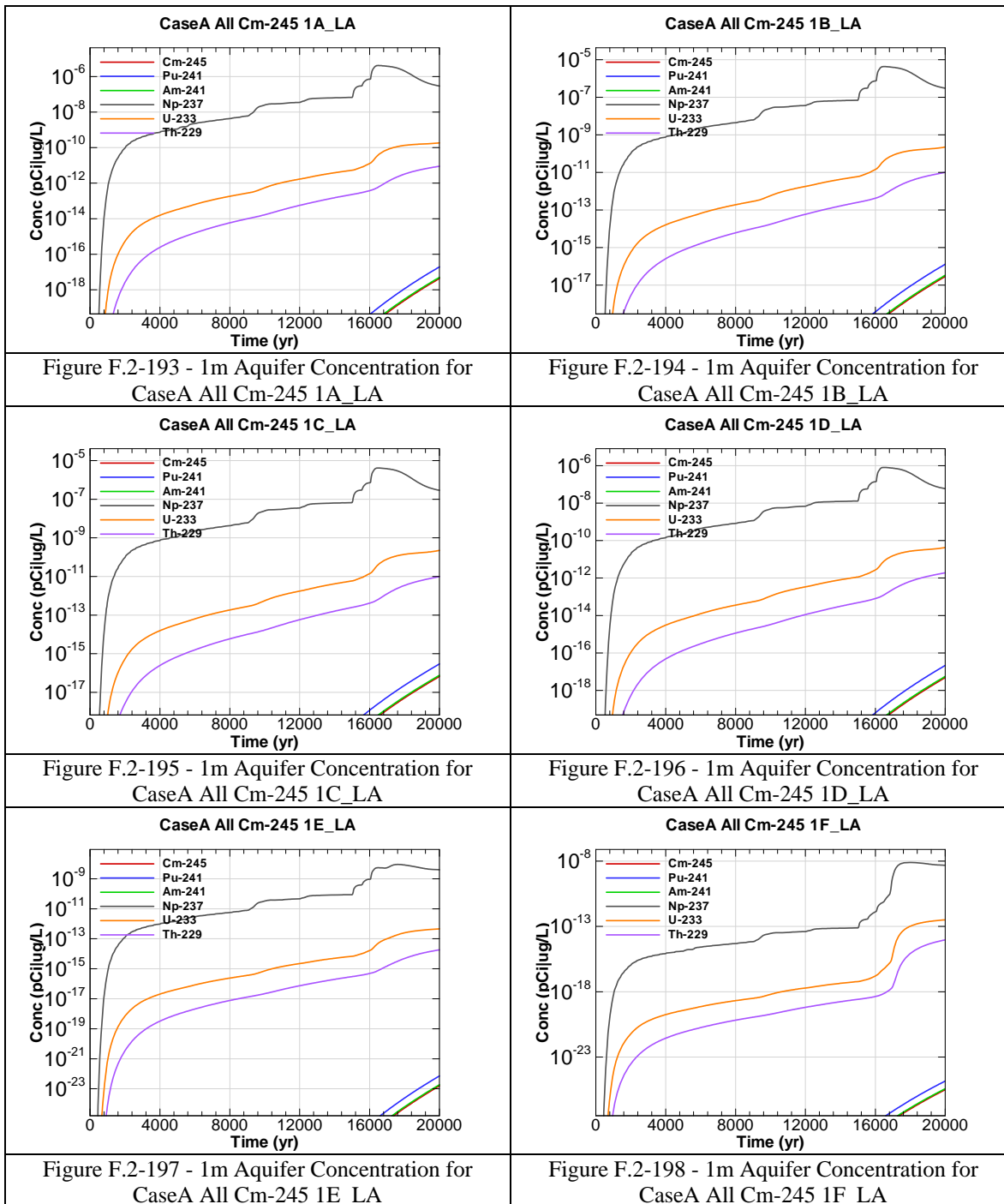
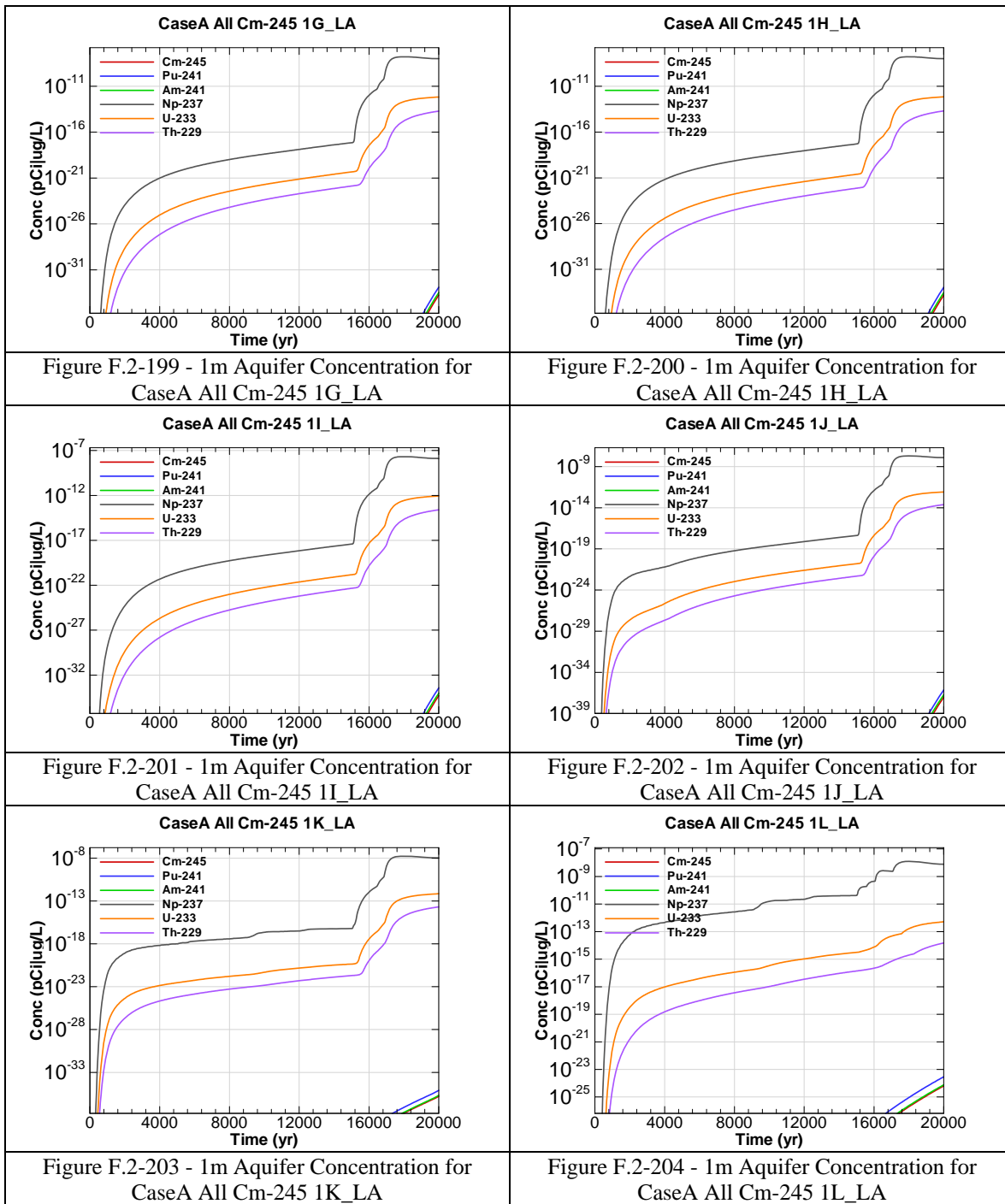


Figure F.2-192 - 1m Aquifer Concentration for
CaseA All Cm-244 1L_LA





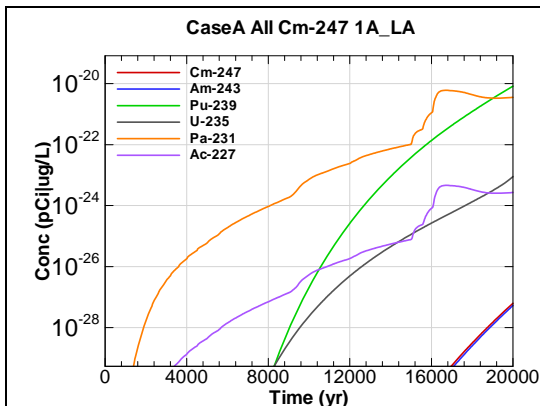


Figure F.2-205 - 1m Aquifer Concentration for
CaseA All Cm-247 1A_LA

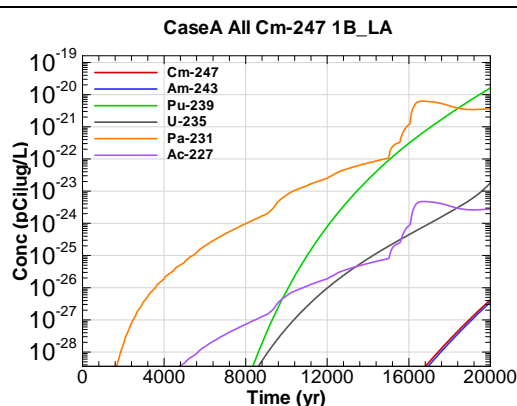


Figure F.2-206 - 1m Aquifer Concentration for
CaseA All Cm-247 1B_LA

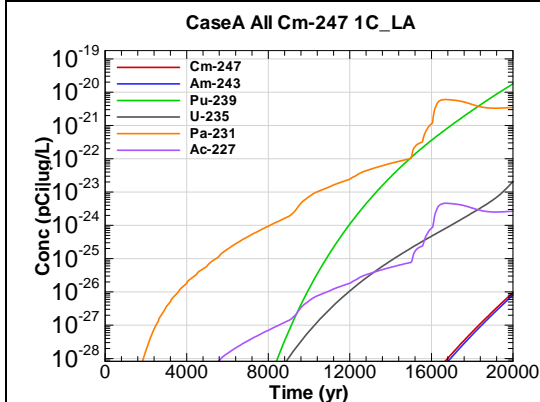


Figure F.2-207 - 1m Aquifer Concentration for
CaseA All Cm-247 1C_LA

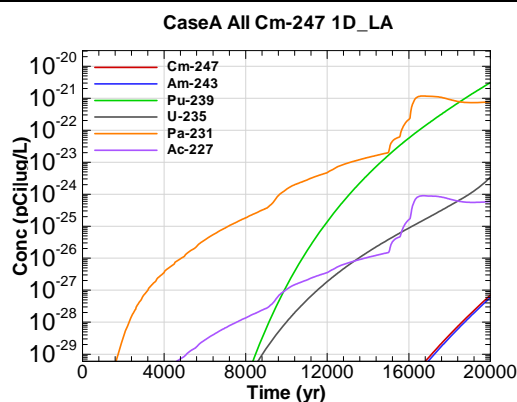


Figure F.2-208 - 1m Aquifer Concentration for
CaseA All Cm-247 1D_LA

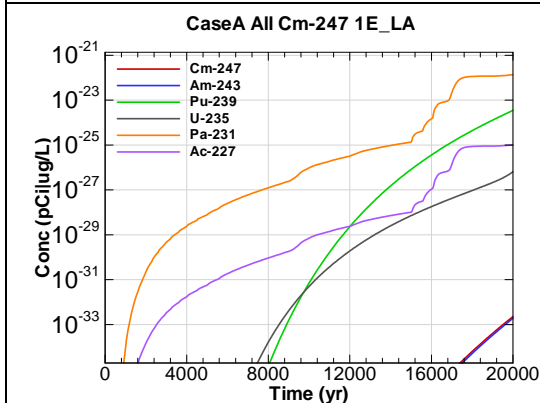


Figure F.2-209 - 1m Aquifer Concentration for
CaseA All Cm-247 1E_LA

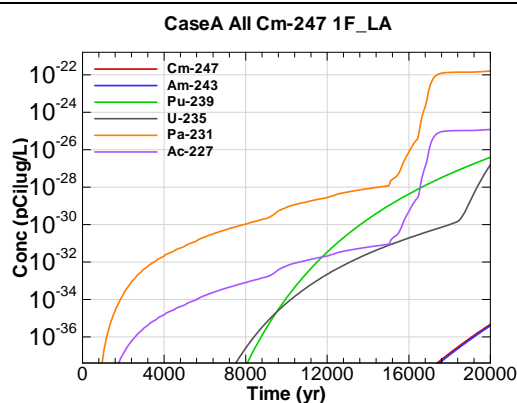
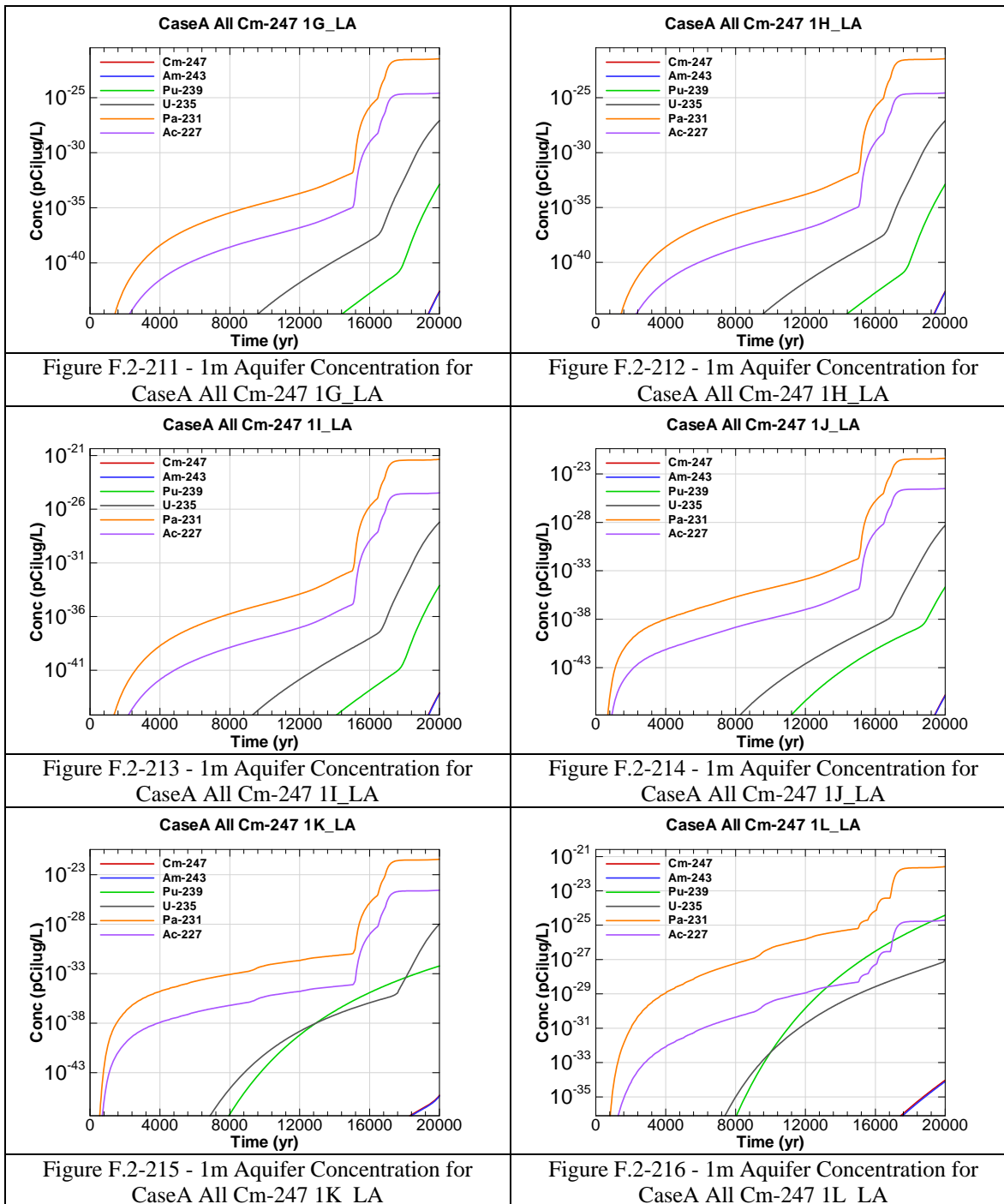
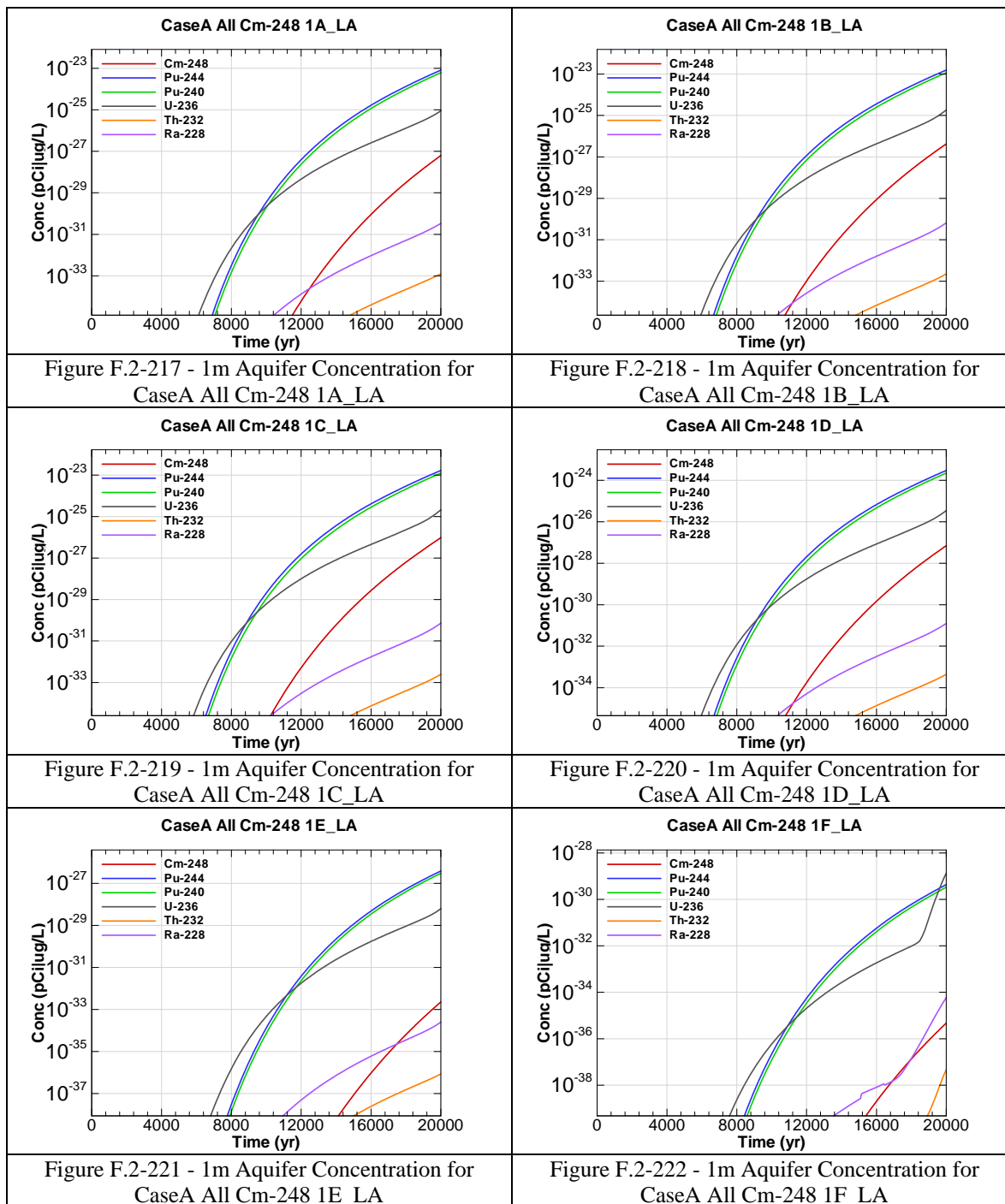
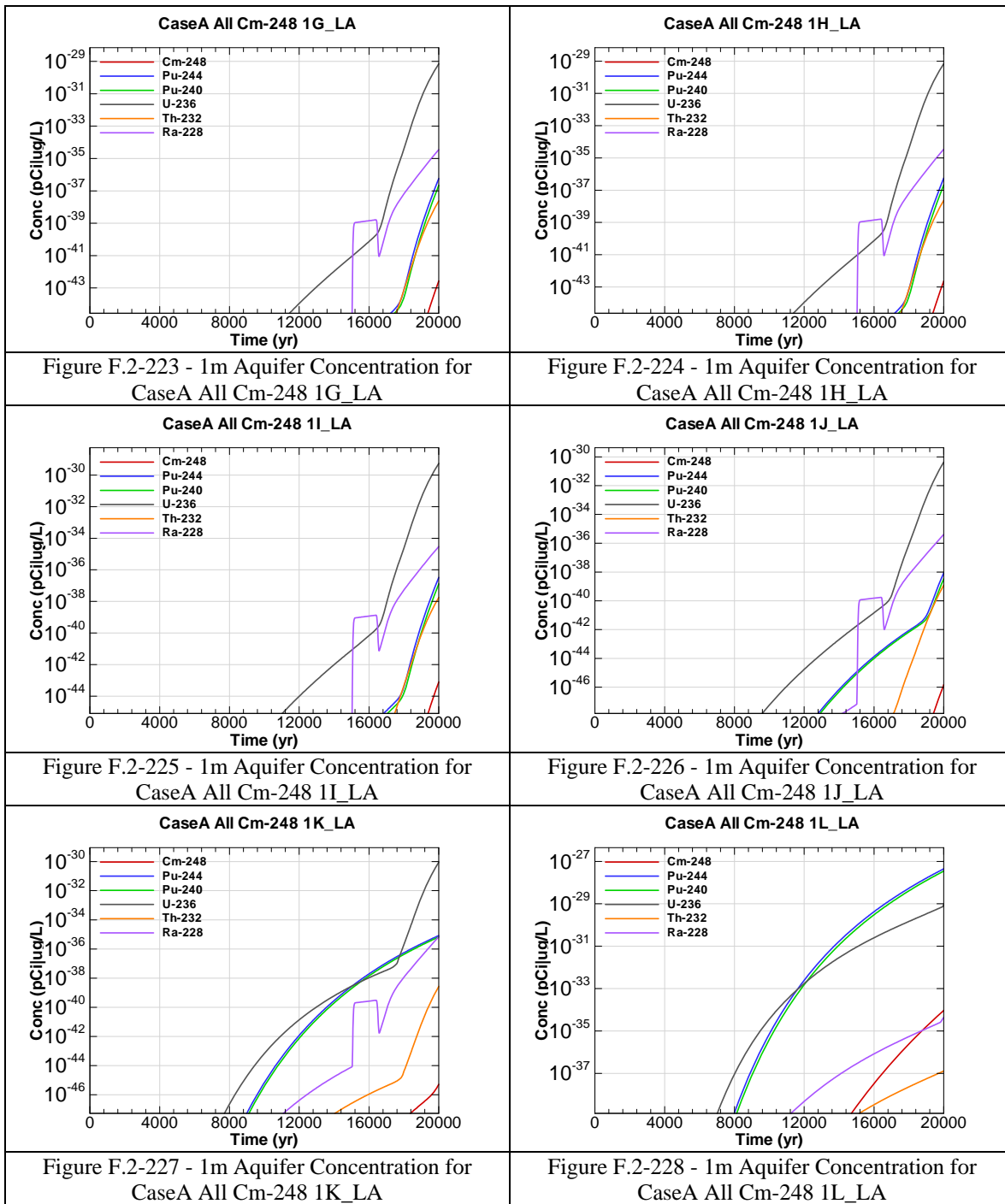
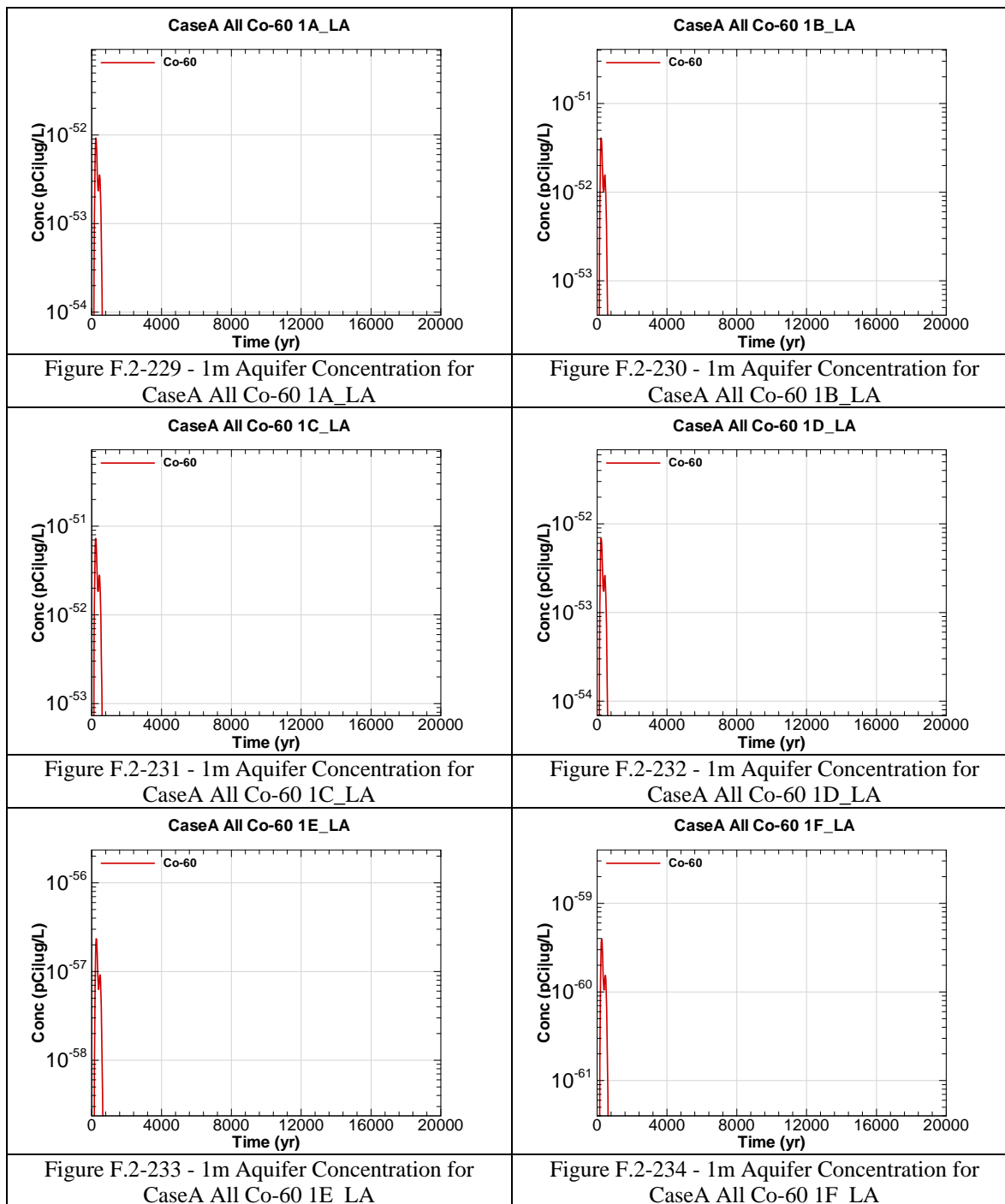


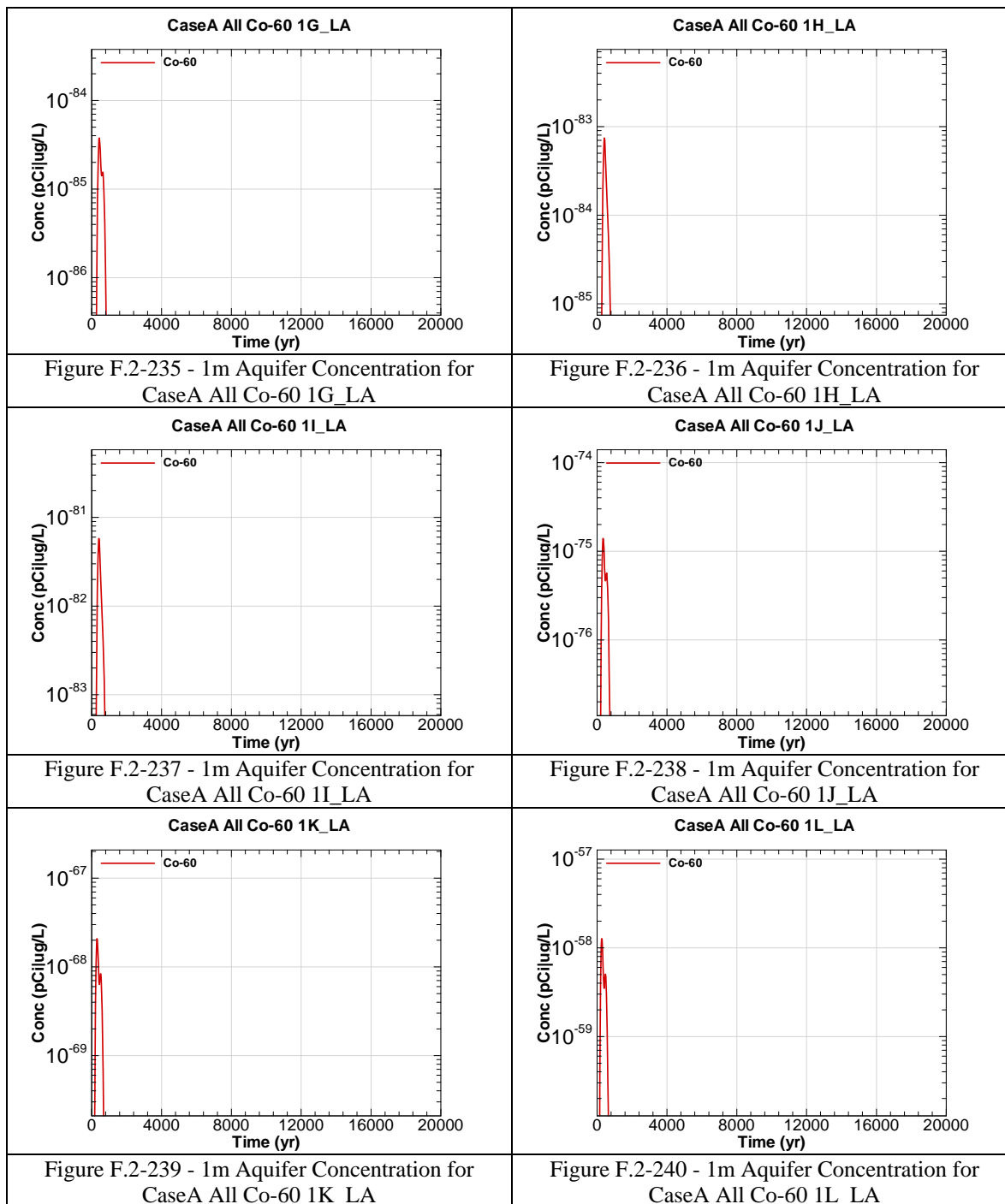
Figure F.2-210 - 1m Aquifer Concentration for
CaseA All Cm-247 1F_LA

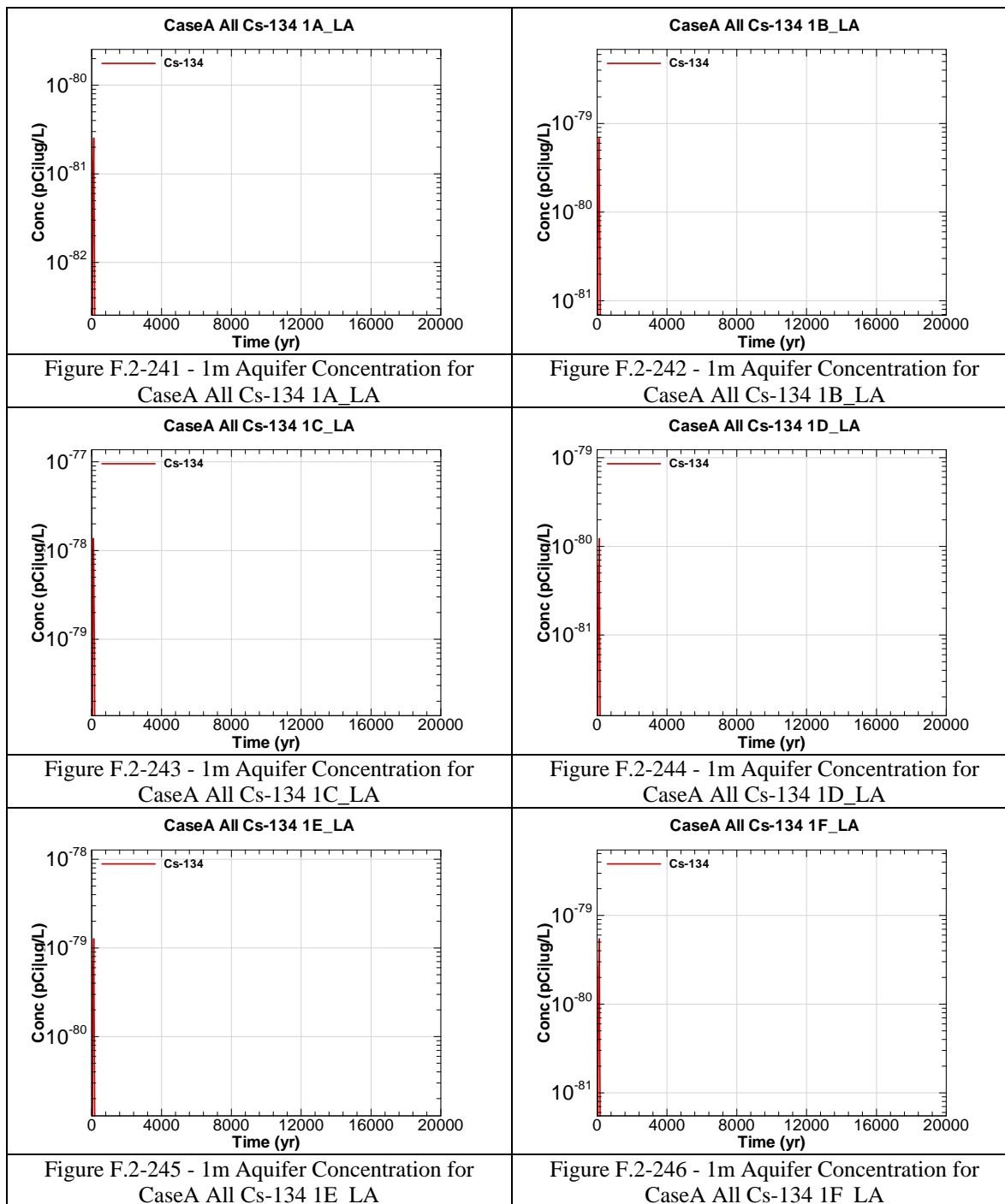


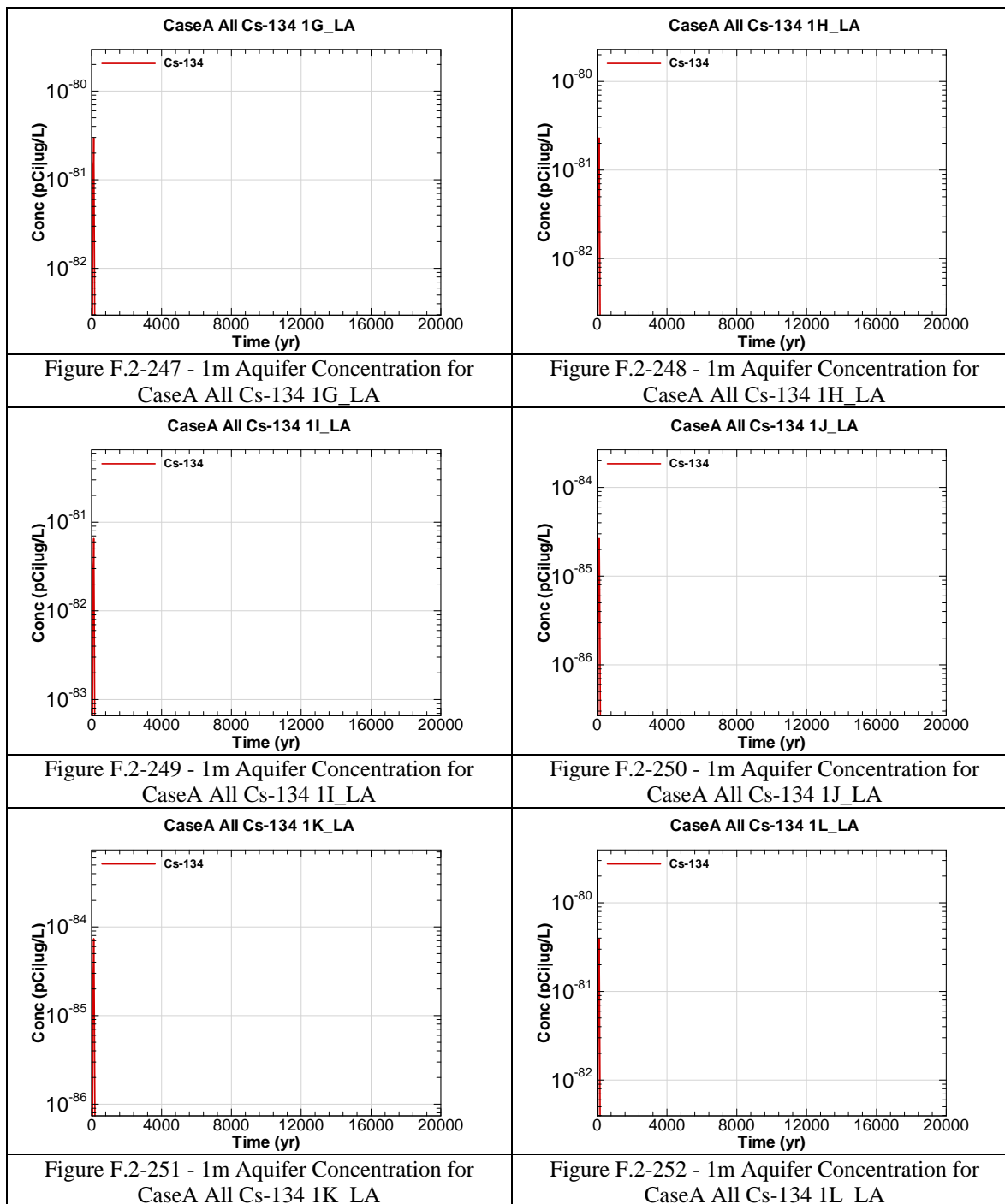


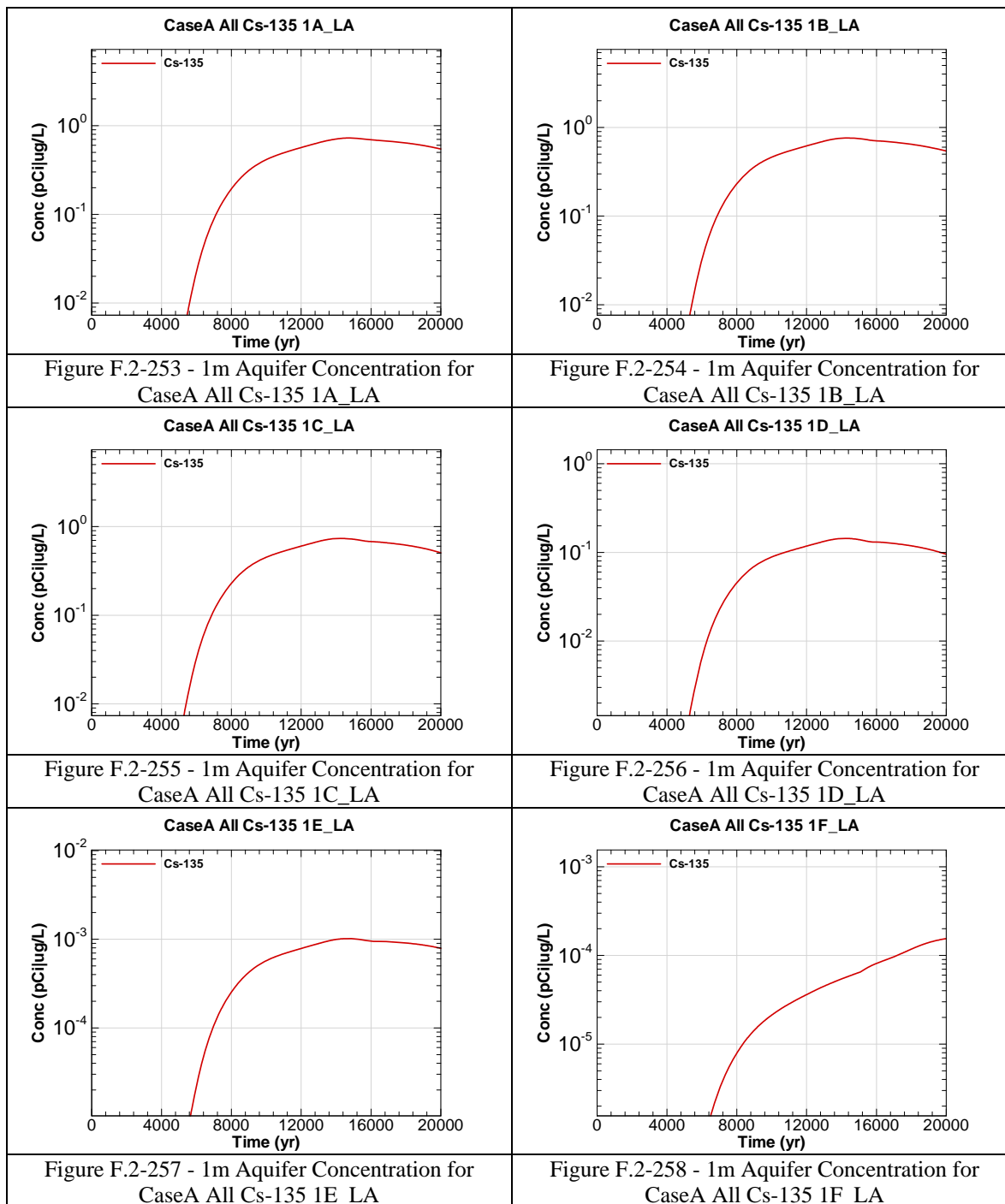


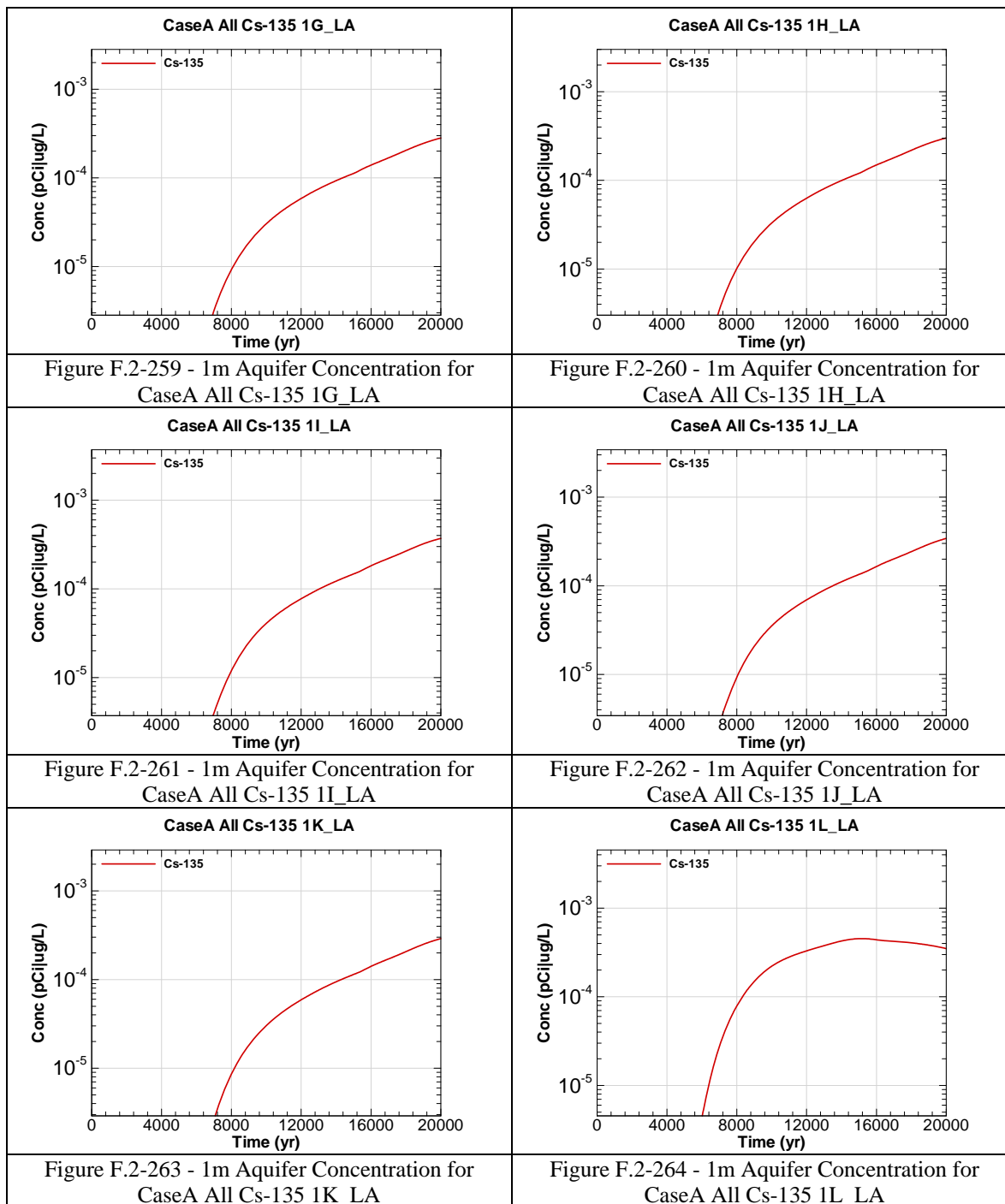


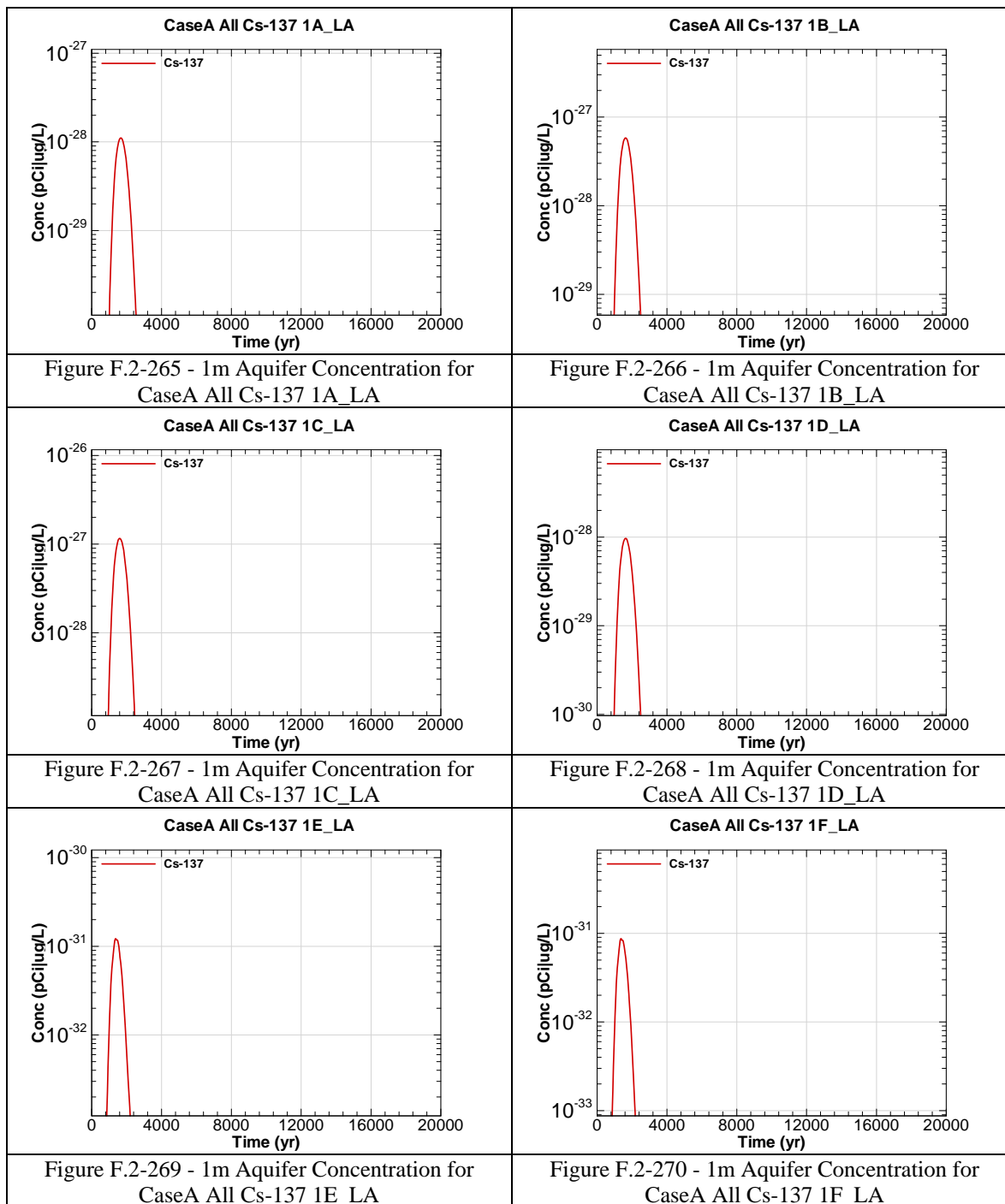


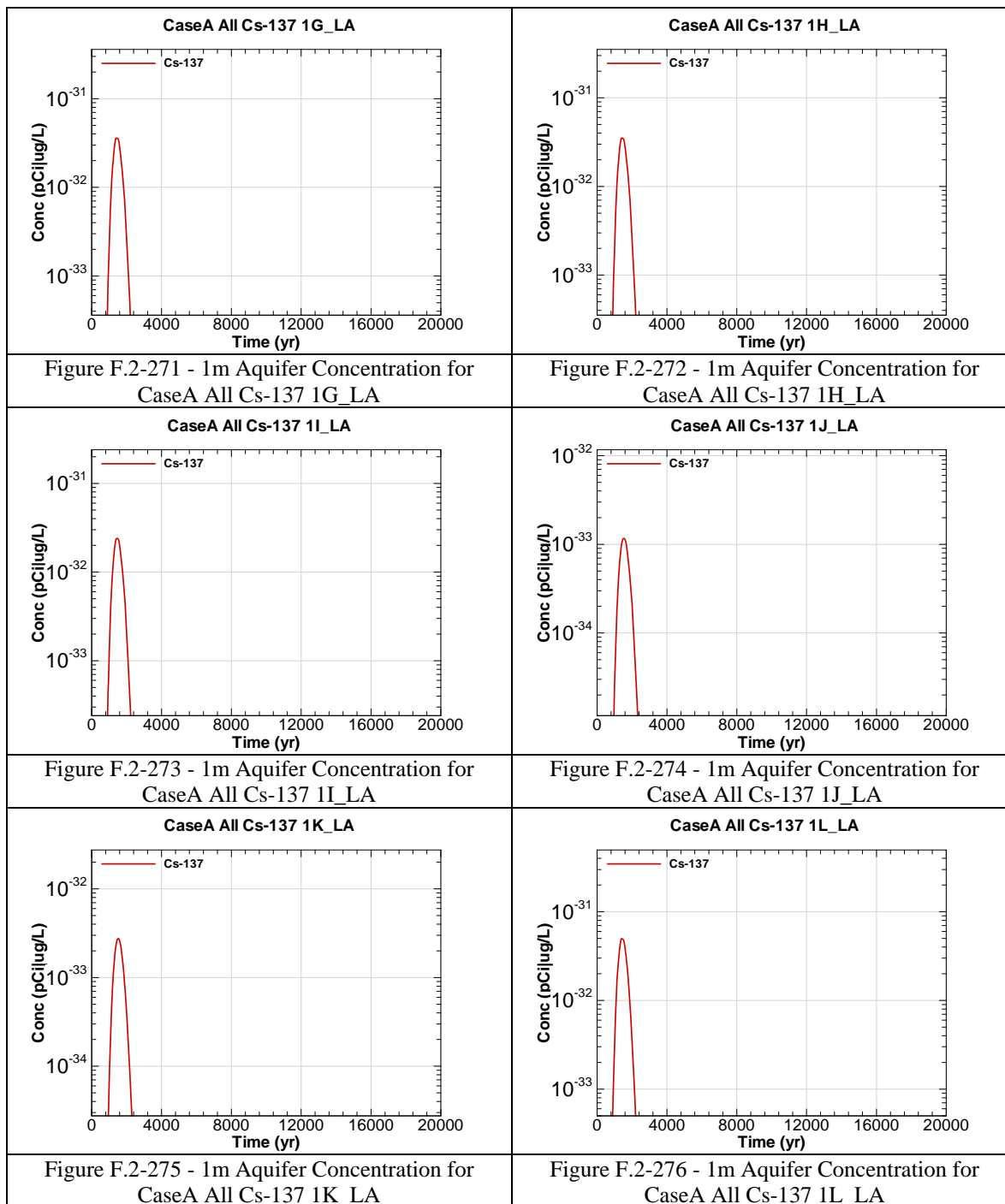


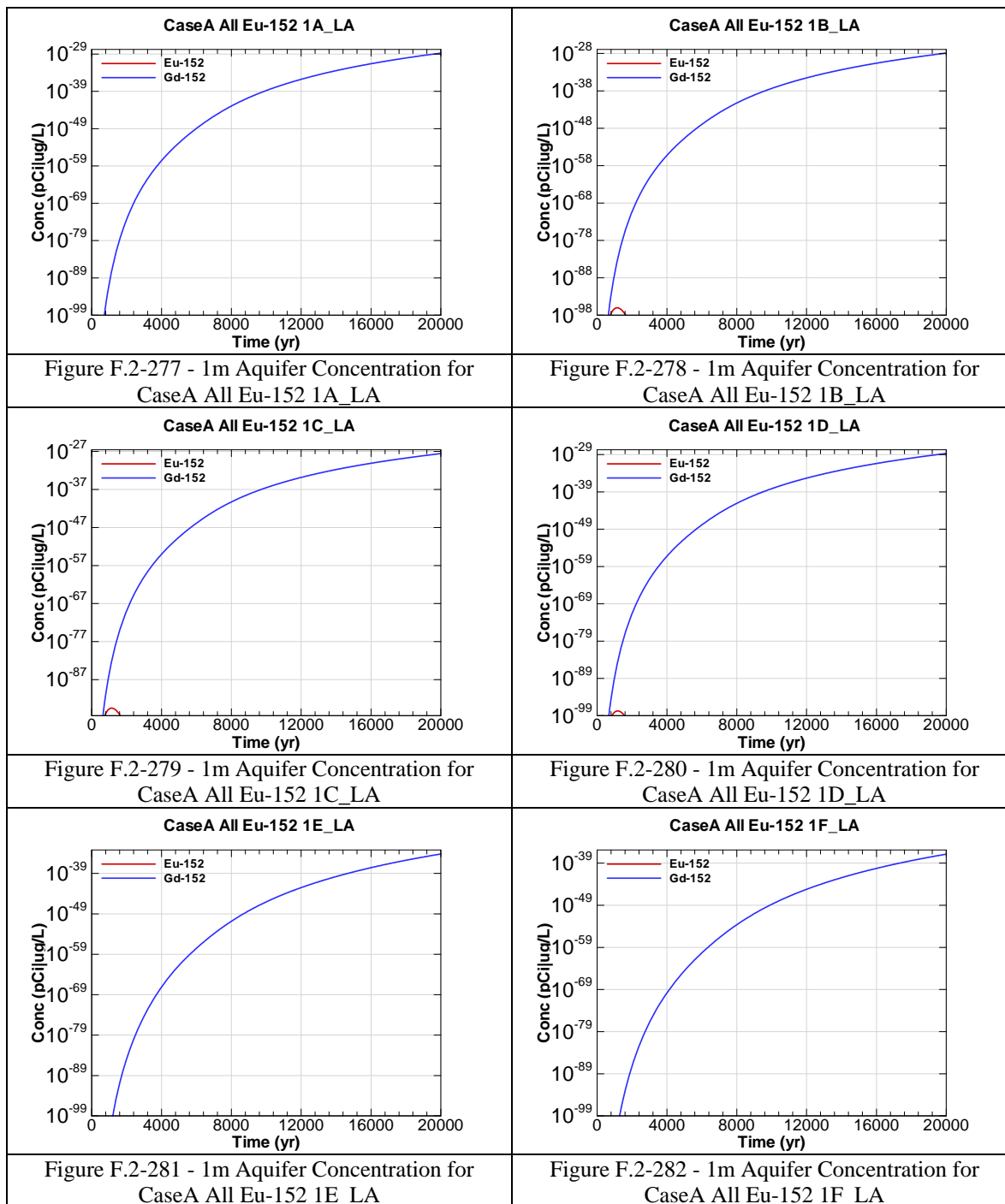


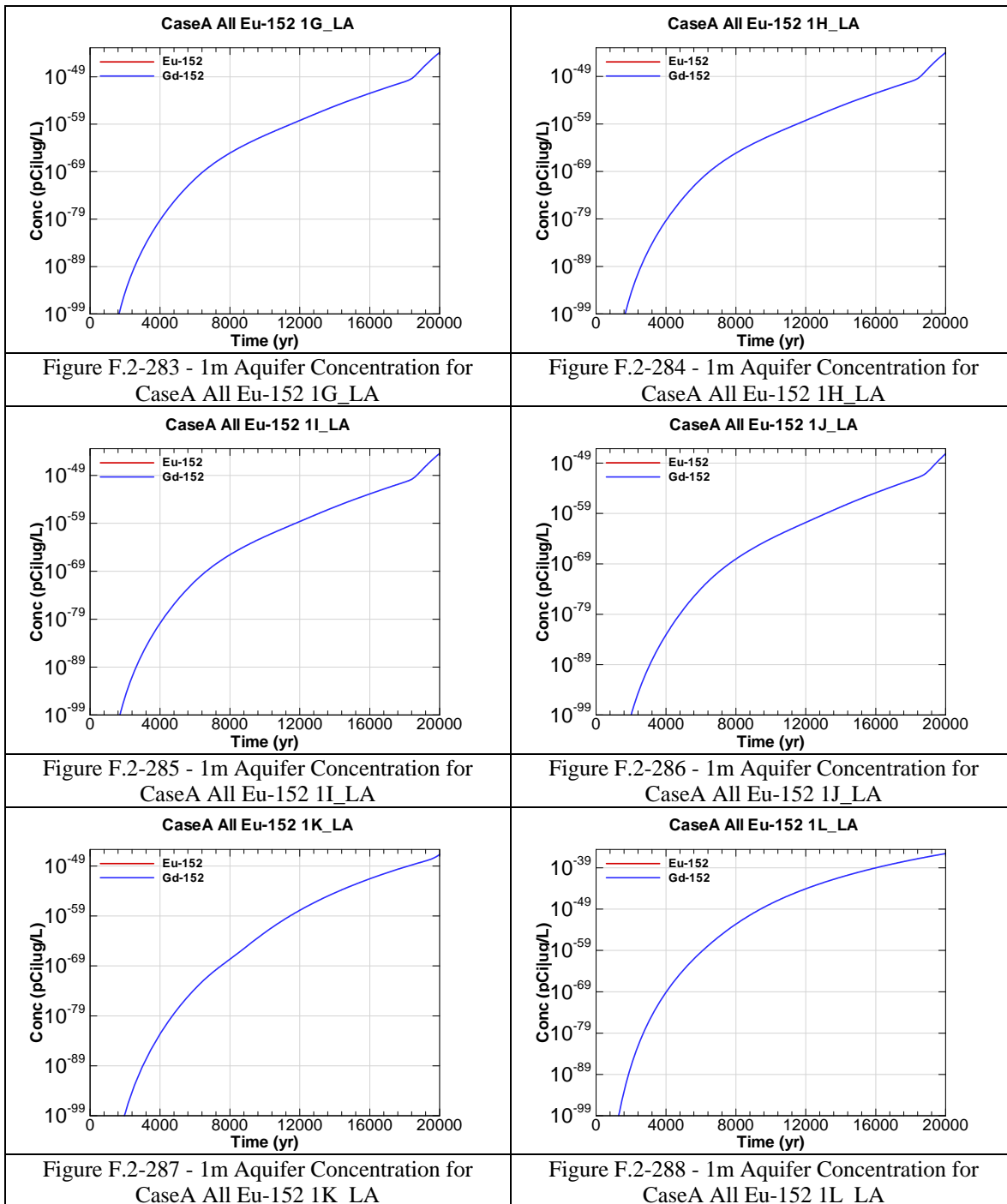


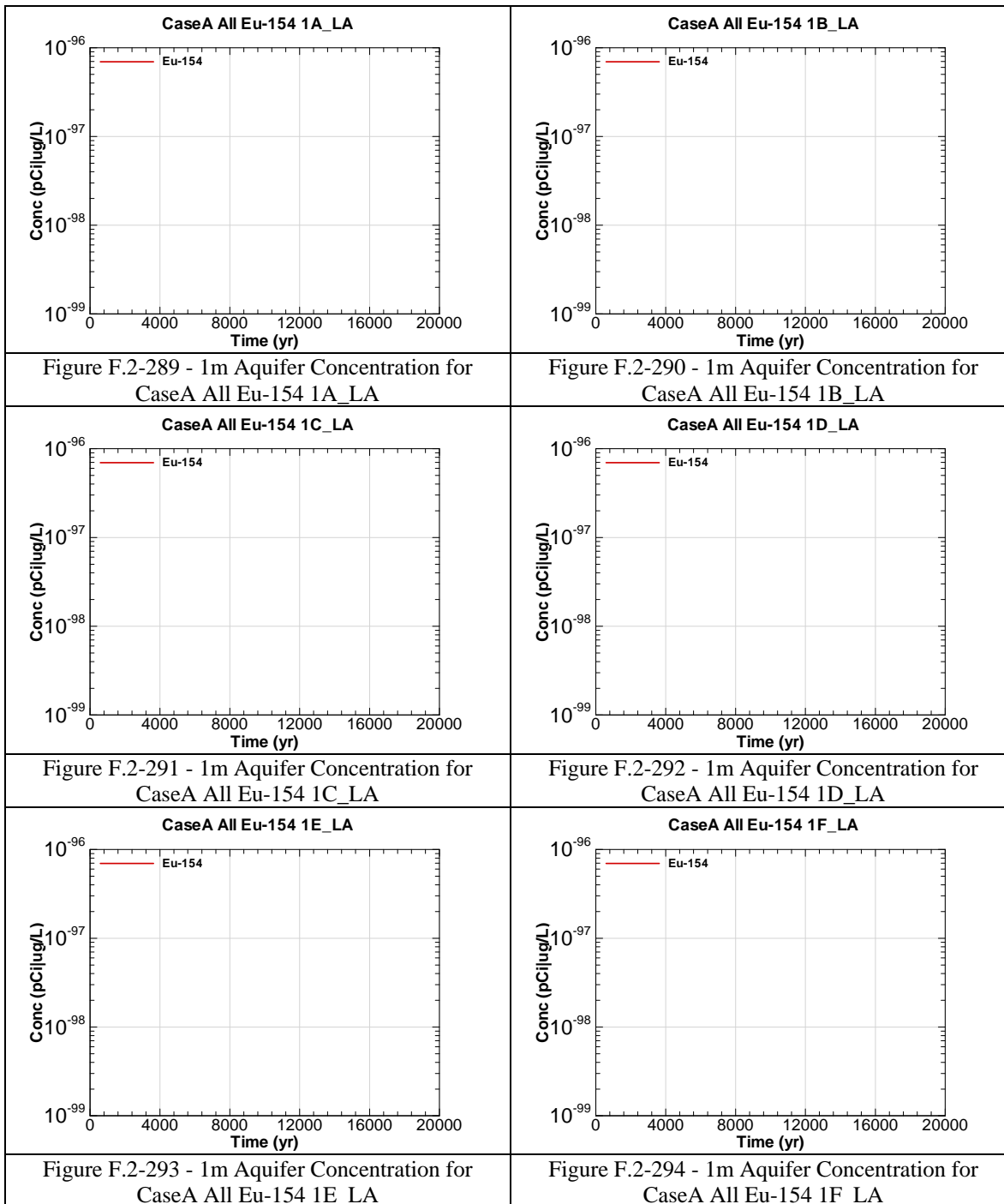


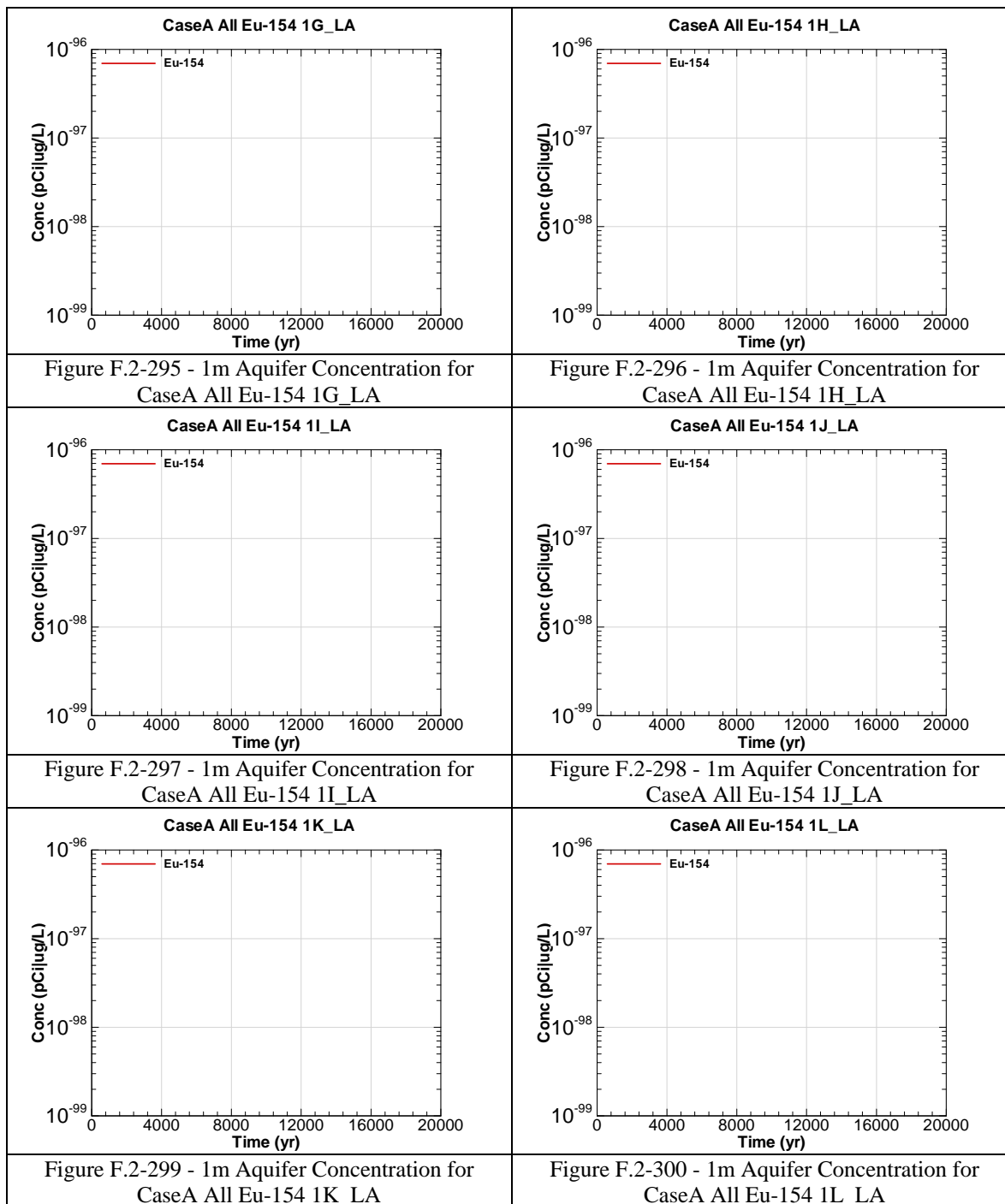


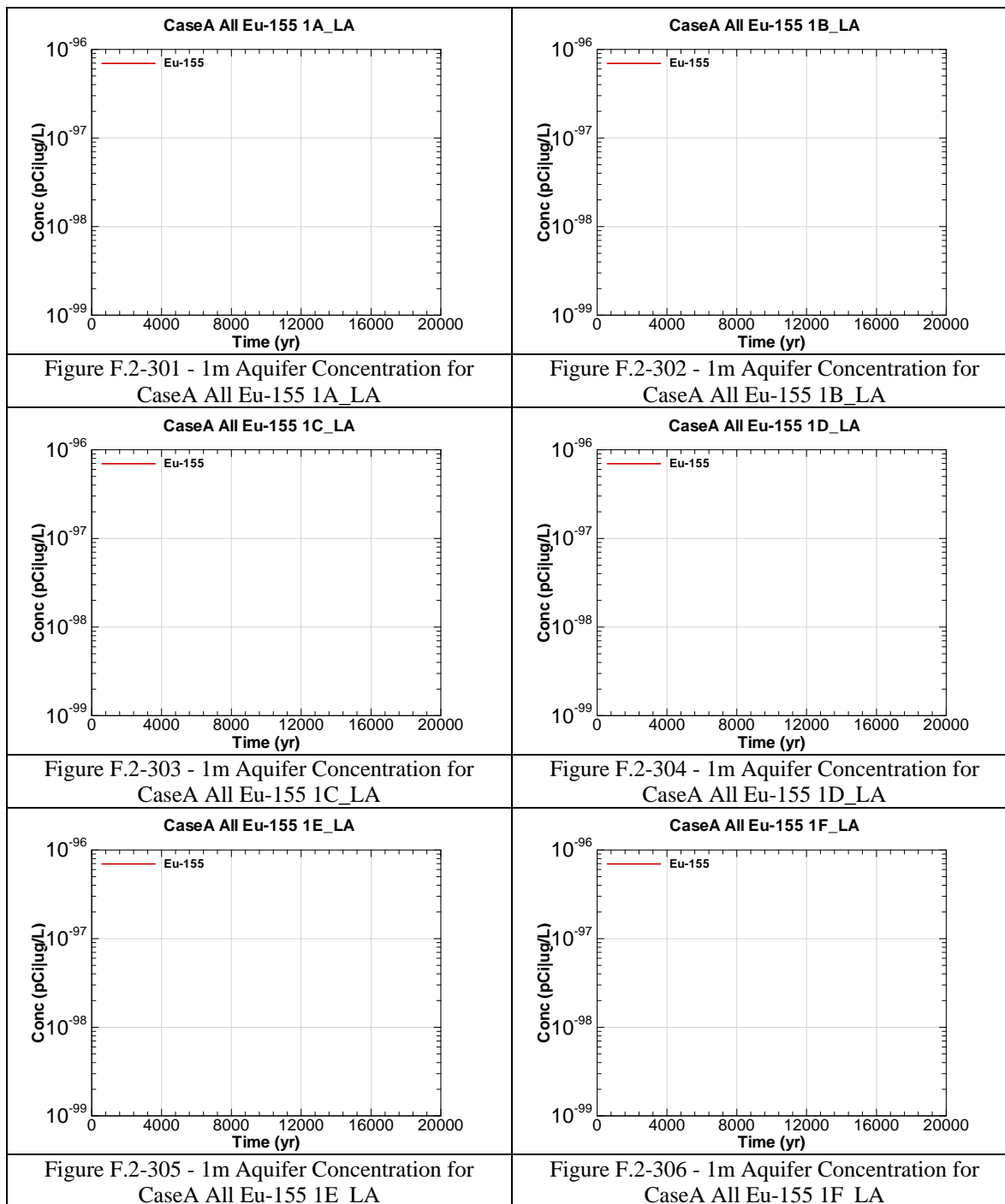


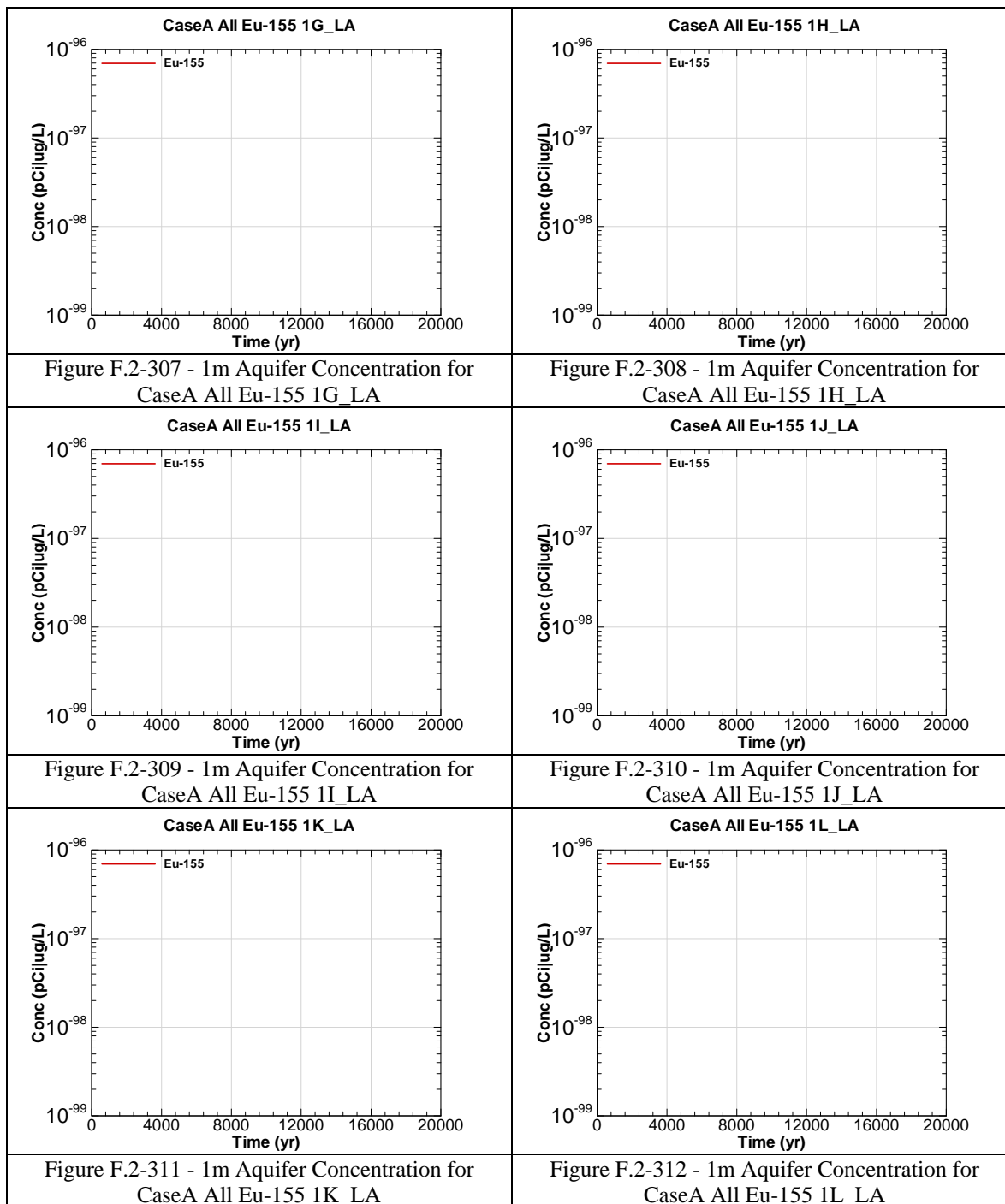


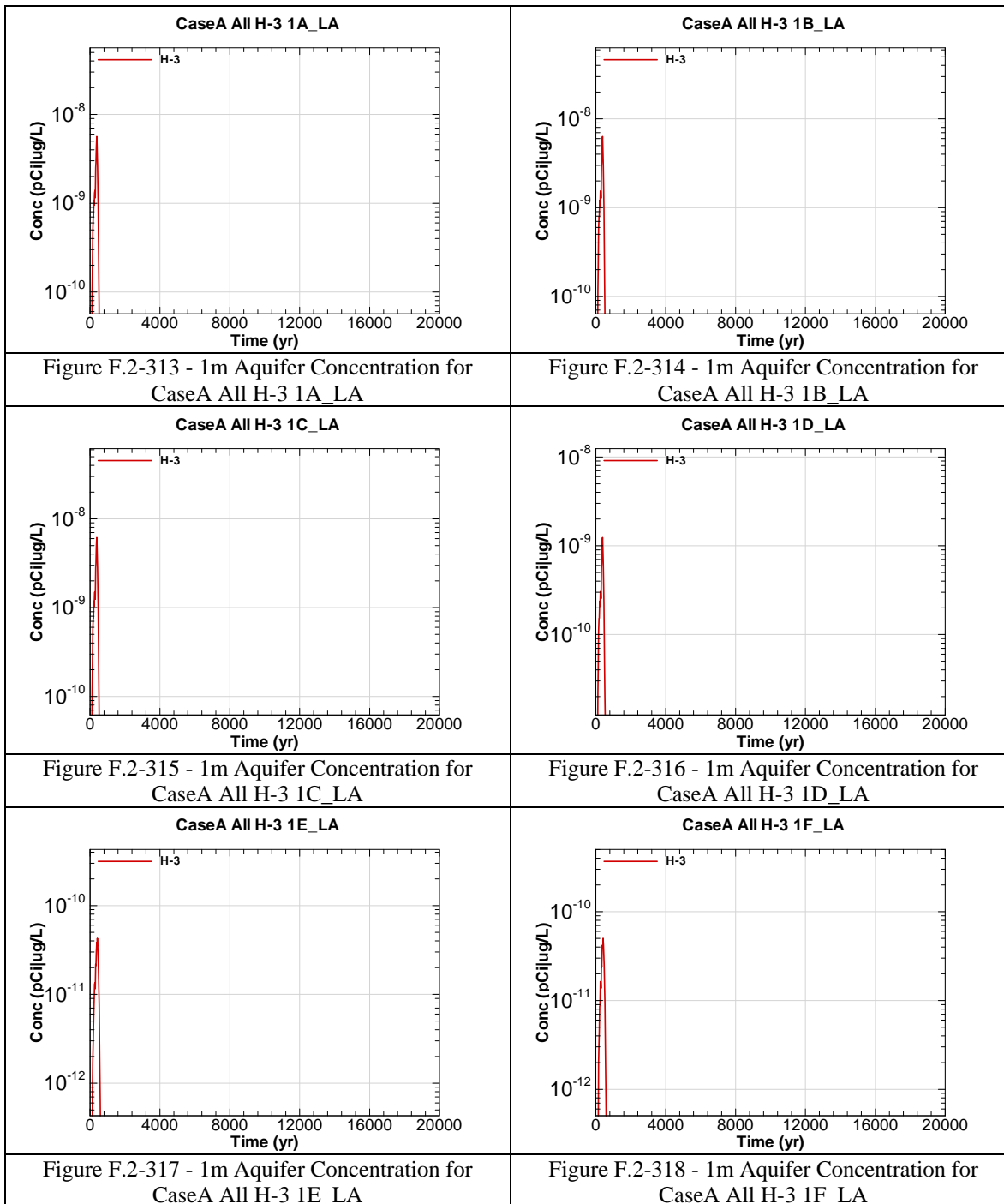


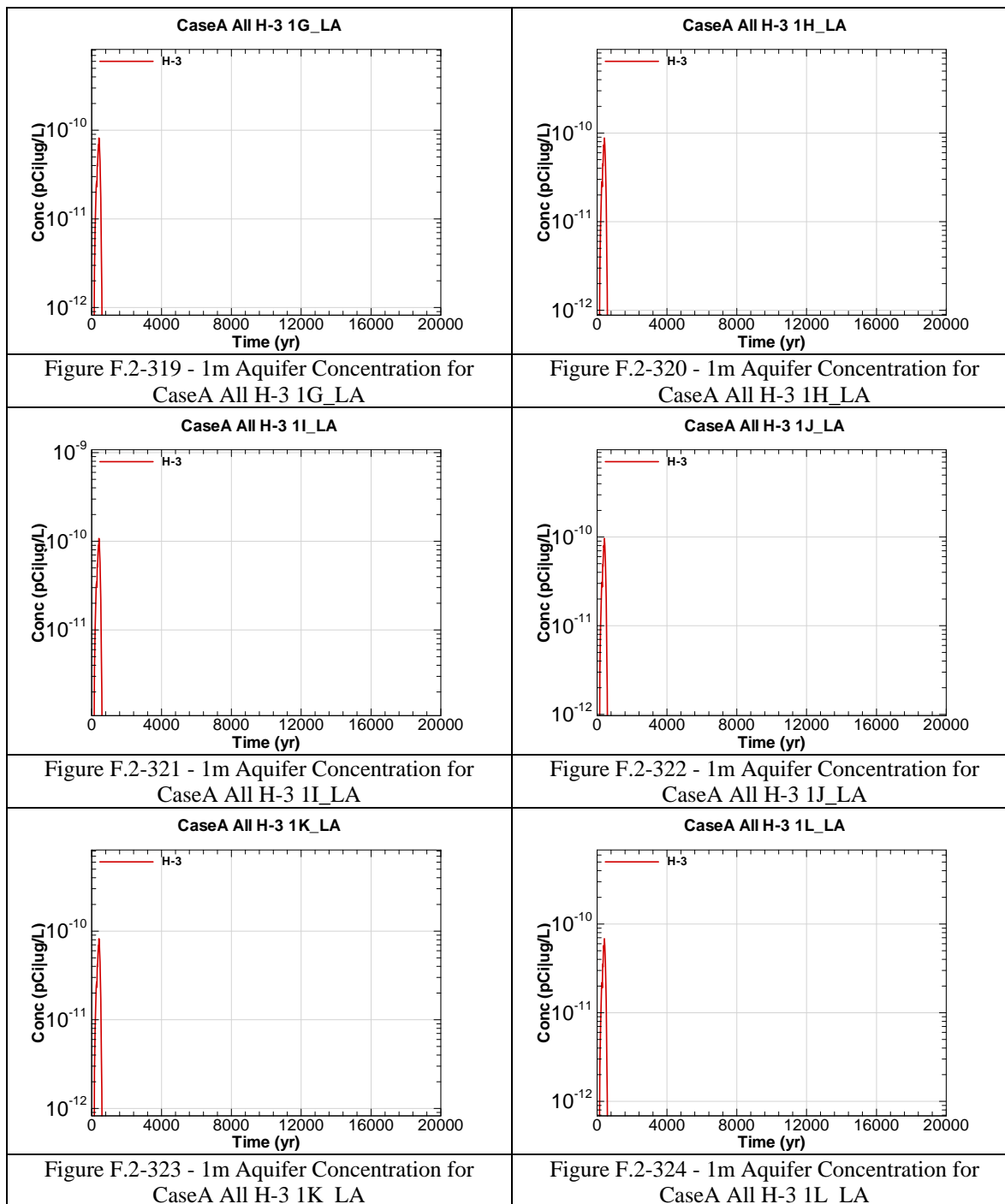


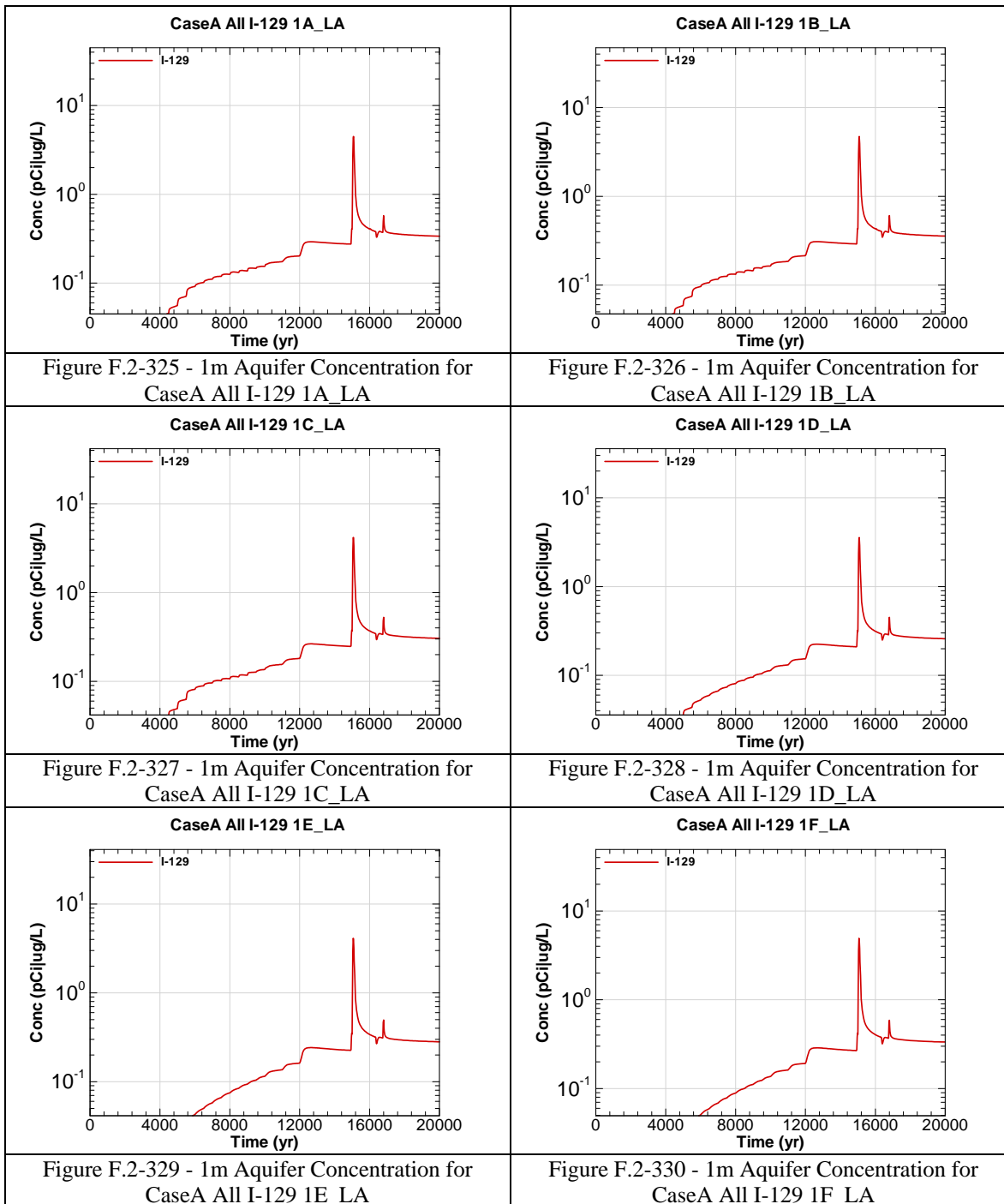


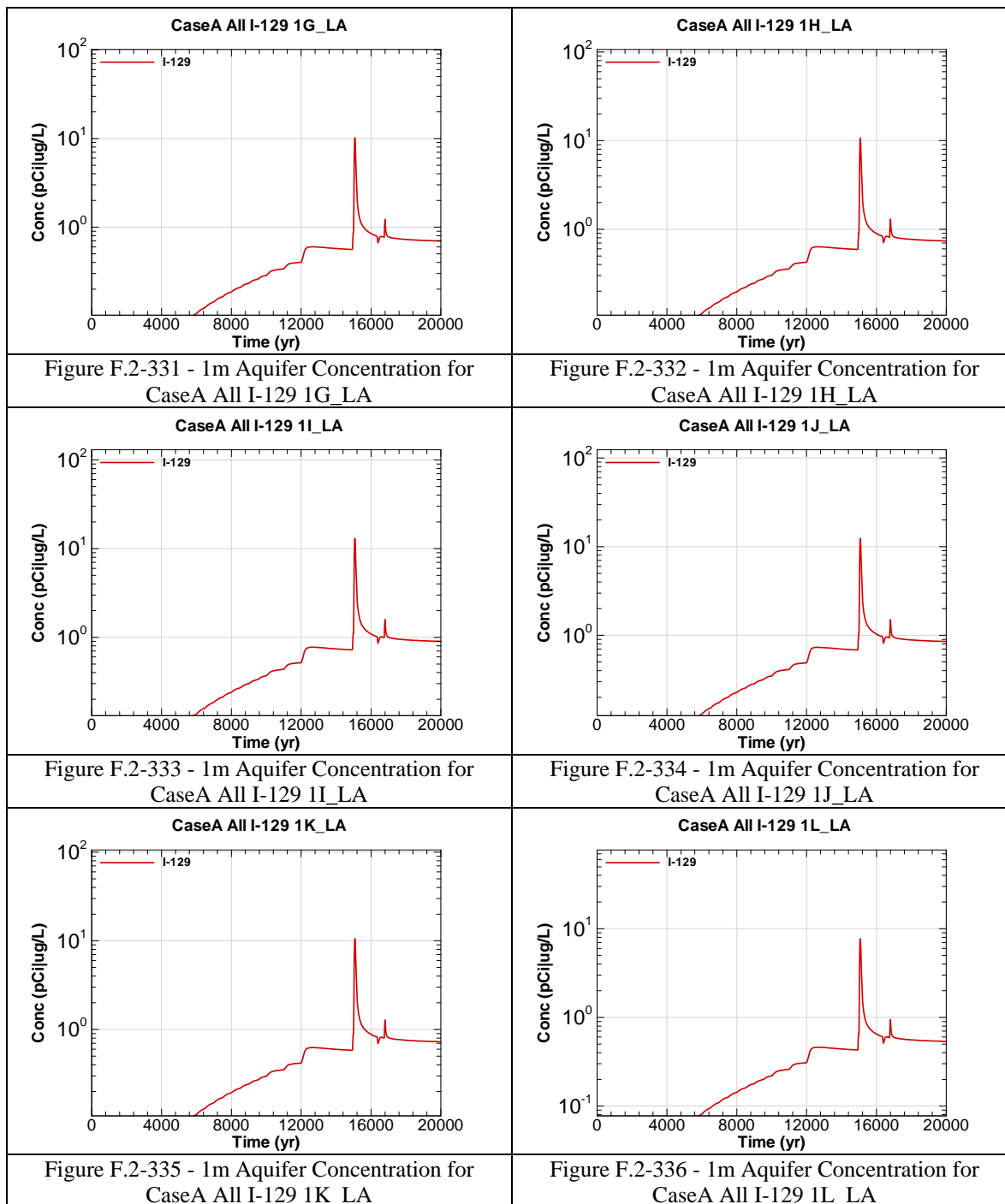


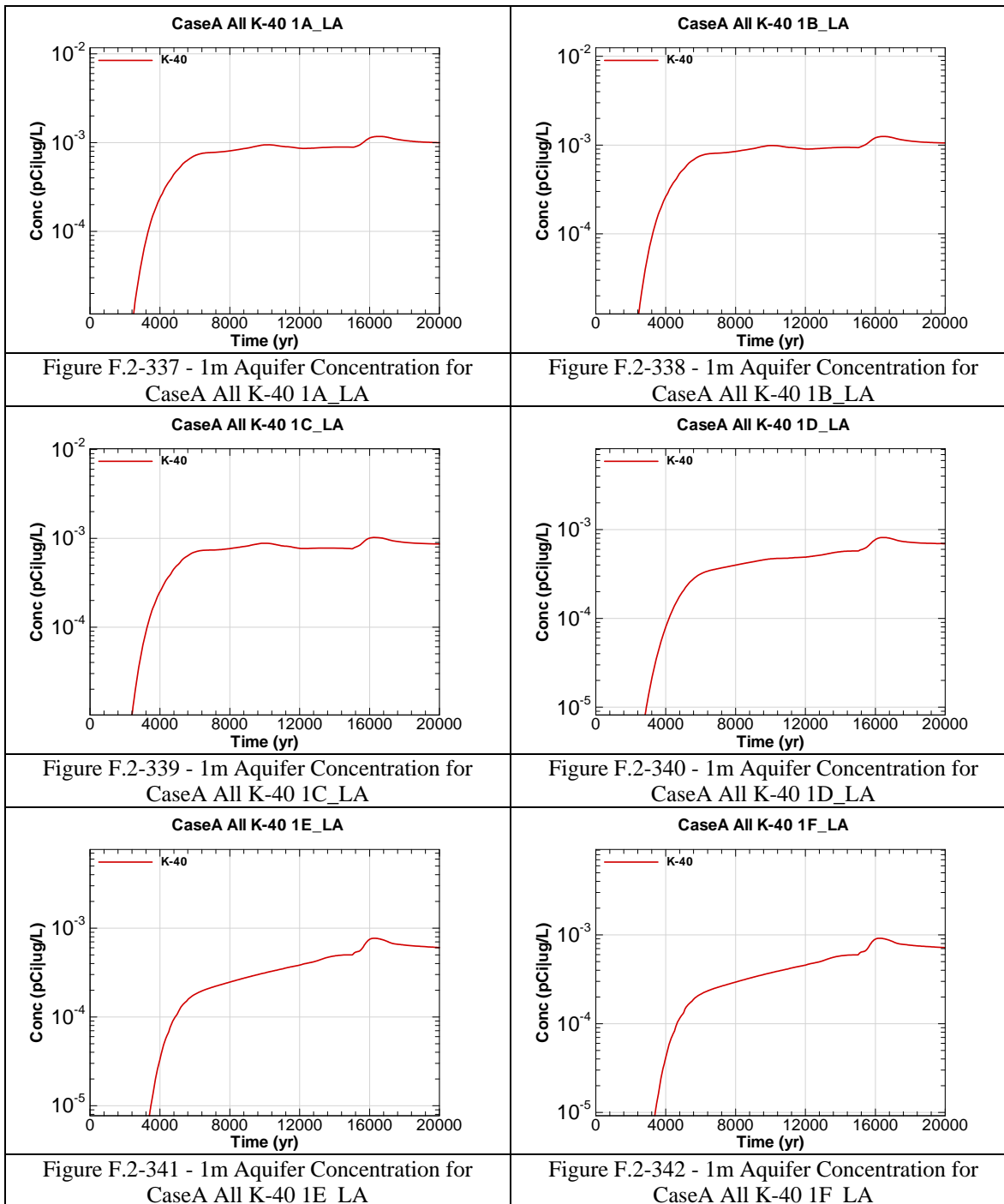


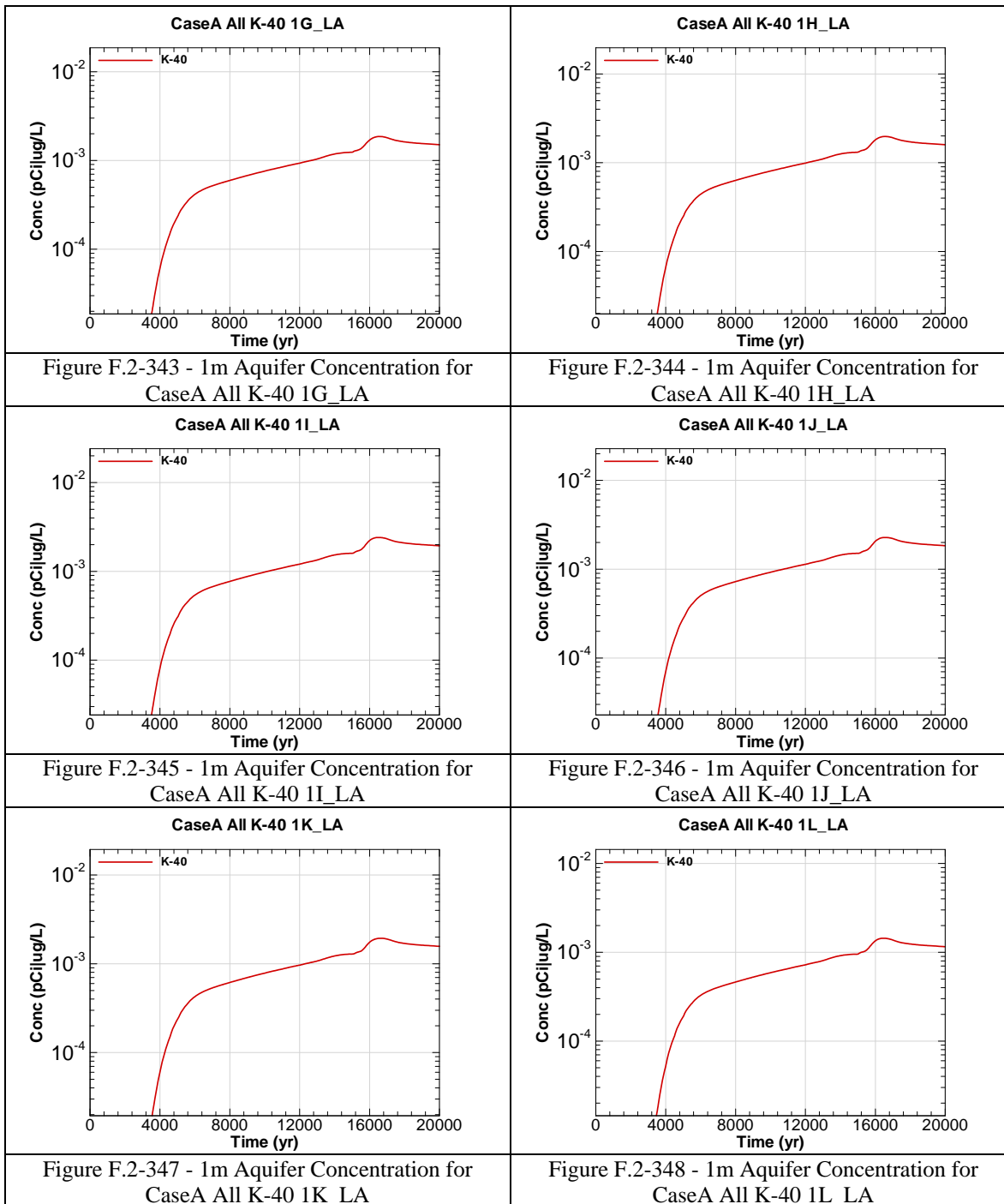


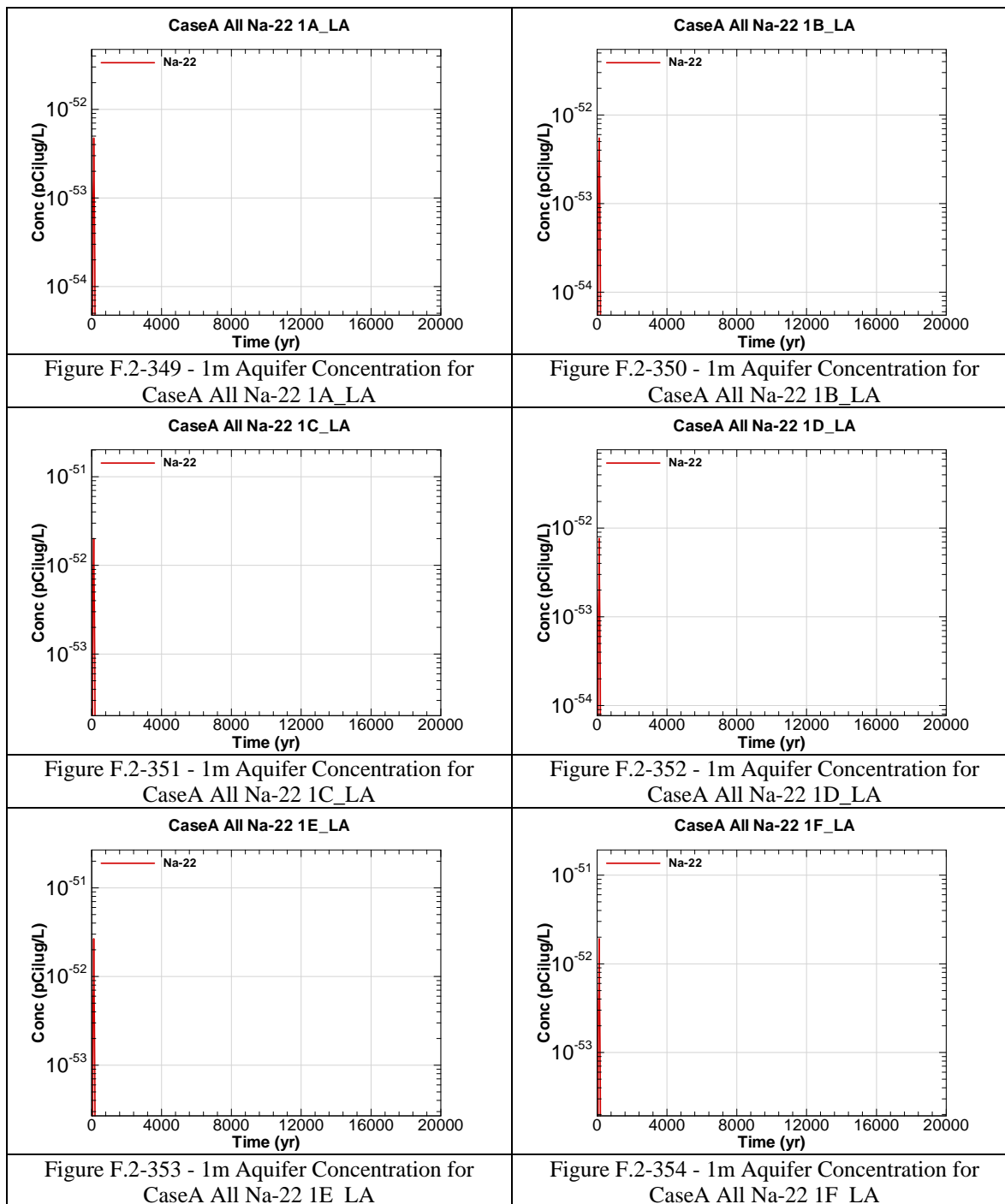


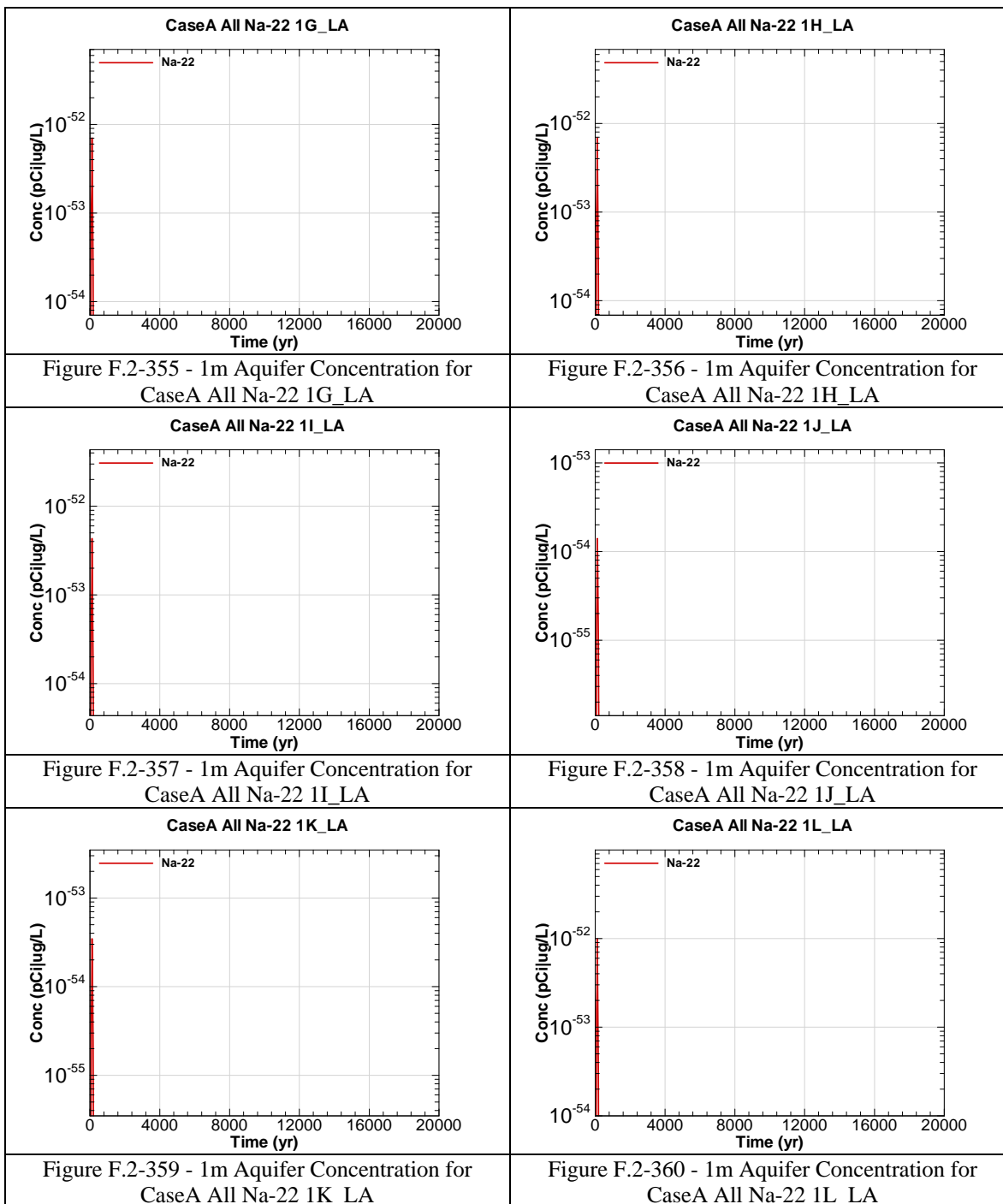


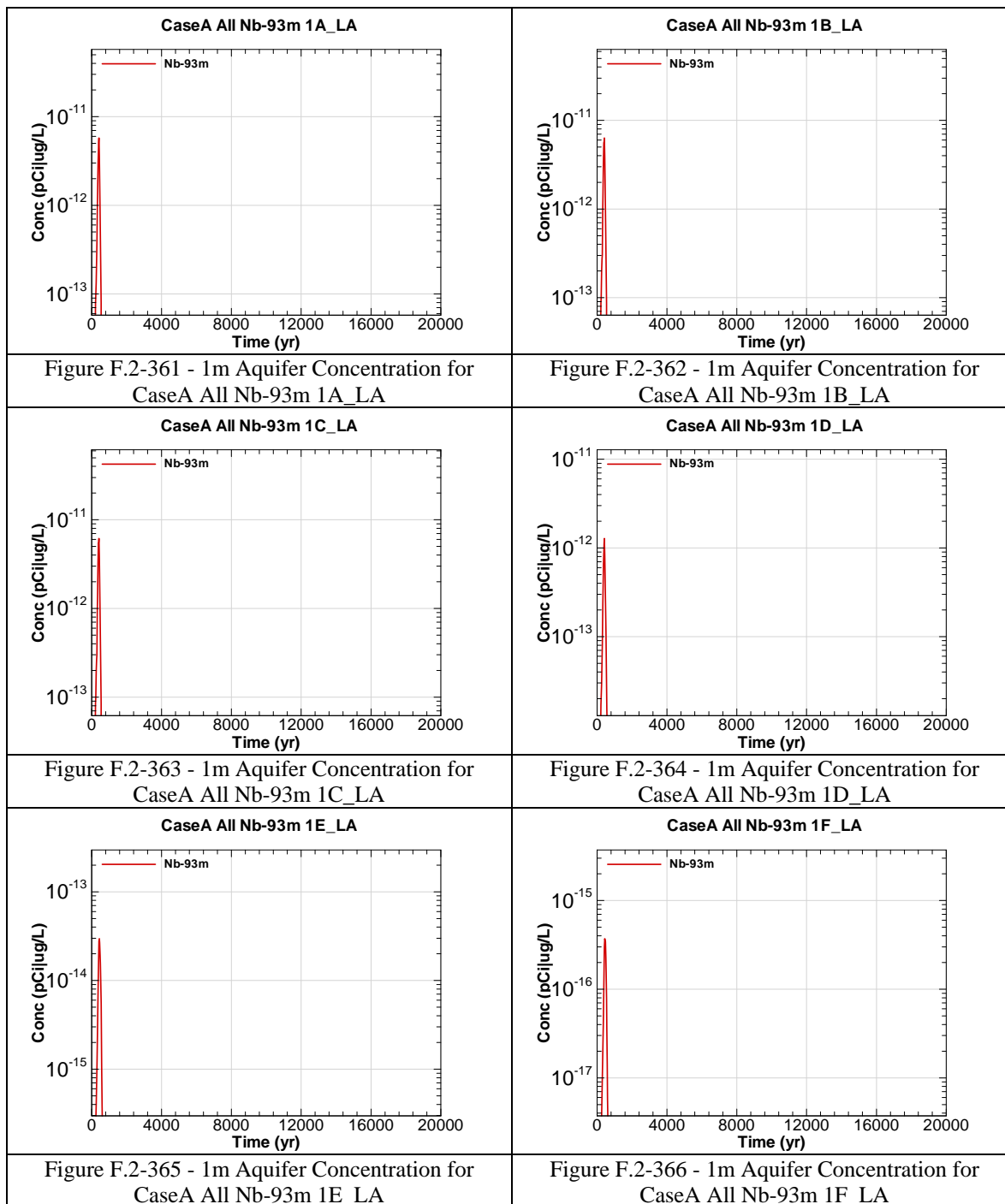


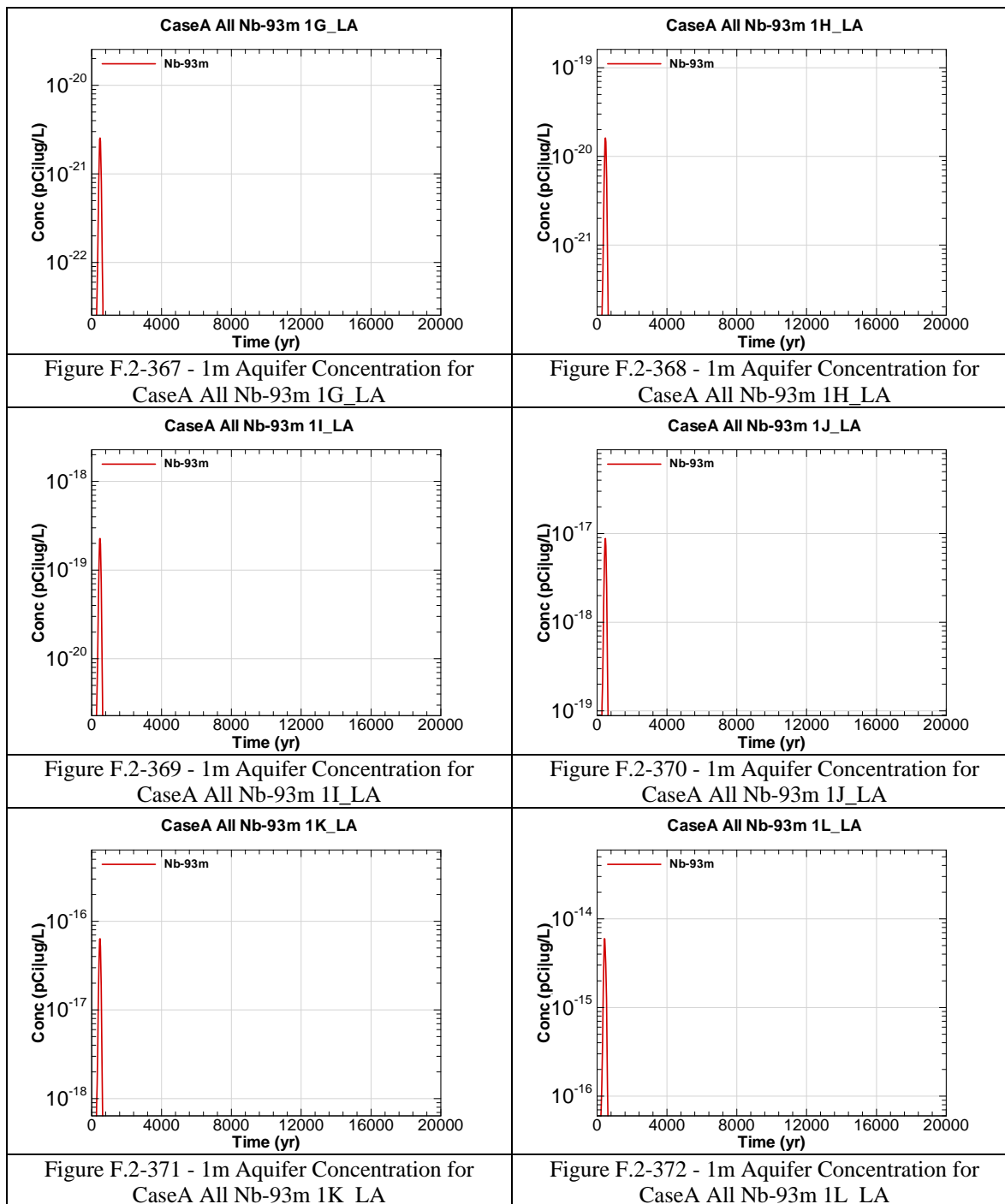


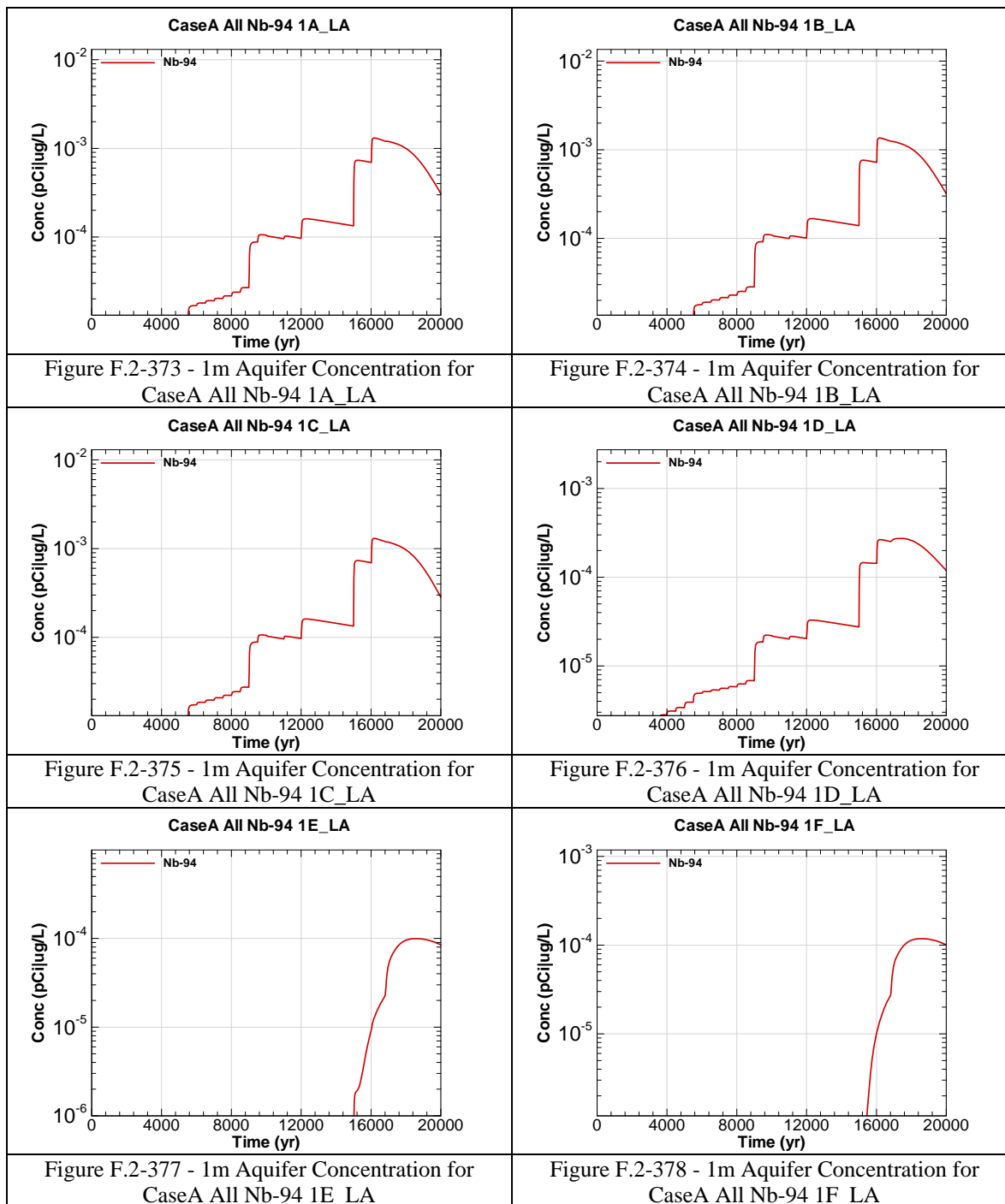


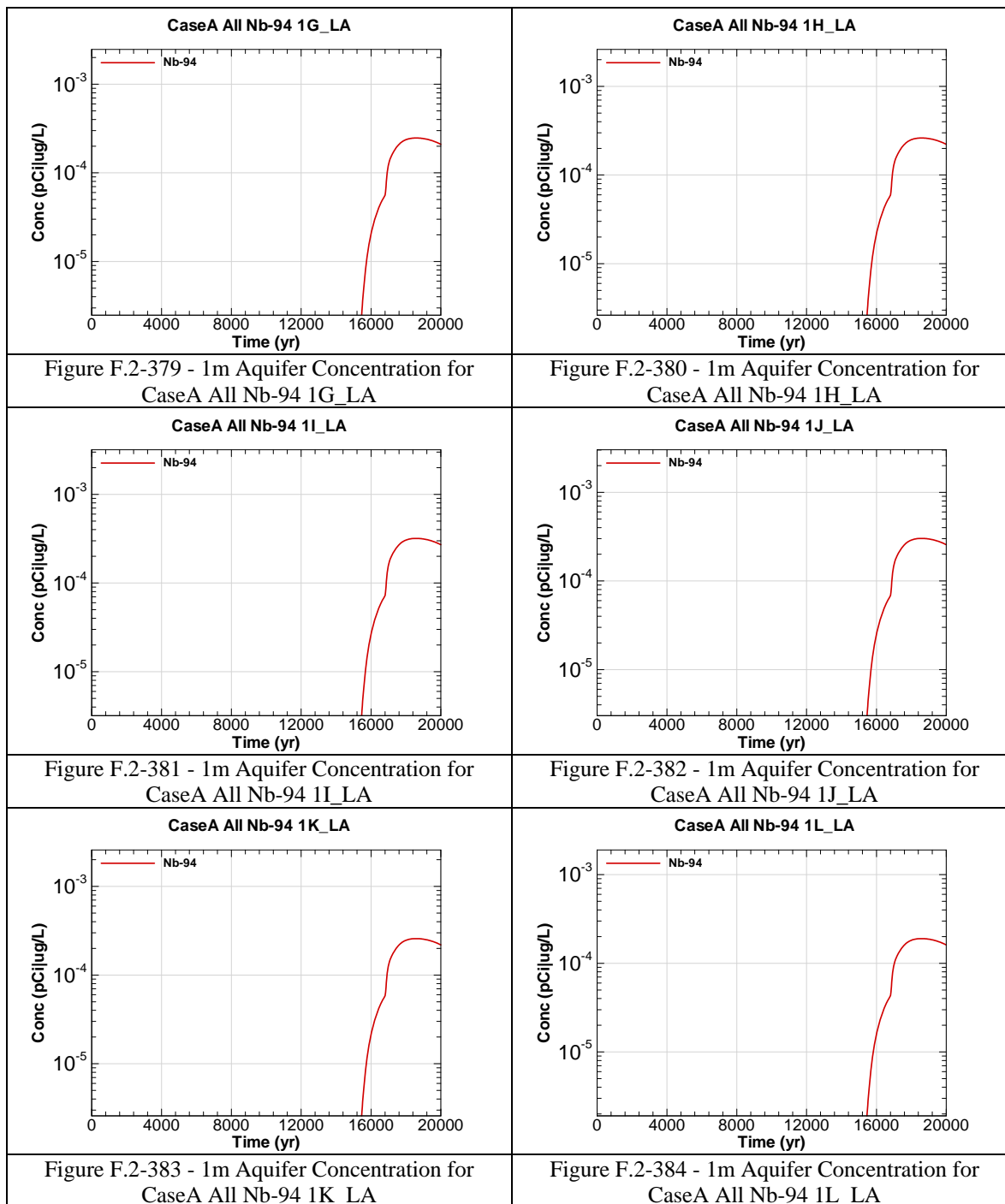


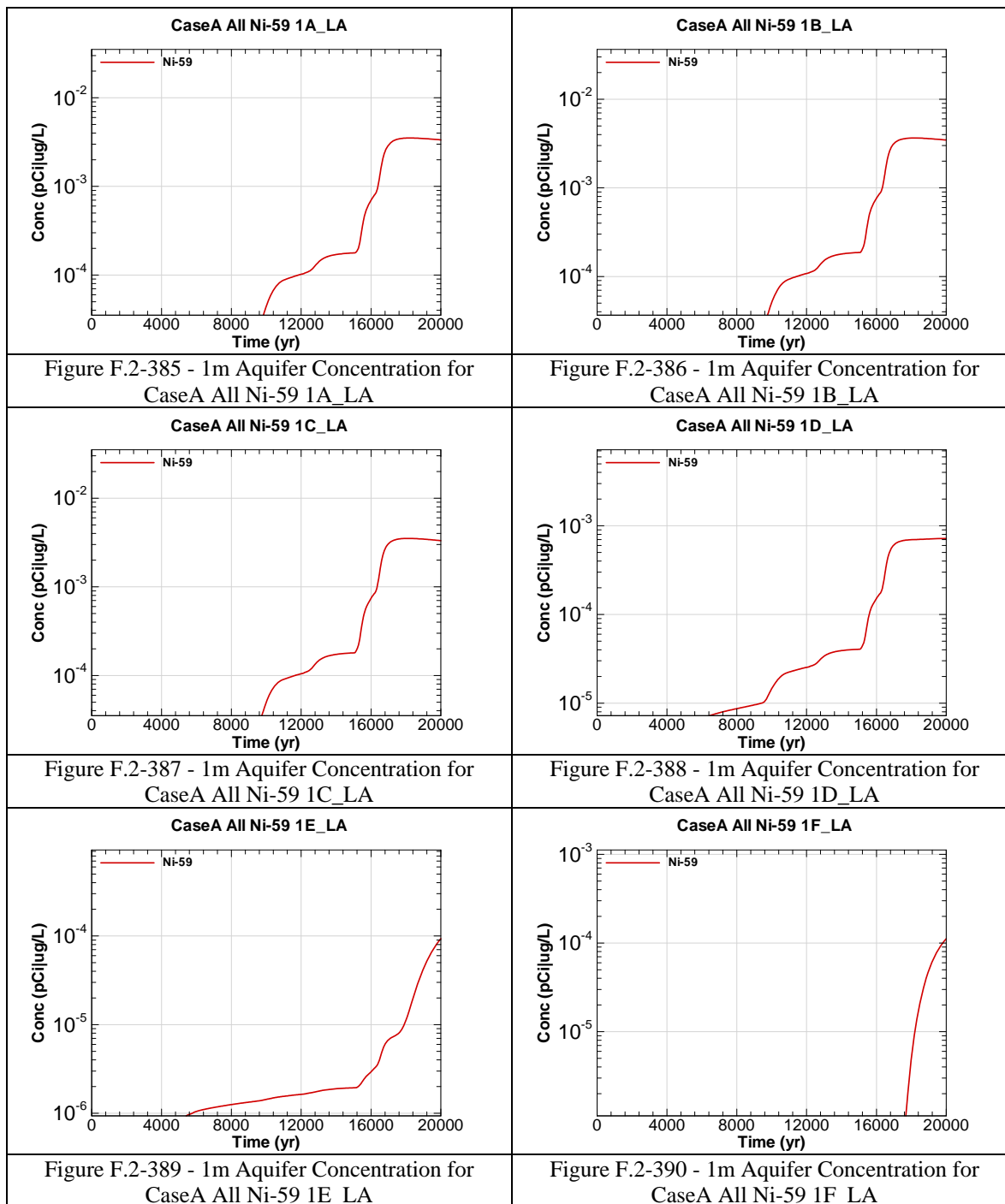


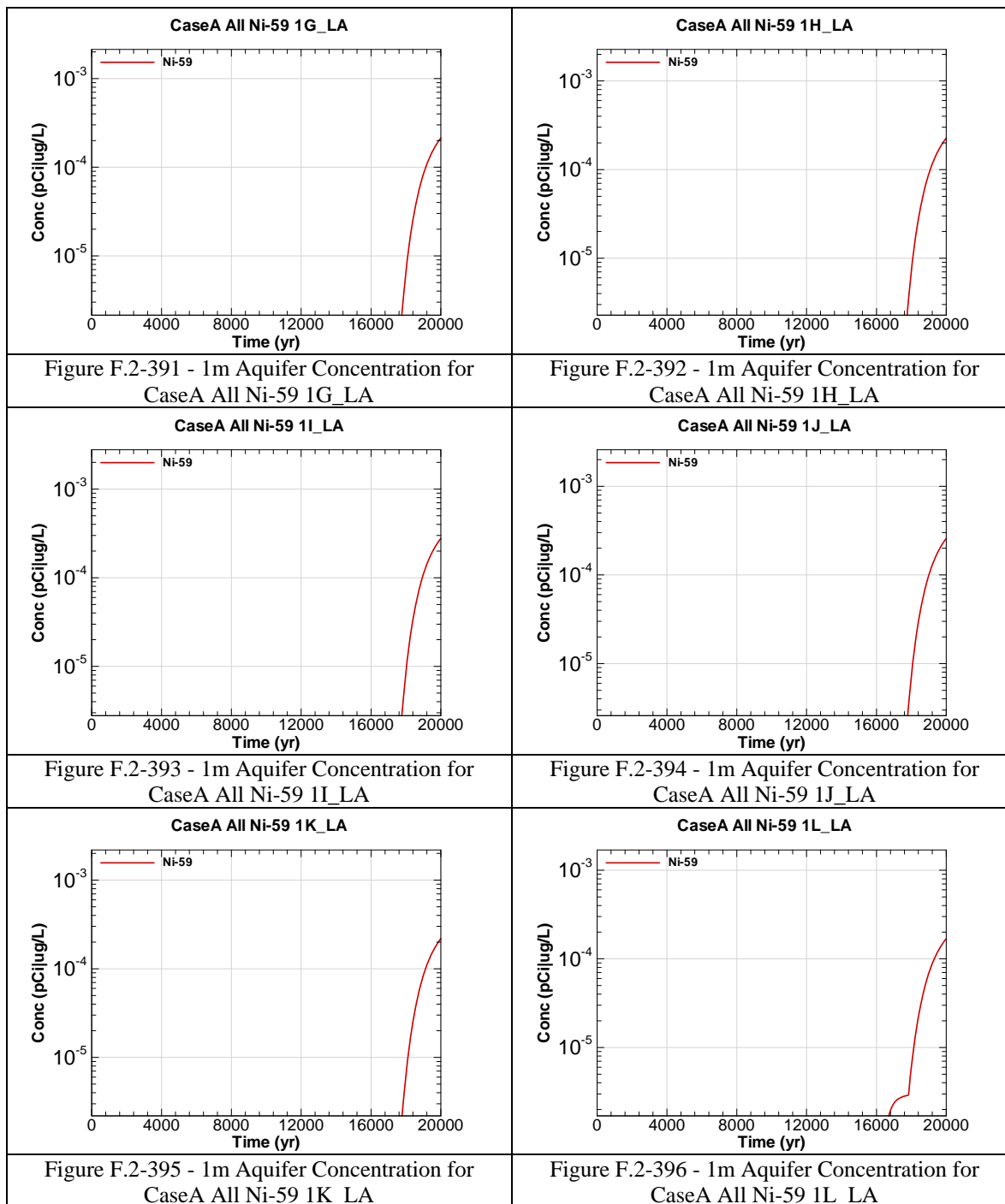


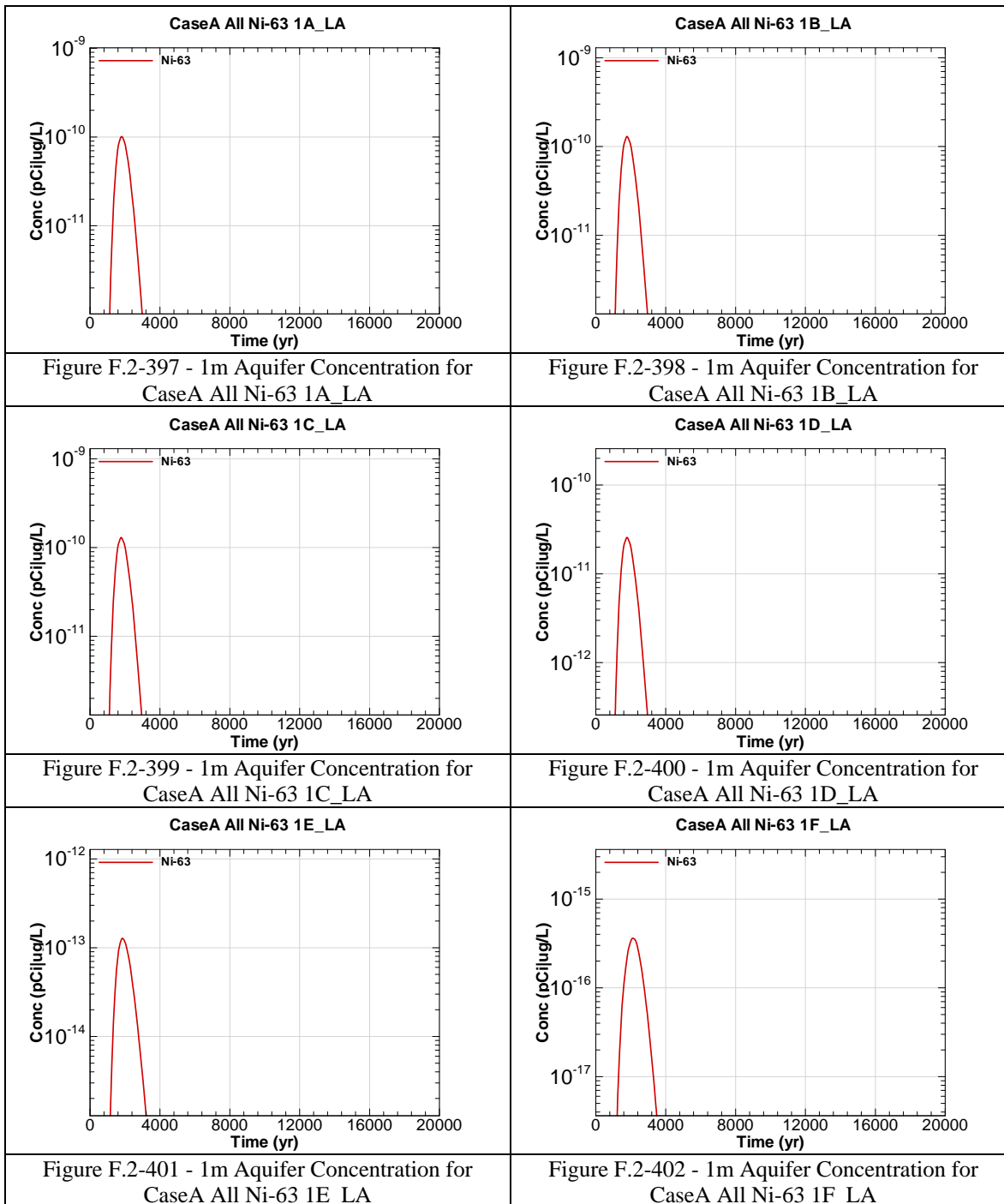


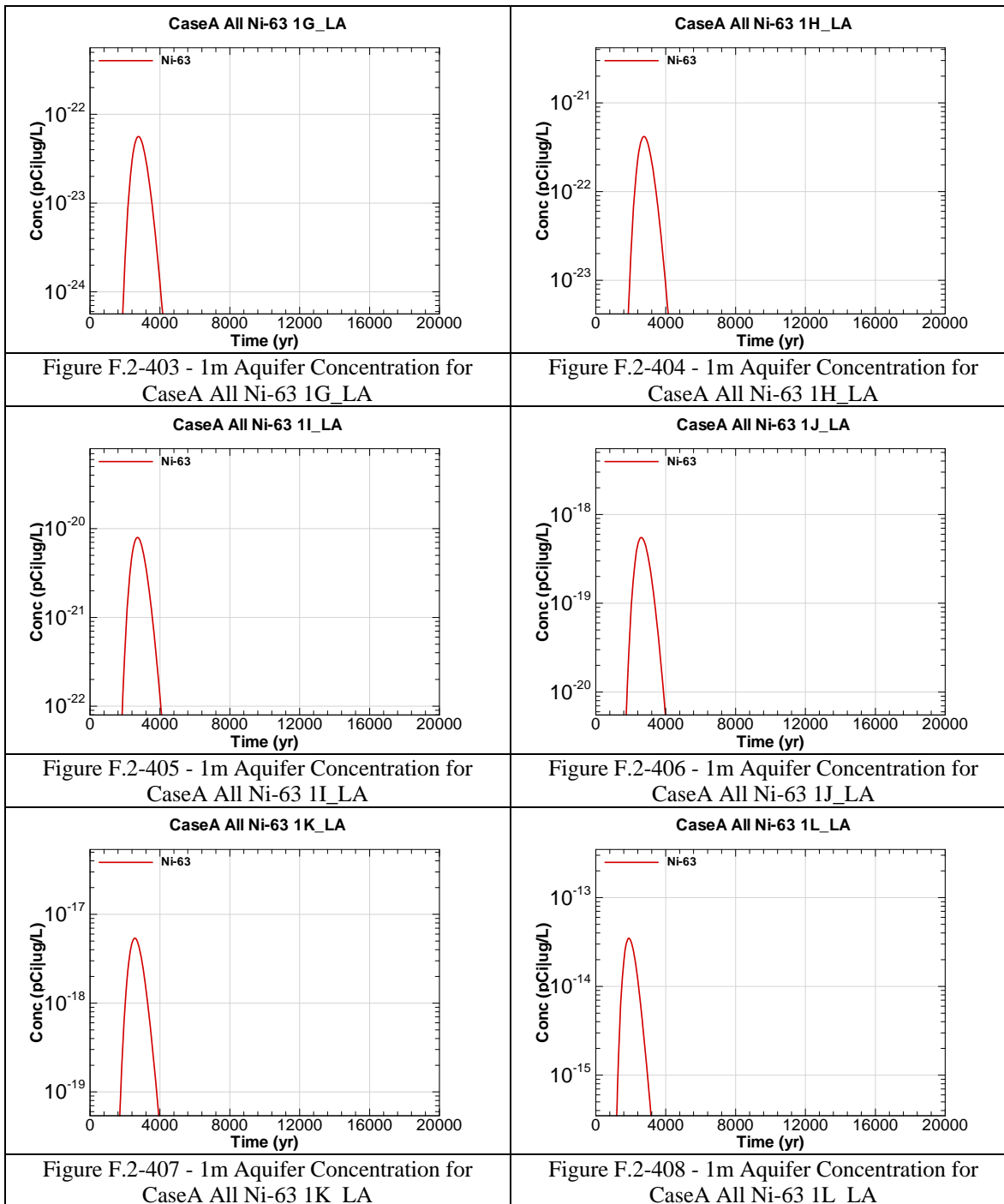












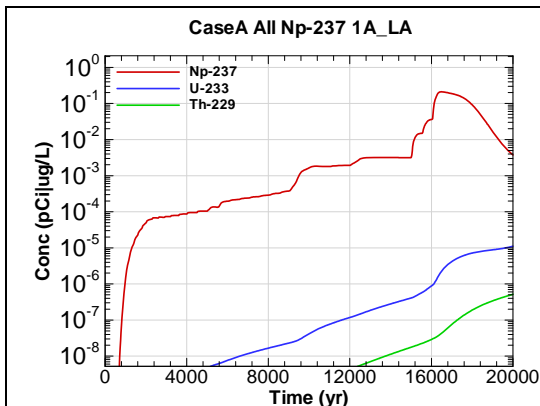


Figure F.2-409 - 1m Aquifer Concentration for
CaseA All Np-237 1A_LA

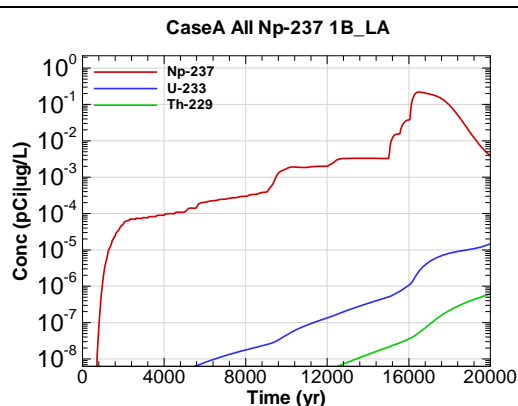


Figure F.2-410 - 1m Aquifer Concentration for
CaseA All Np-237 1B_LA

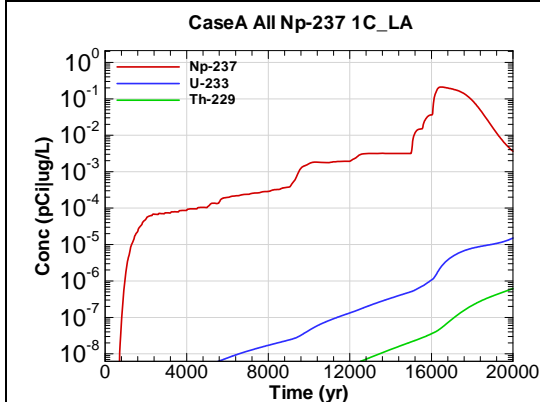


Figure F.2-411 - 1m Aquifer Concentration for
CaseA All Np-237 1C_LA

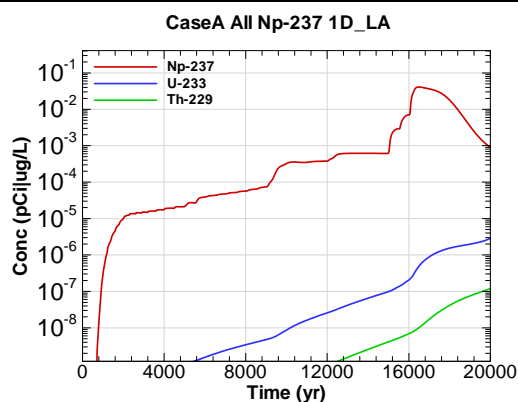


Figure F.2-412 - 1m Aquifer Concentration for
CaseA All Np-237 1D_LA

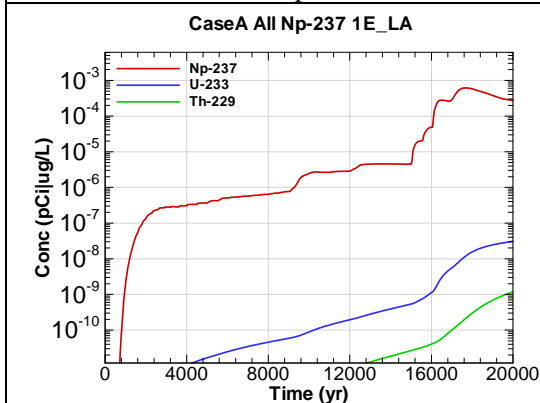


Figure F.2-413 - 1m Aquifer Concentration for
CaseA All Np-237 1E_LA

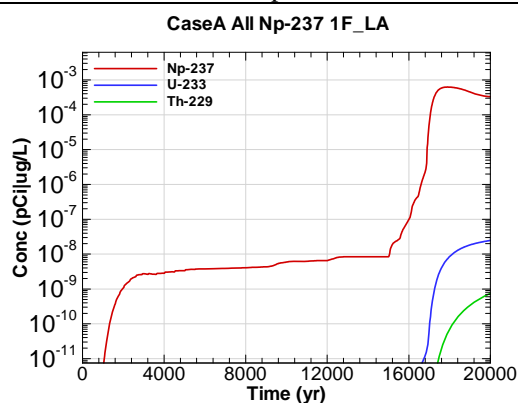
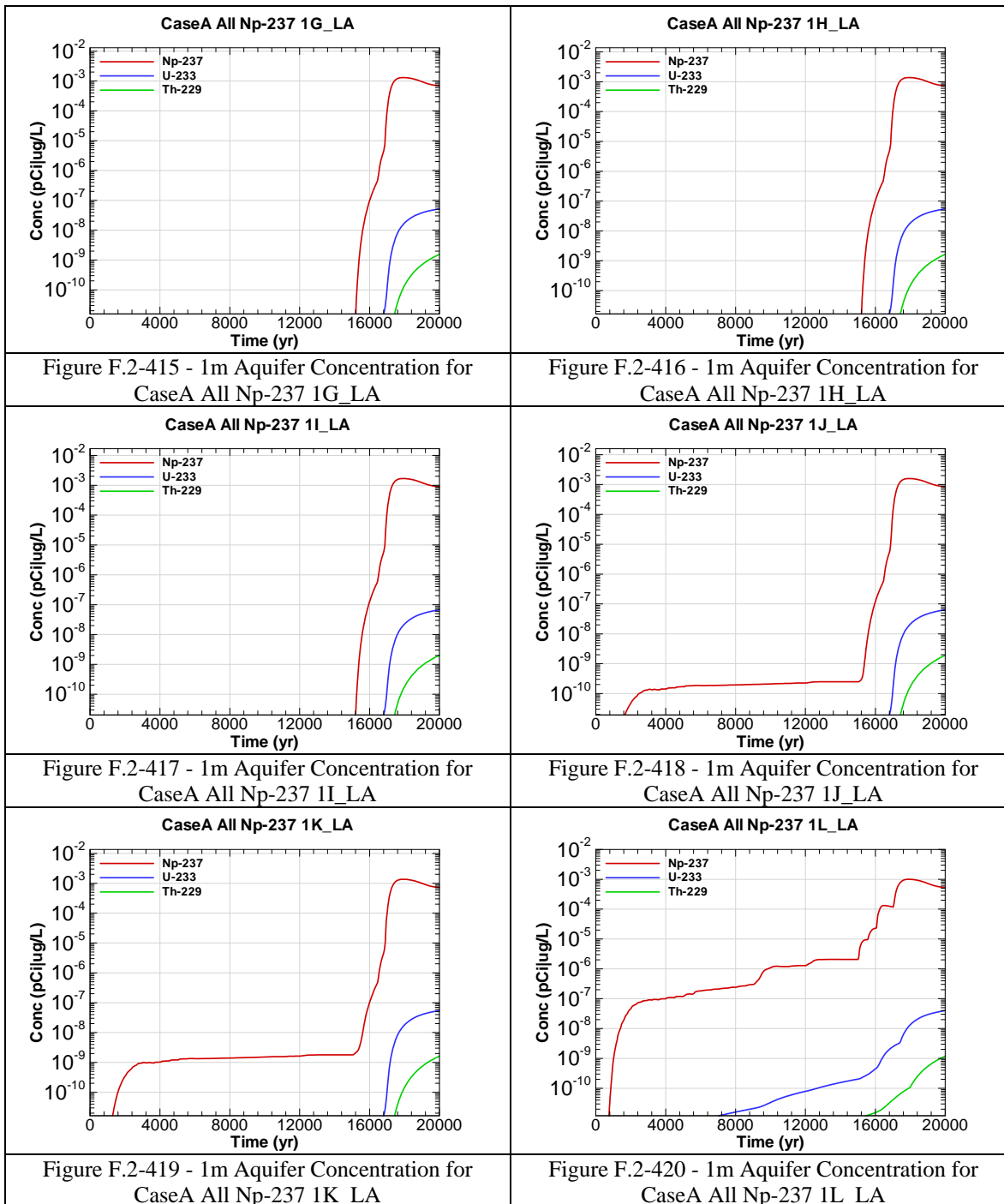
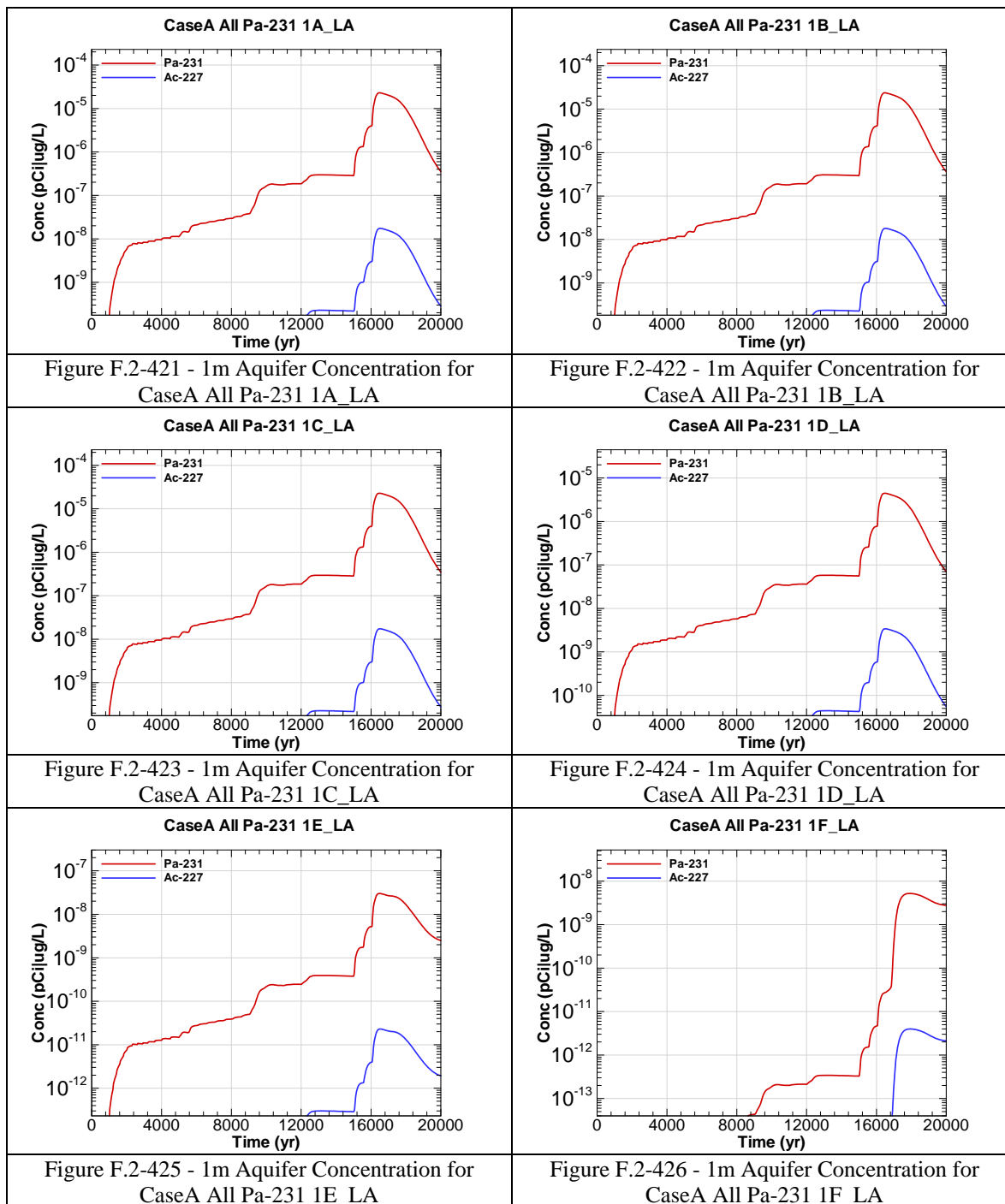
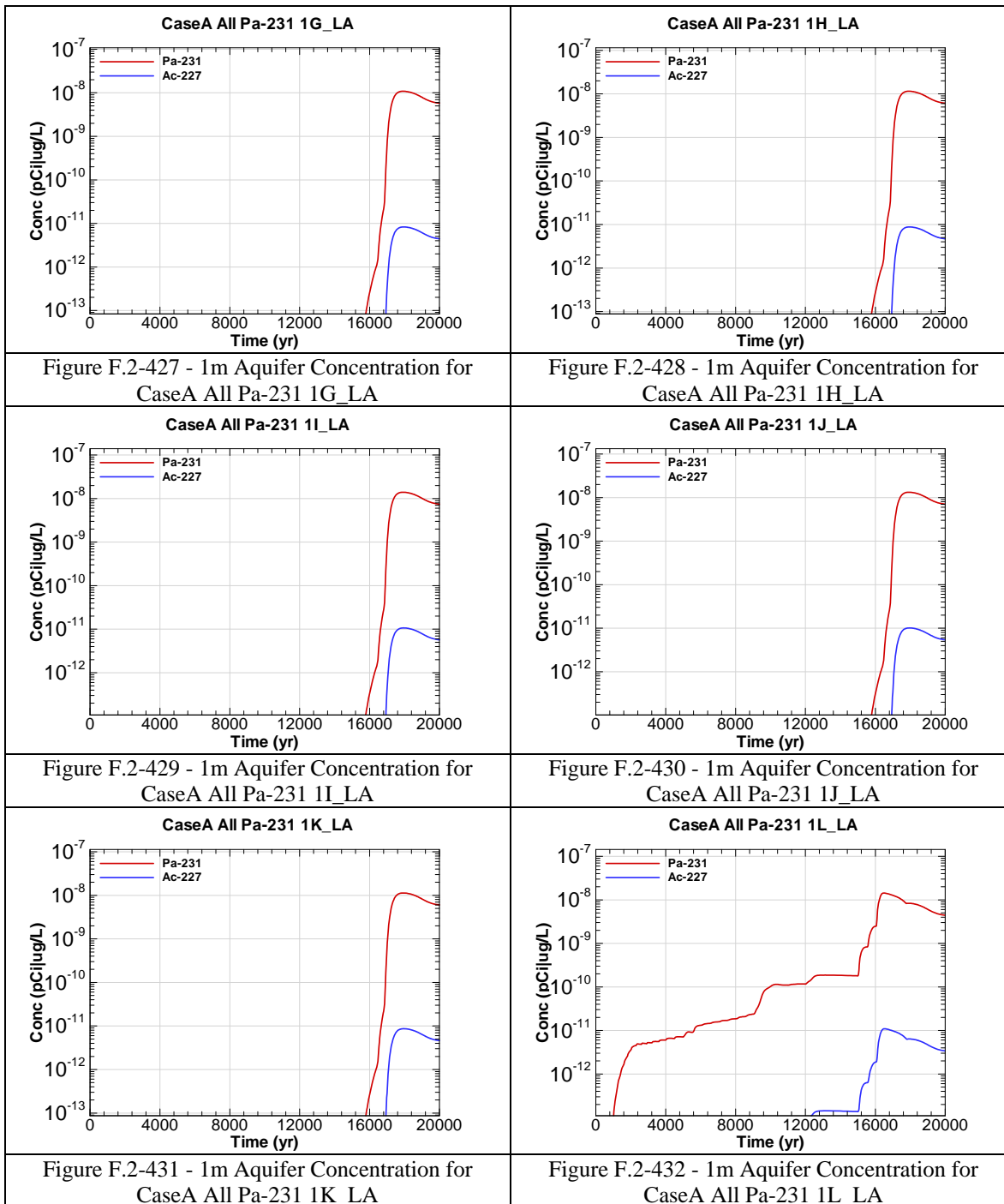
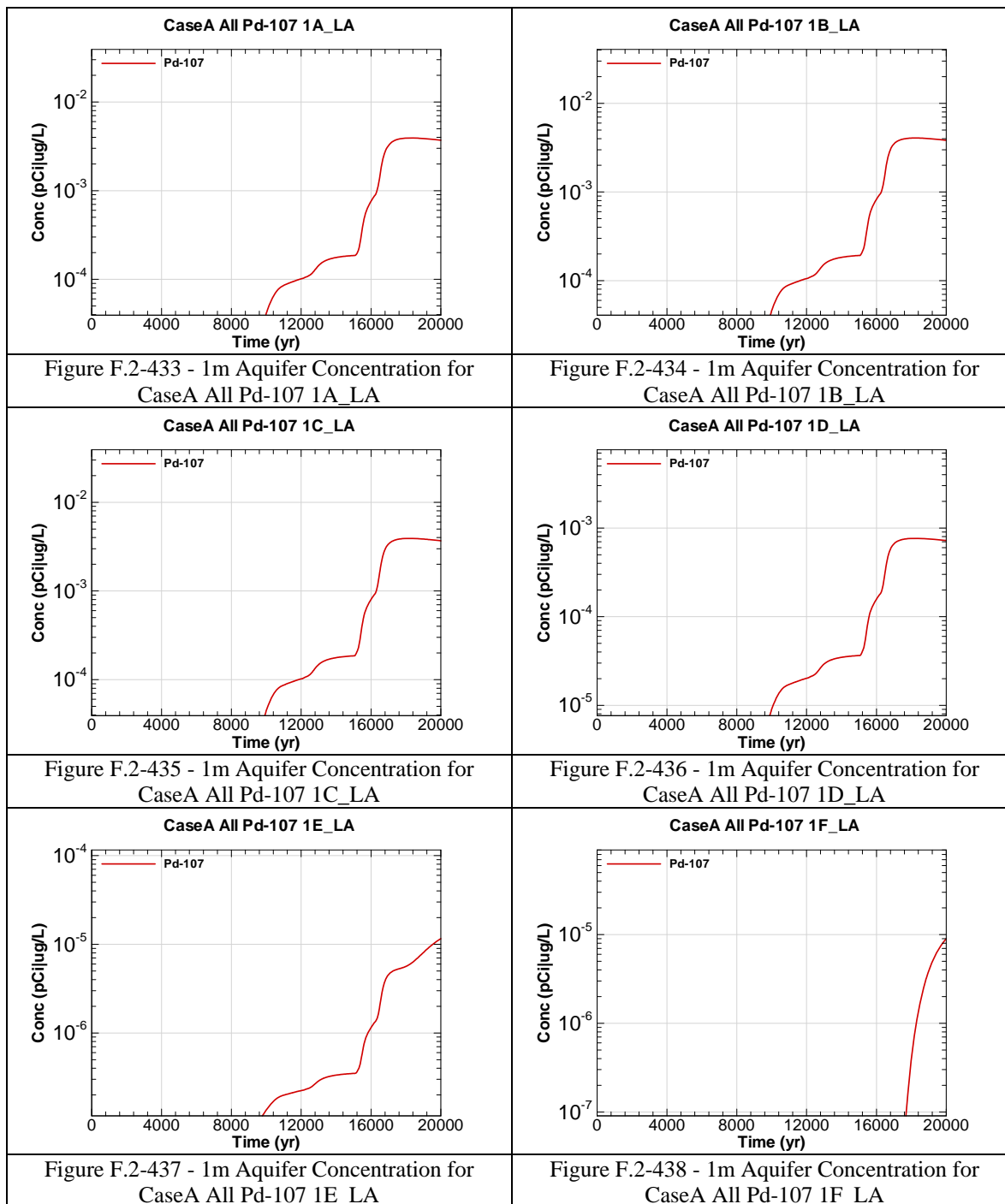


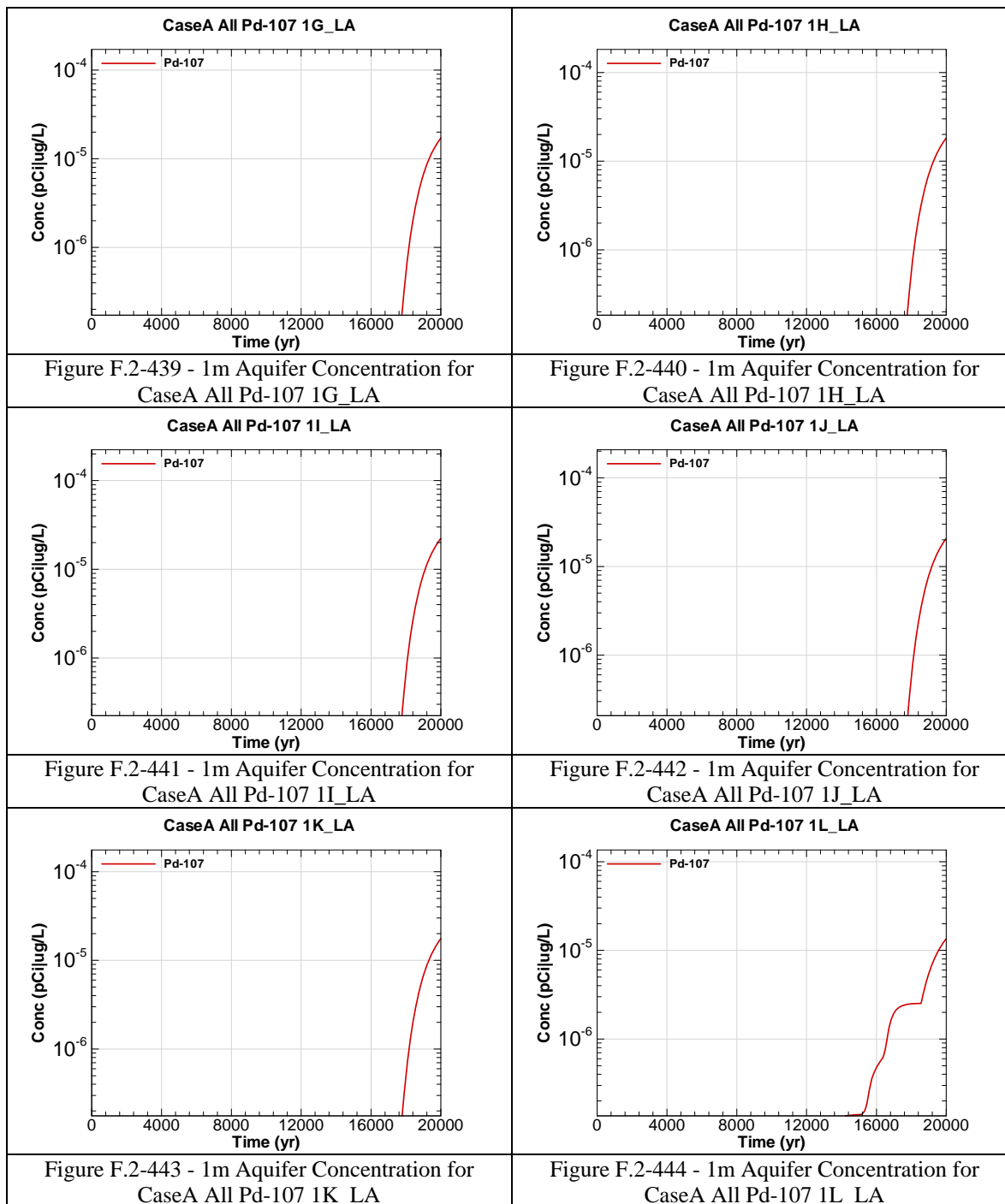
Figure F.2-414 - 1m Aquifer Concentration for
CaseA All Np-237 1F_LA

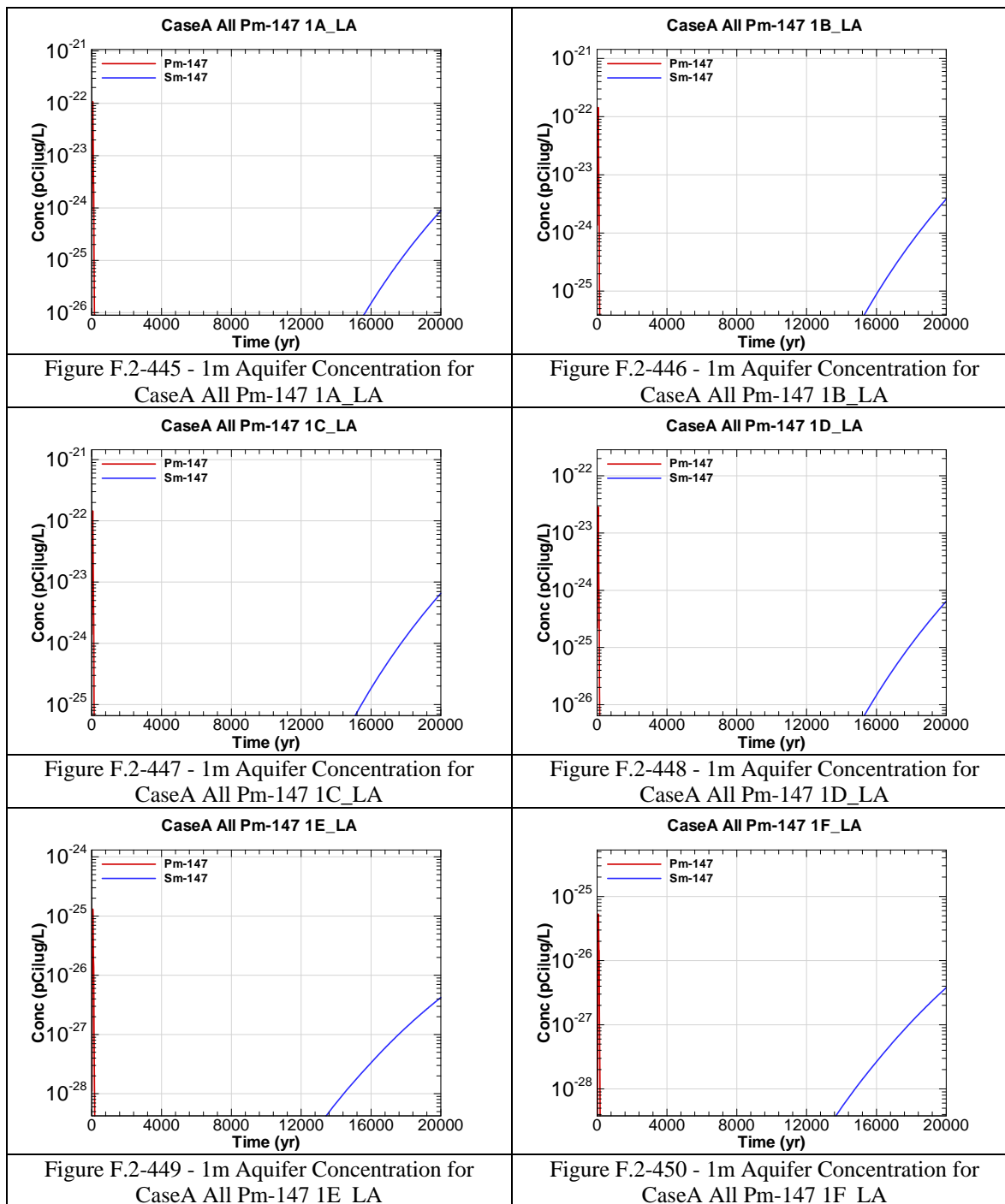


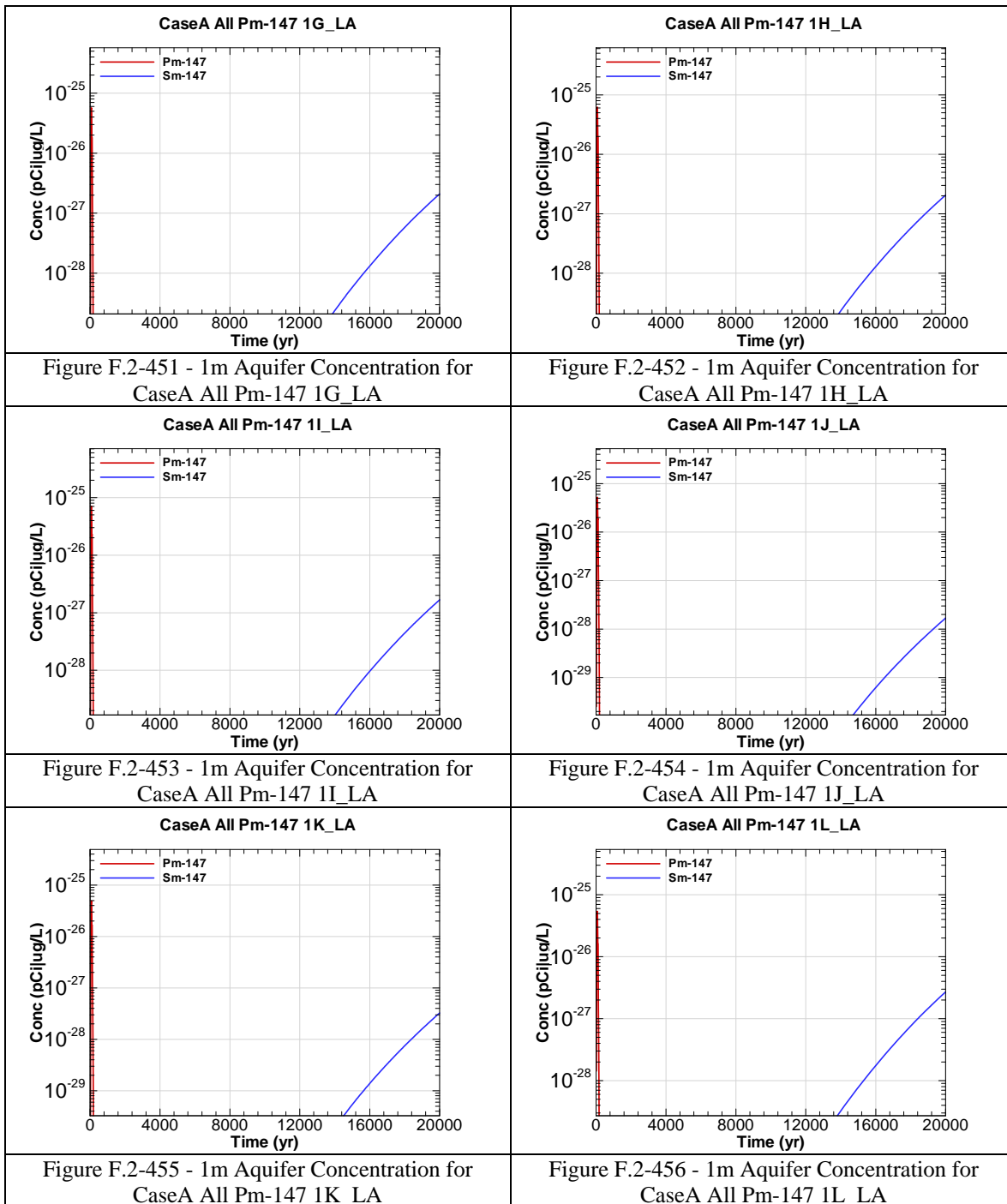


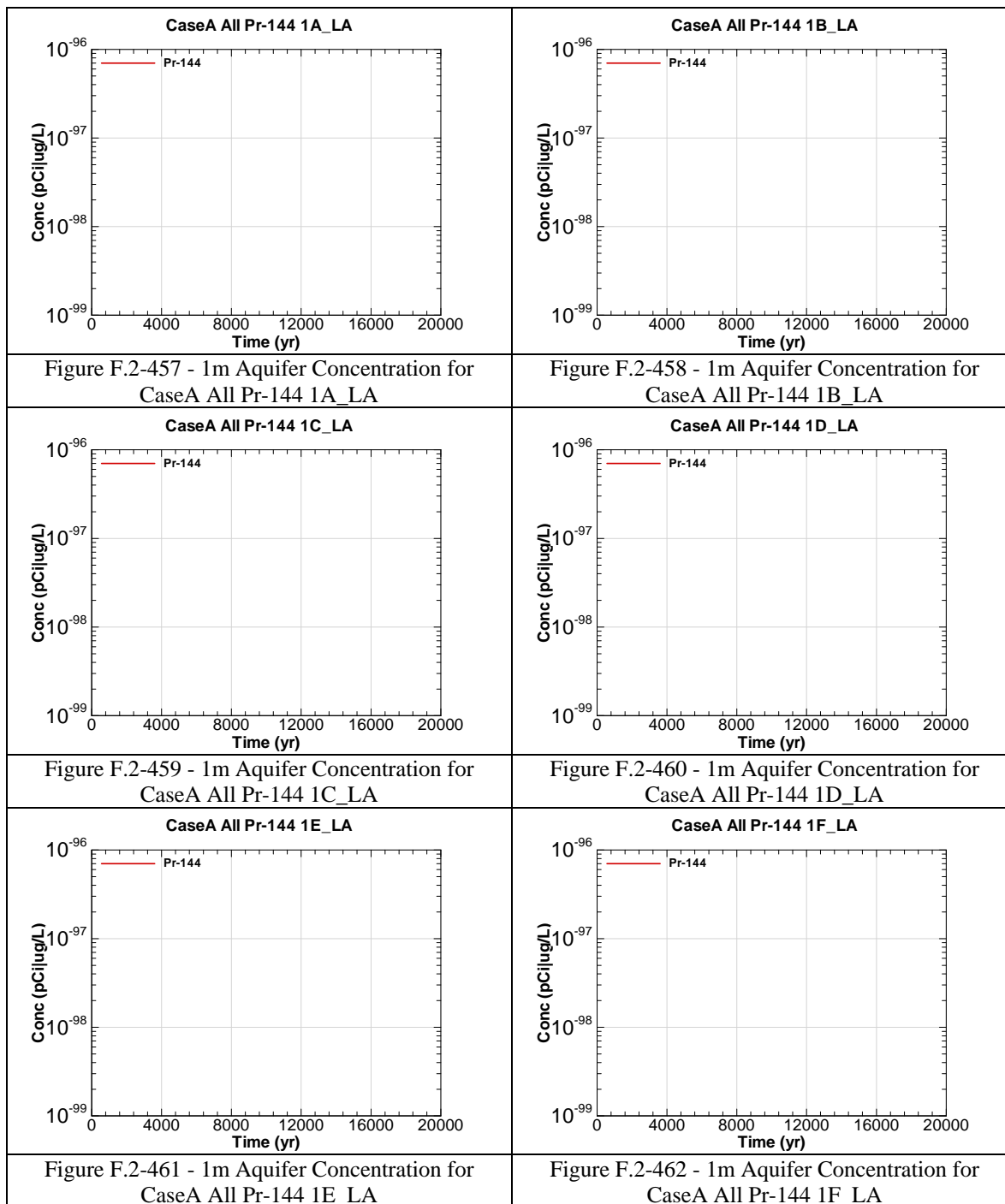


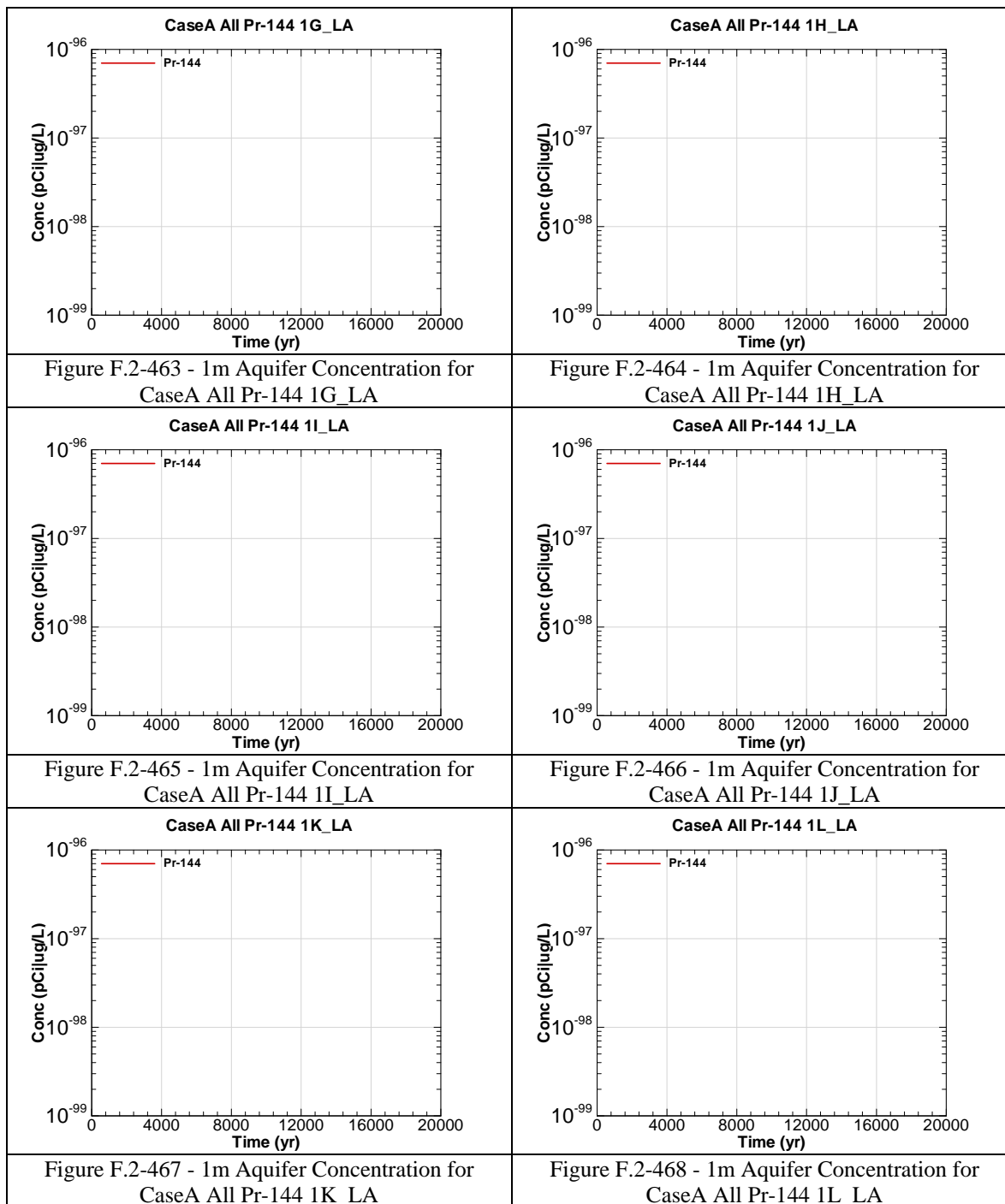


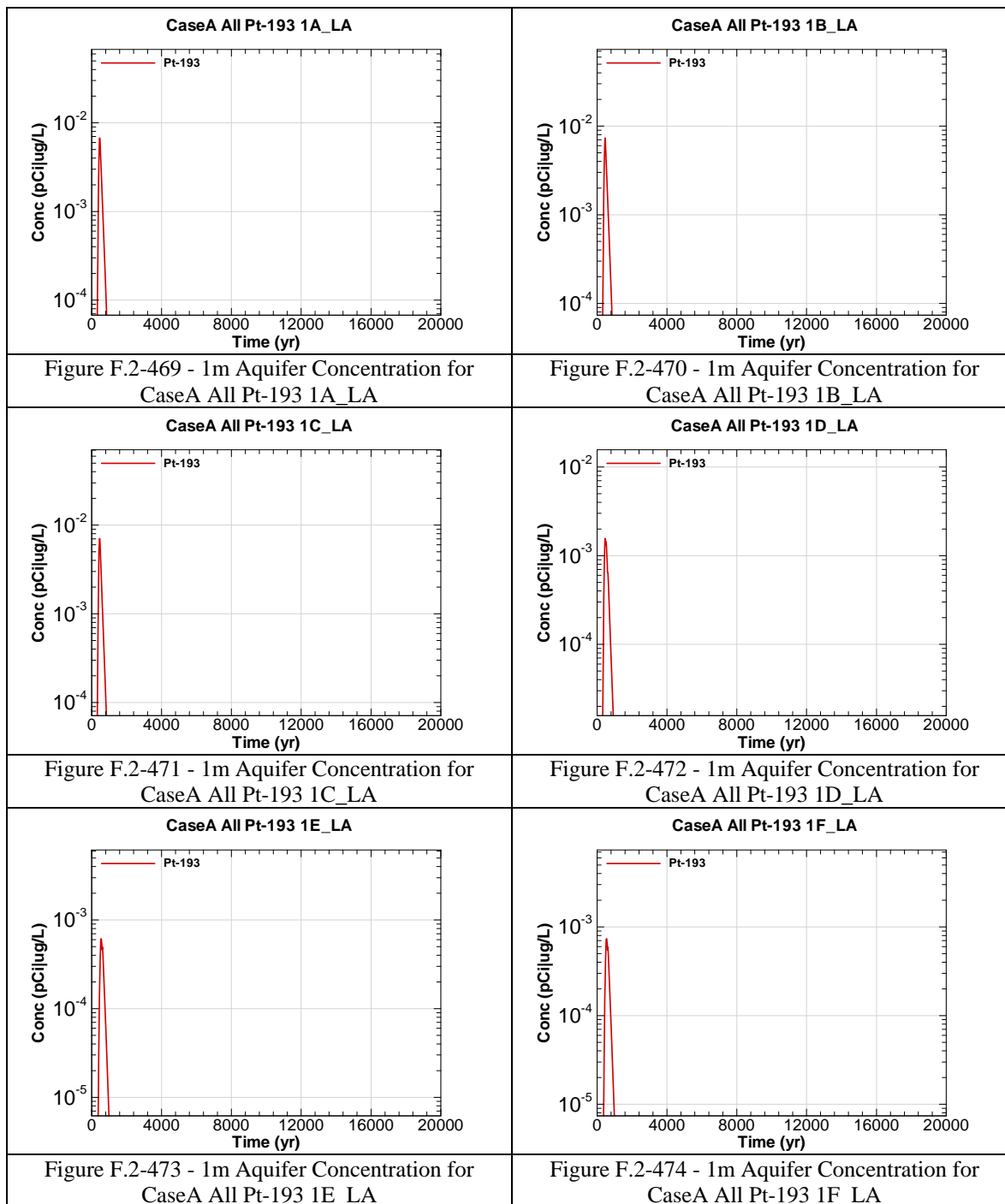


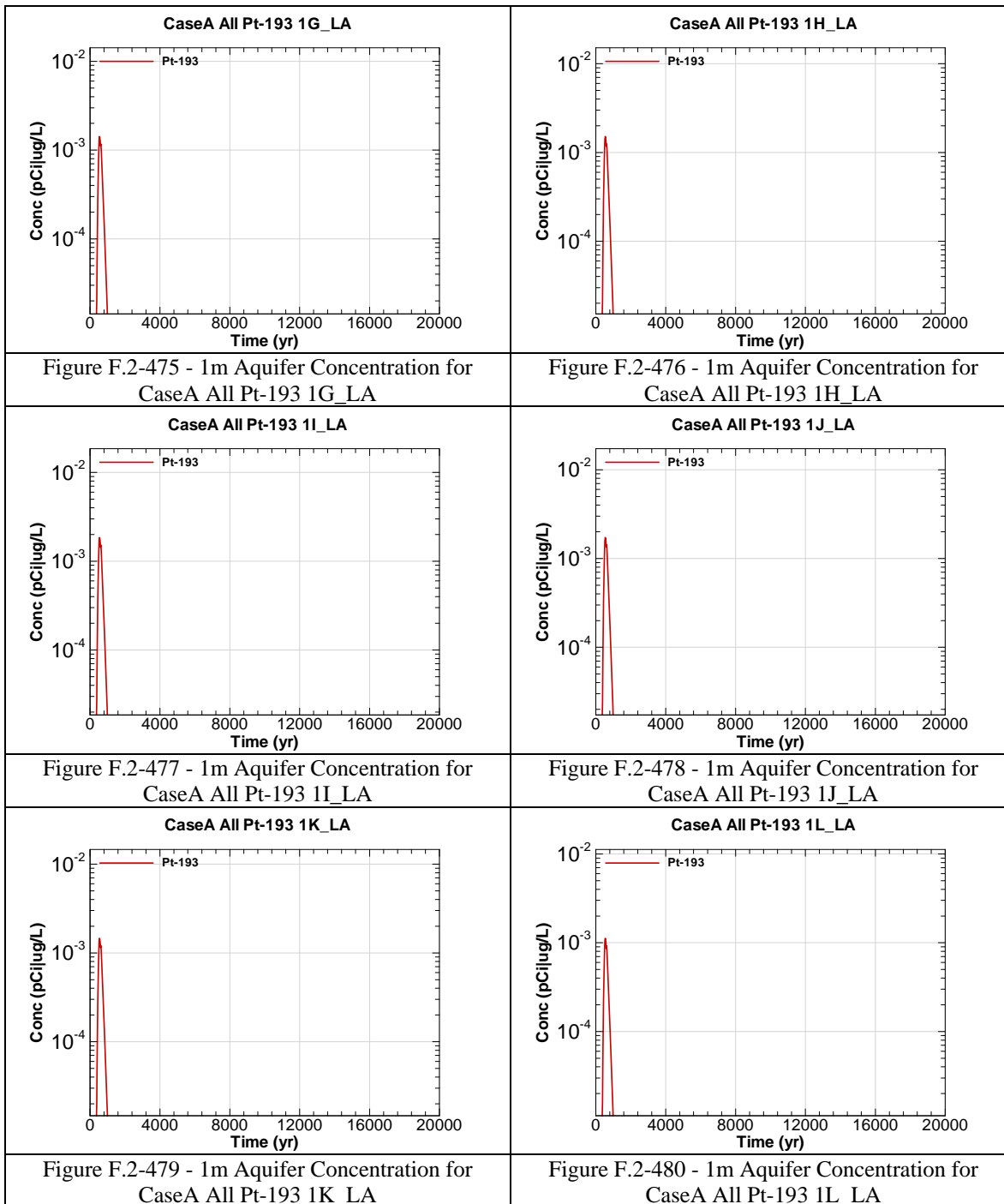












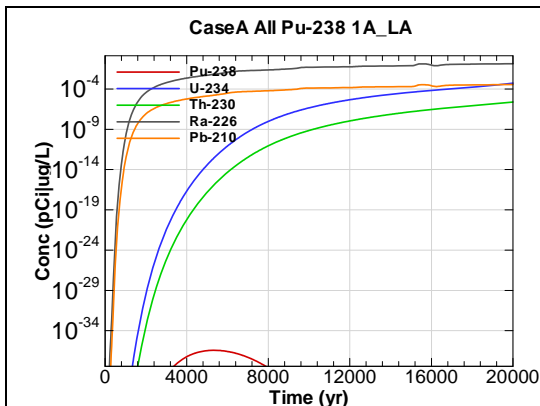


Figure F.2-481 - 1m Aquifer Concentration for
CaseA All Pu-238 1A_LA

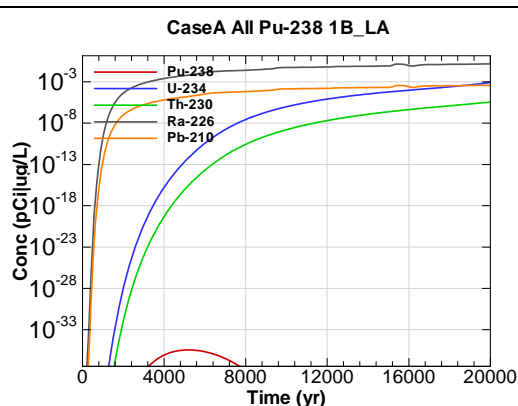


Figure F.2-482 - 1m Aquifer Concentration for
CaseA All Pu-238 1B_LA

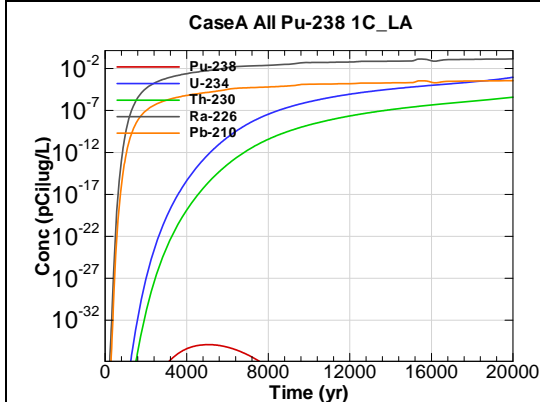


Figure F.2-483 - 1m Aquifer Concentration for
CaseA All Pu-238 1C_LA

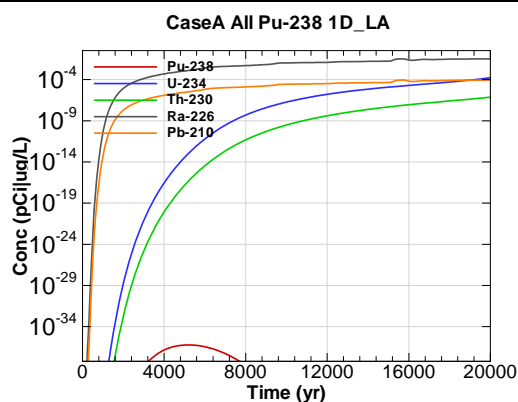


Figure F.2-484 - 1m Aquifer Concentration for
CaseA All Pu-238 1D_LA

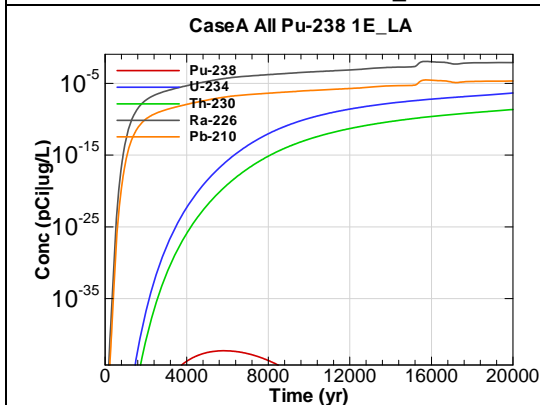


Figure F.2-485 - 1m Aquifer Concentration for
CaseA All Pu-238 1E_LA

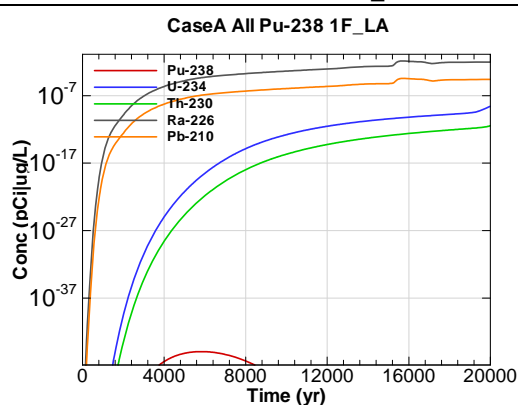


Figure F.2-486 - 1m Aquifer Concentration for
CaseA All Pu-238 1F_LA

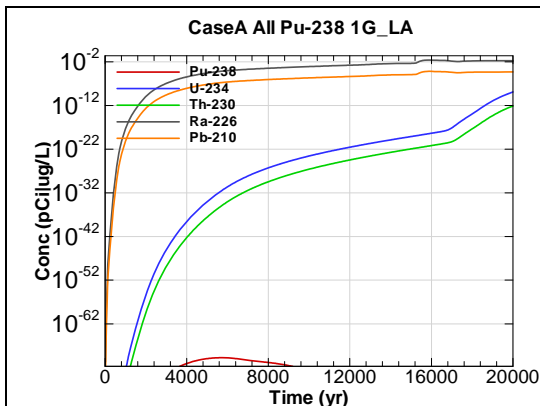


Figure F.2-487 - 1m Aquifer Concentration for
CaseA All Pu-238 1G_LA

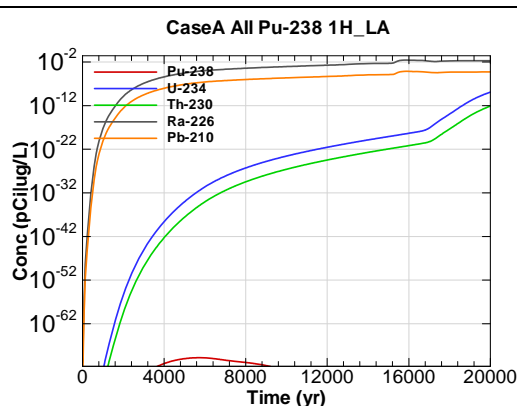


Figure F.2-488 - 1m Aquifer Concentration for
CaseA All Pu-238 1H_LA

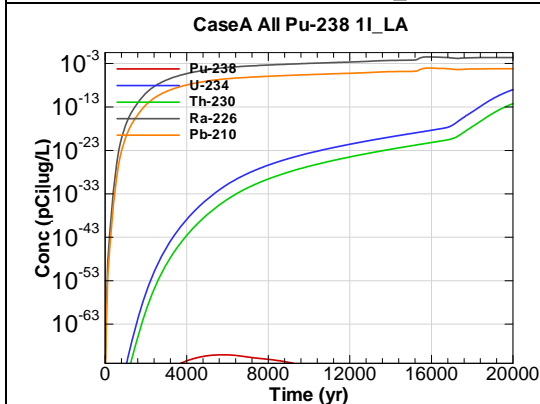


Figure F.2-489 - 1m Aquifer Concentration for
CaseA All Pu-238 1I_LA

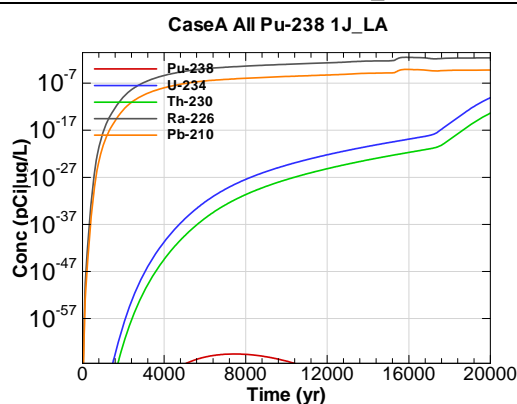


Figure F.2-490 - 1m Aquifer Concentration for
CaseA All Pu-238 1J_LA

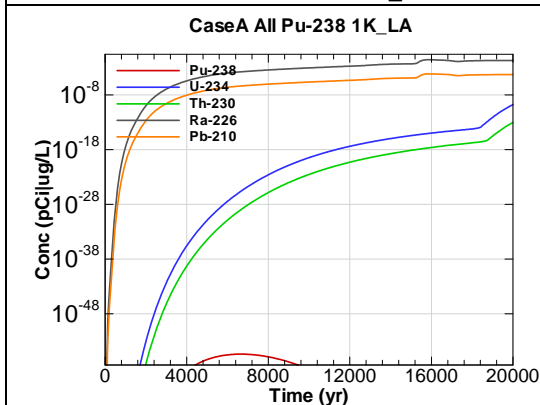


Figure F.2-491 - 1m Aquifer Concentration for
CaseA All Pu-238 1K_LA

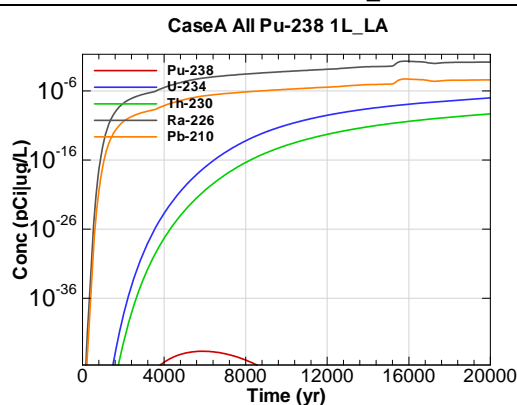


Figure F.2-492 - 1m Aquifer Concentration for
CaseA All Pu-238 1L_LA

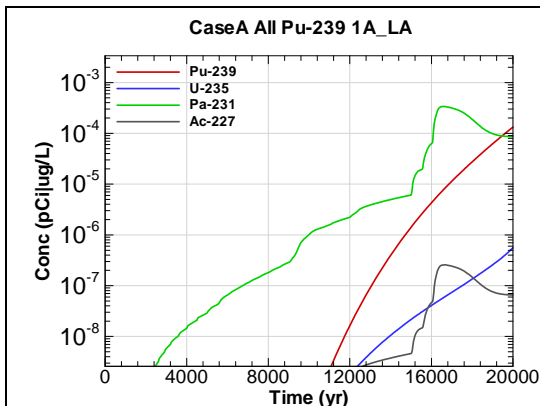


Figure F.2-493 - 1m Aquifer Concentration for
CaseA All Pu-239 1A_LA

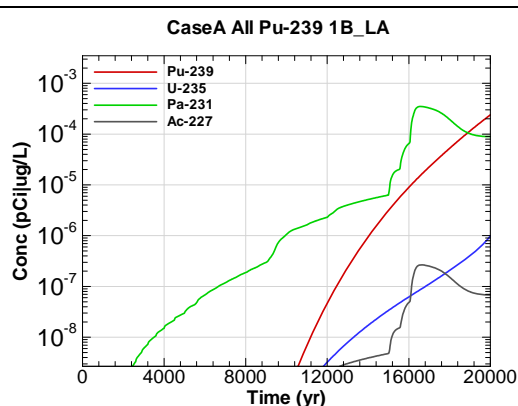


Figure F.2-494 - 1m Aquifer Concentration for
CaseA All Pu-239 1B_LA

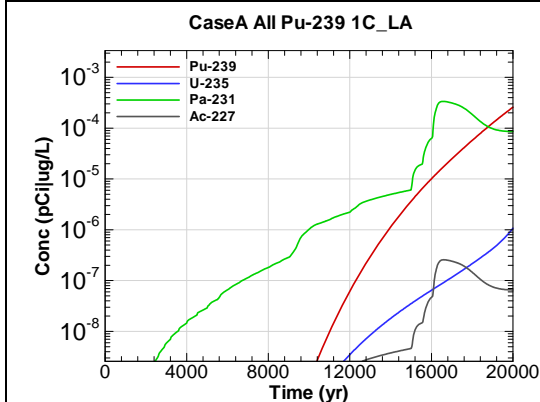


Figure F.2-495 - 1m Aquifer Concentration for
CaseA All Pu-239 1C_LA

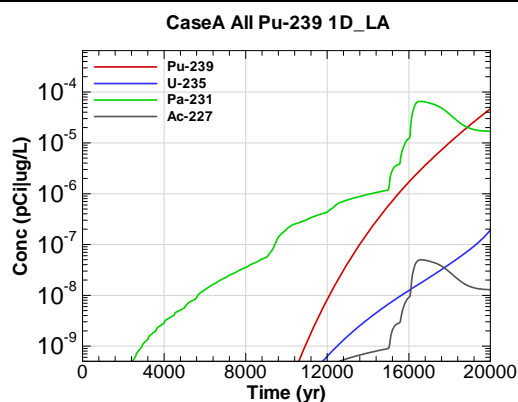


Figure F.2-496 - 1m Aquifer Concentration for
CaseA All Pu-239 1D_LA

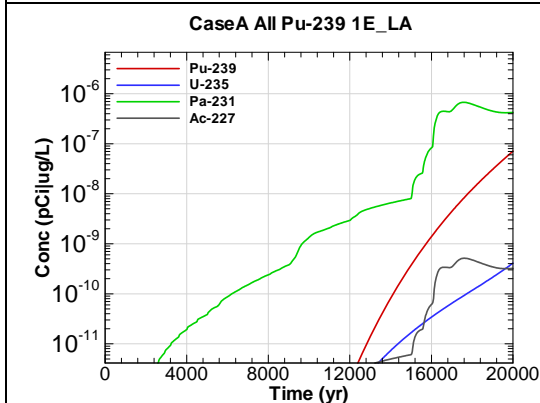


Figure F.2-497 - 1m Aquifer Concentration for
CaseA All Pu-239 1E_LA

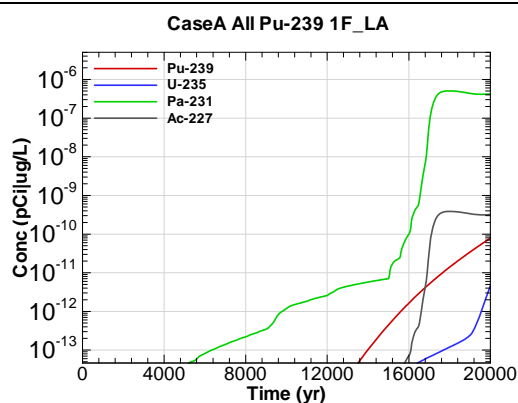


Figure F.2-498 - 1m Aquifer Concentration for
CaseA All Pu-239 1F_LA

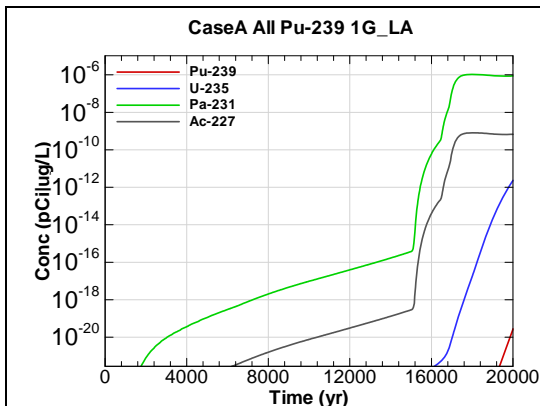


Figure F.2-499 - 1m Aquifer Concentration for CaseA All Pu-239 1G_LA

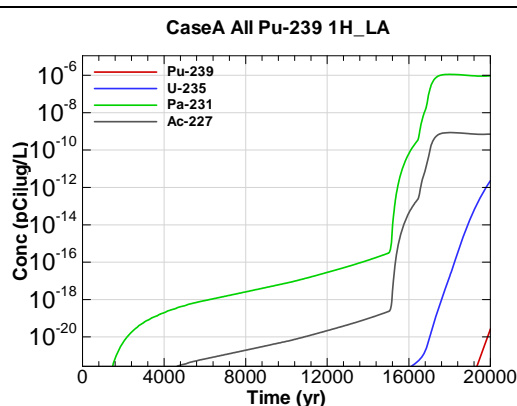


Figure F.2-500 - 1m Aquifer Concentration for CaseA All Pu-239 1H_LA

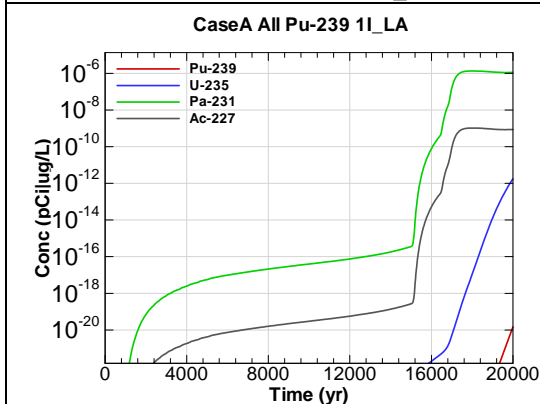


Figure F.2-501 - 1m Aquifer Concentration for CaseA All Pu-239 1I_LA

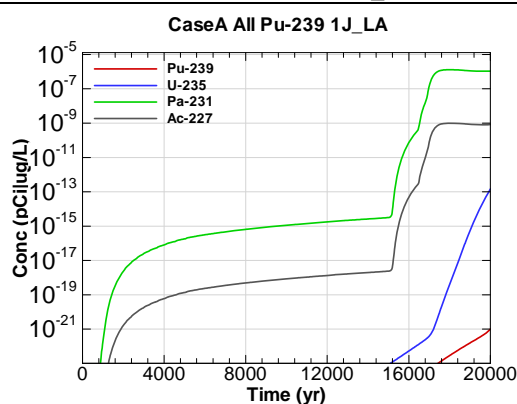


Figure F.2-502 - 1m Aquifer Concentration for CaseA All Pu-239 1J_LA

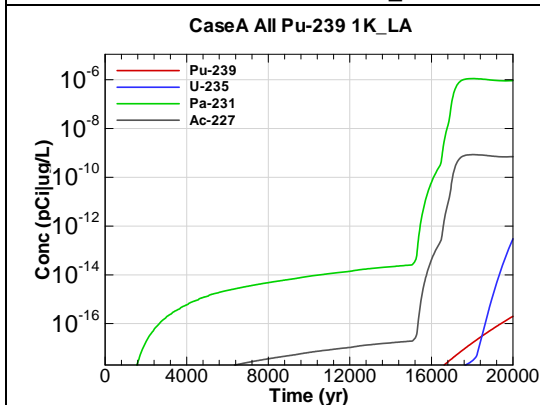


Figure F.2-503 - 1m Aquifer Concentration for CaseA All Pu-239 1K_LA

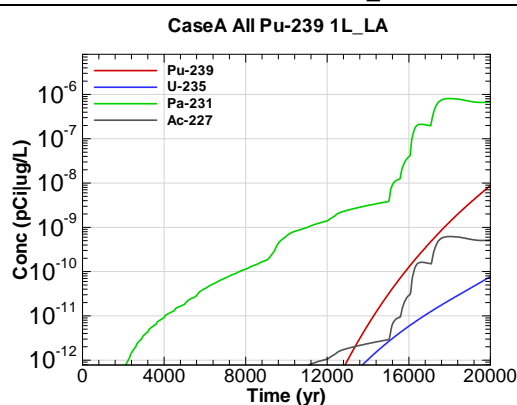
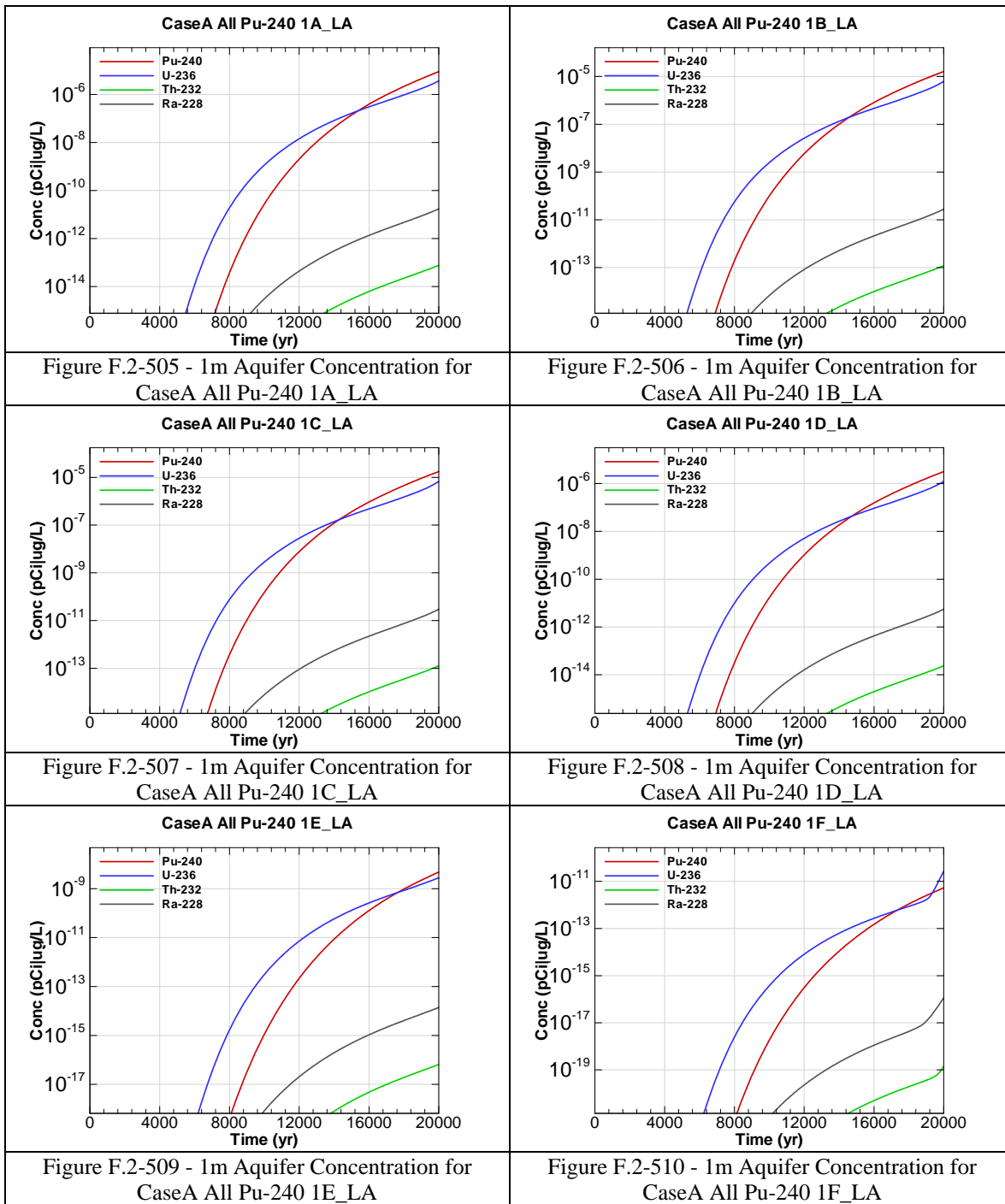
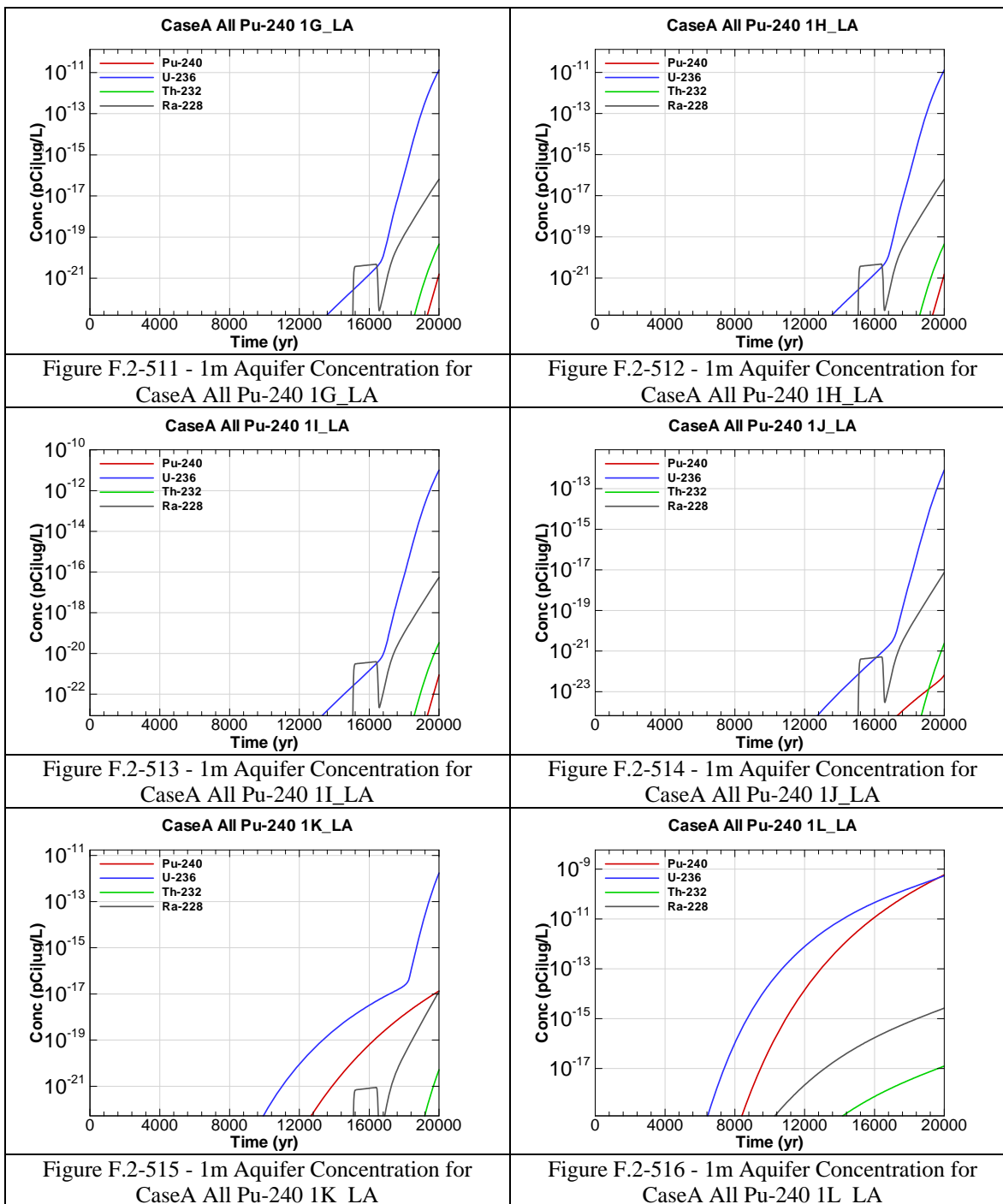


Figure F.2-504 - 1m Aquifer Concentration for CaseA All Pu-239 1L_LA





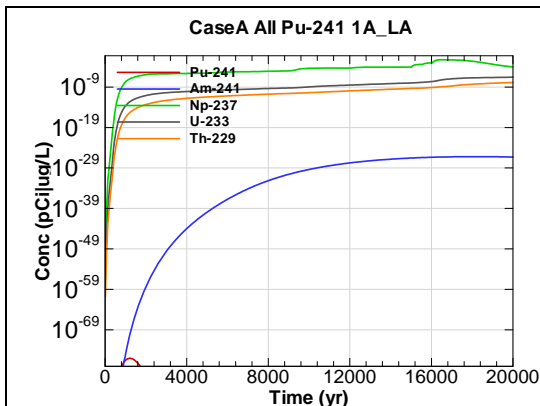


Figure F.2-517 - 1m Aquifer Concentration for
CaseA All Pu-241 1A_LA

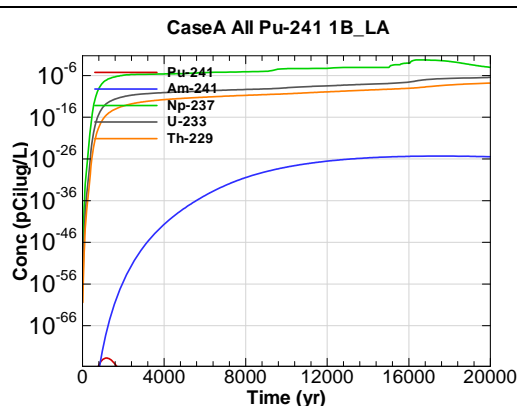


Figure F.2-518 - 1m Aquifer Concentration for
CaseA All Pu-241 1B_LA

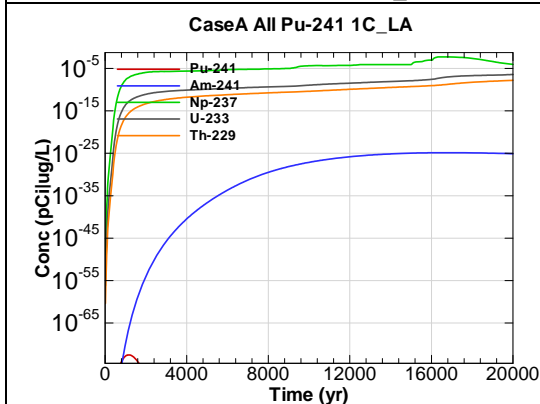


Figure F.2-519 - 1m Aquifer Concentration for
CaseA All Pu-241 1C_LA

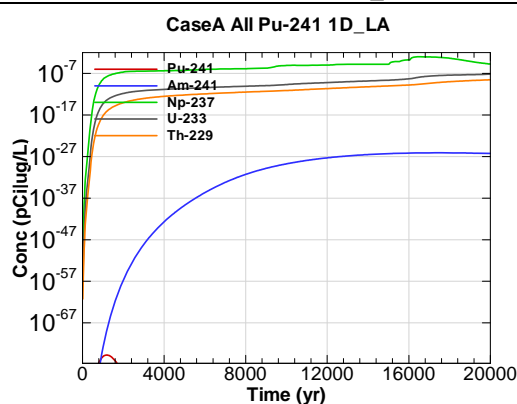


Figure F.2-520 - 1m Aquifer Concentration for
CaseA All Pu-241 1D_LA

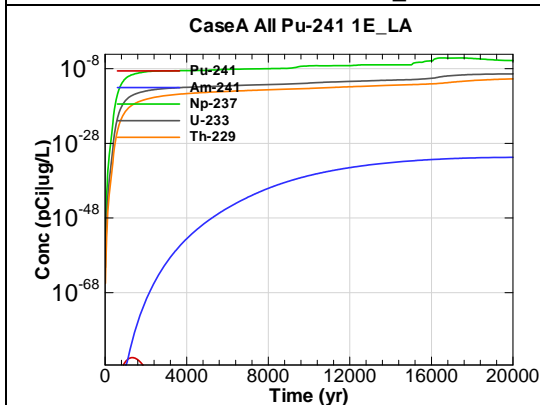


Figure F.2-521 - 1m Aquifer Concentration for
CaseA All Pu-241 1E_LA

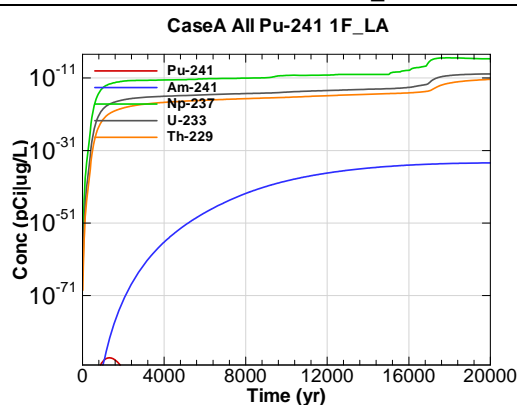
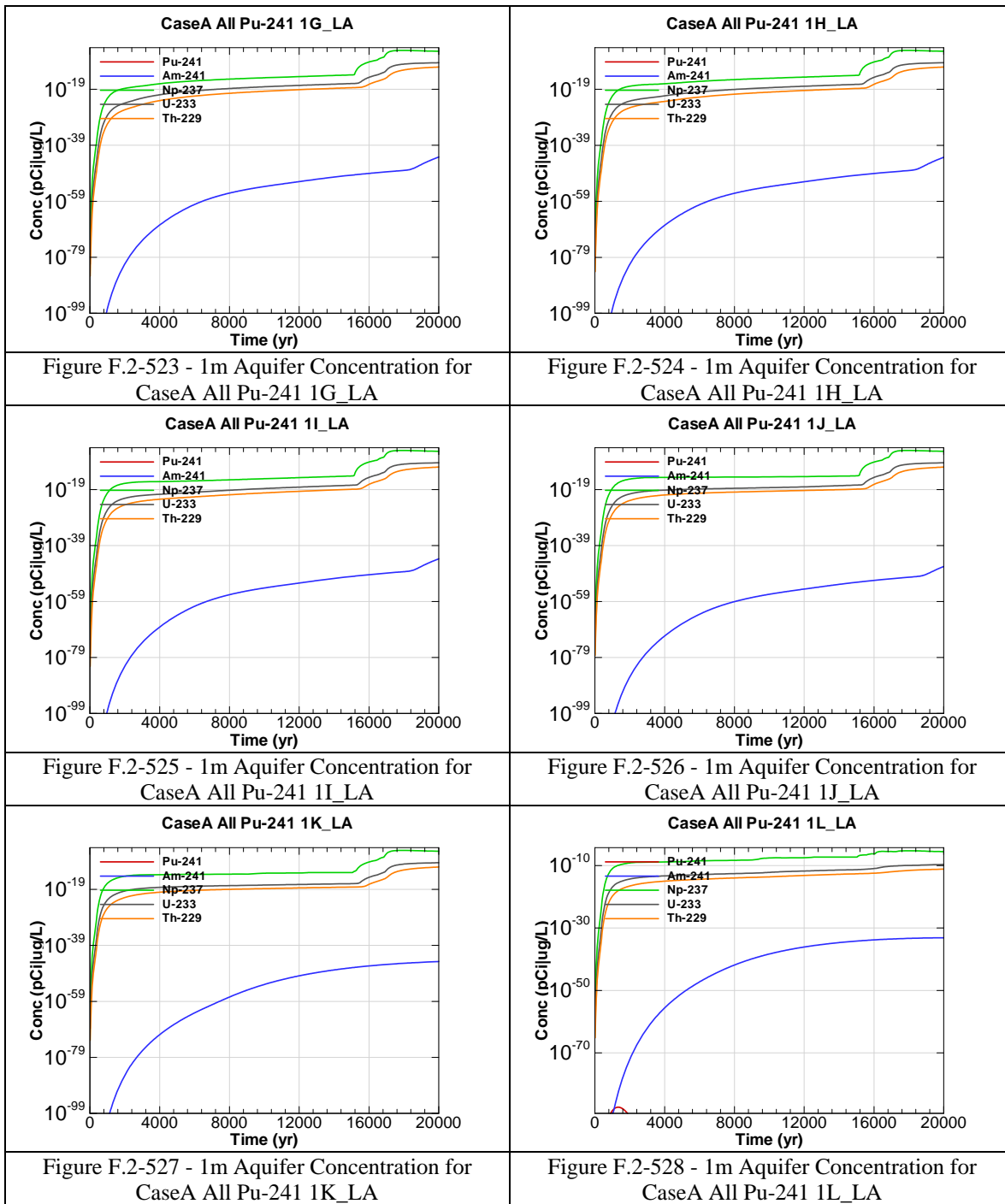


Figure F.2-522 - 1m Aquifer Concentration for
CaseA All Pu-241 1F_LA



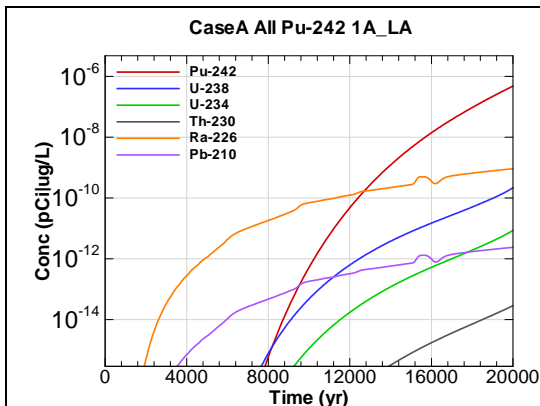


Figure F.2-529 - 1m Aquifer Concentration for
CaseA All Pu-242 1A_LA

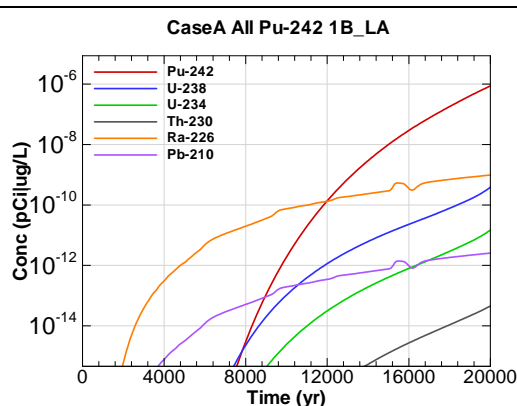


Figure F.2-530 - 1m Aquifer Concentration for
CaseA All Pu-242 1B_LA

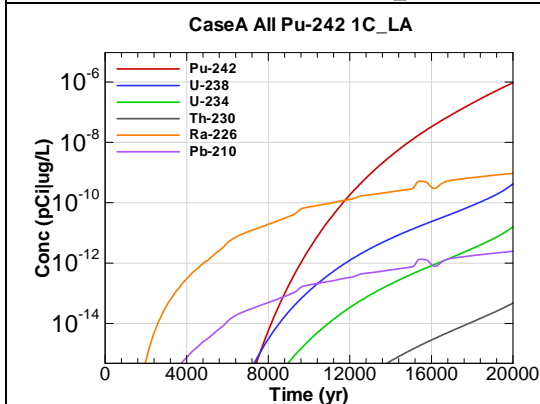


Figure F.2-531 - 1m Aquifer Concentration for
CaseA All Pu-242 1C_LA

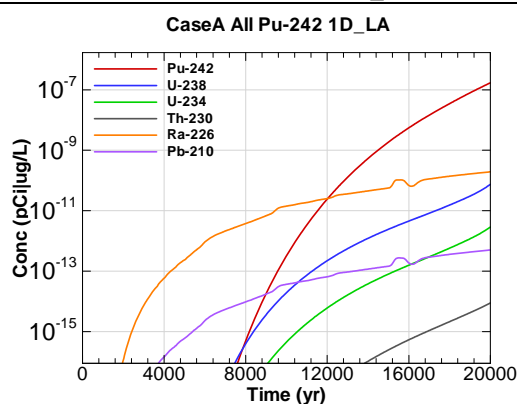


Figure F.2-532 - 1m Aquifer Concentration for
CaseA All Pu-242 1D_LA

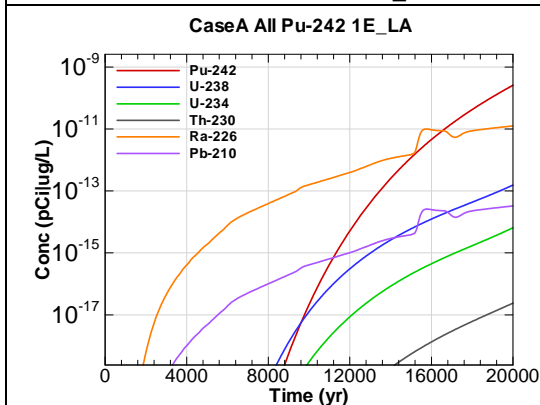


Figure F.2-533 - 1m Aquifer Concentration for
CaseA All Pu-242 1E_LA

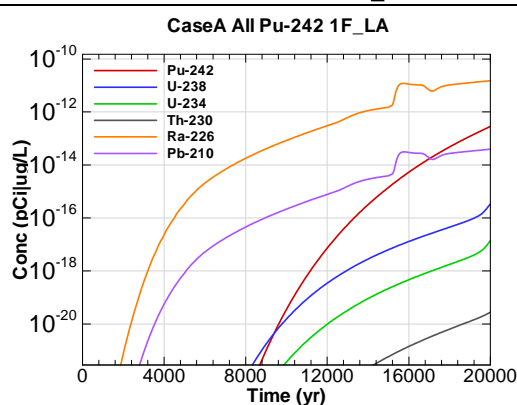
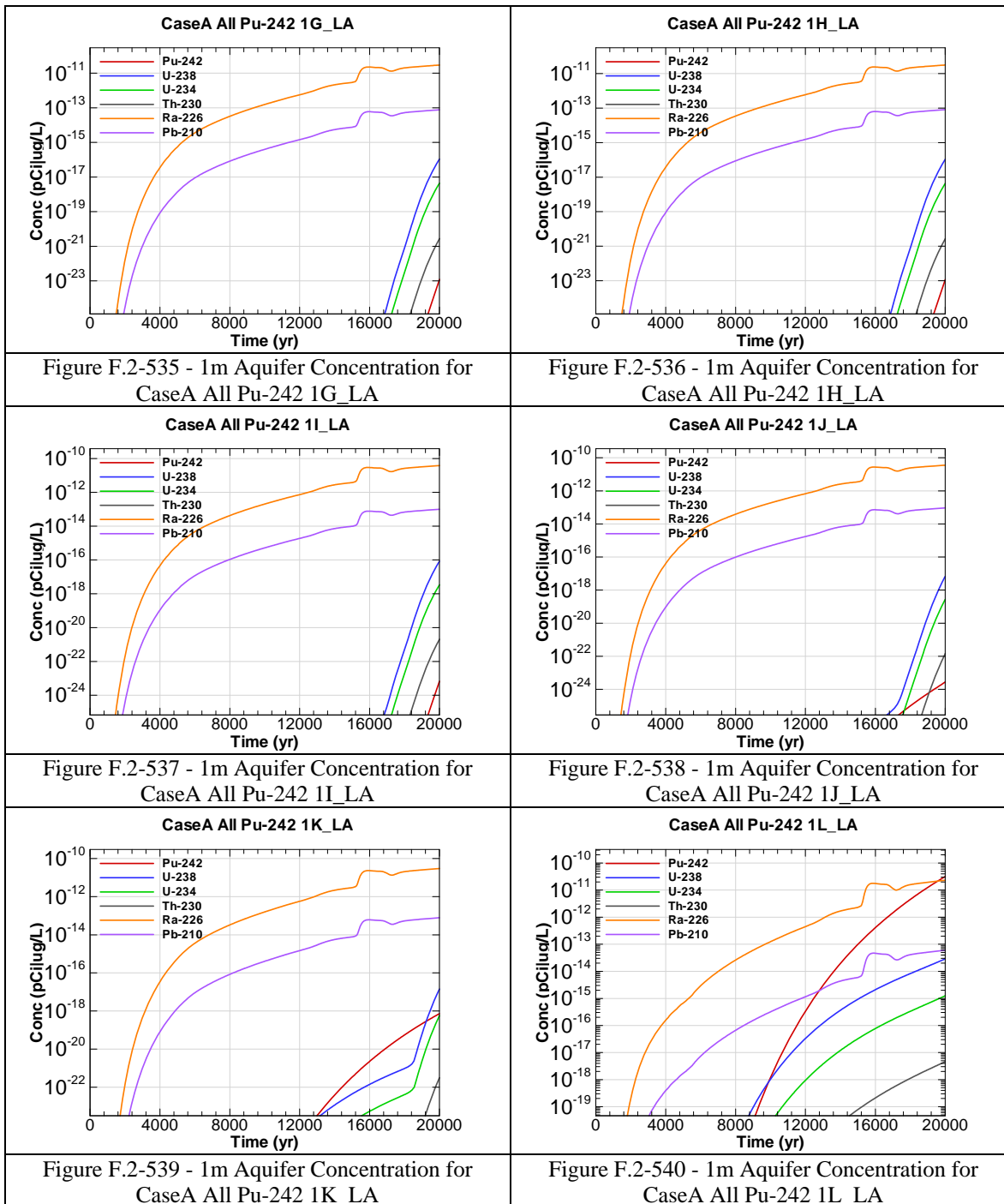
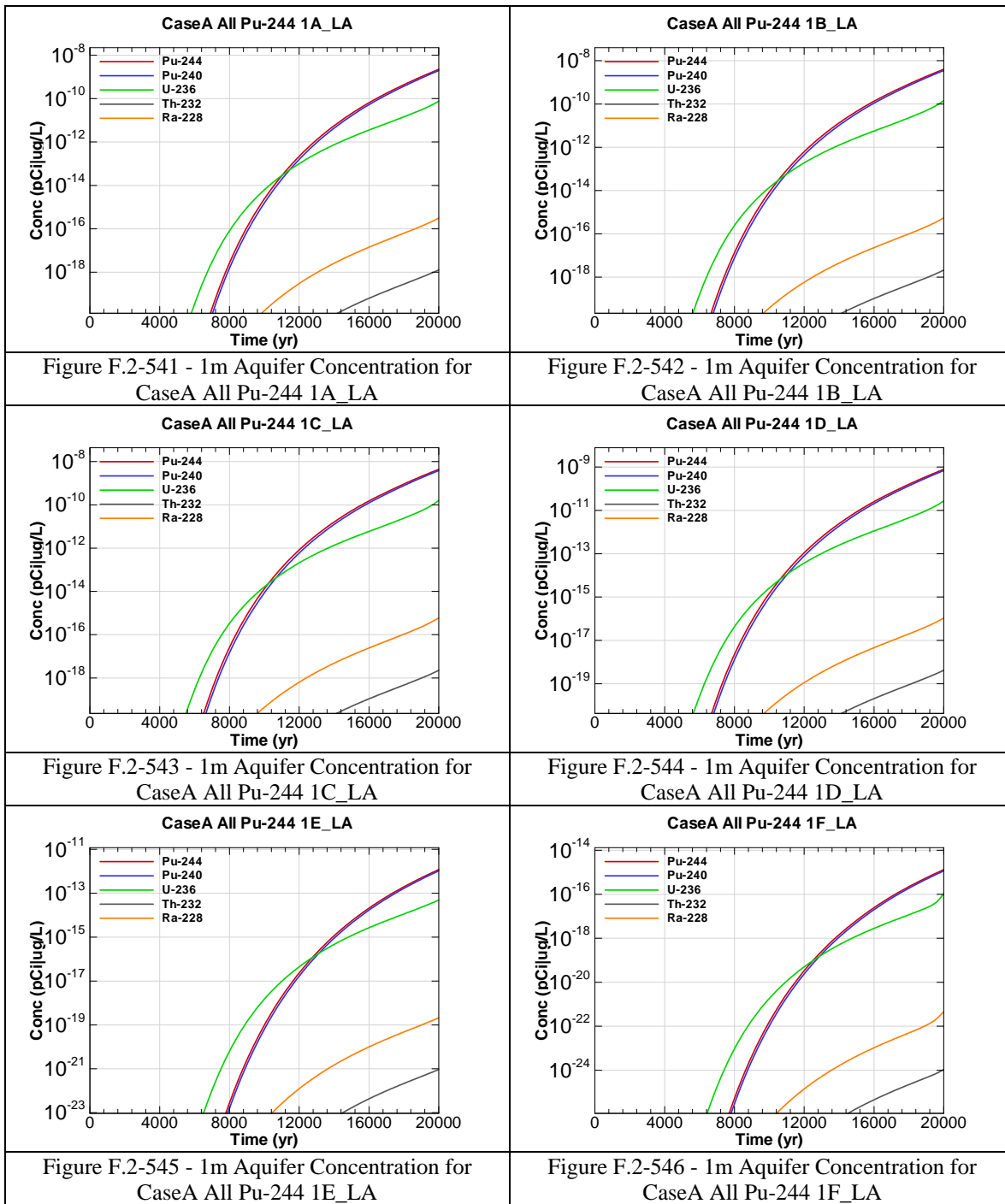
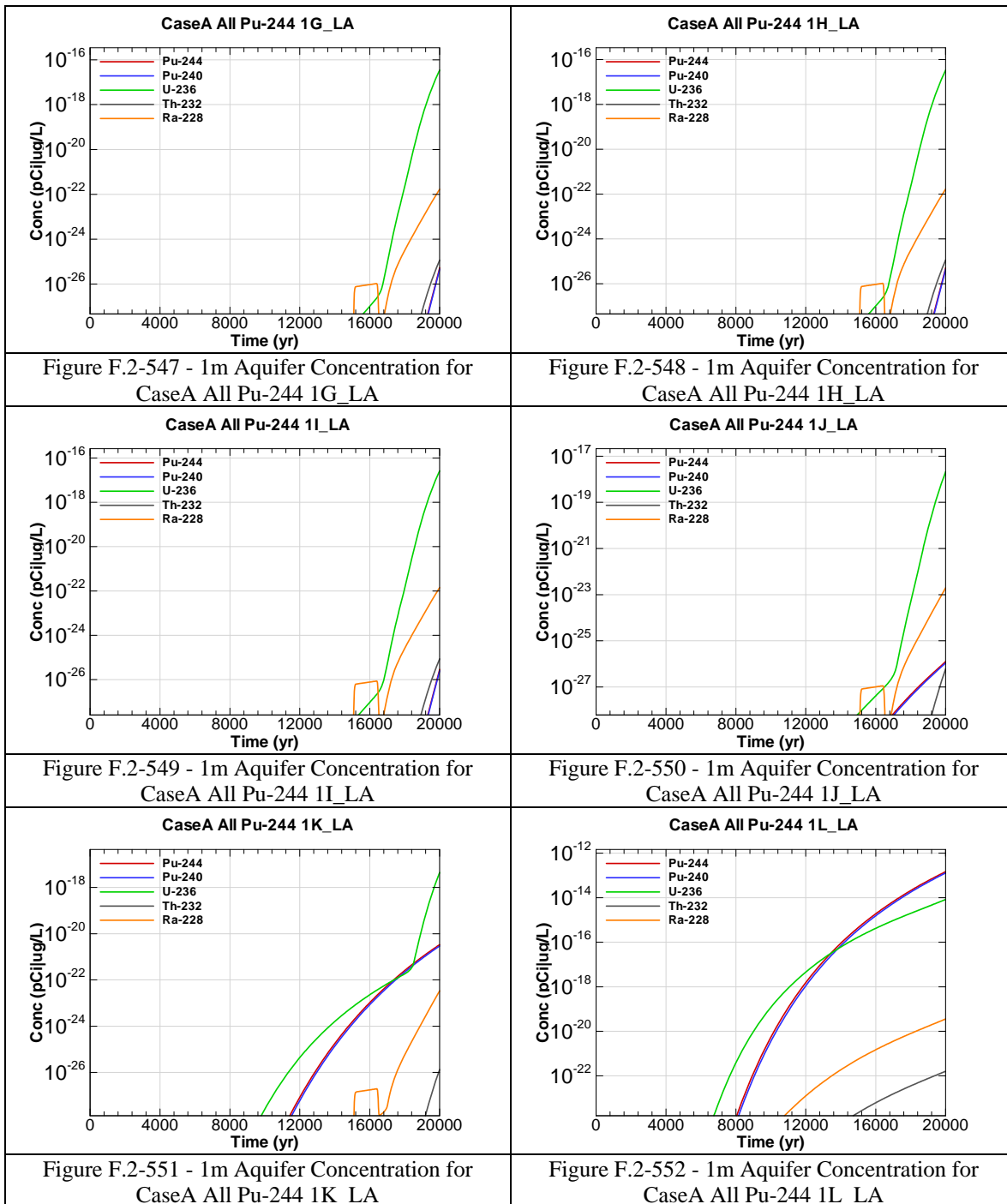
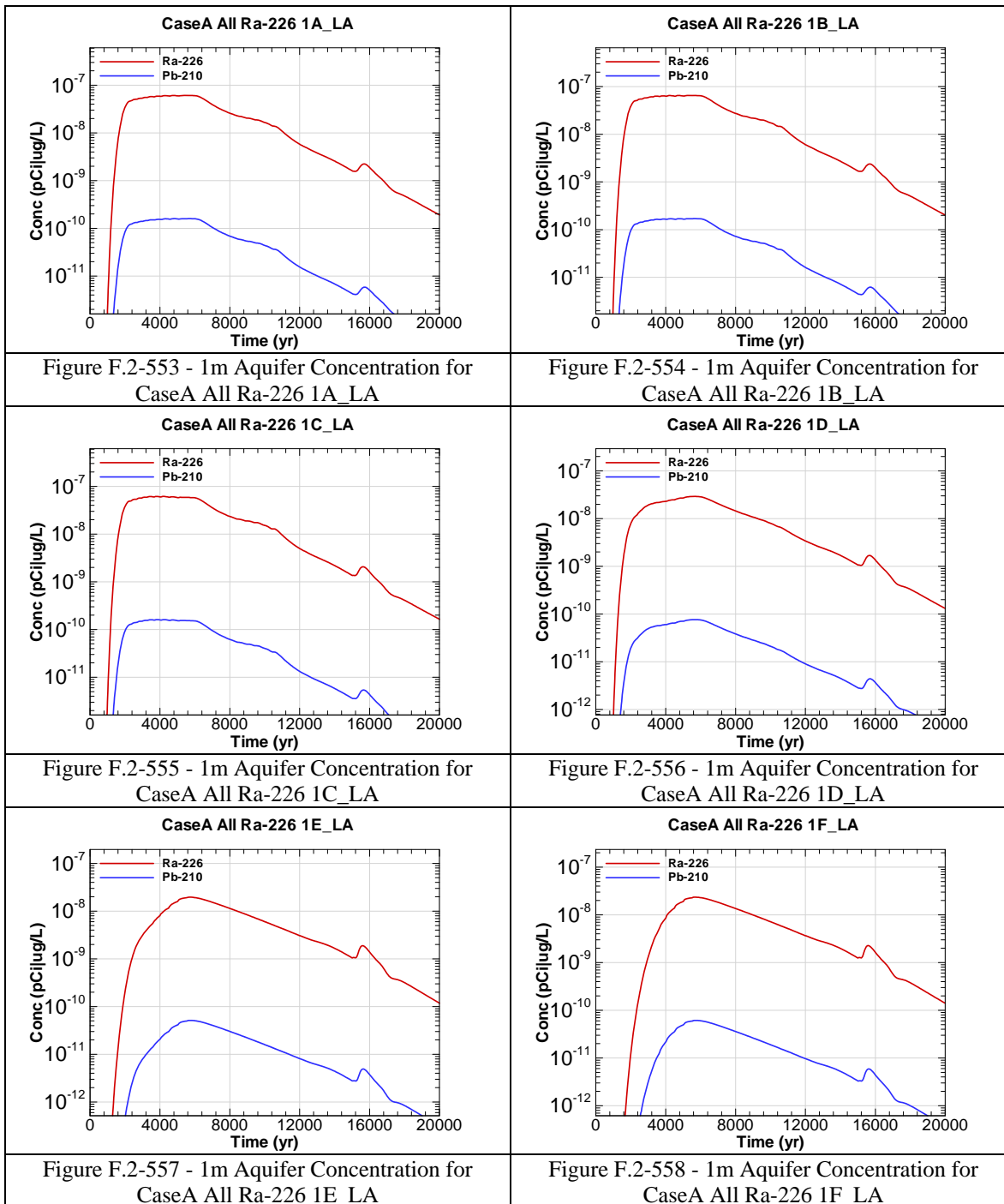


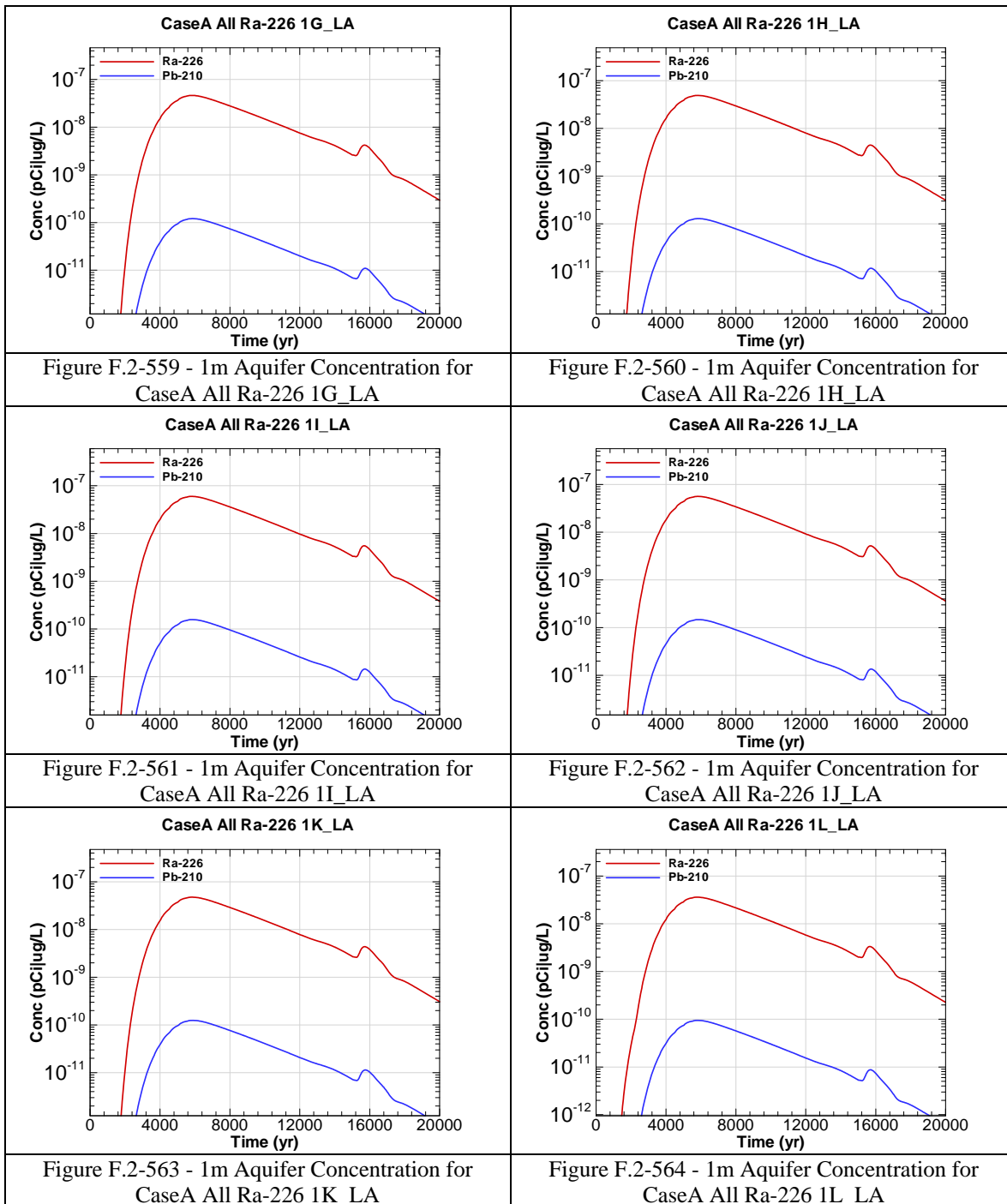
Figure F.2-534 - 1m Aquifer Concentration for
CaseA All Pu-242 1F_LA

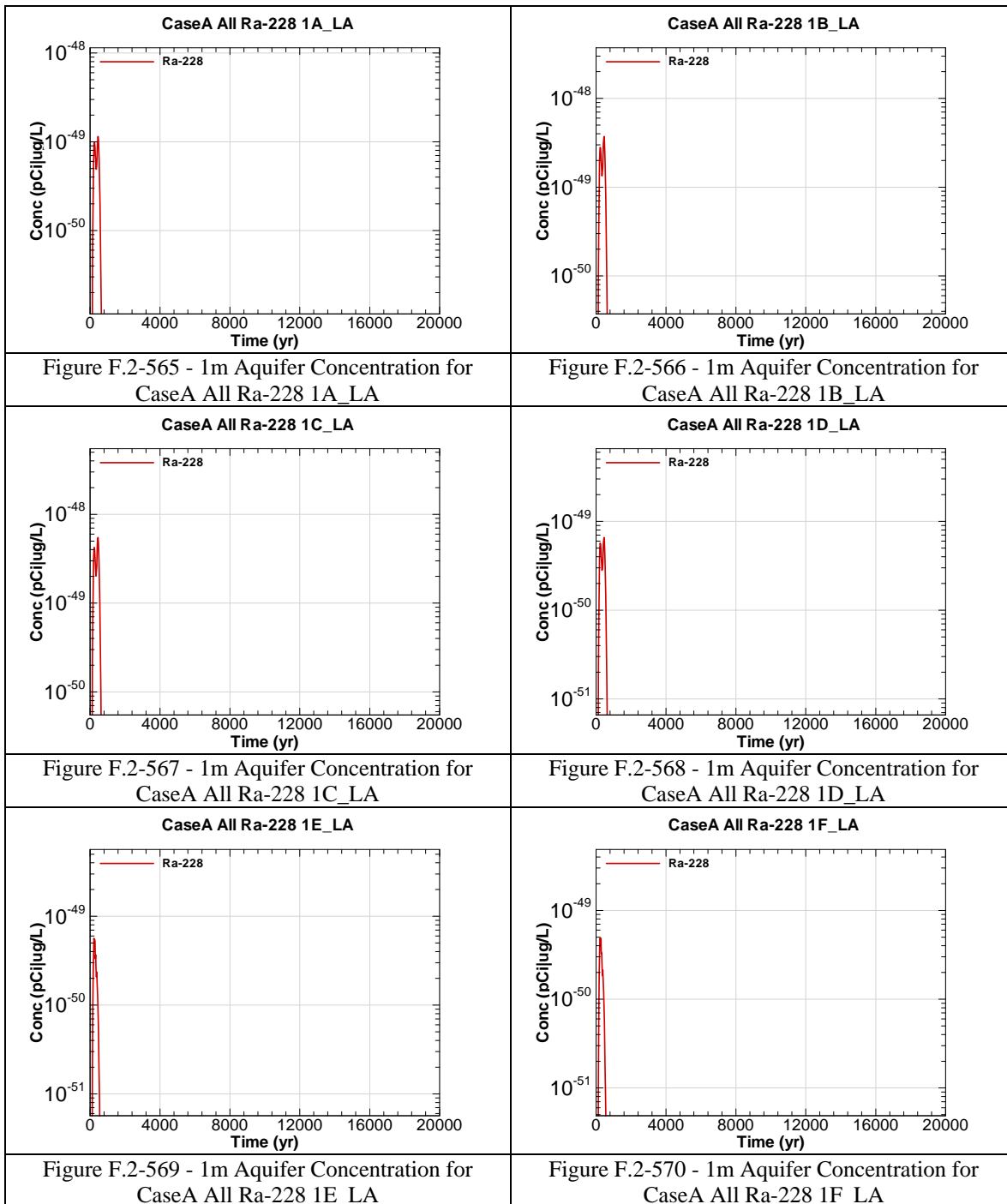


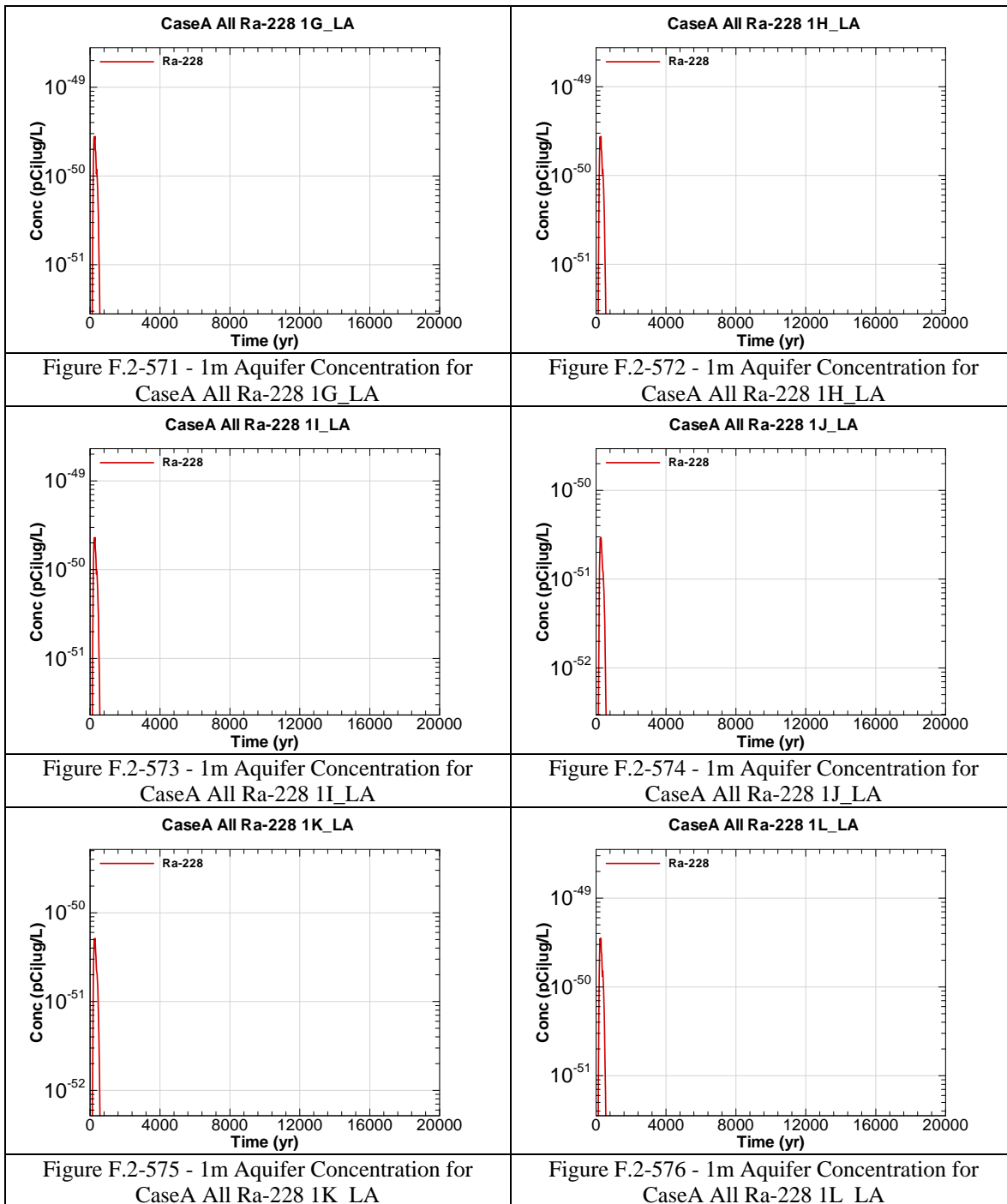


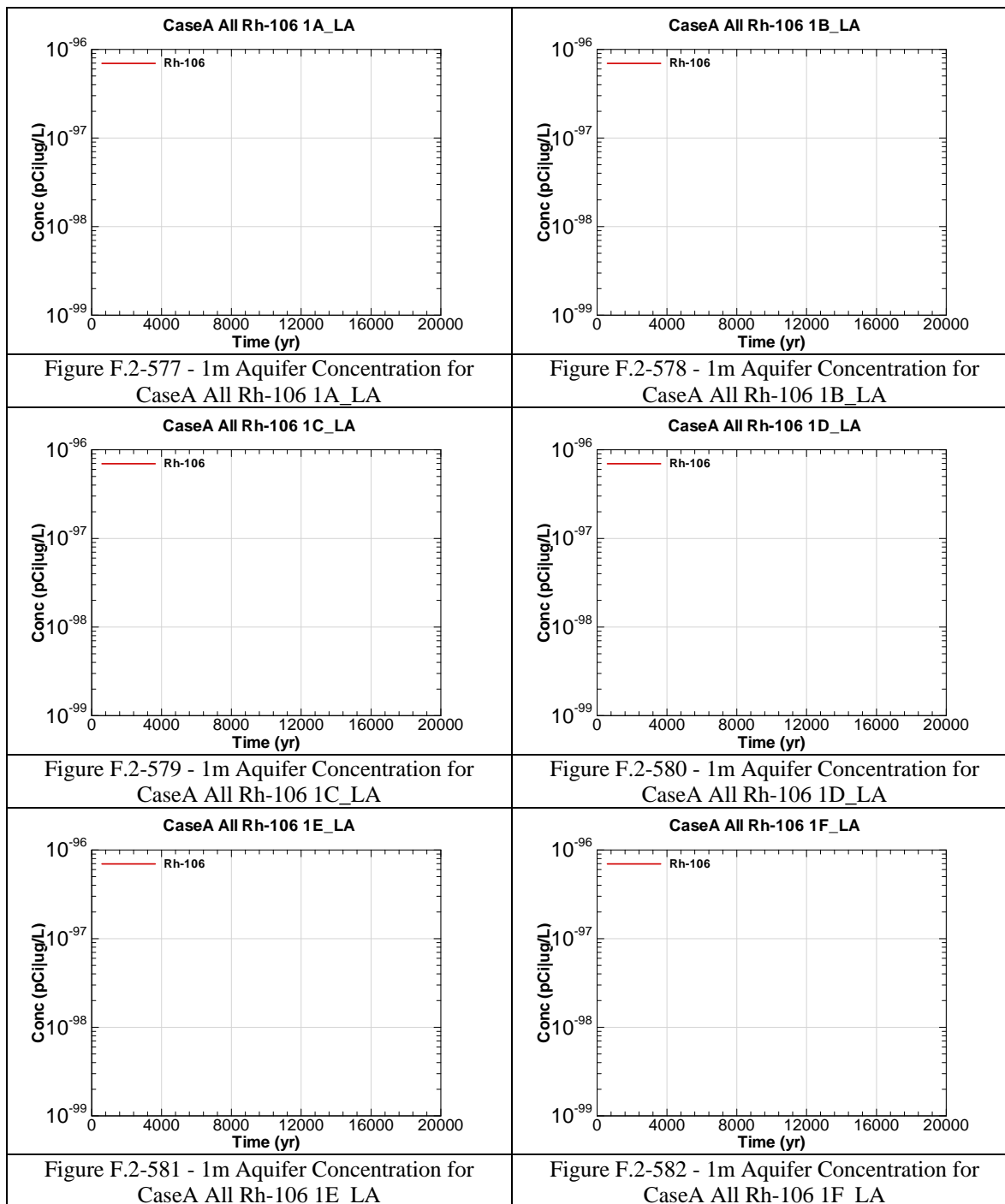


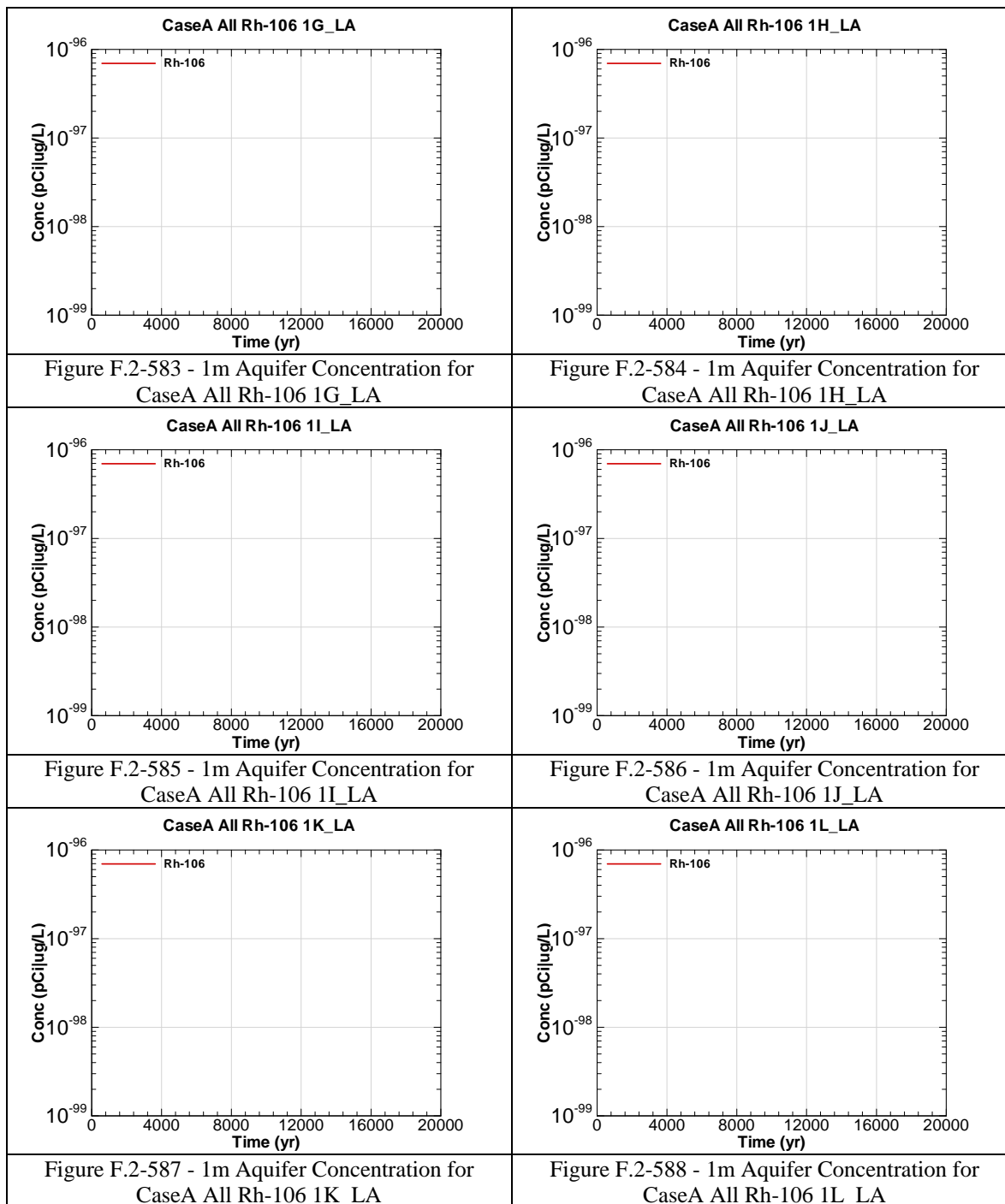


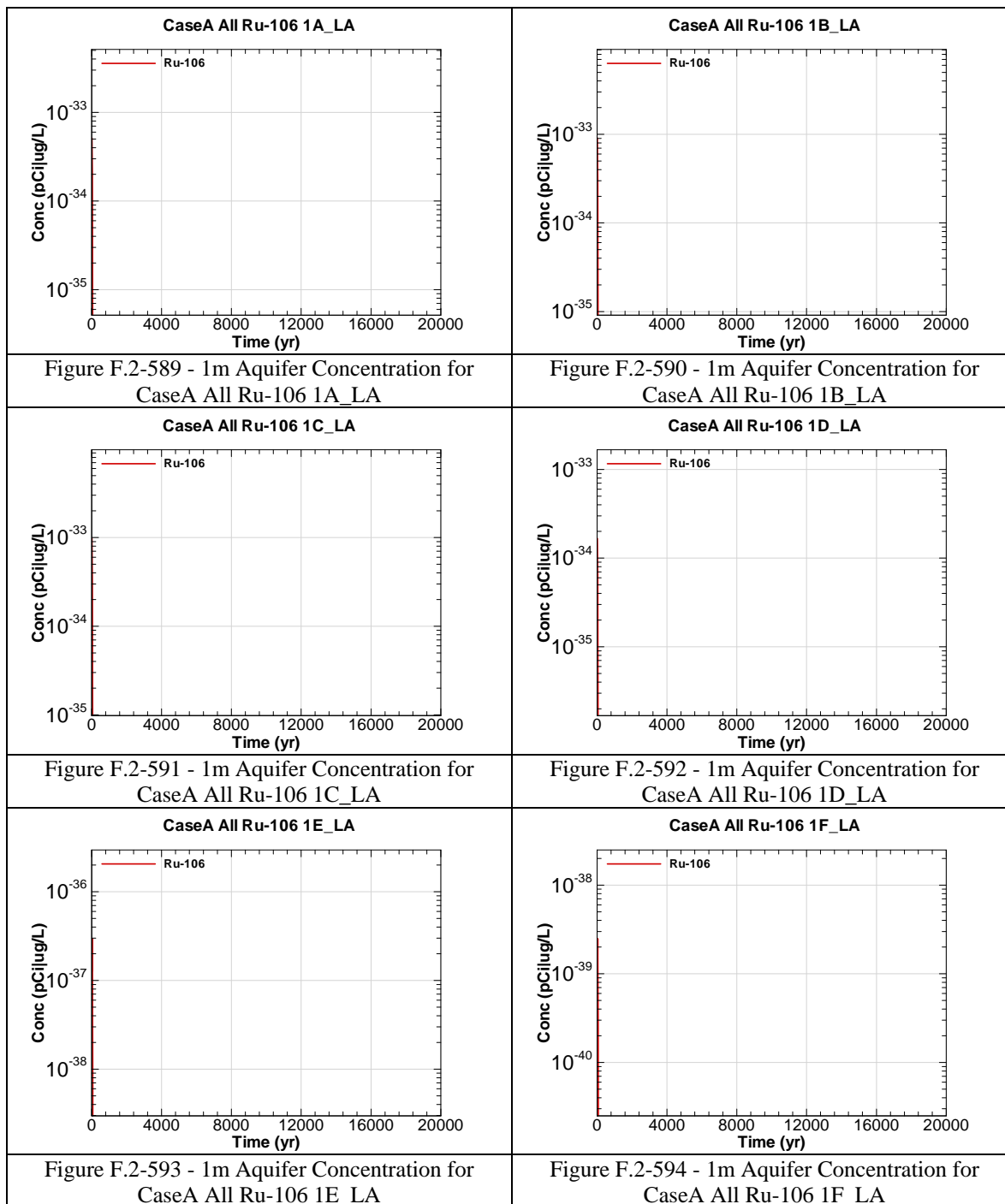


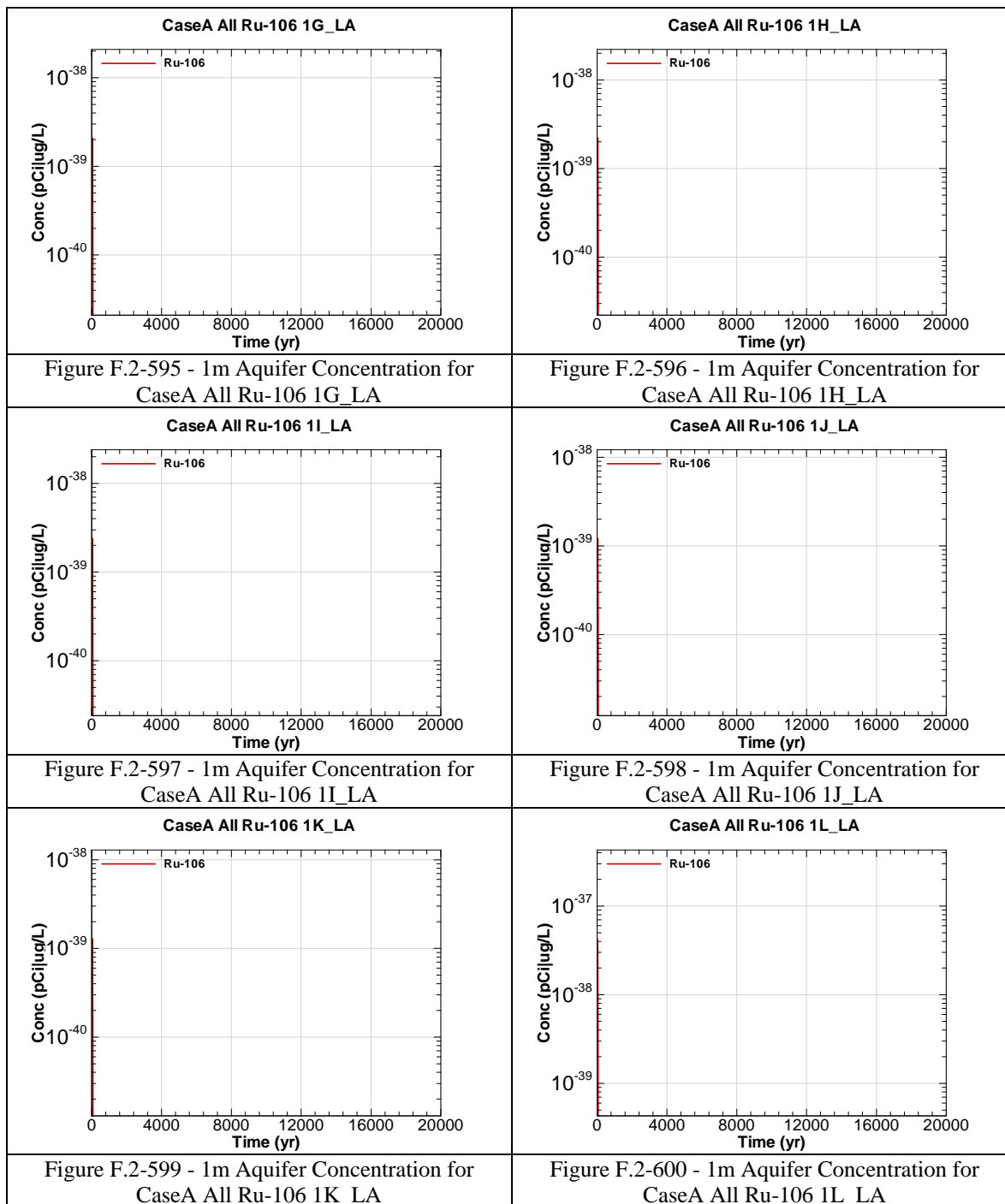


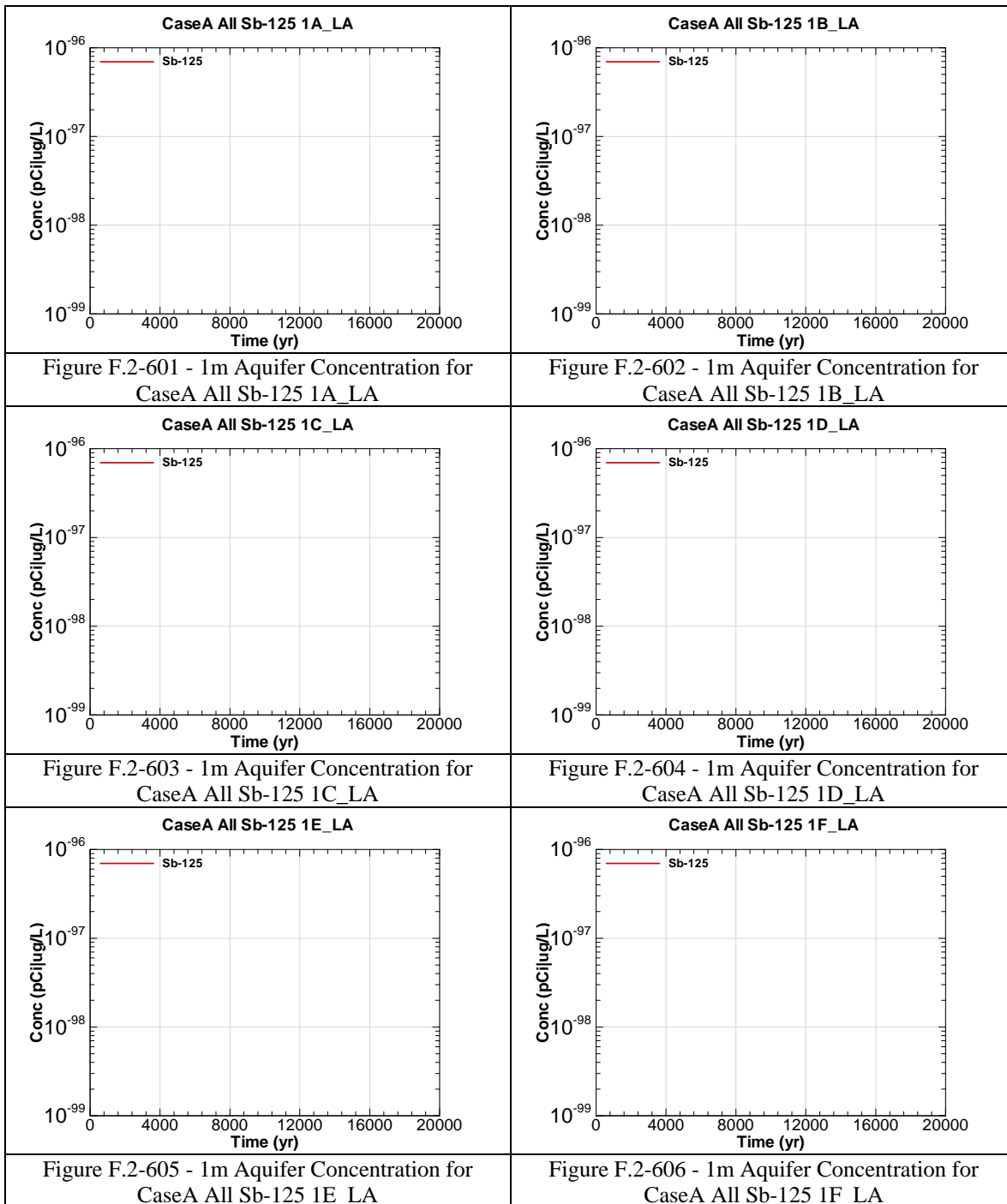


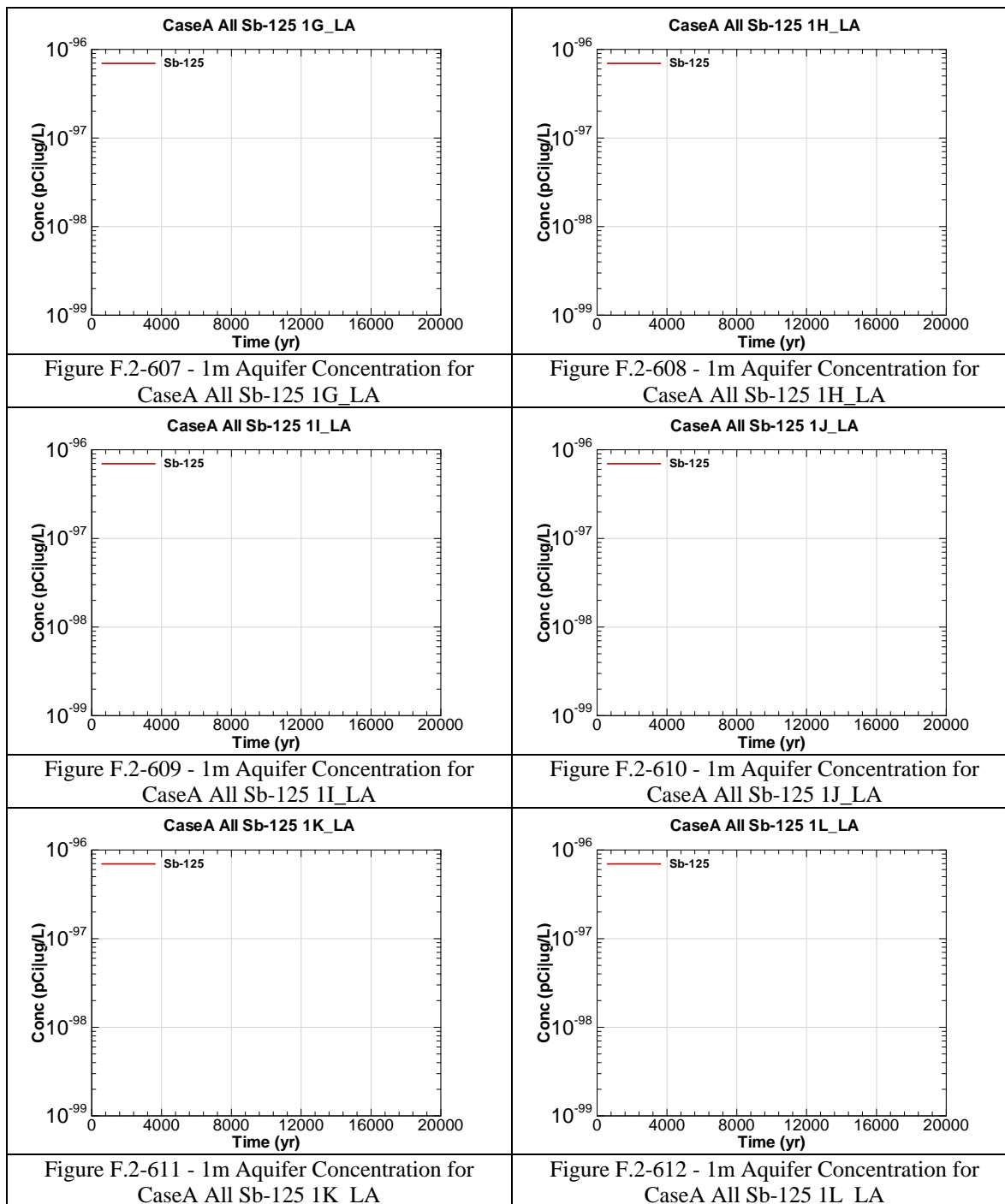


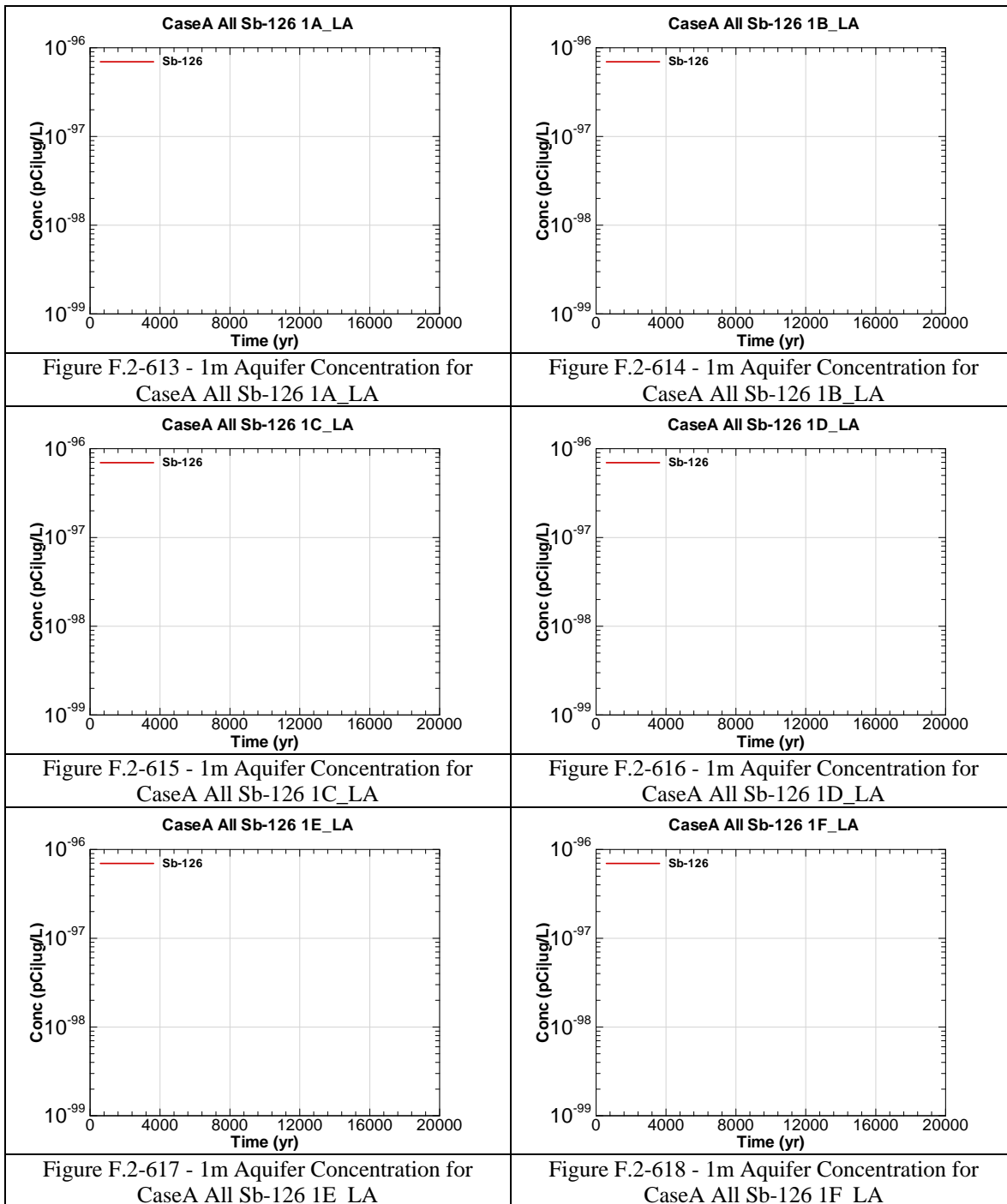


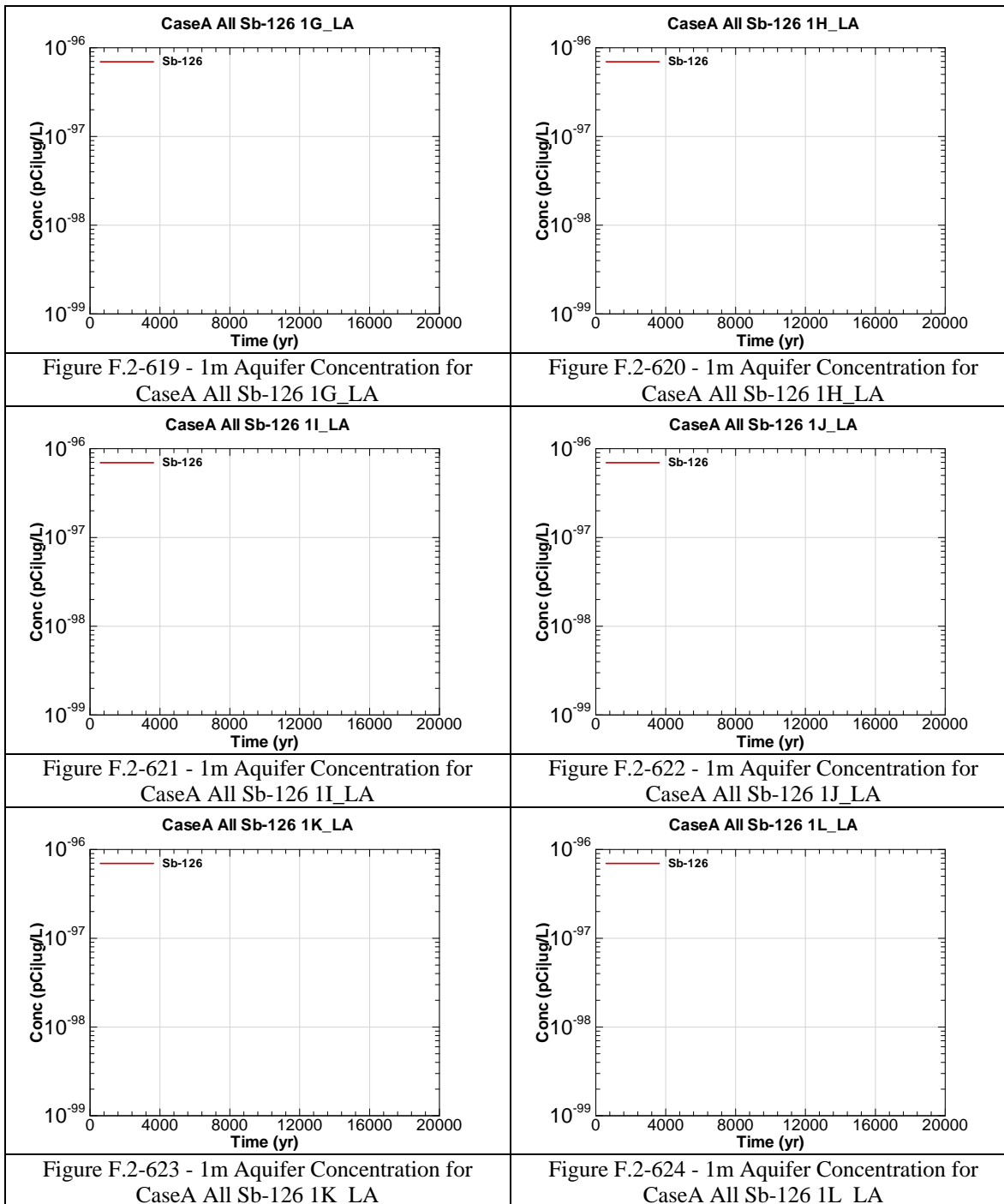


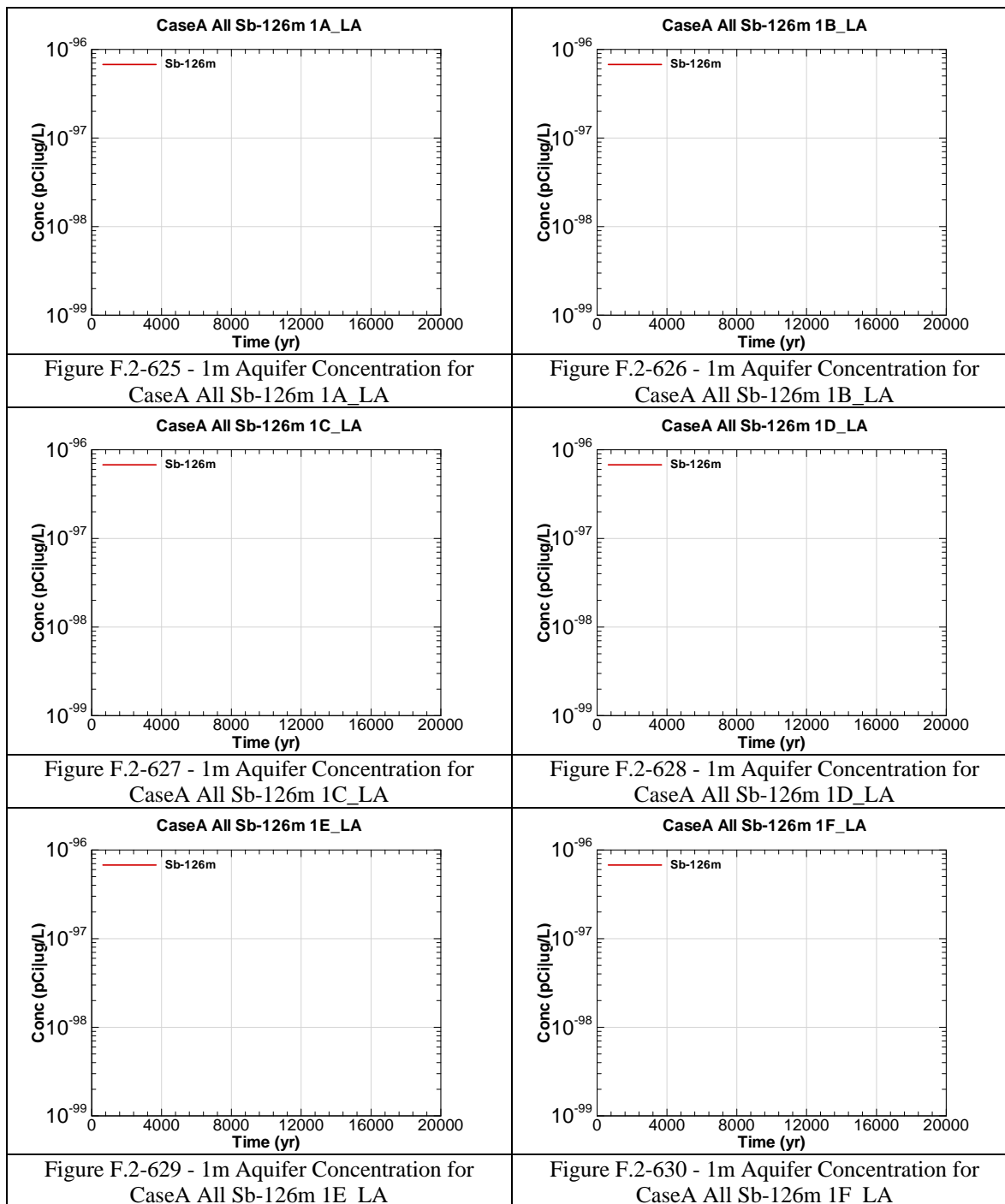


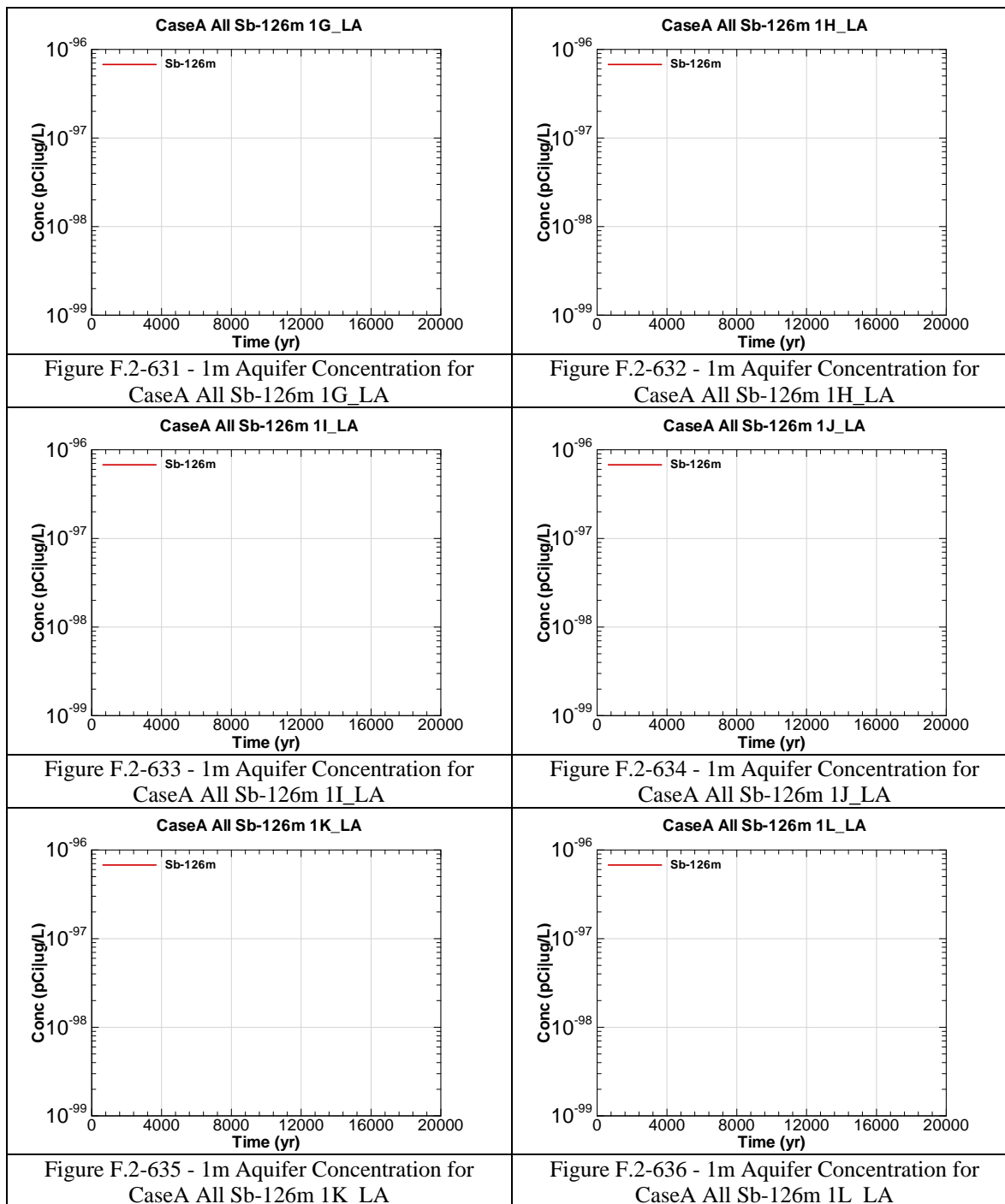


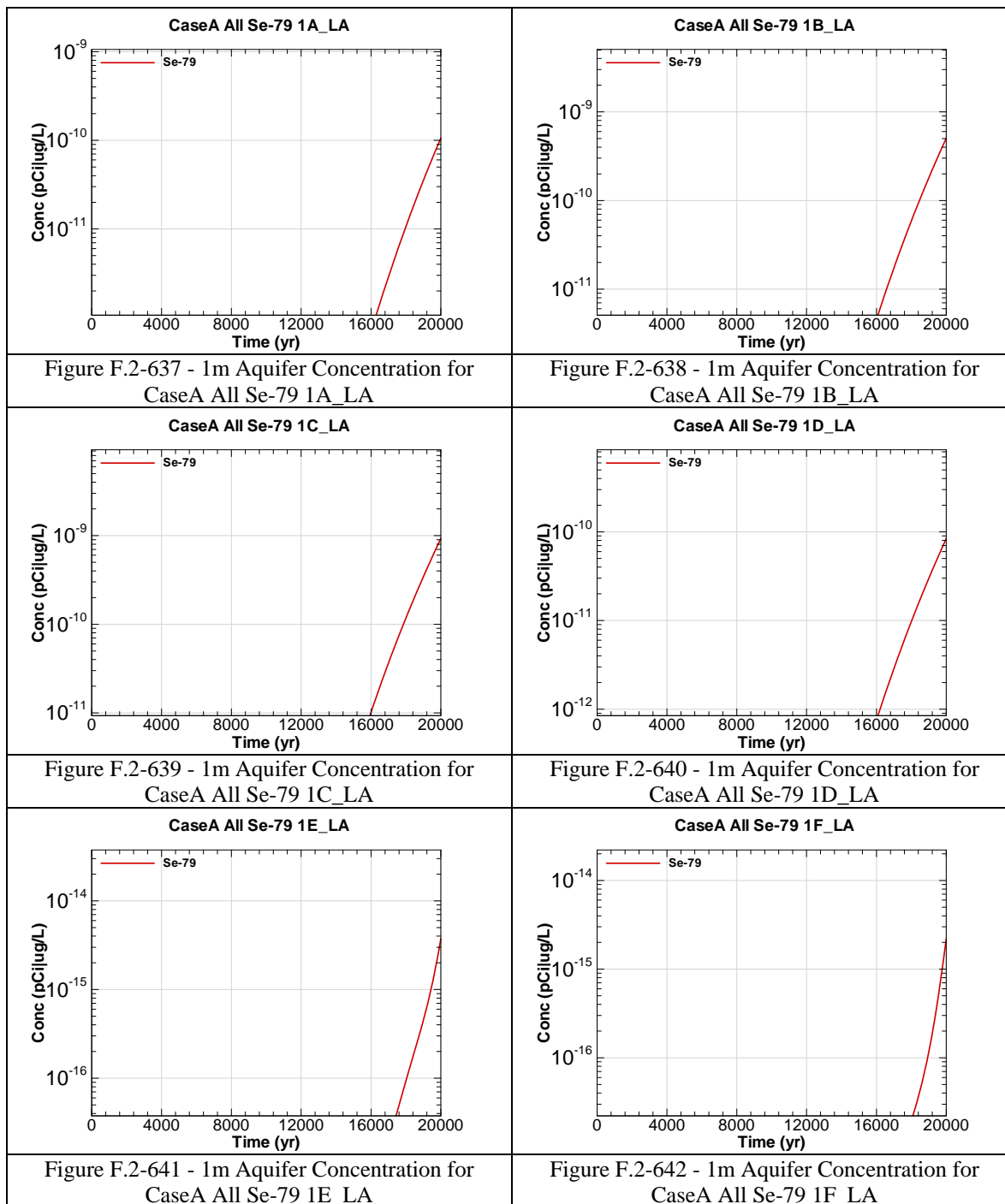


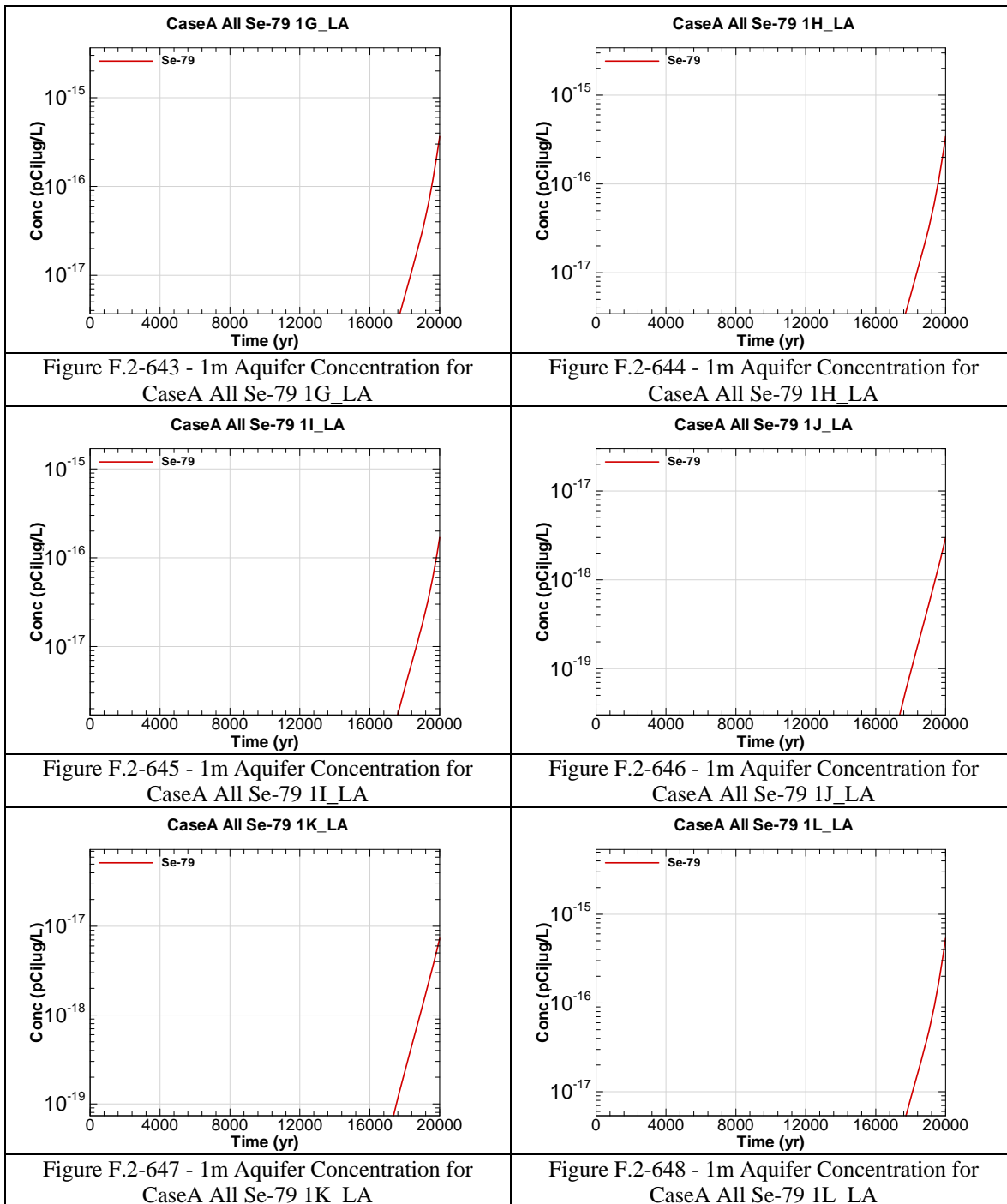


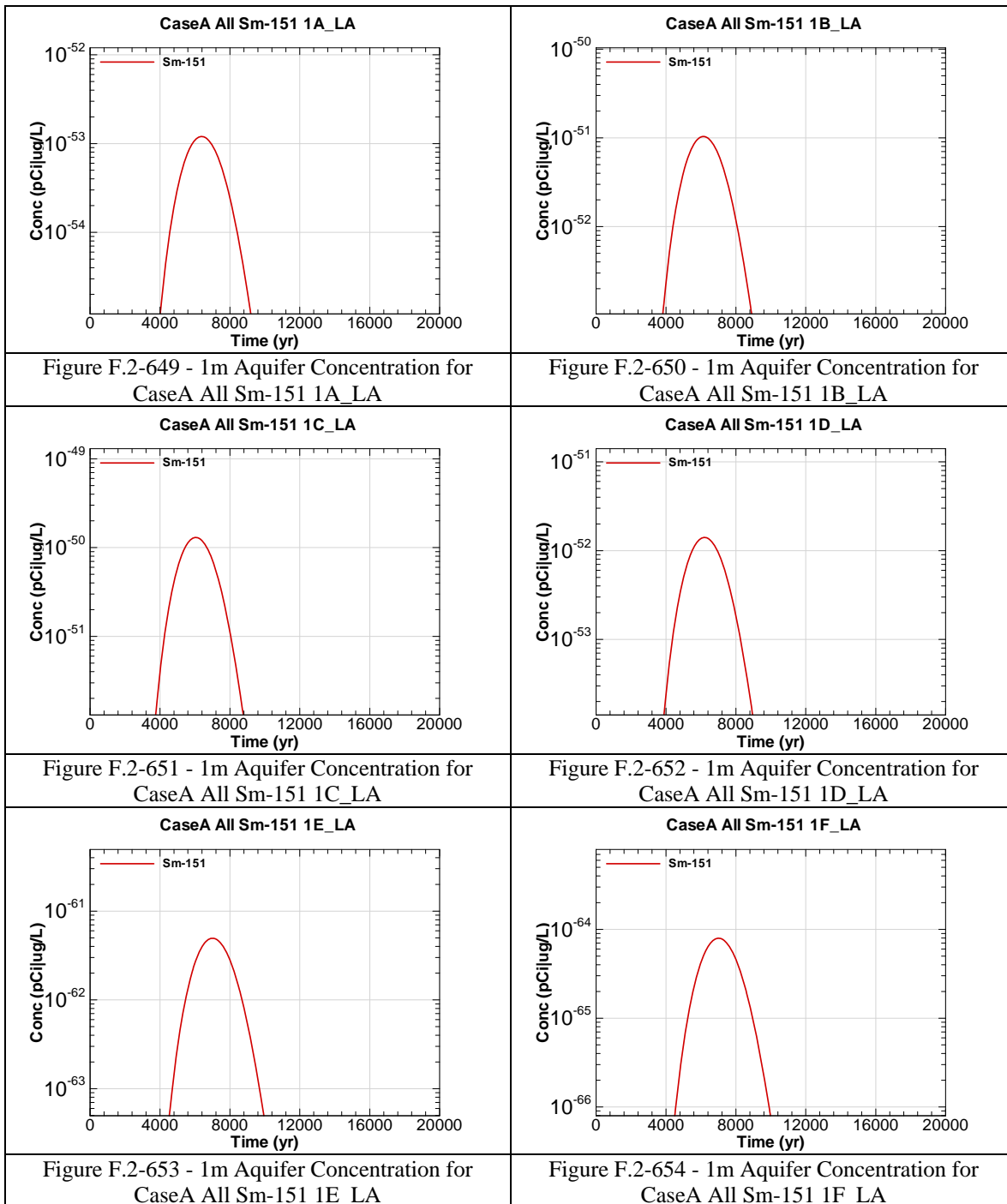


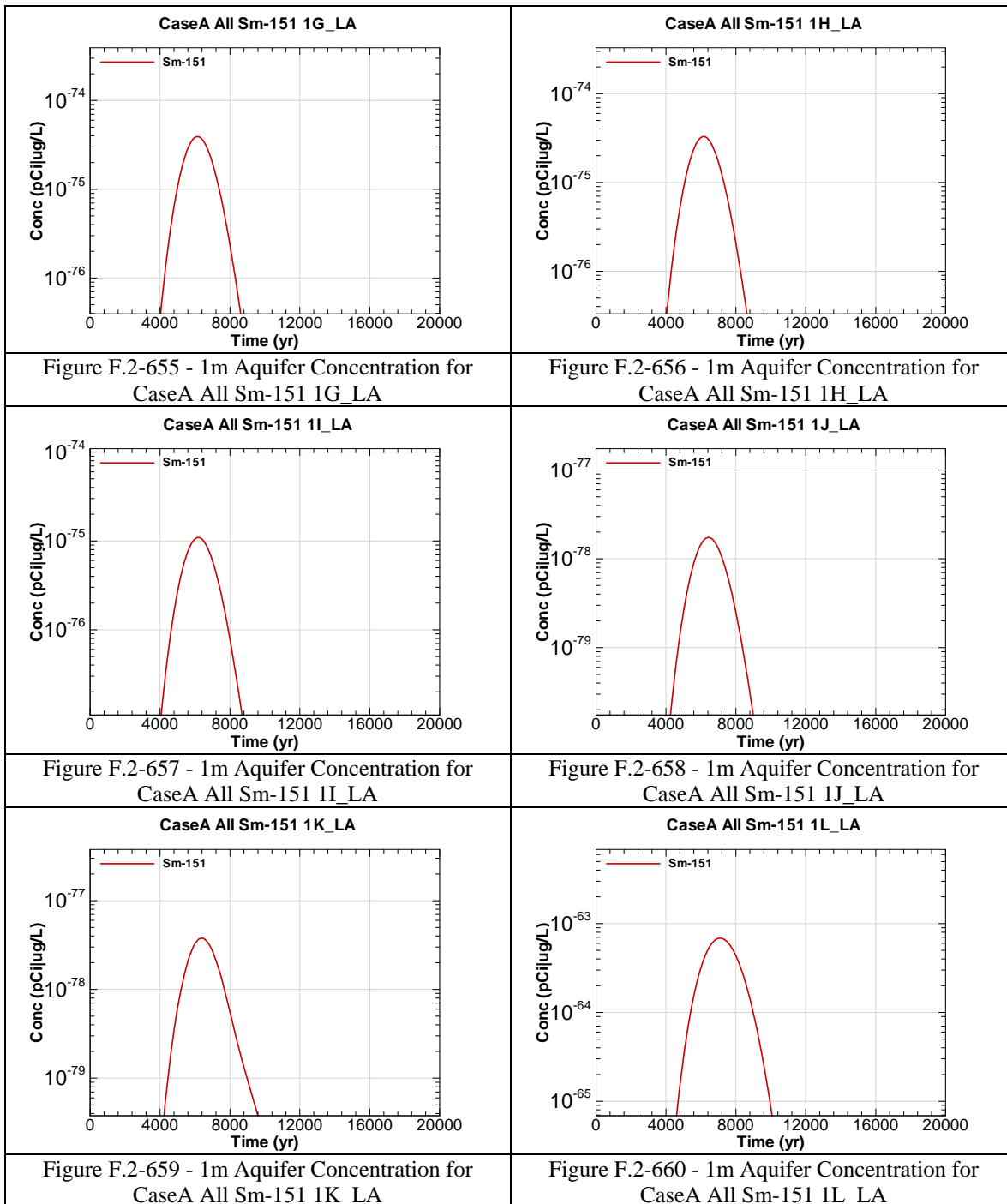


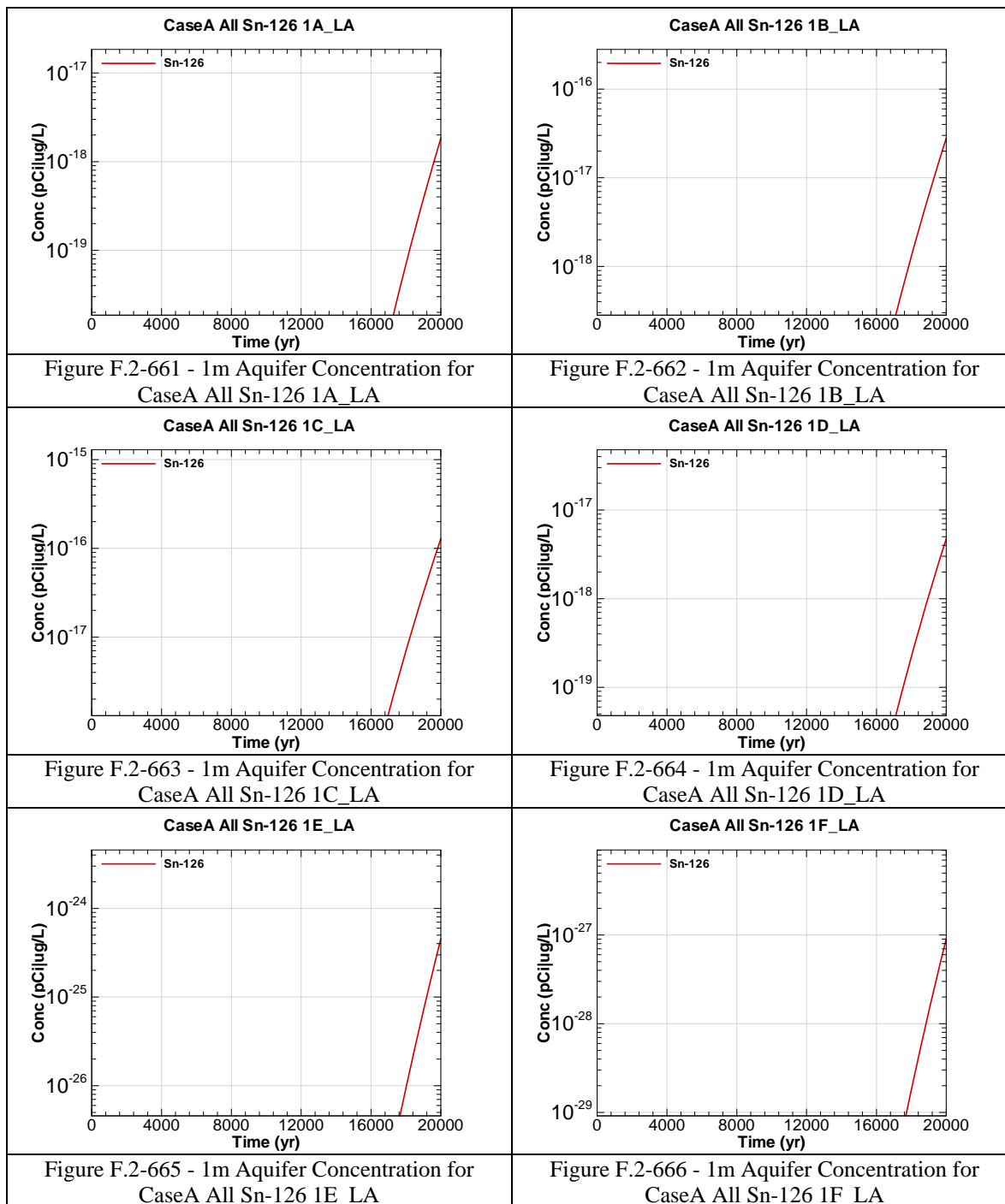


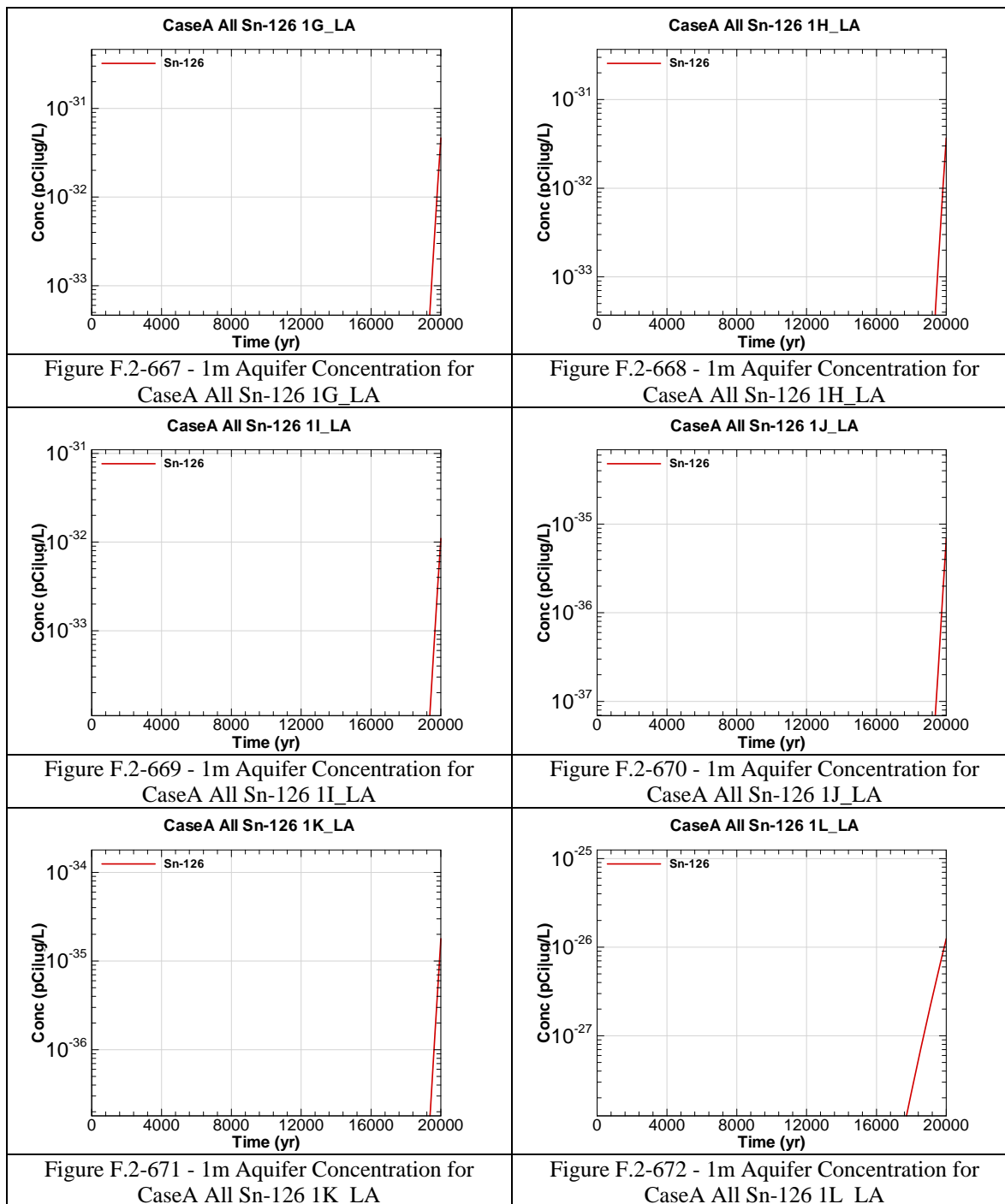


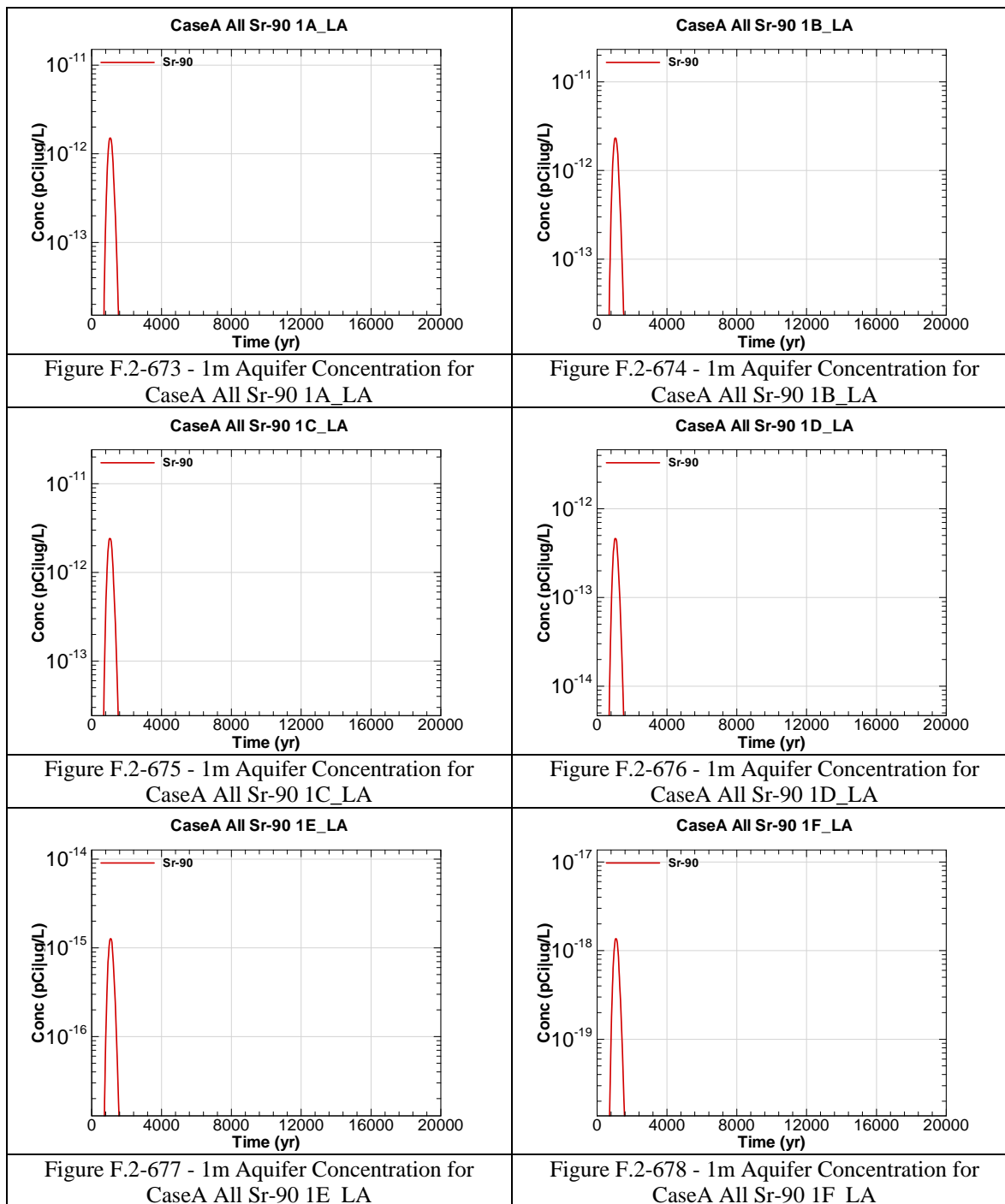


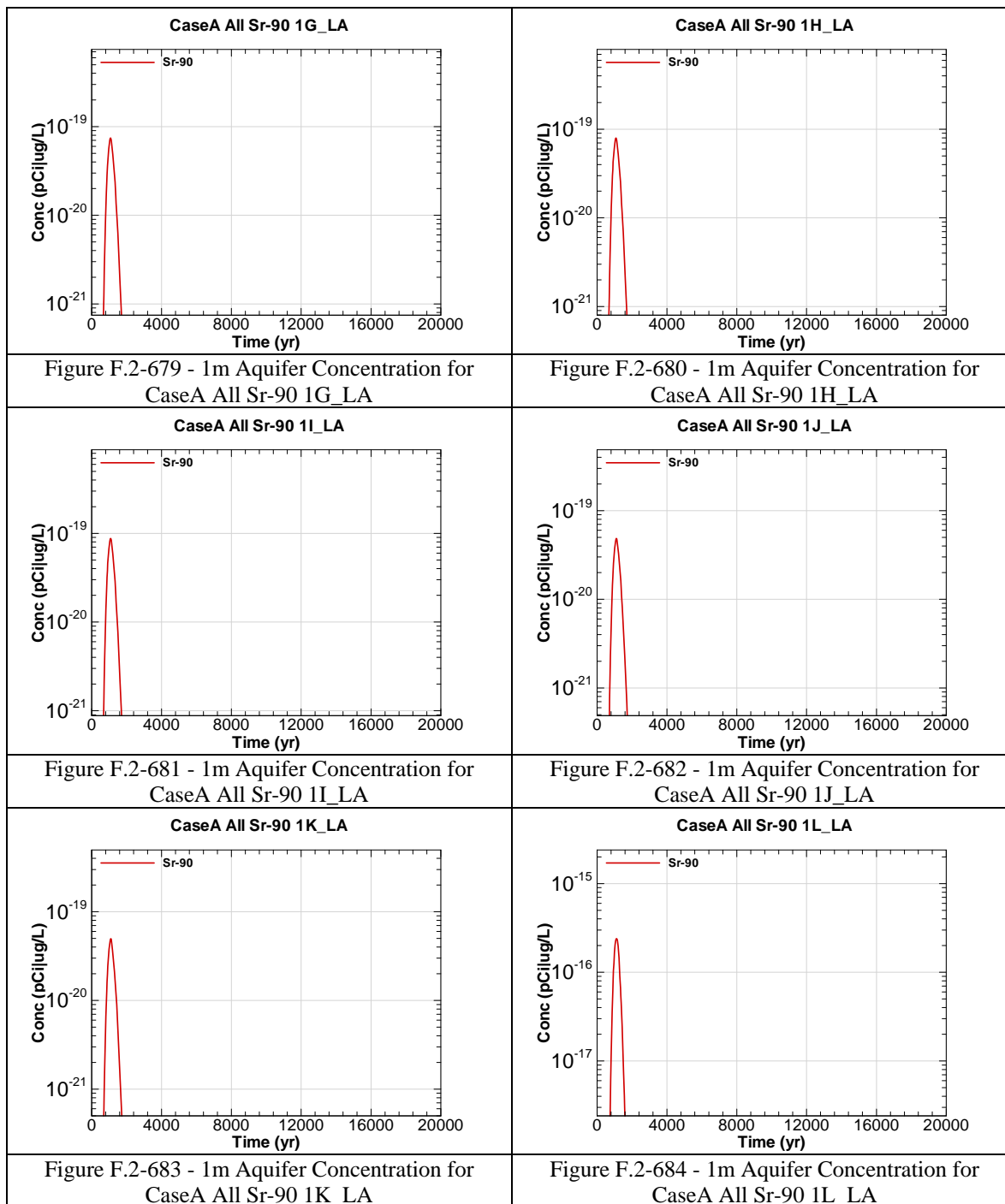


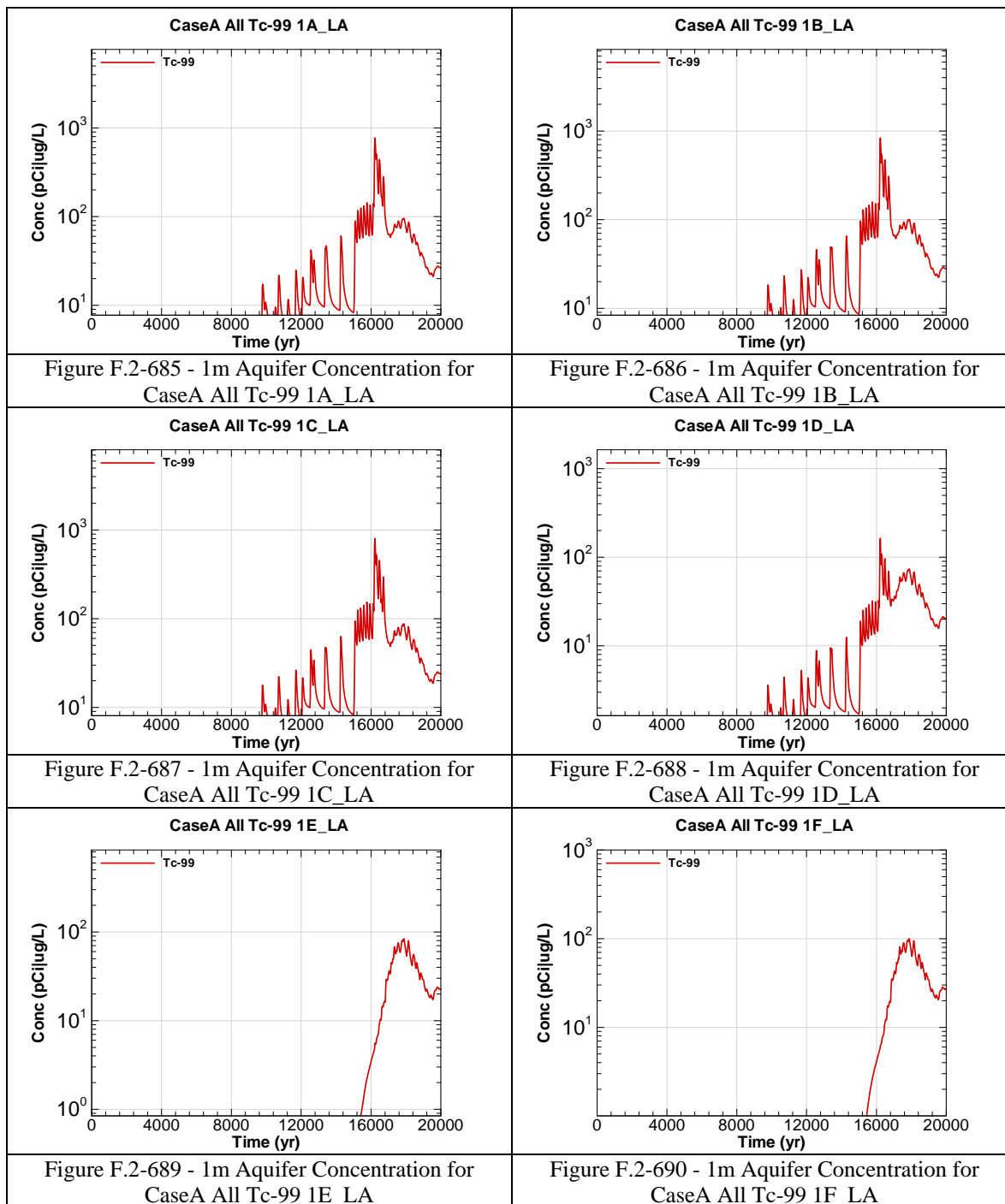


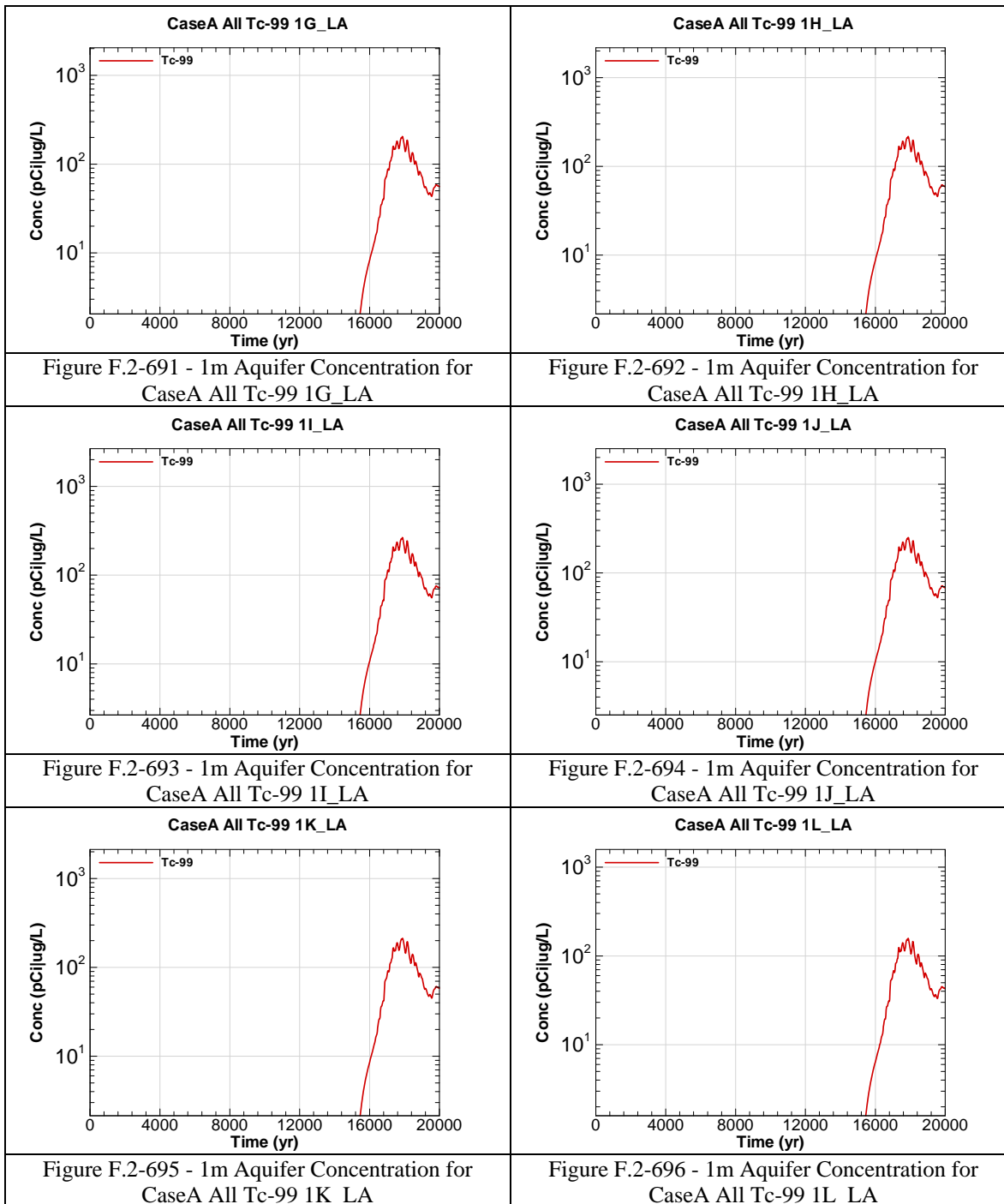


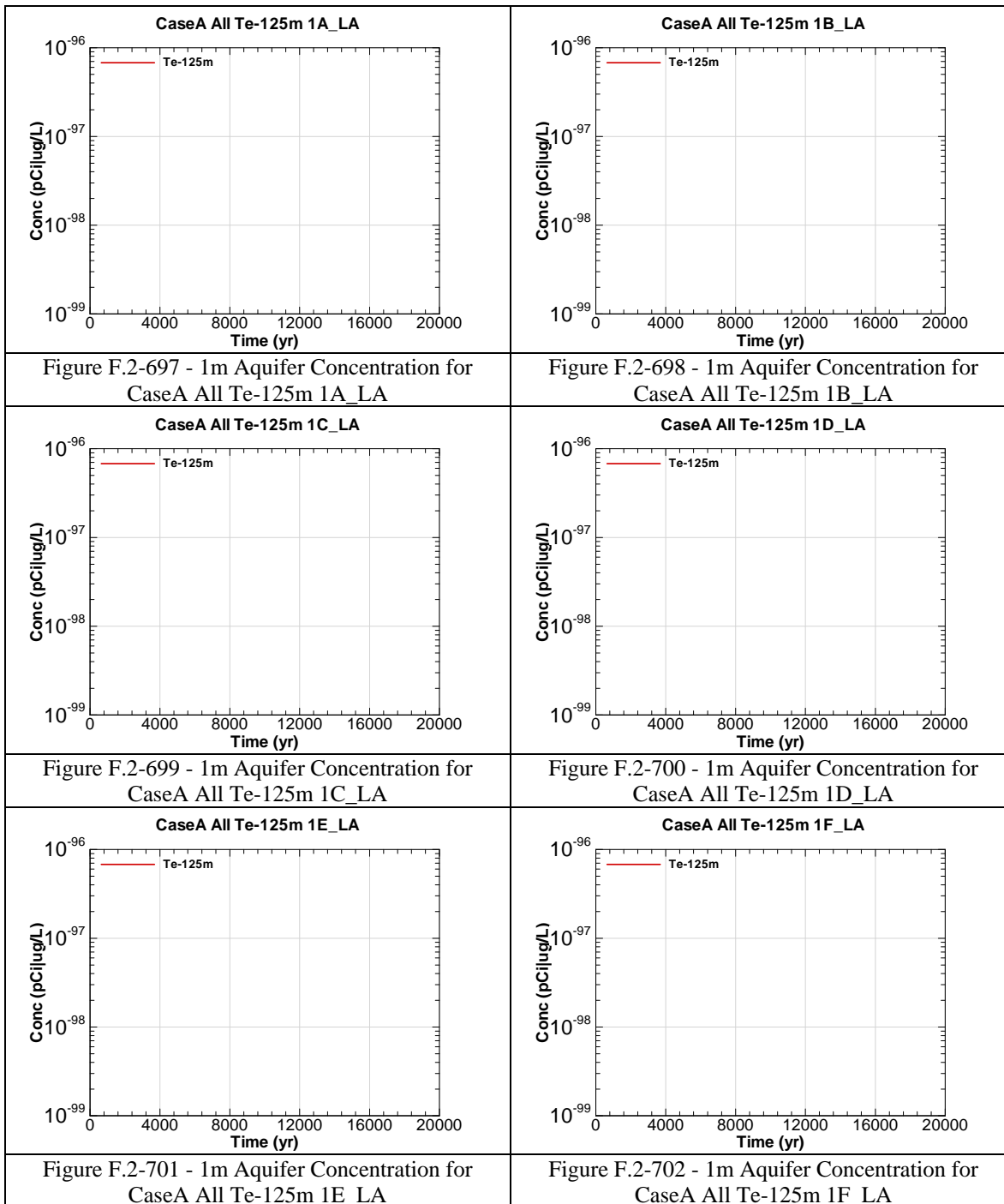


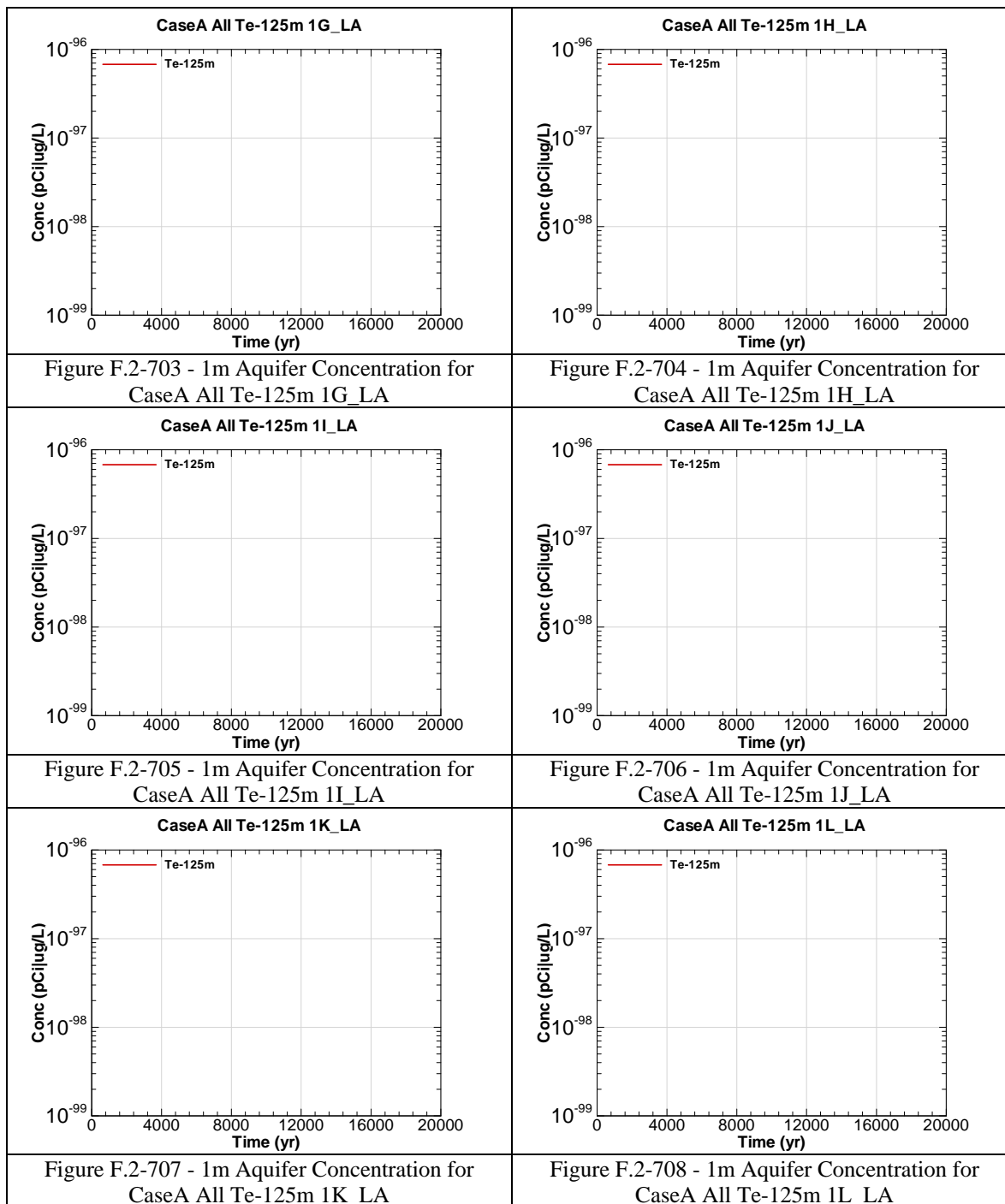


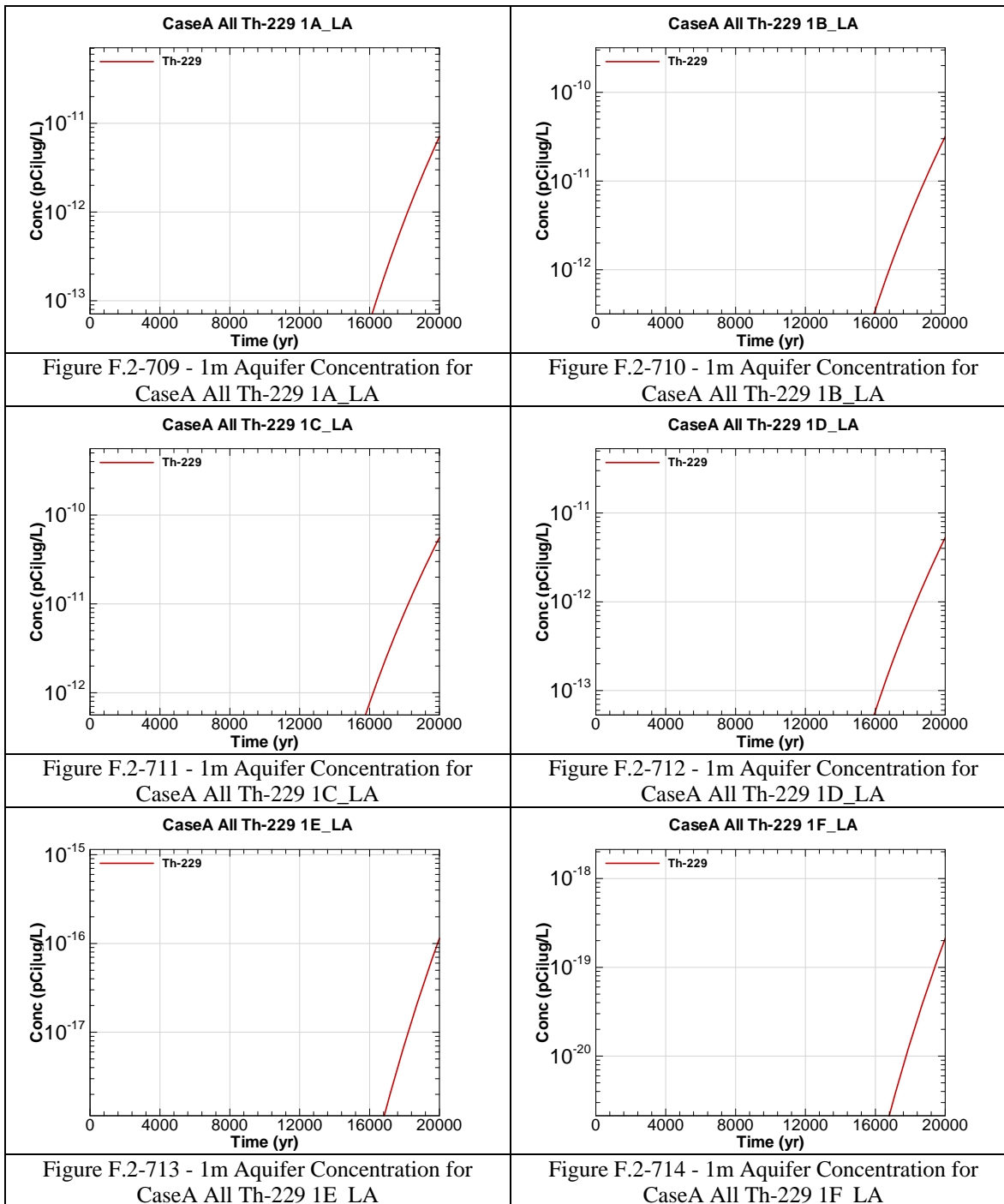


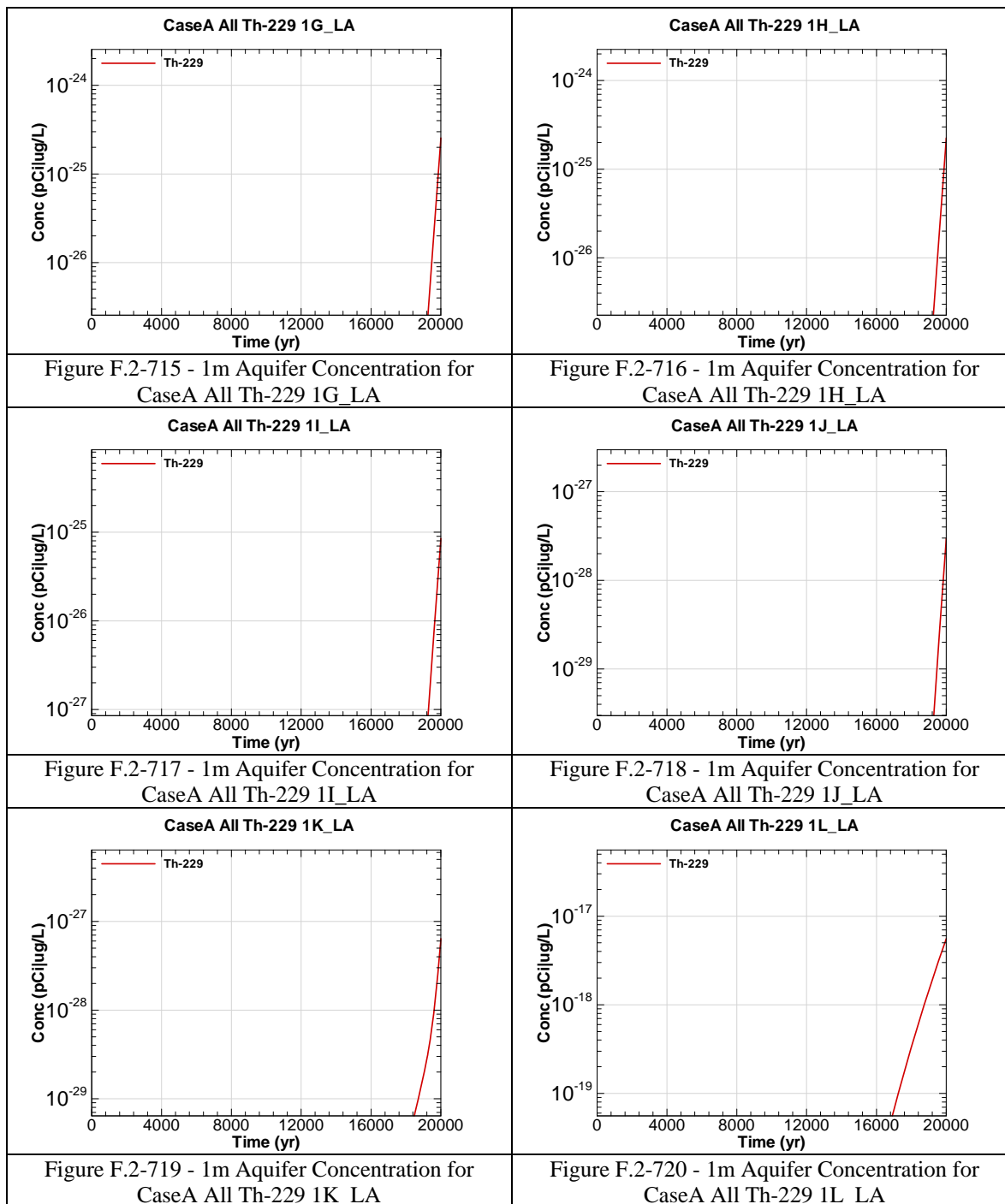












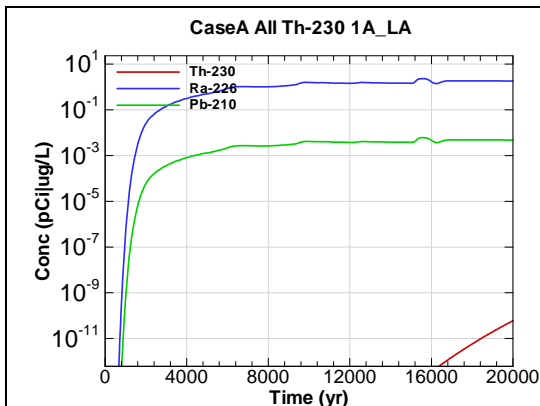


Figure F.2-721 - 1m Aquifer Concentration for
CaseA All Th-230 1A_LA

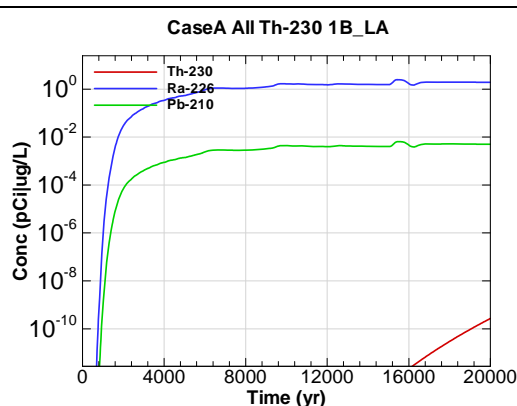


Figure F.2-722 - 1m Aquifer Concentration for
CaseA All Th-230 1B_LA

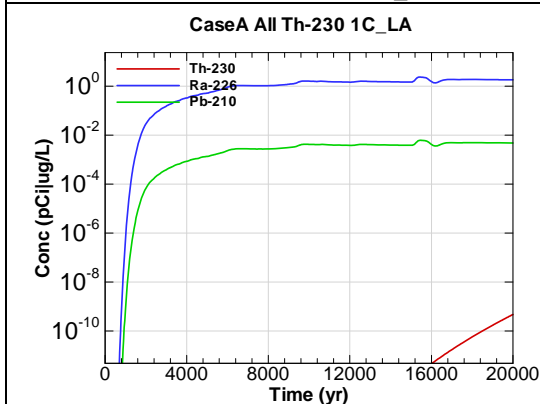


Figure F.2-723 - 1m Aquifer Concentration for
CaseA All Th-230 1C_LA

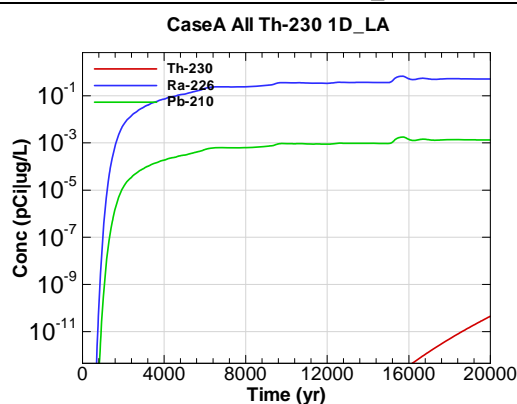


Figure F.2-724 - 1m Aquifer Concentration for
CaseA All Th-230 1D_LA

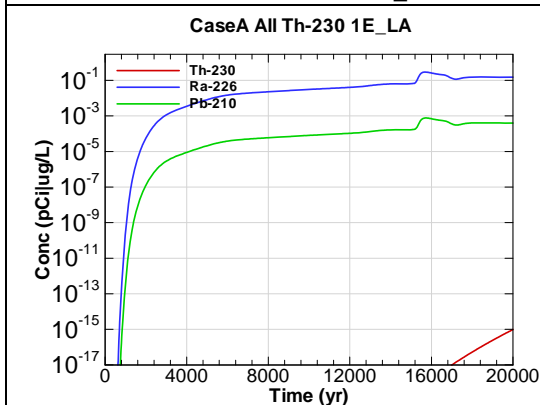


Figure F.2-725 - 1m Aquifer Concentration for
CaseA All Th-230 1E_LA

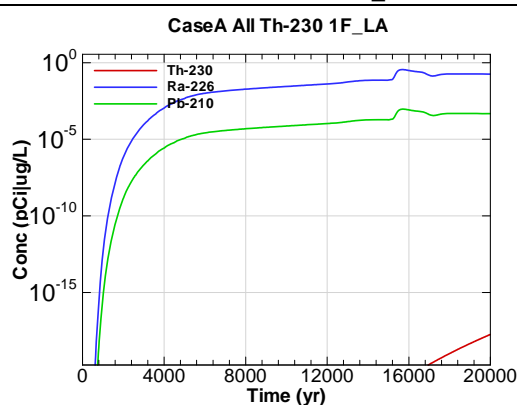


Figure F.2-726 - 1m Aquifer Concentration for
CaseA All Th-230 1F_LA

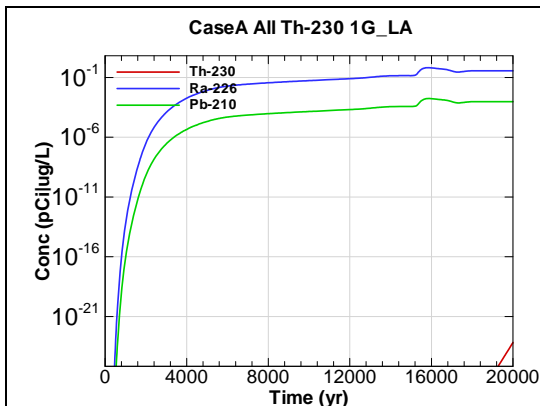


Figure F.2-727 - 1m Aquifer Concentration for
CaseA All Th-230 1G_LA

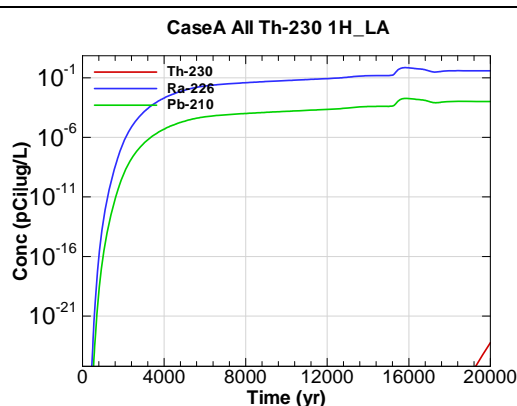


Figure F.2-728 - 1m Aquifer Concentration for
CaseA All Th-230 1H_LA

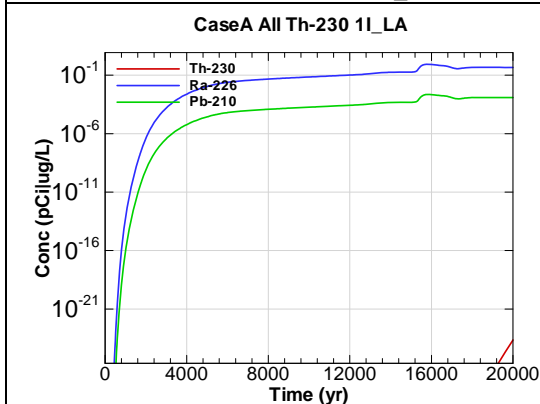


Figure F.2-729 - 1m Aquifer Concentration for
CaseA All Th-230 1I_LA

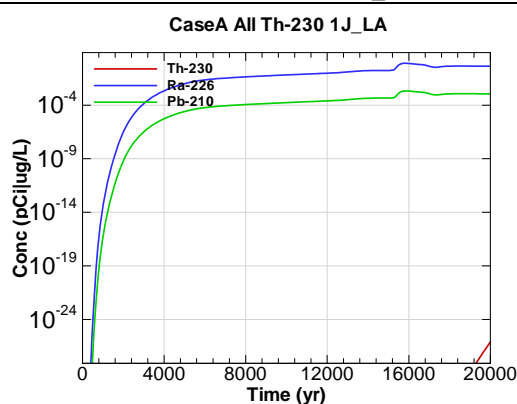


Figure F.2-730 - 1m Aquifer Concentration for
CaseA All Th-230 1J_LA

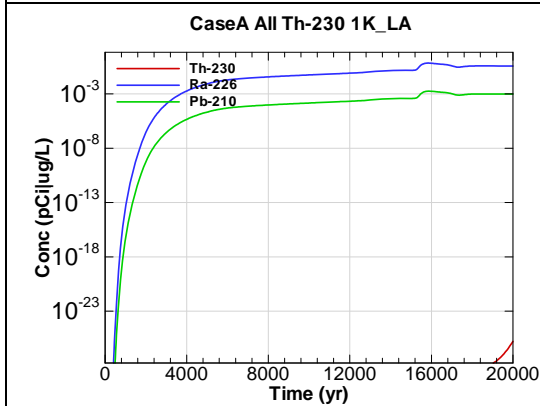


Figure F.2-731 - 1m Aquifer Concentration for
CaseA All Th-230 1K_LA

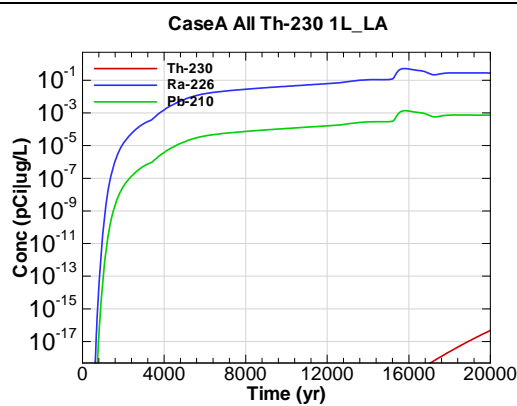


Figure F.2-732 - 1m Aquifer Concentration for
CaseA All Th-230 1L_LA

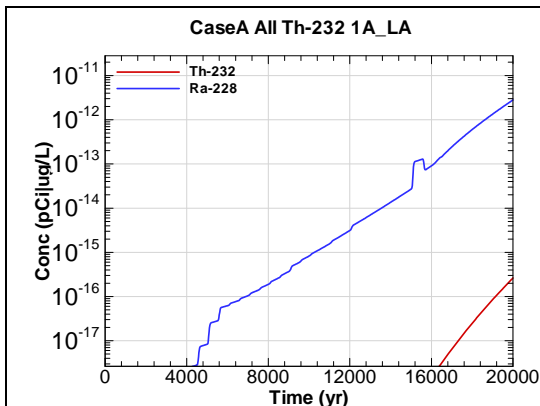


Figure F.2-733 - 1m Aquifer Concentration for
CaseA All Th-232 1A_LA

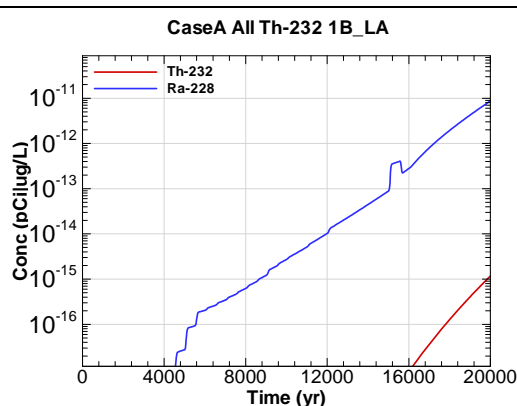


Figure F.2-734 - 1m Aquifer Concentration for
CaseA All Th-232 1B_LA

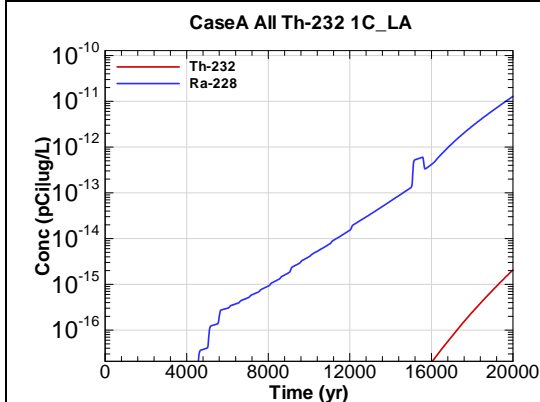


Figure F.2-735 - 1m Aquifer Concentration for
CaseA All Th-232 1C_LA

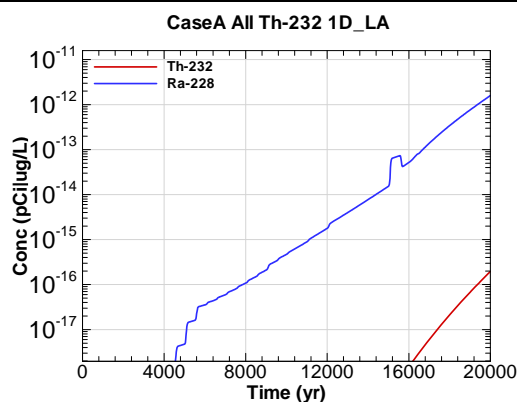


Figure F.2-736 - 1m Aquifer Concentration for
CaseA All Th-232 1D_LA

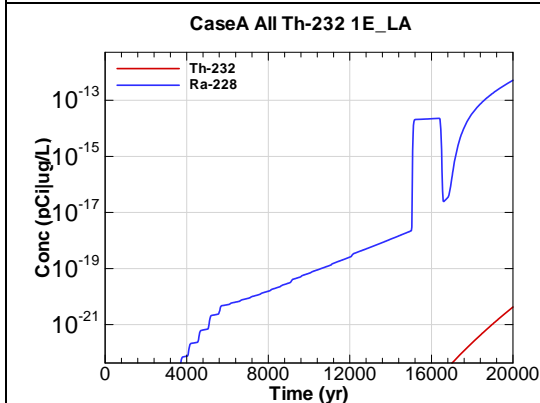


Figure F.2-737 - 1m Aquifer Concentration for
CaseA All Th-232 1E_LA

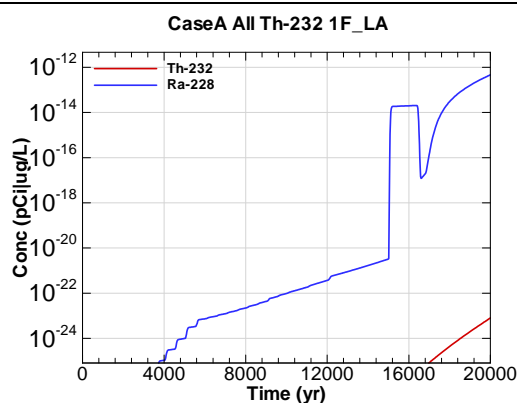


Figure F.2-738 - 1m Aquifer Concentration for
CaseA All Th-232 1F_LA

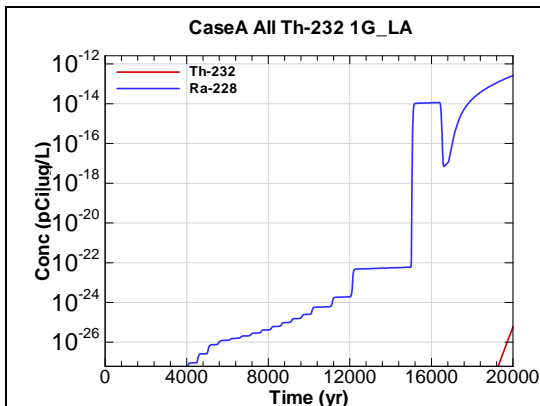


Figure F.2-739 - 1m Aquifer Concentration for
CaseA All Th-232 1G_LA

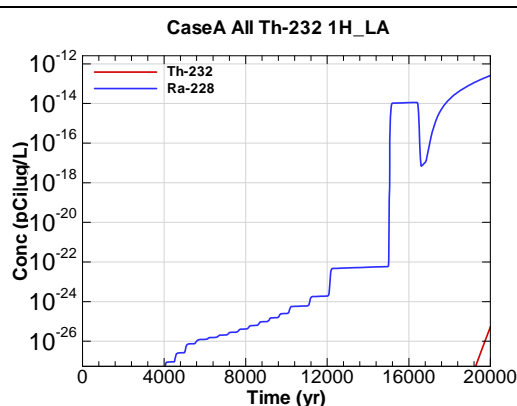


Figure F.2-740 - 1m Aquifer Concentration for
CaseA All Th-232 1H_LA

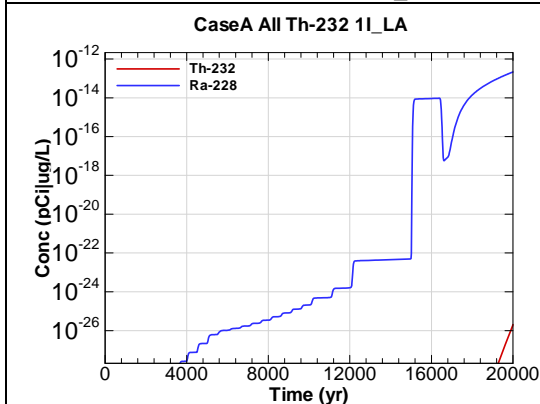


Figure F.2-741 - 1m Aquifer Concentration for
CaseA All Th-232 1I_LA

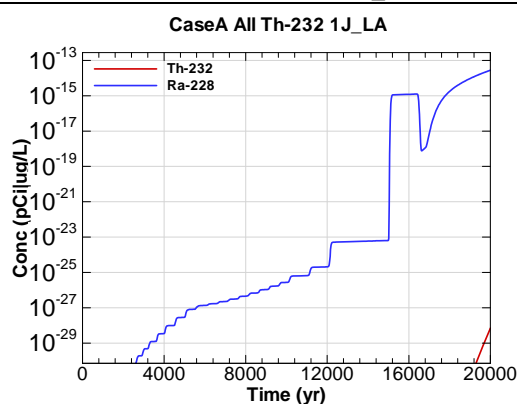


Figure F.2-742 - 1m Aquifer Concentration for
CaseA All Th-232 1J_LA

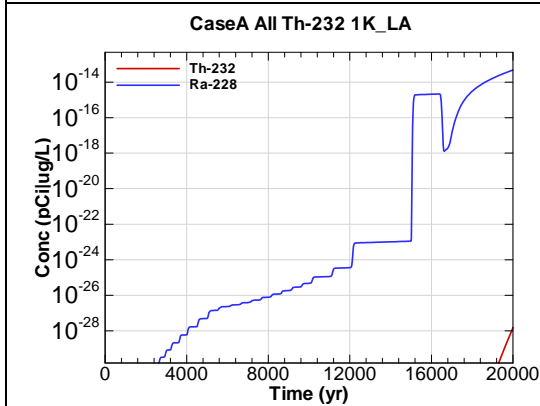


Figure F.2-743 - 1m Aquifer Concentration for
CaseA All Th-232 1K_LA

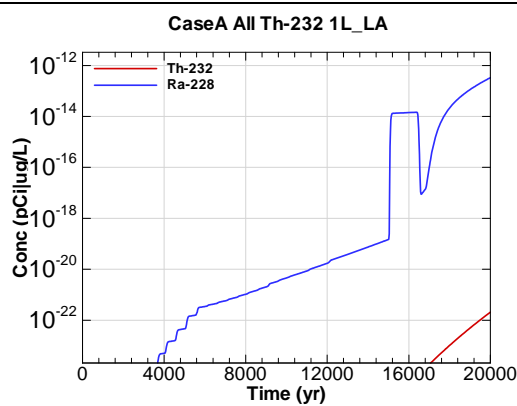
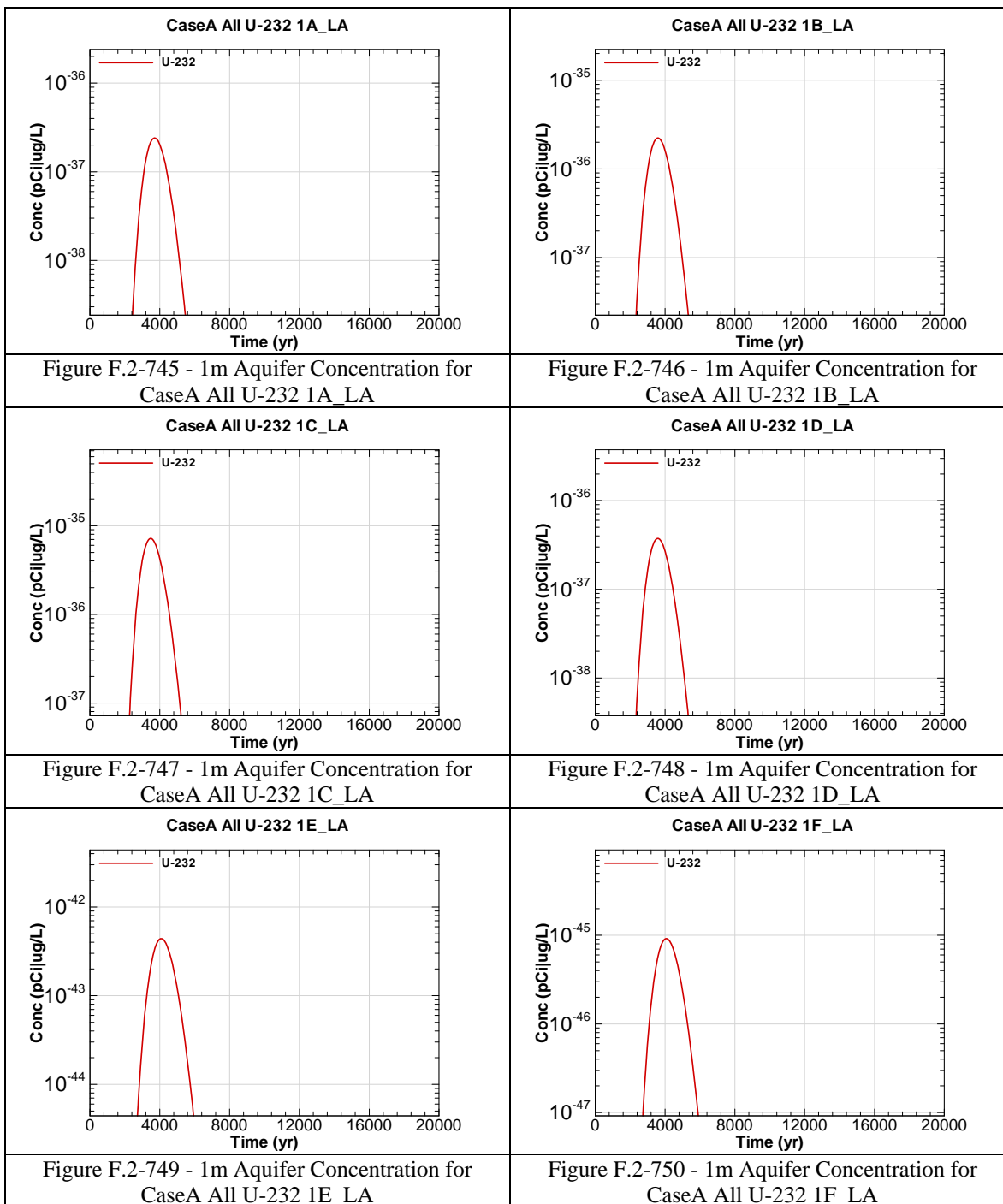
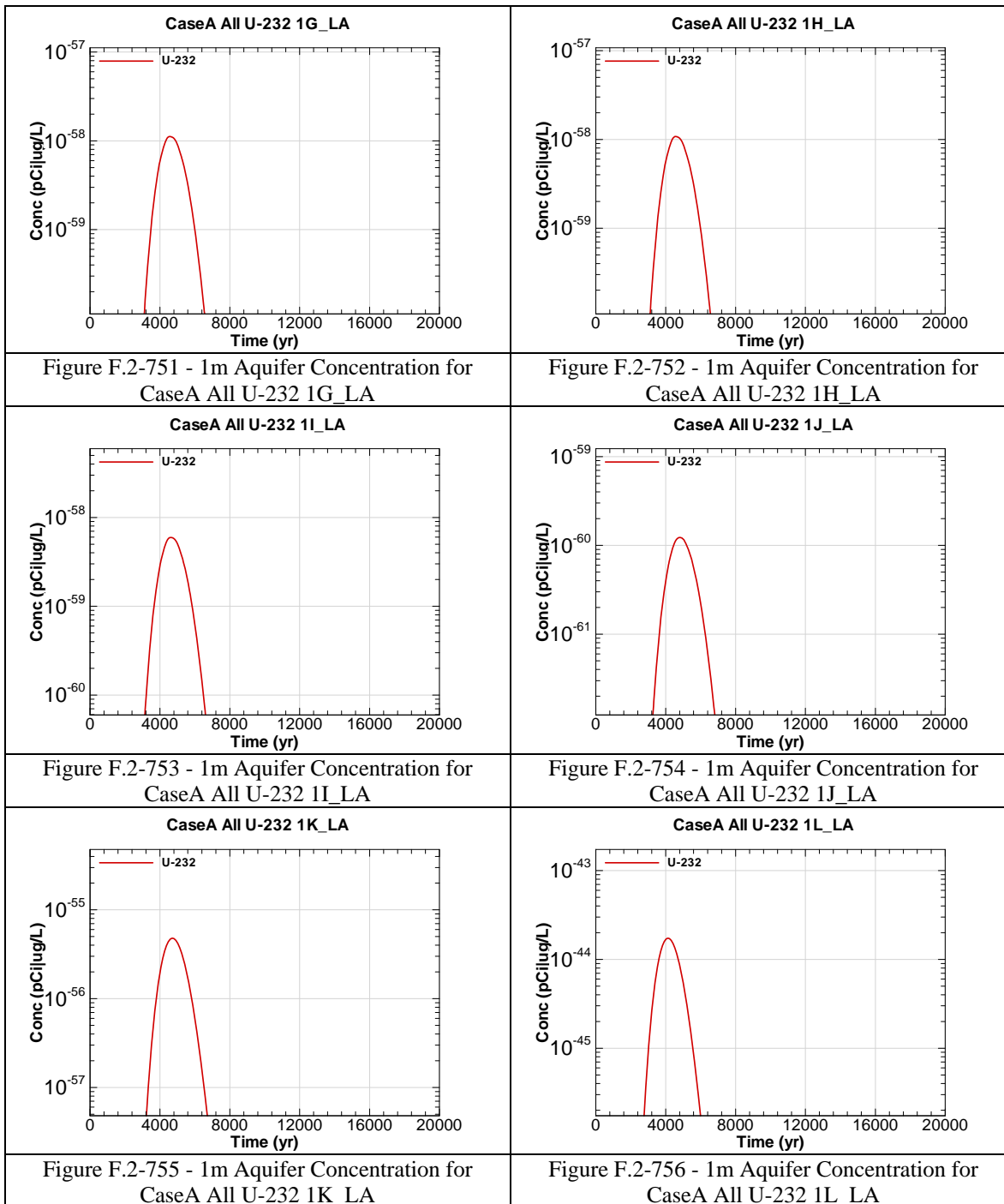
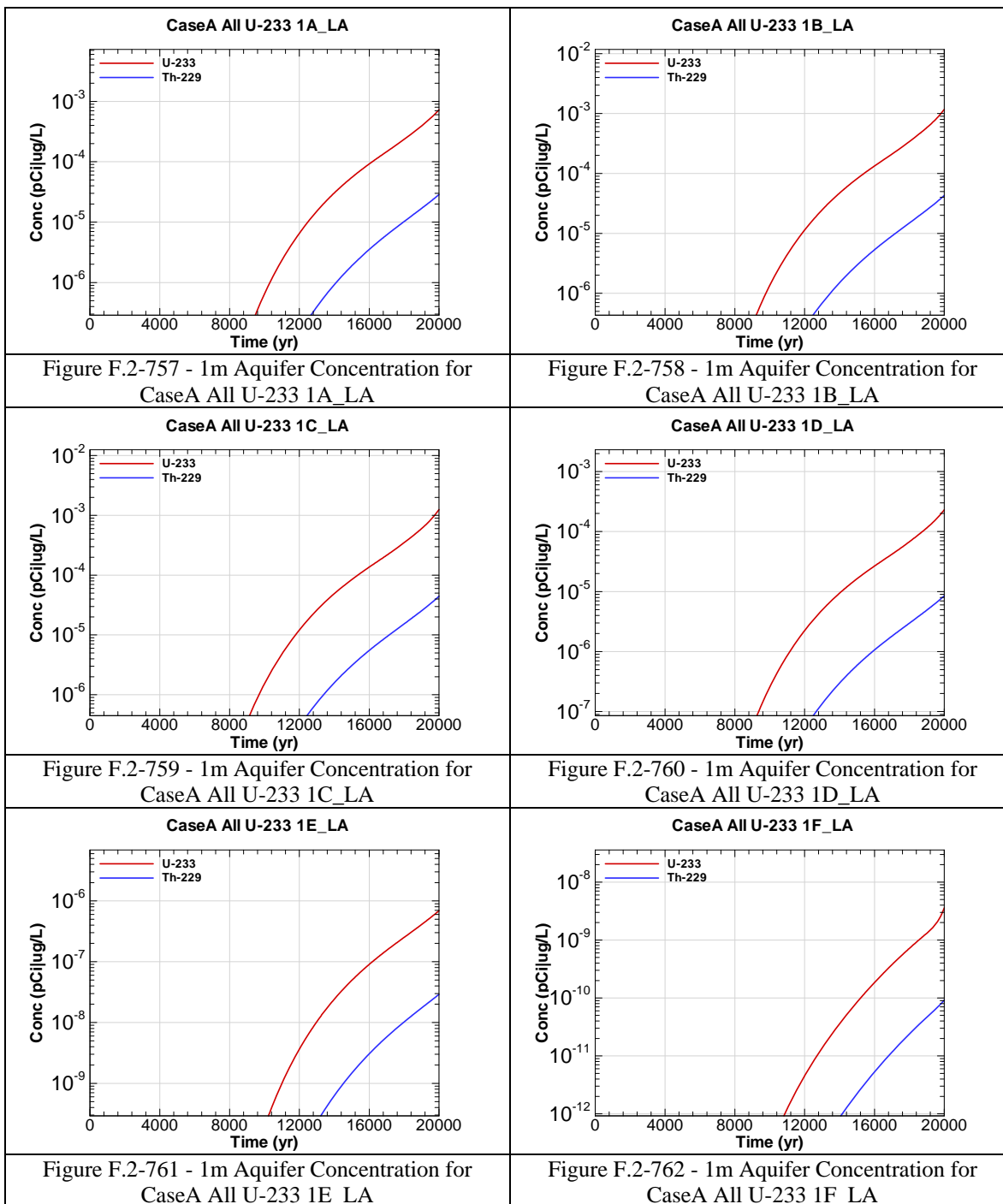
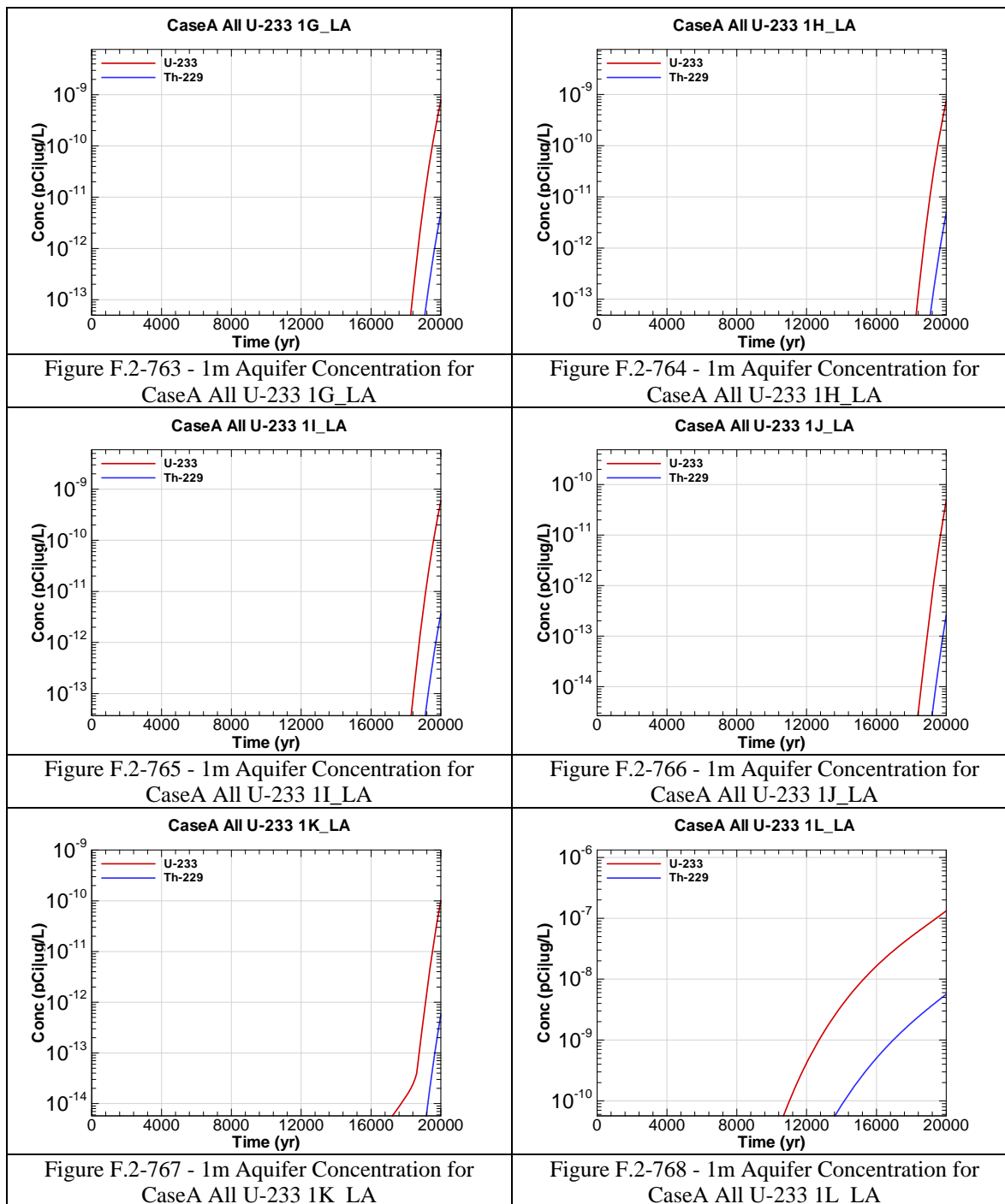


Figure F.2-744 - 1m Aquifer Concentration for
CaseA All Th-232 1L_LA









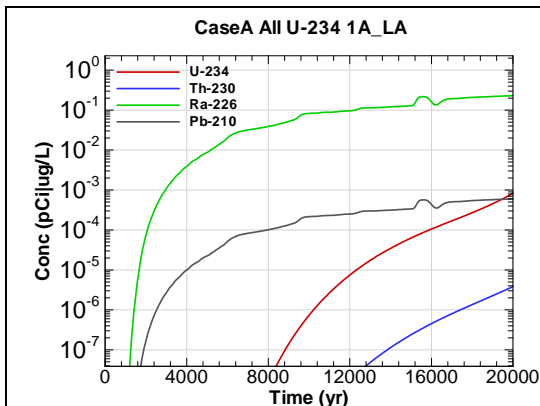


Figure F.2-769 - 1m Aquifer Concentration for
CaseA All U-234 1A_LA

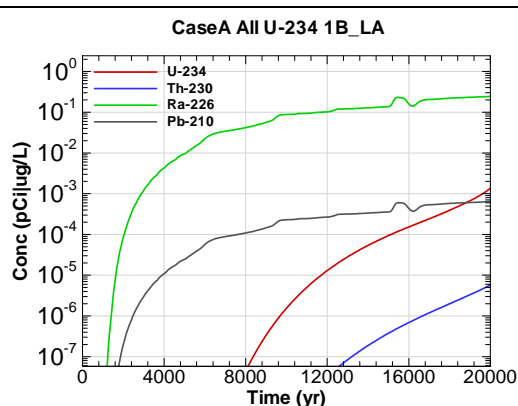


Figure F.2-770 - 1m Aquifer Concentration for
CaseA All U-234 1B_LA

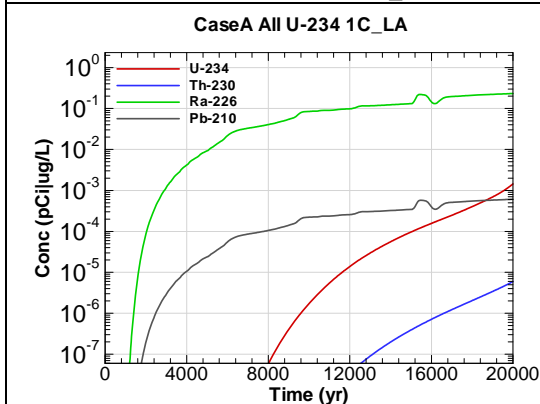


Figure F.2-771 - 1m Aquifer Concentration for
CaseA All U-234 1C_LA

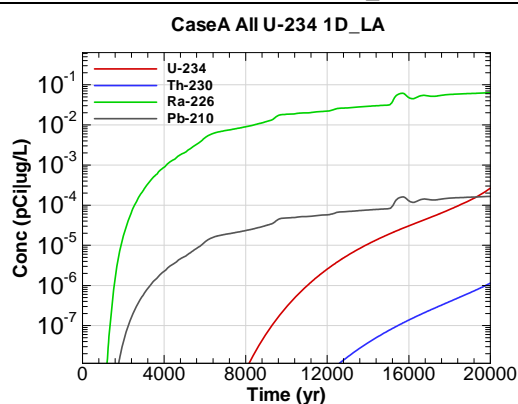


Figure F.2-772 - 1m Aquifer Concentration for
CaseA All U-234 1D_LA

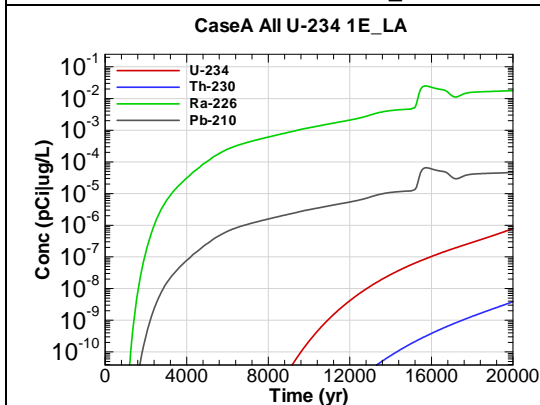


Figure F.2-773 - 1m Aquifer Concentration for
CaseA All U-234 1E_LA

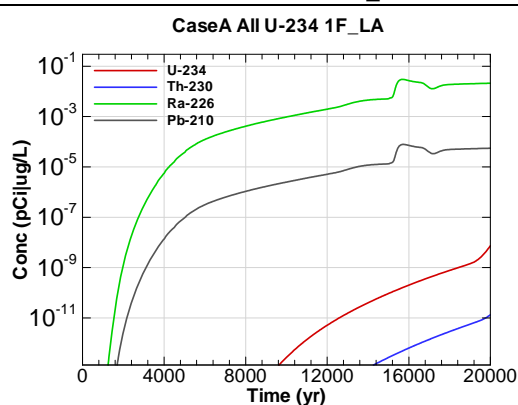
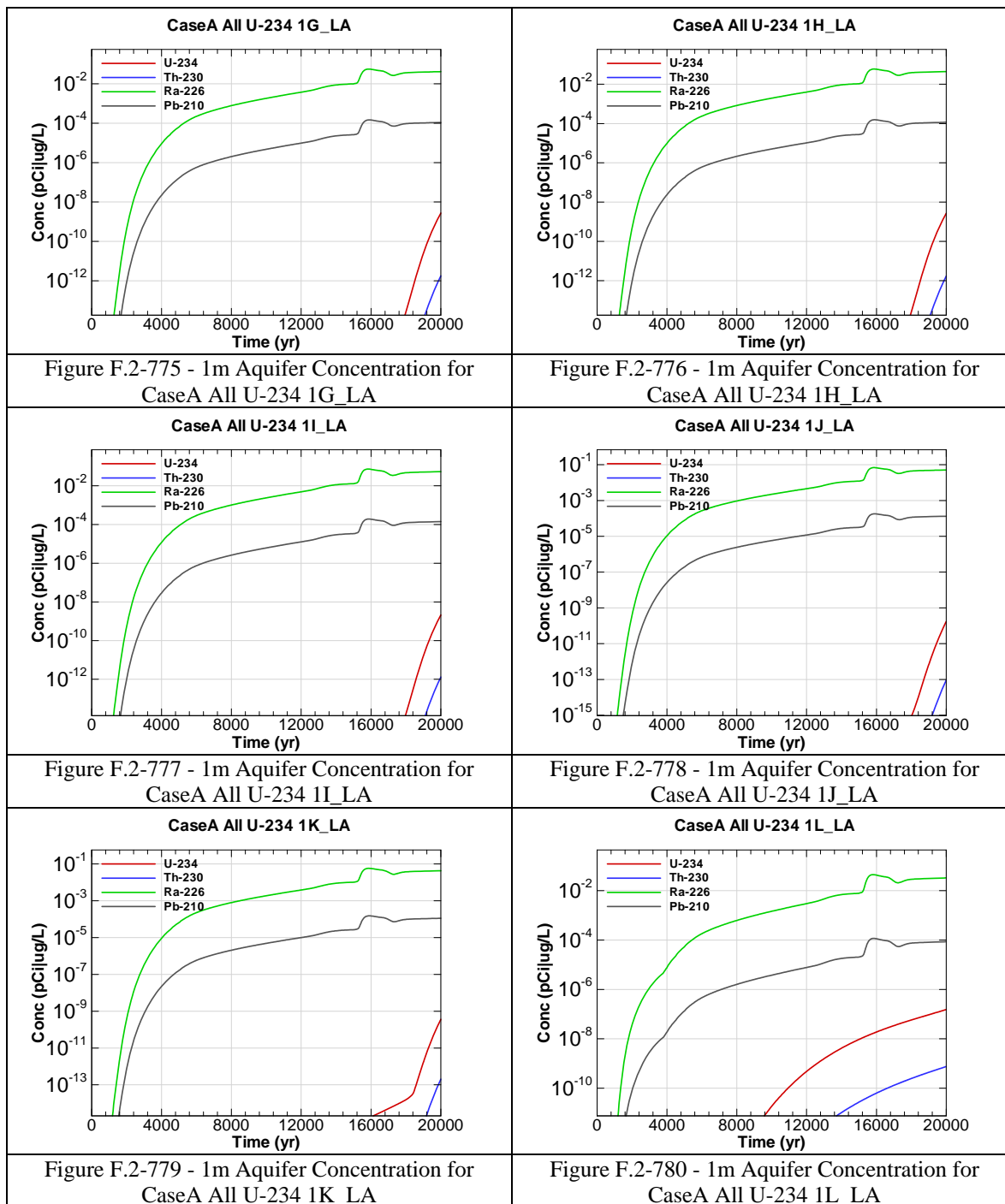
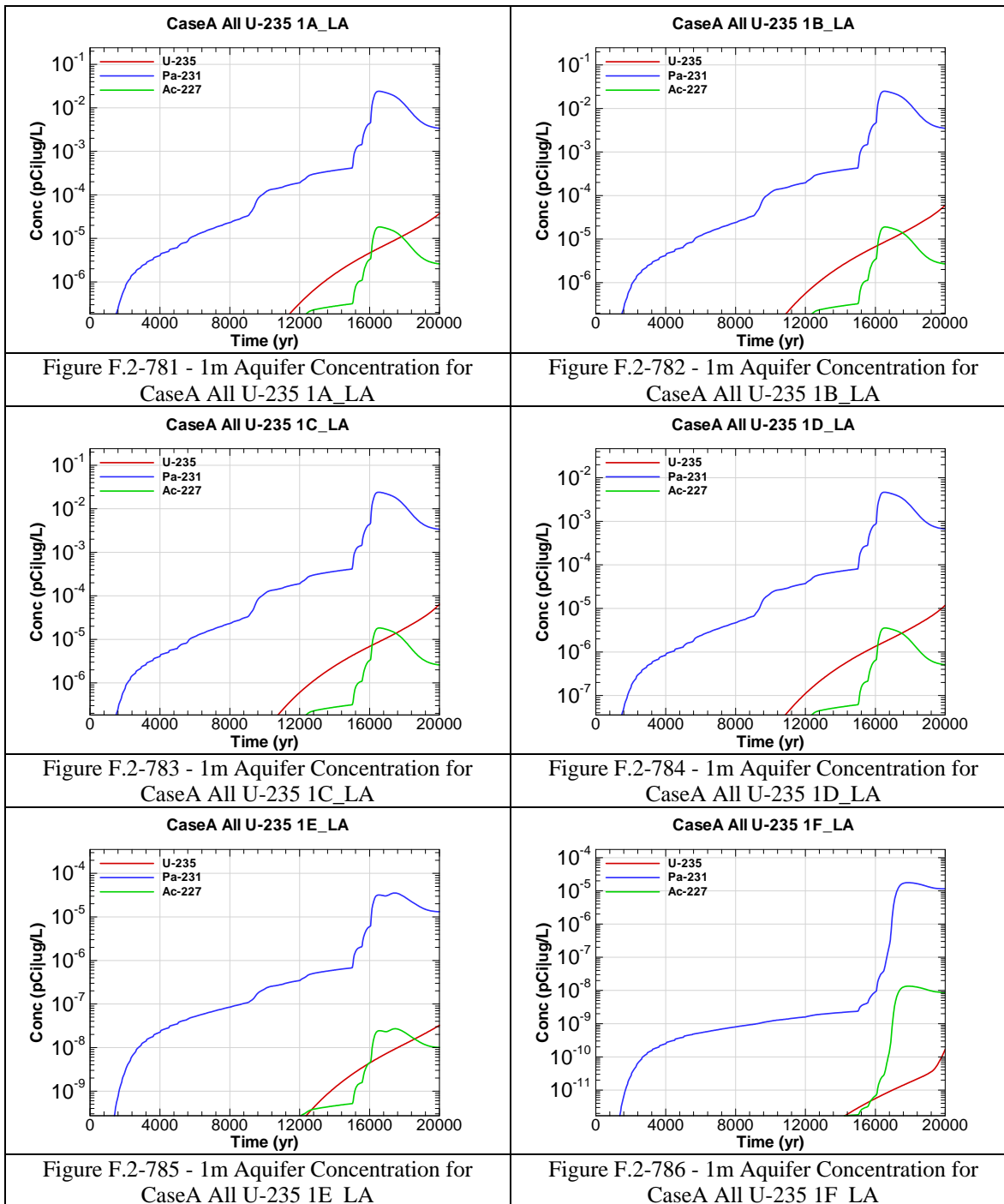
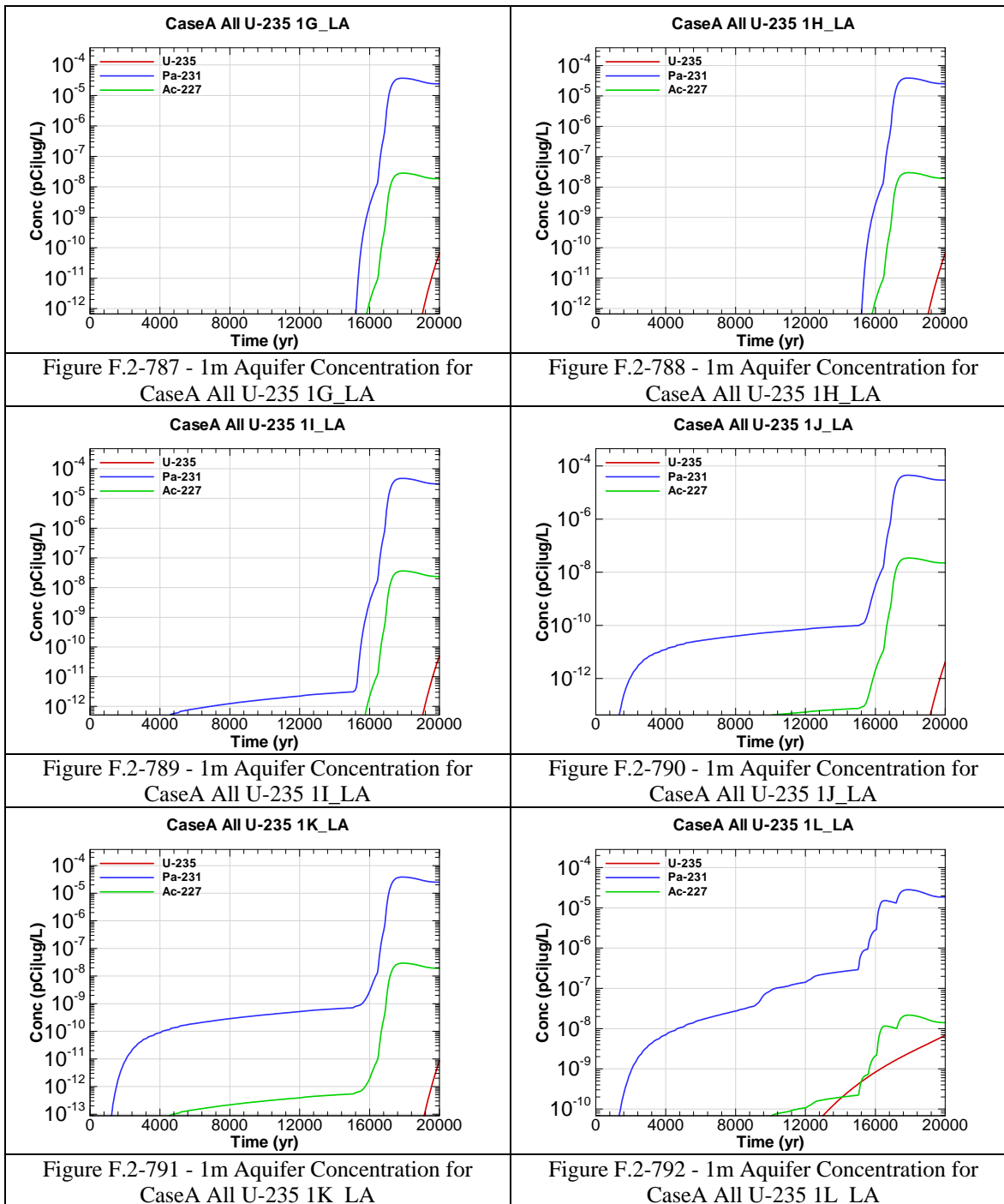
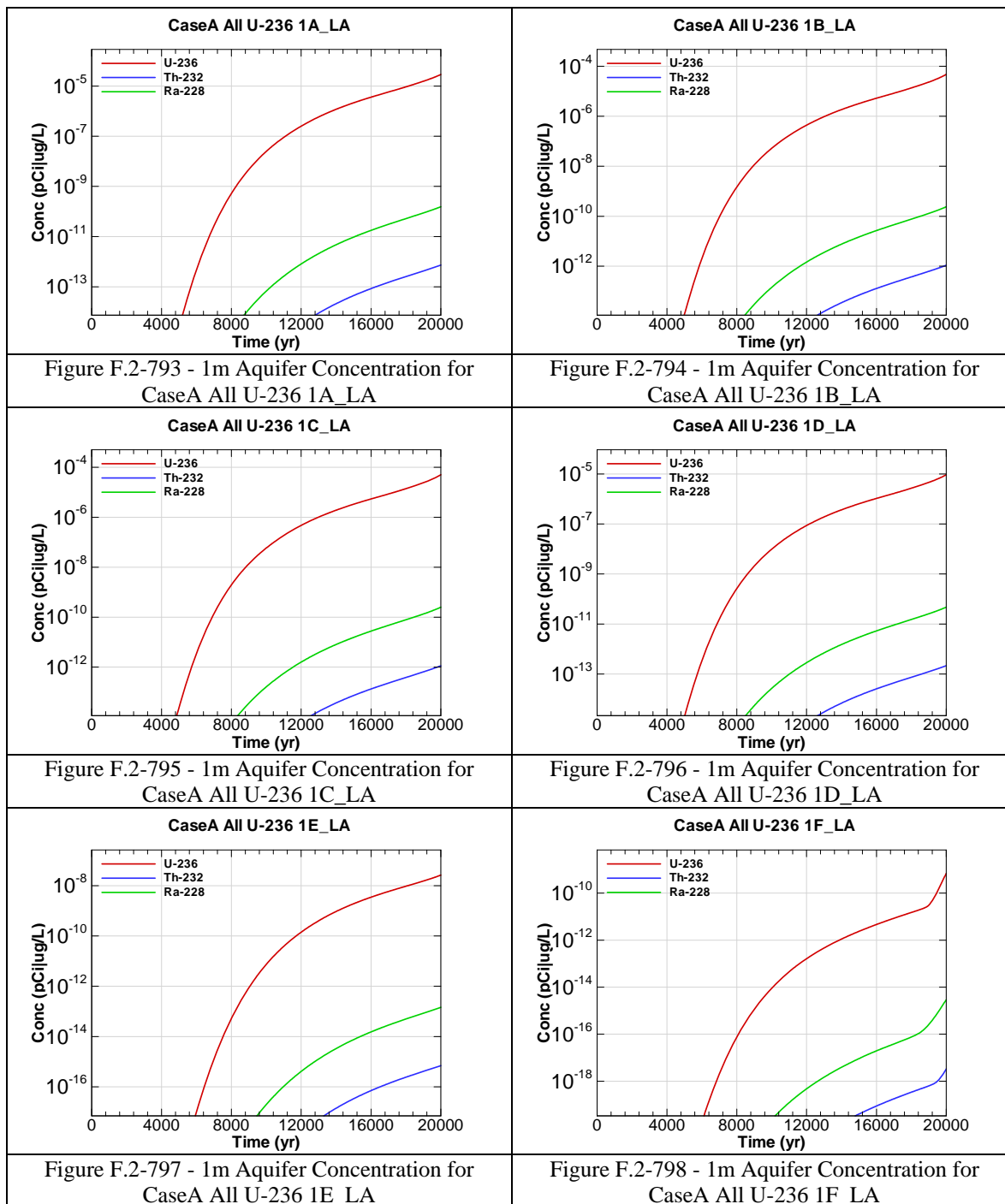


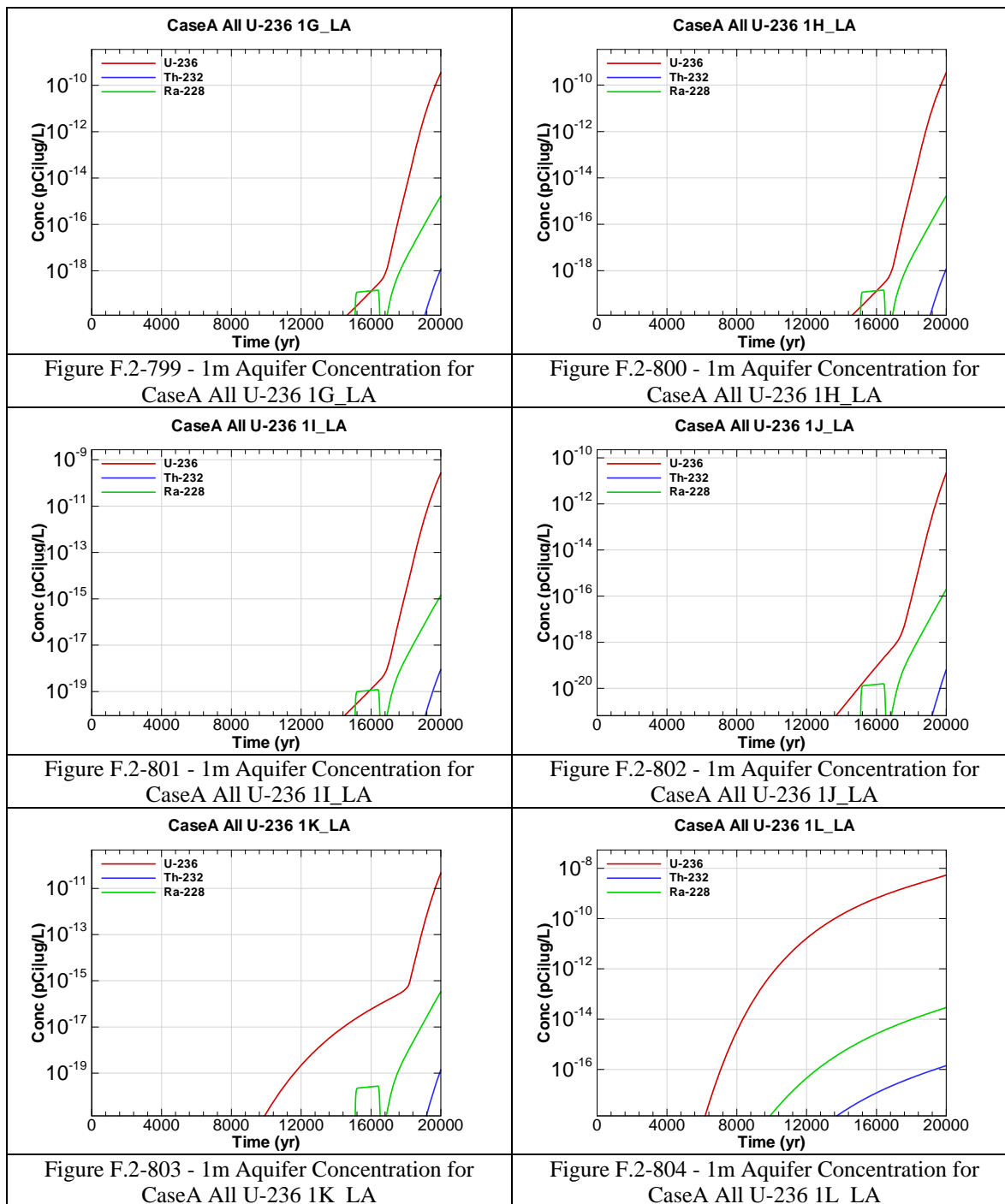
Figure F.2-774 - 1m Aquifer Concentration for
CaseA All U-234 1F_LA











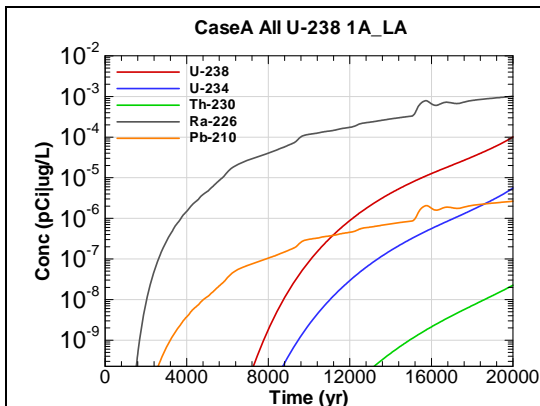


Figure F.2-805 - 1m Aquifer Concentration for
CaseA All U-238 1A_LA

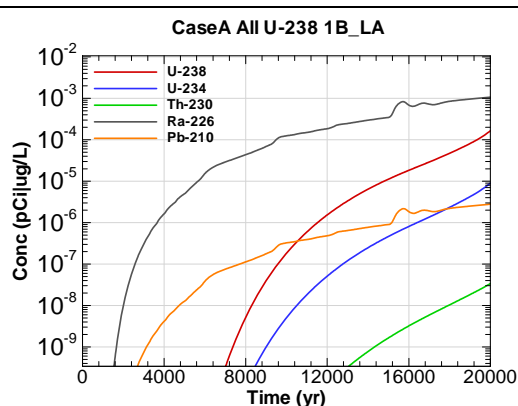


Figure F.2-806 - 1m Aquifer Concentration for
CaseA All U-238 1B_LA

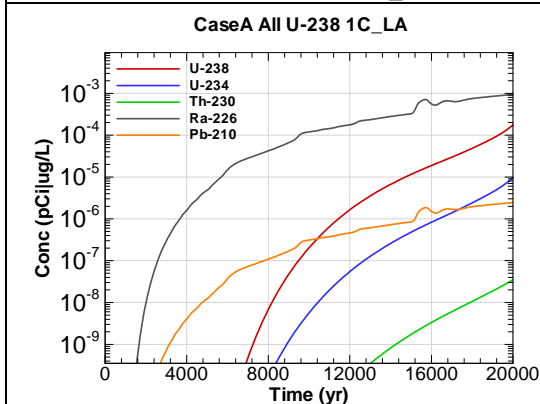


Figure F.2-807 - 1m Aquifer Concentration for
CaseA All U-238 1C_LA

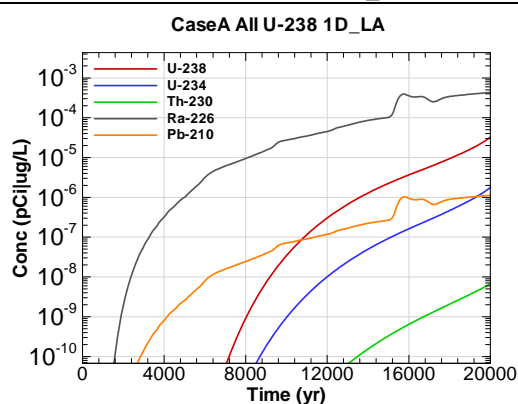


Figure F.2-808 - 1m Aquifer Concentration for
CaseA All U-238 1D_LA

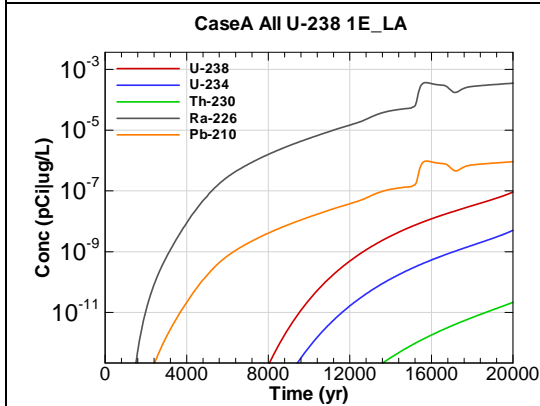


Figure F.2-809 - 1m Aquifer Concentration for
CaseA All U-238 1E_LA

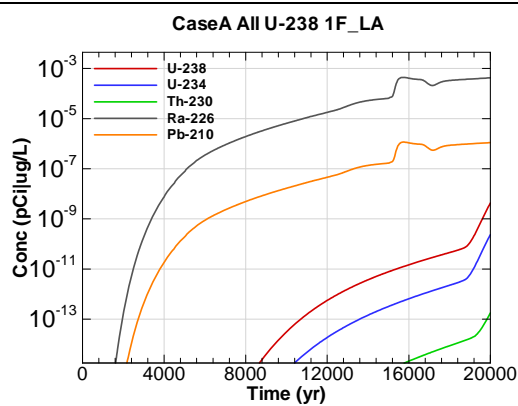
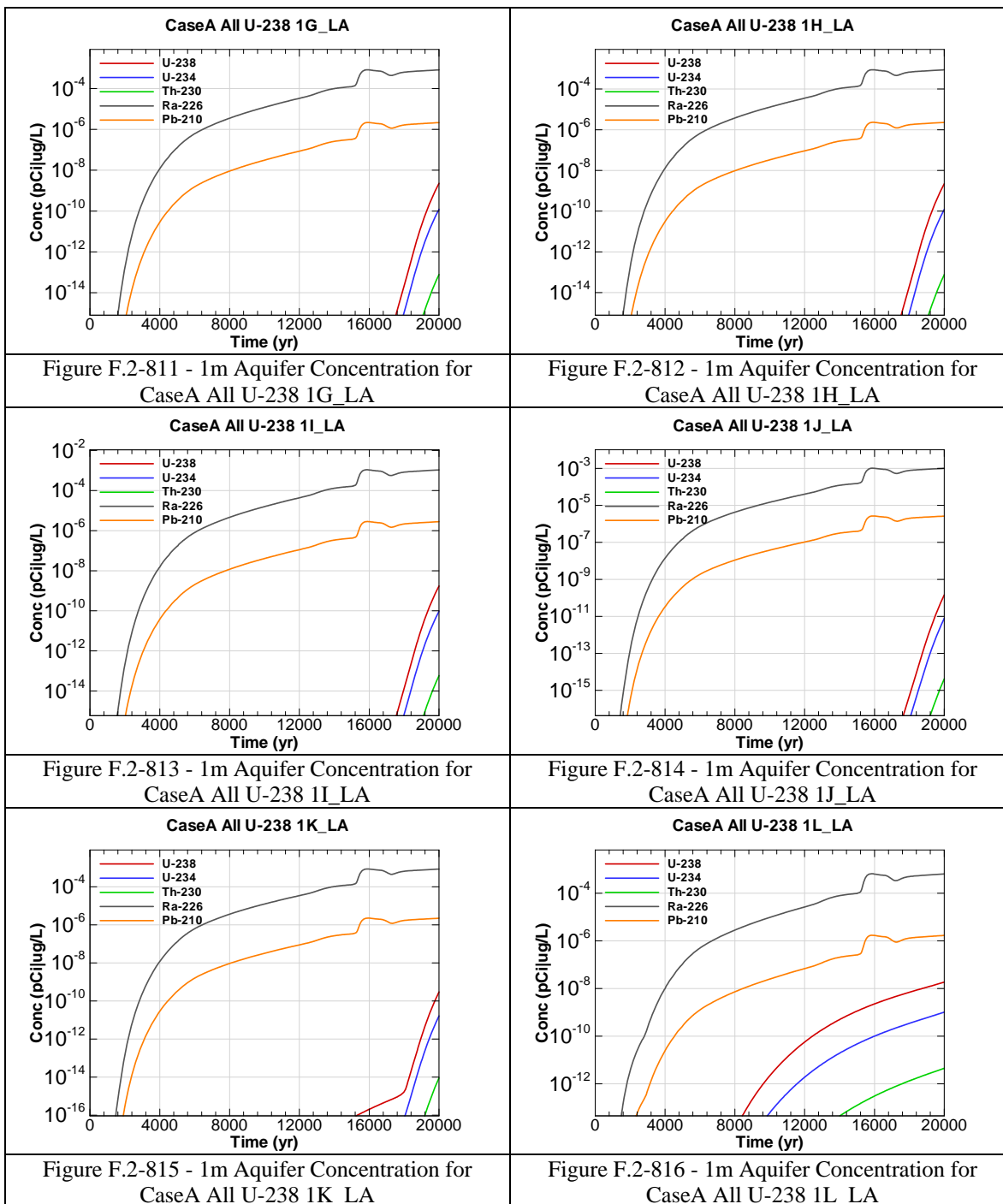
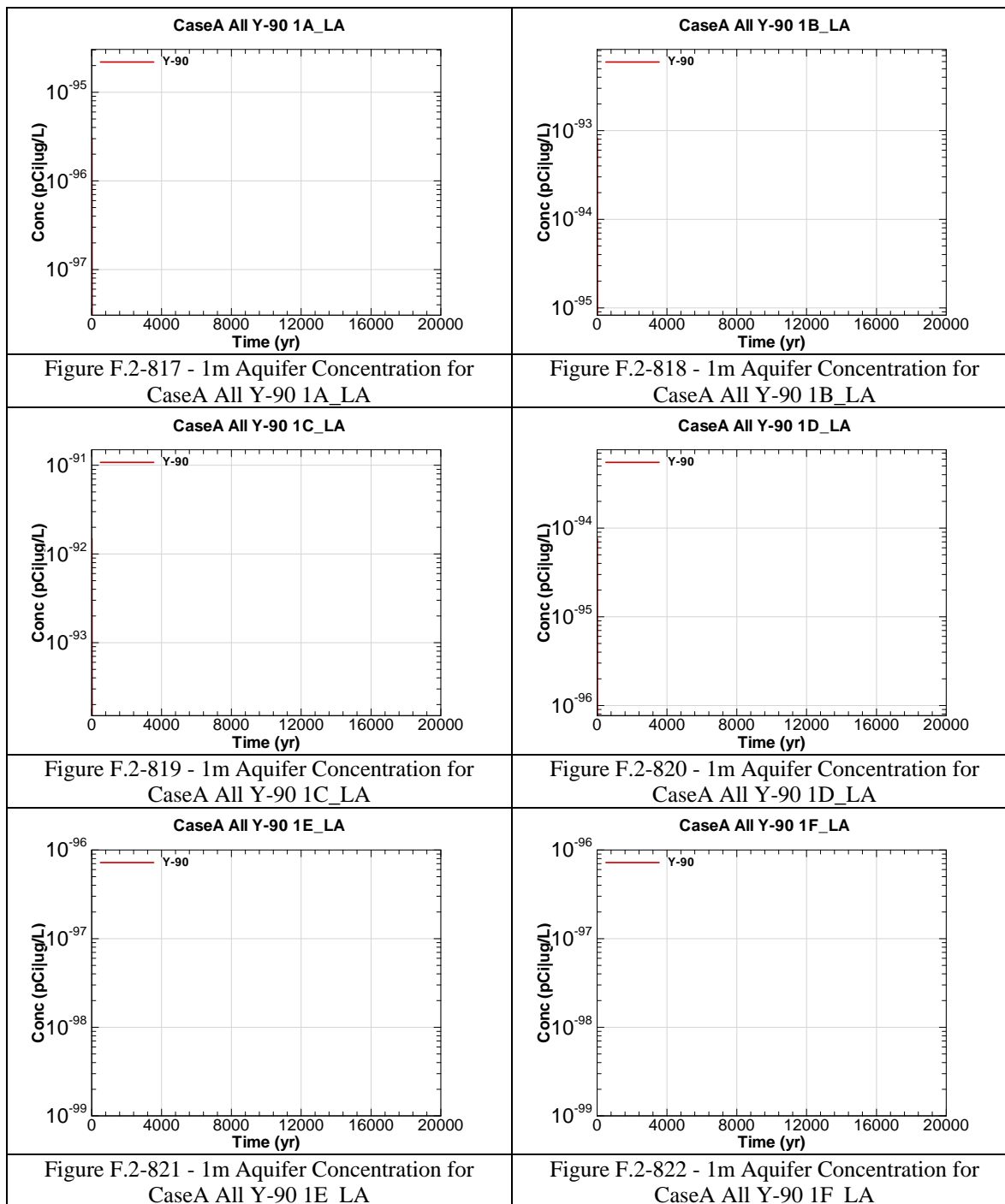
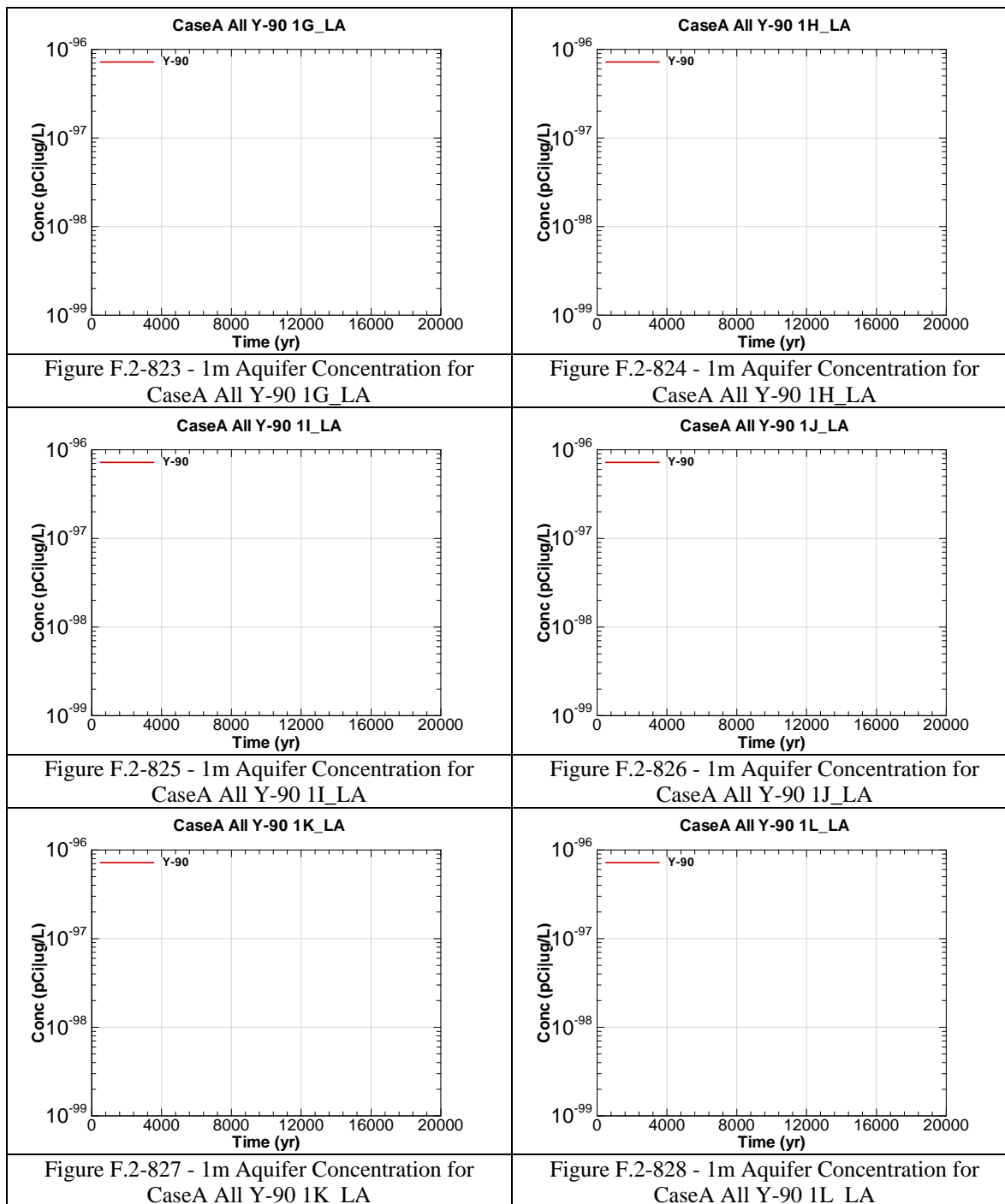
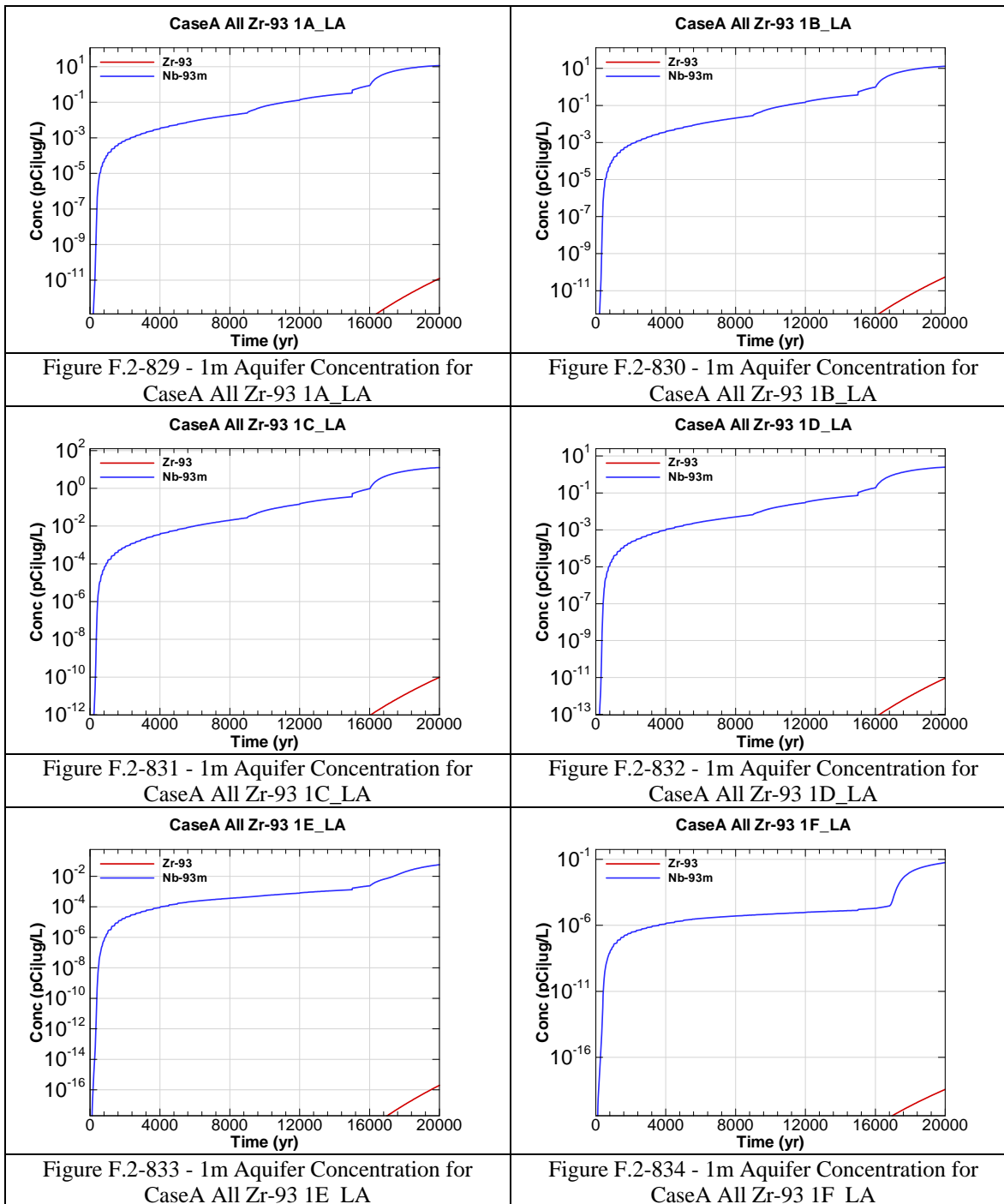


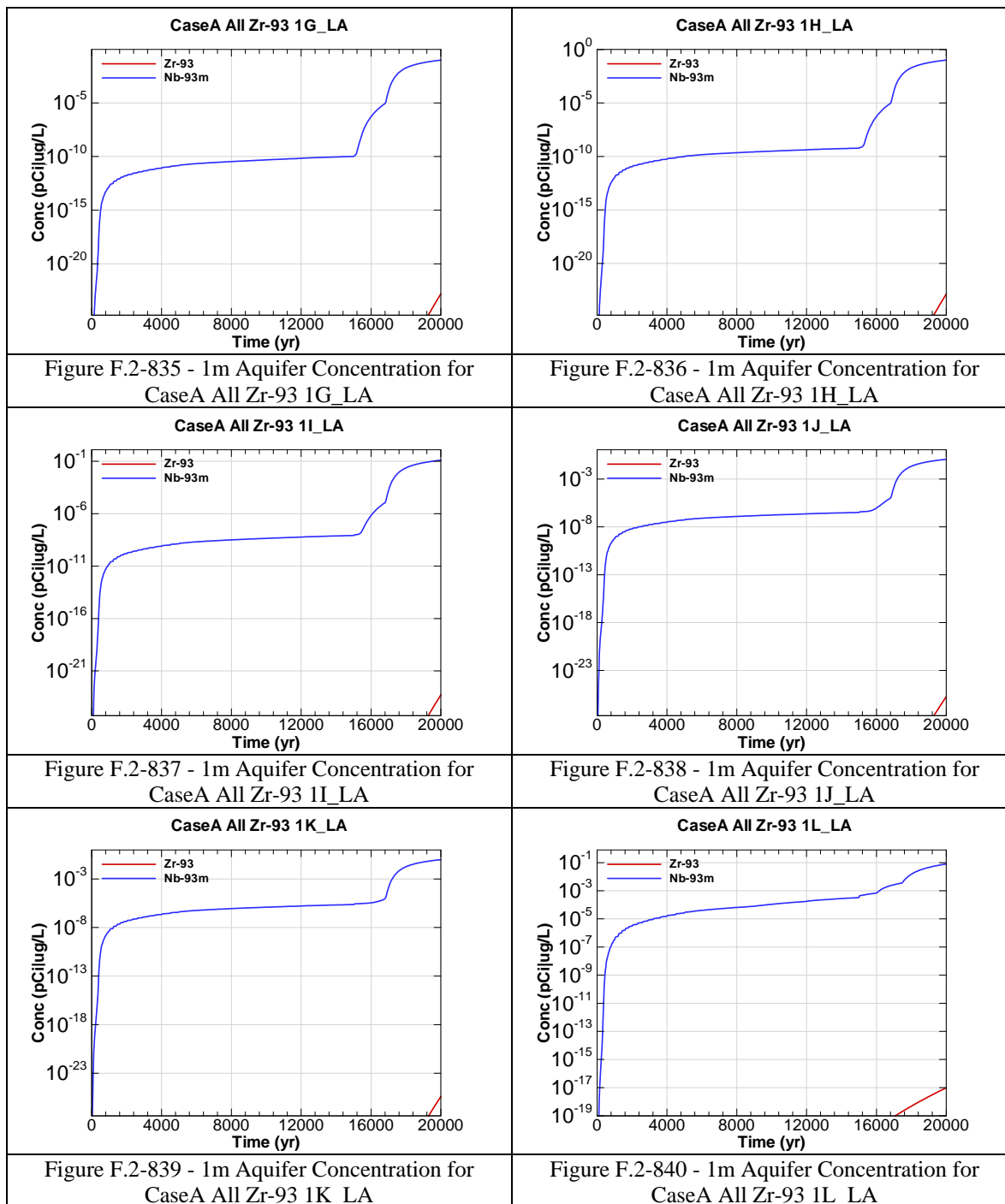
Figure F.2-810 - 1m Aquifer Concentration for
CaseA All U-238 1F_LA





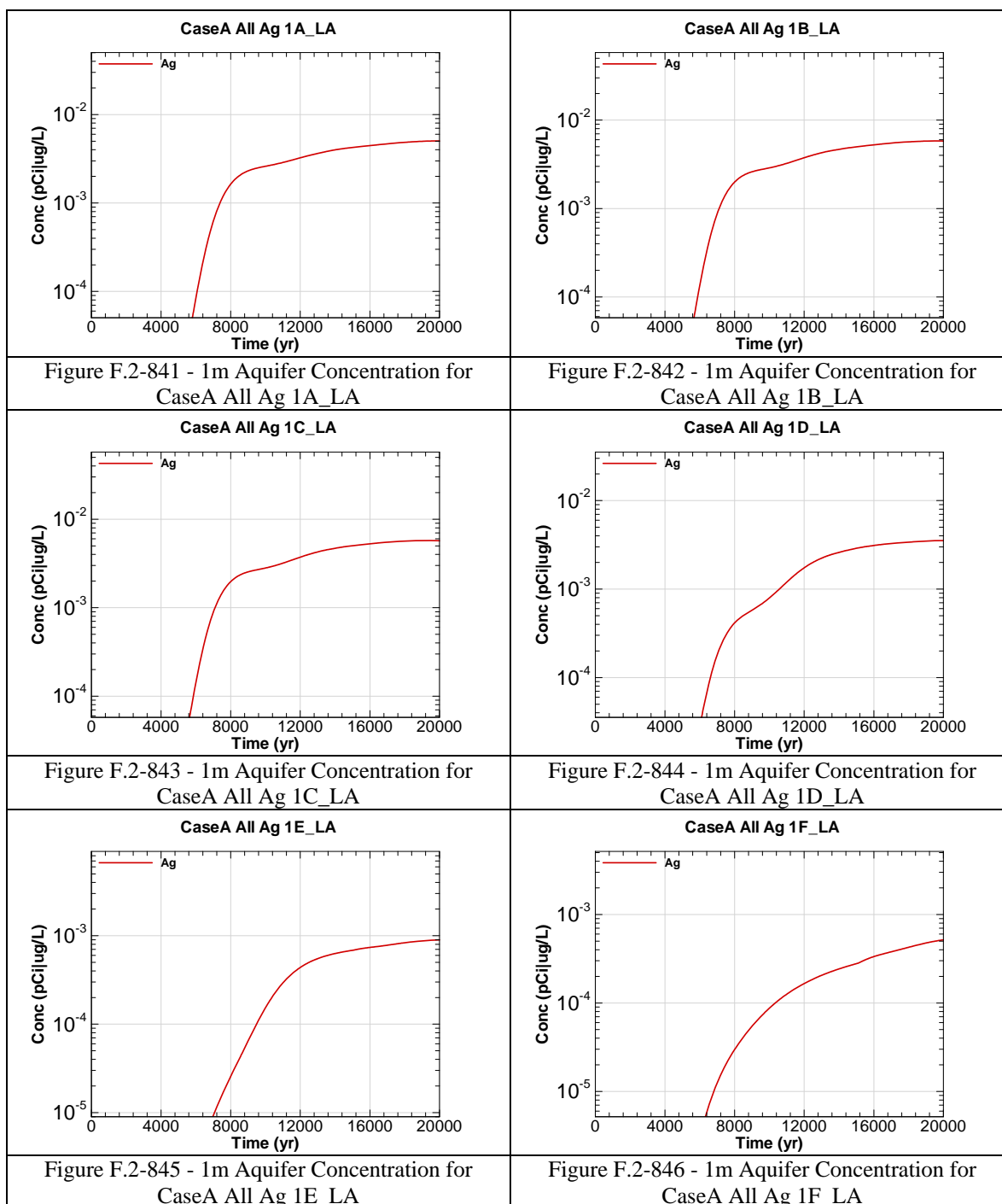


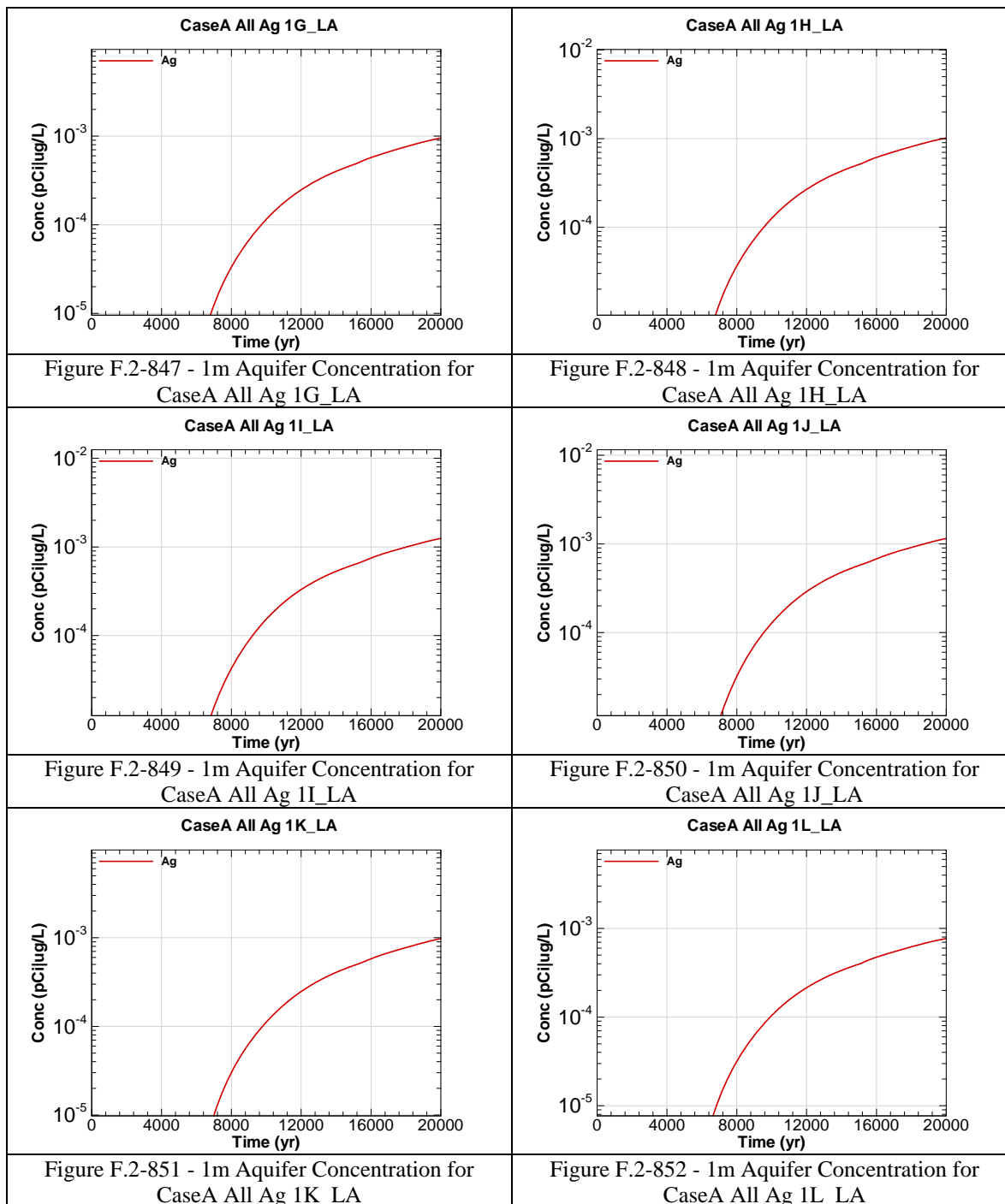


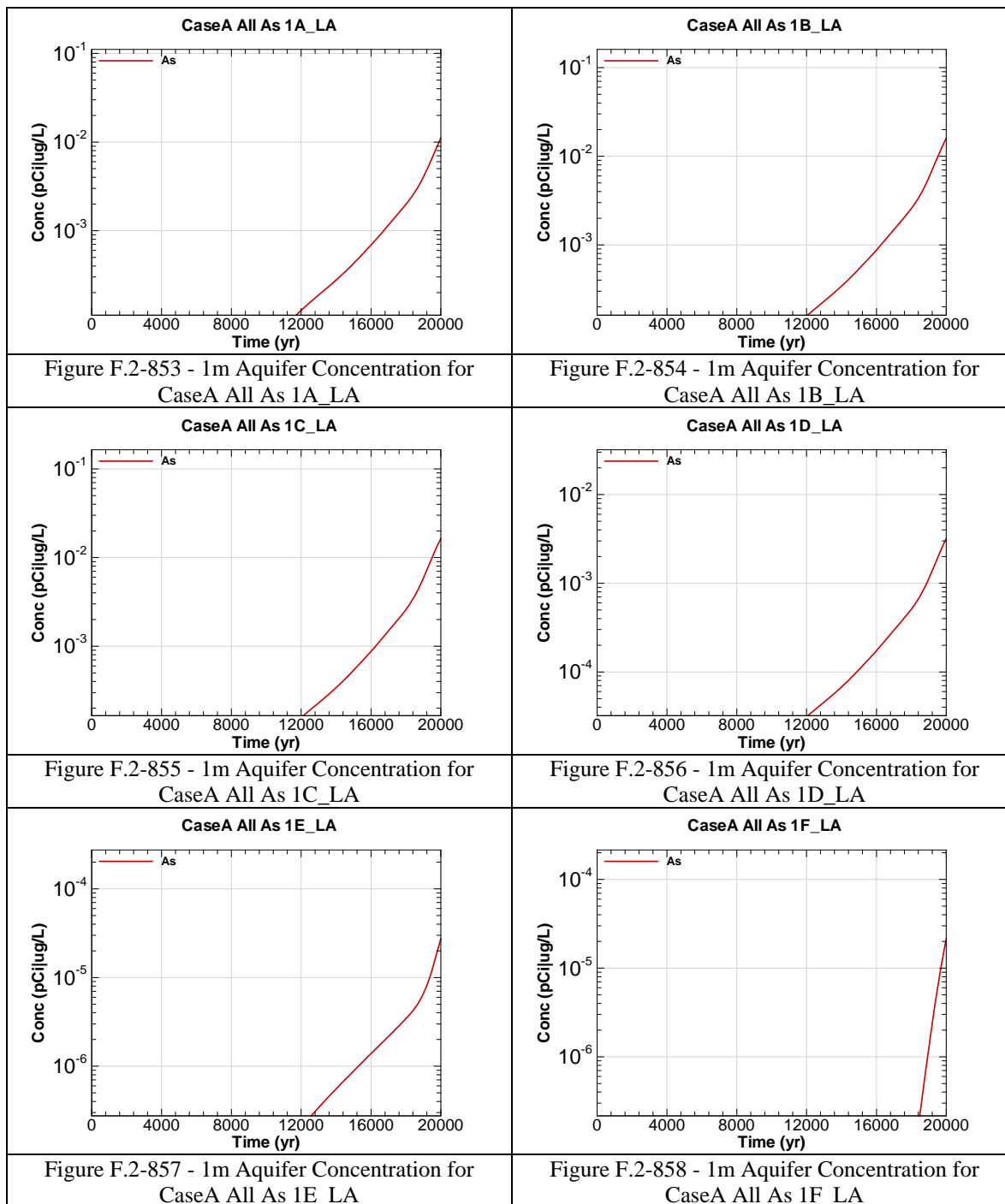


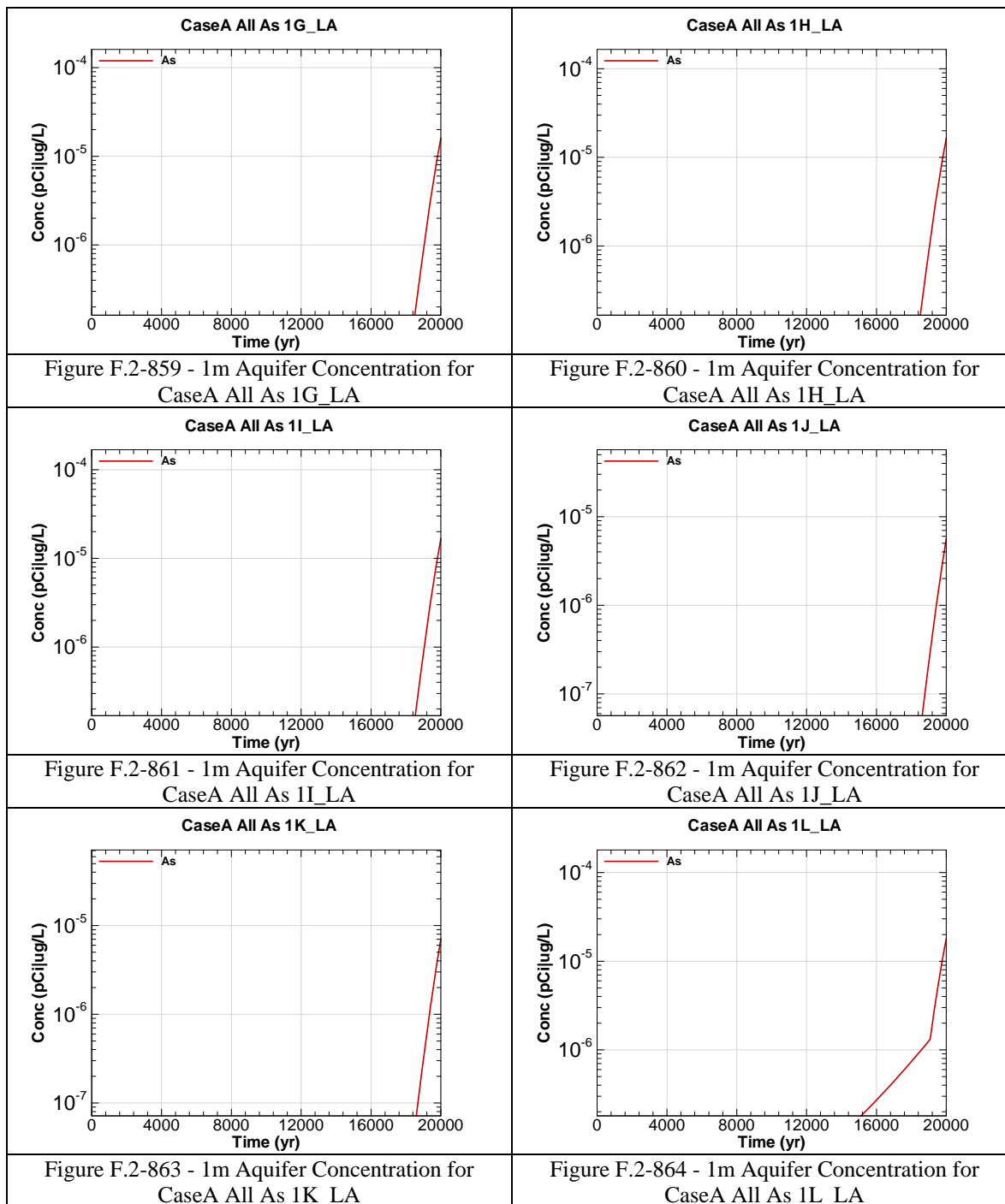
The chemical contaminants were modeled prior to the revision of the final closure inventory calculations presented in Table 3.3-8 for five chemical components: As, Cr, Cu, N and U. The figures that follow represent the concentrations calculated with an initial inventory input. The multipliers in the table below are to be used to determine the final concentrations with respect to time for the impacted chemicals as the inventory has a linear relationship with concentration in the Saltstone model. The groundwater concentration tables in Section 5 have been corrected using the multipliers.

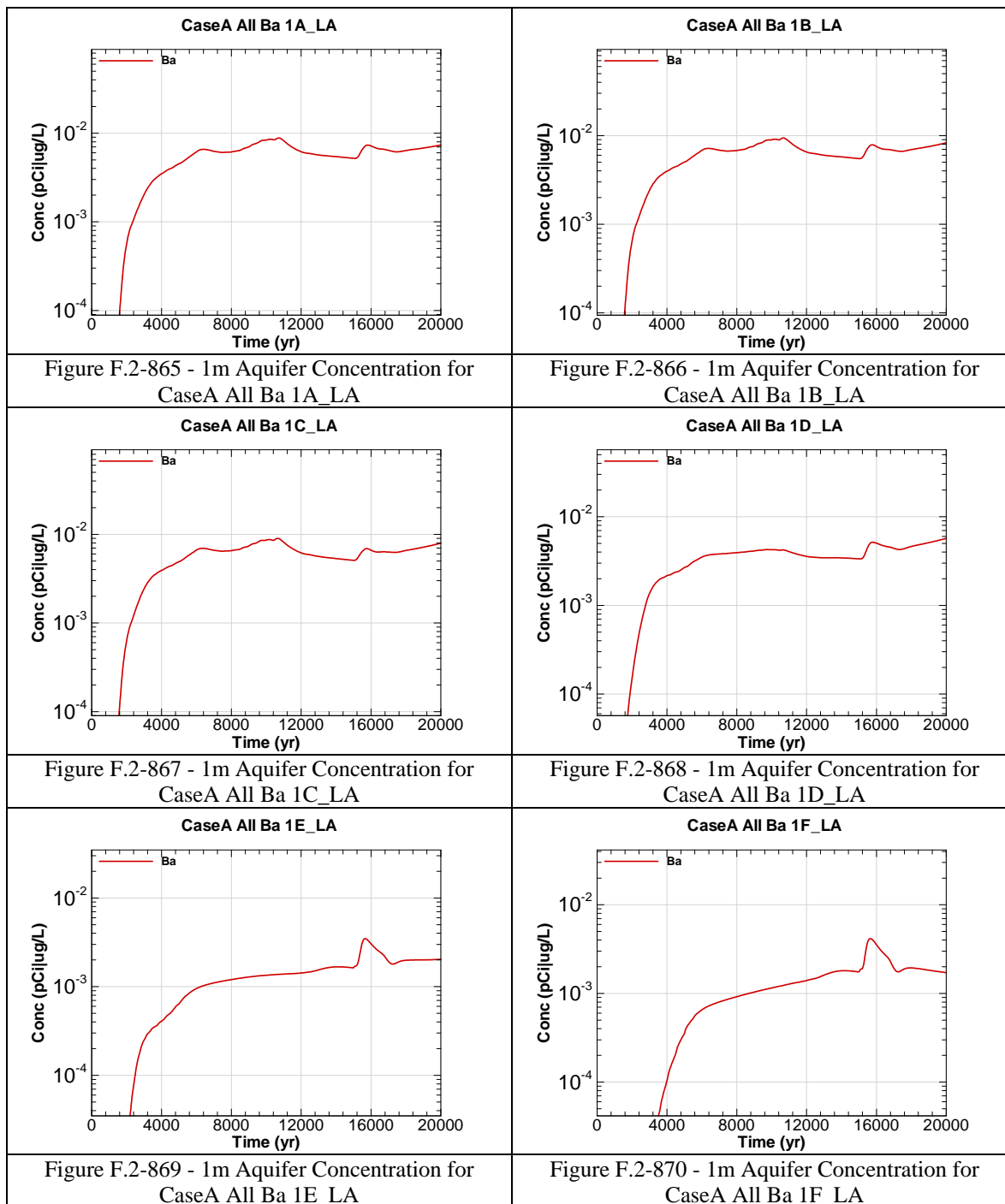
| Chemical Component | Modeled Inventory | Projected Inventory | Percent Increase | Multiplier |
|---------------------------|--------------------------|----------------------------|-------------------------|-------------------|
| Ag | 8.8E+01 | 8.8E+01 | 0.0% | None |
| As | 1.08E+04 | 1.1E+04 | 2.3% | 1.02E+00 |
| Ba | 1.7E+02 | 1.7E+02 | 0.0% | None |
| Cd | 1.3E+03 | 1.3E+03 | 0.0% | None |
| Cr | 2.9E+04 | 3.0E+04 | 1.4% | 1.01E+00 |
| Cu | 1.9E+04 | 1.9E+04 | 0.9% | 1.01E+00 |
| F | 1.7E+04 | 1.7E+04 | 0.0% | None |
| Fe | 2.9E+03 | 2.9E+03 | 0.0% | None |
| Hg | 1.1E+04 | 1.1E+04 | 0.0% | None |
| Mn | 7.3E+03 | 7.3E+03 | 0.0% | None |
| Ni | 1.5E+03 | 1.5E+03 | 0.0% | None |
| Total N | 2.2E+07 | 2.4E+07 | 5.8% | 1.06E+00 |
| Pb | 6.7E+03 | 6.7E+03 | 0.0% | None |
| Se | 4.0E+04 | 4.0E+04 | 0.0% | None |
| U | 8.2E+02 | 8.9E+02 | 8.9% | 1.10E+00 |
| Zn | 2.7E+04 | 2.7E+04 | 0.0% | None |

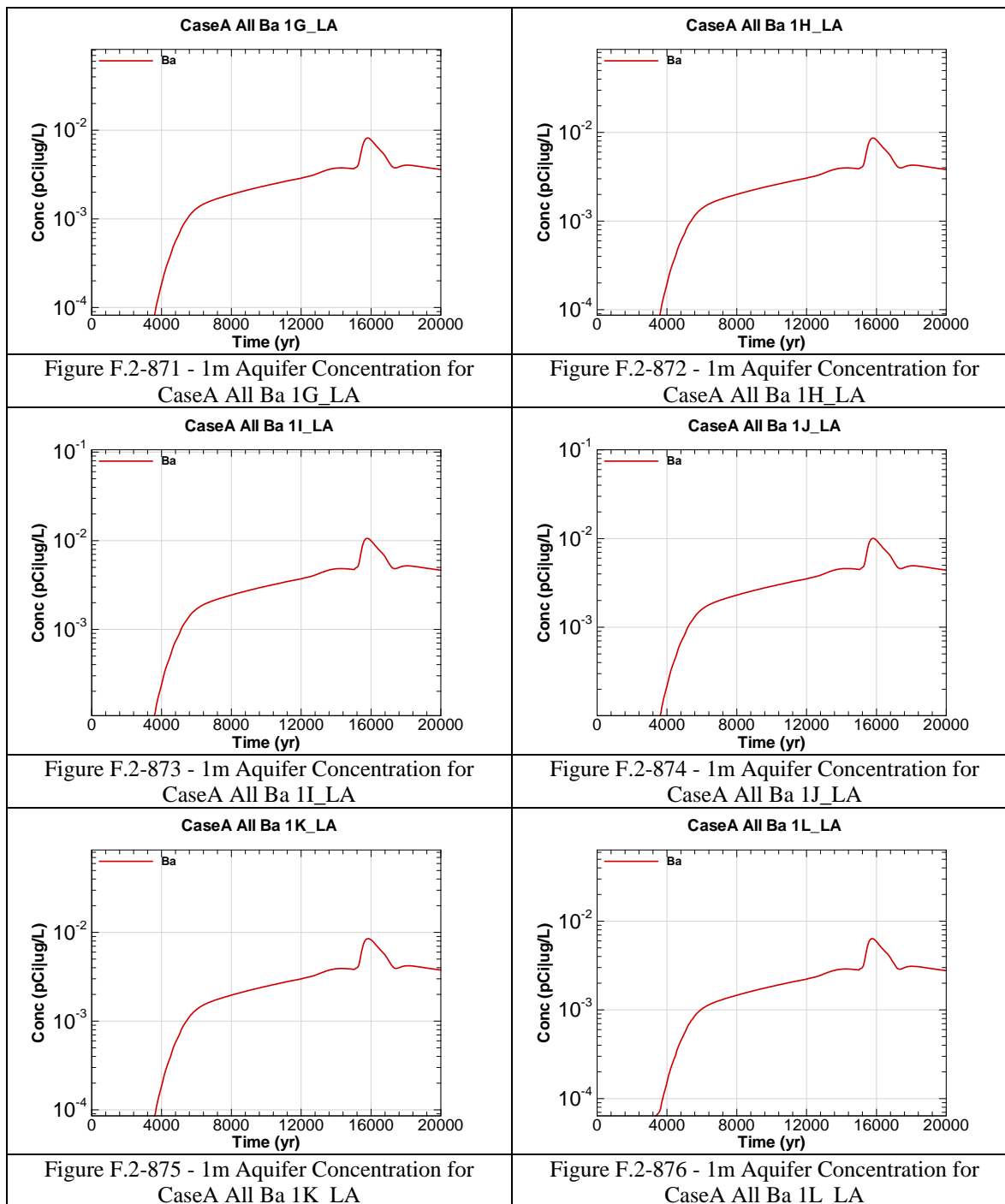


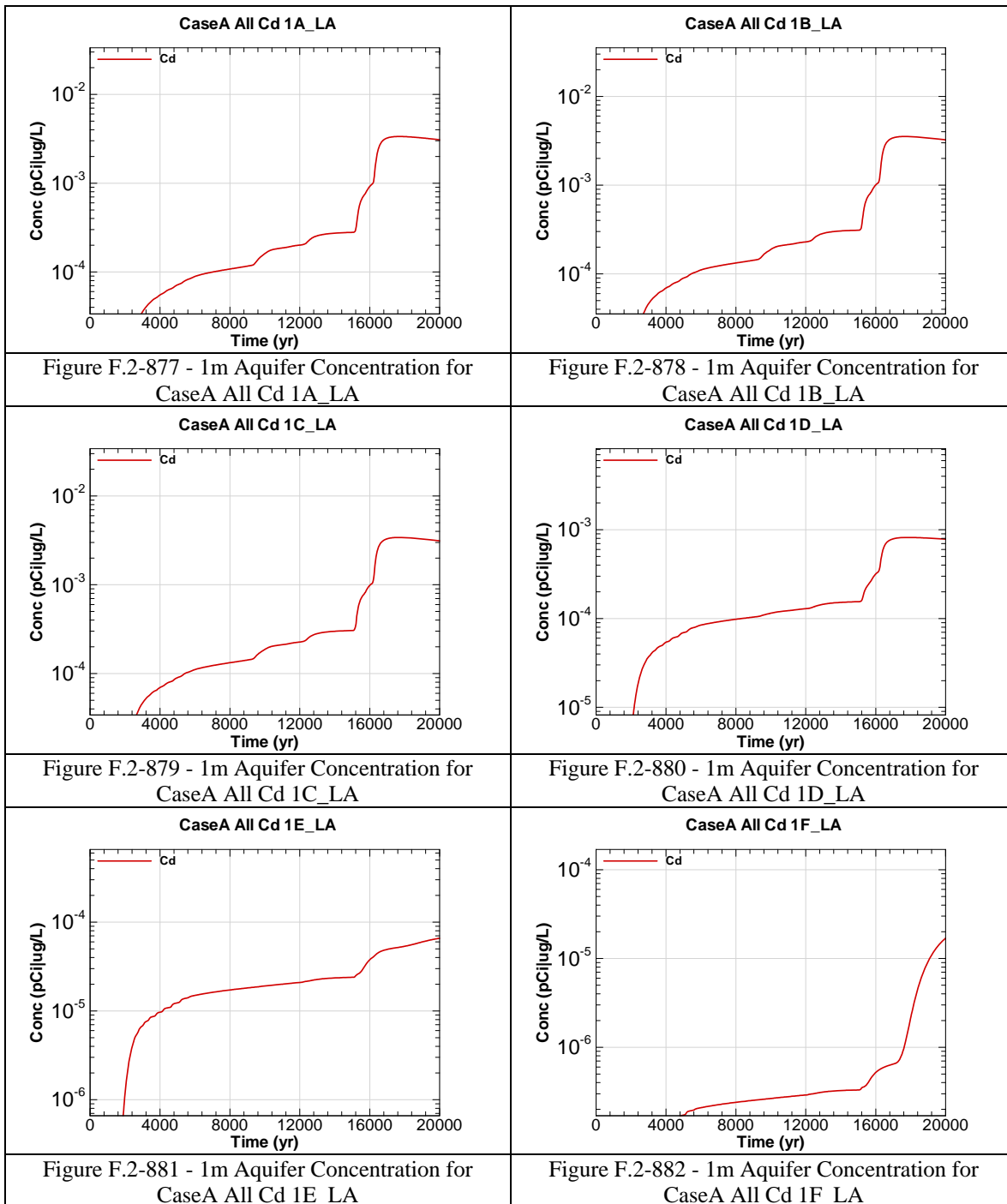


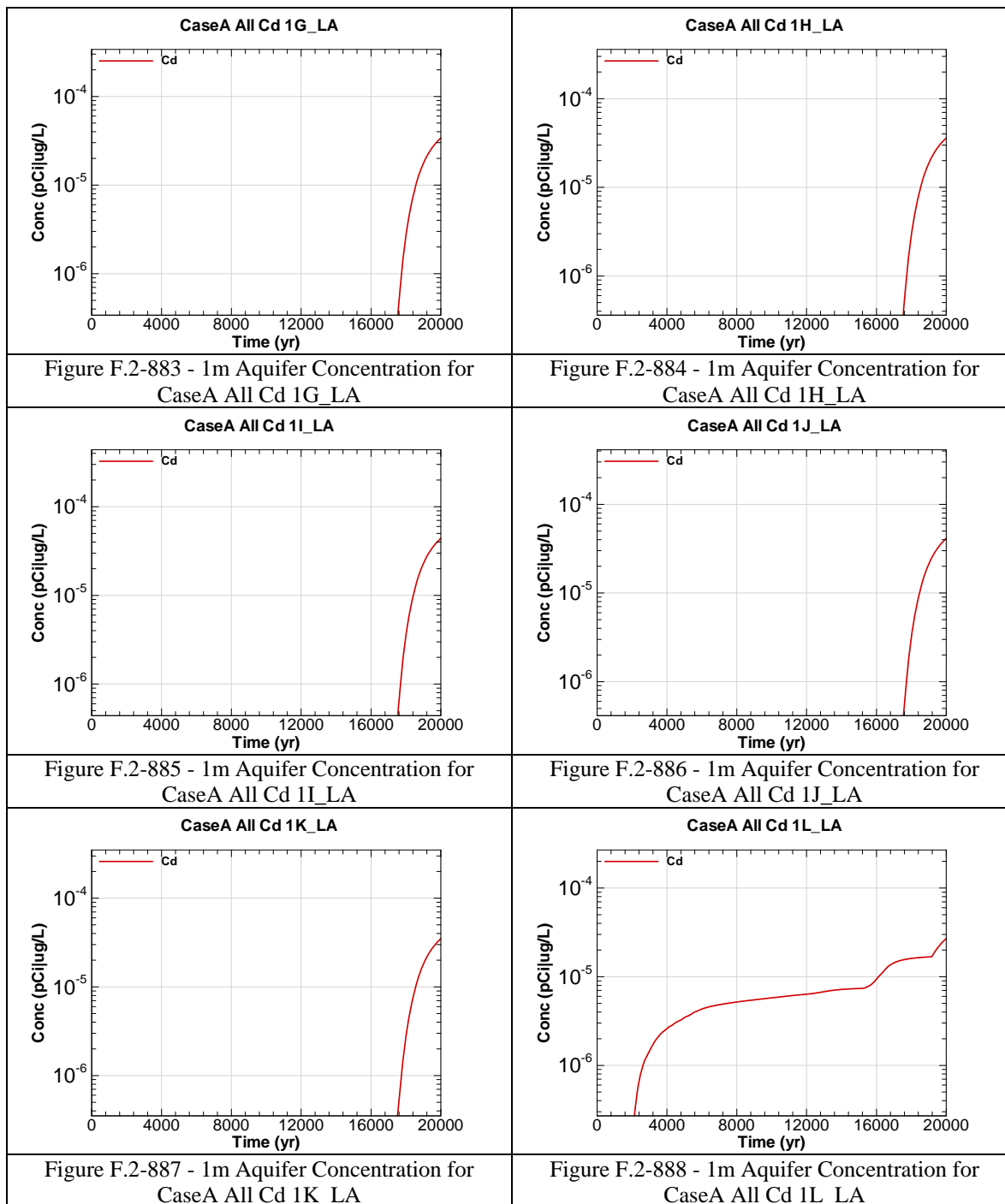


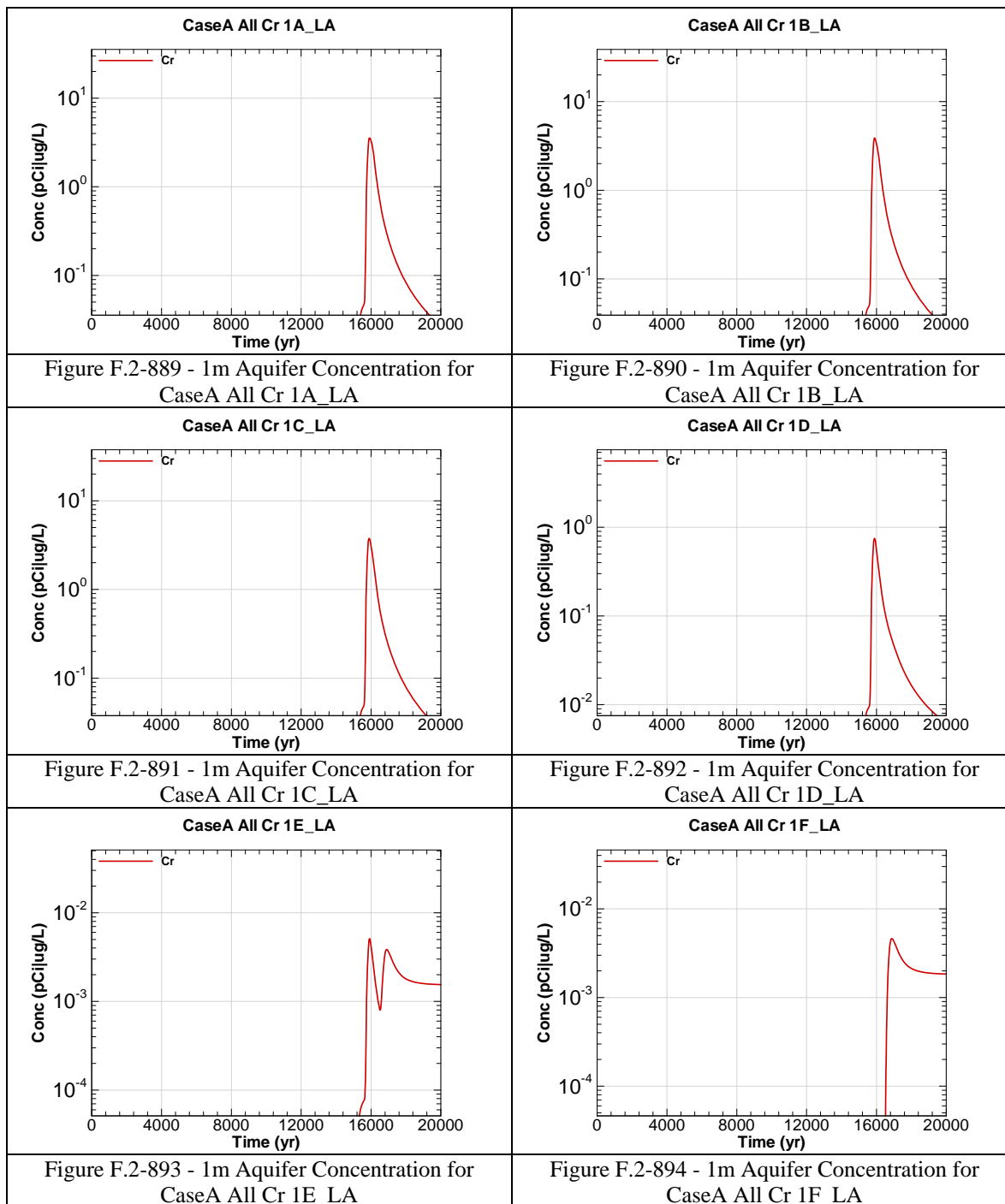


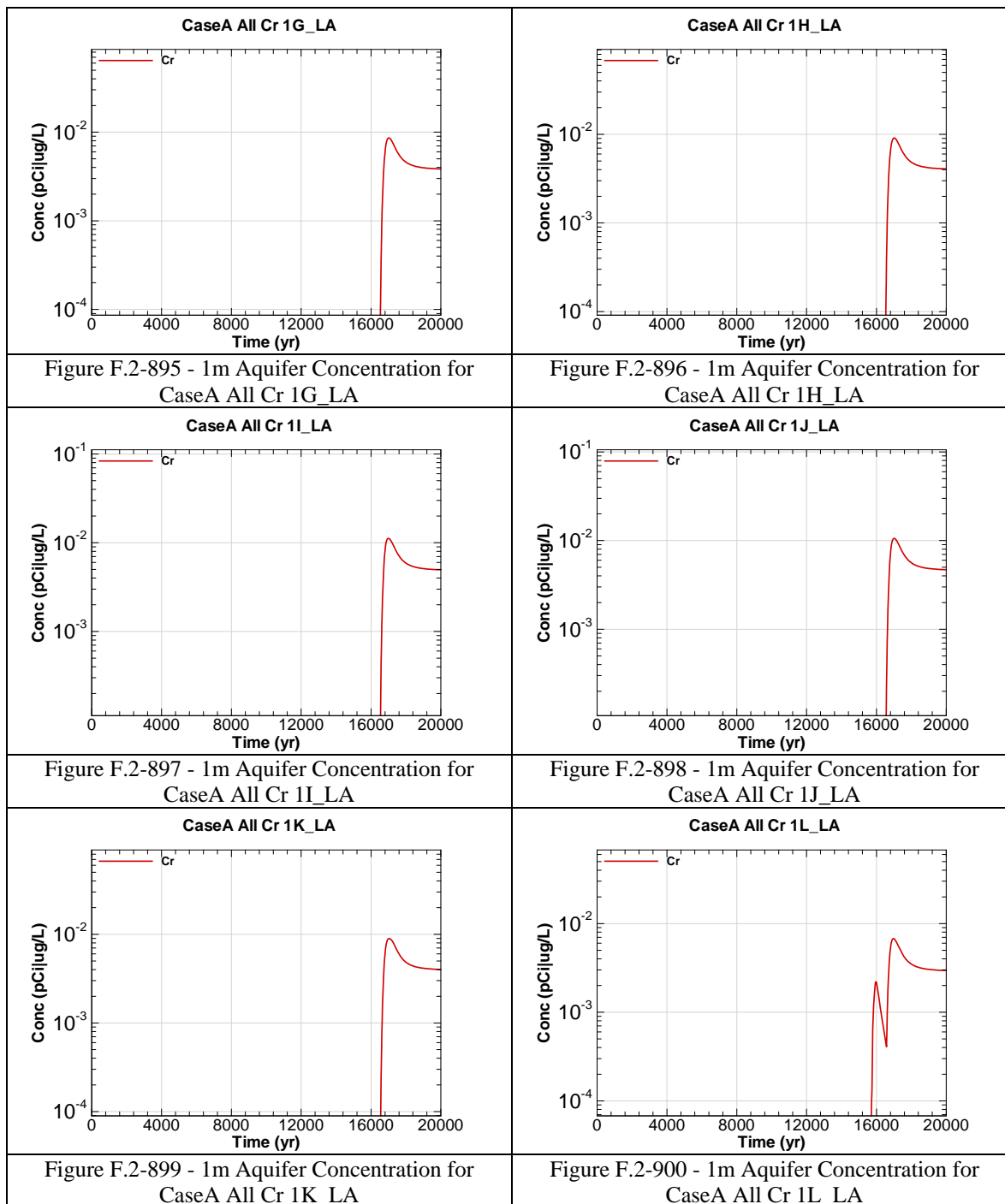


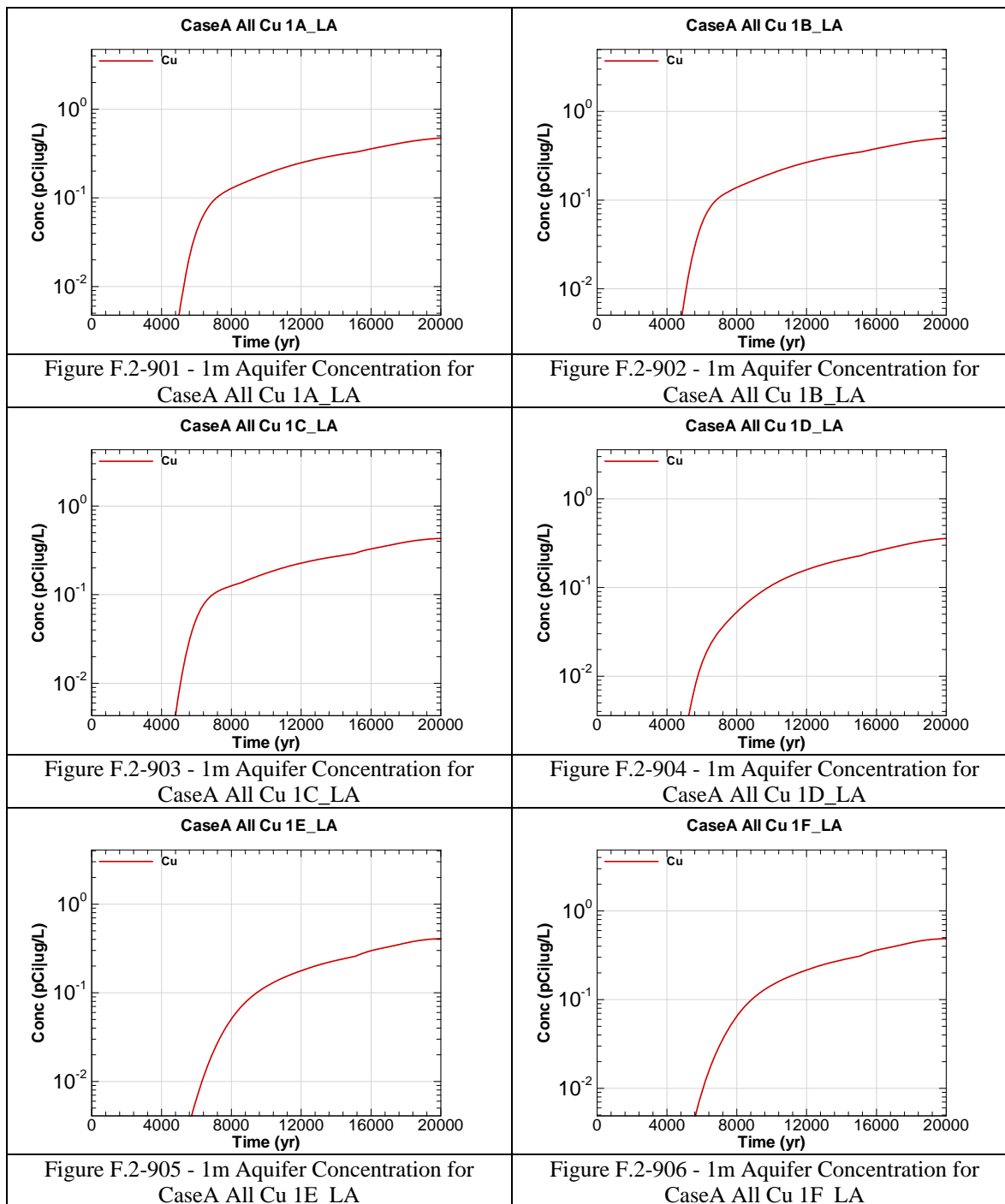


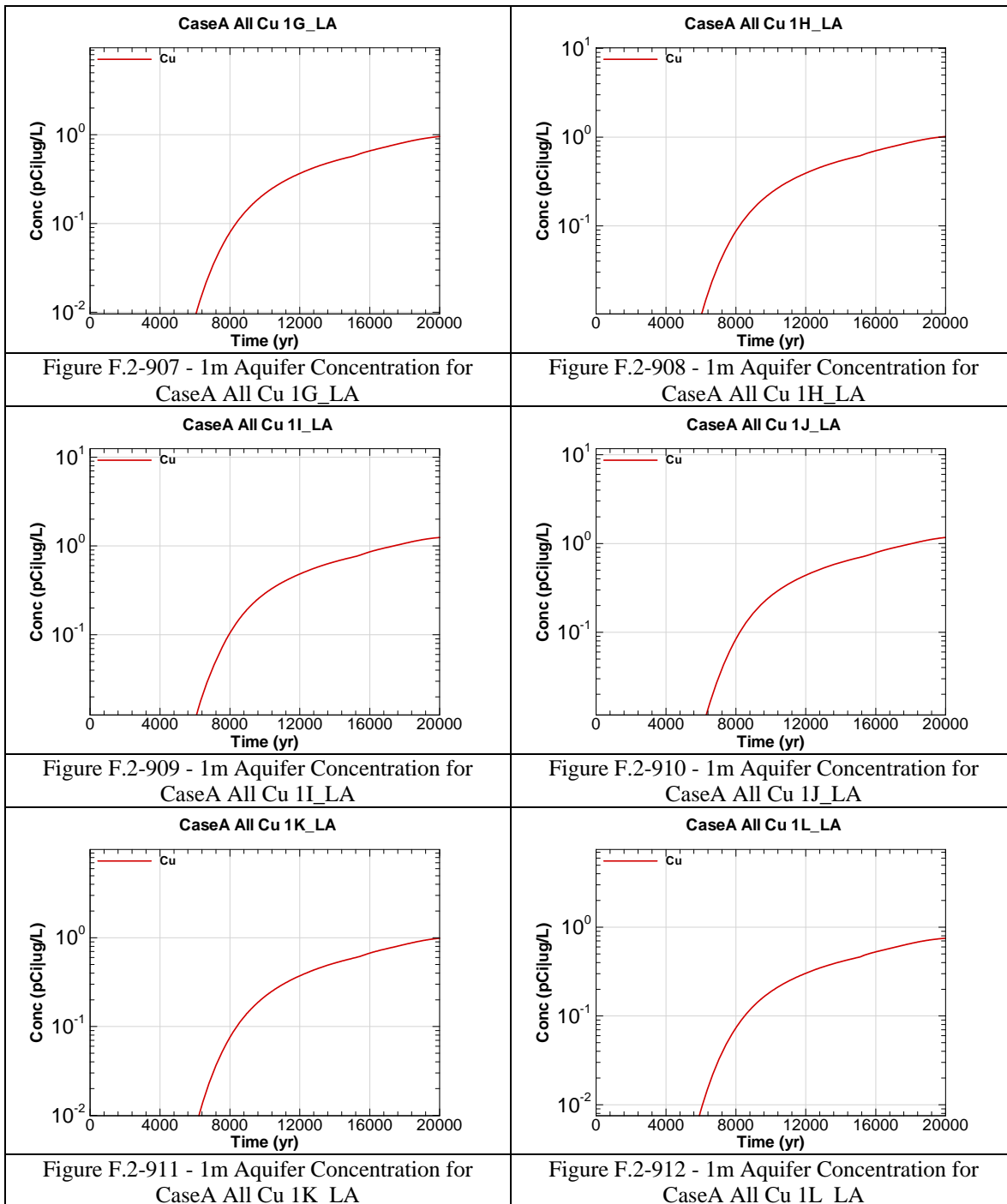


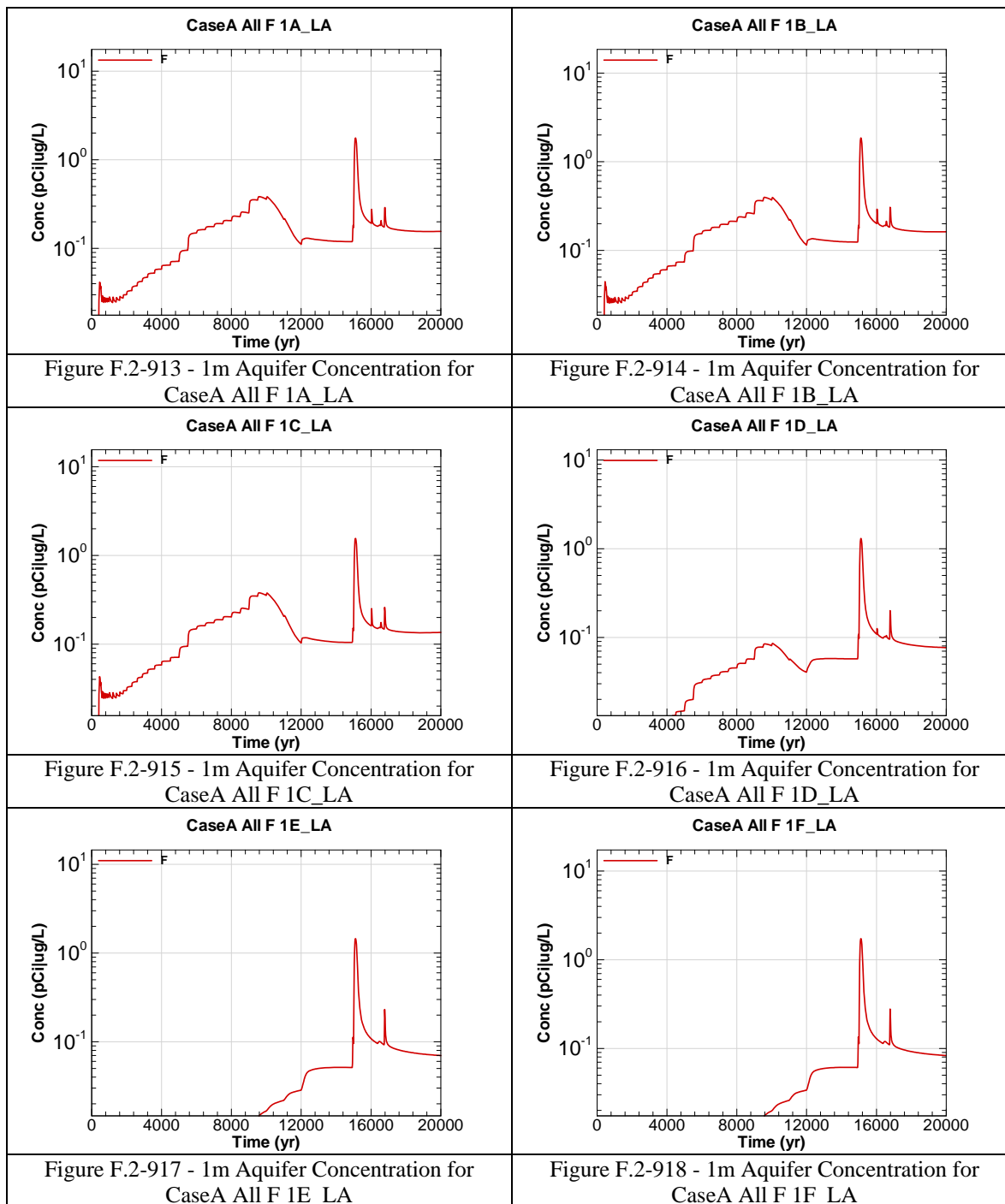


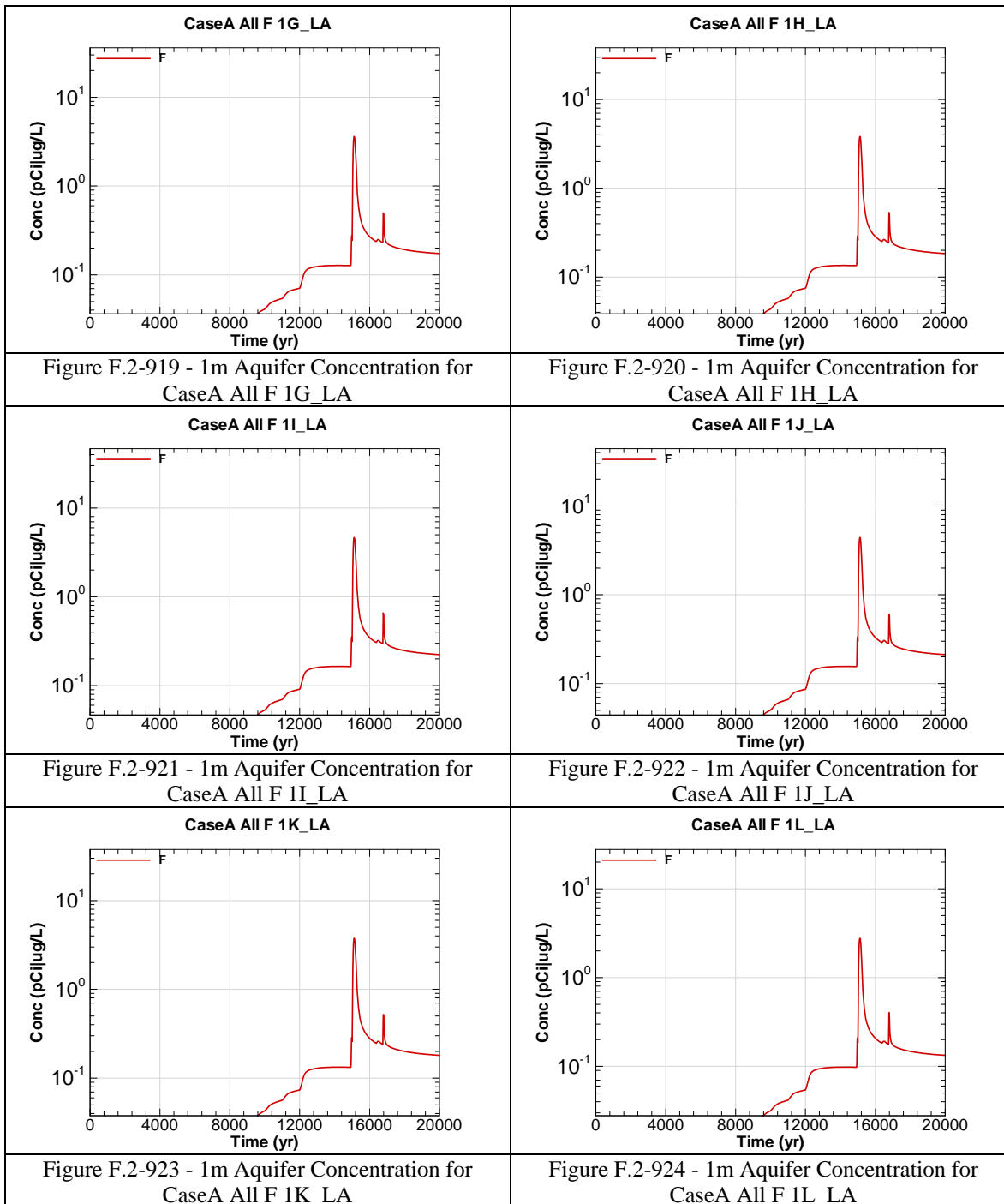


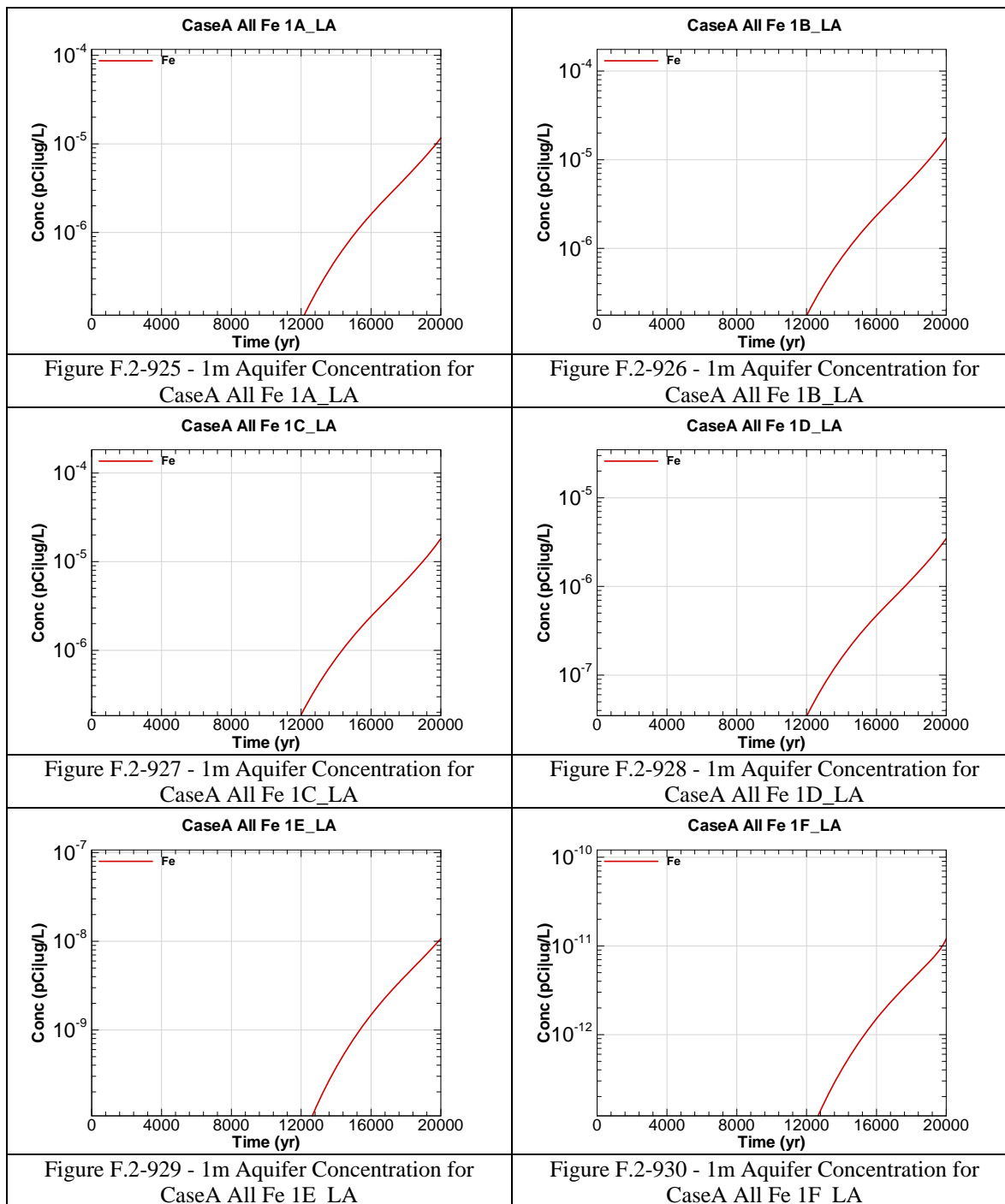


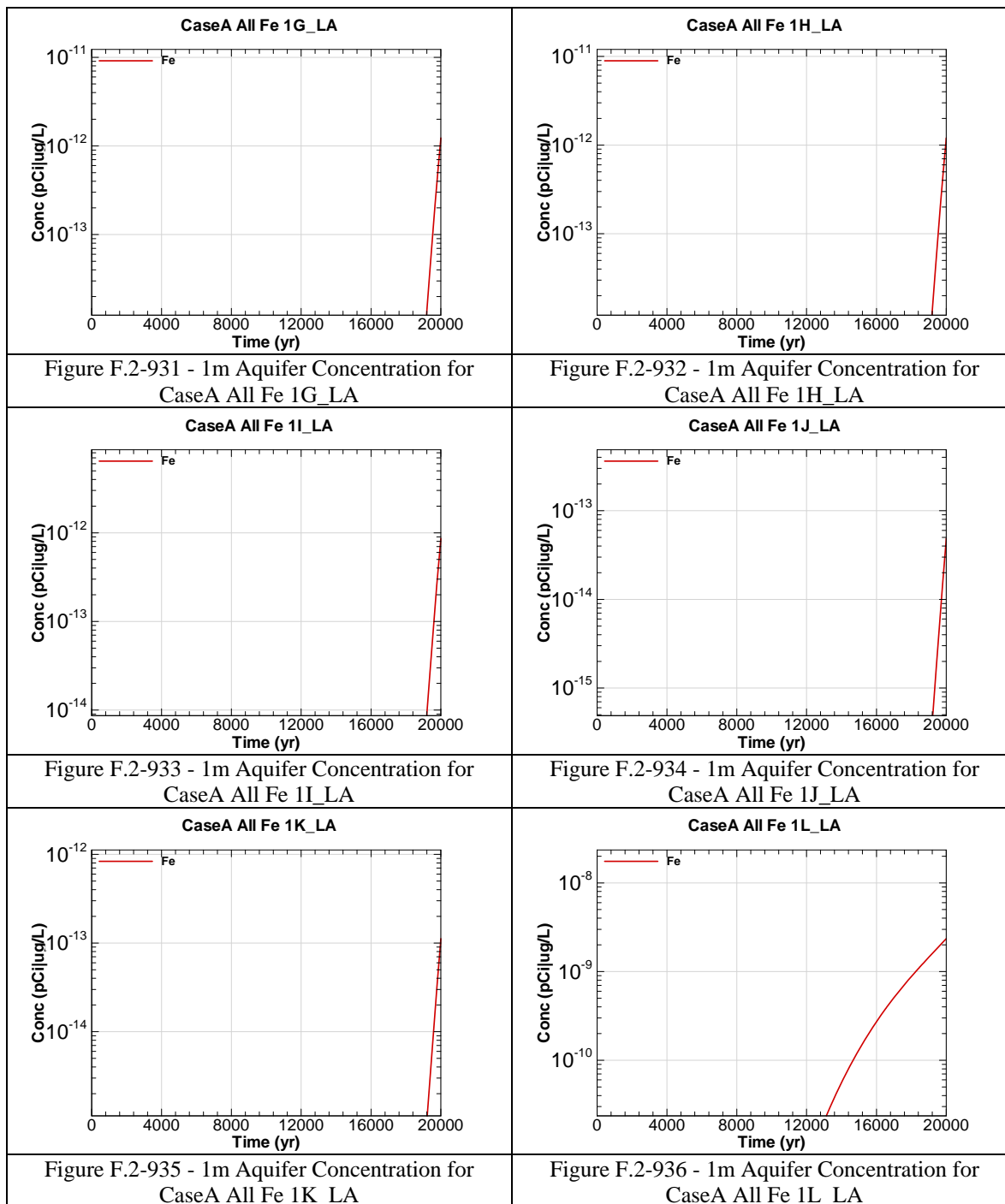


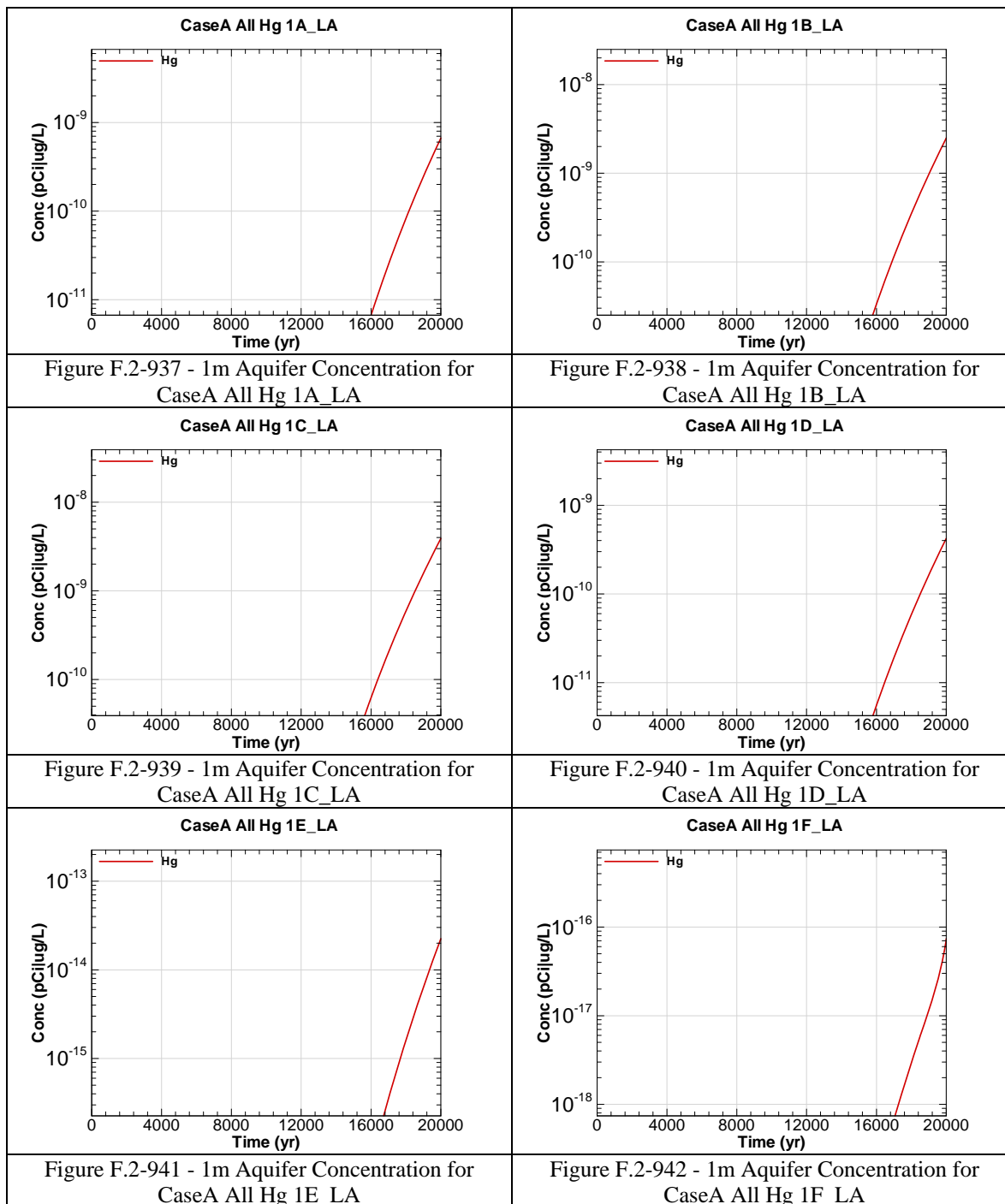


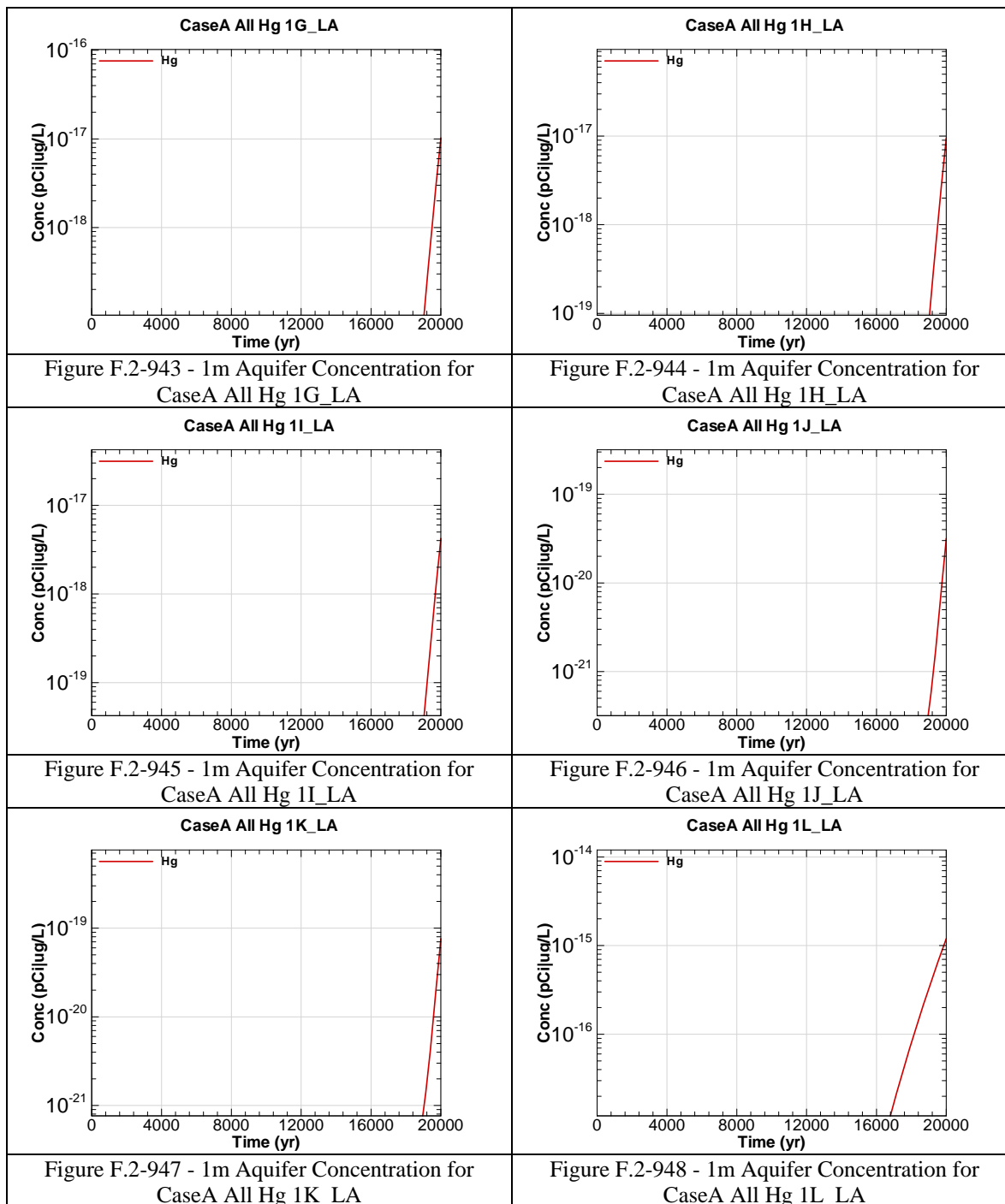


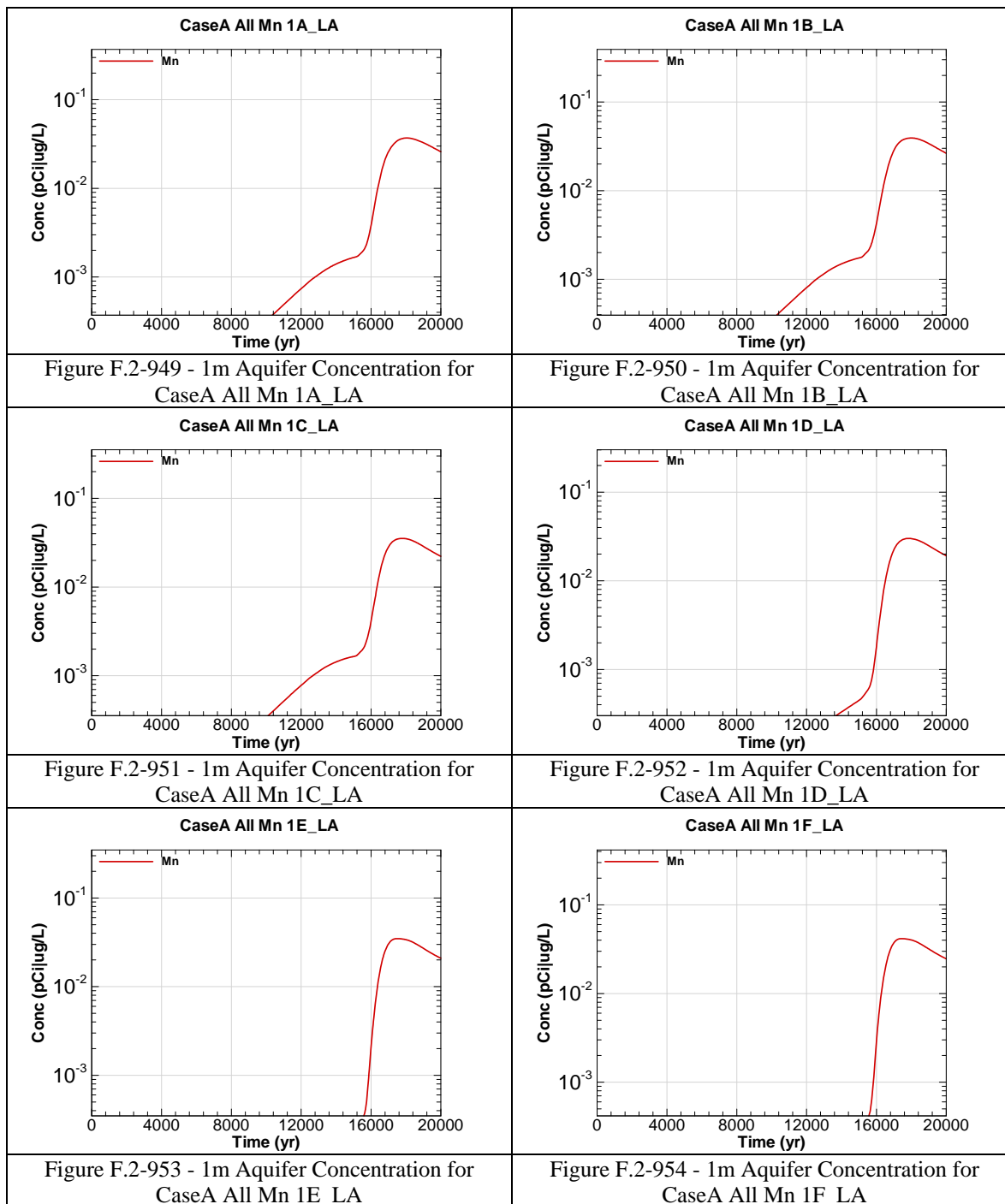


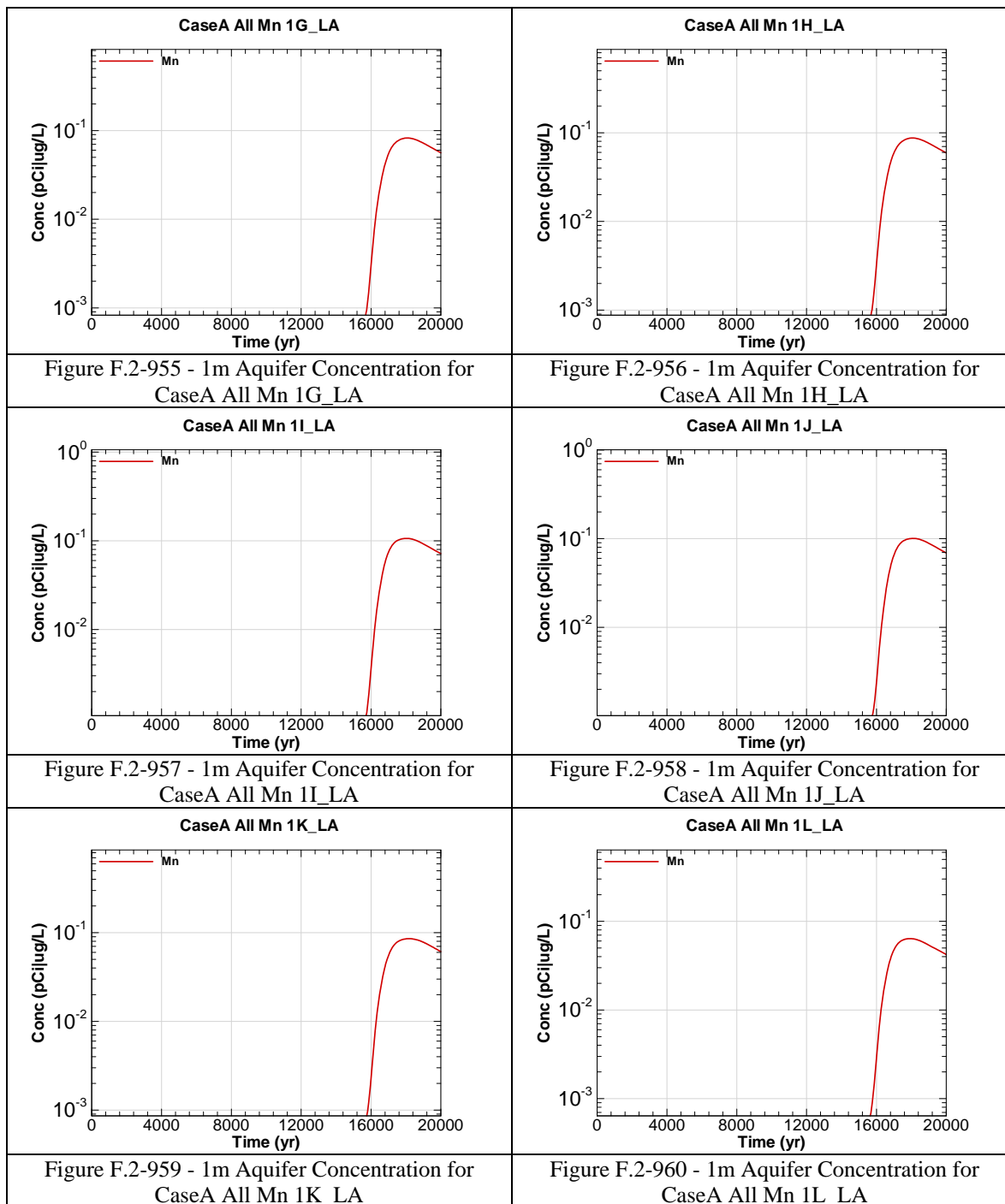


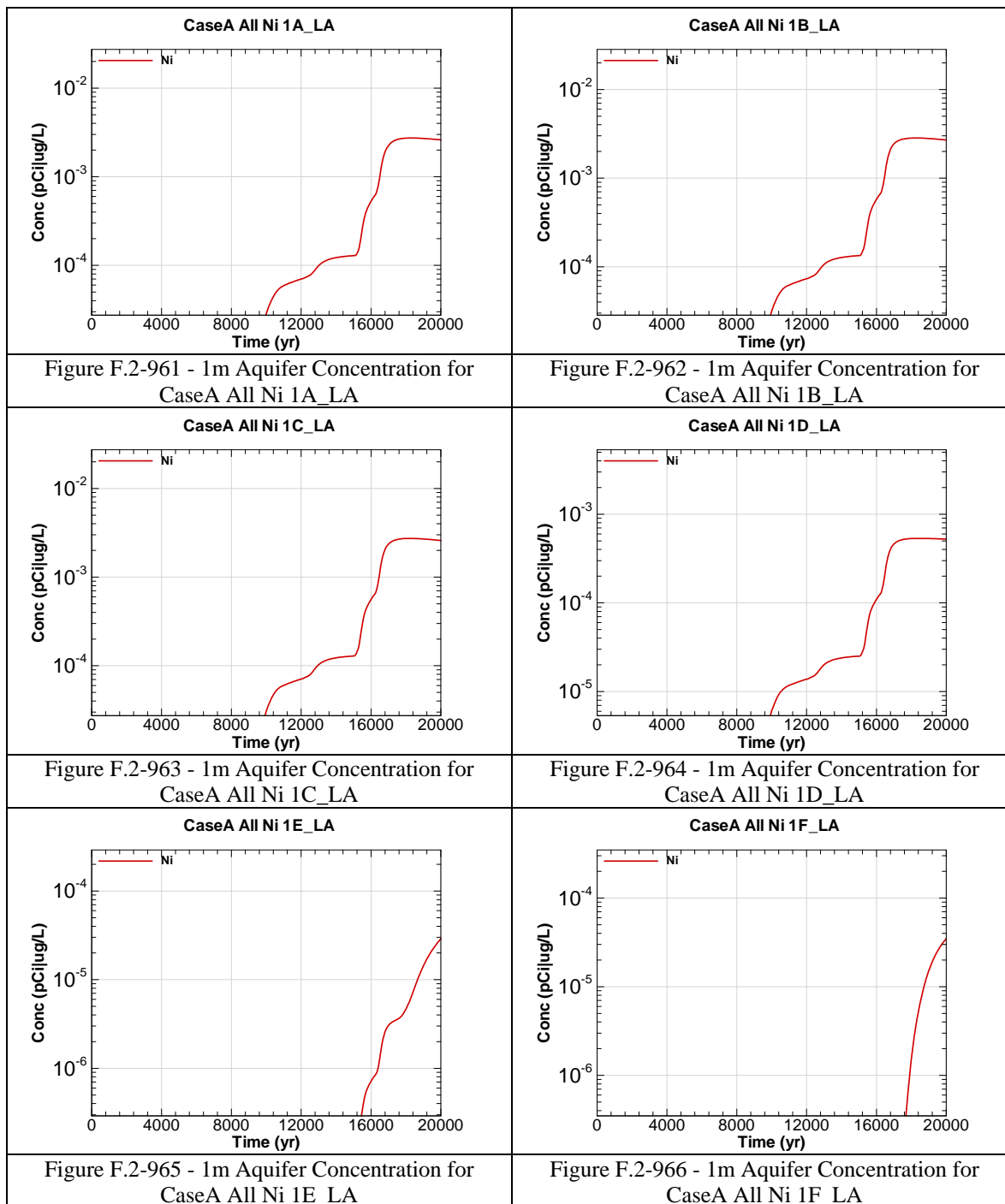


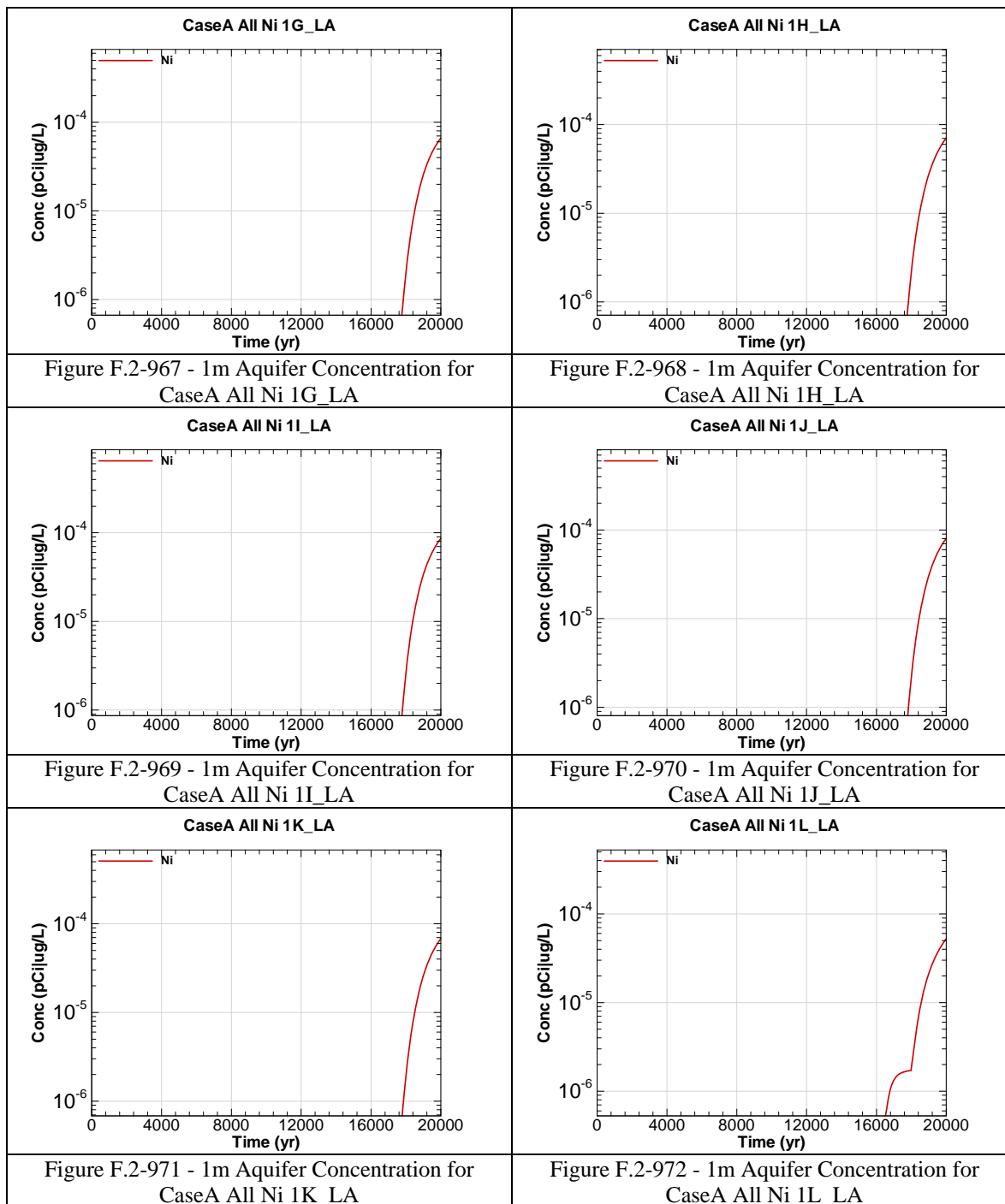


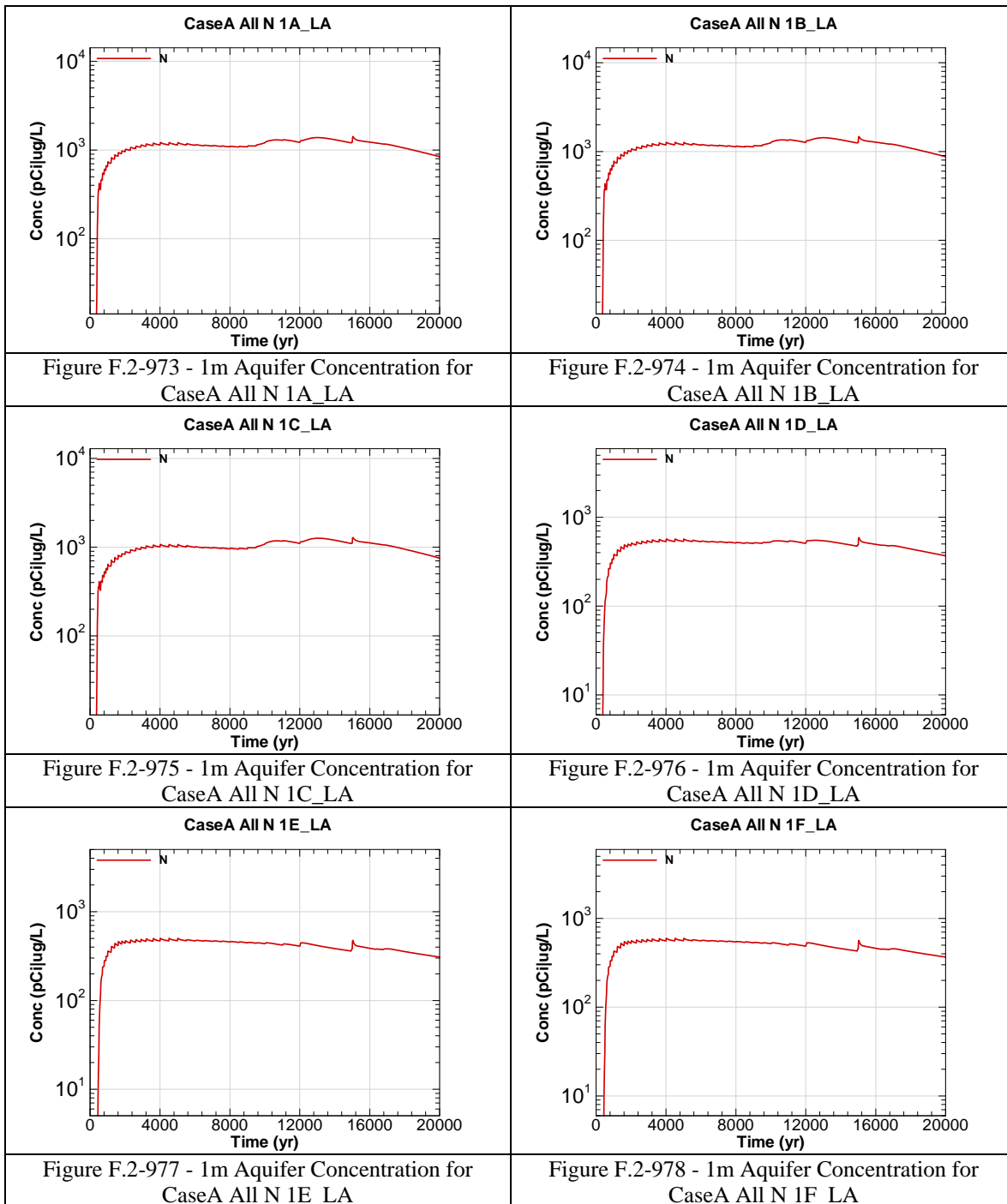


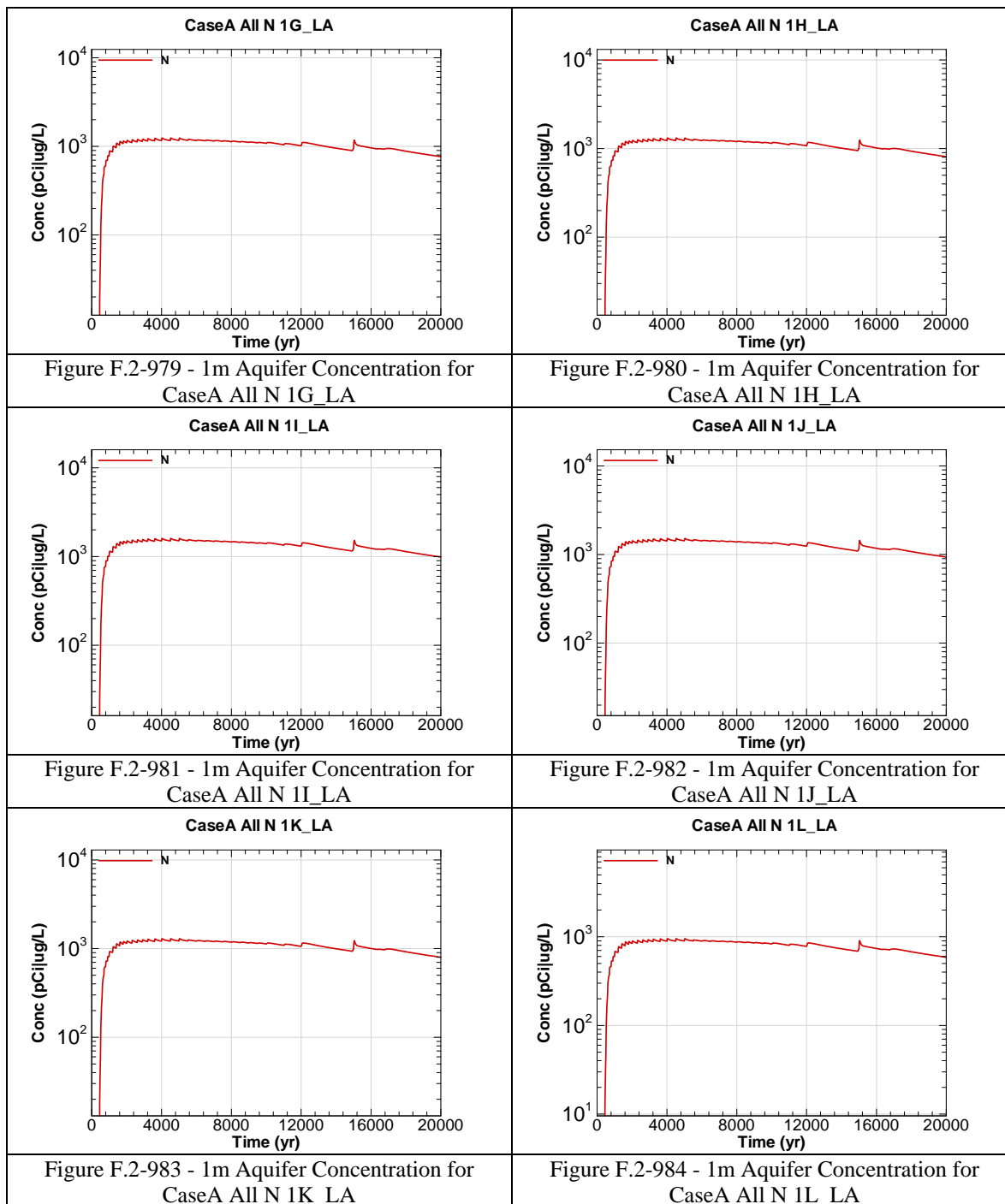


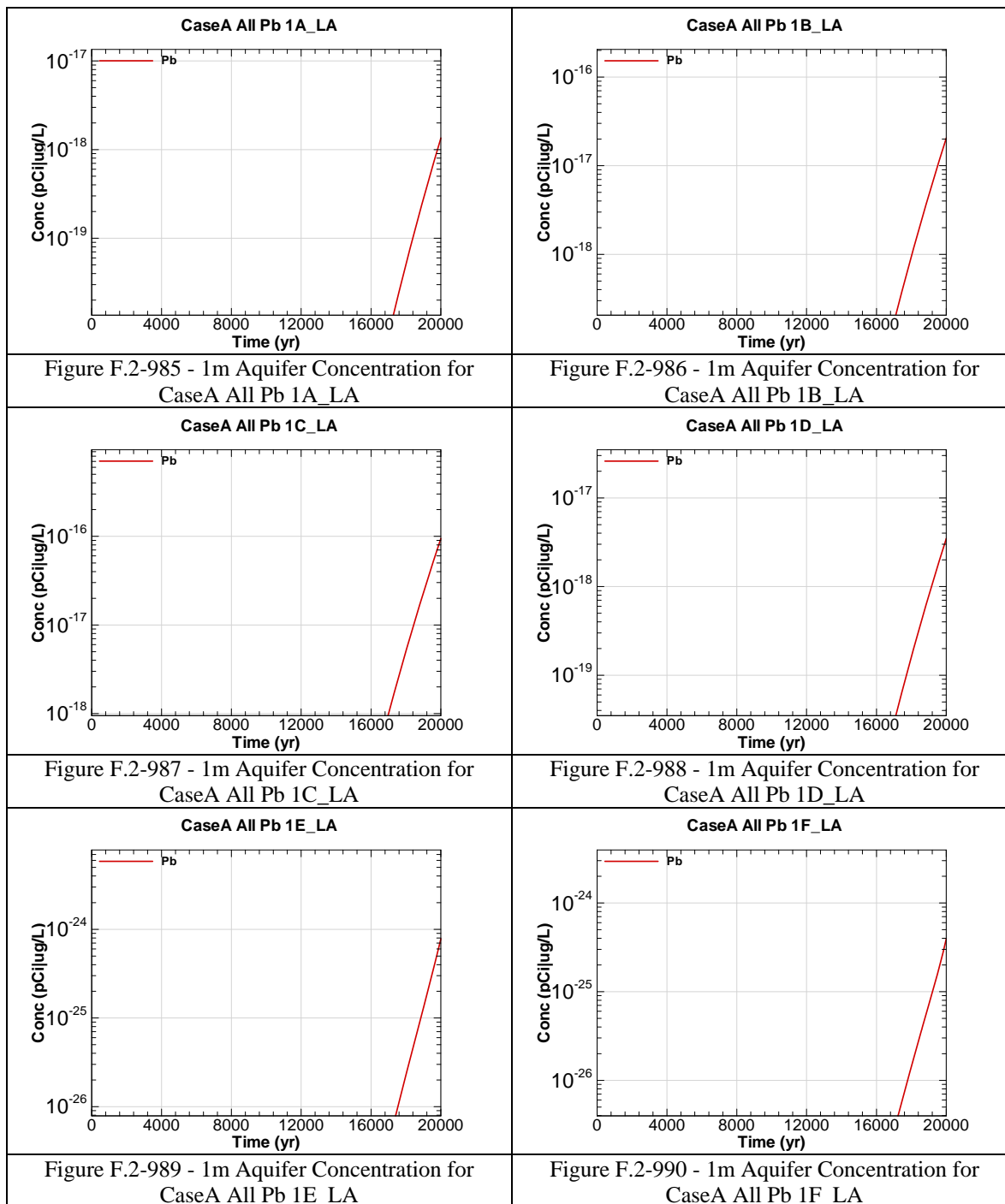


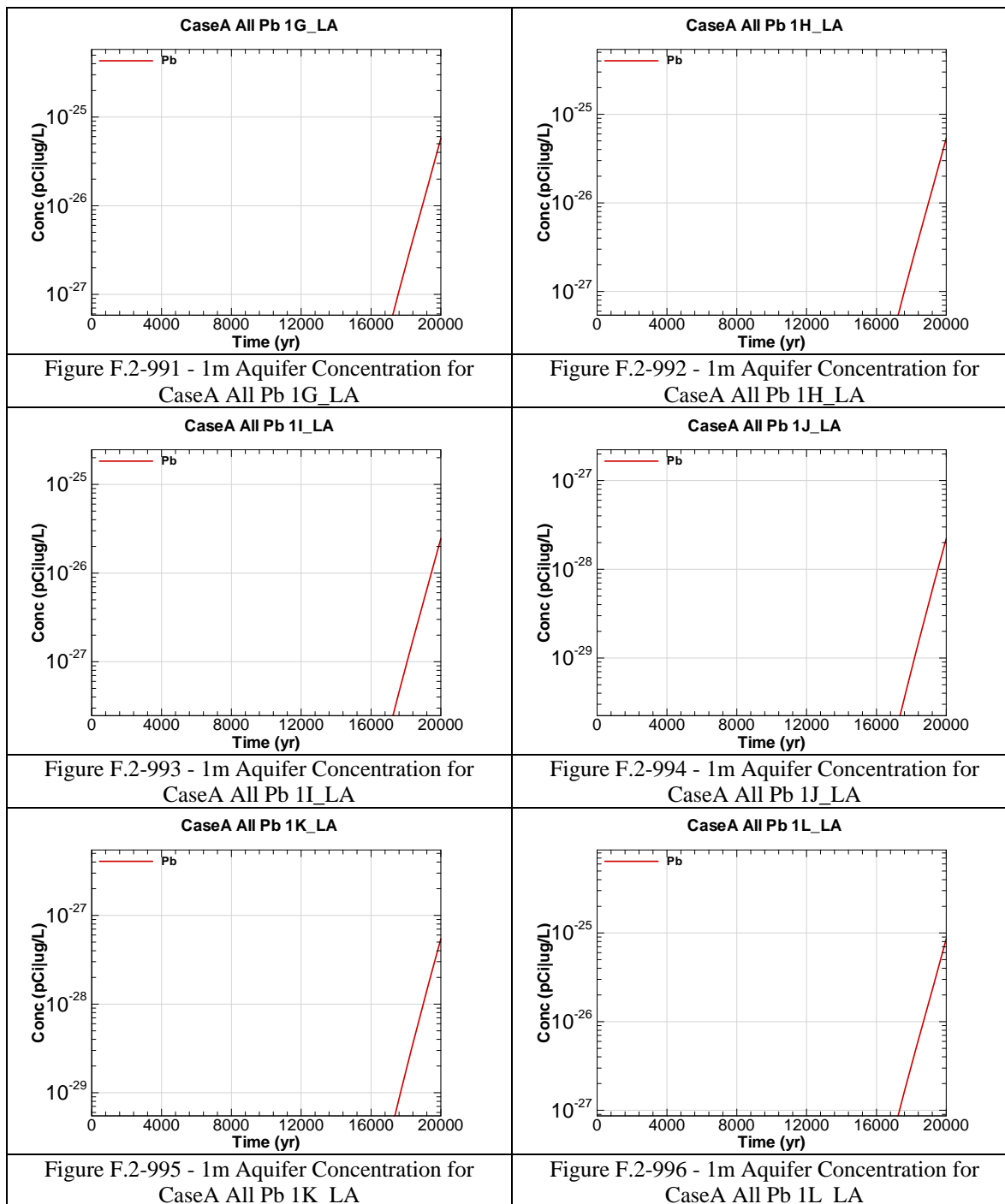


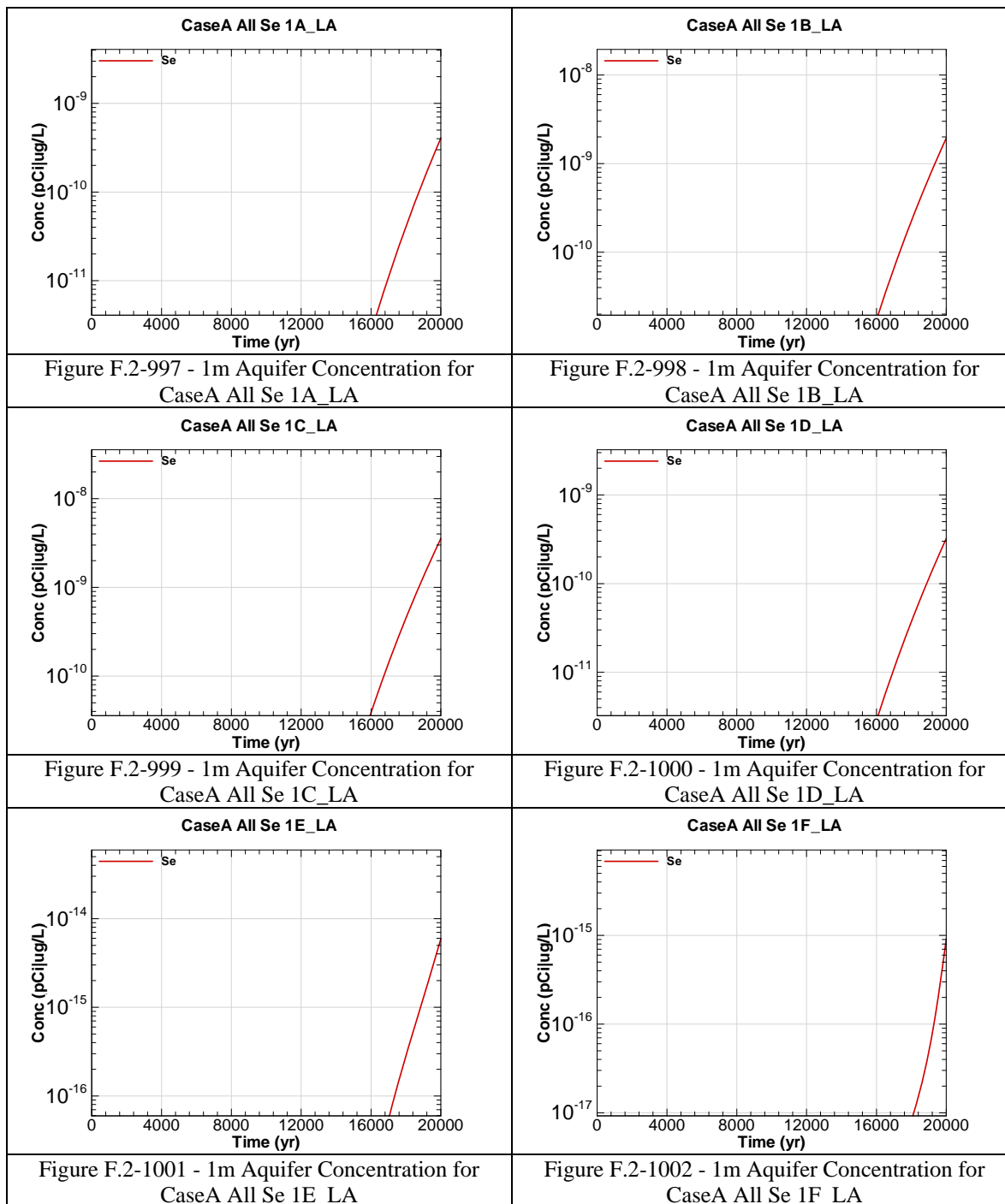


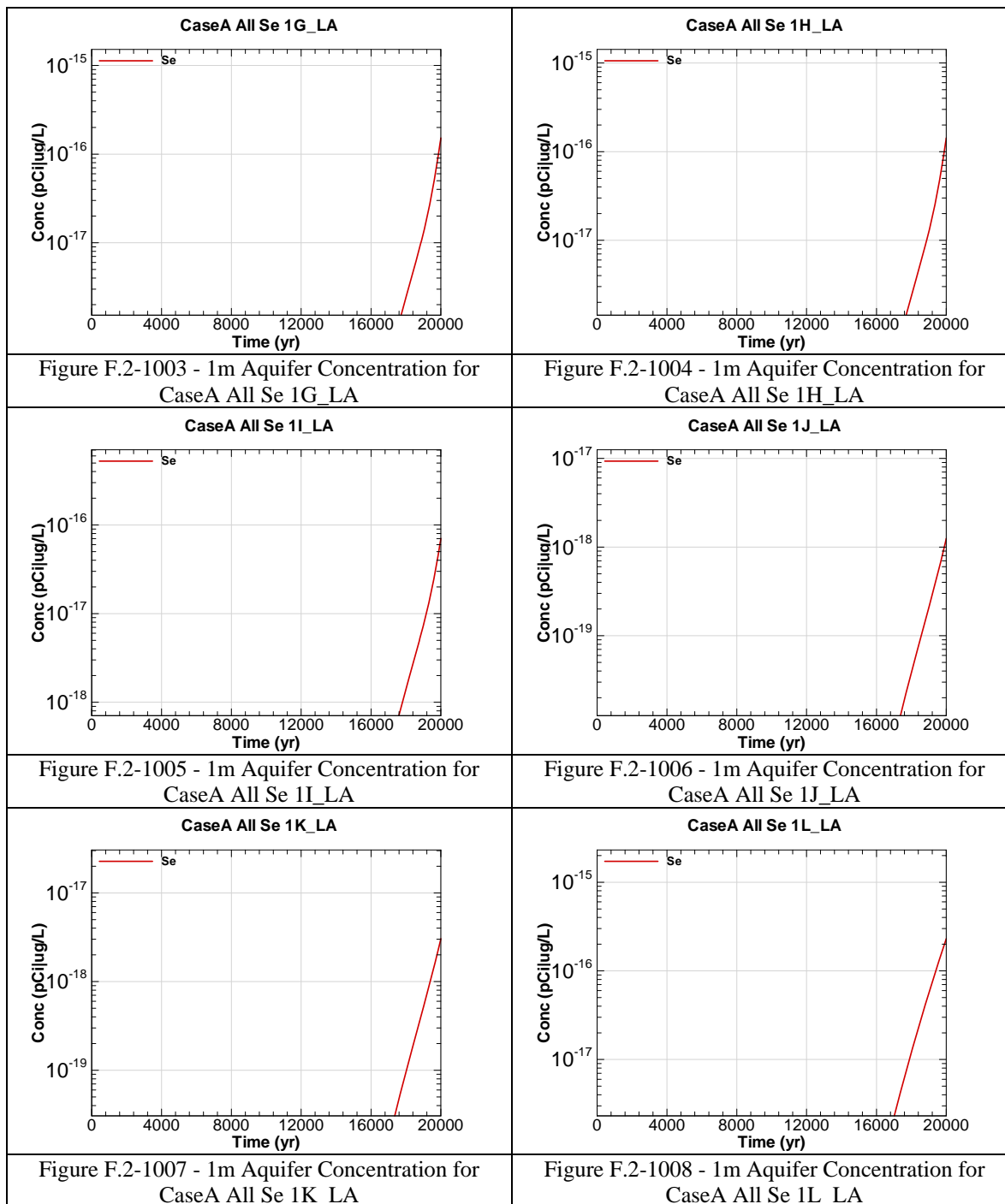


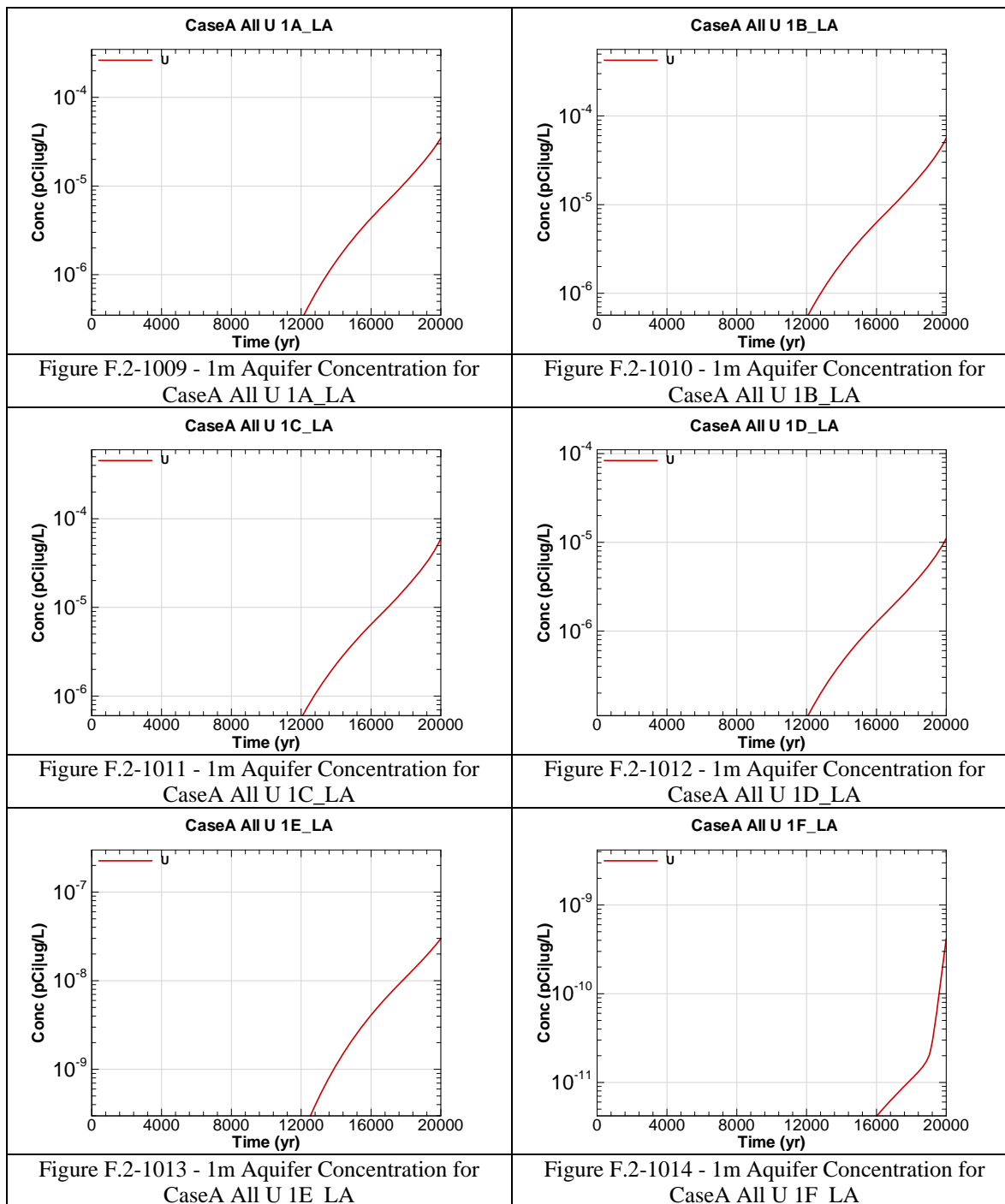


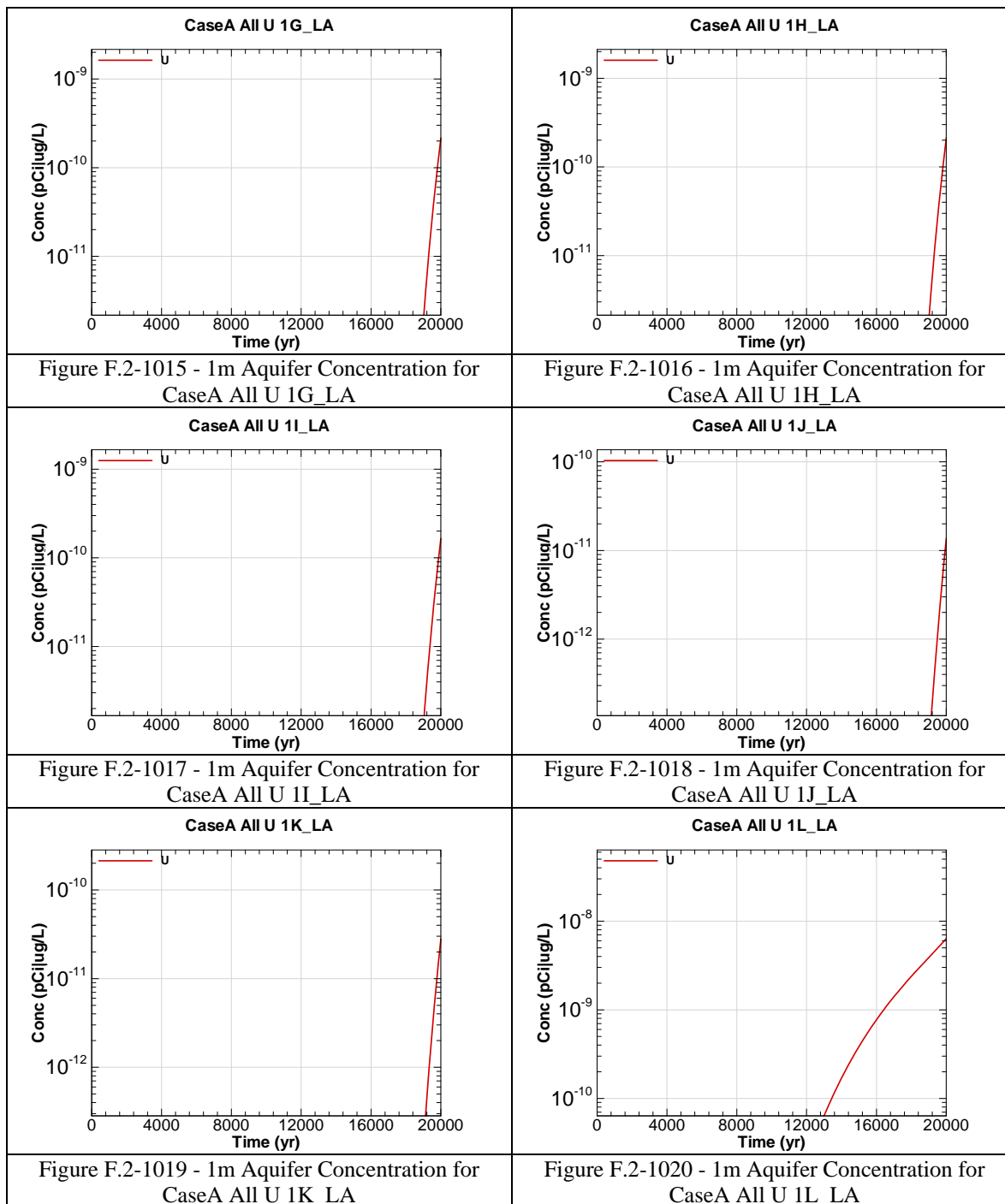


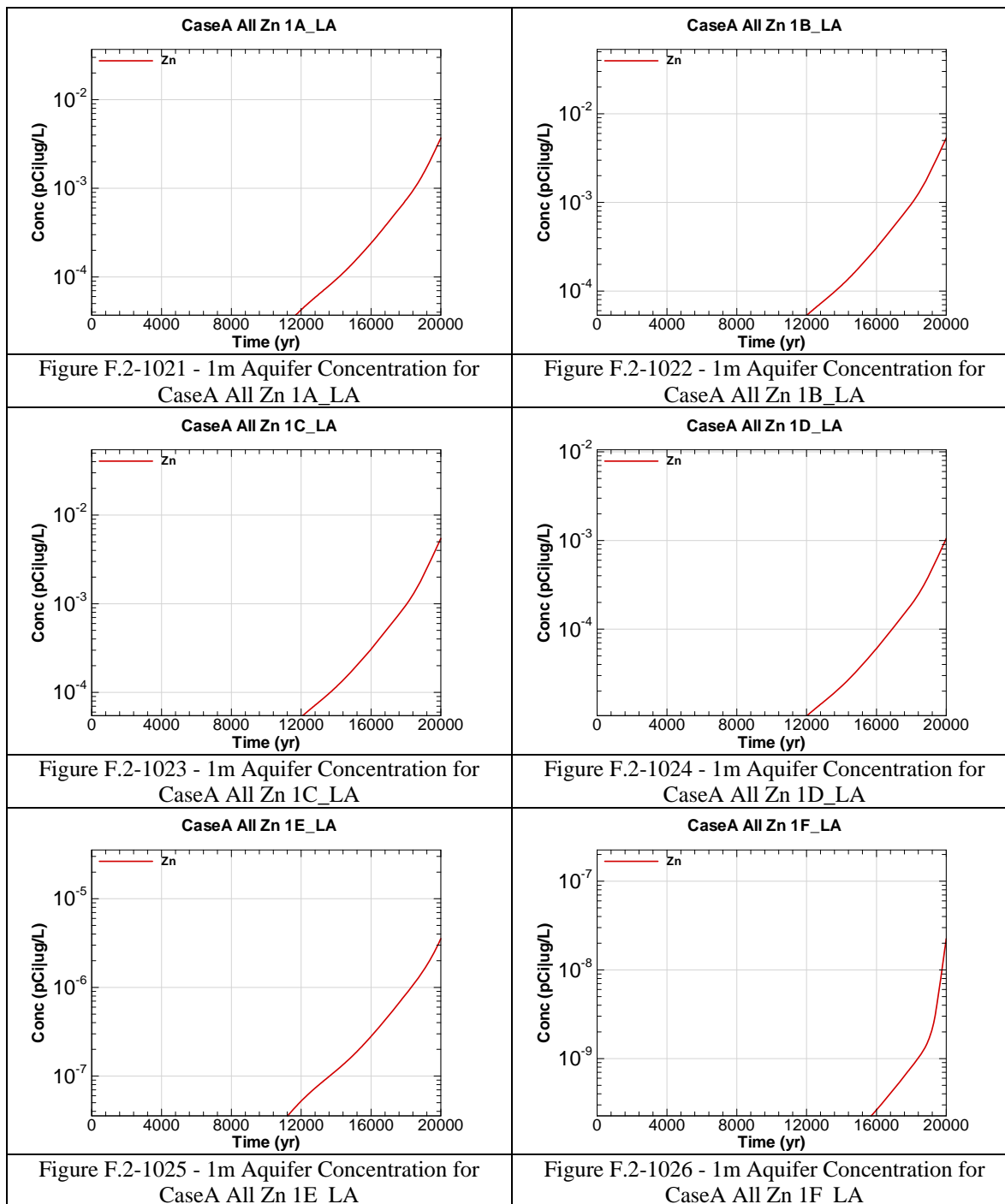


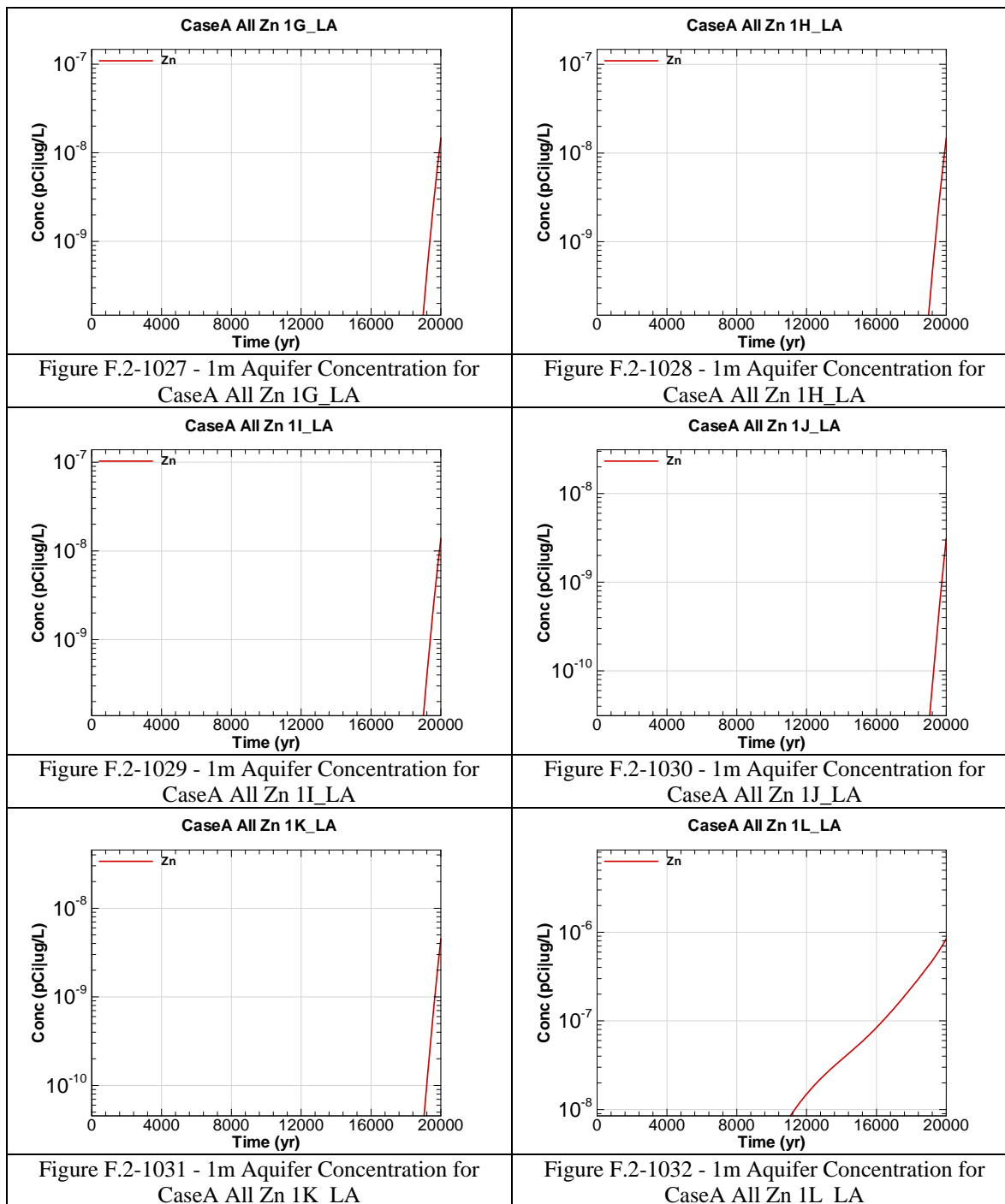












APPENDIX F.3

1-METER RADIOLOGICAL AND CHEMICAL CONCENTRATIONS AT THE GORDON AQUIFER

Appendix F.3 contains curves showing the 1 meter radiological and chemical concentrations for all SDF (vault and FDC inventories) for the Base Case (Case A). 20,000 year concentration results are presented from the Gordon Aquifer for Sectors A through L

Graph heading example "CaseA All Ac-227 1A_GA"

Key

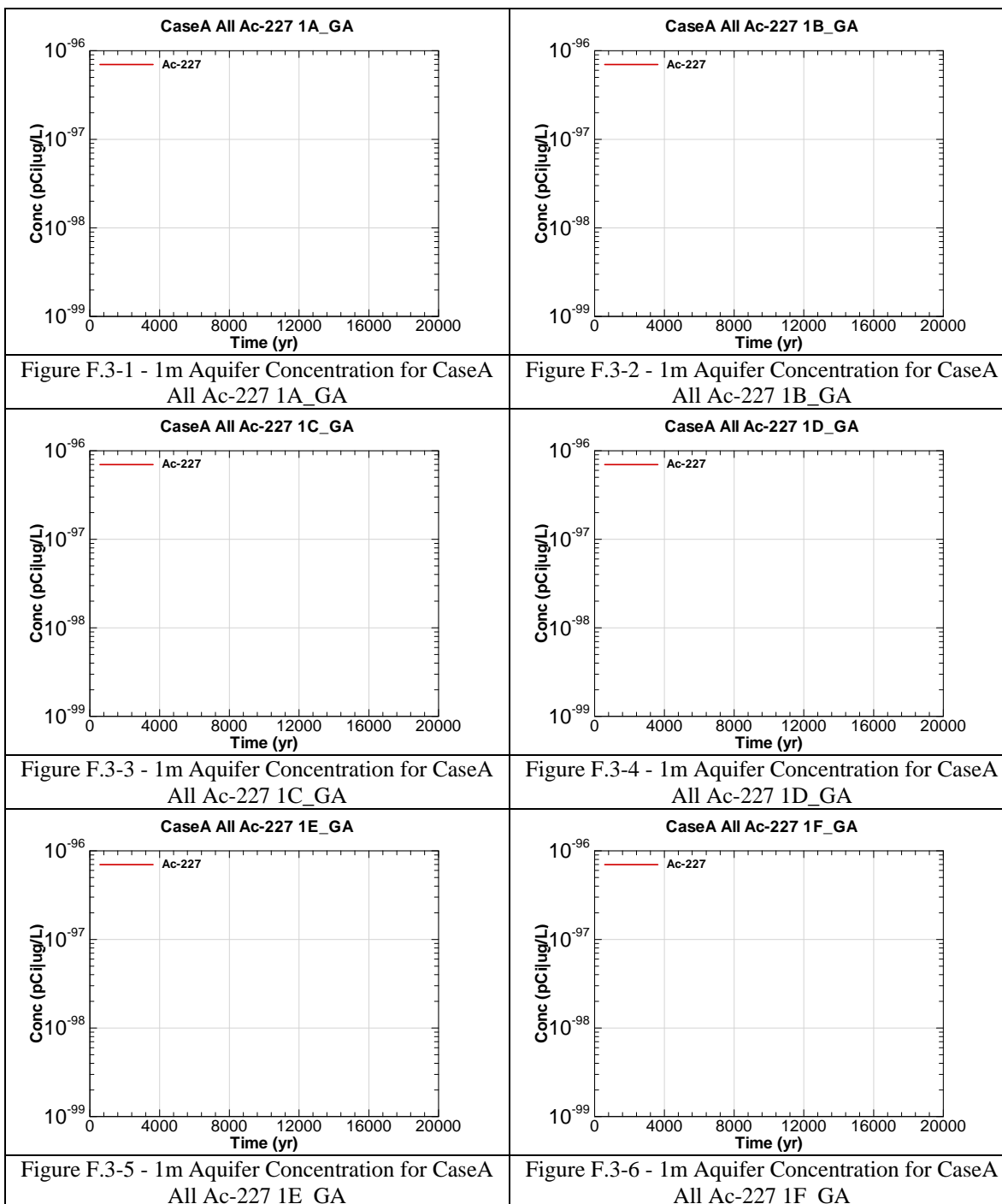
CaseA = Scenario case

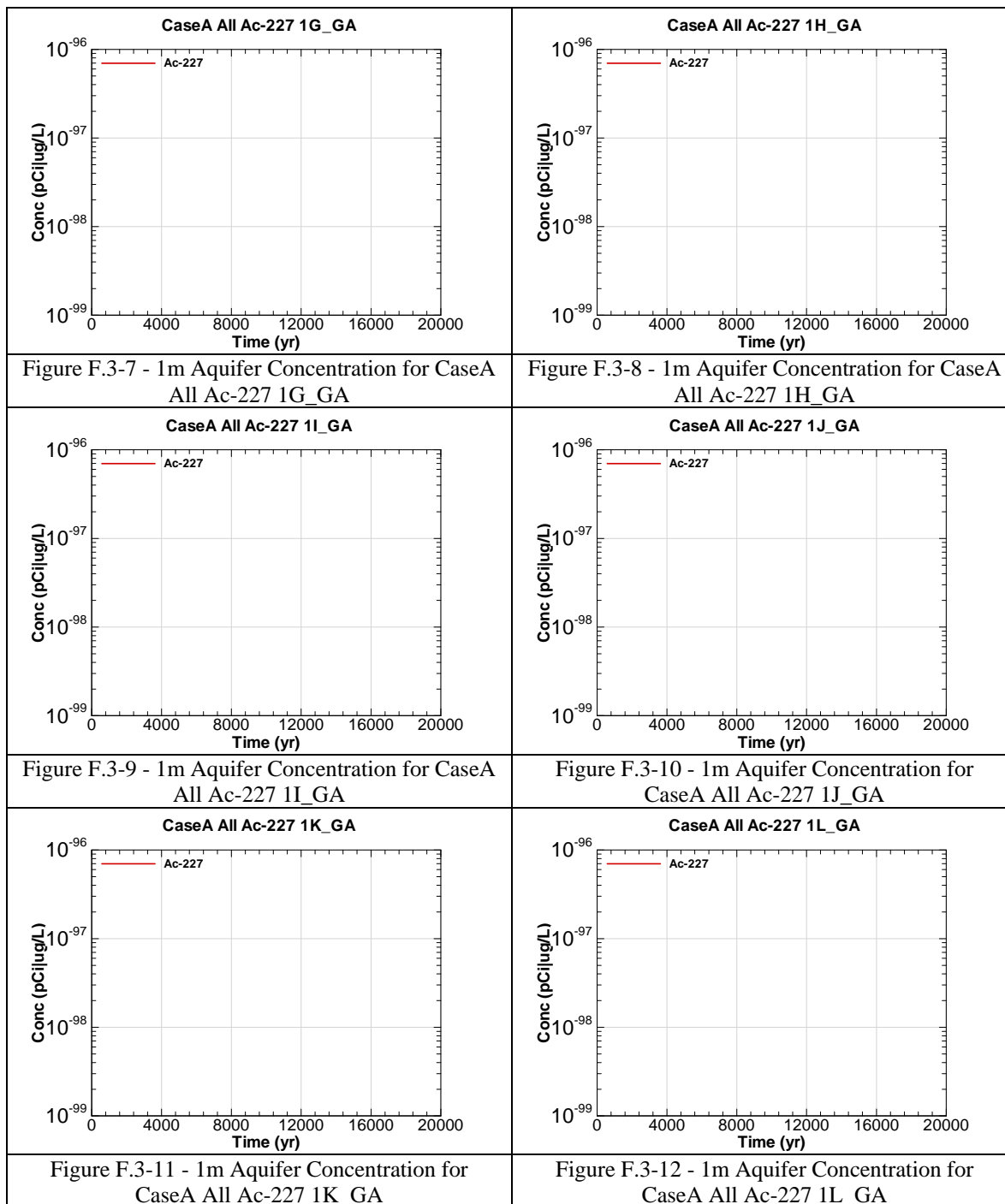
All = Inventory source is all disposal units

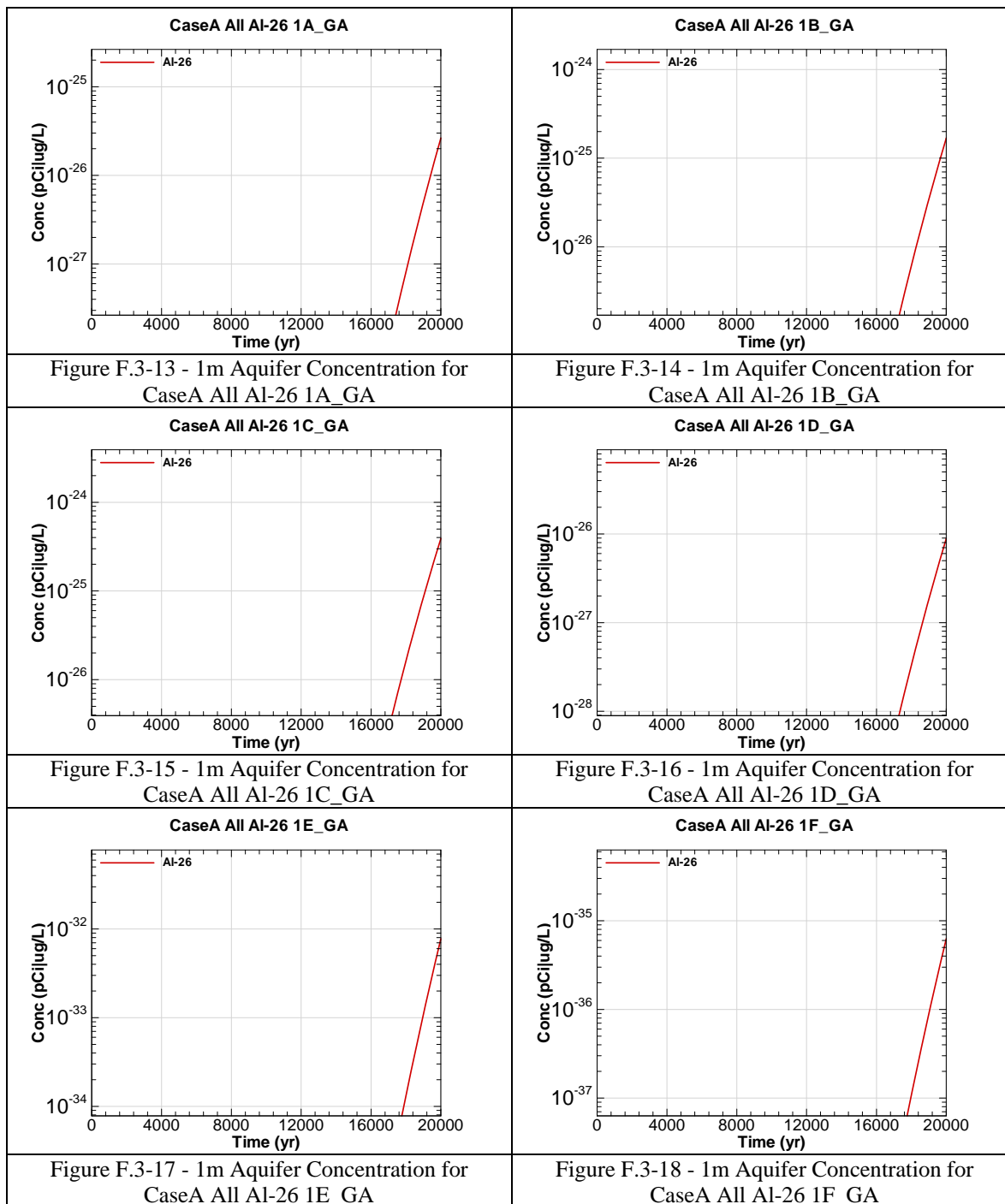
Ac-227 = Radionuclide or chemical of concern

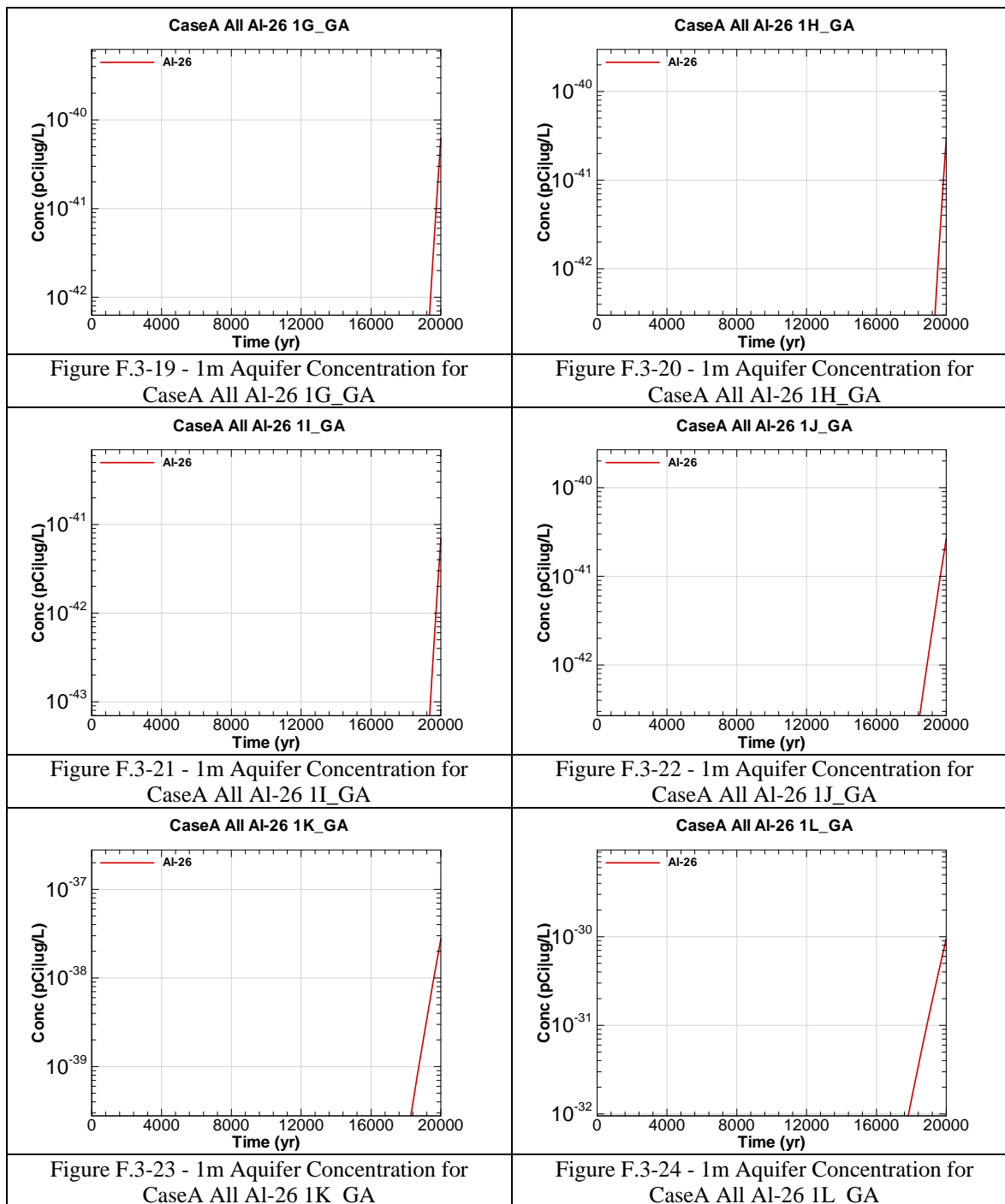
1A = 1 meter evaluation sector of concern

GA = Aquifer of concern is Gordon Aquifer









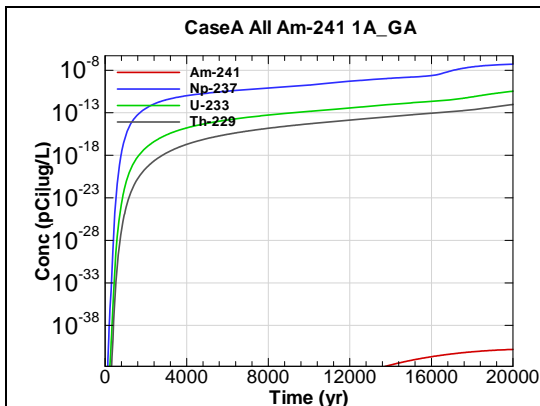


Figure F.3-25 - 1m Aquifer Concentration for
CaseA All Am-241 1A_GA

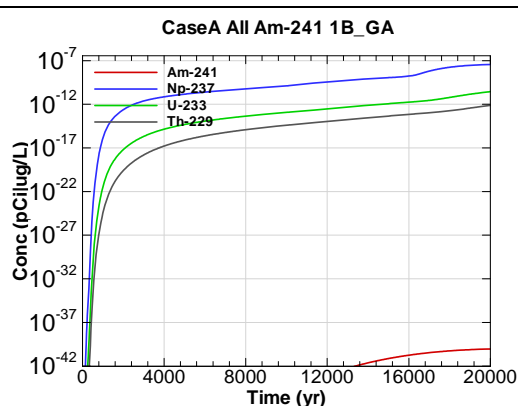


Figure F.3-26 - 1m Aquifer Concentration for
CaseA All Am-241 1B_GA

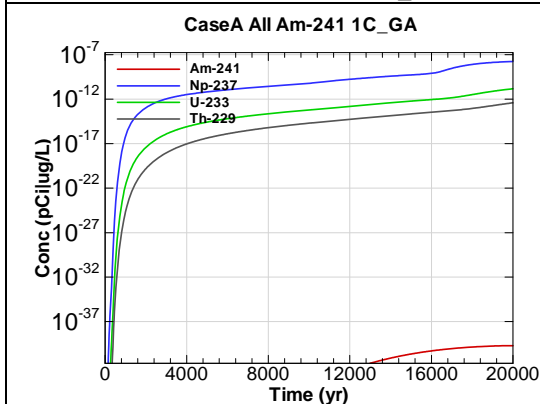


Figure F.3-27 - 1m Aquifer Concentration for
CaseA All Am-241 1C_GA

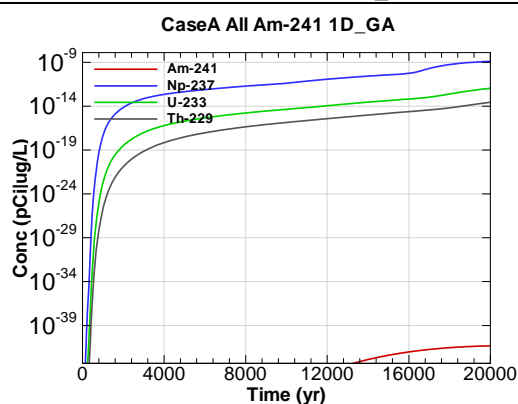


Figure F.3-28 - 1m Aquifer Concentration for
CaseA All Am-241 1D_GA

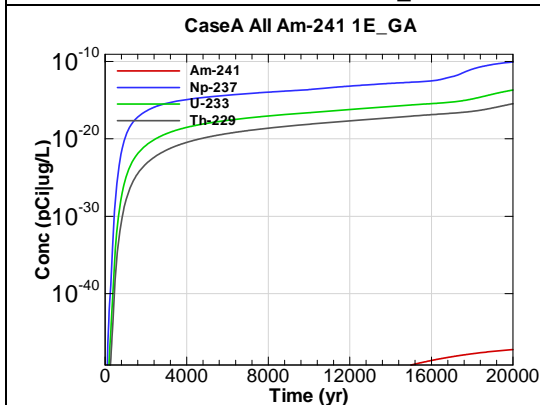


Figure F.3-29 - 1m Aquifer Concentration for
CaseA All Am-241 1E_GA

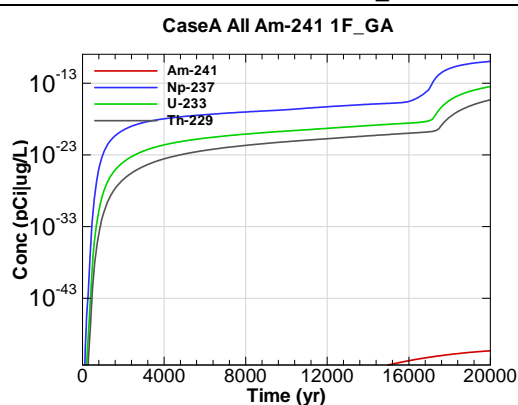
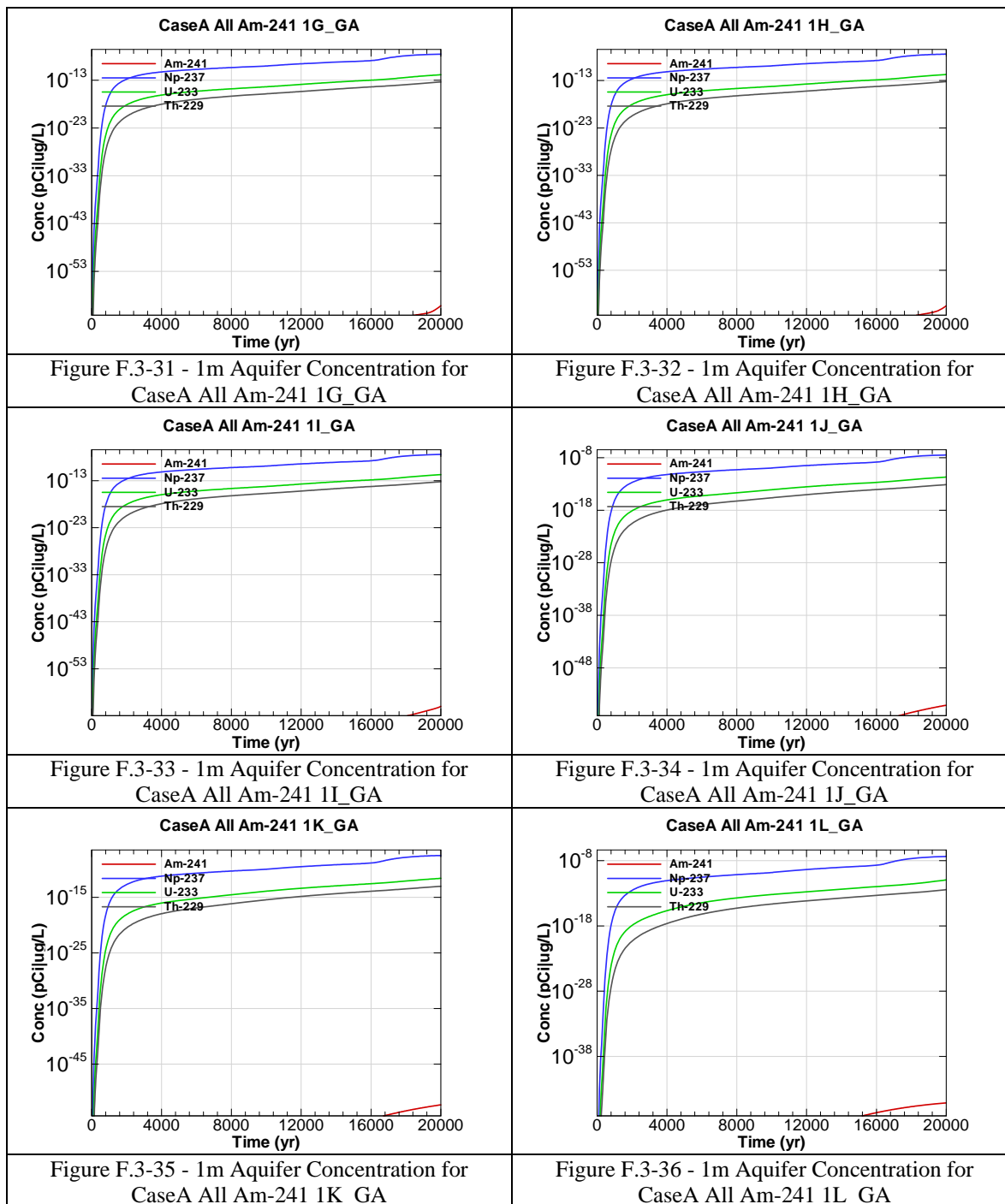


Figure F.3-30 - 1m Aquifer Concentration for
CaseA All Am-241 1F_GA



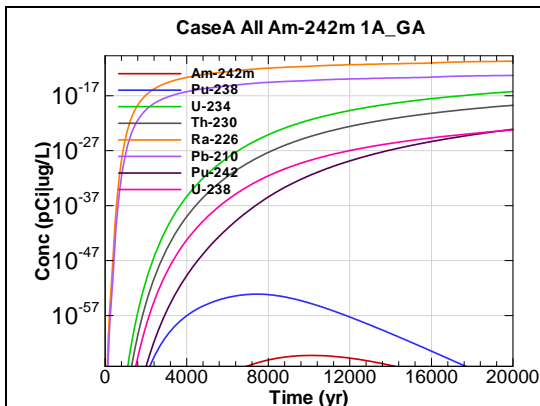


Figure F.3-37 - 1m Aquifer Concentration for
CaseA All Am-242m 1A_GA

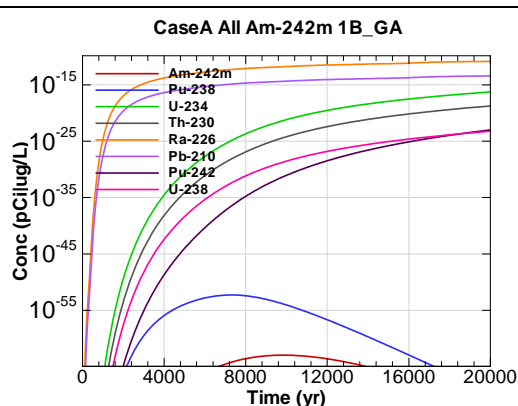


Figure F.3-38 - 1m Aquifer Concentration for
CaseA All Am-242m 1B_GA

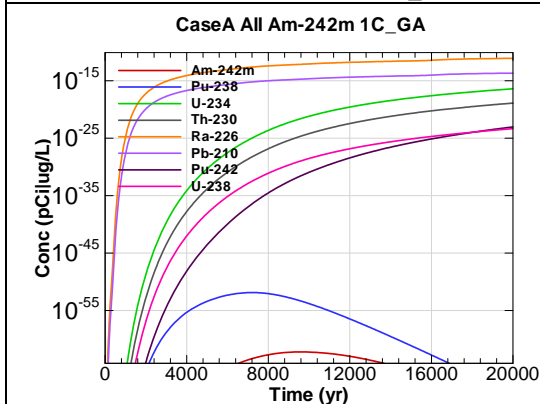


Figure F.3-39 - 1m Aquifer Concentration for
CaseA All Am-242m 1C_GA

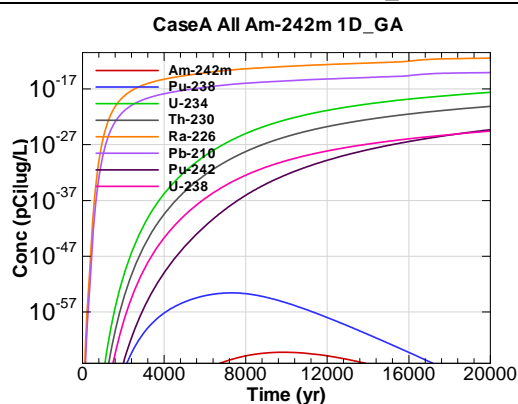


Figure F.3-40 - 1m Aquifer Concentration for
CaseA All Am-242m 1D_GA

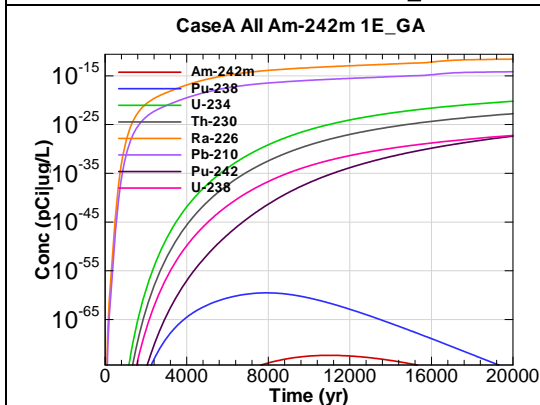


Figure F.3-41 - 1m Aquifer Concentration for
CaseA All Am-242m 1E_GA

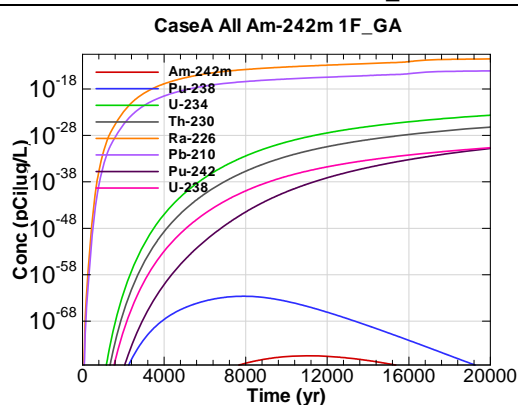


Figure F.3-42 - 1m Aquifer Concentration for
CaseA All Am-242m 1F_GA

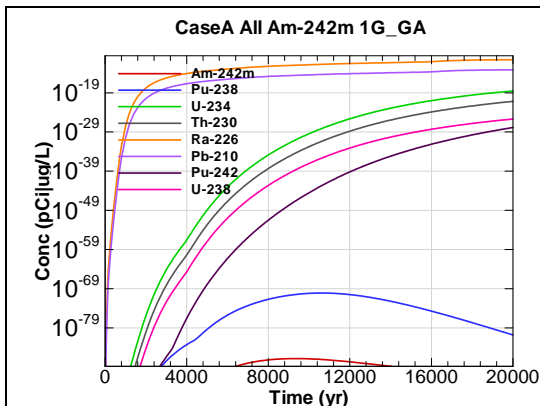


Figure F.3-43 - 1m Aquifer Concentration for
CaseA All Am-242m 1G_GA

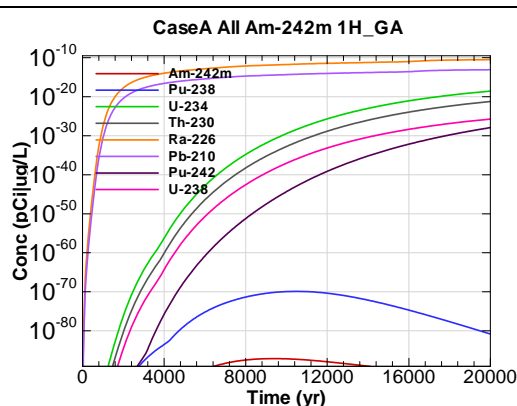


Figure F.3-44 - 1m Aquifer Concentration for
CaseA All Am-242m 1H_GA

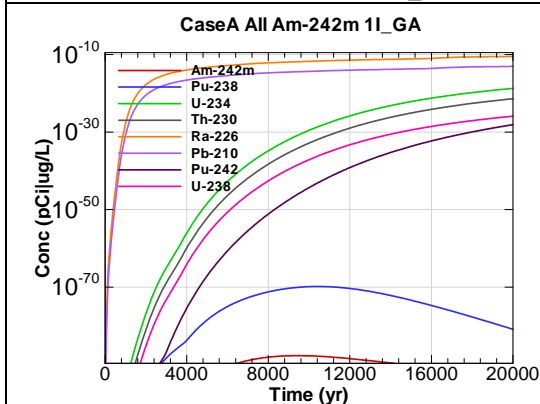


Figure F.3-45 - 1m Aquifer Concentration for
CaseA All Am-242m 1I_GA

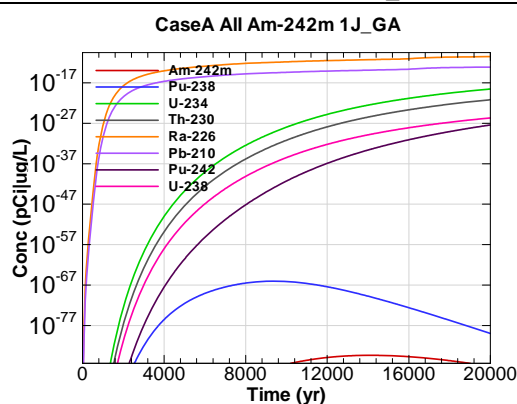


Figure F.3-46 - 1m Aquifer Concentration for
CaseA All Am-242m 1J_GA

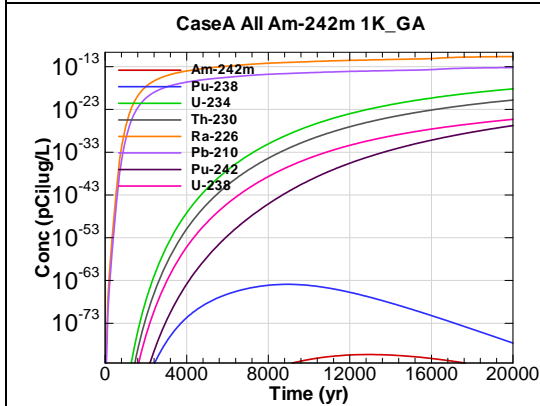


Figure F.3-47 - 1m Aquifer Concentration for
CaseA All Am-242m 1K_GA

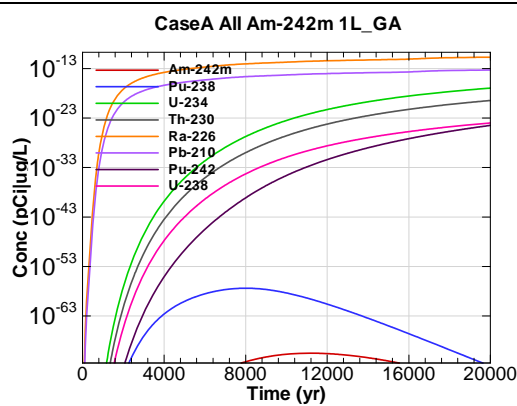


Figure F.3-48 - 1m Aquifer Concentration for
CaseA All Am-242m 1L_GA

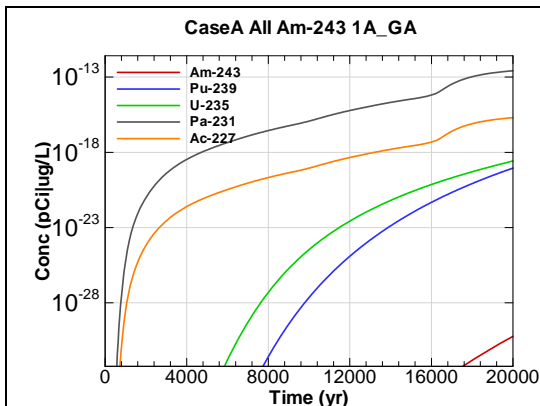


Figure F.3-49 - 1m Aquifer Concentration for
CaseA All Am-243 1A_GA

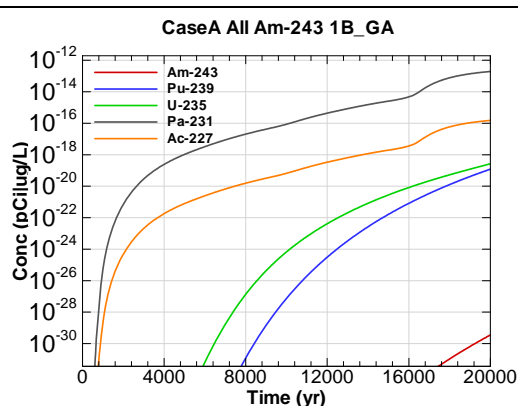


Figure F.3-50 - 1m Aquifer Concentration for
CaseA All Am-243 1B_GA

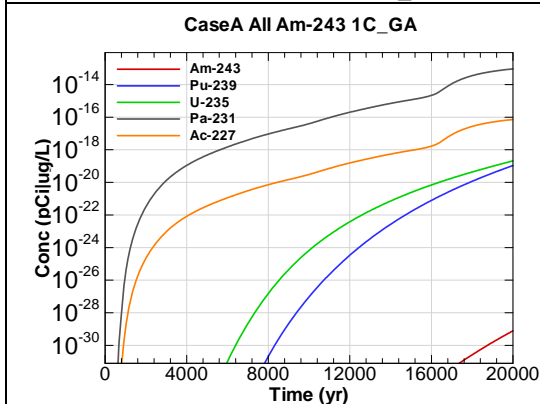


Figure F.3-51 - 1m Aquifer Concentration for
CaseA All Am-243 1C_GA

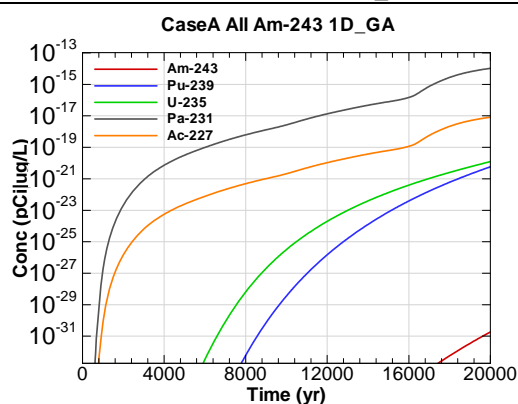


Figure F.3-52 - 1m Aquifer Concentration for
CaseA All Am-243 1D_GA

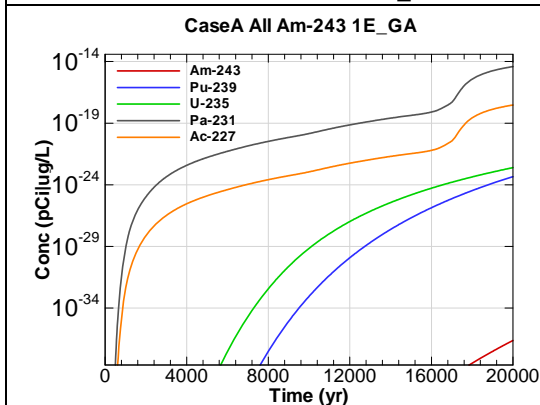


Figure F.3-53 - 1m Aquifer Concentration for
CaseA All Am-243 1E_GA

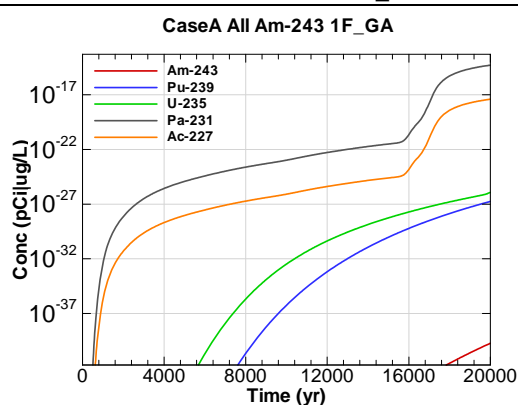


Figure F.3-54 - 1m Aquifer Concentration for
CaseA All Am-243 1F_GA

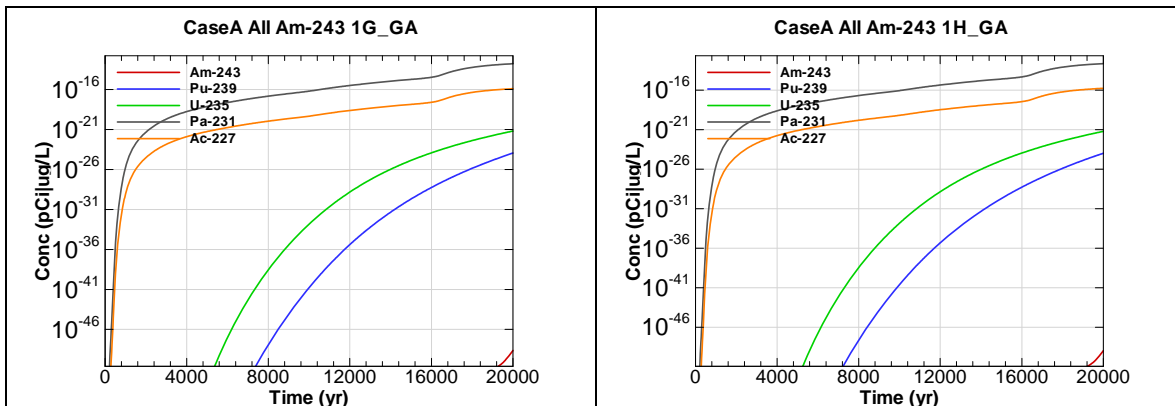


Figure F.3-55 - 1m Aquifer Concentration for
CaseA All Am-243 1G_GA

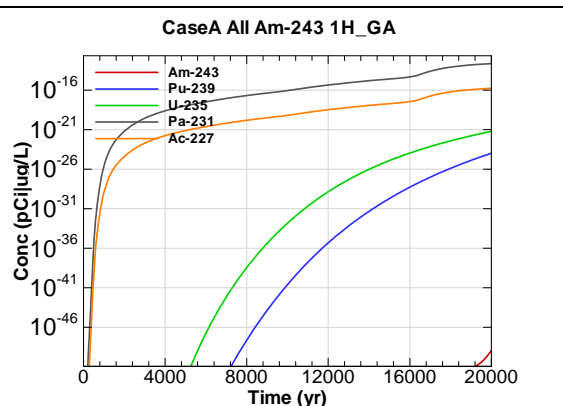


Figure F.3-56 - 1m Aquifer Concentration for
CaseA All Am-243 1H_GA

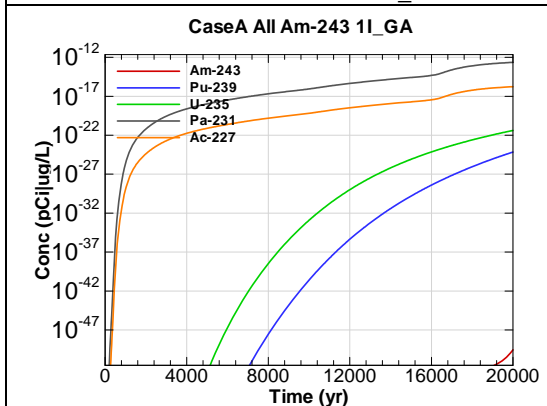


Figure F.3-57 - 1m Aquifer Concentration for
CaseA All Am-243 1I_GA

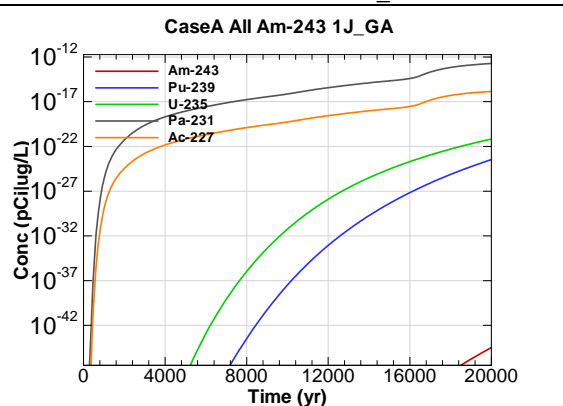


Figure F.3-58 - 1m Aquifer Concentration for
CaseA All Am-243 1J_GA

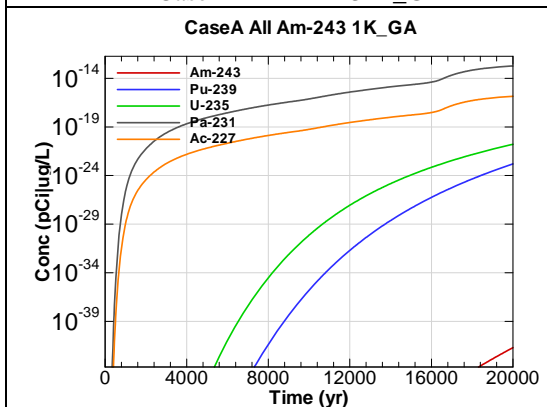


Figure F.3-59 - 1m Aquifer Concentration for
CaseA All Am-243 1K_GA

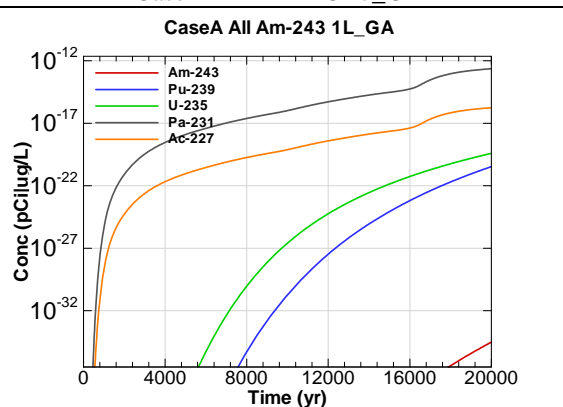
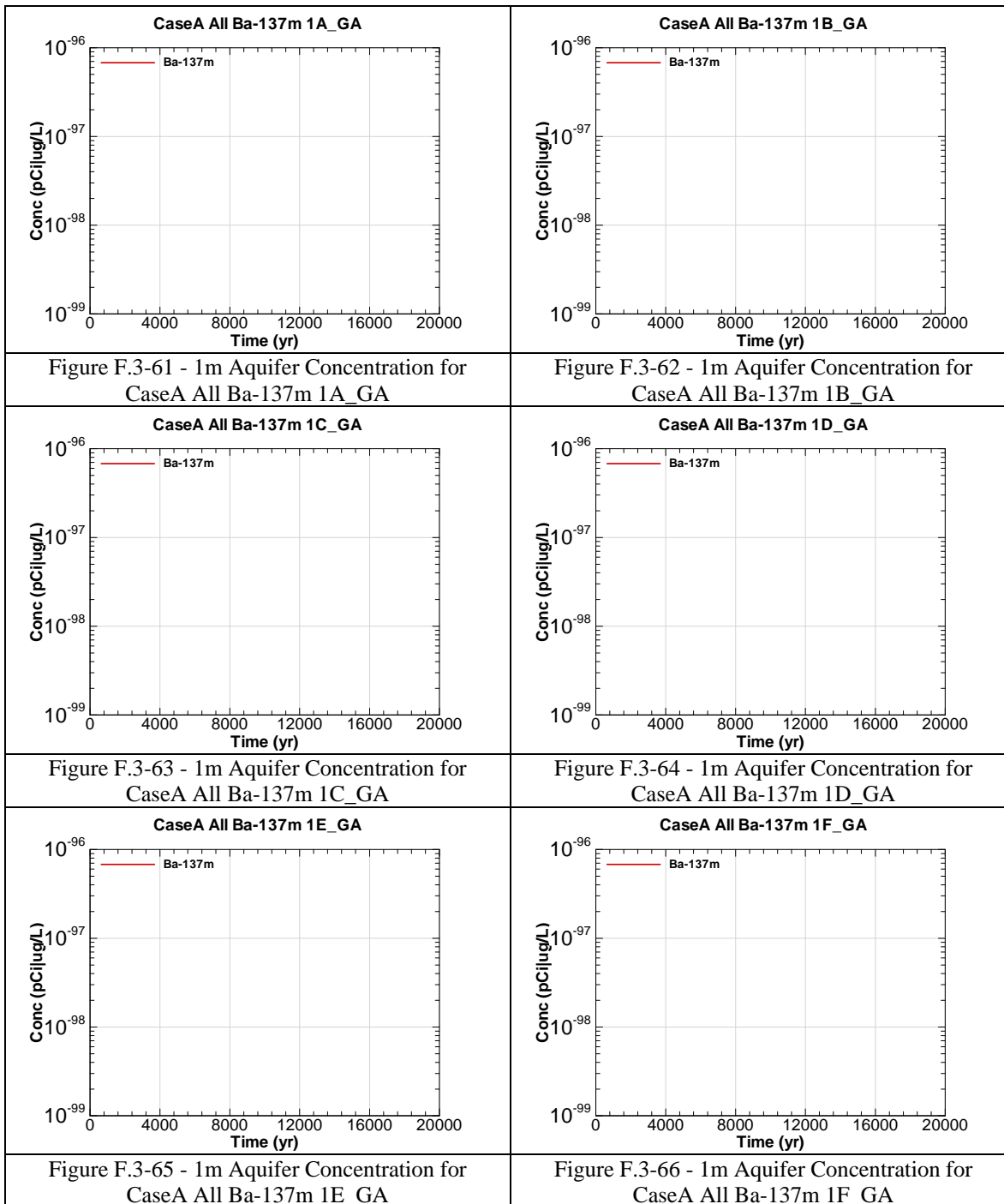
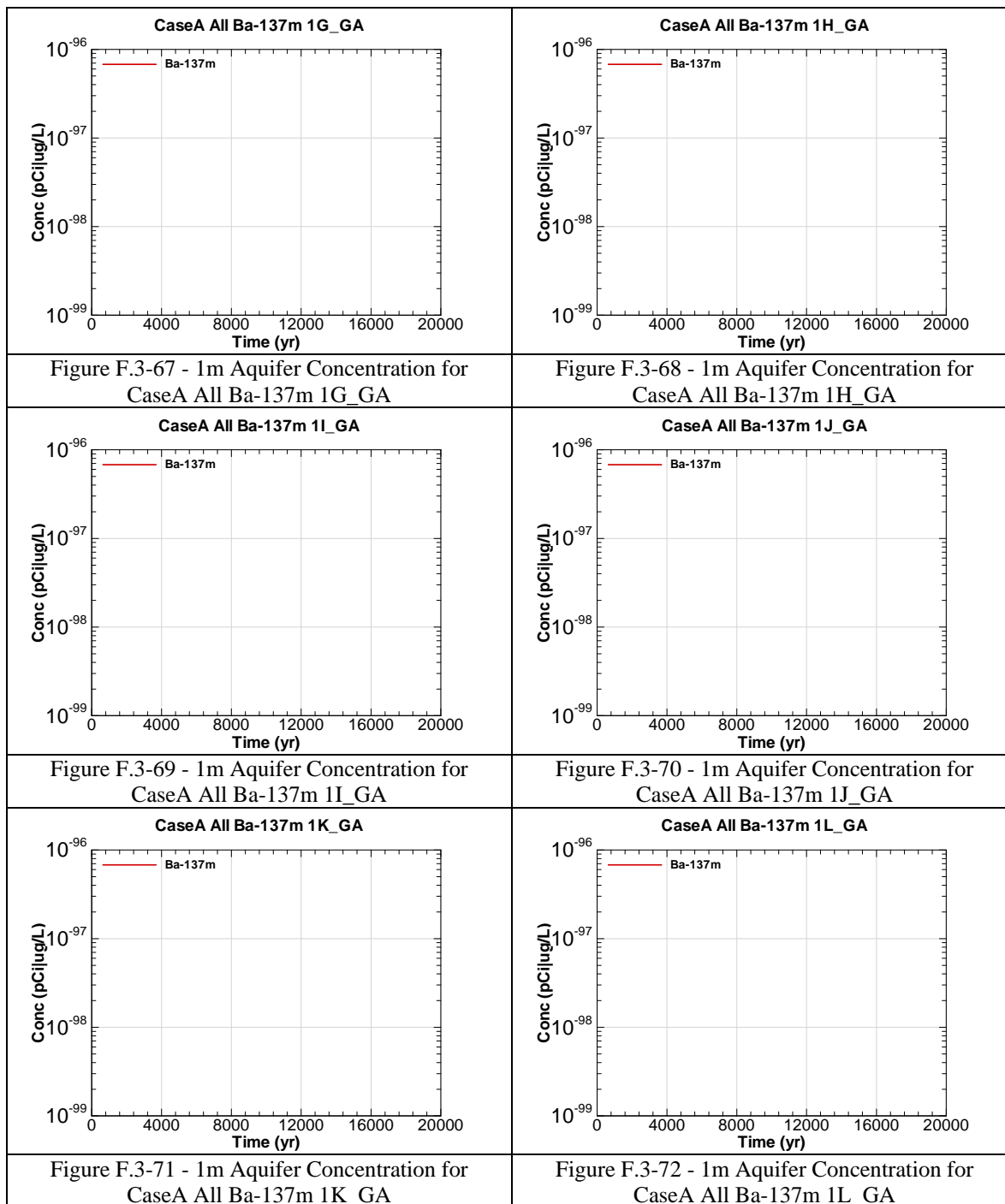


Figure F.3-60 - 1m Aquifer Concentration for
CaseA All Am-243 1L_GA





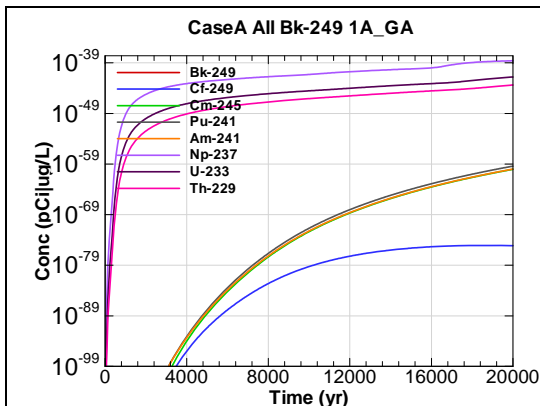


Figure F.3-73 - 1m Aquifer Concentration for
CaseA All Bk-249 1A_GA

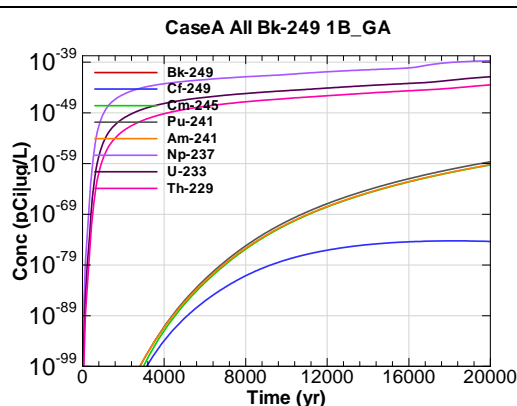


Figure F.3-74 - 1m Aquifer Concentration for
CaseA All Bk-249 1B_GA

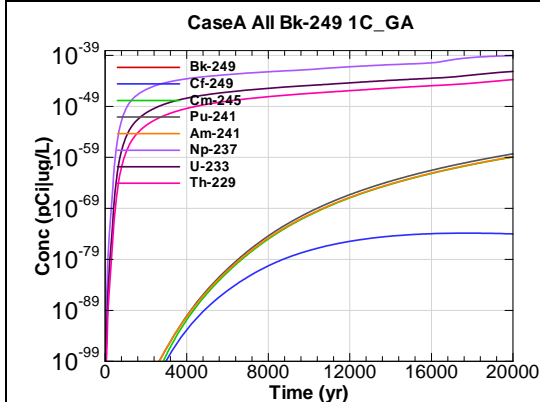


Figure F.3-75 - 1m Aquifer Concentration for
CaseA All Bk-249 1C_GA

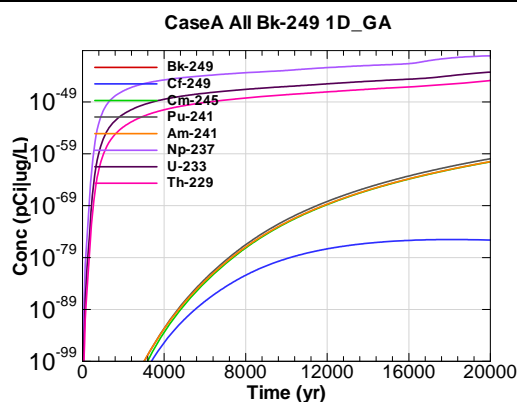


Figure F.3-76 - 1m Aquifer Concentration for
CaseA All Bk-249 1D_GA

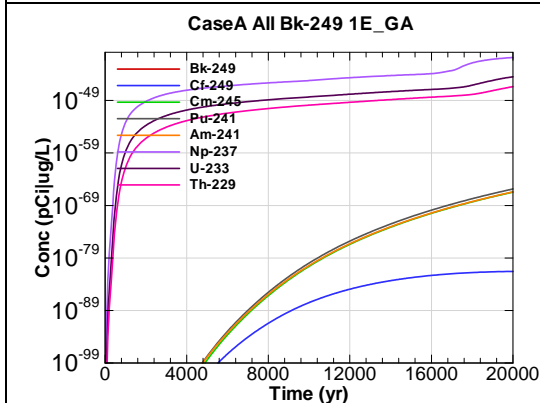


Figure F.3-77 - 1m Aquifer Concentration for
CaseA All Bk-249 1E_GA

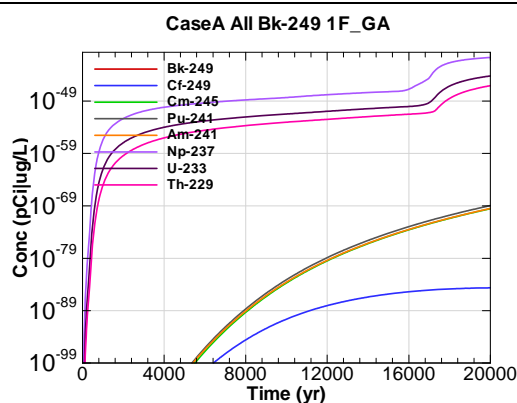


Figure F.3-78 - 1m Aquifer Concentration for
CaseA All Bk-249 1F_GA

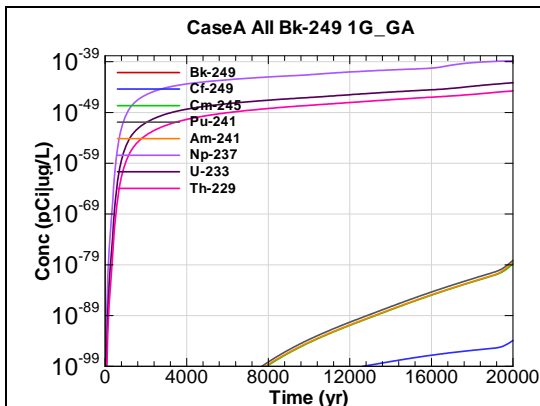


Figure F.3-79 - 1m Aquifer Concentration for
CaseA All Bk-249 1G_GA

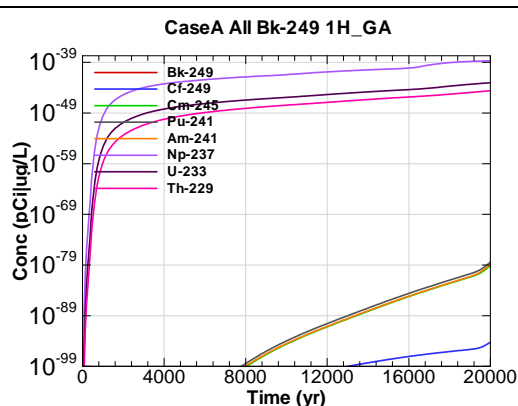


Figure F.3-80 - 1m Aquifer Concentration for
CaseA All Bk-249 1H_GA

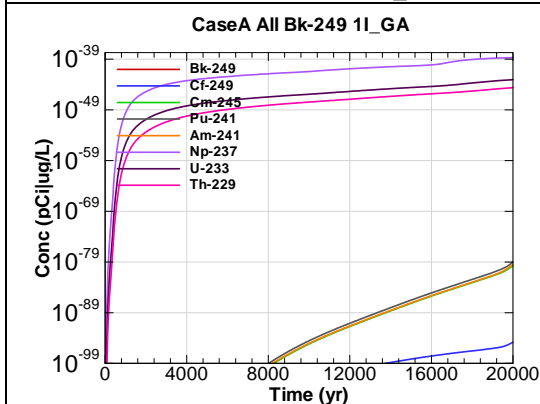


Figure F.3-81 - 1m Aquifer Concentration for
CaseA All Bk-249 1I_GA

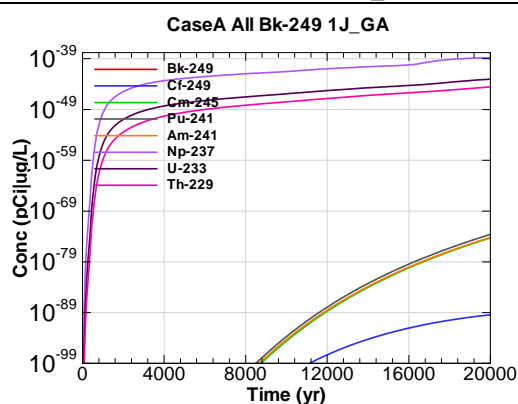


Figure F.3-82 - 1m Aquifer Concentration for
CaseA All Bk-249 1J_GA

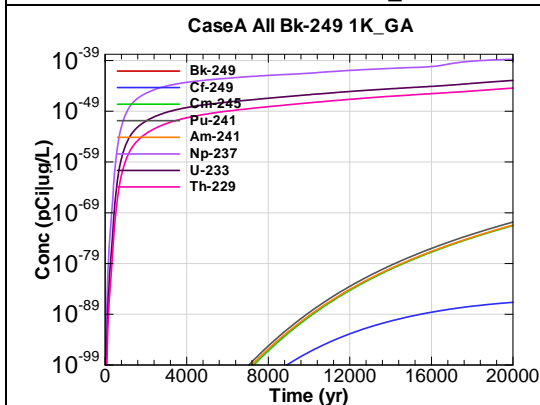


Figure F.3-83 - 1m Aquifer Concentration for
CaseA All Bk-249 1K_GA

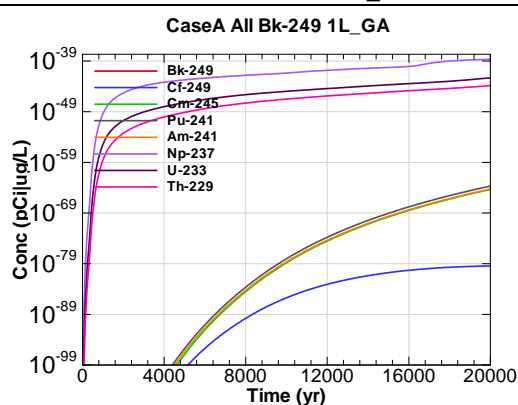
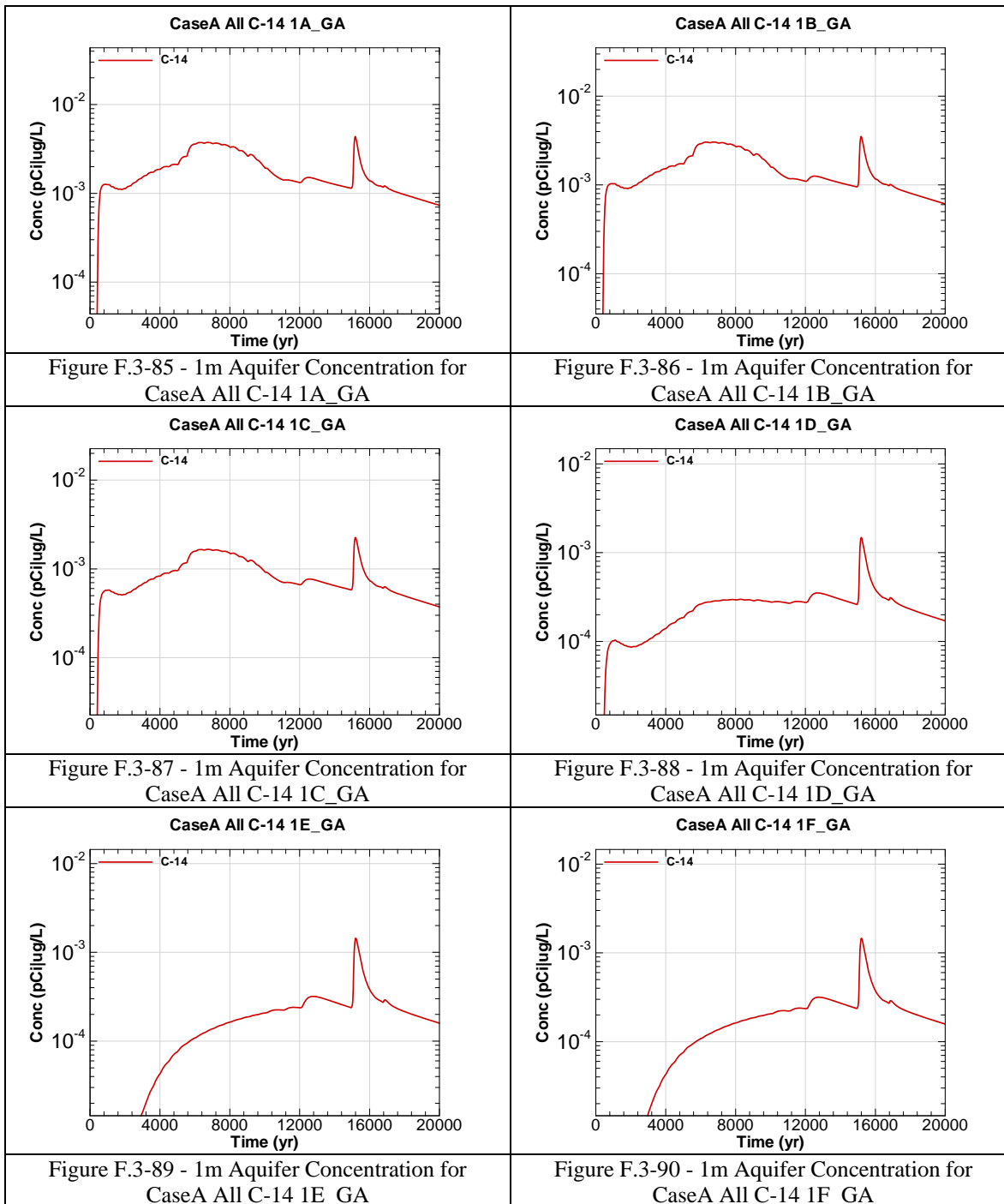
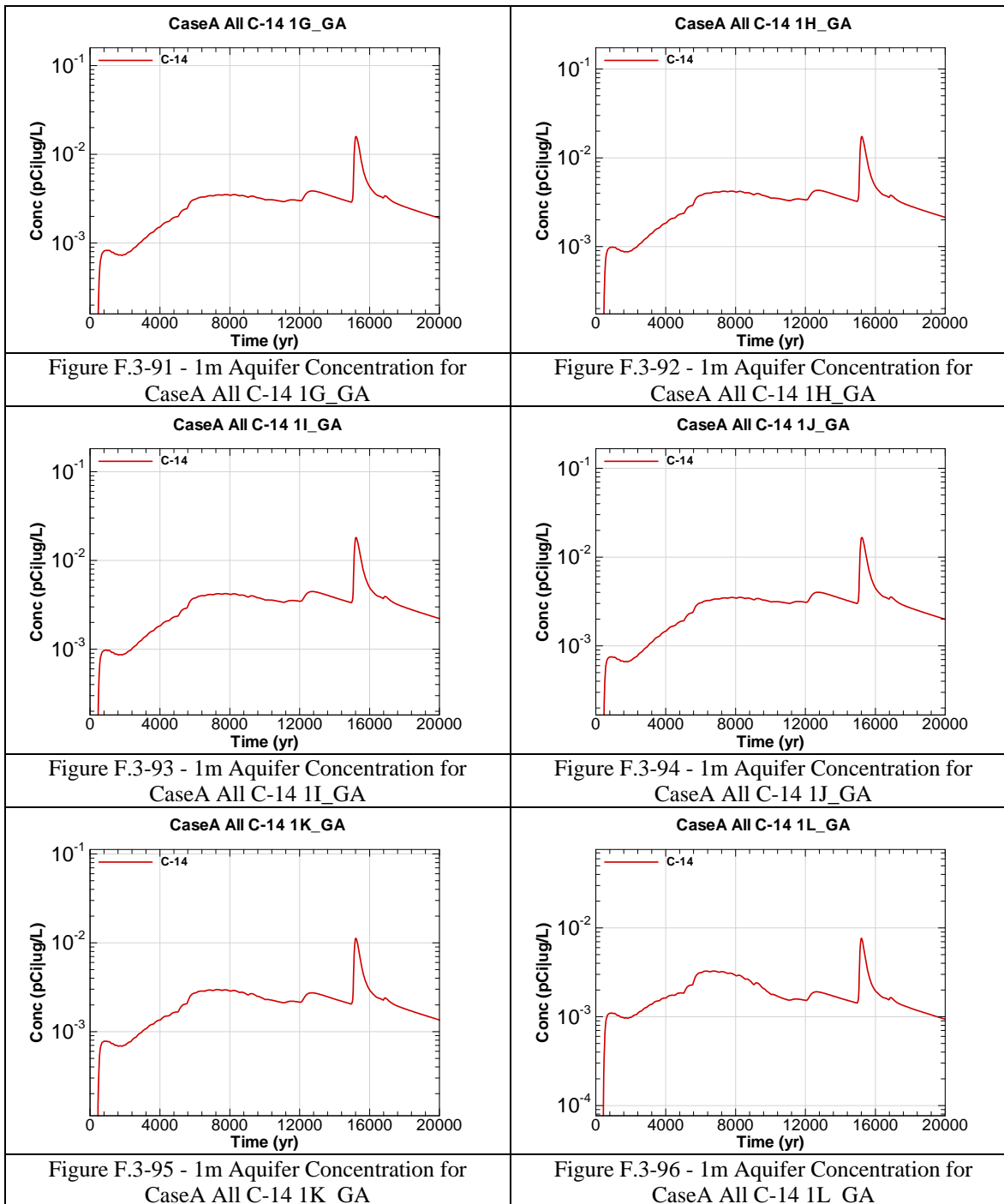
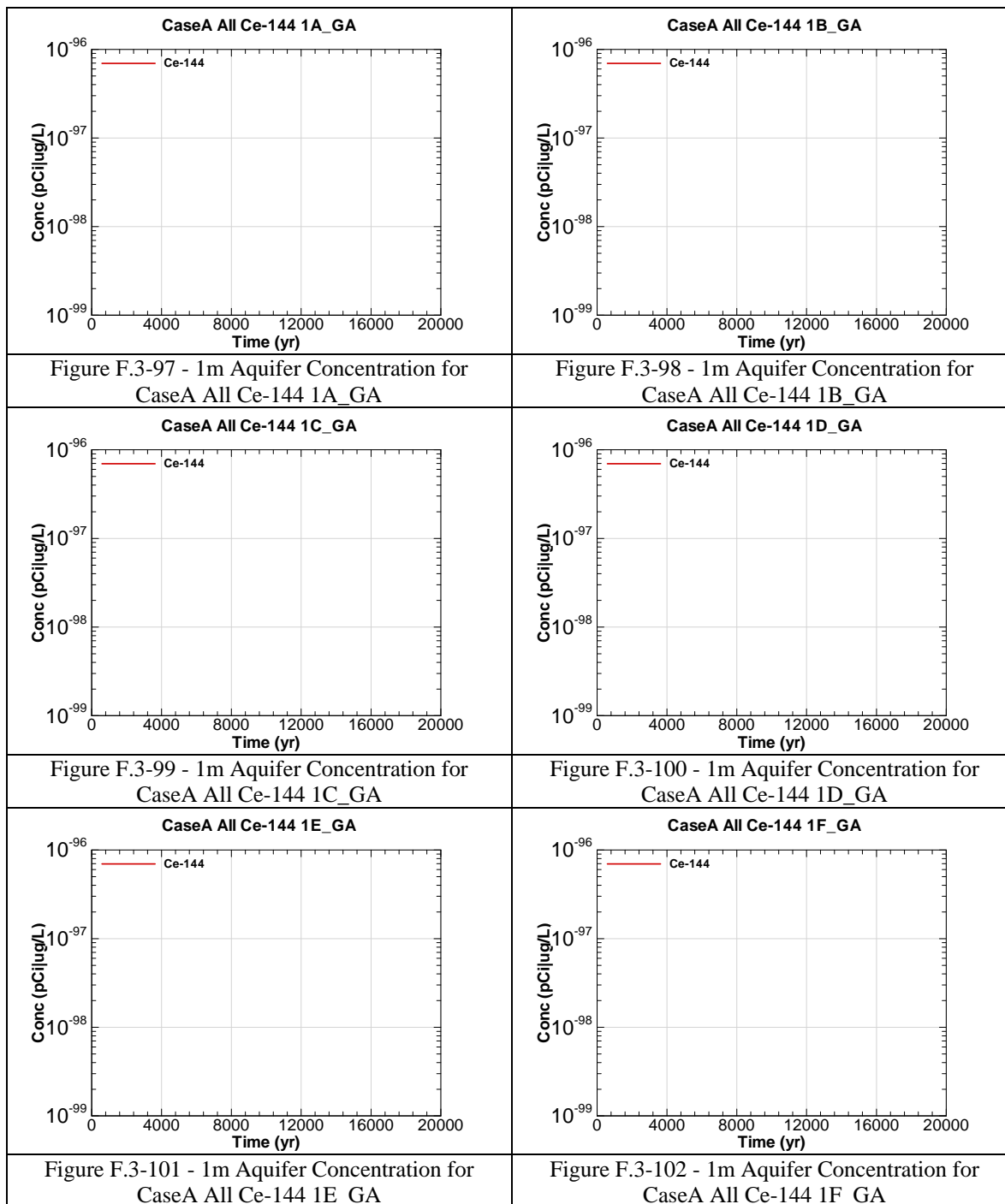
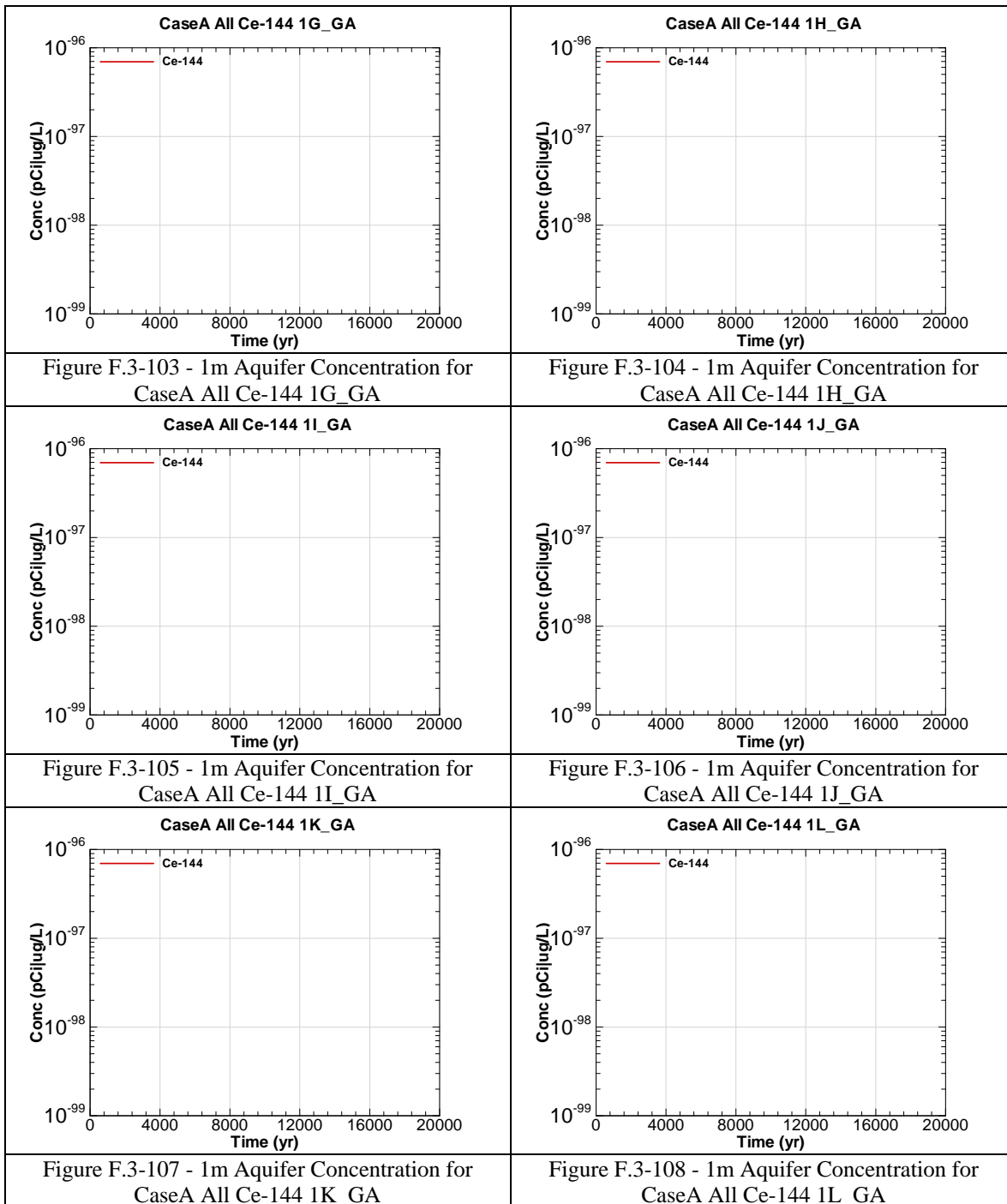


Figure F.3-84 - 1m Aquifer Concentration for
CaseA All Bk-249 1L_GA









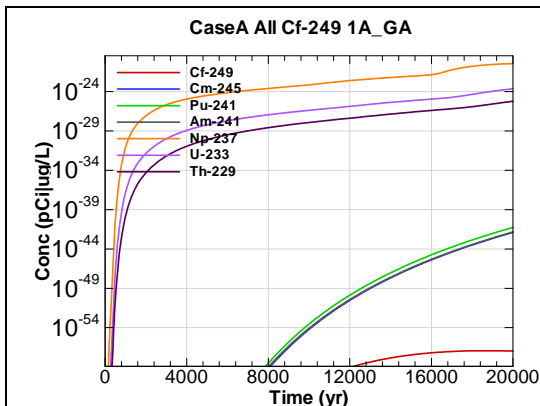


Figure F.3-109 - 1m Aquifer Concentration for
CaseA All Cf-249 1A_GA

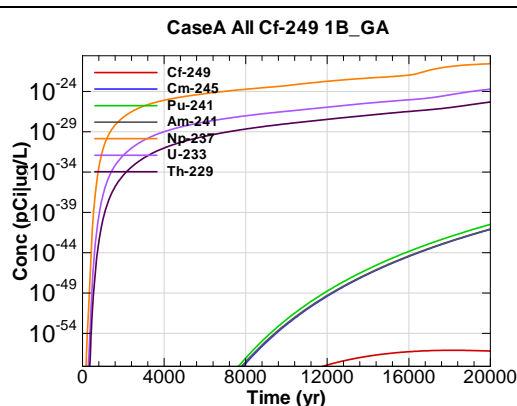


Figure F.3-110 - 1m Aquifer Concentration for
CaseA All Cf-249 1B_GA

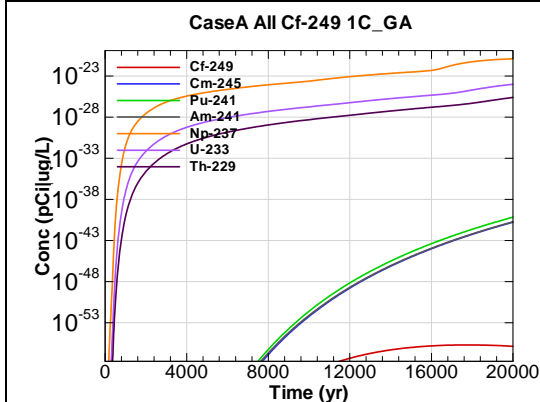


Figure F.3-111 - 1m Aquifer Concentration for
CaseA All Cf-249 1C_GA

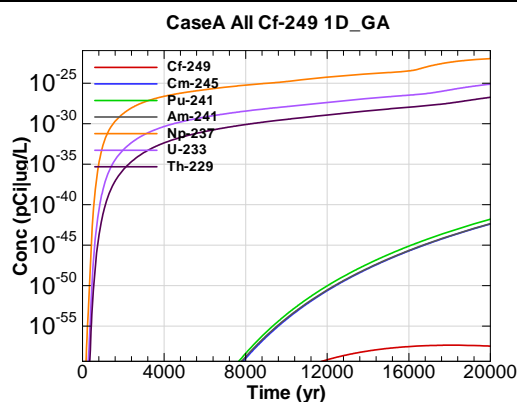


Figure F.3-112 - 1m Aquifer Concentration for
CaseA All Cf-249 1D_GA

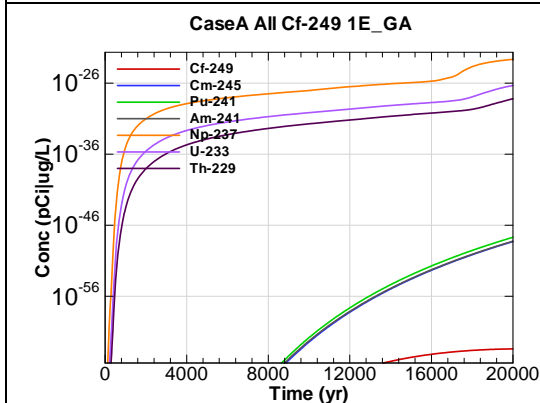


Figure F.3-113 - 1m Aquifer Concentration for
CaseA All Cf-249 1E_GA

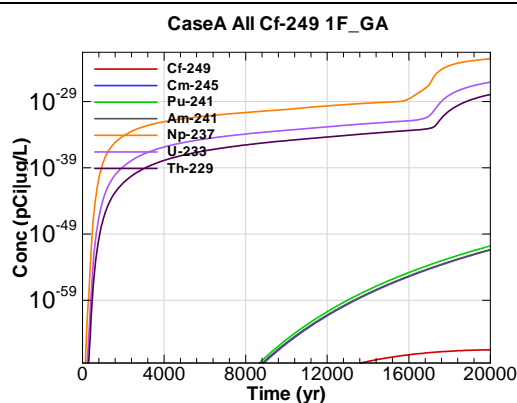


Figure F.3-114 - 1m Aquifer Concentration for
CaseA All Cf-249 1F_GA

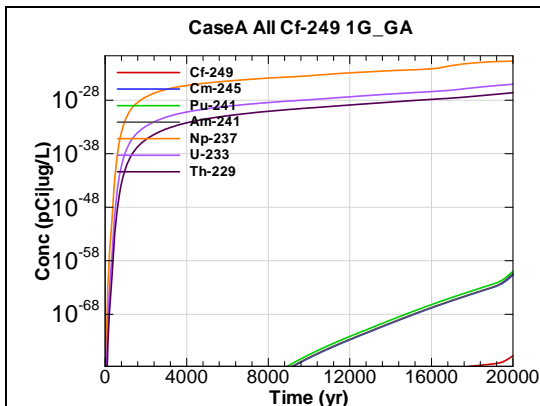


Figure F.3-115 - 1m Aquifer Concentration for
CaseA All Cf-249 1G_GA

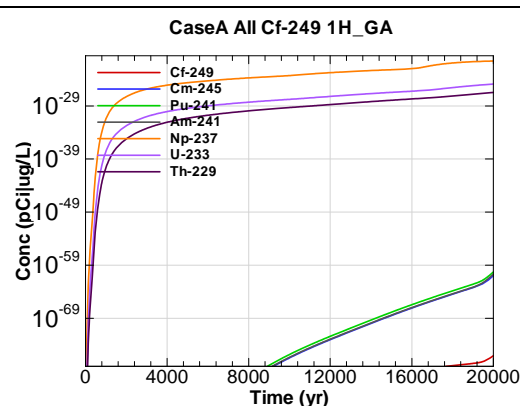


Figure F.3-116 - 1m Aquifer Concentration for
CaseA All Cf-249 1H_GA

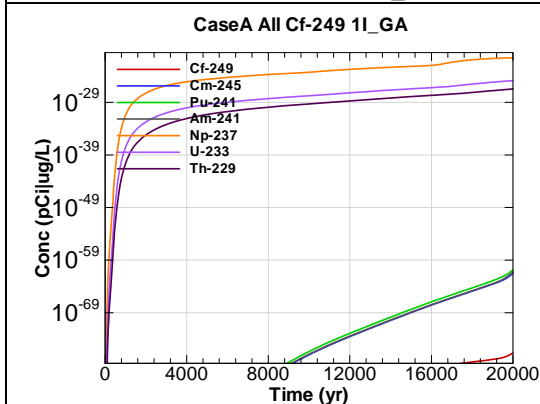


Figure F.3-117 - 1m Aquifer Concentration for
CaseA All Cf-249 1I_GA

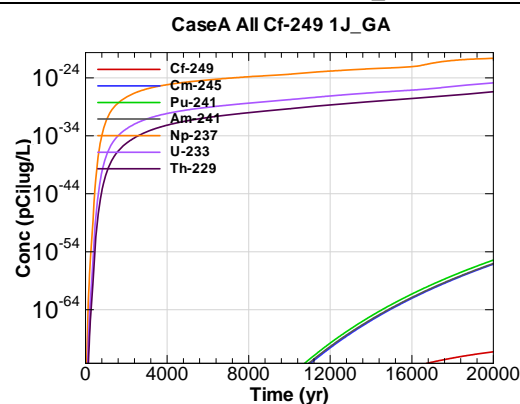


Figure F.3-118 - 1m Aquifer Concentration for
CaseA All Cf-249 1J_GA

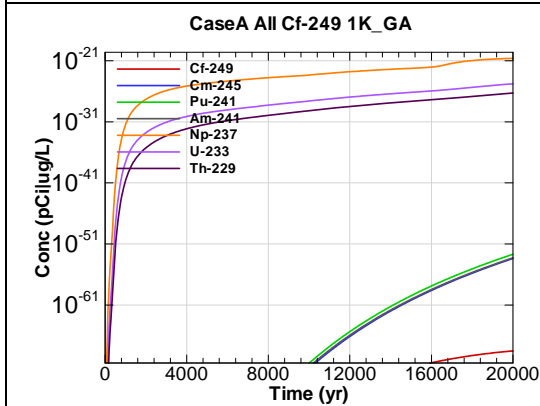


Figure F.3-119 - 1m Aquifer Concentration for
CaseA All Cf-249 1K_GA

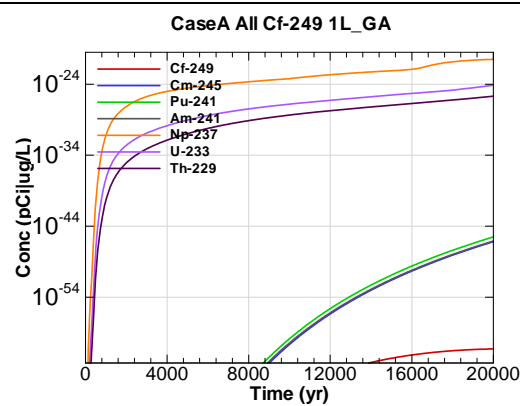
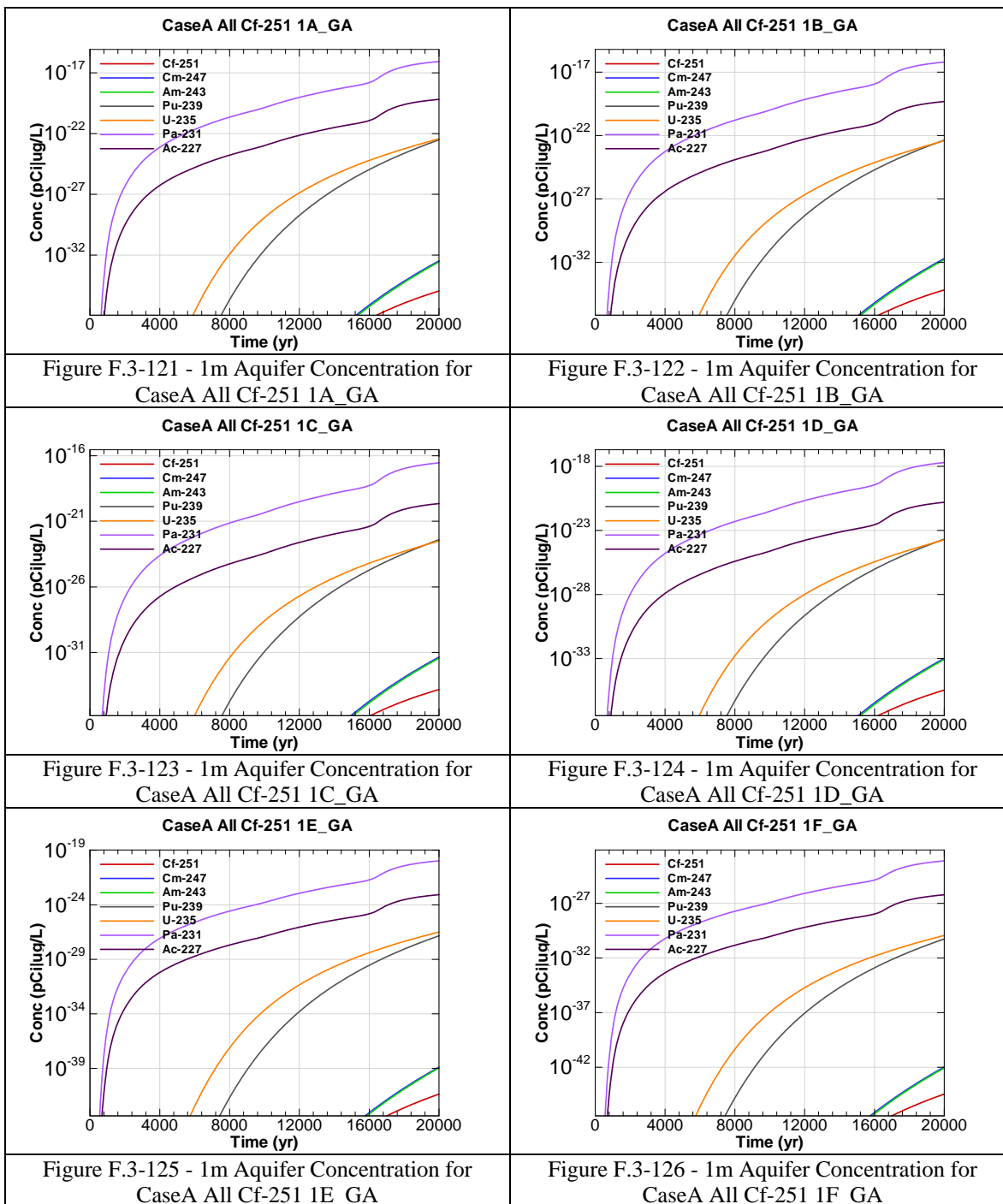


Figure F.3-120 - 1m Aquifer Concentration for
CaseA All Cf-249 1L_GA



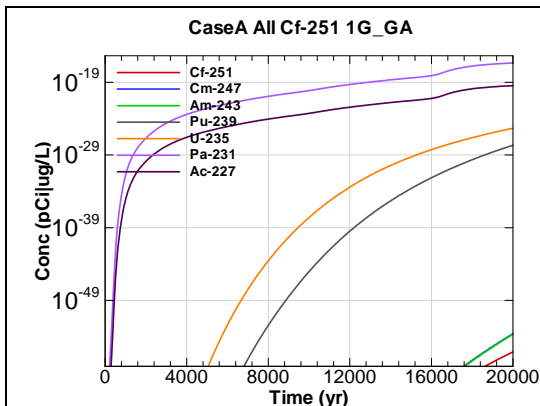


Figure F.3-127 - 1m Aquifer Concentration for CaseA All Cf-251 1G_GA

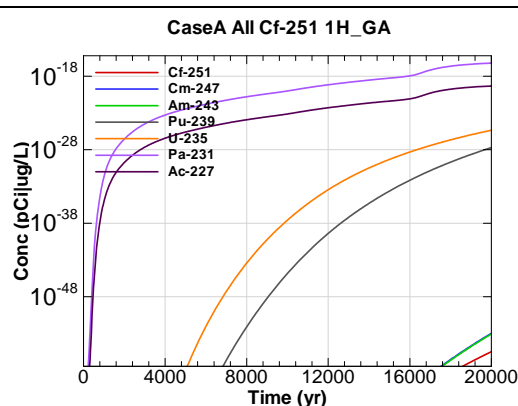


Figure F.3-128 - 1m Aquifer Concentration for CaseA All Cf-251 1H_GA

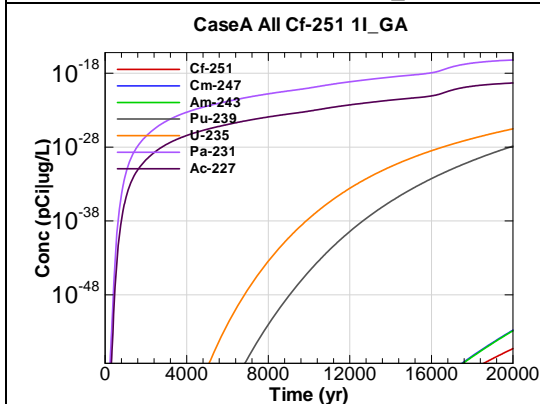


Figure F.3-129 - 1m Aquifer Concentration for CaseA All Cf-251 1I_GA

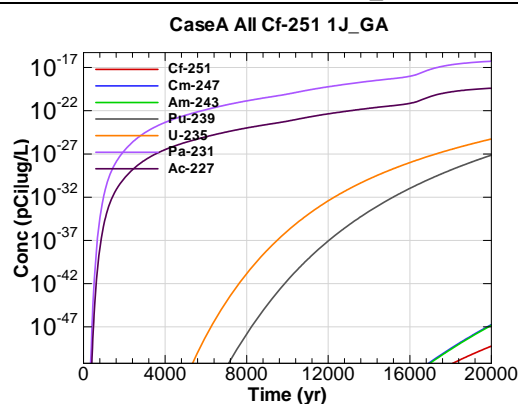


Figure F.3-130 - 1m Aquifer Concentration for CaseA All Cf-251 1J_GA

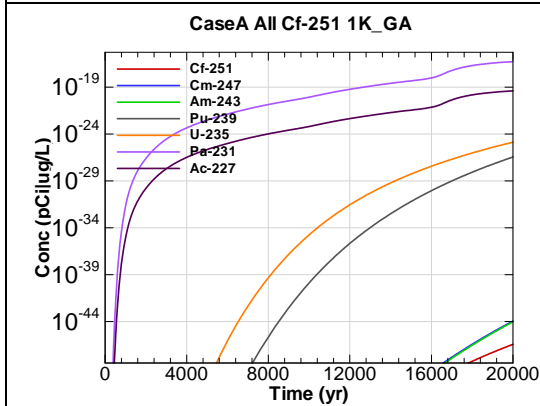


Figure F.3-131 - 1m Aquifer Concentration for CaseA All Cf-251 1K_GA

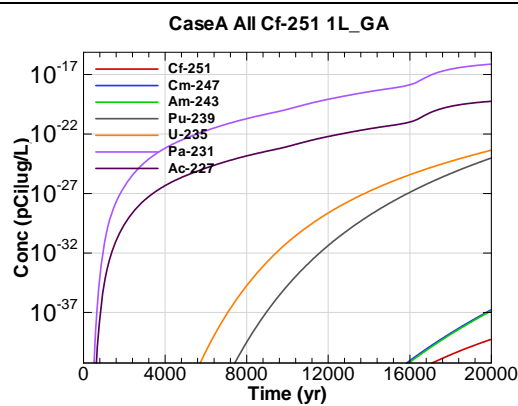


Figure F.3-132 - 1m Aquifer Concentration for CaseA All Cf-251 1L_GA

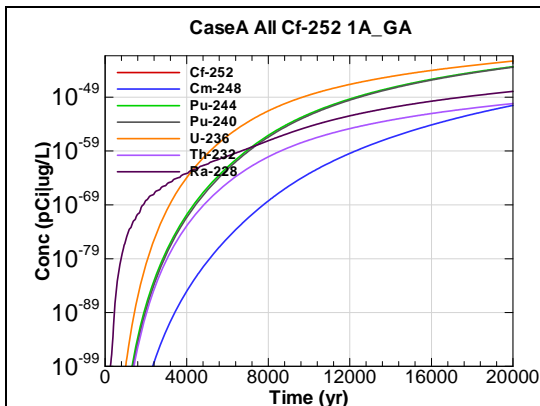


Figure F.3-133 - 1m Aquifer Concentration for
CaseA All Cf-252 1A_GA

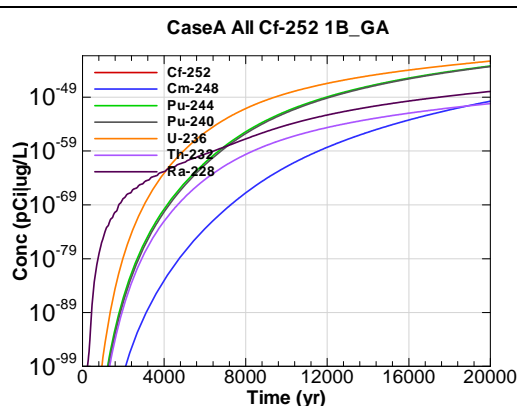


Figure F.3-134 - 1m Aquifer Concentration for
CaseA All Cf-252 1B_GA

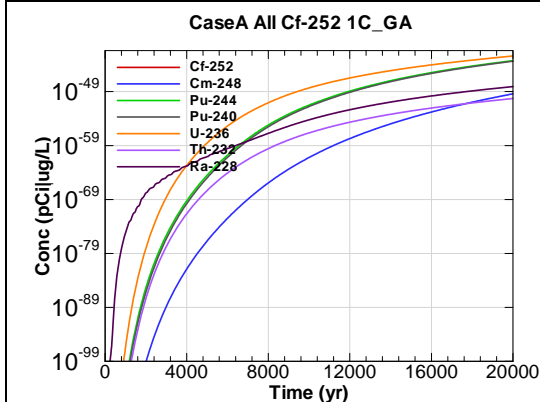


Figure F.3-135 - 1m Aquifer Concentration for
CaseA All Cf-252 1C_GA

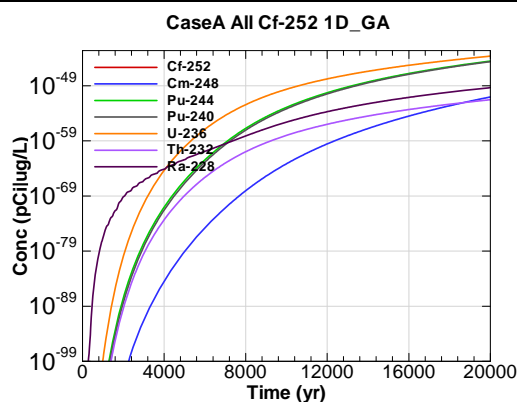


Figure F.3-136 - 1m Aquifer Concentration for
CaseA All Cf-252 1D_GA

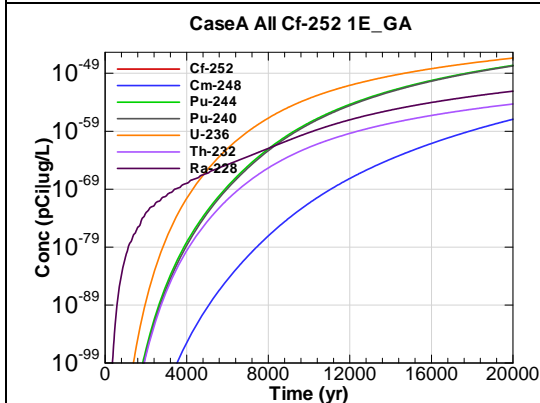


Figure F.3-137 - 1m Aquifer Concentration for
CaseA All Cf-252 1E_GA

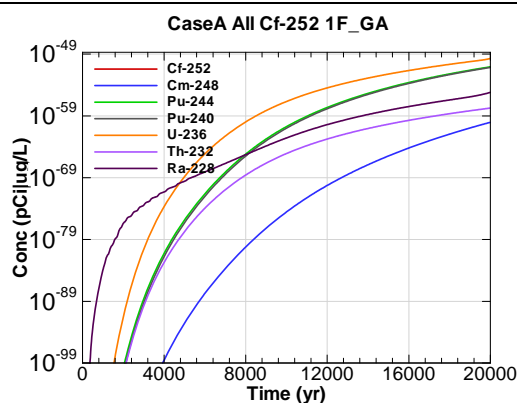
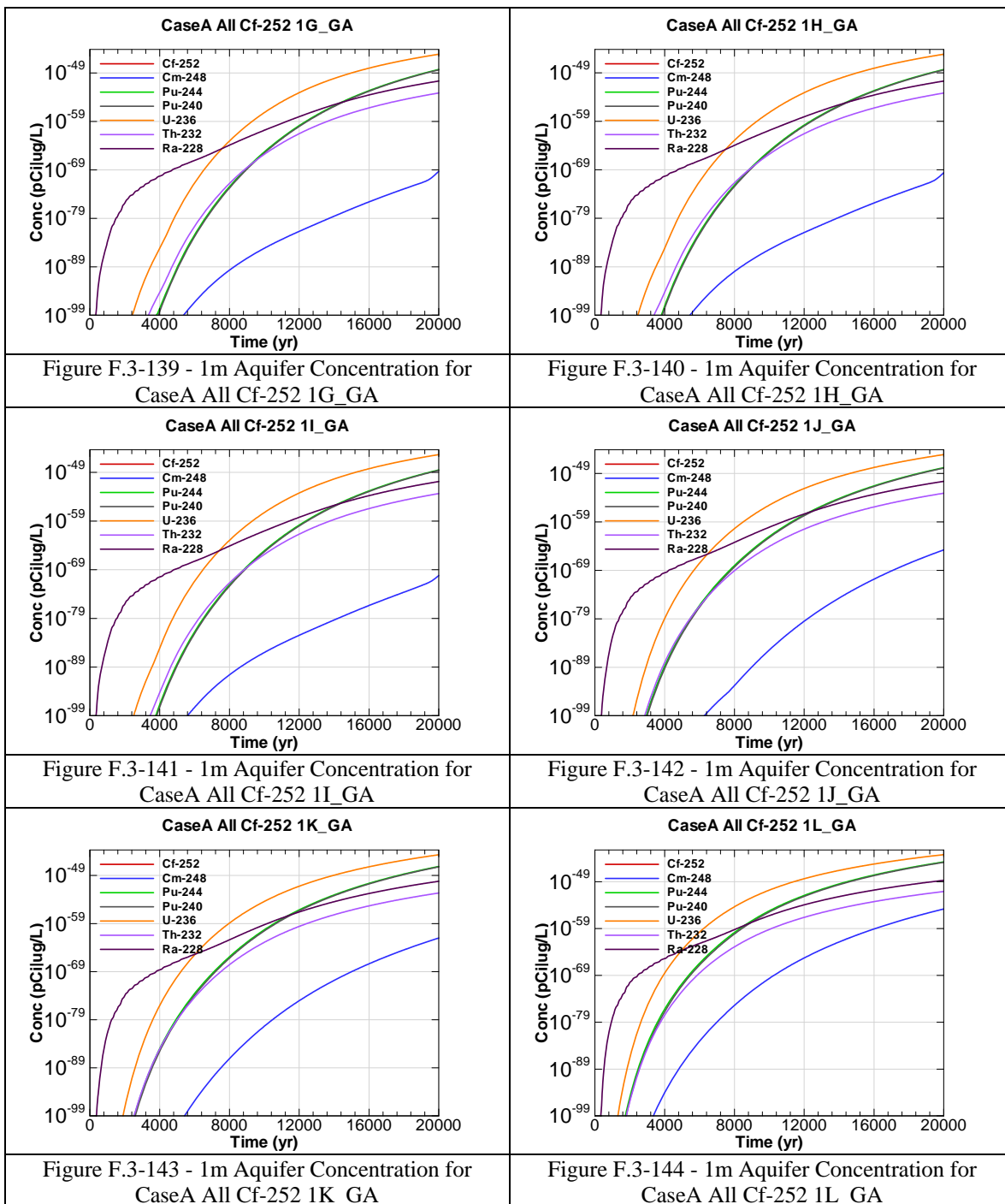
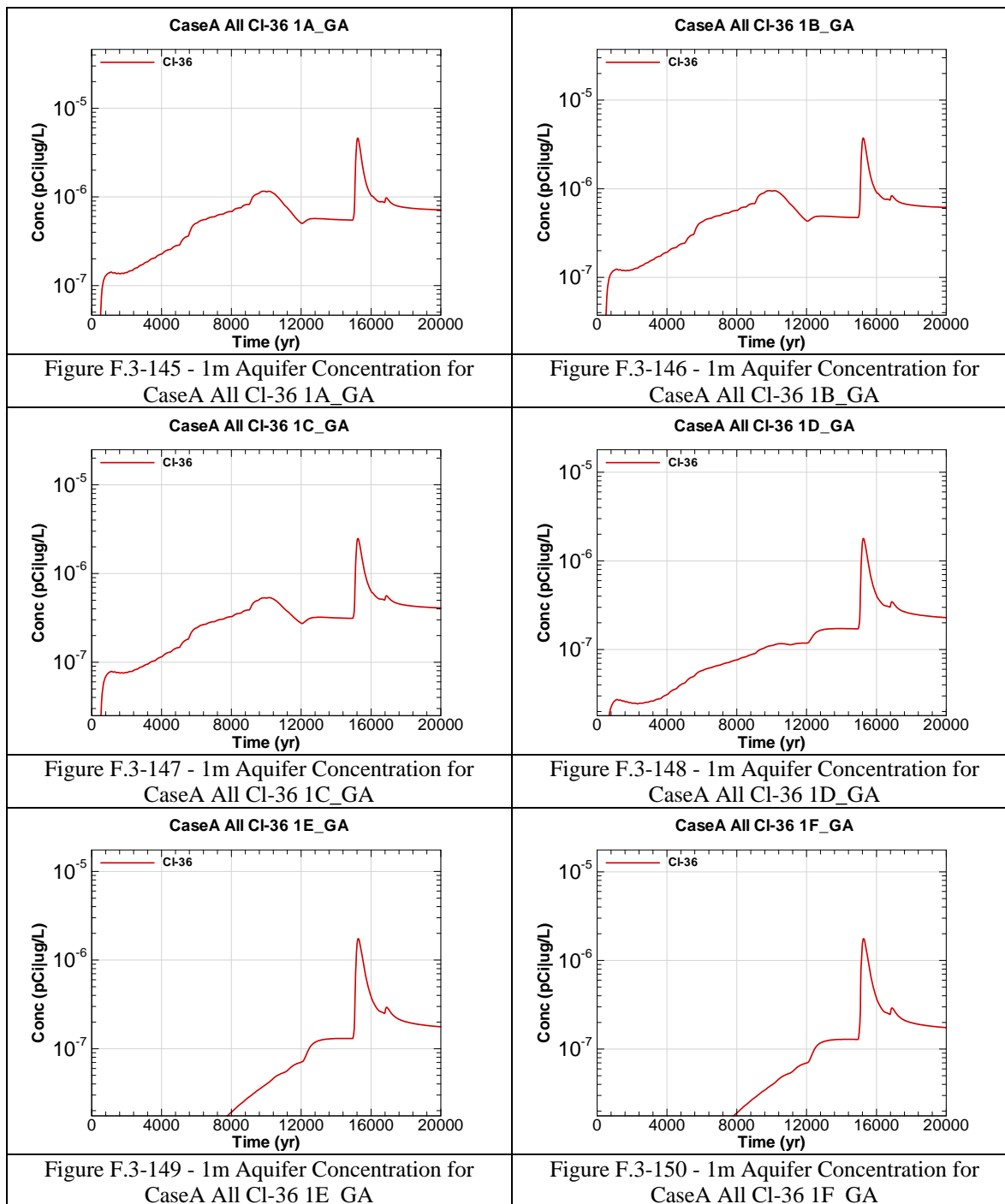
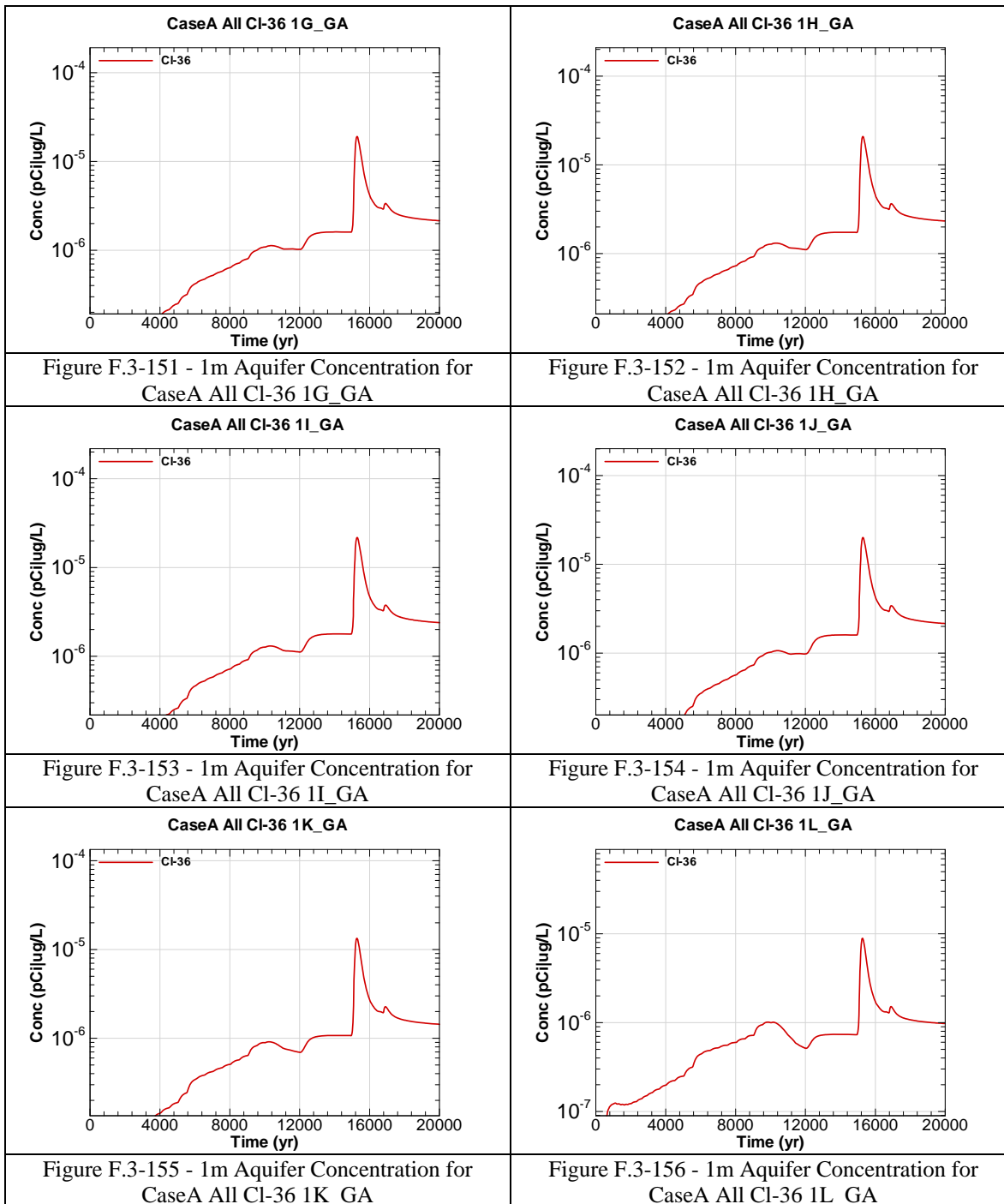


Figure F.3-138 - 1m Aquifer Concentration for
CaseA All Cf-252 1F_GA







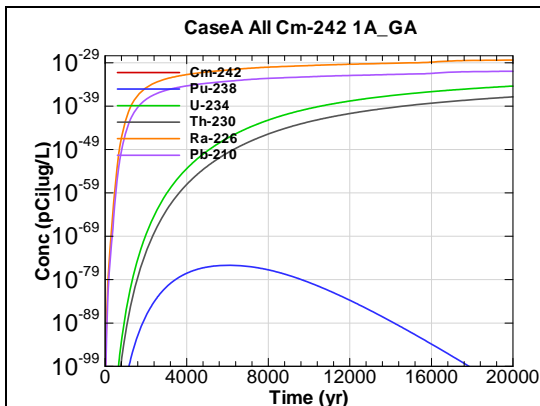


Figure F.3-157 - 1m Aquifer Concentration for
CaseA All Cm-242 1A_GA

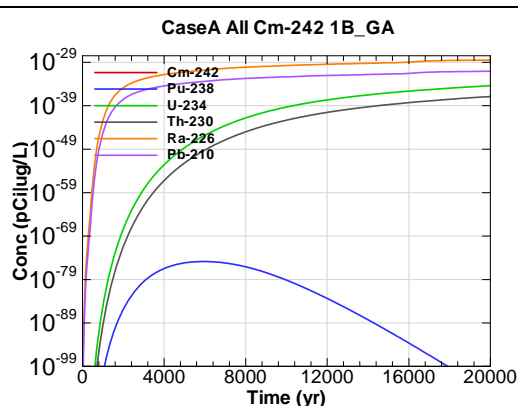


Figure F.3-158 - 1m Aquifer Concentration for
CaseA All Cm-242 1B_GA

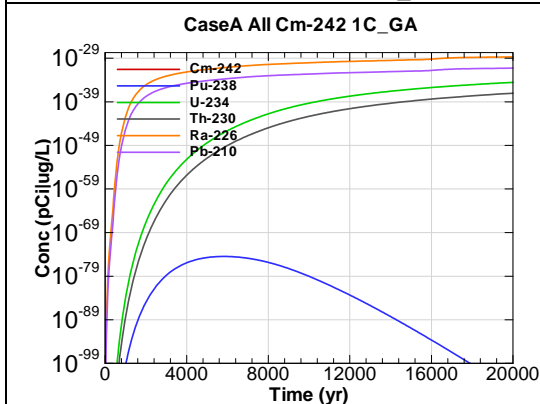


Figure F.3-159 - 1m Aquifer Concentration for
CaseA All Cm-242 1C_GA

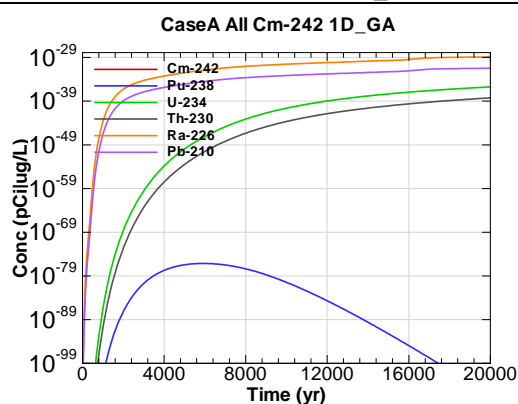


Figure F.3-160 - 1m Aquifer Concentration for
CaseA All Cm-242 1D_GA

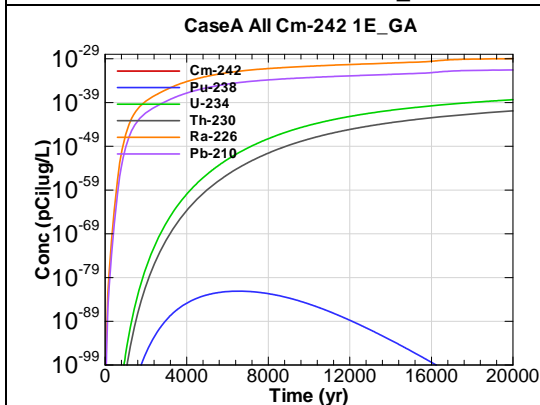


Figure F.3-161 - 1m Aquifer Concentration for
CaseA All Cm-242 1E_GA

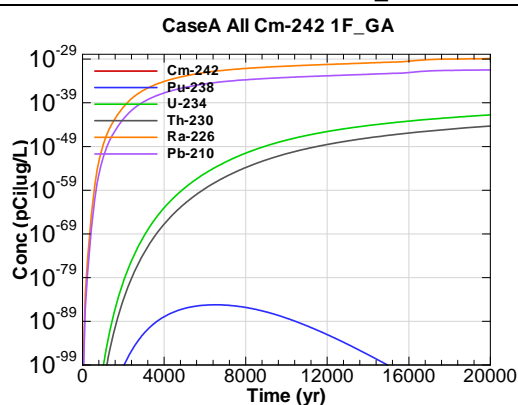
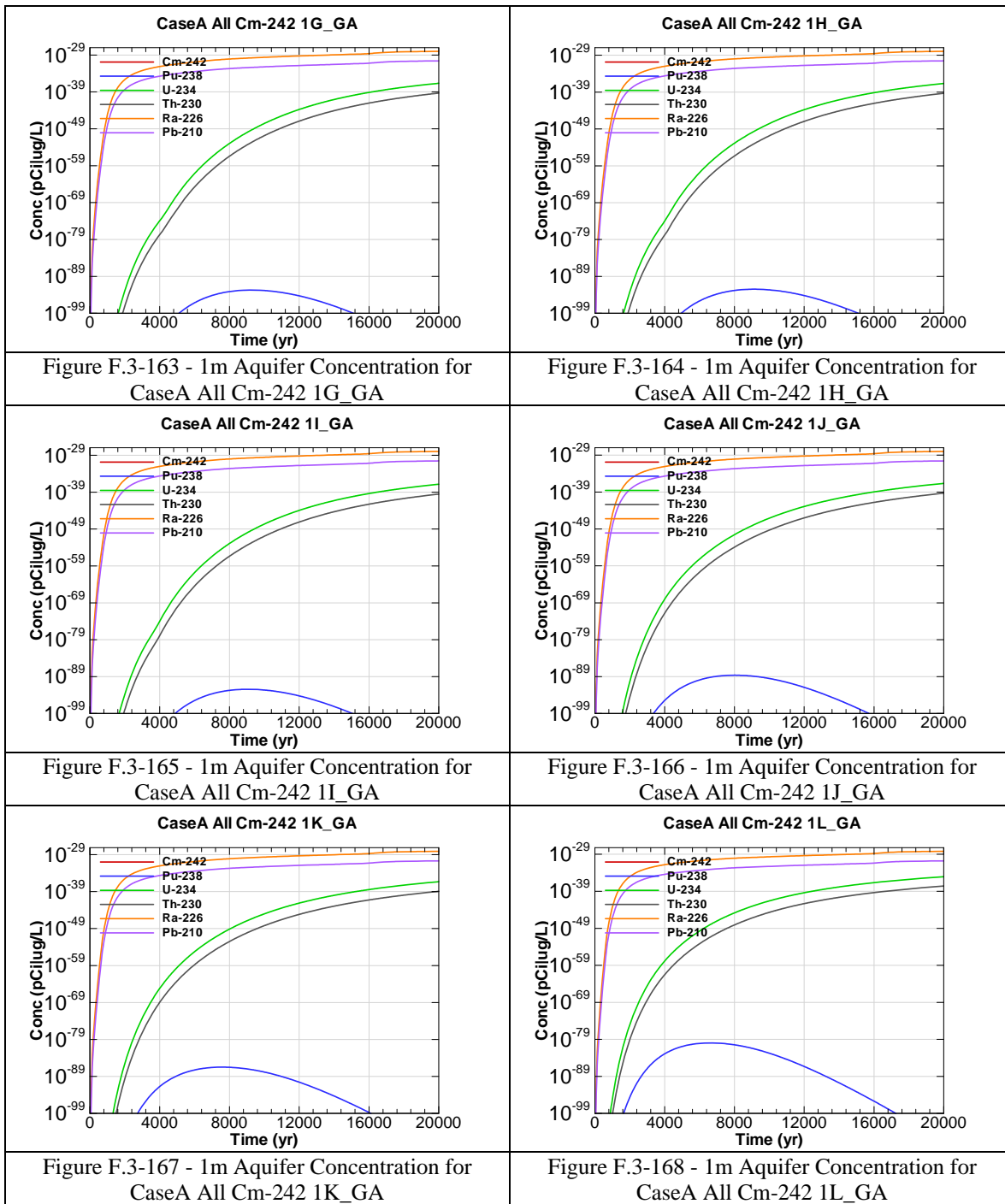


Figure F.3-162 - 1m Aquifer Concentration for
CaseA All Cm-242 1F_GA



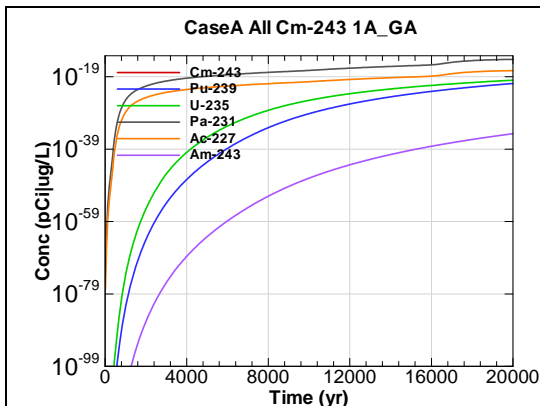


Figure F.3-169 - 1m Aquifer Concentration for
CaseA All Cm-243 1A_GA

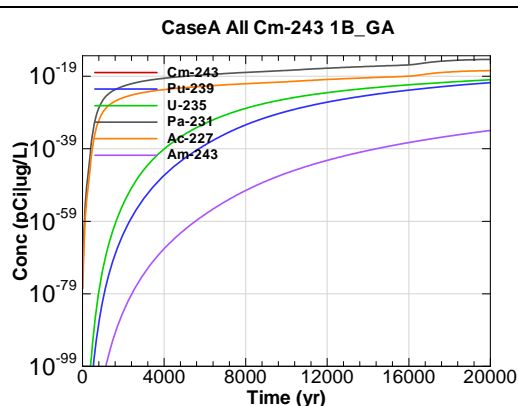


Figure F.3-170 - 1m Aquifer Concentration for
CaseA All Cm-243 1B_GA

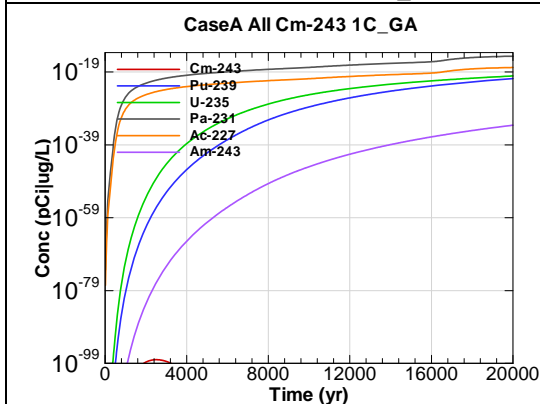


Figure F.3-171 - 1m Aquifer Concentration for
CaseA All Cm-243 1C_GA

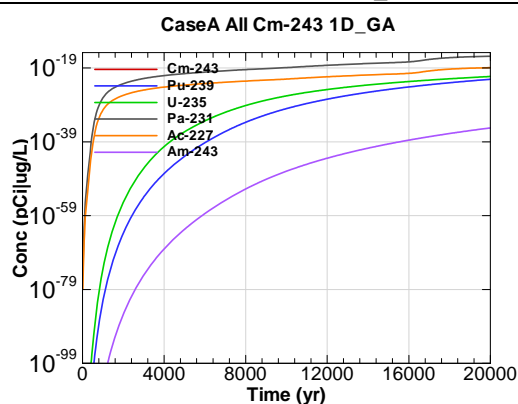


Figure F.3-172 - 1m Aquifer Concentration for
CaseA All Cm-243 1D_GA

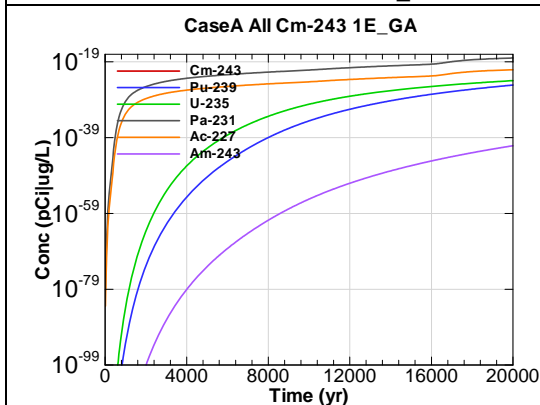


Figure F.3-173 - 1m Aquifer Concentration for
CaseA All Cm-243 1E_GA

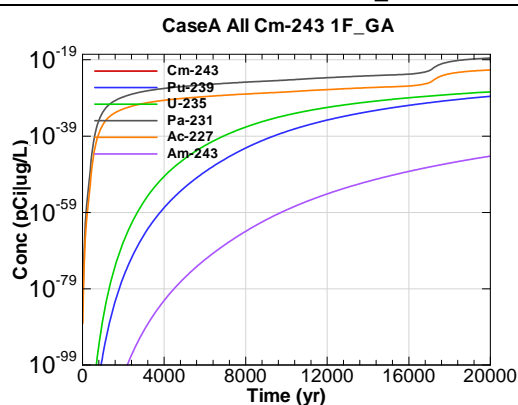
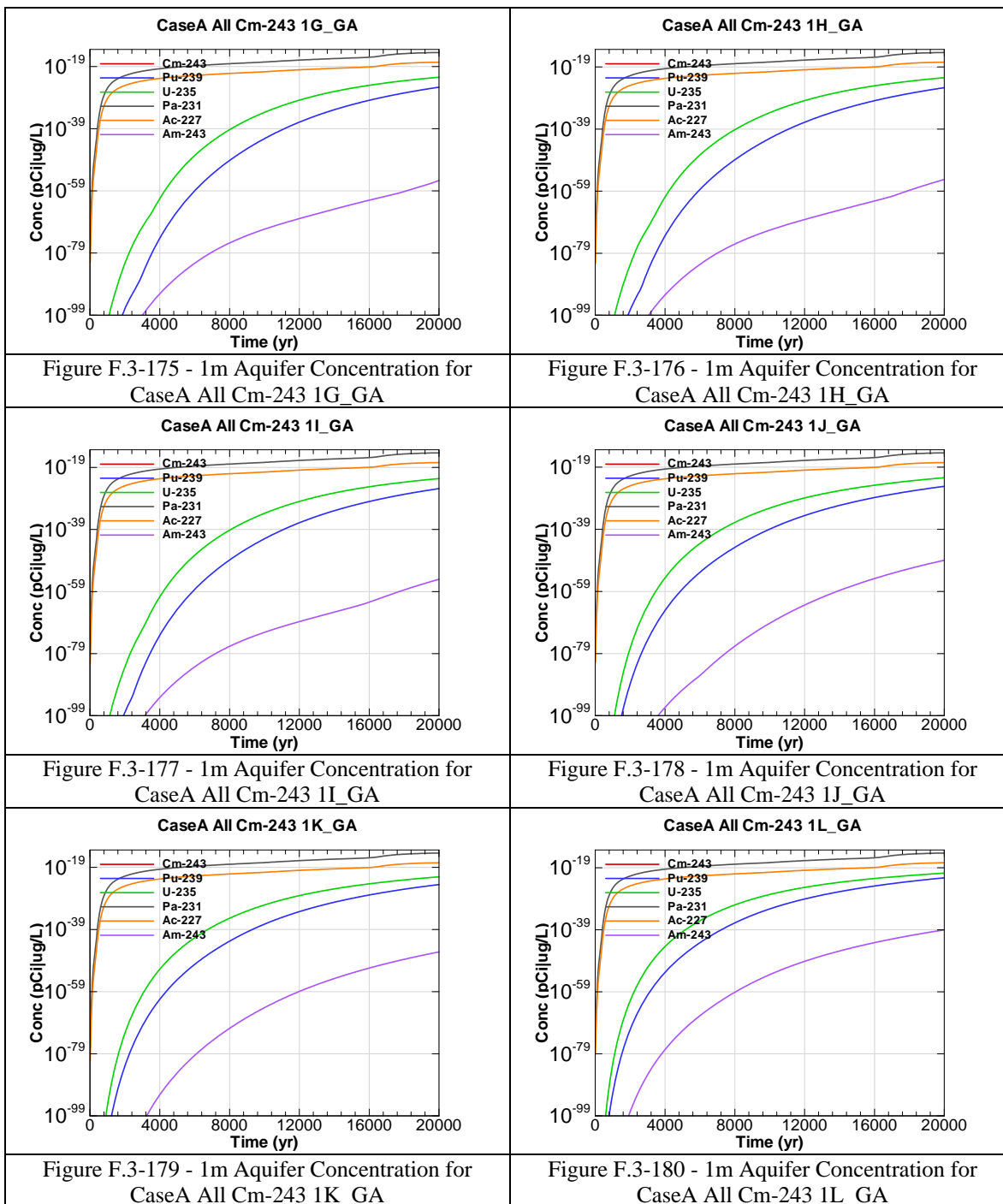
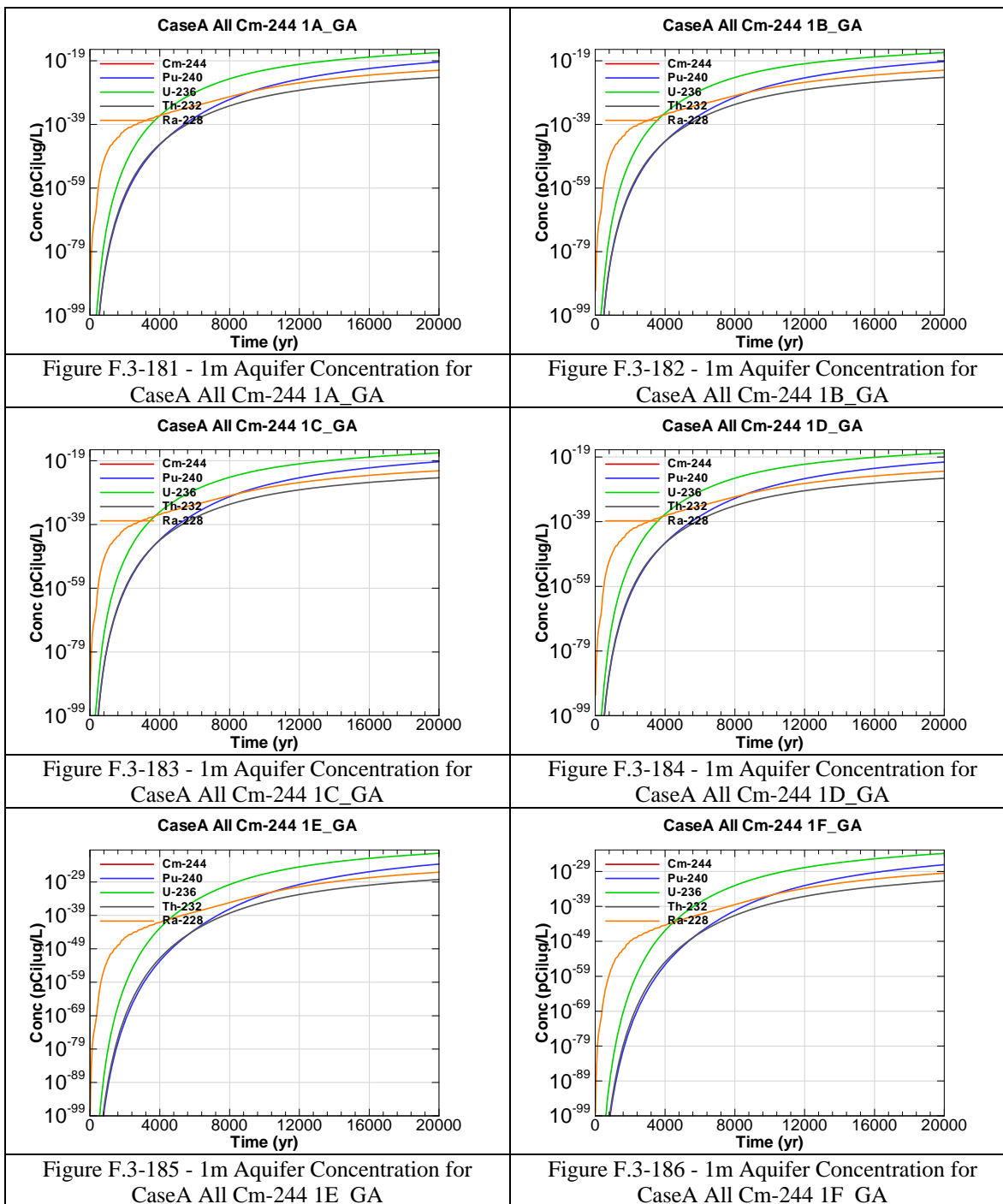
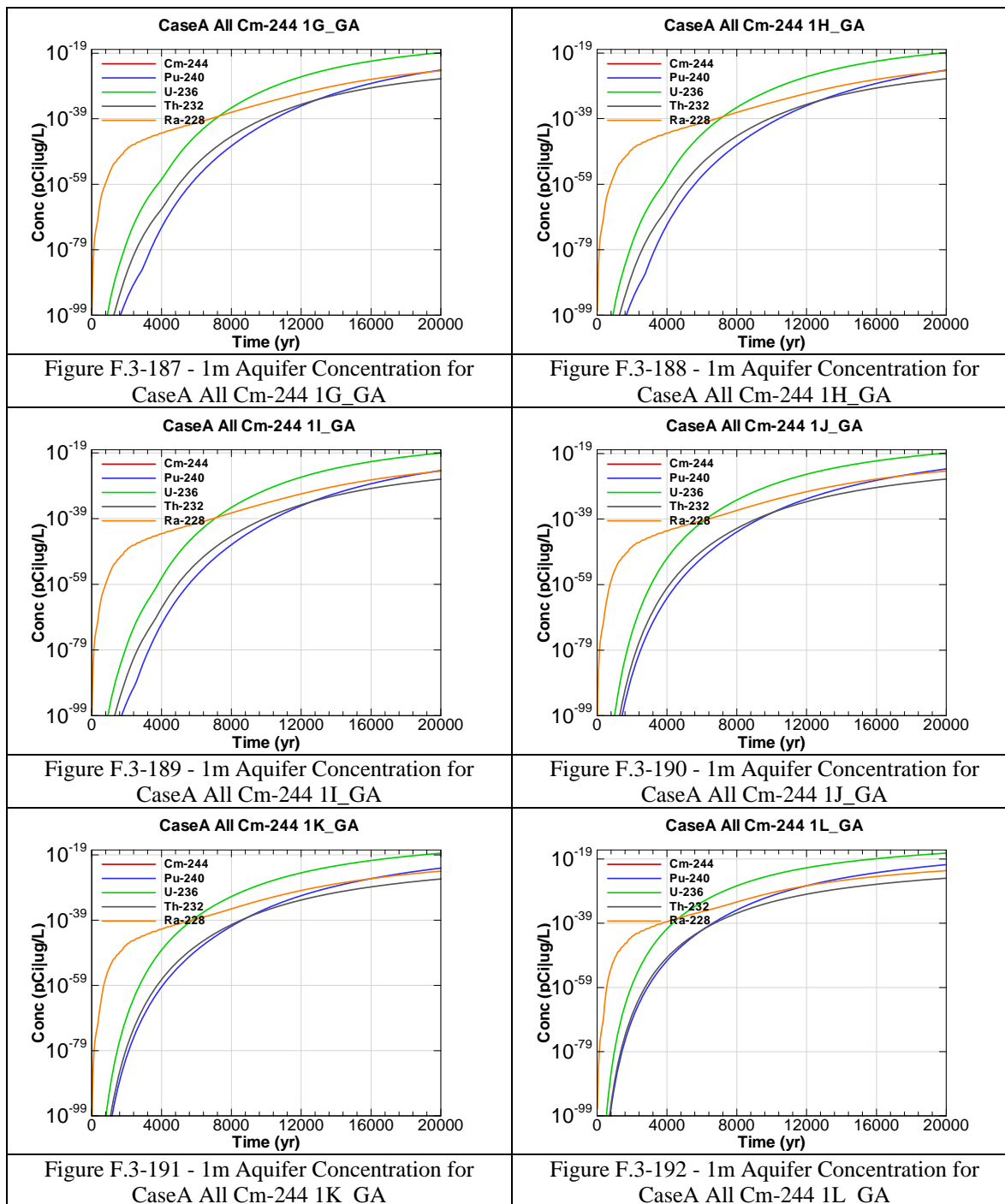
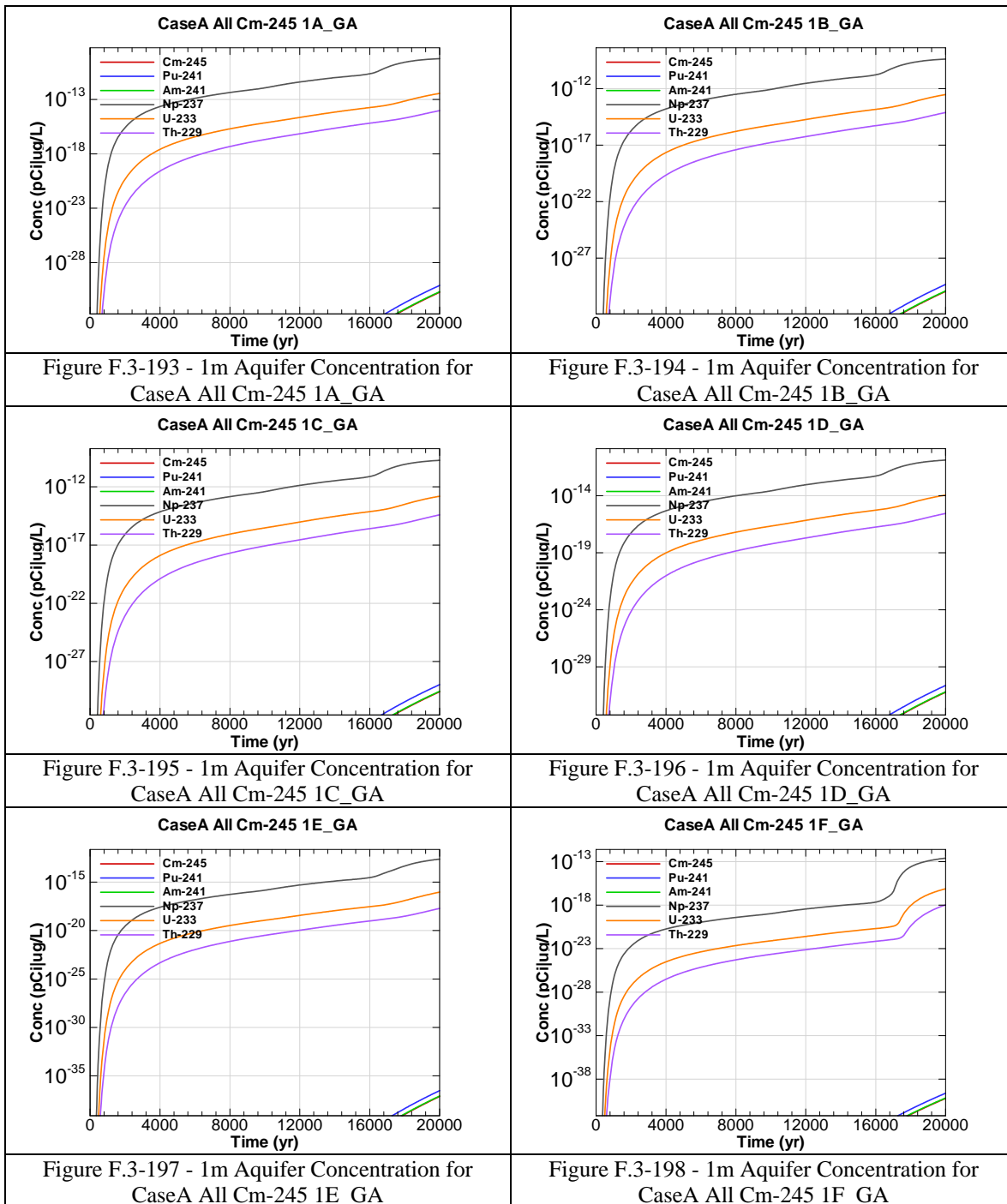


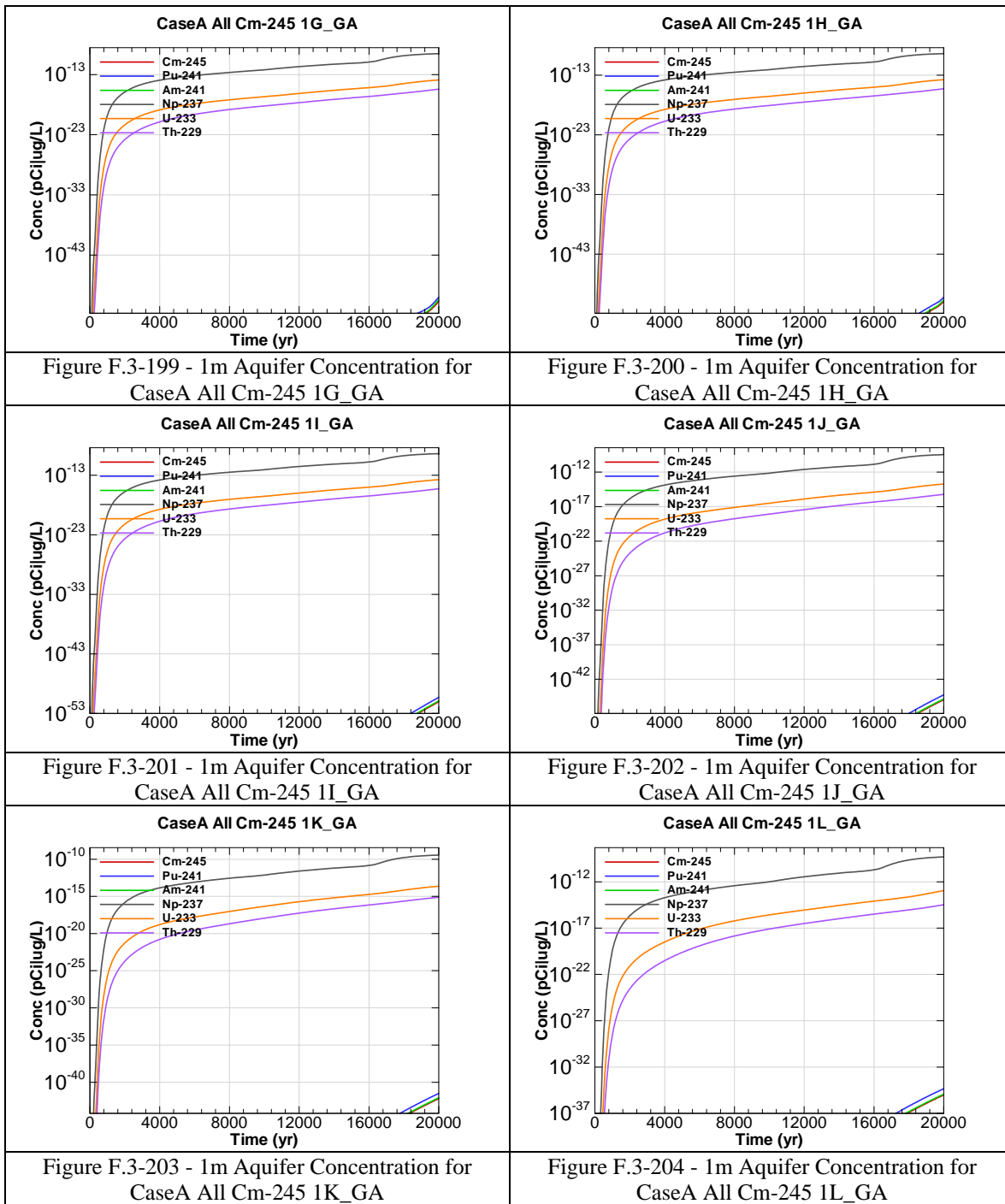
Figure F.3-174 - 1m Aquifer Concentration for
CaseA All Cm-243 1F_GA

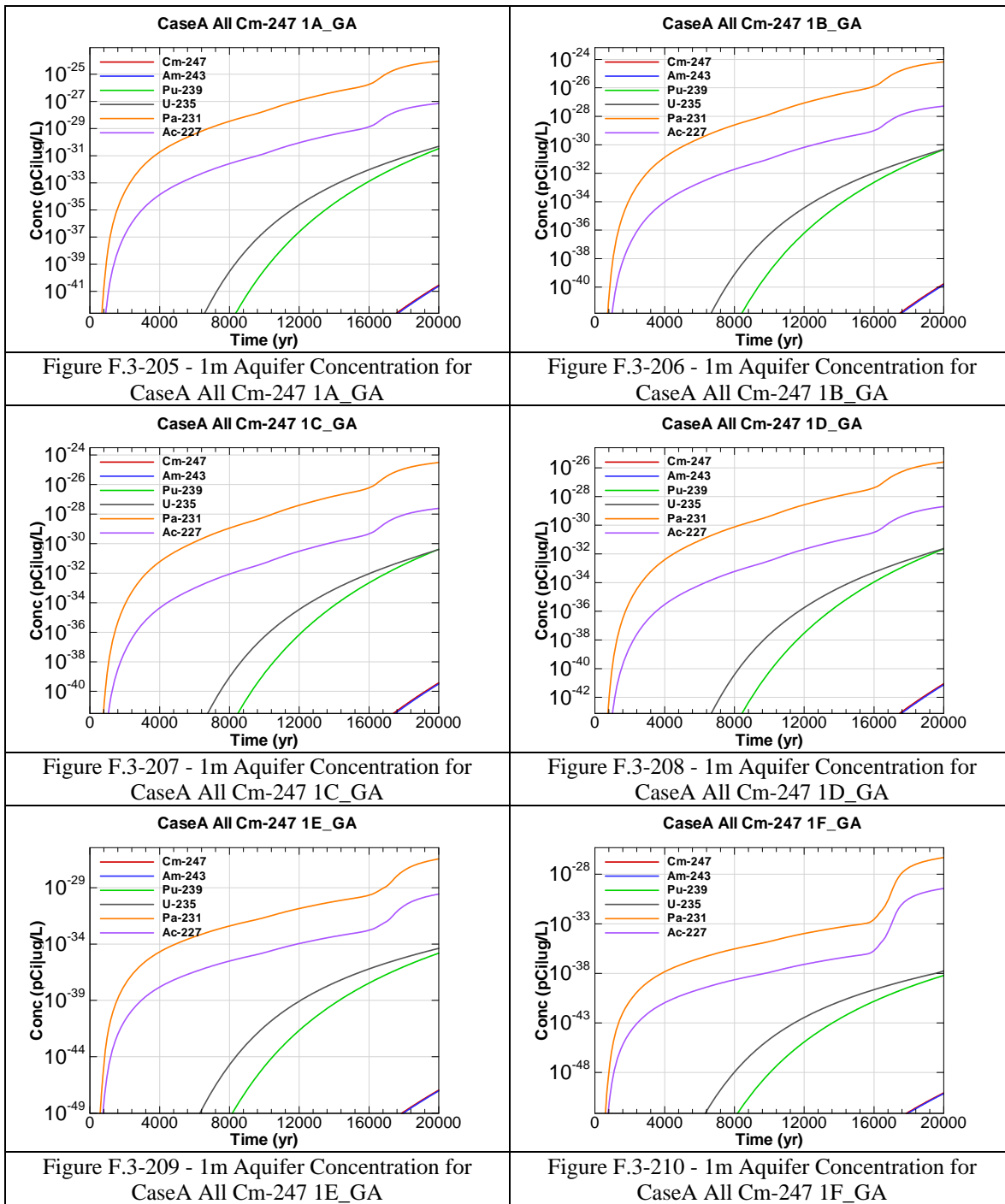


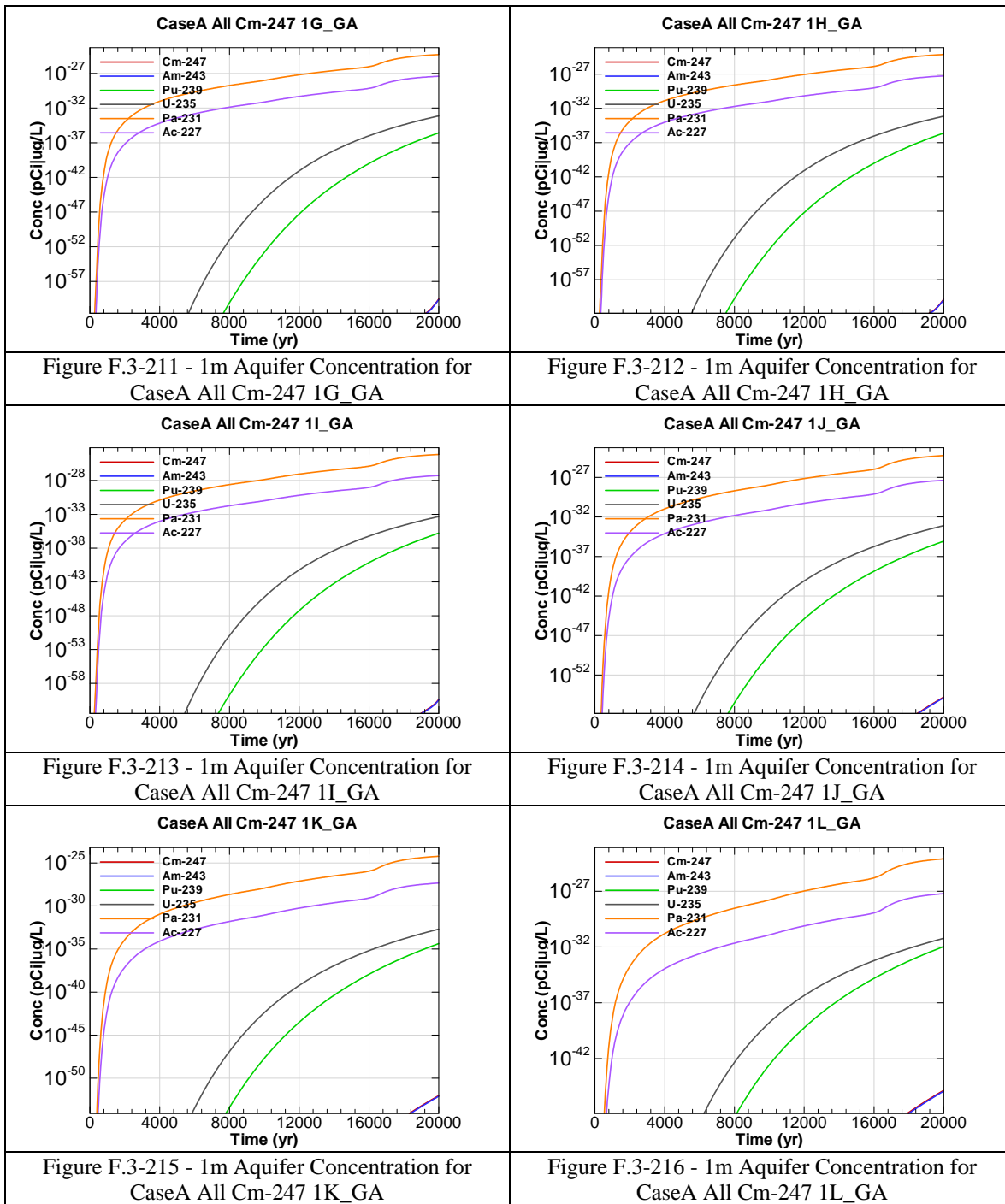


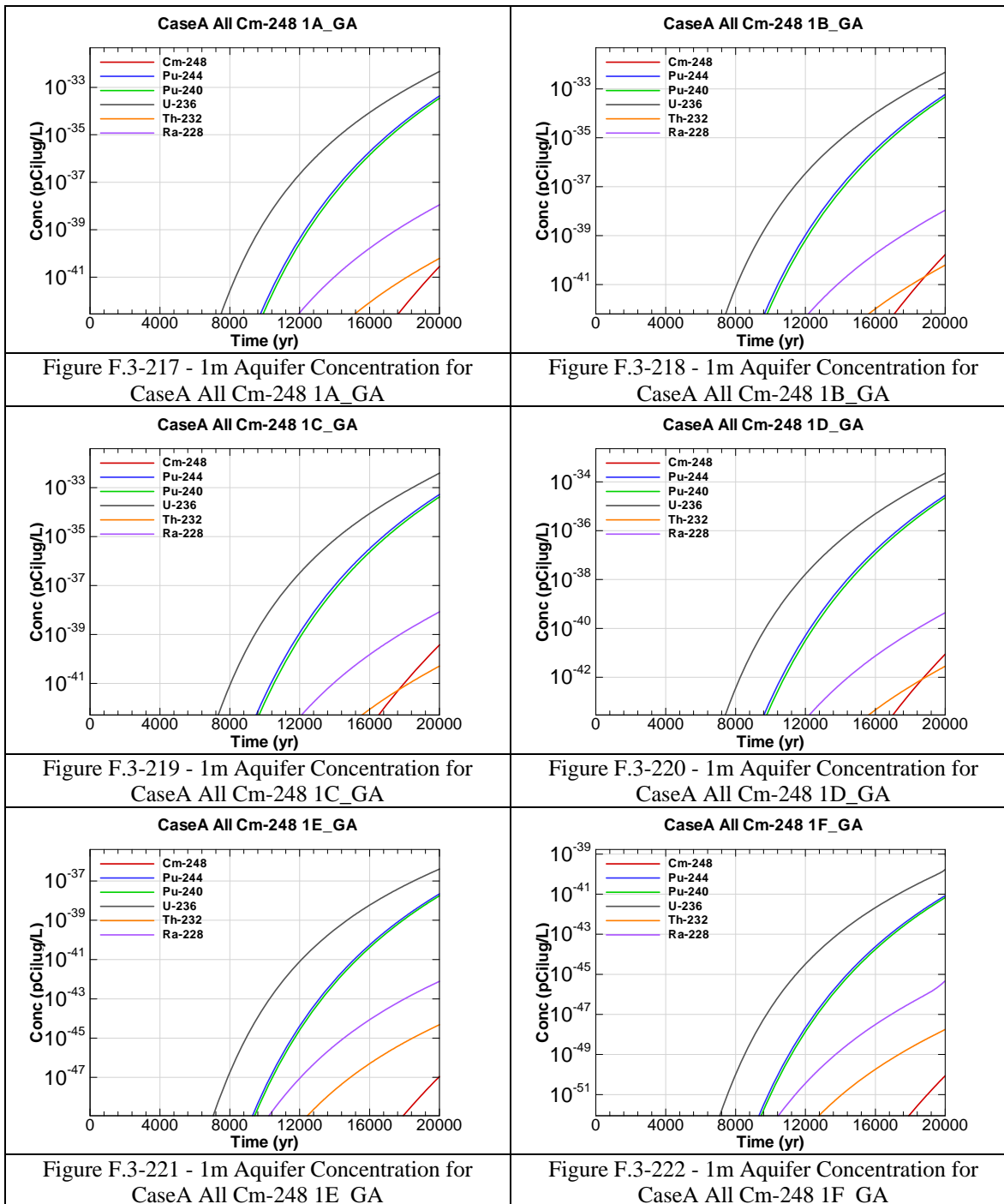












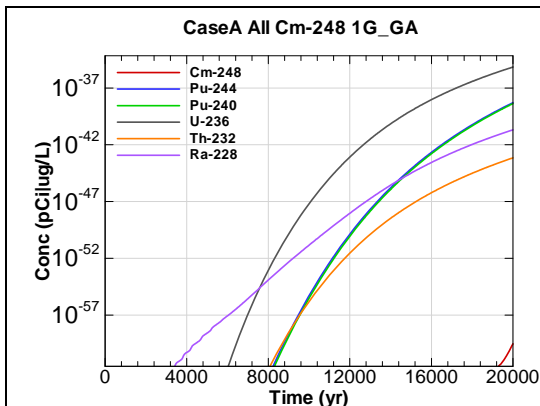


Figure F.3-223 - 1m Aquifer Concentration for
CaseA All Cm-248 1G_GA

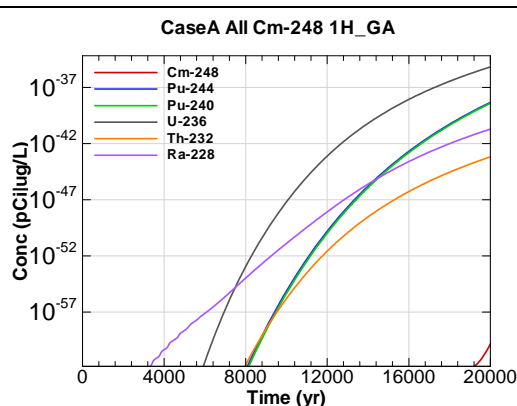


Figure F.3-224 - 1m Aquifer Concentration for
CaseA All Cm-248 1H_GA

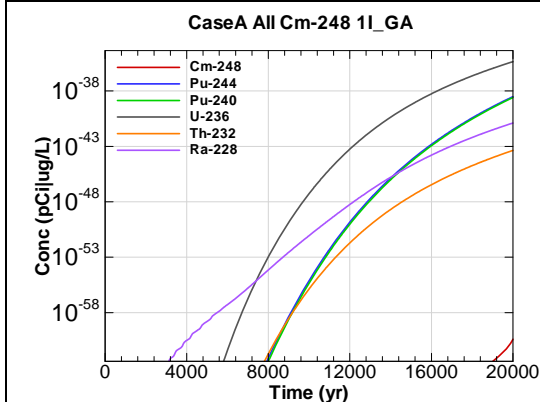


Figure F.3-225 - 1m Aquifer Concentration for
CaseA All Cm-248 1I_GA

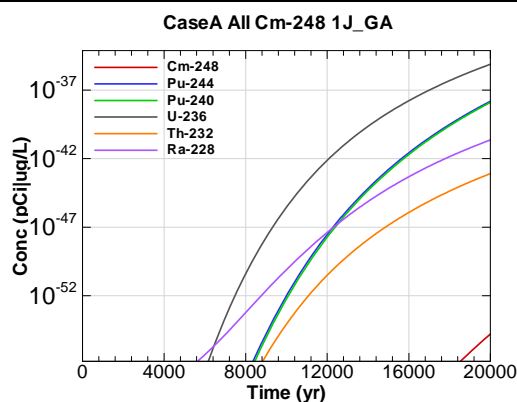


Figure F.3-226 - 1m Aquifer Concentration for
CaseA All Cm-248 1J_GA

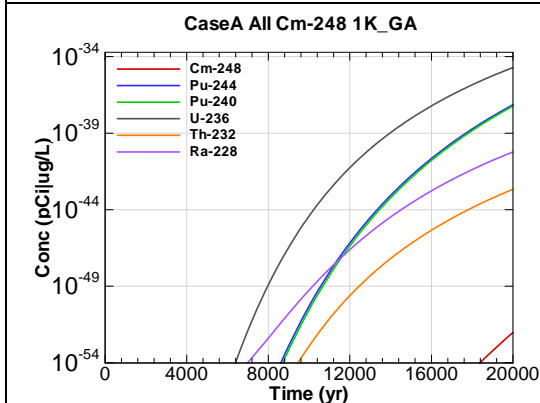


Figure F.3-227 - 1m Aquifer Concentration for
CaseA All Cm-248 1K_GA

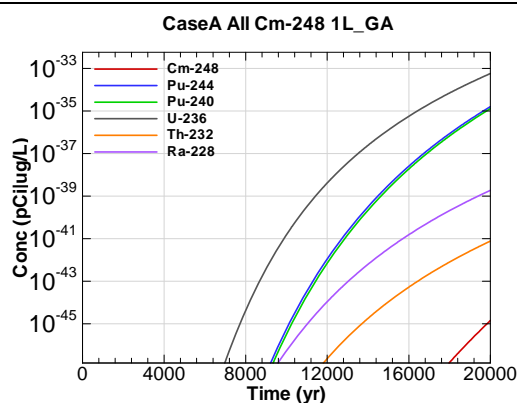
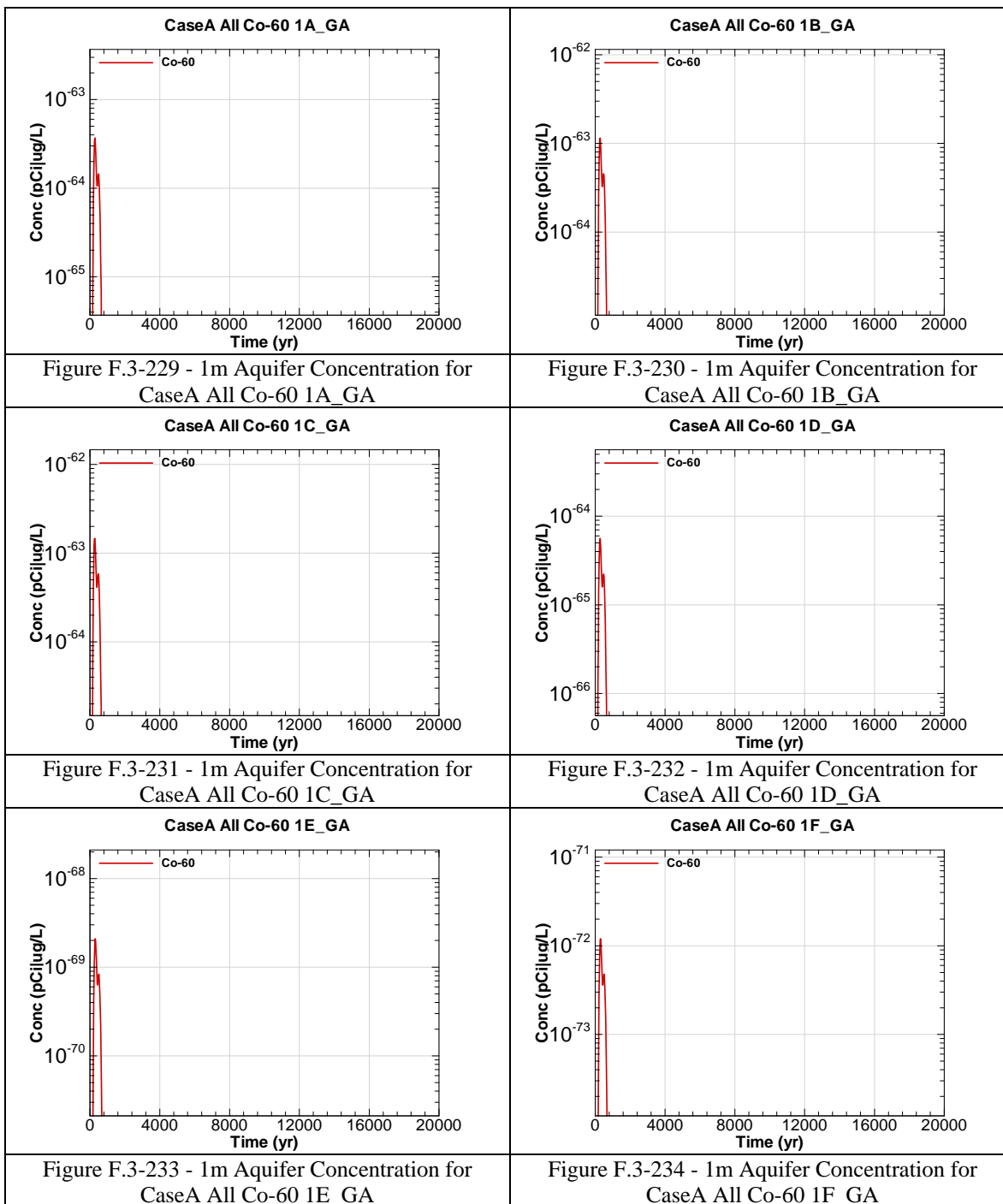
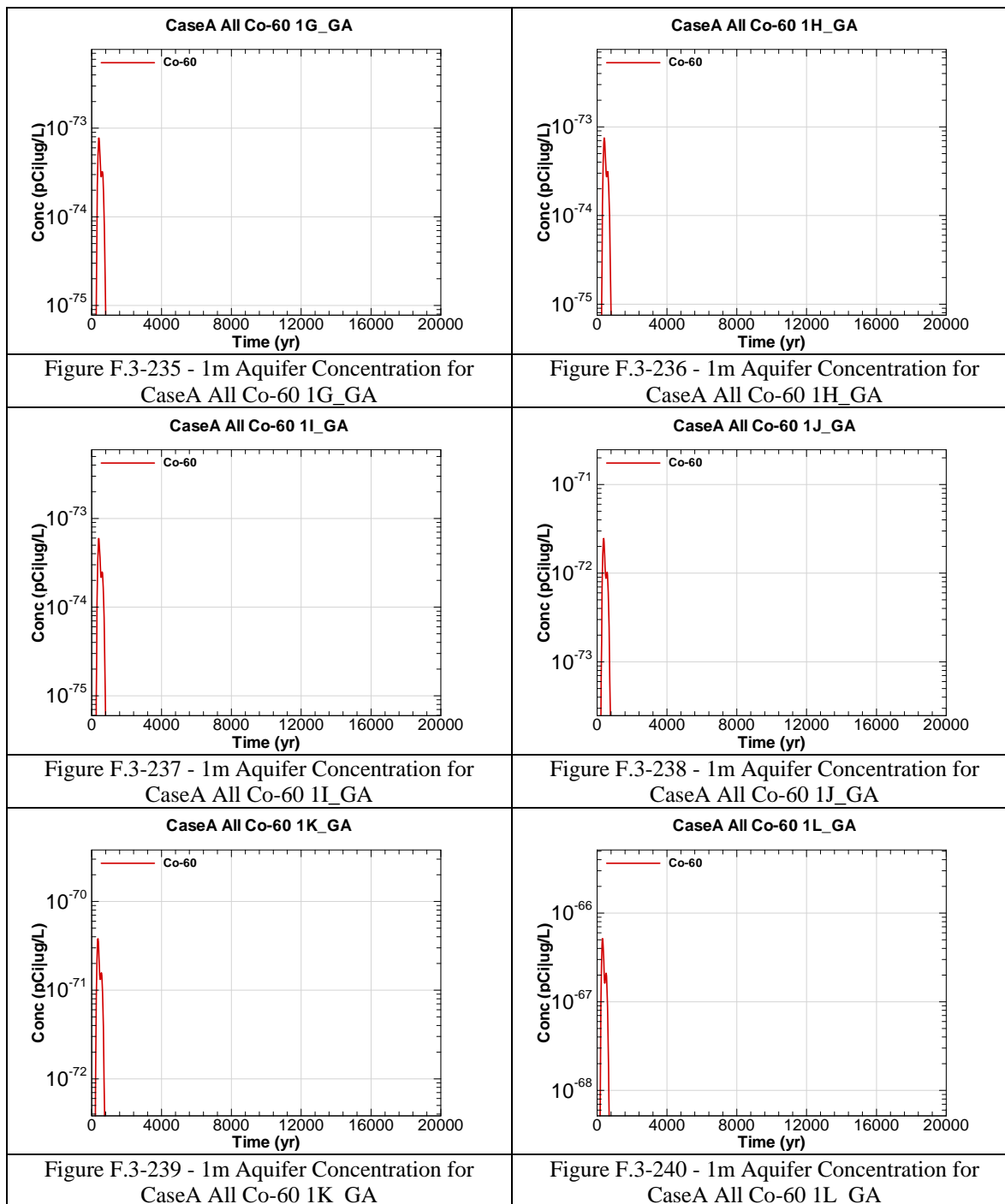
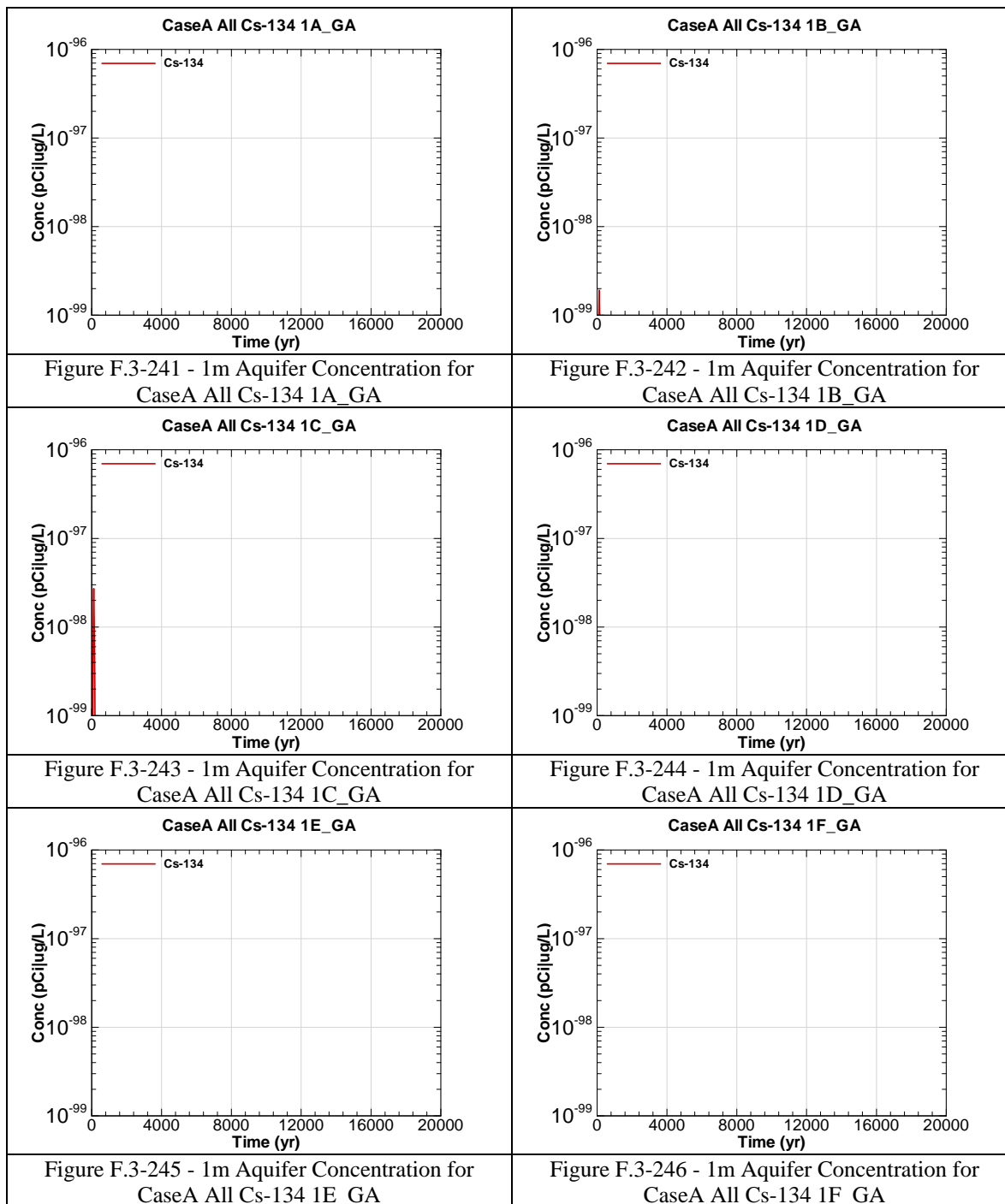
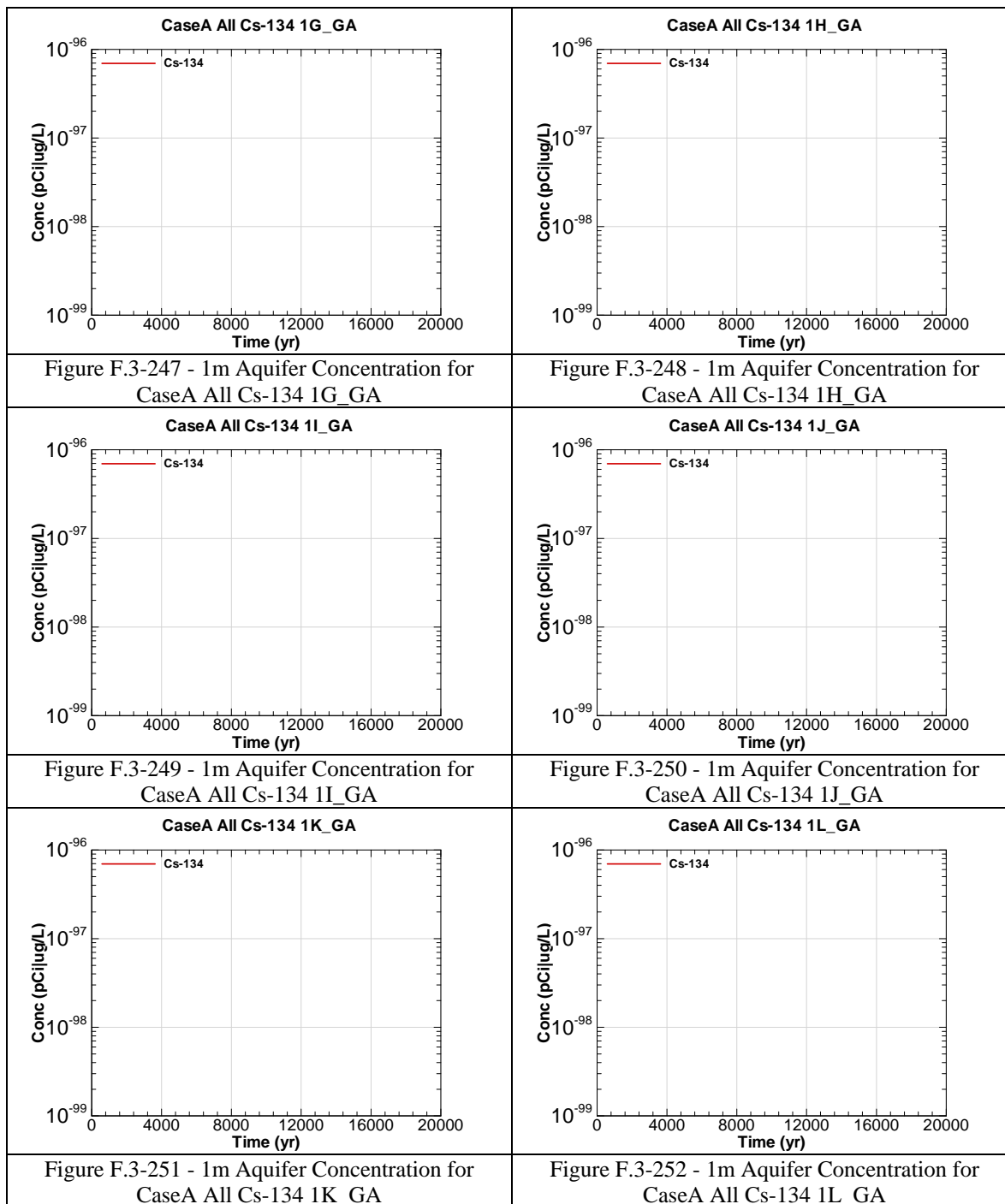


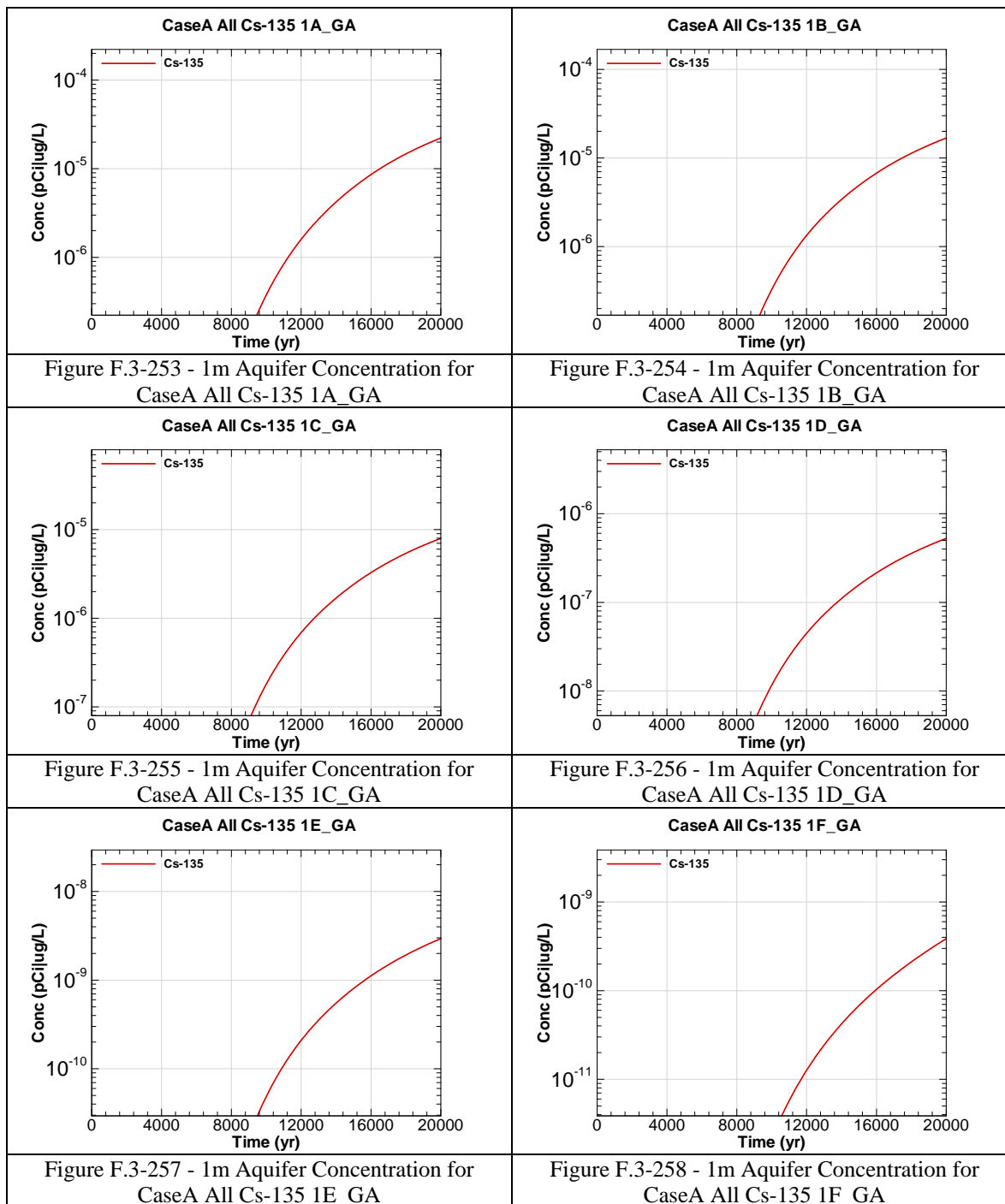
Figure F.3-228 - 1m Aquifer Concentration for
CaseA All Cm-248 1L_GA

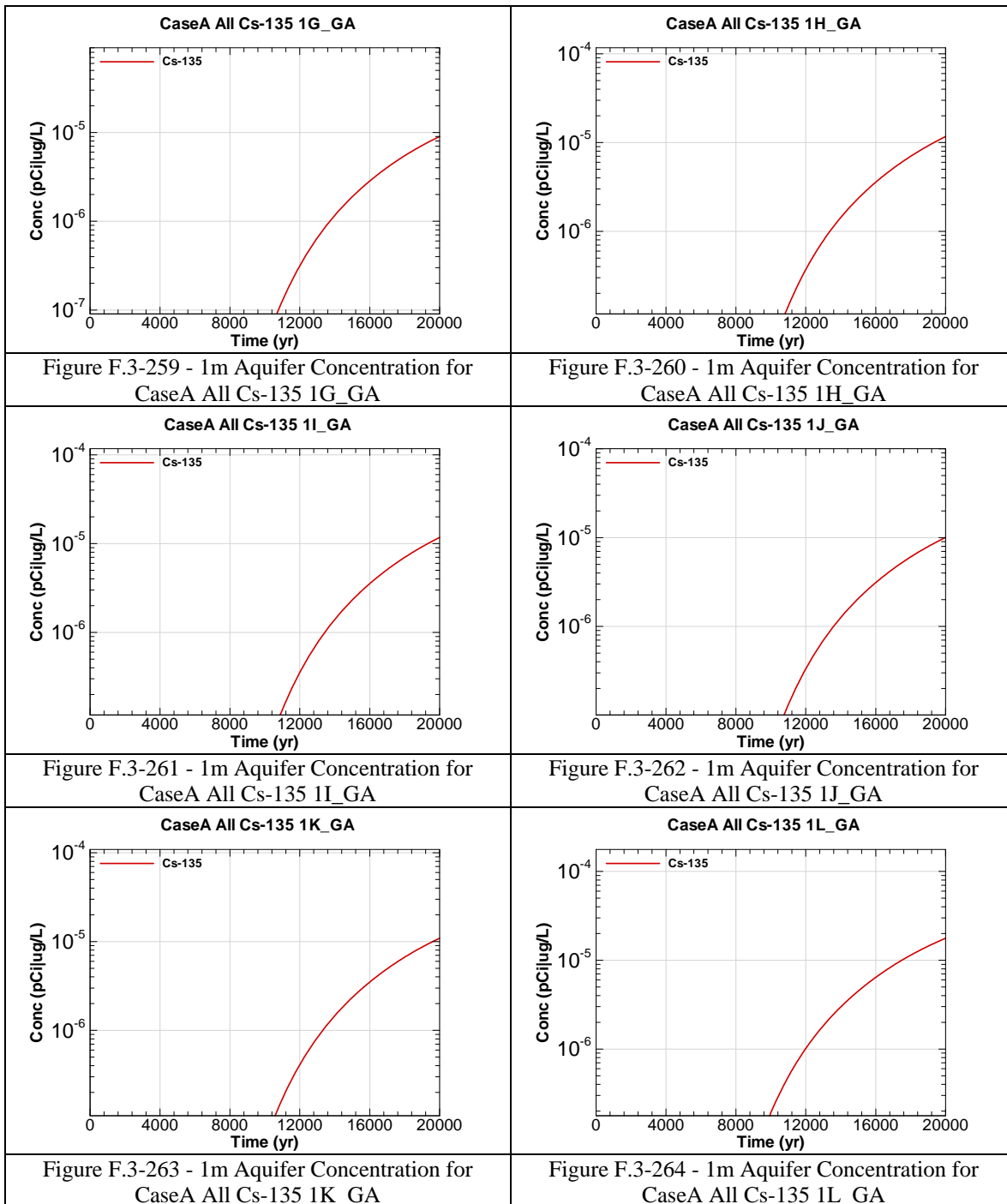


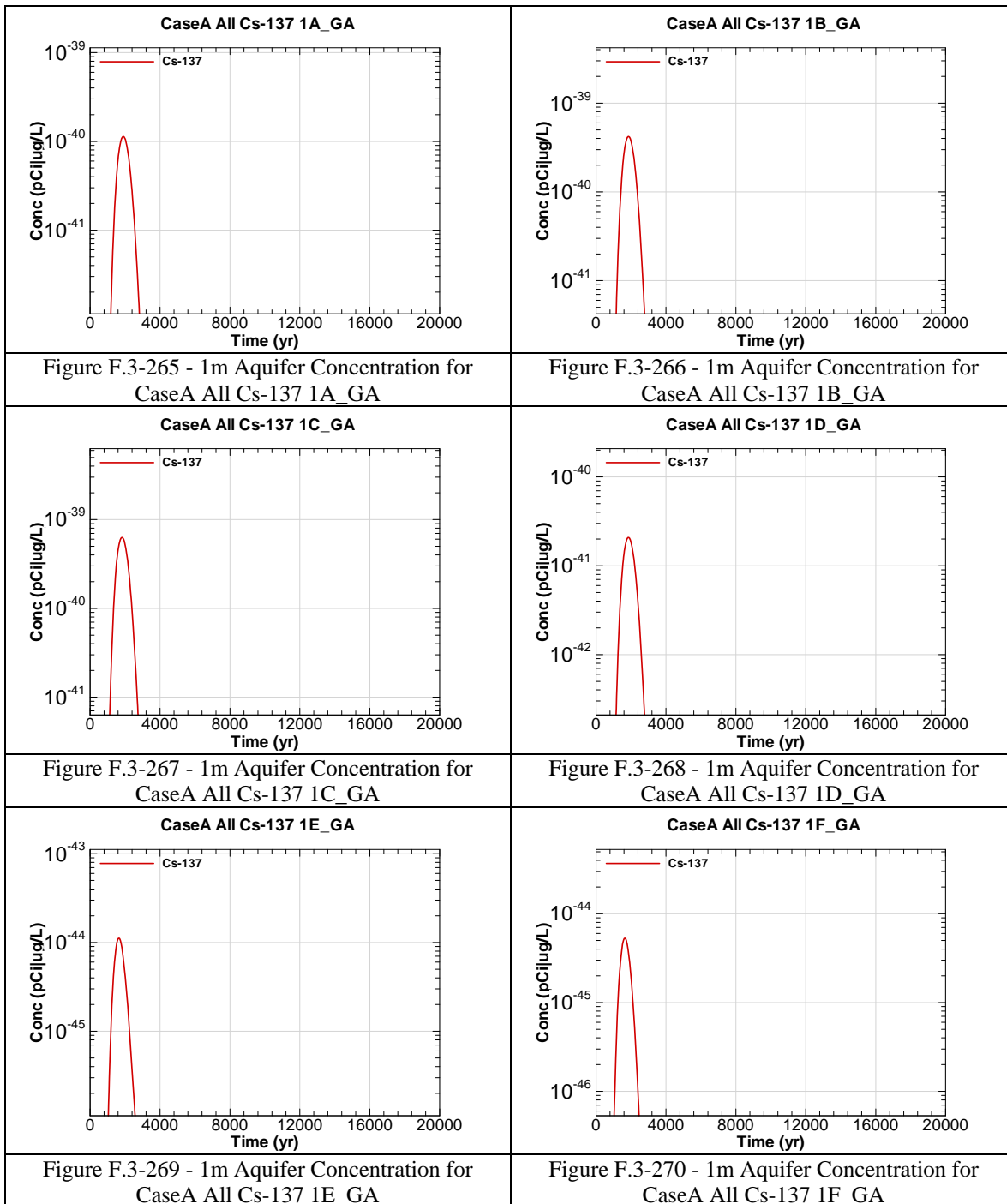


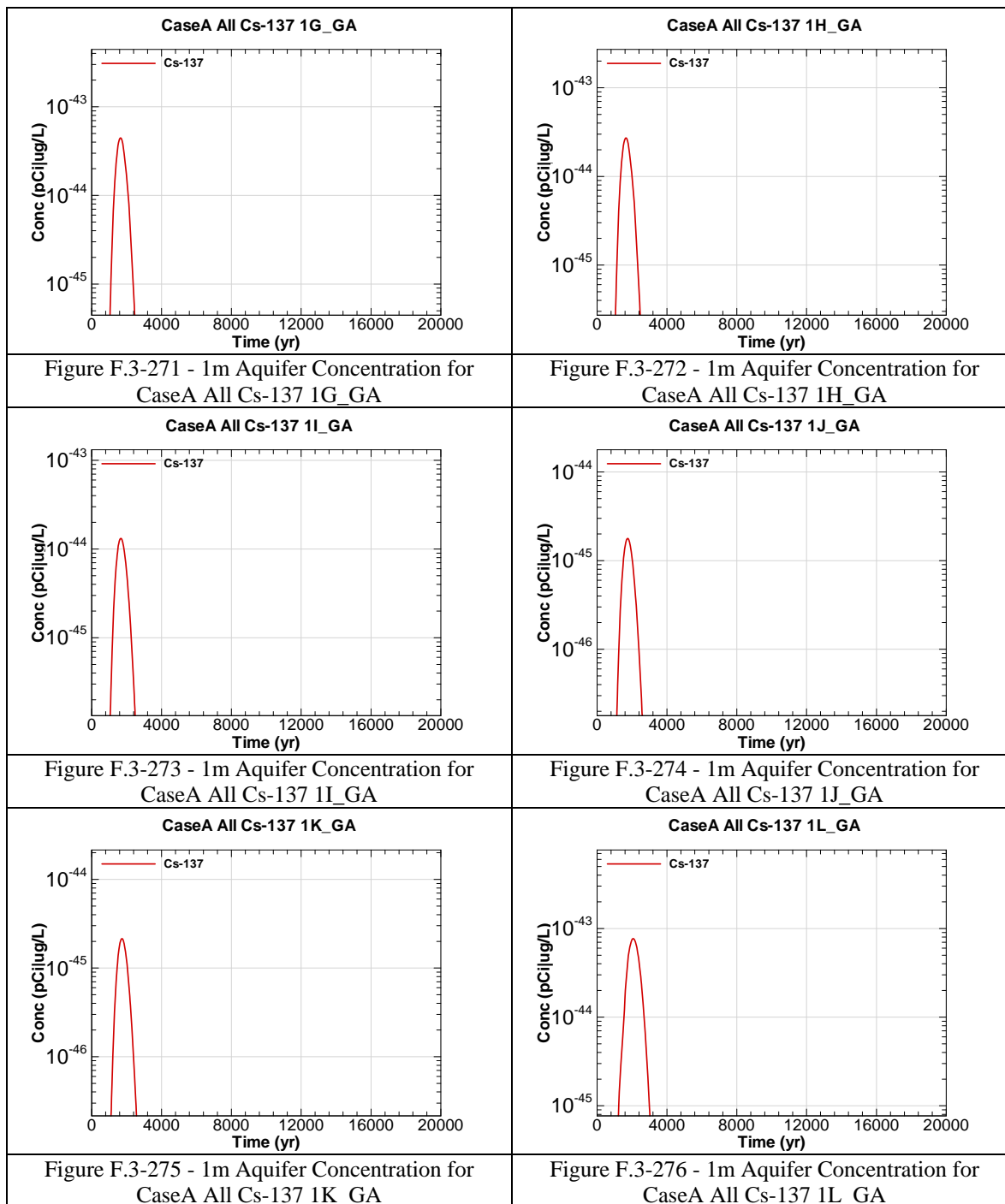


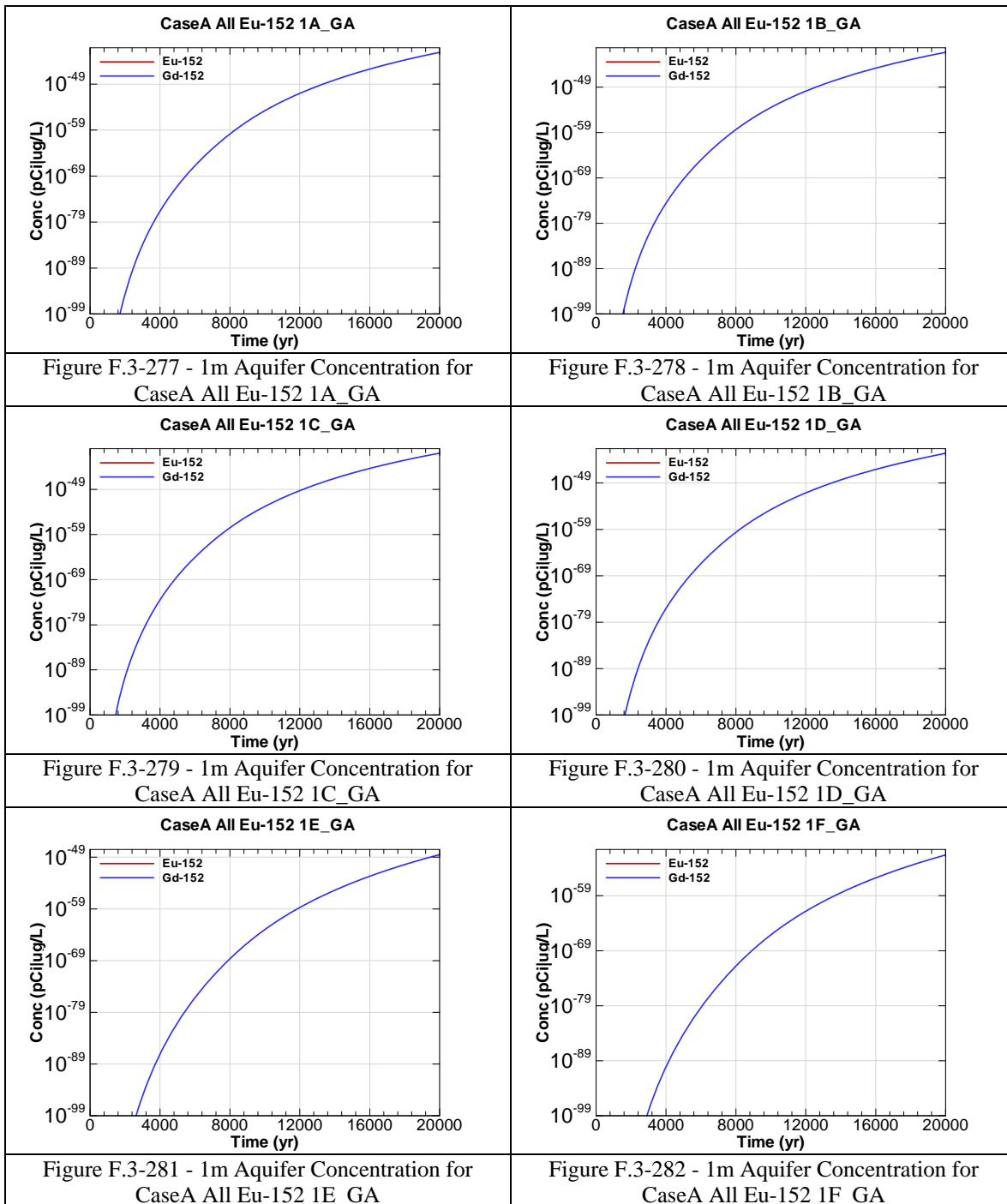


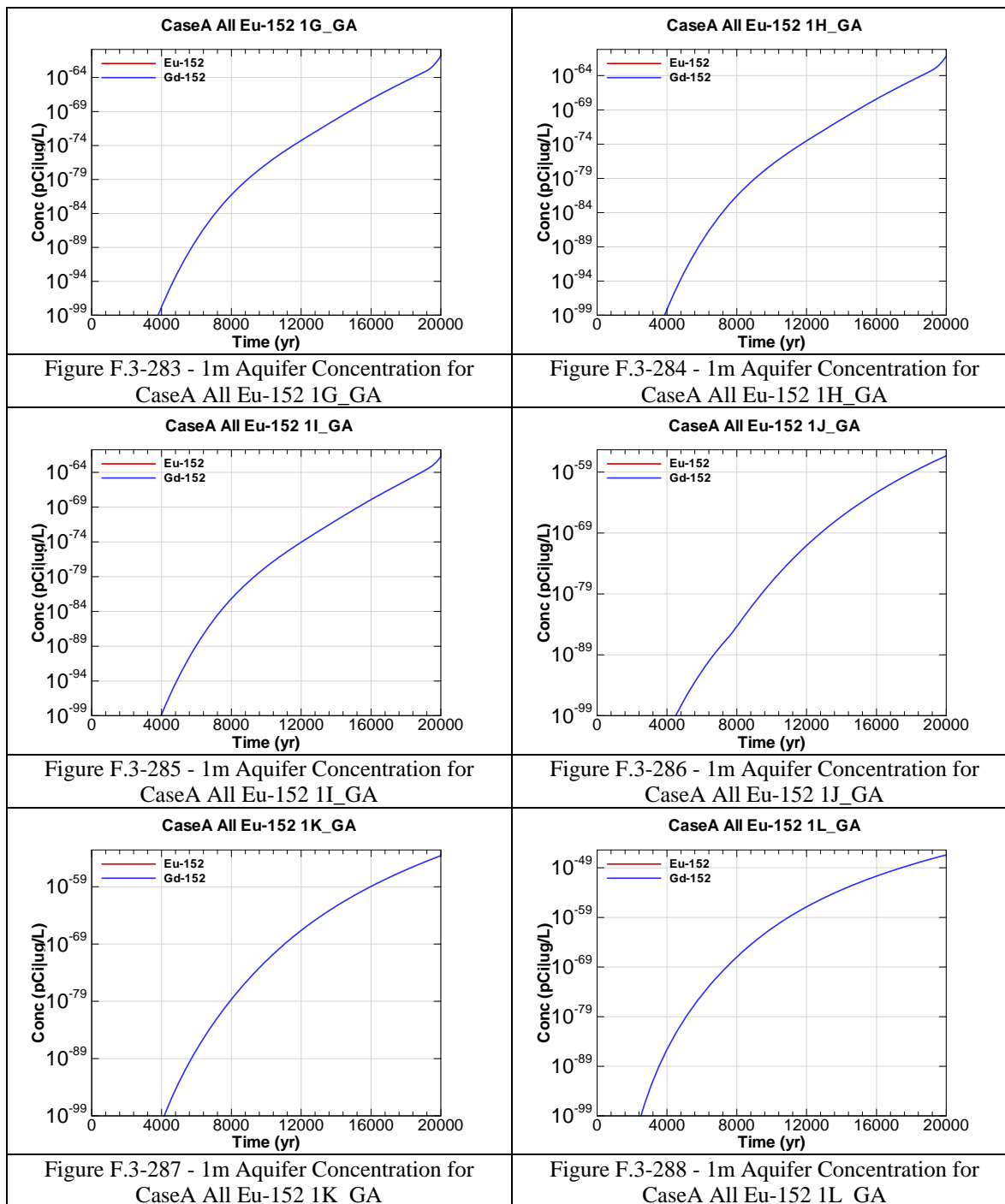


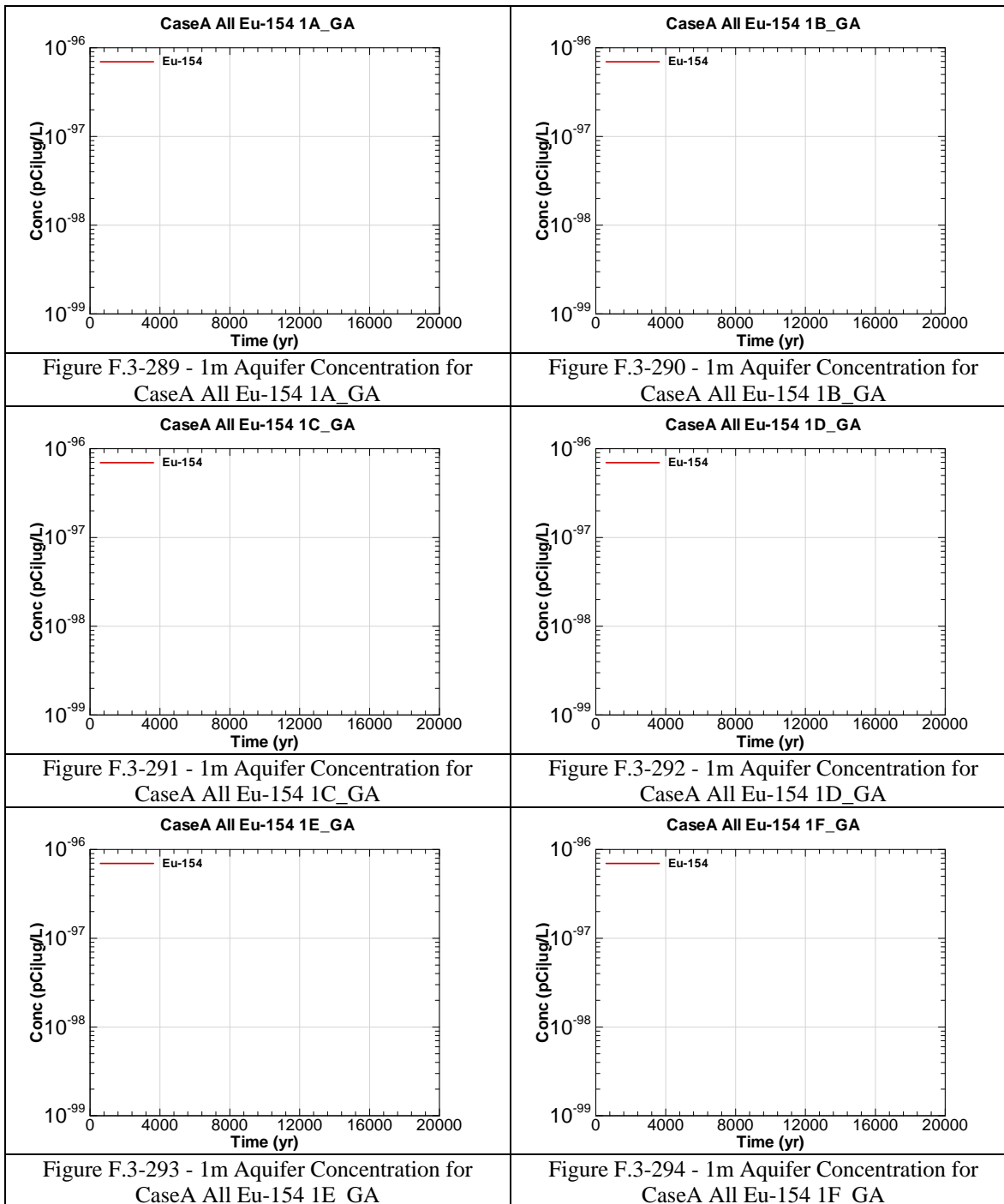


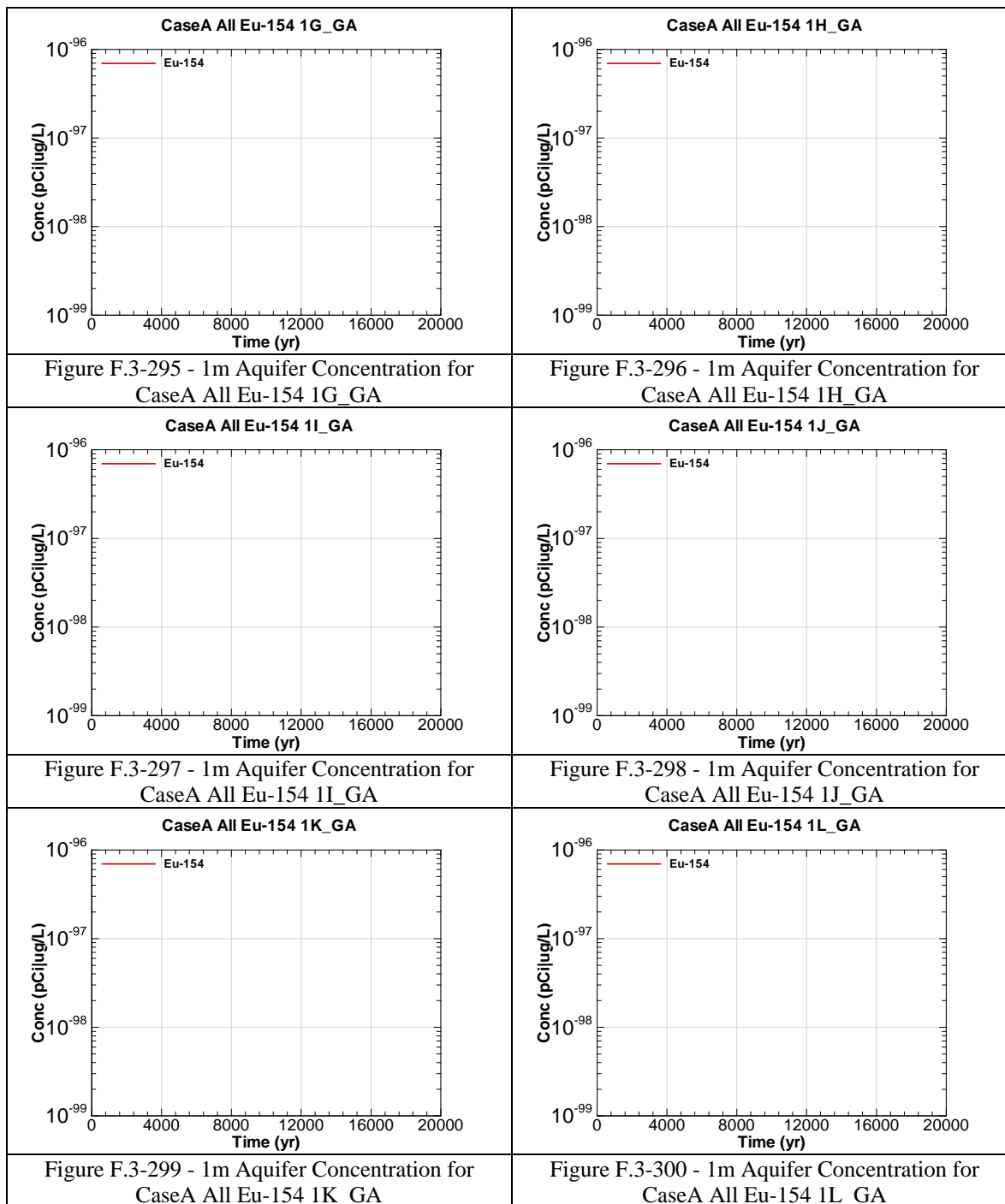


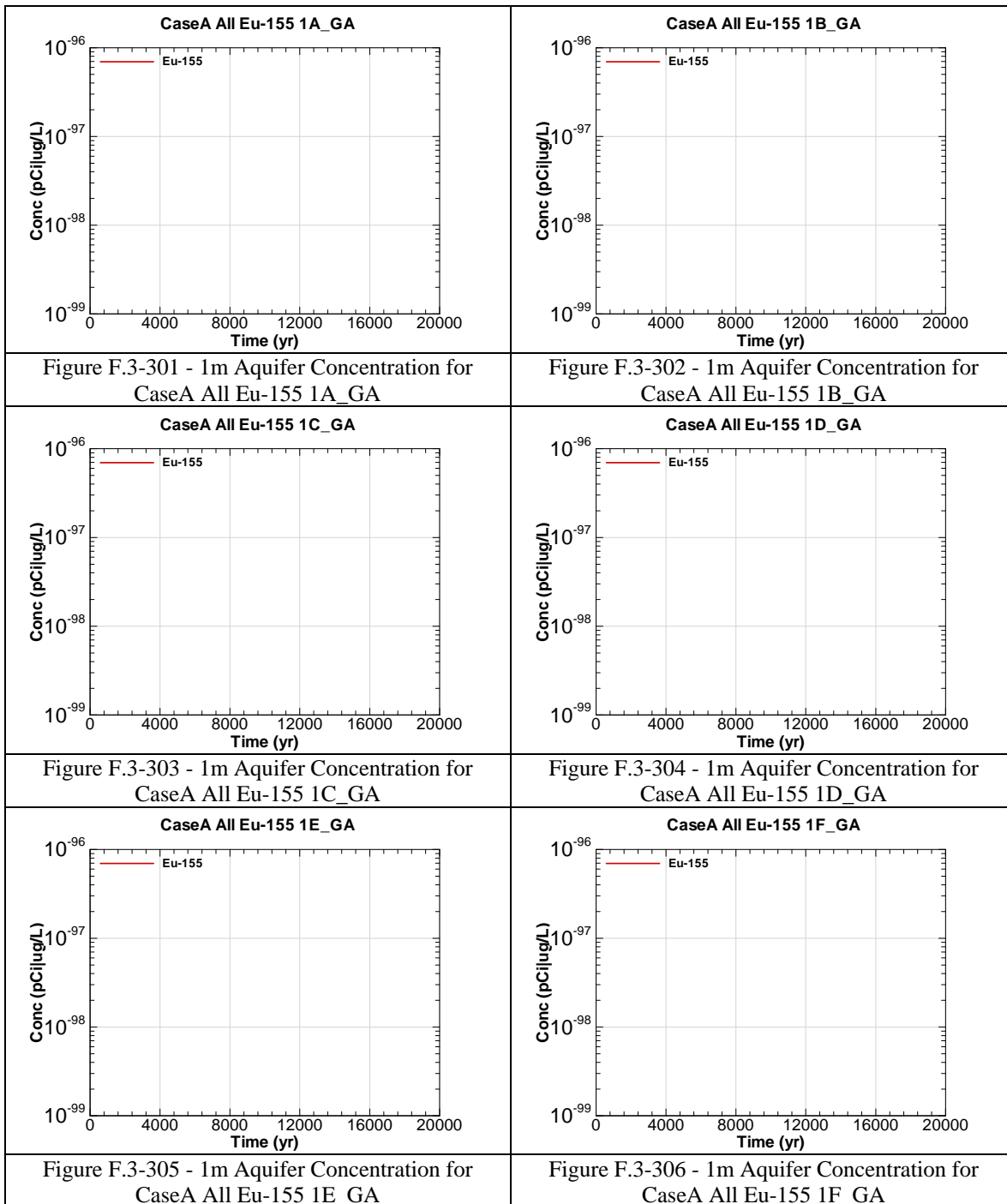


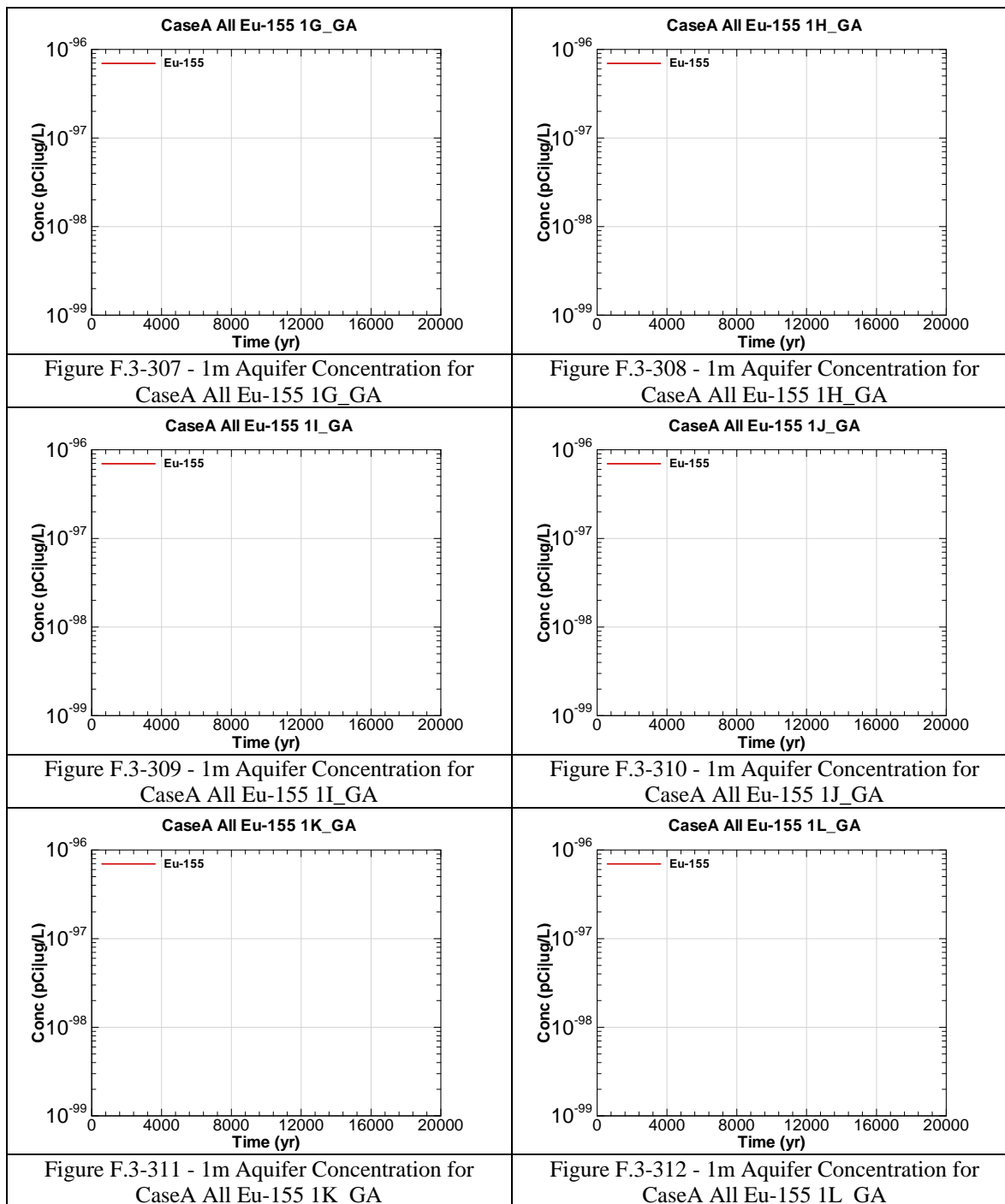


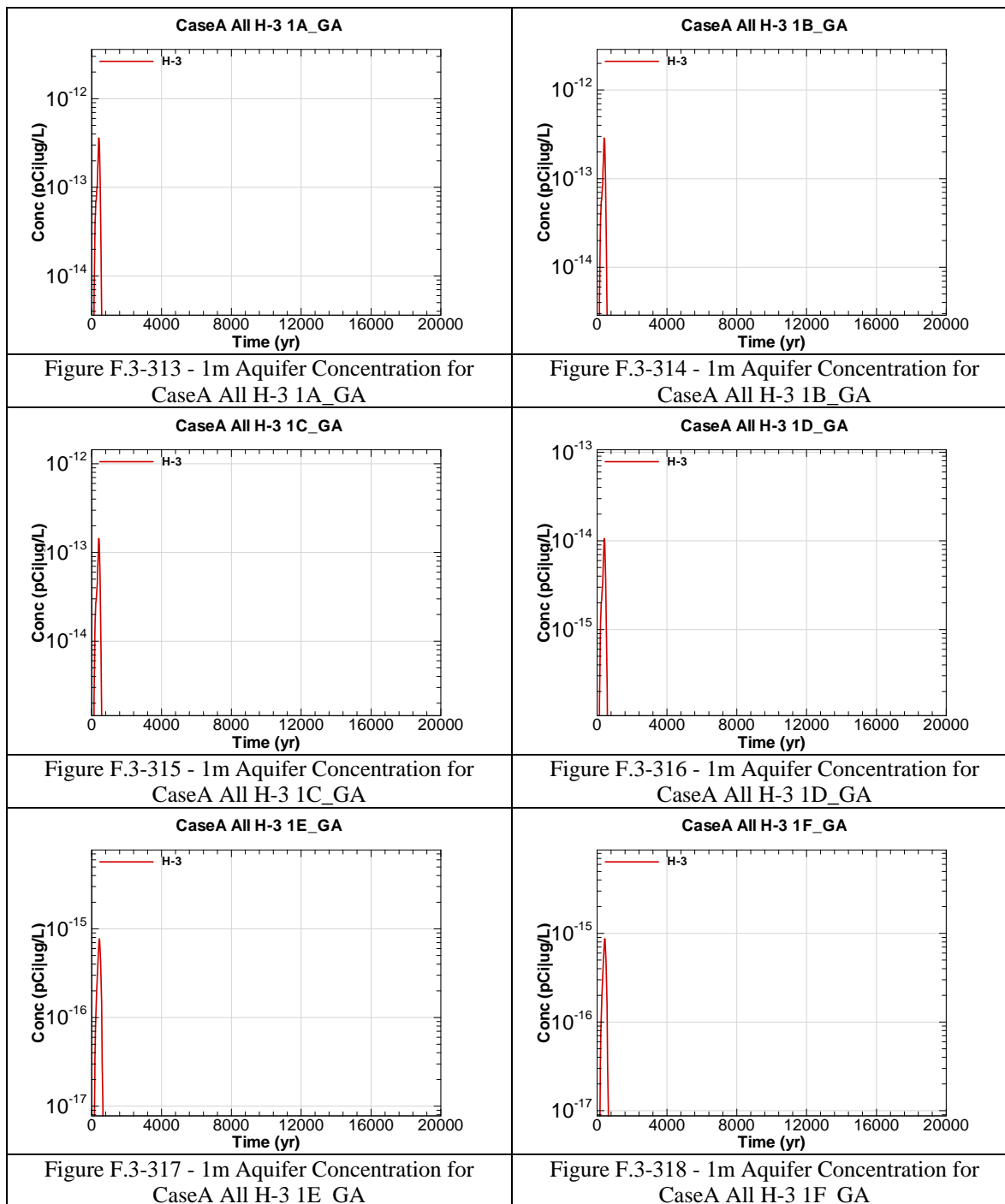


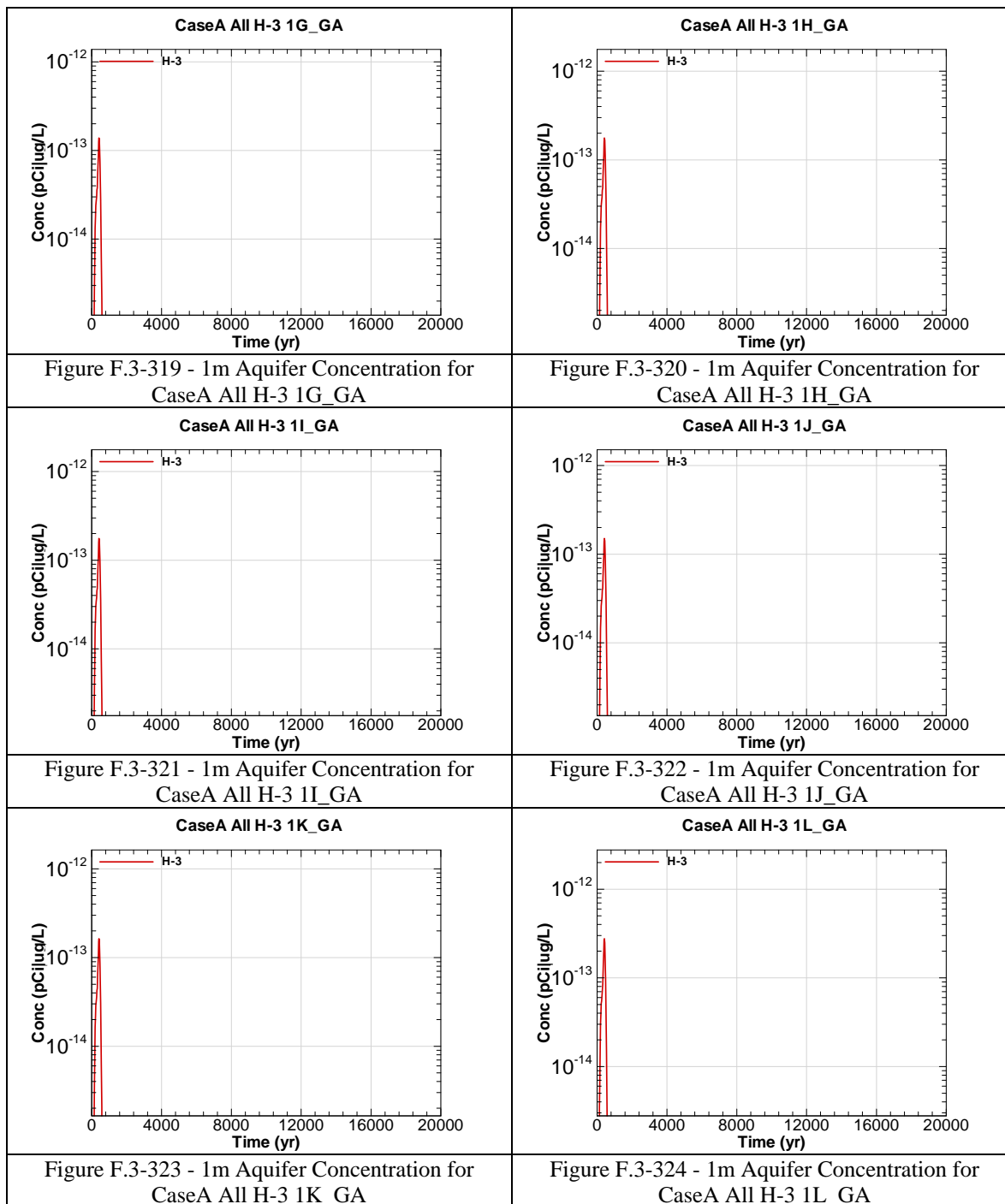


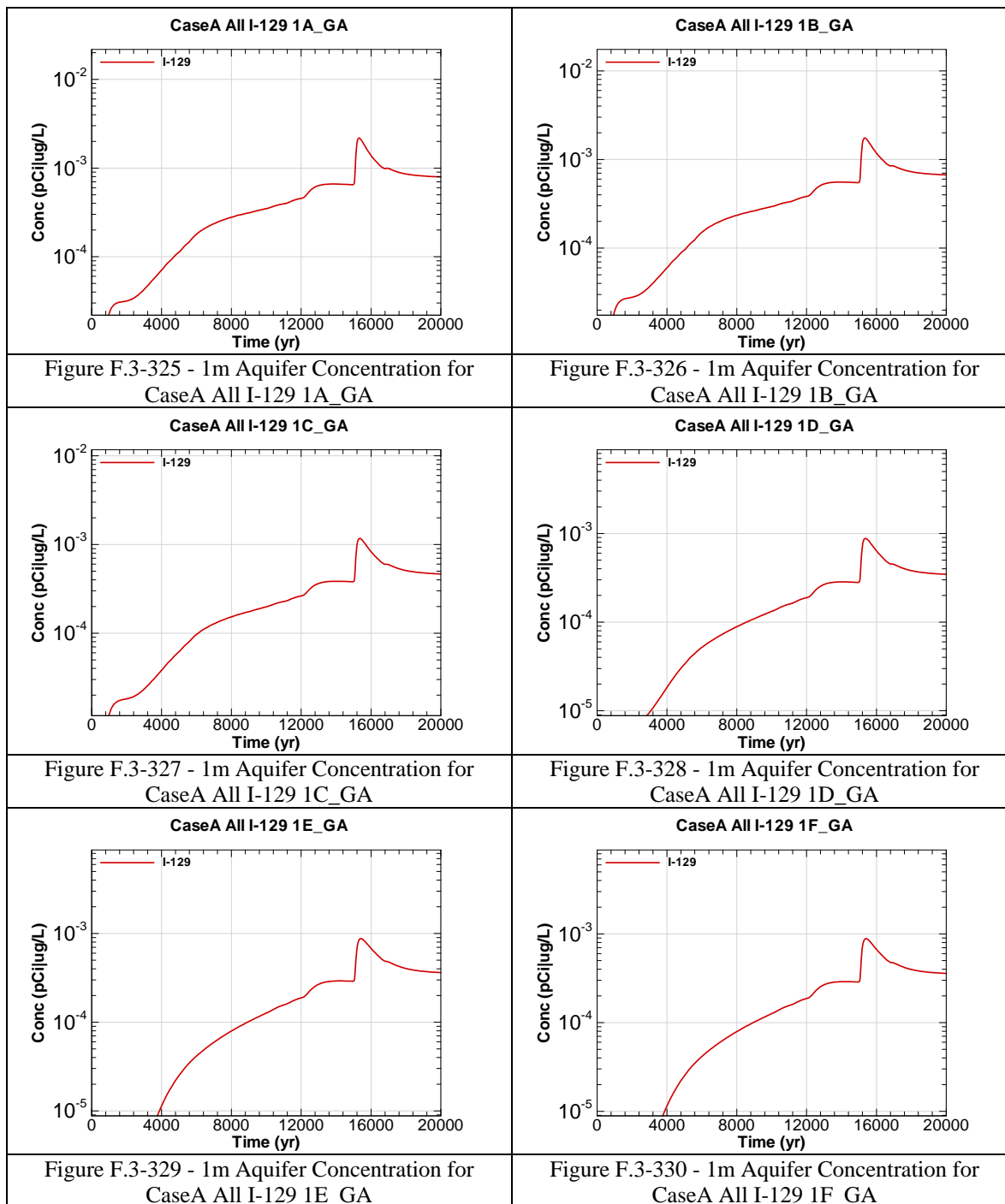


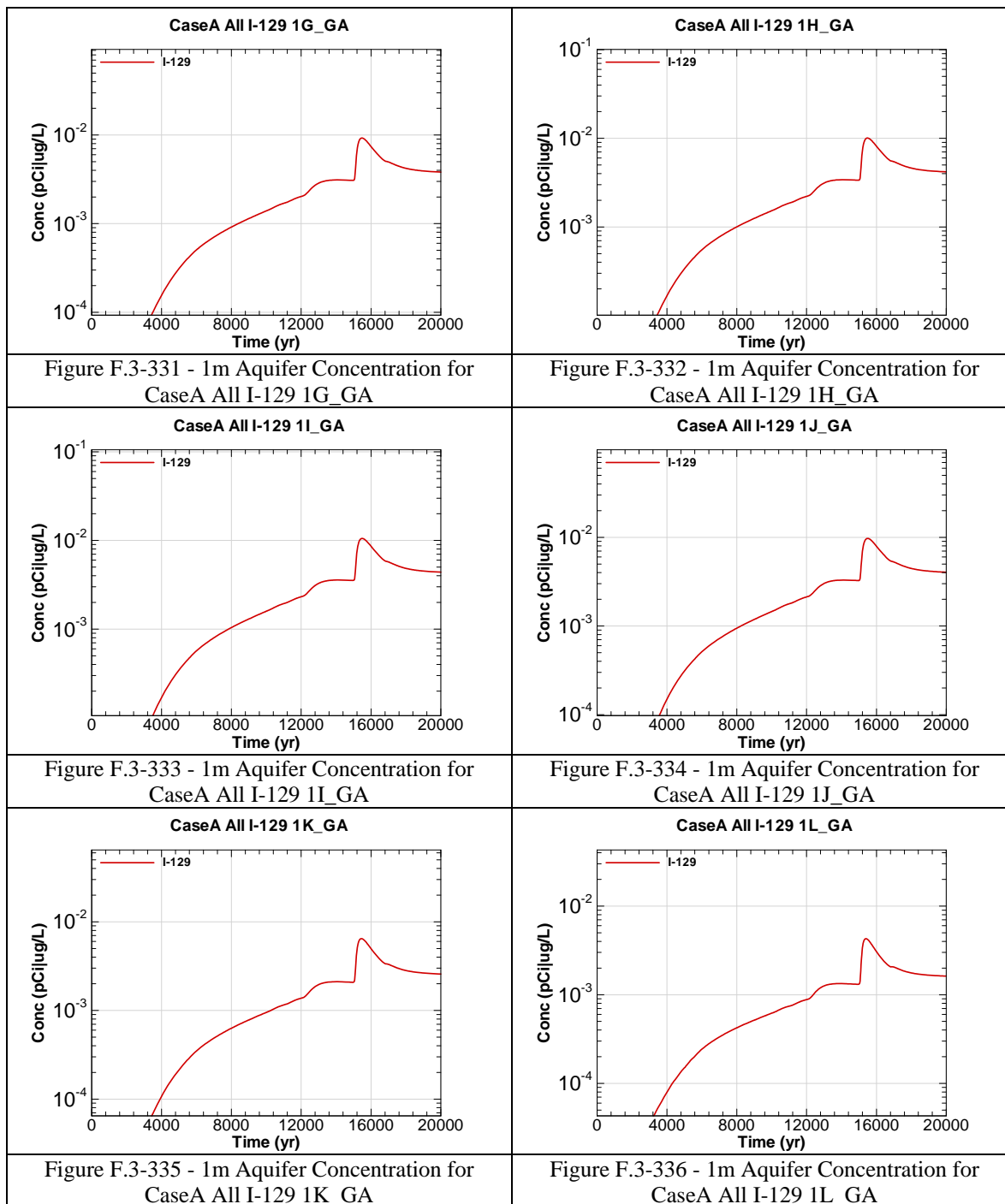


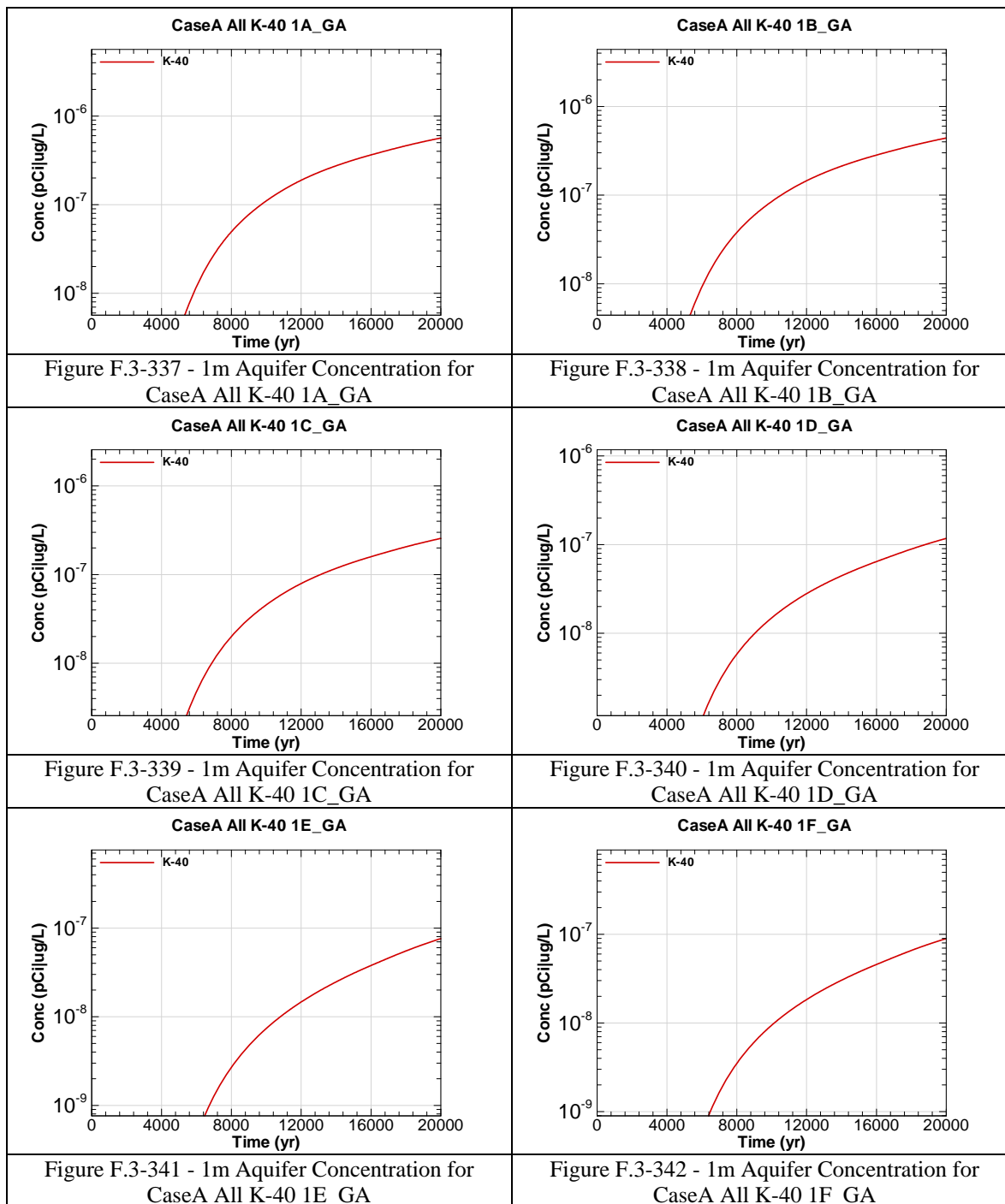


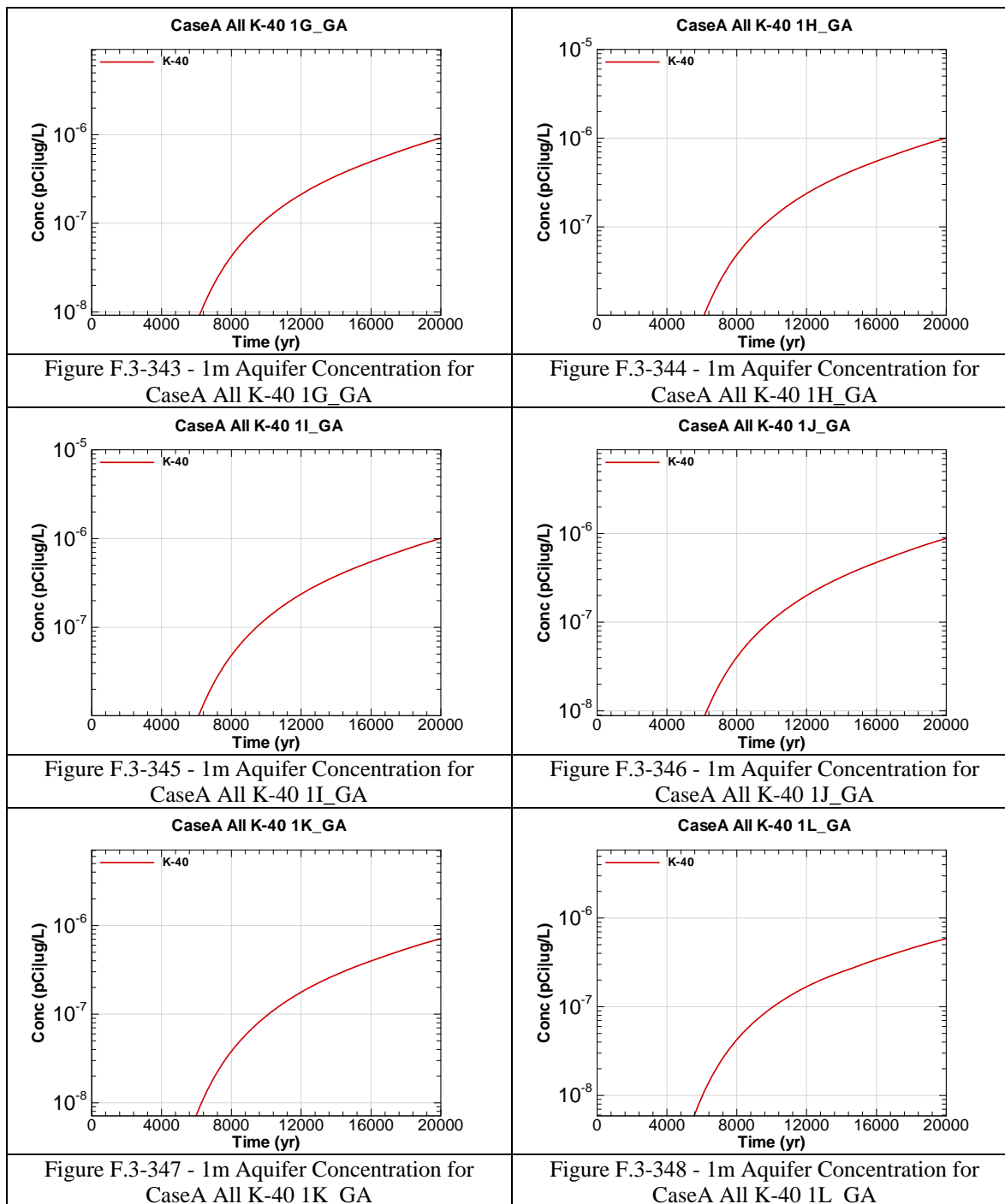


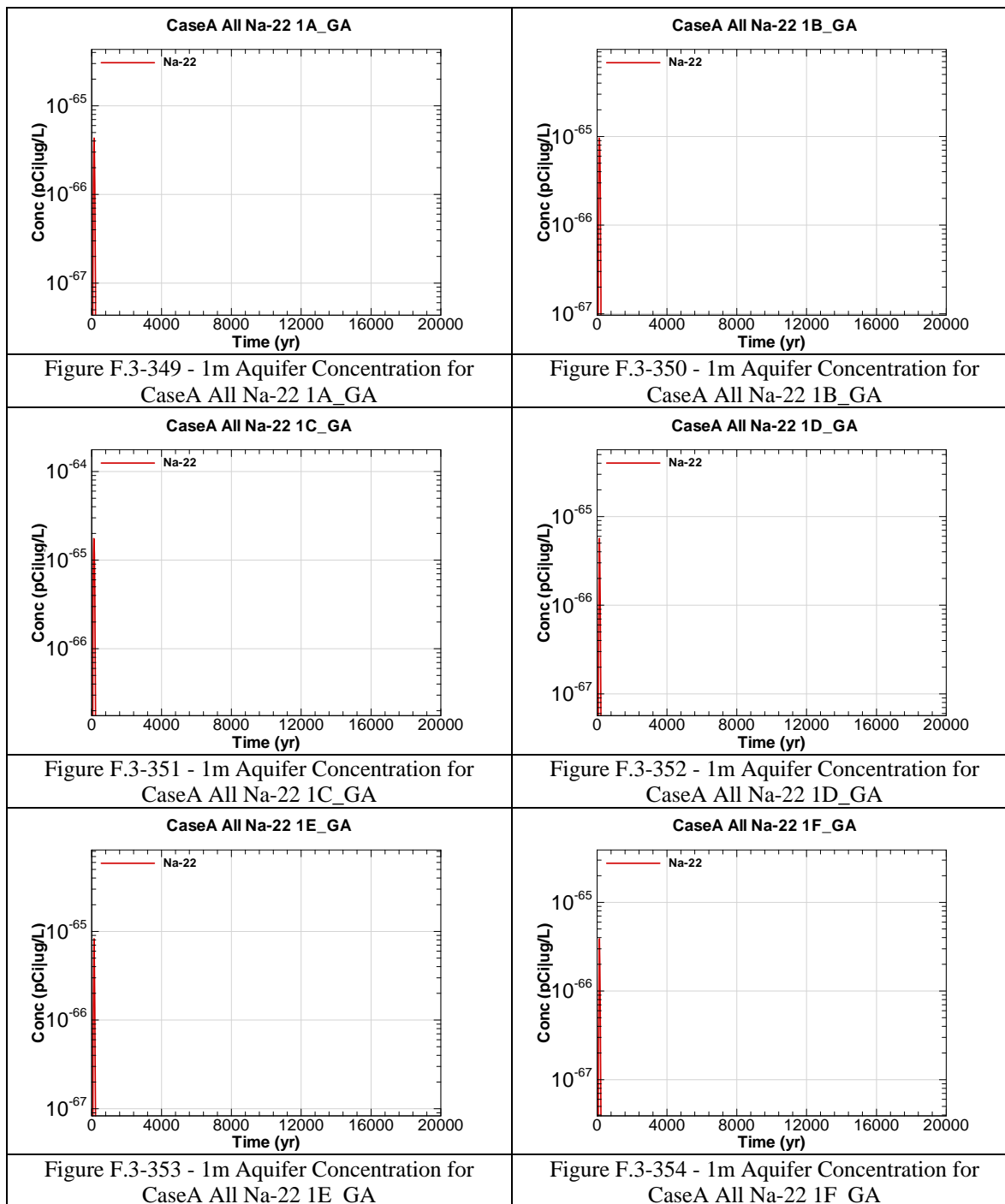


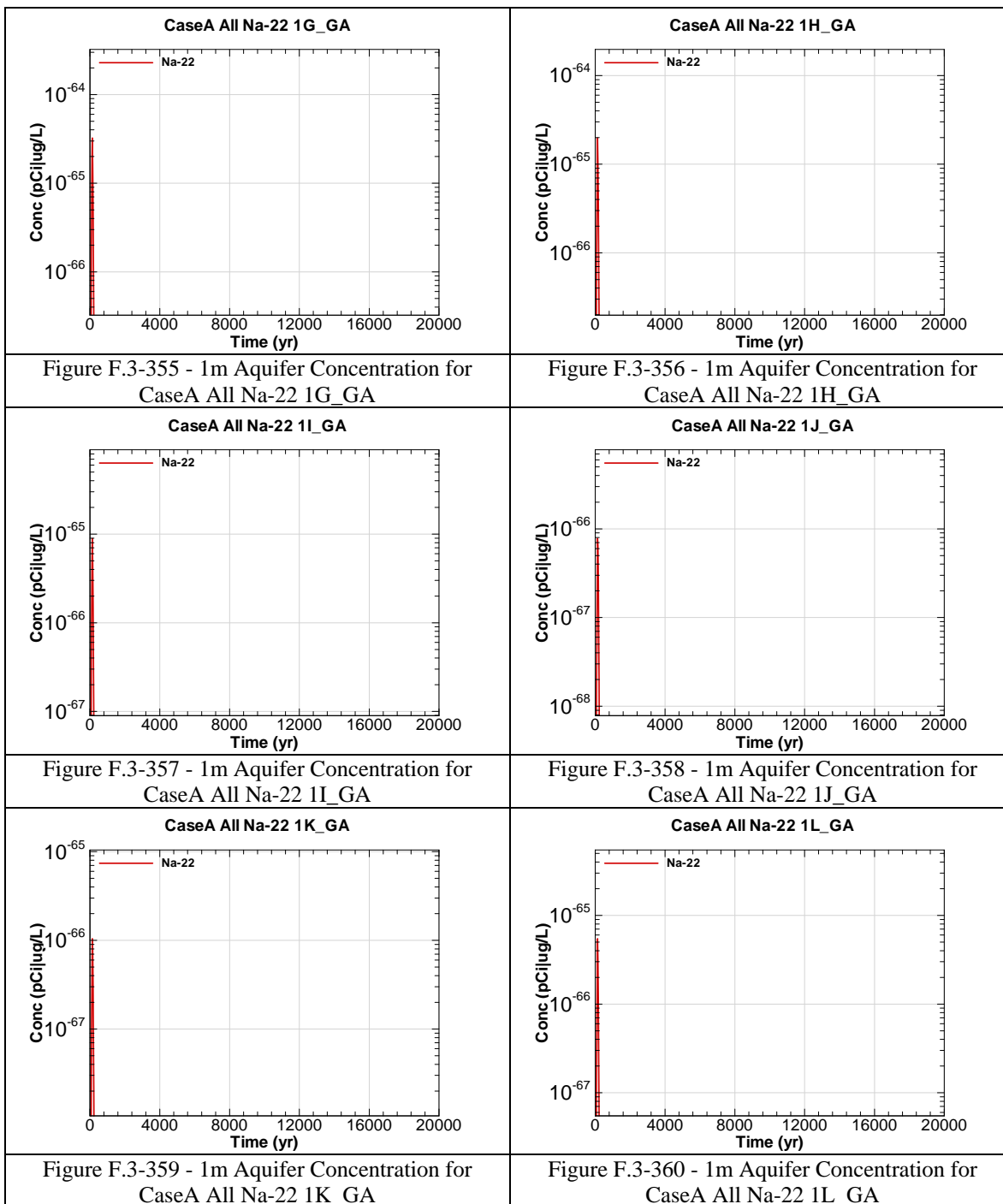


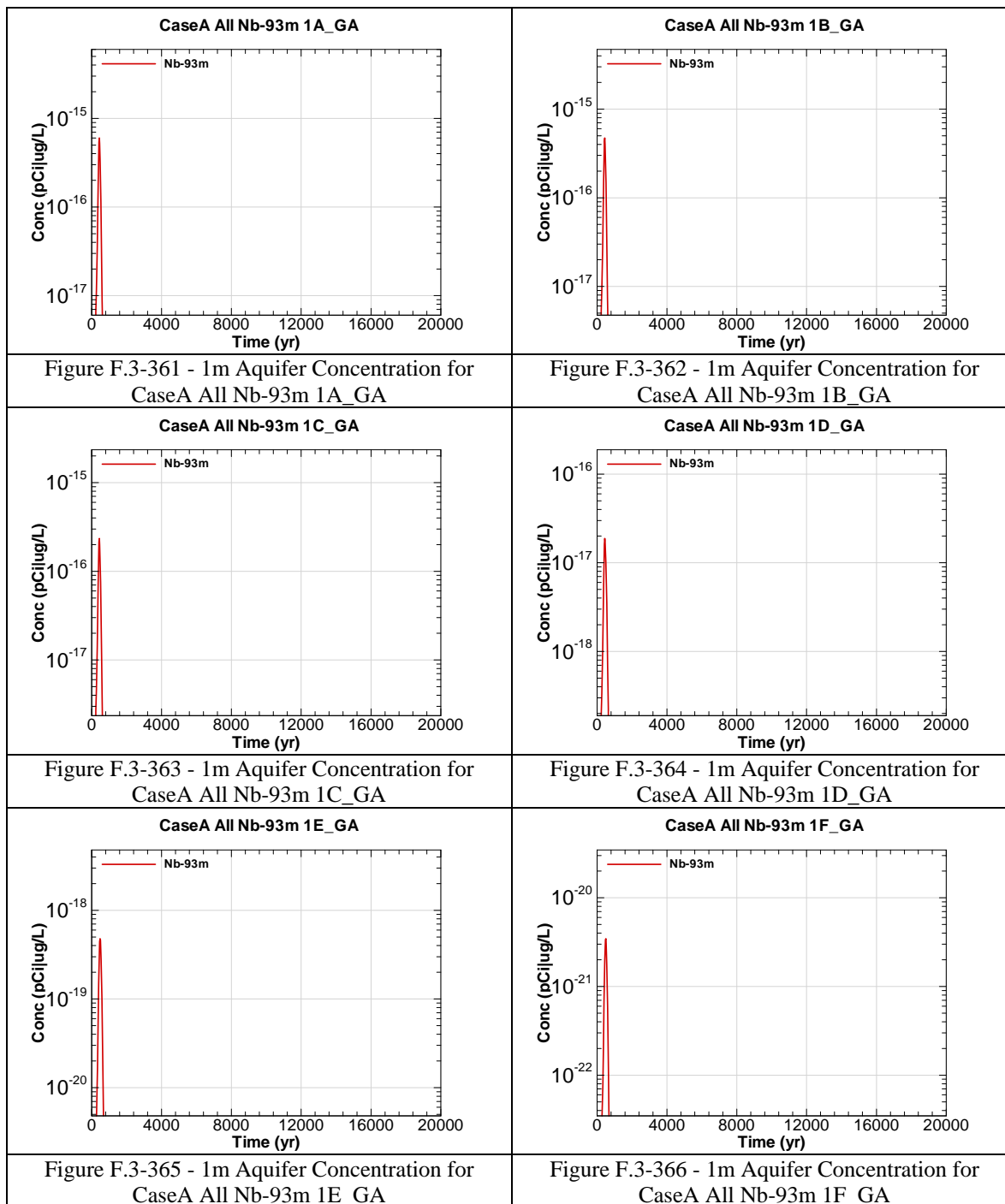


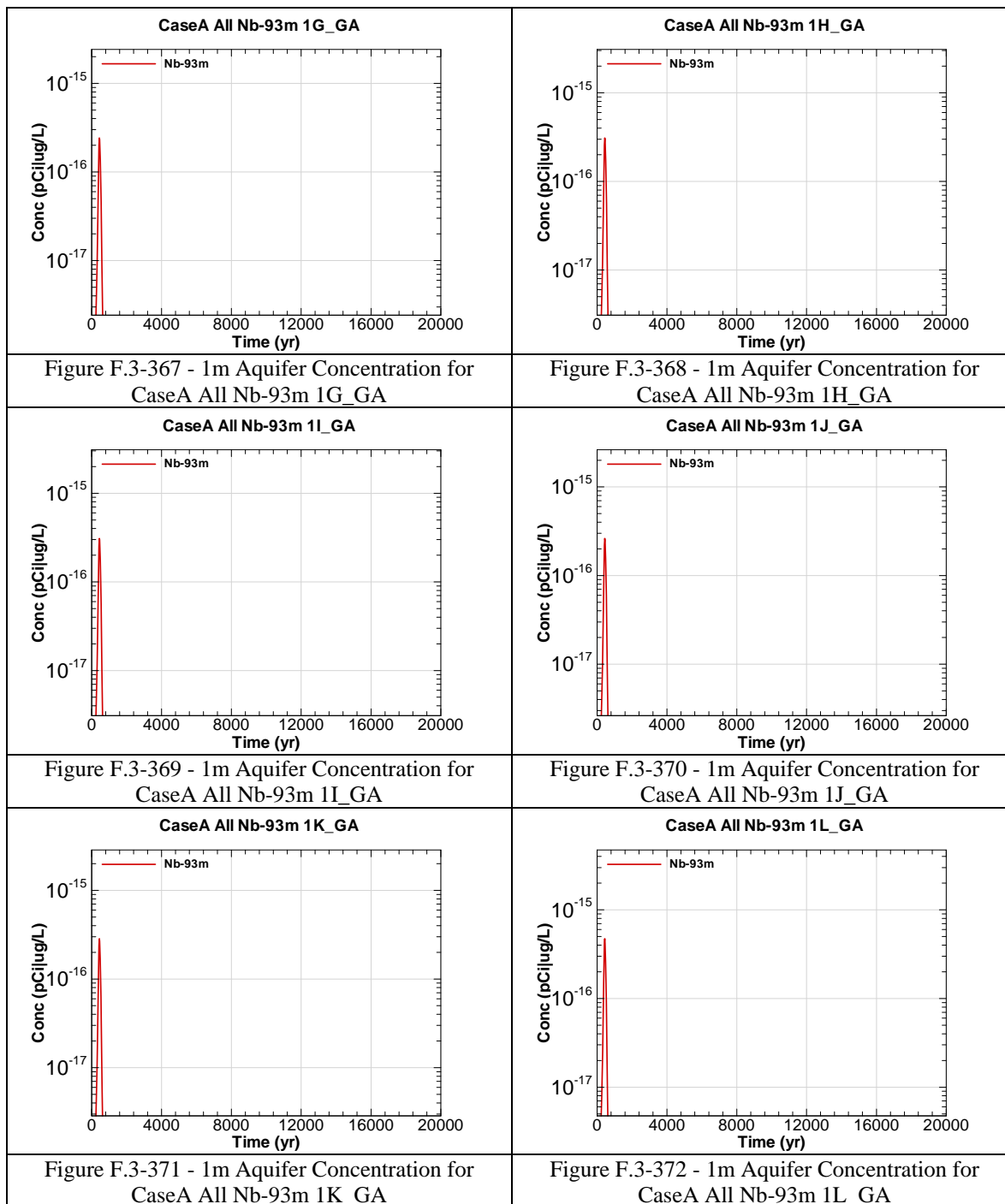


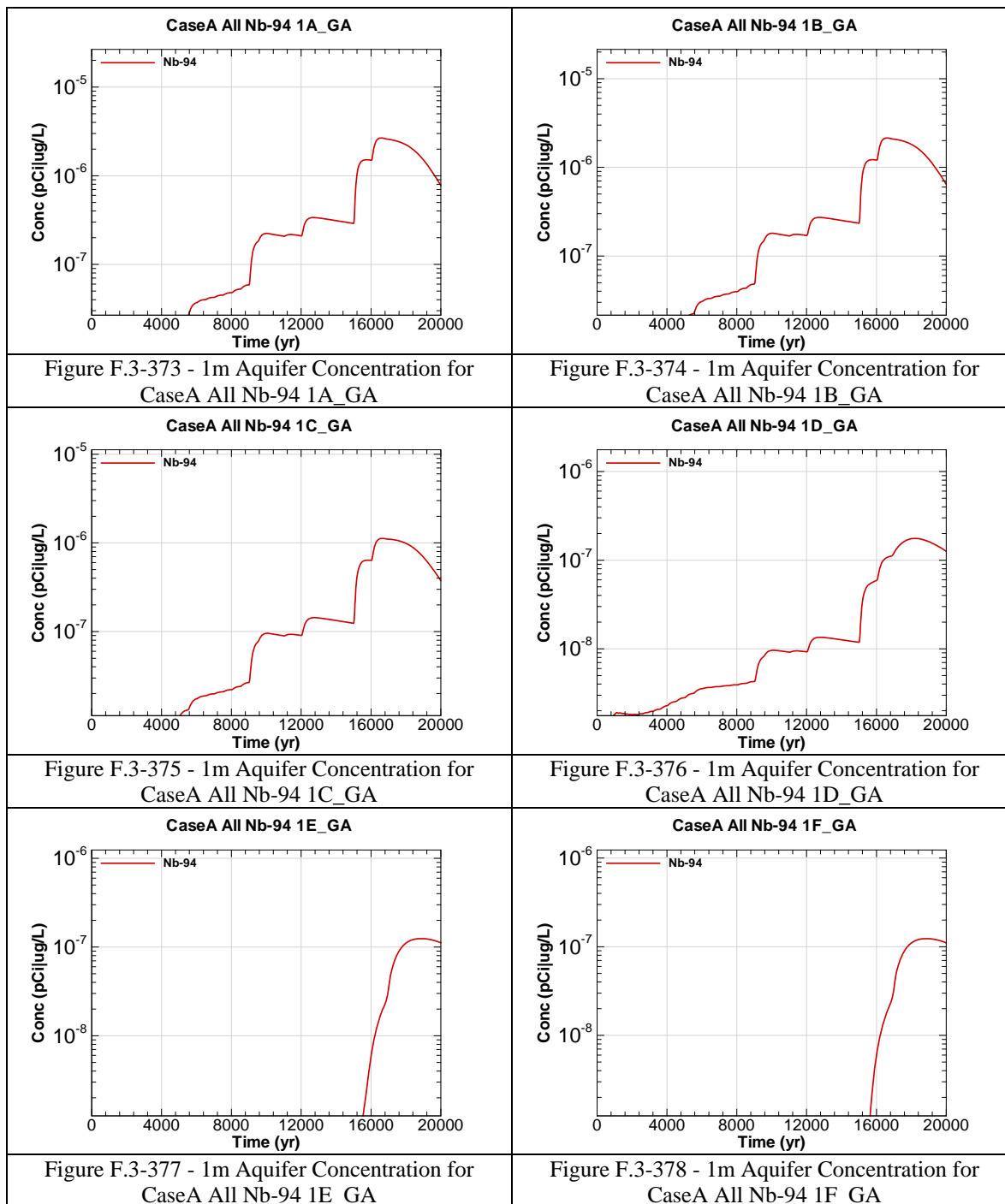


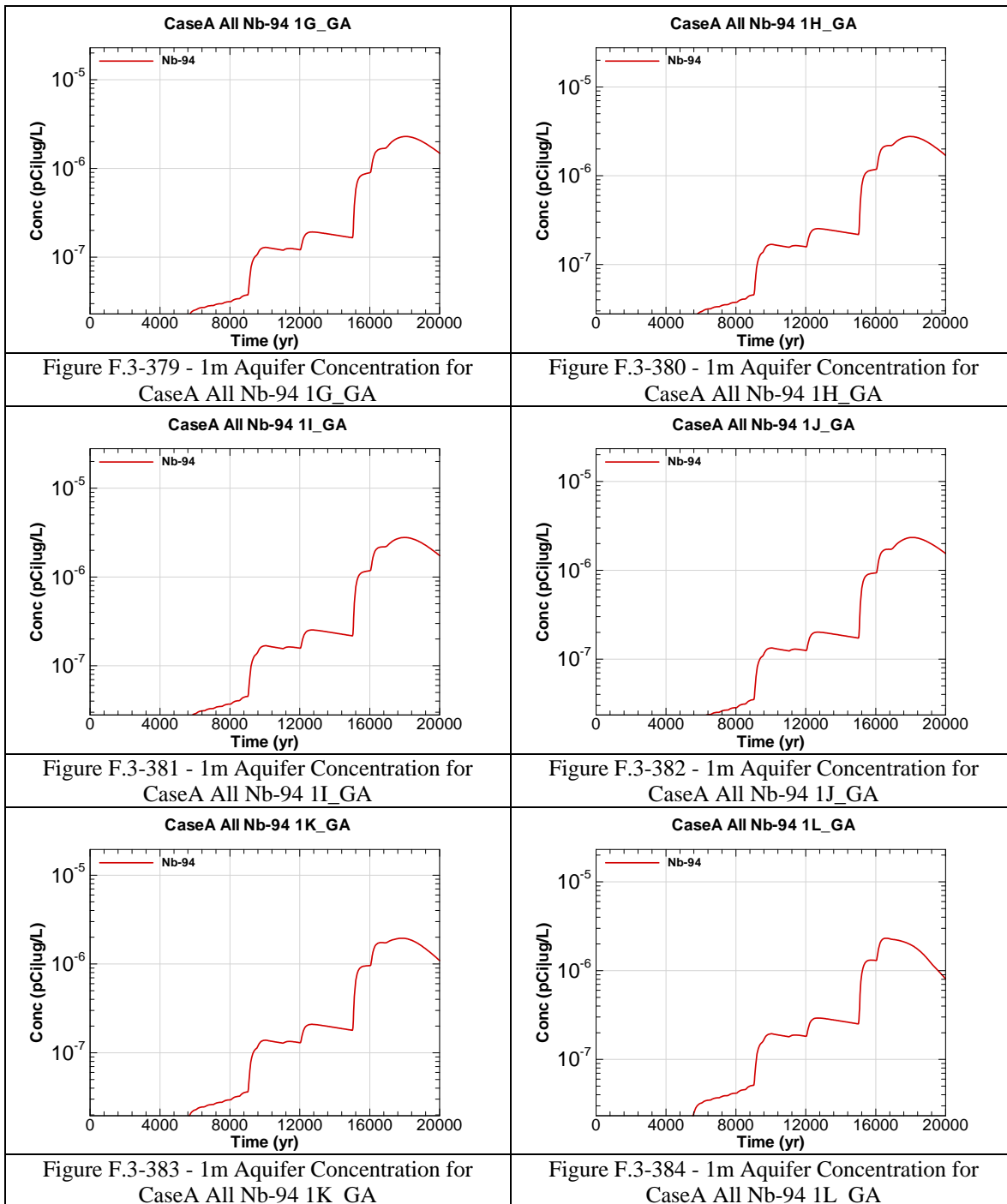


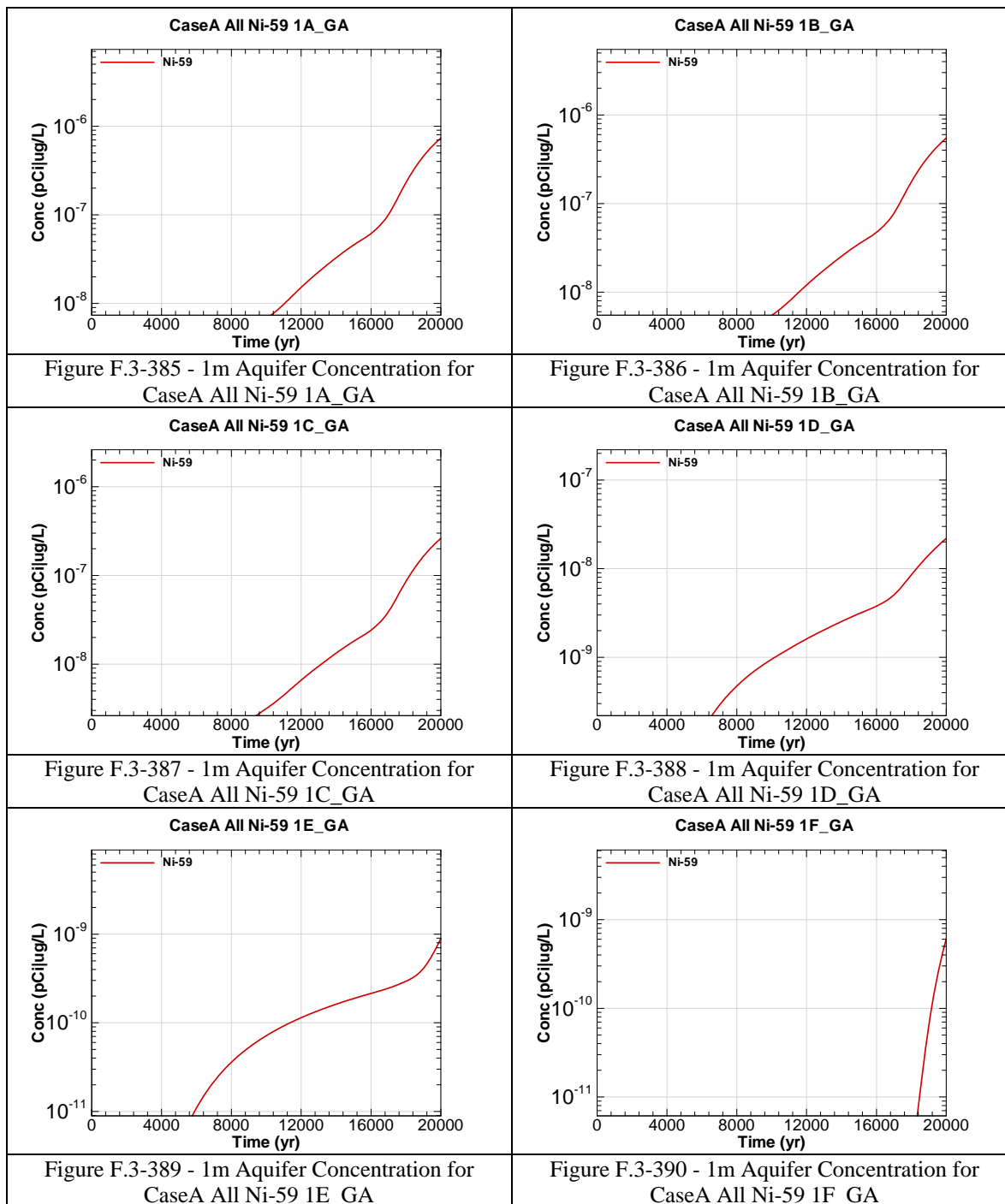


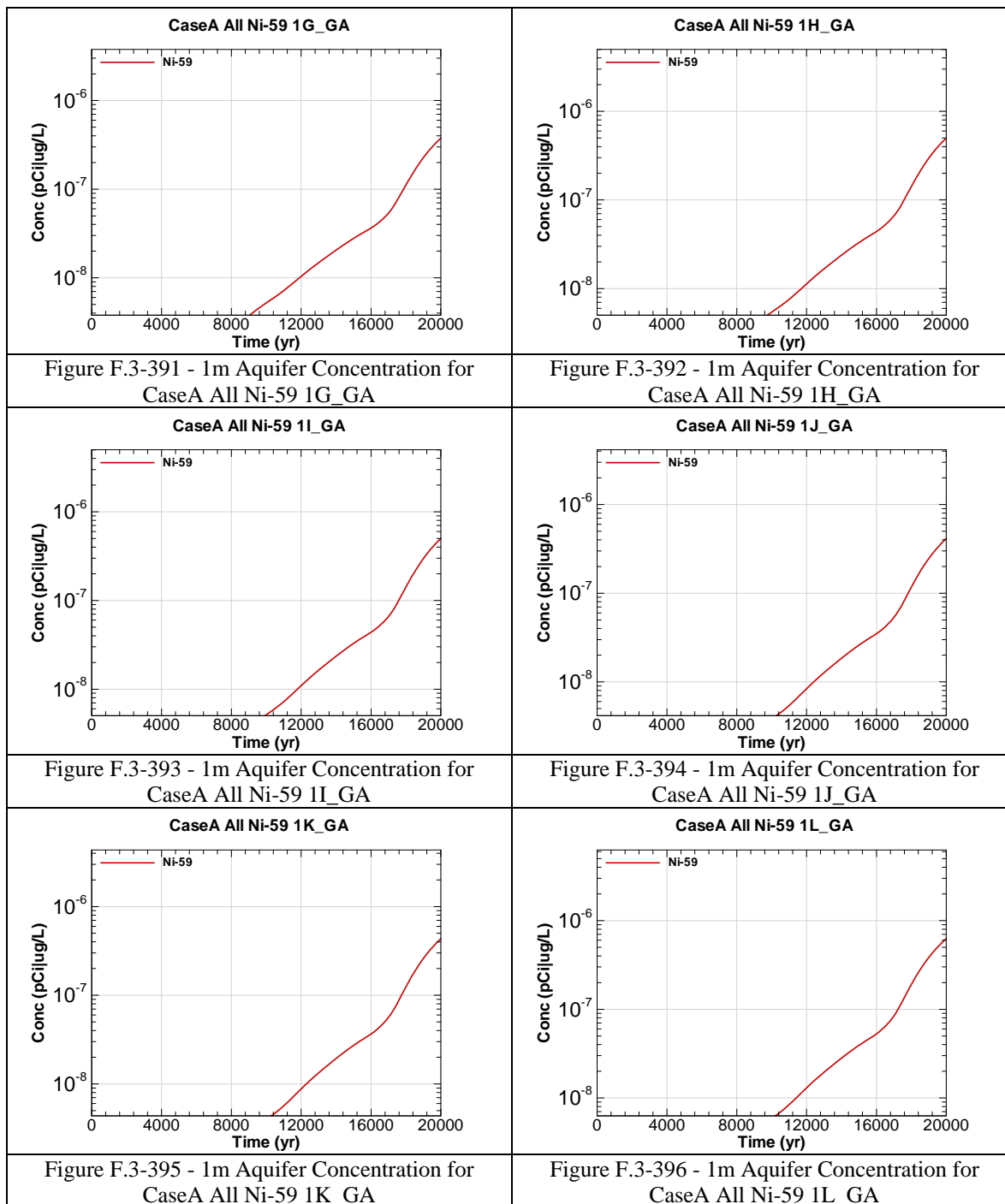


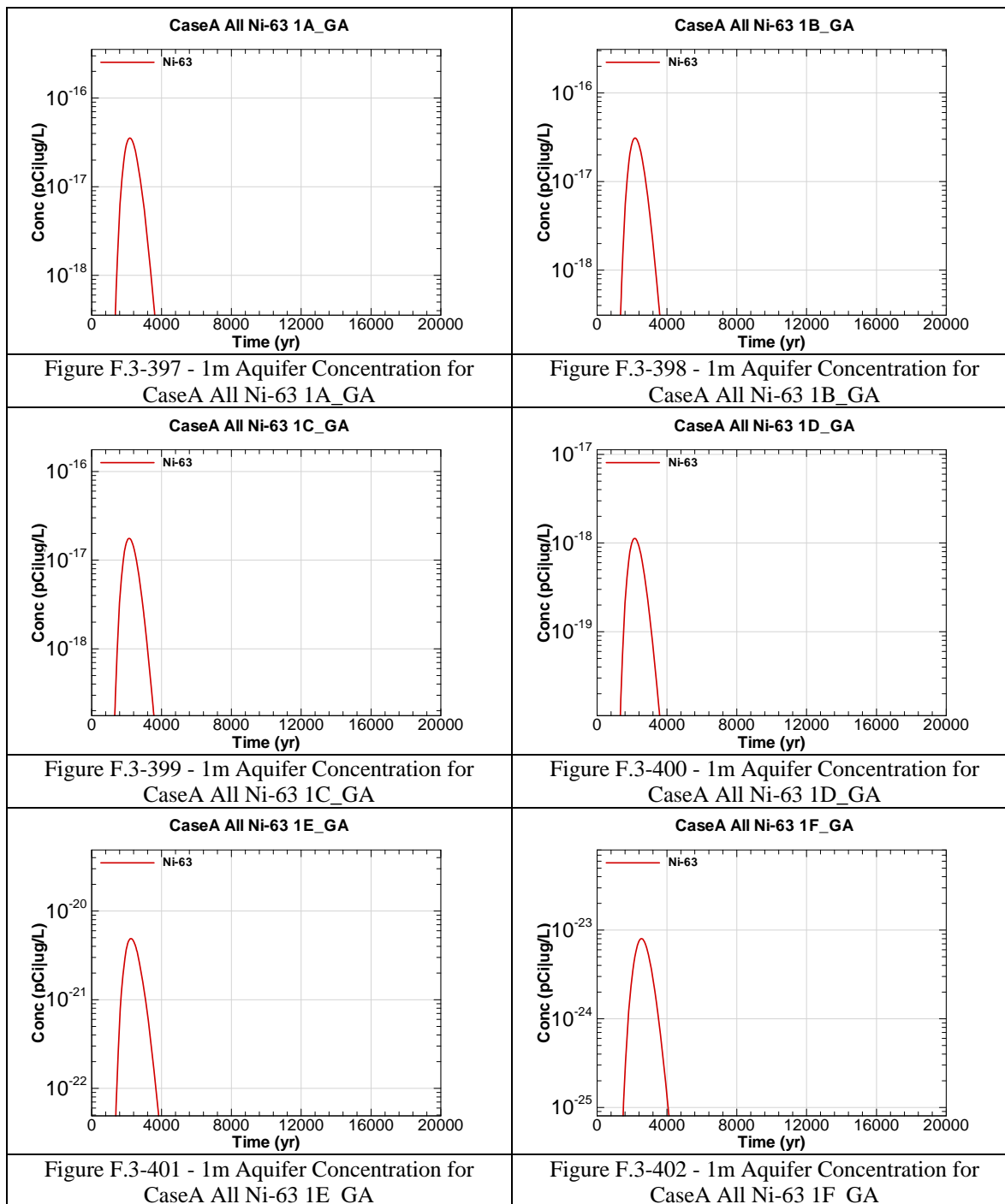


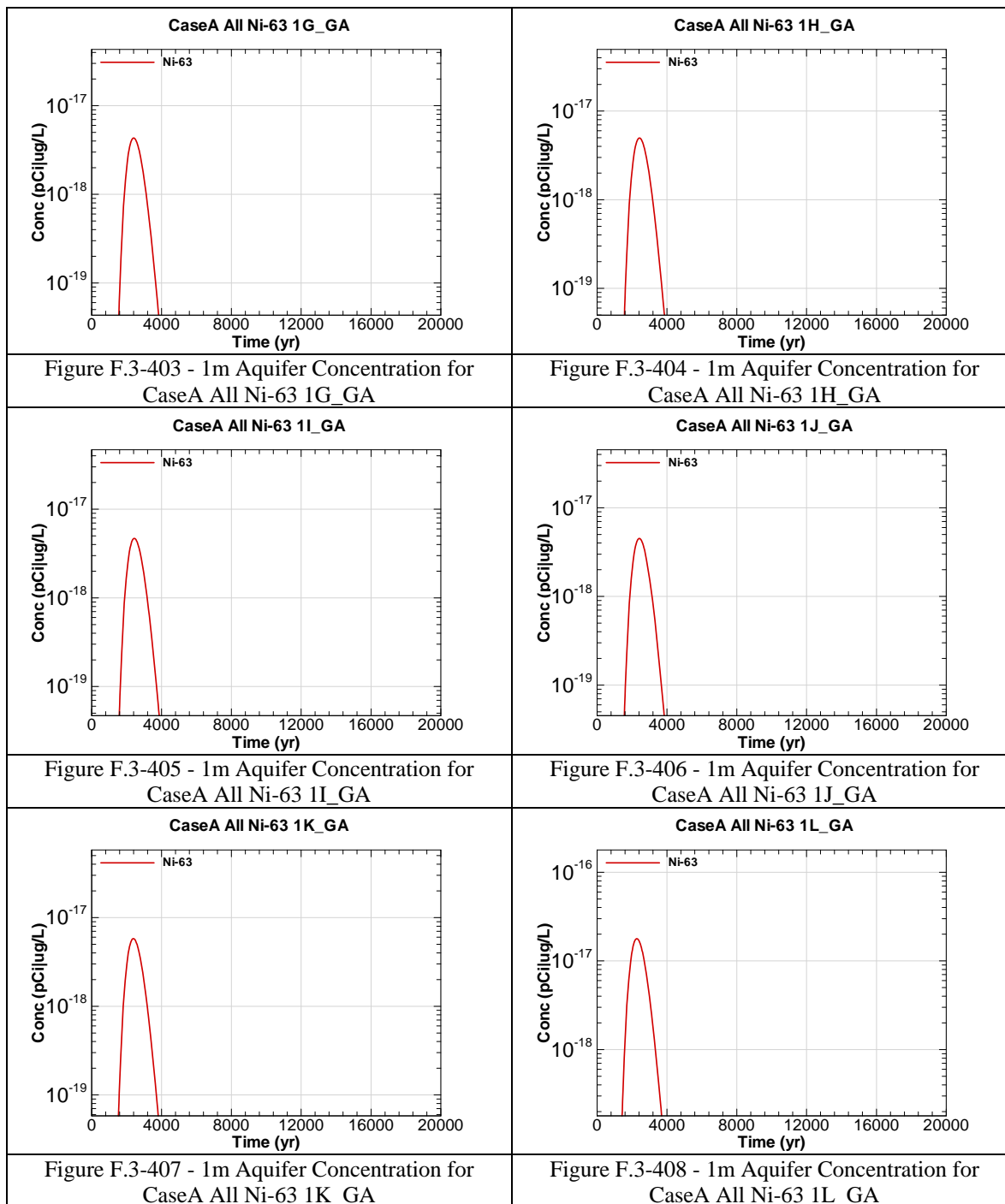


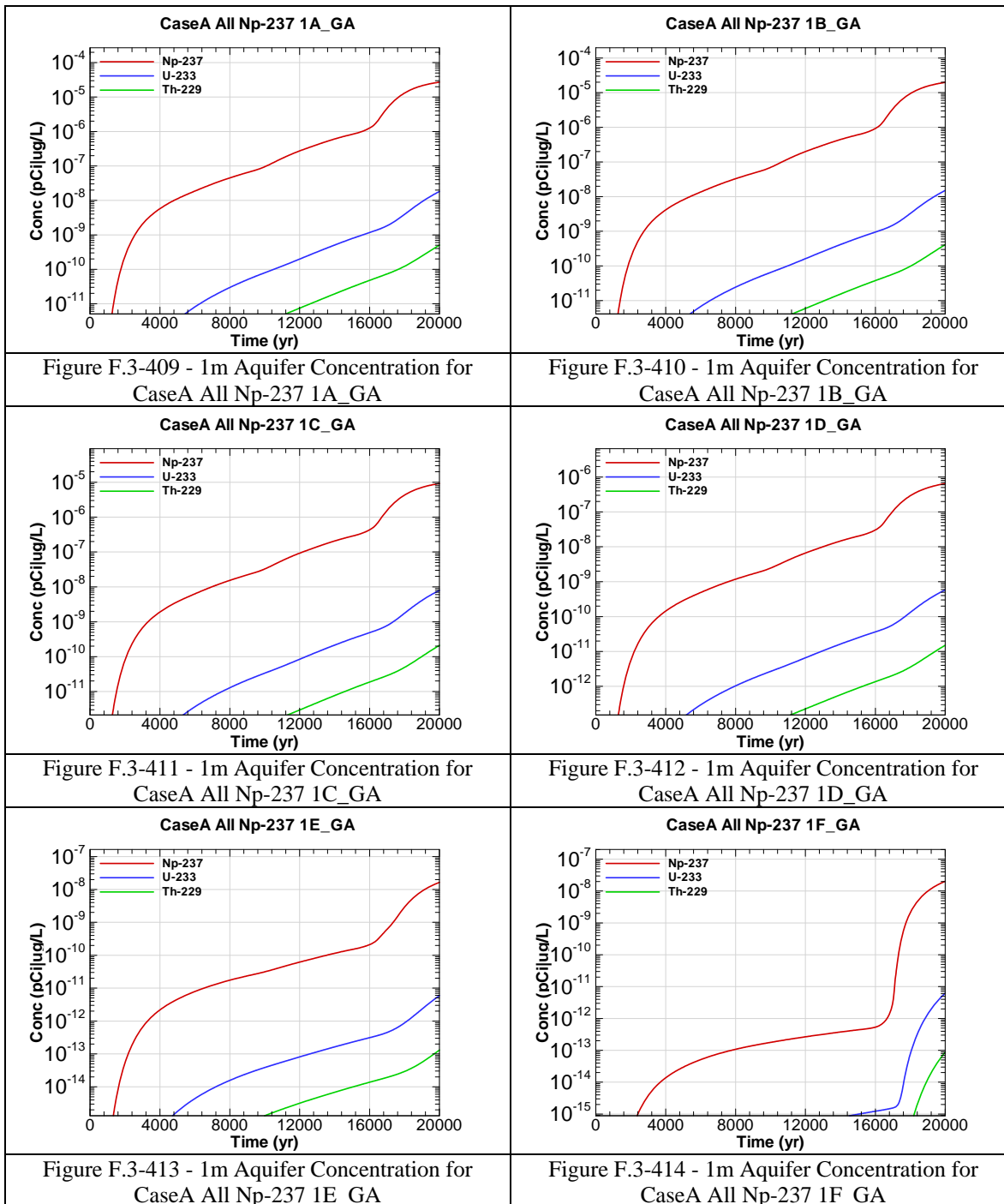












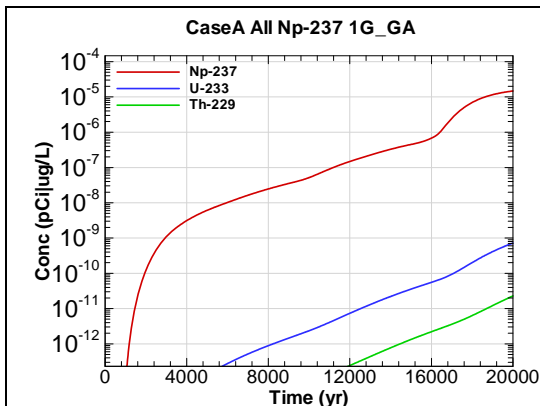


Figure F.3-415 - 1m Aquifer Concentration for
CaseA All Np-237 1G_GA

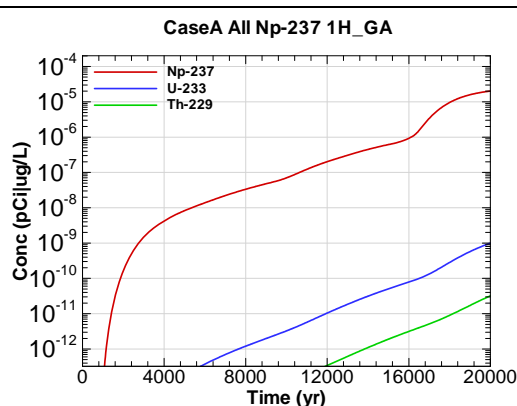


Figure F.3-416 - 1m Aquifer Concentration for
CaseA All Np-237 1H_GA

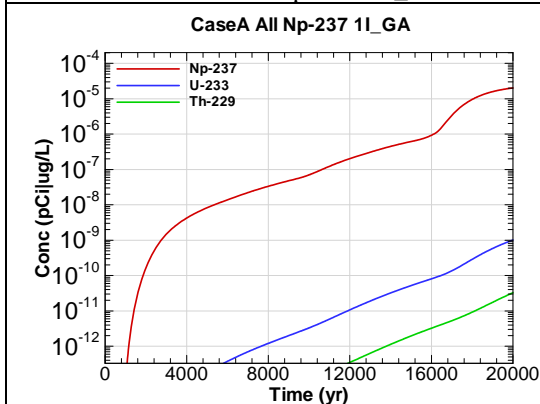


Figure F.3-417 - 1m Aquifer Concentration for
CaseA All Np-237 1I_GA

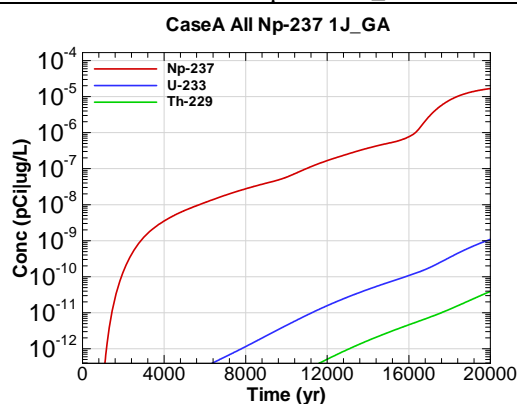


Figure F.3-418 - 1m Aquifer Concentration for
CaseA All Np-237 1J_GA

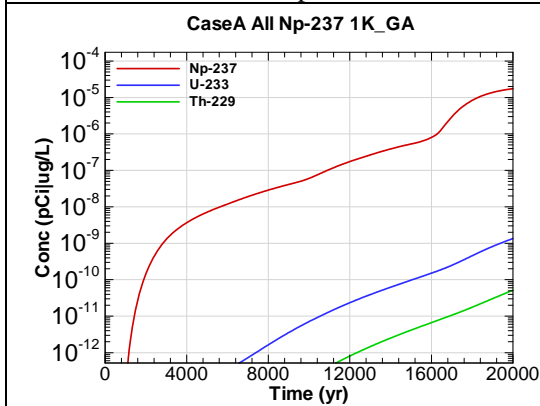


Figure F.3-419 - 1m Aquifer Concentration for
CaseA All Np-237 1K_GA

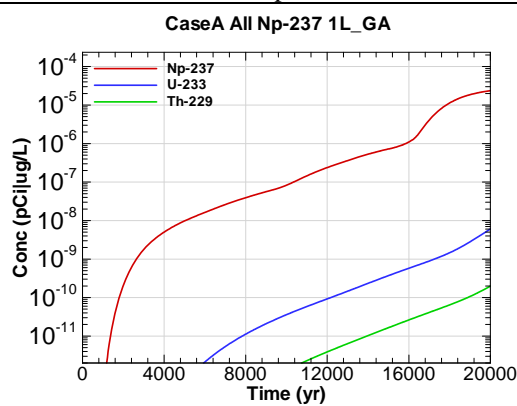
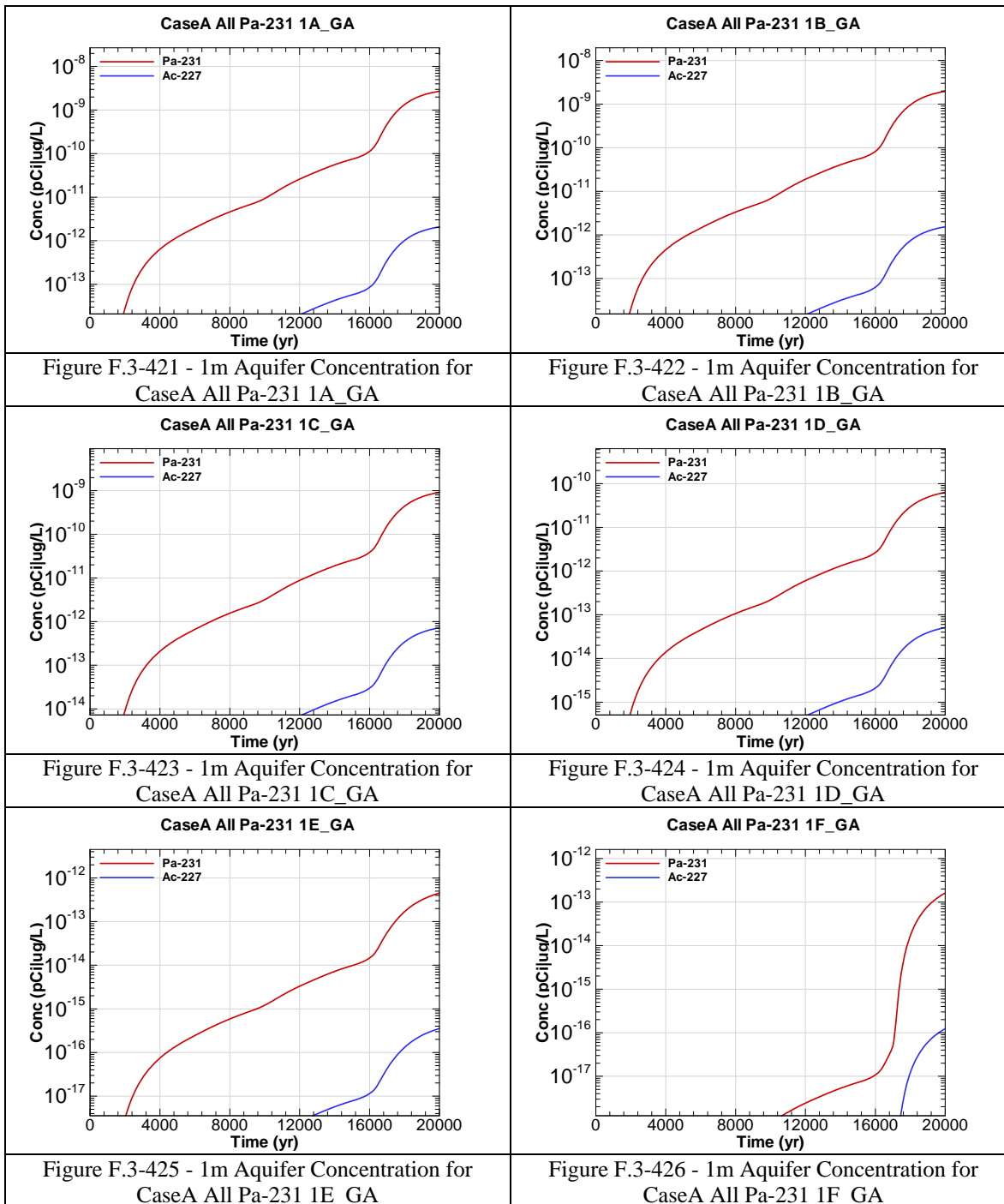
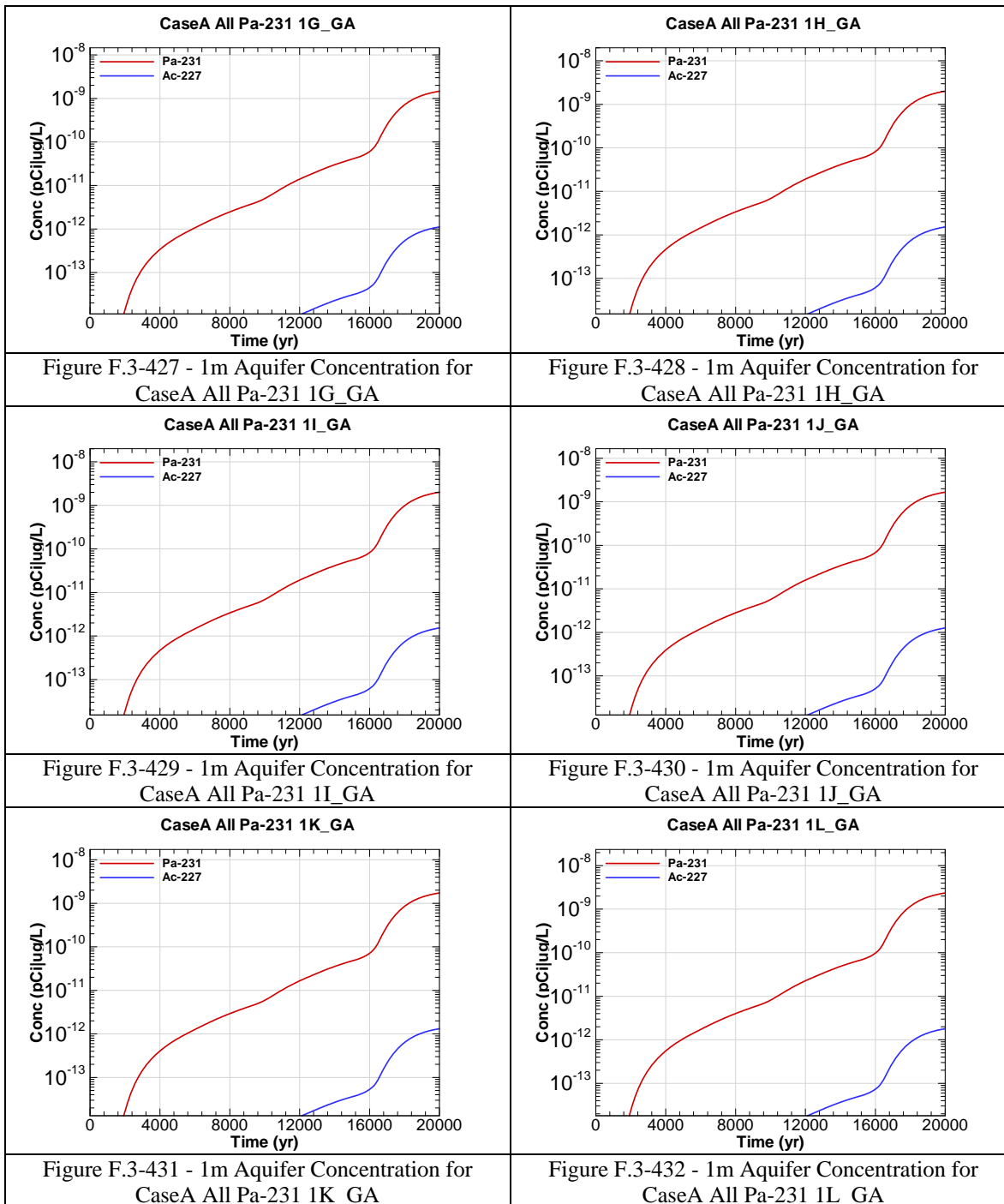
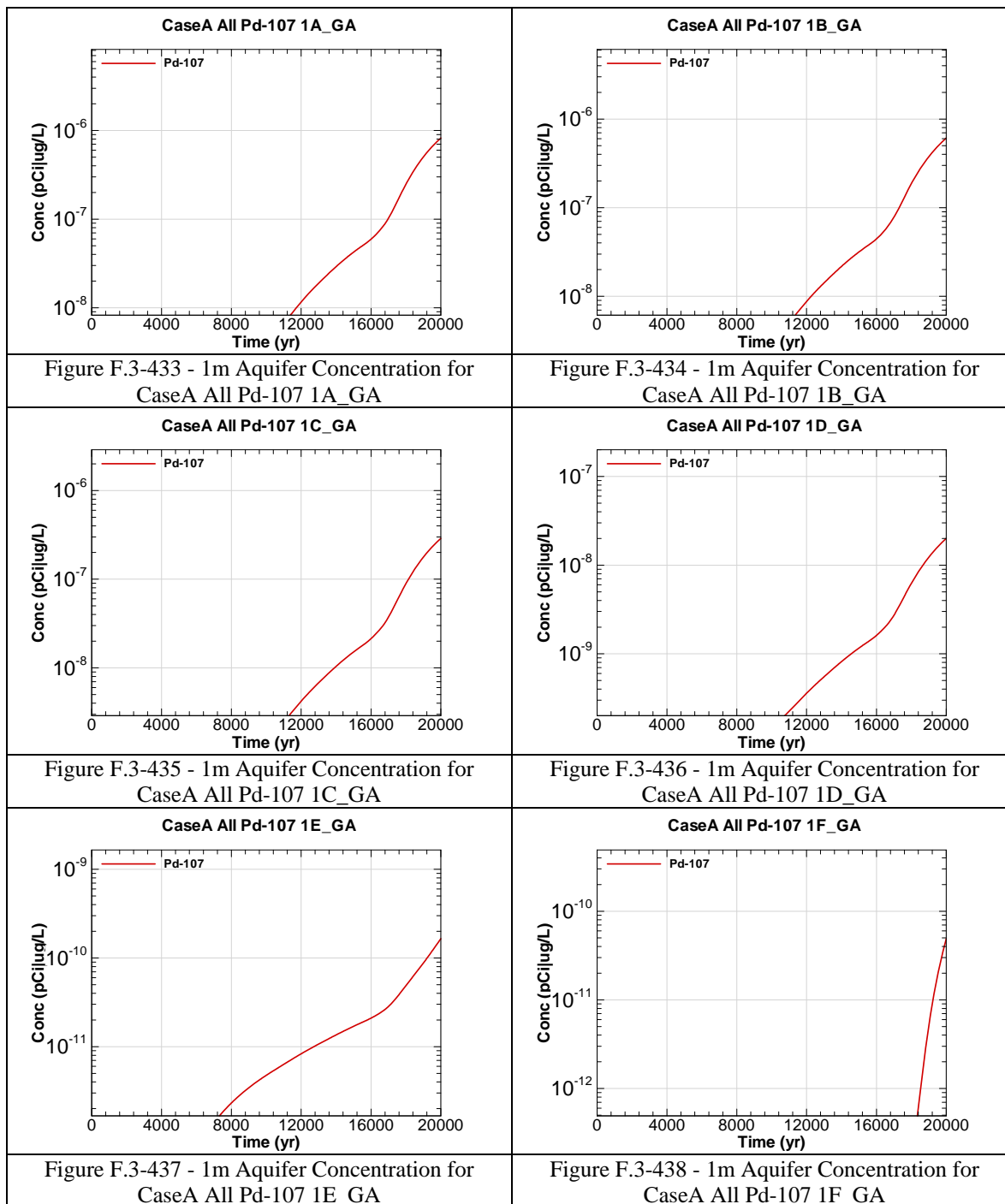
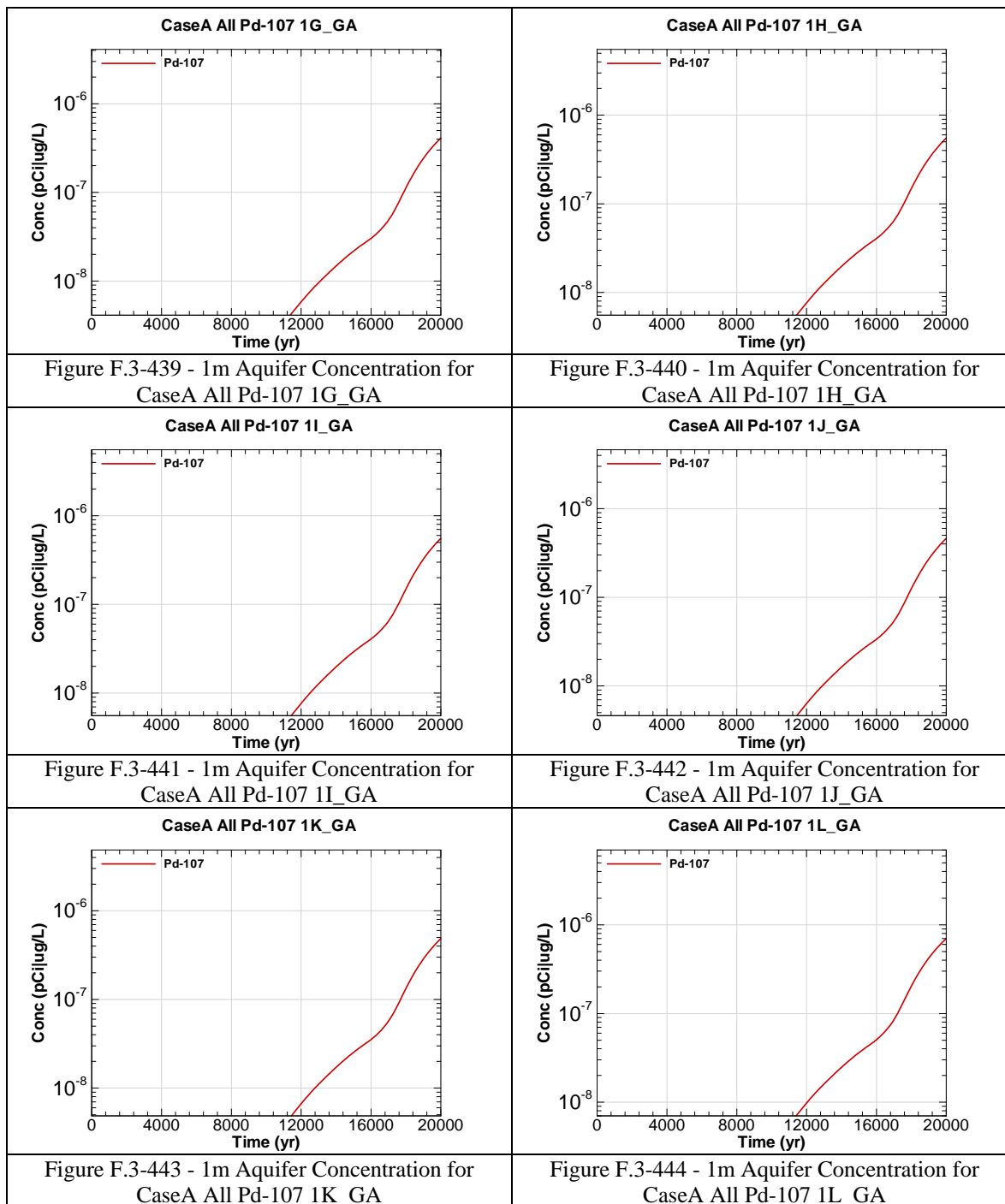


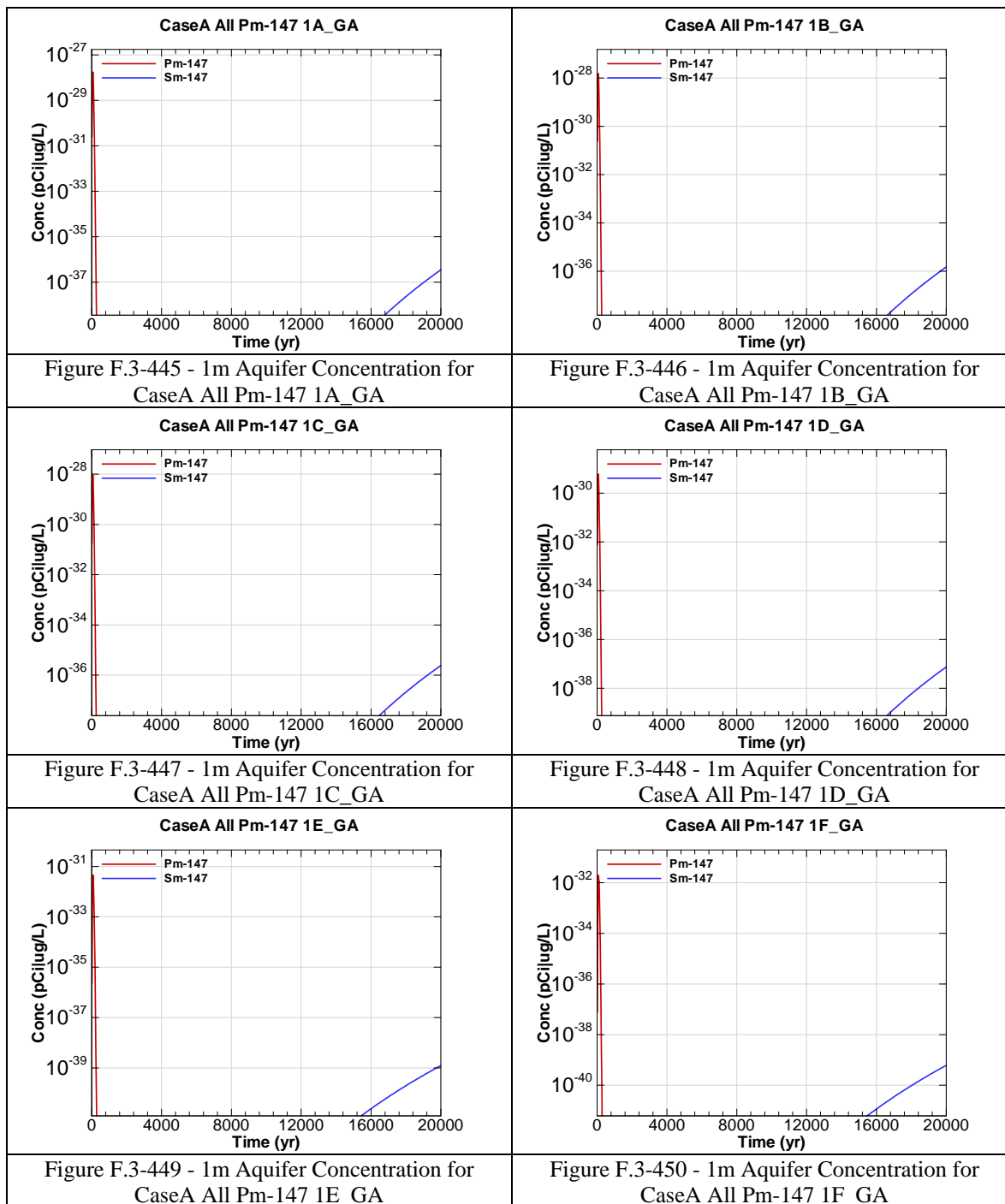
Figure F.3-420 - 1m Aquifer Concentration for
CaseA All Np-237 1L_GA

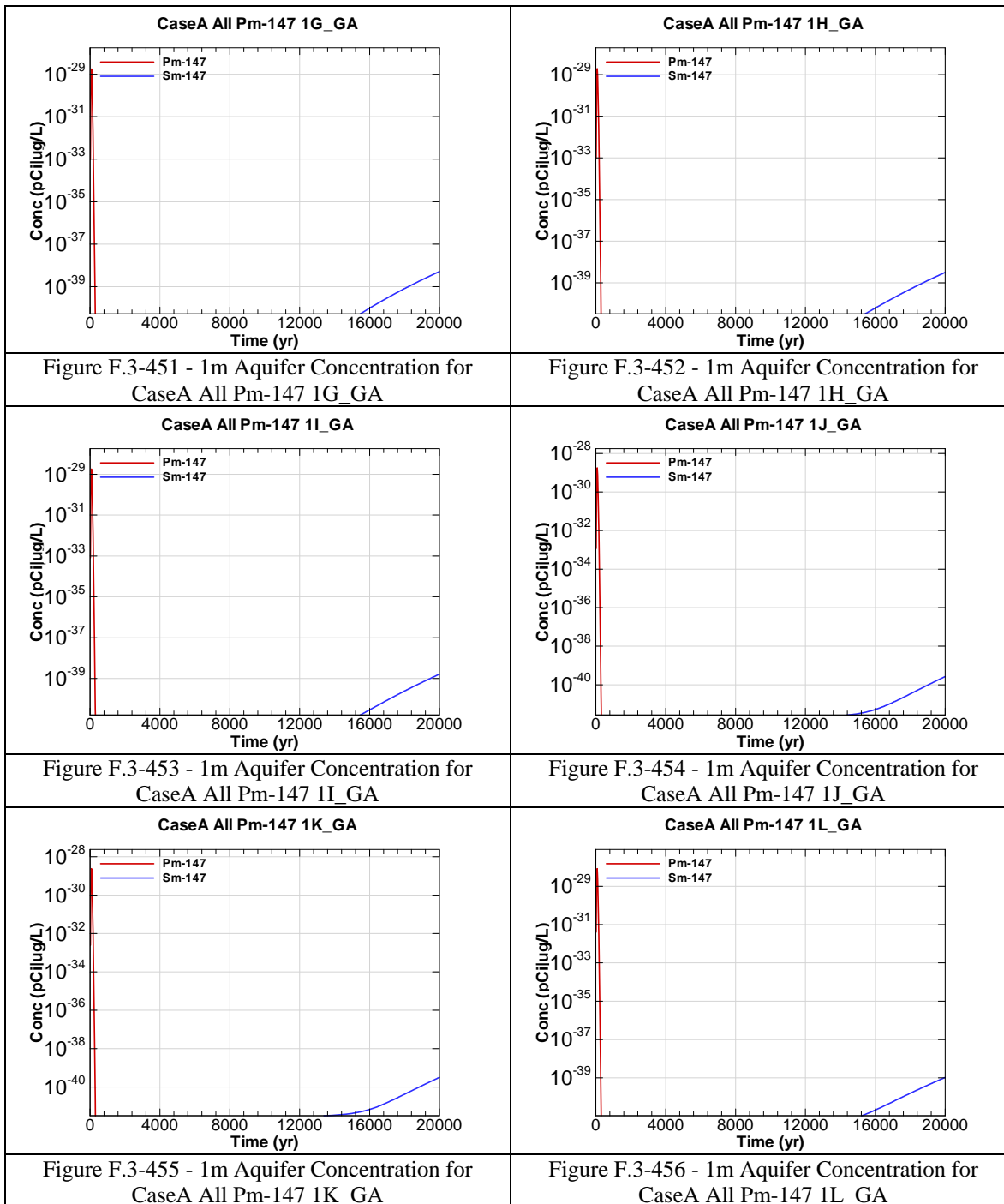


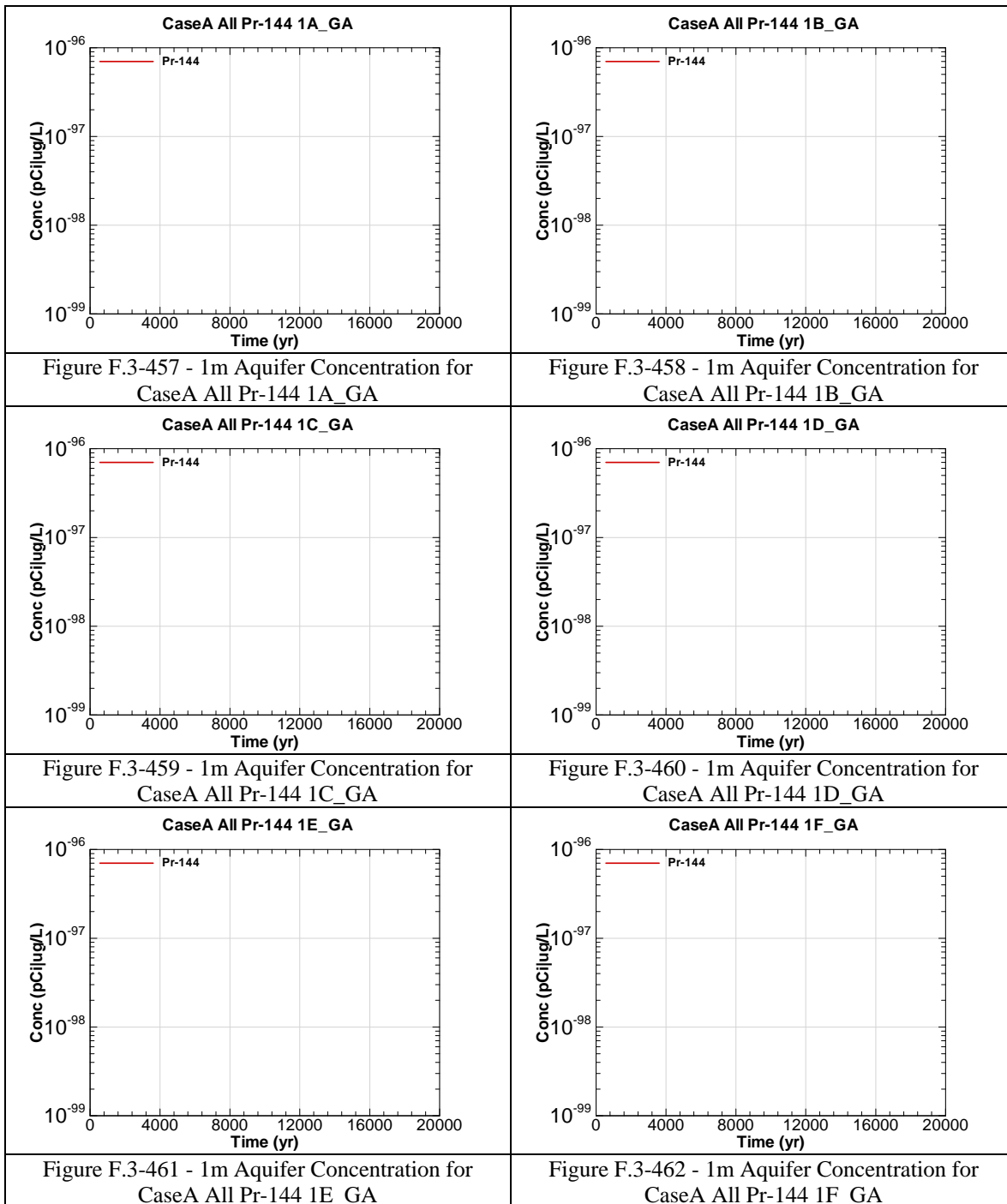


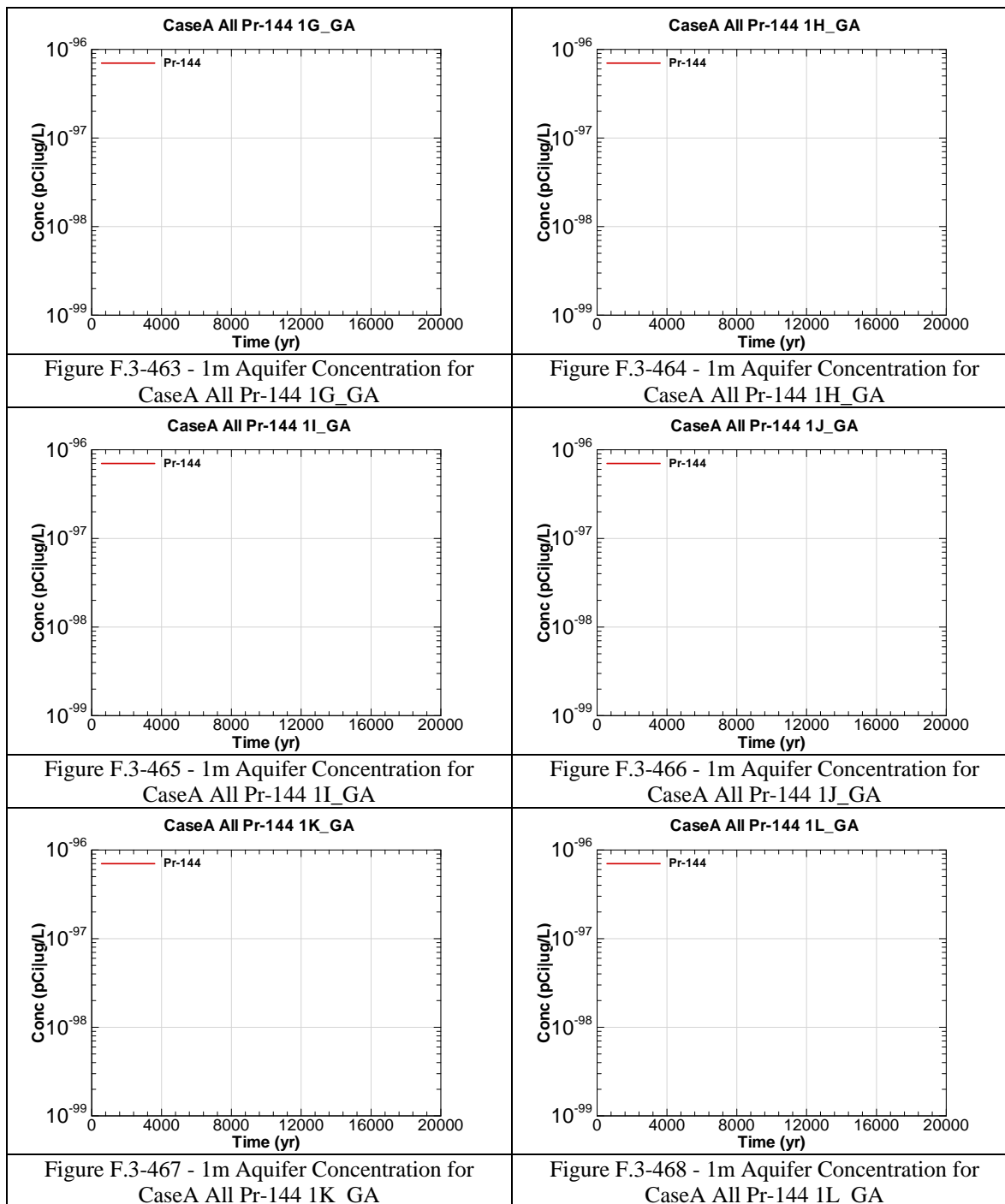


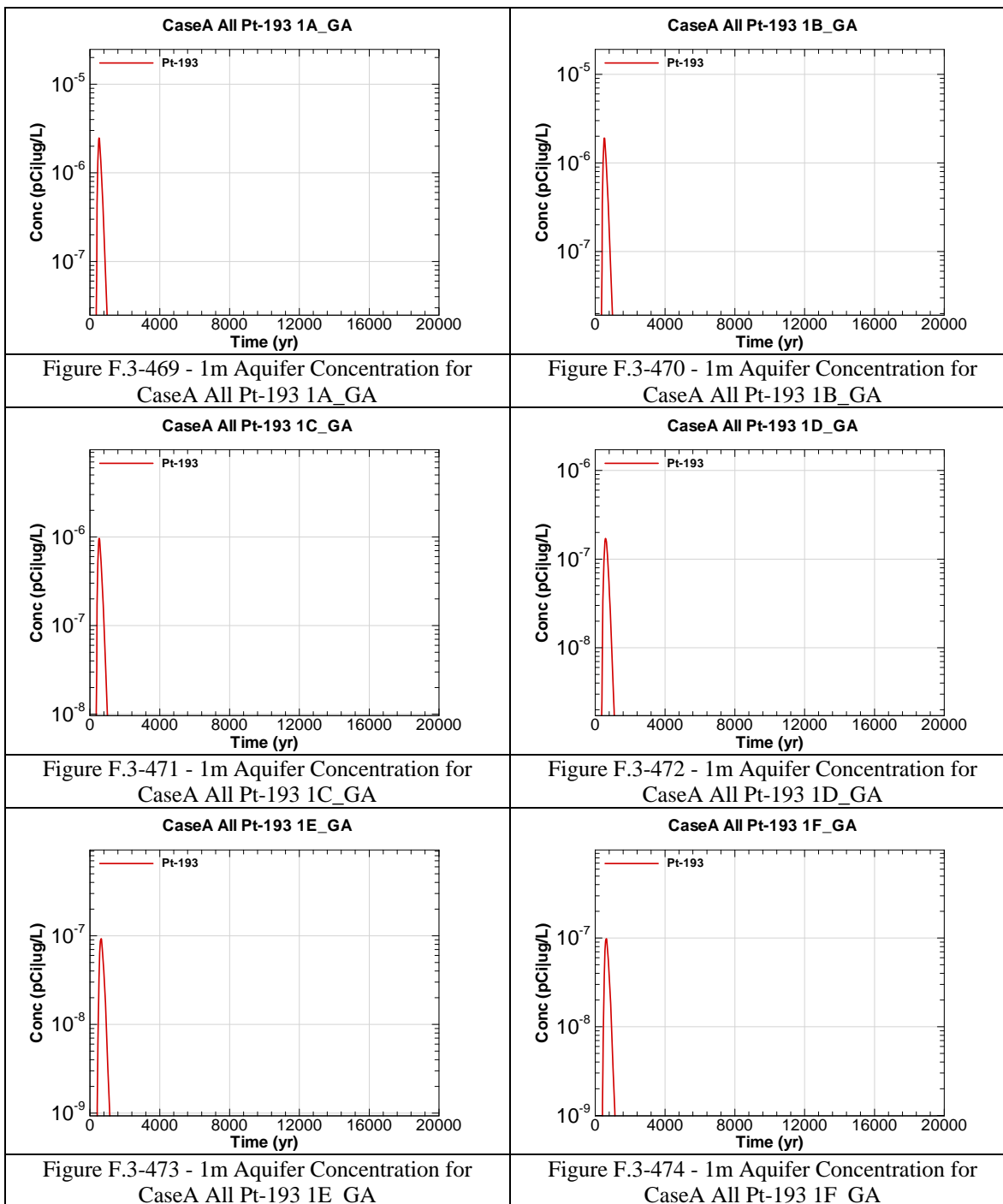


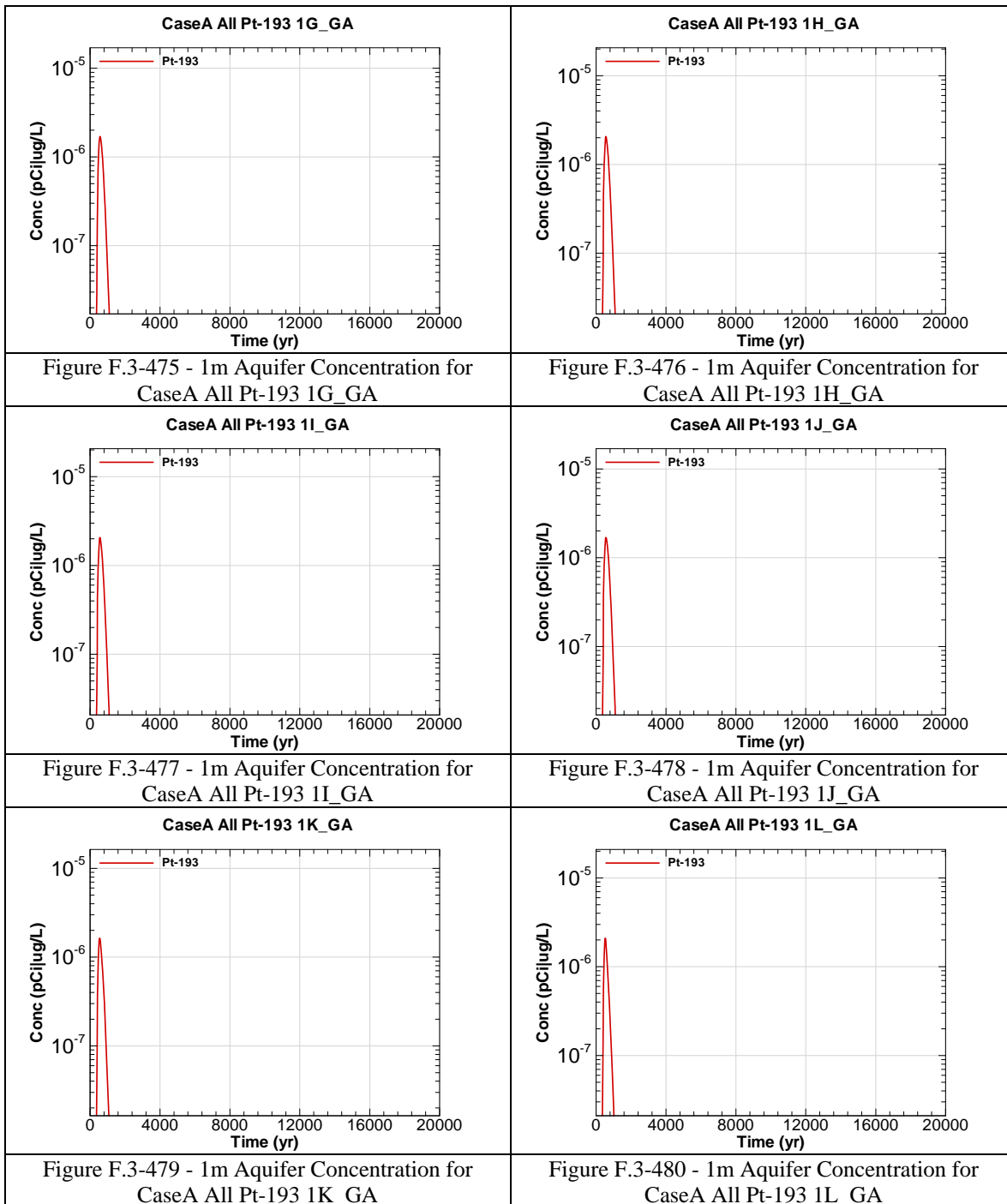












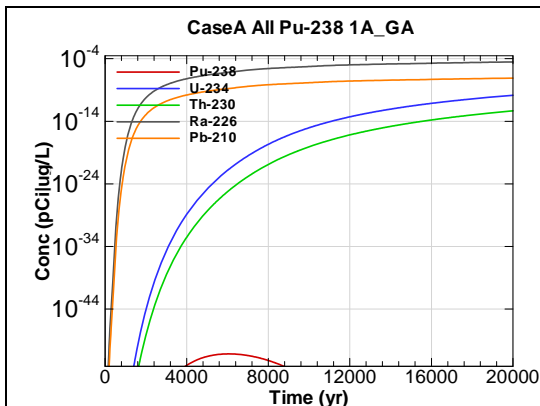


Figure F.3-481 - 1m Aquifer Concentration for
CaseA All Pu-238 1A_GA

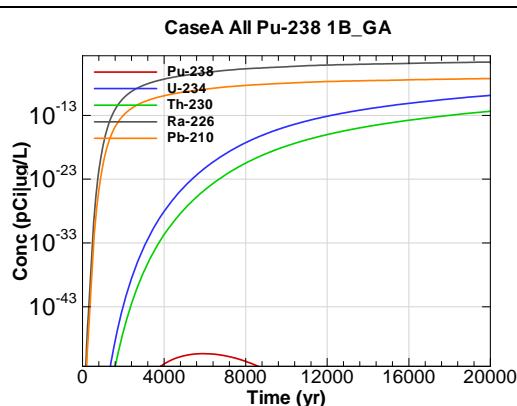


Figure F.3-482 - 1m Aquifer Concentration for
CaseA All Pu-238 1B_GA

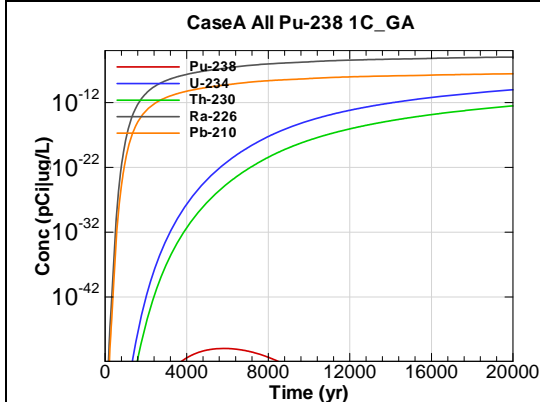


Figure F.3-483 - 1m Aquifer Concentration for
CaseA All Pu-238 1C_GA

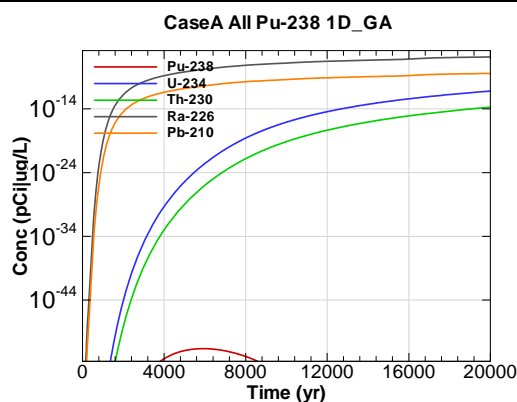


Figure F.3-484 - 1m Aquifer Concentration for
CaseA All Pu-238 1D_GA

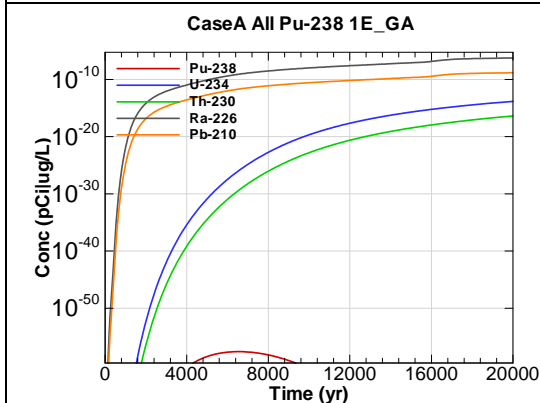


Figure F.3-485 - 1m Aquifer Concentration for
CaseA All Pu-238 1E_GA

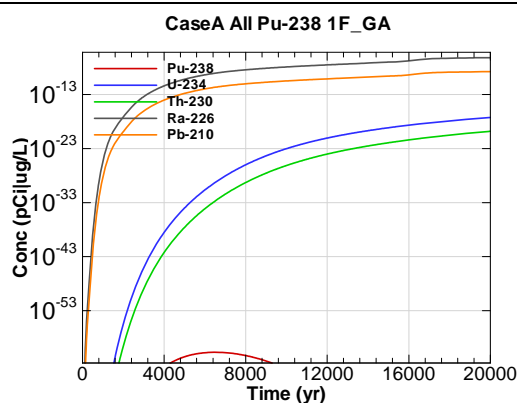
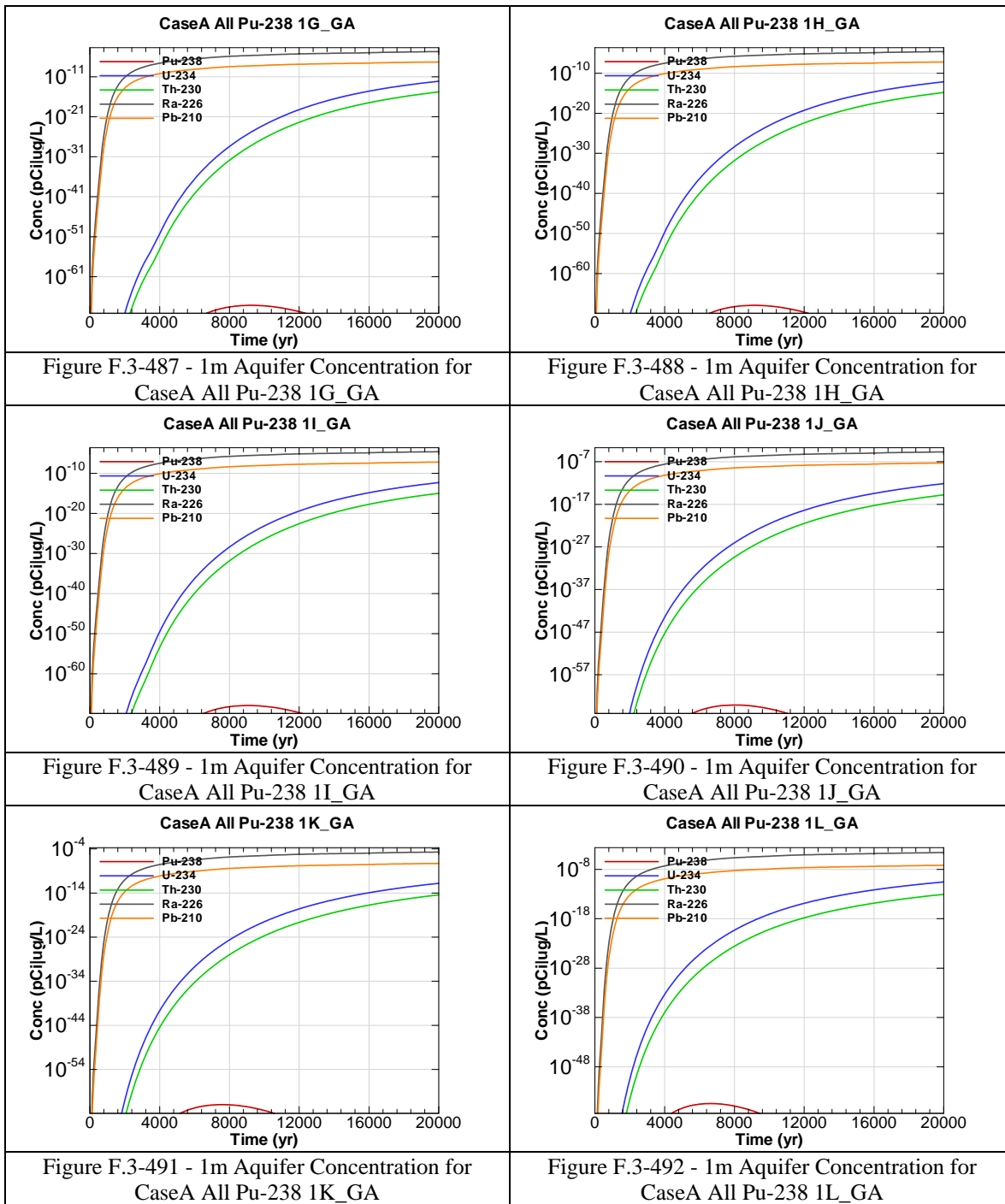
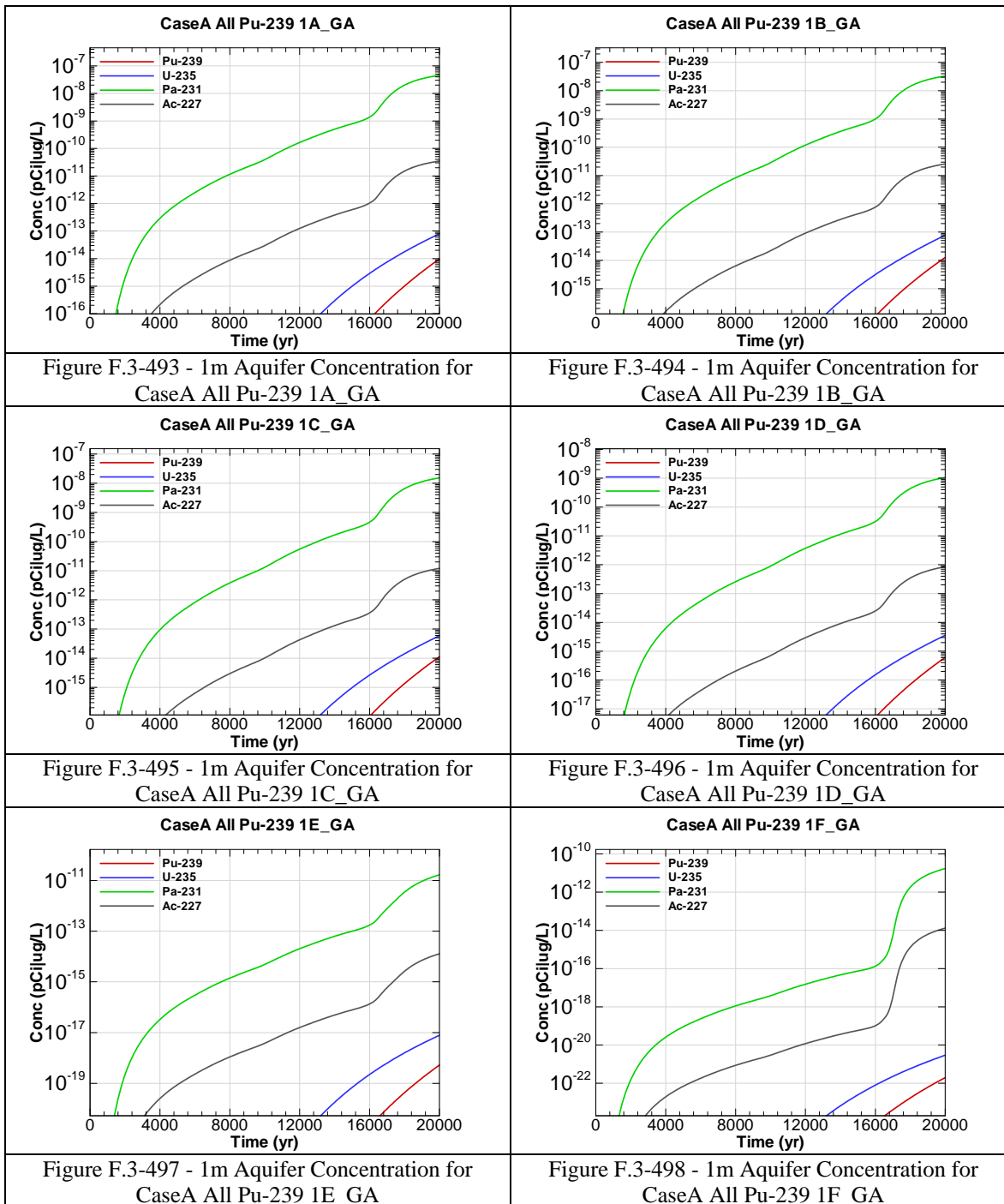
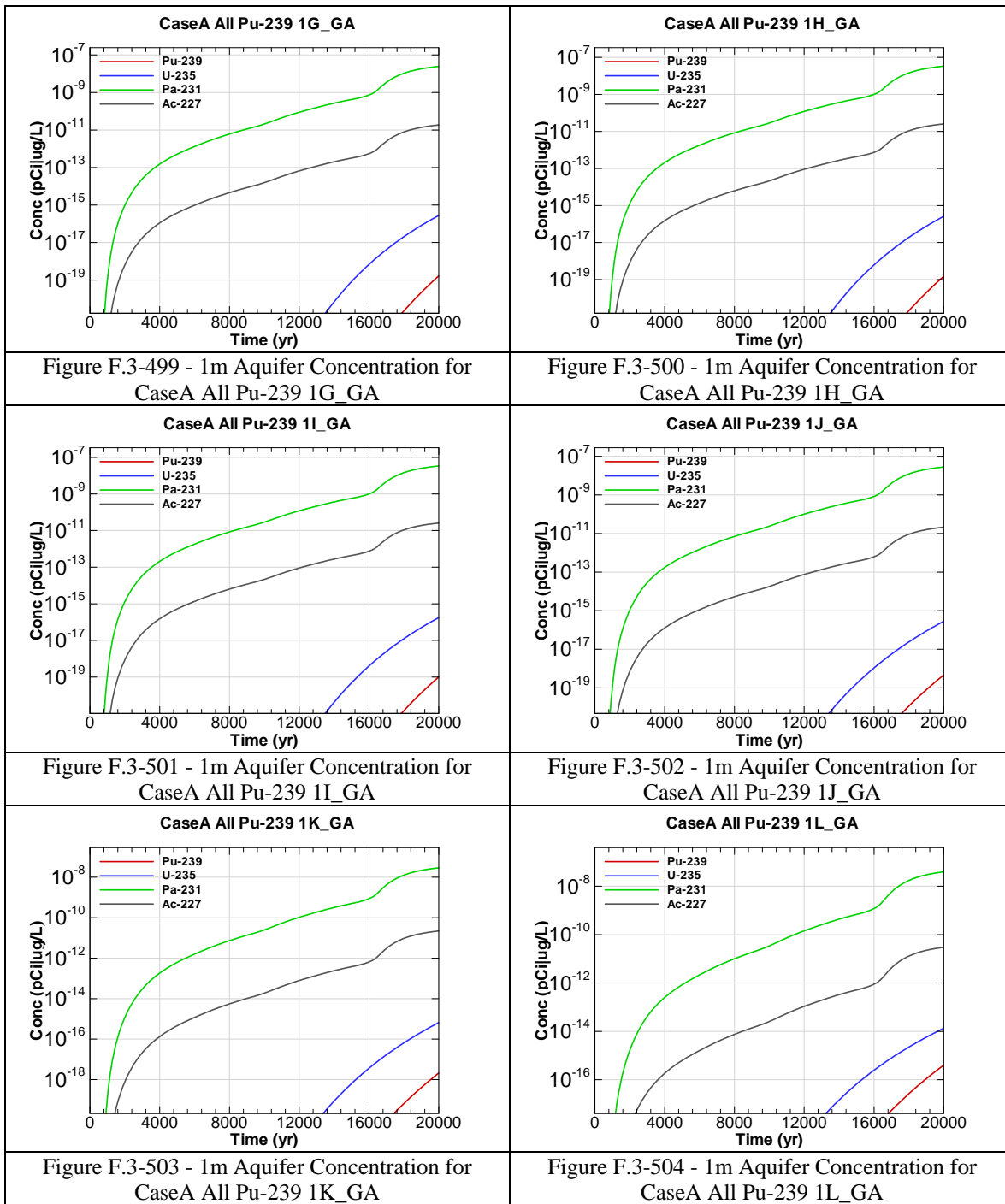
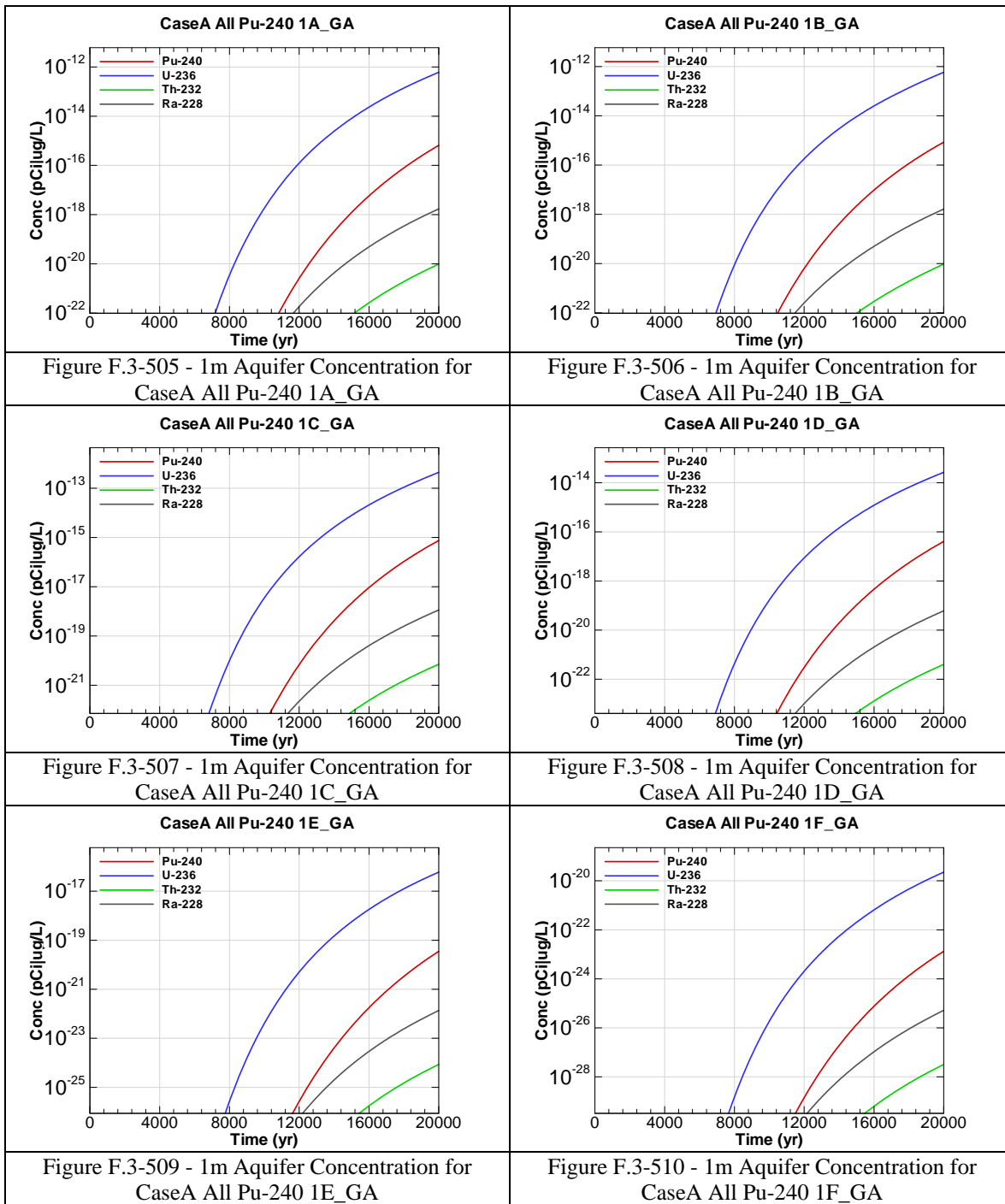


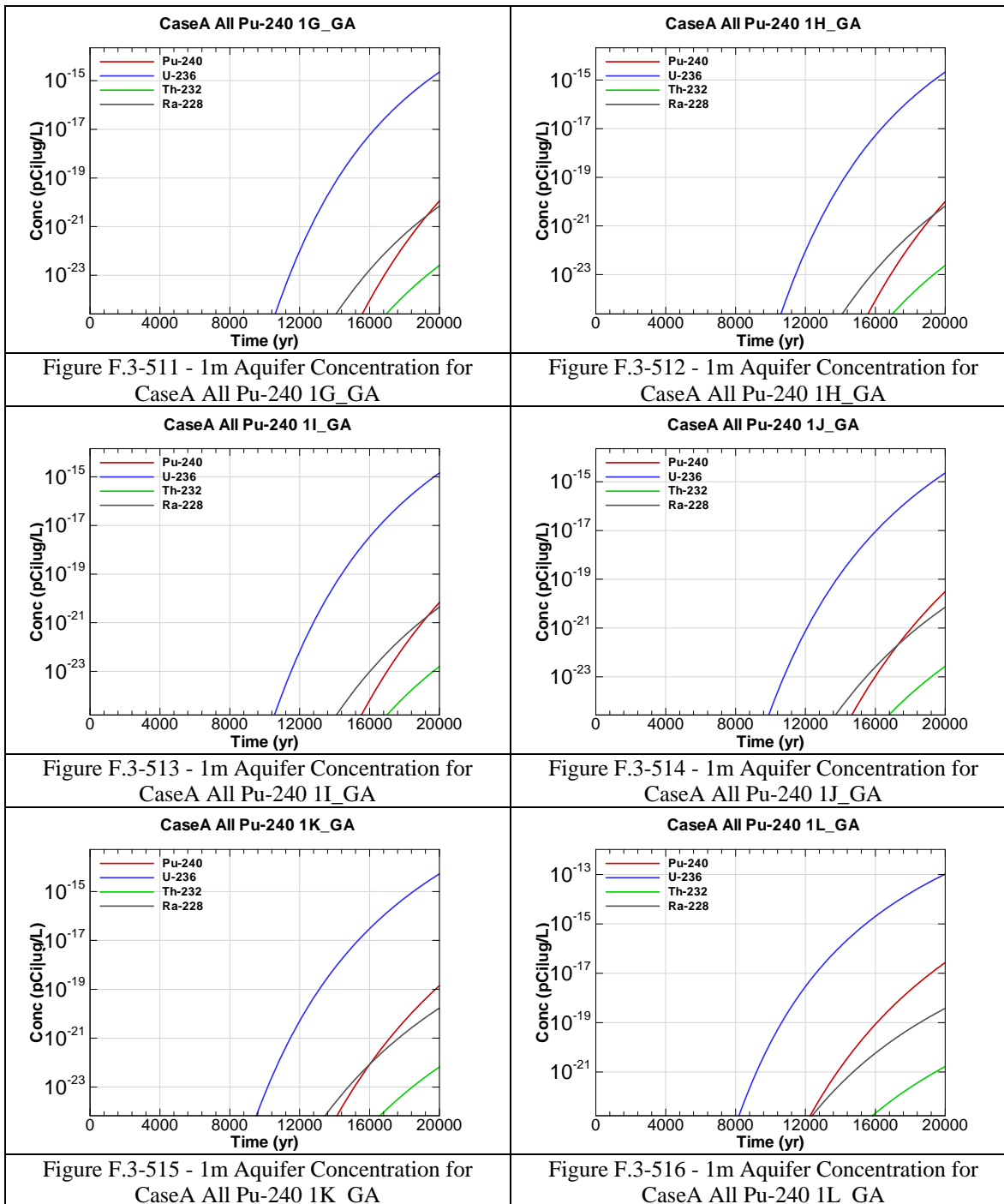
Figure F.3-486 - 1m Aquifer Concentration for
CaseA All Pu-238 1F_GA











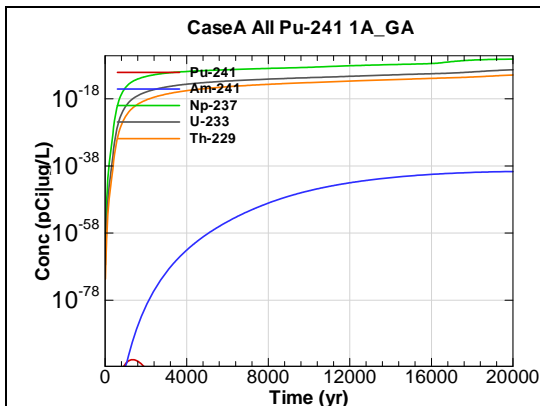


Figure F.3-517 - 1m Aquifer Concentration for
CaseA All Pu-241 1A_GA

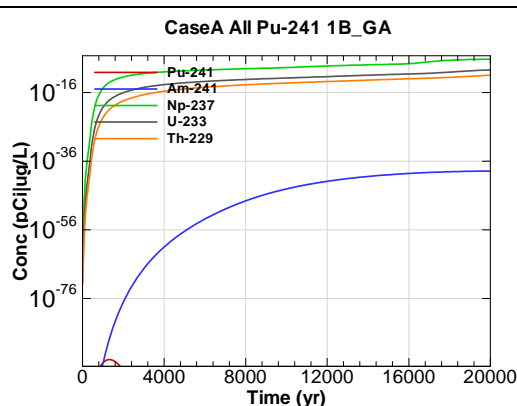


Figure F.3-518 - 1m Aquifer Concentration for
CaseA All Pu-241 1B_GA

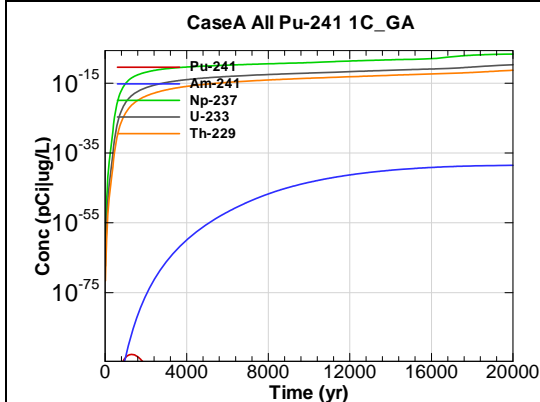


Figure F.3-519 - 1m Aquifer Concentration for
CaseA All Pu-241 1C_GA

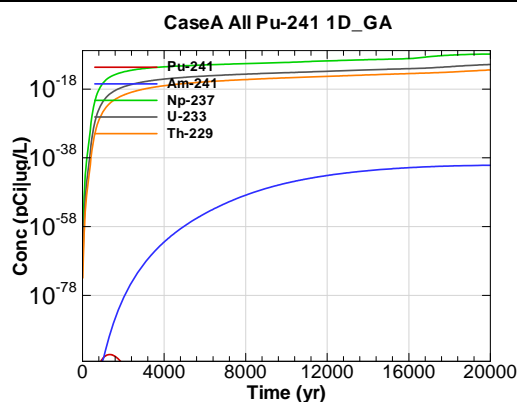


Figure F.3-520 - 1m Aquifer Concentration for
CaseA All Pu-241 1D_GA

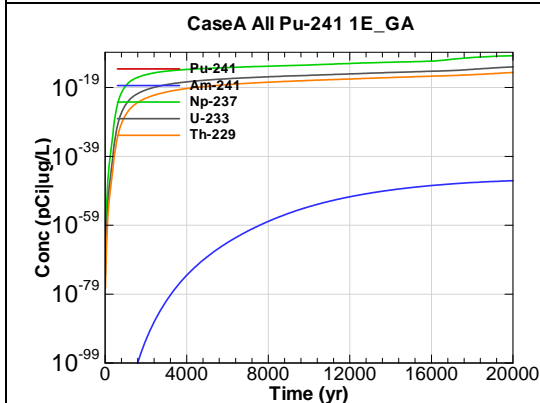


Figure F.3-521 - 1m Aquifer Concentration for
CaseA All Pu-241 1E_GA

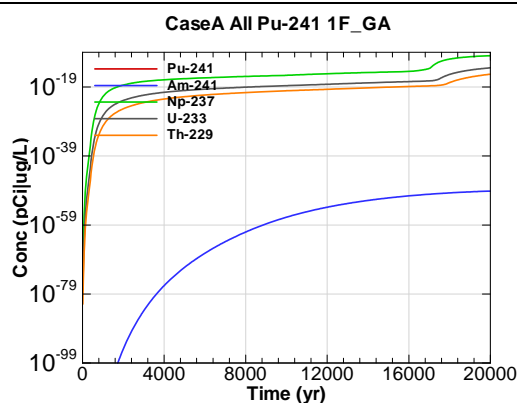
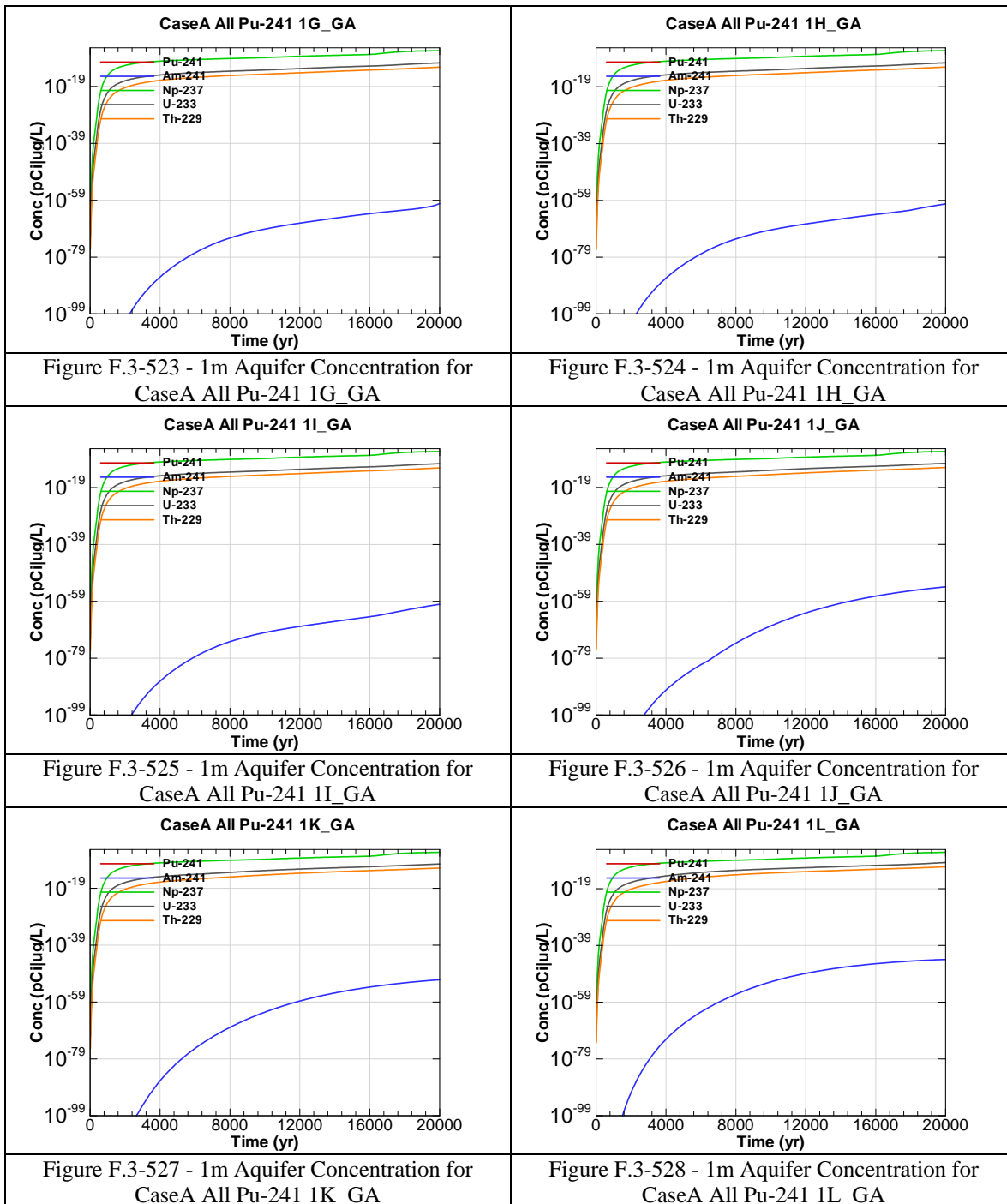
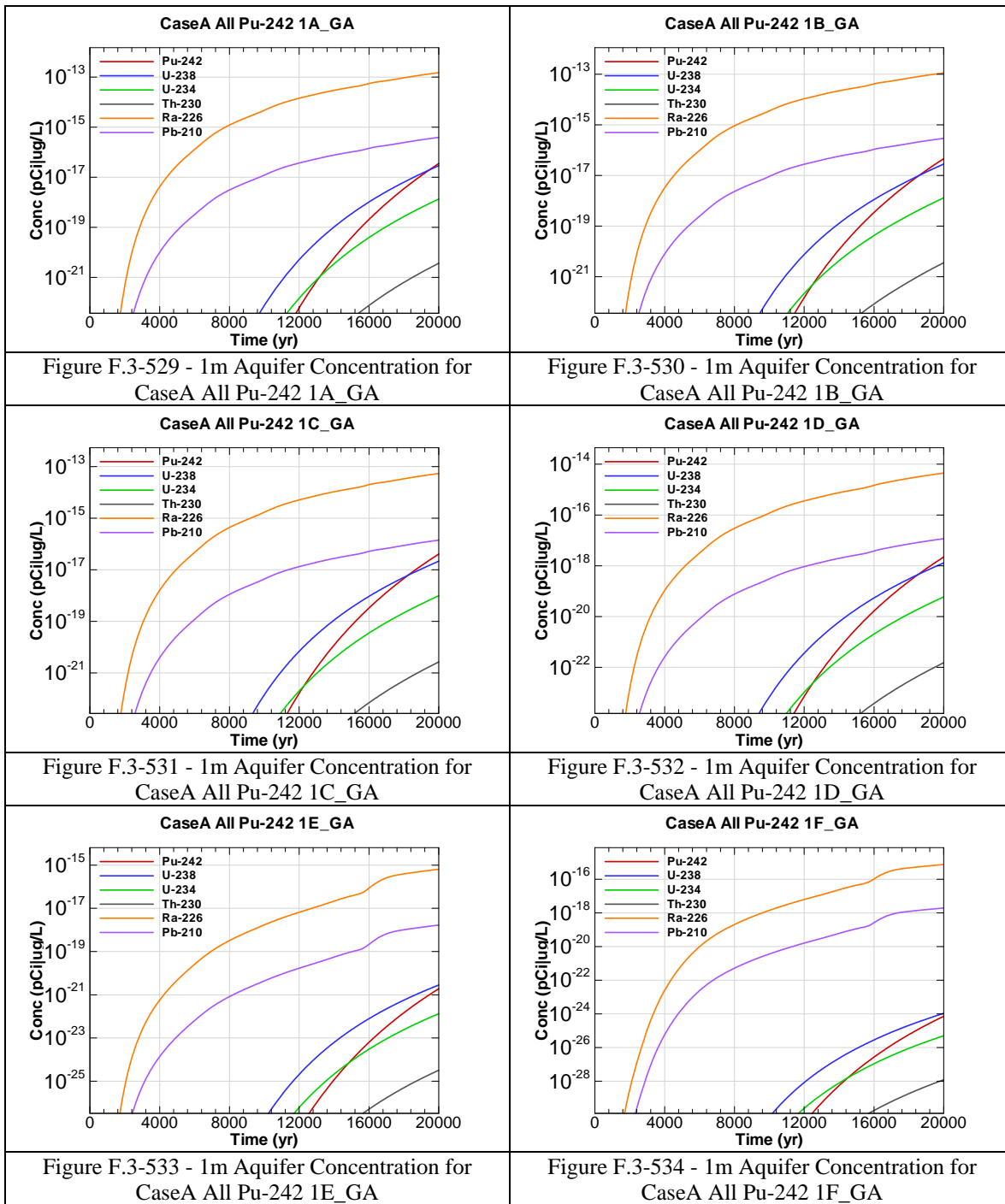


Figure F.3-522 - 1m Aquifer Concentration for
CaseA All Pu-241 1F_GA





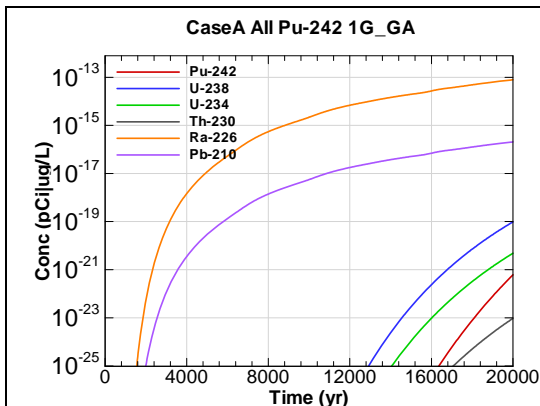


Figure F.3-535 - 1m Aquifer Concentration for
CaseA All Pu-242 1G_GA

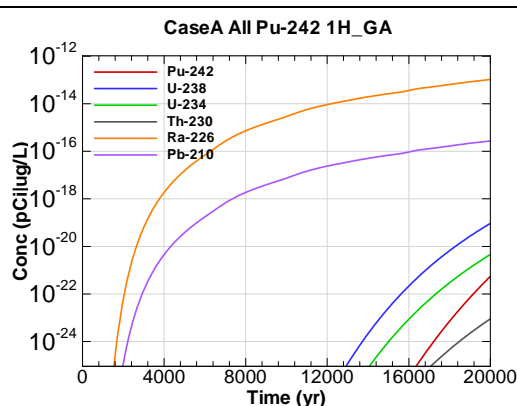


Figure F.3-536 - 1m Aquifer Concentration for
CaseA All Pu-242 1H_GA

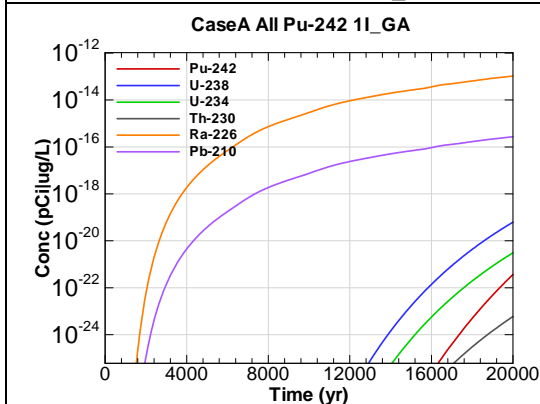


Figure F.3-537 - 1m Aquifer Concentration for
CaseA All Pu-242 1I_GA

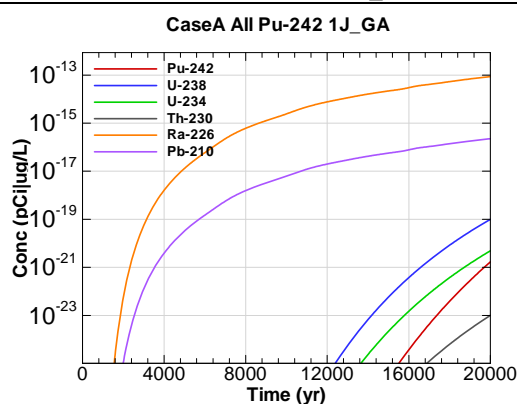


Figure F.3-538 - 1m Aquifer Concentration for
CaseA All Pu-242 1J_GA

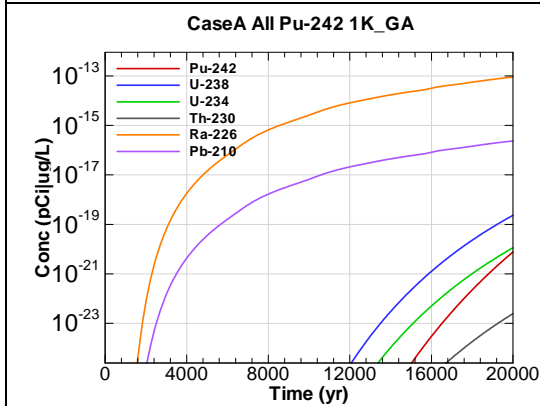


Figure F.3-539 - 1m Aquifer Concentration for
CaseA All Pu-242 1K_GA

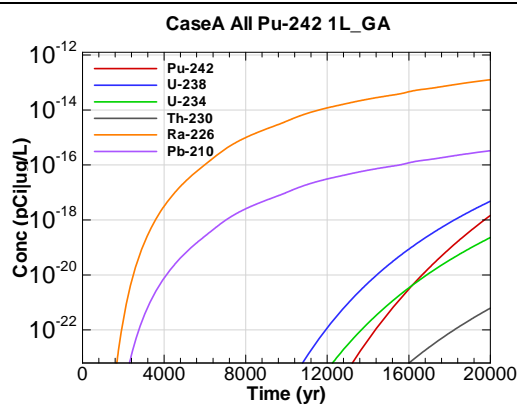
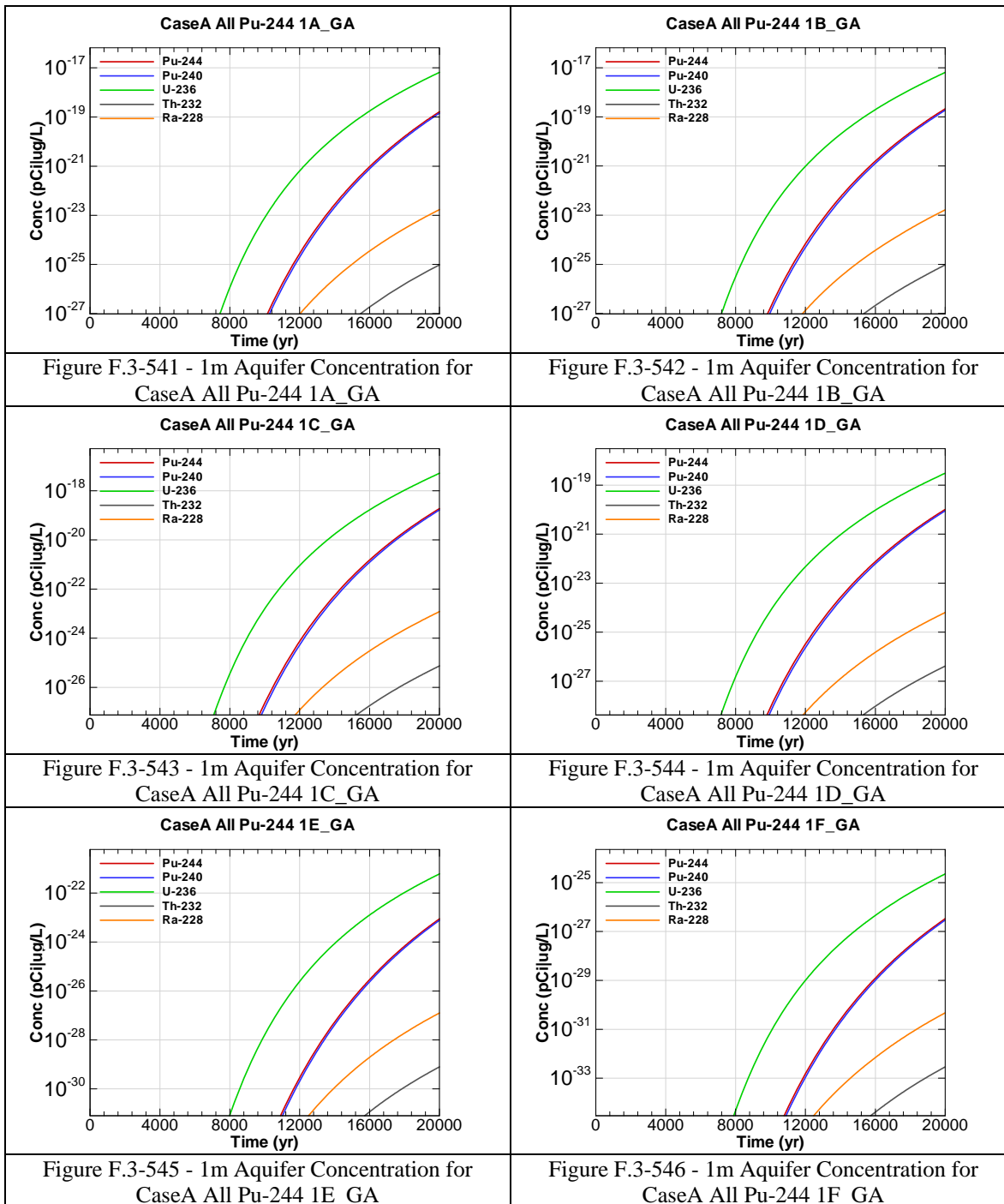
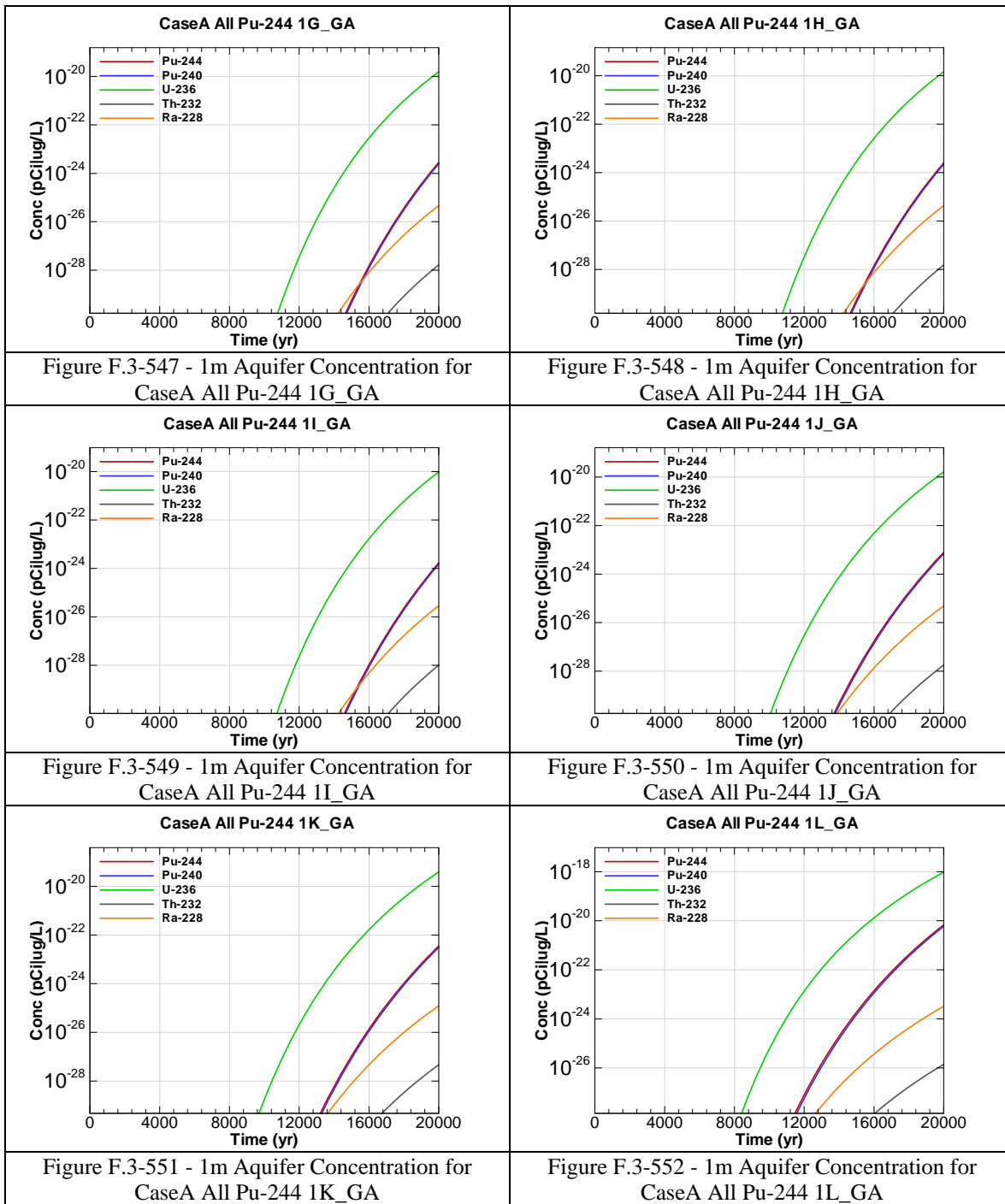
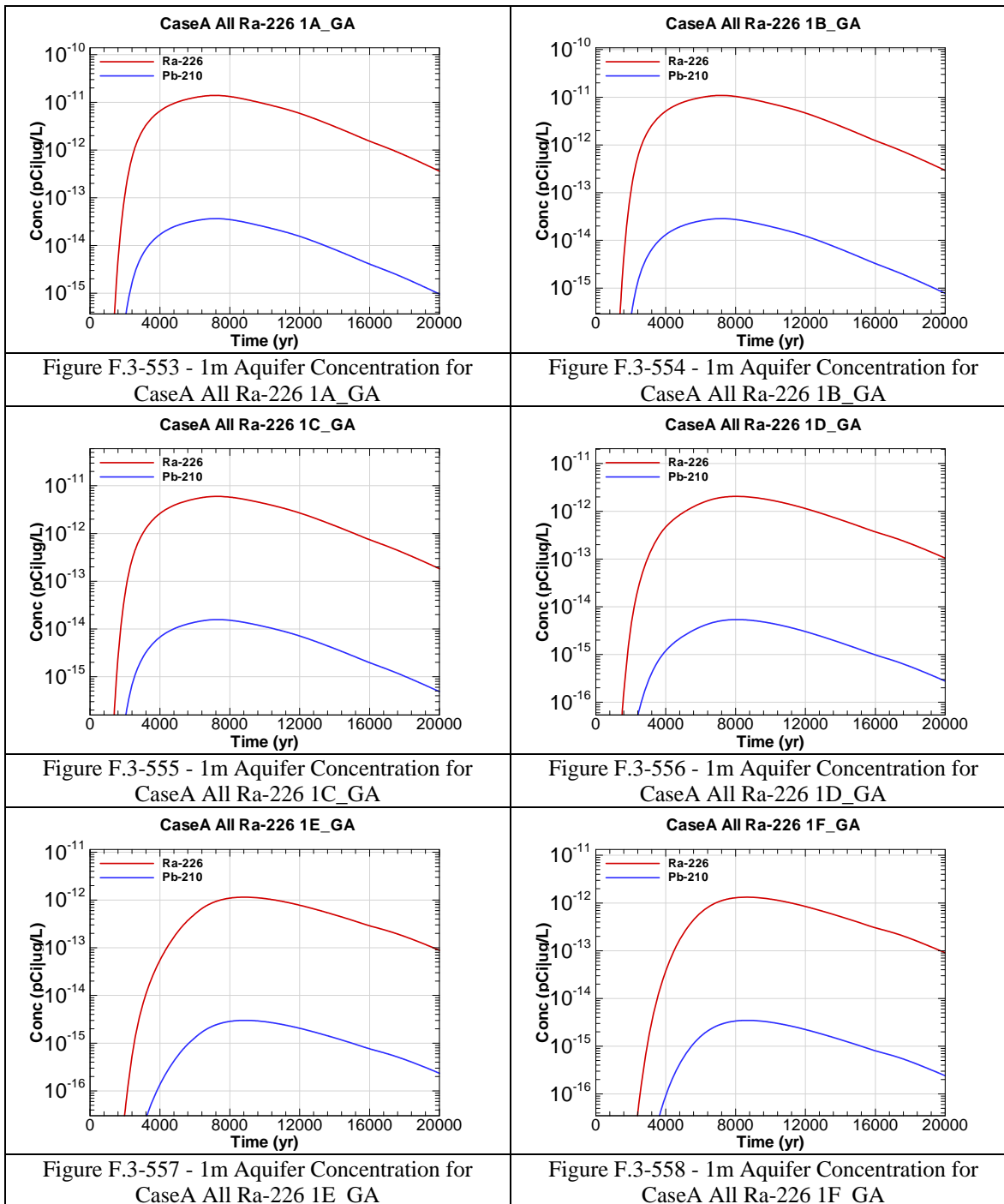


Figure F.3-540 - 1m Aquifer Concentration for
CaseA All Pu-242 1L_GA







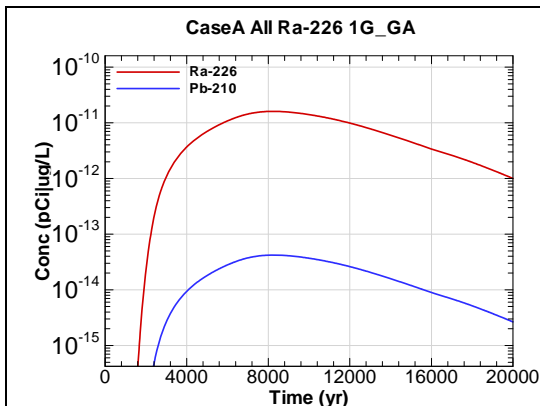


Figure F.3-559 - 1m Aquifer Concentration for
CaseA All Ra-226 1G_GA

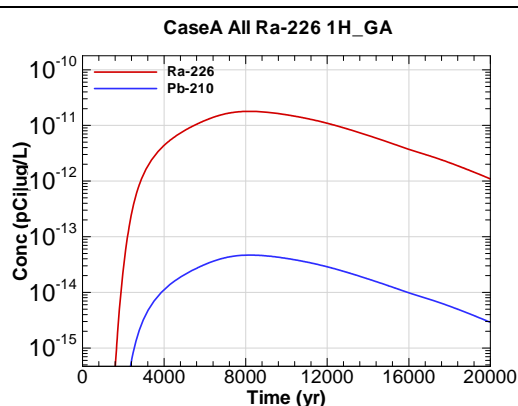


Figure F.3-560 - 1m Aquifer Concentration for
CaseA All Ra-226 1H_GA

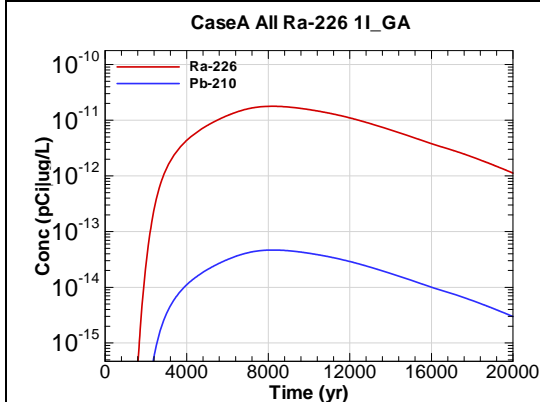


Figure F.3-561 - 1m Aquifer Concentration for
CaseA All Ra-226 1I_GA

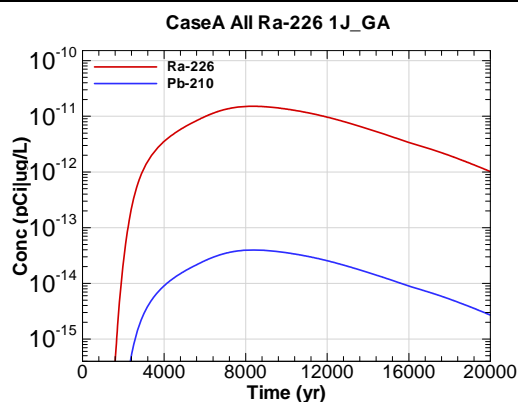


Figure F.3-562 - 1m Aquifer Concentration for
CaseA All Ra-226 1J_GA

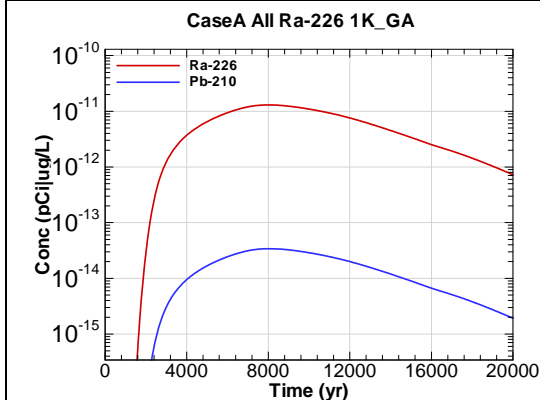


Figure F.3-563 - 1m Aquifer Concentration for
CaseA All Ra-226 1K_GA

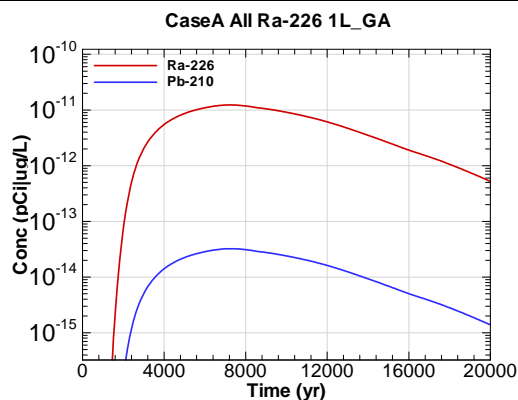
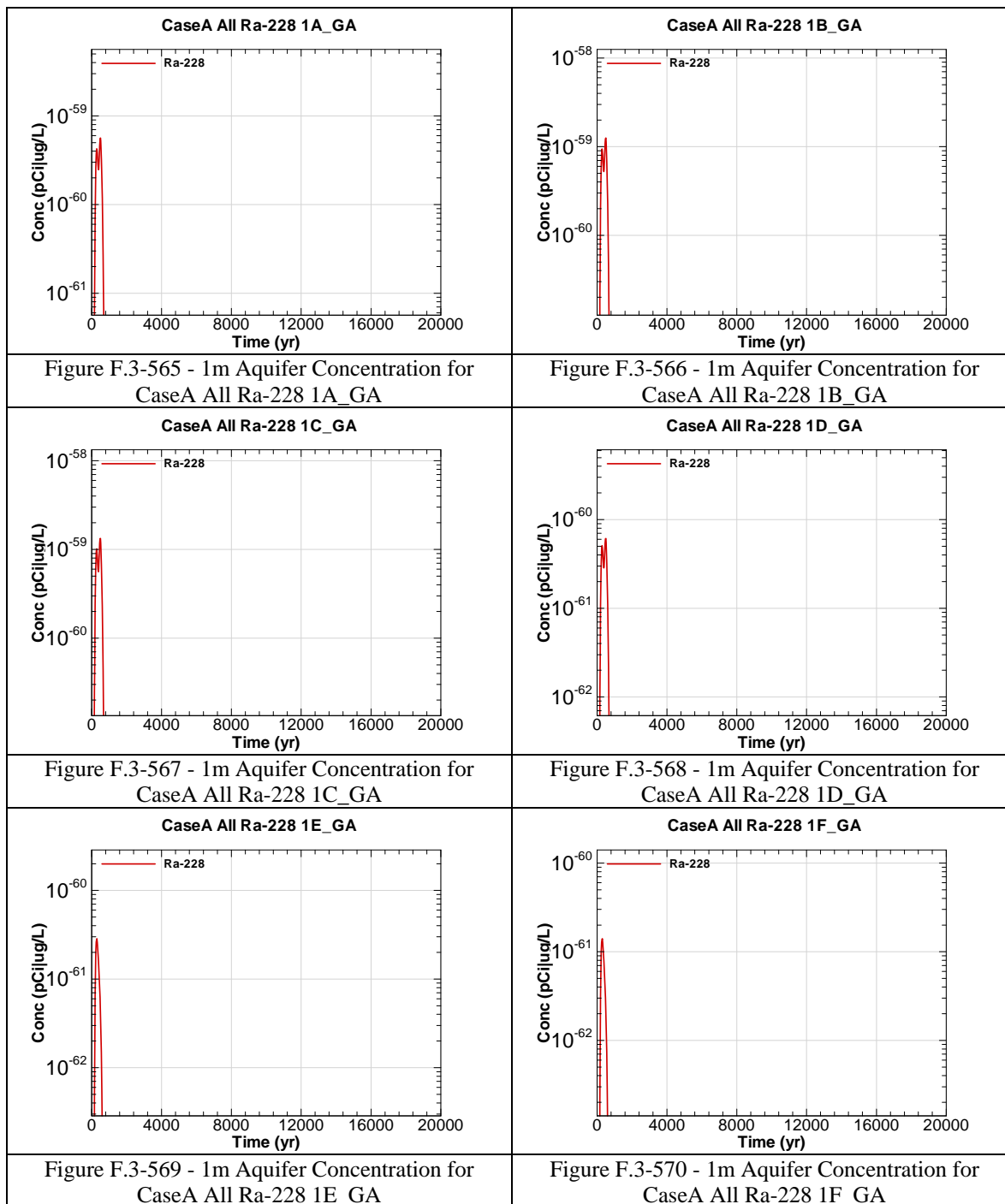
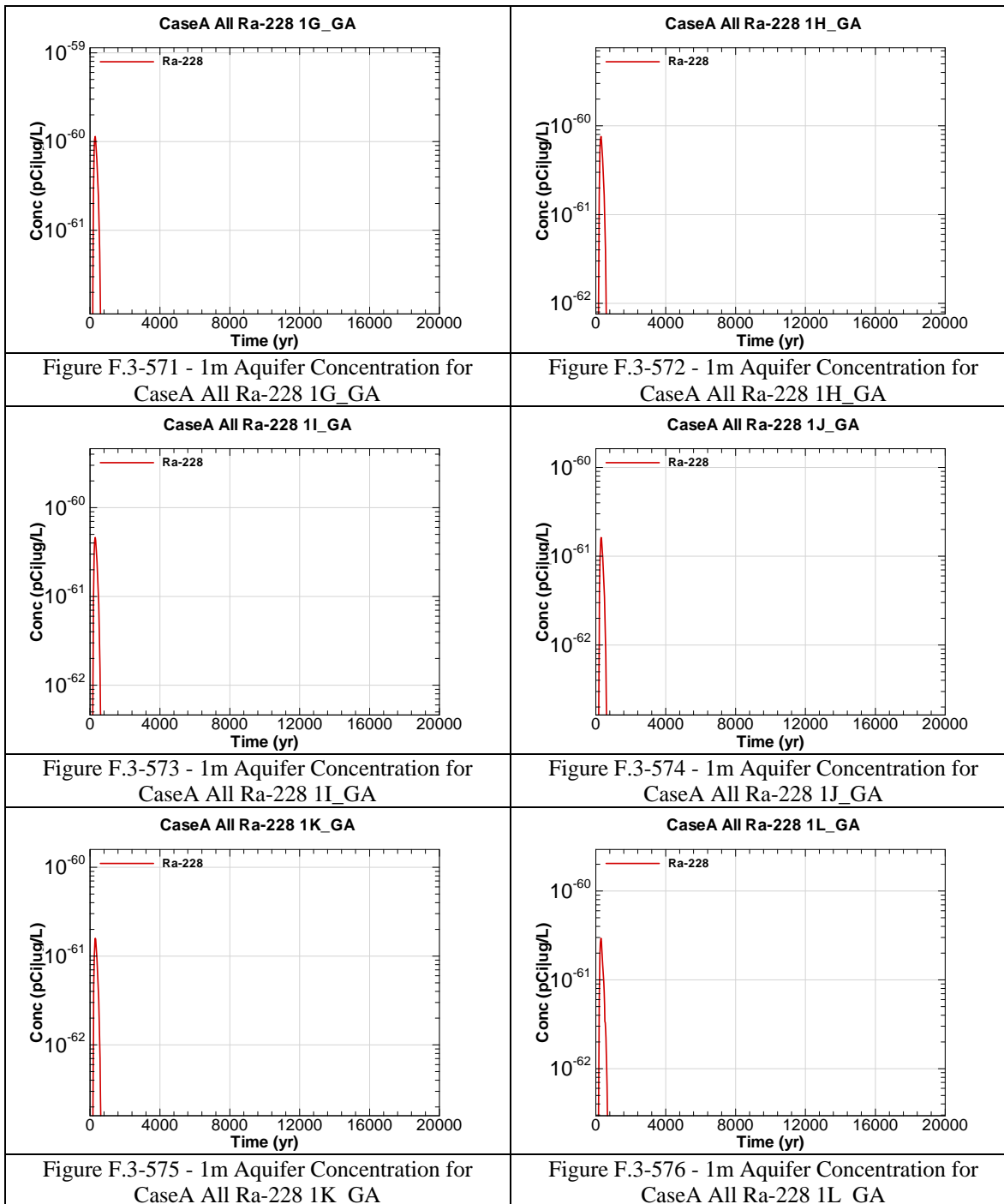
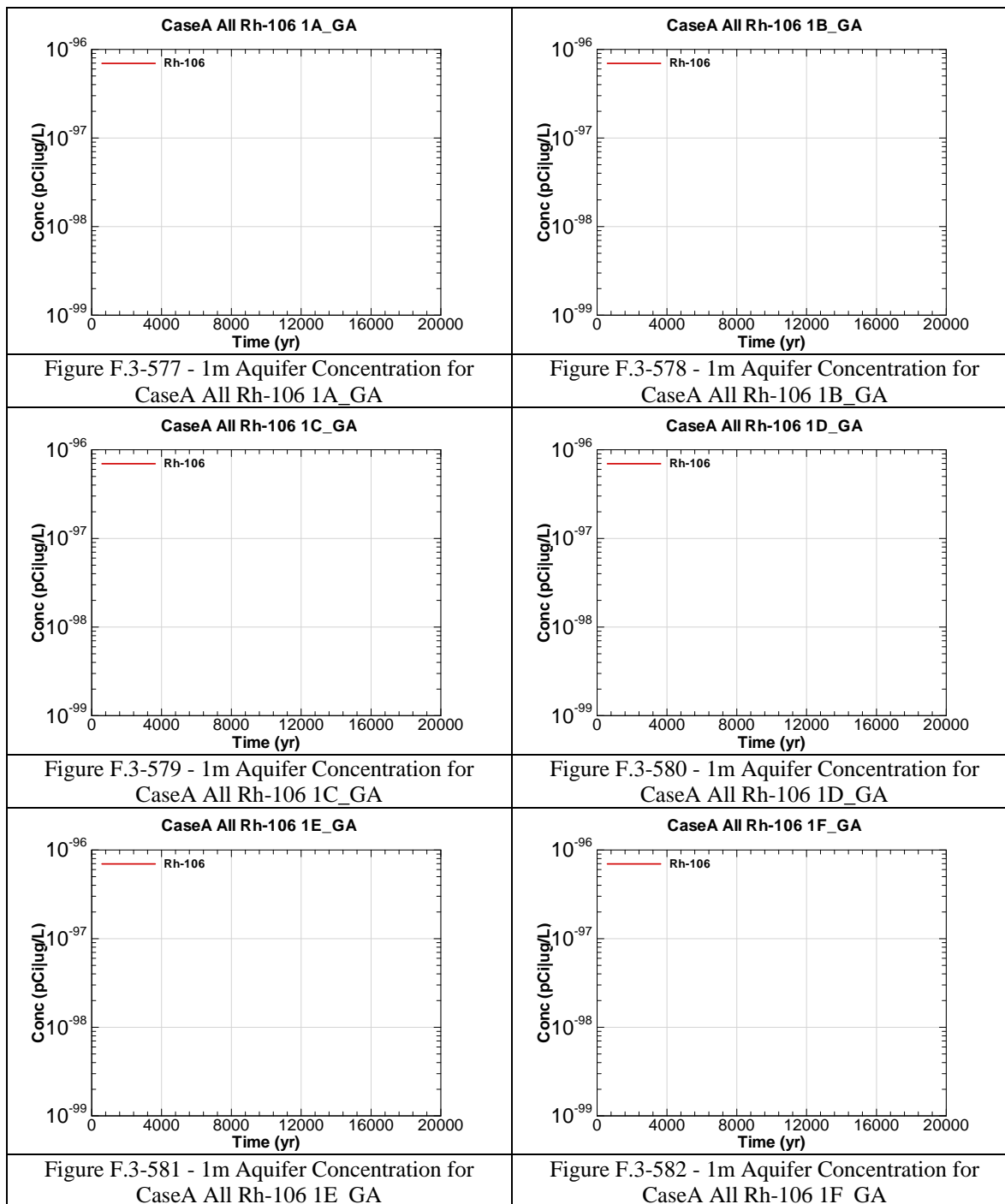
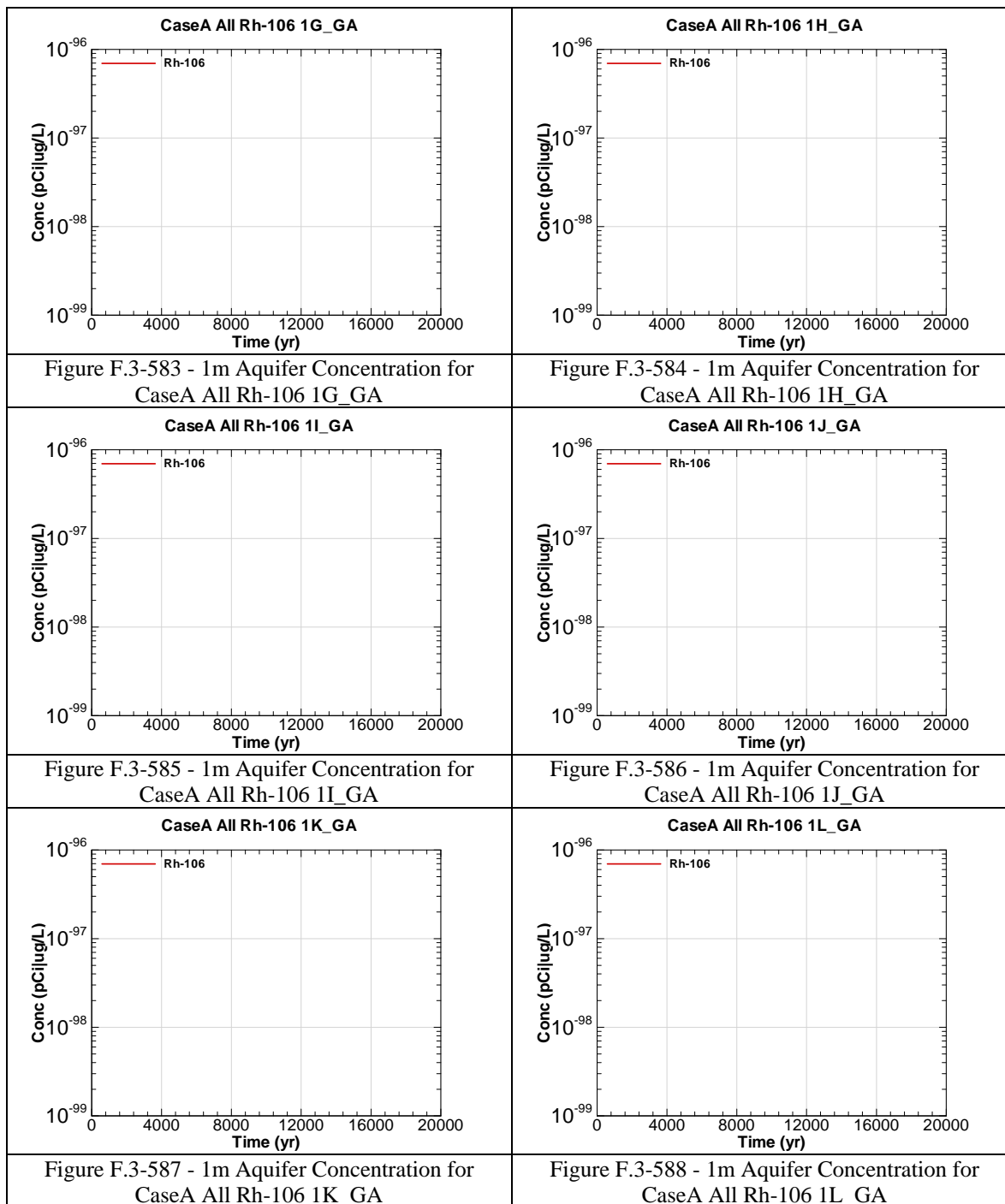


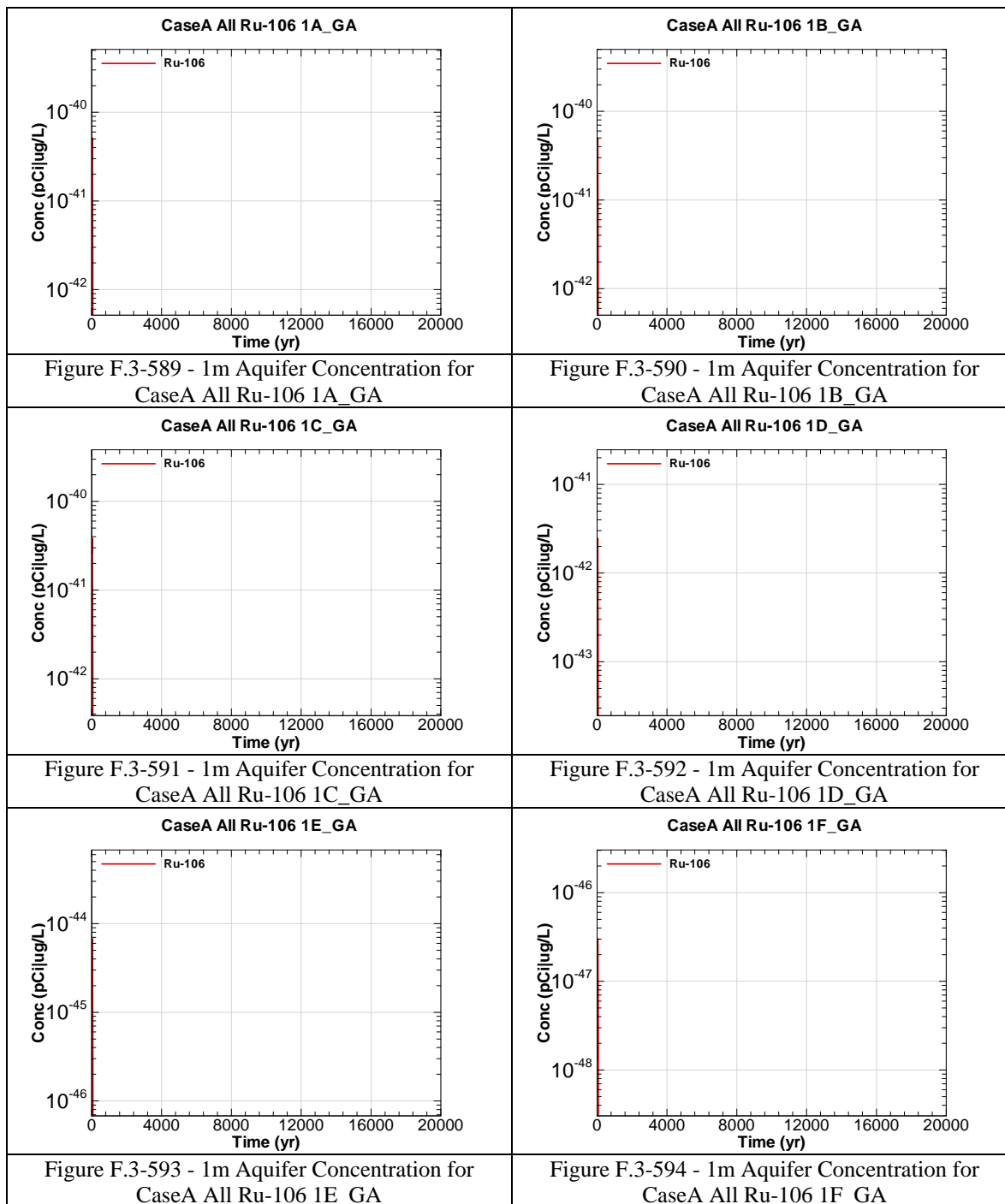
Figure F.3-564 - 1m Aquifer Concentration for
CaseA All Ra-226 1L_GA

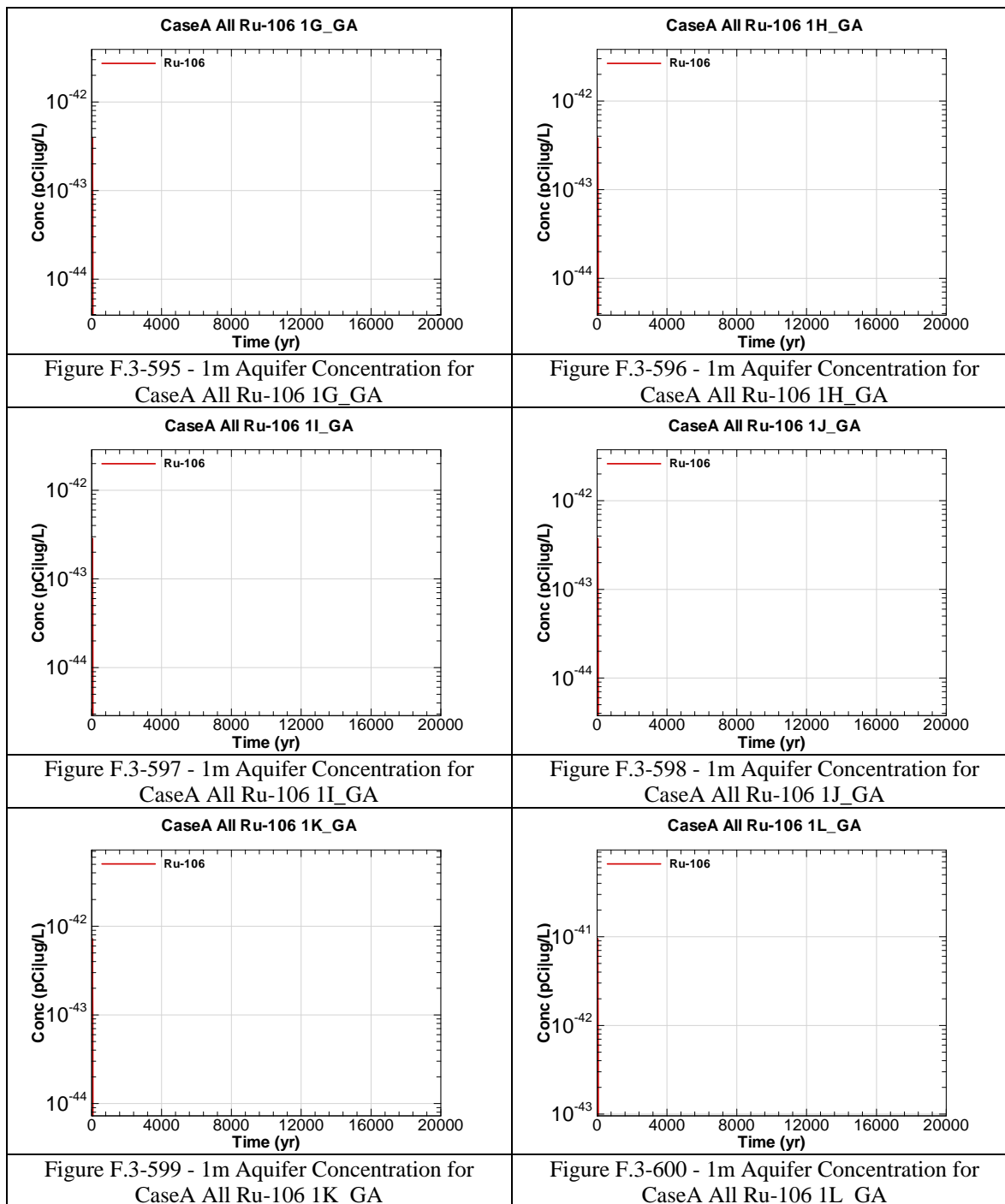


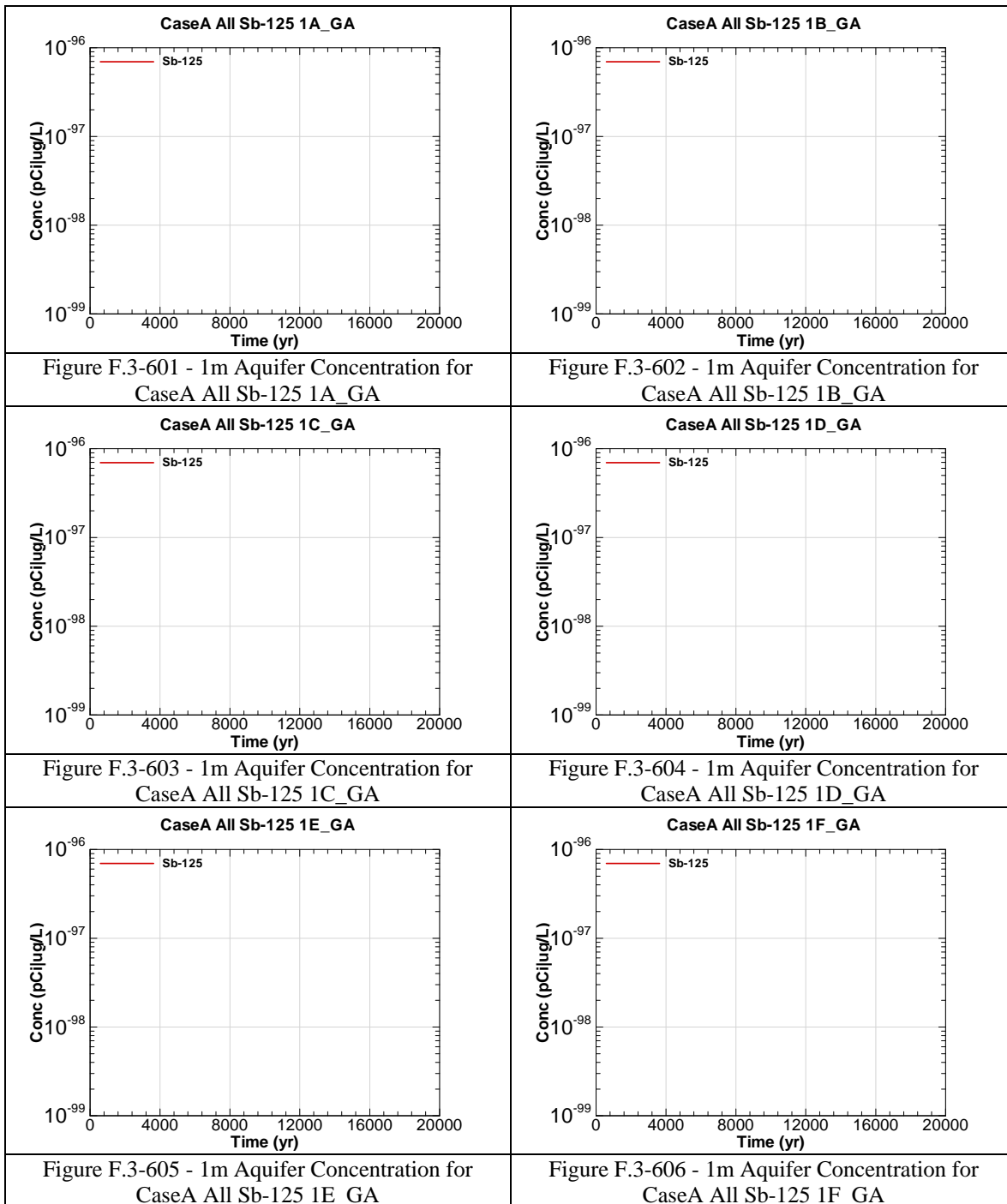


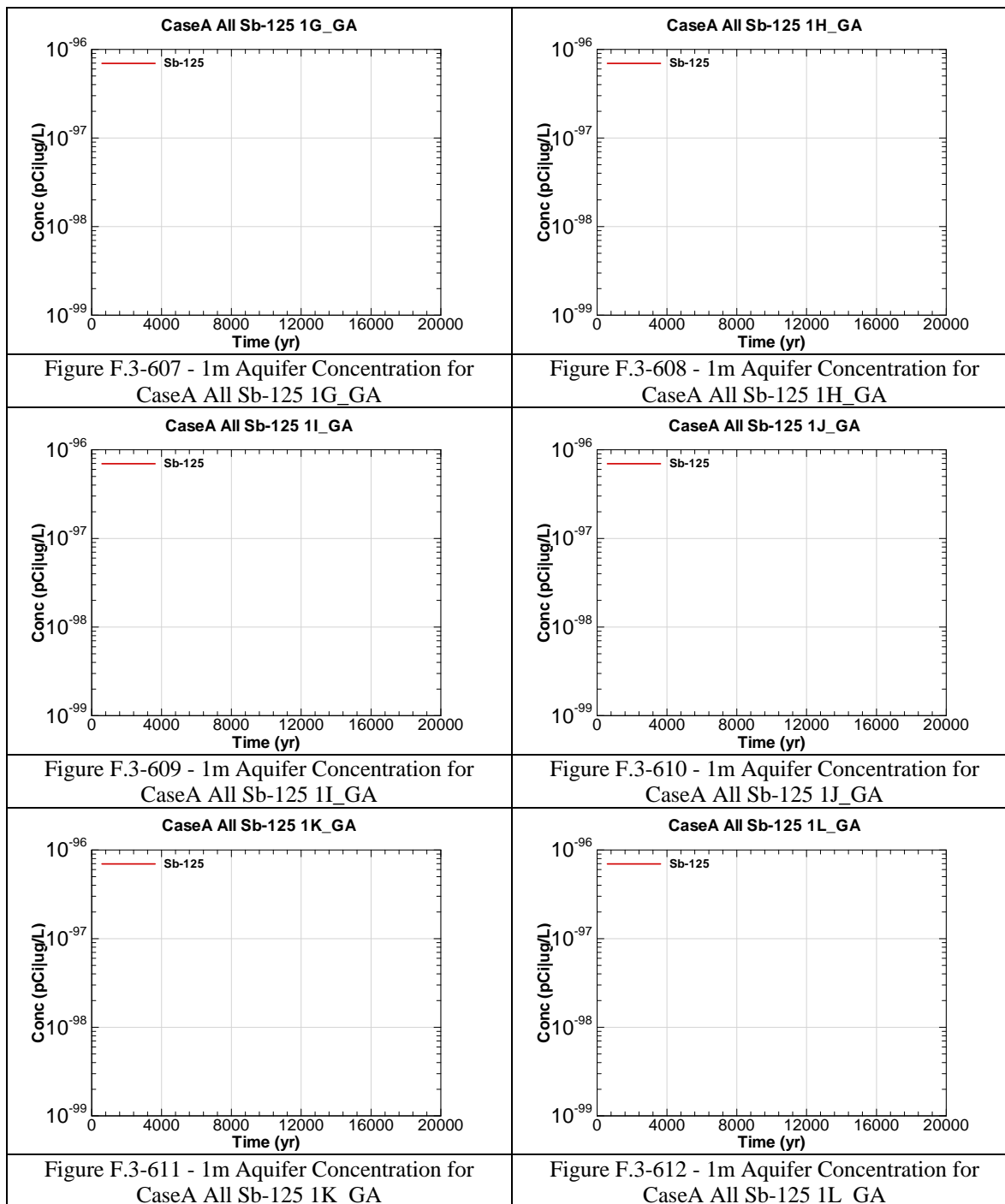


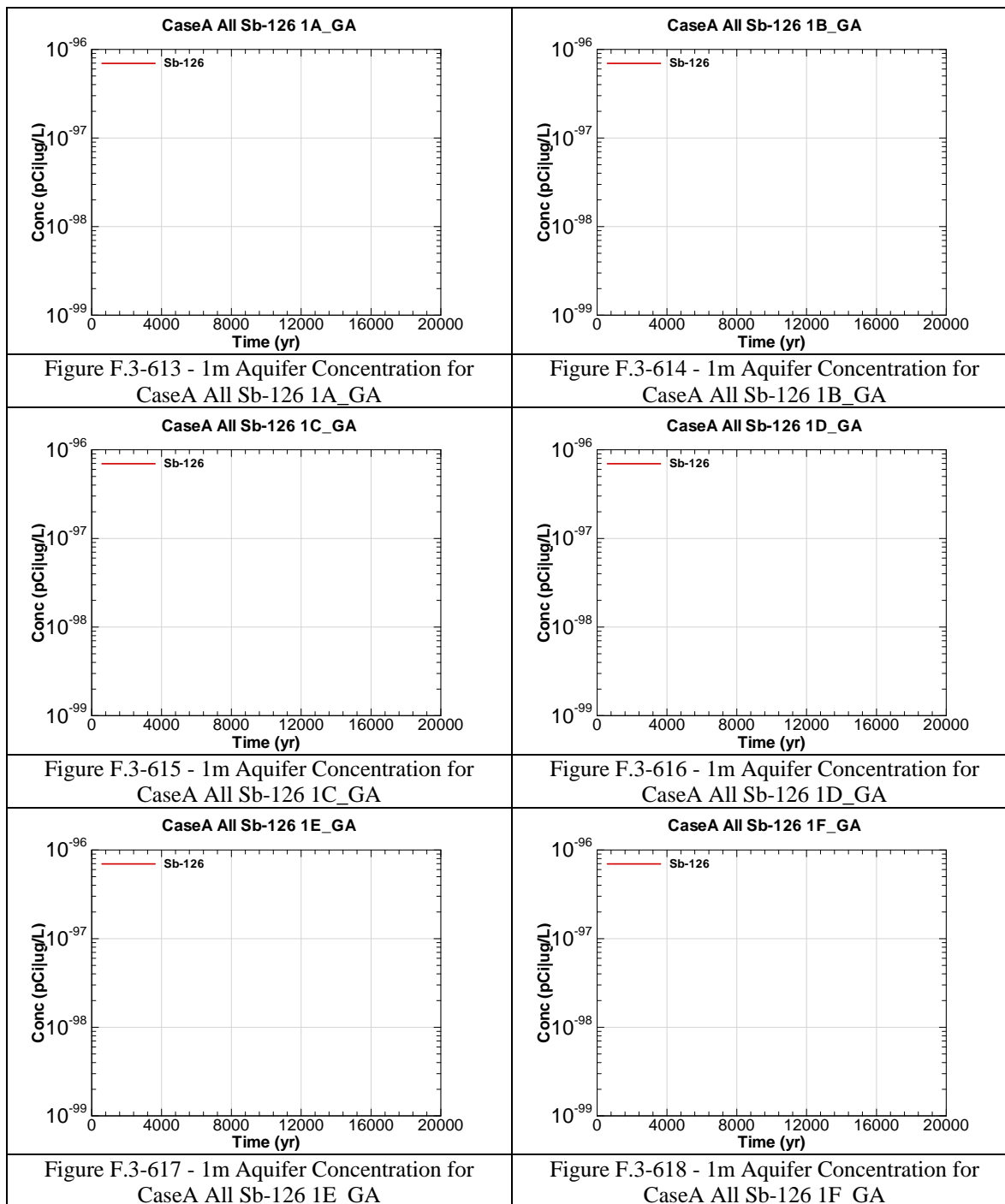


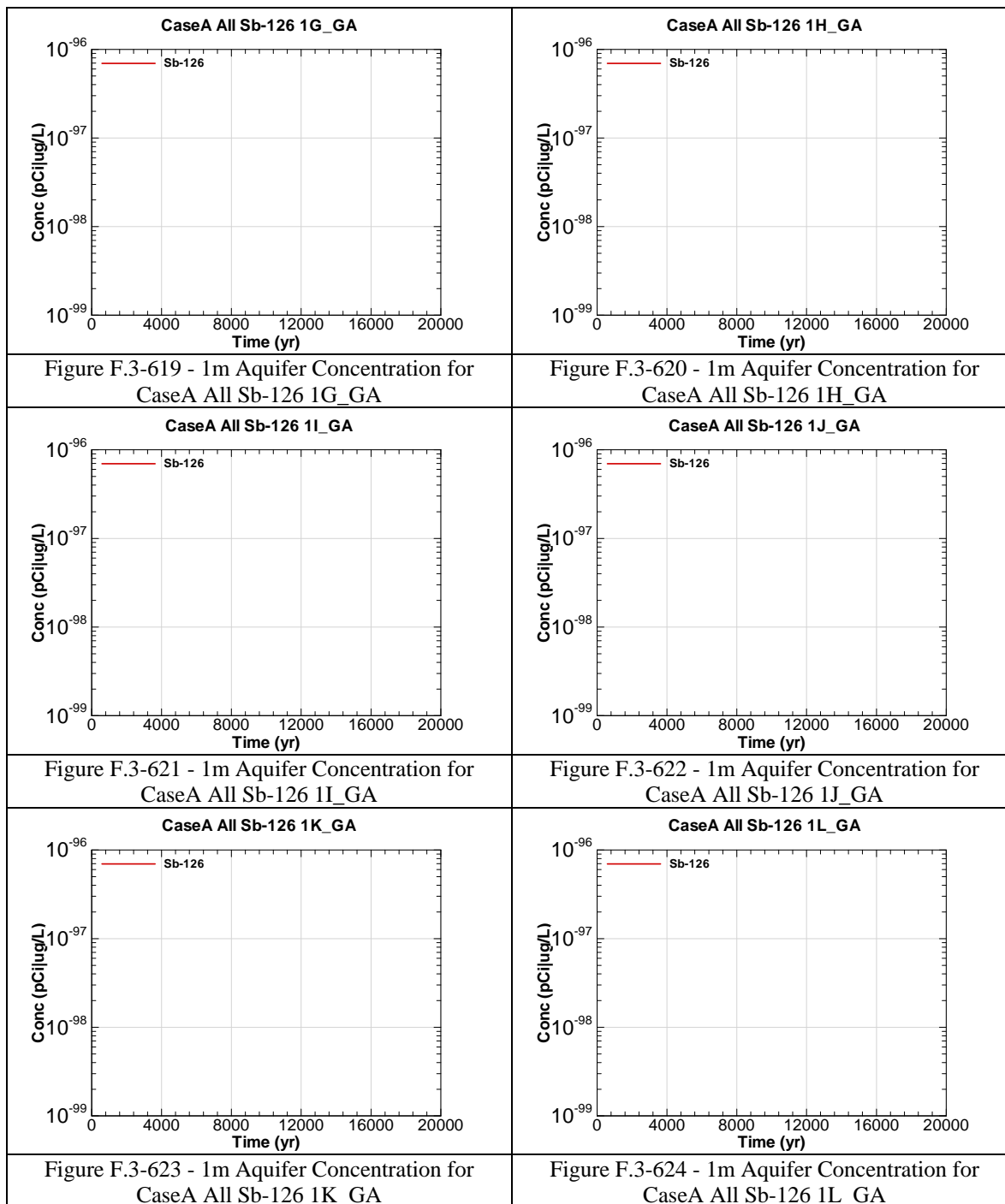


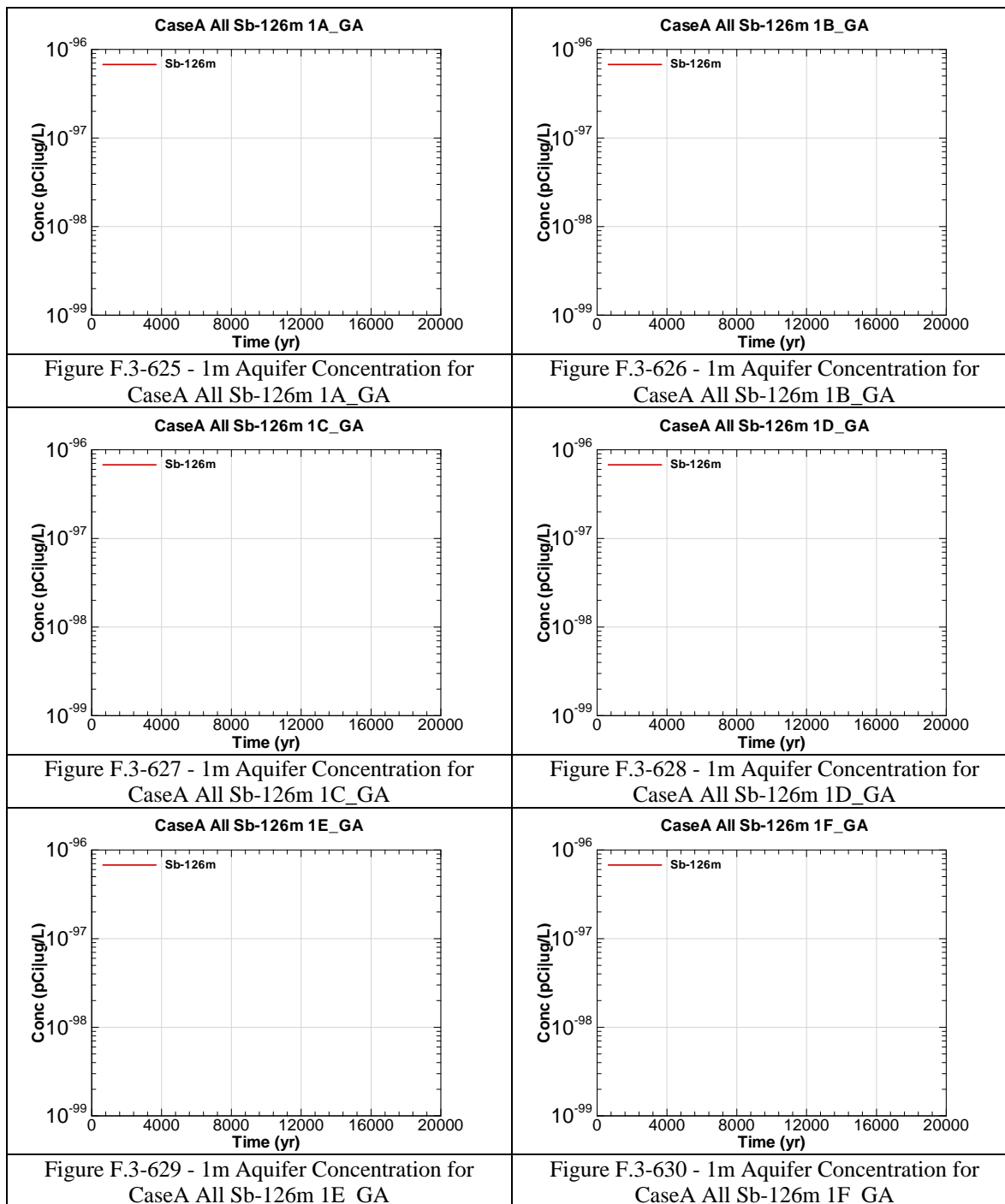


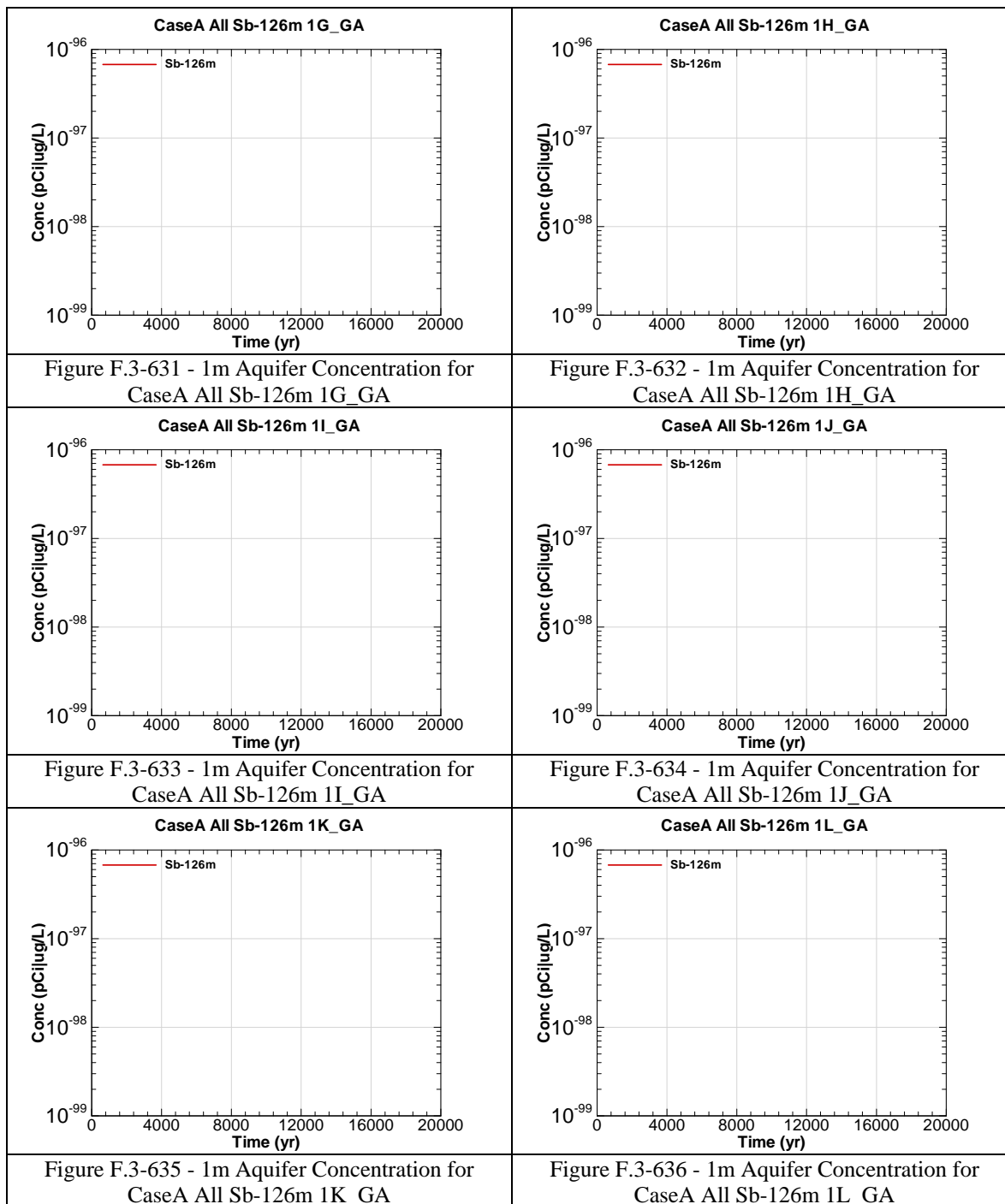


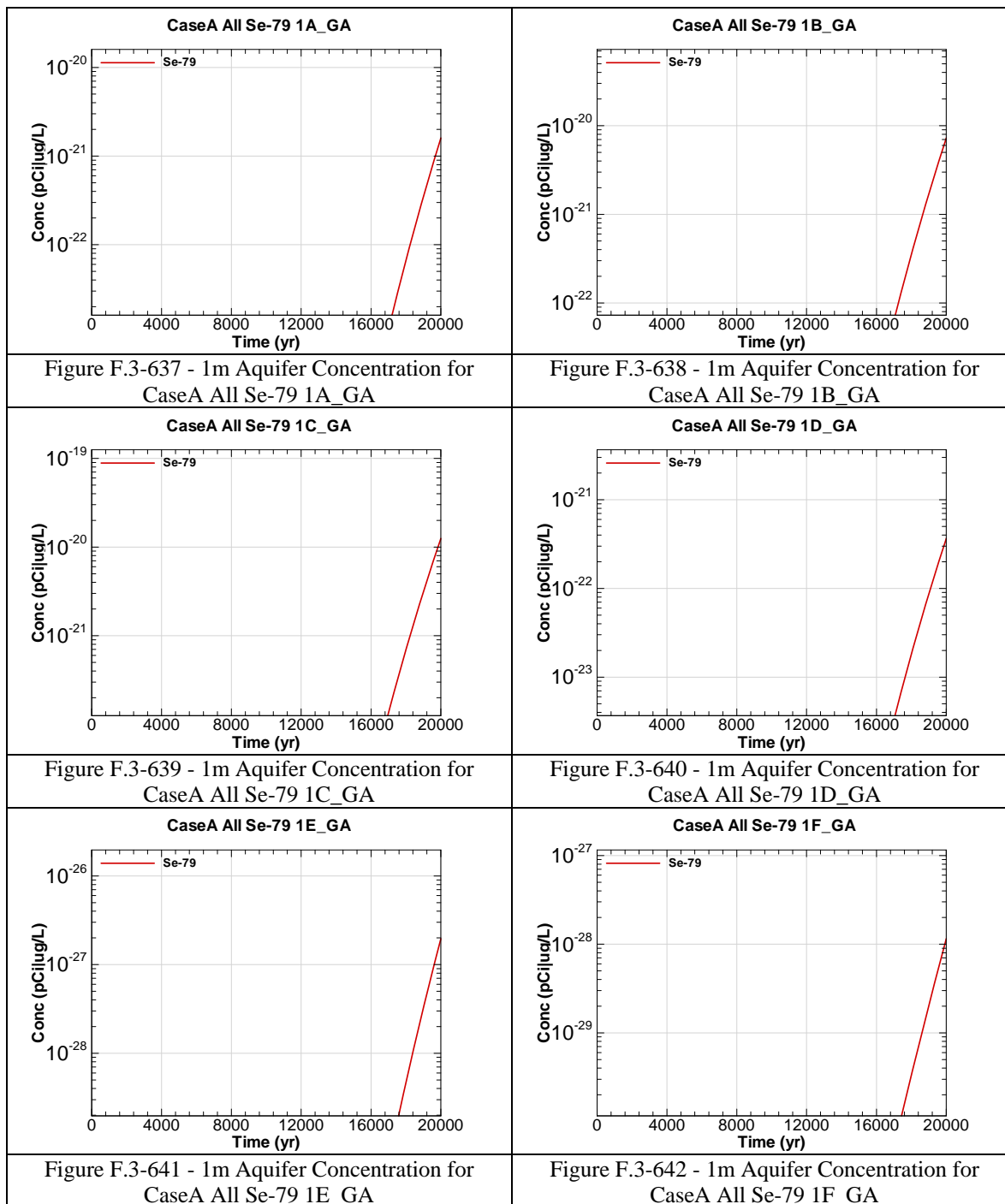


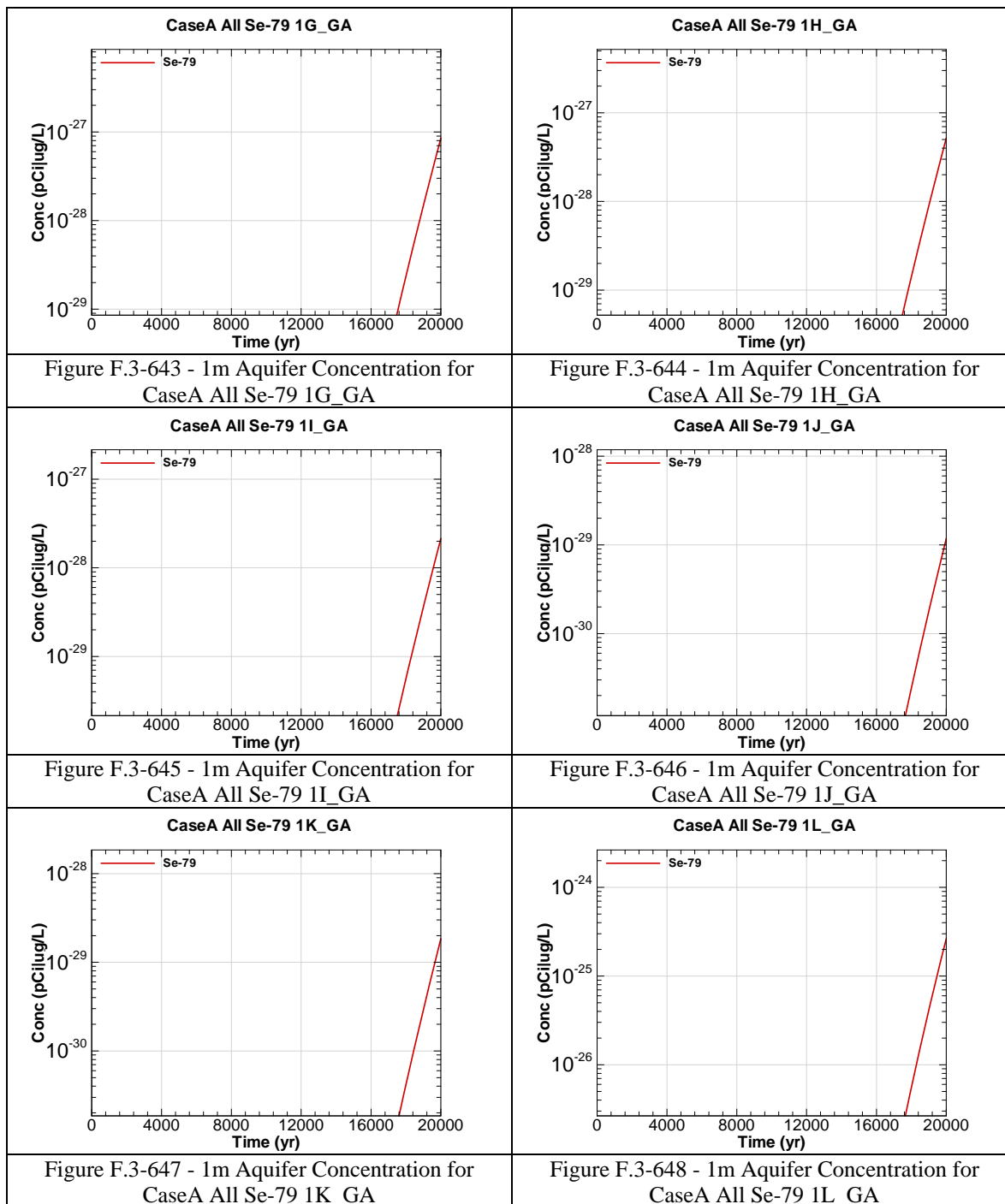


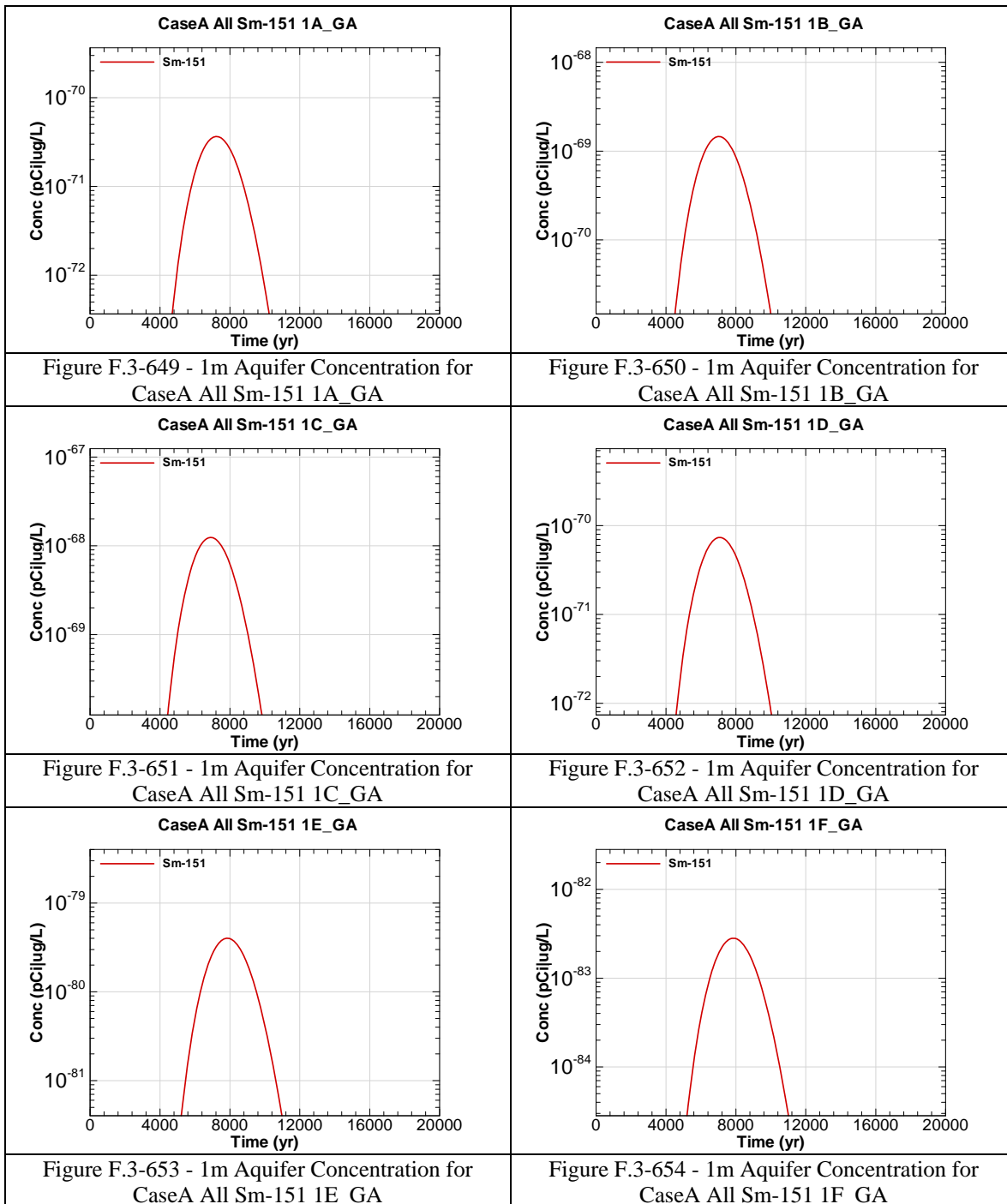


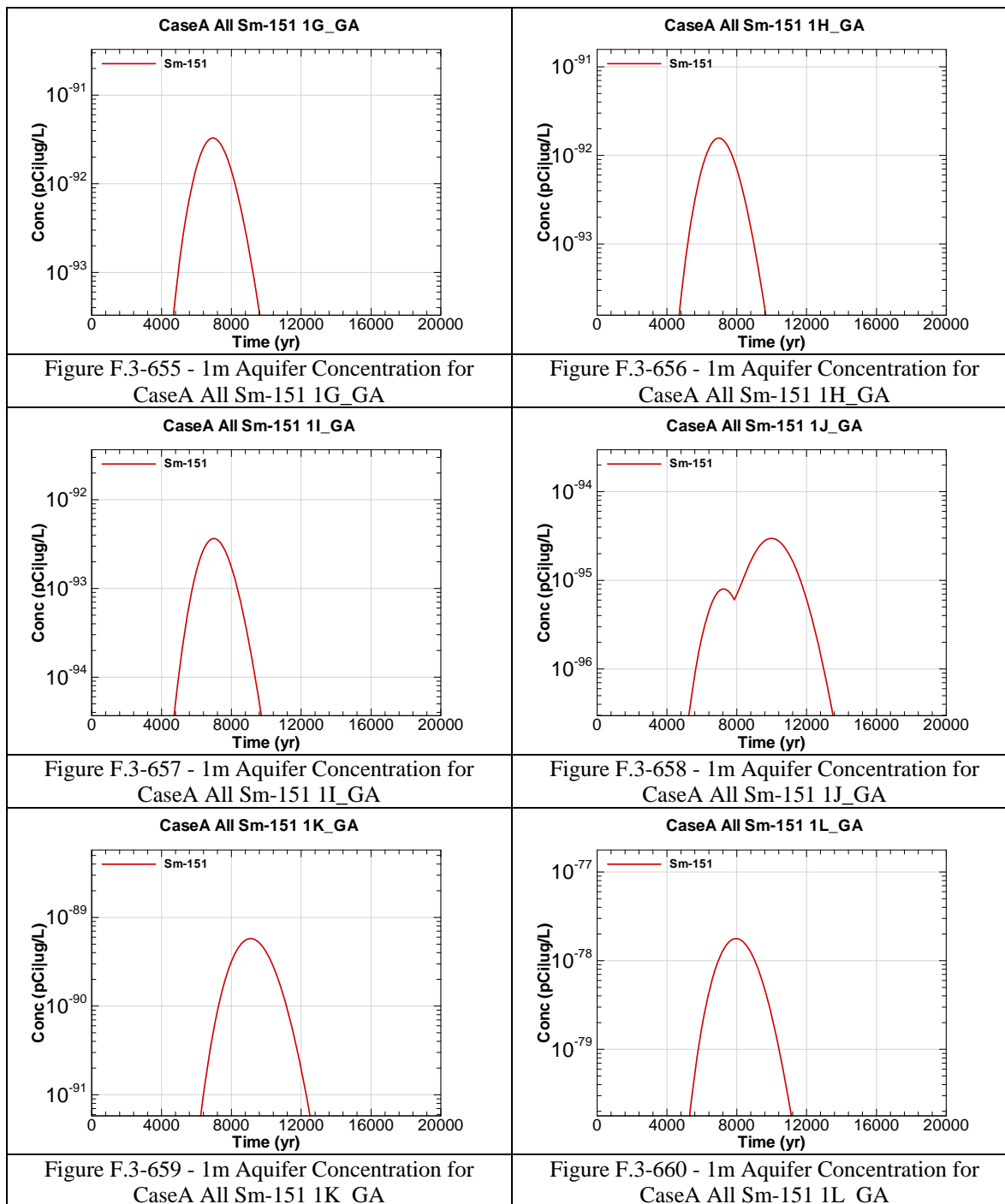


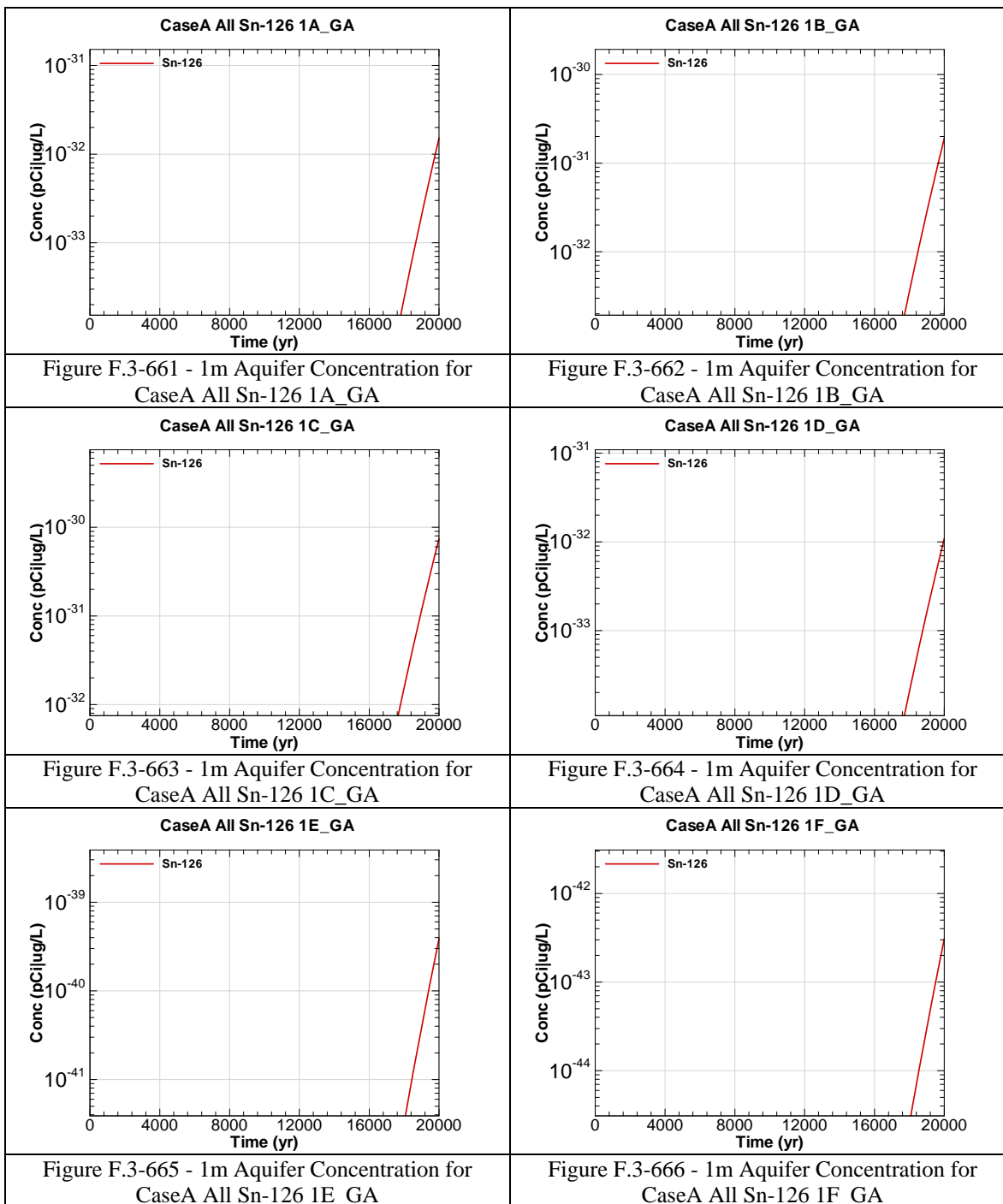


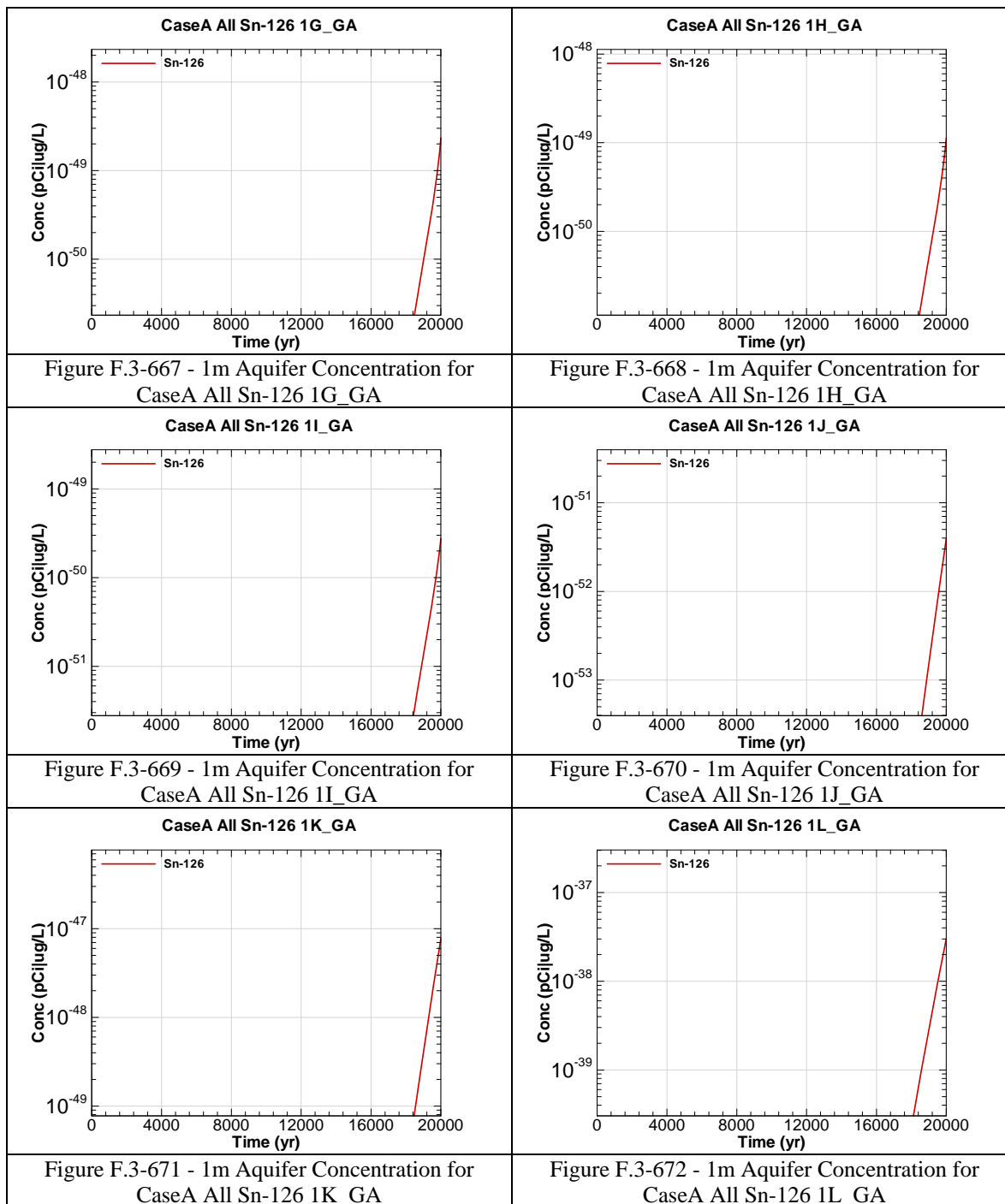


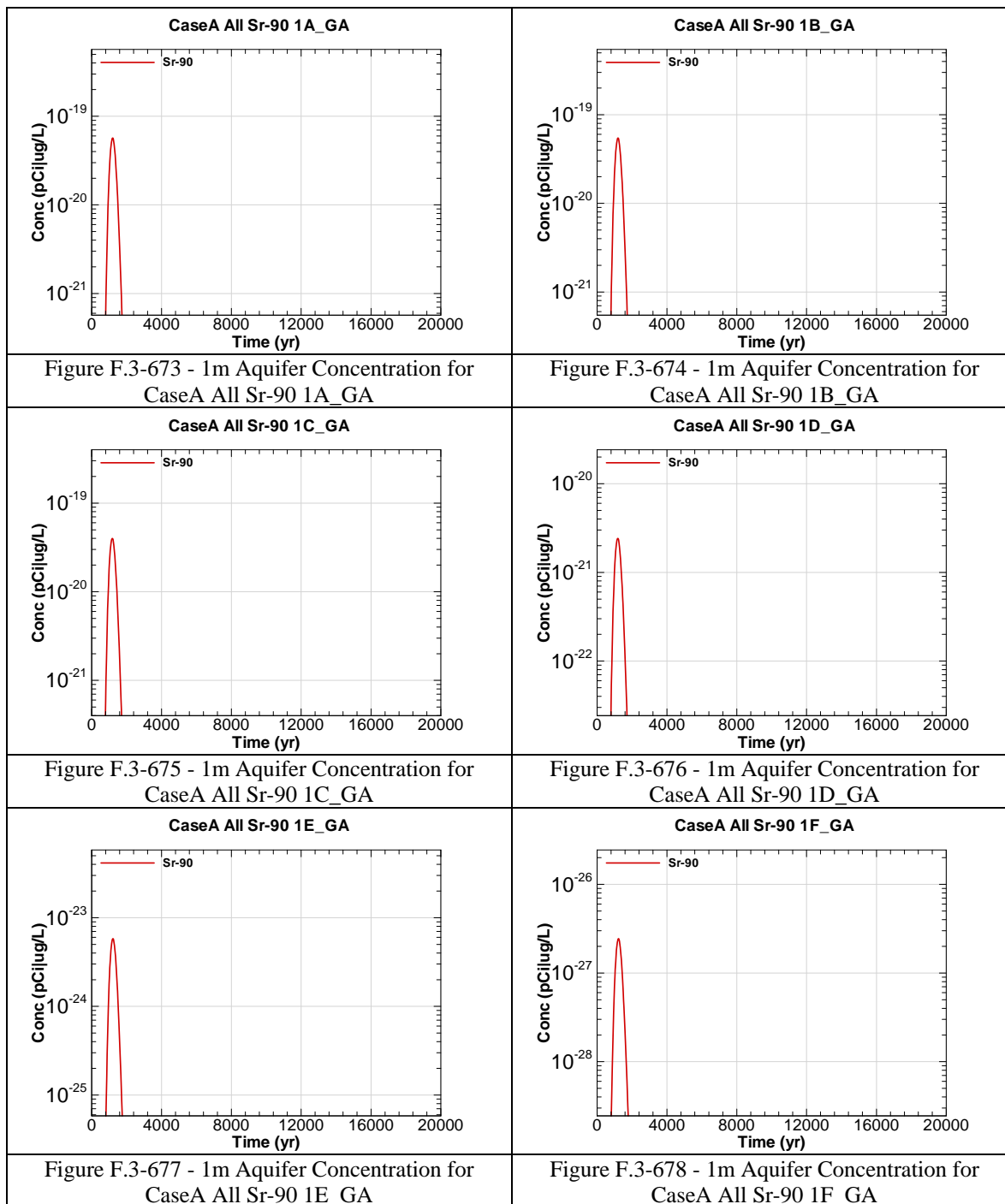


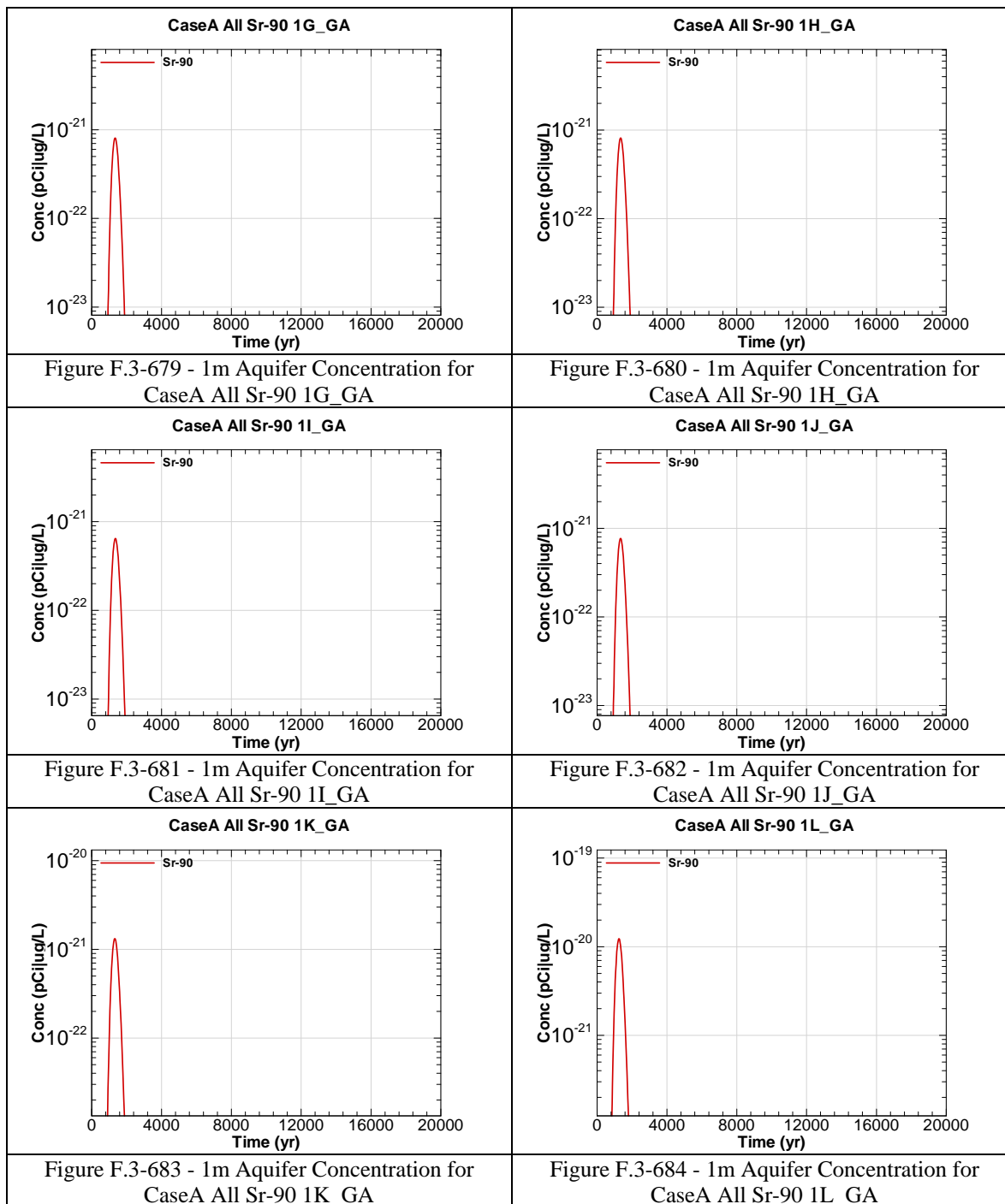


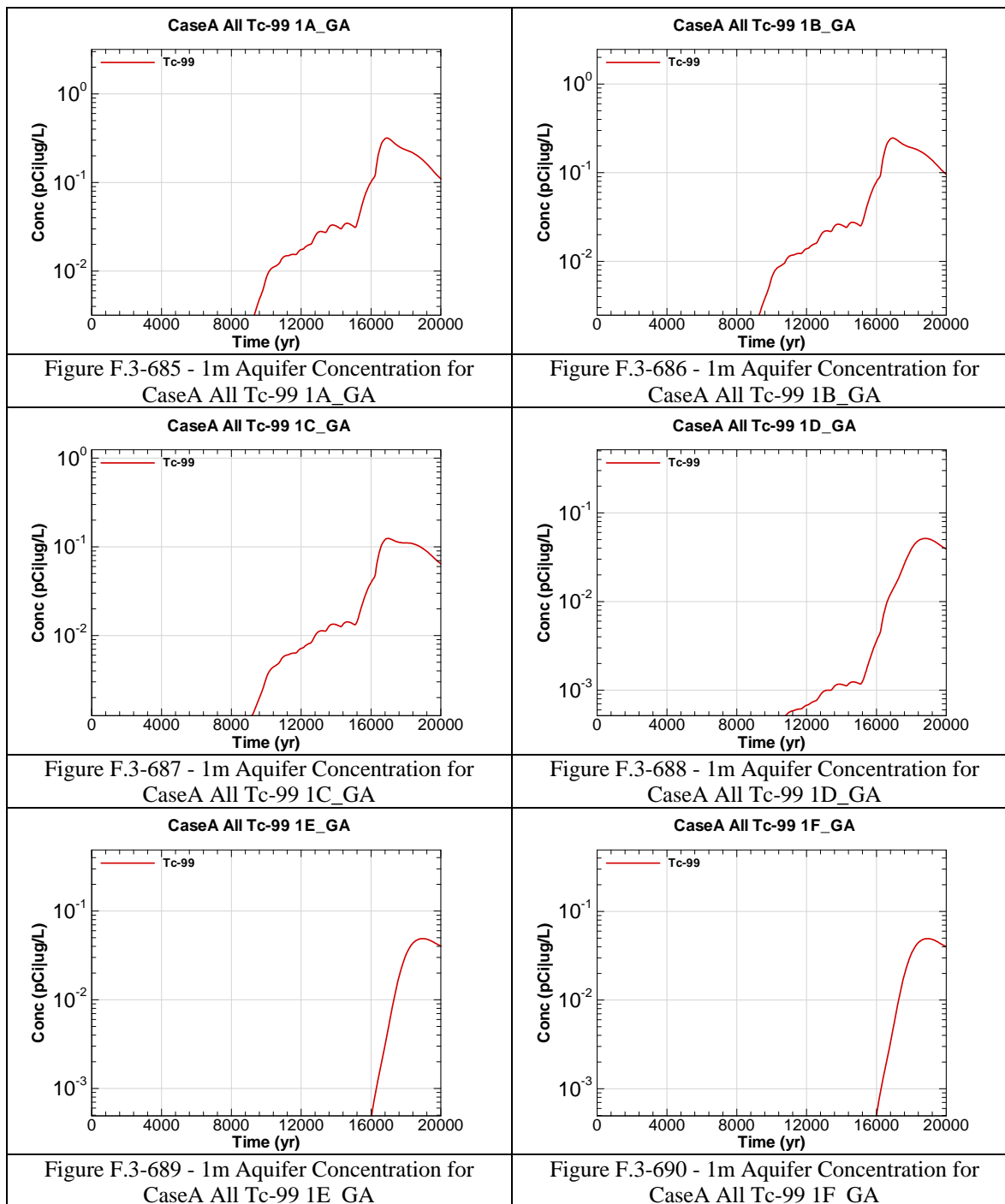


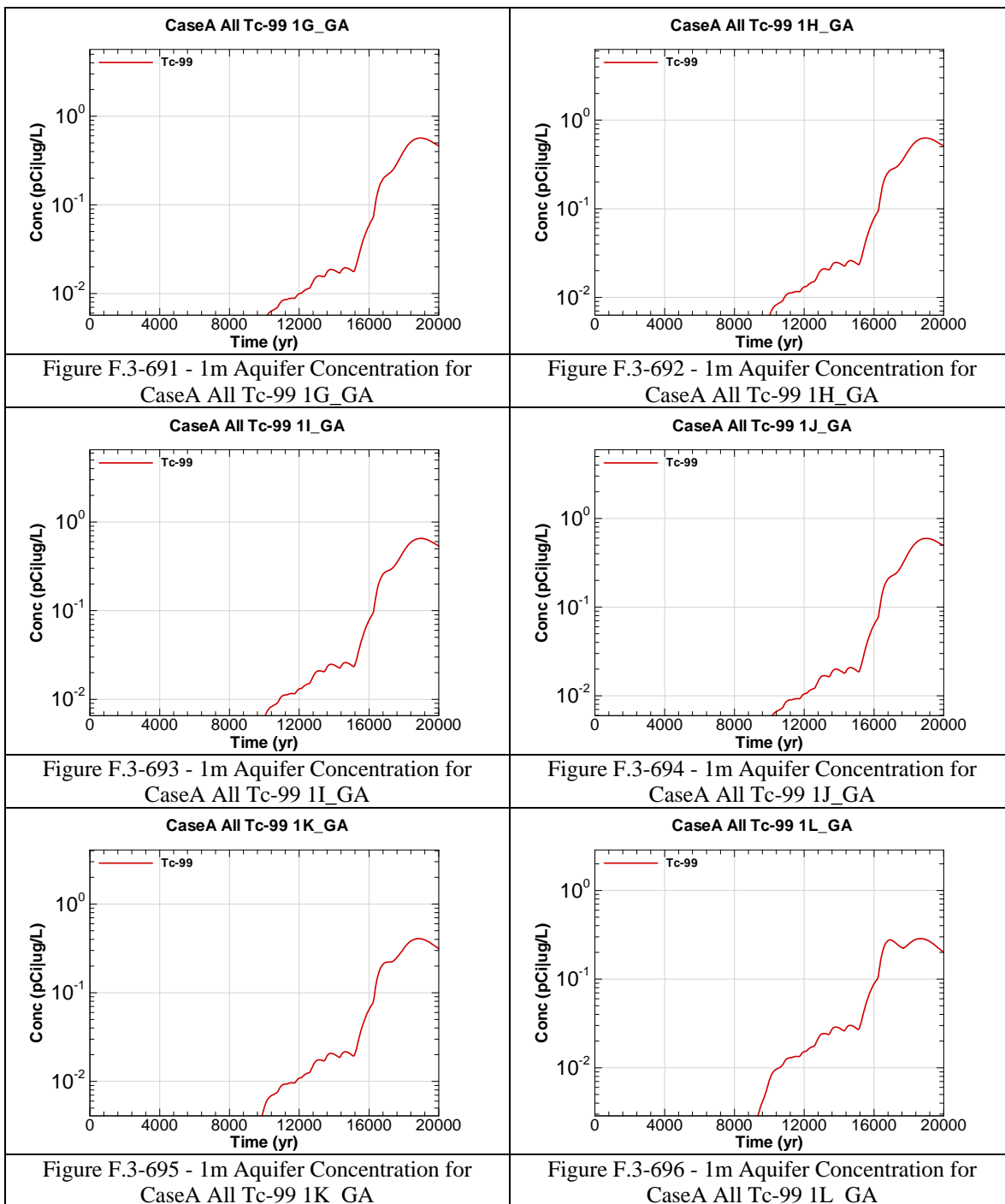


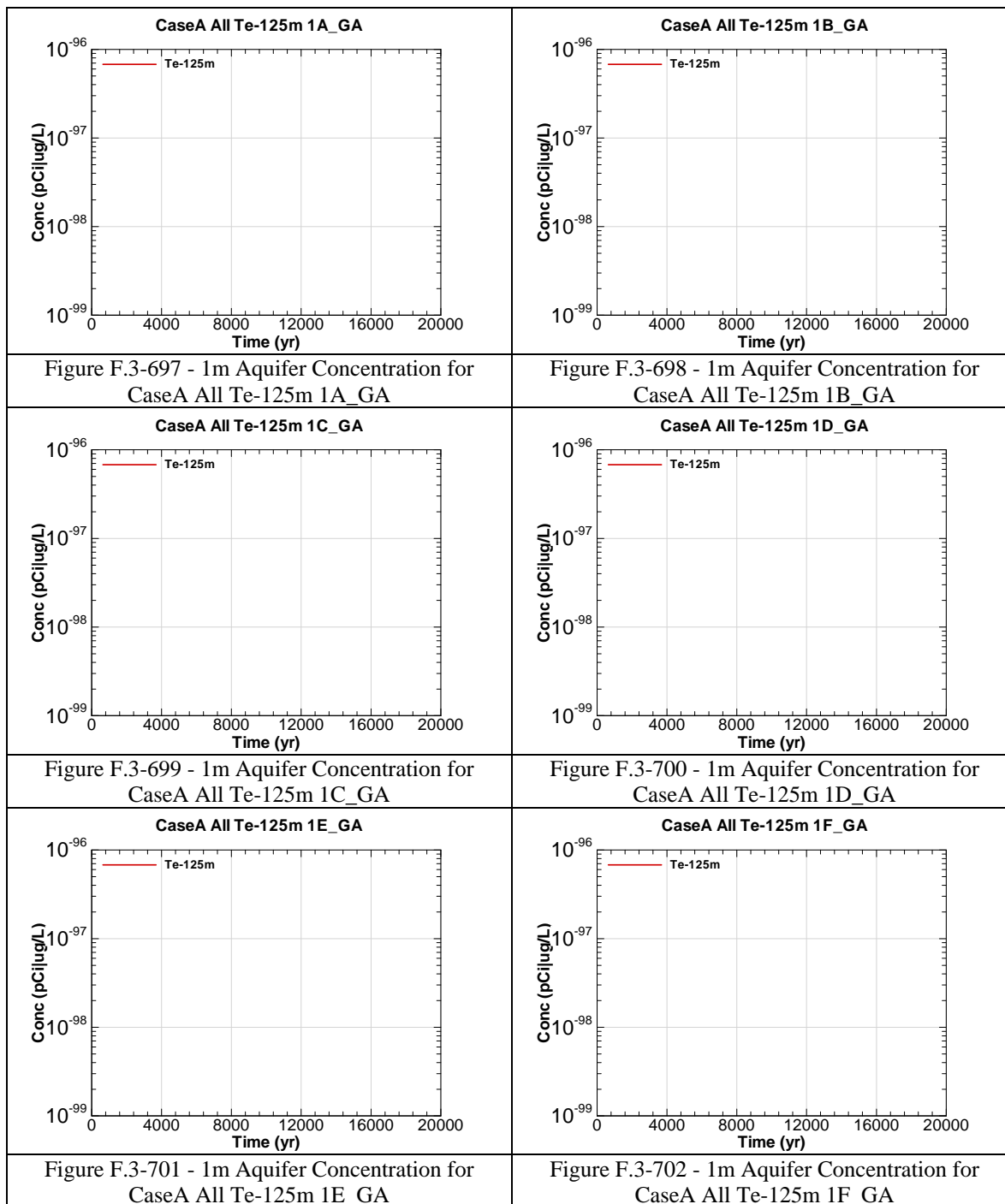


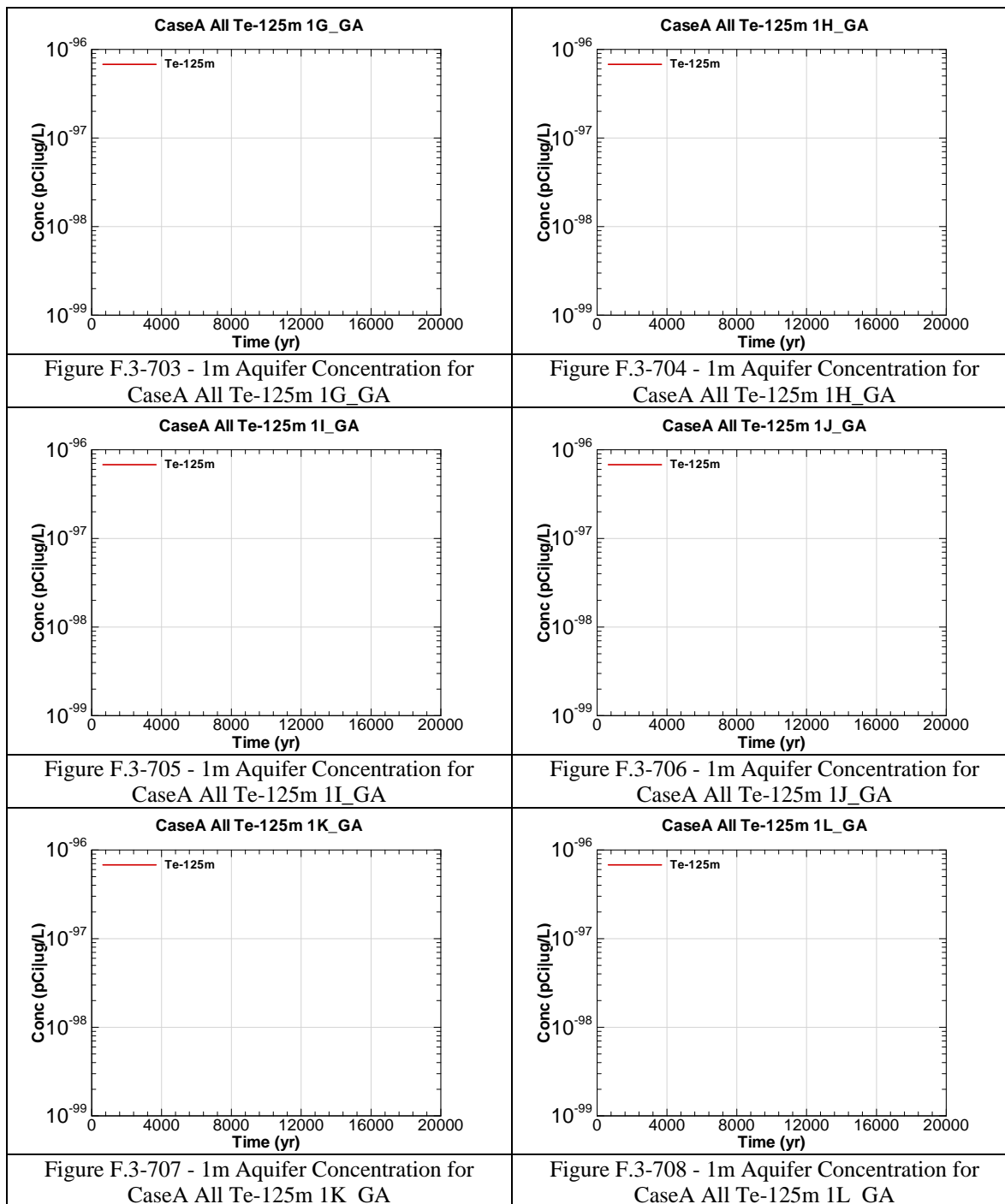


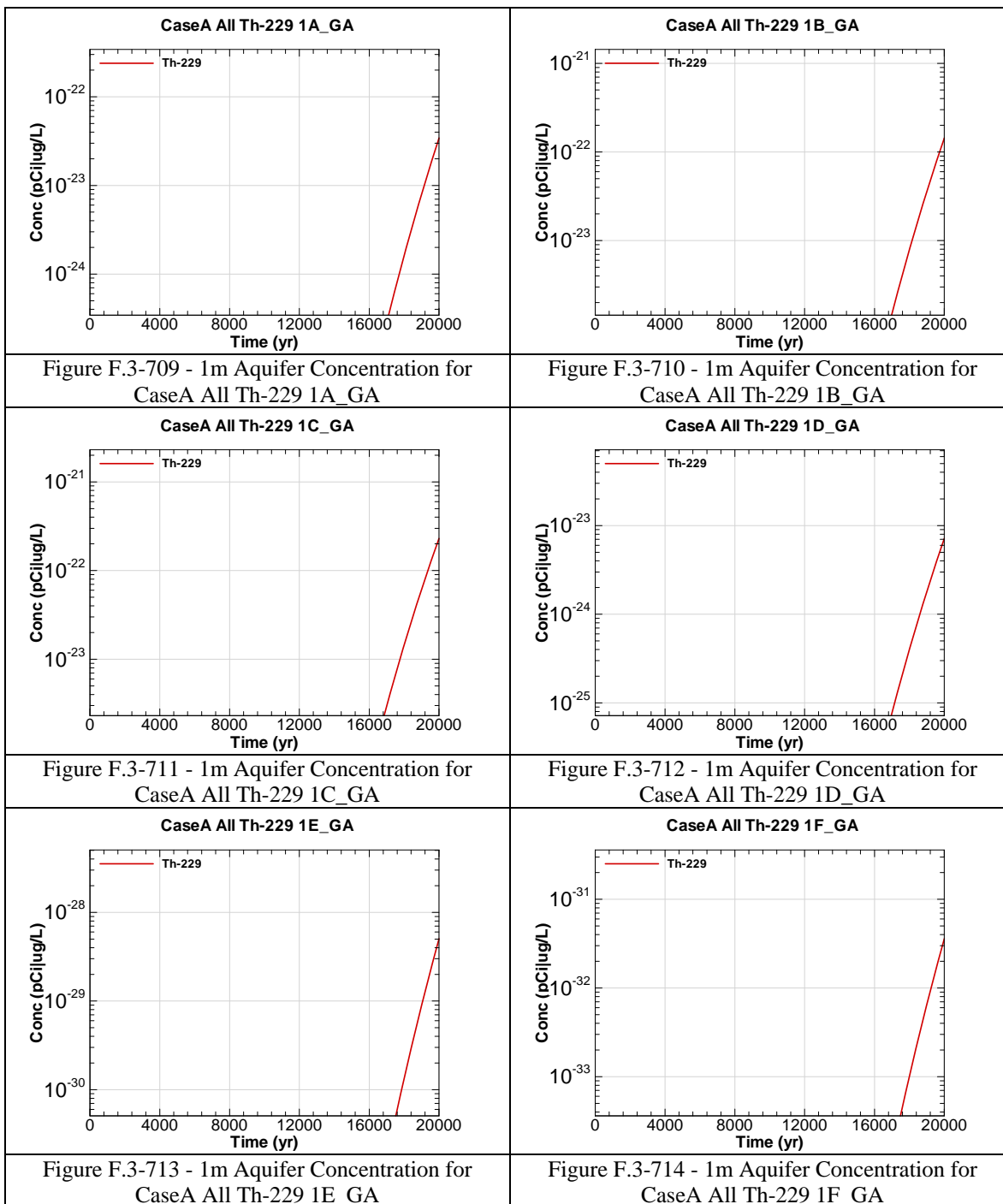


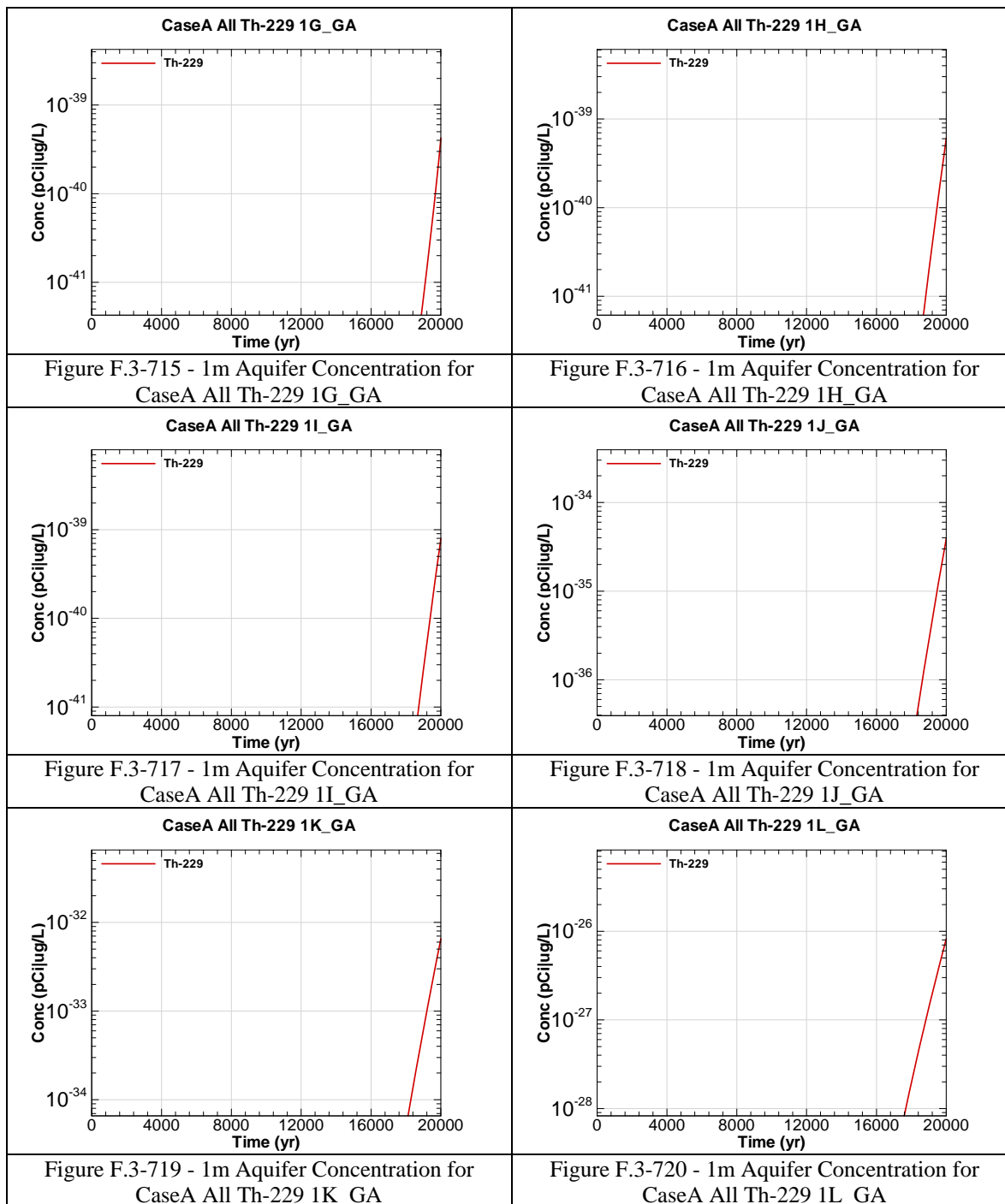


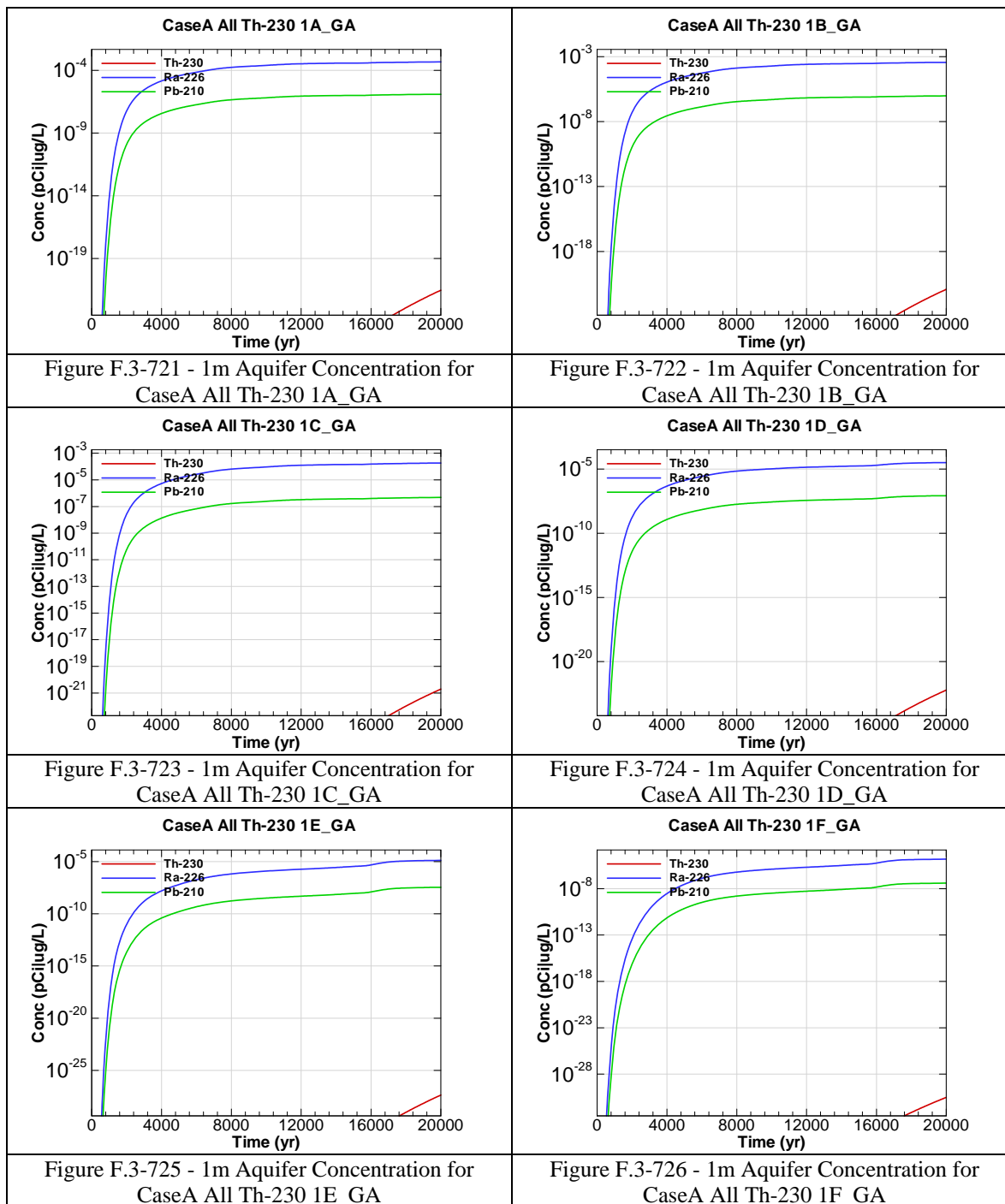


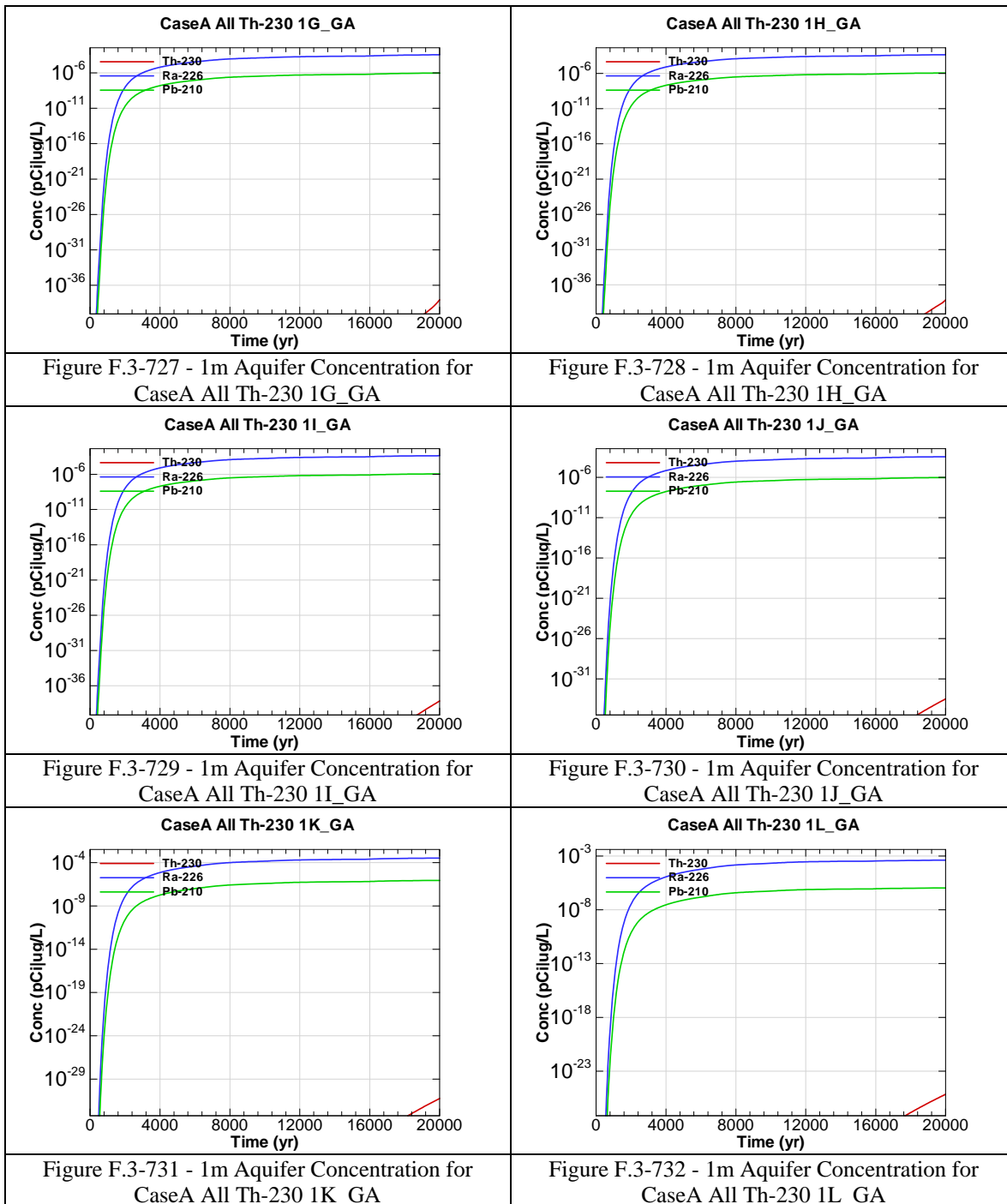


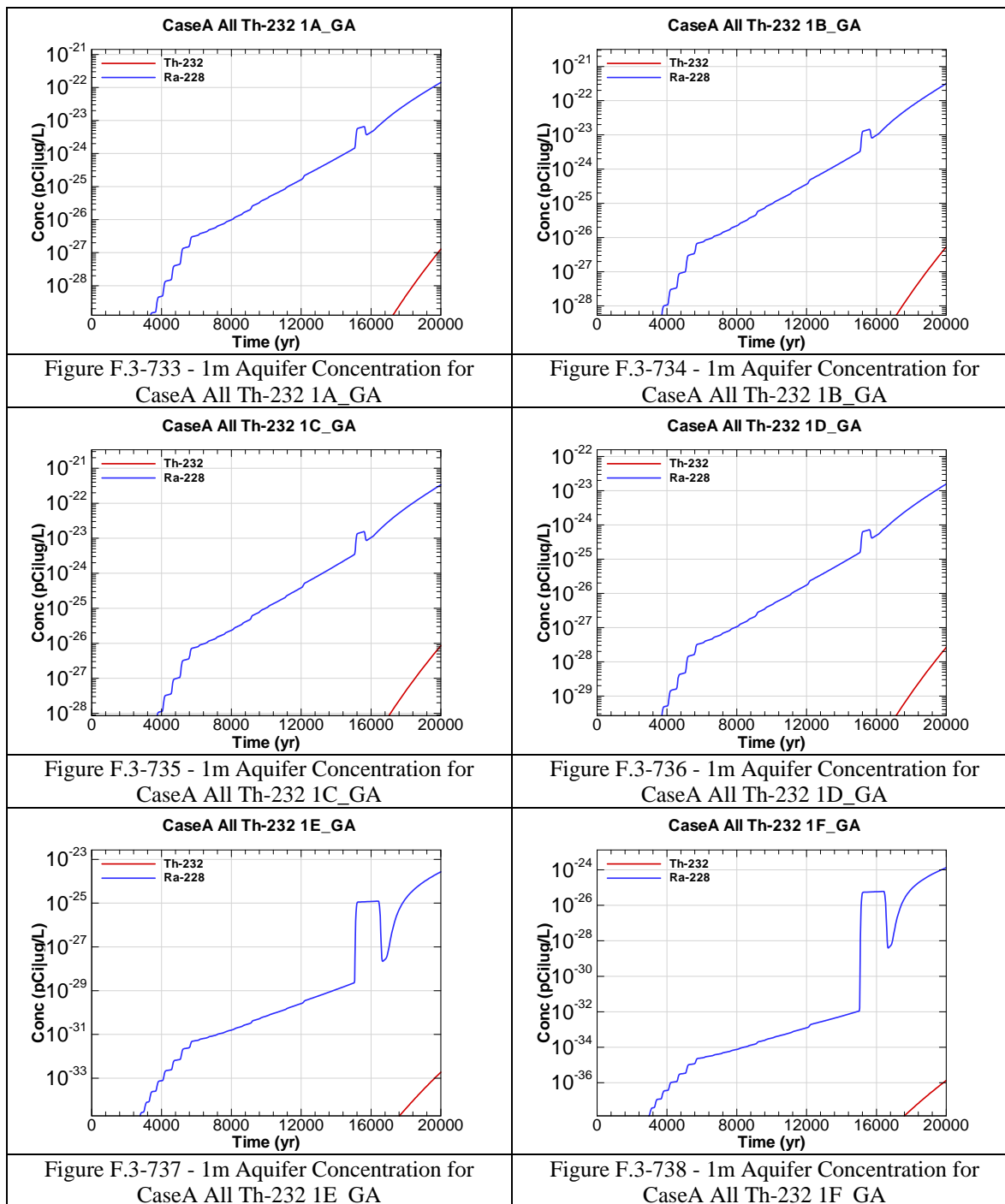


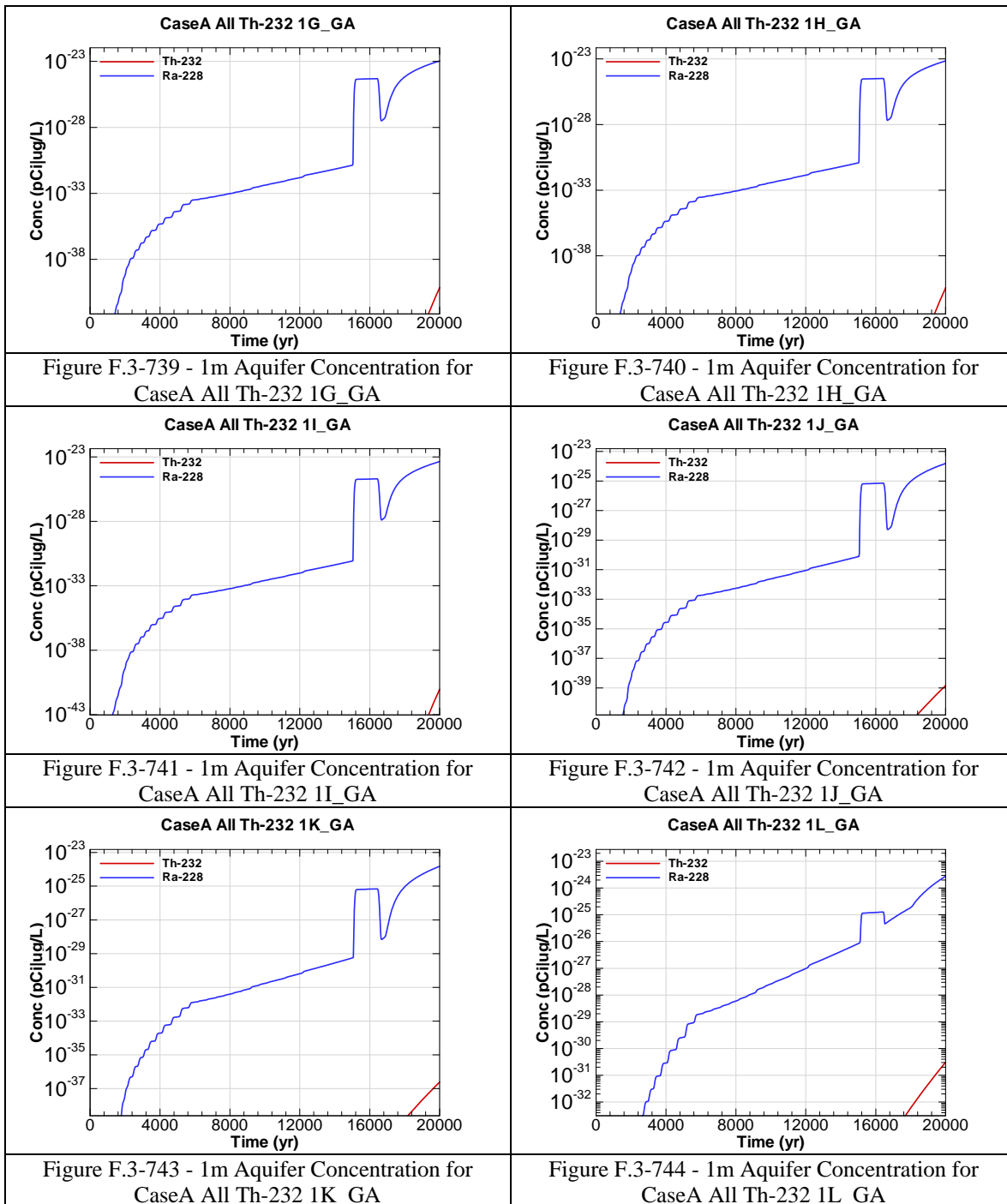


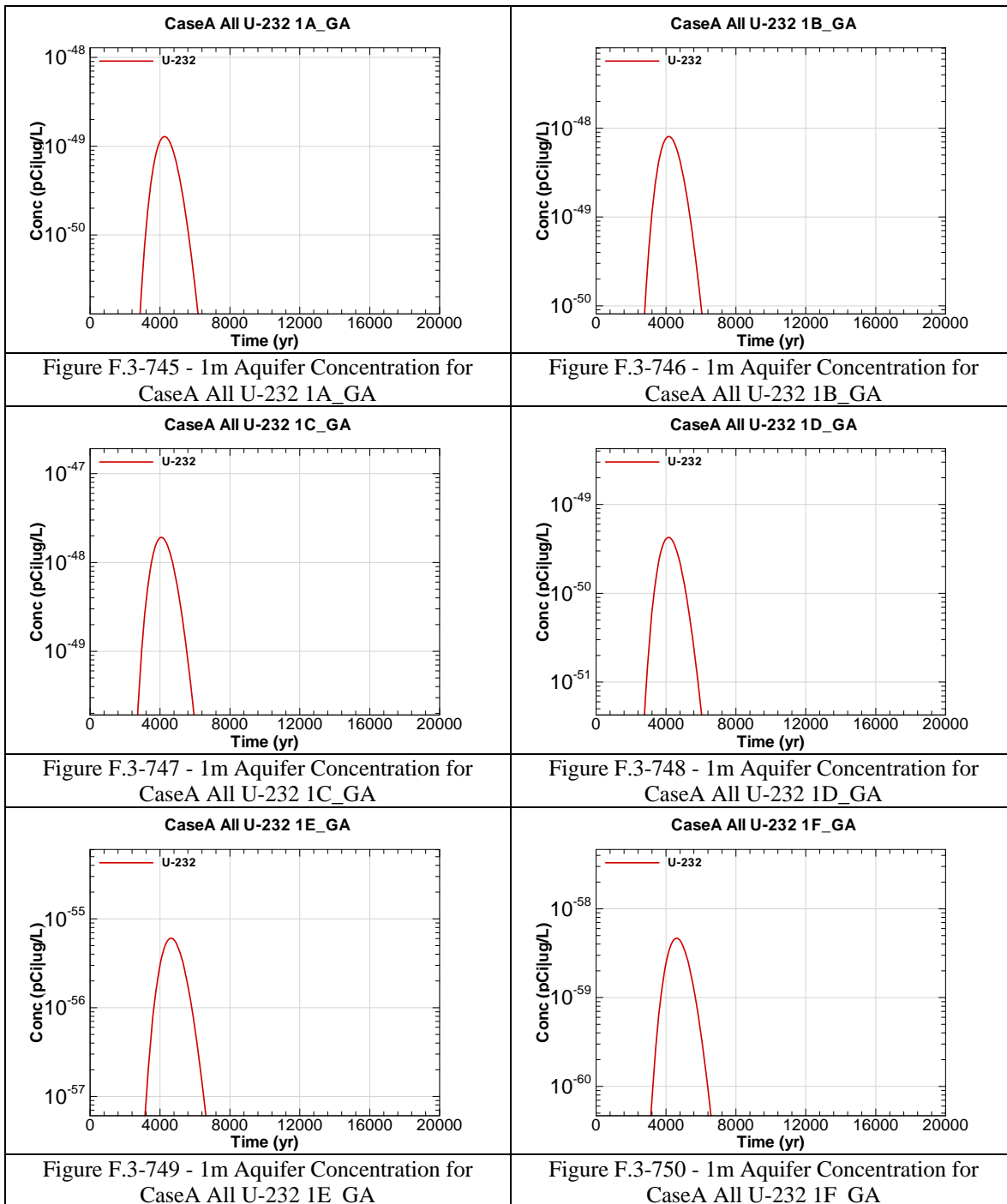


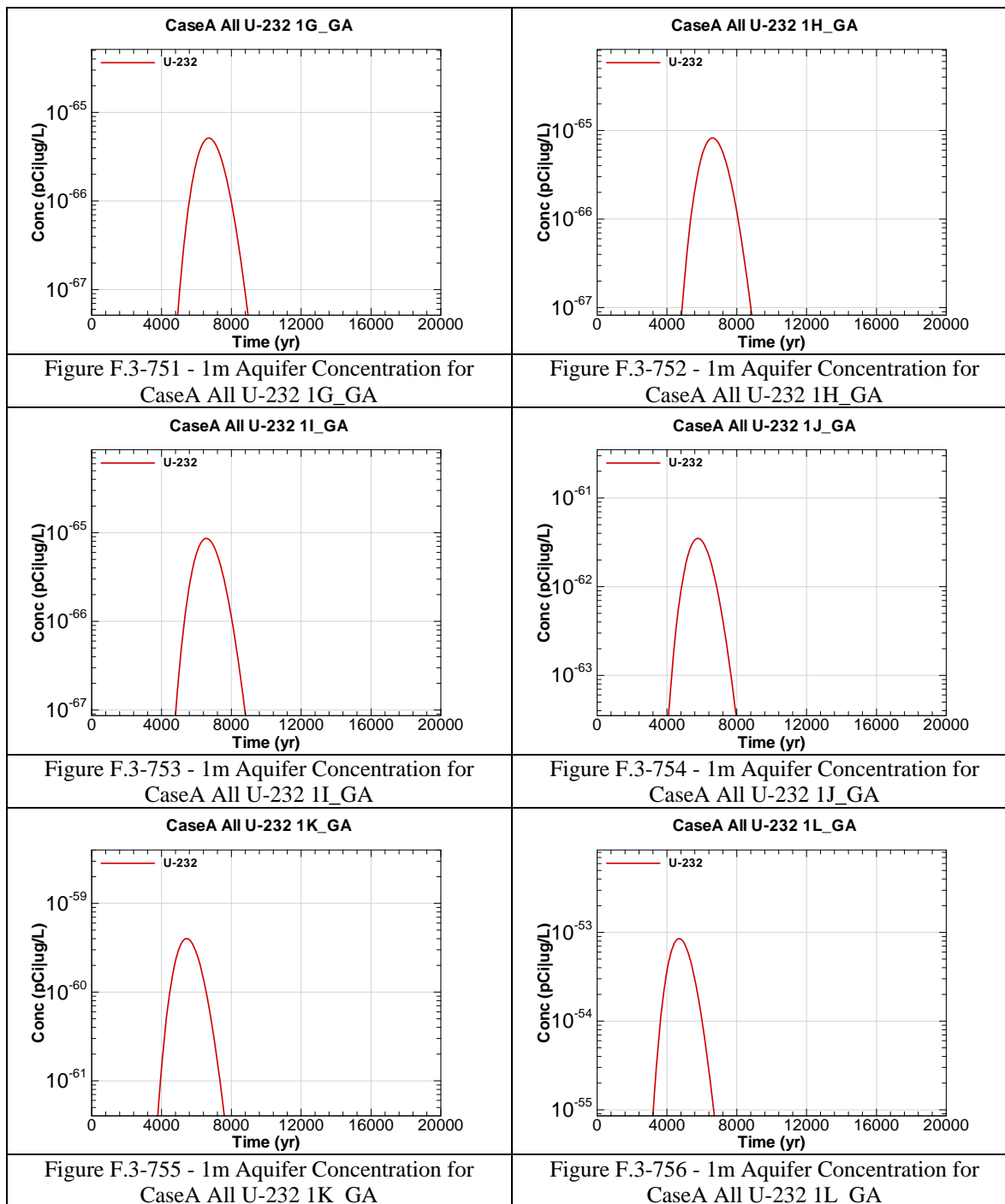


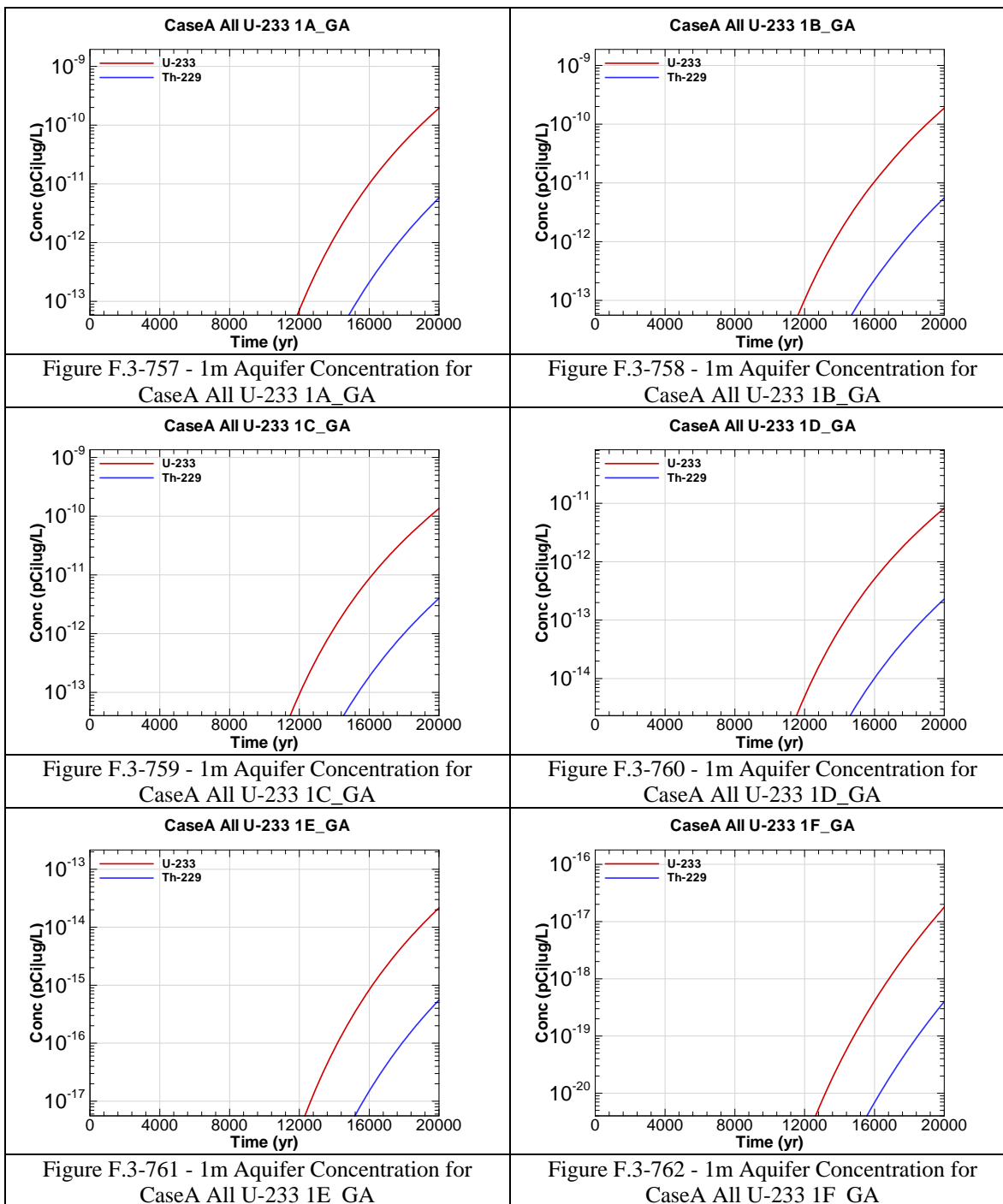


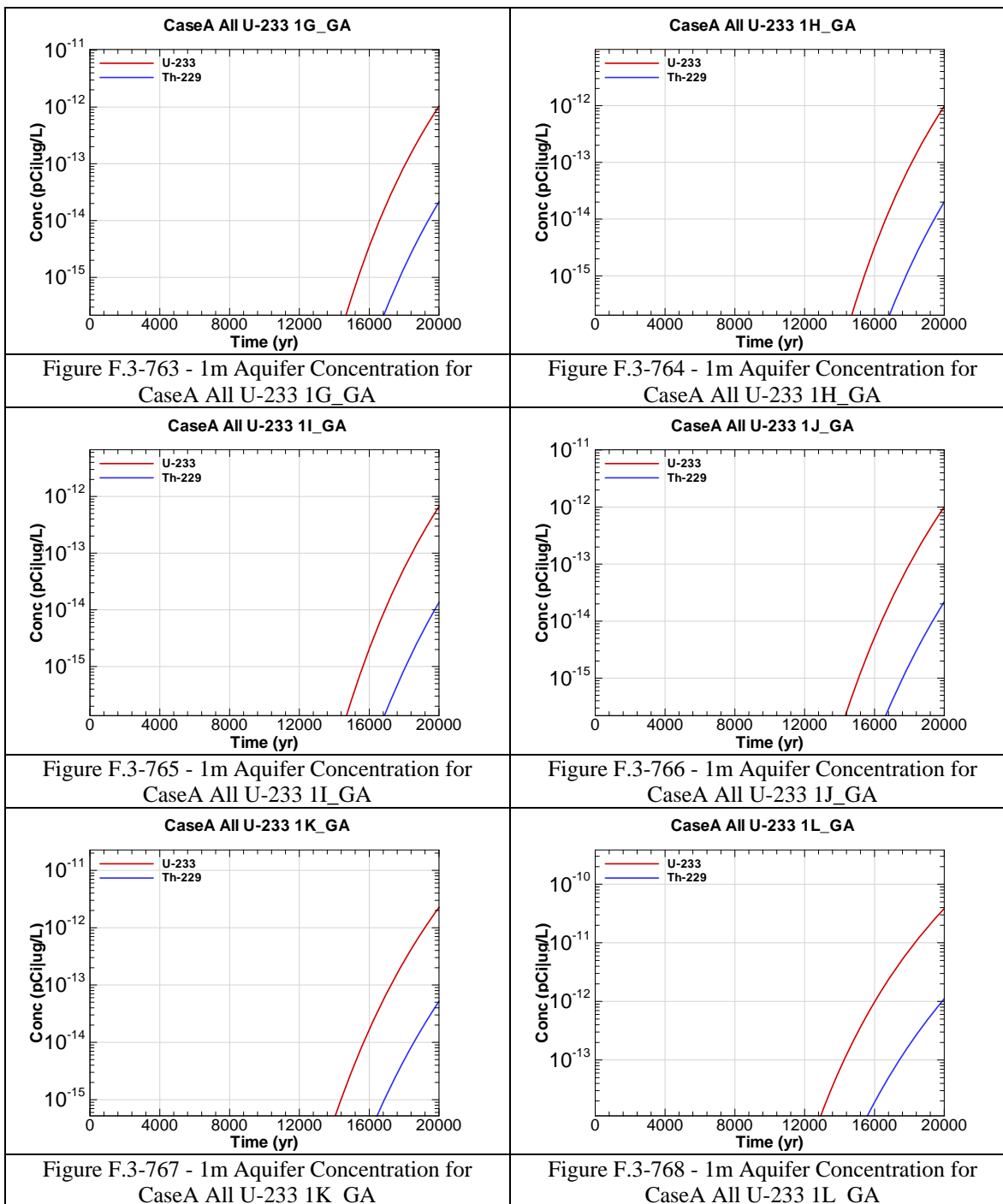


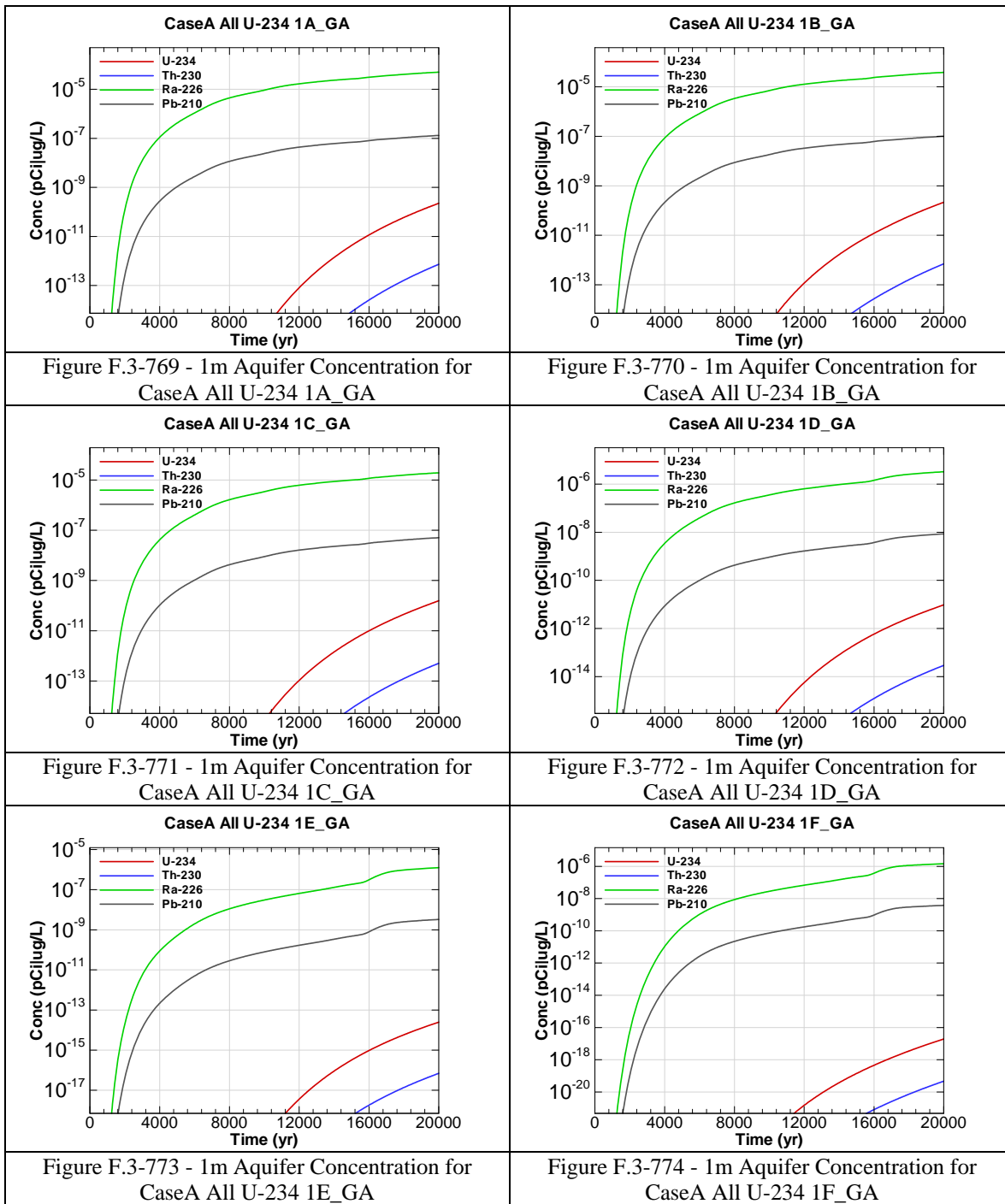


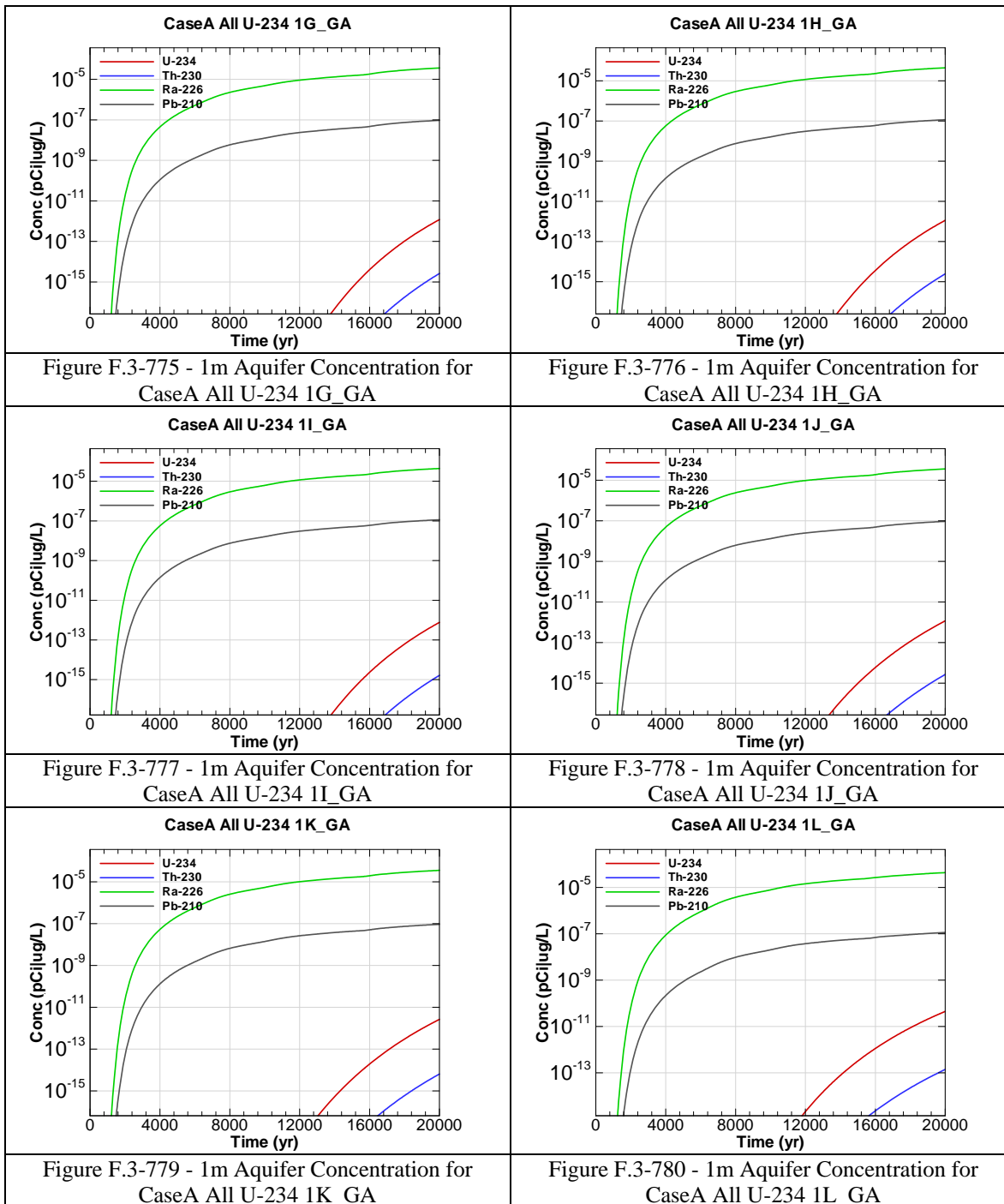


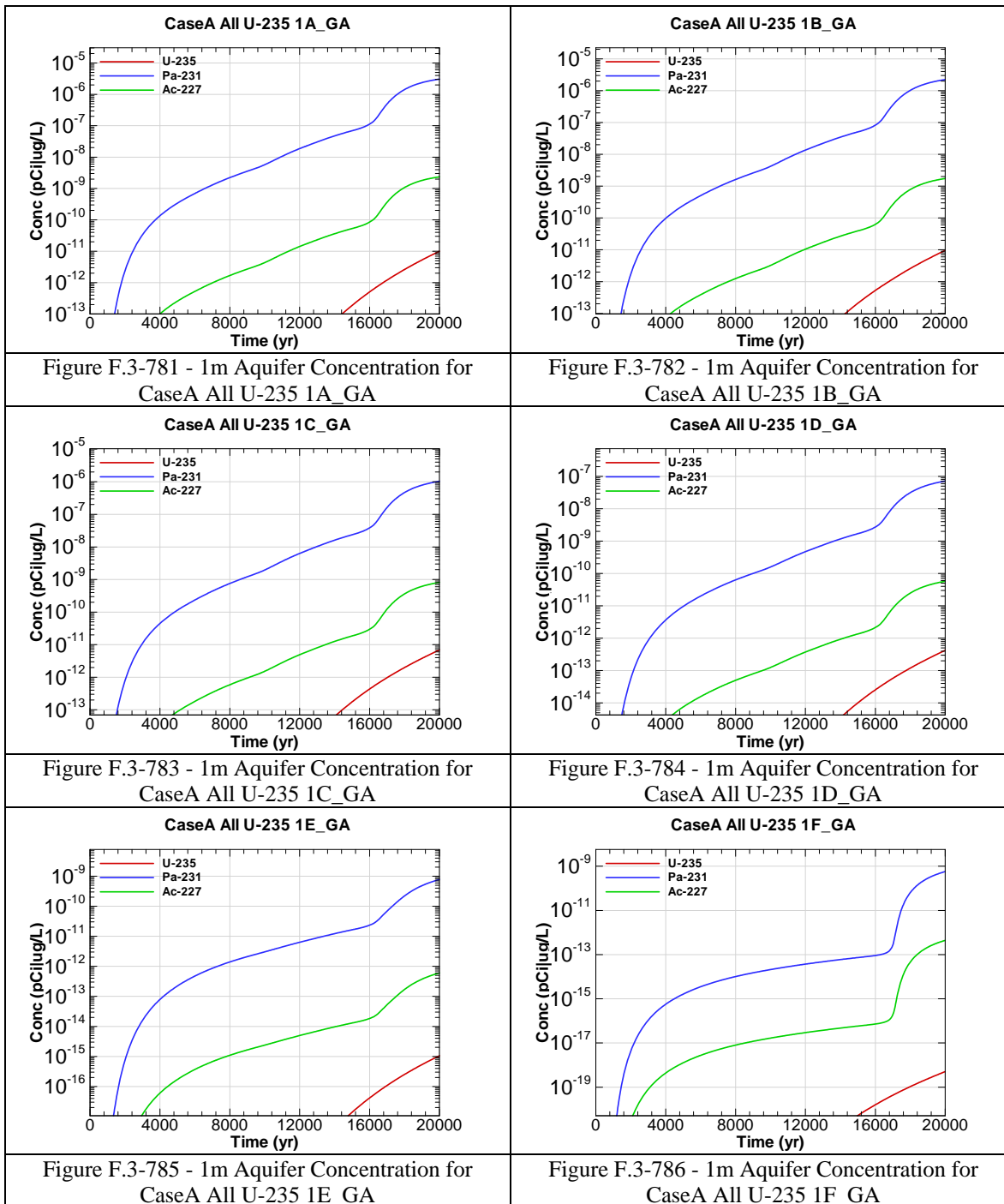


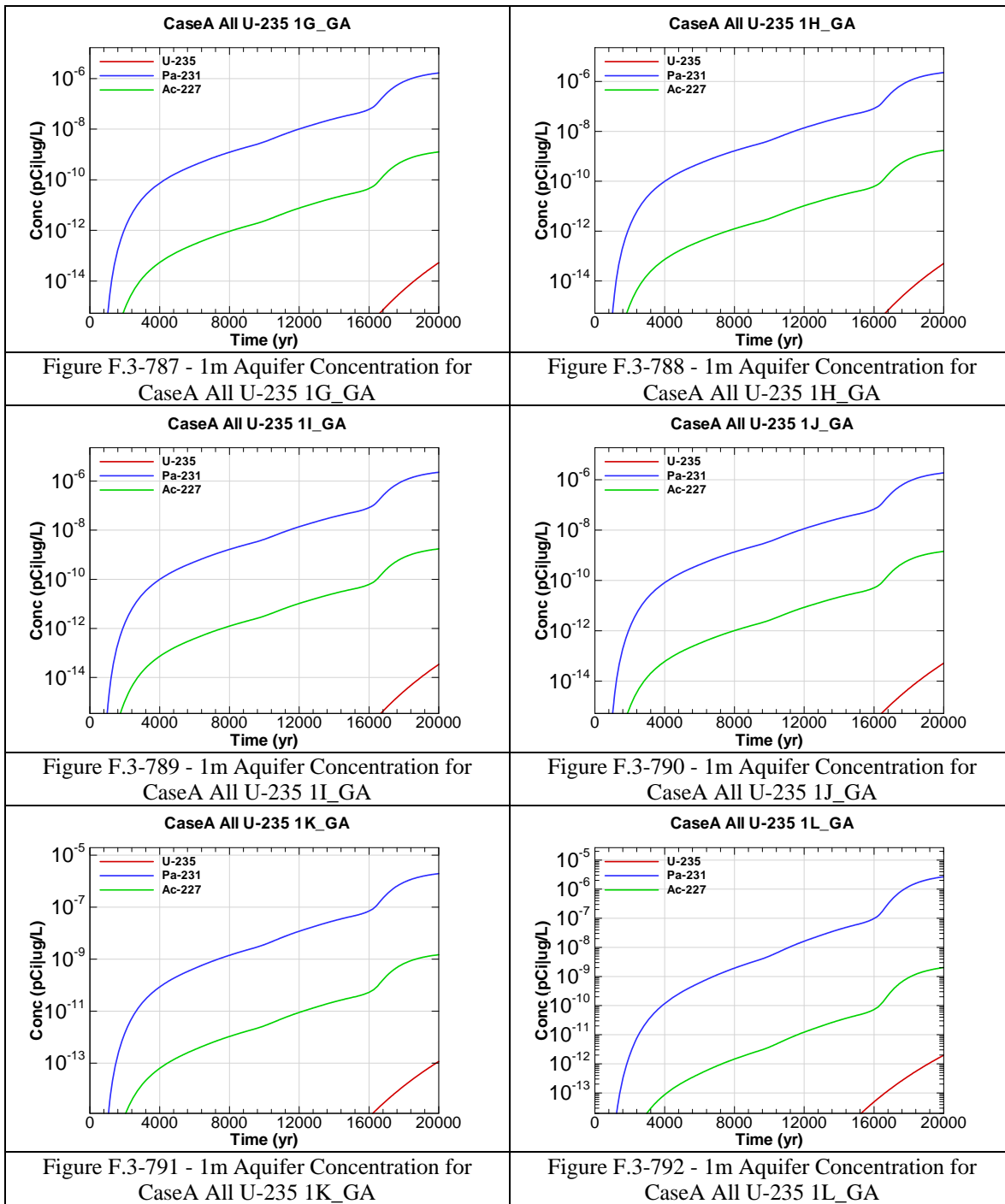


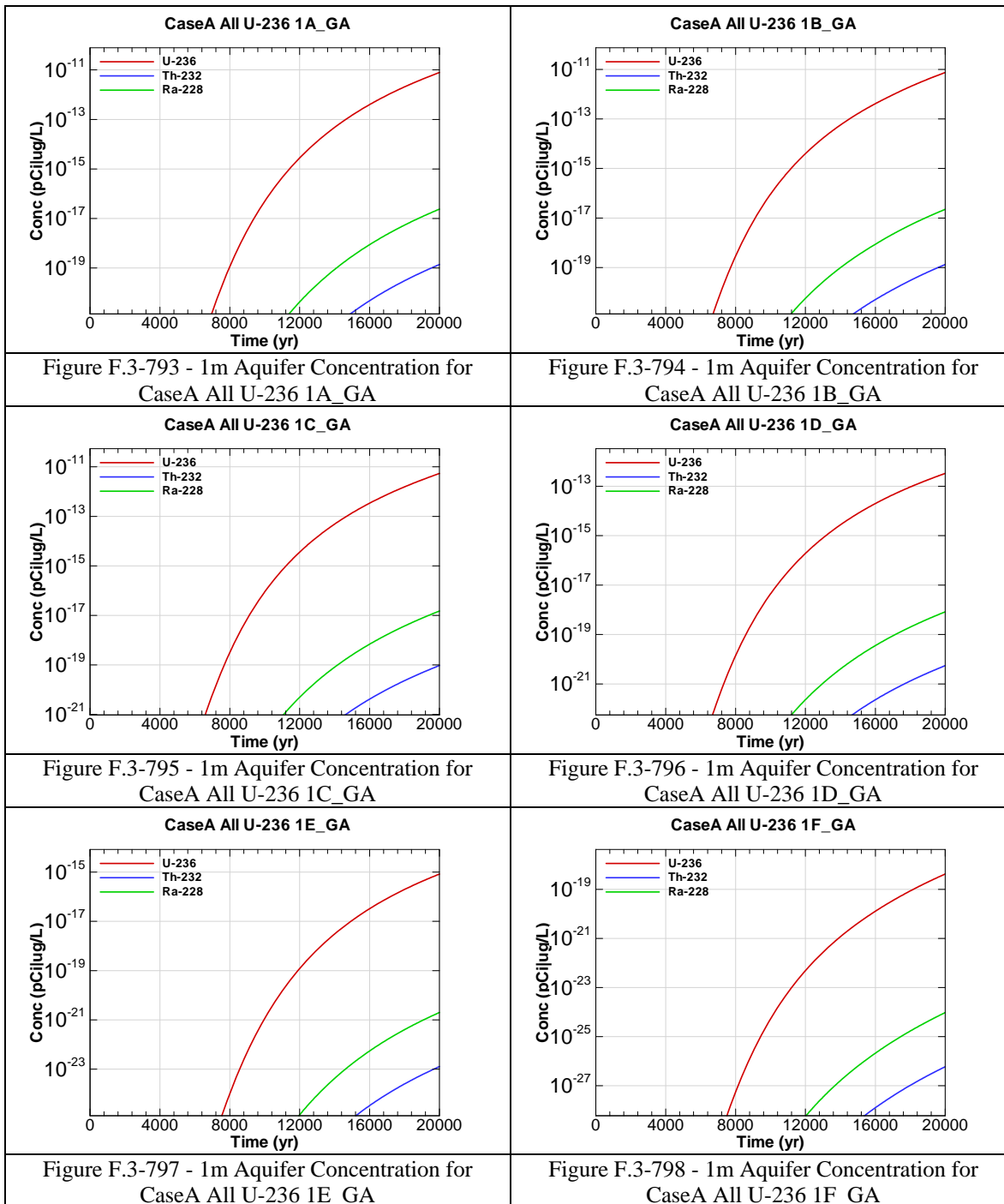


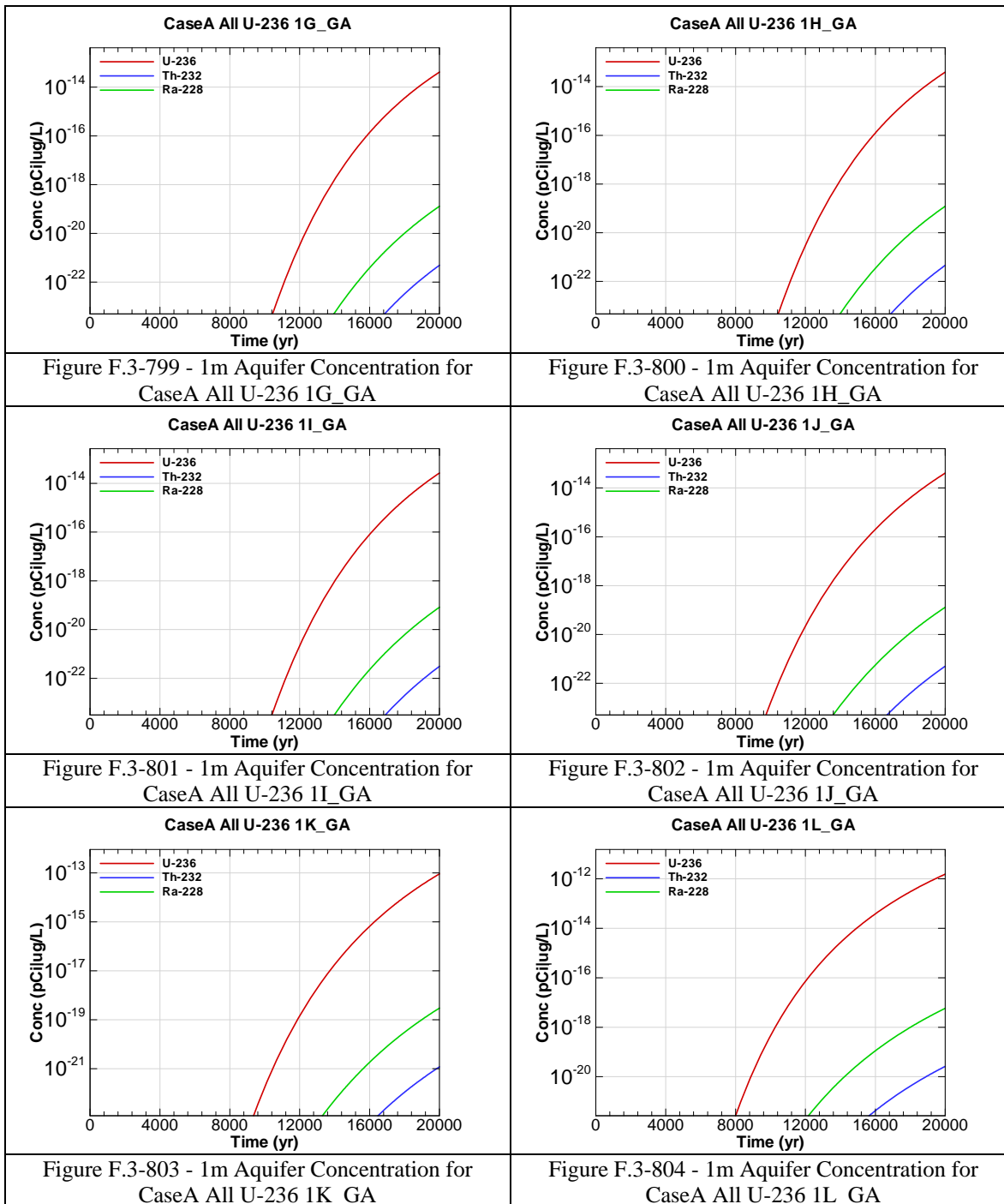


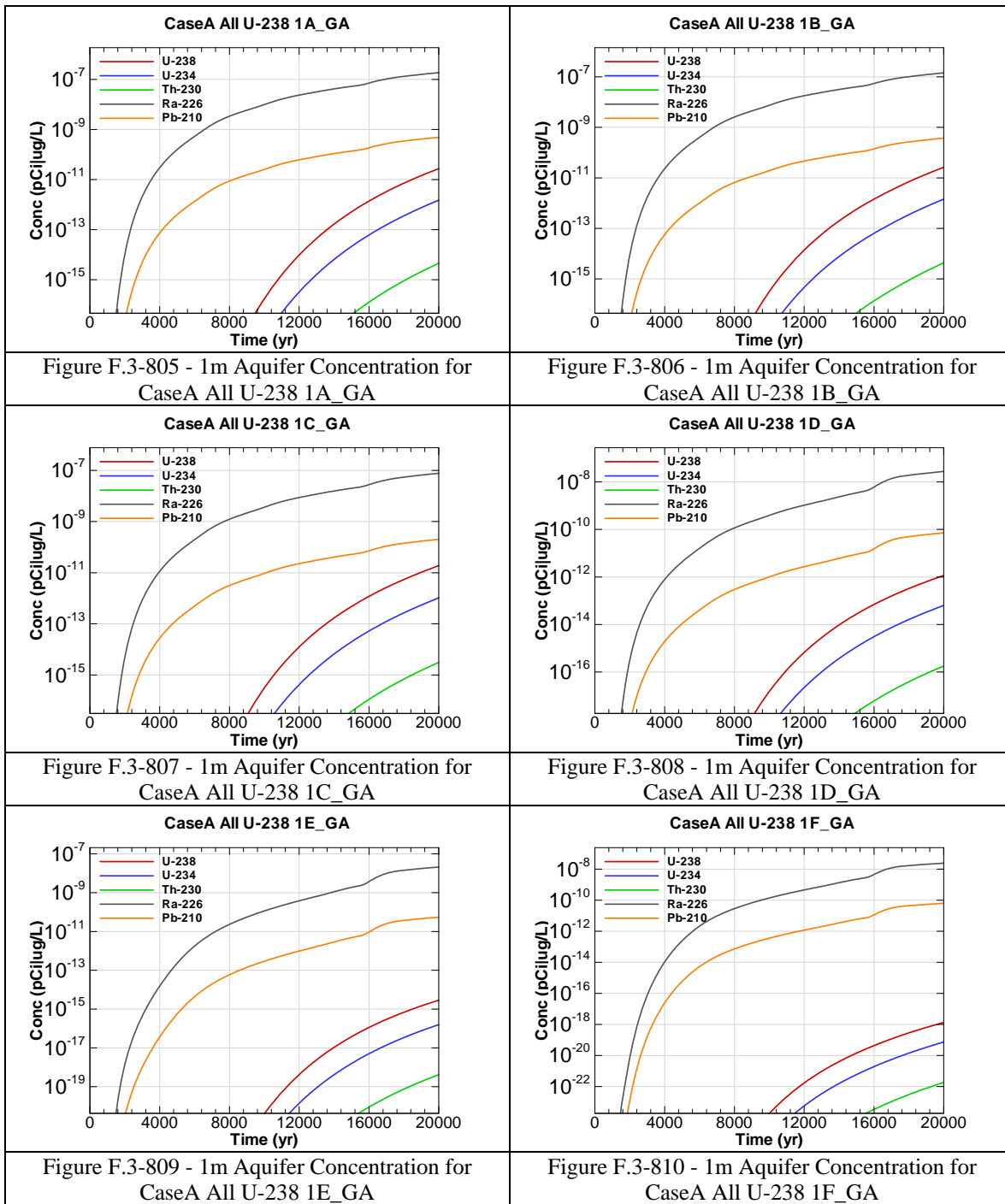


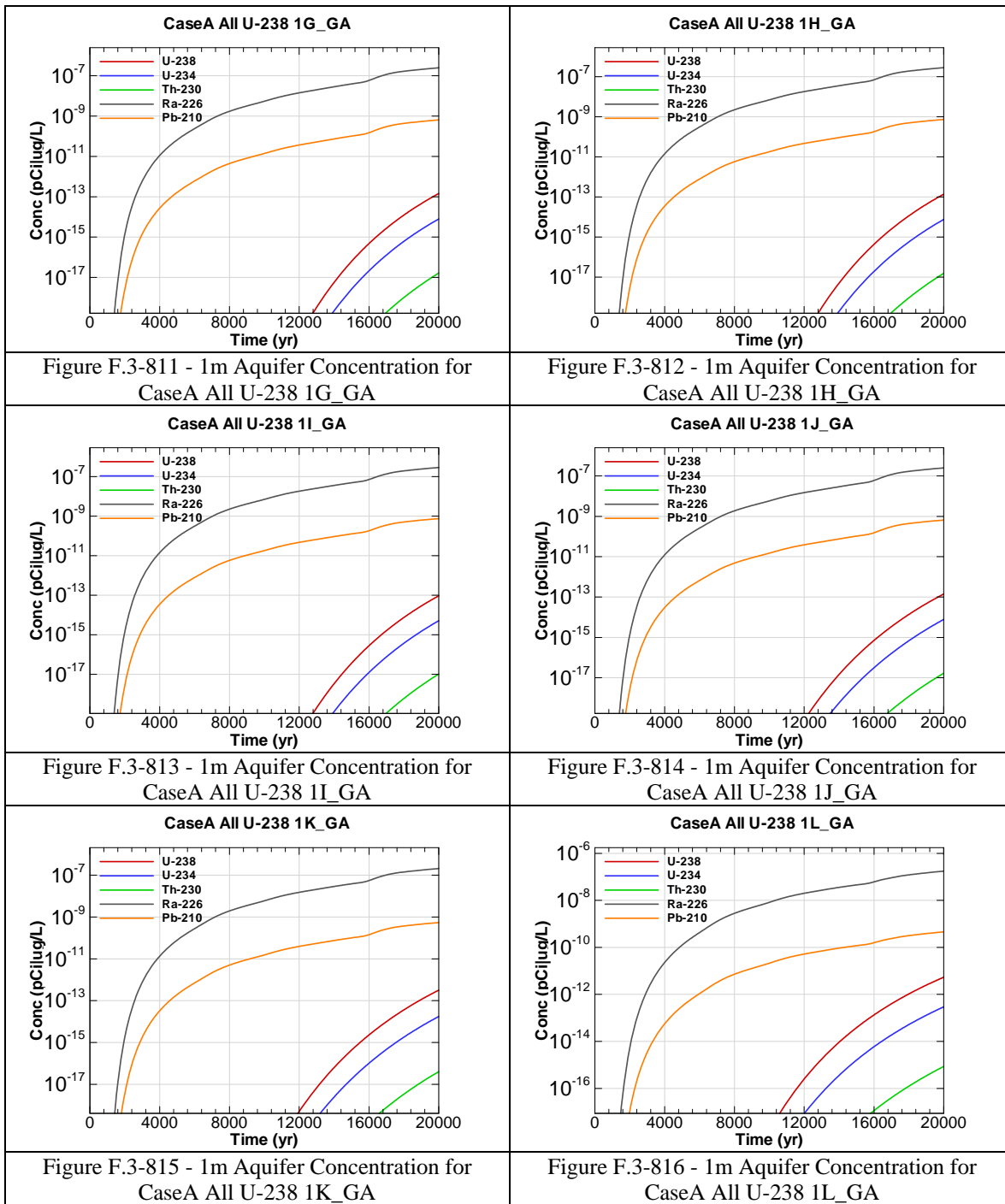


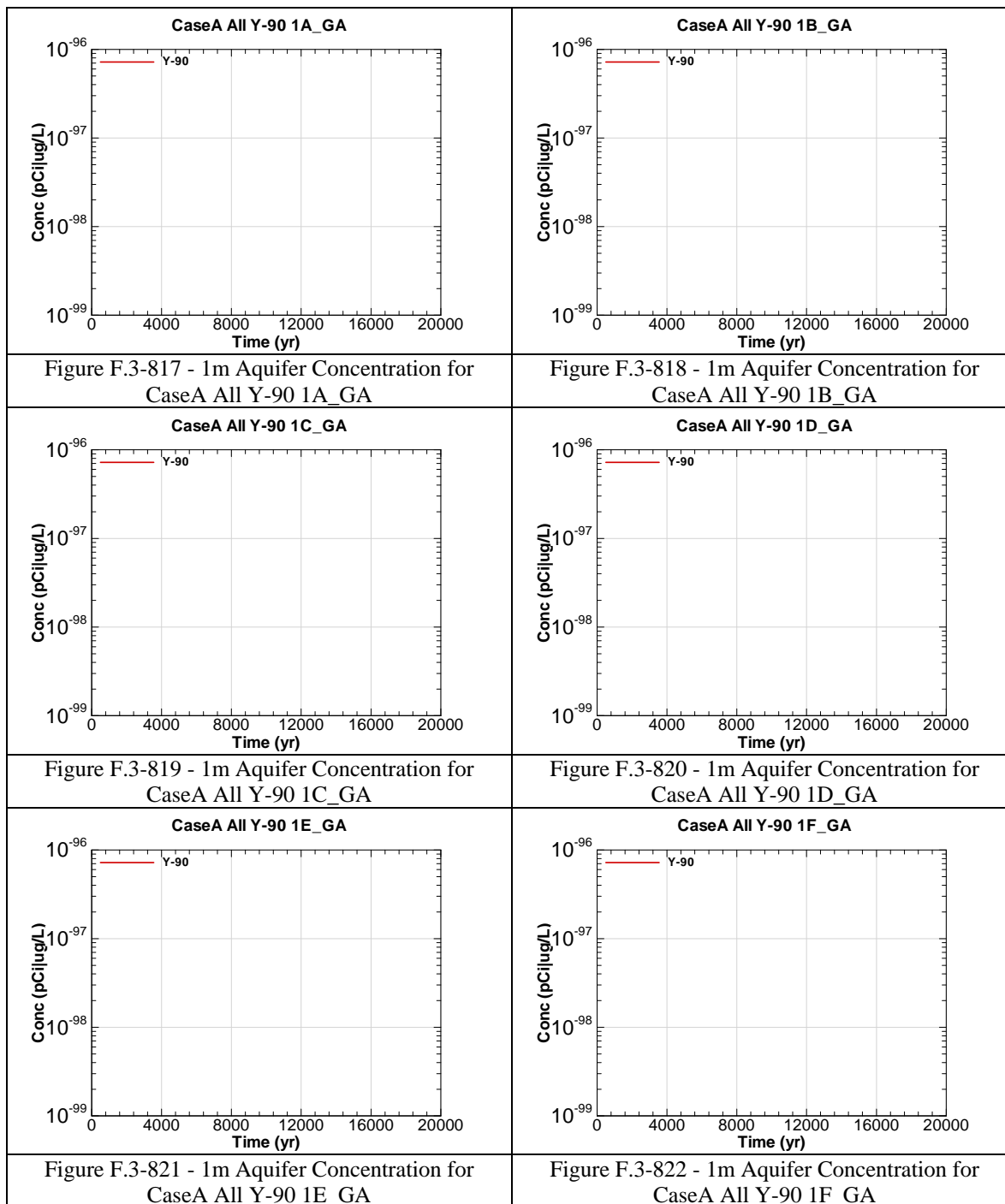


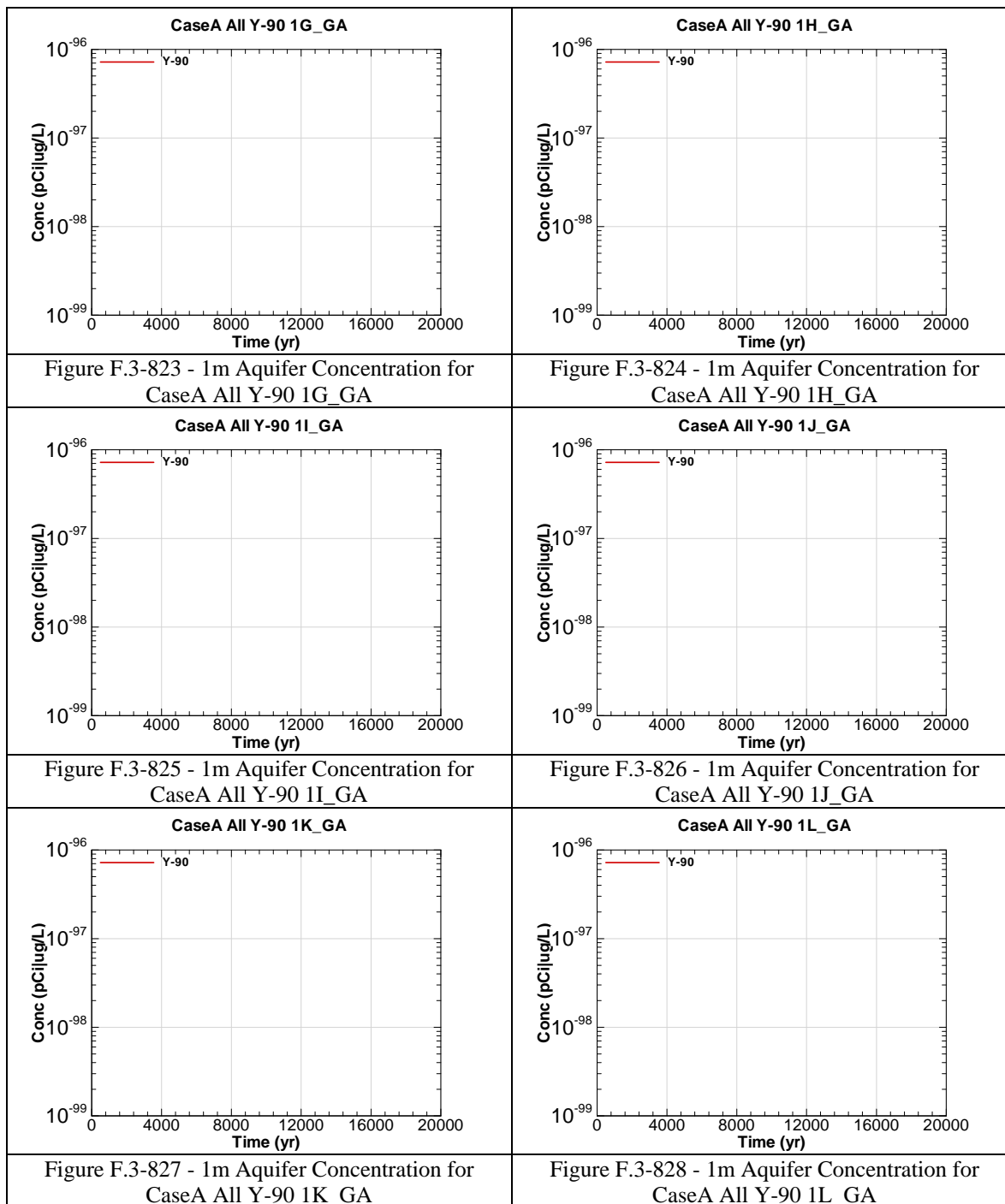


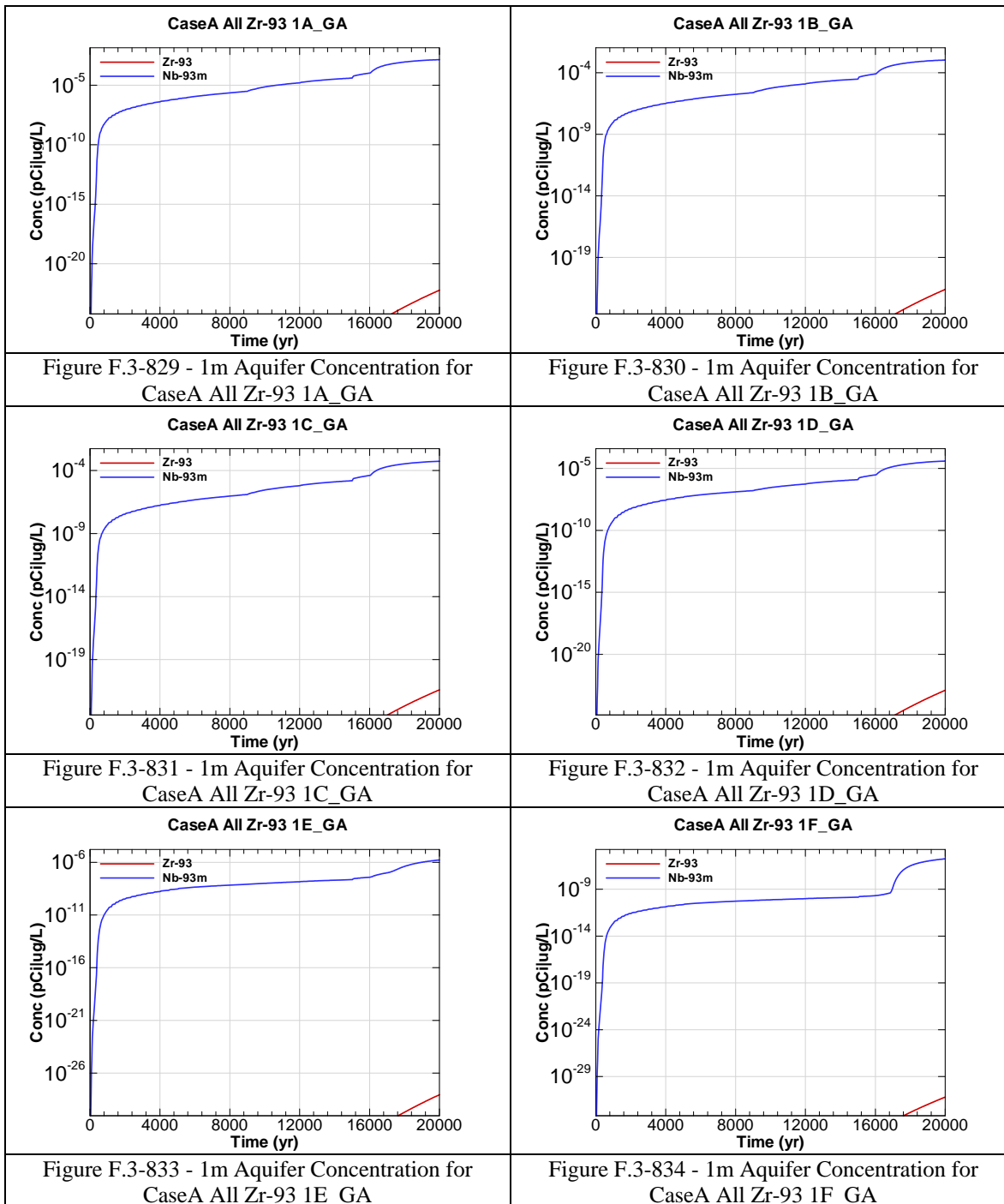


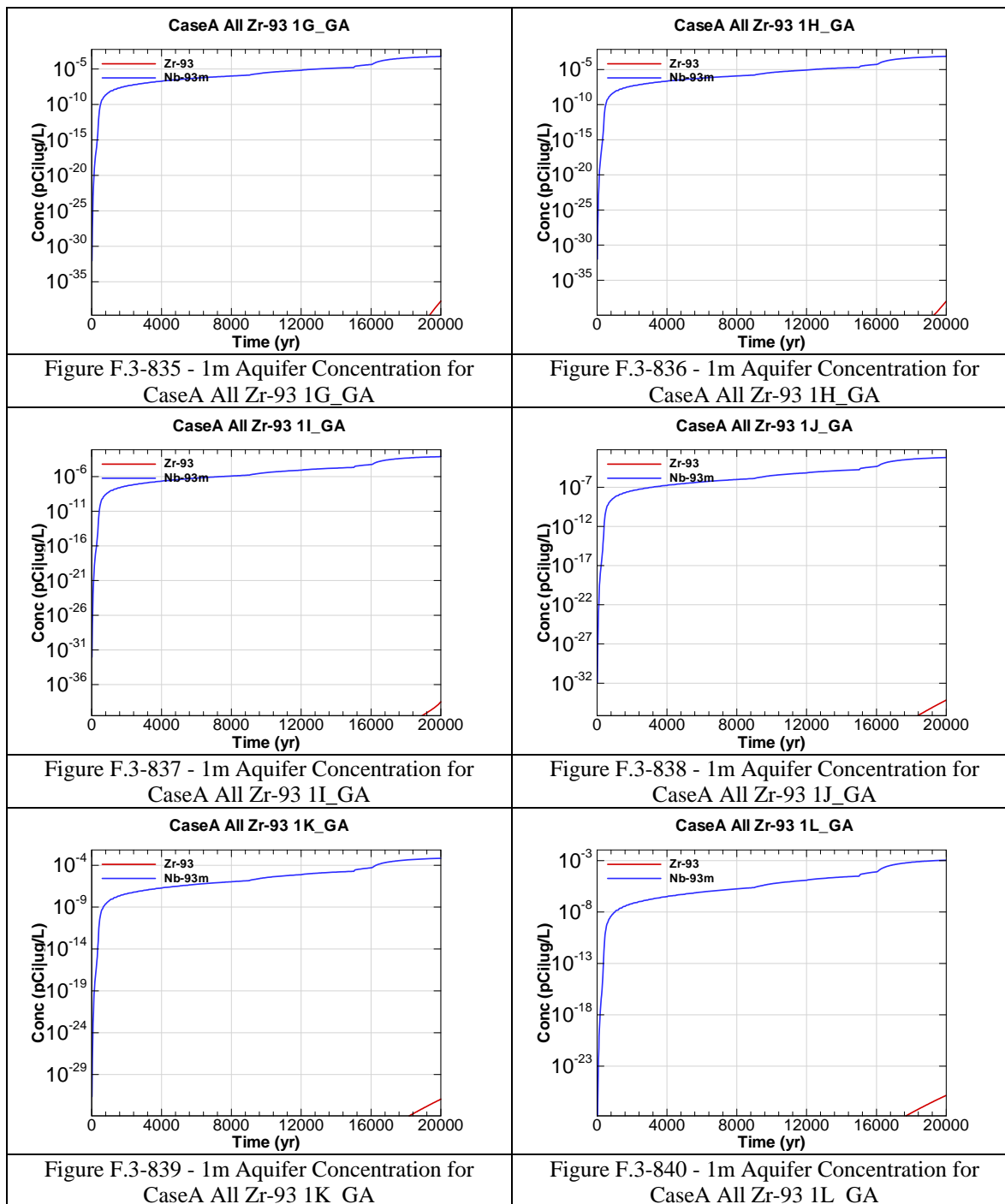






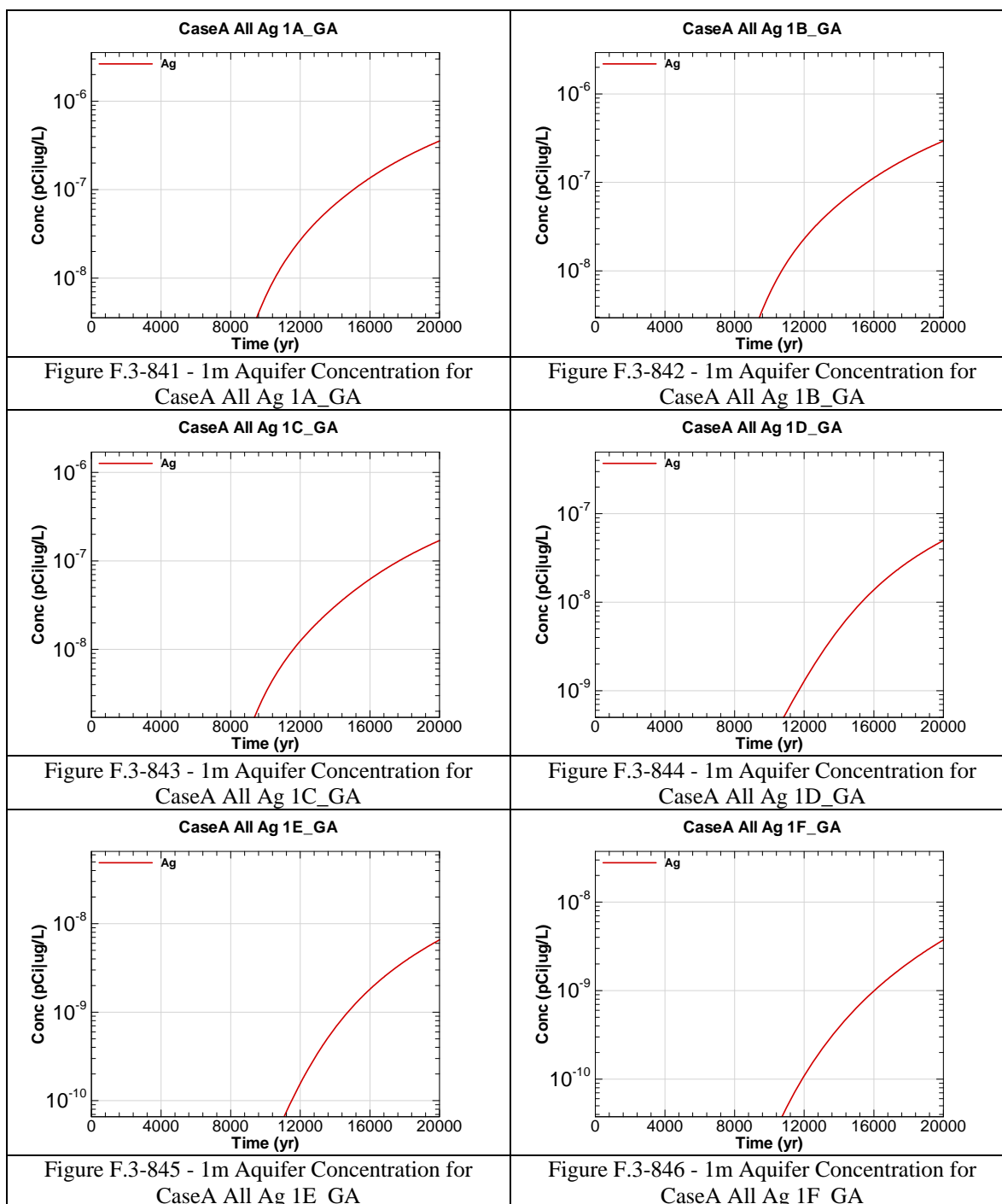


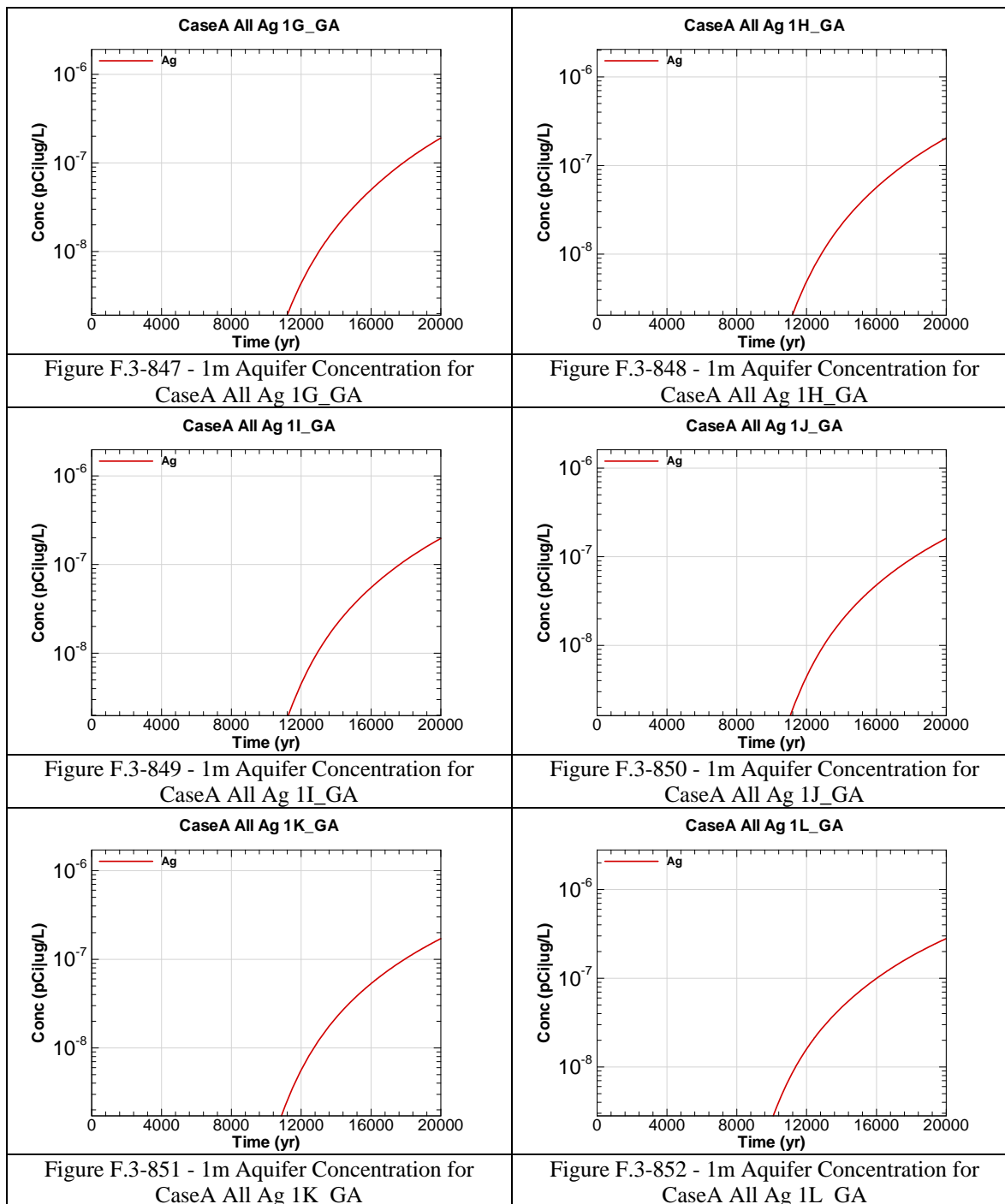


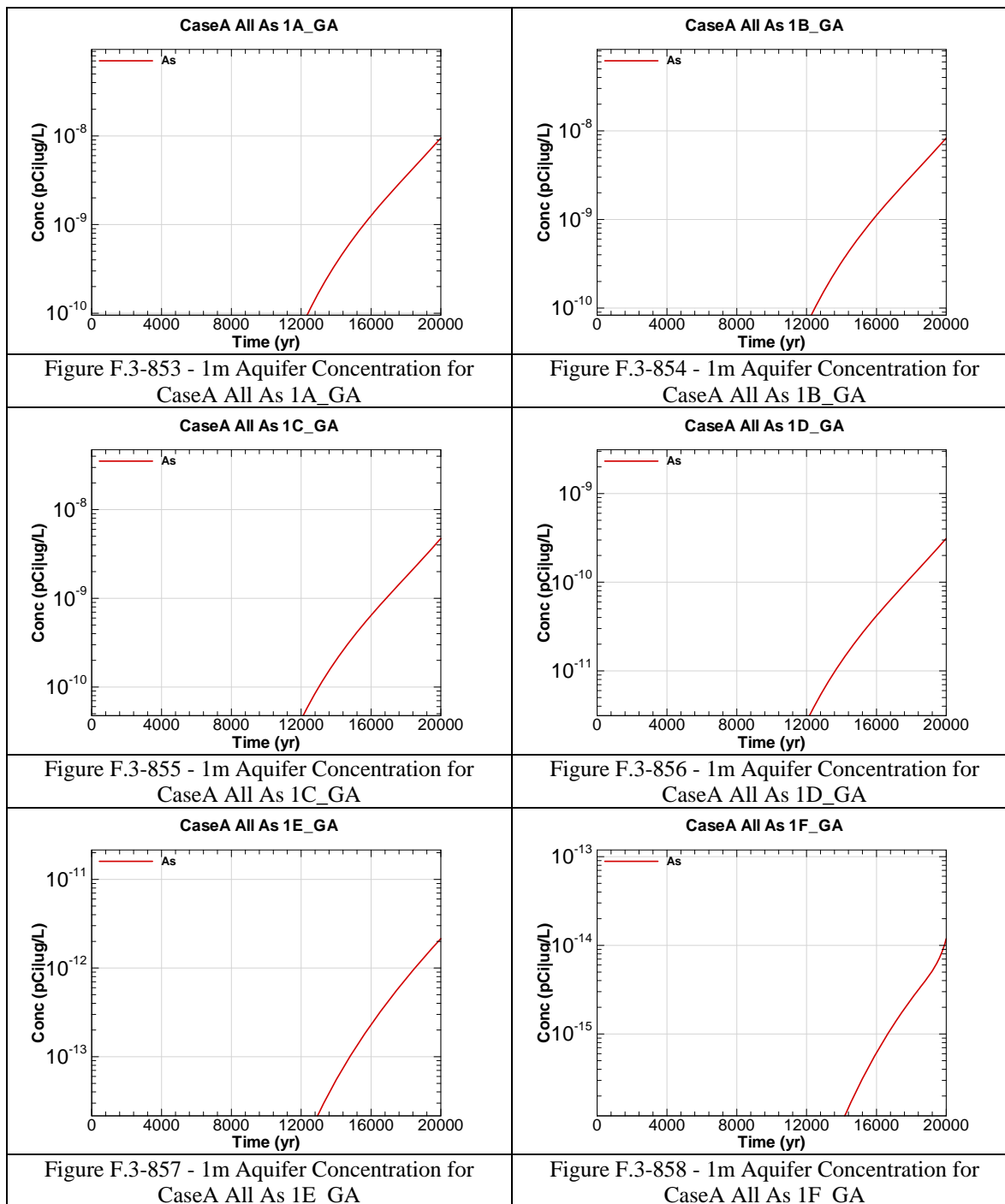


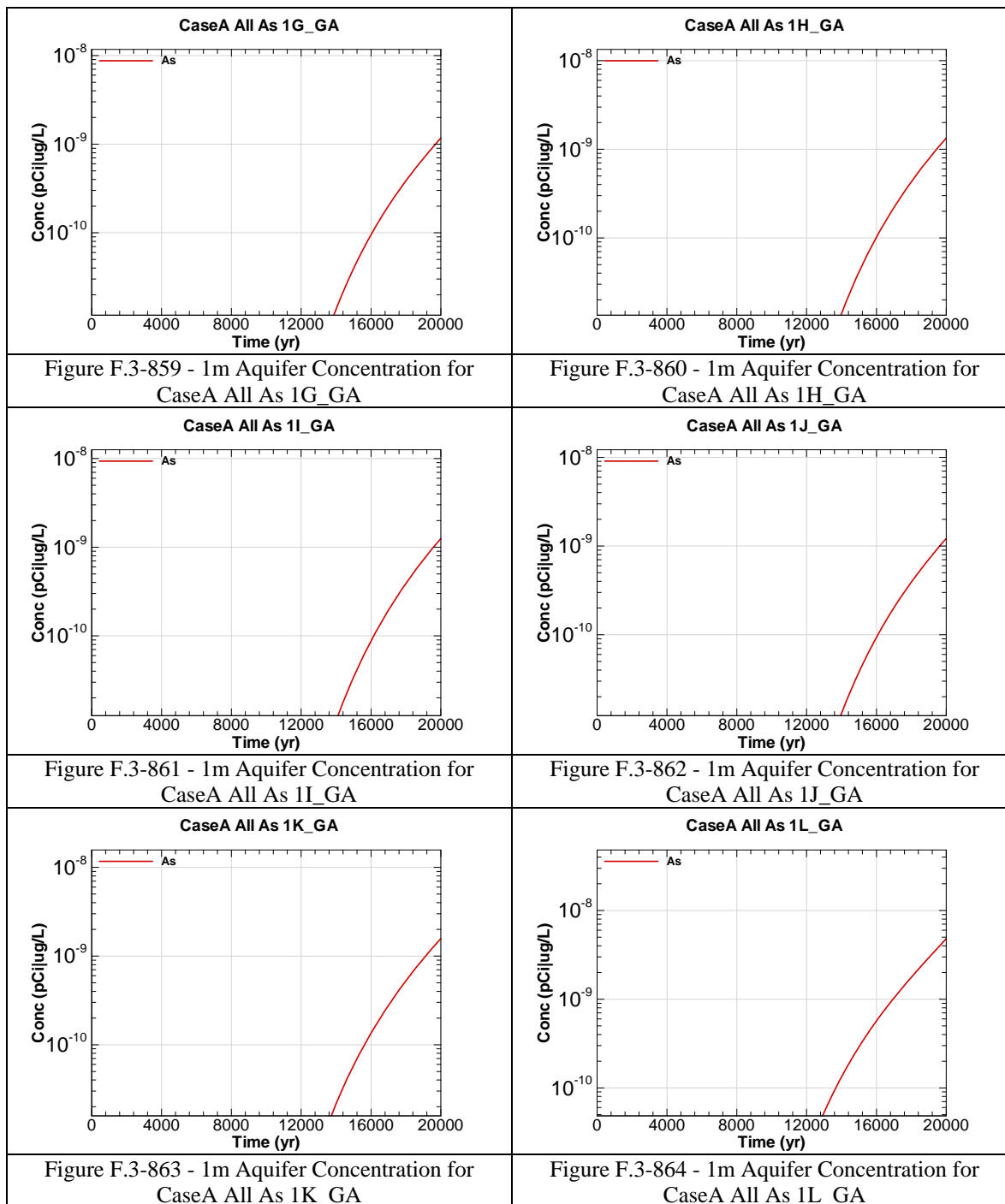
The chemical contaminants were modeled prior to the revision of the final closure inventory calculations presented in Table 3.3-8 for five chemical components: As, Cr, Cu, N and U. The figures that follow represent the concentrations calculated with an initial inventory input. The multipliers in the table below are to be used to determine the final concentrations with respect to time for the impacted chemicals as the inventory has a linear relationship with concentration in the Saltstone model. The groundwater concentration tables in Section 5 have been corrected using the multipliers.

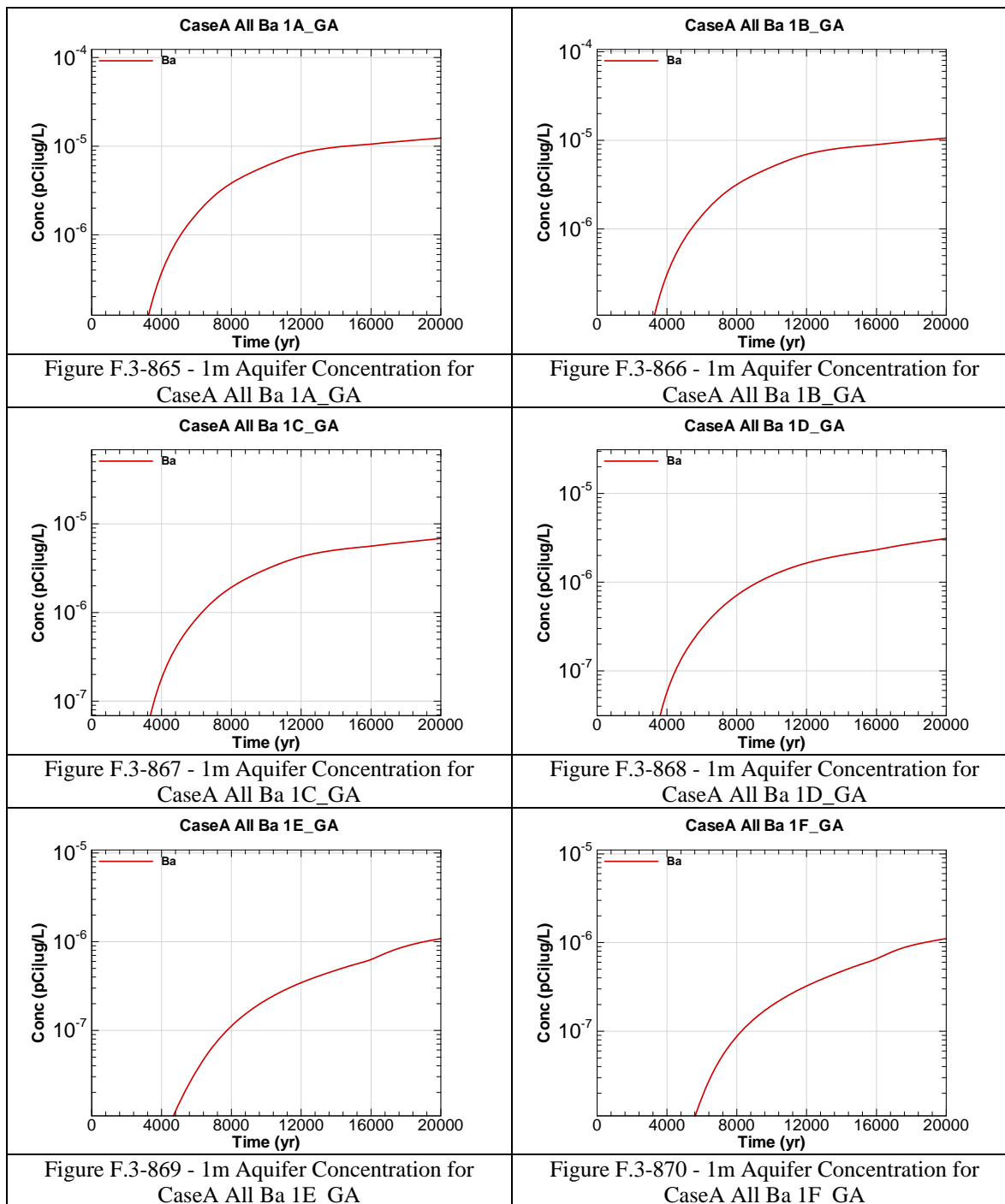
| Chemical Component | Modeled Inventory | Projected Inventory | Percent Increase | Multiplier |
|---------------------------|--------------------------|----------------------------|-------------------------|-------------------|
| Ag | 8.8E+01 | 8.8E+01 | 0.0% | None |
| As | 1.08E+04 | 1.1E+04 | 2.3% | 1.02E+00 |
| Ba | 1.7E+02 | 1.7E+02 | 0.0% | None |
| Cd | 1.3E+03 | 1.3E+03 | 0.0% | None |
| Cr | 2.9E+04 | 3.0E+04 | 1.4% | 1.01E+00 |
| Cu | 1.9E+04 | 1.9E+04 | 0.9% | 1.01E+00 |
| F | 1.7E+04 | 1.7E+04 | 0.0% | None |
| Fe | 2.9E+03 | 2.9E+03 | 0.0% | None |
| Hg | 1.1E+04 | 1.1E+04 | 0.0% | None |
| Mn | 7.3E+03 | 7.3E+03 | 0.0% | None |
| Ni | 1.5E+03 | 1.5E+03 | 0.0% | None |
| Total N | 2.2E+07 | 2.4E+07 | 5.8% | 1.06E+00 |
| Pb | 6.7E+03 | 6.7E+03 | 0.0% | None |
| Se | 4.0E+04 | 4.0E+04 | 0.0% | None |
| U | 8.2E+02 | 8.9E+02 | 8.9% | 1.10E+00 |
| Zn | 2.7E+04 | 2.7E+04 | 0.0% | None |

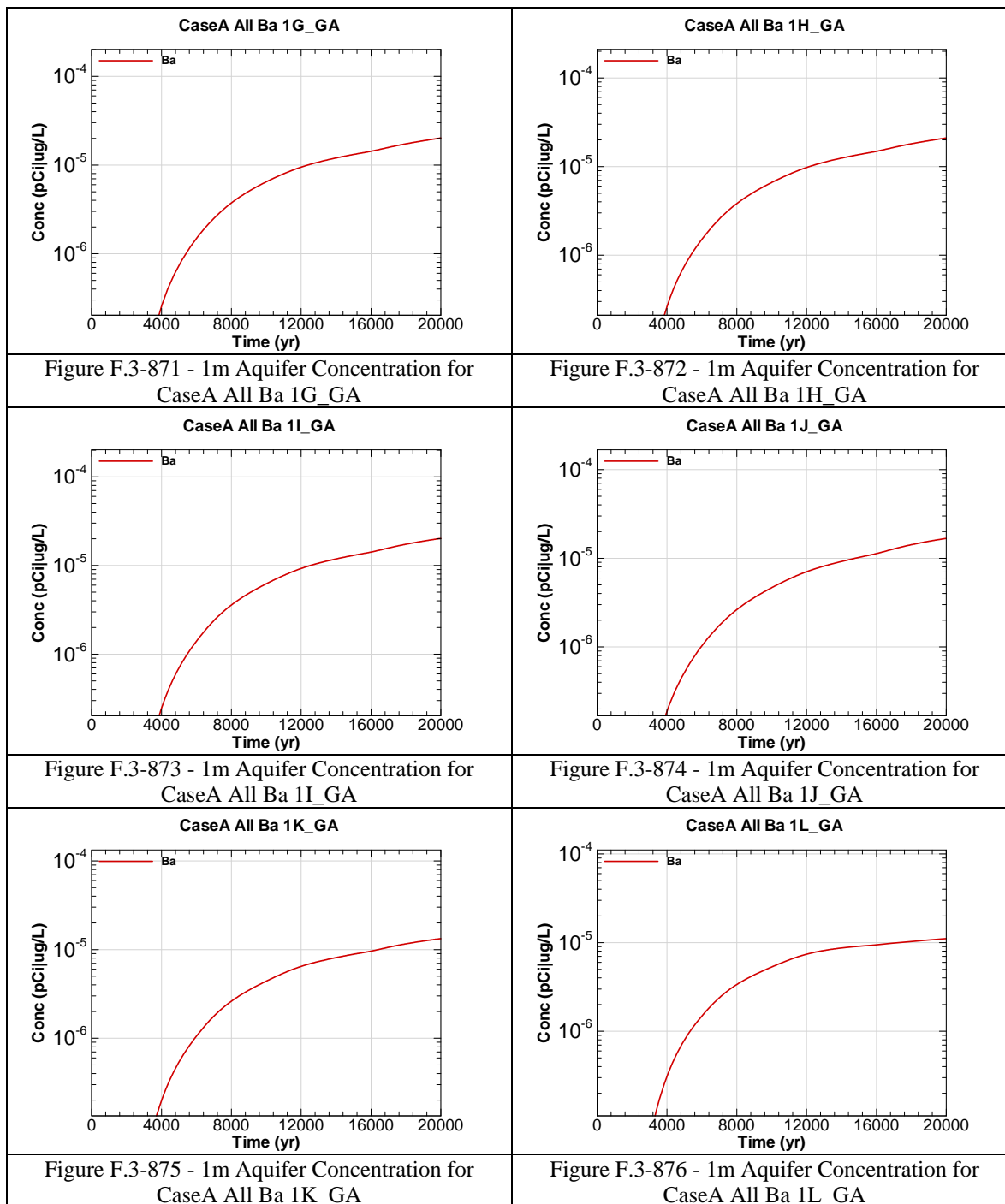


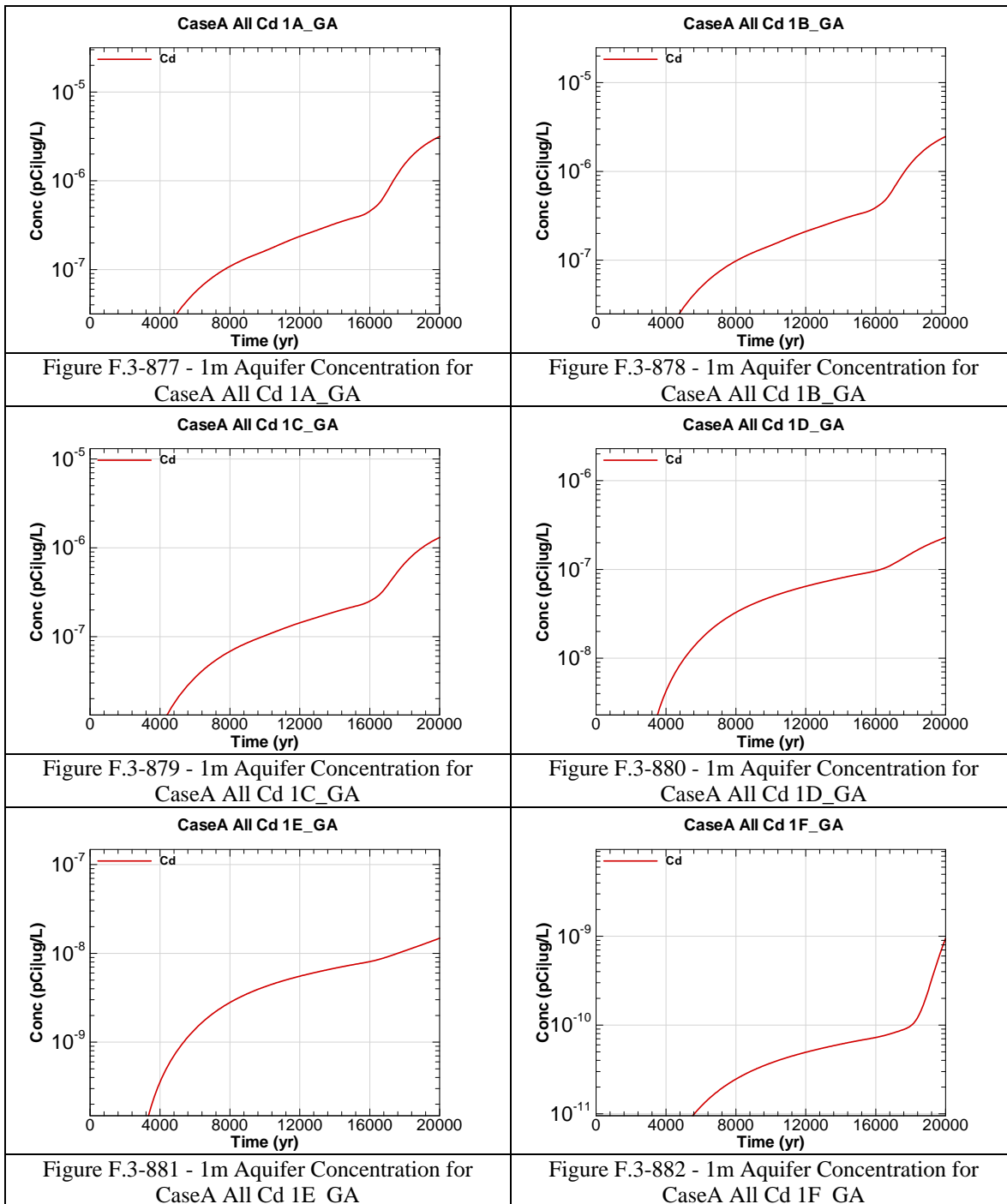


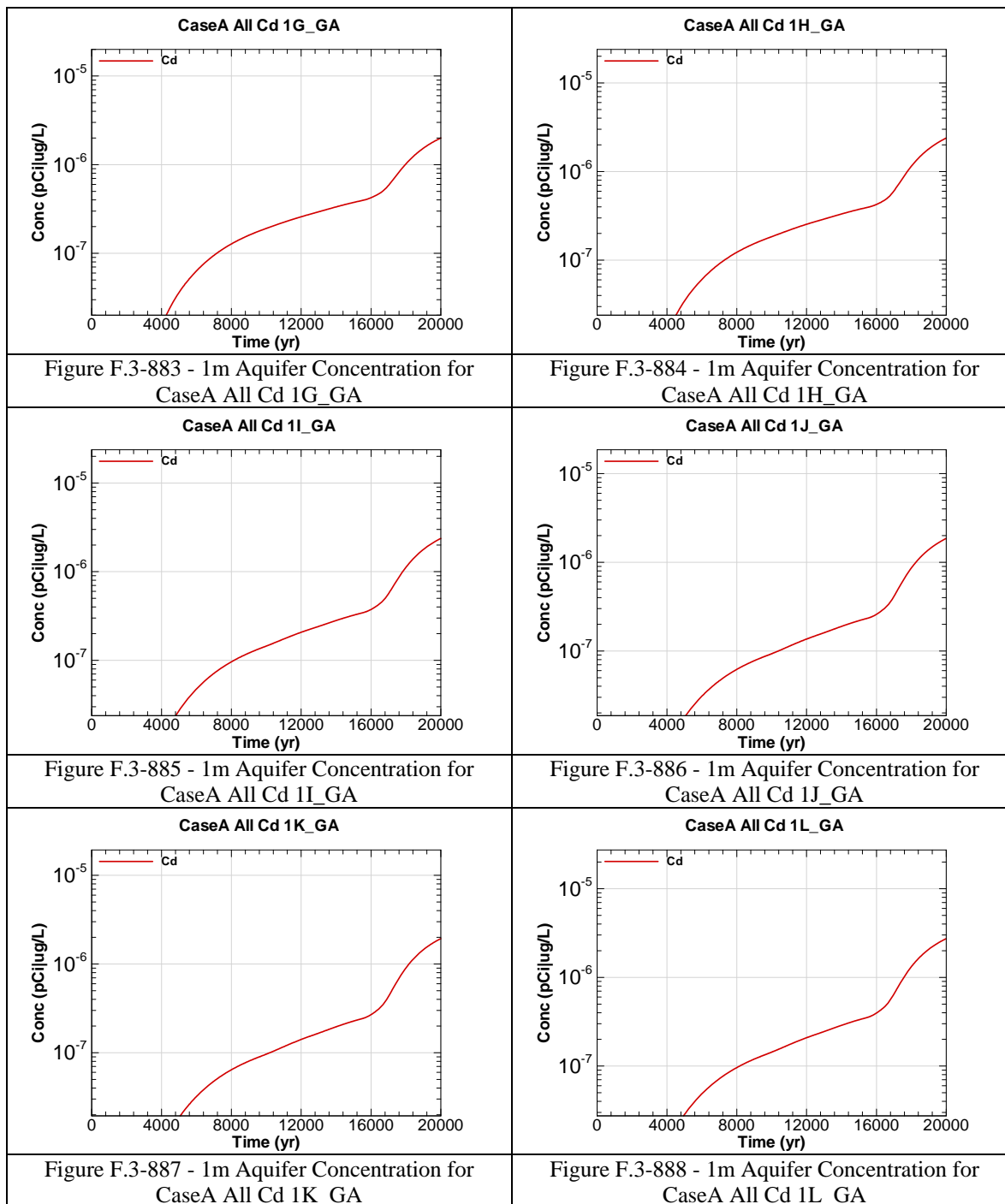


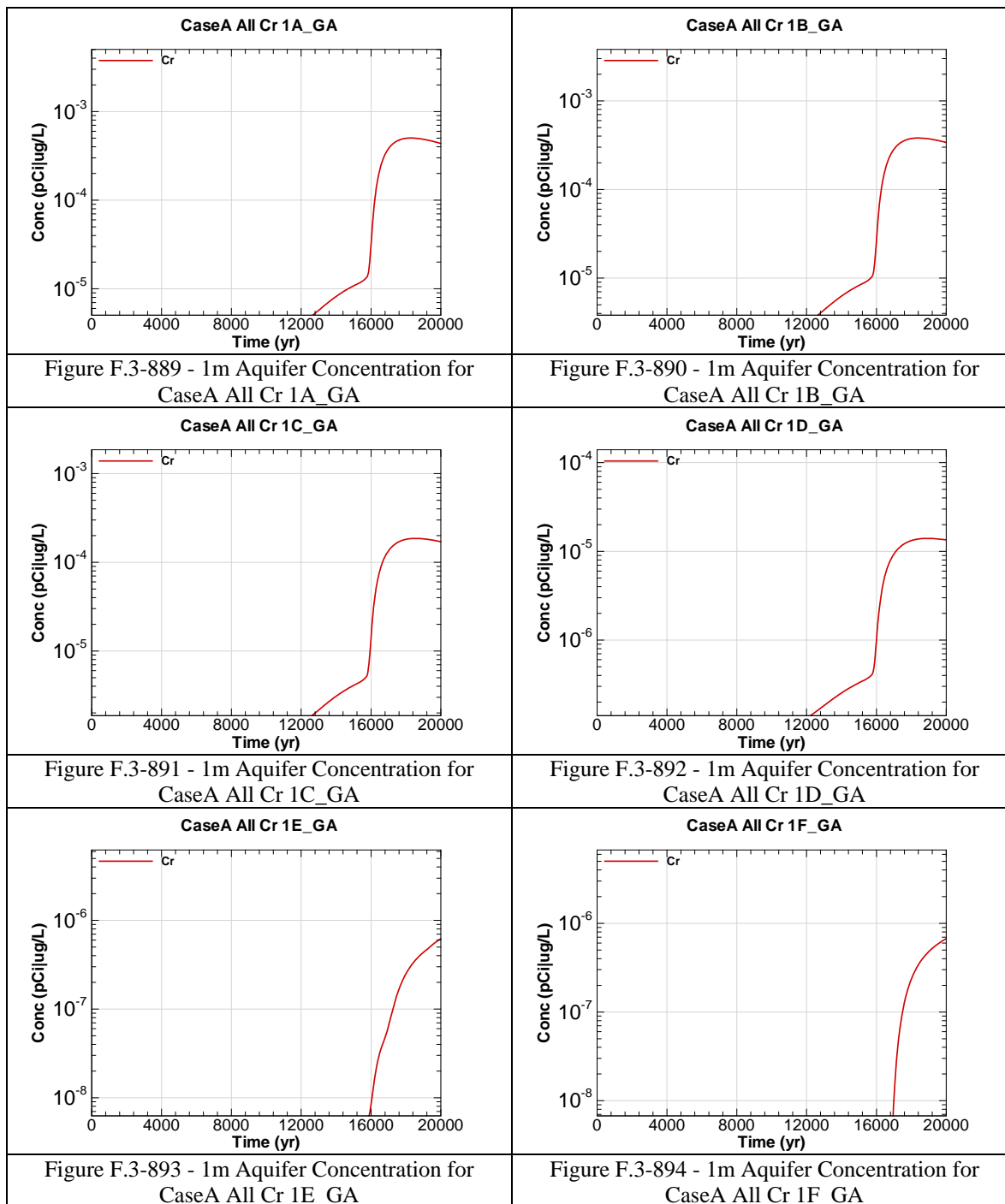


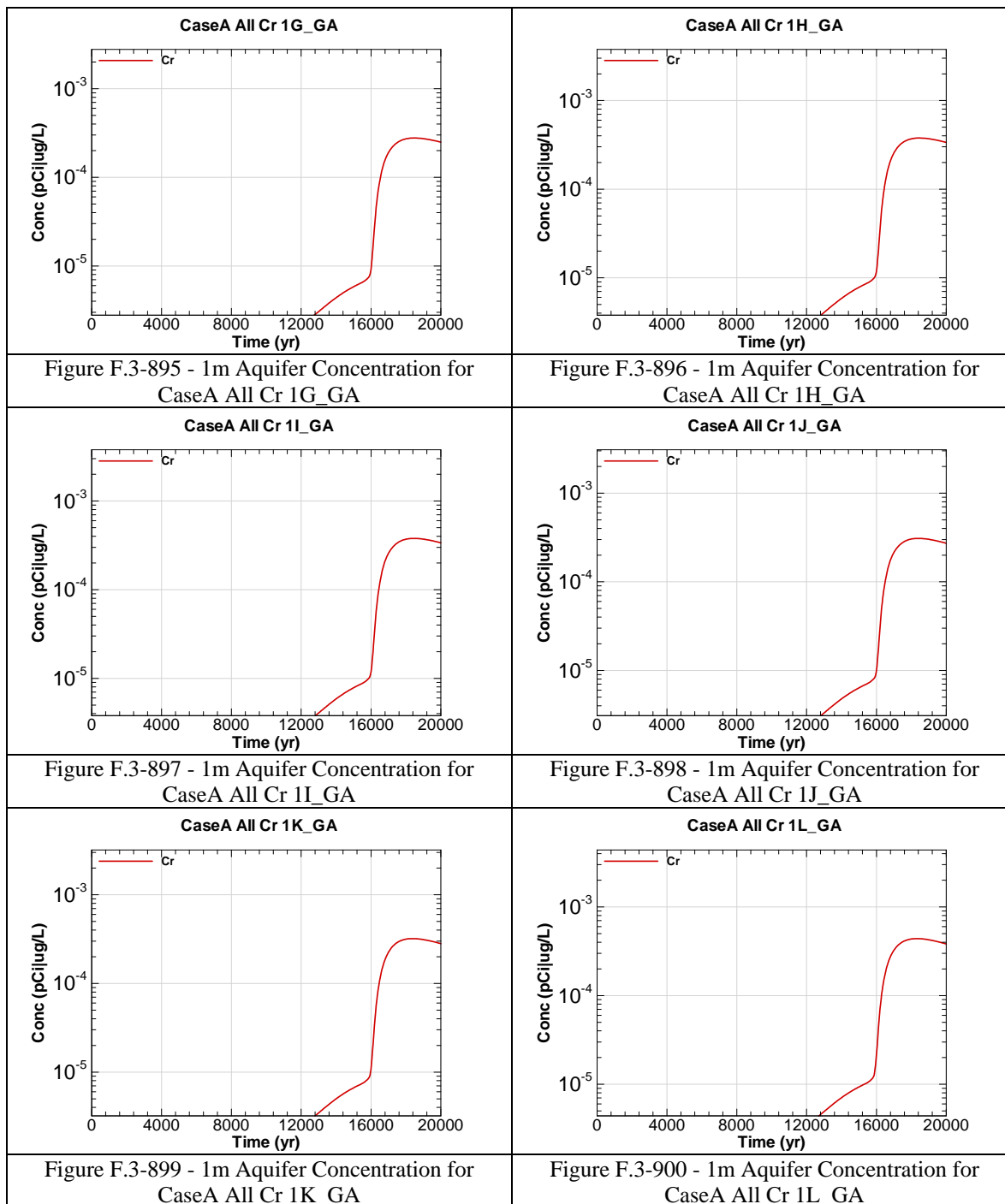


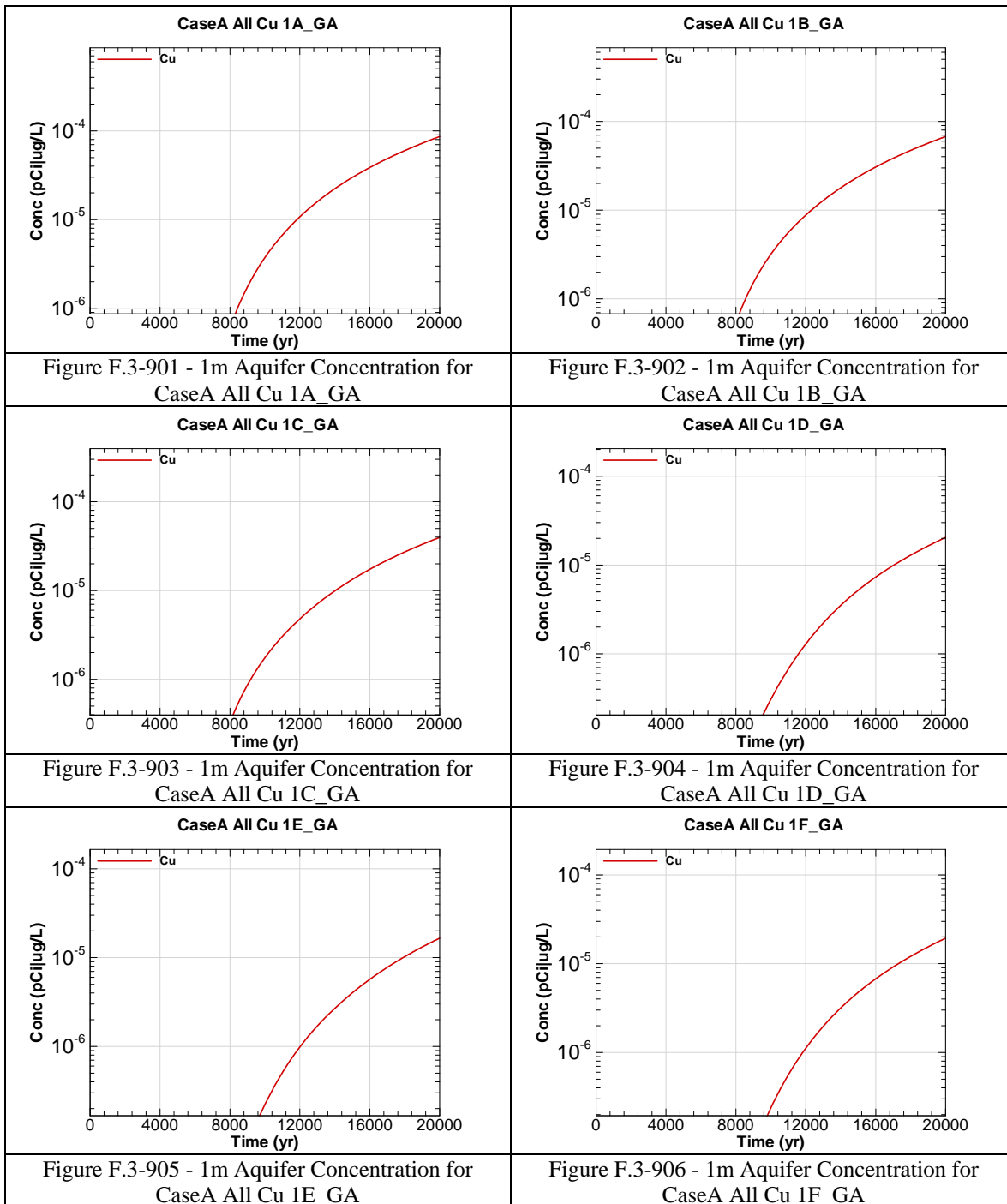


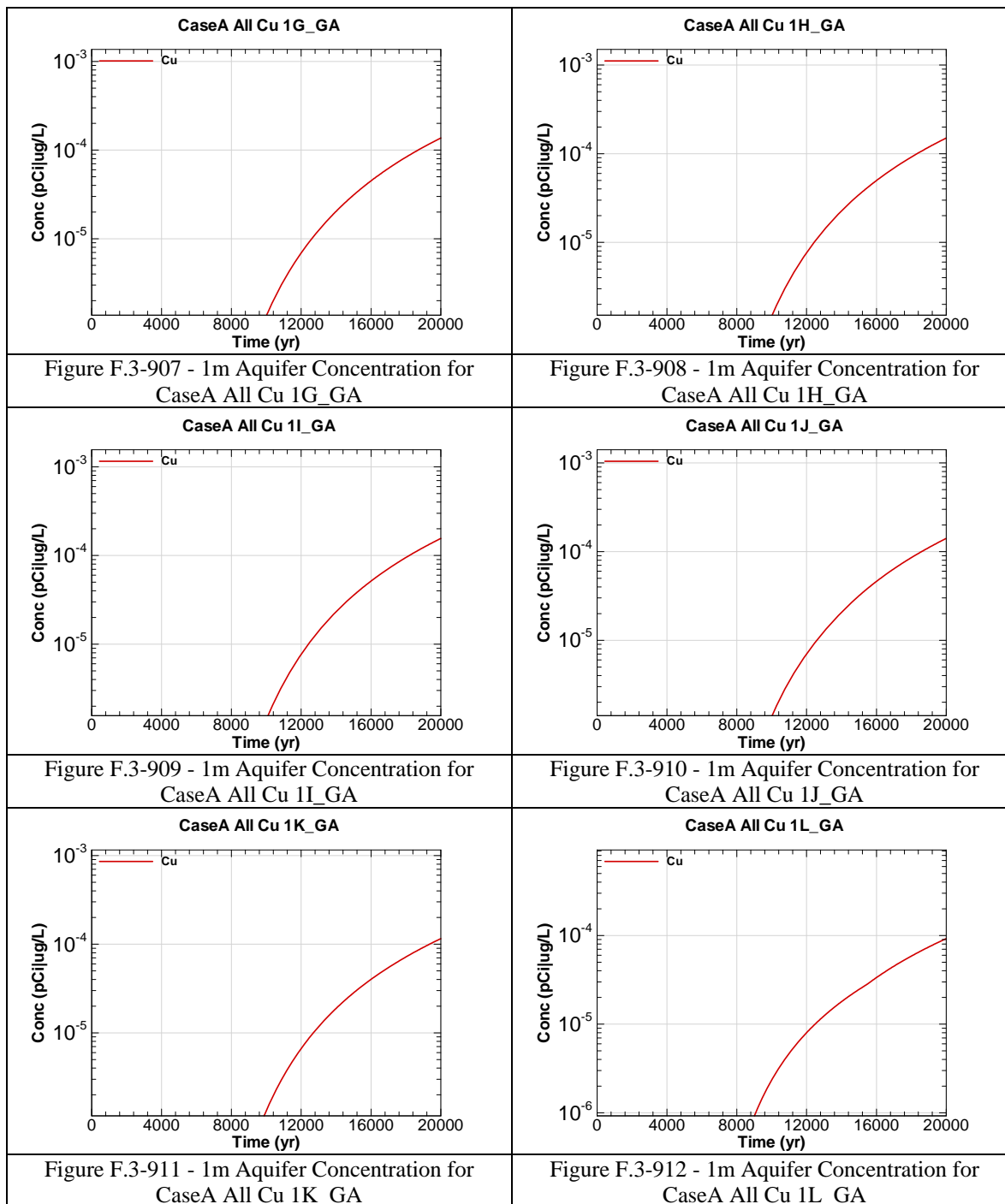


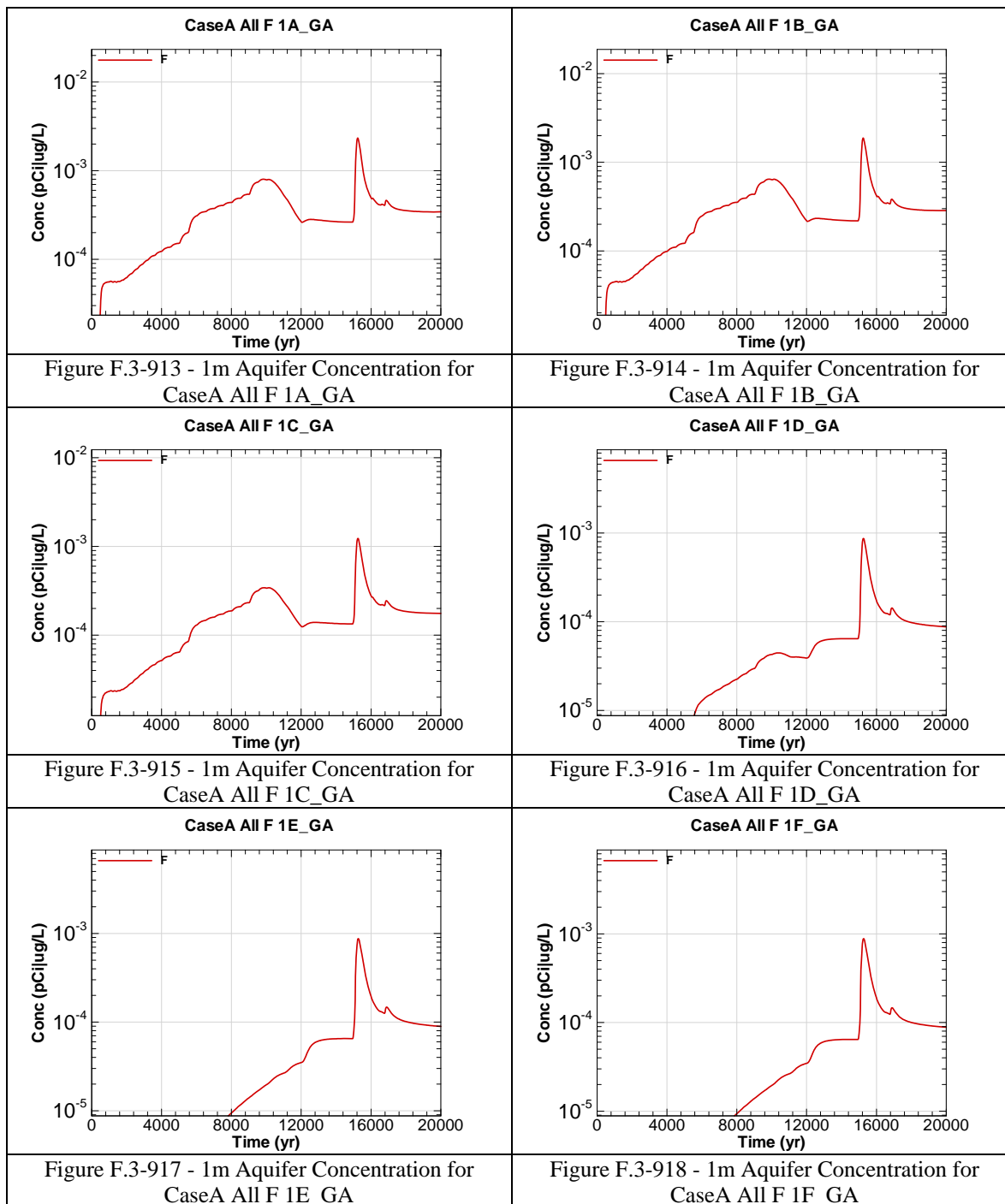


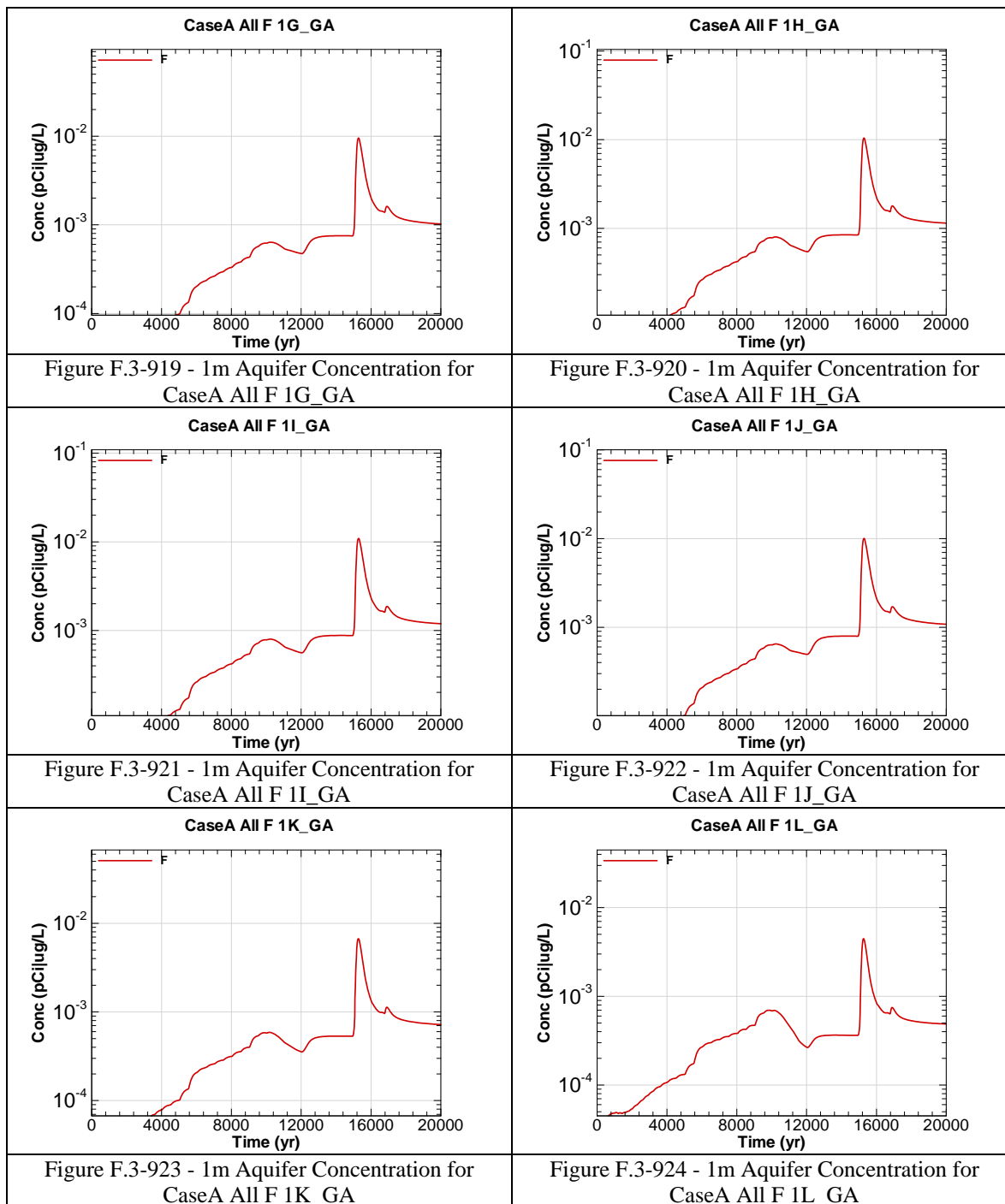


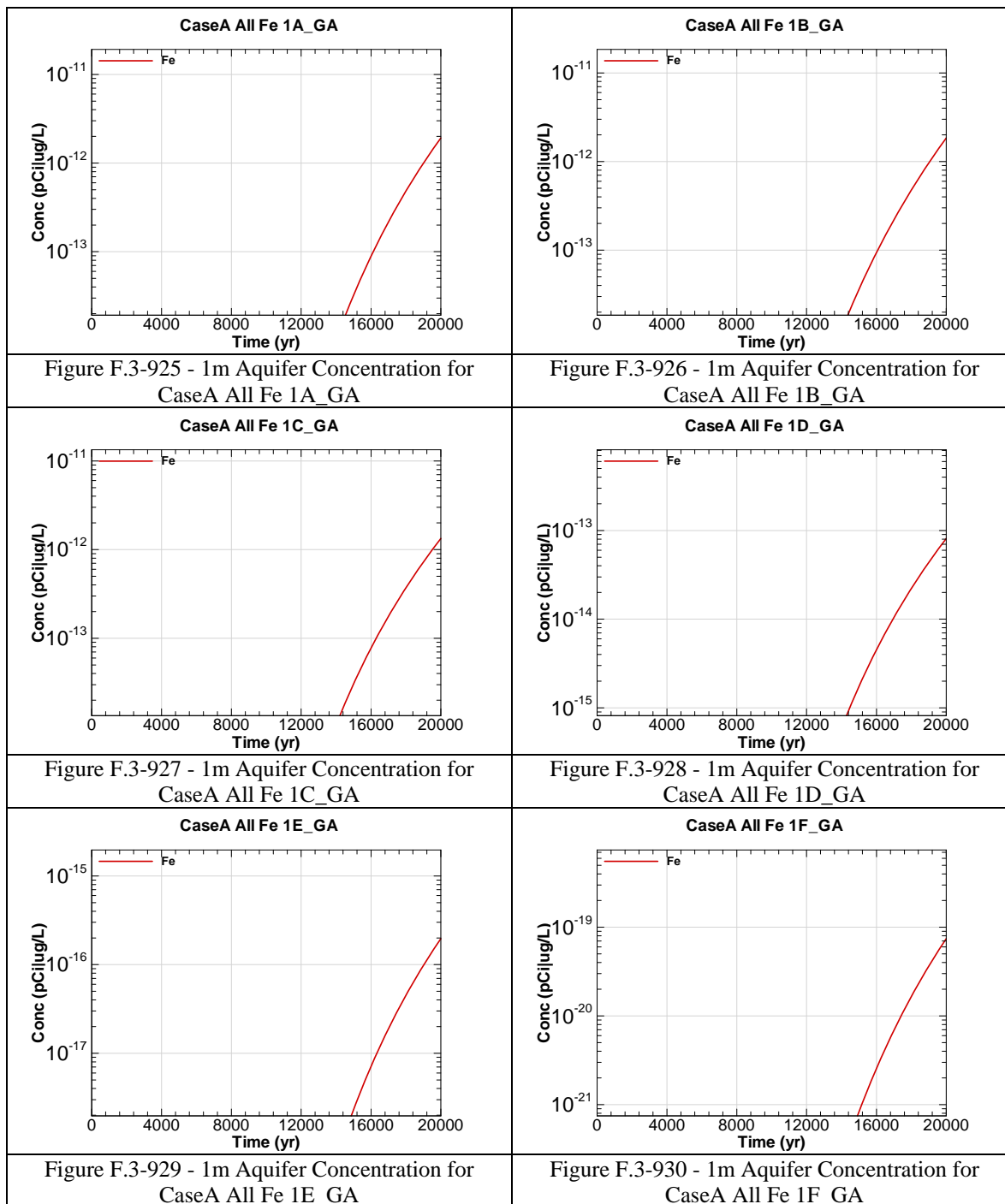


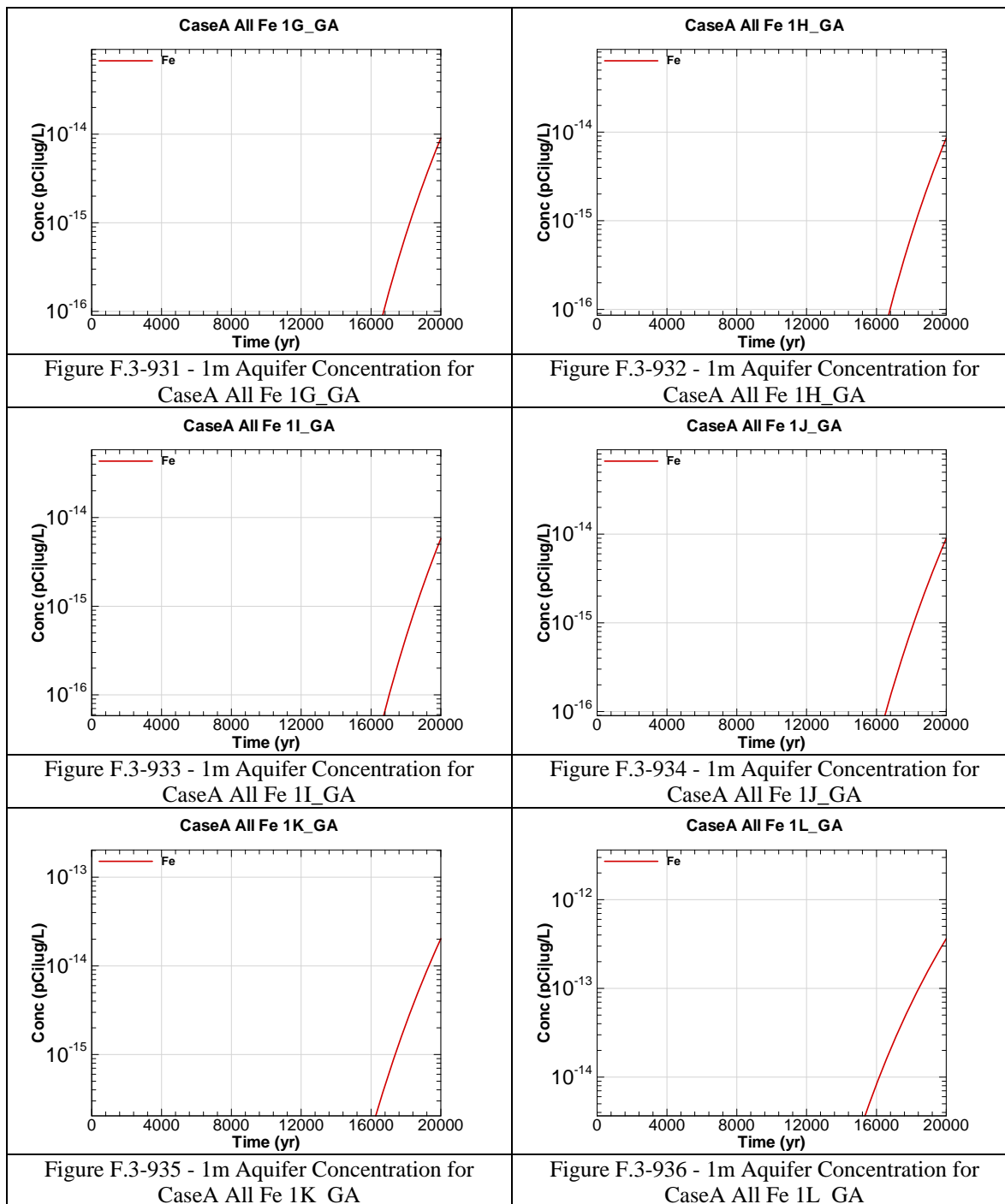


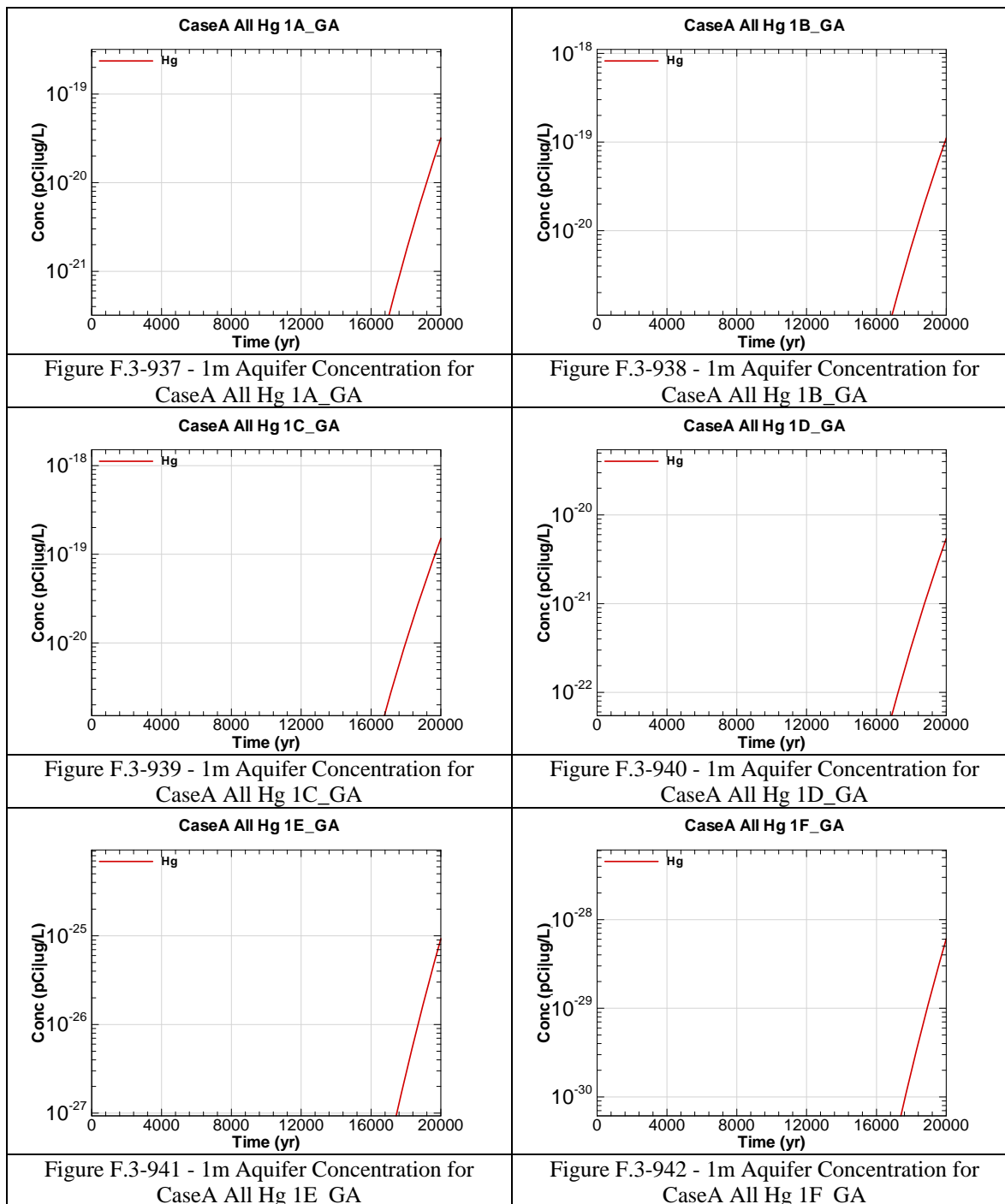


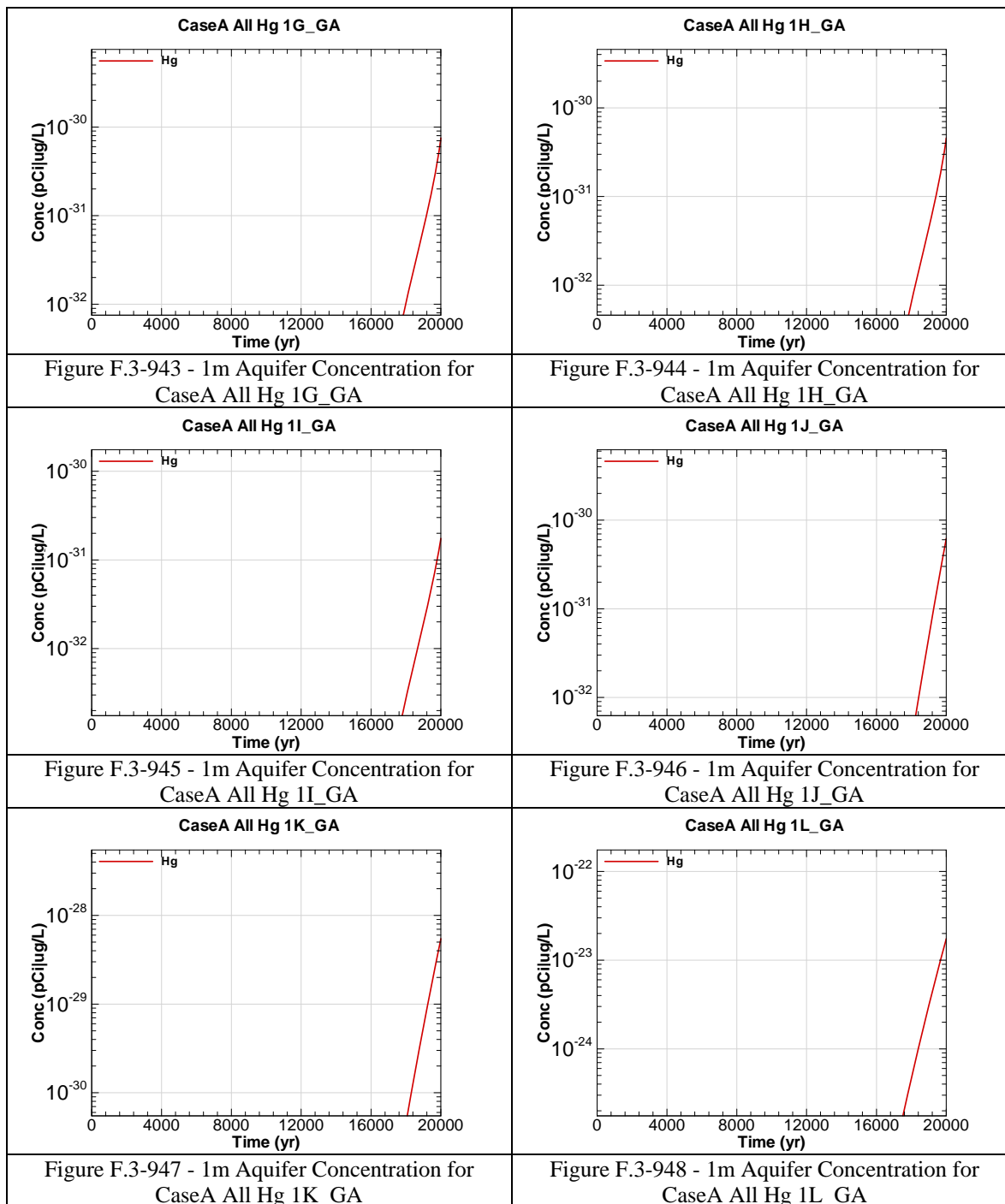


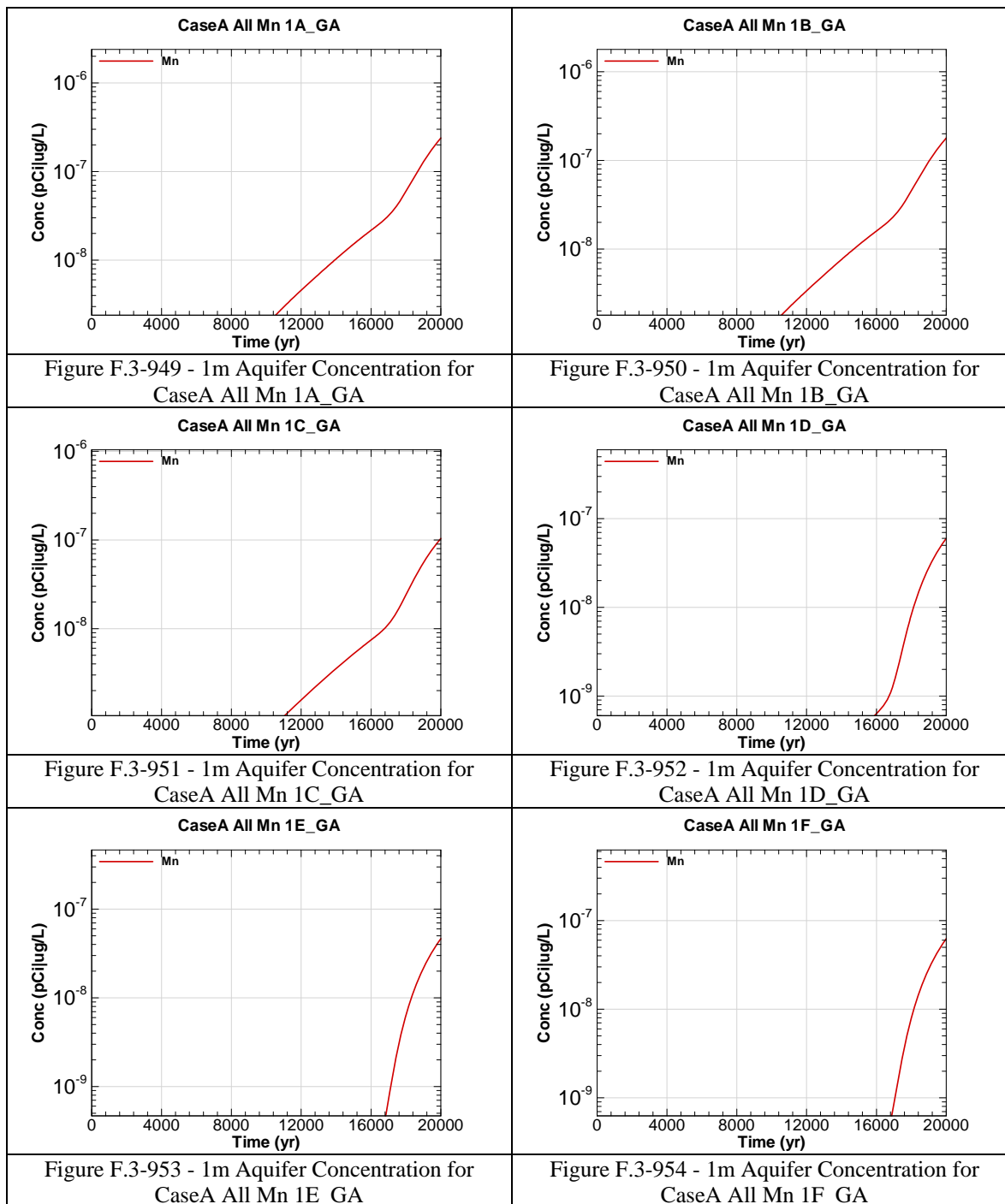


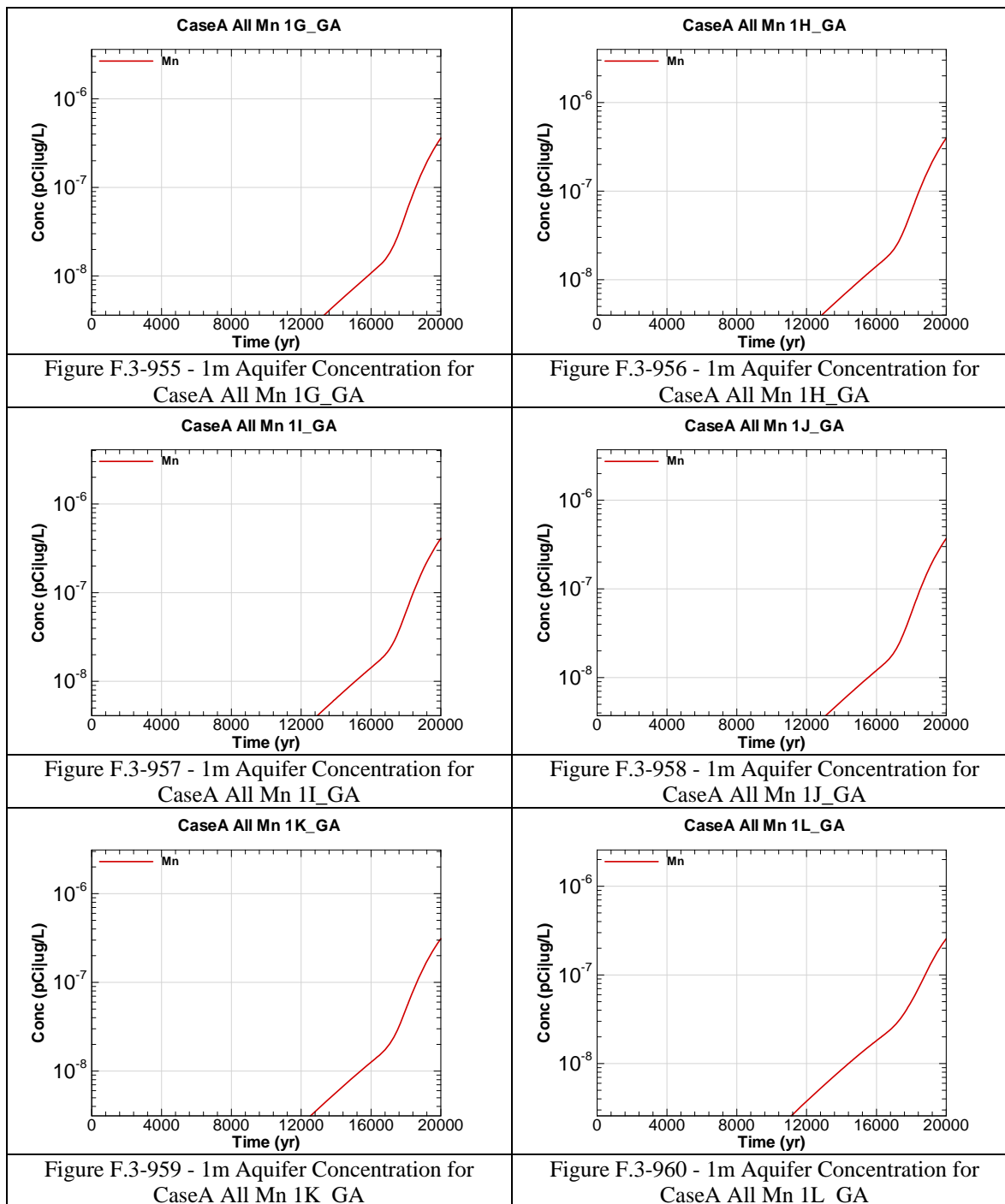


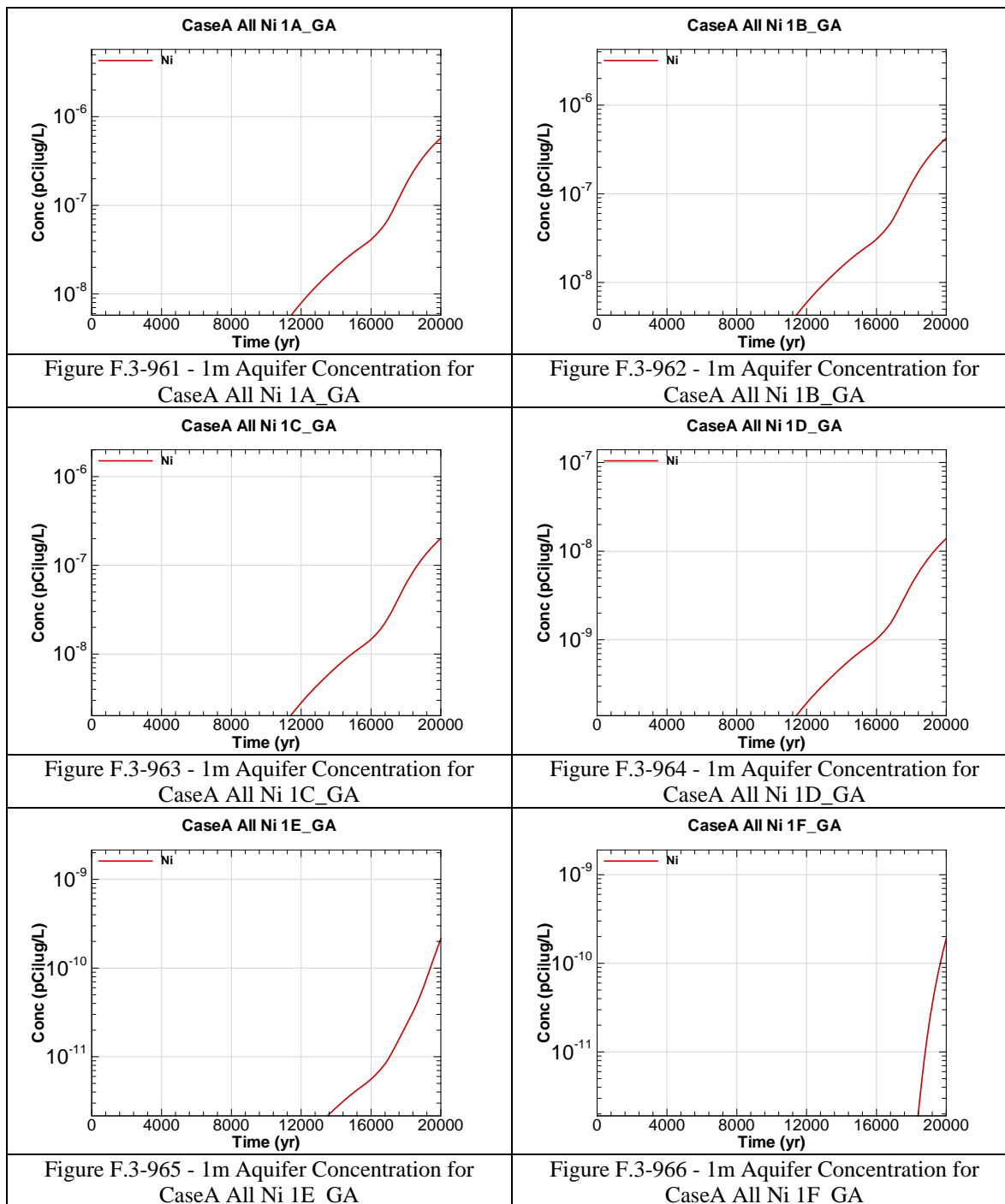


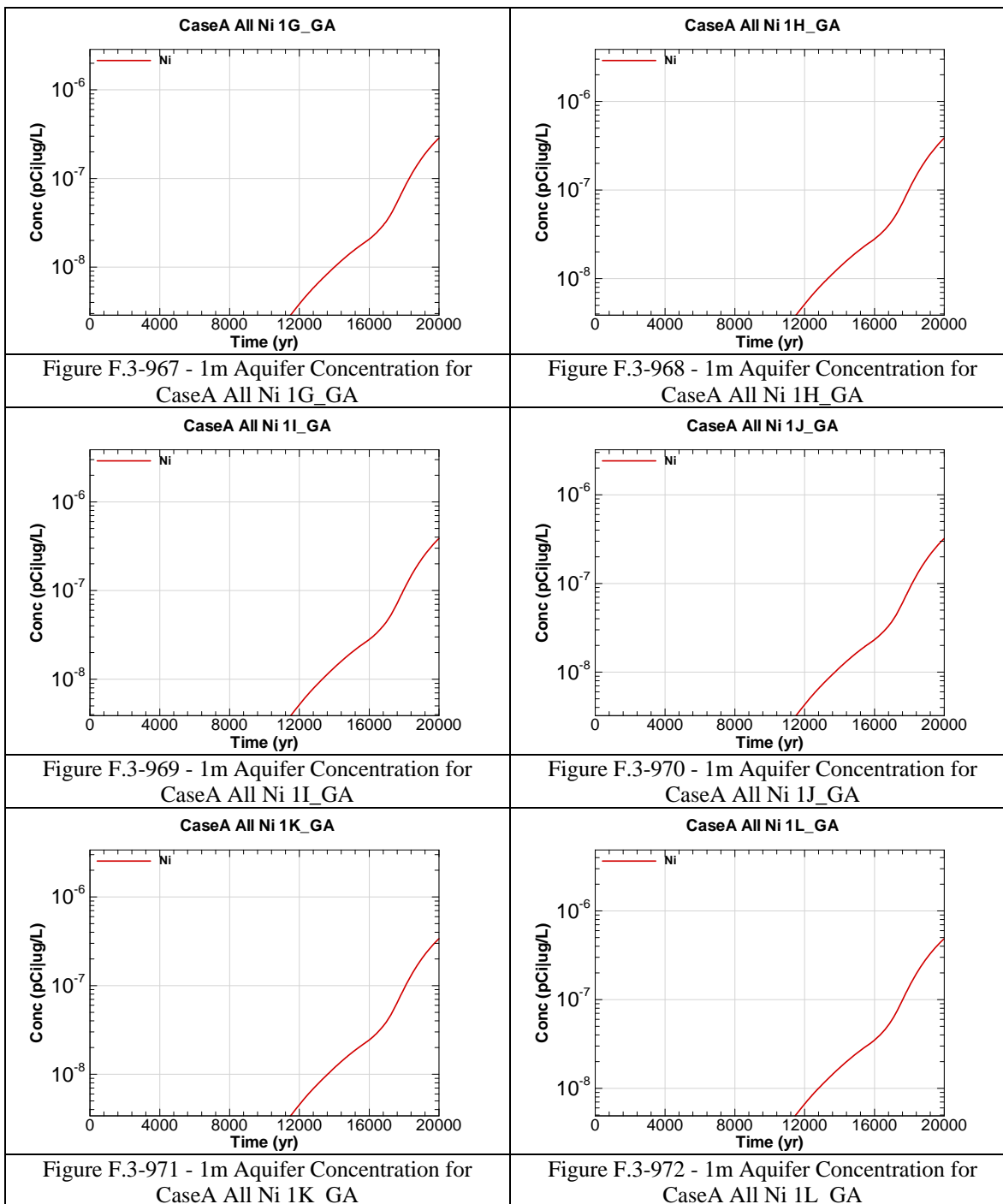


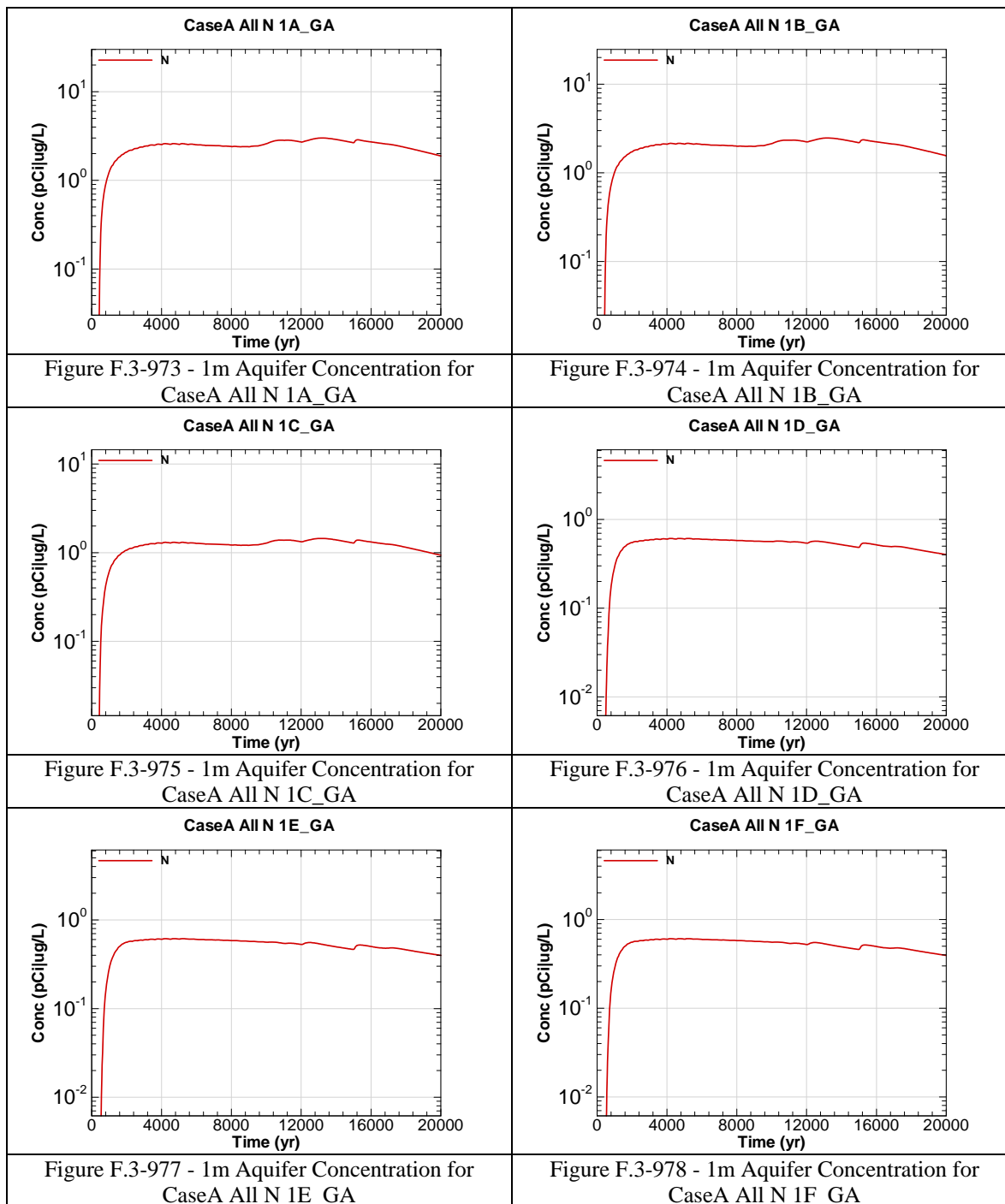


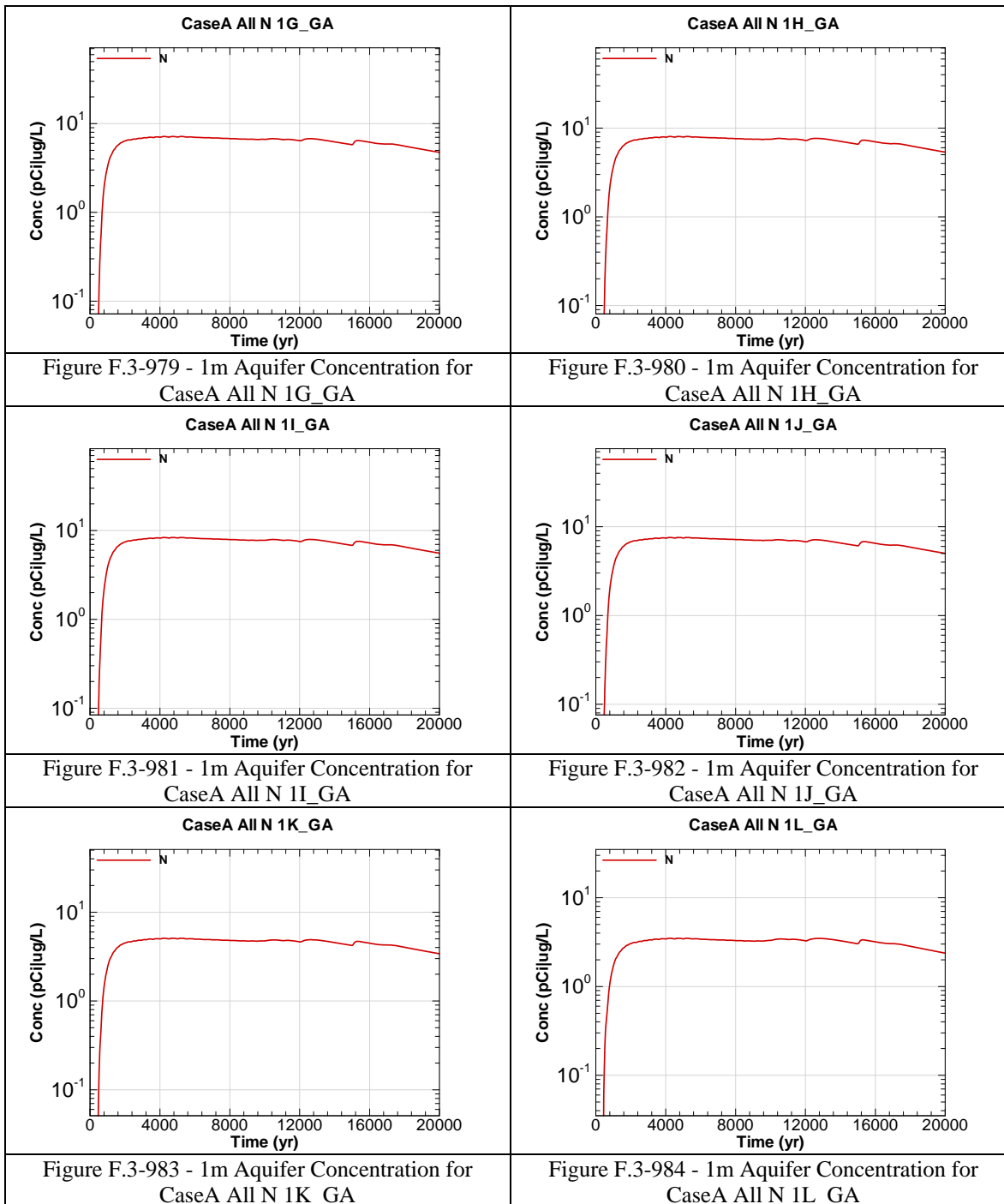


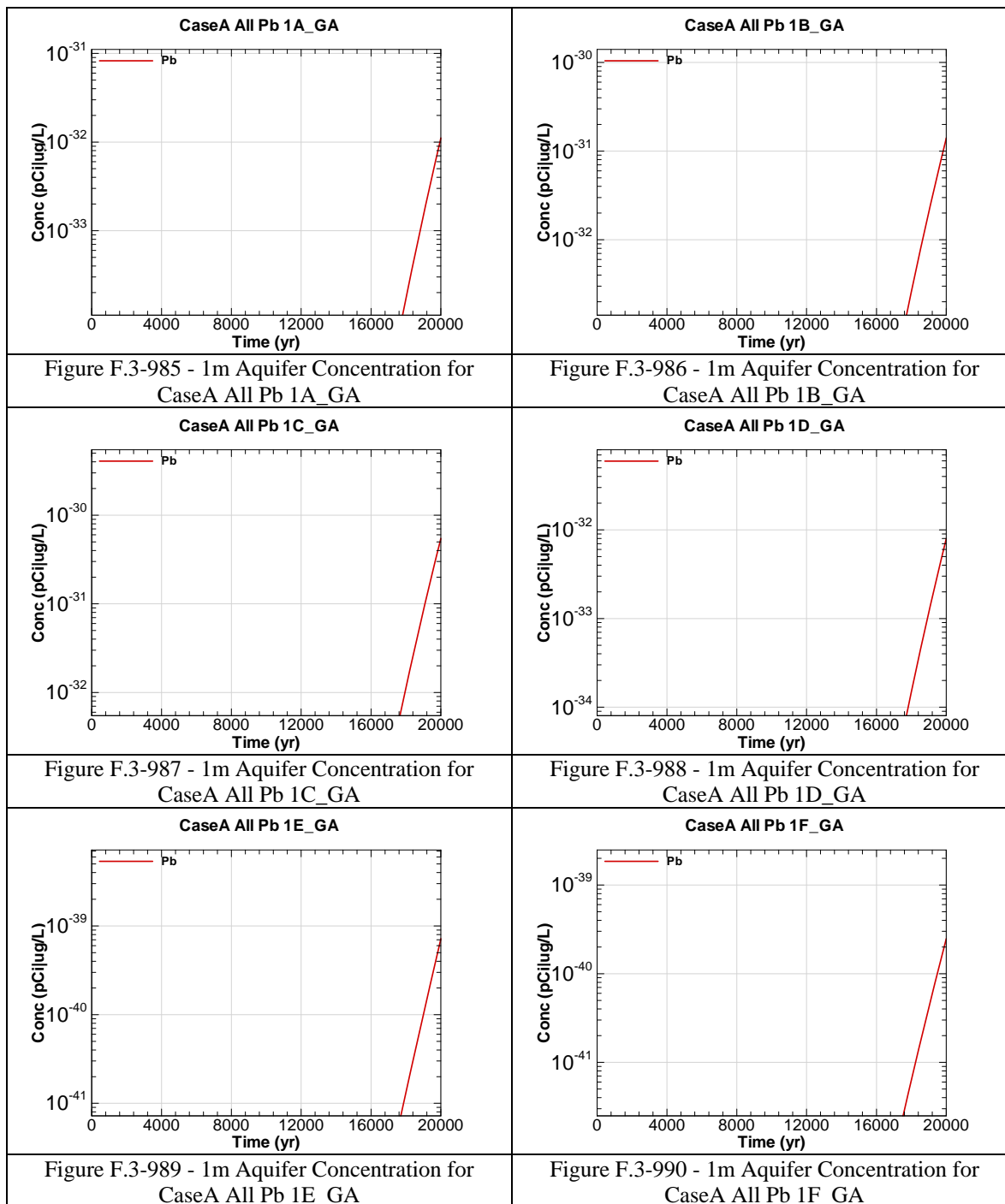


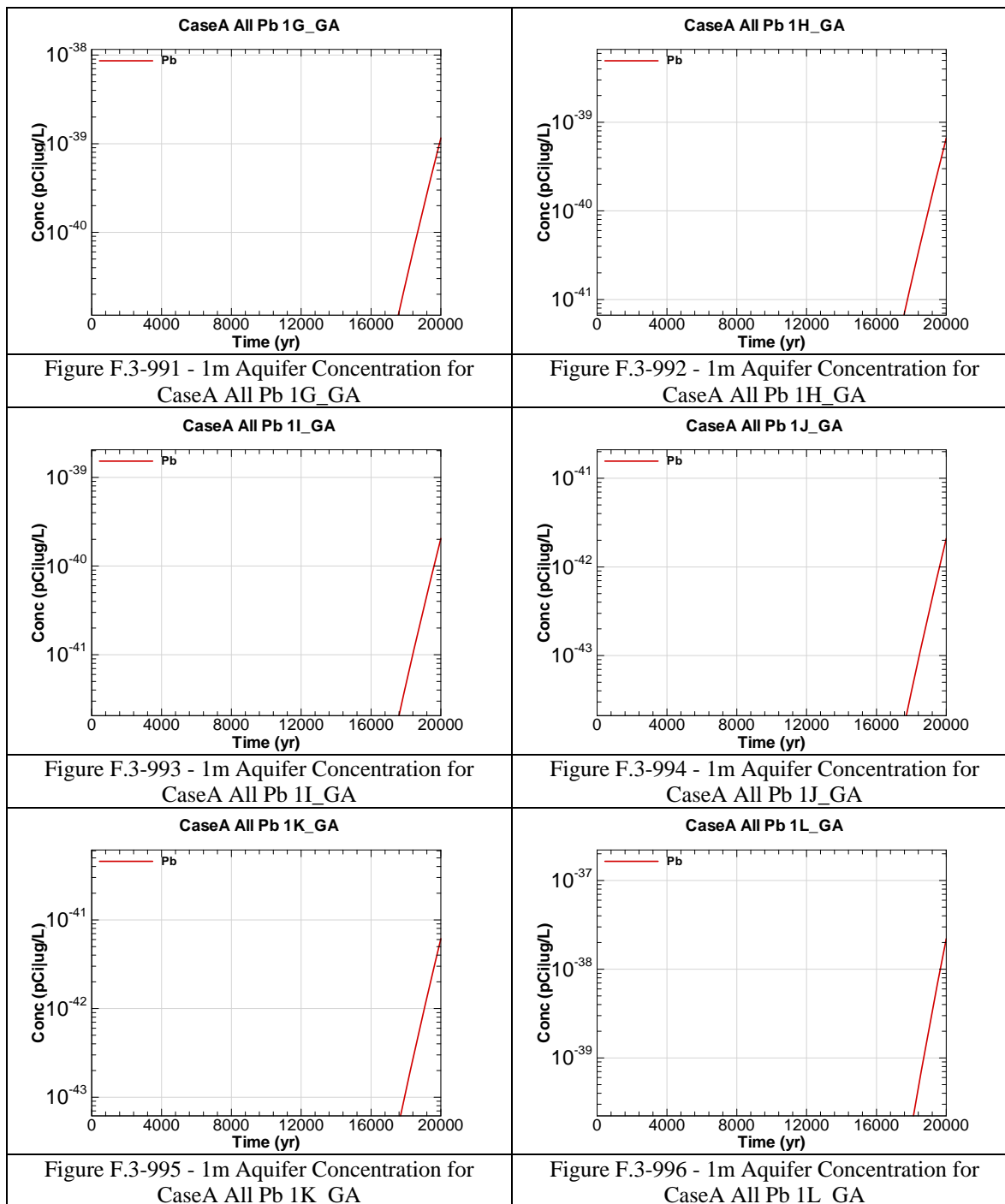


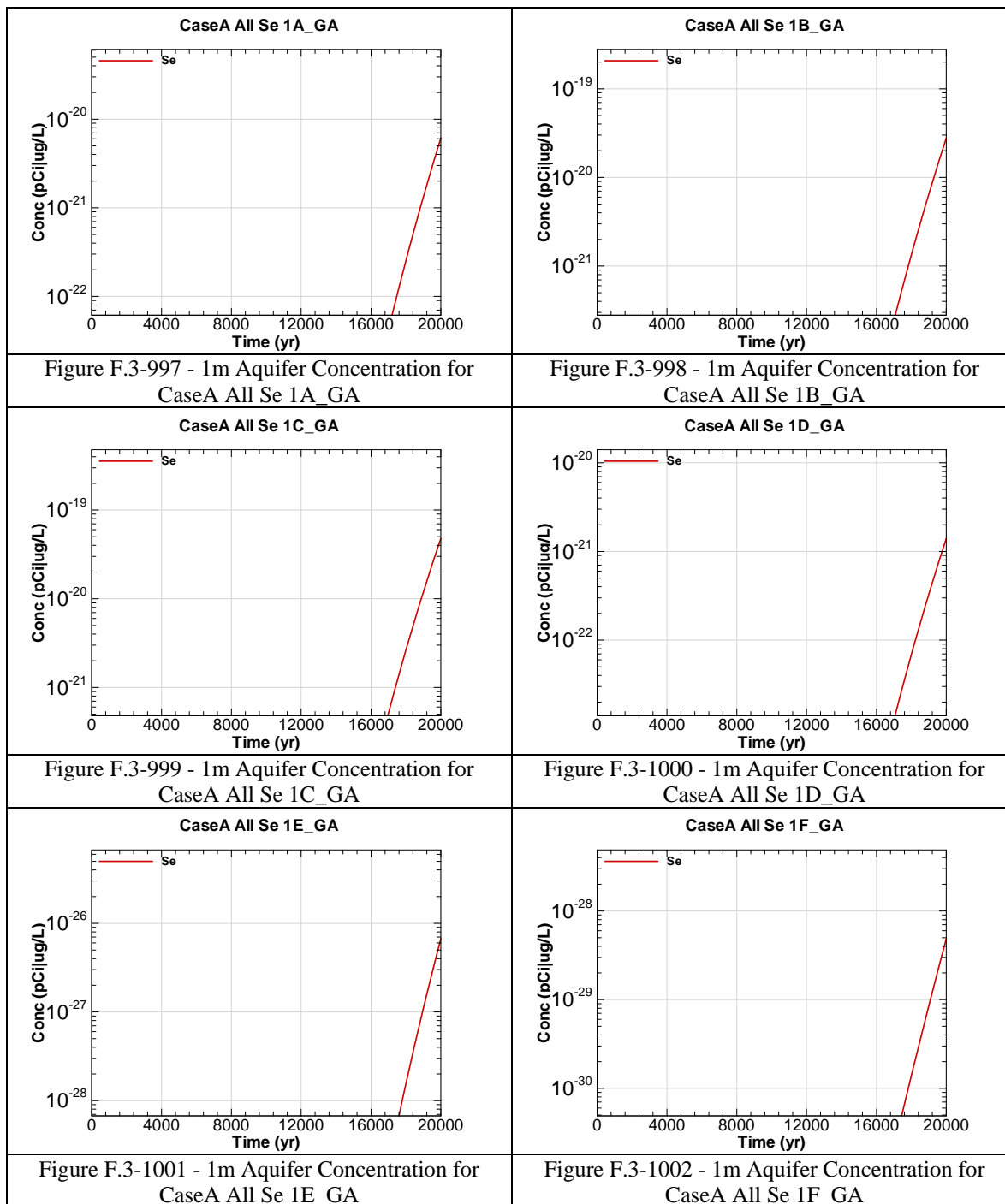


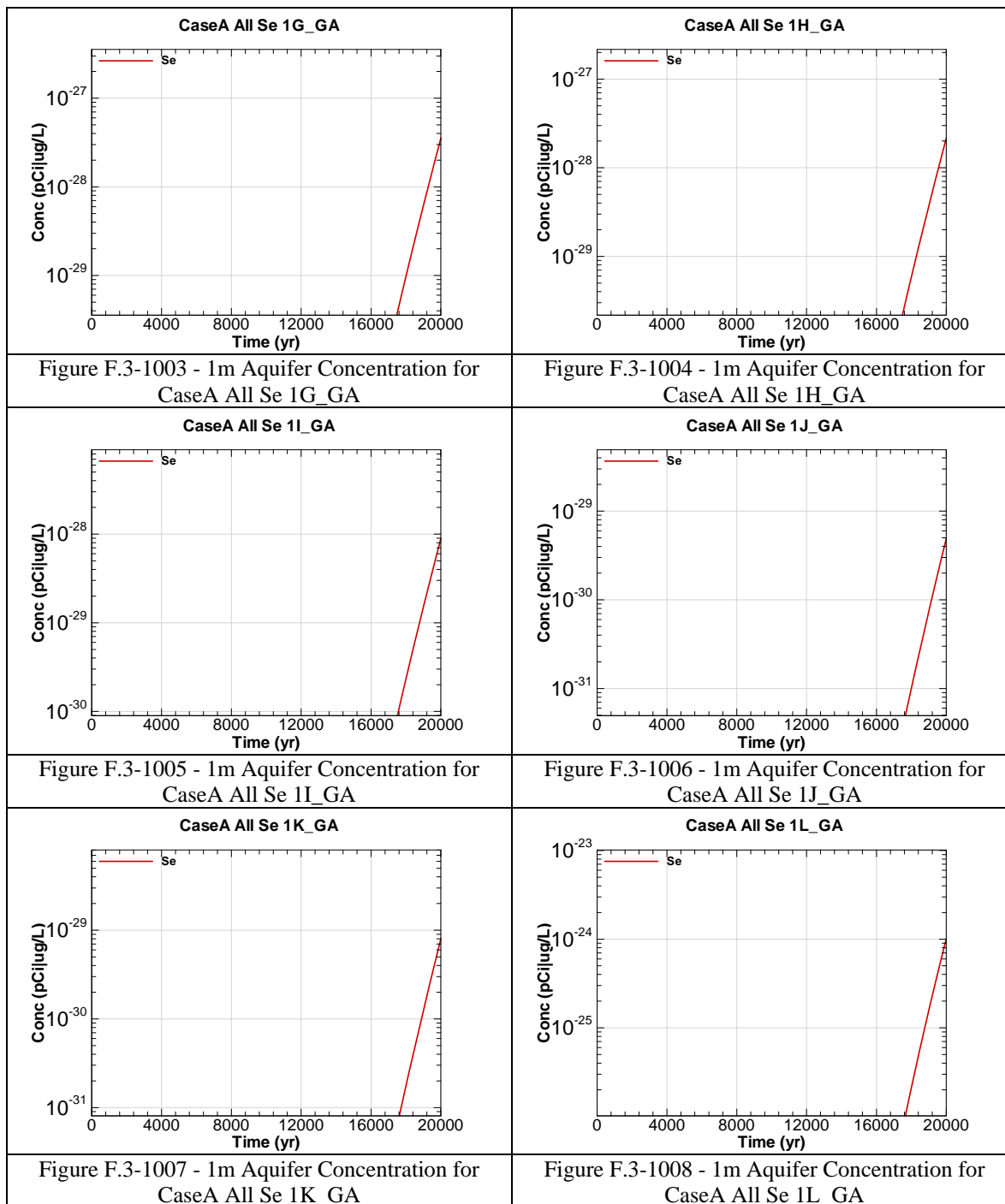


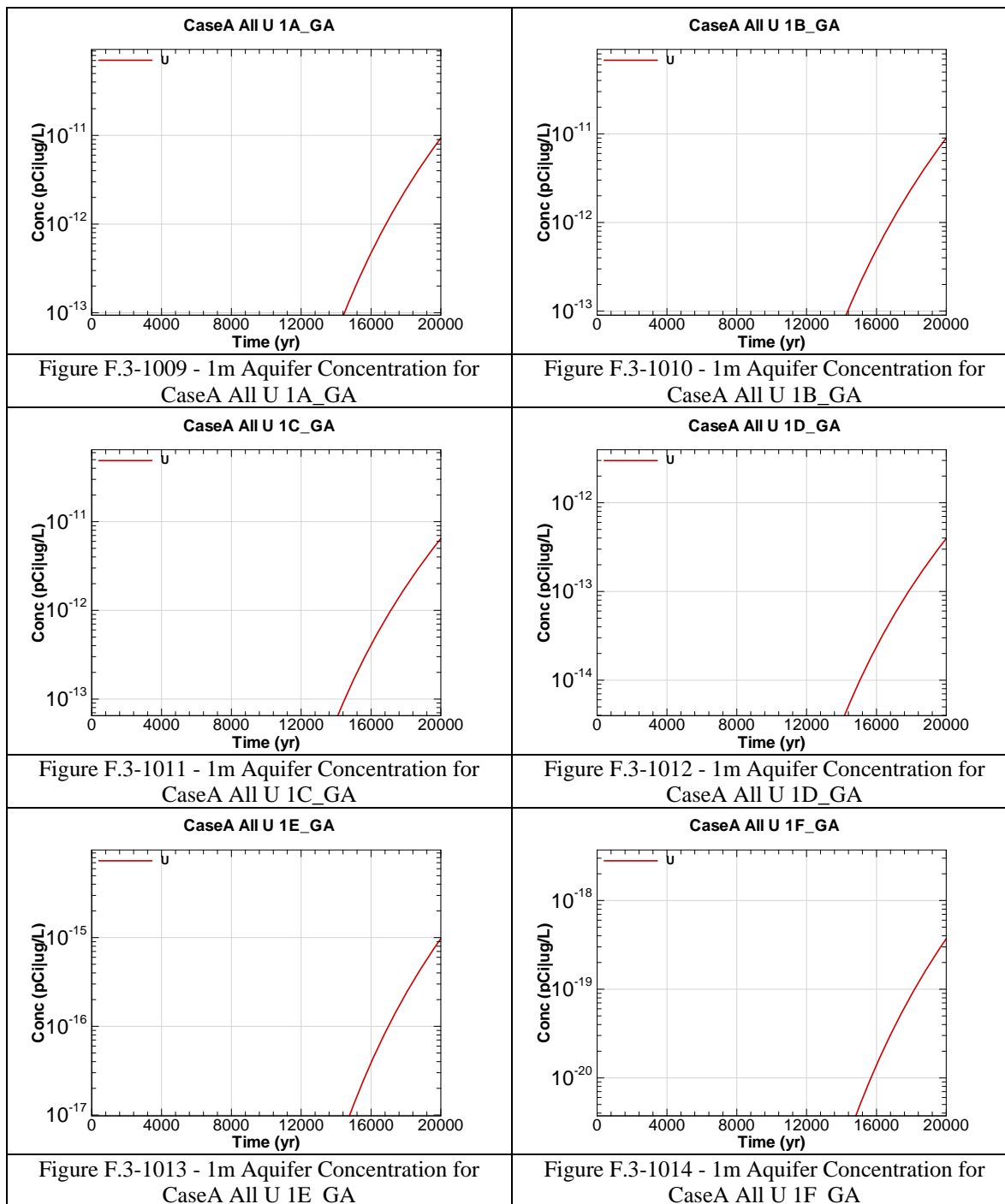


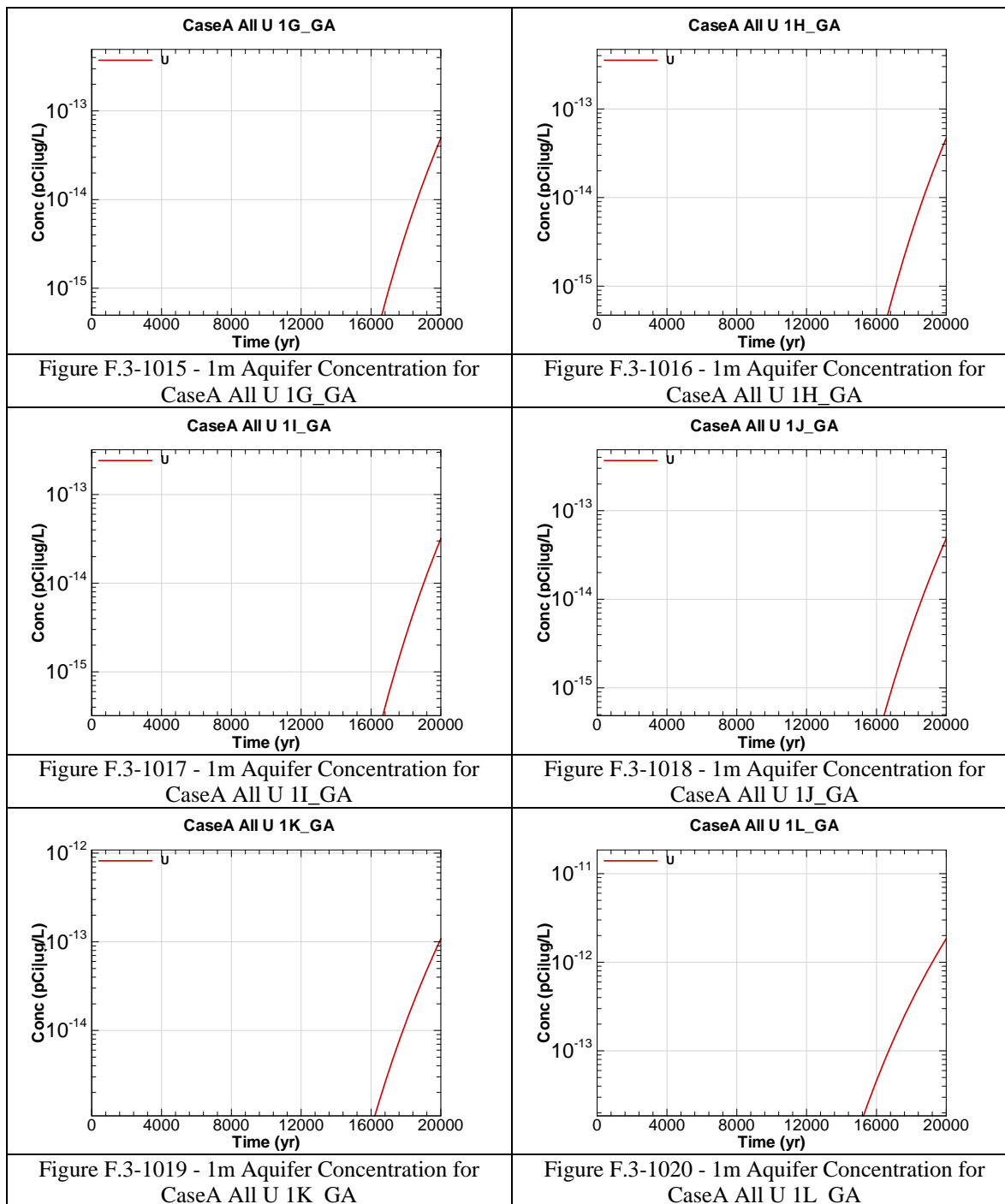


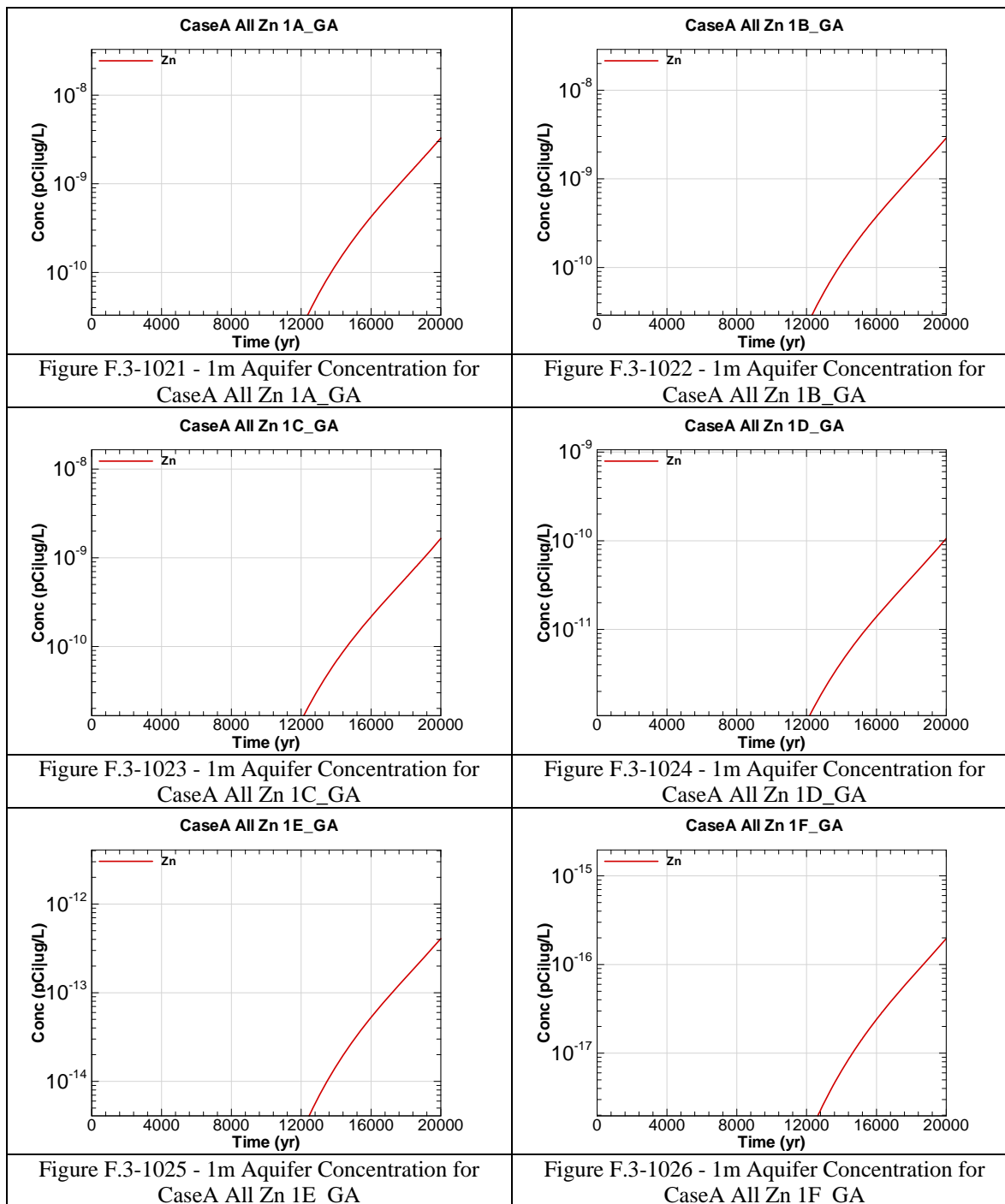


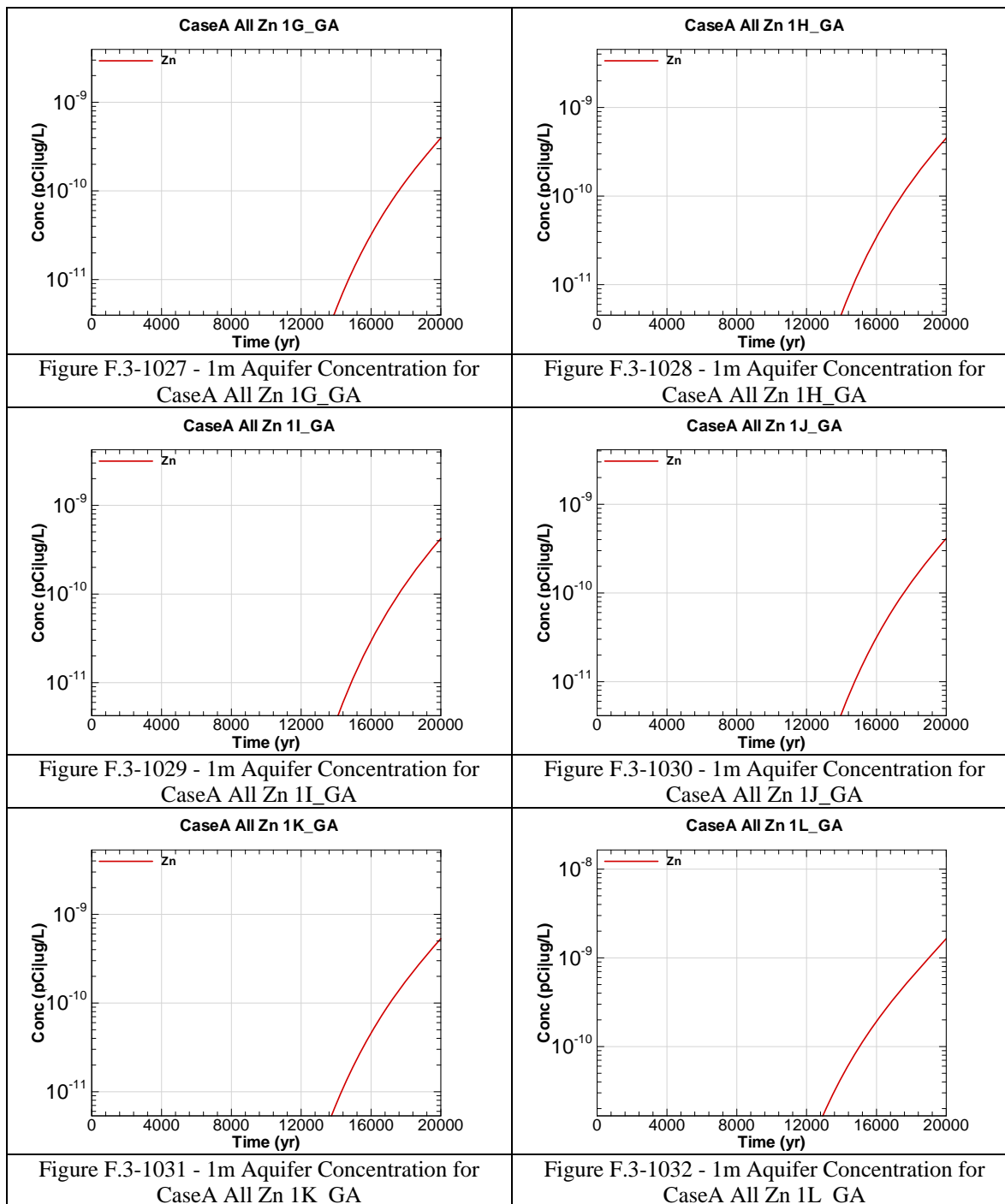












APPENDIX G.1

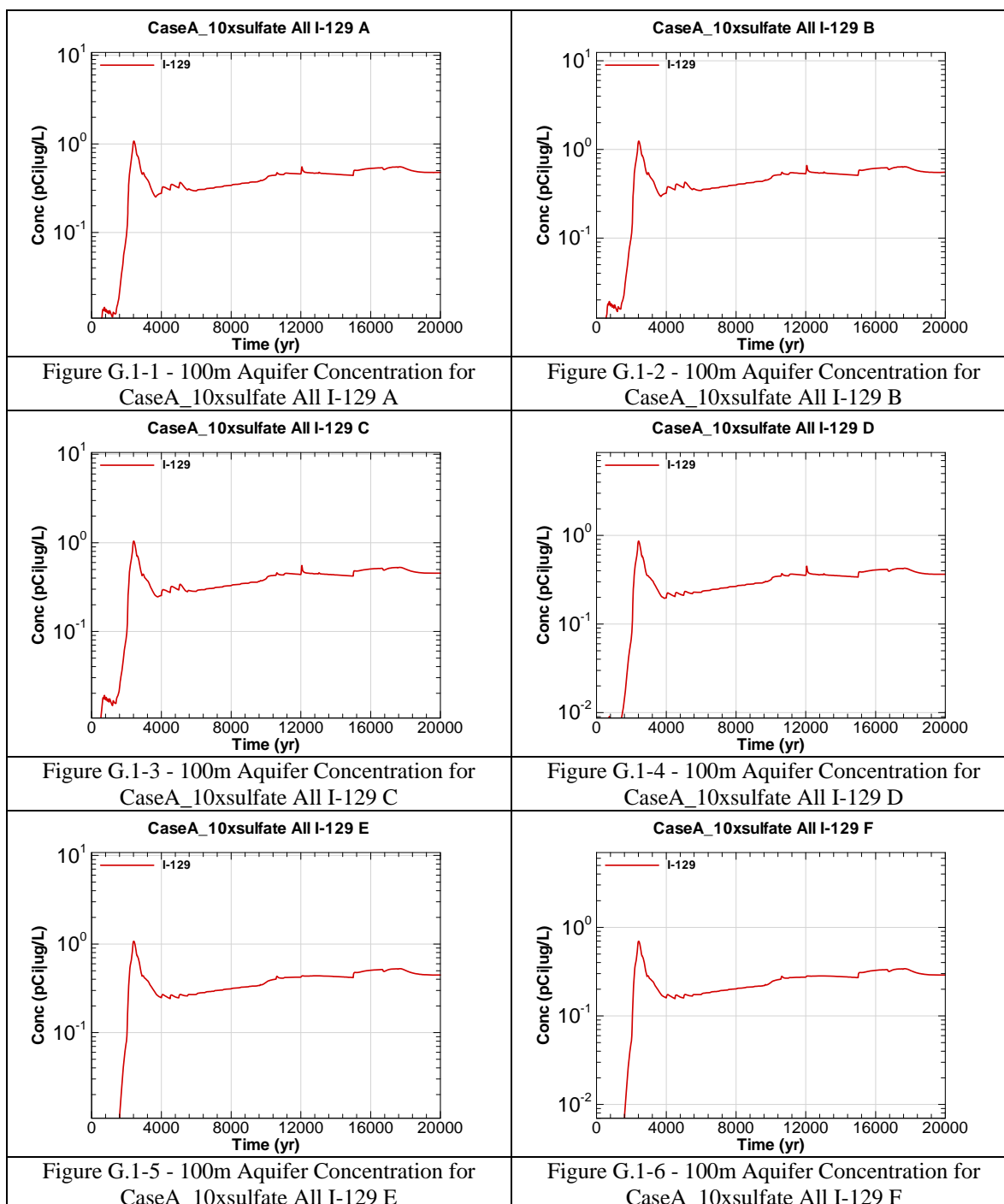
CONCRETE MATERIAL DEGRADATION SENSITIVITY – ACCELERATED DEGRADATION

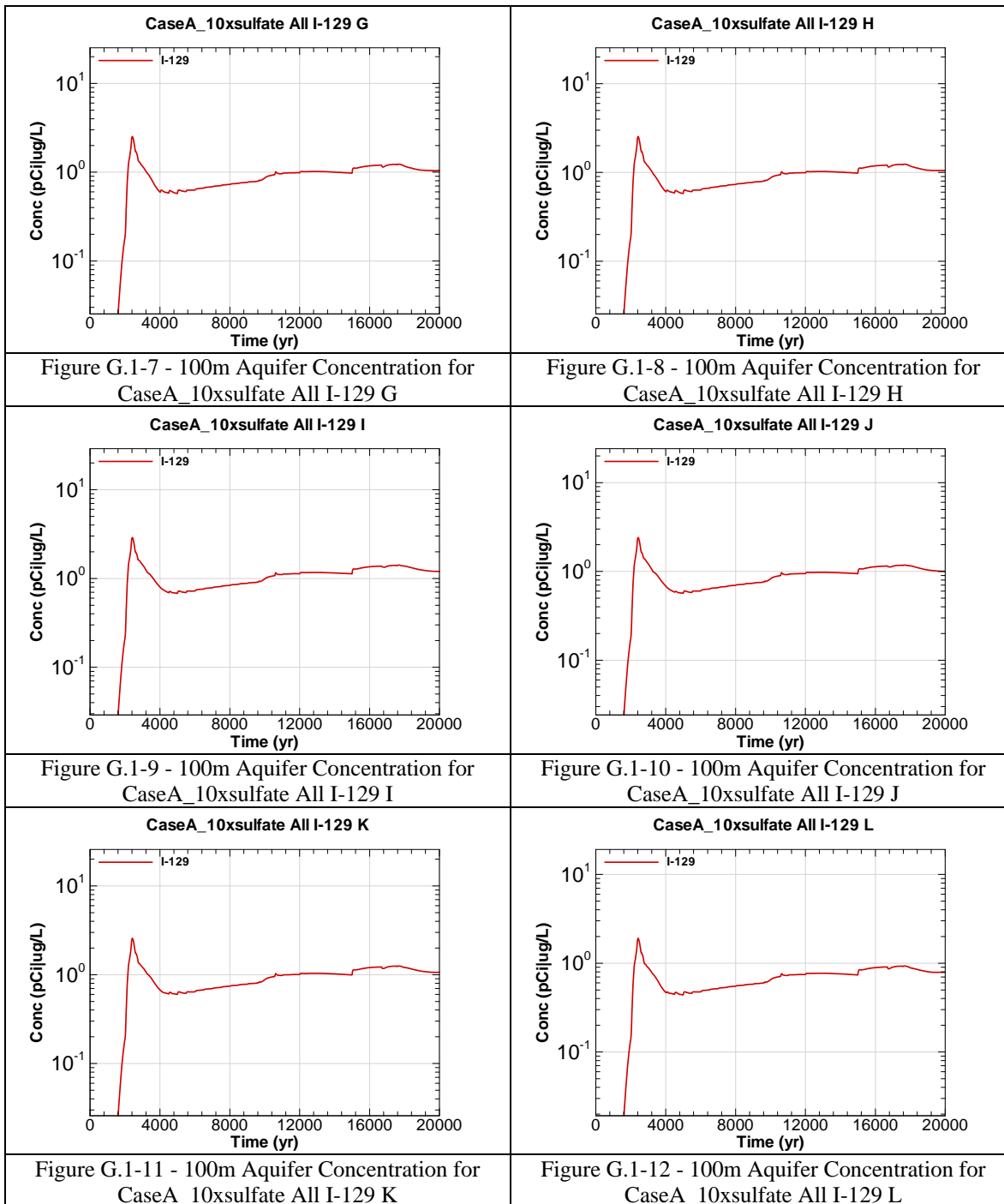
Appendix G.1 contains curves showing the 100 meter concentrations for key radiological and chemical concentrations for all of SDF (vault and FDC inventories) for the Base Case (Case A) for a case of accelerated concrete degradation times (i.e., higher sulfate concentrations in the salt solution than the base case). 20,000 year concentration results are presented for Sectors A through L for the peak concentration per sector regardless of aquifer.

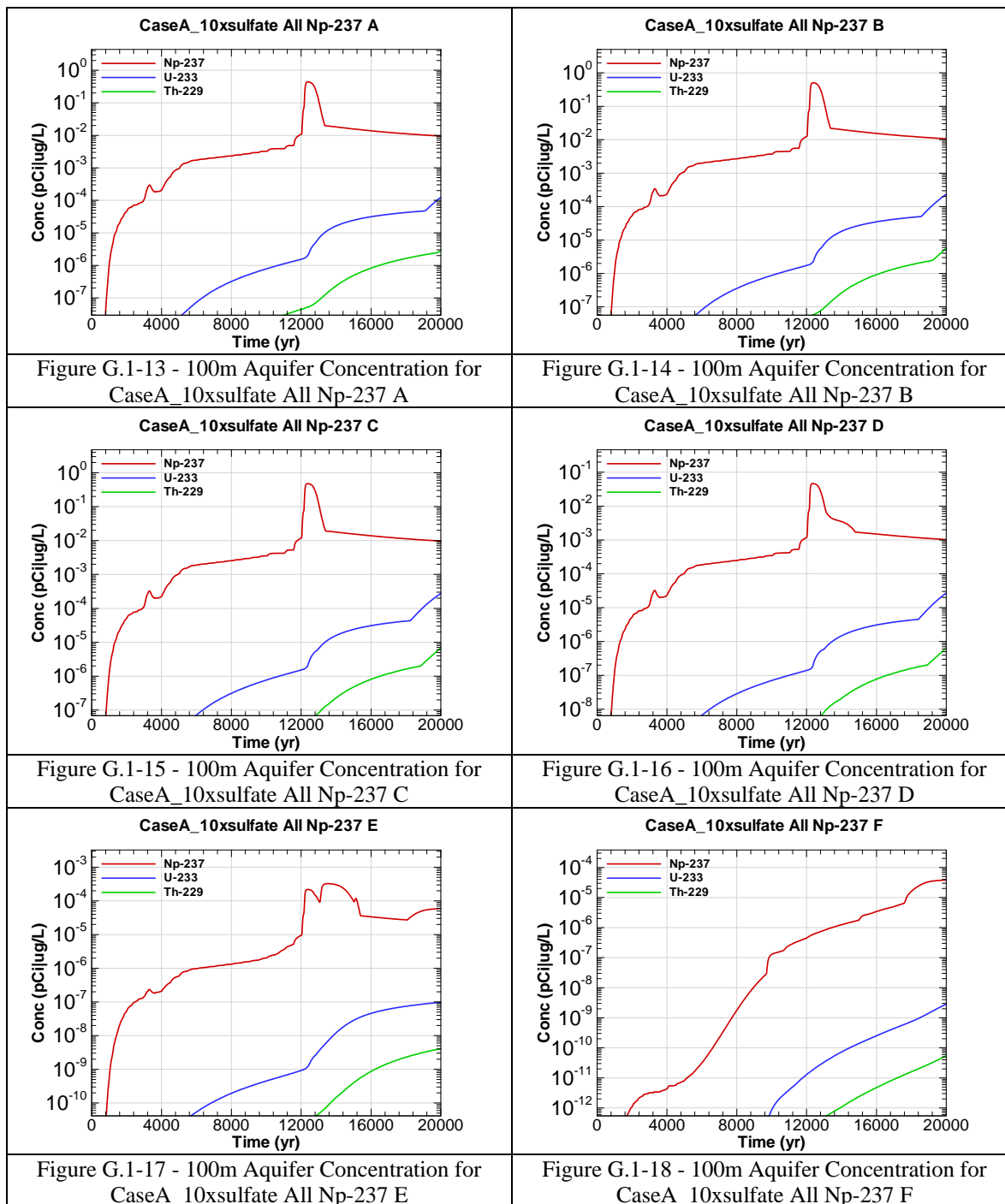
Graph heading example “CaseA_10xsulfate All I-129 A”

Key

CaseA = Scenario case
10xsulfate = Accelerated degradation
All = Inventory source is all disposal units
I-129 = Radionuclide or chemical of concern
A = Evaluation sector of concern







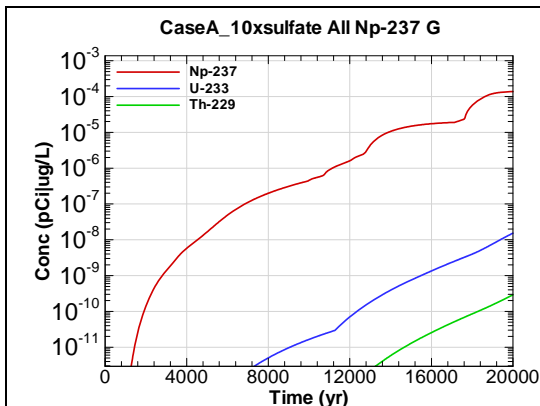


Figure G.1-19 - 100m Aquifer Concentration for
CaseA_10xsulfate All Np-237 G

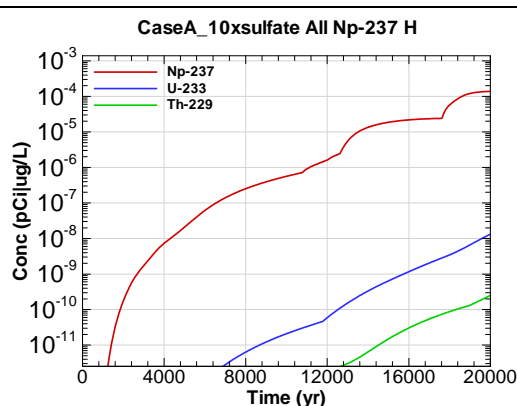


Figure G.1-20 - 100m Aquifer Concentration for
CaseA_10xsulfate All Np-237 H

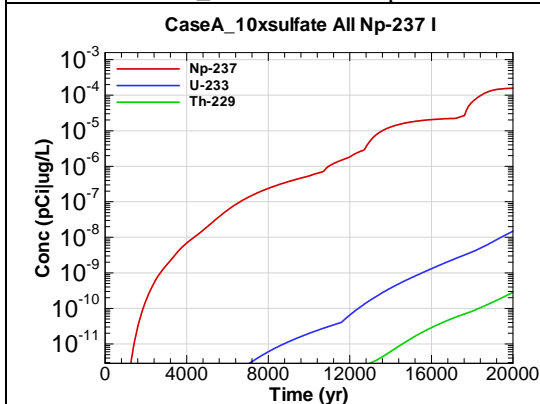


Figure G.1-21 - 100m Aquifer Concentration for
CaseA_10xsulfate All Np-237 I

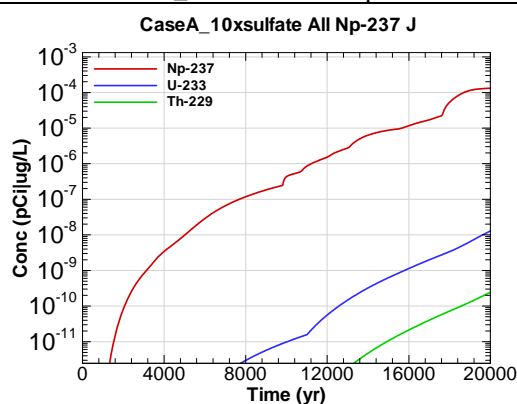


Figure G.1-22 - 100m Aquifer Concentration for
CaseA_10xsulfate All Np-237 J

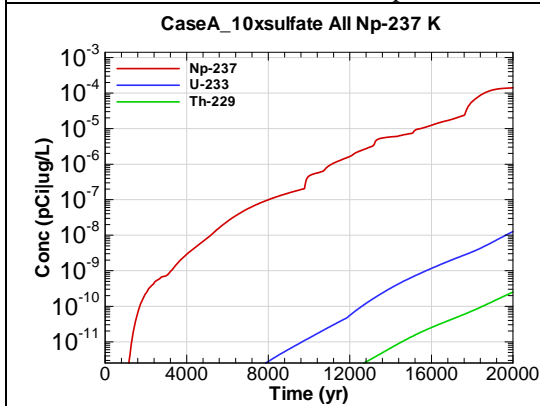


Figure G.1-23 - 100m Aquifer Concentration for
CaseA_10xsulfate All Np-237 K

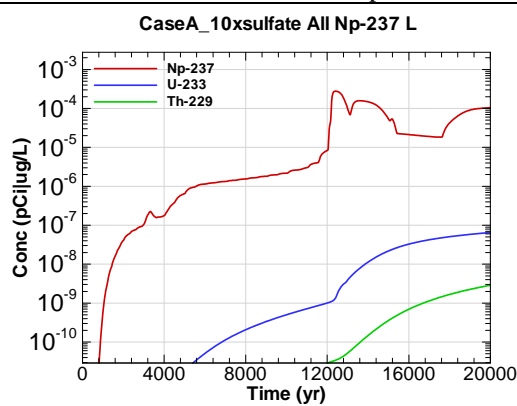


Figure G.1-24 - 100m Aquifer Concentration for
CaseA_10xsulfate All Np-237 L

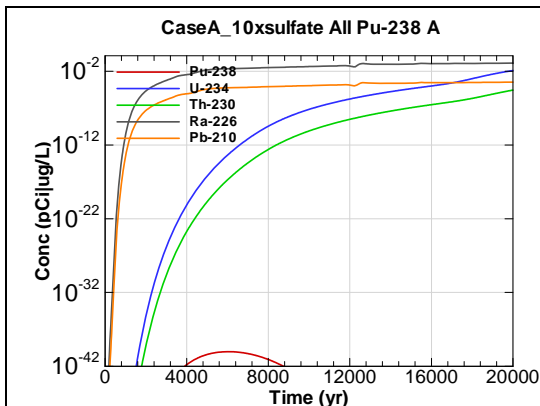


Figure G.1-25 - 100m Aquifer Concentration for CaseA_10xsulfate All Pu-238 A

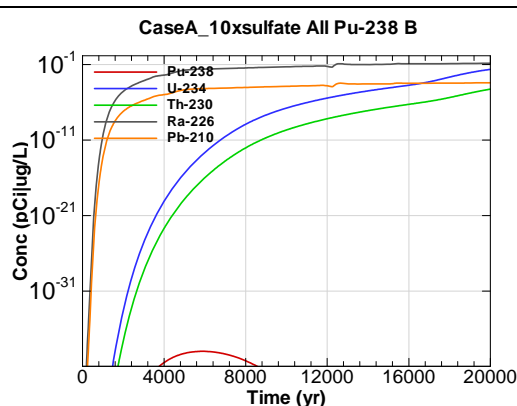


Figure G.1-26 - 100m Aquifer Concentration for CaseA_10xsulfate All Pu-238 B

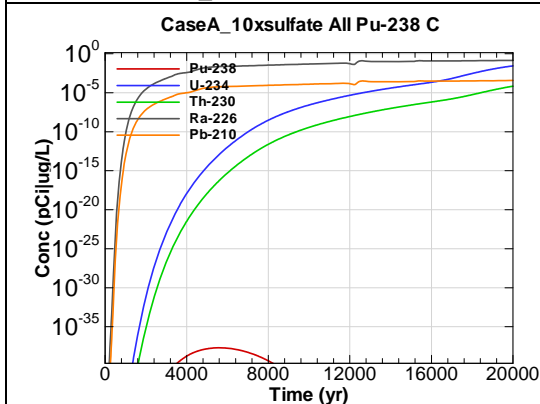


Figure G.1-27 - 100m Aquifer Concentration for CaseA_10xsulfate All Pu-238 C

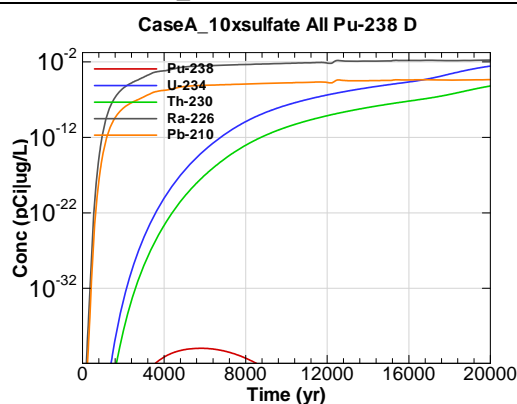


Figure G.1-28 - 100m Aquifer Concentration for CaseA_10xsulfate All Pu-238 D

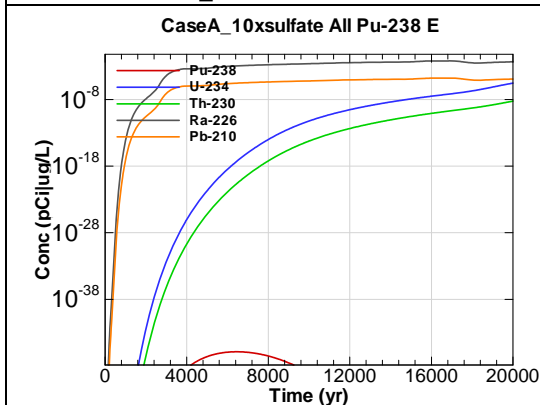


Figure G.1-29 - 100m Aquifer Concentration for CaseA_10xsulfate All Pu-238 E

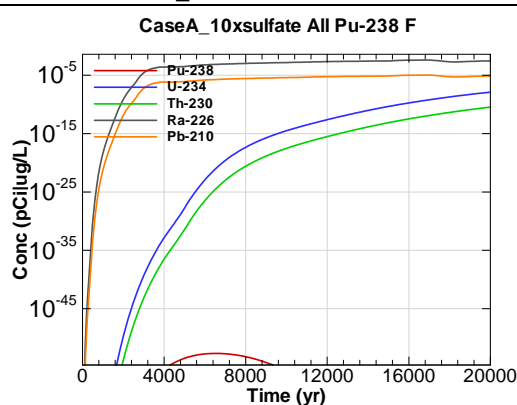


Figure G.1-30 - 100m Aquifer Concentration for CaseA_10xsulfate All Pu-238 F

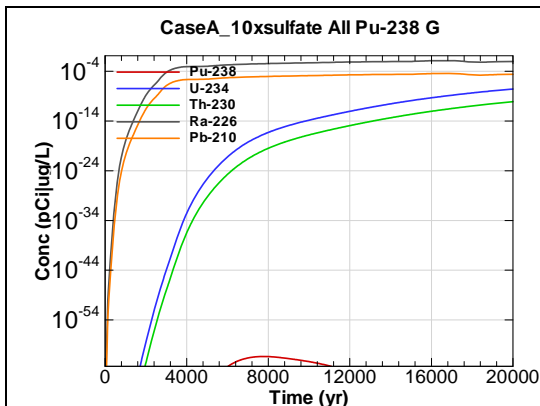


Figure G.1-31 - 100m Aquifer Concentration for CaseA_10xsulfate All Pu-238 G

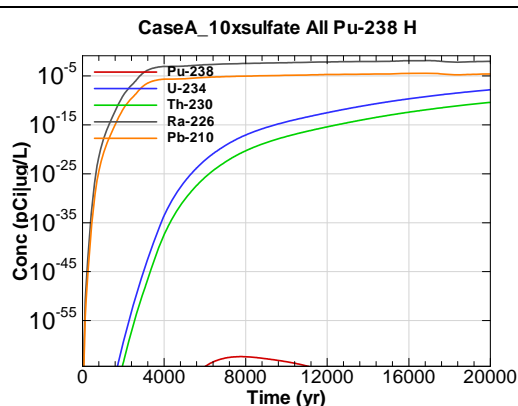


Figure G.1-32 - 100m Aquifer Concentration for CaseA_10xsulfate All Pu-238 H

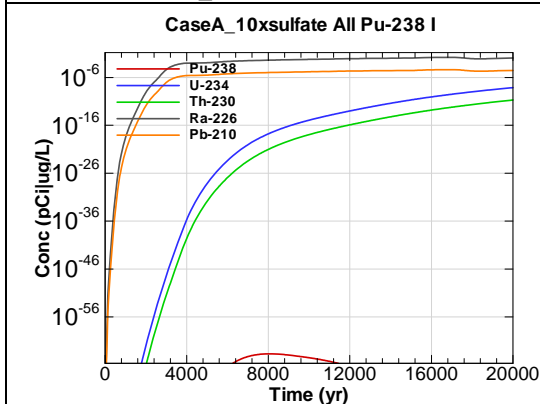


Figure G.1-33 - 100m Aquifer Concentration for CaseA_10xsulfate All Pu-238 I

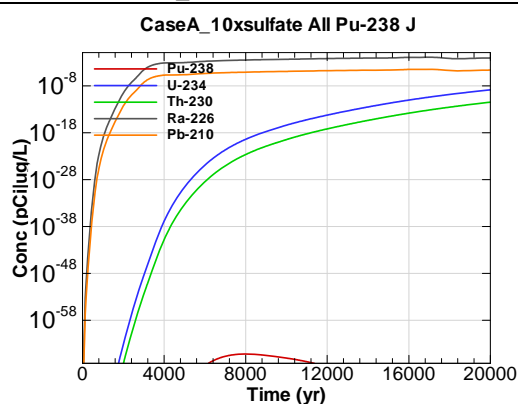


Figure G.1-34 - 100m Aquifer Concentration for CaseA_10xsulfate All Pu-238 J

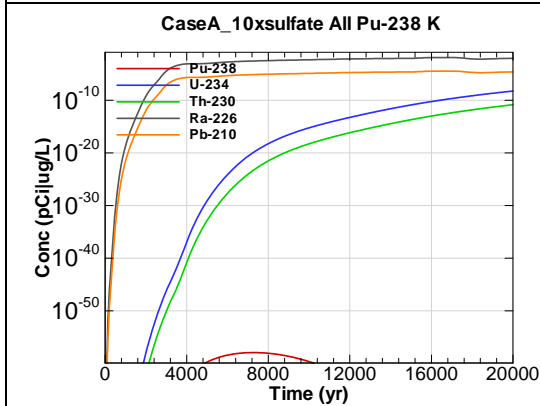


Figure G.1-35 - 100m Aquifer Concentration for CaseA_10xsulfate All Pu-238 K

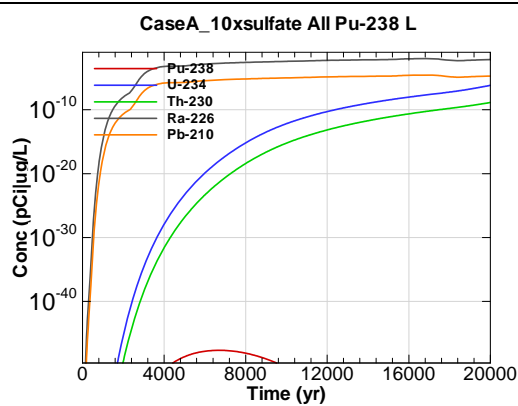
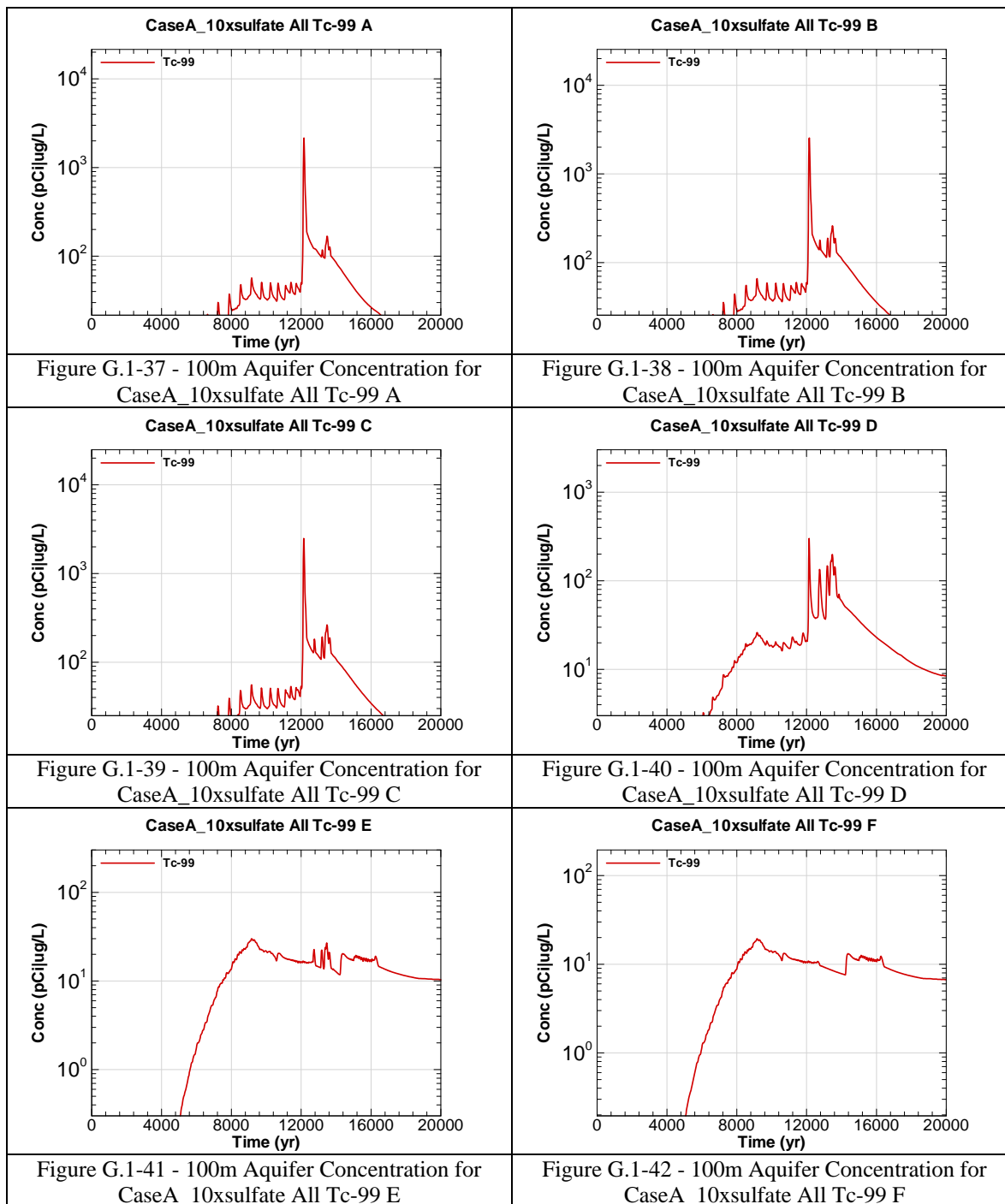
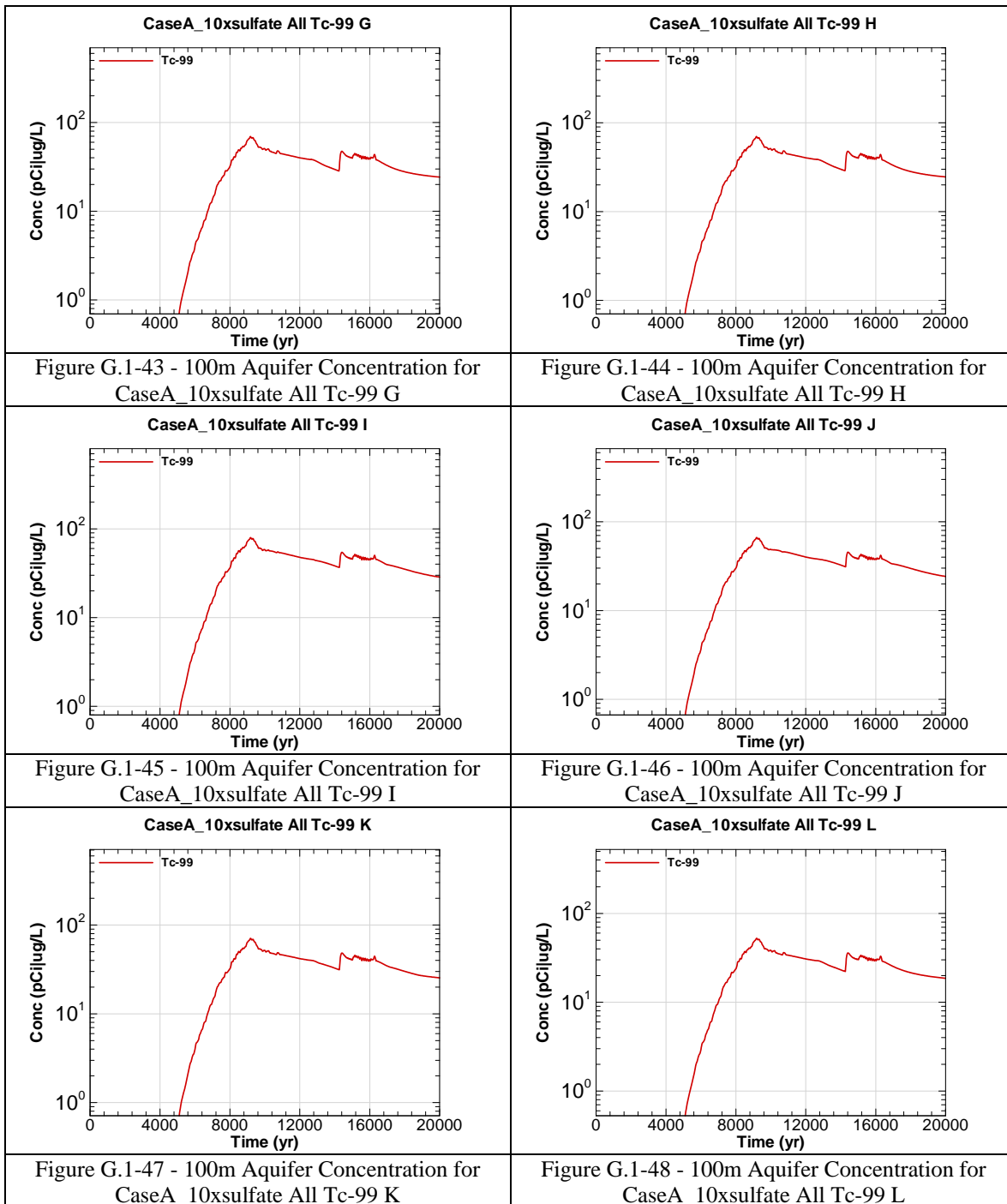
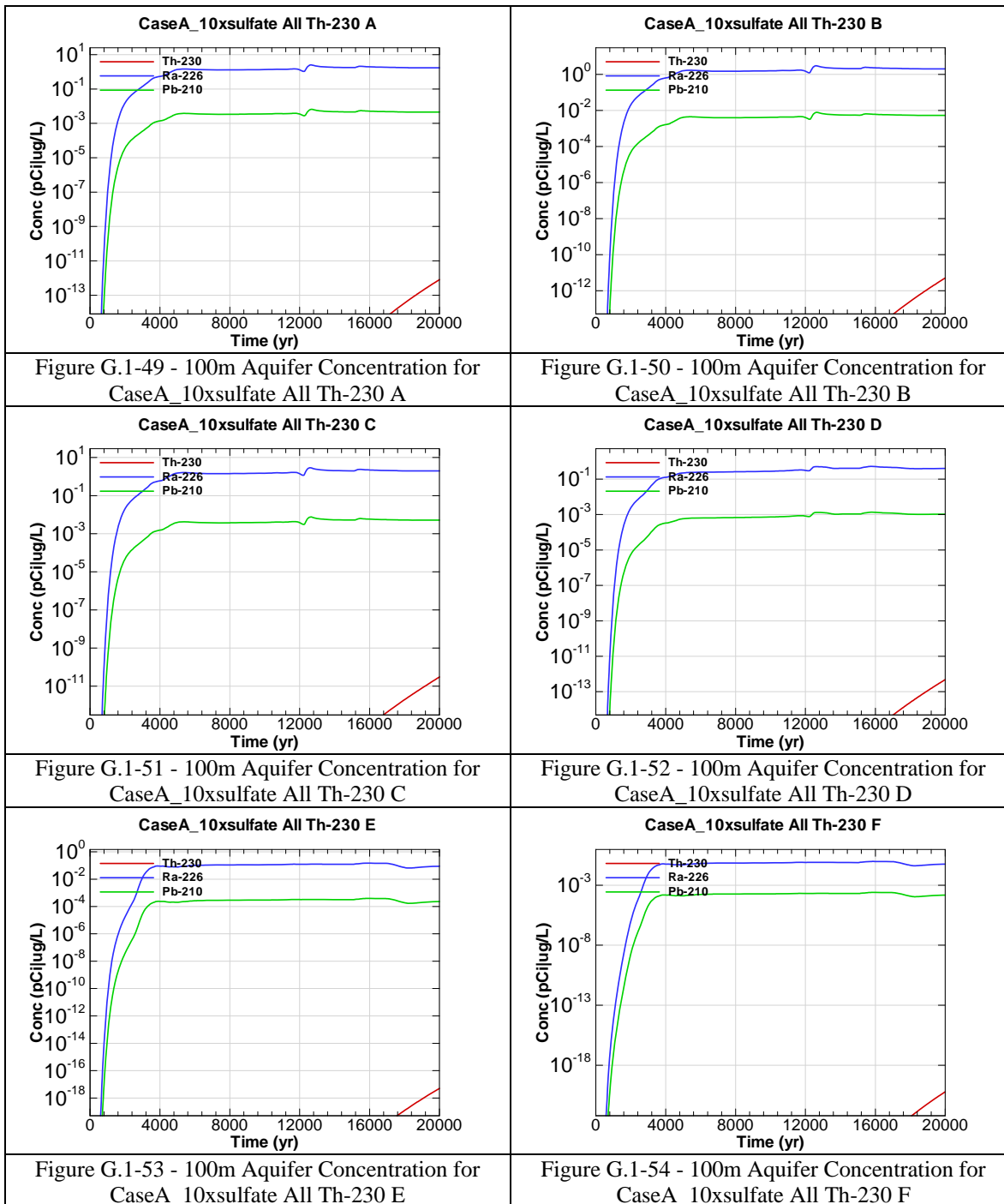


Figure G.1-36 - 100m Aquifer Concentration for CaseA_10xsulfate All Pu-238 L







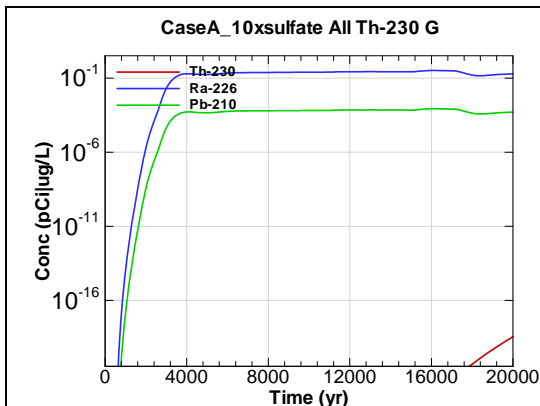


Figure G.1-55 - 100m Aquifer Concentration for CaseA_10xsulfate All Th-230 G

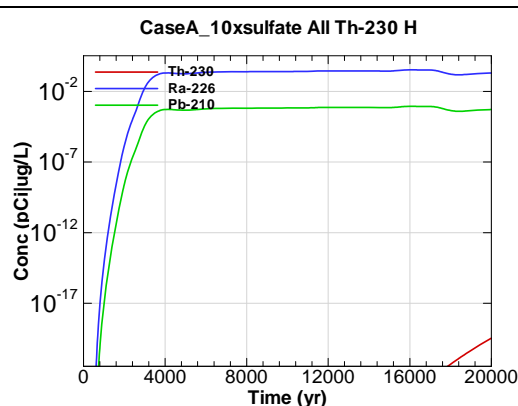


Figure G.1-56 - 100m Aquifer Concentration for CaseA_10xsulfate All Th-230 H

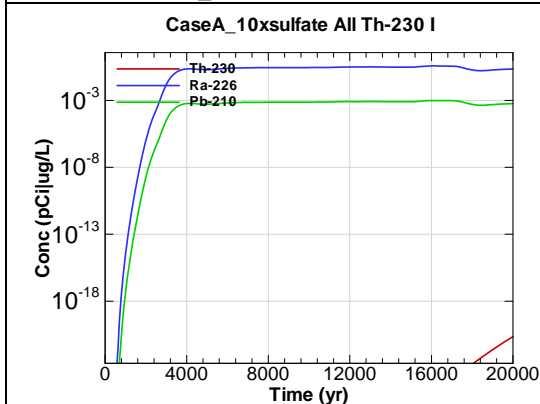


Figure G.1-57 - 100m Aquifer Concentration for CaseA_10xsulfate All Th-230 I

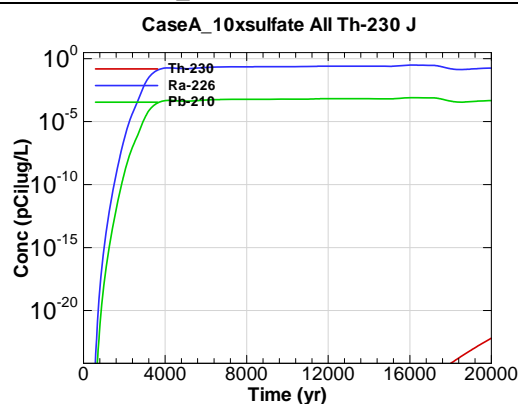


Figure G.1-58 - 100m Aquifer Concentration for CaseA_10xsulfate All Th-230 J

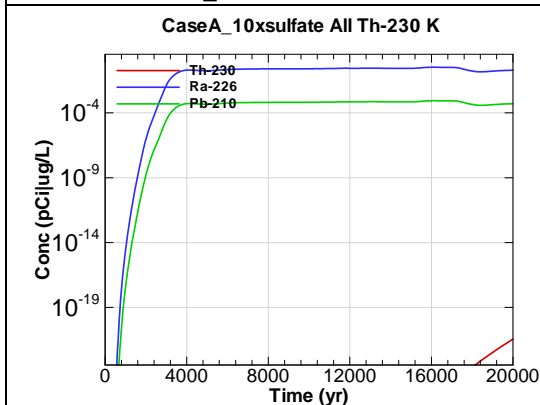


Figure G.1-59 - 100m Aquifer Concentration for CaseA_10xsulfate All Th-230 K

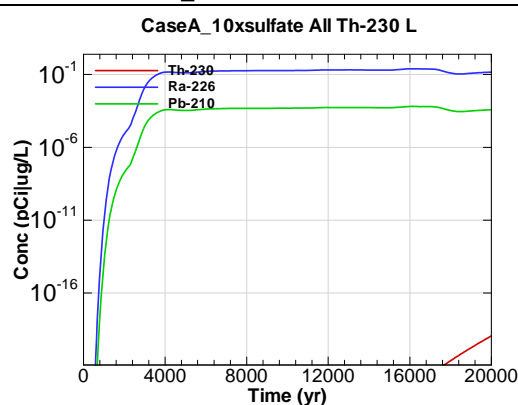
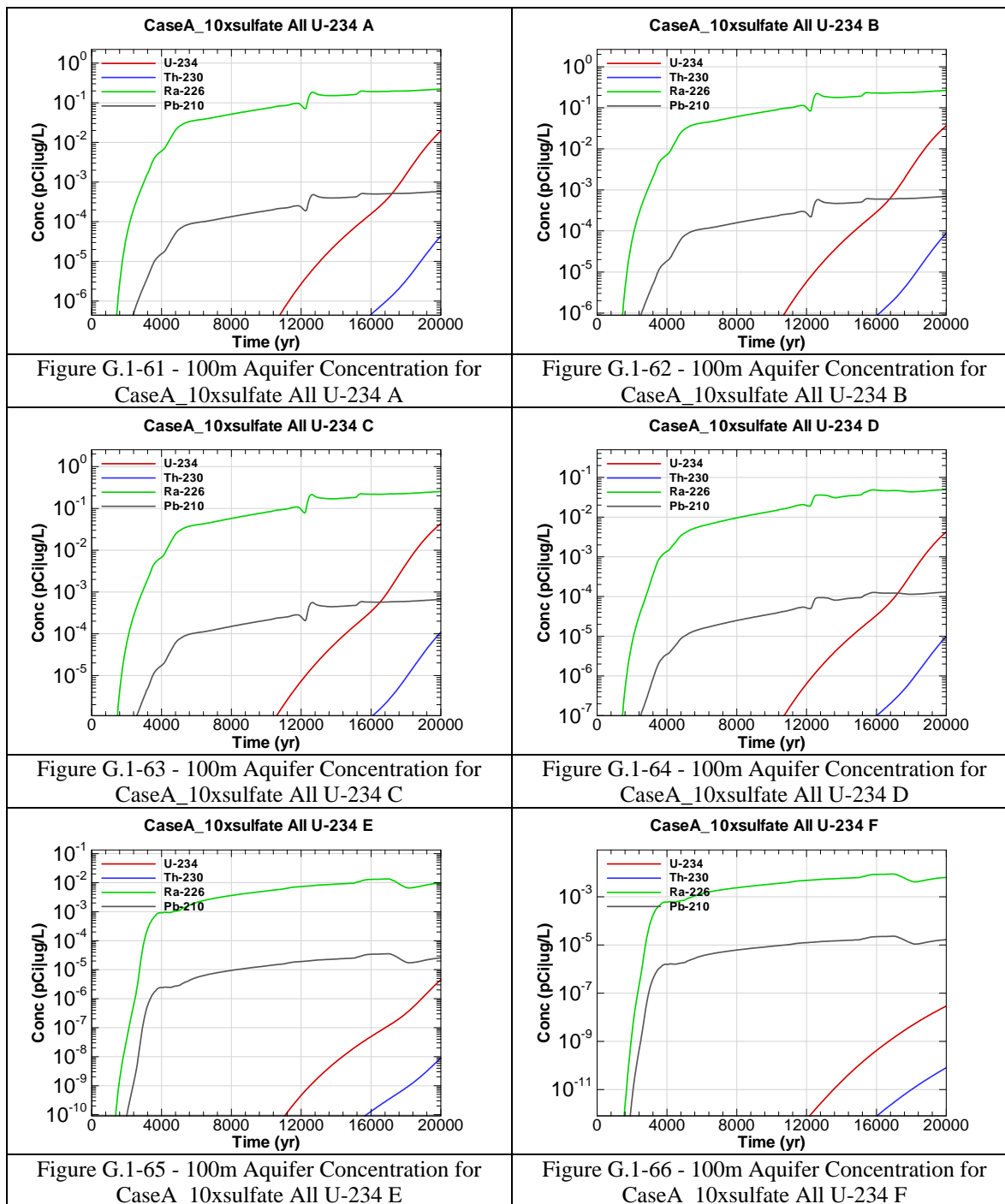
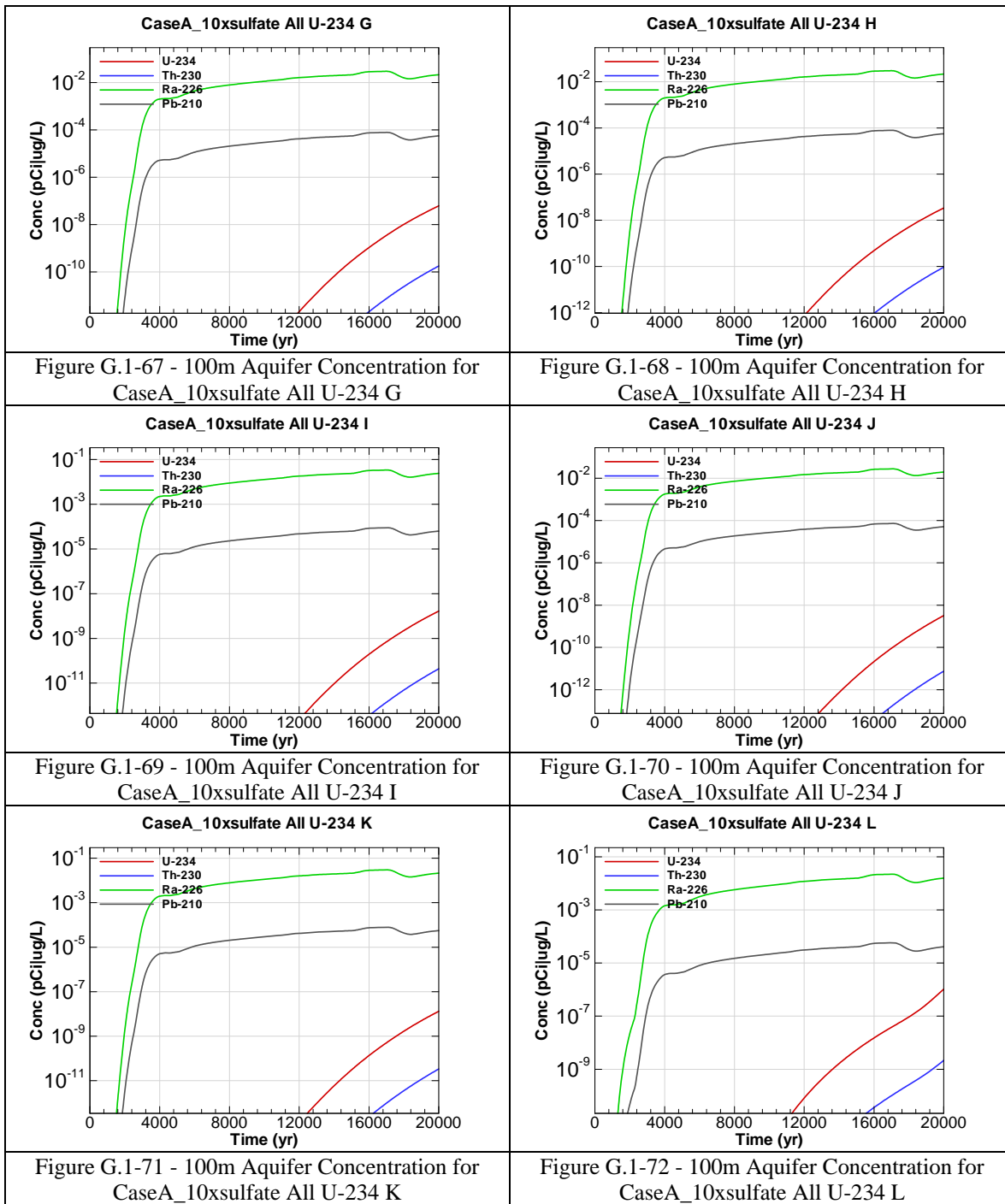
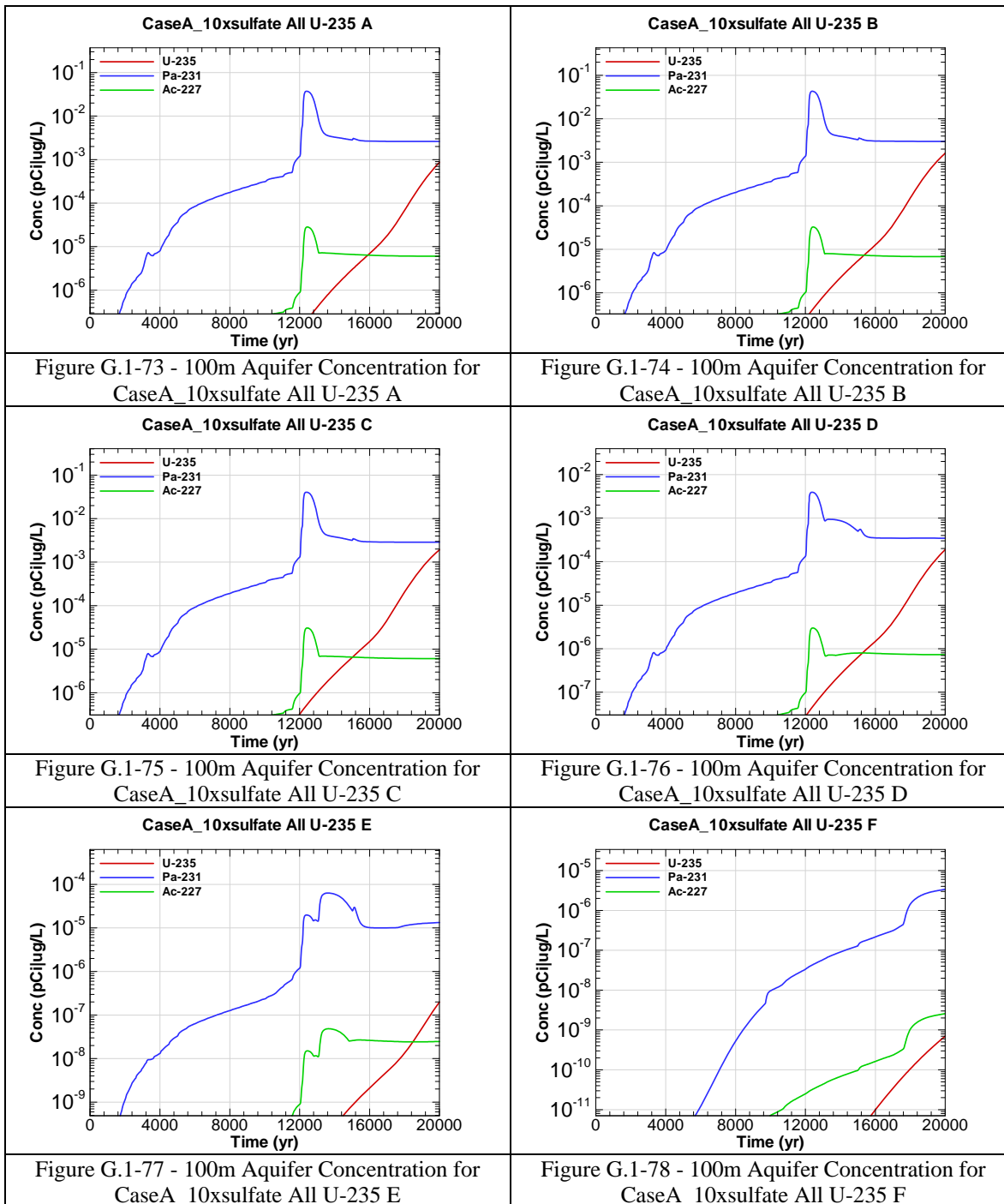
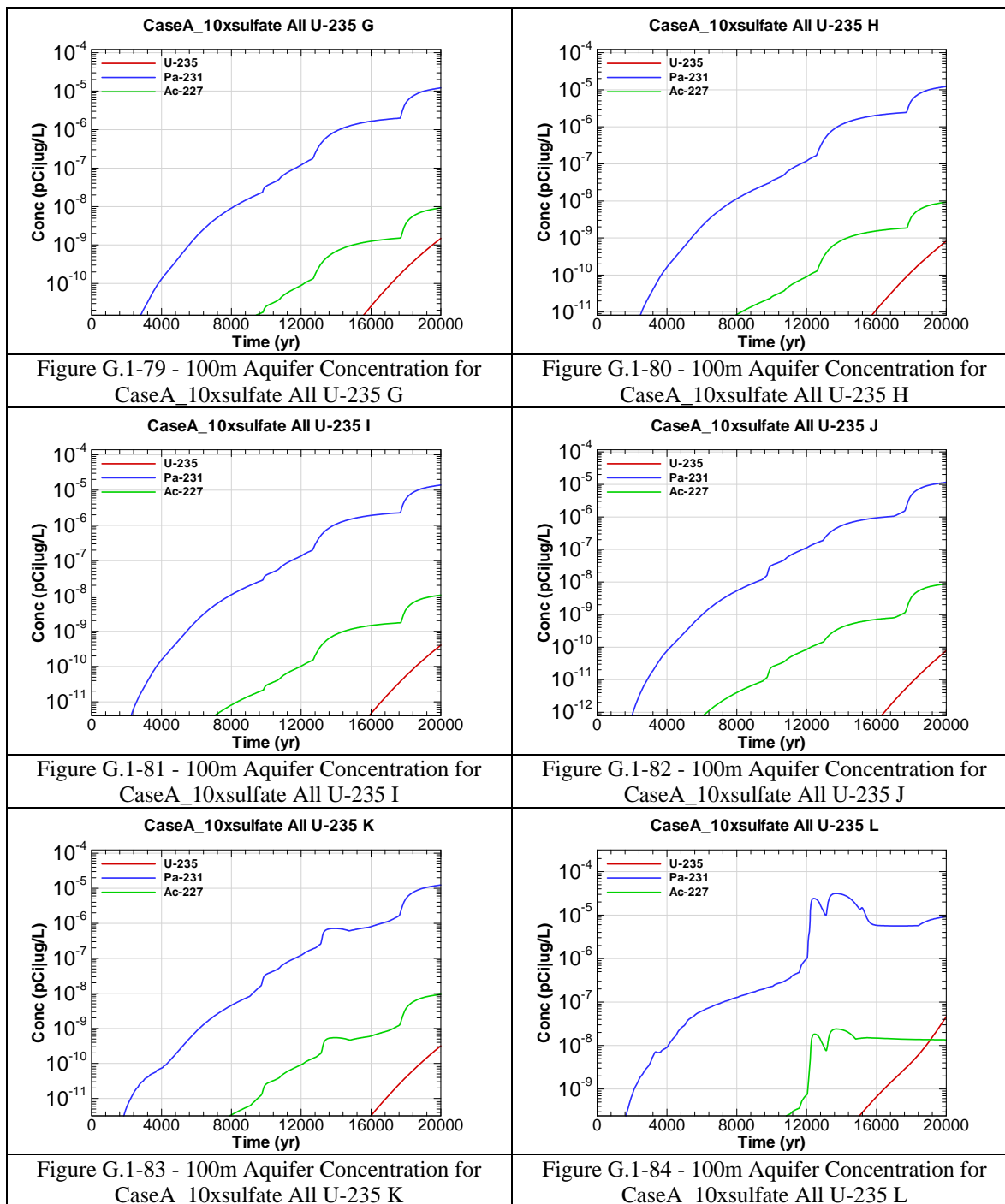


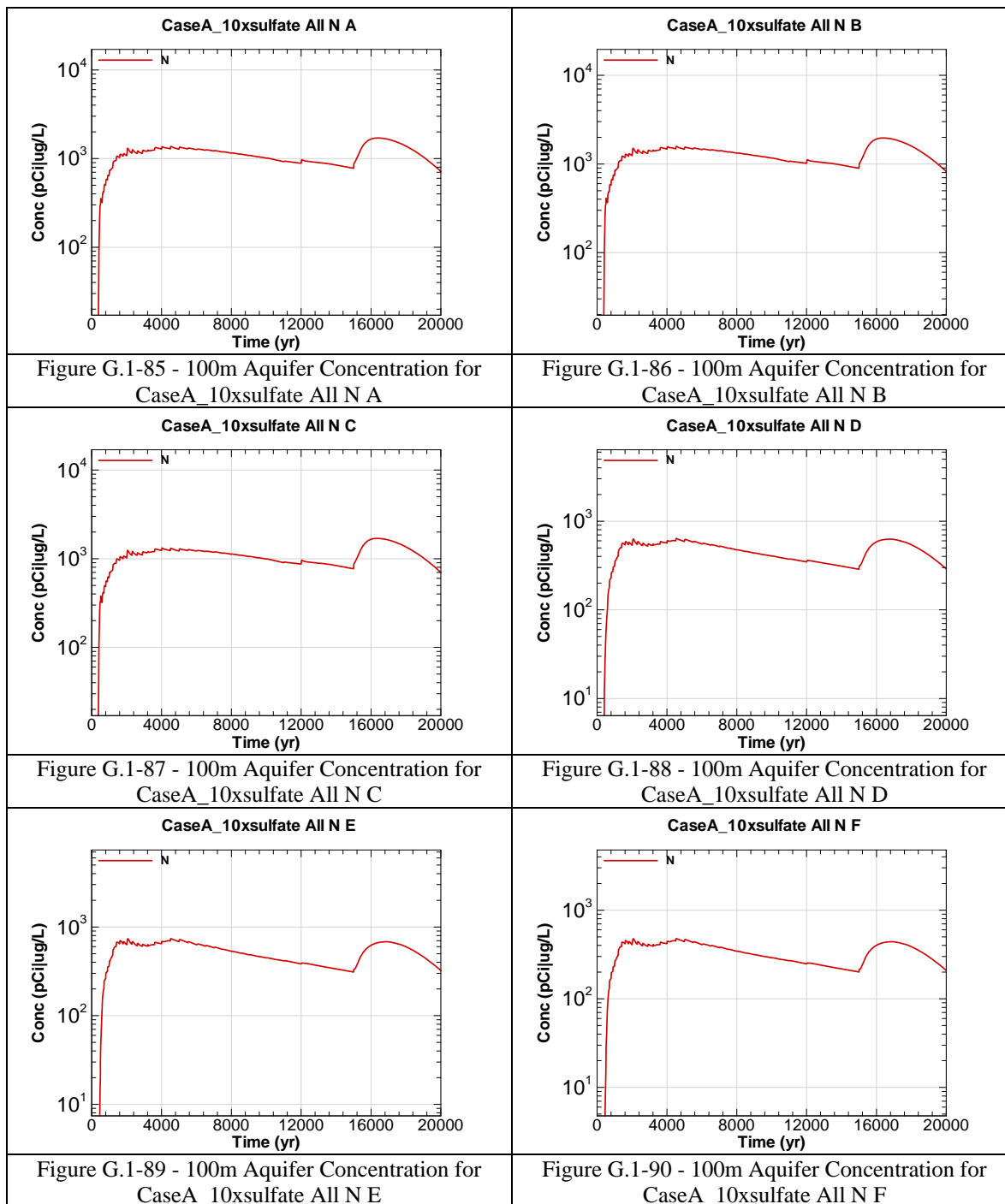
Figure G.1-60 - 100m Aquifer Concentration for CaseA_10xsulfate All Th-230 L

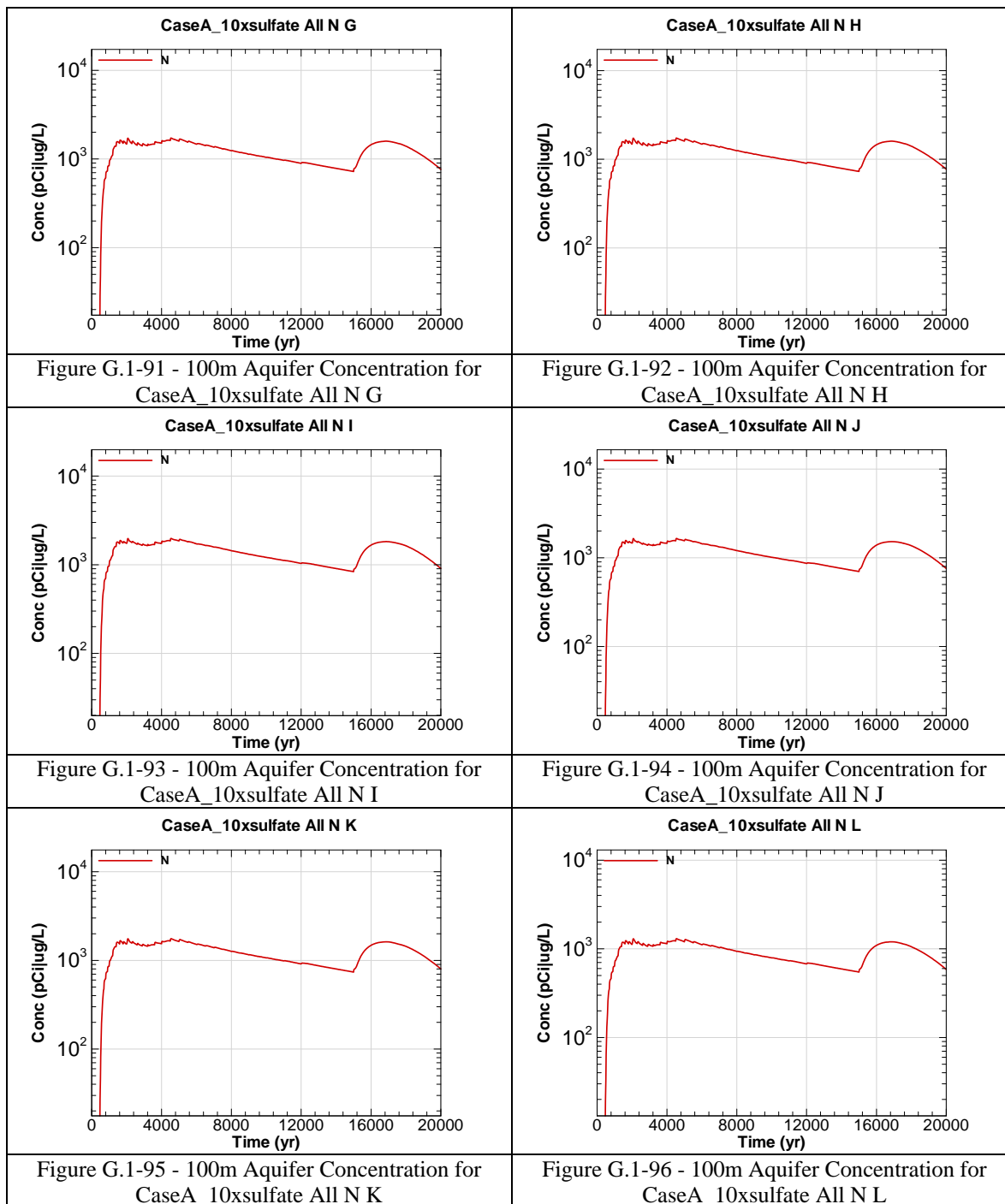












This page intentionally left blank

APPENDIX G.2

CONCRETE MATERIAL DEGRADATION SENSITIVITY – DECREASED DEGRADATION

Appendix G.2 contains curves showing the 100 meter concentrations for key radiological and chemical concentrations for all of SDF (vault and FDC inventories) for the Base Case (Case A) for a case of decreased concrete degradation times (i.e., lower sulfate concentrations in the salt solution than the base case). 20,000 year concentration results are presented for Sectors A through L for the peak concentration per sector regardless of aquifer.

Graph heading example “CaseA_nosulfate All I-129 A”

Key

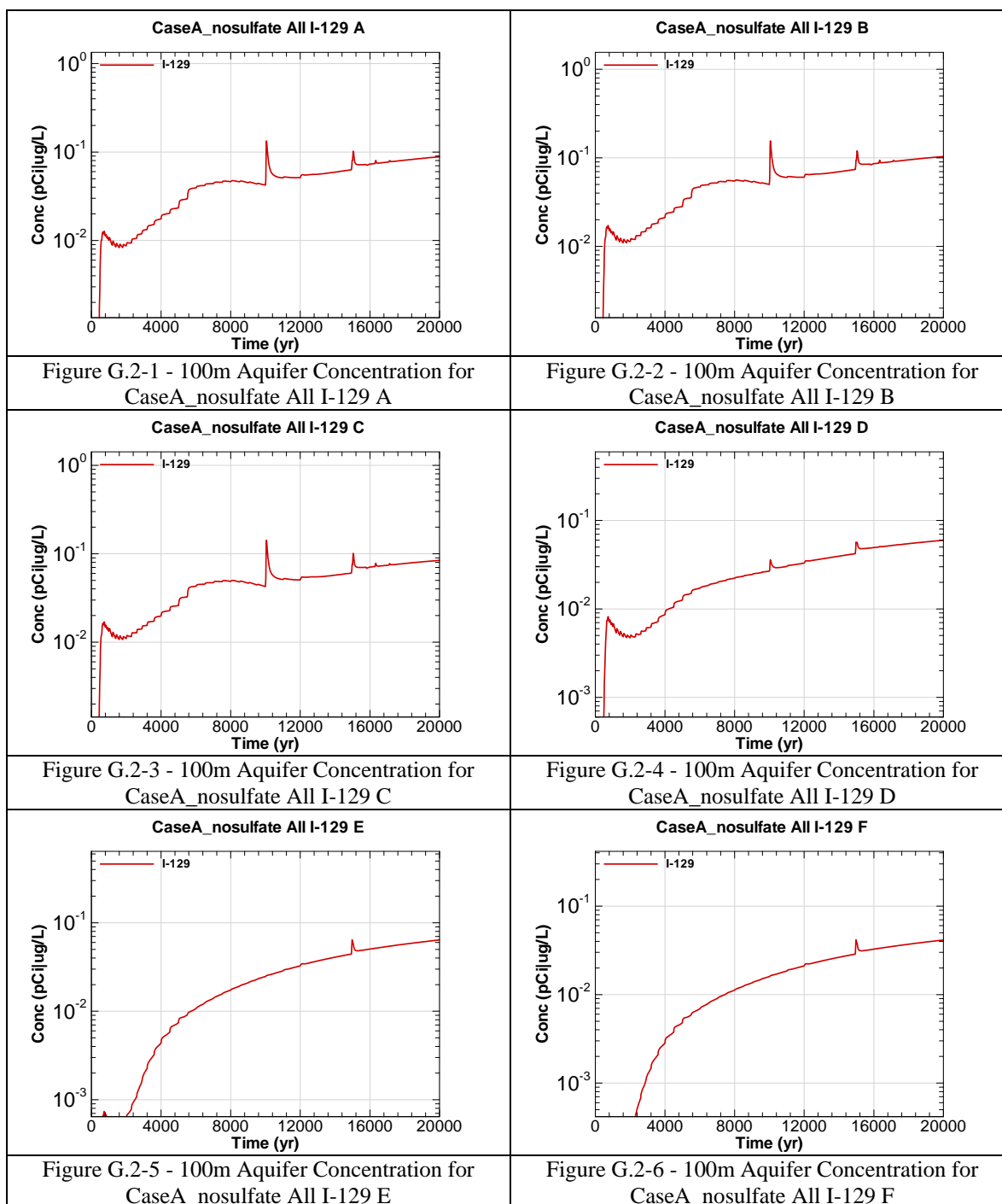
CaseA = Scenario case

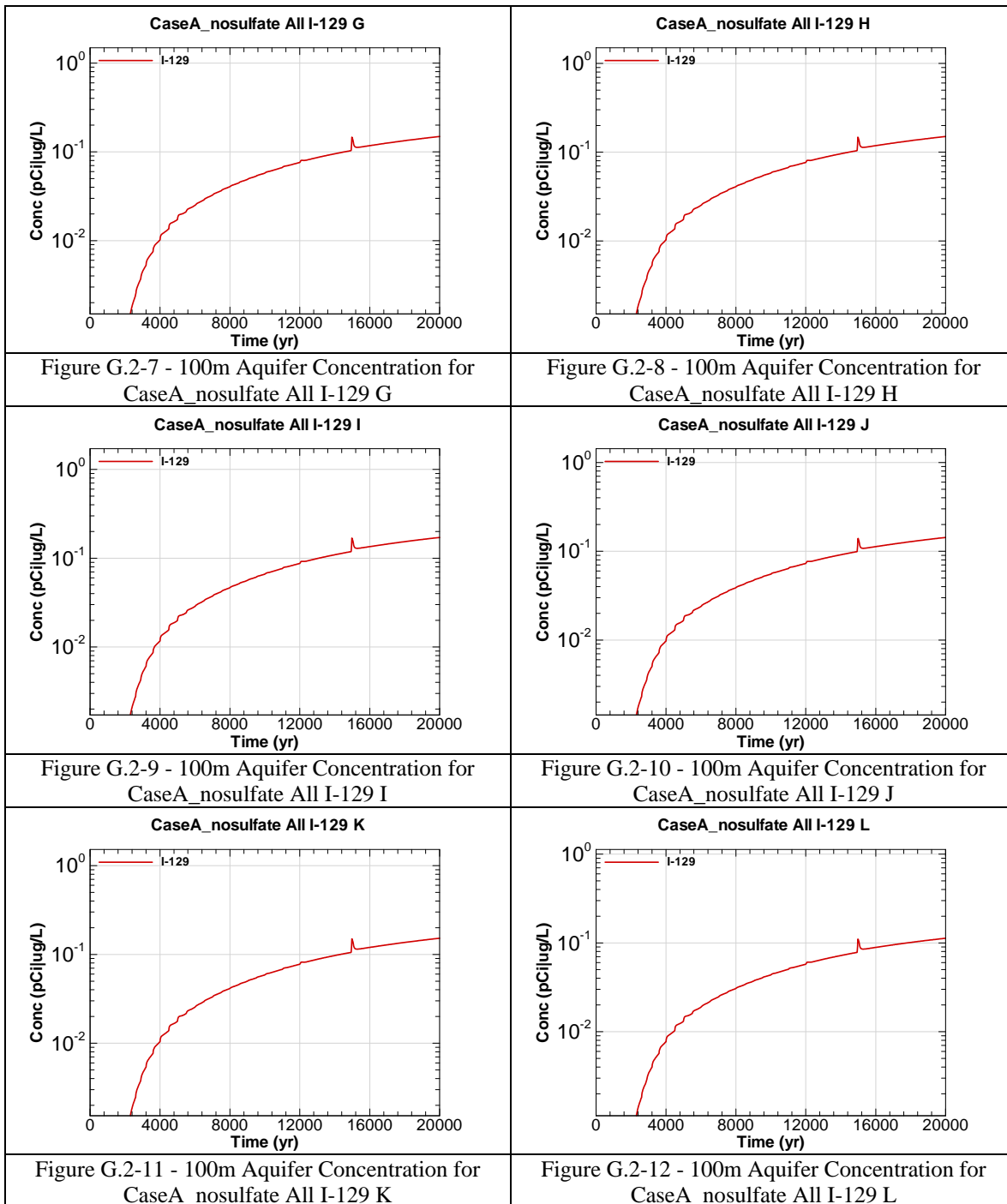
nosulfate = Decreased degradation

All = Inventory source is all disposal units

I-129 = Radionuclide or chemical of concern

A = Evaluation sector of concern





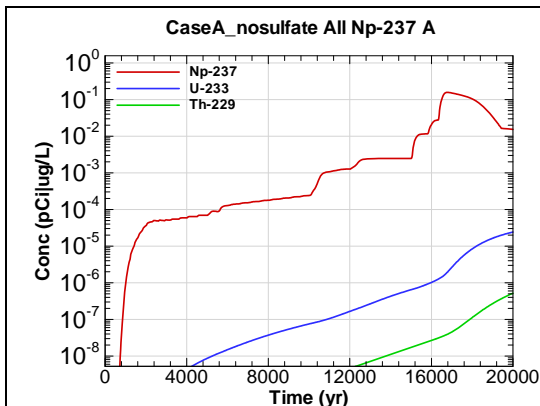


Figure G.2-13 - 100m Aquifer Concentration for CaseA_nosulfate All Np-237 A

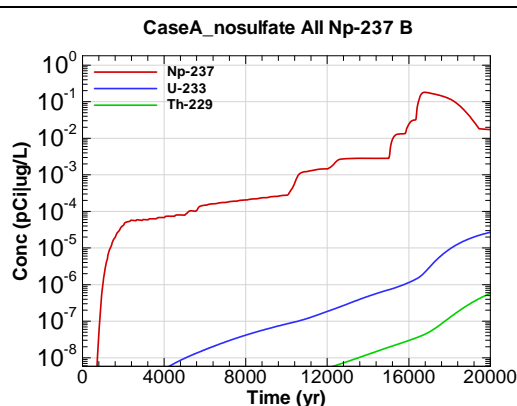


Figure G.2-14 - 100m Aquifer Concentration for CaseA_nosulfate All Np-237 B

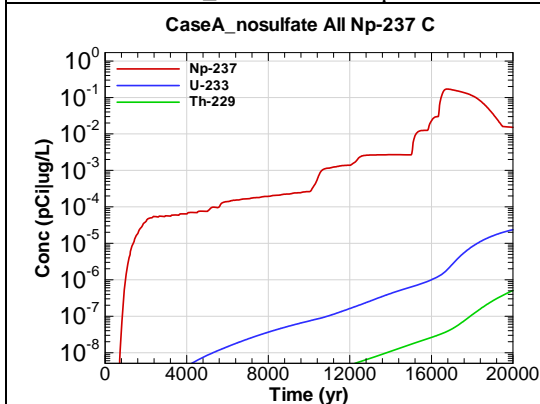


Figure G.2-15 - 100m Aquifer Concentration for CaseA_nosulfate All Np-237 C

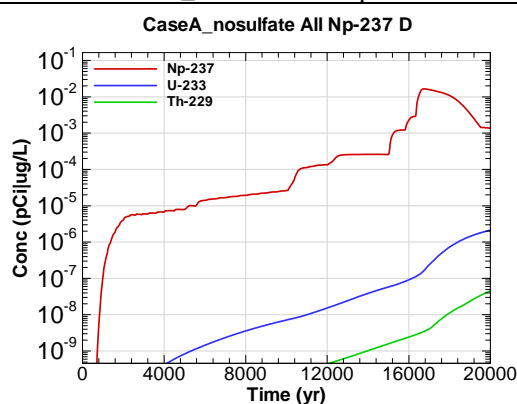


Figure G.2-16 - 100m Aquifer Concentration for CaseA_nosulfate All Np-237 D

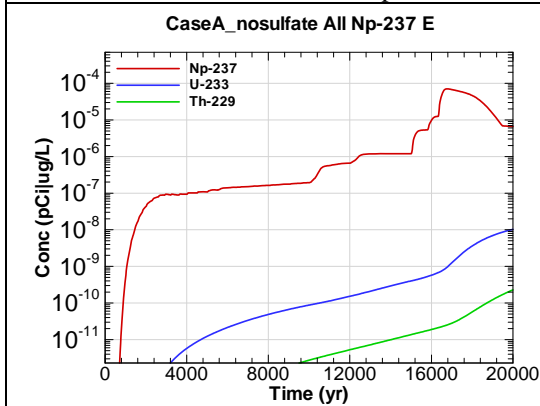


Figure G.2-17 - 100m Aquifer Concentration for CaseA_nosulfate All Np-237 E

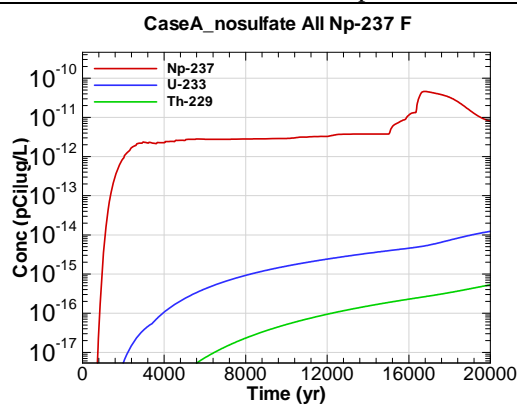


Figure G.2-18 - 100m Aquifer Concentration for CaseA_nosulfate All Np-237 F

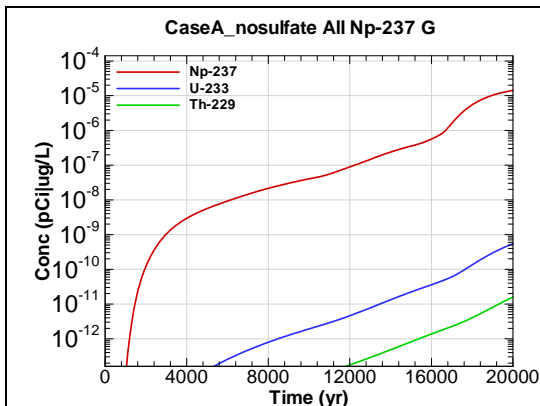


Figure G.2-19 - 100m Aquifer Concentration for
CaseA_nosulfate All Np-237 G

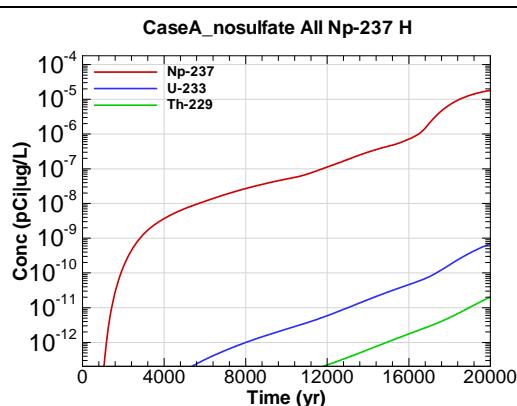


Figure G.2-20 - 100m Aquifer Concentration for
CaseA_nosulfate All Np-237 H

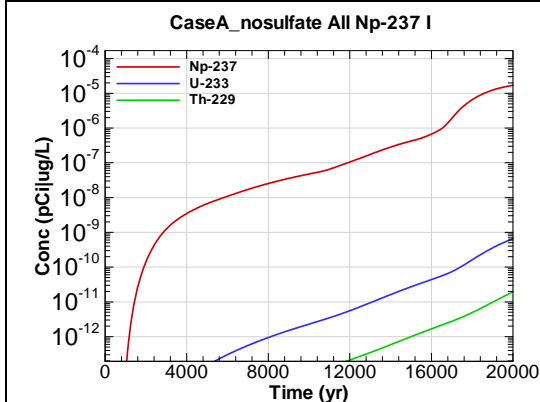


Figure G.2-21 - 100m Aquifer Concentration for
CaseA_nosulfate All Np-237 I

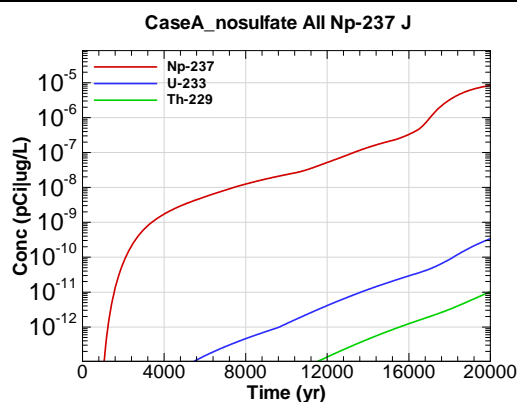


Figure G.2-22 - 100m Aquifer Concentration for
CaseA_nosulfate All Np-237 J

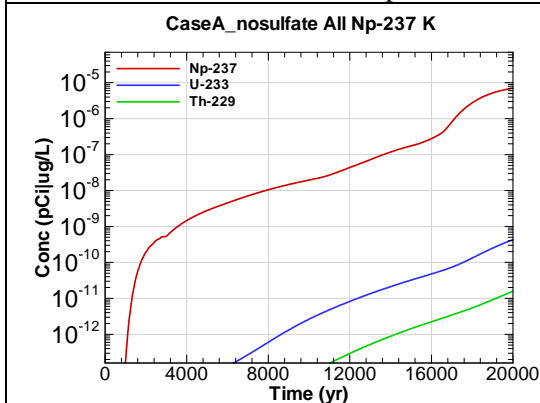


Figure G.2-23 - 100m Aquifer Concentration for
CaseA_nosulfate All Np-237 K

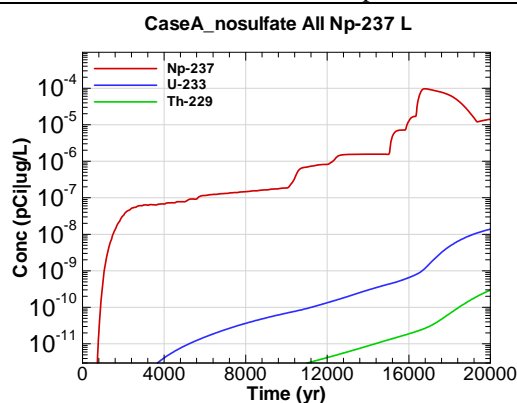


Figure G.2-24 - 100m Aquifer Concentration for
CaseA_nosulfate All Np-237 L

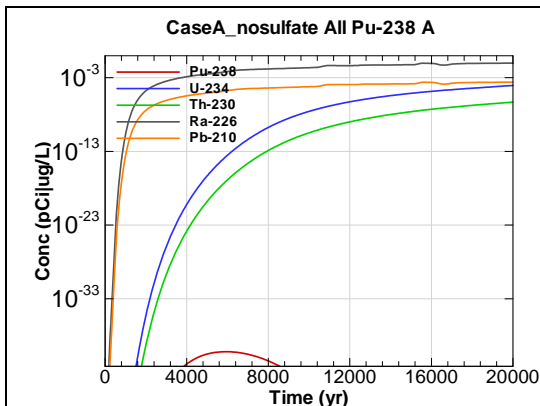


Figure G.2-25 - 100m Aquifer Concentration for CaseA_nosulfate All Pu-238 A

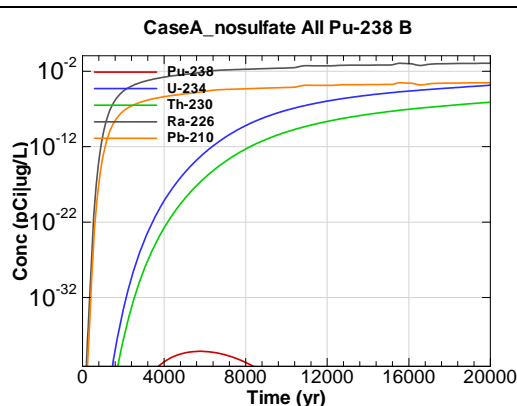


Figure G.2-26 - 100m Aquifer Concentration for CaseA_nosulfate All Pu-238 B

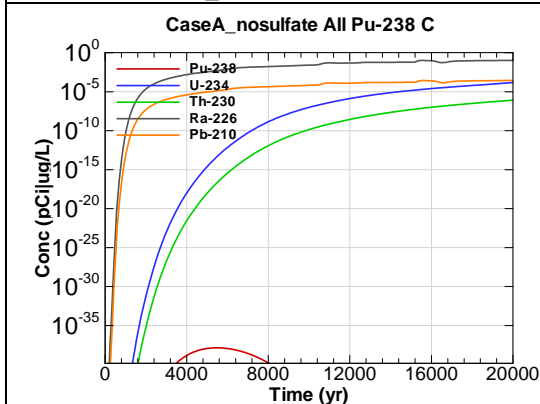


Figure G.2-27 - 100m Aquifer Concentration for CaseA_nosulfate All Pu-238 C

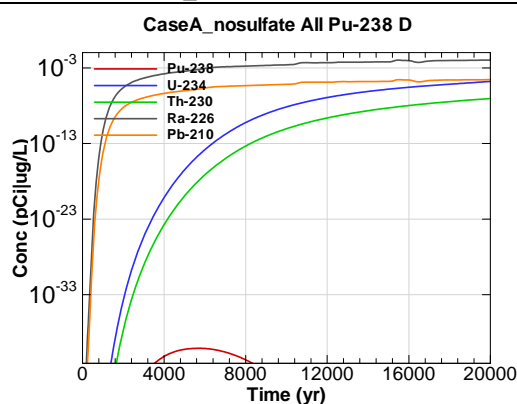


Figure G.2-28 - 100m Aquifer Concentration for CaseA_nosulfate All Pu-238 D

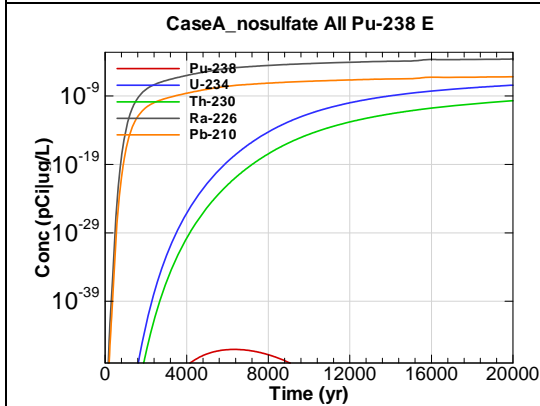


Figure G.2-29 - 100m Aquifer Concentration for CaseA_nosulfate All Pu-238 E

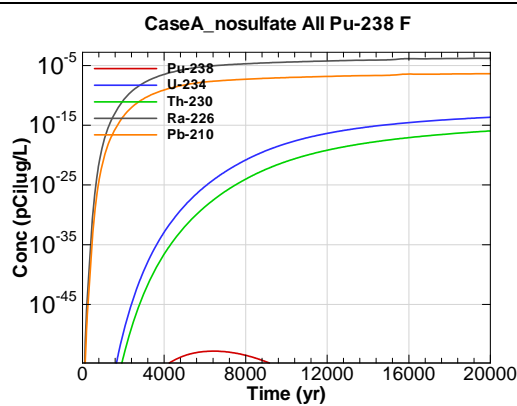
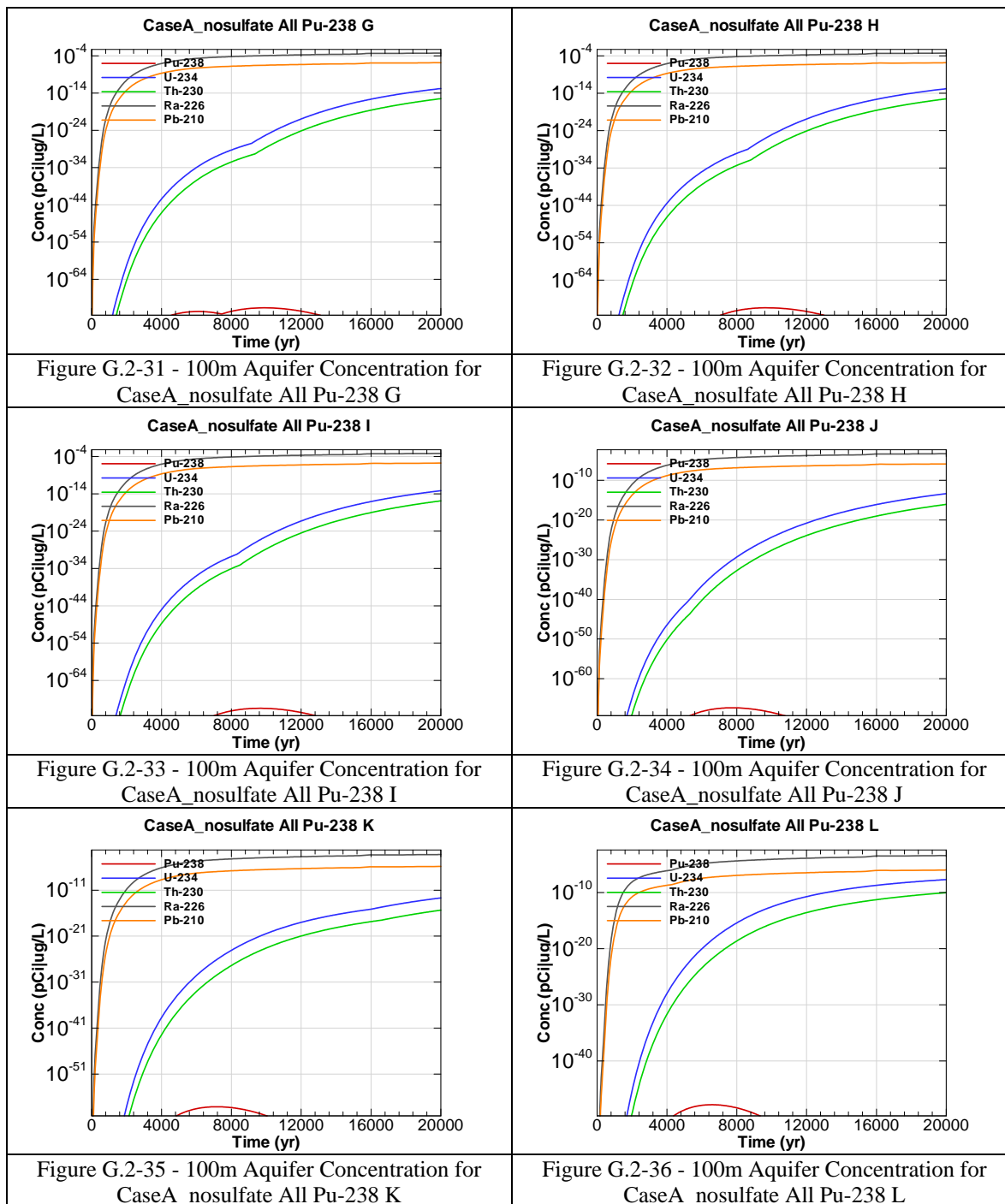
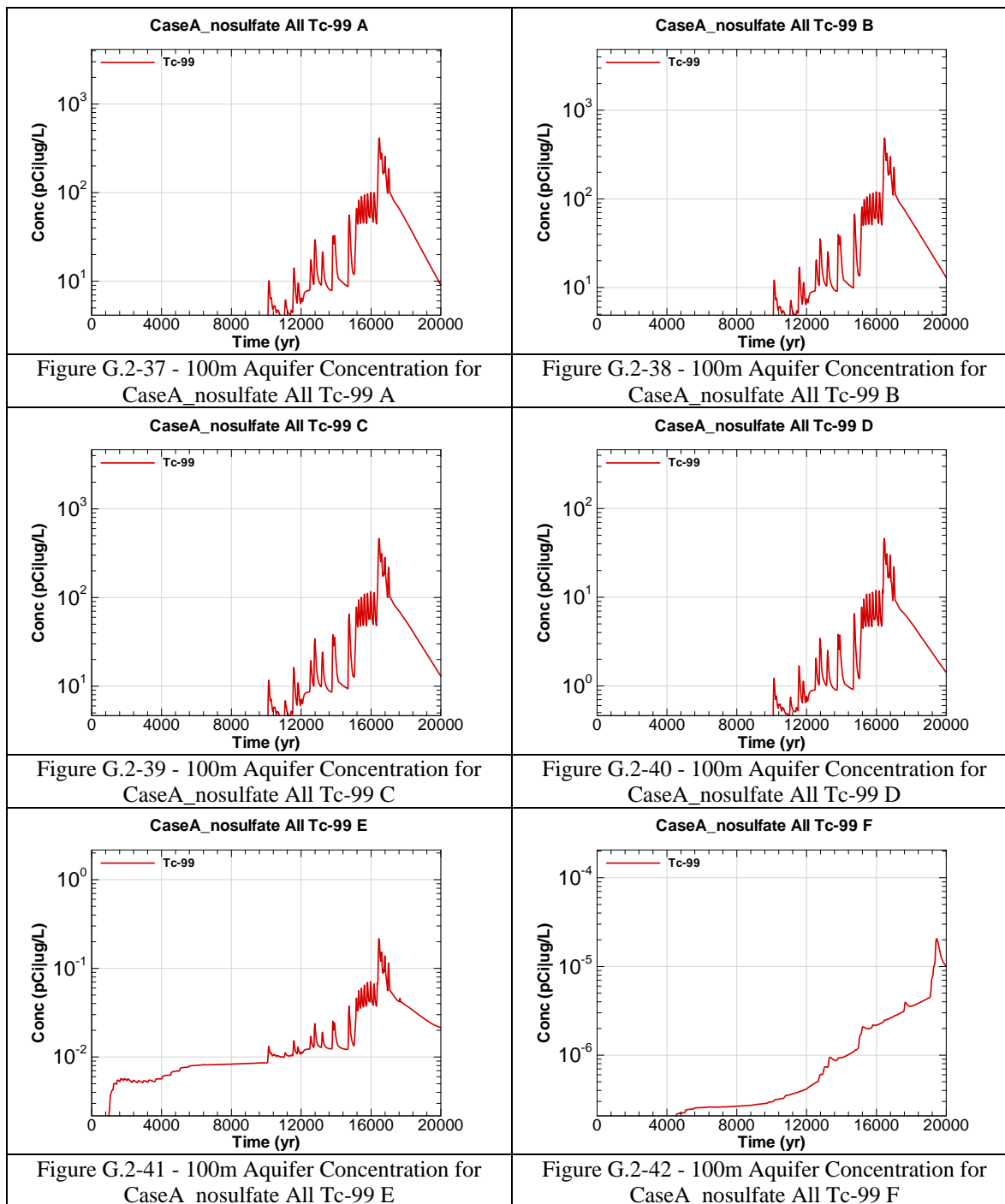
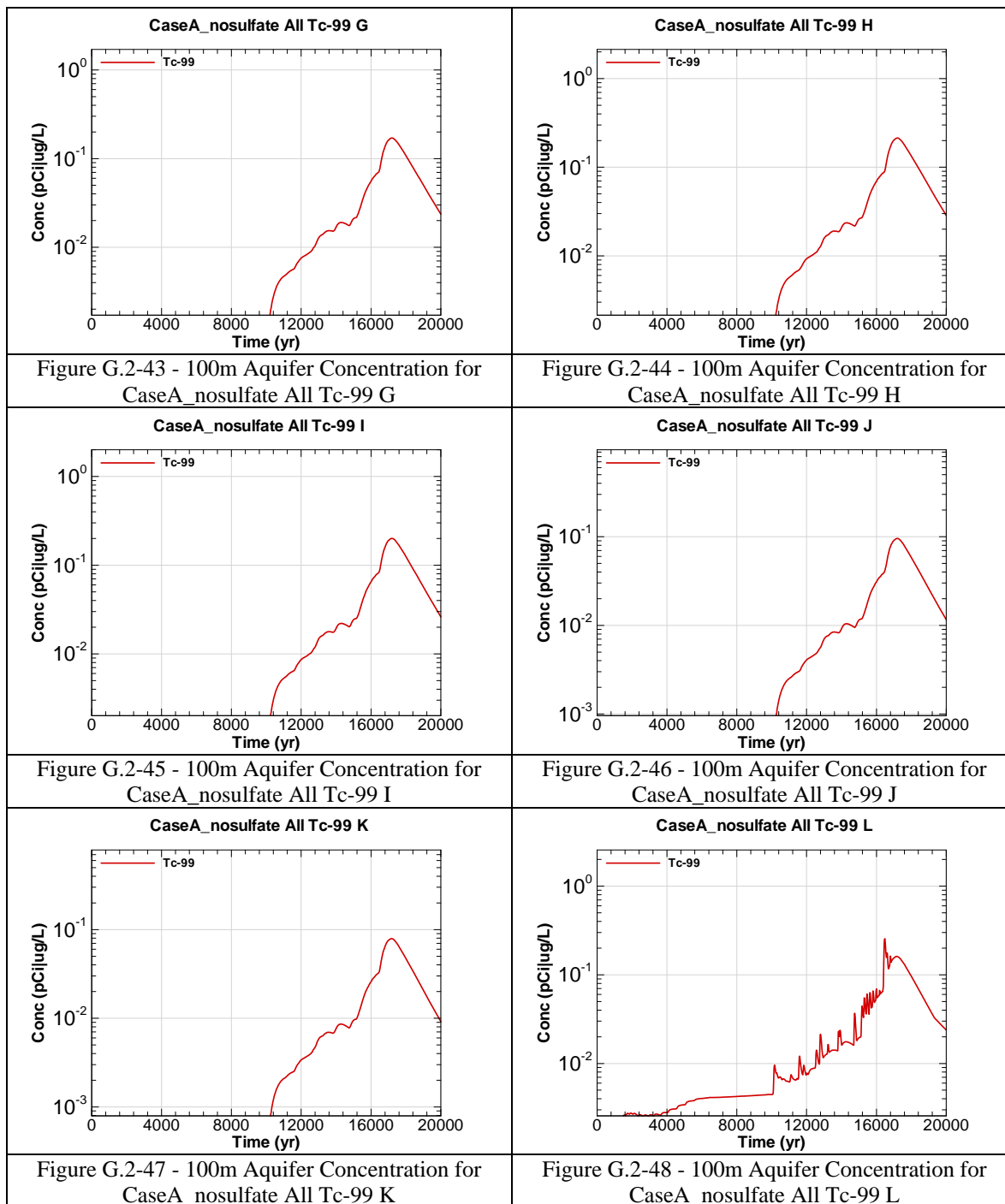


Figure G.2-30 - 100m Aquifer Concentration for CaseA_nosulfate All Pu-238 F







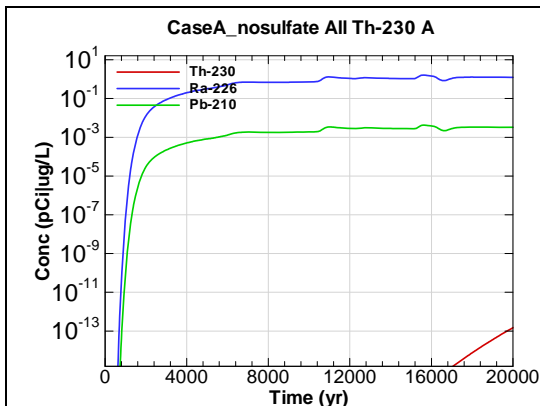


Figure G.2-49 - 100m Aquifer Concentration for CaseA_nosulfate All Th-230 A

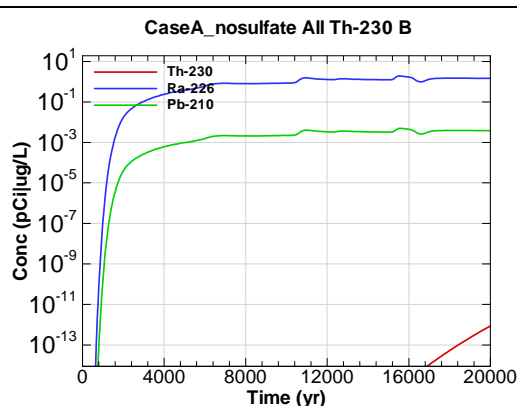


Figure G.2-50 - 100m Aquifer Concentration for CaseA_nosulfate All Th-230 B

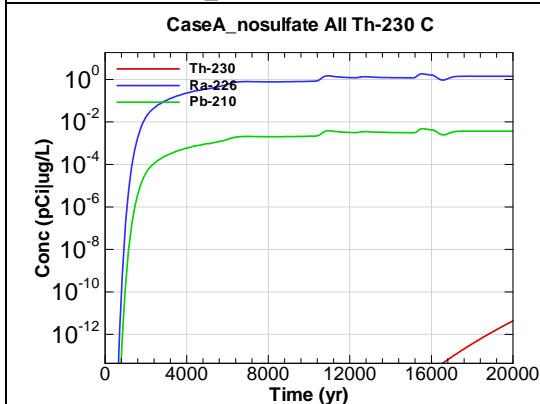


Figure G.2-51 - 100m Aquifer Concentration for CaseA_nosulfate All Th-230 C

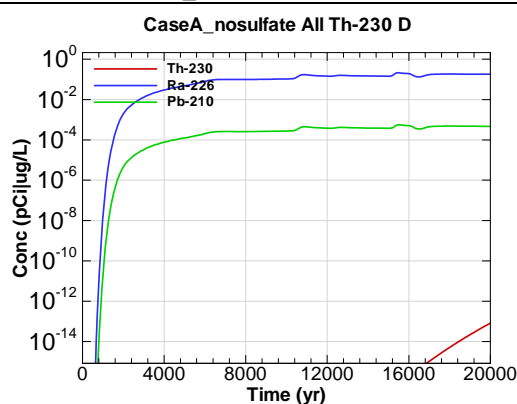


Figure G.2-52 - 100m Aquifer Concentration for CaseA_nosulfate All Th-230 D

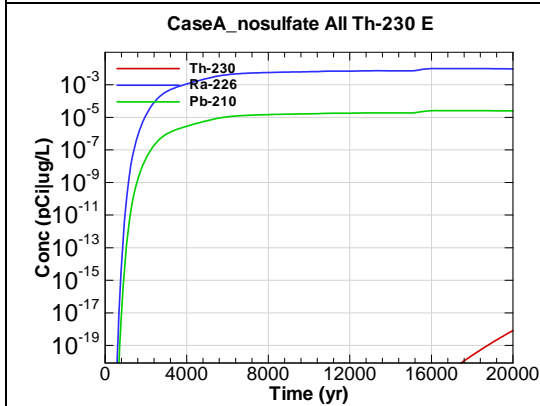


Figure G.2-53 - 100m Aquifer Concentration for CaseA_nosulfate All Th-230 E

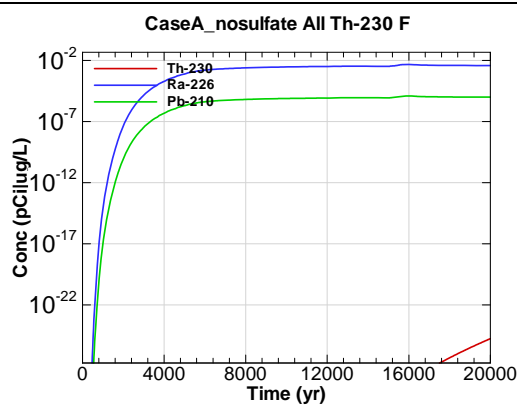
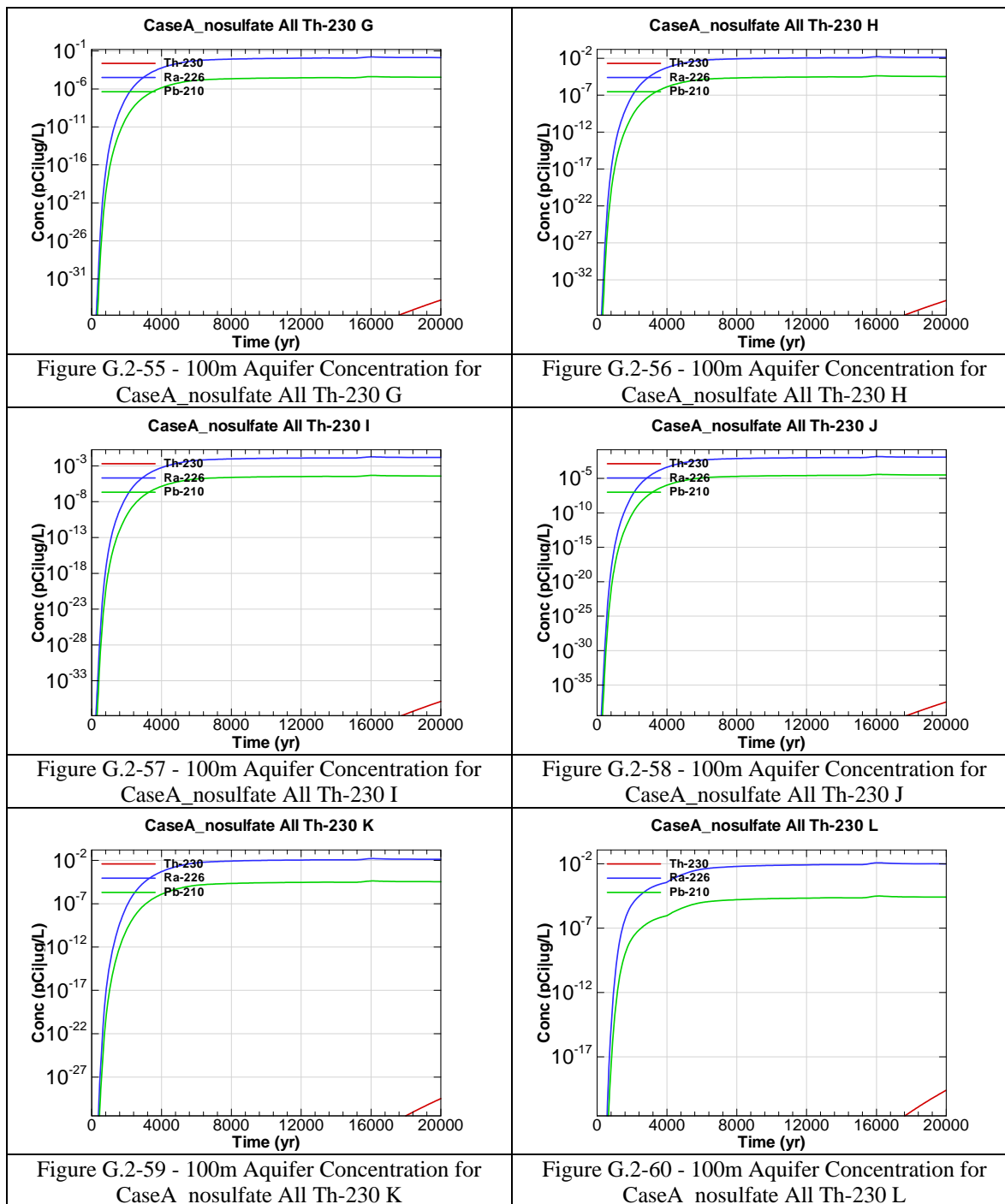


Figure G.2-54 - 100m Aquifer Concentration for CaseA_nosulfate All Th-230 F



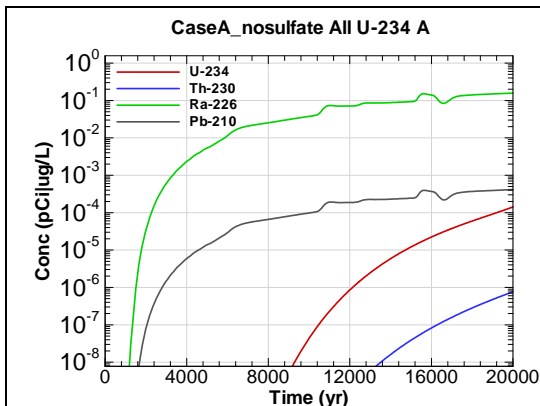


Figure G.2-61 - 100m Aquifer Concentration for CaseA_nosulfate All U-234 A

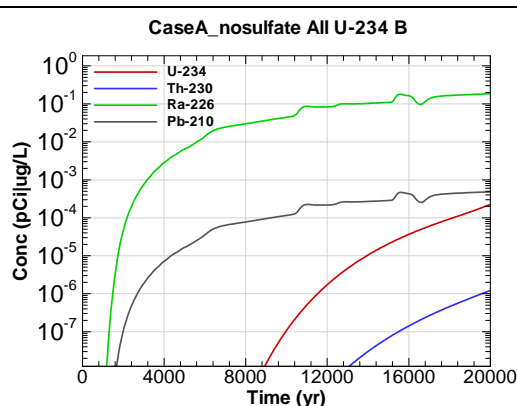


Figure G.2-62 - 100m Aquifer Concentration for CaseA_nosulfate All U-234 B

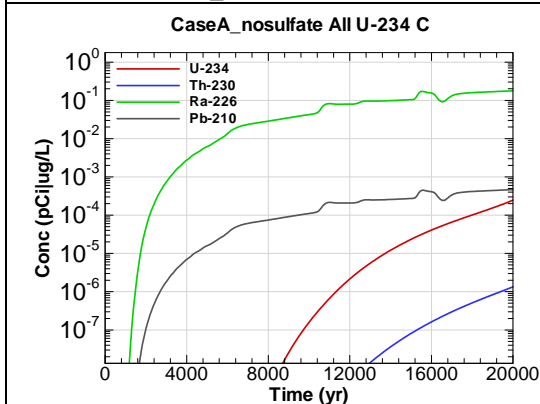


Figure G.2-63 - 100m Aquifer Concentration for CaseA_nosulfate All U-234 C

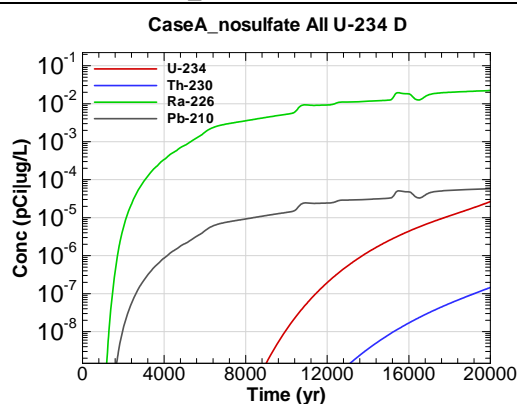


Figure G.2-64 - 100m Aquifer Concentration for CaseA_nosulfate All U-234 D

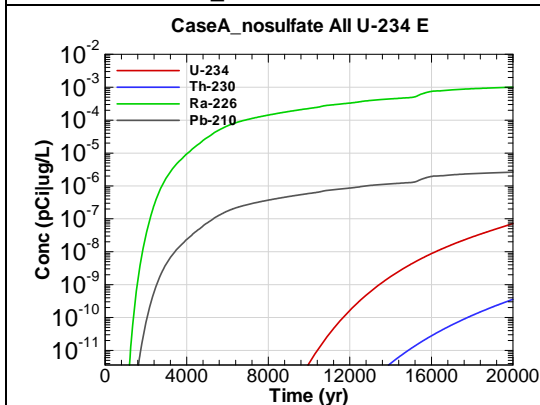


Figure G.2-65 - 100m Aquifer Concentration for CaseA_nosulfate All U-234 E

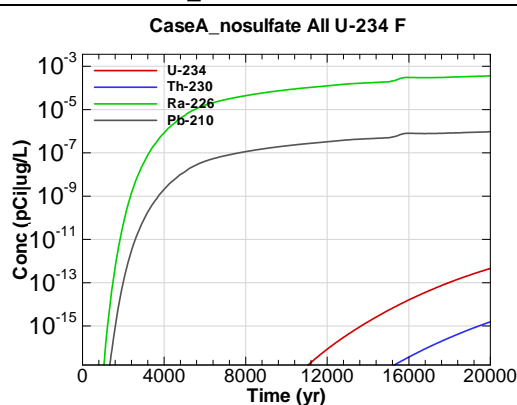
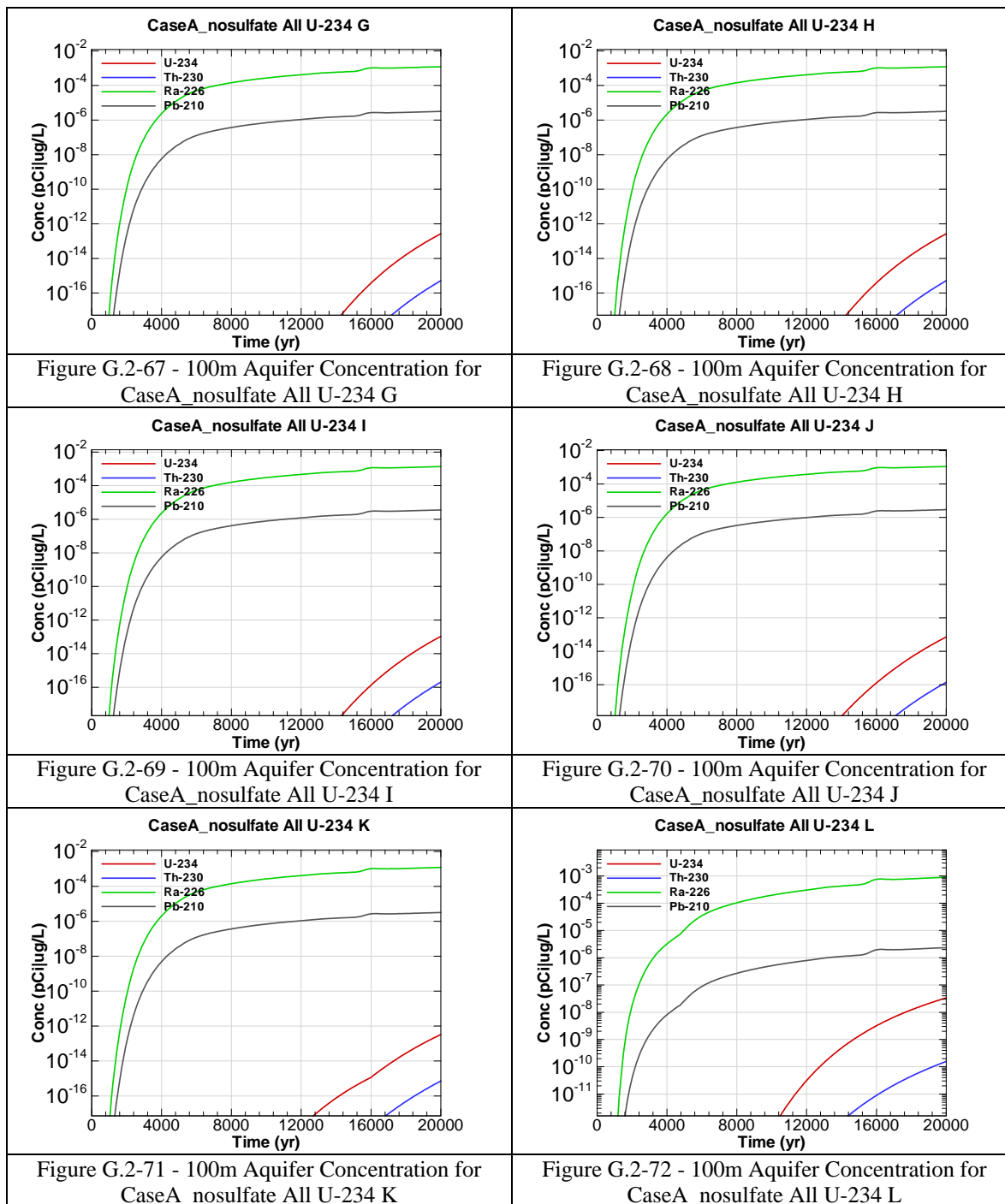
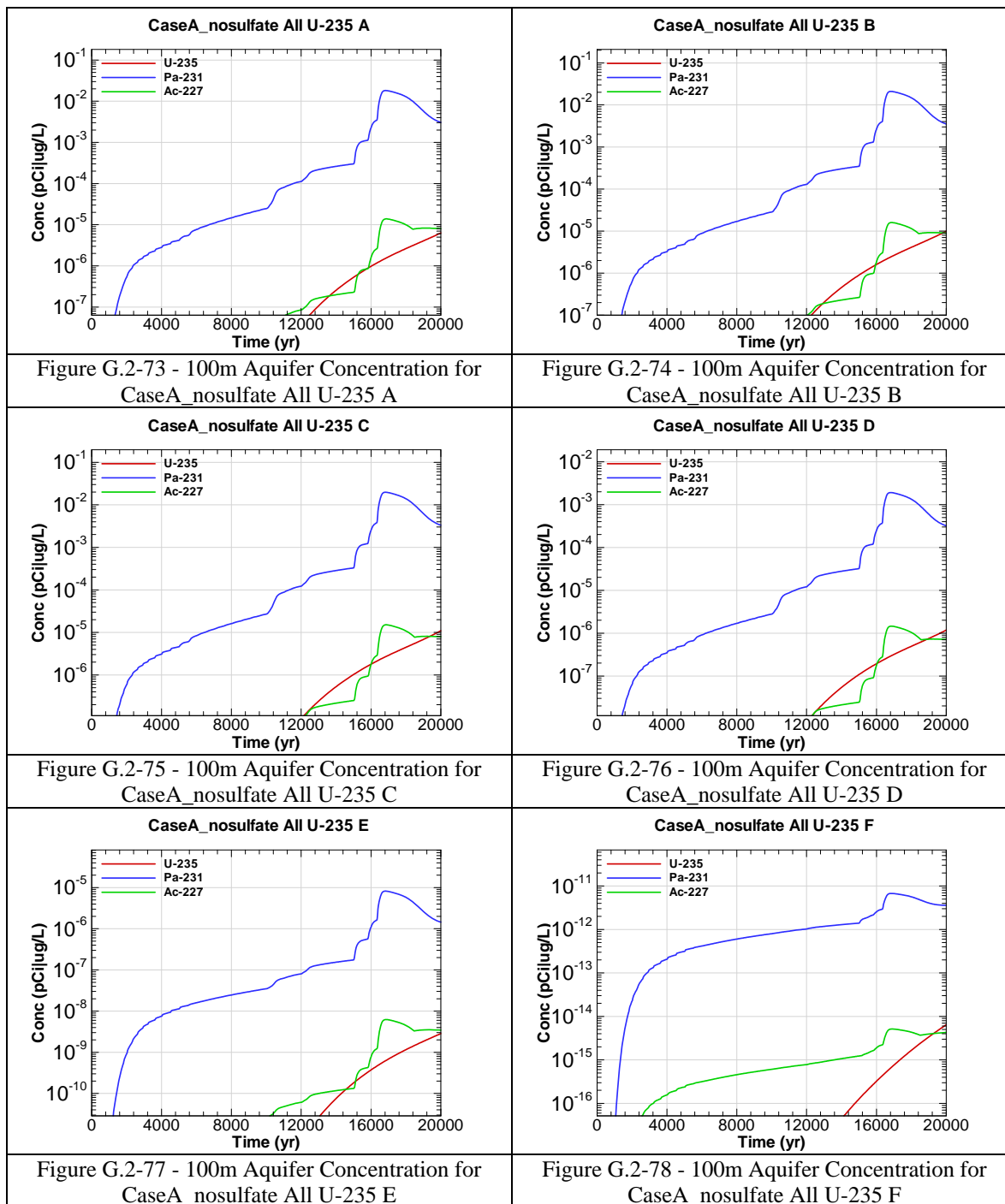
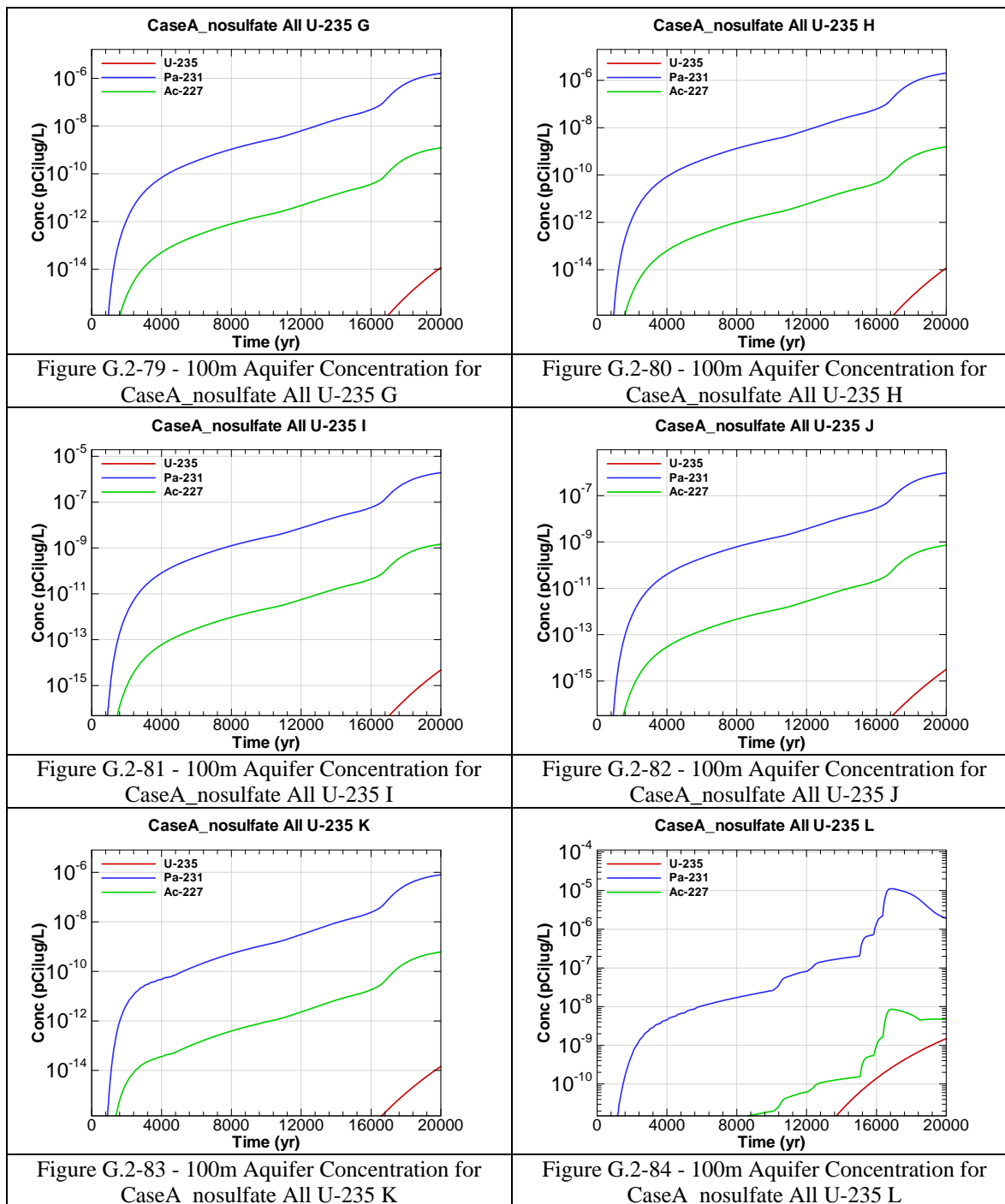
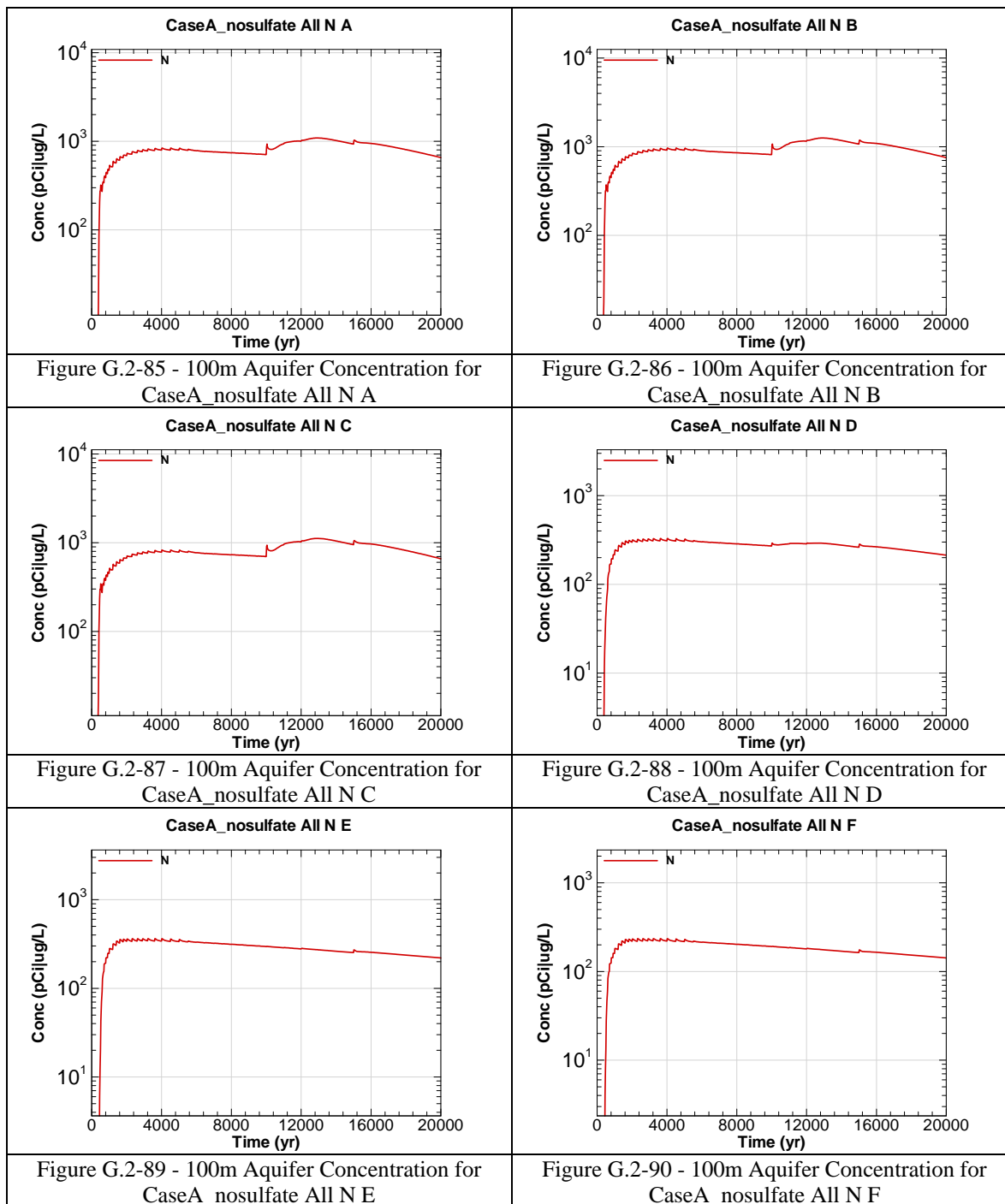


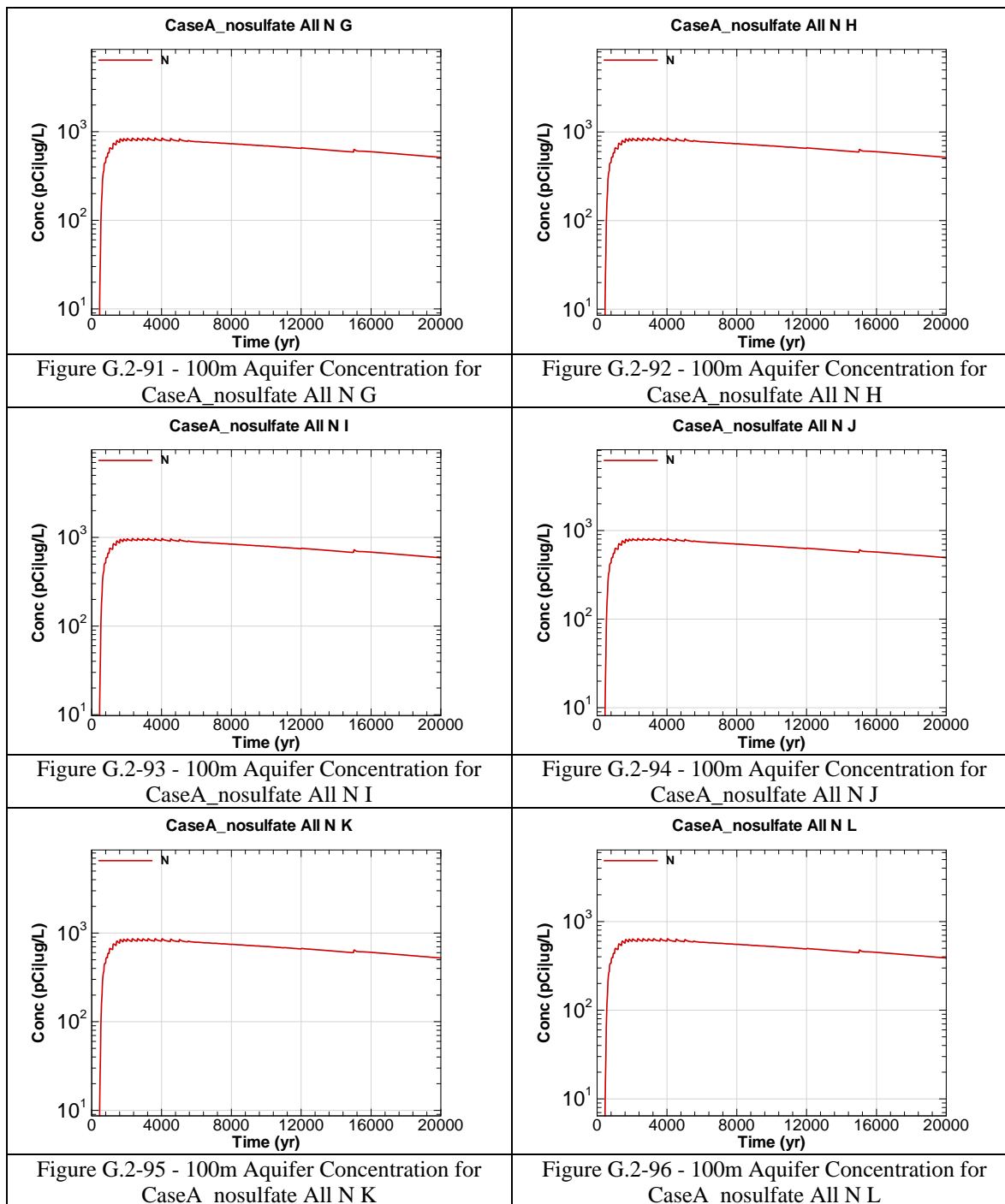
Figure G.2-66 - 100m Aquifer Concentration for CaseA_nosulfate All U-234 F











This page intentionally left blank

APPENDIX H

FLOW SENSITIVITY (NO CLOSURE CAP)

Appendix H contains curves showing the 100 meter concentrations for key radiological and chemical concentrations for all of SDF (vault and FDC inventories) for the Base Case (Case A) for a case of higher flow available to the disposal system (i.e., no engineered closure cap and thus natural soil infiltration rate from year 0). 20,000 year concentration results are presented for Sectors A through L for the peak concentration per sector regardless of aquifer.

Graph heading example “CaseA_nocap All I-129 A”

Key

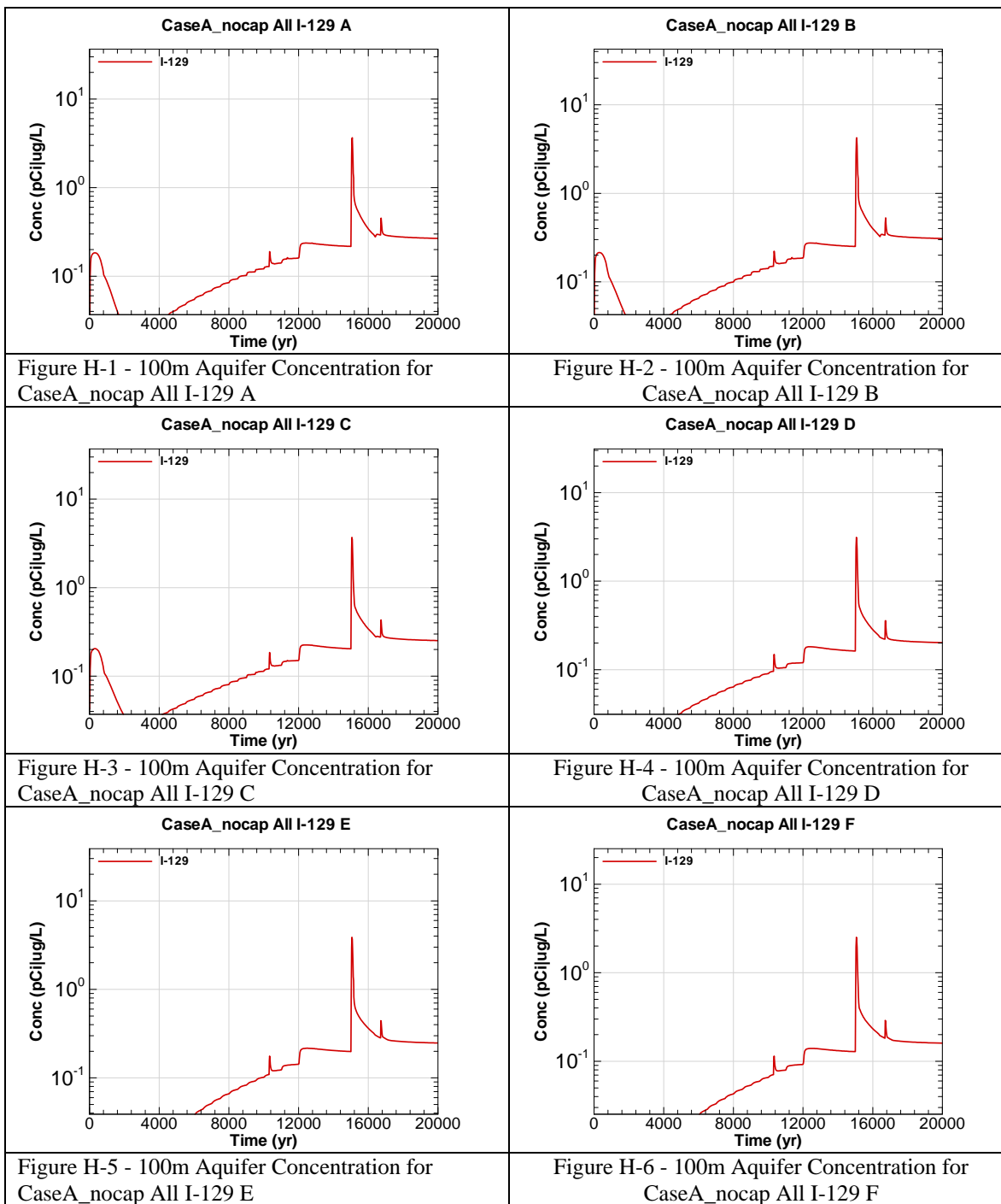
CaseA = Scenario case

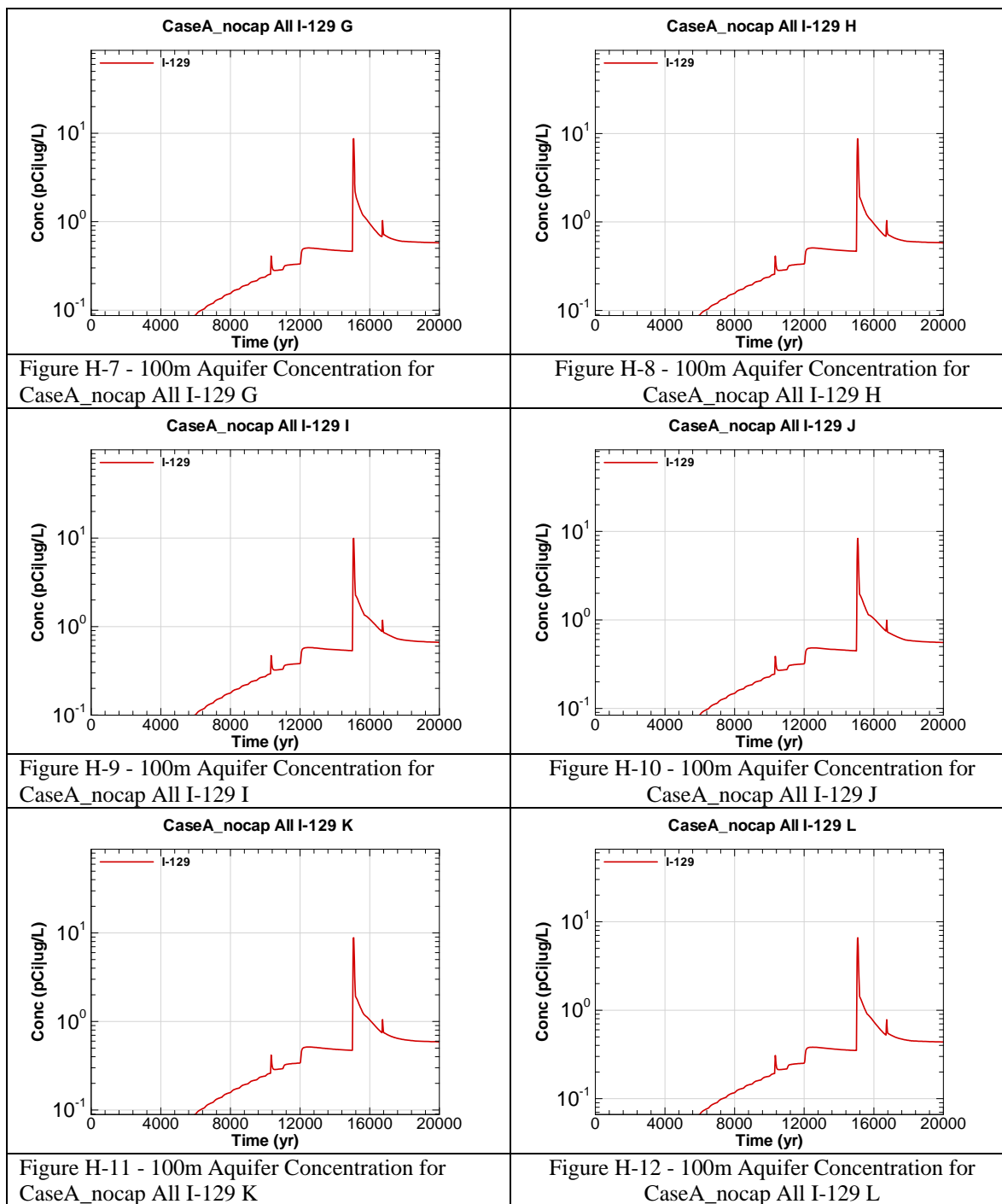
nocap = Higher soil infiltration rate

All = Inventory source is all disposal units

I-129 = Radionuclide or chemical of concern

A = Evaluation sector of concern





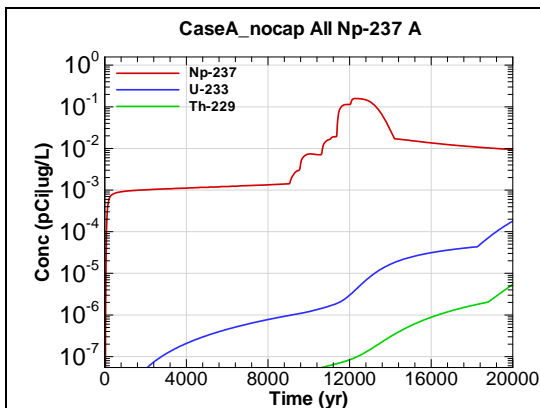


Figure H-13 - 100m Aquifer Concentration for CaseA_nocap All Np-237 A

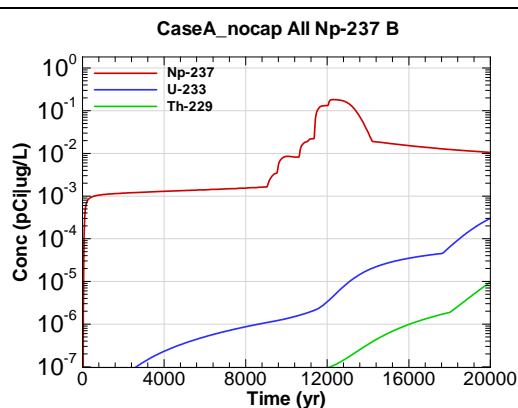


Figure H-14 - 100m Aquifer Concentration for CaseA_nocap All Np-237 B

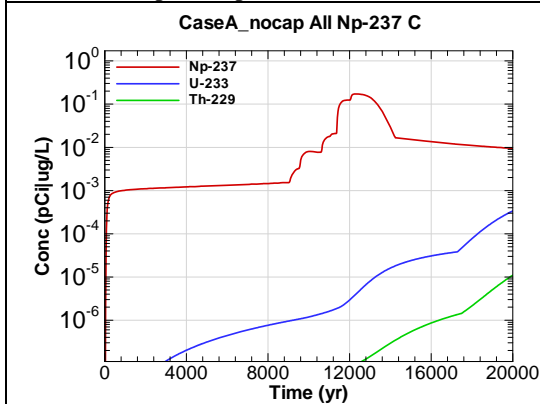


Figure H-15 - 100m Aquifer Concentration for CaseA_nocap All Np-237 C

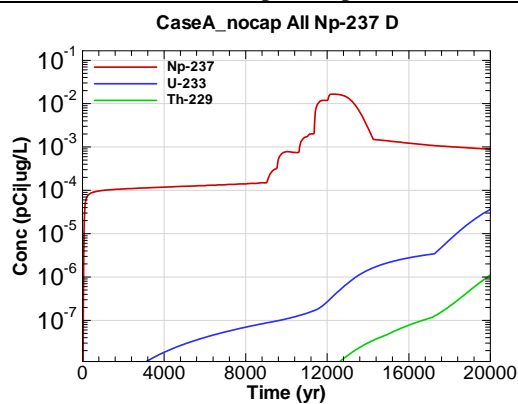


Figure H-16 - 100m Aquifer Concentration for CaseA_nocap All Np-237 D

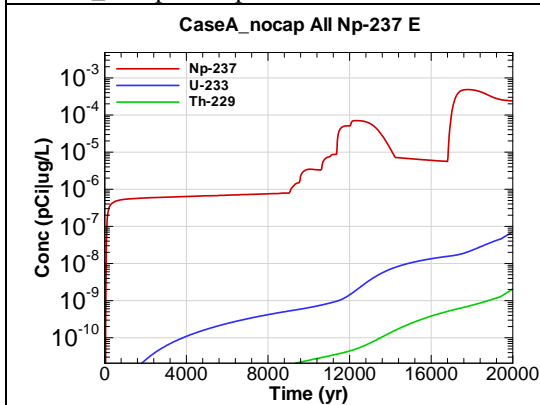


Figure H-17 - 100m Aquifer Concentration for CaseA_nocap All Np-237 E

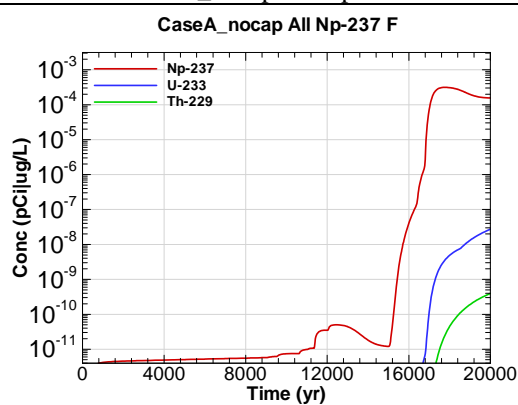


Figure H-18 - 100m Aquifer Concentration for CaseA_nocap All Np-237 F

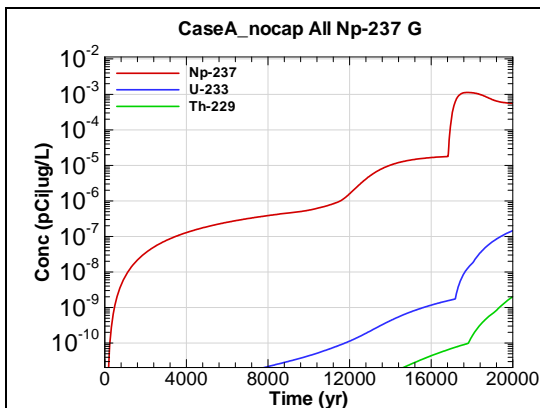


Figure H-19 - 100m Aquifer Concentration for CaseA_nocap All Np-237 G

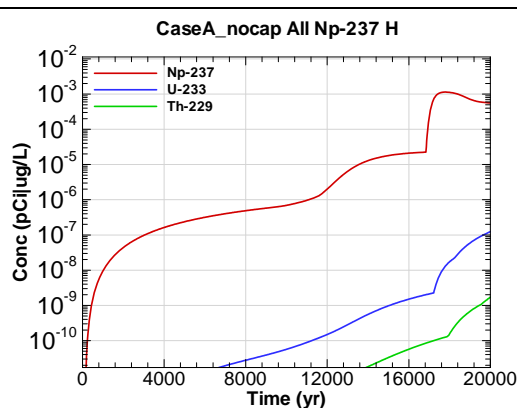


Figure H-20 - 100m Aquifer Concentration for CaseA_nocap All Np-237 H

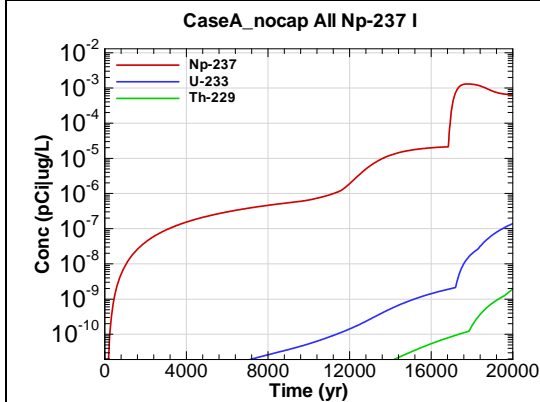


Figure H-21 - 100m Aquifer Concentration for CaseA_nocap All Np-237 I

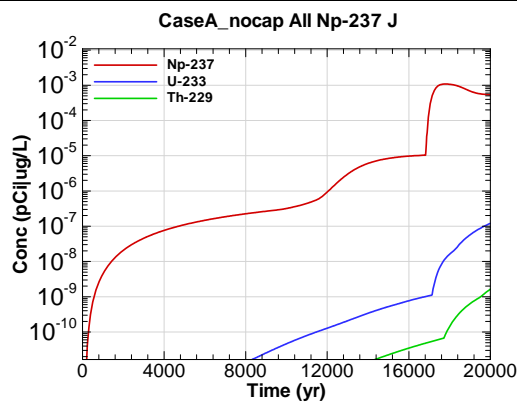


Figure H-22 - 100m Aquifer Concentration for CaseA_nocap All Np-237 J

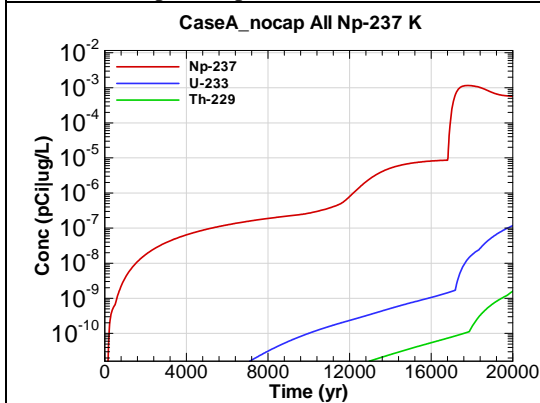


Figure H-23 - 100m Aquifer Concentration for CaseA_nocap All Np-237 K

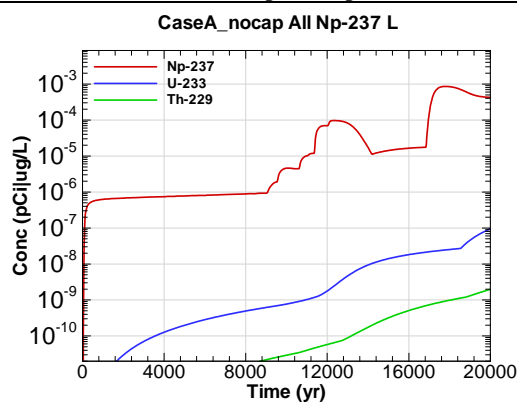


Figure H-24 - 100m Aquifer Concentration for CaseA_nocap All Np-237 L

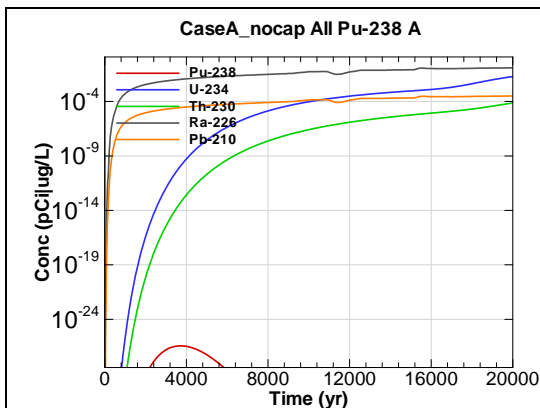


Figure H-25 - 100m Aquifer Concentration for CaseA_nocap All Pu-238 A

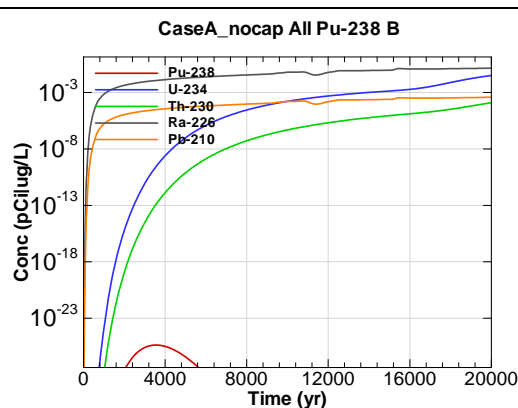


Figure H-26 - 100m Aquifer Concentration for CaseA_nocap All Pu-238 B

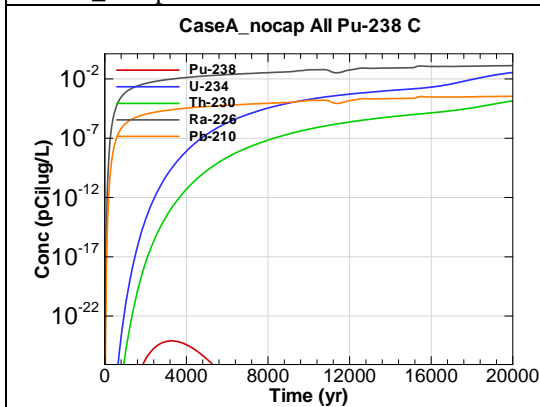


Figure H-27 - 100m Aquifer Concentration for CaseA_nocap All Pu-238 C

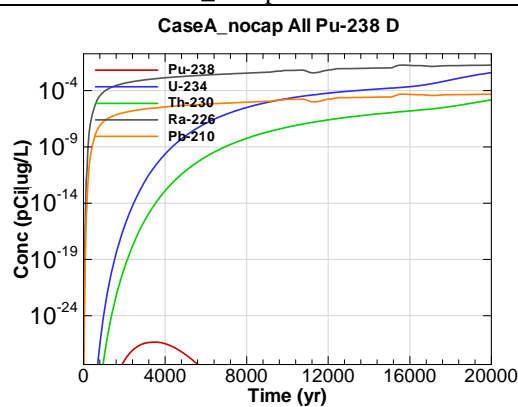


Figure H-28 - 100m Aquifer Concentration for CaseA_nocap All Pu-238 D

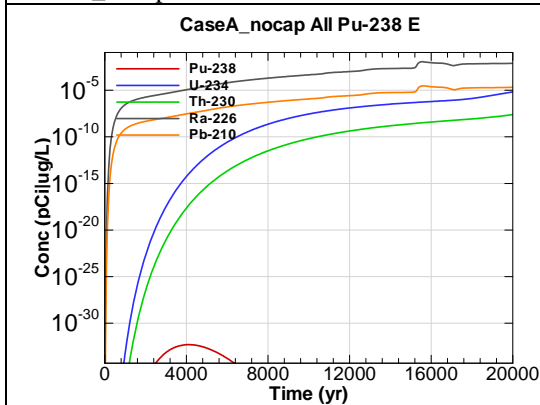


Figure H-29 - 100m Aquifer Concentration for CaseA_nocap All Pu-238 E

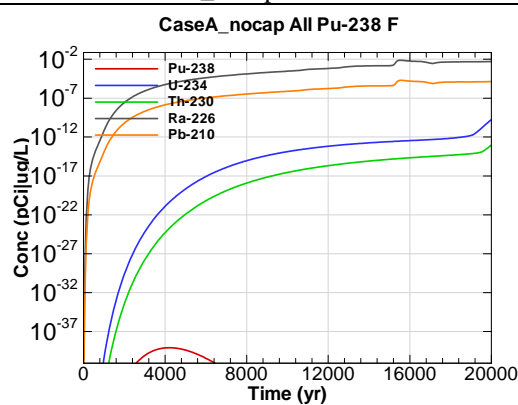


Figure H-30 - 100m Aquifer Concentration for CaseA_nocap All Pu-238 F

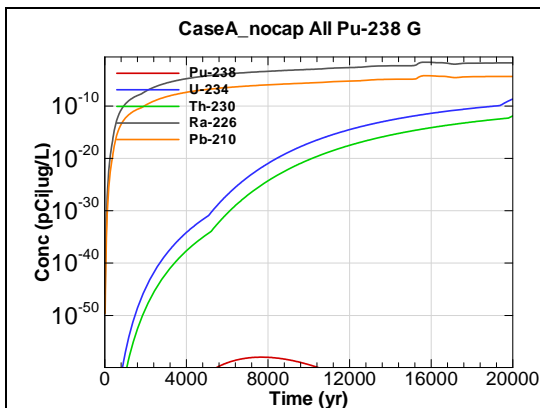


Figure H-31 - 100m Aquifer Concentration for CaseA_nocap All Pu-238 G

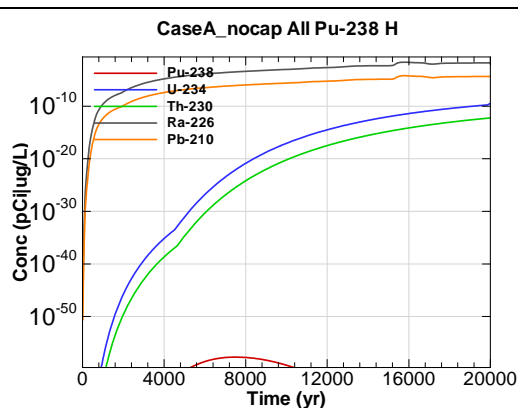


Figure H-32 - 100m Aquifer Concentration for CaseA_nocap All Pu-238 H

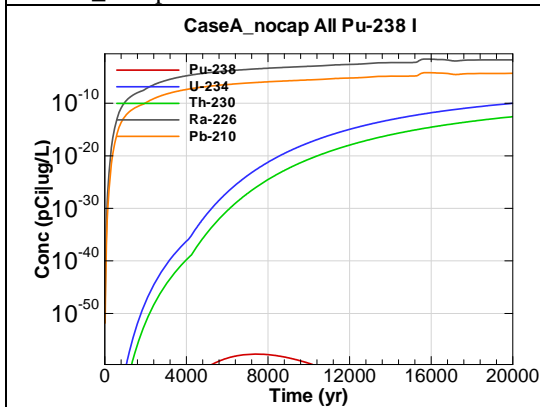


Figure H-33 - 100m Aquifer Concentration for CaseA_nocap All Pu-238 I

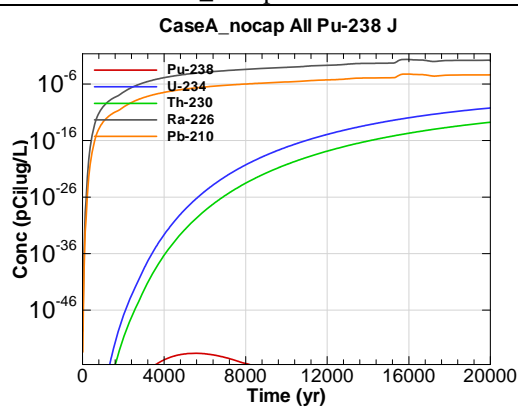


Figure H-34 - 100m Aquifer Concentration for CaseA_nocap All Pu-238 J

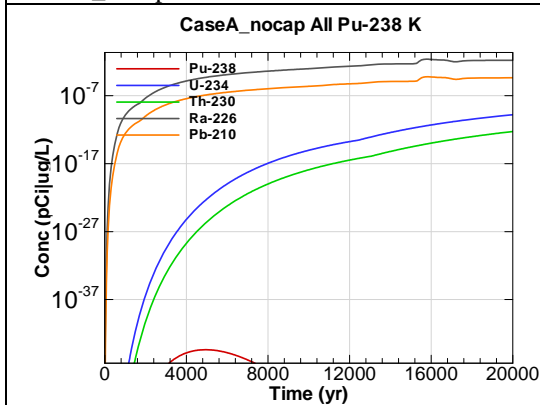


Figure H-35 - 100m Aquifer Concentration for CaseA_nocap All Pu-238 K

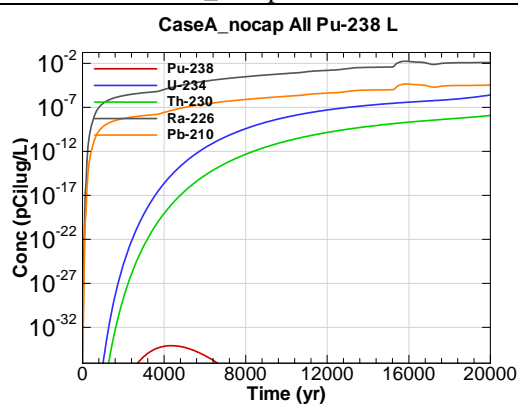


Figure H-36 - 100m Aquifer Concentration for CaseA_nocap All Pu-238 L

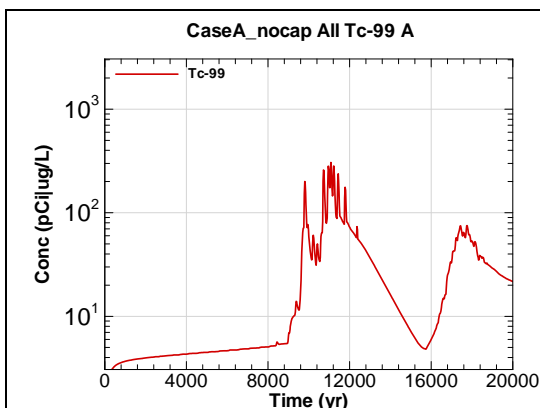


Figure H-37 - 100m Aquifer Concentration for CaseA_nocap All Tc-99 A

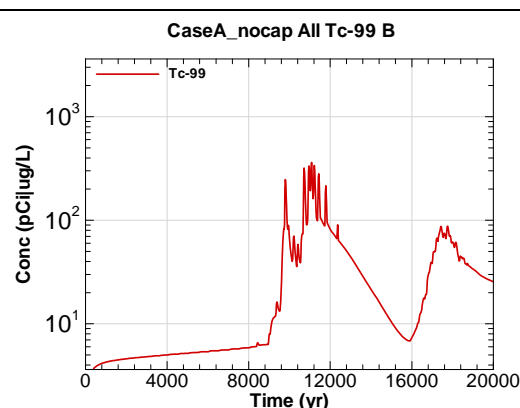


Figure H-38 - 100m Aquifer Concentration for CaseA_nocap All Tc-99 B

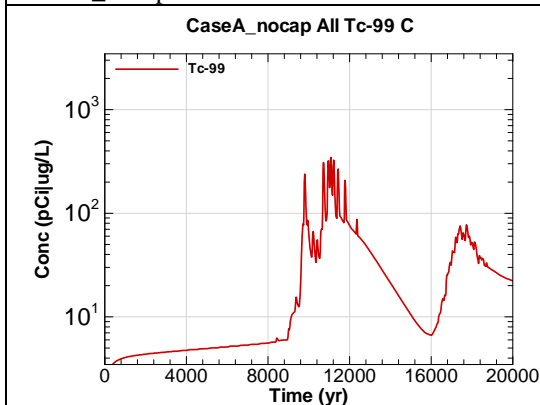


Figure H-39 - 100m Aquifer Concentration for CaseA_nocap All Tc-99 C

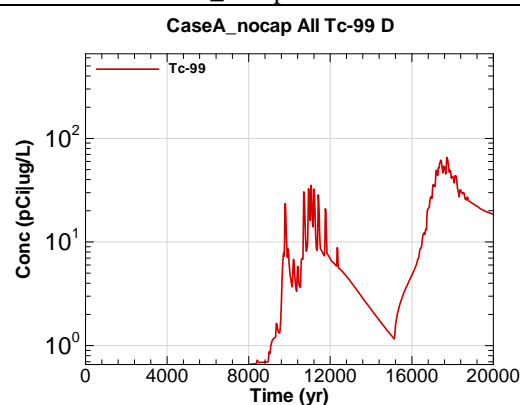


Figure H-40 - 100m Aquifer Concentration for CaseA_nocap All Tc-99 D

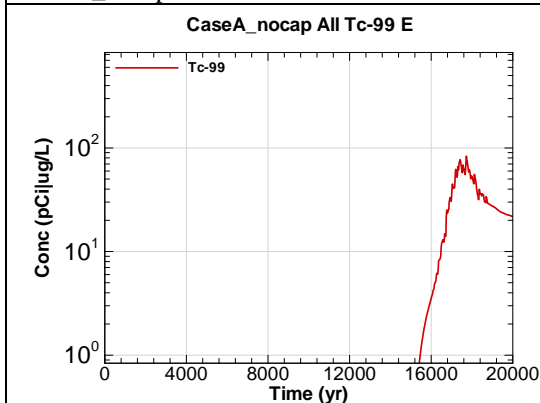


Figure H-41 - 100m Aquifer Concentration for CaseA_nocap All Tc-99 E

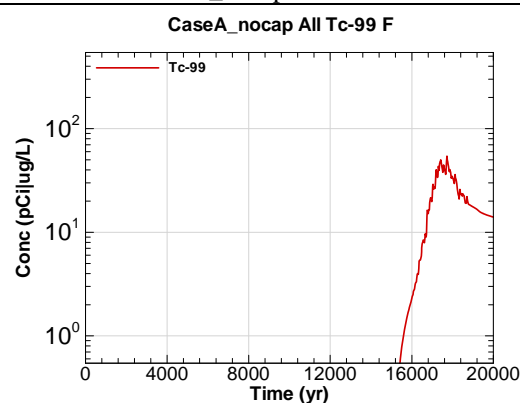
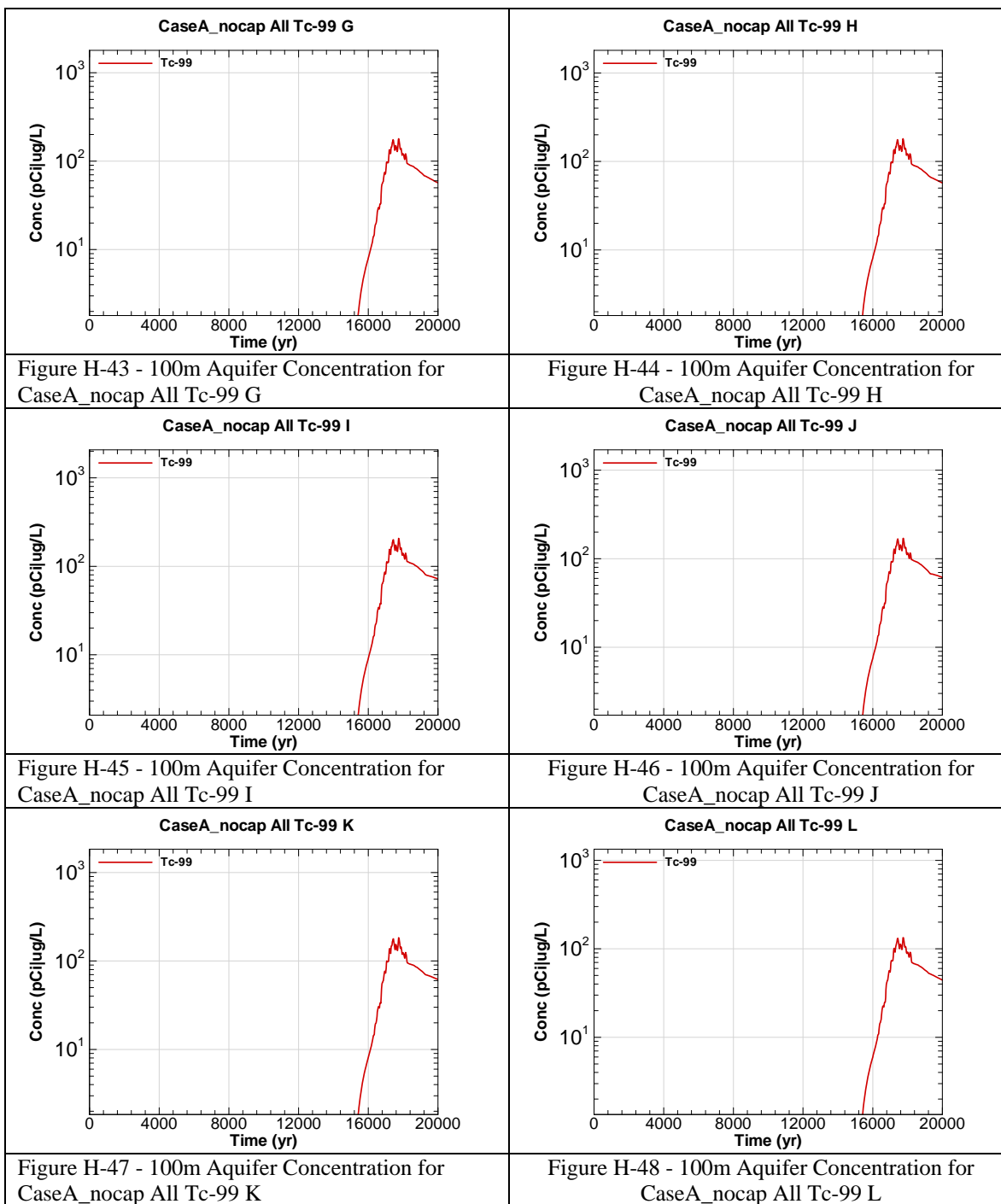


Figure H-42 - 100m Aquifer Concentration for CaseA_nocap All Tc-99 F



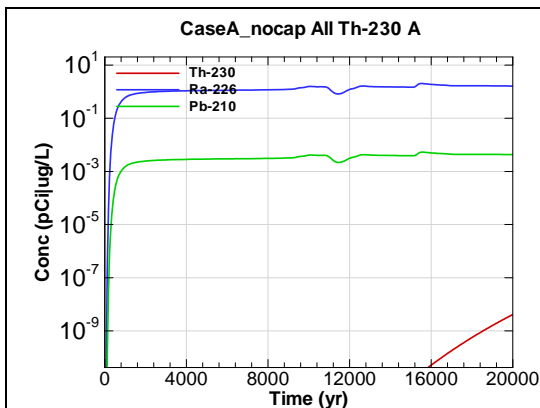


Figure H-49 - 100m Aquifer Concentration for CaseA_nocap All Th-230 A

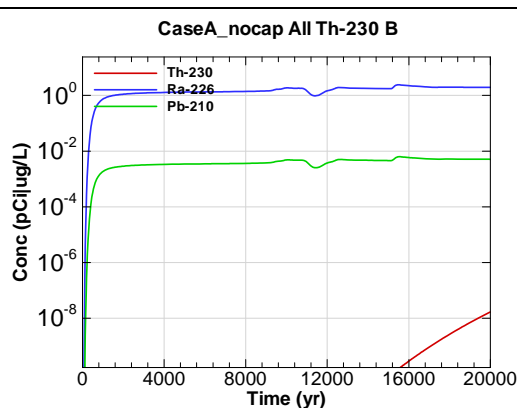


Figure H-50 - 100m Aquifer Concentration for CaseA_nocap All Th-230 B

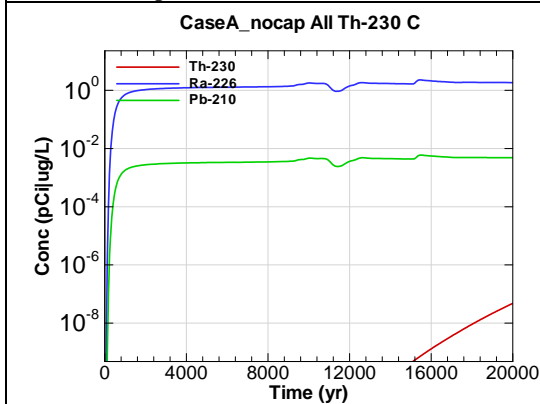


Figure H-51 - 100m Aquifer Concentration for CaseA_nocap All Th-230 C

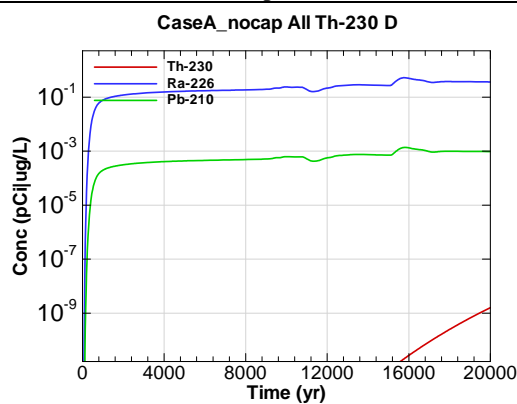


Figure H-52 - 100m Aquifer Concentration for CaseA_nocap All Th-230 D

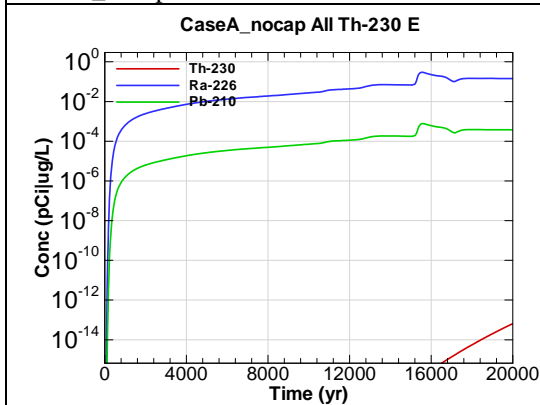


Figure H-53 - 100m Aquifer Concentration for CaseA_nocap All Th-230 E

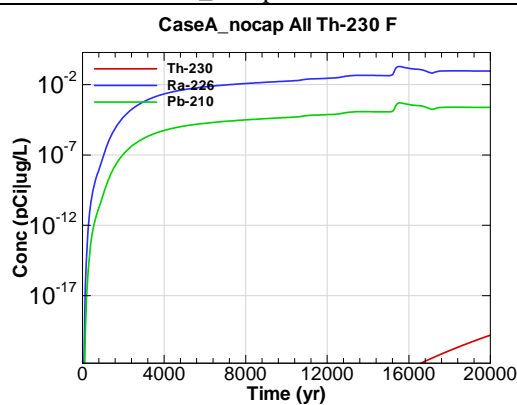


Figure H-54 - 100m Aquifer Concentration for CaseA_nocap All Th-230 F

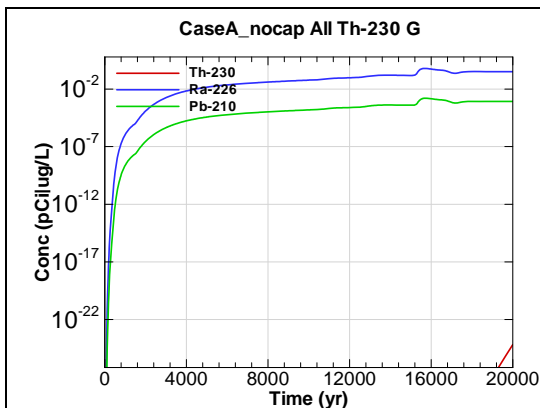


Figure H-55 - 100m Aquifer Concentration for CaseA_nocap All Th-230 G

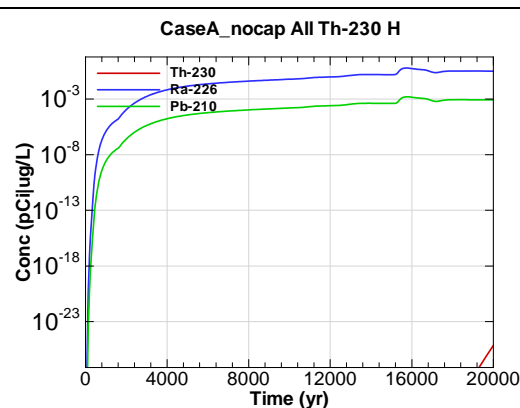


Figure H-56 - 100m Aquifer Concentration for CaseA_nocap All Th-230 H

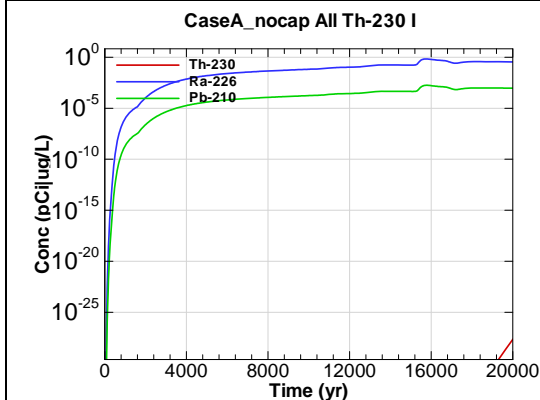


Figure H-57 - 100m Aquifer Concentration for CaseA_nocap All Th-230 I

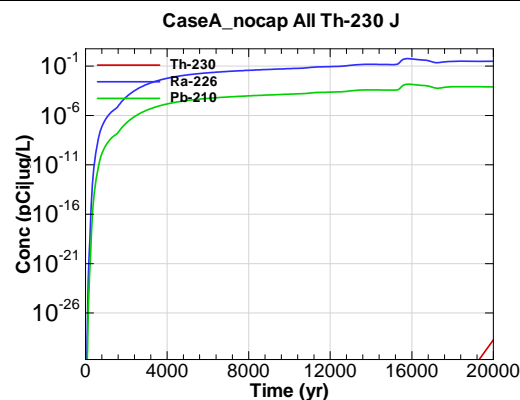


Figure H-58 - 100m Aquifer Concentration for CaseA_nocap All Th-230 J

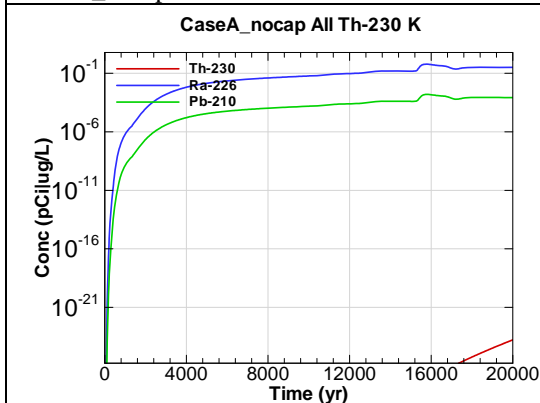


Figure H-59 - 100m Aquifer Concentration for CaseA_nocap All Th-230 K

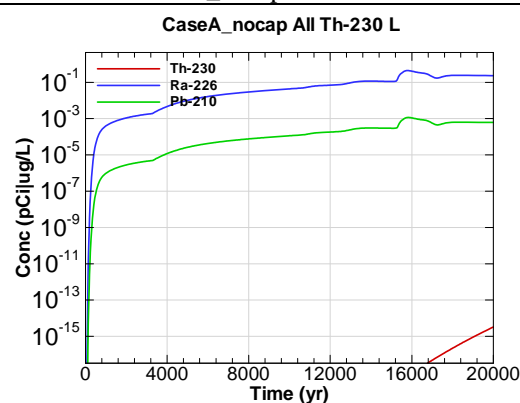


Figure H-60 - 100m Aquifer Concentration for CaseA_nocap All Th-230 L

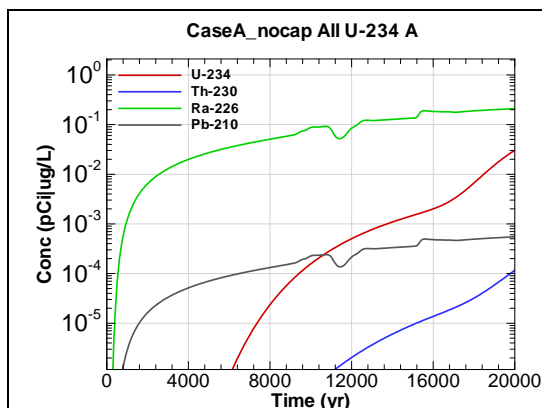


Figure H-61 - 100m Aquifer Concentration for CaseA_nocap All U-234 A

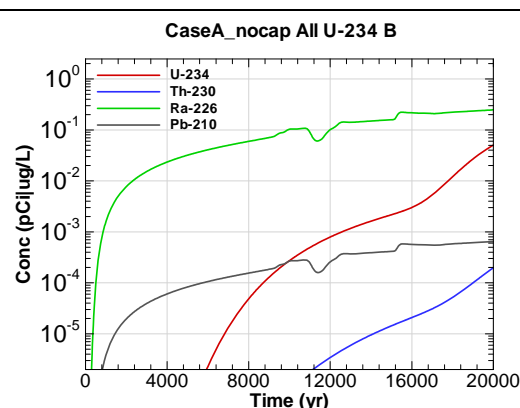


Figure H-62 - 100m Aquifer Concentration for CaseA_nocap All U-234 B

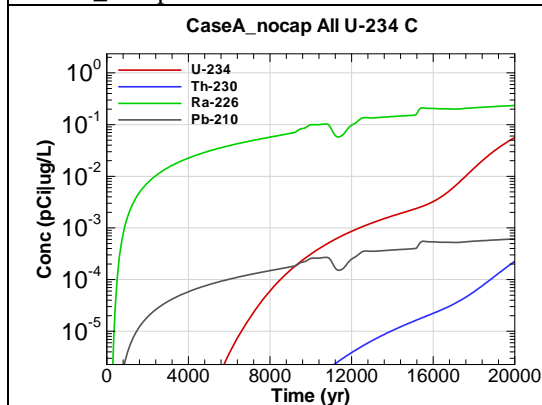


Figure H-63 - 100m Aquifer Concentration for CaseA_nocap All U-234 C

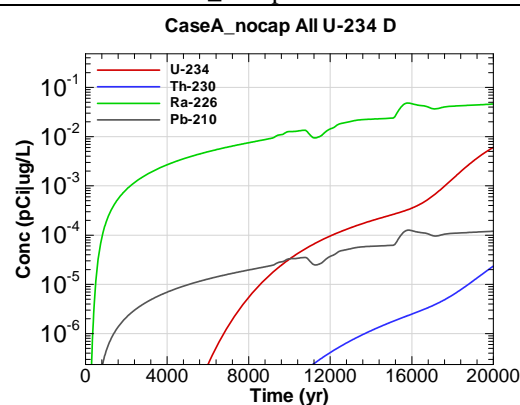


Figure H-64 - 100m Aquifer Concentration for CaseA_nocap All U-234 D

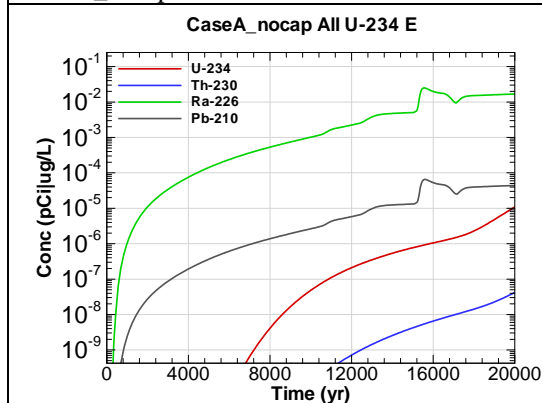


Figure H-65 - 100m Aquifer Concentration for CaseA_nocap All U-234 E

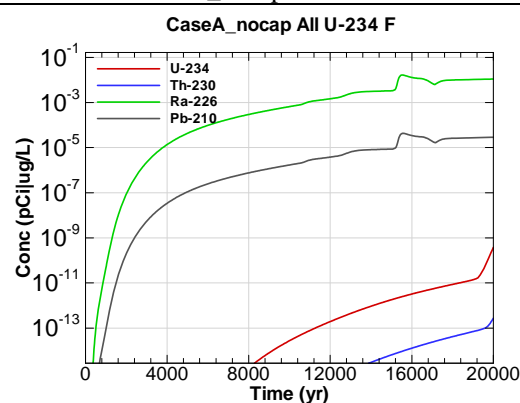


Figure H-66 - 100m Aquifer Concentration for CaseA_nocap All U-234 F

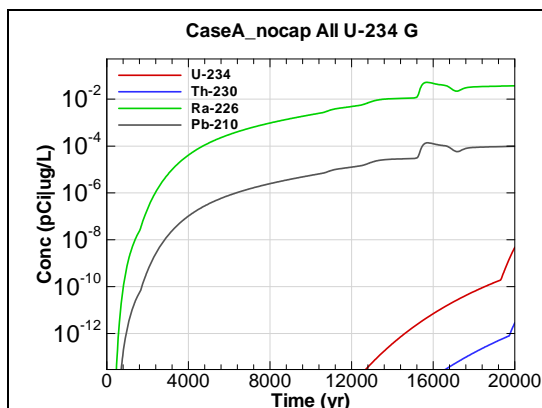


Figure H-67 - 100m Aquifer Concentration for CaseA_nocap All U-234 G

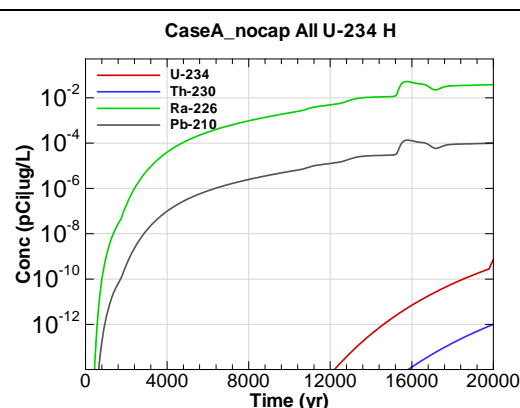


Figure H-68 - 100m Aquifer Concentration for CaseA_nocap All U-234 H

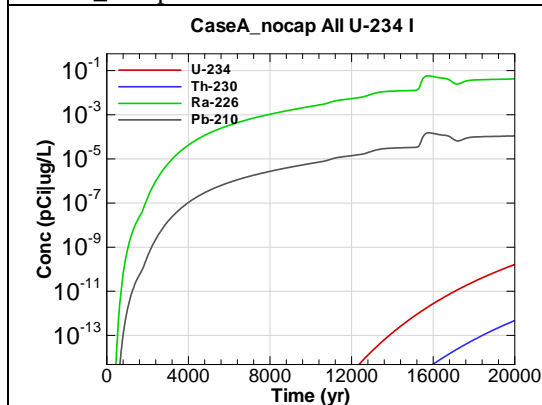


Figure H-69 - 100m Aquifer Concentration for CaseA_nocap All U-234 I

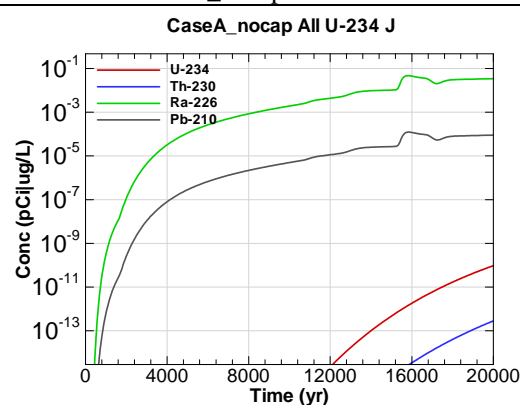


Figure H-70 - 100m Aquifer Concentration for CaseA_nocap All U-234 J

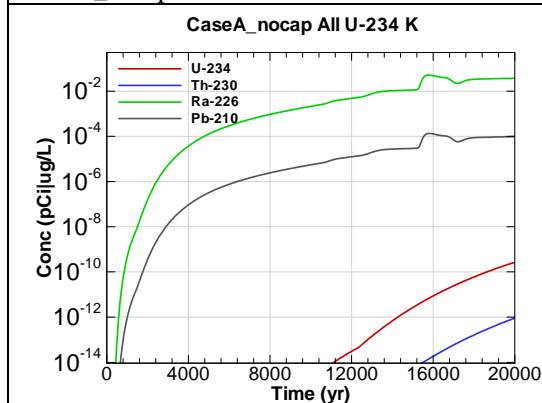


Figure H-71 - 100m Aquifer Concentration for CaseA_nocap All U-234 K

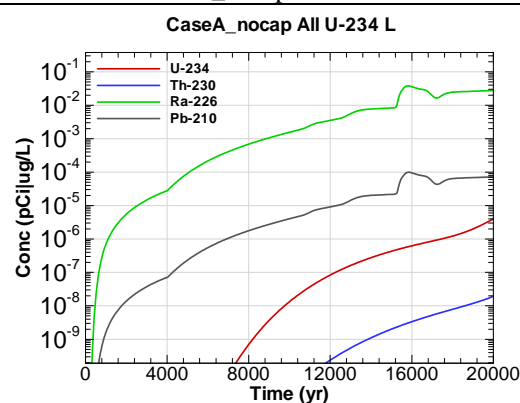
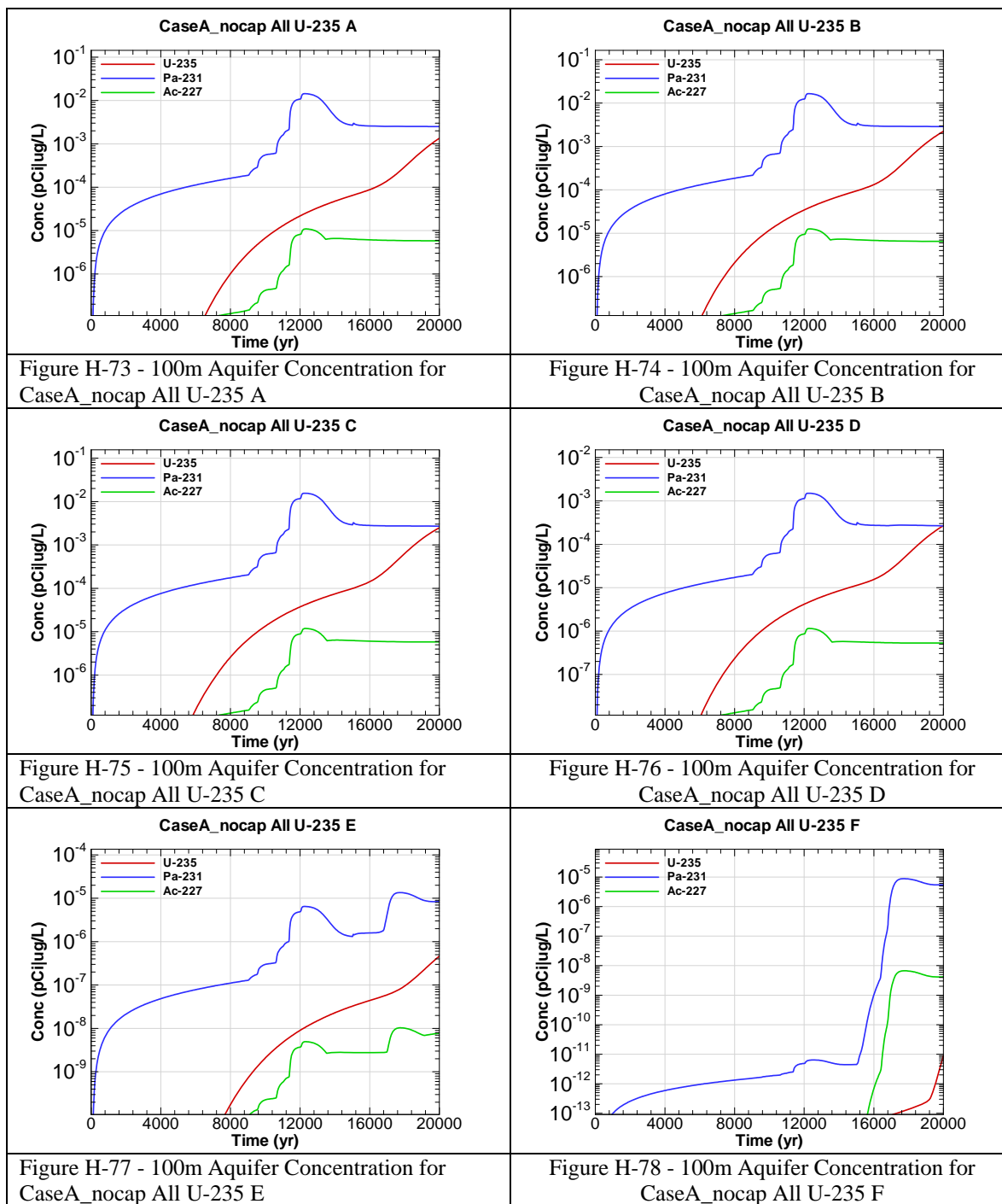


Figure H-72 - 100m Aquifer Concentration for CaseA_nocap All U-234 L



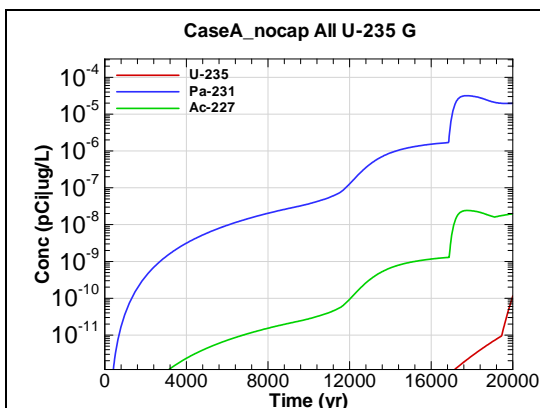


Figure H-79 - 100m Aquifer Concentration for CaseA_nocap All U-235 G

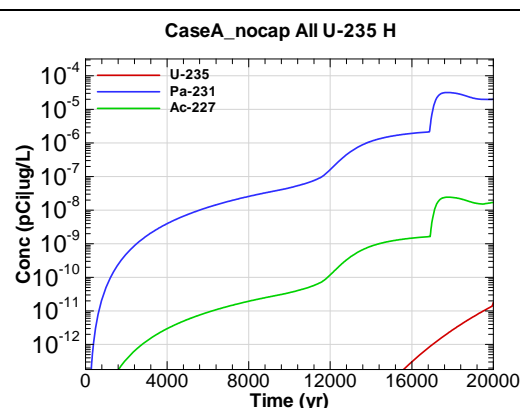


Figure H-80 - 100m Aquifer Concentration for CaseA_nocap All U-235 H

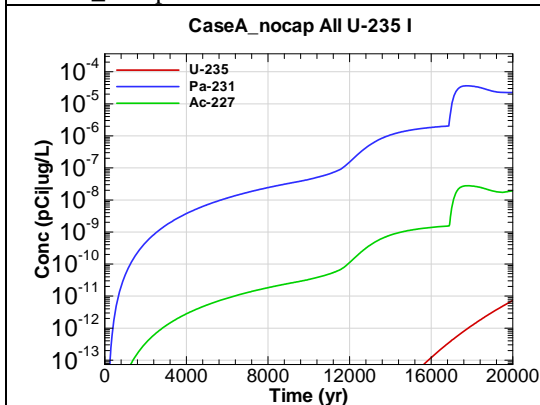


Figure H-81 - 100m Aquifer Concentration for CaseA_nocap All U-235 I

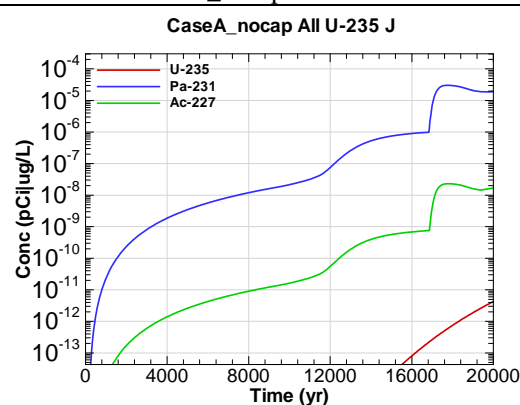


Figure H-82 - 100m Aquifer Concentration for CaseA_nocap All U-235 J

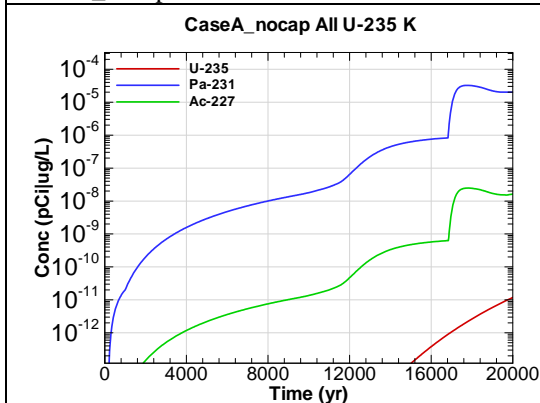


Figure H-83 - 100m Aquifer Concentration for CaseA_nocap All U-235 K

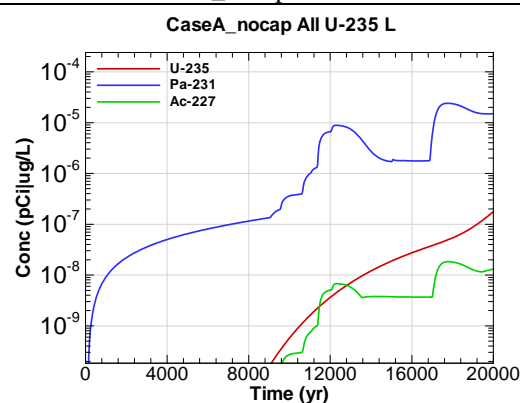
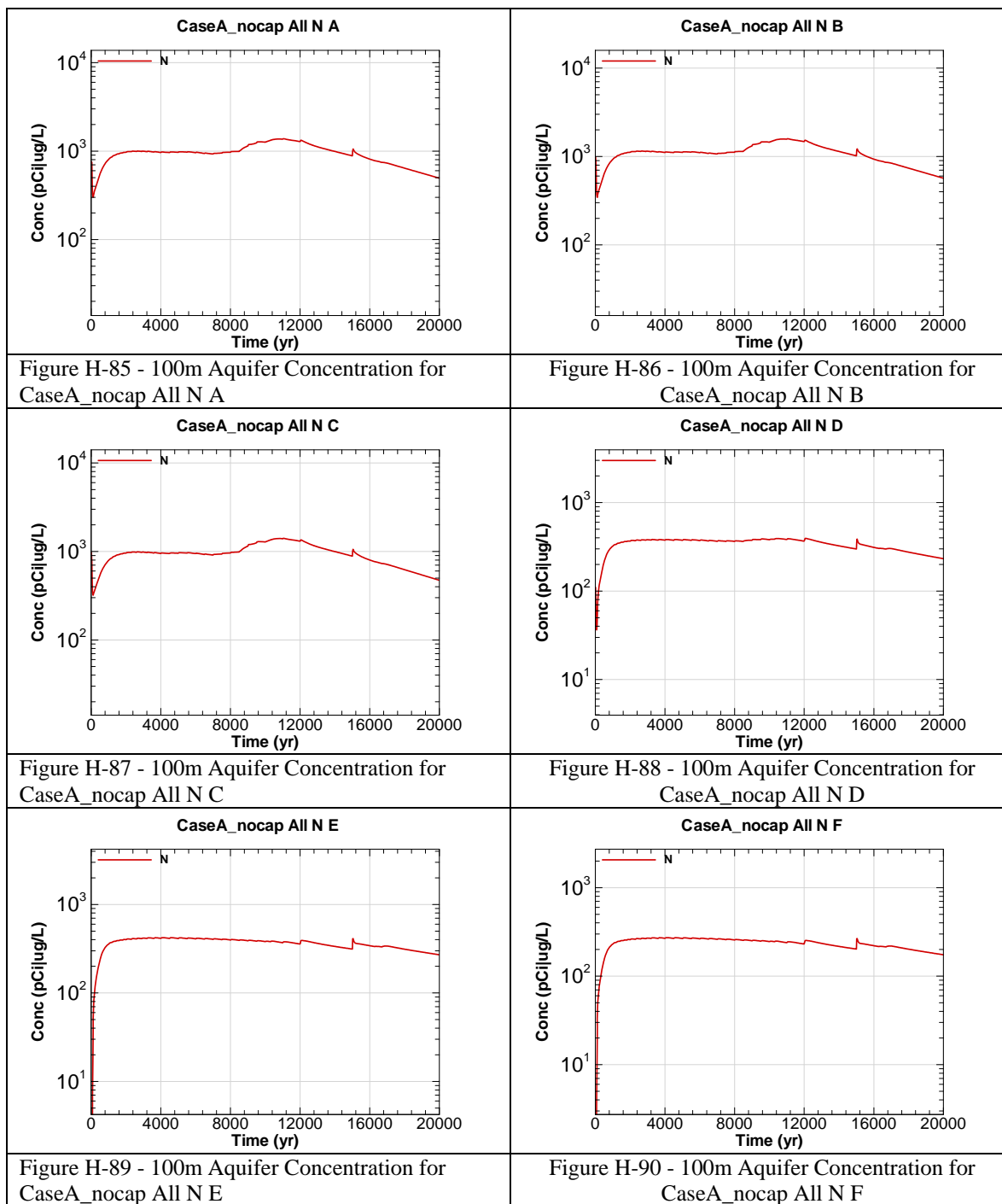
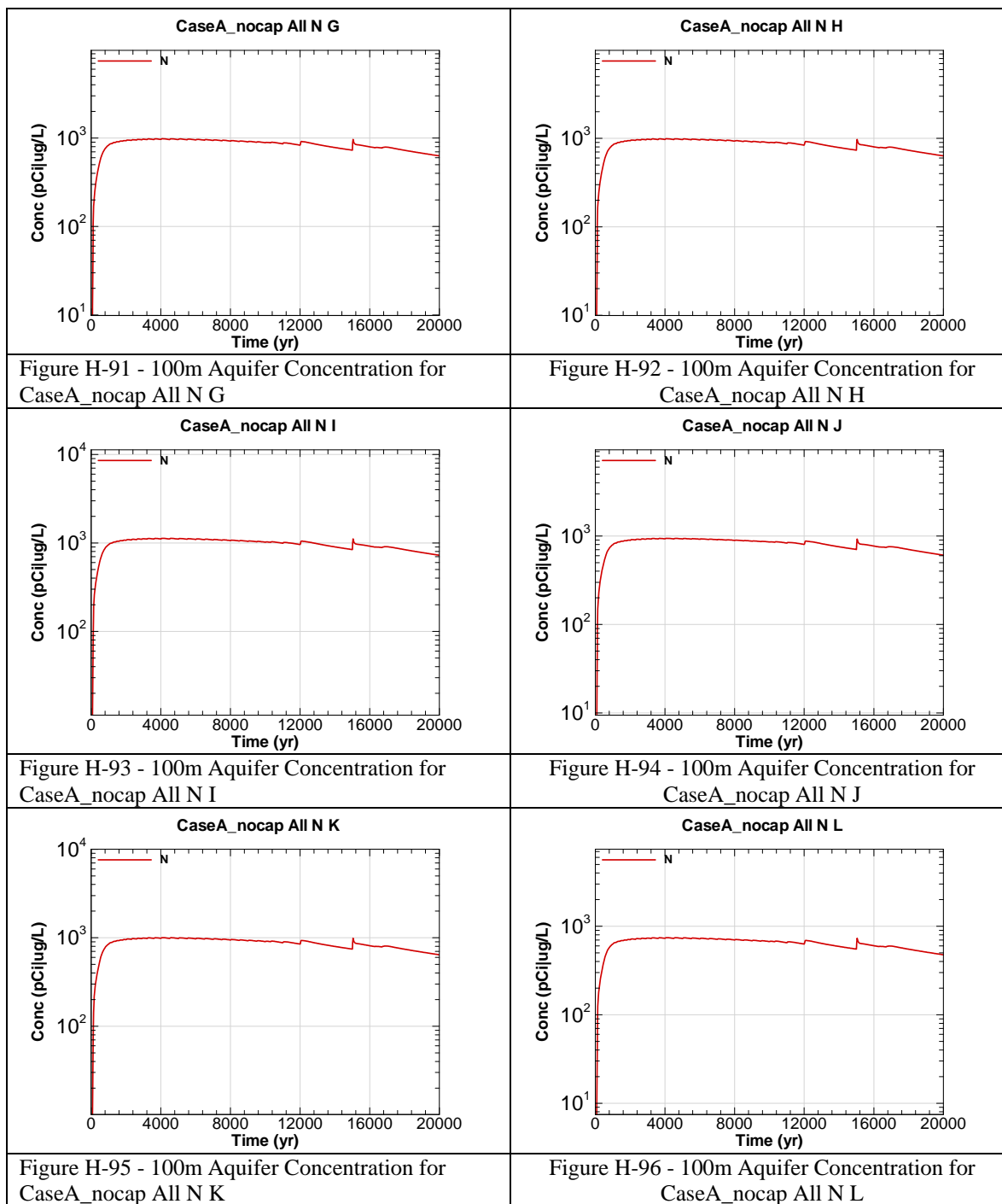


Figure H-84 - 100m Aquifer Concentration for CaseA_nocap All U-235 L





This page intentionally left blank

TABLE OF CONTENTS

| | |
|---|----|
| TABLE OF CONTENTS..... | 1 |
| LIST OF FIGURES | 1 |
| LIST OF TABLES | 2 |
| Purpose..... | 3 |
| Methodology | 3 |
| I1 Infiltration Rate through Engineered Closure Cap | 4 |
| I2 Chemistry Data | 5 |
| I3 Hydraulic Properties of Materials | 9 |
| I4 Disposal Unit Data..... | 13 |
| I5 Configuration Cases..... | 21 |
| I6 Radionuclide and Chemical Inventory..... | 26 |
| I7 Dose Conversion Factors and Dose Pathway Factors..... | 30 |
| I8 Other Stochastics in the GoldSim Probabilistic Model | 41 |
| I9 Summary | 43 |

LIST OF FIGURES

| | |
|--|----|
| Figure I1-1: Infiltration Rate, Analytical Values vs. Model Input | 5 |
| Figure I4-1: Comparison of Analytical Solution and Modeling Steps for FDC Wall Degradation..... | 19 |

LIST OF TABLES

| | |
|---|----|
| Table I1-1: Infiltration Rate from the SDF Engineered Closure Cap | 4 |
| Table I2-1: Pore Volumes for Chemical Transitions | 6 |
| Table I2-2: K_d Values (mL/g) for Elements in Soils and Cementitious Media | 7 |
| Table I2-3: Location of K_d Values in GoldSim v2.0stoch | 9 |
| Table I2-4: K_d Value Distribution | 9 |
| Table I3-1: Hydraulic Properties of Materials and Zones | 11 |
| Table I3-2: Characteristic Curves and Source of Data | 12 |
| Table I3-3: Material Properties in GoldSim | 12 |
| Table I4-1: Vault 1 Design and Modeling Parameters | 14 |
| Table I4-2: Summary of Degradation Analysis for Vault 1 | 15 |
| Table I4-3: Vault 4 Design and Modeling Parameters | 16 |
| Table I4-4: Summary of Degradation Analysis for Vault 4 | 17 |
| Table I4-5: FDC Design and PORFLOW Modeling Parameters | 17 |
| Table I4-6: Summary of Degradation Analysis for FDCs | 19 |
| Table I4-7: Disposal Unit Data in GoldSim v2.0stoch | 20 |
| Table I4-8: Disposal Unit Numbering Differences between SDF PA and GoldSim v2.0stoch | 21 |
| Table I5-1: Cases Postulated for SDF Vaults and FDCs | 22 |
| Table I5-2: Vault 1 Model Changes for Cases A, C, and E | 23 |
| Table I5-3: Vault 4 Model Changes for Cases A through E | 24 |
| Table I5-4: FDC Model Changes for Cases A through E | 25 |
| Table I5-5: Configuration Cases Stochastic in GoldSim v2.0stoch | 26 |
| Table I6-1: Radionuclide Inventory in the Disposal Units at Closure, Curies | 27 |
| Table I6-2: Radionuclide Inventory Uncertainty in the Disposal Units | 28 |
| Table I6-3: Chemical Inventory in the Disposal Units at Closure, Kg | 29 |
| Table I6-4: Chemical Discrepancy in Vault 4 and SDF Total Inventory | 30 |
| Table I7-1: Radionuclides with Roll-Up Dose Factors in GoldSim Models | 31 |
| Table I7-2: Dose Conversion Factors for Ingestion, Inhalation, and External Exposure | 32 |
| Table I7-3: Dissimilar Values in GoldSim Models | 34 |
| Table I7-4: Elemental Transfer Factors | 35 |
| Table I7-5: Crop Exposure Times and Productivity | 37 |
| Table I7-6: Physical Parameters | 38 |
| Table I7-7: Individual Exposure Times and Consumption Rates | 39 |
| Table I8-1: Width of Saturated Zone below the Disposal Units | 43 |

Purpose

The purpose of this appendix is to document the verification of the input data used for the modeling of the PORFLOW analysis being conducted by SRNL personnel for the SDF PA. In addition, parameters originating from this set of data that are utilized by SRNL personnel to conduct GoldSim simulation runs are verified within the GoldSim application. Finally, this data used in PORFLOW and GoldSim is further verified that it has been successfully transcribed into the SDF PA.

Note: Not included in this appendix is the radiological dose pathway methodology used to determine radiological exposure used in GoldSim.

Methodology

Data utilized by SRNL to perform PORFLOW computer simulations is provided in SRNL-STI-2009-00115. The data provided in SRNL-STI-2009-00115 for use in PORFLOW are verified by checking the data from references cited within the SDF PA.

Parameters used in the GoldSim simulation runs are verified by checking the data presented within the SDF PA to the values contained in the files (containers) within GoldSim. These parameters include:

- Disposal unit data
- Waste release parameters and K_d
- Material properties
- Ingestion and immersion dose conversion factors
- Buffer distance from each respective SDF disposal unit to the 100m boundary
- Ranges of values for parameters of interest to develop a stochastic model of potential radiological exposure

Notes:

1. Names of files or containers within the GoldSim application will be presented in *italics*.
2. Because the non-radiological (chemical) PA is based on concentration and not calculated “exposures”, GoldSim is not utilized to determine non-radiological PA. Therefore, input provided in GoldSim related to chemical attributes will not be verified.
3. The following radionuclides are not included in the GoldSim inventory: Ba-137m, Bk-249, Ce-144, Cf-252, Cm-242, Cs-134, Eu-155, Na-22, Pm-147, Pr-144, Rh-106, Ru-106, Sb-125, Sb-126, Sb-126m, Te-125m, and Y-90. These radionuclides are not included for various reasons (e.g., short half life, no dose conversion factor (DCF)) and none of these radionuclides have been shown to be “key radionuclides” to dose (as demonstrated in Section 5.2.2).
4. The data in two GoldSim models were checked for consistency (1) GoldSim model “saltstone v2.009.gsp” (for stochastic analysis) and (2) model “saltstone dose v1.117a.gsp” (a dose calculator using PORFLOW output concentrations). For brevity GoldSim model “saltstone v2.009.gsp” will be identified as “GoldSim v2.0stoch” and “saltstone dose v1.117a.gsp” will be identified as “GoldSim v1.1dose” within this appendix.

I1 Infiltration Rate through Engineered Closure Cap

Two conditions are analyzed in the PORFLOW model, (1) the proposed engineered cap design and (2) a “no closure cap” model, which is used solely as a sensitivity case. Table I1-1 provides the infiltration rate obtained from WSRC-STI-2008-00244. Figure I1-1 illustrates the analytical results presented in Table I1-1 and the PORFLOW model input values obtained from Figure 55 of SRNL-STI-2009-00115.

Table I1-1: Infiltration Rate from the SDF Engineered Closure Cap

| Time After Closure (years) | Annual Average Infiltration Rate | | | |
|----------------------------------|------------------------------------|---------|----------------------------------|---------|
| | With Engineered Cap ⁽¹⁾ | | No Engineered Cap ⁽²⁾ | |
| | (in/yr) | (cm/yr) | (in/yr) | (cm/yr) |
| 0 | 0.00042 | 0.00107 | 16.45 | 41.78 |
| 100 | 0.00333 | 0.00846 | 16.45 | 41.78 |
| 180 | 0.04520 | 0.115 | 16.45 | 41.78 |
| 220 | 0.05676 | 0.144 | 16.45 | 41.78 |
| 300 | 0.17110 | 0.435 | 16.45 | 41.78 |
| 380 | 0.47236 | 1.20 | 16.45 | 41.78 |
| 460 | 0.72342 | 1.84 | 16.45 | 41.78 |
| 560 | 1.0211 | 2.59 | 16.45 | 41.78 |
| 1,000 | 2.2638 | 5.75 | 16.45 | 41.78 |
| 1,800 | 4.340 | 11.02 | 16.45 | 41.78 |
| 3,200 | 6.795 | 17.26 | 16.45 | 41.78 |
| 5,412 | 10.6 | 26.92 | 16.45 | 41.78 |
| 5,600 | 10.6 | 26.92 | 16.45 | 41.78 |
| Thereafter | 10.6 | 26.92 | 16.45 | 41.78 |

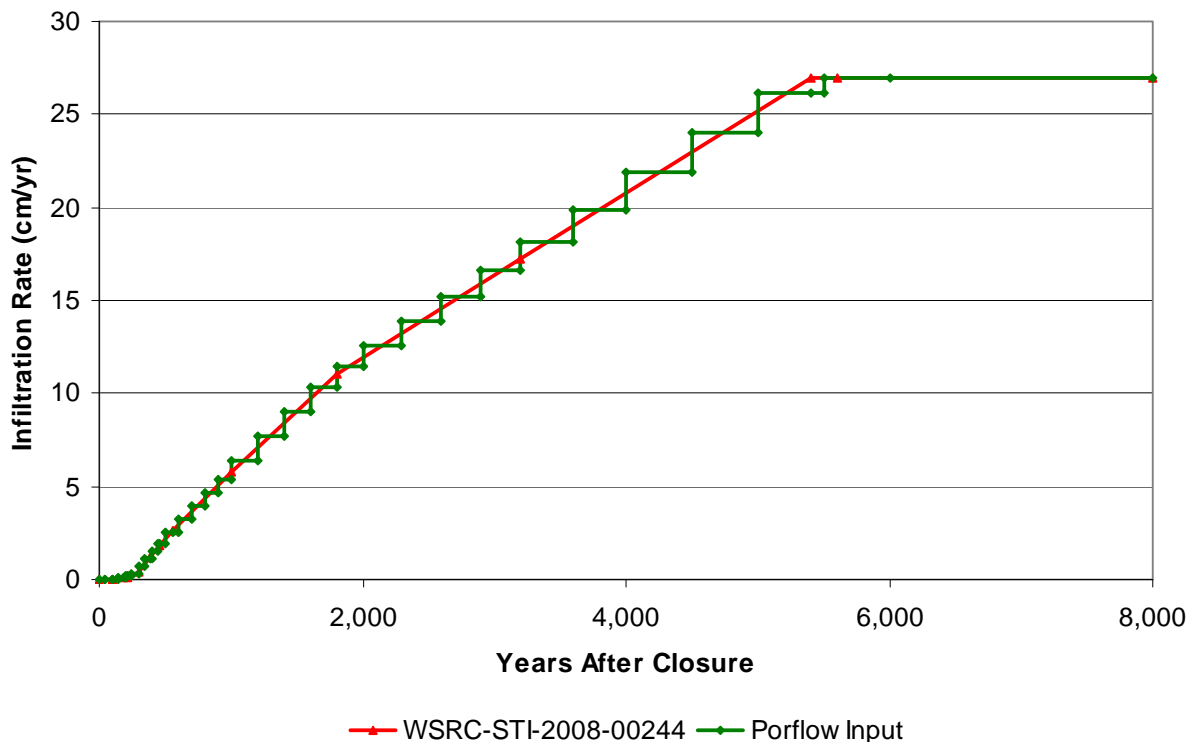
(1) Presented in SDF PA Table 3.2-7, obtained from WSRC-STI-2008-00244, Table 48, in “in/yr”.

(2) Presented in SDF PA Section 5.6.6.2, obtained from WSRC-STI-2008-00244, Section 6.7.3 in “in/yr”.

Note 1: Rate in “cm/yr” obtained by multiplying “in/yr” by 2.54 cm/in.

Note 2: GoldSim does not utilize the cap infiltration rates; rather it uses flow results from PORFLOW.

Figure I1-1: Infiltration Rate, Analytical Values vs. Model Input



I2 Chemistry Data

I2.1 Waste Release

The transport of contaminants from the SDF disposal units to the environment occurs from the leaching of contaminants from the saltstone grout by the pore fluid that infiltrates the saltstone grout. The mechanism generally controlling the release of contaminants from the saltstone is the adsorption characteristic of the saltstone expressed by the K_d value, which is element dependent and differs as the saltstone E_h and pH conditions change over time (e.g., from a reducing cementitious medium to an oxidized cementitious medium). Change in pH, or from reducing to oxidized states, is treated as a function of the pore water volume that travels through the saltstone matrix. The volume of pore water traveling through the saltstone matrix is dependent on the infiltration rate into the saltstone. An analysis documented in SRNL-TR-2008-00283 estimates the pore volume changes required for cementitious material to transition from reducing to oxidizing environments (E_h turns positive), and from middle age to old age (pH less than 11). The results from the SRNL-TR-2008-00283 analysis are provided in Table 4.2-9 of the SDF PA and Table 40 of SRNL-TR-2008-00115. Table I2-1 presents the pore volumes required for the given cementitious material, as shown in SDF PA Table 4.2-9, and the location of these values in GoldSim v2.0stoch. These transitions are used only for the Vault 4 roof, and the FDCs and Vault 4 walls. As indicated in SDF PA Table 4.2-17, the other cementitious material does not reach transition times prior to 20,000 years.

Table I2-1: Pore Volumes for Chemical Transitions

| Material | Transition | Volume | GoldSim v2.0stoch location |
|------------------------|----------------|--------|---|
| Saltstone ¹ | E _h | 2,806 | <i>VaultData : PoreFlushes : Mean_1stss</i> |
| Saltstone ¹ | pH | 10,422 | <i>VaultData : PoreFlushes : Mean_2ndss</i> |
| Vault concrete | E _h | 3,230 | <i>VaultData : PoreFlushes : Mean_1stc</i> |
| Vault concrete | pH | 4,206 | <i>VaultData : PoreFlushes : Mean_2ndc</i> |

(1) The Base Case in the SDF PA assumes no fast flow paths of infiltrate through the saltstone so the pore fluid is assumed to be groundwater equilibrated with CSH as indicated in Section 4.2.2 of the SDF PA.

Note that a stochastic has been included for this parameter, as discussed in SDF PA Section 5.6.3.4, with a range of $\pm 50\%$, as recommended in SRNL-TR-2008-00283. The stochastic parameters are provided in *Flushes_1stss* and *Flushes_2ndss* for saltstone, and *Flushes_1stc* and *Flushes_2ndc* for the vault concrete. These files are located under *VaultData: PoreFlushes*.

I2.2 K_d Values for Elemental Transport

The transport of elements through the various soil and cementitious layers is governed by K_d values that are developed through literature reviews, laboratory studies, and analyses. Table I2-2 provides the K_d values used in the SDF PA. As discussed above, the chemical stage of the cementitious material (reducing or oxidizing, middle age or old age) is affected by the number of pore volume changes within the saltstone grout and the disposal unit concrete. Depending on the chemical stage of the cementitious material, the appropriate K_d value is selected. The K_d values provided in Table I2-2 are provided in SDF PA Table 4.2-15 for soils and SDF PA Table 4.2-18 for cementitious material. The values in Table I2-2 are also found in Table 14 of SRNL-STI-2009-00115. Table I2-3 lists the files where the K_d values are located within GoldSim v2.0stoch. Note that zero K_d values cannot be handled appropriately within the GoldSim application; therefore a small value of 1E-09 is used or is assigned “*Epsilon*”, which is defined as a value of 1E-30. The K_d values in these files have been reviewed and no discrepancy was found.

As indicated in SDF PA Section 4.2.2 and SDF PA Figure 4.2-41, the K_d values for Tc-99 in a reducing medium are based on the reducing capacity within the material. Note that SDF PA Figure 4.2-41 indicates that the maximum K_d value is 1,000 rather than 5,000, as reported in SRNS-STI-2008-00045. This is not a discrepancy, but rather a different approach to the modeling of the release of Tc-99 in a reducing cementitious environment.

Note that in GoldSim v2.0stoch the K_d values for Tc-99 are assigned a value of 5,000 for all stages of reducing concrete with a BMF of 0.3 multiplied to the middle aged reducing concrete K_d value. A BMF of 500 was multiplied to the middle aged and old aged oxidizing concrete K_d values. The use of these BMFs in the GoldSim model are included for completeness, but are not considered a discrepancy.

GoldSim v1.1dose also includes files containing K_d values, but the dose calculator does not use these values and therefore the values in GoldSim v1.1dose have not been reviewed.

Table I2-2: K_d Values (mL/g) for Elements in Soils and Cementitious Media

| Element | Soils Media | | | Oxidizing Cementitious Media | | | | Reducing Cementitious Media | | | |
|---------|-------------|--------|------|------------------------------|------------|---------|------|-----------------------------|------------|---------|------|
| | Sandy | Clayey | Ref. | Young Age | Middle Age | Old Age | Ref. | Young Age | Middle Age | Old Age | Ref. |
| Ac | 1,100 | 8,500 | a | 6,000 | 6,000 | 600 | e | 5,000 | 5,000 | 1,000 | e |
| Ag (x) | 60 | 150 | b | 1 | 1 | 0.1 | e | 1 | 1 | 0.1 | e |
| Al | 1,300 | 1,300 | b | 6,000 | 6,000 | 600 | e | 5,000 | 5,000 | 1,000 | e |
| Am | 1,100 | 8,500 | a | 6,000 | 6,000 | 600 | e | 5,000 | 5,000 | 1,000 | f |
| Ar (x) | 0 | 0 | a | 0 | 0 | 0 | e | 0 | 0 | 0 | e |
| As (x) | 100 | 200 | b | 1,000 | 1,000 | 100 | e | 1,000 | 1,000 | 100 | e |
| At (x) | 0 | 0.6 | a | 8 | 15 | 4 | e | 2 | 10 | 4 | e |
| Ba (x) | 5 | 17 | a | 100 | 100 | 70 | e | 0.5 | 3 | 20 | e |
| Bk (x) | 1,100 | 8,500 | a | 6,000 | 6,000 | 600 | e | 5,000 | 5,000 | 1,000 | e |
| C | 0 | 0 | a | 20 | 10 | 0 | e | 20 | 10 | 0 | e |
| Cd | 4 | 10 | b | 4,000 | 4,000 | 1,000 | e | 5,000 | 5,000 | 1,000 | f |
| Ce (x) | 1,000 | 1,500 | b | 6,000 | 6,000 | 600 | e | 5,000 | 5,000 | 1,000 | f |
| Cf | 1,100 | 8,500 | a | 6,000 | 6,000 | 600 | e | 5,000 | 5,000 | 1,000 | e |
| Cl | 0 | 0 | a | 20 | 20 | 2 | e | 20 | 20 | 2 | e |
| Cm | 1,100 | 8,500 | a | 6,000 | 6,000 | 600 | e | 5,000 | 5,000 | 1,000 | e |
| Co | 7 | 30 | a | 4,000 | 4,000 | 1,000 | e | 5,000 | 5,000 | 1,000 | f |
| Cr | 4 | 10 | b | 20 | 20 | 2 | e | 5,000 | 5,000 | 1,000 | e |
| Cs | 50 | 250 | a | 2 | 20 | 10 | e | 0 | 2 | 10 | f |
| Cu | 50 | 70 | b | 1 | 1 | 0.1 | e | 1 | 1 | 0.1 | e |
| Eu | 1,100 | 8,500 | a | 6,000 | 6,000 | 600 | e | 5,000 | 5,000 | 1,000 | e |
| F | 0 | 0 | b | 20 | 20 | 2 | e | 20 | 20 | 2 | e |
| Fe | 200 | 400 | b | 6,000 | 6,000 | 600 | e | 5,000 | 5,000 | 1,000 | e |
| Fr (x) | 50 | 250 | a | 2 | 20 | 10 | e | 0 | 2 | 10 | e |
| Gd | 1,100 | 8,500 | a | 6,000 | 6,000 | 600 | e | 5,000 | 5,000 | 1,000 | e |
| H | 0 | 0 | a | 0 | 0 | 0 | e | 0 | 0 | 0 | e |
| Hg | 800 | 1,000 | b | 300 | 300 | 300 | e | 1,000 | 1,000 | 300 | f |
| I | 0 | 0.6 | a | 8 | 15 | 4 | e | 5 | 9 | 0 | f |
| K | 10 | 60 | b | 2 | 20 | 10 | e | 0 | 2 | 10 | e |
| Mn (x) | 15 | 200 | b | 100 | 100 | 10 | e | 100 | 100 | 10 | e |
| N | 0 | 0 | b | 0 | 0 | 0 | e | 0 | 0 | 0 | e |
| Na (x) | 5 | 25 | b | 0.5 | 1 | 0.5 | e | 0.5 | 1 | 0.5 | e |
| Nb | 0 | 0 | a | 1,000 | 1,000 | 500 | e | 1,000 | 1,000 | 500 | e |
| Ni | 7 | 30 | a | 4,000 | 4,000 | 1,000 | e | 5,000 | 5,000 | 1,000 | e |
| Np | 0.6 | 35 | a | 1,600 | 1,600 | 250 | e | 4,000 | 4,000 | 3,000 | f |
| Pa | 0.6 | 35 | a | 1,600 | 1,600 | 250 | e | 5,000 | 5,000 | 500 | f |

Table I2-2: K_d Values (mL/g) for Elements in Soils and Cementitious Media (Continued)

| Element | Soils Media | | | Oxidizing Cementitious Media | | | | Reducing Cementitious Media | | | |
|---------|-------------|--------|------|------------------------------|------------|---------|------|-----------------------------|------------|---------|------|
| | Sandy | Clayey | Ref. | Young Age | Middle Age | Old Age | Ref. | Young Age | Middle Age | Old Age | Ref. |
| Pb | 2,000 | 5,000 | a | 500 | 500 | 250 | e | 500 | 500 | 250 | e |
| Pd | 7 | 30 | b | 4,000 | 4,000 | 1,000 | e | 5,000 | 5,000 | 1,000 | e |
| Pm (x) | 0 | 0 | g | 0 | 0 | 0 | g | 0 | 0 | 0 | g |
| Po (x) | 2,000 | 5,000 | a | 500 | 500 | 250 | e | 500 | 500 | 250 | e |
| Pr (x) | 0 | 0 | g | 0 | 0 | 0 | g | 0 | 0 | 0 | g |
| Pt | 0 | 0 | g | 0 | 0 | 0 | g | 0 | 0 | 0 | g |
| Pu | 270 | 5,900 | a | 10,000 | 10,000 | 1,000 | c | 10,000 | 10,000 | 10,000 | c |
| Ra | 5 | 17 | a | 100 | 100 | 70 | e | 0.5 | 3 | 20 | e |
| Rb (x) | 50 | 250 | a | 2 | 20 | 10 | e | 0 | 2 | 10 | e |
| Re (x) | 0.1 | 0.2 | a | 0.8 | 0.8 | 0.5 | e | 5,000 | 5,000 | 5,000 | e |
| Rh (x) | 0 | 0 | g | 0 | 0 | 0 | g | 0 | 0 | 0 | g |
| Rn | 0 | 0 | a | 0 | 0 | 0 | e | 0 | 0 | 0 | e |
| Ru (x) | 0 | 0 | g | 0 | 0 | 0 | g | 0 | 0 | 0 | g |
| Sb | 2,500 | 2,500 | b | 100 | 100 | 2 | e | 5,000 | 5,000 | 1,000 | e |
| Se | 1,000 | 1,000 | a | 300 | 300 | 150 | e | 300 | 300 | 300 | f |
| Sm | 1,100 | 8,500 | a | 6,000 | 6,000 | 600 | e | 5,000 | 5,000 | 1,000 | e |
| Sn | 2,000 | 5,000 | a | 4,000 | 4,000 | 2,000 | e | 5,000 | 5,000 | 2,000 | f |
| Sr | 5 | 17 | a | 3 | 30 | 15 | e | 0.5 | 3 | 20 | f |
| Tc | 0.6 | 1.8 | c | 0.8 | 0.8 | 0.5 | e | 5,000 | 5,000 | 5,000 | e |
| Te (x) | 1,000 | 1,000 | a | 300 | 300 | 150 | e | 300 | 300 | 150 | e |
| Th | 900 | 2,000 | a | 5,000 | 5,000 | 500 | e | 5,000 | 5,000 | 500 | e |
| U | 200 | 300 | a | 250 | 250 | 70 | e | 2,500 | 2,500 | 2,500 | f |
| V (x) | 0 | 0 | g | 0 | 0 | 0 | g | 0 | 0 | 0 | g |
| Y (x) | 0 | 0 | g | 5,000 | 5,000 | 500 | e | 5,000 | 5,000 | 1,000 | f |
| Zn (x) | 100 | 200 | d | 4,000 | 4,000 | 1,000 | e | 5,000 | 5,000 | 1,000 | e |
| Zr | 900 | 2,000 | a | 5,000 | 5,000 | 500 | e | 5,000 | 5,000 | 500 | e |

(a) WSRC-TR-2006-00004, Table 10, Best Value

(b) SRNL-RPA-2007-00006

(c) SRNL-TR-2009-00019

(d) SRS-REG-2007-00036

(e) WSRC-STI-2007-00640

(f) SRNS-STI-2008-00045

(g) Assigned a value of zero (conservative assumption)

The elements annotated with an (x) are not included in GoldSim v2.0stoch, in some cases these elements relate to the isotopes not included in the GoldSim model, as discussed in the beginning of this appendix. The following elements: Ag, Ar, As, At, Fr, Mn, Po, Rb, Re, V, and Zn are either not in the SDF inventory (i.e., Ar, At, Fr, Po, Rb, Re and V), or are evaluated for chemical releases only (i.e., Ag, As, Mn, and Zn).

Table I2-3: Location of K_d Values in GoldSim v2.0stoch

| Material Zone | File Location [Materials :] |
|---------------------------|--|
| Clayey Soils | <i>ClayeySoilKds : Kd_Median</i> |
| Sandy Soils | <i>SandySoilKds : Kd_Median</i> |
| Young Oxidizing Concrete | <i>Concrete_Kds_Oxidizing : young_concrete_kds_ox : Kd_Median</i> |
| Middle Oxidizing Concrete | <i>Concrete_Kds_Oxidizing : middle_concrete_kds_ox : Kd_Median</i> |
| Old Oxidizing Concrete | <i>Concrete_Kds_Oxidizing : old_concrete_kds_ox : Kd_Median</i> |
| Young Reducing Concrete | <i>Concrete_Kds_Reducing : young_concrete_kds_ox : Kd_Median</i> |
| Middle Reducing Concrete | <i>Concrete_Kds_Reducing : middle_concrete_kds_ox : Kd_Median</i> |
| Old Reducing Concrete | <i>Concrete_Kds_Reducing : old_concrete_kds_ox : Kd_Median</i> |

GoldSim v2.0stoch also includes the stochastics associated with potential distribution of K_d values discussed in SDF PA Section 5.6.3.3. Based on SRNL-STI-2009-00150, the distribution selection is predicated on whether the applicable baseline K_d value is less than or greater than a certain value, as shown in Table I2-4. All the distributions are assumed to be lognormal, with their bounds driven by the baseline value, as shown in Table I2-4. The baseline value is defined as the GM of the distribution. The GoldSim files were reviewed and found to utilize the methodology presented in Table I2-4.

Table I2-4: K_d Value Distribution

| Material Zone | Minimum | Maximum | Log-Normal Geometric Standard Deviation | |
|----------------------------------|-----------|-----------|---|--------------------------|
| Clayey Soils (Backfill Layer) | 0.5 x GM | 1.5 x GM | GM < 4.0 mL/g | GM = 4.0 mL/g or greater |
| | | | 1.001 mL/g | 0.25 x GM |
| Sandy Soils (Vadose Zone) | 0.25 x GM | 1.75 x GM | GM < 2.7 mL/g | GM = 2.7 mL/g or greater |
| | | | 1.001 mL/g | 0.375 x GM |
| Cementitious Materials | 0.25 x GM | 1.75 x GM | GM < 2.7 mL/g | GM = 2.7 mL/g or greater |
| | | | 1.001 mL/g | 0.375 x GM |

I3 Hydraulic Properties of Materials

The transport of elements through the various cementitious and soil media is also influenced by the hydraulic properties of the media. Table I3-1 provides the material hydraulic properties for the various media used in the analysis. Included in this table is a cross reference to Table 13 of SRNL-STI-2009-00115 with the material labeled as identified in Table 13 within brackets “[]”.

The model also utilizes characteristic curves (relative permeability and suction head as functions of saturation) for the cementitious media and the soil media. The data used to develop those curves are from either WSRC-STI-2006-00198, WSRC-STI-2007-00649, or SRNL-STI-2009-00115, and are not reproduced here. Table I3-2 provides a cross-reference of the characteristic curves provided in the SDF PA and the source of the data used to generate the curves.

Hydraulic conductivity and the diffusion coefficient change for the various media as the media degrades. For the lower lateral drainage layer that is placed above each disposal unit, SDF PA Section 4.2.3.2.2 provides the change in hydraulic properties based on the analysis described in SRNL-STI-2009-00115, Section 3.2. SDF PA Figures 4.2-15 and 4.2-16 illustrate the change in conductivity and porosity for the lower lateral drainage layer based on Table 22 of SRNL-STI-2009-00115. The HDPE-GCL layer that lies above each FDC also undergoes degradation, as addressed in SDF PA Section 4.2.3.2.2 and evaluated in SRNL-STI-2009-00115, Section 3.4. SDF PA Figure 4.2-19 illustrates the change in conductivity and diffusion coefficient for the HDPE-GCL layer based on SRNL-STI-2009-00115, Table 23, columns 17 and 28, respectively. The degradation of the HDPE liner on the walls of each FDC is addressed in SDF PA Section 4.2.3.2.4, with SDF PA Figure 4.2-42 illustrating the change in conductivity and diffusion coefficient for the HDPE liner based on SRNL-STI-2009-00115, Table 23, columns 12 and 21, respectively. The degradation of the cementitious material via sulfate attack is discussed in Section I4.

Table I3-1: Hydraulic Properties of Materials and Zones

| Material | SDF PA Table | Bulk Density (g/cc) | Particle Density (g/cc) | Effective Porosity | Hydraulic Conductivity (cm/sec) | Diffusion Coefficient (cm²/sec) |
|---|---------------------|----------------------------|--------------------------------|---------------------------|--|---|
| Lower Lateral Drainage Layer ^a [sand_drain] | 4.2-12 | 1.65 | 2.66 | 0.417 | 5.0E-02 | 8.0E-06 |
| Backfill ^b [backfill] | 4.2-14 | 1.71 | 2.63 | 35 % | 7.6E-5 (h) 4.1E-5 (v) | 5.3E-6 |
| Lower Vadose ^b [native_soil] | 4.2-14 4.2-19 | 1.62 | 2.66 | 39 % | 3.3E-4 (h) 9.1E-5 (v) | 5.3E-6 |
| Saturated Zone ^c | 4.2-19 | 1.04 | 1.39 | 25 % | n. a. | Sandy – 5.3E-6 Clayey – 4.0E-6 |
| Gravel ^b [gravel] | 4.4-5 | 1.82 | 2.60 | 30 % | 1.5E-01 | 9.4E-06 |
| Low quality concrete ^d [concrete_mat] | 4.2-16 | 2.06 | 2.61 | 21.1 % | 1.0E-08 | 8.0E-07 |
| Medium quality concrete ^d [vault1_roof] | 4.2-16 | 2.20 | 2.57 | 14.5 % | 5.0E-09 | 1.0E-07 |
| Medium quality concrete ^d [vault4_roof] | 4.2-16 | 2.21 | 2.56 | 13.6 % | 5.0E-09 | 1.0E-07 |
| High quality concrete ^{e, f} [vault1_floor] | 4.2-16 | 2.24 | 2.55 | 12 % | 3.1E-10 | 5.0E-08 |
| Fractured walls in Vault 1 and 4 ^g | 4.2-16 | 2.24 | 2.55 | 12 % | 1.7E-01 | 5.0E-08 |
| High quality concrete ^{e, h} [vault2_roof] | 4.2-16 | 2.22 | 2.49 | 11 % | 9.3E-11 | 5.0E-08 |
| Saltstone and clean cap ^{e, i} | 4.2-16 | 1.01 | 2.40 | 58 % | 2.0E-09 | 1.0E-07 |
| HDPE-GCL layer ^{e, j} [HDPE_GCL] | Note 2 | 1.50 | 2.14 | 30 % | 2.8E-12 | 1.2E-10 |
| HDPE ^{e, j} [HDPE] | Note 3 | 1.50 | 2.14 | 30 % | 2.0E-13 | 4.0E-11 |

Note 1: Material name in Table 13 of SRNL-STI-2009-00115 is provided within brackets “[]”.

Note 2: Data provided in the text in SDF PA Section 4.2.3.2.2.

Note 3: Data provided in the text in SDF PA Section 4.2.3.2.4.

(a) WSRC-STI-2008-00244, after degradation parameters revert to Backfill material. Values for bulk density, particle density, and diffusion coefficient are taken from Table 13 of SRNL-STI-2009-00115 but were not presented in the SDF PA table.

(b) WSRC-STI-2006-00198, Table 5-18, values are shown in Table 13 of SRNL-STI-2009-00115 for “backfill” and “native-soil”, respectively.

(c) WSRC-STI-2006-00198, Section 5.6.1.

(d) Obtained from Table 6-47, WSRC-STI-2006-00198.

(e) Values obtained from Table 13 of SRNL-STI-2009-00115.

(f) Also applicable to [vault4_floor], [vault1_wall_uncracked], and [vault4_wall_uncracked].

(g) Based on analysis presented in SRNL-STI-2009-00115, Section 3.7 and applicable for [vault1_wall] and [vault4_wall].

(h) Values are also applicable to [vault2_wall] and [vault2_floor].

(i) Values are applicable to [saltstone] and [z_clean_cap].

(j) Values for bulk density, particle density, and porosity were not presented in the SDF PA text.

Table I3-2: Characteristic Curves and Source of Data

| Material or Media | SDF PA Figure | Data Source |
|-------------------------|---------------|---|
| Backfill | 4.2-17 | WSRC-STI-2006-00198, Table 5-21 |
| Lateral Drainage Layer | 4.2-18 | WSRC-STI-2006-00198, Table 5-20 (sand) |
| Lower Vadose Zone | 4.2-22 | WSRC-STI-2006-00198, Table 5-19 |
| Low Quality Concrete | 4.2-23 | WSRC-STI-2006-00198, Table 6-48 |
| Medium Quality Concrete | 4.2-24 | WSRC-STI-2006-00198, Table 6-48 (ordinary quality concrete) |
| High Quality Concrete | 4.2-25 | WSRC-STI-2006-00198, Table 6-48 |
| Fractured Concrete | 4.2-26 | SRNL-STI-2009-00115, Appendix D |
| Saltstone | 4.2-27 | WSRC-STI-2007-00649 |
| Gravel | 4.4-5 | WSRC-STI-2006-00198, Table 5-22 (gravel) |
| Degraded Saltstone | 4.4-8 | SRNL-STI-2009-00115, Appendix D |

The GoldSim stochastic and dose calculator models also use some of the hydraulic parameters identified in Table I3-1. Table I3-3 provides the data extracted from GoldSim v2.0stoch and GoldSim v1.1dose. Note that some of the parameters are not the same as used in PORFLOW being that the modeler may elect different values to benchmark the results between PORFLOW and GoldSim and thus the “correctness” of the values provided is not subject to review since the benchmarking process is described in SDF PA Section 5.6.2.

Table I3-3: Material Properties in GoldSim

| GoldSim v2.0stoch Container Materials | Table I3-1 Material/Zone | GoldSim v2.0stoch Value | |
|--|-----------------------------|---------------------------------------|--|
| | | Dry Bulk Density g/cm ³ | Particle Density (Porosity) g/cm ³ |
| <i>ClayeySoilProperties</i> | Backfill | 1.66 | 2.7 |
| <i>SandySoilProperties</i> | Lower Vadose | 1.62 | 2.66 |
| <i>SatSandySoilProperties</i> | Saturated Zone | 1.04 | 1.39 |
| <i>Vault_1_4FloorWall</i> | Fractured Walls | 2.24 | 2.55 |
| <i>Vault_1_Roof</i> | Vault 1 Roof | 2.2 | 2.57 |
| <i>Vault_2Concrete</i> | Vault 2 Concrete | 2.28 | 2.56 |
| <i>Vault_4_Roof</i> | Vault 4 Roof | 2.21 | 2.56 |
| <i>WasteProperties</i> | Saltstone | 1.01 | Porosity = 0.58 |
| GoldSim v1.1dose Container Materials | Table I3-1 Material/Zone | GoldSim v1.1 dose Value | |
| | | Dry Bulk Density | Particle Density (or Porosity) |
| <i>ClayeySoilProperties</i> | Backfill | 2.0 | 2.7 |
| <i>ConcreteProperties</i> | Vault concrete | 2.1 | 2.53 |
| <i>SandySoilProperties</i> | Lower Vadose | 1.62 | 2.66 |
| <i>SatSandySoilProperties</i> | Saturated Zone | 1.0425 | 1.39 |
| <i>WasteProperties</i> | Saltstone | 2.0 | Porosity = 0.259 |

I4 Disposal Unit Data

This section provides the data obtained from various sources for the physical data including site locations, elevations, and structural and material parameters for the disposal units.

I4.1 Disposal Unit Locations and Elevations

SDF PA Figure 3.1-5 and SRNL-STI-2009-00115 Figure 4 provide the anticipated layout for the SDF disposal units. For Vaults 1 and 4 (existing), and the FDCs 2A and 2B (under construction), the locations are obviously known, but for the remaining FDCs, the locations are only currently anticipated and the numbering are only placeholders that may not match the final disposal unit numbering. The model as described in the SDF PA and SRNL-STI-2009-00115 is based on this anticipated layout. Figure 14 of SRNL-STI-2009-00115 provides the anticipated layout for the SDF disposal units with the proposed closure cap configuration that was evaluated in WSRC-STI-2008-00244. SDF PA Figure 4.2-21 provides the average water table elevation. Based on the information provided in these figures, the vadose zone thickness (depth of soil beneath the disposal units) is estimated and presented in SDF PA Table 4.2-13 and SRNL-STI-2009-00115 Table 45.

I4.2 Vault 1 Design and Modeling Parameters

Table I4-1 provides the design and modeling parameters associated with Vault 1. The design parameters are presented in SDF PA Section 3.2.1.1 and the modeling parameters are provided in SDF PA Section 4.4.1.1 and Table 4.4-1. The modeling parameters are further reviewed in SRNL-STI-2009-00115 to verify the information used in the model and to identify any discrepancies.

Table I4-1: Vault 1 Design and Modeling Parameters

| Parameter | Design SDF PA Section 3.2.1.1 | Reference | Modeled SDF PA Section 4.4.1.1 | Verification of Model ¹ |
|---|-------------------------------------|---------------------------------------|---|---------------------------------------|
| Backfill layer ² | Not specified | WSRC-STI-2008-00244 | 4 feet | Figure 59 |
| Lower lateral drainage layer (LLDL) thickness | 24 inches | WSRC-STI-2008-00244, Table 4 | Same as design | Figure 59 |
| Roof thickness | 6 inches (min. with 2% slope) | C-CC-Z-0010 | Same as design | Figure 59, Table 30 |
| Clean grout cap thickness | 6 inches (minimum) | C-CC-Z-0010 | Same as design | Figure 59 |
| Saltstone grout thickness | 24 feet | WSRC-STI-2006-00198, Section 4.6.1 | Same as design | Figure 59 |
| Floor slab thickness | 24 inches | W780625 | Same as design | Figure 59, Table 29 |
| Working slab thickness | 4 inches | W780625 | Not in model | Not applicable |
| Native soil depth beneath vault | 48 feet (SDF PA Table 4.2-13) | See SDF PA Section 4.2.3.2.3 | Same as design | Figure 59 |
| Wall thickness | 18 inches | W780625 | Same as design | Figure 59, Table 28 |
| Vault height | 27 feet | W780625 | Not shown | Section 2.2.1 ³ |
| Vault width | 100 feet | W780625 | Not shown | Section 2.2.1 |
| Vault length | 600 feet | W780625 | Not shown | Section 2.2.1 |

(1) Model verification based on review of SRNL-STI-2009-00115 with cited reference(s).

(2) Backfill layer directly above the vault is based on WSRC-STI-2008-00244, Figure 6.

(3) SRNL-STI-2009-00115 Section 2.2.1 shows a height of 25 feet as measured from the top of the 2 foot thick concrete floor. The 27 foot dimension in SDF PA Section 3.2.1.1 is measured from the bottom of the concrete floor.

Degradation of Vault 1 Cementitious Materials

As described in SDF PA Section 4.2.3.2.4 and evaluated in SRNL-STI-2009-00115, Section 3.5; the vault concrete is susceptible to degradation from sulfate attack, and thus will experience changes in its hydraulic properties of conductivity and diffusion coefficient as it degrades. Table I4-2 summarizes the degradation analysis conducted and the results utilized in the model. SDF PA Figures 4.2-36 and 4.2-37 illustrate the degradation of the Vault 1 concrete relating to the increase in conductivity and diffusion coefficient, respectively, based on the results provided in SRNL-STI-2009-00115, Tables 28, 29, and 30

Table I4-2: Summary of Degradation Analysis for Vault 1

| Vault Concrete | Thickness | Initial Conductivity (cm/sec) | Initial Diffusion Coefficient (cm²/sec) | SRNL-STI-2009-00115 Analysis | Remarks |
|-----------------------|------------------|--------------------------------------|---|-------------------------------------|----------------|
| Wall | 18 inches | 1.7E-01 | 5.0E-08 | Table 28 | Note 1 |
| Floor | 24 inches | 3.1E-10 | 5.0E-08 | Table 29 | None |
| Roof | 12 inches | 5.0E-09 | 1.0E-07 | Table 30 | Note 2 |

Note 1: Table 28 is based on an un-fractured concrete wall (conductivity = 3.1E-10). SDF PA Figure 4.2-36 is based on the degradation factors provided in Table 28, but with the initial conductivity value shown for fractured concrete (1.7E-01).

Note 2: Based on a 2% slope and a 50 foot individual cell width, the roof thickness increases from 6 inches at the edge to 18 inches at the peak of the roof, and averages 12 inches.

I4.3 Vault 4 Design and Modeling Parameters

Table I4-3 provides the design and modeling parameters associated with Vault 4. The design parameters are presented in SDF PA Section 3.2.1.2 and the modeling parameters are provided in SDF PA Section 4.4.1.2 and Table 4.4-2. The modeling parameters are further reviewed in SRNL-STI-2009-00115 to verify the information used in the model and to identify any discrepancies.

Degradation of Vault 4 Cementitious Materials

Table I4-4 summarizes the degradation analysis conducted and the results utilized in the model. The degradation analysis conducted for the Vault 4 concrete is provided in SRNL-STI-2009-00115 Tables 34, 35, and 36. Note that because Tables 34 and 35 provide the same results as Tables 28 and 29, SDF PA Figures 4.2-36 and 4.2-37 also illustrate the changes in conductivity and diffusion coefficient for the Vault 4 wall and floor. Because of the different parameters for the Vault 4 roof, as shown in SRNL-STI-2009-00115 Table 36, Figure 4.2-38 is required to illustrate the changes in conductivity and diffusion coefficient for the Vault 4 roof.

Table I4-3: Vault 4 Design and Modeling Parameters

| Parameter | Design SDF PA Section 3.2.1.2 | Reference | Modeled SDF PA Section 4.4.1.2 | Verification of Model ¹ |
|--|------------------------------------|---------------------------------------|-----------------------------------|---------------------------------------|
| Backfill layer ² | Not specified | WSRC-STI-2008-00244 | 24 feet | Figure 61 |
| LLDL thickness | 24 inches | WSRC-STI-2008-00244 Table 4 | Same as design | Figure 61 |
| Roof thickness ³ | 6 inches (2% slope) | C-CS-Z-0002 | 4 inches | Figure 61, Table 36 |
| Clean grout cap thickness ³ | 15 inches (minimum) | WSRC-STI-2006-00198, Section 4.6.2 | 17 inches (minimum) | Figure 61 |
| Saltstone grout thickness | 24.75 feet | WSRC-STI-2006-00198, Section 4.6.2 | Same as design | Figure 61 |
| Floor slab thickness | 24 inches | W828993 | Same as design | Figure 61, Table 35 |
| Working slab thickness | 4 inches | W828993 | Not in model | Not applicable |
| Native soil depth beneath vault | 38.4 feet (SDF PA Table 4.2-13) | See SDF PA Section 4.2.3.2.3 | Same as design | Figure 61 |
| Wall thickness | 18 inches | W780625 | Same as design | Figure 61, Table 34 |
| Vault height | 30 feet | W828993, C-CC-Z-0013 | Not shown | Section 2.2.2 ⁴ |
| Vault width | 200 feet | W828992 | Not shown | Section 2.2.2 |
| Vault length | 600 feet | W828992 | Not shown | Section 2.2.2 |

(1) Model verification based on review of SRNL-STI-2009-00115 with cited reference.

(2) Backfill layer directly above the vault is based on WSRC-STI-2008-00244, Figure 6.

(3) The roof of Vault 4 is 6 inches thick and comprised of steel decking encapsulated in concrete. The model conservatively assumes that the roof is comprised of 4 inches of concrete with the remaining 2 inches incorporated into the clean grout cap.

(4) SRNL-STI-2009-00115 Section 2.2.2 shows a height of 26 feet. The 30 foot dimension in SDF PA Section 3.2.1.1 is measured from the bottom of the 2 foot thick concrete floor to the peak of the roof. Considering a 2% slope and a 100 foot length, the roof height increases by 2 feet from the wall to the high point of the roof. Thus, the height of the wall as measured from the top of the concrete floor is 26 feet.

Table I4-4: Summary of Degradation Analysis for Vault 4

| Vault Concrete | Thickness | Initial Conductivity (cm/sec) | Initial Diffusion Coefficient (cm ² /sec) | SRNL-STI-2009-00115 Analysis | Remarks |
|----------------|-----------|-------------------------------|--|------------------------------|--------------------------|
| Wall | 18 inches | 1.7E-01 | 5.0E-08 | Table 34 | See Note 1 of Table I4-2 |
| Floor | 24 inches | 3.1E-10 | 5.0E-08 | Table 35 | None |
| Roof | 4 inches | 5.0E-09 | 1.0E-07 | Table 36 | None |

Table I4-5: FDC Design and PORFLOW Modeling Parameters

| Parameter | Design SDF PA Section 3.2.1.3 | Reference | Modeled SDF PA Section 4.4.1.3 | Verification of Model ¹ |
|---|-------------------------------|---|--------------------------------|------------------------------------|
| Backfill layer thickness ² | Not specified | WSRC-STI-2008-00244 | 7 feet | Figure 60 |
| LLDL thickness | 24 inches | WSRC-STI-2008-00244, Table 4 | Same as design | Figure 60 |
| HDPE-GCL layer thickness above roof ³ | 0.3 inch | WSRC-STI-2008-00244, Table 4 and Section 4.4 | 1 inch | Figure 60, Table 23 |
| Roof thickness | 8 inches | WB00001K-004 | Same as design | Figure 60, Table 33 |
| Grout cap thickness | 24 inches (minimum) | WSRC-STI-2006-00198, Section 4.6.3 and WB00001K-004 | Same as design | Figure 60 |
| Saltstone grout thickness | 20 feet | WSRC-STI-2006-00198, Section 4.6.3 | Same as design | Figure 60 |
| Floor slab thickness | 8 inches | WB00001K-004 | Same as design | Figure 60, Table 32 |
| Upper mud mat thickness | 4 inches | WB00001K-004 | Same as design | Figure 60, Table 32 |
| HDPE-GCL layer thickness above lower mud mat ³ | 0.3 inch | C-SPP-Z-00006, Section 02378 and 02379 | 1 inch | Figure 60, Table 23 |
| Lower mud mat thickness | 4 inches | WB00001K-004 | Same as design | Figure 60 |
| Native soil depth beneath FDC | 42 feet (SDF PA Table 4.2-13) | See SDF PA Section 4.2.3.2.3 | Same as design | Figure 60 |

Table I4-5: FDC Design and PORFLOW Modeling Parameters (Continued)

| Parameter | Design SDF PA Section 3.2.1.3 | Reference | Modeled SDF PA Section 4.4.1.3 | Verification of Model ¹ |
|----------------------------------|-------------------------------------|------------------------------|---|---------------------------------------|
| Wall thickness | 8 inches | WB00001K-004 | Same as design | Figure 60, Table 31 |
| Shotcrete thickness ⁴ | 2.3 inches | WB00001K-004 | 6 inches | Figure 60 |
| HDPE liner ⁵ | 0.1 inch | C-SPP-Z-00006, Section 02378 | 1 inch | Figure 60, Table 23 |
| Height | 22 feet | WB00001K-004 | Not shown | Section 2.2.3 |
| Diameter | 150 feet | WB00001K-004 | Not shown | Section 2.2.3 |

- (1) Model verification based on review of SRNL-STI-2009-00115 with cited reference(s).
- (2) Backfill layer directly above the FDCs is based on WSRC-STI-2008-00244, Figures 6 and 7.
- (3) As indicated in SDF PA Section 4.4.1.3, and SRNL-STI-2009-00115 Section 4.5, the use of a 1 inch layer thickness is compensated for by increasing the hydraulic conductivity provided in SDF PA Figure 4.2-19 by 3.33 (= 1/0.3).
- (4) The references cited indicate that shotcrete will cover the exterior of the wall to protect the 26 gauge steel diaphragm and prestress wiring system. Based on these references an average value of 2.3 inches is stated in the PA. The model includes 6 inches of shotcrete, but with hydraulic parameters of backfill. However, the PORFLOW model used Oxidizing Concrete for the material zone to select the K_d values. See Discrepancy I4-1.
- (5) As indicated in SDF PA Section 4.4.1.3 and SRNL-STI-2009-00115 Section 4.5, the use of a 1 inch layer thickness is compensated for by increasing the hydraulic conductivity provided in SDF PA Figure 4.2-42 by 10 (= 1/0.1)

Discrepancy I4-1:

The PORFLOW model assumes a thickness of six inches to the shotcrete zone; however the average value is 2.3 inches. The PORFLOW model assigned “Oxidizing Concrete” as the material zone for the selection of appropriate K_d values for the shotcrete zone. The material zone for assignment of K_d values for the shotcrete zone should be backfill (clayey soil). The impact on this discrepancy is addressed in the Summary, Section I9.

Degradation of FDC Cementitious Materials

Table I4-6 summarizes the degradation analysis conducted and the results utilized in the model. The degradation analysis conducted for the FDC concrete is provided in SRNL-STI-2009-00115 Tables 31, 32, and 33. SDF PA Figure 4.2-39 illustrates the changes in conductivity and diffusion coefficient for the FDC roof and floor (including the upper mud mat) based on SRNL-STI-2009-00115 Tables 32 and 33. SDF PA Figure 4.2-40 illustrates the changes in conductivity and diffusion coefficient for the FDC wall based on SRNL-STI-2009-00115, Table 31.

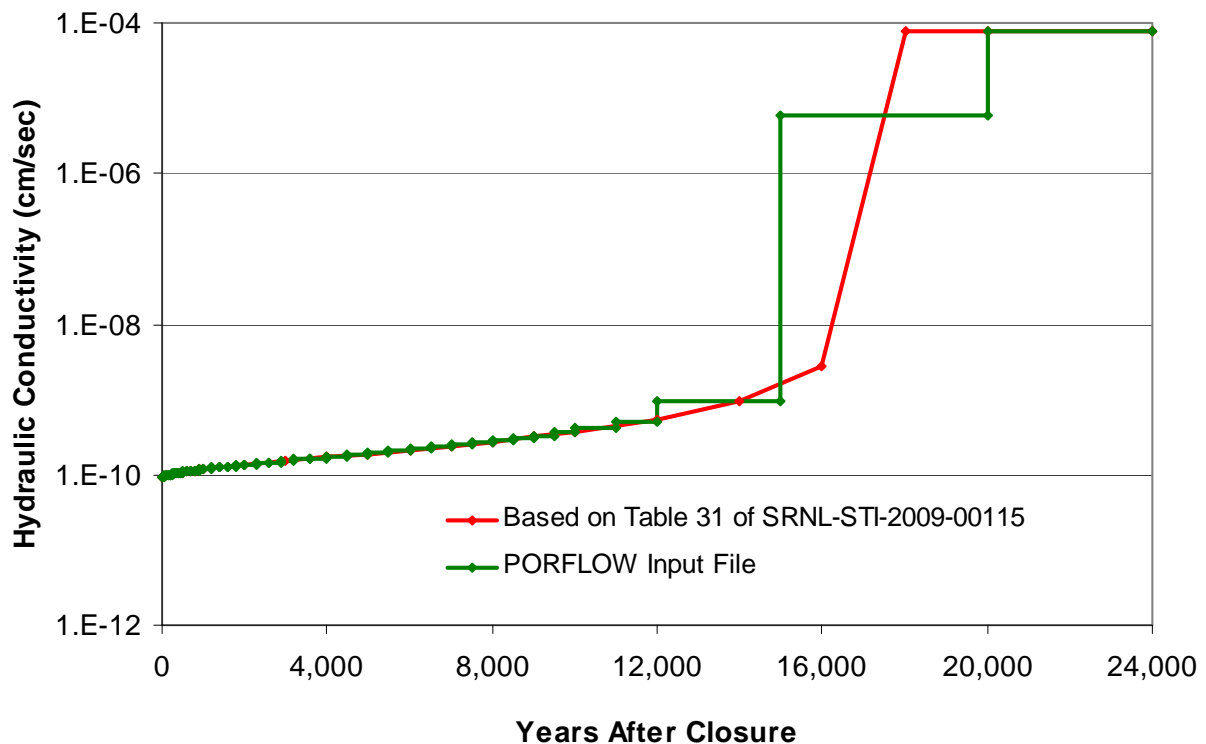
Table I4-6: Summary of Degradation Analysis for FDCs

| Vault Concrete | Thickness | Initial Conductivity (cm/sec) | Initial Diffusion Coefficient (cm ² /sec) | SRNL-STI-2009-00115 Analysis | Remarks |
|----------------|-----------|-------------------------------|--|------------------------------|------------|
| Wall | 8 inches | 9.3E-11 | 5.0E-08 | Table 31 | See Note 1 |
| Floor | 12 inches | 9.3E-11 | 5.0E-08 | Table 32 | See Note 2 |
| Roof | 4 inches | 9.3E-11 | 5.0E-08 | Table 33 | None |

Note 1: As indicated in SDF PA Figure 4.2-40 and SRNL-STI-2009-00115 Table 31, the degradation of the wall is expected 18,000 years after SDF closure. However, review of the modeling input (SRNL-STI-2009-00115, Appendix E) indicates that the time step changes utilized show almost a 60,000 fold increase in the hydraulic conductivity at 15,000 years after closure. Figure I4-1 illustrates the difference between the analytical solution and the step changes in the model.

Note 2: The value of 12 inches is used to acknowledge that the 8 inch thick floor and the 4 inch upper mud mat are both comprised of the same cementitious material. Review of the modeling input (SRNL-STI-2009-00115, Appendices E and F) indicates that the parameters for the floor and upper mud mat are identical.

Figure I4-1: Comparison of Analytical Solution and Modeling Steps for FDC Wall Degradation



I4.5 Disposal Unit Data in GoldSim

GoldSim v2.0stoch is essentially a transport model used to simulate the transport of radionuclides from the SDF disposal units to the saturated zone. The flow results obtained from PORFLOW are utilized by GoldSim v2.0stoch as the transport mechanism; however, GoldSim v2.0stoch uses disposal unit data, transition times, K_d values (described in I2), and hydraulic properties of various materials (described in I3) to perform the radionuclide-specific transport analysis. The disposal unit data used in GoldSim v2.0stoch is identified in Table I4-7.

Table I4-7: Disposal Unit Data in GoldSim v2.0stoch

| Parameter | Vault 1 | Vault 4 | FDCs | Remarks |
|---|-------------|-------------|-----------|---------|
| Data obtained from GoldSim v2.0stoch container <i>TheVaults</i> : <i>VaultData</i> | | | | |
| Height | 27 feet | 28.5 feet | 20 feet | Note 1 |
| Length | 600 feet | 600 feet | NA | None |
| Width | 49.2 feet | 98.4 feet | NA | Note 2 |
| Radius | NA | NA | 75 feet | None |
| Native soil depth beneath disposal unit | 50 feet | 40 feet | 42 feet | Note 3 |
| Data obtained from GoldSim v2.0stoch container <i>TheVaults</i> : | | | | |
| Saltstone grout height | 23.95 feet | 26.25 feet | 20 feet | Note 4 |
| Floor thickness | 23.6 inches | 23.6 inches | 16 inches | Note 5 |
| Wall thickness | 17.7 inches | 17.7 inches | 8 inches | None |

- Note 1: Vault 4 height is 1.5 feet higher than the design value and the height of the FDCs is 2 feet shorter than the design value. These differences are not expected to have a significant effect on the modeling, especially since benchmarking has been performed.
- Note 2: Stated widths for Vault 1 and Vault 4 consider the use of symmetry along the centerline and the interior dimensions.
- Note 3: Stated soil depth for Vault 1 is 2 feet deeper than the design value and the stated soil depth for Vault 4 is 1.6 feet deeper than the design value. These differences are not expected to have a significant effect on the modeling, especially since benchmarking has been performed.
- Note 4: The Vault 4 saltstone grout height is 1.5 feet higher than the design value which is not expected to have a significant effect on the modeling, especially since benchmarking has been performed.
- Note 5: The floor thickness of the FDCs includes the thickness of the floor and the upper and lower mud mat. Because the PORFLOW modeling results are dominated by the flow and transport through the walls, this difference is not expected to have any significant impact, especially since benchmarking has been performed. In addition, the 16 inches of floor is assumed to be reducing cementitious material even though the lower mud mat is oxidizing cementitious material.

In addition to the data presented above, GoldSim requires additional data to simulate the flow of contaminants from the waste zone based on output from PORFLOW. SDF PA Figure 4.4-70 depicts the streaming data from PORFLOW for the various disposal units to the 100m boundary. The shortest distance to the 100m boundary is estimated and provided in SDF PA Table 5.2-2 and in the GoldSim container *DoseAssessment : ExposureMediaConc : SectorLocations : Centerline_Mean* for each of the disposal units. Note that GoldSim v2.0stoch has different disposal unit numbering than provided in SDF PA Figure 4.2-20 and Table 5.2-2. Table I4-8 provides a correspondence between SDF PA Table 5.2-2 and the GoldSim v2.0stoch model where differences exist with the numbering of the disposal units.

Table I4-8: Disposal Unit Numbering Differences between SDF PA and GoldSim v2.0stoch

| GoldSim v2.0stoch | SDF PA Table 5.2-2 | GoldSim v2.0stoch | SDF PA Table 5.2-2 | GoldSim v2.0stoch | SDF PA Table 5.2-2 |
|----------------------|-----------------------|----------------------|-----------------------|----------------------|-----------------------|
| 13A | 3A | 16C | 15C | 19A | 18A |
| 13B | 3B | 16D | 15D | 19B | 18B |
| 14A | 13A | 17A | 16A | 19C | 18C |
| 14B | 13B | 17B | 16B | 19D | 18D |
| 14C | 13C | 17C | 16C | 20A | 19A |
| 14D | 13D | 17D | 16D | 20B | 19B |
| 15A | 14A | 18A | 17A | 21A | 20A |
| 15B | 14B | 18B | 17B | 21B | 20B |
| 16A | 15A | 18C | 17C | 21C | 20C |
| 16B | 15B | 18D | 17D | 21D | 20D |

I5 Configuration Cases

SDF PA Section 4.4.2 describes the conceptual scenario cases associated with the SDF model. SDF PA Table 4.4-4 is repeated below as Table I5-1 for convenience in the following discussion. Because GoldSim v2.0stoch uses the flow results from PORFLOW and the GoldSim v1.1dose uses the radionuclide concentrations from PORFLOW, the PORFLOW modeling input, provided in SRNL-STI-2009-00115, is reviewed for consistency with the description provided in SDF PA Section 4.4.2.

Table I5-1: Cases Postulated for SDF Vaults and FDCs

| Case | Vault 1 | Vault 4 | FDCs |
|------|--|---|--|
| A | <u>Base Case</u> vault wall degraded, saltstone intact | <u>Base Case</u> vault wall degraded, saltstone intact | <u>Base Case</u> disposal unit wall intact, saltstone intact |
| B | N/A (no sheet drains) | <u>Fast flow walls</u> fast flow along walls from roof thru floor, vault wall degraded | <u>Fast flow walls</u> fast flow along walls from roof thru floor (including upper and lower mud mats) |
| C | <u>Fast flow walls & crack</u> fast flow along cracks from roof thru floor, vault wall degraded | <u>Fast flow walls & crack</u> fast flow along walls and cracks from roof thru floor vault wall degraded | <u>Fast flow walls & columns</u> fast flow along walls and columns from roof thru floor (including upper and lower mud mats) |
| D | N/A (no sheet drains) | <u>Capillary break</u> Base Case with capillary break at sheet drains | <u>Capillary break</u> Base Case with capillary break at sheet drains |
| E | <u>Saltstone severely degraded</u> vault wall degraded | <u>Saltstone severely degraded</u> vault wall degraded | <u>Saltstone severely degraded</u> disposal unit wall intact |

Appendices E and F of SRNL-STI-2009-00115 are used to verify the PORFLOW model inputs for the various cases. In the summary tables I5-2, I5-3, and I5-4, the term “Sorption material” refers to the material medium used to determine K_d values and the term “Hydraulic material” refers to the material medium used for hydraulic properties. The hydraulic parameters of horizontal conductivity (k_h) and vertical conductivity (k_v) are specifically included in the summary tables.

I5.1 Vault 1 Configuration Cases

As presented in Table I5-1 and discussed in SDF PA Section 4.4.2.1, Vault 1 does not contain sheet drains, so only Cases A, C, and E are applicable to Vault 1. Using Table 46 and Appendices E and F of SRNL-STI-2009-00115, Table I5-2 provides a summary of the PORFLOW changes between the various cases. Parameters that are unchanged between the different cases are not included in this summary table.

Table I5-2: Vault 1 Model Changes for Cases A, C, and E

| Material Region | Parameter | Case A | Case C | Case E |
|--------------------|-------------------------|------------------------------|-------------------|----------------------------------|
| Crack ¹ | k _h (cm/sec) | 2.0E-09 | 1.5E-01 | 1.7E-03 |
| | k _v (cm/sec) | 5.0E-15 | 1.5E-01 | 5.0E-15 |
| | Hydraulic Material | Saltstone | Gravel | Fractured Saltstone ⁴ |
| | Sorption Material | Reducing Middle ² | None ³ | Reducing Middle ² |
| Saltstone grout | k _h (cm/sec) | 2.0E-09 | 2.0E-09 | 1.7E-03 |
| | k _v (cm/sec) | 2.0E-09 | 2.0E-09 | 1.7E-03 |
| | Hydraulic Material | Saltstone | Saltstone | Fractured Saltstone ⁴ |
| | Sorption Material | Reducing Middle ² | None ³ | Reducing Middle ² |

(1) Material zone within model to simulate fast flow path in Case C.

(2) Reducing middle age concrete

(3) K_d value assumed to be zero

(4) Fractured Saltstone is the material defined for degraded saltstone.

I5.2 Vault 4 Configuration Cases

As presented in Table I5-1 and discussed in SDF PA Section 4.4.2.2, Vault 4 contains sheet drains, so Cases A through E are applicable to Vault 4. Using Table 46 and Appendices E and F of SRNL-STI-2009-00115, Table I5-3 provides a summary of the PORFLOW changes between the various cases. Parameters that are unchanged between the different cases are not included in this summary table.

Table I5-3: Vault 4 Model Changes for Cases A through E

| Material Region | Parameter | Case A | Case B | Case C | Case D | Case E |
|--------------------------|--------------------|------------------------------|------------------------------|------------------------------|------------------------------|----------------------------------|
| Crack ¹ | k_h (cm/sec) | 2.0E-09 | 2.0E-09 | 1.5E-01 | 2.0E-09 | 1.7E-03 |
| | k_v (cm/sec) | 5.0E-15 | 5.0E-15 | 1.5E-01 | 5.0E-15 | 5.0E-15 |
| | Hydraulic Material | Saltstone | Saltstone | Gravel | Saltstone | Fractured Saltstone ⁵ |
| | Sorption Material | Reducing Middle ³ | Reducing Middle ³ | None ⁴ | Reducing Middle ³ | Reducing Middle ³ |
| Sheet Drain ² | k_h (cm/sec) | 2.0E-09 | 1.5E-01 | 1.5E-01 | 5.0E-15 | 1.7E-03 |
| | k_v (cm/sec) | 5.0E-15 | 1.5E-01 | 1.5E-01 | 5.0E-15 | 5.0E-15 |
| | Hydraulic Material | Saltstone | Gravel | Gravel | Saltstone | Fractured Saltstone ⁵ |
| | Sorption Material | Reducing Middle ³ | None ⁴ | None ⁴ | None ⁴ | Reducing Middle ³ |
| Saltstone grout | k_h (cm/sec) | 2.0E-09 | 2.0E-09 | 2.0E-09 | 2.0E-09 | 1.7E-03 |
| | k_v (cm/sec) | 2.0E-09 | 2.0E-09 | 2.0E-09 | 2.0E-09 | 1.7E-03 |
| | Hydraulic Material | Saltstone | Saltstone | Saltstone | Saltstone | Fractured Saltstone ⁵ |
| | Sorption Material | Reducing Middle ³ | Reducing Middle ³ | Reducing Middle ³ | Reducing Middle ³ | Reducing Middle ³ |

(1) Material zone within model to simulate fast flow path in Case C.

(2) Material zone within model to simulate fast flow path in Cases B and C.

(3) Reducing middle age concrete.

(4) K_d value assumed to be zero.

(5) Fractured saltstone is the material defined for degraded saltstone.

I5.3 FDC Configuration Cases

As presented in Table I5-1 and discussed in SDF PA Section 4.4.2.3, the FDCs contain sheet drains, so Cases A through E, are applicable to the FDCs. Using Table 46 and Appendices E and F of SRNL-STI-2009-00115, Table I5-4 provides a summary of the PORFLOW changes between the various cases. Parameters that are unchanged between the different cases are not included in this summary table.

Table I5-4: FDC Model Changes for Cases A through E

| Material Region | Parameter | Case A | Case B | Case C | Case D | Case E |
|--------------------------|-------------------------|------------------------------|------------------------------|------------------------------|------------------------------|----------------------------------|
| Column ¹ | k _h (cm/sec) | 2.0E-09 | 2.0E-09 | 5.0E-04 | 2.0E-09 | 1.7E-03 |
| | k _v (cm/sec) | 5.0E-15 | 5.0E-15 | 2.8E-04 | 5.0E-15 | 5.0E-15 |
| | Hydraulic Material | Saltstone | Saltstone | Sand | Saltstone | Fractured Saltstone ⁵ |
| | Sorption Material | Reducing Middle ³ | Reducing Middle ³ | None ⁴ | Reducing Middle ³ | Reducing Middle ³ |
| Sheet Drain ² | k _h (cm/sec) | 2.0E-09 | 1.5E-01 | 1.5E-01 | 5.0E-15 | 1.7E-03 |
| | k _v (cm/sec) | 5.0E-15 | 1.5E-01 | 1.5E-01 | 5.0E-15 | 5.0E-15 |
| | Hydraulic Material | Saltstone | Gravel | Gravel | Saltstone | Fractured Saltstone ⁵ |
| | Sorption Material | Reducing Middle ³ | None ⁴ | None ⁴ | None ⁴ | Reducing Middle ³ |
| Saltstone grout | k _h (cm/sec) | 2.0E-09 | 2.0E-09 | 2.0E-09 | 2.0E-09 | 1.7E-03 |
| | k _v (cm/sec) | 2.0E-09 | 2.0E-09 | 2.0E-09 | 2.0E-09 | 1.7E-03 |
| | Hydraulic Material | Saltstone | Saltstone | Saltstone | Saltstone | Fractured Saltstone ⁵ |
| | Sorption Material | Reducing Middle ³ | Reducing Middle ³ | Reducing Middle ³ | Reducing Middle ³ | Reducing Middle ³ |

(1) Material zone within model to simulate fast flow path in Case C.

(2) Material zone within model to simulate fast flow path in Cases B and C.

(3) Reducing middle age concrete.

(4) K_d value assumed to be zero.

(5) Fractured Saltstone is the material defined for degraded saltstone.

I5.4 Configuration Cases in GoldSim Model

Because the GoldSim SDF model is used only to model contaminant transport; flow profiles over time are calculated for each of the five cases using the PORFLOW SDF model and the results of the PORFLOW runs are manipulated to simulate a 1-D model that is used by GoldSim v2.0stoch. SDF PA Section 5.6.3.1 discusses the development of the stochastic for the various configuration cases, which is used in GoldSim v2.0stoch. SDF PA Table 5.6-3, reproduced below in Table I5-5, includes the GoldSim v2.0stoch locations, which were verified to contain the same data as the SDF PA table. Within GoldSim 2.0stoch the Cases A through E are labeled as 1 through 5.

Table I5-5: Configuration Cases Stochastic in GoldSim v2.0stoch

| Case | Probability by Disposal Unit Type | | |
|----------------------------------|---|---|---|
| | Vault 1 | Vault 4 | FDCs |
| A | 95 % | 85 % | 85 % |
| B | 0 % | 5 % | 5 % |
| C | 4.9 % | 4.9 % | 4.9 % |
| D | 0 % | 5 % | 5 % |
| E | 0.1 % | 0.1 % | 0.1 % |
| GoldSim v2.0stoch location | <i>TheVaults: Vault_1: VaultFlows: Configurations</i> | <i>TheVaults: Vault_4: VaultFlows: Configurations</i> | <i>TheVaults: Vault_2: VaultFlows: Configurations</i> |

I6 Radionuclide and Chemical Inventory

I6.1 Radionuclide Inventory

Table I6-1 presents the radionuclide inventory in the disposal units presented in SDF PA Tables 3.3-1, 3.3-3, and 3.3-5, which are from SRNS-J2100-2008-00004. Note that the model applies a factor of 2 to the Vault 1 inventory to account for the fact that three of the six cells are available for future disposal of low-level contaminated sources, as stated in SDF PA Section 3.3.

The inventory tables in SRNL-STI-2009-00115 Tables 7, 9, and 11 were reviewed and found to be consistent with the SDF PA tables. Review of other SRNL Saltstone data files confirms that the factor of 2 was applied to the Vault 1 inventory.

GoldSim v2.0stoch contains the inventories for Vaults 1 and 4 in *Inventory: SouthVaultSourceMultipliers : NominalSouthSourceMult*. For the FDCs, the inventory is provided in *Inventory: Tank_to_Vault: NominalMult_Vault2*. The following radionuclides are not input into the GoldSim model: Ba-137m, Bk-249, Ce-144, Cf-252, Cm-242, Cs-134, Eu-155, Na-22, Pm-147, Pr-144, Rh-106, Ru-106, Sb-125, Sb-126, Sb-126m, Te-125m, and Y-90. The inventory for Vault 1 was doubled in the GoldSim v2.0stoch files. All other inventories provided in the GoldSim model have been verified to be consistent with the SDF PA.

I6.2 Radionuclide Inventory Stochastic

SDF PA Section 5.6.3.2 discusses the stochastic analysis associated with the radionuclide inventory in the SDF vaults and FDCs. The data provided in SDF PA Table 5.6-4 is reproduced in Table I6-2, which includes the names of the GoldSim v2.0stoch files that were reviewed to verify the data input into GoldSim v2.0stoch. GoldSim v2.0stoch includes specific uncertainty stochastics for the following radionuclides, which are included in the “All others” category in SDF PA Table 5.6-4 and Table I6-2: I-129, Np-237, and Tc-99. The inventory distribution associated with location variability described in SDF PA Section 5.6.3.2 is coded within the GoldSim v2.0stoch within the container *Tank_to_Vault*.

Table I6-1: Radionuclide Inventory in the Disposal Units at Closure, Curies

| Radionuclide | Vault 1 | Vault 4 | FDC | Radionuclide | Vault 1 | Vault 4 | FDC |
|--------------|---------|---------|---------|--------------|---------|---------|---------|
| Ac-227 | N/A | 1.6E-05 | 1.7E-07 | Pa-231 | N/A | 9.3E-05 | 9.8E-07 |
| Al-26 | N/A | 3.4E-01 | 1.9E-01 | Pd-107 | 1.9E-03 | 5.0E-02 | 5.6E-03 |
| Am-241 | 4.7E-04 | 1.3E+02 | 1.4E+00 | Pm-147 | N/A | 4.1E-01 | 7.7E-02 |
| Am-242m | N/A | 6.7E-02 | 5.9E-04 | Pr-144 | N/A | 1.8E-09 | 3.6E-10 |
| Am-243 | N/A | 1.8E+00 | 3.7E-02 | Pt-193 | 3.7E-01 | 1.0E+01 | 1.1E+00 |
| Ba-137m | 4.1E+00 | 2.8E+05 | 2.2E+01 | Pu-238 | 7.8E-03 | 9.1E+03 | 1.7E+02 |
| Bk-249 | N/A | 1.8E-28 | 1.8E-28 | Pu-239 | 1.2E-02 | 3.8E+02 | 1.5E+01 |
| C-14 | 1.3E+00 | 2.7E+01 | 2.0E+00 | Pu-240 | 1.2E-02 | 1.2E+02 | 4.1E+00 |
| Ce-144 | N/A | 1.8E-09 | 3.6E-10 | Pu-241 | 9.8E-03 | 2.4E+03 | 4.2E+01 |
| Cf-249 | N/A | 6.5E-13 | 6.7E-13 | Pu-242 | 9.0E-04 | 8.1E-01 | 3.9E-03 |
| Cf-251 | N/A | 1.2E+00 | 2.3E-14 | Pu-244 | N/A | 1.6E-02 | 1.6E-05 |
| Cf-252 | N/A | 1.8E-18 | 1.8E-18 | Ra-226 | 6.4E-07 | 4.1E+00 | 7.8E-07 |
| Cl-36 | 7.6E-04 | 3.0E-03 | 4.2E-04 | Ra-228 | N/A | 1.6E-06 | 8.7E-05 |
| Cm-242 | N/A | 6.7E-02 | 6.3E-19 | Rh-106 | 1.5E-10 | 9.1E-07 | 1.2E-06 |
| Cm-243 | N/A | 2.1E-01 | 2.1E-04 | Ru-106 | 1.5E-10 | 9.1E-07 | 1.2E-06 |
| Cm-244 | N/A | 1.3E+02 | 9.5E-01 | Sb-125 | 1.6E-01 | 5.7E+00 | 2.4E-01 |
| Cm-245 | N/A | 9.2E-01 | 2.4E-04 | Sb-126 | 1.4E-01 | 9.0E-01 | 1.2E+00 |
| Cm-247 | N/A | 3.9E-06 | 7.1E-14 | Sb-126m | 1.0E+00 | 6.4E+00 | 8.2E+00 |
| Cm-248 | N/A | 1.2E-13 | 7.4E-14 | Se-79 | 3.0E-01 | 4.6E+01 | 1.4E+00 |
| Co-60 | 8.2E-05 | 4.6E-01 | 5.4E-02 | Sm-151 | N/A | 4.2E+01 | 5.9E+01 |
| Cs-134 | N/A | 5.2E-01 | 1.5E-05 | Sn-126 | 1.0E+00 | 6.4E+00 | 8.2E+00 |
| Cs-135 | N/A | 5.4E+00 | 1.3E-04 | Sr-90 | 6.9E-03 | 2.4E+05 | 3.7E+01 |
| Cs-137 | 4.3E+00 | 3.0E+05 | 2.3E+01 | Tc-99 | 1.1E+02 | 5.8E+02 | 5.4E+02 |
| Eu-152 | 1.8E-03 | 9.7E-02 | 9.8E-02 | Te-125m | 3.8E-02 | 1.4E+00 | 5.8E-02 |
| Eu-154 | 2.3E-04 | 1.2E+01 | 1.8E+00 | Th-229 | 3.0E-01 | 2.5E+01 | 3.9E-02 |
| Eu-155 | N/A | 6.8E-01 | 1.3E-01 | Th-230 | 4.1E-01 | 7.5E+00 | 1.9E-01 |
| H-3 | 6.1E+00 | 2.6E+02 | 3.0E+01 | Th-232 | N/A | 3.2E-04 | 1.4E-03 |
| I-129 | 1.1E-01 | 2.8E-01 | 3.8E-01 | U-232 | N/A | 4.4E-02 | 3.1E-04 |
| K-40 | 7.6E-04 | 3.0E-03 | 4.2E-04 | U-233 | 2.8E-01 | 2.4E+01 | 3.7E-02 |
| Na-22 | N/A | 1.5E-01 | 6.9E-02 | U-234 | 2.8E-01 | 2.6E+01 | 1.3E-01 |
| Nb-93m | 2.5E-01 | 8.4E+00 | 3.7E-01 | U-235 | 3.2E-03 | 4.7E-01 | 3.0E-03 |
| Nb-94 | 2.5E-03 | 8.7E-02 | 3.8E-03 | U-236 | 3.2E-03 | 7.7E-01 | 1.6E-02 |
| Ni-59 | 3.5E-02 | 4.0E-01 | 8.4E-02 | U-238 | 7.4E-03 | 5.9E-01 | 1.0E-01 |
| Ni-63 | 7.8E-01 | 2.2E+01 | 2.4E+00 | Y-90 | 6.9E-03 | 2.4E+05 | 3.7E+01 |
| Np-237 | 4.5E-03 | 6.1E-01 | 5.0E-02 | Zr-93 | 2.4E-01 | 8.4E+00 | 3.7E-01 |

Note 1: Radionuclides that are shaded are not included in the GoldSim v2.0stoch model.

Note 2: The inventory in Vault 1 is doubled in the PORFLOW and GoldSim models to account for future contaminated sources in the three remaining cells of Vault 1.

Table I6-2: Radionuclide Inventory Uncertainty in the Disposal Units

| Radionuclide | Minimum | Maximum | GoldSim File - Vault 1 ^a | GoldSim File - Vault 4 ^b | GoldSim File For FDCs ^c |
|--------------|----------|---------|-------------------------------------|-------------------------------------|---|
| C-14 | x 0.1 | x 10 | <i>C14u</i> | <i>C14u</i> | <i>InventoryUncertainty_dist</i> and data tables providing the minimum and maximum values for each radionuclide |
| Cs-137 | 1 | x 10 | <i>Cs137u</i> | <i>Cs137u</i> | |
| Pu-239 | x 0.1 | x 10 | <i>Pu239u</i> | <i>Pu239u</i> | |
| Sr-90 | x 0.001 | 1 | <i>Sr90u</i> | <i>Sr90u</i> | |
| U-238 | x 0.0001 | x 10 | <i>U238u</i> | <i>U238u</i> | |
| All others | x 0.1 | x 10 | <i>Otheru</i> | <i>Otheru</i> | |

(a) Located in Inventory: InventoryUncertainty: Vault1Uncert

(b) Located in Inventory: InventoryUncertainty: Vault4Uncert

(c) Located in Inventory: InventoryUncertainty: Vault2Uncert

GoldSim v2.0stoch was revised from the earlier versions to reflect the revised uncertainty distribution described in SDF PA Section 5.6.3.2. Review of the GoldSim v2.0stoch files found a discrepancy with the distribution for Tc-99 in Vault 1. This discrepancy is described below. No other discrepancies were found.

Discrepancy I6-1:

The inventory uncertainty of Tc-99 in Vault 1 utilized a GSD of 1.0001 rather than 1.1 as specified in SDF PA Section 5.6.3.2. The impact of this discrepancy is presented in the Summary, Section I9.

I6.3 Chemical Inventory

Table I6-3 presents the chemical inventory in the disposal units presented in SDF PA Tables 3.3-2, 3.3-4, and 3.3-6, which are obtained from SRNS-J2100-2008-00004. Note that the model applies a factor of 2 to the Vault 1 inventory to account for the fact that three of the six cells are available for future disposal of low-level contaminated sources, as stated in SDF PA Section 3.3.

The inventory tables in SRNL-STI-2009-00115 Tables 8, 10, and 12 were reviewed and found to be consistent with the SDF PA tables except for the inventory in Vault 4 for a number of chemicals. Discrepancy I6-1, provided below, gives the details. Review of other SRNL Saltstone data files confirms that the factor of 2 was applied to the Vault 1 inventory. Because GoldSim is not used to evaluate chemical transport, the chemical inventories are not included in the GoldSim models.

Table I6-3: Chemical Inventory in the Disposal Units at Closure, Kg

| Chemical | Vault 1 | Vault 4 | FDC |
|-----------------|---------|---------|---------|
| Ag | 2.0E+01 | 2.7E+01 | 3.4E-01 |
| As | 4.4E+01 | 1.0E+03 | 1.6E+02 |
| Ba | 2.0E+01 | 2.6E+01 | 1.7E+00 |
| Cd | 3.9E+02 | 3.8E+01 | 8.0E+00 |
| Cr | 1.8E+02 | 3.5E+03 | 4.0E+02 |
| Cu | N/A | 8.8E+02 | 2.9E+02 |
| F | N/A | 3.5E+03 | 2.0E+02 |
| Fe | N/A | 6.9E+02 | 3.5E+01 |
| Hg | 1.5E+00 | 9.8E+02 | 1.5E+02 |
| Mn | N/A | 4.1E+02 | 1.1E+02 |
| Ni | N/A | 8.9E+01 | 2.2E+01 |
| NO ₂ | 7.4E-01 | 4.0E+05 | 7.7E+04 |
| NO ₃ | 3.4E+01 | 4.3E+06 | 2.2E+05 |
| Pb | 2.3E+01 | 4.5E+02 | 9.7E+01 |
| Se | 6.1E+01 | 5.2E+03 | 5.5E+02 |
| U | N/A | 2.8E+02 | 9.6E+00 |
| Zn | N/A | 1.3E+03 | 4.0E+02 |

Note: The inventory in Vault 1 is doubled in the PORFLOW model to account for the future contaminated sources in the three remaining cells of Vault 1.

Discrepancy I6-2:

The chemicals identified below in Table I6-4 have inventories provided in SDF PA Table 3.3-4 for Vault 4 that differ from the inventory used in the PORFLOW analysis shown in Table 10 of SRNL-STI-2009-00115. To account for the differences between the current SDF PA chemical inventory and the inventory modeled in PORFLOW, an adjustment factor is applied to concentration results obtained from PORFLOW. The adjustment factor is one plus the percent difference of the SDF PA inventory to the PORFLOW model inventory for the individual chemical. The adjustment factors have been applied to SDF PA Tables 5.2-12 through 5.2-20 for the 100m distance, and SDF PA Tables 6.1-10 through 6.1-18 for the 1m distance.

Table I6-4: Chemical Discrepancy in Vault 4 and SDF Total Inventory

| Chemical | Vault 4 Inventory | | SDF Total Inventory | | |
|-----------------|--------------------|----------|-----------------------------------|----------|-------------------|
| | SDF PA Table 3.3-4 | PORFLOW | SDF PA Model Total ^(a) | PORFLOW | Adjustment Factor |
| As | 1.01E+03 | 7.61E+02 | 1.10E+04 | 1.08E+04 | 1.02 |
| Cr | 3.50E+03 | 3.08E+03 | 2.98E+04 | 2.93E+04 | 1.01 |
| Cu | 8.76E+02 | 7.05E+02 | 1.94E+04 | 1.92E+04 | 1.01 |
| NO ₂ | 4.01E+05 | 4.01E+05 | 5.34E+06 | 5.34E+06 | - - |
| NO ₃ | 4.32E+06 | 2.95E+06 | 1.82E+07 | 1.68E+07 | - - |
| U | 2.80E+02 | 2.00E+02 | 8.95E+02 | 8.15E+02 | 1.10 |
| Total N | 4.72E+06 | 3.35E+06 | 2.35E+07 | 2.22E+07 | 1.06 |

(a) The SDF PA Model Total is the total of the individual chemicals in SDF PA Table 3.3-8 plus the Vault 1 inventory in SDF PA Table 3.3-2 to account for the potential use of the three remaining empty cells in Vault 1.

(b) Total N is used in the model based on the sum of NO₂ and NO₃

I7 Dose Conversion Factors and Dose Pathway Factors

Dose pathway factors and DCFs are used by the GoldSim models v2.0stoch and v1.1dose to compute the dose from various pathways and at various locations. GoldSim model v2.0stoch is used to develop the sensitivity analyses for the various probability distributions of parameters and thus uses the flow results from PORFLOW as the starting point of its analysis. GoldSim model v1.1dose is used to calculate the doses for the various cases by using the actual PORFLOW concentrations of the various radionuclides at discrete locations to determine radiological exposure. Verification of the DCF data and the dose pathway factor data requires the review of both GoldSim models.

I7.1 Dose Conversion Factors

Table I7-1 provides the dose factors for the radionuclides of interest in the SDF PA modeling. SDF PA Table 4.7-1 lists the internal and external DCFs for a large number of radionuclides and Table I7-1 is a subset of SDF PA Table 4.7-1 and only includes those radionuclides in the GoldSim modeling. Thus, the conversion factors for Ba-137m, Bk-249, Ce-144, Cf-252, Cm-242, Cs-134, Eu-155, Na-22, Pm-147, Pr-144, Rh-106, Ru-106, Sb-125, Sb-126, Sb-126m, Te-125m, and Y-90 are not included in Table I7-1.

The dose factors can be found in the following GoldSim files within GoldSim v2.0stoch and GoldSim v1.1dose. The values are the same in either GoldSim model.

| Dose Factor | GoldSim v2.0stoch |
|--------------------------|--|
| Ingestion | <i>DoseFactorIngestionNotRolledUp</i> ¹ |
| Inhalation | <i>InhalationDCFNotRolledUp</i> ¹ |
| External soil (15 cm) | <i>Ex15cmSoilNotRolledUp</i> ² |
| External soil (infinite) | Not used in model |
| Water Submergence | <i>DFSubmergedNotRolledUp</i> ¹ |

(1) Located in *DoseAssessment: DoseParameters: LADTAP_Factors*

(2) Located in *DoseAssessment: IHI*

No discrepancies were found between the data referenced above and the data provided in the SDF PA.

Within the GoldSim models a number of radionuclides have roll-up dose factors to account for the daughters that are not tracked within the model. Therefore, they will have dose factors greater than those presented in Table I7-2. The radionuclides with roll-up dose factors in the GoldSim models are listed below with their daughters identified.

Table I7-1: Radionuclides with Roll-Up Dose Factors in GoldSim Models

| Radionuclides with Roll-ups | Daughters Included in the Rollup Calculation within GoldSim |
|------------------------------------|--|
| Ac-227 | Th-227, Fr-223, Ra-223, Rn-219, Po-215, Pb-211, Bi-211, and Tl-207 |
| Am-242m | Np-238, Am-242, and Cm-242 |
| Am-243 | Np-239 |
| Cm-247 | Pu-243 |
| Cs-137 | Ba-137m |
| Np-237 | Pa-233 |
| Pu-244 | U-240, Np-240m, and Np-240 |
| Ra-228 | Ac-228, Th-228, Ra-224, Rn-220, Po-216, Pb-212, Bi-212, Po-212, and Tl-208 |
| Rn-222 | Po-218, Pb-214, Bi-214, and Po-214 |
| Sn-126 | Sb-126m and Sb-126 |
| Sr-90 | Y-90 |
| Th-229 | Ra-225, Ac-225, Fr-221, At-217, Bi-213, Po-213, Tl-209, and Pb-209 |
| U-235 | Th-231 |
| U-238 | Th-234, Pa-234m, and Pa-234 |

Table I7-2: Dose Conversion Factors for Ingestion, Inhalation, and External Exposure

| Radionuclide | Ingestion (rem/ μ Ci) | Inhalation (rem/ μ Ci) | External Infinite (rem/yr per μ Ci /m ³) | External 15 cm depth (rem/yr per μ Ci /m ³) | Water Immersion (rem/yr per μ Ci /m ³) |
|--------------|------------------------------|-------------------------------|--|---|---|
| Ac-227 | 4.07E+00 | 2.04E+03 | 3.10E-07 | 3.06E-07 | 1.52E-06 |
| Al-26 | 1.30E-02 | 7.40E-02 | 1.09E-02 | 9.03E-03 | 3.43E-02 |
| Am-241 | 7.40E-01 | 1.55E+02 | 2.73E-05 | 2.73E-05 | 2.20E-04 |
| Am-242m | 7.03E-01 | 1.37E+02 | 1.06E-06 | 1.05E-06 | 8.50E-06 |
| Am-243 | 7.40E-01 | 1.52E+02 | 8.88E-05 | 8.88E-05 | 5.77E-04 |
| C-14 | 2.15E-03 | 7.40E-03 | 8.41E-09 | 8.41E-09 | 5.13E-08 |
| Cf-249 | 1.30E+00 | 2.59E+02 | 1.16E-03 | 1.07E-03 | 4.03E-03 |
| Cf-251 | 1.33E+00 | 2.63E+02 | 3.29E-04 | 3.22E-04 | 1.45E-03 |
| Cl-36 | 3.44E-03 | 2.70E-02 | 1.50E-06 | 1.42E-06 | 5.23E-06 |
| Cm-243 | 5.55E-01 | 1.15E+02 | 3.64E-04 | 3.53E-04 | 1.52E-03 |
| Cm-244 | 4.44E-01 | 9.99E+01 | 7.87E-08 | 7.87E-08 | 1.34E-06 |
| Cm-245 | 7.77E-01 | 1.55E+02 | 2.13E-04 | 2.10E-04 | 1.03E-03 |
| Cm-247 | 7.03E-01 | 1.44E+02 | 1.11E-03 | 1.03E-03 | 3.82E-03 |
| Cm-248 | 2.85E+00 | 5.55E+02 | 5.49E-08 | 5.49E-08 | 9.30E-07 |
| Co-60 | 1.26E-02 | 3.70E-02 | 1.01E-02 | 8.47E-03 | 3.20E-02 |
| Cs-135 | 7.40E-03 | 2.55E-03 | 2.39E-08 | 2.39E-08 | 1.28E-07 |
| Cs-137 | 4.81E-02 | 1.70E-02 | 4.70E-07 | 4.60E-07 | 1.74E-06 |
| Eu-152 | 5.18E-03 | 1.55E-01 | 4.38E-03 | 3.76E-03 | 1.44E-02 |
| Eu-154 | 7.40E-03 | 1.96E-01 | 4.80E-03 | 4.11E-03 | 1.55E-02 |
| H-3 | 6.66E-05 | 1.67E-04 | 0.00E+00 | 0.00E+00 | 0.00E+00 |
| K-40 | 2.29E-02 | 7.77E-03 | 6.51E-04 | 5.34E-04 | 2.03E-03 |
| I-129 | 4.07E-01 | 1.33E-01 | 8.09E-06 | 8.09E-06 | 1.04E-04 |
| Nb-93m | 4.44E-04 | 1.89E-03 | 6.51E-08 | 6.51E-08 | 1.21E-06 |
| Nb-94 | 6.29E-03 | 4.07E-02 | 6.05E-03 | 5.29E-03 | 1.95E-02 |
| Ni-59 | 2.33E-04 | 4.81E-04 | 0.00E+00 | 0.00E+00 | 0.00E+00 |
| Ni-63 | 5.55E-04 | 1.78E-03 | 0.00E+00 | 0.00E+00 | 0.00E+00 |
| Np-237 | 4.07E-01 | 8.51E+01 | 4.87E-05 | 4.86E-05 | 2.71E-04 |
| Pa-231 | 2.63E+00 | 5.18E+02 | 1.19E-04 | 1.12E-04 | 4.42E-04 |
| Pb-210 | 2.55E+00 | 4.07E+00 | 1.53E-06 | 1.53E-06 | 1.53E-05 |
| Pd-107 | 1.37E-04 | 2.18E-03 | 0.00E+00 | 0.00E+00 | 0.00E+00 |
| Pu-238 | 8.51E-01 | 1.70E+02 | 9.46E-08 | 9.43E-08 | 1.33E-06 |
| Pu-239 | 9.25E-01 | 1.85E+02 | 1.85E-07 | 1.78E-07 | 1.12E-06 |

**Table I7-2: Dose Conversion Factors for Ingestion, Inhalation and External Exposure
(Continued)**

| Radionuclide | Ingestion (rem/μCi) | Inhalation (rem/μCi) | External Infinite (rem/yr per μCi /m³) | External 15 cm depth (rem/yr per μCi /m³) | Water Immersion (rem/yr per μCi /m³) |
|---------------------|--------------------------------|---------------------------------|--|---|--|
| Pu-240 | 9.25E-01 | 1.85E+02 | 9.17E-08 | 9.16E-08 | 1.30E-06 |
| Pu-241 | 1.78E-02 | 3.33E+00 | 3.69E-09 | 3.68E-09 | 1.89E-08 |
| Pu-242 | 8.88E-01 | 1.78E+02 | 8.00E-08 | 8.00E-08 | 1.09E-06 |
| Pu-244 | 8.88E-01 | 1.74E+02 | 4.72E-08 | 4.72E-08 | 8.13E-07 |
| Ra-226 | 1.04E+00 | 1.30E+01 | 1.99E-05 | 1.93E-05 | 8.12E-05 |
| Ra-228 | 2.55E+00 | 9.62E+00 | 0.00E+00 | 0.00E+00 | 0.00E+00 |
| Rn-222 | 0.00E+00 | 0.00E+00 | 1.47E-06 | 1.33E-06 | 4.86E-06 |
| Se-79 | 1.07E-02 | 4.07E-03 | 1.16E-08 | 1.16E-08 | 6.93E-08 |
| Sm-151 | 3.63E-04 | 1.48E-02 | 6.16E-10 | 6.16E-10 | 9.93E-09 |
| Sn-126 | 1.74E-02 | 1.04E-01 | 9.22E-05 | 9.23E-05 | 5.56E-04 |
| Sr-90 | 1.04E-01 | 1.33E-01 | 4.40E-07 | 4.34E-07 | 1.71E-06 |
| Tc-99 | 2.37E-03 | 1.48E-02 | 7.85E-08 | 7.83E-08 | 3.67E-07 |
| Th-229 | 1.81E+00 | 2.63E+02 | 2.01E-04 | 1.99E-04 | 1.00E-03 |
| Th-230 | 7.77E-01 | 5.18E+01 | 7.56E-07 | 7.46E-07 | 4.60E-06 |
| Th-232 | 8.51E-01 | 9.25E+01 | 3.26E-07 | 3.25E-07 | 2.32E-06 |
| U-232 | 1.22E+00 | 2.89E+01 | 5.64E-07 | 5.57E-07 | 3.76E-06 |
| U-233 | 1.89E-01 | 1.33E+01 | 8.74E-07 | 8.46E-07 | 4.25E-06 |
| U-234 | 1.81E-01 | 1.30E+01 | 2.51E-07 | 2.50E-07 | 2.04E-06 |
| U-235 | 1.74E-01 | 1.15E+01 | 4.51E-04 | 4.38E-04 | 1.86E-03 |
| U-236 | 1.74E-01 | 1.18E+01 | 1.34E-07 | 1.33E-07 | 1.35E-06 |
| U-238 | 1.67E-01 | 1.07E+01 | 6.45E-08 | 6.45E-08 | 9.29E-07 |
| Zr-93 | 4.07E-03 | 3.70E-02 | 0.00E+00 | 0.00E+00 | 0.00E+00 |

I7.2 Dose Pathway Factors

Dose pathway factors are those factors used in the model to simulate the uptake of radionuclides from various pathways and include parameters associated with the transfer of radionuclides from the groundwater to the soil, into the food chain, and human and animal consumption rates. A number of these factors have a distribution associated with them to be used in the stochastic analysis discussed in SDF PA Section 5.6.3.7.

I7.3 Bioaccumulation Transfer Factors

Table I7-4 repeats the transfer factors found in SDF PA Tables 4.6-1 (soil-to-vegetable transfer), 4.6-2 (feed-to-milk transfer), 4.6-3 (feed-to-meat transfer), and 4.6-4 (water-to-fish transfer) for the radionuclides evaluated in the GoldSim models.

The transfer factors can be found in the following GoldSim files within GoldSim v2.0stoch and GoldSim v1.1dose. The values are the same in either GoldSim model except as noted in Table I7-3.

Table I7-3: Dissimilar Values in GoldSim Models

| <u>Transfer Factor</u> | <u>GoldSim v2.0stoch or v1.1dose</u> |
|-------------------------------|---|
| • Soil-to-Plant | • <i>PlantToSoilRatio</i> ¹ |
| • Feed-to-Milk | • <i>TransferFractionMilk</i> ¹ |
| • Feed-to-Meat | • <i>TransferFractionBeef</i> ¹ |
| • Water-to-Fish | • <i>BioaccumulationFactorAq</i> ² |

(1) Located in *DoseAssessment: DoseParameters: IRRIDOSE_Factors*

(2) Located in *DoseAssessment: DoseParameters: LADTAP_Factors*

No discrepancies were found in the GoldSim models with respect to bioaccumulation transfer factors.

Table I7-4: Elemental Transfer Factors

| Element | Soil to Plant (Unitless) | Feed to Meat (d/Kg) | Feed to Milk (d/L) | Water to Fish (L/Kg) |
|---------|-----------------------------|------------------------|-----------------------|-------------------------|
| Ac | 6.83E-05 | 4.00E-04 | 2.00E-05 | 2.50E+01 |
| Al | 1.27E-04 | 1.50E-03 | 2.06E-04 | 5.00E+02 |
| Am | 6.83E-05 | 4.00E-05 | 1.50E-06 | 3.00E+01 |
| C | 1.37E-01 | 3.10E-02 | 1.20E-02 | 3.00E+00 |
| Cf | 6.83E-05 | 4.00E-05 | 1.50E-06 | 2.50E+01 |
| Cl | 1.37E+01 | 2.00E-02 | 1.70E-02 | 5.00E+01 |
| Cm | 8.39E-05 | 4.00E-05 | 2.00E-05 | 3.00E+01 |
| Co | 1.31E-02 | 1.00E-02 | 3.00E-04 | 3.00E+02 |
| Cs | 9.00E-01 | 5.00E-02 | 7.90E-03 | 3.00E+03 |
| Eu | 3.90E-03 | 2.00E-05 | 3.00E-05 | 3.00E+01 |
| Gd | 3.90E-03 | 2.00E-05 | 3.00E-05 | 3.00E+01 |
| H | 4.80E+00 | 1.20E-02 | 1.50E-02 | 1.00E+00 |
| I | 7.80E-03 | 4.00E-02 | 9.00E-03 | 4.00E+01 |
| K | 1.07E-01 | 2.00E-02 | 7.20E-03 | 1.00E+03 |
| Mo | 1.56E-01 | 1.00E-03 | 1.70E-03 | 1.00E+01 |
| Nb | 4.88E-03 | 2.90E-04 | 3.20E-05 | 3.00E+02 |
| Ni | 1.17E-02 | 5.00E-03 | 1.60E-02 | 1.00E+02 |
| Np | 2.54E-03 | 1.00E-03 | 5.00E-06 | 2.10E+01 |
| Pa | 4.18E-04 | 4.47E-04 | 5.00E-06 | 1.00E+01 |
| Pb | 1.17E-03 | 4.00E-04 | 2.60E-04 | 3.00E+02 |
| Pd | 7.80E-03 | 4.00E-03 | 1.00E-02 | 1.00E+01 |
| Pt | 4.88E-03 | 4.00E-03 | 5.15E-03 | 3.50E+01 |
| Pu | 2.15E-04 | 1.00E-05 | 1.10E-06 | 3.00E+01 |
| Ra | 4.64E-03 | 9.00E-04 | 1.30E-03 | 5.00E+01 |
| Rn | 0 | 0 | 0 | 0 |
| Se | 5.14E-02 | 1.50E-02 | 4.00E-03 | 1.70E+02 |
| Sm | 3.90E-03 | 3.16E-04 | 3.00E-05 | 3.00E+01 |
| Sn | 1.17E-03 | 8.00E-02 | 1.00E-03 | 3.00E+03 |
| Sr | 9.75E-02 | 8.00E-03 | 2.80E-03 | 6.00E+01 |
| Tc | 4.68E-02 | 6.32E-03 | 1.87E-03 | 2.00E+01 |
| Th | 6.44E-05 | 4.00E-05 | 5.00E-06 | 1.00E+02 |
| U | 2.34E-03 | 3.00E-04 | 4.00E-04 | 1.00E+01 |
| Zr | 1.95E-04 | 1.84E-04 | 5.50E-07 | 3.00E+02 |

I7-4 Human Health Exposure Parameters

Various parameters associated with crop exposure times and productivity (SDF PA Table 4.6-5), environmental physical parameters (SDF PA Table 4.6-6), and individual exposure times and consumption rates (SDF PA Table 4.6-7) are used in the dose assessment methodology of GoldSim v2.0stoch and GoldSim v1.1dose. A number of the parameters referred to above also have stochastic analyses conducted within the GoldSim v2.0stoch model as shown in SDF PA Tables 5.6-9, 5.6-10, and 5.6-11. These parameters are shown in Table I7-5 through I7-7 with a cross reference to the GoldSim model files. A stochastic, or distribution, is shown in both the GoldSim v2.0stoch and the GoldSim v1.1dose models and in some cases are not the same. The stochastic, or distribution, provided in GoldSim v2.0stoch is used in the SDF stochastic analysis. However, the dose calculator model (v1.1dose) only utilizes the “Deterministic” value shown within the stochastic or distribution file. The recommended value or baseline value presented in the SDF PA tables is labeled as the “Deterministic” value in Tables I7-3 through I7-5.

Table I7-5: Crop Exposure Times and Productivity

| Parameter | Deterministic | Minimum | Maximum | Distribution | GoldSim File |
|--|---------------|----------|----------|--------------|--|
| Pasture exposure time to irrigation (day) | 30 | Not used | Not used | None | <i>GrassExposureTime</i> ¹ |
| Vegetable crop exposure times to irrigation (day) | 70 | 60 | 90 | Normal | <i>VeggieExposureTime</i> ¹ |
| Soil exposure time period to irrigation (day) (Buildup time in soil) | 183 | 60 | 365 | Uniform | <i>SoilBuildupTime</i> ¹ |
| Productivity | | | | | |
| Pasture grass (kg/m ²) | 1.8 | 0.7 | 2 | None | Not used in the model – |
| Agricultural (veg/produce) (kg/m ²) | 0.7 | 0.5 | 4 | None | Agricultural and garden (vegetable) yield assumed equal in the model. |
| Vegetable crop yield (kg/m ²) | 0.7 | 0.2 | 4 | LogNormal | <i>VegetationProductionYield</i> ¹ |
| Fraction of Foodstuff Produced Locally | | | | | |
| Vegetables (MOP) | 0.173 | 0 | 0.5 | Triangular | <i>LocalGrown</i> ^{2,5} |
| Meat (MOP) | 0.306 | 0 | 0.5 | Triangular | <i>FracLocalBeef_MOP</i> ³ <i>LocalMeatFrac_MOP</i> ⁶ |
| Milk (MOP) | 0.207 | 0 | 0.5 | Triangular | <i>FracLocalMilk_MOP</i> ³ <i>LocalMilkFrac_MOP</i> ⁶ |
| Vegetables (Intruder) | 0.308 | 0 | 0.5 | Triangular | <i>FracLocalVeggie</i> ⁴ |
| Meat (Intruder) | 0.319 | 0 | 0.5 | Triangular | <i>FracLocalMeat</i> ⁴ |
| Milk (Intruder) | 0.254 | 0 | 0.5 | Triangular | <i>FracLocalMilk</i> ⁴ |
| Dilution Factor for Mixing of Waste in Vegetable Garden | | | | | |
| Agricultural scenario | 0.2 | 0.2 | 0.2 | None | Not found in model parameters |
| Post-Drilling Scenario | 0.02 | 0.002 | 0.02 | None | Not found in model parameters |

(1) *DoseAssessment: DoseParameters: IRRIDOSE_Factors* in GoldSim v2.0stoch and v1.1dose

(2) *DoseAssessment: Doses_by_Sector: IRRIDOSE: LeeValues* in GoldSim v2.0stoch

(3) *DoseAssessment: Doses_by_Sector: IRRIDOSE* in GoldSim v2.0stoch

(4) *DoseAssessment: IHI* in GoldSim v2.0stoch and v1.1dose

(5) *DoseAssessment: Doses_by_Region: IRRIDOSE: LeeValues* in GoldSim v1.1dose

(6) *DoseAssessment: Doses_by_Region: IRRIDOSE* in GoldSim v1.1dose

Table I7-6: Physical Parameters

| Parameter | Deterministic | Minimum | Maximum | Distribution | GoldSim File |
|--|---------------|----------|----------|--------------|--|
| Areal density of soil (kg/m ²) | 240 | Not used | Not used | None | <i>SurfaceSoilDensity</i> ¹ |
| Atmospheric mass loading of soil (kg/m ³) (while in garden or while in home) | 1.0 E-07 | Not used | Not used | None | <i>AirMassLoadingSoil</i> ² |
| Depth of garden (cm) | 15 | 15 | 61 | Triangular | <i>TillDepth</i> ^{3, 5} |
| Garden irrigation rate (L/d/m ²) | 3.6 | 2.08 | 5.5 | Triangular | <i>IrrigationRate</i> ¹ |
| Fraction of the year that crops are irrigated | 0.2 | 0.2 | 0.25 | Triangular | <i>FracYearIrrigate</i> ¹ |
| Crop weathering constant (L/d) | 0.0495 | Not used | Not used | None | <i>WeatherandDecayConst</i> ¹ |
| Fractional retention of deposition on leaves | 0.25 | Not used | Not used | None | <i>LeafRetention</i> ¹ |
| Area of garden for family of four (m ²) | 100 | 100 | 1,000 | Triangular | <i>GardenSize</i> ^{3, 5} |

(1) *DoseAssessment: DoseParameters: IRRIDOSE_Factors* in GoldSim v2.0stoch and v1.1dose

(2) *DoseAssessment: IHI* in GoldSim v2.0stoch and v1.1dose

(3) *DoseAssessment: IHI: ResidentScenarioOutputs* in GoldSim v2.0stoch

(4) *Materials: SandySoilProperties*, in GoldSim v2.0stoch and v1.1dose see Discrepancy I7-6

(5) *DoseAssessment: IHI: ResidentScenario* in GoldSim v1.1dose

Table I7-7: Individual Exposure Times and Consumption Rates

| Parameter | Deterministic | Minimum | Maximum | Distribution | GoldSim File |
|--|----------------|----------|----------|--------------|--|
| Breathing rate (m ³ /yr) | 5,548 | 1,267 | 11,600 | Normal | <i>AirIntake</i> ¹ |
| Soil consumption (kg/yr) | 0.0365 | Not used | Not used | None | <i>ConsumptionSoil</i> ¹ <i>DirtConsumption</i> ^{2, 8} |
| Leafy vegetable consumption (kg/yr) | 21 | 18 | 43 | Lognormal | <i>Leafy</i> ^{3, 9} |
| Other vegetable consumption (kg/yr) | 163 | 90 | 276 | Lognormal | <i>Veg</i> ^{3, 9} |
| Other vegetable consumption - intruder (kg/yr) | 163 | 90 | 276 | Lognormal | <i>ConsumptionVeggies</i> ¹ |
| Meat consumption (kg/yr) | 43 | 26 | 81 | Lognormal | <i>Beef</i> ^{3, 9} |
| Finfish consumption (kg/yr) | 9 ^b | 2.2 | 19 | Triangular | <i>AnnualAquaticFoodConsumption</i> ^{4, 10} |
| Seafood consumption (kg/yr) | 0 | 0 | 5 | None | Not in model – has no impact since only finfish is consumed from fishing in local streams. |
| Milk consumption (L/yr) | 120 | 73.7 | 230 | Lognormal | <i>Milk</i> ^{3, 9} |
| Water consumption (L/yr) | 337 | 184 | 730 | Triangular | <i>WaterConsumptionRate</i> ^{4, 10} <i>ConsumptionWater</i> ¹ |
| Fodder - Beef cattle (kg/d) | 36 | 27 | 50 | Normal | <i>ConsumptionFodderBeef</i> ⁵ |

Table I7-7: Individual Exposure Times and Consumption Rates (Continued)

| Parameter | Deterministic | Minimum | Maximum | Distribution | GoldSim File |
|--|---------------|----------|----------|--------------|--|
| Fodder - Milk cattle (kg/d) | 52 | 36 | 55 | Normal | <i>ConsumptionFodderMilk</i> ⁵ |
| Fraction of beef-cow intake from pasture | 0.75 | 0.5 | 1 | Triangular | <i>FodderFractionBeef</i> ⁵ |
| Fraction of milk-cow intake from pasture | 0.56 | 0.5 | 1 | Triangular | <i>FodderFractionMilk</i> ⁵ |
| Water (beef cow) (L/d) | 28 | 28 | 50 | Triangular | <i>CattleWaterConsumptionBeef</i> ⁵ |
| Water (milk cow) (L/d) | 50 | 50 | 60 | Triangular | <i>CattleWaterConsumptionMilk</i> ⁵ |
| Shoreline exposure (hr/yr) | 23 | Not used | Not used | None | <i>AnnualUsageFactor</i> ^{4, 10} |
| Swimming exposure (hr/yr) | 8.9 | Not used | Not used | None | <i>AnnualSwimming</i> ^{4, 10} |
| Boating exposure (hr/yr) | 21 | Not used | Not used | None | <i>AnnualBoating</i> ^{4, 10} |
| Showering exposure (min/d) | 10 | 10 | 30 | Triangular | <i>ExposureFractionShower</i> ^{6, 11} |
| Fraction of year working in garden MOP (/yr) | 0.01 | Not used | Not used | None | <i>ExposureFractionGarden</i> ¹² |
| Fraction of year working in garden for intruder(/yr) | 0.01 | 0.01 | 0.08 | Triangular | <i>FractionInGarden</i> ⁷ |
| Fraction of year residing in home (/yr) | 0.7 | Not used | Not used | None | <i>ExposureFractionHome</i> ¹ Parameter provided but is not used in the model |

Table I7-7: Individual Exposure Times and Consumption Rates (Continued)

| Parameter | Deterministic | Minimum | Maximum | Distribution | GoldSim File |
|--|---------------|----------|----------|--------------|---|
| Fraction of time cattle on pasture | 1 | Not used | Not used | None | Not in model – has no impact since the Deterministic value = 1. |
| Vegetable transport time (d) | 6 | Not used | Not used | None | <i>VegetableHoldupTime</i> ⁵ |
| Feed-milk-man transport time (d) | 3 | Not used | Not used | None | <i>MilkTime</i> ⁵ |
| Time from slaughter to consumption (d) | 6 | Not used | Not used | None | <i>BeefTime</i> ⁵ |

- (1) *DoseAssessment: IHI* in GoldSim v2.0stoch and v1.1dose
(2) *DoseAssessment: Doses_by_Sector: IRRIDOSE* in GoldSim v2.0stoch
(3) *DoseAssessment: Doses_by_Sector: IRRIDOSE: LeeValues* in GoldSim v2.0stoch
(4) *DoseAssessment: Doses_by_Sector: LADTAP_Sectors* in GoldSim v2.0stoch
(5) *DoseAssessment: DoseParameters: IRRIDOSE_Factors* in GoldSim v2.0stoch and v1.1dose
(6) *DoseAssessment: Doses_by_Sector: Inhalation* in GoldSim v2.0stoch
(7) *DoseAssessment: IHI: ResidentScenario* in GoldSim v2.0stoch and GoldSim v1.1dose
(8) *DoseAssessment: Doses_by_Region: IRRIDOSE* in GoldSim v1.1dose
(9) *DoseAssessment: Doses_by_Region: IRRIDOSE: LeeValues* in GoldSim v1.1dose
(10) *DoseAssessment: Doses_by_Region: LADTAP_Regions* in GoldSim v1.1dose
(11) *DoseAssessment: Doses_by_Region: Inhalation* in GoldSim v1.1dose
(12) *DoseAssessment: IHI* in GoldSim v2.0stoch

I8 Other Stochastics in the GoldSim Probabilistic Model

SDF PA Section 5.6.3 discusses the stochastic analysis utilized in the probabilistic model in GoldSim v2.0stoch. SDF PA Section 5.6.3.1 discusses the stochastic for the configuration cases and is addressed in I5.4. SDF PA Section 5.6.3.2 discusses the stochastic for the radionuclide inventory and is addressed in I6.2. SDF PA Section 5.6.3.3 discusses the stochastic for the distribution coefficients (K_d values) and is addressed in I2.2. SDF PA Section 5.6.3.4 discusses the stochastic for the transition times between chemical states of cementitious materials and is addressed in I2.1. SDF PA Section 5.6.3.7 discusses the stochastics associated with bioaccumulation factors and human health exposure factors and is addressed in I7.2. This section addresses the remaining stochastics discussed in SDF PA Section 5.6.3.

I8.1 Lower Vadose Zone Thickness

SDF PA Section 5.6.3.5 discusses the stochastic modeling associated with the depth of the vadose zone beneath the SDF vaults and FDCs. A range of ± 16.4 feet (5m) from the baseline depth is considered a reasonable variance of the baseline depth. SDF PA Section 5.6.3.5 identifies the baseline vadose zone depth values of 50 feet for Vault 1, 40 feet for Vault 4, and 42

feet for the FDCs, which differ from the values presented in SDF PA Section 4.2.3.2.3 in order to present the actual GoldSim model. The notes accompanying Table I4-7 addresses these differences. In GoldSim v2.0stoch the distribution of the vadose zone thickness is presented in *UZthicknessDist*, which is located in *TheVaults: VaultData: UZ-Thickness*. The mean shown in *UZthicknessDist* corresponds to the baseline value presented above, Vault 1 15.24m (50 feet); Vault 2 12.8m (42 feet), and Vault 4 12.19m (40 feet).

I8.2 Well Depth

SDF PA Section 5.6.3.6 discusses the impact on dose from the depth of the well that is drilled after SDF closure. The depth of the well determines which aquifer the water would be pumped from. SDF PA Table 5.6-7 provides the percentage of time that a well may be drilled down to a specific depth so as to reach one of the three available aquifers. SDF PA Table 5.6-8 provides the dose ratios with respect to each aquifer based on the 10,000 year results in Sector B, the sector with the highest dose within the 10,000 year period after SDF closure. This data is captured in GoldSim v2.0stoch as *CompletionStratum* located in *Dose Assessment: ExposureMediaConc: WellCompletionDepth*, which provides the data presented in SDF PA Table 5.6-7. A selector labeled *WellConcRatio* also located in *Dose Assessment: ExposureMediaConc: WellCompletionDepth* is used to apply the ratios presented in SDF PA Table 5.6-8 based on the depth (stratum) picked from *CompletionStratum*.

I8.3 Saturated Zone Modeling Parameters

SDF PA Section 5.6.3.8 discusses the stochastic modeling associated with the saturated zone modeling parameters. Of importance in the model is the concentration of contaminants in the aquifers below the vaults and the FDCs. The concentration is based on the saturated zone thickness, the width of the saturated zone below the disposal units, and the Darcy Velocity in the saturated zone. Each of these three parameters has a distribution of potential values that are input into the GoldSim v2.0stoch model.

The distribution for the saturated zone thickness is defined in *SatThickness* located in *Transport: WaterTransport* of GoldSim v2.0stoch and uses a mean value of 12m and a normal distribution with a minimum of 5m and a maximum of 19m as reported in SDF PA Section 5.6.3.8.

The distribution for the width of the saturated zone is defined by the length of the vault (for Vaults 1 and 4), the diameter for the FDCs, and a uniform distribution with a minimum of 80% of the defined value and a maximum of 120% of the defined value. Table I8-1 presents the saturated width distribution used in GoldSim 2.0stoch.

Table I8-1: Width of Saturated Zone below the Disposal Units

| Disposal Unit | Length | GoldSim Distribution | GoldSim v2.0stoch File |
|---------------|---------------------------|--|--|
| Vault 1 | 600 feet (182.9m) | Min = 0.8 x 182.9 Mean = 182.9 Max = 1.2 x 182.9 | <i>TheVaults: Vault_1: Site Geometry: SatWidth</i> |
| Vault 4 | 600 feet (182.9m) | Min = 0.8 x 182.9 Mean = 182.9 Max = 1.2 x 182.9 | <i>TheVaults: Vault_4: Site Geometry: SatWidth</i> |
| FDCs | 150 feet (dia) (45.7m) | Min = 0.8 x 45.7 Mean = 45.7 Max = 1.2 x 45.7 | <i>TheVaults: Vault_2: Site Geometry: SatWidth</i> |

The distribution for the Darcy Velocity is defined in *SatZoneDarcyVelDist* located in *Transport: WaterTransport* and uses a mean value of 45.72 m/yr and a normal distribution with a minimum of 80% of the mean value and a maximum of 120% of the mean value as reported in SDF PA Section 5.6.3.8.

I9 Summary

Review of the input data to PORFLOW and the GoldSim models found a limited number of inconsistencies with the data presented in the SDF PA.

Provided below are the discrepancies that were identified in this review. All the discrepancies noted below are expected to have no significant impact on the conclusions presented in the SDF PA.

Discrepancy I4-1:

The PORFLOW model assumes a thickness of 6 inches to the shotcrete zone; however the average value is 2.3 inches. The PORFLOW model assigned “Oxidizing Concrete” as the material zone for the selection of appropriate K_d values for the shotcrete zone. The material zone for assignment of K_d values for the shotcrete zone should be backfill (clayey soil).

Discussion for Discrepancy I4-1:

The shotcrete layer that surrounds the exterior walls of the FDCs is included in the model with a thickness of 6 inches rather than the average thicknesses of 2.3 inches described in SDF PA Section 3.2.1.3.2. However, the model assigns hydraulic properties associated with backfill (clayey soil), specified in SDF PA Section 4.2.3.2.3, to this shotcrete layer rather than the hydraulic properties associated with cementitious material. Using hydraulic properties associated with backfill essentially removes this material from the model because the FDCs are surrounded with backfill material. Therefore, with respect to the flow of the contaminants leaving the FDCs, the thickness of this layer is of no consequence to the model. On the other hand, the K_d values assigned to this shotcrete layer are associated with middle aged oxidizing concrete specified in SDF PA Table 4.2-18. Thus, with respect to the transport of the contaminants leaving the FDCs, the greater thickness of the shotcrete layer may have an impact on the amount of contaminants released to the groundwater and the

timing of the release. Scoping runs were performed on selected radionuclides which replaced the K_d values associated with middle aged oxidizing concrete with K_d values associated with backfill that are specified in SDF PA Table 4.2-15. The results of these scoping runs found that the peak doses described above would not be affected for the following reasons:

- The peak dose at 10,000 years is located in Sector B and driven by Vault 4 and the shotcrete layer is only associated with the FDCs.
- The greater radionuclide flux occurs earlier in the assessment period and has no adverse impact on the peak dose for the 20,000 year period.

Discrepancy I6-1:

The inventory uncertainty of Tc-99 in Vault 1 utilized a GSD of 1.0001 rather than 1.1 as specified in PA Section 5.6.3.2. The adverse impact of this discrepancy is that the GoldSim model may select an inventory from Vault 1 for Tc-99 that is much narrower than discussed in the SDF PA. Using a GSD of 1.0001, the maximum value of the inventory could be approximately 216 Ci. With the GSD of 1.1, the maximum value of the inventory could be approximately 320 Ci. From Table I6-1, the baseline inventory of Tc-99 in the disposal units are approximately 220 Ci in Vault 1, 580 Ci in Vault 4, and 540 Ci in each of the 64 FDCs. Based on PA Figure 4.4-70, Tc-99 release from Vault 4 is expected to contribute to the Tc-99 concentration in Sectors A through D. Within any one of these sectors the Tc-99 contribution would be from Vault 1, Vault 4, and at least six FDCs. Using the GSD of 1.1 for Vault 4 and the FDCs, the maximum Tc-99 inventory is estimated to be 844 Ci in Vault 4 and 785 Ci in an FDC. Thus, the impact of using a GSD of 1.0001 rather than 1.1 for the inventory uncertainty of Tc-99 in Vault 1 would have minimal impact on the SDF PA stochastic results.

Discrepancy I6-2:

The chemicals identified in Table I6-4 of the text have inventories provided in SDF PA Table 3.3-4 for Vault 4 that differ from the inventory used in the PORFLOW analysis shown in Table 10 of SRNL-STI-2009-00115. To account for the differences between the current SDF PA chemical inventory and the inventory modeled in PORFLOW, an adjustment factor is applied to concentration results obtained from PORFLOW. The adjustment factor is one plus the percent difference of the SDF PA inventory to the PORFLOW model inventory for the individual chemical and they are shown in Table I6-4 of the text. The adjustment factors have been applied to SDF PA Tables 5.2-12 through 5.2-20 for the 100m distance and SDF PA Tables 6.1-10 through 6.1-18 for the 1m distance.

APPENDIX J

SALTSTONE HYDRAULIC CONDUCTIVITY SENSITIVITY

Appendix J contains curves showing the 100 meter concentrations for key radiological and chemical concentrations for all of SDF (vault and FDC inventories) for the Base Case (Case A) for a case of higher initial saltstone hydraulic conductivity (i.e., $1.0\text{E-}7\text{cm/sec}$). 20,000 year concentration results are presented for Sectors A through L for the peak concentration per sector regardless of aquifer.

Graph heading example “CaseA_kgrout All I-129 A”

Key

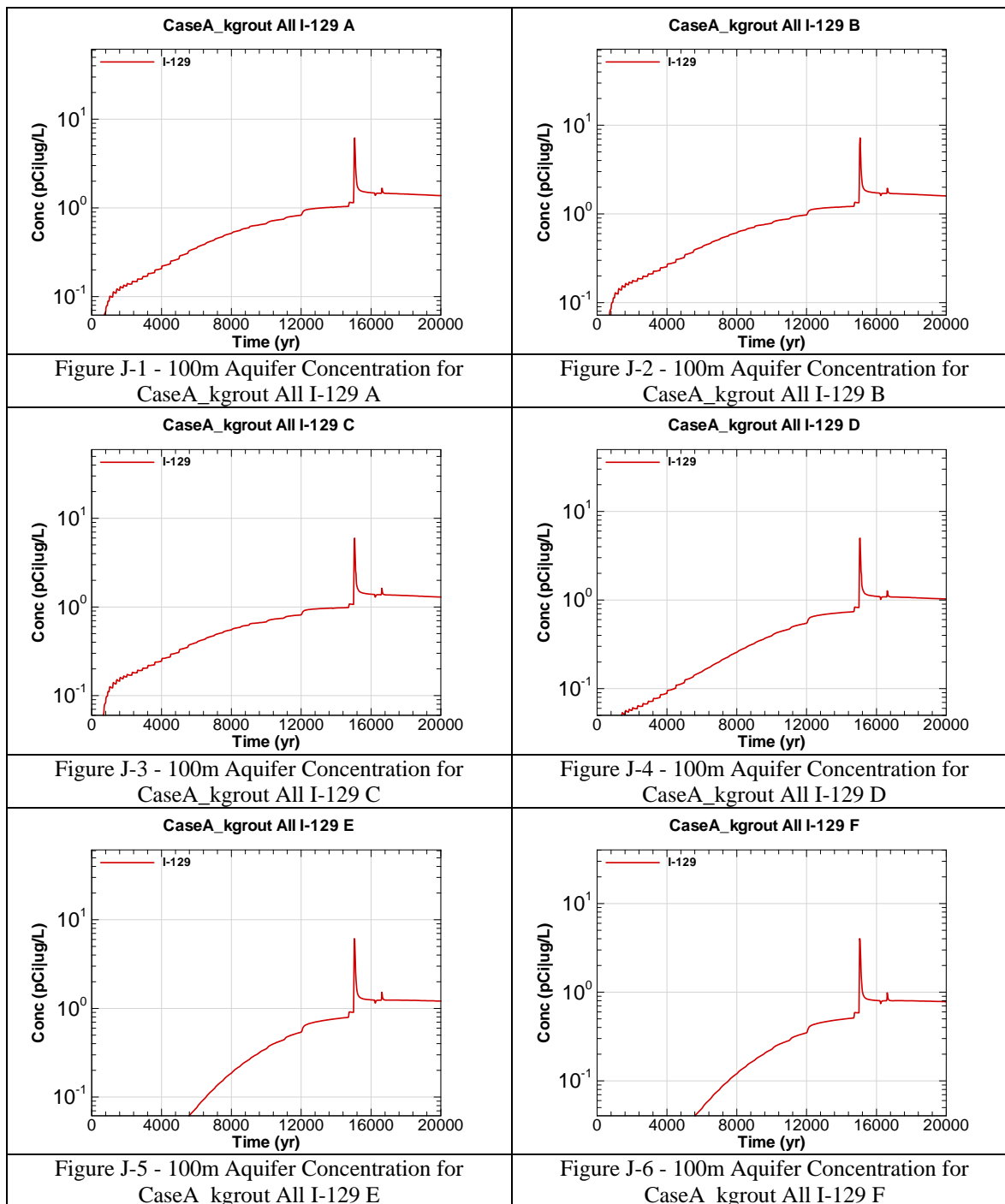
CaseA = Scenario case

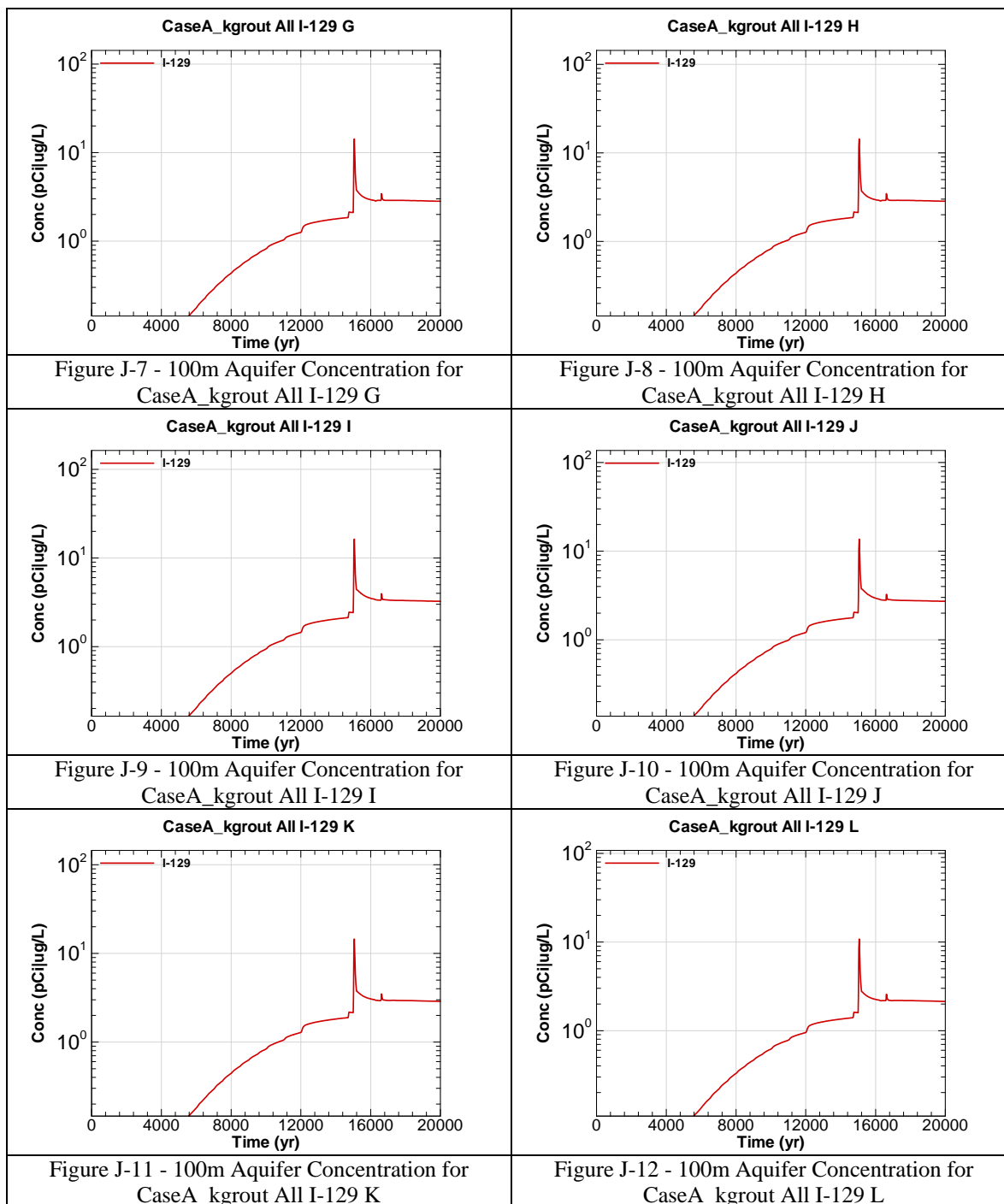
kgrout = Higher saltstone hydraulic conductivity

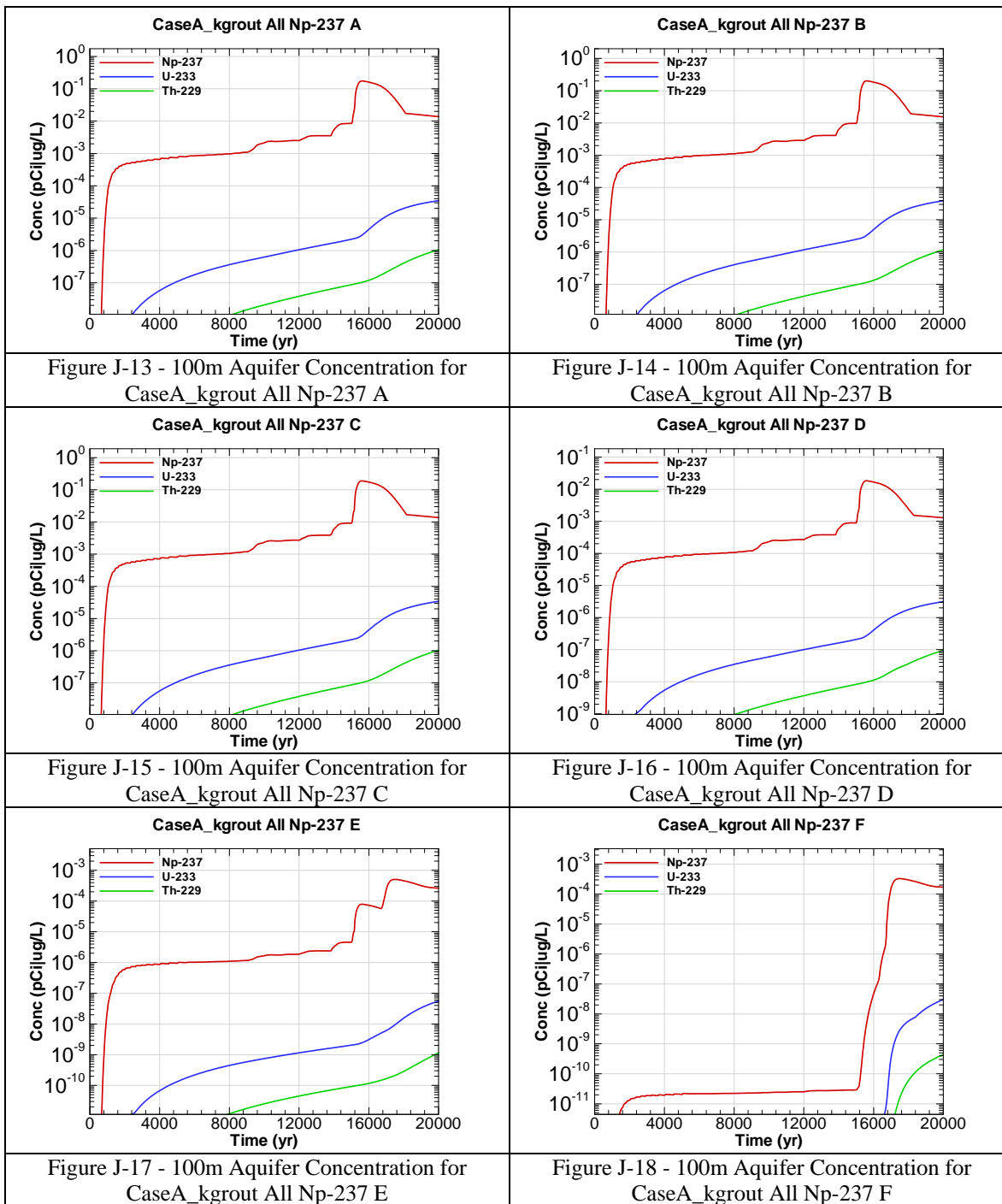
All = Inventory source is all disposal units

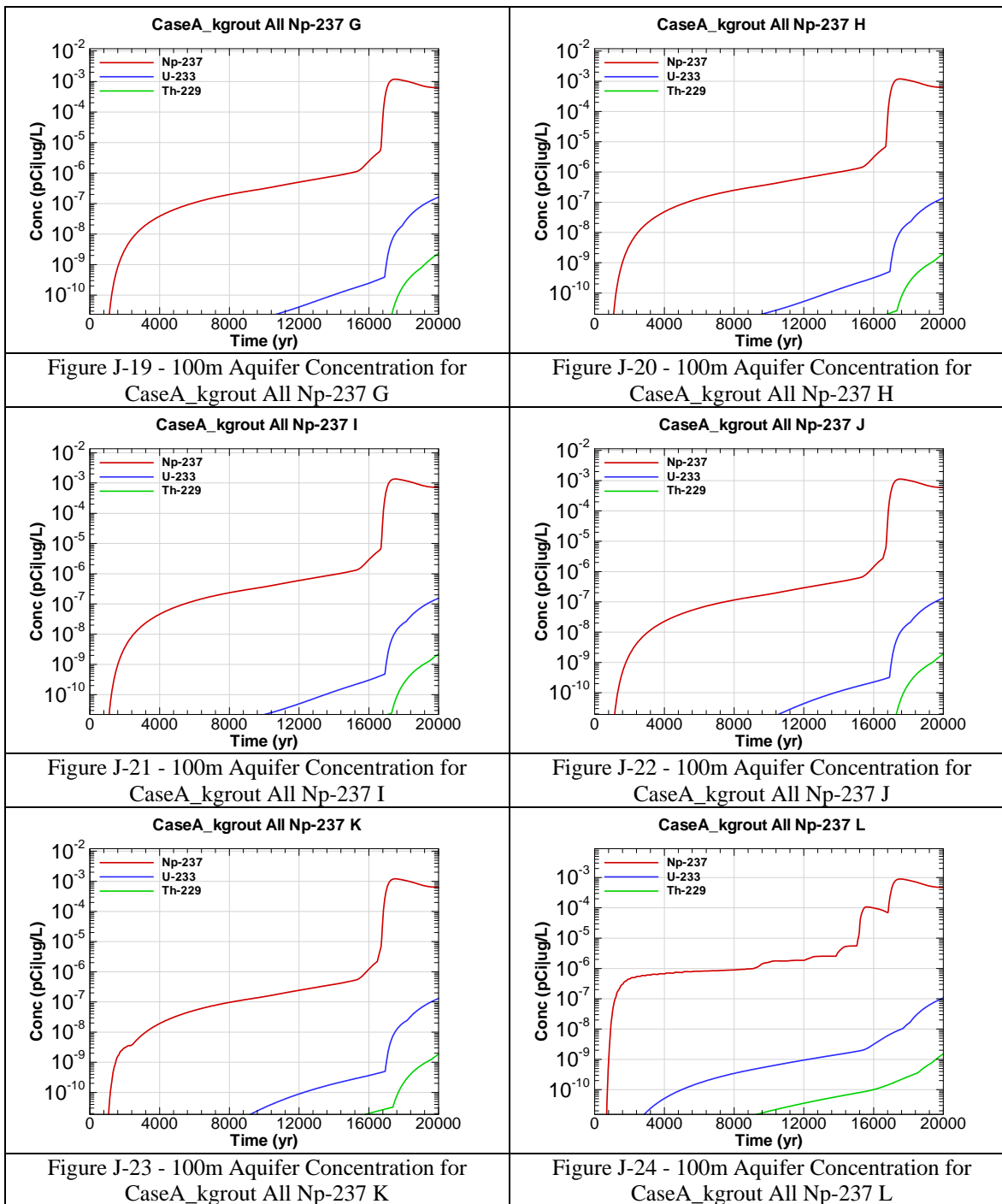
I-129 = Radionuclide or chemical of concern

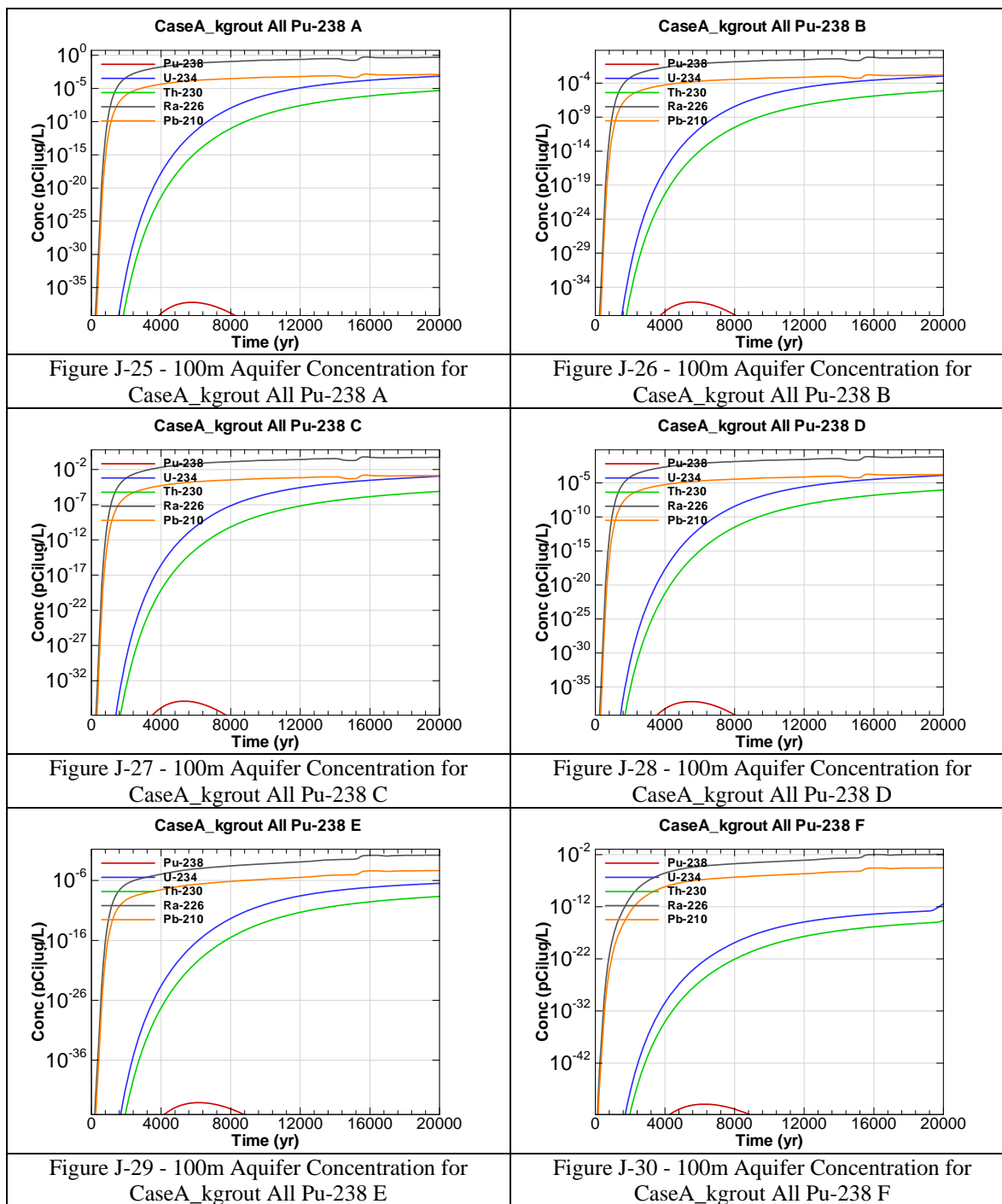
A = Evaluation sector of concern

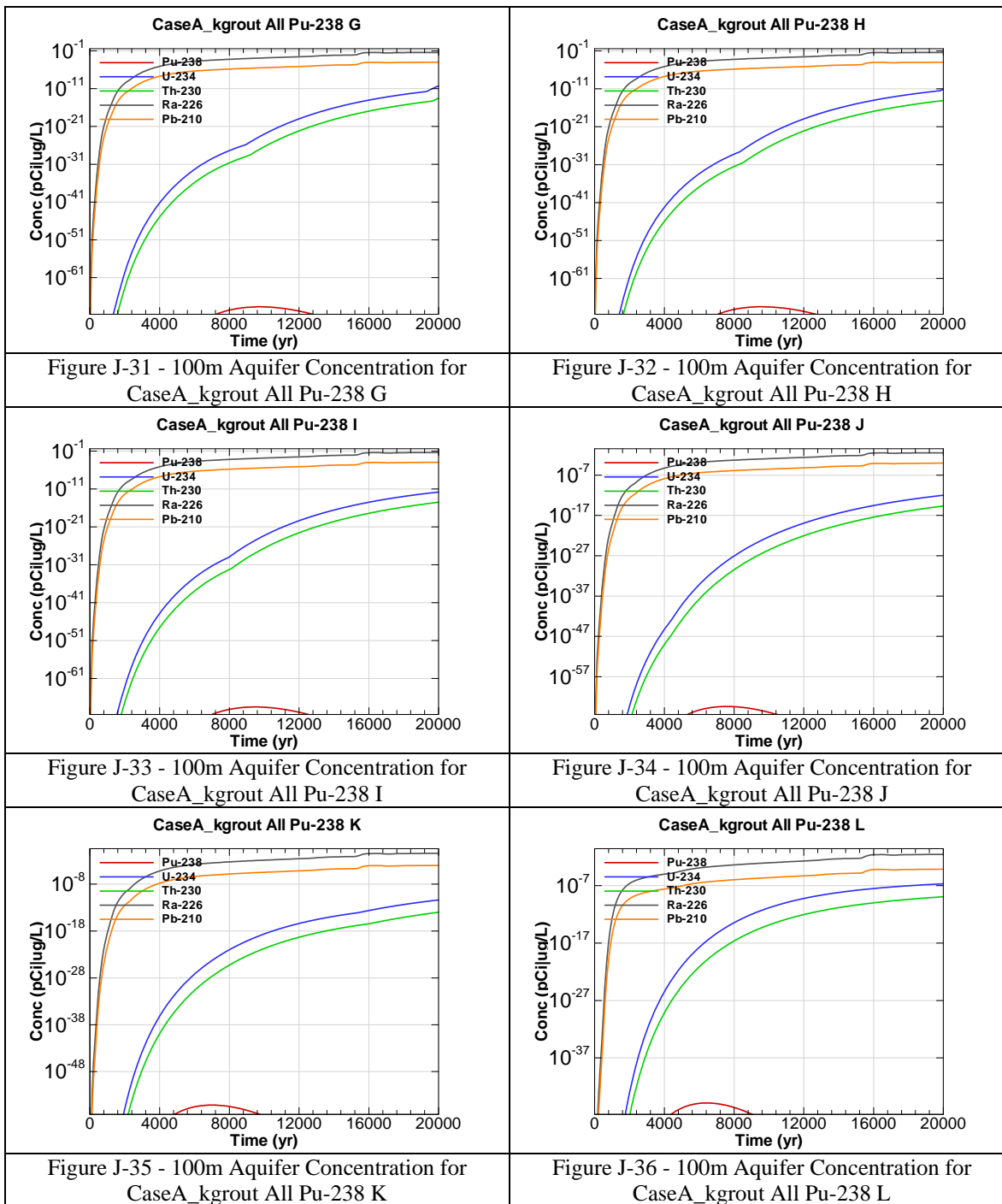


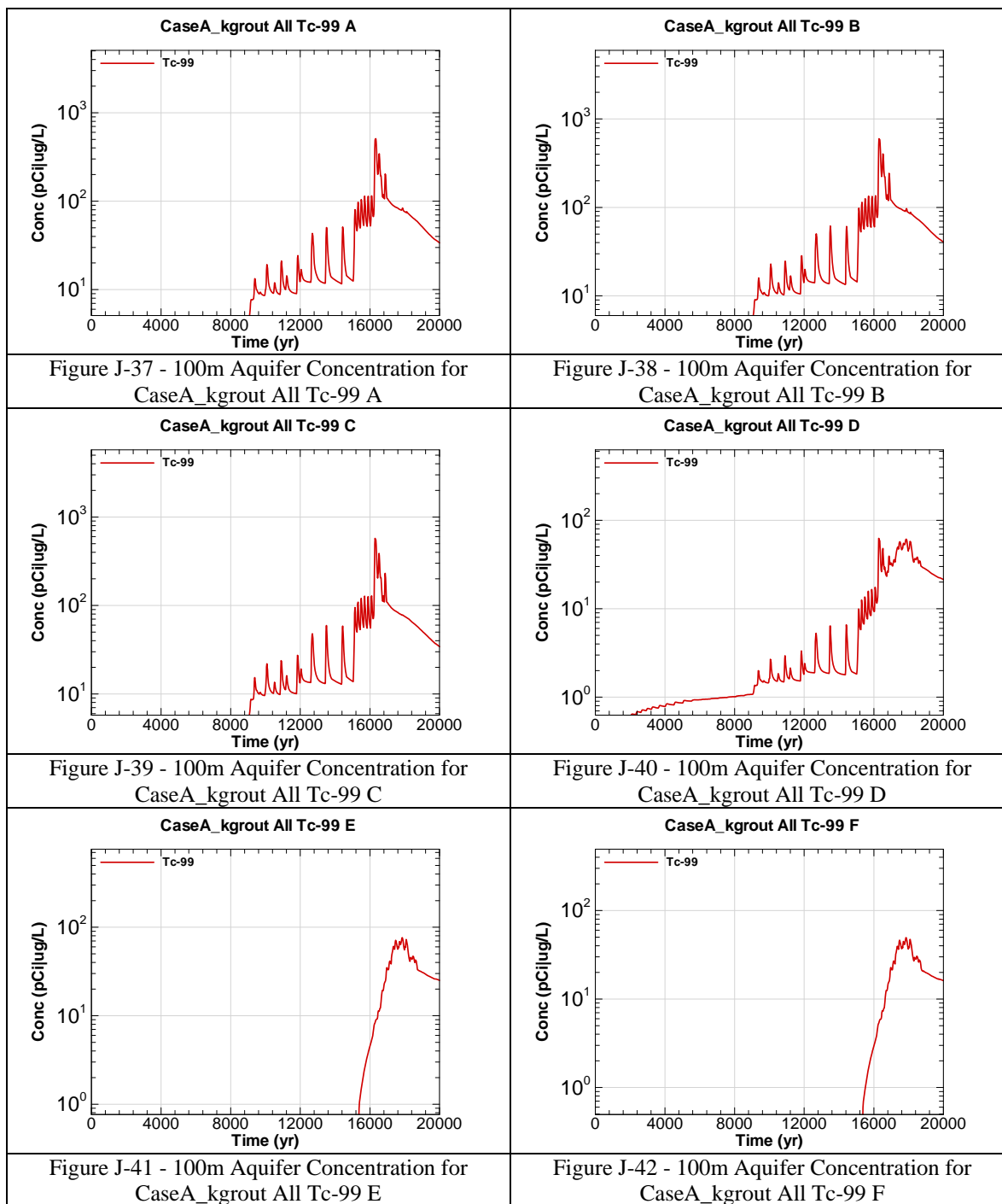


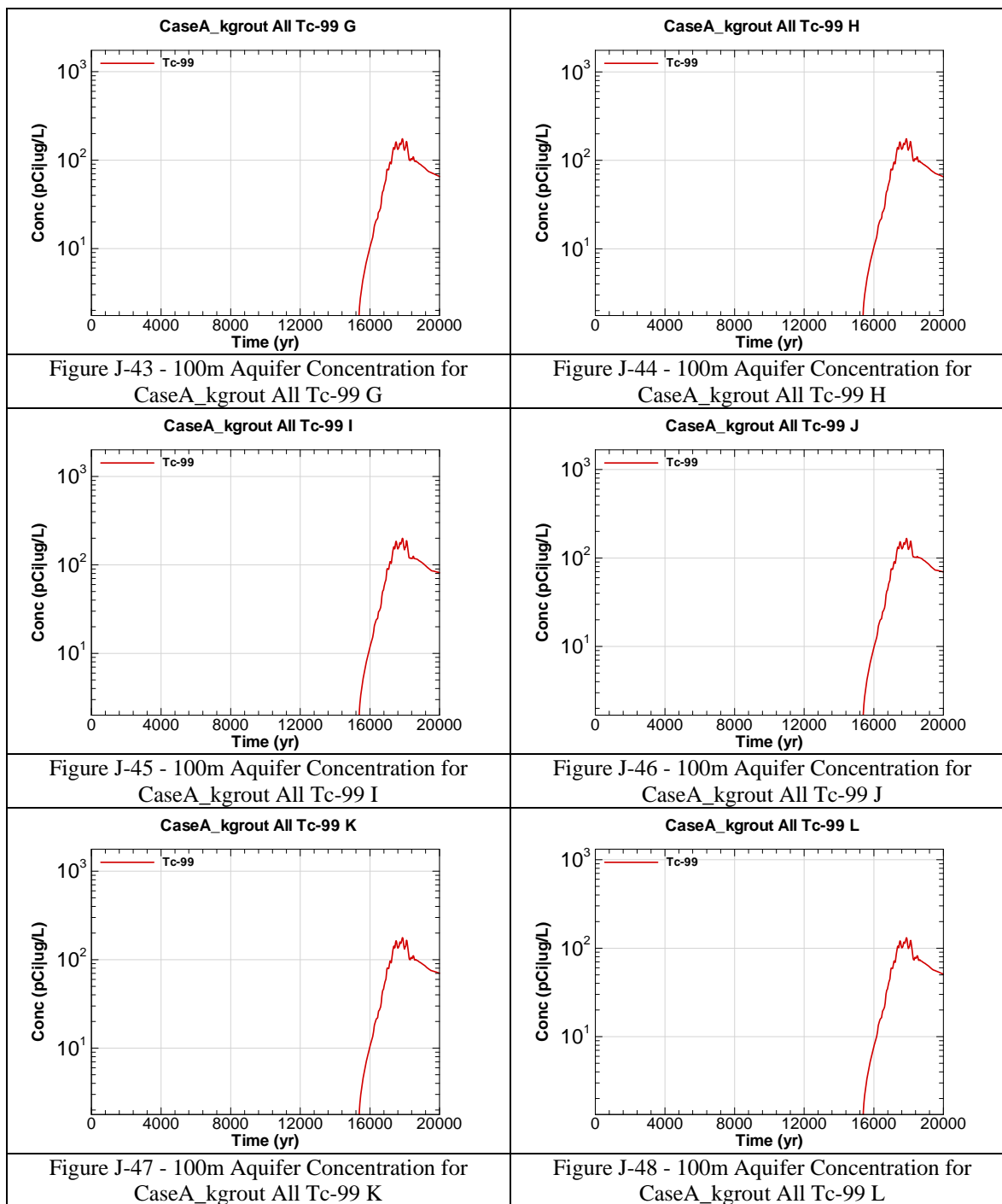


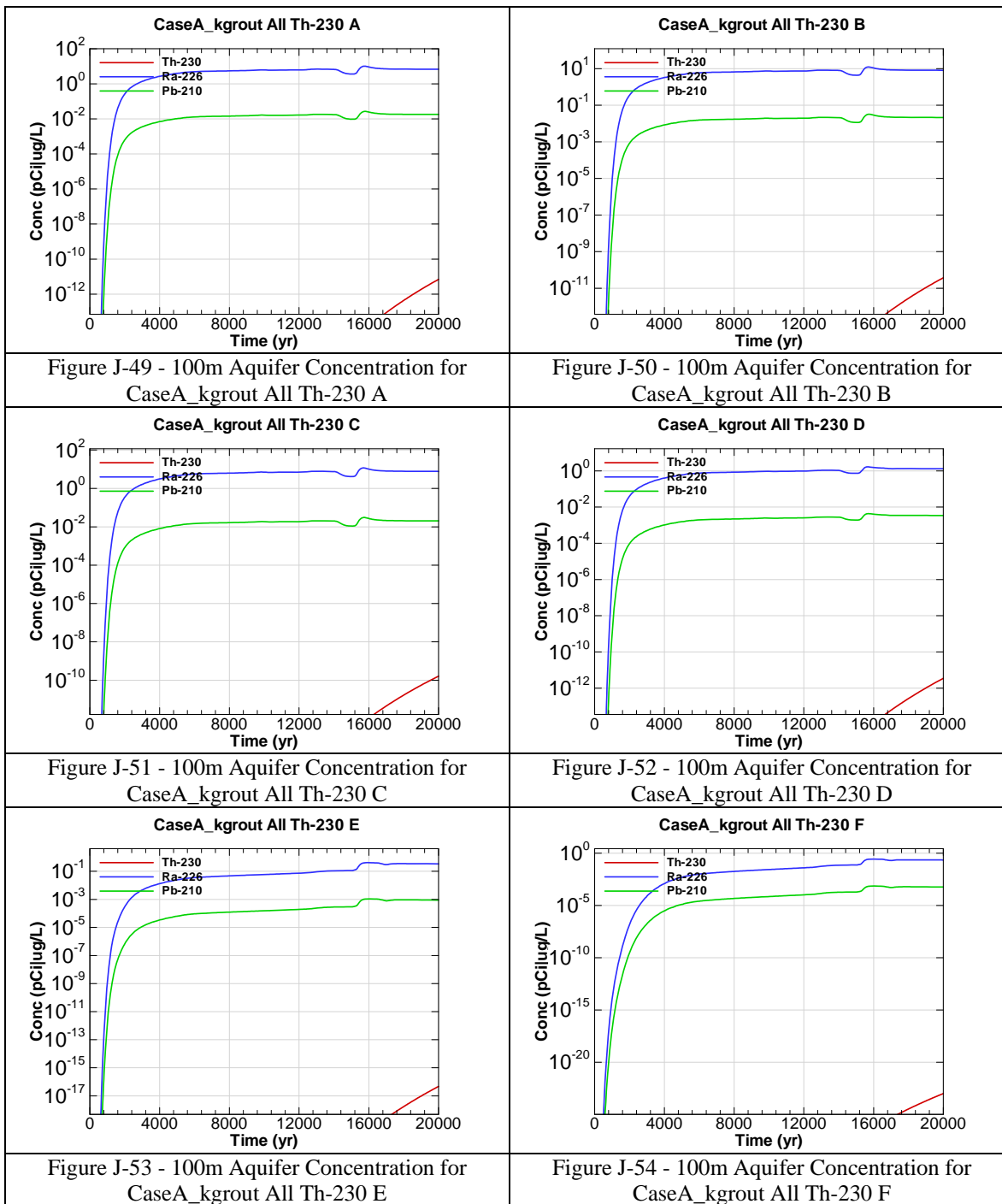


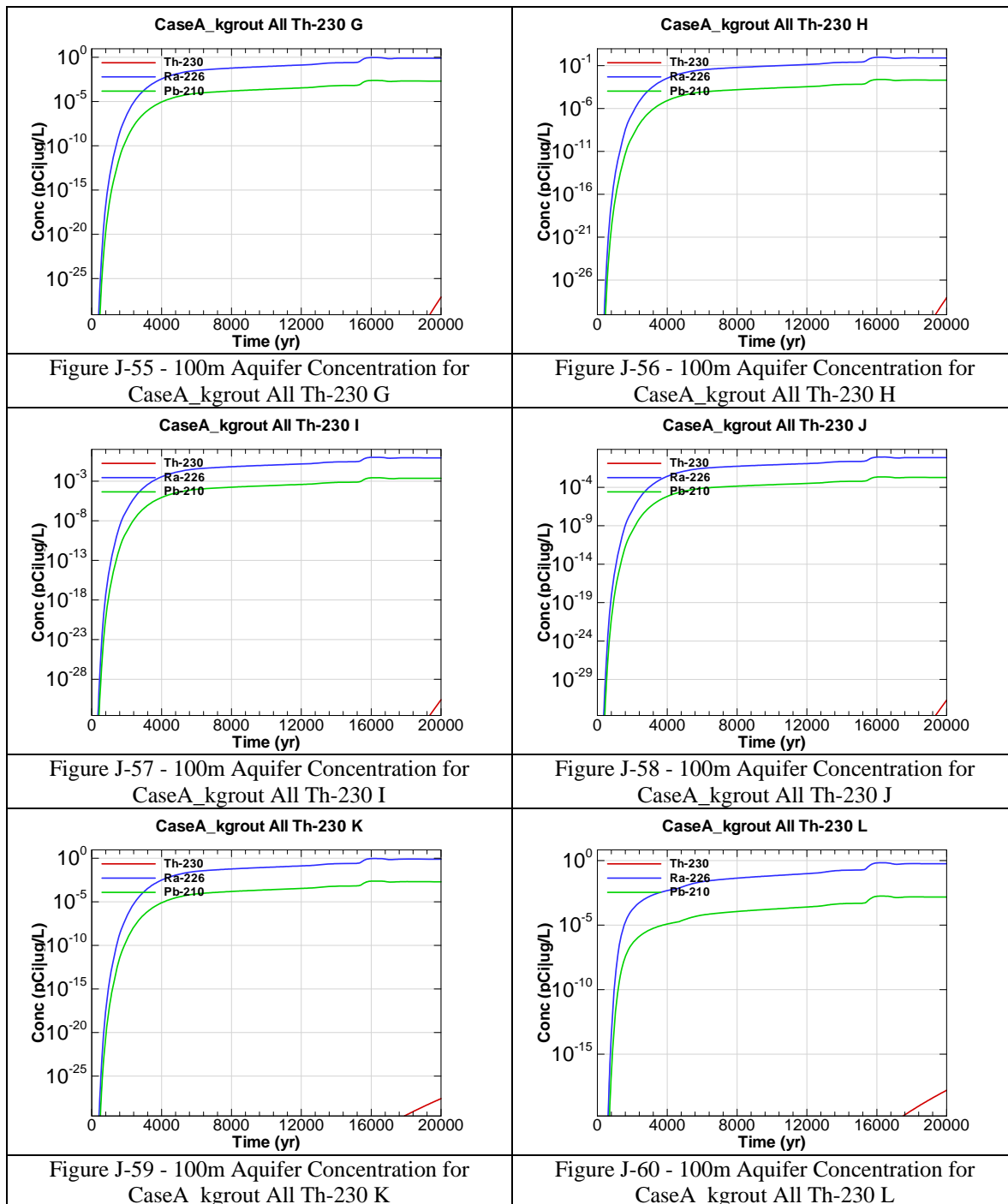


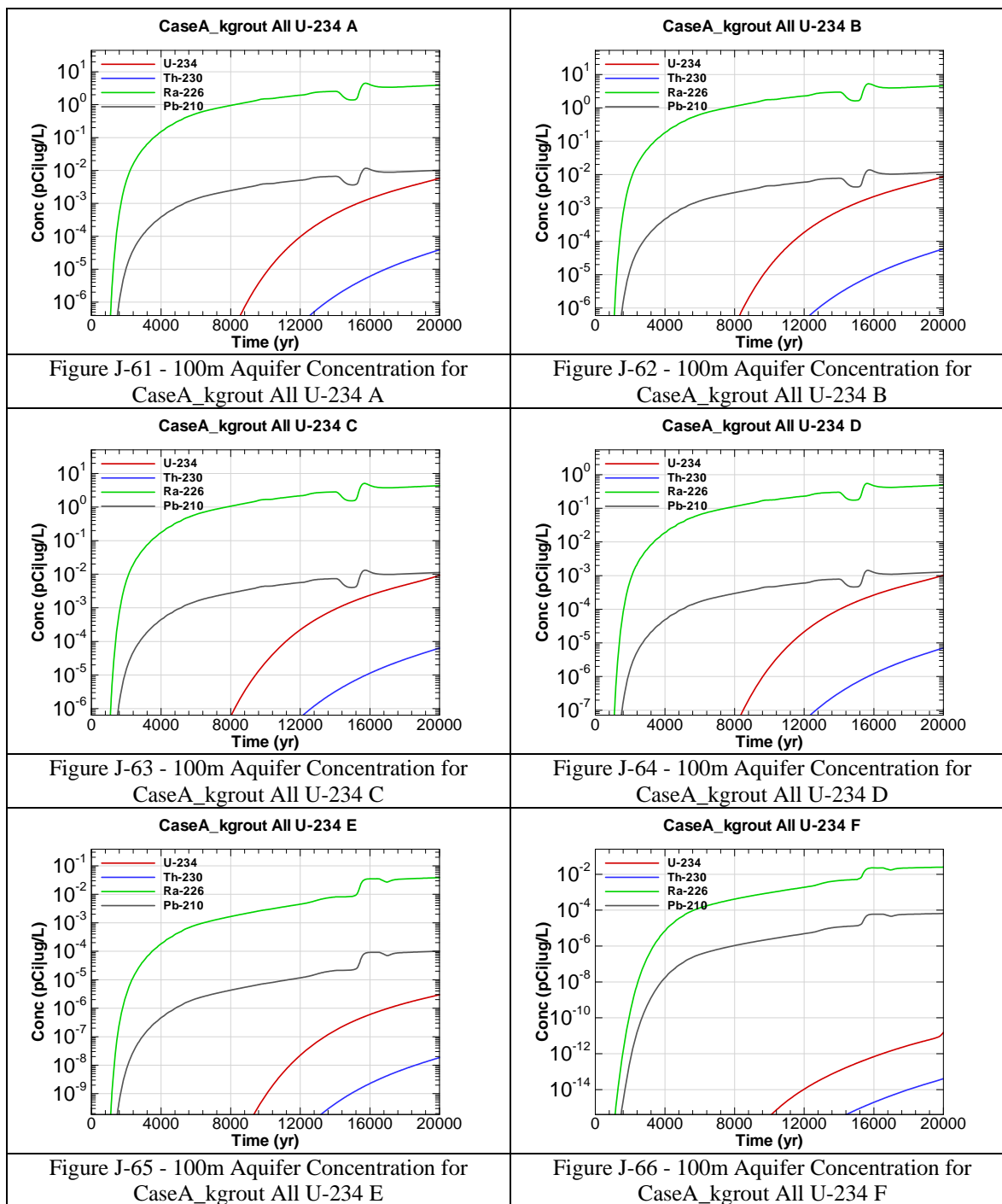


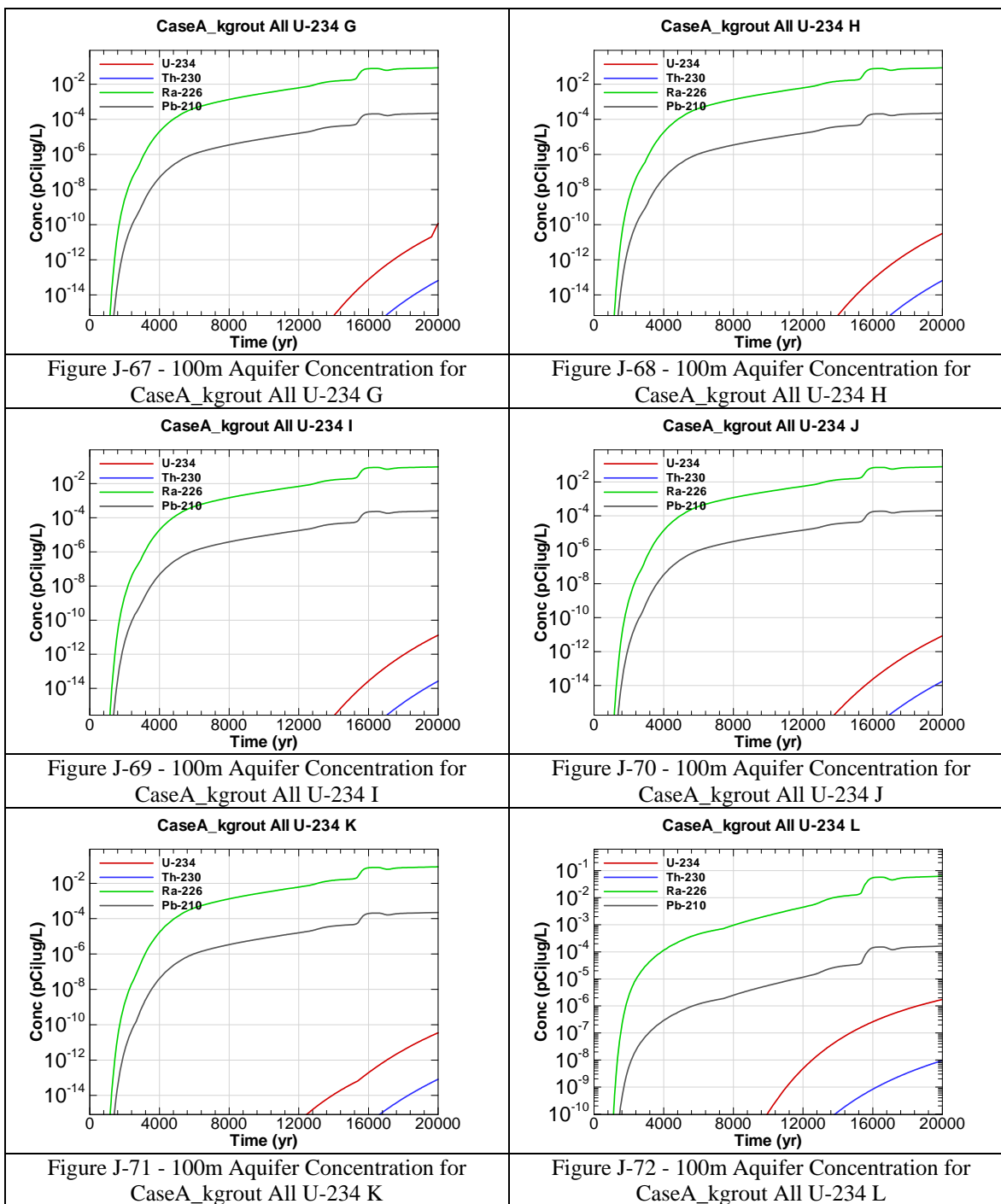


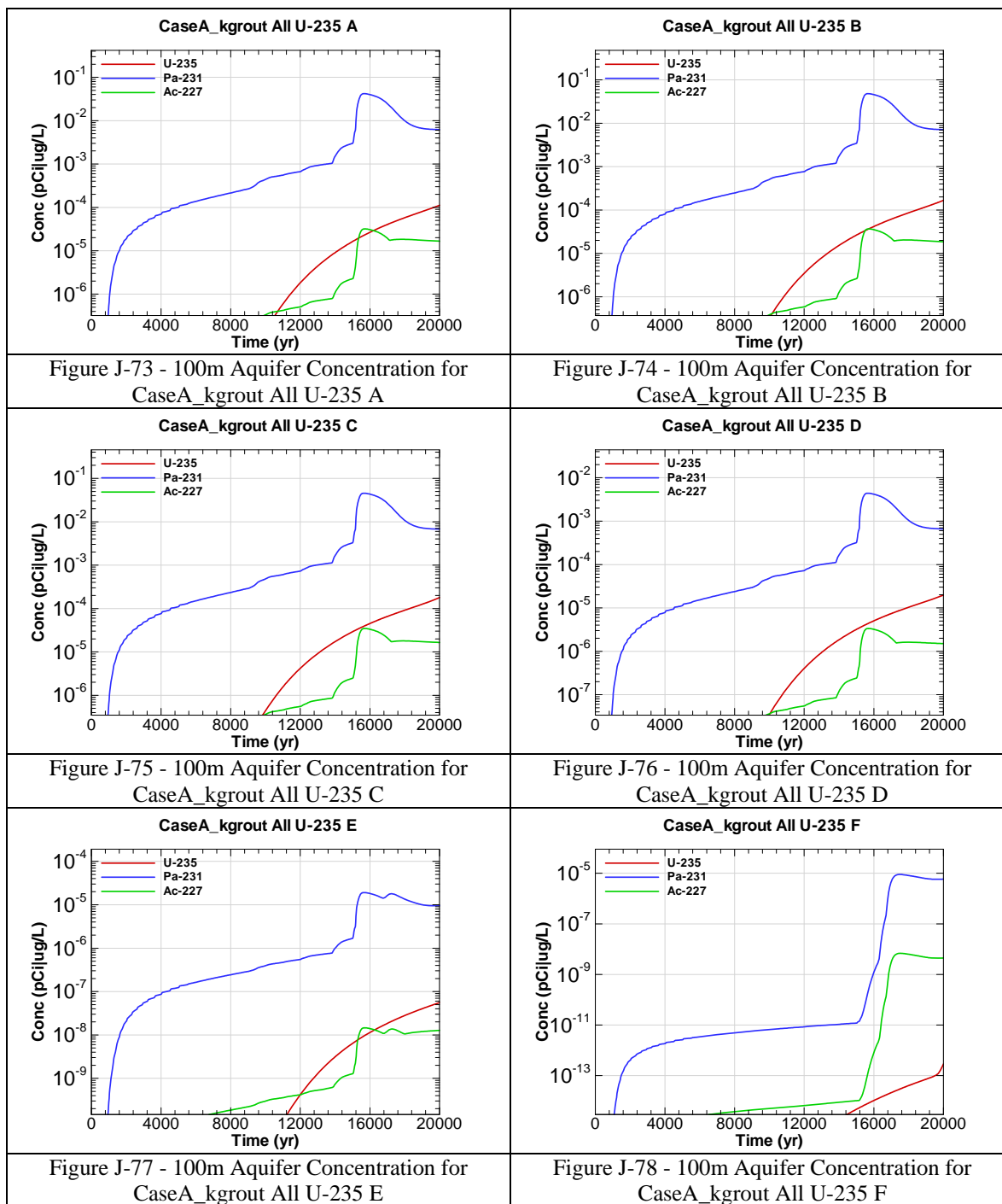


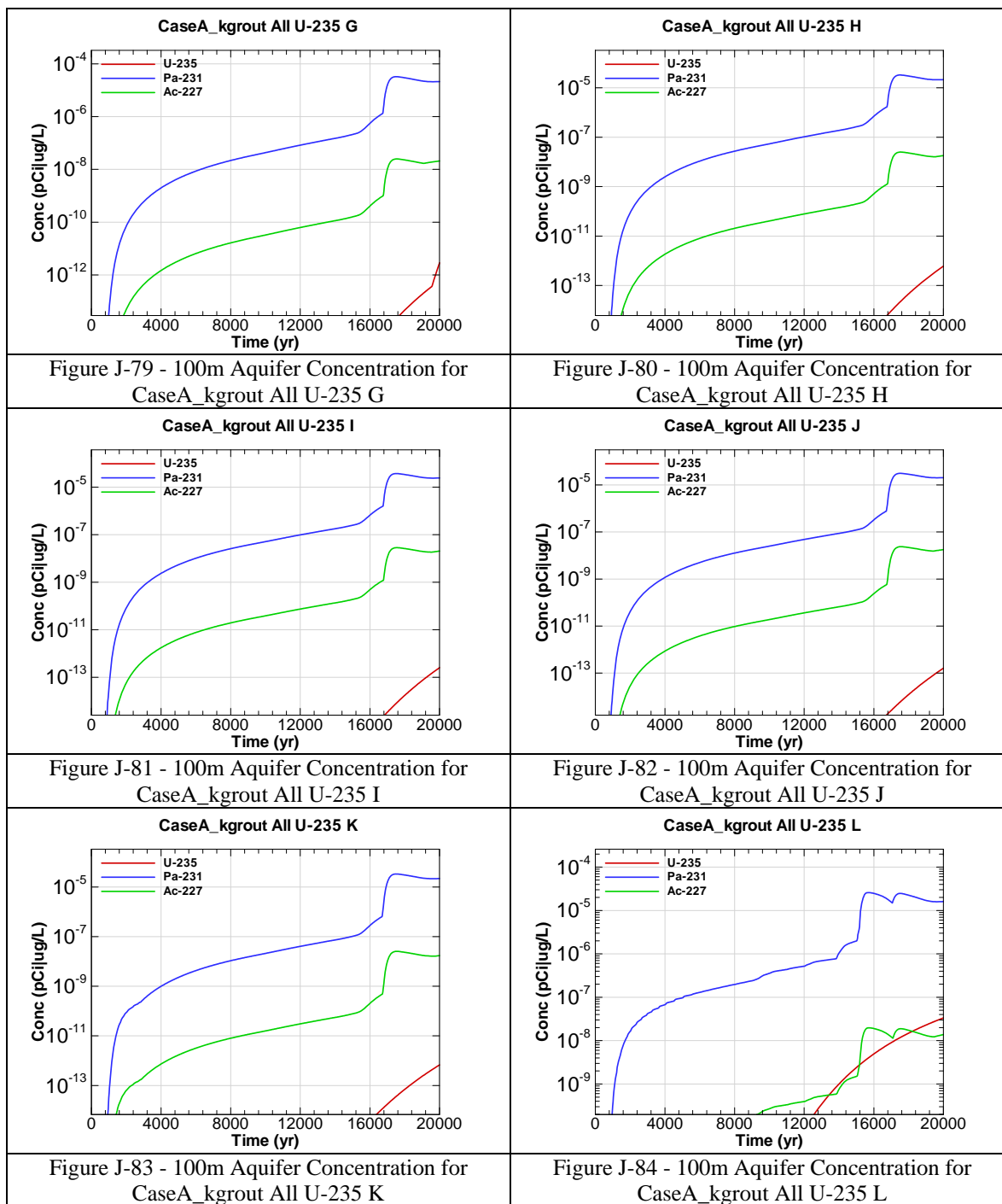


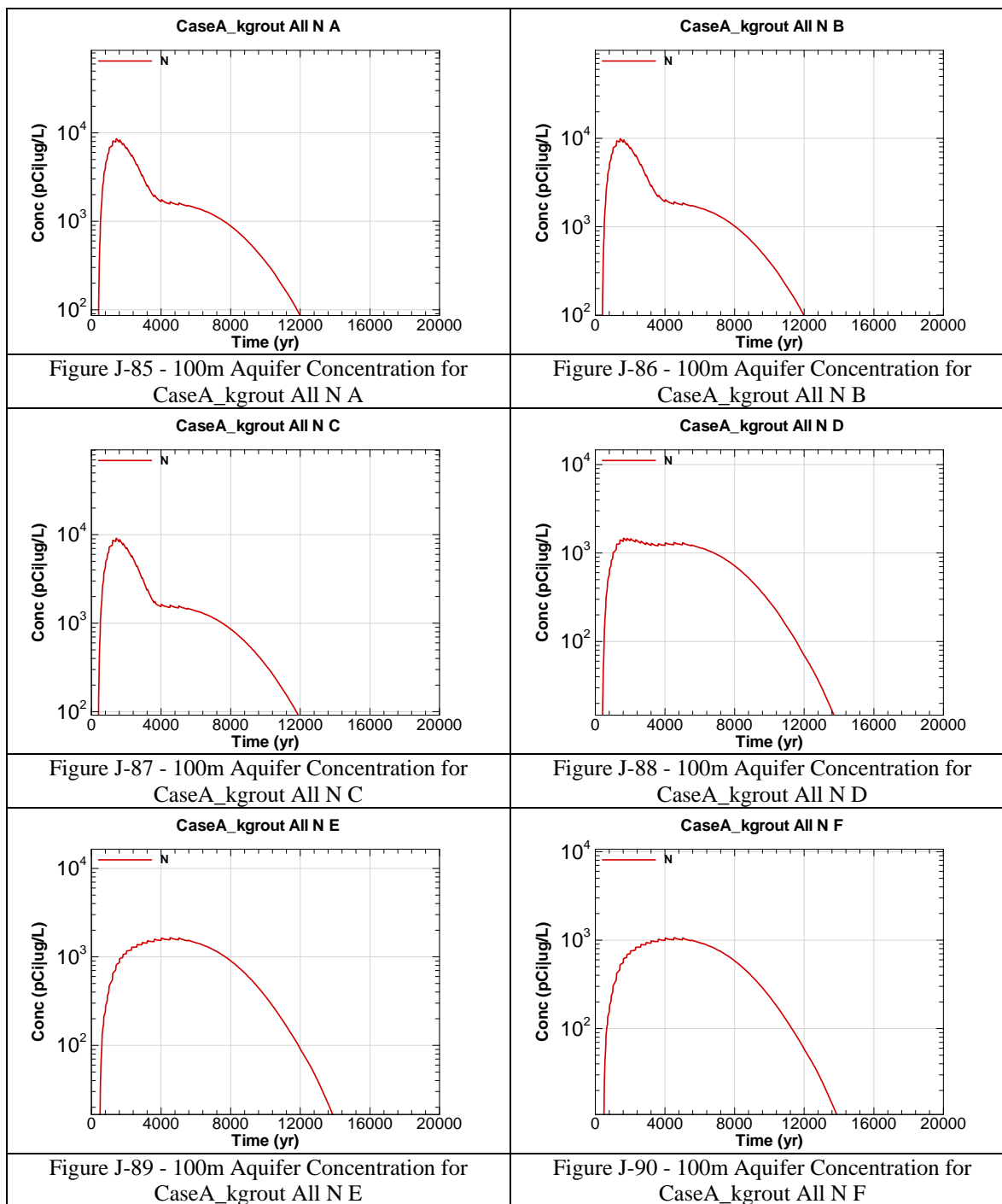


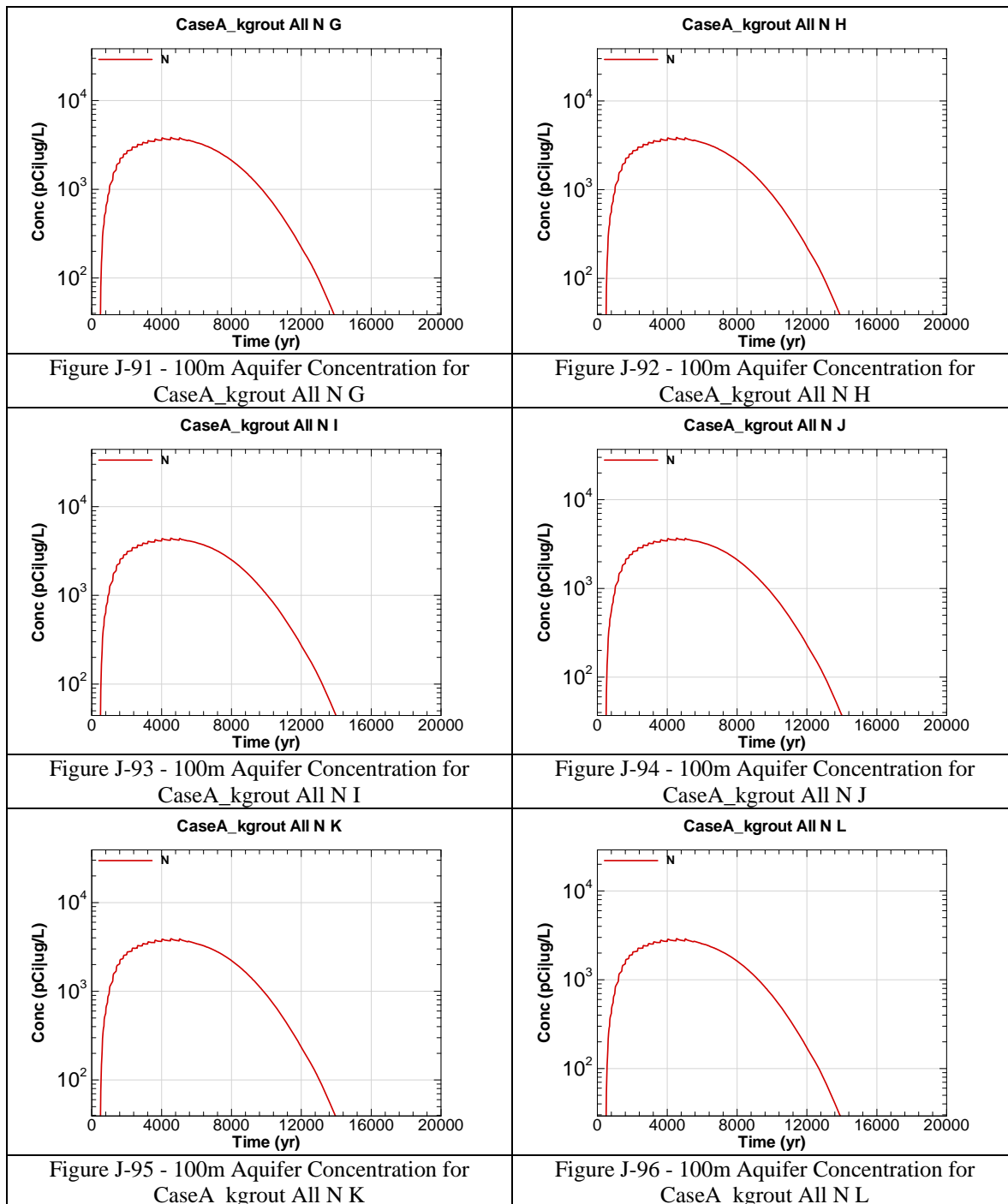












This page intentionally left blank

APPENDIX K

VAULT 1 AND 4 OXIDIZED CONCRETE SENSITIVITY

Appendix K contains curves showing the 100 meter concentrations for key radiological and chemical concentrations for all of SDF (vault and FDC inventories) for the Base Case (Case A) for a case of the concrete walls and floor of Vault 1 and 4 oxidized at time zero. 20,000 year concentration results are presented for Sectors A through L for the peak concentration per sector regardless of aquifer.

Graph heading example "CaseA_ox All I-129 A"

Key

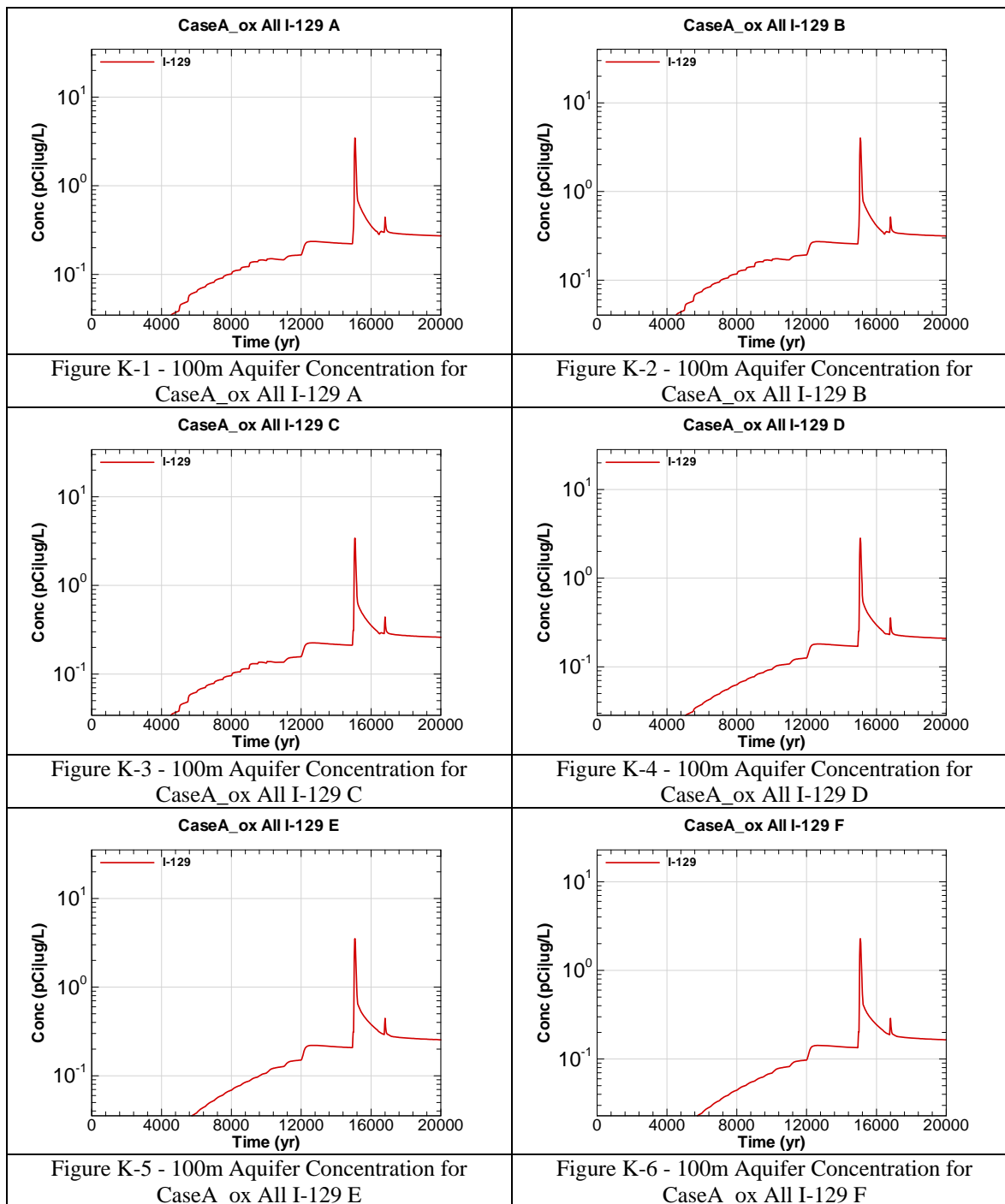
CaseA = Scenario case

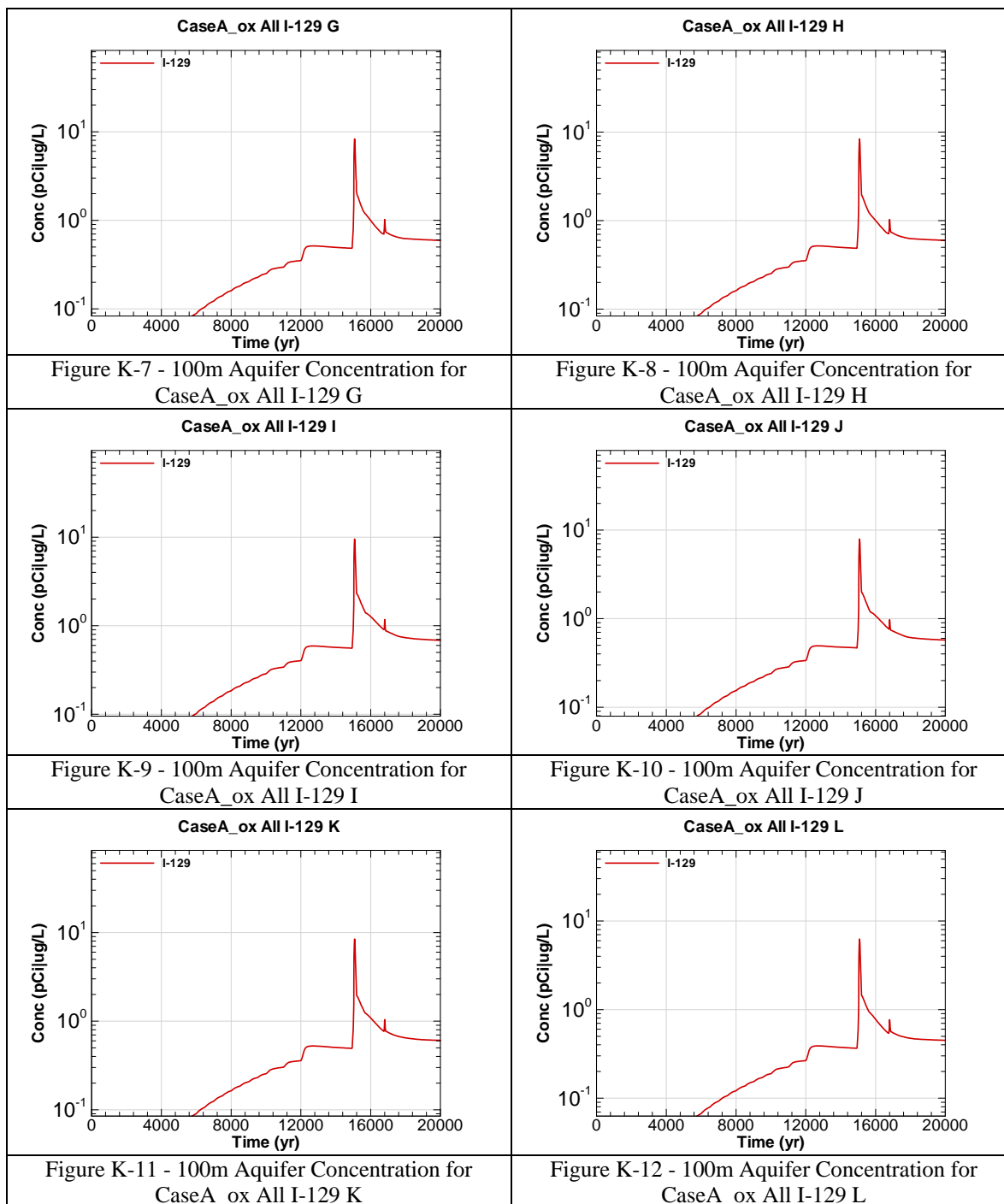
ox = Oxidized Vault 1 and 4 concrete

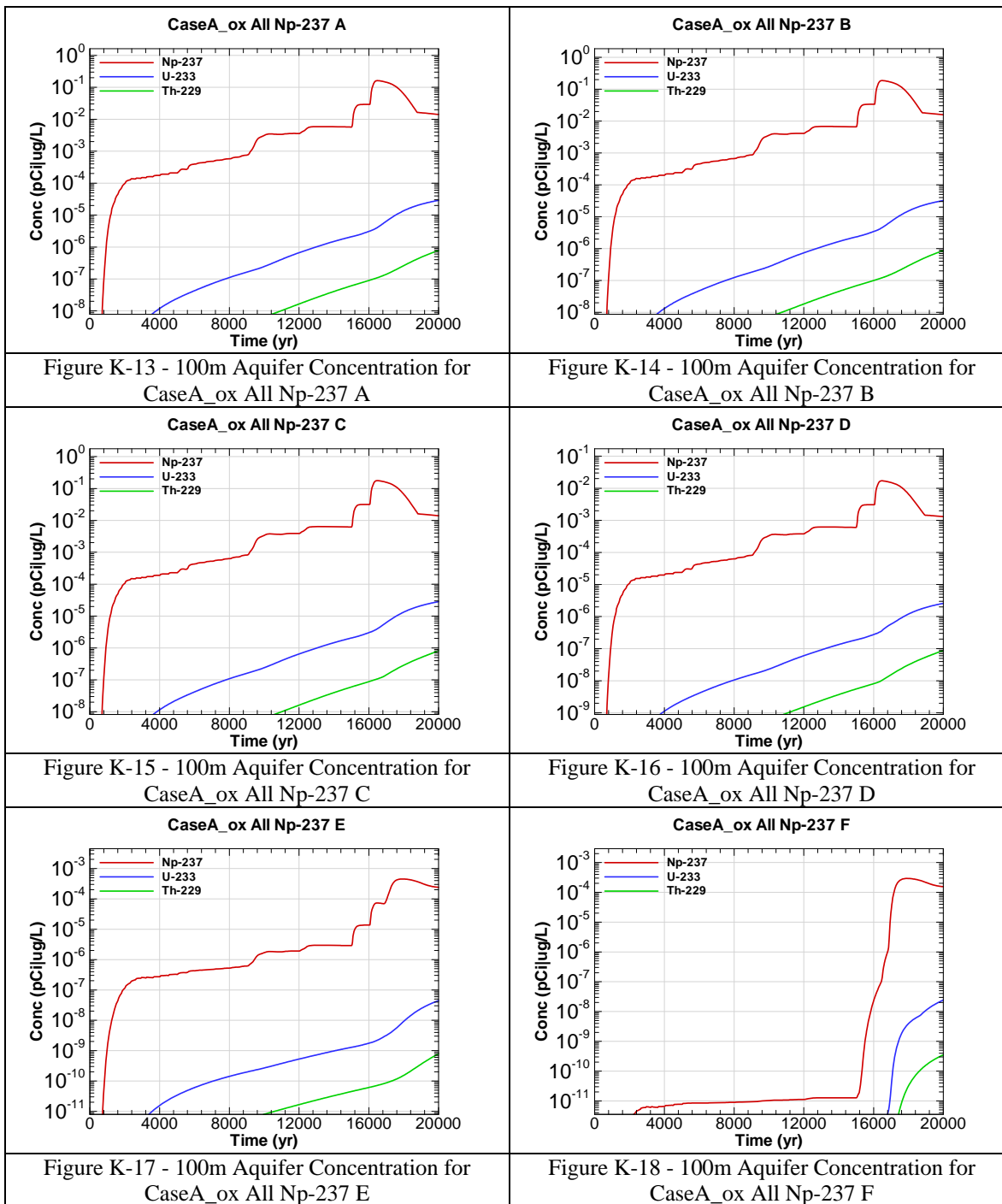
All = Inventory source is all disposal units

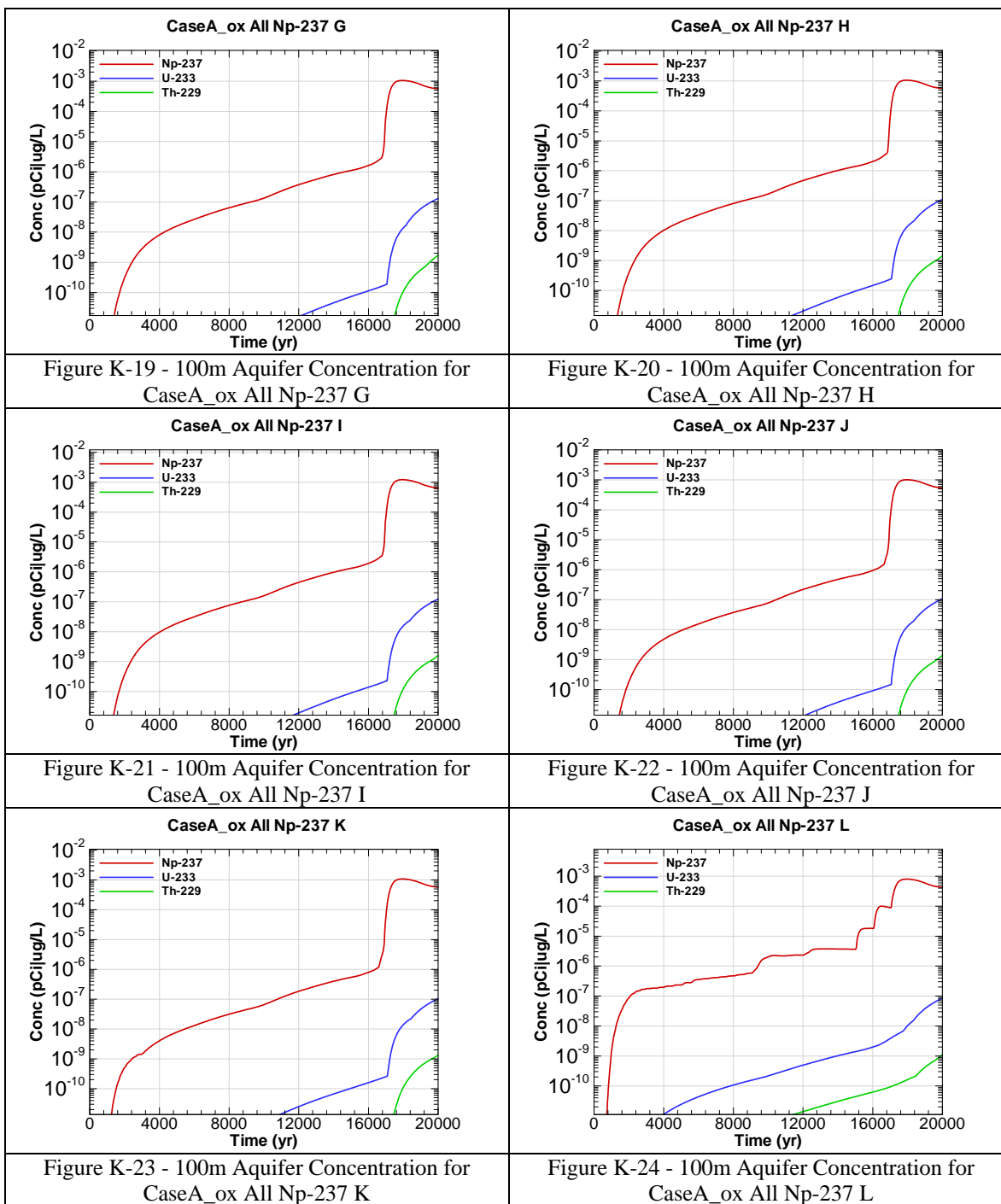
I-129 = Radionuclide or chemical of concern

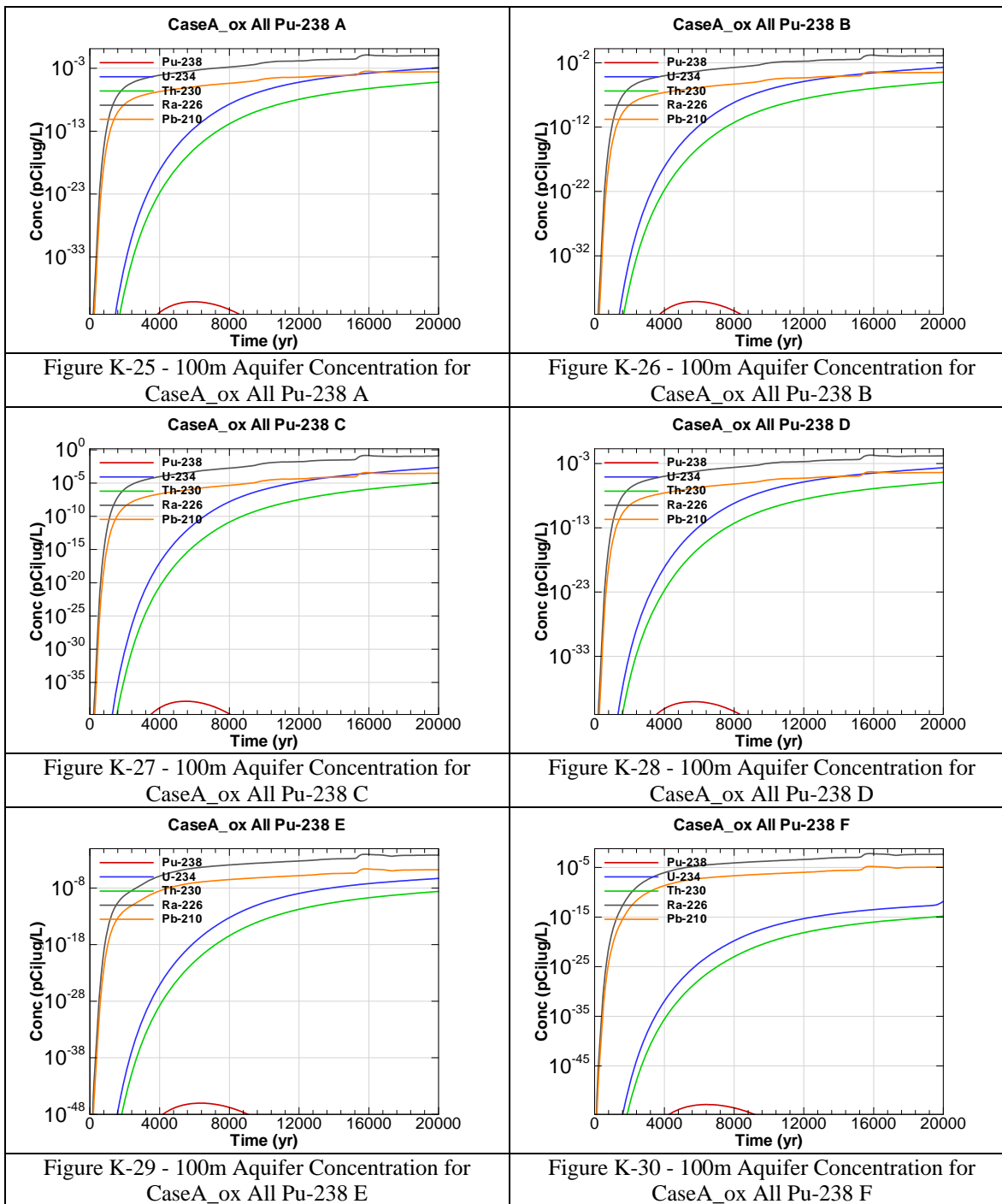
A = Evaluation sector of concern

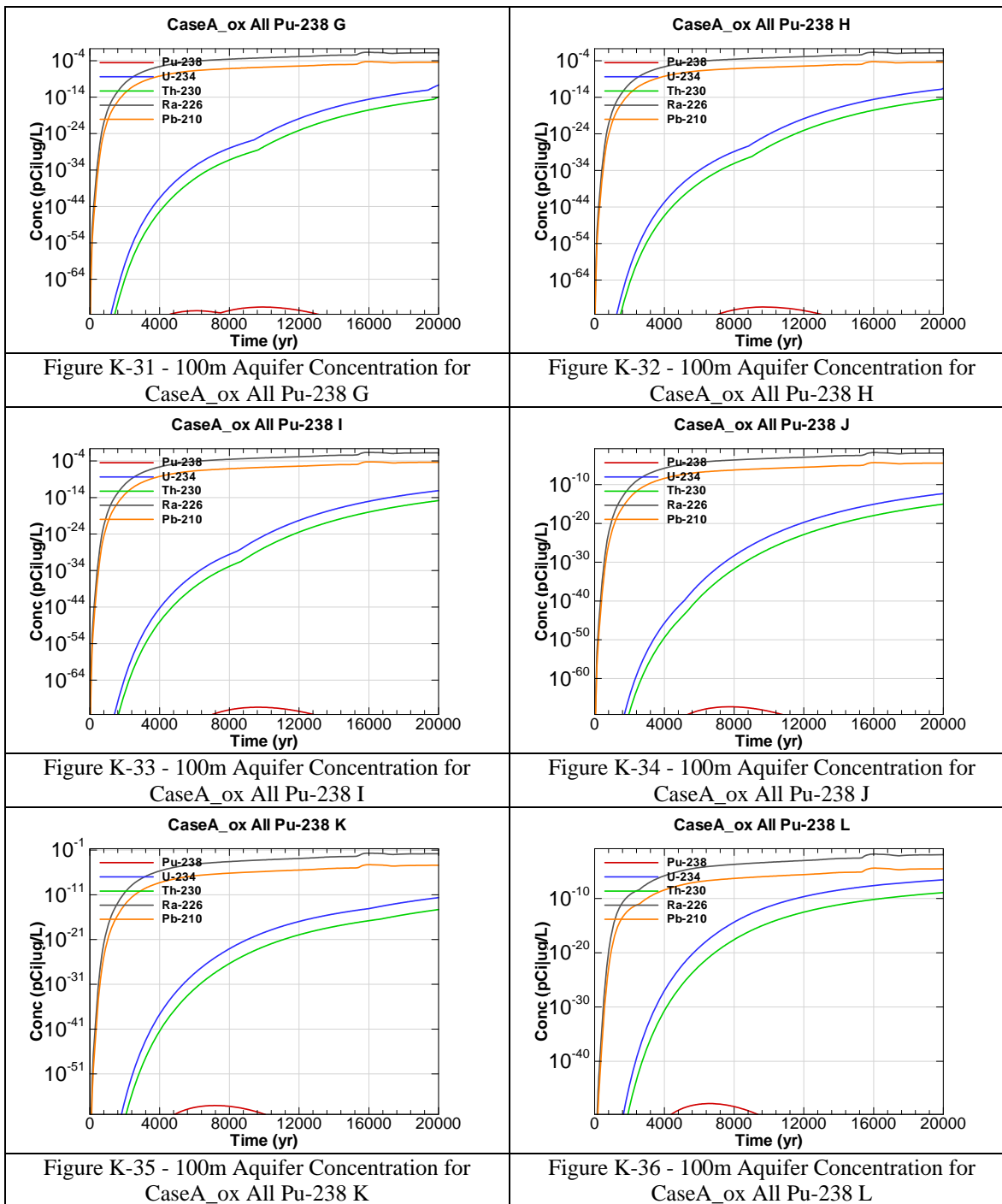


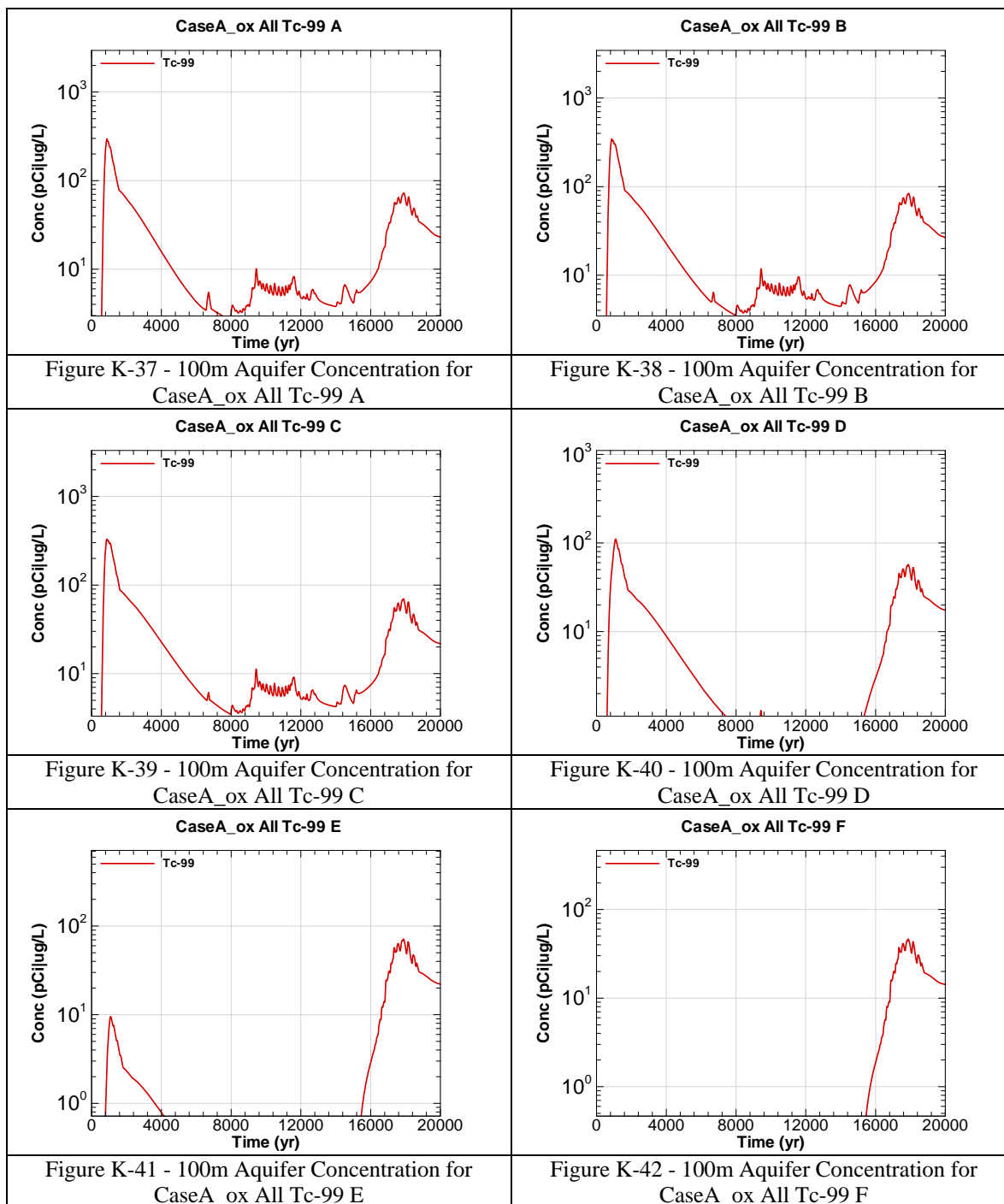


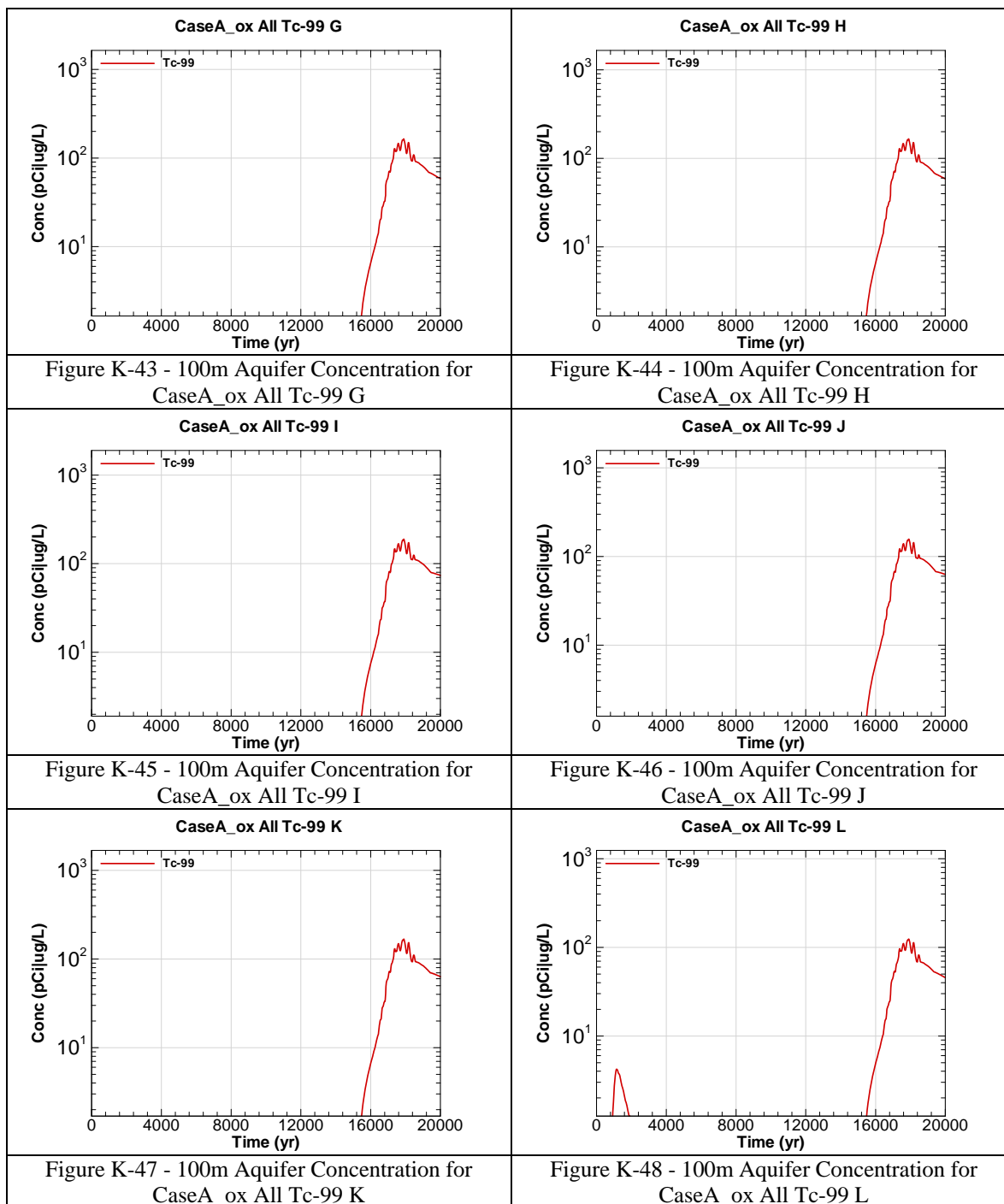


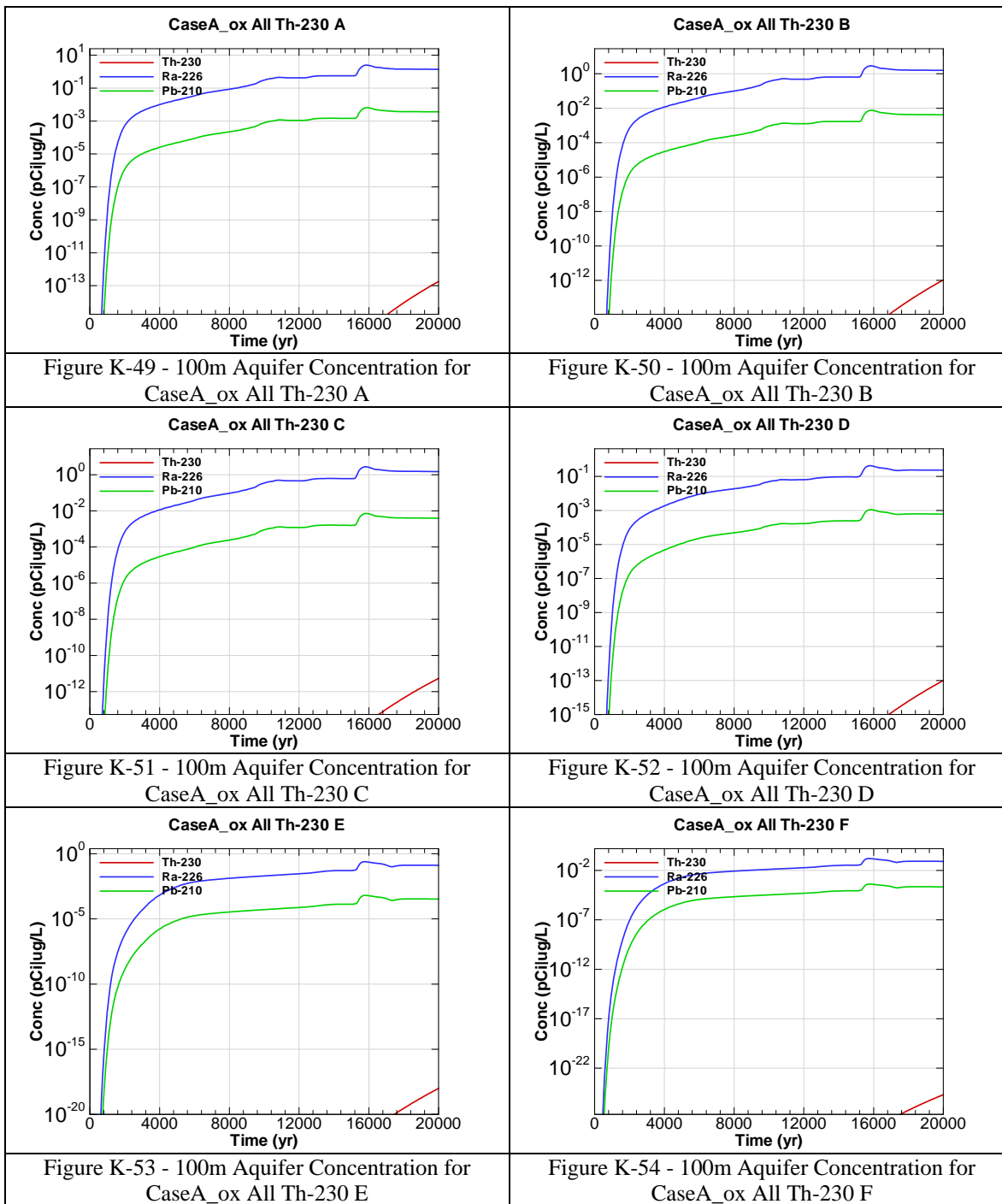


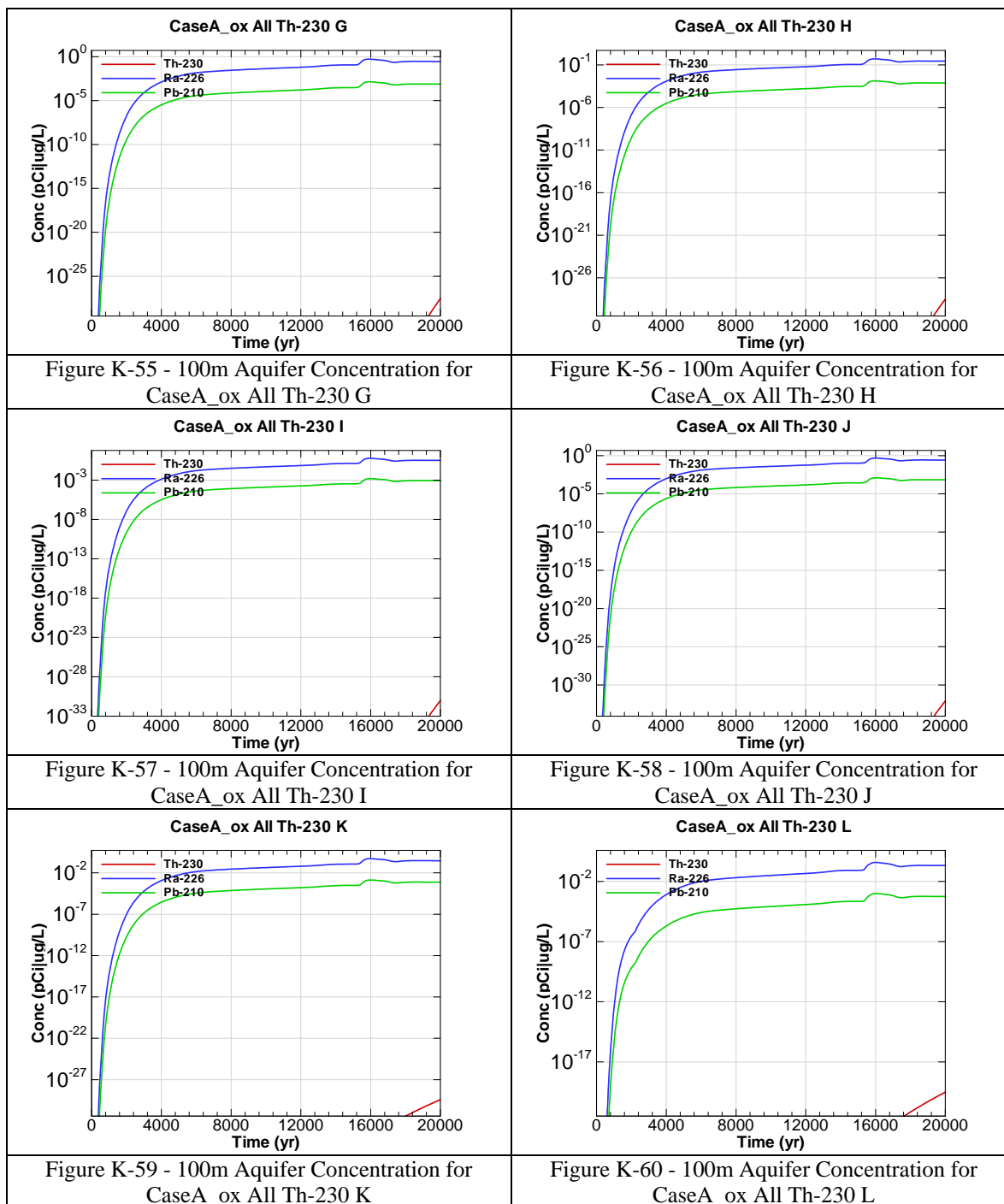


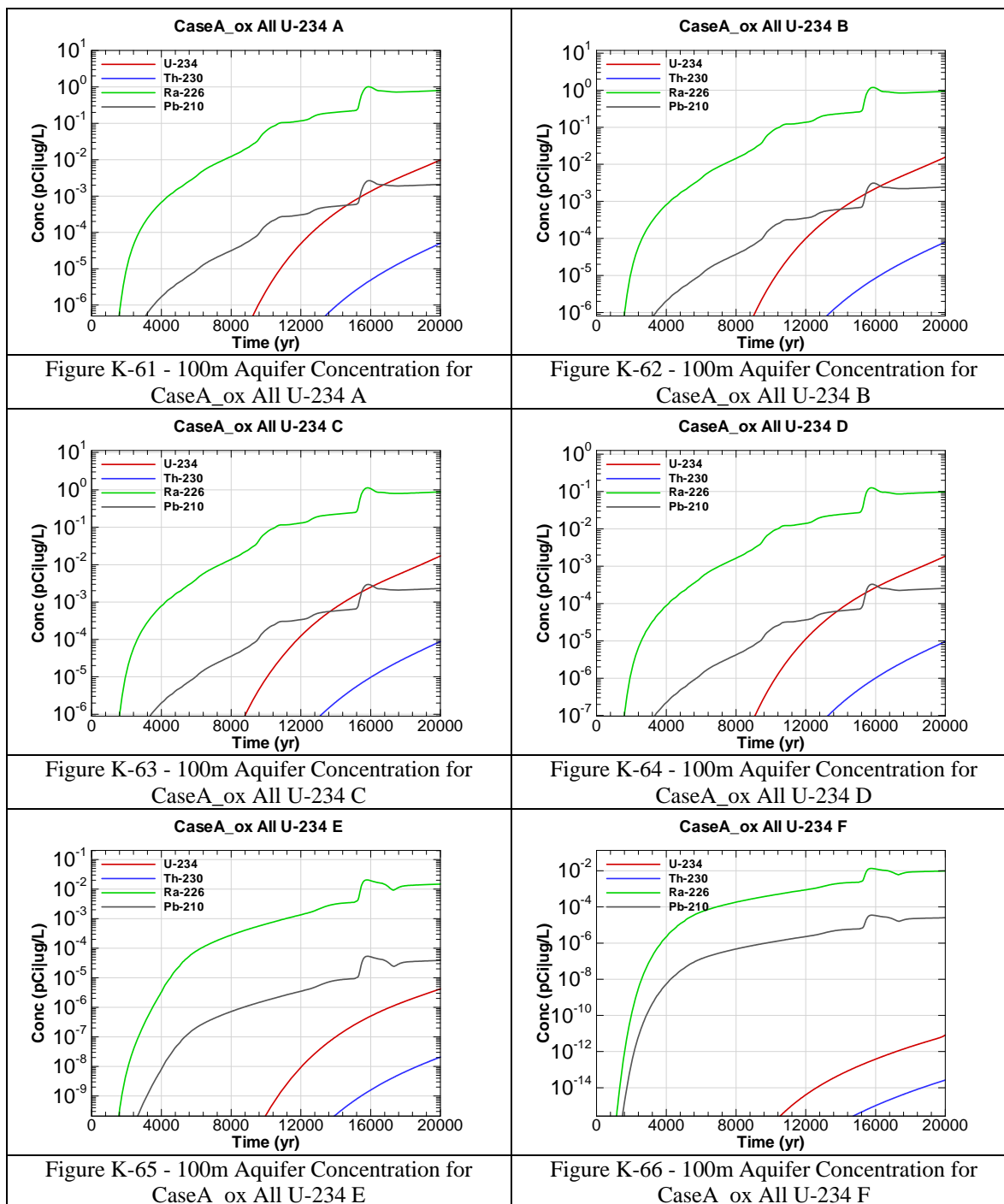


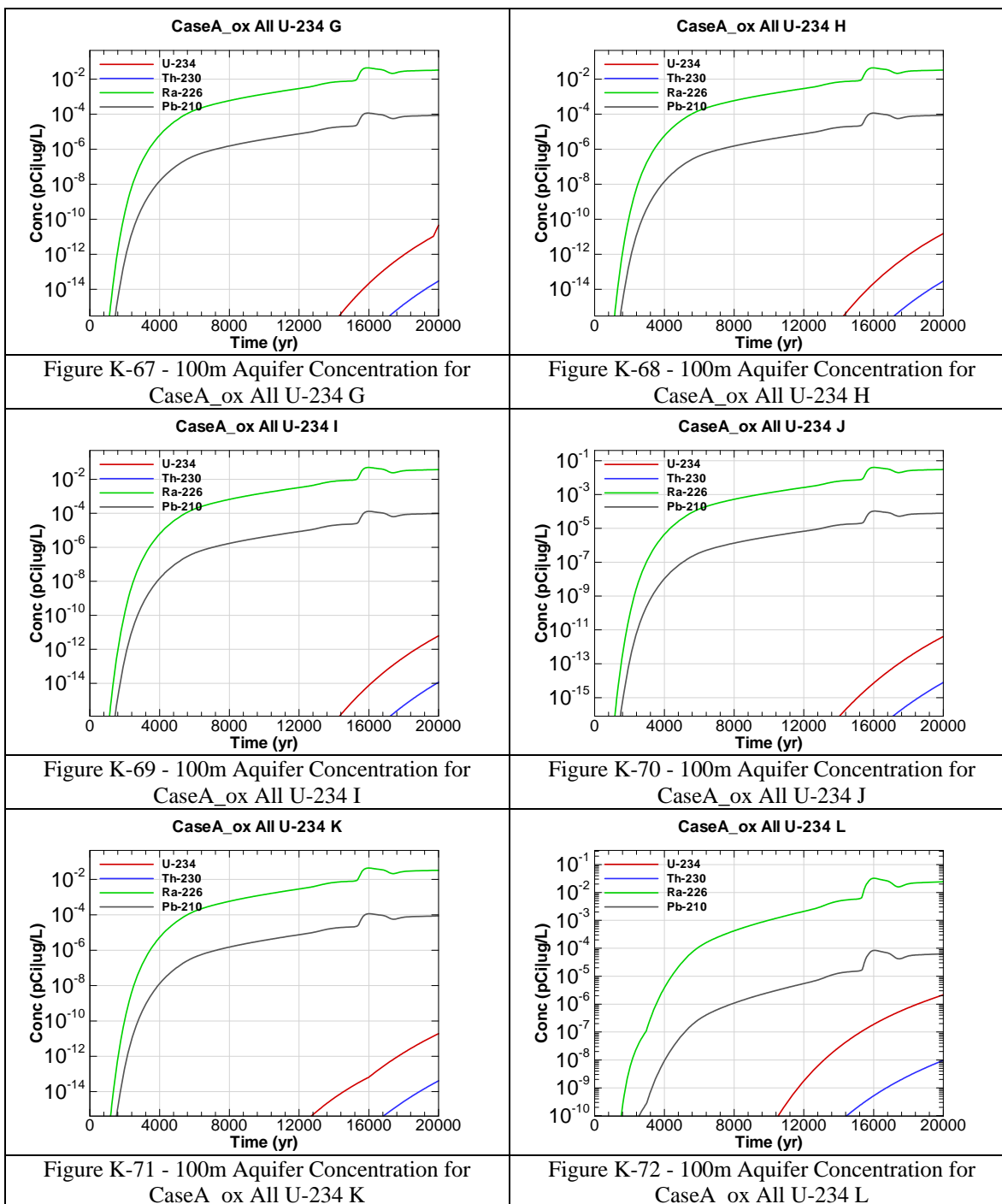


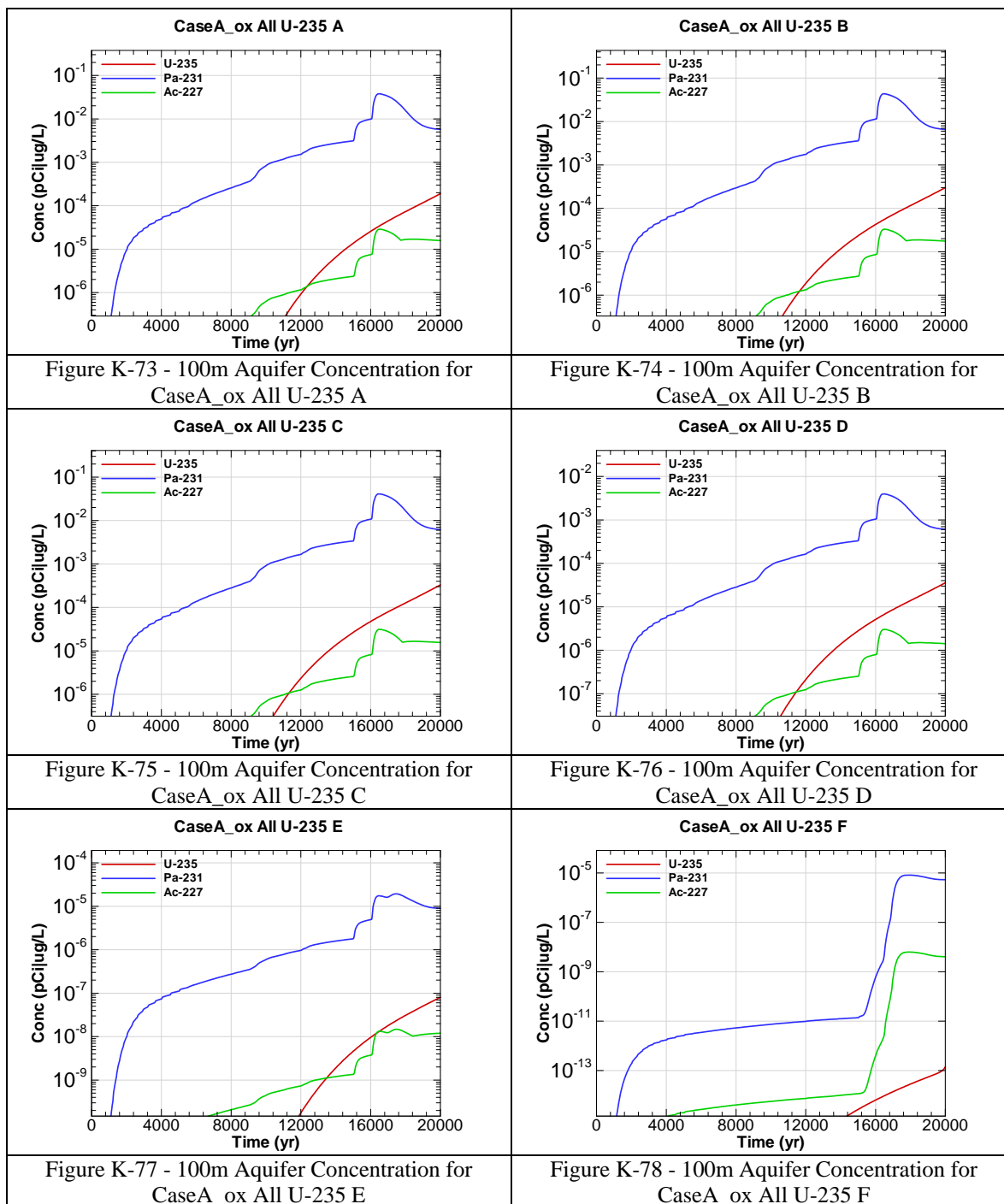


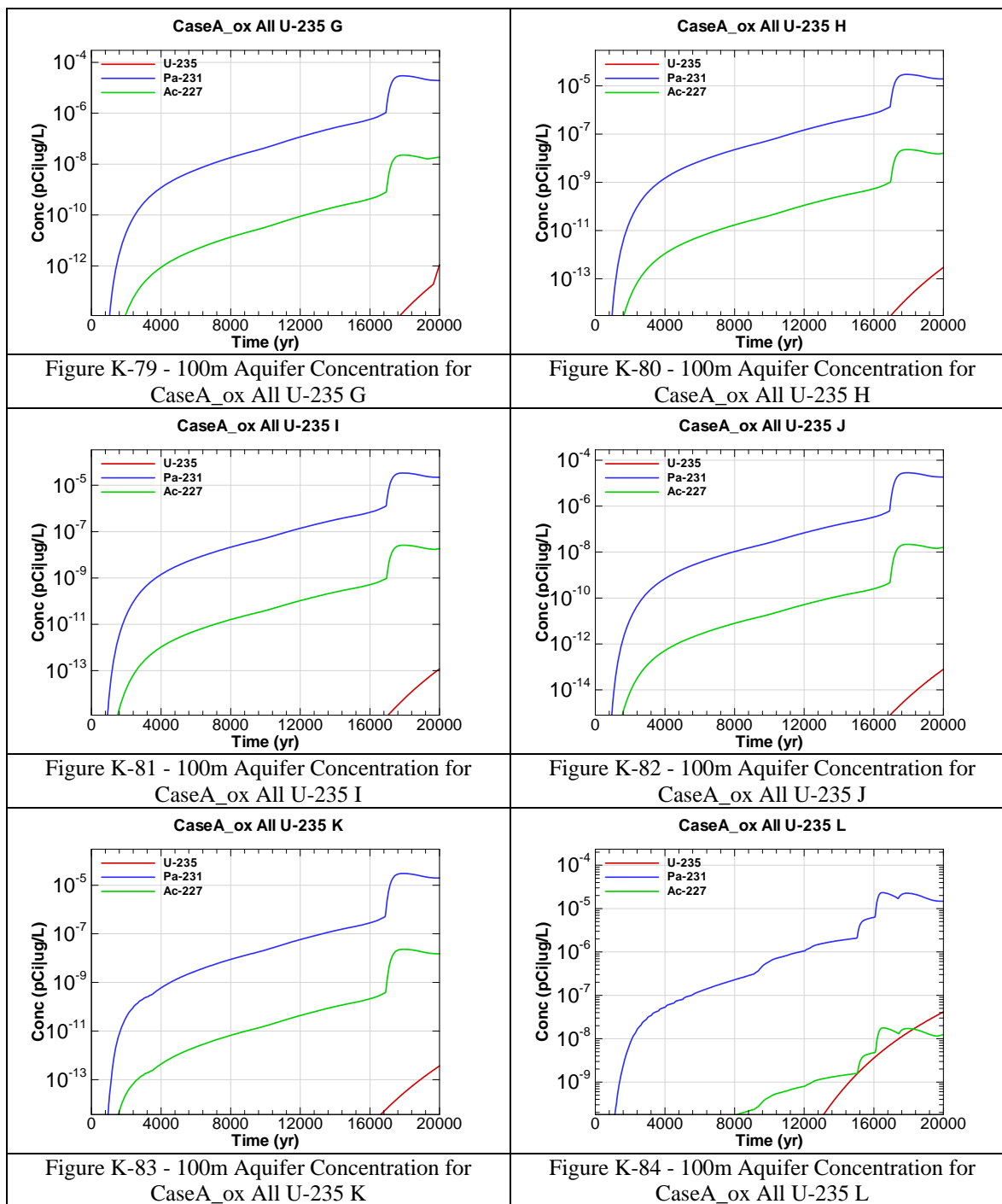


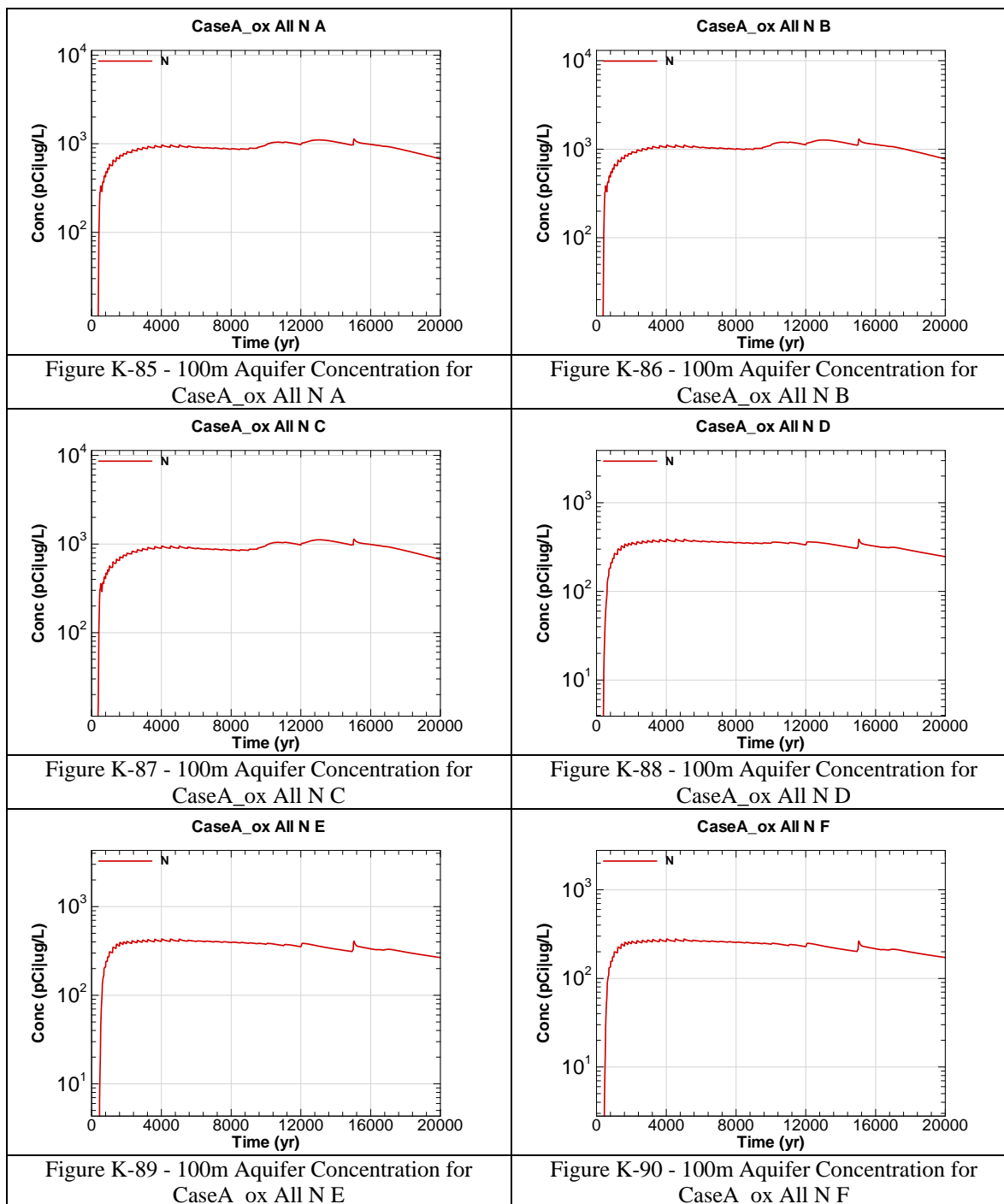


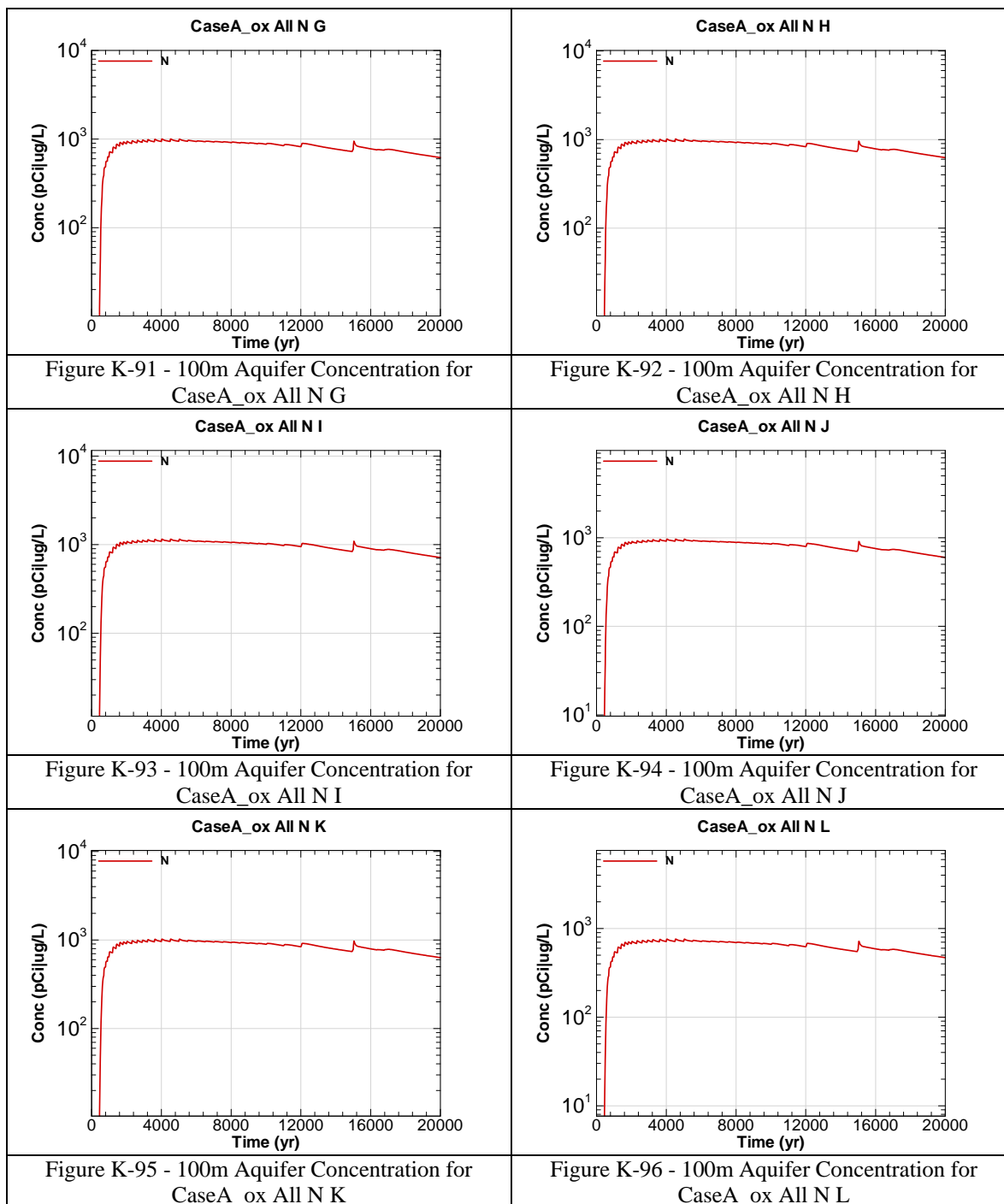












This page intentionally left blank

APPENDIX L

ALTERNATIVE DETERMINISTIC SENSITIVITY CASE

Appendix H contains curves showing the 100 meter concentrations for key radiological and chemical concentrations for all of SDF (vault and FDC inventories) for the alternative case addressing increased cap infiltration, early concrete degradation from rebar corrosion, saltstone cracking, and gaseous oxygen supplied to saltstone for accelerated oxidation. 20,000 year concentration results are presented for Sectors A through L for the peak concentration per sector regardless of aquifer.

Graph heading example “CaseJ All I-129 A”

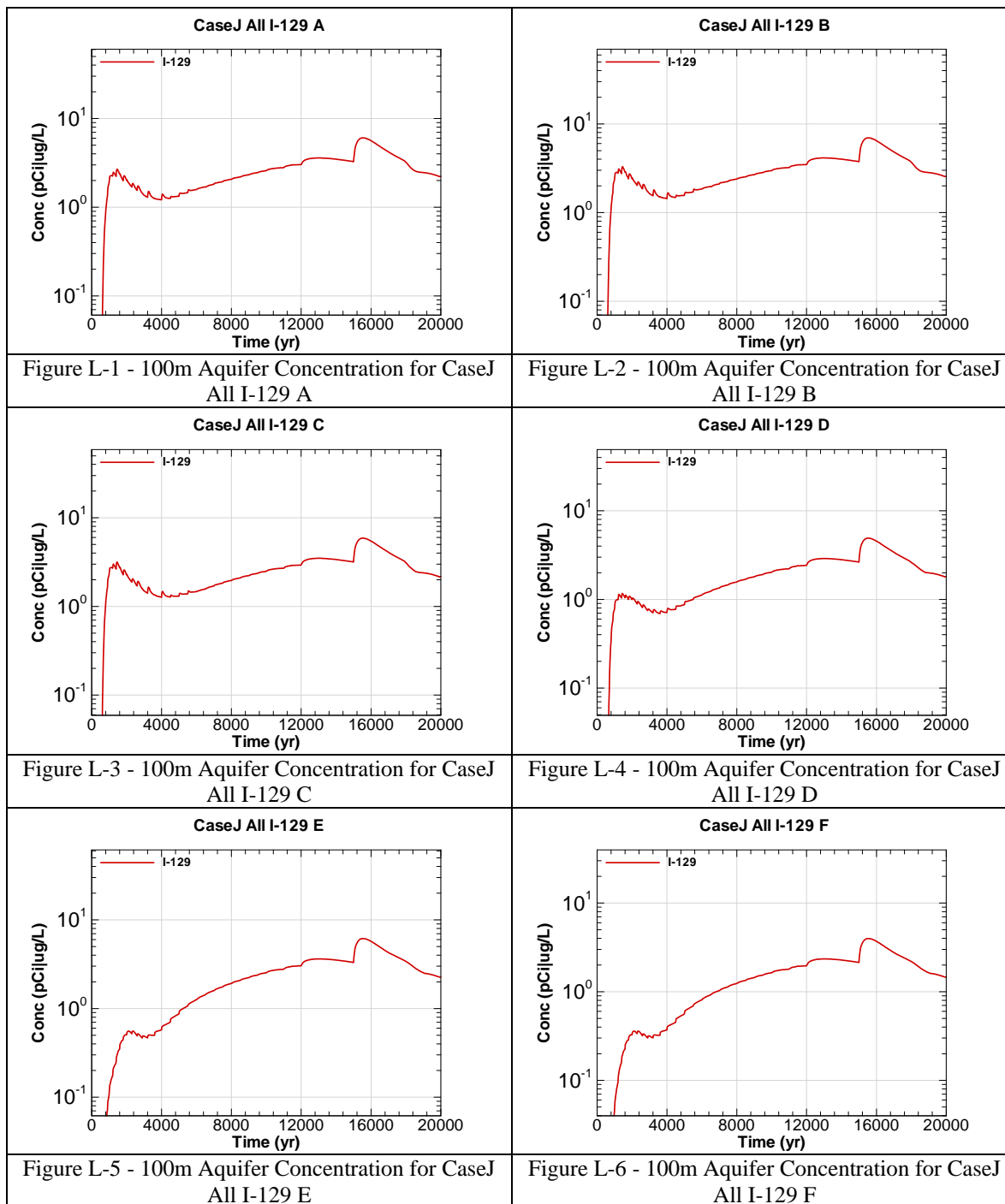
Key

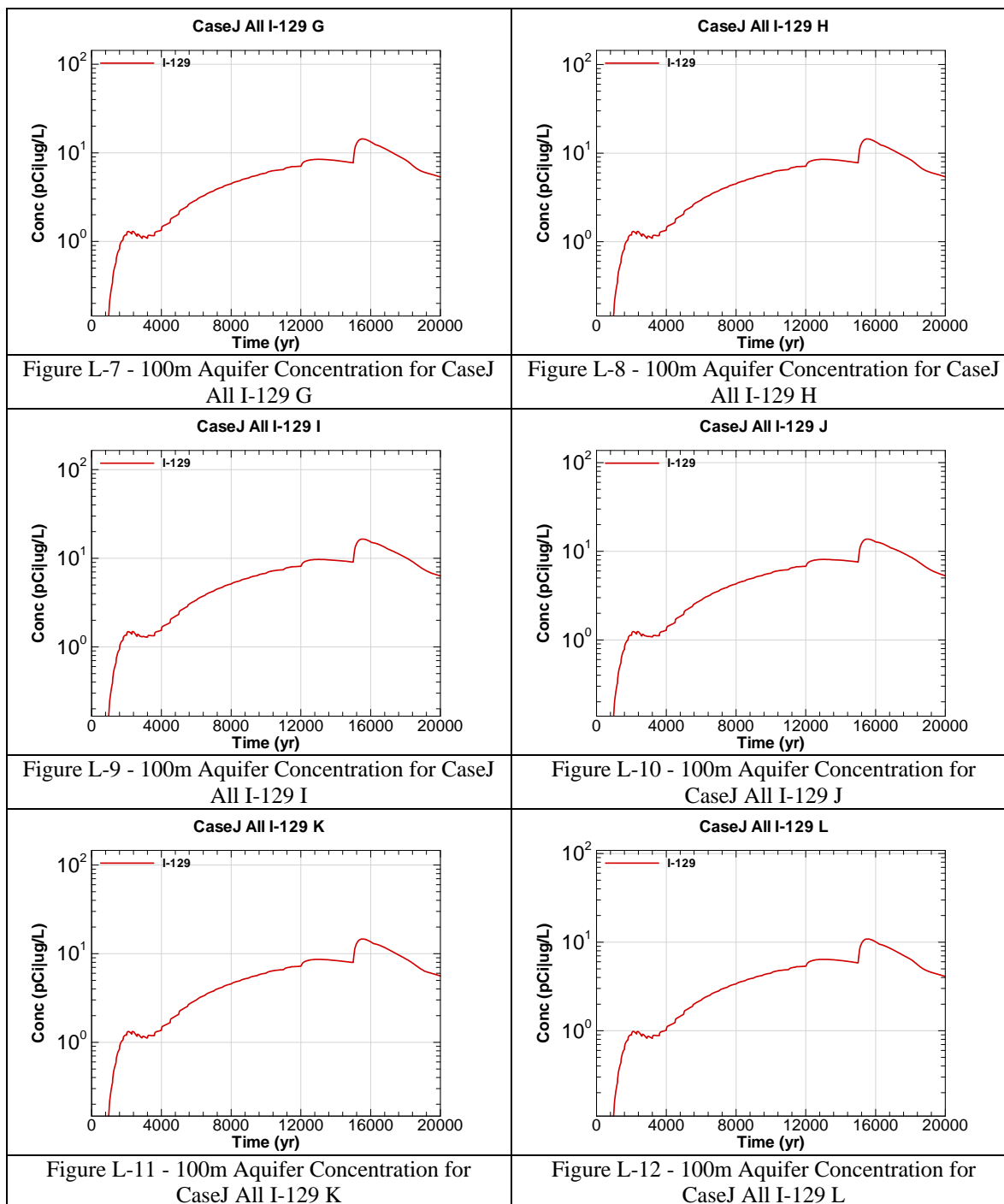
CaseJ = Alternative case

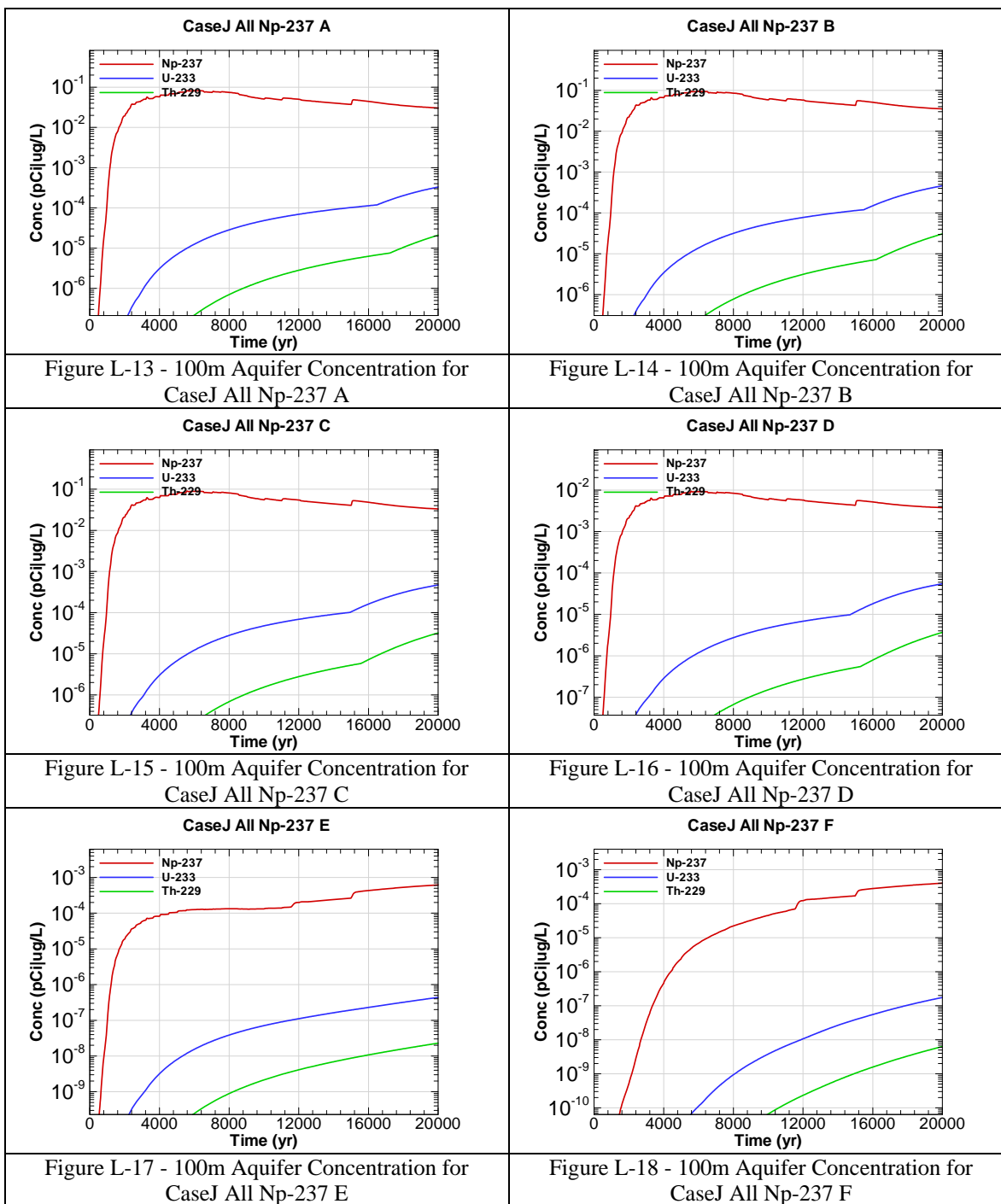
All = Inventory source is all disposal units

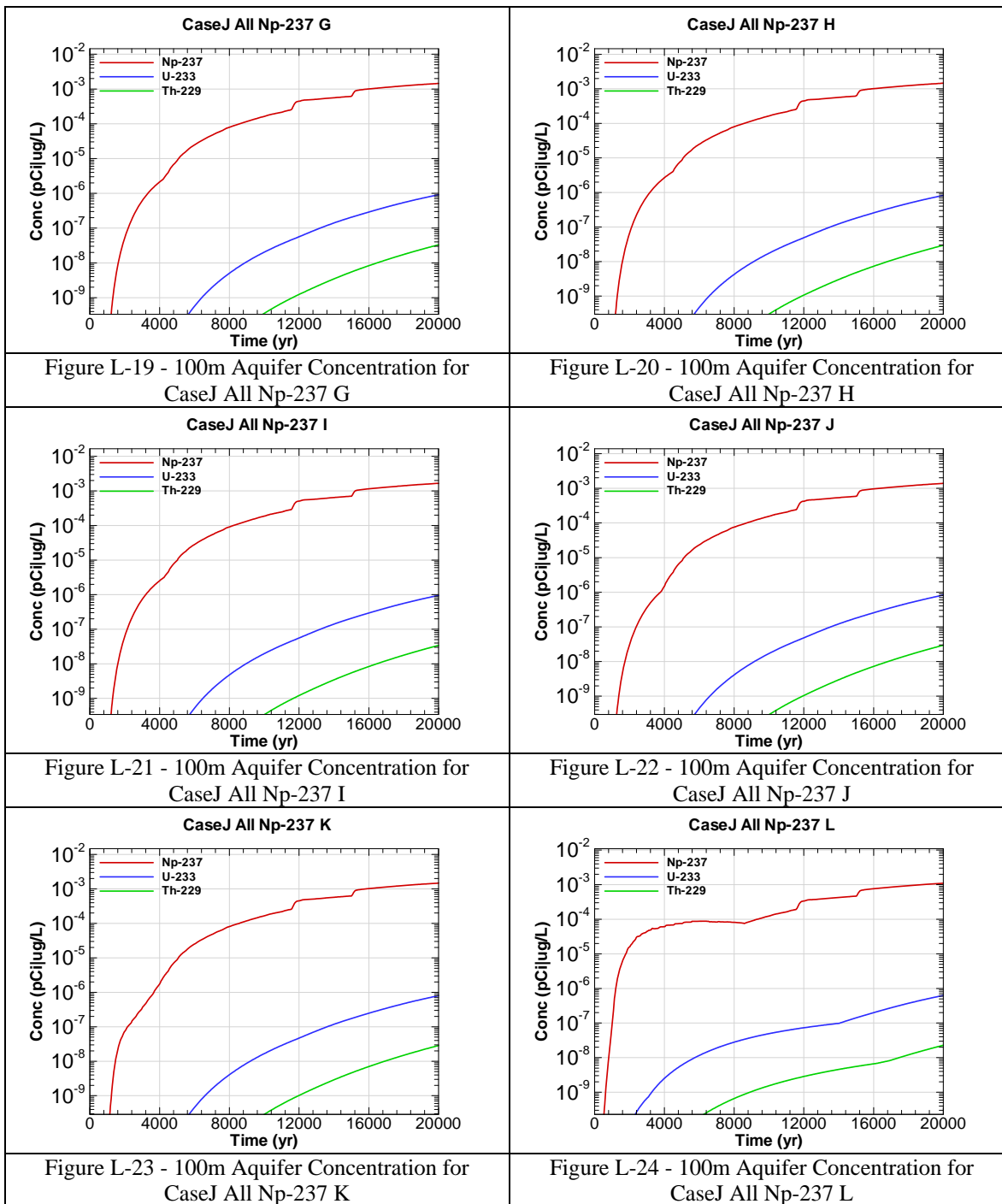
I-129 = Radionuclide or chemical of concern

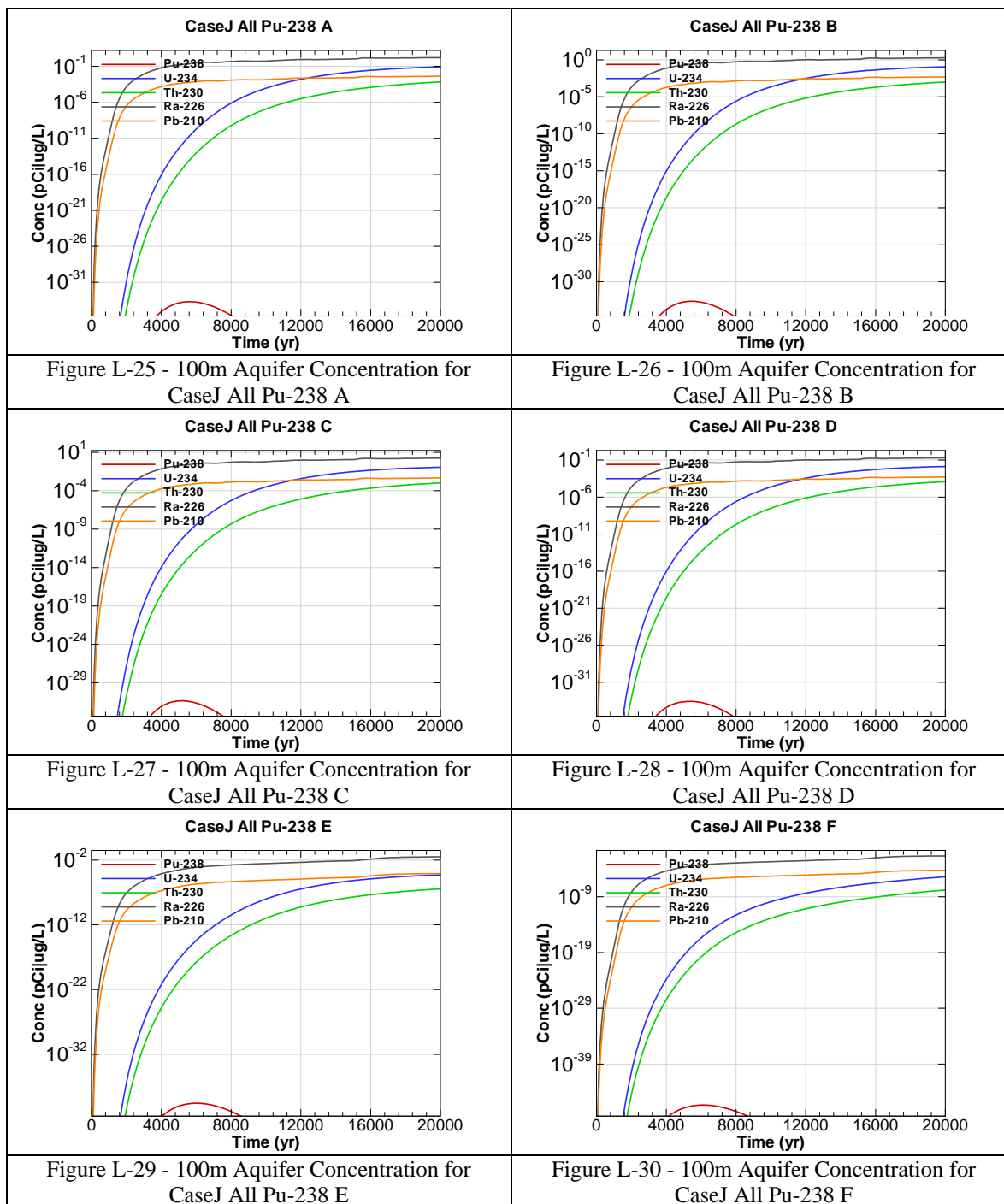
A = Evaluation sector of concern

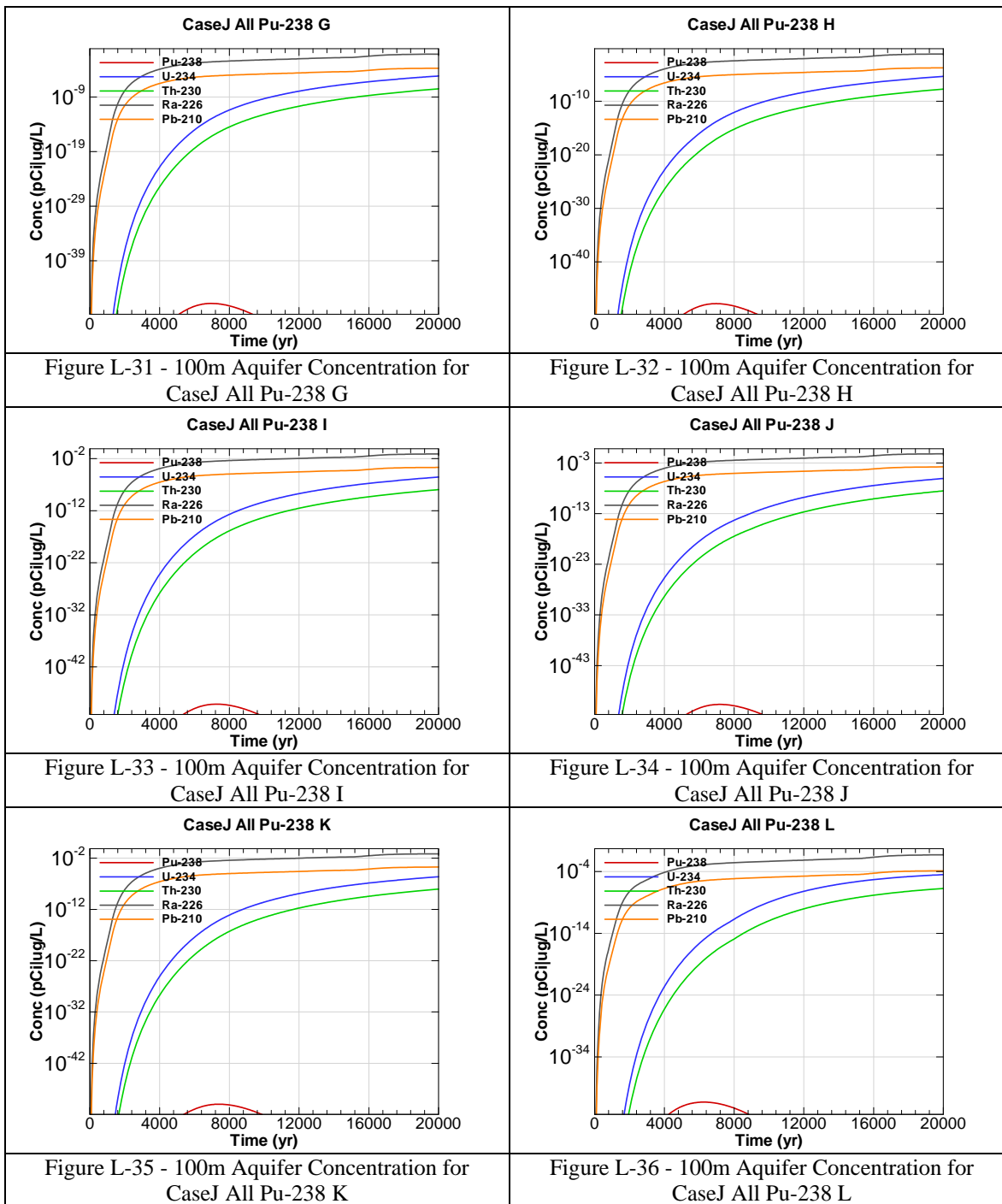


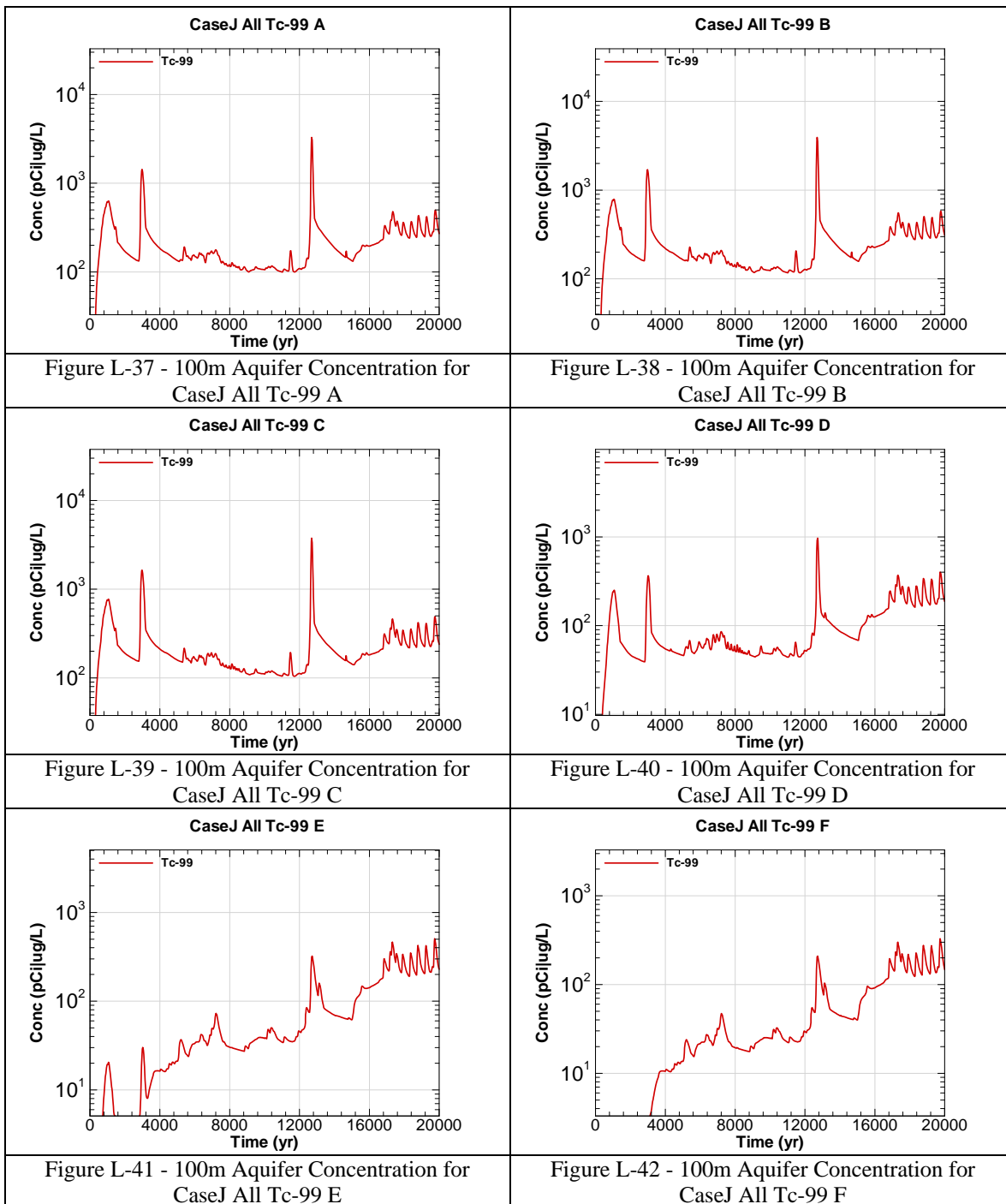


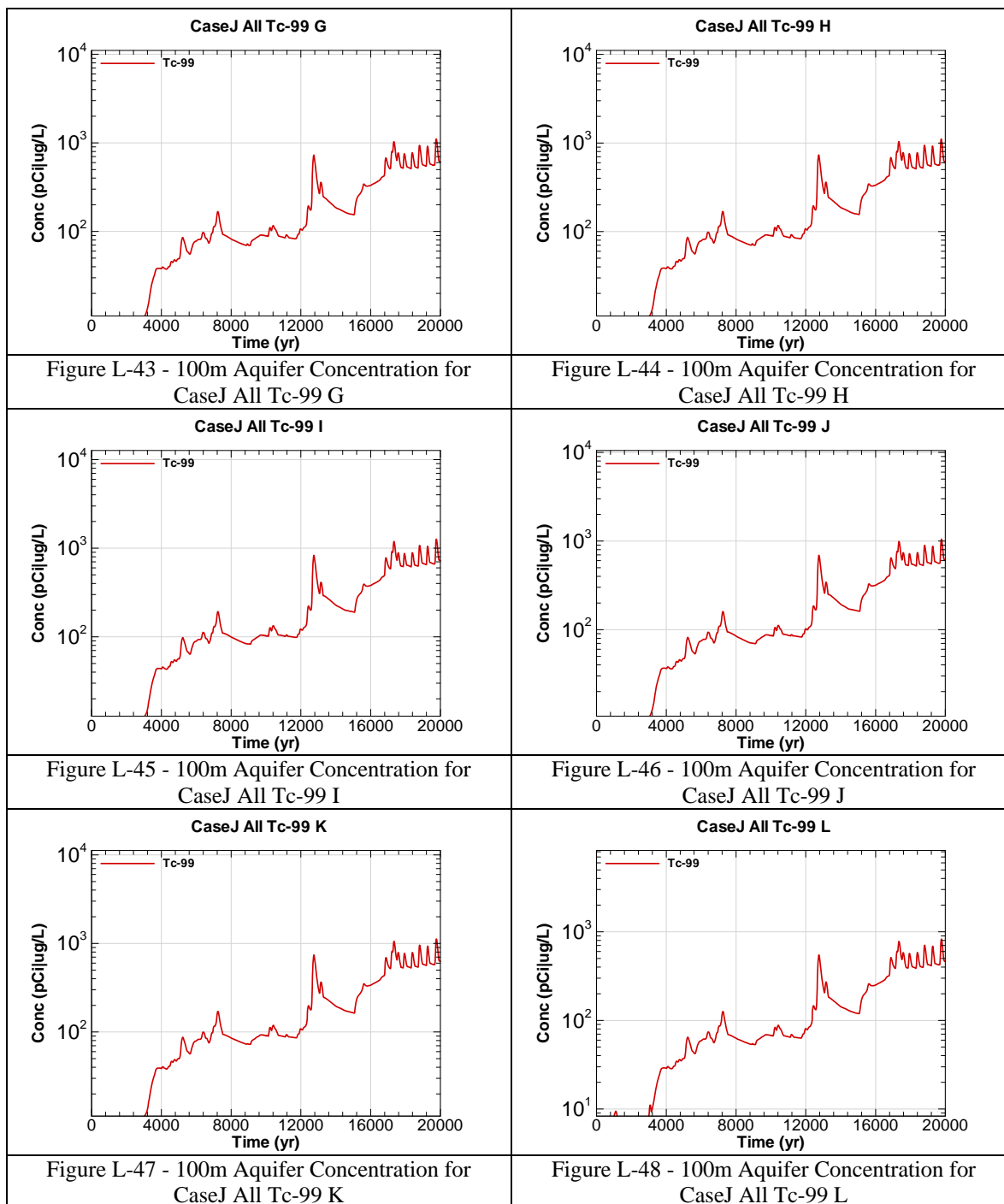


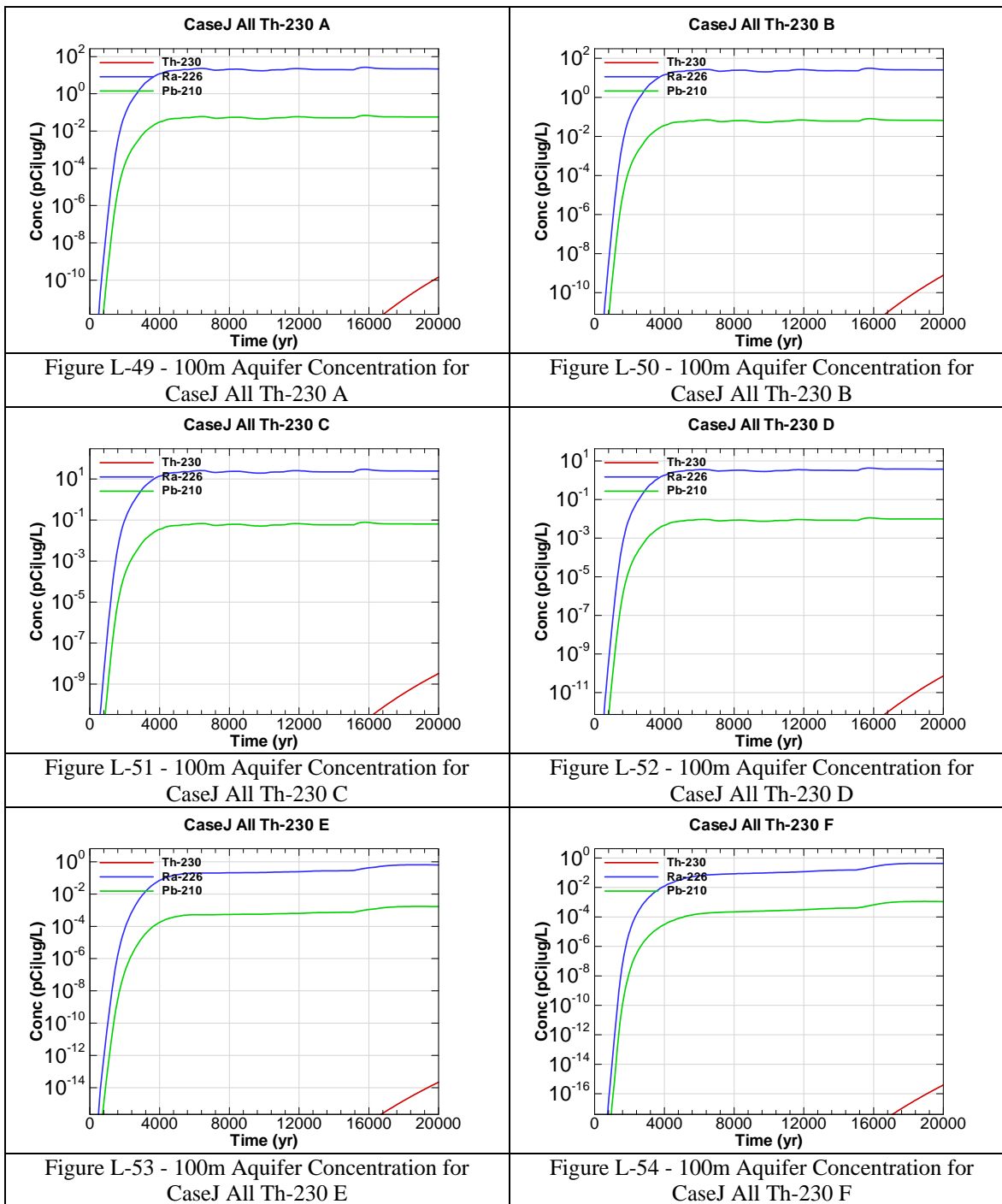


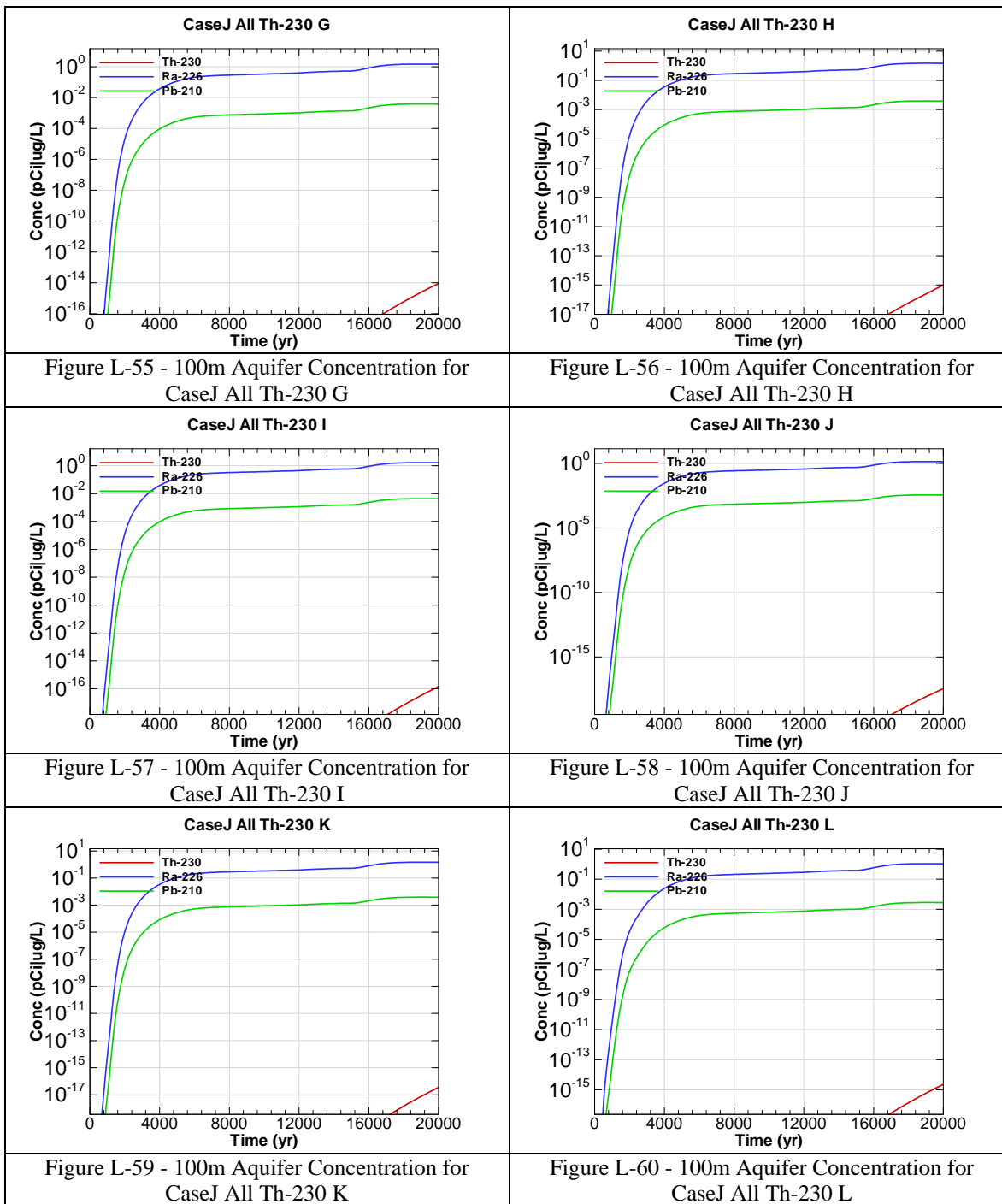


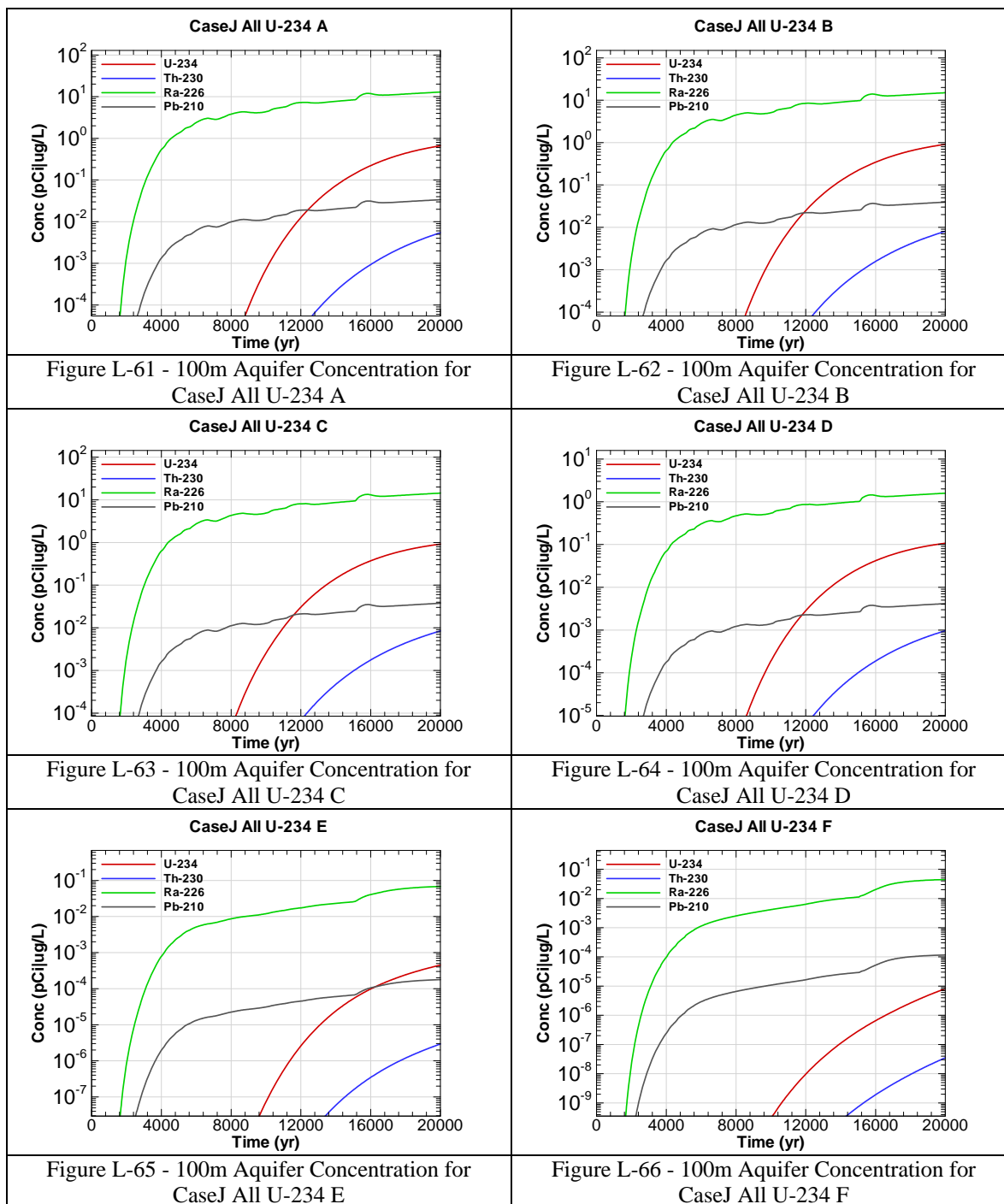


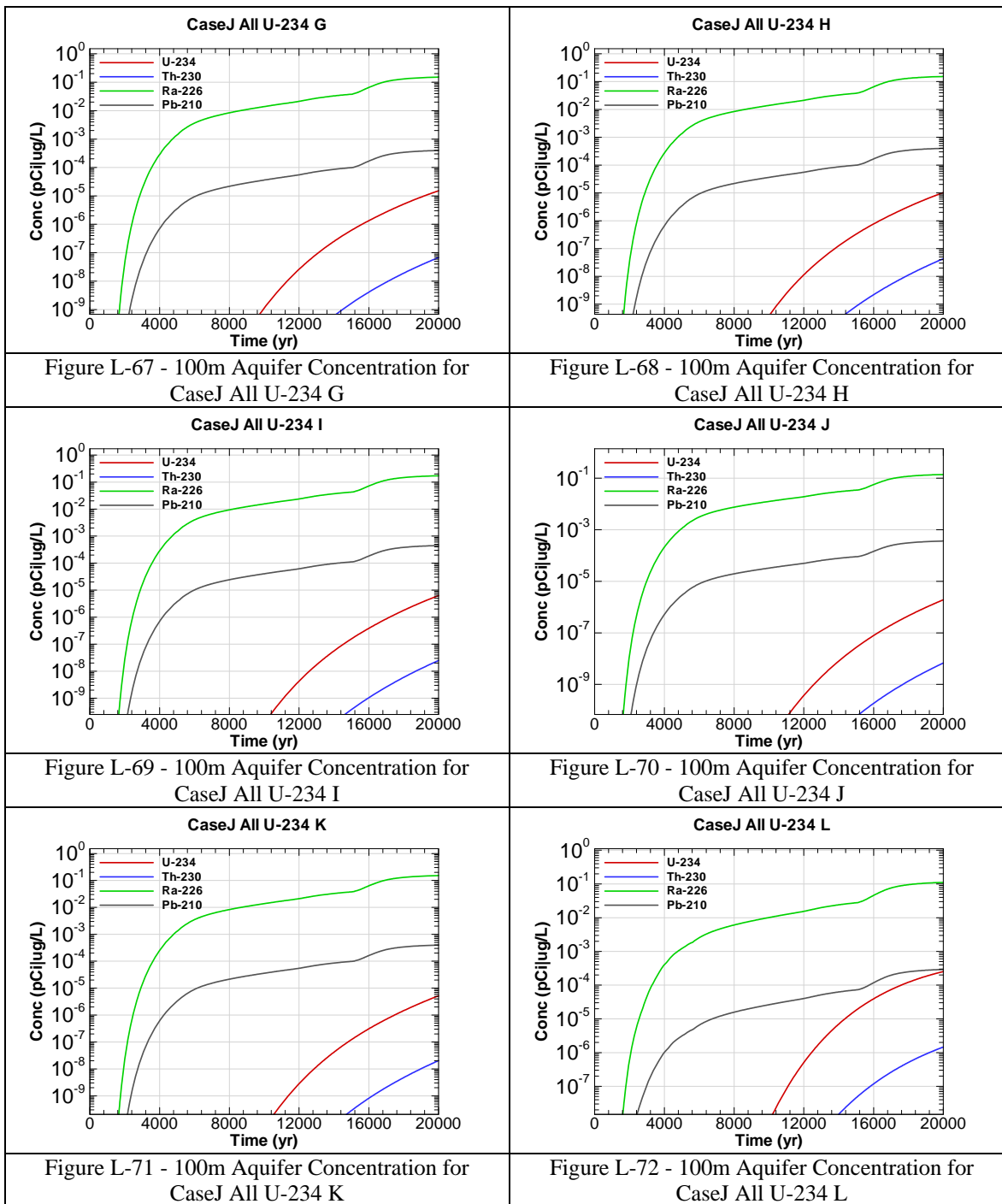


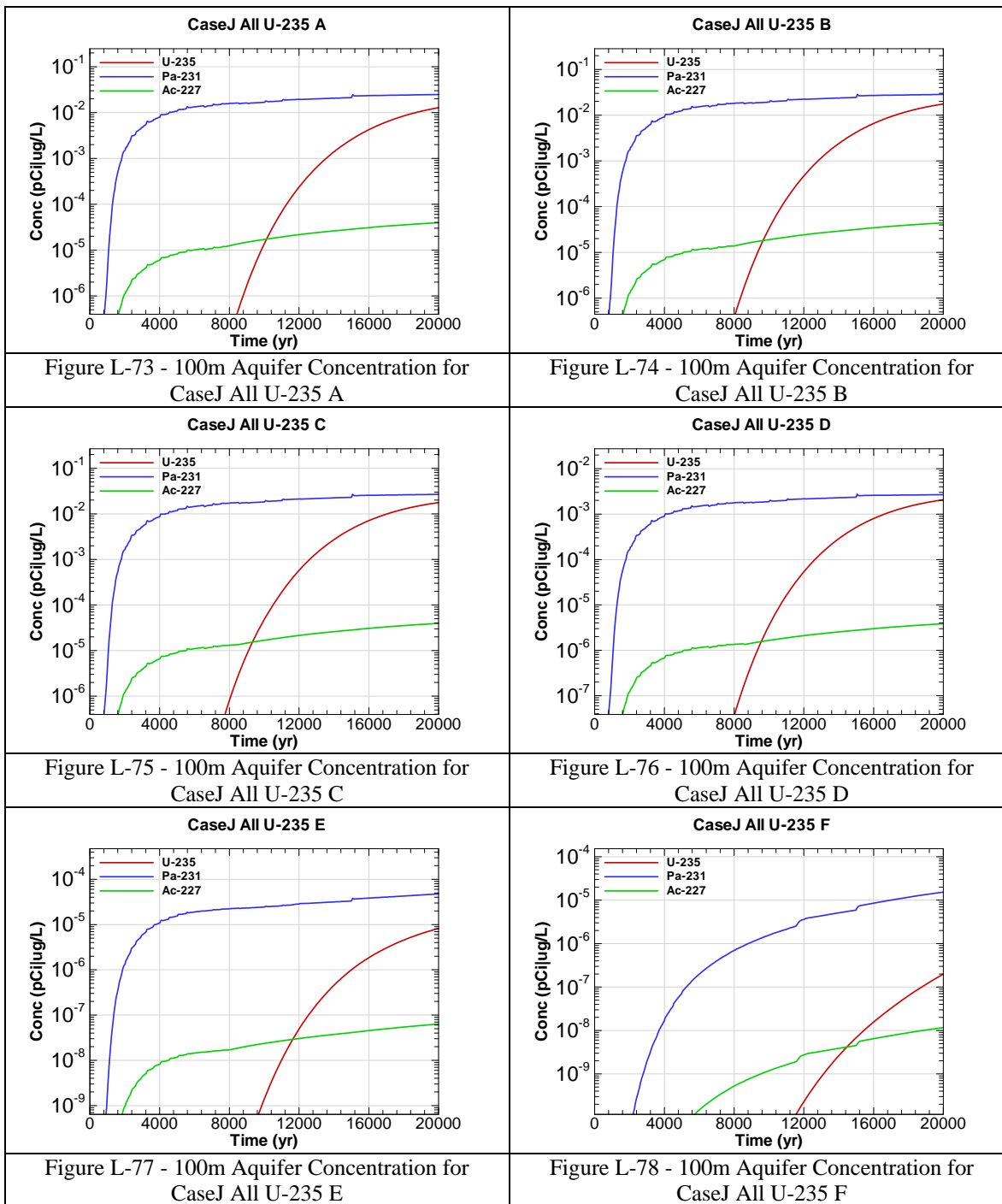


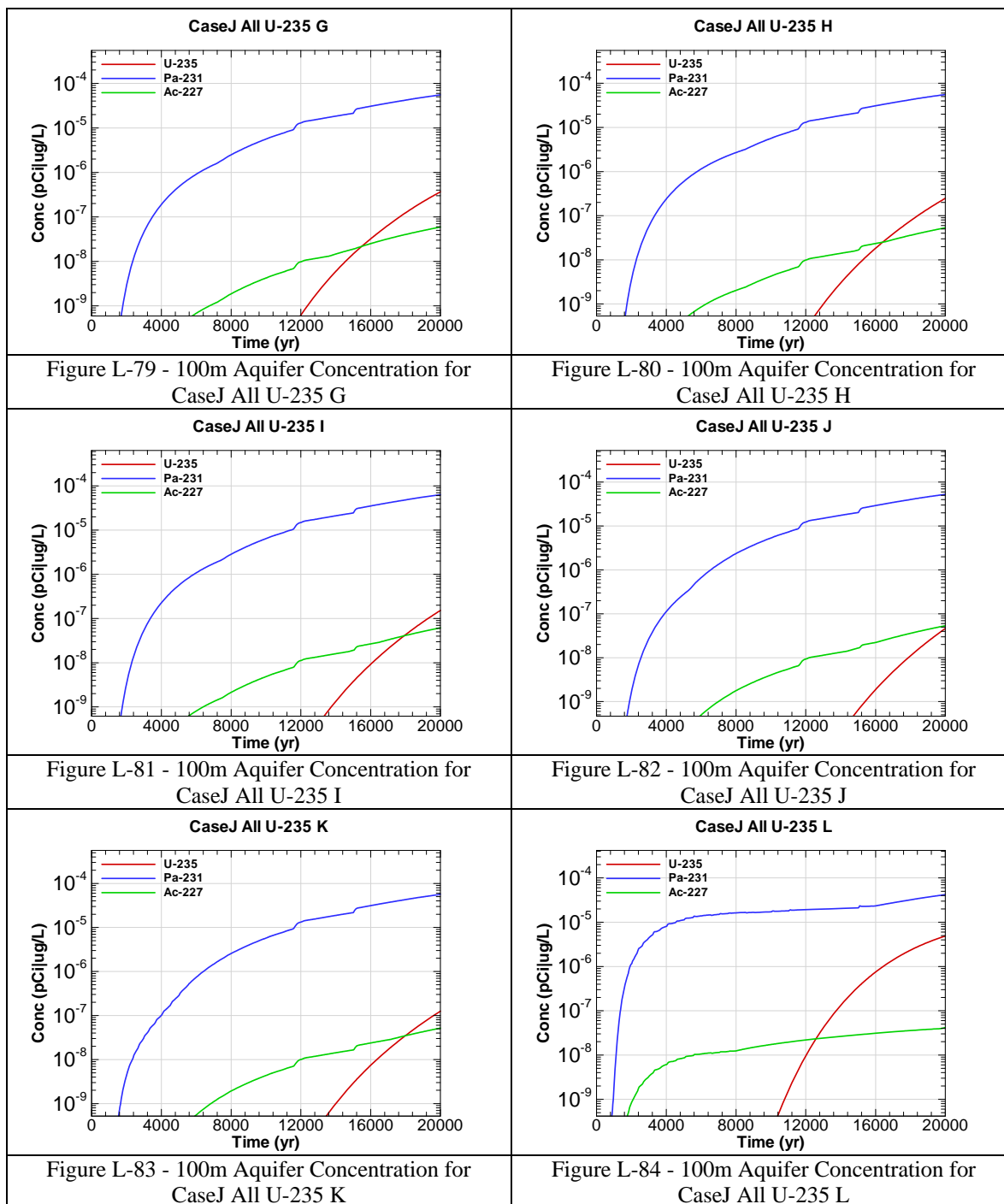


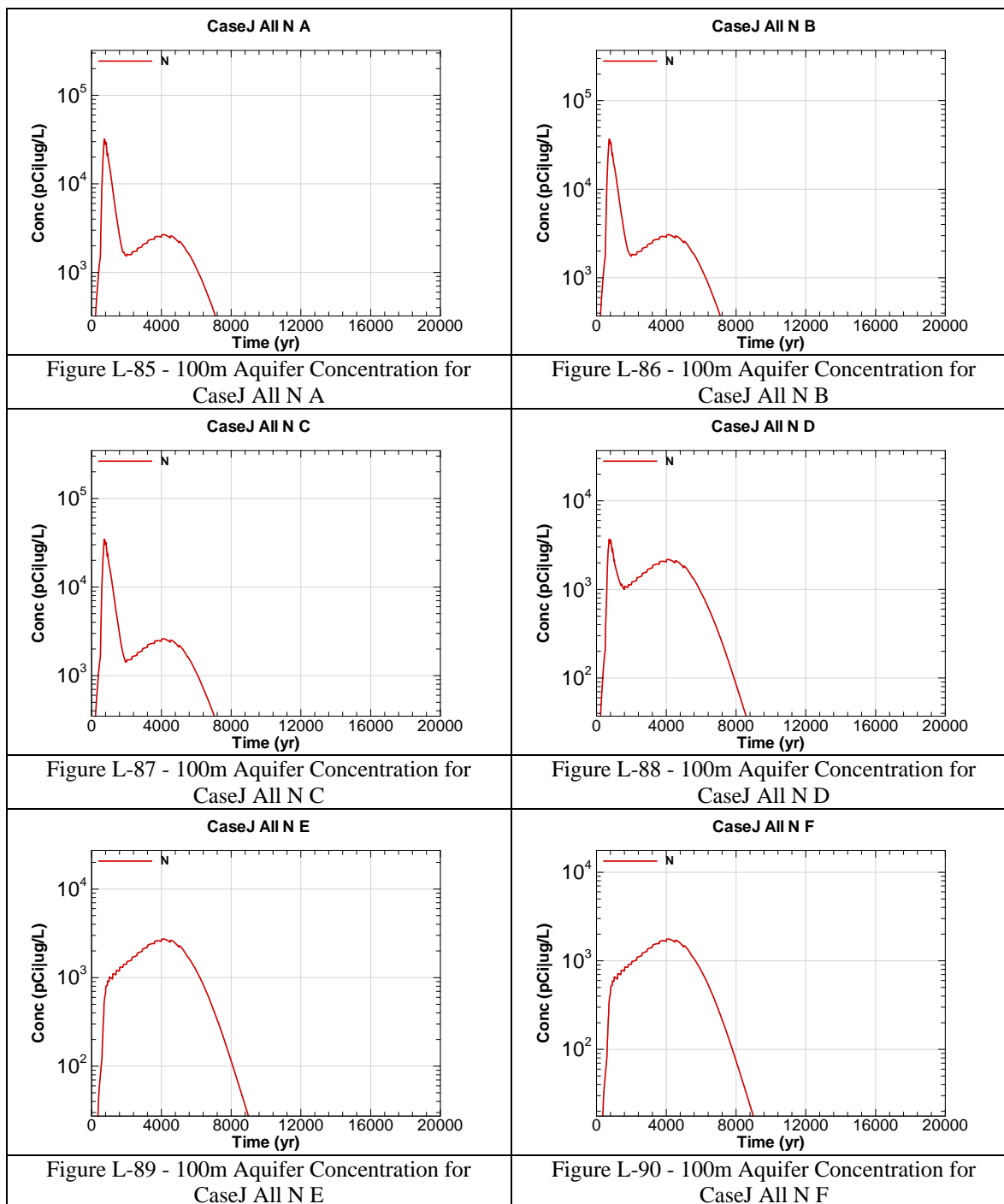


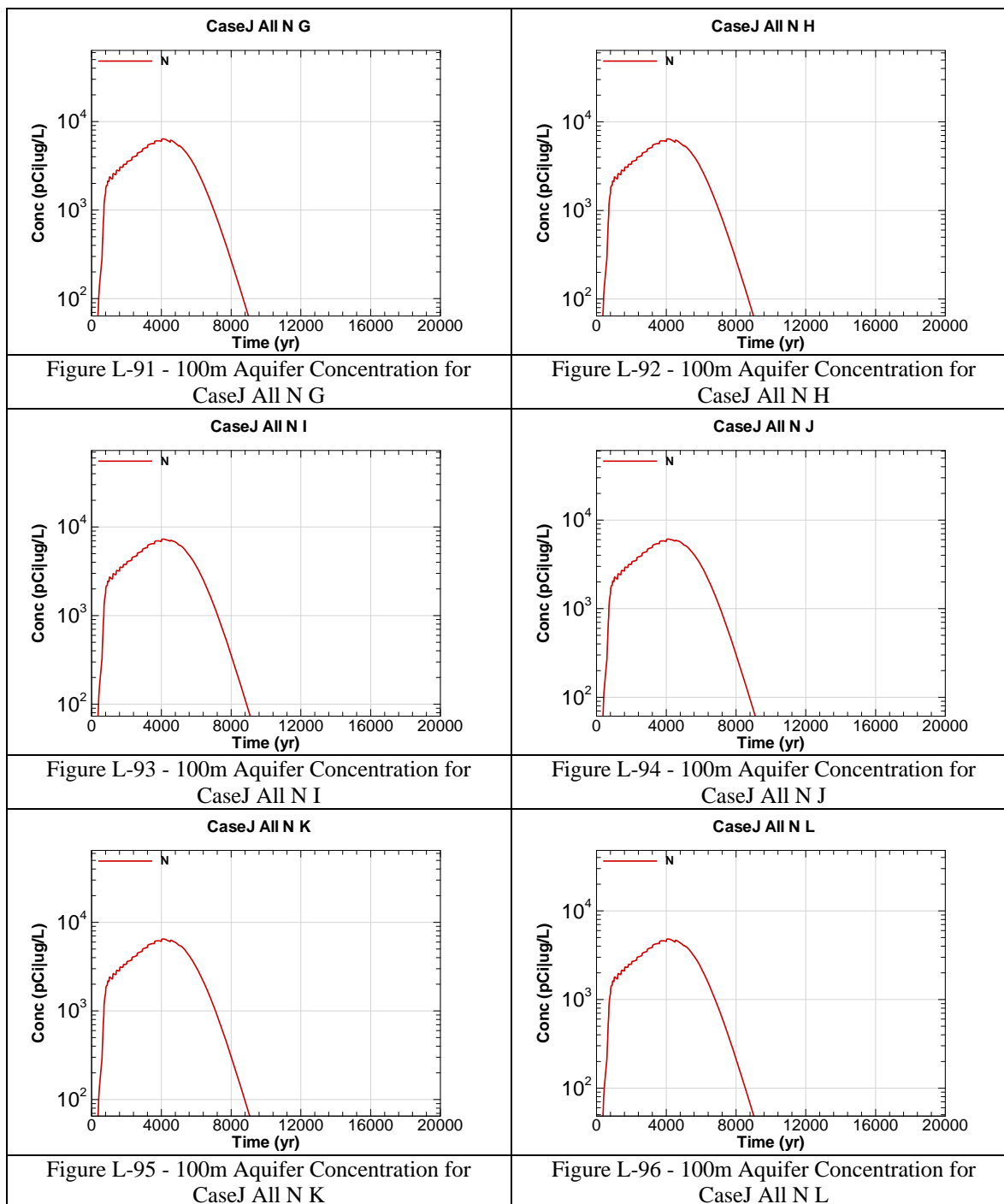












This page intentionally left blank